Canadian Journal of Chemistry

Issued by THE NATIONAL RESEARCH COUNCIL OF CANADA

VOLUME 41 JANUARY 1963 NUMBER 1

Can. J. Chem. Downloaded from www.nrcresearchpress.com by 210.87.254.40 on 09/05/12
For personal use only.

GAS–LIQUID CHROMATOGRAPHY OF TERPENES

PART VII. THE DEHYDRATION OF *p*-MENTHAN-8-OL[1,2,3]

E. VON RUDLOFF

National Research Council of Canada, Prairie Regional Laboratory, Saskatoon, Saskatchewan

Received July 11, 1962

ABSTRACT

Mixtures of *cis*- and *trans*-*p*-menthan-8-ol were prepared by hydrogenation of α-terpineol over platinum or palladium catalysts and the isomer ratios obtained were determined by gas–liquid chromatography. The dehydration of a 1:1 mixture, as well as of the pure stereoisomers, was studied with a number of reagents. Aqueous oxalic and acetic acids, fused potassium hydrogen sulphate, anhydrous oxalic, silicic, and boric acids, and "Florisil" promoted the typical acid-catalyzed dehydration, with *p*-menth-4(8)-ene and smaller amounts of isomeric *p*-menth-8-enes as the primary products, and *p*-menth-3-ene the final product owing to isomerization. With anhydrous silicic acid the latter was obtained in better than 80% yield. With non-acidic alumina, or thionyl chloride in excess pyridine, the main product was *p*-menth-8-ene (up to 90%); no isomerization to *p*-menth-3-ene was obtained. The possible reaction mechanisms are discussed.

INTRODUCTION

Dehydration of suitable terpene alcohols provides a simple means for synthesizing unsaturated terpenes required as reference compounds in gas–liquid chromatography (GLC). In Part II of this series (1) the analysis of the mixture of *p*-menthadienes and oxides obtained in the acid-catalyzed dehydration of α-terpineol (*p*-menth-1-ene-8-ol) was described. More recently (2), the author has reported results obtained in the dehydration of a number of terpene alcohols, including α-terpineol and *p*-menthan-8-ol (dihydro-α-terpineol), with a simple non-acidic reagent, viz., base-modified alumina. The dehydration of *p*-menthan-8-ol by acidic and non-acidic dehydrating agents has now been studied in detail and optimum conditions for the preparation of *p*-menth-3-, -4(8)-, and -8-ene by this means have been determined. Since cis or trans elimination of the elements of water can proceed equally well with *p*-menthan-8-ol, it was hoped that such a study would also provide data on the relative ease of the formation of exocyclic double bonds in cyclohexane derivatives.

In 1910, Béhal (3) hydrogenated α-terpineol over nickel catalyst by the Sabatier–Senderson method and obtained what was then thought to be *cis*-*p*-menthan-8-ol. Shortly afterwards Wallach (4) obtained the solid trans isomer (m.p. 35° C) using colloidal palladium catalyst. Both authors reported that dehydration with acetic acid containing sulphuric acid gave *p*-menth-4(8)-ene. Perkin and Pickles (5) dehydrated *p*-menthan-8-ol

[1]*For Part VI, see Phytochemistry, 1962 (in press).*
[2]*Presented at the 45th Annual Conference of the Chemical Institute of Canada, Edmonton, May 27–31, 1962.*
[3]*Issued as N.R.C. No. 7068.*

Can. J. Chem. Downloaded from www.nrcresearchpress.com by 210.87.254.40 on 09/05/12
For personal use only.

(m.p. 35° C) with fused potassium hydrogen sulphate and reported the isolation of *p*-menth-8-ene. However, Kötz and Busch (6) obtained 87% of theory of *p*-menth-3-ene when this reaction was carried out in a copper autoclave at 200° C for 24 hours. Zeitschel and Schmidt (7) isolated *trans*-p-menthan-8-ol from American pine oil and claim to have obtained the pure cis and trans isomers by fractional distillation. However, their cis isomer was a liquid and gave a phenylurethane, m.p. 90–92° C. Keats (8), on the other hand, obtained solid *cis-p*-menthan-8-ol, m.p. 25° C (phenylurethane m.p. 114° C), and attempted to correlate the stereochemistry of both isomers by conversion, via the chloride, to *cis*- and *trans-p*-menth-8-ene. The above discrepancies were resolved when in 1960 Eastman and Quinn (9) succeeded in obtaining both isomeric alcohols pure (m.p. 35° and 47° C) by fractional distillation through a highly efficient distillation column, and showed that both the pure isomers gave phenylurethanes of m.p. 115–117° C, whereas mixture of these gave phenylurethanes of m.p. 91–97° C. In this study small aliquots of α-terpineol were hydrogenated over either platinum oxide or palladium-on-charcoal and the total product was analyzed by GLC to determine the yield of hydrogenation products and the isomer ratio. The most favorable conditions were then used for preparing a 1:1 mixture of *cis*- and *trans-p*-menthan-8-ol and smaller amounts of the pure isomers. These were then used in the dehydration studies.

EXPERIMENTAL

The gas chromatographic equipment and techniques have been described previously (1, 2, 10). All columns were made up with the stationary phase on Chromosorb W (60–80 mesh) in the weight ratio of 1:6. Retention times were measured from the time of injection to the initial emergence of the peaks (1, 10). The percentage compositions of terpene mixtures were determined by measuring the area under the curves (triangulation method), the error being ±1 to ±5% depending on peak size (see also ref. 11) and degree of separation. Terpene hydrocarbons were analyzed at 65° C (2 m×0.6 mm O.D. columns) or 80° C (4-m columns), and the *p*-menthan-8-ol isomers and unreacted α-terpineol at 100–110° C. The retention times of *p*-menthenes, *p*-cymene, α-terpineol, and the *p*-menthan-8-ols have been described previously (1, 2, 10, 12). The relative rentention times (RRT) of *trans*- and *cis-p*-menthane with respect to limonene (=1.00) were 0.29 and 0.355 on the adipate polyester column (at 65° C) and 0.30 and 0.35 on the polyethylene glycol 1540 column (at 65° C) respectively. Good separation of the hydrocarbons was also obtained on an ethylene glycol bis-(propionitrile)-ether column. With this column *p*-menth-3-ene and camphene were completely separated (RRT 0.33 and 0.42 respectively). Recently, Wilcox *et al.* (13) have shown that in the dehydration of α-terpineol with ethanolic sulphuric acid peak 1 was in fact *p*-menth-3-ene, and not camphene as previously reported (1). This was confirmed by means of this column.

Individual components were isolated by injecting 10- to 50-μl amounts onto the analytical columns and collecting individual peaks, or center cuts thereof, in glass traps which were cooled in an acetone – solid carbon dioxide bath. In preparative runs the detector current was reduced from 250 ma to 100 ma to prevent thermal decomposition (14). The identity of individual components was determined by comparison of infrared spectra and retention data with those of authentic samples. No isomerization of the *p*-menthenes during GLC analysis was encountered. The infrared spectra obtained for *p*-menth-8-, -4(8)-, and -3-ene agreed with those reported by Frank and Berry (15) in all respects. Infrared spectra were recorded as liquid films between sodium chloride plates on a Perkin–Elmer Model 21 double-beam spectrophotometer.

Hydrogenation of α-Terpineol

Commercial α-terpineol (Fisher Scientific Co.), having n_D^{20} 1.4829, $[\alpha]_D^{20}$ +15.1°, was used in all experiments. Small-scale hydrogenation was carried out in a micro hydrogenation apparatus, α-terpineol (10 mg) in solvent (0.5 ml) being reduced in the presence of reduced catalyst (1–5 mg) at room temperature. With platinum oxide (Adam's) catalyst and either methanol or methanol – acetic acid (4:1, v/v) as solvent, the product was found to contain 50–52% *trans*-, 46–48% *cis-p*-menthan-8-ol, and 2% unreacted α-terpineol. Using palladium-on-charcoal catalyst and methanol, the uptake of hydrogen was slower and the product after 48 hours contained 50% unreacted α-terpineol, 35% *trans*-, and 15% *cis-p*-menthan-8-ol. The rate of hydrogenation could be increased by carrying out the reaction at 50–60° C or by adding acetic acid to the solvent, but the product after 48 hours still contained 25% and 10% unreacted α-terpineol respectively. Repeated preparative runs (10-mg scale) on the polyester or polyethylene glycol GLC column gave pure *cis*- and *trans-p*-menthan-8-ol in small amounts. Both crystallized on keeping at 0–2° C, m.p. 33–34° and

42–44° C respectively (lit. m.p. 34.5–35° and 46.7–47° C respectively (9)). No significant optical rotation was recorded.

α-Terpineol (50 g) was added to reduced platinum oxide catalyst (1 g, commercial) in methanol (80 ml) and acetic acid (20 ml). Hydrogenation was continued for 4 days, when the uptake of hydrogen ceased. The mixture was filtered, ether (200 ml) and water (200 ml) were added, and the ether layer was washed repeatedly with a saturated aqueous sodium bicarbonate solution to remove the acetic acid. The neutral ethereal solution was washed with water and the ether was evaporated. The residue (50 g) was shaken with powdered potassium permanganate to remove unreacted α-terpineol. The product was taken up in ether (100 ml), washed with water, and dried over anhydrous sodium sulphate. After evaporation of the ether, the residue (49 g) was distilled at 90 mm pressure to give pure *p*-menthan-8-ol with a ratio of trans to cis isomer of 51:49 (GLC analysis); n_D^{25} 1.4640. The derived phenylurethane had m.p. 90–96° C (lit. 91–91° C (9)).

In another experiment, α-terpineol (100 g) was similarly hydrogenated over reduced palladium-on-charcoal (5 g, 5% commercial). The product (98 g) after neutralization, washing, drying, and removal of solvents was fractionally distilled through a spinning band column (Podbielniak, 8 mm×1 m) at 50 mm pressure and a high reflux ratio. The fraction b.p. 116–118° C (32 g) was redistilled under the same conditions to give practically pure (98%, GLC) *trans-p*-menthan-8-ol (15 g), m.p. 34–35° C, n_D^{25} 1.4622. The derived phenylurethane had m.p. 115–117° C after recrystallization from petrol (b.p. 60–70° C) (lit. m.p. 117° C (9)). Found: C, 73.93; H, 9.06; N, 5.16%. Calculated for $C_{17}H_{25}O_2N$: C, 74.14; H, 9.15; N, 5.09%. By repeated fractional distillation of fractions which contained a high percentage of the cis isomer, the latter was obtained 97% pure (GLC), m.p. 24–28° C, n_D^{25} 1.4658, phenylurethane m.p. 114–116° C (lit. 116° C (9)).

Dehydration Experiments

(1) Aqueous Reagents

p-Menthan-8-ol (1.00 g), oxalic acid dihydrate (3 g), and water (6 ml) were heated under reflux for the desired length of time. The mixture was then steam-distilled for 0.5 hours and the product was extracted with ether (2×5 ml). The ethereal solution was washed with aqueous bicarbonate solution (1 ml), water (2×1 ml), and was dried over anhydrous sodium sulphate. The filtered solution was evaporated to dryness on a steam bath in a flask having a long neck (1). The residue was weighed and analyzed by GLC for the content of hydrocarbons and unreacted starting material. The results obtained are shown in Table I. In the "0" hour experiment the mixture was steam-distilled at once.

TABLE I

Dehydration of *p*-menthan-8-ol with aqueous oxalic acid

Reaction time (hr)	Yield		Unreacted (%)		*p*-Menthenes (%)			
	g	%*	*trans*	*cis*	*trans*-8	*cis*-8	4(8)	3
(*a*) *trans-* + *cis-p*-Menthan-8-ol (51:49)								
0†	0.96	18	43	37	3	2	12	3
1	0.89	74	15	9	8	4	27	35
2	0.915	94	4	2	13	4	33	42
3	0.88	98.5	1	1/2	13	4	29	52
6	0.85	96.5	0	0	11	3	27	58
9	0.82	93	0	0	10	2	20	66
(*b*) *trans-p*-Menthan-8-ol (98%)								
0†	0.98	6	93	—	2	—	3	2
1	0.86	70	25	—	18	—	25	31
2	0.82	89	3	—	19	—	33	45
3	0.84	95.5	1	—	22	—	32	45
6	0.87	99	0	—	20	—	29	51
9	0.83	94.5	0	—	18	—	23	59
(*c*) *cis-p*-Menthan-8-ol (97%)								
3	0.85	96.5	0	0	—	4	28	68

*Percentage yield of hydrocarbons based on theory.
†Direct steam distillation.

In experiments with aqueous acetic acid (50%, v/v) the alcohol (1.0 g) was mixed with the reagent (5.0 ml) and treated as above. The results obtained are shown in Fig. 1.

Can. J. Chem. Downloaded from www.nrcresearchpress.com by 210.87.254.40 on 09/05/12
For personal use only.

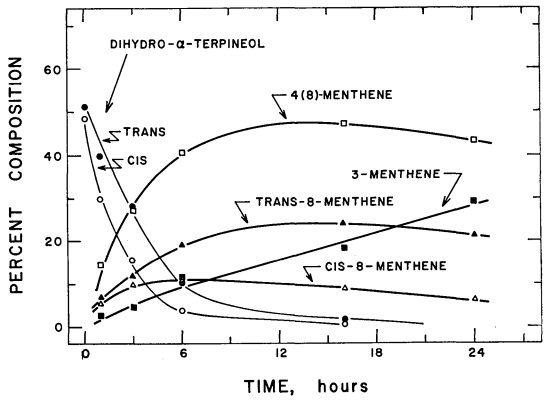

FIG. 1. Dehydration of *p*-menthan-8-ol (51% *trans*, 49% *cis*) with 50% aqueous acetic acid.

(2) Solid Reagents

p-Menthan-8-ol (1.0 g) and the solid reagent (2.0 g) were heated under reflux (210–215° C) for 1 hour. The mixture was steam-distilled and the product isolated and analyzed as above. The results obtained with anhydrous oxalic acid, fused potassium hydrogen sulphate, boric acid, silicic acid, "Florisil" (Floridin Co., Warren, Pa., U.S.A.), sodium sulphate, pyridine-modified alumina (2), and almost neutral alumina (M. Woelm, Eschwege, Germany, activity grade I) are shown in Table II. Because of the low yield of

TABLE II

Dehydration of *p*-menthan-8-ol with solid reagents

	Reaction time (hr)	Yield		Unreacted (%)		*p*-Menthenes (%)			
		g	%*	*trans*	*cis*	*trans*-8	*cis*-8	4(8)	3
(*a*) Acidic reagents									
Anhydrous oxalic acid	1	0.76	89	1	0	19	0	24	56
Anhydrous oxalic acid†	1	0.75	88	0	—	12	0	16	72
Fused $KHSO_4$	1	0.65	75	0	0	20	4	34	42
Boric acid	1	0.64	71	1.5	0.5	28	15	34	21
Anhydrous SiO_2	1	0.73	85	0	0	5	1	11	83
Anhydrous SiO_2	3	0.57	65	0	0	6	1	12	81
Florisil	1	0.71	82‡	0	0	6	1	12	76
Florisil	3	0.56	64§	0	0	5	0	13	51
Florisil	5	0.50	57‖	0	0	3	0	13	38
(*b*) Non-acidic reagents									
Al_2O_3 + 2% pyridine	1	0.87	98	1	0	47	44	8	0
Al_2O_3 (Woelm)	1	0.81	93	1	0	47	40	12	0
Al_2O_3 (Woelm)†	1	0.84	96	0	—	90	0	10	0
Anhydrous Na_2SO_4	1	0.99	5	49	46	2	2	1	0
Anhydrous Na_2SO_4 (×5)	3	0.96	26	42	32	12	9	4	1
[$SOCl_2$–pyridine¶	10 min	0.81	92	0	0	42	33	25	0]

*Percentage yield of hydrocarbons based on theory.
†Reaction with *trans*-*p*-menthan-8-ol (98%).
‡Including 5% *trans*-, 1% *cis*-*p*-menthane, and 2% cymene.
§Including 19% *trans*-, 9% *cis*-*p*-menthane, and 3% *p*-cymene.
‖Including 24% *trans*-, 15% *cis*-*p*-menthane, and 5% *p*-cymene.
¶In solution at room temperature.

dehydration products in the reaction with anhydrous sodium sulphate the reaction was also carried out with five times the amount of reagent. With "Florisil" and alumina the reaction was also carried out for 3 and 5 hours, with heating under reflux, to determine the degree of isomerization and hydrogen transfer.

(3) Dehydration with Thionyl Chloride – Pyridine Reagent (16)

The alcohol (1.00 g) was dissolved in dry pyridine (40 ml) and the solution was cooled to about 5° C. Thionyl chloride (5.0 g) was added dropwise with shaking during 10 minutes. After standing 5 minutes,

Can. J. Chem. Downloaded from www.nrcresearchpress.com by 210.87.254.40 on 09/05/12
For personal use only.

sodium carbonate (3 g) in water (15 ml) was added slowly. The mixture was extracted thrice with ether and the ether layer was washed with saturated tartaric acid solution until all pyridine had been removed. After washing with water the ethereal solution was worked up and analyzed as above (see Table II).

RESULTS AND DISCUSSION

The results obtained in the hydrogenation experiments show that with platinum catalyst at atmospheric pressure α-terpineol is reduced to an approximately 1:1 mixture of *cis*- and *trans*-menthan-8-ol. With palladium catalyst this ratio changes to about 7:2 in favor of the more stable trans isomer. These findings are in accord with those reported for substituted cyclohexenes by Siegel and Smith (17) and also by Sauvage *et al.* (18). Eastman and Quinn (9) report a higher yield of the trans isomer using platinum catalyst, but these authors employed high pressures. Siegel and Smith have shown that the ratio of isomers formed is a function of pressure, as well as of catalyst. The quantitative separation of the two isomers was readily achieved on a milligram scale by GLC on 2-m polyester or polyethylene glycol columns. For larger quantities the less efficient separation by fractional distillation (see ref. 9) was used. However, once preparative GLC in gram amounts has been achieved with the same degree of efficiency as analytical GLC, the preparation and characterization of pure stereoisomeric terpene alcohols of this type should present no more difficulty. Preliminary results in this laboratory indicate that repeated small-scale runs on analytical columns offer a more promising means of achieving this than the use of larger diameter columns (1- to 5-cm diameter) and larger samples (0.1–2 g).

The results of the dehydration of *p*-menthan-8-ol with either aqueous oxalic or acetic acid were similar to those obtained previously with α-terpineol (1), except that with this fully saturated alcohol no side reactions, such as oxide formation, occurred. With aqueous oxalic acid the dehydration was complete in about 3 hours' reaction time, *p*-menth-4(8)- and -3-ene being the major reaction products and the isomeric *p*-menth-8-enes the minor ones (see Table I*a*). As expected, more *trans-p*-menth-8-ene than the cis isomer was formed throughout the reaction. When the reaction was carried out with pure *trans-p*-menthan-8-ol (Table I*b*), no *cis-p*-menth-8-ene was detected, showing that no isomerization from trans to cis isomers occurred during dehydration. Similarly, no isomerization from cis to trans isomer was detected (Table I*c*). With increased reaction time the overall yield of terpenes remained almost constant, but the yield of *p*-menth-3-ene increased at the expense of the other isomers. This is in accord with the findings of Frank and Berry (15), who studied the isomerization of *p*-menth-8-ene. When a mixture of *trans*- and *cis-p*-menth-8-ene (88%) and *p*-menth-4(8)-ene was heated with excess aqueous oxalic acid isomerization to *p*-menth-3-ene proceeded somewhat faster than in the dehydration reaction.

With 50% aqueous acetic acid as dehydrating agent, the reaction not only proceeded very much slower (see Fig. 1) but isomerization was very much reduced. This resulted in an increased yield of *p*-menth-4(8)-ene, e.g. almost 60% in the reaction with *cis-p*-menthan-8-ol. Also, the greater stability of the trans isomers is clearly evident from the slower rate of dehydration of *trans-p*-menthan-8-ol and the higher yield of *trans-p*-menth-8-ene. Both Béhal (3) and Wallach (4) reported that dehydration of *p*-menthan-8-ol with acetic acid containing sulphuric acid gives *p*-menth-4(8)-ene. In the present study, when the alcohol was heated under reflux with glacial acetic acid containing 5% sulphuric acid for 1 hour, the yield of steam-volatile products was low (60%) and polymerization extensive. Since *p*-menth-3-ene was the major hydrocarbon formed (59%) and the 4(8)-isomer was obtained in minor amounts only (6%), this reaction was not investigated

Can. J. Chem. Downloaded from www.nrcresearchpress.com by 210.87.254.40 on 09/05/12
For personal use only.

further. With glacial acetic acid alone the reaction proceeded very slowly (about 50% dehydration in 12 hours) and the product obtained was similar to that formed in the reaction with aqueous acetic acid.

The results obtained with the aqueous acidic reagents can be readily explained by assuming that the dehydration proceeds via carbonium-ion intermediates (E_1 elimination). Protonation of *p*-menthan-8-ol (I) and subsequent loss of the elements of water would lead to carbonium ion II. Loss of a proton can then result in the formation of either *p*-menth-8-ene (III) or the 4(8)-isomer (IV). Rearrangement of the carbonium ion II to one with the charge at carbon 4 (V) followed by loss of a proton could then result in the formation of either *p*-menth-3-ene (VI) or -4(8)-ene (IV). Since these steps are reversible, reprotonation of III, IV, and VI may be assumed to take place. This would account for the isomerization of *p*-menth-8- and -4(8)-ene to *p*-menth-3-ene. Thus, in the initial steps formation of an exocyclic double bond is the preferred reaction route, and only in the subsequent isomerization is the more stable *p*-menth-3-ene formed. This is clearly borne out in the experiments with 50% aqueous acetic acid, where the acid strength has been reduced to such an extent that isomerization proceeds only very slowly (see Fig. 1).

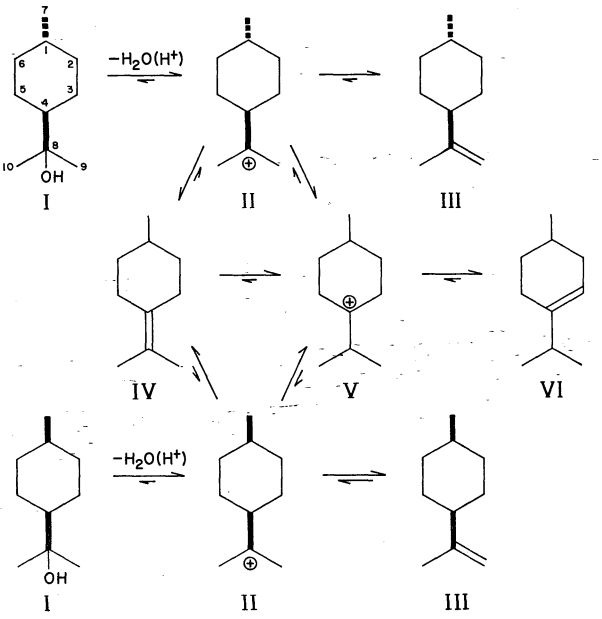

With solid anhydrous acids the reaction proceeds similarly (see Table II*a*) but much faster (especially isomerization), presumably due to the higher temperature of reaction. Fused potassium hydrogen sulphate gave a mixture of hydrocarbons very similar to that obtained with aqueous oxalic acid, confirming in part the findings of Kötz and Busch (6). Semmler and Rimpel (19) have pointed out that this reagent does not give a single product. With boric acid the relative yield of *p*-menth-3-ene was much lower and that of the *p*-menth-8-enes considerably higher, as would be expected for a weak acid. Anhydrous oxalic acid, "Florisil" (a commercial silica containing about 15% MgO, see also ref. 20), and especially anhydrous silica gave high yields of *p*-menth-3-ene. Increased reaction times did not increase the relative yields of this isomer, but caused overall losses due to

Can. J. Chem. Downloaded from www.nrcresearchpress.com by 210.87.254.40 on 09/05/12
For personal use only.

resinification. With "Florisil" a new side reaction occurred, *trans*- and *cis*-*p*-menthane and *p*-cymene being formed in increasing amounts with increasing reaction times. Thus, this reagent not only catalyzes dehydration but causes hydrogen transfer between the monoolefins to give the saturated and aromatic analoges. *p*-Menthadienes were not found in the reaction product. Recently, Wilcox *et al.* (13) have shown that dehydration of α-terpineol with ethanolic sulphuric acid gave, amongst others, *p*-menth-3-ene, and not camphene as previously reported (1) (see also Experimental). The formation of *p*-menth-3-ene in conjunction with *p*-cymene shows that hydrogen transfer can take place readily with acidic reagents.

With the non-acidic reagents the ratio of *p*-menthene isomers obtained is significantly different (see Table II*b*). These reagents give *p*-menth-8-ene as the main reaction product, smaller amounts of the 4(8)-isomer, but no *p*-menth-3-ene. Thus this dehydration proceeds in an anti-Saytzeff (Hofmann) orientation and without isomerization of the resulting olefins. The reaction is similar to the homogeneous elimination with thionyl chloride in excess pyridine (see Table II*b*) and forms an excellent complement to the acid-catalyzed dehydration.

Since pyridine-modified alumina dehydrates *l*-menthol mainly to *p*-menth-2-ene (*trans*) and less *p*-menth-3-ene (2), the reaction does not involve pyrolytic cis elimination of the elements of water (21). Pines and co-workers (22, 23) have proposed for the gas-phase dehydration of alcohols with ammonia-modified alumina a concerted mechanism involving both acidic and basic sites. These authors suggest that isomerization is suppressed by neutralization of the strong acid sites by the weak base. Beranek *et al.* (24) have shown that in gas-phase dehydrations over pyridine-modified alumina the active centers responsible for dehydration differ from those causing isomerization of olefinic double bonds. Since in the present study the dehydration with base-modified alumina was carried out at the boiling point of the alcohol, it is possible that the reaction proceeds by the same mechanism as in gas-phase dehydration. However, even though it seems probable that a concerted E_2 elimination takes place, this in itself does not account for an anti-Saytzeff oriented loss of the elements of water. Anti-Saytzeff orientation in E_2 eliminations is thought by Hughes and Ingold (25, 26) to be due to inductive control. Brown *et al.* (27, 28), on the other hand, propose that steric influences are the deciding factors in determining the direction of elimination. However, these authors have based their proposals on elimination reactions of substituted alcohols (ammonium, sulphonium, and sulphoxonium compounds) and the results obtained in this study with alumina catalyst on the free alcohol could not be correlated with these proposals.

Brown's view (29, 30) that introduction of a trigonal atom is resisted in cyclohexanes would favor the formation of *p*-menth-8-ene. Whereas this view is supported by the results obtained in the dehydration with alumina or thionyl chloride in excess pyridine, it does not hold for the acid-catalyzed reaction. In the latter type of reaction both *p*-menthan-8-ol and α-terpineol (1) give the exocyclic derivative as the primary dehydration product. Thus, there appears to be an inherent contradiction in Brown's proposal. The dehydration of other terpene alcohols is being studied in the hope of obtaining further insight into the reaction mechanism.

The present study has shown that dehydration of *p*-menthan-8-ol with solid reagents is useful for the preparation of either *p*-menth-8-ene or -3-ene. It should be pointed out that the use of solid reagents simplifies experimental procedure since, after reflux, the resulting hydrocarbons may be simply distilled off and used as reference compounds as such. Although *p*-menth-4(8)-ene was formed in every instance, its yield was usually

Can. J. Chem. Downloaded from www.nrcresearchpress.com by 210.87.254.40 on 09/05/12
For personal use only.

low and rose above 50% yield only when aqueous acetic acid was used. For reference purposes in GLC studies it is often quite advantageous to have more than one isomer present in the test mixture, and the product obtained with, for example, boric acid can serve to establish the relative retention times of the four *p*-menthene isomers under discussion.

ACKNOWLEDGMENTS

The helpful discussions with Dr. A. S. Perlin are gratefully acknowledged. Thanks are also due to Mr. M. Granat for technical assistance and Mr. W. C. Haid for recording the infrared spectra.

REFERENCES

1. E. von Rudloff. Can. J. Chem. **39**, 1 (1961).
2. E. von Rudloff. Can. J. Chem. **39**, 1860 (1961).
3. A. Béhal. Compt. Rend. **150**, 1762 (1910); Chem Abstr. 4, 2936² (1910).
4. O. Wallach. Ann. **381**, 55 (1911).
5. W. H. Perkin and J. Pickles. J. Chem. Soc. **87**, 639, 650 (1905).
6. A. Kötz and G. Busch. J. Prakt. Chem. **119**, 1 (1928).
7. O. Zeitschel and H. Schmidt. Ber. **60**, 1376 (1927).
8. G. H. Keats. J. Chem. Soc. 2003 (1937).
9. R. H. Eastman and R. A. Quinn. J. Am. Chem. Soc. **82**, 4249 (1960).
10. E. von Rudloff. Can. J. Chem. **39**, 1190 (1961).
11. J. Jának. J. Chromatog. **3**, 308 (1960).
12. W. J. Zubyk and A. Z. Conner. Anal. Chem. **32**, 912 (1960).
13. C. F. Wilcox, M. F. Wilcox, and S. S. Chibber. J. Org. Chem. **27**, 2285 (1962).
14. E. von Rudloff. Can. J. Chem. **38**, 631 (1960).
15. R. L. Frank and R. E. Berry. J. Am. Chem. Soc. **72**, 2985 (1950).
16. O. Motl, V. Herout, and F. Šorm. Collection Czech. Chem. Commun. **23**, 1293 (1958).
17. S. Siegel and G. V. Smith. J. Am. Chem. Soc. **82**, 6082, 6087 (1960).
18. J. F. Sauvage, R. H. Baker, and A. S. Hussey. J. Am. Chem. Soc. **82**, 6090 (1960).
19. F. W. Semmler and Ch. Rimpel. Ber. **39**, 2582 (1906).
20. R. H. Bible, Jr. and N. W. Atwater. J. Org. Chem. **26**, 1336 (1961).
21. D. H. R. Barton. J. Chem. Soc. 2174 (1949).
22. H. Pines and C. N. Pillai. J. Am. Chem. Soc. **82**, 2401 (1960).
23. H. Pines and W. O. Haag. J. Am. Chem. Soc. **82**, 2471 (1960).
24. L. Beranek, M. Kraus, K. Kochloefl, and V. Bazant. Collection Czech. Chem. Commun. **25**, 2513 (1960).
25. E. D. Hughes and C. K. Ingold. Trans. Faraday Soc. **37**, 657 (1947).
26. C. K. Ingold. Structure and mechanism in organic chemistry. Cornell University Press. 1953. Chap. VIII, especially p. 445.
27. H. C. Brown and I. Moritani. J. Am. Chem. Soc. **78**, 2203 (1956).
28. H. C. Brown. J. Chem. Soc. 1248 (1956).
29. H. C. Brown, J. H. Brewster, and H. Shechter. J. Am. Chem. Soc. **76**, 467 (1954).
30. H. C. Brown. J. Org. Chem. **22**, 439 (1957).

Can. J. Chem. Downloaded from www.nrcresearchpress.com by 210.87.254.40 on 09/05/12
For personal use only.

ELECTRON SPIN RESONANCE OF AN X-RAY IRRADIATED SINGLE CRYSTAL OF DIKETOPIPERAZINE

W. C. LIN AND C. A. MCDOWELL

Department of Chemistry, University of British Columbia, Vancouver, British Columbia

Received August 20, 1962

Can. J. Chem. Downloaded from www.nrcresearchpress.com by 210.87.254.42 on 09/05/12
For personal use only.

ABSTRACT

The electron spin resonance of an X-ray irradiated single crystal of diketopiperazine has been measured at 9 Gc/sec for various orientations of the crystal in the static magnetic field. From an analysis of the hyperfine structure observed we have been able to calculate the components of the hyperfine interaction tensor for the radical produced by the irradiation. The principal values for the hyperfine interaction tensor are similar to those found for the radical produced by the X-ray or γ-ray irradiation of glycylglycine and N-acetylglycine and is therefore attributed to a radical with a C—H fragment. The fine details of the spectrum indicate that the radical responsible for the electron resonance observed probably has the structure

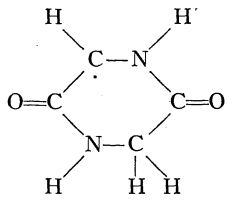

which is formed from diketopiperazine by the loss of a hydrogen atom from one of the CH_2 groups in that molecule.

INTRODUCTION

The study of the electron spin resonance spectra of the long-lived radicals produced in organic crystalline compounds by X-ray and γ-ray irradiation has led to much valuable information on the structures of the various paramagnetic species. In many cases the identity of the radical produced has been unequivocally established and in others the probable nature of the radical has been clearly indicated. Amongst the many examples known mention may perhaps be made of the studies on the radicals produced in single crystals of malonic acid (1), succinic acid (2), glycollic acid (3), glutaric acid (4), glycine (5, 6), *dl*-alanine (7–9), and glutamic acid HCl (10). The e.s.r. spectra of γ-irradiated single crystals of more complex compounds derived from amino acids have been studied by Gordy and his co-workers and several other groups. These works have led to an understanding of the nature of the radicals produced in N-acetylglycine (11), glycylglycine (12–14), and urea oxalate (15). In many of these latter cases it appeared that the radical was formed by the loss of a hydrogen atom during the irradiation process. The resulting radical gave an electron resonance largely dominated by the hyperfine splitting splitting from a CH group. It was, therefore, of interest to study the radical resulting from the X-ray irradiation of diketopiperazine, the anhydride of glycine, and this paper describes the results of our experiments which led to the identification of the radical responsible for the observed electron spin resonance. We have also determined the principal values of the components for the hyperfine interaction tensor and their direction cosines.

EXPERIMENTAL

The single crystals of diketopiperazine grown from aqueous solution by slow evaporation were monoclinic prisms with the 010 face dominant. The cell constants as determined by Bernal (16) and Corey (17) are: space group $P2_1/a$, $a = 5.19$ Å, $b = 11.50$ Å, $c = 3.96$ Å, $\beta = 97°$. There are two molecules per unit cell. Carefully chosen crystals were irradiated at room temperature with 50 kv X rays for several hours. The irradiated crystals were studied at 9 Gc/sec in our e.s.r. spectrometer using 10 kc/sec modulation and a cavity operating on the TE_{012} mode. A 6-inch Varian magnet with pole shims supplied the magnetic field. The angular rotation of the crystals could be measured to about $\pm 2°$, and the hyperfine splitting constants are probably correct to about ± 0.5 gauss.

A diagram of the crystal and its axes is given in Fig. 1, which also shows the reference set of axes a', b', and c' chosen for our studies. With the chosen orthogonal set of axes the alignment of the crystal could be made more accurately than with any other choice.

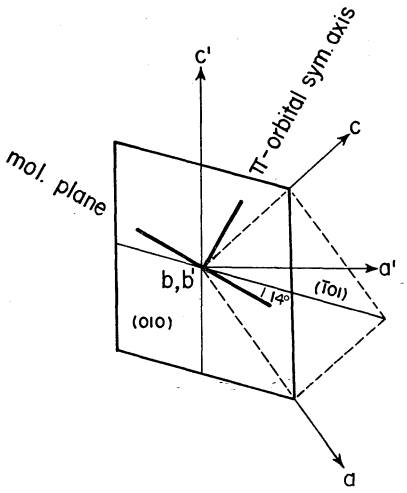

FIG. 1. Relation between crystal axes a, b, c and reference axes a', b', c'. The dotted outline shows the unit cell. The orientation of the radical is also indicated in the figure by the heavy lines. The direction of the CH bond is not indicated in the figure but it is perpendicular to the (010) plane.

RESULTS AND DISCUSSION

The energy levels for an oriented radical in a single crystal in an external magnetic field can be calculated from the spin Hamiltonian

$$[1] \qquad \mathcal{H} = \beta \mathbf{H} \cdot \mathbf{g} \cdot \mathbf{S} + \mathbf{S} \cdot \mathbf{A} \cdot \mathbf{I} - g_n \beta_n \mathbf{H} \cdot \mathbf{I}.$$

Our data can be interpreted in terms of these levels. For most orientations the observed spectra can be regarded as consisting of a main doublet which is split further into triplets of intensity ratio 1:2:1. Figures 2, 3, and 4 show three main types of spectra observed,

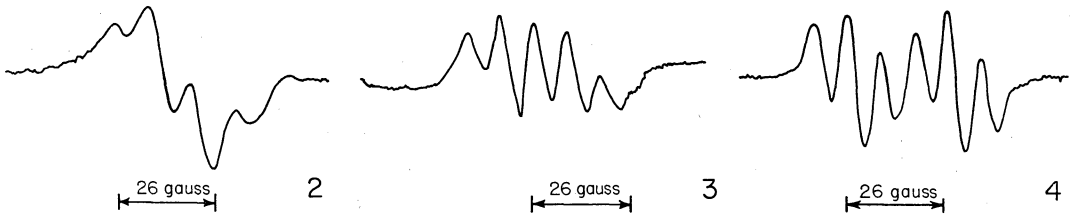

FIG. 2. Electron spin resonance spectrum of an X-ray irradiated single crystal of diketopiperazine (H_0 direction cosines: 0,1,0).

FIG. 3. Electron spin resonance spectrum of an X-ray irradiated single crystal of diketopiperazine (H_0 direction cosines: 0.766,0.643,0).

FIG. 4. Electron spin resonance spectrum of an X-ray irradiated single crystal of diketopiperazine (H_0 direction cosines: 3/2,0,1/2).

Can. J. Chem. Downloaded from www.nrcresearchpress.com by 210.87.254.42 on 09/05/12
For personal use only.

which correspond to four, five, and six lines with intensity ratios 1:3:3:1, 1:2:2:2:1, and 1:2:1:1:2:1 respectively. The splitting of the main doublet is anisotropic and varies between 7 and 27 gauss but the triplet splitting is almost isotropic and approximately 9 gauss in extent. Experimental values of the observed hyperfine interactions at different orientations enabled the hyperfine interaction tensor to be evaluated with respect to the a', b', c' system of axes. The principal values of the hyperfine interaction tensor and the respective direction cosines are given in Table I.

TABLE I

Direction cosines of principal values of the interaction tensor **A** of 1,4-diketopiperazine radical with respect to the a', b', c' system of axes

Principal values (gauss)	Direction cosines		
	l	m	n
7.4	0	1	0
15.9	1/2	0	3/2
26.5	3/2	0	−1/2
Isotropic component = 16.6 gauss			

The theory of the π-electron–σ-proton hyperfine interaction is well known (1, 2). The isotropic portion of the coupling constant is given by $A_H = Q\rho$, where ρ is the π-electron density at the adjacent carbon atom. Using the value of $Q \simeq 23$, it follows from the data in Table I that the π-electron density on the carbon atom of the interacting CH group is approximately 0.72. The principal axis corresponding to the smallest principal value (7.4 gauss) lies parallel to the direction of the σ-CH bond. The intermediate principal value is parallel to the π-orbital symmetry axis, i.e. normal to the 'molecular' plane. These results are similar to those found for the radicals formed in single crystals of N-acetylglycine, glycylglycine, and urea oxalate. The orientation of the radical may now be calculated. It is indicated in Fig. 1 by the heavy lines. This calculated orientation agrees well with the molecular orientation deduced from Corey's (17) results. These indicate that the diagonal joining the two CH_2 groups is approximately parallel to the b-axis and that the molecule is parallel to the $\bar{1}01$ plane, which is also shown in Fig. 1. There is a difference of 14° between the radical plane, as calculated, and the molecular plane, which is taken to be the $\bar{1}01$ plane. There might thus be a slight reorientation of the molecule as the result of X-ray bombardment to form the free radical. It is to be noted that the molecules in this crystal are not extensively hydrogen bonded.

In the crystals of diketopiperazine the molecules are approximately planar hexagonal and possess a center of symmetry. Although the unit cell contains two molecules which are differently orientated, the planes of the two molecules are nearly parallel. The positions of the CH_2 groups are such that the CH bonds of two adjacent radicals would be nearly parallel, and for monoclinic crystals both would be almost parallel to the b-axis. For these reasons only one pair of doublets is observed for all orientations of the crystal. Thus the structure of the free radical formed by the X-ray irradiation of diketopiperazine is that shown in Fig. 5.

The small, almost isotropic triplet splitting observed is attributed to the hyperfine interaction between the odd π-electron and the two protons of the undamaged methylene group. This is the so-called π-electron–π-proton interaction (2) whch is found in various radicals, such as those formed by irradiation of succinic acid (2, 3), glutaric acid (4),

Can. J. Chem. Downloaded from www.nrcresearchpress.com by 210.87.254.42 on 09/05/12
For personal use only.

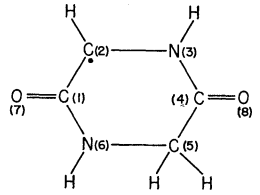

FIG. 5.

glutamic acid HCl (5), etc. Heller and McConnell (2) have proposed that the isotropic interaction b_N due to a π-proton is directly proportional to the spin density ρ_N on the neighboring unsaturated carbon atom, i.e.

$$[2] \qquad b_N = \rho_N B \cos^2 \theta,$$

where B is a constant = 40 gauss (for the $(CH_3)_2COH$ radical), and θ is the angle between the π-orbital and the projection of the π-proton C—H bond along the C—C bond onto the orbital, i.e. $\theta = 0$ when the π-proton CH bond is parallel to the π-orbital symmetry axis. In the present case $\theta = 30°$ and therefore $B \cos^2 \theta = 30$ gauss. The observed triplet splitting of 9 gauss corresponds to an odd π-electron density of 0.3 at the carbon atom adjacent to the methylene group. Of course the odd π-electron density could also be at the adjacent nitrogen atom but then the magnitude would be different as presumably the values of ρ and B would not be the same as for the carbon atom. Nevertheless it seems unlikely that the odd electron density is ever very high at the nitrogen atoms; otherwise a large nitrogen hyperfine interaction would surely have been observed.

The occurrence of an appreciable spin density at carbon atom C(4) can be understood from the following considerations. A possible valence bond structure for the radical is shown below:

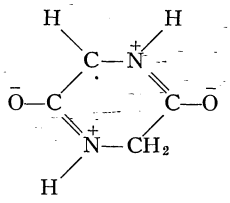

(I)

from which the following structures, II and III, are easily formed:

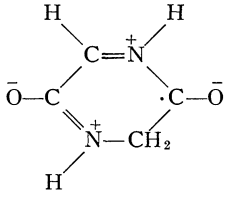

(II)

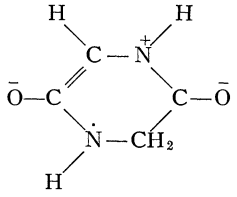

(III)

In these structures it is evident that an appreciable spin density is possible at carbon atom C(4) and nitrogen atom N(6).

It is, of course, also possible to account for a high spin density on carbon atom C(4) on the molecular orbital basis. In this case it is assumed that a delocalized π-orbital is

Can. J. Chem. Downloaded from www.nrcresearchpress.com by 210.87.254.42 on 09/05/12
For personal use only.

formed involving atoms C(2), N(3), C(4), and O(8). Electron spin resonance studies on various amino quinones (18), amine cations (19), and diazine anions (20) have shown that such conjugation systems are common in heterocyclic free radicals. From this molecular orbital viewpoint the radical can be regarded as forming a structure like IV,

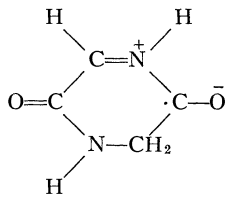

(IV)

which gives a high spin density at carbon atom C(4) because of the assumed π-orbital involving the above-mentioned four atoms, i.e. C(2), N(3), C(4), and O(8).

In both structures II and III it is possible for interaction to occur between the unpaired π-electron and the two methylene protons by the mechanism of hyperconjugation. This type of interaction is known to be almost isotropic and if the two protons are placed symmetrically with respect to the π-orbital symmetry plane (as is the case in the radical from diketopiperazine) the two coupling constants would be equal and a triplet structure with a 1:2:1 intensity ratio would be expected. This is in accord with our experimental observations. Furthermore, as has already been pointed out, it is unlikely that there is an appreciable spin density at the nitrogen atom N(6) and so we must conclude that valence bond structure III predominates in the radical along with structure I.

ACKNOWLEDGMENTS

We are indebted to the Defense Research Board and the National Research Council for generous support of this research work. Professor I. Miyagawa, Institute of Solid State Physics, University of Tokyo, has also studied the e.s.r. spectra of X-ray irradiated single crystals of diketopiperazine and obtained similar results. We are indebted to Professor Miyagawa for sending us a copy of his report in advance of publication.

REFERENCES

1. H. M. McCONNELL, C. HELLER, T. COLE, and R. W. FESSENDEN. J. Am. Chem. Soc. **82**, 766 (1960).
2. C. HELLER and H. M. McCONNELL. J. Chem. Phys. **32**, 1535 (1960).
3. N. M. ATHERTON and D. H. WHIFFEN. Mol. Phys. **3**, 103 (1960).
4. A. J. HORSFIELD, J. R. MORTON, and D. H. WHIFFEN. Mol. Phys. **4**, 169 (1961).
5. D. H. GHOSH and D. H. WHIFFEN. Mol. Phys. **2**, 285 (1959).
6. A. J. HORSFIELD, C. A. McDOWELL, and W. C. LIN. Unpublished experiments. (See Proc. Fourth Intern. Symposium on Free Radicals, Dunbarton College. 1959. p. D-IV-1.)
7. I. MIYAGAWA and W. GORDY. J. Chem. Phys. **32**, 255 (1960).
8. J. R. MORTON and A. J. HORSFIELD. J. Chem. Phys. **35**, 1142 (1961).
9. W. C. LIN and C. A. McDOWELL. Can. J. Chem. **40**, 1060 (1962).
10. W. C. LIN, C. A. McDOWELL, and J. R. ROWLANDS. J. Chem. Phys. **35**, 757 (1961).
11. I. MIYAGAWA, Y. KURITA, and W. GORDY. J. Chem. Phys. **33**, 1595 (1960).
12. W. C. LIN and C. A. McDOWELL. Mol. Phys. **4**, 333 (1961).
13. I. MIYAGAWA, Y. KURITA, and W. GORDY. J. Chem. Phys. **33**, 1599 (1960).
14. H. C. BOX, H. G. FREUND, and K. LILGA. Free radicals in biological systems. Academic Press, New York. 1961. p. 239.
15. D. V. G. L. RAO and W. GORDY. J. Chem. Phys. **35**, 362 (1961).
16. J. D. BERNAL. Z. Krist. **78**, 363 (1931).
17. R. B. COREY. J. Am. Chem. Soc. **60**, 1598 (1938).
18. Y. MATSUNAGA and C. A. McDOWELL. Can. J. Chem. **38**, 1167 (1960).
19. M. T. MELCHIOR and A. H. MAKI. J. Chem. Phys. **34**, 471 (1961).
20. C. A. McDOWELL, J. R. ROWLANDS, and K. F. PAULUS. Proc. Chem. Soc. 60 (1962).

Can. J. Chem. Downloaded from www.nrcresearchpress.com by 210.87.254.42 on 09/05/12
For personal use only.

STEREOCHEMISTRY OF ARSENIC

PART VI. TRI-*p*-TOLYLARSINE

J. TROTTER

Department of Chemistry, University of British Columbia, Vancouver, British Columbia

Received August 7, 1962

ABSTRACT

Crystals of tri-*p*-tolylarsine are rhombohedral, with cell dimensions $a = 9.84$ Å, $\alpha = 80° 2'$, and space group $R\bar{3}$. There are two molecules in the unit cell, and hence the molecule has symmetry C_3. The structure has been determined from a projection along the rhombohedral cell axis, and the bond lengths and valency angles are given. In comparison with an ideal model having maximum interaction between the arsenic lone pair and the aromatic π-electrons, each ring is rotated about its As—C bond by 36°, the three rotations being in the same sense. These displacements increase overcrowded distances in the ideal model to about the normal van der Waals separations, the closest intramolecular contacts between *p*-tolyl groups being C···C = 3.4 Å and H···H = 2.8 Å. All the intermolecular contacts correspond to van der Waals interactions.

INTRODUCTION

The crystal structure of tri-*p*-tolylarsine has been examined as part of a series of investigations of arsenic derivatives. The chief points of interest in this molecule are the values of the C—As—C angles and the rotations of the aromatic rings from the positions which they would occupy in an "ideal" structure (1).

EXPERIMENTAL

Crystals of tri-*p*-tolylarsine are colorless rhombs with {100} forms developed. The density was measured by flotation in aqueous potassium iodide, and the unit cell dimensions and space group were determined from precession films (Mo $K\alpha$ radiation, $\lambda = 0.7107$ Å).

Crystal Data

Tri-*p*-tolylarsine, $C_{21}H_{21}As$; $M = 348.3$; m.p. = 148–149° C

Rhombohedral, $a = 9.84$ Å, $\alpha = 80° 2'$

Volume of the unit cell = 914 Å^3

D_{calc} (with $Z = 2$) = 1.258, D_{meas} = 1.25 g cm^{-3}

Absorption coefficient for X rays, $\lambda = 0.7107$ Å, $\mu = 19.4$ cm^{-1}

$F(000) = 360$

The Laue group is $\bar{3}$ and there are no systematically absent reflections; therefore the space group is $R3$ or $R\bar{3}$.

The intensities of the $hk0$ reflections were recorded on precession films, estimated visually, and the structure amplitudes derived as usual. No absorption corrections were applied, and the absolute scale was established later by correlation with the calculated structure factors.

Structure Analysis

Since there are only two molecules in the cell, they must have symmetry C_3, with their threefold axes coincident with the space group symmetry axis. The arsenic atoms occupy the special positions xxx, $\bar{x}\bar{x}\bar{x}$ (even if the true space group is the one of lower symmetry, the origin can be chosen midway between the arsenic atoms). The arsenic positions were determined from the Patterson line $P(xx0)$, and an electron-density projection along the principal cell axis was computed with signs based on the As contributions only. This map was necessarily centrosymmetric, and it could be interpreted in terms of space group $R\bar{3}$. Carbon atom coordinates —x, y, and z— were derived and refinement proceeded by several cycles of F_o synthesis, the final electron-density projection being shown in Fig. 1. Although the resolution is rather poor, as a result of the trigonal symmetry of the structure the projection is quite sensitive to small changes in orientation of the *p*-tolyl groups. It was possible therefore to determine the carbon atom positions more precisely than the general appearance of Fig. 1 would suggest.

Can. J. Chem. Downloaded from www.nrcresearchpress.com by 210.87.254.42 on 09/05/12
For personal use only.

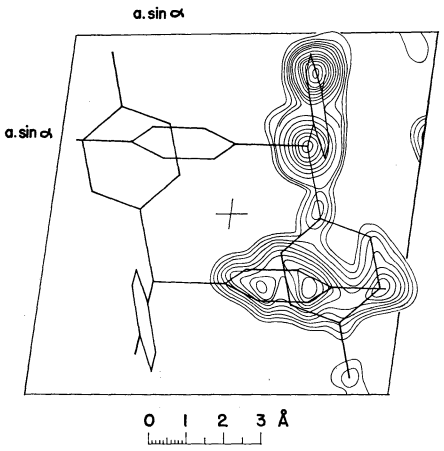

FIG. 1. Electron-density projection along the rhombohedral cell axis; contours at intervals of 1 e Å^{-2} (lowest contour 2 e Å^{-2}) except at the arsenic atom where contours are at 5 e Å^{-2}.

An (F_o—F_c) synthesis was then computed; since many of the atoms were close together in projection, this map was not very useful, but it was possible to make a few small adjustments in the carbon atom positions. The final measured and calculated structure factors are available from the author on request, the discrepancy factor, for the 95 observed reflections, being 0.15. The scattering factors used were those listed by Sagel (2), with $B = 6.5$ Å^2 for all the atoms.

Coordinates and Molecular Dimensions

The final positional parameters of the atoms are listed in Table I, x, y, z being fractional coordinates referred to the rhombohedral crystal axes, and X, Y, Z coordinates in Å with respect to orthohexagonal

TABLE I

Final positional parameters

Atom	x	y	z	X	Y	Z
As	0.1867	0.1867	0.1867	0	0	3.692
C_1	0.251	−0.014	0.192	1.677	−0.537	2.828
C_2	0.392	−0.065	0.151	2.898	0.088	3.144
C_3	0.439	−0.207	0.156	4.094	−0.296	2.551
C_4	0.343	−0.301	0.201	4.075	−1.315	1.602
C_5	0.201	−0.251	0.244	2.853	−1.961	1.285
C_6	0.155	−0.108	0.238	1.664	−1.567	1.879
C_7	0.393	−0.454	0.208	5.359	−1.742	0.969

axes a, b, and c. The standard deviations were calculated from Cruickshank's (3) formulae, the mean values being $\sigma(x) = \sigma(y) = \sigma(z) = 0.007$ Å for As and 0.05 Å for C. These formulae are not strictly applicable in the present case where there is considerable overlap in projection. This factor, however, is probably cancelled out by the fact that each coordinate has effectively been measured twice.

The best plane through the p-tolyl group given in Table I has the equation

$$+0.1546X - 0.6692Y + 0.7268Z = 2.6835$$

and all the atoms listed in Table I, including the As atom, were found to lie within ±0.01 Å from this plane. The other p-tolyl groups are of course related by the trigonal symmetry.

The bond lengths and valency angles in the molecule, calculated from the coordinates of Table I, are shown in Fig. 2. The closest intramolecular contacts between the p-tolyl groups are C_2—C_6' = 3.43 Å and H_2—H_6' = 2.81 Å (assuming that the hydrogen atoms lie on the ring diagonals with C—H = 1.08 Å).

DISCUSSION

Differences between chemically equivalent bond lengths and valency angles are not significant, the mean values, with standard deviations, being:

Can. J. Chem. Downloaded from www.nrcresearchpress.com by 210.87.254.42 on 09/05/12
For personal use only.

As—C	=	1.96±0.05 Å
C_{ar}—C_{ar}	=	1.40±0.03 Å
C_{ar}—CH_3	=	1.49±0.07 Å
∠ C—As—C	=	102.0±2°
∠ As—C—C	=	120±3°
∠ C—C—C	=	120±2°

These dimensions are very similar to those of other arsenic derivatives (4–6).

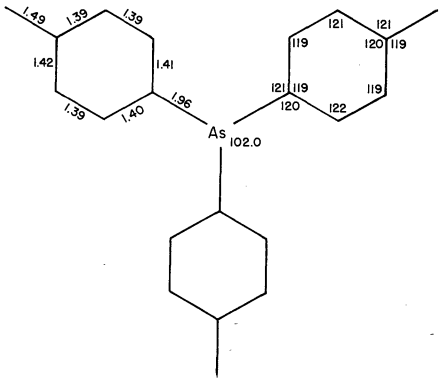

FIG. 2. Measured bond lengths (Å) and valency angles (degrees).

The *p*-tolyl groups are planar, and the arsenic atom lies on the plane of each of the three groups. In the absence of any intramolecular steric interferences between the groups we might expect that the most stable molecular configuration would be that in which there is maximum overlap between the arsenic lone pair and the π-electrons of each of the three *p*-tolyl groups. The arsenic lone pair is directed along the rhombohedral [111] axis and makes an angle of 116° with each of the As—C bonds. An "ideal" model was constructed in which the substituent groups were oriented so that the normals to the aromatic rings lay in the planes defined by the lone pair and the As—C bonds. This model exhibited overcrowding between the *ortho* carbon atoms and between the hydrogen atoms bonded to these carbons.

In comparison with this ideal model the true structure has each ring rotated, in the same sense, about its As—C bond by 36°, the minimum C···C and H···H approaches between adjacent *p*-tolyl groups thereby being increased to 3.4 Å and 2.8 Å respectively, that is to about the normal van der Waals separations. The deviations from the "ideal" model appear to be such as to make the interactions between the lone pair and the aromatic rings as large as possible while increasing the non-bonded intramolecular contacts to the van der Waals distances. The symmetrical deviations may be contrasted with the markedly unsymmetrical displacements in the halogenodiphenylarsines (5, 6).

The intermolecular distances correspond to normal van der Waals interactions.

The author is indebted to the National Research Council and to the President's Research Fund, University of British Columbia, for financial support, to Dr. W. R. Cullen for the crystal sample and for helpful discussion, to Dr. F. R. Ahmed for kindly making available his IBM 1620 programs, and to the staff of the University of British Columbia Computing Centre for assistance with the operation of the computer.

Can. J. Chem. Downloaded from www.nrcresearchpress.com by 210.87.254.42 on 09/05/12
For personal use only.

REFERENCES

1. J. TROTTER. Can. J. Chem. **40**, 1878 (1962).
2. K. SAGEL. Tabellen zur Röntgenstrukturanalyse. Springer-Verlag, Berlin. 1958.
3. D. W. J. CRUICKSHANK. Acta Cryst. **2**, 65 (1949).
4. TABLES OF INTERATOMIC DISTANCES AND CONFIGURATION IN MOLECULES AND IONS. Chem. Soc. Special Publ. No. 11. 1958.
5. J. TROTTER. J. Chem. Soc. 2567 (1962).
6. J. TROTTER. Can. J. Chem. **40**, 1590 (1962).

Downloaded from www.nrcresearchpress.com by 210.87.254.42 on 09/05/12
For personal use only.

SODIUM CHELATES OF ETHYLENEDIAMINETETRAACETIC ACID

VLADIMIR PALATY*
Department of Anatomy, University of British Columbia, Vancouver, British Columbia
Received August 10, 1962

ABSTRACT

The stability constant of the sodium chelate of EDTA was determined by means of a sodium-sensitive glass electrode. It appears that a hydrogen chelate of the formula $NaHY^{2-}$ is formed in the neutral solution of EDTA, but is very unstable. The stability constants, $pK_{NaY} = -2.61$ and $pK_{NaHY} = 0.03$, are comparable to the value obtained by Schwarzenbach and Ackermann under different experimental conditions by a less sensitive method.

INTRODUCTION

Sodium-sensitive glass electrodes, developed by Eisenman and his co-workers (1) in 1957, have been widely employed for the determination of sodium cation activity. This entity is of basic importance in biological studies of sodium metabolism. To test the suitability of the electrode for the determination of stability constants of sodium chelates, an attempt was made to determine this constant for the sodium chelate of ethylenediaminetetraacetic acid. Its value was determined by Schwarzenbach and Ackermann (2) from the shift of the titration curve of EDTA (ethylenediaminetetraacetic acid, usually shortened as EDTA or H_4Y), caused by the addition of sodium chloride. For the reaction (I),

$$Na^{1+} + Y^{4-} = [NaY]^{3-}, \qquad (I)$$

they found $\log_{10} K = 1.66$. They did not observe any formation of a hydrogen chelate.

The sodium-sensitive glass electrode is sluggish at sodium ion activities lower than 5×10^{-3} *M*, and because the most suitable molar ratio is 1 mole EDTA per mole of sodium, experimental conditions different from those of Schwarzenbach and Ackermann (2) had to be used. The activities and the activity coefficients were calculated by means of the Debye–Hückel equation. The ionic strength of the solutions was always less than 0.1 *M* and therefore the use of this equation was justifiable. Because the sodium-sensitive glass electrode exhibits some response to the ions of potassium as well as to those of sodium, tetramethylammonium hydroxide was employed as the titrant.

EXPERIMENTAL

Reagents

The reagents used were 10^{-2} *M* ethylenediaminetetraacetic acid, di(tetramethyl)ammonium salt; 10^{-2} *M* sodium chloride in 10^{-2} *M* di(tetramethyl)ammonium salt of EDTA; and 1 *M* tetramethylammonium hydroxide, standardized by potassium hydrogen phthalate. The usual precautions were taken to guard against contamination by carbon dioxide.

Instruments

The activity of the sodium ion was measured with a bulb-type sodium-sensitive glass electrode, prepared from NAS_{11-18} glass (1). The electrode was filled with 0.1 *M* sodium chloride. A silver – silver chloride electrode served as the internal reference. Standardization of the sodium electrode was made with standard sodium chloride solutions over the whole pH_s range used in the measurements.

For measuring the pH_s value a Beckman Type G glass electrode was employed. It was standardized with NBS standards.

A Cary Electrometer Model 31, equipped with a high-impedance switch, was used for measuring the E.M.F. of both cells. Saturated calomel electrodes were used as reference.

**Permanent address: Institute of Physiology, Czechoslovak Academy of Sciences, Prague, Czechoslovakia.*

Can. J. Chem. Downloaded from www.nrcresearchpress.com by 210.87.254.42 on 09/05/12
For personal use only.

Can. J. Chem. Downloaded from www.nrcresearchpress.com by 210.87.254.42 on 09/05/12
For personal use only.

RESULTS

For the determination of the last two dissociation constants of EDTA, titrations of 10^{-2} *M* EDTA solution were performed. A correction for the small change of volume was made. The following values were used in the calculations: $-\log K_w = 14.167$; $a_{H^+} = 9$ A; $a_{EDTA} = 6$ A (for all ionic forms of EDTA), and $a_{Na^+} = 4.5$ A. The observed and calculated values for the dissociation constants are given in Table I, where pK_c, pK_f, pK_Y, and pK_{HY} were calculated as follows:

$$pK_c = -\log_{10} \frac{c_{H^{1+}} \times c_{H_nY^{-4+n}}}{c_{H_{n+1}Y^{-4+n+1}}} \qquad pK_f = -\log_{10} \frac{f_{H^{1+}} \times f_{H_nY^{4+n}}}{f_{H_{n+1}Y^{4+n+1}}}$$

$$pK_Y = -\log_{10} \frac{a_{H^{1+}} \times a_{Y^{4-}}}{a_{HY^{3-}}} \qquad pK_{HY} = -\log_{10} \frac{a_{H^{1+}} \times a_{HY^{3-}}}{a_{H_2Y^{2-}}}$$

TABLE I

Dissociation constant for the reaction $H_2Y^{2-} = H^{1+} + HY^{3-}$										
$[(CH_3)_4N] \times 100$	2.21	2.32	2.42	2.52	2.63	2.74	2.84			
pH_s	5.90	6.10	6.29	6.48	6.67	6.79	7.12			
pK_c	6.41	6.37	6.40	6.38	6.37	6.35	6.33			
pK_f	0.40	0.42	0.43	0.44	0.45	0.47	0.48			
pK_{HY}	6.80	6.79	6.83	6.82	6.82	6.82	6.81			
Dissociation constant for the reaction $HY^{3-} = H^{1+} + Y^{4-}$										
$[(CH_3)_4N] \times 100$	3.05	3.16	3.26	3.37	3.47	3.58	3.68	3.79	3.89	4.00
pH_s	9.35	9.87	10.13	10.29	10.44	10.59	10.73	10.87	11.00	11.14
pK_c	10.72	10.69	10.69	10.63	10.62	10.61	10.61	10.58	10.56	10.52
pK_f	0.66	0.67	0.69	0.70	0.71	0.72	0.73	0.74	0.75	0.76
pK_Y	11.38	11.36	11.38	11.33	11.33	11.33	11.34	11.32	11.31	11.28

The titrations of EDTA in the presence of 10^{-2} *M* sodium chloride were performed similarly. For two reasons it was assumed that a hydrogen chelate of formula $[NaHY]^{2-}$ was formed. First, the observed activity of the sodium ion was significantly less than the theoretical value in the region where almost no Y^{-4} was present in the solution (pH_s 6.50–8.50) and, besides, it was dependent on the pH_s value. Second, the stability constant K_{NaY}, calculated under the assumption that only $[NaY]^{3-}$ had been formed, fell steeply to a constant value with the disappearance of the HY^{3-} from the solution. When a new calculation was performed, assuming the formation of the hydrogen chelate, the value of K_{NaY} appeared to be constant through the whole pH region. The observed and calculated values are given in Table II. The observed activities of the sodium ion are illustrated in Fig. 1.

TABLE II

Stability constant for the reaction $Na^{1+} + Y^{4-} = [NaY]^{3-}$								
pH_s	9.20	9.55	9.95	10.10	10.25	10.55	10.75	11.30
$-\log a_{Na^+}$	2.119	2.132	2.154	2.167	2.177	2.205	2.223	2.256
$-\log c_{Na^+}$	2.023	2.034	2.055	2.067	2.076	2.103	2.120	2.150
$-pK_c$	1.91	1.92	1.89	1.85	1.83	1.82	1.82	1.84
$-pK_f$	0.70	0.72	0.73	0.74	0.75	0.77	0.78	0.80
$-pK_{NaY}$	2.61	2.64	2.62	2.59	2.58	2.59	2.60	2.64
Stability constant for the reaction $Na^{1+} + HY^{3-} = [NaHY]^{2-}$								
pH_s	6.80	7.35	8.55					
$-\log_{10} a_{Na^+}$	2.108	2.112	2.115					
$-\log_{10} c_{Na^+}$	2.016	2.017	2.019					
pK_c	0.36	0.35	0.37					
$-pK_f$	0.32	0.33	0.34					
pK_{NaHY}	0.04	0.02	0.03					

NOTE: pK_{NaHY}, pK_{NaY}, pK_f, and pK_c have the meaning analogous to those symbols in Table I.

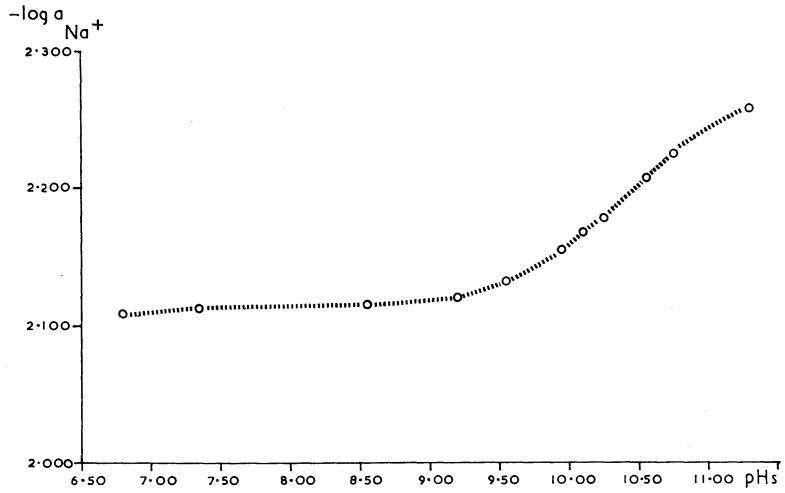

FIG. 1. The sodium cation activity in the presence of an equimolar concentration EDTA ($10^{-2}M$) as the function of pH_s.

DISCUSSION

The results presented here indicate that the sodium-sensitive glass electrode (1) is very suitable and precise for the determination of stability constants of sodium chelates. This method is much more sensitive than the pH shift method, as described in reference 2, but attention must be paid to the properties of the electrode, especially to the low sensitivity and sluggishness at sodium activities lower than 5×10^{-3} M. Apparently, the assumption that only the normal chelate $[NaY]^{3-}$ is formed by EDTA is not correct, as there is evidence for formation of a hydrogen chelate, $[NaHY]^{2-}$, an analogue to those of calcium and magnesium. The most important evidence is considered to be the dependence of the stability constant value on pH, when calculated according to the assumption that only the $[NaY]^{3-}$ chelate is formed. This was not observed by Schwarzenbach and Ackermann (2), because the pH shift method is very insensitive in the case of weak chelates. The stability constants $pK_{NaY} = -2.61$ and $pK_{NaHY} = 0.03$ are comparable to the value given in reference 2, if different experimental conditions are considered.

ACKNOWLEDGMENTS

This work was done while the author was Visiting Research Associate at the University of British Columbia. The author is indebted to the Leon and Thea Koerner Foundation of the University of British Columbia for making this visit possible, and wishes to express his appreciation to Professor S. M. Friedman for his kind hospitality and many helpful discussions during his stay.

REFERENCES

1. G. EISENMAN, D. O. RUDIN, and J. U. CASBY. Science, **126**, 831 (1957).
2. G. SCHWARZENBACH and H. ACKERMANN. Helv. Chim. Acta, **30**, 1798 (1947).

Can. J. Chem. Downloaded from www.nrcresearchpress.com by 210.87.254.42 on 09/05/12
For personal use only.

NEW APPROACHES TO THE STUDY OF ELECTROCHEMICAL DECARBOXYLATION AND THE KOLBE REACTION

PART I. THE MODEL REACTION WITH FORMATE

B. E. Conway and M. Dzieciuch
Department of Chemistry, University of Ottawa, Ottawa, Canada
Received June 29, 1962

ABSTRACT

The kinetics of electrochemical decarboxylation of formate ions has been studied in detail for the first time as a model reaction for examination of the decarboxylation and radical coupling that occurs with higher aliphatic acids. Current–potential curves have been obtained which show a sharp transition region, not diffusion controlled, which is characteristic of passivation phenomena. The behavior is observed with gold, palladium, platinum, and gold–palladium alloys. Tafel slopes and exchange currents have been evaluated for the reaction and possible reaction mechanisms are examined in relation to the experimental results.

Galvanostatic charging, reverse pulse discharging, and open-circuit decay transients have been obtained which indicate formation of films of adsorbed intermediates on the surface. The transition regions in the current–potential curves are associated with formation of this ad-layer. The galvanostatic results enable distinctions to be made between some of the possible reaction mechanisms proposed and estimates to be made of the extent of film formation by adsorbed intermediates formed in the reaction.

Can. J. Chem. Downloaded from www.nrcresearchpress.com by 210.87.254.40 on 09/05/12
For personal use only.

GENERAL INTRODUCTION

The following introduction is intended to cover material presented in this paper and in Parts II and III.

Despite the discovery by Kolbe many years ago (1) of a coupling reaction at the anodic electrode during electrolysis of aliphatic carboxylic acids R.COOH to give derivatives R_2 and some oxidation by-products (Hofer–Moest reaction), rather little is known of the mechanism of this reaction from a fundamental electrochemical point of view, e.g. with regard to the primary anodic step (see ref. 2, p. 398). The reaction has been the subject of organic chemical studies for many years, including uses for chain extension of semi-esters of dicarboxylic acids, dimerization of certain compounds, and other modifications of the reaction which have been adequately reviewed (2) in the literature of organic chemistry.

In this present series of papers (Parts I–III), it is the aim to examine the basic electrochemical behavior of reactions involving anodic decarboxylation by choosing, initially, two systems in which side reactions are minimized, so that the electrochemical kinetics of a single reaction can be studied. In the first case we examine the mechanism of the apparently simplest anodic decarboxylation that can occur, viz., that of formic acid or the formate ion. No other papers have evidently been published previously on the electrochemical kinetics of this reaction, and other work (e.g. ref. 3) has been concerned only with the problem of coulombic yields of CO_2 at the anode, the absence of hydrogen as an anodic product, and the production of hydrogen at the cathode. This reaction is ideally suited for electrochemical study since (*a*) the reaction pathway is very largely the simple decarboxylation to give hydrogen ions and carbon dioxide, and (*b*) the reaction is an essential model reaction for studies on the Kolbe reaction itself. It is also of interest in relation to the fuel-cell oxidation of methanol, where formic acid is the limiting product under certain conditions and diminishes cell efficiency.

In the second case (Part II), we examine a true coupling reaction but one which is virtually free from complications caused by the formation of side products.* Such a reaction is that occurring in the electrolysis of trifluoroacetates, where C_2F_6, and the stoichiometric quantity of carbon dioxide, are almost exclusively the reaction products. Since the C-atom at the trifluoromethyl function is in a high state of oxidation, oxidative side reactions, such as occur in the acetate case, are absent and the electrochemical mechanism can be examined under ideal conditions.

The approaches made have been as follows: evaluation of the Tafel parameters determining the current–potential relationship and examination, where possible, of the significance of these parameters in terms of rate-controlling steps; examination of the role of adsorbed intermediates by galvanostatic charging† and open-circuit decay measurements (18) with evaluation of electrode capacitance (19) and surface charge; examination of the role of anodic barrier layer films in the reaction as in the case of the oxygen evolution reaction (20); comparison between the kinetics of the model reactions in non-aqueous solvents (where oxygen evolution or production of oxide intermediates is eliminated) and in water.

Previous proposals regarding the mechanism of the Kolbe reaction are summarized below; none is entirely satisfactory and, as we shall show, most previous theories are based on an inadequate recognition of basic factors governing the kinetics of electrochemical and, in particular, anodic reactions.

In earlier theories by Schall (4) and Fichter (5) it was postulated that an acyl peroxide intermediate was involved which was formed by oxidation of carboxylate ions by electrochemically generated nascent oxygen simultaneously formed. This theory is now untenable since the Kolbe reaction proceeds, in fact, more efficiently in non-aqueous solutions, where no direct oxygen evolution is possible, than in aqueous solutions, where some simultaneous oxygen evolution from the solvent usually occurs; also no evidence for peroxide intermediates can be cited, although their steady-state concentration in an heterogeneous reaction might, of course, be small.

An alternative theory, proposed by Glasstone and Hickling (6), involves the assumption that hydroxyl radicals or hydrogen peroxide generated at the anode initiates the decomposition of the carboxylate ion. The peroxide or OH radical is assumed to produce an acyl-peroxide intermediate which then decomposes to either CO_2 and the Kolbe hydrocarbon or other oxidation products, e.g. alcohols, which are commonly formed as side products. This theory is subject to the same objections as mentioned above for the acyl peroxide theory (and is, in fact, a variant of it) and no hydrogen peroxide or peracids can be detected in the Kolbe reaction. In general, oxidizing intermediates, e.g., OH, which may be formed during the aqueous Kolbe reaction are only incidental to the reaction and in fact complicate it by forming side oxidation products and other species on the electrode surface (see Part II).

The most satisfactory general theory of the reaction is undoubtedly the discharged ion or adsorbed free radical mechanism originally discussed by Crum-Brown and Walker (8) and supported by Walker and co-workers (9, 10) and others in the field (11–14). In this theory, the carboxylate ion is regarded as being discharged onto the electrode surface,

*The literature on the Kolbe reaction is, in fact, almost as much concerned with the chemistry of the side reactions as with the coupling reaction itself. The side reactions are not necessary steps for the coupling process and arise only from choice of system and conditions in the earlier work.

†Recently a similar original approach to the aqueous acetate Kolbe reaction was made by Dickenson and Wynne-Jones (14). However, our preliminary description (16) of the application of this method to anodic decarboxylation was, in fact, published prior to the submission of their papers and described earlier (21). These approaches were evidently made independently and at about the same time.

Can. J. Chem. Downloaded from www.nrcresearchpress.com by 210.87.254.40 on 09/05/12
For personal use only.

where it subsequently decomposes* to give the Kolbe products (and any other side products); the reaction is thus essentially

$$2R.COO^- \rightarrow 2RCOO\cdot(M) + 2e$$
$$2RCOO\cdot(M) \rightarrow 2R\cdot(M) + 2CO_2$$
$$R\cdot(M) + R\cdot(M) \rightarrow R_2,$$

where M signifies a metal site at which the radical is adsorbed. In this scheme, no mention has previously been made concerning which step is rate determining. In the present work we present some conclusions concerning the identity of the rate-determining step and report information on surface coverage (Part III) and anode film formation by adsorbed intermediates. The corresponding sequence for formate discharge is different from the above and must involve steps such as

$$H.COO^- \rightarrow HCOO\cdot(M) + e$$
$$H.COO\cdot(M) \rightarrow H\cdot(M) + CO_2 \text{ or } H.COO\cdot(M) \rightarrow CO_2 + H^+ + e.$$

Normally, in the formate reaction, no coupling is possible to form the "Kolbe" product H_2 since the $H\cdot$ can ionize very rapidly to give H^+ ions in solution at the high anodic potentials required for carboxylate ion discharge to occur at significant rates.

The origin of side products such as CH_4, alcohols, and esters in the acetate case has been examined (11, 12) by deuteration techniques and discussed in terms of carbonium ion intermediates (15) and H-atom abstraction steps (11, 12).

Since the present work was commenced and our preliminary results on determination of the extent of coverage with intermediates by galvanostatic and decay techniques was published (16, 17), Dickenson and Wynne-Jones (14) have published anodic polarization and charging curves for acetate solutions in water. Their results serve to demonstrate the complicated nature of the reaction in aqueous media when oxide film formation and oxygen evolution are concomitant processes in the Kolbe reaction.

In most work, it has been recognized that a critical potential (6, 7), or a critical current density (14), is required for significant Kolbe yields in aqueous solutions. The significance of this potential will be further elucidated in the present work, developing our earlier observations (17), and it will be shown that this potential is apparently not unique to aqueous alkyl carboxylate systems but applies in non-aqueous solutions and also to the simple decarboxylation of formate.

EXPERIMENTAL

(a) General

General techniques for electrochemical kinetic measurements under high purity conditions were used, as previously described (22, 23). The cell, equipped with solution-sealed stopcocks and joints, was similar to that used previously (20, 23) and could be thermostated by circulation of coolant through glass coils sealed into the cell. Provision was made for runs on five or six electrodes in a given purified solution by the usual technique (20, 22, 23). Most of the experimental details described below also apply to the work reported in Parts II and III, except where otherwise stated.

(b) Solutions

Formic acid (98–100%) was first dried over anhydrous cupric sulphate for 3 days and then distilled under vacuum at room temperature. Only the middle fraction was retained. Final traces of water were removed by allowing the acid to remain in contact with boric anhydride for at least 1 week with continuous stirring. Purity of the acid was checked by the freezing point method (observed 8.2(3)° C; literature (24) 8.2(5)° C).

Reagent grade potassium formate was purified by dissolving the salt in hot conductivity water and filtering through decolorizing charcoal. The salt was then recrystallized twice from conductivity water at 0° C,

**Such a reaction is also consistent with the known behavior of carboxyl radicals in the gas phase, e.g., in the decomposition of organic acid peroxides.*

Can. J. Chem. Downloaded from www.nrcresearchpress.com by 210.87.254.40 on 09/05/12
For personal use only.

washed with ethanol, and dried at 120° C under vacuum. Solutions of potassium formate in formic acid were prepared by adding formic acid, freshly vacuum distilled from the boric anhydride, to a known weight of the purified salt.

In all experimental measurements, pre-electrolysis of the solutions (22) was carried out on a sacrificial anode for a minimum of 24 hours at a current density of 10^{-2} amp cm^{-2}.

(c) Gases

Hydrogen used for the reference electrodes was purified as previously described (23).

Medical grade carbon dioxide free from hydrogen sulphide, carbon monoxide, and sulphur dioxide was used to saturate all solutions and was further purified by passing the gas through a purification train. The use of the train was discontinued when experimental results showed no significant differences when the highly purified gas was substituted by that passed through a molecular sieve material only (Union Carbide, type 13X).

Nitrogen gas, used for bubbling through the solutions during pre-electrolysis, was purified by passing the gas through a deoxygenation train, as described previously (20, 23).

(d) Electrodes

Satisfactory reproducibility of measurements was obtained by adopting a standardized method of electrode preparation. The electrodes used for kinetic runs were prepared from spectroscopically pure wires of gold, palladium, and platinum, 0.5-mm diameter, which were first cleaned in alcoholic potassium hydroxide, washed in conductivity water, and dried with redistilled acetone. Electrodes were then sealed under oxygen-free nitrogen in glass bulbs following our previous procedures (25). Electrodes of larger area required for low current density coulombic efficiency determinations were cut from sheets of the metal foil and spot-welded to a wire of the same type of metal; subsequent purification was as described above, except for sealing in the bulbs.

Hydrogen reference electrodes were used in all the work both in non-aqueous and aqueous solutions (see Part II), and were prepared without addition agents. Electrodes were always used in pairs and their potentials were checked frequently. Reversibility of hydrogen electrodes in pure aliphatic acids has been demonstrated previously (26).

(e) Coulombic Efficiency Measurements

Coulombic efficiency studies were carried out in a cell consisting of two compartments separated by a solution-sealed stopcock. The cathode compartment was vented directly to the atmosphere while the anode compartment could be vented either to the atmosphere or to a gas collecting system. Provision was also made to allow gas to be bubbled through each compartment to presaturate the solutions, e.g. with CO_2.

The number of coulombs passed during electrolysis was evaluated by means of a copper coulometer, using well-known procedures.

Solutions and electrodes were prepared as described above. The cell was filled with solution, saturated with carbon dioxide, and allowed to come to thermal equilibrium at 5° C. The flow of gas through the solution was then stopped, and the solution electrolyzed for approximately 30 minutes at the required current density, the gas evolved being vented to the atmosphere. This procedure ensured that the system was saturated with the anticipated product gas. Measurements were then made by placing the copper coulometer in the electrolysis circuit and connecting the cell to a previously evacuated gas collecting burette, where the gas was then collected by displacement of mercury at constant pressure and temperature in an air thermostat at 30±0.2° C. At the commencement of electrolysis, the evolved gas was allowed to accumulate so that the solution was not sucked into the evacuated gas collecting system when the stopcock to the burette was opened. When a sufficient volume of gas had been collected and the electrolysis terminated, the pressure was adjusted in the system and the total volume of evolved gas recorded, and corrected to s.t.p. after making allowance for the partial pressure of solvent vapor.

(f) Gas Analysis

Carbon dioxide was determined in an Orsat absorption pipette by absorption in 40% aq. KOH. Remaining gases were then transferred to a sampling bulb and analyzed by gas phase chromatography (Perkin–Elmer Model 154) using a silica gel column. The fractograms of the unknown mixture were compared against calibration curves for H_2, O_2, CF_4,* C_2F_6,* and the quantity of unknown gases determined by comparing either peak heights or half widths.

(g) Electrical Measurements

Currents were measured by means of a Sensitive Research milliammeter (Model S) with ranges from 0.01 to 1000 ma full scale. The accuracy of the instrument was certified by the manufacturer as 0.5% of full scale deflection.

Potential measurements were made by one of the following procedures: (i) Potentials were read directly from a recording potentiometer (Philips model PR2210A) with a high input impedance ($\sim 10^{14}$ ohms)

See Part II.

Can. J. Chem. Downloaded from www.nrcresearchpress.com by 210.87.254.40 on 09/05/12
For personal use only.

electrometer (Keithly model 610A) between the recorder and test electrode. (ii) Alternatively, potential measurements were made by means of a manual high-impedance potentiometer (Radiometer model PHM-4b or a Doran pH–mV meter).

(h) Polarization Measurements

Potential measurements vs. the hydrogen electrode in the same solution were conducted over the current density range of 5×10^{-7} to 10^{-2} amp cm^{-2} at 5° C.* This temperature was chosen in order to eliminate slight attack of the metal which otherwise occurs at room and elevated temperatures. Successive measurements were made with the five other electrodes in the same solution. Potentials were either recorded on a recording potentiometer using the Keithly electrometer as an impedance converter or obtained on the high-impedance Doran pH–mV meter.

Potential measurements were conducted by either the rapid method (22), in which the potential was measured as quickly as possible (beyond the short period of double-layer charging) after setting the current to successive desired values, or by waiting until the potential had reached a steady value. The latter procedure was used in the film-forming or transition region of the Tafel lines observed (see below).

(i) Galvanostatic Measurements

General conditions were as described above. When pre-electrolysis was terminated, overpotential measurements were carried out on one electrode over the current density range of 10^{-7}–10^{-2} amp cm^{-2}. If the potential measurements were unsatisfactory, galvanostatic measurements were not carried out, and pre-electrolysis was continued for a further period or a fresh solution was prepared until satisfactory current–potential relations were obtained.

Potential–time relationships, for the anodic charging process, open-circuit decay, and forced cathodic decay were then obtained at each remaining electrode.

Galvanostatic charging curves were obtained by previously setting the current at the desired value, and impressing it on the test electrode by activating a mercury-wetted vacuum relay having an extremely short switching time. Details of the circuit are given in Part III. The resulting transient was then recorded photographically on the oscilloscope, the input to which was circuited through the Keithly high-impedance electrometer.

Potential–time relationships for the open-circuit decay process were obtained by either polarizing the test electrode at the desired current density until a steady potential was reached or by polarizing the electrode successively for several controlled increments of time (1–300 seconds) with decay transients taken after each period of time, the current being terminated by activating the relay; the resulting open-circuit decay transient was recorded.

Galvanostatic forced decay studies were carried out by anodically polarizing the test electrode at the desired current density for controlled intervals of time (1–300 seconds), reversing the current at the same numerical value by activating the vacuum relay, and recording the resulting transient on a calibrated oscilloscope (see Part III).

In all runs, the electrode was allowed to return to within 5–10 mv of its original rest potential before further transients were taken.

RESULTS

(a) Current–Potential Curves

Current density (i) – potential (V) curves in the form of Tafel lines over a current density range of five to six powers of 10 are shown in Fig. 1(a, b, c) for the system potassium formate (0.1, 1.0, 5.0 M) – 100% formic acid at Pt, Au, and Pd electrodes. From previous work (20), we had available some Pd–Au alloys and as a matter of interest, in relation to the electronic configuration of the alloys (23), runs were also carried out on these materials. The results are shown in Fig. 2(a, b, c). In all these experiments, the data presented are based on runs on at least 12 electrodes studied in at least two separately prepared solutions. A typical assembly of points is shown for one series of runs in Fig. 1(b) but in the other figures referred to above, the data are shown as the best straight lines drawn over the linear regions of the $V - \log [i]$ plots. In most cases very satisfactory reproducibility was observed and it was unnecessary to make statistical calculations of the lines of best fit.

In all cases, the $V - \log [i]$ plots showed a sharp inflection at a critical current density. At first it was suspected that this might have been due to presence of traces of anodic

**That is, below the freezing point of the pure solvent. No trouble was encountered in the non-aqueous solution with freezing of the solution as the presence of electrolyte lowers the freezing point.*

Can. J. Chem. Downloaded from www.nrcresearchpress.com by 210.87.254.40 on 09/05/12
For personal use only.

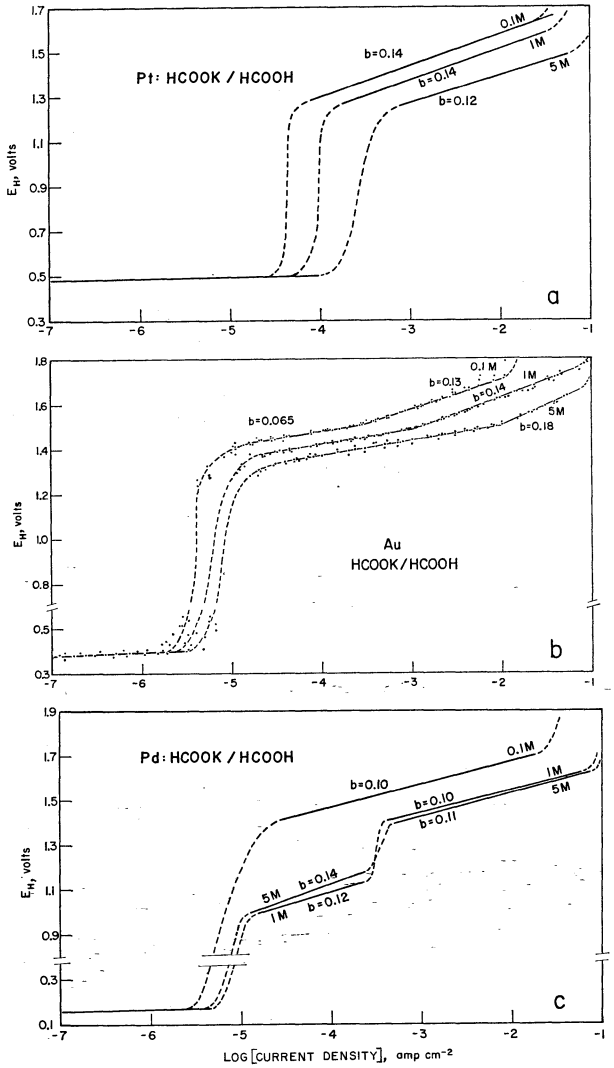

FIG. 1. Current–potential curves for anodic decarboxylation at platinum, gold, and palladium in solutions of HCOOK in 100% HCOOH (5° C).

depolarizers, e.g. formaldehyde, so that the critical current was simply a diffusion-controlled oxidation current. Rigorous purification of the solutions did not modify the effect. Addition of formaldehyde and other likely impurities had the effect of lowering the critical current rather than raising it. The effect is hence due to a general activation-controlled process and is also found in the aqueous solutions (Part II) and in the case of trifluoroacetate decarboxylation (Part II). Its significance will be further discussed below. The critical currents are generally increased with increasing formate concentration; analogous effects were also observed first in potentiostatic work on the aqueous acetate Kolbe reaction (27) and reported again subsequently (14) for steady-state current-potential curves. In these measurements (14, 27), however, the critical currents increased with *decreasing* carboxylate concentration. The critical currents observed in the acetate

Can. J. Chem. Downloaded from www.nrcresearchpress.com by 210.87.254.40 on 09/05/12
For personal use only.

Can. J. Chem. Downloaded from www.nrcresearchpress.com by 210.87.254.40 on 09/05/12
For personal use only.

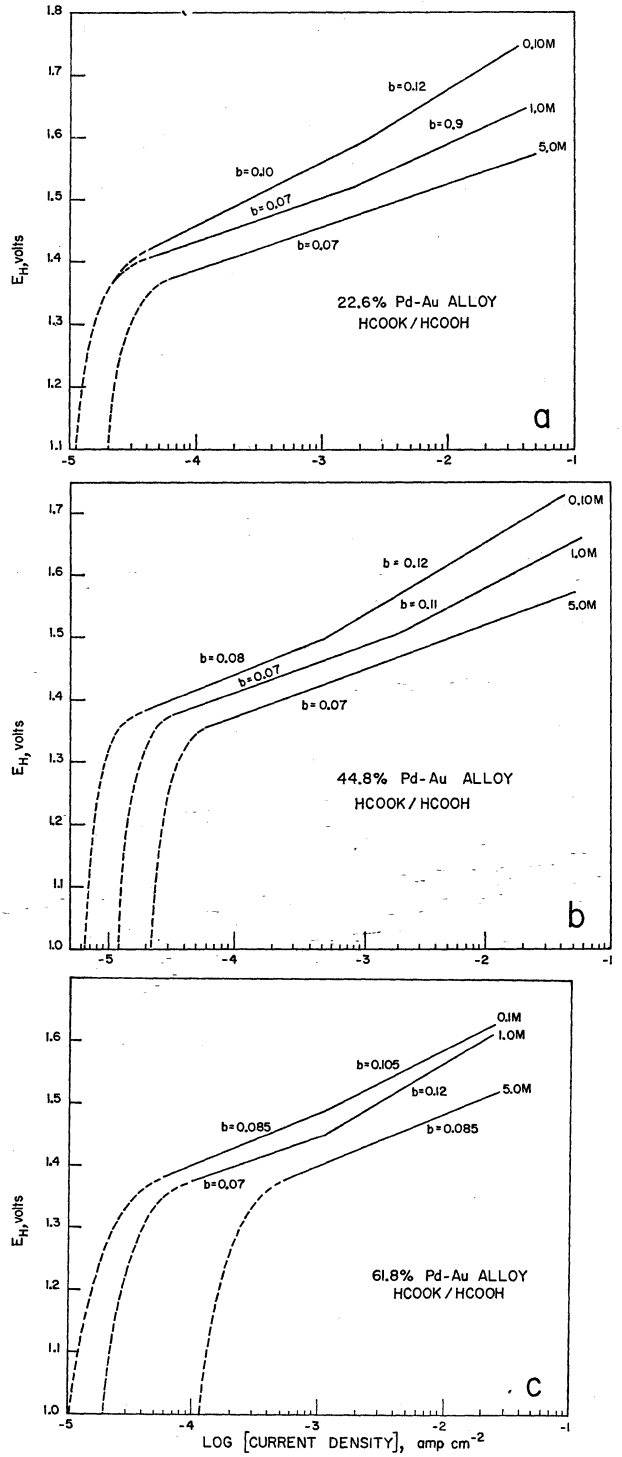

Fig. 2. Current–potential curves for anodic decarboxylation at Pd–Au alloys in solutions of HCOOK in 100% formic acid (5° C). (*a*) 22.6 wt% Pd–Au; (*b*) 44.8 wt% Pd–Au; (*c*) 61.8 wt% Pd–Au.

work may correspond to a process different from that leading to the critical behavior in the formate system, since already in the acetate work the anodic potentials are very high (viz. $E_H \doteqdot 2$ v). We suspect, in relation to the present results and those for trifluoroacetate in aqueous solution (Part II), that another critical region may exist at current densities lower than those used in the acetate work and would correspond to our critical behavior, which occurs at 10^{-5}–10^{-4} amp cm^{-2}. In the Russian work (27), the data appear to be expressed in current rather than current densities, so quantitative comparison of their results with other data is not possible.

At palladium and platinum, the Tafel slopes approach $2.3(2RT/F)$ in the upper region. In the lower region at Pt and Pd, the current density is, at first, almost independent of potential. At gold, in the upper region, two Tafel regions are observed with slopes of about 0.065 (ca. $2.3RT/F$) and 0.13 to 0.18 ($>2.3(2RT/F)$) depending on the concentration of the electrolyte. Two Tafel slopes are also observed in the upper region for the Pd–Au alloys and the lower slopes have varying values dependent upon the alloy composition.

(b) Galvanostatic Transients and Decay Behavior

The sharp transitions from a lower to an upper region in the current–potential curves described above suggested that a phenomenon similar to passivation with anodic film formation was occurring in the decarboxylation reaction. This was supported by the observation of: (*a*) periodic fluctuations of potential at constant current, near the critical current for transition in the current–potential plot (such periodic phenomena are characteristic of changes of an anode from an active to a passive, back to an active state, etc., and are well known in anodic oxidation of metals (28)) and (*b*) "overshoot" and "undershoot" transients in the potential when the current was either being raised or lowered, respectively, near the critical current; the latter effects were observed particularly in the aqueous solution reaction.

Further information was sought on the nature of the transition behavior in the current–voltage curves, in the light of the above observations, by examining charging, discharging, and open-circuit decay behavior of the anodes in formic acid containing potassium formate. Typical curves obtained galvanostatically for anodic charging and reverse cathodic discharging after polarization are shown in Figs. 3 and 4, which are copies of oscilloscope photos; (related open-circuit decay curves will be discussed in Part III; e.g. see Figs. 6, 10, 11, Part III). For the three metals studied in the present work, gold, palladium, and platinum, there is clear evidence of an arrest in the transients corresponding to the charge associated with a film of adsorbed intermediates produced in the anodic reaction. The arrests only appear after moderate and high anodic polarizations and confirm that the transition behavior in the current–potential plot is associated with a critical condition for formation of an anodic product (an anodic passive film) on the electrode surface, which can be removed either by a self-discharge process (18, 29) on open-circuit or by a reverse cathodic pulse, as with adsorbed O or H (30). Following our initial observations in a preliminary paper (16, 17), we believe this is the first direct proof of the role of an adsorbed layer of intermediates in electrochemical decarboxylation reactions. Similar layers are formed in the case of the Kolbe reaction itself (with CF_3COO^-) and will be discussed in Part II.

The arrest behavior in the formic acid/formate system is characteristic not only of the current density of the initial anodic polarization, but also depends on the *time* of prior anodic polarization at this current density, as shown in Fig. 5 for cathodic discharge. Similar behavior on open-circuit decay at Pd will be seen in Fig. 6, Part III. The time

Can. J. Chem. Downloaded from www.nrcresearchpress.com by 210.87.254.40 on 09/05/12
For personal use only.

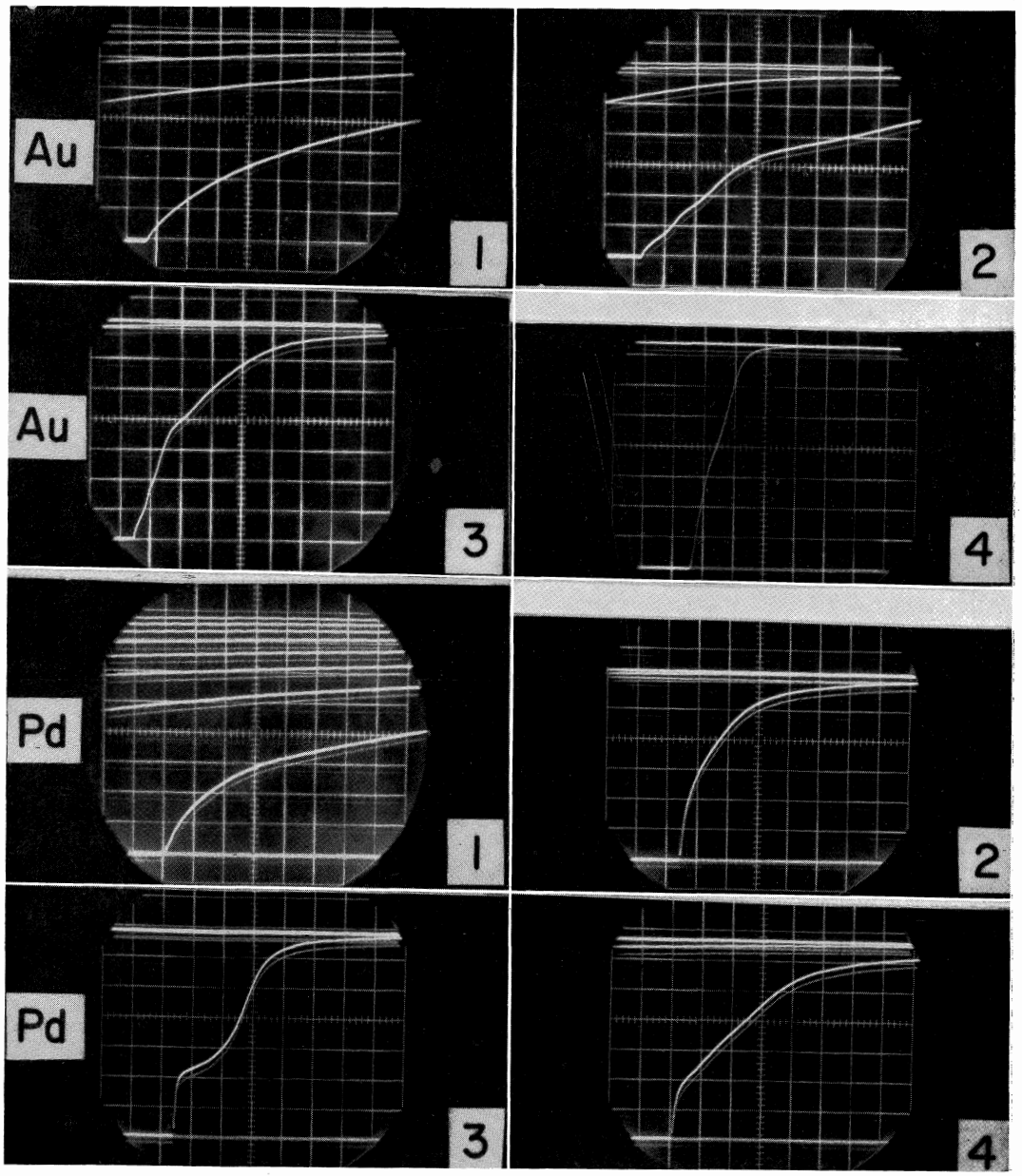

FIG. 3.

NOTE: For explanation of Figs. 3–5 see p. 37.

Can. J. Chem. Downloaded from www.nrcresearchpress.com by 210.87.254.40 on 09/05/12
For personal use only.

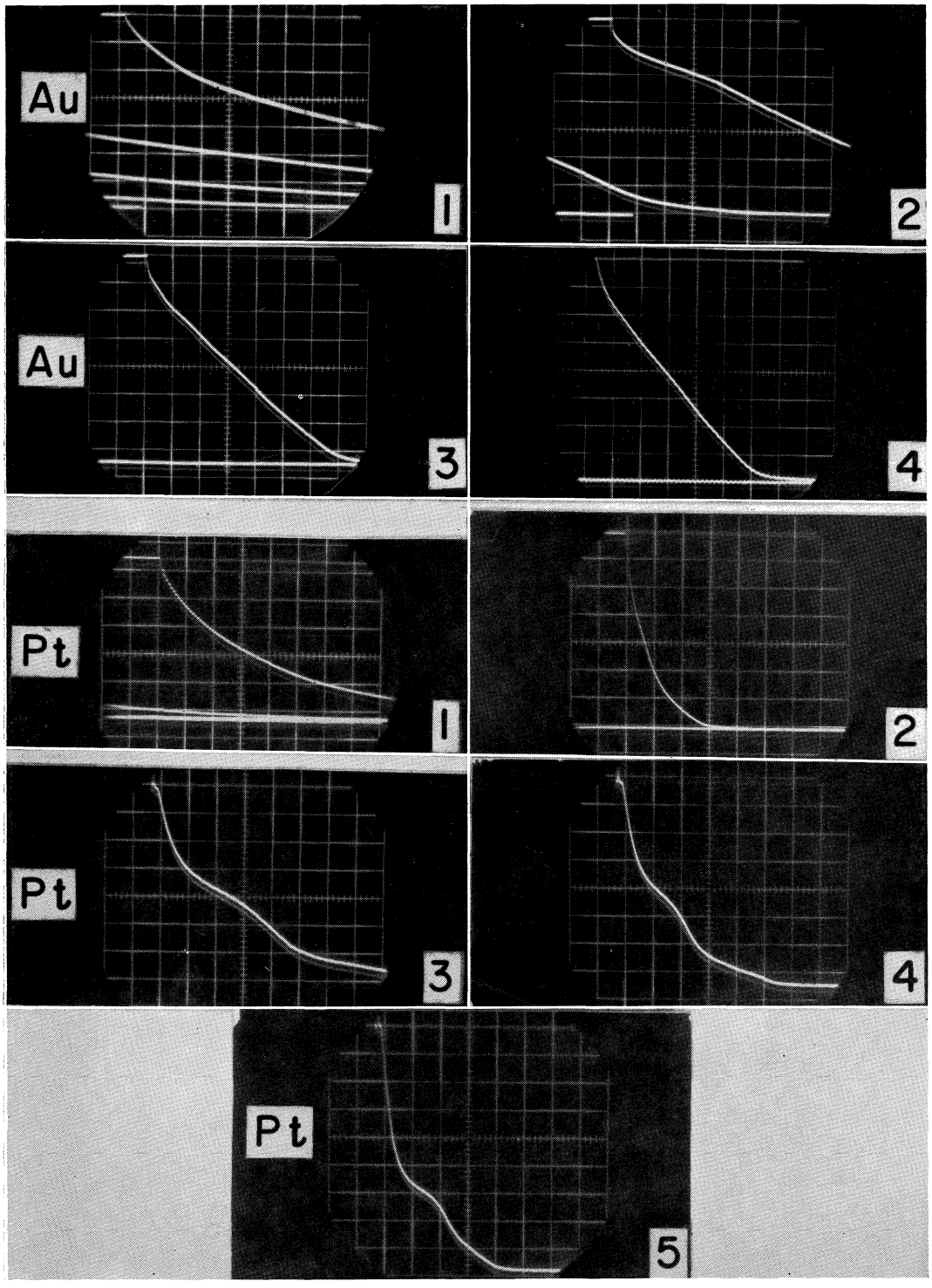

FIG. 4.

Can. J. Chem. Downloaded from www.nrcresearchpress.com by 210.87.254.40 on 09/05/12
For personal use only.

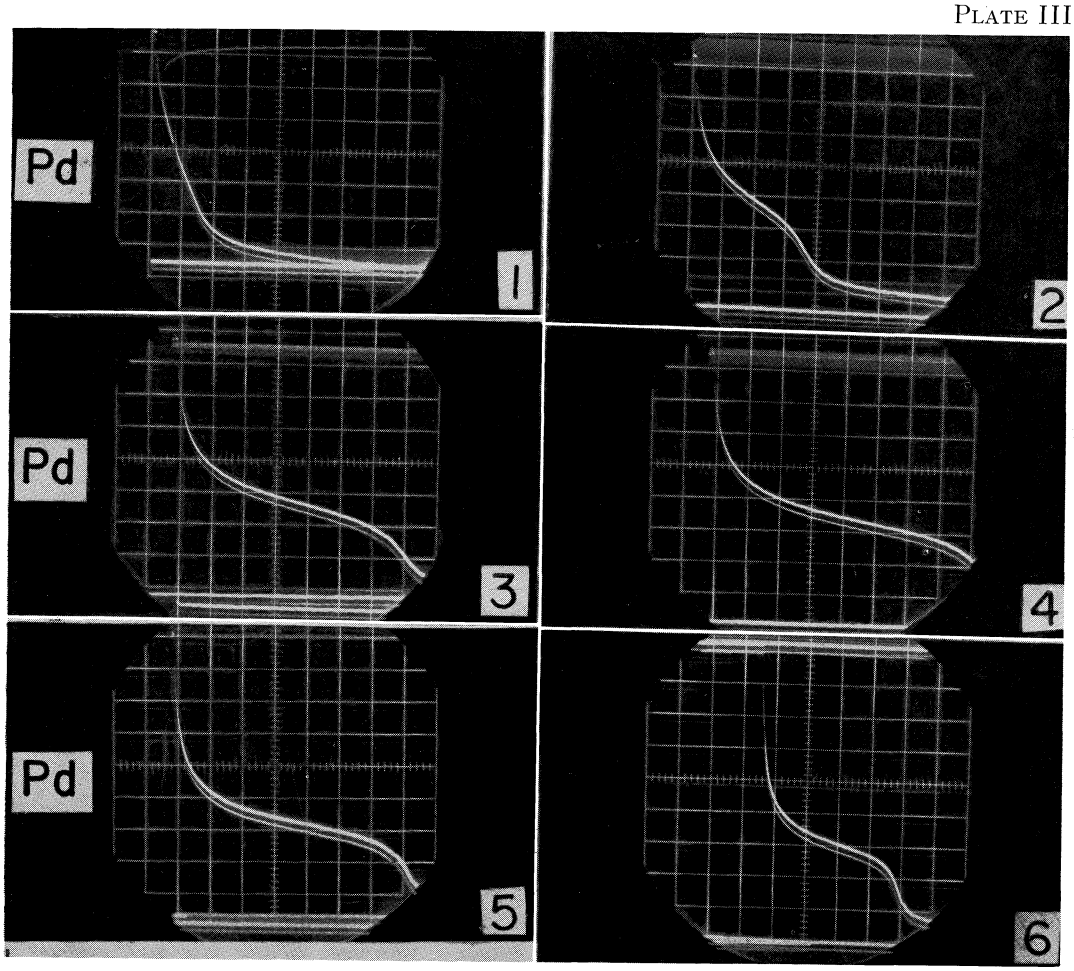

FIG. 5.

Can. J. Chem. Downloaded from www.nrcresearchpress.com by 210.87.254.40 on 09/05/12
For personal use only.

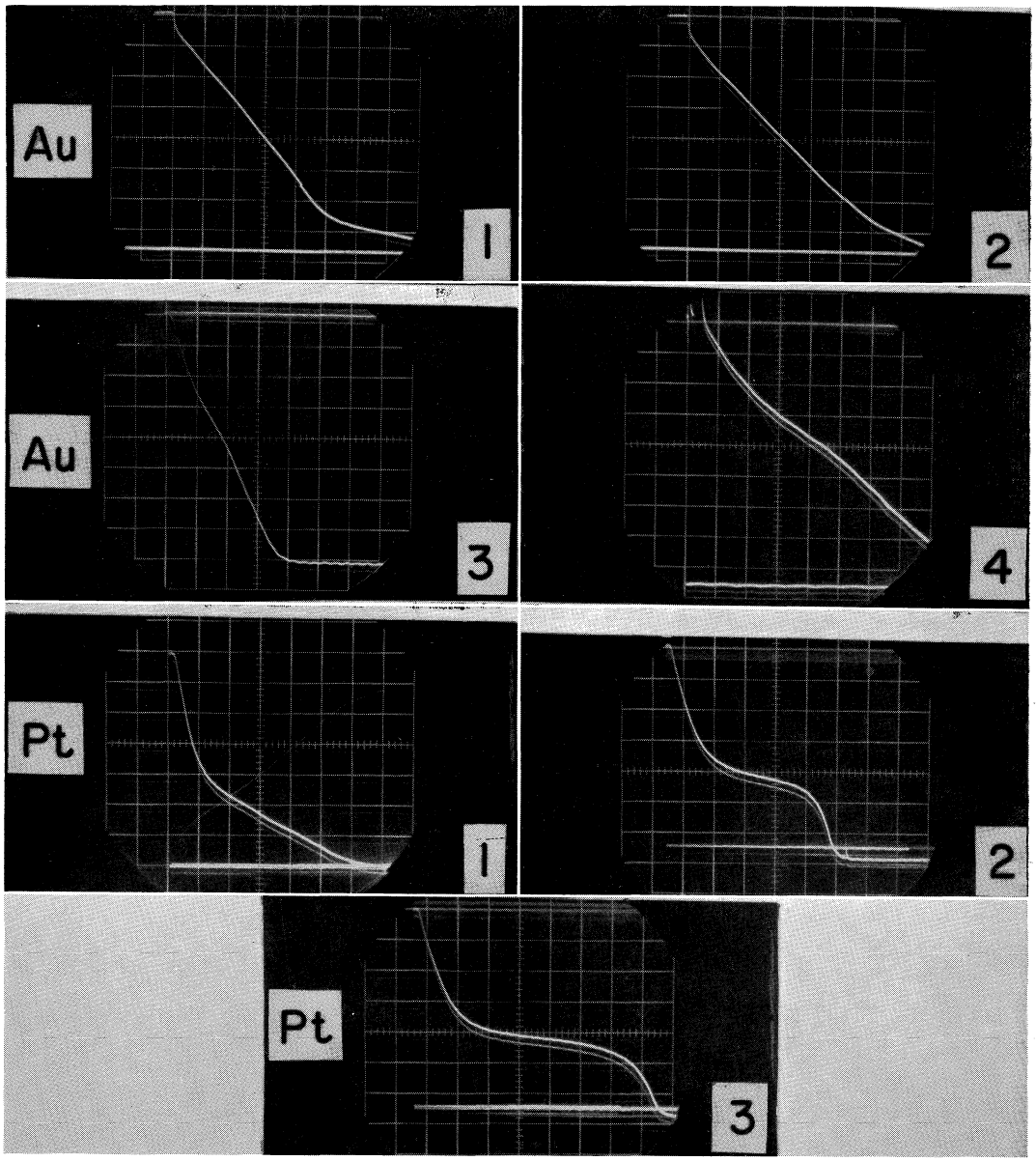

FIG. 5.

Can. J. Chem. Downloaded from www.nrcresearchpress.com by 210.87.254.40 on 09/05/12
For personal use only.

effects increase in the order Pd > Pt > Au and are associated with buildup of thicker, or more extensive, layers of the anodic product with time as will be discussed quantitatively in Part III.

(c) Coulombic Efficiency in the Anodic Decarboxylation

Results of the coulombic efficiency runs are shown in Table I. Provided the solution is presaturated with CO_2, the coulombic yield approaches 1 mole of CO_2 per 2 Faradays at

TABLE I

Current efficiencies for CO_2 production in anodic decarboxylation in formic acid
(1 *M* HCOOK/HCOOH, 5° C)

Electrode	Current density, amp cm^{-2}	Products	Efficiency, %
Pt	1×10^{-2}	CO_2	86
	2.5×10^{-3}	CO_2	79
	5×10^{-4}	CO_2	65
Pd	1×10^{-2}	CO_2	84
	1.2×10^{-3}	CO_2	75
	5×10^{-4}	CO_2	56
Au	1×10^{-2}	CO_2	86
	1×10^{-3}	CO_2	62
	5×10^{-4}	CO_2	55

high current densities. The actual values vary from about 86% to 55% of the theoretically expected yields based on the reaction

$$HCOO^- \rightarrow CO_2 + H^+ + 2e. \qquad [I]$$

This discrepancy from 100% is due to some attack on the metal, which is visible as a colloidal suspension after prolonged coulombic-yield electrolyses. It is minimized by operating at low temperatures (5° C in the present work). The low yields at low current densities where there is little visible bubble formation may be due to supersaturation of the solution by CO_2. No other gases, including oxygen, can be detected from the formate decarboxylation and, in particular, no hydrogen (the "Kolbe analogue") is present and peroxides were shown to be absent. The above coulombic yields justify interpretation of the observed electrochemical behavior largely in terms of steps which may be involved in the overall anodic reaction [I], particularly at the higher current densities.

DISCUSSION

(a) Kinetic Parameters

The parameters i_0 (the exchange current) and b, the Tafel slope, which characterize the kinetics of the rate-determining step, can be obtained from the current–potential relations of Figs. 1 and 2. Evaluation of i_0 values requires calculation of the reversible potential for reaction [I] on the hydrogen scale, since the reaction itself is not practically reversible. The half-cell reactions involving the hydrogen electrode are

$$CO_2 + 2H^+ + 2e \rightarrow HCOOH$$

and

$$H_2 \rightarrow 2H^+ + 2e,$$

i.e.

$$HCOOH \rightarrow CO_{2(g)} + H_{2(g)}.$$

Can. J. Chem. Downloaded from www.nrcresearchpress.com by 210.87.254.40 on 09/05/12
For personal use only.

The equilibrium constant is

$$K = f_{CO_2} f_{H_2} / a_{HCOOH}$$

in terms of the fugacities of the gases and the activity of formic acid. The free energy change is

$$\Delta G = \Delta G^0 + RT \ln f_{CO_2} f_{H_2} - RT \ln a_{HCOOH}$$

and the e.m.f. of the hydrogen – formic acid cell is hence, at unit fugacity (pressure) of the gases (the standard state),

$$E = E^0 - (RT/2F) \ln a_{HCOOH}.$$

The ΔG^0 value for the above reaction is obtained from the standard free energies of formation of HCOOH (liq.) and CO_2 (g) as 10.622 kcal mole^{-1} (31) for a standard state of unit mole fraction of HCOOH and unit fugacity (in atm) of CO_2 (here unit pressure is actually taken). The value of E^0 is hence -0.230 (European convention) on the hydrogen scale in pure formic acid. The observed log current–potential behavior can hence be extrapolated to the theoretical reversible potential and the log $[i_0]$ evaluated or log $[i_0]$ can be calculated from the observed overpotential and Tafel slope. Values of log $[i_0]$ and b are summarized in Table II. The formic acid decarboxylation is seen to be highly irreversible

TABLE II

Mean Tafel parameters in anhydrous HCOOK/HCOOH
(From data for a minimum of 10 electrodes; temp. 6±1° C)

Electrode	Concn., M	b (±1%)	i_0 (calc.),* amp cm^{-2} (±40%)	Current density, amp cm^{-2}
Pt	0.1	0.14	1.2×10^{-15}	1×10^{-4}–3×10^{-2}
	1	0.14	5.2×10^{-15}	2×10^{-4}–3×10^{-2}
	5	0.12	3.2×10^{-16}	9×10^{-4}–1×10^{-1}
Pd	0.1	0.10	1.0×10^{-21}	4×10^{-5}–2×10^{-2}
		0.12†	1.0×10^{-15}	1.5×10^{-5}–2.5×10^{-4}
	1	0.10	1.8×10^{-20}	5×10^{-4} –1×10^{-1}
		0.14†	2.1×10^{-14}	1.5×10^{-5}–2.5×10^{-4}
	5	0.11	1×10^{-18}	5×10^{-4}–6×10^{-2}
Au‡	0.1	0.065	5×10^{-31}	1.8×10^{-5}–3×10^{-4}
		0.13	1.2×10^{-17}	3×10^{-4}–2.5×10^{-2}
	1	0.065	3.5×10^{-30}	2.5×10^{-5}–1×10^{-3}
		0.14	4.8×10^{-16}	1×10^{-3}–5×10^{-2}
	5	0.065	2.0×10^{-29}	5×10^{-5}–9×10^{-3}
		0.18	2.3×10^{-12}	9×10^{-3}–6×10^{-2}
22.6% Pd–Au‡	0.1	0.10	1.3×10^{-21}	4.5×10^{-5}–1.5×10^{-3}
		0.12	1.3×10^{-18}	1.5×10^{-3}–4.5×10^{-2}
	1	0.07	1.7×10^{-28}	4.5×10^{-5}–1.6×10^{-3}
		0.09	5.8×10^{-23}	1.6×10^{-3}–4×10^{-2}
	5	0.07	6.2×10^{-28}	5.5×10^{-5}–4.5×10^{-2}
44.8% Pd–Au‡	0.1	0.08	1.3×10^{-25}	1.5×10^{-5}–5.5×10^{-4}
		0.12	1.9×10^{-18}	5.5×10^{-4}–4.5×10^{-2}
	1	0.07	3.5×10^{-28}	3×10^{-5}–1.6×10^{-3}
		0.11	3.5×10^{-19}	1.6×10^{-3}–5×10^{-2}
	5	0.07	1.3×10^{-27}	6×10^{-5}–4.5×10^{-2}
61.8% Pd–Au‡	0.1	0.085	6.8×10^{-24}	6×10^{-5}–1.3×10^{-3}
		0.11	4.7×10^{-20}	1.3×10^{-3}–2.5×10^{-2}
	1	0.07	1.2×10^{-27}	7.5×10^{-5}–1×10^{-3}
		0.12	1.1×10^{-17}	1×10^{-3}–2.5×10^{-2}
	5	0.085	6.8×10^{-23}	4.5×10^{-4}–2.5×10^{-2}

*Based on calculated extrapolations to the theoretical reversible potential $E_H = -0.230$ v with respect to the hydrogen electrode in the same solution. The i_0 values have been referred to this E_H value at 25° C. From the entropy change in the overall reaction, which is approximately 51 e.u., the reversible potential at 5° C will differ from the above value by ca. 21 mv.
†Intermediate potential region; see Fig. 1.
‡Two slopes in the upper region are observed here; see Figs. 1 and 2.

Can. J. Chem. Downloaded from www.nrcresearchpress.com by 210.87.254.40 on 09/05/12
For personal use only.

and this can offer a kinetic explanation of the difficulty of obtaining useful rapid oxidation beyond the formate stage to CO_2, encountered in the fuel cell oxidation of methanol.

(b) Reaction Mechanism

No previous studies of the mechanism of the reaction have been made although the production of $HCOO^{\cdot}$ radicals as intermediates has been recognized (3). The following steps corresponding to the overall reaction [I] can be envisaged (equivalent steps involving the molecule HCOOH can, of course, be written but involve the same intermediates):

$$M + HCOO^- \rightarrow HCOO^{\cdot}(M) + e \qquad [II]$$
$$HCOO^{\cdot}(M) \rightarrow CO_2 + H^{\cdot}(M) \qquad [III]$$
$$H^{\cdot}(M) \rightarrow H^+ + e \qquad [IV]$$
$$[H^+ + HCOO^- \rightleftarrows HCOOH],$$

scheme A

where (M) indicates a site on the metal surface to which the ad-species is bound; or

$$M + HCOO^- \rightarrow HCOO^{\cdot}(M) + e \qquad [II]$$
$$HCOO^{\cdot}(M) \rightarrow CO_2 + H^+ + e \qquad [V]$$

scheme B

or

$$M + HCOO^- \rightarrow M + CO_2 + H^+ + 2e, \qquad [VI]$$

scheme C

i.e. the overall reaction in one step involving two electrons.

A pathway involving

$$HCOO^{\cdot}(M) \rightarrow CO_2 + H(M) \qquad [III]$$

followed by

$$2H(M) \rightarrow H_2 \text{ (Kolbe analogue product)}$$

or

$$H(M) + HCOO^- \rightarrow H_2 + CO_2 + e$$

is not observed presumably since if [III] occurs, the desorption ionization [IV] will tend to be very rapid at the high anodic potentials involved, and steady-state coverage by H(M) will be very small.

Radical–ion desorption steps (cf. the case of the hydrogen evolution reaction) such as

$$HCOO^{\cdot}(M) + HCOO^- \rightarrow (HCOO)_2 + e,$$

or recombination of the $HCOO^{\cdot}$ radicals, could lead to diformyl peroxide. Experimentally peroxides are not detectable.

Step [VI] (the scheme C) or a radical desorption step such as

$$HCOO^{\cdot}(M) + HCOO^- \rightarrow 2H^+ + 2CO_2 + 3e$$

is unlikely since they involve more than one electron in a single rate-determining step. Similarly, such a step as

$$HCOO^- + H(M) \rightarrow 2H^+ + CO_2 + 3e$$

is kinetically improbable as a single electrochemical step. Schemes A and B are hence the likely pathways in CO_2 evolution and are examples of the "discharged ion" theory of decarboxylation.

The Tafel slopes for Langmuir conditions (i.e. at limitingly low or limitingly high surface coverage by intermediates; cf. refs. 18, 32) are readily apparent for various rate-determining steps in the above schemes and have been derived by now well-known

Can. J. Chem. Downloaded from www.nrcresearchpress.com by 210.87.254.40 on 09/05/12
For personal use only.

principles of analysis of consecutive electrochemical reactions (33, 29). The following limiting values are obtained.

Scheme A	
(*a*) Ion discharge [II]	$2.3(2RT/F)$
(*b*) First-order decomposition of HCOO·(M), [III], with [II] in quasi-equilibrium and surface coverage of HCOO·(M) potential dependent	$2.3RT/F$
(*c*) HCOO·(M) approaching full coverage and its surface concentration potential independent	Limiting current
(*d*) H(M) ionization [IV] (steps [II] and [III] in quasi-equilibrium)—unlikely to be rate controlling at high anodic potentials	$2.3(2RT/3F)$
H·(M) ionization at full coverage by H·—unlikely to be rate controlling at high anodic potentials	$2.3(2RT/F)$
Scheme B	
(*a*) Ion discharge [II] (as in scheme A)	$2.3(2RT/F)$
(*b*) HCOO·(M) ionization and decomposition	
(i) Full coverage by HCOO·	$2.3(2RT/F)$
(ii) Potential-dependent coverage with [II] in quasi-equilibrium	$2.3(2RT/3F)$

In order to make as complete an analysis as possible of the theoretically predictable results, we now examine cases where effects of coverage by the intermediates on their respective heats of adsorption are significant and introduce these effects in the free energies of activation of the various steps, as in previous papers (34, 19); this treatment is necessary since we show here and in Part III that the electrode surface is appreciably covered by the adsorbed intermediates. We obtain for scheme A

$$v_2 = k_2(1-\theta_F)a_{F^-}\exp -[\Delta G_2^{\ddagger}-\beta VF+\beta r_1\theta]/RT, \quad [1]$$

where subscripts F^- and F represent the formate ion and adsorbed radical, respectively, the latter at a total coverage θ; r_1 is a term similar* to that used previously (34) to allow for the variation of heat of adsorption of F with coverage, and β is the usual symmetry factor (19). Similarly

$$v_{-2} = k_{-2}\theta_F \exp -[\Delta G_{-2}^{\ddagger}+(1-\beta)VF-(1-\beta)r_1\theta]/RT \quad [2]$$

$$v_3 = k_3\theta_F(1-\theta_H) \exp -[\Delta G_3^{\ddagger}-\beta r_1\theta+(1-\beta)r_2\theta]/RT \quad [3]$$

$$v_{-3} = k_{-3}\theta_H(1-\theta_F) \exp -[\Delta G_{-3}^{\ddagger}-\beta r_2\theta+(1-\beta)r_1\theta]/RT, \quad [4]$$

**This term arises (cf. ref. 34) in the expression for the variation of heat of adsorption ΔH of the intermediate with coverage θ in the equation*

$$\Delta H_F = \Delta H_F^0 - r_1\theta.$$

An equation of this form originates if there is heterogeneity of adsorption sites or if there are surface induction effects (37) associated with change of the work function of the metal with coverage. Two-dimensional interaction effects will not generally give rise to a linear equation for ΔH as a function of θ and the magnitude of the r values for such a model are usually too small to account for the observed fall of heat of adsorption with coverage, e.g. of O, N, *and* H *from the gas phase at various metals (37, 38). The general case for the simultaneous adsorption of several species at comparable coverages has been worked out elsewhere (19).*

Can. J. Chem. Downloaded from www.nrcresearchpress.com by 210.87.254.40 on 09/05/12
For personal use only.

where r_2 is a term similar to r_1, but referring to the variation of heat of adsorption of H with coverage. The velocity of [IV] is

$$v_4 = k_4\theta_H \exp -[\Delta G_4^{\neq} - \beta VF - \beta r_2\theta]/RT. \quad [5]$$

We now examine limiting cases assuming, with Thomas (34), that at coverages sufficient to influence the exponential terms ("Temkin" conditions) the pre-exponential terms are of the order of magnitude of unity and will not be very potential dependent (cf. ref. 34). If [II] were rate determining we obtain the same result as in the Langmuir case, namely $dV/d \ln i_2 = 2RT/F$.

When [III] is rate determining, and [II] in quasi-equilibrium, so that

$$VF = r_1\theta + \text{constants}, \quad [6]$$

and θ_H is small (since [IV] will tend to be fast under these conditions and particularly at the high anodic potentials involved here), we obtain

$$v_3 = k'\theta_F \exp -\left[\Delta G_3^{\neq} + \frac{r_2 - r_1}{2r_1} VF\right]/RT, \quad [7]$$

and the Tafel slope as

$$dV/d \ln i_3 = \frac{2RT}{F}\left(\frac{r_1}{r_1 - r_2}\right)(\beta \rightarrow \tfrac{1}{2}). \quad [8]$$

As in previous calculations (19, 36), we are faced with the problem of assignment of values to r_1 and r_2; it is clear that we actually only require the ratio r_2/r_1. Since [IV] will tend to be fast at the high anodic potentials, $\theta_H \rightarrow 0$ so that $\theta \rightarrow \theta_F$. In the case of the radicals "F" and H, we note that their areas are quite different and from space-filling models it may be calculated that the area of "F" is about 14.2 Å^2 and that of H (e.g. for one atom of H per surface hexagonal hole or per surface metal atom) about 6 Å^2. For purely steric reasons the effective value of r_1 will be some 2.5 times larger than that of r_2 and we may anticipate that if r_1 and r_2 are also associated with some two-dimensional dipole-layer induction effects (37) in the interphase, r_1 will be greater than r_2 owing to greater surface dipole moment, since presumably the adsorbed H.COO$^-$ will be appreciably more polar than the adsorbed H. The steric effect in the ratio of effective r_1 and r_2 values arises since, if reaction [III] were allowed to proceed for a unit surface fully covered with "F" to produce the equivalent coverage by H (assuming no further antecedant reactions), the latter species would, in fact, only cover approximately 1/2.5 of the surface. Thus, when any "F" radical decomposes it effectively locally creates for the resulting H a relatively uncovered region of the surface.

We may hence anticipate values of r_1 about 3 to 4 times r_2; $dV/d \ln v_3$ will hence be in the range $3RT/F$ to $2.7RT/F$; when $r_1 \gg r_2$, $dV/d \ln v_3 \rightarrow 2RT/F$ as a *minimum* value. The observed slopes lower than $2RT/F$ cannot be explained by taking, for example, $r_1 < r_2$ since negative values of $dV/d \ln v_3$ then result, which have no physical significance. The lower slopes (ca. RT/F) at Au and the Pd–Au alloys hence cannot be explained in terms of reaction [III] proceeding at appreciable coverages under "Temkin" conditions.

Finally, for the unlikely case of [IV] being rate determining at potentials substantially anodic to the hydrogen electrode potential, and with [II] (and [III]) in resulting quasi-equilibrium, the limiting result is

$$v_4 = k_4' \exp -\left[\Delta G_4^{\neq} - \beta VF - \beta\left(\frac{r_2}{r_1}\right) VF\right]/RT \quad [9]$$

Can. J. Chem. Downloaded from www.nrcresearchpress.com by 210.87.254.40 on 09/05/12
For personal use only.

or

$$= k_4' \exp -\left[\Delta G_4^{\neq} - \beta VF\left(1 + \frac{r_2}{r_1}\right)\right]/RT \qquad [10]$$

and

$$dV/d \ln i_4 = \frac{2RT}{F}\left(\frac{r_1}{r_1+r_2}\right). \qquad [11]$$

In scheme B, the result for [II] is the same as above and for [V], rate determining

$$v_5 = k_5\theta_F \exp -[\Delta G_5^{\neq} - \beta VF - \beta r_1\theta]/RT. \qquad [12]$$

If [II] is in quasi-equilibrium and equation [6] applies,

$$dV/d \ln i_5 = RT/F \ (\beta \doteqdot 1/2) \qquad [13]$$

except for limitingly full coverage by HCOO· when the Langmuir result applies ($dV/d \ln i_5 = 2RT/F$) in any case.

Barrier layer film effects, which are important in some anodic reactions (20, 35), are evidently not significant in the present reaction since the maximum Tafel slopes observed are not abnormally high. There is some possibility, however, of the role of such effects in the Kolbe reaction itself and in aqueous solutions (see Parts II and III).

The polarization behavior at all three electrodes at low current densities (below the critical current) is associated with an unusually low slope. This is characteristic of a process occurring at a current less than or close to its exchange current. The apparent overpotential referred to the hypothetical standard formate reversible potential is quite appreciable at these low current densities, so it is not the formate decomposition reaction itself which determines this behavior. Since the current efficiency for CO_2 production at the lowest current densities is only about 55–60%, and metal dissolution visibly occurs (by formation of colloidal metal in prolonged low current density polarization) we suggest that this low-slope region is associated with the "active" attack of the metal which occurs simultaneously with reactions [II] and [III] at low coverage. This is consistent with the subsequent "passive" behavior at the critical current, at higher current densities. Such low slopes are not observed in the aqueous solutions (Part II).

(c) Galvanostatic Results

Some possibility for distinction between the various reaction mechanisms envisaged above is afforded by the galvanostatic charging results. It is seen that at appreciable current densities (Figs. 3 and 4) there is a significant arrest amounting to 200–250 μcoulombs/cm^2 at Pt or Au and up to 1770 μcoulombs/cm^2 both on the charging and forced discharge transients (and implicit in the open-circuit decay curves) at appreciable anodic current densities (16, 17). The charging arrest cannot be a diffusion-controlled transient since: (*a*) at the current density used, the transition time for $HCOO^-$ oxidation is some 10^3 to 10^4 times larger than that observed; (*b*) the arrest is also seen both on the reverse transient and on open-circuit decay. The magnitude of the arrests at platinum and gold correspond to an initial coverage of about one monolayer by some more or less reversibly removable ad-species, presumably produced in the discharge step. This calculation is based on an assumed area of the HCOO· radical of 14.2 Å^2 (from Courtauld models). It is reasonable to assume this ad-species is the HCOO· radical discussed above; it is unlikely to be H· since any adsorbed H would tend to be removed at a very high rate (ca. $10^{10}\theta_H$ amp cm^{-2}) at the high anodic potentials (ca. 1–1.5 v) used so that its steady-

Can. J. Chem. Downloaded from www.nrcresearchpress.com by 210.87.254.40 on 09/05/12
For personal use only.

state coverage in an *anodic* reaction could hardly be significant and certainly not experimentally measurable in a slow transient such as observed here. The charging results therefore indicate an appreciable coverage presumably by HCOO· radicals; it may hence be concluded that, at least for the upper potential region (Figs. 1 and 2), discharge from or to which gives the arrest in the transients, a radical desorption step is the rate-controlling process, i.e. either process [III] (scheme A) or [V] (scheme B) is involved. Reaction [III] gives $dV/d \ln i = RT/F$ under "Langmuir" conditions or $(2RT/F)\cdot(r_1/r_1-r_2)$ under "Temkin" conditions while V gives $2RT/F$ for full coverage, or for potential-dependent coverage conditions, $2RT/3F$ ("Langmuir") or RT/F ("Temkin" conditions). The slope $2RT/3F$ is *not* observed under any of the conditions examined, but slopes of approximately RT/F and $2RT/F$ are found for Au and the Au–Pd alloys while slopes of about $2RT/F$ are found for Pt and Pd. At gold, the change of slope from a low to a higher value with increasing current density is explicable formally in terms either of a transition from one rate-determining step to another in a *consecutive* reaction sequence, or in terms of a transition from "Langmuir" to "Temkin" conditions (e.g. for reactions [III] or [V]); the corresponding change for reaction [V] is from $2RT/3F$ (Langmuir) to RT/F (Temkin) to $2RT/F$ (full coverage). The first transition is not observed. We believe the latter type of transition may be applicable in the present case, since a second *consecutive* step (e.g. [IV]) is not plausible in this scheme. Alternatively [III] (Langmuir) followed by [V] (at full coverage)—which is really a related path involving the same initial state—is also consistent with the results for gold and some of the alloys. For Pt or Pd, the results are consistent with [III] (Temkin) or [V] (full coverage) over the whole current density range in the upper region. We have outlined plausible reaction mechanisms here consistent with the experimental behavior but it is premature to propose any further final conclusions at the present stage. The behavior of possible intermediates,-e.g. the HCOO· is further discussed in Part III in terms of the e.m.f. decay behavior.

(d) The Transition Behavior

The transition behavior observed in the present system is quite analogous to that observed in oxygen evolution (20) and, in general, in anodic passivation. In the present work, no oxygen evolution or oxide film formation is possible and we must presume that the passivation behavior is associated with formation of a film of "formate" or formate radicals on the metal surface. This is supported by the form of the observed galvanostatic transients and by the open-circuit decay behavior (Fig. 5). Under certain conditions, visible decomposition of the film at Pd occurs on open circuit when it has been formed to an appreciable thickness (16); the metal then returns to an "active" condition and the film layer can be repeatedly re-formed by anodic polarization. Periodic phenomena commonly associated with critical conditions for passivation were also observed in the present work. The critical potentials previously referred to (6, 7, 14) in work on the Kolbe reaction are probably related to this condition of passivation and formation of a carboxylate film (HCOO·(M) in the present case). Further evidence that the transition region corresponds to completion of an ad-layer is afforded by the quantitative analysis of the e.m.f. decay transients in terms of surface charge and adsorption pseudocapacity to be discussed in Part III.

Time Dependence of Electrode Potential

In the present non-aqueous system, very little time variation of potential was noted except near the critical current in the transition region where, under rather critical

Can. J. Chem. Downloaded from www.nrcresearchpress.com by 210.87.254.40 on 09/05/12
For personal use only.

conditions of current adjustment, periodic oscillations of the potential occurred of the kind well known near the critical condition for passivation. In the upper potential region, steady potential values were attained within 10–20 seconds. Extended logarithmic time dependence of the overpotential of the kind reported in Part III for the aqueous solutions of potassium formate was not observed for the reaction in the 100% formic acid solutions.

Dependence of Kinetic Parameters on the Metal

In Table II are shown the Tafel slopes and exchange currents for the various metals used. Basically, the same type of transition behavior is observed at all three metals and the highest Tafel slopes are all of the order of $2.3(2RT/F)$. Gold and the gold-rich Au–Pd alloys, however, differ from platinum and palladium in that a slope of about $2.3RT/F$ is observed in the upper potential region followed by the slope of $2.3(2RT/F)$. As we have discussed on p. 35, this could arise from a change of coverage conditions, since at the top of the transition region, the pseudocapacity data indicate coverage by $HCOO^{\cdot}$ to only about 0.5 monolayer. As in the case of the oxygen evolution reaction at alloys (20), no direct relationships to metal *d*-band configuration are observed since the anodic reactions are proceeding, at the higher current densities, on a film of an anodic intermediate, so that the kinetic parameters will not necessarily be expected to reflect properties of the metal itself.

ACKNOWLEDGMENT

Grateful acknowledgment is made to the National Research Council for support of this work.

REFERENCES

1. H. KOLBE. Ann. **69**, 257 (1849).
2. B. C. L. WEEDON. Quart. Rev. (London), **6**, 380 (1952).
3. E. BAUR. Helv. Chim. Acta, **11**, 372 (1928).
4. C. SCHALL. Z. Elektrochem. **3**, 83 (1896).
5. F. FICHTER. Trans. Electrochem. Soc. **75**, 309 (1939).
6. S. GLASSTONE and A. HICKLING. J. Chem. Soc. 1878 (1934); 820 (1936).
7. G. S. PANDE and S. N. SHUKLA. Electrochim. Acta, **4**, 215 (1961).
8. A. CRUM-BROWN and O. J. WALKER. Ann. **261**, 107 (1891).
9. S. N SHUKLA and O. J. WALKER. Trans. Faraday Soc. **27**, 722 (1931).
10. D. A. FAIRWEATHER and O. J. WALKER. J. Chem. Soc. 3111 (1926).
11. K. CLUSIUS and P. HOLEMAN. Z. Physik. Chem. B, **35**, 261 (1937).
12. K. CLUSIUS and W. SCHANZER. Z. Physik. Chem. A, **192**, 223 (1943); A, **190**, 241 (1941).
13. C. C. WILSON and W. J. LIPPINCOTT. J. Electrochem. Soc. **103**, 672 (1956); J. Am. Chem. Soc. **78**, 4290 (1956).
14. T. DICKENSON and W. F. K. WYNNE-JONES. Trans. Faraday Soc. **58**, 382, 388, 400 (1962).
15. N. L. BAULD. Thesis, University of Illinois, Urbana, Ill. 1959.
16. B. E. CONWAY and M. DZIECIUCH. Nature, **189**, 914 (1961).
17. B. E. CONWAY and M. DZIECIUCH. Proc. Chem. Soc. 121 (1962).
18. B. E. CONWAY and P. L. BOURGAULT. Trans. Faraday Soc. **58**, 593 (1962).
19. B. E. CONWAY and E. GILEADI. Trans. Faraday Soc. In press (1963).
20. B. E. CONWAY and J. J. MACDONALD. Proc. Roy. Soc. (London), Ser. A, **269**, 419 (1962).
21. B. E. CONWAY and M. DZIECIUCH. Abstracts of the Meeting of the Electrochemical Society, Chicago. J. Electrochem. Soc. **107** No. 199, 760 (1960).
22. A. M. AZZAM, J. O'M. BOCKRIS, B. E. CONWAY, and M. ROSENBERG. Trans. Faraday Soc. **46**, 918 (1950).
23. B. E. CONWAY, E. M. BEATTY, and P. A. D. DE MAINE. Electrochim. Acta, **7**, 39 (1962); Proc. Roy. Soc. (London), Ser. A, **256**, 128 (1960).
24. R. R. DREISBACH and R. A. MARTIN. Ind. Eng. Chem. **41**, 2875 (1949).
25. J. O'M. BOCKRIS, B. E. CONWAY, and W. MEHL. J. Sci. Instr. **33**, 400 (1956); cf. J. Sci. Instr. **25**, 283 (1948) and Rev. Sci. Instr. **28**, 209 (1957).
26. J. O'M. BOCKRIS. Discussions Faraday Soc. **1**, 95 (1947); Trans. Faraday Soc. **43**, 417 (1947).
27. M. R. FIOSHIN and I. B. VASILEV. Dokl. Akad. Nauk SSSR, **134**, 879 (1960).
28. K. F. BONHOEFFER and H. GERISHER. Z. Elektrohem. **52**, 149 (1948).
29. B. E. CONWAY and P. L. BOURGAULT. Can. J. Chem. **37**, 292 (1959).
30. A. SLYGIN and B. V. ERSHLER. Acta Physicochim. URSS, **11**, 45 (1939). A. SLYGIN and A. N. FRUMKIN. Acta Physicochim. URSS, **3**, 791 (1935).

Can. J. Chem. Downloaded from www.nrcresearchpress.com by 210.87.254.40 on 09/05/12
For personal use only.

31. W. L. LATIMER. Oxidation potentials. 2nd ed. Prentice Hall, New York. 1952.
32. J. O'M. BOCKRIS and H. KITA. J. Electrochem. Soc. **108**, 678 (1961).
33. J. O'M. BOCKRIS. J. Chem. Phys. **24**, 817 (1956).
34. J. G. N. THOMAS. Trans. Faraday Soc. **57**, 1603 (1961). B. E. CONWAY and E. GILEADI. Trans. Faraday Soc. In press (1962).
35. L. YOUNG. Proc. Roy. Soc. (London), Ser. A, **263**, 395 (1961).
36. B. E. CONWAY and P. BOURGAULT. Can. J. Chem. **40**, 1960 (1962).
37. M. BOUDART. J. Am. Chem. Soc. **72**, 3556 (1952).
38. G. HALSEY and H. S. TAYLOR. J. Chem. Phys. **15**, 624 (1947).

EXPLANATION OF FIGURES 3–5

FIG. 3. Anodic charging curves for gold and palladium electrodes at various current densities in 1 *M* HCOOK/100% HCOOH (5° C), starting at the potentials indicated.

Au: 1. 7×10^{-6} amp cm^{-2}, 180 mv, 0.05 v cm^{-1}, 0.2 sec cm^{-1}
2. 1.7×10^{-5} amp cm^{-2}, 180 mv, 0.2 v cm^{-1}, 1 sec cm^{-1}
3. 6×10^{-5} amp cm^{-2}, 180 mv, 0.2 v cm^{-1}, 1 sec cm^{-1}
4. 9×10^{-4} amp cm^{-2}, 180 mv, 0.2 v cm^{-1}, 0.1 sec cm^{-1}

Pd: 1. 1.2×10^{-5} amp cm^{-2}, 160 mv, 0.1 v cm^{-1}, 0.2 sec cm^{-1}
2. 1.4×10^{-4} amp cm^{-2}, 160 mv, 0.2 v cm^{-1}, 0.2 sec cm^{-1}
3. 4.07×10^{-4} amp cm^{-2}, 160 mv, 0.2 v cm^{-1}, 0.2 sec cm^{-1}
4. 2.33×10^{-3} amp cm^{-2}, 160 mv, 0.2 v cm^{-1}, 0.2 sec cm^{-1}

FIG. 4. Cathodic reverse pulse discharge curves for gold electrodes at various current densities in 1 *M* HCOOK/100% HCOOH (5° C), starting at the potentials indicated.

Au: 1. 7.1×10^{-6} amp cm^{-2}, 560 mv, 0.2 v cm^{-1}, 0.5 sec cm^{-1}
2. 2.7×10^{-5} amp cm^{-2}, 1355 mv, 0.2 v cm^{-1}, 0.5 sec cm^{-1}
3. 6×10^{-3} amp cm^{-2}, 1420 mv, 0.2 v cm^{-1}, 0.5 sec cm^{-1}
4. 3.1×10^{-4} amp cm^{-2}, 1460 mv, 0.2 v cm^{-1}, 0.2 sec cm^{-1}

Pt: 1. 2.4×10^{-5} amp cm^{-2}, 1110 mv, 0.2 v cm^{-1}, 0.2 sec cm^{-1}
2. 2.7×10^{-4} amp cm^{-2}, 1165 mv, 0.2 v cm^{-1}, 0.2 sec cm^{-1}
3. 7.8×10^{-4} amp cm^{-2}, 1360 mv, 0.2 v cm^{-1}, 50 msec cm^{-1}
4. 1.8×10^{-3} amp cm^{-2}, 1410 mv, 0.2 v cm^{-1}, 50 msec cm^{-1}
5. 4.5×10^{-3} amp cm^{-2}, 1480 mv, 0.2 v cm^{-1}, 50 msec cm^{-1}

(Data for Pd at various current densities and times of polarization are given in Fig. 5 (Part I) and in Figs. 2 and 4, Part III, and open-circuit decay behavior is shown in Fig. 6, Part III.)

FIG. 5. Cathodic discharge transients as a function of time of previous anodic polarization, starting at the potentials indicated (1 *M* HCOOK/HCOOH, 5° C).

Pd: 1. 5.9×10^{-3} amp cm^{-2}, 3.9 sec, 1115 mv, 50 msec cm^{-1}, 0.2 v cm^{-1}
2. 5.9×10^{-3} amp cm^{-2}, 20.6 sec, 1295 mv, 50 msec cm^{-1}, 0.2 v cm^{-1}
3. 5.9×10^{-3} amp cm^{-2}, 65.7 sec, 1395 mv, 50 msec cm^{-1}, 0.2 v cm^{-1}
4. 5.9×10^{-3} amp cm^{-2}, 50 sec, 1400 mv, 50 msec cm^{-1}, 0.2 v cm^{-1}
5. 5.9×10^{-3} amp cm^{-2}, 505 sec, 1415 mv, 0.1 sec cm^{-1}, 0.2 v cm^{-1}
6. 5.9×10^{-3} amp cm^{-2}, 1050 sec, 1560 mv, 0.2 sec cm^{-1}, 0.2 v cm^{-1}

(Note change in time scale in 4, 5, and 6.)

Au: 1. 6.65×10^{-5} amp cm^{-2}, 29.2 sec, 1410 mv, 0.5 sec cm^{-1}, 0.2 v cm^{-1}
2. 6.65×10^{-5} amp cm^{-2}, 66.5 sec, 1410 mv, 0.5 sec cm^{-1}, 0.2 v cm^{-1}
3. 1.1×10^{-3} amp cm^{-2}, 212 sec, 1480 mv, 20 msec cm^{-1}, 0.2 v cm^{-1}
4. 1.1×10^{-3} amp cm^{-2}, 310 sec, 1480 mv, 50 msec cm^{-1}, 0.2 v cm^{-1}

(Note almost constant capacity of 160 μF cm^{-1} over ca. 1.0 v in 1 and 2.)

Pt: 1. 1.1×10^{-3} amp cm^{-2}, 15.9 sec, 1420 mv, 50 msec cm^{-1}, 0.2 v cm^{-1}
2. 1.1×10^{-3} amp cm^{-2}, 105 sec, 1430 mv, 50 msec cm^{-1}, 0. 2 v cm^{-1}
3. 1.1×10^{-3} amp cm^{-2}, 310 sec, 1410 mv, 50 msec cm^{-1}, 0.2 v cm^{-1}

Can. J. Chem. Downloaded from www.nrcresearchpress.com by 210.87.254.40 on 09/05/12
For personal use only.

NEW APPROACHES TO THE STUDY OF ELECTROCHEMICAL DECARBOXYLATION AND THE KOLBE REACTION

PART II. THE MODEL REACTION WITH TRIFLUOROACETATE AND COMPARISONS WITH AQUEOUS SOLUTION BEHAVIOR

B. E. CONWAY AND M. DZIECIUCH
Department of Chemistry, University of Ottawa, Ottawa, Canada

Received June 29, 1962

Can. J. Chem. Downloaded from www.nrcresearchpress.com by 210.87.254.40 on 09/05/12
For personal use only.

ABSTRACT

Electrochemical kinetic studies on the Kolbe reaction have been carried out in the trifluoroacetate – 100% trifluoroacetic acid system, where the reaction can be examined from an electrochemical viewpoint with minimum complication by oxidative side reactions. High yields of the Kolbe products C_2F_6 and CO_2 are obtained and current–potential curves exhibiting transition behavior and linear Tafel regions are found. Tafel slopes are deduced for "Langmuir" and "Temkin" conditions of surface coverage by intermediates and compared with the experimental observations. Plausible reaction mechanisms are proposed, which are supported by galvanostatic discharge transients; the latter indicate that the coverage by adsorbed intermediates in the trifluoroacetate reaction approaches a monolayer. In the aqueous formate systems, multilayer formation is indicated, including deposition of layers of different species corresponding to different arrest regions in the galvanostatic discharge transients. It is suggested that these layers may consist of oxide and the discharged carboxylate and that the transition behavior and critical potentials in the Kolbe reaction correspond to conditions for passivation of the metal by oxide and carboxylate species.

INTRODUCTION

A general introduction to the problem has been given in Part I (1), where the model decarboxylation reaction involving formate in formic acid was examined. In the present paper, studies of the kinetics of the Kolbe decarboxylation and coupling reaction with the trifluoroacetate ion in 100% trifluoroacetic acid are reported. Comparisons are made with the kinetics of this reaction and of the formate decarboxylation in aqueous media. The system has been chosen as one giving minimal side reactions owing to the difficulty of further oxidation of the trifluoromethyl function and also since complications due to oxygen evolution or anodic oxide formation (cf. ref. 2) are absent under non-aqueous conditions. The system can hence be studied from a fundamental electrochemical viewpoint with minimum ambiguity. The results demonstrate that in aqueous media the decarboxylations are more complex than in non-aqueous media and probably involve surface films both of oxide and carboxylate species.

EXPERIMENTAL

(a) General

General methods of approach through current–potential studies, galvanostatic charging and discharging experiments, and coulombic yield determinations have been described in Part I (1) and were applied to the present system.

(b) Solutions

Trifluoroacetic acid (b.p. 70–72° C) was first gently* refluxed over phosphorus pentoxide for 1 hour, and distilled (3). A second distillation from fresh phosphorus pentoxide was then carried out and only the fraction distilling at 71.1° C was kept for preparation of the experimental solutions. The acid was stored in glass-stoppered vessels until required. Prior to use, the acid was again distilled from fresh phosphorus pentoxide in order to eliminate water completely and thus avoid the consequent possibility of direct oxygen evolution.

**The formation of the anhydride is minimized by keeping the temperature of the mixture as low as possible. In any case it is readily separated in the subsequent distillation.*

Potassium trifluoroacetate was prepared by neutralizing previously purified trifluoroacetic acid with potassium hydroxide. The salt was then recrystallized twice from conductivity water, washed with ethanol, and exhaustively dried under vacuum at 100° C for 24 hours.

Solutions of potassium trifluoroacetate in the 100% trifluoroacetic acid were prepared from the freshly dried salt by redistilling (see above) the purified trifluoroacetic acid directly from the desiccant under vacuum near room temperature. Pre-electrolysis was for 24 hours at 10^{-2} amp cm^{-2} on a sacrificial electrode.

(c) Electrical Measurements

These were as described in Part I. The details of the galvanostatic circuit are given in Part III. Hydrogen reference electrodes were used as in the pure formic acid solutions and were satisfactorily reversible.

(d) Current Efficiency for CO_2 and C_2F_6 Production

The expected gases were CO_2 and C_2F_6 (CF_4 was also found in traces). The CO_2 was determined as described in Part I and C_2F_6 by gas chromatography using standard records obtained with known samples of Matheson C_2F_6. Gas collection and total charge passed were determined as in Part I.

(e) Measurements in Aqueous Solutions

In order to compare the kinetic behavior of the trifluoroacetate and formate decarboxylations under aqueous and non-aqueous conditions, a number of runs were performed in 1 *M* aqueous solutions of the potassium salts of the two acids and in solutions also containing 1 *M* KOH. The latter was used to stabilize the pH and also possibly to facilitate simultaneous oxygen evolution or oxide film formation in the aqueous systems. All other conditions were as described above and in Part I; the water used was conductivity water which had been redistilled in purified nitrogen. During the runs, the solutions were saturated with pure carbon dioxide. All runs were carried out at 5° C.

RESULTS

(a) Current–Potential Curves

The Tafel lines for Pt, Pd, and Au in 1 *M* CF_3COOK in 100% CF_3COOH are shown in Fig. 1(*a*, *b*, *c*). The lines are already in a high-potential region (>2.0 v) at 10^{-5} amp cm^{-2} and the transition behavior previously observed in the formate system occurs between 10^{-6} and 10^{-5} amp cm^{-2} in the trifluoroacetate system (see Fig. 2 for comparison). It is also observed on the open-circuit decay and the cathodic galvanostatic discharge. The Tafel lines in the upper region at all three metals are striking on account of their high slopes of $4RT/F$ to about $6RT/F$, depending on metal and current density. These high slopes are not impurity controlled and are maintained with the most carefully purified solutions and electrodes. Similar high slopes are known for the oxygen evolution reaction when oxide films are present (4) and, in some cases, are associated with barrier layer charge transfer processes (5). Comparison between the current–potential behavior in the trifluoroacetate and formate decarboxylation reactions is shown in Fig. 2.

Comparative runs were carried out in aqueous solutions and are shown in Fig. 3(*a*, *b*, *c*). The current–potential behavior is again complex but Tafel slopes only exceed $2RT/F$ for Pt, except in the transition regions, which cover a range of potential of about 1.5 v. At high current densities the slopes at Pd and Au are about 0.08 v, i.e. much lower than in the non-aqueous solutions. In general, the Tafel regions are well defined and remarkably reproducible, e.g. the data for Pt and Pd, except near the transition region, where presumably film formation is either not complete or has not reached a steady state. At Pt, two transition regions are observed: a main one at $10^{-5.5}$ amp cm^{-2}, analogous to that observed at Pd and Au and in the formate system, and a smaller one at $10^{-2.9}$ amp cm^{-2} with hysteresis between the upper and lower regions. The significance of the Tafel lines will be discussed after the coulombic yields have been reported in the following section.

The time variation of electrode potential in the aqueous Kolbe reaction is relatively small except at low current densities ($< 10^{-5}$ amp cm^{-2}), where the potential increases initially in an approximately logarithmic manner with time, as also shown in Part III, and becomes constant after about 10–20 minutes. At higher current densities beyond the

Can. J. Chem. Downloaded from www.nrcresearchpress.com by 210.87.254.40 on 09/05/12
For personal use only.

Can. J. Chem. Downloaded from www.nrcresearchpress.com by 210.87.254.40 on 09/05/12
For personal use only.

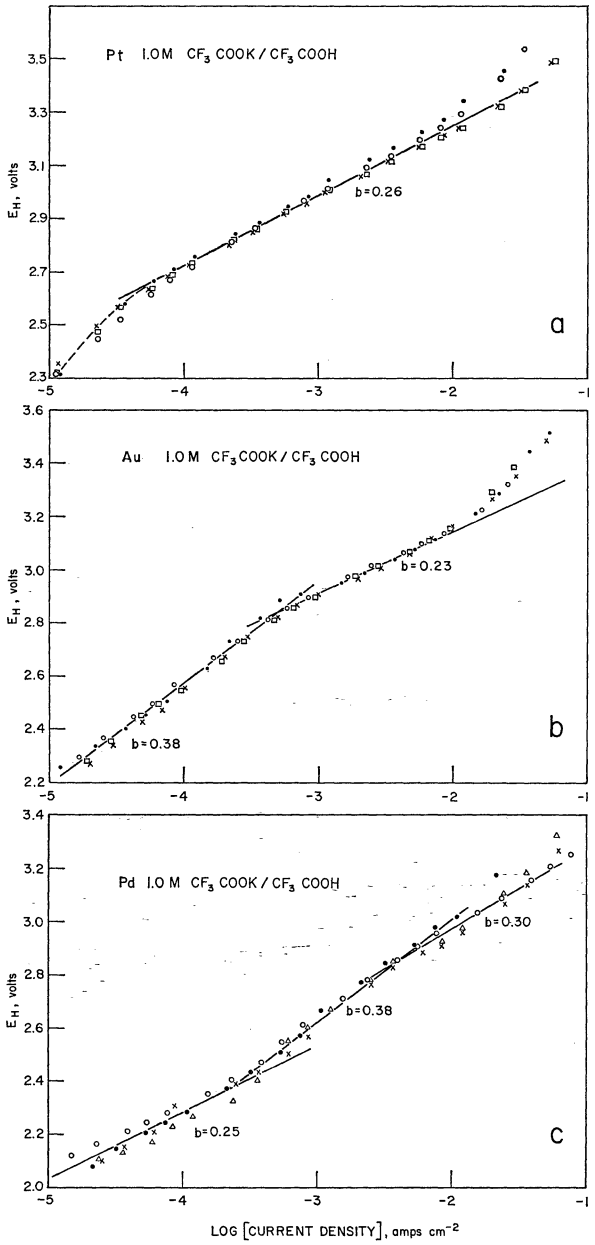

FIG. 1. Current–potential curves at 5° C for the trifluoroacetate Kolbe reaction in 100% trifluoroacetic acid.

limiting current, the time variation is small and sensibly constant electrode potentials are reached in about 2 minutes in the direction of both increasing and decreasing current densities.

In order to compare the behavior observed with trifluoroacetate in water with that for formate under the same conditions, a number of current–potential curves were obtained for the system 1 *M* H.COOK in water. The results were more difficult to reproduce than

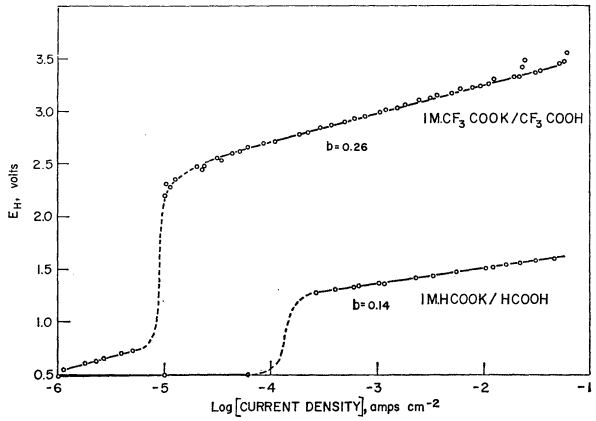

FIG. 2. Comparison between the current–potential curves for trifluoroacetate and formate decarboxylation in the respective pure acids (1 *M* potassium salts; 5° C).

those obtained in the 100% formic acid, particularly at Pd. By carrying out the reactions in the presence of 1 *M* (and 5 *M*) KOH, reproducibility was much improved. The current–potential curves are shown in Fig. 4 for aqueous formate and aqueous formate plus KOH at 5° C.

(b) Coulombic Yields

Coulombic yields in the 100% trifluoroacetic acid are very satisfactory and amount to 96% of the theoretical yields based on the reaction

$$2CF_3COO^- \rightarrow C_2F_6 + 2CO_2 + 2e. \qquad [I]$$

Also, the correct ratio of C_2F_6 (except for small traces (less than 2%) of CF_4 at low current densities) to CO_2 for 2 Faradays is observed in CO_2-saturated solutions. The yields are better than those in the formate system owing, probably, to a smaller attack on the metal. The coulombic yields are recorded in Table I. It is this observation of high coulombic yields that allows the kinetics in the pure trifluoroacetic acid to be discussed almost

TABLE I

Coulombic efficiencies for gas evolution in the trifluoroacetate Kolbe reaction (100% trifluoroacetic acid, 5° C)

Metal	Current density, amp cm^{-2}	Coulombic efficiencies, %	
		CO_2	C_2F_6
Pt	1×10^{-2}	94	96
	2.5×10^{-3}	93	92
	5×10^{-4}	93	85
Pd	1×10^{-2}	96	95
	2.5×10^{-3}	94	91
	5×10^{-4}	93	83
Au	1×10^{-2}	91	92
	2.5×10^{-3}	90	89
	5×10^{-4}	89	80

NOTE: At low current densities ($< 10^{-3}$ amp cm^{-2}), traces of CF_4 were identified in amounts less than 1–2% of the total volume of gas evolved and analyzed.

Can. J. Chem. Downloaded from www.nrcresearchpress.com by 210.87.254.40 on 09/05/12
For personal use only.

Can. J. Chem. Downloaded from www.nrcresearchpress.com by 210.87.254.40 on 09/05/12
For personal use only.

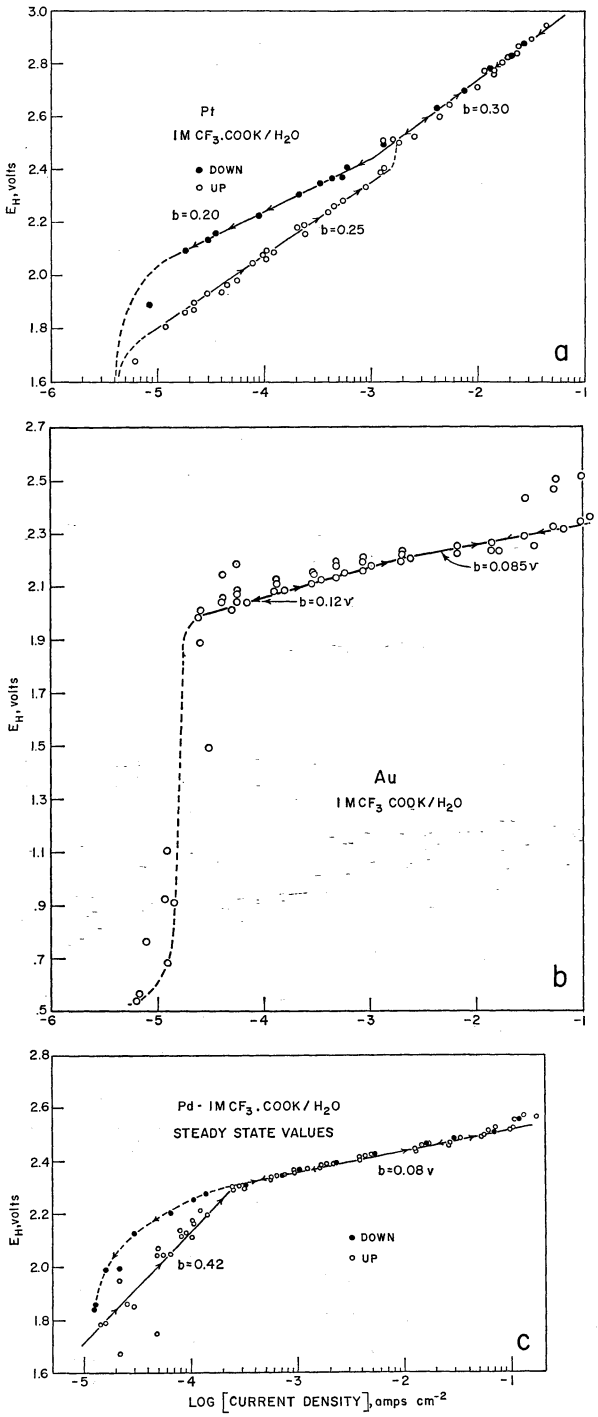

FIG. 3. Current–potential curve at 5° C for the trifluoroacetate Kolbe reaction in aqueous solution (1 *M* potassium trifluoroacetate).

Can. J. Chem. Downloaded from www.nrcresearchpress.com by 210.87.254.40 on 09/05/12
For personal use only.

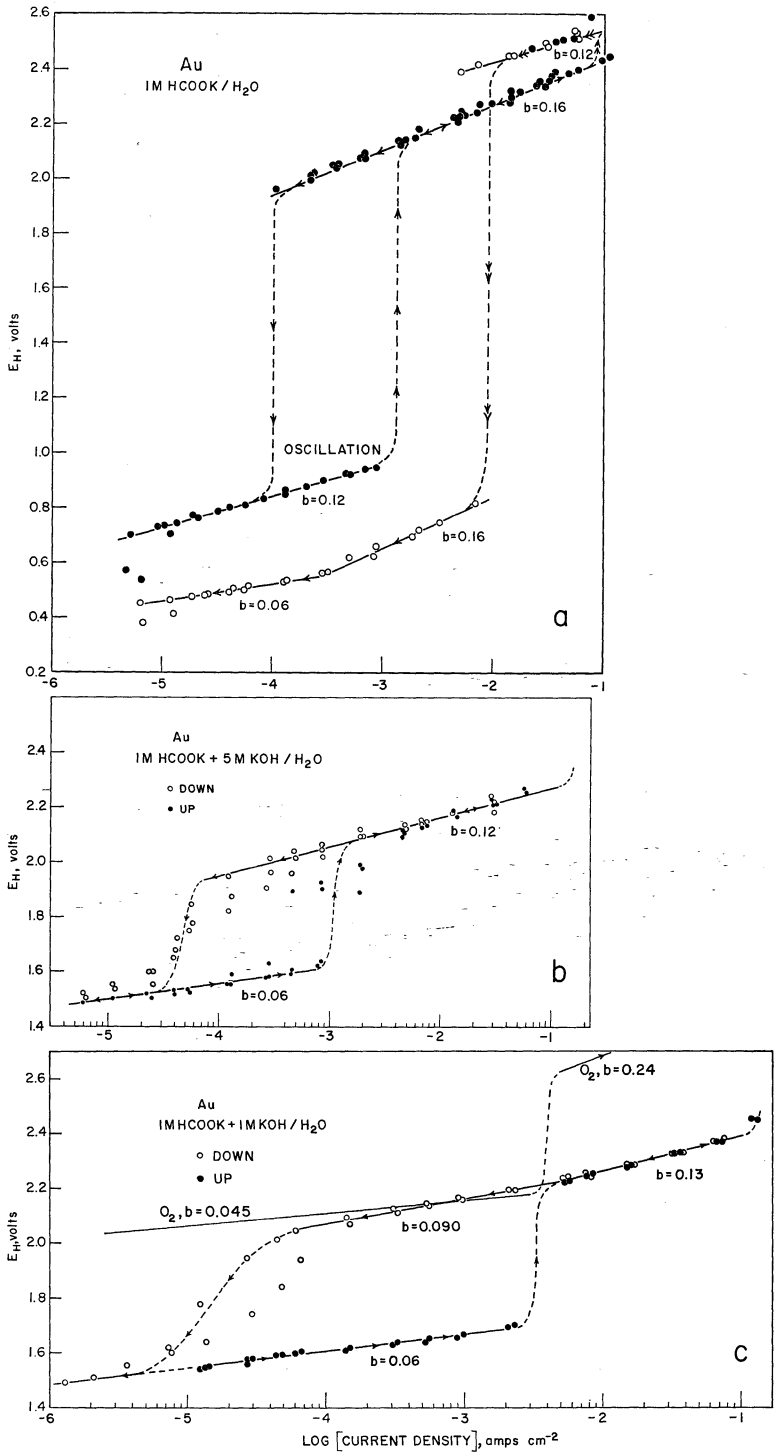

FIG. 4. Comparative current–potential curves for formate decarboxylation in aqueous 1 *M* HCOOK and 1 *M* HCOOK + KOH (5° C). (In *h* results in absence of alkali are not reproducible.)

Can. J. Chem. Downloaded from www.nrcresearchpress.com by 210.87.254.40 on 09/05/12
For personal use only.

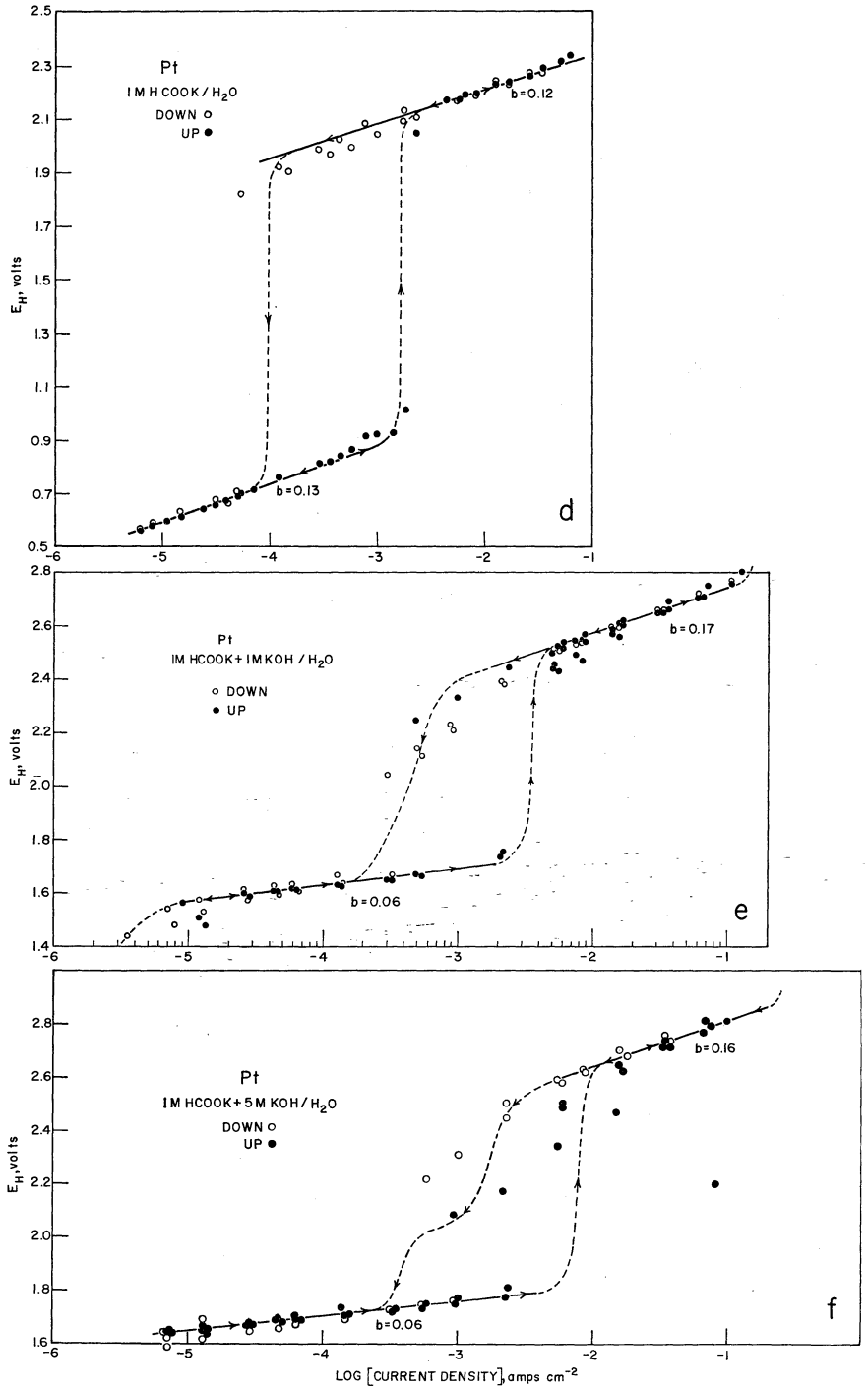

FIG. 4.

exclusively in terms of the overall reaction [I] above. Coulombic yields for the anodic formate decarboxylation reaction in aqueous solutions are given in Table II. Oxygen is also evolved under the aqueous conditions, so that the coulombic percentages have been

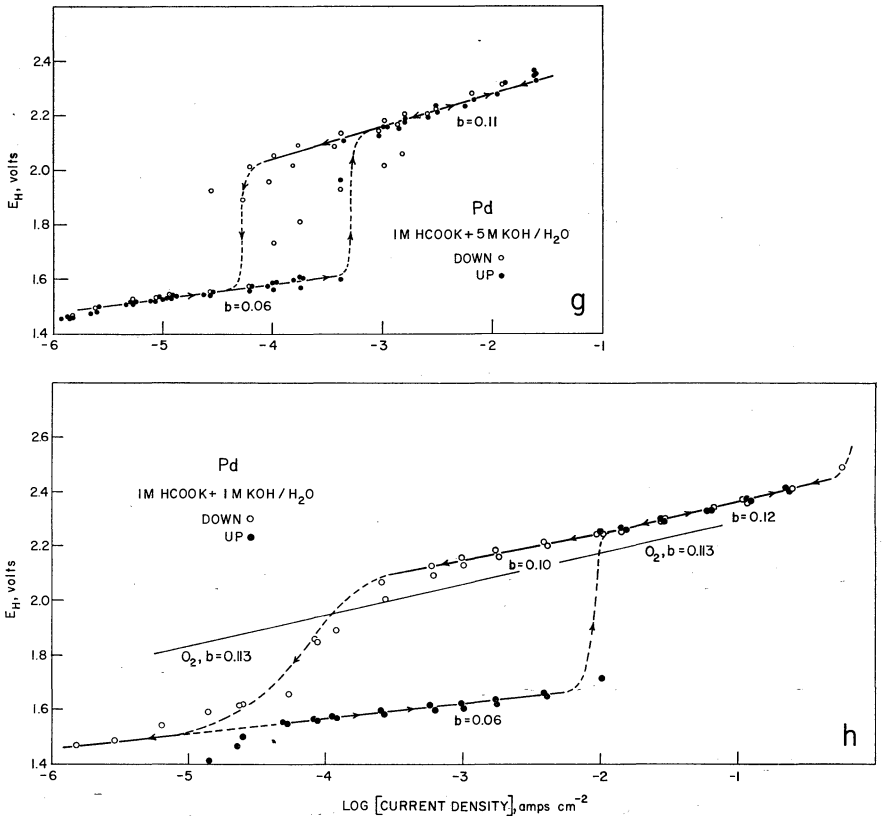

FIG. 4.

TABLE II

Coulombic yields for CO_2 and O_2 production in the anodic decarboxylation in aqueous potassium formate (1 *M* HCOOK, H_2O, 5° C)

Electrode	Current density, amp cm^{-2}	Coulombic yields, % CO_2	Coulombic yields, % O_2
Pt	1×10^{-1}	93	6
	2.5×10^{-2}	72	24
	5×10^{-3}	65	33
Pd	1×10^{-1}	74	21
	2.5×10^{-2}	63	27
	5×10^{-3}	52	33
Au	2.5×10^{-2}	24	55
	3.1×10^{-3}	22	38

calculated for CO_2 and O_2 assuming that 2 F per mole CO_2 and 4 F per mole O_2 are involved in the evolution of the gas mixture. From the measured volumes of each of the two gases evolved and the total number of coulombs passed as determined in the copper coulometer, the coulombic percentage yields may be calculated. The coulombic percentage yields do not necessarily add up to 100%, since the reactions leading to gas evolution are themselves not necessarily 100% coulombically efficient with respect to volumes of the gases evolved. Thus, visible surface films are formed at gold and palladium in the aqueous

Can. J. Chem. Downloaded from www.nrcresearchpress.com by 210.87.254.40 on 09/05/12
For personal use only.

formate system but not under non-aqueous (100% formic acid) conditions. The films may hence be surface oxides (see below).

The anodic reaction at Pd and Au in aqueous potassium trifluoroacetate, which was studied for comparative purposes only and in less detail than the corresponding non-aqueous reaction gives 87–96% O_2 and only 5–10% CO_2 with very little C_2F_6. The results are striking in so far as at Au and Pd, the decarboxylation reaction is almost completely inhibited by the oxygen evolution process which proceeds with quite high coulombic efficiency (and visible oxide films can be seen at Au), and the Tafel plots in Fig. 3(*b*, *c*) are hence principally for O_2 evolution from the trifluoroacetate solution. At Pt the Kolbe coupling reaction to give C_2F_6 still occurs but only at a moderate efficiency of ca. 25% with oxygen evolution. This disparity of behavior is probably connected with the stability and extent of growth of oxide films at Au and Pd in comparison with that at Pt. This result can also offer an explanation of why oxidation products are more predominant in the acetate Kolbe reaction at Au than at Pt.

(c) Galvanostatic Transients

The qualitative features of the transients (Fig. 5) were similar to those observed in the formate – formic acid system except that the arrests were generally shorter at a given current density, indicating a rather smaller surface concentration of ad-species. However, in the aqueous formate system, anodic films of appreciable thickness are indicated, as shown below (Fig. 6). Considerable complexity in the transients was observed in the aqueous systems, indicating formation of several electrochemically distinct species on the surface. These transients are discussed in more detail below.

(d) Exchange Currents

Exchange current densities, i_0, could not be evaluated for the trifluoroacetate reaction owing to lack of the appropriate thermodynamic data and to the low coulombic yields in the aqueous media. However, for the aqueous formate decarboxylation, i_0 values can be evaluated, since the standard reversible potential can be calculated (9); values are recorded in Table III for the various aqueous solutions used. The i_0 values are based on the reversible potentials given in Table IV.

DISCUSSION

(a) Reaction Mechanisms

By analogy with the reaction with formate, we may envisage the following steps in the overall reaction [I]:

$$CF_3COO^- \rightarrow CF_3COO^{\cdot}(M) + e \qquad [II]$$

$$CF_3COO^{\cdot}(M) \rightarrow CF_3^{\cdot}(M) + CO_2 \qquad [III]$$

$$2CF_3^{\cdot} \rightarrow C_2F_6. \qquad [IV]$$

Side reactions could lead to the production of the peroxide $(CF_3.COO)_2$ or the ester $CF_3.COOCF_3$; the coulombic yields indicate that these pathways are insignificant, although *adsorbed* peroxide could be an intermediate which quantitatively decomposes to C_2F_6 and CO_2. A reaction involving two ions, decarboxylation, coupling, and two-electron transfer in one step is unlikely. The above scheme is hence believed to be the most reasonable pathway on which to base a more definitive treatment of reaction mechanism. At full coverage by $CF_3COO^{\cdot}$ in [III], potential-dependent radical–ion desorption paths such as

$$CF_3^{\cdot} + CF_3COO^- \rightarrow C_2F_6 + CO_2 + e \qquad [V]$$

or

$$CF_3COO^{\cdot} + CF_3COO^- \rightarrow C_2F_6 + 2CO_2 + e \qquad [VI]$$

Can. J. Chem. Downloaded from www.nrcresearchpress.com by 210.87.254.40 on 09/05/12
For personal use only.

Can. J. Chem. Downloaded from www.nrcresearchpress.com by 210.87.254.40 on 09/05/12
For personal use only.

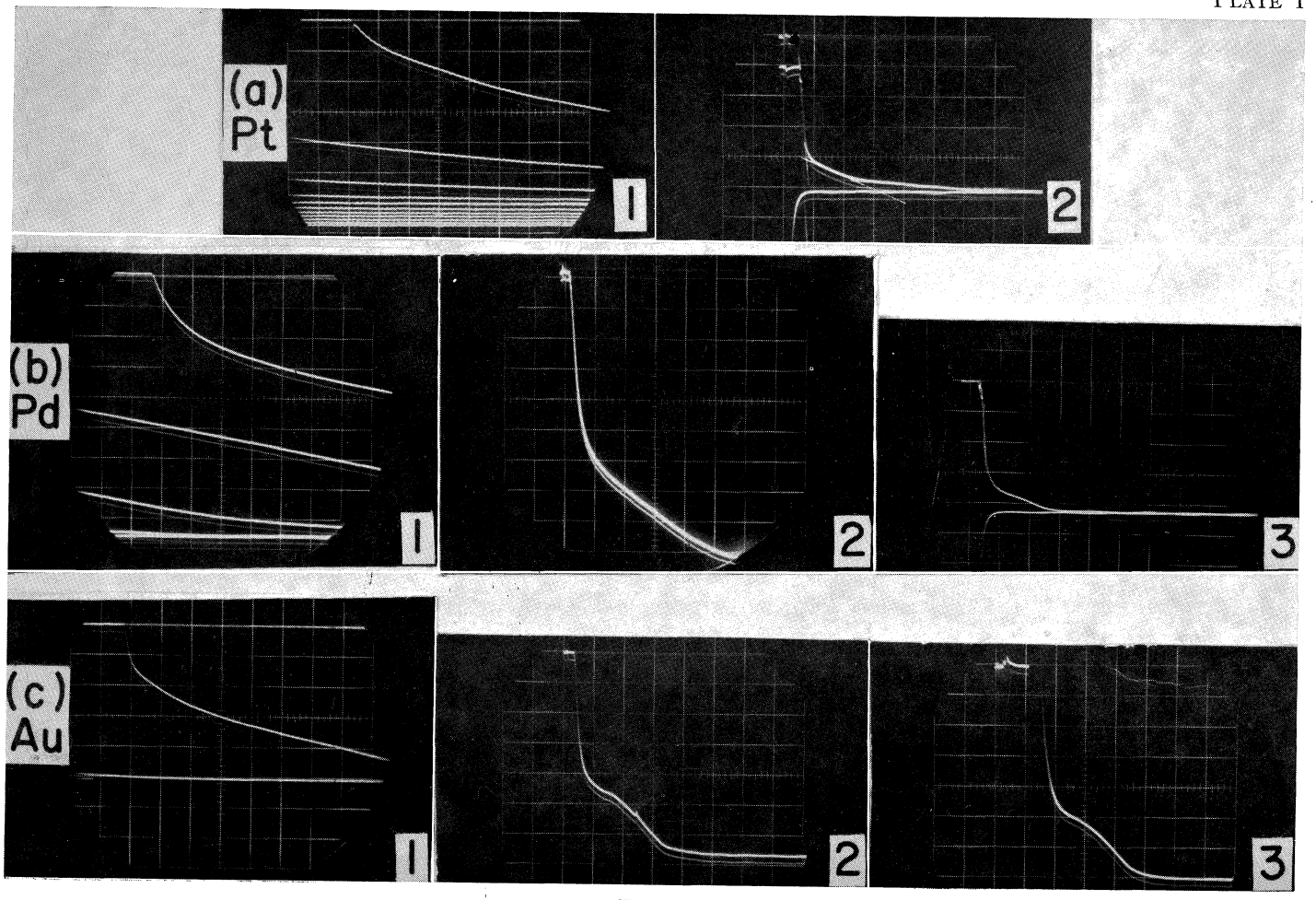

FIG. 5.

NOTE: For explanation of Figs. 5 and 6 see p. 54.

Can. J. Chem. Downloaded from www.nrcresearchpress.com by 210.87.254.40 on 09/05/12
For personal use only.

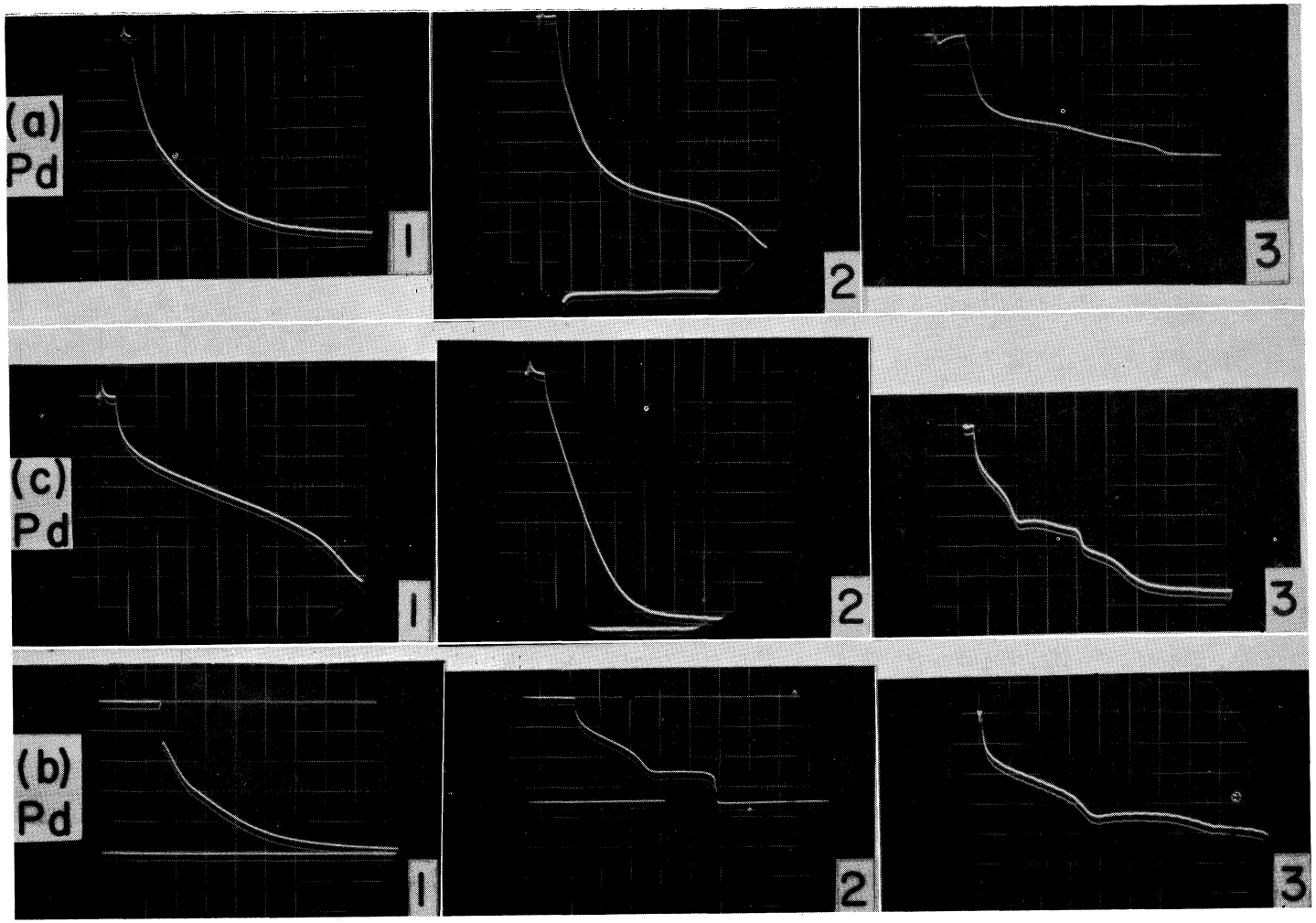

FIG. 6.

Can. J. Chem. Downloaded from www.nrcresearchpress.com by 210.87.254.40 on 09/05/12
For personal use only.

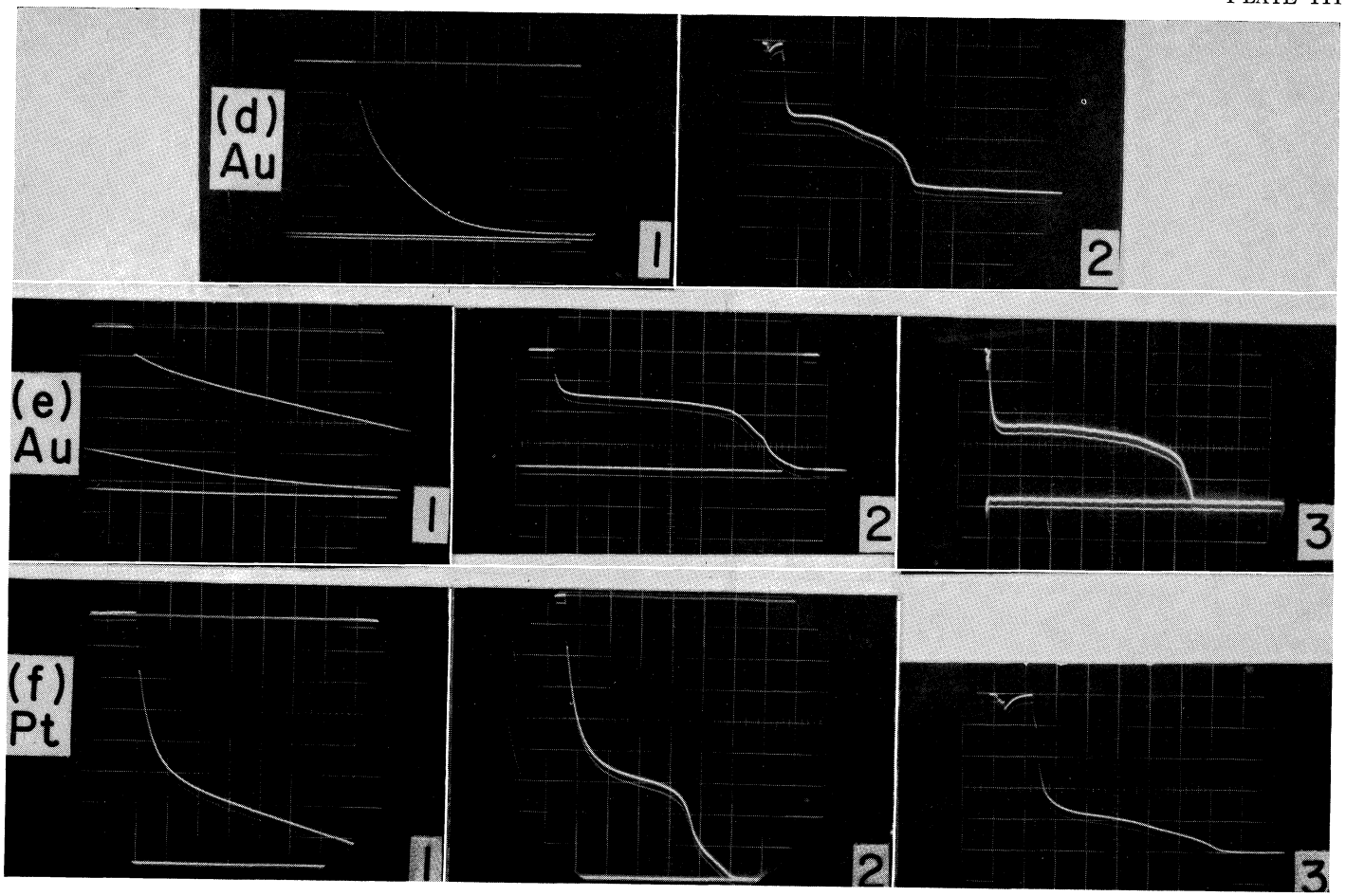

FIG. 6.

Can. J. Chem. Downloaded from www.nrcresearchpress.com by 210.87.254.40 on 09/05/12
For personal use only.

TABLE III

Mean Tafel parameters for the aqueous formate decarboxylation reaction (5° C)
(minimum of 10 electrodes in two solutions)

Electrode	Concentration	$b(\pm 1\%)$, v	$i_0(\pm 40\%)$ amp cm^{-2}	Current density range, amp cm^{-2}
Pt	1 *M* HCOOK/H_2O	0.13 (lower)	1×10^{-10}	6×10^{-6}–1×10^{-2}
		0.12 (upper)	1.7×10^{-21}	2×10^{-4}–5×10^{-2}
Au	"	0.12 (lower)	3.9×10^{-11}	5×10^{-6}–1×10^{-3}
		0.16 (upper)	3.9×10^{-17}	1.5×10^{-4}–5×10^{-2}
Pt	1 *M* HCOOK + 1 *M* KOH/H_2O	0.06 (lower)	4×10^{-30}	9×10^{-6}–2×10^{-3}
		0.17 (upper)	3.2×10^{-17}	1.5×10^{-3}–1.1×10^{-1}
Pd	"	0.06 (lower)	4×10^{-29}	1.5×10^{-6}–5×10^{-3}
		0.12 (above hysteresis)	1.3×10^{-20}	1.5×10^{-2}–5×10^{-1}
		0.10 (in hysteresis region)	4×10^{-24}	2.5×10^{-4}–1.5×10^{-2}
Au	"	0.06 (lower)	8×10^{-26}	1.5×10^{-6}–2.5×10^{-3}
		0.13 (above hysteresis region)	4×10^{-19}	5×10^{-3}–1.1×10^{-1}
		0.09 (in hysteresis region)	6×10^{-26}	5×10^{-5}–5×10^{-3}
Pt	1 *M* HCOOK + 5 *M* KOH/H_2O	0.06 (lower)	5×10^{-31}	7×10^{-6}–3×10^{-3}
		0.16 (upper)	2×10^{-18}	5×10^{-3}–2×10^{-1}
Pd	"	0.06 (lower)	1×10^{-29}	2×10^{-6}–4×10^{-4}
		0.11 (upper)	2×10^{-22}	8×10^{-5}–2.5×10^{-2}
Au	"	0.06 (lower)	2×10^{-28}	5×10^{-6}–9×10^{-4}
		0.12 (upper)	1×10^{-19}	6×10^{-5}–5×10^{-2}

NOTE: Exchange currents are calculated with respect to the reversible potential estimated from the thermodynamic free energy for 25° C; see Table IV.

The apparent i_0 values for Au are based on the overall current. The values given are hence correct to within about a third of an order of magnitude, taking into account the observed current efficiencies. The uncertainty is not seriously different from that involved in the extrapolation to the reversible potential. At Pt and Pd the errors are correspondingly less.

TABLE IV

Reversible potentials for the reaction
$HCOOH \rightleftarrows 2H^+ + CO_2 + 2e$ on the hydrogen scale
in the same solution indicated

Solution	E_H, v
1 *M* aq. HCOOK	−0.047
1 *M* aq. HCOOK + 1 *M* aq. KOH	+0.105
1 *M* aq. HCOOK + 5 *M* aq. KOH	+0.125

NOTE: Data are calculated from thermodynamic data for 25° C. Standard state HCOOH = unit activity, 1 atm pressure of CO_2 and H_2. The reversible potential of the reaction shown depends on KOH concentration since the extent of hydrolysis of the potassium formate by $H_2O + HCOO^- \rightarrow HCOOH + OH^-$ depends on KOH activity. The reversible potentials calculated for 5° C will differ from the above values by approximately 17 mv since the standard entropy change for the reaction HCOOH (aq.) $\rightleftarrows CO_2 + H_2$ is approximately 43 e.u.

may also be envisaged analogous to the reaction $H^{\cdot} + H^+ + e \rightarrow H_2$ in the hydrogen evolution reaction. However, reaction [VI] is probably not exclusively the desorption path since, in the acetate case, methylations as well as acetoxylations of suitable substrates can be achieved (15, 16), indicating that steps such as [III] must be involved. The pathway [II], [VI] would, of course, not involve any alkyl radicals.

By analogy with the treatment given in Part I for the formate decarboxylation and with that for the hydrogen and oxygen evolution reactions, the limiting Tafel slopes for the above steps under Langmuir conditions (6, 7) are obviously $dV/d \ln i_2 = 2RT/F$

Can. J. Chem. Downloaded from www.nrcresearchpress.com by 210.87.254.40 on 09/05/12
For personal use only.

($\beta = 0.5$); $dV/d \ln i_3 = RT/F$ or a limiting current as the coverage by $CF_3COO^{\cdot}$ tends to unity; $dV/d \ln i_4 = RT/2F$ or a recombination controlled limiting current as the coverage by $CF_3^{\cdot}$ tends to unity. For reaction [V], when $\theta_{CF_3COO\cdot}$ is potential independent at full coverage, the Tafel slope would be $dV/d \ln i_5 = 2RT/F$. Similarly for reaction [VI], the Langmuir slopes are $2RT/3F$ or $2RT/F$ and the slopes at intermediate coverage will be $2RT/3F$ or RT/F as in the analogous hydrogen evolution case (6).

The step corresponding to reaction [IV] in Part I, viz. ionization of H and decarboxylation in one stage, is unlikely here since this would lead to the formation of the carbonium ion CF_3^+, which presumably will give $CF_3.COOCF_3$ (or CF_3OH in water) as a final product. This pathway is insignificant. The corresponding slopes under conditions (cf. refs. 6, 7) where coverage-dependent activation energies must be considered are

$$dV/d \ln i_2 = 2RT/F; \; dV/d \ln i_3 = \frac{2RT}{F} \cdot \frac{r_1}{r_1 - r_2},$$

as in the corresponding formate reaction, where r_1 now refers to changes of adsorption energy of $CF_3.COO^{\cdot}$ with coverage and r_2 to corresponding changes for $CF_3^{\cdot}$ (see Part I). The same limitations apply to the values of the Tafel slope *under these conditions* as have been discussed for the unimolecular formate decomposition; the minimum value of this slope for reaction [III] is $2RT/F$.

At low coverage by $CF_3^{\cdot}$, step [IV] will be associated with a slope of $RT/2F$ while at high coverage by $CF_3^{\cdot}$ or $CF_3COO^{\cdot}$, where activated adsorption of $CF_3^{\cdot}$ from C_2F_6 might consequently arise (cf. the hydrogen case (6, 7)), the recombination slope would be RT/F. The Tafel slopes ($dV/d \ln i$) deduced are summarized below:

Reaction	"Langmuir" conditions	Intermediate coverage ("Temkin" conditions)
[II]	$2RT/F$	$2RT/F$
[III]	RT/F or limiting current as $\theta_{CF_3COO\cdot} \rightarrow 1$	$\frac{r_1}{r_1 - r_2} \cdot \frac{2RT}{F}$
[IV]	$RT/2F$ or limiting current as $\theta_{CF_3\cdot} \rightarrow 1$	$r_1RT/2Fr_2$ or r_1RT/Fr_2 for activated adsorption of C_2F_6 as $2CF_3^{\cdot}$
[V]	$2RT/F$ (at full coverage by $CF_3COO^{\cdot}$)	$\frac{2RT}{F} \cdot \frac{r_1}{r_1+2r_2}$ or $\frac{2RT}{F} \frac{r_1}{r_1+r_2}$ for activated adsorption
[VI]	$2RT/F$ ($\theta_{CF_3COO\cdot} \rightarrow 1$) or $2RT/3F$ (low coverage)	$2RT/3F$ or RT/F for activated adsorption

FOOTNOTE ADDED IN PROOF: In a forthcoming publication, we deduce the Tafel slopes for these reactions under conditions where the variation of free energy of adsorption of intermediates with coverage originates from induced heterogeneity (ref. 37, Part I) rather than intrinsic heterogeneity effects. For such a case, Tafel slopes are derived which are related to those given in the above table but not specifically involving the two r parameters.

The observed slopes (for non-aqueous conditions; Fig. 1(*a*, *b*, *c*)) above the transition region are consistently above $2RT/F$ and approach values between 0.24 and 0.38 v (i.e. between about $4RT/F$ or $6RT/F$ respectively for the Naperian Tafel slopes). Slopes higher than $2RT/F$ can, in principle, be explained in terms of barrier layer films as discussed previously for processes at anodic oxide films (4, 5); under such conditions, the slope is proportional to the thickness of the film and the transfer coefficient for a single-electron charge-transfer step becomes δ/D where δ is the half-jump distance or barrier half-width

Can. J. Chem. Downloaded from www.nrcresearchpress.com by 210.87.254.40 on 09/05/12
For personal use only.

and D is the thickness of the film. The observed slopes thus would correspond, as in the oxygen evolution reaction at gold and gold–palladium alloys (4), to film thicknesses of the order of two to three monolayers.

The galvanostatic cathodic discharge curves (Fig. 5) indicate arrests of about 30–100 μcoulombs cm^{-2} which, with an area of the species $CF_3COO^{\cdot}$ taken as 25 Å^2 from Courtauld models, correspond to apparent fractional coverages of about 0.36–1.7; with a real to apparent area factor (cf. ref. 8) of about 3, these coverages would all become *less* than a monolayer. This conclusion will be seen subsequently to be of importance in the discussion of the kinetics. The detailed data are shown in Table V. Extended polarization prior to discharge increases the coverage and pseudocapacity somewhat as seen from the table; the capacity and coverage also depend on current density (or potential), as expected.

TABLE V

Surface charge q_s, coverage θ, and mean pseudocapacity C in the trifluoroacetate reaction (from cathodic reversed pulse discharge transients)

i, amp cm^{-2}	E_H, v	q_s μcoulomb cm^{-2}	θ	C, μF cm^{-2}	Previous polarization time, sec.
Pd, 1 *M* CF_3COOK/CF_3COOH system					
7.9×10^{-6}	0.960	23	0.36	47	75.6
	1.030	45	0.70	80	159
	1.070	40	0.76	83	304
9.15×10^{-4}	1.860	41	0.64	147	7.2
	2.070	58	0.89	122	87.5
	2.120	83	1.02	171	164
6.7×10^{-3}	2.310	70	1.1	185	18.1
	2.340	80	1.25	259	91.2
	2.345	80	1.25	244	163
	2.345	100	1.25	400	326
Pt, 1 *M* CF_3COOK/CF_3COOH system					
7.7×10^{-4}	2.050	20	0.31	82	188
	2.050	22	0.33	86	311
6.05×10^{-3}	2.13	54	1.1	362	13.6
	2.14	67	1.3	211	78
	2.13	74	1.4	255	159
	2.13	90	1.7	276	310
	2.13	90	1.7	264	314
Au, 1 *M* CF_3COOK/CF_3COOH					
1.76×10^{-3}	2.91	26	0.41	85	14.8
	2.93	27	0.43	75	19.1
	3.02	29	0.45	107	78
	3.04	30	0.47	142	121
	3.05	30	0.47	113	204
7.15×10^{-3}	3.175	36	0.56	97	2.3
	3.200	39	0.61	197	33
	3.215	43	0.67	295	79
	3.220	43	0.67	143	115
	3.220	47	0.72	111	203
	3.220	72	0.78	82	304

NOTES: 1. θ values are based on an area of 25 Å^2 for the $CF_3COO^{\cdot}$ radical assuming no free area between groups. The corresponding effective molecular area for a square lattice arrangement will be $4/\pi$ times larger and value of the charge for $\theta = 1$ will be $4/\pi$ times smaller. 2. The values quoted in this table are all calculated for the *apparent* electrode area. 3. θ and C values are calculated from the arrest region in the transients. 4. The derived data recorded in this table were calculated from measurements on 10× enlargements of the oscilloscope photographs.

The appreciable coverages observed are inconsistent with reaction [II] being rate determining and indicate a relatively slow desorption step. The recombination slopes $RT/2F$ (or RT/F) for [IV] are not observed under any conditions, so that it can be stated

Can. J. Chem. Downloaded from www.nrcresearchpress.com by 210.87.254.40 on 09/05/12
For personal use only.

fairly unambiguously that the radical coupling reaction [IV] cannot be rate determining. The nature of the products does not indicate a carbonium ion desorption mechanism, so that [III] or [V] are probably the only rate-determining steps which can be formulated in accordance with all the experimental data. The coverage results indicate appreciable values of θ so that the kinetic treatment for appreciable coverages ($\theta \doteqdot 0.5$) must probably be preferred. For [III], this predicts Tafel slopes of $r_1/(r_1-r_2)\times 2RT/F$. All observed slopes (see Fig. 1(*a*, *b*, *c*)) are much greater than $2RT/F$ (with $\beta = 1/2$) and could in principle (but see below) be explained with values of r_1 which are about 1.5–2 times r_2; thus for $r_2 = (1/2)r_1$ the Tafel slope is $4RT/F$ and with $r_2 = (2/3)r_1$ the slope is $6RT/F$. As in the formate case, it is reasonable to suppose that r_1 for the adsorption of the bulky polar $CF_3COO^{\cdot}$ group is greater than that for the smaller $CF_3^{\cdot}$ group. As we have mentioned above, it should be noted that high anodic slopes could, in principle, be explained on the basis of charge transfer across barrier layer films (4, 5) as in the formation of anodic oxide layers in oxygen evolution. However, for the present reaction, with the observed real fractional coverages of less than unity in most cases, this explanation is inconsistent with the experimental data as it implies a barrier film thickness D of at least four to six times the half-jump distance δ ($\beta \doteqdot \delta/D$). It will be noted that the high slopes always occur *above* the transition region, that is, where the surface, as in the formate case, is probably filled by the carboxylate radicals (see Parts I and III). In such a case, the "Temkin" slope deduced for reaction [III] is actually inapplicable since the coverage by $CF_3COO^{\cdot}$ is either high (Langmuir conditions) or unity and hence independent of potential. A potential-dependent desorption step such as [V] proceeding on the more or less completely covered surface appears therefore to be indicated as the likely mechanism in the upper Tafel region. The metal–solution interface can then be represented electrically as a complex double layer with a potential difference across the layer of $CF_3COO^{\cdot}$ plus $CF_3^{\cdot}$ radicals and a further potential difference across an ionic double layer. The potential profile will hence be as qualitatively shown in Fig. 7, i.e. with a surface dipole double layer and an ionic double layer beyond its limit at the interface with the solution. The effective symmetry factor is then appreciably less than 0.5 if the activated state ($\ddagger$) in the charge transfer desorption reaction [V] falls within the ionic double layer and an appreciable fraction of the total metal–solution potential difference falls across the dipole double layer.* The same effects need *not* arise in the formate reaction, where the rate of decomposition of the adsorbed radical layer itself can be potential dependent at high coverage by the reaction

$$HCOO^{\cdot} \rightarrow CO_2 + H^+ + e, \qquad [VI]$$

as discussed in Part I. This is consistent with the normal (ca. $2RT/F$) slopes observed in the upper Tafel region in the formate decomposition.

(b) Reactions in Aqueous Solution

Much of the earlier work on the Kolbe reaction has been carried out in aqueous media. Several experiments were hence performed in aqueous solutions of potassium trifluoroacetate in order to compare the kinetic behavior under the idealized conditions in the wholly non-aqueous trifluoroacetate system with that in the aqueous solutions. The current potential curves are shown in Fig. 3(*a*, *b*, *c*). Comparisons were also made with the behavior of 1 *M* formate in aqueous and aqueous 1 *M* KOH solutions (Fig. 4).

**This model is actually a variant of the barrier layer model except that no separate process of potential-dependent activated transport of charge carriers within a film of significant thickness is involved.*

Can. J. Chem. Downloaded from www.nrcresearchpress.com by 210.87.254.40 on 09/05/12
For personal use only.

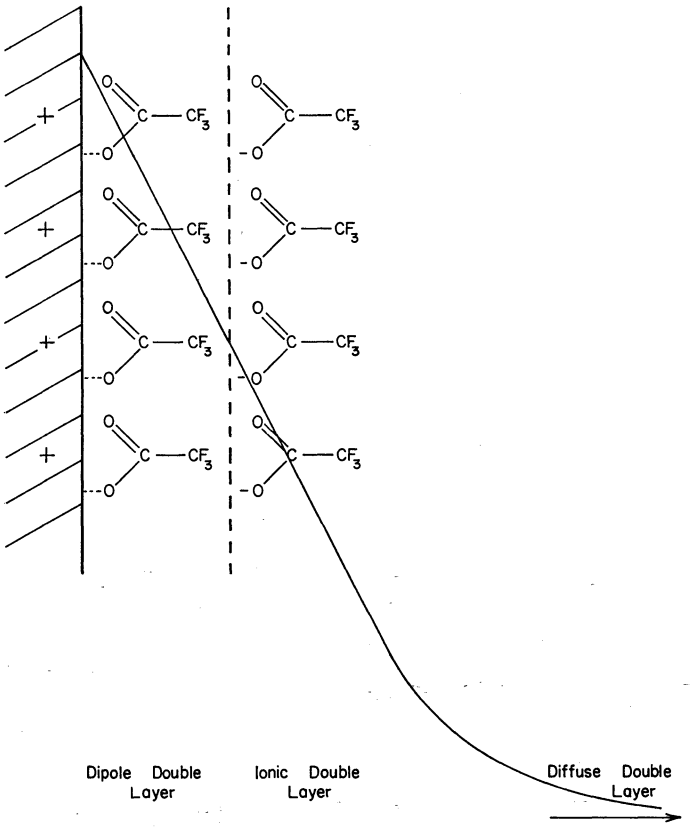

FIG. 7. Schematic representation of surface layer at electrode with adsorbed trifluoroacetate radicals.

The runs in aqueous CF_3COOK exhibit slopes greater than $2.3(2RT/F)$ (0.25–0.30 v) in the upper region only at platinum electrodes, while at gold or palladium the slopes are between 0.12 and 0.08 v. There is usually hysteresis, near the transition region, between the results obtained for increasing polarizing currents and decreasing currents, suggesting irreversibility in the film-forming process. At platinum, there appears to be a small second transition region at a current density of 2×10^{-3} amp cm^{-2} possibly corresponding to that mentioned for the acetate case by Dickenson and Wynne-Jones (2). This is not observed at palladium or gold. At platinum and gold, the Tafel regions are well defined and extend over two or three decades of current density.

The coulombic yields observed (see p. 46) indicate that under aqueous conditions the trifluoroacetate Kolbe reaction only proceeds with appreciable efficiency at Pt, and the current–potential curves shown in Fig. 3 for Au and Pd are therefore essentially those for oxygen evolution from the trifluoroacetate solution. This difference of behavior between Pt, and Au and Pd on the other hand, is consistent with the observed Tafel slopes which are only greater than $2.3(2RT/F)$ in the Pt case and are comparable with those observed in the non-aqueous trifluoroacetic acid at Pt. At Au and Pd in the aqueous case, the reaction is largely oxygen evolution so that the Tafel parameters will not be expected to be comparable with those in the non-aqueous solutions where the Kolbe reaction proceeds with high efficiency at these metals (Table I). It must be supposed that for chemical

Can. J. Chem. Downloaded from www.nrcresearchpress.com by 210.87.254.40 on 09/05/12
For personal use only.

reasons the oxide films are more stable and thicker at Au and Pd than at Pt and cause the inhibition of the trifluoroacetate discharge. Such oxide films cannot, of course, be formed in the pure trifluoroacetic acid.

The runs in aqueous formate and aqueous KOH – formate solutions (Fig. 4) all demonstrate well-defined transition regions, and the lower-slope region is well developed since the limiting transition current density is higher here than in the formate – 100% formic acid system (Part I). At palladium, gold, and platinum, the lower Tafel region consistently has a slope of $0.06(2.3RT/F)$ and the upper regions* have slopes of about 0.12 $[2.3(2RT/F)]$ or somewhat larger. In Part III we show that the transition region in most cases corresponds to the filling up of the surface with adsorbed radicals, so that the lower-slope region probably corresponds to the rate-determining step

$$HCOO^{\cdot} \rightarrow H^{\cdot} + CO_2$$

associated with the unimolecular decomposition slope of $2.3RT/F$ (see Part I). The upper region then probably corresponds to discharge of the formate radicals (reaction [VI]) at high coverage, or discharge of further formate ions onto the layer or film of adsorbed formate, e.g. in a way analogous to the oxygen evolution reaction which often occurs on an oxide layer. Typical transition region behavior (i.e. oscillation) is observed in the aqueous system as in the non-aqueous one.

It is of interest that addition of KOH in the aqueous formate decarboxylation reaction diminishes the "height" of the transition region. Inspection of the curves (Fig. 4), indicates that this is mainly due to a shift of the lower Tafel line to higher overpotentials† (or lower exchange currents; see Table III) in the presence of KOH. This effect, which is very marked, is seemingly general, since it is observed at Pt, Au, and also Pd, although the reproducibility of the results in pure aqueous formate solutions is bad at the latter metal. We suggest that this striking effect arising upon addition of the KOH is due either to adsorption of OH^- ions competitive with that of $HCOO^{\cdot}$ radicals or to facilitation of formation of an oxide film‡ in the lower Tafel region; the overall process in this region is not oxygen evolution and the Tafel parameters for this region, if they were calculated for oxygen evolution with respect to the reversible oxygen potential, are not at all comparable with those we have reported elsewhere for oxygen evolution at gold or palladium (4) in pure 1 *M* KOH solutions, or which are available (13) for platinum. The process in the lower-slope region is hence not simply oxygen evolution or oxide film formation, as is also apparent from the significant evolution of CO_2 (in the absence of KOH). The data of MacDonald and Conway (4) for oxygen evolution at Au and Pd in 1 *M* aq. KOH are shown in Fig. 4(*c*, *h*) for comparison. It is evident from these figures that the formate decarboxylation at Au in the presence of 1 *M* KOH proceeds over most of the current density range at potentials less than those for the oxygen evolution reaction in 1 *M* KOH in the absence of formate. In the case of Pd, which shows no transition region in the oxygen evolution Tafel line, it will be noted that a transition region is developed (as in the non-aqueous solutions) in the formate/KOH system. This transition region, and probably that at Au in the formate solution, is hence not specifically connected with the oxygen evolution process. In considering the role of simultaneous reactions of formate decomposition and

**The Tafel lines shown for the aqueous formate reaction are based on the observed total current. Corrections for the O_2 evolution co-current do not seriously affect the shape of the Tafel lines or the slopes except at gold, where the current efficiencies are lowest (Table II).*

†This result will be of interest in connection with the fuel-cell oxidation of methanol, where formate oxidation is the last step. In alkaline solution, this step is obviously kinetically much more difficult than in neutral (or acid) solutions.

‡The galvanostatic results, shown below, indicate, for example, complex film formation in the aqueous formate decarboxylation reaction.

Can. J. Chem. Downloaded from www.nrcresearchpress.com by 210.87.254.40 on 09/05/12
For personal use only.

oxygen evolution, it must be borne in mind that formation of formate radicals at the surface will almost certainly modify the oxygen evolution kinetics, and the present results show that formation of oxygen-containing species substantially inhibits the formate kinetics and no simple relationship between the kinetics of the two reactions, when they can occur together, can be proposed. At intermediate current densities, e.g. in the case of gold (Table II), oxygen evolution is appreciable and occurs simultaneously with CO_2 evolution.

(c) Galvanostatic Transients and Reaction Mechanism

The reversed pulse cathodic transients for the trifluoroacetate and aqueous formate systems have been shown in Figs. 5 and 6. The results for the anhydrous trifluoroacetate system at the three metals Pt, Pd, and Au consistently indicate fairly short arrest regions (Fig. 5) not exceeding about 100 μcoulombs cm^{-2} of apparent electrode area (a monolayer of $CF_3COO^{\cdot}$ (25 Å^2) corresponds to about 66 μcoulombs cm^{-2} of real area). By contrast, the formate reaction in aqueous solutions and in alkaline aqueous solutions (1 *M* KOH) evidently proceeds at anodic films of appreciable thickness (5–20 monolayers), as indicated by the transients shown in Fig. 6. In general, at the three metals, the film thickness increases with current density (as also at Pd in 100% HCOOH; see Part I). With all three metals, and particularly with Pd, the arrest behavior in the aqueous and aqueous KOH media is more complex than in the pure formic acid system. At Pd, three arrest regions are developed at high current densities which suggest relatively thick (20–30 monolayers) anodic films in various valence states of the metal, or possibly both oxide and formate film formation over different potential ranges. Some evidence for this is seen in the current–potential curve (Fig. 4) for Pt, where at the highest current densities the behavior of the current with decreasing potential is quite different from that found for decreasing current if the polarization has not reached the highest values. The critical potentials referred to in the work on the Kolbe reaction (e.g. refs. 2, 10; cf. 11) are, we believe, associated with the upper potentials (or related critical currents for film formation) in the film-forming region of the transients. Both in the aqueous and non-aqueous solutions a critical film-forming region occurs at a certain limiting current and it is evidently this film formation or "passivation" which has been regarded as necessary for occurrence of the Kolbe reaction at appreciable efficiencies. Actually, under non-aqueous conditions (in the CF_3COOH system), this film formation is actually not a prerequisite since we have found that the coupling reaction also occurs at currents less than the critical current, i.e. in the lower Tafel region. However, in aqueous solutions, it is usually found (12, 2) that some oxygen evolution precedes Kolbe coupling, so it appears that the electrode requires to be "passivated" by a carboxylate film (possibly on top of an oxide film, e.g. see Fig. 6(*b*, *c*) for the formate case) before significant coupling can occur. Presumably so long as a film of reactive oxygen-containing species (e.g. $OH^{\cdot}$ or $O^{\cdot}$) is present at the interface, some oxidative degradation of discharged alkyl carboxylate radicals tends to occur, leading to "Hofer-Moest" products; we suggest that only when this film is superseded by a complete carboxylate film does the coupling reaction occur efficiently. In the 100% trifluoroacetic or formic acid systems, no oxide film formation can occur (for example, no double arrests are seen in the transients) and the decarboxylation reaction occurs only on a simple film of the adsorbed carboxylate at high current density, and on a partially covered metal surface (see Part III) at current densities below the critical current.

The results of the present comparisons between the behavior in aqueous and non-aqueous solutions and our conclusions on the role of adsorbed intermediates serve, we believe, to clarify some of the points which were actively under discussion by various contributors in 1947 (14).

Can. J. Chem. Downloaded from www.nrcresearchpress.com by 210.87.254.40 on 09/05/12
For personal use only.

ACKNOWLEDGMENT

Grateful acknowledgment is made to the National Research Council for support of this work.

REFERENCES

1. B. E. CONWAY and M. DZIECIUCH. Can. J. Chem. **41**, 21 (1963).
2. T. DICKENSON and W. F. K. WYNNE-JONES. Trans. Faraday Soc. **58**, 382, 388, 400 (1962).
3. R. E. BUCKLES and J. F. MILLS. J. Am. Chem. Soc. **75**, 552 (1953).
4. J. J. MACDONALD and B. E. CONWAY. Proc. Roy. Soc. (London), Ser. A, **269**, 419 (1962).
5. R. E. MEYER. J. Electrochem. Soc. **107**, 847 (1960).
6. J. G. N. THOMAS. Trans. Faraday Soc. **57**, 1603 (1961).
7. B. E. CONWAY and E. GILEADI. Trans. Faraday Soc. In press (1963).
8. J. O'M. BOCKRIS and B. E. CONWAY. J. Chem. Phys. **28**, 707 (1958).
9. W. M. LATIMER. Oxidation potentials. 2nd ed. Prentice Hall, New York. 1952.
10. G. S. PANDE and S. N. SHUKLA. Electrochim. Acta, **4**, 215 (1961).
11. B. E. CONWAY and M. DZIECIUCH. Proc. Chem. Soc. 121 (1962).
12. S. GLASSTONE and A. HICKLING. J. Chem. Soc. 1878 (1934); 820 (1936).
13. J. O'M. BOCKRIS and A. K. M. S. HUQ. Proc. Roy. Soc. (London), Ser. A, **237**, 277 (1956).
14. A. HICKLING. Discussions Faraday Soc. **1**, 227 (1947). Contributions in general discussion, Discussions Faraday Soc. **1**, 248–251 (1947).
15. L. F. FIESER, R. C. CLAPP, and W. H. DAUDT. J. Am. Chem. Soc. **64**, 2052 (1942).
16. W. G. SMITH and H. G. GILDE. J. Am. Chem. Soc. **81**, 5325 (1960).

EXPLANATION OF FIGURES 5 AND 6

FIG. 5. Galvanostatic reversed pulse discharge curves for the Kolbe reaction with trifluoroacetate in 100% trifluoroacetic acid (5° C).

(*a*) Pt, anhydrous CF_3COOH, 1 *M* CF_3COOK: (1) 7.3×10^{-6} amp cm^{-2} (166 sec); 0.2 v cm^{-1}; 0.1 sec cm^{-1} (no arrest region); (2) 6×10^{-3} amp cm^{-2} (314 sec); 0.5 v cm^{-1}; 10 msec cm^{-1}; $C = 264$ μF; $q = 90$ μcoulombs cm^{-2}.

(*b*) Pd, anhydrous CF_3COOH, 1 *M* CF_3COOK: (1) 7.9×10^{-6} amp cm^{-2} (304 sec); 0.1 v cm^{-1}; 0.2 sec cm^{-1}; $C = 83$ μF; $q = 40$ μcoulombs cm^{-2}; (2) 9.2×10^{-4} amp cm^{-2} (164 sec); 0.2 v cm^{-1}; 20 msec cm^{-1}; $C = 171$ μF; $q = 83$ μcoulombs cm^{-2}; (3) 6.7×10^{-3} amp cm^{-2} (326 sec); 0.5 v cm^{-1}; 10 msec cm^{-1}; $C = 400$ μF; $q = 100$ coulombs cm^{-2}.

(*c*) Au, anhydrous CF_3COOH, 1 *M* CF_3COOK: (1) 6×10^{-5} amp cm^{-2} (204 sec); 0.5 v cm^{-1}; 0.2 sec cm^{-1}; $C = 64$ μF; $q = 96$ μcoulombs cm^{-2}; (2) 1.8×10^{-3} amp cm^{-2} (309 sec); 0.5 v cm^{-1}; 20 msec cm^{-1}; $C = 70$ μF; $q = 88$ μcoulombs cm^{-2}; (3) 7.2×10^{-3} amp cm^{-2} (304 sec); 0.5 v cm^{-1}; 5 msec cm^{-1}; $C = 82$ μF; $q = 72$ μcoulombs cm^{-2} (intermediate region at inflection gives capacity approx. 200 μF cm^{-2}).

FIG. 6. Galvanostatic reversed pulse cathodic discharge curves for the aqueous formate decarboxylation (5° C). (NOTE: In Plate II, "(*a*) Pd" should read "(*a*) Pt"; also "(*c*) Pd" and "(*b*) Pd" should be interchanged.)

(*a*) Pt, 1 *M* $HCOOK/H_2O$: (1) 6.8×10^{-4} amp cm^{-2} (159 sec); 0.1 v cm^{-1}; 20 msec cm^{-1}; over all $q = 95$ μcoulombs cm^{-2} (no arrest capacity); (2) 1.1×10^{-2} amp cm^{-2} (67.1 sec); 0.2 v cm^{-1}; 10 msec cm^{-1}; $C = 1900$ μF; $q = 495$ μcoulombs cm^{-2}; (3) 4.2×10^{-2} amp cm^{-2} (175 sec); 0.5 v cm^{-1}; 5 msec cm^{-1}; two regions of arrest; $q_1 \doteqdot 645$ μcoulombs cm^{-2}, $q_2 = 600$ μcoulombs cm^{-2}.

(*b*) Pd, 1 *M* $HCOOK/H_2O$: (1) 8.5×10^{-4} amp cm^{-2} (328 sec); 0.1 v cm^{-1}; 10 msec cm^{-1}; $C = 40$ μF; $q = 30$ μcoulombs cm^{-2}; (2) 7.5×10^{-3} amp cm^{-2} (164 sec); 0.2 v cm^{-1}; 10 msec cm^{-1}; $C = 660$ μF; $q = 525$ μcoulombs cm^{-2}; (3) 5.3×10^{-2} amp cm^{-2} (162 sec); 0.5 v cm^{-1}; 20 msec cm^{-1}. Note complex structure (reproducible) developed at high current densities. This behavior is *not* observed in 100% formic acid at comparable current densities. $q_1 \doteqdot 1500$ μcoulombs cm^{-2} (note undershoot), $q_2 \doteqdot 2200$ μcoulombs cm^{-2}, $q_3 \doteqdot 1700$ μcoulombs cm^{-2}.

(*c*) Pd, 1 *M* HCOOK, 1 *M* KOH/H_2O: (1) 5×10^{-5} amp cm^{-2} (152 sec); 0.1 v cm^{-1} 0.1 sec cm^{-1} (little arrest region); (2) 9.9×10^{-4} amp cm^{-2} (154 sec); 0.5 v cm^{-1}; 0.2 sec cm^{-1}; $q_1 \doteqdot 400$ μcoulombs cm^{-2}, $q_2 \doteqdot 400$ μcoulombs cm^{-2} (approx. potential-independent region); (3) 8.6×10^{-3} amp cm^{-2} (345 sec); 0.5 v cm^{-1}; 50 msec cm^{-1}; $q_1 \doteqdot 1290$ μcoulombs cm^{-2} (note undershoot), $q_2 \doteqdot 1720$ μcoulombs cm^{-2}, q_3—uncertain.

(*d*) Au, 1 *M* $HCOOK/H_2O$: (1) 1.4×10^{-4} amp cm^{-2} (309 sec); 0.1 v cm^{-1}; 0.1 sec cm^{-1}; no arrest region; (2) 5.7×10^{-2} amp cm^{-2} (166 sec); 0.5 v cm^{-1}; 10 msec cm^{-1}; complex arrest behavior.

(*e*) Au, 1 *M* HCOOK, 1 *M* KOH/H_2O: (1) 3.7×10^{-5} amp cm^{-2} (501 sec); 0.2 v cm^{-1}; 0.2 sec cm^{-1}; no arrest region; (2) 2.6×10^{-4} amp cm^{-2} (504 sec); 0.5 v cm^{-1}; 0.5 sec cm^{-1}; mean $C \doteqdot 7800$ μF; $q = 780$ μcoulombs cm^{-2}; (3) 6.4×10^{-3} amp cm^{-2} (514 sec); 0.5 v cm^{-1}; 50 msec cm^{-1}; mean $C \doteqdot 4000$ μF; $q = 1920$ μcoulombs cm^{-2}.

(*f*) Pt, 1 *M* HCOOK, 1 *M* KOH/H_2O: (1) 3×10^{-4} amp cm^{-2}; (436 sec); 0.1 v cm^{-1}; 0.1 sec cm^{-1}; $C = 700$ μF; $q = 210$ μcoulombs cm^{-2}; (2) 8.7×10^{-4} amp cm^{-2} (327 sec); 0.2 v cm^{-1}; 0.2 sec cm^{-1}; (3) 6×10^{-2} amp cm^{-2} (526 sec); 0.5 v cm^{-1}; 5 msec cm^{-1}; *C* variable but large; total $q = 1590$ μcoulombs cm^{-2}.

Can. J. Chem. Downloaded from www.nrcresearchpress.com by 210.87.254.40 on 09/05/12
For personal use only.

NEW APPROACHES TO THE STUDY OF ELECTROCHEMICAL DECARBOXYLATION AND THE KOLBE REACTION

PART III. QUANTITATIVE ANALYSIS OF DECAY AND DISCHARGE TRANSIENTS AND THE ROLE OF ADSORBED INTERMEDIATES

B. E. CONWAY AND M. DZIECIUCH
Department of Chemistry, University of Ottawa, Ottawa, Canada

Received June 29, 1962

Can. J. Chem. Downloaded from www.nrcresearchpress.com by 210.87.254.6 on 09/05/12
For personal use only.

ABSTRACT

Galvanostatic cathodic discharge and open-circuit decay transients have been obtained for the decarboxylation of formate in formic acid and interpreted quantitatively in terms of the adsorption of intermediates in the reaction. These intermediates are identified with $HCOO^{\cdot}$ radicals. Extended anodic polarization at platinum and particularly at palladium leads to the formation of films of an anodic product which are considerably thicker than a monolayer. After relatively long times (>100 seconds) of anodic polarization, the film growth obeys the inverse logarithmic rate law deduced by Mott and Cabrera. The thick films which are formed at palladium are believed to be responsible, upon autocatalytic decomposition, for the delayed gas evolution phenomenon observed at this metal.

A new method for deduction of adsorption pseudocapacitance and charge associated with the ad-layer from open-circuit decay curves and Tafel parameters is used to obtain the pseudocapacitance and charge associated with the transition region in the current–potential curves for the formate decarboxylation. It is shown that this region corresponds to filling of the surface with adsorbed intermediates formed in the reaction. These observations are shown to support the reaction mechanism proposed in Part I.

INTRODUCTION

The mechanisms of consecutive reactions can always be elucidated more definitively if knowledge of the behavior and concentrations of intermediates is available. Steady-state current–potential curves for electrochemical reactions can lead to an understanding of the reaction mechanism only to a limited extent, through evaluation of Tafel slopes; non-steady-state measurements by means of analysis of transients can lead, in favorable cases, to important complementary information on: (*a*) the coverage of the electrode by reaction intermediates as a function of potential and (*b*) the associated adsorption pseudocapacitance (1); interpretation of the potential dependence of the latter (2) can then lead to information on the adsorption behavior (e.g. the type of isotherm applying) of the intermediates at the surface. In the case of anodic film formation, the extent of film growth can be examined as a function of time and current density, if the film can be formed and removed (cathodically) in a more or less reversible manner.

In the present paper, we examine the behavior of the adsorbed intermediates formed in the formate decarboxylation by a quantitative analysis of the discharge and e.m.f. decay transients.

EXPERIMENTAL

(1) General Conditions

Experimental conditions, methods of preparation of solutions and electrodes, etc. were identical with those described in Parts I and II.

(2) Electrical Circuits

A general circuit was devised whereby anodic d-c. charging, reversed pulse cathodic discharging following steady anodic polarization, and open-circuit e.m.f. decay could be followed with the same apparatus. High-speed mercury-wetted vacuum relays were used and activated by a microswitch. A bank of accumulators provided the polarizing current. The arrangement of resistors to provide various constant currents to the

cell is shown in Fig. 1 and the galvanostatic relay circuit is illustrated in Fig. 2 with the appropriate connections shown for anodic charging, cathodic discharging, and open-circuit decay. Potential measurements were made with respect to two hydrogen electrodes in the same solution, provided with a Luggin capillary to the anode compartment of the cell. The potential difference between the transiently polarized anode and the reference electrodes was fed to a calibrated Hewlett–Packard oscilloscope through a Keithley

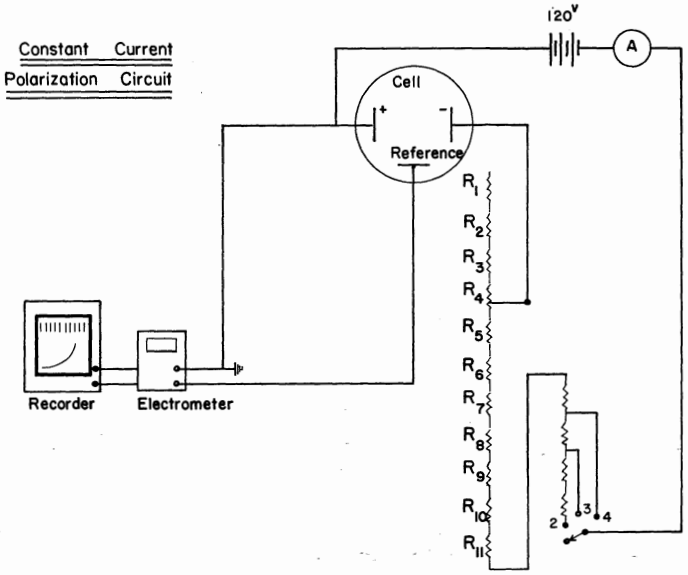

FIG. 1. Circuit for control of current in galvanostatic charging and discharging.

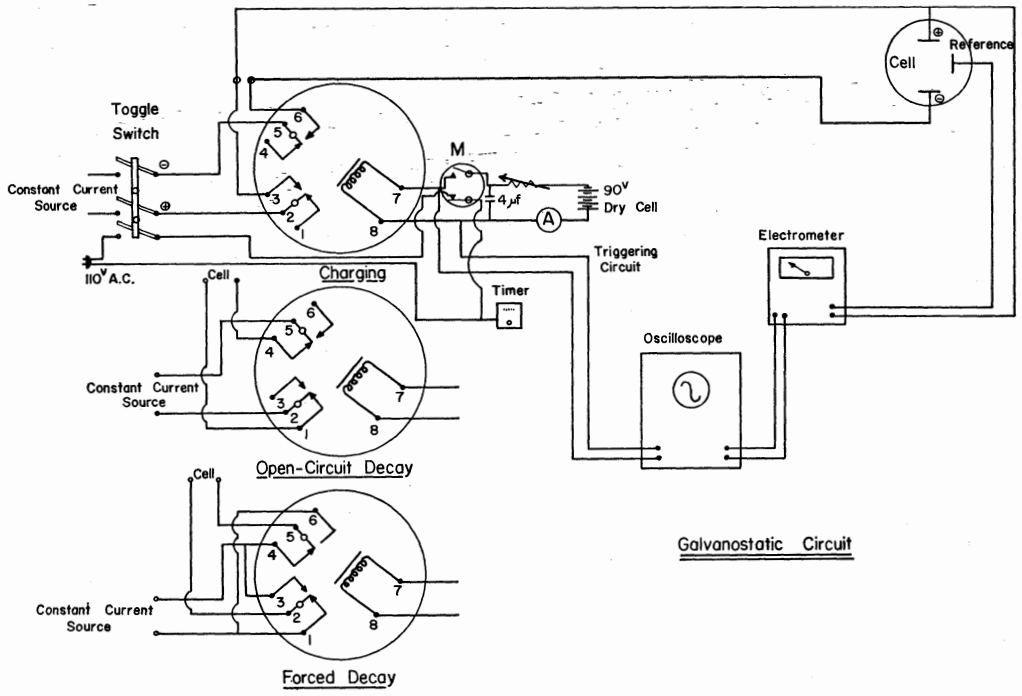

FIG. 2. Circuits for d-c. charging, reverse discharging, and open-circuit decay.

Can. J. Chem. Downloaded from www.nrcresearchpress.com by 210.87.254.6 on 09/05/12
For personal use only.

electrometer (input impedance up to 10^{14} ohm). Transients were recorded on a Polaroid film by means of a Polaroid Land Camera and subsequently enlarged some 8 to 10 times for quantitative analysis of the potential–time traces.

RESULTS AND DISCUSSION

Three types of derived information were required:

(i) Film thickness or associated charge, as a function of current density and time of anodic polarization in the anhydrous formic acid system, where remarkable delayed gas evolution effects (at Pd) had previously indicated (3) extensive formation of an unstable anodic film which decomposed after a delay time related to the duration of prior anodic film formation, and hence probably to its thickness.

(ii) Initial capacity at the polarization potential at the commencement of an e.m.f. decay transient.

(iii) The variation of pseudocapacity (probably associated with adsorbed $HCOO^{\cdot}$) with potential over the range of potentials examined in the steady-state current–potential studies, and the total charge corresponding to formation of the ad-layer associated with the region of significant[1] pseudocapacity (2).

(i) Anodic Film Formation

Following the observation (3) of a delayed gas evolution (CO_2) in the e.m.f. decay at a palladium electrode, and which was dependent on the time of previous anodic polarization, a number of experiments were carried out to evaluate, by cathodic galvanostatic discharge, the extent of film formation in the anodic decomposition of formate in 100% formic acid as a function of the time and current density of previous polarization. The results for palladium, gold, and platinum are shown in Fig. 3 in terms of the delay time in the arrest region of the galvanostatic cathodic discharge transients as a function of the logarithm of the time of previous anodic polarization. In Figs. 4 and 5 the corresponding charges associated with the arrest region are plotted reciprocally in terms of the log at the previous anodic polarization time and in Fig. 6 are shown the arrests on open circuits after anodic polarization of Pd for various times. Choice of the logarithmic plot was suggested by theories of film growth (4) in which, under high-field conditions (i.e. with thin films as in the present case), with metal ion transfer from the metal into the anodic film the rate-controlling process in film growth, a reciprocal relation should exist between film thickness and the logarithm of time of growth. In the present case, the thickness is assumed to be proportional to the charge associated with the film. In the formate case, this charge amounts to about 120 μcoulombs cm^{-2} per monolayer of $HCOO^{\cdot}$ (area 14.2 $Å^2$). The parabolic growth law (4) in which the film thickness should vary with the square root of time of growth for low-field conditions, when metal ion diffusion in the film is rate controlling for film growth, does not fit the present results so well as the reciprocal log plot.

At palladium, the charge associated with the arrest region increases with time of anodic polarization and reaches about 4000 μcoulombs cm^{-2} or about 35 layers in thickness. If this were a layer of a palladium formate which decomposed on open circuit, about 0.01 ml of CO_2 would be liberated at a 10 cm^2 electrode. This is presumably the gas[2] which is observed in the delayed gas evolution (3). The film growth rate cannot be

[1]*That is, where the adsorption pseudocapacity is appreciably greater than the anticipated anodic ion double layer capacity of about 40–80 $\mu F\ cm^{-2}$.*

[2]*We have previously reported (3) that the gas produced in periodically interrupted electrolysis, in which an appreciable volume of the total gas evolved arises from delayed evolution, is chemically indistinguishable from that evolved continuously. We have hence concluded that the gas evolved after delay is also* CO_2.

Can. J. Chem. Downloaded from www.nrcresearchpress.com by 210.87.254.6 on 09/05/12
For personal use only.

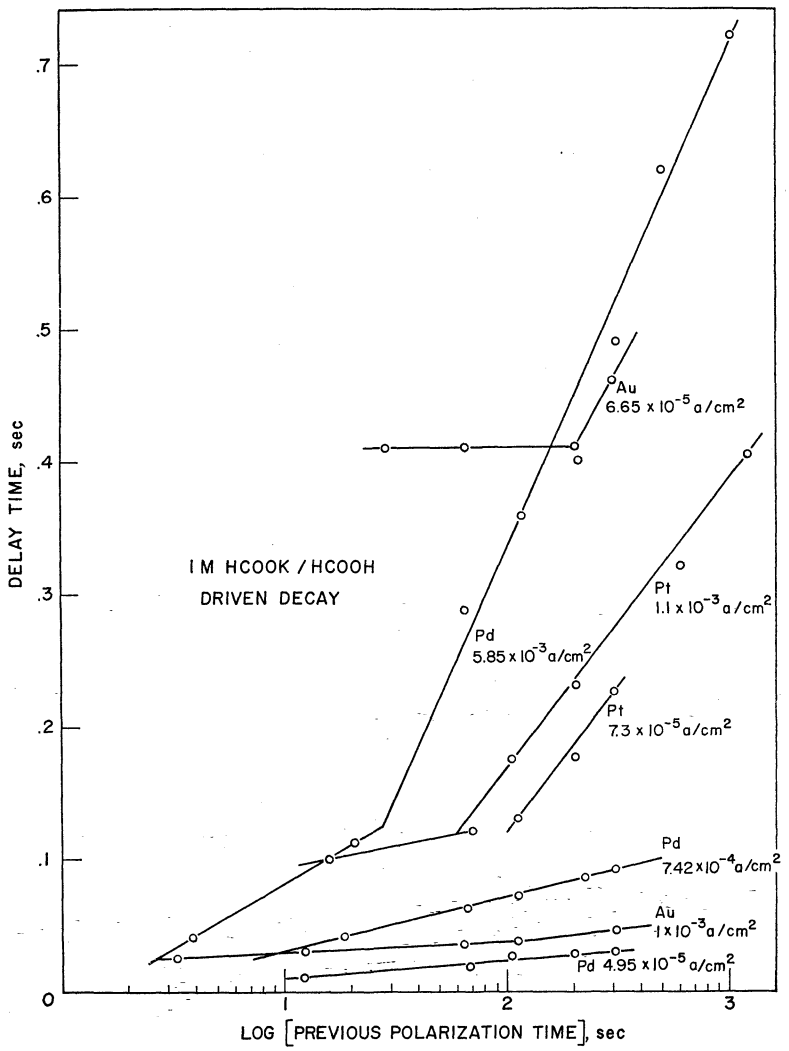

FIG. 3. Delay times in the arrest region as a function of the log of the time of previous polarization at Au, Pt, and Pd (1 *M* HCOOK/HCOOH, 5° C).

directly related to the current passing, since most of the current is associated with the overall Faradaic process of CO_2 evolution in the formate electrolysis; only a small fraction of the total current is evidently involved in increasing the anode film thickness with time. The maximum charge of about 4000 μcoulombs cm^{-2} at the palladium electrode is just sufficient to produce a visible gas evolution if the layer is a formate of palladium[3] which decomposes to give CO_2[4] autocatalytically after a delay period or, equivalently, after the electrode potential has fallen to a critical value (3). No delayed gas evolution is seen at platinum or gold or in the Kolbe reaction itself and this is consistent with the 10 times smaller film thickness (or charge) observed at the platinum electrode (Fig. 5) in the same formate/formic acid system.

[3]*No stable palladium formate compounds appear to exist and this is consistent with the present observations that such a compound, if formed under strongly oxidizing conditions, decomposes as soon as the potential has fallen to lower anodic values.*

[4]*See footnote 2 of previous page.*

Can. J. Chem. Downloaded from www.nrcresearchpress.com by 210.87.254.6 on 09/05/12
For personal use only.

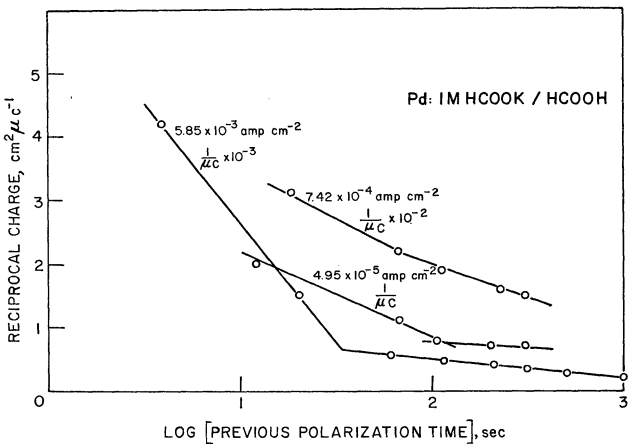

FIG. 4. Reciprocal charge associated with the arrest region at palladium as a function of the log of the time of previous anodic polarization (1 *M* HCOOK/HCOOH, 5° C; from galvanostatic discharge).

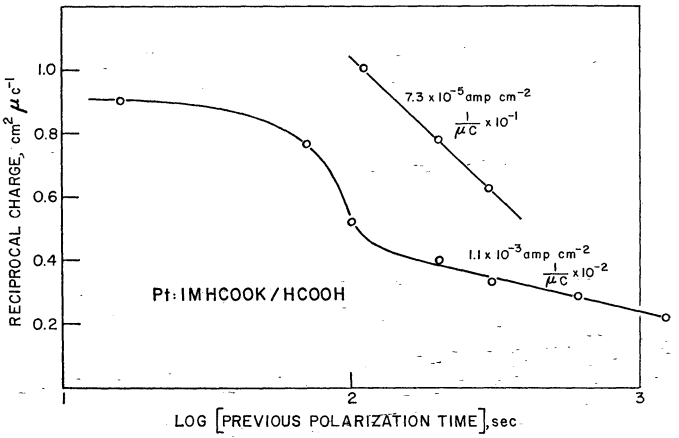

FIG. 5. Reciprocal charge associated with the arrest region at platinum as a function of the log of the time of previous polarization (1 *M* HCOOK/HCOOH, 5° C; from galvanostatic discharge).

In the trifluoroacetic acid Kolbe reaction, a similar buildup of an adsorbed layer with time is observed (Fig. 7) but this does not exceed 50–80 μcoulombs cm^{-2}—the limit for a monolayer. This is further confirmation (see Part II) that for the trifluoroacetate reaction in anhydrous trifluoroacetic acid, the process occurs on a more or less completely filled surface at current densities above that for the transition behavior, or passivation, and barrier layer films of appreciable thickness are not involved.

(ii) Anodic Film Formation in Aqueous Solutions

The anodic film formation in the *aqueous* formate reaction is also quite extensive, as previously shown in Part II. Arrests in the galvanostatic transient up to 2000 μcoulombs cm^{-2} were measured, indicating films of about 20 monolayers per apparent cm^2. In the polarization measurements made in obtaining the current–potential curve, it was noticed that near the transition region there was considerable time variation of electrode potential, which was not observed at lower or higher current densities. As the current was either increased or decreased the potential would "overshoot" or "undershoot", respectively,

Can. J. Chem. Downloaded from www.nrcresearchpress.com by 210.87.254.6 on 09/05/12
For personal use only.

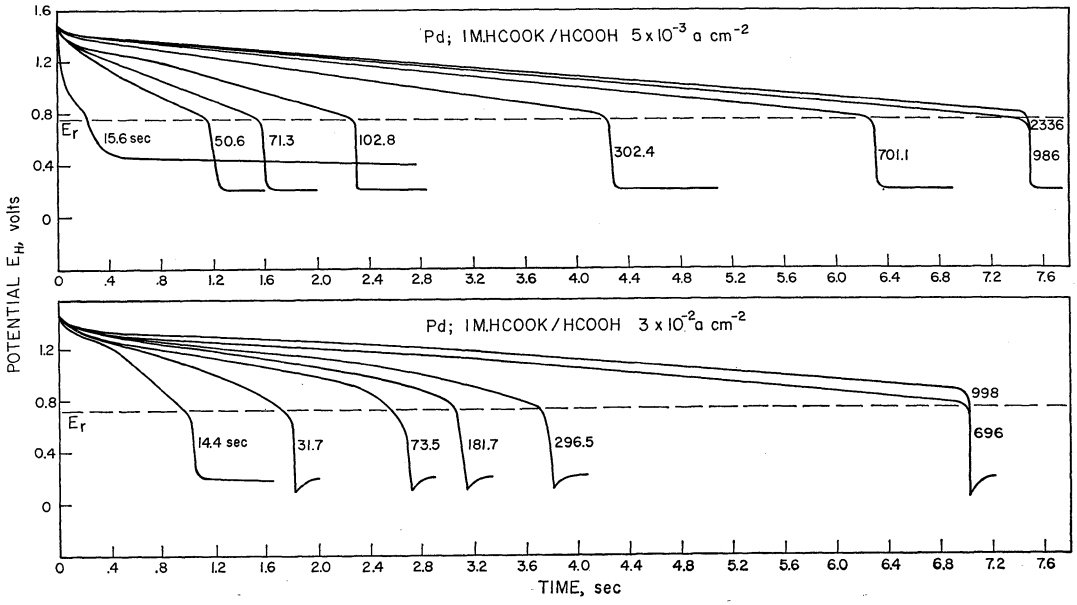

FIG. 6. Open-circuit e.m.f. decay curves for the anodic polarization of Pd (1 *M* HCOOK in 100% HCOOH, 5° C) for various times.

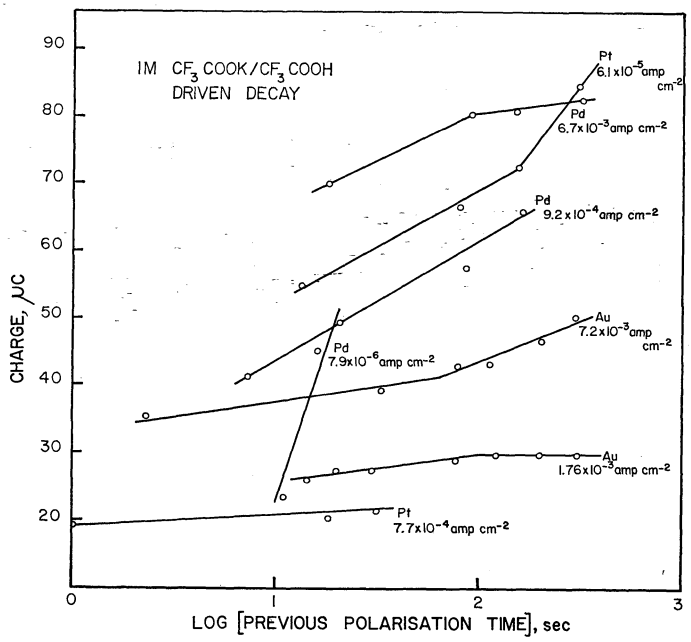

FIG. 7. The surface charge associated with the arrest region in the trifluoroacetic acid Kolbe reaction (1 *M* potassium trifluoroacetate, 5° C) as a function of time of previous anodic polarization.

and then return to a steady value. Similar behavior has been observed previously in the oxygen evolution reaction (5) and at barrier layer film electrodes (6). The phenomenon is characteristic of slow readjustment of space charge in a barrier layer film when the field is changed. Some typical plots of the logarithmic change of potential with time near the transition region and of e.m.f. recovery after "undershoot" are shown in Figs. 8 and 9.

Can. J. Chem. Downloaded from www.nrcresearchpress.com by 210.87.254.6 on 09/05/12
For personal use only.

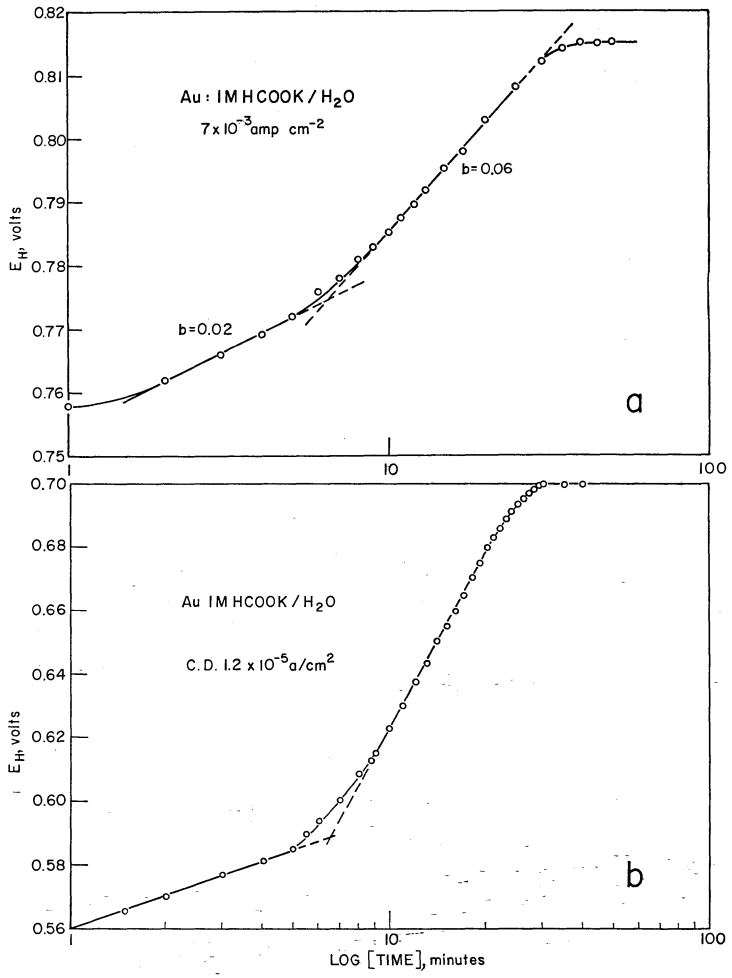

FIG. 8. Typical buildup curves plotted logarithmically in time for the aqueous formate reaction: (*a*) Au, 1 *M* HCOOK/H_2O; 7×10^{-3} amp cm^{-2} (near the transition region); (*b*) Au, 1 *M* HCOOK/H_2O; 1.2×10^{-5} amp cm^{-2} (below the transition region).

The buildup curves are similar to those found in the anodic evolution of oxygen at platinum and are probably associated with the same type of process (7), viz. deactivation of sites on the metal surface by adsorption of a product (probably $HCOO^{\cdot}$ in the present case) of one of the steps in the reaction. The logarithmic recovery after "overshoot" or "undershoot", also observed in the oxygen evolution reaction (5) at palladium, is probably associated with a first-order readjustment of space charge (6) in the multilayer film following a sudden change of field as the potential (or current density) is changed.

(iii) The Charge and Pseudocapacity Associated with Adsorbed Intermediates Calculated from Open-circuit Decay Transients

Here we examine the case of the formate decomposition only in 100% formic acid near the transition region. The behavior in aqueous solution is probably too complex (see Part II) for the simple non-steady-state analysis described below to be applicable.

It is well known (8, 9) that the capacitance of an electrode can be deduced from the *initial* rate of fall of potential at the potential V_1 (assumed free of ohmic or concentration

Can. J. Chem. Downloaded from www.nrcresearchpress.com by 210.87.254.6 on 09/05/12
For personal use only.

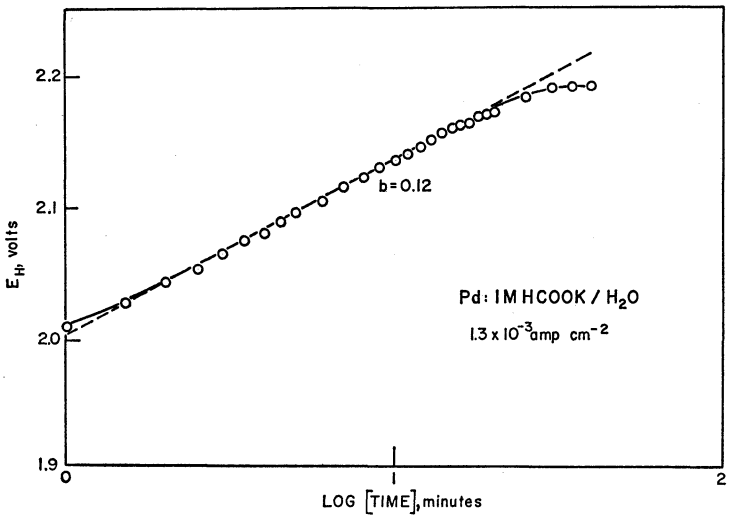

FIG. 9. Recovery from "undershoot" in the aqueous formate reaction. Pd, 1 *M* HCOOK/H_2O; 1.3×10^{-4} amp cm^{-2}.

polarization effects) corresponding to the moment of commencement of decay. The current passing is then, momentarily, the initial polarizing current i_1 and

$$[1] \qquad i_1 = -C_{V_1}(dV/dt)_1,$$

so that the *initial* capacitance can be calculated. The capacitance as a function of potential V could then in principle (cf. ref. 9) be evaluated as a function of potential by using various initial polarizing currents as we have suggested previously (12).

The kinetics of e.m.f. decay are normally expressed (8, 11, 12) by an equation,

$$[2] \qquad i_V = -C_V(dV/dt) = i_0e^{V/b},$$

at any potential (where b is the Naperian Tafel slope), and $i_0e^{V/b}$ is, in fact, the self-discharge current passing at the potential V; it is clear then (as we show elsewhere (10)) that C_V can be obtained at any potential in the decay curve if the corresponding Tafel expression is known over the same range of potentials, since the Tafel equation defines the term $i_0e^{V/b}$ at any potential. In this discussion, it is assumed, as usual (8, 11, 12), that on open circuit the same process as that during steady polarization is the rate-determining one. The charge associated with the capacity C_V is hence obviously

$$[3] \qquad \Delta q = \int_{V_1}^{V_2} \frac{-i_0e^{V/b}}{dV/dt}\cdot dV,$$

where we keep the term dV/dt in the denominator for convenience in order to evaluate $i_0 \exp [V/b]/dV/dt$ experimentally and integrate the result over a range of values of V. The value of Δq obtained is obviously that corresponding to the change of q over the potential range V_1 to V_2. If C_V corresponds to a pseudocapacity associated with the adsorption of reaction intermediates (1, 2, 13), it will usually be large (12, 13) compared with the double-layer capacity when the coverage θ by intermediates is $0.2 < \theta < 0.9$, so that integration, in equation [3], over the potential region of appreciable values of C_V will give, approximately, the actual value of q associated with the adsorbed intermediates,

Can. J. Chem. Downloaded from www.nrcresearchpress.com by 210.87.254.6 on 09/05/12
For personal use only.

and hence θ the extent of coverage, if we assume that one electron is required for Faradaic discharge to produce each adsorbed group ($HCOO^{\cdot}$ in the present case) and also assume an effective molecular area for the adsorbed species, as discussed previously (Parts I and II).

The above treatment has been applied to the evaluation of the pseudocapacity and coverage associated with the adsorbed species in the formate decarboxylation, particularly near the critical current or transition region where we suspect that formation of a passivating layer is occurring. Values of dV/dt have been obtained from the decay curves and values of $i_0 e^{V/b}$ from the actual current–potential relationships (see Part I).

The decay curves are shown in Fig. 10 for gold, platinum, and palladium taken from potentials above the transition region, and in Fig. 11 for palladium taken in a separate experiment from a potential corresponding to a lower current density. The arrests in the decay curves in Fig. 10 are related to the arrests obtained on galvanostatic forced discharge mentioned in Part I, and correspond to an appreciable pseudocapacity. The data for platinum and palladium are taken for a current density and time below that for which multilayer formation sets in (see Fig. 4).

The capacity curves (calculated from equation [2]) over the transition regions are shown in Fig. 12 as a function of the overpotential for the reaction (see Part I) and the integral charges associated with this region are shown in Fig. 13 for Pt and Pd.

The capacity curve for the higher current density arrest region at Pd has almost the correct *shape* (2, 13) for the case of Langmuir adsorption of the intermediates. Its maximum value is, however, too low (particularly bearing in mind that the real to apparent area factor for the metal surface must be greater than 1), since for the adsorption of formate radicals, the maximum theoretically expected "Langmuir" value is $kF/4RT$, where k is the charge associated with $\theta = 1$, i.e. 120 μcoulombs cm^{-2} in the present case for a molecular area of 14.2 Å^2 for $HCOO^{\cdot}$; C_{max} is hence 1200 μF cm^{-2} for the present system. The actual observed capacity behavior as a function of potential fits the general equation

$$\frac{k}{C} = \frac{dV}{d\theta} = \frac{RT}{F}\frac{d \ln [\theta/1-\theta]}{d\theta} + r_1/F,$$

deduced previously (2) taking into account variation of heat of adsorption of $HCOO^{\cdot}$ with coverage (14, 15) through the term r_1 (defined in Part I). The observed capacity curve (Fig. 12(*b*)) and the charge as a function of potential are consistent with $r_1 \doteqdot 3$ kcal $mole^{-1}$ for Pd.

At palladium, two transition regions are observed in the current–potential plots (Fig. 1 in Part I) for 1 *M* and 5 *M* potassium formate solutions in formic acid. Correspondingly, two pseudocapacity regions are observed as shown in Fig. 12(*a*,*b*). The lower-region capacity exhibits a wider region of potential dependence than the upper one, which approaches (but is not identical with) ideal Langmuir behavior (cf. Fig. 13). This behavior suggests that an anodic film is first formed at the lower current density and then suffers an oxidation at higher potentials. A surface redox step can, of course, formally exhibit the same type of pseudocapacity as a direct adsorption process since, if a Nernst type of relation applies to the potential associated with this layer as a function of activity of "oxidized" and "reduced" species, an appreciable pseudocapacity will arise over the potential region where the ratio of the activities of "oxidized" and "reduced" forms varies from about 0.1 to 10. Similar considerations have been discussed previously for the surface phase at the nickel oxide electrode (12).

Can. J. Chem. Downloaded from www.nrcresearchpress.com by 210.87.254.6 on 09/05/12
For personal use only.

Can. J. Chem. Downloaded from www.nrcresearchpress.com by 210.87.254.6 on 09/05/12
For personal use only.

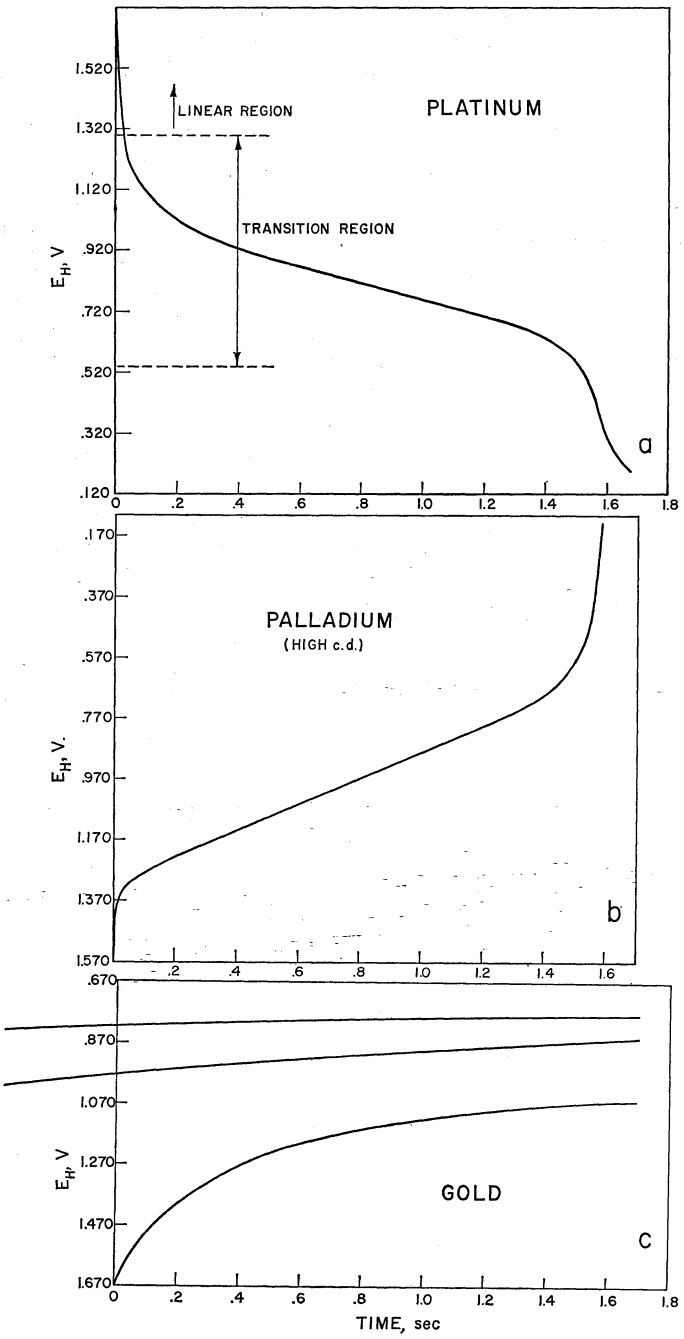

FIG. 10. E.m.f. decay curves taken from potentials above the transition region for formate decarboxylation (1 *M* HCOOK/100% HCOOH, 5° C): (*a*) platinum; (*b*) palladium; (*c*) gold.

The corresponding data for platinum indicate a larger value of r_1 (viz. 7 kcal mole^{-1}) since C and q (or θ) depend on potential over a wider range of potentials than for the case of Pd on the ideal Langmuir case. Since in both of these cases, the θ values vary from

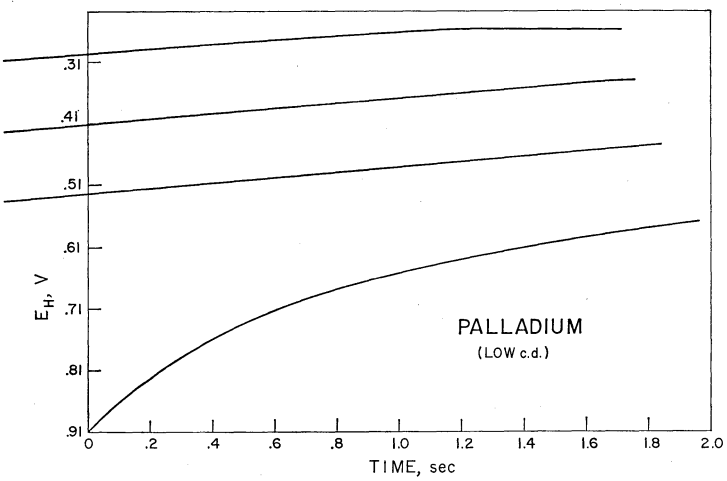

FIG. 11. E.m.f. decay curve at Pd at a lower current density than that used for Fig. 10(*b*).

ca. 0.1 to 1, but different r_1 values are found for the *same* reaction (and hence presumably for the same intermediates), we conclude that r_1 may be predominantly determined by heterogeneity of energies of adsorption at various sites rather than by two-dimensional interaction effects within the ad-layer. It is recognized, however, that different orientations of the adsorbed species at Pt and Pd could also lead to different two-dimensional interactions and hence to different r_1 values. The linear variation of heat of adsorption with coverage assumed in this treatment and elsewhere (14, 15) is actually best accounted for (2) in terms of the model discussed by Boudart (16) and based on induced heterogeneity effects through the surface potential arising from the ad-layer and its effect on the electronic work function of the metal.

Significance of the Transition Region

The above results give rather direct evidence regarding the behavior of the adsorbed intermediates, which we must presume to be $HCOO^{\cdot}$ radicals. It is clear that the transition from lower current density behavior to that at high current density, associated with a sharp change of potential, must be ascribed to filling up of the surface by the adsorbed species. This suggests that the primary discharge of formate ions is not the rate-controlling step, as was also deduced in Parts I and II. Beyond a certain critical current, decomposition of the radicals can no longer support the current and a limiting current is observed. This suggests that the rate-controlling reaction at low current densities is

$$HCOO^{\cdot} \rightarrow H + CO_2,$$

which gives a limiting current, rather than

$$HCOO^{\cdot} \rightarrow H^+ + CO_2 + e,$$

which is always potential dependent. Once the transition region is completed, further potential-dependent reactions can continue by

$$HCOO^{\cdot}{}_{\theta \rightarrow 1} \rightarrow H^+ + CO_2 + e$$

at the higher current densities. The transition behavior, which shows all the characteristics of a "passivation" phenomenon, may thus be directly ascribed to formation of a monolayer of adsorbed reaction intermediates. The corresponding "active" region is that

Can. J. Chem. Downloaded from www.nrcresearchpress.com by 210.87.254.6 on 09/05/12
For personal use only.

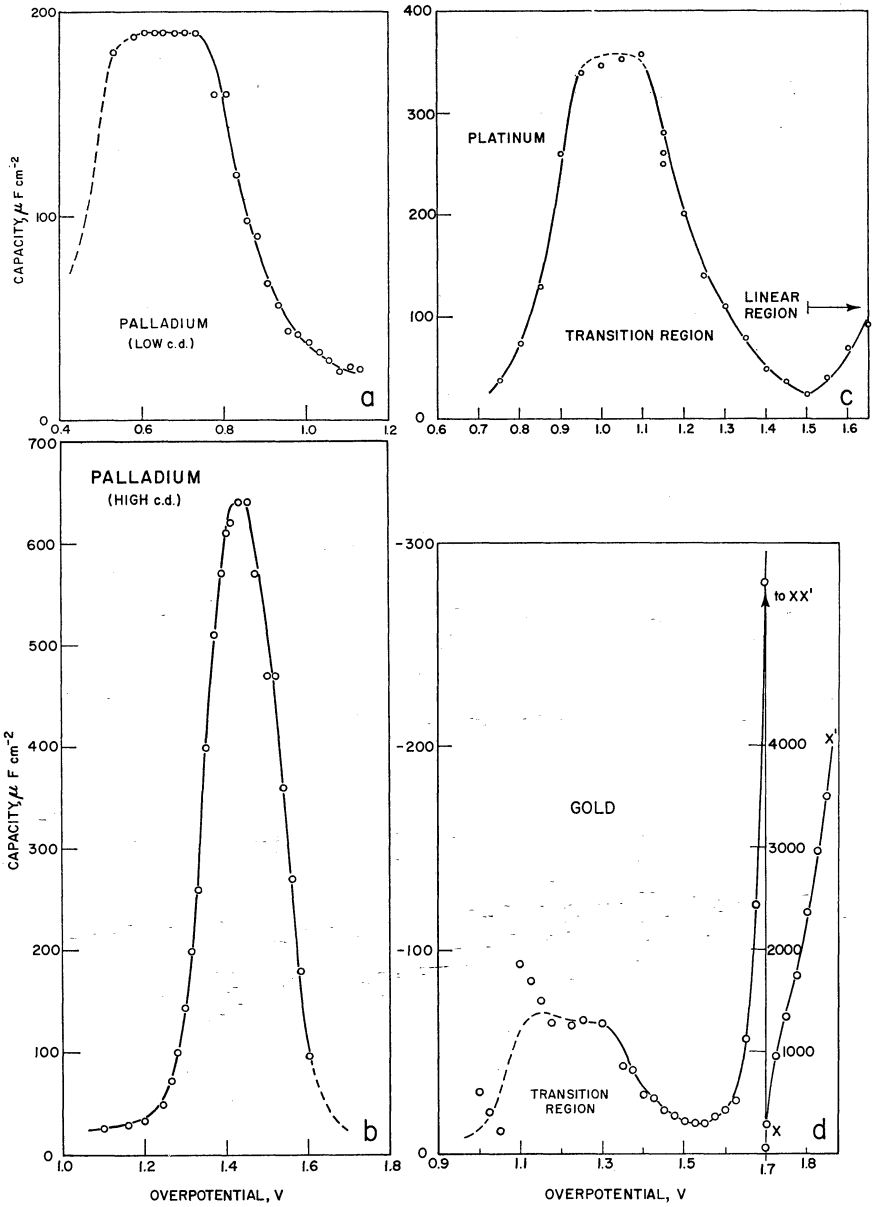

FIG. 12. Capacity curves for the formate decarboxylation in the transition region as a function of overpotential (1 *M* HCOOK/100% HCOOH, 5° C; from open-circuit decay and Tafel-line parameters): (*a*) palladium, low current density; (*b*) palladium, high current density; (*c*) platinum; (*d*) gold.

at low current densities, i.e., less than the transition current densities, where we have shown (Part I) that some attack of the electrode occurs and the coulombic yields of CO_2 are appreciably less than those expected for the quantitative occurrence of the formate decarboxylation.

Beyond the transition region at higher current densities, the pseudocapacity again increases with increasing current density (or potential, see Fig. 12(*d*)) and time owing to formation of thicker films as discussed above and shown in Figs. 4 and 5.

Can. J. Chem. Downloaded from www.nrcresearchpress.com by 210.87.254.6 on 09/05/12
For personal use only.

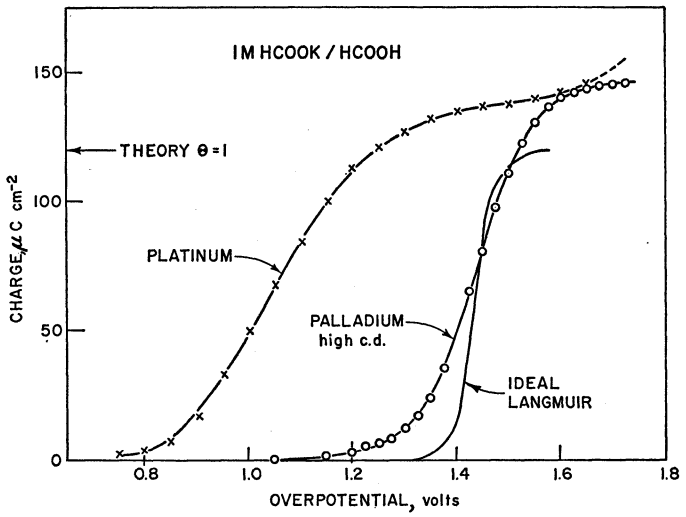

FIG. 13. Integral charges associated with the adsorbed species, deduced from Figs. 10 and 12. ($\theta_{HCOO^-} = 1$ corresponds to 120 μcoulomb cm^{-2} for a real to apparent area factor of 1.)

Further work is in progress on the quantitative treatment of the transition behavior in the Kolbe reaction itself.

ACKNOWLEDGMENT

Grateful acknowledgment is made to the National Research Council for support of this work.

REFERENCES

1. A. EUCKEN and B. WEBLUS. Z. Elektrochem. **55**, 114 (1951).
2. B. E. CONWAY and E. GILEADI. Trans. Faraday Soc. In press (1963).
3. B. E. CONWAY and M. DZIECIUCH. Nature, **189**, 914 (1961).
4. N. CABRERA and N. F. MOTT. Rept. Progr. Phys. **12**, 163 (1948–49).
5. B. E. CONWAY and J. J. MACDONALD. Proc. Roy. Soc. (London), Ser. A, **269**, 419 (1962).
6. L. YOUNG. Proc. Roy. Soc. (London), Ser. A, **263**, 395 (1961).
7. J. O'M. BOCKRIS and A. K. M. S. HUQ. Proc. Roy. Soc. (London), Ser. A, **237**, 277 (1956).
8. H. B. MORLEY and F. E. W. WETMORE. Can. J. Chem. **34**, 359 (1956).
9. V. E. PAST and Z. A. JOFA. Zh. Fiz. Khim. **33**, 913 (1955).
10. B. E. CONWAY, M. DZIECIUCH, and E. GILEADI. Electrochim. Acta. In press (1963).
11. G. ARMSTRONG and J. A. V. BUTLER. Trans. Faraday Soc. **29**, 1261 (1933).
12. B. E. CONWAY and P. BOURGAULT. Trans. Faraday Soc. **58**, 593 (1962).
13. J. O'M. BOCKRIS and H. KITA. J. Electrochem. Soc. **108**, 676 (1961).
14. J. G. N. THOMAS. Trans. Faraday Soc. **57**, 1603 (1961).
15. M. I. TEMKIN. Zh. Fiz. Khim. **15**, 296 (1941).
16. M. BOUDART. J. Am. Chem. Soc. **74**, 3556 (1952).

Can. J. Chem. Downloaded from www.nrcresearchpress.com by 210.87.254.6 on 09/05/12
For personal use only.

HYDROGEN CHEMISORPTION ON NICKEL–MAGNESIA CATALYSTS

N. RAMASUBRAMANIAN[1] AND L. M. YEDDANAPALLI
Chemistry Department, Loyola College, Madras, India
Received July 16, 1962

ABSTRACT

The hydrogen adsorption activities, per gram of nickel, of two nickel–magnesia catalysts are compared and explained on the basis of different types of nickel being present. The application of the Elovich equation to interpret the kinetic data shows the possibility of the presence of three kinetic stages in the temperature and pressure range studied. A study of the effect, on the hydrogen adsorption, of deliberate oxygen addition to and re-reduction of the catalyst surface shows that the nature of the oxygen contamination in the catalyst is different from that of the added oxygen.

Can. J. Chem. Downloaded from www.nrcresearchpress.com by 210.87.254.5 on 09/05/12
For personal use only.

It is evident from the work of Schuit and de Boer (1) that an imperfect reduction of the catalyst affects the fast and slow chemisorption of hydrogen on nickel. Taylor *et al.* (2) observed breaks in the Elovich plots of the data obtained on the aged nickel – Kieselguhr catalyst but not on the freshly prepared catalyst and it was suggested that oxygen contamination might be the cause of the occurrence of multiple kinetic stages. In the case of hydrogen chemisorption on nickel–magnesia catalysts the presence of more than a single stage of adsorption is shown by the Elovich plots (3). Nickel being the active adsorbent for hydrogen chemisorption in nickel–magnesia catalysts, it is felt that the nature of the sites, reduced and unreduced, can be better understood from a comparison of the chemisorptive capacity of nickel in catalysts of varying nickel content. Two catalysts of nickel content 79% and 18% were studied and the Elovich equation was applied to interpret the kinetic data. The results were analyzed to find out how the amounts of fast and slow adsorption and the rates of slow adsorption, calculated per gram of nickel in the catalysts, vary.

On the nickel–magnesia catalysts it was observed (3) that breaks on the Elovich plots appeared in either direction depending on the temperature and pressure conditions. Low (4) from his work on rhodium and palladium catalysts reported that the time of appearance and temporal range of existence of the individual kinetic stages are affected by initial pressure and by temperature. Therefore, the chemisorption on catalyst II was studied more extensively at different temperatures and initial pressures. In an attempt to determine the role of oxygen contamination, a study of the influence of oxygen introduced deliberately and re-reduction of the catalyst surface on the adsorption process was made on catalyst II.

EXPERIMENTAL

The method employed, preparation, and analysis of the catalysts, etc., have been described elsewhere (3). The catalyst II was prepared from 18 g of nickel nitrate and 50 g of magnesium nitrate and the precipitated, dried hydroxides were reduced in a stream of pure hydrogen at 390±5° C for 60 hours. Eight grams of nickel nitrate and 70 g of magnesium nitrate were used for preparing catalyst III and the drying and reduction conditions were the same as those for catalyst II. The nickel content of the catalysts II and III were 79.06% and 18.02%, respectively.

RESULTS

The algebraic method of Sarmousakis and Low (5) was used to evaluate the Elovich parameters. The q vs. log t plots were linear and showed discontinuities. The data obtained

[1]*Present address: Division of Applied Chemistry, National Research Council, Ottawa, Canada.*

on the two catalysts are presented in Table I, where q_1 stands for the amount adsorbed in the first minute (the fast adsorption); $q_{100}-q_1$, the difference in the amounts adsorbed

TABLE I

Comparison, per gram of nickel, of the activity of the two nickel–magnesia catalysts

Run No.	Temp. (°C)	Press. (cm Hg)	q_1 (cc, NTP)	$q_{100}-q_1$ (cc, NTP)	α_1	α_2
Catalyst II, 5.875 g, 79.06% Ni						
81	280	54.95	1.195	0.185	27.79	22.32
80	260	54.91	1.222	0.165	32.58	28.15
79	240	55.00	1.286	0.150	30.09	30.09
78	220	55.01	1.344	0.157	26.49	29.14
77	200	55.26	1.308	0.198	22.74	28.44
82	180	55.20	1.271	0.219	18.59	27.87
83	30	54.95	0.888	0.355	11.47	18.76
Catalyst III, 5.329 g, 18.02% Ni						
122	300	54.83	0.573	0.541	11.58	7.49
127	240	54.90	0.479	0.292	17.13	11.99
126	200	54.78	0.448	0.250	24.02	12.75
128	160	54.81	0.260	0.188	36.08	18.04
124	30	54.86	0.042	0.125	27.74	—

at the 100th and 1st minutes (the slow adsorption); and α_1 and α_2 the α values of the observed adsorption stages, respectively. A distinct difference in behavior with increasing temperature is readily seen from a comparison of the results on the two catalysts. The fast adsorption is higher on catalyst II and at lower temperatures the difference is more marked. On the other hand, the slow adsorption becomes considerably higher on catalyst III with increasing temperature. These observations point out that relative to one another, on the two catalysts II and III, respectively, sites active for high-temperature slow adsorption and lower-temperature fast adsorption are less. The difference in the activity of the chemisorption sites available on the catalysts could be seen from the α values also. When a α is very large, i.e. the q vs. log t plot is linear, the constant α in the Elovich equation becomes inversely proportional to the rate of adsorption at a time t. In contrast to catalyst II, on catalyst III the ratio α_2/α_1 is less than unity at and below 240° C and at higher temperatures both the α values are low. On catalyst III a higher degree of dispersion of nickel in magnesia and hence a higher activity is expected. It is interesting to note that it is less active than catalyst II towards total adsorption.

It is seen from Table I that at lower temperatures $\alpha_2 > \alpha_1$, whereas at higher temperature $\alpha_2 < \alpha_1$. It was pointed out by Low (4) that comparison of the kinetic stages on the basis of their temporal order of appearance resulted in misleading conclusions and, in general, low initial gas pressure and high temperature favor the early appearance of any one stage. The Elovich plot is a straight line for the adsorption carried out on catalyst II at 55 cm Hg and 240° C for about 3 hours; above or below this temperature α_2 is less or greater than α_1 (Table I). Therefore the temperatures 280 and 200° C were chosen to study the initial pressure effect. The variation of the α values with initial pressure at these two temperatures is shown in Fig. 1. At the higher temperature of 280° C there is a change in the value of α_2 relative to α_1, around 15 cm Hg. Then, according to Low's (4) generalization, this means that in the pressure range studied at 280° C the stages observed below 15 cm Hg are the first and second $\alpha_1 < \alpha_2$ and above this pressure are the second and third $\alpha_2 < \alpha_1$. At 200° C the stages observed are the first and second throughout the pressure range studied.

Can. J. Chem. Downloaded from www.nrcresearchpress.com by 210.87.254.5 on 09/05/12
For personal use only.

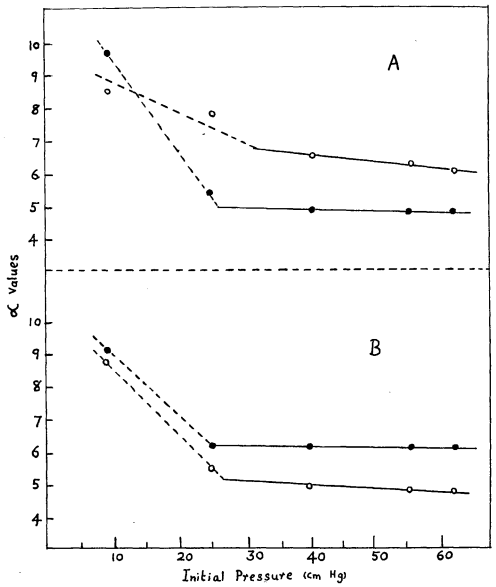

FIG. 1. Variation with initial pressure of α values; hydrogen adsorption at (A) 280 and (B) 200° C on catalyst II; ○, α_1 and ●, α_2.

It was then of interest to study the chemisorption at the lower pressure of 10 cm Hg at the other temperatures too. In Fig. 2 are shown the plots of the α values against

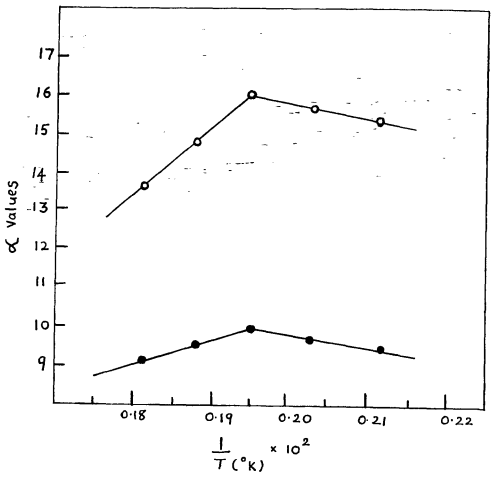

FIG. 2. Variation with temperature of α_1, ●, and α_2, ○; hydrogen adsorption at 10 cm Hg on catalyst II.

temperature and it is readily seen that first and second stages show up. As pointed out earlier, at 240° C the Elovich plot is a straight line for the data obtained at 55 cm Hg and the observed kinetic stage has to be the second. On the basis of more than two kinetic stages being present, though mostly only two of these are observed depending on the temperature and pressure conditions, a comparison points out that the temperature range of appearance of the kinetic stages is different on the two catalysts.

Can. J. Chem. Downloaded from www.nrcresearchpress.com by 210.87.254.5 on 09/05/12
For personal use only.

It is suspected that oxygen contamination might be the cause of the occurrence of multiple kinetic stages (2). To find out how the two stages of adsorption were affected by oxygen, introduced deliberately, the catalyst II was evacuated as usual for 8 hours at 380±5° C and cooled to room temperature. A small quantity of pure oxygen (0.3 cc at NTP) was sent into the catalyst vessel and the temperature raised gradually to 380° C over a period of 2 hours. The mercury levels on the manometer became equal, which indicated that the oxygen was taken up almost completely. The catalyst was evacuated for ½ hour at 380° C and a few experiments were carried out under conditions similar to those of an experiment on the usual starting surface S_I. The Elovich plots of the kinetic data are shown in Fig. 3, where A represents the run on the surface S_I and B, C, D, E,

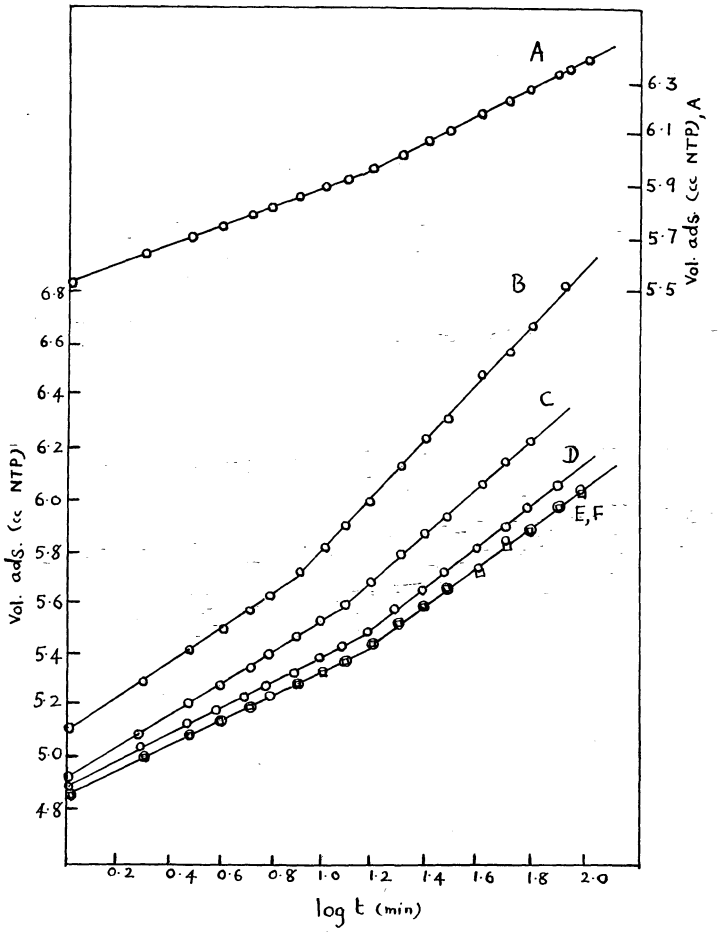

FIG. 3. The effect of oxygen contamination; hydrogen adsorption on catalyst II at 55 cm Hg and 280° C; A, normal run 81; B, C, D, E, and F, the successive runs 92 to 96 subsequent to oxygen contamination.

and F the successive experiments after oxygen addition. The values of the Elovich parameters, the fast adsorption q_1, and the slow adsorption $q_{100}-q_1$ are given in Table II. The oxygen contamination is seen to result in an increased slow adsorption, as is evidenced by the decreased α values, at the expense of the fast adsorption, a behavior similar to

Can. J. Chem. Downloaded from www.nrcresearchpress.com by 210.87.254.5 on 09/05/12
For personal use only.

TABLE II

Hydrogen chemisorption on Ni–MgO catalyst II, 5.875 g, 79.06% Ni, and effect of oxygen contamination and re-reduction of the catalyst surface

Surface	Run No.	Initial press. (cm Hg)	Temp. (°C)	α_1	α_2	q_1 (cc, NTP)	$q_{100}-q_1$ (cc, NTP)
S_I	81	54.95	280	6.413	4.807	5.544	0.841
	79	55.00	240	6.479	6.479	5.977	0.651
	77	55.26	200	4.897	6.124	6.059	0.911
				0.3 cc NTP oxygen added			
	92	54.71	280	2.804	1.980	5.086	1.824
	93	54.98	280	3.542	2.530	4.923	1.507
	94	54.87	280	4.487	2.804	4.874	1.296
	95	54.87	280	5.098	3.059	4.893	1.184
	96	54.80	280	5.174	3.059	4.923	1.157
S_{II}	97	54.80	280	5.174	3.059	4.923	1.157
	98	54.50	240	5.399	5.399	5.348	0.811
	99	54.74	200	4.897	6.124	5.419	0.892
				Re-reduced at 410° C with hydrogen			
S_{III}	106	54.60	280	6.119	4.807	5.699	0.834
	107	54.38	240	6.170	6.170	6.023	0.632
	108	54.30	200	4.710	6.124	6.318	0.917

that observed by Schuit and de Boer (1) on nickel–silica catalysts. The increase in the slow adsorption is nearly twice the decrease in the fast adsorption and is to a higher extent on the observed second kinetic stage. It is seen that after three repeated experiments reproducible results are obtained and the catalyst surface will be referred to as S_{II} to distinguish it from S_I. The break in the Elovich plot occurs earlier subsequent to oxygen addition but in the succeeding experiments there is a gradual shift towards and to the time of occurrence of break obtained on surface S_I. During the course of the repeated experiments at 280° C the slow adsorption decreases and the fast adsorption remains nearly constant at the decreased value.

The catalyst was re-reduced by heating at 410° C in hydrogen at atmospheric pressure for 12 hours. It was subsequently evacuated for 8 hours at 410° C and this procedure of heating in hydrogen and evacuation was repeated twice. After a couple of adsorption measurements at 280° C and 55 cm Hg reproducible results were obtained. This surface will be referred to as S_{III}. The results of a set of experiments on the surfaces S_{II} and S_{III} are compared with those on S_I in Table II. Compared to S_I, the α_1 and α_2 values on S_{II} show a slight decrease or $(q_{100}-q_1)$ a slight increase. It is evident from the results on S_{III} that on re-reduction at a higher temperature the fast adsorption has increased and the values of q_1, α_1, and α_2 are closer to those on S_I. On all the three surfaces the trend in the variation of the two α values with temperature is the same.

DISCUSSION

Of the two catalysts, the room-temperature fast adsorption is much less, the high-temperature slow adsorption is greater, and the total adsorption is less on the higher magnesia content catalyst III than on catalyst II. If unreduced nickel in the catalyst was mainly responsible for the activated or high-temperature slow adsorption of hydrogen (1) then the observation that the high-temperature slow adsorption is greater on catalyst III would mean that there is more nickel in the unreduced state in catalyst III than in catalyst II. A higher adsorptive capacity due to a higher degree of dispersion of nickel in magnesia is expected on the former catalyst. The fact that it is less active indicates

Can. J. Chem. Downloaded from www.nrcresearchpress.com by 210.87.254.5 on 09/05/12
For personal use only.

the possibility of some of the nickel becoming unavailable for chemisorption purposes with increase in magnesia content. Thus there seems to be a similarity to nickel–silica catalysts, the hydrogen adsorptive capacity of which was explained by the proposal of the presence of different types of nickel, viz., pure or relatively pure, unreduced, and unavailable nickel made by Schuit (6). The analysis of the kinetic data using the Elovich equation brings out the characteristics of the catalyst, seen from the study, on catalyst II, of the variation of α with temperature and pressure, which shows that there is every likelihood of at least three kinetic stages being present and that the temperature range of existence of the stages is different on the two catalysts.

The fact that oxygen contamination has a marked influence on the rates of adsorption and on the occurrence of kinetic stages is readily seen from the immediate effect of added oxygen. However, it is observed that this effect is not lasting; during the repeated adsorption measurements at 280° C there is a steady approach to the previous usual behavior, and hydrogen treatment at 410° C restores it. This would mean that there is the possibility that the added oxygen is being removed by hydrogen at a decreasing rate, a process faster and complete at the higher temperature. Then, the reproducibility obtained at 280° C only shows the drastic lowering of the reduction rate. The results on S_I and S_{II} show that the added oxygen, whatever amount that was left, has changed the fast and slow adsorption rates considerably but not the time of occurrence of the break and the general trend in the variation of the α values with temperature. Thus it appears that, though the catalyst has been heated in oxygen over the reduction temperature range employed in its preparation and the added oxygen affects the occurrence of the kinetic stages and to a greater extent the rates of adsorption, compared to the oxygen contamination in the catalyst, the added oxygen behaves differently in the sense that it can be relatively easily removed by hydrogen reduction.

REFERENCES

1. G. C. A. Schuit and N. H. de Boer. Rec. Trav. Chim. **70**, 1067 (1951).
2. M. J. D. Low, L. Leibowitz, and H. A. Taylor. J. Phys. Chem. **62**, 471 (1958).
3. N. Ramasubramanian and L. M. Yeddanapalli. J. Phys. Chem. **66**, 1222 (1962).
4. M. J. D. Low. Can. J. Chem. **38**, 588 (1960).
5. J. N. Sarmousakis and M. J. D. Low. J. Chem. Phys. **25**, 178 (1956).
6. G. C. A. Schuit and L. L. Von Reijen. Advances in catalysis. Vol. X. Academic Press Inc., New York. 1958. p. 243.

Can. J. Chem. Downloaded from www.nrcresearchpress.com by 210.87.254.5 on 09/05/12
For personal use only.

METABOLITES OF PATHOGENIC FUNGI

III. THE STRUCTURE OF XANTHOMEGNIN[1-4]

GEORGE JUST AND WILLIAM C. DAY[5]
Department of Chemistry, McGill University, Montreal, Que.

AND

FRITZ BLANK[6]
Department of Bacteriology, McGill University, Montreal, Que.

Received August 3, 1962

ABSTRACT

Xanthomegnin, a pigment isolated from *Trichophyton megnini*, was shown to be (−) 3,3′-bis-[2-methoxy-5-hydroxy-7-(2-hydroxypropyl)-8-carboxy-1,4-naphthoquinone lactone]. Application of the Hudson–Klyne lactone rule (C. S. Hudson, J. Am. Chem. Soc., **32**, 338 (1910); W. Klyne, Chem. Ind. (London), 1198 (1954)) gave results which supported the proposed stereochemistry.

Xanthomegnin, a yellow pigment, is one of the metabolites we have isolated[1] from the mycelium of *Trichophyton megnini*. The isolation of the compound was effected by deionization of the crude extract, followed by subsequent Soxhlet extraction, column chromatography, and fractional crystallization procedures. Xanthomegnin represented about 0.10% of the dried mycelium.

The pigment crystallized from a chloroform–benzene solution as orange platelets which did not melt but cindered at 264°. It was insoluble in hydroxylic solvents, only slightly soluble in acetone, ethyl acetate, or benzene, and moderately soluble in chloroform.

The empirical formula of xanthomegnin was originally established as $C_{15}H_{12}O_6$ based on the elemental analysis. However, the proton count by n.m.r. showed only 11 hydrogen atoms in the pigment, and the odd number persisted for the derivatives. On further investigation it was shown that the formula was actually $(C_{15}H_{11}O_6)_2$, where the molecule consisted of two identical halves joined into a dimeric structure. Zeisel, Kuhn–Roth, and active hydrogen determinations indicated one methoxyl, one methyl, and one hydroxyl group respectively per monomeric unit.

The infrared spectrum[7] showed a broad absorption at 3389 cm^{-1} ($CHCl_3$) for a bonded hydroxyl, and two carbonyl peaks, one at 1716 cm^{-1} and one at 1680 cm^{-1}. There was an additional band at 1622 cm^{-1} and a strong aromatic absorption at 1600 cm^{-1}.

The n.m.r. showed peaks at the following τ values:[8] −2.55, bonded hydroxyl; 2.83,

[1] *Part II. F. Blank, W. C. Day, and G. Just. J. Invest. Dermatol. In press.*
[2] *Presented at the 141st Meeting of the American Chemical Society, Washington, D.C., March 1962; Abstracts, p. 13-O.*
[3] *This investigation was supported by a PHS research grant, AI 04050-02, National Institute of Allergy and Infectious Diseases, Public Health Service, and grants from the Brown-Hazen Fund and the National Research Council of Canada.*
[4] *From the thesis presented to McGill University in partial fulfillment of the requirements for the Ph.D. degree by W. C. D., 1962.*
[5] *Holder of a National Research Council Scholarship, 1960–1961.*
[6] *Present address: Skin and Cancer Hospital, Departments of Dermatology and Microbiology, Temple University School of Medicine, Philadelphia, Pa.*
[7] *Unless specified, infrared data refer to potassium bromide pellets.*
[8] *Tetramethylsilane (0 c.p.s., τ = 10) as internal standard.*

Can. J. Chem. Downloaded from www.nrcresearchpress.com by 210.87.254.42 on 09/05/12
For personal use only.

aryl hydrogen; 5.53, $\diagdown$C—H, multiplet; 6.03, methoxyl; 7.08, Ar—CH_2—, doublet; and 8.51, methyl, doublet. The respective splitting of the alkyl constituents and the chemical shift of the methine suggested the moiety Ar—CH_2—CH(O$\diagup$)—CH_3.

The ultraviolet spectrum of the compound in dioxane exhibited a maximum at 228 mμ (ε 24,500), an inflection at 289 mμ (ε 7,900), and a peak at 389 mμ (ε 4,500).

Xanthomegnin formed a diacetate, and the single infrared absorption peak at 1775 cm^{-1} indicated that both esters were vinyl acetates. The aromatic maximum, poorly resolved in the pigment itself, appeared as a well-defined absorption at 262.5 mμ (ε 21,300) in the acetylated compound. Acetylation produced a hypsochromic shift of the chromophore from 389 to 344 mμ.

When the diacetate was subjected to catalytic hydrogenation in ethyl acetate with Adam's catalyst 2 mole-equiv of hydrogen were absorbed rapidly. In the infrared spectrum of the product, the 1680 cm^{-1} peak was no longer present and the 1716 cm^{-1} carbonyl band was shifted to 1658 cm^{-1}. Reacetylation returned the carbonyl absorption to 1716 cm^{-1}, thus indicating the hydrogen-bonded character of the quinol hydroxyl to the carbonyl. The bonded hydroxyl appeared at -2.64 τ and a free hydroxyl at 3.91 τ in the n.m.r. spectrum. The hydrogenated compound, upon acetylation, produced the same hexaacetate obtained by reductive acetylation of the pigment.

The quinone nature of the chromophore was therefore established, and comparison of the ultraviolet spectrum of xanthomegnin diacetate with that of 1,4-naphthoquinone and 2-methoxy-1,4-naphthoquinone showed marked similarities.

The pigment underwent reversible color changes at various pH's, being yellow in acidic and neutral media, and violet in basic solutions. This behavior is typical of certain hydroxy quinones.

The results of color tests conducted on the pigment with alkali solutions, methanolic lead acetate, and sulphuric acid suggested the 5-hydroxynaphthoquinone structure for xanthomegnin (2).

The position and the phenolic nature of the hydroxyl in the monomer could be postulated from the following information: (i) acetylation gave a vinyl acetate; (ii) the hydroxyl was bonded to the quinone as shown by absorption at 3389 and 1622 cm^{-1}, and -2.55 τ; (iii) hypsochromic shifts upon acetylation is a behavior of *peri*-hydroxy quinones (3); and (iv) the color reactions were consistent with those of 5-hydroxynaphthoquinones.

At this point we endeavored to establish the nature of the 1716 cm^{-1} carbonyl. In order to satisfy the double-bond equivalents of the formula of the pigment, a naphthoquinone derivative would have to have an additional ring. Since n.m.r. suggested the Ar—CH_2—CH(O$\diagup$)—CH_3 grouping, it seemed fitting that this structure was incorporated

into a δ-lactone ring. In order to test whether or not the carbonyl was a lactone, a sample of xanthomegnin was dissolved in aqueous alkali and the barium salt precipitated by the addition of barium chloride. The infrared spectrum of the barium salt showed the disappearance of the 1716 cm^{-1} band and the appearance of the carboxylate bands at 1410 and 1550 cm^{-1}.

Can. J. Chem. Downloaded from www.nrcresearchpress.com by 210.87.254.42 on 09/05/12
For personal use only.

Since the lactone was hydrogen bonded to a quinol hydroxyl in the reduced product, there were only three possible orientations (A, B, C) for the lactone ring attached to a

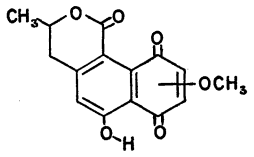

A.

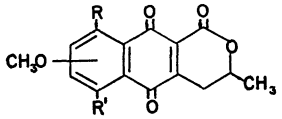

B. R = OH; R' = H
C. R = H; R' = OH

naphthoquinone structure. The problem remained to establish whether the methoxyl or the lactone was on the quinone ring of the naphthoquinone.

Oxidative cleavage of the quinone nucleus in xanthomegnin with alkaline peroxide gave a $C_{12}H_{10}O_7$ acid, m.p. 194–195°, $[\alpha]_D^{23}$ −76.7, −78.0 (*c* 0.34, 0.29 in acetonitrile), λ_{max}^{EtOH} 254, 337 mμ (ε 7,300, 5,500). The n.m.r. spectrum (in trideuteroacetic acid) showed the presence of the Ar—CH_2—CH—CH_3 group but no peak for the OCH_3 substituent.

The infrared absorption (acetonitrile solution) showed what appeared to be two carbonyl bands overlapping at 1725 cm^{-1} and a single carbonyl peak at 1680 cm^{-1}. These data were consistent for the structure of 4-hydroxy-6-(2′-hydroxypropyl)-hemimellitic acid δ-lactone (I). The carboxyl group flanked by another carboxyl and the lactone structure is apparently twisted out of planarity with the aromatic ring. It thus exhibited an infrared absorption like a non-aryl acid which placed its band high enough to overlap with the δ-lactone absorption peak. The other carboxyl, ortho to the phenol, behaved like salicyclic acid.

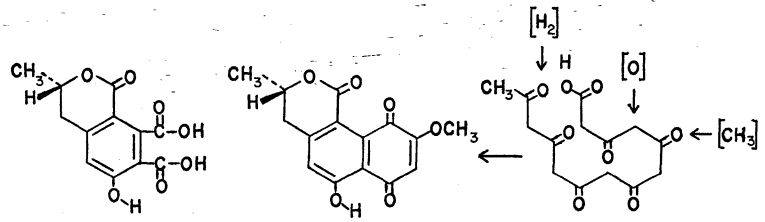

I II III

Sublimation of acid I resulted in dehydration and formation of a $C_{12}H_8O_6$ compound which had the spectral characteristics of a phthalic anhydride. Hydrolysis of the anhydride regenerated the original $C_{12}H_{10}O_7$ acid.

With I as the structure of the phthalic acid, II could then be drawn as the structure of the parent naphthoquinone. The 2-position for the methoxyl was chosen in accordance with the acetate hypothesis (see III) for natural products (3) and has not been established on chemical evidence.

A small amount of crotonic acid was isolated from the oxidation reaction. This apparently arose from the oxidative cleavage of the phenolic ring to produce β-hydroxybutyric acid, which readily dehydrates to crotonic acid.

Can. J. Chem. Downloaded from www.nrcresearchpress.com by 210.87.254.42 on 09/05/12
For personal use only.

One problem which remained to be solved was the odd number of protons in the n.m.r. spectra. In the spectra of xanthomegnin, the diacetate, and the hexaacetate, the apparent number of protons was 11, 13, and 19, respectively. In no instance was there evidence of the hydrogen atom in the 3-position of the naphthoquinone structure.

When the molecular weight determination was conducted on xanthomegnin diacetate using the ebullioscopic method with chloroform as the solvent, a value of 655 was obtained. An alternate determination[9] by measurements of the vapor pressure lowering of benzene solutions at 38° gave an average value of 877. Since the calculated molecular weight of the monomeric structure would be 330, the data would indicate the dimeric nature of the pigment.

Considering the remarkable insolubility of xanthomegnin in organic solvents, its failure to melt, and its inability to sublime *in vacuo* at elevated temperatures, it was apparent that the physical properties of the pigment were inconsistent with the monomeric structure. The absence of the hydrogen at the 3-position together with the molecular weight findings leads us to propose the following dimeric structures for xanthomegnin and the diacetate as the only ones which satisfy all the spectroscopic and analytical data:

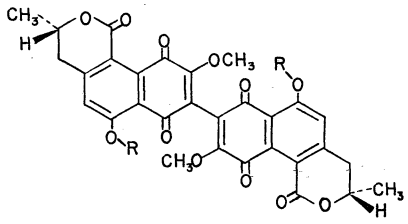

IV. XANTHOMEGNIN, R = H

V. XANTHOMEGNIN DIACETATE, R = AC

The final question to be settled was the absolute configuration of the asymmetric center in the δ-lactone. Klyne (1) has shown that the Hudson lactone rule can be applied to determine the absolute stereochemistry of the asymmetric center of the potential alcohol of the 5- and 6-membered-ring lactones. The direction of rotation induced by the formation of the lactone ring from the hydroxy acid is determined by the stereochemistry of the carbon atom bearing the hydroxyl group.

When acid I was dissolved in aqueous potassium hydroxide (*c* 2.05), the initial specific rotation was −98°. After 30 minutes it had risen to a constant value of −35°. Acidification of the solution resulted in a return of the rotation to −81°. The rotational increment passing from the acid to the lactone is hence −63°, establishing the absolute stereochemistry as depicted in I, and subsequently, IV and V.

No reference could be found in the literature to compounds where the double bond in the α,β-position had been studied in relation to the lactone rule. It is felt that the conclusion is most probably valid, although for this reason, the proposed configuration is advocated with reservation until verification is made of the fact that the lactone rule also applies to dihydroisocoumarins.

EXPERIMENTAL

All melting points were observed on a Kofler microscope hot-stage and are corrected. Rotations were measured with a Hilger Standard Polarimeter or a Zeiss Automatic Polarimeter using a 0.5-dm tube. The

[9]*Performed by Dr. A. F. Siriani, National Research Council, Ottawa, Canada.*

Can. J. Chem. Downloaded from www.nrcresearchpress.com by 210.87.254.42 on 09/05/12
For personal use only.

ultraviolet spectra were obtained in absolute ethanol or dioxane on the Beckman DK-1 recording spectrophotometer. The infrared spectra were recorded on a Perkin–Elmer model 21 using a potassium bromide pellet unless noted to the contrary. All n.m.r. spectra were taken at 60 Mc in deuterated chloroform with tetramethylsilane (0 c.p.s., $\tau = 10$) as an internal standard with the single exception when trideuteroacetic acid was used as the solvent. All analyses were carried out by Dr. C. Daesslé, Montreal, Que., and Dr. A. Bernhardt, Mülheim, Germany.

The Isolation of Xanthomegnin

A yellow matabolite, xanthomegnin, was isolated from the crude pigment extract of the mycelium of *Trichophyton megnini* by a sequence of deionization, Soxhlet extraction, column chromatography, and fractional crystallization procedures. The isolation has been reported separately.[1] The compound crystallized from a chloroform–benzene solution as orange platelets which did not melt but cindered at 264°.

Anal. Calc. for $(C_{15}H_{11}O_6)_2$: C, 62.72; H, 3.86; O, 33.42; methoxyl, 10.80 (2); methyl, 5.23 (2); active hydrogen, 0.35 (2). Found: C, 62.50; H, 3.92; average of four concordant analyses; O, 32.52; methoxyl, 10.87, 12.40; methyl, 3.01; active hydrogen, 0.75, 0.55.

Xanthomegnin Diacetate (V)

A mixture of 100 mg of xanthomegnin, 2 ml of acetic anhydride, and 10 drops of pyridine was allowed to stand at room temperature for 18 hours in the dark. The solution was poured onto ice to hydrolyze the excess anhydride, and the yellow flocculent solid was collected and recrystallized twice from ethanol–chloroform, m.p. 227–228°; ν 1775 cm^{-1} (vinyl acetate); λ_{max}^{diox} 262.5, 344 mμ (ϵ 21,300, 4,700); 7.40 τ, 3 protons per acetate.

Anal. Calc. for $(C_{17}H_{13}O_7)_2$: C, 62.01; H, 3.98. Found: C, 61.50; H, 3.97.

Tetrahydroxanthomegnin Diacetate

An ethyl acetate solution of 10.1 mg of xanthomegnin diacetate (V) absorbed 0.630 ml (1.84 mole-equiv, 2 mole-equiv = 0.685 ml), of hydrogen at room temperature and atmospheric pressure in the presence of 12 mg of prereduced platinum oxide.

Reduction was then carried out on a larger scale by stirring a solution of 89 mg of the acetate under hydrogen with 20 mg of platinum oxide until the uptake of hydrogen was complete. After the removal of the catalyst by filtration, the ether-soluble fraction of the product was crystallized from carbon tetrachloride, yielding 63 mg of bead-like crystals, m.p. 192–193°. The infrared spectrum showed no carbonyl absorption at 1716 and 1680 cm^{-1} but exhibited a new band at 1658 cm^{-1}. The n.m.r. spectrum showed a bonded hydroxyl at -2.64 τ and a free hydroxyl at 3.91 τ.

Anal. Calc. for $(C_{17}H_{15}O_7)_2$: C, 61.63; H, 4.56. Found: C, 60.52; H, 4.40. It proved to be very difficult to free the compound of water and solvents.

Tetrahydroxanthomegnin Hexaacetate

The 94 mg of hydrogenated xanthomegnin diacetate from the combined fractions was acetylated by dissolving the material in 2 ml of acetic anhydride, adding 10 drops of pyridine, and then allowing the solution to stand overnight in the dark. The reaction mixture was poured onto ice and after 1 hour the precipitate was collected by filtration and air dried. This product was chromatographed on silica gel, yielding 59 mg of nearly colorless solid from the benzene–ether (1:1 v/v) eluate. Recrystallization from isopropyl alcohol gave a pale yellow, amorphous precipitate, m.p. 191–192°; $[\alpha]_D^{23}$ -86.4, -82.2 (c, 0.72, 0.51 in chloroform); ν 1716 cm^{-1}; λ_{max}^{diox} 262 mμ (ϵ 37,000).

Anal. Calc. for $(C_{22}H_{19}O_9)_2$: C, 60.72; H, 4.61. Found: C, 60.55; H, 4.64.

Reductive Acetylation of Xanthomegnin Diacetate

Upon stirring a mixture of 27 mg of xanthomegnin diacetate (V), 27 mg of zinc dust, 2 ml of acetic anhydride, and two drops of pyridine for 10 minutes, the initially yellow solution became colorless. The reaction mixture was stirred vigorously for an additional 60 minutes and then allowed to stand overnight. Solid materials were filtered off and the filtrate was poured onto ice. After 2 hours the pale yellow precipitate was collected and recrystallized from isopropyl alcohol, m.p. 191–193°. Admixture of the product with tetrahydroxanthomegnin hexaacetate did not result in a lowering of the melting point, and the infrared spectra of the two compounds were superimposable.

Anal. Calc. for $(C_{21}H_{19}O_9)_2$: C, 60.72; H, 4.61. Found: C, 60.95; H, 4.64.

4-Hydroxy-6-(2′-hydroxypropyl)-hemimellitic acid δ-Lactone (I)

An alkaline peroxide oxidation of 500 mg of xanthomegnin was carried out in 50 ml of 10% aqueous sodium hydroxide. Ten milliliters of 30% hydrogen peroxide was added dropwise to the stirred solution while the reaction temperature was maintained below 10° with an ice bath. After ½ hour, an additional 2 ml of peroxide was added, the ice bath was removed, and the reaction mixture was allowed to stand at room temperature for 2 hours.

The solution was acidified to pH 4 with concentrated hydrochloric acid (approx. 10.5 ml). A slight excess of sodium bicarbonate was then added and the solution extracted twice with chloroform; only 2 mg of unreacted pigment was recovered.

Can. J. Chem. Downloaded from www.nrcresearchpress.com by 210.87.254.42 on 09/05/12
For personal use only.

The solution was reacidified and extracted for 2 days with ether in a liquid–liquid extractor. Part of the material thus obtained was an easily sublimable product, which was separated by collecting it on a cold finger adjusted into the flask. By leaving the flask in a water bath at 45° for 20 hours, 32 mg of white sublimate was collected at atmospheric pressure. On further investigation this sublimate, m.p. 58–60°, proved to be predominantly crotonic acid (reported (4) m.p. 72°). Comparison of the R_f values of the sublimate with pure samples on Whatman No. 1 paper with ethanol – ammonium hydroxide – water (16:1:3 v/v) and bromocresol purple as developer confirmed the presence of crotonic and oxalic acids.

The main product was dissolved in ethyl acetate and washed six times with water, each wash being re-extracted five times with ethyl acetate. The small amount of water-soluble material was chiefly oxalic acid, as shown by a paper chromatogram using *n*-propanol – eucalyptol – formic acid (5:5:2 v/v), with water added to persistent cloudiness and using an ammoniacal silver nitrate developer.

The residue recovered upon evaporation of the ethyl acetate was recrystallized from acetone–benzene, yielding 163 mg of slightly colored, stubby needles (I), m.p. 194–195°. Two additional recrystallizations did not raise the melting point.

Anal. Calc. for $C_{12}H_{10}O_7$: C, 54.14; H, 3.79. Found: C, 54.49, 54.45; H, 4.07, 3.97.

3-Carboxy-6-hydroxy-4-(2′-hydroxypropyl)-phthalic anhydride Lactone

Sublimation of 40 mg of acid I at 165° and 2 mm gave 29 mg of pale yellow, stout needles of the anhydride, m.p. 227–229°; ν 1780 and 1855 cm^{-1} (phthalic anhydride); λ_{max}^{diox} 270, 352 mμ (ϵ 5,050, 7,760).

Anal. Calc. for $C_{12}H_8O_6$: C, 58.07; H, 3.25. Found: C, 58.16; H, 3.30.

Five milligrams of the anhydride was dissolved in 10 drops of acetic acid. The solution was diluted by approximately 20% with water, one drop of concentrated hydrochloric acid was added, and the mixture was allowed to stand overnight. Water was then added to force precipitation of the hydrolyzed product. The white solid was collected by filtration and dried, m.p. 196–197°. Admixture of this product and a sample of acid I gave no depression of the melting point. The infrared spectra were superimposable.

Rotation Studies on Acid I to Determine the Δ Value of the Lactone

The initial rotation of the acid was determined in 5% potassium hydroxide solution and was found to be $[\alpha]_D^{20}$ −98° (*c* 0.20). The rotation then decreased until it reached a constant value of −35°, after ½ hour and at room temperature; Δ value, −63°. Upon the addition of hydrochloric acid the rotation returned to −81° (*c* 0.14).

The rotation of the acid was determined again in 5% potassium hydroxide solution, giving −94° (*c* 0.20), changing to the constant value −29°; Δ value, −65°.

ACKNOWLEDGMENTS

The authors are indebted to Dr. R. Fraser of the University of Ottawa and to Mr. J. Nicholson of the National Research Council for obtaining the n.m.r. spectra and for valuable consultations concerning the interpretations thereof.

REFERENCES

1. C. S. Hudson. J. Am. Chem. Soc. **32**, 338 (1910). W. Klyne. Chem. Ind. (London), 1198 (1954).
2. R. Kuhn and K. Wallenfels. Chem. Ber. **72**, 1411 (1939). H. R. V. Arnstein and A. H. Cook. J. Chem. Soc. 1021 (1947).
3. A. J. Birch and F. W. Donovan. Australian J. Chem. **6**, 360 (1953); **8**, 529 (1955).
4. K. v. Auwers and H. Wissebach. Chem. Ber. **56**, 715 (1923).

Can. J. Chem. Downloaded from www.nrcresearchpress.com by 210.87.254.42 on 09/05/12
For personal use only.

THE ACIDITY FUNCTION, H_0, IN AQUEOUS CONCENTRATED ACID AND SALT SOLUTIONS

DONALD ROSENTHAL* AND JAMES S. DWYER
Department of Chemistry, The University of Chicago, Chicago, Ill., U.S.A.

Received August 17, 1962

ABSTRACT

Some H_0 measurements in concentrated LiCl solutions are reported. It is shown that the H_0 values in 1–9 *M* LiCl, 1–9 *M* $HClO_4$, and 1–11 *M* HCl solutions can be calculated using the equation

$$H_0 = pCH + n \log a_w - BC,$$

where a_w is the activity of water, C is either the molar or molal concentration, and n and B are least-squares constants. Values of $n = 2$ (molar equation) and $n = 1$ (molal equation) fit the experimental data better than does $n = 4$. With the molar equation a non-integral value of n for $HClO_4$ is required to give reasonable H_0 values. The adequacy and significance of integral and non-integral values of n are considered. The nature of the constant B is also discussed. A more general equation is developed which under certain conditions reduces to the simpler equation. The more general equation is based upon a model which assumes the existence of more than one hydrated form of the indicator base, its conjugate acid, and H_3O^+. Some of the implications of this more general equation are considered.

INTRODUCTION

H_0 is defined as

$$H_0 \equiv pK_{BH^+} - \log (C_{BH^+}/C_B) \quad [1]$$

for the reaction $BH^+ \rightleftarrows B + H^+$, where B is a suitable uncharged indicator base (usually a substituted aniline) (1, 2). It is implicitly assumed that the proton and perhaps also B and BH^+ are solvated by water molecules in aqueous solutions. If, as seems reasonable, the number of water molecules required to solvate BH^+ is not equal to the number of water molecules required to solvate B and H^+, the above chemical equation can be more adequately represented as

$$BH^+ + nH_2O \rightleftarrows B + H^+.$$

Indeed, Bascombe and Bell (3) have indicated they could account for the H_0 values of less than 8 *M* strong acid solutions by assuming $n = 4$ and therefore that

$$H_0 = -\log [H^+](f_{H^+}f_B/f_{BH^+}a_w^4) = pMH + 4 \log a_w - \log (f_{H^+}f_B/f_{BH^+}). \quad [2]$$

Values of H_0 can be evaluated by assuming that

$$\log (f_{H^+} f_B/f_{BH^+}) = BM, \quad [3]$$

where B is a constant whose value depends upon the nature of the acid or salt and M is the molar concentration of electrolyte (acid or salt). That value of B which best fits the data is selected. Equation [3] is not unreasonable, since $\log f_B = B'M$ is valid for most non-electrolytes over a rather extended range of concentrations (4, 5), and $\log f_{H^+}/f_{BH^+}$ is relatively small in magnitude and for the present purposes can be adequately represented by $B''M$, so that $B = B' + B''$ (4, 6).

**Present address: Department of Chemistry, Clarkson College, Potsdam, N.Y.*

Can. J. Chem. Downloaded from www.nrcresearchpress.com by 210.87.254.105 on 09/05/12
For personal use only.

The present study was initiated to examine the adequacy of various equations in the calculation of H_0 values, and to consider what is the detailed nature of the acid–base equilibrium which defines H_0. In addition to published data on H_0 in hydrochloric and perchloric acid solutions, the results of some H_0 measurements we have made on slightly acidified lithium chloride solutions were used.

EXPERIMENTAL DETAILS OF LiCl H_0 MEASUREMENTS

Reagents

Baker Analyzed Reagent grade LiCl and reagent grade HCl were used. The indicators used were Eastman Kodak Co. white label brand compounds recrystallized twice from alcohol and once from water. The following melting points were obtained after the above purification: for *p*-nitroaniline 147–148° C, for *o*-nitroaniline 71.5–71.7° C, for 4-chloro-2-nitroaniline 116–117° C.

Solutions

Lithium chloride solution was made up roughly to 10.5 *M* and allowed to stand from 4 to 7 days until the insoluble impurities settled out. The clear supernatant was then siphoned off or filtered and standardized with a silver nitrate solution. The titer was adjusted to within one part per thousand of 10.00 *M*. Stock solutions (4×10^{-4} *M*) of the indicators and HCl solutions (0.1000 *M* and 1.000 *M*) were prepared.

All solutions used in the spectrophotometric measurements were prepared from the LiCl, HCl, and indicator stock solutions using calibrated volumetric glassware and diluting to 100 ml in a calibrated volumetric flask. The temperature of the solutions and glassware was maintained at 25±0.5° C.

Spectrophotometric Measurements

Measurements were made using a Beckman DU Quartz Spectrophotometer with 10-cm fused silica cells. The solutions and cells were maintained at 25±0.5° C. In each instance the reference solution was identical in composition with the corresponding indicator solution except for the absence of the indictor. The molar absorptivity of the indicators in the basic form was obtained with indicator solutions of concentration sufficient (ca. 10^{-5} *M*) that the absorbance was about one at the absorption maximum. To make sure the indicators were completely in the basic form, each solution was 0.001 *M* in NaOH. The wavelength of maximum absorbance and the molar absorptivity of the basic form of the indicators were different for water and the various LiCl solutions, and so were determined for each salt concentration used. The absorption maximum and molar absorptivity of the basic form changed as follows in going from water to the most concentrated LiCl solution: *p*-nitroaniline–water (0.001 *M* NaOH), 382 mμ, 1.30×10^4 liters $mole^{-1}cm^{-1}$; 8 *M* LiCl, 386 mμ, 1.264×10^4; *o*-nitroaniline–water (0.001 *M* NaOH), 412 mμ, 4.46×10^3; 9 *M* LiCl, 420 mμ, 4.23×10^3; 10 *M* LiCl, 423 mμ, 4.21×10^3; 4-chloro-2-nitroaniline–water (NaOH), 425 mμ, 4.52×10^3; 9 *M* LiCl, 431 mμ, 4.35×10^3. In general, the change in the wavelength maximum and molar absorptivity was not a linear function of concentration, but for *p*-nitroaniline the error made in assuming a linear function is negligible. Measurements made in aqueous solutions revealed the indicators conform to Beer's law in the concentration range employed in these studies. The results obtained in the LiCl solutions are consistent with the assumption that the indicators conform to Beer's law in these solutions.

The absorbance was zero in aqueous solutions in which the indicators were in their acid forms. It was assumed the molar absorptivity of the acid forms of the indicators was zero in all the LiCl solutions.

A series of absorbance measurements was made in 4 *M* LiCl using *p*-nitroaniline and *o*-nitroaniline, and in 8 *M* LiCl using *o*-nitroaniline and 4-chloro-2-nitroaniline. Hydrochloric acid concentrations varied from 5×10^{-3} *M* to 8×10^{-2} *M* and C_{BH^+}/C_B (equation [1]) varied from 0.5 to 3. The total indicator concentration was such that the absorbance of the solutions was between 0.3 and 1.6. H_0 was calculated from the absorbance measurements and the appropriate molar absorptivities using equation [1] and Paul and Long's pK_{BH^+} values for the indicators (2).

$H_0-pM\mathrm{H}$ was found to be a constant (1.054, $n = 5$, $S.D_{\bar{x}} = 0.012$) in the 4 *M* LiCl, and equal to 2.488 ($n = 7$, $S.D_{\bar{x}} = 0.004$) in the 8 *M* LiCl solutions (7). Having demonstrated the existence of *an* acidity function, H_0, in 4 and 8 *M* LiCl solutions, measurements were made with *p*-nitroaniline in 1–7 *M* LiCl solutions which were 5×10^{-3} *M* in HCl, and with *o*-nitroaniline in 9 *M* LiCl solutions. These H_0 results are summarized in Table III.

DISCUSSION

Least-squares H_0 Calculations

Using the expression

$$H_0 = pM\mathrm{H}+n\log a_w-BM, \qquad [4]$$

where $n = 4$, least-squares values of B were obtained for HCl, $HClO_4$, and LiCl from

Can. J. Chem. Downloaded from www.nrcresearchpress.com by 210.87.254.105 on 09/05/12
For personal use only.

H_0 data for 1–11 M HCl, 1–9 M $HClO_4$, and 1–9 M LiCl solutions (the range of concentrations for which there are both H_0 values and activity of water data). Columns 5 and 6 of Tables I, II, and III contain values of H_0 calculated from equation [4] using the least-squares B values. Where an attempt is made to fit all the data (column 6), many of the calculated H_0 values are significantly different from the corresponding experimental values. Where only the 1–6 M data is fitted (column 5), the differences between the calculated and experimental values are comparable in magnitude to the errors in the H_0 measurements (2). Extrapolation of the least-squares straight line to concentrations greater than 6 M (data in parentheses column 5) leads to systematic deviations between calculated and experimental H_0 values. These deviations might be explained in terms of a competition between the hydrogen or lithium ion, chloride or perchlorate ion, indicator base and conjugate acid for water of solvation in these more concentrated acid or salt solutions, which results in a value of n less than four. (In some instances there is insufficient water to provide the "normal hydration numbers" for all species which are present.) In addition, there may be systematic deviations from equation [3] in very concentrated solutions (5).

In using and interpreting a value of $n = 4$ in equation [4], Bascombe and Bell assumed (3) that B and BH^+ were either unhydrated or hydrated to the same extent. There is evidence that both B (8, 9) and BH^+ (8, 10, 11, 12) are hydrated in aqueous solution and further that they are not hydrated to the same extent.

Instead of assigning a value to n, least-squares values of n and B were obtained using equation [4], and the H_0 values given in columns 7 and 8 of Tables I, II, and III were calculated. With an additional adjustable parameter it is not surprising that a better fit to the experimental data is obtained. However, the remarkable thing is that the deviation, between the experimental and calculated H_0 values (column 8), is in every case less than the magnitude of the experimental error expected for such measurements. If equation [4] is to be regarded as anything more than an empirical expression, the values of B and n obtained as a result of the least-squares calculations (column 8) need to be interpreted. The magnitude and sign of the values of B are not inconsistent with equation [3] and the previous relevant discussion (13). The non-integral values of n obtained for $HClO_4$ and LiCl, and the magnitude and the difference in n values for HCl and $HClO_4$ are not so readily explained.

Integral Values of n

Perhaps as reasonable as the assumption that n equals four (3) is the assumption that, at least where there is excess water available, there are three water molecules in the primary hydration shells of BH^+ and H_3O^+ and one (or no) water molecules in the primary hydration shell of B (8–12). (This model of the H_0 determining reaction assumes that B is a primary amine. This is true of many of the indicators used in establishing the H_0 values for HCl and $HClO_4$, and all the indicators in the LiCl measurements. Errors due to the fact that the n (and B) values of the indicators may differ are partially compensated for by the procedure by which pK_{BH^+} values are assigned and by the fact that any one indicator is only used over a small range of acid (or salt) concentration and thus a small range of activity of water. However, some of the deviation between calculated and experimental H_0 values may be attributed to this source of error.) This would give a value for n of two (or one). Such values are in better agreement with the n values from the least-squares calculations. The H_0 values calculated using equation [4] with $n = 2$ are given in columns 9 and 10 of Tables I–III. Considering just the 1–6 M data (column 9),

Can. J. Chem. Downloaded from www.nrcresearchpress.com by 210.87.254.105 on 09/05/12
For personal use only.

Can. J. Chem. Downloaded from www.nrcresearchpress.com by 210.87.254.105 on 09/05/12
For personal use only.

TABLE I
Comparison of observed and calculated H_0 values in HCl solutions at 25° C

Molarity HCl	Molality*	Activity of water (a_w)†	H_0 (exptl.)‡	Calculated H_0 using equation [4]					
				$n = 4$ 1–6 M	$n = 4$ 1–11 M	1–6 M	1–11 M	$n = 2$ 1–6 M	$n = 2$ 1–11 M
1	1.022	0.9623	−0.20	−0.16	−0.12	−0.18	−0.19	−0.18	−0.19
2	2.086	0.9137	−0.69	-0.63_5	−0.57	−0.67	−0.68	−0.68	−0.68
3	3.197	0.8529	−1.05	−1.02	−0.93	−1.06	−1.08	−1.07	−1.07
4	4.356	0.7811	−1.40	−1.39	−1.26	−1.41	−1.43	−1.42	−1.42
5	5.570	0.7004	−1.76	-1.76_5	−1.60	−1.76	−1.77	−1.76	−1.77
6	6.843	0.6133	−2.12	-2.16_5	−1.97	−2.11	−2.12	−2.11	−2.12
7	8.180	0.5241	−2.50	(−2.59)§	−2.36	(−2.48)§	−2.47	(−2.46)§	−2.47
8	9.590	0.4375	−2.86	(−3.05)	−2.79	(−2.85)	−2.83	(−2.82)	−2.83
9	11.081	0.3587	−3.22	(−3.54)	−3.24	(−3.24)	−3.21	(−3.19)	−3.21
10	12.664	0.2880	−3.59	(−4.05)	−3.73	(−3.65)	−3.60	(−3.58)	−3.60
11	14.349	0.2250	−3.99	(−4.61)	−4.25	(−4.07)	−4.01	(−3.99)	−4.01
			B	0.08924	0.05667	0.14226	0.15353	0.15024	0.15211
			$S.D_B$	0.00413	0.00656	0.01046	0.00424	0.00163	0.00085
			n			2.2617	1.9702		
			$S.D_n$			0.3381	0.0870		

*Calculated from density data found in "International Critical Tables", Vol. III, McGraw-Hill Book Co., Inc., New York, N.Y., 1928, p. 54; and British Standards, No. 976, 1957.
†Calculated from osmotic coefficient data found in R. A. Robinson and R. H. Stokes, "Electrolyte Solutions", Butterworths Publications Ltd., London, England, 1959, pp. 483, 504.
‡M. A. Paul and F. A. Long, Chem. Rev., **57**, 12 (1957).
§Calculated using the least-squares value of B (and n in column 7) obtained for the 1–6 M HCl data.

Can. J. Chem. Downloaded from www.nrcresearchpress.com by 210.87.254.105 on 09/05/12
For personal use only.

TABLE II

Comparison of observed and calculated H_0 values in $HClO_4$ solutions at 25° C

Molarity $HClO_4$	Molality*	a_w†	H_0 (exptl.)‡	Calculated H_0 using equation [4]					
				$n = 4$ 1–6 M	$n = 4$ 1–9 M	1–6 M	1–9 M	$n = 2$ 1–6 M	$n = 2$ 1–9 M
1	1.050	0.9611	−0.22	−0.20	−0.15	−0.22	−0.24	−0.25	−0.27
2	2.201	0.9058	−0.78	−0.73	−0.63	−0.77	−0.80	−0.82	−0.85
3	3.468	0.8286	−1.23	−1.19	−1.04	−1.24	−1.28	−1.30	−1.34
4	4.864	0.7260	−1.72	−1.67	−1.47	−1.71	−1.74	−1.75	−1.81
5	6.408	0.6002	−2.23	−2.23	−1.98	−2.23	−2.24	−2.23	−2.31
6	8.120	0.4589	−2.84	−2.91	−2.60	−2.84	−2.80	−2.76	−2.85
7	10.024	0.3178	−3.50	(−3.74)§	−3.38	(−3.56)§	−3.45	(−3.37)§	−3.47
8	12.165	0.1950	−4.22	(−4.78)	−4.36	(−4.44)	−4.22	(−4.07)	−4.18
9	14.603	0.1039	−5.11	(−6.05)	−5.59	(−5.50)	−5.14	(−4.88)	−5.01
			B	0.12911	0.07812	0.17095	0.19966	0.21798	0.23293
			$S.D_B$	0.00493	0.01495	0.00383	0.00621	0.00551	0.00447
			n			3.0583	2.4296		
			$S.D_n$			0.0834	0.0758		

*Calculated from density data from A. E. Markham, J. Am. Chem. Soc., **63**, 874 (1941); and L. H. Brickwedde, J. Res. Natl. Bur. Stand., **42**, 309 (1949).
†R. A. Robinson and R. H. Stokes, "Electrolyte Solutions", Butterworths Publications Ltd., London, England, 1959, pp. 483, 504.
‡M. A. Paul and F. A. Long, Chem. Rev., **57**, 12 (1957). 7, 8 and 9 M values from T. G. Bonner and J. C. Lockhart, J. Chem. Soc., 2840 (1957).
§Calculated using the least-squares value of B (and n for column 7) obtained for the 1–6 M $HClO_4$ data.

Can. J. Chem. Downloaded from www.nrcresearchpress.com by 210.87.254.105 on 09/05/12
For personal use only.

TABLE III

Comparison of observed and calculated H_0 values in LiCl solutions at 25° C

Molarity LiCl	Molality*	a_w†	H_0 (exptl.)§ = pMH+	Calculated H_0 using equation [4]					
				$n = 4$ 1–6 M H_0 = pMH+	$n = 4$ 1–9 M H_0 = pMH+	$n = 2$ 1–6 M H_0 = pMH+	$n = 2$ 1–9 M H_0 = pMH+	$n = 2$ 1–6 M H_0 = pMH+	$n = 2$ 1–9 M H_0 = pMH+
1	1.022	0.9631	-0.21_9	−0.209	−0.194	−0.238	−0.229	−0.236	−0.243
2	2.086	0.9169	-0.47_5	−0.440	−0.409	−0.485	−0.471	−0.483	−0.497
3	3.197	0.8590	-0.74_1	−0.697	−0.650	−0.745	−0.731	−0.743	−0.764
4	4.360	0.7888	-1.05_4	−0.989	−0.927	−1.022	−1.013	−1.021	−1.048
5	5.579	0.7078	-1.30_5	−1.322	−1.244	−1.319	−1.322	−1.319	−1.353
6	6.860	0.6190	-1.63_5	−1.699	−1.606	−1.636	−1.659	−1.639	−1.680
7	8.205	0.5253	-1.98_4	(−2.129)‡	−2.019	(−1.979)‡	−2.029	(−1.985)‡	−2.033
8	9.620	0.4345	-2.48_8	(−2.603)	−2.479	(−2.343)	−2.428	(−2.354)	−2.408
9	11.110	0.3502	-2.84_3	(−3.122)	−2.982	(−2.728)	−2.857	(−2.745)	−2.806
			B	0.14437	0.12877	0.20640	0.18703	0.20372	0.21056
			$S.D_B$	0.00510	0.00490	0.01264	0.00967	0.00192	0.00265
			n			1.90981	2.57520		
			$S.D_n$			0.41963	0.23102		

*Calculated from density data found in "International Critical Tables", Vol. III, McGraw-Hill Book Co., Inc., New York, N.Y., 1928, p. 77.
†Calculated from osmotic coefficient data found in R. A. Robinson, and R. H. Stokes, "Electrolyte Solutions", Butterworths Publications Ltd., London, England, 1959, pp. 483, 504.
‡Calculated using the least-squares value of B (and n in column 7) obtained for the 1–6 M LiCl data.
§(H_0−pMH) was shown to be constant for a particular LiCl solution over a wide range of dilute HCl concentration (see Experimental Details). H_0 equals pMH plus the value listed in the column.

the results obtained for HCl and LiCl with $n = 2$ were in better agreement with the experimental H_0 values than the results obtained with $n = 4$. For $HClO_4$ the results obtained with $n = 2$ were no better than those obtained with $n = 4$. Where all the data given in Tables I–III are considered (column 10), the deviations between the calculated and experimental H_0 values are less than the uncertainties in the H_0 values for HCl and LiCl. The $HClO_4$ deviations can probably not be explained merely in terms of the errors in the experimental H_0 values. For HCl, LiCl, and $HClO_4$ deviations were less with $n = 2$ (column 10) than with $n = 4$ (column 6). The value of n is significantly closer to two than to one for HCl, LiCl, and $HClO_4$. (However, see Discussion in final section.)

The large deviations which occur for $HClO_4$ (column 10, Table II) and some of the other deviations (columns 7–10, Tables I–III) might be explained in terms of an effective change in n in going from dilute to more concentrated solutions. It may be unreasonable to attempt to use a model in which n has a constant value for all acid (or salt) concentrations. However, there is no convincing evidence that n equals four even in the more dilute solutions. Table IV contains the values of the least-squares constants for equation [4] when only portions of the concentration–H_0 values in Tables I–III are used (see also

TABLE IV

Results of least-squares calculations for portions of the H_0 data

Range of concn., M	Values of equation [4] least-squares constants for: HCl		$HClO_4$		LiCl	
	n	B	n	B	n	B
1–3	−1.521 (0.067)*	0.225 (0.001)*	2.372 (0.752)	0.186 (0.019)	4.000 (1.131)	0.160 (0.024)
4–6	2.694 (0.114)	0.128 (0.004)	2.964 (0.106)	0.176 (0.005)	1.236 (0.872)	0.228 (0.027)
7–9	1.673 (0.062)	0.170 (0.003)	2.188 (0.078)	0.222 (0.007)	2.850 (1.242)	0.175 (0.058)
9–11	1.711 (0.122)	0.167 (0.007)				
1–5	1.910 (0.583)	0.151 (0.016)	3.068 (0.176)	0.171 (0.007)	1.983 (0.808)	0.205 (0.022)
5–9			2.309 (0.080)	0.211 (0.007)	2.849 (0.390)	0.175 (0.017)
7–11	1.662 (0.043)	0.170 (0.002)				

*Values in parentheses are standard deviations.

columns 7 and 8, Tables I–III). H_0 is not a very sensitive function of n at low concentrations where the logarithm of the activity of water is very small, and errors in the experimental H_0 values can be 0.05 or greater. This explains the negative n value for HCl in the 1–3 M range and the large $S.D_n$ values at these low concentrations. In general n values are closer to two than four, but not always significantly so. There is no case in which n is significantly closer to four than to two.

Non-integral and Variable Values of n

In sufficiently concentrated salt solutions there is insufficient water to satisfy the "normal hydration numbers" of all the species present. This means that in addition to species like $H_3O^+.3H_2O$ (3), $B.H_2O$, and $BH^+.3H_2O$, species like $H_3O^+.2H_2O$, $H_3O^+.H_2O$, H_3O^+, B, $BH^+.2H_2O$, $BH^+.H_2O$, and BH^+ must also be present (14). A series of chemical

Can. J. Chem. Downloaded from www.nrcresearchpress.com by 210.87.254.105 on 09/05/12
For personal use only.

equations and equilibrium constant expressions of the following general form can then be written:

$$H_3O^+.mH_2O \rightleftarrows H_3O^+.(m-1)H_2O + H_2O$$

$$K_{Hmw} = \frac{[H_3O^+.(m-1)H_2O]a_w}{[H_3O^+.mH_2O]} \frac{f_{H(m-1)w}}{f_{Hmw}}; \quad [5]$$

$$BH^+.pH_2O \rightleftarrows BH^+.(p-1)H_2O + H_2O$$

$$K_{BHpw} = \frac{[BH^+.(p-1)H_2O]a_w}{[BH^+.pH_2O]} \frac{f_{BH(p-1)w}}{f_{BHpw}}; \quad [6]$$

$$B.qH_2O \rightleftarrows B.(q-1)H_2O + H_2O$$

$$K_{Bqw} = \frac{[B.(q-1)H_2O]a_w}{[B.qH_2O]} \frac{f_{B(q-1)w}}{f_{Bqw}}; \quad [7]$$

and

$$nH_2O + BH^+.dH_2O \rightleftarrows B.(n+d-b)H_2O + H_3O^+.bH_2O$$

$$K^i_{BH^+} = \frac{[B.(n+d-b)H_2O][H_3O^+.bH_2O]}{[BH^+.dH_2O]a_w^n} \frac{f_{B(n+d-b)w}f_{Hbw}}{f_{BHdw}}. \quad [8]$$

In the above, the subscript w refers to water. Where H appears as the first subscript it refers to H_3O^+, and the subscript of f identifies the species to which the molar activity coefficient refers. Only one particular $K^i_{BH^+}$, K'_{BH^+} corresponding to particular n, d, and b values need be explicitly defined. All other equilibrium constants of form [8] can be expressed as a function of K'_{BH^+}, equilibrium constants of form [5]–[7], a_w, and activity coefficients quotients.

It is assumed that operationally

$$H_0 = pK_{BH^+} - \log \frac{([BH^+]+[BH^+.H_2O]+[BH^+.2H_2O]+\ldots)}{([B]+[B.H_2O]+\ldots\ldots\ldots\ldots)}, \quad [9]$$

where the numerator and denominator of the log term are each equivalent to an absorbance divided by a molar absorptivity. (This assumption is probably correct for the LiCl H_0 measurements, because the molar absorptivities were determined in each of the salt solutions. In HCl and $HClO_4$ solutions this assumption implies the further assumption that the molar absorptivities of each of the solvated species in the numerator are equivalent, and similarly for the denominator.) For convenience, it is further assumed that only those species indicated at the beginning of this section need be considered, i.e., m = 1–3 in equation [5], p = 1–3 in equation [6], and q = 1 in equation [7]. The treatment could be made more general by postulating additional solvated species, but this would only make the resulting equations more cumbersome without changing the essential form of the result. There may be differences in the secondary hydration shells of each of the species postulated. These differences, if important, are assumed to be adequately incorporated into the activity coefficients. Finally, this model does not specifically consider the consequences of solvation of Li^+ or the anions by B, the sharing of a water molecule by the ions, the structure of these solutions (15), and the decrease in the static dielectric constant with increasing salt (or acid) concentration, etc. (7, 16).

Having made the above indicated assumptions, the concentration of each of the four species in the numerator of the log term of equation [9] can be expressed as a function of the $BH^+.3H_2O$ concentration by using the equation [6] type equilibrium constants. The

Can. J. Chem. Downloaded from www.nrcresearchpress.com by 210.87.254.105 on 09/05/12
For personal use only.

two terms in the denominator can be expressed as a function of $B.H_2O$ concentration (equation [7]). The equilibrium constant K'_{BH^+} (equation [8]) for the reaction in which $n = 2$, $d = 3$, and $b = 3$ is then used to express $[BH^+.3H_2O]/[B.H_2O]$ as a function of a_w and $[H_3O^+.3H_2O]$. Finally $[H_3O^+.3H_2O]$ is expressed as a function of total acid concentration using equation [5]. This leads to

$$H_0 = (pK_{BH^+} - pK'_{BH^+}) + pMH - \log \frac{1}{a_w^2} \frac{f_{Bw} f_{H3w}}{f_{BH3w}} \times \underset{A}{\frac{\left[1 + \frac{K_{BH3w} f_{BH3w}}{a_w f_{BH2w}} + \frac{K_{BH2w} K_{BH3w} f_{BH3w}}{a_w^2 f_{BHw}} + \frac{K_{BHw} K_{BH2w} K_{BH3w} f_{BH3w}}{a_w^3 f_{BH}}\right]}{\left[1 + \frac{K_{H3w} f_{H3w}}{a_w f_{H2w}} + \frac{K_{H2w} K_{H3w} f_{H3w}}{a_w^2 f_{Hw}} + \frac{K_{Hw} K_{H2w} K_{H3w} f_{H3w}}{a_w^3 f_H}\right]\left[1 + \frac{K_{Bw} f_{Bw}}{a_w f_B}\right]}}_{B \qquad C} \quad [10]$$

This equation is more general than the previous expressions [2] and [4] and gives additional insight into possible H_0 functionality. Equation [10] will reduce to equation [4] whenever only one equilibrium K''_{BH^+} (equation [8]) is important over the concentration range of interest, i.e., when one term in each of the sums of terms in A, B, and C (square brackets, equation [10]) is large compared to all the other terms, and provided equation [3] is valid. To obtain equation [4] it must also be assumed that $pK_{BH^+} = pK''_{BH^+}$. Because of the way pK_{BH^+} is evaluated (2) this assumption may not always be true. Where two or more terms in A, B, or C (equation [10]) are comparable in magnitude over any portion of the acid (or salt) concentration range, *in general*, equation [4] will not adequately describe H_0 as a function of concentration over an extended range of concentrations and different values of n will be obtained over different, more limited ranges.

It has already been shown that the H_0 data for HCl, $HClO_4$, and LiCl can be calculated using equation [4]. However, a non-integral value of n must be used to satisfactorily fit the $HClO_4$ data. This could be interpreted as evidence for the necessity of using a more general form of equation [10], since integral values of n are to be expected. Presumably equation [4] appears adequate with non-integral values of n because the experimental H_0 values are inherently rather inaccurate (2), H_0 is relatively insensitive to n values at low acid concentrations, the activity of water changes by less than an order of magnitude for the data, and there are two adjustable parameters in equation [4]. Even for HCl and LiCl, where integral values of n ($n = 2$) are adequate, it seems probable that two or more terms in A, B, or C (equation [10]) are important (see discussion at the beginning of this section). Depending upon which terms in A, B, or C are important, the apparent value of n in equation [4] might increase, decrease, or change very little, when calculations over a limited range at low concentrations are compared with the results at higher concentrations. For example, there are some indications (8) that B is rather weakly solvated. If $B.H_2O$ were the predominant species in the less concentrated solutions and B the predominant species in concentrated solutions, the last term in C would become important in more concentrated solutions and n would change from two towards one. At higher concentrations where H_3O^+ and BH^+ are competing for water the second term in A ($BH^+.2H_2O$) might be more important than the second term in B ($H_3O^+.2H_2O$), in which case n would then increase. If the second term in A were comparable to the second term in B, there would be little or no change in n. It is difficult to draw any general conclusions from the data.

Can. J. Chem. Downloaded from www.nrcresearchpress.com by 210.87.254.105 on 09/05/12
For personal use only.

The fact that equation [4] best fits the HCl data (smallest a_w range) and seems least adequate for the $HClO_4$ data (largest a_w range) is at least consistent with what would be expected if equation [10] applies.

For the reduction of equation [10] to equation [4] it was necessary to assume the validity of equation [3]. In the earlier discussion equation [3] was shown to be reasonable. The experimental justification of equation [3] is that equation [4] is adequate for the explanation of the H_0 values of HCl and LiCl, and gives reasonable n and B values. The inadequacy of equation [4] in explaining $HClO_4$ H_0 values has been interpreted as evidence for the necessity of using a more general form of equation [10]. Alternatively, the $HClO_4$ results, at least in part, might be interpreted as evidence for the inadequacy of equation [3]. If

$$\log f_B f_{H^+}/f_{BH^+} = BM+g \log a_w, \quad [11]$$

the values of n obtained by equation [4] are theoretically interpretable in terms of equation [10] only if the empirical constant g is small. The possibility that g is large can not entirely be ruled out (see next section).

Related Expressions for H_0

The following modified versions of equation [4] were used to obtain least-squares values of B and n:

$$H_0 = pMH+n \log a_w-Bm \quad [12]$$

$$H_0 = pmH+n \log a_w-Bm \quad [13]$$

$$H_0 = pmH+n \log a_w-BM, \quad [14]$$

where m refers to molal concentrations. (Differences between H_0 on the molal and molar scales are negligible.) The results are summarized in Table V. In each instance the calculated value of H_0 obtained utilizing the least-squares values of B and n was not significantly different from the experimental value. The utilization of pmH rather than pMH did not lead to significantly different values of n (compare the results for equations [4] with [14], and [12] with [13]), but the utilization of molality rather than molarity in expressing the total electrolyte concentration (salt or acid) did lead to different values of n (compare the results for equations [4] with [12], and [13] with [14]).

TABLE V

Least-squares values of B and n

Equation used	n	$S.D_n$	B	$S.D_B$
1–11 M HCl				
4	1.9702	0.0870	0.1535	0.0042
12	0.8205	0.1456	0.1703	0.0058
13	0.8383	0.1479	0.1613	0.0059
14	1.9266	0.0891	0.1455	0.0043
1–9 M $HClO_4$				
4	2.4296	0.0758	0.1997	0.0062
12	1.3734	0.0695	0.1933	0.0039
13	1.4509	0.0752	0.1736	0.0042
14	2.3999	0.0762	0.1793	0.0062
1–9 M LiCl				
4	2.5752	0.2310	0.1870	0.0097
12	1.4152	0.2938	0.1991	0.0104
13	1.4399	0.2949	0.1899	0.0105
14	2.5461	0.2321	0.1784	0.0097

Can. J. Chem. Downloaded from www.nrcresearchpress.com by 210.87.254.105 on 09/05/12
For personal use only.

The least-squares B values obtained using integral values of n are summarized in Table VI. In no instance were the values of H_0 calculated with $n = 4$ in reasonable agreement with the experimental values. The differences between the experimental and calculated H_0 values for HCl, $HClO_4$, and LiCl obtained with equations [12] and [13] when

TABLE VI

Least-squares values of B

Equation used	$n = 1$		$n = 2$		$n = 4$	
	B	$S.D_B$	B	$S.D_B$	B	$S.D_B$
1–11 M HCl						
4	0.1998	0.0032	0.1521	0.0008	0.0567	0.0066
12	0.1632	0.0009	0.1239	0.0024	0.0452	0.0062
13	0.1550	0.0009	0.1156	0.0024	0.0370	0.0061
14	0.1897	0.0031	0.1420	0.0009	0.0467	0.0067
1–9 M $HClO_4$						
4	0.3103	0.0186	0.2329	0.0045	0.0781	0.0150
12	0.2136	0.0019	0.1592	0.0030	0.0503	0.0120
13	0.1981	0.0023	0.1437	0.0027	0.0350	0.0117
14	0.2876	0.0134	0.2102	0.0042	0.0557	0.0152
1–9 M LiCl						
4	0.2515	0.0053	0.2106	0.0026	0.1288	0.0049
12	0.2136	0.0019	0.1786	0.0021	0.1086	0.0058
13	0.2052	0.0019	0.1702	0.0020	0.1003	0.0057
14	0.2416	0.0052	0.2007	0.0026	0.1189	0.0050

$n = 1$ were less than the error in the experimental H_0 values. A value of $n = 2$ in equation [12] or [13] yielded reasonable H_0 values for LiCl, but not for HCl and $HClO_4$. A value of $n = 2$ in equation [14] (and equation [4]) yielded reasonable H_0 values for HCl and LiCl, but not for $HClO_4$.

If it is assumed that

$$\log f_B f_{H^+}/f_{BH^+} = Bm \qquad [15]$$

in equations [12] and [13], then the n values could be interpreted in a manner similar to that employed in the discussion of equation [4], i.e., in terms of equations [8] and [10]. When the activity coefficients in equation [15] are on the molal scale (as in equation [13]), equation [15] can be justified by arguments similar to those employed to justify equation [3] (17). (Most of the reservations expressed in the discussion of the interpretation of equations [3] and [4] (preceding section) are also applicable to equations [12] and [13].)

The interpretation of integral values of n for equations [13] and [4] in terms of equation [8] leads to the expectation that the same n values will be obtained using these two equations. However, the H_0 data can be fitted with $n = 1$ for equation [13] or [12] but not for equation [4] or [14]. A value of $n = 2$ is satisfactory for LiCl and HCl H_0 calculations with equation [4] or [14], but is not satisfactory for HCl or $HClO_4$ calculations using equation [12] or [13]. This anomaly can only be resolved if equations [4] and [14], and/or equations [12] and [13], are regarded as empirical in nature. One reason for this might be that equations [3] and/or [15] are not valid. There is no compelling reason for preferring either equation (4, 17). Another possible explanation is that a form of equation [10] more general than equation [4], [12], [13], or [14] should really be employed. Consistent with the latter interpretation is the fact that the values of n given in Table V are, at least in some instances, significantly different from integers.

Can. J. Chem. Downloaded from www.nrcresearchpress.com by 210.87.254.105 on 09/05/12
For personal use only.

ACKNOWLEDGMENTS

This work was supported in part by grants from Research Corporation principally in the form of a Research Corporation Fellowship for one of us (J. S. D.), and in part is taken from his Ph.D. research. The authors wish to thank the Chemistry Division of the Argonne National Laboratory for permission to use their IBM 610 Computer and Dr. George H. Winslow of that laboratory for his assistance.

REFERENCES

1. L. P. HAMMETT and A. J. DEYRUP. J. Am. Chem. Soc. **54**, 2721 (1932).
2. M. A. PAUL and F. A. LONG. Chem. Rev. **57**, 1 (1957).
3. K. N. BASCOMBE and R. P. BELL. Discussions Faraday Soc. **24**, 158 (1957).
4. F. A. LONG and W. F. MCDEVIT. Chem. Rev. **51**, 119 (1952).
5. M. A. PAUL. J. Am. Chem. Soc. **75**, 2513 (1953).
6. M. A. PAUL. J. Am. Chem. Soc. **76**, 3236 (1954).
7. D. ROSENTHAL and J. S. DWYER. J. Phys. Chem. To be published.
8. G. BRIEGLEB. Z. Elektrochem. **53**, 350 (1949).
9. D. PRESSMAN and M. SIEGEL. J. Am. Chem. Soc. **79**, 994 (1957).
10. R. W. TAFT, JR. J. Am. Chem. Soc. **82**, 2965 (1960).
11. A. F. TROTMAN-DICKENSON. J. Chem. Soc. 1293 (1949).
12. H. K. HALL, JR. J. Am. Chem. Soc. **79**, 5441 (1957).
13. R. L. BERGEN, JR. and F. A. LONG. J. Phys. Chem. **60**, 1131 (1956).
14. P. A. H. WYATT. Discussions Faraday Soc. **24**, 162 (1957). K. B. WIBERG and R. J. EVANS. J. Am. Chem. Soc. **80**, 3019 (1958). S. BRUCKENSTEIN. J. Am. Chem. Soc. **82**, 307 (1960). M. T. EMERSON, E. GRUNWALD, M. L. KAPLAN, and R. A. KROMHOUT. J. Am. Chem. Soc. **82**, 6307 (1960). J. F. BUNNETT. J. Am. Chem. Soc. **83**, 4965 (1961).
15. G. W. BRADY. J. Chem. Phys. **28**, 464 (1958). J. BECK. Z. Physik, **40**, 474 (1939).
16. J. B. HASTED, D. M. RITSON, and C. H. COLLIE. J. Chem. Phys. **16**, 1 (1948). J. B. HASTED and G. W. RODERICK. J. Chem. Phys. **29**, 17 (1958).
17. H. S. HARNED and B. B. OWEN. The physical chemistry of electrolyte solutions. Reinhold Publishing Corp., New York, N.Y. 1943. p. 532.

Can. J. Chem. Downloaded from www.nrcresearchpress.com by 210.87.254.105 on 09/05/12
For personal use only.

PAPER CHROMATOGRAPHY OF ETHYLENEDIAMINE DIHYDROCHLORIDE AND DIACETATE IN ACIDIC SOLVENT SYSTEMS[1]

R. A. B. BANNARD AND A. A. CASSELMAN
Defence Research Chemical Laboratories, Ottawa, Ontario
Received August 2, 1962

ABSTRACT

Quantitative chromatography of ethylenediamine dihydrochloride on *unwashed* Whatman No. 17 paper in *t*-butanol:acetic acid:water (2:1:1) resulted in a 1% conversion to ethylenediamine diacetate (R_F 0.51) and a 98% recovery of the dihydrochloride (R_F 0.28). The cause of the multiple zoning, which was not observed on acid-washed papers, was traced to minor quantities of alkaline earth metals which are present as impurities in *unwashed* papers. Ion exchange mechanisms are suggested to account for the observed conversion. Quantitative chromatography of ethylenediamine diacetate on *unwashed* or acid-washed Whatman No. 17 paper in *t*-butanol:0.5% hydrochloric acid (3:1) resulted in quantitative recovery of the dihydrochloride due to displacement of the weak acid in the substrate by the strong acid in the solvent system.

Can. J. Chem. Downloaded from www.nrcresearchpress.com by 210.87.254.40 on 09/05/12
For personal use only.

In an earlier communication (1) we reported that paper chromatography of clam poison dihydrochloride on *unwashed* Whatman No. 1 paper in the solvent system *t*-butanol: acetic acid:water (2:1:1) gave two Weber-positive components, R_F 0.32 and 0.53. Repetition of the experiments using Whatman No. 1 paper which had been washed with hydrochloric or acetic acid or specially pretreated (1) for removal of extractable impurities gave only one Weber-positive component, R_F 0.32, which was identified as clam poison dihydrochloride. The faster-moving component observed on *unwashed* paper (substance X) was not identified but was concluded to differ from clam poison diacetate (R_F 0.53 on *unwashed* Whatman No. 1 paper in the same solvent system). It was also concluded that substance X is not a different ionic species or a tautomer of clam poison. Since our supply of clam poison was limited, it seemed worthwhile to examine the behavior of another diacid base during paper chromatography in the same solvent system to determine whether multizoning would occur and disappear under similar conditions and, if possible, to establish the cause of these phenomena. Results obtained during chromatography of ethylenediamine dihydrochloride and diacetate are reported herein.

Qualitative chromatograms were performed on *unwashed* Whatman No. 1 and No. 17 papers and on the same papers which had been pretreated by chromatographic washing with 0.01 *N* hydrochloric acid, 0.6 *N* acetic acid, 0.01 *N* sulphuric acid, or by the method described earlier for removal of extractable impurities (1). Two solvent systems were used, namely, *t*-butanol:acetic acid:water (2:1:1) and *t*-butanol:0.5% hydrochloric acid (3:1). Amines were detected by spraying with ninhydrin. Chloride ion was revealed by spraying with 5% silver nitrate followed by washing with water and ultraviolet irradiation. Acetate ion was detectable as deep blue spots by dipping chromatograms performed on Whatman No. 1 paper in an alcoholic lanthanum nitrate – iodine solution, followed by dipping in 5 *N* ammonium hydroxide. Incomplete removal of solvent during drying masked the test for acetate ion when Whatman No. 17 paper was used.

Results of the experiments in *t*-butanol:acetic acid:water (2:1:1) are summarized in Table I, from which it is evident that multizoning similar to that previously observed

[1]*Issued as D.R.C.L. Report No. 383.*

Can. J. Chem. Downloaded from www.nrcresearchpress.com by 210.87.254.40 on 09/05/12
For personal use only.

TABLE I

Paper chromatography of ethylenediamine dihydrochloride and diacetate on Whatman No. 1 and No. 17 papers in *t*-butanol:acetic acid:water (2:1:1)

Compound	Whatman No. 1						Whatman No. 17			
	Unwashed			Acid washed¶			Unwashed		Acid washed¶	
Ethylenediamine dihydrochloride	0.24 (f)*	0.31 (s)*†	0.37 (f)*†	0.44 (f)*	0.54 (s)*‡‖	0.34 (s)*†	0.30 (s)*†	0.50 (s)*‖	0.28 (s)*†	
Ethylenediamine diacetate	0.24 (f)*			0.44 (f)*	0.57 (s)*‡	0.55 (s)*‡§		0.52 (s)*		0.57 (s)*§

NOTE: s = strong; f = faint.
*Ninhydrin positive.
†Positive for chloride ion.
‡Positive for acetate ion.
§Spot exhibits strong tailing to R_F 0.35.
‖Spot exhibits faint ninhydrin-positive shadow to R_F 0.37.
¶See experimental section for details.

with clam poison dihydrochloride occurs when ethylenediamine dihydrochloride is chromatographed on the *unwashed* papers. The two principal ninhydrin-positive spots at R_F 0.30–0.31 and 0.50–0.54 were observed on all chromatograms of the dihydrochloride on *unwashed* papers but frequently the very faint spots at R_F 0.24, 0.35, and 0.44 on Whatman No. 1 paper were not discernible. These spots were never observed on Whatman No. 17 paper. Since chloride ion was coincident with the strong ninhydrin-positive spot at R_F 0.30–0.31 and there was no marked tailing or bearding of the spot with either chromogen it was tentatively concluded that this substance was an ethylenediamine mono- or di-hydrochloride. Similarly, since acetate ion was coincident with the strong ninhydrin-positive material at R_F 0.54 (Whatman No. 1) it was tentatively concluded that this substance was an ethylenediamine mono- or di-acetate. It is noteworthy that the latter material was followed by a very faint and diffuse ninhydrin-positive shadow extending back to R_F 0.37. The principal ninhydrin-positive spot obtained by chromatography of ethylenediamine diacetate under similar conditions on Whatman No. 1 paper (and this was the only material ever observed on the heavier paper) was at R_F 0.57 and was coincident with acetate ion. This material was obtained as a somewhat elongated dense spot which did not exhibit strong tailing or diffuse shadowing. It was tentatively concluded that this material was probably identical with the substance of R_F 0.50–0.54 resulting from chromatography of the dihydrochloride under similar conditions.

Chromatography of the dihydrochloride on the acid-washed papers gave only one compact ninhydrin- and chloride-positive spot, R_F 0.28–0.34. Under identical conditions, the diacetate gave one ninhydrin- and acetate-positive spot, R_F 0.55 on Whatman No. 1 paper, and one ninhydrin-positive spot, R_F 0.57 on Whatman No. 17 paper. Both of these spots exhibited strong tailing back to R_F 0.35.

Chromatography of both salts in *t*-butanol:0.5% hydrochloric acid (3:1) gave only one compact ninhydrin- and chloride-positive spot, R_F 0.12–0.14, on both papers regardless of whether the paper was acid washed or *unwashed*. This material was considered to be ethylenediamine mono- or di-hydrochloride.

The similarity of the forementioned R_F values suggested that some conversion of ethylenediamine hydrochloride to acetate occurs when the dihydrochloride is chromatographed on *unwashed* Whatman No. 1 or No. 17 papers using *t*-butanol:acetic acid:water (2:1:1) as developer, and that total conversion to hydrochloride results when ethylenediamine diacetate is chromatographed on *unwashed* or pretreated Whatman No. 1 or No. 17 papers when *t*-butanol:0.5% hydrochloric acid (3:1) is used as developer.

To demonstrate the validity of these tentative conclusions, quantitative chromatography of ethylenediamine dihydrochloride and diacetate was studied using *unwashed* Whatman No. 17 paper. Whatman No. 1 paper was judged unsuitable for this purpose since it could not be loaded sufficiently heavily and because of the multiplicity of ninhydrin-positive spots which it sometimes produced (see Table I).

Ethylenediamine dihydrochloride (3 g) was chromatographed on six sheets of *unwashed* Whatman No. 17 paper using *t*-butanol:acetic acid:water (2:1:1) as developer. The two bands, R_F 0.28 and 0.51, which were located on the air-dried chromatograms by ultraviolet irradiation were recovered by aqueous elution, yielding 3.45 g and 0.4 g respectively of crude products which occupied total areas of 402 and 393 sq. in. respectively on the chromatograms. Vacuum sublimation of the slower-moving band followed by recrystallization of the sublimate gave 2.94 g (98.0%) of ethylenediamine dihydrochloride, which

Can. J. Chem. Downloaded from www.nrcresearchpress.com by 210.87.254.40 on 09/05/12
For personal use only.

Can. J. Chem. Downloaded from www.nrcresearchpress.com by 210.87.254.40 on 09/05/12
For personal use only.

was identified by its infrared spectrum and elemental analysis. Vacuum sublimation of the faster-moving band, followed by recrystallization of the sublimate from ethanol, gave 40 mg (1.0%) of ethylenediamine diacetate, which was identified by its infrared spectrum and its melting point in admixture with an authentic specimen. It is therefore evident that the ninhydrin-positive material appearing at R_F 0.28 during quantitative chromatography of ethylenediamine dihydrochloride on *unwashed* Whatman No. 17 paper in *t*-butanol:acetic acid:water (2:1:1) is unchanged dihydrochloride, i.e. the substance applied to the chromatogram moves as an ion pair. The latter conclusion agrees with that reported by Waldron-Edward (2) following qualitative chromatography of ethylenediamine dihydrochloride and sulphate in butanol:acetic acid:water (4:1:5) on *unwashed* Whatman No. 1 paper, during which multiple spotting was also observed. It is clear that the substance which appears at R_F 0.51 on the quantitative chromatogram referred to above is ethylenediamine diacetate which has been formed from the dihydrochloride during chromatography. The amount of dihydrochloride thus converted cannot exceed 2%. This result was unanticipated because the areas covered by the two bands were almost identical. Furthermore, although there was a difference in intensity of the two bands (as revealed by ultraviolet irradiation or spraying with ninhydrin) the difference was not proportional to the quantities of substances present. Thus, when multiple spots are observed on paper chromatograms it is unsafe to conclude either that impurities in the starting material are responsible or that extensive conversion of the latter to another substance is involved without careful quantitative investigation. Possible explanations for this multizoning effect are considered below.

Ethylenediamine diacetate (400 mg) was chromatographed on four sheets of *unwashed* No. 17 paper using *t*-butanol:0.5% hydrochloric acid (3:1) as developer. Ultraviolet irradiation of the air-dried chromatograms revealed only one band, R_F 0.13. This material was recovered by aqueous elution and purified by sublimation *in vacuo*, yielding 284 mg (96.0%) of ethylenediamine dihydrochloride as colorless needles, which was identified by its infrared spectrum. Clearly, based on the R_F values observed in this experiment, the diacetate has been converted quantitatively to the dihydrochloride during chromatography by the action of the stronger acid in the developing solvent.

The occurrence of multiple zones or spots during chromatography of pure substances is now a frequently observed phenomenon. In a recent review article on the subject Keller and Giddings (3) list the following possible causes: (i) chemical reaction of the substrate prior to or during chromatography, (ii) impurities in the solution chromatographed, (iii) discontinuities in the immobile phases, (iv) discontinuities in the mobile phase, (v) charged species and complexes, and (vi) equilibrium between two species. It is frequently difficult, however, to demonstrate which of these causes is responsible for a particular case of multiple spotting. From the purity of the dihydrochloride used and the nature of the solvent system employed, it seemed unlikely that causes other than (i), (v), or (vi) could be responsible for formation of ethylenediamine diacetate from the dihydrochloride during chromatography. Since the phenomenon was observed only on *unwashed* paper it appeared probable that a complexing (3, 4) or ion exchange (3, 5) mechanism involving impurities in the paper was responsible. Some support for this view resulted from the observation that ethylenediamine diacetate exhibits strong tailing during chromatography on the acid-washed papers but *not* on the *unwashed* papers. It was previously reported (4–6) that acid washing removes trace quantities of calcium and magnesium ions which otherwise remain bound to the paper. The presence of these

ions can lead to troublesome tailing during chromatography of phosphate esters in basic solvent systems (4) and their absence can lead to equally troublesome tailing during chromatography of aminoacids and peptides (6). We observed the latter phenomenon during chromatography of clam poison dihydrochloride on acid-washed paper and for this reason subsequent washing with calcium acetate and water was used to restore a small amount of calcium ion to the paper and eliminate the tailing (cf. Connell, Dixon, and Hanes (6)).

Acid-washed Whatman No. 17 paper was washed chromatographically with 0.1 *N* calcium acetate for 2 days, then with water for 2 days, followed by air drying. Ethylenediamine dihydrochloride and diacetate were then chromatographed on these papers using *t*-butanol:acetic acid:water (2:1:1) as developer. For the diacetate, results were identical with those observed on *unwashed* paper, i.e. tailing was eliminated. From the dihydrochloride under the same conditions, however, two ninhydrin-positive spots, R_F 0.32 and 0.54, were obtained. The latter spot exhibited a faint ninhydrin-positive shadow back to R_F 0.37, i.e. *the results obtained were identical with those observed on unwashed papers.* Thus, restoration of calcium ion to the paper regenerated the multiple-spot phenomenon in acid-washed paper. Similar results were also obtained on acid-washed No. 17 papers to which a small amount of magnesium ion had been restored by washing with 0.1 *N* magnesium acetate and water. It is therefore concluded that alkaline earth metals present in small amounts in *unwashed* paper are responsible for the observed effect.

Formation of diacetate from dihydrochloride could readily result from an ion exchange process. It is known that alkaline earth metals present in paper are bound as salts of residual carboxylic acid groups in cellulose (7). Several years ago Schute (5) suggested a cation exchange mechanism involving trace amounts of metallic ions such as Na^+, K^+, Ca^{++}, and Mg^{++} bound to carboxyl groups in the paper to explain absorption of alkaloids by paper when acidic solvent systems are employed. A simple extension of this mechanism could account for the hydrochloride-to-acetate conversion observed in the present investigation. A carboxylate salt of type II could be formed by partial acetolysis of the dicarboxylate salt I (where M^{++} is an alkaline earth metal cation) under the influence of the solvent

$$\underset{\text{I}}{\text{COO}^-\text{M}^{++}\,^-\text{OOC}} + \text{HOAc} \rightarrow \underset{\text{II}}{\text{COO}^-\text{M}^{++}\text{AcO}^-} + \text{HOOC}$$

system used (7). Sites of type II in the paper could then readily effect conversion of the dihydrochloride to the diacetate by anion exchange. Clearly, the extent to which such a mechanism could operate is governed by the number of carboxylate groups and alkaline earth metal cations present in the paper, both of which are small (7), and also by the rapidity with which complete acetolysis of the salt II leads to restriction of the phenomenon to an early stage in development of the chromatogram by destroying the anion exchange sites. Were it not for the latter factor, intervention of the suggested mechanism would be expected to lead to pronounced bearding of the dihydrochloride band as it moves down the paper. Such an effect is not observed. However, generation of a small amount of acetate during a very early stage in the development of the chromatogram, before all the active sites for ion exchange are eliminated by the acid in the solvent system, could account for the diffuse band of diacetate recovered in the quantitative experiment in which conversion was observed.

An alternative mechanism which would accomplish conversion of dihydrochloride to

Can. J. Chem. Downloaded from www.nrcresearchpress.com by 210.87.254.40 on 09/05/12
For personal use only.

diacetate involves ion exchange between the alkaline earth metal cation in the dicarboxylate salt I and the ethylenediammonium ion present in the dihydrochloride, with formation of III. By this means a small amount of chloride ion from the salt would be removed when the dihydrochloride is first applied to the paper. Development with the acid solvent system would then release the ethylenediammonium cation, forming a small quantity of ethylenediamine diacetate. Again by this mechanism the effect would be limited to an early stage in development of the chromatogram since alkaline earth metals would be removed from active sites of type I by the acid in the solvent system.

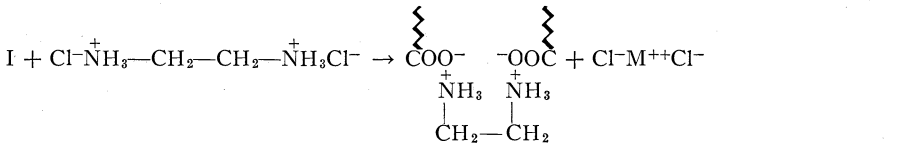

III

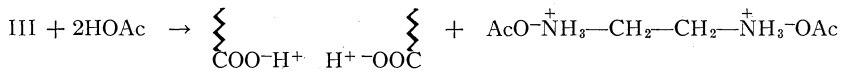

Both ion exchange mechanisms mentioned above are in agreement with the experimental observations but it is not possible on the basis of the data currently available to distinguish between them. The possibility also exists that the observed conversion of dihydrochloride to diacetate occurs via intervention of a chelated metal complex, since it is well known that ethylenediamine has a great tendency toward formation of such complexes (8, p. 519). If complex formation is responsible it appears probable that an alkaline earth metal rather than a transition metal is involved, since washing the papers with acid does not remove the latter (4) yet causes the multizoning to disappear. However, formation of complexes between ethylenediamine and alkaline earth metals has not been reported (8, p. 184; 9; 10). There would thus appear to be no basis for assuming intervention of a complexing mechanism at present.

It is suggested that the formation of 1% of ethylenediamine diacetate during chromatography of ethylenediamine dihydrochloride on *unwashed* Whatman No. 17 paper in *t*-butanol:acetic acid:water (2:1:1) results from chemical reaction of the dihydrochloride via an ion exchange mechanism with traces of alkaline earth metals present in the paper as impurities. It is not clear whether the ion exchange occurs directly on application of the substrate to the paper, during an early stage in development of the chromatogram, or at both these times. On the other hand, complete conversion of ethylenediamine diacetate to the dihydrochloride during chromatography of the former on *unwashed* or pretreated Whatman No. 17 paper in *t*-butanol:0.5% hydrochloric acid (3:1) is ascribed to displacement of the weaker acid from the salt by the stronger acid in the solvent system.

The similarity in chromatographic behavior of clam poison dihydrochloride and ethylenediamine dihydrochloride in *t*-butanol:acetic acid:water (2:1:1) on *unwashed* papers, together with the positive identification of ethylenediamine diacetate as the minor component produced during chromatography of ethylenediamine dihydrochloride under such conditions, indicates the desirability of careful re-examination of the minor component from chromatography of clam poison dihydrochloride (1) to determine whether or not it is the diacetate salt.

Can. J. Chem. Downloaded from www.nrcresearchpress.com by 210.87.254.40 on 09/05/12
For personal use only.

EXPERIMENTAL[2,3]

Ethylenediamine Dihydrochloride

Ethylenediamine (6.01 g, 0.100 mole) was placed in a 250-ml round-bottom flask, ether (15 ml) was added, and the resultant solution was mechanically stirred in an ice bath while a solution of hydrochloric acid (37%, 33 ml, 0.4 mole) in ether (50 ml) was added dropwise over a period of 30 minutes. The resultant colorless precipitate was collected, washed with anhydrous ether (5×10 ml), and recrystallized from water–methanol (4:1), yielding 12.6 g (94.7%) of ethylenediamine dihydrochloride as colorless needles, which sublimed without melting. Calc. for $C_2H_{10}N_2Cl_2$: C, 18.06; H, 7.58; N, 21.06; Cl, 53.31%. Found: C, 18.28; H, 7.53; N, 20.96; Cl, 53.44%.

Ethylenediamine Diacetate

The procedure was identical with that used for preparation of the dihydrochloride except that acetic acid (23.1 ml, 99.7%, 0.4 mole) was employed instead of hydrochloric acid. The resultant solid was recrystallized from absolute ethanol, yielding 16.0 g (88.8%) of ethylenediamine diacetate as colorless needles, m.p. 117–118°. Calc. for $C_6H_{16}N_4O_4$: C, 39.99; H, 8.95; N, 15.55%. Found: C, 39.80; H, 8.79; N, 15.64%.

Qualitative Paper Chromatography

(1) Using Whatman No. 1 Paper

Strips of Whatman No. 1 paper (6.25×22.5 in.) were pretreated by chromatographic washing (*a*) with 0.01 *N* hydrochloric acid (3 days) and water (3 days), (*b*) with 0.6 *N* acetic acid (3 days) and water (3 days), (*c*) with 0.01 *N* sulphuric acid (3 days) and water (3 days), and (*d*) by the method described previously for elimination of extractable impurities from papers employed for quantitative paper chromatography of clam poison (1). To a strip of each of these pretreated papers, together with untreated Whatman No. 1 paper, 7.5 λ (150 γ), spots of 2% aqueous solutions of ethylenediamine dihydrochloride and ethylenediamine diacetate were applied. The chromatograms were developed in *t*-butanol:acetic acid:water (2:1:1) and in *t*-butanol:0.5% hydrochloric acid (3:1). After drying in a forced air oven at 60° to remove as much solvent as possible, the chromatograms were treated with reagents for detection of amine (ninhydrin), chloride ion (5% silver nitrate followed by ultraviolet irradiation), and acetate ion (lanthanum nitrate – ammonia).

(2) Using Whatman No. 17 Paper

The experiments described above were repeated using untreated and pretreated Whatman No. 17 paper employing 200 γ of the ethylenediamine salts per spot.

Lanthanum Nitrate Test for Acetate Ion

This test is a modification of the spot test for acetate reported by Feigl (11). Resublimed iodine (0.2 g) was dissolved in ethanol (75 ml), lanthanum nitrate (5 g) was added, and the solution made up to 100 ml with water. The chromatogram or test strip was dipped into the lanthanum nitrate solution and allowed to stand 1.5 to 2 minutes at room temperature before being dipped into a 5 *N* ammonium hydroxide developer. Acetate ion was revealed by the appearance of deep blue spots in 2–5 minutes. The minimum quantity of ethylenediamine diacetate detectable by this method was 5 γ (1 γ of ethylenediamine diacetate was detectable by dipping chromatograms in a 0.4% solution of ninhydrin in water-saturated *n*-butanol).

Quantitative Paper Chromatography

(a) Chromatography of Ethylenediamine Dihydrochloride in t-Butanol:Acetic Acid:Water (2:1:1)

Ethylenediamine dihydrochloride (500 mg) was applied as a streak from 25% aqueous solution to each of six sheets of *unwashed* Whatman No. 17 paper ($18\frac{1}{4}\times22\frac{1}{2}$ in.). The chromatograms were suspended by the stirrup method (12) in a Model A 300 Chromatocab (Research Equipment Corp., Oakland, Calif.) and developed simultaneously by the descending method in *t*-butanol:acetic acid:water (2:1:1) for 38 hours, using a single wick of Whatman No. 3 paper as solvent feed. After air drying, ultraviolet irradiation revealed the presence of two bands, R_F 0.28 and 0.51, which, after elution with water (40 ml each), combination of corresponding eluates, filtration through a fine-porosity fritted-glass funnel, concentration, and drying *in vacuo*, gave 3.45 g and 0.4 g respectively of crude product, which occupied areas of 402 and 393 sq. in. respectively on the chromatograms.

Sublimation of the slower-moving band at 185° at 10^{-3} mm pressure gave 3.1 g of colorless solid which, after recrystallization from water–methanol (4:1), yielded 2.94 g (98.0%) of colorless needles with an infrared spectrum (KBr pellet) identical with that of an authentic sample of ethylenediamine dihydrochloride and possessing the following analytical data: C, 18.32; H, 7.64; N, 20.84; Cl, 53.05%.

The dried material from the faster-moving band was washed with boiling absolute ethanol (3×5 ml). Sublimation of the dried ethanol-soluble fraction at 120° at 10^{-3} mm pressure gave 50 mg of colorless solid, recrystallization of which from ethanol gave 40 mg (1.0%) of colorless needles, m.p. 116.5–117.5° alone and in admixture with an authentic sample of ethylenediamine diacetate. The infrared spectra (KBr pellet) of the two samples were also identical.

[2] *Melting points are uncorrected.*
[3] *Microanalysis by J. G. Helie of these laboratories.*

Can. J. Chem. Downloaded from www.nrcresearchpress.com by 210.87.254.40 on 09/05/12
For personal use only.

(b) Chromatography of Ethylenediamine Diacetate in t-Butanol:0.5% Hydrochloric Acid (3:1)

Ethylenediamine diacetate (100 mg) was applied as a streak from 10% aqueous solution to each of four sheets of *unwashed* Whatman No. 17 paper ($18\frac{1}{4}\times22\frac{1}{2}$ in.) and developed as described above except that *t*-butanol:0.5% hydrochloric acid (3:1) was used as developer (48 hours). Each chromatogram exhibited one band at R_F 0.13 under ultraviolet irradiation. The total area covered by the combined bands was 251 sq. in. The bands were recovered as described above, yielding 0.528 g of crude product, recrystallization of which from water–methanol (4:1) yielded 0.284 g (96.0%) of colorless needles, the infrared spectrum of which (KBr pellet) was identical with that of an authentic sample of ethylenediamine dihydrochloride.

REFERENCES

1. A. A. Casselman, R. Greenhalgh, H. H. Brownell, and R. A. B. Bannard. Can. J. Chem. **38**, 1277 (1960).
2. D. M. Waldron-Edward. Chem. Ind. (London), 104 (1954).
3. R. A. Keller and J. C. Giddings. J. Chromatog. **3**, 205 (1960).
4. C. S. Hanes and F. A. Isherwood. Nature, **164**, 1107 (1949).
5. J. B. Schute. Nature, **171**, 839 (1953).
6. G. E. Connell, G. H. Dixon, and C. S. Hanes. Can. J. Biochem. Physiol. **33**, 416 (1955).
7. C. B. Purves. *In* High polymers. Vol. V. Cellulose and cellulose derivatives. *Edited by* E. Ott. Interscience Publishers Inc., New York. 1946. p. 123.
8. A. E. Martell and M. Calvin. Chemistry of the metal chelate compounds. Prentice-Hall Inc., New York. 1952.
9. R. D. Johnson and C. F. Callis. *In* The chemistry of the coordination compounds. *Edited by* J. C. Bailar. Reinhold Publishing Corp., New York. 1956. p. 777.
10. T. Moeller. Inorganic chemistry an advanced textbook. John Wiley and Sons. Inc., New York. 1952. p. 236.
11. F. Feigl. Spot tests. Vol. II. Organic applications. Elsevier Publishing Co., New York. 1954. p. 247.
12. H. H. Brownell, J. G. Hamilton, and A. A. Casselman. Anal. Chem. **29**, 550 (1957).

Downloaded from www.nrcresearchpress.com by 210.87.254.40 on 09/05/12
For personal use only.

Can. J. Chem. Downloaded from www.nrcresearchpress.com by 210.87.254.40 on 09/05/12
For personal use only.

PHOTOCHEMICAL SYNTHESES

5. SULPHENES AS PHOTOCHEMICAL INTERMEDIATES[1]

J. F. KING, P. DE MAYO, E. MORKVED,[2] A. B. M. A. SATTAR, AND A. STOESSL[3]
Department of Chemistry, University of Western Ontario, London, Ontario

Received August 23, 1962

ABSTRACT

The present status of sulphenes ($R'R''C{:}SO_2$) as stable entities or chemical intermediates is discussed. The early report by Locher and Fierz (Helv. Chim. Acta, **10**, 642 (1927)) of the preparation of a stable crystalline sulphene has been investigated; it is concluded that their claim is unfounded.

The irradiation of unsaturated sultones in the presence of methanol is shown to give sulphonic esters: the corresponding thermal reaction of sultones is known to lead to sulphonic acid derivatives. It is proposed that the irradiation of unsaturated sultones yields sulphenes, which then react with the medium.

The preparation and properties of ketenes have been studied over many years, but investigations directed towards a similar study of the sulphonyl analogue, the sulphene, $R'R''C = SO_2$, have been but sporadic and inconclusive.

Zincke and Brune reported in 1908 (2) that treatment of I with sodium acetate in acetone gave a yellow color, formulated as II, which rapidly faded with deposition of polymer. Not long after, Wedekind and Schenk (3) found that treatment of benzylsulphonyl chloride with triethylamine yielded stilbene together with triethylamine hydrochloride. They proposed the following mechanism to account for the formation of stilbene: (*a*) abstraction of hydrogen chloride from the sulphonyl chloride forming the "sulphene" (the term was first proposed by these authors in this connection), (*b*) decomposition of

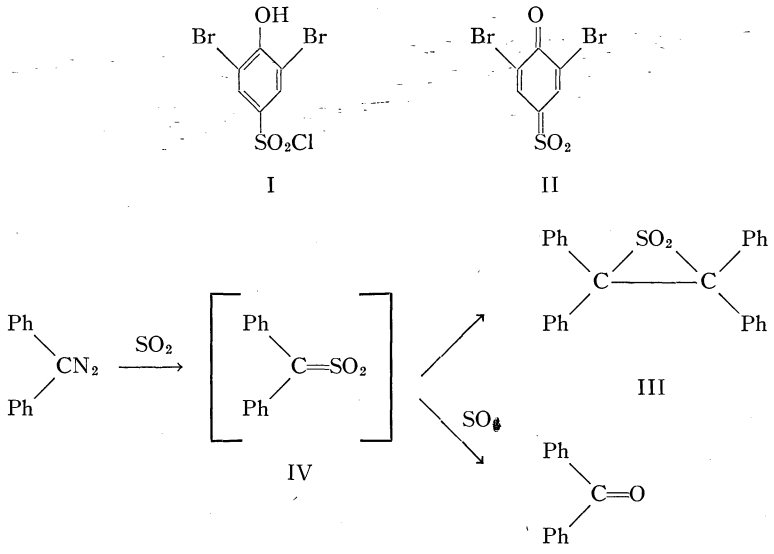

[1]*Part of the material here reported has been described in a preliminary communication (1).*
[2]*Nee E. Henmo.*
[3]*Present address: Research Institute, Canada Department of Agriculture, London, Ontario.*

the phenylsulphene to phenylcarbene and sulphur dioxide, and (*c*) coupling of two phenylcarbene molecules to form stilbene. Subsequent studies by Wedekind and co-workers (4, 5) and much more recent work in this laboratory (6) with these and analogous materials have yielded sulphur-containing compounds readily derivable from sulphene intermediates.

Recently (7, 8) it has been found that enamines react with methanesulphonyl and benzylsulphonyl chlorides in the presence of base to give four-membered ring aminosulphones. It has been suggested that the sulphene, formed as in the Wedekind reaction, might be an intermediate.

A process akin to Wedekind's step (*b*) was first reported by Staudinger and Pfenninger (9), who observed that diphenyldiazomethane in an inert solvent readily reacts with sulphur dioxide, giving tetraphenylethylene sulphone (III), or when the sulphur dioxide is in excess, benzophenone. The mechanism put forward by these authors involved, in both cases, initial formation of diphenylsulphene (IV) followed in the former case by reaction with a second molecule of diphenyldiazomethane with subsequent loss of nitrogen, and in the latter case by addition of sulphur dioxide to the sulphene followed by loss of "S_2O_3". When the reaction was carried out in hydroxylic solvents the products were those derivable by direct addition of solvent to the sulphene in the manner of ketenes: in water, the sulphonic acid; in methanol, the methyl ester; and in ethanol, the ethyl ester of the sulphonic acid. More recently the reaction of diphenyldiazomethane and sulphur dioxide in the presence of an amine has been shown (10) to yield the sulphonamide. The reaction of other diazo compounds with sulphur dioxide shows the generality of the Staudinger and Pfenninger process. Stilbestrol and a number of analogues have been synthesized by pyrolysis of the sulphone initially formed by reacting the phenylethyldiazomethane with sulphur dioxide (12), and ethylene sulphone—previously unknown—has been prepared (11) from diazomethane and sulphur dioxide.

The only record of the preparation of a stable crystalline sulphene is that of substance V by Locher and Fierz (13), who report that it is formed in poor yield on heating the

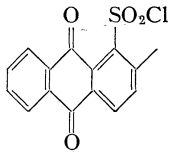

VI

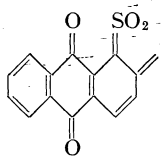

V

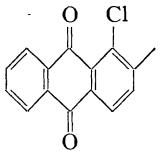

VII

acid chloride (VI) in chlorobenzene. Because of the intrinsically unlikely nature of this transformation (though it is not entirely without some chemical analogy (15)), we have reinvestigated their claim.

Exact replication of their experiments was difficult because these authors did not present adequate evidence for their conclusions as to the character of either the sulphonic acid, its acid chloride, nor the so-called anilide said to be derived from the "sulphene". Further, they did not specify quantities or reaction times for the alleged sulphene-forming reaction. We have prepared the sulphonic acid by the method of Locher and Fierz and find that it may exist in both hydrated and anhydrous forms, which are interconvertible; the anhydrous form melts at 220–221°. Significantly, Locher and Fierz report that the sulphene melts at 221–222° (they report no melting point for the acid).

The acid chloride can be prepared from the acid using phosphorus oxychloride and phosphorus pentachloride as described by Locher and Fierz, but is made much more

Can. J. Chem. Downloaded from www.nrcresearchpress.com by 210.87.254.40 on 09/05/12
For personal use only.

cleanly using thionyl chloride. They reported a melting point of "ca. 165°" for this material and asserted that the compound was difficult to crystallize owing to instability; they reported no analyses. We find the compound to be readily purified, providing normal precautions are taken to exclude moisture. It melts at 181–183° in an evacuated capillary; heating on a Kofler block in the air leads to hydrolysis and when only small samples are used the melting point obtained is that of the anhydrous sulphonic acid. On heating in chlorobenzene for short periods (e.g. 2 hours or less) little reaction takes place. On refluxing for longer periods (14 hours or more) there is both hydrolysis and loss of sulphur dioxide with formation of 1-chloro-2-methylanthraquinone (VII); the latter transformation has precedent in simpler systems in which sulphene formation is impossible (14 and work referred to, especially, F. Ullmann and P. Kertesz, Ber., **52**, 546 (1919)). To ascertain whether the sulphonic acid produced might be formed by rapid addition of water to the sulphene during isolation, the reaction product—immediately after refluxing for 14 hours—was treated with D_2O. Quantitative examination of the infrared spectrum in the methyl symmetrical deformation region (1375 cm^{-1}) showed the absence of significant $—CH_2D$ formation in the deuterated material.

Locher and Fierz report that the "sulphene" on treatment with aniline yields the sulphanilide as small yellow needles melting at 132–133°.[4] We have attempted to make the anilide by heating the sulphonyl chloride with aniline in chlorobenzene as described briefly by these authors but have isolated only aniline hydrochloride by this method. Attempts to prepare the anilide by heating the sulphonyl chloride with aniline followed by pouring into dilute hydrochloric acid gave, surprisingly, only the anilinium salt of the sulphonic acid.[5] The latter compound is prepared more cleanly directly from the sulphonic acid and aniline; it is obtained from chlorobenzene solution as small yellow needles melting around 235° with decomposition.

In view of the above results, and the similarity between the alleged sulphene and the anhydrous sulphonic acid, the claim of Locher and Fierz to have prepared a stable sulphene cannot be credited.

Although sulphenes may well be intermediates in some of the reactions discussed, alternative rationalizations are possible. If the sulphene can have but an ephemeral existence, it seemed that in order to prove it to be an intermediate in a reaction, one would have to generate it under mild, and possibly specific, conditions, so as to reduce the chance of producing the final product by other routes. From another area of work (16) there was available in these laboratories the cyclic unsaturated sultone VIII. This contains the cyclic homannular dienic system, known, in a number of cases, to open to the acyclic triene on irradiation (for a review see ref. 17). The present case contained the so far unique feature of two heteroatoms situated where the bond fission would be expected to occur.

Irradiation of VIII in methanol gave the expected ester (IX), which structure followed by analogy with the following simpler instance, XI → XIII, and which was confirmed by alkaline cleavage to benzoic acid (1 mole) and the known sodium sulphonate (X) (16).

In view of the apparent success of the photochemical transformation, the sultone XI (18) was prepared and irradiated in methanol. The product (XII) was an unstable oil

[4]*In view of the high melting points of all other compounds in this series, this is an unlikely melting point for the most stable crystal form of either a sulphonamide or a salt derived from this sulphonic acid. Though not established, it is attractive and reasonable, nonetheless, to suggest that the material which Locher and Fierz actually had in hand was the anilinium salt and that the reported melting point is either a misprint or—less likely—that the melting point is that of a low-melting crystal form or solvate (see Experimental).*

[5]*The ease of hydrolysis of the acid chloride and the failure to form the anilide under these conditions suggest that both of these reactions may involve attack on the sulphur atom by the oxygen of the adjacent carbonyl group. We plan further study of this point.*

Can. J. Chem. Downloaded from www.nrcresearchpress.com by 210.87.254.40 on 09/05/12
For personal use only.

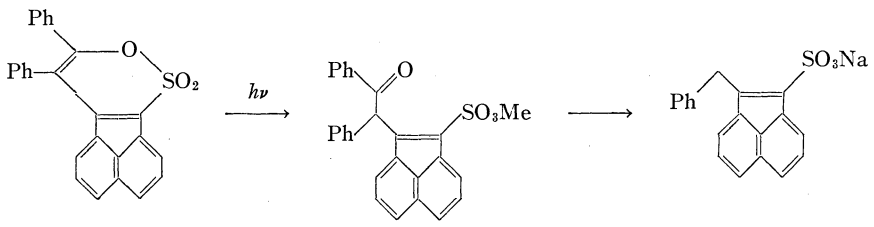

VIII IX X

which had, however, the expected spectroscopic properties. It showed λ_{max} 234 mμ (ϵ 8500) in the ultraviolet for the unsaturated ketone, and had a band at 1696 cm^{-1} ($CHCl_3$) in the infrared[6] to be attributed to the conjugated carbonyl. The n.m.r. spectrum showed a singlet (3 H) at τ 7.8 for the methyl ketone and a closely spaced doublet at τ 7.9 for the allylic methyl group, the vinyl proton appearing at τ 3.68. A singlet (3 H) at τ 6.14 is attributed to the methoxyl group whilst another singlet (2 H) at τ 5.44 is due to the methylene group. All peaks and all protons are thereby accounted for. The isomeric structure XIV is excluded by ultraviolet and infrared spectral evidence, but XIII and XII are not distinguished. The oily methyl ester was characterized as the 2,4-dinitrophenylhydrazone. This showed bands in the n.m.r. spectrum (apart from the aromatic

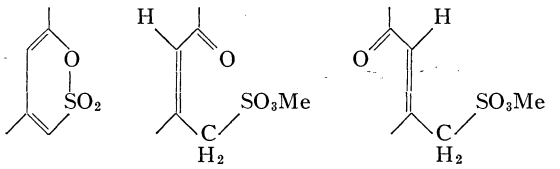

XI XII XIII

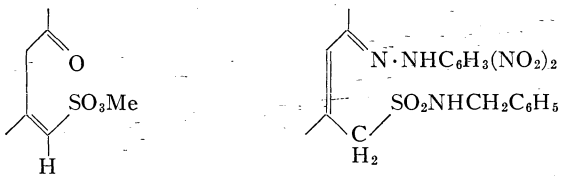

XIV XV

hydrogens) at τ 4.2 (1 H), 5.4 (2 H, singlet), 6.25 (3 H, singlet), and a close doublet and singlet (6 H) at τ 7.75, in agreement with the expected structure.

Irradiation of the sultone XI in ether containing two equivalents of benzylamine gave an oil which was converted to the 2,4-dinitrophenylhydrazone. Chromatography on bentonite–Celite gave the sulphonamide (XV). This showed λ_{max} 375 mμ (ϵ 25,000), appropriate for a conjugated ketone derivative, and showed peaks in the n.m.r. spectrum at τ 7.8 (3 H, singlet, CH_3CO—), 7.66 (3 H, close doublet, CH_3—C(H)=C—), 4.0 (1 H, unresolved, —C(H)=C—), 6.17 (2 H, singlet, —CH_2—SO_2—), 5.61 (2 H, apparent doublet, benzyl CH_2), and ca. 5.16 (1 H, unresolved, NH).

[6]*Mesityl oxide has* λ_{max} *238 m*μ *(*ϵ *11,300),* ν_{max} *1685 cm*$^{-1}$ *(*$CHCl_3$*).*

Can. J. Chem. Downloaded from www.nrcresearchpress.com by 210.87.254.40 on 09/05/12
For personal use only.

Finally, irradiation of the sultone XVI (19) in methanol gave the corresponding ester of the phenol (XVII). The n.m.r. spectrum indicated that it was a mixture of the geometrical isomers XVII*a* and XVII*b*, and the mixture was hydrogenated to the homogeneous dihydro compound XVIII.

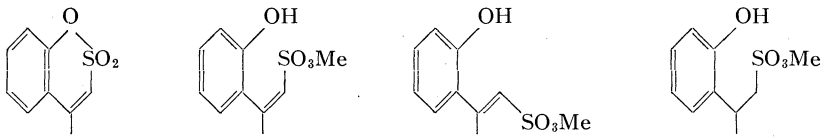

XVI XVII*a* XVII*b* XVIII

Appropriate controls clearly established that all these transformations were photochemically induced. Furthermore, although slow reaction with the solvent occurred in the absence of light, the products were in that case entirely acidic and no trace of the sulphonic esters could be detected. It would thus appear that these photolyses, like those in related systems (17), proceed by bond rearrangement, that is, in the present instance, through the sulphene XIX. In the absence of any suitable base, recyclization to the

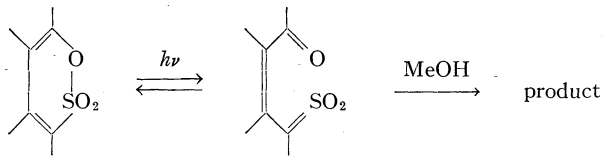

XIX

sultone would be expected, as occurs with the equivalent ketene system (20). By analogy with the experiments of Wedekind it was thought possible that competitive thermal dissociation of the sulphene might be induced. In the event, irradiation in dry diglyme with warming gave up to 25% sulphur dioxide, in agreement with the present view.

EXPERIMENTAL

Unless otherwise stated melting points were determined on a Kofler hot stage. The light source for the irradiation experiments was a Hanovia CH-3 lamp (80 watts). If not otherwise indicated infrared spectra refer to Nujol mulls, ultraviolet spectra to solutions in 95% ethanol, and n.m.r. spectra (determined on a Varian HR 60 spectrometer) to solutions in deuterochloroform using tetramethylsilane as internal standard. Petroleum ether refers to the fraction of boiling range 30–60°. The quartz immersion apparatus used in some of the irradiation experiments is that previously described (21).

Irradiation of Sultone VIII

Irradiations were carried out for periods varying from 30 to 100 minutes in methanol solution contained in a stoppered Pyrex flask cooled by a stream of air. The reaction mixture was worked up by pouring into excess water and extracting with chloroform; the extracts were washed successively with dilute sodium bicarbonate solution and water, and dried over sodium sulphate. Evaporation of the solvent left a brown semicrystalline residue from which most of the color was removed by washing with a small amount of ether. In a typical experiment, irradiation of 474 mg of the sultone (VIII) in 700 ml of methanol for 40 minutes, in two equal lots, yielded 348 mg (73%) of the crude sulphonic ester (IX).

The analytical specimen was prepared by chromatography of the crude ester on silica gel followed by four recrystallizations from chloroform–ether; m.p. 162–179°. Calc. for $C_{27}H_{20}O_4S$: C, 73.63%; H, 4.58%; S, 7.27%; OCH_3, 7.05%. Found: C, 73.87%; H, 4.59%; S, 7.53%; OCH_3, 6.56%.

Alkaline Hydrolysis of the Sulphonic Ester IX

(*a*) Sulphonic ester IX (150 mg) was added to a solution of sodium hydroxide (4 g) in a mixture of water (30 ml) and 95% ethanol (90 ml), and the solution refluxed under nitrogen for 2 hours. The mixture was cooled and acidified, and the crude sodium salt isolated as previously described (16). This was washed successively with small amounts of ether and ethyl acetate and recrystallized from ethanol, giving yellow crystals identified as X by the infrared and ultraviolet spectra.

Can. J. Chem. Downloaded from www.nrcresearchpress.com by 210.87.254.40 on 09/05/12
For personal use only.

(*b*) In another experiment the sulphonic ester (IX) (17.7 mg, 0.040 mmole) was refluxed for ½ hour under nitrogen with a solution of potassium hydroxide (0.45 g) in water (3 ml) and ethanol (9 ml). The solution was cooled and made acid to Congo red with 6 *N* sulphuric acid. The acidic solution was then slowly distilled, constant volume being maintained by addition of water. The distillate was titrated with *N*/100 sodium hydroxide using phenolphthalein as indicator. The titer consumed by the first 55 ml of distillate (after correction for the blank) corresponded to 0.041 mmole of acid. Continued distillation yielded no more acid. In a separate experiment the acidic material of the distillate was identified as benzoic acid by melting point, mixed melting point, and infrared spectrum.

Irradiation of Sultone XI in Anhydrous Methanol

A solution of XI (3.50 g) in methanol dried by the magnesium methoxide procedure (182 ml) was irradiated in the quartz immersion apparatus for 3½ hours. The product was poured into dilute sodium chloride solution (800 ml) and extracted with carbon tetrachloride. The extract was washed with sodium bicarbonate solution and with water, dried with sodium sulphate, and evaporated. The crude product was distilled *in vacuo*, yielding a yellow oil which deposited crystals on cooling. Calc. for $C_7H_{12}O_4S$: C, 43.75%; H, 6.29%; O, 33.31%; S, 16.65%; OCH_3, 16.13%. Found: C, 44.70%; H, 6.06%; O, 32.90%; S, 16.25%; OCH_3, 14.91%.

A solution of the distilled product (169 mg) in methanol (2 ml) was added to a solution of 2,4-dinitrophenylhydrazine (212 mg) in methanol (12 ml) containing hydrochloric acid. After standing at room temperature for 20 minutes the solution was poured into water and extracted with chloroform as usual. The crude product was dissolved in benzene and poured onto a column of bentonite (8 g) mixed with three times its volume of Celite. The crystalline dinitrophenylhydrazone was eluted slowly with benzene. The fractions were combined and recrystallized twice from chloroform – ethyl acetate; m.p. 143–145°. Calc. for $C_{13}H_{16}O_7N_4S$: C, 41.92%; H, 4.33%; O, 30.07%; N, 15.04%; OCH_3, 8.33%. Found: C, 42.37%; H, 4.42%; O, 30.08%; N, 15.00%; OCH_3, 8.64%.

Irradiation of Sultone XI in Ether containing Benzylamine

A solution of XI (320 mg) in ether (160 ml) containing benzylamine (0.43 ml) was irradiated in the quartz immersion apparatus under nitrogen for 140 minutes. The ether solution was washed respectively with *N* hydrochloric acid, water, saturated sodium bicarbonate solution, and water, and then evaporated. The gummy product (347 mg) was dissolved in methanol (4 ml) and water (1 ml), and added to a solution of 2,4-dinitrophenylhydrazine (490 mg) in methanol (15 ml) containing concentrated hydrochloric acid. The mixture was poured into water, giving a precipitate which was filtered off and washed with water, and taken up in methanol, which was then evaporated. The orange-red gummy product (543 mg) was dissolved in benzene and placed on a column consisting of bentonite (20 g) mixed with three times its volume of Celite. The material eluted with chloroform and 10% ethanol in chloroform was recrystallized four times from chloroform – petroleum ether; m.p. 157–158°. Calc. for $C_{19}H_{21}O_6N_5S$: C, 51.00%; H, 4.73%; N, 15.65%; S, 7.15%. Found: C, 51.04%; H, 4.76%; N, 15.39%; S, 6.74%.

Elimination of Sulphur Dioxide during Irradiation of Sultone XI

A sample of the sultone (XI) was dissolved in diethyleneglycol dimethyl ether ("diglyme", previously distilled over sodium) contained in a 50-ml round-bottomed quartz flask placed approximately 2.5 cm from the light source. During the irradiation the temperature rose rapidly to the temperature recorded. A slow stream of nitrogen was passed through the solution and led into a trap containing a solution of iodine in aqueous potassium iodide. After an interval the irradiation was stopped and the loss of iodine in the trap determined by titration with *N*/10 sodium thiosulphate. In each case a blank experiment was run with approximately the same weight of sultone and with other conditions identical except that the solution was heated in an oil bath without irradiation to the same temperature as that of the irradiation experiment.

Wt. of sultone irradiated (mg)	Wt. of sultone in blank (mg)	Vol. diglyme (ml)	Temp. (0° C)	Time (hr)	Loss of I_2; irradiation (mmole)	Loss of I_2; blank* (mmole)	Net mole% sulphur dioxide
197	209	15	80	11	0.36	0.08	23
144	166	15	130	9.5	0.24	0.06	20
622	582	20	110	5.5	0.585	0.075	13

*In a blank experiment carried out by heating the solvent for 12 hours at 120° without the sultone, the loss of iodine was 0.03 mmole.

Irradiation of Sultone XVI

A solution of XVI (1.18 g) in methanol (160 ml) was irradiated in the immersion apparatus for 7¼ hours. The product was worked up by evaporating the methanol to a small volume, pouring into water, and extracting with chloroform. The chloroform extract was washed with water and then extracted with 1% sodium hydroxide solution, which in turn was washed with chloroform, acidified with hydrochloric acid, and

Can. J. Chem. Downloaded from www.nrcresearchpress.com by 210.87.254.40 on 09/05/12
For personal use only.

extracted with chloroform. The chloroform extract was washed with water and evaporated, yielding 485 mg of acidic product, which was chromatographed on silica gel. The major fractions (300 mg) showed sharp bands in the n.m.r. at τ 7.77, 7.51, 6.30, and 6.11, consistent with the presence of the geometrical isomers XVII*a* and XVII*b*.

Some (138 mg) of this material was dissolved in ethyl acetate and hydrogenated in the presence of palladium on charcoal catalyst until approximately 1 mole of hydrogen was taken up. Evaporation of the solvent left a colorless oil which was distilled *in vacuo* at 100–110° C. Calc. for $C_{10}H_{14}SO_4$: C, 52.17%; H, 6.13%; OCH_3, 13.48%. Found: C, 51.80%; H, 6.13%; OCH_3, 13.06%. $\lambda\lambda_{max}$ 273 mμ (ϵ 2280) and 278 mμ (ϵ 2090); singlet τ 6.27, doublet τ 8.49 (J = 6 cycles/sec), unresolved bands at ca. τ 3.0 (aromatic H), τ 4.4 (benzylic H), and τ 6.5 (doublet due to CH_2).

2-Methylanthraquinone-1-sulphonic Acid

This compound was prepared from the barium salt followed by recrystallization from concentrated hydrochloric acid, as described by Locher and Fierz (13), who concluded that this material is a dihydrate. On drying *in vacuo* at 70–80°, recrystallization from benzene, or heating to 200° in air, the hydrated acid loses water, giving the anhydrous acid as yellow crystals (parallelogram-shaped plates from benzene) which rapidly turn a dirty greenish color on exposure to light; m.p. 220–221° (Kofler or vacuum capillary). Considerable sublimation was observed on the Kofler block, especially above 200°; the sublimate has a highly characteristic "shingled" appearance which is particularly striking when viewed with polarized light. On cooling below 160°, the melted sample solidified, and on heating, it melted again at 215–220°. A sample was recrystallized twice from benzene. Calc. for $C_{15}H_{10}O_5S$: C, 59.61%; H, 3.34%; S, 10.58%. Found: C, 59.75%; H, 3.43%; S, 10.15%.

The infrared spectra of the hydrated and anhydrous forms of the acid are distinctly different and serve as a ready means of identifying the compounds. On standing for a few hours in an open test tube enclosed in a flask containing a few drops of water and filled with nitrogen (or simply on standing for a day in the air), the anhydrous acid is converted to the hydrated form. When a few drops of D_2O are placed in the flask instead of H_2O, a material is obtained which has the same infrared spectrum as the hydrated acid except that the broad band at 3600 cm^{-1} is diminished and a new broad band at 2500 cm^{-1} is present. A sample of twice-recrystallized anhydrous acid was allowed to equilibrate for 3 days in the air of the laboratory. Calc. for $C_{15}H_{10}O_5S.1\frac{1}{2}H_2O$: C, 54.71%; H, 3.98%; S, 9.72%; H_2O, 8.21%. Found: C, 54.07%; H, 3.89%; S, 9.34%; loss on drying, 8.2%.

2-Methylanthraquinone-1-sulphonyl Chloride (VI)

2-Methylanthraquinone-1-sulphonic acid (hydrate, 540 mg) was dissolved in freshly distilled thionyl chloride (10 ml) and the solution refluxed for 1 hour. The excess thionyl chloride was evaporated under reduced pressure, leaving a brownish crystalline residue which readily recrystallized from methylene chloride – petroleum ether, giving well-formed pale yellow blades melting at 181–183° (vacuum capillary). Calc. for $C_{15}H_9SO_4Cl$: C, 56.17%; H, 2.83%; S, 10.00%; Cl, 11.06%. Found: C, 55.76%; H, 2.96%; S, 9.54%; Cl, 10.63%.

Action of Heat on 2-Methylanthraquinone-1-sulphonyl Chloride

(a) In Dry Chlorobenzene

A solution of the sulphonyl chloride (VI) (131 mg) in thrice-distilled chlorobenzene (6 ml) was refluxed for 18 hours in a dry 10-ml round-bottomed flask fitted with an air condenser bearing a drying tube containing Drierite. The solvent was then removed *in vacuo*, leaving a yellow crystalline solid. Methylene chloride (ca. 2 ml) dissolved all but 23 mg of this material; the infrared spectrum of the undissolved material showed it to be the sulphonic acid (hydrate). The infrared spectrum of the solution was similar to that of 1-chloro-2-methylanthraquinone except for a band at 1185 cm^{-1} characteristic of the anhydrous sulphonic acid (in CH_2Cl_2). The methylene chloride solution was washed with water and both phases evaporated separately. The aqueous phase yielded 32 mg of a pale yellow solid whose infrared spectrum ($CHCl_3$) was identical with that of the sulphonic acid. The methylene chloride phase gave 45 mg of pale yellow crystals which, after two recrystallizations from glacial acetic acid, melted at 169–170°; melting point on admixture with an authentic sample of 1-chloro-2-methylanthraquinone, 169–171°; its infrared spectrum (CH_2Cl_2) was identical with that of 1-chloro-2-methylanthraquinone.

Another solution of the sulphonyl chloride (178 mg) in chlorobenzene (6 ml) was heated just below reflux temperature (bath temperature 132°) for 2 hours and the solvent evaporated as above. The infrared spectrum (CH_2Cl_2) of the product (163 mg) indicated it to be substantially unchanged starting material; all differences from the spectrum of pure starting material were readily ascribable to the presence of approximately equal amounts of the sulphonic acid and 1-chloro-2-methylanthraquinone.

In a third experiment a solution of the sulphonyl chloride (119 mg) in dry chlorobenzene (5 ml) was refluxed for 14 hours as before. It was allowed to cool for 5 minutes, D_2O (0.5 ml) was then added, the mixture shaken for 5 minutes and allowed to stand for 20 minutes. It was then poured into methylene chloride and extracted with water. Evaporation of the methylene chloride phase yielded 64 mg of a yellow crystalline solid whose infrared spectrum (CH_2Cl_2) showed it to be impure 1-chloro-2-methylanthraquinone. The

Can. J. Chem. Downloaded from www.nrcresearchpress.com by 210.87.254.40 on 09/05/12
For personal use only.

aqueous phase gave 44 mg of a pale yellow crystalline solid, which was recrystallized from benzene. The infrared spectrum (KBr) was virtually identical with that of an authentic sample of the sulphonic acid run at the same time; in particular, the band at 1385 cm^{-1} showed precisely the same intensity relative to the other bands in both spectra.

(b) On Kofler Block (in Air)

About 3 or 4 mg of the sulphonyl chloride was placed on a microscope slide (without cover glass) and set on the Kofler block at 125°, and the temperature increased gradually. At ca. 145° the transparent blades became opaque. Heating was continued until the temperature reached 200°; no melting had taken place. The infrared spectrum was identical with that of the anhydrous acid.

When one or two crystals of the sulphonyl chloride were placed on a microscope slide (with cover glass) and placed on the Kofler block at <130°, the same crystal change at ca. 140° was observed followed by sublimation gradually around 150° and rapidly above 200°; the sublimate was identical in appearance with the characteristic sublimate formed on heating the sulphonic acid. The material melted sharply at 218–220°, yielding a transparent yellow melt. On cooling below 160° the melt crystallized; on heating again it showed the characteristic sublimation above 200° and melted around 210–219°.

Reaction of the Sulphonyl Chloride VI with Aniline

The sulphonyl chloride (VI) (106 mg) was heated at 135° with aniline (2 ml) for 100 minutes. The mixture was allowed to cool and then poured into excess dilute hydrochloric acid. The reddish precipitate was filtered off, washed with dilute hydrochloric acid, dried, and recrystallized from toluene, giving a brownish crystalline solid whose infrared spectrum was identical with that of the anilinium salt.

Anilinium 2-Methylanthraquinone-1-sulphonate

Aniline (0.1 ml) was added to a solution of the sulphonic acid (90 mg) in water (2 ml). A yellowish crystalline precipitate formed within 20 seconds. This was filtered off and recrystallized three times from water, giving pale yellow blades which on heating on the Kofler block changed crystal form with partial melting around 148–150°, apparently changed crystal form again at 200–210°, and finally melted around 230–238° with decomposition. Calc. for $C_{21}H_{17}O_5NS.H_2O$: C, 61.01%; H, 4.63%; N, 3.39%. Found: C, 61.06%; H, 4.63%; N, 3.49%.

Adding aniline to a hot solution of the sulphonic acid in chlorobenzene gave fine yellow needles which (after recrystallization from chlorobenzene) apparently changed crystal form below 160°, then around 200°, and finally melted at 235–238° with decomposition. The infrared spectrum was identical with that of the material obtained from aqueous solution.

ACKNOWLEDGMENTS

The authors would like to thank Mr. R. E. Klinck for the determination of the n.m.r. spectra. They are indebted for financial support to the U.S.A.F. under Grant No. AF-AFOSR-61-6.

REFERENCES

1. E. Henmo, P. de Mayo, A. B. M. A. Sattar, and A. Stoessl. Proc. Chem. Soc. 238 (1961).
2. T. Zincke and R. Brune. Ber. **41**, 902 (1908).
3. E. Wedekind and D. Schenk. Ber. **44**, 198 (1911).
4. E. Wedekind, D. Schenk, and R. Stüsser. Ber. **56**, 633 (1923).
5. E. Wedekind and R. Stüsser. Ber. **56**, 1557 (1923).
6. J. F. King and T. Durst. Unpublished observations.
7. G. Stork and I. J. Borowitz. J. Am. Chem. Soc. **84**, 313 (1962).
8. G. Opitz and H. Adolph. Angew. Chem. **74**, 77 (1962).
9. H. Staudinger and F. Pfenninger. Ber. **49**, 1941 (1916).
10. H. Kloosterziel, M. H. Deinema, and H. J. Backer. Rec. Trav. Chim. **71**, 1228 (1952).
11. G. Hesse, E. Reichold, and S. Majmudar. Ber. **90**, 2106 (1957).
12. L. von Vargha and E. Kovács. Ber. **75**, 794 (1942).
13. A. Locher and H. E. Fierz. Helv. Chim. Acta, **10**, 642 (1927). A. Locher. Thesis. Swiss Federal Institute of Technology, Zürich, Switzerland. 1925.
14. F. Muth. *In* Methoden der organischen Chemie (Houben-Weyl). Vol. 9. 4th ed. Georg Thieme Verlag, Stuttgart. 1955. p. 595.
15. H. Hart and R. W. Fish. J. Am. Chem. Soc. **82**, 749 (1960).
16. P. de Mayo and A. Stoessl. Can. J. Chem. **40**, 57 (1962).
17. P. de Mayo and S. T. Reid. Quart. Rev. (London), **15**, 393 (1961).
18. T. Morel and P. E. Verkade. Rec. Trav. Chim. **68**, 619 (1949).
19. E. M. Philbin, E. R. Stuart, R. F. Timoney, and T. S. Wheeler. J. Chem. Soc. 4414 (1956).
20. D. H. R. Barton and G. Quinkert. J. Chem. Soc. 1 (1960).
21. P. de Mayo. Advances in organic chemistry. Vol. 2. Interscience Pub. Inc. 1960. p. 370.

Can. J. Chem. Downloaded from www.nrcresearchpress.com by 210.87.254.40 on 09/05/12
For personal use only.

OXIDATION STATES OF MANGANESE IN FUSED ALKALI NITRATES

RUTH M. BENNETT* AND OWEN G. HOLMES

University of Saskatchewan, Regina Campus, Regina, Saskatchewan

Received August 7, 1962

ABSTRACT

When dissolved in fused alkali nitrate, manganese (II) is oxidized to MnO_2. In the same solvent MnO_4^- decomposes to MnO_2. Peroxide ion arrests the decomposition at MnO_4^{2-}, while the presence of hydroxide ion results in the formation of MnO_4^{3-}. The spectra of MnO_4^{2-} and MnO_4^{3-} in molten nitrate show great similarity to their spectra in alkaline aqueous solution.

Can. J. Chem. Downloaded from www.nrcresearchpress.com by 210.87.254.5 on 09/05/12
For personal use only.

Fused nitrate salts form useful and interesting solvents due to the variety of reactions which they undergo with different solutes. The nitrate ion is capable of participating in oxidation–reduction processes and acid–base reactions. Duke (1) has interpreted the latter on the basis of the dissociation of nitrate ion in the melt into nitronium ion and oxide ion, analogous in many respects to the ionic dissociation of water.

In this report we present some observations on the chemistry of manganese when its compounds are dissolved in molten alkali nitrates. Spectrophotometric methods were used for identification and analysis of species of different oxidation states which occurred under various experimental conditions.

EXPERIMENTAL

In the experiments reported here, a eutectic mixture of $NaNO_3$–KNO_3, 45.5 mole% $NaNO_3$, melting point 218° C, was used as solvent. The nitrate melts were maintained at 260±15° C both during the periods of chemical reaction with solutes and during the periods of spectrophotometric examination.

Manganese was introduced into the nitrate melt either as anhydrous manganese (II) sulphate or as potassium permanganate. The manganese was approximately 4×10^{-4} *M* in all cases reported.

Anhydrous sodium peroxide, 96.0% Na_2O_2, was used as a source of peroxide ions, while hydroxide ions were added in the form of sodium hydroxide which assayed at 99.0% NaOH.

The compounds $NaNO_3$, KNO_3, $MnSO_4$, $KMnO_4$, Na_2O_2, and NaOH used in these experiments were Fisher Reagent grade.

Aqueous solutions of manganate ion were prepared for spectrophotometric analysis by dissolving potassium permanganate in 4 *M* sodium hydroxide and heating for several minutes until no further color changes were observed.

Absorption spectra of liquid solutions were measured with a Beckman DU spectrophotometer. For the fused salt solutions, the 1-cm pyrex absorption cells were housed and heated in a small electrical furnace through which an optical path had been cleared. This assembly was placed between the source and the optical system of the instrument rather than behind the dispersing unit as in the conventional Beckman DU arrangement.

Reflectance spectra were measured with a reflectance accessory attached to the spectrophotometer. For reference, instead of the usual $MgSO_4$ block, a quenched eutectic $NaNO_3$–KNO_3 mixture was used. Both quenched pure solvent and solution were powdered by a mechanically driven mortar and pestle prior to reflectance measurement.

RESULTS AND DISCUSSION

The chemistry of manganese in fused $NaNO_3$–KNO_3 can be summarized as follows:

**Holder of a Bursary from the National Research Council.*

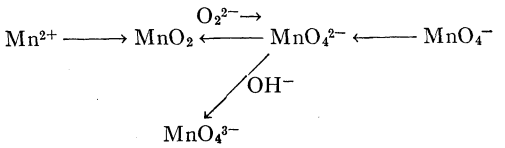

Each of the indicated reactions is discussed separately below.

(1) Oxidation of Mn^{2+}

Manganese (II) is rapidly oxidized to MnO_2, which precipitates from the molten nitrate solution. Simultaneously NO_2 is expelled. These observations can be accounted for by:

$$Mn^{2+} + 2NO_3^- \rightarrow MnO_2 + 2NO_2. \quad [1]$$

In the presence of excess O_2^{2-}, MnO_2 is further oxidized to manganate ion:

$$MnO_2 + O_2^{2-} \rightleftharpoons MnO_4^{2-}. \quad [2]$$

(2) Decomposition of MnO_4^-

In fused $NaNO_3$–KNO_3 at 260° C, permanganate ion slowly decomposes ultimately to MnO_2 and O_2. However, green manganate ion is an intermediate of several minutes' duration. Figure 1 shows the reflectance spectrum of the cooled and powdered solid obtained

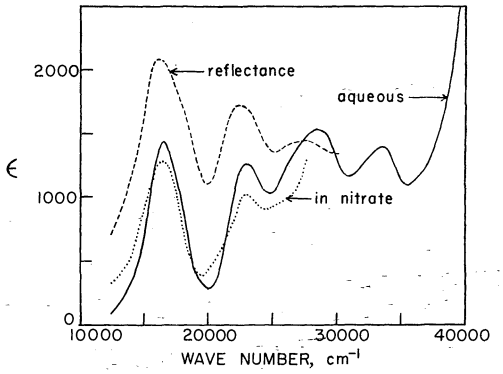

FIG. 1. Spectra of MnO_4^{2-}.

on filtering a solution of MnO_4^{2-} containing MnO_2 through glass wool. The absorption scale for this reflectance spectrum is only relative. Equations [3]–[6] are suggested for the reduction of MnO_4^- to MnO_2 in this system.

$$4MnO_4^- + 2NO_3^- \rightarrow 4MnO_4^{2-} + 2NO_2^+ + O_2 \quad [3]$$

$$2MnO_4^{2-} \rightarrow 2MnO_2 + 2O^{2-} + O_2 \quad [4]$$

$$MnO_4^{2-} \rightleftharpoons MnO_2 + O_2^{2-} \quad [5]$$

$$2MnO_4^{2-} + 2NO_2^+ \rightarrow 2MnO_2 + 2NO_3^- + O_2 \quad [6]$$

Equation [3] shows the decomposition in nitrate melt of MnO_4^- into MnO_4^{2-} and O_2, a process in which the NO_3^- acts as a base to provide the necessary oxides. The pyrolysis of $KMnO_4$ above 200° C yields a mixture of K_2MnO_4 and MnO_2 (2), as there is not enough oxygen content to allow K_2MnO_4 alone.

Equations [4], [5], and [6] present alternatives for the decomposition of MnO_4^{2-}. In [4] the decomposition is direct, yielding oxide ions; in [5], peroxide ions. Equation [6]

Can. J. Chem. Downloaded from www.nrcresearchpress.com by 210.87.254.5 on 09/05/12
For personal use only.

suggests that nitronium ion could play an acidic role in this decomposition by accepting the oxides released when MnO_4^{2-} is converted into MnO_2.

(3) Stabilization of MnO_4^{2-} by O_2^{2-}

Peroxide ion present in the melt in excess of the MnO_4^{2-} concentration prevents further decomposition to MnO_2. This observation is consistent with that summarized in equation [2]. Peroxide ion would destroy the NO_2^+ necessary for the process in equation [6] by neutralization:

$$2NO_2^+ + 2O_2^{2-} \rightarrow 2NO_3^- + O_2. \qquad [7]$$

The absorption spectrum of MnO_4^{2-} preserved in molten nitrate solution by O_2^{2-} is shown in Fig. 1. The ultraviolet spectrum was inacccessible due to interference of the nitrate ion (3).

(4) MnO_4^{3-} in Fused Nitrate

The addition of NaOH to manganate ion in fused nitrate causes a rapid change in color from green to blue. The spectrum of the blue solution is shown in Fig. 2, along with

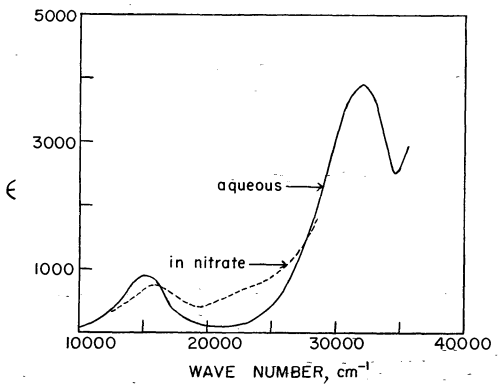

FIG. 2. Spectra of MnO_4^{3-}.

the spectrum of MnO_4^{3-} reported by Carrington and Symons (4). Although attempts to chemically identify the blue species were unsuccessful, its spectrum and a previous report (5) of the production of $Na_3MnO_4.10H_2O$ by oxidation of manganese (II) with alkaline nitrate indicate that it is hypomanganate, MnO_4^{3-}. In the spectrum of MnO_4^{3-} in nitrate solution shown in Fig. 2, the absorption in the region 20,000–25,000 cm^{-1} was probably due to residual MnO_4^{2-}.

The introduction of OH^- raises a number of possibilities for the stabilization of MnO_4^{3-}. Further experimental evidence is required before the role of OH^- in the chemistry of molten nitrate solutions can be understood.

(5) Spectra of MnO_4^{2-} and MnO_4^{3-} in Fused Nitrate

In Table I a summary is given of the band maxima and molar extinction coefficients for MnO_4^{2-} and MnO_4^{3-}.

It is apparent that the aqueous and nitrate spectra are remarkably similar, as is generally observed for solutes in these solvents (3, 6).

The formulas given here, MnO_4^{2-} and MnO_4^{3-}, are those suggested by Carrington and Symons (4), who give arguments in support of them.

Can. J. Chem. Downloaded from www.nrcresearchpress.com by 210.87.254.5 on 09/05/12
For personal use only.

TABLE I

Spectra of MnO_4^{2-} and MnO_4^{3-}

		Aqueous	Nitrate solution	Reflectance
Spectra of MnO_4^{2-}				
Band 1	Maximum, cm^{-1}	16,500	16,300	16,000
	Extinction coefficient	1,430	1,290	—
Band 2	Maximum, cm^{-1}	22,800	22,700	22,200
	Extinction coefficient	1,260	1,025	—
Band 3	Maximum, cm^{-1}	28,800		27,400
	Extinction coefficient	1,530		—
Band 4	Maximum, cm^{-1}	33,500		
	Extinction coefficient	1,400		
Spectra of MnO_4^{3-}				
Band 1	Maximum, cm^{-1}	15,000*	15,900	
	Extinction coefficient	900*	750	
Band 2	Maximum, cm^{-1}	32,000*		
	Extinction coefficient	3,900*		

*Reference 4.

The authors wish to acknowledge the support of the National Research Council in the form of research grants.

REFERENCES

1. F. R. DUKE. J. Chem. Educ. **39**, 57 (1962).
2. N. V. SIDGWICK. The chemical elements and their compounds. Oxford, Clarendon Press. 1950.
3. G. P. SMITH and C. R. BOSTON. Ann. N.Y. Acad. Sci. **79**, 930 (1960).
4. A. CARRINGTON and M. C. R. SYMONS. J. Chem. Soc. 3373 (1956).
5. B. JEZOWSKA-TRZEBIATOWSKA, J. NAWOJSKA, and M. WRONSKA. Roczniki Chem. **25**, 405 (1951).
6. G. HARRINGTON and B. R. SUNDHEIM. Ann. N.Y. Acad. Sci. **79**, 950 (1960).

Can. J. Chem. Downloaded from www.nrcresearchpress.com by 210.87.254.5 on 09/05/12
For personal use only.

LIQUID–LIQUID EXTRACTION OF BERYLLIUM

II. STUDIES OF BERYLLIUM–THIOCYANATE EXTRACTION

WENDELL J. BIERMANN AND ROBERT MCCORKELL
Department of Chemistry, University of Manitoba, Winnipeg, Manitoba
Received April 9, 1962

ABSTRACT

The partition of beryllium and aluminum between aqueous thiocyanate solutions and several organic solvents was determined under a variety of experimental conditions. From these batch studies it was concluded that a two-solvent countercurrent extraction of beryllium from a thiocyanate solution should give good recovery of beryllium with effective separation from aluminum and, by inference, other inert gas configuration cations.

Can. J. Chem. Downloaded from www.nrcresearchpress.com by 210.87.254.40 on 09/05/12
For personal use only.

In the first paper of this series (1), it was shown that the thiocyanate ion was particularly useful as a ligand for forming an extractable complex with beryllium, showing considerable selectivity with inert gas configuration ions, as represented by Al^{+3}. It also appeared that the organic solvent played an active role in forming the extractable species, methyl isobutyl ketone, isoamyl acetate, 2-octanol, and 1-hexanol being among the inexpensive and efficient solvents.

There being no indication that quantitative separation of beryllium from other metals could be achieved except through a series of extractions, it was evident that studies of the beryllium–thiocyanate extraction would ultimately require a continuous-extraction technique. Because of the relative simplicity of batch extraction studies on a separatory funnel scale, it seemed desirable to first study the effects of the several variables concerned on the efficiency of extraction and separation in this manner. Such information would then considerably facilitate later continuous-extraction studies.

This paper, therefore, concerns itself with the determination of distribution coefficients, in the convenient guise of percentages extracted, of systems whose behavior will be relevant to a continuous countercurrent extraction based on the beryllium–thiocyanate–solvent complex and associated stripping and reagent-recovery steps. As in the previous work, separation from aluminum is used as the criterion of specificity, since generally this is the most common and difficult separation involving beryllium.

EXPERIMENTAL

The percentages of metal ion extracted were determined by shaking the mixtures in separatory funnels, equal volumes of organic and aqueous phases being used. Metal concentrations were determined as previously described and thiocyanate was determined by titration with standardized mercury (II) nitrate solutions, neither beryllium nor aluminum causing any interference. pH measurements were made with a conventional glass electrode – calomel pH meter and hydrogen ion concentrations have been approximated as $[H^+]$ = antilog $(-pH)$.

The organic solvents were obtained by fractional distillation of commercial grade materials, the fractions being retained were: methyl isobutyl ketone, 114.5–115.5° C; 1-hexanol, 155–157° C; and 2-octanol, 176–179° C.

EXPERIMENTAL RESULTS

As would be anticipated, the percentage of beryllium extracted at constant ammonium thiocyanate concentration shows a maximum as the pH is varied. These results, collected in Table I, show a maximum extraction in the interval pH 2 to pH 3 regardless of the solvent, indicating that the solvent is not involved in the pH-sensitive process.

TABLE I

The extraction of beryllium from aqueous ammonium thiocyanate solutions as a function of pH before extraction

pH	Percent beryllium extracted by: 1-Hexanol	Methyl isobutyl ketone	Isoamyl acetate
0.5	20.4	11.6	6.8
1.0	39.7	34.5	21.7
2.0	55.3	45.4	29.9
3.0	54.2	42.3	30.8
4.0	26.3	30.7	11.3
5.0	11.0	1.8	1.1

NOTE: The concentration of ammonium thiocyanate was initially 2.0 *M* and the beryllium concentration 0.10 *M* in all the above.

Schwartzenback (2, p. 2) reports that the p*K* for the process $Be^{++} + H_2O = BeOH^+ + H^+$ is -3.63, from which it can be shown that the hydroxy complex becomes the predominate species between pH 3 and pH 4, in agreement with our postulate that hydroxylation is the cause of the falloff of extraction above pH 3.

The falloff of extraction below pH 2 is not so simply explained. Schwartzenback (2, p. 37) reports the p*K* for thiocyanic acid to be -0.85, from which the thiocyanate ion concentration is calculated to be 1.8 *M* at pH 2.0 and 1.2 *M* at pH 1.0 in these solutions. In all three solvents, the falloff of extraction between these two pH values is in the same ratio as the thiocyanate ion concentration, suggesting that only one thiocyanate ion is coordinated per beryllium ion, making it difficult to envision the nature of the extracted species. If the species extracted were $(NH_4)_2Be(CNS)_4$, analogous to transitional metal thiocyanates extracted by Bock and Watkins or Welt and Diamond (3), or $Be(CNS)_2$·$(solvent)_2$, which we had anticipated, extraction should fall off much more rapidly with pH. As all our other data indicate a ligand number of about 2 for the thiocyanate bound to beryllium, it is probable that either the p*K* value for thiocyanic acid is not reliable, or that some other effect is operating simultaneously, for example, an enhanced solubility of the solvents at lower pH.

pH variation is of little use in the separation of beryllium and aluminum, as the formation constant of the first hydroxy aluminum complex is very close to that for beryllium. Results not included here confirm this to be the situation.

The effect of thiocyanate ion concentration on the extraction of beryllium and aluminum is shown in Table II, the extraction generally showing a decrease with lower thiocyanate concentration, the pH being held constant.

The percentage extraction of beryllium should be proportional to the activity of the extracted species $Be(CNS)_n^{2-n}$ in the aqueous phase, which should, in turn, be proportional to the activity product $a_{Be^{++}}a^n_{CNS^-}$. An approximate value of n can be derived by making two simplifying assumptions: (1) that the activity coefficient ratio $\gamma_{Be(CNS)_n^{2-n}}/\gamma_{Be^{++}}\gamma^n_{CNS^-}$ remains constant in both phases over the range of concentrations used, and (2) that the formation constant of the thiocyanato beryllium complex is sufficiently small that the concentration of free beryllium ion can be approximated as the concentration of unextracted beryllium. It was found that the product $[Be^{++}][CNS^-]^2$ varies linearly with the percentage extraction up to 4 *M* ammonium thiocyanate within an average deviation of $\pm 5\%$ for 1-hexanol and 2-octanol and $\pm 10\%$ for methyl isobutyl ketone. Extraction with the last-named solvent increases more rapidly than the concentration function, which is indicative of an average ligand number slightly greater than 2.

Can. J. Chem. Downloaded from www.nrcresearchpress.com by 210.87.254.40 on 09/05/12
For personal use only.

TABLE II

Extraction of beryllium and aluminum as a function of ammonium thiocyanate concentration

[NH_4CNS], moles/liter	Percentage metal extracted using:					
	Methyl isobutyl ketone		1-Hexanol		2-Octanol	
	Be	Al	Be	Al	Be	Al
0.5	2.9	0.2	8.0	0.0	2.3	0.0
1.0	14.4	1.1	23.6	0.1	10.9	0.0
1.5	29.4	1.6	41.8	9.0	21.9	1.0
2.0	43.2	3.7	52.3	19.3	34.1	1.5
2.5	59.3	7.0	64.8	30.8	43.9	4.7
3.0	71.0	12.7	72.1	41.2	56.1	10.3
4.0	78.8		83.0			
5.0	83.1		88.7			
6.0	85.1		91.5			
7.0	86.6		94.5			

NOTE: The above were determined by using an aqueous solution initially 0.100 *M* in the metal, the pH adjusted to 3.00 by sulphuric acid. Equal volumes of aqueous and organic phases were used.

Aluminum extraction tends to fall off more rapidly than beryllium as the thiocyanate concentration is lowered, being proportional to the third power of the thiocyanate concentration.

Tables IIIA and IIIB are a summary of experiments measuring the extraction of thiocyanate ion at different concentrations of thiocyanate, metal, and hydronium ions.

TABLE IIIA

Extraction of thiocyanate ion by methyl isobutyl ketone at pH 3.00

[NH_4CNS], moles/liter	[Metal ion], moles/liter	Total CNS^- extracted, %	Free CNS^- extracted, %
1.0	—	2.0	2.0
2.0	—	2.2	2.2
3.0	—	2.1	2.1
4.0	—	2.2	2.2
1.0	Be^{++} 0.100	6.6	3.8
2.0	Be^{++} 0.100	7.0	2.7
3.0	Be^{++} 0.100	6.8	2.3
4.0	Be^{++} 0.100	5.9	2.0
1.0	Al^{+++} 0.100	3.2	2.9
2.0	Al^{+++} 0.100	3.3	2.7
3.0	Al^{+++} 0.100	3.8	2.5
4.0	Al^{+++} 0.100	4.6	—

TABLE IIIB

Extraction of thiocyanate ion by several solvents at varying pH in the presence of 0.100 *M* beryllium sulphate

pH	Percent thiocyanate extracted by:		
	1-Hexanol	2-Octanol	Methyl isobutyl ketone
0.3	51.0	51.4	—
0.6	31.7	29.4	40.2
1.0	12.6	3.4	13.4
2.0	6.3	2.8	7.3

Can. J. Chem. Downloaded from www.nrcresearchpress.com by 210.87.254.40 on 09/05/12
For personal use only.

These were done to determine whether any appreciable extraction of uncoordinated thiocyanate took place, an important consideration if multistage extraction is used, and also to establish the feasibility of stripping excess thiocyanate from the raffinate.

Where the water phase contained metal ions, the amount of uncomplexed thiocyanate extracted was computed from the data of Table II, on the assumption that each mole of beryllium ion extracted had complexed 2 moles of thiocyanate ion and aluminum, 3. In view of the contributing experimental errors and approximations, the data are consistent with the conclusion that about 2% of the excess ammonium thiocyanate would be removed by methyl isobutyl ketone per stage of extraction at pH 3 and somewhat less for the alcohols, based on their relative behavior at pH 2.

The rapid rise of extraction of thiocyanate at lower pH values would permit stripping excess thiocyanate from raffinates by any of the three solvents with little contamination by excess aluminum, the extraction of which becomes small when both the pH and thiocyanate concentrations are low.

For convenience, the initial beryllium ion concentration had been kept at 0.100 *M* in all the preceding work. Where the chemistry of the extraction process is only partially understood, it is not justifiable to assume that the partition will not be affected by concentration. In Table IV is shown the dependence of beryllium extraction on initial

TABLE IV

Effect of beryllium concentration on the extraction from ammonium thiocyanate at pH 3.00 with methyl isobutyl ketone

Initial $[NH_4CNS]$	Initial $[Be^{++}]$	Percent Be extracted	$[CNS^-]$ at equilibrium	Percent extraction from Table II
3.00	0.10	71	2.86	—
3.00	0.20	70	2.72	—
3.00	0.40	58	2.54	59
3.00	0.80	50	2.20	49
3.00	1.00	45	2.10	46

beryllium concentration, at constant pH and initial ammonium thiocyanate concentration. As the thiocyanate concentration is appreciably reduced when larger amounts of beryllium are extracted, the equilibrium concentration of thiocyanate in the aqueous layer was calculated on the basis of two thiocyanate ions extracted with each beryllium ion, and the percentage beryllium extraction predicted at each of these equilibrium concentrations was obtained by linear interpolation of Table II. The close agreement shows that the distribution coefficient is independent of concentration over a wide range and, incidentally, confirms a ligand number of 2 for the coordination of thiocyanate by beryllium in the extracted species.

As a matter of interest, it was decided to examine the effect of changing the cation associated with the thiocyanate ion, leading to the information of Table V. It is evident that small radii considerably enhance extraction; this is probably a "salting-out" effect, but could indicate that the tendency of formation of complexes containing beryllium in anionic forms, which was noted in the discussion of Table II, is enhanced by the presence of high-field ions. No practical import is associated with this effect as economic considerations indicate the use of ammonia as the associated cation.

Stripping of beryllium from the organic phase does not seem to offer any difficulty. A single extraction with dilute ammonia water quantitatively removes the beryllium, and

Can. J. Chem. Downloaded from www.nrcresearchpress.com by 210.87.254.40 on 09/05/12
For personal use only.

TABLE V

Effect of associated cation on beryllium–thiocyanate extraction

Solvent	Percent Be extracted from solution 1.5 *M* in:			
	NH_4CNS	KCNS	NaCNS	LiCNS
Methyl isobutyl ketone	28.3	30.6	34.3	47.8
1-Hexanol	38.7	40.1	48.0	56.4
2-Octanol	21.3	21.5	28.4	33.6
Isoamyl acetate	15.2	18.4	21.3	33.0

NOTE: Initial beryllium concentration 0.100 *M*, pH 3.00.

either water or dilute sulphuric acid could be used for stripping in a column, as both remove about 30%, per extraction stage, of the beryllium in the organic phase with a solvent ratio of 1.

DISCUSSION

In order to obtain high purity of beryllium in the extract and at the same time have only small losses in the raffinate, a two-solvent countercurrent extraction process is indicated as neither single solvent countercurrent nor crosscurrent extractions are particularly suited to this system (4). The extraction solvent might be any one of those which was found suitable in the exploratory work described earlier and the wash solvent would be a suitable ammonium thiocyanate solution, such as 2 *M* adjusted to pH 3 by sulphuric acid.

Based on a column having eight stages with feed at the center, using the above wash solvent and methyl isobutyl ketone as the extraction solvent, and postulating the feed to contain equimolecular amounts of beryllium and aluminum, and a solvent ratio of 4, an approximation based on the Kremser equation predicts a raffinate containing only about 1% of the beryllium in the feed, and the beryllium in the extract from the wash section would contain less than 0.01 mole% aluminum.

Studies of such a continuous-extraction system are presently underway in this laboratory, as are studies designed to give a more adequate description of the extracted species and the equilibria involved in its formation.

REFERENCES

1. W. J. BIERMANN and R. MCCORKELL. Can. J. Chem. **40**, 1368 (1962).
2. G. SCHWARTZENBACH, J. BJERRUM, and L. SILLEN. Stability constants. Part II: Inorganic ligands. The Chemical Society, London. 1958.
3. R. M. DIAMOND and D. G. TUCK. Extraction of inorganic compounds. *In* Progress in inorganic chemistry. Vol. II. *Edited by* F. A. Cotton. Interscience, New York. 1960. p. 179.
4. L. ALDERS. Liquid–liquid extraction. Elsevier, Amsterdam. 1959. Chap. V.

Can. J. Chem. Downloaded from www.nrcresearchpress.com by 210.87.254.40 on 09/05/12
For personal use only.

Can. J. Chem. Downloaded from www.nrcresearchpress.com by 210.87.254.42 on 09/05/12
For personal use only.

THE ORIGIN OF CARBON ATOMS 2, 3, AND 7 OF RICININE[1]

P. F. JUBY[2] AND LÉO MARION
Division of Pure Chemistry, National Research Council, Ottawa, Canada

Received September 14, 1962

ABSTRACT

The isolation of carbon atoms 2 and 3 of the α-pyridone nucleus of ricinine is described. Evidence is provided to support the suggestion that succinic acid or a closely related four-carbon dicarboxylic acid provides carbon atoms 2, 3, and 7 in the biosynthesis of the ricinine molecule.

In a preliminary communication (1) evidence was presented to support proposals (2, 3) that in the higher plants the pyridine ring and related α-pyridone ring of such compounds as nicotine and ricinine (I) (see Fig. 1) may be synthesized directly from simple metabolic intermediates related to acetate, succinate, glycerol, and propionate. From the percentage activities found at the nitrile group of ricinine isolated from *Ricinus communis* L. plants that had been fed various simple labelled substances, it was suggested that succinic acid, or a closely related four-carbon dicarboxylic acid found in the Krebs tricarboxylic acid cycle, provided carbon atoms 2, 3, and 7 of ricinine. If such be the case, the four-carbon acid would be incorporated in such a way that one of the carboxyl groups (C-1) would provide the carbon for the nitrile group of ricinine (C-7), and the 2- and 3-carbon atoms would give rise to carbons 3 and 2 respectively of the pyridone ring. The other carboxyl group would be lost by decarboxylation either before or after incorporation into the pyridone ring or its precursor.

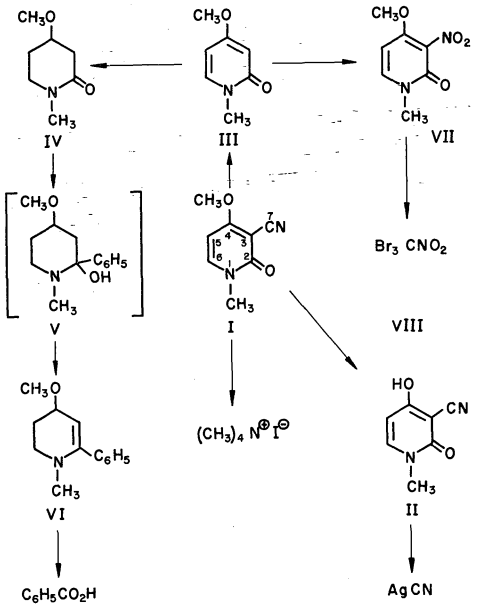

FIG. 1. Degradation schemes for ricinine.

[1]*Issued as N.R.C. No. 7082.*
[2]*National Research Council Postdoctorate Fellow.*

Can. J. Chem. Downloaded from www.nrcresearchpress.com by 210.87.254.42 on 09/05/12
For personal use only.

In order to test this suggestion it is therefore necessary to isolate carbons 2 and 3 from the remaining carbons in ricinine. Carbon atom 2 was isolated in the form of the carboxyl group of benzoic acid. Removal of the nitrile group from ricinine (I) by hydrolysis followed by decarboxylation gave rise to 4-methoxy-1-methyl-2-pyridone (III), which was reduced easily to the corresponding piperidone (IV) with hydrogen and Adams' catalyst. The action of phenyl magnesium bromide on the piperidone (IV) gave the carbinol (V), which lost the elements of water spontaneously and produced the unstable 4-methoxy-1-methyl-2-phenyl-2-piperideine (VI). The product (VI) was treated immediately with potassium permanganate, and the benzoic acid containing carbon 2 of ricinine as its carboxyl group was isolated and burnt in a combustion train. The carbon dioxide was collected as barium carbonate.

The observation (4) that nitrophenols react with calcium hypobromite to yield tribromonitromethane (bromopicrin) in which the carbon atom is the one that carried the nitro group prompted the application of this degradative procedure to the ricinine molecule. Nitration of 4-methoxy-1-methyl-2-pyridone (III) gave a mononitroderivative, the nuclear magnetic resonance spectrum of which contained two doublets centered at τ values of 3.90 and 2.55 p.p.m. with a coupling constant of 8.0 c.p.s. The product, therefore, must contain a proton on each of two adjacent carbon atoms. Accordingly, the nitro group must be located on carbon 3 and the product is 4-methoxy-1-methyl-3-nitro-2-pyridone (VII). Treatment of VII with calcium hypobromite liberated carbon 3 of ricinine as bromopicrin (VIII), which was purified by gas–liquid chromatography. The pure bromopicrin was converted by combustion to carbon dioxide, which was collected as barium carbonate.

To determine the activity of the nitrile group, the methoxy group of ricinine was first hydrolyzed and the resulting ricinic acid (II) oxidized as previously described by Böttcher (5). The liberated hydrogen cyanide was precipitated as silver cyanide and its activity measured.[3]

The methyl groups attached to oxygen and to nitrogen were each isolated as tetramethylammonium iodide.

These methods of determination were applied to two samples of ricinine obtained from plants of *R. communis* L. that had been fed succinic acid-2,3-^{14}C and sodium acetate-2-^{14}C. Quantities of the radioactive ricinine to be used for the determinations were diluted initially with varying quantities of inactive ricinine. The results obtained are recorded in Table I, which gives the activity at each carbon atom in terms of a percentage of the total activity of ricinine.

TABLE I

Location of radioactivity in ricinine

Position		Percentage of activity of ricinine from plants fed succinic acid-2,3-^{14}C	Percentage of activity of ricinine from plants fed sodium acetate-2-^{14}C
OCH_3	(as $(CH_3)_4NI$)	0.55	0.66
NCH_3	(as $(CH_3)_4NI$)	0.58	0.65
7	(as AgCN)	19.1	20.8
2	(as $BaCO_3$ from $C_6H_5CO_2H$)	38.6	38.9
3	(as $BaCO_3$ from Br_3CNO_2)	36.9	38.3
	Total	95.7	99.3

[3]*The method of determination of the activity of the nitrile group by difference gave erratic results and was abandoned.*

The results given in Table I for ricinine obtained from plants fed succinic acid-2,3-^{14}C show that the sum of the activities of carbon atoms 2, 3, and 7 (nitrile) and the carbon atoms of the two methyl groups represents 95.7% of the total activity of the ricinine molecule. Thus, within experimental error, all the activity of the ricinine is accounted for when the plants are fed succinic acid-2,3-^{14}C. Moreover, both carbon atoms 2 and 3 are approximately equally labelled as would be expected if they were derived from carbons 3 and 2 respectively of succinic acid-2,3-^{14}C. The nitrile carbon of ricinine is derived from carbon 1 of succinic acid. This carbon becomes labelled as a result of randomization of activity in the Krebs cycle.

Feeding of sodium acetate-2-^{14}C to *Ricinus* plants gave rise to ricinine labelled similarly to that obtained from succinic acid-2,3-^{14}C. The results (see Table I) may be explained by assuming that the acetate-2-^{14}C enters the Krebs cycle with the subsequent formation of succinic acid-2,3-^{14}C. Strong experimental evidence is thus provided to support the proposal that succinic acid or a closely related four-carbon dicarboxylic acid found in the Krebs cycle is an intermediate in the biosynthesis of ricinine.

Recently, Waller and Henderson (6) have reported that most of the activity in ricinine obtained from young *Ricinus* plants fed succinate-1,4-^{14}C was located on the nitrile carbon. This is in agreement with the present observations, since the activity of carboxyl-labelled succinate will not be randomized amongst carbon atoms 2 and 3 (of succinate) as a result of the operation of the Krebs cycle.

The high extent of incorporation of such compounds as nicotinic acid and nicotinamide (7) into ricinine suggests that these compounds are closer to ricinine than succinic acid in the biosynthetic pathway. The results obtained with ricinine may well be applicable to the pyridine ring of such compounds as nicotine and the related tobacco alkaloid anabasine, since nicotinic acid has been shown (8) to be an important intermediate in the biosynthesis of nicotine. Ricinine (1) and nicotine (9, 10) isolated from the plants after feeding acetate-1-^{14}C as well as acetate-2-^{14}C to *Ricinus* and *Nicotiana* plants, respectively, show labelling patterns which are compatible with the conclusion that succinic acid (or a closely related four-carbon dicarboxylic acid) is a common precursor of the intermediate nicotinic acid.

EXPERIMENTAL

Melting points were determined on a Kofler block and are corrected. Radioactive samples were counted as thin layers on aluminum planchets in either a Radiation Counter Laboratories Inc. internal sample proportional counter or a Baird-Atomic, Inc. end window proportional counter, as indicated in the text. Appropriate corrections were made for background count and sample self-absorption. Succinic acid-2,3-^{14}C and sodium acetate-2-^{14}C were supplied by Merck and Company Ltd., Montreal.

Growth of Ricinus Plants and Administration of the Tracers

Seeds of *R. communis* L., after removal of the outer shells, were planted just beneath the surface of moist sand contained in glass trays placed in a dark cabinet in a greenhouse kept at 20–25°. The sand was kept moist with distilled water. After 12 days the trays were brought out into the light for about 16 hours each day, and the sand kept moist with an inorganic nutrient solution containing $MgSO_4.7H_2O$ (0.85 g), KH_2PO_4 (0.14 g), $NH_4H_2PO_4$ (0.071 g), KNO_3 (0.072 g), $Ca(NO_3)_2.4H_2O$ (0.21 g), $Fe(NH_4)_2(SO_4)_2.6H_2O$ (0.036 g) per liter of distilled water. On the 22nd day of growth, when the plants had reached a height of 15–20 cm, and when the primary leaves were just emerging, an aqueous solution (total 1.0 ml) of succinic acid-2,3-^{14}C (0.85 mg) was introduced into 56 plants by means of glass capillary tubes (partly filled with the solution by capillary rise) inserted into the base of each plant stem. Uptake of the solution by each plant was usually complete within a few minutes. The succinic acid-2,3-^{14}C fed had a total activity of 9.1×10^7 d.p.m. measured on the Radiation Counter Laboratories instrument.

In a like manner an aqueous solution (0.7 ml) of sodium acetate-2-^{14}C (6.05 mg) was fed to 42 *Ricinus* plants grown under conditions similar to those described for the succinic acid feeding experiment. The acetate-2-^{14}C fed had a total activity of 3.58×10^8 d.p.m. (Radiation Counter Laboratories instrument).

Can. J. Chem. Downloaded from www.nrcresearchpress.com by 210.87.254.42 on 09/05/12
For personal use only.

Isolation of Ricinine

The tubes were left in the stems until the plants were harvested 72 hours after insertion. The wet stems and leaves were powdered by grinding in the presence of liquid nitrogen. After evaporation of the nitrogen, the ground material was extracted with absolute ethanol in a Soxhlet extractor for 12 hours. The extract was evaporated, the residue suspended in water and washed with petroleum ether (30–60°), and the aqueous solution extracted continuously for 12 hours with chloroform.

Removal of the solvent from this last extract yielded crystalline ricinine, which was purified to constant count by alternate crystallization from methanol and by sublimation at 180° and 5×10^{-4} mm.

Ricinine (415 mg), m.p. 202° (11), with radioactivity of 8000 d.p.m./mg (Radiation Counter Laboratories instrument, previously reported (1) in c.p.m./mg) was obtained from plants fed succinic acid-2,3-^{14}C, which represents an incorporation of 3.6%.

The plants fed acetate-2-^{14}C gave ricinine (353 mg), m.p. 202°, with activity of 65,000 d.p.m./mg (Radiation Counter Laboratories instrument, previously reported (1) in c.p.m./mg), which represents an incorporation of 6.6%.

Degradations of Ricinine from the Succinic Acid-2,3-^{14}C Feeding Experiment

Activities of the OMe and NMe Groups

Active ricinine (52.28 mg) from the succinic acid-2,3-^{14}C feeding experiment (8000 d.p.m./mg) was diluted with pure inactive ricinine (28.1 mg) obtained from *Ricinus* plants not fed any radioactive precursor. The two methyl groups were successively removed by a modification of the Herzig–Meyer method (12). The liberated methyl iodide in each case was trapped in 15% methanolic solutions of trimethylamine and the precipitated tetramethylammonium iodide was crystallized from methanol to constant activity. The tetramethylammonium iodide from the OMe group had an activity of 23.5 d.p.m./mg, and that from the NMe group, 24.8 d.p.m./mg, both measured on the Radiation Counter Laboratories instrument.

Determination of the Activity of the Nitrile Group

Ricinine (5.75 mg) from the feeding experiment was diluted with pure inactive ricinine (ca. 95 mg). The mixture was recrystallized from methanol. A small sample of this diluted ricinine was subjected to combustion and the resulting carbon dioxide collected in a barium hydroxide solution. The barium carbonate thus produced had an activity of 34.2 d.p.m./mg, measured on the Baird-Atomic instrument.

The remainder of the diluted active ricinine was hydrolyzed with dilute aqueous potassium hydroxide to the corresponding hydroxy compound, ricinic acid (II), which was oxidized with chromic acid according to the procedure described by Böttcher (5). The liberated hydrogen cyanide was collected in a solution of silver nitrate acidified with nitric acid. The precipitated silver cyanide (35 mg) had an activity of 77.0 d.p.m./mg (Baird-Atomic instrument).

Dilution of Active Ricinine

All the following experiments were carried out with active ricinine from the succinic acid-2,3-^{14}C feeding which was diluted with pure, inactive ricinine by a factor of approximately 11. The active ricinine was co-crystallized with the inactive sample. A small sample of the diluted ricinine was converted by combustion to carbon dioxide, which was converted to barium carbonate as usual. The barium carbonate, counted on the Baird-Atomic instrument, had an activity of 56.0 d.p.m./mg.

Removal of the Nitrile Group from Ricinine

The diluted ricinine (550 mg) was hydrolyzed and decarboxylated (13) with 57% sulphuric acid solution to 4-methoxy-1-methyl-2-pyridone (350 mg) (III). The product was purified by sublimation at 80° and 5×10^{-4} mm and had m.p. 114–116°.

Reduction of 4-Methoxy-1-methyl-2-pyridone to the Corresponding Piperidone (IV)

A solution of the pyridone (III) (195 mg) in methanol (25 ml) was shaken in an atmosphere of hydrogen with Adams' catalyst at room temperature and under pressure of a small head of mercury, until no further uptake of hydrogen was observed. The 4-methoxy-1-methyl-2-piperidone (IV) was worked up in the usual manner and distilled, b.p. 60–64° at 1 mm. In the ultraviolet the oily product showed end absorption only. Found: C, 58.83; H, 9.29; N, 9.63. Calc. for $C_7H_{13}O_2N$: C, 58.72; H, 9.15; N, 9.78%.

4-Methoxy-1-methyl-2-phenyl-2-piperideine (VI)

Phenyl magnesium bromide was prepared in dry ether (25 ml) in the usual manner using magnesium (400 mg) and bromobenzene (2.62 g). A portion (5 ml) of the ethereal solution of the Grignard reagent was added to 4-methoxy-1-methyl-2-piperidone (170 mg) dissolved in dry ether (6 ml) and the reaction mixture was heated under reflux for 16 hours. The complex was decomposed with dilute hydrochloric acid, the aqueous layer saturated with sodium carbonate, and the mixture shaken. The ether layer was removed and the aqueous layer re-extracted exhaustively with chloroform. The ether and chloroform extracts were combined, the solvents removed, and the residue subjected to a short-path distillation at 12 mm. The fraction distilling at 80–120° (air-bath temperature) was collected. It consisted of a colorless oil that rapidly turned red-brown on exposure to air. The product showed a maximum at 247 mμ (ϵ = 4000) in its ultraviolet absorption spectrum. An infrared spectrum (liquid film) of the product showed no O—H stretching absorption, but contained strong absorption in the 1580–1640 cm^{-1} region, indicative of unsaturation, together with strong C—H deformation bands in the 700–800 cm^{-1} region. The product failed to form either a crystalline hydro-

Can. J. Chem. Downloaded from www.nrcresearchpress.com by 210.87.254.42 on 09/05/12
For personal use only.

chloride or a satisfactory picrate. It was not further characterized, but used immediately in the next step.

Oxidation of the Piperideine (VI) to Benzoic Acid

The distilled piperideine was heated under reflux with potassium permanganate (2.0 g) in water (40 ml) for 2 hours. Ethanol was added to the cooled mixture to destroy the excess permanganate, and the filtered solution was acidified with concentrated hydrochloric acid. Extraction with ether gave an extract which on evaporation left a solid residue (80 mg). This residue was purified to constant count by crystallization from water and sublimation, after which it consisted of a colorless crystalline product, m.p. 121–122°, either alone or in admixture with an authentic specimen of benzoic acid. Comparison of infrared spectra confirmed the identity. A sample of the active benzoic acid was converted by combustion to carbon dioxide, which by collection in a barium hydroxide solution was obtained as barium carbonate, with an activity of 24.7 d.p.m./mg (Baird-Atomic instrument).

Nitration of 4-Methoxy-1-methyl-2-pyridone

The pyridone (III) (140 mg) was dissolved in concentrated sulphuric acid (1.0 ml) and the solution cooled in an ice-water bath. A solution of fuming nitric acid (0.2 ml) in concentrated sulphuric acid (2.0 ml) was added to the pyridone solution and the mixture allowed to stand at room temperature for 20 minutes. It was neutralized with aqueous sodium hydroxide and extracted several times with chloroform. The 4-methoxy-1-methyl-3-nitro-2-pyridone (VII) produced was purified by recrystallization from benzene, m.p. 172–173°. Found: C, 45.75; H, 4.35; N, 15.39. Calc. for $C_7H_8O_4N_2$: C, 45.65; H, 4.38; N, 15.21%. A nuclear magnetic resonance spectrum (60 Mc) of the product (VII) in $CDCl_3$ using tetramethylsilane as an internal reference showed signals at τ values of 6.48 and 6.08 p.p.m. and two doublets centered at 3.90 and 2.55 p.p.m. with $J = 8.0$ c.p.s. The nitropyridone gradually decomposed when exposed to light.

Preparation of Tribromonitromethane (VIII) from 4-Methoxy-1-methyl-3-nitro-2-pyridone

A paste was prepared from calcium hydroxide (10 g), water (40 ml), both at 0°, and bromine (3.3 ml). The nitropyridone (VII) (150 mg) was well mixed with the paste. The mixture was gently warmed for several minutes, then strongly heated until about 6.0 ml of distillate had been collected. The crude tribromonitromethane (bromopicrin) (200 mg) was separated by centrifuging, washed with distilled water, and distilled over a short path at 12 mm and an air-bath temperature of 60–70°. The distilled product was purified in two batches by gas–liquid chromatography. A 2 m long, 0.635 cm diameter silicone grease column was used at 80°, with the helium carrier gas at a pressure of 25 p.s.i., giving a flow rate of approximately 150-cc/min. A retention time (peak maximum) of about 36 minutes was observed for the bromopicrin. The bromopicrin (70 mg) was collected in a small U-tube cooled with an ice–water mixture. An infrared spectrum of the purified bromopicrin showed absorption in good agreement with reported absorption maxima (14). The spectrum was also superimposable upon a spectrum obtained from bromopicrin prepared from picric acid by a similar procedure (15). Gas–liquid chromatography of a small sample of the purified bromopicrin showed only one component with a retention time almost identical with that obtained for authentic bromopicrin. The pure bromopicrin was converted by combustion to carbon dixoide, which was collected in a barium hydroxide solution as barium carbonate. The barium carbonate had an activity of 165.5 d.p.m./mg (Baird-Atomic instrument).

Degradations of Ricinine Obtained from the Acetate-2-^{14}C Feeding Experiment

Activities of the OMe and NMe Groups

The O-methyl and N-methyl groups were isolated as described for ricinine from the succinic acid-2,3-^{14}C feeding experiment. The active ricinine (30.4 mg) was first diluted with pure inactive ricinine (48.6 mg). The tetramethylammonium iodide from the OMe group had an activity of 135.0 d.p.m./mg and that from the NMe group, 132.5 d.p.m./mg, both measured on the Radiation Counter Laboratories instrument.

Determination of the Activity of the Nitrile Group

Ricinine (29.2 mg) from the feeding experiment was diluted with pure inactive ricinine (83.5 mg). The nitrile group was isolated as silver cyanide as before. The silver cyanide had an activity of 4300.0 d.p.m./mg (Radiation Counter Laboratories instrument).

Degradations to Isolate Carbon Atoms 2 and 3

Active ricinine was diluted approximately 20 times by the usual method. A small sample of the diluted ricinine was converted by combustion to carbon dioxide and collected as barium carbonate, which had an activity of 229.0 d.p.m./mg (Baird-Atomic Instrument).

By methods outlined in Fig. 1 and described above, carbon atoms 2 and 3 were isolated as the carboxyl group of benzoic acid and as bromopicrin respectively. Both derivatives were converted by combustion to carbon dioxide, which was collected in a barium hydroxide solution as barium carbonate. The barium carbonate from C-2 had an activity of 71.7 d.p.m./mg, and that from C-3, 701.0 d.p.m./mg (Baird-Atomic instrument).

ACKNOWLEDGMENTS

The authors thank Mr. M. Lesage for running the gas–liquid chromatograms and Mr. H. Seguin for the microanalyses and sample combustions.

Can. J. Chem. Downloaded from www.nrcresearchpress.com by 210.87.254.42 on 09/05/12
For personal use only.

REFERENCES

1. P. F. JUBY and L. MARION. Biochem. Biophys. Res. Commun. **5**, 461 (1961).
2. T. GRIFFITH. K. P. HELLMAN, and R. U. BYERRUM. J. Biol. Chem. **235**, 800 (1960).
3. G. R. WALLER and L. M. HENDERSON. Biochem. Biophys. Res. Commun. **5**, 5 (1961).
4. H. WERBIN and C. HOLOWAY. J. Biol. Chem. **223**, 651 (1956).
5. B. BÖTTCHER. Ber. **51**, 673 (1918).
6. G. R. WALLER and L. M. HENDERSON. Biochem. Biophys. Res. Commun. **6**, 398 (1961).
7. G. R. WALLER and L. M. HENDERSON. J. Biol. Chem. **236**, 1186 (1961).
8. R. F. DAWSON, D. R. CHRISTMAN, A. F. D'ADAMO, M. L. SOLT, and A. P. WOLF. J. Am. Chem. Soc. **82**, 2628 (1960).
9. T. GRIFFITH and R. U. BYERRUM. Science, **129**, 1485 (1959).
10. T. GRIFFITH, K. P. HELLMAN, and R. U. BYERRUM. Biochemistry, **1**, 336 (1962).
11. E. C. TAYLOR and A. J. CROVETTI. J. Am. Chem. Soc. **78**, 214 (1956).
12. F. PREGL. Quantitative organic microanalysis. 4th ed. Blakiston Co., Philadelphia. 1945. p. 156.
13. E. WINTERSTEIN, J. KELLER, and A. B. WEINHAGEN. Arch. Pharm. **255**, 513 (1917).
14. J. MASON, J. BANUS, and J. DUNDERDALE. J. Chem. Soc. 759 (1956).
15. J. BADDILEY, G. EHRENSVÄRD, E. KLEIN, L. REIO, and E. SALUSTE. J. Biol. Chem. **183**, 777 (1950).

Can. J. Chem. Downloaded from www.nrcresearchpress.com by 210.87.254.42 on 09/05/12
For personal use only.

THE S^{32} (n,p) P^{32} REACTION AS A FAST-NEUTRON FLUX MONITOR[1]

D. C. SANTRY AND J. P. BUTLER
Research Chemistry Branch, Atomic Energy of Canada Limited, Chalk River, Ontario
Received August 24, 1962

ABSTRACT

An extensive study is made of the use of sulphur as a monitor for neutrons with energies from 2 to 20 Mev. Irradiated disks of pressed sulphur are burnt before counting to increase the efficiency and reproducibility of determining the P^{32} activity. It was established that on burning irradiated sulphur 95.5±0.5% of the P^{32} activity is retained with a reproducibility of ±1.0%. Measurements of relative cross sections for the S^{32} (n,p) P^{32} reaction have been extended to 20.3 Mev using the T (d,n) He^4 and D (d,n) He^3 reactions to produce monoenergetic neutrons. Neutron production using Zr–T targets is examined as is the effect of extraneous neutrons from the D (d,np) D process on the S^{32} (n,p) reaction.

INTRODUCTION

By counting the 1.71 Mev beta particles from P^{32} (half-life 14.22 days) the S^{32} (n,p) P^{32} reaction may be used as a standard to monitor a high-energy neutron flux. It is suitable for the measurement of either a continuous neutron spectrum, as in a nuclear reactor, or for the measurement of a monoenergetic-neutron flux. Reactor cross-section values for the sulphur reaction have been summarized by Mellish (1). He has used the reaction to normalize and compare other fast-reactor cross sections which had been measured by different investigators. Allen *et al.* (2) have measured the cross section for the S^{32} (n,p) reaction as a function of neutron energy from 1.59 to 9.56 Mev and from 13.38 to 14.95 Mev. In addition to having its cross section well established, various techniques have been developed by Reinhardt and Davis (3), Fujita *et al.* (4), and Parker (5) for using the sulphur reaction for fast-neutron dosimetry.

We have been using sulphur as a monitor in measuring excitation curves for fast-neutron reactions (6), and in this paper describe a study of this convenient method for fast-neutron monitoring. The procedures for sample preparation and activity measurements are given. In addition, we have extended the measurements of the S^{32} (n,p) cross section to 20.3 Mev.

EXPERIMENTAL AND RESULTS

A. Monitor Material

For the monitor we have chosen elemental sulphur in the form "flowers of sulphur". It is readily available, inexpensive, and relatively pure. Any impurities which may be present appear to have low activation cross sections. Powdered sulphur has been pressed into disks of known and reproducible area with diameters of 3/16 in. to 1 1/8 in. using a briquetting[2] or disk[3] press. Disks of a desired thickness can be rapidly produced by packing powdered sulphur into a short hollow tube of a predetermined volume, then tapping it out into the press. Under pressure sulphur packs into firm disks and requires no extraneous binding agent. Disks thicker than 0.015 in. do not powder or crack under normal handling and irradiation conditions. We use a pressure of 25 tons/in^2 and produce 0.040-in. disks 3/16 in. in diameter, which weigh about 34 mg. The relatively small size of the disks enables one to determine a flux more accurately in a position where flux gradients exist.

B. Irradiations

Sulphur was irradiated with neutrons produced with an accelerator using the (D + D) and (D + T) reactions. The spread in energy of neutrons produced in this manner depends on the angle the sample subtends at the neutron source. By using samples with a small diameter and irradiating at a distance, the angle

[1]*Issued as A.E.C.L. No. 1648.*
[2]*Applied Research Lab (Glendale, Calif.).*
[3]*Research & Industrial Inst. Co. (London, England).*

Can. J. Chem. Downloaded from www.nrcresearchpress.com by 210.87.254.5 on 09/05/12
For personal use only.

subtended can be made small. Consequently, the sulphur was irradiated with essentially a monoenergetic flux of fast neutrons of known energy.

Irradiations were also carried out in the Chalk River NRX reactor in positions which had a fast-neutron contribution.

In all irradiations thin aluminum foil served to protect the sulphur disks from contamination during irradiations. For reactor irradiations several samples were also enclosed in 0.030-in. cadmium foil to reduce the effect of thermal neutrons.

C. Counting and Calibration

Using a technique suggested by Reinhardt and Davis (3), the sulphur disks, after an irradiation, were weighed and placed on suitable aluminum counting trays. The trays were then placed on a hot plate heated to 370° C. The sulphur melts, self-ignites, and burns off, leaving the P^{32} activity behind on the tray as a weightless source. This burning method has several desirable features: (i) it increases the counting efficiency of P^{32}, (ii) it removes any S^{35} which may have formed as a contaminating activity by the (n,γ) reaction on sulphur, (iii) it eliminates discrepancies which might arise from variations in the thickness and surface texture of the samples, and (iv) by producing a thin source, it permits an easy standardization of a counting system for the absolute counting of the P^{32} activity produced.

In our work an end-window beta proportional counter was used with an aluminum window of 1 1/2-in. diameter and 0.00075-in. thickness. Samples were positioned very near the counter window. Under these conditions the efficiency for counting a weightless source of P^{32} was 51.5%. This was measured by counting high specific activity P^{32} which had been standardized by 4π-absolute beta counting.

D. Examination of the Method

1. It was necessary to determine if any P^{32} activity was lost in the burning of sulphur. Samples which had been irradiated in a uniform flux were weighed and counted as disks. After burning, the samples were recounted as thin sources. The ratio of [residual activity after burning] to [activity of disks] is plotted against the [weight of disk] as curve A in Fig. 1. An extrapolation of this linear curve to zero weight indicates that 93% of the P^{32} activity remains after burning. This is in agreement with measurements made by other investigators (3, 5) who used much thicker samples. Curve B in Fig. 1 shows the same measurements made

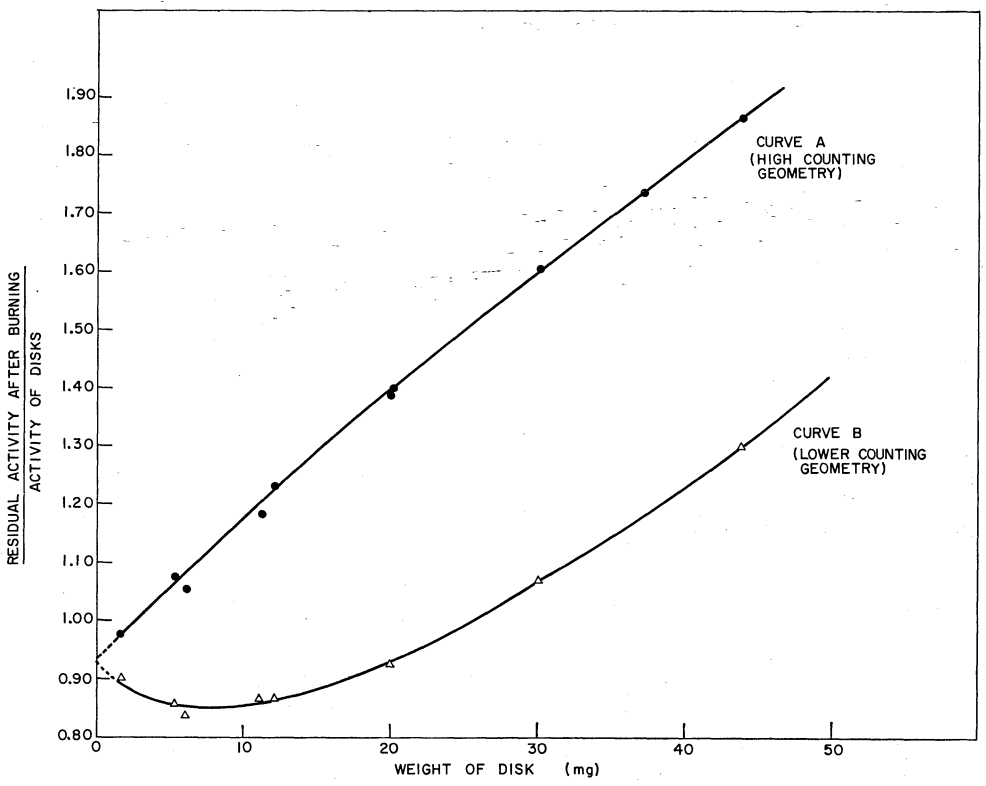

FIG. 1. Variation in the ratio of observed P^{32} activity in burnt and unburnt samples with sample weight (3/16 in. diam. sulphur disks).

Can. J. Chem. Downloaded from www.nrcresearchpress.com by 210.87.254.5 on 09/05/12
For personal use only.

at lower counting geometry. The curve is not linear at low sample weight. The initial increase in counting efficiency of a disk with increasing weight, which reduces the ratio, is due to self-scattering effects (7). For thin wide sources there is an enhanced scattering of beta particles out of the sample plane and into the counter. At greater thicknesses self-absorption predominates and the standard absorption curve is observed. Although self-scattering is more noticeable at low counting geometry with a window-type detector, it may also exist at higher geometry. Because of this, the extrapolation over the region where thin disks cannot be prepared may not be exact. A further check on the retention of P^{32} on burning was made by irradiating simultaneously disks of sulphur and Li_2SO_4 in a uniform flux. The Li_2SO_4 was dissolved in 0.05 N nitric acid containing phosphate carrier. The P^{32} activity was determined by 4π-absolute beta counting. This activity when compared with the P^{32} activity from the burnt sulphur disks indicated a value of $95.5\pm0.5\%$ retention (the average of four separate determinations). On the basis of this value and the unburnt activity measurements, an efficiency curve is drawn in Fig. 2 for counting P^{32} in sulphur disks. Included in the

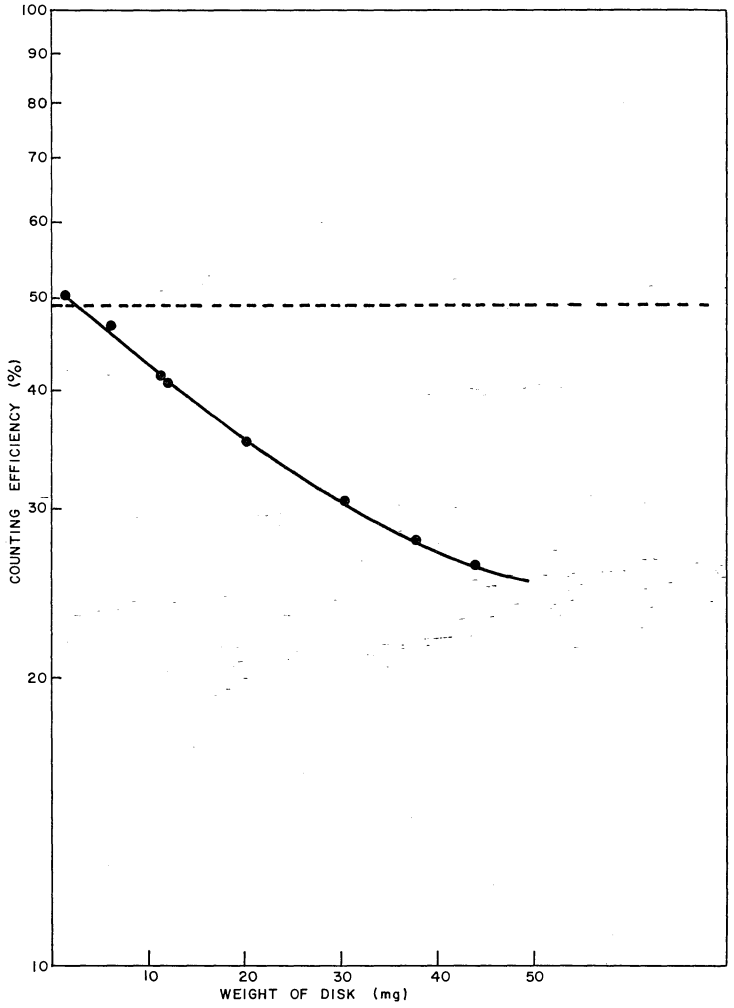

FIG. 2. Counting efficiency of P^{32} for irradiated sulphur disks 3/16-in. diam. —— disks, - - - burnt samples.

graph is the efficiency curve for counting burnt samples, i.e. $(51.5\times0.955)\%$. The difference between the two curves represents the gain in counting efficiency using the burning technique.

2. To test the reproducibility of the burning process samples of different diameters and thicknesses were irradiated in a uniform flux, burnt, and counted. After 2 minutes of heating, burning was complete. Further heating had no effect on the remaining activity. The counting rate per mg of sulphur irradiated was constant

Can. J. Chem. Downloaded from www.nrcresearchpress.com by 210.87.254.5 on 09/05/12
For personal use only.

to within a standard deviation of ±1.0%. A thin dark residue which remains after the sulphur is burnt does not interfere with the P^{32} determination. To check this a thin P^{32} source was deposited on an aluminum tray and counted. Then a sulphur disk was placed over the source and burnt. No change in activity of the sample was observed. Larger sulphur samples when burnt and reweighed indicated that an average source was less than 2 $\mu g/cm^2$, i.e., essentially weightless.

3. Since elemental sulphur melts at about 110° C it cannot be used in a high-temperature region of a nuclear reactor. For such positions we have irradiated pressed disks of $Li_2SO_4.H_2O$ encased in cadmium. The hydrate appeared to press better than the anhydrous salt. Since there may be partial conversion of the hydrate at reactor temperatures it was necessary to complete the conversion by heating the disks after an irradiation to 150° C for at least 1 hour. The samples were then weighed to determine the amount of sulphate irradiated. As mentioned previously, the disks were dissolved in a known amount of dilute acid and a suitable aliquot deposited on a counting tray as a weightless source. The reduced counting efficiency of this sulphur compound is partially offset by the higher fast-neutron flux associated with a high-temperature position in a reactor. Lithium sulphate when pressed into disks is not as robust as are elemental sulphur disks.

4. Irradiated sulphur was analyzed for impurities by following its radioactive decay. Samples counted immediately after an irradiation show some short-lived impurities, the most important of which is the 2.62-hour Si^{31} formed by the S^{34} (n,α) Si^{31} reaction. Allowing the samples to decay for at least 1 day eliminates these activities. Irradiated samples when counted as disks or burnt samples decay with a half-life of 14.2 days, indicating that only P^{32} activity is present. However, when sulphur is irradiated in the presence of a high thermal-neutron flux (not encased in cadmium), 87-day S^{35} is observed. It constitutes a small percentage of the net activity in a sulphur disk at the end of an irradiation. From decay analysis it is possible to apply the small correction for this impurity. The burning of the sulphur sample before counting effectively removes this contaminant. Due to the low isotopic abundance of S^{33} and its low counting efficiency, 25-day P^{33} is not observed.

E. Cross-Section Measurements

To use the S^{32} (n,p) P^{32} reaction as a flux monitor, it is desirable to have a complete curve of cross section vs. neutron energy. However, from 9.56 to 13.38 Mev and above 14.95 Mev neutron energies there are no cross-section data available.

By using the differential cross-section data for the D (d,n) He^3 and T (d,n) He^4 reactions we were able to complete the S^{32} (n,p) cross-section curve up to 20.3 Mev.

The energy and intensity of neutrons produced with an accelerator depend on the angle at which the neutrons are emitted relative to the incident deuteron beam. Consequently, the saturation activity S_1 produced in a sulphur monitor irradiated at a given angle, i.e. at an energy En_1, is given by

$$S_1 = N_1\phi_1\sigma_1.$$

Another monitor S_2 irradiated at a different angle, i.e. at an energy En_2, is given by

$$S_2 = N_2\phi_2\sigma_2.$$

N_1 and N_2 are the number of S^{32} atoms irradiated at each angle, ϕ_1 and ϕ_2 are the neutron fluxes, σ_1 and σ_2 are the cross-section values for the sulphur (n,p) reaction at the neutron energies En_1 and En_2 respectively. By irradiating the sulphur monitors simultaneously at two different angles, we can combine the above equations. Thus,

$$\sigma_2 = \frac{S_2N_1}{S_1N_2}\frac{\phi_1}{\phi_2}\sigma_1.$$

That is, the cross section at one energy can be expressed relative to a previously measured cross section at another energy.

Cross sections were measured at 10.40, 11.00, and 11.60 Mev using the D (d,n) He^3 reaction. The irradiation conditions were similar to those described previously (6). A gas target 1.6 cm in diameter and 1.27 cm in length was filled to a pressure of 225 cm of Hg with deuterium gas (>99.5% D_2). The deuteron beam from a Tandem Van de Graaff Accelerator enters the gas cell through a 0.00025-in. tantalum window and after traversing the cell is stopped in a gold end plate. Sulphur disks of 1/2-in. diameter and 0.060-in. thickness were irradiated at 0° and 55° on both sides of the axis of the deuteron beam. The disks were accurately positioned 12.2 cm from the end of the gas cell and subtended a half angle of 2.9° at the point of origin of neutrons. The deuteron energy was chosen to produce neutrons in the forward direction at an energy where the sulphur (n,p) cross section was not known. At 55° the corresponding neutrons were produced at energies where the cross section had been measured previously (2). The energies involved are listed in Table I together with the values of the relative neutron intensities as listed by Brolley and Fowler (8). Corrections were applied to the P^{32} activities for the presence of extraneous neutrons (see Table II). Background neutrons at both angles were determined by counting the P^{32} activity obtained in irradiations with the gas cell evacuated. The effect of breakup neutrons produced by the D (d,np) D reaction was calculated from the cross-section and angular distribution measurements of Cranberg *et al.* (9) and Anderson *et al.* (10). A more

Can. J. Chem. Downloaded from www.nrcresearchpress.com by 210.87.254.5 on 09/05/12
For personal use only.

TABLE I

Neutron intensity ratios for the D (d,n) He^3 reaction

Deuetron energy (Mev)	Neutron energy (Mev)		Intensity (55°/0°)
	0° *	55°	
7.25±0.04	10.40	7.18	0.0912
7.88±0.04	11.00	7.53	0.0891
8.51±0.03	11.60	7.88	0.0867

*An effective angle of 2° was used.

TABLE II

Typical corrections applied to the P^{32} activity for extraneous neutrons

Deuteron energy (Mev)	Angle (deg)	Neutron energy (Mev)	% correction	
			Background neutrons	Breakup neutrons
D (d,n) He^3 reaction				
7.25	0	10.40	2.6	7.3
	55	7.18	9.2	—
7.88	0	11.00	4.2	15.0
	55	7.53	15.7	—
8.51	0	11.60	2.0	25.8
	55	7.88	12.4	—
T (d,n) He^4 reaction				
3.70	0	20.3	13.7	—
	25	19.8	7.9	—
	50	18.5	7.7	—
	75	16.6	6.5	—
	105	14.42	3.3	—
	140	12.53	1.3	—

detailed discussion of these corrections is included in Section G of this paper. Irradiations were performed away from the floor and walls so that the effect of scattered neutrons on the sulphur could be considered small.

For cross-section measurements above 12 Mev, neutrons were produced using the T (d,n) He^4 reaction. This irradiation assembly was also described in a previous paper (6). Zirconium–tritium targets (1.2 cm^3/cm^2 of tritium at NTP) were bombarded with 125 kev deuterons from a Texas Nuclear Neutron Generator, and with 4.00 Mev deuterons from the tandem accelerator. Sulphur disks of 3/16-in. diameter and 0.040-in. thickness were irradiated at angles of 25°, 50°, 75°, 105°, and 140° on both sides of the axis of the deuteron beam and at 0°. The sulphur disks were 1.4 cm from the target and subtended a half angle of 9°. Monoenergetic neutrons from 13.58 to 14.76 Mev were obtained using 125 kev deuterons. The energies and relative neutron intensity values used (11, 12) are listed in Table III. These irradiations were normalized

TABLE III

Relative neutron intensities for the T (d,n) He^4 reaction

Angle (deg)	125 kev deuterons		3.70±0.20 Mev deuterons	
	Neutron energy (Mev)	Relative neutron intensity	Neutron energy (Mev)	Relative neutron intensity
0*	14.76	1.000	20.3	1.000
25	14.68	0.995	19.8	0.738
50	14.50	0.983	18.5	0.466
75	14.24	0.965	16.6	0.316
105	13.89	0.941	14.42	0.267
140	13.58	0.918	12.53	0.309

*An effective angle of 6.8° was used.

Can. J. Chem. Downloaded from www.nrcresearchpress.com by 210.87.254.5 on 09/05/12
For personal use only.

at 14.50 Mev to the cross-section value for the sulphur (n,p) reaction as measured by Allen *et al.* (2). No corrections for background or breakup neutrons were required.

Monoenergetic neutrons of energies from 12.53 to 20.3 Mev (Table III) were produced using the T (d,n) He^4 reaction and a 4.00 Mev deuteron beam. Again the data were normalized at 14.50 Mev to the sulphur cross-section data. Sulphur samples were irradiated using Zr targets containing no tritium to measure the background contribution at various angles (see Table II). Corrections for breakup neutrons were negligible.

The results for the cross sections measured and the values to which they were normalized are listed in Table IV. The cross-section values are plotted in Fig. 3 together with the data of Allen *et al.* (2). Our measure-

TABLE IV

S^{32} (n,p) P^{32} cross-section data

Neutron source	En (Mev)	Cross section (millibarns)
D (d,n) He^3	7.18±0.48	339*
	7.53±0.51	342*
	7.88±0.54	345*
	10.40±0.05	422±25
	11.00±0.04	371±22
	11.60±0.04	422±24
T (d,n) He^4	12.53±0.26	324±15
	12.6±0.5	321±15
	13.58±0.06	277±6
	13.89±0.08	263±6
	14.24±0.08	235±5
	14.50±0.06	226*
	14.68±0.06	219±5
	14.76±0.06	216±5
	16.6±0.6	130±6
	17.5±1.0	123±6
	18.5±0.5	95±4
	19.2±0.8	88±7
	19.8±0.3	87±5
	20.3±0.3	68±5

*Cross-section values used for normalization (2).

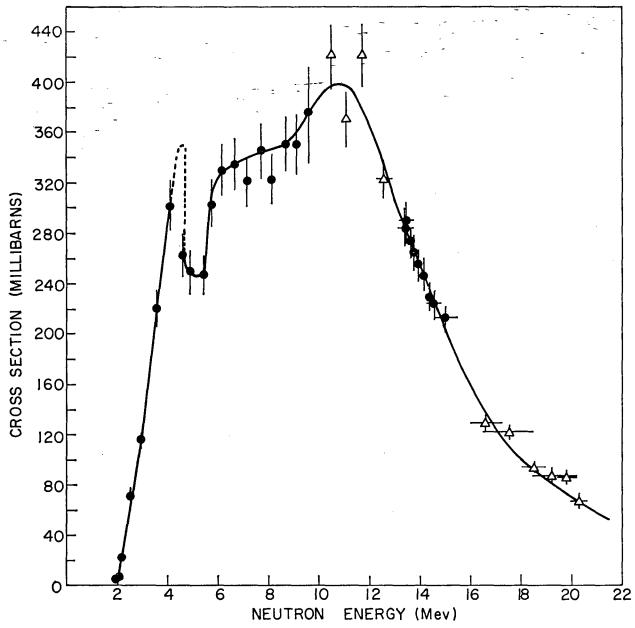

FIG. 3. S^{32} (n,p) P^{32} cross section versus neutron energy. ● Allen *et al.* (2), △ this work.

Can. J. Chem. Downloaded from www.nrcresearchpress.com by 210.87.254.5 on 09/05/12
For personal use only.

ments from 13.58 to 14.76 Mev have not been included in Fig. 3. They confirm the shape of the cross-section curve in this region as that given by Allen. The values we measured at 10.4, 11.0, and 11.6 Mev do not fall on a smooth curve. The measurements were reproducible and may indicate either discontinuities in the excitation curve similar to that observed at 4.5 Mev or incorrect angular distribution data upon which the determinations were based. The values at the three energies were averaged together and the curve drawn through an average value in this region.

The errors in the cross-section values include:

(*a*) standard deviation in the observed counting rates (1 to 3%);
(*b*) corrections for activity produced by extraneous neutrons (up to 5%);
(*c*) burning of sulphur disks (1.4%);
(*d*) irradiation geometry (2%);
(*e*) relative flux intensity values (1% for 125 kev deuteron irradiations and 3.5 to 5% for the others).

The error in the cross-section values listed in Table IV is the root-mean-square deviation and does not include any error in the sulphur cross-section value to which the data were normalized. The neutron energies given are average values and the spread in energy represents the error in energy as seen by the sulphur samples.

F. An Examination of Neutron Production Using Zr–T Targets

Since the energies of neutrons emitted and the relative neutron intensity values depend on the effective deuteron bombarding energy, it is important to know the thickness of the Zr–T layer. The targets supplied[4] were listed as having about 9 mg/cm² of zirconium metal. While this thickness can be measured optically, as described below, it cannot be assumed that the tritium is distributed uniformly throughout the zirconium. As a check on the calculated value of the effective deuteron energy for these Zr–T targets, neutron spectra were measured as a function of angle for targets irradiated with 4.00 Mev deuterons. A 1-in.×1-in. plastic scintillator of polyvinyltoluene was used as a neutron detector. This technique has been described by Swartz and Owen (13) and Cross (14). The energy of recoiling protons produced in the scintillator by neutrons was analyzed on a 100-channel pulse-height analyzer. From the pulse-height spectra measured at various angles, relative neutron energies were obtained. The neutron energy scale was normalized at 14.42 Mev by viewing neutrons emitted at an angle of 105° to the incident deuteron beam. At this angle the neutron energy is insensitive to the energy of the bombarding deuterons over the energy range expected, as seen in Table V.

TABLE V

Deuteron energy (Mev)	Neutron energy at 105° (Mev)
3.00	14.26
3.50	14.38
4.00	14.50

Values for the relative neutron intensities were also determined from the spectra. The results are given in Tables VI and VII for two Zr–T targets. The calculated neutron energies were from the tables of Fowler

TABLE VI

Neutron energies (Mev) for Zr–T targets

	Target A (9.8 mg/cm² of Zr) (average deuteron energy = 3.62±0.25 Mev)		Target B (7.8 mg/cm² of Zr) (average deuteron energy = 3.70±0.20 Mev)		En calc. for Ed (assumed) = 2.75
Angle (deg)	En calc.	En obs.	En calc.	En obs.	
0*	20.3	20.7	20.4	19.2	19.2
50	18.5	18.4	18.5	17.2	17.5
105	14.4	14.4	14.4	14.1	14.1
140	12.5	12.6	12.5	12.7	12.6

*A effective angle of 1.8° was used.

and Brolley (15) and the intensities were from Bame and Perry (11). The thickness of zirconium and the rate of energy loss of deuterons in zirconium were used to determine the average deuteron energy. The

[4]*Radiochemical Centre, Amersham, Bucks, England.*

Can. J. Chem. Downloaded from www.nrcresearchpress.com by 210.87.254.5 on 09/05/12
For personal use only.

TABLE VII

Relative angular neutron intensities for Zr–T targets

Angle (deg)	Target A		Target B	
	Calculated intensity	Observed intensity	Observed intensity	Calculated for Ed = 2.75 Mev
0*	1.000	1.00	1.00	1.00
50	0.450	0.47	0.66	0.61
105	0.260	0.25	0.42	0.40
140	0.300	0.29	0.37	0.39

*An effective angle of 1.8° was used.

calculated and observed neutron energies and intensities for target A are in excellent agreement, but not so for target B. In the last column of Tables VI and VII are the values calculated for target B if the average deuteron energy was 2.75 Mev. The agreement here implies that the deuteron beam was striking a section of the target which was about four times thicker than expected. Such a thick source gives a greater spread in energy of the deuterons, and hence a greater spread in the neutron energy at a particular angle, with the exception of the back angles 105° and 140°. Photomicrographs of traverse sections cut through the center of several sources showed many to have unevenly deposited zirconium. Source B discussed above did appear to be three times thicker than source A when measured optically. In all sources there appeared to have occurred an interaction between the zirconium layer and the tungsten substrate. This has the effect of altering the rate of energy loss of deuterons in the target material. Variations in thickness and composition of these Zr–T targets have little effect on neutron production for very low energy (<300 kev) deuteron irradiations, but for higher deuteron energies, where one must calculate the effective deuteron energy producing neutrons, caution should be exercised. At present we still use these sources since they have the highest tritium content of any solid targets on the market and do not involve the health hazard associated with using tritium gas under pressure in a cell.

G. Corrections for the D (d,np) D Reaction

A source of monoenergetic neutrons for energies greater than 2.5 Mev is the D (*d,n*) He^3 reaction. However, for neutrons above 7.7 Mev there is associated with the monoenergetic group a continuum of neutrons produced by the D (*d,np*) D or breakup reaction. Sulphur used to monitor neutrons produced by the D + D process will also be activated by the presence of these breakup neutrons. Since there is no other source of monoenergetic neutrons with energies in the region of 8.0 to 12.5 Mev, calculations have been made for a breakup correction required when using the S^{32} (*n,p*) P^{32} reaction as a neutron monitor.

The data of Cranberg *et al.* (9) and Anderson *et al.* (10) were used to calculate the relative amounts of P^{32} activity produced at a given deuteron energy from the D (*d,n*) He^3 and D (*d,np*) D reactions. For both reactions the activity produced is proportional to the product of the sulphur (*n,p*) cross section and the neutron intensity. Since the neutron intensity is proportional to the cross section for neutron production, an effective cross section, $\hat{\sigma}_{S(n,p)}$, for the reaction of breakup neutrons on sulphur can be calculated from the following equation

$$\hat{\sigma}_{S(n,p)} = \frac{\int_{0.95\ \mathrm{Mev}}^{E_{max}} \sigma_{S(n,p)}\sigma_{D(d,np)}dE}{\int_{0.95\ \mathrm{Mev}}^{E_{max}} \sigma_{D(d,np)}dE},$$

where $\sigma_{S(n,p)}$ is the cross section for the sulphur (*n,p*) reaction and $\sigma_{D(d,np)}$ is the cross section for producing breakup neutrons of a given energy *E*. Both of these cross sections are energy dependent. The integral extends from the calculated maximum neutron energy in the spectrum down to 0.95 Mev, where $\sigma_{S(n,p)}$ is zero. Values for $\hat{\sigma}_{S(n,p)}$ and the various quantities used in the equation are given in Table VIII. Also listed in the last column of the same table are values for

$$\frac{\hat{\sigma}_{S(n,p)} \int \sigma_{D(d,np)}dE \times 100}{\hat{\sigma}_{S(n,p)} \int \sigma_{D(d,np)}dE + \sigma_{S(n,p)}\sigma_{D(d,n)}}.$$

This is the percentage correction that must be applied to the observed P^{32} activity to account for breakup neutrons when using sulphur to monitor neutrons from the D + D reaction. The term $\int \sigma_{D(d,np)}dE$ is the denominator of the preceding equation and expresses the total number of neutrons of all energies in the spectrum, and $\sigma_{D(d,n)}$ is the cross section for monoenergetic neutron production. The percentage corrections are plotted against deuteron energy in Fig. 4 and have an estimated error of ±5%.

To test the calculated corrections, the Al^{27} (*n,α*) Na^{24} cross section was measured at 13.6 Mev with sulphur as a flux monitor (16). Neutrons of this energy were produced in two different ways. In one case, the

Can. J. Chem. Downloaded from www.nrcresearchpress.com by 210.87.254.5 on 09/05/12
For personal use only.

Can. J. Chem. Downloaded from www.nrcresearchpress.com by 210.87.254.5 on 09/05/12
For personal use only.

TABLE VIII

The effect of breakup neutrons on the S^{32} (n,p) P^{32} reaction

Monoenergetic neutrons				Breakup neutrons			
Deuteron energy (Mev)	Neutron energy (Mev)	D (d,n) He^3 0° cross section (millibarns/sterad)	S^{32} (n,p) P^{32} cross section (millibarns)	Max. neutron energy (Mev)	D (d,np) D 0° integrated cross section (millibarns/sterad)	S^{32} (n,p) P^{32} effective cross section (millibarns)	Correction at 0° (%)
5.78	8.99	76.6	352	2.4	5.4	7.35	0.15
6.31	9.49	80.0	356	2.98	12.9	35.3	1.57
6.80	9.98	82.8	360	3.47	19.8	52.5	3.37
7.16	10.30	84.8	358	3.80	30.2	78.2	7.22
7.33	10.49	85.7	356	4.00	32.0	834	8.05
8.90	11.99	91	342	5.57	68.0	226	33.0
11.75	14.63	97	222	8.55	160.	296	68.8

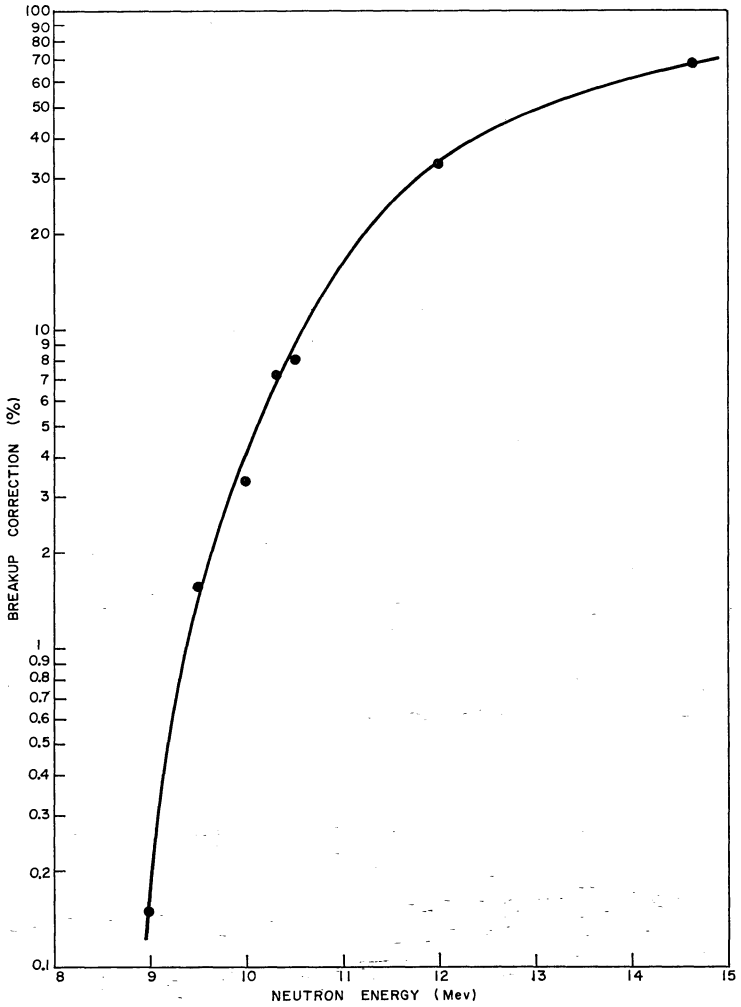

FIG. 4. Breakup correction applied to the P^{32} activity when using sulphur to monitor D + D neutrons emitted at zero degrees.

D (d,n) He^3 reaction was used with samples placed at 0° to a 10.6-Mev deuteron beam. Calculated corrections applied to the observed activities in sulphur and aluminum samples to account for breakup neutrons were 57% and 0.9% respectively. The measured Al^{27} (n,α) Na^{24} cross section was 123 ± 9 millibarns. In the other case, 125 kev deuterons and the T (d,n) He^4 reaction were used with samples placed at 140°. No breakup corrections were required. This time a measured cross section for the Al^{27} (n,α) reaction was 127 ± 5 millibarns.[5] The confirmation of the breakup correction at this energy gives one confidence in applying the correction at lower energies where sulphur was used as a monitor.

DISCUSSION

The use of sulphur for monitoring high-energy neutrons appears to be satisfactory. The ease with which the irradiated material can be converted to a form which can be counted efficiently without involving chemical separations and purification make it ideal for routine monitoring. The half-life of the product is a good compromise. It is long enough that counting immediately after an irradiation is not necessary and short enough that sufficient activity is produced even with a relatively low neutron flux.

[5] *A recent value of 131±6 millibarns was measured at this energy by Bayhurst and Prestwood (17).*

Can. J. Chem. Downloaded from www.nrcresearchpress.com by 210.87.254.5 on 09/05/12
For personal use only.

The difficulty of determining an absolute cross section makes it necessary to use a monitor and give a measured cross section relative to that of the monitor. Mellish (1) suggested using the sulphur reaction for such a monitor in measuring fast-reactor cross sections and establishing its effective cross-section value as 60 millibarns. We would like to suggest that the sulphur reaction be also used as a standard for comparison when monitoring monoenergetic fast neutrons. For the present, cross-section values taken from a smooth curve through Allen's data and ours could be used. The S^{32} (n,p) cross-section data appear to be reliable since excitation curves for other fast-neutron reactions determined by us, using sulphur as a monitor, are in agreement with measurements monitored in other ways (16).

REFERENCES

1. C. E. MELLISH. Nucleonics, **19**, No. 3, 114 (1961).
2. L. ALLEN, JR., W. A. BIGGERS, R. J. PRESTWOOD, and R. K. SMITH. Phys. Rev. **107**, 1363 (1957).
3. P. W. REINHARDT and F. J. DAVIS. Physics, **1**, 169 (1958).
4. M. FUJITA, J. AKAISHI, and H. YAMAMOTO. Radioisotopes (Tokyo), **9**, 102 (1960).
5. B. H. PARKER. AERE Report R-3443. 1960.
6. J. P. BUTLER and D. C. SANTRY. Can. J. Chem. **39**, 689 (1961).
7. W. E. NERVIK and P. C. STEVENSON. Nucleonics, **10**, No. 3, 18 (1952).
8. J. E. BROLLEY, JR. and J. L. FOWLER. *In* Fast neutron physics. Part 1. *Edited by* J. B. Marion and J. L. Fowler. Interscience, New York. 1960. p. 80.
9. L. CRANBERG, A. H. ARMSTRONG, and R. L. HENKEL. Phys. Rev. **104**, 1639 (1956). L. CRANBERG. Private communications.
10. ANDERSON, GARDNER, MCCLURE, NAKADA, and WONG. Livermore Laboratory. Private communication (1958) as listed in ref. 8, pp. 97–101.
11. S. J. BAME, JR. and J. E. PERRY, JR. Phys. Rev. **107**, 1616 (1957).
12. J. D. SEAGRAVE. Neutron source handbook. LAMS-2162. 1957.
13. C. D. SWARTZ and G. E. OWEN. *In* Fast neutron physics. Part 1. *Edited by* J. B. Marion and J. L. Fowler. Interscience, New York. 1960. Chap. IIB.
14. W. G. CROSS. To be published.
15. J. L. FOWLER and J. E. BROLLEY, JR. Rev. Mod. Phys. **28**, 103 (1956).
16. J. P. BUTLER and D. C. SANTRY. Can. J. Phys. In press. 1963.
17. B. P. BAYHURST and R. J. PRESTWOOD. Los Alamos Report LA-2493. 1961.

Can. J. Chem. Downloaded from www.nrcresearchpress.com by 210.87.254.5 on 09/05/12
For personal use only.

Can. J. Chem. Downloaded from www.nrcresearchpress.com by 210.87.254.105 on 09/05/12
For personal use only.

METALLO-ORGANIC COMPOUNDS CONTAINING METAL–NITROGEN BONDS

PART IV. SOME BIS-(PRIMARY AMINO)-TITANIUM COMPOUNDS[1]

D. C. Bradley and E. G. Torrible[2]
Department of Chemistry, University of Western Ontario, London, Ontario

Received August 8, 1962

ABSTRACT

The aminolysis reactions involving primary amines with either $Ti(NMe_2)_4$ or $Ti(NEt_2)_4$ have been studied. The primary amines behave as bifunctional reactants, forming colored, insoluble, non-volatile bis-(primary amino)-titanium compounds $Ti(NR)_2$ which (except for $R = C_6H_5$) are highly reactive towards water or alcohols. With *n*-butylamine some soluble polymers of the general formula $Ti_x(NBu^n)_{2x-2}(NEt_2)_4$ were isolated. With *tert*-butylamine the dimers $Ti_2(NBu^t)_2(NMe_2)_4$ and $Ti_2(NBu^t)_2(NHBu^t)_2(NMe_2)_2$ were obtained. The structures of these polymeric metal–nitrogen compounds are discussed.

INTRODUCTION

In a previous communication the preparation of a number of dialkylamino derivatives of titanium and zirconium was reported (1). The titanium compounds $(TiNR_2)_4$ were monomeric and could be distilled *in vacuo*. The monomeric nature of these compounds was significant in view of the tendency of titanium to expand its coordination number and the presence of donor nitrogen atoms in the dialkylamino groups. The absence of coordination–polymerization in these compounds and the limitation of aminolysis (e.g. $Ti(NMe_2)_4 + 3HNEt_2 \rightarrow Ti(NMe_2)(NEt_2)_3 + 3HNMe_2$) were ascribed to steric hindrance.

Since the steric effects of primary amines RNH_2 must be considerably less than those of secondary amines R_2NH it was considered worthwhile to investigate the aminolysis of dialkylamino-titanium compounds with primary amines:

$$Ti(NR_2)_4 + 2RNH_2 \rightarrow Ti(NR)_2 + 4HNR_2. \qquad [1]$$

Moreover, the primary amino derivatives were expected to be polymeric since the primary nitrogen is potentially bifunctional and could lead to the formation of a metal–nitrogen chain, 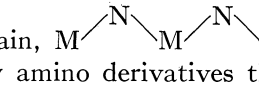 . There was also the additional possibility that in the primary amino derivatives the titanium might be able to achieve a coordination number of six as a result of coordination–polymerization. We now report the results of the reactions of several primary amines with tetrakis-(dialkylamino)-titanium compounds.

RESULTS AND DISCUSSION

When either $Ti(NMe_2)_4$ or $Ti(NEt_2)_4$ was treated with an excess of the primary amine RNH_2, where R = Pr^n, Pr^i, Bu^i, Bu^s, cyclohexyl, or phenyl, the deeply colored insoluble bis-(monoalkylamino)-titanium compound $Ti(NR)_2$ was obtained (viz. equation [1]), with the primary amines being bifunctional. With the exception of the anilino derivative, which was black and relatively stable towards hydrolysis, the new compounds were red and extremely vigorously hydrolyzed. The difference in chemical

[1]*Part III, D. C. Bradley and I. M. Thomas, Can. J. Chem.*, **40**, *1355 (1962).*
[2]*Present address: Department of Chemistry, Queen's University, Kingston, Ontario.*

reactivity between the anilino derivative and the cyclohexylamino derivative was remarkable and in view of the similarity in size of the ligands suggests that electronic factors must be of predominant importance. The most likely factor to favor resistance to hydrolysis would be covalency expansion by the titanium involving donation of the lone pair of electrons from nitrogen. This could occur either by σ-bonding, which would cause coordination–polymerization, or by π-bonding, and in either case the increased electron density on the titanium would lower its susceptibility to nucleophilic attack by water. However, covalency expansion by σ-coordination should be assisted by electron release by the alkyl or aryl group attached to nitrogen and this would be greater for the cyclohexylamino derivative than for the anilino derivative. Covalency expansion by π-bonding (II) would be enhanced in the anilino derivative because of interaction with the ring π-orbitals and we are inclined to favor this as an explanation for the striking difference in behavior of cyclohexylamino and anilino derivatives. It is hoped to gain further information on this point as a result of infrared and n.m.r. studies now in progress on metallo-organic compounds containing metal–nitrogen bonds.

The insolubility and non-volatility of the bis-(monoalkylamino)-titanium compounds suggest that they are high polymers and it is evident that an infinite linear polymer (I) is feasible in which each unit of the polymer is joined by a double nitrogen bridge.

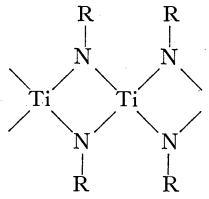

I

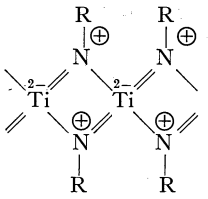

II

A notable feature of I is that the titanium atoms are 4-coordinated and that covalency expansion by σ-coordination would produce a 3-dimensional polymer.

Experiments in which *n*-butylamine was added to tetrakis-(diethylamino)-titanium showed that soluble polymers containing both diethylamino and *n*-butylamino groups could be obtained. An attempt to prepare the dimer $Ti_2(NBu^n)(NEt_2)_6$ by means of the reaction depicted in equation [2] gave a dark red liquid containing some solid. Heating

$$2Ti(NEt_2)_4 + Bu^nNH_2 \rightarrow Ti_2(NBu^n)(NEt_2)_6 + 2Et_2NH \qquad [2]$$

this inhomogeneous product caused disproportionation and $Ti(NEt_2)_4$ distilled over at 110–120° at 0.1 mm, leaving a non-volatile dark red solid whose analysis was near to the requirements of $Ti(NBu^n)_2$ but which still contained a small proportion of diethylamino groups. Further experiments in which $Ti(NEt_2)_4$ was treated with an excess of *n*-butylamine gave products having the general formula $Ti_x(NBu^n)_{2x-2}(NEt_2)_4$ (x = 6–14). These compounds were soluble in boiling cyclohexane and molecular weights were determined ebulliometrically in this solvent. The more polymeric compounds were noticeably less soluble in cyclohexane at room temperature and although quite soluble when hot they would not crystallize on cooling but gave gels instead. Surprisingly these compounds appeared to be insoluble in such "donor" solvents as pyridine, dioxane, or acetonitrile. All of the butylamino-titanium polymers contained residual diethylamino groups which resisted disproportionation at 130° at 0.1 mm and the molecular weights in boiling cyclohexane were in reasonable agreement with the structural formula III.

Can. J. Chem. Downloaded from www.nrcresearchpress.com by 210.87.254.105 on 09/05/12
For personal use only.

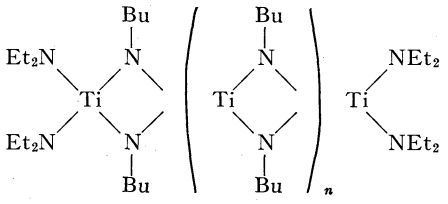

III

According to this model the polymers contain the repeating unit I with the double metal–nitrogen bridge but finite polymers are produced because the diethylamino groups act as chain stoppers. Assuming that the titaniums are tetrahedrally bonded to nitrogen then a rigid linear polymer results. We have explored the possibility that 6-coordinated titanium might be involved in these polymers but it appears to be impossible to formulate such low polymers in terms of octahedrally coordinated titanium. It is possible that the metal–nitrogen bridges shown in formula III are reinforced by π-bonding due to intramolecular covalency expansion by titanium as shown in II.

An attempt was made to study the formation of polymers by the addition of primary amine to a solution of $Ti(NEt_2)_4$ in boiling diethylamine:

$$x\mathrm{RNH_2} + \mathrm{Ti(NEt_2)_4} \rightarrow \frac{1}{n}[\mathrm{Ti(NR)}_x(\mathrm{NEt_2})_{4-2x}]_n + 2x\mathrm{Et_2NH}. \qquad [3]$$

Experiments showed that $Ti(NEt_2)_4$ is monomeric in boiling diethylamine; hence the degree of polymerization n of the polymer produced in reaction [3] could in principle be determined ebulliometrically. However, the addition of either cyclohexylamine, isobutylamine, or *n*-butylamine to the $Ti(NEt_2)_4$ in boiling diethylamine gave no evidence of immediate reaction. After about 3 hours a slight red coloration had developed but it was concluded that reaction [3] must be reversible and in the presence of excess of diethylamine is forced to the left-hand side. To test the reversibility of equation [3] some bis-(isopropylamino)-titanium was refluxed with diethylamine and with di-*n*-propylamine but the replacement of isopropylamino groups was very slow. It appears that once the solid infinite polymer $[Ti(NR)_2]_\infty$ is formed it is resistant to aminolysis by secondary amines. Nevertheless, treatment of $Ti(NPr^i)_2$ with excess of *n*-butylamine caused slow replacement of isopropylamino by *n*-butylamino groups and a soluble *n*-butylamino-titanium polymer was formed.

Finally, we report some interesting results from the treatment of tetrakis-(dimethylamino)-titanium with excess boiling *tert*-butylamine. After about 2 hours of reaction the volatile materials were evaporated off *in vacuo* and a dark red solid (IV) remained. Analysis of IV and a molecular weight determination suggested that it was $Ti_2(NBu^t)_2(NMe_2)_4$, for which the bridged structure IV is proposed. Prolonged treatment of $Ti_2(NBu^t)_2(NMe_2)_4$ with excess boiling *tert*-butylamine gave another dimer, $Ti_2(NBu^t)_2(HNBu^t)_2(NMe_2)_2$ (V), which sublimed readily at 140–160° at 0.1 mm as a dark red

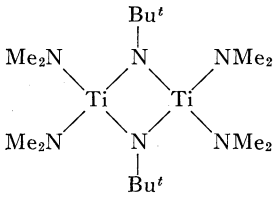

IV

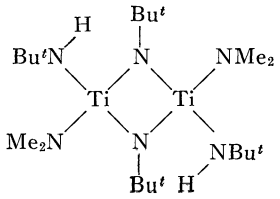

V

Can. J. Chem. Downloaded from www.nrcresearchpress.com by 210.87.254.105 on 09/05/12
For personal use only.

solid. The results suggest that the development of the double metal–nitrogen bridged linear polymer I is prevented in the case of *tert*-butylamino groups by the strong steric hindrance of the *tert*-butyl groups. It does not seem to be possible by the aminolysis reaction to arrange four Bu^tN-groups around each titanium, as required in I.

EXPERIMENTAL

Special precautions were taken to exclude water from the apparatus and chemicals and all reactions were conducted in an atmosphere of oxygen-free nitrogen. The amines and solvents were dried over sodium and distilled immediately before use.

Analysis

(a) For titanium.—The alkylamino derivative was weighed into a platinum crucible, hydrolyzed cautiously, and the hydrated oxide dried under an infrared lamp and then ignited to TiO_2.

(b) For nitrogen.—In the case of derivatives of the low-boiling amines the sample was hydrolyzed in alkali, the amine steam distilled and titrated with standard acid. For the less volatile amines the nitrogen was determined by the Kjeldahl method.

Molecular Weight Determinations

Measurements were carried out in boiling cyclohexane in the previously described (2) all-glass ebulliometer employing a differential water thermometer using the method of internal calibration (3) with fluorene.

Preparation of Bis-(alkylamino)-titanium Compounds

The preparation of bis-(isopropylamino)-titanium is described to illustrate the general technique, and the essential details of the other preparations carried out similarly are summarized in Table I.

TABLE I

Preparation of bis-(primary alkylamino)-titaniums

Compound	Color	Reaction time (hr)	Found (%)		Calc. (%)	
			Ti	N	Ti	N
$Ti(NPr^n)_2$*	Orange	0.25	29.6	16.9	29.6	16.9
$Ti(NPr^i)_2$*	Red	1	29.2	16.5	29.6	16.9
$Ti(NBu^i)_2$†	Red	6	25.3	14.0	25.2	14.7
$Ti(NBu^s)_2$†	Red	8	25.6	14.1	25.2	14.7
$Ti(NC_6H_{11})_2$†	Scarlet	2	21.0	—	19.8	—
$Ti(NC_6H_5)_2$*	Black	2	20.8	11.8	20.8	12.2

*From $Ti(NMe_2)_4$.
†From $Ti(NEt_2)_4$.

An excess of isopropylamine (ca. 20 ml) added to tetrakis-(dimethylamino)-titanium (4.4 g prepared by Bradley and Thomas' method (1)) caused a deep red coloration with deposition of some red solid. The mixture was refluxed for 1 hour and allowed to cool overnight. Evaporation of the amines *in vacuo* followed by drying at 140° left a red solid which was vigorously hydrolyzed and reacted with alcohols to form titanium alkoxides. Found: Ti, 29.2; N, 16.5. $Ti(NPr^i)_2$ requires: Ti, 29.6; N, 16.9%. Gas chromatographic analysis of the volatile product of *n*-propanolysis showed the presence of isopropylamine but no dimethylamine. In some of the other preparations a small amount of $Ti(NMe_2)_4$ or $Ti(NEt_2)_4$ was distilled out of the product during drying *in vacuo* at 100–140° but dialkylamino groups were not detected in the final product.

Preparation of n-Butylamino-titanium Diethylamide Polymers

Addition of excess *n*-butylamine (15.0 g) to tetrakis-(diethylamino)-titanium (6.15 g prepared by Bradley and Thomas' method (1)) caused precipitation of an orange solid which dissolved when heated, giving a red solution. After refluxing for 4 hours the solution was allowed to cool but nothing crystallized. After evaporating off the amines the product was dried at 130° at 0.1 mm, and a small amount (ca. 0.2 g) of $Ti(NEt_2)_4$ distilled over at 110–120°. The final product was a dark red solid (3.25 g) which was shown by gas chromatographic analysis of the volatile products of *n*-butanolysis to contain both *n*-butylamino and diethylamino groups. In some cases the polymeric product was treated further with boiling *n*-butylamine to displace more diethylamino groups. The results are summarized in Table II.

Reaction Between Bis-(isopropylamino)-titanium and n-Butylamine

Excess of *n*-butylamine was added to bis-(isopropylamino)-titanium (3.0 g) and the scarlet solid became orange colored and slowly dissolved during 44 hours of heating at 100°. Evaporation of the amines followed

Can. J. Chem. Downloaded from www.nrcresearchpress.com by 210.87.254.105 on 09/05/12
For personal use only.

TABLE II

Polymeric *n*-butylamino-titanium diethylamides

Compound	Found			Calc.		
	Ti	N	M.W.	Ti	N	M.W.
$Ti_6(NBu^n)_{10}(NEt_2)_4$	22.9	15.4	1,280	22.4	15.25	1,286
$Ti_{14}(NBu^n)_{26}(NEt_2)_4$	24.0	15.1	2,770	23.9	15.0	2,806
$Ti_{16}(NBu^n)_{30}(NEt_2)_4$	24.1	15.1	3,120	24.05	14.9	3,188
$Ti_{100}(NBu^n)_{198}(NEt_2)_4$	25.0	14.8	3,920	25.0	14.8	19,136

by drying at 140° at 0.1 mm left a brown solid (3.75 g). Found: Ti, 24.8; N, 15.0. $Ti(NBu)_2$ requires: Ti, 25.2; N, 14.7%. Gas chromatographic analysis of the volatile product of *n*-butanolysis revealed only the presence of *n*-butylamine. The product was soluble in *n*-butylamine.

Reaction Between Tetrakis-(dimethylamino)-titanium and tert-Butylamine

Addition of excess *tert*-butylamine to $Ti(NMe_2)_4$ (10.3 g) caused a moderate reaction, with liberation of dimethylamine. After approximately 2 hours' fractional distillation to remove more dimethylamine, slowly formed during continued heating, during which time some solid was precipitated and the solution became dark red, the amines were evaporated off *in vacuo*. Final drying *in vacuo* at 120° gave no $Ti(NMe_2)_4$ and left a dark red solid (9.2 g). Found: Ti, 23.3; N, 20.3; M.W., 365. $Ti_2(NBu^t)_2(NMe_2)_4$ requires: Ti, 23.2; N, 20.3%; M.W., 414. The compound reacted vigorously on ethanolysis, liberating both *tert*-butylamine and dimethylamine.

The foregoing product (7.9 g) was treated with excess boiling *tert*-butylamine under a fractionating column for 3 hours and then the solution was evaporated to dryness *in vacuo*. On heating the product to 140–160° at 0.1 mm a dark red sublimate (4.2 g) was obtained. Found: Ti, 20.5; N, 17.2; M.W., 540. $Ti_2(NBu^t)_2(NHBu^t)_2(NMe_2)_2$ requires: Ti, 20.4; N, 17.9%; M.W., 470.

In another experiment in which $Ti(NMe_2)_4$ (8.9 g) was treated with excess *tert*-butylamine as before the residue (8.6 g) remaining after removal of amines and drying at 115° *in vacuo* was close in analysis to the composition of the sublimate obtained in the previous experiment. Found: Ti, 20.9; N, 17.9%; M.W., 530. A good yield of sublimate (6.0 g from 7.6 g) was obtained at 140–150° at 0.1 mm. Found: Ti, 20.8; N, 18.0%; M.W., 510.

ACKNOWLEDGMENTS

We are indebted to the U.S. Air Force for supporting this research through the Wright Air Development Division, Air Research and Development Command.

REFERENCES

1. D. C. Bradley and I. M. Thomas. J. Chem. Soc. 3857 (1960).
2. D. C. Bradley, R. Gaze, and W. Wardlaw. J. Chem. Soc. 3977 (1955).
3. D. C. Bradley, W. Wardlaw, and A. Whitley. J. Chem. Soc. 5 (1956).

Can. J. Chem. Downloaded from www.nrcresearchpress.com by 210.87.254.105 on 09/05/12
For personal use only.

THE CHEMISTRY OF THE AMINOCHROMES

PART V. REARRANGEMENTS IN THE PRESENCE OF SODIUM HYDROXIDE AND ZINC ACETATE[1, 2, 3]

R. A. HEACOCK AND G. L. MATTOK
The Psychiatric Research Unit, University Hospital, Saskatoon, Saskatchewan

Received September 10, 1962

ABSTRACT

The rates of rearrangement of several aminochromes have been measured in: (1) water, (2) aqueous sodium hydroxide, and (3) aqueous zinc acetate. The rates were found to be first order with respect to aminochrome concentration in each reaction medium, and to zinc acetate concentration. However, no simple kinetic relationship between the rate of rearrangement and alkali concentration was detected. The rate increased very rapidly with increasing alkali concentration.

Mechanisms for these rearrangements are suggested, based on the influence of substituents in the 1-, 2-, and 3-positions of the aminochrome molecule on the kinetic and thermodynamic features of the reaction.

INTRODUCTION

The ease with which the red solutions obtained on oxidation of the catecholamines could be decolorized was recognized long before the structures of the compounds involved were established (see ref. 1 for references). As a result of studies on the oxidation of 3,4-dihydroxyphenylalanine (DOPA) carried out over 30 years ago, Raper proposed what was essentially the correct explanation of the changes that occurred, namely that the oxidation of DOPA (I: $R_1 = R_3 = H$; $R_2 = COOH$) resulted in the initial formation

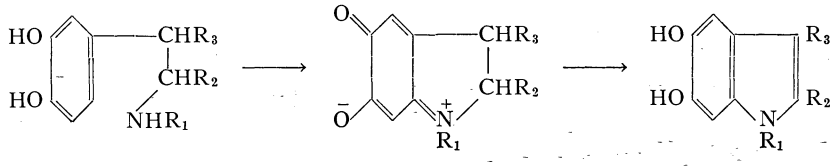

I II III

of an aminochrome,* i.e. a 2,3-dihydroindole-5,6-quinone derivative (II: $R_1 = R_3 = H$; $R_2 = COOH$),† which subsequently underwent a spontaneous internal oxidation–reduction process, forming the colorless 5,6-dihydroxyindole (III: $R_1 = R_2 = R_3 = H$). The rate of decolorization of the intermediate pigment could be increased by the action of either base or acid. In the latter case, however, the rearrangement product was not 5,6-dihydroxyindole, but 5,6-dihydroxyindole-2-carboxylic acid (III; $R_1 = R_3 = H$; $R_2 = COOH$) (3). This general picture has subsequently been confirmed spectroscopically, manometrically, and paper chromatographically (4–6).

Solutions of adrenaline (I: $R_1 = CH_3$; $R_2 = H$; $R_3 = OH$) and certain related catecholamines with a hydroxyl group in the β-position that have undergone oxidation in

[1]*This investigation was supported by grants from the Government of Saskatchewan (Department of Public Health) and the Department of National Health and Welfare (Ottawa).*

[2]*Presented in part at the 45th Annual Conference of the Chemical Institute of Canada, Edmonton, Alberta, May, 1962.*

[3]*Part IV: Can. J. Chem.* **38**, *516 (1960).*

**The term "aminochrome" as a general name for the highly colored cyclic oxidation products of the catecholamines was not introduced until 1951 by Sobotka and Austin (2).*

†*The chemical and physical properties of these compounds suggest that the zwitterionic form of the molecule, as shown above, makes the major contribution to the aminochrome structure (cf. ref. 1).*

Can. J. Chem. Downloaded from www.nrcresearchpress.com by 210.87.254.5 on 09/05/12
For personal use only.

alkaline media exhibited a transient but intense yellow-green fluorescence (see ref. 1 for references). The fluorescent derivative of adrenaline was, in fact, 5,6-dihydroxy-*N*-methylindoxyl* (i.e. adrenolutin; IV), first isolated and characterized by Lund in 1949

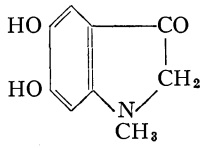

IV

(7, 8) and obtained by the alkaline rearrangement of the initially formed aminochrome (i.e. adrenochrome; II: $R_1 = CH_3$; $R_2 = H$; $R_3 = OH$). Rearrangement of aminochromes to 5,6-dihydroxyindole or 5,6-dihydroxyindoxyl derivatives is catalyzed by certain metallic ions, particularly Zn^{2+} and Al^{3+} (9, 10).

Although speculative mechanisms, notably those of Trautner and Bradley (11), Sobotka, Barsel, and Chanley (12), and Bu'Lock and Harley-Mason (13), have been advanced to explain certain aspects of the manner by which the rearrangement of the aminochromes to 5,6-dihydroxy-indole or -indoxyl derivatives occurs, none is based on a systematic physico-organic chemical investigation.

A number of reports of an essentially qualitative nature dealing with the stability of adrenochrome solutions has appeared in the literature, and these have been summarized previously (1). Zambotti and Moret studied the effects of pH and temperature on the stability of adrenochrome solutions in phosphate buffer polarographically and manometrically and reported that, in the relatively limited range studied, the decomposition of adrenochrome follows first-order kinetics and that the rate of disappearance of aminochrome varied linearly with the pH at 37° and exponentially with temperature at pH = 7.38 (14–16).

It appeared to the authors that a systematic study of the kinetic and thermodynamic features of the rearrangement of a number of different aminochromes would enable a more satisfactory explanation of the mechanisms of these reactions to be formulated.

EXPERIMENTAL

Aminochromes

Adrenochrome (17), *N*-isopropylnoradrenochrome (18), and adrenochrome methyl and ethyl ethers (18) were prepared as pure crystalline solids by the methods described in the literature. However, in the cases of epinochrome, 2-methyladrenochrome, *N*-ethyl-2-methylnoradrenochrome, and noradrenochrome, where it was either not possible to isolate a pure sample of the aminochrome or where only limited quantities of the relevant catecholamines were available, the aminochrome was prepared in aqueous solution by oxidation of the appropriate catecholamine hydrochloride (25 mg in 3 ml water) with freshly prepared silver oxide (2×0.2 g) (finally filtering the oxidation mixture through a small Dowex-1 (Cl^-) (200/400 mesh) resin bed to ensure complete removal of colloidal and ionic silver (cf. ref. 17). The rates of rearrangement obtained for adrenochrome prepared in this way showed satisfactory agreement with those determined using crystalline adrenochrome. Solutions of noradrenochrome prepared in this manner were not entirely satisfactory, since the visible absorption spectra of these solutions frequently showed a shift in λ_{max} accompanied by an increase in the intensity of absorption at this wavelength. This phenomenon is possibly due to the relatively slow cyclization of the initially formed "noradrenaline quinone" (i.e. 1-(α-hydroxy-β-aminoethyl)-3,4-benzoquinone) to noradrenochrome (cf. refs. 19, 20). However, it is not unreasonable to assume that the rates obtained represent the relative order of reactivity of this compound.

Kinetic Measurements

The rearrangements of the various aminochromes were studied in three reaction media: (*a*) water, (*b*) aqueous sodium hydroxide, (*c*) aqueous zinc acetate. The reactions were followed by measuring the decrease in absorbance at λ_{max} (ca. 480–495 mμ) with time using a Beckmann DK-2 spectrophotometer equipped with

**Often formulated in the enolic form, i.e. as 3,5,6-trihydroxy-N-methylindole.*

Can. J. Chem. Downloaded from www.nrcresearchpress.com by 210.87.254.5 on 09/05/12
For personal use only.

a temperature-regulated cell holder. (The absorption maxima and minima of the aminochromes used are given in Table I.) The initial concentrations of the reagents are given in Table II. In all cases the solutions

TABLE I

Absorption spectra of some aminochromes in water
(in the range 250–650 mμ)

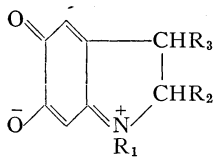

R_1	R_2	R_3	Absorption maxima (mμ)		Absorption minima (mμ)	
H	H	OH	281	484	253	370
CH_3	H	OH	301	487	262	361
C_2H_5	H	OH	303	490	261	368
i-C_3H_7	H	OH	303	495	261	366
CH_3	CH_3	OH	301	487	260	365
C_2H_5	CH_3	OH	303	490	260	367
CH_3	H	H	303	475	258	369

of the reagents were preheated to the reaction temperature in the cell holder. The reaction mixtures were prepared by the admixture of 2 ml of the aminochrome solution with 1 ml of the catalyst solution, care being taken to ensure rapid and complete mixing of the reagents.

There was a good linear relationship between the aminochrome concentration and the absorbance at λ_{max}.

The Reaction of Adrenochrome Methyl Ether with Zinc Acetate

A saturated solution of zinc acetate (1.5 ml) was added to a solution of adrenochrome methyl ether (73 mg) in water (2.2 ml). The reaction mixture was left to stand for 1 hour and the dark blue precipitate which formed was filtered off, washed with water and ether, and dried in air. The weight of the dry precipitate was 60.2 mg. The aqueous filtrate, which was initially yellow but which quickly became blue-green in color, gave, after standing for an hour, on the addition of more zinc acetate solution (3 ml) a blue precipitate, which was filtered, washed with water and ether, and dried in air. The weight of this dry residue was 29.8 mg.

The aqueous filtrate (30 ml) was extracted with ether (3×10 ml). Concentration of the dried (Na_2SO_4) ether extract afforded a white crystalline residue (5.5 mg). A paper chromatographic examination of this residue indicated that it was probably 5,6-dihydroxy-*N*-methylindole (i.e. III: $R_1 = CH_3$; $R_2 = R_3 = H$ (cf. ref. 21)). Assuming that this was in fact the product, the expected yield of a complex composed of one zinc atom and one aminochrome unit would be 90.4 mg, and that for 1:2 complex, 78.9 mg. The total weight of complex obtained was 85.7 mg.

Analyses of several different samples of these products for carbon, hydrogen, nitrogen, and zinc were inconclusive. (Found: C, 47.57, 47.38, 43.20, 43.19, 42.52, 49.53, 51.06; H, 5.32, 4.08, 4.07, 3.83, 4.15, 4.61, 4.70; N, 5.96, 5.90, 4.07, 5.63; Zn, 12.57, 12.57%.) The calculated composition of 1:1 zinc/aminochrome complex would be C, 46.41; H, 4.29; N, 5.42; Zn, 25.28%; and that for a 1:2 zinc/aminochrome complex would be C, 53.16; H, 4.91; N, 6.20; Zn, 14.47%. It is therefore difficult to say whether the experimentally determined percentage composition of the complex supports a 1:1 or a 1:2 complex.

It is interesting to note that the averages of the experimental values (i.e. C, 46.35; H, 4.69; N, 5.39; Zn, 12.57%) fit the calculated composition of a hydrated 1:2 complex (4 molecules of water) (i.e. $C_{20}H_{26}N_2O_{10}Zn$ requires C, 46.21; H, 5.04; N, 5.39; Zn, 12.58%).

Since these products are insoluble in the usual reagents, it was not possible to purify them further by recrystallization.

In view of the formation of insoluble precipitates in this case, the reaction was not followed spectroscopically beyond approximately 10% reaction, since clouding of the cell walls that resulted would have given anomalous results.

RESULTS

The rearrangements of adrenochrome and its methyl ether were first order with respect to aminochrome concentration in all three reaction media (see Figs. 1, 2, 3, and 4). In the

Can. J. Chem. Downloaded from www.nrcresearchpress.com by 210.87.254.5 on 09/05/12
For personal use only.

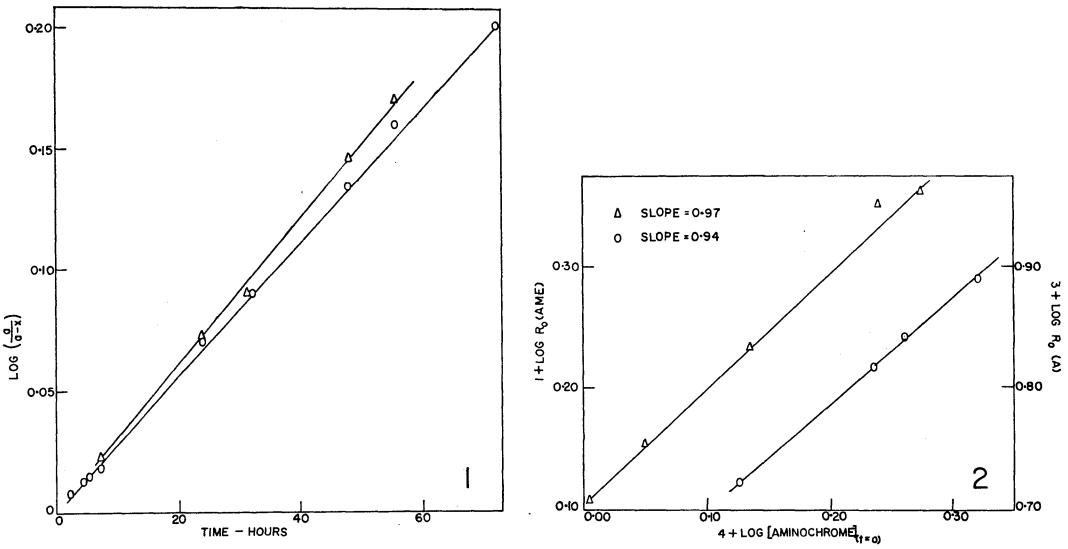

FIG. 1. Rearrangement of: adrenochrome (△), at 28.9°, and adrenochrome methyl ether (○), at 30.2°, in water. First-order plots (k_1 (for adrenochrome) = 1.10×10^{-4} min^{-1}; k_1 (for adrenochrome methyl ether) = 0.96×10^{-4} min^{-1}).

FIG. 2. Rearrangement of: adrenochrome (△), at 29.7°, 4.5×10^{-5} *N* NaOH, and adrenochrome methyl ether (○), at 42.6°, 8.5×10^{-5} *N* NaOH, in the presence of sodium hydroxide. Order with respect to aminochrome concentration. (A = adrenochrome; AME = adrenochrome methyl ether.)

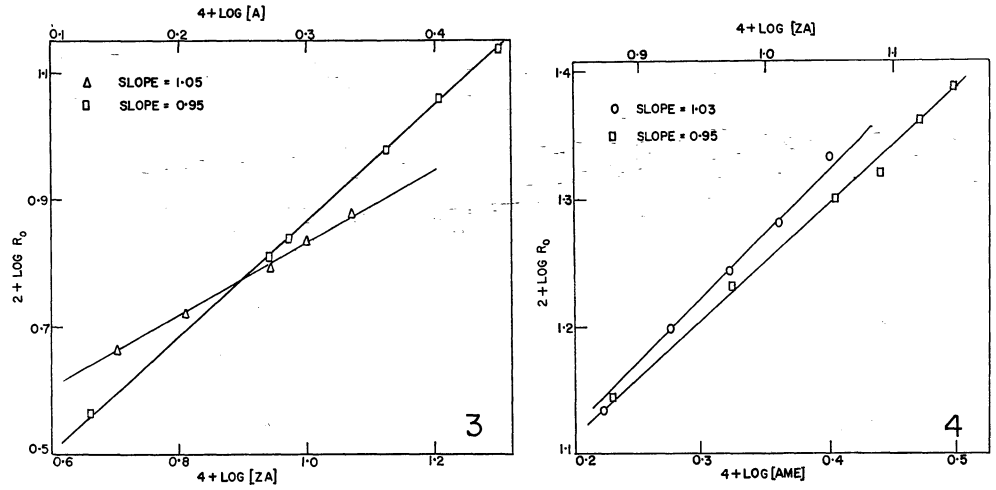

FIG. 3. Rearrangement of adrenochrome in the presence of zinc acetate, at 28.8°. Order in: adrenochrome (△), zinc acetate 9.4×10^{-4} *M*, and zinc acetate (□), adrenochrome 2.0×10^{-4} *M*. (A = adrenochrome; ZA = zinc acetate.)

FIG. 4. Rearrangement of adrenochrome methyl ether in the presence of zinc acetate, at 42.6°. Order in: adrenochrome methyl ether (○) and zinc acetate (□). (AME = adrenochrome methyl ether; ZA = zinc acetate.)

presence of zinc acetate the rearrangements also obeyed first-order kinetics with respect to zinc acetate. Rearrangements in the presence of sodium hydroxide, whilst being first order with respect to aminochrome concentration, did not show any simple dependency on

Can. J. Chem. Downloaded from www.nrcresearchpress.com by 210.87.254.5 on 09/05/12
For personal use only.

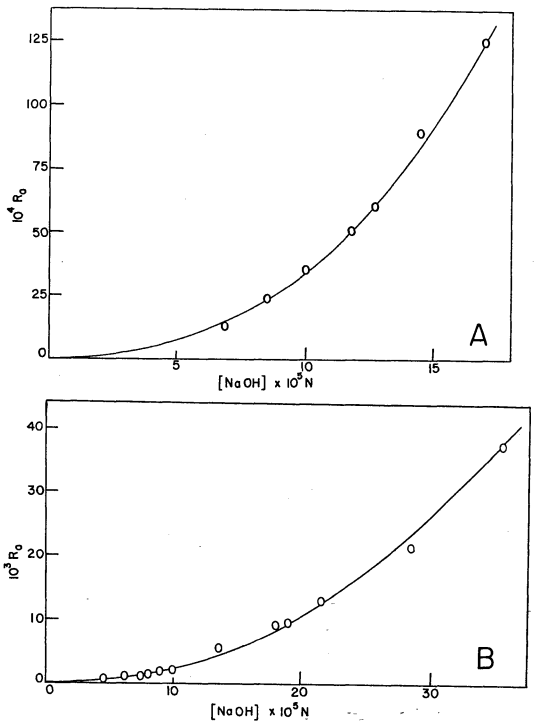

FIG. 5. Effect of sodium hydroxide concentration on the rate of rearrangement of: (A) adrenochrome, at 29.7°, initial concentration of adrenochrome 1.90×10^{-4} *M*, and (B) adrenochrome methyl ether, at 42.6°, initial concentration of adrenochrome methyl ether 1.91×10^{-4} *M*.

alkali concentration (see Fig. 5). The rate of rearrangement in the presence of sodium hydroxide increased rapidly with alkali concentration.

With the exception of experiments which were carried out to determine the order of the reaction, they were all performed with standardized zinc acetate and sodium hydroxide concentrations. The first-order rate constants were calculated by the method of initial slopes to avoid errors due to any secondary reactions.

The rates of rearrangement, at 35°, of some aminochromes are given in Table II. When the substituent on carbon atom 3 only is varied the sequence of reactivity is: H > OH > OCH_3 > OC_2H_5. Further, when the substituent on the nitrogen atom only is varied the sequence of reactivity is *i*-C_3H_7 > CH_3 > H. Variation of the substituent on C_2 from H to CH_3 had little effect on the rate of reaction (see Table II). These generalizations are true for rearrangements in water, alkali, and zinc acetate solution. An incidental observation is that OH^- is about 10 times better a catalyst for the rearrangement than Zn^{2+} (on a molar basis). It is also of interest to note that solutions of noradrenochrome are not as unstable as they are generally considered to be.

The effect of temperature in the range 30–50° on the rates of some of these reactions was also investigated, and the thermodynamic functions (at 35°) for these rearrangements are given in Table III. In each of the three reaction media, the activation energy decreases as the rate of rearrangement increases. In general, the entropy term is fairly constant. However, with epinochrome, which carries two hydrogen atoms on C_3, the entropy term is consistently more favorable than for adrenochrome. Although this difference is small, it is probably significant.

Can. J. Chem. Downloaded from www.nrcresearchpress.com by 210.87.254.5 on 09/05/12
For personal use only.

TABLE II

Rearrangement of several aminochromes in various reaction media
(Rate constants at 35°)

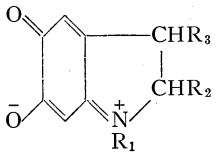

Aminochrome*	R_1	R_2	R_3	$k_1\times10^4$ (min^{-1}) in: H_2O	NaOH*	$Zn(OAc)_2$*
Epinochrome	CH_3	H	H	14.6	72.1	126
Adrenochrome	CH_3	H	OH	2.04	22.4	13.4
Adrenochrome methyl ether	CH_3	H	OCH_3	1.26	15.3	10.4
Adrenochrome ethyl ether	CH_3	H	OC_2H_5	0.76	10.2	9.77
N-Isopropylnoradrenochrome	i-C_3H_7	H	OH	3.72	41.7	19.5
Noradrenochrome†	H	H	OH	1.48	12.3	11.9
2-Methyladrenochrome	CH_3	CH_3	OH	1.80	17.3	16.3
N-Ethyl-2-methylnoradrenochrome	C_2H_5	CH_3	OH	1.80	19.3	18.8

*Initial concentrations of reagents: NaOH = 8.50×10^{-5} *M*, $Zn(OAc)_2$ = 9.50×10^{-4} *M*, aminochrome = 2.05×10^{-4} *M*.
†See experimental section dealing with preparation of aminochromes.

TABLE III

Rearrangement of aminochromes in (i) water, (ii) aqueous sodium hydroxide, and (iii) aqueous zinc acetate
(Thermodynamic functions at 35°)

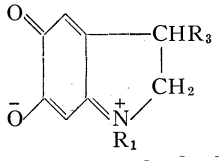

Substituents		Water			NaOH (1.5×10^{-5} *M*)			$Zn(OAc)_2$ (9.5×10^{-4} *M*)		
R_1	R_3	E_{exp}*	$\Delta S^{\ddagger}$†	$\Delta F^{\ddagger}$*	E_{exp}	$\Delta S^{\ddagger}$	$\Delta F^{\ddagger}$	E_{exp}	$\Delta S^{\ddagger}$	$\Delta F^{\ddagger}$
CH_3	H	18.0	−23.6	24.7	17.3	−23.6	23.9	17.5	−20.8	23.3
CH_3	OH	18.9	−24.8	25.9	17.6	−24.0	24.4	17.9	−24.2	24.9
CH_3	OCH_3	20.0	−21.8	26.2	17.9	−23.8	24.6	18.4	−23.7	25.1
CH_3	OC_2H_5	20.7	−22.2	26.9	18.6	−22.4	24.9	19.0	−21.6	25.1
i-C_3H_7	OH	18.3	−25.8	25.6	16.8	−25.4	24.1	17.3	−25.2	24.5

*E_{exp} and $\Delta F^{\ddagger}$ in kcal/mole.
†$\Delta S^{\ddagger}$ in e.u.

DISCUSSION

Rearrangements in Water and Alkali

The overall reaction consists of removal of protons from the 2- and 3-positions in the five-membered ring of the aminochrome molecule (II) and the addition of a proton to each of the C_5- and C_6-carbonyl oxygen atoms on the *o*-benzoquinone ring. The primary reaction center must therefore be either C_2 or C_3. The following lines of evidence suggest that the primary reaction center is, in fact, C_3: (i) In the cases investigated, substituents in the 3-position had a marked effect on the reaction rates, whilst those in the 2-position had little effect; (ii) the entropy term for epinochrome (II: $R_1 = CH_3$; $R_2 = R_3 = H$) is slightly more favorable for rearrangement than for the other aminochromes. This would be expected if the rate-determining process is removal of a proton from carbon 3.

Can. J. Chem. Downloaded from www.nrcresearchpress.com by 210.87.254.5 on 09/05/12
For personal use only.

The reaction in water is first order with respect to aminochrome concentration. (This is the case for at least 40% reaction.) In aqueous alkali, the rearrangement is also first order with respect to aminochrome; however, the order with respect to sodium hydroxide concentration is not simple, indicating that alkali probably plays a multiple role in the reaction.

The rate-controlling process would then be the loss of a proton from the three position, resulting in a transition state involving one aminochrome molecule.

The two carbonyl groups in *o*-quinonoid structures tend to promote electromeric changes in opposite directions, resulting in the high reactivity associated with these structures, which have a tendency to revert to structures in which the tension of the opposed electromeric effects has been relieved (22). The tendency of the C_5-carbonyl group to polarize effectively lowers the electron density on C_3, by the series of electromeric changes as shown below, thus facilitating the removal of the proton from the 3-position. Electron-attracting substituents at C_3 will diminish the supply of electrons available for the

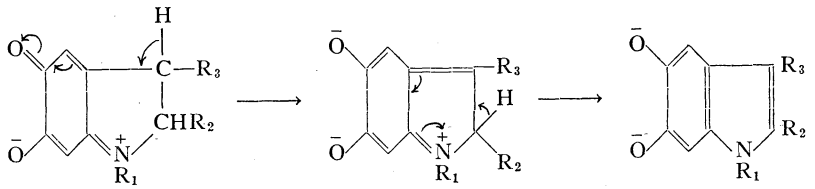

electromeric shifts, resulting in the polarization of the C_5-carbonyl group. The rate of rearrangement will therefore decrease with an increase in electron-attracting capacity of the C_3-substituent (R_3), and this is, in fact, observed for the following series of compounds: epinochrome (R_3 = H) > adrenochrome (R_3 = OH) > adrenochrome methyl ether (R_3 = OCH_3) > adrenochrome ethyl ether (R_3 = OC_2H_5).

The rate-determining stage is then followed by a second series of electronic shifts in the pyrrole moiety of the molecule, resulting in the loss of a proton from C_2 and the formation of a fully aromatic structure.

Electron-donating groups on the nitrogen atom will promote further polarization of the C_6-carbonyl group, resulting in an increase in the already high contribution of the zwitterionic form of the aminochrome molecule to the ground-state resonance hybrid. This results in a raising of the ground-state free energy of the molecule. The observed sequence of reactivity for the *N*-substituted aminochromes is: *N*-*i*-C_3H_7 > *N*-CH_3 > *N*-H. This would be expected on the basis of the inductive effects of these groups. This effect is also probably associated with the observed shift towards longer wavelengths of the main absorption peak (see Table I) of the *N*-substituted aminochromes with increasing electron-donating capacity of the *N*-substituent.

The rapid increase in the rate of rearrangement of the aminochromes with increasing alkali concentration indicates that the catalyst does not play a single role in the reaction, but presumably assists several processes simultaneously. The hydroxyl ions will act as proton scavengers, and the presence of alkali will also tend to stabilize the enolate anion of the transition state. Furthermore, interaction of the hydroxyl ions with the quaternary nitrogen center will localize the positive charge of the zwitterionic system and thus destabilize the molecule by limiting the possibilities for resonance.

Rearrangements in the Presence of Zinc Acetate

Several of the observed kinetic features of these rearrangements are similar to those in the alkali-catalyzed and uncatalyzed rearrangements. The same sequence of reactivity for substituents in the 1-, 2-, and 3-positions is observed. The thermodynamic aspects of

Can. J. Chem. Downloaded from www.nrcresearchpress.com by 210.87.254.5 on 09/05/12
For personal use only.

the rearrangements are similar. However, there are some important differences. Firstly, there is a good first-order dependency with respect to the zinc acetate concentration, whilst there is no simple relationship to alkali concentration. Secondly, rearrangement of the various aminochromes in the presence of sodium hydroxide leads to analogous products in every case. However, when zinc acetate is the catalyst, rearrangement of the aminochromes with R_3 = H or OH leads to the formation of the same products as with alkali, whereas when R_3 = *O*-alkyl (i.e. the aminochrome ethers) these aminochromes react with zinc acetate solution to form an insoluble dark blue precipitate (cf. ref. 21), which forms relatively slowly. The composition of these precipitates is uncertain. Analysis of the product derived from adrenochrome methyl ether did not confirm either a 1:1 or 1:2 zinc/aminochrome composition but suggested a hydrated 1:2 complex. It was impossible to obtain a pure sample of this material, since it is probable that the product is contaminated with insoluble melanitic materials which are formed at the same time as the complex. Insoluble precipitates were never obtained initially in the cases where R_3 = H or OH.

Bu'Lock and Harley-Mason have suggested, by analogy with the products formed during the oxidation of catechol in the presence of zinc acetate, that the rearrangement of aminochromes in the presence of zinc acetate proceeds via an intermediate composed of one zinc unit and two aminochrome units (13). Our results do not rule out the formation of such a complex as the final product with the aminochrome ethers, but, the transition state for the zinc ion catalyzed rearrangement must, from the kinetic data, involve only one zinc ion and one aminochrome molecule.

The bimolecular process required to form a 1:1 complex is more likely than the three-body collision necessary for the formation of the 1:2 complex proposed by Bu'Lock and Harley-Mason. Further, it is difficult to rationalize the pronounced effect of the C_3-substituent, in the case of the aminochrome ethers, on the solubility and stability of this complex.

From the kinetic data, there will be a primary interaction between one Zn^{2+} ion and one aminochrome molecule. Presumably, the zinc ion approaches the dicarbonyl function of the benzoquinone moiety. The polarization of the C_6-carbonyl group will assist this approach. The proximity of the Zn^{2+} ion to the C_5-carbonyl will induce polarization in this group, thus providing the driving force for the same electromeric shifts, resulting in the removal of the C_3-proton, as proposed for the hydroxyl ion catalyzed rearrangement. The C_2-proton is removed by the second series of shifts as described previously.

The mechanisms of rearrangement of the aminochromes in the presence of alkali or zinc acetate therefore differ mainly in the method by which the two catalysts bring about the same electronic changes in the aminochrome molecule. This is in accord with the fact that, apart from catalytic aspects, the same general kinetic features are observed for the two types of rearrangement.

ACKNOWLEDGMENTS

The authors wish to express their thanks to Burrough-Wellcome and Co. (Canada) Ltd., for a generous gift of epinine hydrochloride and to Mrs. B. D. Scott for the preparation of samples of 3,4-dihydroxyephedrine hydrochloride and *N*-ethyl-3,4-dihydroxynorephedrine hydrochloride.

REFERENCES

1. R. A. Heacock. Chem. Rev. **59**, 181 (1959).
2. H. Sobotka and J. Austin. J. Am. Chem. Soc. **73**, 3077 (1951).
3. H. S. Raper. Biochem. J. **21**, 89 (1927).

Can. J. Chem. Downloaded from www.nrcresearchpress.com by 210.87.254.5 on 09/05/12
For personal use only.

4. H. S. MASON. J. Biol. Chem. **172**, 83 (1947).
5. H. S. MASON and C. WRIGHT. J. Biol. Chem. **180**, 235 (1949).
6. S. BOUCHILLOUX and A. KODJA. Bull. Soc. Chim. Biol. **42**, 65 (1960).
7. A. LUND. Acta Pharmacol. Toxicol. **5**, 75 (1949).
8. A. LUND. Acta Pharmacol. Toxicol. **5**, 121 (1949).
9. P. FISCHER, G. DEROUAUX, H. LAMBOT, and J. LECOMTE. Bull. Soc. Chim. Belges, **59**, 72 (1950).
10. J. HARLEY-MASON and J. D. BU'LOCK. Nature, **166**, 1036 (1950).
11. E. M. TRAUTNER and T. R. BRADLEY. Australian J. Biol. Sci. **4B**, 303 (1951).
12. H. SOBOTKA, N. BARSEL, and J. D. CHANLEY. Fortschr. Chem. Org. Naturstoffe, **14**, 217 (1957).
13. J. D. BU'LOCK and J. HARLEY-MASON. J. Chem. Soc. 2248 (1951).
14. V. ZAMBOTTI and V. MORET. Arch. Sci. Biol. (Bologna), **33**, 522 (1949).
15. V. ZAMBOTTI and V. MORET. Arch. Sci. Biol. (Bologna), **34**, 272 (1950).
16. V. MORET. Giorn. Biochim. **3**, 210 (1954).
17. R. A. HEACOCK, C. NERENBERG, and A. N. PAYZA. Can. J. Chem. **36**, 853 (1958).
18. R. A. HEACOCK and B. D. SCOTT. Can. J. Chem. **38**, 516 (1960).
19. A. KODJA and S. BOUCHILLOUX. Compt. Rend. Soc. Biol. **153**, 1407 (1959).
20. A. KODJA and S. BOUCHILLOUX. Biochim. Biophys. Acta, **41**, 345 (1960).
21. R. A. HEACOCK. Chem. Ind. (London), 752 (1959).
22. J. R. JOHNSON. *In* Organic chemistry. Vol. II. *Edited by* H. Gilman. John Wiley & Sons Inc., New York. 1957. p. 1922.

Can. J. Chem. Downloaded from www.nrcresearchpress.com by 210.87.254.5 on 09/05/12
For personal use only.

A NUCLEAR MAGNETIC RESONANCE INVESTIGATION OF THE PROTONATION OF AMIDES IN FLUOROSULPHURIC ACID

R. J. GILLESPIE AND T. BIRCHALL
Department of Chemistry, McMaster University, Hamilton, Ontario
Received August 30, 1962

ABSTRACT

The proton resonance spectra of solutions of acetamide, *N,N*-dimethylacetamide, formamide, and *N,N*-dimethylformamide in fluorosulphuric acid have been studied at temperatures between 25° and −98°. At low temperatures a new peak appears in the spectra of solutions of all four compounds which is not present at room temperatures and which, from peak areas and other considerations, may be assigned with certainty to the $\rangle C{=}\overset{+}{O}H$ group. It is thereby unambiguously established that these amides protonate on the carbonyl oxygen and not on the nitrogen atom.

Can. J. Chem. Downloaded from www.nrcresearchpress.com by 210.87.254.5 on 09/05/12
For personal use only.

The structure of the ion formed when amides are protonated has been the subject of discussion since Hantzsch (1) first presented evidence for *O*-protonation of benzamide in concentrated sulphuric acid from ultraviolet absorption spectra studies. A variety of other evidence has since been put forward by other workers in support of *O*-protonation but much evidence has also been adduced in favor of *N*-protonation (II). All this previous work has been summarized by Katritzky and Jones (2), who conclude that the evidence as a whole strongly indicates that amides are predominantly protonated at the oxygen atom.

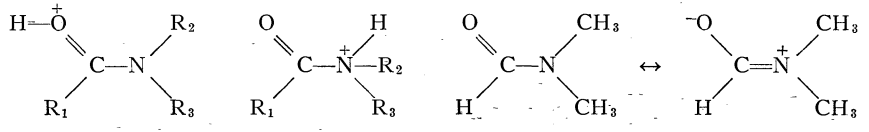

I II III

Perhaps the strongest evidence for *O*-protonation has come from proton magnetic resonance studies. For example, the spectrum of pure liquid dimethylformamide shows two peaks of equal area for the *N*-methyl groups (3, 4). It is concluded that the two methyl groups have different environments because of restricted rotation about the OC—NMe_2 bond, due to its partial double-bond character (III). Fraenkel and Niemann (5) have shown that these two peaks remain unchanged in solution in aqueous strong acids and in 100% H_2SO_4 and D_2SO_4. They assume that in the *O*-protonated form (I) rotation around the OC—NMe_2 bond would still be restricted, while in the *N*-protonated form (II) the $NHMe_2^+$ group should be free to rotate; thus they concluded that the *O*-protonated form predominates in these strong acid solutions. For *N*-methylformamide the signal from the *N*-methyl protons is a doublet attributed to spin–spin coupling with the single hydrogen attached directly to nitrogen. This doublet collapses to a single peak in basic or weakly acidic solutions but reappears again as a doublet, and not a triplet, in strongly acidic media, which rules out the possibility of an NH_2Me^+ group. Similar results have been obtained for *N*-methylacetamide (6). A solution of acetamide in 100% sulphuric acid gives a spectrum consisting of two signals of relative areas 3:2 which have been interpreted as being due to the CH_3 and NH_2 peaks of an *O*-protonated cation (7).

Spinner, who obtained infrared evidence for *N*-protonation (8),* has suggested, however, that the n.m.r. results can also be explained on this basis (9). For example, he attributes the doublet *N*-methyl group signal observed in the spectrum of protonated *N*-methylacetamide to the non-equivalent hydrogen atoms H_a and H_b resulting from restricted rotation about the C—N bond in the *N*-protonated form (IV). However, this

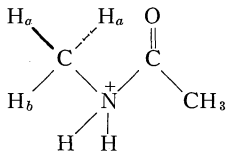

IV

would give components of the methyl group signal of relative areas 1:2 and not the equal areas observed. It must also be assumed that the expected spin–spin coupling between the *N*-methyl group and the two hydrogens directly attached to nitrogen is too weak to be observed. Spinner does, however, make the important point that all the n.m.r. evidence is rather indirect as in no case has a signal been observed in the spectrum from the proton supposedly captured by the oxygen atom in the *O*-protonated form. This has been attributed by other workers to rapid exchange of this proton with the solvent.

It is evident that the site of protonation could be determined unambiguously if the rate of exchange of the captured proton with the solvent could be slowed down sufficiently so that a separate signal for this proton could be observed in the spectrum. Earlier n.m.r. studies of the protonation of amides have been carried out at room temperature in aqueous acid solutions or in 100% sulphuric acid. In the present work we have studied solutions of formamide, acetamide, and their *N*,*N*-dimethyl derivatives in anhydrous fluorosulphuric acid. Fluorosulphuric acid is a stronger acid and a weaker base than 100% sulphuric acid (10) and has the added important advantage of a low freezing point of −89.0° (11). By recording the spectra of the fluorosulphuric acid solutions of these amides at sufficiently low temperatures it has been possible to observe for the first time the signal from the captured proton and thus to determine unambiguously the site of protonation.

EXPERIMENTAL

Materials

The amides were commercial samples which in the case of the solids were recrystallized. The n.m.r. spectra run at high gain showed no peaks that could be attributed to impurities. Fluorosulphuric acid was distilled twice in a dry atmosphere before use. The solutions of the amides in fluorosulphuric acid were approximately 6 mole%.

The n.m.r. spectra were recorded with a Varian H.R. 60 spectrometer equipped with a variable temperature probe and an integrator. Chemical shifts were measured from an external reference of tetramethylsilane using the audio side-band technique. No correction was made for differences in the bulk diamagnetic susceptibilities of the solution and the reference compound.

RESULTS AND DISCUSSION

Table I summarizes the chemical shifts and spin–spin coupling constants for the protonated forms of all four of the compounds studied.

Acetamide

The proton magnetic resonance spectrum of a 6 mole% solution of acetamide in fluorosulphuric acid at 25° consists of two peaks of relative areas 3.00:2.04 in addition to the

**Recent work (15) has shown, however, that Spinner's interpretation of the infrared data is probably not correct.*

Can. J. Chem. Downloaded from www.nrcresearchpress.com by 210.87.254.5 on 09/05/12
For personal use only.

TABLE I
Chemical shifts of amides in fluorosulphuric acid

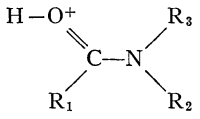

Amide	Temperature (°C)	−δ (p.p.m.) from external T.M.S. OH	CR_1	NR_2	NR_3	J (cycles/sec)
Acetamide	+25	—	2.76	8.28	8.28	
	−80	10.72	2.67	8.24	8.36	
	−92	10.40	2.67	8.26	8.36	
N,N-Dimethylacetamide	+25	—	2.73	3.55	3.55	
	−79	9.80	2.64	3.45	3.45	
Formamide	+25	—	8.55	8.68	8.68	$J_{N,R_{2,3}}$ 62±5 J_{R_1,R_3} 8.5
	−84.5	10.81	8.60	8.60	8.60	
	−98	10.69	8.60	8.60	8.60	
N,N-Dimethylformamide	+25	—	8.38	3.49	3.59	J_{R_1,R_3} 1.1 J_{R_1,R_2} 0.7
	−80	9.98	8.38	3.43	3.53	$J_{R_1,OH}$ 4.7

signals due to the solvent and the external tetramethylsilane reference (Fig. 1*a*). Essentially the same spectrum has been obtained previously for an aqueous solution of pH 7

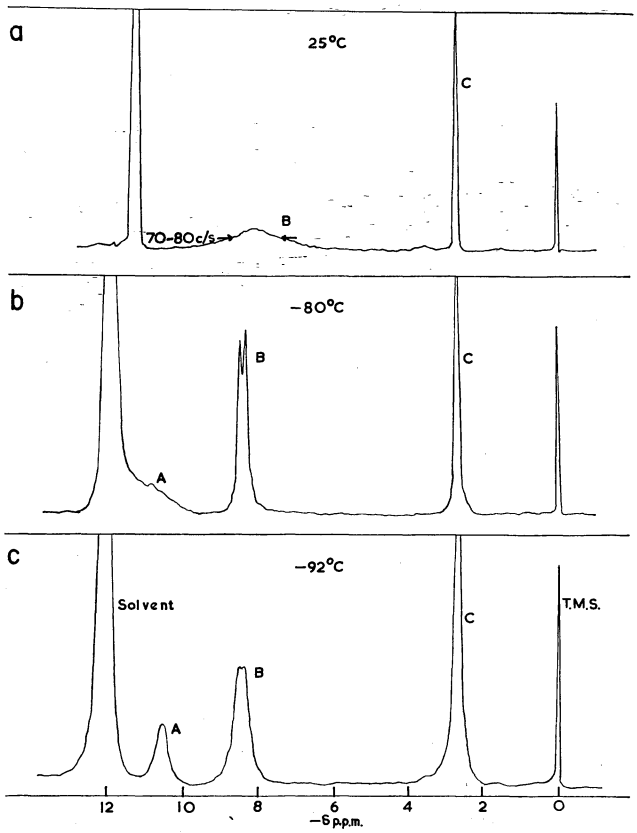

FIG. 1. Nuclear magnetic resonance spectra of a solution of acetamide in fluorosulphuric acid.

Can. J. Chem. Downloaded from www.nrcresearchpress.com by 210.87.254.5 on 09/05/12
For personal use only.

Can. J. Chem. Downloaded from www.nrcresearchpress.com by 210.87.254.5 on 09/05/12
For personal use only.

and for a solution in 100% sulphuric acid (7), and the peaks have been assigned to the CH_3 and NH_2 groups. The NH_2 peak B is approximately 70–80 cycles/sec wide, due to quadrupole relaxation of the N^{14} nucleus. As the temperature is lowered the NH_2 peak becomes sharper and eventually splits into a doublet. At −80° another peak, A, becomes visible on the high-field side of the large solvent peak (Fig. 1*b*) and shifts to higher field as the temperature is further decreased until at −92° it was recorded as a separate well-resolved peak (Fig. 1*c*). This new peak can only be assigned to a proton on the carbonyl oxygen, and in agreement with this conclusion the relative areas of the three peaks were found to be A:B:C::1.07:2.10:3.00, confirming their assignment to the OH, NH_2 and CH_3 groups respectively. Protonation on nitrogen with no exchange would give a spectrum consisting of two peaks of equal area.

The splitting of the NH_2 resonance may be attributed to non-equivalence of the two hydrogens as a consequence of restricted rotation about the C—N bond due to its partial double-bond character. The loss of resolution in the NH_2 doublet at −92° can probably be attributed to the increased viscosity of the solution, which is very close to the freezing point or possibly slightly supercooled. Even at −90° the OH peak has a width of 23.2 cycles/sec and although some of this broadening is perhaps due to the increased viscosity of the solutions much of it can probably be attributed to the fact that at this temperature slow OH-solvent proton exchange is still occurring.

N,N-Dimethylacetamide

The spectrum of a solution of dimethylacetamide in fluorosulphuric acid at 25° contains only two signals, B and C, due to the $N(CH_3)_2$ and $C{:}CH_3$ groups respectively (Fig. 2*a*).

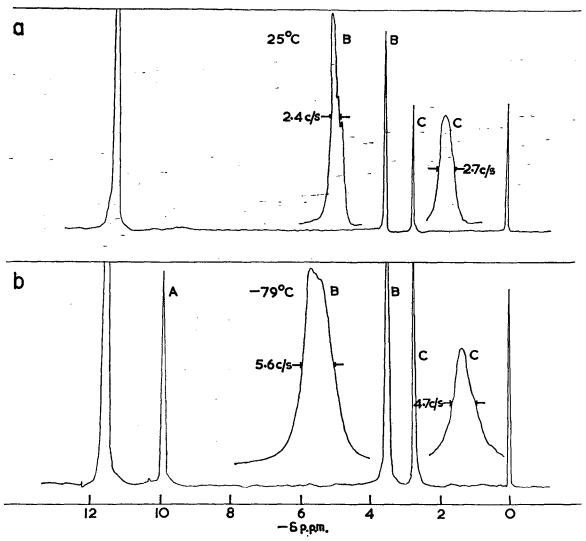

FIG. 2. Nuclear magnetic resonance spectra of a solution of *N,N*-dimethylacetamide in fluorosulphuric acid.

On decreasing the temperature a new peak, A, appears with a chemical shift of approximately −10 p.p.m. which is at first broad and then gradually narrows until it has a width of only 2.8 cycles/sec at −79° (Fig. 2*b*). This peak may be assigned to the protonated oxygen atom by comparison with the similar peak which occurs in the spectrum of acetamide at low temperatures. No further change in the spectrum occurs below −79°,

indicating that exchange of the captured proton with the solvent has become very slow. The relative areas of the three peaks at −79° were found to be A:B:C::0.96:5.91:3.00 and they are assigned to the OH, $N(CH_3)_2$, and $C.CH_3$ groups respectively. We may note that if *N*-protonation occurred three peaks of relative area 1:6:3 would be expected as for *O*-protonation. However, the new peak due to the captured proton has a chemical shift of −9.80 p.p.m., which is close to the chemical shift of −10.40 p.p.m. for the analogous peak in the acetamide spectrum which can be unambiguously assigned to the $=\overset{+}{O}H$ group. Moreover, A is a single sharp line showing no evidence of any fine structure, although if *N*-protonation occurred spin–spin coupling between the NH and $N(CH_3)_2$ protons would be expected since in a neutral aqueous solution of *N*-methylacetamide $J_{NH.NCH_3} = 3.8$ cycles/sec (5). At all temperatures the $N(CH_3)_3$ signal is essentially a single peak, although its width (2.4 cycles/sec at 25° and 5.6 cycles/sec at −79°), its unsymmetrical shape, and the presence of several ill-defined shoulders strongly indicate that it has an unresolved fine structure. This can presumably be attributed to a very small chemical shift between the two methyl groups, their non-equivalence being due to restricted rotation about the central C—N bond, and mutual spin–spin coupling. There is possibly also some coupling with the OH and $C.CH_3$ protons. The greater width of the $N(CH_3)_2$ signal at −79° can perhaps be attributed to a small increase in the chemical shift between the two methyl groups with decreasing temperature. In the pure liquid and in solution in various organic solvents the signals from the two *N*-methyl groups are clearly separated at room temperature (12). However, in 100% sulphuric acid Fraenkel and Franconi (7) were unable to resolve the two separate methyl groups. They attributed this to the broadening of the peaks caused by the high viscosity of sulphuric acid. However, as the viscosity of fluorosulphuric acid is only 1/10 that of sulphuric acid (11), this cannot be the only factor involved. Presumably the chemical shift between the *N*-methyl groups is smaller in the protonated than in the neutral amide. It is interesting to note that a recent study of the spectra of solutions of dimethylacetamide in a variety of organic solvents has shown that the chemical shift between the two methyl groups is solvent and concentration dependent and can become zero or even change sign in suitable solvents (12).

Formamide

The spectrum of pure liquid formamide at room temperature is shown in Fig. 3*a*. The broad peak C can be attributed to the NH_2 protons and the peak B to the formyl proton H_1 split by coupling with the H_3 proton (V) (13). The chemical shifts between the three

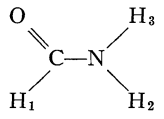

V

protons are relatively small and they will not therefore give rise to a simple first-order spectrum, which is the reason for the unsymmetrical nature of the formyl-proton doublet. In solution in fluorosulphuric acid the spectrum changes to that shown in Fig. 3*b*. It seems clear that the broad NH_2 peak has now split into the triplet expected for N^{14}—H coupling and that the middle peak of this triplet lies beneath the sharper doublet that can be attributed to H_1. Unresolved splitting due to coupling with H_2 in addition to H_3 is evident in the form of shoulders on the center peak. The observed separation of the outer components of the NH_2 triplet gives $J_{NH} = 62 \pm 5$ cycles/sec, which is in good

Can. J. Chem. Downloaded from www.nrcresearchpress.com by 210.87.254.5 on 09/05/12
For personal use only.

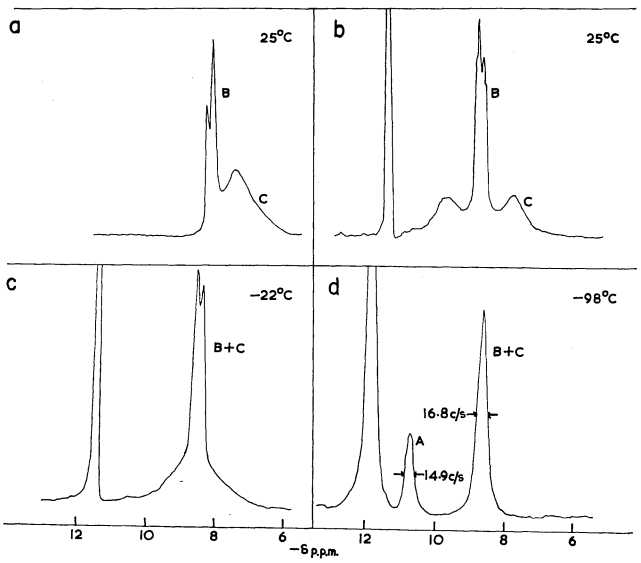

FIG. 3. Nuclear magnetic resonance spectra of (*a*) liquid formamide and (*b*, *c*, *d*) a solution of formamide in fluorosulphuric acid.

agreement with the value of 60±4 cycles/sec obtained by Roberts (14) for pure liquid formamide at temperatures above 50°. An integrated spectrum gave relative areas for the three peaks of 0.74:1.55:0.71, which is in reasonable agreement with the expected values of 0.67:1.66:0.67 in view of the extensive overlap of the broad peaks.

With decreasing temperature the NH_2 signal collapses to a single peak that is coincident with the peak due to the formyl proton (Fig. 3*c*). At −80° a new peak, A, appears at low field which may be attributed to the $C{=}\overset{+}{O}H$ group. At −98° the A peak has a chemical shift of −10.69 p.p.m. and integration of the spectrum gave relative peak areas A:B+C::1.00:3.03, in agreement with their assignment to the $C{=}\overset{+}{O}H$ and NH_2 plus CH groups respectively. The width of the $C{=}\overset{+}{O}H$ peak (14.9 cycles/sec) presumably indicates that exchange of this proton with the solvent is still occurring at −98°, although some of the broadening could be due to the increased viscosity of the solvent at this temperature.

N,N-Dimethylformamide

The spectrum of a solution of dimethylformamide in fluorosulphuric acid at 25° consists of the peak B, due to the formyl proton, and the doublet C, due to the two *N*-methyl groups (Fig. 4). For the pure liquid dimethyformamide and for solutions in a large number of organic solvents it has been found that two peaks are obtained for the *N*-methyl groups and it has been shown that this is because they are non-equivalent as a consequence of hindered rotation about the OC—N bond (3, 4, 12). The peak at higher field is split into a doublet of separation 1.1 cycles/sec and the lower field peak is split into a doublet of separation 0.7 cycle/sec. These splittings are almost exactly twice as large as those found by Hatton and Richards (12) for the pure liquid (0.65 and 0.3 cycle/sec respectively). The splitting is attributed to coupling of the *N*-methyl groups with the formyl proton, and the high-field peak has been assigned to the $CH_3{}^a$ group trans to the formyl hydrogen and the low-field peak to the $CH_3{}^b$ group cis to the formyl proton (VI). The greater

Can. J. Chem. Downloaded from www.nrcresearchpress.com by 210.87.254.5 on 09/05/12
For personal use only.

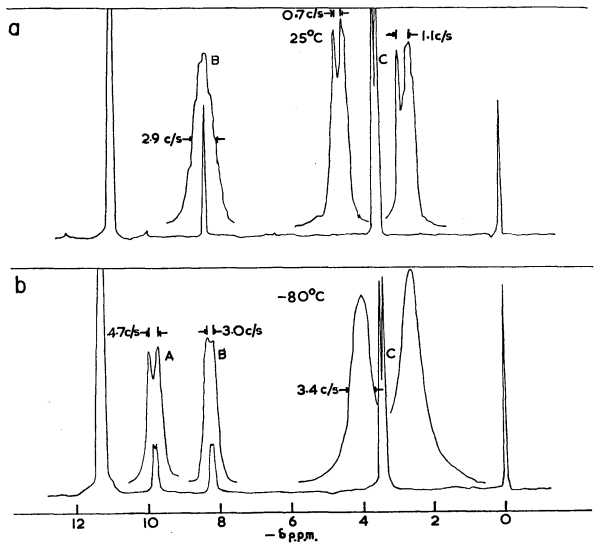

FIG. 4. Nuclear magnetic resonance spectra of a solution of *N*,*N*-dimethylformamide in fluorosulphuric acid.

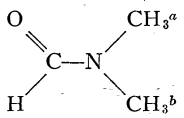

VI

coupling between the formyl proton and the *N*-methyl groups in the protonated form than in the neutral amide may reasonably be associated with a greater double-bond character of the central C—N bond in the protonated form. In solutions of dimethylformamide in 100% H_2SO_4 Fraenkel and Franconi (7) found rather larger splittings of the *N*-methyl resonances of 1.2 and 1.7 cycles/sec respectively. The reason for the difference between their results and ours is not clear. The resonance of the formyl proton is somewhat broad (2.9 cycles/sec) and a number of shoulders on the line strongly indicate unresolved fine structure. This must arise from spin–spin coupling between the formyl proton and the *N*-methyl groups. At low temperatures a new peak, A, appears in the spectrum at low field (−9.98 p.p.m.) which can evidently be attributed to the OH group of the *O*-protonated form. At −80° the relative areas of the peaks were found to be A:B:C::1.04:0.96:6.00, in agreement with the suggested assignment. The OH and CH peaks are both doublets due to mutual spin–spin coupling, $J_{CH,OH} = 4.7$ cycles/sec. That the resolution of the CH doublet is poorer than that of the OH doublet is presumably due to weak spin–spin coupling of the CH proton with the two *N*-methyl groups. The reason for the loss of fine structure in the doublet C due to the *N*-methyl groups is, however, not clear.

Benzamide and N-Methylbenzamide

A preliminary investigation of these amides in fluorosulphuric acid has been carried out and it has been found that proton exchange is sufficiently slow at low temperatures to allow the observation of a separate peak due to the captured proton. The *N*-methyl resonance in *N*-methylbenzamide is a doublet due to coupling with the single NH proton, $J \approx 5$ cycles/sec, but the position of the resonance due to the NH protons is uncertain and work on these and other amides is continuing.

Can. J. Chem. Downloaded from www.nrcresearchpress.com by 210.87.254.5 on 09/05/12
For personal use only.

Quadrupole Relaxation

The signal from protons bonded to N^{14} may be a broad single line or have a triplet structure (14). A sharp triplet is obtained when the electronic configuration around the nitrogen nucleus is symmetrical as in NH_4^+. This arises from spin–spin coupling of the protons with the N^{14} nucleus, which has a spin of unity. Rapid relaxation of the N^{14} nucleus occurs, however, when its quadrupole moment interacts sufficiently strongly with fluctuating electric-field gradients and the triplet structure of the proton resonance then collapses to a single peak. Roberts (14) has found in a number of cases that the fluctuating field-gradients become less effective as the temperature is increased, i.e. with increase in the rate of molecular motions, and the relaxation rate correspondingly decreases and the broad single proton resonance tends to become a triplet. Conversely as the temperature is lowered the relaxation rate increases, leading to collapse of the triplet structure to a single peak. This was observed in the present work in the case of a formamide solution in fluorosulphuric acid. The triplet structure observed for the NH_2 proton resonance at room temperature collapses to a single peak on lowering the temperature. It is interesting to note also that the NH_2 signal changes from a broad single peak in pure formamide (13) to a triplet in a dilute solution in fluorosulphuric acid. Evidently quadrupole relaxation is less effective in the latter solution but the reason for this is not clear. Indeed, protonation on oxygen must, surely, increase the C—N double-bond character and thereby increase the electrical asymmetry around the nitrogen nucleus, which would be expected to lead to more effective rather than less effective quadrupole relaxation.

The broad NH_2 peak of acetamide also narrows as the temperature is lowered, the relaxation of the N^{14} nucleus eventually becoming sufficiently great that it is effectively decoupled from the protons. The proton signal then becomes relatively sharp, allowing the observation of separate signals from the two non-equivalent NH protons.

Can. J. Chem. Downloaded from www.nrcresearchpress.com by 210.87.254.5 on 09/05/12
For personal use only.

ACKNOWLEDGMENTS

We thank the Petroleum Research Fund of the American Chemical Society for generous financial aid and Mr. James Bacon for his able assistance with the operation and maintenance of the n.m.r. spectrometer.

REFERENCES

1. A. Hantzsch. Ber. **64**, 661 (1931).
2. R. A. Y. Jones and A. R. Katritzky. Chem. Ind. (London), 722 (1961).
3. W. D. Phillips. J. Chem. Phys. **23**, 1363 (1955).
4. H. S. Gutowsky and C. H. Holm. J. Chem. Phys. **25**, 1228 (1956).
5. G. Fraenkel and C. Niemann. Proc. Natl. Acad. Sci. U.S. **44**, 688 (1958).
6. A. Berger, A. Loewenstein, and S. Meiboom. J. Am. Chem. Soc. **81**, 62 (1959).
7. G. Fraenkel and C. Franconi. J. Am. Chem. Soc. **82**, 4478 (1960).
8. E. Spinner. Spectrochim. Acta, **15**, 95 (1959).
9. E. Spinner. J. Phys. Chem. **64**, 275 (1960).
10. J. Barr, R. J. Gillespie, and E. A. Robinson. Can. J. Chem. **39**, 1266 (1961).
11. J. Barr, R. J. Gillespie, and R. C. Thompson. Unpublished.
12. J. V. Hatton and R. E. Richards. Mol. Phys. **5**, 139 (1962).
13. L. H. Piette, J. D. Ray, and R. A. Ogg. J. Mol. Spectry. **2**, 66 (1958).
14. J. D. Roberts. J. Am. Chem. Soc. **78**, 4495 (1956).
15. R. Stewart and L. J. Muenster. Can. J. Chem. **39**, 401 (1961).

STÉROÏDES

CCXIX. PRÉPARATION ET PROPRIÉTÉS DE QUELQUES 17-ISO-PREGNANES ET 17-ISO-PREGNÈNES SUBSTITUÉS EN C-16*†

PIERRE CRABBÉ, MAGDALENA PÉREZ ET GLORIA VERA
Laboratoires de Recherches, Syntex, S.A., Mexico D.F., Mexico

Reçu le 14 Juin, 1962

ABSTRACT

The preparation of 16β-carboxy-(5α)-17α-pregnane-3β-ol-20-one and 16β-carbomethoxy-3β-fluoro-17α-Δ5-pregnene-20-one, as well as several of their derivatives, is described. The stereochemistry of these compounds is deduced from their optical rotatory dispersion curves.

Can. J. Chem. Downloaded from www.nrcresearchpress.com by 210.87.254.40 on 09/05/12
For personal use only.

Il a été montré précédemment (1) que, douée d'une réactivité particulière, la liaison éthylénique 16,17 du 3β-hydroxy 20-oxo pregna-5,16-diène (I)‡ se prête aisément aux réactions d'addition. C'est ainsi que le 3β-hydroxy 16α-cyano 20-oxo pregna-5-ène (IX), produit de la réaction du cyanure de potassium sur la diènone (I), a ouvert la voie à de larges possibiltés de synthèses (1). Dans un mémoire précédent (2), on a décrit la préparation et discuté la stéréochimie des dérivés du pregna-5-ène et 17-iso-pregna-5-ène substitués en C-16 présentant les différentes configurations possibles aux positions 16 et 17. La présente note a pour objet, d'une part, de généraliser certaines observations faites dans la série du 17-iso-pregna-5-ène (2) par des résultats identiques obtenus avec l'iso-pregnane substitué en C-16; et de signaler, d'autre part, la synthèse du 16β-méthoxycarbonyl 3β-fluoro 20-oxo (17α)pregna-5-ène (XVI*a*).

Le 3β-acétoxy 20-oxo 16:17α-époxy pregna-5-ène (II), d'accès aisé (3), a été choisi comme composé de départ pour la synthèse du 16β-carboxy 3β-hydroxy 20-oxo (5α,17α)-pregnane (VIII*a*). On s'est adressé à cet époxyde car, tout en rappellant la diènone (I), la double liaison réactive 16–17 s'y trouve protégée d'une manière adéquate (II). La réduction catalytique sur charbon palladié de la liaison éthylénique 5,6 du composé (II) conduit au 3β-acétoxy 20-oxo 16:17α-époxy (5α)pregnane (III), dont les constantes physiques sont en accord avec celles du composé décrit antérieurement (4).

L'étape suivante consiste à régénérer la liaison éthylénique 16,17. Tandis que différentes méthodes permettent de réduire une fonction époxyde du type (III) en énone correspondante (IV), c'est la technique au chlorure de chromyle§ qui a donné les résultats les plus satisfaisants. L'époxyde (III), soumis à ce procédé, fournit un mélange réactionnel qui a été séparé par chromatographie en quatre constituants différents. Le premier composé, élué à l'hexane et obtenu avec un rendement d'environ 3%, répond à la structure de la dièneone (VI). Ce composé résulte vraisemblablement de la déshydratation de la fonction hydroxyle en position 3 de l'alcool (IV*a*), identifié également parmi les produits secondaires de cette réaction (*vide infra*). Le second composé, produit principal de la réaction, obtenu avec environ 80% de rendement et élué au mélange hexane–benzène, est le 3β-acétoxy 20-oxo (5α)pregna-16-ène (IV*b*) attendu. Une élution ultérieure de la

*Communication précédente dans cette série: Stéroïdes. CCXVIII. A. Bowers, J. A. Edwards et J. C. Orr. *J. Org. Chem.* **27**, 3378 (1962).

†*Ce travail constitue une partie de la thèse de license soumise par M. P. à l'Université de Mexico et par G. V. à l'Université de Guanajuato.*

‡*On adopte dans ce travail la nomenclature proposée par J. P. Mathieu et A. Petit dans Pouvoir Rotatoire Naturel, Stéroïdes, Masson et Cie, Paris, 1956, pp. 3f et suivantes.*

§*Pour une discussion du mécanisme de cette réaction ainsi que pour une référence de base, voir référence 5.*

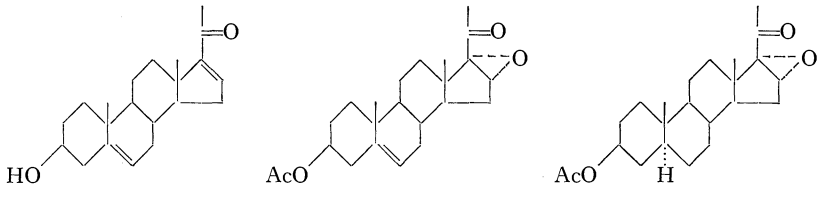

I II III

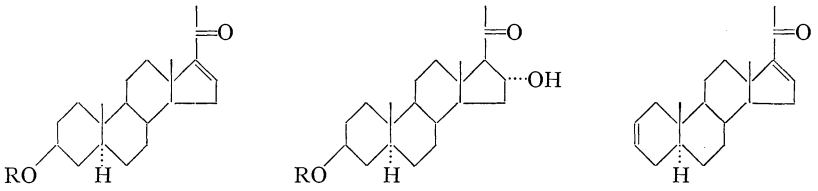

IV V VI

a, R = H
b, R = Ac

a, R = H
b, R = Ac

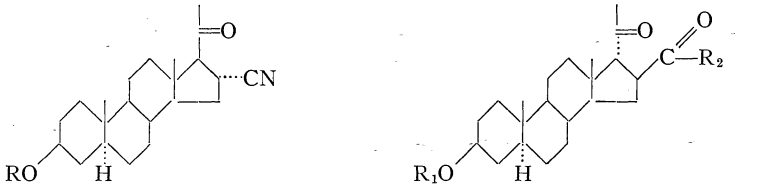

VII VIII

a, R = H
b, R = Ac

a, R_1 = H, R_2 = OH
b, R_1 = Ac, R_2 = OH
c, R_1 = Ac, R_2 = NH_2

colonne de chromatographie par un mélange benzène–chloroforme permet d'isoler, avec 5%, le 16α-hydroxy 3β-acétoxy 20-oxo (5α)pregnane (V*b*). Ce composé est l'acétate en position 3 du 3β,16α-dihydroxy 20-oxo (5α)pregnane (V*a*), facteur d'excrétion du sodium du cortex surrénal (6). Le même mélange, benzène–chloroforme, élue finalement 2% environ de 3β-hydroxy 20-oxo (5α)pregna-16-ène (IV*a*). L'hydrolyse alcaline d'un échantillon de l'acétate (IV*b*) obtenu ci-dessus conduit à un composé identique, confirmant la structure (IV*a*) assignée à la substance isolée du mélange réactionnel.

L'addition de Michael des éléments de l'acide cyanhydrique sur la double liaison 16,17 de l'acétate (IV*b*) fournit quantitativement le 3β-hydroxy 16α-cyano 20-oxo (5α)pregnane (VII*a*). La configuration β assignée à la chaîne latérale en position 17 résulte de l'effet Cotton positif présenté par la courbe de dispersion rotatoire de ce composé (VII*a*) et de son dérivé acétylé (VII*b*) (7), comme l'indique la Fig. 1. Par analogie avec d'autres additions sur cette liaison éthylénique 16,17 (8), on assigne la configuration α au groupement cyano de ce dérivé d'addition (VII*a*). L'attaque de l'anion CN^-, qui s'effectue par la face α stériquement la moins encombrée, justifie cette attribution de configuration qui s'est trouvé confirmée par l'examen du spectre de résonance magnétique nucléaire du cyano-acétate (VII*b*).* Cette conclusion est en accord avec la configuration assignée à cette fonction dans le composé (IX) obtenu dans la série du pregna-5-ène (2).

**Une étude détaillé des spectres de résonance magnétique nucléaire des composés obtenus dans ces séries (2) est actuellement en préparation (9).*

Can. J. Chem. Downloaded from www.nrcresearchpress.com by 210.87.254.40 on 09/05/12
For personal use only.

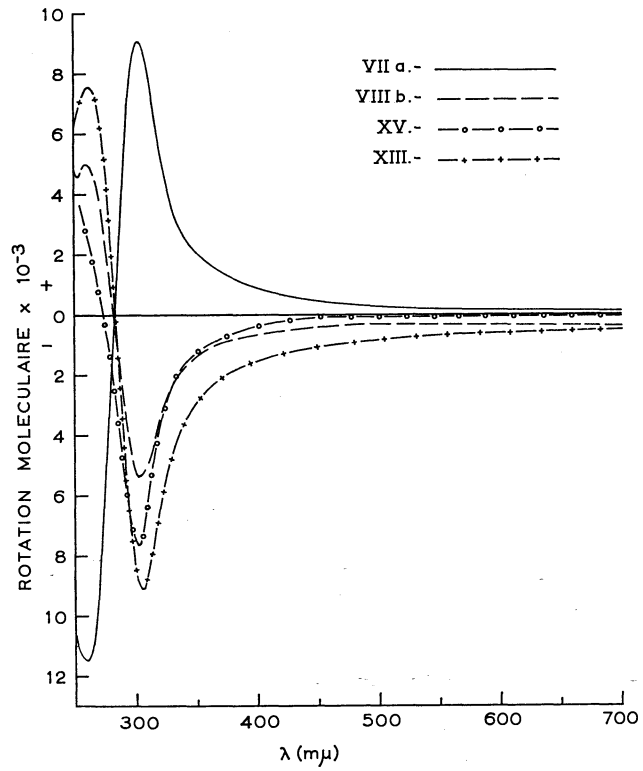

FIG. 1. Courbes de dispersion rotatoire du 3β-hydroxy 16α-cyano 20-oxo (5α)pregnane (VII*a*), 16β-carboxy 3β-acétoxy 20-oxo (5α,17α)pregnane (VIII*b*), 16α-méthoxycarbonyl 3β-acétoxy 20-oxo (5α,17α)-pregnane (XIII) et 16β-méthoxycarbonyl 6,20-dioxo 3α:5-cyclo (5α,17α)pregnane (XV).

Le groupement cyano de ce composé d'addition (VII*a*) est ensuite hydrolysé en milieu fortement alcalin (1, 2) en acide correspondant (VIII*a*). Lorsque l'acide (VIII*a*) est acétylé à température ordinaire, l'acétate correspondant (VIII*b*) est obtenu, qui, traité successivement par le chlorure de thionyle puis par l'ammoniac, conduit au 16β-carbamoyl 3β-acétoxy 20-oxo (5α,17α)pregnane (VIII*c*). Comme dans la série du pregna-5-ène, l'hydrolyse de (VII*a*) en (VIII*a*) est accompagnée d'une double inversion de configuration en C-16 et C-17 (1(*c*), 2). Ceci se déduit aisément de l'examen des courbes de dispersion rotatoire de l'acétoxy-acide (VIII*b*) et de l'acétoxy-amide (VIII*c*). L'effet Cotton négatif présenté par la courbe de dispersion rotatoire de l'acétoxy-acide (VIII*b*) (Fig. 1) conduit à assigner la configuration β à la chaîne carboxylée en position 16. En effet, les courbes de dispersion rotatoire des composés de la série (VIII) sont superposables à celles des composés correspondants obtenus dans la série de l'iso-pregna-5-ène (X) (7). En outre, comme l'indique la Fig. 1, l'intensité du creux qui caractérise l'acétate-acide (VIII*b*) est moins négative que celle associée au creux de la courbe de dispersion rotatoire de l'ester (XIII), appartenant à la série 16α,17α, dont la préparation est signalée ci-dessous. L'acide (VIII*a*) présente par conséquent la stéréochimie du 16β-carboxy (17α)pregnane, en accord avec les observations faites dans la série du pregna-5-ène (2).

Il a été montré antérieurement (2, 10) que le traitement de l'acide (X*a*) dans des conditions particulières conduit à la lactone d'énol (XI). En outre, lorsque cette lactone (XI)

Can. J. Chem. Downloaded from www.nrcresearchpress.com by 210.87.254.40 on 09/05/12
For personal use only.

est portée à reflux dans le méthanol en présence de bicarbonate de potassium, le 16α-méthoxycarbonyl 3β-acétoxy 20-oxo (17α)pregna-5-ène (XII) est obtenu (2). L'hydrogénation sélective sur platine de la double liaison 5,6 fournit le (5α,17α)pregnane correspondant (XIII). La courbe de dispersion rotatoire de l'ester (XIII), dont l'effet Cotton négatif intense est caractéristique de la substitution 16α-carboxy 17α-acétyle du noyau stéroïde (7), est l'image spéculaire (Fig. 1) de la courbe de dispersion rotatoire du composé d'addition (VII*a*).

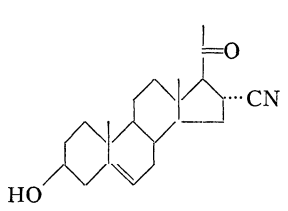

IX

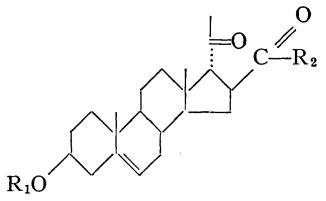

X

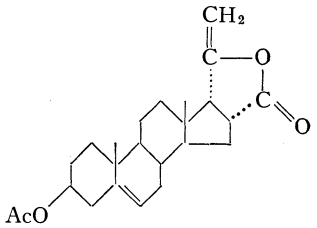

XI

a, R_1 = H, R_2 = OH
b, R_1 = H, R_2 = OCH_3
c, R_1 = Tos, R_2 = OCH_3

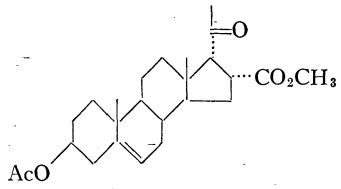

XII

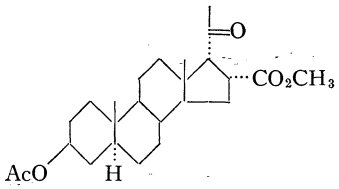

XIII

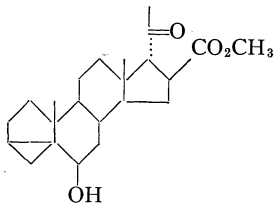

XIV

Par suite de l'importante activité progestative présentée par le 3β-fluoro 20-oxo pregna-5-ène (11), il semblait intéressant de préparer l'homologue correspondant dans la série du 16β-carboxy iso-pregna-5-ène. Le 16β-carbamoyl 3β-fluoro 20-oxo (17α)pregna-5-ène (XVI*c*) a été préparé par l'intermédaire du 6β-hydroxy cyclo-stéroïde (XIV). Le composé de départ utilisé pour cette synthèse est le 16β-méthoxycarbonyl 3β-hydroxy 20-oxo (17α)pregna-5-ène (X*b*), obtenu par la suite de réactions I $\rightarrow$ IX $\rightarrow$ X*a* $\rightarrow$ X*b*, décrite antérieurement (1, 2). Le traitement de l'alcool (X*b*) par le chlorure de l'acide *p*-toluène sulfonique dans la pyridine fournit le tosylate correspondant (X*c*). La solvolyse de ce tosylate (X*c*) dans l'acétone en présence d'acétate de potassium conduit par le jeu d'un réarrangement classique (12) au cyclo-stéroïde (XIV).

La preuve de la structure de ce 16β-méthoxycarbonyl 6β-hydroxy 20-oxo 3α:5-cyclo (5α,17α)pregnane (XIV) résulte de l'oxydation de ce composé, par l'acide chromique dans l'acétone en présence d'acide sulfurique (13), en 6,20-dicétone correspondante (XV). Ce composé (XV) ne présente aucune absorption en ultraviolet dans la région de 240 mμ, même après traitement alcalin. En outre, sa courbe de dispersion rotatoire, illustrée sur la Fig. 1, confirme la structure et la stéréochimie représentée en (XV). L'allure générale de cette courbe est caractérisée par l'absence d'effets Cotton multiple associés à un système Δ^4-3-cétonique. Par ailleurs, l'effet Cotton fortement négatif présenté par cette dicétone résulte de la combinaison (14) de l'amplitude du pouvoir rotatoire moléculaire

Can. J. Chem. Downloaded from www.nrcresearchpress.com by 210.87.254.40 on 09/05/12
For personal use only.

(15) du groupement cétonique en position 6, caractérisé par un effet Cotton *négatif* (16), et de la fonction 17α-acétyle.

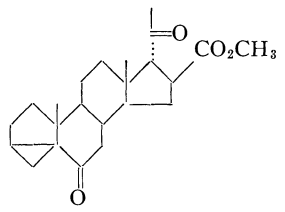

XV

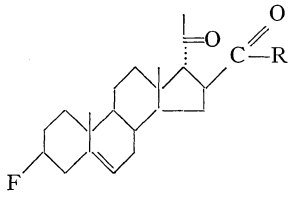

XVI

a, R = OCH_3
b, R = OH
c, R = NH_2

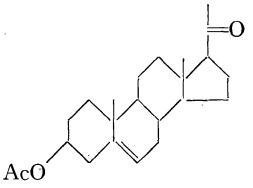

XVII

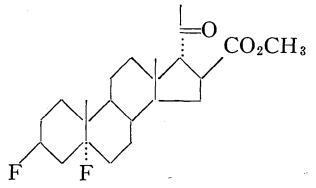

XVIII

Le traitement du 6β-hydroxy cyclo-stéroïde (XIV) par l'acide fluorhydrique conduit à un mélange qui, séparé par chromatographie, a permis d'identifier trois contituants. Le produit principal de la réaction, obtenu avec un rendement de 65%, est élué en premier lieu et répond aux propriétés du 16β-méthoxycarbonyl 3β-fluoro 20-oxo (17α)pregna-5-ène (XVI*a*). Ce dérivé fluoré (XVI*a*) résulte d'une attaque nucléophile en position 3 du composé (XIV) par l'ion F^- (17). L'analyse élémentaire du second constituant du mélange (11%), légèrement plus polaire sur la colonne que le composé principal de la réaction (XVI*a*), répond à la formule empirique $C_{23}H_{34}O_3F_2$. Par analogie avec la remarquable addition d'acide fluorhydrique sur la liaison éthylénique 5,6 de l'acétate de pregnénolone (XVII), observée dans des conditions expérimentales identiques (18), la structure (XVIII) est proposée pour ce composé difluoré. Ce 3β,5α-difluoro-stéroïde (XVIII) résulte vraisemblablement de l'addition d'acide fluorhydrique sur la liaison éthylénique 5,6 du fluoro-ester (XVI*a*), grâce à la présence du tétrahydrofuranne, qui, jouant le rôle d'accepteur de protons, augmente ainsi la concentration en ions fluorures dans le milieu réactionnel (19). Enfin, le troisième produit de cette réaction (isolé avec 8%) répond aux propriétés du 3β-hydroxy-ester (X*b*), produit probable de l'hydrolyse du 3β-fluoro-ester (XVI*a*) dans les conditions de l'expérience.

A partir de l'ester (XVI*a*), la fluoro-amide (XVI*c*) est préparée par hydrolyse alcaline, traitement de l'acide libre (XVI*b*) au chlorure de thionyle, suivi de réaction avec l'ammoniac. La configuration assignée aux dérivés fluorés (XVI*a*), (XVI*c*) et (XVIII) résulte également de l'examen de leurs courbes de dispersion rotatoire. Celles-ci, caractérisées par un effet Cotton négatif, sont superposables aux courbes des composés correspondants de la série oxygénée en position 3 (X) (7). Dès lors, la stéréochimie 16β-carboxy 17α-acétyle est attribuée à ces dérivés fluorés (XVI*a*), (XVI*c*) et (XVIII).

PARTIE EXPÉRIMENTALE

Les microanalyses ont été effectuées par le Dr. A. Bernhardt, Max Planck Institut, Mühlheim (Allemagne), et par les Laboratoires Midwest, Forest Lane, Indianapolis (Etats Unis).

Les pouvoirs rotatoires sont mesurés à 16–22° avec un tube de 1 dm pour la raie jaune du sodium (589 mμ).

Can. J. Chem. Downloaded from www.nrcresearchpress.com by 210.87.254.40 on 09/05/12
For personal use only.

Les courbes de dispersion rotatoire ont été prises avec un spectropolarimètre enregistreur Rudolph. Les pouvoirs rotatoires reportés sur la Fig. 1 et dans cette section sont exprimés en pouvoirs rotatoires moléculaires [Φ] (15).

Les points de fusion ont été mesurés en tubes capillaires à l'aide d'un appareil "Mel-temp"; ils ne sont pas corrigés.

Les spectres infra-rouges ont été obtenus avec un spectrophotomètre Perkin–Elmer, modèle 21, prisme NaCl.

Les spectres ultraviolets ont été déterminés avec un spectrophotomètre Beckman, modèle DU; EtOH: alcool éthylique à 95%.

Nous remercions M. J. C. Matthews pour les déterminations spectroscopiques et les pouvoirs rotatoires.

3β-Acétoxy 20-oxo 16:17α-époxy (5α)pregnane (III)

On dissout 1 g de l'époxy-pregnène (II) (3) dans 10 ml d'acétate d'éthyle et cette solution est hydrogénée en présence de 400 mg de palladium sur charbon (à 5%), jusqu'à absorption d'une molécule d'hydrogène. Après filtration du catalyseur, lavage au chloroforme et évaporation des solvents sous vide, on obtient 1.040 mg de (III), p.f. 178–181°. On recristallise par dissolution dans l'acétone, dilution avec l'hexane et évaporation de l'acétone; p.f. 183–185°; $[\alpha]_D$ +48° (*c*, 0.2; $CHCl_3$). Spectre UV: λ_{max}^{EtOH} 295 mμ (log ε: 1.56). Spectre IR: ν_{max}^{KBr} 1739 et 1242 cm^{-1} (acetate), 1706 cm^{-1} (20-cétone). (Plattner *et al.* (4(*b*)): p.f. 186–187°; $[\alpha]_D$ +52° (*c*, 1.2; $CHCl_3$).)

Traitement de l'époxyde (III) par le chlorure de chromyle

On dissout 1 g de l'époxyde (III) dans 20 ml d'acétone, ajoute 20 ml d'acide acétique glacial et agite cette solution durant 10 minutes à température ambiante. A ce mélange homogène, on additionne lentement une solution de chlorure de chromyle préparée comme suit (5): on mélange 15 g de zinc, 20 ml d'eau, 1.2 g de chlorure mercurique et 1 ml d'acide chlorhydrique concentré et agite ce mélange jusqu'à obtention d'une solution claire, qui est décantée; l'amalgame est ensuite lavé à l'eau. On ajoute alors à cet amalgame 25 ml d'eau, puis 6 ml d'acide chlorhydrique concentré. On fait ensuite passer un lent courant d'anhydride carbonique à travers cette solution. Le chlorure chromique (8 g) est ajouté par petites portions, tandis que le mélange réactionnel est agité vigoureusement jusqu'au virage de la coloration verte au bleu. Après addition de cette solution à la solution contenant le stéroïde, le mélange réactionnel est agité vigoureusement durant 30 minutes. On ajoute alors de l'eau et de la glace et extrait plusieurs fois le composé organique au chloroforme. La phase organique est concentrée sous vide, 100 ml d'acétone sont ajoutés, puis 1 ml d'acide chlorhydrique concentré. Après 2 heures de chauffage à reflux, le mélange réactionnel est repris par l'eau et le composé organique est extrait plusieurs fois au chloroforme. On lave à l'eau à neutralité, sèche sur sulfate de sodium anhydre et évapore les solvants sous vide.

Le produit brut obtenu (95%) est chromatographié sur 50 g d'alumine neutre. L'élution de la colonne par l'hexane fournit 35 mg de *20-oxo (5α)pregna-2,16-diène* (VI), qui, recristallisé dans un mélange acétone–hexane, présente les constantes physiques: p.f. 148–151°; $[\alpha]_D$ +48° (*c*, 0.2; $CHCl_3$). Spectre UV: λ_{max}^{EtOH} 240 mμ (log ε: 3.94), 318 mμ (log ε: 1.77). Spectre IR: ν_{max}^{KBr} 1656 et 1582 cm^{-1} (Δ^{16}-20-cétone). Anal. Calc. pour $C_{21}H_{30}O,1/2CH_3COCH_3$: C, 82.51; H, 10.16. Trouvé: C, 82.46; H, 10.53.

L'élution par un mélange hexane–benzène (98:2) conduit à 780 mg du composé (IV*b*), qui, recristallisé dans un mélange de chlorure de méthylène et hexane, fournit l'échantillon analytique de *3β-acétoxy 20-oxo (5α)pregna-16-ène* (IV*b*); p.f. 164–165°; $[\alpha]_D$ +43° (*c*, 1; $CHCl_3$). Spectre UV: λ_{max}^{EtOH} 240 mμ (log ε: 4.0), 318 mμ (log ε: 1.76). Spectre IR: ν_{max}^{KBr} 1730 et 1248 cm^{-1} (acétate), 1656 et 1587 cm^{-1} (Δ^{16}-20-cétone). (Plattner *et al.* (4(*b*)): p.f. 166–167°; $[\alpha]_D$ +42° (*c*, 1.2; $CHCl_3$).) Anal. Calc. pour $C_{23}H_{34}O_3$: C, 77.16; H, 9.57; O, 13.41. Trouvé: C, 76.81; H, 9.33; O, 13.42.

L'élution ultérieure de la colonne de chromatographie par un mélange benzène–chloroforme (3:1) conduit ensuite à 50 mg de *16α-hydroxy 3β-acétoxy 20-oxo (5α)pregnane* (V*b*), dont l'échantillon analytique, obtenu par recristallisation dans un mélange acétone–hexane, présente les constantes suivantes: p.f. = 185–187°; $[\alpha]_D$ +48° (*c*, 0.8; $CHCl_3$). Spectre UV: λ_{max}^{EtOH} 280 mμ (log ε: 1.77). Spectre IR: ν_{max}^{KBr} 3333 cm^{-1} (OH), 1730 et 1248 cm^{-1} (acétate), 1701 cm^{-1} (20-cétone). (Neher *et al.* (6): p.f. 184–186°.) Anal. Calc. pour $C_{23}H_{36}O_4$: C, 73,36; H, 9.64. Trouvé: C, 72.79; H, 9.48.

Enfin, le dernier composé, de polarité très voisine de celle de (V*b*), est élué peu après celui-ci par le même mélange benzène–chloroforme (3:1). On obtient ainsi 15 mg de l'hydroxy-ènone (IV*a*); p.f. 182–185°. Ce composé s'est avéré identique au *3β-hydroxy 20-oxo (5α)pregna-16-ène* (IV*a*) obtenu ci-dessous par hydrolyse alcaline de l'acétate (IV*b*) (pas de dépression du point de fusion, et les spectres infra-rouges sont superposables).

Hydrolyse alcaline de l'acétate (IVb)

On abandonne 20 heures à la température ambiante la solution de 200 mg de (IV*b*) (p.f. 143–145°) et 200 mg d'hydroxyde de potassium dans 10 ml de méthanol. On dilue à l'eau, extrait à l'acétate d'ethyle, lave à neutralité, sèche et évapore à sec pour obtenir 160 mg; p.f. 183–186°. Après recristallisation dans un mélange acétone–hexane, on obtient le *3β-hydroxy 20-oxo (5α)pregna-16-ène* (IV*a*); p.f. 187–190°; $[\alpha]_D$ +36° (*c*, 0.4; $CHCl_3$). Spectre UV: λ_{max}^{EtOH} 240 mμ (log ε: 3.92), 320 mμ (log ε: 1.73). Spectre IR: ν_{max}^{KBr} 3413 cm^{-1} (OH), 1658 et 1590 cm^{-1} (Δ^{16}-20-cétone). Anal. Calc. pour $C_{21}H_{32}O_2$: C, 79.70; H, 10.19. Trouvé: C, 79.72; H, 9.83.

Can. J. Chem. Downloaded from www.nrcresearchpress.com by 210.87.254.40 on 09/05/12
For personal use only.

3β-Hydroxy 16α-cyano 20-oxo (5α)pregnane (VIIa)

Un mélange de 1 g de (IV*b*) dans 20 ml de méthanol contenant 1 g de cyanure de potassium et 2 ml d'eau est chauffé à reflux durant 2 heures. Le mélange réactionnel est repris par l'eau et le précipité qui se forme est filtré, lavé à l'eau et sèché. On récolte 1.1 g de (VII*a*), p.f. 195–202°, qui est recristallisé dans un mélange chlorure de méthylène et méthanol; p.f. 226–227°; $[\alpha]_D$ +75° (*c*, 2; $CHCl_3$). DR: méthanol (*c*, 0.023): $[\Phi]_{700}$ +135°; $[\Phi]_{589}$ +165°; $[\Phi]_{302.5}$ +9060°; $[\Phi]_{262.5}$ −11,500°; $[\Phi]_{250}$ −10,650°. Spectre UV: λ_{max}^{EtOH} 272 mμ (log ε: 1.61). Spectre IR: ν_{max}^{KBr} 3436 cm^{-1} (OH), 2222 cm^{-1} (cyano), 1701 cm^{-1} (20-cétone). Anal. Calc. pour $C_{22}H_{33}O_2N$: C, 76.92; H, 9.68; O, 9.32; N, 4.08. Trouvé: C, 77.03; H, 9.69; O, 9.20; N, 4.07.

3β-Acétoxy 16α-cyano 20-oxo (5α)pregnane (VIIb)

Une solution de 500 mg de (VII*a*) dans 2 ml de pyridine anhydre et 1 ml d'anhydride acétique est abandonnée 16 heures à 22°. On dilue à l'eau, filtre le précipité que s'est formé, lave plusieurs fois avec une solution diluée d'acide chlorhydrique (5%), puis à l'eau et sèche ensuite sur sulfate de sodium anhydre. On obtient ainsi 550 mg de l'acétate (VII*b*), p.f. 166–169°. Une recristallisation dans un mélange chloroforme–méthanol donne de longs cristaux soyeux; p.f. 172–174°; $[\alpha]_D$ +62° (*c*, 1; $CHCl_3$). DR: méthanol (*c*, 0.060): $[\Phi]_{700}$ +182°; $[\Phi]_{589}$ +231°; $[\Phi]_{305}$ +9250°; $[\Phi]_{260}$ −1610°. Spectre UV: λ_{max}^{EtOH} 281 mμ (log ε: 1.68). Spectre IR: ν_{max}^{KBr} 2217 cm^{-1} (cyano), 1727 et 1250 cm^{-1} (acétate), 1701 cm^{-1} (20-cétone). Anal. Calc. pour $C_{24}H_{35}O_3N$: C, 74.76; H, 9.15; O, 12.45; N, 3.63. Trouvé: C, 74.68; H, 9.18; O, 12.66; N, 3.67.

16β-Carboxy 3β-hydroxy 20-oxo (5α,17α)pregnane (VIIIa)

On porte à reflux durant 1 heure, une solution contenant 1 g du dérivé cyané (VII*a*) dans 60 ml d'alcool éthylique, 4 g d'hydroxyde de potassium et 15 ml d'eau. Le mélange réactionnel est repris par l'eau, et extrait à l'acétate d'éthyle afin d'éliminer le composé de départ (VII*a*) (120 mg). La phase aqueuse est neutralisée à l'aide d'une solution diluée d'acide chlorhydrique (10%) et le précipité que se forme est filtré, lavé à pH neutre et sèché; p.f. 218–221° (695 mg). Après recristallisation dans le méthanol contenant quelques gouttes d'eau, on obtient l'échantillon analytique de l'acide (VIII*a*), p.f. 219–222°, $[\alpha]_D$ −38° (*c*, 0.4; CH_3OH). Spectre UV: λ_{max}^{EtOH} 281 mμ (log ε: 1.60). Spectre IR: $\nu_{max}^{CHCl_3}$ 3333 cm^{-1} (OH), 1720–1705 cm^{-1} (bande large et intense: 16-carboxy et 20-cétone). Anal. Calc. pour $C_{22}H_{34}O_4$: C, 72.89; H, 9.45; O, 17.66. Trouvé: C, 72.73; H, 9.49; O, 17.95.

16β-Carboxy 3β-acétoxy 20-oxo (5α,17α)pregnane (VIIIb)

On abandonne 18 heures à la température ambiante la solution de 500 mg de l'hydroxy-acide (VIII*a*) dans 1 ml de pyridine anhydre et 0.5 ml d'anhydride acétique. On dilue à l'eau, filtre le composé cristallin qui précipite, lave et sèche. Après recristallisation dans un mélange de chlorure de méthylène et hexane, l'acétate (VIII*b*) présente les caractéristiques physiques suivantes: p.f. 195–198°; $[\alpha]_D$ −51° (*c*, 1; $CHCl_3$). DR: méthanol (*c*, 0.060): $[\Phi]_{700}$ −348°; $[\Phi]_{589}$ −384°; $[\Phi]_{302.5}$ −5370°; $[\Phi]_{260}$ +4950°; $[\Phi]_{252.5}$ +4580°; $[\Phi]_{250}$ +4860°. Spectre IR: ν_{max}^{KBr} 3344 cm^{-1} (OH), 1733 et 1241 cm^{-1} (acétate), 1704 cm^{-1} (16-carboxyle et 20-cétone). Anal. Calc. pour $C_{24}H_{36}O_5$: C, 71.25; H, 8.97; O, 19.78. Trouvé: C, 71.03; H, 8.89; O, 19.82.

16β-Carbamoyl 3β-acétoxy 20-oxo (5α,17α)pregnane (VIIIc)

On dissout 1 g de l'acétoxy-acide (VIII*b*) dans 30 ml de benzène anhydre, puis distille lentement 10 ml de benzène pour éliminer toute trace d'humidité. Cette solution est ensuite refroidie dans la glace et 0.9 ml de chlorure de thionyle fraîchement distillé est ajouté lentement. Après 2 heures de chauffage à reflux, le mélange réactionnel est évaporé à sec, sous vide. On ajoute ensuite 30 ml de tétrahydrofuranne anhydre à ce chlorure de l'acide (VIII*b*). La solution est laissée au repos durant 15 minutes à 0°, puis on ajoute 25 ml d'hydroxyde d'ammonium. On conserve le mélange réactionnel, agité magnétiquement, 16 heures à la température ambiante. On dilue ensuite à l'eau, extrait à l'acétate d'éthyle, lave à neutralité, sèche et évapore à sec pour obtenir, après deux cristallisations dans un mélange de chlorure de méthylène et méthanol, 210 mg de l'amide (VIII*c*); p.f. 207–209°; $[\alpha]_D$ −57° (*c*, 1; $CHCl_3$). DR: méthanol (*c*, 0.060): $[\Phi]_{700}$ −230°; $[\Phi]_{589}$ −262°; $[\Phi]_{302.5}$ −5480°; $[\Phi]_{257.5}$ +5560°; $[\Phi]_{252.5}$ +5250°. Spectre IR: ν_{max}^{KBr} 3344 cm^{-1} (NH_2), 1656 et 1618 cm^{-1} (amide), 1730 et 1252 cm^{-1} (acétate), 1701 cm^{-1} (20-cétone). Anal. Calc. pour $C_{24}H_{37}O_4N$: C, 71.43; H, 9.24; O, 15.86; N, 3.47. Trouvé: C, 71.68; H, 9.23; O, 15.60; N, 3.36.

16α-Méthoxycarbonyl 3β-acétoxy 20-oxo (5α,17α)pregnane (XIII)

L'acétate-ester (XII) (200 mg) (2) dans 30 ml de méthanol est hydrogéné en présence de 50 mg d'oxyde de platine, préalablement réduit dans 10 ml de méthanol. En 2 heures on a fixé la quantité théorique d'hydrogène. Après filtration et lavage du catalyseur, le solvant est évaporé. On récolte 170 mg de (XIII), p.f. 197–200°. Pour analyse, on recristallise dans un mélange de chlorure de méthylène et hexane; p.f. 203–205°; $[\alpha]_D$ −79° (*c*, 0.6; $CHCl_3$). DR: Méthanol (*c*, 0.027): $[\Phi]_{700}$ −528°; $[\Phi]_{589}$ −587°; $[\Phi]_{305}$ −9100°; $[\Phi]_{262.5}$ +7530°; $[\Phi]_{250}$ +6190°. Spectre UV: λ_{max}^{EtOH} 283 mμ (log ε: 1.79). Spectre IR: ν_{max}^{KBr} 1739 et 1250 cm^{-1} (acétate), 1730 cm^{-1} (16-méthoxycarbonyl), 1701 cm^{-1} (20-cétone). Anal. Calc. pour $C_{25}H_{38}O_5$: C, 71.74; H, 9.15; O, 19.11. Trouvé: C, 71.68; H, 9.24; O, 19.15.

16β-Méthoxycarbonyl 3β-p-toluènesulfonate 20-oxo (17α)pregna-5-ène (Xc) (avec H. Barrera)

On laisse reposer 92 heures à la température ambiante la solution de 1.8 g de l'ester (X*b*) (p.f. 198–199°), préparé à partir de l'énone (I) suivant la séquence I → IX → X*a* → X*b*, décrite précédemment (1, 2),

Can. J. Chem. Downloaded from www.nrcresearchpress.com by 210.87.254.40 on 09/05/12
For personal use only.

et 4.12 g de chlorure de l'acide *p*-toluènesulfonique recristallisé, dans 70 ml de pyridine anhydre. Après réaction, on dilue à l'eau, extrait à l'acétate d'éthyle, lave à neutralité, sèche sur sulfate de sodium anhydre et concentre le solvant sous vide, pour obtenir 1.55 g du tosylate (X*c*), p.f. 145–148°. Après recristallisation dans un mélange de chlorure de méthylène et hexane, on obtient l'échantillon analytique; p.f. 148–149°; $[\alpha]_D$ −86° (*c*, 0.9; $CHCl_3$). Spectre UV: λ_{max}^{EtOH} 224 mμ (log ε: 4.09), 256 mμ (log ε: 2.65), 262 mμ (log ε: 2.74), 267 mμ (log ε: 2.69), 274 mμ (log ε: 2.57). Spectre IR: ν_{max}^{KBr} 1733 cm^{-1} (16-ester), 1709 cm^{-1} (20-cétone), 1603, 1351 et 1174 cm^{-1} (tosylate). Anal. Calc. pour $C_{30}H_{40}O_6S$: C, 68.14; H, 7.63; O, 18.16; S, 6.07. Trouvé: C, 68.09; H, 7.58; O, 18.46; S, 5.92.

16β-Méthoxycarbonyl 6β-hydroxy 20-oxo 3α:5-cyclo (5α,17α)pregnane (XIV) (avec H. Barrera)

Une solution contenant 822 mg de tosylate (X*c*) et 910 mg d'acétate de potassium dans 31 ml d'acétone aqueux (50%) est maintenue à reflux durant 24 heures. Ensuite, l'acétone est évaporé sous vide, et le précipité qui se forme est collecté sur filtre et séché. Le produit brut ainsi obtenu est chromatographié sur 50 g d'alumine neutre. Le benzène élue 465 mg de (XIV), p.f. 187–189°, qu'on recristallise dans un mélange de chlorure de méthylène et hexane; p.f. 191–192°; $[\alpha]_D$ −36° (*c*, 1; $CHCl_3$). DR: méthanol (*c*, 0.030): $[\Phi]_{700}$ −64°; $[\Phi]_{589}$ −157°; $[\Phi]_{300}$ −5400°; $[\Phi]_{255}$ +7740°; $[\Phi]_{250}$ +7510°. Spectre IR: ν_{max}^{KBr} 3509 cm^{-1} (OH), 1733 cm^{-1} (16-ester), 1701 cm^{-1} (20-cétone). Anal. Calc. pour $C_{23}H_{34}O_4$: C, 73.76; H, 9.15; O, 17.09. Trouvé: C, 73.84; H, 9.10; O, 17.16.

16β-Méthoxycarbonyl 6,20-dioxo 3α:5-cyclo (5α,17α)pregnane (XV) (avec H. Barrera)

On ajoute goutte à goutte 0.35 ml de solution 8 *N* d'acide chromique dans l'acide sulfurique dilué (13) à 374 mg de l'alcool (XIV) dans 15 ml d'acétone (distillé sur permanganate), le mélange étant maintenu à 0°. On agite à l'aide d'un barreau magnétique 5 minutes à 0°. On verse dans l'eau, ajoute une solution diluée de bicarbonate de sodium (10%), extrait le précipité à l'acétate d'éthyle, lave à neutralité, sèche et évapore. Ce composé brut, passé sur 5 g d'alumine neutre, est élué par un mélange hexane–benzène (4:1). L'échantillon analytique de la dicétone (XV) est obtenu par recristallisation dans un mélange de chlorure de méthylène et hexane; p.f. 154–155°; $[\alpha]_D$ −25° (*c*, 1; $CHCl_3$). DR: méthanol (*c*, 0.063): $[\Phi]_{700}$ −18°; $[\Phi]_{589}$ −54°; $[\Phi]_{302.5}$ −7620°; $[\Phi]_{255}$ +3640°. Spectre UV: λ_{max}^{EtOH} 282 mμ (log ε: 1.92) (identique en milieu alcalin). Spectre IR: ν_{max}^{KBr} 1739 cm^{-1} (16-ester), 1712 cm^{-1} (6-cétone), 1698 cm^{-1} (20 cétone). Anal. Calc. pour $C_{23}H_{32}O_4$: C, 74.16; H, 8.66; O, 17.18. Trouvé: C, 74.48; H, 8.46; O, 17.30.

16β-Méthoxycarbonyl 3β-fluoro (17α)pregna-5-ène (XVIa) et 16β-méthoxycarbonyl 3β,5α-difluoro (17α)-pregnane (XVIII)

Dans un récipient en polyéthylène, muni d'un barreau magnétique, et contenant un mélange d'un gramme de l'alcool (XIV) dans 50 ml de chlorure de méthylène anhydre et maintenu à −70°, on ajoute goutte à goutte, avec agitation, une solution refroidie à −70° de 4 g d'acide fluorhydrique dans 30 ml de tétrahydrofuranne anhydre. Le mélange réactionnel est ensuite laissé 24 heures à 0°. On verse alors prudemment cette solution dans un large excès de carbonate de sodium (solution à 10%) et extrait au chloroforme. Après traitement habituel on obtient 880 mg d'un mélange, p.f. 138–150°. Ce mélange est chromatographié sur 30 g d'alumine neutre. L'hexane élue 90% tandis que les derniers 10% sont élués au benzène–chloroforme (9:1); p.f. 201–203°; $[\alpha]_D$ −110° (*c*, 0.7; $CHCl_3$). Le point de fusion de mélange avec un échantillon du 16β-méthoxycarbonyl 3β-hydroxy (17α)pregna-5-ène (X*b*)(2) ne donne pas de dépression et les spectres infra-rouges sont superposables.

Le produit cristallisé obtenu par élution à l'hexane présente: p.f. 142–158°; $[\alpha]_D$ −71° (*c*, 0.8; $CHCl_3$). Une rechromatographie minutieuse de 200 mg de ce mélange sur 25 g d'alumine a permis une meilleure séparation des deux constituants. L'hexane élue 165 mg d'un composé, p.f. 141–145°, $[\alpha]_D$ −83° (*c*, 0.7; $CHCl_3$), qui, recristallisé dans un mélange de chlorure de méthylène et hexane, fournit l'échantillon analytique du composé fluoré (XVI*a*): cristaux primatiques; p.f. 146–146.5°; $[\alpha]_D$ −116° (*c*, 0.8; $CHCl_3$). DR: méthanol (*c*, 0.065): $[\Phi]_{700}$ −128°; $[\Phi]_{589}$ −271°; $[\Phi]_{302.5}$ −6330°; $[\Phi]_{260}$ +3140°. Spectre IR: ν_{max}^{KBr} 1735 cm^{-1} (16-ester), 1701 cm^{-1} (20-cétone). Anal. Calc. pour $C_{23}H_{33}O_3F$: C, 73.36; H, 8.84; F, 5.05. Trouvé: C, 73.35; H, 8.71; F, 5.57.

L'élution ultérieure de la colonne de chromatographie par un mélange hexane–benzène (9:1) conduit à environ 25 mg d'un composé; p.f. 181–189°; $[\alpha]_D$ −59° (*c*, 0.2; $CHCl_3$). Par recristallisation de cette substance dans un mélange de chlorure de méthylène et hexane, on obtient le composé difluoré (XVIII), p.f. 192–194°; $[\alpha]_D$ −59° (*c*, 0.4; $CHCl_3$). DR: méthanol (*c*, 0.065): $[\Phi]_{700}$ −187°; $[\Phi]_{589}$ −285°; $[\Phi]_{302.5}$ −6605°; $[\Phi]_{265}$ +3780°. Spectre IR: ν_{max}^{KBr} 1734 cm^{-1} (16-ester), 1701 cm^{-1} (20-cétone). Anal. Calc. pour $C_{23}H_{34}O_3F_2$: C, 69.74; H, 8.60; F, 9.63. Trouvé: C, 70.00; H, 8.56; F, 9.94.

16β-Carbamoyl 3β-fluoro 20-oxo (17α)pregna-5-ène (XVIc)

On porte à reflux durant 2 heures une solution contenant 1 g du fluoro-ester (XVI*a*), 8 g d'hydroxyde de potassium dans 5 ml d'eau et 160 ml de méthanol. Le mélange réactionnel est repris par l'eau, acidifié par une solution d'acide chlorhydrique (10%), extrait, lavé et séché. Le spectre infra-rouge du produit brut présente une large bande carboxyle dans la région de 1720 cm^{-1}, correspondant à l'acide (XVI*b*). Cet acide n'est pas isolé mais immédiatement traité, 2 heures à reflux dans 30 ml de benzène anhydre, par 0.9 ml de chlorure de thionyle fraîchement distillé. On évapore ensuite, sous vide poussé, le benzène et le chlorure de thionyle en excès. Le chlorure d'acide sec, ainsi obtenu, est additioné de 20 ml de tétrahydrofuranne anhydre,

Can. J. Chem. Downloaded from www.nrcresearchpress.com by 210.87.254.40 on 09/05/12
For personal use only.

puis à 0° de 25 ml d'hydroxyde d'ammonium. On agite ce mélange réactionnel 16 heures à la température ambiante, dilue à l'eau, extrait et lave. L'amide (XVI*c*) ainsi obtenue, après distillation des solvants sous vide et chromatographie sur 30 g de silice (B.D.H. Laboratory, Angleterre), est éluée au mélange benzène–chloroforme (1:3). L'échantillon analytique est préparé par recristallisation dans un mélange de chlorure de méthylène et méthanol, p.f. 198–200°; $[\alpha]_D$ −115° (*c*, 0.3; $CHCl_3$). DR: méthanol (*c*, 0.046): $[\Phi]_{700}$ −210°; $[\Phi]_{589}$ −292°; $[\Phi]_{302.5}$ −5415°; $[\Phi]_{270}$ −242°. Spectre IR: ν_{max}^{KBr} 3390, 3300 et 3175 cm^{-1} (NH_2, libre et associé), 1701 cm^{-1} (20-cétone), 1669 et 1645 cm^{-1} (amide). Anal. Calc. pour $C_{22}H_{32}O_2FN$: C, 73.08; H, 8.92; N, 3.88; F, 5.26. Trouvé: C, 72.97; H, 8.88; N, 4.04; F, 4.78.

BIBLIOGRAPHIE

1. (*a*) J. Romo. Tetrahedron, **3**, 37 (1958).
   (*b*) B. Ellis, V. Petrow et D. Wedlake. J. Chem. Soc. 3748 (1958).
   (*c*) R. H. Mazur et J. A. Cella. Tetrahedron, **7**, 130 (1959).
2. P. Crabbé, L. M. Guerrero, J. Romo et F. Sánchez-Viesca. Tetrahedron. Sous presse.
3. P. L. Julian, E. W. Meyer, W. J. Karpel et I. R. Waller. J. Am. Chem. Soc. **72**, 5145 (1950).
4. (*a*) R. E. Marker, E. M. Jones et E. L. Wittbecker. J. Am. Chem. Soc. **64**, 468 (1942).
   (*b*) P. A. Plattner, L. Ruzicka, H. Heusser et E. Angliker. Helv. Chim. Acta, **30**, 385 (1947).
5. W. Cole et P. L. Julian. J. Org. Chem. **19**, 131 (1954).
6. R. Neher, P. Desaulles, E. Vischer, P. Wieland et A. Wettstein. Helv. Chim. Acta, **41**, 1667 (1958).
7. P. Crabbé. Tetrahedron. Sous presse.
8. D. K. Fukushima et T. F. Gallagher. J. Am. Chem. Soc. **73**, 196 (1951). J. Romo, M. Romero, C. Djerassi et G. Rosenkranz. J. Am. Chem. Soc. **73**, 1528 (1951). H. Hirschmann, F. B. Hirschmann et M. A. Daus. J. Am. Chem. Soc. **74**, 539 (1952). D. Gould, F. Gruen et E. B. Hershberg. J. Am. Chem. Soc. **75**, 2510 (1953). G. P. Mueller et B. Riegel. J. Am. Chem. Soc. **76**, 3686 (1954). D. Gould, E. L. Shapiro, L. E. Finckenor, F. Gruen et E. B. Hershberg. J. Am. Chem. Soc. **78**, 3158 (1956).
9. A. D. Cross et P. Crabbé. En préparation.
10. P. Crabbé et J. Romo. Chem. Ind. (London), 408 (1962); Ciencia (Mex.), **22**, 29 (1962).
11. O. Halpern, J. A. Edwards et J. A. Zderic. Chem. Ind. (London), 1571 (1962).
12. A. Stoll. Z. Physiol. Chem. **207**, 147 (1932). E. S. Wallis, E. Fernholtz et F. T. Gephart. J. Am. Chem. Soc. **59**, 137 (1937). L. F. Fieser et M. Fieser. Steroids. Reinhold Publ. Corp., New York. 1959. pp. 314 et suivantes.
13. K. Bowden, I. M. Heilbron, E. R. H. Jones et B. C. L. Weedon. J. Chem. Soc. 39 (1946). C. Djerassi, R. R. Engel et A. Bowers. J. Org. Chem. **21**, 1547 (1956).
14. C. Djerassi. Optical rotatory dispersion. McGraw-Hill, New York. 1960. p. 71. C. Djerassi et W. Closson. J. Am. Chem. Soc. **78**, 3761 (1956).
15. W. Klyne. *Dans* Advances in organic chemistry. Vol. I. *Edité par* T. A. Raphael, E. C. Taylor et H. Wynberg. Interscience Publ. Inc. 1960. p. 250. C. Djerassi. Optical rotatory dispersion. McGraw-Hill, New York. 1960. p. 17.
16. A. E. Lippman, E. W. Foltz et C. Djerassi. J. Am. Chem. Soc. **77**, 4364 (1955). C. Djerassi. Bull. Soc. Chim. France, 741 (1957); Optical rotatory dispersion. McGraw-Hill, New York. 1960. p. 43.
17. L. C. King. J. Am. Chem. Soc. **70**, 2685 (1948). R. M. Dodson et B. Riegel. J. Org. Chem. **13**, 424 (1948). S. Winstein et E. M. Kosower. J. Am. Chem. Soc. **81**, 4401 (1959).
18. A. Bowers, P. G. Holton, E. Denot, M. C. Loza et R. Urquiza. J. Am. Chem. Soc. **84**, 1050 (1962). C. S. Barnes et C. Djerassi. J. Am. Chem. Soc. **84**, 1962 (1962).
19. R. F. Hirschmann, R. Miller, J. Wood et R. E. Jones. J. Am. Chem. Soc. **78**, 4956 (1956).

Can. J. Chem. Downloaded from www.nrcresearchpress.com by 210.87.254.40 on 09/05/12
For personal use only.

THE STRUCTURE OF PULCHERRIMINIC ACID[1]

J. C. MacDonald
The National Research Council of Canada, Prairie Regional Laboratory, Saskatoon, Saskatchewan
Received August 7, 1962

ABSTRACT

The red pigment pulcherrimin was isolated from three strains of *Candida pulcherrima* and converted to pulcherriminic acid. The properties of derivatives of this acid and the products obtained from its reduction indicate that it differs from pulcherriminic acid isolated by other workers. A probable structure for the new pulcherriminic acid is 2,5-diisobutyl-3,6-dihydroxypyrazine-1,4-dioxide. The structures of the compounds obtained from its reduction were also investigated.

INTRODUCTION

Pulcherrimin, the red pigment of *Candida pulcherrima*, was first isolated by Kluyver *et al.* (1), who proposed structure I for the compound. Early work by Cook and Slater (2) supported this structure, and it was shown that pulcherrimin could be converted to a dibasic acid, pulcherriminic acid, which gave L-leucine anhydride (2,5-diisobutyl-3,6-dioxopiperazine) on reduction with zinc and acetic acid, which in turn gave L-leucine on hydrolysis. Structure II was proposed for pulcherriminic acid, but when the same workers later prepared synthetic (racemic) 2,5-diisobutyl-1,4-dihydroxy-3,6-dioxopiperazine (3)

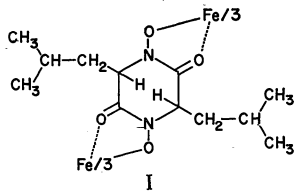

I

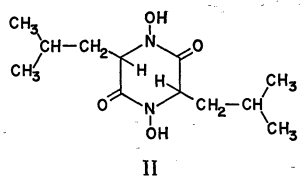

II

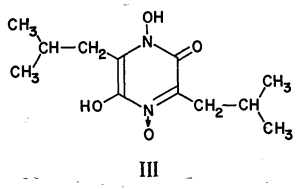

III

and found that it was not identical with natural pulcherriminic acid, further investigations were carried out which led to the proposal of structure III for pulcherriminic acid (4). In this structure the isobutyl substituents are attached to carbons-2 and -5 of the ring, and these carbon atoms should become carbon-2 of leucine on degradation by zinc – acetic acid reduction followed by hydrolysis. One would not expect optically active leucine from this degradation if structure III were correct, and the present work was undertaken to try and resolve this discrepancy. However, it was not possible to do this, because the pulcherriminic acid obtained in the present work appeared to differ in its properties and in its reactions from that described by Cook and Slater. The pulcherriminic acid, and especially its morpholinium and cyclohexylammonium salts, had lower solubilities than the corresponding compounds described by Cook and Slater (2). The latter salts could not be recrystallized from butanol–morpholine or butanol–cyclohexylamine, respectively, as described by these workers. The cyclohexylammonium salt of pulcherriminic acid obtained in this study was more soluble in water than in organic solvents, whereas Cook and Slater found that their salt was sparingly soluble in water, but soluble in common organic solvents. In an attempt to obtain pulcherriminic acid with the properties described by these workers, two strains of *C. pulcherrima*, other than the one

[1]*Issued as N.R.C. No. 7053.*

Can. J. Chem. Downloaded from www.nrcresearchpress.com by 210.87.254.105 on 09/05/12
For personal use only.

supplied by Dr. A. H. Cook, were used to produce pulcherrimin. However, the pulcherriminic acid isolated from all three strains had the same melting point and infrared spectra (Fig. 1), and the morpholinium and cyclohexylammonium salts showed the same

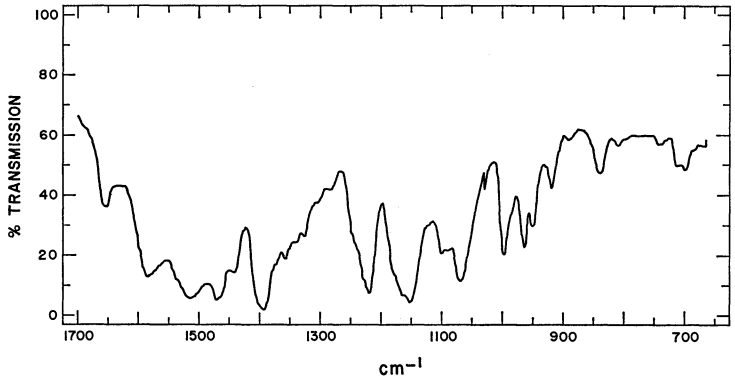

FIG. 1. Infrared spectrum of pulcherriminic acid. Solid in KBr.

low solubility in organic solvents. Therefore the work described below is concerned primarily with the properties and reactions of this new pulcherriminic acid.

The yield of purified pulcherriminic acid from pulcherrimin was quite good. For example, 81.7 mg of pulcherriminic acid, purified through its morpholinium salt, was obtained from 145 mg of pulcherrimin isolated from *C. pulcherrima*. This yield, together with the finding that crude pulcherrimin and the ferric salt made from the isolated pulcherriminic acid had identical infrared spectra (Fig. 2), indicates that the pulcherriminic acid isolated

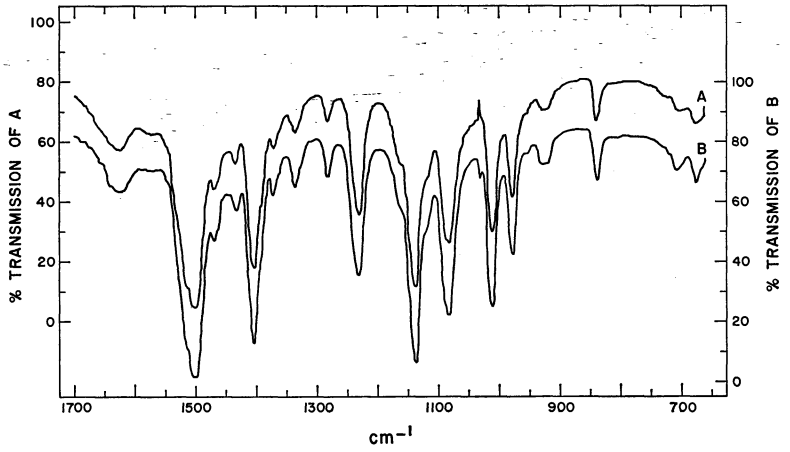

FIG. 2. Infrared spectrum of pulcherrimin (A) and the ferric salt of pulcherriminic acid (B). Solid in KBr. The absorption at 1625 cm^{-1} is due to an impurity in the KBr.

was the free acid whose ferric salt is pulcherrimin, and was not merely a minor constituent of the natural pigment pulcherrimin. Values for the percentage of iron in the ferric salt of pulcherriminic acid were, in general, too high, until a modification of a procedure used by Kluyver *et al.* (1) to prepare material of constant analysis from crude pulcherrimin

Can. J. Chem. Downloaded from www.nrcresearchpress.com by 210.87.254.105 on 09/05/12
For personal use only.

was adopted. The procedure presumably removed coprecipitated ferric ions and consisted of heating the freshly precipitated ferric salt with acidic ethanol, while Kluyver *et al.* used strong acid and longer periods of heating.

The pulcherriminic acid isolated here had the empirical formula $C_{12}H_{20}N_2O_4$, and was dibasic, as shown by the titration of its morpholinium salt, and the elemental analysis of its morpholinium and cyclohexylammonium salts. The percentage of carbon found by analysis of these salts differs somewhat from that expected; this difference may be due to their instability and may indicate that it is difficult to obtain them absolutely pure. The pulcherriminic acid probably contains no asymmetric carbon atoms, because it was reduced to DL-leucine anhydride with zinc and acetic acid. The proton magnetic resonance spectra of pulcherriminic acid (Table I) indicated that the acid has two isobutyl side chains, and no ring hydrogen atoms. This evidence indicates that the pulcherriminic acid has structure IV or possibly a tautomer of this structure, III.

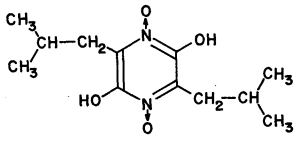

IV

TABLE I

Analysis of functional groups by proton magnetic resonance spectrometry

Compound*	Number of protons in functional groups†					
		Isobutyl group	Isobutylidene group			
	CH_3	$CH + CH_2$	CH	=CH	Ring H	NH
Pulcherriminic acid	12 (9.37, 9.26)	6.1 (CH multiplet 8.0; CH_2 7.35, 7.22)	0	0	0	0
Pulcherriminic acid sodium salt in D_2O	12 (9.14, 9.03)	6.3 (CH multiplet 7.8; CH_2 7.27, 7.16)	0	0	0	0
Compound A	12 (9.28, 9.17)	0	1.8 (multiplet 7.6)	1.8 (4.08, 3.90)	0	0
Compound B	12 (9.40, 9.32, 9.28, 9.17)	3.3 (8.53, 8.46)	1.3 (multiplet 7.6)	1.1 (4.07, 3.91)	1.1 (5.92)	1.2 (1.75)
DL-Leucine anhydride	12 (9.37, 9.30)	6.4 (8.50, 8.43)	0	0	1.8 (5.97)	1.9 (1.98, 1.80)

*The solvent was trifluoroacetic acid unless otherwise stated.
†This was calculated from the integral curve or from the areas under the peaks, setting the value for CH_3 protons equal to 12. Figures in parentheses represent the τ values (9) of the major peaks. Data were obtained with a Varian model A-60 n.m.r. spectrometer with tetramethylsilane as an external reference.

The reduction of pulcherriminic acid by phosphorus and iodine in acetic acid yielded at least three products, one of which was leucine anhydride. While pulcherriminic acid itself has no exocyclic double bonds, the other two products, compounds A and B, did have such bonds (see below). This indicates that there is a migration of double bonds during the reduction and that the structure of these derivatives could lead to a misinterpretation of the structure of the parent compound.

Can. J. Chem. Downloaded from www.nrcresearchpress.com by 210.87.254.105 on 09/05/12
For personal use only.

Compound A resembled a compound which Kluyver *et al.* (1) obtained from the pyrolysis of pulcherrimin in the presence of zinc dust. Both the compound obtained here and that obtained by Kluyver *et al.* had the empirical formula $C_{12}H_{18}N_2O_2$ and their ultraviolet spectra showed a single absorption maximum near 280 mμ (Fig. 3). The proton magnetic resonance spectrum of compound A (Table I) indicated that it has two isobutylidene substituents on the ring and no NH groups, which is consistent with structure V.

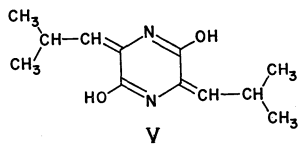

V

The results of degradation of compound A are also compatible with this structure. On hydrolysis, α-keto isocaproic acid (1.7 moles of derivative per mole of A) was formed, undoubtedly by decomposition of dehydroleucine released on hydrolysis (5). Ozonolysis of compound A yielded isobutyraldehyde, and reduction, leucine anhydride. Compound A was obtained in much higher yield from the reduction of pulcherriminic acid with phosphorus and iodine when acetic anhydride was added to the reaction mixture.

The proton magnetic resonance spectrum of compound B (Table I) indicates that it has an isobutyl side chain, an isobutylidene side chain, one ring hydrogen atom, and one NH group. This, together with its empirical formula $C_{12}H_{20}N_2O_2$ and the fact that it gave leucine anhydride on hydrogenation, indicates that its structure is either VI or VII.

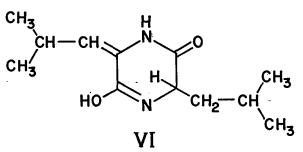

VI

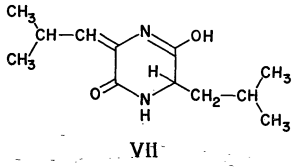

VII

Compound B yielded, on hydrolysis, DL-leucine (0.9 mole per mole of B) and α-keto isocaproic acid (0.7 mole of crude derivative per mole of B), and on ozonolysis isobutyraldehyde. These results are compatible with either structure.

The structure proposed here for pulcherriminic acid (IV, 2,5-diisobutyl-3,6-dihydroxypyrazine-1,4-dioxide) is well supported by the proton magnetic resonance spectra and the fact that DL-leucine anhydride is formed by zinc – acetic acid reduction. However, since the pulcherriminic acid isolated by Cook and Slater (2) gave L-leucine anhydride on reduction, it probably had a structure similar to II, with optically active centers of L-configuration at positions 2 and 5 of the ring. The empirical formula for their compound (4) would require that either the 2- or 5-substituent contained a double bond, which might lead to the formulation of their product as either 2-isobutyl-5-(2-methyl-1-propenyl)-1,4-dihydroxy-3,6-dioxopiperazine or 2-isobutyl-5-(2-methyl-2-propenyl)-1,4-dihydroxy-3,6-dioxopiperazine. It is possible that the pigment pulcherrimin is not necessarily a single compound but that its structure might vary slightly depending on the strain and the growth conditions used. However, only the one compound could be isolated in the experiments done here, and no further attempts to obtain a different compound are contemplated. The infrared spectra of pulcherrimin and pulcherriminic acid (Figs. 1 and 2) may prove of value to other workers in establishing whether the pulcherrimin isolated from other strains is the same as that described in this paper.

Can. J. Chem. Downloaded from www.nrcresearchpress.com by 210.87.254.105 on 09/05/12
For personal use only.

Can. J. Chem. Downloaded from www.nrcresearchpress.com by 210.87.254.105 on 09/05/12
For personal use only.

EXPERIMENTAL

Origin and Maintenance of Cultures

Candida pulcherrima PRL 2019 was a strain kindly supplied by Dr. A. H. Cook, Brewing Industry Research Foundation, Nutfield, Surrey, England. *C. pulcherrima* PRL 1933 was a red-pigmented mutant isolated from *C. pulcherrima* ATCC 7696. *C. pulcherrima* PRL 2007 was obtained from the Centraalbureau voor Schimmelcultures, C.B.S. number 1901, and was the strain used by Kluyver *et al.* (1) for the production of pulcherrimin. All cultures were maintained on slants of the agar medium described by Kluyver *et al.* (1), except that 1 g of Difco yeast extract replaced 1 ml of yeast autolyzate, and distilled water replaced tap water.

Production of the Pigment

C. pulcherrima PRL 1933 was grown 1 week at 28° C in Petri dishes containing Difco potato dextrose agar plus 0.21% ferric ammonium citrate. *C. pulcherrima* PRL 2007 was grown 4 days at 28° C in Petri dishes containing the agar medium used for the maintenance of cultures. Pulcherrimin was isolated from agar cultures as described by Cook and Slater (2). *C. pulcherrima* PRL 2019 was grown on the liquid medium described by Cook and Slater (2), except that Difco yeast extract replaced yeastrel, 60% sodium lactate replaced 50% potassium lactate, 0.1 mg calcium chloride was used instead of a 'trace', and distilled water replaced tap water. The organism was grown in 500-ml Erlenmeyer flasks each containing 100 ml of medium for 2 to 5 days at 28° C on a rotary shaker operating at 240 r.p.m. with a radius of motion of 1 in. Larger amounts of cells were produced by using 300 ml of culture grown on the liquid medium to inoculate 20 liters of medium contained in a stainless steel fermentor, which was a larger version of that described by Roxburgh *et al.* (6). This fermentor was operated at 28° C for 5 days with constant stirring at 300 r.p.m. and aeration at the rate of 6 liters per minute. The cells (1660 g) were collected with a Sharples centrifuge, suspended in 1.5 liters of methanol and centrifuged, prior to extraction with methanolic potash and isolation of pulcherrimin (yield 8.1 g) by the method of Cook and Slater (2).

Morpholinium Salt of Pulcherriminic Acid

Pulcherrimin (217 mg) was triturated with 5 ml of 2 *M* sodium hydroxide, the ferric hydroxide centrifuged off, and the supernatant liquid filtered. The ferric hydroxide was resuspended in 5 ml of sodium hydroxide and the process repeated. The combined filtrates were acidified with hydrochloric acid to precipitate crude pulcherriminic acid (buff or rust color), which was filtered and washed with water. The wet solid was dissolved in 2 ml of 2 *M* ammonium hydroxide, 4 ml of morpholine added, and the solution cooled at −8° C overnight. The morpholinium salt was filtered off, washed with cold *n*-butanol, and transferred to a centrifuge tube. The salt was suspended in an equal volume of butanol, heated in a steam bath for 1 minute, cooled in an ice bath for approximately 5 minutes, centrifuged, and the reddish supernatant liquid discarded. This procedure was repeated until the supernatant liquid had no reddish tinge and the morpholinium salt was a bright yellow color. The salt was suspended in ether and centrifuged, the ether discarded, and this ether washing repeated. Ether was removed from the salt by a stream of nitrogen, and then by evaporation *in vacuo*. The product (226 mg, m.p. 119–121° C) contained: C, 56.6%; H, 8.8%; N, 13.0%. $C_{20}H_{38}N_4O_6$ requires: C, 55.8%; H, 8.9%; N, 13.0%. The salt dissolved in water was titrated with standard hydrochloric acid to a pH of 3.80. The molecular weight, assuming the salt was dibasic, was 436. $C_{20}H_{38}N_4O_6$ requires 430.

The salt decomposed slowly when stored at room temperature, with lowering of the melting point and change to an oily liquid within 2 weeks of its preparation. The salt was soluble in water but insoluble in ether and in butanol–morpholine, 1:1, from which it could not be recrystallized. It could be recrystallized from butanol alone, but the yield was poor and the product had the same melting point and infrared spectrum as the product from the procedure described above.

Pulcherriminic Acid

The morpholinium salt of pulcherriminic acid (151 mg) was dissolved in approximately 10 ml of water and then acidified with hydrochloric acid. The flocculent precipitate was centrifuged down, the supernatant liquid discarded, the precipitate resuspended in water, and centrifuged down again. The washing with water was repeated in this manner until the supernatant liquid was no longer acidic, and then the pulcherriminic acid was collected by filtration and dried over sulphuric acid *in vacuo*. The product (81.7 mg) was a cream-colored or pale yellow solid, m.p. 162–164° C (decomposes). Analysis: C, 56.0%; H, 7.7%; N, 11.0%. $C_{12}H_{20}N_2O_4$ requires: C, 56.2%; H, 7.9%; N, 10.9%.

Ferric Salt of Pulcherriminic Acid

A solution of 30 mg of ferric chloride in 2 ml of trifluoroacetic acid was added to 50.2 mg of pulcherriminic acid dissolved in 1 ml of trifluoroacetic acid, mixed well, and then 3 ml of water added. The precipitate was collected by filtration, washed with water, and then heated for about 1 hour at 70° C with several milliliters of ethanol – 2 *M* hydrochloric acid (1:1). The solid was collected by centrifuging, and the heating with ethanol–acid repeated. The solid was finally washed with ethanol and dried *in vacuo*. The yield of the ferric salt was 51.2 mg, which contained: C, 49.3%; H, 6.2%; N, 9.7%; Fe, 12.8%. $C_{12}H_{18}N_2O_4 \cdot 2/3Fe$ requires: C, 49.4%; H, 6.2%; N, 9.6%; Fe, 12.8%. The infrared spectrum of the salt was identical with that of crude pulcherrimin (Fig. 2).

Cyclohexylammonium Salt of Pulcherriminic Acid

Pulcherriminic acid (53.8 mg) was dissolved in 2 ml of 2 *M* ammonium hydroxide, and 0.2 ml of cyclohexylamine added. A yellow precipitate formed immediately. About 4 ml of acetone was added to the suspension, which was then centrifuged, and the clear supernatant discarded. Such acetone washings were repeated until the supernatant liquid was no longer basic. The precipitate was then dried *in vacuo*. Yield 92.0 mg, m.p. 161–161.5° C (decomposition). Analysis: C, 62.9%; C, 62.7%; H, 10.2%; H, 10.3%; N, 12.5%. $C_{24}H_{46}N_4O_4$ requires: C, 63.4%; H, 10.2%; N, 12.3%.

The solubility of the salt was tested by shaking weighed samples with varying amounts of solvent overnight at room temperature (approximately 25° C). The solubility in water was between 1 and 2 mg/ml, in ethanol between 0.4 and 0.7 mg/ml, and in benzene or acetone less than 0.1 mg/ml.

The melting point of various freshly prepared samples differed, although the individual samples melted with decomposition sharply within a range of 1° C. Preparations were obtained melting as low as 157° C and as high as 171° C, although the infrared spectrum of all samples was the same. The salt decomposed on storage at room temperature and within a week had become a semiplastic solid with no definite melting point.

Reduction of Pulcherriminic Acid with Zinc and Acetic Acid

Pulcherriminic acid (215 mg) was reduced as described by Cook and Slater (2). After treatment with hydrogen sulphide and filtration, the solution was evaporated to dryness and the solid sublimed at 150° C and 0.02 mm to give 115 mg of leucine anhydride (60% yield), identified by its infrared spectrum. The product had no appreciable optical rotation (*c*, 0.52, ethanol, 4-decimeter tube). A sample from a similar experiment was recrystallized from ethanol for analysis. Found: C, 63.6%; H, 9.6%; N, 12.1%. $C_{12}H_{22}N_2O_2$ requires: C, 63.7%; H, 9.8%; N, 12.4%.

A yellow insoluble solid was obtained along with unreacted zinc from the reduction. This solid had the same infrared spectrum as pulcherrimin and was assumed to be the zinc salt of pulcherriminic acid. It was dissolved in 1.0 *M* sodium hydroxide, a solution of sodium sulphide added, and the precipitate of zinc sulphide filtered off. The filtrate was acidified and the solid which precipitated filtered off and washed with water. The solid was dissolved in 2.0 *M* ammonium hydroxide, reprecipitated by acidifying the solution with hydrochloric acid, washed with water, and dried *in vacuo*. The product (57 mg) had an infrared spectrum identical with that of pulcherriminic acid.

Leucine anhydride (105 mg) from the above reduction was hydrolyzed with 10 ml of 42% hydrobromic acid in a sealed tube for 16 hours at 100° C. After evaporation of the hydrobromic acid *in vacuo*, the amino acid was desalted, and sublimed (7). The product (114 mg or 96% of theory) had no measurable optical rotation (*c*, 0.54, 6 *M* hydrochloric acid, 4-decimeter tube), and had an infrared spectrum identical with that of DL-leucine.

Reduction of Pulcherriminic Acid with Phosphorus and Iodine in Acetic Acid

Pulcherriminic acid (1.50 g) was added to a flask containing 900 mg red phosphorus, 300 mg iodine, and 30 ml glacial acetic acid. The flask, fitted with a reflux condenser, was heated in a 150° C oil bath for $2\frac{1}{4}$ hours. The contents were filtered while hot into a cold solution of 3 g sodium metabisulphite in 240 ml water, whereon a flesh-colored precipitate formed. This precipitate was filtered off, and more material recovered from the filtrate by extraction several times with chloroform, and evaporation of the chloroform. To remove traces of acetic acid and colored material, the combined solids were suspended in water, sufficient sodium hydroxide solution added to make the suspension alkaline, and the material extracted by shaking with several portions of chloroform. The product (705 mg) obtained after evaporation of the chloroform was chromatographed on an alumina column (Merck chromatographic grade) 41 cm long and 6.5 cm in diameter. Chloroform was used in packing the column and dissolving the sample. The column was first eluted with approximately 3 liters of 1% ethanol in chloroform and 20-ml fractions collected. Portions of various fractions were evaporated, the residue dissolved in ethanol, and the ultraviolet spectrum of the solution determined with a Beckman DK2 spectrophotometer. The spectra of the three compounds obtained, compounds A, B, and C (Fig. 3), had been determined from previous experiments on a smaller scale and were used as a guide to the purity of the collected fractions. Fractions containing compound A were eluted first, followed by fractions containing compounds A and B. The column was then eluted with 4 liters of 2% ethanol in chloroform and compound B obtained in these fractions. The column was then eluted with chloroform and increasing amounts of ethanol to give first fractions containing compounds B and C, and then fractions containing compound C. Fractions containing only compounds A, B, or C were evaporated to dryness while fractions containing a mixture of two of these compounds were discarded.

Compound A was purified by sublimation at 140° C and 0.02 mm, followed by recrystallization from ethanol. The product (66.5 mg) contained: C, 64.7%; H, 8.1%; N, 12.7%. $C_{12}H_{18}N_2O_2$ requires: C, 64.8%; H, 8.2%; N, 12.6%. The compound was insoluble in water and very slightly soluble in organic solvents at room temperature. Decomposition point (sealed capillary) was 301–303° C. The ultraviolet spectrum in ethanol had a single peak at 278 mμ, ϵ = 24,400 (Fig. 3).

Compound B was purified in the same manner as compound A. The product (223 mg) contained C, 64.4%; H, 9.0%; N, 12.6%. $C_{12}H_{20}N_2O_2$ requires: C, 64.3%; H, 9.0%; N, 12.6%. Decomposition point

Can. J. Chem. Downloaded from www.nrcresearchpress.com by 210.87.254.105 on 09/05/12
For personal use only.

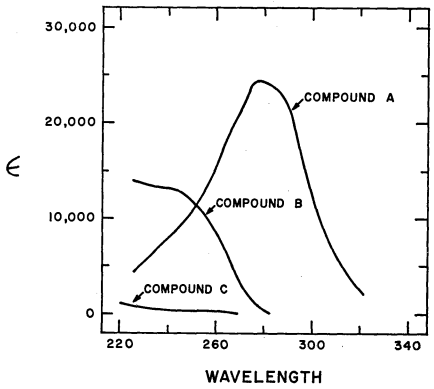

FIG. 3. Ultraviolet spectra for compounds A, B, and C. Solvent, absolute ethanol.

(sealed capillary) was 263–266° C. The ultraviolet spectrum in ethanol showed no single absorption peak but $\epsilon = 13{,}200$ at 240 mμ (Fig. 3).

Compound C was purified in the same manner as compound A. The product (76 mg) had an infrared spectrum identical with that of leucine anhydride, and a decomposition point of 266–267° C (sealed capillary).

Reduction of Pulcherriminic Acid with Phosphorus and Iodine in Acetic Acid Containing Acetic Anhydride

A mixture containing 1.00 g of pulcherriminic acid, 600 mg red phosphorus, 200 mg iodine, 6 ml acetic anhydride, and 54 ml glacial acetic acid was refluxed on a 155° C oil bath for 2¼ hours, and then filtered into a cold solution of 2 g of sodium metabisulphite in 160 ml of cold water, whereon a precipitate formed. After the solution had been allowed to stand overnight at −8° C, the suspension was filtered and the precipitate recrystallized from ethanol. The product (305 mg) had infrared and ultraviolet spectra identical with that of compound A. No compound A, B, or C could be found in chloroform extracts of the aqueous filtrate, which gave only gummy material on evaporation of the chloroform.

Reactions of Compound A

Hydrolysis.—A suspension of 30.9 mg of compound A in 3 ml of 6 *M* hydrochloric acid was heated in a sealed tube at 100° C for approximately 40 hours. The small amount of solid left was filtered off and 30 ml of 2,4-dinitrophenylhydrazine solution (concentration 1 mg/ml of 2 *M* hydrochloric acid) added to the filtrate. A yellow precipitate formed, and after the suspension had been kept at −8° C overnight, it was filtered off, washed with a little 0.1 *M* hydrochloric acid, and dried *in vacuo*. Yield 45.8 mg, m.p. 156–158.5° C. To the filtrate 30 ml more of the 2,4-dinitrophenylhydrazine solution was added to obtain 26.9 mg more of the compound, m.p. 153–156° C. The compound was soluble in 0.1 *M* sodium carbonate and its melting point was not depressed by mixture with the 2,4-dinitrophenylhydrazone of α-keto isocaproic acid, m.p. 156–157° C. Analysis: C, 46.7%; H, 4.7%. $C_{12}H_{14}N_4O_6$ requires: C, 46.5%; H, 4.6%.

Reduction.—Compound A (12.0 mg) was added to a mixture of 30 mg red phosphorus, 11 mg iodine, and 3 ml of glacial acetic acid and refluxed for 40 minutes. The reaction mixture was filtered into 24 ml of water containing 300 mg sodium metabisulphite. No precipitate formed until the solution was made alkaline by the addition of sodium carbonate. The suspension was then extracted three times with an equal volume of chloroform, the chloroform extracts evaporated to dryness, and the product sublimed at 140° C and 0.02 mm. Yield 11.4 mg (93% of theory) of leucine anhydride, identified by its infrared spectrum.

Ozonolysis.—Compound A (29.9 mg) and 36 ml dichloromethane were cooled in a dry ice – ethanol bath and ozone passed through until a faint blue solution was obtained. The solution was warmed slightly and 60 ml of 2,4-dinitrophenylhydrazine solution added. The flask was warmed to room temperature and shaken vigorously. The dichloromethane layer was removed and the aqueous layer extracted with 30 ml dichloromethane. The combined dichloromethane extracts were evaporated to dryness, the solid suspended in 60 ml 2 *M* hydrochloric acid and extracted six times with 30 ml petroleum ether (b.p. 60–80° C). The petroleum ether extracts were evaporated to dryness and the solid chromatographed on a silicic acid – celite column (8). The first colored band, eluted from the column with 2% ether in petroleum ether, was collected, the solvent evaporated off, and the solid recrystallized twice from petroleum ether. Yield 10.2 mg of isobutyraldehyde dinitrophenylhydrazone, m.p. 177–180° C. Analysis: C, 47.9%; H, 4.9%. $C_{10}H_{12}N_4O_4$ requires: C, 47.6%; H, 4.8%.

Reactions of Compound B

Hydrolysis.—Compound B (30.7 mg) and 3 ml 42% hydrobromic acid were heated in a sealed tube for 16 hours at 100° C. Dinitrophenylhydrazine solution (15 ml) was added and the solution cooled at −8° C

Can. J. Chem. Downloaded from www.nrcresearchpress.com by 210.87.254.105 on 09/05/12
For personal use only.

overnight. The precipitate was collected as mentioned for the hydrolysis of compound A. Yield 22.0 mg, m.p. 155–158° C. Analysis: C, 46.7%; H, 4.9%. $C_{12}H_{14}N_4O_6$ requires: C, 46.5%; H, 4.6%. The melting point was not significantly changed by mixing with the 2,4-dinitrophenylhydrazone of α-keto isocaproic acid. A second crop (8.3 mg) of this derivative was obtained by adding more dinitrophenylhydrazine solution to the filtrate, but it was discarded since its melting point (151–155° C) was low.

The filtrate, after the removal of the dinitrophenylhydrazone, was extracted several times with ether, and the aqueous layer, which contained leucine as shown by circular paper chromatography (solvent, *sec*-butanol – 3% ammonium hydroxide, 3:1), evaporated to dryness. The solid was extracted with water, the aqueous solution desalted (7), and the leucine purified by sublimation at 130° C and 0.02 mm. The product, 16.9 mg, had an infrared spectrum identical with that of DL-leucine and no measurable optical rotation (*c*, 0.52, 6 *M* hydrochloric acid, 2-decimeter tube).

Reduction.—Compound B (12.1 mg) was reduced for 100 minutes and the product isolated by the same methods as were used for the reduction of compound A. Yield 11.8 mg of leucine anhydride, identified by its infrared spectrum.

Ozonolysis.—Compound B (29.1 mg) was subjected to ozonolysis and isobutyraldehyde isolated as its 2,4-dinitrophenylhydrazone derivative by the same methods as were used for the ozonolysis of compound A. Yield 13.0 mg., m.p. 177–180.5° C. Analysis: C, 47.5%; H, 4.9%. $C_{10}H_{12}N_4O_4$ requires: C, 47.6%; H, 4.8%. The product had the same R_f (approximately 0.3) as authentic isobutyraldehyde dinitrophenylhydrazone when subjected to thin layer chromatography on silica gel G (E. Merck, Darmstadt, Germany) with benzene as the developing solvent.

Melting points were done with a Fisher-John's hot stage except for compounds which sublimed readily, in which case a sealed capillary and a metal heating block were used. Melting points were corrected by calibrating the melting point apparatus with appropriate reference compounds of known melting point.

ACKNOWLEDGMENTS

The author is grateful to Dr. R. U. Lemieux, Department of Chemistry, University of Alberta, for proton magnetic resonance spectra. Cultures for the isolation of pulcherrimin were grown by Dr. R. H. Haskins and Dr. J. F. T. Spencer of this laboratory. Analyses were done by Mr. M. Mazurek and infrared spectra by Mr. W. C. Haid. The author is also indebted to Mr. D. M. Tenaschuk for technical assistance and to Dr. L. C. Vining for valuable advice.

REFERENCES

1. A. J. KLUYVER, J. P. VAN DER WALT, and A. J. VAN TRIET. Proc. Natl. Acad. Sci. U.S. **39**, 583 (1953).
2. A. H. COOK and C. A. SLATER. J. Inst. Brewing, **51**, 213 (1954).
3. A. H. COOK and C. A. SLATER. J. Chem. Soc. 4130 (1956).
4. A. H. COOK and C. A. SLATER. J. Chem. Soc. 4133 (1956).
5. A. MEISTER and J. P. GREENSTEIN. J. Biol. Chem. **195**, 849 (1952).
6. J. M. ROXBURGH, J. F. T. SPENCER, and H. R. SALLANS. Can. J. Technol. **34**, 389 (1956).
7. J. C. MACDONALD. Can. J. Microbiol. **6**, 27 (1960).
8. B. E. GORDON, F. WOPAT, JR., H. D. BURNHAM, and L. C. JONES, JR. Anal. Chem. **23**, 1754 (1951).
9. L. M. JACKMAN. Applications of nuclear magnetic resonance spectroscopy in organic chemistry. Pergamon Press, New York. 1959. p. 47.

Can. J. Chem. Downloaded from www.nrcresearchpress.com by 210.87.254.105 on 09/05/12
For personal use only.

CHARACTERISTIC VIBRATIONAL FREQUENCIES OF OXYGEN COMPOUNDS OF PHOSPHORUS AND CHLORINE: CORRELATION OF SYMMETRIC AND ASYMMETRIC STRETCHING FREQUENCIES OF PO AND ClO BONDS

E. A. ROBINSON
Department of Chemistry, University of Toronto, Toronto, Ontario
Received August 28, 1962

ABSTRACT

Linear relationships have been established between the symmetric and asymmetric stretching frequencies of PO_2 and ClO_2 groups that are useful in the assignment of the characteristic vibrational frequencies of these groups in the Raman and infrared spectra of phosphorus and chlorine compounds containing two or more oxygen ligands. The values of the frequencies depend, in a systematic manner, on the electronegativities of the groups attached to the central atom.

INTRODUCTION

For a variety of inorganic and organic compounds containing the sulphuryl group, it was shown originally by Bellamy and Williams (1), and more recently by the present author (2), that any change in the symmetric stretching frequency is accompanied by a proportional change in the asymmetric stretching frequency. The latter work extended the relationship to include ionic species such as the anions of sulphuric acid and substituted sulphuric acids, and more recently we have shown that it is also applicable to the $S(OH)_2$ group (3). Such a relationship is reasonable since the SO_2 stretching frequencies are expected to be relatively free from mass and coupling effects. Recently a similar correlation has been obtained between the symmetric and asymmetric stretching frequencies of the UO_2 group in uranyl complexes (4).

Because of the rather similar chemical nature of oxygen compounds of phosphorus, sulphur, and chlorine it might be expected that similar relationships would apply also to compounds containing PO_2 and ClO_2 groups, as indeed is shown to be the case in the present paper. In the case of phosphorus compounds the correlation is restricted to species containing groups such as PO_2^-, since neutral compounds containing two double bonds between phosphorus and oxygen (e.g. PO_2X) are not known. In the same way that the previous correlation was shown to apply not only to simple sulphuryl compounds $XYSO_2$ but also to ions such as XSO_3^- and SO_4^{2-}, the present correlations include species such as $XYPO_2^-$, XPO_3^{2-}, and PO_4^{3-}, and $XYClO_2$, $XClO_3$, ClO_2^-, ClO_3^-, and ClO_4^-, that is, any species with two or more oxygen ligands attached to the central phosphorus or chlorine atom. The relationship also applies to compounds containing $P(OH)_2$ groups.

ClO STRETCHING FREQUENCIES

Data collected from the literature for ClO stretching frequencies of several oxychlorine compounds and ions are shown in Table I and plotted in Fig. 1.

In tetrahedral molecules of the type $XClO_3$ there should be one symmetric ClO_3 stretch and two asymmetric stretches which are degenerate. In the case of perchloric acid two asymmetric stretches have been observed and this is attributed to loss of tetrahedral symmetry in the molecule (5), but for fluorine perchlorate (6) and perchloryl fluoride (7) only one band has been observed in the asymmetric stretching region of the infrared

Can. J. Chem. Downloaded from www.nrcresearchpress.com by 210.87.254.105 on 09/05/12
For personal use only.

TABLE I

Cl—O stretching frequencies

		ν_{sym}	ν_{asym}	Ref.
Perchloric acid	$HO.ClO_3$	1050	1326, 1263 } 1296	5
Fluorine perchlorate	$FO.ClO_3$	1049	1298	6
Perchloryl fluoride	$FClO_3$	1061	1315	7
Chlorine dioxide	ClO_2	943	1110	20
Chlorite ion	ClO_2^-	860	952	21
Chlorate ion	ClO_3^-	930	975	9
		930	1087	*
Perchlorate ion	ClO_4^-	935	1110	22
Perchloric anhydride	Cl_2O_7	1034, 1057 } 1045	1260, 1270, 1295 } 1275	23

*Present assignment.

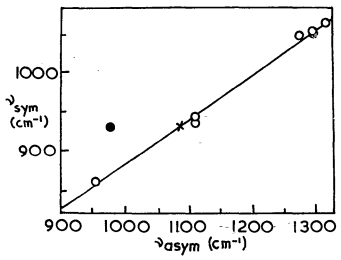

FIG. 1. Correlation of symmetric and asymmetric Cl—O stretching frequencies.

spectrum. In the case of perchloric acid the mean of the asymmetric stretching frequencies is taken as the frequency this vibration would have in the absence of resonance splitting. Recently, by comparison with the spectrum of the chlorosulphate ion (8), we cast doubt on the previous assignment of the frequency at 1315 cm^{-1} in the spectrum of perchloryl fluoride to the asymmetric ClO stretch (7). In view of the present correlation this doubt appears to be unfounded.

In the case of the chlorate ion the symmetric and asymmetric stretches have been assigned by several workers (e.g. see refs. 9, 10) near 930 and 975 cm^{-1}, respectively. These values, however, do not fit the correlation (the point marked ● in Fig. 1). However, if the line at 1082 cm^{-1} observed in the infrared spectrum of potassium chlorate by Ramdas (9) is assigned as the ClO asymmetric stretch, rather than 975 cm^{-1}, then the fit is good (the point marked × in Fig. 1). The line at 975 cm^{-1} can then be reinterpreted as an overtone of the bend at 486 cm^{-1} ($2\times486 = 972$ cm^{-1}). This view appears to be supported by the work of Rocchicciaoli (10), who observed a splitting of the low-frequency bend into two lines in the spectra of several solid chlorates, which was accompanied by a similar splitting of the line near 975 cm^{-1}. In all cases the two lines near 975 cm^{-1} can be interpreted as combination or overtone bands of the doublet in the region of the bending mode.

As can be seen from Fig. 1, when the symmetric stretch is plotted against the asymmetric stretch a good straight line results which can be represented by the equation

$$\nu_{sym} = 0.56\nu_{asym} + 322. \quad [1]$$

Can. J. Chem. Downloaded from www.nrcresearchpress.com by 210.87.254.105 on 09/05/12
For personal use only.

In the case of the previous correlation of the symmetric and asymmetric stretches (2) of the SO_2 group, the straight-line equation was not given. It is now given for comparison:

[2] $$\nu_{sym} = 0.62\nu_{asym} + 329,$$

and is very similar in form to equation [1]. As in the previous correlation the exact positions of ν_{sym} and ν_{asym} depend on the electronegativities of the attached ligands, the highest frequencies being observed for the ligand of highest electronegativity, i.e. fluorine.

P—O STRETCHING FREQUENCIES

Unfortunately, very few reliable or complete measurements of the spectra or complete assignments of spectral frequencies to normal modes of vibration of such ions have been made. However, a small amount of reliable data is available. The ions $H_2PO_2^-$, HPO_3^{2-}, and $CH_3OPO_3^-$ have been examined by Tsuboi (11) and P—O symmetric and asymmetric stretches assigned; a complete assignment of the spectrum of the $P_2O_6^{4-}$ ion has recently been made by Palmer (12), and the symmetric and asymmetric stretches in the phosphate ion are also known (13). The data for the above ions is shown in Table II and the symmetric and asymmetric stretches are plotted in Fig. 2. As can be seen a good straight-line cor-

TABLE II

Well-established P—O stretching frequencies in phosphorus oxyanions

Ion	ν_{sym}	ν_{asym}	Ref.
PO_4^{3-}	980	1082	13
$H_2PO_2^-$	1050	1200	11
HPO_3^{2-}	980	1100	11
$CH_3OPO_3^{2-}$	985	1100	11
$P_2O_6^{4-}$	1062, 942 } 1002	1088, 1168 } 1128	12

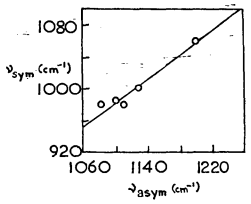

FIG. 2. Correlation of well-established P—O stretching frequencies.

relation is suggested on the basis of this rather limited amount of data, although the information is not sufficient to establish a definite general correlation.

It is of interest to note that the P—O stretching frequencies of $H_2PO_2^-$ are at higher frequency than those of HPO_3^{2-}, $CH_3OPO_3^{2-}$, and $[O_3P—PO_3]^{4-}$, which are in turn at higher frequencies than the stretching frequencies of the PO_4^{3-} ion. This is consistent with reduced double-bond character in the P—O bonds as the charge per phosphorus atom increases.

Having established a possible straight-line correlation between the P—O stretching frequencies for these oxyanions it was of interest to see if supporting evidence could be obtained from some of the published spectra for which complete assignments have not been given.

Can. J. Chem. Downloaded from www.nrcresearchpress.com by 210.87.254.105 on 09/05/12
For personal use only.

Fluorophosphates

Corbridge and Lowe (14) measured the infrared spectra of the sodium, potassium, barium, and silver salts. Two bands were observed in each case in the PO stretching region and the lower frequency of each pair can be assigned as the symmetric stretch and the higher as the asymmetric stretch. Pustinger and co-workers (15) examined the spectra of the sodium, potassium, and silver salts and assignments very similar to those made above are possible. The frequencies so assigned agree well with the linear correlation between symmetric and asymmetric stretches.

Difluorophosphates

The only measurement of the spectrum of the difluorophosphate ion appears to be that of the ammonium salt by Corbridge and Lowe (14). Three bands were observed in the P—O stretching region at 1005 cm^{-1} (weak), 1125 cm^{-1} (strong), and 1262 cm^{-1} (strong). It seems reasonable to assign the latter two to the symmetric and asymmetric PO stretches, respectively.

Dimethylphosphonates

Only the sodium salt was examined. By assigning 1028 cm^{-1} as the frequency of the symmetric stretch and 1168 cm^{-1} as the frequency of the asymmetric stretch a good correlation with the straight line in Fig. 2 is obtained.

Dihydrogenphosphates

From the infrared spectra of the ammonium, sodium, potassium, and calcium salts, the mean frequencies of 1076 and 1271 cm^{-1} may be assigned as the symmetric and asymmetric stretches respectively. It is also possible to assign frequencies at 870 and 963 cm^{-1} in the spectrum of the sodium salt to the symmetric and asymmetric $P(OH)_2$ stretching frequencies. Similarly 877 and 935 cm^{-1} for the calcium salt and 890 and 963 cm^{-1} for the hydrated calcium salt may be assigned as the frequencies of these vibrations. All these assignments are consistent with the original correlation.

Phosphites

Infrared bands were observed at 1006, 1022, 1082, and 1130 cm^{-1} in the spectrum of the barium salt. If we assume that the first pair of frequencies can be assigned to the symmetric PO stretch and the latter pair to the asymmetric stretch, both frequencies being split by crystal forces, and take the mean value of each pair as the symmetric and asymmetric stretches, respectively, in the absence of crystal splitting, then the pair of frequencies so obtained (1014 and 1106 cm^{-1}) is in reasonable agreement with the relationship.

Peroxydiphosphates

Corbridge and Lowe (14) have also examined the infrared spectrum of lithium peroxydiphosphate. Lines in their spectrum at 998 and 1115 cm^{-1} may be assigned as the symmetric and asymmetric PO stretches, respectively, and these frequencies fit the straight-line correlation well. Theoretically the symmetric and asymmetric stretches of the $P_2O_8^{4-}$ ion should occur as a maximum of six lines in the spectrum. We asume, as only two lines are observed, that the three symmetric stretches and three assymmetric stretches are degenerate.

Phosphoramidates

Corbridge and Lowe report bands at 994 and 1158, 993 and 1162, and 994 and 1143 cm^{-1} in the infrared spectra of sodium, potassium, and ammonium phosphoramidates, respectively. The infrared spectrum of $NH_4.PO_3NH_3$ is also reported by Steger (16), who

Can. J. Chem. Downloaded from www.nrcresearchpress.com by 210.87.254.105 on 09/05/12
For personal use only.

assigns the P—O symmetric stretch at 993 cm^{-1} and the asymmetric stretch at 1170 cm^{-1}. However, in his published spectrum there is a distinct shoulder at approximately 1130 cm^{-1} which could possibly be reassigned as the asymmetric stretch. The pair of frequencies 993 and 1130 cm^{-1} fits the correlation well.

Other values for the symmetric and asymmetric P—O stretches in oxyanions of phosphorus which also support the present correlation can be deduced from spectra reported by other workers. Steger (16) gives lines at 1000 and 1125 cm^{-1} in the spectrum of $BaPO_3NH_2$ and at 1023 and 1183 cm^{-1} in the spectrum of the magnesium salt. Several workers report the spectrum of diphosphates. In the $P_2O_7^{4-}$ ion a maximum of three symmetric and three asymmetric P—O stretches are theoretically expected, and in the $H_2P_2O_7^{2-}$ ion two symmetric and two asymmetric stretches. Hanwick and Hoffmann (17) report lines at 1018 and 1128 cm^{-1} in the Raman spectrum of $K_4P_2O_7$, at 1018 and 1138 cm^{-1} in the spectrum of $K_2Na_2P_2O_7$, at 1087 and 1253 cm^{-1} in the spectrum of $K_2H_2P_2O_7$, and at 1105 and 1244 cm^{-1} in the spectrum of $Na_2H_2P_2O_7$. If the former of these pairs is taken as the frequency of P—O symmetric stretches (assumed degenerate), and the latter as that of the asymmetric stretches (assumed degenerate) correlation with the straight line of Fig. 2 is good. MacArthur and Beevers (18) give 987 and 1030 cm^{-1} as the symmetric P—O stretches and 1121 and 1152 cm^{-1} as the asymmetric P—O stretches of the $P_2O_7^{4-}$ ion. The mean symmetric stretch (1008 cm^{-1}) and mean asymmetric stretch (1137 cm^{-1}) are in good agreement with the frequencies of the single lines reported by Hanwick and Hoffmann. It is significant that the pair of stretches in the $H_2P_2O_7^{2-}$ ion come at relatively higher frequencies than the pair of frequencies in the $P_2O_7^{4-}$ ion, which is consistent with greater double-bond character of the P—O bonds in the former ion than in the latter.

Daasch and Smith (19) have measured the infrared spectra of several compounds containing the $P(OH)_2$ group. They do not give the exact frequencies of the bands in the spectra but approximate frequencies may be estimated from their published spectra. In the spectrum of benzenephosphonic acid ($C_6H_5.P(O)(OH)_2$) there are lines at approximately 920 and 1000 cm^{-1}, which can be assigned as the symmetric and asymmetric P—OH stretches and are in good agreement with the straight-line correlation. Pairs of lines which can be assigned as symmetric and asymmetric P—OH stretching frequencies were also observed in the spectrum of *p*-chlorobenzenephosphonic acid (at 925 and 1005 cm^{-1}). In the spectrum of dideuterobenzenephosphonic acid lines were observed at 925, 945, and 1030 cm^{-1}. If it is assumed that the lines at 925 and 945 cm^{-1} are the symmetric P—OD stretch split in the spectrum and the mean frequency of 935 cm^{-1} is taken as the value of the P—OD symmetric stretch and 1030 cm^{-1} as the frequency of the asymmetric stretch, then another pair of frequencies is obtained which fits the correlation.

The symmetric and asymmetric P—O stretches discussed above are plotted against each other in Fig. 3, which also shows the frequencies used in the preliminary correlation. The data is collected in Table III. The straight-line correlation is given by the equation

$$[3] \qquad \nu_{sym} = 0.65\nu_{asym} + 270.$$

It is interesting to note that anions containing highly electronegative ligands attached to the central phosphorus atom, e.g. $PO_2F_2^-$, have higher stretching frequencies than those containing less electronegative ligands, e.g. $PO_2(OH)_2^-$, carrying the same formal charge. P—OH stretching frequencies occur at even lower frequencies than the P—O stretches in the ions. These trends are consistent with increasing double-bond character of the P—O bonds as the electronegativity of the central phosphorus atom increases.

Can. J. Chem. Downloaded from www.nrcresearchpress.com by 210.87.254.105 on 09/05/12
For personal use only.

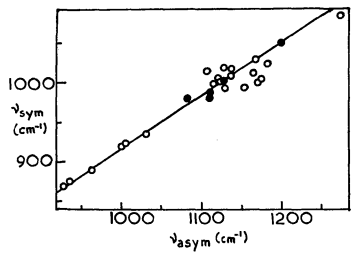

FIG. 3. Correlation of symmetric and asymmetric P—O stretching frequencies (● indicates data used in original correlation).

TABLE III

Symmetric and asymmetric PO stretching frequencies in phosphorus oxyanions and acids

	ν_{sym}		ν_{asym}		Ref.	
Fluorophosphates						
Na_2PO_3F	1005		1175		15	
K_2PO_3F	1000		1170		15	
Ag_2PO_3F	1002		1123		15	
Na_2PO_3F	1010		1170		14	
K_2PO_3F	1013		1166		14	
$BaPO_3F$	1005		1163		14	
Ag_2PO_3F	1018		1162		14	
Difluorophosphates						
$NH_4PO_2F_2$	1125		1262		14	
Dimethylphosphonates						
$Na(CH_3)_2PO_2$	1028		1168		14	
Dihydrogenphosphates						
$NH_4PO_2(OH)_2$	1084		1275		14	
$NaPO_2(OH)_2$	1045	1076	1284	1271	14	
$KPO_2(OH)_2$	1085		1285		14	
$Ca(PO_2(OH)_2)_2$	1090		1240		14	
$NaPO_2(OH)_2$	870		927		14	P—OH
$Ca(PO_2(OH)_2)_2$	877		935		14	P—OH
$Ca(PO_2(OH)_2)_2$ hydrate	890		963		14	P—OH
Phosphites						
$BaHPO_3$	1006	1014	1082	1106	14	
	1022		1130			
Peroxydiphosphates						
$Li_2P_4O_8$	998		1115		14	
Phosphoramidates						
$NaPO_3NH_3$	994		1158		14	
KPO_3NH_3	993	994	1162	1154	14	
$NH_4PO_3NH_3$	994		1143		14	
	993		1130		15	Present assignment
$BaPO_3NH_2$	1000		1125		16	
$MgPO_3NH_2$	1023		1183		16	
Pyrophosphates						
$K_4P_2O_7$	1018		1128		17	
	1018		1138		17	
$Na_4P_2O_7$	987	1008	1121	1137	18	
	1030		1152			
$K_2H_2P_2O_7$	1087		1253		17	
$Na_2H_2P_2O_7$	1105		1244		17	
Benzenephosphonic acids						
$C_6H_5PO(OH)_2$	920		1000		19	P—OH
$Cl.C_6H_4PO(OH)_2$	925		1005		19	P—OH
$C_6H_5PO(OD)_2$	925	935	1030		19	P—OD
	945					

Can. J. Chem. Downloaded from www.nrcresearchpress.com by 210.87.254.105 on 09/05/12
For personal use only.

The correlation appears to be relatively well established but it is clear that more work is required to establish the assignment of P—O stretching frequencies definitely in some of the species discussed. However, the present correlation should prove useful in such a task.

The slopes of the straight-line relationship for symmetric and asymmetric P—O, S—O, and Cl—O stretching frequencies are 0.65, 0.62, and 0.56, respectively, and the intercepts are quite similar in magnitude (270, 322, and 329, respectively). The small decrease in the slopes in the series PO_2, SO_2, ClO_2 is probably due to a decrease in the double-bond character, which results in a decrease in the coupling between the symmetric and asymmetric stretches.

ACKNOWLEDGMENTS

Professor R. J. Gillespie of the Chemistry Department, McMaster University, is thanked for useful discussion of the manuscript, and the financial support of the National Research Council of Canada is gratefully recognized.

REFERENCES

1. L. J. Bellamy and R. L. Williams. J. Chem. Soc. 863 (1957).
2. E. A. Robinson. Can. J. Chem. **39**, 247 (1961).
3. R. J. Gillespie and E. A. Robinson. Unpublished.
4. S. P. McGlynn, J. K. Smith, and W. C. Neely. J. Chem. Phys. **35**, 105 (1961).
5. P. A. Giguère and R. Savoie. Can. J. Chem. **40**, 495 (1962).
6. H. Agahigian, A. P. Gray, and G. D. Vickers. Can. J. Chem. **40**, 157 (1962).
7. D. R. Lide and D. E. Mann. J. Chem. Phys. **25**, 1128 (1956).
8. R. J. Gillespie and E. A. Robinson. Can. J. Chem. **40**, 655 (1962).
9. A. K. Ramdas. Proc. Indian Acad. Sci. Sect. A, **35**, 249 (1952); Sect. A, **36**, 55 (1952); Sect. A, **37**, 451 (1953).
10. Cl. Rocchicciaoli. Compt. Rend. **242**, 2922 (1956).
11. M. Tsuboi. J. Am. Chem. Soc. **79**, 1351 (1957).
12. W. G. Palmer. J. Chem. Soc. 1552 (1961).
13. G. Herzberg. Molecular spectra and molecular structure. Vol. II. Van Nostrand, New York. 1945. p. 167.
14. D. E. C. Corbridge and E. J. Lowe. J. Chem. Soc. 493, 4555 (1954).
15. J. V. Pustinger, W. T. Cave, and M. L. Nielsen. Spectrochim. Acta, **15**, 909 (1959).
16. E. Steger. Z. Electrochem. **61**, 1004 (1957).
17. T. I. Hanwick and P. O. Hoffmann. J. Chem. Phys. **19**, 708 (1951).
18. D. M. MacArthur and C. A. Beevers. Acta Cryst. **10**, 428 (1957).
19. L. W. Daasch and D. C. Smith. Anal. Chem. **23**, 853 (1951).
20. A. H. Nielsen and P. J. H. Woltz. J. Chem. Phys. **20**, 1878 (1952).
21. Cl. Duval, J. Lecomte, and J. Morandat. Bull. Soc. Chim. France, **18**, 745 (1951).
22. H. Cohn. J. Chem. Soc. 4282 (1952).
23. P. A. Giguère and R. Savoie. Can. J. Chem. **40**, 991 (1962).

Can. J. Chem. Downloaded from www.nrcresearchpress.com by 210.87.254.105 on 09/05/12
For personal use only.

STRUCTURE OF PYROLYZED POLYVINYLIDENE CHLORIDE

J. R. Dacey and R. G. Barradas
Department of Chemistry, Royal Military College of Canada, Kingston, Ontario
Received July 23, 1962

ABSTRACT

Systematic infrared analyses, using the standard KBr pellet technique, of samples ranging from the pure polymer (Saran) to the fully carbonized charcoal have been examined in an attempt to clarify the structural changes and mechanism of decomposition of the polymer on pyrolysis. A complementary technique has been investigated for obtaining homogeneous samples of the carbon and of the partially pyrolyzed polymer which will transmit infrared radiation without the use of any halide dispersal medium. The significance, possible applications, and limitations of these spectral studies are discussed. Pore volumes have been examined by means of a modified helium displacement densitometer and also through the adsorption of argon in a McBain–Bakr balance. Porosity measurements based on the adsorption of argon at its saturation vapor pressure are more satisfactory and they contribute towards a better understanding of the microstructure of Saran charcoal and of its partially carbonized antecedents. The influence of pelletizing pressure has been found to play an important role in the determination of pore volumes.

INTRODUCTION

Carbons derived from synthetic organic polymers are often porous; however, they may not always inherit a uniform pore size from the regular structure of the polymer predecessors because few valence angles and distances survive thermal decomposition unchanged during the course of their preparation by pyrolysis. Their porosities have been established as owing to capillaries ranging from a few angstroms to several microns.

The presence of ultrafine capillaries of the order of molecular size are of interest to surface chemists since these pores are responsible for the behavior of many such solids as partial molecular sieves, namely materials through which small molecules can penetrate more readily than larger ones.

Adsorption and kinetic studies on "Saran charcoal", a carbon produced by the complete pyrolytic decomposition of polyvinylidene chloride, have been extensively studied in our laboratory (1–5) and elsewhere (6–8). Less attention has been focused on the correlation of adsorption with the structure and mechanism of formation of the charcoal. One can tacitly assume that any variation in physical properties will depend upon fundamental structural parameters which are generally characteristic of composition, molecular geometry, and nature of the porosity.

In the present work we have carried out systematic infrared analyses, by means of the standard potassium bromide technique, of a large number of samples ranging from pure polymer to the fully carbonized charcoal in an attempt to clarify the structural changes of the polymer on pyrolysis. A technique has been concurrently established for obtaining homogeneous samples of Saran charcoal and of the partially pyrolyzed polymer in the form of thin wafers which will transmit infrared radiation without the use of potassium bromide or any other customary dispersal medium. The applications and limitations of these wafers in adsorption studies will be discussed.

Porosity measurements based on the adsorption of argon in a McBain–Bakr balance are compared with similar determinations utilizing a helium dilatometric technique.

EXPERIMENTAL

Method of Preparation of Samples

(a) Circular Wafer Samples

Pure polyvinylidene chloride (Dow Chemical Co.) was pressed into the form of a thin wafer in a stainless

Can. J. Chem. Downloaded from www.nrcresearchpress.com by 210.87.254.105 on 09/05/12
For personal use only.

steel die (2-cm diameter) under a pressure of 15,000 lb/in² by means of a Carver hydraulic press. In general, the weight of the polymer used for the production of the wafers was 58±1 mg. The compressed wafers were 0.13±0.01 mm in thickness. The fully decomposed wafer (calculated on the basis of $(CH_2CCl_2)_n = 2nC + 2n$HCl, representing 75.3% weight loss) was 14 mm in diameter and 0.09±0.01 mm in thickness. The stoichiometric weight loss of hydrogen chloride in relation to the carbon percentage composition during the course of pyrolysis is conveniently demonstrated in Fig. 1.

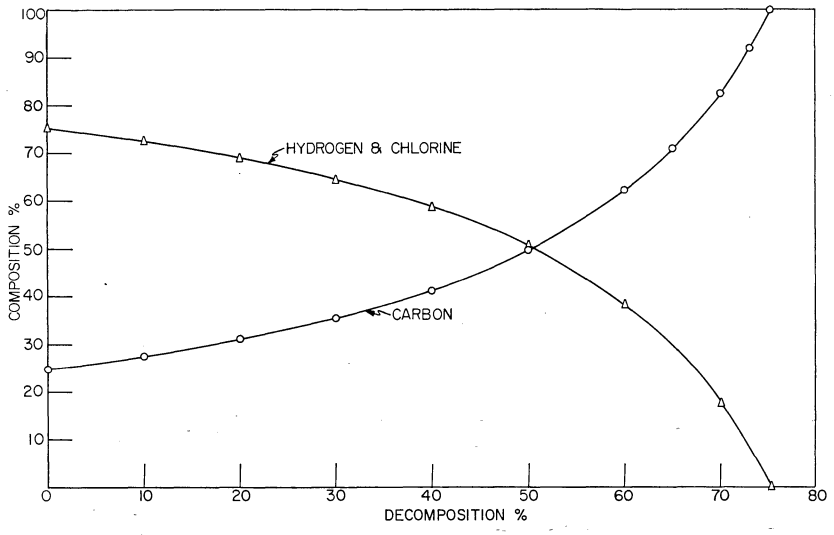

FIG. 1. Composition of polyvinylidene chloride during the course of pyrolysis.

(b) Samples Used in the McBain–Bakr Balance and Helium Densitometer

Disks prepared within the range of 0 to 75.3% decomposition were used in the sorption balance; their weights were approximately 100 to 150 mg. Larger disks of approximately 500-mg weight were prepared in a similar manner for use in the helium densitometer. All disks were compressed under a pressure of 10,000 lb/in².

(c) Pyrolysis

The disks and wafers were placed between flat porous plates and heated gradually to 195° C in a vacuum oven over a period of several days. Slow heating ensures the formation of a uniform composition, a regular surface, and an even pore structure. Rapid heating results in fast evolution of hydrogen chloride, which tends to give samples of uneven shape and texture, and an additional disadvantage is the formation of visible large-scale cracks.

To obtain a uniform sample of the partially decomposed polymer it is necessary to heat the pure polymer at the appropriate temperature for a considerable time; the degree of decomposition achieved is a function of the temperature. By using the data previously obtained by Dacey and Cadenhead (9) it is possible to produce uniform samples of any desired decomposition. The oven was set for various temperatures and pre-determined periods of heating using an Intermatic timing device (International Register Co.). After each heating period and temperature setting, the oven was automatically switched off and allowed to cool to room temperature, when one or more wafers and disks were removed. The percentage decomposition of the samples was determined by weighing.

For temperatures up to 195° C a conventional vacuum oven was used and for higher temperatures the samples were heated under vacuum in a quartz tube in an electric furnace capable of attaining temperatures in excess of 800° C. The hydrogen chloride liberated during pyrolysis was condensed in liquid air traps and removed periodically. Fully carbonized samples were obtained at a temperature of 700° C, since no significant weight loss occurred through heating the samples for another few hours at 725° C.

(d) Potassium Bromide Pellets

A range of samples of carbonized Saran prepared as described above was intimately ground together with dry potassium bromide (Analar Reagent grade). Mixtures containing 1% and in some cases 0.1% of the polymer were compressed into pellets of 170-mg weight and 0.5-mm thickness through application of 20,000 lb/in² pressure in a Carver press.

(e) Instrumentation and Apparatus

In general the spectra were recorded on a Perkin–Elmer 137B spectrophotometer, and where necessary the precise location of wave bands were checked by use of a Perkin–Elmer Model 21 instrument.

Can. J. Chem. Downloaded from www.nrcresearchpress.com by 210.87.254.105 on 09/05/12
For personal use only.

The true density and degree of porosity were measured in a modified Franklin (11) volumetric adsorption apparatus through displacement of helium (Air Reduction (Canada) Ltd.) by the carbonized sample. A known weight of the carbon was outgassed and then exposed to helium in a conventional manner. By simple application of the gas laws, the volume of helium in the dead space was calculated. The true volume occupied by the carbon was thus obtained, and hence the actual density of the carbon. From a known apparent volume of the carbon disk (measured accurately by means of a vernier caliper) the percentage porosity was computed. The degree of porosity or pore volume was also obtained by the adsorption of argon (British Oxygen (Canada) Ltd.) at its saturation vapor pressure at $-195°$ C using a sensitive helical quartz spiral (12).

RESULTS

Spectra of Pyrolyzed Saran Dispersed in Potassium Bromide

The spectrum of a compressed compact wafer of the pure polymer agrees reasonably well with that reported by Krimm and Liang (13) for thin solid films, although in our case transmissions at wavelengths below 670 cm^{-1} could not be examined because of the limitations of the spectrophotometers available.

On partial carbonization the most apparent changes are in the diminution of the intensity of the CCl_2 stretching frequency at 750 cm^{-1} and also of the 1045 and 1070 cm^{-1} doublet attributed to the combination of an overtone of a CCl_2 stretching mode at 531 cm^{-1} ($2\times531 = 1061$ cm^{-1}) in resonance with the chain skeletal vibration at about 1070 cm^{-1}. This is quite consistent with the progressive removal of hydrogen chloride on pyrolysis.

Other striking observations include the formation of new bands at 1460 cm^{-1}, a doublet at 1570 and 1620 cm^{-1}, and one at 1710 cm^{-1}. The doublet and the band at 1710 cm^{-1} persist up to 42% weight loss (see Fig. 2), and at higher carbon percentage composition only two sharp bands, at 1570 and 1710 cm^{-1}, appear to dominate with medium intensities within this region of the spectrum.

The 1460 cm^{-1} band has been reported as one of four characteristic frequencies for C—H vibrations of extinite and vitrinite coals (21, 22). It is noteworthy to point out that although this band appears at an early stage of carbonization in our work, its intensity decreases as the other bands become stronger, and this is again consistent with the progressive elimination of hydrogen as hydrogen chloride.

It was noticed that even at a carbon composition of 83.1% the two bands at 1570 and 1710 cm^{-1} were clearly evident, although their intensities have apparently reduced considerably. This is not unreasonable as it is to be expected that at higher carbon percentage the amount of infrared radiation lost by scattering will have increased. This is more obviously manifested in the fully carbonized sample where the scattering is so great that only the stronger band at 1570 cm^{-1} appeared to be feebly perceptible. A reduction of the charcoal content of the KBr pellets and the use of fluorolube served to emphasize the distinct presence of the 1570 cm^{-1} band in the fully carbonized samples without equivocation (see Fig. 3). The spectral data obtained in this work for decomposed polymers of high carbon content show many features of similarity with those reported for coals of varying carbon composition (20–23).

Spectra of Pyrolyzed Saran Wafers in the Absence of a Dispersion Medium

Using thin wafers a similar set of spectra have been recorded (see Fig. 4). Here the pattern of spectral behavior is almost identical with those of the above series except that the losses of radiation through scattering have been increased at least twofold. In order to obtain any reasonable spectra, the reference beam intensity of the spectrophotometer was reduced by approximately a half through the use of a fine wire screen. It was later found that with considerable care and improvement in technique thinner wafers of pyrolyzed Saran could be obtained without sacrificing too much in structural texture and

Can. J. Chem. Downloaded from www.nrcresearchpress.com by 210.87.254.105 on 09/05/12
For personal use only.

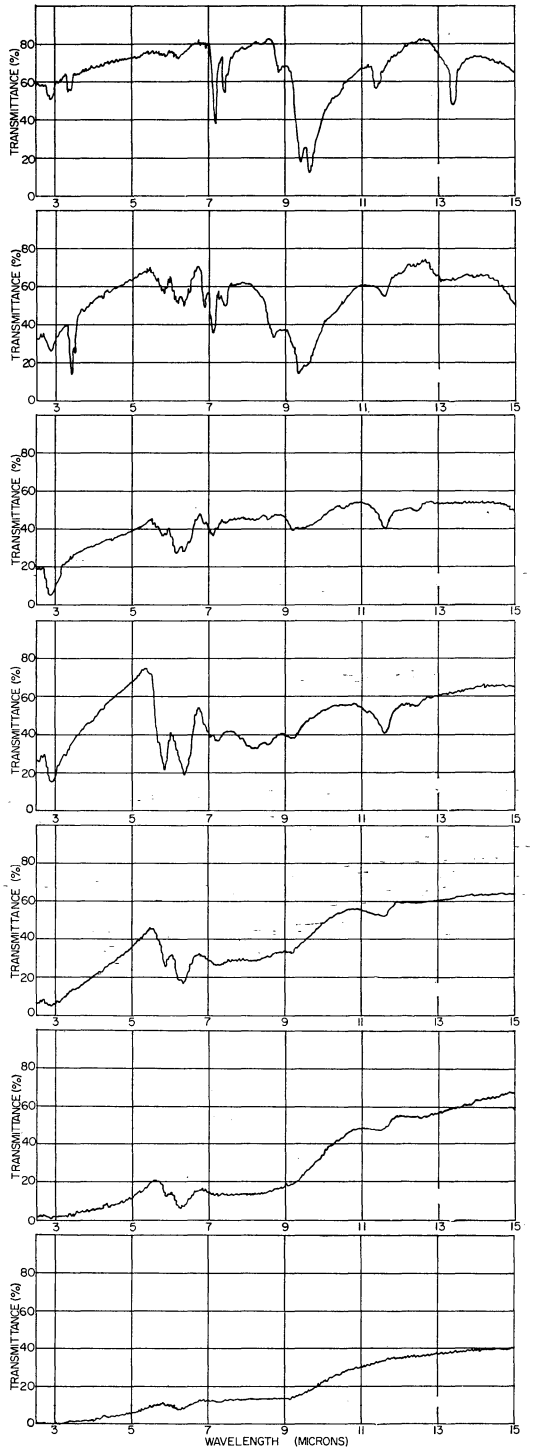

FIG. 2. Infrared spectra using KBr pellet technique. Top to bottom: pure Saran, 20.0%, 42.0%, 56.0%, 66.4%, 70.0%, and 75.3% weight loss respectively.

Can. J. Chem. Downloaded from www.nrcresearchpress.com by 210.87.254.105 on 09/05/12
For personal use only.

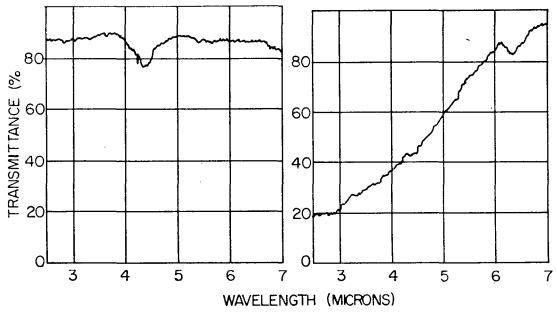

FIG. 3. Left: Infrared spectrum of fluorolube. Right: Infrared spectrum of a fully carbonized Saran charcoal coated with fluorolube.

rigidity. These new samples were approximately one third less in weight and thickness than those reported above and slightly better spectra could be obtained, and in some cases (carbon composition of less than 80%) even by dispensing with the reduction of the intensity of the reference beam in the spectrophotometer. However, it was noted that the reduction in thickness of the wafers was not proportional to the increase in optical transmittance, e.g., a diminution of an extra 10% in thickness for a sample already reduced by 20% in thickness did not show any noticeable gain in transmittance.

Determination of Pore Volumes

(a) Porosity Measurements by Means of Argon Adsorption

The following values of x/m (the ratio of the weight of adsorbate to adsorbent) were determined for Sarans of varying percentage decomposition. Using the density of liquid argon $\rho_A = 1.4$ at $-186°$ C, we can calculate the pore volumes as listed on the last column of Table I. Samples ranging from 0.1 to 0.12 g in weight were used in these experiments. A plot of porosity versus percentage decomposition is illustrated in Fig. 5.

TABLE I

Porosity values by argon adsorption

Percentage decomposition	x/m (g/g)	Pore volume (cc/g)
75.3	0.570	0.410
73.1	0.507	0.362
72.3	0.500	0.357
67.0	0.384	0.275
59.3	0.183	0.131
50.0	0.000	—
40.0	0.000	—

(b) Porosity Measurements by Means of Helium Displacement

Disks of approximately 0.5 g were used in this series of determinations. In view of their considerably increased size as compared with those used in the argon adsorption experiments their apparent volumes could be estimated with good accuracy by means of a vernier caliper. A plot of the experimentally evaluated pore volumes versus percentage decomposition determined at room temperature by the helium dilatometric technique is also shown in Fig. 5.

(c) Regular Reduction of Volume of the Samples on Pyrolysis

An interesting observation is the regular diminution of volume of the disks with

Can. J. Chem. Downloaded from www.nrcresearchpress.com by 210.87.254.105 on 09/05/12
For personal use only.

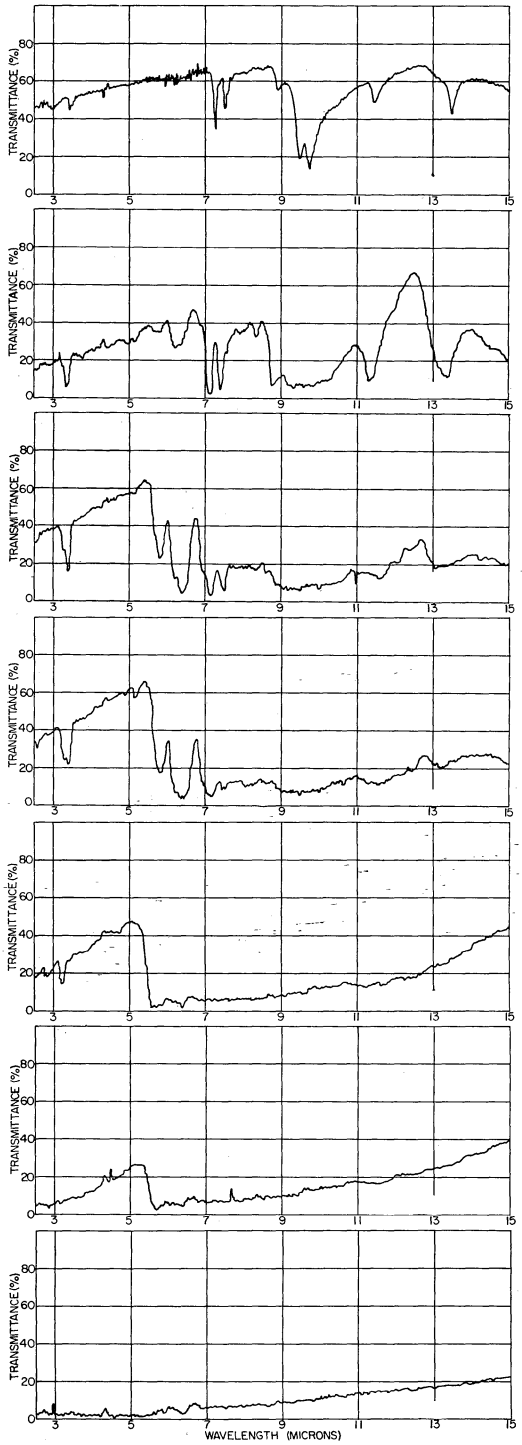

FIG. 4. Infrared spectra of thin wafers without KBr. Top to bottom: pure Saran, 3.9%, 23.6%, 34.0%, 60.5%, 66.0%, and 75.3% weight loss respectively.

Can. J. Chem. Downloaded from www.nrcresearchpress.com by 210.87.254.105 on 09/05/12
For personal use only.

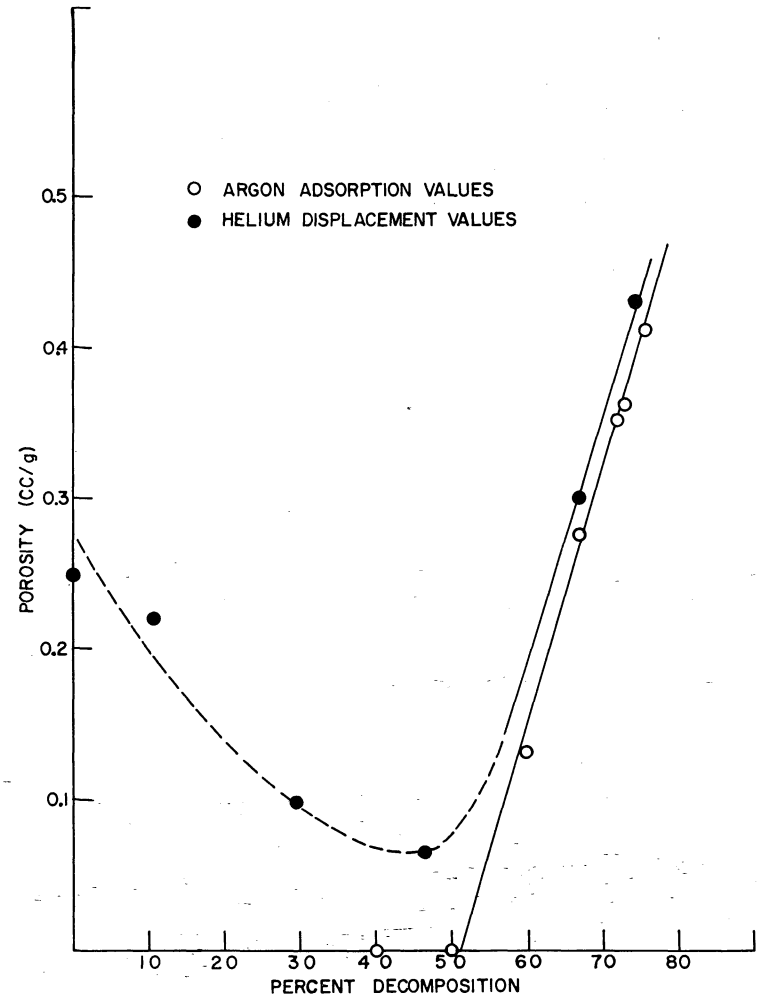

FIG. 5. Porosity values versus percentage decomposition: O argon adsorption values, ● helium displacement values.

progressive pyrolysis. This is shown in Fig. 6, where the total volume exhibits a linear decrease with increasing percentage decomposition.

DISCUSSION

Origin and Nature of Pore Structure

Saran charcoal falls into the category of Franklin's definition (14) as a "non-graphitising" carbon; it does not show any trace of homogeneous development of the three-dimensional graphitic structure even when heated up to temperatures of about 3000° C. Non-graphitizing carbons have been shown by X-ray studies to possess a characteristic open structure and a strongly cross-linked system of randomly orientated crystallites. Such an architecture of carbon atoms naturally favors the existence of large porosity and internal surface area.

The importance of cross-linking in the structure of the porous carbons is also revealed by their physical properties. Saran charcoal is hard and strong. The greater hardness of

Can. J. Chem. Downloaded from www.nrcresearchpress.com by 210.87.254.105 on 09/05/12
For personal use only.

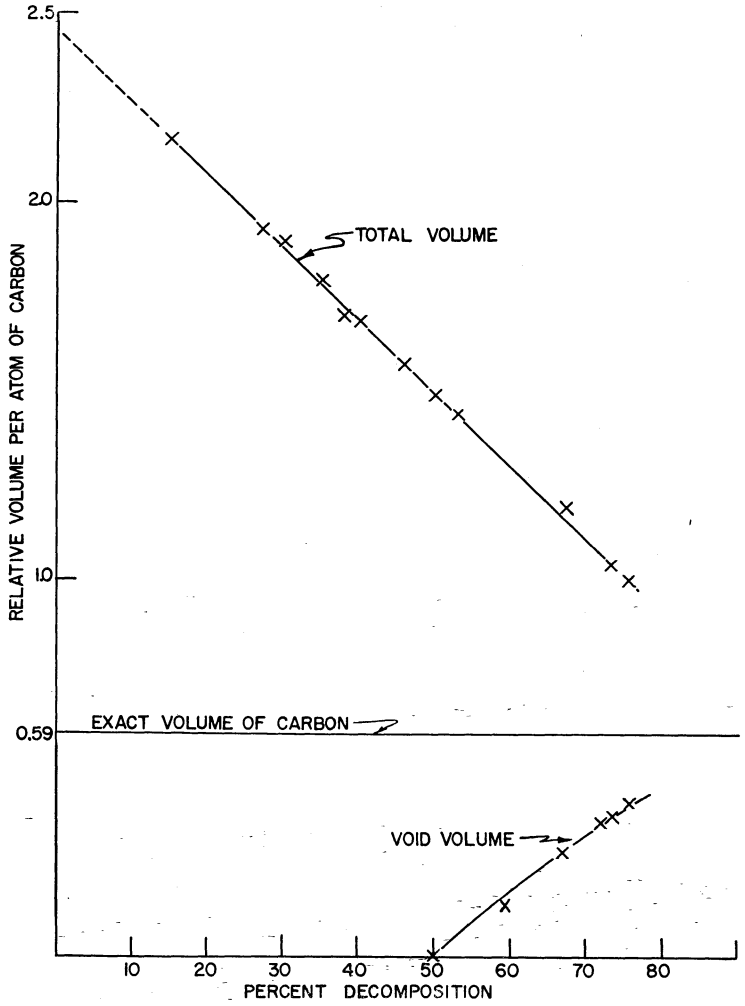

FIG. 6. Relative volume per atom of carbon versus percentage decomposition. Void volume values refer to those obtained by argon adsorption.

the non-graphitizing as compared with the graphitizing carbons must be attributed to greater regularity and strength of the bonding between neighboring crystallites.

Correlation Between Spectral Data, Structure, and Mechanism of Carbonization

The 1710 cm^{-1} band is the weaker of the two which persist up to 70% decomposition (83.1% carbon) but it is coincident with the carbonyl stretching frequency encountered in cyclohexanone and other six-membered ketonic ring compounds (cf. ref. 16, p. 142 *et seq.*). Standard precautions were taken to avoid entry of oxygen during the formation of the wafers and disks, but this does not guarantee the *total* exclusion of oxygen. In the event of trace contamination due to oxygen one could accept the possibility that certain aromatic quinonoid compounds may be formed. The 1710 cm^{-1} band could not be detected at full carbonization (75.3% decomposition) but this cannot be construed as proof of its absence in view of the intense scattering effect associated with the spectra. It should be emphasized that extreme care must be taken to avoid chemisorbed oxygen in the preparation of any pyrolytic carbon sample before reliance can be placed on its use in other experimental measurements.

Can. J. Chem. Downloaded from www.nrcresearchpress.com by 210.87.254.105 on 09/05/12
For personal use only.

The persistence of the lone band at 1570 cm^{-1} may hence be interpreted as being due to the C=C stretching vibrations commonly found in aromatic conjugated rings. Thus the spectral evidence would tend to support earlier speculations (10(*a*), 10(*b*)) that the polymer decomposed according to a Diels–Alder mechanism as depicted in Fig. 7, whereby

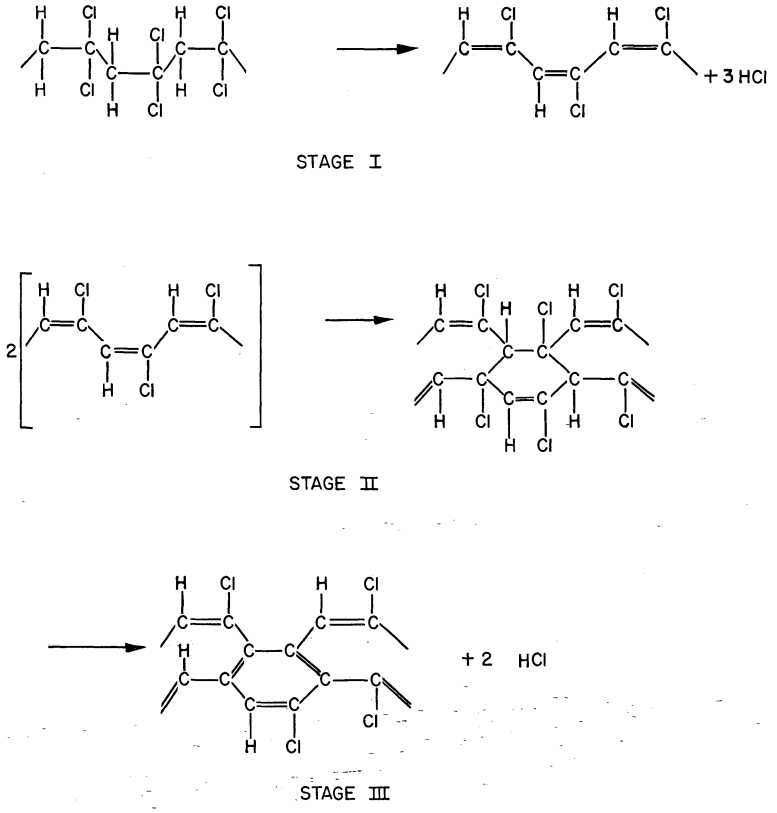

FIG. 7. Suggested Diels–Alder mechanism for the decomposition of polyvinylidene chloride.

a linear polyacetylene is first produced with successive release of adjacent HCl groups along the polymer chain, followed by a possible cyclization of adjacent polyene chains ending with the growth of fused rings. The presence of unpaired electrons in Saran charcoal has been demonstrated by microwave adsorption experiments (17), and in particular Franklin's evidence from X-ray diffraction patterns (14) is concordant with the above decomposition hypothesis.

The rate of HCl evolution also lends support to the suggested mechanism of carbonization. For temperatures between 150° C and 200° C hydrogen chloride is released at a very rapid rate up to about two-fifth decomposition by weight of the polymer. For temperatures in excess of 200° C the rate slows down progressively when adjacent hydrogen and chloride atoms may then be more than one or two carbon-to-carbon distances apart (Fig. 7, stage III). The internal surface ruptures and high temperatures of the final carbonization may provide conducive circumstances for distantly separated individual hydrogen and chlorine atoms to "hop" from carbon atom to carbon atom before reaching favorable sites for mutual interaction. During the last stages of pyrolysis

Can. J. Chem. Downloaded from www.nrcresearchpress.com by 210.87.254.105 on 09/05/12
For personal use only.

one can visualize that HCl molecules may then escape through established pore channels or slowly created new ones.

It must be accepted that obvious hazards are inherent in any mechanistic interpretation of the pyrolysis based on classical organic chemistry, but on the evidence reviewed (including the present work) it would appear that there are strong grounds for accepting the Diels–Alder mechanism. Moreover, it is equally plausible that the fully carbonized polymer may well comprise of a compact homogeneous network of aromatic cross-links.

Interpretation of Porosity Data

Figure 5 relates Saran at various percentage decompositions with the porosities obtained by argon adsorption and helium displacement. No argon was observed to be adsorbed with samples of less than 50% decomposition whereas the values obtained from the helium displacement experiments indicate the presence of fine pores at all compositions. This is not an entirely surprising result, since it has been previously found (1, 5) that Saran charcoal (100% carbon) consists of a series of fine pores accessible to a wide range of small and relatively flat molecules but not to such bulky molecules as α-pinene, sulphur hexafluoride, and tetraethylmethane, which do not enter the pore too readily. Inspection of Table II in terms of the molecular geometry of the adsorbates

TABLE II

Saturation values of various adsorbates on samples of completely pyrolyzed saran

Adsorbate	cm^3/g	Adsorbate	cm^3/g
Nitrogen	0.43	Naphthalene	0.37
n-Pentane	0.42	Neopentane	0.34
Benzene	0.42	Cyclohexane	0.34
Toluene	0.43	Tetraethylmethane	0.27*
cis-Butene-2	0.43	α-Pinene	Negligible
trans-Butene-2	0.43		
Argon	0.41		

*Non-equilibrium value after 6 days.

listed will confirm the view that the pores are fine and probably slot-like in cross section, and between 12 and 15 Å in width in their narrowest dimension. It would appear that with samples of the polymer below 50% decomposition, there may be pores which are so small that they deny penetration of argon but will allow the passage of helium.

The porosity values obtained with helium for samples above 66% decomposition are comparable although slightly higher than the argon adsorption values. With samples below 50% decomposition a marked divergence was clearly evident from Fig. 5, and there may be at least two possible sources of explanation:

(i) The apparently anomalous helium values may be due to "natural" pores existing in the pure polymer disks prior to pyrolysis. Helium pore volume values were later found to vary according to the pressure applied in the preparation of the disks (see Table III). The preliminary results in Table III introduce an additional parameter for consideration in the calculation of pore volumes of partially pyrolyzed samples. The effect of the compactness of the disks is being further pursued and will be reported in more detail elsewhere. It suffices for the present to point out that helium porosity values at low polymer decompositions are variable:

(ii) An additional complicating factor which would invalidate the helium values is the assumption that adsorption of helium is always negligible when the gas is used as a

Can. J. Chem. Downloaded from www.nrcresearchpress.com by 210.87.254.105 on 09/05/12
For personal use only.

TABLE III

Effect of pelletizing pressures on pure polyvinylidene chloride disks

Porosity (cm^3/g)	Pressure applied (lb/in^2)	Apparent density
0.296	5,000	1.65
0.257	10,000	1.64
0.125	15,000	1.75

dilatometric fluid (18). Once again our preliminary investigations (19) of this problem with Saran charcoal have revealed that appreciable adsorption of helium occurs even at room temperatures. This work is presently being carried out in a more thorough manner and will be reported later.

ACKNOWLEDGMENTS

Grateful thanks are due to the Department of Chemistry, Queen's University, Kingston, for permission to use their Perkin–Elmer Model 21 infrared spectrophotometer and also to Canadian Industries Limited, Ammonia Works, Millhaven, Ontario, for a gift of liquid nitrogen. Finally, we wish to thank the Defence Research Board for their generous financial support through DRB Grant No. 8220/12.

REFERENCES

1. J. R. DACEY and D. G. THOMAS. Trans. Faraday Soc. **50**, 740 (1954).
2. J. R. DACEY and D. G. THOMAS. Can. J. Chem. **33**, 344 (1955).
3. J. R. DACEY and J. A. FENDLEY. Proc. Symp. Colston Res. Soc. **10**, 142 (1960).
4. J. R. DACEY, J. C. CLUNIE, and D. G. THOMAS. Trans. Faraday Soc. **54**, 250 (1958).
5. J. R. DACEY. Advan. Chem. Ser. No. 33, 172 (1961).
6. C. PIERCE, J. W. WILEY, and R. N. SMITH. J. Phys. Colloid Chem. **53**, 669 (1949).
7. R. V. CULVER and N. S. HEATH. Trans. Faraday Soc. **51**, 1569 (1955).
8. D. A. CADENHEAD and D. H. EVERETT. Ind. Carbon Graphite. Papers Conf. London, 272 (1958).
9. D. A. CADENHEAD and J. R. DACEY. Proc. Conf. Carbon, 4th, Buffalo, 315 (1960).
10. (*a*) F. H. WINSLOW, W. O. BAKER, and W. A. YAGER. Proc. Conf. Carbon, 1st 2nd, Buffalo, 93 (1956). (*b*) F. H. WINDLOW, W. MATREYEK, and W. A. YAGER. Ind. Carbon Graphite. Papers Conf. London, 190 (1958).
11. R. E. FRANKLIN. Trans. Faraday Soc. **45**, 274 (1949).
12. J. W. MCBAIN and A. M. BAKR. J. Am. Chem. Soc. **48**, 690 (1926).
13. S. KRIMM and C. Y. LIANG. J. Polymer Sci. **22**, 95 (1956).
14. R. E. FRANKLIN. Acta Cryst. **3**, 107 (1950).
15. R. N. JONES and C. SANDORFY. Techniques of organic chemistry. Vol. IX. *Edited by* A. Weissberger. Interscience. 1956. p. 368 *et seq.*
16. L. J. BELLAMY. Infra red spectra of complex molecules. 2nd. ed. Methuen. 1958.
17. F. H. WINSLOW, W. O. BAKER, and W. A. YAGER. J. Am. Chem. Soc. **77**, 4751 (1955).
18. F. A. P. MAGGS, P. H. SCHWABE, and J. H. WILLIAMS. Nature, **186**, 956 (1960).
19. R. G. BELEC. B.Sc. Thesis, Royal Military College, Kingston, Ontario. 1962.
20. R. BENT and J. K. BROWN. Fuel, **40**, 47 (1961).
21. J. K. BROWN. Fuel, **38**, 55 (1959).
22. J. K. BROWN. J. Chem. Soc. 744, 752 (1955).
23. H. A. VAN VUCHT, B. J. RIETVELD, and D. W. VAN KREVELEN. Fuel, **34**, 50 (1955).

Can. J. Chem. Downloaded from www.nrcresearchpress.com by 210.87.254.105 on 09/05/12
For personal use only.

Can. J. Chem. Downloaded from www.nrcresearchpress.com by 210.87.254.105 on 09/05/12
For personal use only.

NOTES

STEREOCHEMISTRY OF ARSENIC
PART VII. IODODIPHENYLARSINE

J. TROTTER

Crystals of iododiphenylarsine are isomorphous with those of the bromo and chloro derivatives (1); the molecular configurations of the three compounds are very similar, and this study of the iodo compound has been confined to a measurement of the As—I bond distance.

The unit cell dimensions and space group were determined from precession films (Mo $K\alpha$, $\lambda = 0.7107$ Å). The crystal data are: Iododiphenylarsine, $C_{12}H_{10}AsI$; M, 356; m.p. 37–39°. Monoclinic, $a = 11.01 \pm 0.04$, $b = 8.82 \pm 0.03$, $c = 12.34 \pm 0.04$ Å, $\beta = 91°$ $37' \pm 5'$. Volume of the unit cell = 1198 Å^3. D_c (with $Z = 4$) = 1.962, $D_m \sim 1.9$ g cm^{-3}. Absorption coefficient for X rays, $\lambda = 0.7107$ Å, $\mu = 57$ cm^{-1}. Total number of electrons per unit cell = $F(000) = 672$. Absent spectra: $h0l$ when h is odd, $0k0$ when k is odd. Space group is $P2_1/a$.

Intensity data for the $h0l$ and $0kl$ reflections were recorded on precession films, estimated visually, and the structure amplitudes derived from the usual formulae, no absorption corrections being applied. The signs of the structure factors were derived by the isomorphous replacement method, and Fourier series then summed; the coordinates of the arsenic and iodine atoms, derived from the resulting electron-density maps, are given in Table I, expressed as fractions of the unit cell edges. The As—I bond length calculated

TABLE I
Positional parameters

Atom	x	y	z
As	−0.0173	0.1789	0.2755
I	0.0837	−0.4120	0.2000

from these parameters is 2.53 Å, which is, of course, longer than the distances As—Cl = 2.26 Å and As—Br = 2.40 Å in the chloro and bromo derivatives, but very similar to the As—I bond lengths in AsI_3 (2.52 Å) and $(CH_3)_2AsI$ (2.54 Å) (2). The other features of the molecular geometry do not differ significantly from those of the other halogen derivatives (3).

Structure factor data are not listed, but are available from the author.

The author thanks Dr. W. R. Cullen for the crystal sample and for helpful discussion, and the National Research Council of Canada and the President's Research Fund, University of British Columbia, for financial support.

1. W. R. CULLEN and J. TROTTER. Can. J. Chem. **39**, 2602 (1961).
2. TABLES OF INTERATOMIC DISTANCES AND CONFIGURATION IN MOLECULES AND IONS. Chem. Soc. Special Publ. No. 11. 1958.
3. J. TROTTER. Can. J. Chem. **40**, 1590 (1962).

RECEIVED AUGUST 7, 1962.
DEPARTMENT OF CHEMISTRY,
UNIVERSITY OF BRITISH COLUMBIA,
VANCOUVER 8, BRITISH COLUMBIA.

POLAROGRAPHIC REDUCTION OF ORTHO ALKYL NITROBENZENES

OWEN H. WHEELER

Nitrobenzenes are reduced at the dropping mercury electrode in neutral or alkaline solution to phenylhydroxylamines or anilines (1). It has been shown (2) that methyl substitution ortho to the nitro group results in an increase in half-wave reduction potential ($E_{1/2}$ more negative) at pH 7.2 (in 80% water–dioxane). Alkyl groups larger than methyl were not investigated. This paper reports polarographic data (see Table I) for *ortho*-methyl-, -ethyl-, -isopropyl-, and -*t*-butyl-nitrobenzenes and the corresponding para

TABLE I

Polarographic data of nitrobenzenes*

Substituent	$-E_{1/2}$		$i_d/cm^{2/3}t^{1/6}$†	
—	0.62	(0.62)	5.6	(5.7)
p-Methyl	0.59	(0.62)	5.7	(5.2)
o-Methyl	0.66	(0.66)	5.5	(5.5)
o,*o*-Dimethyl	0.73		4.9	
p-Ethyl	0.59		5.0	
o-Ethyl	0.62		4.9	
p-Isopropyl	0.59		5.0	
o-Isopropyl	0.61		4.8	
p-*t*-Butyl	0.62		4.8	
o-*t*-Butyl	0.65		4.0	

*Half-wave potentials against saturated calomel electrode, taken at pH 7.2. Values in parenthesis taken from ref. 2.
†In μamp mmole^{-1}mg$^{-2/3}$sec$^{-1/6}$.

substituent where the effect of the substituent can only be electronic. These ortho alkyl nitrobenzenes show marked decreases in intensity and hypsochromic displacements of the wavelengths of ultraviolet absorption (3, 4) (see Table II) attributable to steric inhibition of resonance between the nitro group and the aromatic ring.

TABLE II

Ultraviolet spectra of nitrobenzenes

Substituent	λ_{max}*	
—	252	(8,620)
p-Methyl	264	(10,250)
o-Methyl	250	(5,950)
p-Isopropyl	265	(10,430)
o-Isopropyl	247	(3,760)
	280	(1,500)†
p-*t*-Butyl	265	(10,720)
o-*t*-Butyl	265	(800)†

*Wavelengths in mμ, molar extinction coefficient in parenthesis, from ref. 3 in isooctane.
†Inflections, read from curves.

The values at pH 7.2 in 80% water–dioxane (Table I) for the ortho-substituted compounds are higher than those of the para isomers (increases of 0.07, 0.03, 0.02, and 0.03 v for Me, Et, *i*-Pr, and *t*-Bu), the increase for *o*,*o*-dimethylnitrobenzene being particularly large (0.014 v compared to *p*-nitrotoluene) and of the same order as that found for nitro-

Can. J. Chem. Downloaded from www.nrcresearchpress.com by 210.87.254.40 on 09/05/12
For personal use only.

mesitylene and nitrodurene (0.13 v in both cases (2)). The potential increases, however, do not increase with increasing size of the substituent as might be expected. The diffusion current constants ($i_d/cm^{2/3}t^{1/6}$) were all smaller for the substituted nitrobenzenes and were generally less for the ortho than the para compounds.

The overall differences found were rather small and the results probably do not warrant a detailed analysis. However, the inductive and hyperconjugative effects of alkyl groups, by increasing the negative charge on the nitro group, will cause a higher reduction potential. The fact that these electronic effects increase and decrease, respectively, in the series methyl, ethyl, isopropyl, and *t*-butyl probably accounts for the increase in the reduction potential of *p*-*t*-butylnitrobenzene. In the case of ortho substitution these effects will be more directly felt by the nitro group. However, electronic effects cannot entirely explain the observed results, and steric hindrance must play a large role.

Steric hindrance has been shown to increase the reduction potential of aliphatic nitro compounds (5) and of aromatic aldehydes, ketones, and nitro compounds (6). Steric hindrance may arise from steric inhibition of resonance between the aromatic ring and the nitro substituent (2) and by steric hindrance to adsorption of the nitro group on the charged mercury surface. Both these effects would be expected to increase the reduction potential, the first by increasing the effective charge on the nitro group (by inhibiting resonance charge sharing with the ring) and the second by increasing the energy barrier to addition of electronic charge to the nitro group. Prevost and co-workers (6) have suggested that the first effect is predominant, since the $E_{1/2}$ values are nearly independent of substituent size. However, the spectra (Table II) show a steady increase in steric hindrance with increasing substituent size, an effect that can only be due to steric inhibition of resonance. Recent work on the polarographic reduction of aliphatic halides (7) has shown the importance of the steric requirements of both the reducible group and the electrode surface.

It must be concluded from the present work that polarographic reduction potentials are not a sensitive indication of steric hindrance.

EXPERIMENTAL

Nitrobenzenes

Nitrobenzene, *o*- and *p*-nitrotoluene, and 2,6-dimethylnitrobenzene were Eastman-Kodak white label samples. *o*- and *p*-Nitroethylbenzene and *o*- and *p*-nitroisopropylbenzene were prepared by nitration of the corresponding hydrocarbons (7, 8) and were separated by fractional distillation. *o*- and *p*-Nitro-*t*-butylbenzene were supplied by Professor H. C. Brown (9). Their physical constants are given in Table III.

TABLE III

Physical constants of nitrobenzenes

	B.p. (°C), at 18 mm	n_D^{20}
p-Ethyl	126	1.5400
o-Ethyl	115	1.5345
p-Isopropyl	142	1.5370
o-Isopropyl	125	1.5255
p-*t*-Butyl	150	1.5336
o-*t*-Butyl	130	1.5178

Polarography

Dioxane was purified by refluxing with and distilling from sodium. The buffer (pH 7.2, 0.2 *M* disodium hydrogen phosphate and 0.18 sodium dihydrogen phosphate) was prepared in 80% water–dioxane (v/v) (2). The polarographic reductions were carried out using Sargent model XI and XV polarographs. The capillary

Can. J. Chem. Downloaded from www.nrcresearchpress.com by 210.87.254.40 on 09/05/12
For personal use only.

had a drop-time of 3.3 seconds (open circuit in 0.1 *N* potassium chloride solution) and a flow of 1.63 mg of mercury/sec. The solutions (ca. 2×10^{-4} *M*) contained several drops of 0.1% gelatin in 80% water–dioxane and were deoxygenated by passing nitrogen, previously saturated with the same solvent, for 20 minutes. Voltages were measured against a Beckman calomel electrode (with capillary collar) dipping into the solution. No correction was necessary for the voltage drop in the cell since at this low internal resistance and low concentration the error was <0.005 v. The polarograms were run three or four times and the average values are reported in Table I.

ACKNOWLEDGMENTS

A gift of *t*-butylnitrobenzenes from Professor H. C. Brown is gratefully acknowledged. Some of the data were checked by Cesar Reyes, under a National Science Foundation undergraduate research participation grant.

1. I. M. KOLTHOFF and J. J. LINGANE. Polarography. Interscience Publishers, Inc., New York. 1954.
2. M. FIELDS, C. VALLE, and M. KANE. J. Am. Chem. Soc. **71**, 421 (1949).
3. W. G. BROWN and H. REAGAN. J. Am. Chem. Soc. **69**, 1032 (1947).
4. B. M. WEPSTER. Rec. Trav. Chim. **76**, 335 (1957).
5. G. W. GOWARD, C. E. BRICHER, and W. C. WILDMAN. J. Org. Chem. **20**, 378 (1955).
6. C. PREVOST, P. SOUCHAY, and C. MALEN. Bull. Soc. Chim. France, 78 (1953).
7. D. A. SHIRLEY. Preparation of organic intermediates. John Wiley and Sons, New York, N.Y. 1951. pp. 220, 223.
8. H. C. BROWN and W. H. BONNER. J. Am. Chem. Soc. **76**, 605 (1954).
9. K. L. NELSON and H. C. BROWN. J. Am. Chem. Soc. **73**, 5605 (1951).

RECEIVED MAY 7, 1962.
DEPARTMENT OF CHEMISTRY,
UNIVERSITY OF PUERTO RICO,
MAYAGUEZ, PUERTO RICO.

Can. J. Chem. Downloaded from www.nrcresearchpress.com by 210.87.254.40 on 09/05/12
For personal use only.

2,3-DIPHENYLBUTANE-2,3-DIOL. SOLVENT EFFECTS

H. AGAHIGIAN, J. F. MORAVECK, AND H. GAUTHIER

The effect of concentration on the chemical shift of the hydroxyl resonance of alcohols has been reported (1(*a*); 1(*b*) and references cited therein) and the position of the hydroxyl proton is an estimate of the extent and nature of the hydrogen bonding. The use of different solvents may lend some insight into the nature of the hydrogen bonding, as has been suggested by Jardetsky (2).

The n.m.r. studies on the butanes have been quite comprehensive (3, 4) in an effort to establish the rotamer population as well as the coupling constants of the protons in possible rotamer configuration; however, butanediols, in particular the meso- and the *dl*-2,3-diphenylbutane-2,3-diols, have not been investigated with respect to solvent effects. Various diastereomeric alcohols have been studied (5) and the hydroxyl resonances have been determined and evidence was given to show the extent hydrogen bonding is dependent on the stereochemistry.

The meso- and *dl*-2,3-diphenylbutane-2,3-diol isomers were characterized (6) by their infrared spectra. An interesting feature of the infrared spectrum of the *dl*-2,3-diphenylbutane-2,3-diol was the broad hydroxyl band. Molecular models indicate that the intramolecular hydrogen bonding is enhanced in the *dl* form whereas in the meso form the intramolecular hydrogen bonding is not sterically favored.

The proton n.m.r. spectra of the *dl*- and meso-2,3-diphenylbutane-2,3-diol in benzene,

had a drop-time of 3.3 seconds (open circuit in 0.1 *N* potassium chloride solution) and a flow of 1.63 mg of mercury/sec. The solutions (ca. 2×10^{-4} *M*) contained several drops of 0.1% gelatin in 80% water–dioxane and were deoxygenated by passing nitrogen, previously saturated with the same solvent, for 20 minutes. Voltages were measured against a Beckman calomel electrode (with capillary collar) dipping into the solution. No correction was necessary for the voltage drop in the cell since at this low internal resistance and low concentration the error was <0.005 v. The polarograms were run three or four times and the average values are reported in Table I.

ACKNOWLEDGMENTS

A gift of *t*-butylnitrobenzenes from Professor H. C. Brown is gratefully acknowledged. Some of the data were checked by Cesar Reyes, under a National Science Foundation undergraduate research participation grant.

1. I. M. KOLTHOFF and J. J. LINGANE. Polarography. Interscience Publishers, Inc., New York. 1954.
2. M. FIELDS, C. VALLE, and M. KANE. J. Am. Chem. Soc. **71**, 421 (1949).
3. W. G. BROWN and H. REAGAN. J. Am. Chem. Soc. **69**, 1032 (1947).
4. B. M. WEPSTER. Rec. Trav. Chim. **76**, 335 (1957).
5. G. W. GOWARD, C. E. BRICHER, and W. C. WILDMAN. J. Org. Chem. **20**, 378 (1955).
6. C. PREVOST, P. SOUCHAY, and C. MALEN. Bull. Soc. Chim. France, 78 (1953).
7. D. A. SHIRLEY. Preparation of organic intermediates. John Wiley and Sons, New York, N.Y. 1951. pp. 220, 223.
8. H. C. BROWN and W. H. BONNER. J. Am. Chem. Soc. **76**, 605 (1954).
9. K. L. NELSON and H. C. BROWN. J. Am. Chem. Soc. **73**, 5605 (1951).

RECEIVED MAY 7, 1962.
DEPARTMENT OF CHEMISTRY,
UNIVERSITY OF PUERTO RICO,
MAYAGUEZ, PUERTO RICO.

Can. J. Chem. Downloaded from www.nrcresearchpress.com by 210.87.254.5 on 09/05/12
For personal use only.

2,3-DIPHENYLBUTANE-2,3-DIOL. SOLVENT EFFECTS

H. AGAHIGIAN, J. F. MORAVECK, AND H. GAUTHIER

The effect of concentration on the chemical shift of the hydroxyl resonance of alcohols has been reported (1(*a*); 1(*b*) and references cited therein) and the position of the hydroxyl proton is an estimate of the extent and nature of the hydrogen bonding. The use of different solvents may lend some insight into the nature of the hydrogen bonding, as has been suggested by Jardetsky (2).

The n.m.r. studies on the butanes have been quite comprehensive (3, 4) in an effort to establish the rotamer population as well as the coupling constants of the protons in possible rotamer configuration; however, butanediols, in particular the meso- and the *dl*-2,3-diphenylbutane-2,3-diols, have not been investigated with respect to solvent effects. Various diastereomeric alcohols have been studied (5) and the hydroxyl resonances have been determined and evidence was given to show the extent hydrogen bonding is dependent on the stereochemistry.

The meso- and *dl*-2,3-diphenylbutane-2,3-diol isomers were characterized (6) by their infrared spectra. An interesting feature of the infrared spectrum of the *dl*-2,3-diphenylbutane-2,3-diol was the broad hydroxyl band. Molecular models indicate that the intramolecular hydrogen bonding is enhanced in the *dl* form whereas in the meso form the intramolecular hydrogen bonding is not sterically favored.

The proton n.m.r. spectra of the *dl*- and meso-2,3-diphenylbutane-2,3-diol in benzene,

deuterochloroform, and acetone were studied. The meso compound in deuterochloroform had a methyl resonance at 8.45 τ, hydroxyl resonance at 7.70 τ, and an aromatic peak at 2.83 τ while the *dl* mixture in deuterochloroform had resonances at 8.55 τ (methyl), 7.32 τ (hydroxyl), and 2.83 τ (aromatic). The slight high-field resonance of the methyl in the *dl* mixture may be due to the anisotropy associated with the phenyl ring in the preferred rotamer orientation.

The hydroxyl resonance of the *dl* isomer is at lower field than the meso, which is consistent with the infrared data. A twofold dilution of the deuterochloroform solutions of both the *dl* and meso isomers caused the hydroxyl resonance to be shifted to high field by 3 c.p.s. and the methyl resonance by 2.4 c.p.s. In benzene solution the methyl resonances of the meso and *dl* isomers are the same and the expected shift to high field occurred (8.62 τ). The hydroxyl resonances were 7.94 and 7.55 τ for the meso and *dl* isomers respectively.

In acetone solution the spectrum of the meso compound exhibited an interesting effect. In addition to the low-field shift of the hydroxyl due to hydrogen bonding (6.10 τ), the phenyl resonance was split into two multiplets in a ratio of 2:3, 2.63 and 2.85 τ respectively. From the molecular models, it appears that the ortho protons are deshielded because of the steric interaction (7) of the phenyl rings in the preferred configuration due to the hydrogen bonding of the diol with the acetone. There appears to be formation of a solute–solvent "dimer" which is forcing the diol into a geometry where there is steric hindrance. Although the possibility that hydrogen bonding of the aromatic protons with acetone may cause this effect, it is unlikely. The exchange of the hydroxyl proton with deuterium to obtain the deuterated diol and a subsequent proton spectrum in acetone under identical conditions indicated the same splitting of the aromatic protons. There appears to be no isotope effect or at least the changes in bond length due to isotopic substitution had little or no effect on the geometry of the phenyl groups of the meso isomer.

The proton spectrum of the *dl* isomer in acetone (50 mg in 0.5 ml of acetone) was studied and the hydroxyl resonance was 5.87 τ; however, dilution to 1 ml and successive dilution in 0.5-ml increments showed no change in the resonance position of the hydroxyl proton. In a solution of the *dl* isomer in acetone (100 mg in 0.5 ml) the hydroxyl resonance is 5.83 τ.

An identical series using deuterochloroform demonstrated a high-field shift of the hydroxyl upon successive dilutions. This indicates that the intermolecular hydrogen bonding present in the acetone–diol dimer is large compared to the intramolecular hydrogen bonding. Because of the steric interaction of the phenyl groups in the meso diol in acetone one would expect the chemical shift of the hydroxyl resonance to be slightly higher than that of the *dl* isomer in the same solvent, the steric requirements favoring hydrogen bonding of the *dl* isomer. The *dl* isomer resonance is 5.83 τ and that of the meso isomer 6.10 τ, the steric repulsion accounting for the high shift of the meso compound.

Preparations of 2,3-diphenylbutane-2,3-diol have been described (8, 9, 10). In addition to these, there are many others too numerous to mention. Generally, the methods involved the reaction of acetophenone and ethyl benzoate in sodium dispersion; the reaction of acetophenone in alcohol and benzene in the presence of aluminum foil and mercuric chloride; or the reaction of acetophenone in isopropanol in the presence of sunlight for several months. However, when a quartz cell in the presence of ultraviolet light was used good yields of the meso and *dl* isomers of 2,3-diphenylbutane-2,3-diol were obtained in 5 days.

Can. J. Chem. Downloaded from www.nrcresearchpress.com by 210.87.254.5 on 09/05/12
For personal use only.

EXPERIMENTAL

In a typical run 2,3-diphenylbutane-2,3-diol was prepared by the reaction of 160 g (1.33 mole) of acetophenone, which was dried with calcium hydride and freshly distilled in 850 ml of isopropanol, and a drop of acetic acid in the presence of ultraviolet light (100 watt Hanovia Ultraviolet Lamp) for 20 days with stirring. The solvent was removed and a 95% yield of the isomer mixture was obtained, m.p. 92–117° C. The *dl* isomer was obtained pure by repeated crystallizations from petroleum ether – benzene, m.p. 125° C. The meso-2,3-diphenylbutane-2,3-diol was isolated by elution from an alumina column with benzene. By using the quartz cell the time of irradiation was limited to 5 days, with the yield of the isomers being approximately the same as those in the experiment in which a pyrex reaction vessel was used.

The n.m.r. spectra were obtained using the Varian A-60 spectrometer. The chemical shifts are reported in "τ" values. Tetramethylsilane was used as the internal standard. The concentrations were identical for the pure *dl* and meso measurements. In addition, known concentrations of synthetic mixtures gave essentially the same chemical shifts as those exhibited by the meso or the *dl* isomers at that concentration.

The infrared spectra were obtained as fluorolube–nujol mulls as well as KBr pellets.

ACKNOWLEDGMENTS

The authors wish to thank Mr. Warren Harple for the infrared spectral data and Mr. George D. Vickers for his assistance in this work.

1. (*a*) M. Saunders and J. B. Hyne. J. Chem. Phys. **29**, 253 (1958).
   (*b*) L. M. Jackman. Applications of NMR spectroscopy in organic chemistry. Pergamon Press, New York. 1959. pp. 66–72.
2. O. Jardetsky. Private communication.
3. A. A. Bothner-By and C. Naar-Colin. J. Am. Chem. Soc. **84**, 743 (1962).
4. F. A. L. Anet. J. Am. Chem. Soc. **84**, 747 (1962).
5. J. L. Mateos and D. J. Cram. J. Am. Chem. Soc. **81**, 2759 (1959).
6. D. J. Cram and K. R. Kopecky. J. Am. Chem. Soc. **81**, 2745 (1959).
7. C. Reid. J. Mol. Spectry. **1**, 18 (1957).
8. R. Shishido and H. Nozaki. J. Am. Chem. Soc. **70**, 776 (1948).
9. L. Mamlock and J. Wiemann. Bull. Soc. Chim. France, 1424 (1945).
10. C. F. H. Allen, C. G. Eliot, and A. Bell. Can. J. Res. B, **17**, 75 (1939).

Received July 18, 1962.
Olin Mathieson Chemical Corporation,
Research Center,
New Haven, Conn.

Can. J. Chem. Downloaded from www.nrcresearchpress.com by 210.87.254.5 on 09/05/12
For personal use only.

N-β-D-GLUCOPYRANOSYLTHIOUREA

M. H. Benn

Recently, on the basis of a successful nucleoside synthesis in which D-glucosylthiourea was converted into 1-N-β-D-glucopyranosylthymine and by analogy with glucosylurea (1, 2), Naito and Sano (3) have assigned glucosylthiourea the N-β-D-pyranosyl structure.[1] As an extension of earlier studies of the glycosylureas (1) we are re-examining the chemistry of the glycosylthioureas and in view of the lingering controversy (1, 4, 5, 6) as to whether this type of compound has a Schiff's base or N-glycosidic structure, we wish to present our own independent observations, which support the conclusions of the Japanese workers.

[1]*The reported conversion of the pentabenzoate of glucosylthiourea into the pentabenzoate of glycosylurea, by the action of mercuric oxide (4), is additional evidence supporting this assignment.*

EXPERIMENTAL

In a typical run 2,3-diphenylbutane-2,3-diol was prepared by the reaction of 160 g (1.33 mole) of acetophenone, which was dried with calcium hydride and freshly distilled in 850 ml of isopropanol, and a drop of acetic acid in the presence of ultraviolet light (100 watt Hanovia Ultraviolet Lamp) for 20 days with stirring. The solvent was removed and a 95% yield of the isomer mixture was obtained, m.p. 92–117° C. The *dl* isomer was obtained pure by repeated crystallizations from petroleum ether – benzene, m.p. 125° C. The meso-2,3-diphenylbutane-2,3-diol was isolated by elution from an alumina column with benzene. By using the quartz cell the time of irradiation was limited to 5 days, with the yield of the isomers being approximately the same as those in the experiment in which a pyrex reaction vessel was used.

The n.m.r. spectra were obtained using the Varian A-60 spectrometer. The chemical shifts are reported in "τ" values. Tetramethylsilane was used as the internal standard. The concentrations were identical for the pure *dl* and meso measurements. In addition, known concentrations of synthetic mixtures gave essentially the same chemical shifts as those exhibited by the meso or the *dl* isomers at that concentration.

The infrared spectra were obtained as fluorolube–nujol mulls as well as KBr pellets.

ACKNOWLEDGMENTS

The authors wish to thank Mr. Warren Harple for the infrared spectral data and Mr. George D. Vickers for his assistance in this work.

1. (*a*) M. Saunders and J. B. Hyne. J. Chem. Phys. **29**, 253 (1958).
   (*b*) L. M. Jackman. Applications of NMR spectroscopy in organic chemistry. Pergamon Press, New York. 1959. pp. 66–72.
2. O. Jardetsky. Private communication.
3. A. A. Bothner-By and C. Naar-Colin. J. Am. Chem. Soc. **84**, 743 (1962).
4. F. A. L. Anet. J. Am. Chem. Soc. **84**, 747 (1962).
5. J. L. Mateos and D. J. Cram. J. Am. Chem. Soc. **81**, 2759 (1959).
6. D. J. Cram and K. R. Kopecky. J. Am. Chem. Soc. **81**, 2745 (1959).
7. C. Reid. J. Mol. Spectry. **1**, 18 (1957).
8. R. Shishido and H. Nozaki. J. Am. Chem. Soc. **70**, 776 (1948).
9. L. Mamlock and J. Wiemann. Bull. Soc. Chim. France, 1424 (1945).
10. C. F. H. Allen, C. G. Eliot, and A. Bell. Can. J. Res. B, **17**, 75 (1939).

Received July 18, 1962.
Olin Mathieson Chemical Corporation,
Research Center,
New Haven, Conn.

Can. J. Chem. Downloaded from www.nrcresearchpress.com by 210.87.254.5 on 09/05/12
For personal use only.

N-β-D-GLUCOPYRANOSYLTHIOUREA

M. H. Benn

Recently, on the basis of a successful nucleoside synthesis in which D-glucosylthiourea was converted into 1-N-β-D-glucopyranosylthymine and by analogy with glucosylurea (1, 2), Naito and Sano (3) have assigned glucosylthiourea the N-β-D-pyranosyl structure.[1] As an extension of earlier studies of the glycosylureas (1) we are re-examining the chemistry of the glycosylthioureas and in view of the lingering controversy (1, 4, 5, 6) as to whether this type of compound has a Schiff's base or N-glycosidic structure, we wish to present our own independent observations, which support the conclusions of the Japanese workers.

[1]*The reported conversion of the pentabenzoate of glucosylthiourea into the pentabenzoate of glycosylurea, by the action of mercuric oxide (4), is additional evidence supporting this assignment.*

D-Glucosylthiourea was best prepared from 2:3:4:6-tetra-O-acetyl-D-glucosylisothiocyanate (7). The product was homogeneous when examined by paper chromatography.[2] The direct, acid-catalyzed condensation of glucose with thiourea (8) gave poor yields of glucosylthiourea, which is difficult to obtain pure.

In unbuffered solution, pH 3–4, in the dark, at 4°, glucosylthiourea rapidly consumed 2 moles mole^{-1} of periodate (within 4 hours), after which slow "overoxidation" (1, 6) took place (2.6 moles mole^{-1} periodate were consumed in 24 hours).

This rules out the Schiff's base structure and establishes the pyranosyl configuration of the sugar moiety.

The β-configuration at the anomeric center was inferred from the following, mainly spectral evidence. The infrared spectrum of glucosylthiourea, in a potassium bromide disk, shows strong absorption at 900 cm^{-1}, weak absorption at 775 cm^{-1}, and absence of absorption at 844 cm^{-1}, features considered as characteristic of glucosides possessing the β-configuration (6, 9).

Proton magnetic resonance spectroscopy of glucosylthiourea itself was inconclusive, but the tetra-O-acetyl glucosylisothiocyanate precursor gave a spectrum at 60 Mc/s in chloroform, practically identical with that of tetra-O-acetyl-β-D-glucopyranosyl chloride (10), in which the signal for the anomeric hydrogen was submerged in the signal due to the secondary hydrogens at τ 4.84. The chemical shift of protons adjacent to an isothiocyanate group is very close to that produced by an adjacent chlorine atom (11) and tetra-O-acetyl-α-D-glucopyranosyl chloride shows a clearly resolved signal for the anomeric hydrogen, τ 3.75 (10). It was therefore concluded that the tetra-O-acetyl glucosyl isothiocyanate has the β-D-pyranosyl configuration—as would be expected from its mode of preparation from tetra-O-acetyl-α-D-glucopyranosyl bromide. The preparation of glucosylthiourea from the isothiocyanate was performed under conditions unlikely to result in inversion of configuration.

N-β-D-Glucopyranosylthiourea does not mutarotate. In aqueous solution it shows intense ultraviolet light absorption at 242 mμ, log ϵ 4.19. Thiourea itself exhibits similar intense absorption at 254 mμ, log ϵ 4.2 (12).

1. M. H. BENN and A. S. JONES. J. Chem. Soc. 3837 (1960).
2. T. NAITO, M. HIRATA, T. KAWAKAMI, and M. SANO. Chem. Pharm. Bull. (Tokyo), **9**, 703 (1961).
3. T. NAITO and M. SANO. Chem. Pharm. Bull. (Tokyo), **9**, 709 (1961).
4. I. GOODMAN. Advan. Carbohydrate Chem. **13**, 215 (1958).
5. L. SEGAL, R. T. O'CONNER, and F. G. EGGERTON. J. Am. Chem. Soc. **82**, 2807 (1960).
6. A. S. JONES and G. W. ROSS. Tetrahedron, **18**, 189 (1962).
7. E. FISCHER. Ber. **47**, 1377 (1914). S. MULLER and A. WILHELMS. Ber. **74**, 698 (1941).
8. B. HELFERICH and W. KOSCHE. Ber. **59**, 69 (1926).
9. S. A. BARKER, E. J. BOURNE, and D. H. WIFFEN. *In* Methods of biochemical analysis. Vol. 3. Interscience Publishers. 1962. p. 213.
10. R. U. LEMIEUX, R. K. KULLNIG, H. J. BERNSTEIN, and W. G. SCHNEIDER. J. Am. Chem. Soc. **80**, 6098 (1958).
11. Unpublished experimental results. See also G. V. D. TIERS. Compilation of proton magnetic resonance shielding values. Minnesota Mining and Manufacturing Co. 1958.
12. A. CLOW and N. L. HELMRICH. Trans. Faraday Soc. **36**, 685 (1940).
13. I. W. GROTE. J. Biol. Chem. **93**, 25 (1931).
14. W. E. TREVELYAN, D. P. PROCTER, and J. S. HARRISON. Nature, **166**, 144 (1950).

RECEIVED JUNE 28, 1962.
DEPARTMENT OF CHEMISTRY,
UNIVERSITY OF ALBERTA, CALGARY,
CALGARY, ALBERTA.

[2]*n-Butanol – acetic acid – water (4:1:5), upper phase, R_F 0.15, purple to Grote's reagent (13), grey with Trevelyan's silver nitrate reagent (14).*

Can. J. Chem. Downloaded from www.nrcresearchpress.com by 210.87.254.5 on 09/05/12
For personal use only.

HYDROGEN BONDING IN HALOFORM SOLUTIONS[1]

W. G. PATERSON AND D. M. CAMERON

Although it has not been possible to demonstrate a quantitative correlation of n.m.r. intermolecular hydrogen-bond shifts with hydrogen-bond strength and other physical properties, the trend of recent results has been encouraging (1). In this note some n.m.r. and infrared measurements are reported on chloroform–ether and chloroform–ketone solutions, which in the former case follow a simple qualitative correlation pattern, but which in the latter case apparently do not. Additional n.m.r. measurements on bromoform and iodoform solutions are also reported.

EXPERIMENTAL

The n.m.r. spectra were obtained at approximately 40° C on a Varian A-60 Analytical n.m.r. spectrometer operating at 60 Mc/s. Line positions were measured by the customary side-band technique (2), using a Hewlett–Packard Model 200AB audio-oscillator and a Hewlett–Packard Model 521C frequency counter. Tetramethylsilane (<0.5% by weight) was used as an internal reference and was accounted for in the mole fraction calculation. The precision in measurement of line position was approximately 0.2 c.p.s.

The infrared spectra were recorded on a Perkin–Elmer Model 421 infrared spectrophotometer. At the low concentrations which were used, only the hydrogen-bonded species was visible in the infrared spectrum. The instrument was calibrated using carbon monoxide. The infrared half-band-width measurements were considered to be accurate to less than 2 cm^{-1}. All materials were reagent grade or better and were used without further purification.

RESULTS AND DISCUSSION

The experimental results are summarized in Table I. In the n.m.r. measurements, the CHX_3 (X = Cl, Br) proton shifts in solutions of different concentration were extrapolated to infinite dilution. The CHX_3 hydrogen-bond shift δ_H was taken as the difference between the CHX_3 proton shift in cyclohexane, extrapolated to infinite dilution, and the

TABLE I

Summary of nuclear magnetic resonance and infrared data

Solvent	δ_H ($CHCl_3$), p.p.m.*	δ_H ($CHBr_3$), p.p.m.*	ν_{CD}, cm^{-1} (stretching)	$\Delta\nu$,† cm^{-1}	$\delta\nu_{\frac{1}{2}}$,‡ cm^{-1}	Concn.,‖ mole/l.
1. Cyclohexane	0	0	2252.5	11.0	~9††	0.100
2. Diethyl ether	0.76§	0.639	2243.5	20.0	16.2¶	0.099
3. Di-*n*-propyl ether	0.632	0.514	2242.6	20.9	15.9	0.099
4. Diisopropyl ether	0.713	0.639	2238.2	25.3	16.5	0.101
5. Di-*n*-butyl ether	0.502	0.452	2241.9	21.6	15.2¶	0.102
6 Tetrahydrofuran	0.900**	0.785	2243.9	19.6	18.0	0.100
7. 1,4-Dioxane	0.587	0.520	2247.8	15.7	16.8¶	0.100
8. Acetone	0.897	0.815	2252.4	11.1	14.7¶	0.104
9. 4-Heptanone	0.911	0.828	2253.5	10.0	16.7	0.098
10. 2,6-Dimethyl-4-heptanone	0.864	0.782	2254.4	9.1	20.7	0.101
11. 5-Nonanone	0.851	—	2253.4	10.1	19.9	0.103

*Nuclear magnetic resonance hydrogen-bond shift expressed in p.p.m. from the CHX_3 signal in cyclohexane at infinite dilution.
†Infrared frequency shift from $CDCl_3$ vapor; ν_{CD} = 2263.5 cm^{-1} (ref. 7).
‡Infrared half-band width; average of two determinations.
§Reference 3.
‖Infrared samples.
¶References 4 and 9 report 16, 15, 14, 15 cm^{-1}, respectively (reading down column).
**Reference 8 reports 0.88 p.p.m.
††Partially obscured by solvent.

[1]*Taken in part from the B.Sc. Research Report of D. M. Cameron, University of Alberta, 1962.*

Can. J. Chem. Downloaded from www.nrcresearchpress.com by 210.87.254.6 on 09/05/12
For personal use only.

corresponding shift in the solvent under investigation (3). A plot of the n.m.r. hydrogen-bond shifts of $CHCl_3$ against those of $CHBr_3$, in a variety of solvents (Fig. 1), indicates

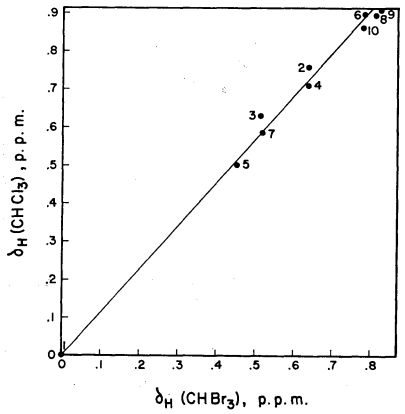

FIG. 1. Comparison of $CHCl_3$ hydrogen-bond shifts with $CHBr_3$ hydrogen-bond shifts in various solvents, relative to CHX_3 proton signal in cyclohexane. The numbering of points corresponds with the list of solvents in Table I.

that the solute–solvent interaction is essentially the same in all cases. The lack of gross deviation from linearity suggests the absence of significant steric hindrance to intermolecular association.

Although fairly well-defined correlations between n.m.r. hydrogen-bond shifts and the corresponding infrared frequency shifts have recently been demonstrated (11–15), sometimes the correlation has been poor or even nonexistent (3, 4; see also Table I). It was claimed by Huggins and Pimentel (4) that a better indication of hydrogen-bond strength, in their case for chloroform solutions, was the infrared band intensity, approximated by the half-band width. This is supported in part by the more quantitative treatment of Reid (16), who predicted enhancement in infrared band intensities for *weak* hydrogen bonds, such as those reported in this note.

Although $CHCl_3$ cannot be used for the infrared measurements because of solvent interference, the comparison of $CDCl_3$ infrared data with $CHCl_3$ n.m.r. data is probably justifiable (3–5). The relationship between the $CHCl_3$ n.m.r. hydrogen-bond shift and the $CDCl_3$ infrared half-band width in a variety of ethers and ketones is shown in Fig. 2. A crude correlation seems evident for the cyclohexane and monobasic ether solutions but not for the other solutions. It is possible that variable anisotropic effects in the carbonyl group of the ketones give rise to anomalous n.m.r. hydrogen-bond shifts (6).

A measure of the hydrogen-bond strength in CHX_3–ether systems should be given by the proton-acceptor or base strength of the ether. A comparison of observed n.m.r. hydrogen-bond shifts with recently measured (10) base strengths of monobasic ethers, given by the appropriate pK_a, is shown in Fig. 3. An approximate correlation is apparent, and the graph also indicates that increasing base strength is accompanied by an increased n.m.r. hydrogen-bond shift. This relationship is being examined currently in greater detail.

Finally it may be noted that the n.m.r. hydrogen-bond shift of $CHCl_3$ is always greater than that of $CHBr_3$. A few measurements on dilute solutions of CHI_3 showed that the magnitude of n.m.r. hydrogen-bond shifts was always in the order $CHCl_3 > CHBr_3 > CHI_3$. This is the anticipated result on the simple basis of electronegativity differences among the halogens.

Can. J. Chem. Downloaded from www.nrcresearchpress.com by 210.87.254.6 on 09/05/12
For personal use only.

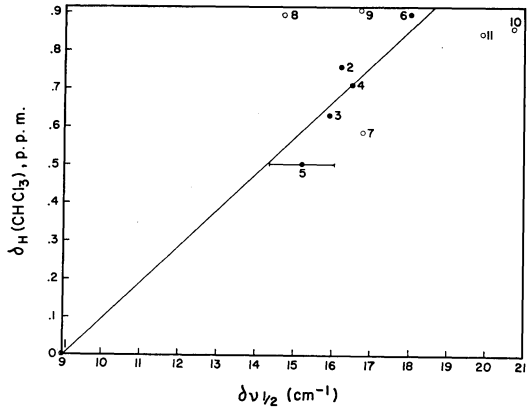

FIG. 2. Comparison of $CHCl_3$ hydrogen-bond shifts, relative to $CHCl_3$ proton signal in C_6H_{12}, with infrared half-band widths of $CDCl_3$ in various solvents. The numbering of points corresponds with the list of solvents in Table I.

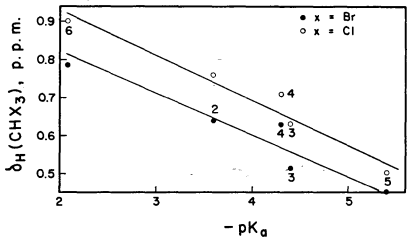

FIG. 3. Comparison of CHX_3 hydrogen-bond shift δ_H with pK_a of the solvent. The numbering of points corresponds with the list of solvents in Table I.

ACKNOWLEDGMENTS

This work was supported in part by the National Research Council of Canada, whose financial assistance is gratefully appreciated. The authors are indebted to Mr. R. Swindlehurst and Miss G. B. Stayura for recording most of the spectra, and to Dr. R. J. Crawford for several helpful discussions.

1. J. A. POPLE, W. G. SCHNEIDER, and H. J. BERNSTEIN. High-resolution nuclear magnetic resonance. McGraw-Hill, New York. 1959. Chap. 15.
2. J. T. ARNOLD and M. E. PACKARD. J. Chem. Phys. **19**, 1608 (1951).
3. G. KORINEK and W. G. SCHNEIDER. Can. J. Chem. **35**, 1157 (1957).
4. C. M. HUGGINS and G. C. PIMENTEL. J. Chem. Phys. **23**, 896 (1955).
5. G. L. CALDOW. D.Phil. Thesis, Oxford University. 1959.
6. L. M. JACKMAN. Applications of NMR spectroscopy in organic chemistry. Pergamon Press, London. 1959. Chap. 7.
7. M. L. JOSIEN, J. P. LEICKNAM, and N. FUSON. Bull. Soc. Chim. France, 188 (1958).
8. Z. PAJAK and F. PELLAM. Compt. Rend. **251**, 79 (1960).
9. R. C. LORD, B. NOLIN, and H. D. STIDHAM. J. Am. Chem. Soc. **77**, 1365 (1955).
10. E. M. ARNETT and C. Y. WU. J. Am. Chem. Soc. **84**, 1680, 1684 (1962).
11. I. GRANACHER. Helv. Phys. Acta, **34**, 272 (1961).
12. E. A. ALLAN and L. W. REEVES. J. Phys. Chem. **66**, 613 (1962).
13. L. W. REEVES, E. A. ALLAN, and K. O. STRØMME. Can. J. Chem. **38**, 1249 (1960).
14. H. S. GUTOWSKY, A. L. PORTE, and I. M. HUNSINGER. J. Am. Chem. Soc. **82**, 5057 (1960).
15. J. R. MERRILL. J. Phys. Chem. **65**, 2023 (1961).
16. C. REID. J. Chem. Phys. **30**, 182 (1959).

RECEIVED JUNE 25, 1962.
DEPARTMENT OF CHEMISTRY,
UNIVERSITY OF ALBERTA,
EDMONTON, ALBERTA.

Can. J. Chem. Downloaded from www.nrcresearchpress.com by 210.87.254.6 on 09/05/12
For personal use only.

THE PREPARATION OF ALKALI DITHIONATES

D. W. LARSON, R. W. O'DONNELL, A. B. VANCLEAVE, AND R. L. EAGER

The dithionates of lithium, sodium, potassium, rubidium, cesium, and ammonium have been prepared using an ion exchange technique. Barium dithionate was first prepared by the method given by Blitz (1). Sulphur dioxide was passed through an aqueous suspension of manganese dioxide to form manganese dithionate. Repeated attempts to use the procedure outlined by Blitz always resulted in very unsatisfactory yields and much of the manganese dioxide remained unreacted even after a number of hours. However, when the aqueous suspension was cooled in an ice-water bath and agitated with a magnetic stirrer, the manganese dioxide dissolved completely in a few hours and very satisfactory yields were obtained.

The final procedure adopted for the preparation of barium dithionate was as follows: Sulphur dioxide gas was passed through a cooled, continuously agitated suspension of 50 g of powdered manganese dioxide (Merck, precipitated reagent) in 250 ml of water until the powder had all dissolved (2 to 5 hours). The resulting solution was diluted to 1500 ml with distilled water and boiled to remove excess sulphur dioxide. Solid barium hydroxide (200 g) was added to the boiling solution and the precipitated manganese (II) hydroxide was removed by filtration. The absence of manganese (II) ion in the solution was confirmed with ammonium sulphide. Carbon dioxide gas was bubbled through the filtrate to remove the excess of barium hydroxide, the barium carbonate precipitate being removed by filtration. The solution was then evaporated to about 400 ml, more carbon dioxide was bubbled through the solution, which was then filtered and allowed to cool slowly while crystallization of barium dithionate occurred. Further evaporation of the decantate to about 200 ml yielded another crop of crystalline product. The barium dithionate product was further recrystallized twice from aqueous solution. The final yield of crystalline $BaS_2O_6.2H_2O$, was 106 g. Calculated on the basis of the MnO_2 used, the yield was 55% of the theoretical value. It would, of course, be possible to recover more product from the mother liquor.

Pure alkali dithionates were prepared from the recrystallized barium dithionate by an ion exchange technique. An ion exchange column was assembled with Amberlite 1R-120 cation exchange resin (16–50 mesh, styrene base, nuclear sulphonic acid type) in a glass column 6 mm in inside diameter and 70 cm in length. The resin, originally in the acid form, was eluted with 200 ml of distilled water to remove any free acid prior to loading the column with the desired alkali chloride. A saturated solution of the appropriate alkali chloride (analytical reagent grade) was passed slowly through the column until the effluent was of the same pH as the entering chloride solution. Complete loading of the column was necessary since the presence of any hydrogen ions on the resin would lead to the production of unstable dithionic acid and contamination in the final product. After flushing the loaded resin with distilled water to remove free salt, a saturated solution of barium dithionate was passed into the column. Liquid flow was restricted to 20 drops per minute, the effluent being collected in small samples. The effluent was frequently checked for the presence of barium ion using sulphuric acid as a test reagent; collection of effluent was stopped at the first detection of barium ion. After appropriate effluent samples were combined, the solution was carefully concentrated by evaporation and allowed to stand until a suitable crop of crystals of alkali dithionate had formed. Some

Can. J. Chem. Downloaded from www.nrcresearchpress.com by 210.87.254.5 on 09/05/12
For personal use only.

difficulty was encountered in crystallizing lithium dithionate, but this was circumvented by using vacuum desiccation. All of the alkali dithionates were obtained as well-formed colorless crystals; ammonium dithionate always occurred as a mass of finely textured material. None of the dithionates prepared by the above method gave any indication of the presence of sulphate on the addition of barium ion to their aqueous solutions.

Yields of dithionate varied from 12 to 19%, based on the amount of the corresponding chloride required to load the column. However, much of the alkali chloride used could be recovered by evaporating to dryness the acidic effluent collected as the column was being loaded, and heating the salt to 500° C to remove hydrochloric acid. About 50% of the rubidium and cesium chlorides used were recovered in this manner. Taking this fact into account, the dithionate yields could be said to vary from 24 to 38%, based on the amount of alkali chloride on the loaded resin. Since no recrystallization is necessary to get a product of high purity by this method, these yields are quite satisfactory. The main advantage of this method of preparation lies in the ease with which a product of high purity is obtained.

Infrared spectra of the dithionates showed a broad absorption band between 1200 and 1280 cm^{-1} and a fairly narrow band at 1000 cm^{-1}. The former band was often split into two peaks. These spectra compare well with the spectra for dithionates given by Golding (2), who lists five strong bands and one medium band between 1196 and 1266 cm^{-1}, and a strong band and a very strong band at 1035 cm^{-1} and 1015 cm^{-1} respectively. Differences appear to lie in the degree of resolution.

Refractive indices of the salts were measured by the Becke method, using calibrated refractive index oils. In all cases, the observed values were in excellent agreement with those quoted by Mellor (3). Table I shows the comparison between observed and literature values for refractive indices.

TABLE I

Refractive indices of dithionates

	Measured	Literature
$BaS_2O_6.2H_2O$	$\beta=1.594$	$\beta=1.595$
$Li_2S_2O_6.2H_2O$	$\beta=1.561$	$\beta=1.5602$
$Na_2S_2O_6.2H_2O$	$\beta=1.495$	$\beta=1.4953$
$K_2S_2O_6$	$\omega=1.456$	$\omega=1.4550$
	$\epsilon=1.515$	$\epsilon=1.5153$
$Rb_2S_2O_6$	$\omega=1.457$	$\omega=1.4574$
	$\epsilon=1.509$	$\epsilon=1.5078$
$Cs_2S_2O_6$	$\omega=1.522$	$\omega=1.5230$
	$\epsilon=1.544$	$\epsilon=1.5438$

ACKNOWLEDGMENT

One of us (D. W. L.) wishes to acknowledge with thanks the receipt of a fellowship from the International Nickel Company of Canada.

1. H. Biltz and W. Biltz. Laboratory methods of inorganic chemistry. J. Wiley and Sons, New York. 1909. p. 131.
2. R. M. Golding. J. Phys. Chem. **33**, 1666 (1960).
3. J. W. Mellor. A comprehensive treatise on inorganic and theoretical chemistry. Vol. X. Longmans Green and Co., London. 1930. pp. 582–599.

Received September 13, 1962.
Department of Chemistry and Chemical Engineering,
University of Saskatchewan,
Saskatoon, Saskatchewan.

Can. J. Chem. Downloaded from www.nrcresearchpress.com by 210.87.254.5 on 09/05/12
For personal use only.

THE SYSTEM LITHIUM SULPHATE – ZINC SULPHATE – WATER AT 30° C

G. ARAVAMUDAN[1]

INTRODUCTION

Solubility and phase relationships were investigated in this system in continuation of the lithium sulphate – magnesium sulphate – water system, the results of which were reported recently (1). The binary (anhydrous) system Li_2SO_4–$ZnSO_4$ is of the simple eutectic type and is without the formation of either definite compounds or solid solutions in any part of the polytherm, according to Evseeva and Bergman (2).

EXPERIMENTAL

The mode of prepartion of the 'complexes' and their after-treatment during the present study were exactly similar to the pattern followed for the earlier system (1) except that the respective isomorphous zinc salts were used in place of the several forms of magnesium sulphate taken in the previous work. The saturated solutions were separated from the wet residues after equilibrium was attained, which generally took less than 24 hours. Chemical analysis of the two parts involved the determination of water by evaporation and drying at 400° to constant weight and the determination of zinc by the oxine method. The composition of the saturating phases was found from the analytical data using the algebraic variation of the Schreinemaker method.

RESULTS AND DISCUSSION

The results of the study are recorded in Table I. $ZnSO_4.7H_2O$ and $Li_2SO_4.H_2O$ are the stable phases at 30°, whereas $ZnSO_4.6H_2O$ appears in the isotherm, as can be seen in Fig. 1, as a metastable phase in the entire region of its existence. It was noticed that addition of $Li_2SO_4.H_2O$ crystals to supersaturated solutions of zinc sulphate brings about

TABLE I

The system Li_2SO_4–$ZnSO_4$–H_2O at 30° C

Amount contained in 100 g saturated solution		Amount contained in 100 g wet residue		Composition of solid phase
Li_2SO_4	$ZnSO_4$	Li_2SO_4	$ZnSO_4$	
25.39	—			$Li_2SO_4.H_2O$
22.85	5.04	69.74	1.312	"
19.83	11.19	67.79	3.074	"
17.84	15.24	68.31	3.923	"
15.53	19.75	65.89	5.651	"
12.75	25.39	64.66	7.439	"
10.22	30.66	63.32	9.168	"
—	38.02			$ZnSO_4.7H_2O$
2.01	36.49	0.63	49.86	"
3.67	35.20	1.12	49.65	"
5.59	33.83	1.83	48.87	"
7.57	32.48	2.38	48.54	"
8.36	31.99	2.60	48.63	"
9.31	31.39	3.09	48.00	"
10.14	30.89	40.20	23.87	$ZnSO_4.7H_2O$ + $Li_2SO_4.H_2O$
—	39.44			$ZnSO_4.6H_2O$
2.05	37.66	0.67	52.85	"
3.49	36.46	1.19	51.97	"
5.03	35.22	1.59	51.85	"
7.07	33.62	2.29	51.43	"
8.21	32.80	2.77	50.66	"
9.79	31.66	37.84	26.79	$ZnSO_4.6H_2O$ + $Li_2SO_4.H_2O$

[1]*Present address: Department of Chemistry, Indian Institute of Technology, Madras-36, India.*

Can. J. Chem. Downloaded from www.nrcresearchpress.com by 210.87.254.42 on 09/05/12
For personal use only.

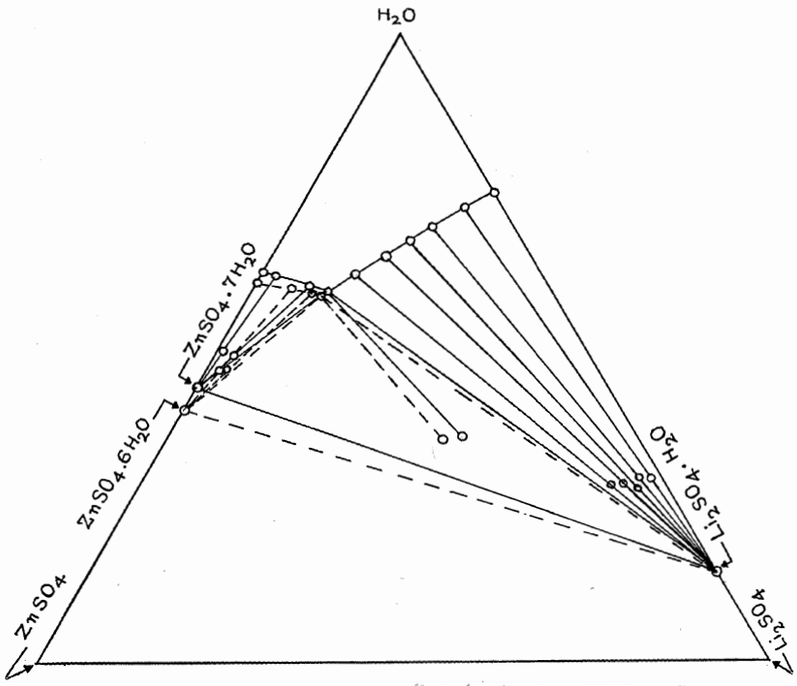

FIG. 1. The system Li_2SO_4–$ZnSO_4$–H_2O at 30° C.

the separation of the metastable phase, $ZnSO_4.6H_2O$, and not of the stable phase, $ZnSO_4.7H_2O$. Microscopic examination of crystals that separated on controlled evaporation, in the range 0–45° C, of solutions containing different proportions of lithium sulphate and zinc sulphate did not reveal any new solid phases.

ACKNOWLEDGMENTS

The author wishes to thank Professor K. R. Krishnaswami for his keen interest in the work and the Government of India for financial assistance.

1. G. ARAVAMUDAN. Can. J. Chem. **40**, 1035 (1962).
2. N. N. EVSEEVA and A. G. BERGMAN. Zh. Obshchei. Khim. **21**, 1763 (1951); Chem. Absts. **49**, 705g (1955).

RECEIVED AUGUST 14, 1962.
DEPARTMENT OF INORGANIC AND PHYSICAL CHEMISTRY,
INDIAN INSTITUTE OF SCIENCE,
BANGALORE, INDIA.

CONFORMATIONAL EQUILIBRIUM IN ESTERS OF CYCLOHEXANOL BY PROTON MAGNETIC RESONANCE

V. ADJACENT DEUTERATION

E. A. ALLAN, E. PREMUZIC, AND L. W. REEVES

Low-temperature proton resonance studies of some cyclohexyl ethers in the second paper of this series (1) were unsuccessful in distinguishing the axial and equatorially

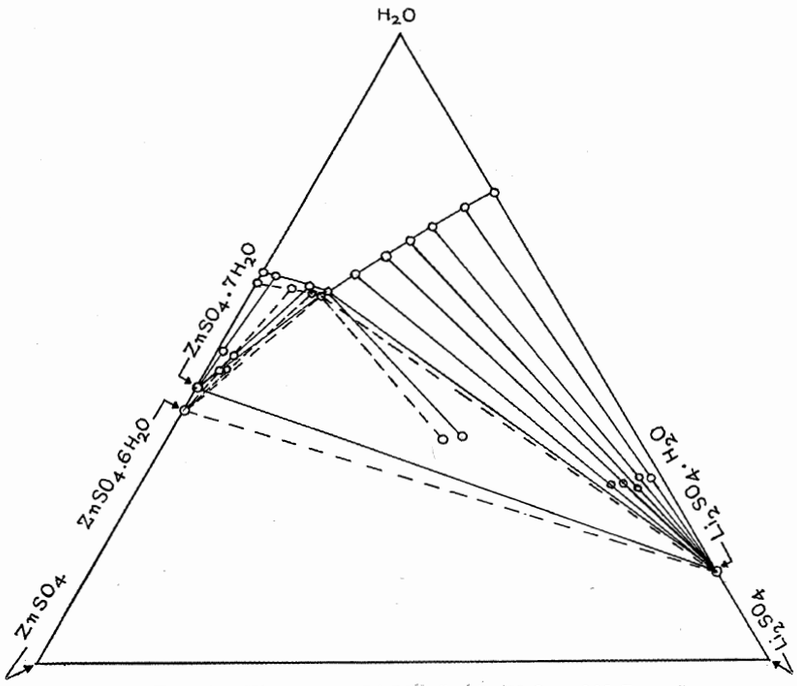

FIG. 1. The system Li_2SO_4–$ZnSO_4$–H_2O at 30° C.

the separation of the metastable phase, $ZnSO_4.6H_2O$, and not of the stable phase, $ZnSO_4.7H_2O$. Microscopic examination of crystals that separated on controlled evaporation, in the range 0–45° C, of solutions containing different proportions of lithium sulphate and zinc sulphate did not reveal any new solid phases.

ACKNOWLEDGMENTS

The author wishes to thank Professor K. R. Krishnaswami for his keen interest in the work and the Government of India for financial assistance.

1. G. ARAVAMUDAN. Can. J. Chem. **40**, 1035 (1962).
2. N. N. EVSEEVA and A. G. BERGMAN. Zh. Obshchei. Khim. **21**, 1763 (1951); Chem. Absts. **49**, 705g (1955).

RECEIVED AUGUST 14, 1962.
DEPARTMENT OF INORGANIC AND PHYSICAL CHEMISTRY,
INDIAN INSTITUTE OF SCIENCE,
BANGALORE, INDIA.

CONFORMATIONAL EQUILIBRIUM IN ESTERS OF CYCLOHEXANOL BY PROTON MAGNETIC RESONANCE

V. ADJACENT DEUTERATION

E. A. ALLAN, E. PREMUZIC, AND L. W. REEVES

Low-temperature proton resonance studies of some cyclohexyl ethers in the second paper of this series (1) were unsuccessful in distinguishing the axial and equatorially

oriented ether groupings. The halides (1, 2) and various other compounds of the saturated six-membered-ring type (3, 4) have been successfully studied from the point of view of conformational equilibrium and in one case (3), of the kinetics of interconversion, from low-temperature n.m.r. spectra. In this communication the study of 2,6-tetradeuterocyclohexyl esters has shown that compounds with oxygen attached to the cyclohexane ring have an adjacent proton which has a much smaller axial-to-equatorial chemical shift difference than that observed in the halides. It is therefore necessary to deuterate these compounds in the 2 and 6 position in order to resolve separate resonances at low temperature and 40 Mc/s for the axial and equatorial —CH— proton at the point of substitution.

There are now many other studies of conformational processes in the six-membered-ring series at low temperature in the literature (5–11). Deuteration of the six-membered-ring series to simplify the complex spectra obtained was first achieved by Calvin and co-workers (12), followed recently by Anet (13) and Premuzic and Reeves (4).

The 2,6-tetradeuterated cyclohexyl esters were obtained by exchange of the α hydrogen atoms of cyclohexanone in basic D_2O solutions, followed by reduction with lithium aluminum hydride in ether. The formate, acetate, trifluoroacetate, and nitrate were prepared from 2,6-tetradeuterocyclohexanol. These compounds were dissolved in carbon disulphide (2) and a small amount of tetramethylsilane added to serve as an internal reference peak. Proton resonance studies at 40 Mc/s were performed in the temperature region −100° C to +25° C and special attention has been paid to the adjacent —CH—O— resonance peak. The substitution of deuterium for hydrogen in the 2 and 6 positions reduces the value of the vicinal coupling constants by approximately 1/6 but increases the number of theoretical first-order splittings. The —CHO— peak at 25° C appears as a relatively narrow line 4 c.p.s. in half width with no resolvable splittings and symmetrical in shape. The position of this peak can be determined with a maximum error of 0.15 c.p.s. by repeated bracketing between side bands generated from audio modulations on the tetramethylsilane resonance. Concentrations of the acetate, trifluoroacetate, nitrate, and formate in CS_2 were 30, 15, 16, and 15 mole% respectively. The data is presented in tabular form (Table I). Careful chemical shift measurements

TABLE I

Chemical shifts of the —CHO— proton in four esters of 2,6-tetradeuterocyclohexanol at various temperatures

Compound	Temp. (°C)	δ_a (c.p.s.)	δ_e (c.p.s.)	$\delta_{e,a\ av}$ (c.p.s.)	% equatorial ester group	Coalescence temp. °(C)	$\delta_a-\delta_e$ (c.p.s.)
Acetate	−96	−179.4	−191.7				
	−65 → +25			−182.4	76	−72±5	12.3
Formate	−92	−184.0	−198.9				
	−60 → +25			−189.9	61	−77±5	14.9
Trifluoroacetate	−100	−189.6	−203.9				
	−50 → +25			−193	76	−74±5	14.3
Nitrate	−105	−188.7	−203.0				
	+25			−192.6	73	−82±5	14.3

were made and the percentage of equatorial ester group present obtained assuming rapid time averaging of the axial and equatorial environments (14) at the higher temperatures. The point at which the separate axial and equatorial resonance peaks become

Can. J. Chem. Downloaded from www.nrcresearchpress.com by 210.87.254.5 on 09/05/12
For personal use only.

a single broad line, i.e. the coalescence temperature, is noted in the table. The percentage of equatorial acetate group in this particular ester agrees well with the value obtained by Anet in the same solvent (13). The formate has a detectably smaller proportion of the compound in the equatorial form, presumably because of smaller steric repulsions involving the free rotations of the ester grouping in the axial position. The dominant steric repulsions must involve the oxygen adjacent to the ring and the 3,5-axial protons, with the ester group axially oriented. The chloro- and bromo-cyclohexanes are 77% and 82% axial under the same conditions (2).

ACKNOWLEDGMENTS

This research has been supported by the Petroleum Research Fund of the American Chemical Society. We wish to thank Mr. R. Louie for assistance in esterifying the deuterated alcohol.

1. L. W. Reeves and K. O. Strømme. Trans. Faraday Soc. **57**, 390 (1961).
2. L. W. Reeves and K. O. Strømme. Can. J. Chem. **38**, 1241 (1960).
3. L. W. Reeves and K. O. Strømme. J. Chem. Phys. **34**, 1711 (1961).
4. E. Premuzic and L. W. Reeves. Can. J. Chem. **40**, 1870 (1962).
5. L. W. Reeves and E. J. Wells. Discussions Faraday Soc. In press. 1962.
6. F. R. Jenson, D. S. Noyce, C. H. Sederholm, and A. J. Berlin. J. Am. Chem. Soc. **84**, 386 (1962).
7. G. Van Dyke Tiers. Proc. Chem. Soc. 389 (1960).
8. W. B. Moniz and J. A. Dixon. J. Am. Chem. Soc. **83**, 1671 (1961).
9. R. K. Harris and N. Sheppard. Proc. Chem. Soc. 418 (1961).
10. S. Brownstein. Can. J. Chem. **40**, 870 (1962).
11. A. Lutteringhaus, S. Kafuss, W. Maier, and H. Freibolin. Z. Naturforsch. **16b**, 761 (1961).
12. G. Claeson, G. H. Androes, and M. Calvin. J. Am. Chem. Soc. **82**, 4428 (1960).
13. F. A. L. Anet. J. Am. Chem. Soc. **84**, 1053 (1962).
14. H. S. Gutowsky and A. Saika. J. Chem. Phys. **21**, 1688 (1953).

Received September 4, 1962.
Department of Chemistry,
University of British Columbia,
Vancouver, British Columbia.

Can. J. Chem. Downloaded from www.nrcresearchpress.com by 210.87.254.5 on 09/05/12
For personal use only.

THE EFFECT OF AGITATION ON THE RATE OF NATTA TYPE PROPYLENE POLYMERIZATION*

T. Keii,† M. Taira, and T. Takagi

According to Natta *et al.* (1), the stationary rate of propylene polymerization in the presence of titanium trichloride and triethyl aluminum is expressed by

$$r_\infty = AGP \exp(-10 \text{ kcal}/RT),$$

where A is the frequency factor, G the weight of titanium trichloride, and P the pressure of propylene. The value of the activation energy, 10 kcal/mole, suggests that the rate-determining step of the reaction is not physical but chemical in nature. On the basis that the reaction is observed to be second order, the rate-determining step may be further supposed as a surface reaction which is either of the Twigg–Rideal type (between a propylene molecule in the solution and the titanium trichloride surface covered completely

*Issued as N.R.C. No. 7102.
†Visiting Scientist, May–November, 1962, National Research Council, from Tokyo Institute of Technology.

a single broad line, i.e. the coalescence temperature, is noted in the table. The percentage of equatorial acetate group in this particular ester agrees well with the value obtained by Anet in the same solvent (13). The formate has a detectably smaller proportion of the compound in the equatorial form, presumably because of smaller steric repulsions involving the free rotations of the ester grouping in the axial position. The dominant steric repulsions must involve the oxygen adjacent to the ring and the 3,5-axial protons, with the ester group axially oriented. The chloro- and bromo-cyclohexanes are 77% and 82% axial under the same conditions (2).

ACKNOWLEDGMENTS

This research has been supported by the Petroleum Research Fund of the American Chemical Society. We wish to thank Mr. R. Louie for assistance in esterifying the deuterated alcohol.

1. L. W. Reeves and K. O. Strømme. Trans. Faraday Soc. **57**, 390 (1961).
2. L. W. Reeves and K. O. Strømme. Can. J. Chem. **38**, 1241 (1960).
3. L. W. Reeves and K. O. Strømme. J. Chem. Phys. **34**, 1711 (1961).
4. E. Premuzic and L. W. Reeves. Can. J. Chem. **40**, 1870 (1962).
5. L. W. Reeves and E. J. Wells. Discussions Faraday Soc. In press. 1962.
6. F. R. Jenson, D. S. Noyce, C. H. Sederholm, and A. J. Berlin. J. Am. Chem. Soc. **84**, 386 (1962).
7. G. Van Dyke Tiers. Proc. Chem. Soc. 389 (1960).
8. W. B. Moniz and J. A. Dixon. J. Am. Chem. Soc. **83**, 1671 (1961).
9. R. K. Harris and N. Sheppard. Proc. Chem. Soc. 418 (1961).
10. S. Brownstein. Can. J. Chem. **40**, 870 (1962).
11. A. Lutteringhaus, S. Kafuss, W. Maier, and H. Freibolin. Z. Naturforsch. **16b**, 761 (1961).
12. G. Claeson, G. H. Androes, and M. Calvin. J. Am. Chem. Soc. **82**, 4428 (1960).
13. F. A. L. Anet. J. Am. Chem. Soc. **84**, 1053 (1962).
14. H. S. Gutowsky and A. Saika. J. Chem. Phys. **21**, 1688 (1953).

Received September 4, 1962.
Department of Chemistry,
University of British Columbia,
Vancouver, British Columbia.

Can. J. Chem. Downloaded from www.nrcresearchpress.com by 210.87.254.6 on 09/05/12
For personal use only.

THE EFFECT OF AGITATION ON THE RATE OF NATTA TYPE PROPYLENE POLYMERIZATION*

T. Keii,† M. Taira, and T. Takagi

According to Natta *et al.* (1), the stationary rate of propylene polymerization in the presence of titanium trichloride and triethyl aluminum is expressed by

$$r_\infty = AGP \exp(-10 \text{ kcal}/RT),$$

where A is the frequency factor, G the weight of titanium trichloride, and P the pressure of propylene. The value of the activation energy, 10 kcal/mole, suggests that the rate-determining step of the reaction is not physical but chemical in nature. On the basis that the reaction is observed to be second order, the rate-determining step may be further supposed as a surface reaction which is either of the Twigg–Rideal type (between a propylene molecule in the solution and the titanium trichloride surface covered completely

*Issued as N.R.C. No. 7102.
†Visiting Scientist, May–November, 1962, National Research Council, from Tokyo Institute of Technology.

with triethyl aluminum) or the Langmuir–Hinshelwood type (between the triethyl aluminum adsorbed strongly and a propylene molecule adsorbed weakly). Accordingly, the rate of this reaction can be considered as independent of physical factors, such as degree of agitation.

However, we have found the existence of an effect of agitation on the rate of this polymerization. Using an apparatus with a stroboscope (Fig. 1), we carried out the

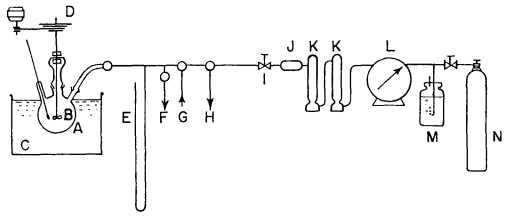

FIG. 1. Experimental apparatus. A, reaction vessel (500 ml); B, magnetic stirrer; C, thermostat; D, stroboscope; E, manometer; F, pump; G, nitrogen; H, purge; I, needle valve; J, P_2O_5; K, NaOH; L, wet gas meter; M, manostat; N, propylene.

polymerization of propylene in the system $TiCl_3$ (ARA of Stauffer Co. Ltd.) – $(C_2H_5)_3Al$ (obtained from Stauffer Co. Ltd. and redistilled) – *n*-heptane (Philips Co. Ltd.). The observed rate of propylene absorption in our system changed exponentially with reaction time from the large initial value to the stationary one, as reported by Natta *et al.* (1). Figure 2, shows the result obtained from the experiment with reaction conditions 44° C,

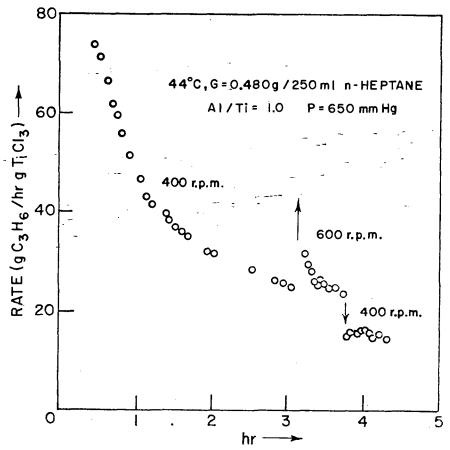

FIG. 2. The dependence of the rate on the rotational speed of the stirrer.

G = 0.48 g/250 ml *n*-heptane, Al/Ti = 1.0, P = 650 mm Hg. In order to examine the behavior in detail, the experiment was repeated, changing randomly the rotational speed of the stirrer within the range 300–600 r.p.m. Figure 3 shows the results obtained at 44° C and 27° C. The variation of the rate with the change of the rotational speed was found to be reproducible, giving an abrupt increase (decrease) followed by a gradual decrease (increase) in rate as the rotational speed is instantly changed to a higher (lower) one. The latter gradual decrease or increase always approaches the rate curve (smooth curve in Fig. 3), which is observed with a constant speed of rotation. It can be seen from the

Can. J. Chem. Downloaded from www.nrcresearchpress.com by 210.87.254.6 on 09/05/12
For personal use only.

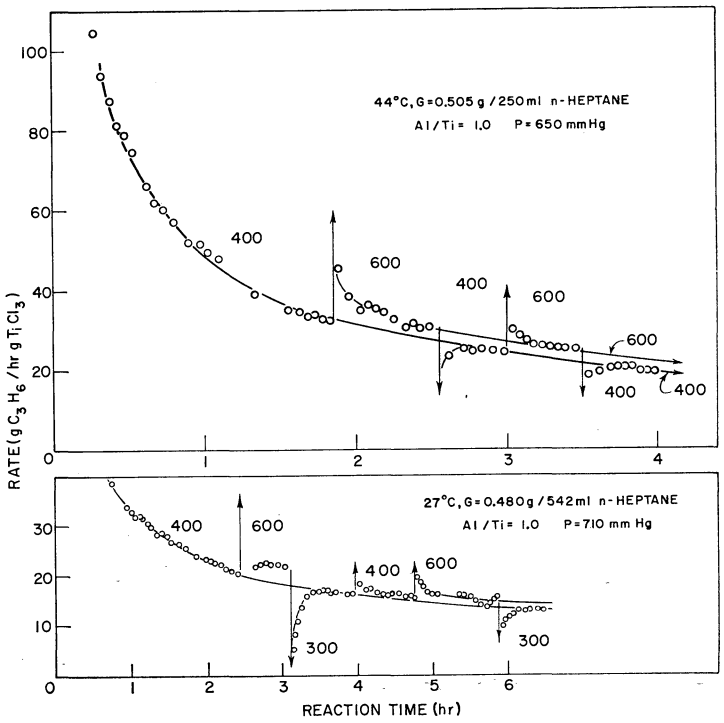

FIG. 3. The dependence of the rate on the rotational speed of the stirrer.

curves in Fig. 3 that the stationary rate of this propylene polymerization is a function of the rotational speed of the stirrer as well as the rate of the initial stage of polymerization. The dependence of the former rate is clearly smaller than the usual one of physical absorption of a gas by a liquid, rate $\propto$ (r.p.m.)^3. Therefore, the other step of mass transfer, i.e., that between liquid phase and solid phase, must be taken into account for the rate-determining step.

Further experiments are being carried out on the chemico-engineering aspects of the reaction.

The authors wish to thank Drs. R. J. Cvetanović, S. Bywater, S. Affrossman, and Y. Amenomiya for their kind discussions. T. K. thanks Dr. I. E. Puddington, Director, for the splendid hospitality afforded him by the Division of Applied Chemistry.

1. G. NATTA and I. PASQON. Advan. Catalysis, **9**, 1 (1959).

RECEIVED SEPTEMBER 4, 1962.
DEPARTMENT OF CHEMICAL ENGINEERING,
TOKYO INSTITUTE OF TECHNOLOGY,
MEGURO, TOKYO, JAPAN,
AND
DIVISION OF APPLIED CHEMISTRY,
NATIONAL RESEARCH COUNCIL,
OTTAWA, CANADA.

Can. J. Chem. Downloaded from www.nrcresearchpress.com by 210.87.254.6 on 09/05/12
For personal use only.

KINETICS AND MECHANISM OF THE PERSULPHATE OXIDATION OF 2-PROPANOL AND 2-BUTANOL

L. S. Levitt and Barbara W. Levitt

INTRODUCTION

Edwards *et al.* (1) have reported that the disodium salt of ethylenediaminetetraacetic acid (EDTA) decreases the first-order rate constant for the oxidation of 2-propanol by potassium persulphate to a value equal to or lower than that observed when $K_2S_2O_8$ is allowed to decompose in water or buffer solution, in the absence of organic compounds. This fact was interpreted as evidence for the chelating agent (EDTA) having removed traces of Cu^{++} which might be present as an impurity in analytical grade persulphate and might conceivably function as a catalyst in persulphate oxidations.

This questionable conclusion, unsupported by any direct evidence for the presence of Cu^{++}, led Edwards to believe that all previous investigations in the kinetics and mechanisms of persulphate oxidations of both inorganic and organic substrates were grossly in error due to the previously unsuspected presence of Cu^{++}.

It was also concluded by Edwards *et al.* that O_2 affects the rate of persulphate oxidations in two different ways: usually, as an inhibitor of a radical-chain process, but in the presence of EDTA, as a catalytic accelerator. The mechanism presented by these authors for the case where O_2 is excluded from the reaction environment[1] is given by the following sequence:

$$S_2O_8^{=} \xrightarrow{k_1} 2SO_4^{-}$$

$$SO_4^{-} + R_2CHOH \xrightarrow{k_2} HSO_4^{-} + R_2\dot{C}OH$$

$$R_2\dot{C}OH + S_2O_8^{=} \xrightarrow{k_3} R_2CO + HSO_4^{-} + SO_4^{-}$$

$$R_2\dot{C}OH + SO_4^{-} \xrightarrow{k_4} R_2CO + HSO_4^{-}$$

From the above series of reactions, the derived rate law (1) is $v = (k_1k_2k_3/k_4)^{1/2}[S_2O_8^{=}] \times [ROH]^{1/2}$, which implies kinetics first order with respect to persulphate and half order with respect to alcohol, or overall 3/2 order.

Wiberg (2) has reported that allyl acetate decreases the first-order rate constant for the oxidation of 2-propanol (0.02 *M*) by potassium persulphate (0.02 *M*) from the value 0.84 hr^{-1} at 60° and pH 5 to the value observed in the absence of 2-propanol (0.014 hr^{-1}). This fact was likewise interpreted as an "inhibition" by allyl acetate of a radical-chain process, and the oxidation mechanism was represented by the following sequence of five irreversible free-radical reactions, from which was derived the final rate law, $v = (2k_1k_2k_4/k_5)^{1/2}[S_2O_8^{=}]$:

$$S_2O_8^{=} \xrightarrow{k_1} 2SO_4^{-}$$

$$SO_4^{-} + H_2O \xrightarrow{k_2} HO\cdot + HSO_4^{-}$$

$$HO\cdot + R_2CHOH \xrightarrow{k_3} H_2O + R_2\dot{C}OH$$

[1]*It is impossible to rigorously exclude oxygen since oxygen is constantly being produced during the course of the reaction by means of the slow oxidation of water.*

Can. J. Chem. Downloaded from www.nrcresearchpress.com by 210.87.254.6 on 09/05/12
For personal use only.

$$R_2\dot{C}OH + S_2O_8^{=} \xrightarrow{k_4} R_2C{=}O + HSO_4^{-} + SO_4^{-}$$

$$R_2\dot{C}OH + SO_4^{-} \xrightarrow{k_5} R_2C{=}O + HSO_4^{-}$$

When we compare the Wiberg mechanism with that proposed by Edwards we note that whereas Edwards invokes a direct attack of SO_4^{-} radicals on an alcohol molecule, Wiberg shows the intermediate formation of HO· radicals and their subsequent reaction with the alcohol molecules.

Edwards' purpose in adding the chelating agent (EDTA) was to attempt to demonstrate that the observed decrease in the rate constant could be attributed to the removal of trace amounts of Cu^{++} which might be present and possibly function as a catalyst in persulphate oxidations. Wiberg's purpose in adding the "radical trap", allyl acetate, to the reaction mixture was to attempt to demonstrate the radical nature of the reaction.

Both of these attempted demonstrations of mechanism are invalidated, however, by the fact that the phenomenon of retardation in the rate of persulphate oxidations can be brought about by the addition to the alcohol–persulphate solution of any one of hundreds of organic compounds which are in no way either chelating agents or radical traps, but simply compounds which are themselves oxidized at a relatively slow rate by persulphate under the same conditions (3).

EXPERIMENTAL RESULTS

We have carried out kinetic experiments[2] in which various organic compounds, notably 2-butanol, allyl acetate, and thiodiglycol sulphoxide, were separately added to the persulphate and isopropyl alcohol in buffered aqueous solution. In each case, the overall disappearance of $S_2O_8^{=}$, measured by iodometric titration, was considerably slower than the oxidation of 2-propanol itself. The rate constants, which always remained strictly first order with respect to persulphate,[3] were nearly identical with those observed when the added compound was oxidized in the buffer solution in the absence of 2-propanol.

Our results strongly suggest that the oxidation mechanisms of both Wiberg and Edwards are incorrect, for the following reasons. First of all, it is not true that allyl acetate, as stated by Wiberg, reduces the first-order rate constant to that observed in the buffer solution alone. We have found that 0.04 *M* allyl acetate reduces the rate constant only to approximately the value (0.063 hr^{-1}) observed when it itself reacts with 0.02 *M* persulphate at pH 7 and 60°. This is 4.5 times the rate of disappearance of persulphate in the buffer alone. The results of Kolthoff, Meehan, and Carr (4) also show that the reaction with allyl acetate is significantly faster (by about 40% at the half-time) than that with the buffer alone.

What is more significant, however, is the fact that 2-butanol (which hardly can be considered a "radical trap") produces the same type of result. Thus 0.02 *M* 2-butanol gives $k = 0.22$ hr^{-1} when alone in the buffer solution, and 0.02 *M* 2-propanol alone gives 0.84 hr^{-1}, but the two together in the same solution give 0.30 hr^{-1}. We have obtained similar results when various sulphoxides (3) or other alcohols are mixed with the 2-propanol, or with one another. We find, in general, that the more slowly the added compound is oxidized by persulphate, the more effective it is in diminishing the overall rate of disappearance of persulphate in solutions of mixed substrates.

[2]*The experimental procedure was identical with that previously described (11). It should be noted that we encountered no difficulty in obtaining reproducible data, though such difficulty was reported by Edwards et al. (1).*

[3]*It is seen from the first-order plots in Fig. 1 that the lines are perfectly straight, with no evidence of the sigmoid character reported in reference 1.*

Can. J. Chem. Downloaded from www.nrcresearchpress.com by 210.87.254.6 on 09/05/12
For personal use only.

When 0.020 *M* 2-propanol is oxidized and, at the half-time of this oxidation, a quantity of 2-butanol required to make the solution 0.01 *M* with respect to the latter is injected into the reaction flask, the first-order rate plot (Fig. 1D) changes immediately from its

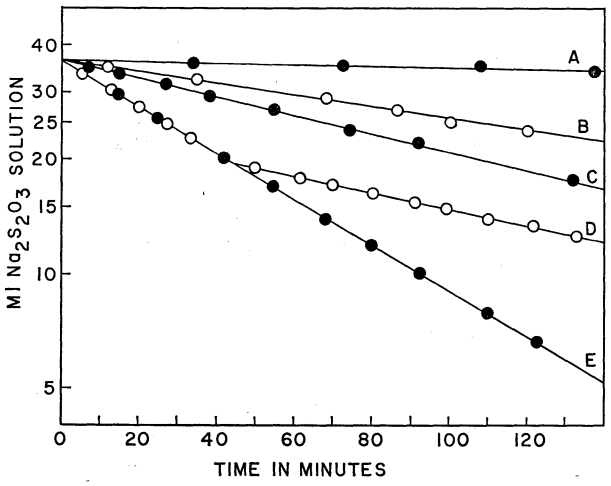

FIG. 1. First-order plot of persulphate (0.02 *M*) oxidations in buffer solution (pH 8.0) at 60°: A, buffer alone; B, 0.02 *M* 2-butanol; C, 0.02 *M* 2-butanol + 0.02 *M* 2-propanol; D, 0.02 *M* 2-propanol with 0.01 *M* 2-butanol added at the half-time; E, 0.02 *M* 2-propanol alone.

previous slope corresponding to $k = 0.84\ hr^{-1}$ to that corresponding to the much smaller value $k = 0.29\ hr^{-1}$. In the reverse situation, however, when 0.02 *M* 2-butanol is oxidized and 0.01 *M* 2-propanol is injected at the half-time, the first-order rate plot increases only slightly in slope ($k = 0.22\ hr^{-1} \rightarrow k = 0.26\ hr^{-1}$). These data are summarized in Table I and some of them plotted in Fig. 1.

TABLE I

First-order rate constants for the disappearance of 0.02 *M* $K_2S_2O_8$ in buffered aqueous solutions of various organic compounds at 60° and pH 8.0

Substrate	k (hr^{-1})
Buffer solution alone	0.018
2-Propanol (0.02 *M*)	0.84
Allyl acetate (0.04 *M*) (pH 7.0)	0.060
Allyl acetate (0.04 *M*) + 2-propanol (0.02 *M*) (pH 7.0)	0.063
2-Butanol (0.02 *M*)	0.22
2-Butanol (0.02 *M*) + 2-propanol (0.02 *M*)	0.30
2-Butanol (0.02 *M*) + 2-propanol (0.01 *M*) injected at the half-time	0.22 (→ 0.26)
2-Propanol (0.02 *M*) + 2-butanol (0.01 *M*) injected at the half-time	0.84 (→ 0.29)

DISCUSSION

It is apparent from the above results that the diminution in the rate, when a compound which is more slowly oxidized[4] by persulphate is added to the isopropyl alcohol – persulphate solution, is due to the formation, by the competing substrate, of a stronger intermediate complex with the active oxidizing species (possibly sulphur tetroxide, $^{+}\ddot{O}{:}SO_3^{-}$)

[4]*It was, indeed, found that persulphate slowly oxidized the sequestering agent (1).*

Can. J. Chem. Downloaded from www.nrcresearchpress.com by 210.87.254.6 on 09/05/12
For personal use only.

(5) than that which isopropyl alcohol forms with the oxidant. The mechanism appears, then, to involve an equilibrium of the type (3, 6)

$$R_2CHOH + S_2O_8^{=} \rightleftharpoons \text{complex} \rightarrow R_2CO + 2HSO_4^{-}$$

The complex is very likely one of the possible persulphate esters, formed as unstable intermediates analogous to the formation of chromate esters in the chromic acid oxidation of alcohols (7). One alcohol apparently can displace another from this complex, as demonstrated by the present results: when 2-butanol is added to the 2-propanol solution, the k immediately decreases from 0.84 to 0.29 hr^{-1}; on the other hand, 2-propanol is not able to displace 2-butanol since the k increases only slightly from 0.22 to 0.26 hr^{-1} when 2-propanol is added to the 2-butanol solution. We may be dealing here with a type of ester interchange, which can be represented as:

$$R'OH + \text{R-ester} \rightleftharpoons ROH + \text{R}'\text{-ester},$$

and which is entirely analogous to the ester interchange postulated by Westheimer (7) in the chromic acid oxidation of 2-propanol in the presence of *t*-butyl alcohol, where the latter compound was observed to retard the rate markedly (8). In persulphate oxidations, the esters[5] are probably of the structure $RO—SO_2—O—O—SO_3^{-}$ (an alkyl peroxidisulphate) or $RO—O—SO_3^{-}$ (an alkyl peroxymonosulphate). The latter might be formed by the displacement of $SO_4^{=}$ from $S_2O_8^{=}$ by the alcohol molecule (6). It is interesting to note that chloride ion (9) also effects a marked retardation in the rate of persulphate oxidations, and this may be due to displacement of $SO_4^{=}$ from $S_2O_8^{=}$ by Cl^{-} to give $ClOSO_3^{-}$. This, too, is analogous to the effect of Cl^{-} on chromic acid oxidations, due to formation of $ClCrO_3^{-}$ (10).

In view of these experimental observations it would seem that the "inhibition" of the persulphate oxidation of alcohols by EDTA, reported by Edwards (1), has no more to do with the elimination of trace metal catalysis than the "inhibition"[6] by allyl acetate, reported by Wiberg (2), has to do with removal of SO_4^{-} or $HO\cdot$ radicals. Further evidence against a radical-chain mechanism for the persulphate oxidation of organic compounds is the relatively high activation energy (11, 12) of approximately 26 kcal/mole for these reactions, and the fact that molecular oxygen has no effect on the rate of the persulphate oxidation of sulphides (11), sulphoxides (11), or toluene (13); even in the Ag^{+}-catalyzed persulphate cleavage of glycols strong evidence has been presented by Greenspan and Woodburn (14) for the absence of free-radical intermediates.[7]

The original proposal of a free-radical chain mechanism for persulphate oxidation of alcohols was made by Bartlett (15, 16). The first step in the oxidation of thiols was considered by Eager and Winkler (17) to be the reversible dissociation of persulphate into sulphate ion radicals:

$$S_2O_8^{=} \rightleftharpoons 2SO_4^{-}$$

The mechanisms proposed by Wiberg and by Edwards, however, consider this first step as an *irreversible* process because rate equations of the form required by these authors cannot be derived without this assumption. Now, it is well known that persulphate is

[5]*We assume that* $S_2O_8^{=}$ *and* SO_4 *and their derivatives in the solution all titrate iodometrically as equivalent oxidizing agents, in the same fashion as do t-Bu-hypochlorite and the chromate esters.*

[6]*The competing organic compound is erroneously referred to as the "inhibitor" in Wiberg's paper (2).*

[7]*It is noteworthy that these authors found that* Cu^{++} *failed to catalyze the persulphate cleavage of glycols.*

Can. J. Chem. Downloaded from www.nrcresearchpress.com by 210.87.254.6 on 09/05/12
For personal use only.

prepared by the anodic oxidation of aqueous bisulphate solutions, where the mechanism is, of necessity, either

$$HSO_4^- - e^- \rightarrow SO_4^- + H^+$$
$$2SO_4^- \rightarrow S_2O_8^=$$

or (5)

$$HSO_4^- - 2e^- \rightarrow SO_4 + H^+$$
$$SO_4 + SO_4^= \rightarrow S_2O_8^=$$

It is therefore clear that if SO_4^- is formed by dissociation of $S_2O_8^=$ as shown in the Wiberg or Edwards mechanism, it is quite impossible for such dissociation to be irreversible. Thus the mechanisms in question are also quite impossible, since the introduction of the $SO_4^- \cdot$ recombination step into the kinetic scheme leads to a completely altered rate expression which is not in accord with experiment.[8]

Turning now to Wiberg's rate expression for these oxidations, we note that this equation does not involve the constant k_3, which represents the rate of direct attack of the $HO \cdot$ radical on the alcohol molecule. Since this reaction is depicted as the only one in which an intact alcohol molecule participates, one might expect little or no variation of the rate when secondary alcohols other than 2-propanol are oxidized under the same conditions by persulphate.[9] This is not what is observed experimentally, however, since the structure of the alcohol has a marked effect on the rate (18, 19), as shown by the above-mentioned rate constants for 2-propanol and 2-butanol.

Returning finally to Edwards' kinetic scheme for the case where oxygen is excluded from the reaction, we noted above that the rate equation predicts an overall 3/2-order reaction. Therefore, when the initial concentrations of persulphate and alcohol are equal, a given kinetic run should plot as a 3/2-order reaction with respect to the disappearance of persulphate. However, as is well known, this is certainly not the case, for the reactions are strictly first order with respect to persulphate regardless of the initial concentrations.

In any case, the proposed radical-chain mechanisms do not in any way lead to the remarkable dependence of the initial first-order rate constant on the initial concentrations of alcohol and persulphate, which we have shown (6) to be of the form

$$k = k_{max}[ROH]_0[S_2O_8^=]_0/(b+[ROH]_0)(c+[S_2O_8^=]_0),$$

where b and c are empirical constants. As already pointed out in a previous article (3, 6), there is a close, but not exact, analogy between this rate expression and that for enzyme kinetics, thus strongly suggesting the existence of at least one equilibrium step in the reaction sequence leading to a reactive intermediate complex (20, 12) which decomposes irreversibly to the observed oxidation products, as discussed above.

ACKNOWLEDGMENT

The authors are indebted to Mr. Henry J. Helble for obtaining some of the kinetic data, and for verifying the kinetic constants for some of the runs.

[8]*Wiberg's own data on the induced exchange of radioactive sulphate with persulphate in the presence of 2-propanol confirm those of others (R. L. Eager and K. J. McCallum. Can. J. Chem.* **32**, *692 (1954); P. C. Riesebos and A. H. W. Aten, Jr. J. Am. Chem. Soc.* **74**, *2440 (1952)) that a significant, though small, exchange does occur, strongly suggesting that at least one of the two steps of Wiberg's postulated reaction sequence which directly involve* $S_2O_8^=$ *should be reversible, unless the exchange is to be attributed to a possible side reaction.*

[9]*It is true that the rate constants* k_4 *and* k_5 *do appear in Wiberg's rate equation and these represent reactions of radicals formed by abstraction of a hydrogen atom from the carbinol carbon of the secondary alcohol. However, the bond dissociation energies of all these secondary alcohol radical species, and hence their reactivities, are nearly identical.*

Can. J. Chem. Downloaded from www.nrcresearchpress.com by 210.87.254.6 on 09/05/12
For personal use only.

1. D. L. BALL, M. M. CRUTCHFIELD, and J. O. EDWARDS. J. Org. Chem. **25**, 1599 (1960).
2. K. B. WIBERG. J. Am. Chem. Soc. **81**, 252 (1959).
3. L. S. LEVITT, B. W. LEVITT, and E. R. MALINOWSKI. J. Org. Chem. **27**, 2917 (1962).
4. I. M. KOLTHOFF, E. J. MEEHAN, and E. M. CARR. J. Am. Chem. Soc. **75**, 1439 (1953).
5. L. S. LEVITT. Can. J. Chem. **31**, 915 (1953).
6. E. R. MALINOWSKI and L. S. LEVITT. J. Am. Chem. Soc. **80**, 5334 (1958).
7. F. H. WESTHEIMER *et al.* J. Chem. Phys. **11**, 506 (1943); J. Am. Chem. Soc. **73**, 65 (1951); Chem. Rev. **45**, 419 (1949).
8. H. KWART and P. S. FRANCIS. J. Am. Chem. Soc. **77**, 4907 (1955).
9. L. S. LEVITT and D. Z. DENNEY. Unpublished observations.
10. M. COHEN and F. H. WESTHEIMER. J. Am. Chem. Soc. **74**, 4387 (1952).
11. E. HOWARD, JR. and L. S. LEVITT. J. Am. Chem. Soc. **75**, 6170 (1953).
12. L. S. LEVITT and E. R. MALINOWSKI. J. Am. Chem. Soc. **77**, 4517 (1955).
13. A. KAILEN and L. OLBRICH. Monatsh. **47**, 449 (1926).
14. F. P. GREENSPAN and H. M. WOODBURN. J. Am. Chem. Soc. **76**, 6345 (1954).
15. P. D. BARTLETT and J. COTMAN. J. Am. Chem. Soc. **71**, 1419 (1949).
16. I. M. KOLTHOFF and I. K. MILLER. J. Am. Chem. Soc. **73**, 3055 (1951).
17. R. L. EAGER and C. A. WINKLER. Can. J. Res. B, **26**, 527 (1948).
18. B. W. LEVITT and L. S. LEVITT. Abstracts of Papers, Chicago Meeting, American Chemical Society, September, 1958. p. 5P.
19. B. W. LEVITT and L. S. LEVITT. Abstract of Papers, Cleveland Meeting, American Chemical Society, April 5, 1960. p. 94-O.
20. L. S. LEVITT. J. Org. Chem. **20**, 1297 (1955).

RECEIVED IN ORIGINAL FORM JULY 27, 1961;
AS REVISED JULY 24, 1962.
CHEMISTRY DEPARTMENTS,
SETON HALL UNIVERSITY,
SOUTH ORANGE, N.J.,
AND
STEVENS INSTITUTE OF TECHNOLOGY,
HOBOKEN, N.J.

Can. J. Chem. Downloaded from www.nrcresearchpress.com by 210.87.254.6 on 09/05/12
For personal use only.

DEGRADATION OF D-RIBONO-1 → 4-LACTONE TO D-ERYTHRONO-1 → 4-LACTONE

D. L. MITCHELL

D-Erythrono-1 → 4-lactone (I) can be readily prepared by the alkaline bromine oxidation of D-erythrose. A convenient source of the D-erythro-alcohol grouping occurs at carbons 4 and 5 of D-glucose, and various procedures which employ glycol cleaving reagents have been described for the selective degradation of D-glucose (1), 4,6-*O*-ethylidene-D-glucose (2), and starch (3) to D-erythrose. An analogous degradation of L-rhamnose to L-erythrono-1 → 4-lactone has also been described (4). Most other preparations which have been described are manipulatively more difficult and give less satisfactory yields (see refs. 1 and 5 for a summary of methods).

Sodium 2,3-*O*-isopropylidene-D-ribonate (II), conveniently obtained from 2,3-*O*-isopropylidene-D-ribono-1 → 4-lactone (6), was selectively cleaved between carbons 4 and 5, by sodium metaperiodate, to form sodium 2,3-*O*-isopropylidene-L-erythruronate (III) *in situ*. After selective sodium borohydride reduction of the newly formed aldehyde group at carbon 4, D-erythrono-1 → 4-lactone was obtained in 76% yield with loss of the *O*-isopropylidene group occurring during the lactonization. In this sequence of reactions, the four carbon atoms of D-erythrono-1 → 4-lactone have originated from carbons 1 to 4 of D-ribono-1 → 4-lactone, and, therefore, subsequently from carbons 1 to 4 of D-ribose. Application of this reaction to C^{14}-labelled D-ribose could be useful in obtaining a partial degradation of this pentose.

D-Erythrono-1 → 4-lactone readily forms the derived 2,3-*O*-isopropylidene-D-erythrono-1 → 4-lactone with the reaction being easily followed polarimetrically. The molecular

1. D. L. BALL, M. M. CRUTCHFIELD, and J. O. EDWARDS. J. Org. Chem. **25**, 1599 (1960).
2. K. B. WIBERG. J. Am. Chem. Soc. **81**, 252 (1959).
3. L. S. LEVITT, B. W. LEVITT, and E. R. MALINOWSKI. J. Org. Chem. **27**, 2917 (1962).
4. I. M. KOLTHOFF, E. J. MEEHAN, and E. M. CARR. J. Am. Chem. Soc. **75**, 1439 (1953).
5. L. S. LEVITT. Can. J. Chem. **31**, 915 (1953).
6. E. R. MALINOWSKI and L. S. LEVITT. J. Am. Chem. Soc. **80**, 5334 (1958).
7. F. H. WESTHEIMER *et al.* J. Chem. Phys. **11**, 506 (1943); J. Am. Chem. Soc. **73**, 65 (1951); Chem. Rev. **45**, 419 (1949).
8. H. KWART and P. S. FRANCIS. J. Am. Chem. Soc. **77**, 4907 (1955).
9. L. S. LEVITT and D. Z. DENNEY. Unpublished observations.
10. M. COHEN and F. H. WESTHEIMER. J. Am. Chem. Soc. **74**, 4387 (1952).
11. E. HOWARD, JR. and L. S. LEVITT. J. Am. Chem. Soc. **75**, 6170 (1953).
12. L. S. LEVITT and E. R. MALINOWSKI. J. Am. Chem. Soc. **77**, 4517 (1955).
13. A. KAILEN and L. OLBRICH. Monatsh. **47**, 449 (1926).
14. F. P. GREENSPAN and H. M. WOODBURN. J. Am. Chem. Soc. **76**, 6345 (1954).
15. P. D. BARTLETT and J. COTMAN. J. Am. Chem. Soc. **71**, 1419 (1949).
16. I. M. KOLTHOFF and I. K. MILLER. J. Am. Chem. Soc. **73**, 3055 (1951).
17. R. L. EAGER and C. A. WINKLER. Can. J. Res. B, **26**, 527 (1948).
18. B. W. LEVITT and L. S. LEVITT. Abstracts of Papers, Chicago Meeting, American Chemical Society, September, 1958. p. 5P.
19. B. W. LEVITT and L. S. LEVITT. Abstract of Papers, Cleveland Meeting, American Chemical Society, April 5, 1960. p. 94-O.
20. L. S. LEVITT. J. Org. Chem. **20**, 1297 (1955).

RECEIVED IN ORIGINAL FORM JULY 27, 1961;
AS REVISED JULY 24, 1962.
CHEMISTRY DEPARTMENTS,
SETON HALL UNIVERSITY,
SOUTH ORANGE, N.J.,
AND
STEVENS INSTITUTE OF TECHNOLOGY,
HOBOKEN, N.J.

Can. J. Chem. Downloaded from www.nrcresearchpress.com by 210.87.254.42 on 09/05/12
For personal use only.

DEGRADATION OF D-RIBONO-1 → 4-LACTONE TO D-ERYTHRONO-1 → 4-LACTONE

D. L. MITCHELL

D-Erythrono-1 → 4-lactone (I) can be readily prepared by the alkaline bromine oxidation of D-erythrose. A convenient source of the D-erythro-alcohol grouping occurs at carbons 4 and 5 of D-glucose, and various procedures which employ glycol cleaving reagents have been described for the selective degradation of D-glucose (1), 4,6-*O*-ethylidene-D-glucose (2), and starch (3) to D-erythrose. An analogous degradation of L-rhamnose to L-erythrono-1 → 4-lactone has also been described (4). Most other preparations which have been described are manipulatively more difficult and give less satisfactory yields (see refs. 1 and 5 for a summary of methods).

Sodium 2,3-*O*-isopropylidene-D-ribonate (II), conveniently obtained from 2,3-*O*-isopropylidene-D-ribono-1 → 4-lactone (6), was selectively cleaved between carbons 4 and 5, by sodium metaperiodate, to form sodium 2,3-*O*-isopropylidene-L-erythruronate (III) *in situ*. After selective sodium borohydride reduction of the newly formed aldehyde group at carbon 4, D-erythrono-1 → 4-lactone was obtained in 76% yield with loss of the *O*-isopropylidene group occurring during the lactonization. In this sequence of reactions, the four carbon atoms of D-erythrono-1 → 4-lactone have originated from carbons 1 to 4 of D-ribono-1 → 4-lactone, and, therefore, subsequently from carbons 1 to 4 of D-ribose. Application of this reaction to C^{14}-labelled D-ribose could be useful in obtaining a partial degradation of this pentose.

D-Erythrono-1 → 4-lactone readily forms the derived 2,3-*O*-isopropylidene-D-erythrono-1 → 4-lactone with the reaction being easily followed polarimetrically. The molecular

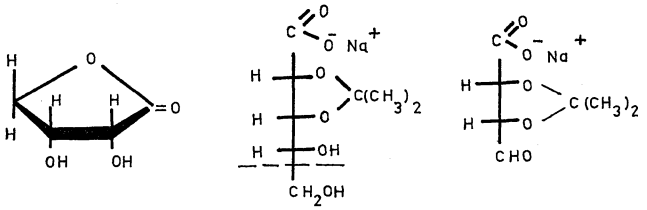

I II III

rotational difference between the product and the reactant is large ($[\Delta M]_D$ ca. 100). This observation is in agreement with the optical rotational differences previously recorded between 2,3-*O*-isopropylidene-D-ribono-1 → 4-lactone and D-ribono-1 → 4-lactone (6) and for other 2,3-*O*-isopropylidene-1 → 4-lactones prepared in this laboratory (7).

The following new derivatives were also prepared: (i) 2,3-*O*-isopropylidene-D-ribonamide, (ii) 2,3-*O*-isopropylidene-D-erythronamide, (iii) a mono-*O*-toluene-*p*-sulphonyl-D-erythrono-1 → 4-lactone, and (iv) a di-*O*-toluene-*p*-sulphonyl-D-ribono-1 → 4-lactone.

EXPERIMENTAL

Solutions were concentrated under reduced pressure (ca. 15 mm). Melting points were uncorrected and optical rotations were determined in water, unless otherwise stated. Paper chromatography was carried out by the descending method on Whatman No. 1 filter paper using the solvent system (v:v) ethyl acetate – acetic acid – formic acid – water (18:3:1:4). Unsubstituted 1 → 4-lactones were detected on paper chromatograms with an alkaline silver nitrate spray reagent (8).

Conversion of D-*Ribono-1 → 4-lactone to* D-*Erythrono-1 → 4-lactone*

2,3-*O*-Isopropylidene-D-ribono-1 → 4-lactone (5.20 g, 0.028 mole) was hydrolyzed with 1 molar equivalent of 0.1 *N* sodium hydroxide at room temperature. The optical rotation, $[\alpha]_D^{20}$ 56°, did not change appreciably over a period of 15 hours. The solution was adjusted to pH 7 with acetic acid, diluted to 2 liters with water, and finely powdered potassium metaperiodate (7.01 g, 0.029 mole) was added and the solution was stored in the dark for 2 hours.* A solution of lead acetate (15.3 g) in water (100 ml) was added with stirring and the insoluble lead salts were separated by filtration and washed thoroughly with cold water (50 ml). The combined filtrates were added dropwise, with stirring, to an excess of sodium borohydride (3 g). The solution was filtered free from a small deposit of metallic lead, and the filtrate was acidified with dilute acetic acid and passed down a column of Amberlite IR-120 (H) resin. The eluate was concentrated to dryness and the syrupy acid was lactonized by repeated additions of acetic acid and ethanol and reconcentration to dryness. The residue was extracted with boiling acetone and the solution concentrated to a crystalline mass (3.28 g, 76%) of m.p. 102° (from ethanol), ν_{max} 1753 cm^{-1} (nujol) and $[\alpha]_D^{20}$ −74° (*c*, 1.1). Lit. m.p. 103° C and $[\alpha]_D^{20}$ −73.3° (H_2O) (9). The rates of movement on paper chromatograms for D-erythrono-1 → 4-lactone and D-ribono-1 → 4-lactone were R_{Rh} 1.7 and R_{Rh} 1.4 respectively. Anal. Calc. for $C_4H_6O_4$: C, 40.7; H, 5.1. Found: C, 40.9; H, 5.2.

*2,3-O-Isopropylidene-*D-*erythrono-1 → 4-lactone*

A solution of D-erythrono-1 → 4-lactone (0.105 g) in acetone (5 ml) containing concentrated hydrochloric acid (3 drops) was observed polarimetrically (Table I). After 4 hours, the neutralized solution (silver carbonate) was filtered from inorganic salts and the filtrate was concentrated. The product spontaneously crystallized and was purified twice by sublimation (1–3 mm, 55–60° C) to yield a product (0.105 g, 74%) of m.p. 68–68.5° C, $[\alpha]_D^{20}$ −112° (*c*, 1.5) (Table I) and ν_{max} 1740 cm^{-1} (nujol). Lit. m.p. 65–67.5° C and $[\alpha]_D^{22}$ −116° (10). No hydroxyl absorption was detected. Anal. Calc. for $C_7H_{10}O_4$: C, 53.2; H, 6.4. Found: C, 53.4; H, 6.4.

*2,3-O-Isopropylidene-*D-*erythronamide*

A solution of 2,3-*O*-isopropylidene-D-erythrono-1 → 4-lactone (0.031 g) in liquid ammonia (2 ml) was stored in a sealed ampoule at room temperature for 48 hours (11). After the ampoule was chilled to −80° C, it was opened and stored in a desiccator over evaporating dishes containing concentrated sulphuric acid and solid sodium hydroxide. The solid had m.p. 107–109° C and ν_{max} 3300, 3250, 3150, 1670, and 1630 cm^{-1} (nujol). No lactone carbonyl absorption was detected. Anal. Calc. for $C_7H_{13}NO_4$: C, 48.0; H, 7.5; N, 8.0. Found: C, 47.8; H, 7.6; N, 8.2.

**Sodium metaperiodate was used for some preparations.*

Can. J. Chem. Downloaded from www.nrcresearchpress.com by 210.87.254.42 on 09/05/12
For personal use only.

TABLE I

Optical rotations of 1 → 4-lactones

D-Erythrono-1 → 4-lactone*								
Hours	0	0.25	0.5	0.74	1.0	1.5	3.25	4.0
$[\alpha]_D^{20}$ (deg)	−19	−53	−74	−82.5	−92	−102	−114	−115
2,3-*O*-Isopropylidene-D-erythrono-1 → 4-lactone†								
Hours	0	0.4	1.0	1.45	2.25			
$[\alpha]_D^{20}$ (deg)	−112	−87	−62.5	−52	−37.5			

*Acidified acetone (*c*, 2.1).
†Water (*c*, 1.5).

2,3-O-Isopropylidene-D-ribonamide

2,3-*O*-Isopropylidene-D-ribono-1 → 4-lactone (0.26 g) was dissolved in liquid ammonia and stored at room temperature in a sealed ampoule for 3 days. The ammonia-free syrup solidified on trituration with ethanol and was recrystallized from acetone–ether, m.p. 108–110° C. $[\alpha]_D^{21}$ 58° (*c*, 0.5, ethanol), ν_{max} 3250, 3150 (broad peak), 1650, and 1630 cm^{-1} (nujol). No lactone carbonyl absorption was detected. Anal. Calc. for $C_8H_{15}NO_5$: C, 46.8; H, 7.4; N, 6.8. Found: C, 47.1; H, 7.5; N, 6.6.

Periodate oxidation (unbuffered) indicated a periodate uptake of 0.54 mole/mole (5 minutes) and 0.70 mole/mole (8 hours). The solution after 8 hours' oxidation gave a positive test for formaldehyde with the chromotropic acid reagent.

Mono-O-toluene-p-sulphonyl-D-erythrono-1 → 4-lactone

Solid toluene-*p*-sulphonyl chloride (0.650 g) was added in one portion to a cold (0° C) solution of D-erythrono-1 → 4-lactone (0.095 g) in dry pyridine. After storage for 0.5 hour, excess sulphonyl chloride was decomposed by the addition of water (0.3 ml), and the solution poured into a slurry of chipped ice and water (75 ml). The solid was collected, dried (0.105 g, 85%), and recrystallized from methanol (4 ml) to yield fine needles first melting at 172–173° C, then solidifying at ca. 178° C in strongly birefringent prismatic flakes, and remelting at 183–184° C. ν_{max} 3300 cm^{-1} and ν_{max} 1760 cm^{-1} (nujol). Anal. Calc. for $C_{11}H_{12}SO_6$: C, 48.2; H, 4.4; S, 11.8. Found: C, 48.6; H, 4.5; S, 11.7. Attempts to prepare the di-*O*-toluene-*p*-sulphonyl derivative were unsuccessful.

Di-O-toluene-p-sulphonyl-D-ribono-1 → 4-lactone

D-Ribono-1 → 4-lactone (2.53 g) and toluene-*p*-sulphonyl chloride (16.6 g) in pyridine (20 ml) were stored in the refrigerator for 1.5 hours. Water (0.5 ml) was added to the solution to decompose the excess sulphonyl chloride, and after standing for 0.5 hours, the dark red solution was poured into a slurry of chipped ice and water (1.5 liters). The precipitated gum was extracted with chloroform and the chloroform extracts were washed successively with dilute mineral acid, dilute sodium bicarbonate solution, and finally with water. The crude tarry product was dissolved in methanol, warmed, treated with charcoal and the solution filtered through a pad of cellulose. The filtrate, upon dilution with a small volume of light petroleum, deposited crystals (3.36 g, 43%). A specimen, which was recrystallized from methanol – light petroleum (b.p. 60–80° C), melted at 123–125° C and had $[\alpha]_D^{25}$ 9° (*c*, 2.1, ethanol). ν_{max} 3350 cm^{-1} and ν_{max} 1780 cm^{-1} (nujol). Anal. Calc. for $C_{19}H_{20}O_9S_2$: C, 50.0; H, 4.4; S, 14.1. Found: C, 50.2; H, 4.5; S, 14.3.

A sample (61 mg) was dissolved in acetone (10 ml) and 0.01 *N* sodium hydroxide (50 ml). At intervals, aliquots (5 ml) were withdrawn and the remaining alkali was titrated with 0.01 *N* sulphuric acid using phenolphthalein as the indicator.

Time (minutes)	1	5	10	180	24 hr
Moles of alkali consumed/mole of compound	1.2	1.3	1.8	1.9	2.0

Attempts to prepare mono-*O*-toluene-*p*-sulphonyl-D-ribono-1 → 4-lactone by using equimolar quantities of reactants according to the method described above resulted in producing the di-*O*-toluene-*p*-sulphonyl derivative, m.p. 124–125° C, $[\alpha]_D^{25}$ 9° (*c*, 1.13, ethanol), in very low yield (9%). Found: C, 50.2; H, 4.6; S, 14.3.

Attempts to prepare the tri-*O*-toluene-*p*-sulphonyl-D-ribono-1 → 4-lactone by using a large excess of toluene-*p*-sulphonyl chloride and a warmer reaction temperature (one experiment at 37° C, a second experiment at room temperature) yielded a black tarry product that could not be crystallized.

Can. J. Chem. Downloaded from www.nrcresearchpress.com by 210.87.254.42 on 09/05/12
For personal use only.

ACKNOWLEDGMENTS

The author wishes to thank the Central Research Grants Committee, Makerere University College, for a maintenance grant and also the Royal Military College of Canada, Kingston, Ontario, for a gift of chemicals.

1. A. S. Perlin and C. Brice. Can. J. Chem. **33**, 1216 (1955).
2. R. Barker and D. L. MacDonald. J. Am. Chem. Soc. **82**, 2301 (1960).
3. A. Jeanes and C. S. Hudson. J. Org. Chem. **20**, 1565 (1955).
4. J. N. Baxter and A. S. Perlin. Can. J. Chem. **38**, 2217 (1960).
5. W. G. Overend, M. Stacey, and L. F. Wiggins. J. Chem. Soc. 1358 (1949).
6. L. Hough, J. K. N. Jones, and D. L. Mitchell. Can. J. Chem. **36**, 1720 (1958).
7. D. L. Mitchell. Unpublished experiments.
8. W. E. Trevelyan, D. P. Proctor, and J. S. Harrison. Nature, **166**, 444 (1950).
9. O. Ruff. Ber. **32**, 3672 (1899).
10. R. Schaffer. J. Res. Natl. Bur. Stand. A, **65**, 507 (1961).
11. V. C. Jelinek and F. W. Upson. J. Am. Chem. Soc. **60**, 355 (1938).

Received August 7, 1962.
Department of Chemistry,
Makerere University College,
The University College of East Africa,
Kampala, Uganda.

Can. J. Chem. Downloaded from www.nrcresearchpress.com by 210.87.254.42 on 09/05/12
For personal use only.

Canadian Journal of Chemistry

Issued by THE NATIONAL RESEARCH COUNCIL OF CANADA

VOLUME 41 FEBRUARY 1963 NUMBER 2

X-RAY DIFFRACTION DATA FOR ALKALI DITHIONATES

D. W. LARSON[1] AND A. B. VANCLEAVE[2]

Departments of Chemistry and Chemical Engineering, University of Saskatchewan, Saskatoon, Saskatchewan

Received September 13, 1962

ABSTRACT

X-Ray powder diffraction patterns have been recorded for the alkali dithionates and for barium and ammonium dithionate. The patterns have been indexed and unit cell dimensions determined for lithium dithionate dihydrate, sodium dithionate (anhydrous), and rubidium dithionate. Previously determined cell dimensions have been confirmed in other cases.

INTRODUCTION

X-Ray crystal structure studies have previously been carried out on all the alkali dithionates (1–4) except lithium dithionate; however, the only ones for which X-ray powder diffraction patterns are available are sodium dithionate dihydrate (5) and cesium dithionate (4, 6). Also lacking are powder data for barium dithionate and ammonium dithionate.

EXPERIMENTAL

The dithionates of lithium, sodium, potassium, rubidium, cesium, and ammonium were prepared in a high state of purity from barium dithionate using an ion exchange technique (7). X-Ray powder diffraction patterns were obtained on a General Electric XRD-5 X-Ray Diffraction Unit, using a copper target tube operated at a potential of 50 kv and a tube current of 16 ma. A 0.0007-inch nickel foil filter was used to absorb Cu K_β radiation, and intensities of the diffraction maxima were determined by using a krypton-filled proportional counter. The spectra were recorded at 24° C. A 1° beam slit and a 0.02° detector slit were employed. A protractor speed of 0.2°/min was used in conjunction with a recorder speed of 30 in./hr at a time constant of 4. Instrumental errors were minimized by calibration with reference to sodium chloride (ASTM data card 5-0628). The 2θ angles were measured with an estimated accuracy of $\pm 0.02°$.

The crystalline salt samples were powdered to -325 mesh and carefully packed into $24 \times 19 \times 2$ mm cavities in flat lucite sample holders for the recording of spectra. Relative intensities were determined by determination of peak height above background, both by direct count and by estimation from chart recordings, and also by determination of integrated peak areas. Since good agreement between the different methods of estimating relative intensities was observed, only those values estimated from chart recordings are given. No large variation in relative intensity of spectral lines was observed when a flat sample spinner was employed.

Potassium, rubidium, and cesium dithionate ($K_2S_2O_6$, $Rb_2S_2O_6$, and $Cs_2S_2O_6$) form hexagonal crystals (2–4). Unit cell dimensions for potassium dithionate have been determined by Stanley (2) as $a = 9.785$ Å and $c = 6.295$ Å. For rubidium dithionate and cesium dithionate, unit cell dimensions have been determined by analysis of the powder patterns; these values are $a = 10.17$ Å and $c = 6.42$ Å, and $a = 6.35$ Å and $c = 11.55$ Å respectively. Hagg (4) has studied cesium dithionate and gives the unit cell dimensions as $a = 6.326$ Å and $c = 11.535$ Å; corrected to the present standards of X-ray wavelengths, Hagg's dimensions are $a = 6.338$ Å and $c = 11.558$ Å. The indexed powder patterns for the above three salts are given in Tables I–III.

The powder pattern for ammonium dithionate ($(NH_4)_2S_2O_6$) is presented in Table IV, indexed as that of an hexagonal crystal with unit cell dimensions $a = 10.22$ Å and $c = 6.47$ Å. This indexing must be

[1]*Graduate student. Present address: Department of Chemistry, University of Toronto, Toronto, Ontario.*
[2]*Present address: University of Saskatchewan, Regina Campus, Regina, Saskatchewan.*

Can. J. Chem. Downloaded from www.nrcresearchpress.com by 210.87.254.6 on 09/05/12
For personal use only.

Can. J. Chem. Downloaded from www.nrcresearchpress.com by 210.87.254.6 on 09/05/12
For personal use only.

TABLE I

X-Ray powder data for potassium dithionate ($K_2S_2O_6$)

d(Å)	I/I_1	hkl	d(Å)	I/I_1	hkl	d(Å)	I/I_1	hkl	d(Å)	I/I_1	hkl
5.05	14	101	2.577	5	301	1.928	10	113	1.491	4	403
4.89	100	110	2.528	3	202	1.881	2	312	1.479	3	511
3.86	64	111	2.352	10	310	1.857	13	321	1.426	5	323
3.52	21	201	2.279	14	221	1.774	4	411	1.412	6	600
3.203	4	210	2.246	13	212	1.755	4	213	1.387	1	413
2.950	17	102	2.202	7	311	1.631	8	330	1.371	2	512
2.845	22	211	2.103	7	302	1.594	3	412	1.357	3	520
2.825	40	300	2.037	9	103	1.565	3	313			
2.647	45	112	1.944	5	320	1.522	2	510			

TABLE II

X-Ray powder data for rubidium dithionate ($Rb_2S_2O_6$)

d(Å)	I/I_1	hkl	d(Å)	I/I_1	hkl	d(Å)	I/I_1	hkl	d(Å)	I/I_1	hkl
5.08	16	110	2.365	18	221	1.928	9	321	1.478	2	422
3.99	100	111	2.312	9	212	1.841	6	411	1.468	1	600
3.63	23	201	2.283	6	311	1.699	4	501	1.431	1	601
3.329	12	210	2.168	9	302	1.665	1	420	1.419	1	512
3.018	6	102	2.083	5	401	1.649	1	412	1.410	1	520
2.954	6	211	2.020	6	320	1.639	1	331	1.344	1	610
2.936	38	300	1.995	1	222	1.611	1	421	1.315	1	611
2.715	29	112	1.975	8	113	1.582	3	510	1.235	1	531
2.443	7	310	1.945	1	312	1.535	3	403	1.200	1	620

TABLE III

X-Ray powder data for cesium dithionate ($Cs_2S_2O_6$)

d(Å)	I/I_1	hkl	d(Å)	I/I_1	hkl	d(Å)	I/I_1	hkl	d(Å)	I/I_1	hkl
4.98	10	101	2.557	8	104	1.835	10	300	1.476	7	312
3.99	100	102	2.485	34	202	1.830	2	213	1.413	8	216
3.179	50	110	2.239	8	203	1.817	19	106	1.392	4	224
3.153	23	103	2.137	24	114	1.589	6	220	1.314	3	118
2.887	33	004	2.047	5	211	1.577	7	206	1.201	2	410
2.678	8	201	1.957	17	212	1.548	10	304	1.109	2	414

Can. J. Chem. Downloaded from www.nrcresearchpress.com by 210.87.254.6 on 09/05/12
For personal use only.

TABLE IV

X-Ray powder data for ammonium dithionate $(NH_4)_2S_2O_6$)

d(Å)	I/I_1	hkl	d(Å)	I/I_1	hkl	d(Å)	I/I_1	hkl	d(Å)	I/I_1	hkl
5.22	17	101	2.951	10	300	2.325	3	212	1.619	1	421
5.10	100	110	2.733	14	112	2.295	3	311	1.544	1	403
4.01	11	111	2.684	2	301	2.094	6	103	1.475	1	600
3.65	10	201	2.611	2	202	1.937	5	321	1.417	1	520
3.235	5	002	2.554	2	220	1.850	2	411	1.350	1	610
3.036	10	102	2.454	2	310	1.812	4	213	1.321	1	611
2.971	9	211	2.376	3	221	1.703	2	330	1.279	1	513

TABLE V

X-Ray powder data for barium dithionate dihydrate ($BaS_2O_6.2H_2O$)

d(Å)	I/I_1	d(Å)	I/I_1	d(Å)	I/I_1	d(Å)	I/I_1	d(Å)	I/I_1	d(Å)	I/I_1
5.26	9	3.183	3	2.628	16	2.180	3	1.926	5	1.559	5
4.54	4	3.104	3	2.384	11	2.164	4	1.888	8	1.544	3
4.43	80	2.978	5	2.335	7	2.144	17	1.808	1	1.521	3
4.29	100	2.957	8	2.300	5	2.033	3	1.769	3	1.499	1
3.79	11	2.905	18	2.245	1	1.991	4	1.753	3	1.490	7
3.53	13	2.890	8	2.210	5	1.966	7	1.726	3	1.480	1
3.35	9	2.765	12	2.190	8	1.938	1	1.582	4	1.428	1
3.329	5										

Can. J. Chem. Downloaded from www.nrcresearchpress.com by 210.87.254.6 on 09/05/12
For personal use only.

TABLE VI

X-Ray powder data for lithium dithionate dihydrate ($Li_2S_2O_6.2H_2O$)

d(Å)	I/I_1	hkl	d(Å)	I/I_1	hkl	d(Å)	I/I_1	hkl	d(Å)	I/I_1	hkl
7.27	50	110	3.107	37	221	2.503	23	212	1.932	9	151
2.51	92	020	2.992	4	031	2.424	8	330	1.922	8	501
5.16	16	101	2.945	6	301	2.336	17	401	1.891	9	511
5.07	27	200	2.881	17	131	2.325	13	141	1.884	8	332
4.62	41	111	2.833	5	311	2.317	18	240	1.738	3	060
3.87	14	201	2.768	23	112	2.310	16	222	1.706	2	133
3.67	30	121	2.606	12	040	2.279	15	420	1.687	3	152
3.64	100	220	2.586	9	231	2.267	6	032	1.554	21	442
3.286	6	130	2.564	9	321	2.241	4	302			
3.218	6	310	2.537	6	400	2.192	4	312			

TABLE VII

X-ray powder data for sodium dithionate dihydrate ($Na_2S_2O_6.2H_2O$)

d(Å)	I/I_1	hkl	d(Å)	I/I_1	hkl	d(Å)	I/I_1	hkl	d(Å)	I/I_1	hkl
7.58	93	110	2.691	46	040	2.057	2	113	1.686	4	620
5.38	54	020			321	2.051	1	402			522
5.34	29	200	2.660	57	400	1.983	10	203	1.632	4	333
4.89	89	111			212			332			621
4.10	21	201	2.523	5	330	1.952	1	123	1.596	2	243
3.84	91	121	2.462	20	401			213			352
3.79	100	220	2.447	5	222	1.861	2	223	1.592	1	423
3.38	6	310	2.400	37	240	1.831	4	530	1.508	5	710
3.262	45	221			411	1.786	2	052	1.483	2	452
3.003	73	131	2.349	11	331	1.762	1	152			
2.953	68	112	2.325	9	312			531			

regarded as tentative, since optical observations indicate deviation from hexagonal symmetry; the optical interference figure is a black cross which appears to separate into two isogyres when the microscope stage is rotated. There seems to be no evidence for ammonium dithionate being a hemihydrate, as reported by Mellor (8). Infrared studies indicate no water of hydration, and there is no observable weight loss when the powder is heated at 100° C.

Barium, lithium, and sodium dithionate crystallize as dihydrates ($BaS_2O_6 \cdot 2H_2O$, $Li_2S_2O_6 \cdot 2H_2O$, and $Na_2S_2O_6 \cdot 2H_2O$), forming orthorhombic crystals (9, 8, 1). In Tables V, VI, and VII the powder data for these three salts are given. Unit cell dimensions for lithium dithionate dihydrate have been determined as $a = 10.15$ Å, $b = 10.43$ Å, and $c = 5.99$ Å; for sodium dithionate dihydrate, $a = 10.65$ Å, $b = 10.76$ Å, and $c = 6.41$ Å. The above values for the sodium salt compare well with those given by Martinez, Garcia-Blanco, and Rivoir (1). When the powders of these three dihydrates are heated at 90° C, loss of the two molecules of water of hydration occurs. With sodium dithionate dihydrate, efflorescence takes place even at room temperature when the crystals are ground to a powder. Loss of water was confirmed by weight loss measurements and infrared spectra on the powders before and after heating. Anhydrous sodium dithionate yielded a good powder spectrum; this has been indexed as that of an hexagonal crystal with unit cell dimensions $a = 9.08$ Å and $c = 5.91$ Å (refer to Table VIII). No significant maxima were observed in the diffraction spectrum of the dehydrated barium dithionate, and the pattern for anhydrous lithium dithionate (see Table IX) was too brief to be indexed.

TABLE VIII

X-Ray powder data for dehydrated sodium dithionate ($Na_2S_2O_6$)

d(Å)	I/I_1	hkl	d(Å)	I/I_1	hkl
4.54	100	110	2.119	5	221
3.60	31	111	1.960	4	302
3.271	3	201	1.911	3	103
2.957	17	002	1.807	3	113
2.621	18	300	1.648	6	411
2.477	41	112	1.575	2	303
2.396	24	301			

TABLE IX

X-Ray powder data for dehydrated lithium dithionate ($Li_2S_2O_6$)

d(Å)	I/I_1	d(Å)	I/I_1	d(Å)	I/I_1	d(Å)	I/I_1
4.54	40	3.94	15	2.713	100	2.146	10
4.02	35	3.004	40	2.179	10		

ACKNOWLEDGMENT

This work was carried out under a fellowship from the International Nickel Company of Canada; grateful acknowledgment is made of this assistance.

REFERENCES

1. S. MARTINEZ, S. GARCIA-BLANCO, and L. RIVOIR. Acta Cryst. **9**, 145 (1956).
2. E. STANLEY. Acta Cryst. **9**, 897 (1956).
3. W. H. BARNES and A. V. WENDLING. Z. Krist. **99**, 153 (1938).
4. G. HAGG. Z. Physik. Chem. Sect. B, **18**, 327 (1932).
5. ASTM X-RAY POWDER DATA FILE. Card 5-0357.
6. ASTM X-RAY POWDER DATA FILE. Card 3-0277.
7. D. W. LARSON, R. W. O'DONNELL, A. B. VANCLEAVE, and R. L. EAGER. Can. J. Chem. **41**, 201 (1963).
8. J. W. MELLOR. A comprehensive treatise on inorganic and theoretical chemistry. Vol. X. Longmans, Green and Co., London. 1930. pp. 582–599.
9. S. GARCIA-BLANCO and V. GOMIS. Chem. Abstr. **48**, 7974 (1954).

Can. J. Chem. Downloaded from www.nrcresearchpress.com by 210.87.254.6 on 09/05/12
For personal use only.

PRESSURE-INDEPENDENT FLOW SYSTEM PYROLYSIS OF DIMETHYL MERCURY

M. KRECH AND S. J. PRICE
Department of Chemistry, Essex College, Assumption University of Windsor, Windsor, Ontario
Received August 20, 1962

ABSTRACT

The pyrolysis of $HgMe_2$ has been investigated in a benzene carrier system using temperatures from 693° K to 800° K and pressures from 0.36 cm to 26.0 cm. High-pressure limiting rate constants were obtained above approximately 10 cm pressure. The high-pressure activation energy, E_0, of 53.7±0.5 kcal/mole is identified with D(MeHg—Me) within the limits $D < E_0 < D+RT$.

INTRODUCTION

Many investigations of the pyrolysis of dimethyl mercury have been made (1–10). Several of these have given estimates of D(MeHg—Me) and, by combination of kinetic and thermodynamic data, D(Me—Hg). Russel and Bernstein (8) have questioned all previous work in static systems because of complexities in the mechanism of the pyrolysis. They also reject previous estimates of D(MeHg—Me) from flow system work because of the low total pressures used. However, Russel and Bernstein's work has also been questioned (9) because of the accumulation of H_2 during their inhibited experiments. The present work has utilized the efficient energy transfer properties of benzene to extend flow system results to a high-pressure limit.

EXPERIMENTAL

Materials

(*a*) Dimethyl mercury was prepared by adding an ether solution of methyl magnesium iodide to an ether slurry of $HgCl_2$. The reverse Grignard removes the difficulty of adding a solid during the reaction and gives an excellent yield (75%). The excess Grignard was hydrolyzed, the organic layer separated and dried over $CaCl_2$, the bulk of the ether stripped, and the remaining solution fractionally distilled (b.p. 92° C at 750 mm).

(*b*) Spectro grade benzene was prepared for use by refluxing over sodium for 24 hours and then degassing twice by bulb-to-bulb distillation.

Apparatus and Procedure

The apparatus used was a modified Szwarc toluene carrier system designed to work at pressures up to 2 atm. Pressures were measured using a mercury manometer for pressures above 4 cm and a mercury – dioctyl phthalate differential manometer for pressures below 4 cm. Dimethyl mercury vapor was injected into the carrier stream through a capillary sealed to the barrel of the stopcock at the top of the alkyl reservoir. The alkyl and benzene vessels were weighed at the end of each run to determine the amounts used. In each experiment, a pre-run of 2–5 minutes during which benzene only was passed was used to stabilize flow conditions. A similar post-run was used to remove all products from the reaction zone while conditions were still stabilized. The quartz reaction zone had a volume of 171 cc. Contact times were controlled by a capillary sealed in at the outlet of the reaction vessel. A dry ice – acetone trap removed benzene, unreacted alkyl, and diphenyl. The remaining products were continuously transferred by a diffusion pump via a Le Roy still at −160° C and a Toepler pump to a gas burette. On completion of a run the gaseous products were measured and then transferred to a sampling vessel for analysis by gas chromatography on a 1-m silica gel column at 40° C using a flow rate of helium of approximately 20 cc/min.

RESULTS

The results are shown in Table I. Rate constants were calculated from the usual first-order equation assuming

$$\text{fraction decomposed} = \frac{1/2(\text{moles } CH_4) + \text{moles } C_2H_6}{\text{moles } HgMe_2}.$$

Can. J. Chem. Downloaded from www.nrcresearchpress.com by 210.87.254.5 on 09/05/12
For personal use only.

TABLE I

Pyrolysis of dimethyl mercury

Temp. (° K)	Contact time (sec)	Total pressure (cm)	Length of run (min)		$Hg(Me)_2$ (10^{-4} mole)	CH_4 (10^{-4} mole)	C_2H_6 (10^{-4} mole)	k (sec^{-1})
			Total	Alkyl				
800	1.10	21.8	8	5	18.3	13.9	7.2	1.35
799	0.89	15.4	8	5	8.06	5.47	2.23	1.10
800	1.06	13.0	8	5	6.05	4.41	2.16	1.20
800	1.45	8.0	20	10	5.47	3.23	2.78	1.13
798	1.18	7.4	8	5	5.17	3.58	2.26	1.30
784	1.09	26.0	8	5	20.4	8.42	3.67	0.617
784	1.09	18.6	8	5	15.3	7.17	4.17	0.642
784	1.14	10.6	8	5	24.2	9.54	6.94	0.579
783	1.18	8.0	8	5	13.7	5.13	4.72	0.644
784	1.17	7.8	8	5	13.5	5.01	4.72	0.653
783.5	1.65	2.9	20	15	16.3	3.74	4.89	0.348
783.5	1.53	2.8	20	15	20.8	5.15	7.68	0.376
783	1.83	2.3	20	15	6.2	2.03	1.81	0.333
783.5	2.46	1.89	20	15	5.42	1.43	1.64	0.243
783.5	2.90	1.10	40	30	6.95	2.78	4.03	0.212
783	3.06	1.05	20	15	6.42	1.29	2.10	0.182
771	1.04	13.44	8	5	10.89	3.30	1.897	0.378
771	1.04	12.36	8	5	10.05	3.095	1.502	0.348
760	1.19	15.65	8	5	18.8	3.67	2.39	0.221
760	1.17	13.72	8	5	16.05	2.90	1.60	0.216
760	1.08	11.25	8	5	13.84	2.44	1.60	0.226
760	1.19	7.86	10	7	13.54	2.32	1.78	0.213
760	1.28	5.02	10	7	10.55	1.53	1.42	0.179
760	1.67	2.71	20	15	13.68	1.59	1.87	0.129
760	3.34	1.02	30	20	9.25	0.585	0.957	0.0434
760	12.42	0.36	30	20	7.82	0.772	1.398	0.0238
752	1.147	10.0	8	5	11.20	1.608	0.828	0.1374
753	1.143	9.90	8	5	11.87	1.762	0.895	0.152
753	1.135	9.60	8	5	11.29	1.655	0.878	0.144
744	1.21	11.40	8	5	12.50	1.36	0.669	0.0939
743	1.12	10.70	10	7	12.56	1.71	0.683	0.117
724	1.158	10.6	10	7	11.54	0.565	0.2138	0.0378
723	1.187	10.4	8	5	11.02	0.426	0.1705	0.02985
724	1.158	10.3	10	7	25.24	0.856	0.453	0.03108
724	1.124	9.8	10	7	14.1	0.658	0.284	0.0395
723	1.16	9.4	8	5	12.47	0.462	0.182	0.02908
720	1.14	12.74	8	5	15.75	0.538	0.223	0.0282
720	1.13	10.0	10	7	18.02	0.651	0.297	0.0304
720	1.235	7.9	15	10	13.95	0.506	0.193	0.0261
720	1.126	5.4	20	15	13.64	0.454	0.225	0.0285
720	2.018	2.48	20	17	6.21	0.168	0.115	0.01595
720	8.89	0.41	30	20	7.13	0.197	0.233	0.0117
708	1.17	12.20	10	7	15.74	0.328	0.135	0.0163
706	1.098	17.8	8	5	5.68	1.183	0.250	0.01362
706	1.12	11.8	8	5	11.90	0.1945	0.716	0.01358
706	1.075	11.4	8	5	12.68	0.234	0.0889	0.0152
695	1.305	14.26	12	8	24.5	0.26	0.144	0.00846
695	1.285	7.5	20	15	18.8	0.187	0.0823	0.00734
696	1.77	2.65	20	15	13.98	0.1142	0.0607	0.00468
695.5	2.02	2.00	20	15	4.73	0.0473	0.0146	0.00410
695	5.72	0.75	30	20	5.52	0.0299	0.0394	0.00173
693	1.268	9.46	10	7	17.59	0.173	0.0551	0.00636
693.5	1.278	9.12	8	5	11.8	0.101	0.0349	0.00569
693	1.255	8.80	10	7	22.35	0.135	0.0427	0.00403

The times listed under alkyl represent the portion of the total run during which alkyl was passed. The analyses showed traces of C_2H_4 in most runs but no C_3 or C_4 hydrocarbons were observed. (The Le Roy still was warmed to $-100°$ C after several runs to allow any C_3 or C_4 hydrocarbons to be collected with the other gaseous products.)

Can. J. Chem. Downloaded from www.nrcresearchpress.com by 210.87.254.5 on 09/05/12
For personal use only.

The rate constant was studied as a function of pressure at four temperatures. From these studies it appears that when benzene is used as a carrier the first-order rate constant is independent of pressure above 10 cm at all temperatures used in the present work. Previous work (6) and preliminary investigations following the present work indicate that toluene is somewhat less than half as efficient as benzene in maintaining the rate of alkyl decomposition. However, benzene is a less efficient radical scavenger than toluene. To test for possible side reactions, runs were carried out under the unfavorable conditions of low benzene pressure and high temperature. When corrected for slight differences in total pressure, the first-order rate constants obtained at approximately 2.5 cm at 783° K using alkyl concentrations of 6.6×10^{-9} to 20.8×10^{-9} mole/cc show little variation.

Figure 1 shows the Arrhenius plots for the high-pressure limit and for 16 mm. The lines may be represented respectively by $\log k\ (\text{sec}^{-1}) = 14.8-53{,}700/2.303RT$ and $\log k\ (\text{sec}^{-1}) = 13.6-51{,}000/2.303RT$.

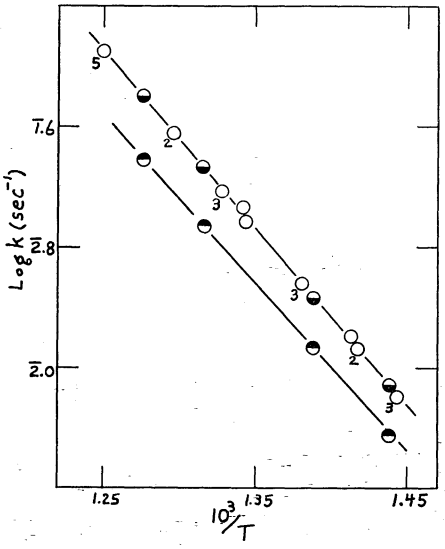

FIG. 1. Arrhenius plots for the decomposition of dimethyl mercury at the high-pressure limit (○, ◒) and at 16 mm (◓). Subscripts refer to number of experiments averaged to obtain a point. Half-filled circles are points taken from log k vs. log p curves.

DISCUSSION

The present results may be represented by a mechanism similar to that previously proposed for the decomposition of $HgMe_2$ in the presence of toluene (6):

$$Hg(CH_3)_2 \rightarrow HgCH_3 + CH_3 \quad [1]$$

$$HgCH_3 \rightarrow Hg + CH_3 \quad [2]$$

$$CH_3 + C_6H_6 \rightarrow CH_4 + C_6H_5 \quad [3]$$

$$2CH_3 \rightarrow C_2H_6 \quad [4]$$

$$2C_6H_5 \rightarrow C_{12}H_{10}. \quad [5]$$

The results at 783° K using low benzene concentrations apparently rule out any appreciable contribution from reaction [6] under the experimental conditions used. Since k_6 is

$$CH_3 + C_6H_5 \rightarrow C_6H_5{-}CH_3 \quad [6]$$

probably at least four times k_3, this result must be attributed to the removal of approximately 67% of the CH_3 by reaction [4] and to the 100- to 200-fold excess of benzene over the maximum C_6H_5 concentration.

Can. J. Chem. Downloaded from www.nrcresearchpress.com by 210.87.254.5 on 09/05/12
For personal use only.

Since reaction [2] is extremely fast in comparison to reaction [1], the observed high-pressure activation energy may be placed within the limits $D(\text{MeHg—Me}) < 53{,}700$ cal mole$^{-1} < D(\text{MeHg—Me}) + RT$ or, if $h\nu/kT$ is taken as approximately unity, $D(\text{MeHg—Me}) \approx 53{,}000$ cal mole^{-1}. This is in good agreement with an estimated value of 52,500 cal mole^{-1} obtained by applying Slater's theory to low-pressure flow system results, taking $n = 9$ (11). Taking $D(\text{CH}_3\text{—H}) = 102.5$ kcal mole^{-1} in conjunction with ΔHf^0_{298} ($HgMe_2$, g) = 22.4 kcal mole^{-1} (12, 13) yields 57.2 kcal mole^{-1} for the sum of the two metal–carbon bond dissociation energies in mercury dimethyl. To be consistent, this value should be corrected to 0° K, where it would have a value of approximately 56 kcal mole^{-1}, giving $D(\text{Me—Hg}) = 3.0 \pm 1.0$ kcal mole^{-1}.

In Table II the present results are compared with previous determinations of the Arrhenium parameters for the pyrolysis of dimethyl mercury. Since A and E tend to be

TABLE II

Summary of dimethyl mercury pyrolysis data

Pressure (mm)	Temperature range (° C)	E (kcal mole^{-1})	log A	k^* (sec^{-1})	Method	Ref.
10	489–552	51.5±2.0	13.5	5.6×10^{-4}	Flow, CO_2 + 3 mm toluene	2
16	465–608	50.1±1.0	13.1	5.5×10^{-4}	Flow, toluene	6
16	420–523	51.0±1.0	13.6	1.0×10^{-3}	Flow, benzene	‡
>100	420–519	53.7±0.5	14.8	2.0×10^{-3}	Flow, benzene	‡
38†	294–333	51.3±0.5	14.3	4.0×10^{-3}	Static	4
360	290–376	57.9±1.4	15.7	6.8×10^{-4}	Static, cyclopentane inhibited	8

*Values calculated for 400° C from A and E.
†Initial pressure, pressure at end of runs 70–80 mm.
‡Present work.

self-compensating, calculated values of the rate constants at 400° C have been included. The differences in total pressure and in the composition of the gaseous mixtures used make direct comparison difficult. However, when due allowance is made for the relative efficiencies of benzene, carbon dioxide, and toluene in energy transfer, good agreement is obtained between the three flow system studies. The static system work of Laurie and Long (4) is in fair agreement with the flow system data. Possible errors in the cyclopentane-inhibited studies have previously been discussed (9).

ACKNOWLEDGMENTS

This work has been supported by a grant from the National Research Council of Canada.

REFERENCES

1. J. P. Cunningham and H. S. Taylor. J. Chem. Phys. **6**, 359 (1938).
2. B. G. Gowenlock, J. C. Polanyi, and E. Warhurst. Proc. Roy. Soc. (London), Ser. A, **218**, 269 (1953).
3. L. M. Yeddanapalli, R. Srinivasan, and V. J. Paul. J. Sci. Ind. Res. (India), Sect. B, **13**, 232 (1954).
4. C. M. Laurie and L. H. Long. Trans. Faraday Soc. **51**, 665 (1955).
5. L. H. Long. J. Chem. Soc. 3410 (1956).
6. S. J. W. Price and A. F. Trotman-Dickenson. Trans. Faraday Soc. **53**, 939 (1957).
7. R. Srinivasan. J. Chem. Phys. **28**, 895 (1958).
8. M. E. Russel and R. B. Bernstein. J. Chem. Phys. **30**, 607 (1959).
9. J. Cattanach and L. H. Long. Trans. Faraday Soc. **56**, 1286 (1960).
10. B. G. Gowenlock. Z. Naturforschung. **15b**, 137 (1960).
11. S. J. W. Price. Ph.D. Thesis, Edinburgh University, Edinburgh, Scotland. 1958.
12. K. Hartley, H. O. Pritchard, and H. A. Skinner. Trans. Faraday Soc. **46**, 1019 (1950).
13. A. S. Carson, E. M. Carson, and B. Wilmshurst. Nature, **170**, 320 (1952).

Can. J. Chem. Downloaded from www.nrcresearchpress.com by 210.87.254.5 on 09/05/12
For personal use only.

SYNTHESIS OF SOME PHENAZINE DERIVATIVES[1]

CHAIM STAMMER[2] AND ALFRED TAURINS
Department of Chemistry, McGill University, Montreal, Que.
Received August 15, 1962

ABSTRACT

Nitration of 2-amino-, 2-N-methylamino-, and 1-amino-phenazine resulted in the formation of 2-amino-1-nitro-, 2-N-methylamino-1-nitro-, and 1-amino-4-nitro-phenazine, respectively. Nitration of 2-aminophenazine was shown to proceed via the intermediate nitramine, which was isolated and identified. 2-Hydroxy-1-nitrophenazine was found to exist in the solid state exclusively in the hydroxy form, and 4-nitro-1(5H)-phenazinone was the only solid obtained on acidification of a 1-hydroxy-4-nitrophenazine salt solution.

DISCUSSION

In a continuation of the studies dealing with the structure and reactivity of aza-aromatic nitramines (1–3), an investigation of the behavior of phenazine nitramine derivatives was undertaken.

2-Aminophenazine (I) (4) was nitrated in concentrated sulphuric acid with 70% nitric acid at temperatures between −50° and −15°. This resulted in the formation of 2-nitraminophenazine, in an almost quantitative yield. The nitramine obtained in this way was found to be a mixture of the monohydrate (II) and anhydrous (III) forms, the former being the main component. On prolonged drying, II was gradually transformed into the anhydrous form (III). The pure monohydrate was prepared by slow crystallization from a dilute acidic solution of the mixture. When dried by benzene distillation at 50°, both the monohydrate and the mixture of the two forms yielded the anhydrous nitramine.

Both the monohydrate and the anhydrous nitramine decomposed rapidly when heated to 150–160°. No differences in the chemical behavior of the two forms were observed. They were weakly acidic, dissolved in dilute alkali, and could be reprecipitated from solution with dilute acids. When treated with concentrated sulphuric acid, the nitramines (II, III) were rearranged to 2-amino-1-nitrophenazine (IV).

The infrared spectra of the two forms were in agreement with the proposed structures. In the spectrum of the monohydrate (II), the broad band with maxima at 3540, 3400, and 3200 cm^{-1} indicated the presence of water of crystallization. Absorption which could be attributed to $\overset{+}{N}$—H stretching and to —NO_2 symmetrical vibrations were present in the spectra of the two forms, and the absorption patterns in the range 900–700 cm^{-1} were in agreement with a phenazine substituted in position 2. Distinguishing features between the spectra of II and III were the presence of peaks at 855 and 790 cm^{-1} in the spectrum of III which did not appear in that of II and the difference in the frequency and shape of the bands assigned to the $\overset{+}{N}$—H stretching vibrations (a broad weak band at 2700 cm^{-1} in the spectrum of II and a broad unresolved band between 3100 and 2700 cm^{-1} in that of III). The presence of an $\overset{+}{N}$—H absorption in the spectra of both forms and the

[1]*This investigation received financial assistance from the National Research Council of Canada, Ottawa. Abstracted from a portion of the thesis submitted by C. Stammer to the Faculty of Graduate Studies and Research, McGill University, November 1961, in partial fulfillment of the requirements for the Ph.D. degree.*
[2]*Holder of a Canadian Industries (1954) Limited Fellowship 1960-61.*

Can. J. Chem. Downloaded from www.nrcresearchpress.com by 210.87.254.6 on 09/05/12
For personal use only.

FORMULAE SHEET

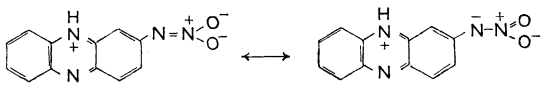

III

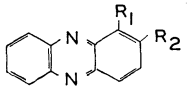

I: $R_1=H$; $R_2=NH_2$
IV: $R_1=NO_2$; $R_2=NH_2$
V: $R_1=R_2=NH_2$
VIII: $R_1=H$; $R_2=NH-CH_3$
IX: $R_1=H$; $R_2=N(CH_3)(COCH_3)$
X: $R_1=NO_2$; $R_2=NHCH_3$
XI: $R_1=NH_2$; $R_2=H$

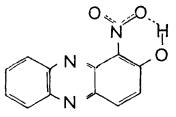

VI

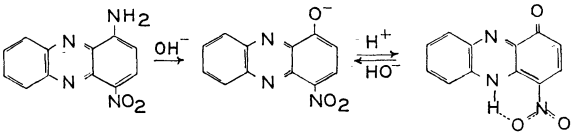

XIV XVI XVII

shift of the $-NO_2$ symmetric vibrations to higher frequencies suggested a nitriminophenazinium inner-salt structure for the nitramines (II, III). Such a structure had been proposed previously (5) for other aza-aromatic nitramines.

Rearrangement of 2-nitraminophenazine was carried out in concentrated sulphuric acid at 0°. After 3 hours, isomerization was complete and 2-amino-1-nitrophenazine (IV), the main rearrangement product, was obtained in a 55% yield. The aminonitro compound (IV) was basic, and dissolved readily in 5% hydrochloric or sulphuric acid. Direct nitration of 2-aminophenazine (I) performed under conditions similar to those of rearrangement resulted in the formation of IV in a slightly lower yield. Thus it would appear that in direct nitration, formation of IV occurred via rearrangement of the intermediate nitramine.

Proof for the structure of the aminonitro derivative (IV) was obtained in several ways. When IV was oxidized in an alkaline medium with potassium permanganate, the production of quinoxaline-2,3-dicarboxylic acid showed that only one carbocyclic ring in IV was substituted. Reduction of IV provided a diamine, of necessity 1,2-diaminophenazine (V). The aminonitro compound IV on being refluxed with concentrated hydrochloric acid or boiled with 1% aqueous sodium hydroxide was converted into 2-hydroxy-1-nitrophenazine (VI) (6, 7). In the infrared spectrum of IV there were bands at 3430, 3290, and 3170 cm^{-1} in the N—H stretching region, and peaks at 1520 and 1280 cm^{-1} which could be correlated with the asymmetric and symmetric vibrations of the nitro group. The lack of any bands between 900 and 850 cm^{-1} and the presence of a peak at 802 cm^{-1} were consistent with 1,2-substitution.

1,2-Diaminophenazine (V) was prepared both by zinc – acetic acid reduction and by

Can. J. Chem. Downloaded from www.nrcresearchpress.com by 210.87.254.6 on 09/05/12
For personal use only.

catalytic reduction of 2-amino-1-nitrophenazine (IV). When a methanolic solution of IV was reduced with hydrogen in the presence of a platinum catalyst, the color of the liquid changed from brown, to deep red, to colorless. On exposure to air, the colorless liquid became deep red again, and a product, identical with the diamine (V) obtained by zinc – acetic acid reduction, was isolated. The colorless methanolic solution was considered to contain a product of further reduction, most probably 1,2-diamino-5,10-dihydrophenazine (VII).

Hydrolytic replacement of the amino group of 2-amino-1-nitrophenazine (IV) in acidic medium was very slow. On the other hand, the replacement reaction in alkaline medium proceeded in a straightforward fashion. It was complete within $1\frac{1}{2}$ hours, and a nearly quantitative yield of 2-hydroxy-1-nitrophenazine was obtained.

When *o*-nitroaniline and methylaniline hydrochloride were allowed to react in the presence of fused zinc chloride according to a modified Wohl–Lange procedure (4), a mixture consisting of approximately 15% 2-aminophenazine (1) and 85% 2-N-methylaminophenazine (VIII) was obtained. Separation of the amines was achieved by chromatography. Acetylation of VIII provided 2-N-acetyl-N-methylaminophenazine (IX). Nitration of the N-methylamine (VIII) in concentrated sulphuric acid with nitric acid (70% excess) at temperatures below −20° resulted in the immediate formation of 2-N-methylamino-1-nitrophenazine (X).

It has been established (8–11) that nitration of electron-deficient aza-aromatic amines proceeded mainly by an "indirect route", and that in cases in which the intermediate nitramine was not formed, the amine resisted nitration. Since the nitration of the N-methylamine (VIII) took place under such mild conditions, it was believed that 2-methylamino-1-nitrophenazine (X) was produced by the intramolecular rearrangement of an unstable intermediate nitramine. Had a direct nitration occurred, much more vigorous reaction conditions would have been necessary and different products would likely have been formed. The nitration of 2-aminophenazine (I) had been considered to proceed by the same reaction mechanism. In the case of the N-methylamine (VIII), however, nitration occurred at a much faster rate, and the reaction resulted in a higher yield of product, 65% versus 55%, being obtained. The increased rate of rearrangement was expected since 2-nitraminophenazine (II, III) had already rearranged readily, and because it had been demonstrated in the pyridine series that introduction of a methyl group into the amino function decreased the stability of the intermediate nitramine in the rearrangement reaction. The fact that the nitro groups in both instances, migrated to position 1 of the phenazine nucleus provided additional support for the assumption that the same mechanism was operative in each case.

The structure proposed for the methylaminonitro compound (X) was substantiated by the infrared spectrum, which had bands indicating the presence of an N—H group, a methyl group, a nitro group, and 1,2-substitution. Further evidence for the structure of X was obtained by its transformation to 2-hydroxy-1-nitrophenazine (VI) on treatment with a 1% sodium hydroxide solution.

1-Aminophenazine (XI) was prepared at first by the deamination of 1,3-diaminophenazine (XII) (12). The difficulties encountered in the deamination led to an investigation of alternative procedures for the synthesis of the amine. 1-Aminophenazine (XI) was reported (13) to have been obtained in a 50% yield by refluxing 2,2′-diaminodiphenylamine (XIII) with nitrobenzene. However, no details of procedure were given in the report and attempts to duplicate the published results failed. After considerable effort had been directed toward determining the exact reaction conditions for the oxidation,

Can. J. Chem. Downloaded from www.nrcresearchpress.com by 210.87.254.6 on 09/05/12
For personal use only.

it was found that by heating the diamine (XIII) with nitrobenzene in a nitrogen atmosphere, and removing the water formed in the reaction by distillation, 1-aminophenazine (XI) was obtained in a 40% yield.

The main mononitration product of 1-aminophenazine in concentrated sulphuric acid was found to be 1-amino-4-nitrophenazine (XIV). Nitration with a 30% excess of nitric acid for 1 hour was complete, but a considerable amount of a substance soluble in ammonia was produced simultaneously with XIV. The former was assumed to be 1-nitramino-4-nitrophenazine on the basis of its solubility in ammonia, rapid decomposition at the melting temperature, relative stability with respect to dilute acids, and the infrared spectrum of the crude product. Complete nitration of 1-aminophenazine with no detectable formation of polynitro compounds soluble in ammonia was achieved when a 70% excess of nitric acid was used and the reaction was terminated after 2 minutes. The structure of the aminonitro compound XIV was demonstrated by oxidation and reduction reactions, by its infrared spectrum, and by replacement of the amino group with an hydroxyl function.

Oxidation of 1-amino-4-nitrophenazine (XIV) in alkaline medium with potassium permanganate provided quinoxaline-2,3-dicarboxylic acid. Reduction of a methanolic solution of the aminonitro compound (XIV) with hydrogen and using a platinum catalyst resulted in a change in the color of the solution from brown to blue to colorless. The colorless solution, on exposure to air, became blue then changed to brown, and a brown solid precipitated. It was assumed that the final reduction product, which gave the colorless solution, was 1,4-diamino-5,10-dihydrophenazine. The colorless solution was rapidly oxidized by air back to the blue solution containing 1,4-diaminophenazine (XV). This sequence of reactions excluded the possibility of 1,2-substitution for the amino nitrophenazine (XIV), since 1,2-diaminophenazine (V) had been identified previously, and of 1,3-substitution because a methanolic solution of 1,3-diaminophenazine (XII) was red. The behavior of the aminonitro compound (XIV) on reduction with zinc – acetic acid provided further confirmation of 1,4-substitution, insofar as the solution of the reduction product in acetic acid was violet while the solutions of the 1,2-diamine (V) and the 1,3-diamine (XII) were brown and green respectively. The 1,4-diaminophenazine (XV) was isolated from the acetic acid solution in the form of blue needles when the acidic solution was rendered alkaline with ammonia in a nitrogen atmosphere. The substance did not melt below 300°, and in solution on exposure to air formed a brown unidentified product.

Additional evidence in favor of the proposed structure was accumulated when, on boiling of 1-amino-4-nitrophenazine (XIV) with aqueous alkali, 1-hydroxy-4-nitrophenazine (XVI), as its alkali salt, was produced. By acidifying the aqueous solution of the alkali salt (XVI), 4-nitro-1(5H)-phenazinone (XVII) was obtained. The alkaline solution of 2-hydroxy-1-nitrophenazine (VI), when acidified, gave the phenazinol tautomer exclusively.

The formation of XVII as the only solid tautomer, and the sole existence of the hydroxy tautomer of 2-hydroxy-1-nitrophenazine (VI) in the solid state, were explained by a hydrogen-bonding effect and formation of a stable six-membered chelate ring. The stability of the hydroxy tautomer in VI required the nitro group to be located in position 1, likewise in the case of XVII the nitro group must be in position 4.

Confirmatory evidence for the structure proposed for the phenazinone (XVII) was based on the reversible transformation of the compound into the ammonium salt of 1-hydroxy-4-nitrophenazine (XVI), the infrared spectra of XVI and XVII, and the

Can. J. Chem. Downloaded from www.nrcresearchpress.com by 210.87.254.6 on 09/05/12
For personal use only.

ultraviolet spectrum of XVII in aqueous solution. The general absorption pattern in the 900–700 cm^{-1} region of the infrared spectrum of XVI was similar to that of 1-amino-4-nitrophenazine (XIV) and constituted a clear indication of analogous structures. The absorption pattern in the same region for the phenazinone (XVII), however, was completely different, the two very characteristic bands at 820 ± 10 and 750 ± 15 cm^{-1}, which appeared in all the other phenazines studied, being absent.

4-Nitro-1(5H)-phenazinone (XVII) was soluble in water at 25° to the extent of 0.5 mg/ml. The red solution, on 10-fold dilution, became yellow in color. When this yellow solution was evaporated, red crystals of XVII were recovered. In acidic medium (pH 2.0) the phenazinone (XVII) was much less soluble, and the solution was red. These observations could be explained by an equilibrium in water solution between the phenazinone (XVII) and the hydroxy tautomer in its anionic form (XVI), the phenazinone being red and the anion yellow in color. This equilibrium was studied by means of ultraviolet spectroscopy. The aqueous solution of phenazinone (XVII) (4.15×10^{-5} mole/liter) absorbed at 425 mμ with a molar extinction coefficient of 13,970; no absorption occurred at wavelengths above 530 mμ. An alkaline solution of XVII of an equivalent concentration gave the same absorption curve, and it was concluded that at the given concentration, the phenazinone was already fully converted to the anion. An acidic solution of XVII (2 drops of 3.7% hydrochloric acid per 4 ml of solution) of the same concentration displayed a maximum at 400 mμ and a molar extinction coefficient of 12,050. It also absorbed markedly at 530 mμ ($\epsilon = 3370$). Assuming that the compound in acidic solution existed completely in the phenazinone form, the absorption at 530 mμ could be used to measure the amount of phenazinone (XVII) present in equilibrium in water solutions of different concentrations. Because of the high absorbance exhibited by the solutions studied, the differential method of measurement was applied. The reference cells were filled with alkaline solutions of phenazinone (XVII) of the same concentration, and the differential absorbance shown at 530 mμ was attributed to the presence of phenazinone (XVII) in equilibrium. The approximate ratio of phenazinone (XVII) to anion (XVI) in a saturated aqueous solution of 4-nitro-1(5H)-phenazinone (XVII) was 7:93; on 5-fold dilution the ratio dropped to 2:98, and on 10-fold dilution no detectable amount of XVII was found.

In the nitrations of 2-amino-, 2-N-methylamino-, and 1-amino-phenazines, the nitro groups entered the α-positions of the ring. No β-substituted products were isolated, although in each case the β-position of the ring was available. These results were in agreement with those observed for other electrophilic reactions in the phenazine series such as chlorination (14) and direct nitration (15) in which only α-substituted products were obtained. Such behavior provided confirmatory evidence for the theoretical predictions which had been based on molecular orbital calculations (16, 17).

NOTE ADDED IN PROOF: A. Gray and F. G. Holliman (Tetrahedron, **18**, 1095 (1962)) have claimed the preparation of 1-amino-4-nitro-, 1-hydroxy-4-nitro-, and 1,4-diaminophenazine. On the basis of our present work we suggest that these compounds actually are: 1-amino-2-nitro-, 1-hydroxy-2-nitro-, and 1,2-diamino-phenazine, respectively.

EXPERIMENTAL

The melting points were determined in a Gallenkamp melting point apparatus and are uncorrected. The analyses were carried out in the C. Daesslé Laboratory, Montreal. Infrared spectra were determined on a Perkin–Elmer Model 21 double-beam instrument equipped with a sodium chloride prism. The ultraviolet absorption spectra were measured by means of a Beckman recording spectrophotometer Model DK1. Neutral, activity I Woelm aluminum oxide was used for chromatography unless otherwise noted.

Can. J. Chem. Downloaded from www.nrcresearchpress.com by 210.87.254.6 on 09/05/12
For personal use only.

2-Nitraminophenazine (II, III) (2-Nitrimino-(10H)phenazinium Betaine)

2-Aminophenazine (I) (200 mg; m.p. 279°) was powdered and dissolved in concentrated sulphuric acid (2 ml). The brown solution was cooled to −50° and formed a thick paste. Nitric acid (0.073 ml; sp. gr. 1.42; 70% nitric acid) was added at once, and the reaction mixture was stirred for 1–2 minutes until an orange liquid had formed. The temperature rose to about −20°. The solution was poured onto crushed ice (12.5 g) and was stirred until the ice had melted. The orange precipitate which formed was filtered, and the wet solid cake was suspended in water (100 ml). The addition of concentrated ammonia (16 drops) effected solution of the solid material and brought the pH of the solution to 8.0. The solution was filtered through a sintered-glass plate, then was heated to 50°. On addition of aqueous acetic acid (1:1; 20 drops) to the filtrate, fine yellow needles (243 mg) separated from solution. A portion of this material (100 mg) was dissolved in water (200 ml) and ammonia (6 drops) at 75°. The hot solution was acidified with aqueous acetic acid (1:2; 15 drops). On gradual cooling, gold needles deposited, and were isolated. A yield of 98 mg of 2-nitraminophenazine monohydrate (II), m.p. 150–160° (explodes), was obtained. $\bar{\nu}_{max}^{KBr}$ 3540, 3400, 3200, 2700, 1515, 1315, 1300, 880, 835, 820, 765, 755, 745 cm^{-1}. Anal. Calc. for $C_{12}H_8N_4O_2.H_2O$: C, 55.80; H, 3.95. Found: C, 55.22; H, 4.16%.

2-Nitraminophenazine monohydrate (II) (100 mg) was ground and suspended in dry benzene (50 ml). The suspension was heated to 50° for 2 hours with occasional swirling, then approximately 35 ml of the benzene was distilled off under reduced pressure at a temperature not exceeding 50°. The solid 2-nitraminophenazine (III) (60 mg) was separated by filtration, m.p. 150–160° (decomp.). $\bar{\nu}_{max}^{KBr}$ 3100–2700, 1510, 1320, 1295, 880, 855, 830, 820, 790, 765, 750, 740 cm^{-1}. Anal. Calc. for $C_{12}H_8N_4O_2$: C, 59.98; H, 3.36; N, 23.33. Found: C, 59.56; H, 3.40; N, 23.35%.

2-Amino-1-nitrophenazine (IV)

2-Nitraminophenazine (II, III) (0.5 g) was added gradually to concentrated sulphuric acid (5 ml) which had been cooled to −40°. The thick paste was stirred continuously. When all the substance had dissolved, the viscous brown liquid was kept in an ice-water bath for 3 hours. The reaction mixture was diluted with ice water (200 ml), and the precipitate (90 mg) which formed was filtered. The acidic filtrate was heated to 60°, then neutralized with ammonia, yielding 390 mg of a yellow-green substance. The crude material (400 mg) was dissolved in chloroform (500 ml), and the solution was chromatographed on alumina (90 g). Elution with methanol–chloroform (1:21) provided 2-amino-1-nitrophenazine (IV) (344 mg), yellow needles, m.p. 264–265°. $\bar{\nu}_{max}^{KBr}$ 3430, 3290, 3170, 1520, 1280, 845, 835, 802, 795, 770, 755, 740 cm^{-1}. Anal. Calc. for $C_{12}H_8O_2N_4$: C, 60.00; H, 3.40; N, 23.30. Found: C, 60.25; H, 3.43; N, 23.53%.

1,2-Diaminophenazine (V)

A suspension of 2-amino-1-nitrophenazine (IV) (50 mg) in glacial acetic acid (9 ml) was prepared by grinding the substance with acid in a mortar. The suspension was diluted with water (1.5 ml), and zinc powder (excess) was added in three small portions at 30°. The mixture was shaken vigorously; the yellow suspension became orange-brown and formed a clear solution. The excess zinc was filtered off and washed with water (8 ml). The filtrate was made alkaline by the gradual addition of concentrated ammonia (50 ml), whereupon the liquid became purple and brown lustrous needles were deposited from solution. The mixture was refrigerated for 3 hours, then the crystalline product (41 mg) was isolated. This material after two sublimations (1 mm at 130–135°) provided 1,2-diaminophenazine (V), purple needles, m.p. 189–191°. $\bar{\nu}_{max}^{KBr}$ 3390, 3300, 3170, 825, 785, 755 cm^{-1}. Anal. Calc. for $C_{12}H_{10}N_4$: N, 26.64. Found: N, 26.68%.

2-Amino-1-nitrophenazine (IV) (17 mg) was suspended in methanol (5 ml) and reduced with hydrogen in the presence of Adams' catalyst (14 mg PtO_2). The suspended particles dissolved and color changes from brown to purple to almost colorless were observed. The colorless solution on exposure to air became purple again and on evaporation of the solvent 13 mg of a brown solid was obtained. Sublimation of this material provided 1,2-diaminophenazine (V) in the form of purple needles.

2-Hydroxy-1-nitrophenazine (VI)

2-Amino-1-nitrophenazine (IV) (50 mg) was refluxed with 0.8% sodium hydroxide solution (25 ml). After 40 minutes, the solid dissolved, forming an orange solution. Refluxing was continued for 1 hour. The hot solution was filtered and treated dropwise with 3.7% hydrochloric acid at 60° until the pH was 2.0. Yellow crystals precipitated and, after standing overnight in a refrigerator, were filtered and washed with slightly acid water. The material was dissolved in hot water (20 ml) to which concentrated ammonia (4 drops) had been added. The orange solution was filtered hot and acidified to pH 2.0 by the dropwise addition of 3.7% hydrochloric acid at 80°. After standing overnight, the yellow needles which had precipitated were isolated. A yield of 46 mg of 2-hydroxy-1-nitrophenazine (VI), m.p. 238, was obtained. $\bar{\nu}_{max}^{KBr}$ 3040, 1550, 1530, 1250, 840, 802, 755 cm^{-1}. Anal. Calc. for $C_{12}H_7N_3O_3$: C, 59.75; H, 2.93; N, 17.42. Found: C, 59.67; H, 3.29; N, 17.49%.

2-Amino-1-nitrophenazine (IV) (22 mg) was dissolved in concentrated hydrochloric acid (15 ml). The solution was refluxed for 24 hours, during which time the liquid changed in color from red to orange to deep brown. It was filtered and ammonia was added to the hot filtrate until the pH was 3.0. The yellow needles (6 mg) which precipitated were isolated and identified as starting material (IV). After 2 days' standing at

Can. J. Chem. Downloaded from www.nrcresearchpress.com by 210.87.254.6 on 09/05/12
For personal use only.

room temperature, an orange crystalline substance precipitated from solution. This material was isolated and identified by its infrared spectrum as 2-hydroxy-1-nitrophenazine (VI), m.p. 223°.

2-N-Methylaminophenazine (VIII)

Methylaniline hydrochloride (1.45 g) and *o*-nitroaniline (1.40 g) were heated together. The mixture melted at 80–90°; at 135° fused zinc chloride (4.5 g) was added and the temperature was raised to 170° during ½ hour. A vigorous reaction ensued, with vapors of water and *o*-nitroaniline being evolved. The reaction subsided after a few seconds but the mixture was stirred at 170° for 25 minutes longer. Hot water (20 ml) was added carefully and stirring was continued until the mixture had cooled to room temperature. The aqueous layer was decanted, and the tarry residue was washed twice with water (3 ml), then was ground with 2% hydrochloric acid (20 ml). The acidic extract was filtered and the residue on the filter was washed with 0.5% hydrochloric acid. The combined filtrates were cooled and made alkaline with 20% sodium hydroxide (20 ml). A voluminous brown precipitate formed, which, after standing overnight, was filtered and washed with water until the latter gave a neutral reaction. The brown powder (1.2 g) was sublimed. At a temperature up to 120° under reduced pressure, unchanged *o*-nitroaniline was obtained; *in vacuo* with the temperature being gradually raised to 160°, an orange sublimate (0.35 g) was collected. Several batches of the latter (1.2 g) were combined and resublimed. At 125–130°, a sublimate consisting of *o*-nitroaniline and an oily material was obtained, and at 150–160° a mixture of orange and deep red crystals (0.77 g) sublimed. The latter mixture (1.76 g) was taken up in chloroform (176 ml) and filtered, leaving a residue (0.16 g) of 2-aminophenazine (I). The filtrate was chromatographed on alumina (450 g). Elution with chloroform provided 1.43 g of orange needles. Purification of these by sublimation afforded 2-N-methylaminophenazine (VIII), m.p. 199–201°. $\bar{\nu}_{max}^{KBr}$ 3260, 855, 815, 805, 755, 750, 735 cm^{-1}. Anal. Calc. for $C_{13}H_{11}N_3$: C, 74.62; H, 5.30; N, 20.08. Found: C, 74.73; H, 5.64; N, 20.16%. On further elution, 2-aminophenazine (I) (90 mg) was recovered.

2-N-Acetyl-N-methylaminophenazine (IX)

2-N-Methylaminophenazine (VIII) (100 mg) was dissolved in glacial acetic acid (0.5 ml), and acetic anhydride (0.5 ml) was added. The solution was allowed to remain at room temperature for 24 hours, then was diluted with water (2 ml) and evaporated to dryness under reduced pressure. Recrystallization of the residue from aqueous ethanol provided 2-N-acetyl-N-methylaminophenazine (IX) (75 mg), m.p. 155°. $\bar{\nu}_{max}^{KBr}$ 2980, 2900, 1665, 860, 830, 765, 760, 745 cm^{-1}. Anal. Calc. for $C_{15}H_{13}N_3O$: N, 16.69. Found: N, 16.78%.

2-N-Methylamino-1-nitrophenazine (X)

2-N-Methylaminophenazine (VIII) (200 mg) was dissolved in concentrated sulphuric acid (2 ml). The brown solution was cooled to −50° and solidified to a paste. Nitric acid (0.11 ml; sp. gr. 1.42) was added at once, and the mixture was stirred until a red liquid was obtained (10–20 seconds). The liquid was poured onto crushed ice (12.5 g), and the brown solution which formed was filtered. The filtrate was treated with ammonia at 0° until the pH was 3.0–4.0. A brown mass precipitated; it was filtered and washed with water until the wash water gave a neutral reaction. The crude product (200 mg) was taken up in chloroform (45 ml) and chromatographed on alumina (80 g). Elution with methanol–chloroform (1:20) and recrystallization from chloroform gave 162 mg of 2-N-methylamino-1-nitrophenazine (X), m.p. 278–280°. The analytical sample was sublimed *in vacuo* at a temperature above 200°. $\bar{\nu}_{max}^{KBr}$ 3340, 2900, 1515, 1265, 830, 802, 800, 785, 760 cm^{-1}. Anal. Calc. for $C_{13}H_{10}N_4O_2$: N, 22.04. Found: N, 22.14%.

1-Aminophenazine (XI)

Crude 2,2′-diaminodiphenylamine (m.p. 85–90°) (20 g) was heated and stirred with nitrobenzene (200 ml). A stream of nitrogen (3 bubbles/sec) was passed through the reaction vessel during the process. The reaction was controlled in such a way that as the nitrobenzene slowly distilled off, it was replaced continuously by the addition of fresh nitrobenzene (Table I). When the reaction was complete after 5 hours, the product (150 ml) was diluted with benzene (850 ml) and shaken with 3.7% hydrochloric acid (500 ml). The emulsion which formed was filtered and the residue was washed with the same acid (200 ml). The blue acidic layer of the combined filtrates was separated from the brown benzene layer, and the latter was extracted twice with the acid (300 ml). The combined acidic extracts (1 l.) were filtered, diluted with water (1 l.), and boiled

TABLE I

Progress of the oxidation reaction of 2,2′-diaminodiphenylamine with nitrobenzene

Time, hr	Amount of nitrobenzene, distilled off, ml	Amount of fresh nitrobenzene added, ml	Appearance of distillate
1	40	40	Yellow, cloudy
2	55	40	Orange, cloudy
3	48	40	Orange, slightly turbid
4	55	40	Orange, clear
5	52	40	Orange, clear

Can. J. Chem. Downloaded from www.nrcresearchpress.com by 210.87.254.6 on 09/05/12
For personal use only.

until no odor of nitrobenzene could be detected. Then the liquid (1.2 l.) was cooled and filtered. The gradual addition of anhydrous sodium acetate (150 g), with stirring, at room temperature, resulted in the formation of a precipitate. After standing for 3 hours in the refrigerator, the solid product was isolated. The red crystalline material (9.7 g) was sublimed twice, providing 1-aminophenazine (XI) (7.76 g), red crystals, m.p. 181–182°. Reported m.p. 179–181° (18). $\bar{\nu}_{max}^{KBr}$ 3480, 3340, 820, 765, 735 cm^{-1}.

1-Amino-4-nitrophenazine (XIV)

1-Aminophenazine (XI) (600 mg; m.p. 181–182°) was ground and dissolved in concentrated sulphuric acid (6 ml). The solution was cooled to a paste (−50°) and nitric acid (0.324 ml; sp. gr. 1.42) was added with stirring. The mixture was placed in an ice-water bath and stirring was continued for approximately 2 minutes until a drop of the liquid nitration mixture when added to ice water dissolved to form a yellow solution. Then the nitration mixture was poured onto crushed ice (300 g). The yellow suspension obtained was extracted with four portions of chloroform, the temperature being maintained near 0°. The chloroform extracts were combined (400 ml) and allowed to pass through a column of alumina (500 g; activity IV). Elution with chloroform provided a brown solution (600 ml) from which, on evaporation, was obtained 320 mg of 1-amino-4-nitrophenazine (XIV), orange needles, m.p. 281–282° (sublimes). $\bar{\nu}_{max}^{KBr}$ 3430, 3290, 1520, 1285, 820, 802, 775, 770, 765 cm^{-1}. Anal. Calc. for $C_{12}H_8O_2N_4$: N, 23.30. Found: N, 23.11%. Concentration of the mother liquor provided an additional 17 mg of (XIV), m.p. 274–278°, and when the mother liquor from this material was rechromatographed on alumina a further 7 mg of (XIV), m.p. 278–281°, was collected. In the latter instance, evaporation of the mother liquor to dryness left 95 mg of a brown crystalline powder, m.p. 140–145° (decomp.), which was distinguished by a strong band at 2150 cm^{-1} in the infrared spectrum.

4-Nitro-1(5H)-phenazinone (XVII)

1-Amino-4-nitrophenazine (XIV) (200 mg; m.p. 281–282°) was refluxed with a 1% solution of sodium hydroxide (80 ml). The solid dissolved completely after 20 minutes and the brown solution which formed was refluxed for another hour, then was allowed to cool slowly for 2 hours. A yellow precipitate settled out of solution, then redissolved when the mixture was heated to 60°. The hot liquid was filtered and the filtrate was acidified at room temperature to pH 2.0 by the dropwise addition of 3.7% hydrochloric acid. After standing for 3 hours at room temperature, the red crystalline material (180 mg) which formed was isolated. The latter (75 mg) was heated to 40° with water (150 ml), cooled to room temperature, and filtered. The filtrate was acidified with 3.7% hydrochloric acid (15 ml) at room temperature, and allowed to stand; a red crystalline substance precipitated and was isolated. A yield of 60 mg of 4-nitro-1(5H)-phenazinone (XVII), m.p. 200° (decomp.), was obtained.

1-Hydroxy-4-nitrophenazine Ammonium Salt (XVI)

Crude 4-nitro-1(5H)-phenazinone (XVII) (50 mg) was dissolved in water (20 ml) and rendered alkaline with ammonia (3 drops). The solution was filtered and treated with concentrated ammonia (14 drops) at 60°. The mixture was allowed to stand overnight in the refrigerator. Isolation of the precipitate which formed afforded 1-hydroxy-4-nitrophenazine ammonium salt (XVI) (22 mg) as light yellow needles, which decomposed at 280°. $\bar{\nu}_{max}^{KBr}$ 3400, 3100, 1540, 1530, 1510, 1320, 1265, 820, 805, 765 cm^{-1}. Anal. Calc. for $C_{12}H_{10}N_4O_3$: N, 21.70. Found: N, 21.45%.

ACKNOWLEDGMENT

The authors are grateful to Dr. Barbara G. Ketcheson for the preparation of the manuscript.

REFERENCES

1. S. O. Harris and A. Taurins. To be published.
2. A. Blaga and A. Taurins. To be published.
3. S. Kasman and A. Taurins. Can. J. Chem. **34**, 1261 (1956).
4. A. Wohl and M. Lange. Ber. **43**, 2186 (1910).
5. A. Taurins. Can. J. Chem. **36**, 465 (1958).
6. B. Hegedüs. Jubilee Vol. Emil Barrel, 388 (1946); Chem. Abstr. **41**, 6262 (1947).
7. H. Otomasu. Pharm. Bull. (Tokyo), **2**, 283 (1954); Chem. Abstr. **50**, 1033*a* (1956).
8. A. E. Tschitschibabin and B. Rasorenow. J. Russ. Phys. Chem. Soc. **47**, 1286 (1915).
9. A. E. Tschitschibabin and A. W. Kirsanov. Ber. **61**, 1223 (1928).
10. E. Plazek and E. Sucharda. Ber. **61**, 1813 (1928).
11. E. Plazek, A. Marcinkow, and C. Stammer. Roczniki Chem. **15**, 365 (1935).
12. F. Kehrman and P. Prunier. Helv. Chim. Acta, **7**, 984 (1924).
13. A. Gray, G. Gertner, and F. G. Holliman. Tetrahedron Letters, **7**, 24 (1959).
14. S. Maffei and M. Aymon. Gazz. Chim. Ital. **83**, 327 (1953).
15. S. Maffei and M. Aymon. Gazz. Chim. Ital. **84**, 667 (1954).
16. H. C. Longuet-Higgins and C. A. Coulson. J. Chem. Soc. 971 (1949).
17. M. J. S. Dewar and P. M. Maitlis. J. Chem. Soc. 2521 (1957).
18. B. Hegedüs. Helv. Chim. Acta, **33**, 766 (1950).

Can. J. Chem. Downloaded from www.nrcresearchpress.com by 210.87.254.6 on 09/05/12
For personal use only.

CONCURRENT ION–MOLECULE REACTIONS IN ETHYLENE AND PROPYLENE

A. G. HARRISON
Department of Chemistry, University of Toronto, Toronto, Ontario
Received September 7, 1962

ABSTRACT

The ion–molecule reactions occurring in ethylene and in propylene at high pressures in the mass spectrometer ion source have been studied. It has been shown that two of the six secondary ions in ethylene and four of the nine secondary ions studied in propylene are products of more than one ion–molecule reaction. The cross sections for the separate reactions at 10 v/cm field strength are reported.

INTRODUCTION

The identification of the reactant ion in ion–molecule reactions by appearance potential measurements provides information on the reactant ion of lowest appearance potential. Due to the limited sensitivity of such determinations, particularly for ions of low abundance, concurrent reactions involving ions of higher appearance potential will frequently remain undetected. If such is the case the measured reaction cross sections will be in error.

Pobo and Hutchinson (1) have outlined a method whereby the contribution of concurrent ion–molecule reactions leading to the same product ion in binary systems may be estimated. A recent communication from this laboratory (2) has extended this method and has shown that four of the seven secondary ions studied in cyclopropane are the product of more than one ion–molecule reaction.

The principles of the method can be briefly reiterated. Consider the two ion–molecule reactions leading to the same product ion,

$$P_1^+ + M \rightarrow S^+ + N_1$$
$$P_2^+ + M \rightarrow S^+ + N_2.$$

The total secondary ion current, I_s, can be expressed as the sum of two independent contributions in the usual fashion:

$$[1] \qquad I_s = f_1Q_1d[M]I_{P_1} + f_2Q_2d[M]I_{P_2},$$

where [M] is the concentration of molecules, d is the distance from the electron beam to exit slit, f_x is the collision efficiency, and Q_x is the reaction cross section. Equation [1] on rearrangement gives two similar equations:

$$[2] \qquad \frac{I_s}{I_{P_1}} = f_1Q_1d[M] + f_2Q_2d[M]\frac{I_{P_2}}{I_{P_1}}$$

$$[3] \qquad \frac{I_s}{I_{P_2}} = f_1Q_1d[M]\frac{I_{P_1}}{I_{P_2}} + f_2Q_2d[M].$$

The plot of the ion current ratios indicated by equations [2] and [3] should lead to linear relations, the relevant cross sections being obtained from the slopes and intercepts. As pointed out previously (2) the variation of ion current ratios is achieved by varying the electron energy. The success of the method therefore depends on two assumptions, first, that the reaction cross sections do not change with electron energy, and, second, that the relative collection efficiencies for the primary and secondary ions do not change with electron energy. The present study of the ion–molecule reactions of ethylene and of

Can. J. Chem. Downloaded from www.nrcresearchpress.com by 210.87.254.6 on 09/05/12
For personal use only.

propylene was undertaken in part to obtain further evidence concerning these assumptions.

The ion–molecule reactions in ethylene were studied briefly by Schissler and Stevenson (3, 4) and, in detail, by Field *et al.* (5) and Fuchs (6). Although general agreement has been obtained on the reactions occurring and their cross sections, the present work presents evidence that two of the secondary ions, $C_4H_2^+$ and $C_4H_5^+$, are produced in more than one ion–molecule reaction.

Two of the ion–molecule reactions in propylene were reported by Schissler and Stevenson (3, 4); a more detailed study has been made by Fuchs (6). Again the present results suggest that several of the secondary ions are the product of more than one reaction.

EXPERIMENTAL

The experimental work was carried out using an A.E.I. Ms-2 mass spectrometer. The instrument and general experimental procedure have been described previously (2). In the present work reaction cross sections have been measured at 50 v electron energy and at low electron energy near the appearance potential threshold for the reactant ion. The cross sections at 50 v were determined in the usual fashion by measurement of the ion current ratio I_s/I_P as a function of the source pressure [M]. At the source concentrations used in this work (maximum of less than 1×10^{13} molecules/cc) such a small fraction of the primary ions disappears by ion–molecule reactions, or by charge-transfer reactions such as reported by Field for ethylene (7), that corrections to the measured primary ion currents are negligible. In these measurements it was assumed that only one reaction was occurring. The reaction identification was taken from previous work (5, 6). At low electron energies the results for each secondary ion were treated in the manner of equations [2] and [3]. The choice of a first reactant ion was dictated by appearance potential measurements. The choice of a second possible reactant ion was dictated from thermochemical considerations, the assumption being made that endothermic reactions do not occur. In general, for ethylene no more than two reactions to form each secondary ion are thermochemically possible. For propylene several exothermic reactions can be postulated for most of the secondary ions. The choice of the second reactant ion was dictated, in part, by the results found for the similar system cyclopropane (2) and, in part, by the relative abundances of the primary ions at the low electron energies.

For secondary ions which are formed by only one reaction, equation [1] predicts a linear relation between secondary and primary ion currents at constant source concentration. Several studies (8, 9) have not found such a relation at low field strengths. Since the success of the method outlined above depends on a linear relation, this factor was investigated in some detail. Satisfactory linear plots were obtained at field strengths of 10 v/cm or greater, although deviations were observed at lower field strengths. Typical results are shown in Fig. 1, where the ratio I_s/I_P is plotted against I_P for the reaction

$$C_2H_4^+ + C_2H_4 \rightarrow C_3H_5^+ + CH_3.$$

It is probable that the deviations at lower field strengths are caused by changes in the ionic residence time due to varying space-charge effects as the electron energy is varied. All results in the present work were obtained at a field strength of 10 v/cm.

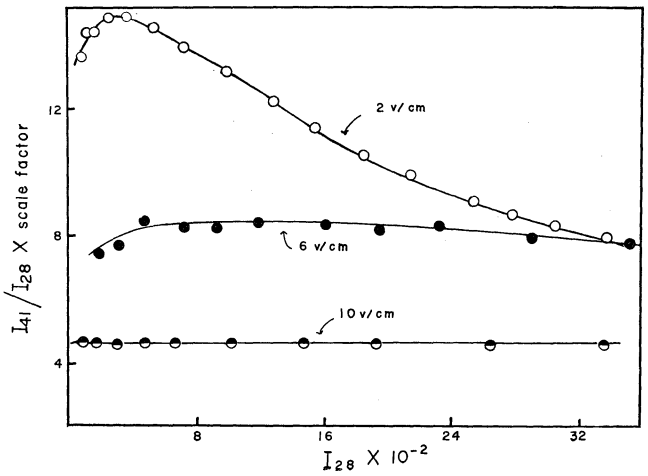

FIG. 1. I_{41}/I_{28} as a function of I_{28} in ethylene. Scale factors: ○ 10^{+2}, ● 10^{+3}, ◓ 10^{+3}.

Can. J. Chem. Downloaded from www.nrcresearchpress.com by 210.87.254.6 on 09/05/12
For personal use only.

The ethylene and propylene were research grade chemicals of 99.9+% purity and were used without further purification.

RESULTS AND DISCUSSION

The results obtained for ethylene are summarized in Table I. The cross sections at 50 v electron energy and 10 v/cm field strength are in good agreement with previous

TABLE I

Ion–molecule reactions in ethylene

Reaction No.	Secondary ion (m/e)	Reaction	$-\Delta H$ reaction (kcal/mole)	$fQ\times10^{16}$ (cm²/molecule) Low energy	High energy This work	High energy Ref. 5
1	39	$C_2H_2^+ + C_2H_4 \rightarrow C_3H_3^+ + CH_3$	24	17.5	25.3	22
2	39	$C_2H_3^+ + C_2H_4 \rightarrow C_3H_3^+ + CH_4$	42	<2		
3	41	$C_2H_4^+ + C_2H_4 \rightarrow C_3H_5^+ + CH_3$	6	42.3	36.2	43
4	50	$C_2^+ + C_2H_4 \rightarrow C_4H_2^+ + H_2$	163	54.8	145	89
5	50	$C_2H^+ + C_2H_4 \rightarrow C_4H_2^+ + H_2 + H$	25	21.0		
6	51	$C_2H^+ + C_2H_4 \rightarrow C_4H_3^+ + H_2$	124	34.9	36.2	34
7	51	$C_2^+ + C_2H_4 \rightarrow C_4H_3^+ + H$	158	<1		
8	53	$C_2H_2^+ + C_2H_4 \rightarrow C_4H_5^+ + H$	18	10.2	11.5	14
9	53	$C_2H_3^+ + C_2H_4 \rightarrow C_4H_5^+ + H_2$	32	1.7		
10	55	$C_2H_4^+ + C_2H_4 \rightarrow C_4H_7^+ + H$	12	3.5	3.8	4

results (5) with the exception of reaction 4 leading to the $C_4H_2^+$ ion. This discrepancy will be discussed below.

At low electron energies both reactions 4 and 5 were found to contribute to the formation of $C_4H_2^+$ and both reactions 8 and 9 to the formation of $C_4H_5^+$. Figures 2 and 3

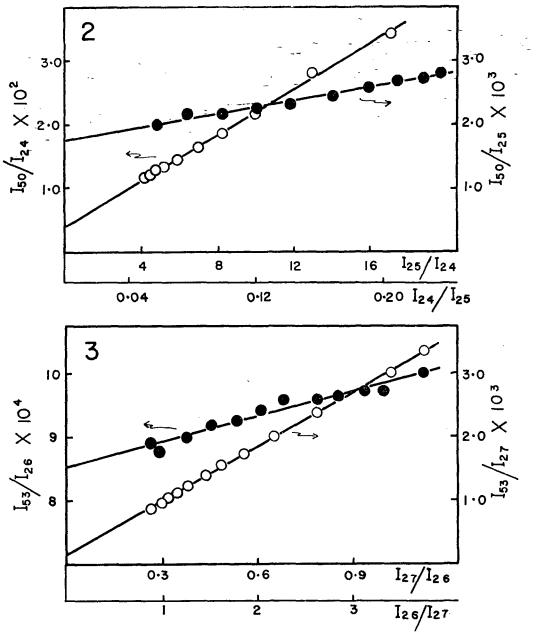

FIG. 2. Dependence of I_{50} ($C_4H_2^+$) on I_{24} (C_2^+) and I_{25} (C_2H^+). Ethylene [M] = 7.00×10^{12} molecules/cc.
FIG. 3. Dependence of I_{53} ($C_4H_5^+$) on I_{26} ($C_2H_2^+$) and I_{27} ($C_2H_3^+$). Ethylene [M] = 6.80×10^{12} molecules/cc.

Can. J. Chem. Downloaded from www.nrcresearchpress.com by 210.87.254.6 on 09/05/12
For personal use only.

show the experimental results for these two ions plotted in the manner of equations [2] and [3]. The non-zero intercepts and slopes clearly show that two reactions are involved in each case. The cross sections calculated from these data are given in Table I. The concurrent charge-transfer reaction

$$C_2H_2^+ + C_2H_4 \rightarrow C_2H_4^+ + C_2H_2,$$

reported by Field (7), cannot explain the variation of I_{53}/I_{26} since at constant source pressure this reaction would cause only a constant, if small, diminution in the measured $C_2H_2^+$ ion current.

Although both reactions 1 and 2 leading to the $C_3H_3^+$ ion are thermochemically permitted, no evidence could be found for the occurrence of reaction 2. An estimate of the sensitivity of the method suggests that if reaction 2 does occur the cross section must be less than 2×10^{-16} cm^2/molecule. The $C_4H_3^+$ ion can be formed by both reactions 6 and 7. No evidence could be found for reaction 7 and it is estimated that the cross section for this reaction must be less than 1×10^{-16} cm^2/molecule. The $C_3H_5^+$ and $C_4H_7^+$ ions can be formed by only one exothermic reaction.

The cross section obtained at 50 ev for reaction 4 (assuming that this is the only reaction resulting in $C_4H_2^+$) is considerably larger than previously obtained. The present result is in agreement with the results at low electron energy. Considering equation [1], a plot of I_{50}/I_{24} against [M], which is the usual method for obtaining cross sections, gives a slope,

$$f_4Q_4d+f_5Q_5d\frac{I_{25}}{I_{24}},$$

rather than the simple quantity f_4Q_4d. Using $I_{25}/I_{24} = 4.1_5$, determined experimentally at 50 ev, and the individual cross sections obtained at low energy (Table I) a cross section of 142×10^{-16} cm^2/molecule is calculated for reaction 4 at 50 ev. The cross section obtained for reaction 4 at higher electron energies will obviously be strongly dependent on the ion current ratio I_{25}/I_{24}, which may explain the discrepancy between the present result and earlier results. It is interesting to note that the rate constants for the ion–molecule reactions in ethylene calculated by Field *et al.* (5) were all reasonably constant with the exception of that for reaction 4, which was unexplainably high. This is undoubtedly due to the undetected contribution from reaction 5; the cross section obtained in the present work for reaction 4 alone brings all the rate constants into line.

The agreement between the cross sections at low electron energy and the cross sections obtained at 50 or 70 ev is within experimental error for all secondary ions which are formed by one reaction only. This result provides support for the assumptions that the cross sections and the relative ion collection efficiencies do not vary with electron energy.

The results obtained for propylene are summarized in Table II. In addition to the nine secondary ions reported in Table II secondary ions at m/e = 68 ($C_5H_8^+$), 77 ($C_6H_5^+$), 79 ($C_6H_7^+$), and 81 ($C_6H_9^+$) were reported by Fuchs (6) but were not investigated in the present work because of their low intensity. The secondary ion at m/e = 52 ($C_4H_4^+$) was not reported by Fuchs. The cross sections obtained at 50 ev are compared in Table II with the results obtained by Fuchs (6) at 70 ev and ~13 v/cm field strength. The cross sections obtained in the present work are somewhat higher, as would be expected. The reactions given in Table II do not comprise a comprehensive listing of possible exothermic reactions but only those for which positive evidence was found for their occurrence.

Four of the secondary ions, $C_4H_3^+$, $C_4H_4^+$, $C_4H_7^+$, and $C_6H_5^+$, were found by low-energy studies to be formed by two ion–molecule reactions each. The experimental results

Can. J. Chem. Downloaded from www.nrcresearchpress.com by 210.87.254.6 on 09/05/12
For personal use only.

TABLE II

Ion–molecule reactions in propylene

Reaction No.	Secondary ion (m/e)	Reaction	$-\Delta H$ reaction (kcal/mole)	$fQ\times10^{16}$ (cm²/molecule) Low energy	High energy This work	High energy Ref. 6
11	51	$C_3H^+ + C_3H_6 \rightarrow C_4H_3^+ + C_2H_4$	105	46.4	58.3	28
12	51	$C_3H_2^+ + C_3H_6 \rightarrow C_4H_3^+ + C_2H_5$	8	2.6		
13	52	$C_3H^+ + C_3H_6 \rightarrow C_4H_4^+ + C_2H_3$	61	6.4	24.3	
14	52	$C_3H_2^+ + C_3H_6 \rightarrow C_4H_4^+ + C_2H_4$	30	18.2		
15	53	$C_3H_3^+ + C_3H_6 \rightarrow C_4H_5^+ + C_2H_4$	15	15.5	18.6	11
16	54	$C_3H_4^+ + C_3H_6 \rightarrow C_4H_6^+ + C_2H_4$	34	16.3	16.5	
17	55	$C_3H_5^+ + C_3H_6 \rightarrow C_4H_7^+ + C_2H_4$	19	32.2		
18	55	$C_3H_6^+ + C_3H_6 \rightarrow C_4H_7^+ + C_2H_5$	28	9.9	59.3	44
19	56	$C_3H_6^+ + C_3H_6 \rightarrow C_4H_8^+ + C_2H_4$	35	13.8	14.0	11
20	65	$C_2H_2^+ + C_3H_6 \rightarrow C_5H_5^+ + H_2 + H$	44	34.1	89.3	51
21	65	$C_3H_2^+ + C_3H_6 \rightarrow C_5H_5^+ + CH_3$	107	30.6		
22	67	$C_3H_5^+ + C_3H_6 \rightarrow C_5H_7^+ + CH_4$	36	6.6	5.7	4
23	69	$C_3H_6^+ + C_3H_6 \rightarrow C_5H_9^+ + CH_3$	−4 to 7	11	8	6

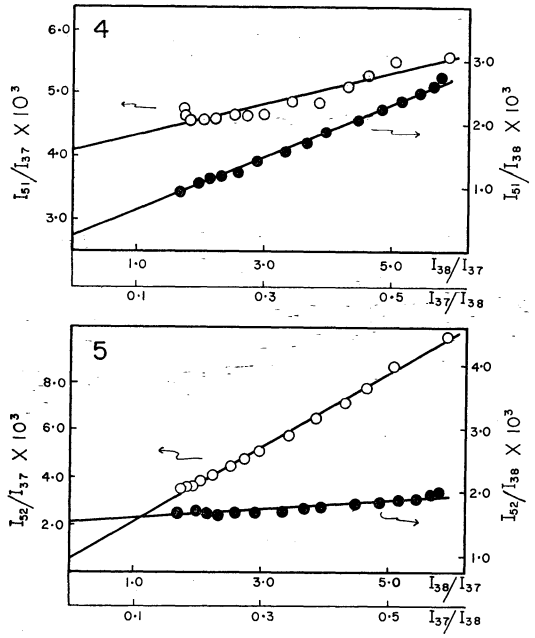

FIG. 4. Dependence of I_{51} ($C_4H_3^+$) on I_{37} (C_3H^+) and I_{38} ($C_3H_2^+$). Propylene [M] = 6.86×10^{12} molecules/cc.

FIG. 5. Dependence of I_{52} ($C_4H_4^+$) on I_{37} (C_3H^+) and I_{38} ($C_3H_2^+$). Propylene [M] = 6.86×10^{12} molecules/cc.

for these cases are shown in Figs. 4–7. The cross sections calculated from these figures are reported in Table II. Reactions 11 and 12 resulting in $C_4H_3^+$ are the same as found for cyclopropane (2); however, the cross section for reaction 12 is lower by a factor of 10 compared to cyclopropane. This is consistent with the considerably lower abundance of $C_4H_3^+$ in the high-pressure mass spectrum of propylene. The formation of $C_4H_4^+$ by

Can. J. Chem. Downloaded from www.nrcresearchpress.com by 210.87.254.6 on 09/05/12
For personal use only.

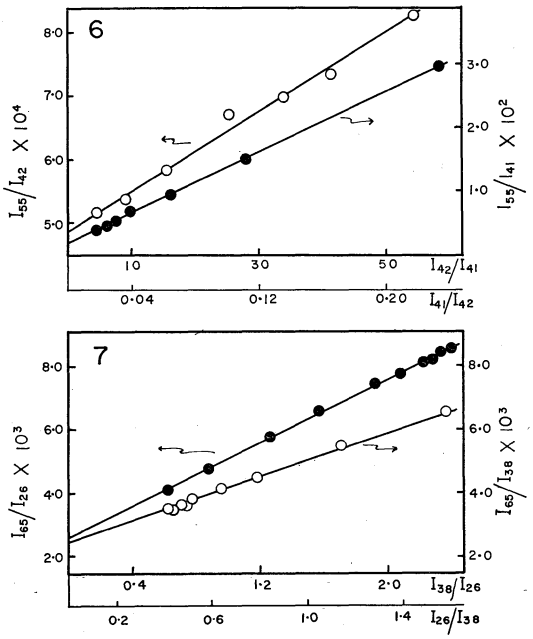

FIG. 6. Dependence of I_{55} ($C_4H_7^+$) on I_{42} ($C_3H_6^+$) and I_{41} ($C_3H_5^+$). Propylene [M] = 3.74×10^{12} molecules/cc.

FIG. 7. Dependence of I_{65} ($C_5H_5^+$) on I_{26} ($C_2H_2^+$) and I_{38} ($C_3H_2^+$). Propylene [M] = 6.12×10^{12} molecules/cc.

reaction 13 is in contrast to the results for cyclopropane (2), where the reaction

$$C_2H_2^+ + C_3H_6 \rightarrow C_4H_4^+ + CH_4$$

was found in addition to reaction 14. The results for propylene were not consistent with reaction of $C_2H_2^+$. Reactions 17 and 18 to form $C_4H_7^+$ are identical with the assignments made for cyclopropane, although the cross sections are considerably higher for propylene.

For the $C_4H_5^+$, $C_4H_6^+$, $C_4H_8^+$, $C_5H_7^+$, and $C_5H_9^+$ ions only one reaction leading to each ion was found. Reaction 16 leading to the $C_4H_6^+$ ion is in contrast to the reaction

$$C_3H_6^+ + C_3H_6 \rightarrow C_4H_6^+ + C_2H_6$$

proposed by Fuchs (6). No evidence could be found for this reaction in the present work. Reaction 16 has also been postulated for cyclopropane (2, 10). For these five reactions the cross sections obtained at low electron energies are in quite satisfactory agreement with the results obtained at higher energies. This agreement suggests again that the reaction cross sections and the relative collection efficiencies are not varying with electron energy and further that any contributions from undetected reactions must be quite small.

The 50 ev cross sections reported in Table II for reactions 11, 13, 18, and 20 are based on the erroneous assumption that these are the only reactions leading to the respective secondary ions. As discussed above for the $C_4H_2^+$ ion from ethylene these composite cross sections can be calculated from the individual cross sections obtained at low energy and the observed ion current ratios at 50 ev. The calculated and experimental cross sections are compared in Table III. In each case satisfactory agreement is obtained between the calculated and experimental results. This agreement again suggests that contributions from undetected reactions are small.

Can. J. Chem. Downloaded from www.nrcresearchpress.com by 210.87.254.6 on 09/05/12
For personal use only.

TABLE III

Comparison of calculated and experimental composite cross sections

Reaction No.	$fQ\times10^{16}$	
	Calculated	Experimental
11	51.0	58.3
13	22.1	24.3
18	55.1	59.3
20	100	89.3

ACKNOWLEDGMENTS

The author is indebted to the National Research Council for financial support and to Mr. J. M. S. Tait for assistance with some of the preliminary work on propylene.

REFERENCES

1. L. Pobo and D. Hutchinson. Paper presented at A.S.T.M. Committee E-14 meeting, Chicago. June, 1961.
2. A. G. Harrison and J. M. S. Tait. Can. J. Chem. **40**, 1986 (1962).
3. D. O. Schissler and D. P. Stevenson. J. Chem. Phys. **24**, 926 (1956).
4. D. P. Stevenson. J. Phys. Chem. **61**, 1453 (1957).
5. F. H. Field, J. L. Franklin, and F. W. Lampe. J. Am. Chem. Soc. **79**, 2419 (1957).
6. R. Fuchs. Z. Naturforsch. **16a**, 1026 (1961).
7. F. H. Field. J. Am. Chem. Soc. **83**, 1523 (1961).
8. D. P. Stevenson and D. O. Schissler. J. Chem. Phys. **29**, 282 (1958).
9. J. H. Beynon, G. R. Lester, R. A. Saunders, and A. E. Williams. Trans. Faraday Soc. **57**, 1259 (1961).
10. R. F. Pottie, A. J. Lorquet, and W. H. Hamill. J. Am. Chem. Soc. **84**, 529 (1962).

Can. J. Chem. Downloaded from www.nrcresearchpress.com by 210.87.254.6 on 09/05/12
For personal use only.

THERMOGRAVIMETRY OF THE DEHYDRATION OF $Mg(OH)_2$[1]

R. C. TURNER, I. HOFFMAN, AND D. CHEN
Research Branch, Canada Department of Agriculture, Ottawa, Ontario
Received August 3, 1962

ABSTRACT

The DTG curves for the dehydration of a number of preparations of $Mg(OH)_2$ were determined. Equations necessary to calculate energies of activation and rate constants from these curves were derived on the basis of a two-thirds-order process for dehydration. It was found that the energy of activation was about 5 kcal greater for naturally occurring than for precipitated $Mg(OH)_2$. This was interpreted to mean that there was a difference in the energy levels of the two preparations, and therefore a difference in their apparent solubility products. Differences obtained in the DTG curves for four different preparations of $Mg(OH)_2$ indicated the probability of a series of energy levels for $Mg(OH)_2$.

Can. J. Chem. Downloaded from www.nrcresearchpress.com by 210.87.254.40 on 09/05/12
For personal use only.

An investigation (1) of reactions responsible for certain characteristics of potentiometric titration curves of clays, saturated with Al^{3+} and then titrated with MgO, led to the suggestion that $Mg(OH)_2$ was precipitated at a pH below that expected if the solubility product were near $10^{-11.0}$ (2). Although more recent work (3) indicated that precipitation of a double hydroxide may account for the phenomenon, the possibility that $Mg(OH)_2$ can be formed with a solubility product considerably less than $10^{-11.0}$ was supported by the work of Quartaroli and Belofoiri (4). They observed that naturally occurring $Mg(OH)_2$ (brucite) had the same solubility as precipitated $Mg(OH)_2$, when it was first suspended in an aqueous solution. After the suspension was allowed to settle and the supernatant liquid replaced with fresh solution, however, the apparent solubility product decreased, and, with successive replacements of the supernate, it continued to decrease to a minimum significantly less than $10^{-11.0}$. When this procedure was tried in this laboratory, it was found that after a number of replacements of the supernate in a CO_2-free system the apparent solubility product of a sample of brucite was about $10^{-13.5}$.

Although the results in this laboratory agreed in general with the work of Quarteroli and Belofoiri, it was realized that with successive replacements of the supernatant liquid the smallest, more rapidly dissolved crystals might have been selectively removed, leaving only larger crystals requiring more than the time allowed in our experiment (8 days) to come to equilibrium with the solution. Consequently, other properties of the precipitated and naturally occurring $Mg(OH)_2$ were studied. This paper deals with the thermogravimetry of the two materials.

THEORETICAL

It was found that the kinetic treatment for a first-order reaction, which applied to the thermogravimetry of the decomposition of soil organic matter (5), could not be used for the dehydration of $Mg(OH)_2$. It was necessary to derive equations for the two-thirds-order process, which was the order reported by Gregg and Razouk (6).

The kinetics of a first-order reaction applied to thermogravimetry was developed from the basic equation

$$[1] \qquad -\frac{dw}{dT} = \frac{k_0}{b} e^{-A/T} w,$$

[1]*Contribution No. 65 and 34 from Soil Research Institute and Analytical Chemistry Research Service, respectively.*

where w is the weight remaining to be lost at temperature T, k_0 ($k_0 = ke^{A/T}$) is the frequency factor, b is the constant rate of heating, and A is E/R, where E and R are the energy of activation and gas constant respectively. The corresponding equation for a two-thirds reaction is

$$-\frac{dw}{dT} = \frac{k_0}{b} e^{-A/T} w^{2/3}. \qquad [2]$$

After integration, equation [2] can be put in the form

$$F = \left[-\epsilon \int_0^p e^{-1/p} dp + 1 \right]^3, \qquad [3]$$

where w/w_0, $(k_0 A)/(3bw_0^{1/3})$, and T/A are given the symbols F, ϵ, and p respectively. Differentiation of equation [3] gives

$$\frac{dF}{dp} = -3\epsilon e^{-1/p} \left[-\epsilon \int_0^p e^{-1/p} dp + 1 \right]^2. \qquad [4]$$

Using the expansion of Schlömilch (7) for $-E_i(-x)$, it can be shown that

$$\int_0^p e^{-1/p} dp = pe^{-1/p} \left(\frac{p}{(p+1)} - \frac{p^2}{(p+1)(p+2)} + \frac{2p^3}{(p+1)\ldots(p+3)} - \frac{4p^4}{(p+1)\ldots(p+4)} + \frac{14p^5}{(p+1)\ldots(p+5)} - \ldots \right). \qquad [5]$$

The expression enclosed in parentheses in equation [5] is an infinite series, but when p is small, all terms after a given one can be ignored without affecting the result materially. With p less than 0.04 (which applies in this work) ignoring all but the first two terms has no effect on the first three significant figures of the result and introduces an error less than 0.06%. With this approximation equation [5] becomes

$$\int_0^p e^{-1/p} dp = e^{-1/p} \frac{2p^2}{(p+1)(p+2)} \qquad [6]$$

and equations [3] and [4] can be written, respectively,

$$F = \left[-\epsilon e^{-1/p} \frac{2p^2}{(p+1)(p+2)} + 1 \right]^3 \qquad [7]$$

and

$$\frac{dF}{dp} = -3\epsilon e^{-1/p} \left[-\epsilon e^{-1/p} \frac{2p^2}{(p+1)(p+2)} + 1 \right]^2. \qquad [8]$$

It can be shown by a treatment similar to that used for a first-order reaction (5) that

$$\epsilon = \frac{e^{1/p_m} (p_m+1)(p_m+2)}{2p_m^2[(p_m+1)(p_m+2)+1]}, \qquad [9]$$

where the subscript m denotes maximum rate of reaction.

From equations [7], [8], and [9] it is possible to calculate dw/dT, w/w_0, w, and k_0 if T_m and A are known. T_m can usually be measured from experimental DTG curves but some other means of calculating A from experimental data is necessary. It was found graphically (5) that, for a first-order reaction, a fairly simple relation existed between A, T_m, and

Can. J. Chem. Downloaded from www.nrcresearchpress.com by 210.87.254.40 on 09/05/12
For personal use only.

δT,[2] where δT is the temperature required to reduce the rate of decomposition to half its value on either side of the maximum rate. For the two-thirds-order reaction the corresponding relation was

$$[10] \qquad \log A = \log T_m - \log \frac{\delta T}{T_m} + 0.2998 - \left[\frac{T_m}{A}\right]^{1.35}.$$

Table I shows the properties of equation [4] and therefore of equation [8] which were required to obtain equation [10] or are needed in the application of the equations to experimental results. The first three terms of the infinite series in equation [5] were used to calculate p_1 and p_2 to ensure sufficient significant figures.

TABLE I

Some characteristics of the curves represented by equation [8]

p_m	p_1*	p_2†	p_2-p_1	$\frac{\delta p}{p_m}$	$\frac{p_m-p_1}{p_2-p_m}=\frac{T_m-T_1}{T_2-T_m}$
0.01	0.009872	0.010070	0.000198	0.0198	1.83
0.02	0.019490	0.020274	0.000784	0.0392	1.86
0.03	0.028870	0.030615	0.001745	0.0582	1.84
0.04	0.03802	0.04109	0.00307	0.0768	1.82

*p_1 is the value of p at one half the maximum rate before the maximum is reached.
†p_2 is the value of p at one half the maximum rate after the maximum is passed.

EXPERIMENTAL

The brucite used in the experiments was a high-quality sample available in these laboratories. The only impurities that were detected in it were Mn (less than 0.02%) and Fe (0.05%). It was ground to pass a $\frac{1}{2}$-mm sieve. The precipitated $Mg(OH)_2$ was produced by adding NaOH to a solution of $MgCl_2$. The solid was separated from the solution, washed free from chlorides, and air dried.

The apparatus used was a Stanton Thermo-Recording Balance of 0.1 mg sensitivity, modified by the installation of a current chopper (purchased from the manufacturer) and the introduction of a rheostat to control the current entering the furnace. A linear rate of 5.4° C per minute was maintained over the entire temperature range by following a program of previously determined settings. Samples (100.0 mg) were weighed in platinum crucibles on an ordinary analytical balance. Automatic arresting of the thermobalance at 5-minute intervals recorded the time scale on the weight curve. The rate of weight change per 2.5-minute interval as obtained by simple difference was plotted vs. temperature to give differential thermogravimetric (DTG) curves. Prolonged heating at constant temperature was effected without the use of the current chopper by manual operation of the main furnace switch over short intervals.

RESULTS

The DTG curves from 600 to 770° K for the precipitated and naturally occurring $Mg(OH)_2$ (Fig. 1) indicated some loss in weight with both materials at all temperatures in this range. Near 373° K, the precipitated material also lost about 0.5 mg, presumably free or adsorbed H_2O. The natural material did not lose any weight until 600° K was reached. Both samples continued to lose weight until the temperature reached nearly 1273° K (6, 8). The maximum rate of weight loss occurred at 689° for the precipitated and at 745° K for the natural material.

The value for δT measured from the DTG curve for the precipitated material was 36°. When this value along with 689° for T_m were substituted into equation [10], A was found to be 25,860. With this value for A, dF/dp was calculated by means of equations [9] and [8] for a number of temperatures, including that at which the experimental was at a maximum. Since dw/dT is equal to $(w_0^{1/3}/A)(dF/dp)$, it was possible to calculate w_0 at the maximum rate of dehydration. With this value for w_0, dw/dT was calculated from

[2]*This was given the symbol ΔT in the previous publication (5).*

Can. J. Chem. Downloaded from www.nrcresearchpress.com by 210.87.254.40 on 09/05/12
For personal use only.

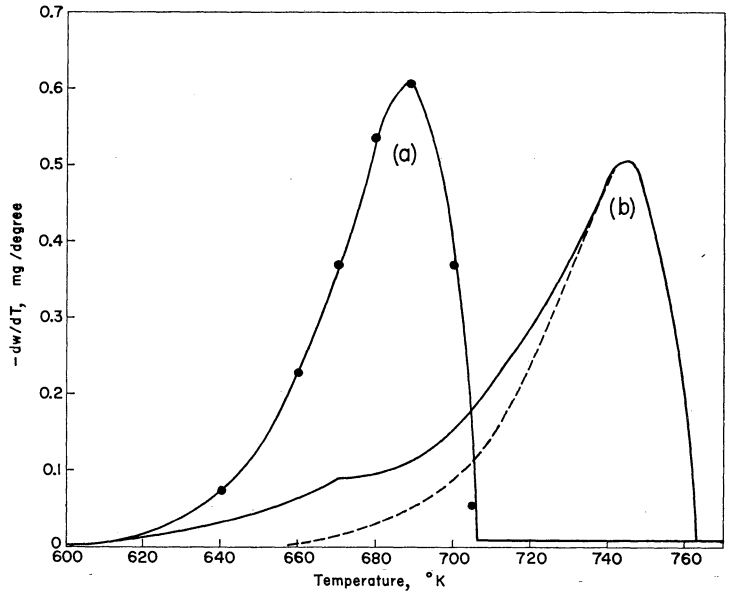

FIG. 1. DTG curves for (*a*) precipitated $Mg(OH)_2$ and (*b*) naturally occurring $Mg(OH)_2$.

the values for dF/dp for the other temperatures. These values, shown as filled circles in Fig. 1, agreed well with the experimental curve.

For the brucite, a value for δT was calculated by multiplying the fraction to the right of the maximum rate of dehydration by 1.85 (see Table I) to find the theoretical value to the left of the maximum; the sum of the two fractions was 38°. This value with 745° K for T_m gave a value of 28,660 for A when substituted into equation [10]. Values for dw/dT were then calculated as before and the theoretical DTG curve was constructed (broken line in Fig. 1). Comparison of the calculated with the experimental curve showed that there was considerable loss in weight between 600 and 730° K not accountable by the main reaction.

From the definitions in the theoretical part, E, k_0, and k for a number of temperatures were calculated from the theoretical DTG curves in Fig. 1. These results (Table II)

TABLE II

Summary of values calculated from the theoretical DTG curves

Material	E (kcal)	k_0 ($mg^{1/3}min^{-1}$)	Temperature (°K): 653	689	728	745
			k ($mg^{1/3}min^{-1}$)			
Precipitated	51.4	$10^{16.2378}$	0.11	0.87	6.46	14.6
Brucite	57.0	$10^{16.4531}$	0.0025	0.024	0.23	0.56

showed that the energy of activation for dehydration was 5.6 kcal higher for the natural than for the precipitated material. The values of k_0 for the two materials were very similar. The values for k, however, were much greater at a given temperature for the precipitated material than for brucite because of the difference in activation energy.

Can. J. Chem. Downloaded from www.nrcresearchpress.com by 210.87.254.40 on 09/05/12
For personal use only.

A number of independent experiments were made to check the validity of the kinetic treatment. Since the kinetic treatment was based on the assumption that dehydration of $Mg(OH)_2$ proceeds by a two-thirds-order process, the rate of the reaction was followed at constant temperature. The temperature of the precipitated material was raised from room temperature at the rate of 5.4° per minute until it reached 653° K. It was then held constant and the loss in weight followed as a function of time with the automatic recorder, until the rate of loss in weight was too small to measure. A plot of $(w/w_0)^{1/3}$, with w_0 equal to the total loss in weight during the isothermal treatment, against time was made. Since the two-thirds-order reaction can be represented by

$$[11] \qquad \left[\frac{w}{w_0}\right]^{1/3} = -\frac{kt}{3w_0^{1/3}} + 1,$$

the above plot should be a straight line with slope equal to $-(k/3w_0^{1/3})$. Figure 2 shows that the plot for the precipitated material (curve *a*) followed a straight line until well

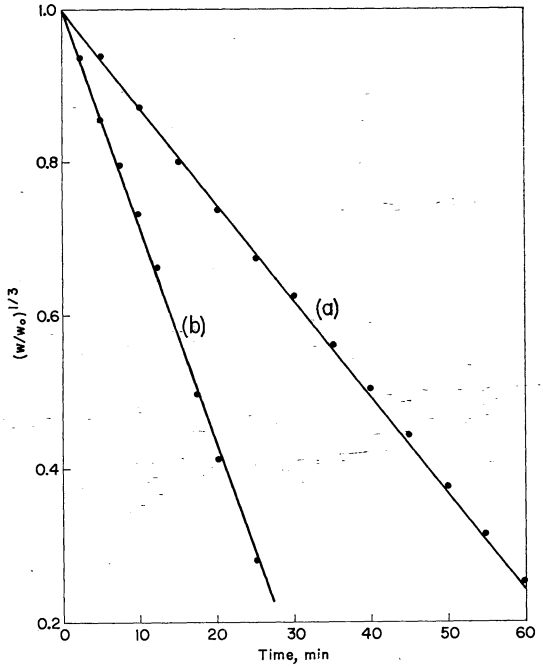

FIG. 2. Rates of dehydration of $Mg(OH)_2$: (*a*) precipitated $Mg(OH)_2$ at 653° K, (*b*) naturally occurring $Mg(OH)_2$ at 728° K.

over 95% of the reaction was completed. From the slope of the line, k was found to be 0.11 $mg^{1/3}min^{-1}$, the same as that calculated from the theoretical DTG curve (Table II).

The same procedure was followed with brucite except that the temperature was raised to 648° K and held at this temperature until the rate of weight loss was negligible, then raised to 668°, and again held constant until the rate of weight loss was very small. It was then raised to 728° K and the progress of the reaction followed, as before, at this temperature. The plot was also a straight line (curve *b*, Fig. 2); from the slope of the line, k was equal to 0.22 $mg^{1/3}min^{-1}$, which is in good agreement with the value in Table II.

Can. J. Chem. Downloaded from www.nrcresearchpress.com by 210.87.254.40 on 09/05/12
For personal use only.

There does not seem to be any doubt about the order of the reaction or the magnitude of the rate constants calculated from the theoretical DTG curves.

As pointed out above, it appeared from the theoretical and experimental DTG curves for brucite (Fig. 1) that much of the loss in weight between 600 and 730° K could not be ascribed to the main reaction. This was supported by results from the experiment described in the last paragraph concerning the rate of dehydration of brucite at constant temperature. When the temperature was held at 648° a considerable decrease in rate of weight loss with time, even more pronounced at 668° K, was observed (Fig. 3). Dehydration of an homogeneous material would have proceeded at rates essentially constant at

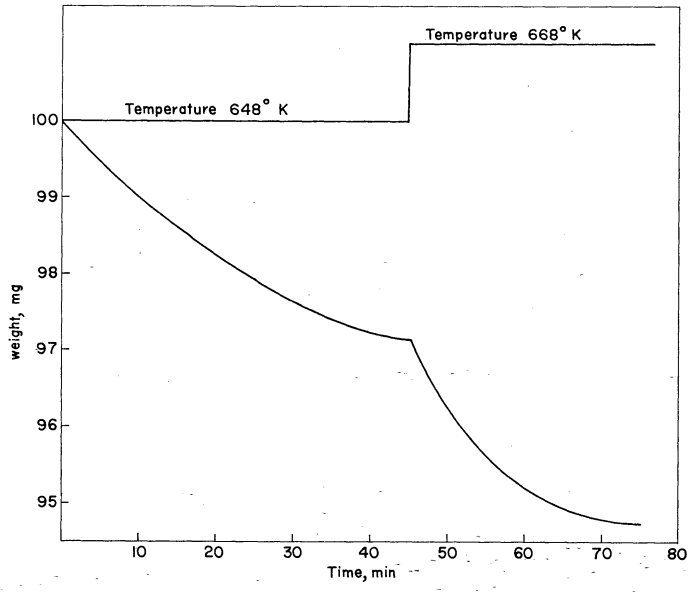

FIG. 3. Weight loss as a function of time at two temperatures for naturally occurring $Mg(OH)_2$.

each of these temperatures, since the difference between $w^{2/3}$ at the beginning and end of each interval was very small.

As a check on the validity of equation [8] for calculating A and thus the activation energy, an alternate method was used for its calculation from the experimental DTG curve for the precipitated material. Values of $(\log \Delta w/\Delta T)/w^{2/3}$, with $\Delta w/\Delta T$ calculated for each 2.5-minute interval and w the average weight remaining to be lost in the corresponding intervals, were plotted against $1/T$, with T the mean temperature in each interval. The plot, which should be a straight line in accordance with equation [2], is shown in Fig. 4. The slope of the line, equal to $-A/3.026$, was $-10{,}900$, which makes A equal to 2.51×10^4 and E about 50 kcal, a value in good agreement with the one given in Table II.

From the DTG curves in Fig. 1, it appeared that there were at least two forms of $Mg(OH)_2$. Further information on this point was gained by studying the thermogravimetry of $Mg(OH)_2$ prepared by two other methods. One preparation was obtained by reacting Mg metal with hot H_2O and the other was prepared by utilizing a KOH melt according to directions given by Mellor (9). The DTG curves for all four preparations are shown in Fig. 5. The Mg plus H_2O and Mellor preparations each showed two maximum

Can. J. Chem. Downloaded from www.nrcresearchpress.com by 210.87.254.40 on 09/05/12
For personal use only.

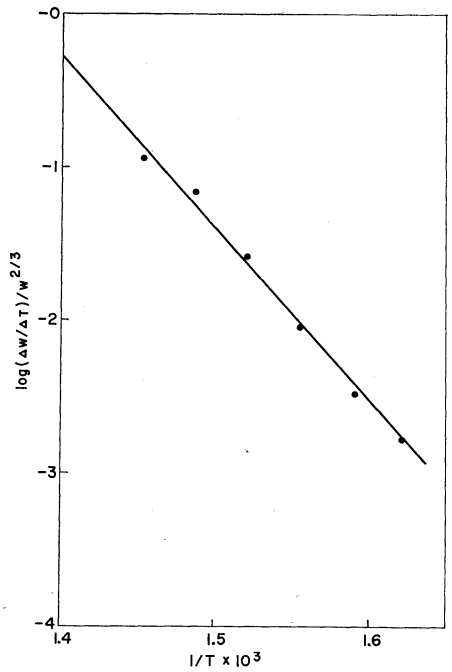

FIG. 4. Energy of activation for dehydration of precipitated $Mg(OH)_2$.

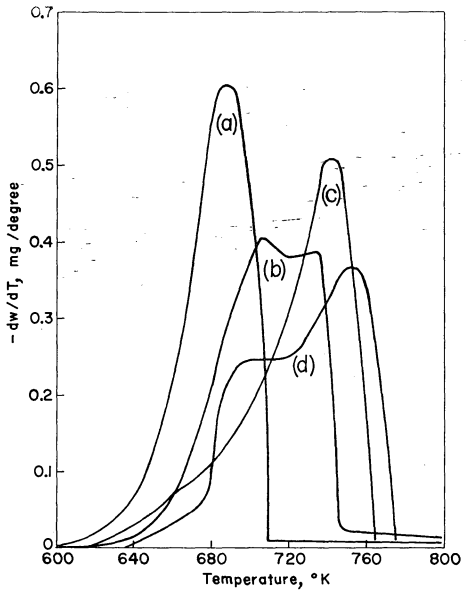

FIG. 5. DTG curves for a number of preparations of $Mg(OH)_2$: (*a*) precipitated, (*b*) Mg reacted with H_2O, (*c*) naturally occurring, (*d*) Mellor preparation.

rates of dehydration but none of these, with the possible exception of the second for the Mellor preparation, corresponded with those for the precipitated or natural $Mg(OH)_2$. The higher temperature for the maximum rate for the Mellor preparation was not greatly different from that for brucite.

Can. J. Chem. Downloaded from www.nrcresearchpress.com by 210.87.254.40 on 09/05/12
For personal use only.

Can. J. Chem. Downloaded from www.nrcresearchpress.com by 210.87.254.40 on 09/05/12
For personal use only.

DISCUSSION

Since the results from the isothermal experiments agreed with those calculated from the equations derived in the theoretical section for DTG curves, interpretations based on this theoretical treatment were considered justified. For instance, the theoretical treatment shows a difference of about 5 kcal between the energies of activation for dehydration of precipitated and naturally occurring $Mg(OH)_2$. Admittedly, this is a small difference when considered in the light of the magnitude of the error usually involved in measuring activation energies at these relatively high temperatures. The fact, however, that the rate constants determined at constant temperature for the two materials agreed with those calculated from the DTG curves, calculations that depended almost entirely on this difference in activation energies for the differences in rate constants (Table II), is rather convincing evidence that there was a difference of the order of 5 kcal.

The total loss of H_2O per gram was the same for the two preparations and they both had the characteristic brucite X-ray diffraction pattern. Consequently, the difference in activation energy for dehydration was attributed to a difference in energy levels of materials with the same crystal form, rather than to two different ones. This difference could be caused by differences in surface energy and crystal lattice defects (10). With the reasonable assumption that the activated complex for dehydration was the same for the two preparations, it can be concluded that the difference in energy levels was about 5 kcal.

Apparent solubility products of $10^{-11.0}$ for the precipitated and $10^{-13.5}$ for naturally occurring $Mg(OH)_2$ were mentioned in the introduction. Since these are equilibrium constants for dissolving $Mg(OH)_2$ at 25° C (assuming that activities of the solids can be put equal to unity), the difference indicates a change in free energy of about 3.4 kcal in going from one to the other. This difference in free energy is in the same order of magnitude as the 5 kcal difference in energy levels mentioned above. The difference in energy levels also includes any difference in entropy between the two materials, so that the two differences, 5 and 3.4 kcal, are not strictly comparable. The fact that they are of the same order of magnitude, however, supports the conclusion of Quartaroli and Belofoiri (4) that the naturally occurring $Mg(OH)_2$ has a solubility product lower than $10^{-11.0}$, which is generally found for the precipitated material (2).

Furthermore, the DTG curves in Fig. 1 indicate why the natural material showed the same solubility as the precipitated material when it was equilibrated with water the first time. Presumably it contained some of the more soluble material, i.e. material that was dehydrated at the same temperature as precipitated $Mg(OH)_2$. When this material had been dissolved and removed, the lower solubility became apparent.

The DTG curves for the four different preparations of $Mg(OH)_2$ (Fig. 5) indicate that there is a series of energy levels and the possibility that different levels can be found for still other preparations cannot be excluded. A series of apparent solubility products would, therefore, be expected. According to the DTG curves, however, all preparations should show about the same solubility when equilibrated with H_2O for the first time, since all showed some decomposition at the temperature of maximum rate of decomposition of precipitated $Mg(OH)_2$.

REFERENCES

1. R. C. Turner and W. E. Nichol. Soil Sci. **94**, 58 (1962).
2. K. W. Sykes. Stability constants. Part 11. Inorganic ligands. Special Publication No. 7 of the Chemical Society, London, England. Metcalf and Cooper Ltd., London. 1957.
3. R. C. Turner and J. E. Brydon. Science, **136**, 1652 (1962).
4. A. Quartaroli and O. Belofiori. Ann. Chim. Applicata, **33**, 56 (1941).
5. R. C. Turner and M. Schnitzer. Soil Sci. **93**, 225 (1962).

6. S. J. GREGG and R. I. RAZOUK. J. Chem. Soc. S36 (1949).
7. O. SCHLÖMILCH. Vorlesungen über hoheren Analysis. 2nd ed. Braunschweig. 1874. p. 226. *Taken from* D. W. Van Krevelen, C. Van Hurden, and F. J. Huntjens. Fuel, **30**, 253 (1951).
8. M. P. JOLIBOIS and M. BERGES. Compt. Rend. **224**, 78 (1947).
9. J. W. MELLOR. A comprehensive treatise on inorganic and theoretical chemistry. Vol. IV. Longmans and Co., 39 Palermaster Row, London, England. 1923. p. 290.
10. C. N. R. RAO, S. R. YOGANARASIMHAN, and M. P. LEWIS. Can. J. Chem. **38**, 2359 (1960).

Can. J. Chem. Downloaded from www.nrcresearchpress.com by 210.87.254.40 on 09/05/12
For personal use only.

HINDERED DIPHENYL ETHERS RELATED TO THE BISBENZYLISOQUINOLINE ALKALOIDS[1]

MARJORIE ALLEN[2] AND R. Y. MOIR
Department of Chemistry, Queen's University, Kingston, Ontario
Received in original form August 31, 1961; as revised August 28, 1962

ABSTRACT

Sixteen steps from vanillin led to syntheses of (*a*) dimethyl 3-(4′-carbomethoxyphenoxy)-4,5-dimethoxyphthalate (I*c*), a known degradation product of isochondrodendrine, and (*b*) the more hindered dimethyl 3-(4′-carbomethoxy-2′-methoxyphenoxy)-4,5-dimethoxyphthalate (I*a*), which has not been derived from any alkaloid, though the usual concepts of biosynthesis do not rule out the occurrence of alkaloids which could lead to it. Diphenyl ethers related to I*a* would be expected to show the effects of steric hindrance, but even with the most hindered member of the group, 7-(4′-carboxy-2′-iodophenoxy)metameconine (VA*e*), no evidence for an appreciable half-life of rotational isomers could be obtained. Attempts to make diphenyl ethers through the condensation of phenols with dicyclohexylcarbodiimide led to other products.

Diphenyl ethers of type I are of interest both because of their relationship to the bisbenzylisoquinoline alkaloids, and because of their place in the study of steric effects in diphenyl ethers. For example, the ester I*a* would be expected to arise from the hypothetical alkaloid II*a* in the same reactions that actually gave I*c* as the degradation product of the dimethyl ether of isochondrodendrine (II*b*) (1). Indeed, our whole study of diphenyl ethers arose from the efforts of Dr. J. A. McRae and his students to form the ester I*a*, the same biosynthetic argument[3] that had succeeded for the structure of isochondrodendrine leading them to suppose II*a* to be a probable structure for the alkaloid cularine (2, 3). The synthesis of I*a* proved unexpectedly difficult, and the challenge presented by the difficulty maintained our interest even when it became apparent many years ago that I*a* was not in fact closely related to cularine (III) (3).

The early efforts of Dr. McRae and his students to synthesize I*a* had several practical results. Prolonged attempts to use the Ullmann reaction directly led to the independent discovery of the transmethylation side reaction (5–7). Attempts to use the phthalide group as a guarded source of carboxyl groups led to two lines of attack continued in the present work: a study of the place of steric hindrance in the synthesis of diphenyl ethers (5, 9, 10, 13), and an extensive development of the chemistry of metameconine (IV*a*) (5, 8–12). Oxidation of the metameconines yielded phthalic acids. One of these (9) was related to pellotine (14) and to capaurine (15, 16), and another (11), an essential link in determining the structure of the bisbenzylisoquinoline alkaloids bebeerine and tubocurarine (17, 18), was synthesized by methods which added greatly to the security of its proof of structure.

[1]*Most of the material is taken from a thesis written by Mrs. J. R. Allen as part of the requirements for the degree of Doctor of Philosophy, Queen's University, May, 1961.*

[2]*Holder of a Scholarship from the National Research Council of Canada, 1960–61.*

[3]*To exclude structure II*a*, the argument based on accepted biosynthetic pathways must be supplemented by the observation that with one or two exceptions no bisbenzylisoquinoline alkaloid is known which bears, on a benzyl moiety, a methoxyl or hydroxyl meta to the methylene group (4). Groups so situated are a commonplace in the benzylisoquinoline alkaloids, and it is interesting that the extra meta groups in the known exceptions are at positions involving little steric interference about the diphenyl ether linkage.*

Can. J. Chem. Downloaded from www.nrcresearchpress.com by 210.87.254.42 on 09/05/12
For personal use only.

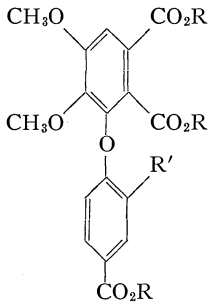

Ia: R = Me; R′ = OMe
Ib: R = H; R′ = H
Ic: R = Me; R′ = H
Id: R = H; R′ = OMe

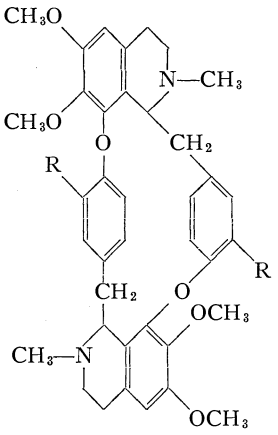

IIa: R = OMe
IIb: R = H

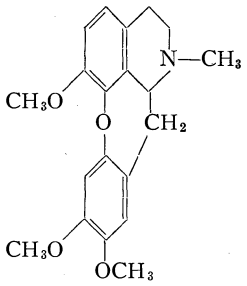

III

Synthesis of Ia

Success was made possible by the application of a method of synthesis discovered by Hems and his co-workers (19). Many years ago we took the decisive step for the preparation of I*a* in using the Hems synthesis to convert 7-hydroxymetameconine (IV*c*) into the diphenyl ether VA*a*, in which all the groups were correctly placed (9). The principal difficulty in completing the work lay in the (indirect) replacement of the nitro group of VB*a* by the methoxyl group of VA*d*. Once this was accomplished, the ester I*a* was fairly easily obtained by oxidation and methylation of the intermediate VA*d*.

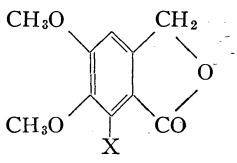

IVa: X = H
IVb: X = I
IVc: X = OH

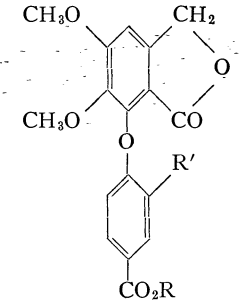

V

Substituent code

a: R′ = NO_2 A: R = H
b: R′ = NH_2 B: R = Me
c: R′ = H
d: R′ = OMe
e: R′ = I
f: R′ = OH

Replacement of the nitro group by the methoxyl group was made especially difficult by the fact that the first step of the conversion, reduction of the nitro group of VB*a* to the amino group of VB*b*, took place in low yields only. We were therefore restricted to the trial of only three methods of converting the amino acid group to methoxyl:

Can. J. Chem. Downloaded from www.nrcresearchpress.com by 210.87.254.42 on 09/05/12
For personal use only.

(*a*) The obvious treatment of the diazotized amine with methanol led to the replacement of the diazonium group with hydrogen rather than with methoxyl. The resulting product VB*c* was itself of considerable interest since on oxidation it gave the acid I*b*; this acid and the methyl ester appeared to be identical with the compounds obtained by Faltis and Frauendorfer (1) from the dimethyl ether of isochondrodendrine (II*b*). They also synthesized the acid and the ester with the use of the Ullmann reaction, which succeeded because of the presence of only two groups ortho to the diphenyl ether linkage (1, 10).

(*b*) Attempts to proceed via the diazonium fluoborate and the acetoxy compound failed. No attempt was made to proceed via the phenol by hydrolysis of the diazonium derivative because of the uniformly negative results obtained with this reaction in the metameconine series.

(*c*) The method that finally succeeded had been previously used by us in the metameconine series (5, 9), and had also been recommended by Blair and Newbold (20). Diazotization of the amino ester VB*b*, followed by the treatment with potassium iodide and iodine over chloroform (21), gave the iodo ester VB*e*. After many trials, themselves interesting in outlining the capabilities of the Ullmann reaction in this series, the iodo group of VBe was converted to the free phenolic group of VA*f*. An easy methylation then completed the conversion of VA*f* to VA*d*, the desired methoxy acid from which I*a* was made by oxidation and methylation.

The 16 steps by which vanillin was converted to the final product I*a* included 7 reactions of substitution on the benzene ring. Five of these occurred in the synthesis of VB*a*, and were shown in our previous work to take place without rearrangement (5, 8–12). Of the two remaining substitution reactions, one (in the conversion of the amino group in VB*b* to the iodo group in VB*e*) has been used so often in synthetic and structural work that there seems no point in discussing the possibility of rearrangement in it. Some attention must be given to the possibility of rearrangement in the final substitution reaction, the Ullmann reaction in which the iodo compound VB*e* was converted to the phenolic acid VA*f*, since a restricted class of Ullmann reactions is known which involves some rearrangement. Such a possibility is no light matter, since the structures given for almost all the known bisbenzylisoquinoline alkaloids rest either on the tacit assumption of the lack of rearrangement in the Ullmann reaction (22), or upon a similar assumption in the degradation of diphenyl ethers with metals and amines, a reaction that has also been called into question (23).

However, the following considerations seem to show that the possibility of rearrangement is not of concern in the present work. The expected rearrangement reaction would occur through a benzyne intermediate, and would require (in the present series) the presence of a hydrogen atom ortho to the halogen undergoing displacement (24). In related reactions, 4-bromoveratrole reacted with ethylamine without rearrangement, though ortho protons were available (25), and the iodometameconines (e.g. IV*b*) reacted easily in Ullmann reactions with hydroxide, methoxide, or ethoxide ions, though no ortho protons were available (5, 9). A still closer experimental parallel is the rather high-temperature Ullmann reaction by which Lowenthal and Pepper (26) converted 5-bromosalicylic acid without rearrangement into 2,5-dihydroxybenzoic acid. From a wider point of view, the fact that although the rearrangement as a side reaction was discovered a long time ago (27), the known examples are confined to aryl halides bearing, at most, alkyl groups as other substituents suggests that there is a limitation to the rearranging mechanism. This conclusion is supported to some extent by the fact that no inconsis-

Can. J. Chem. Downloaded from www.nrcresearchpress.com by 210.87.254.42 on 09/05/12
For personal use only.

tencies have arisen in the widespread and uncritical use of the Ullmann reaction in structural investigation of alkaloids. Perhaps most convincing is the consideration that the rearrangement reaction belongs to the class of benzyne reactions in which an ortho proton must be removed by a base (24). Ionization of the proton would be made very difficult by the presence on the ring of a negatively charged group, and in fact no example of a benzyne reaction has ever been observed with any aryl halide bearing a negatively charged group on the ring, even when bases much stronger than aqueous sodium hydroxide have been used (24). It is shown in the experimental part that the Ullmann reaction with VB*e* was preceded by saponification of the carbomethoxy group to give the negatively charged carboxyl ion. Bottini and Roberts (23) showed that the formation of cresols from hydroxide ion and halogenated toluenes gave a much lower ratio of "rearranging" to "non-rearranging" reaction at 250° than at 350°. The rearranging reaction could scarcely be predominant at the still lower temperature (175°) of our reaction in which the charge situation was less favorable to it.

*Attempted Resolution of the Triply Ortho-substituted Diphenyl Ether VA*e

Two characteristics made 7-(2′-iodo-4′-carboxyphenoxy)metameconine (VA*e*) an attractive compound for an attempt to demonstrate rotational isomerism in the series. First, it formed a well-characterized strychnine salt. Secondly, it possessed in the iodine atom a more promising blocking group than the nitro group previously used (10); as Trotter has shown in a series of papers (28), the nitro group is rather easily twisted out of coplanarity with the ring to which it is attached.

The behavior to be expected from such a salt depends on the half-life of the rotational isomers. With a half-life of the order of minutes or less, separation into diastereoisomers becomes too difficult, but a compensating factor appears. Usually one diastereoisomer is less soluble than the other, so that at equilibrium (now quickly reached because of the short half-life) the crystals deposited from the solution consist of one diastereoisomer only, and this diastereoisomer may be obtained pure in yields much greater than the maximum of 50% possible with stable isomers. The possibility of distinguishing a resolution of this type from a simple failure to resolve again depends on the half-life of the rotational isomers in solution. With half-lives of the order of several minutes, dissolution of the crystals is followed by an easily observable mutarotation; examples are known in the diphenyl series (29). However, half-lives much less than the time required for dissolution would give mutarotations observable only by the closest attention to experimental errors.

The properties of the strychnine salt of VA*e* showed it to be a single substance; the yield in which it was obtained was too large to allow it to be regarded as one of a pair of stable diastereoisomers. Failure to resolve would then have been due either to double-salt formation or to maintenance in the crystal of free rotation about the diphenyl ether linkage; with the bulky and irregular molecule of VA*e*, both possibilities seem sufficiently unlikely to make further discussion worthwhile. No mutarotation was observed on dissolution of the salt, and as shown in the experimental part, the necessary attention to the precision of the measurements ensured that the mutarotation, if it occurred, must have had a half-life much less than the 3 minutes required for dissolution and initial observation. As a check on the work, it may be noted that both a failure to resolve, or rapid racemization, should give solutions of specific rotations appropriate to the strychnine salt of an inactive acid. Such a check was obtained with the brucine salt of the previous work (10), but the strychnine salt of VA*e* had a specific rotation very different

Can. J. Chem. Downloaded from www.nrcresearchpress.com by 210.87.254.42 on 09/05/12
For personal use only.

from that expected. This anomalous result may be compared with the wide variation of rotations recorded for strychnine salts, as noted in the experimental part.

Further progress in attempts to demonstrate rotational isomerism in this series can only be made if the techniques of X-ray crystallography and nuclear magnetic resonance spectroscopy become available to us. The effects of the ortho substitution upon the infrared and ultraviolet spectra of the ethers of this series will be reported in another paper.

An Attempted New Synthesis of Diphenyl Ethers

In accord with a suggestion of Dr. J. K. N. Jones, an attempt was made to condense phenols to diphenyl ethers by the action of dicyclohexylcarbodiimide. Highly activated phenols, such as VI, VII, and VIII, reacted readily with the reagent, but under the conditions used, the less acidic phenol salicylaldehyde did not react, nor could cross reaction with more reactive phenols be induced with it. Since there is general agreement (30) that the first step in such reactions is the formation of an isoureide, the proposed synthesis amounted to setting up a competition between external and internal nucleophilic attacks on the activated benzene ring of the isoureide: external attack by a phenol or phenoxide ion to give a diphenyl ether, and internal attack by a nitrogen atom of the isoureide to give an N-phenylurea. A similar competition occurs in the well-known reaction of carbodiimides with carboxylic acids; anhydrides are not formed if the intermediate acylisourea undergoes sufficiently rapid rearrangement to the acylurea (30). Busch, Blume, and Pungs (31) found that diphenylcarbodiimide and certain activated phenols (not those of the present work) gave rearranged triphenylureas. It was not surprising, then, that the highly activated phenols VI and VII with dicyclohexylcarbodiimide gave 1:1 addition products whose infrared spectra showed the bands expected for ester groups and for

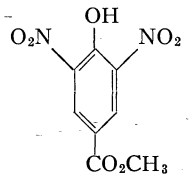

VI

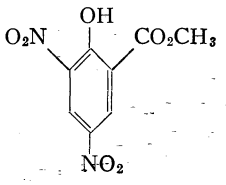

VII

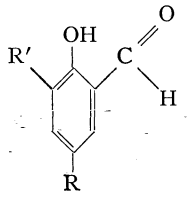

VIII*a*: R = R′ = NO_2
VIII*b*: R = NO_2; R′ = H
VIII*c*: R = H; R′ = NO_2

amides of the type AcNHR. The absence of dicyclohexylurea in the reaction products confirmed the fact that no diphenyl ether had been formed, and when the addition product from VI was heated strongly with another mole of VI, it was recovered unchanged.

The reactions of the nitrosalicylaldehydes VIII*a*, VIII*b*, and VIII*c* were of special interest since, in our hands, the Hems synthesis has failed when applied to highly substituted salicylaldehydes. In fact, dicyclohexylurea was obtained in the reaction of dicyclohexylcarbodiimide with each of VIII*a*, VIII*b*, and VIII*c*, but the condensation so indicated was not that of diphenyl ether formation. With 3,5-dinitrosalicylaldehyde (VIII*a*), the initial crude product became warm when treated with methanol; recrystallized from methanol the product was shown by analysis to correspond to a 1:1 addition product which had undergone the loss of water and the addition of methanol.

No doubt the interpretation of these results is obvious, but since analysis and spectra showed that the reaction product from 5-nitrosalicylaldehyde (VIII*b*) was quite different in character from that with dinitrosalicylaldehyde (VIII*a*), we prefer to regard our results

Can. J. Chem. Downloaded from www.nrcresearchpress.com by 210.87.254.42 on 09/05/12
For personal use only.

as merely establishing the fact that the reaction cannot be expected to offer a route to diphenyl ethers. New observations on the nitration of salicylaldehyde are reported in the experimental part.

EXPERIMENTAL

Melting points and infrared spectra were determined as previously described (11) but the wavelength values quoted are uncorrected.

7-(4′-Carbomethoxy-2′-nitrophenoxy)metameconine (VBa)

This material was made in nine steps from vanillin as previously described (9, 10).

7-(2′-Amino-4′-carbomethoxyphenoxy)metameconine (VBb)

7-(4′-Carbomethoxy-2′-nitrophenoxy)metameconine (2.0 g) was kept at 60–70° for 30 minutes with iron powder (1.0 g) and glacial acetic acid (50 ml). A small amount of insoluble material was removed by filtration and washed with a little acetic acid; the combined filtrates were evaporated to a black sticky residue which gave a white precipitate when treated with water. The white precipitate was recovered and very thoroughly washed with water. As five recrystallizations did not give a pure product, the material was then extracted with dilute hydrochloric acid; the small amount of insoluble material was recovered as usual and identified as unchanged starting material by melting point and mixture melting point. The acid extract was carefully neutralized with sodium bicarbonate and the precipitated solid twice recrystallized from ethanol to give white fluffy needles which partially melted at 200°, resolidified, and melted again at 209–211°. Two more recrystallizations gave the analytical material with the same partial melting point at 200°, and final melting point of 210–212°. Found: C, 60.19, 60.22; H, 4.79, 4.87; N, 4.04, 3.97%. Calc. for $C_{18}H_{17}O_7N$: C, 60.17; H, 4.73; N, 3.90%.

In two similar experiments, the nitro compound (8.15 g) was reduced to give the amine having a final melting point of 210–211° in a yield of 3.03 g or 40%. In five further runs the relative amount of acetic acid was doubled and the temperature of reduction increased to 85–90°; the crude yield was 12.2 g, or 59% from 22.4 g of starting material, but purification of a portion of the amine showed that the overall yield of reasonably pure material was only 43%.

7-(2′-Amino-4′-carboxyphenoxy)metameconine (VAb)

7-(2′-Amino-4′-carbomethoxyphenoxy)metameconine (0.2 g) was heated on the steam bath for 30 minutes with aqueous sodium hydroxide (10 ml, 10%). The solution was cooled and acidified and the resulting precipitate recovered and twice recrystallized, once from aqueous methanol, and once from methanol, to give a product of m.p. 269.5–270.5°. The melting point reported previously (9) for material made in a different way was 268.4–268.8°.

7-(4′-Carbomethoxy-2′-iodophenoxy)metameconine (VBe)

(*a*) The method is that used by Chalmers, Dickson, Elks, and Hems (21) in the synthesis of a precursor of thyroxine. Sodium nitrite (0.5 g) was dissolved in concentrated sulphuric acid (10 ml) with gentle warming; the solution was then cooled to 0° and diluted with glacial acetic acid (10 ml). A second solution, prepared from 7-(2′-amino-4′-carbomethoxyphenoxy)metameconine (2.0 g, m.p. 210–211°), concentrated sulphuric acid (20 ml), and glacial acetic acid (20 ml), was cooled to 0° and then added over the course of 2 hours to the first solution while the reaction mixture was vigorously stirred and kept between −2° and 1°. Stirring was continued for 1 hour after the addition was complete, the diazonium solution was then poured, with vigorous stirring but without cooling, into a mixture of chloroform (50 ml), water (100 ml), potassium iodide (5.0 g), iodine (5.0 g), and urea (2.0 g); the temperature rose to 40°. Stirring was continued for an additional hour; the layers were then separated and the aqueous layer twice extracted with chloroform (100-ml portions). The chloroform solutions were combined, twice washed with water, and then covered with a solution of sodium sulphite (10 g) in water. Sulphur dioxide was bubbled into the mixture until the color due to the iodine had been discharged; the pale yellow chloroform layer was separated, twice washed with water, dried with magnesium sulphate, and evaporated. The dry residue was recrystallized from ethanol (150 ml) to give white needles, m.p. 208–209°, in a yield of 1.03 g or 39%. It was found (after the product had been recovered unchanged from a second attempt at diazotization) that the needles were insoluble in hydrochloric acid, contained halogen but not nitrogen, and that admixture with the starting material markedly depressed the melting point. Three more recrystallizations of the needles from ethanol gave the analytical sample of VB*e*, m.p. 206.5–207.5°. Found: C, 45.99, 46.10; H, 3.27, 3.19; I, 27.24, 27.34%. Calc. for $C_{18}H_{15}O_7I$: C, 45.97; H, 3.22; I, 26.99%.

In two other runs the crude amino compound (6.0 g, m.p. 196–200°) was converted to purified iodo compound (only one diazotization step being performed for each run!), m.p. 206–207°, in a yield of 3.96 g or 50%.

(*b*) The crude amino compound (2.0 g) was diazotized at 20° with butyl nitrite, hydrogen chloride, and acetic acid, and the mixture poured into a mixture of potassium iodide, water, iodine, and chloroform. Crude product, m.p. 201–209°, was isolated in a yield of only 0.51 g, but one recrystallization from ethanol gave the pure iodo compound VB*e*, m.p. 206–207°.

Can. J. Chem. Downloaded from www.nrcresearchpress.com by 210.87.254.42 on 09/05/12
For personal use only.

(*c*) Attempts to proceed via the isolated diazonium fluoborate failed. In the first attempt, the amine failed to dissolve in a mixture of hydrochloric acid and aqueous sodium fluoborate, and eventually most of it was recovered unchanged. In the second attempt, modelled on a different preparation of Niemann and McCasland (32), the amine was first diazotized with butyl nitrite and hydrogen chloride in acetic acid solution; sodium fluoborate solution (33) and hydrochloric acid were then added but no precipitate formed even when the solution was held 60 hours below 0°. A diazonium compound still remained at the end of this time, since the solution gave a bright red precipitate with a solution of β-naphthol. It is not unusual for this method to fail with ortho-substituted amines (34).

Reaction of 7-(4′-Carbomethoxy-2′-iodophenoxy)metameconine with Bases

In this section, the increasing severity of the conditions demonstrates the relative reactivities of the iodo and carbomethoxy groups towards alkali. Saponification occurred in all the experiments, but the Ullmann reaction only under the most severe conditions used.

(*a*) 7-(4′-Carbomethoxy-2′-iodophenoxy)metameconine (2.0 g, m.p. 204–206°) and a trace of copper catalyst were heated under reflux with the solution made from potassium (1.0) and dry methanol (50 ml) for 12 hours, the preparation being protected from atmospheric moisture. A very long isolation procedure gave crude starting material (m.p. 200–206°, undepressed by admixture) and crude 7-(4′-carboxy-2′-iodophenoxy)metameconine (0.24 g, m.p. 249–252°), easily identified since, when treated with diazomethane in ether, it gave the starting material (after one recrystallization the m.p. being 206–208°, undepressed by admixture).

(*b*) 7-(4′-Carbomethoxy-2′-iodophenoxy)metameconine (0.95 g) was heated under reflux for 2 hours with acetone (10 ml) and aqueous potassium hydroxide (20 ml of 5%); the solution was then cooled and acidified, and the oily mixture extracted with ether. Evaporation of the ethereal extract and recrystallization of the residue from ethanol gave a product (0.56 g) of m.p. 256–258°. Two more recrystallizations yielded white crystals (0.3 g) of 7-(4′-carboxy-2′-iodophenoxy)metameconine which melted sharply at 260°.

(*c*) 7-(4′-Carbomethoxy-2′-iodophenoxy)metameconine (0.3 g), aqueous sodium hydroxide (5 ml of 10%), and a trace of copper catalyst (Kahlbaum's copper bronze #02219) were heated under reflux with stirring. After 1 hour, more sodium hydroxide (5 ml) was added, and after a second hour acetone (5 ml) and water (5 ml) were added to dissolve the insoluble material; heating and stirring were continued for an hour longer. The copper was then removed by filtration, and the filtrate acidified; it deposited a sticky precipitate which solidified when strongly cooled; after recrystallization from ethanol (10 ml) the precipitate weighed 0.2 g, m.p. 256–259°. A second recrystallization yielded crystals of two types; as one type did not depress the other's melting point on admixture, the two forms were reunited and recrystallized to give the analytical sample, m.p. 260.5–261.0°, of 7-(4′-carboxy-2′-iodophenoxy)metameconine (VA*e*). Found: C, 45.45, 45.28; H, 3.05, 2.85%. Calc. for $C_{17}H_{13}O_7I$: C, 44.76; H, 2.87%.

Methylation of a portion of the analytical sample with diazomethane gave a product which after one recrystallization from ethanol had m.p. 205–207°, undepressed by admixture with authentic 7-(4′-carbomethoxy-2′-iodophenoxy)metameconine, the starting material.

(*d*) 7-(4′-Carbomethoxy-2′-iodophenoxy)metameconine (0.5 g) was heated under reflux with aqueous sodium hydroxide (15 ml of 10%) until a clear solution was obtained (2 hours). The solution was transferred to a copper test tube, and copper catalyst (0.5 g) was added. The copper test tube was then placed, upright, inside a glass tube sealed at one end; the system was cooled strongly, evacuated, sealed, heated slowly to 120° (bath temp.), held at this temperature for 1 hour, cooled, and opened. The contents of the tube was filtered, the filtrate acidified, and the precipitate recrystallized from ethanol to give 0.28 g of a product whose melting point (251–257°) was not depressed by admixture with the 7-(4′-carboxy-2′-iodophenoxy)metameconine of (*c*) part.

(*e*) Conditions were the same as those in (*d*) part, except that the reaction temperature was 170–180°. In three runs 7-(4′-carbomethoxy-2′-iodophenoxy)metameconine (2.3 g) was converted into crude 7-(4′-carboxy-2′-hydroxyphenoxy)metameconine (1.42 g or 84%), m.p. near 255°, markedly depressed on admixture with the analytical sample of the iodo acid from (*c*) part. The product was interesting in being almost insoluble in either ethanol or water, though quite soluble in a mixture of the two. Two recrystallizations of a small portion of the crude material raised the melting point of the supposed 7-(4′-carboxy-2′-hydroxyphenoxy)metameconine (VA*f*) to 282–288°, but the recovery was very small. Because of this difficulty of purification, and because of the great scarcity of material, the substance was characterized and purified as its methyl ether methyl ester, as shown in the next section.

7-(4′-Carbomethoxy-2′-methoxyphenoxy)metameconine (VBd)

Supposed 7-(4′-carboxy-2′-hydroxphenoxy)metameconine (0.6 g, crude, from (*e*) part of the previous section) was suspended in methanol while a solution of diazomethane in ether was slowly added in excess. During the addition the crystals at first slowly dissolved; later, a precipitate formed. Next morning the precipitate was recovered (m.p. 190–192°; yield 0.25 g); two recrystallizations from aqueous methanol gave the analytical sample, m.p. 189.6–190.2°. Found: C, 61.24, 61.18; H, 5.10, 5.08%. Calc. for $C_{19}H_{18}O_8$: C, 60.96; H, 4.85%. In two more runs, 0.74 g starting material was converted to crude product, m.p. 185–188°, in a yield of 0.35 g or 44%.

Can. J. Chem. Downloaded from www.nrcresearchpress.com by 210.87.254.42 on 09/05/12
For personal use only.

Dimethyl 3-(4′-Carbomethoxy-2′-methoxyphenoxy)-4,5-dimethoxyphthalate (Ia)

(a) Oxidation

7-(4′-Carbomethoxy-2′-methoxyphenoxy)metameconine (0.10 g, m.p. 185–188°) was heated on the steam bath with aqueous potassium hydroxide (5 ml of 10%) until solution was obtained (1 hour). Potassium permanganate (0.30 g) in water (5 ml) was added and the heating continued for 30 minutes. Sulphur dioxide was then passed into the cooled reaction mixture until it was colorless; a few drops of concentrated sulphuric acid were added and a trace of solid removed by filtration. The filtrate was cooled in an ice bath; the crystals which separated were recovered (m.p. 241–246°) and recrystallized from water (5 ml) to give colorless plates (0.06 g) which first melted and then resolidified as fine needles at 208–210°, and then melted again at 264–265°, when observed between cover glasses on the hot stage of the microscope. A second oxidation of 0.25 g of starting material gave two crops of acid, final m.p. 264–265°, in a combined yield of 0.17 g, or 65%, of the supposed 3-(4′-carboxy-2′-methoxyphenoxy)-4,5-dimethoxyphthalic acid (I*d*). Because of the unsatisfactory nature of the free phthalic acids as derivatives, we followed the usual policy (11, 13) of characterizing the acid through its methyl ester.

(*b*) *Esterification*

Treatment of the acid product of the oxidation (0.14 g, as just above) with an excess of diazomethane gave a vigorous reaction. Next morning the solution was evaporated and the residue recrystallized from methanol to give small, diamond-shaped plates, m.p. 156.0–157.5°. One more recrystallization gave the first analytical sample, m.p. 157.0–157.2°. Found: C, 58.80, 58.50; H, 5.29, 5.24%. In a second experiment, the acid (0.09 g) was methylated in the same way; after four recrystallizations from methanol the second analytical sample had m.p. 157–158°. Found: 57.71, 57.71; H, 4.97, 5.23%. Calc. for $C_{21}H_{22}O_{10}$: C, 58.06; H, 5.11%.

7-(4′-Carbomethoxyphenoxy)metameconine (VBc)

The method was similar to the general method of Hodgson and Walker (35). Sodium nitrite (0.25 g) was dissolved in concentrated sulphuric acid (5 ml) with gentle warming. The solution was then cooled to 0° and glacial acetic acid (5 ml) was added with stirring and cooling. 7-(2′-Amino-4′-carbomethoxyphenoxy)metameconine (VB*b*) (1.0 g, m.p. 209.0–210.5°) was stirred with acetic acid (5 ml), and sufficient sulphuric acid (2 ml) was added to give a pale yellow, viscous solution; this second solution was cooled and added over a period of 90 minutes to the first solution with vigorous stirring. Stirring was then continued for another 90 minutes, the temperature being maintained at −2 to 0°. Methanol (50 ml) was then added; the temperature rose to 10°, and some frothing occurred. The mixture was gradually warmed and finally heated under reflux for 90 minutes. Some solvent (about 30 ml) was removed by distillation; the cooled residue was poured onto ice (100 g), the resulting orange precipitate recovered and recrystallized from ethanol to give short orange needles (0.38 g or 40%), m.p. 162–172°. Four more recrystallizations from ethanol gave the pale orange analytical sample, m.p. 194–195°. Found: 62.57, 62.54; H, 4.69, 4.70%. Calc. for $C_{18}H_{16}O_7$: C, 62.79; H, 4.68%. A second run using the same quantities and conditions gave 0.5 g of once-recrystallized material as remarkable lenticular plates, m.p. 191–193°; after another recrystallization the crystals (0.36 g, m.p. 194.0–195.5°) still had slightly curved edges.

Dimethyl 3-(4′-Carbomethoxyphenoxy)-4,5-dimethoxyphthalate (Ic)

(a) Oxidation

7-(4′-Carbomethoxyphenoxy)metameconine (0.36 g, m.p. 194.0–195.5°) was heated with water (10 ml) and aqueous potassium hydroxide (2 ml of 10%) for 1 hour, a clear red solution being obtained. Potassium bicarbonate (1 g) was added, and while the mixture was heated on the water bath, solid potassium permanganate (0.35 g) was added until a permanent pale purple color remained. Heating was continued for 45 minutes in all; the mixture was then cooled and filtered, and the precipitate washed with a little water. The combined filtrates were decolorized with sulphur dioxide and acidified with hydrochloric acid. A precipitate slowly settled out; it was recovered and recrystallized from water to give a product (crystals "A") which melted at 141–146°, resolidified, and melted again over the range 171–191°, yield 0.16 g or 42%. This product was purified as its ester (see below). The aqueous mother liquors from this experiment and from another experiment (in which 0.16 g of starting material had given no crystalline precipitate) were continuously extracted with ether; the ethereal extract was evaporated; the solid residue dissolved in potassium hydroxide solution, reprecipitated with acid, recovered, and twice recrystallized from water to give fine needles which on the hot stage of the microscope melted at 138–140° with effervescence, resolidified at 151–154°, and slowly melted again at 245–259°. The acid, 3-(4′-carboxyphenoxy)-4,5-dimethoxyphthalic acid (I*b*), has previously been reported to form a dihydrate (36), first m.p. 207°, second 245°; and a monohydrate (1), first m.p. 178° or 188°, second m.p. 245° (less stable form) and 254–255°, or sinters 247°, melts 250–253° (more stable form) (in a capillary). This interesting dependence on the rate of heating adds to the unsatisfactory properties of the free phthalic acid as a characteristic derivative; our main attention was accordingly given to the methyl ester.

(*b*) *Esterification*

The crystals "A" above (0.16 g) were almost dissolved in ether (5 ml) and an excess of an ethereal solution of diazomethane (20 ml) was slowly added, the mixture being cooled in ice. A vigorous reaction occurred;

Can. J. Chem. Downloaded from www.nrcresearchpress.com by 210.87.254.42 on 09/05/12
For personal use only.

after 3 hours, the ether was removed, the residue crystallized by solution in methanol followed by evaporation, and then recrystallized from aqueous methanol. Long needles, m.p. 116.0–116.5°, were obtained in a yield of 0.14 g. A second recrystallization gave the analytical sample, m.p. 115.6–116.2°. Found: C, 59.78, 59.65; H, 4.92, 5.16%. Calc. for $C_{20}H_{20}O_9$: C, 59.40; H, 4.99%. Faltis and Frauendorfer (1) reported that the substance sintered at 111° and melted at 113–114°; King (36) did not obtain a crystalline ester.

Attempted Resolution of 7-(4′-Carboxy-2′-iodophenoxy)metameconine (VAe)

7-(4′-Carboxy-2′-iodophenoxy)metameconine (0.6 g, m.p. 257–258°) suspended in chloroform (100 ml) was dissolved by the addition of ethanol (10 ml). Strychnine (0.44 g, m.p. 279–282°, from the nitrate) in chloroform (20 ml) was added to the solution. After 24 hours, the solution was concentrated to 20 ml and diluted with petroleum ether to precipitate a colorless oil which gradually hardened; the precipitate was recovered and recrystallized from ethanol to give a white product, m.p. 174–178°, in a yield of 0.82 g or 79%; three more recrystallizations from ethanol gave white crystals (0.38 g), m.p. 178.5–179.5°, and a fifth recrystallization left the melting point unchanged. Found: C, 57.34, 57.63; H, 4.97, 5.03; N, 3.51, 3.42%. Calc. for $C_{38}H_{35}O_9N_2I$: C, 57.73; H, 4.46; N, 3.54%. The ethanol mother liquors from the first three recrystallizations were combined and concentrated; they deposited crystals (0.31 g, m.p. 161–166°, mixture m.p. with the anal. sample 177–181°) which after one recrystallization had m.p. 176–177°; thus a second diastereoisomer did not seem to be present.

The strychnine salt (analytical sample, 0.3023 g) was dissolved in chloroform to give a solution volume of 5 ml. At age 3 minutes for the solution, a single reading showed a rotation of −0.49°; the mean for 10 readings taken before age 10 minutes was −0.470°, while that for 10 readings at 20 hours was −0.471°; sets of 10 readings at ages 1 hour, 2.25 hours, and 5 hours showed no deviation of the mean from these larger than 0.006°. The zero point was 0.032°. From these readings $[M]_D = -650°$ (0.077 M in chloroform). The lack of mutarotation showed that dynamic interchange of the stereoisomers did not occur at an observable rate, but time did not permit us to investigate further the following anomaly in our results. Strychnine itself has $[M]_D^{18} = -465°$ (0.067 M in chloroform) (37, 38), but while our salt showed a molecular rotation apparently significantly more negative than this, known salts of strychnine have much less negative molecular rotations than does the free base. Thus aqueous solutions of the salts of mineral acids (39) and organic acids (40) show molecular rotations close to −110°, while solutions of organic salts of strychnine in organic solvents show numerically very small molecular rotations, which may be either positive or negative in sign (39, 41, 42).

Nitration of Salicylaldehyde

(a) Preparation of the Crude Mixture of 3- and 5-Nitrosalicylaldehydes (VIIIb and VIIIc)

The method of von Miller (43) was followed, but the yield obtained (58%) was much less than those (90–100%) reported by others (43–47).

(b) Separation of the Mononitro Derivatives

(i) Via the sodium salts.—Von Miller (43) reported an easy separation by fractional crystallization of the yellow sodium salt of the 5-nitro derivative from the red salt of the 3-derivative. The method has often been used without comment; there are two reports (44, 46) of easy and almost quantitative separations (though the reported proportions of the isomers differed very greatly!), and three (47–49) in which the method was difficult or inefficient. In our work fractions enriched in one or other of the components were obtained, but in very prolonged, careful, and repeated fractional crystallizations of the sodium salts, only two small crops of the pure yellow salt of the 5-isomer; the other fractions were all mixtures of the yellow and red salt. There seemed to be little difference in their solubilities, and the successes reported previously presumably were based on the maintenance of suitably supersaturated solutions.

(ii) Via the sodium bisulphite addition compounds.—Taege (50) found that 5-nitrosalicylaldehyde formed a stable crystalline addition compound, and that the derivative of 3-nitrosalicylaldehyde did not crystallize. Our results did not agree with this. In fact, when a mixture of the sodium salts, enriched in the 3-isomer, was treated with sodium bisulphite, a small amount of a crystalline precipitate was obtained which on treatment with aqueous acid gave directly almost pure 3-nitrosalicylaldehyde, m.p. 108.5–110.5°. The 5-isomer could also be obtained almost pure (see below).

(iii) By partial acidification.—One quarter of a mother liquor saturated in both salts was treated cautiously with dilute hydrochloric acid until the color just changed; the rest of the mother liquor was then added with shaking, and next morning the precipitate was recovered; its melting point of 103–109° showed that it was almost entirely 3-nitrosalicylaldehyde. But later crops were mixtures much less rich in the 3-isomer. Presumably the selective precipitation of the 3-isomer was a solubility effect, since the difference in their acidity constants is small and in the wrong direction (51).

(iv) By a combination of methods.—The most elementary theory suggests that separations of this type are best carried out with at least two methods having different separation coefficients. The following work demonstrated that the intractable mixture of salts could be broken by the use of this principle, though the separation was tedious. Salicylaldehyde (100 g) was nitrated in the usual way (43) and the mixed product was treated at 70° with water (300 ml) and sodium bisulphite (88.4 g); all but a few milligrams dissolved. Next morning, the light yellow crystals which had separated from the chilled solution were recovered (from mothor liquor A), washed with sodium bisulphite solution, resuspended in water, treated with hydrochloric

Can. J. Chem. Downloaded from www.nrcresearchpress.com by 210.87.254.42 on 09/05/12
For personal use only.

Can. J. Chem. Downloaded from www.nrcresearchpress.com by 210.87.254.42 on 09/05/12
For personal use only.

acid and a stream of air, the crystals recovered, washed, and dried, yield 28.2 g (20% on salicylaldehyde) of almost pure 5-nitrosalicylaldehyde, m.p. 124.5–128.5°. The acid mother liquor B was subjected to an air stream for a long time, and four successive crops of mixed aldehydes were obtained. Thus the crystalline addition product must have been a mixture, and the recovery from it of 5-isomer was due at least as much to the faster decomposition in acid of the 5-derivative as to its lesser solubility in water. Mixed aldehydes were also recovered from mother liquor A; the mixed aldehydes from A and B were separately converted to their sodium salts and subjected to very long and careful fractional crystallizations from water. A gave two small crops of the pure yellow salt from which almost pure 5-nitrosalicylaldehyde was obtained directly by acidification; m.p. 126.5–127° and 126–126.5°, yield 7.8 g or 5.6% in all. All other fractions were mixtures; one of the mother liquors from B was used to establish the results in (iii) above (and therefore also confirmed the previous demonstration of the crystalline bisulphite addition product of the 3-isomer). The remaining salts and mother liquors from A and B were now united in one aqueous solution for the demonstration of the differential separation. The combined solution was treated as in (iii) with one quarter of the amount of hydrochloric acid required for neutralization, and the precipitate (B1) recovered. The filtrate was then concentrated until (as it was judged) enough water had been removed to bring it back to saturation, in the cold, in the 3-isomer; after being chilled, it deposited a salt (C1). The double separation was then repeated several times to obtain the "less soluble acids" B2, B3, and B4, and the "less soluble salts" C2 and C3. One recrystallization of C2 and C3 gave a pure yellow salt which on treatment with acid gave almost pure 5-nitrosalicylaldehyde, m.p. 125.5–125.8°, yield 3.2 g or 2.3%. The deep orange C1 gave mainly the 3-isomer. The fractions B1, B2, B3, and B4 were somewhat impure 3-isomer, yield 14.2 g or 10%. Two recrystallizations from aqueous acetic acid and one from ethanol of the united fractions of the crude 3-isomer, with charcoal, gave large, bright, sandy-yellow crystals, m.p. 108.5–109.5°, of pure 3-nitrosalicylaldehyde, yield 18.2 g or 13%. One recrystallization of its united fractions from aqueous acetic acid gave beautifully shaped, very light yellow crystals of pure 5-nitrosalicylaldehyde, m.p. 125.4–126.4°, yield 33.7 g or 24%. Mixed fractions (useful for further nitration) were also obtained in a yield of 15%.

(c) Dinitration

The crude mixture of mononitrosalicylaldehydes (43.4 g) obtained as in (*a*) part was treated according to the method of Lovett and Roberts (52) to give crude 3,5-dinitrosalicylaldehyde (VIII*a*) in a yield of 90%. Three recrystallizations from benzene and one from aqueous acetic acid gave 6.7 g of bright yellow crystals, m.p. 72.1–74.4°. A slightly better sample, m.p. 72.3–73.7°, was recovered from the mother liquors in a yield of 1.0 g. A second crop, 26.4 g, m.p. 72.9–73.4°, was obtained as a light yellow powder and a third crop, 0.78 g, m.p. 70.6–72.1°, as a darker powder. There was, therefore, little evidence of fractionation, supporting the correctness of our melting point, which was much higher than those recorded before, viz., 56° (53), 58–60° (52), and 62–63° (45).

Reactions of Dicyclohexylcarbodiimide

(a) With Methyl 2-Hydroxy-3,5-dinitrobenzoate (VII)

Dicyclohexylcarbodiimide (2.0 g) was added to a warm solution of methyl 2-hydroxy-3,5-dinitrobenzoate (54) (4.0 g, m.p. 124–125°) in dry ethyl acetate (40 ml). A precipitate began to form immediately. Next morning the precipitate was recovered and the solid residue from the evaporation of the mother liquor to dryness was added to it. One crystallization from methanol and two from benzene gave small bright yellow needles whose melting point of 205–207° was raised to 211–212° by two more recrystallizations from methanol and one from aqueous acetone. A final recrystallization from methanol gave the analytical sample of the 1:1 addition compound, m.p. 211.6–212.2°. Found: C, 56.08, 56.26; H, 6.21, 6.32; N, 12.46, 12.30%. Calc. for $C_{21}H_{28}O_7N_4$: C, 56.24; H, 6.29; N, 12.49%. Dicyclohexylurea could not be found in the mother liquors, though a little phenolic starting material was recovered.

(b) With Methyl 3,5-Dinitro-4-hydroxybenzoate (VI)

Methyl 3,5-dinitro-4-hydroxybenzoate (54) (10 g), dissolved in dry ethyl acetate (75 ml), was treated with dicyclohexylcarbodiimide (5 g). The mixture became warm and a precipitate began to form in a few minutes; after 2 days it was recovered and recrystallized from benzene to give a yellow product (6.89 g), m.p. 191–201°. Two more recrystallizations from benzene and one from methanol gave prisms which exhibited dimorphism at the melting point: the prisms partially melted at 190°, the melt resolidified as needles, the remaining prisms melted at 196–200°, and the needles sharply at 200°. Another recrystallization from methanol gave a mixture of needles (0.96 g) and prisms (0.34 g) which were separated by hand; the needles melted at 199–200° and the prisms behaved as before; in chloroform solution the infrared spectra of the two forms were identical. One more recrystallization from methanol gave a pure sample of the 1:1 addition compound, which separated originally as needles but which after 3 days had completely changed to prisms; they showed the same double melting point as before, and two more recrystallizations from methanol produced no change in the melting point. Found: C, 56.18, 56.26; H, 6.36, 6.20; N, 12.75, 12.69%. Calc. for $C_{21}H_{28}O_7N_4$: C, 56.24; H, 6.29; N, 12.49%. The reaction mixture filtrate and the mother liquors gave, after one recrystallization of the crude crystals from methanol, an excellent product showing the double melting point in the range 190–200°, in a yield of 8.39 g, as well as a fraction (m.p. 97–112°, 2.29 g) thought to be impure phenolic starting material since, when the reaction was repeated in dry benzene at the reflux temperature, 9.62 g of crude addition product, m.p. 195–198°, was obtained as well as 2.4 of

material, m.p. 107–111°, undepressed by admixture with methyl 3,5-dinitro-4-hydroxybenzoate. No dicyclohexylurea could be found in the mother liquor.

The addition product (2.25 g, m.p. 190–200°) was recovered unchanged in a yield of 1.85 g after it had been heated at 170° for 2 hours with methyl 3,5-dinitro-4-hydroxybenzoate and dimethylformamide, the mixture poured into water, and the precipitate recrystallized from methanol. No substituted diphenyl ether could be recovered.

(c) With Unactivated Phenols

When methyl 3,5-dinitro-4-hydroxybenzoate (2.4 g), dicyclohexylcarbodiimide (2.2 g), and methyl salicylate (20 ml) were heated 8 hours on the steam bath, the only insoluble compound produced was the same addition product observed in (*b*) just above, identified by melting point and infrared spectrum. Cyclohexylcarbodiimide failed to react on prolonged contact with methyl *p*-hydroxybenzoate in dry ethyl acetate.

(d) With 3,5-Dinitrosalicylaldehyde (VIIIa)

A solution of 3,5-dinitrosalicylaldehyde (8.4 g, m.p. 55–58°) and dicyclohexylcarbodiimide (4.4 g) in dry ethyl acetate (80 ml) was heated under reflux for 4 hours and then evaporated to dryness. Light-sensitive crystals, m.p. 186–206°, were obtained by recrystallization of the residue from benzene, yield 4.78 g. The benzene mother liquor was evaporated to dryness and the residual gum triturated with methanol; significantly, the mixture became quite warm. A solid (0.82 g, m.p. 171–186°) separated from the cooled methanol; it was added to the previous solid fraction, and efforts to purify these solids failed. The methanolic mother liquor, however, yielded prisms (2.47 g, m.p. 156–186°) which after two more recrystallizations from methanol and two from aqueous acetone gave the analytical sample, which seemed also to be dimorphic (m.p. 192.5–193.5° with a little previous melting and resolidification at 188°). Found: C, 58.46, 58.26; H, 6.59, 6.52; N, 12.98, 13.25%; mol. wt., 415. Calc. for $C_{21}H_{28}O_6N_4$: C, 58.32; H, 6.53; N, 12.96%; mol. wt., 432. In a second experiment, the methanolic mother liquors gave dicyclohexylurea as white crystals (0.7 g), separated by virtue of its low solubility in benzene; after one recrystallization it was pure. It was identified by its melting point (233.2–234.0°), mixture melting point, and infrared spectrum.

(e) With 5-Nitrosalicylaldehyde (VIIIb)

Two experiments very similar to those above, but using purified 5-nitrosalicylaldehyde as the phenolic component, were performed. From the first experiment, pure dicyclohexylurea (m.p. 233.0–233.4°, with an abrupt change of crystal form but no melting at 222°) was obtained. Found: C, 69.92; H, 10.64; N, 11.08%. $C_{13}H_{24}ON_2$ requires: C, 69.65; H, 10.72; N, 12.50%. In the second experiment, five recrystallizations of the entire solid reaction mixture from ethanol gave the analytical sample of the principal reaction product, m.p. 142–143°. Found: C, 62.94, 62.74; H, 6.54, 6.63; N, 11.12, 11.27%.

(f) With 3-Nitrosalicylaldehyde (VIIIc)

In two experiments using purified 3-nitrosalicylaldehyde as the phenolic component, small amounts of unchanged 3-nitrosalicylaldehyde were recovered and identified by mixture melting point. The only other pure product obtained was dicyclohexylurea (identified by m.p., mixture m.p., and infrared spectrum), which separated spontaneously from the dry ethyl acetate of the first experiment.

(g) Infrared Spectra

The values given are uncorrected. The addition products, A with methyl 2-hydroxy-3,5-dinitrobenzoate and B with methyl 4-hydroxy-3,5-dinitrobenzoate, showed bands at the same position (near 3320 cm^{-1}) as the N—H stretching band of dicyclohexylurea (C) in potassium bromide disks; in a chloroform solution of B, the band was weakened and raised to 3440 cm^{-1}. This band was completely absent in D, the condensation product with 3,5-dinitrosalicylaldehyde, and in E, the condensation product with 5-nitrosalicylaldehyde. A and B showed an ester carbonyl stretching band at 1730 and 1737 cm^{-1}, absent in the others; all the compounds showed bands in the "amide I" region; 1650 (A), 1640 (B), 1630 (C), 1682 (D), and 1660 cm^{-1} (E) in potassium bromide (aldehyde C—H stretching bands being absent in the spectra of D and E); in chloroform the band for B was *raised* to 1670 cm^{-1}, as would be expected for a band of this type. A, B, D, and E showed strong bands near 1620 cm^{-1}, extremely strong in the latter pair. The "amide II" region (near 1550 cm^{-1}) was occupied also by the nitro groups' frequency; in A and B the two sources overlapped to form a wide band, in potassium bromide disks, but in the spectrum of a chloroform solution of B the bands were resolved, one component moving to a lower frequency (as would be expected for a true "amide II" frequency). In agreement with the loss of the N—H stretching bands, the spectra of D and E both showed narrower bands (with potassium bromide disks) having the shape of the nitro groups' band alone. As expected, a strong, moderately broad band near 1290 cm^{-1} in the spectra of A and B was absent in that of D; the differences between D and E suggested by the elementary analysis were most clearly supported in the spectra by the presence in the spectrum of E, but not of D, of an extremely strong, broad band between 1330 and 1290 cm^{-1}, and by the presence in the spectrum of E of two moderately strong, very sharp, and well-resolved bands at 1480 and 1380 cm^{-1}, present at most as weak shoulders in the spectra of the other compounds.

ACKNOWLEDGMENTS

The present work was undertaken as a tribute to Professor J. A. McRae and to all the many research students at Queen's who have worked upon the problem. It is hard to have

Can. J. Chem. Downloaded from www.nrcresearchpress.com by 210.87.254.42 on 09/05/12
For personal use only.

to report that Dr. McRae died nearly a year before the completion of our own work. We wish to thank Dr. R. H. Manske for the suggestions which led to the beginning of this work nearly 25 years ago, for his advice as to the early concepts of the biosynthesis of cularine, and for his long continued interest in the problem. Miss Shelagh Courtney determined most of the infrared spectra, Miss Lorna Craig and Mr. Stephen Safe made our work possible by the production of very large amounts of the necessary intermediates, and Dr. C. A. Sankey gave us the large amounts of vanillin needed as starting material. The National Research Council of Canada supported the work by a research grant, and by the grant of a scholarship to one of us.

Can. J. Chem. Downloaded from www.nrcresearchpress.com by 210.87.254.42 on 09/05/12
For personal use only.

REFERENCES

1. F. Faltis and H. Frauendorfer. Ber. Sect. B, **63**, 806 (1930).
2. R. H. F. Manske. Can. J. Res. Sect. B, **16**, 81 (1938).
3. R. H. F. Manske. J. Am. Chem. Soc. **72**, 55 (1950).
4. M. Kulka. *In* The alkaloids. Vol. IV. *Edited by* R. H. Manske. Academic Press, New York. 1954. p. 199.
5. J. A. McRae, R. B. VanOrder, F. H. Griffiths, and T. E. Habgood. Can. J. Chem. **29**, 482 (1951).
6. H. King and E. V. Wright. J. Chem. Soc. 1168 (1939).
7. A. G. Davies and J. Kenyon. Quart. Rev. (London), **9**, 203 (1955).
8. R. H. Manske, J. A. McRae, and R. Y. Moir. Can. J. Chem. **29**, 526 (1951).
9. J. A. McRae, R. Y. Moir, J. J. Ursprung, and H. H. Gibbs. J. Org. Chem. **19**, 1500 (1954).
10. M. Allen and R. Y. Moir. Can. J. Chem. **37**, 1799 (1959).
11. M. Allen, A. L. Promislow, and R. Y. Moir. J. Org. Chem. **26**, 2906 (1961).
12. J. A. McRae, M. Allen, and R. Y. Moir. Can. J. Chem. **39**, 995 (1961).
13. F. Faltis, L. Holzinger, P. Ita, and R. Schwarz. Ber. Sect. B, **74**, 79 (1941).
14. E. Späth. Ber. Sect. B, **65**, 1778 (1932).
15. R. H. Manske and H. L. Holmes. J. Am. Chem. Soc. **67**, 95 (1945).
16. R. H. Manske, A. E. Ledingham, and H. L. Holmes. Can. J. Res. Sect. B, **23**, 100 (1945).
17. H. King. J. Chem. Soc. 1157 (1939).
18. H. King. J. Chem. Soc. 265 (1948).
19. E. T. Borrows, J. C. Clayton, B. A. Hems, and A. G. Long. J. Chem. Soc. S190 (1949).
20. J. Blair and G. T. Newbold. J. Chem. Soc. 3935 (1954).
21. J. R. Chalmers, G. T. Dickson, J. Elks, and B. A. Hems. J. Chem. Soc. 3424 (1949).
22. H. E. Ungnade. Chem. Rev. **38**, 405 (1946).
23. A. T. Bottini and J. D. Roberts. J. Am. Chem. Soc. **79**, 1458 (1957).
24. J. F. Bunnett. J. Chem. Ed. **38**, 278 (1961).
25. R. Y. Moir and C. B. Purves. Can. J. Res. Sect. B, **26**, 694 (1948).
26. J. Lowenthal and J. M. Pepper. J. Am. Chem. Soc. **72**, 3292 (1950).
27. V. E. Meharg and I. Allen. J. Am. Chem. Soc. **54**, 2920 (1932).
28. J. Trotter. Can. J. Chem. **39**, 1638 (1961).
29. H. C. Yuan and R. Adams. J. Am. Chem. Soc. **54**, 2966 (1932).
30. H. G. Khorana. Chem. Rev. **53**, 145 (1953).
31. M. Busch, G. Blume, and E. Pungs. J. Prakt. Chem. Ser. 2, **79**, 513 (1909).
32. C. Niemann and G. E. McCasland. J. Am. Chem. Soc. **66**, 1870 (1944).
33. C. M. Suter, E. J. Lawson, and P. G. Smith. J. Am. Chem. Soc. **61**, 161 (1939).
34. A. Roe. *In* Organic reactions. Vol. V. Wiley and Sons, New York. 1949. p. 193.
35. H. H. Hodgson and J. Walker. J. Chem. Soc. 1620 (1933).
36. H. King. J. Chem. Soc. 1276 (1936).
37. K. Warnat. Helv. Chim. Acta, **14**, 997 (1931).
38. A. C. Oudemans, Jr. Ann. **166**, 76 (1873).
39. F. L. Shinn. J. Phys. Chem. **11**, 201 (1907).
40. H. Tykociner. Rec. Trav. Chim. **I**, 144 (1882).
41. J. Minguin. Compt. Rend. **140**, 243 (1905).
42. T. C. James and J. J. Sudborough. J. Chem. Soc. **95**, 1538 (1909).
43. W. von Miller. Ber. **20**, 1927 (1887).
44. H. Biltz. Ann. **305**, 187 (1899).
45. P. Hill and R. Robinson. J. Chem. Soc. 486 (1933).
46. K. C. Pandya, O. S. Saxena, and J. D. Tinku. J. Indian Chem. Soc. **24**, 437 (1947).
47. C. C. Hach, L. M. Ligett, and H. Diehl. Iowa State Coll. J. Sci. **21**, 316 (1947); Chem. Abstr. **42**, 1240 (1948).
48. R. Stoermer. Ber. **44**, 637 (1911).
49. H. Ichibagase and S. Terada. J. Pharm. Soc. Japan, **72**, 878 (1952); Chem. Abstr. **47**, 6413 (1953).
50. C. Taege. Ber. **20**, 2109 (1887).
51. J. G. Jones, J. B. Poole, J. C. Tompkinson, and R. J. P. Williams. J. Chem. Soc. 2001 (1958).
52. A. B. E. Lovett and E. Roberts. J. Chem. Soc. 1975 (1928).
53. L. N. Gilliland, Jr., J. P. Hart, and M. R. Everett. Proc. Oklahoma Acad. Sci. **21**, 119 (1941); Chem. Abstr. **36**, 438 (1942).
54. G. W. K. Cavill. J. Soc. Chem. Ind. **64**, 212T (1945).

DIELECTRIC EVIDENCE FOR ACETONE HYDRATE[1]

G. J. WILSON[2] AND D. W. DAVIDSON
Division of Applied Chemistry, National Research Council, Ottawa, Canada
Received August 16, 1962

ABSTRACT

The phase diagram of the acetone–water system shows that acetone hydrate decomposes at an incongruent melting point. The existence of acetone hydrate is confirmed by a study of the low-frequency dielectric properties of this system. A dispersion region, related to the relaxation of water molecules in the clathrate structure, is characterized by a "static" dielectric constant and an activation energy about half as large as the corresponding values for ice, and by a limiting high-frequency dielectric constant of about 7 at 200° K. The magnitude of the latter is attributed to orientation of acetone molecules within the larger cavities of the hydrate structure.

Can. J. Chem. Downloaded from www.nrcresearchpress.com by 210.87.254.42 on 09/05/12
For personal use only.

It is now well-established that a cubic form of ice which is stable at low temperatures for long periods of time can be formed by condensation of water vapor on a sufficiently cold surface (1). Since 1896 several workers have reported that an isotropic form of ice could be formed by cooling aqueous solutions of a large number of organic substances, including acetone (for summary, see ref. 2). In particular, Cohen and van der Horst (3) suggested the formation of "ice VIII" in cooled concentrated solutions of acetone and other organic liquids. They inferred that acetone was found in their analyses of the crystals as a result of their inability to separate the crystals completely from the acetone-rich mother liquor. Recently an X-ray study by Quist and Frank (4) clearly suggested that the cubic solid obtained at high acetone concentrations was acetone hydrate rather than ice VIII. The diffraction patterns were identical with those reported by von Stackelberg and Müller (5) for "hydrates of structure II" like those of $CHCl_3$ and C_2H_5Cl. In these structures, first proposed by Claussen (6), the organic molecules (A) occupy the larger of two different-sized cavities formed by a lattice of hydrogen-bonded water molecules. Since there are eight large cavities to the 136 water molecules in the unit cell, the maximum A content is given by $A.17H_2O$. The oxygen atoms of the water molecules belong to space group O_h^7—$Fd3m$ and the side of the unit cell is 17.2 Å.

In view of the uncertainty of the conditions of existence of acetone hydrate and our interest in molecular motions in clathrate structures of this type, we have studied the acetone–water system at low temperatures by means of low-frequency dielectric measurements, as well as by thermal analysis.

EXPERIMENTAL METHODS

Dielectric measurements were made on solutions of four concentrations (15.5, 27.0, 27.5, and 97.7 wt%) of distilled Reagent Grade acetone (conductivity 1.2×10^{-7} ohm^{-1} cm^{-1}) in conductivity water. Temperatures were between −194 and −15° and frequencies between 0.050 and 500 kc/sec, with instrumentation as previously indicated (7, 8). The cell was a three-terminal type with vertical coaxial stainless steel electrodes. Samples of known composition slowly frozen in this type of cell were found in the course of preliminary work on other hydrates (9) to be as satisfactory as those frozen *ex situ* and compressed hydraulically into disks before insertion between the parallel plate electrodes of the usual type of cell for solids. To the inconvenience of pressing the sample at low temperatures in the second method must be added a considerable uncertainty in the proper value of the cell constant to be used at different temperatures. When, as for many of the present measurements, liquid and solid phases are both present, vertical electrodes are less subject to the trapping of air pockets and incomplete filling of the interelectrode region than horizontal ones. We believe

[1]*Issued as N.R.C. No. 7122.*
[2]*N.R.C. Postdoctoral Fellow, 1961–62.*

the effect of possible air gaps to be small, except below the eutectic temperature, in the method we have used. Temperatures were measured to within about ±0.2° with a copper–constantan thermocouple.

Ten-gram samples for thermal analyses were inserted in a glass tube fitted with a thermocouple and an evacuated jacket. Because of relatively fast heating and cooling rates (1 to 2° per minute) and inadequate stirring of the samples, temperatures of inflection points in the curves were possibly uncertain by 1 to 2°.

RESULTS

Phase Diagram

Figure 1 summarizes the results of the thermal analyses. The liquidus curve divides into two branches at concentrations greater than about 31% acetone: the lower branch

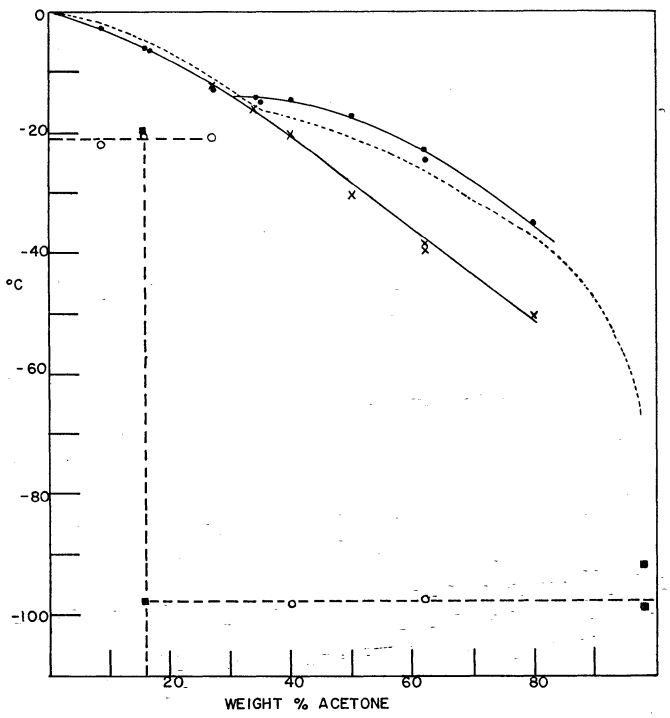

FIG. 1. Suggested phase diagram for the acetone–water system: × freezing points, ● melting points, ○ plateaus in heating and cooling curves, ■ discontinuities in dielectric heating curves.

marks the beginning of freezing, the upper the end of melting. The lower branch, continuous with the curve for lower concentrations, is assigned to the freezing of ice, the upper to the melting (and final decomposition) of acetone hydrate. Under our conditions practically all samples froze originally as ice but showed the later formation of acetone hydrate, during cooling to dry ice temperature and subsequent heating, either by a higher melting than freezing point (for large acetone concentrations) or by an inflection in the heating curve near −21° (for small concentrations). This latter temperature is some 6° lower than the intersection point of the ice and hydrate liquidus curves. Except for this feature, the behavior is that of a solid compound of acetone and water with an incongruent melting point. In fact, such a hydrate is a solid solution of guest molecules in a host lattice which can only exist when more than a critical fraction of the cavities are occupied (10). The composition of the hydrate will therefore depend on the activity of the acetone in the liquid phase present and may well depend also on the thermal

Can. J. Chem. Downloaded from www.nrcresearchpress.com by 210.87.254.42 on 09/05/12
For personal use only.

history of the sample. The vertical line in Fig. 1 at 15.9% acetone refers to the ideal composition given when all the cavities are occupied.

Most of the earlier studies of the acetone–water system (11) appear to have made use of freezing point measurements alone and do not show the upper branch of Fig. 1. However, the results of Benjamin, although reported (11) as freezing temperatures, are qualitatively in agreement with our hydrate decomposition temperatures. They are shown as the broken curve in Fig. 1. Our eutectic temperature (−99°) is somewhat higher than Benjamin's (−105°).

Dielectric Behavior

The complex plane locus of Fig. 2 is typical of the dispersion and absorption behavior shown by acetone hydrate at audio and low radio frequencies. Superimposed on a region

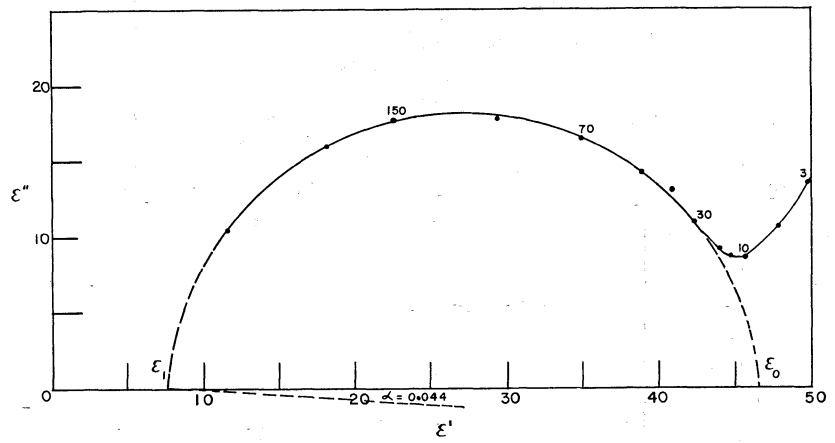

FIG. 2. Complex dielectric locus of 15.48 wt% acetone sample at −54.8°. Numbers beside points are frequencies in kc/sec.

usually marked by a well-defined absorption maximum is an additional absorption region at relatively low frequencies. Typically, the values of ϵ' and ϵ'' associated with this low-frequency absorption region continued to rise with decreasing frequency until the latter exceeded the range of the bridge. There is a similar effect in "slightly impure" ice (12).

As in ice (12), the low-frequency absorption was considerably reduced by application of a d-c. field, though in our case never completely eliminated. Figure 3 illustrates the effect on the sample of heating to −50°, followed by recooling in a field of some 1000 v/cm over a period of several hours. The absorption region occurring at higher frequencies is unaffected by the d-c. "fore-field". We attribute this latter region to orientational relaxation of the water molecules in the hydrate lattice.

Water Relaxation Region

It is difficult to define exactly the shape of the dispersion–absorption region associated with the rotational orientation of water molecules because of the low-frequency polarization mentioned above. It is slightly broader than would correspond to a single relaxation time. We have analyzed the results in terms of the time corresponding to the frequency of maximum absorption, as in a Cole–Cole type of representation (13), to which the data approximately conform. There is a definite tendency for the dispersion to become broader and for the Cole–Cole α to increase (cf. Fig. 2 with Fig. 3) as the temperature gets lower. In common with the hydrate of ethylene oxide (9), there is some indication that this

Can. J. Chem. Downloaded from www.nrcresearchpress.com by 210.87.254.42 on 09/05/12
For personal use only.

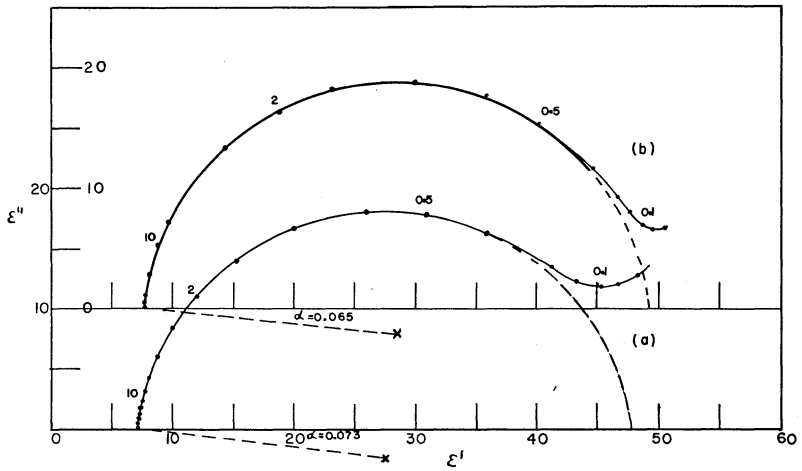

FIG. 3. Loci of same sample (27.45% acetone) (*a*) at −111.5° before and (*b*) at −107.0° after application of a d-c. field of 1000 v/cm.

dispersion region may be resolvable, particularly at low temperatures, into two or three single relaxation processes, but such a procedure is by no means unambiguous. For most samples the low-frequency polarization tends to overlap the water dispersion region more seriously as the temperature decreases, a relative temperature dependence which is the reverse of that found in ice.

The behavior of the real part ϵ' of the dielectric constant at a fixed frequency (100 kc/sec) is shown on the composite plot in Fig. 4. The points represent data obtained on samples in thermal equilibrium, the solid curves data on the 15.5% sample, which had been initially rapidly cooled and subsequently heated through the eutectic and acetone hydrate decomposition temperature ranges at a rate of ca. 0.5° per minute.

The ϵ' values at 100 kc/sec approximate to ϵ_1, the limiting high-frequency intercept, at low temperatures, increase rapidly with rising temperature through the dispersion region, and approach the static dielectric constant ϵ_0 near the hydrate-decomposition temperature. At this temperature, ϵ' falls, since the ice in the ice – aqueous acetone liquid mixture has an ϵ' value of not much more than 3 at this frequency (14).

Examination of a 97.7 wt% acetone solution above the eutectic temperature revealed no liquid phase dispersion to interfere with that attributed to acetone hydrate.

Limiting High-frequency Dielectric Constant: ϵ_1

The behavior of this quantity at different temperatures is illustrated for three samples in Fig. 5. Below the eutectic temperature the sample containing 15.5% acetone showed a lower value of ϵ_1 when rapidly cooled than when slowly cooled, which reflects either a "freezing-in" of some ice, a lower fraction of occupied cavities, or the presence of a larger air gap in the former. The ϵ_1 data for the slowly cooled case showed only a slight rise as the temperature rises through the eutectic point, followed by a fall at higher temperatures, which suggests very little liquid is in coexistence with the acetone hydrate for this composition. This roughly supports the stoichiometry provided by the X-ray formula, $A.17H_2O$, since the above composition represents 97% of the acetone content of the hydrate with fully occupied cavities. The samples of higher acetone content showed a rapid rise of ϵ_1 with increasing temperature above the eutectic point as more liquid phase was formed.

Can. J. Chem. Downloaded from www.nrcresearchpress.com by 210.87.254.42 on 09/05/12
For personal use only.

Can. J. Chem. Downloaded from www.nrcresearchpress.com by 210.87.254.42 on 09/05/12
For personal use only.

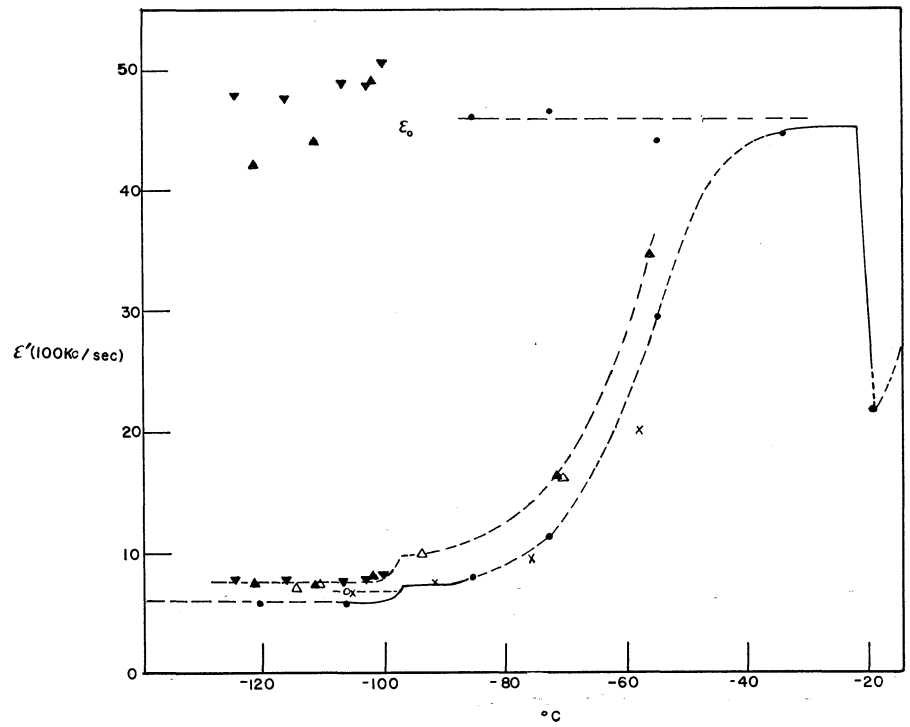

FIG. 4. Plot of ϵ' as measured at 100 kc/sec for various samples and temperatures. 15.48% acetone: ● sample cooled rapidly to −140° and reheated, × cooling measurements, ○ heated through eutectic temperature and recooled; 27.45% acetone: ▲▼ different runs; 27.0% acetone: △. Upper points are estimated ϵ_0 values.

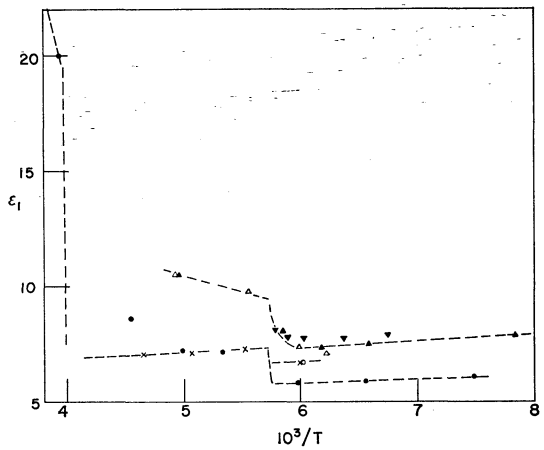

FIG. 5. Temperature dependence of ϵ_1. Points are identified in caption of Fig. 4.

These results suggest a true value of ϵ_1 somewhat in excess of 7 at temperatures near 200° K.

Limiting Low-frequency Dielectric Constant: ϵ_0

We have approximately evaluated the limiting low-frequency dielectric constant appropriate to the water relaxation by fitting a circular arc to the experimental points for

frequencies sufficiently high that the low-frequency polarization may be assumed to make only a minor contribution (cf. Figs. 2 and 3). This procedure is somewhat uncertain where there is serious overlap of the two polarization regions. Moreover, the presence of an air gap acting in series with the sample results in a measured ϵ_0 which is smaller than the true one, an effect which is greatest at low temperatures. Above the eutectic temperature the apparent value of ϵ_0 depends, in addition, upon the quantity, concentration, and distribution within the sample of the liquid phase. For samples of relatively high acetone content, ϵ_0 increases rapidly with rise of temperature.

Except for the samples with 27% acetone above the eutectic temperature, the experimental values of ϵ_0 tended to lie between 40 and 50 (see upper part of Fig. 4). We believe that the true static dielectric constant of acetone hydrate near its decomposition temperature is not likely to be greater than 60 and therefore no more than one-half the ϵ_0 value of ice at comparable temperatures (14).

Relaxation Times τ_0

These are plotted vs. $1/T$ in Fig. 6. They show no dependence upon sample composition to within the accuracy with which they have been derived (4 to 20%, depending upon sample and temperature). The activation energy derived from the straight line drawn in Fig. 6 is 6.3 kcal/mole, again about one-half of the corresponding figure for ice (14). As for ethylene oxide hydrate (9), there are signs that the dependence of τ_0 on $1/T$ may become less at low temperatures.

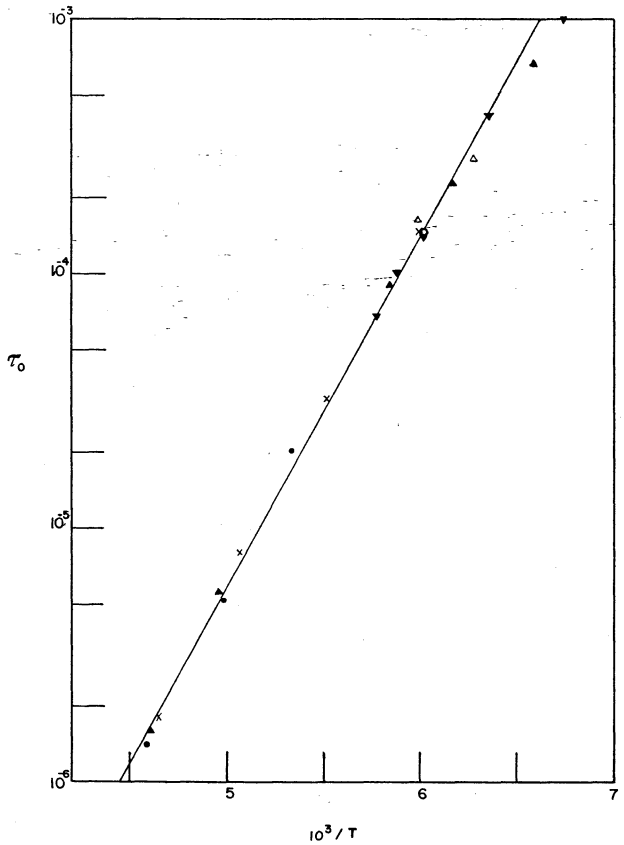

FIG. 6. Temperature dependence of τ_0. Points are identified in caption of Fig. 4.

Can. J. Chem. Downloaded from www.nrcresearchpress.com by 210.87.254.42 on 09/05/12
For personal use only.

Space-charge Polarization

In attributing the increasing values of ϵ'' and ϵ' at relatively low frequencies to space-charge polarization associated with the presence of impurity ions, we have been guided by the previous experience with ice and by the effect of application of a d-c. field. Since the ϵ'' values exceeded the range of the bridge at low frequencies we have tried to define qualitatively the amplitude of this dispersion by making photographic transient studies of the sample containing 15.5% acetone at temperatures corresponding to those of bridge measurements.

The results of one such measurement, along with the corresponding bridge results, are shown in Fig. 7. The transient curve represents the sample charging current, expressed

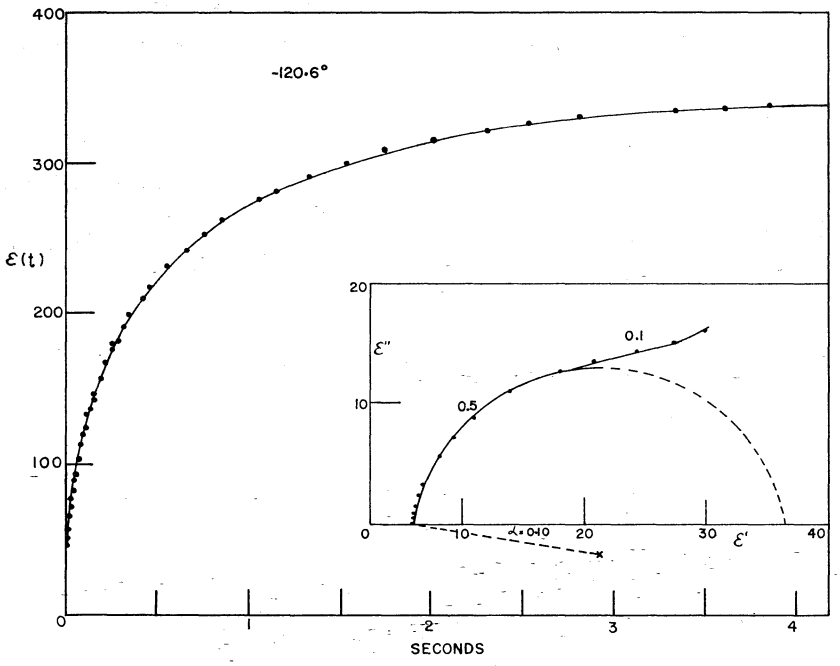

FIG. 7. Transient and bridge results for sample containing 15.48% acetone at −120.6°.

in units of capacitance equal to the cell constant, following application of a voltage rising linearly with time (15, 16). The linear contribution of a d-c. conductivity of 1.1×10^{-10} $ohm^{-1}cm^{-1}$ has been subtracted.

It is apparent that at times of the order of 5 seconds the polarization approaches a value equivalent to a dielectric constant some 10 times as great as that characteristic of the circular arc dispersion, for which τ_0 is of the order of 1 millisecond. The polarization curve rises somewhat more rapidly at the beginning, and less rapidly at the end, than the exponential, which rises to a fraction $(1-1/e)$ of its final value in the same time. In fact, the curve of Fig. 7 is fitted by $\epsilon(t) = 32+284t^{1/2}$ up to times of about 0.3 second, and by an exponential with a time constant of 0.81 second for times greater than 0.5 second. Such initial proportionality to $t^{1/2}$ and subsequent exponential behavior has been reported by Gränicher *et al.* (17) for the change of d-c. conductance of ice. Initial proportionality to $t^{1/2}$ was also found (12) for the rise in the low-frequency values of ϵ' and ϵ'' after removal of a d-c. fore-field. Extrapolation of relaxation data for higher temperatures (14) indicates that ordinary ice would have a relaxation time of the order of 4×10^3 seconds at this temperature.

Can. J. Chem. Downloaded from www.nrcresearchpress.com by 210.87.254.42 on 09/05/12
For personal use only.

DISCUSSION

The properties of the dielectric dispersion which we have attributed to the water molecules in acetone hydrate are qualitatively similar to those of other hydrates of the clathrate type that we have examined, in particular to those of ethylene oxide (9). These include values of ϵ_1 too large to be explained on the basis of induced polarization alone, values of ϵ_0 of the order of one-half those of ice, relaxation times intermediate between those of ice and liquid water, and an increase in breadth with decreasing temperature of a dispersion region which is slightly broader than the Debye type.

Calculation of ϵ_1

There seems little doubt that values of ϵ_1 considerably greater than 3 are related to the ability of the acetone molecules in the cavities to undergo orientation in the field. The magnitude of ϵ_1 to be expected on this basis may be estimated by a simple extension of the Onsager cavity method (18).

We consider a polar molecule at the center of a spherical cavity of radius a in a continuous medium of dielectric constant ϵ_∞. The reorientation rate of the molecule in the cavity is taken to be much greater than that of the water molecules in the surrounding medium, so that only polarizability effects in the latter contribute to ϵ_∞. The average component of the central molecule in the direction of the field is

$$\overline{\overline{m}}_E = \frac{3\epsilon_\infty}{2\epsilon_\infty+1}\frac{E}{1-f}\left[\alpha + \frac{\mu_0^2}{3kT(1-f)}\right],$$

in which E is the applied field, α and μ_0 the polarizability and dipole moment of the occluded molecule, and $f = 2(\epsilon_\infty-1)\alpha/(2\epsilon_\infty+1)a^3$. For the 16-faced cavities of von Stackelberg's structure II, a may be taken as 3.45 Å, one-half of the cavity diameter (5).

For acetone specifically, $\mu_0 = 2.88\times10^{-18}$ e.s.u. and, from the molar refraction, $\alpha = 6.4\times10^{-24}$ cm^3/molecule (19). With $\epsilon_\infty = 3$ one finds $f = 0.089$, $\overline{\overline{m}}_E = 1.64\times10^{-22}E$ e.s.u. at 200° K. The contribution to the Maxwell polarization arising from the permanent dipoles in the cavities is $P_2 = \nu y\overline{\overline{m}}_E$, where ν is the number of large cavities per cm^3 and y is the fraction of these cavities occupied by molecules. For eight cavities in a unit cube of side 17.16 Å (4) $\nu = 1.58\times10^{21}$ cavities per cm^3 and $P_2 = 0.260yE$. Under the further assumption that this polarization may simply be added to that of the continuum (i.e., to the polarizability contribution specified by ϵ_∞),

$$\epsilon_1 = 3+4\pi P_2/E = 3+3.3y,$$

which has a maximum value of 6.3 when all the cavities are occupied.

This value agrees well with the experimental value of about 7 at 200° K (Fig. 5). The calculated value of ϵ_1 is greatly dependent on the value assumed for ϵ_∞, which can only be determined experimentally at frequencies sufficiently high that rotations of the molecules in the cavities no longer contribute to the dielectric constant. In our frequency range, we have been unable to find the absorption region related to rotation of molecules in the cavities even at temperatures as low as −194°.

When y approaches unity there should be an approximately linear dependence of ϵ_1 on the square of the dipole moments of the occluded molecules. Such a dependence has been noted by Dryden (20) for some of the quinol clathrates, to which a similar model may be applied.

Values of ϵ_0

It is necessary to account for the relatively low values of ϵ_0, in comparison with those of ice or water, in terms of the structure built up in the hydrate by hydrogen bonding of

Can. J. Chem. Downloaded from www.nrcresearchpress.com by 210.87.254.42 on 09/05/12
For personal use only.

the water molecules. Detailed calculations of the type attempted by Powles (21) for ice, already laborious, are made more so by the presence of three types of water molecule with non-identical environments and of some angles which depart considerably from tetrahedral if all the distances between water molecules are taken as equal (5). Furthermore, even for the simplest Pauling model, computational difficulties due to the interdependence of legs leading out from a central molecule as the number of layers of neighbors grows, which appeared first on consideration of third-nearest neighbors in ice, appear now as soon as the group of molecules considered includes second-nearest neighbors (lying in the same pentagonal ring).

There are, however, a number of factors which should lead to values of ϵ_0 which are lower for the hydrates than for ice. The first of these is the presence of pentagonal rings which, in the hydrates of structure II, outnumber the hexagonal rings in a ratio of 9 to 1. A simple analysis of the probabilities of the occurrence of hydrogen atoms at different positions around the ring, subject to the conditions that the positions of the hydrogen atoms on one molecule be fixed and that there be one hydrogen atom in each bond, shows that the most likely arrangement is that in which the resultant moment of the OH bonds adds vectorially to zero. The next most likely configurations give rise only to small resultant moments. There is a similar but smaller tendency within hexagonal rings.

The second factor arises from the lower density of water molecules in the hydrates. The X-ray parameters of Quist and Frank (4) at ca. $-37°$ lead to a number of water molecules per cm^3 which is some 15% less than that for ice at a comparable temperature.

Finally, an important factor in determining the value of ϵ_0 is the quantity $(\epsilon_\infty+2)^2$, to which ϵ_0 is proportional (cf. equation 1.2 of reference 20). It is clear that if the refractive index of the hydrate were appreciably less than that of ice, a considerable reduction in ϵ_0 would occur.

It seems likely that the combined effect of the above factors is sufficient to reduce the static dielectric constant to roughly half its value in ice.

Relaxation of the Water Molecules

The faster relaxation rate and lower activation energy for water reorientation in acetone hydrate is consistent with a looser hydrogen-bonded structure than is found in ice. According to von Stackelberg and Müller (5) the distance between oxygen atoms in neighboring water molecules is 2.78 Å compared with 2.76 Å in ice, and some of the angles between hydrogen bonds are considerably distorted from tetrahedral values. If the water molecules were able to undergo reorientation independently of one another, one might expect three discrete dispersion regions characteristic of the three types of environment of the water molecules; the amplitudes of dispersion would be greatly different since the numbers of water molecules in the three environments are in the ratio 1:4:12. The more likely relaxation mechanism, the diffusion of rotational defects of the Bjerrum (22) type, should also lead to a broadening of the dispersion character, since presumably some diffusion paths through the hydrate are more likely than others.

The relaxation rate may also be affected by the degree of occupancy of adjacent cavities. It will be interesting to determine the effect on the relaxation of different types of occluded molecules.

Dielectric Evidence of the Existence of Acetone Hydrate

"High-frequency" dielectric constants of acetone–water mixtures which are greatly in excess of 3 below the eutectic temperature can only be accounted for by the presence of a hydrate structure containing cavities within which the acetone molecules are capable

Can. J. Chem. Downloaded from www.nrcresearchpress.com by 210.87.254.42 on 09/05/12
For personal use only.

of orientation at rates considerably faster than the measuring frequencies. Values no greater than 3 would be expected for mixtures of ice and solid acetone.

The relaxation properties of the dispersion region described above are greatly different from those of ice and are independent of concentration of acetone. They therefore must be attributed to the existence of a structure present at all appreciable acetone concentrations, rather than to an ice structure perturbed to an extent which depends upon the quantity of acetone present. These properties are qualitatively similar to those of the ethylene oxide hydrate, whose existence has been well established (cf. ref. 23 and references cited therein).

The dielectric behavior appears to be in accord with the suggested phase diagram in all respects.

Can. J. Chem. Downloaded from www.nrcresearchpress.com by 210.87.254.42 on 09/05/12
For personal use only.

ACKNOWLEDGMENT

We are indebted to Gordon Young for assistance with the measurements.

REFERENCES

1. M. BLACKMAN and N. D. LISGARTEN. Proc. Roy. Soc. (London), Ser. A, **239**, 93 (1957).
2. H. GRÄNICHER. Z. Krist. **110**, 432 (1958).
3. E. COHEN and C. J. G. VAN DER HORST. Z. Physik. Chem. Sect. B, **40**, 231 (1938).
4. A. S. QUIST and H. S. FRANK. J. Phys. Chem. **65**, 560 (1961).
5. M. VON STACKELBERG and H. R. MÜLLER. Z. Elektrochem. **58**, 25 (1954).
6. W. F. CLAUSSEN. J. Chem. Phys. **19**, 259 (1951).
7. D. W. DAVIDSON. Can. J. Chem. **35**, 458 (1957).
8. R. F. GRANT, D. W. DAVIDSON, and P. GRAY. J. Chem. Phys. **33**, 1713 (1960).
9. D. W. DAVIDSON and G. J. WILSON. Unpublished results.
10. J. H. VAN DER WAALS and J. C. PLATTEEUW. *In* Advances in chemical physics. Vol. II. 1959. p. 1.
11. J. TIMMERMANS. The physico-chemical constants of binary systems in concentrated solutions. Vol. 4. Interscience Publishers, New York. 1960. p. 39.
12. H. GRÄNICHER, C. JACCARD, P. SCHERRER, and A. STEINEMANN. Helv. Phys. Acta, **28**, 300 (1955).
13. K. S. COLE and R. H. COLE. J. Chem. Phys. **9**, 341 (1941).
14. R. P. AUTY and R. H. COLE. J. Chem. Phys. **20**, 1309 (1952).
15. D. W. DAVIDSON, R. P. AUTY, and R. H. COLE. Rev. Sci. Instr. **22**, 678 (1951).
16. D. W. DAVIDSON. Can. J. Chem. **39**, 571 (1961).
17. H. GRÄNICHER, C. JACCARD, P. SCHERRER, and A. STEINEMANN. Discussions Faraday Soc. **33**, 50 (1957).
18. L. ONSAGER. J. Am. Chem. Soc. **58**, 1486 (1936).
19. A. A. MARYOTT and F. BUCKLEY. Tables of dielectric constants and electric dipole moments of substances in the gaseous state. NBS Circ. 537. 1953.
20. J. S. DRYDEN. Trans. Faraday Soc. **49**, 1333 (1953).
21. J. G. POWLES. J. Chem. Phys. **20**, 1302 (1952).
22. N. BJERRUM. Kgl. Danske Videnskab. Selskab, Mat. Fys. Medd. **27**, No. 1 (1951).
23. M. VON STACKELBERG and B. MEUTHEN. Z. Elektrochem. **62**, 130 (1958).

Can. J. Chem. Downloaded from www.nrcresearchpress.com by 210.87.254.42 on 09/05/12
For personal use only.

REACTIONS OF PHENYL-SUBSTITUTED HETEROCYCLIC COMPOUNDS

I. NITRATION OF 2-PHENYL-1,2,3,2H-TRIAZOLE[1]

BRIAN M. LYNCH[2] AND TZE-LOCK CHAN[3]
Chemistry Department, Memorial University of Newfoundland, St. John's, Newfoundland

Received September 27, 1962

ABSTRACT

Structures have been assigned to the mono-, di-, and tri-nitration products of 2-phenyl-1,2,3,2H-triazole, on the basis, partly, of ultraviolet absorption spectra. The pattern of nitration closely resembles that of 1-phenylpyrazole. A compound previously described as 2-(*o*-nitrophenyl)-1,2,3,2H-triazole is actually 4-nitro-2-*p*-nitrophenyl-1,2,3,2H-triazole.

Riebsomer (1) investigated the nitration of 2-phenyl-1,2,3,2H-triazole (I) by mixed acids at 20°, and obtained two products, having m.p. 183° and 125°. He suggested that the higher-melting compound was 2-*p*-nitrophenyl-1,2,3,2H-triazole, and that the lower-melting compound was the ortho isomer. We required these substances as intermediates in the syntheses of 2-*p*-biphenylyl-1,2,3,2H-triazole (II) and 2-*o*-biphenylyl-1,2,3,2H-triazole (III), so Riebsomer's experiments were repeated.

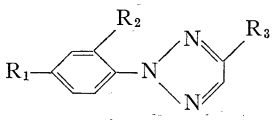

I: $R_1 = R_2 = R_3 = H$

II: $R_1 = Ph$; $R_2 = R_3 = H$

III: $R_1 = R_3 = H$; $R_2 = Ph$

IV: $R_1 = R_3 = Ph$; $R_2 = H$

The higher-melting compound had the characteristics reported by Riebsomer, and its ultraviolet absorption was closely similar to that of 1-*p*-nitrophenylpyrazole (see Table I).

TABLE I

Ultraviolet absorption maxima of corresponding phenyltriazoles and phenylpyrazoles

1,2,3,2H-Triazole	λ_{max} (mμ)	log ε	Pyrazole	λ_{max} (mμ)	log ε
2-Phenyl	263	4.13	1-Phenyl	252	4.13
2-*p*-Nitrophenyl	306	4.09	1-*p*-Nitrophenyl*	312–314	4.24
4-Nitro-2-*p*-nitrophenyl	304	4.36	4-Nitro-1-*p*-nitrophenyl*	306	4.37
2-*p*-Biphenylyl	286	4.50	1-(2,4-Dinitrophenyl)	306	3.85
			1-*p*-Biphenylyl	280	4.50

*From DalMonte *et al.* (4).

Since the replacement of —CH: by —N: in heteroaromatic systems generally has little influence on ultraviolet absorption (2), correspondingly substituted 1-phenylpyrazoles and 2-phenyl-1,2,3,2H-triazoles should have similar electronic spectra, and assignments

[1]*Financial assistance for this work was received from the National Research Council.*
[2]*To whom requests for reprints should be addressed, at the Department of Chemistry, St. Francis Xavier University, Antigonish, Nova Scotia.*
[3]*Summer Research Assistant, 1962. Present address: Department of Chemistry, University of Kansas City, Kansas City, Missouri, U.S.A.*

of structure can be based on such similarities. Further, the infrared spectra of the higher-melting compound showed strong bands at 1345 and 1530 cm^{-1}, corresponding to the symmetric and asymmetric N—O stretching vibrations, closely similar in frequency to those noted for 1-*p*-nitrophenylpyrazole (1341 and 1527 cm^{-1}). Present work (3) indicates that these band positions are characteristic of a *p*-nitro substituent in N-phenylated pyrazoles and imidazoles, and it seems likely that the correlation extends to phenyltriazoles.

Additional evidence in support of Riebsomer's assignment for the compound of m.p. 183° was obtained after reduction to the corresponding amine, followed by diazotization of the amine and Gomberg arylation of benzene. This yielded a biphenylyltriazole with ultraviolet absorption closely resembling that of 1-*p*-biphenylylpyrazole (3; see Table I), and showing strong infrared absorption in the C—H out-of-plane deformation region at 700, 765–770 (phenyl group), 850 (para substitution), and 950–965 cm^{-1} (triazole ring), to which structure II is assigned.

The lower-melting compound mentioned by Riebsomer was also obtained in our nitrations, although the melting point was raised to 140° by adsorption chromatography and crystallization. The ultraviolet absorption of this product differed markedly from that of 1-*o*-nitrophenylpyrazole, thus excluding the structure suggested by Riebsomer. Furthermore, the analytical results reported previously (nitrogen analyses) (1) do not distinguish between a mono- and a di-nitrophenyltriazole. Our analytical figures show that the compound, m.p. 140°, is a dinitro-2-phenyl-1,2,3,2H-triazole. Ultraviolet absorption data do not distinguish unequivocally between the two most likely structures, i.e., 4-nitro-2-*p*-nitrophenyl-1,2,3,2H-triazole and 2-(2,4-dinitrophenyl)-1,2,3,2H-triazole, since the spectra of the correspondingly substituted pyrazoles are fairly similar to one another and to the spectra of the compound of m.p. 140° (see Table I).

However, 2-(2,4-dinitrophenyl)-1,2,3,2H-triazole should readily undergo nucleophilic fission of the inter-ring C—N bond (compare 1-(2,4-dinitrophenyl)pyrazole (5, 6)), and the dinitrophenyltriazole, m.p. 140°, was unaffected by boiling with methanolic sodium methoxide, thus leading to the conclusion that the compound of m.p. 140° is 4-nitro-2-*p*-nitrophenyl-1,2,3,2H-triazole. Reduction of 4-nitro-2-*p*-nitrophenyl-1,2,3,2H-triazole as for 2-*p*-nitrophenyl-1,2,3,2H-triazole, followed by tetrazotization and Gomberg arylation of benzene, yielded 2-*p*-biphenylyl-4-phenyl-1,2,3,2H-triazole (IV).

Further nitration of 2-*p*-nitrophenyl-1,2,3,2H-triazole at 25° was found to yield 4-nitro-2-*p*-nitrophenyl-1,2,3,2H-triazole (compare the behavior of 1-*p*-nitrophenylpyrazole (5)), while nitration of the mono- or di-nitro compounds at 80°, or of the dinitro compound at 25°, yielded 2-(2,4-dinitrophenyl)-4-nitro-1,2,3,2H-triazole. Proof of structure of the trinitro compound was obtained by fission with methanolic sodium methoxide to yield 2,4-dinitroanisole.

Exclusive mononitration of 2-phenyl-1,2,3,2H-triazole to the *p*-nitrophenyltriazole can be effected in good yield by nitric acid in acetic anhydride, a more selective attacking reagent than nitric acid – sulphuric acid.

The general conditions necessary for the stepwise nitration of 2-phenyl-1,2,3,2H-triazole thus show close correspondence with those for 1-phenylpyrazole (5), notwithstanding the presence of an additional electron-attracting nitrogen atom in the triazole.

EXPERIMENTAL

General

Analyses were by the Schwarzkopf Microanalytical Laboratory, Woodside, N.Y., U.S.A. Infrared spectra were recorded using a Unicam SP100 spectrophotometer (samples were examined using the potassium chloride

Can. J. Chem. Downloaded from www.nrcresearchpress.com by 210.87.254.42 on 09/05/12
For personal use only.

disk technique) and ultraviolet spectra were measured in 95% ethanol using a Beckman DK-2A Ratio-Recording spectrophotometer; melting points were determined on a Fisher–Johns melting point apparatus and are uncorrected.

2-Phenyl-1,2,3,2H-triazole (I)

This compound, b.p. 228°, was prepared by oxidation of glyoxal bisphenylhydrazone with copper (II) sulphate (Riebsomer (1)).

Nitrations

(a) Of the Phenyltriazole (I) by Mixed Acids at 20°

The conditions employed were essentially those reported previously (1). 2-Phenyl-1,2,3,2H-triazole (7 g) in sulphuric acid (*d* 1.84, 20 ml) was nitrated by addition of nitric acid (*d* 1.42, 10 ml) over 1 hour at 20°. The reaction mixture was poured onto crushed ice and the precipitate was collected and washed repeatedly with cold ethanol. Crystallization from ethanol gave light yellow needles (5.5 g) of 2-*p*-nitrophenyl-1,2,3,2H-triazole, m.p. 183°. Anal. Calc. for $C_8H_6N_4O_2$: C, 50.53; H, 3.18%. Found: C, 50.33; H, 2.90%. Ultraviolet absorption: see Table I.

The ethanol washings and the mother liquor from the crystallizations were combined and the solvent was removed under reduced pressure. The residue was dissolved in benzene and chromatographed on alumina. Removal of solvent from the eluate, followed by crystallization from ethanol, yielded light yellow needles, m.p. 140° (0.98 g), presumed to be 4-nitro-2-*p*-nitrophenyl-1,2,3,2H-triazole. Anal. Calc. for $C_8H_5N_5O_4$: C, 40.86; H, 2.14; N, 29.78%. Found: C, 41.01; H, 2.34; N, 29.85%. Ultraviolet absorption: see Table I.

(b) Of the Phenyltriazole (I) by Nitric Acid – Acetic Anhydride

To 2-phenyl-1,2,3,2H-triazole (5 g) in acetic anhydride (50 ml) was added nitric acid (*d* 1.52, 25 ml) in acetic anhydride (25 ml) at ca. 15°. Precipitation commenced almost immediately; after 1 hour, the mixture was poured onto ice, and the product was collected and crystallized from ethanol, giving 2-*p*-nitrophenyl-1,2,3,2H-triazole (5.3 g), m.p. 183°. No lower-melting nitration products were isolated.

(c) Of 2-Nitrophenyl-1,2,3,2H-triazole by Mixed Acids at 25°

2-*p*-Nitrophenyl-1,2,3,2H-triazole (1.4 g) was nitrated at 25° using the general conditions of part (*a*) above. Repeated crystallization of the reaction product from ethanol yielded 4-nitro-2-*p*-nitrophenyl-1,2,3,2H-triazole (1.3 g), m.p. 140°, identical in all respects with the lower-melting product from the nitration of I. Anal. Found: C, 41.14; H, 2.01; N, 29.60%.

(d) Of 2-p-Nitrophenyl-1,2,3,2H-triazole or 4-Nitro-2-p-nitrophenyl-1,2,3,2H-triazole at 80°, or of 4-Nitro-2-p-nitrophenyl-1,2,3,2H-triazole at 25°

These reactions were carried out using the conditions noted in part (*a*) above. Both the mono- and the di-nitro compounds (in sulphuric acid) gave a blue color on addition of nitric acid: completion of reaction was indicated by a color change to yellow. The products of all three reactions were needles, m.p. 104°, of 2-(2,4-dinitrophenyl)-4-nitro-1,2,3,2H-triazole. Anal. calc. for $C_8H_4N_6O_6$: C, 34.30; H, 1.44%. Found: C, 34.02; H, 1.52%. Ultraviolet absorption: λ_{max} 285 mμ, log ϵ 4.24. Yields were as follows: 2.4 g from 2.5 g mononitro compound at 80°, 0.65 g from 0.80 g dinitro compound at 80°, and 0.30 g from 1.0 g dinitro compound at 25°.

Proof of Structure of 2-(2,4-Dinitrophenyl)-1,2,3,2H-triazole

The trinitro compound (1.0 g) in methanol (25 ml) was heated under reflux with 0.6 *N* methanolic sodium methoxide (20 ml) for 10 minutes. The reaction mixture was poured onto ice, and the resulting precipitate was collected, dried, dissolved in benzene, and chromatographed on alumina. Evaporation of the eluate yielded 2,4-dinitroanisole (0.45 g), m.p. 87°, identical (m.p., mixed m.p., infrared and ultraviolet absorption) with an authentic sample.

2-p-Biphenylyl-1,2,3,2H-triazole (II)

2-*p*-Nitrophenyl-1,2,3,2H-triazole (2.0 g) was quantitatively reduced to the corresponding amine by tin and hydrochloric acid, and converted into the diazonium chloride by standard procedures. The diazo solution thus obtained was stirred vigorously with benzene at 5°, after buffering to pH 5 with sodium acetate. The mixture was allowed to reach room temperature with continuous stirring, and the benzene layer was chromatographed on alumina. Evaporation of the eluate, followed by crystallization from ethanol, yielded 2-*p*-biphenylyl-1,2,3,2H-triazole (0.5 g), m.p. 90°. Anal. Calc. for $C_{14}H_{11}N_3$: C, 76.00; H, 5.01%. Found: C, 75.80; H, 5.30%. Ultraviolet absorption: see Table I.

2-p-Biphenylyl-4-phenyl-1,2,3,2H-triazole (IV)

Similar reduction of 4-nitro-2-*p*-nitrophenyl-1,2,3,2H-triazole by tin and hydrochloric acid, followed by tetrazotization and reaction of the buffered tetrazonium salt solution with benzene, gave 2-*p*-biphenylyl-4-phenyl-1,2,3,2H-triazole, m.p. 124°, in poor yield. Anal. Calc. for $C_{20}H_{15}N_3$: C, 80.80; H, 5.08%. Found: C, 80.58; H, 5.69%. Ultraviolet absorption: λ_{max} 308 mμ, log ϵ 4.52.

Can. J. Chem. Downloaded from www.nrcresearchpress.com by 210.87.254.42 on 09/05/12
For personal use only.

ACKNOWLEDGMENTS

We thank the National Research Council for generous support through Operating and Equipment Grants, Mr. M. A. Khan for furnishing reference samples, and Miss J. Murphy for skilled assistance with spectrophotometry.

REFERENCES

1. J. L. RIEBSOMER. J. Org. Chem. **13**, 815 (1948).
2. A. E. GILLAM and E. S. STERN. An introduction to electronic absorption spectroscopy in organic chemistry. Edward Arnold, London. 1954. p. 134.
3. M. A. KHAN and B. M. LYNCH. To be published.
4. D. DALMONTE, A. MANGINI, and R. PASSERINI. Gazz. Chim. Ital. **86**, 797 (1956).
5. I. L. FINAR and R. J. HURLOCK. J. Chem. Soc. 3024 (1957).
6. H. P. CROCKER and R. H. HALL. J. Chem. Soc. 4489 (1955).

Can. J. Chem. Downloaded from www.nrcresearchpress.com by 210.87.254.42 on 09/05/12
For personal use only.

APPLICATION OF QUASI-LATTICE THEORY TO ALCOHOL – CARBON TETRACHLORIDE SYSTEMS[1]

B. DACRE[2] AND G. C. BENSON
Division of Pure Chemistry, National Research Council, Ottawa, Canada
Received August 24, 1962

ABSTRACT

Values of heats of mixing are reported for methanol, *n*-butanol, and *n*-octanol with carbon tetrachloride at 25° C. The experimental results are combined with data from other sources and an analysis of the excess thermodynamic functions for carbon tetrachloride solutions of methanol, ethanol, *n*-propanol, *n*-butanol, and *n*-octanol in terms of Barker's theory of solutions is described. The behavior of these systems can be reproduced fairly well by the Barker model.

INTRODUCTION

A method for calculating the thermodynamic properties of solutions from a quasi-lattice model which allows for the effects of cooperative orientation has been described by Barker and co-workers (1, 2, 3). Application of the theory involves the assumption of certain volume and contact relations for the molecules and the adjustment of energy parameters to fit the experimental data. Despite these somewhat empirical aspects, the theory provides a useful approach to the study of associated solutions, and data for a number of binary systems have been analyzed by this approach. Quite recently Goates, Snow, and James (4) applied Barker's theory to the systems ethanol–cyclohexane, methanol–benzene, and ethanol–benzene and were able to find a set of contact interaction energies which were consistent with their enthalpy values.

The present paper reports the results of measurements of the heat of mixing of methanol, *n*-butanol, and *n*-octanol with carbon tetrachloride at 25° C. During an analysis of the results in terms of Barker's theory, values of the free energy, heat, and volume of mixing for a number of alcohol – carbon tetrachloride systems were published by Missen and co-workers (5, 6). These new data and information from other sources have been employed, together with the results obtained in the present work, in a comprehensive series of Barker calculations for mixtures of methanol, ethanol, *n*-propanol, *n*-butanol, and *n*-octanol with carbon tetrachloride (subsequently referred to as systems I, II, ···, V respectively). The object of the computations was to find a consistent set of interaction energies which would reproduce the thermodynamic mixing functions for the five systems. In the dilute concentration region where comparison could be made with values obtained from infrared and n.m.r. studies, alcohol monomer fractions were also calculated.

EXPERIMENTAL

The main features of the adiabatic calorimeter used for the heat of mixing determinations have been described previously (7). For the present work a pyrex mixing cell in which the two components were separated initially by mercury was supported inside the metal calorimeter vessel and the intervening space filled with water to improve the thermal contact.

Refractive indices and boiling points characterizing the pure components used to form the binary solutions are summarized in Table I. Spectrochemical grade methanol (Matheson, Coleman and Bell) and carbon tetrachloride (Eastman Organic Chemicals) were used directly. The *n*-butanol and *n*-octanol were reagent grade materials (British Drug Houses) which were distilled from sodium prior to use. A second distillation had a negligible effect on the values of the physical properties listed in Table I.

[1]*Issued as N.R.C. No. 7123.*
[2]*National Research Council of Canada Postdoctoral Fellow 1960–1962. Present address: Royal Military College of Science, Shrivenham, Wilts, England.*

Can. J. Chem. Downloaded from www.nrcresearchpress.com by 210.87.254.42 on 09/05/12
For personal use only.

TABLE I

Physical properties of component liquids

Component	n_D^{20}	B.p. (760 mm)
Methanol	1.3287	—
n-Butanol	1.3992	117.6–117.8
n-Octanol	1.4292	194.6
Carbon tetrachloride	1.4600	—

An analysis of the precision of the various experimental quantities indicates that under the existing operating conditions the accuracy of the result depends mainly on the measurement of the changes in thermocouple e.m.f. during the mixing and calibration periods. A reasonable estimate of the error in these voltages is 0.15 μv, which corresponds to an error of about 0.5 cal mole^{-1} in the heat of mixing. The free vapor volumes in the mixing cell were quite small (0.1 to 0.2 cm^3) and no vapor space corrections were made since calculations showed that these were negligible compared to the estimated error of the results.

RESULTS

The experimental results for the heat of mixing at constant pressure H_p^E (stated in cal mole^{-1} of solution[3]) are given in Table II for the three alcohol – carbon tetrachloride

TABLE II

Experimental values of heats of mixing for alcohol – carbon tetrachloride systems at 25° C

CH_3OH–CCl_4		C_4H_9OH–CCl_4		$C_8H_{17}OH$–CCl_4	
Mole fraction of alcohol	H_p^E (cal mole^{-1})	Mole fraction of alcohol	H_p^E (cal mole^{-1})	Mole fraction of alcohol	H_p^E (cal mole^{-1})
0.0465	66.7	0.0329	71.7	0.0030	13.4
0.1274	80.6	0.0902	103.2	0.0116	40.9
0.1346	81.2	0.1374	115.9	0.0990	107.8
0.1796	82.4	0.2228	120.5	0.1669	121.6
0.2072	80.5	0.2974	120.4	0.2054	127.9
0.2705	75.5	0.4132	104.2	0.2935	127.2
0.3010	74.3	0.4950	84.9	0.4191	115.1
0.3040	74.8	0.7235	26.7	0.5704	92.4
0.4195	59.8	0.8540	6.1	0.7158	58.1
0.4892	47.4	0.9427	0.2	0.7596	50.3
0.6034	29.0			0.8877	23.6
0.8577	−2.2				
0.9127	−6.0				

systems at 25° C. It was not possible to represent the concentration dependence of H_p^E properly by a Margules type of equation, as employed by Scatchard *et al.* (8), using powers of the mole fraction difference as high as 4. The inadequacy of the Margules form for alcohol systems presumably is due to the marked asymmetric character of the curves and has been noted by other workers (5, 6, 9). Otterstedt and Missen (10) have suggested a square root relation but this too failed to represent the data satisfactorily and graphical procedures were adopted. It was possible to draw, through large-scale plots of the results, acceptable smooth curves from which the standard deviations of the experimental points were 0.6, 0.8, and 0.7 cal mole^{-1} for systems I, IV, and V respectively. Values of H_p^E read from the curves at concentration intervals of 0.05 are collected in Table III. Heats of mixing for some of the same systems have been reported by several previous investigators (6, 8, 11, 12, 13). However, none of the measurements were made at 25° C and it

[3]*The defined thermochemical calorie, equal to 4.184 absolute joules, is used throughout this paper.*

Can. J. Chem. Downloaded from www.nrcresearchpress.com by 210.87.254.42 on 09/05/12
For personal use only.

TABLE III

Values of H_p^E at rounded concentrations for alcohol – carbon tetrachloride systems at 25° C

Mole fraction of alcohol	H_p^E (cal mole^{-1})		
	CH_3OH–CCl_4	C_4H_9OH–CCl_4	$C_8H_{17}OH$–CCl_4
0.05	67.7	82.5	89.1
0.10	78.4	107.0	108.0
0.15	81.9	116.2	120.3
0.20	81.6	120.0	126.5
0.25	78.6	121.2	127.8
0.30	74.1	120.2	126.6
0.35	68.9	115.3	123.0
0.40	62.4	108.0	117.7
0.45	54.4	96.3	111.4
0.50	45.4	83.3	104.2
0.55	37.0	70.5	95.9
0.60	29.4	57.2	86.2
0.65	22.6	44.0	75.3
0.70	16.0	32.0	63.5
0.75	10.0	22.0	52.2
0.80	4.0	13.8	41.8
0.85	−1.4	7.0	31.7
0.90	−5.6	2.6	21.0
0.95	−5.0	0.1	10.2

appears that a reliable interpolation can be made only in the case of the data of Otterstedt and Missen (6). Using the cubic form suggested by these authors, values of H_p^E at 25° C were calulated for systems I and V at the 19 concentrations given in Table III; the standard deviation from the values in Table III was 2.4 cal mole^{-1} for system I and 1.5 cal mole^{-1} for system V. This agreement is quite satisfactory since the standard deviations are of the same magnitude as those quoted in reference 6.

DATA FOR SYSTEMS I–V

Experimental results obtained at constant pressure must be corrected to constant volume before comparison with values calculated for a lattice model of the solution. Theoretically this means that the volume for each molecule should be constant for the mixing process (14, 15); however, it is common practice to evaluate the correction on the basis of constant volume for the system as a whole and this course was followed in the present work. The excess energy U_v^E (at constant volume) was calculated from values of the enthalpy H_p^E (at constant pressure) using the formula

$$U_v^E = H_p^E - T(\alpha/\beta)V^E \quad [1]$$

derived by Scatchard (16). In this equation V^E is the volume of mixing, T the absolute temperature, α the coefficient of thermal expansion for the solution, and β the isothermal compressibility.

Values of the excess entropy S_v^E were obtained from the relation

$$TS_v^E = U_v^E - G_p^E, \quad [2]$$

where G_p^E is the excess Gibbs free energy. This expression neglects the difference between the Gibbs and Helmholtz free energies since it depends on the square of V^E and is small for the systems considered.

A fit between theory and experiment can be attempted with most confidence at 25° C since the present enthalpy measurements for systems I, IV, and V were made at this temperature and values of V^E (for all five systems) are also available. Data for evaluating

Can. J. Chem. Downloaded from www.nrcresearchpress.com by 210.87.254.42 on 09/05/12
For personal use only.

the ratio α/β at 25° C have been published for the pure components (17, 18) and estimates for solutions were made assuming additivity. The excess Gibbs free energies have not been determined at 25° for any of the systems but the temperature coefficient of the free energy is fairly small, particularly for the longer-chain alcohol systems. Values of G_p^E at 25° could therefore be estimated with reasonable accuracy from data at other temperatures.

The methods employed to obtain the "experimental" points, plotted in Figs. 1–5, are summarized in the following paragraphs. For clarity each of the five systems is considered individually.

Can. J. Chem. Downloaded from www.nrcresearchpress.com by 210.87.254.42 on 09/05/12
For personal use only.

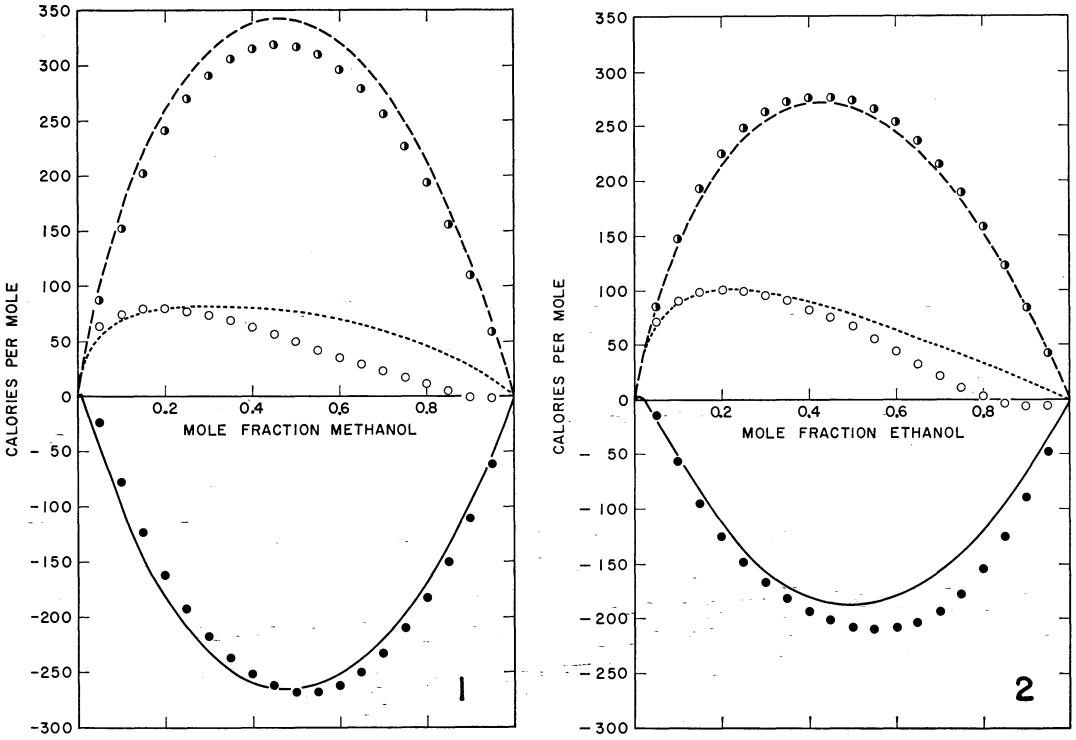

FIG. 1. Excess thermodynamic functions for methanol – carbon tetrachloride solutions at 25° C. Experimental points: ◑, G_p^E, ○, U_v^E, and ●, TS_v^E. Curves calculated from theory.

FIG. 2. Excess thermodynamic functions for ethanol – carbon tetrachloride solutions at 25° C. Experimental points: ◑, G_p^E, ○, U_v^E, and ●, TS_v^E. Curves calculated from theory.

(I) Methanol – Carbon Tetrachloride

G_p^E at 25° C was calculated from the equation given by Scatchard and Ticknor (19). More recent vapor pressure measurements (5, 12) are in fairly good agreement with these earlier data. Values of H_p^E were taken from the present work; data for V^E due to Paraskevopoulos and Missen (5), which are more extensive than the results given in reference 19, were used in making the correction to constant volume.

(II) Ethanol – Carbon Tetrachloride

The values of G_p^E at 45° and 65° C, reported by Barker, Brown, and Smith (2) were extrapolated to 25° assuming a linear variation with temperature. For H_p^E only the data of Otterstedt and Missen (6) at 35° C are available. In order to estimate values at 25° C it was assumed that the temperature variation at a given concentration was the mean of that for systems I and III at the same concentration. As a check on this method, values

of H_p^E estimated at 45° C were found to agree reasonably well with the experimental data of Brown and Fock (13) over the very limited concentration range studied by those authors. V^E was calculated from densities given in reference 2.

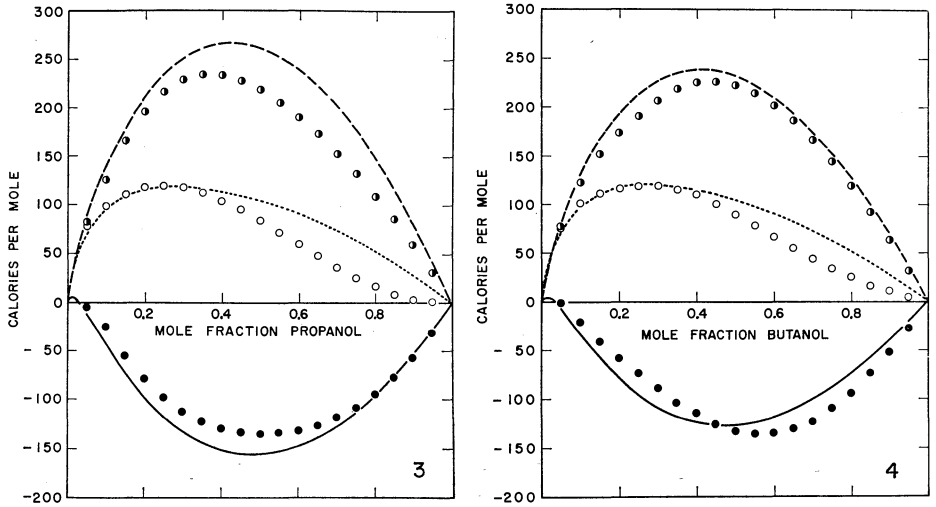

FIG. 3. Excess thermodynamic functions for propanol – carbon tetrachloride solutions at 25° C. Experimental points: ◑, G_p^E, ○, U_v^E, and ●, TS_v^E. Curves calculated from theory.

FIG. 4. Excess thermodynamic functions for butanol – carbon tetrachloride solutions at 25° C. Experimental points: ◑, G_p^E, ○, U_v^E, and ●, TS_v^E. Curves calculated from theory.

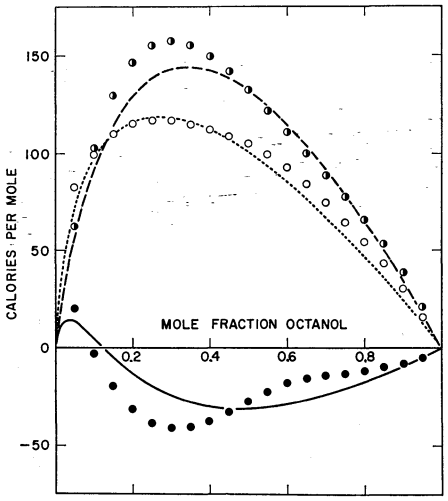

FIG. 5. Excess thermodynamic functions for octanol – carbon tetrachloride solutions at 25° C. Experimental points: ◑, G_p^E, ○, U_v^E, and ●, TS_v^E. Curves calculated from theory.

(III) n-Propanol – Carbon Tetrachloride

All the quantities G_p^E, H_p^E, and V^E were estimated at 25° C from the data of Missen and co-workers (5, 6).

(IV) n-Butanol – Carbon Tetrachloride

Values of G_p^E at 25° were calculated from data at 35° C (5) assuming a linear temperature dependence for H_p^E as determined from the present results at 25° and those of

Can. J. Chem. Downloaded from www.nrcresearchpress.com by 210.87.254.42 on 09/05/12
For personal use only.

reference 6 at 35° C. The excess enthalpies from the present work were corrected to constant volume with values of V^E given in reference 5.

(V) n-Octanol – Carbon Tetrachloride

The temperature dependence of H_p^E given by Missen and co-workers (6) was used to calculate G_p^E at 25° from data at 60° C (5). Values of H_p^E were taken from the present work and V^E data from reference 5.

THEORY

In applying Barker's theory (1) a quasi-lattice with coordination number $z = 4$ is assumed. Values used for the other geometric factors, i.e. r_μ, the number of sites occupied by a molecule of species μ, and Q_i, the number of contact points of type i, are summarized in Table IV. Alcohol molecules (component A) are assumed to have three kinds of contact

TABLE IV

Geometric characteristics of component molecules

Component	r_μ	Q_H	Q_O	Q_I	Q_S
CH_3OH	2	1	2	3	—
C_4H_9OH	5	1	2	9	—
$C_8H_{17}OH$	9	1	2	17	—
CCl_4	5	—	—	—	12

area; these are associated with the hydroxyl hydrogen, the oxygen atom, and the alkyl chain and are indicated by subscripts H, O, and I respectively. The carbon tetrachloride solvent (component B) has a single type of contact S. The interaction energy U_{i-j} is defined in such a way that $2U_{i-j}$ is the increase in energy when two $(i–j)$ contacts are formed from a pair of $(i–i)$ and $(j–j)$ contacts. Thus $U_{i-i} = U_{j-j} = 0$ and only six contact energies must be specified for each system. This number is further reduced by imposing the condition

$$U_{H-I} = U_{O-I} = U_{O-S} = U_{I-S}. \qquad [3]$$

In subsequent description it is convenient to write each of the above energies as U_3 and to denote U_{H-O} and U_{H-S} by U_1 and U_2 respectively. Use of equation [3] neglects differences between some of the contact energies on the assumption that they are relatively less significant than the H–O and H–S interactions.

The excess energy and Helmholtz free energy (at constant volume) are given by the formulae

$$U_v^E = -2RT\{[X_H X_O - xX_H' X_O']\eta_1 \ln \eta_1 + [X_I(X_H + X_O) - xX_I'(X_H' + X_O')]\eta_3 \ln \eta_2 + X_S[X_H\eta_2 \ln \eta_2 + (X_O + X_I)\eta_3 \ln \eta_3]\} \qquad [4]$$

$$A^E = RT\left\{x \ln x + (1-x)\ln(1-x) + Q_H \ln\left(\frac{X_H}{xX_H'}\right) + Q_O \ln\left(\frac{X_O}{xX_O'}\right) + Q_I \ln\left(\frac{X_I}{xX_I'}\right) + Q_S \ln\left(\frac{X_S}{(1-x)X_S'}\right) + r_B\left(\frac{z}{2} - 1\right)\ln\left(\frac{r_A x + r_B(1-x)}{r_B}\right)\right\}, \qquad [5]$$

Can. J. Chem. Downloaded from www.nrcresearchpress.com by 210.87.254.42 on 09/05/12
For personal use only.

Volume 41, 1963

Page 283. In the last term of the first line of equation [4] "η_2" should read "η_3".

where x is the mole fraction of alcohol and

$$[6] \qquad \eta_i = \exp(-U_i/RT).$$

The parameters X_H, X_O, X_I, and X_S are determined by solving the set of equations

$$[7] \qquad \begin{aligned} X_H(X_H+\eta_1X_O+\eta_3X_I+\eta_2X_S) &= xQ_H/2, \\ X_O(\eta_1X_H+X_O+\eta_3X_I+\eta_3X_S) &= xQ_O/2, \\ X_I(\eta_3X_H+\eta_3X_O+X_I+\eta_3X_S) &= xQ_I/2, \\ X_S(\eta_2X_H+\eta_3X_O+\eta_3X_I+X_S) &= (1-x)Q_S/2. \end{aligned}$$

The quantities X_H', X_O', and X_I' in equation [4] and X_S' in equation [5] are the solutions of the set [7] for the special cases $x = 1$ and $x = 0$ respectively.

Numerical calculations were carried out on an IBM 1620 computer; an iterative Newton–Raphson procedure was used to obtain values of X_H, X_O, X_I, and X_S from the set of equations [7] and these were subsequently employed in the evaluation of U_v^E, A_v^E, and TS_v^E. In the computations U_1 was identified with the hydrogen bond strength and a value, -5000 cal mole^{-1}, based on data for solutions of alcohols in carbon tetrachloride (20) was used. U_3 was put equal to zero in the preliminary calculations and U_2 was varied until an approximate fit could be obtained for the minimum of TS_v^E. Except in the case of the methanol system, the values of U_2 were very similar and an average (-1800 cal mole^{-1}) was adopted for systems II–V. Finally U_3 was adjusted until the maximum of U_v^E could be reproduced. The values of the energy parameters selected are given in Table V; these were used to construct the "theoretical" curves in Figs. 1–5.

TABLE V

Values of the contact energies

System	U_1 (cal mole^{-1})	U_2 (cal mole^{-1})	U_3 (cal mole^{-1})
CH_3OH–CCl_4	−5000	−1400	25
C_2H_5OH–CCl_4	−5000	−1800	0
C_3H_7OH–CCl_4	−5000	−1800	13
C_4H_9OH–CCl_4	−5000	−1800	11
$C_8H_{17}OH$–CCl_4	−5000	−1800	7

In certain instances a better fit of the "experimental" points could have been obtained by adjusting both U_2 and U_3. However, it seems preferable to attempt to reproduce the general features of the data with as small a number of parameters as possible. It is clear that the methanol system does not fit into the general scheme followed by the higher members of the homologous series.[4]

The fit of U_v^E at high alcohol concentrations is poor and the change of sign observed experimentally for the lower alcohols is not reproduced by the theory using the energy values of Table V.

For small alcohol mole fractions the theory predicts a region of positive values for TS_v^E which Barker (1) has attributed to the breaking of hydrogen bonds. This region extends to higher concentrations as the chain length of the alcohol is increased and is observed experimentally for the *n*-octanol system. In very dilute solutions the mole

[4] *After this manuscript was completed a paper by J. R. Goates, R. L. Snow, and J. B. Ott, J. Phys. Chem., **66**, 1301 (1962), appeared which presents an application of Barker's theory to a series of alcohol–benzene systems. It is interesting to note that these workers also had difficulty in fitting the methanol systems with the set of parameters used for the higher alcohols.*

Can. J. Chem. Downloaded from www.nrcresearchpress.com by 210.87.254.42 on 09/05/12
For personal use only.

fraction of alcohol present as polymer is given approximately by $2X_{H}X_{O}\eta_{1}$ and thus α, the monomer fraction, may be estimated from the formula

$$\alpha = 1-(2X_{H}X_{O}\eta_{1}/x). \quad [8]$$

Values of α calculated for systems II–V from the energies in Table V are very nearly the same for mole fractions below 0.1 and are shown as a single curve in Fig. 6. Similar

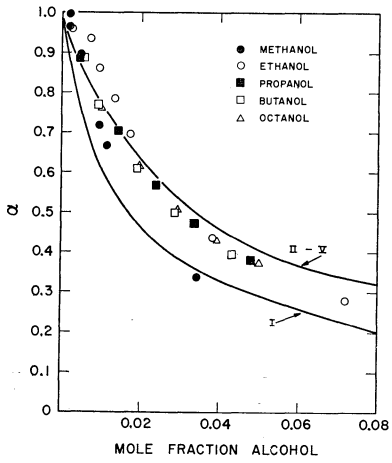

FIG. 6. Comparison of experimental results with theoretical curves for the monomer fraction in alcohol – carbon tetrachloride solutions.

calculations for the methanol system give somewhat lower results. An examination of Fig. 6 shows that there is fair agreement between the theoretical curves and the points which represent the results of infrared and n.m.r. studies (21, 22, 23).

CONCLUSION

In view of the number of interactions involved in the present set of systems (i.e. six) and considering the approximations made in the theoretical treatment, the agreement between experiment and theory is probably as good as can be expected. The numerous calculations that have been carried out in the course of the present work indicate that it is unlikely that any other set of three reasonably consistent energy parameters can improve the agreement and at this stage the introduction of additional parameters does not appear to be justified.

ACKNOWLEDGMENTS

The authors wish to thank Mr. P. D'Arcy for invaluable assistance in the calorimetric determinations. They are also indebted to the staff of the Computation Centre, N.R.C., for use of their facilities.

REFERENCES

1. J. A. BARKER. J. Chem. Phys. **20**, 1526 (1952).
2. J. A. BARKER, I. BROWN, and F. SMITH. Discussions Faraday Soc. **15**, 142 (1953).
3. J. A. BARKER and F. SMITH. J. Chem. Phys. **22**, 375 (1954).
4. J. R. GOATES, R. L. SNOW, and M. R. JAMES. J. Phys. Chem. **65**, 335 (1961).
5. G. C. PARASKEVOPOULOS and R. W. MISSEN. Trans. Faraday Soc. **58**, 869 (1962).
6. J.-E. A. OTTERSTEDT and R. W. MISSEN. Trans. Faraday Soc. **58**, 879 (1962).
7. G. C. BENSON and G. W. BENSON. Rev. Sci. Instr. **26**, 477 (1955).
8. G. SCATCHARD, L. B. TICKNOR, J. R. GOATES, and E. R. MCCARTNEY. J. Am. Chem. Soc. **74**, 3721 (1952).

Can. J. Chem. Downloaded from www.nrcresearchpress.com by 210.87.254.42 on 09/05/12
For personal use only.

9. R. V. MRAZEK and H. C. VAN NESS. A.I.Ch.E.J. **7**, 190 (1961).
10. J.-E. A. OTTERSTEDT and R. W. MISSEN. Can. J. Chem. Eng. **40**, 12 (1962).
11. R. MECKE. Z. Elektrochem. **52**, 107 (1948).
12. E. A. MOELWYN-HUGHES and R. W. MISSEN. J. Phys. Chem. **61**, 518 (1957).
13. I. BROWN and W. FOCK. Australian J. Chem. **8**, 361 (1955).
14. R. L. SCOTT. J. Phys. Chem. **64**, 1241 (1960).
15. M. L. MCGLASHAN, K. W. MORCOM, and A. G. WILLIAMSON. Trans. Faraday Soc. **57**, 601 (1961).
16. G. SCATCHARD. Trans. Faraday Soc. **33**, 160 (1937).
17. H. BENNINGA and R. L. SCOTT. J. Chem. Phys. **23**, 1911 (1955).
18. W. P. MCKINNEY, G. F. SKINNER, and L. A. K. STAVELEY. J. Chem. Soc. 2415 (1959).
19. G. SCATCHARD and L. B. TICKNOR. J. Am. Chem. Soc. **74**, 3724 (1952).
20. G. C. PIMENTEL and A. L. MCCLELLAN. The hydrogen bond. W. H. Freeman and Co., San Francisco. 1960. pp. 355–356.
21. E. G. HOFFMANN. Z. Physik. Chem. Sect. B, **53**, 179 (1943).
22. E. D. BECKER, U. LIDDEL, and J. N. SHOOLERY. J. Mol. Spectry. **2**, 1 (1958).
23. N. D. COGGESHALL and E. L. SAIER. J. Am. Chem. Soc. **73**, 5414 (1951).

Can. J. Chem. Downloaded from www.nrcresearchpress.com by 210.87.254.42 on 09/05/12
For personal use only.

FLUORESCENCE EFFICIENCY OF CYCLOPENTANONE VAPOR AND ITS RELATION TO PHOTOLYSIS

S. R. La Paglia and B. C. Roquitte*

Aeronautical Research Laboratories, Office of Aerospace Research, Wright-Patterson Air Force Base, Ohio

Received August 3, 1962

Can. J. Chem. Downloaded from www.nrcresearchpress.com by 210.87.254.40 on 09/05/12
For personal use only.

ABSTRACT

Cyclopentanone vapor, when excited by light of wavelength 3130 Å, gives rise to four different photoproducts and fluorescence. The photochemistry of the molecule has been investigated by Srinivasan (J. Am. Chem. Soc. **81**, 1546 (1959); **83**, 4344, 4348 (1961)). In the present work the fluorescence spectrum and fluorescence efficiency of cyclopentanone vapor are reported for the first time. The fluorescence spectrum is identical with that obtained from liquid solutions of cyclopentanone, with a maximum at 4100 Å. Time, temperature, oxygen, and inert gases do not affect the spectrum, which contains no component ascribable to phosphorescence, maximum 4450 Å. Beer's law is obeyed.

The fluorescence efficiency is also found to be independent of the variables temperature and pressure of inert gas, cyclopentanone, and oxygen. This is in marked contrast with the behavior of the photochemical yields (see work by Srinivasan). The yields of cyclobutane and ethylene tend to increase at high vibrational energy content of the excited molecule (low pressure, high temperature, short exciting wavelengths), while the yield of pentenal increases under conditions of decreasing vibrational energy content (high pressures, etc.). The fact that fluorescence stabilization does not occur in cyclopentanone can be related to the results of photolysis.

INTRODUCTION

The photodecomposition of cyclopentanone has been investigated extensively (1–3). Recently it was reinvestigated by Srinivasan (4(*a*)) and it was shown that, in addition to the two primary processes postulated by Benson and Kistiakowsky, a third primary process is quite important. The product 4-pentenal was isolated by Srinivasan, who suggested that it results from a rearrangement process, whereas the products carbon monoxide, ethylene, and cyclobutane are obtained as a result of molecular splitting. All three primary processes were postulated to be molecular since radical scavengers do not inhibit them. A detailed study of these three primary processes was published in a subsequent paper by Srinivasan (4(*b*)). The effect of inert gases on the decomposition of cyclopentanone was reported. The amount of cyclopentanone undergoing photolysis was not affected by inert gas addition whereas the ratio of pentenal to carbon monoxide changed sharply. On the other hand the ratio of ethylene to cyclobutane changed much less markedly. These experimental evidences led Srinivasan to postulate that the three primary processes are occurring from three different vibrational levels of the first excited singlet state and that the vibrational energy is being transferred during collisions at the rate of one or a few quanta per collision, which affects the products formed.

In view of the fact that fluoroscence and phosphorescence have been observed in condensed phases (5) and the quantum yield of the dissociation of cyclopentanone (gas phase) is less than unity, it is quite possible that part of the energy of the excited molecule is emitted in the gas phase as fluorescence and/or phosphorescence. Hence the study of cyclopentanone emission in the gas phase was undertaken to get a better understanding of the mechanism of photodecomposition.

In this article the fluorescence of cyclopentanone in the gas phase is reported. The effect of temperature, pressure, oxygen, and inert gas on the relative fluorescence yield

**Present address: National Research Council, Ottawa, Canada.*

has been studied and attempts are made to correlate the dissociation processes with the emission process of the cyclopentanone molecule.

EXPERIMENTAL

Materials

The cyclopentanone used in these experiments was an Eastman White Label chemical. Vapor phase chromatographic analysis showed the material to consist of only one component. In addition, it was distilled through a 1-m, well-packed column, and a middle fraction was taken. This fraction was further subjected to bulb-to-bulb distillation on the vacuum line, and stored behind a mercury cutoff at dry ice – acetone temperature. It is the same material used in our spectroscopic studies (5). The other materials used in these studies were Matheson's best quality gases, and were used directly from lecture bottles without further treatment.

Fluorescence Efficiency Measurements

The fluorescence cell was T-shaped and made of quartz. Its overall length was 14 cm, the end windows were 5 cm in diameter, while the T window was 2.5 cm in diameter. All windows were double in order to maintain a uniform temperature distribution. The cell was housed in an aluminum block oven, wound with nichrome wire and covered with layers of asbestos. Temperature was read from a copper–constantan thermocouple sunk into the aluminum block. Dead space existed between the cell and the first stopcock, where a condensation finger was located. The volume of the dead space was about 14 cc, but it was entirely wire wound and heated.

The light from a Hanovia high-pressure arc (No. 30600) was prefiltered by a Corning 7-54 filter and allowed to fall on the entrance slit (1 mm) of a Gaertner quartz prism monochromator. The monochromator was focused for the 3130 Å lines of the arc. These lines were collimated by two quartz lenses and allowed to pass through the cell. An air-cooled photomultiplier was placed behind the exit window of the cell in order to intercept and measure the intensity of the transmitted radiation. This photomultiplier was an RCA 1P28, powered by a Furst Electronics, constant voltage, d-c. power supply at 1000 v. The transmitted intensity (called I_t if cyclopentanone is present in the cell, or I_t^0 if it is absent) was reduced by the use of neutral density filters so that the I_t^0 photocurrent was no greater than 0.2 μa. An air-cooled 1P21 photomultiplier, similarly powered, was placed at the T window of the cell. The radiation passing through this window was filtered by a Corning 0-52 filter to remove scattered 3130 Å light. The amount of scattered light was small since the incident beam was well collimated and the cell walls partially blackened.

The fluorescent light was focused onto the 1P21 photomultiplier, which then gave the fluorescence intensity in the presence of cyclopentanone (I_f), and in its absence (I_f^0). Pressures of the ketone (of order 50 mm, 25° C) were used such that I_t was some five times greater than I_f^0. The actual magnitude of the I_f^0 photocurrent was 0.02 μa. The photocurrents were easily amplified and were recorded by a Leeds and Northrup Speedomax G, especially modified for use with photomultipliers.

There are four quantities to be measured in order to determine the fluorescence efficiency under a given set of conditions, I_f, I_f^0, I_t, and I_t^0. The zero quantities were measured either from the evacuated cell, or with the cell filled with an inert gas. Either method gave the same readings. Cyclopentanone was then passed in to fill the cell to its vapor pressure at room temperature, 10 mm. This amount of cyclopentanone in the cell was quantitatively transferred to another portion of the line and the procedure repeated. Five fillings followed by quantitative transfer back to the cell of all the material gave, in this case, a working concentration of 50 mm (25° C). The cell temperature was then brought up to 70–80° C and the quantities I_t and I_f were measured.

For addition of small amounts of inert gases the ketone was condensed into a side arm before the gas was added. After addition the ketone was evaporated by warming and the two gases were allowed to mix by diffusion for several hours. This method was found to be quite reliable because of the small dead space. However, for the addition of inert gases which greatly exceeded the pressure of cyclopentanone, a slow and careful leakage into the cell containing the uncondensed ketone gave very reliable results, with a minimum of diffusion time being necessary for complete mixing.

The fluorescence efficiency, Q, is taken as the fluorescence intensity ($I_f - I_f^0$) divided by the fraction of incident light absorbed, I_a. I_a is taken to be $(I_t^0 - I_t)/I_t^0$. Under the usually employed conditions, I_a was approximately one third of the incident intensity. The intensity of the incident light was found to vary by only a few percent over the period of a run. Such variations are accounted for by using the quantity I_a rather than merely $(I_t^0 - I_t)$. A detailed consideration of the possible sources of experimental error shows that any given value of Q can be in error by as much as 15%. However, the reproducibility of the experiments was much better than this. As a result we claim an accuracy for the relative yields, Q/Q_0, of about 5%.

Fluorescence Spectrum

The light from an Osram, 100 watt, high-pressure mercury arc was focused into the fluorescence cell by a quartz lens, after having been filtered by a Corning 7-54 filter and 5 cm of $NiSO_4$–$CoSO_4$ solution. This filter combination had an O.D. of about 0.7 at 3130 Å and was completely opaque (O.D. > 3) beyond 3600 Å. The cell contained about 100 mm of cyclopentanone at 130° C. Viewed at right angles to the exciting

Can. J. Chem. Downloaded from www.nrcresearchpress.com by 210.87.254.40 on 09/05/12
For personal use only.

light the blue-violet fluorescence of cyclopentanone in the ultraviolet beam was quite evident to the unaided eye. A lens combination focused an image of the fluorescing beam onto the slit (0.1 mm wide) of a Hilger and Watts small quartz prism spectrograph, with a dispersion of about 110 Å/mm at 4000 Å. Kodak 103-F or 103-O plates were exposed for several hours, then the slit was partially masked and a mercury spectrum recorded for positive wavelength identification. The plates were developed for 4 minutes in D-19.

RESULTS AND DISCUSSION

Effect of Temperature, Vapor Pressure, Inert Gas Pressure, and Oxygen

Measurement of I_t/I_t^0 (λ_{ex}, 3130 Å) over the range of cyclopentanone concentrations 10 to 80 mm (25° C) at a vapor temperature of 100° C showed that the vapor obeyed Beer's law, at least under the conditions used in these studies.

The relative fluorescence yield, Q/Q_0, of a sample at 20 mm (25° C) of cyclopentanone was measured at eight temperatures over the range 54° to 134° C. The relative yield was constant, at 0.96 ± 0.05 over the entire range, where Q_0 is the fluorescence efficiency of the sample at 54° C. This indicates that the fluorescence efficiency is independent of the vapor temperature in the region of photochemical interest.

The fluorescence efficiency was found to be independent of cyclopentanone pressure. Indeed, the effect of pressure (cyclopentanone, inert gases, or oxygen) on the fluorescence efficiency was the same for all these gases, nil. We illustrate the situation in Fig. 1, where

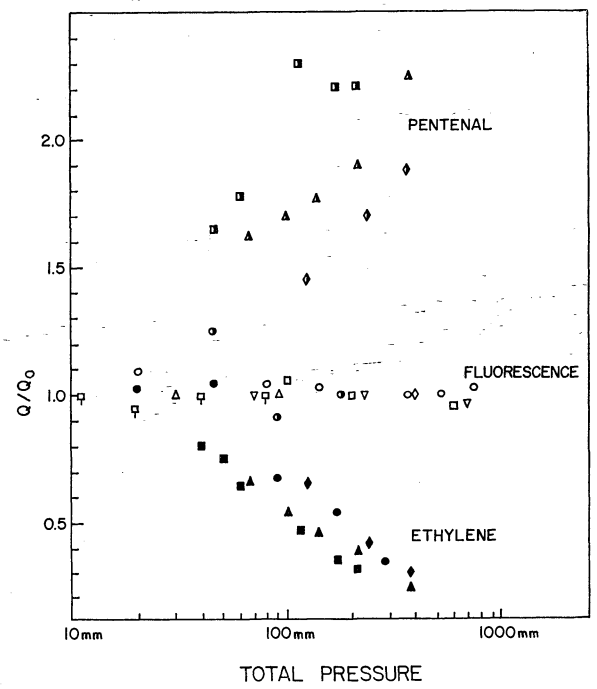

FIG. 1. Relative yields as defined in the text versus total pressure (inert gas plus cyclopentanone). Filled symbols are yields of ethylene, unfilled symbols are fluorescence yields, and half-filled symbols are the yields of pentenal. Symbol code is ⊓ cyclopentanone, ○ oxygen, □ methane, ▽ hydrogen, △ carbon dioxide, ◇ argon. Ethylene and pentenal yields are taken from the work of Srinivasan (4) (see text).

the relative fluorescence yields for all pressures up to 1 atm lie along the horizontal axis. The relative decomposition yields as a function of the pressure of the very same gases are included for the sake of comparison and discussion (4). For the yield as a function of cyclopentanone pressure, Q_0 is the efficiency at 10 mm (25° C) of cyclopentanone vapor

Can. J. Chem. Downloaded from www.nrcresearchpress.com by 210.87.254.40 on 09/05/12
For personal use only.

at 100° C. For the other gases, including oxygen, Q_0 is usually the efficiency at 50 mm (25° C) and vapor temperature 70–80° C (for the low-pressure yields Q_0 refers to 10 mm of the ketone). In the case of the decomposition yields, Q_0 is the yield of ethylene in μmoles (filled symbols) or pentenal in μmoles (half-filled symbols), at room temperature and approximately 10 mm of cyclopentanone. Q is then the decomposition yield in μmoles under the same conditions but with added gas. Several of the decomposition yields at nearly the same total pressure have been averaged for the sake of clarity.

Fluorescence Spectrum of Cyclopentanone Vapor

As stated previously, in recording the fluorescence spectrum of cyclopentanone vapor the exciting lines were mainly 3130 Å of Hg. The fluorescence spectrum was photographed at different temperatures and in the presence of inert gas and oxygen. The results were always the same and as shown in the microdensitometer tracing Fig. 2. The spectrum is

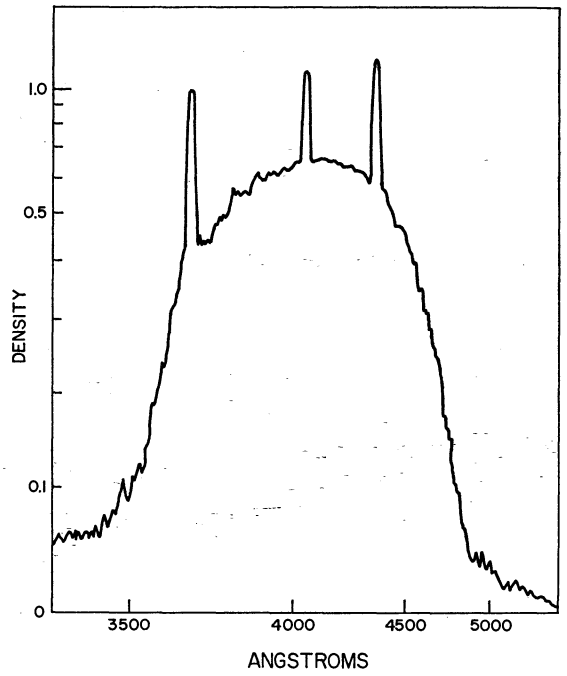

FIG. 2. Microdensitometer tracing of fluorescence of cyclopentanone vapor. Approximately 100 mm of cyclopentanone at 130° C recorded on a Kodak 103-O plate with 12 hours' exposure. The prominent peaks are the groups of mercury lines at 3660, 4047, and 4358 Å respectively.

in agreement with the fluorescence spectrum reported previously for solutions of cyclopentanone (5). The maximum is located at about 4100 Å. There is no evidence of phosphorescence emission from the vapor (maximum 4400–4500 Å) (5).

Connection with Photolysis

In spite of the variety and quantity of experimentation which have been performed on the photochemical and luminescence behavior of cyclopentanone it is not possible to unambiguously formulate a kinetic mechanism for these processes. Explicitly, the experiments to date leave undecided what role, if any, is played by the triplet state in the photoreactions of cyclopentanone. Although the existence of this state has been established (5),

Can. J. Chem. Downloaded from www.nrcresearchpress.com by 210.87.254.40 on 09/05/12
For personal use only.

the results of photolysis in the presence of oxygen 4(*b*)) have been interpreted as supporting the idea that the triplet state is not important in the photochemistry of this molecule. If this is the case one must assume that any ^3C formed by intersystem crossing does not lead to observable amounts of photoproduct. Then it is simple to extend the mechanism proposed by Srinivasan (4(*b*)). The new information which must be added is that, while fluorescence does occur, the fluorescence spectrum and fluorescence efficiency are independent of temperature and pressure. Since the fluorescence spectrum and efficiency do not change with time we assume that decomposition products do not contribute and fluorescence arises solely from the excited singlet state of cyclopentanone, ^1C. The steps needed are fluorescence, intersystem crossing, and some steps dealing with the final fate of ^3C:

$$1.\ C + h\nu \rightarrow {}^1C \qquad I_a$$

2. $^1C_n \rightarrow D_1$	k_{D1}	6. $^1C_m \rightarrow D_2$	k_{D2}
3. $^1C_n \rightarrow C + h\nu$	k_{F1}	7. $^1C_m \rightarrow C + h\nu$	k_{F2}
4. $M + {}^1C_n \rightarrow {}^1C_m + M$	k_{M1}	8. $M + {}^1C_m \rightarrow {}^1C_p + M$	k_{M2}
5. $^1C_n \rightarrow {}^3C$	k_{IS1}	9. $^1C_m \rightarrow {}^3C$	k_{IS2}

10. $^1C_p \rightarrow D_3$	k_{D3}
11. $^1C_p \rightarrow C + h\nu$	k_{F3}
12. $^1C_p \rightarrow {}^3C$	k_{IS3}
13. $^3C \rightarrow C$	
14. $^3C + Q \rightarrow C + Q$	

where subscripts n, m, and p denote decreasing vibrational levels of the excited state, M is an inert molecule, Q is a quencher.

On this basis, the fluorescence yield is found to be independent of pressure (independent of [M]) if the rate constants are the same for all vibrational levels of the excited state, that is, (1) $k_{D1} = k_{D2} = k_{D3}$, (2) $k_{F1} = k_{F2} = k_{F3}$, (3) $k_{IS1} = k_{IS2} = k_{IS3}$, (4) $k_{M1} = k_{M2}$. Then the fluorescence yield is

$$Q_F = \frac{k_F}{k_F + k_D + k_{IS}},$$

as for a much simpler model, one possessing only one vibrational level. From the viewpoint of our ignorance, conditions (2) to (4) are acceptable, but (1) seems rather stringent if not improbable.

Unlike some other photoexcited species, cyclopentanone does not undergo "fluorescence stabilization" in the presence of inert gas (6, 7). In fluorescence stabilization the excited molecule is vibrationally deactivated by collisions with inert molecules. By thus removing some of the excitation energy the probability of decomposition is decreased (the molecule is stabilized) and the molecule has more time to re-emit (fluorescence is enhanced). Fluorescence stabilization will *not* occur if fluorescence must compete with decomposition (at nearly the same rate) at every vibrational level, down to the very lowest vibrational level of the excited state. This is the situation implicit in the above mechanism, subject to the given conditions. In this case, the emission spectrum (being continuous in the present degree of resolution) need not necessarily suffer an observable change or shift with pressure of added gas. Fluorescence stabilization also will not occur if decomposition or intersystem crossing take place so rapidly upon absorption of light that collisional deactivation cannot compete even at high pressures. However, in this case the fluorescence spectrum, if observable, would be a resonance spectrum.

One cannot even begin to consider the numerous possibilities for intrusion of the triplet state more directly into the photodecomposition; such considerations would be mere

Can. J. Chem. Downloaded from www.nrcresearchpress.com by 210.87.254.40 on 09/05/12
For personal use only.

speculation at the present time. However, in this regard it may be worth noting that while photolysis in the presence of oxygen affects the yield of ethylene and cyclobutane, as would the corresponding pressure of any inert gas, the yield of pentenal is not increased by addition of even 275 mm of oxygen (4(*b*)) (Fig. 1).

ACKNOWLEDGMENTS

The authors gratefully acknowledge the suggestions of Dr. B. Stevens, Sheffield University, and the help of Dr. J. T. Dubois, Aeronautical Research Laboratories.

REFERENCES

1. O. D. Saltmarch and R. G. W. Norrish. J. Chem. Soc. 455 (1935).
2. S. W. Benson and G. B. Kistiakowsky. J. Am. Chem. Soc. **64**, 80 (1942).
3. F. E. Blacet and A. Miller. J. Am. Chem. Soc. **79**, 4327 (1957).
4. (*a*) R. Srinivasan. J. Am. Chem. Soc. **81**, 1546 (1959).
   (*b*) R. Srinivasan. J. Am. Chem. Soc. **83**, 4344, 4348 (1961).
5. S. R. La Paglia and B. C. Roquitte. J. Phys. Chem. **66**, 1739 (1962).
6. H. Okabe and E. W. R. Steacie. Can. J. Chem. **36**, 137 (1958).
7. M. Boudart and J. T. Dubois. J. Chem. Phys. **23**, 223 (1955).

Can. J. Chem. Downloaded from www.nrcresearchpress.com by 210.87.254.40 on 09/05/12
For personal use only.

THE DETECTION AND ESTIMATION OF BRANCHING IN DEXTRAN BY PROTON MAGNETIC RESONANCE SPECTROSCOPY[1]

W. M. PASIKA AND L. H. CRAGG
Department of Chemistry, University of Alberta, Edmonton, Alberta
Received September 20, 1962

ABSTRACT

The proton magnetic resonance spectrum of branched dextran contains a peak, not found in the spectrum of linear dextran, which is assigned to C_1 protons at non-1,6-linkages—linkages which in most branched dextrans form the branch points. A quantitative measure of the extent of branching—the ratio of 1,6-linkages to non-1,6-linkages—is obtained by taking the ratio of the areas of the peaks associated with these two types of linkages. The value so obtained agrees well with that obtained by periodate analysis.

For polysaccharides in which the non-1,6-linkages are known to be at branch points, n.m.r. spectroscopy thus affords a means of detecting and estimating branching which is more convenient than methods currently in use.

A. INTRODUCTION

Despite continuing research by many investigators, the methods available for the detection, characterization, and estimation of branching in polymers still leave much to be desired. In our investigation of the viscosity behavior of dextran and of polyelectrolytes derived from it we, like others before us, wished for a convenient physical method of detecting and measuring the degree of branching in these compounds. In the unsubstituted dextran, 1,3-branching can be detected by infrared spectroscopy (1) but in sulphated dextran the 1,3-branching peak is completely masked by a large broad peak attributed, by Orr (2), to sulphate. Even in the unsubstituted compound, the branching peak is not too pronounced (Fig. 1).

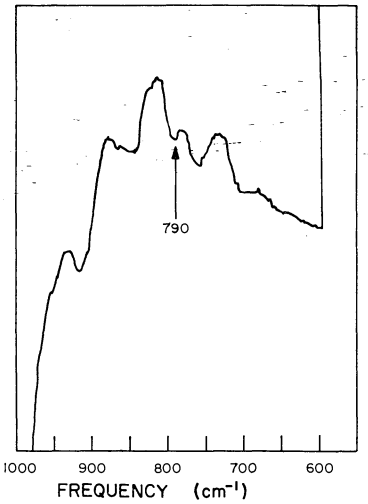

FIG. 1. Infrared adsorption at 790 cm^{-1} indicative of 1,3-branching in NRRL B-742. (Ordinate expansion 5×.)

The structures of linear and 1,3-branched dextran, which have been established on accumulated chemical evidence (3–7), are shown diagrammatically in Fig. 2. Examination

[1]*Based on research work done by W. M. Pasika for the Ph.D. degree, University of Alberta.*

Can. J. Chem. Downloaded from www.nrcresearchpress.com by 210.87.254.105 on 09/05/12
For personal use only.

Can. J. Chem. Downloaded from www.nrcresearchpress.com by 210.87.254.105 on 09/05/12
For personal use only.

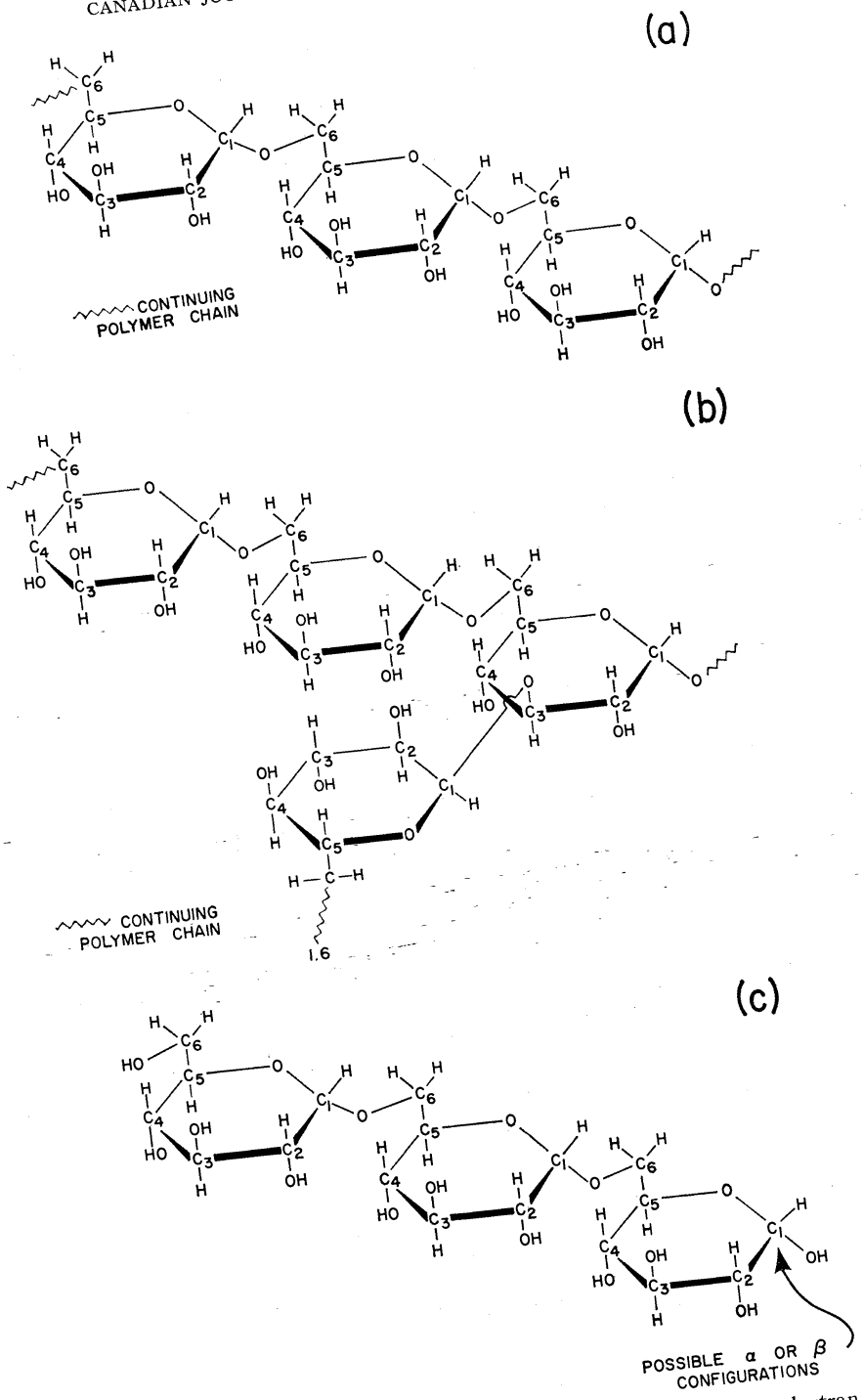

FIG. 2. (*a*) Schematic representation of a portion of the polymer chain of linear dextran NRRL B-512. (*b*) Schematic representation of a portion of the polymer of branched dextran NRRL B-742 showing a branch emanating from the 3 position of an anhydroglucose unit of the backbone chain. (*c*) Schematic representation of the isomaltotriose molecule.

of these suggests that, because of differences in proton environments in the two compounds, proton magnetic resonance spectra might exhibit significant differences which could be related to branching. In this paper we present evidence that n.m.r. spectroscopy can indeed be used to detect branching, and to estimate its extent, in dextran. (Later we shall report extension of the method to dextran sulphate.)

B. RESULTS AND DISCUSSION

Isomaltotriose

Isomaltotriose was selected as a model compound to aid in peak assignments because of its close structural similarity to linear dextran (see Fig. 2). Its n.m.r. spectrum is reproduced in Fig. 3. Peak 4 at −4.80 p.p.m. is due to the proton of deuterium hydroxide,

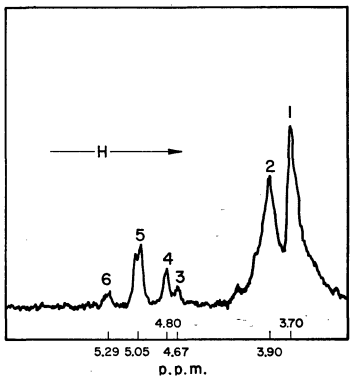

FIG. 3. The n.m.r. spectrum of isomaltotriose. (The external standard here, as in the succeeding n.m.r. spectra, was tetramethylsilane.)

DOH, which is present in small concentration in the solvent deuterium oxide. The relatively intense signals at 1 and 2 (−3.70 and −3.90 p.p.m.) may be attributed to the C_5 and C_6 protons and the C_2, C_3, and C_4 protons respectively. (The protons with the higher electron density environment would give the signal at the higher field.) The other signals, then, would be due to the anomeric C_1 protons, the signal at 5 (−5.05 p.p.m.) to the protons on the two C_1 carbons involved in the 1,6-linkages, and those at 3 and 6 (−4.67 and −5.29 p.p.m.) to the protons on the hemiacetal anomeric carbon. (Signals 3 and 6 can be assigned to the β and α configurations, respectively; cf. refs. 8 and 9.)

If these assignments are correct, the ratio of the sum of the areas of peaks 1 and 2 to the area of peak 5 should be 18/2 or 9, and the ratio of the area of peak 5 to the sum of the areas of 3 and 6 should be 2. The measured ratios, 9.0 and 2.2, are in satisfactory accord with these predictions. (The sides of the peaks were extrapolated to the base line and the areas so enclosed were measured with a planimeter.)

Linear Dextran

The spectrum of the linear dextran NRRL B-512 is reproduced in Fig. 4. In this high-polymeric polyglucose the contribution to the n.m.r. spectrum of the anomeric proton on the reducing end would be vanishingly small. We should expect, therefore, that peaks 3 and 6 would not appear. In fact, they do not. The three signals that are observed correspond to signals 1, 2, and 5 of the isomaltotriose spectrum, and are so labelled. Making an assignment analogous to that for isomaltotriose, one would predict that the ratio of the

Can. J. Chem. Downloaded from www.nrcresearchpress.com by 210.87.254.105 on 09/05/12
For personal use only.

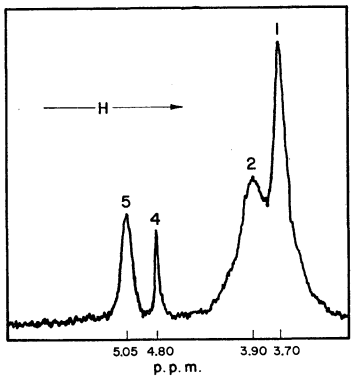

FIG. 4. The n.m.r. spectrum of NRRL B-512 "linear" dextran.

sum of the areas of peaks 1 and 2 to the area of peak 5 would be 6/1 or 6. The value obtained from area measurements was 5.9.

Branched Dextran

The n.m.r. spectrum for branched dextran NRRL B-742, reproduced in Fig. 5, contains peaks corresponding to those in Fig. 4, but, in addition, has a peak, 7, at −5.40 p.p.m.

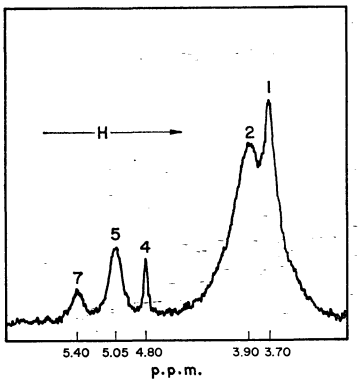

FIG. 5. The n.m.r. spectrum of NRRL B-742 branched dextran.

whose counterpart does not occur in the spectrum of isomaltotriose or linear dextran. (In the three spectra, corresponding peaks are labelled with the same number. That such peaks are indeed counterparts of one another is evident from the data of Table I. Differences in structure of the three compounds have affected very little, indeed, the chemical shift values.) This new peak can only be due to the one structural feature—non-1,6-linkages—known to be present in B-742 dextran (3, 4, 6, 10) but absent from isomaltotriose and present only to a very small extent (less than 5%) in B-512 dextran. (In Fig. 2, these "non-1,6-linkages" are represented by a 1,3-linkage.) The proton responsible for the signal at 7 must be either the one on the C_1, or else that on the C_3, of the 1,3-linkage (or the C_4 if the linkage is 1,4). Of the two alternatives, the first seems the more probable. The signal at 7 must arise at the expense of the signal at 5 (C_1 proton at the 1,6-linkage), which would mean a small shift from −5.05 to −5.40 p.p.m.; or else it is produced at the expense of the signal at 2 (C_2, C_3, C_4 protons), which would mean a much larger shift

Can. J. Chem. Downloaded from www.nrcresearchpress.com by 210.87.254.105 on 09/05/12
For personal use only.

TABLE I

Spectrum	Peak	Protons responsible	Chemical shift* (p.p.m.)	
Isomaltotriose	1	C_5, C_6	−3.69	
B-512 dextran	1		−3.70	
B-742 dextran	1		−3.72	−3.70
Isomaltotriose	2	C_2, C_3, C_4	−3.88	
B-512 dextran	2		−3.96	
B-742 dextran	2		−3.90	−3.90
Isomaltotriose	5	C_1 (1,6-linkage)	−5.05	
B-512 dextran	5		−5.05	
B-742 dextran	5		−5.05	−5.05
B-742 dextran	7	C_1 (non-1,6-linkage) *branch*	−5.40	−5.40
Isomaltotriose	4	DOH	−4.78	
B-512 dextran	4		−4.80	
B-742 dextran	4		−4.80	−4.80

*All of the shifts were to the left of the external standard (T.M.S.) and therefore are recorded as negative values. Values in the figures are to be read as negative values.

from −3.90 to −5.40 p.p.m. For neither the C_1 nor the C_3 proton would one expect a change in proton environment sufficient to produce a large shift. Tentatively, then, we assign the signal at 7 to the C_1 proton at the non-1,6-linkage.

If this assignment is correct, it should follow that, if comparisons are made at the same concentrations in grams per liter (i.e. with the same number of anhydroglucose units in a given volume of solution), (*a*) the combined intensities of signals 1 and 2 should be the same for the linear and branched dextrans and (*b*) the intensity of signal 5 for the linear dextran should equal the sum of the intensities of signals 5 and 7 for the branched dextran (anhydroglucose units that are joined by 1,3- or 1,4-linkages in the branched dextran would have been joined by 1,6-linkages had the dextran been linear).

To test these predictions, n.m.r. spectra for the B-512 and B-742 dextrans were obtained at several different concentrations under otherwise identical conditions. In Fig. 6 the sum of the areas of peaks 1 and 2 is plotted against concentration for both dextrans. In accordance with prediction (*a*) above, the points for the two dextrans fall on the same line. In Fig. 7 are plotted, against concentration: A, the area of peak 5 (1,6-linkage) for the linear dextran; B, the area of peak 5 for the branched dextran; and C, the area of peak 7 (the "branching peak") for branched dextran. Also plotted are the sums of the areas of 5 and 7 for branched dextran. These last points fall on the same line as do the points representing the peak 5 areas for linear dextran, in accordance with prediction (*b*) above. Thus the assignment of peak 7 to the C_1 proton of the non-1,6-linkage is confirmed.

Further confirmation is afforded by a comparison of peak areas in the branched dextran spectrum. From periodate oxidation and methylation studies (4), it is known that in this particular branched dextran the ratio of 1,6-linkages to non-1,6-linkages is 70/30 or 2.3 (10). Assignment of peak 5 to the protons on the C_1 carbons involved in 1,6-linkages and of peak 7 to the C_1 protons at the non-1,6-linkages would require, therefore, that the ratio of these signal intensities be 2.3. The ratio calculated as a ratio of the measured peak areas is 2.4.

It may be concluded then that n.m.r. spectra may be used not only to detect the branching in this dextran but also to make a reasonably good estimate of the extent of branching. (The ratio of 1,6-linkages to non-1,6-linkages calculated from the ratio of

Can. J. Chem. Downloaded from www.nrcresearchpress.com by 210.87.254.105 on 09/05/12
For personal use only.

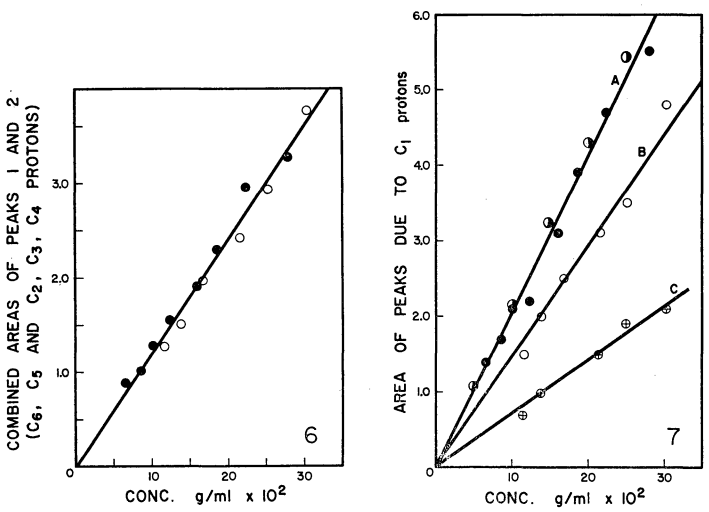

FIG. 6. Combined peak areas 1 and 2 for (●) linear (B-512) and (○) branched (B-742) dextran vs. concentrations.

FIG. 7. Areas of peaks due to C_1 protons of linear and branched dextrans: curve C (⊕) due to C_1 proton of non-1,6-linkage of B-742 dextran; curve B (○) due to C_1 proton of 1,6-linkage of B-742 dextran; curve A (●) due to C_1 proton of 1,6-linkage of B-512 dextran; curve A(◑) due to sum of curve C (⊕) and curve B (○).

peak areas, i.e. from the n.m.r. data, is 71:29 as compared to the 70:30 ratio obtained by other and much more tedious means.)

The method, as we have used it, does not distinguish between 1,2-, 1,3-, and 1,4-linkages, all of which occur at branch points in one form or another of branched dextran. As mentioned earlier, the proportions of 1,3-linkages can be detected, approximately, by infrared spectroscopy. Combining infrared and n.m.r. measurements would then give a convenient estimate of the extent of non-1,6-linkages other than 1,3-linkages (i.e. of 1,2 and 1,4 combined).

It is reasonable to predict that n.m.r. spectra may similarly be used to measure the extent of branching in other branched polysaccharides. It should perhaps be emphasized that what is detected is the existence of different kinds of linkage (in dextran, non-1,6- as compared to 1,6-linkages). These could be in the main chain (4) and, therefore, would not necessarily indicate branch points. But if it is known that in the family of compounds under study the different kinds of linkage occur only at branch points, the n.m.r. method would, as with our dextran, measure the extent of branching. Indeed, the method should in principle be applicable to polymers other than polysaccharides.

C. EXPERIMENTAL

Materials

The dextran samples have been described by Jeanes (10). Characterizing properties are as follows:

NRRL B-512 F: $\bar{M}_w$, 71,000; [η], 0.250 dl/g; % 1,6, 96; % 1,3, 4.
NRRL B-742: $\bar{M}_w$, 61,000; [η], 0.153 dl/g; % 1,6, 70; % 1,3, 18; % 1,4, 12.
Isomaltotriose was a purified sample prepared by Dr. D. H. Hutson.
Deuterium oxide (Merck, Sharp and Dohme of Canada): minimum isotopic purity 99.7 atom% D.

Methods

Spectra were obtained on a Varian A60 analytical proton nuclear magnetic resonance spectrophotometer which operated at 60 Mc/s. Tetramethylsilane (T.M.S.) was used throughout as the external standard.

Can. J. Chem. Downloaded from www.nrcresearchpress.com by 210.87.254.105 on 09/05/12
For personal use only.

Before introduction into the spectrometer, all samples were treated, to exchange labile protons of the hydroxyl groups with deuterons, by a thrice repeated process of dissolving in deuterium oxide and freeze-drying.

ACKNOWLEDGMENTS

We are grateful to Dr. R. U. Lemieux of the Department of Chemistry, University of Alberta, for helpful discussions, to Dr. D. H. Hutson, Royal Holloway College, University of London, for the sample of pure isomaltotriose, and to Dr. Allene Jeanes, Northern Utilization Research and Development Division, United States Department of Agriculture, Peoria, Illinois, for the samples of linear and branched dextran. We are grateful, too, for financial assistance, in the form of research grants, from the Defence Research Board of Canada.

REFERENCES

1. S. C. Burket and E. H. Melvin. Science, **115**, 516 (1952).
2. S. F. D. Orr. Biochim. Biophys. Acta, **14**, 171 (1954).
3. W. B. Neely. Advances in carbohydrate chemistry. Academic Press, New York. 1960. pp. 344, 351.
4. DeW. Stetten, Jr. and M. R. Stetten (*Editor*). *In* Polysaccharides in biology. Transactions of the Third Conference, The Josiah Macy Jr. Foundation. May, 1957. p. 138.
5. J. W. Van Cleave, W. C. Schaefer, and C. E. Rist. J. Am. Chem. Soc. **78**, 4435 (1956).
6. A. Jeanes *et al.* J. Am. Chem. Soc. **76**, 5041 (1954).
7. J. W. Sloan *et al.* J. Am. Chem. Soc. **76**, 4429 (1954).
8. R. U. Lemieux. Trans. Roy. Soc. Can. LII, Series III.
9. R. U. Lemieux, R. K. Kulling, H. J. Bernstein, and W. G. Schneider. J. Am. Chem. Soc. **80**, 6098 (1958).
10. A. Jeanes. Private communication.

Can. J. Chem. Downloaded from www.nrcresearchpress.com by 210.87.254.105 on 09/05/12
For personal use only.

Can. J. Chem. Downloaded from www.nrcresearchpress.com by 210.87.254.40 on 09/05/12
For personal use only.

OXYGEN-18 TRACER EVIDENCE FOR THE TERMINATION MECHANISM IN THE PHOTOCHEMICAL OXIDATION OF ACETALDEHYDE

C. A. McDowell and S. Sifniades

Department of Chemistry, University of British Columbia, Vancouver, British Columbia

Received July 30, 1962

ABSTRACT

The chain-terminating step in the photochemical oxidation of acetaldehyde in the gas phase has earlier been established to be the reaction

$$2AcOO = AcOOAc + O_2.$$

Using oxygen-18 of 99.4% purity in the form of molecular oxygen we have made a careful study of the variation of the isotopic ratios of the various oxygens, by mass spectrometry, during the course of the photooxidation. The results show conclusively that the mechanism of the termination step is:

$$AcOO + AcO^*O^* = AcOO^*Ac + OO^*,$$

where O* represents O^{18}. Thus the recombination terminating reaction takes place with the elimination of one oxygen atom from each reacting peroxy AcOO radical. The mechanism of this elimination process is thought to be as follows:

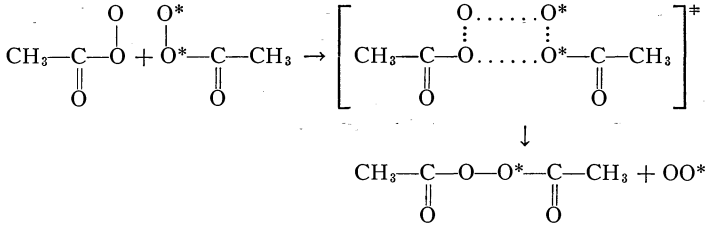

INTRODUCTION

The thermal and photochemical oxidations of acetaldehyde in the gas phase both lead to the main product peracetic acid. It has also been established (1–4) that the terminating step in these oxidation reactions is the recombination of chain carrier and that the radical involved is the peroxyacetyl radical CH_3CO_3. In the case of the low temperature phase photooxidation of acetaldehyde the following kinetic mechanism (2–4) has been found to be in agreement with the experimental data for the processes leading to peroxide formation:

$$CH_3CHO \xrightarrow[3130\ Å]{h\nu} CH_3 + CHO \qquad [1a]$$

$$CH_3CHO \xrightarrow[3130\ Å]{h\nu} CH_3CHO' \qquad [1b]$$

$$\left.\begin{matrix} CH_3 + O_2 \\ CHO + O_2 \end{matrix}\right\} = R \qquad [1c]$$

$$\left.\begin{matrix} R + CH_3CHO = RH + CH_3CO \\ CH_3CHO' + O_2 = CH_3CO + HO_2 \end{matrix}\right\} \phi_2 I_a \qquad [1d]$$

$$CH_3CO + O_2 = CH_3CO_3 \qquad [2]$$

$$CH_3CO_3 + CH_3CHO = CH_3CO_3H + CH_3CO \qquad [3]$$

$$2CH_3CO = (CH_3CO)_2 \qquad [4]$$

$$CH_3CO + CH_3CO_3 = (CH_3CO)_2O_2 \quad [5]$$

$$2CH_3CO_3 = (CH_3CO)_2O_2 + O_2 \quad [6]$$

Since it has been shown (4) that the photochemical oxidation is proportional to $I_a^{1/2}$, where I_a is the number of quanta absorbed, and independent of the oxygen pressure, it is probable that reaction [2] is rather fast and it is also likely that at the oxygen pressures usually used in the experiments (greater than 5 mm HgO_2) reactions [4] and [5] are negligible compared with reaction [6]. Earlier work relied on simple titrations to detect the formation of the second peroxide other than peracetic acid. Paper chromatographic methods do confirm that diacetyl peroxide is a product of the oxidation (5). This observation has now been conclusively confirmed by gas chromatographic methods which will be described later in this paper. It is thus now clear that apart from the radical-initiation step, the important reactions leading to the production of the peroxides in the gas phase photooxidation of acetaldehyde at low temperatures are reactions [2], [3], and [6].

The determination of the absolute values for the recombination reactions of both the peroxyacetyl and the peroxypropionyl radicals showed that both processes are quite efficient (6). Why the processes represented by equation [6] should be so very efficient is not clear; but the experimental evidence (6) shows that in the case of the peroxyacetyl radical one collision in every two is effective and one collision in every four is effective in the case of the recombination of peroxypropionyl radicals. Nor is the chemistry of process [6] clear. There are obviously two possible mechanisms: (i) It could be that when the two peracetyl radicals interact, the oxygen molecule which is formed is produced by the elimination of an oxygen atom from each of the interacting radicals. (ii) The oxygen molecule formed in equation [6] could come exclusively from one of the interacting radicals by a radical displacement reaction which was previously suggested (6):

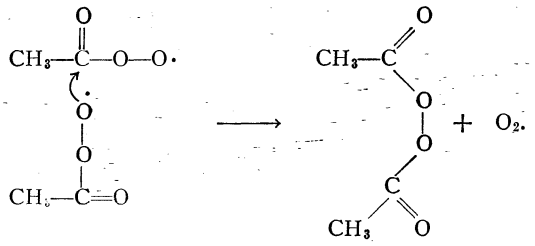

In the earlier work to which we have referred it was pointed out (see ref. 6, p. 277) that the use of isotopically enriched oxygen might enable the chemistry of process [6] to be elucidated. We shall now describe the results of such experiments using O^{18} as a tracer which do enable a decision to be made between the alternative mechanism outlined above. Here we should mention that similar studies using O^{18} as a tracer carried out by Traylor and Bartlett (7) have shown that in the liquid phase autooxidation of cumene, the termination step proceeds by mechanism (i), i.e.

$$ROO + RO^*O^* = ROO\cdots O^*O^*R = R—O—O^*—R \text{ (or } RO + RO^*) + OO^*,$$

where O^* represents an O^{18} atom.

EXPERIMENTAL

The acetaldehyde was purified gas chromatographically, using a 5 ft long column packed with dinonyl phthalate on firebrick. O^{18}, in the form of molecular oxygen, of 98.35% purity was obtained from the Isotope Department, Weismann Institute of Science, Rehovoth, Israel.

Can. J. Chem. Downloaded from www.nrcresearchpress.com by 210.87.254.40 on 09/05/12
For personal use only.

The experimental conditions were essentially the same as those described by McDowell and Sharples (4, 6). Somewhat higher light intensities were used to provide a short chain length so that the equilibration with oxygen-34 could be followed easily. In a typical experiment 60 mm Hg of gas composed of O_2^{32}, O_2^{36}, and argon in the ratio 106.4:6.13:5.00 were introduced into the 75-ml quartz reaction vessel, followed by 150 mm Hg of acetaldehyde. After the gases were allowed to mix for some 15 minutes, the vessel was illuminated with light from a G.E.C. AH6 high-pressure water-cooled mercury lamp. Light filters were used to permit the passage of radiation of wavelength 3130 Å. All the experiments were carried out at 25° C.

At the end of an experiment the products were separated into two portions, one of which was the materials condensable at 77° K. This condensable portion was analyzed by gas chromatography using a 2-ft column packed with dinonyl phthalate in firebrick at 0° C. This column separates hydroperoxides (8) and we found it gave a satisfactory separation of peracetic acid and diacetyl peroxide (see Fig. 1). The gaseous portion not

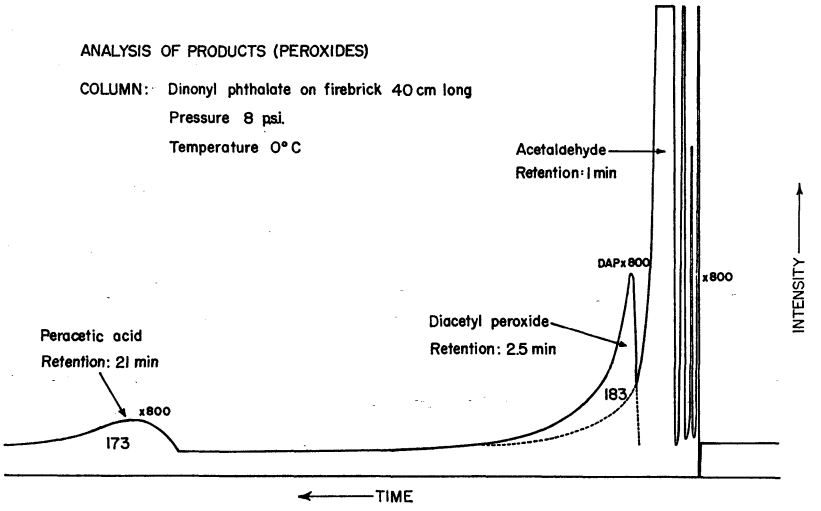

FIG. 1. Gas chromatogram for condensable products from photooxidation of acetaldehyde showing the presence of peracetic acid and diacetyl peroxide.

condensable at 77° K was analyzed mass spectrometrically and the intensities of the peaks at masses 32, 34, 36, and 40 recorded. The analyses beyond the first one were evaluated relative to the argon concentration, which was constant at 1.01×10^{-5} moles based on the original composition of the oxygen mixture at 25°. Two complete sets of experiments were run using the same concentrations of the reactants but at light intensities of 100 and 36.4 (arbitrary units). The results obtained are given in Tables I and II. It is to be

TABLE I

Analysis of products during the photochemical oxidation of 150 mm Hg of acetaldehyde and 60 mm Hg of O_2–Ar mixture at 25° (Intensity of illumination = 100 arbitrary units; all data are in units of moles$\times10^5$; P = peracetic acid, D = diacetyl peroxide)

Time, sec	O_2^{32} (x)	O_2^{34} (y)	O_2^{36} (z)	$W = (x+y+z)$	O^{18}, %	P	D	P/D
0	21.71	0.123	1.220	23.05	5.55	0	0	—
90	19.57	0.230	1.053	20.85	5.60	1.26	1.15	1.095
180	15.79	0.331	0.764	16.84	5.52	2.86	2.88	0.993
240	13.10	0.392	0.579	14.07	5.51	4.16	3.82	1.088
300	12.93	0.407	0.568	13.90	5.55	4.78	4.37	1.094
360	11.62	0.409	0.505	12.53	5.66	5.58	5.58	1.000
								Mean 1.054±0.052

noted that the analytical data for the various isotopic oxygens have been corrected for the natural abundance of O^{18} in ordinary oxygen and also for the O^{17} present in the 98.35% oxygen-18. In making these corrections it was assumed that the O^{18} is statistically distributed with the other isotopic species.

Can. J. Chem. Downloaded from www.nrcresearchpress.com by 210.87.254.40 on 09/05/12
For personal use only.

TABLE II

Analysis of products during the photochemical oxidation of 150 mm Hg of acetaldehyde and 60 mm Hg of O_2–Ar mixture at 25° (Intensity of illumination = 34.6 arbitrary units; all data are in units of moles$\times 10^5$; P = peracetic acid, D = diacetyl peroxide)

Time, sec	O_2^{32} (x)	O_2^{34} (y)	O_2^{36} (z)	$W = (x+y+z)$	O^{18}, %	P	D	P/D
0	21.71	0.123	1.220	23.05	5.55	0	0	—
60	21.12	0.154	1.180	22.45	5.60	0.315	0.161	1.96
120	20.31	0.184	1.110	21.60	5.57	0.882	0.460	1.92
180	19.65	0.200	1.048	20.90	5.49	1.344	0.702	1.92
300	17.68	0.241	0.926	18.85	5.55	2.50	1.473	1.70
420	15.71	0.284	0.805	16.80	5.60	3.64	2.10	1.73
600	12.87	0.312	0.617	13.80	5.60	6.26	3.16	1.98
								Mean 1.87±0.12

It will be convenient to express the two possible mechanisms for the production of oxygen in reaction [6] by the following scheme:

$$\begin{array}{c} AcO^{16}O^{18}Ac + O^{16}O^{18} \\ \uparrow \\ [AcO^{16}O^{16} \cdots O^{18}O^{18}Ac]^{\mp} \\ \Uparrow \qquad\qquad [6a] \\ AcO^{16}O^{16} + AcO^{18}O^{18} \\ \Downarrow \qquad\qquad [6b] \\ [AcO^{16}O^{16} \cdots AcO^{18}O^{18}]^{\mp} \text{ or } [AcO^{18}O^{18} \cdots AcO^{16}O^{16}]^{\mp} \\ \downarrow \qquad\qquad \downarrow \\ AcO^{16}O^{16}Ac + O^{18}O^{18} \text{ or } AcO^{18}O^{18}Ac + O^{16}O^{16} \end{array}$$

Mechanism [6a], involving a head-to-head approach of the two types of isotopically substituted peroxyacetyl radicals, must produce the asymmetrical oxygen-34, whereas mechanism [6b] will produce only oxygen-32 or oxygen-36 without any resulting equilibration with oxygen-34.

From Tables I and II it is evident that oxygen-34 appears during the course of the reaction. Since no equilibration among the species O_2^{32}, O_2^{34}, and O_2^{36} occurs (i) on long standing, (ii) during the photooxidation of rubene, (iii) from the thermal decomposition of rubene peroxide, or (iv) during the decomposition of unlabelled t-butylhydroperoxide (7), the appearance of oxygen-34 must be attributed to the formation of oxygen molecules by the mechanism indicated by [6a]. This interpretation is supported by a detailed kinetic analysis of the results given below.

Under the experimental conditions the chain length of the reaction is constant for each intensity of illumination. This is shown by the figures in the last column of Tables I and II. Moreover, the ratio of the means of the chain lengths is equal to the square root of the ratio of the light intensities used, which is in agreement with the generally accepted mechanism for the reaction (1, 4, 6). Assuming the mechanism outlined earlier, plus path [6a] for the chain-terminating reaction, we can derive equations which relate the chain length, C, and the change in the concentration of the isotopic oxygen during a reaction.

THEORETICAL

According to mechanism given by equations [2]–[6], for each mole of peracetic acid, CH_3CO_3H, produced, the equivalent of M_y moles of O_2^{34} are consumed (M_y = mole fraction of O_2^{34}; it is to be noted that $M_y = 1/2(M_{O_2}{}^{32}+M_{O_2}{}^{36})$, where $M_{O_2}{}^{32}$ and $M_{O_2}{}^{36}$ are the mole fractions of O_2^{32} and O_2^{36} consumed in the formation of peracetic acid. Note $M_{O_2}{}^{36}$ is later represented by M_z. For each mole of diacetyl peroxide produced via mechanism [6a], $2M_y$ moles of O_2^{34} are consumed and f_y moles of O_2^{34} are generated. f_y is the probability that a terminating collision will be between a labelled and an unlabelled peracetyl radical. In our terminology the peroxy radical $RO^{16}O^{18}$ is labelled.

We can write

$$y = y(P,D), \qquad [7]$$

Can. J. Chem. Downloaded from www.nrcresearchpress.com by 210.87.254.40 on 09/05/12
For personal use only.

where y is the total amount, in moles, of O_2^{34}, P = the amount of peracetic acid, and D = the diacetyl peroxide produced in the reaction.

Partial differentiation of equation [7] yields

$$dy = (\partial y/\partial P)_D dP + (\partial y/\partial D)_P dD. \quad [8]$$

But

$$(\partial y/\partial P)_D = -M_y \text{ and } (\partial y/\partial D)_P = -2M_y + f_y$$

and substitution of these in equation [8] leads to

$$dy = -M_y dP + (f_y - 2M_y) dD. \quad [9]$$

Under our experimental conditions P/D = the chain length, C, which is constant, so we may write $dP = CdD$. Substituting in equation [9] we get

$$dy = \{f_y - (C+2)M_y\} dD. \quad [10]$$

M_y is, however, equal to y/W, where W = total oxygen concentration. But $W = W_0 - (D+P)$ so we now have the following equation for M_y:

$$M_y = \frac{y}{W_0 - (C+1)D}. \quad [11]$$

Substituting this expression for M_y into equation [10] yields the result that

$$dy + \left\{\frac{(C+2)y}{W_0 - (C+1)D} - f_y\right\} dD = 0. \quad [12]$$

Equation [12] may be integrated to give the following expression in which the substitution $M_y = y/W$ has been made,

$$f_y - M_y = \{f_y - (M_y)_0\}\left(\frac{W}{W_0}\right)^{1/C+1}, \quad [13]$$

or taking logarithms this becomes

$$\ln (f_y - M_y) = \ln \{f_y - (M_y)_0\} + \frac{1}{C+1} \ln W/W_0. \quad [14]$$

A similar expression can be derived relating f_z and M_z, and C:

$$\ln (M_z - f_z) = \ln \{(M_z)_0 - f_y\} + \frac{1}{C+1} \ln W/W_0. \quad [15]$$

f_y is the probability that a terminating collision of two peracetyl radicals will be between a labelled and an unlabelled radical and can, if isotope effects are neglected, be taken as equal to $2\alpha(1-\alpha)$, where α is the atom-fraction of O^{18} in the total oxygen. Similarly, f_z is the probability that a terminating collision will take place between two labelled peracetyl radicals. Again neglecting isotope effects it is apparent that $f_z = \alpha^2$. M_z is the mole fraction of O_2^{36}.

DISCUSSION

The validity of the above theory and, *ipso facto*, the mechanism for the termination reactions, namely equation [6*a*], can be tested by applying equations [14] and [15] to our results. In Tables III and IV we outline the values for the various parameters in equations

Can. J. Chem. Downloaded from www.nrcresearchpress.com by 210.87.254.40 on 09/05/12
For personal use only.

TABLE III
Variation of oxygen isotopes during oxidation of acetaldehyde
(Intensity of illumination = 100 units (arbitrary))

Time, min	$M_y \times 10^2$	$f_y - M_y$	W/W_0	$M_z \times 10^2$	$M_z - f_z$
0	0.533	0.0995	1.000	5.29	0.0498
90	1.10	0.0938	0.904	5.05	0.0474
180	1.97	0.0851	0.730	4.54	0.0423
240	2.79	0.0769	0.610	4.12	0.0381
300	2.93	0.0755	0.602	4.09	0.0378
360	3.26	0.0722	0.543	4.03	0.0372

TABLE IV
Variation of oxygen isotopes during oxidation of acetaldehyde
(Intensity of illumination = 34.6 units (arbitrary))

Time, min	$M_y \times 10^2$	$f_y - M_y$	W/W_0	$M_z \times 10^2$	$M_z - f_z$
0	0.533	0.0995	1.000	5.29	0.0498
60	0.686	0.0979	0.975	5.26	0.0495
120	0.852	0.0963	0.938	5.14	0.0483
180	0.957	0.0952	0.907	5.01	0.0470
300	1.28	0.0920	0.217	4.91	0.0460
520	1.69	0.0879	0.729	4.79	0.0448
600	2.26	0.0822	0.599	4.47	0.0416

[14] and [15] as calculated from the experimental data given in Tables I and II. Figures 2 and 3 show that both equations [14] and [15] are satisfied by the experimental results.

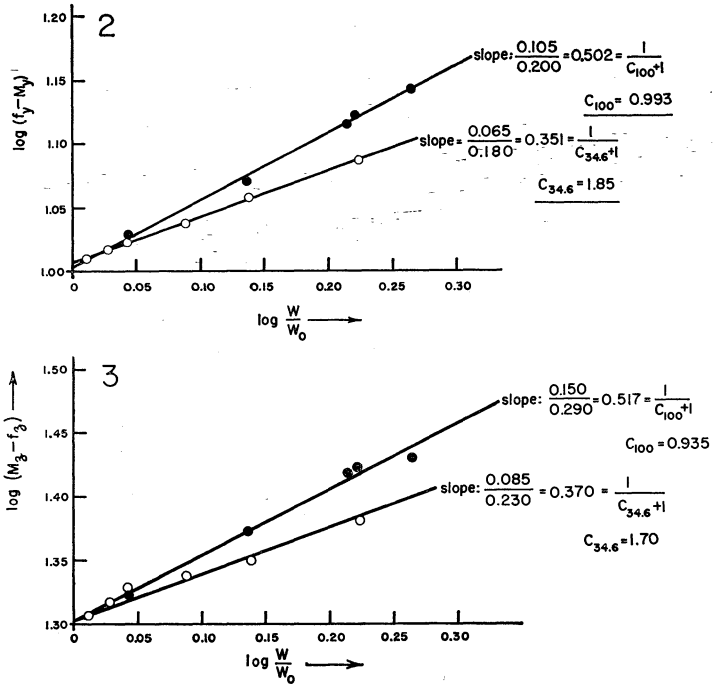

FIG. 2. Plot of equation [14] using experimental data on analysis of variation of O_2^{34} and values of f_y from Table III. ●, intensity = 100 units; ○, intensity = 34.6 units.

FIG. 3. Plot of equation [15] using experimental data on analysis of variation of O_2^{36} and values of f_z from Table IV. ●, intensity = 100 units; ○, intensity = 34.6 units.

Can. J. Chem. Downloaded from www.nrcresearchpress.com by 210.87.254.40 on 09/05/12
For personal use only.

There can therefore be no doubt but that the mechanism [6*a*] given for the terminating process is indeed the correct one. Furthermore, indirectly, the overall mechanism outlined for the production of peroxides in this photooxidation reaction is likewise confirmed.

It is also possible to show that both the isotopic and the peroxide analytic results are self-consistent and this again is further confirmation of the correctness of the mechanisms put forward. Perhaps the best way of showing the self-consistent nature of the results is that displayed in Table V.

TABLE V

Kinetic analysis of data in Tables I and II
($\alpha = 0.0555, f_y = 0.1048, f_z = 0.0031$)

C_{100} from equation [14], Fig. 1	= 0.993
C_{100} from equation [15], Fig. 1	= 0.935
C_{100} calc. from P/D	= 1.054±0.052
$C_{34.6}$ from equation [14], Fig. 2	= 1.85
$C_{34.6}$ from equation [15], Fig. 2	= 1.70
$C_{34.6}$ calc. from P/D	= 1.87±0.12

Since we have now shown conclusively that the recombination of peroxyacetyl radicals takes place according to equation [6*a*] with the elimination of one oxygen atom from each reacting peroxyacetyl radical, it now remains for us to suggest a detailed mechanism for this process. A satisfactory reaction scheme is that shown below in Fig. 4 which involves a transition state, marked with the symbol ‡, in which a planar four-centered oxygen atomic system is the site of chemical reactivity.

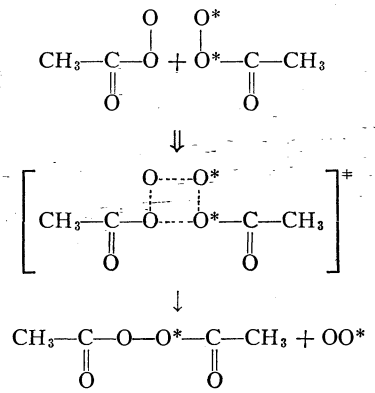

FIG. 4. Suggested mechanism for the recombination of peroxyacetyl radicals.

As the work of Traylor and Bartlett (7) and that now reported both show that the mechanism of the recombination of the peroxy radicals derived from cumene in the liquid phase is the same as that for the peroxy radicals from acetaldehyde in the gas phase, it may reasonably be assumed that this is a general mechanism for this type of reaction. If this is so, it is then of interest to compare the absolute values for the velocity constants from such reactions in both the gas and liquid phases. The absolute value for k_6 for the recombination of peroxyacetyl radicals is known to be $2.69(\pm 1.35)\times 10^{10}$ l. mole^{-1}sec^{-1} from the work of McDowell and Sharples (6). Unfortunately, no values are available for velocity constants for the recombination of these radicals in the liquid phase though there are data in the literature for the recombination of other peroxy

Can. J. Chem. Downloaded from www.nrcresearchpress.com by 210.87.254.40 on 09/05/12
For personal use only.

radicals in the liquid phase. These values for k_6 for various radicals in the liquid phase vary from 0.95×10^6 l. mole^{-1}sec^{-1} for the cyclohexylperoxy radicals (9) to 2.10×10^8 l. mole^{-1}sec^{-1} for the peroxy radical from benzaldehyde (10). This latter datum can be taken as approximating to within an order of magnitude to the value of k_6 expected for the recombination of peroxyacetyl radicals in solution. It would then be seen that k_6 for the gas phase recombination of peroxyacetyl radicals is between 10 and 100 times as great as the anticipated value for the liquid phase reaction. This difference seems to be what might reasonably be expected on theoretical grounds. Presumably the smaller value expected for k_6 for the liquid phase process would be due to entropy factors associated with possible solvation of the peroxy radical. Recombination of two solvated peroxy radicals would, of course, be expected to be a somewhat less rapid process than the gas phase recombination of the same peroxy radicals.

ACKNOWLEDGMENTS

We wish to thank the National Research Council of Canada for generous grants in aid of this research work. One of us (S. S.) is also indebted to that body for the award of a Studentship.

REFERENCES

1. C. A. McDowell and J. B. Farmer. Fifth Symposium (International) on Combustion. Reinhold Publishing Co., New York. 1955. p. 453.
2. E. G. Bowen and E. L. Jietz. J. Chem. Soc. 234 (1930).
3. A. Combe, M. Niclause, and M. Letort. Rev. Inst. Franc. Petrole. Ann. Combust. Liquides, **10**, 786, 929 (1955).
4. C. A. McDowell and L. K. Sharples. Can. J. Chem. **36**, 251 (1958).
5. C. A. McDowell and J. Black. Unpublished results.
6. C. A. McDowell and L. K. Sharples. Can. J. Chem. **36**, 268 (1958).
7. T. G. Traylor and P. D. Bartlett. Tetrahedron Letters, No. 24, 30 (1960).
8. K. M. Bell and C. A. McDowell. Can. J. Chem. **39**, 1424 (1961).
9. L. Bateman and G. Gee. Proc. Roy. Soc. (London), Ser. A, **195**, 391 (1948).
10. T. A. Inglis and H. W. Melville. Proc. Roy. Soc. (London), Ser. A, **218**, 175 (1952).

Can. J. Chem. Downloaded from www.nrcresearchpress.com by 210.87.254.40 on 09/05/12
For personal use only.

THE ABSOLUTE CONFIGURATION OF *dextro*-1-DEUTERIOETHANOL[1]

R. U. LEMIEUX[2] AND J. HOWARD[3]
Department of Chemistry, University of Ottawa, Ottawa, Ontario
Received August 31, 1962

ABSTRACT

Reduction of 1,2-*O*-isopropylidene-3-*O*-benzyl-5-oxo-α-D-xylofuranose with lithium aluminum deuteride followed by removal of the isopropylidene and benzyl groups provided 5-deuterio-D-xylose. Nuclear magnetic resonance examination of the 5-deuterio-β-D-xylopyranose tetraacetate showed the isomer with the 5-carbon in the R-configuration (deuterium equatorial) to be present in 30% excess. The substance was degraded to 1-deuterioethanol, which possessed a dextrorotation of the magnitude expected and which necessarily possessed the R-configuration. This result confirmed the prediction made by Brewster (Tetrahedron Letters, **20**, 23 (1959)).

Can. J. Chem. Downloaded from www.nrcresearchpress.com by 210.87.254.5 on 09/05/12
For personal use only.

Recently, Althouse, Ueda, and Mosher (1) have reported on the reduction of 1-deuteriotrimethylacetaldehyde by actively fermenting yeast and have reviewed the results of the investigations by Westheimer, Vennesland, and their respective co-workers on the alcohol dehydrogenase catalyzed reduction of both acetaldehyde by monodeuterio-reduced diphosphopyridine nucleotide (DPND) and of 1-deuterioacetaldehyde by unlabelled DPNH to form optically pure samples of 1-deuterioethanol. Furthermore, the various lines of conflicting reasoning applied by Vennesland, Streitweiser, Kaplan, Brewster, and their respective co-workers to predict the absolute configuration of optically active 1-deuterioethanol and other optically active primary alcohols rendered dissymmetric by monodeuteration of the 1-carbon are discussed. The speculations presented by Mosher and his collaborators (1) on the configurational relationship between the 1-deuterioneopentyl alcohol, obtained by reduction using actively fermenting yeast, and the 1-deuterioethanol prepared by the DPNH reduction of 1-deuterioacetaldehyde (2), overlook the fact that Lemieux and Giguere (3) found that, whereas the reduction of β-keto-*n*-caproic and β-keto-*n*-caprylic acids by actively fermenting yeast yielded the corresponding D-β-hydroxyacids, the similar reduction of β-ketobutyric acid gave L-β-hydroxybutyric acid. Evidently, at least two mechanisms for the reduction of a carbonyl group are present in actively fermenting yeast and the procedure does not provide a reliable means for the establishment of configurational relationships. The purpose of this communication is to report an unequivocal proof for the absolute configuration of *dextro*-1-deuterioethanol.

The 3-*O*-benzyl derivative (II) of 1,2:5,6-di-*O*-isopropylidene-α-D-glucofuranose (I) was subjected to simultaneous preferential hydrolysis of the 5,6-*O*-isopropylidene group and periodate oxidation of the resulting 5,6-glycol by treatment in 90% aqueous acetic acid with 0.08 *M* periodic acid at room temperature for 25 minutes. The 1,2-*O*-isopropylidene-3-*O*-benzyl-5-oxo-α-D-xylofuranose (III) thus obtained was purified by distillation and reduced at room temperature in ether by slow addition (over 1 hour) of lithium aluminum deuteride in ether. The product (IV) was subjected to catalytic hydrogenolysis to remove the benzyl group and form 1,2-*O*-isopropylidene-5-deuterio-α-D-xylofuranose (V). Acid

[1]*Presented at the XXIXth Congrès de l'Association Canadienne-Française pour l'Avancement des Sciences, Ottawa, 1961.*
[2]*Present address: Department of Chemistry, University of Alberta, Edmonton, Alberta.*
[3]*National Research Council of Canada Postdoctoral Fellow 1959–61. Present address: Research Division, Rayonier Canada (B.C.) Limited, Vancouver, British Columbia.*

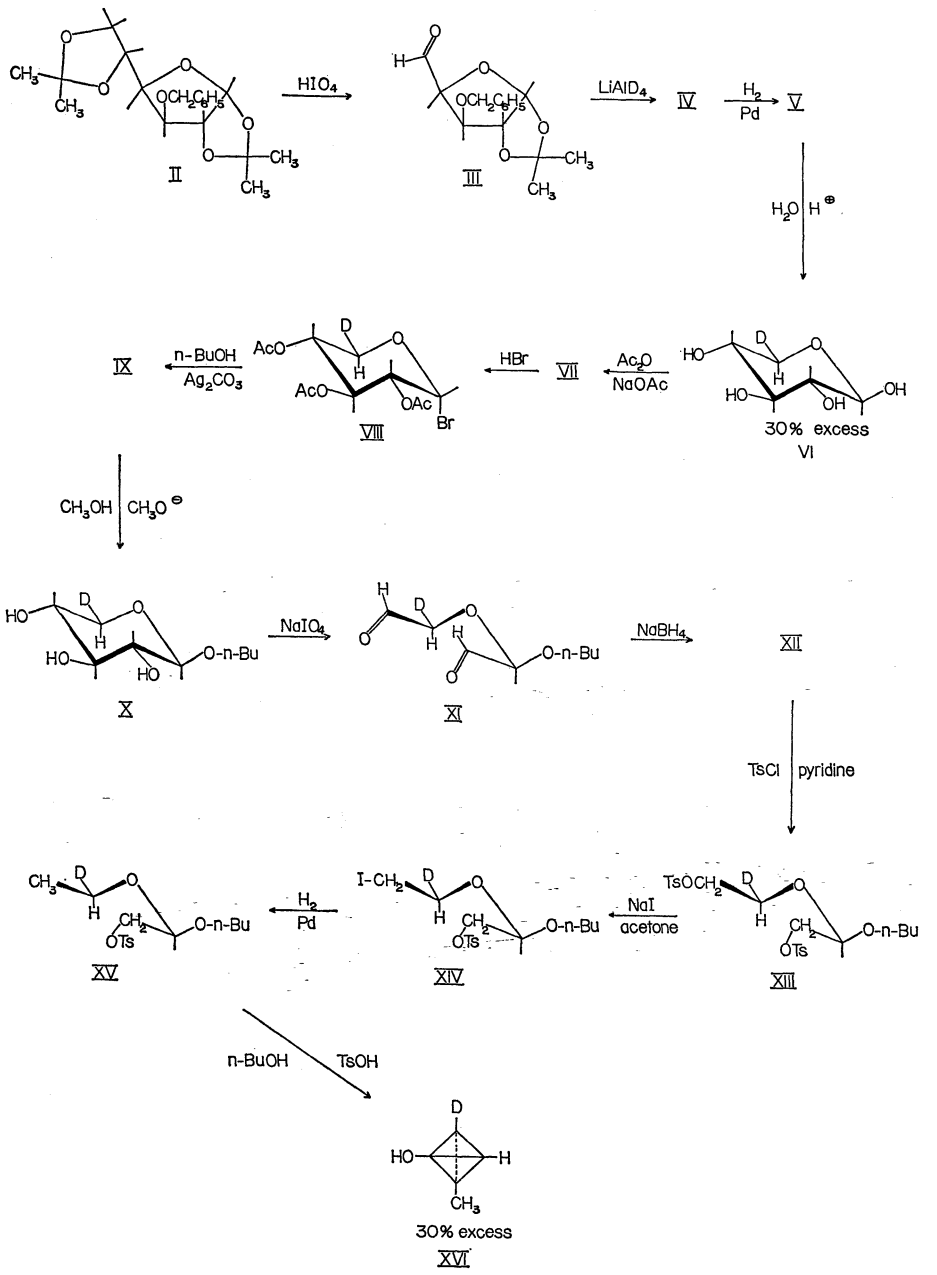

hydrolysis of the latter compound gave 5-deuterio-D-xylose (VI), which was acetylated using sodium acetate and acetic anhydride to form 5-deuterio-β-D-xylopyranose tetraacetate (VII). The nuclear magnetic resonance signals produced by the hydrogen at the 5-carbon of this product, which is the mixture of diastereoisomers differing in the configuration of the 5-carbon depicted in Fig. 1B, are compared in Fig. 1 with those of the methylene group in undeuterated β-D-xylopyranose tetraacetate (Fig. 1A). Lemieux and his collaborators (4) have already made the assignment of the signals for the methylene

Can. J. Chem. Downloaded from www.nrcresearchpress.com by 210.87.254.5 on 09/05/12
For personal use only.

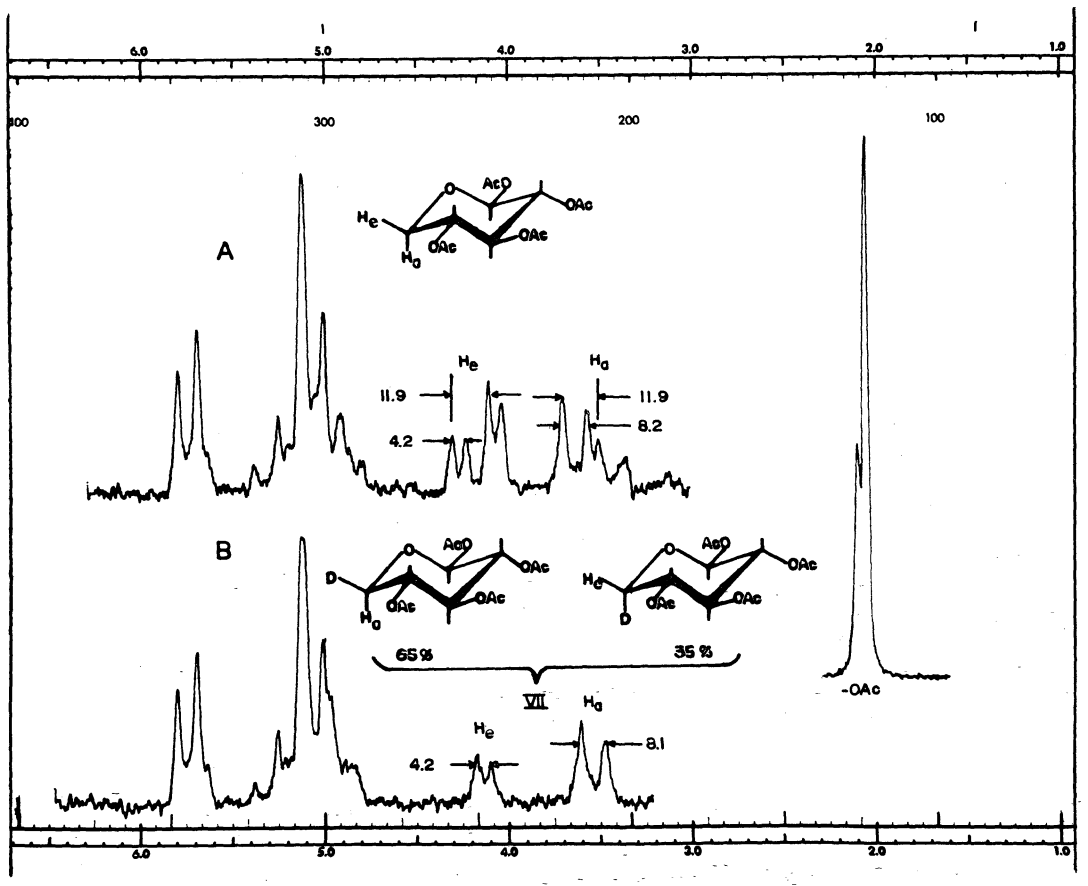

FIG. 1. Nuclear magnetic resonance spectra measured in chloroform. A. β-D-xylopyranose tetraacetate. B. Mixture of the diastereoisomeric tetraacetates (VII) of 5-deuterio-β-D-xylopyranose.

hydrogens in β-D-xylopyranose tetraacetate. In the case of the 5-deuterio derivatives (VII) the 5-hydrogen (either H_a or H_e) is coupled strongly only with the hydrogen at the 4-position. Therefore, the appearance of the two rough doublets (because of coupling with the deuterium atom) is in accord with expectation. Undoubtedly, the signal at low field, $\tau = 5.87$, with a spacing of 4.2 c.p.s. arose from the molecules in which the hydrogen is equatorial and the one at high field, $\tau = 6.46$, with a spacing of 8.1 c.p.s. arose from the molecules in which the hydrogen is axial (4). A comparison of the relative intensities of these two signals showed that the isomer which has the 5-hydrogen in axial orientation was 1.85 times more abundant than the other. Since the absolute configuration of β-D-xylopyranose tetraacetate is known to be that depicted in Fig. 1, the absolute configuration of the 5-carbon in the more abundant isomer of VII possesses, in terms of the Cahn–Ingold–Prelog designation (5), the R-configuration. Therefore, degradation of VII to 1-deuterioethanol by way of a sequence of reactions that does not disturb any of the four bonds of the 5-carbon would yield R-1-deuterioethanol (XVI) of about 30% optical purity. The degradation was accomplished as follows.

The tetraacetate (VII) was converted to tri-*O*-acetyl-5-deuterio-β-D-xylopyranosyl bromide (VIII) and this compound was reacted with *n*-butanol in the presence of silver

Can. J. Chem. Downloaded from www.nrcresearchpress.com by 210.87.254.5 on 09/05/12
For personal use only.

carbonate and anhydrous calcium sulphate to give *n*-butyl tri-*O*-acetyl-5-deuterio-β-D-xylopyranoside (IX) (6). Deacetylation provided *n*-butyl 5-deuterio-β-D-xylopyranoside (X), which was oxidized with sodium periodate at pH 5 to 6. The resulting dialdehyde (XI) was reduced with sodium borohydride at pH about 8 to afford the diol (XII). On subjecting the ditosylate (XIII) of the diol to a treatment with a refluxing solution of sodium iodide in dry acetone for 3 hours, the 2-tosyloxy-1-deuterioethyl group of XIII was transformed to the 2-iodo-1-deuterioethyl group of XIV. Hydrogenolysis of the iodo compound using palladium–hydrogen in methanol containing an excess of diethylamine gave the *n*-butyl 1-deuterioethyl mixed acetal of *O*-tosyl glycolaldehyde (XV). This substance was heated under conditions for distillation with dry *n*-butanol containing *p*-toluenesulphonic acid. The 1-deuterioethanol in the distillate was isolated by fractional distillation using the Podbielniak semimicro, spinning-band column. Four successive, about 0.35-ml fractions were collected in the boiling point range expected for ethanol. Examination of these fractions by gas–liquid partition chromatography and nuclear magnetic resonance spectroscopy showed the first three fractions, which distilled at the same temperature, to be virtually pure 1-deuterioethanol. Although the n.m.r. spectra of the fractions indicated the presence of water, the amount certainly was no more than is present in the ethanol–water azeotropic mixture. Levy, Loewus, and Vennesland (ref. 2, footnote 12) have shown that the drying of optically active 1-deuterioethanol does not change the sign of rotation. Consequently, the samples were not dried before measuring their rotations at the D-line of sodium. The fact that the samples were the expected 1-deuterioethanol is clear from the spectra shown in Fig. 2. Spectrum A is for a commercial grade of anhydrous ethanol and spectrum B is for a sample of ethanol–water azeotropic mixture. Spectrum C is of the combined fractions of 1-deuterioethanol after their individual rotations and n.m.r. spectra had been measured. The essentially doublet character of the signal for the methyl group clearly requires the deuterium to be at the 1-position of the ethanol.

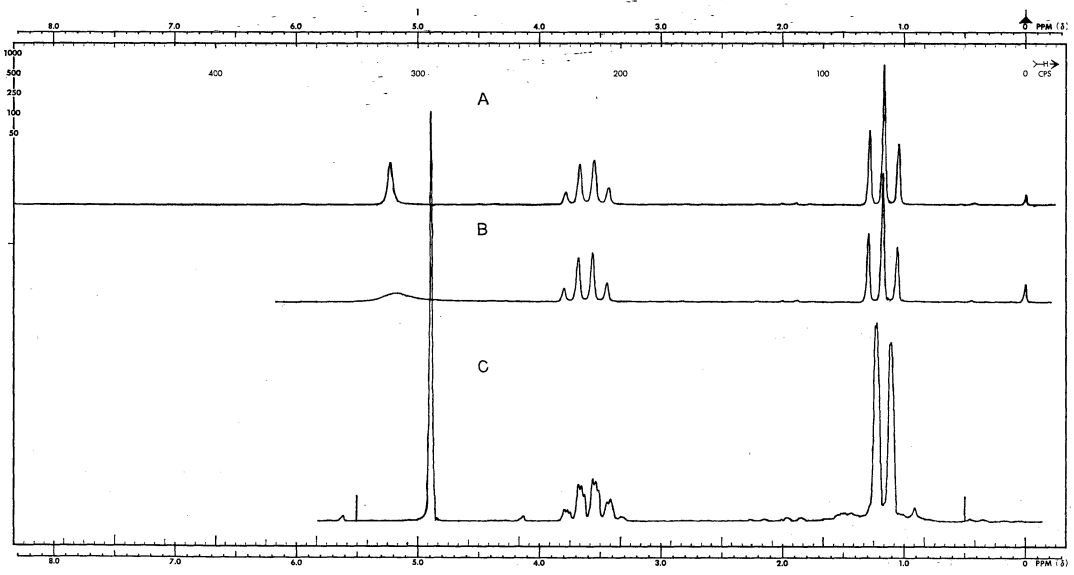

FIG. 2. Nuclear magnetic resonance spectra of ethanol (A), ethanol–water azeotrope (B), and the sample of *dextro*-1-deuterioethanol (C).

Can. J. Chem. Downloaded from www.nrcresearchpress.com by 210.87.254.5 on 09/05/12
For personal use only.

The optical rotations of the three fractions of 1-deuterioethanol were measured under conditions of replication whereby a solution which was expected to produce a rotation of $-0.052°$ different from the commercial alcohol used as a blank actually gave a rotation of $-0.057 \pm 0.02°$. The observed optical rotations of the first three 1-deuterioethanol fractions were found to be $+0.061°$, $+0.066°$, and $+0.069°$, respectively. From the known (2) rotation of an optically pure sample of 1-deuterioethanol, the expected magnitude for the rotation was $\pm 0.066°$. It is inconceivable that these fractions would contain an optically active compound other than the deuterioethanol. Nevertheless, should the distillate possess such a compound and it, rather than the deuterioethanol, was responsible for the optical rotation, the substance would have to be present in about the same trace quantity in each of the three fractions and be present in just sufficient quantity to produce the magnitude of rotation expected if all of the optical activity came from the deuterioethanol. This event is too unlikely to warrant consideration. It is therefore concluded that, as anticipated both by Brewster (7) and by van Eys and Kaplan (8), dextrorotatory 1-deuterioethanol has the R-configuration shown in XVI. Therefore, since the reduction of 1-deuterioacetaldehyde by DPNH leads to the formation of levorotatory S-1-deuterioethanol (2), it is now definite that the acetaldehyde accepts the hydride ion in the manner depicted in XVII.

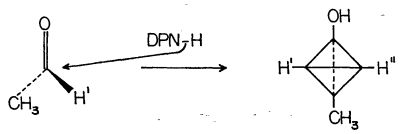

XVII

Of the variety of reducing conditions studied for the reduction of the aldehyde (III) using a deuterated reducing agent, the conditions reported herein gave the largest extent of partial asymmetric synthesis. The effects of temperature and order of addition using lithium aluminum deuteride have already appeared in Table III of the paper recently published by Haubenstock and Eliel (9) and require no further comment. Of real interest is the fact that a solution of deuterated isobornylmagnesium bromide which rapidly (2 hours) reduced benzaldehyde (10) left the aldehyde III unchanged even after prolonged (3 days) reaction times. Other attempts to make the aldehyde enter into a Meerwein–Ponndorf–Verley type of reduction were unsuccessful. Most likely these results are due to ready enolization of the aldehyde and the consequent formation of an enolate which resists reduction. Schaffer and Isbell (11) have demonstrated that 1,2-*O*-isopropylidene-5-oxo-α-D-xylofuranose undergoes aldol condensation and we observed (paper chromatography) the formation of the *arabo*-configuration in the reduction of one of our preparations of the 3-*O*-benzyl derivative (III). Whatever the reason for the resistance to reduction by alkoxides, displayed by the aldehyde III, this property precluded our ability to prepare optically pure 1-deuterioethanol.

EXPERIMENTAL

The melting points were determined on a Leitz microstage and are uncorrected. Unless otherwise stated, the optical rotations were measured at room temperature to $0.01 \pm 0.01°$. The nuclear magnetic resonance spectra were measured on high-resolution Varian Associates spectrometers operating at 60 Mc/s.

1,2:5,6-Di-O-isopropylidene-α-D-glucofuranose (I)

The compound was prepared under the conditions described by Mehltretter and co-workers (12) except that the glucose was ground to pass through a 100-mesh sieve and no temperature control was used. A study of the progress of the reaction showed that the yield passed through a maximum after about 45 minutes' reaction time. At this time, only 3% of the glucose remained undissolved and the yield of product, melting

Can. J. Chem. Downloaded from www.nrcresearchpress.com by 210.87.254.5 on 09/05/12
For personal use only.

at 93–104° and giving pure product after one recrystallization from 80–100° petroleum ether, was 80% based on the glucose which had reacted. Since these experiments were performed Recondo and Rinderknecht (13) reported the use of acetic acid to help solubilize the glucose and evolved a procedure which appears equivalent to the best conditions developed in this investigation.

1,2:5,6-Di-O-isopropylidene-3-O-benzyl-α-D-glucofuranose (II)

The procedure reported by Adams, Reeves, and Goebel (14) was followed and the product was distilled at 170–180° and 0.1 mm pressure. The yield was 95%.

1,2-O-Isopropylidene-3-O-benzyl-5-oxo-α-D-xylofuranose (III)

1,2:5,6-Di-*O*-isopropylidene-3-*O*-benzyl-α-D-glucofuranose, 30 g (0.086 *M*), was dissolved in 1 liter of glacial acetic acid. A solution of 21 g of periodic acid (H_5IO_6, 0.092 *M*) in 150 ml of water was added. After thorough mixing, the reaction was allowed to continue at 25°. After 25 minutes, the reaction was quenched by the addition of 60 g of sodium acetate dissolved in 2 liters of water. The aqueous solution was extracted using five 200-ml volumes of benzene, and the combined extracts were washed free of iodine with 0.1 *N* sodium thiosulphate solution. The yellowish oily residue, 20 g, which remained after the benzene was removed by distillation *in vacuo*, was dried by azeotropic distillation with benzene. The infrared spectrum showed weak carbonyl and very strong hydroxyl stretching vibrations and, consequently, the aldehyde was in the aldehydrol form. The oil was distilled in a high vacuum using a flask and condensing unit which had both been washed previously with concentrated nitric acid and distilled water to remove surface basicity in order to minimize the possibility for enolization. The faintly yellow viscous liquid, 16 g (67% yield), boiled at 140° at 0.15 mm pressure and its infrared spectrum showed no hydroxyl, but very strong carbonyl stretching vibrations. However, on exposure to moisture in the atmosphere the substance soon reverted to the aldehydrol form. The semicarbazone of the aldehyde was prepared, and melted at 170–173°. Anal. Calc. for $C_{16}H_{21}N_5O_3$: C, 57.29; H, 6.31%. Found: C, 57.71; H, 6.49%.

1,2-O-Isopropylidene-3-O-benzyl-5-deuterio-α-D-xylofuranose (IV)

Lithium aluminum deuteride (purchased from Metal Hydrides Inc., Beverly, Mass.), 0.923 g (0.022 *M*) (98% pure), was dissolved in 200 ml of ether (dried over lithium aluminum hydride) contained in a two-neck flask fitted with a condenser and calcium chloride tube, serum cap, and magnetic stirrer. As soon as the lithium aluminum deuteride had dissolved in the ether, 20-ml portions were slowly added, using a large hypodermic syringe, to 1,2-*O*-isopropylidene-3-*O*-benzyl-5-oxo-α-D-xylofuranose (III), 21.7 g (0.078 *M*), dissolved in 500 ml of dry ether contained in a liter flask fitted with a magnetic stirrer, serum cap, condenser, and calcium chloride tube. The time taken for the addition of all the deuteride was 60 minutes. After allowing the reaction mixture to stand for a further 15 minutes, a small portion of the solution was added to water. A moderate evolution of gas indicated that a slight excess of lithium aluminum deuteride had been added. Water, 5 ml, was then added with stirring. The precipitate was removed by filtration with the aid of Celite and the ether was removed *in vacuo*. The clear colorless oil, 21 g (96% yield), which remained was dried by azeotropic distillation with benzene. The infrared spectrum indicated strong hydroxyl and C—D stretching vibrations but no signal characteristic of the carbonyl group. No purification was achieved as could be judged by infrared spectroscopy on distilling the substance at 160° and 0.1 mm pressure. The material, $[\alpha]_D^{27} = -31.3°$ (*c*, 6 in ethanol), resisted crystallization as did the 2,4-dinitrobenzoate ester.

1,2-O-Isopropylidene-5-deuterio-α-D-xylofuranose (V)

Substance IV, 21 g (0.075 *M*), was dissolved in 150 ml of absolute alcohol and hydrogenolyzed at room temperature and 4 atm pressure using a 10% palladium on charcoal catalyst (purchased from Engelhard Industries Inc., Newark 2, N.J.). The uptake of hydrogen was complete after 9 hours. The catalyst was removed by filtration and the filtrate was evaporated to a thick colorless syrup, 13.5 g (95% yield). The infrared spectrum showed that removal of the benzyl group was complete. The compound was characterized through its hydrolysis to 5-deuterio-α-D-xylose (VI) as described below.

5-Deuterio-α-D-xylose (VI)

The deuterioisopropylidene xylose (V), 13.5 g (0.071 *M*), was dissolved in 100 ml of 0.1 *N* sulphuric acid and the solution was heated on a steam bath for 45 minutes. After this time, the optical rotation was constant. The hot solution was neutralized with aqueous 0.1 *N* barium hydroxide and, after cooling, the barium sulphate was removed by filtration with the aid of Celite. The filtrate was evaporated *in vacuo* and the residue was dried by azeotropic distillation with benzene and ethanol. The colorless clear syrup after seeding with a small amount of undeuterated D-xylose and treatment with a little absolute ethanol crystallized completely within an hour. The dried crystals, 10.4 g (97% yield), melted at 142–143°. Pure α-D-xylose melts at 145°. A sample was chromatographed on paper using an ethyl acetate – pyridine – benzene – water (5:3:1:3) solvent system. Only one spot for xylose ($R_f = 0.36$) was detected using aniline phthalate as the spray reagent.

Tetra-O-acetyl-5-deuterio-β-D-xylopyranose (VII) (15)

The deuterated xylose (VI), 10.4 g (0.069 *M*), and 12 g of fused sodium acetate were mixed and cautiously heated, with efficient stirring, with 50 ml of acetic anhydride. The temperature of the initial reaction was

Can. J. Chem. Downloaded from www.nrcresearchpress.com by 210.87.254.5 on 09/05/12
For personal use only.

kept below 100° by cooling but after the initial strong liberation of heat had subsided, the mixture was kept at 100° for a period of 30 minutes, cooled, and poured into 200 ml of stirred water. Within a short time, the oil that separated began to crystallize and after 1 hour the mixture was cooled to 5° and the colorless product, 11 g (55% yield), melting at 122–125°, was collected by filtration. The filtrate was extracted with two 50-ml volumes of benzene and the combined extracts were washed with saturated sodium bicarbonate solution. Evaporation provided 8.4 g of a brown syrup which only partially crystallized. This material was retained and combined with the same syrups obtained in three subsequent acetylations of deuterated xylose. The mixture of α- and β-D-xylose tetraacetates, 26 g, was then deacetylated in 250 ml of anhydrous methanol made alkaline with a methanolic solution of potassium methoxide. The methanol was then evaporated to leave 14 g of syrupy deuterated xylose, which was immediately reacetylated using fused sodium acetate and acetic anhydride in the manner described above. The overall yield of tetra-*O*-acetyl-5-deuterio-β-D-xylopyranose (VII) was 78%.

The n.m.r. spectrum of the purified substance is shown in Fig. 1. Integration of the signals for the hydrogens on the 5-carbon, doublets centered at $\tau = 5.87$ (spacing 4.2 c.p.s.) and $\tau = 6.46$ (spacing 8.1 c.p.s.), showed the latter (high-field) signal to have an intensity 1.85 times that of the low-field signal.

Tri-O-acetyl-5-deuterio-α-D-xylopyranosyl Bromide (VIII)

The dry deuterated β-D-xylose tetraacetate (VII), 10.5 g (0.033 *M*), was dissolved in 100 ml of dry, ethanol-free chloroform. A 34-ml amount of 32% hydrobromic acid in acetic acid which contained 4 ml of acetic anhydride was then added to the chloroform solution at 10°. After 45 minutes, the optical rotation had become constant and the mixture was plunged into 300 ml of ice water contained in a separatory funnel. After thorough washing, first with ice water and then with saturated sodium bicarbonate solution at 0°, the chloroform solution was dried over sodium sulphate. The total time taken for washings was approximately 20 minutes. After filtration, the chloroform was evaporated *in vacuo* at a temperature not exceeding 50° to reduce the volume to 50 ml. This solution was used directly to prepare the butyl xyloside (IX) as described below. In a control experiment, removal of the chloroform gave a 91% yield of colorless crystalline product (VIII) melting in the range 95–100°. Pure tri-*O*-acetyl-α-D-xylopyranosyl bromide melts at 102° (16).

n-Butyl Tri-O-acetyl-5-deuterio-β-D-xylopyranoside (IX)

Hori (6) prepared this compound in 43% yield from the bromide VIII. The yield was improved to 53% by maintaining anhydrous conditions throughout the addition over a period of 4 hours of the bromide (VIII), dissolved in chloroform (see above), to a slurry of silver carbonate in *n*-butanol containing anhydrous calcium sulphate. The reaction and work-up conditions were otherwise similar to those reported by Hori (6). The yield was 9.5 g of a syrup which crystallized spontaneously and gave only a faint Fehling test. Recrystallization from 3 parts of methanol–water (2:1) gave 6 g of crystalline product (IX) melting at 95–99°. The overall yield from the tetraacetate (VII) was 53%.

Crystalline *n*-butyl 5-deuterio-β-D-xylopyranoside (X) was obtained in quantitative yield by deacetylation in dry methanol using sodium methoxide as catalyst in the usual manner. After one recrystallization from ethyl acetate and petroleum ether, the compound melted at 89–90°. Hori (6) reported the substance (X) to melt at 90–91°.

Periodate Oxidation of n-Butyl 5-Deuterio-β-D-xylopyranoside (X) to the Ditosylate XIII

The deuterated butyl xyloside (X), 10.3 g (0.0475 *M*), was dissolved in 210 ml of water containing 5 g of sodium acetate and 25.8 g of sodium metaperiodate (0.12 *M*) added over a 5-minute period to the stirred solution, kept at room temperature in a water bath. After approximately 15 minutes, the optical rotation was constant. The solution was filtered and extracted nine times using 50-ml portions of ethyl acetate. The combined extracts were dried over sodium sulphate and evaporated *in vacuo* to give 9.1 g of the syrupy hydrated dialdehyde XI. The infrared spectrum of the material showed strong absorptions in the hydroxyl, carbonyl, and C—D stretching regions.

The hydrated dialdehyde XI, 9.1 g, was dissolved in 100 ml of water, and 4 g of sodium borohydride in approximately 0.25-g portions was added over a period of 15 minutes to the stirred solution, which was kept at 0°. During the reduction the pH was kept at approximately 8.0 by the addition of glacial acetic acid. After 1 hour, the excess sodium borohydride was destroyed by the addition of glacial acetic acid to maintain a pH of 7. The solution was then extracted using six 60-ml portions of ethyl acetate and the combined extracts were dried over sodium sulphate. Filtration and solvent removal left 7.0 g of an oil which was distilled to give 5.4 g (64% yield) of clear colorless oil which boiled at 110° and 0.1 mm pressure. The n.m.r. spectrum of this compound in heavy water showed a triplet of 6 c.p.s. spacing at 5.25 τ. The spectrum showed two bands, one in the region 6.0 to 6.5 τ due to the hydrogens of the methylene groups attached to oxygen and the other in the region 8.2 to 9.3 τ due to the propyl group of the *n*-butyl group. The relative intensities of these bands was 1:1, as expected for the monodeuterio derivative. The specific rotation of the undeuterated compound was too small to measure in water but was $-11.7°$ in ethyl acetate ($c = 4$).

The deuterated diol XII, 5.3 g (0.03 *M*), was dissolved in 80 ml of dry pyridine. Tosyl chloride, 35 g (0.183 *M*), was dissolved in 80 ml of ethanol-free, dry chloroform. The two solutions were mixed at 0° and kept at this temperature for 1 hour. The reaction mixture was allowed to stand at room temperature for 3 hours and 8 ml of water was added with cooling. After 30 minutes, 200 ml of chloroform was added and the

Can. J. Chem. Downloaded from www.nrcresearchpress.com by 210.87.254.5 on 09/05/12
For personal use only.

solution was extracted successively using two 400-ml portions of ice-cold water, one 400-ml portion of 2 *N* hydrochloric acid at 0°, and one 50-ml portion of a saturated solution of sodium bicarbonate. The chloroform solution was then dried over magnesium sulphate, filtered, and evaporated *in vacuo* to a 14.5 g syrupy residue of the deuterated ditosylate XIII. The n.m.r. spectrum in carbon tetrachloride showed the presence of two tosyl groups per butyl group and a triplet of 5 c.p.s. spacing at 5.43 τ. The hydrogens of the methylene groups attached to oxygen produced their signals in a wide band ranging from 5.7 to 6.9 τ. The intensity of this band relative both to the signals for aromatic hydrogens and the signals of the hydrogens in the propyl group showed the deuterated compound (XIII) to possess one hydrogen less than the undeuterated normal substance prepared in the same way but from normal D-xylose. The compound (XIII) showed absorption in the region of the infrared, 2200 cm^{-1}, characteristic of the C—D bond stretch. The signal was not present in the absence of the deuteration.

The n-Butyl 1-Deuterioethyl Acetal of O-Tosylglycolaldehyde (XV)

The deuterated ditosylate (XIII), 14.4 g (0.02 *M*), was dissolved in a solution of 20 g of dry sodium iodide in 400 ml of dry acetone. On standing at room temperature overnight, 3.8 g of sodium *p*-toluenesulphonate precipitated. The filtrate was kept at a reflux temperature for 1½ hours and a further 2.2 g of the salt precipitated. The total amount, 6.0 g, corresponds to the replacement of 1.04 tosyloxy groups per mole of XIII. The reaction mixture was then filtered and evaporated at 35° *in vacuo* to a salt cake. Water, 100 ml, was added and the mixture was extracted with three 50-ml portions of ether. The combined ethereal extracts were washed first with a solution of sodium thiosulphate and then with water. After drying over magnesium sulphate, the solvent was removed *in vacuo* to leave 12.2 g of colorless product (XIV). The substance was dissolved in 50 ml of dry methanol which contained 5 ml of diethylamine and 1.5 g of 10% palladium on charcoal. The solution was hydrogenolyzed at an initial pressure of 3 atm. The hydrogen uptake (1 mole per mole of XIV) was complete after 30 minutes. The catalyst was removed by filtration and the filtrate was evaporated to a semisolid mass, which was dissolved in 100 ml of water, and the mixture was extracted with two 100-ml portions of ether. After drying over magnesium sulphate, the ether was removed *in vacuo* to leave 8.2 g of a colorless oil (XV). Although the n.m.r. spectrum of this product was not determined, that of the ethyl *n*-butyl acetal of *O*-tosylglycolaldehyde prepared in the same manner from D-xylose was in complete agreement with the structure expected for the compound.

dextro-1-Deuterioethanol (XVI)

The 1-deuterioethyl *n*-butyl acetal of *O*-tosylglycolaldehyde (XV), 8.0 g (0.025 *M*), and 1.36 g of *p*-toluenesulphonic acid were dissolved in 70 ml of pure dry *n*-butanol contained in a 100-ml flask which was fitted with a take-off condenser and a dropping funnel containing *n*-butanol. The *n*-butanol was dried by fractional distillation and was found to be devoid of optical activity when examined in a 2-dm tube. The flask was immersed in an oil bath which was maintained at 140°. Slow distillation resulted and 26 ml of distillate boiling in the range 100–114° was collected over a period of 5½ hours. Gas–liquid partition chromatography on an Apiezon column at 68° indicated that the distillate contained only ethanol and *n*-butanol. A second 4-ml fraction of distillate, which boiled over at 114°, was collected over a period of 1 hour. Analysis of this fraction showed only *n*-butanol to be present. The main fraction was then fractionally distilled using a Podbielniak, semimicro, spinning-band column under conditions which had previously been found to effect a sharp separation of ethanol from *n*-butanol. Three successive fractions were collected of 0.35-, 0.39-, and 0.36-ml volumes, respectively, boiling in the range 77–78° (uncorrected). A fourth fraction, 0.55 ml, boiled at 76–85° and was found by gas–liquid partition chromatography to contain a very small amount of *n*-butanol. However, the first three fractions appeared pure and represent a 74% yield.

The optical rotations of the above three fractions were measured separately in a 1-dm tube at the D-line of sodium. The fields were matched by one investigator and the readings were taken by someone else. This was done 10 times for each fraction, once with the tube pointing in one direction and once with the tube pointing in the opposite direction in order to be sure that there was no contribution to rotation arising from the glass windows. The investigators then changed positions and repeated the operation. The zero point was taken as the average reading obtained using the tube filled with pure synthetic ethanol. This reading coincided with the air blank. In this way, a minimum of 20 readings was made on each of the fractions and the blanks without the observer knowing the readings of the polarimeter. Thus, the results were kept as free as possible from subjective error. In no single reading (in over 100 readings) was the sign of rotation determined for a sample of 1-deuterioethanol not found to be positive relative to the blank. The averages of the rotations observed for the three fractions were +0.061°, +0.066°, and +0.069°, respectively. In taking these averages, the root mean square deviations were calculated in order to exclude some of the readings. The n.m.r. spectra of the fractions indicated that the samples contained less water than is present in the ethanol–water azeotrope. The three fractions were combined to obtain the n.m.r. spectrum of 1-deuterioethanol shown in Fig. 2. These spectra were taken with a Varian A60 spectrometer and show beyond doubt that the sample represents virtually pure 1-deuterioethanol. The only impurities evident in this sample are a trace of *n*-butanol and about 6% water. Most of the water present was undoubtedly introduced during several transfers of the 1-deuterioethanol which were made before the spectrum was taken. On the basis of the known observed rotation of optically pure 1-deuterioethanol (2), $\pm 0.22 \pm 0.02°$, and the fact that the sample prepared in this work could be expected to be 30% pure, the rotation of the sample should be $\pm 0.066°$. The

Can. J. Chem. Downloaded from www.nrcresearchpress.com by 210.87.254.5 on 09/05/12
For personal use only.

observed rotation of a 0.25% solution of β-D-xylopyranose tetraacetate in ethanol would be expected to be −0.052°. When the rotation was measured, using the procedure described above to measure the rotation of the samples of 1-deuterioethanol, a value of -0.057 ± 0.02 was obtained. Thus, there can be no doubt that *dextro*-1-deuterioethanol was prepared.

ACKNOWLEDGMENTS

This research was supported by the National Research Council of Canada through a grant-in-aid for research to R. U. L. The n.m.r. spectra were measured by Mrs. A. Westland (U. of O.) and R. Swindlehurst (U. of A.) and the microanalyses were made by Miss E. Busk.

REFERENCES

1. V. E. Althouse, K. Ueda, and H. S. Mosher. J. Am. Chem. Soc. **82**, 5938 (1960).
2. H. R. Levy, F. A. Loewus, and B. Vennesland. J. Am. Chem. Soc. **79**, 2949 (1957).
3. R. U. Lemieux and J. Giguere. Can. J. Chem. **29**, 678 (1951).
4. R. U. Lemieux, R. K. Kulling, H. J. Bernstein, and W. G. Schneider. J. Am. Chem. Soc. **80** 6098 (1958).
5. R. S. Cahn, C. K. Ingold, and V. Prelog. Experientia, **12**, 81 (1956).
6. R. Hori. Yakugaku Zasshi, **78**, 523 (1958); Chem. Abstr. **52**, 17118 (1958).
7. J. H. Brewster. Tetrahedron Letters, **20**, 23 (1959).
8. J. van Eys and N. O. Kaplan. J. Am. Chem. Soc. **79**, 2782 (1957).
9. H. Haubenstock and E. L. Eliel. J. Am. Chem. Soc. **84**, 2363 (1962).
10. A. Streitwieser, Jr., J. R. Wolfe, Jr., and W. D. Schaeffer. Tetrahedron, **6**, 338 (1959).
11. R. Schaffer and H. S. Isbell. J. Am. Chem. Soc. **80**, 756 (1958).
12. C. L. Mehltretter, B. H. Alexander, R. L. Mellies, and C. E. Rist. J. Am. Chem. Soc. **73**, 2424 (1951).
13. E. Recondo and H. Rinderknecht. Helv. Chim. Acta, **43**, 1653 (1960).
14. M. H. Adams, R. E. Reeves, and W. F. Goebel. J. Biol. Chem. **140**, 653 (1941).
15. H. Appel. J. Chem. Soc. 425 (1935).
16. J. K. Dale. J. Am. Chem. Soc. **37**, 2745 (1915).

Can. J. Chem. Downloaded from www.nrcresearchpress.com by 210.87.254.5 on 09/05/12
For personal use only.

PERFLUOROALKYL ARSENICALS

PART VI. SOME REACTIONS OF TRISTRIFLUOROMETHYLARSINE AND DICHLOROTRIFLUOROMETHYLARSINE

W. R. CULLEN

Department of Chemistry, University of British Columbia, Vancouver, British Columbia

Received July 30, 1962

Can. J. Chem. Downloaded from www.nrcresearchpress.com by 210.87.254.105 on 09/05/12
For personal use only.

ABSTRACT

Tristrifluoromethylarsine reacts with arsenic trichloride at 210° to give dichlorotrifluoromethylarsine. Attempts to prepare trifluoromethyl derivatives of mercury, boron, and aluminum by interaction of tristrifluoromethylarsine with halides of these elements have been unsuccessful. Tristrifluoromethylarsine is stable to phosphorus at 220° but reacts with nitric oxide at 70° to give nitrogen and low yields of trifluoronitroso- and trifluoronitro-methane. It probably forms a weak 1:2 complex with pyridine.

Dichlorotrifluoromethylarsine is easily reduced, at 20°, to trifluoromethylarsine by shaking with hydrogen chloride in the presence of mercury. Pyridine reacts with the chloroarsine at 20°.

DISCUSSION AND RESULTS

Walachewski reports (1) that tristrifluoromethylarsine reacts with arsenic triiodide at 220° to give iodotrifluoromethylarsines. It has now been found that chlorotrifluoromethylarsines are produced when tristrifluoromethylarsine interacts with arsenic trichloride at 210°, the major product being dichlorotrifluoromethylarsine:

$$2AsCl_3 + (CF_3)_3As \rightarrow 3CF_3AsCl_2.$$

This reaction provides a convenient source of the reactive chloroarsine, and is similar to that reported (2) for triphenylarsine:

$$(C_6H_5)_3As + AsCl_3 \rightarrow C_6H_5AsCl_2 + (C_6H_5)_2AsCl.$$

Furthermore, since there is evidence (3) that triphenylarsine will yield its phenyl groups in exchange for halogen atoms of several inorganic halides, attempts were made to prepare trifluoromethyl derivatives of boron, aluminum, and mercury by interacting their halides with tristrifluoromethylarsine.

Tristrifluoromethylarsine and boron triiodide at 130° give boron trifluoride, trifluoroiodomethane, iodobistrifluoromethylarsine, and arsenic triiodide. The products suggest that the boron triiodide mainly acts as a source of iodine since, apart from the boron trifluoride, the products are those obtained from tristrifluoromethylarsine and iodine at temperatures above 100° (1, 4). The formation of boron trifluoride could, however, indicate that some exchange of trifluoromethyl groups takes place since trifluoromethyl boron compounds are expected to be unstable with respect to the formation of boron trifluoride (5).

The slow reaction of tristrifluoromethylarsine with aluminum triiodide at 115° also produces trifluoroiodomethane and iodotrifluoromethylarsines. At 150°, however, the reaction is rapid and the tristrifluoromethylarsine is decomposed to carbon tetrafluoride, hexafluoroethane, arsenic trifluoride, and arsenic metal. The thermal decomposition of tristrifluoromethylarsine, which is reported (6) to take place at temperatures above 350°, can be represented by the equation

$$(CF_3)_3As \rightarrow As + 3/2C_2F_6,$$

only minor amounts of carbon tetrafluoride and arsenic trifluoride being produced. Therefore the decomposition of the arsine by aluminum triiodide at 150° is not simply a catalyzed thermal reaction. In producing carbon tetrafluoride and arsenic trifluoride the reaction bears a close resemblance to the fluorination of tristrifluoromethylarsine either by fluorine or cobalt trifluoride (4).

Tristrifluoromethylarsine and mercuric iodide do not react at 175°, although it is reported (7) that at this temperature bistrifluoromethylmercury reacts with mercuric iodide:

$$(CF_3)_2Hg + HgI_2 \rightarrow 2CF_3HgI.$$

Like tristrifluoromethylarsine, bistrifluoromethylmercury does not seem to take part in exchange reactions involving the trifluoromethyl group and the halogens of metals and metalloids (8, 9) even though reactions of this type are very common for alkyl and aryl mercury compounds.

These results support the view that fluoroalkyl groups readily exchange for halogen attached to other elements only when the group is attached to the more electropositive elements, for example (10)

$$(CH_3)_2SiCl_2 + 2C_3F_7Li \rightarrow (CH_3)_2Si(C_3F_7)_2 + 2LiCl.$$

A reaction which possibly involves exchange of a trifluoromethyl group for oxygen has recently been described by Griffiths and Burg (11). These authors report that tristrifluoromethylphosphine interacts with mercuric oxide at 100° to give bistrifluoromethylmercury:

$$2(CF_3)_3P + 2HgO \rightarrow (CF_3)_2Hg + \text{"}Hg[P(O)(CF_3)_2]_2\text{"}.$$

The exact nature of the other reaction product is not established. The corresponding reaction using tristrifluoromethylarsine has now been investigated. At 95° reaction occurs to only a very small extent and even at 165° recovery of the arsine is almost quantitative. At 95° a very low yield of bistrifluoromethylarsine oxide and trifluoronitrosomethane is obtained. The latter is also obtained from the reaction at 165°, though the arsine oxide, even if produced, would not be stable at this temperature (1). Griffiths and Burg could not isolate any of the diphosphorane, $(CF_3)_2POP(CF_3)_2$, from their reaction. The low yield and nature of the products obtained from the arsine reaction suggest that the reaction which occurred was with an impurity, probably mercuric nitrate, and not with the mercuric oxide.

The transfer of perfluoroalkyl groups from one metal or metalloid to another element has been described in two publications (12, 13):

$$(CH_3)_3SnCF_3 + BF_3 \rightarrow (CH_3)_3SnBF_3(CF_3)$$

$$(C_2F_5)_2Hg + 3S \rightarrow (C_2F_5)_2S_2 + HgS.$$

Bistrifluoromethylmercury on the other hand does not transfer its trifluoromethyl groups to metals such as zinc and magnesium (7). Since triphenylarsine reacts with phosphorus to give triphenylphosphine (14):

$$(C_6H_5)_3As + P \rightarrow (C_6H_5)_3P + As,$$

the reaction of tristrifluoromethylarsine with phosphorus was investigated. The arsine was found to be inert to phorphorus at temperatures up to 220°, the temperature at which both tristrifluoromethyl-arsine and -phosphine are formed from the appropriate element and trifluoroiodomethane (4). The transfer of phenyl groups from arsenic to phorphorus could be due to an increased stability of triphenylphosphine over that of

Can. J. Chem. Downloaded from www.nrcresearchpress.com by 210.87.254.105 on 09/05/12
For personal use only.

triphenylarsine due to the greater possibility of overlap of the "lone pair" electron on the phorphorus with the π-orbitals on the phenyl groups. This sort of stabilization would of course not be operative in the trifluoromethyl derivatives of these elements.

The transfer of trifluoromethyl groups from arsenic to nitrogen has been achieved by Jander and Haszeldine (15). These authors found that tristrifluoromethylarsine and nitrosyl chloride react at 100° to give chloroarsines and a small amount of trifluoronitrosomethane, a reaction which is formally analogous to the exchange reactions discussed above. They also found that tristrifluoromethylarsine and nitric oxide react to give low yields (5%) of trifluoronitrosomethane when irradiated with ultraviolet light.

In the present investigation the thermal reaction between the arsine and nitric oxide has been investigated. Reaction occurs slowly at 70°, a white solid first forms which later disappears. Analysis of this solid shows a surprisingly low percentage of CF_3, a result which is confirmed in magnitude by the carbon analysis, and it is unlikely that any possible single product containing arsenic and trifluoromethyl could give such an analysis. The volatile reaction products are also complex: nitrogen is produced and small amounts of trifluoronitromethane and trifluoronitrosomethane can be isolated. The usual method for the preparation of trifluoronitrosomethane is by the reaction of nitric oxide with trifluoromethyl radicals (16). However, since the arsine is thermally stable at 70° (6) and since no hexafluoroethane is produced in the reaction of the arsine with nitric oxide at 70°, it seems improbable that a free-radical mechanism involving dissociation of the arsine to trifluoromethyl radicals is operating in this case to produce the trifluoronitrosomethane. The formation of trifluoronitromethane in this reaction is also unusual since trifluoronitrosomethane is stable at 70° (15, 16), a fact which suggests that the nitro compound is produced by interaction of the arsine with nitrogen dioxide. This would account for the formation of nitrogen and also for the observation that the gas in the reaction tube turns red before turning blue.

Arsenic trichloride seems to have the ability to act as an electron acceptor in forming 1:1 and 1:2 complexes with pyridine (17). Antimony trihalides are also electron acceptors and tristrifluoromethylstibine forms a moderately stable 1:1 pyridine adduct (18). Tristrifluoromethylarsine does not form a stable 1:1 adduct with pyridine, though Fig. 1 shows that possibly a weak 1:2 complex, $(CF_3)_2As,2C_5H_5N$, may exist.

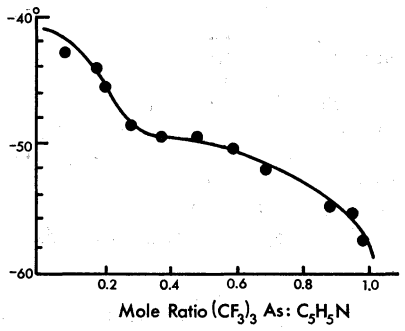

FIG. 1.

Dichlorotrifluoromethylarsine reacts with pyridine at 20°. Analysis of the solids produced indicates that the pyridine unit is decomposed.

Dichlorotrifluoromethylarsine reacts with hydrogen chloride in the presence of mercury to give trifluoromethylarsine in good yield:

$$CF_3AsCl_2 + Hg + 2HCl \rightarrow CF_3AsH_2 + HgCl_2.$$

Can. J. Chem. Downloaded from www.nrcresearchpress.com by 210.87.254.105 on 09/05/12
For personal use only.

This reaction provides a more convenient source of the arsine than reduction of the diiodoarsine using a zinc–copper couple and hydrochloric acid (4). Bistrifluoromethylarsine has recently been obtained from chlorobistrifluoromethylarsine using the same method (19).

EXPERIMENTAL

The apparatus and techniques used in this investigation were the same as have been described in earlier papers in this series.

Reaction of Tristrifluoromethylarsine with Arsenic Trichloride

Tristrifluoromethylarsine (11.566 g) and arsenic trichloride (16 g) did not react after 9 hours at 165° and 14 hours at 195°. Reaction took place at 210° (20 hours). The contents of the reaction tube were distilled in a nitrogen atmosphere and gave tristrifluoromethylarsine (2.0 g, b.p. 33°, lit. value, 33.3° (4)), a small fraction, b.p. 33–70°, and 4.5 g of slightly impure dichlorotrifluoromethylarsine, b.p. 70–80° (lit. value, 71° (1)). Infrared examination of the last fraction showed the presence of chlorobistrifluoromethylarsine, which was removed by trap-to-trap distillation. All the volatile material except the dichlorotrifluoromethylarsine was shaken with excess mercury for 4 days at 20°. This produced 0.608 g of tetrakistrifluoromethyldiarsine (identified by its infrared spectrum) corresponding to the production of at least 0.85 g of chlorobistrifluoromethylarsine by the original reaction.

Reaction of Tristrifluoromethylarsine with Aluminum Triiodide

The arsine (3.535 g) and aluminum triiodide (1.5 g) were heated for 14 hours at 45° and quantitative recovery of the arsine was obtained. When the same reactants were heated to 115° for 14 hours reaction took place and the following fractions were isolated: −132° fraction, trifluoroiodomethane (0.201 g; found: M, 202; calc.: M, 196), which was shown by infrared examination to contain traces of tristrifluoromethylarsine and other unidentified impurities; −96° fraction, tristrifluoromethylarsine (3.272 g; found: M, 287; calc.: M, 282); −46° fraction, a pale green liquid (0.097 g) which hydrolyzed to give fluoroform (found: CF_3 (as CF_3H), 48%) and a hydrolyzate which contained arsenic but no aluminum.

The solid remaining in the reaction tube was heated with the recovered tristrifluoromethylarsine for 1 hour at 150°. Rapid reaction took place and the following fractions were isolated: −196° fraction (1.146 g; M, 98.2), shown by its infrared spectrum to be mainly carbon tetrafluoride together with traces of silicon tetrafluoride, hexafluoroethane, and other unidentified impurities; −160° fraction, shown by infrared examination to be mainly hexafluoroethane and silicon tetrafluoride (0.324 g; M, 125); −64° fraction, 0.598 g of arsenic trifluoride (found: M, 142; calc.: M, 142). The infrared spectrum of the last fraction showed very strong absorption in the region of 700 cm^{-1}, the As—F stretching region, and also indicated the presence of impurities. Alkaline hydrolysis yielded fluoride, arsenic (found: As, 55%; calc. for AsF_3: As, 57%), but no fluoroform. The solid residue in the original reaction tube was stable to alkaline hydrolysis at 20° (no fluoroform evolved) and an X-ray powder photograph showed the presence of arsenic metal and the absence of any unreacted aluminum triiodide.

Reaction of Tristrifluoromethylarsine with Boron Triiodide

When boron triiodide (1.6 g) and the arsine (3.062 g) were heated at 130° for 48 hours the most volatile fraction produced (0.137 g) was identified as being mainly boron trifluoride on the evidence of its infrared spectrum and molecular weight (found: M, 69.4; calc.: M, 67.0). The other volatile fractions isolated were trifluoroiodomethane (0.646 g; found: M, 198; calc.: M, 196), tristrifluoromethylarsine (2.225 g; found: M, 282; calc.: M, 282), and iodobistrifluoromethylarsine (0.259 g; found: M, 330; calc.: M, 340). The identity in each case was confirmed by the infrared spectrum. An X-ray powder photograph of the solid from the reaction tube showed the presence of arsenic triiodide. Alkaline hydrolysis of the most volatile fraction failed to produce any fluoroform though the hydrolyzate contained boron. The hydrolyzate of the least volatile fraction contained arsenic but not boron.

Reaction of Tristrifluoromethylarsine with Mercuric Iodide

The arsine (1.996 g) and mercuric iodide (19 g) did not react after 2 days at 105° and, in a separate experiment, 1 day at 175°.

Reaction of Tristrifluoromethylarsine with Mercuric Oxide

The arsine (2.156 g) and mercuric oxide (21.0 g) when heated to 95° for 17 hours gave 0.010 g of bistrifluoromethylarsine oxide, 2.126 g of tristrifluoromethylarsine (M, 282), and a trace of a blue gas, trifluoronitrosomethane. The identity of the fractions was confirmed by their infrared spectra. The recovered tristrifluoromethylarsine was heated with the mercuric oxide for 19 hours at 125°, and for 18 hours at 165°. In both cases trap-to-trap distillation showed that very little reaction had taken place. The weight of the tristrifluoromethylarsine finally recovered was 1.996 g (M, 282).

Reaction of Tristrifluoromethylarsine with Red Phosphorus

The arsine (1.050 g) failed to react with red phosphorus (2.01 g) when heated to 220° for 24 hours. Infrared examination of the volatile material recovered (100%) showed it to be only tristrifluoromethylarsine.

Can. J. Chem. Downloaded from www.nrcresearchpress.com by 210.87.254.105 on 09/05/12
For personal use only.

Reaction of Tristrifluoromethylarsine with Nitric Oxide

When 1.999 g of the arsine and 0.441 g of nitric oxide were heated to 70° for 4 days a white solid was produced and the gas in the tube became red and finally blue. The solid on the tube walls disappeared after the tube had been left for 5 days at 20°, and did not re-form on heating the tube to 70° for a further 24 hours. A non-condensable gas was produced which was identified as nitrogen by means of its infrared spectrum, its molecular weight of 29.9, and its inertness to alkaline pyrogallol. The remaining volatile contents of the tube on trap-to-trap distillation gave a most volatile fraction (ca. 60 cc of gas at S.T.P.) which consisted of a blue gas, trifluoronitrosomethane (ca. 30 cc of gas at S.T.P.), and at least one other unidentified colorless substance which sublimed in the vacuum system. The fraction which condensed at −130° was identified as slightly impure trifluoronitromethane (0.25 g) by means of its molecular weight (found: M, 112; calc.: M, 115) and its infrared spectrum. Tristrifluoromethylarsine (0.855 g; found: M, 277; calc.: M, 282) was recovered and a small unidentified least volatile fraction (0.13 g; M, 132) was also obtained. In a separate experiment the reaction was stopped after the white solid had formed. Analysis of this solid gave C, 4.58; H, 1.97; CF_3 (as CF_3H), 26.4%; arsenic was present in the hydrolyzate.

Reaction of Tristrifluoromethylarsine with Pyridine

A 1:1 mixture of pyridine (0.328 g) and the arsine (1.176 g) failed to react to give a solid phase on warming to 20°. Similarly a 2:1 mixture of the arsine and pyridine showed no evidence of stable complex formation. The melting point diagram, Fig. 1, was obtained by the direct method for the range indicated.

Reaction of Dichlorotrifluoromethylarsine with Pyridine

The arsine (0.630 g) and excess pyridine (5.0 g) were miscible at 20°, giving a yellow solution which became red after 24 hours. The volatile contents of the reaction tube were taken into the vacuum system, leaving a viscous red oil and a small amount of a white sublimable solid. The infrared spectrum of this solid showed the absence of any bands associated with a pyridine fragment. The remaining red oil was soluble in pyridine and when the solvent was removed it slowly solidified. Analysis of the solid gave C, 25.5; H, 2.16; N, 12.12%.

Reaction of Dichlorotrifluoromethylarsine with Hydrogen Chloride in the Presence of Mercury

The chloroarsine (0.614 g), mercury (100 g), and hydrogen chloride (0.850 g) were shaken at 20° for 48 hours. Trap-to-trap distillation showed that only hydrogen chloride and trifluoromethylarsine (0.330 g, 79% yield; found: M, 147; calc. for CF_3AsH_2: M, 146) were present. The identity of the arsine was confirmed by its infrared spectrum.

ACKNOWLEDGMENTS

The author is indebted to Professor H. J. Emeléus, F.R.S., for his interest in and encouragement of this work, part of which was carried out in the University Chemical Laboratories, Cambridge. Financial assistance from the National Research Council of Canada is gratefully acknowledged.

REFERENCES

1. E. G. Walachewski. Ber. **86**, 272 (1953).
2. W. J. Pope and E. E. Turner. J. Chem. Soc. 1452 (1920).
3. F. Challenger, F. Pritchard, and J. R. A. Jinks. J. Chem. Soc. 864 (1924).
4. H. J. Emeléus, R. N. Haszeldine, and E. G. Walachewski. J. Chem. Soc. 1552 (1953).
5. J. J. Lagowski. Quart. Rev. (London), **13**, 233 (1959).
6. P. B. Ayscough and H. J. Emeléus. J. Chem. Soc. 3381 (1954).
7. H. J. Emeléus and R. N. Haszeldine. J. Chem. Soc. 2953 (1949).
8. J. J. Lagowski. Ph.D. Dissertation, University of Cambridge, Cambridge, England. 1959.
9. H. Pugh and H. J. Emeléus. Unpublished results.
10. O. R. Pierce, E. T. McBee, and G. F. Judd. J. Am. Chem. Soc. **76**, 474 (1954).
11. J. E. Griffiths and A. B. Burg. J. Am. Chem. Soc. **82**, 5759 (1960).
12. R. D. Chambers, H. C. Clark, and C. J. Willis. Proc. Chem. Soc. 114 (1960).
13. C. G. Krespan. U.S. Patent No. 2,844,614 (1958).
14. C. W. Raiziss and J. L. Gavron. Organic arsenic compounds. The Chemical Catalogue Co., Inc., New York. 1923.
15. J. Jander and R. N. Haszeldine. J. Chem. Soc. 912 (1954).
16. R. N. Haszeldine. J. Chem. Soc. 2075 (1953).
17. S. Gibson, J. D. A. Johnson, and D. C. Vining. J. Chem. Soc. 1710 (1930).
18. J. W. Dale, H. J. Emeléus, R. N. Haszeldine, and J. H. Moss. J. Chem. Soc. 3708 (1957).
19. W. R. Cullen. Can. J. Chem. **39**, 1855 (1961).

Can. J. Chem. Downloaded from www.nrcresearchpress.com by 210.87.254.105 on 09/05/12
For personal use only.

Can. J. Chem. Downloaded from www.nrcresearchpress.com by 210.87.254.105 on 09/05/12
For personal use only.

PERFLUOROALKYL ARSENICALS

PART VII. SOME REACTIONS OF CHLOROBISTRIFLUOROMETHYLARSINE AND RELATED COMPOUNDS[1]

W. R. CULLEN

Department of Chemistry, University of British Columbia, Vancouver, British Columbia

Received August 31, 1962

ABSTRACT

Chlorobistrifluoromethylarsine reacts with mercury at 20° to give tetrakistrifluoromethyldiarsine. The diarsine is also the major product when this reaction is carried out using trifluoroiodomethane as solvent. Iodobistrifluoromethylarsine, mercury, and trifluoroiodomethane, however, give tristrifluoromethylarsine in good yield. Dichlorotrifluoromethylarsine reacts similarly to give the compounds $(CF_3)_3As$, $(CF_3)_2AsCl$, and $((CF_3)_2As)_2$. The mechanism of reactions of this type is discussed.

Chlorobistrifluoromethylarsine and bistrifluoromethylarsine react at 100° to give tetrakistrifluoromethyldiarsine. Chlorodimethylarsine and bistrifluoromethylarsine react similarly to give the unsymmetrical diarsine $(CF_3)_2As—As(CH_3)_2$. The same diarsine is produced in low yield from chlorobistrifluoromethylarsine and dimethylarsine though in this reaction bistrifluoromethylarsine and other compounds are formed. These results are interpreted in terms of a series of equilibria involving a non-random addition of hydrogen chloride across the unsymmetrical As—As bond.

Dimethylarsine and hydrogen chloride react at low temperatures to give dimethylarsonium chloride. The compound decomposes reversably on warming. The thermal stability of bistrifluoromethylarsine and tetrakistrifluoromethyldiarsine is described.

DISCUSSION AND RESULTS

The reaction of alkyl- and aryl-iodoarsines with trifluoroiodomethane in the presence of mercury at 20° gives alkyl- and aryl-trifluoromethylarsines in good yield (1, 2). It has now been found that iodobistrifluoromethylarsine reacts similarly to give tristrifluoromethylarsine (62% yield), the other product of reaction being tetrakistrifluoromethyldiarsine. The diarsine is probably produced by the direct reaction of iodobistrifluoromethylarsine with mercury (3):

$$(CF_3)_2AsI + Hg + CF_3I \rightarrow (CF_3)_3As + HgI_2$$

$$2(CF_3)_2AsI + Hg \rightarrow (CF_3)_2As—As(CF_3)_2 + HgI_2.$$

Iododimethylarsine also reacts easily with mercury at 20°. However, no volatile products are obtained if the reaction tube is pumped out at 20°. Small amounts of tetramethyldiarsine can be obtained only if the reaction products are strongly heated. Tetramethyldiarsine interacts completely with hexafluorobutyne-2 and bromotrifluoroethylene at 20°; yet the butyne and ethylene are recovered quantitatively after being shaken with iododimethylarsine and mercury (4). These results indicate that no free diarsine is produced in the reaction of the iodoarsine with mercury and suggest that a diarsine mercuric iodide complex, probably $(CH_3)_2As—As(CH_3)_2 \cdot HgI_2$, is formed which liberates the diarsine in strong heating:

$$2(CH_3)_2AsI + Hg \rightarrow (CH_3)_2As—As\ (CH_3)_2 \cdot HgI_2 \rightarrow (CH_3)_2As—As(CH_3)_2 + HgI_2.$$

After some diarsine has been obtained in this way part of the solid reaction residue is sublimable in a vacuum. Analysis of this yellow sublimate indicates that it is probably a mixture of the diarsine complex and its decomposition products. It has been found that

[1]*Presented at the Second International Symposium on Fluorine Chemistry, Estes Park, Colorado, July, 1962.*

other iododialkylarsines interact with mercury to give diarsine complexes (5). The diarsine melts at 0–0.5°. The previously recorded melting point was −6° (6).

Chlorobistrifluoromethylarsine, mercury, and trifluoroiodomethane give only traces of tristrifluoromethylarsine. The main product in this reaction is the diarsine, which has been found to be produced quantitatively from the reaction of chlorobistrifluoromethylarsine and mercury:

$$2(CF_3)_2AsCl + Hg \rightarrow (CF_3)_2As—As(CF_3)_2 + HgCl_2.$$

A similar difference in reactivities has been found for the compounds $(CH_3)_2AsX$ (X = Cl or I) (1). Dichlorotrifluoromethylarsine reacts with mercury and trifluoroiodomethane to give chlorobistrifluoromethylarsine (36%), tristrifluoromethylarsine (32%), and tetrakistrifluoromethyldiarsine (8%). This result suggests that the reaction can go by at least two paths, one resulting in the replacement of two chlorine atoms to give tristrifluoromethylarsine and the other resulting in the replacement of one chlorine atom and the production of chlorobistrifluoromethylarsine and ultimately the diarsine:

$$CF_3AsCl_2 + 2CF_3I + Hg \rightarrow CF_3As(CF_3)_2$$

$$CF_3AsCl_2 + CF_3I + Hg \rightarrow (CF_3)_2AsCl \xrightarrow{Hg} (CF_3)_2As—As(CF_3)_2.$$

The first step seems necessary because of the low yield of tristrifluoromethylarsine obtained from chlorobistrifluoromethylarsine, mercury, and trifluoroiodomethane. This result together with the result that a much higher yield of tristrifluoromethylarsine is obtained from iodobistrifluoromethylarsine, mercury, and trifluoroiodomethane suggests that the source of the tristrifluoromethylarsine in experiments of this sort is not the diarsine, a conclusion which is substantiated by the result that tetrakistrifluoromethyldiarsine, mercury, and trifluoroiodomethane give only minor amounts (2%) of tristrifluoromethylarsine at 20°. The diarsine is, however, readily cleaved by trifluoroiodomethane at 75° (1):

$$(CF_3)_2As—As(CF_3)_2 + CF_3I \rightarrow (CF_3)_3As + IAs(CF_3)_2.$$

Thus it seems likely that these reactions involving halotrifluoromethylarsines, mercury, and trifluoroiodomethane proceed through intermediates of the type $(CF_3)_2AsHgX$:

$$(CF_3)_2AsX + Hg \rightarrow (CF_3)_2AsHgX \begin{cases} \xrightarrow{CF_3I} (CF_3)_2AsCF_3 \\ \xrightarrow[XAs(CF_3)_2]{} (CF_3)_2As—As(CF_3)_2 \end{cases}$$

When X = I, the intermediate is reactive enough to interact with the CF_3I, which in these reactions is in large excess. However, when X = Cl the less active intermediate can react easily only with the very active halobistrifluoromethylarsine.

In the reaction of dichlorotrifluoromethylarsine with mercury and trifluoroiodomethane no unchanged chloroarsine was recovered. The reaction products account for only 75% reaction of the starting material and the remaining 25% probably reacts directly with the mercury to give polymers of the type $(CF_3As)_x$. Such polymers appear to be formed from the reaction of diiodotrifluoromethylarsine and mercury (7).

Bistrifluoromethylarsine is reported to be unstable at 220°, decomposing according to (8)

$$3(CF_3)_2AsH \rightarrow (CF_3)_3As + 2As + 3CF_3H.$$

Can. J. Chem. Downloaded from www.nrcresearchpress.com by 210.87.254.105 on 09/05/12
For personal use only.

In the present investigation a more detailed study of the thermal stability of this compound has been made. The arsine is stable up to 165°, and only slight decomposition is found after 20 hours at 200°; fluoroform is liberated but no volatile solid is produced. The thermal stability of tetrakistrifluoromethyldiarsine has also been investigated. In the gas phase at 210° decomposition gives tristrifluoromethylarsine and a brown solid. On the basis of the diarsine recovered and the tristrifluoromethylarsine produced, the reaction seems to be best represented by the equation

$$3(CF_3)_2As—As(CF_3)_2 \rightarrow 4(CF_3)_3As + 2As.$$

Another possible reaction route is the following:

$$x(CF_3)_2As—As(CF_3)_2 \rightarrow x(CF_3)_3As + (CF_3As),$$

which would probably be favored by small reaction volumes. When the diarsine is heated in a small tube such that liquid phase is always present no reaction is detected at 150° and only slight decomposition to tristrifluoromethylarsine and an involatile black solid occurs at 180°. Decomposition in the small tube is faster at 220°, though the rate is slower than when the diarsine is heated in the gas phase. Thus, in a closed system, the thermal decomposition of both bistrifluoromethylarsine and tetrakistrifluoromethyldiarsine failed to give volatile polymers of the type $(CF_3As)_x$. Mahler and Burg report (9) that thermal decomposition of the corresponding phosphorus compounds yields the volatile polymers $(CF_3P)_4$ and $(CF_3P)_5$.

Dehn and Wilcox (10) have reported that the reaction of chlorodimethylarsine with dimethylarsine at 100° produces tetramethyldiarsine and hydrogen chloride. In the present investigation when this reaction was first repeated it was found that the diarsine is produced in low yield (25%) after 3 days at 100°; hydrogen is also produced, but no hydrogen chloride could be isolated by trap-to-trap distillation. This result suggested that either the diarsine was formed by thermal decomposition of dimethylarsine with elimination of hydrogen, or that the hydrogen was formed by reaction of hydrogen chloride with dimethylarsine giving chlorodimethylarsine and hydrogen. On checking both of these possibilities negative results were obtained. However, in the reaction of dimethylarsine with hydrogen chloride it was found that at low temperatures a compound is formed between the two reactants which prohibits their separation by trap-to-trap distillation. This compound, which can be formulated as dimethylarsonium chloride, sublimes in the vacuum system, melts at −46°, exists as a liquid above this temperature, and is completely dissociated in the vapor phase at 20°. This behavior is in marked contrast with the

$$(CH_3)_2AsH + HCl \rightleftharpoons (CH_3)_2AsH_2Cl$$

reaction of dimethylarsine with hydrogen bromide and iodide, where the onium compound appears to be formed but then decomposes to hydrogen and the halodimethylarsine (10).

$$(CH_3)_2AsH + HX \rightarrow (CH_3)_2AsH_2X \rightarrow (CH_3)_2AsX + H_2 \qquad (X = Br, I)$$

In a second reaction hydrogen chloride was identified, by means of its mass spectrum, as a reaction product of dimethylarsine and chlorodimethylarsine, so the main reaction appears to be

$$(CH_3)_2AsH + ClAs(CH_3)_2 \rightleftharpoons (CH_3)_2As—As(CH_3)_2 + HCl.$$

The reaction must be represented as an equilibrium since the diarsine reacts with hydrogen chloride at 20° to give dimethylarsine. The mechanism of the production of hydrogen is still in doubt.

Can. J. Chem. Downloaded from www.nrcresearchpress.com by 210.87.254.105 on 09/05/12
For personal use only.

Chlorobistrifluoromethylarsine and bistrifluoromethylarsine react at 100° to give tetrakistrifluoromethyldiarsine in good yield. Minor amounts of chlorotrifluoromethane are produced which could arise from disproportionation of the chloroarsine, a reaction well established for iodobistrifluoromethylarsine (11). Again the main reaction is best represented as an equilibrium,

$$(CF_3)_2AsCl + (CF_3)_2AsH \rightleftharpoons (CF_3)_2As—As(CF_3)_2 + HCl,$$

since the reaction of the diarsine with hydrogen chloride in the presence of mercury gives a high yield of bistrifluoromethylarsine at 20° (12). This last reaction is probably described by the following equations:

$$(CF_3)_2As—As(CF_3)_2 + HCl \rightleftharpoons (CF_3)_2AsH + ClAs(CF_3)_2$$
$$2(CF_3)_2AsCl + Hg \rightarrow (CF_3)_2As—As(CF_3)_2 + HgCl_2,$$

the only function of the mercury being to displace the equilibrium and so produce more starting material.

The experimental observation that bistrifluoromethylarsine and hydrogen chloride can be separated must mean that any onium compound formed from these two reactants is less stable than that formed from dimethylarsine and hydrogen chloride. This result would be qualitatively expected, in view of the strong electron-withdrawing power of the trifluoromethyl group. The relative reactivities are possibly quantitatively measured by the first ionization potential of 9.0 ev for dimethylarsine and 10.9 ev for bistrifluoromethylarsine (13).

Bistrifluoromethylarsine and chlorodimethylarsine react at 100° to give hydrogen chloride. The reaction again seems to be an equilibrium, since if the hydrogen chloride is removed more is produced by the remaining reactants. The bistrifluoromethylarsine recovered corresponds well with the hydrogen chloride produced according to the equation

$$(CF_3)_2AsH + ClAs(CH_3)_2 \rightleftharpoons (CF_3)_2As—As(CH_3)_2 + HCl.$$

Thus the reaction almost undoubtedly produces the new unsymmetrical diarsine 1,1-dimethyl-2,2-bis(trifluoromethyl)diarsine, though it has not yet been possible to isolate and characterize this compound. Neither dimethylarsine nor tetrakistrifluoromethyldiarsine is produced so that the addition of hydrogen chloride to the As—As bond in the unsymmetrical diarsine seems to be orientated by the overall polarity of the molecule. The same unsymmetrical diarsine is produced by the reaction of dimethylarsine with chlorobistrifluoromethylarsine at 100°; other reaction products are hydrogen, bistrifluoromethylarsine, chlorodimethylarsine, tetramethylarsine, and probably hydrogen chloride. Minor amounts of chlorotrifluoromethane and silicon tetrafluoride are also produced. The formation of the main reaction products can be accounted for by the following reactions:

$$(CH_3)_2AsH + ClAs(CF_3)_2 \rightarrow (CH_3)_2As—As(CF_3)_2 + HCl \quad [1]$$
$$(CH_3)_2As—As(CF_3)_2 + HCl \rightleftharpoons (CH_3)_2AsCl + HAs(CF_3)_2 \quad [2]$$
$$(CH_3)_2AsCl + HAs(CH_3)_2 \rightleftharpoons (CH_3)_2As—As(CH_3)_2 + HCl. \quad [3]$$

Reactions [1] and [2] involve the formation of the unsymmetrical diarsine, which because of the polarity effect reacts with hydrogen chloride to give bistrifluoromethylarsine. This accounts for the absence of chlorobistrifluoromethylarsine and consequently of tetrakistrifluoromethyldiarsine (by reaction [4]) from the equilibrium mixture. Reaction [3] simply

$$(CF_3)_2AsH + ClAs(CF_3)_2 \rightleftharpoons (CF_3)_2As—As(CF_3)_2 + HCl \quad [4]$$

accounts for the production of tetramethyldiarsine.

Can. J. Chem. Downloaded from www.nrcresearchpress.com by 210.87.254.105 on 09/05/12
For personal use only.

Recently Grant and Burg (14) have synthesised, at low temperature, the unsymmetrical diphosphine 1,1-dimethyl-2,2-bis(trifluoromethyl)diphosphine by the reaction

$$(CF_3)_2PCl + HP(CH_3)_2 \rightarrow (CF_3)_2P—P(CH_3)_2$$

and find that at higher temperatures this reaction gives $(CF_3)_2PH$. The unsymmetrical diphosphine is also cleaved by hydrogen chloride to give $(CF_3)_2PH$. These results are comparable to those described above, though Grant and Burg suggest that the production of bistrifluoromethylphosphine could be due to attack by the hydrogen chloride on the more basic phosphorus atom followed by a rearrangement of the products:

$$(CH_3)_2P—P(CF_3)_2 + HCl \rightarrow (CH_3)_2PH + ClP(CF_3)_2$$
$$(CH_3)_2PH + ClP(CF_3)_2 \rightarrow (CH_3)_2PCl + HP(CF_3)_2.$$

A similar explanation could be used to account for the results of the present investigation; however, the idea that the overall polarity of the molecular influences the direction of addition seems more attractive.

EXPERIMENTAL

Apparatus and Technique

The methods used in the present investigation have been described in earlier parts of this series. All starting materials were prepared by methods described in the literature.

Reaction of Chlorobistrifluoromethylarsine with Mercury

When chlorobistrifluoromethylarsine (1.855 g) was shaken with 30 g of mercury for 24 hours at 20°, 1.578 g (99% yield) of tetrakistrifluoromethyldiarsine was obtained (found: M, 417; calc.: M, 426). The identity of the diarsine was confirmed by infrared examination. A single distillation through a trap at −46° brought the molecular weight up to the theoretical value of 426.

Reaction of Iodobistrifluoromethylarsine with Trifluoroiodomethane in the Presence of Mercury

The iodoarsine (1.568 g), mercury (80 g), and trifluoroiodomethane (13.0 g) when shaken at 20° for 6 days gave trifluoroiodomethane (12.2 g), tristrifluoromethylarsine (0.831 g, 62% yield), and tetrakistrifluoromethyldiarsine (0.308 g, 32% yield). The fractions were separated by trap-to-trap distillation and identified by their infrared spectra.

Reaction of Chlorobistrifluoromethylarsine with Trifluoroiodomethane in the Presence of Mercury

The arsine (0.714 g), mercury (64 g), and trifluoroiodomethane (12.7 g) were shaken at 20° for 6 days. Trap-to-trap distillation gave tetrakistrifluoromethyldiarsine (0.455 g; 75% yield; M, 414) and a small fraction which condensed at −96°. This fraction (M, 257) on infrared examination was found to be largely unreacted chlorobistrifluoromethylarsine (calc.: M, 249) together with a trace of tristrifluoromethylarsine. The fraction was shaken with excess mercury for 2 days at 20° and only a trace of tristrifluoromethylarsine could be isolated from the tetrakistrifluoromethyldiarsine produced by reaction of the chloroarsine.

Reaction of Dichlorotrifluoromethylarsine with Trifluoroiodomethane in the Presence of Mercury

The arsine (0.942 g), trifluoroiodomethane (17.672 g), and mercury (60 g) were shaken at 20° for 4 days. The following fractions were obtained: 16.621 g of trifluoroiodomethane; 0.391 g (32% yield) of tristrifluoromethylarsine (found: M, 280; calc.: M, 282); chlorobistrifluoromethylarsine (0.396 g); and slightly impure tetrakistrifluoromethyldiarsine (0.079 g) identified by its low vapor pressure at 20° and its infrared spectrum. Because of the similarity of the boiling points of tristrifluoromethylarsine and chlorobistrifluoromethylarsine these were not separated by trap-to-trap distillation but were separated by reacting the fraction which condensed at −96° with excess mercury. This converted the chlorobistrifluoromethylarsine (whose presence in the −96° fraction was indicated by the infrared spectrum of that fraction) into tetrakistrifluoromethyldiarsine (0.352 g; M, 432), which was easily separated from the unchanged tristrifluoromethylarsine. The identity of these fractions was confirmed by their infrared spectra.

Reaction of Tetrakistrifluoromethyldiarsine with Trifluoroiodomethane in the Presence of Mercury

The diarsine (1.563 g), mercury (100 g), and trifluoroiodomethane (12.5 g) were shaken at 20° for 6 days. A small amount of mercuric iodide was produced. Trap-to-trap distillation and infrared examination of the fractions isolated showed that only 0.035 g of tristrifluoromethylarsine had been produced (2% yield); 1.506 g of the diarsine was recovered.

Reaction of Chlorobistrifluoromethylarsine with Bistrifluoromethylarsine

The chloroarsine (0.274 g) and bistrifluoromethylarsine (0.203 g) when heated to 100° for 16 hours gave

Can. J. Chem. Downloaded from www.nrcresearchpress.com by 210.87.254.105 on 09/05/12
For personal use only.

0.023 g of hydrogen chloride (M, 39.8), which on the evidence of its infrared spectrum contained a little chlorotrifluoromethane. Tetrakistrifluoromethyldiarsine (0.205 g, 51% yield) was also isolated and identified by its infrared spectrum and molecular weight (M, 426). Infrared examination of the fraction of intermediate volatility showed that this was mainly unchanged starting materials.

Thermal Stability of Tetrakistrifluoromethyldiarsine

The diarsine (0.597 g) was heated in the gas phase to 210° for 60 hours. After 12 hours at this temperature a brown film had formed on the walls of the reaction tube. Trap-to-trap distillation gave tristrifluoromethylarsine (0.451 g; M, 285), and the remaining liquid (0.065 g; M, 373) was identified as being mainly unreacted diarsine containing a little tristrifluoromethylarsine. In a second experiment the diarsine (0.564 g) was heated in a small tube (5 ml) for 4 days at 150°. The molecular weight and vapor pressure of the sample were unchanged after this treatment. After 48 hours at 180° a small amount of a black solid had formed and after a further 48 hours at this temperature 0.067 g of tristrifluoromethylarsine and 0.445 g of mainly unreacted diarsine (M, 380) were obtained. The diarsine fraction was heated to 220° for 48 hours. More black solid was formed and tristrifluoromethylarsine (0.174 g; M, 283) was isolated.

Thermal Stability of Bistrifluoromethylarsine

A sample of the arsine (0.210 g) showed no signs of decomposition after 3 months at 20° in a sealed tube. The arsine was not affected by heating at 100° for 3 weeks, or at 165° for 6 hours. After 20 hours at 200° slight decomposition with the formation of a trace of fluoroform was detected. The extent of reaction was checked in all cases by trap-to-trap distillation and infrared examination of the fractions isolated.

Reaction of Bistrifluoromethylarsine with Chlorodimethylarsine

When 0.782 g of bistrifluoromethylarsine and 0.512 g of chlorodimethylarsine were heated to 100° for 24 hours, 0.057 g of hydrogen chloride (M, 36.6) was produced. The hydrogen chloride was removed and when the rest of the reaction mixture was heated to 100° for 1 week a further 0.231 g of hydrogen chloride (M, 37.0) was formed. The infrared spectrum of this fraction showed the absence of any compounds containing C—F groups. The hydrogen chloride was again removed and the reaction mixture was heated to 100° for another week to give 0.011 g of hydrogen chloride. The total yield of hydrogen chloride was thus 69%. Trap-to-trap distillation recovered 0.210 g of bistrifluoromethylarsine (73% reaction), which did not condense at −78° and which was identified by its infrared spectrum. No other compounds were detected in this fraction. The remaining fraction, the least volatile one, on the evidence of its infrared spectrum contained chlorodimethylarsine and a trace of bistrifluoromethylarsine. No bands attributable to tetrakistrifluoromethyldiarsine were observed. The spectrum in the C—F stretching region included weak bands in the same positions as are reported below for the involatile product obtained from dimethylarsine and chlorobistrifluoromethylarsine. The fraction was rapidly oxidized by air.

Reaction of Dimethylarsine with Chlorobistrifluoromethylarsine

When dimethylarsine (1.442 g) and the chloroarsine (0.879 g) were heated at 100° for 3 days a small amount of hydrogen was produced which was identified by its mass spectrum. Trap-to-trap distillation together with infrared examination of the fractions isolated gave the following: −196° fraction, 0.146 g of a mixture of chlorotrifluoromethane and silicon tetrafluoride (M, 101); −23° fraction, 0.072 g of tetramethyldiarsine, m.p. −2–1°; and intermediate fractions which contained bistrifluoromethylarsine, chlorodimethylarsine, and a substance whose vapor phase infrared spectrum in the C—F region corresponded with that obtained from the involatile fraction isolated in the preceding experiment with bands at 1171, 1150, and 1100 cm^{-1}. No chlorobistrifluoromethylarsine was detected.

Reaction of Iododimethylarsine with Mercury

The iodoarsine (18 g) and mercury (200 g) were shaken for 5 days at 20°. A yellow solid was produced and on strong heating 1.374 g of a colorless involatile liquid was obtained. The bulk of the mercury was removed and the remaining solid was sublimed in a vacuum to give a yellow solid, insoluble in all common organic solvents. Anal. Found: C, 2.58; H, 0.55; As, 17.0%. Mercury and iodine were also present. The involatile liquid was identified as tetramethyldiarsine by its melting point of −1–0° (lit. value, −6° (6)) and by its reactions with excess iodomethane (7.75 g). This reaction gave pale yellow crystals at 0° and when the reaction tube was heated to 100° for 1 hour a black solid was obtained. The excess iodomethane was removed and the resulting solid was extracted with acetone, leaving 1.7 g of colorless crystals which were identified as tetramethylarsonium iodide, m.p. 325° (decomp.) (lit. value, 328° (15)), mercuriiodide, m.p. 183° (lit. value, 184° (16)). The acetone solution was evaporated *in vacuo* to give violet crystals of tetramethylarsonium triiodide, m.p. 133° (lit. value, 133° (15)). The yield of tetramethyldiarsine was 17%.

When the reaction was carried out in acetic acid as solvent the reaction followed substantially the same path. The acetic acid was recovered quantitatively, and tetramethyldiarsine was obtained (10% yield) only by strongly heating the reaction tube. The diarsine was identified as above.

Reaction of Chlorodimethylarsine with Dimethylarsine

Chlorodimethylarsine (0.679 g) and dimethylarsine (0.751 g) were heated to 100° for 3 days. Hydrogen was produced (identified by its mass spectrum) and trap-to-trap distillation failed to isolate any hydrogen

Can. J. Chem. Downloaded from www.nrcresearchpress.com by 210.87.254.105 on 09/05/12
For personal use only.

chloride. The unreacted dimethylarsine was separated only with difficulty from the other fractions. Tetramethyldiarsine (0.3 g; 26% yield) was isolated as a fraction which condensed at −23° and was identified by its melting point of 0–0.5°. In a second experiment the chloroarsine (2.162) and excess dimethylarsine (3.154 g) were heated to 100° for 1 day. Hydrogen was again produced and tetramethyldiarsine (0.7 g; 22% yield; m.p., −1–0°) was isolated as above. The more volatile fractions were allowed to expand into a large volume and a mass spectrum of the vapor showed the presence of hydrogen chloride.

Reaction of Tetramethyldiarsine with Hydrogen Chloride

The diarsine (0.114 g) and hydrogen chloride (0.071 g) were left at 20° for 2 days. Trap-to-trap distillation followed by infrared examination of the fractions isolated showed the presence of dimethylarsine.

Thermal Stability of Dimethylarsine

The arsine (1.195 g) was unchanged after 2 days at 100°.

Reaction of Dimethylarsine with Hydrogen Chloride

The arsine (1.195 g) and hydrogen chloride (0.440 g) were heated to 104° for 2 days. No hydrogen was produced. Trap-to-trap distillation isolated only 0.005 g of hydrogen chloride. The remaining reaction products sublimed in the vacuum system and condensed at −130°. The molecular weight of this fraction was 68 at 20° (calc. for a 1:1 mixture of $(CH_3)_2AsH$ and HCl: M, 71). The vapor pressure of the solid was 0 mm at −130°, 1 mm at −96°, 3 mm at −78°. The solid melted at −46° under a pressure of 81 mm. The substance seemed to be stable as a liquid at temperatures above −46°. The vapor pressure values were reproducible on warming and cooling the sample.

ACKNOWLEDGMENTS

The author wishes to acknowledge financial assistance from the National Research Council of Canada. He is also indebted to Professor H. J. Emeléus for his encouragement of this work. Some of the reactions described above were carried out in the University Chemical Laboratories, Cambridge.

REFERENCES

1. W. R. Cullen. Can. J. Chem. **38**, 439 (1960).
2. W. R. Cullen. Can. J. Chem. **38**, 445 (1960); **39**, 2486 (1961).
3. G. R. A. Brandt, H. J. Emeléus, and R. N. Haszeldine. J. Chem. Soc. 2552 (1952).
4. W. R. Cullen and N. K. Hota. Unpublished observations.
5. G. E. Coates. Private communication.
6. R. W. Bunsen. Ann. **42**, 14 (1842).
7. W. R. Cullen. Ph.D. Dissertation, University of Cambridge, Cambridge, England. 1958.
8. H. J. Emeléus, R. N. Haszeldine, and E. G. Walachewski. J. Chem. Soc. 1552 (1953).
9. W. Mahler and A. B. Burg. J. Am. Chem. Soc. **79**, 251 (1957); **80**, 6161 (1958).
10. W. M. Dehn and B. B. Wilcox. Am. Chem. J. **35**, 1 (1906).
11. E. G. Walachewski. Ber. **86**, 272 (1953).
12. W. R. Cullen. Can. J. Chem. **39**, 1855 (1961).
13. W. R. Cullen and D. C. Frost. Can. J. Chem. **40**, 390 (1962).
14. L. R. Grant and A. B. Burg. J. Am. Chem. Soc. **84**, 1834 (1962).
15. W. Steinkopf and G. Schwenn. Ber. **54**, 1437 (1921).
16. E. Mannheim. Ann. **341**, 182 (1905).

Can. J. Chem. Downloaded from www.nrcresearchpress.com by 210.87.254.105 on 09/05/12
For personal use only.

THE ZINC CHLORIDE CATALYZED MIGRATION OF HALOGEN IN THE CLAISEN REARRANGEMENT[1]

E. PIERS AND R. K. BROWN
Department of Chemistry, University of Alberta, Edmonton, Alberta
Received September 17, 1962

ABSTRACT

The zinc chloride catalyzed rearrangement of allyl 2,6-dichlorophenyl ether in nitrobenzene solution gave a good yield of 2-allyl-4,6-dichlorophenol along with some 2,6-dichlorophenol and 2-methyl-5,7-dichlorocoumaran. The coumaran increased at the expense of the 2-allyl-4,6-dichlorophenol. This is in contrast to the thermal rearrangement of this ether, which gave mainly 4-allyl-2,6-dichlorophenol along with smaller amounts of 2-allyl-6-chlorophenol and 2-allyl-4,6-dichlorophenol.

INTRODUCTION

In a paper published some time ago, Carlin and Fisher (1) pointed out the formal analogy between the mechanism proposed by Robinson and Robinson (2, 3) for the Fischer indole synthesis and that established to explain the Claisen rearrangement (4–8). Furthermore, Carlin and Fisher (1) found that five 2,6-dichlorophenylhydrazones, subjected to the conditions of the Fischer indole synthesis in the presence of zinc chloride, gave the corresponding 5,7-dichloroindoles, products which resulted from the migration of one of the chlorine atoms. The migration is believed to be due to the formation of a dienonimine intermediate which undergoes a zinc halide promoted allylic shift of the halogen atom (9, 10). These conversions appear to have no recorded analogy among the examples of the Claisen rearrangement, although Carlin and Fisher (1) suggested that they might indeed occur but to such a small extent as to have escaped detection.

It was felt that, since zinc chloride appeared to be necessary for the halogen shift in the indole synthesis (1, 9, 10), the application of this Lewis acid might catalyze the Claisen rearrangement as well as bring about a similar halogen migration. Accordingly experiments were performed to determine the effect of zinc chloride on the rearrangement of allyl 2,6-dichlorophenyl ether.

Examination of the literature has shown that a great deal of work has been published concerning the thermal rearrangement of allyl aryl ethers (4–8) but only a small number of investigations have been concerned with the effect of acidic reagents on this reaction. That the Claisen rearrangement might be catalyzed by acid was first shown by Tarbell and Kincaid. A kinetic study of the rearrangement of allyl 2,6-dimethylphenyl ether in diphenyl ether revealed that the addition of 1% and of 2% acetic acid increased the rate 28% and 42% respectively (11).

Later observations disclosed that the rearrangement of allyl aryl ethers occurred at a much lower temperature, when Lewis acids were present, than that required for thermal reaction. For example, treatment of the allyl ether of guaiacol with $BF_3.2CH_3CO_2H$ at 68° gave 38% of eugenol as well as some guaiacol, 6-allylguaiacol, and the allyl ether of allylguaiacol or eugenol (12). Also, allyl phenyl ether at −80° was converted by boron trichloride exclusively to *o*-allylphenol (13). Furthermore, a recent study (14) showed that boron trichloride effected the intramolecular rearrangement in high yields (90–98%)

[1]*Taken from the thesis of E. Piers to be submitted to the Graduate School of the University of Alberta in partial fulfillment of the requirements for the degree of Doctor of Philosophy.*

Can. J. Chem. Downloaded from www.nrcresearchpress.com by 210.87.254.105 on 09/05/12
For personal use only.

of allyl phenyl ether to 2-allylphenol, allyl *p*-tolyl ether to 2-allyl-4-methylphenol, allyl 2,6-dimethylphenyl ether to a mixture of 2,6-dimethyl-3-allylphenol and 2,6-dimethyl-4-allylphenol, and also allyl mesityl ether to 3-allylmesitol.

RESULTS AND DISCUSSION

In the present work, heating a mixture of zinc chloride and allyl 2,6-dichlorophenyl ether (2:1) in nitrobenzene revealed that this Lewis acid also had a catalytic effect on the Claisen rearrangement since the reaction could be carried out to completion at 145° over a 24-hour period in the presence of zinc chloride whereas in its absence, under otherwise identical conditions, about 40% of the original ether was recovered (compare expt. 2, Table I, and expt. 5, Table II). Furthermore, as in the case of the Fisher cyclization of

TABLE I

The zinc chloride catalyzed rearrangement of allyl 2,6-dichlorophenyl ether in nitrobenzene

Expt. No.	Reaction conditions	Composition of reaction mixture* (%)			
		Allyl 2,6-dichlorophenyl ether	2,6-Dichlorophenol	2-Allyl-4,6-dichlorophenol	2-Methyl-5,7-dichlorocoumaran
1	130–135° 28 hr	13.4	4.2	82.4	Trace
2	140–145° 24 hr	Trace	4.4	90.9	4.7
3	150–155° 20 hr	Nil	4.1	88.3	7.7
4	180–185° 1 hr	Nil	15.8	77.0	7.2
	5 hr	Nil	16.1	30.1	53.8

*No 2-allyl-6-chlorophenol was detected.

2,6-dichlorophenylhydrazones (1), halogen migration occurred here also since the zinc chloride catalyzed rearrangement of allyl 2,6-dichlorophenyl ether in nitrobenzene at 140–160° gave a mixture of 2,6-dichlorophenol (4–5%), 2-allyl-4,6-dichlorophenol (88–91%), and 2-methyl-5,7-dichlorocoumaran (4–8%). Lower temperatures required longer reaction times and gave, as well, unreacted starting material. Higher temperatures reduced the time necessary for complete reaction of the original ether but produced more of the cleavage product, 2,6-dichlorophenol, and of the coumaran (expts. 1–4, Table I). The coumaran increased at the expense of the 2-allyl-4,6-dichlorophenol as reaction time was extended, but the amount of cleavage product remained essentially enchanged (expt. 4, Table I).

Products were analyzed by V.P.C. and the retention times compared with those of authentic samples. Careful fractionation of the reaction mixture from experiment 4, Table I, permitted the isolation of all three products indicated. Elemental analysis and comparison of n.m.r. and infrared spectra proved the coumaran to be identical with the compound obtained by ring closure of 2-allyl-4,6-dichlorophenol according to Claisen's general method (15). Nuclear magnetic resonance analysis of this compound was in agreement with the structure designated as 2-methyl-5,7-dichlorocoumaran.

Repeated extraction of the phenolic products from an ethereal solution of the reaction mixture with Claisen's alkali (16), a procedure employed in a recent report concerning the Claisen rearrangement (17) although generally Claisen alkali extractions are made from hydrocarbon solvents (18), still left a considerable portion of the 2-allyl-4,6-dichloro-

Can. J. Chem. Downloaded from www.nrcresearchpress.com by 210.87.254.105 on 09/05/12
For personal use only.

TABLE II

Thermal rearrangement of allyl 2,6-dichlorophenyl ether

Expt. No.	Reaction conditions	Composition of reaction mixture* (%)				
		Allyl 2,6-dichlorophenyl ether	2-Allyl-6-chlorophenol	2-Allyl-4,6-dichlorophenol	4-Allyl-2,6-dichlorophenol	2-Methyl-5,7-dichlorocoumaran
1	No solvent 193–200° 90 min	Nil	6.7	2.0	91.3	Trace
2	In diphenyl ether 180–185° 5.5 hr	Nil	3.2	Nil	96.8	Nil
3	In nitrobenzene 180–185° 3 hr	Nil†	10.8	7.6	81.6	Nil
	10 hr	Nil	10.6	7.7	81.7	Nil
4	Nitrobenzene + LiCl 180–185° 3 hr	Nil	15.5	10.6	73.9	Nil
5	In nitrobenzene 140–145° 24 hr	39.9	8.2	3.3	48.6	Nil
6	In nitrobenzene + LiCl 140–145° 24 hr	42.1	14.9	4.3	38.7	Nil

*No 2,6-dichlorophenol was detected.
†It took 3 hours under these conditions for all the original ether to disappear, whereas expt. 4, Table I, shows that with $ZnCl_2$ present, all the ether had disappeared in 1 hour.

phenol in the neutral fraction. In fact, synthetic mixtures of 2-allyl-4,6-dichlorophenol, diethyl ether, and diphenyl ether extracted three times with Claisen's alkali also gave incomplete separation of the phenol, although phenol extraction from this solvent was better than that from the nitrobenzene–ether solvent. Accordingly, in the present work, to avoid such loss of phenol, alkaline treatment was omitted and analyses were performed, quite satisfactorily, directly on samples of the total reaction mixture.

Thermal rearrangement of allyl 2,6-dichlorophenyl ether, either as the pure liquid or in nitrobenzene or diphenyl ether solution, yielded a mixture of products somewhat different from that obtained from the zinc chloride catalyzed reaction (Table II). The main product of the thermal reaction, 4-allyl-2,6-dichlorophenol, was accompanied by much smaller amounts of 2-allyl-6-chlorophenol and 2-allyl-4,6-dichlorophenol, but *none* of the 2,6-dichlorophenol or the coumaran (expts. 1 and 3, Table II). The formation of the monohalogenated phenol agrees with similar observations by previous workers (15, 19). For example, Tarbell and Wilson (19) have found that heating pure allyl 2,6-dichlorophenyl ether at 193–200° gave a mixture of 2-allyl-6-chlorophenol and 4-allyl-2,6-dichlorophenol. Our repetition of this experiment disclosed that, in addition, a small amount (2%) of 2-allyl-4,6-dichlorophenol was formed (expt. 1, Table II). In nitrobenzene solvent, the yield of both the 2-allyl-4,6-dichlorophenol and 2-allyl-6-chlorophenol increased. The addition of lithium chloride to the nitrobenzene solution further enhanced both the amount of halogen migration product and halogen elimination product, although no catalysis of the decomposition of the original ether appeared to occur. In the solvent

Can. J. Chem. Downloaded from www.nrcresearchpress.com by 210.87.254.105 on 09/05/12
For personal use only.

diphenyl ether only half as much of the monochlorophenol was obtained and *none of the product of halogen migration* (expt. 2, Table II). When a naphthalene was employed as solvent results were very much similar to those found with diphenyl ether. However, in this case difficulty was experienced in obtaining clear separations by V.P.C. of the solvent naphthalene and 2-allyl-6-chlorophenol, hence the results are not recorded in Table II.

The above facts indicate that both halogen elimination and halogen migration are assisted by a polar reaction medium.

The formation of the products from the zinc chloride catalyzed reaction can be explained by the following scheme.

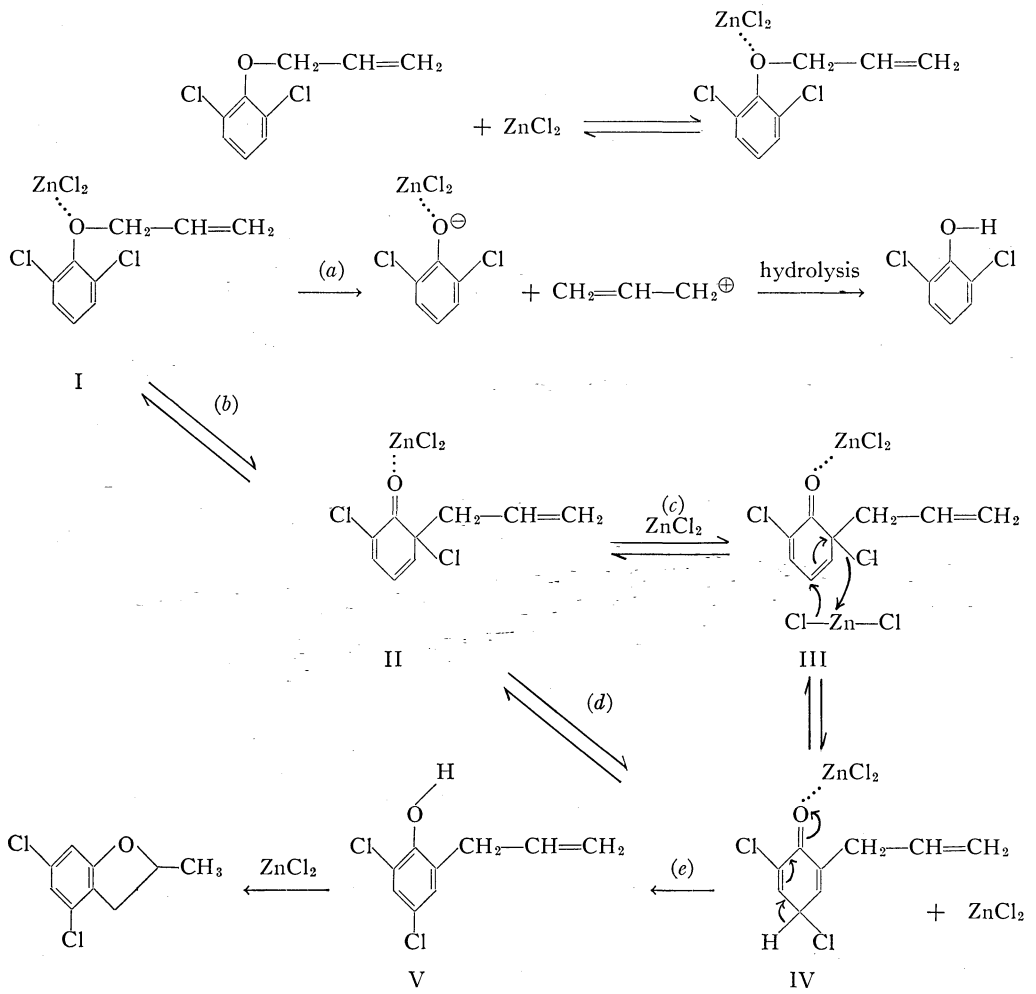

The zinc chloride – allyl 2,6-dichlorophenyl ether complex (I) cleaved in the usual manner via route *a* under the influence of the Lewis acid (20) to form 2,6-dichlorophenol. Simultaneously there occurred a preferential intramolecular rearrangement of I by route *b* to form the intermediate dienone II (7). The dienone then underwent a migration of halogen via an allylic shift, to a small extent by route *d*, but chiefly through the agency of a zinc chloride bridge, III (route *c*). Aromatization of IV gave the 2-allyl-4,6-dichloro-

Can. J. Chem. Downloaded from www.nrcresearchpress.com by 210.87.254.105 on 09/05/12
For personal use only.

phenol V, which cyclized to the coumaran in the presence of zinc chloride. Since replacement of zinc chloride by lithium chloride gave under otherwise identical conditions only a

Page 333. In lines 3 and 4, "15.5%" and "10.6%" should read "10.6%" and "7.6%" respectively.

halogen by a zinc chloride bridge is favored.

EXPERIMENTAL

Allyl 2,6-Dichlorophenyl Ether

To a solution of 0.5 mole of 2,6-dichlorophenol (21) in 200 ml of water containing 30 g of sodium hydroxide was added 300 ml of acetone. Allyl bromide (0.7 mole) was added and the solution was refluxed with stirring for 3 hours. The material was then poured into 700 ml of ice water, the resulting mixture extracted twice with ether, and the combined ether extracts dried over anhydrous magnesium sulphate. Removal of the ether afforded an oil which upon distillation under reduced pressure through a short Vigreux column gave 91 g (90%) of allyl 2,6-dichlorophenyl ether. B.p. 69–70° at 1 mm. Lit. b.p. 89–90° at 2 mm (19).

Zinc Chloride Catalyzed Rearrangement of Allyl 2,6-Dichlorophenyl Ether. General Procedure

Anhydrous powdered zinc chloride (41 g, 0.3 mole) was stirred into 150 ml of dry ether. While the mixture was gently heated to permit evaporation of the ether, redistilled nitrobenzene (123 g, 1 mole) was slowly added. After the resulting solution was heated to the desired temperature for the rearrangement, allyl 2,6-dichlorophenyl ether (30 g, 0.15 mole) was slowly added. The mixture was then stirred and heated under an atmosphere of purified, dry nitrogen for the specified time. The cooled material was then poured into a mixture of water and ether. After filtration, the ether layer was separated and washed several times with water, then dried ($MgSO_4$). Removal of the ether gave the mixture of reaction products, which was analyzed directly by V.P.C.

2-Methyl-5,7-dichlorocoumaran

The general procedure reported in the literature (15) was employed to obtain this compound. From 18.3 g (0.09 mole) of 2-allyl-4,6-dichlorophenol there was obtained 8.8 g (48%) of 2-methyl-5,7-dichlorocoumaran, b.p. 81° at 0.7 mm. Anal. Calc. for $C_9H_8Cl_2O$: C, 53.23; H, 3.97; Cl, 34.92%. Found: C, 52.91; H, 4.08; Cl, 35.20%.

Gas Chromatography

A Burrell Model K-2 Kromo-Tog, with helium as the carrier gas, was used for all analyses. A 2-m column, packed with 22% Apiezon L adsorbed on Gas Chrom P (60–80 mesh) afforded good separation of components into clearly resolved peaks. The paper areas of these peaks were measured by means of a planimeter. An analysis of carefully weighed authentic mixtures of the reaction products showed that these paper areas could be used as a direct measure of molar compositions of the reaction mixtures.

ACKNOWLEDGMENT

The authors wish to thank the National Research Council of Canada for their financial support during the course of this work.

Page 332. In the reaction scheme, the lower left structure

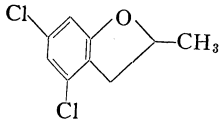

should read

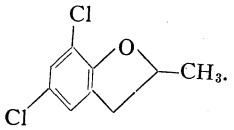

7. H. CONROY and R. A. FIRESTONE. J. ...
8. L. F. FIESER and M. FIESER. Advanced organic chemistry. Reinhold Publishing Corporation, New York. 1961. p. 768.
9. R. B. CARLIN, J. G. WALLACE, and E. E. FISHER. J. Am. Chem. Soc. **74**, 990 (1952).
10. R. B. CARLIN and G. W. LARSON. J. Am. Chem. Soc. **79**, 934 (1957).
11. D. S. TARBELL and J. F. KINCAID. J. Am. Chem. Soc. **62**, 728 (1940).
12. L. YA BRYUSOVA and M. L. IOFFE. J. Gen. Chem. USSR (Eng. Transl.), **11**, 722 (1941); Chem. Abstr., **36**, 430 (1942).
13. W. GERRARD, M. F. LAPPERT, and H. B. SILVER. Proc. Chem. Soc. 19 (1957).
14. P. FAHRNI, A. HABICH, and H. SCHMID. Helv. Chim. Acta, **43**, 448 (1960).
15. C. D. HURD and C. N. WEBB. J. Am. Chem. Soc. **58**, 2190 (1936).

Can. J. Chem. Downloaded from www.nrcresearchpress.com by 210.87.254.105 on 09/05/12
For personal use only.

16. L. F. FIESER. Experiments in organic chemistry. 3rd ed. revised. D. C. Heath and Co., Boston. 1957. p. 310.
17. W. N. WHITE and B. E. NORCROSS. J. Am. Chem. Soc. **83**, 1968 (1961).
18. D. S. TARBELL and S. S. STRADLING. J. Org. Chem. **27**, 2724 (1962).
19. D. S. TARBELL and J. W. WILSON. J. Am. Chem. Soc. **64**, 1066 (1942).
20. R. L. BURWELL, JR. Chem. Rev. **54**, 615 (1954).
21. D. S. TARBELL, J. W. WILSON, and P. E. FANTA. Organic syntheses. Coll. Vol. III. John Wiley and Sons, Inc., New York. 1955. p. 267.

Can. J. Chem. Downloaded from www.nrcresearchpress.com by 210.87.254.105 on 09/05/12
For personal use only.

THE MERCURY-PHOTOSENSITIZED DECOMPOSITION OF PROPANE A MASS SPECTROMETRIC STUDY AT LOW PRESSURES

PART I

P. KEBARLE AND M. AVRAHAMI[1]
Chemistry Department, University of Alberta, Edmonton, Alberta
Received June 26, 1962

ABSTRACT

It is found that the primary decomposition involves the cleavage of a C—H bond. Both primary and secondary hydrogen atoms are lost. The relative rates of the two processes could not be determined accurately but are estimated to be approximately 1:1. It is found that at least 70% of the secondary reactions involves the interaction of hydrogen atom with a propyl radical. The main reaction is the re-formation of propane. An important disproportionation of hydrogen atoms with propyl radicals leading to propylene is shown to occur. The atomic cracking reaction $H + C_3H_7 \rightarrow C_3H_8^* \rightarrow C_2H_5 + CH_3$ is also observed. Using mixtures of C_3H_8 and C_3D_8 the relative cracking rate of *n*-propyl- to isopropyl-derived propane is determined to be equal to 5. This result is compared with theoretical predictions.

INTRODUCTION

The mercury-photosensitized decomposition of propane has been studied by several investigators (1–5). The results from previous work have established the main features of the reaction. The primary decomposition leads to isopropyl radicals and hydrogen atoms (1). At high propane pressures the secondary reactions are: abstraction of hydrogen from the unreacted propane by the hydrogen atom and recombination–disproportionation of the propyl radicals. This simple scheme leads to an expected quantum yield for hydrogen formation equal to 1. The experimentally observed values are considerably lower but it has been pointed out by Back (5) that hydrogen atoms are lost by addition to the propylene formed by the disproportionation of the propyl radicals.

When the mercury-photosensitized decomposition of propane is studied at low pressures a new secondary reaction is found to occur. If the recombination product of propyl + H is not stabilized by collisions it decomposes to ethyl and methyl free radicals (2). The recombinations of the radicals produced by this "atomic cracking" lead to butane, ethane, and methane.

The present mass spectrometric investigation developed from an interest in the atomic cracking reaction and its suppression by the addition of inert gas (He). In the course of this work, it was discovered that in addition to the known primary decomposition to isopropyl and H there occurs also an equally important split leading to *n*-propyl. The secondary reactions also involved some new features. These results together with some findings on the atomic cracking reaction are described in the first paper.

For the elucidation of some of the secondary reactions, it was convenient to use deuterated propanes. It was found that the primary decomposition of the various isotopic propanes showed some interesting and important differences. The results from these studies are described in the subsequent paper.

EXPERIMENTAL

The apparatus used is shown in Fig. 1. It consists of a flow reaction system coupled to a mass spectrometer. The original design of such a system is due to Lossing (6). The modifications incorporated in the

[1]*University of Alberta Postdoctoral Fellow 1960–62.*

Can. J. Chem. Downloaded from www.nrcresearchpress.com by 210.87.254.5 on 09/05/12
For personal use only.

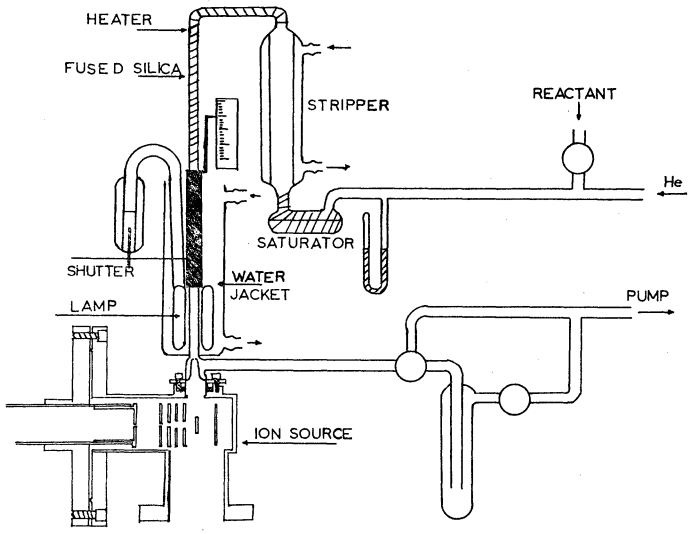

FIG. 1. Apparatus. Flow system for mercury-photosensitized decomposition attached to mass spectrometer.

present apparatus have been described elsewhere (7). For this reason, only the features pertinent to the work to be described will be mentioned. Propane is added to the carrier gas (He). The mixture is saturated with mercury vapor at 52° C in the saturator and stripper. The reaction zone is kept at 55° C. The length of the reaction zone, corresponding approximately to the length of the annular Hg resonance lamp, is close to 3.5 cm. For the flow velocity used, this results in a contact time of approximately 1.5 milliseconds. A sampling pinhole is located immediately below the reaction zone. A small portion of the reaction stream leaks through it into the mass spectrometer ion source. The predominant part of the reaction stream is either pumped out directly or passed through an efficient trap, where the condensables at liquid nitrogen temperature are collected for subsequent gas chromatographic separation. The pressure of the carrier gas was 10 mm Hg unless otherwise stated. The pressure of propane was 5 μ. The intensity of unreversed 2537 radiation has been estimated (6) in excess of 10^{-5} einsteins.

Analysis of the reaction mixture emerging from the reaction zone can be obtained directly by the mass spectrometer. With this method one may detect, in addition to the stable reaction products, the presence of free radicals. For positive detection, the radical concentration in the reaction stream should be more than 0.05 μ. The detection limit for the stable reaction products depends on the nature of the compound and the composition of the mixture. For an "average" compound the concentration should be not much less than one volume percent. For a substrate pressure of 5 μ this corresponds also to 0.05 μ. A much higher analytical sensitivity for the stable reaction products can be obtained through collection of the reaction products in the liquid nitrogen trap and subsequent gas chromatographic separation. The fractions separated by gas chromatography could be reintroduced into the mass spectrometer for analysis. In order to check the reliability of the freezing-out technique, control runs were made by using a synthetic mixture of composition similar to that of the reaction mixture. The analytical results showed that the recovery was in the average about 90%. The light reaction products ethane and ethylene were recovered with the even lower efficiency of 60–70%. The reason for this low recovery of the light products is specific to the reaction conditions of the system. Since one works at a very low propane pressure, the partial pressures of the products ethane and ethylene are of the same order or less than their saturation vapor pressures at the temperature of liquid nitrogen. Although appropriate corrections were applied to the results for ethane and ethylene, analytical results for these compounds cannot be considered very accurate.

Materials Used

The light propane (Philips research grade) was checked by gas chromatography for trace impurities. The heavy propane C_3D_8 (Merck and Dohme) was checked by mass spectrometry for completeness of deuterium substitution. It was found that it contained 6% of the lighter isotope C_3D_7H. Corrections to the analytical results for the presence of this isotope were made.

Mass Spectrometric Analysis of Deuteroisomers

Since spectral standards were not available for the deuteroisomers one had to rely mainly on the parent (molecular) peaks. This method of analysis can be employed if the parent peak is quite isolated, i.e. if there are no fragment peaks due to loss of one or a few hydrogen, correspondingly deuterium atoms, which would overlap with parent peaks of lighter deuteroisomers. This is the case with the *n*-pentane and the

Can. J. Chem. Downloaded from www.nrcresearchpress.com by 210.87.254.5 on 09/05/12
For personal use only.

three hexanes, and their analyses were obtained in this manner. The method depends very much on the purity of the samples, and for the hexanes and the *n*-pentane great care was taken with the gas chromatographic purification. Fragment peaks in the mass spectra were only checked for consistency with the composition predicted by the parent peaks and indication of impurities.

The propylenes and other olefins were analyzed at low electron energies where only the parent peaks appear. These analyses are the most accurate.

The analytical procedure did not give reproducible results for the *n*-butanes. Only some very tentative results could be obtained for the isobutane due to fragment peak interference.

RESULTS AND DISCUSSION

a. Specific Conditions of the Reaction System

The low pressure of the substance decomposed and the relatively high light intensity result in a radical to substrate ratio which is very much higher than that in conventional systems. Under these conditions radical–radical or excited mercury – radical reactions have been shown (6, 8, 9) to be the only important secondary processes inside the reactor. In the experiments where downstream collection was employed, downstream reactions must be considered. Evidence is given in the subsequent discussion that radical molecule reactions are unimportant also downstream. Disproportionation and recombination of the radicals emerging from the reactor should be the main reactions occurring before collection. A more detailed analysis of the situation (7) has shown that such downstream reactions cannot add more than several percent to the stable products emerging from the reactor. This is further verified by experiments described in Section *b* in which the lamp was moved with respect to the mass spectrometer sampling leak.

In view of this the discrepancy between the propylene measured with the mass spectrometer (5%) and the collection technique (3.5%) (Table I) should not be due to downstream reactions but probably to some deficiency in the analytical technique.

b. Primary and Secondary Reactions in the Decomposition of Propane

The products from the decomposition of propane are given in Table I. Only propylene, hydrogen, and methane were determined directly with the mass spectrometer. The remaining compounds were analyzed with the collection technique described in the experimental part. The propane decomposition which was measured directly with the mass spectrometer was approximately 100 per mille of the initial propane. Thus the concentrations given in Table I are in per mille of the initial propane and in percentage of the propane decomposed.

The minor products are shown in Table I in two different columns. The first group includes: ethane, *n*-butane and isobutane, *n*-pentane and isopentane, and the three hexanes 2,3-dimethylbutane, 2-methylpentane, and *n*-hexane. Considering the importance of radical–radical reactions mentioned in the preceding section we can interpret the formation of these products as due to the recombination reactions of methyl, ethyl, *n*-propyl, and isopropyl radicals. The mentioned products correspond exactly to the straight and cross recombination products of these radicals. The following reaction scheme may now be considered:

$$C_3H_8 + Hg^* \rightarrow n\text{-}C_3H_7 + H + Hg \qquad [1a]$$

$$\rightarrow \text{iso-}C_3H_7 + H + Hg \qquad [1b]$$

$$C_3H_7 + H \rightarrow C_3H_8^* \qquad [2]$$

$$C_3H_8^* + M \rightarrow C_3H_8 \qquad [3]$$

$$C_3H_8^* \rightarrow CH_3 + C_2H_5 \qquad [4]$$

$$C_2H_5 + H \rightarrow C_2H_6^* \rightarrow 2CH_3 \qquad [5]$$

$$H + CH_3 + C_2H_5 + C_3H_7 \rightarrow \text{recombination and disproportionation products.}$$

Can. J. Chem. Downloaded from www.nrcresearchpress.com by 210.87.254.5 on 09/05/12
For personal use only.

TABLE I

Composition of reaction mixture from mercury-photosensitized decomposition of propane

Initial propane	1000 (5 μ)		
Propane decomposed	100		
Hydrogen	60.0*	Allene	1.0
Methane	2.0*	Butene-1	0.8
Ethane	3.0	Pentene-1	0.15
Ethylene	2.0	Hexene-1	0.4
Propylene	50,* 35	4-Methylpentene-1	0.4
n-Butane	2.15		
i-Butane	2.0		
n-Pentane	0.5		
i-Pentane	0.5		
n-Hexane	0.6		
2-Methylpentane	1.0		
2,3-Dimethylbutane	0.5		

*From direct mass spectrometric determination.

The most direct confirmation for the reactions given in the reaction scheme comes from the results of the decomposition of mixtures of C_3H_8 and C_3D_8. In these runs mixtures of C_3H_8 and C_3D_8 in a concentration ratio 1:1 were decomposed. The reaction products after separation by gas chromatography were analyzed for isotopic composition with the mass spectrometer. The results from such runs are shown in Tables II–IV. The hexanes should result from recombination of propyl radicals originating from the primary decomposition. Therefore the hexanes should consist exclusively of the deuteroisomers $(C_3H_7)_2$, $C_3H_7 \cdot C_3D_7$, and $(C_3D_7)_2$. It can be seen in Table II that this is indeed the case. The

TABLE II

Hexanes from decomposition of 1:1 mixtures of C_3H_8 and C_3D_8

Deuteroisomer	% *n*-hexane	Ratio C_3H_7/C_3D_7	% 2-methylpentane + 2,3-dimethylbutane*	Ratio C_3H_7/C_3D_7
(*a*) $C_3D_7C_3D_7$	9	$\sqrt{(c/a)} = 2.3$	10	$\sqrt{(c/a)} = 2.1$
(*b*) $C_3D_7C_3H_7$	43	$0.5b/a = 2.4$	44	$0.5b/a = 2.2$
(*c*) $C_3H_7C_3H_7$	48	$c/0.5b = 2.2$	46	$c/0.5b = 2.1$

*The gas chromatographic separation of the two hexanes was not complete so that they were collected and analyzed together.

absence of deuteroisomers like $C_3H_6D \cdot C_3H_7$ shows that no significant part of the C_3H_7 radicals is formed by the addition of D (and by analogy, of H) to propylene, as is observed in the high-pressure decomposition of propane.[2] The ratio of the deuteroisomers $(C_3H_7)_2$:$C_3H_7C_3D_7$:$(C_3D_7)_2$ is not 1:2:1 as may have been expected on basis of an identical behavior of the C_3H_8 and C_3D_8. Instead the ratios are close to 4:4:1. Assuming equal behavior on recombination this means that the concentration ratio C_3H_7:C_3D_7 was close to 2. It will be shown in the succeeding paper, which deals specifically with the various propane deuteroisomers, that the difference of steady-state radical concentrations must be caused by different rates in the primary decomposition of the propane-H_8 and propane-D_8.

[2]*The absence of addition should also mean that there is no significant hydrogen abstraction from the propane since the addition competes successfully with the abstraction even at lower propylene to propane concentration ratios (5).*

Can. J. Chem. Downloaded from www.nrcresearchpress.com by 210.87.254.5 on 09/05/12
For personal use only.

The ethyl and methyl radicals are produced by the "atomic cracking" reactions [4] and [5]. The isobutane should then result from the recombination of methyl with isopropyl radicals, the *n*-pentane and isopentane from the recombination of ethyl with *n*-propyl and isopropyl radicals. Since the ethyls and methyls result from a cracking reaction the C_3H_8–C_3D_8 mixture should produce the following ethyl and methyl radical isomers: C_2H_5, C_2H_4D, C_2D_4H, C_2D_5, and all four methyl isomers. These recombine with C_3H_7 and C_3D_7. It can be seen that the experimentally measured butanes and pentanes (Table III and IV) consist of the isomers required by the scheme. Moreover, since a ratio C_3H_7:C_3D_7 = 2.2 was found in the hexanes, essentially the same ratio should be found in corresponding isomers in the butanes and pentanes. The ratios given in the tables are in agreement with this requirement. The actual numerical results for the composition of the deuteropentanes will be used later, in Section *c*, in an attempt to obtain some details on the cracking reaction.

The products of the propane decomposition given in Table I include a group of unsaturated compounds: allene, butene-1, pentene-1, hexene-1, and 4-methylpentene-1. These products are present in relatively small amounts, and are set apart in Table I because they originate from the mercury-photosensitized decomposition of propylene—the major hydrocarbon product of the propane decomposition. The mercury-photosensitized decomposition of propylene at low pressures has been studied by the mass spectrometric method (6, 10). It has been shown that the primary decomposition leads to allyl radicals and hydrogen atoms and that a significant portion of the allyl radicals react further to give allene. The amount of allene found in the present results roughly corresponds to what might be expected considering the low concentration of propylene. The other products, butene-1, pentene-1, hexene-1, and 4-methylpentene-1, must be the recombination products of the allyl radical with the methyl, ethyl, *n*-propyl, and isopropyl radicals coming from the propane decomposition. This scheme is confirmed by the deuterium content of the products obtained from the decomposition of the C_3H_8–C_3D_8 mixture. For example, since the 1-hexene should be formed by the recombination of *n*-C_3H_7 and *n*-C_3D_7 with the allyl radical, the expected deuteroisomeric 1-hexenes should be $C_3H_7C_3H_5$, $C_3H_7C_3D_5$, $C_3D_7C_3H_5$, and $C_3D_7C_3D_5$. These are the major products found (Table IV). Moreover, since a ratio of *n*-C_3H_7:*n*-C_3D_7 = 2:1 was found in the *n*-hexane and *n*-pentane, a similar ratio should also be observed here. It can be seen that this is exactly the case.

The following alternate schemes can be considered responsible for the formation of the major products—propylene and hydrogen: the direct hydrogen elimination from propane in a primary reaction, [6]; the further decomposition of propyl radicals by collision with excited mercury, [7], followed by a recombination of hydrogen atoms, [8]; and finally the disproportionation of propyl radicals with hydrogen atoms, [9].

$$C_3H_8 + Hg^* \rightarrow C_3H_6 + H_2 + Hg \qquad [6]$$

$$C_3H_7 + Hg^* \rightarrow C_3H_6 + H + Hg \qquad [7]$$

$$H + H \rightarrow H_2 \qquad [8]$$

$$C_3H_7 + H \rightarrow C_3H_6 + H_2 \qquad [9a]$$

$$\rightarrow C_3H_8^* \rightarrow C_3H_6 + H_2 \qquad [9b]$$

The direct split [6] is unlikely but cannot be eliminated completely on the basis of information in the literature (5). In order to establish whether [6] occurs to any significant extent, runs with variable C_3H_8 and C_3D_8 concentrations were made and the hydrogen

Can. J. Chem. Downloaded from www.nrcresearchpress.com by 210.87.254.5 on 09/05/12
For personal use only.

Can. J. Chem. Downloaded from www.nrcresearchpress.com by 210.87.254.5 on 09/05/12
For personal use only.

TABLE III

Pentanes from decomposition of 1:1 mixtures of C_3H_8 and C_3D_8

Deuteroisomer	% *n*-pentane	% *i*-pentane	Ratio								
			C_3H_7/C_3D_7			C_2H_5/C_2H_4D			C_2D_4H/C_2D_5		
				n-Pentane	*i*-Pentane		*n*-Pentane	*i*-Pentane		*n*-Pentane	*i*-Pentane
(*a*) $C_3D_7C_2D_5$	3.2	3.5	*h/d*	2.3	2.4	*h/g*	4	4.3	*f/e*	0.57	0.62
(*b*) $C_3D_7C_2D_4H$	2.1	2.6	*g/c*	2.0	2.5	*d/c*	3.5	4.5	*b/a*	0.66	0.74
(*c*) $C_3D_7C_2H_4D$	5.7	4.4	*f/b*	2.0	1.7						
(*d*) $C_3D_7C_2H_5$	19.7	19.6	*e/a*	2.3	2.0						
(*e*) $C_3H_7C_2D_5$	7.4	7.0									
(*f*) $C_3H_7C_2D_4H$	4.2	4.3									
(*g*) $C_3H_7C_2H_4D$	11.5	11.0									
(*h*) $C_3H_7C_2H_5$	46.3	47.9									

TABLE IV

Deuteroisomers of some products from decomposition of 1:1 mixtures of C_3H_8 and C_3D_8

Isobutane*		Propylene		1-Hexene and 4-methylpentene-1†			
						Ratio	
Deuteroisomer	%	Deuteroisomer	%	Deuteroisomer	%	C_3H_7/C_3D_7	C_3H_5/C_3D_5
$C_3D_7CD_3$	4	C_3D_6	26	(*a*) $C_3D_7C_3D_5$	5	*d/b* = 2	*d/c* = 4.9
$C_3D_7CD_2H$	2	C_3D_5H	2	$C_6D_{11}H$	1	*c/a* = 2	*b/a* = 4.8
$C_3D_7CH_2D$	4	C_3DH_5	5	$C_6D_{10}H_2$	4		
$C_3D_7CH_3$	21	C_3H_6	67	(*b*) $C_3D_7C_3H_5$	24		
$C_3H_7CD_3$	12			(*c*) $C_3H_7C_3D_5$	10		
$C_3H_7CD_2H$	6			$C_6H_8D_4$	3		
$C_3H_7CH_2D$	8			$C_6H_{11}D$	4		
$C_3H_7CH_3$	42			(*d*) $C_3H_7C_3H_5$	49		

*Due to analytical difficulties explained in the experimental part the butane analysis is only an estimate.
†The analytical results for the two hexenes were the same within the experimental error.

formed was analyzed directly with the mass spectrometer. The results are given in Table V and Fig. 2. That [6] could not occur to any significant extent follows from Fig. 2. The plot of H_2:HD versus the initial propane ratio C_3H_8:C_3D_8 gives a straight line which

TABLE V

Isotopic composition of hydrogen formed in the decomposition of C_3H_8–C_3D_8 mixtures*

$\mu\times20$				$\frac{C_3H_8}{C_3D_8}$	$\frac{H_2}{HD}$
C_3H_8	C_3D_8	H_2	HD		
0	92	0	0.1	0	—
21.6	82	0.66	1.86	0.25	0.37
23.2	70	0.82	1.53	0.33	0.55
33.0	69.4	1.1	1.8	0.486	0.61
48.0	50.8	2.2	2.0	0.95	1.1
67.4	38.0	2.5	0.92	1.77	2.7
78.0	24.6	2.7	0.72	3.2	3.8
100	0	6.4	—	—	—

*The D_2 formed could not be measured since its mass overlaps the mass of the He carrier gas.

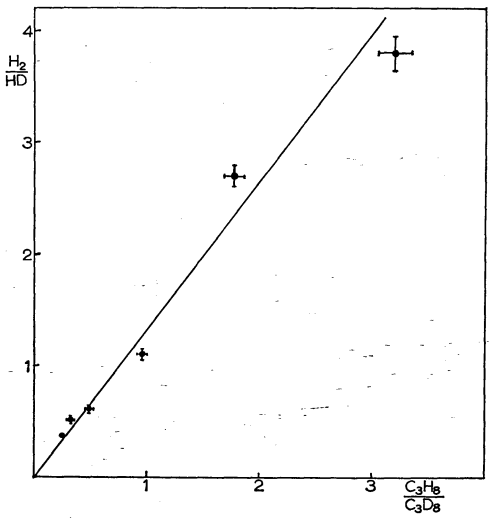

FIG. 2. Hydrogen product from decomposition of C_3H_8–C_3D_8 propane mixtures.

goes through the origin. Consider that a fraction of the hydrogen equal to f is formed by [6] and a fraction equal to g is formed by [8] or [9]. Then in the limit, as the ratio C_3H_8: C_3D_8 approaches zero, all hydrogen atoms reacting according to [8] or [9] will produce HD. Thus the intersection of the curve with the ordinate should give directly the ratio f:g. Since the curve goes through the origin, f must be equal to zero within the experimental error. A maximum possible intersection of the curve with the ordinate may be estimated at $H_2/HD = 0.05$ or 5% as a maximum for the contribution of [6] to the hydrogen-producing reactions.

The importance of the decomposition of free radicals by excited mercury as in [7] was suggested by Lossing (6, 8, 9, 11). If [7] were the major reaction forming propylene then the hydrogen atom recombination [8] should be the main source of the hydrogen. However, this recombination is third body restricted. To obtain information on the rate of H-atom recombination in the experimental system mixtures of H_2 and D_2 were mercury

Can. J. Chem. Downloaded from www.nrcresearchpress.com by 210.87.254.5 on 09/05/12
For personal use only.

photosensitized. The details of these experiments are given elsewhere (12). It was found that the H (and D) atoms recombine by a first-order reaction. Since the recombination is first order, it must be occurring on the wall (13). In these experiments it was also observed that when the lamp was in the position closest to the sampling leak only about 60% of the H atoms produced in the illuminated zone had recombined before reaching the leak. This percentage of recombination was found independent of the concentration of hydrogen. The hydrogen atoms were found almost completely recombined when the lamp was moved 12 cm upstream. If, in the propane decomposition, the hydrogen was formed predominantly by H-atom recombination then one may expect that the hydrogen detected when the lamp is in the bottom position should be only about 60% of the amount detected with the lamp in the upper position. Experiments were made in which the hydrogen and propylene were determined for both positions. It was found that the hydrogen was only about 6% less when the lamp was in the bottom position. Moreover the propylene was also found to be about 6% less, so that the hydrogen to propylene ratio was unchanged. This experiment shows that the majority of the hydrogen could not have been formed by H-atom recombination. The 6% difference for the two positions of the lamp most probably reflects slight differences in the transparency (cleanliness) of the silica reactor wall for the two positions and also some small amount of downsteam reactions.

The reaction that must be considered as the main source of the propylene and hydrogen formation is thus the disproportionation of H atoms with propyl radicals, reactions [9*a*] and [9*b*]. It was suggested that this reaction may be occurring in part as a "straight" disproportionation, [9*a*], and in part as a decomposition of excited propane formed by the recombination of H and propyl. A reaction closely related to these is of course the recombination leading, after stabilization, to propane. The extent of this reaction can be approximately determined by using C_3H_8–C_3D_8 mixtures of variable concentration and determining the amounts of cross recombination product C_3H_7D and C_3D_7H. Using this technique, it was found, in the succeeding paper, that about 40% of the primary decomposition ends up in recombination to propane. This means that the 100‰ observed decomposition given in Table I represents only the net decomposition, the actual primary decomposition is 100/0.6 = 166‰ and the recombination to propane 66‰ of the initial propane. The recombined propane is thus the major "product" followed by the hydrogen and propylene. In this light, the formation of the propylene by the disproportionation reactions [9*a*] and [9*b*] does not appear so unusual.

It is possible now to make a summary of the various reactions participating in the propane decomposition and their relative importance. The reactions are given below and are followed by the estimated number of molecules reacting per 100 molecules propane decomposed in the primary step.

$C_3H_8 + Hg^* \rightarrow n\text{-}C_3H_7 + H + Hg$		[1*a*]
$\rightarrow i\text{-}C_3H_7 + H + Hg$	100 [a+b]	[1*b*]
$C_3H_7 + H \rightarrow C_3H_8^*$		[2]
$C_3H_8^* + M \rightarrow C_3H_8$	40	[3]
$C_3H_8^* \rightarrow C_2H_5 + CH_3$	3.4	[4]
$C_3H_7 + Hg^* \rightarrow C_3H_6 + H + Hg$	30 mainly by [9]	[7]
$C_3H_7 + H \rightarrow C_3H_6 + H_2$		[9]
$C_3H_7 + \text{alkyl} \rightarrow C_3H_7\cdot\text{alkyl}$	5	
$H + H \rightarrow H_2$		

Can. J. Chem. Downloaded from www.nrcresearchpress.com by 210.87.254.5 on 09/05/12
For personal use only.

The relative extent of reactions [1*a*] and [1*b*] cannot be determined from the present results. It can be seen from the recombination products of the propyl radicals (Table I) that the steady-state concentration ratio of *n*-propyl:isopropyl was equal to 1. This ratio cannot be assumed to represent accurately the relative rates of the two primary steps. Thus about 30% of the C_3H_7 radicals react further to form propylene and the rates of this reaction will be at least somewhat different for the *n*-propyl and isopropyl radicals. Since all the remaining accounted reactions involving propyl are recombination reactions and thus not selective, we can estimate that the ratio of the two primary reactions should vary from about 1:1 to 1:2.[3]

c. Atomic Cracking of n-Propyl and Isopropyl Radicals

The excited propane decomposing by the atomic cracking reaction [4] may have been formed by the recombination of *n*-propyl or isopropyl radicals with hydrogen atoms. From the bond dissociation energies $D(n\text{-}C_3H_7\text{—}H) = 99$, $D(i\text{-}C_3H_7\text{—}H) = 94$, and $D(C_2H_5\text{—}CH_3) = 82$ kcal/mole (14), one calculates 17 and 12 kcal excess energy contained in the two recombination products. The recombination product of *n*-propyl should decompose more rapidly. An estimate of the relative decomposition rates of the two excited propanes is of considerable interest since data of this type are needed for the development of the theory of unimolecular reaction rates. The unimolecular decomposition of the excited isopropyl recombination product has been treated theoretically by Marcus (15). Extrapolating his data from an energy excess of 12 to 17 kcal one finds that the lifetime of the *n*-propyl recombination product should be about five times shorter than that of the isopropyl. It is shown in the subsequent text that an estimate of this ratio can be obtained from the isotopic composition of the pentanes formed in the decomposition of a 1:1 mixture of C_3H_8 and C_3D_8.

In the following reaction scheme, I stands for the *i*-propyl and N for the *n*-propyl radical.

$$H + I \rightarrow HI^* \rightarrow C_2H_5 + CH_3 \qquad [20, 20a]$$

$$\xrightarrow{M} HI \qquad [20b]$$

$$D + I \rightarrow DI^* \rightarrow C_2H_4D + CH_3 \qquad [21, 21a]$$

$$\xrightarrow{M} DI \qquad [21b]$$

$$H + N \rightarrow HN^* \rightarrow C_2H_5 + CH_3 \qquad [22, 22a]$$

$$\xrightarrow{M} HN \qquad [22b]$$

$$D + N \rightarrow DN^* \rightarrow \tfrac{1}{2}C_2H_5 + \tfrac{1}{2}CH_2D + \tfrac{1}{2}C_2H_4D + \tfrac{1}{2}CH_3 \qquad [23, 23a]$$

$$\xrightarrow{M} DN \qquad [23b]$$

Reaction [23*a*] expresses the fact that C—C bond cleavage can occur either α or β to the newly formed C—D bond. It is assumed that the two bond ruptures are equally probable.

Some of the ethyl radicals recombine with propyl to form pentanes, i.e.

$$C_2H_5 + \text{propyl} \rightarrow C_2H_5\cdot\text{propyl} \qquad [30]$$

$$C_2H_4D + \text{propyl} \rightarrow C_2H_4D\cdot\text{propyl}. \qquad [31]$$

Assuming that $k_{30} = k_{31}$ we have

$$\frac{R_{30}}{R_{31}} = \frac{(C_2H_5)}{(C_2H_4D)} = r = 4 \quad \text{(see Table III)}.$$

[3]*A more accurate estimate showing that the ratio is close to 1:1 is given in the succeeding paper.*

Can. J. Chem. Downloaded from www.nrcresearchpress.com by 210.87.254.5 on 09/05/12
For personal use only.

Since the ethyl radicals disappear mainly by recombination reactions it is reasonable to assume that the steady-state concentration ratio r is equal to the ratio of the rates of formation of the two radicals, i.e.

$$r = \frac{k_{20a}(\mathrm{HI}^*)+k_{22a}(\mathrm{HN}^*)+\frac{1}{2}k_{23a}(\mathrm{DN}^*)}{k_{21a}(\mathrm{DI}^*)+\frac{1}{2}k_{23a}(\mathrm{DN}^*)}. \qquad [1]$$

With the usual steady-state assumption for (HI*), correspondingly (HN*), one obtains $(\mathrm{HI}^*) = k_{20}(\mathrm{H})(\mathrm{I})/k_{20a}+k_{20b}(\mathrm{M})$ and an analogous set involving [21], [22] etc. From the reaction scheme given in Section *b* it can be seen that the stabilization reaction [*b*] is very much more important than the cracking reaction [*a*]; thus we can write:

$$(\mathrm{HI}^*) = k_{20}(\mathrm{H})(\mathrm{I})/k_{20b}(\mathrm{M}) \qquad [20]$$

$$\vdots \qquad \vdots$$

$$(\mathrm{DI}^*) = k_{23}(\mathrm{D})(\mathrm{I})/k_{23b}(\mathrm{M}). \qquad [23]$$

The following further assumptions can be made:

The isopropyl should recombine equally fast with (H) or (D), but for the higher thermal velocity of H. Thus we can assume

$$k_{20} = \sqrt{2}k_{21} \text{ and analogously } k_{22} = \sqrt{2}k_{23}. \qquad [2]$$

The unimolecular decomposition of the excited protoisopropane should be nearly as fast as that of the deuteroisopropane. The bond energy difference C—D to C—H should be about 1.1 kcal/mole. Using the energy dependence of excited propane derived by Marcus one finds that this should cause a difference by a factor of 1.3 in the unimolecular rate constants, i.e.

$$k_{21a} = 1.3k_{20a} \text{ and analogously } k_{23a} = 1.3k_{22a}. \qquad [3]$$

It should be pointed out that the numerical factors in equations [2] and [3] happen to appear on opposing sides in the subsequent derivation and thus (approximately) cancel. The treatment is equivalent to assuming both these factors equal to unity.

Since the excitational energy in the propanes is nearly 100 kcal/mole the 5 kcal difference for the *n*-propyl- and isopropyl-derived propanes should make little difference in the quenching efficiency of the collisions with the third body. Thus one can assume:

$$k_{20b} = k_{21b} = k_{22b} = k_{23b}. \qquad [4]$$

In Section *b* it was found that:

$$(\mathrm{I}) = (\mathrm{N}). \qquad [5]$$

Substituting [2]–[5] and [20]–[23] into [1] one obtains after rearrangement:

$$x_{\mathrm{H}} = \frac{r-y}{y+0.5(1-r)}, \qquad [6]$$

where $y = (\mathrm{H})/(\mathrm{D})$ and $x_{\mathrm{H}} = k_{22}k_{22a}/k_{20}k_{20a}$. In an analogous manner a reaction set for the pair C_2D_4H and C_2D_5 can be written. Solving the resulting equations one obtains:

$$x_{\mathrm{D}} = \frac{y-r'}{r'+0.5y(r'-1)}, \qquad [7]$$

Can. J. Chem. Downloaded from www.nrcresearchpress.com by 210.87.254.5 on 09/05/12
For personal use only.

where x_D is analogous to x_H but involves the rate constants of the C_2D_4H and C_2D_5 radicals and $r' = (C_2D_4H)/(C_2D_5) = 0.63$ (Table III).

It is reasonable to assume that $x_H = x_D$.[4] Solving the two simultaneous equations [6] and [7] one obtains

$$y = (H)/(D) = 1.93 \text{ and } x_H = x_D = 4.8.$$

The rate constants for recombination of H with *n*-propyl or isopropyl, k_{22} and k_{20}, may not be the same but they should be quite similar. If they are assumed the same then $x_H = k_{22a}/k_{20a} \sim 5$ or the *n*-propyl-derived propane decomposes about five times faster. This result agrees well with the prediction based on the calculations by Marcus mentioned previously. Considering the many assumptions that had to be made, the very close agreement obtained has no significance.

The treatment just given is admittedly very speculative. In particular a number of assumptions concerning the equality of radical rate constants had to be made which, while reasonable, are of course not proved. It is therefore of interest to show that there is one independent check of the calculation.

A ratio for $y = (H)/(D)$ very close to the calculated one can be obtained from data in Section *b*. Figure 2 gives the relationship

$$R_{H_2}/R_{HD} = 1.3(C_3H_8)/(C_3D_8).$$

In our case $(C_3H_8) = (C_3D_8)$, so that $R_{H_2}/R_{HD} = 1.3$. It was also shown that the most likely reaction leading to the hydrogen formation was the disproportionation [9]. We can write:

$$R_{H_2}/R_{HD} = 1.3 = \frac{k(H)(C_3H_7)}{k'(H)(C_3D_7)+k''(D)(C_3H_7)}. \quad [50]$$

From Tables II and III it was found that

$$(C_3D_7) = (C_3H_7)/2.2. \quad [51]$$

The propylene ratio given in Table IV is $C_3H_6/C_3D_6 = 2.6$. This suggests that $k(C_3H_7)/k'(C_3D_7) = 2.6$ and using [51] one obtains:

$$k' = 2.2k/2.6. \quad [52]$$

Assuming

$$k = \sqrt{2}k'', \quad [53]$$

where the square root takes into account the higher thermal velocity of H, one obtains by combining [50]–[53]

$$(H)/(D) = 2.$$

A very similar estimate for this ratio can be obtained also if it is assumed that the hydrogen was formed by the direct recombination of hydrogen atoms.

REFERENCES

1. E. W. R. Steacie and D. J. Dewar. J. Chem. Phys. **8**, 571 (1940).
2. B. de B. Darwent and E. W. R. Steacie. J. Chem. Phys. **13**, 563 (1945).
3. C. R. Masson and E. W. R. Steacie. J. Chem. Phys. **18**, 210 (1950).

[4]*The assumption $x_H = x_D$ implies that the rate constant ratio k_{22a}/k_{20a} in the "light" propanes is equal to the corresponding ratio in the "heavy" propanes. It should be noted that the assumed equality of the ratios does not require that, for instance, the k_{22a} should be the same for the "light" and "heavy" propanes. This is less likely to be true.*

Can. J. Chem. Downloaded from www.nrcresearchpress.com by 210.87.254.5 on 09/05/12
For personal use only.

4. S. BYWATER and E. W. R. STEACIE. J. Chem. Phys. **19**, 313 (1951).
5. R. A. BACK. Can. J. Chem. **37**, 1834 (1959).
6. F. P. LOSSING, D. H. MARSDEN, and J. B. FARMER. Can. J. Chem. **34**, 701 (1956).
7. P. KEBARLE. J. Phys. Chem. To be published.
8. F. P. LOSSING. Can. J. Chem. **35**, 305 (1957).
9. P. KEBARLE and F. P. LOSSING. Can. J. Chem. **37**, 389 (1959).
10. M. AVRAHAMI and P. KEBARLE. To be published.
11. R. F. POTTIE and F. P. LOSSING. Can. J. Chem. **39**, 1900 (1961).
12. P. KEBARLE and M. AVRAHAMI. To be published.
13. K. E. SHULER and K. J. LAIDLER. J. Chem. Phys. **17**, 1212 (1949).
14. A. F. TROTMAN-DICKENSON. Gas kinetics. Butterworths. 1955. p. 15.
15. R. A. MARCUS. J. Chem. Phys. **20**, 352 (1952).

Can. J. Chem. Downloaded from www.nrcresearchpress.com by 210.87.254.5 on 09/05/12
For personal use only.

THE MERCURY-SENSITIZED PRIMARY DECOMPOSITION OF DEUTERATED PROPANES
A MASS SPECTROMETRIC STUDY AT LOW PRESSURES
PART II

M. AVRAHAMI[1] AND P. KEBARLE
Chemistry Department, University of Alberta, Edmonton, Alberta
Received June 26, 1962

ABSTRACT

The primary decomposition of C_3H_8, $CD_3CH_2CD_3$, $CH_3CD_2CH_3$, and C_3D_8 was found equal to: 10, 8, 5.5, and 5%.

The primary reactions were

$$\text{propane} \rightarrow \text{isopropyl} + \text{hydrogen atom} \quad (a)$$
$$\rightarrow n\text{-propyl} + \text{hydrogen atom.} \quad (b)$$

The ratio a/b was strongly affected by deuterium substitution. The numerical values of the ratio for the compounds in the order given above are: 1.2, 6.8, 0.2, 0.9. Elucidation of the underlying reasons for this surprisingly large isotope effect might throw new light on the excited mercury – paraffin interaction.

Can. J. Chem. Downloaded from www.nrcresearchpress.com by 210.87.254.6 on 09/05/12
For personal use only.

INTRODUCTION

It is known that the interaction of Hg $^3P_1$ with molecules containing π electrons leads to the formation of excited molecules which may decompose, but which can also be deactivated by collisions with a third body. The clearest evidence for the formation of excited molecules is the decrease of primary quantum yield with increase of pressure. Excited mercury is quenched by such molecules already at appreciable distances. The situation with the paraffins is quite different. Their quenching cross sections are an order of magnitude smaller. The primary quantum yields of the higher paraffins are believed to be equal or close to unity and are not demonstrably affected by the increase of pressure. These facts suggest that a different type of process must be involved. A chemical interaction of the mercury with one or two of the hydrogen atoms surrounding the carbon skeleton may be suspected since all known Hg-sensitized decompositions of paraffins lead to C—H bond cleavage.

Some chance observations, made during the study of the decomposition of propane described in the preceding paper, led to an investigation of the primary decomposition of deuterium-substituted propanes. The results of these experiments pose some interesting questions and might provide a clue to a better understanding of the nature of the mercury–paraffin interaction.

EXPERIMENTAL

The apparatus, experimental techniques, and conditions are described in the preceding paper.

RESULTS AND DISCUSSION

Table I gives the percentage decomposition of the four deuteroisomers measured at identical experimental conditions. The secondary reactions do not consume any propane, but there is some recombination of H, correspondingly D, with propyl so that the

[1]*University of Alberta Postdoctoral Fellow 1960–62.*

TABLE I

Decomposition of propane isomers

Propane decomposed	% net decomposition*	% propylene product
C_3H_8	10	5.5
$CD_3CH_2CD_3$	8	5.8
$CH_3CD_2CH_3$	5.5	2.8
C_3D_8	5.0	2.9

*In % of initial propane. The initial propane pressure and all other experimental conditions were the same in all cases.

decomposition is less than the primary reaction. It is shown in the Appendix that the recombination is roughly proportional to the primary reaction. Therefore, the figures in Table I may be considered also as roughly proportional to the primary decomposition. The results exhibit a specific pattern. The compounds with deuterium in the secondary position decompose only half as much as the hydrogen-containing compounds. Deuterium substitution in the primary position also decreases the decomposition but the effect is very much smaller.

Even more interesting is the influence of deuterium on the relative importance of the primary splits to *n*-propyl or isopropyl radicals. The relative rates of these reactions can be traced by examining the recombination products of the propyl radicals. It was shown in the preceding paper that the propyl contained in the recombination products originated only from the primary reactions. This was also verified in the present experiments by determining the deuterium content in the hexanes. The relative amounts of the three hexanes are given in Table II. The isopropyl:*n*-propyl ratios calculated in

TABLE II

Hexanes and resulting propyl ratios

	% of total hexanes			*i*-Propyl:*n*-propyl ratio			
Propane decomposed	*n*-Hexane (*a*)	2-Methyl-pentane (*b*)	2,3-Dimethyl-butane (*c*)	$(c/a)^{1/2}$	$2c/b$	$b/2a$	Average
C_3H_8	28	48	24	0.91	1.0	0.86	0.92
$CD_3CH_2CD_3$	5	34	62	3.5	3.7	3.4	3.5
$CH_3CD_2CH_3$	62	34	4	0.25	0.23	0.27	0.23
C_3D_8	31	49	20	0.8	0.81	0.79	0.8

the table should relate to steady-state concentrations of the radicals. Very similar ratios could be obtained from the butanes and pentanes, which are also recombination products of the propyl radicals. These ratios will correspond to the primary rates of radical production only if the radical removal reactions are not specific to the nature of the *n*- or *i*-radical. The main removing reaction—the recombination to propane—should not be selective. The next most important reaction leading to propylene may be expected to be somewhat selective no matter what is the mechanism of propylene formation. Thus we may conclude that the propyl ratios from the hexanes, while not giving a quantitative measure, should at least indicate the trends of the primary reactions.

To obtain more conclusive information, a different experiment was made. Instead of allowing the hydrogen to recombine with the propyl radicals and lead to a "product" in which the nature of the *n*- or *i*-radical cannot be recognized, the propyls were forced

Can. J. Chem. Downloaded from www.nrcresearchpress.com by 210.87.254.6 on 09/05/12
For personal use only.

to recombine with an excess of methyl radicals (CD_3) produced by the simultaneous decomposition of mercury dimethyl-D_6. A sufficient methyl radical excess, by reducing the propyl radical concentration, should also suppress all other reactions of the propyl radical and lead almost exclusively to methyl–propyl recombination and disproportionation.[2] The results from such a methyl saturation experiment are shown in Fig. 1. Given

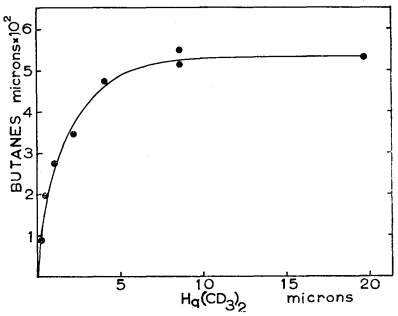

FIG. 1. Combined *n*-butane and isobutane resulting from the recombination of CD_3 with C_3H_7.

is the total recombination products *n*-butane and isobutane with gradually increasing pressure of initial $Hg(CD_3)_2$. It can be seen that the butane formation soon levels off to a constant value. This must correspond to essentially total removal of the propyl by methyl radicals. The position of the lamp in this experiment was 12 cm above the mass spectrometer leak.

The relative amounts of *n*-butane and isobutane could not be determined accurately by direct mass spectrometric analysis of the reaction stream. Therefore a set of runs was made with an initial mercury dimethyl concentration corresponding to saturation (mercury dimethyl pressure = 8 μ) and the products of the decomposition trapped out and analyzed by gas chromatography. The butanes and propylene obtained from these runs are given in Table III. Besides the butanes and the propylene, no other products due to the propane decomposition could be detected. The butanes, obtained from the light propane, were analyzed on the mass spectrometer and found to consist completely of the expected deuteroisomers $C_4H_9D_3$. The propylene, surprisingly, consisted not entirely of the expected C_3H_6 but contained 20% of the isomer C_3H_5D.

The only reasonable mechanism leading to the formation of propylene is the disproportionation of C_3H_7 with CD_3 radicals.[3] Initially it was believed that the C_3H_5D must have resulted from a deuterium exchange in the disproportionation reaction. In a later study, propylene (1 μ) and mercury dimethyl-D_6 (8 μ) were decomposed. The isolated propylene was found to contain about 10% C_3H_5D. The nature of the reaction leading to this product is still under investigation. Results up to the present suggest that such deuterium exchange may be occurring in reactions of excited triplet olefins (produced by mercury photosensitization) with the CD_3 radicals.

Since the butane ratios (Table III) were obtained from collection experiments, evidence

[2]*This technique has been developed by Lossing (1).*

[3]*The propylene to combined butanes ratio is equal to about 0.5 (Table III). This figure should express the disproportionation to recombination ratio of a mixture of the two propyls with methyl radicals. As is shown later from the experimental results one can conclude that the disproportionation ratio for isopropyl is quite similar to that for n-propyl. The disproportionation to recombination ratio of isopropyl with methyl measured by Heller (2) is 0.17. Thus the present results are out of line. However, the disproportionation in the present system may involve vibrationally excited propyl radicals. The excess energies should be initially around 13 and 18 kcal for n-propyl and isopropyl. Since this is equivalent to only a few vibrational quanta above the ground state, the spacing of the levels will be wide and the quenching by helium very inefficient. At the pressure of* CH_3 *1 μ and* He *10 mm the propyl radicals will have about 10,000 collisions with* He *before colliding with a methyl radical. These may not be sufficient for a complete vibrational deactivation (3).*

Can. J. Chem. Downloaded from www.nrcresearchpress.com by 210.87.254.6 on 09/05/12
For personal use only.

Can. J. Chem. Downloaded from www.nrcresearchpress.com by 210.87.254.6 on 09/05/12
For personal use only.

TABLE III

Products from propanes codecomposed with excess of mercury dimethyl

Propane decomposed	% products							$\left(\frac{\text{Propylene}}{\text{Butanes}}\right)$	$\left(\frac{i\text{-Butane}}{n\text{-Butane}}\right)$	$\left(\frac{i\text{-Propyl}}{n\text{-Propyl}}\right)^*$
	Propylene	*i*-Butane	*n*-Butane	Total	Total*	*i*-Propyl*	*n*-Propyl*			
C_3H_8	2.36	2.32	2.68	7.36	7.67	4.15	3.52	0.47	0.87	1.2
$CD_3CH_2CD_3$	2.91	3.44	0.68	7.03	7.05	6.15	0.90	0.69	5.0	6.8
$CH_3CD_2CH_3$	1.22	0.36	2.48	4.06	3.90	0.65	3.25	0.42	0.145	0.2
$CD_3CD_2CD_3$	1.18	0.95	1.36	3.49	3.49	1.70	1.79	0.50	0.71	0.9

*Calculated.

Can. J. Chem. Downloaded from www.nrcresearchpress.com by 210.87.254.6 on 09/05/12
For personal use only.

should be given that no complicating reactions occur downstream of the illuminated zone. One may argue that some of the butanes are formed by downstream hydrogen abstraction from propane by methyl radicals followed by methyl–propyl recombination. One can calculate that the downstream methyl radical decay due to recombination to ethane is too rapid to allow any significant abstraction to occur; however, the following experimental proofs are more direct. The experiment with variable mercury dimethyl concentration (Fig. 1) was done with the ultraviolet lamp 12 cm (~4 milliseconds) upstream of the mass spectrometer sampling leak. The methyl concentration should fall in 4 milliseconds to a small fraction of its original value. The absence of abstraction reactions is evidenced by the levelling off of the butane formation. In the propylene experiment mentioned above, the formation of *i*-pentane should have been observed if methyl radical addition followed by recombination occurred. No *i*-pentane was found in the trapped out reaction mixture.

The information obtained from the methyl addition experiments is in agreement with the results from the decomposition of the propanes alone. It provides also a more accurate estimate of the relative primary rates leading to isopropyl or *n*-propyl radicals. A ratio for these reactions can be obtained directly from the isobutane and *n*-butane products. These ratios are given in Table III. Since propylene is an appreciable product, amounting to about half of the combined butanes, the butane ratio still does not give a complete picture of the primary rates. One can correct the ratio by determining what fractions of the propylene originate from the *n*-propyl and isopropyl radicals. This can be done on the basis of a procedure which is outlined in the Appendix. The isopropyl to *n*-propyl ratios obtained by the calculation are given in the table. Comparing them with the direct isobutane to *n*-butane ratios one finds that the changes introduced by the correction are not very significant.

The experimental results may be briefly summarized as follows. Deuterium substitution affects the mercury-sensitized decomposition in two ways. First, it produces changes in the total primary decomposition. Second, it produces changes in the relative importance of the two primary processes leading to *n*-propyl or isopropyl radicals. The influence of the deuterium is to block bond cleavage in the position of substitution. The deuterium effects are very large.

The change in the primary decomposition can be due to changes of any of the following parameters: cross section for quenching of Hg $^3P_1$ to $^3P_0$, cross section for quenching of $^3P_1$ to ground state, primary quantum yield for reaction with $^3P_1$, primary quantum yield for reaction with $^3P_0$. Obviously a choice between these possibilities on the basis of the present experiments would be impossible. Information available in the literature is quite incomplete. The total quenching cross sections of only three deuterated species, D_2O, ND_3, and PD_3, have been measured (5, 6). The deuterated water and ammonia have cross sections which are only one half as large as those of the light compounds, while PD_3 has a cross section which is somewhat larger than that of PH_3. The differences resulting from deuteration have been explained on the basis of quenching to the metastable state. The energy change for this transition corresponds to 1767 cm^{-1}. In ammonia and water the closest vibrational frequencies (for resonance transfer) shift away from 1767 cm^{-1} with deuteration, while in the phosphine a shift towards this frequency occurs. Cross section measurements of deuterated paraffins are not available; however, measurements of the deuterated propanes are at present being made by Gunning and Rousseau.[4]

[4]*Gunning and Rousseau (7) have undertaken these measurements as an extension of the work quoted in reference 4. The preliminary results were kindly communicated by the authors.*

The preliminary results show that the total quenching cross sections follow the pattern of the total decomposition, observed in the present work, but are much more pronounced, i.e. $(C_3H_8) = 1.2$ Å^2, $(C_3D_6H_2) = 1.0$, $(C_3H_6D_2) = 0.17$, $(C_3D_8) = 0.09$. In analogy with the interpretations used for the deuterated ammonia, water, and phosphine, one might suppose that in this case also differences in quenching to the metastable state are the overriding factors. There are, however, reasons to argue against such an assumption. If one examines the available quenching cross sections of the paraffins (8), one is immediately impressed by their strong structural dependence. A significant increase of the cross section occurs when a secondary and then again when a tertiary hydrogen atom is introduced. At the same time, no specific correlation with normal modes of vibration in the region 1767 cm^{-1} can be made. It is therefore not unreasonable to suppose that the overriding process determining the total quenching cross section of the paraffins is the quenching of the $^3P_1$ excited atom to the ground state, which involves a chemical mercury–hydrogen atom interaction and followed by C—H bond cleavage in the paraffin. The findings of Cvetanović (9) on competitive quenching of nitrous oxide and *n*-butane are in essential support of such a picture. If this view were correct then deuterium should in some way hinder the process. It is difficult to conceive why deuterium should have such a large effect, since considerable excess energy for the final C—H break is available. However, essentially nothing is known about the nature of the mercury–paraffin activated complex and its energy requirements for decomposition. The strong shift of the decomposition from primary to secondary bond cleavage or the reverse, produced by deuterium substitution, also supports the view that the effects are not due to quenching to the metastable state but to a specific mercury–hydrogen, correspondingly deuterium, interaction.

Before being able to utilize the information contained in the deuterium effects, one would also require information on the primary quantum yields of the deuterium-substituted propanes. It is now known that the primary quantum yield for ethane, propane (10), and *n*-butane (9) is unity or close to unity. Since the structural changes from ethane to butane are drastic compared with the change from H to D in the propane, one might suppose that the primary quantum yields for the deuteropropanes should be also unity. If this does not happen to be the case, the operation of some specific effect, like quantum mechanical tunnelling of the hydrogen and deuterium atoms, might have to be invoked.

Can. J. Chem. Downloaded from www.nrcresearchpress.com by 210.87.254.6 on 09/05/12
For personal use only.

REFERENCES

1. R. F. Pottie, A. G. Harrison, and F. P. Lossing. Can. J. Chem. **39**, 102 (1961).
2. C. A. Heller. J. Chem. Phys. **35**, 1711 (1961).
3. H. S. Massey and E. H. S. Burhop. Electronic and ionic impact phenomena. Oxford-Clarendon Press, Oxford. 1956. p. 460.
4. H. E. Gunning and G. Woodall. To be published.
5. M. G. Evans. J. Chem. Phys. **2**, 445 (1934).
6. H. W. Melville, J. L. Bolland, and H. L. Roxburgh. Proc. Roy. Soc. (London), Ser. A, **160**, 406 (1937).
7. H. E. Gunning and Y. Rosseau. To be published.
8. W. A. Noyes and P. A. Leighton. The photochemistry of gases. Reinhold Publishing, New York. 1941. p. 221.
9. R. J. Cvetanović, W. E. Flaconer, and K. R. Jennings. J. Chem. Phys. **35**, 1225 (1961).
10. R. A. Back. Can. J. Chem. **37**, 1834 (1959).

APPENDIX

a. Recombination Reaction Leading to Propane

Mixtures of C_3H_8 and C_3D_8 in which the mole fraction $X_{C_3H_8}$ was varied from 0 to 1 were decomposed and the disappearance of C_3H_8 and C_3D_8 and the formation of the

recombination products C_3H_7D and C_3D_7H measured with the mass spectrometer. The results are shown in Fig. 2. In Fig. 2A the percentage decomposition of C_3D_8 is shown.

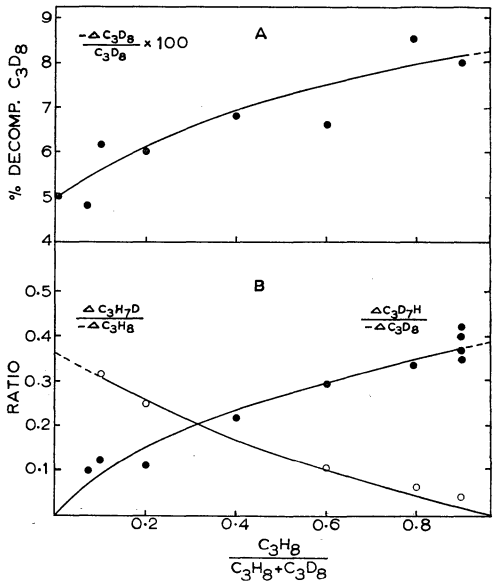

FIG. 2. A: Increase of C_3D_8 decomposition with $X_{C_3H_8}$ due to enhanced formation of recombination product C_3D_7H.
B: Cross recombination products to decomposition ratio as a function of $X_{C_3H_8}$.

The decomposition gradually increases as $X_{C_3H_8}$ is increased, since more and more of the recombination proceeds with H rather than D atoms. The decomposition extrapolated to $X_{C_3H_8} = 1$ is about 8.5% and should at this point correspond to the primary decomposition of C_3D_8. Unfortunately, the corresponding plot which would have given the primary decomposition of the C_3H_8 could not be obtained with any accuracy due to excessive mass interference at mass 44—the molecular mass of C_3H_8. However, the plots in Fig. 2B do provide at least a partial answer as to the extent of the primary decomposition in the two compounds. A plot is shown of $\Delta C_3D_7H/\Delta C_3D_8$ as a function of $X_{C_3H_8}$. In the limit of $X_{C_3H_8} = 1$ all C_3D_7 recombines with H and the intercept gives directly the fraction of the total decomposition ending in recombination. The curve extrapolates to a value of 40%, which agrees well with the predictions from Fig. 2A, where the primary minus the net decomposition was $8.5-5 = 3.5\%$, or the percentage recombination was $3.5\times100/8.5 = 41\%$. The corresponding plot $\Delta C_3H_7D/\Delta C_3H_8$ could be obtained in this case but involves a considerable error due to mass spectral interference. The shape of the curve is somewhat different from that of the deuterated propane. This is due to the fact that the primary decomposition of the C_3D_8 is slower. Thus, on a concentration basis the C_3D_8 is a less efficient provider of (D) atoms for the cross recombination product. The intercept for $X_{C_3H_8} = 0$ occurs at about 36% recombination. This is similar to the 40% obtained for the C_3D_8. The two values cannot be expected to agree. Thus, for example, the C_3D_7H extrapolation gives the recombination of C_3D_7 with H atoms at a concentration level determined by the mechanism of the C_3H_8 decomposition. What one may conclude from the experimental results is that the recombination to primary decomposition ratio in C_3H_8 and C_3D_8, when these substances are decomposed alone, is roughly the same.

Can. J. Chem. Downloaded from www.nrcresearchpress.com by 210.87.254.6 on 09/05/12
For personal use only.

b. Fraction of Propyl Radicals Forming Propylene

The constancy of the propylene to butanes ratio given in Table III shows that the reaction by which propyl is converted into propylene does not show any strong dependence on deuterium substitution. Making the assumption that in the first approximation the propylene-forming reaction depends only on whether the radical is *n*-propyl or isopropyl but not on the deuterium substitution, one can determine what proportion of the propylene originates from isopropyl or *n*-propyl radicals and in this way obtain also the original amounts of these radicals. A good fit of the data is obtained by assuming that 0.56 and 0.76 of the original isopropyl and *n*-propyl end up as isobutane and *n*-butane. A check of the procedure is obtained by comparing the calculated with the measured total propylene plus butanes. The calculated total is obtained by dividing the measured isobutane and *n*-butane by 0.56 and 0.76, respectively, and adding. Equally "good" agreement can be obtained with slightly different factors, so that the procedure is somewhat arbitrary.

Can. J. Chem. Downloaded from www.nrcresearchpress.com by 210.87.254.6 on 09/05/12
For personal use only.

A NEW TECHNIQUE FOR THE STUDY OF HIGH-POLYMER DEGRADATION REACTIONS*

H. H. G. JELLINEK AND J. E. CLARK
Department of Chemistry, Essex College, Assumption University of Windsor, Windsor, Ontario
Received September 17, 1962

ABSTRACT

A quartz spoon gauge, recording pressures automatically, is described. The gauge, representing a closed reaction system, can be used for investigations of the degradation of polymers. It has been tested by degrading polymethylmethacrylate over a temperature range of 300 to 400° C. The important features of the gauge are as follows: (1) The pressure exerted by gases during degradation is continuously recorded at appropriate chart speeds via an electrical transducer (maximum displacement ±0.038 cm; spoon gauges used in this work had sensitivities in the region of 0.035 cm/atm). (2) Only small quantities of polymers are needed; 20 to 40 mg of polymer in the form of films was deposited on the walls of the reaction vessels; however, much smaller samples could be used, the limit being given by mechanical vibrations set up in the system. (3) Temperature equilibrium between the reaction vessels and a thermostated bath is reached within about 30 seconds.

Useful results for polymethylmethacrylate were obtained up to 400° C, which is a temperature about 100° higher than that reached by previous workers, not neglecting the initial parts of the reactions. The reproducibility of the results has been indicated by average curves obtained from several runs at any one particular temperature and their standard deviations.

Can. J. Chem. Downloaded from www.nrcresearchpress.com by 210.87.254.6 on 09/05/12
For personal use only.

The new technique for the study of polymer degradation reactions consists essentially of an automatic recording quartz spoon gauge, which can be used for thermal reactions or any other reactions such as photodegradation as long as volatiles are produced. The present paper deals with this technique as applied to thermal degradation processes. These reactions can be studied with this apparatus at higher temperatures than before because of the short time needed to reach temperature equilibrium between the reaction vessel and a thermostated bath. The method should in principle also be useful for the study of ceiling temperatures. Only small quantities of polymer are required; the smallest amount employed in this work was 20 mg but there is no reason why smaller quantities (ca. 1 mg) could not be used. The lower limit would essentially be given by mechanical vibrations set up in the system.

Thermal degradation of high polymers is quite well understood at relatively low temperatures where the rates of degradation are slow enough to be measured by instruments such as a thermobalance; but, once the rates become appreciable, different methods are needed. One attempt in this direction is reported in the present paper. There is scarcely any kinetic data in the literature for degradation reactions whose rates are high, although there is quite substantial information available from analytical experiments on the degradation of polymers at high temperatures (1).

The new apparatus described here has been evaluated using polymethylmethacrylate, which is known to degrade primarily into monomer. Useful rate measurements were obtained up to 400° C, which is about 100° C higher than the temperature used by other authors (2, 3, 4).

EXPERIMENTAL

(a) Apparatus and Procedure

The apparatus is shown in Fig. 1. The reaction vessel consists of a quartz spoon gauge (1) of about 15 cm^3 capacity. The top of the spoon's pointer has a sensitivity of about 0.035 cm/atm. This, of course, is only a

**Paper presented at the Eleventh Canadian High Polymer Forum, Windsor, Ontario, September 5–7, 1962.*

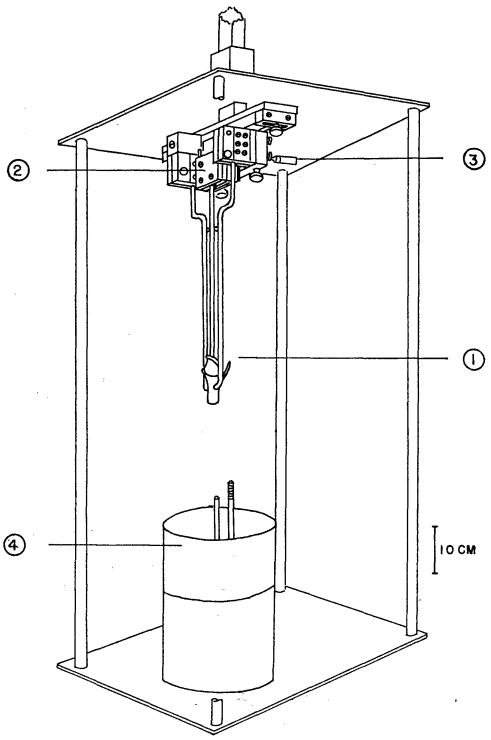

FIG. 1. Quartz spoon gauge apparatus: (1) quartz spoon gauge, (2) Statham transducer, (3) micrometer screw and holder, (4) furnace.

representative value; each individual spoon is calibrated by introducing air of known pressure. The sensitivity of spoons can vary within wide limits. The gauge is fixed in a clamping device (2) and, by means of a micrometer screw (3), contact can be made between the quartz pointer and the lever of a Statham transducer (strain gauge), Model G1OB-0.3-350. The transducer has a maximum displacement of ±0.038 cm and is connected to a two-channel Sanborn recorder, Model 150 (with carrier preamplifier, Model 150-1100, and a low-level preamplifier, Model 150-1500). Pressures, under conditions employed in this work, could be read within ±1 mm Hg; temperatures could be recorded simultaneously.

Polymer was deposited in the form of thin films (for 20-mg samples, the thickness was approximately 5×10^{-3} cm) on the walls of the reaction vessel. The films were formed by introducing into the reaction vessel the requisite volume of a 2% w/v solution of the polymer in acetone. The latter was evaporated slowly at slightly elevated temperatures (ca. 50° C) and the reaction vessel was eventually connected to a high-vacuum system (10^{-5} to 10^{-6} mm Hg). Finally, the film was baked out under high vacuum for at least 24 hours at 65±5° C. The spoon reaction vessel was then sealed off and inserted into the arrangement as shown in Fig. 1. Contact was made with the transducer and the whole assembly was rapidly lowered, so that the spoon reaction vessel was immersed in a thermostated 50:50 by weight lead–tin bath, which was regulated by a platinum resistance thermometer (Sunvic, Type PRT-4, in conjunction with a Sunvic resistance thermometer controller, Type RT-2) to within ±0.5° C at any one particular location of the bath. The temperature profile is given below:

Temperature (°C)	262	281	283	285	284	283
Location (in.)	At surface	−1	−2 to −4	−5 to −8	−9	−10

The reaction vessel was located approximately in the region 4 to 6 in. below the surface of the bath.

Figure 2 shows that it did not take longer than 30 seconds to reach temperature equilibrium between the reaction vessel and the bath. The chart of the Sanborn recorder could be run at various speeds (0.25, 0.5, 2.5, 5, 10, 25, 50, 100 mm/sec) to suit the rate of the reaction. Spoon reaction vessels of various sensitivities were employed; they were calibrated, as already indicated above, by introducing air of known pressures into the spoon gauge and recording by means of the Statham transducer. Characteristic calibration curves are

Can. J. Chem. Downloaded from www.nrcresearchpress.com by 210.87.254.6 on 09/05/12
For personal use only.

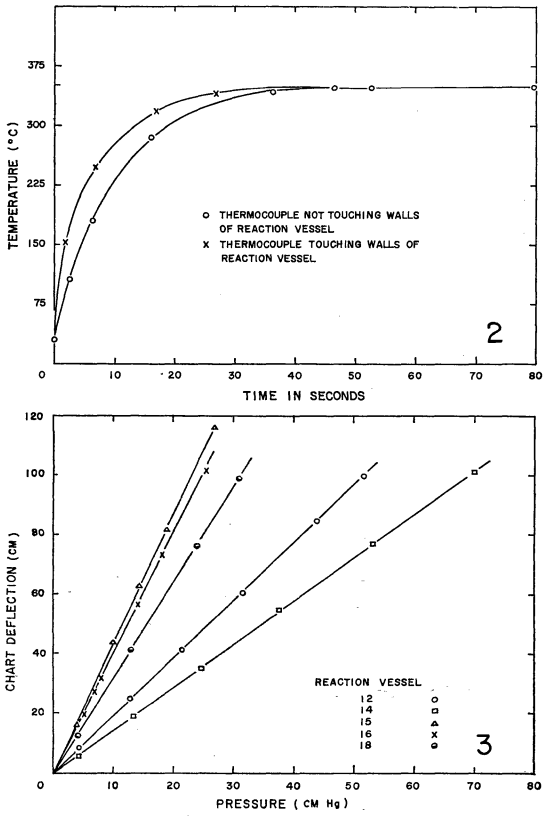

FIG. 2. Attainment of temperature equilibrium for the reaction vessel at 350° C.
FIG. 3. Calibration curves for various spoon gauges.

shown in Fig. 3. The calibration gave the same results whether it was carried out with the spoon in the bath at elevated temperatures or outside the bath at room temperature. The pressure versus chart divisions relationship is linear over the entire range employed.

(b) Materials

All solvents were of analytical reagent grade.

Methylmethacrylate (Rohm and Haas) containing 0.006% hydroquinone was treated as described in Riddle's book (5). Polymerization was carried out with 0.5% benzoylperoxide under vacuum for 30 minutes at 60° C (conversion approximately 5%). The reaction was stopped by pouring the polymer–monomer mixture into five times its volume of methanol. The polymer was filtered off, redissolved in acetone, and and precipitated by dropwise addition of methanol. It was eventually dried to constant weight in a vacuum desiccator. The intrinsic viscosity of the polymer in chloroform was found to be 2.01 dl g^{-1}.

A 2% w/v stock solution in acetone was prepared and aliquots of it were used in all subsequent experiments.

(c) Experimental Results

The experimental results are given in moles of gas produced as a function of time. The assumption that only monomer is produced is not quite correct since it was observed that especially at higher temperatures the remaining polymer showed a yellow to brown color and at 400° C small amounts of charred residue were also found. This may also explain the observation that usually somewhat more than the theoretical number of moles in terms of monomer was found on complete degradation. It is also possible that there is still some residual solvent in the polymer. The moles of gas produced were calculated by using the measured volume of the spoon reaction vessel and the ideal gas law.

Figure 4 shows curves representing average percentage values of a number of runs obtained with 20-mg and 40-mg films respectively at 300° C. Standard deviations are indicated. It is apparent that the degradation is slower for the larger polymer sample. Brockhaus and Jenckel (4) observed a pressure effect for the degradation, which also seems to be apparent in our results. Whether this effect is due only to a diffusion process or also to a chemical reaction remains to be seen.

Can. J. Chem. Downloaded from www.nrcresearchpress.com by 210.87.254.6 on 09/05/12
For personal use only.

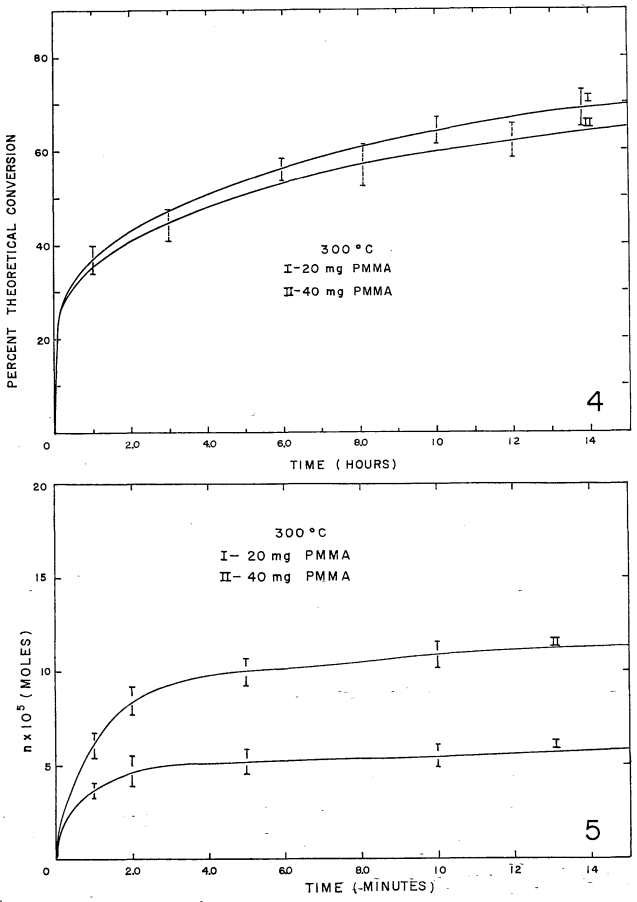

FIG. 4. Percentage conversion of PMMA at 300° C, average curves: I, 20 mg; II, 40 mg. Standard deviations are indicated.

FIG. 5. Degradation of PMMA at 300° C, initial parts only: I, 20 mg; II, 40 mg. Average curves, standard deviations are indicated.

A number of degradation experiments with 20-mg samples was carried out at various temperatures in addition to the runs at 300° C. These are shown in Figs. 5 to 9. The curves again represent average values of several runs. The vertical lines indicate standard deviations.

A number of average values and their standard deviations are given in Table I.

It is seen that satisfactory results are obtained with this apparatus.

There is some uncertainty in the recordings for the very initial parts of the process. Some vibrations are set up when the reaction vessel on being lowered comes into contact with the liquid, but these persist only for 1 or 2 seconds. Sometimes there is also a small jump in the recorded curves on immersion, making the actual pressure values somewhat uncertain. However, the main interest as far as a kinetic analysis is concerned lies in the rates of degradation (slopes) as a function of conversion and not in the actual pressure or mole values. Figure 10 shows plots of the rate of gas production as a function of the moles of gas produced at 300° C (20-mg samples). It is apparent that two different reactions take place.

DISCUSSION

The purpose of this paper is not to present a kinetic analysis but only to give an evaluation of the performance of the apparatus. The experiments show that satisfactory accuracy can be obtained. At higher temperatures, where the reaction is very fast, the

Can. J. Chem. Downloaded from www.nrcresearchpress.com by 210.87.254.6 on 09/05/12
For personal use only.

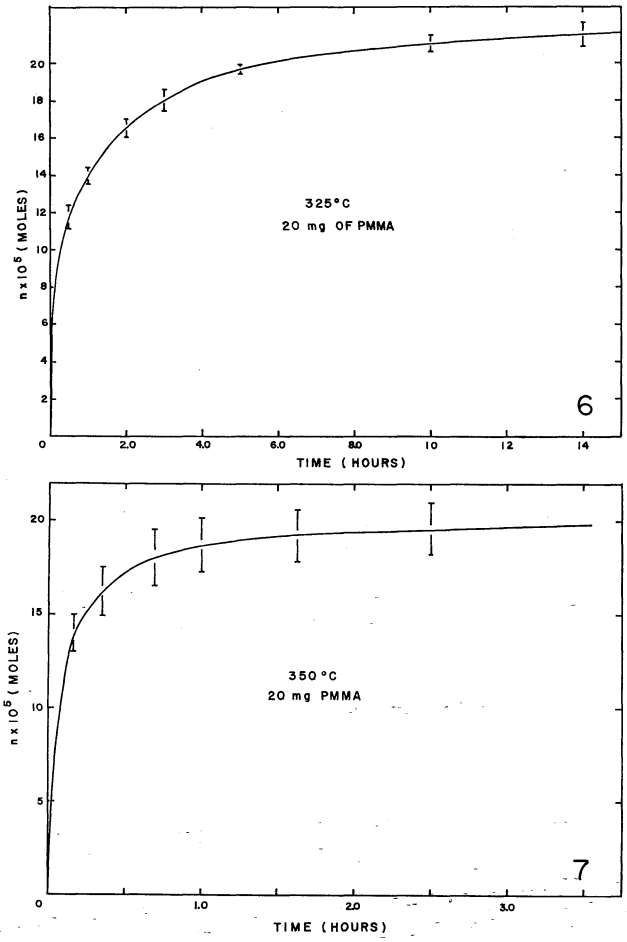

FIG. 6. Degradation of PMMA at 325° C. Average curve, standard deviations are indicated, 20 mg.
FIG. 7. Degradation of PMMA at 350° C. Average curve, standard deviations are indicated, 20 mg.

reproducibility decreases, as is to be expected. The heating period alone at such temperatures represents a large portion of the total reaction time. However, even for experiments at 400° C useful results can be obtained if a sufficiently large number of runs are carried out.

A few observations may be made relating to work on polymethylmethacrylate by other workers. Grassie and Melville (2) were the first to establish that a chain reaction, a depolymerization process, takes place. Jellinek (6), on the basis of their kinetic data, pointed out that two reactions occur simultaneously. Brockhaus and Jenckel (4) extended the work to higher temperatures and showed clearly that two reactions are involved. Madorsky (3) gave extensive analytical data on the products of the degradation. Bywater (7) studied the thermal degradation using mainly emulsion polymerizates.

Brockhaus and Jenckel (4) carried their experiments up to 350° C, but their minimum time for reaching temperature equilibrium was about 5 minutes; thus, about 60% of the polymer was degraded before the equilibrium was reached at 350° C. They give no indications as to the accuracy of their experiments. For our experiments, the heating

Can. J. Chem. Downloaded from www.nrcresearchpress.com by 210.87.254.6 on 09/05/12
For personal use only.

Can. J. Chem. Downloaded from www.nrcresearchpress.com by 210.87.254.6 on 09/05/12
For personal use only.

TABLE I
Arithmetic mean values of gas moles produced and standard deviations at various times and temperatures (20-mg films)

300° C (4 runs)			325° C (5 runs, including 1 up to 1 hr, 1 up to 3 hr, and 1 up to 5 hr)			350° C (5 runs, including 1 up to 10 min)			375° C (4 runs, including 1 up to 2 min)			400° C (10 runs)		
Time	Arithmetic mean $\times 10^5$	Standard deviation $\times 10^5$	Time	Arithmetic mean $\times 10^5$	Standard deviation $\times 10^5$	Time	Arithmetic mean $\times 10^5$	Standard deviation $\times 10^5$	Time	Arithmetic mean $\times 10^5$	Standard deviation $\times 10^5$	Time	Arithmetic mean $\times 10^5$	Standard deviation $\times 10^5$
30 sec	2.9	±0.36	30 sec	4.50	±0.65	30 sec	4.3	±1.02	30 sec	8.6	±1.02	30 sec	12.8	±2.92
1 min	3.6	0.40	1 min	6.0	0.63	1 min	5.5	0.95	1 min	12.4	1.16	40 "	15.1	2.76
2 "	4.7	0.81	2 "	6.8	0.61	3 "	8.6	1.01	1.5 "	14.4	1.33	50 "	16.7	2.54
30 "	6.6	0.70	5 "	7.9	0.62	5 "	10.8	0.88	2 "	16.0	1.30	70 "	18.5	1.97
1 hr	7.5	0.58	30 "	11.8	0.67	10 "	14.0	1.01	2.5 "	17.7	0.85	90 "	19.7	1.74
3 "	9.5	0.14	1 hr	14.3	0.52	20 "	16.2	1.29	3 "	18.4	0.86			
6 "	11.3	0.47	2 "	16.5	0.49	40 "	18.0	1.54						
15 "	13.9	0.58	3 "	17.8	0.65	1 hr	18.7	1.45						
			5 "	19.6	0.19									
			10 "	21.0	0.45									
			14 "	21.5	0.69									

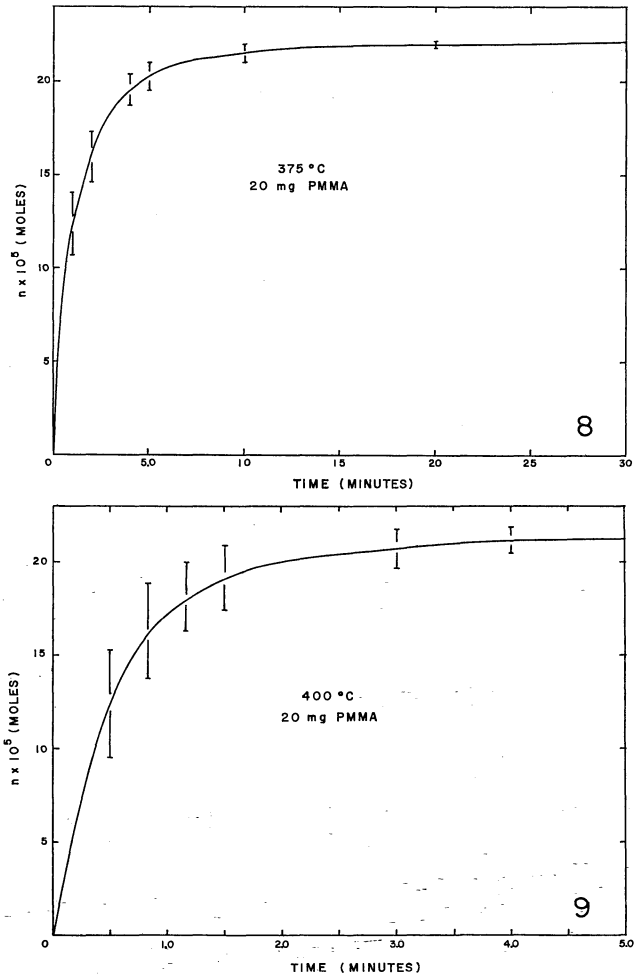

FIG. 8. Degradation of PMMA at 375° C. Average curve, standard deviations are indicated, 20 mg.
FIG. 9. Degradation of PMMA at 400° C. Average curve, standard deviations are indicated, 20 mg.

period was only 30 seconds and useful results could still be obtained at 400° C. These authors also ascertained, as already pointed out, that the rate of degradation is a function of monomer pressure in the system. Our experiments show a similar behavior.

As already mentioned, two degradation reactions take place simultaneously (see Fig. 10). Polymer, prepared under conditions as used in this work, consists of chains of which 50% have double bonds at the ends whereas the other 50% have only single bonds. Brockhaus and Jenckel (4) concluded from their experiments that one depolymerization process was operative which initiated at the double-bond chain ends and another slower one initiated at random in the chains. Gordon (8), however, fitted Brockhaus and Jenckel's results by assuming that both processes are initiated at chain ends, the double-bond chain ends having a rate constant of initiation greater than that for the initiation at the single-bond chain ends. Our results also clearly show that two reactions are operative.

Work concerning the kinetics of degradation of polymethylmethacrylate is in progress and will be published in due course.

Can. J. Chem. Downloaded from www.nrcresearchpress.com by 210.87.254.6 on 09/05/12
For personal use only.

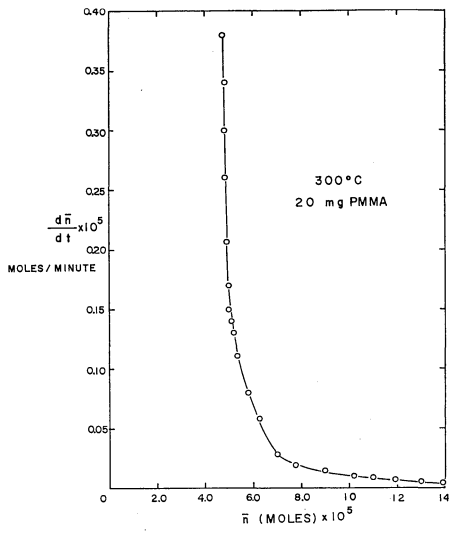

FIG. 10. Rate of monomer production against conversion for PMMA at 300° C, derived from average curve.

ACKNOWLEDGMENT

Thanks are due to the National Research Council of Canada for a grant, which made this work possible.

REFERENCES

1. H. H. G. JELLINEK. Pure Appl. Chem. **4**, 419 (1962).
2. N. GRASSIE and H. W. MELVILLE. Proc. Roy. Soc. (London), Ser. A, **199**, 1, 14, 24, 39 (1949).
3. S. L. MADORSKY. J. Polymer Sci. **11**, 491 (1953).
4. A. BROCKHAUS and E. JENCKEL. Makromol. Chem. **18/19**, 262 (1956).
5. E. H. RIDDLE. Monomeric acrylic esters. Reinhold Publ. Co., New York. 1954. p. 15 ff.
6. H. H. G. JELLINEK. Degradation of vinyl polymers. Academic Press Inc., New York. 1955. pp. 74–76.
7. S. BYWATER. J. Phys. Chem. **57**, 879 (1953).
8. M. GORDON. J. Phys. Chem. **64**, 19 (1960).

Can. J. Chem. Downloaded from www.nrcresearchpress.com by 210.87.254.6 on 09/05/12
For personal use only.

INTRAMOLECULAR HYDROGEN BONDING AND THE ANHARMONICITY OF THE NH_2 STRETCHING VIBRATIONS IN SUBSTITUTED ANILINES[1]

P. J. KRUEGER
Department of Chemistry, University of Alberta, Calgary, Alberta
Received September 10, 1962

ABSTRACT

The fundamental and first overtone NH_2 stretching bands in 55 ortho-, meta-, and para-substituted anilines, measured in dilute carbon tetrachloride solution, have been compared. For all ortho-substituted compounds (except *o*-alkyl, *o*-$COCH_3$, and *o*-$COOCH_2CH_3$) splitting of the symmetric band is observed in the first overtone region. On the basis of unusually low mechanical anharmonicity the high-frequency component is assigned to a vibration arising in an intramolecularly bonded NH_2 group. The mechanical anharmonicity of the "free" NH_2 group is found to be more dependent on the electronic nature of meta and para substituents for the symmetric mode than for the asymmetric mode, with minor changes on ortho substitution. The relative electrical anharmonicities for both modes have been estimated from changes in the ratio of the integrated intensity of the fundamental band to that of the first overtone band. For the asymmetric mode the electrical anharmonicity is independent of the electronic nature of the substituents, but depends on their ring position. For the symmetric mode the electrical anharmonicity decreases as charge separation increases in the molecule, with no significant difference for ortho-substituted compounds. These results are in qualitative agreement with a mechanism previously proposed for these vibrations.

INTRODUCTION

In several previous publications (1, 2) we have investigated the effect of ring substituents on the fundamental NH_2 stretching frequencies, half intensity band widths, and integrated absorption intensities in anilines, as measured in dilute carbon tetrachloride solution. Correlations with the Hammett (3) and Taft (4, pp. 618 ff.) substituent constants were established, and the systematic deviation of ortho-substituted anilines could be interpreted in terms of a vibrational mechanism taking into account the direction of the transition moment, the extent of nitrogen lone pair and aromatic π-electron participation, and the direct field effect of the ortho substituent for each of the two vibrational modes (5).

In an attempt to get a more complete understanding of the vibrational behavior of this group, its anharmonic nature has now been investigated. This paper reports a comparative study of the available data for the fundamental vibrations (5) and the measurements in the first overtone region recently published by Whetsel (6). Additional measurements in the overtone region on selected compounds are presented. Due to extensive overlapping of bands in the overtone region only the peak frequencies and the peak molar absorptivities instead of the integrated intensities can be obtained.

EXPERIMENTAL METHOD

The methods used to obtain the experimental data on the fundamental bands have already been described (5).

The additional overtone data required were obtained with a Beckman DK-1A spectrophotometer with a linear absorbance attachment, operating with a slit height of 13 mm, and at a scanning speed of 50 mμ/min. A pair of matched cylindrical 10-cm fused quartz cells were used to keep the amine concentrations down to below 0.07 *M*. Recent cryoscopic measurements by Rao and co-workers (7) show that theoretical molecular weights are obtained for aniline in carbon tetrachloride solution up to concentrations as high as 0.075 *M*, so that intermolecular hydrogen bonding can be neglected. Slit widths of about 5–8 cm^{-1} were obtained under the operating conditions.

Commercial carbon tetrachloride of spectroscopic quality was used, and all solutions were made up volumetrically and used immediately. The data reported represent averages obtained from at least two

[1]*Presented at the 45th Annual Conference of the Chemical Institute of Canada, Edmonton, May 28-30, 1962.*

Can. J. Chem. Downloaded from www.nrcresearchpress.com by 210.87.254.42 on 09/05/12
For personal use only.

solutions which were prepared independently, except for a few cases where the limited amount of material precluded this. Scale expansion was employed for the spectra of a few difficultly soluble amines. The amines were largely the same samples used in previous work in this laboratory.

Following the method of Whetsel (6), background corrections were applied to all spectra by drawing a line between the low absorbance levels at 1590 and 1415 mμ. Peak molar absorptivities in liter mole^{-1}cm^{-1} were calculated from the expression

$$\epsilon_{02} = a/cx,$$

where a is the corrected absorbance, c is the concentration in moles/liter, and x is the pathlength in cm.

The wavelength scale of the instrument was checked against mercury emission lines, and trial measurements of wavelength and absorbance on selected amines showed that good agreement with the results of Whetsel (6) could be obtained.

To obtain an estimate of the absorption intensity of the minor band component in those cases where band splitting occurred, the major component was reflected about an ordinate through the absorption maximum, and the image subtracted from the observed curve. Where the two components were of comparable intensity, the corrected peak absorbances were used directly to estimate the percentage of intramolecularly bonded molecules.

RESULTS AND DISCUSSION

Figure 1 shows some typical first overtone amine spectra in dilute carbon tetrachloride solution. The numerical data are summarized in Table I. As a first approximation the

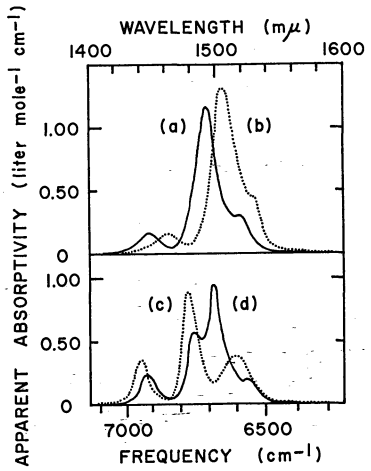

FIG. 1. Near-infrared spectra of some primary aromatic amines in dilute CCl_4 solution (~0.06 M) in 10-cm cells: (*a*) aniline, (*b*) N,N-dimethyl-*p*-phenylenediamine, (*c*) ethyl anthranilate, (*d*) *o*-iodoaniline.

substituent constant scale ($\sum\sigma$) was employed to relate the total electronic effect of the aromatic ring substituents on the NH_2 group (5).

The Band at 6580 cm^{-1}

All of the anilines examined have a relatively weak absorption band at about 6580±20 cm^{-1}, regardless of the substitution type. In *o*-trifluoromethylaniline this band was observed as high as 6645 cm^{-1}. This is probably a combination band.

Amino Group Stretching Frequencies

The overtone frequencies for both NH_2 stretching modes for meta- and para-substituted anilines increase smoothly as the electron-withdrawing character of the ring substituents increases, as shown in Figs. 2 and 3. The basis for these shifts has already been discussed in connection with the corresponding fundamental bands (5). The complex deviation of the frequency data for ortho-substituted compounds is a reflection of factors such as changes in the HNH bond angle, the effective charge on the N atom, and the mechanical anharmonicity on ortho substitution.

Can. J. Chem. Downloaded from www.nrcresearchpress.com by 210.87.254.42 on 09/05/12
For personal use only.

Can. J. Chem. Downloaded from www.nrcresearchpress.com by 210.87.254.42 on 09/05/12
For personal use only.

TABLE I

First overtone NH_2 absorption data for substituted anilines (CCl_4 solution)
(Symmetric ϵ_{02} values refer to molecules with "free" amino groups)

			Asymmetric vibration				Symmetric vibration					
No.*	Substituent(s)	$\Sigma\sigma$†	ν_{01} (cm^{-1})	ν_{02} (cm^{-1})	$x_e\times10^2$	$A_{01}/\epsilon_{02}\times10^{-6}$ (cm^2/liter, $\log_e$)	ν_{01} (cm^{-1})	ν_{02} (cm^{-1})	$x_e\times10^2$	$A_{01}/\epsilon_{02}\times10^{-6}$ (cm^2/liter, $\log_e$)	Doublet separation (cm^{-1})	Percent amine bonded
1	4-$N(CH_3)_2$	−0.83	3456.5	6842	1.01	14.2	3379.5	6643	1.66	1.25		
3	4-NH_2	−0.66	3453	6849	0.81	13.2	3377	6656	1.41	1.32		
4	2-NH_2	(−0.7)‡	3437.5	6821	0.77	11.7	3351.5	6579	1.80	1.21	98	38
								6677	0.38			
5	2,4,6-Tri-$C(CH_3)_3$	−(0.6)‡	3517.5	(6973)	0.86	34.3	3442.5	6767	1.66	1.44	(0)	0
6	2,4,6-Tri-CH_3	−0.51§	3479.5	6910	0.69	15.5	3399.5	6701	1.41	1.33	(0)	0
7	2,4,6-Tri-$CH(CH_3)_2$	−0.45‡	3481.5	6891	1.01	16.0	3405	6689	1.72	1.00	(0)	0
8	2-OCH_3	−0.39§	3487	6916	0.82	27.0	3396	6697	1.36	2.41	46	6
								6743	0.71			
9	2-OCH_2CH_3	−0.35§	3486	6912	0.85	26.9	3396	6696	1.37	2.41	47	6
								6743	0.71			
10	2,6-Di-CH_3	−0.34§	3487.5	6912	0.85	13.9	3405	6701	1.52	1.63	(0)	0
11	2,5-Di-$C(CH_3)_3$	(−0.3)‡	3493.5	—	—	—	3402	6678	1.79	1.02	76	(33)?
								(6754)	0.72			
12	2,5-Di-OCH_3	−0.27§	3492.5	6921	0.90	24.1	3399	6700	1.40	2.37	46	8
								6746	0.75			
13	4-OCH_3	−0.268	3460	6862	0.82	16.7	3382	6667	1.39	1.58		
14	4-OCH_2CH_3	−0.24	3459	6861	0.81	15.7	3381	6657	1.51	1.50		
16	2,5-Di-OCH_2CH_3	−0.20§	3492	6919	0.91	27.2	3399	6699	1.41	2.94	46	7
								6745	0.76			
17	2-$C(CH_3)_3$	(−0.2)‡	3496.5	6927	0.93	13.4	3404	6694	1.62	1.25	81	(22)?
								6775	0.57			
18	4-$C(CH_3)_3$	−0.197	3474	6879	0.97	15.5	3391.5	6673	1.57	1.74		
19	2-CH_3	−0.17§	3482.5	6900	0.90	15.8	3398	6697	1.42	1.81	(0)	0
20	4-CH_3	−0.170	3471	6883	0.81	15.6	3389.5	6684	1.38	1.82		
21	4-$CH(CH_3)_2$	−0.151	3474	6893	0.78	13.7	3392.5	6686	1.42	1.78		
22	2-$CH(CH_3)_2$	(−0.15)	3481	6892	0.99	14.8	3397.5	6686	1.55	1.63	(0)	0
24	4-C_6H_5	−0.01	3485.5	6909	0.82	13.1	3399	6701	1.36	2.53		
25	2-C_6H_5	(−0.01)‡	3483.5	6890	1.13	26.5	3394.5	6675	1.64	2.56	33	10
								6708	1.17			
26	H	0	3481	6900	0.82	17.8	3395.5	6696	1.37	2.35		
31	3-OCH_2CH_3	+0.1	3482	6906	0.82	17.8	3397	6701	1.33	2.45		
32	3-OCH_3	+0.115	3483	6911	0.78	17.2	3398	6700	1.37	2.76		
33	4-I	+0.18	3490	6926	0.76	14.1	3402	6712	1.32	2.82		
34	2-Cl	+0.20§	3494	6933	0.77	20.9	3401	6707	1.36	3.14	69	15
								6776	0.38			
35	2-Br	+0.21§	3491	6925	0.80	20.3	3397	6695	1.42	3.04	53	15
								6748	0.66			

Can. J. Chem. Downloaded from www.nrcresearchpress.com by 210.87.254.42 on 09/05/12
For personal use only.

TABLE I (*Concluded*)

No.*	Substituent(s)	$\Sigma\sigma$†	Asymmetric vibration				Symmetric vibration					
			ν_{01} (cm^{-1})	ν_{02} (cm^{-1})	$x_e \times 10^2$	$A_{01}/\epsilon_{02} \times 10^{-6}$ (cm^2/liter, $\log_e$)	ν_{01} (cm^{-1})	ν_{02} (cm^{-1})	$x_e \times 10^2$	$A_{01}/\epsilon_{02} \times 10^{-6}$ (cm^2/liter, $\log_e$)	Doublet separation (cm^{-1})	Percent amine bonded
36	2-I	+0.21§	3485	6930	0.57	18.5	3387.5	6685	1.29	2.60	67	25
								6752	0.34			
37	4-Cl	+0.227	3482	6910	0.76	18.3	3398	6706	1.29	2.95		
38	4-Br	+0.232	3485	6919	0.72	15.3	3399	6707	1.30	3.13		
39	2-F	+0.24§	3493.5	6919	0.95	19.5	3404	6699	1.55	2.80	52	7
								6751	0.68			
40	3-F	+0.337	3492	6936	0.68	20.5	3405	6719	1.30	3.58		
41	3-Cl	+0.373	3490	6923	0.80	17.3	3402	6713	1.30	3.14		
42	3-$COCH_3$	+0.376	3486	6920	0.73	19.1	3400	6709	1.30	3.43		
43	3-Br	+0.391	3492.5	6924	0.86	15.3	3404	6714	1.34	2.89		
44	2,4-Di-Cl	+0.43§	3496	6938	0.76	19.0	3402	6708	1.37	3.21	58	17
								6766	0.55			
45	3-CF_3	+0.43	3492	6930	0.76	19.1	3404	6720	1.26	3.59		
46	4-SCN	+0.52	3500	6942	0.82	15.8	3410	6730	1.29	4.56		
47	2-CF_3	(+0.54)‡	3515.5	6976	0.77	18.4	3426	6752	1.42	4.11	67	13
								6819	0.48			
49	2,4,6-Tri-Cl	+0.63§	3503	6960	0.65	19.5	3404	6722	1.23	4.35	58	15
								6780	0.41			
52	2,4,6-Tri-Br	+0.65§	3492	6927	0.80	19.2	3394	6688	1.43	4.02	61	13
								6749	0.57			
53	4-$COOCH_2CH_3$	+0.678‖	3500	6943	0.80	14.0	3408	6721	1.36	4.28		
54	2-$COOCH_2CH_3$	(+0.68)‡	3506	6944	0.95	25.8	3378	No free band				100
								6765	−0.13	10.64	(0)	
55	3-NO_2	+0.710	3497	6938	0.79	17.6	3407	6725	1.27	4.19		
56	4-$COCH_3$	+0.874‖	3502	6947	0.80	13.4	3410	6732	1.26	4.07		
57	2-$COCH_3$	(+0.9)‡	3502.5	6939	0.92	16.3	3345	No free band			(0)	100
								6764	−1.13	8.81		
58	4-CN	+1.00‖	3505	6956	0.76	16.1	3412	6738	1.23	5.31		
60	2-NO_2	+1.22§	3522	6986	0.81	21.5	3500	6690	1.57	3.48	106	56
								6796	0.06			
61	4-NO_2	+1.27‖	3509	6964	0.76	10.3	3416	6743	1.27	5.84		
62	2,6-Di-Cl-4-NO_2	+1.67§‖	3519	6991	0.66	17.4	3412	6736	1.26	7.00	61	24
								6797	0.39			
63	2,6-Di-NO_2	+2.44§	3478	6915	0.58	56.2	3362	6624	1.44	5.01	53	43
								6677	0.69			
64	2,4-Di-NO_2	+2.49§‖	3520	6993	0.66	—¶	3395	6679	1.58	—¶	120	—
								6799	−0.13			

*Compounds are numbered as in the earlier study on the fundamental bands (5).
†Unless otherwise indicated the values used are from the critical analysis of Hammett substituent constants by McDaniel and Brown (8).
‡Estimated on the basis that $\sigma_{ortho} \simeq \sigma_{para}$.
§Involving σ_{ortho} values according to Taft (4, pp. 618 ff.).
‖Involving special Hammett substituent constants for anilines according to Jaffe (9).
¶Compound extremely insoluble in CCl_4.

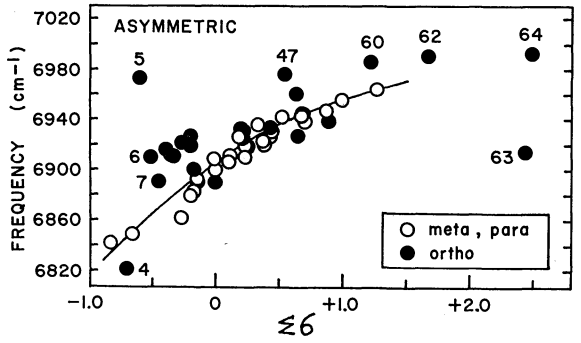

FIG. 2. The dependence of the first overtone asymmetric NH_2 stretching frequencies in anilines on the electronic nature of the substituents.

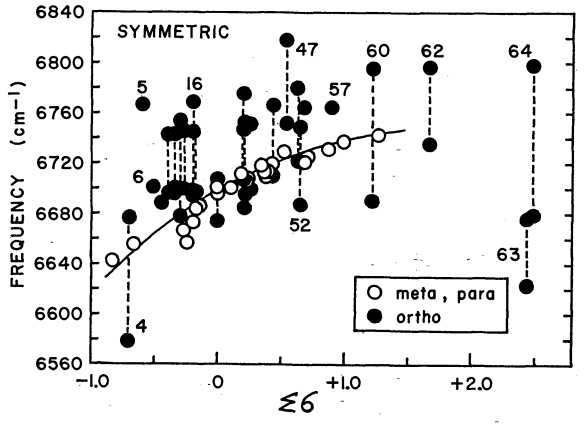

FIG. 3. The dependence of the first overtone symmetric NH_2 stretching frequencies in anilines on the electronic nature of the substituents. Vertical tie lines join the frequency of the intramolecularly bonded species (top point) to that of the free species (bottom point).

A further complication is introduced into the symmetric overtone frequencies by a splitting of the absorption band into two components, which appears to be quite general on ortho substitution. Exceptions are *o*-aminoacetophenone, ethyl anthranilate, and the *o*-alkyl anilines. Whetsel *et al.* (10) have previously pointed out such splitting for three ortho-substituted anilines, and assigned the high-frequency bands to free NH_2 groups and the low-frequency components to NH_2 groups bonded to ortho substitution. Both components of the symmetric band, joined by tie lines, are shown in Fig. 3 for those cases where the splitting permitted the evaluation of two frequencies. In some cases only distinct shoulders were observed on the high-frequency side of the main symmetric band, and graphical resolution was employed.

Mechanical anharmonicity calculations suggest that the *high*-frequency component of this symmetric doublet is due to bonded NH_2 groups, whereas the low-frequency component arises from free NH_2 groups in an equilibrium of the type

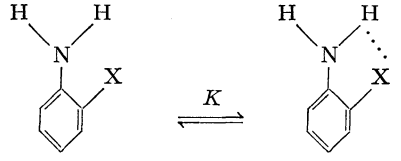

[1]

Can. J. Chem. Downloaded from www.nrcresearchpress.com by 210.87.254.42 on 09/05/12
For personal use only.

This concept rationalizes the anomalous overtone spectra of ortho-substituted anilines with respect to the meta- and para-substituted derivatives. It is supported by temperature studies, deuteration shifts, and the expected solvent dependence.*

The absence of splitting in the fundamental symmetric NH_2 band must mean that the hydrogen bonding interaction is too weak to be observed, except in the overtones. Sheppard (12) has concluded that the vibrational amplitude is an important factor in hydrogen bonded XH vibrations. Both the increase in the equilibrium NH bond lengths and in the vibrational amplitudes for the overtone vibrations would favor stronger interaction than for the fundamental vibrations. It is known that the overtones are in general more sensitive to interaction effects than the fundamental vibrations. Moritz (13) has shown that the asymmetric NH_2 stretching vibration is relatively insensitive to the effects of intramolecular hydrogen bonding involving only one proton, and the recent work of Wolff and Staschewski (14) shows that this is also true for intermolecular hydrogen bonding of primary amines.

Mechanical Anharmonicity

It is well known that the mechanical harmonic oscillator, characterized by a parabolic potential function, is only a useful approximation for very small displacements of the nuclei from the equilibrium position (r_e). As a better approximation cubic, quartic, and higher terms must be introduced (15, pp. 90–92) to give a potential function of the form

$$U = f(r-r_e)^2 - g(r-r_e)^3 + h(r-r_e)^4 + \ldots \quad [2]$$

where $h \ll g \ll f$. The vibrating motion, although still strictly periodic, will no longer have a pure sine form for any amplitude. For a diatomic anharmonic oscillator, the frequencies of the fundamental (ν_{01}) and the first overtone vibration (ν_{02}) lead directly to the mechanical anharmonicity (x_e) for the vibration if cubic and higher terms are neglected, from the expressions (15, pp. 94–96)

$$\nu_{01} = \omega_e(1-2x_e) \quad [3]$$

$$\nu_{02} = 2\omega_e(1-3x_e), \quad [4]$$

where ω_e is the mechanical frequency of the oscillator for very small displacements if anharmonicity could be neglected.

These expressions were applied directly to the experimental data to get the mechanical anharmonicity for the two complex NH_2 vibrational modes. The results are tabulated in Table I, and presented as a function of $\sum\sigma$ in Fig. 4. For ortho-substituted anilines with a split symmetric band, each of the ν_{02} frequencies was coupled with the corresponding ν_{01} band to get two x_e values. The mechanical anharmonicities were found to be normal for the low-frequency component, but unusually low for the high-frequency component. Pimentel and McClellan (16) have summarized the available information concerning the mechanical anharmonicity of XH stretching vibrations involved in hydrogen bonding, and conclude that it may be unusually low. On this basis the high-frequency component is assigned to a vibration arising in an intramolecularly bonded NH_2 group. For very strongly bonded systems negative x_e values have been reported (17). Our work agrees with this, since negative x_e values were found for the single sharp symmetric overtone peak observed for ethyl anthranilate and *o*-aminoacetophenone. Only bonded NH_2

**After this work was completed, Moritz (11) demonstrated that the spectra of monodeuterated ortho-substituted anilines can be interpreted in terms of cis–trans isomerism of the* NHD *group and the relative strengths of intramolecular hydrogen and deuterium bonds.*

Can. J. Chem. Downloaded from www.nrcresearchpress.com by 210.87.254.42 on 09/05/12
For personal use only.

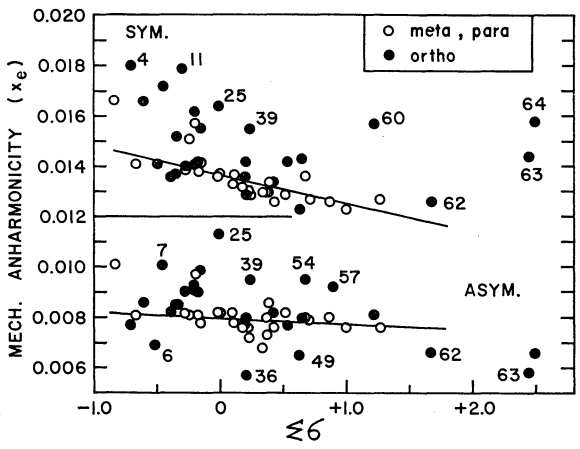

FIG. 4. The mechanical anharmonicity of the NH_2 stretching vibrations and the effect of substituents. The anharmonicities for the intramolecularly bonded species are not shown in this graph.

groups would be expected due to the favorable N—H · · · O distance, and the geometry of the six-membered chelate ring. A negative x_e value was also found for the high-frequency component of the doublet in 2,4-dinitroaniline.

The existence of a "free" form in equilibrium [1] probably implies a certain amount of torsional motion of the NH_2 group, this being one way in which the H atom can get away from the adjacent X group.

The mechanical anharmonicity for the symmetric mode of the "free" NH_2 group exceeds that for the asymmetric mode (average of approximately 0.014 as opposed to 0.008). The slight decrease of x_e with increasing electron-withdrawing power of substituent groups in meta- and para-substituted anilines is most pronounced for the symmetric mode. Ortho substitution introduces no systematic deviation of x_e for the asymmetric mode, but the corresponding values for the symmetric vibration of the "free" NH_2 group appear to be somewhat enhanced (Fig. 4).

Temperature Studies

The intensity ratio of the symmetric doublet was found to be temperature independent, within experimental error, over the range 0–60° C for *o*-nitroaniline, *o*-iodoaniline, and *o*-phenylenediamine, and no "free" band could be induced in ethyl anthranilate by raising the temperature to 60° C. We believe this does not contradict the intramolecular equilibrium proposed since the N · · · X distance is fixed. With the amino group oriented so that nitrogen lone pair – π electron overlap is favored, rotation of 180° about the C—N bond, if permissible in hydrogen-bonded systems like this, brings the other H atom into the interacting position. This is unlike the "free" trans $\rightleftharpoons$ "bonded" cis equilibrium observed in the infrared spectra of ortho-substituted phenols, where temperature dependence is observed (18).

Deuteration Shifts

Since the possibility of an accidental resonance between the overtone symmetric NH_2 vibration and some other vibration of the aniline molecule could not be overlooked, a sample of N,N-dideutero-*o*-nitroaniline, prepared by repeated equilibrium with methanol-*d*, was examined. The asymmetric band was found at 5263 cm^{-1}, and the symmetric doublet at 5072 cm^{-1} ("bonded") and 5039 cm^{-1} ("free"). The intensity ratio

Can. J. Chem. Downloaded from www.nrcresearchpress.com by 210.87.254.42 on 09/05/12
For personal use only.

of the doublet was identical with that found in ordinary *o*-nitroaniline. The deuteration shifts (ν_H/ν_D) are 1.33, 1.34, and 1.33 respectively. These are in agreement with the corresponding shifts observed for OH/OD stretching vibrations in a large number of monomeric, dimeric, and polymeric hydroxylic compounds (16), where no systematic difference from the normal ν_H/ν_D value could be detected for bonded species.

Equilibrium Constants

By making the assumption that the symmetric molar extinction coefficient of an intramolecularly bonded NH_2 group is the same as that for a free NH_2 group,* the percentage of bonded NH_2 groups was estimated for all ortho-substituted compounds. These values are listed in Table I. They range from zero for ortho-alkyl anilines to 56% in *o*-nitroaniline to 100% in ethyl anthranilate and *o*-aminoacetophenone. The lower stability of five-membered chelate rings is readily apparent.

These results indicate that it is difficult for both H atoms of the NH_2 group to hydrogen-bond simultaneously to acceptor atoms (or groups) in the 2,6-positions. Thus in *o*-chloroaniline the percentage of bonded molecules (15%) is the same as it is in 2,4,6-trichloroaniline (15%), whereas in 2,6-dichloro-4-nitroaniline it is increased slightly (24%) due to the strongly electron-withdrawing character of the nitro group in the para position, which increases the HNH angle and brings the H atom closer to the adjacent substituent. In *o*-bromoaniline the percentage of bonded molecules (15%) is also the same as in 2,4,6-tribromoaniline (15%). Since the method used to obtain these values is relatively crude, even in *o*-nitroaniline and 2,6-dinitroaniline the percentage of bonded molecules must be considered to be approximately equal (56% and 43% respectively).

For ortho-halo anilines the order of increased bonding appears to be $F < Cl \approx Br < I$, which agrees with the order of increasing apparent HNH angle calculated for these compounds from the fundamental NH_2 stretching frequencies (5). The low bonding ability of fluorine, the most electronegative element, must be related to the fixed NH $\cdots$ X separation in the intramolecular hydrogen bond. For *o*-fluorophenol n.m.r. evidence (20) indicates that the proton–fluorine separation in the cis isomer is too great for hydrogen bond formation.

Using probable bond lengths and angles, the H$\cdots$X and N$\cdots$X distances can be estimated and compared with covalent atomic radii (Table II). The difference between the H$\cdots$X distance and the sum of the covalent radii for the H and X atoms decreases as the size of the halogen increases. The N$\cdots$X distance is considerably less than the limiting N—H$\cdots$N distance (3.5 Å) and the limiting N—H$\cdots$O distance (3.4 Å), where intermolecular hydrogen bonding has been estimated to vanish (16, pp. 285–293). The hydrogen atom is appreciably off the N$\cdots$X axis, but hydrogen bonding in non-linear systems is well known (16, pp. 304–305).

Frequency Shifts on H-Bond Interaction

The separation between the symmetric band doublet (in those cases where the presence of distinct bands could be established) ranges from 33 cm^{-1} in *o*-aminodiphenyl to 120 cm^{-1} in 2,4-dinitroaniline. Since it is not valid in this case to assume that this frequency displacement is a direct measure of the strength of the hydrogen bond because the NH$\cdots$X distance is fixed by the system, no direct correlation exists with the proportion of the bonded species present.

**This is not unreasonable, since it has been argued (19) that in relatively weak bent intramolecular hydrogen bonds involving five-membered rings the electrostatic interaction is most important, whereas the charge-transfer effects, which are responsible for large intensity increases, are only of secondary importance where the acceptor atom is halogen, oxygen, or nitrogen.*

Can. J. Chem. Downloaded from www.nrcresearchpress.com by 210.87.254.42 on 09/05/12
For personal use only.

TABLE II

Estimated molecular geometry for *o*-haloanilines

Dimensions (Å)	F	Cl	Br	I
(*a*) H · · · X distance	2.46	2.53	2.57	2.63
(*b*) Sum of covalent radii for H and X	1.09	1.36	1.51	1.70
(*a*) − (*b*)	1.37	1.17	1.06	0.93
N · · · X distance	2.73	2.94	3.03	3.15
Data used in the above calculations:				
C—X distance	1.30	1.70	1.85	2.05
Covalent radius of X	0.72	0.99	1.14	1.33

Aromatic C—C distance: 1.395 Å
C—N distance: 1.43
N—H distance: 1.02
Covalent radius of H: 0.37
HNH angles were taken from Table I of ref. 5

Solvent Dependence

Whetsel (6) has observed that in *o*-nitroaniline and *o*-methylsulphonylaniline, where the symmetric band is split into two well-defined components, the high-frequency component falls at nearly the same position in both CCl_4 and $CHCl_3$, but the low-frequency component shifts toward higher frequencies by 10 to 25 cm^{-1} in $CHCl_3$. Our measurements confirm this for a large number of ortho-substituted anilines. Because the CH band of chloroform at 1409 mμ (7097 cm^{-1}) shifts to lower frequencies in the presence of amines Whetsel has interpreted the bonding to the solvent to be of the type

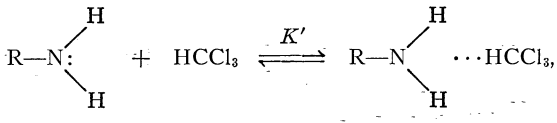

[5]

in agreement with our earlier suggestion based on other spectroscopic evidence (1). Equilibrium [5] appears to be important only in those aniline molecules in which one of the H atoms is not already bonded to an ortho substituent. The partial shift of lone-pair electrons away from the N atom when the amine becomes bonded to $CHCl_3$ increases the electronegativity of the N atom, and the hydrogen atoms of the amino group are bound more firmly, thus raising the overtone symmetric frequency (low-frequency component). In the intramolecularly bonded molecules the apparent HNH angle opening must be accompanied by charge delocalization from the N atom, decreasing the basicity and hindering complex formation with $CHCl_3$. This is not in agreement with the suggestion of Farmer and Thompson (21) that negative charge is induced on the N atom on hydrogen bond formation.

The results of Whetsel show further that for *o*-methylsulphonylaniline the percentage of intramolecularly bonded molecules decreases in $CHCl_3$. This can be understood in terms of the competition between equilibria [5] and [1].

For ethyl anthranilate, where all molecules are held to be intramolecularly bonded, no pronounced frequency shift for the symmetric singlet is expected on going from CCl_4 to $CHCl_3$. Experimentally a small increase in frequency (< 10 cm^{-1}) is observed, but part of this may be due to overlapping with the 6580 cm^{-1} band, which moves up to 6667 cm^{-1} in $CHCl_3$ and becomes very broad.

Can. J. Chem. Downloaded from www.nrcresearchpress.com by 210.87.254.42 on 09/05/12
For personal use only.

The o-tert-Butyl Group

Splitting of the symmetric band was observed for *o-tert*-butylaniline, 2,5-di-*tert*-butylaniline, but not for 2,4,6-tri-*tert*-butylaniline or for any of the other ortho-alkyl anilines examined. In previous work (5) enhanced HNH angles were found for all three of the above compounds. This can probably be ascribed to a steric interaction, the mechanism of which is not yet understood. It is interesting to note that Zanker and Wittwer (22) report a splitting of the asymmetric methyl CH stretching vibration in *o*-toluidine, but not in the meta and para analogues. They suggest hindered rotation of the CH_3 group as a possible cause.

Molar Absorptivities

The overtone molar absorptivities are shown in Figs. 5 and 6 as a function of $\sum\sigma$.

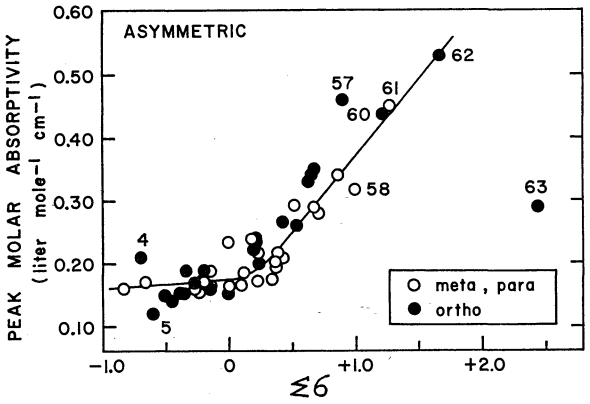

FIG. 5. The molar absorptivity of the first overtone asymmetric NH_2 stretching vibration in CCl_4 solution vs. substituent constants.

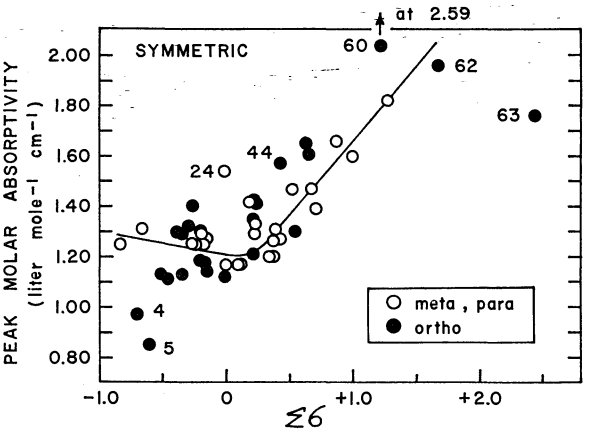

FIG. 6. The molar absorptivity of the first overtone symmetric NH_2 stretching vbiration in CCl_4 solution vs. substituent constants. The absorptivities for ortho-substituted compounds refer to the "free" NH_2 group.

Electron-withdrawing groups increase the intensities for both modes linearly for meta- and para-substituted anilines. As substituents become electron donating in character the asymmetric overtone absorptivity falls slightly, whereas the symmetric overtone absorptivity rises slightly.

Can. J. Chem. Downloaded from www.nrcresearchpress.com by 210.87.254.42 on 09/05/12
For personal use only.

For the asymmetric mode the absorptivities found for ortho-substituted anilines are in good agreement with the results for meta- and para-anilines (Fig. 5). For the symmetric mode a reasonable correlation of all the results is obtained if the observed absorptivity of the low-frequency component is corrected for the estimated percentage in the bonded form now absorbing at a different frequency (Fig. 6). This can be considered as further evidence for the assignment of the low-frequency component to the free NH_2 group.

For ethyl anthranilate and *o*-aminoacetophenone (compounds 54 and 57), which are considered to be 100% bonded, it appears that the symmetric overtone intensity is reduced on intramolecular hydrogen bond formation. Such behavior in the overtones is not unknown (16).

The principal differences in the substituent dependence of the overtone molar absorptivities in relation to the fundamental integrated intensities are:

(*a*) As substituent groups become better electron donors the A_{01} values for both modes continue to fall, whereas ϵ_{02} for the symmetric mode appears to rise slightly.

(*b*) For electron-donating groups A_{01} (asym) > A_{01} (sym), whereas for electron-withdrawing groups this inequality is reversed. For the first overtones the symmetric absorptivities are always between 3 and 6 times as great as the corresponding asymmetric absorptivities.

(*c*) Ortho substitution introduces no general differences into the $\epsilon_{02}/\sum\sigma$ correlation for both modes, provided only the molecules with free NH_2 groups are considered for the overtone measurements. In most cases (except *o*-alkyl) ortho substitution enhances A_{01} for the asymmetric mode.

Electrical Anharmonicity

An approach to the partial interpretation of the above points in terms of the vibrational mechanism previously proposed (5) can be made through the electrical anharmonicity of the vibrations. The presence of electrical anharmonicity in a diatomic molecule implies that the variation of dipole moment M with internuclear distance r as the bond vibrates is not strictly linear, but that M must be replaced by the expression

$$M = M_0+M_1r+M_2r^2+M_3r^3+\ldots \qquad [6]$$

as has been described (15, pp. 94–96).

The fundamental/overtone intensity ratio is actually governed by both the electrical and the mechanical anharmonicity of the vibration. Neglecting terms higher than quadratic in [6], Russell and Thompson (23) have shown that for a diatomic oscillator approximation with $x_e \ll 1$, both the methods of Dunham (24) and of Heaps and Herzberg (25) lead to

$$(A_{02}/A_{01}) = x_e[1-(2B/ar_e)]^2, \qquad [7]$$

where $B = M_2/M_1$, and a is the constant in the Morse potential function

$$V = D_e\{1-\exp[-a(r-r_e)]\}^2 \qquad [8]$$

with vibrational energy levels given by

$$G(v) = (v+\tfrac{1}{2})\omega_e-(v+\tfrac{1}{2})^2x_e\omega_e. \qquad [9]$$

Figures 7 and 8 show that the A_{01}/ϵ_{02} ratio is a function of the electronic effect of the substituents, and that the nature of the dependence varies for the two vibrational modes. For the symmetric mode there is no dependence on the position of the substituent(s), whereas for the asymmetric mode ortho substitution appears to play a large additional

Can. J. Chem. Downloaded from www.nrcresearchpress.com by 210.87.254.42 on 09/05/12
For personal use only.

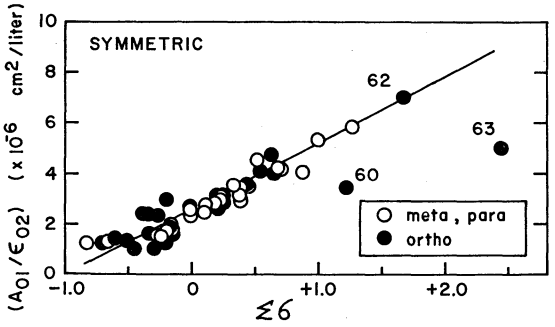

FIG. 7. The fundamental/first overtone symmetric intensity ratio for "free" NH_2 groups and its dependence on the electronic nature and position of ring substituents.

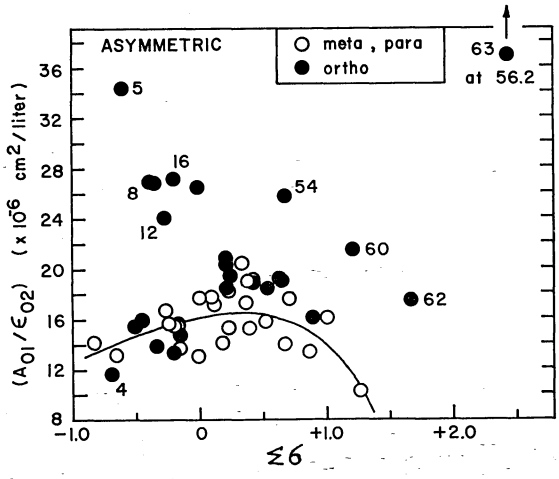

FIG. 8. The fundamental/first overtone asymmetric intensity ratio and its dependence on the electronic nature and position of ring substituents.

role in virtually all those cases where the ortho substituent(s) can accept or donate electrons through a resonance mechanism. Ortho-alkyl compounds (except 2,4,6-tri-*tert*-butyl) behave normally, as expected. The normal behavior of *o*-phenylenediamine suggests a relative orientation of the NH_2 groups so that the lone-pair orbitals would be on opposite sides of the aromatic ring. The positive deviation of the other ortho-anilines from the meta–para correlation in Fig. 8 increases approximately with the absolute value of the Taft σ_R values (4, pp. 594–597) for mono-ortho-substituted compounds. This may be connected with the reversal of sign of the dipole moment during one complete vibrational cycle in this mode.

For a series of secondary amines of widely differing type, Russell and Thompson (23) found a to be $\sim 2\times 10^8$ cm^{-1} and $r_e \sim 1$ Å. Assuming the same values for the aniline series, and letting the product ar_e be a constant as a first approximation, equation [7] becomes

$$B \approx 1-\sqrt{[(1/x_e)(A_{02}/A_{01})]}. \qquad [10]$$

By replacing (A_{02}/A_{01}) by (ϵ_{02}/A_{01}), relative values of the square root quantity were estimated from the experimental data. The results are shown graphically in Figs. 9 and

Can. J. Chem. Downloaded from www.nrcresearchpress.com by 210.87.254.42 on 09/05/12
For personal use only.

10. Since the (ϵ_{02}/A_{01}) ratios have relative significance only, a scale adjustment factor must be introduced before the square root quantity is subtracted from unity. If the same

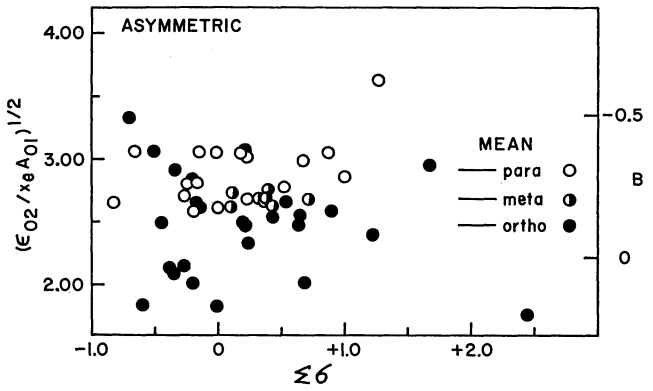

FIG. 9. The relative electrical anharmonicity for the asymmetric NH_2 stretching vibration in substituted anilines. The left-hand ordinate scale units are liter$^{1/2}$ cm^{-1} ($\times 10^3$).

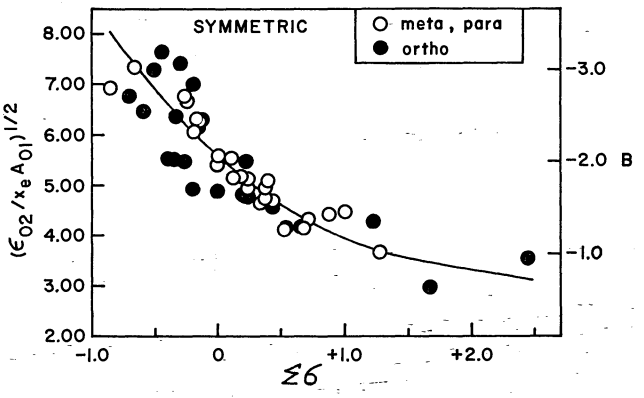

FIG. 10. The relative electrical anharmonicity for the symmetric NH_2 stretching vibration in substituted anilines. The data for ortho-substituted anilines refer to molecules with "free" NH_2 groups. The left-hand ordinate scale units are liter$^{1/2}$ cm^{-1} ($\times 10^3$).

band shape (such as a Lorentz shape) is assumed for both the fundamental and the overtone bands, the ratio

$$(A_{01}/A_{02}) \approx (\epsilon_{01}/\epsilon_{02})(\Delta\nu_{1/2}^{01}/\Delta\nu_{1/2}^{02}) \qquad [11]$$

or approximately 75 and 10 for the asymmetric and symmetric modes respectively.* This is equivalent to multiplying the left-hand ordinate scale in Fig. 9 by $\sqrt{[(15\times10^6)/75]} = 4.5\times10^2$, and the corresponding scale in Fig. 10 by $\sqrt{[(3.0\times10^6)/10]} = 5.5\times10^2$. The right-hand ordinate B scale established by this method in both diagrams is clearly a gross approximation, but the relative values should have significance.

For the asymmetric mode, B appears to be essentially independent of the nature of the substituent, but dependent on its ring position. If the positive square root is taken in [10], the mean ortho, meta, and para B values are -0.1, -0.2, and -0.3 respectively, suggesting that the quadratic term in the dipole moment expansion becomes less important

Both the symmetric and asymmetric first overtone bands have $\Delta\nu_{1/2}^{a}$ values of 80–90 cm^{-1}.

Can. J. Chem. Downloaded from www.nrcresearchpress.com by 210.87.254.42 on 09/05/12
For personal use only.

as the substituents move into a position closer to the direction of the transition moment.

For the symmetric mode a smooth correlation is found for ortho-, meta-, and para-anilines, with estimated B values ranging from -3.0 for strongly electron-donating substituents to -1.0 for strongly electron-withdrawing groups, suggesting that non-linearity in the dipole moment change arises primarily in the lone-pair orbital, decreasing as it becomes delocalized over the ring.

Calculations of dipole moment functions based on infrared intensities suffer from the disadvantage of multiple solutions, and decisions as to the most appropriate expression cannot always be made without recourse to some additional information about bond properties. For secondary amines, Russell and Thompson (23) found that the dipole moment expansion for the NH bond became more linear as the degree of ionic character of the bond increased. For a completely ionic bond B should be zero.

These calculations support the vibrational mechanism previously described (5). The contribution of nitrogen lone pair pulsations to the transition moment in the symmetric mode would be expected to lead to increased non-linearity in the dipole moment change, as is observed by comparing the experimental data in Figs. 9 and 10. However, as the lone-pair electrons become more extensively involved in conjugation with a very mobile π-electron system due to electron-withdrawing substituents, the molecules have greater charge separation in the ground state and in vibrationally excited states and hence the symmetric vibration becomes more "ionic". This is reflected in a decrease in $|B|$. Ortho substitution introduces no significant perturbation since the major contribution to the transition moment in this mode is due to the lone-pair component and the π-electron component.

In the asymmetric vibration the dipole moment function is determined primarily by movement of the charge centroids in the NH bonds as the equilibrium NH distances change. Because of their position with respect to the direction of the transition moment, and due to the reversal of sign of the dipole moment during the vibrational cycle, ortho substituents increase the "ionic character" of this vibration. The overall change in B is smaller than in the symmetric mode because of the relatively small amount of charge movement in the NH bonds themselves.

The Potential Energy Curve for the Hydrogen-Bonded Proton

Recent work by Barrow and his associates (26) has demonstrated experimentally the existence of energy level splitting resulting from a double minimum in the potential energy curve for the intermolecularly hydrogen-bonded proton in some systems. In order to account for the pair of solvent-dependent absorption bands in the first overtone OH stretching region for alcohols, the second minimum would have to lie in the region of the $v = 2$ vibrational level. No experimental evidence for such splitting in intramolecularly hydrogen-bonded systems appears to have been presented, and it is not clear how such a phenomenon would affect the symmetric and asymmetric vibrational modes of the NH_2 group. The experimental data and their interpretation presented here cannot, however, definitely rule out the double minimum explanation for these systems, and further work on the nature of the proton potential energy function is in progress.

ACKNOWLEDGMENTS

The author is indebted to Professor B. M. Wepster (Technische Hogeschool, Delft) and Professor L. R. C. Barclay (Mt. Allison University, Sackville, New Brunswick) for some samples of ortho-substituted amines. The overtone measurements were made by Mrs. G. D. Brown.

Can. J. Chem. Downloaded from www.nrcresearchpress.com by 210.87.254.42 on 09/05/12
For personal use only.

REFERENCES

1. P. J. KRUEGER and H. W. THOMPSON. Proc. Roy. Soc. (London), Ser. A, **243**, 143 (1957).
2. P. J. KRUEGER and H. W. THOMPSON. Proc. Roy. Soc. (London), Ser. A, **250**, 22 (1959).
3. L. P. HAMMETT. Physical organic chemistry. McGraw Hill, New York. 1940. Chap. VII.
4. R. W. TAFT, JR. *In* Steric effects in organic chemistry. *Edited by* M. S. Newman. John Wiley and Sons, New York. 1956.
5. P. J. KRUEGER. Can. J. Chem. **40**, 2300 (1962).
6. K. B. WHETSEL. Spectrochim. Acta, **17**, 614 (1961).
7. B. D. NAGESWARA RAO, P. VENKATESWARLU, A. S. N. MURTHY, and C. N. R. RAO. Can. J. Chem. **40**, 963 (1962).
8. D. H. MCDANIEL and H. C. BROWN. J. Org. Chem. **23**, 420 (1958).
9. H. H. JAFFE. Chem. Rev. **53**, 191 (1953).
10. K. B. WHETSEL, W. E. ROBERSON, and M. W. KRELL. Anal. Chem. **30**, 1598 (1958).
11. A. G. MORITZ. Spectrochim. Acta, **18**, 671 (1962).
12. N. SHEPPARD. *In* Hydrogen bonding. *Edited by* D. Hadzi. Pergamon Press, New York. 1959. p. 105.
13. A. G. MORITZ. Spectrochim. Acta, **16**, 1176 (1960).
14. H. WOLFF and D. STASCHEWSKI. Z. Elektrochem. **66**, 140 (1962).
15. G. HERZBERG. Molecular spectra and molecular structure. I. Spectra of diatomic molecules. 2nd ed. D. Van Nostrand, Inc., New York. 1950.
16. G. C. PIMENTEL and A. L. MCCLELLAN. The hydrogen bond. W. H. Freeman and Co., San Francisco. 1960.
17. E. GREINACHER, W. LUETTKE, and R. MECKE. Z. Elektrochem. **59**, 23 (1955).
18. D. A. K. JONES and J. G. WATKINSON. Chem. Ind. (London), 661 (1960).
19. A. W. BAKER and W. W. KAEDING. J. Am. Chem. Soc. **81**, 5904 (1959).
20. E. A. ALLAN and L. W. REEVES. J. Phys. Chem. **66**, 613 (1962).
21. V. C. FARMER and R. H. THOMPSON. Spectrochim. Acta, **16**, 559 (1960).
22. V. ZANKER and A. WITTWER. *In* Hydrogen bonding. *Edited by* D. Hadzi. Pergamon Press, New York. 1959. p. 277.
23. R. A. RUSSELL and H. W. THOMPSON. Proc. Roy. Soc. (London), Ser. A, **234**, 318 (1956).
24. J. L. DUNHAM. Phys. Rev. **34**, 438 (1929); **35**, 1347 (1930).
25. H. S. HEAPS and G. HERZBERG. Z. Physik, **133**, 48 (1952).
26. C. L. BELL and G. M. BARROW. J. Chem. Phys. **31**, 300, 1158 (1959). G. M. BARROW. Spectrochim. Acta, **16**, 799 (1960).

Can. J. Chem. Downloaded from www.nrcresearchpress.com by 210.87.254.42 on 09/05/12
For personal use only.

PROTON MAGNETIC RESONANCE ABSORPTION IN ETHYL STEARATE

R. F. GRANT[1]
British Columbia Research Council, University of British Columbia, Vancouver, British Columbia
AND
D. LLEWELYN WILLIAMS
Physics Department, University of British Columbia, Vancouver, British Columbia
Received August 8, 1962

ABSTRACT

The proton magnetic resonance absorption in ethyl stearate has been investigated at −77, 0, and 24° C in the solid β-phase and at 28° C in the solid α-phase. Spin-lattice proton magnetic resonance relaxation times were measured in the liquid up to 75° C and in the solid α-phase. The results suggest that the α-phase is composed partly of molecules in a liquid-like state and partly of molecules constrained to rotate about their longitudinal axes. The results also support the proposal that the dielectric dispersion observed in the β-phase is due to molecular motion in crystal defects.

INTRODUCTION

Ethyl stearate is dimorphic and may freeze into the translucent α-phase, in which the long hydrocarbon chains of the molecules are perpendicular to the plane formed by the end groups. The α-phase is unstable and changes irreversibly into the stable β-phase, in which the hydrocarbon chains are tilted with respect to the plane of the end groups (1).

Dielectric studies on ethyl stearate in the α-phase and β-phase have been interpreted in terms of molecular motion (2–4). In the β-phase this motion is generally thought to be associated with crystal defects, although there is some difference of opinion as to the kind of motion involved (3, 4).

Proton magnetic resonance absorption studies in some solid, long-chain hydrocarbons have revealed the presence of various kinds of molecular motion (5, 6). The following is a similar study of the molecular motion in ethyl stearate.

EXPERIMENTAL METHOD

The proton magnetic resonance absorption line shapes were measured with a spectrometer of conventional design employing a marginal oscillator (7). The magnetic field of 4000 gauss was supplied by a regulated Newport Type A electromagnet.

Spin-lattice relaxation times T_1 in the liquid and in the solid α-phase were measured by the Hahn method using two 90° pulses (8). The pulse spectrometer used for these measurements has been described previously (9).

The purified ethyl stearate used in this study was kindly supplied by Dr. D. W. Davidson of the National Research Council. In the β-phase, this ethyl stearate melted at 33.1° C. The sample used for T_1 measurements was degassed under vacuum by the freeze–pump–thaw method in order to remove the dissolved oxygen, which would otherwise affect the value of T_1; this procedure was carried out 15 times before the sample tube was sealed.

The sample was enclosed in a brass case and was maintained at −77° C by immersing the case in dry ice; an ice bath was used for 0° C. The temperatures above 20° C were held within ±0.1° C by circulating water from a large thermostated bath through copper tubing surrounding the sample case. Temperatures were measured by a copper–constantan thermocouple attached to the top of the sample tube.

RESULTS

The derivative curves of the proton magnetic resonance absorption in the β-phase of ethyl stearate observed at −77, 0, and 24° C, are shown in Fig. 1 These curves each

[1]*Present address: Canadian Services College, Royal Roads, Victoria, British Columbia.*

Can. J. Chem. Downloaded from www.nrcresearchpress.com by 210.87.254.5 on 09/05/12
For personal use only.

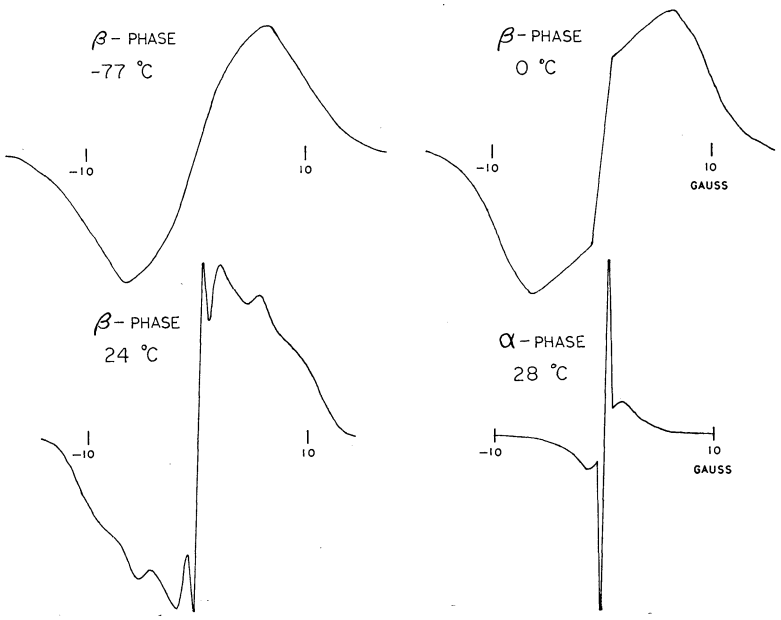

FIG. 1. Averaged derivative absorption curves from ethyl stearate in the α-phase and the β-phase.

represent the average of six traces. The second moments of the curves were calculated by a graphical method (10) and were corrected for the effects of modulation. The second moments are 25.8 gauss^2 at $-77°$ C, 24.3 gauss^2 at 0° C, and 21.0 gauss^2 at 24° C. The derivative of the resonance absorption in the α-phase of ethyl stearate observed at 28° C is also shown in Fig. 1; the second moment is 6.6 gauss^2.

The widths of the narrow peaks on the derivative curves found at 24° C in the β-phase and 28° C in the α-phase seem to be limited by the magnetic field inhomogeneity and modulation amplitude.

The spin-lattice relaxation times T_1 found in liquid ethyl stearate are shown in Fig. 2;

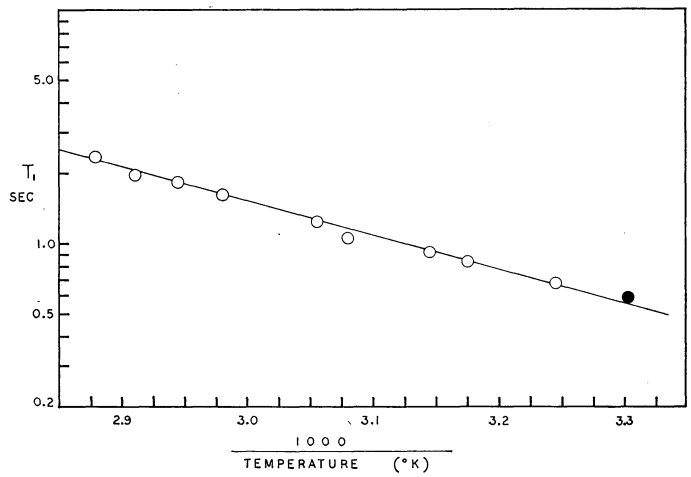

FIG. 2. Spin-lattice relaxation times for ethyl stearate as a function of inverse temperature. Open circles from liquid; filled circle from solid α-phase.

Can. J. Chem. Downloaded from www.nrcresearchpress.com by 210.87.254.5 on 09/05/12
For personal use only.

they range from 2.34 sec at 74.4° C to 0.68 sec at 35.0° C. A T_1 of 0.59 sec was observed in the solid α-phase at 29.1° C, or about one degree below the α-phase freezing point. The same T_1 of 0.59 sec was found at 28.0° C and the normalized amplitude of the first pulse decay was observed to decrease with time. At 28.0° C the first pulse decay decreased to one half of its original intensity in 30 minutes and to one quarter in 50 minutes. Throughout this time there was no change in T_1. The sample was inspected before and after this experiment; it was definitely in the α-phase and it did not change in appearance.

DISCUSSION

The rigid lattice second moment, S, of the proton magnetic resonance for a polycrystalline sample can be calculated by a modification of Van Vleck's formula:

$$S = \frac{716}{N} \sum_{j>k} r_{jk}^{-6},$$

where N is the number of protons considered and r_{jk} is the distance between two protons j and k in angstrom units (11). The intramolecular proton distances in ethyl stearate were calculated by assuming that the dimensions of the molecule are the same as those obtained from electron diffraction studies of simple paraffin molecules (12). For convenience in calculation, the carboxyl group was treated as if it were part of the carbon skeleton of the paraffin chain. The intramolecular contribution to the second moment was found to be 18.5 gauss^2. The unit cell parameters for β-phase ethyl stearate suggested by Fitzgerald (13) were used in calculating the intermolecular second moment; it was found to be 9.0 gauss^2. The predicted rigid lattice second moment for β-phase ethyl stearate is 27.5 gauss^2.

According to the theory of Gutowsky and Pake, the second moment of the resonance absorption line should decrease when molecular reorientation becomes sufficiently rapid (14). Therefore some molecular motion should occur in ethyl stearate at −77° C or higher. Other studies have indicated that in simple long-chain hydrocarbons, the end methyl groups may be free to rotate about their C_3 axes at low temperatures (15). If this motion occurs in ethyl stearate the second moment should be reduced to 23.1 gauss^2. The results show that the methyl end groups probably do not rotate at −77° C or even at 0° C, and it is suggested that the difference between the rigid lattice and experimental second moments at these temperatures is due to torsional oscillation about the long axis of each chain (5, 16). At 24° C the proton resonance absorption line has a complicated structure and it is apparent that motion other than torsional oscillation is taking place. The innermost component of this line is similar to those narrow components that have been found in the resonance absorption spectra of several long-chain hydrocarbon compounds a few degrees below their melting points (5, 6, 15). These narrow peaks are thought to be due to the somewhat unhindered and random motion of molecules or parts of molecules in crystal lattice defects (6). Since the correlation frequency of the motion associated with such narrow peaks is usually in the order of several megacycles (14, 16), it seems likely that this motion contributes to the radio-frequency dielectric dispersion observed in β-phase ethyl stearate.

It can be seen from Fig. 2 that there is no abrupt change in T_1 as ethyl stearate passes from the liquid to the solid α-phase. Thus the freshly formed α-phase seems to contain molecules in a state of motion similar to that of the liquid. As the α-phase ages the amplitude of the first pulse decay decreases, while T_1 remains constant. This could be explained if the molecules in rapid, random motion gradually become part of another structure in

Can. J. Chem. Downloaded from www.nrcresearchpress.com by 210.87.254.5 on 09/05/12
For personal use only.

which the motion is much more restricted, for the resonance line may then have a width too broad to be observed with the pulse apparatus available. These rapidly moving molecules may represent included liquid or zones of disorder associated with the α-phase crystals. It was assumed that the narrow component of the α-phase resonance absorption curve shown in Fig. 1 represented these separate zones in the sample; therefore only the broad component was used to obtain the experimental second moment for the solid.

Ethyl stearate in the α-phase has been shown by X-ray investigation to possess hexagonal symmetry with the hydrocarbon chains arranged parallel and about 4.12 Å apart (1). A rigid lattice intermolecular second moment of 7.7 gauss^2 and a total second moment of 26.2 gauss^2 was found for this model. If the molecules rotate about their long axes, as is generally believed (1), then the second moment should be 7.8 gauss^2. This is larger than the experimentally observed value of 6.6 gauss^2; however, a slight flexing of the rotating chains could qualitatively account for this difference (5). Alternatively, a predicted value of 6.6 gauss^2 is obtained if the methyl groups at the ends of the rotating chains move independently about their C_3 axes.

ACKNOWLEDGMENTS

The authors are indebted to E. P. Jones and E. Sawatzsky for their valuable assistance.

REFERENCES

1. T. MALKIN. Progress in the chemistry of fats and other lipids. Vol. I. Pergamon Press. 1952. p. 1.
2. W. O. BAKER and C. P. SMYTH. J. Am. Chem. Soc. **60**, 1229 (1938).
3. M. G. BROADHURST and E. R. FITZGERALD. J. Chem. Phys. **33**, 210 (1960).
4. D. W. DAVIDSON. Can. J. Chem. **39**, 1321 (1961).
5. E. R. ANDREW. J. Chem. Phys. **18**, 607 (1950).
6. R. F. GRANT and B. A. DUNELL. Can. J. Chem. **38**, 359 (1960).
7. G. D. WATKINS. Ph.D. Thesis, Harvard University, Cambridge, Mass. 1952.
8. E. L. HAHN. Phys. Rev. **80**, 980 (1950).
9. M. LIPSICAS and M. BLOOM. Can. J. Phys. **39**, 881 (1961).
10. J. G. POWLES. Brit. J. Appl. Phys. **9**, 299 (1958).
11. J. H. VAN VLECK. Phys. Rev. **74**, 1168 (1948).
12. B. K. VAINSHTEIN and A. N. LOBACHEV. Dokl. Akad. Nauk SSSR, **120**, 3 (1958).
13. E. R. FITZGERALD. J. Chem. Phys. **32**, 771 (1960).
14. H. S. GUTOWSKY and G. E. PAKE. J. Chem. Phys. **18**, 162 (1950).
15. F. A. RUSHWORTH. Proc. Roy. Soc. (London), Ser. A, **222**, 526 (1954).
16. R. F. GRANT and B. A. DUNELL. Can. J. Chem. **38**, 2395 (1960).

Can. J. Chem. Downloaded from www.nrcresearchpress.com by 210.87.254.5 on 09/05/12
For personal use only.

THE BEHAVIOR OF D-GLUCURONIC, D-GALACTURONIC, AND D-MANNURONIC ACID IN DILUTE AQUEOUS SODIUM HYDROXIDE

I. R. SIDDIQUI[1] AND C. B. PURVES

Division of Industrial and Cellulose Chemistry, McGill University, and Wood Chemistry Division, Pulp and Paper Research Institute of Canada, Montreal, Que.

Received October 3, 1962

ABSTRACT

Two percent aqueous sodium hydroxide at room temperature, preferably for 24 hours, was used to obtain the Lobry de Bruyn – van Ekenstein transformation products. The transformations proceeded much more slowly than in the case of the hexoses; complex changes in specific rotation occurred, and equilibrium among the products was not attained, probably because acidic non-reducing substances formed at a comparable rate. After 24 hours, 39% of D-glucurone was recovered unchanged, together with 9% of D-mannuronic acid and 2% of keto acid probably based on fructose. D-Mannurone gave the same products, but unchanged starting material once more predominated. D-Galacturonic acid was recovered in 58% yield together with 12% of D-taluronic acid, a new substance characterized as a crystalline monohydrated brucine salt. A trace of a keto acid, presumably derived from D-tagatose, was also formed.

INTRODUCTION

During a recent study (1) it was incidentally noticed that D-galacturonic acid appeared to be much more resistant to the oxidizing action of chlorous acid, and also to the Lobry de Bruyn – van Ekenstein transformation in 1% aqueous sodium hydroxide, than was an aldohexose. It was also known (2) that glycosides of uronic acids were unusually resistant to acid hydrolysis. These observations suggested that the chemical behavior of the aldehyde group in uronic acids should be studied in its own right, and this article is concerned with the behavior of uronic acids in cold, dilute alkali. Applications of the Lobry de Bruyn – van Ekenstein transformation to reducing carbohydrates and a few polyuronides have been reviewed (3, 4); more drastic conditions were necessary to epimerize the aldonic acids (3, 5, 6) and galactaric acid (7). D-Galacturonic acid with aqueous calcium or strontium hydroxide was reported to yield some 5-keto-L-galactonic acid, but other reducing substances were produced with baryta. D-Glucuronic acid behaved similarly (8), but lime water converted the 4-O-methyl derivative into a dicarboxylic acid (2).

Preliminary work, carried out by our former colleague E. W. H. Böhme, involved keeping D-glucurone in 1% aqueous sodium hydroxide at room temperature for various times, then removing cations on an ion-exchange resin and chromatographing the effluent on paper. Glucuronic acid or glucurone appeared to be almost completely stable under the conditions cited. The present research therefore employed 2, 6, and 12% aqueous sodium hydroxide at room temperature for periods of 2, 5, 7, and 24 hours. When the chromatograms were developed with naphthoresorcinol a faint blue spot indicated the presence of a keto acid, while a subsequent treatment with water vapor at 70° brought out two new blue spots. This behavior was characteristic of uronic acids (9), and control experiments showed that the greater of these two spots was unchanged glucuronic acid. The acidic nature of these products was substantiated by their negligible movement on paper chromatograms eluted by a basic solvent system. After the glucurone had been in

[1]*Harold Hibbert Memorial Fellow 1961–62. Present address: Food Research Institute, Central Experimental Farm, Ottawa, Ontario.*

Can. J. Chem. Downloaded from www.nrcresearchpress.com by 210.87.254.5 on 09/05/12
For personal use only.

the alkali for a week, the naphthoresorcinol and *o*-aminodiphenyl sprays failed to develop any spots on the paper chromatograms; other chromatograms developed with a bromophenol blue spray, however, contained five or six spots corresponding to non-reducing acids of lower molecular weight. It appeared, therefore, that the Lobry de Bruyn – van Ekenstein transformation was accompanied by a rather rapid sequence of degradation reactions. These reactions were not investigated in the present research.

Since the experiments showed that 2% aqueous sodium hydroxide at room temperature for about 24 hours produced maximum amounts of the two new spots, these conditions were used in subsequent work. D-Mannurone produced a chromatographic pattern superposable on that from D-glucurone, with the exception that the major component was unchanged mannuronic acid. Thus the results suggested that glucurone and mannurone did not yield the same equilibrium mixture of glucuronic, mannuronic, and fructuronic acids, probably because side reactions competed on approximately equal terms with the Lobry de Bruyn – van Ekenstein transformation.

Under the same conditions, D-galacturonic acid yielded a chromatographic spot corresponding to the starting material, together with a minor spot. D-Galacturonic acid was then isomerized on a larger scale and preparative paper chromatography was used to recover from the product both unchanged galacturonic acid (58%) and D-taluronic acid (12%), the former being isolated in a crystalline condition and the latter, a new compound, as a crystalline, monohydrated brucine salt. The crude brucine taluronate contained traces of another brucine salt which gave the naphthoresorcinol test for the salt of a keto acid, presumably the unknown D-tagaturonic acid. To investigate this possibility, the isomerized product was converted to a methyl ester methyl glycoside mixture which was then reduced with lithium aluminum hydride and finally hydrolyzed with aqueous acid. When separated by paper chromatography, the product yielded crystalline D-galactose and an uncrystallized D-talose which was characterized as the crystalline methylphenylhydrazone. The chromatogram also yielded a substance responding to the naphthoresorcinol test and having an R_F value in the range expected for keto sugars. Only a trace, however, could be isolated, and its identity with D-tagatose was not definitely proved.

A larger-scale isomerization of D-glucurone, followed by quantitative paper chromatography, yielded 39%, 8.5%, and 1.9% of glucuronic, mannuronic, and presumably fructuronic acid, the mole ratio being approximately 20:5:1. Reduction and subsequent hydrolysis of the corresponding mixture of methyl glycoside methyl esters gave a mixture of neutral sugars from which paper chromatography recovered D-glucose and D-mannose. The former, which crystallized, was also identified as N-*p*-nitrophenyl-β-D-glucosylamine dihydrate; the latter, which failed to crystallize, was characterized as the corresponding crystalline derivative of mannose. Fructose was recovered in amounts too small for positive identification.

Since control experiments showed that glucose readily yielded both mannose and fructose when kept dissolved in 1% sodium hydroxide for 2 hours, glucuronic, mannuronic, and galacturonic acids differed from the hexoses by failing to yield substantial quantities of keto isomers. Fischer and Schmidt (10), however, recently showed that when sodium salts of the above uronic acids were heated in aqueous solution at pH 7 and 100° for 2 hours or more, the Lobry de Bruyn – van Ekenstein transformation at C_2 was suppressed in favor of isomerism at C_5, D-glucuronic acid, for example, yielding 40% or more of L-iduronic acid. The influence of temperature and hydrogen ion concentration on the uronic acids thus appears to be complex, and worthy of further study.

Can. J. Chem. Downloaded from www.nrcresearchpress.com by 210.87.254.5 on 09/05/12
For personal use only.

EXPERIMENTAL

The following mixtures (v/v ratios) were used for paper chromatograms: (A) ethyl acetate:acetic acid:water (9:2:2); (B) *n*-butanol:formic acid:water (500:115:383); (C) ethyl acetate:pyridine:water (8:2:1); (D) ethyl acetate:acetic acid:water (3:3:1). Reducing sugars were detected with A, an *o*-aminodiphenyl spray (11); keto sugars with B naphthoresorcinol; after development, the latter chromatograms were treated with water vapor at 70° to reveal uronic acids (9). Spray C, bromophenol blue in 95% ethanol, was used to detect acids (12). To remove formic or acetic acid completely, the chromatograms were dried *in vacuo* at 110° for 8 hours before being sprayed. Whatman No. 3MM paper with a wick of No. 1 paper was used in preparative paper chromatography, the sheets measuring 46.5 cm by 57 cm.

Optical rotations were measured on a photoelectric precision polarimeter to 0.005° and were equilibrium values unless otherwise stated. All specific rotations were measured at 25±1° and at the sodium D line wavelength. Evaporations were carried out at 35° in a rotary film evaporator. All the uronic acid samples used for control purposes were chromatographically pure. Amberlite IR-120 resin (Rohm and Haas Company) was used to deionize the solutions.

Preliminary Experiments

Samples, 25 mg, of D-glucurone were kept dissolved in 10-ml volumes of 2%, 6%, and 8% aqueous sodium hydroxide at room temperature. After 2, 5, 7, and 24 hours, 1-ml aliquots were mixed with 2 ml of the ion-exchange resin and were then spotted on chromatograph paper. The use of solvents A and B with spray A in each case revealed D-glucuronic acid as the major component, and small amounts of two other substances ($R_{glucurone}$, 0.47, 0.38 in solvent A; 0.50 and 0.42 in solvent B). Spray B detected only the component of $R_{glucurone}$ 0.47, 0.50 and this reaction for a fructuronic acid was very weak; subsequent development with water vapor at 70° yielded blue spots for all the components but that for the keto acid was still weakest. No movement occurred in the basic solvent C. When the action of the alkali was prolonged for 7 days, paper chromatography showed the presence of no reducing products whatever. Solvent B and spray C yielded faint spots of R_F 0.26, 0.34, 0.40, 0.45, 0.55, and 0.65, which were thought to be those of non-reducing acids of lower molecular weight. The maximum production of new reducing substances occurred when the 2% sodium hydroxide acted for 24 hours.

A similar treatment of D-mannuronic acid ended in paper chromatograms with spots superposable on those in similar chromatograms from D-glucurone, with the difference that D-mannuronic acid instead of D-glucuronic acid was the major component. An examination of D-galacturonic acid under the same conditions gave chromatograms showing much unchanged starting material and a small amount of a compound with $R_{glucurone}$ 0.49 in solvent A, a blue spot being developed by spray B followed by the water vapor treatment. The accompanying changes in specific rotation (Table I) were complex.

TABLE I

Specific rotation of uronic acids in alkali

D-Glucurone*												
Hours	0.16	0.5	2	5	7	24						
$[\alpha]_D^{25}$	+11.5°	+10.1°	+7.9°	+6.8°	+5.3°	−0.5°						
D-Glucurone†												
Hours	0.16	0.4	0.55	0.75	1	2.2	3	4	7.5	9.3	11	21
$[\alpha]_D^{25}$	+9.8°	+9.5°	+8.5°	+8.5°	+9.0°	+8.7°	+7.9°	+7.6°	+6.3°	+5.9°	+3.3°	0
D-Mannurone*												
Hours	0.16	0.5	2	4	6	24						
$[\alpha]_D^{25}$	−10.3°	−9.2°	−8.9°	−7.1°	−6.3°	−3.5°						
D-Galacturonic*												
Hours	0.5	2	4	5	7	24						
$[\alpha]_D^{25}$	+14.3°	+9.3°	+8.7°	+6.3°	+4.3°	−0.9°						

*One percent solutions in 2% aqueous sodium hydroxide at room temperature.
†Four percent solution in 3% sodium hydroxide.

Isolation of Talose and Taluronic Acid

(*a*) A solution of D-galacturonic acid, 1 g, in 100 ml of 2% aqueous sodium hydroxide, was kept at room temperature, the specific rotation decreasing from +14.3 after 30 minutes to −0.9 after 24 hours. The solution was then deionized with 50 ml of Amberlite IR-120 resin and was evaporated to a syrup, 900 mg. This syrup was separated on eight sheets of chromatographic paper with solvent A and elution of the appropriate strips gave 454 mg of galacturonic acid and 95 mg of the uronic acid of $R_{glucurone}$ 0.49. These products were separately heated under reflux for 8 hours with 2% methanolic hydrogen chloride, and the resulting methyl ester methyl glycosides were separately reduced with an excess of lithium aluminum hydride (13) in tetrahydrofurane. The methyl glycosidic groups were hydrolyzed from the products in *N* sulphuric acid for 10

Can. J. Chem. Downloaded from www.nrcresearchpress.com by 210.87.254.5 on 09/05/12
For personal use only.

hours at 100°, and paper chromatography of the two syrups yielded one spot with the R_F and staining properties of galactose in one case and of talose in the other. Crystallization from 95% ethanol gave D-galactose, m.p. 167–170°, and specific rotation +85.5° (*c*, 4.17 in water).

Since the recovery of talose was too small to permit identification, the experiment was repeated with 5 g of D-galacturonic acid. After hydrolysis of the mixture of methyl hexosides, 2.2 g, the product was separated on 12 sheets of paper to yield 1.6 g of D-galactose, 0.15 g of uncrystallized talose, and traces of ketose. A solution of all of the talose fraction in 1 ml of water was mixed with 1 ml of a solution made from 25 g of 1-methyl-1-phenylhydrazine, 100 ml of ethanol, and 3 ml of glacial acetic acid (14). After being kept for 12 hours at 37°, the mixture was cooled to 0°, and 24 hours later 7 mg of crystals was removed. These crystals had m.p. 154–155° and a specific rotation of −4.6° (*c*, 0.63 in methanol), whereas the recorded melting points of the methylphenylhydrazone of talose were 154° (15) and 220–222° (16).

The trace of a ketose recovered from the chromatograms had an R_F value and staining properties appropriate to a ketohexose and therefore appeared to be tagatose.

(*b*) A second 5-g sample of D-galacturonic acid was treated with aqueous sodium hydroxide, the solution was freed of cations, all as described above, and was then chromatographed on 36 sheets of paper, using solvent A. Elution of the appropriate strips gave 2.74 g of galacturonic acid and 0.56 g of taluronic acid. After allowing 6% for locating the strips, these yields corresponded to 58% and 12% respectively. The galacturonic acid had m.p. 103–107° and specific rotation +50.5° (*c*, 1.97 in water), after crystallization from aqueous ethanol, whereas the original sample had m.p. 103–107° and a rotation of 47.9° (*c*, 2.94 in water).

Attempts to crystallize the taluronic acid were unsuccessful. A 200-mg sample was therefore heated at 100° for 10 minutes in 60 ml of water containing 480 mg of brucine. After cooling the solution, excess brucine was removed by three extractions with chloroform, the aqueous residue was concentrated to about 10 ml, and was diluted with acetone. A slight turbidity was removed on the centrifuge, and concentration of the clear liquor yielded a syrup which was dissolved in aqueous ethanol. The slow evaporation of this solution deposited crystals of brucine taluronate monohydrate; m.p. (decomp.) 151–154° with softening at 145°; specific rotation −20.5° (*c*, 1.02 in water). Anal. Calc. for $C_{29}H_{36}O_{11}N_2,H_2O$: C, 57.2; H, 6.2; N, 4.62%. Found: C, 57.0; H, 6.14; N, 4.76%.

The minute amount of acetone-insoluble material removed from the above brucine salt, when chromatographed on paper with naphthoresorcinol as the spray, yielded a single blue spot. This behavior suggested that a trace of the unknown tagaturonic acid was present.

Products from the Transformation of D-*Glucurone*

(*a*) A solution of 1 g of D-glucurone in 100 ml of 2% aqueous sodium hydroxide was decationized after 24 hours and was concentrated to a syrup, 1.1 g, which was quantitatively chromatographed on 16 sheets of paper using solvent A. Fraction 1, 284 mg, was glucuronic acid; fraction 2, 87 mg, mannuronic acid; fraction 3, 18 mg, an unidentified keto acid; fractions 4 and 5, traces of unidentified material; fraction 6, 80 mg, glucurone. After correction for a 6% loss in the guide strips of the chromatograms, the yields were: glucuronic acid plus glucurone, 39%; mannuronic acid, 9.2%; unknown keto acid, 1.9%.

Fractions 4 and 5 were not investigated. The others were separately converted to the methyl ester glycosides, reduced, and hydrolyzed to the free sugars as previously described. Chromatography in solvents A, C, and D with sprays A and B showed that fractions 1 and 6 contained glucose; fraction 2, mannose with traces of glucose and a ketose; fraction 3, like the trace of ketose in fraction 2, had staining properties (naphthoresorcinol) and an R_F value identical with those of fructose, and a trace of mannose was also present.

The combined syrup, 150 mg, from fractions 1 and 6 was heated under reflux for 15 minutes with 3 ml of a solution made from 9 g of *p*-nitroaniline, 200 ml of methanol, and 0.14 ml of concentrated hydrochloric acid. After being filtered while hot, the solution deposited crystals which were twice recrystallized from methanol. The product, m.p. 184–185° and specific rotation −215° (*c*, 1.09 in dry pyridine), was N-*p*-nitrophenyl-β-D-glucopyranosylamine dihydrate, the reported constants (17) of which were m.p. 184° and $[\alpha]_D^{20}$ −201° (*c*, 1.0 in dry pyridine).

(*b*) To identify mannose, a 5-g sample of D-glucurone was treated as described in (*a*) to yield 2 g of the neutral sugars. Of this mixture, 1.2 g was separated on 12 sheets of paper (solvent D) to yield 0.52 g of glucose and 70 mg of uncrystallized mannose, together with a minute amount of fructose. The glucose crystallized and after recrystallization from aqueous ethanol had the correct melting point and specific rotation. The syrupy mannose fraction, 70 mg, was converted to the crystalline N-*p*-nitrophenyl-β-D-mannosylamine dihydrate, which had the specific rotation −335° (*c*, 0.185 in dry pyridine) and m.p. 219°. The recorded rotation was $[\alpha]_D^{20}$ −325° (*c*, 0.16 in dry pyridine) and m.p. 219°. A mixed melting point with an authentic sample was not depressed.

ACKNOWLEDGMENTS

The authors wish to thank Professor J. Riechlein for a sample of D-talose, Mr. A. E. Castagne for carrying out the microcombustions, and the National Research Council of Canada for a grant in aid of research.

Can. J. Chem. Downloaded from www.nrcresearchpress.com by 210.87.254.5 on 09/05/12
For personal use only.

REFERENCES

1. R. H. ZIENIUS and C. B. PURVES. Can. J. Chem. **37**, 1820 (1959).
2. R. N. WHISTLER and G. N. RICHARDS. J. Am. Chem. Soc. **80**, 4888 (1958).
3. J. C. SPECK, JR. Advan. Carbohydrate Chem. **13**, 66 (1958).
4. R. L. WHISTLER and J. N. BEMILLER. Advan. Carbohydrate Chem. **13**, 289 (1958).
5. W. N. HAWORTH and C. W. LONG. J. Chem. Soc. 345 (1929).
6. H. T. BONNETT and F. W. UPSON. J. Am. Chem. Soc. **55**, 1245 (1933).
7. T. PASTERNAK. Naturwissenschaften, **23**, 287 (1935).
8. F. EHRLICH and R. GUTTMAN. Ber. **67**, 573 (1934).
9. S. M. PARTRIDGE. Biochem. J. **42**, 238 (1948).
10. F. G. FISCHER and H. SCHMIDT. Ber. **92**, 2184 (1959).
11. T. E. TIMELL, C. P. J. GLAUDEMANS, and A. L. CURRIE. Anal. Chem. **28**, 1916 (1956).
12. B. S. LUKE and H. J. PLIAFF. Arch. Biochem. Biophys. **51**, 103 (1954).
13. M. A. ABDEL-AKHER and F. SMITH. Nature, **166**, 1037 (1950).
14. E. L. HIRST, J. K. N. JONES, and E. A. WOODS. Modern Methods of Plant Analysis, **2**, 35 (1955); J. Chem. Soc. 1048 (1947).
15. J. J. BLANKSMA and W. A. VAN EKENSTEIN. Chem. Zentr. **II**, 1584 (1908).
16. J. v. BRAUN and O. BAYER. Ber. **58**, 2215 (1925).
17. F. WEYGAND, W. PERKOW, and P. KUHNER. Chem. Ber. **84**, 594 (1951).

Can. J. Chem. Downloaded from www.nrcresearchpress.com by 210.87.254.5 on 09/05/12
For personal use only.

THE PROTON RESONANCE SPECTRA OF BENZYL ACETONE

STEVEN S. DANYLUK[1]
Department of Chemistry, University of Toronto, Toronto, Ontario
Received September 12, 1962

ABSTRACT

The proton resonance spectra of benzyl acetone (4-phenyl-2-butanone) are reported in a variety of solvents at 23° C. A marked solvent dependence is noted for the CH_3 group and the methylene protons adjacent to the keto group. The shifts to high field in aromatic solvents are interpreted in terms of a specific dipole-induced interaction with solvent molecules.

The signals for the two non-equivalent pairs of methylene protons show changes in coupling constant with temperature. From this it is concluded that rapid rotation occurs about the C—C bond in the temperature range investigated with an increase in population of the trans conformation at low temperature. Significant changes in relative chemical shifts are also noted with temperature change for the two pairs of methylene protons and are attributed to the formation of weak molecular complexes in aromatic solvents.

Can. J. Chem. Downloaded from www.nrcresearchpress.com by 210.87.254.40 on 09/05/12
For personal use only.

INTRODUCTION

The rate of interconversion about the C—C bond in 1,2-disubstituted ethanes of the type CH_2XCH_2Y is generally quite rapid (1, 2, 3) and the averaged chemical shifts and coupling constants are observed under normal conditions. A substantial decrease in the rotation rate and a preferential population of one conformation can be effected either by lowering the temperature sufficiently or by introducing bulky substituents on the ethane-like skeleton. Solvents may also exert an influence on the rotation rate, particularly in cases where specific intermolecular interactions are possible between solvent molecules and substituent groups.

In this work we report the proton resonance spectra for benzyl acetone in a number of solvents at 23° C and over the temperature range −85° to 95° C in several solvents. It might be expected that introduction of bulky substituents such as the phenyl and keto groups would strongly hinder or block entirely rotation about the "ethane-like" C—C bond in this compound. The proton resonance spectrum would then consist of superimposed A_2B_2 and ABCD type spectra (4) corresponding to the trans, I, and equivalent gauche II, III conformations respectively.

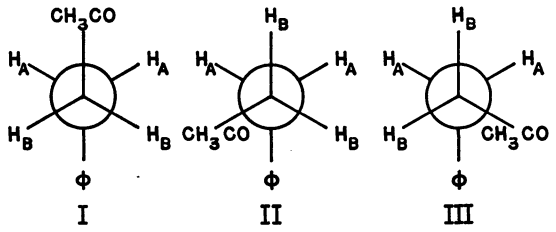

An additional effect arising from interactions between the polar carbonyl group in benzyl acetone and solvent molecules would also influence the spectrum for benzyl acetone.

[1]*This work was initiated during the tenure of an N.R.C. postdoctoral fellowship, 1958–60.*

EXPERIMENTAL

All of the chemicals used were of White label or reagent grade; benzyl acetone was obtained from the Aldrich Chemical Company and was redistilled before use. The concentration of benzyl acetone was 10 mole% in each of the solutions investigated. No significant changes in chemical shift (i.e. greater than 0.5 c/s) were noted for more dilute solutions. Spectra were recorded at 23±1° C with a Varian DP60 spectrometer operating at 60 Mc/s and equipped with a flux stabilizer. The signal separations were measured relative to internal tetramethylsilane by the audio side-band technique (5) and are accurate to ±0.3 c.p.s. Spectra were recorded for several solutions over a temperature range of −85° to 95° C using a thermostatted temperature control device described previously (6).

The proton resonance spectrum for the partially deuterated benzyl acetone, $C_6H_5CH_2CD_2COCD_3$, prepared by Dr. Leitch of the National Research Council, was measured in several solvents and aided in the assignment of the methylene proton signals.

RESULTS AND DISCUSSION

The proton resonance spectrum for benzyl acetone shows a marked dependence on the type of solvent used. This is clearly illustrated in Fig. 1, which shows the signals for the

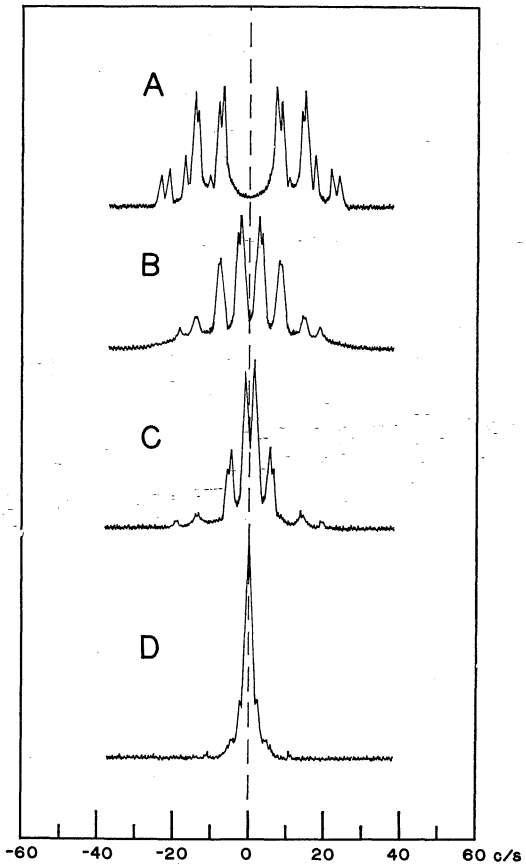

FIG. 1. Proton resonance spectra of benzyl acetone at 23° C. (A) 10 mole% in benzene; (B) pure benzyl acetone; (C) 10 mole% in carbon disulphide; (D) 10 mole% in acetone.

two magnetically non-equivalent pairs of methylene protons in several different solvents. A well-defined A_2B_2 type spectrum is observed in benzene solution while an almost completely collapsed spectrum results in acetone.

Can. J. Chem. Downloaded from www.nrcresearchpress.com by 210.87.254.40 on 09/05/12
For personal use only.

A summary of the chemical shifts and coupling constants obtained by a first order analysis of the A_2B_2 spectra is given in Table I. The two AB coupling constants were

TABLE I

Chemical shifts and coupling constants for benzyl acetone at 23° C

Solvent	δ_A*	δ_B*	$\delta_B-\delta_A$	J_{AB}	δ_{CH_3}
	c/s				
	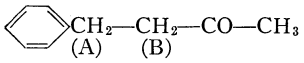 (A) (B)				
Benzyl acetone (pure)	−166.5	−150.7	15.8	8.0	−112.2
n-Hexane	−168.8	−154.3	14.8	8.1	−115.0
Benzene	−166.0	−133.0	32.9	8.1	−96.5
Toluene	−162.7	−133.5	29.2	8.0	−99.3
Pyridine	−170.7	−156.7	13.8	7.9	−117.0
Carbon disulphide	−166.8	−156.6	10.8	8.0	−117.5
Chloroform	−172.9	−163.8	9.0	7.3	−125.4
Methylene chloride	−168.1	−159.5	8.6	7.9	−123.0
Acetonitrile	−168.7	−163.9	4.8	7.9	−123.0
Methanol	−168.8	−164.8	4.0	7.8	−124.0
Acetone	−169.0	−167.0	2.0	7.9	−123.0
	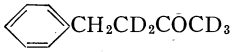				
n-Hexane	−165.9				
Carbon disulphide	−165.1				
Benzene	−163.3				
Acetone	−168.4				
Benzyl acetone (pure)	−166.2				

*Chemical shifts are reported for 10 mole% solutions relative to internal tetramethylsilane and are accurate to ±0.3 c/s. The J_{AB} values are accurate ±0.2 c/s.

assumed to be equal on the basis of the 14-line spectrum observed in benzene solution (7). The signals to the low field side of the A_2B_2 midpoint are assigned to the proton pair (A) adjacent to the phenyl ring on the basis of chemical shifts observed for the methylene protons of $C_6H_5CH_2CD_2COCD_3$. Only a very slight solvent dependence is noted for the chemical shift of the proton pair (A) closest to the ring. On the other hand, the proton pair (B) adjacent to the carbonyl group shows fairly large chemical shift changes. Aromatic solvents, with the exception of pyridine, shift the B protons to high field while polar aliphatic solvents such as acetone and acetonitrile act in the opposite direction. Thus, for example, the relative shifts ($\delta_B-\delta_A$) are 32.9 c/s in benzene, 2.0 c/s in acetone, and 14.8 c/s in an inert non-polar solvent *n*-hexane. The relative shift $\delta_B-\delta_A$ for pure benzyl acetone is somewhat larger than an earlier value of 12.6 c/s reported by Braillon (8).

The internal shift changes with solvent for the CH_3 group, Table I, parallel those observed for the B proton pair. For example, in benzene the shift to high field relative to the *n*-hexane value, 18.5 c/s, is very similar to that observed for the B protons, 21.3 c/s.

The coupling constant J_{AB} is identical in all of the solvents investigated at 23° C and is close to the mean value of J_{trans} and J_{gauche} coupling constants observed for other disubstituted ethanes (7). The present J_{AB} value of 8.0±0.2 c/s is slightly lower than the J_{AB} value reported for dibenzyl acetone, 8.6 c/s (8).

The proton resonance spectra for pure benzyl acetone and solutions in CS_2, *n*-hexane, and toluene were of the A_2B_2 type over a fairly wide temperature range, −85° to 95° C. No indication of ABCD spectra corresponding to gauche conformations II and III was evident even at low temperatures, −85° C. These results indicate that rapid rotation

Can. J. Chem. Downloaded from www.nrcresearchpress.com by 210.87.254.40 on 09/05/12
For personal use only.

occurs about the C—C bond even at low temperatures despite the presence of bulky substituents.

A small but detectable decrease of J_{AB} from 8.3 c/s at −20° C to 7.3 c/s at 95° C was noted in toluene solutions. The measured coupling constant represents, in the present case, the weighted average of the trans J_T and gauche J_G coupling constants (7, 9) and is given by $J_{AB} = pJ_T+(1-p)J_G$, where p is the population of the trans conformation. Accordingly, the increase of J_{AB} with decreasing temperature is indicative of a preferential population of the trans conformation at lower temperatures; $J_T > J_G$ for disubstituted ethanes (7). A satisfactory estimate of the energy barrier could not be determined, however, since the temperature dependence did not follow the expected exponential behavior.

The relative shift $\delta_B-\delta_A$ also shows significant changes with temperature in the solvents investigated, Fig. 2. In aliphatic solvents, both polar and non-polar, the relative shift

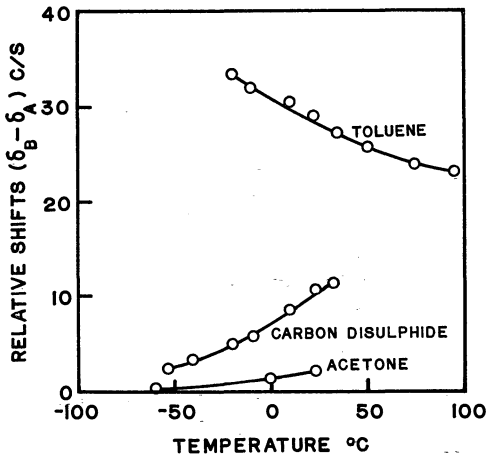

FIG. 2. Temperature variation of the relative shifts for the methylene protons.

increases in each case with increasing temperature. Thus, in carbon disulphide $\delta_B-\delta_A$ increases from 2.5 c/s at −53° C to 12.2 c/s at 45° C. Although the change of $\delta_B-\delta_A$ with temperature in the inert solvents *n*-hexane and carbon disulphide is a good indication of population changes for the trans and gauche conformations, it is not a satisfactory parameter for estimating rotational energy barriers in the present system because of the possibility of complicating solute–solute interactions.

In non-polar aromatic solvents, on the other hand, $\delta_B-\delta_A$ shows a substantial decrease with increasing temperature; for example, in toluene, $\delta_B-\delta_A$ decreases from 33.0 c/s at −20° C to 23.1 c/s at 95° C. A similar change is noted in benzene. The internal shift change with temperature for the CH_3 group parallels the behavior of the B protons in toluene and benzene. In contrast, the chemical shift for the A protons is relatively insensitive to temperature changes.

The preceding internal shift changes with temperature are very similar to those observed recently by Schneider and Hatton (10) for acetonitrile, *p*-benzoquinone, and N,N-dimethylformamide in toluene. Temperature coefficients, $d\delta/dT$, ranging from −0.02 to −0.18 c/s per °C were observed to be dependent upon the concentration and nature of the solute. These low field shifts with increasing temperature have been attributed to the

Can. J. Chem. Downloaded from www.nrcresearchpress.com by 210.87.254.40 on 09/05/12
For personal use only.

formation of molecular complexes between polar solute molecules and aromatic solvent molecules (10).

The formation of weak molecular complexes between polar solutes and aromatic solvents has been conclusively shown for a large number of systems (11,* 12, 13).

Both the high field shifts for the CH_3 protons and B protons in benzene and toluene as compared with aliphatic solvents (Table I) and the $\delta_B - \delta_A$ changes with temperature in the aromatic solvents can be interpreted in terms of weak complex formation. Accordingly, a specific dipole-induced interaction between benzyl acetone and the aromatic solvent molecule results in the formation of a molecular complex whose configuration is illustrated in Fig. 3. In this complex the carbonyl group is directed away from the aromatic ring

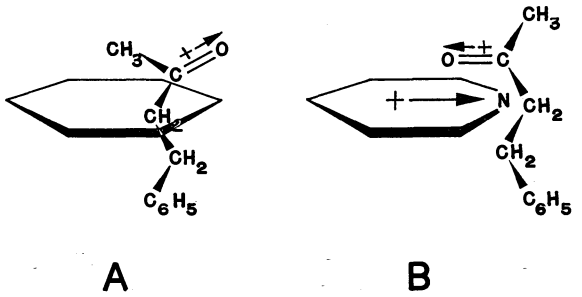

FIG. 3. (A) Configuration of the 1:1 complex between benzyl acetone and benzene; (B) Configuration of the 1:1 complex of benzyl acetone and pyridine.

forcing both the CH_3 group and the B methylene protons to lie above the plane of the ring. Both the CH_3 protons and B protons will therefore be shifted to high field in benzene and toluene solutions as compared with aliphatic solvents. Furthermore, an increase in temperature would favor dissociation of the molecular complex and a shift to low field as observed. On the other hand, the A protons lie off the aromatic ring and only a small shift to high field would occur in toluene (approximately 6 c/s) as compared with the shift in aliphatic solvents.

The internal shifts $\delta_B - \delta_A$ in a polar aromatic solvent such as pyridine appear to be anomalous. However, in this case it is likely that the carbonyl group aligns itself along the polar pyridine ring as illustrated in Fig. 3. On this model the CH_3 group and B protons lie off the plane of the ring and will therefore not be influenced significantly by the ring current of pyridine.

An estimate of the effect of different solvents on the rate of rotation is complicated by polar and association effects on the chemical shifts. Qualitatively, the onset of "free" rotation about the C—C bond at 23° C as indicated by the averaging of δ_B and δ_A is favored, according to the present results, in strongly polar aliphatic solvents such as acetone, methanol, and acetonitrile, while aromatic solvents have the opposite effect.

ACKNOWLEDGMENTS

The financial support of the National Research Council is gratefully acknowledged. The author wishes to express his appreciation to Dr. L. C. Leitch, who synthesized the deuterated compound, and to Dr. W. G. Schneider for his continued interest and helpful comments.

The author is indebted to Dr. Schneider for a preprint of his paper.

Can. J. Chem. Downloaded from www.nrcresearchpress.com by 210.87.254.40 on 09/05/12
For personal use only.

REFERENCES

1. J. A. POPLE, W. G. SCHNEIDER, and H. J. BERNSTEIN. Can. J. Chem. **35**, 1060 (1957).
2. D. M. GRAHAM and J. S. WAUGH. J. Chem. Phys. **27**, 968 (1957).
3. P. M. NAIR and J. D. ROBERTS. J. Am. Chem. Soc. **79**, 4565 (1957).
4. J. A. POPLE. Mol. Phys. **1**, 3 (1958).
5. J. T. ARNOLD and M. E. PACKARD. J. Chem. Phys. **19**, 1608 (1951).
6. W. G. SCHNEIDER, H. J. BERNSTEIN, and J. A. POPLE. J. Chem. Phys. **28**, 601 (1958)
7. J. A. POPLE, W. G. SCHNEIDER, and H. J. BERNSTEIN. High-resolution nuclear magnetic resonance. McGraw-Hill Book Co., New York, N.Y. 1959.
8. B. BRAILLON and R. ROMANET. Bull. Soc. Chim. France, 842 (1961).
9. R. J. ABRAHAM and H. J. BERNSTEIN. Can. J. Chem. **39**, 39 (1961).
10. J. V. HATTON and W. G. SCHNEIDER. Can. J. Chem. **40**, 1285 (1962).
11. W. G. SCHNEIDER. J. Phys. Chem. In press.
12. J. V. HATTON and R. E. RICHARDS. Mol. Phys. **5**, 139 (1962).
13. J. V. HATTON and R. E. RICHARDS. Mol. Phys. **5**, 153 (1962).

Can. J. Chem. Downloaded from www.nrcresearchpress.com by 210.87.254.40 on 09/05/12
For personal use only.

THE O-INSIDE CONFORMATION OF 1,3:2,4-DI-O-METHYLENE-L-THREITOL[1]

R. U. LEMIEUX[2] AND J. HOWARD[3]
Department of Chemistry, University of Ottawa, Ottawa, Ontario
Received September 25, 1962

ABSTRACT

1,3:2,4-Di-*O*-methylene-L-threitol was shown by measurement of its dipole moment and nuclear magnetic resonance spectrum to exist in the so-called *O*-inside conformation as would have been predicted by Mills.

Can. J. Chem. Downloaded from www.nrcresearchpress.com by 210.87.254.40 on 09/05/12
For personal use only.

The cyclic methylene acetals obtained as products of the reaction of sugar alcohols (glycitols) with formaldehyde in the presence of hydrochloric acid were extensively studied by Hudson and his co-workers in the 1940's. The results were extended and reviewed by Zissis and Richtmyer in 1954 (1). A set of simple empirical rules was devised in order to relate the structures of the products obtained with the configurations of the sugar alcohols. Barker, Bourne, and Whiffen (2) in 1952 refined the rules by viewing the sugar alcohol in the planar zigzag arrangement for the carbon chain rather than the Fischer projection formulas used by Hudson and his associates. In 1955, Mills (3) pointed out that the configurations of the sugar alcohols used as reactants is only incidental in these considerations. The composition of the product which is obtained in these reversible acetalation reactions is dependent only on the relative thermodynamic stabilities under the prevailing conditions of the many possible acetals which may form. Therefore, unless the product is one of kinetic rather than thermodynamic control, a rationalization of the courses of reaction should proceed from a consideration of the various possible products rather than from the starting material.

On the basis of a near-planar conformation for the 1,3-dioxolane ring, Mills (3) could conclude that, in general, *O*-methylene cyclic acetals will tend to exist in the staggered arrangement provided by the 1,3-dioxane type of structure. The polyhydric, straight-chained sugar alcohols can afford, depending on their configurations, both *trans*-(I) and cis-fused, six-membered, bicyclic structures. The cis structure can exist with each of the 1,3-dioxane rings in the chair conformation in two possible conformations which have been termed (3) the *H*-inside (II) and *O*-inside (III) conformations. As would be expected from the general principles of conformational analysis, these bicyclic structures would

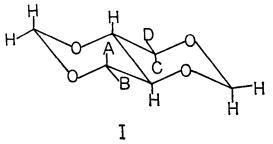

I

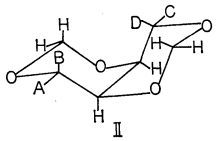

II

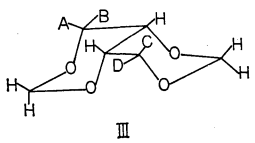

III

be most favorable when the axial substituents are hydrogens. Mills' survey (3) of the known facts related to the main products formed in acetalation reactions of carbohydrates led him to the conclusion that the *O*-inside conformation is inherently more favorable

[1]*Presented at the 43rd National Meeting of the Chemical Institute of Canada, Ottawa (see Chem. Can.* **12**, *No. 4, 65 (1960)).*
[2]*Present address: Department of Chemistry, University of Alberta, Edmonton, Alberta.*
[3]*National Research Council of Canada postdoctoral fellow, 1959–61.*

than the *H*-inside conformation. Although the arguments presented by Mills in drawing this conclusion were exceedingly convincing, all the evidence presented was indirect. In view of the considerable importance of this matter to conformational analysis in carbohydrate chemistry, it seemed desirable to gain direct evidence by determining the conformation of the 1,3:2,4-di-*O*-methylene derivative of L-threitol wherein, for structures II and III, A, B, C, and D are all hydrogen atoms. Direct evidence seemed desirable especially since the driving force for the formation of the *O*-methylene derivative of the sugar alcohols under the reaction conditions used by Hudson and his collaborators is great and the formation of a given derivative need not reflect the favorableness of its structure so much as the unfavorableness of the other possible derivatives. Thus, for example, the formation of 1,3:2,4-di-*O*-methylene-ribitol (I, A = B = C = H and D = CH_2OH) in only 18% yield (4) could not have been anticipated on the basis of an inherently unfavorable structure.

1,3:2,4-Di-*O*-methylene-L-threitol was readily prepared by reaction of L-threitol with methylal in the presence of sulphuric acid. The nuclear magnetic resonance spectrum (Fig. 1) for the compound provided an indication of the presence of 1,3-dioxane rather

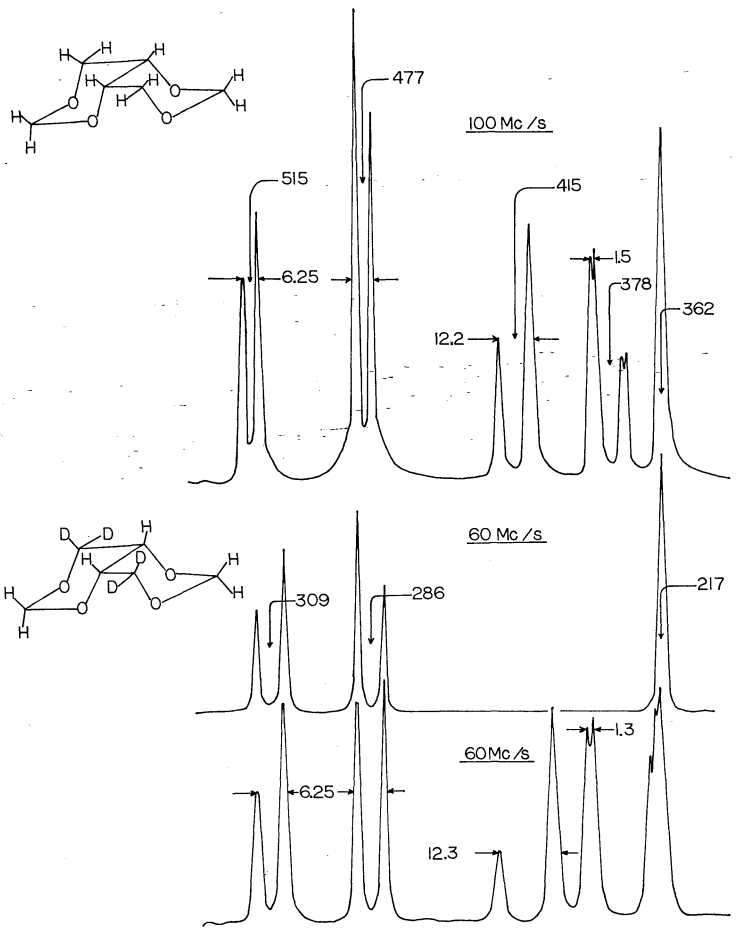

FIG 1. The proton magnetic resonance spectra of 1,3:2,4-di-*O*-methylene-L-threitol (top spectrum at 100 Mc/s and lower at 60 Mc/s) and the 1,1,4,4-tetradeuterio derivative (60 Mc/s) in chloroform. The chemical shifts are in cycles per second from tetramethylsilane.

Can. J. Chem. Downloaded from www.nrcresearchpress.com by 210.87.254.40 on 09/05/12
For personal use only.

Can. J. Chem. Downloaded from www.nrcresearchpress.com by 210.87.254.40 on 09/05/12
For personal use only.

than 1,2-dioxolane rings since the strong chemical shift (0.4 p.p.m.) observed for the *gem*-hydrogens of the *O*-methylene groups is not expected for the flexible dioxolane ring but can arise (5) in a conformationally rigid 1,3-dioxane wherein the axial hydrogen is diamagnetically shielded by the gauche C—O bonds. High conformational rigidity was also indicated by the high melting point, 174.5–175°, for such a simple, low-molecular-weight compound. Definitive evidence for the structure of the compound was obtained through the observation that the compound in 2 *N* sulphuric acid and 0.08 *N* periodic acid at 45° underwent hydrolysis to the extent of 0.65 mole of formaldehyde per mole *without* the consumption of a detectable amount of the oxidant. Under the same conditions, dioxolane rapidly underwent hydrolysis with the simultaneous consumption of 1 mole of periodic acid per mole of dioxolane. Therefore, the di-*O*-methylene-L-threitol could not have the 1,2:3,4-bicyclic ring structure since this structure would inevitably liberate vicinal glycol which would be rapidly attacked by the periodate ion.

The dipole moments for the two possible conformations for 1,3:2,4-di-*O*-methylene-L-threitol (II and III with A = B = C = D = H) were calculated by vector analysis (6). Using the tetrahedral angle of 109°28′ for the carbon valence angles, 105° for the oxygen valence angles, and bond lengths of 1.43 Å and 1.54 Å for the C—O and C—C bonds, respectively, a dipole moment of 4.2 D units was estimated for the *O*-inside conformation and 1.9 D units for the *H*-inside conformation. The main uncertainties in these calculations likely would arise from the oxygen valence angle and the assumed carbon–oxygen bond moment. The dipole moment of 1,3-dioxane in benzene of 2.13 D units at 25° observed by Walker and Davidson (7) was used in the calculations in preference to the individual bond moments reported from measurements made on other ethers. Our calculations showed that variation of the oxygen valence angle in the range 102° to 111° would affect the dipole moment of the *O*-inside conformation by only about 0.7% and that of the *H*-inside conformation by about 8%. The dipole moment of the compound was found to be 4.00±0.07 D units at 25°, in excellent agreement with the calculated value for the *O*-inside conformation.

The results indicate that 1,3:2,4-di-*O*-methylene-L-threitol exists in benzene solution at 25° to an extent of at least 90% in the *O*-inside conformation. A gauche interaction between two methylene groups on a carbon bridge can be expected to destabilize a compound by 0.9 kcal/mole (8). On the other hand, a gauche interaction between oxygen atoms appears to be in the range 0.35–0.55 kcal/mole (9, 10). Mills (3) anticipated the relative magnitudes of these interaction energies on the basis of the van der Waal radii of the atoms involved and assigned the greater stability of the *O*-inside conformation on this basis. It is to be noted, however, that two of the gauche interactions between the methylene groups in the *H*-inside conformation are by way of C—O bridging atoms. In view of the fact that the C—O bond is about 0.11 Å shorter than the C—C bond, these interaction energies can be expected to be substantially greater than the 0.9 kcal/mole estimated as the non-bonded interaction energy of gauche methylene groups in a hydrocarbon. Recently, Foster and his co-workers (11) have established the *O*-inside conformation for 1,3:2,4-di-*O*-benzylidene-L-threitol.

The n.m.r. spectrum of the hydrogens in the threitol residue of 1,3:2,4-di-*O*-methylene-L-threitol in the *O*-inside conformation (III) arises from a six-spin proton system which can be classified as $A_2M_2X_2$ (12). A comparison of the spectra at 60 Mc/s in Fig. 1 allows the conclusion that the bridgehead hydrogens produce their signal at highest field, 3.62 p.p.m., and therefore comprise the X-protons. The doublet centered at 4.15 p.p.m. can be assigned to equatorial hydrogens (A-protons) since these hydrogens, those at positions

B and D in III, are less shielded by C—C and C—O bonds in gauche relationship than are the axial hydrogens at positions A and C in III. (5). The quartet centered at 3.78 p.p.m. must on this basis be assigned to these latter hydrogens, which become the M-protons of the $A_2M_2X_2$ system.

The coupling constants J_{AX} and J_{MX} can be expected (13) to be about 2 c.p.s. if the compound is in the *O*-inside conformation (III) but about 2 and 10 c.p.s., respectively, if the compound is in the *H*-inside conformation. Thus, a decision as to the conformation of the compound can be made on the basis of the magnitude of J_{MX}. The spacings for the quartet centered at 3.78 p.p.m. (M-protons) do not reflect the coupling constants since their values are different for the spectra (Fig. 1) measured at different applied magnetic fields. An appreciation of the second-order effects which may arise in such a system in view of the lack of chemical shift between the X-protons could only be properly ascertained by the calculation of theoretical spectra (14). A number of calculations were kindly provided by Dr. C. A. Reilly of the Shell Development Company. The spectrum was anticipated with reasonable accuracy with $J_{AX} = 0.3$ c.p.s., $J_{MX} = 1.6$ c.p.s., and J_{XX} very nearly zero. It is therefore clear that the compound is in the *O*-inside conformation as indicated by the dipole moment measurements. On the basis of the assignments, the bridgehead hydrogens are more strongly coupled with the axial than with the equatorial hydrogens of the C-methylene groups. This result, on the basis of the Karplus curve (13), can be taken as evidence that the compound exists in an *O*-inside conformation which is distorted in order to relieve the gauche interactions between the oxygen atoms. Since the relative magnitudes of J_{AX} and J_{MX} are opposite to those expected on the basis of a time-averaged spectrum made up of contributions from *O*- and *H*-inside conformations, the results further suggest that the concentration of the latter conformation must be exceedingly small.

From the point of view of n.m.r. spectroscopy it is of interest to note that the signals for the equatorial hydrogens of the *O*-methylene groups of 1,3:2,4-di-*O*-methylene-L-threitol are substantially broader (double the half-band width) than those of the geminal but axial hydrogens. This difference partially disappeared on deuteration of the terminal carbons of the threitol residue. Therefore, these results clearly show that there must exist an orientation effect in the long-range coupling of hydrogens over four bonds in the manner now well established for the coupling of hydrogens over three bonds (5, 13).

The experimental portion describes the preparation of L-threitol. This procedure in our hands was more convenient than published methods (15, 16).

EXPERIMENTAL

Diethyl L-Tartrate

A mixture of L-tartaric acid, 151 g (1 mole), 400 ml of dry ethanol, and 1.5 g of *p*-toluenesulphonic acid was refluxed in a Soxhlet extractor which contained 80 g of Linde Type 4*a* molecular sieves (heated at 400° prior to use) in the extraction chamber to serve as a drying agent. After 24 hours, the ester, 179 g (87% yield), b.p. 142° at 10 mm pressure, $[\alpha]_D^{25°}$ +8.5° (liquid), was isolated by fractional distillation. These constants are in agreement with the literature values (17).

Diethyl 2,3-O-Cyclohexylidene-L-tartrate

A mixture of diethyl L-tartrate, 52 g (0.25 mole), 150 ml of cyclohexanone, 1.5 g *p*-toluenesulphonic acid, and 150 ml of ligroin (30–60°) was refluxed in a Soxhlet extractor containing molecular sieves as described above. After 48 hours, the optical rotation of the mixture had reached a constant value. The mixture was washed with 10% aqueous sodium carbonate and the residue was submitted to fractional distillation *in vacuo* after removal of the ligroin. A fraction, 64 g, b.p. 105° at 2 mm pressure, was identified as 1-cyclohexylidenecyclohexane-2-one (20). A second fraction, 41 g (58% yield), b.p. 152° at 2 mm pressure, was the expected product, $[\alpha]_D^{26°}$ −27.1° (liquid). Calc. for $C_{14}H_{22}O_6$: C, 58.80; H, 7.40%. Found: C, 58.76; H, 7.38%.

Can. J. Chem. Downloaded from www.nrcresearchpress.com by 210.87.254.40 on 09/05/12
For personal use only.

2,3-O-Cyclohexylidene-L-threitol

A solution of 28.6 g (0.1 mole) of diethyl 2,3-*O*-cyclohexylidene-L-tartrate in 50 ml of dry tetrahydrofuran was added to a stirred solution of 9 g of lithium aluminum hydride (0.24 mole) in 250 ml of dry tetrahydrofuran at such a rate as to maintain the reflux temperature. The addition was complete in 15 minutes and the stirring was continued an additional 15 minutes. The excess hydride was then destroyed by the slow addition, with stirring, of 20 ml of ethyl acetate. A solution of 28 g of potassium hydroxide in 100 ml of water was added. After stirring, the solids were isolated by decantation and triturated twice with 20-ml portions of diethyl ether. The solutions were combined and washed with 25 ml of water. Evaporation left a viscous oil, 20 g. A small portion was distilled at 140° and 0.5 mm pressure to give a colorless oil which crystallized after standing. Two recrystallizations from a 1:1 mixture of ether–ligroin (30–60°) provided the analytical sample, m.p. 49–50°; $[\alpha]_D^{25°}$ −3.35° (*c*, 8.2 in ethanol). Calc. for $C_{10}H_{18}O_4$: C, 59.75; H, 8.97%. Found: C, 59.33; H, 8.99%. The remainder of the viscous oil was hydrolyzed to L-threitol without further purification.

L-*Threitol*

The crude 2,3-*O*-cyclohexylidene-L-threitol, 15 g, was dissolved in 200 ml of 0.1 *N* hydrochloric acid and the solution was refluxed for 2 hours. After cooling, the aqueous solution was extracted with 50 ml of ether to remove the cyclohexanone and then concentrated under reduced pressure to about 20 ml. A 1:1 mixture of ether:ethanol, 100 ml, was added and after standing for 7 hours at 5°, L-threitol, 4.1 g, crystallized out. Addition of 200 ml of ether to the mother liquor provided a further 1 g of material. The total yield was 57% of colorless crystals, m.p. 86–88°, $[\alpha]_D^{25°}$ −4.1 (*c*, 4.2 in water). These constants agree with those published by Klosterman and Smith (16).

1,3:2,4-Di-O-methylene-L-threitol

L-Threitol, 5 g (0.041 mole), was added to 250 ml of methylal containing 0.17 g of concentrated sulphuric acid. The mixture was then refluxed in a Soxhlet extractor which contained 60 g of calcium chloride to remove methanol formed in the condensate. After 12 hours, the L-threitol had dissolved. The refluxing was continued for a further 12 hours. The methylal solution was then shaken with 1 g of sodium carbonate until moistened indicator paper showed the solution to be neutral. The solution was clarified by filtration and the methylal was removed by evaporation under reduced pressure to leave an oily liquid. The oil was distilled at 6 mm pressure. The first fraction was a small amount of liquid and this was followed at 150° (bath temperature) by a substance which condensed as long crystalline needles. The yield was 3.5 g (59% yield) of material melting at 173–175°. Recrystallization from 1:1 chloroform–ligroin (60–80°) raised the melting point to 174.5–175°, $[\alpha]_D^{25°}$ −4.1° (*c*, 2.1 in water). Calc. for $C_6H_{10}O_4$: C, 49.31; H, 6.84%. Found: C, 49.11; H, 6.84%.

The di-*O*-methylene-L-threitol, 82 mg (0.566 mmole), was dissolved in 25 ml of 0.16 *M* periodic acid. Ten milliliters of 9.5 *N* sulphuric acid was then added and the solution was diluted to 50 ml with water. The solution, together with a reagent blank, was kept at 45°, and 5-ml aliquots were analyzed after various intervals of time.

No uptake of periodate could be detected over a period of 6 days when the solution was analyzed using the standard arsenite procedure. The formaldehyde content was determined according to the procedure described by Reeves (18) except that the periodate was reduced by iodide at pH 4.75 in order to prevent further hydrolysis of the acetal. No detectable amount of the dimedone derivative of formaldehyde was obtained after 1 day. However, after a 6-day reaction time, 11.6 mg of the derivative melting at 188–189° was obtained. This amount corresponds to the liberation of 0.65 mole of formaldehyde per mole of the di-*O*-methylene-L-threitol.

1,1,4,4-Tetradeuterio-1,3:2,4-di-O-methylene-L-threitol

The compound, m.p. 171–173°, $[\alpha]_D^{25°}$ −5.9° (*c*, 3.7 in water), was prepared on a reduced scale using the same procedures as outlined above starting from L-tartaric acid except that lithium aluminum deuteride was used to reduce the diethyl 2,3-*O*-cyclohexylidene-L-tartrate.

Dipole Moment Measurements

The measurements were made using the equipment described by Davidson (19) and the dipole moments were calculated as described by Walker and Davidson (7). Measurements were made on five independent solutions of different concentrations. The dipole moment determined for 1,3:2,4-di-*O*-methylene-L-threitol in benzene at 25° was 4.00±0.07 units.

ACKNOWLEDGMENTS

The authors are deeply indebted to Dr. D. W. Davidson for the use of his facilities to measure the dipole moments reported herein and the guidance he provided in the calculations and interpretations. The 100 Mc/s spectra were kindly provided by Drs. J. N. Shoolery and L. F. Johnson of Varian Associates. The research was supported by the National Research Council of Canada.

Can. J. Chem. Downloaded from www.nrcresearchpress.com by 210.87.254.40 on 09/05/12
For personal use only.

REFERENCES

1. E. Zissis and N. K. Richtmyer. J. Am. Chem. Soc. **76**, 5515 (1954).
2. S. A. Barker, E. J. Bourne, and D. H. Whiffen. J. Chem. Soc. 3865 (1952). See also, S. A. Barker and E. J. Bourne. Advan. Carbohydrate Chem. **7**, 137 (1952).
3. J. A. Mills. Advan. Carbohydrate Chem. **10**, 1 (1955).
4. R. M. Hann and C. S. Hudson. J. Am. Chem. Soc. **66**, 1906 (1944).
5. R. U. Lemieux, R. K. Kullnig, H. J. Bernstein, and W. G. Schneider. J. Am. Chem. Soc. **80**, 5098 (1958).
6. E. J. Corey and R. A. Sneen. J. Am. Chem. Soc. **77**, 2505 (1955).
7. R. Walker and D. W. Davidson. Can. J. Chem. **37**, 492 (1959).
8. C. W. Beckett, K. S. Pitzer, and R. Spitzer. J. Am. Chem. Soc. **69**, 2488 (1947).
9. S. J. Angyal and D. J. McHugh. Chem. Ind. (London), 1147 (1956).
10. R. U. Lemieux and N. J. Chü. Abstract of Papers, 133rd Meeting of the American Chemical Society. San Francisco, Calif. April 13–18, 1958. 31 N.
11. A. B. Foster, A. H. Haines, and J. Lehmann. J. Chem. Soc. 5011 (1961).
12. H. J. Bernstein, J. A. Pople, and W. G. Schneider. Can. J. Chem. **35**, 65 (1957).
13. M. Karplus. J. Chem. Phys. **30**, 11 (1959).
14. F. A. L. Anet. Can. J. Chem. **39**, 2262 (1961). J. I. Musher and E. J. Corey. Tetrahedron, **18**, 791 (1962).
15. H. J. Lucas and W. Baumgarten. J. Am. Chem. Soc. **63**, 1653 (1941).
16. H. Klosterman and F. Smith. J. Am. Chem. Soc. **74**, 5336 (1952).
17. T. M. Lowry and T. W. Dickson. J. Chem. Soc. **107**, 1173 (1915).
18. R. E. Reeves. J. Am. Chem. Soc. **63**, 1476 (1941).
19. D. W. Davidson. Can. J. Chem. **35**, 458 (1957).
20. J. Reese. Ber. **75B**, 384 (1942).

Can. J. Chem. Downloaded from www.nrcresearchpress.com by 210.87.254.40 on 09/05/12
For personal use only.

FORMATION OF DIASTEREOISOMERIC ORTHOACETATES OF D-MANNOSE: N.M.R. SPECTRAL EVIDENCE[1]

A. S. PERLIN

National Research Council of Canada, Prairie Regional Laboratory, Saskatoon, Saskatchewan

Received October 9, 1962

ABSTRACT

Diastereoisomeric 1,2-orthoacetates of D-mannose are formed under conditions of the Königs–Knorr synthesis. This is shown by the isolation of two crystalline isomers of β-D-mannose 1,2-(benzyl orthoacetate), and also by examination of the nuclear magnetic resonance (n.m.r.) spectra of several D-mannose orthoacetates. The diastereoisomers show notable differences in respective chemical shifts for the *C*-methyl and other protons and these variations, together with isomer-ratio data, suggest that the major isomer of a given pair possesses the configuration in which the *C*-methyl group is *endo*- and the OR group is *exo*-. On acid hydrolysis the orthoacetates yield mainly 2-*O*-acetyl-D-mannose, the structure of which is confirmed by n.m.r. spectral evidence.

Can. J. Chem. Downloaded from www.nrcresearchpress.com by 210.87.254.105 on 09/05/12
For personal use only.

The Königs–Knorr condensation of a 1,2-*trans*-acetohalogen sugar (I) with an alcohol leads to the formation of a 1,2-orthoacetate, frequently in high yield (1, 2, 3, 4). Although two stereoisomeric forms (II and III) of the orthoester are possible, only one isomer has usually been obtained in the many syntheses recorded (3). The single exception is the isolation by Talley, Reynolds, and Evans (5) of two disaccharide orthoacetates from the reaction of 2,3,4,6-tetra-*O*-acetyl α-D-mannosyl bromide with 1,2,3,4-tetra-*O*-acetyl-β-D-glucose. However, additional evidence has now been obtained showing that diastereoisomeric orthoacetates of D-mannose are formed under conditions of the Königs–Knorr synthesis.

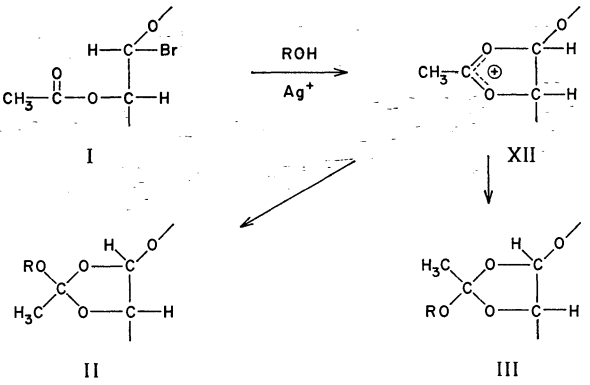

One of the first carbohydrate orthoesters to be characterized was β-D-mannose 1,2-(methyl orthoacetate)3,4,6-triacetate (2, 6), prepared by the silver-catalyzed condensation of tetra-*O*-acetyl α-D-mannosyl bromide with methanol. In the current study, examination of the crude product from this reaction by nuclear magnetic resonance (n.m.r.) spectroscopy showed that two non-equivalent *C*-methyl and *O*-methyl groups were present (Fig. 1B), and indicated that the product contained two orthoacetates in

[1]*Issued as N.R.C. No. 7114.*

Presented in part to the Organic Chemistry Division, 45th Annual Conference of the Chemical Institute of Canada in Edmonton, Alberta, June, 1962.

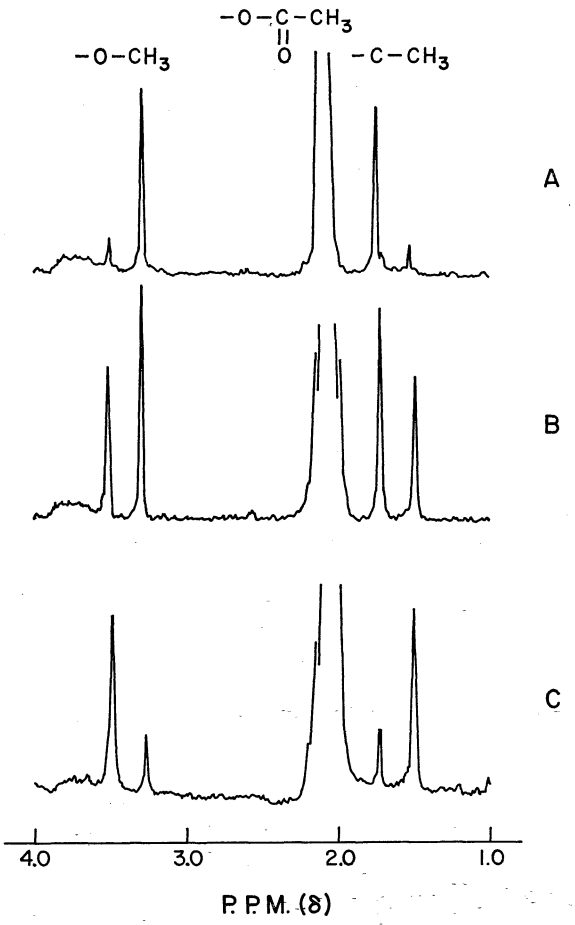

FIG. 1. Partial n.m.r. spectrum of β-D-mannose 1,2-(methyl orthoacetate) 3,4,6-triacetate: A, purified crystalline isomer; B, crude reaction product; and C, syrupy isomer.

a ratio of about 3:2. The relative intensity of these signals was different for the crystalline material isolated from the product, and repeated recrystallization afforded two fractions (one, as a syrup), each of which accounted primarily for one of the *C*-methyl and *O*-methyl chemical shifts (Fig. 1A and 1C). From the physical constants of the crystalline fraction (IV), it was clear that the material used for structural studies by Bott, Haworth, and Hirst (6) consisted essentially of this one isomer. The syrupy isomer (V) remains to be fully characterized.

More definitive evidence for the formation of diastereoisomeric orthoacetates was provided by preparation of the benzyl derivatives. The crude reaction product in this instance also showed chemical shifts for two distinct *C*-methyl groups, in a ratio of about 2:1. A crystalline triacetate (VI) isolated appeared to consist of a single isomer (n.m.r. spectrum), and on deacetylation yielded a crystalline orthoacetate (VII) ($[\alpha]_D$ +27°) which clearly showed one *C*-methyl signal (Fig. 2A). By deacetylating the material contained in the mother liquor from VI, a second crystalline D-mannose benzyl orthoacetate (VIII) ($[\alpha]_D$ −15°) was then obtained. The n.m.r. spectra of these two orthoacetates (Fig. 2A and 2B) differed substantially in the respective chemical shifts found

Can. J. Chem. Downloaded from www.nrcresearchpress.com by 210.87.254.105 on 09/05/12
For personal use only.

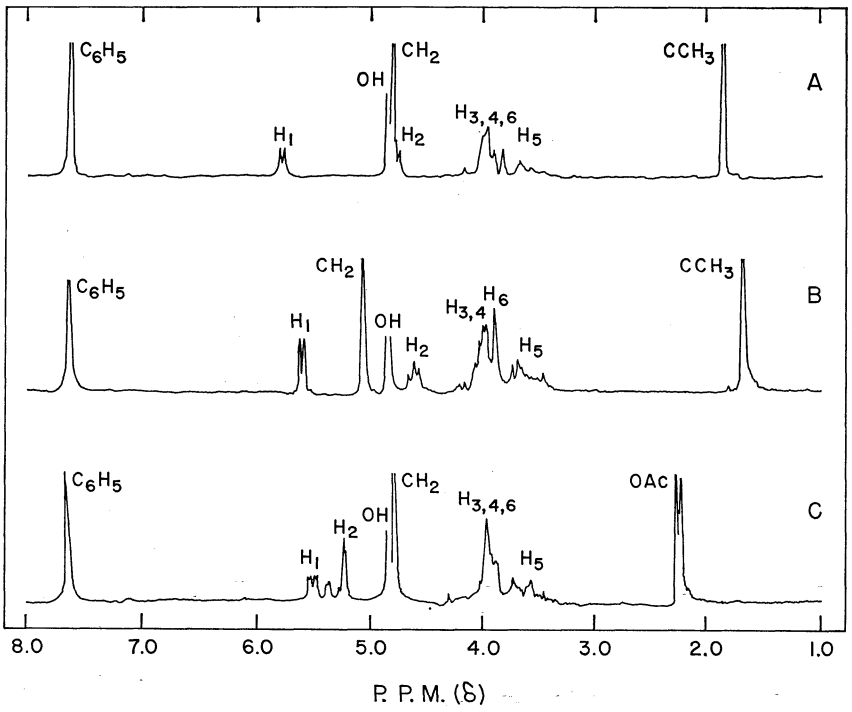

FIG. 2. The n.m.r. spectra of: A, β-D-mannose 1,2-(benzyl orthoacetate) (VII); B, β-D-mannose 1,2-(benzyl orthoacetate) (VIII); and C, 2-*O*-acetyl-D-mannose, prepared from VII or VIII by acid hydrolysis.

for the *C*-methyl, *O*-methylene, and anomeric protons. That both possess the 1,2-orthoacetate structure was shown by the fact that each isomer rapidly consumed only 1 mole of lead tetraacetate in pyridine (7, 8). Molecular models suggest that the α-D-bromide (I) could alternatively yield a 1,6-orthoacetate; however, such a compound would be expected to consume close to 3 moles of the oxidant (7).

Further evidence for the close steric relationship of orthoacetates VII and VIII was provided by acid hydrolysis, which converted each to the same monoacetate (IX) (Fig. 2C). Formation of the latter was clearly apparent in the rapid disappearance of the *C*-methyl signal (Fig. 2A and 2B) and its replacement by a signal attributable to the acetoxyl group (Fig. 2C). This group undoubtedly was at carbon-2 of IX as shown by the following observations: (*a*) the chemical shift for the anomeric proton at relatively high field (see (9)) indicated that the acetoxyl group was not on carbon-1;* (*b*) the appearance of a signal at 5.2 p.p.m. could be ascribed to the paramagnetic effect of the newly formed acetoxyl group on an adjacent secondary proton† (see ref. 10); (*c*) the relatively low chemical shift for the acetoxyl protons is indicative of an axial orientation (i.e., the 2-acetate) (9); (*d*) the monoacetate preparations were resistant to oxidation by lead tetraacetate, which is to be expected only of the 2- (or 1-) isomer (11). Although these observations agree with an early proposal by Pacsu (3) that acid hydrolysis of a 1,2-orthoacetate should yield a 2-acetate, they need not apply for orthoacetates in

**A small percentage of the 1-acetate was sometimes produced, for in certain of the hydrolysis experiments the n.m.r. spectrum showed a weak doublet at 5.9 p.p.m., consistent with the presence of the β-anomeric acetate (9).*

†*The cis-orientation of the 2- and 3-hydroxyl groups makes for the possibility of acetyl migration from position 2 to 3.*

Can. J. Chem. Downloaded from www.nrcresearchpress.com by 210.87.254.105 on 09/05/12
For personal use only.

general. Thus, it has been shown recently (12) that opening of a 1,2-orthoacid ring in the D-glucose series leads to formation of a 1-*O*-acetyl derivative.

The n.m.r. spectroscopy is well suited to the characterization of orthoacetates because the chemical shift for the *C*-methyl protons generally is at higher field than that of protons encountered in other types of carbohydrate structures (9). Also, ready differentiation from other *C*-methyl groups* is possible because of the marked acid lability of orthoesters and (as noted above) the characteristic spectral changes produced during the *C*-methyl → acetoxyl interconversion. However, satisfactory detection of the appropriate signal sometimes may be dependent on the solvent used. Thus the spectrum of IV in chloroform clearly showed the presence of a *C*-methyl group, but this was not apparent with pyridine as solvent. The spectrum of the deacetylated material (V), also in pyridine, indicated that this effect was due to screening of the *C*-methyl signal by that of the acetoxyl protons of the parent triacetate. Integration of the proton signal areas may provide useful analytical data for compounds of this class much more readily than the conventional methods. For example, the n.m.r. spectrum of an acetylated dimeric D-mannose orthoacetate (14) (also see below) shows that one *C*-methyl group and seven acetoxyl groups are present, confirming the earlier data obtained by hydrolytic and saponification procedures.

Coupling constants for the anomeric protons of the various orthoacetates (either in chloroform, deuterium oxide, or pyridine) were found to be 2.7–3.0 c.p.s. According to the Karplus relationship (15), these values correspond to a dihedral angle of about 50° for the H—C_1—C_2—H structure, reflecting the distortion of the chair towards a half-chair conformation, which is to be expected from fusion of the 5-member orthoester group at positions 1 and 2 of the sugar molecule. Molecular models suggest that this distortion should be somewhat greater, and the resulting projected angle perhaps 35–40°. The agreement with theory is much better when the orthoester structure is fused to the D-glucose ring, since a coupling constant of 5.0 c.p.s. is found for the anomeric proton of D-glucose ethyl 1,2-orthoacetate (16), which corresponds to a dihedral angle of about 35°. Hence, although such variation may indicate that the Karplus relationship cannot be applied accurately to some ring systems (see ref. 17), it is possible also that the D-mannose ring of these orthoesters is somewhat closer to possessing a regular chair conformation than might have been anticipated.

Chemical shifts for protons of the orthoester ring in each compound appear to fall into one of two patterns (Fig. 3), providing a possible basis for relating the diastereoisomeric orthoacetates. Thus the anomeric proton, the 2-proton, and the *C*-methyl protons are appreciably *less* shielded, and the OR protons (R = methyl or methylene) *more* shielded, in IV and VII than in V and VIII. Because of the differences in relative orientation of substituents on the orthoester ring, factors which contribute to shielding of a given substituent may have little effect on others more remotely situated. Comparing the diastereoisomers, therefore, it is understandable that for one, the *C*-methyl shift may be to lower field and the OR shift to higher field, and that the situation will be reversed for the other isomer. Hence these data suggest that the configuration of the orthoester group is the same in IV and VII, and that isomers V and VIII possess the opposite configuration.

Protons of the *O*-methyl and *O*-methylene groups of IV and VIII have chemical shifts equivalent to those of the corresponding protons of the parent alcohols (compare Fig. 2B and 2C; similarly, the signal for the *O*-methyl protons, both of deacetylated IV and

**The n.m.r. spectral characteristics of a wide variety of C-methyl groups have been described recently by Anet (13).*

Can. J. Chem. Downloaded from www.nrcresearchpress.com by 210.87.254.105 on 09/05/12
For personal use only.

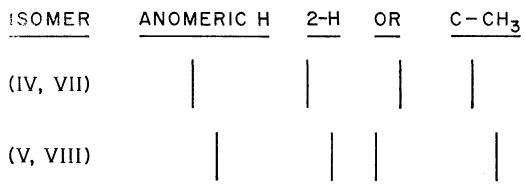

FIG. 3. Schematic representation of relative chemical shifts for various protons of diastereoisomeric orthoacetates of D-mannose.

of the methanol liberated on addition of acid, is at 3.45 p.p.m.). Therefore, they appear to be affected little by other parts of the orthoacetate molecule. In V and VIII, however, these protons are less shielded and the shift is 0.25–0.30 p.p.m. to lower frequencies. Molecular models indicate that the OR group is located further from possible shielding effects when in the *exo*-orientation than in the *endo*-, leading to the suggestion that isomers IV and VII are more likely to have structure X, and isomers V and VIII, structure XI. On the same basis, relative shielding of the *C*-methyl protons should follow the inverse relationship, and the chemical shift at lower field for IV and VII than for V and VIII is also in accord therefore with these assigned configurations. Since chemical shifts for the anomeric protons and 2-protons are in the same direction as that of the *C*-methyl protons (Fig. 3) it may be pertinent that in X all of these protons appear to

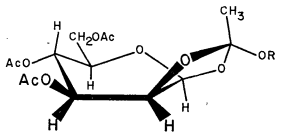

X

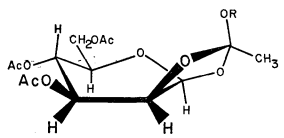

XI

lie in close proximity to three oxygen atoms.* In XI, however, the environment about these protons would appear to be less electronegative and therefore less likely to contribute to decreased shielding.

Other data also are not inconsistent with these assignments of configuration. Lemieux and Cipera (16) have pointed out that nucleophilic attack on the cyclic intermediate ion (XII) should be favored from the side trans (exo) to the pyranose ring. The isomeric ratios of 3:2 and 2:1 (found for the methyl and benzyl derivatives respectively) indicate only moderate stereoselectivity, but compounds IV and VII are nonetheless the major components. An even higher degree of selectivity would be expected on this basis with a hydroxylic component more hindered than the primary carbinols used. One example in which a secondary (anomeric) position is involved in orthoester formation is found in the Königs–Knorr "side reaction" of tetra-*O*-acetyl α-D-mannosyl bromide (14). The mixture of oligomeric orthoacetates produced gives *only one* detectable *C*-methyl signal, indicating that diastereoisomers are not formed; and the dimeric orthoester isolated from this mixture is known to possess a 1,2,1′-structure (14). Further, the n.m.r. spectrum of the dimer shows it to be a steric counterpart of IV, as seen from the virtual equivalence of the anomeric, 2-, and *C*-methyl protons of the two compounds (Table I).†

**Courtauld atomic models indicate that the C-methyl protons are close to the three ring-oxygen atoms, and that simultaneously the anomeric protons and 2-protons are adjacent to the three oxygen atoms of the orthoester structure.*

†Incidentally, these spectral data confirm that the linkage of the dimer is between the orthoester unit and position 1 of the second unit. In any other arrangement an acetoxyl group would be present at C-1 and a highly characteristic shift at low field (about 6.0 p.p.m. (9)) should result; but such a signal is absent from the spectrum of this orthoester.

Can. J. Chem. Downloaded from www.nrcresearchpress.com by 210.87.254.105 on 09/05/12
For personal use only.

TABLE I

Chemical shifts of some proton frequencies for 1,2-orthoacetates (δ, p.p.m.)*

Compound	Anomeric H	2-H	OR	C—CH_3
IV	5.52	4.63	3.29†	1.75
V	5.42	4.40	3.48†	1.51
Dimer	5.55	4.62	—	1.74
VI	5.62	4.74	4.66‡	1.85

*In chloroform.
†R = methyl.
‡R = methylene.

Although these various considerations are speculative, together they favor the tentative assignment of structure X for IV and VII, and of XI for the diastereoisomers V and VIII.

EXPERIMENTAL

Melting points are corrected. Optical rotations were measured at 25°±2° C.

Evaporations were carried out *in vacuo* at 40° C.

The n.m.r. spectra were prepared wtih a Varian A-60 high-resolution spectrometer. The concentration of solute was usually about 10%, and tetramethylsilane was used as the reference standard.

β-D-Mannose 1,2-(Methyl Orthoacetate) 3,4,6-Triacetate

A solution of 2,3,4,6-tetra-*O*-acetyl α-D-mannopyranosyl bromide (0.20 g) in benzene (1 ml) was added dropwise with stirring to a mixture of anhydrous methanol (0.2 ml), benzene (1 ml), and silver oxide (0.20 g). After 1 hour the suspension was filtered, and the filtrate concentrated to a syrup (0.18 g), which partially crystallized. The n.m.r. spectrum of the total product in chloroform showed two *O*-methyl and two *C*-methyl signals (Fig. 1B), indicating the presence of two orthoacetates in a ratio of about 3:2.

A crude crystalline sample of the orthoacetate, m.p. 102–105° C, prepared on a larger scale according to the procedure of Dale (2), gave spectral data similar to that shown in Fig. 1B. After four recrystallizations from cold ether the product had m.p. 106° C and $[\alpha]_D$ −22° (*c*, 5 chloroform); the n.m.r. spectrum of this material is represented by Fig. 1A. Calculated for $C_{15}H_{22}O_{10}$: C, 57.53%; H, 5.98%. Found: C, 57.47%; H, 5.94%.

The ether-soluble product (examined by paper chromatography after deacetylation with sodium methoxide) contained acetates of methyl β-D-mannoside, D-mannose, and an orthoester. By using mixtures of ether–hexane the former two products were crystallized out almost completely, together with additional orthoester. The final syrupy product, $[\alpha]_D$ +12° (*c*, 2.6 chloroform), gave the n.m.r. spectrum represented in Fig. 1C.

Reaction of Tetra-O-acetyl α-D-Mannosyl Bromide with Benzyl Alcohol

The reaction conditions and quantities used above (paragraph 1) were repeated except that benzyl alcohol (0.15 ml) was substituted for the methanol. The partially crystalline crude product (0.21 g) gave an n.m.r. spectrum showing two *C*-methyl signals in a ratio of approximately 2:1.

β-D-Mannose 1,2-(Benzyl Orthoacetate) 3,4,6-Triacetate (VI)

A solution of 2,3,4,6-tetra-*O*-acetyl α-D-mannopyranosyl bromide (15 g) in benzene (50 ml) was added slowly with stirring to benzyl alcohol (10 g) in benzene (25 ml) containing 20 g of suspended silver carbonate. After 4 hours, the suspension was filtered and the benzene evaporated from the filtrate. The thin syrup remaining was taken up in acetone (100 ml) and ether (25 ml), and hexane was added to turbidity affording a product (5.1 g) having m.p. 143–146° C. Recrystallized from acetone–ether–hexane the material had m.p. 146–147° C and $[\alpha]_D$ −1° (*c*, 2.4 chloroform). The integrals of the n.m.r. spectral lines (in chloroform solution) showed the presence of one *C*-methyl group and three acetoxyl groups; the presence of phenyl and acetoxyl groups was confirmed by the infrared absorption spectrum. Calculated for $C_{21}H_{26}O_{10}$: C, 57.53%; H, 5.98%. Found: C, 57.47%; H, 5.94%.

A second crop of crystals (4.2 g) was obtained by further addition of hexane to the mother liquors and, after recrystallization as above, had m.p. 146–147° C and $[\alpha]_D$ −1° (*c*, 1.8 chloroform).

β-D-Mannose 1,2-(Benzyl Orthoacetate) (VIII)

The combined mother liquors from VI were evaporated and excess benzyl alcohol removed by distillation *in vacuo* at 90–100° (bath temp.). Methanol was added to the syrupy residue, the solution was cooled to 5° C, and excess sodium methoxide was added slowly. The solution was stored at 3° for 18 hours, then neutralized with carbon dioxide, filtered, and evaporated. Paper chromatographic examination of the

Can. J. Chem. Downloaded from www.nrcresearchpress.com by 210.87.254.105 on 09/05/12
For personal use only.

residue showed the presence of orthoester, benzyl mannoside, and mannose. The residue was extracted thrice with ether, the extract was filtered and concentrated to a syrup which was extracted in turn with acetone (this procedure eliminated most of the mannose). Addition of ether and hexane to the acetone extract promoted crystallization at room temperature. Yield: 1.5 g; m.p. 115–117° C; $[\alpha]_D$ −14.8° (*c*, 1.1 water); $[\alpha]_D$ −17.8° (*c*, 1.9 pyridine). The n.m.r. spectrum (in deuterium oxide) of the product (Fig. 2B) showed the presence of one *C*-methyl group. Calculated for $C_{15}H_{20}O_7$: C, 57.68%; H, 6.46%. Found: C, 57.92%; H, 6.73%.

The orthoester (12 mg) in pyridine (3 ml) was treated at 0° C with a solution of lead tetraacetate (50 mg) in pyridine (3 ml). The uptake of oxidant (moles/mole (minute)), measured iodometrically as described previously (8) was: 0.92 (2), 0.92 (5), 0.96 (10), 1.05 (30), and 1.10 (45).

In a separate oxidation experiment (room temperature), lead tetraacetate solution equivalent to only 0.8 mole/mole was added, and when the solution became colorless it was concentrated. The residue in water was treated with excess oxalic acid, lead oxalate was filtered off, the supernatant solution was neutralized by ion exchange and added to excess sodium borohydride solution. After removal of sodium and borate, the reduction product was found chromatographically to contain glycerol (derived presumably from both halves of the oxidation product) and mannitol; only minor amounts of unidentified compounds were detected.

β-D-Mannose 1,2-(Benzyl Orthoacetate) (VII)

To a solution of VI (1.0 g) in methanol (20 ml) an excess of sodium methoxide was added and the solution was stored at 3° C for 18 hours. The solution was neutralized with carbon dioxide and concentrated, the residue taken up in acetone, and ether and hexane added. A crystalline product was obtained in the cold (yield, 0.65 g) which, after recrystallization from acetone–ether, had m.p. 128–130° C and $[\alpha]_D$ +26.6° (*c*, 1.2 water); $[\alpha]_D$ +42.2° (*c*, 1.9 pyridine). The n.m.r. spectrum (in deuterium oxide) (Fig. 2A) showed the presence of one *C*-methyl group. Calculated for $C_{15}H_{20}O_7$: C, 57.68%; H, 6.46%. Found: C, 57.80%; H, 6.56%. The orthoester was treated at 0° C with lead tetraacetate in pyridine, as above, affording oxidation rate data virtually identical with those for isomer VIII. Reduction of the oxidized orthoester, as above, yielded mainly glycerol and mannitol (paper chromatogram).

Acid Hydrolysis of VII and VIII

The orthoacetate (VII or VIII) (100 mg) was dissolved in deuterium oxide (1 ml), the solvent was evaporated off, and this treatment repeated twice. The deuterated product in deuterium oxide (1 ml) (Fig. 2A or 2B) was treated with one drop of 0.1 *N* hydrochloric acid. Within 2 minutes, examination of the n.m.r. spectrum (Fig. 2C) showed that the signal for the *C*-methyl group was absent and a new signal (acetoxyl protons) at lower field present. Examination of the hydrolyzate by paper chromatography showed the presence (in each) of a product at $R_{rhamnose}$ 1.17, and a minor proportion of mannose (solvent, butanol–ethanol–water (40:11:19); spray, aniline phthalate). (The parent orthoacetates did not chromatograph well in this solvent, but in butanol–pyridine–water (3:1:1) had $R_{rhamnose}$ 2.05 (isomer VII) and 2.15 (isomer VIII), respectively.)

A portion of each hydrolyzate (0.1 ml) was taken up in acetic acid (5 ml) and a solution of lead tetraacetate (30 mg) in acetic acid (5 ml) was added. At 5 and 15 minutes' reaction time the uptake of oxidant by VII was less than 0.1 mole/mole, and by VIII was 0.2 mole/mole.

ACKNOWLEDGMENTS

Nuclear magnetic resonance spectra were measured by Mr. M. Mazurek and Mr. W. C. Haid at the University of Saskatchewan, through the kind cooperation of Prof. K. J. McCallum and Dr. R. A. Abramovitch. The author is indebted also to Prof. R. U. Lemieux and Dr. K. L. McEwen for helpful discussion. Microanalyses were performed by Mr. M. Mazurek.

REFERENCES

1. E. Fischer, M. Bergmann, and A. Rabe. Ber. **53**, 2362 (1920).
2. J. K. Dale. J. Am. Chem. Soc. **46**, 1046 (1924).
3. E. Pacsu. Advan. Carbohydrate Chem. **1**, 77 (1945).
4. R. U. Lemieux. Advan. Carbohydrate Chem. **9**, 1 (1954).
5. E. A. Talley, D. D. Reynolds, and W. L. Evans. J. Am. Chem. Soc. **65**, 575 (1943).
6. H. G. Bott, W. N. Haworth, and E. L. Hirst. J. Chem. Soc. 1395 (1930).
7. R. C. Hockett and D. F. Mowery, Jr. J. Am. Chem. Soc. **65**, 403 (1943).
8. H. R. Goldschmid and A. S. Perlin. Can. J. Chem. **38**, 2280 (1960).
9. R. U. Lemieux, R. K. Kullnig, H. J. Bernstein, and W. G. Schneider. J. Am. Chem. Soc. **80**, 6098 (1958).
10. L. M. Jackman. Applications of nuclear magnetic resonance spectroscopy in organic chemistry. Pergamon Press. 1959. p. 55.
11. A. J. Charlson and A. S. Perlin. Can. J. Chem. **34**, 1200 (1956).

Can. J. Chem. Downloaded from www.nrcresearchpress.com by 210.87.254.105 on 09/05/12
For personal use only.

12. R. U. LEMIEUX. Private communication.
13. F. A. L. ANET. Can. J. Chem. **39**, 2262 (1961).
14. H. R. GOLDSCHMID and A. S. PERLIN. Can. J. Chem. **39**, 2025 (1961).
15. M. KARPLUS. J. Chem. Phys. **30**, 11 (1959).
16. R. U. LEMIEUX and J. D. T. CIPERA. Can. J. Chem. **34**, 906 (1956).
17. F. A. L. ANET. Can. J. Chem. **39**, 789 (1961).

Can. J. Chem. Downloaded from www.nrcresearchpress.com by 210.87.254.105 on 09/05/12
For personal use only.

VAPOR–LIQUID EQUILIBRIA, DENSITIES, AND REFRACTIVITIES IN THE SYSTEM ACETIC ACID – CHLOROFORM – WATER AT 25° C

A. N. CAMPBELL, E. M. KARTZMARK, AND J. M. T. M. GIESKES
Department of Chemistry, University of Manitoba, Winnipeg, Manitoba
Received July 26, 1962

ABSTRACT

The volume changes on mixing of the two binary mixtures acetic acid – water and acetic acid – chloroform and of the ternary mixture acetic acid – chloroform – water have been determined. In the system acetic acid – water a volume contraction occurs, showing a minimum excess molar volume at 50 mole%. Partial molal volume determinations suggest the formation of a mixed association of one molecule of water with one molecule of acetic acid. In the system acetic acid – chloroform the excess molar volume function is positive over the complete concentration range and this suggests the probability of a positive deviation from Raoult's law.

The refractivities of the two binary systems show that the true molecular volumes of acetic acid, water, and chloroform are additive on mixing.

Studies of the vapor–liquid equilibria show that in all three constituent binary systems there is positive deviation from Raoult's law but if the dimerization of acetic acid in the vapor phase is taken into account the vapor pressure behavior of the system acetic acid – chloroform is virtually ideal. The vapor pressures in the ternary system show strong positive deviations from Raoult's law over the complete concentration range. This shows that the line of pseudo-ideality in terms of zero excess molar volume does not really represent ideal behavior. Zero excess molar volume is caused by the counteracting effects of water and of chloroform molecules on acetic acid molecules.

In the two binary systems investigated the experimental data satisfy the Gibbs–Duhem–Margules equation. This proves that treatment for dimerization of acetic acid in the vapor phase is not merely permissible but necessary.

Can. J. Chem. Downloaded from www.nrcresearchpress.com by 210.87.254.105 on 09/05/12
For personal use only.

The system acetic acid – chloroform – water is a promising subject of study for the student of the theory of solutions. Acetic acid is highly, perhaps completely, dimerized in the pure liquid state but the addition of water and of chloroform causes the dimer to dissociate. Water, with its high dielectric constant, has the greater effect. Chloroform has a dielectric constant about twice that of benzene, the typical non-dissociating solvent, and the effect of chloroform on the dimerization of acetic acid is not negligible, though much less than that of water. The very low degree of miscibility in the water–chloroform system indicates high repulsion between the molecules of these two substances. This repulsion continues to show itself as a relatively large two-liquid area in the three-component system. The ternary system seemed therefore very suitable for the study of non-ideality from the thermodynamic viewpoint.

The thermodynamic implications of determinations of vapor pressure are well known. In such a system as the present one, vapor pressure determinations should give a more or less quantitative measure of the non-ideality of the system. On the other hand, accurate determinations of density yield partial molal volumes of the constituents, again a presumed measure of non-ideality.

Of the component binary systems, the system acetic acid – water has been frequently investigated, in respect to densities, isobaric boiling points, and isothermal vapor pressures of mixtures of varying composition. The latest data on densities are due to Woodman (1) and to Kohner and Gressman (2), the latter of whom determined the refractive index at 25° C for the helium D-line. Redlich and Nielsen (3) report the apparent molal volumes up to 4 *M* acetic acid.

Isobaric studies have been carried out by numerous workers, usually at atmospheric pressure. Arich and Tagliavini (4) give a bibliography of the subject. Chalov and

Aleksandrova (5) have investigated the boiling point diagram at different constant pressures, and thus deduced the isotherms between 20° and 80°, but the extrapolation methods used for the lower temperature make the results doubtful. Wrewsky *et al.* (6) determined directly the isothermal vapor pressure curves, at 42° and 60°, by an air displacement method essentially the same as that used in the present work. Their results show positive deviations from Raoult's law. The same conclusion results from the work of Arich and Tagliavini (4), who investigated the isotherms at 69.7, 79.9, and 89.9° C. Fredenhagen and Liebster (7), also using the air displacement method, have determined the partial pressures of acetic acid in water at 25° up to 2.545 *N* solutions while Giacalone *et al.* (8) report the partial pressures of water at 34.45° up to a concentration of 0.1529 mole fraction acetic acid. Campbell and Kartzmark (9) report the relative viscosities at 25° C over the complete concentration range.

The system water–chloroform shows a large miscibility gap at 25° C, the limits being 0.8 wt% water and 99.4 wt% water according to Brancker, Hunter, and Nash (10) while Reinders and de Minjer (11) give the lower limit as 0.9 wt% water at 25° C. The latter authors, when investigating the isobaric boiling point diagram, found a minimum boiling point at 56.12° and 2.8% water, under a pressure of 760 mm. There appear to be no data on the vapor pressures or densities of the system acetic acid – chloroform.

The ternary system acetic acid – chloroform – water shows a large area of partial miscibility at 25°, as was first pointed out by Wright (12). The limits of the area for 25° have been most accurately defined by Brancker *et al.* (10). The composition of the plait point can be determined from the law of rectilinear diameters and also by a method recently developed by Tarasenkov (13). The composition at 25° is $CHCl_3$ = 42.3%, CH_3COOH = 42.4%, H_2O = 15.3%. Tarasenkov's rule, though it lacks theoretical justification, appears to work in practice and is worth explaining since it has not received the publicity it deserves. According to Tarasenkov, if the tie lines of the miscibility gap, as represented in Fig. 1, are produced they will intersect on the extension of the base

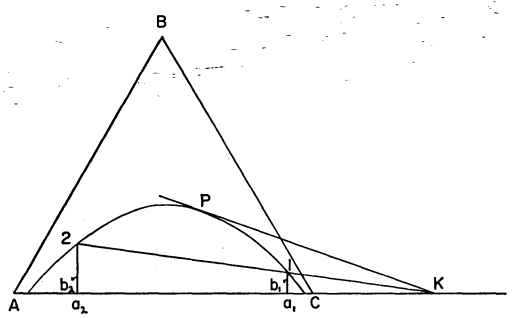

FIG. 1. The method of Tarasenkov to find the plait point in the ternary system. a_1, concentration of A in 1; a_2, concentration of A in 2; b_1, concentration of B in 1; b_2, concentration of B in 2. The origin is chosen at C.

AC at the point K. Slight deviations are considered to be experimental error. The tangent from K to the binodal curve will touch the binodal curve at P, where P is the plait point. It follows also that the ratio of the amounts of the codissolving constituent B in the two layers, for any given tie line, is given by the equation

$$\frac{b_2}{b_1} = \frac{K-a_2}{K-a_1}. \qquad [1]$$

Can. J. Chem. Downloaded from www.nrcresearchpress.com by 210.87.254.105 on 09/05/12
For personal use only.

If the codissolving constituent is not associated in either layer, the above equation gives the distribution coefficient, but this condition is not complied with in the system acetic acid – chloroform – water because acetic acid is largely dimerized in the chloroform layer. Hand (14) discusses the distribution of acetic acid monomers and dimers in the water and chloroform layers.

EXPERIMENTAL

The acetic acid was freed from water by distilling with acetic anhydride, when its density and freezing point were found to be those of pure anhydrous acetic acid. Commercial chloroform is liable to contain a trace of alcohol, added as a stabilizer. To remove this the chloroform was shaken with concentrated sulphuric acid and distilled over calcium chloride. The chloroform so obtained had a density in good agreement with the accepted value. Very pure chloroform is not very stable. It may be preserved in the dark for several days but after that decomposition becomes evident from the acrid smell. Small amounts were therefore prepared at frequent intervals. Distilled water having a specific conductance of 5×10^{-6} mhos/cm at 25° was used.

Analysis of Mixtures

Analyses of mixtures were made by determination of acetic acid content in conjunction with physical properties, viz. density and refractive index. Any ternary mixture can theoretically be analyzed by the determination of two physical properties. Calibration is first done by determining the values of each physical property for a large number of binary and ternary mixtures at a constant temperature. The results are then plotted as curves of "iso-values" (equal density or equal refractive index) against composition on a triangular diagram. For accuracy, it is necessary that the "iso" lines of the two physical properties should intersect at an angle considerably less than 180°. Further necessary requirements are the obvious ones that the physical properties chosen must be such that they can be measured with accuracy and secondly that they should alter markedly with change of composition. In order to analyze a mixture of unknown composition it is only necessary to determine the values of the physical properties for the given mixture: the intersection of the two "iso-curves" then gives the composition. The present problem was simplified by the fact that one component, acetic acid, is readily estimated by titration with standard alkali. If the apex of the composition triangle represents acetic acid, determination of the acetic acid content places the mixture on a line parallel to the base of the triangle. One physical property, e.g. refractive index, is then sufficient to determine the position of the mixture on the horizontal. We measured the refractive index for the D-line (5893 Å) at 25° with an accuracy of ±0.0001. The results of our calibration curve are shown in Fig. 2.

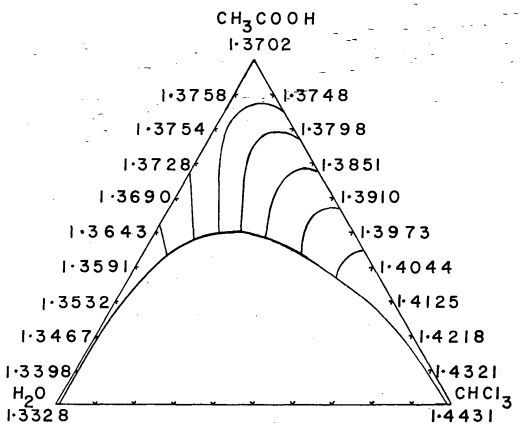

FIG. 2. Curves of equal refractive index at 25° C in the system acetic acid – chloroform – water.

This accuracy enables concentrations in the binary system chloroform – acetic acid to be determined with an accuracy of 0.2 wt%. In the binary system acetic acid – water the accuracy is again 0.2% up to a concentration of 70% acetic acid; at higher acid concentrations the curve of refractive index exhibits a maximum.

For the analysis of ternary mixtures, which is carried out by determining the intersection of the refractive index curve with the horizontal line representing the acetic acid content, the greatest accuracy is obtained in the middle of the triangle but all mixtures can be brought into this area by the addition of a known amount of acetic acid. The overall accuracy is about ±0.5% by weight.

Can. J. Chem. Downloaded from www.nrcresearchpress.com by 210.87.254.105 on 09/05/12
For personal use only.

Densities

The densities were determined with an Ostwald–Sprengel type pyknometer in a thermostat controlled at 25±0.005° C. Densities were reproducible to ±0.0002 g/ml. The density data were used in the calculation of molar volume, thus:

[2] $$V_{exp} = \frac{x_1M_1 + x_2M_2 + x_3M_3}{d}$$

whereas the so-called "ideal volume" results as

$$V_{ideal} = x_1\frac{M_1}{d_1} + x_2\frac{M_2}{d_2} + x_3\frac{M_3}{d_3}.$$

Vapor Pressures and Vapor Compositions

The composition of the vapor given off by a given liquid mixture was determined by the air-bubbling method and the total vapor pressure, manometrically: from these data the partial pressures are calculated. Pearce and Snow (15) point out that the air-bubbling method has sources of error which may be serious. The main source of error lies in the fact that it is difficult to measure accurately and conveniently the large volume of air required. Since, at room temperature, the vapor pressures of acetic acid and of water are low, about 24 hours would be necessary to attain a reasonable amount of distillate, at an air speed of 1 liter per hour: this makes it difficult to measure the volume of air exactly. We therefore decided to follow the procedure of Parks and Chaffee (16), in which the vapor pressures are measured with a manometer (static method) and the vapor compositions by isothermal distillation using the air displacement method: this obviates the necessity of measuring the volume of air.

Little need be said about the air saturation method except to draw attention to the design of the saturators. We used those described by Pearce and Snow (15) and by Von Bichowski and Storch (17). The temperature of our measurements was always 25.00±0.05°. In order to ensure saturation we made use of a presaturator maintained at 30.0° C. The presaturator consisted of four units of the type used in the equilibrium bath. The equilibrium bath itself contained eight saturators. After leaving the last unit the air passes into a tube leading to the trap. In order to avoid condensation of vapor in this tube, it is wound with resistance wire right into the trap, as shown in Fig. 3: the current supplied by a copper oxide rectifier maintains this tube at 50–60°. The trap is kept in an acetone – dry ice mixture.

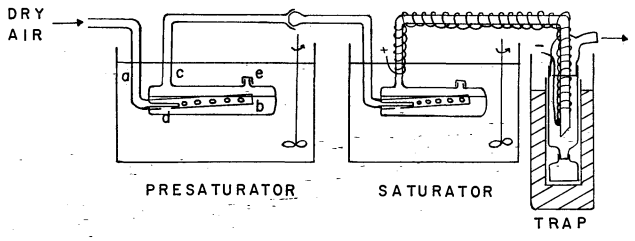

FIG. 3. The isothermal distillation apparatus. *a*, air inlet tube; *b*, slanting tube; *c*, outlet tube; *d*, hole in slanting tube; *e*, filling tube (glass-stoppered).

In the literature it is stated that air speeds up to 10 liters per hour give satisfactory results but we used a speed not exceeding 2 liters per hour. Varying the speed between 0.5 and 2.0 liters per hour gave no larger deviation than 1% by weight, which we believe to represent our experimental error.

EXPERIMENTAL RESULTS AND CALCULATIONS

DENSITY AND VOLUME

Acetic Acid – Water

Table I gives the density and molar excess volume data in terms of concentration.

The molar excess volumes have been calculated using the density data for the pure liquids of Kohner and Gressman (2) and of Woodman (1). When V^E is plotted against mole fraction a minimum of −1.145 ml at 0.5 mole fraction acetic acid is observed.

The partial molal volumes were calculated from our own density data, those of Woodman (1), Kohner and Gressman (2), and Redlich and Nielsen (3). These data are given in Table II.

Can. J. Chem. Downloaded from www.nrcresearchpress.com by 210.87.254.105 on 09/05/12
For personal use only.

TABLE I

Density data for system acetic acid – water

Wt% HAc	Mole% HAc	d_4^{25}	s.v., ml^{-1}	V^E, ml mole^{-1} (negative)
100.00	100.00	1.0440	0.9577	—
96.06	87.97	1.0535	0.9493	0.571
93.75	81.82	1.0567	0.9464	0.751
89.32	71.51	1.0611	0.9424	0.974
84.93	62.84	1.0636	0.9402	1.088
78.96	52.97	1.0648	0.9391	1.137
69.31	40.39	1.0635	0.9402	1.101

TABLE II

Partial molal volumes in the system acetic acid – water

Mole fraction HAc	v_{HAc}, ml mole^{-1}	$(v-v^0)_{HAc}$,* ml mole^{-1} (negative)	v_{H_2O}, ml mole^{-1}	$(v-v^0)_{H_2O}$,† ml mole^{-1} (negative)
0.0	51.88	5.63	18.07	0.00
0.1	53.37	4.14	17.95	0.12
0.2	54.53	2.98	17.78	0.29
0.3	55.38	2.13	17.57	0.50
0.4	55.98	1.53	17.29	0.78
0.5	56.40	1.11	16.92	1.15
0.6	56.74	0.77	16.47	1.60
0.7	52.02	0.49	15.90	2.17
0.8	57.24	0.27	15.19	2.88
0.9	57.39	0.12	14.01	4.06
1.0	57.51	0.00	12.71	5.36

*Partial molal excess volume of HAc.
†Partial molal excess volume of water.

Chloroform – Acetic Acid

Table III gives the concentrations of chloroform, densities, and molar excess volumes at 25° C. A maximum value for V^E of 0.555 ml exists at 0.45 mole fraction chloroform. Table IV gives the partial molal volumes.

TABLE III

Density data for the system acetic acid – chloroform

Wt% $CHCl_3$	Mole% $CHCl_3$	d_4^{25}	s.v., ml^{-1}	ΔV^E, ml mole^{-1}
0.00	0.00	1.0440	.9579	0.000
2.83	1.44	1.0522	.9504	0.033
14.80	8.03	1.0879	.9192	0.204
26.70	15.48	1.1279	.8866	0.286
37.84	23.44	1.1668	.8570	0.447
49.74	33.23	1.2141	.8237	0.504
59.86	42.86	1.2574	.7953	0.555
69.39	53.27	1.3035	.7672	0.486
76.03	61.47	1.3366	.7482	0.489
82.76	70.71	1.3738	.7279	0.386
89.65	81.33	1.4118	.7083	0.397
93.89	88.54	1.4408	.6941	0.157
100.00	100.00	1.4806	.6754	0.000

Acetic Acid – Chloroform – Water

In Table V the densities and excess molar volumes are represented with the corresponding concentrations. The excess volumes were plotted as functions of the composition at

Can. J. Chem. Downloaded from www.nrcresearchpress.com by 210.87.254.105 on 09/05/12
For personal use only.

TABLE IV

Partial molal volumes in the system acetic acid – chloroform

Mole fraction $CHCl_3$	v_{CHCl_3}, ml mole^{-1}	$(v-v^0)_{CHCl_3}$, ml mole^{-1}	v_{HAc}, ml mole^{-1}	$(v-v^0)_{HAc}$, ml mole^{-1}
0.0	83.86	3.22	57.51	0.00
0.1	82.66	2.02	57.54	0.03
0.2	82.09	1.45	57.64	0.11
0.3	81.68	1.02	57.78	0.27
0.4	81.33	0.69	57.95	0.44
0.5	81.06	0.42	58.15	0.64
0.6	80.88	0.22	58.40	0.89
0.7	80.77	0.13	58.67	1.16
0.8	80.71	0.07	59.01	1.50
0.9	80.67	0.03	59.35	1.84
1.0	80.64	0.00	59.69	2.18

TABLE V

Density data for the system water – acetic acid – chloroform

	H_2O		HAc			
No.	Wt%	Mole%	Wt%	Mole%	d_4^{25}	ΔV^E,* ml mole^{-1}
1	9.76	31.60	50.34	48.91	1.1913	0.593
2	20.99	51.06	54.97	40.12	1.1376	0.804
3	30.43	60.86	60.82	36.50	1.0885	1.016
4	5.52	21.40	40.35	46.94	1.2447	0.285
5	10.89	31.68	67.32	58.76	1.1286	0.795
6	20.43	49.06	61.71	44.47	1.1181	0.997
7	10.68	30.70	71.23	61.45	1.1164	0.882
8	19.05	47.59	58.75	44.04	1.1319	0.911
9	20.50	50.51	54.24	40.10	1.1416	0.878
10	9.91	29.89	64.68	58.54	1.1403	0.739
11	9.98	31.42	54.94	51.91	1.1738	0.644
12	14.81	43.12	44.79	39.13	1.1941	0.680
13	8.07	29.40	36.89	40.33	1.2502	0.404
14	1.95	9.53	24.87	36.48	1.3282	+0.080
15	9.48	33.08	37.00	38.74	1.2444	0.462
16	13.18	34.91	76.94	61.14	1.0921	0.964
17	50.11	77.95	44.58	20.81	1.0672	0.798
18	5.50	16.61	89.57	81.15	1.0707	0.677
19	3.98	12.21	94.73	87.19	1.0572	0.559
20	53.22	79.38	45.38	20.31	1.0547	0.799
21	57.50	82.16	40.72	17.46	1.0519	0.915
22	62.97	85.23	35.73	14.51	1.0443	0.611
23	17.99	43.28	75.06	54.19	1.0847	1.061
24	67.40	87.61	30.94	12.07	1.0419	0.559
25	60.58	83.94	37.80	15.72	1.0489	0.679
26	57.63	82.21	40.72	17.43	1.0516	0.733
27	61.39	84.65	35.56	14.71	1.0516	0.643
28	45.84	74.66	49.50	24.19	1.0687	0.869
29	32.89	13.25	64.20	86.17	1.0711	1.086
30	5.17	16.47	79.90	76.36	1.1007	0.547
31	9.76	28.15	75.69	65.52	1.1045	0.819
32	9.64	27.29	80.74	68.60	1.0890	0.856
33	7.09	20.94	85.49	75.76	1.0798	0.747
34	25.96	54.54	70.15	44.23	1.0758	1.101
35	34.49	64.63	60.27	33.89	1.0769	1.013
36	12.78	33.46	82.12	64.52	1.0775	0.995
37	14.72	37.60	77.52	59.41	1.0863	1.012
38	9.99	27.57	84.85	70.28	1.0758	0.909
39	25.09	55.32	60.07	39.74	1.1081	0.985
40	21.70	50.17	65.30	45.30	1.1030	1.015
41	30.05	61.57	55.00	33.81	1.1066	0.944
42	26.69	57.15	60.01	38.56	1.1031	0.993
43	21.14	49.24	66.30	46.34	1.1017	1.016
44	14.95	41.50	55.24	46.01	1.1570	0.803

Can. J. Chem. Downloaded from www.nrcresearchpress.com by 210.87.254.105 on 09/05/12
For personal use only.

TABLE V (*Concluded*)

Density data for the system water – acetic acid – chloroform

No.	H_2O		HAc		d_4^{25}	ΔV^E,* ml mole^{-1}
	Wt%	Mole%	Wt%	Mole%		
45	10.61	32.12	59.89	54.40	1.1545	0.717
46	9.57	31.86	45.74	45.69	1.2095	0.549
47	5.02	18.67	50.49	56.35	1.2051	0.311
48	4.43	16.74	50.99	57.83	1.2047	0.262
49	5.16	19.65	45.51	52.00	1.2244	0.281
50	5.67	21.21	45.78	51.39	1.2220	0.335
51	4.92	20.06	35.29	43.16	1.2686	0.215
52	4.25	13.07	92.69	85.51	1.0628	0.565
53	38.66	69.59	51.21	27.66	1.0884	0.905
54	25.62	56.92	54.76	36.50	1.1223	0.917
55	36.98	66.75	59.73	32.35	1.0703	1.004
56	22.08	52.03	57.67	40.77	1.1253	0.932
57	15.03	41.14	58.19	47.80	1.1467	0.835
58	20.21	50.71	50.98	38.38	1.1530	0.827
59	26.33	57.67	55.02	36.16	1.1181	0.897
60	34.98	66.52	52.26	29.82	1.0978	0.914
61	45.28	74.61	47.98	23.72	1.0747	0.855
62	30.70	62.64	52.65	32.23	1.1114	0.913
63	23.33	53.23	59.85	40.98	1.1144	0.938
64	42.07	71.82	52.06	26.67	1.0746	0.913
65	22.40	8.13	75.72	91.53	1.0702	1.286
66	29.70	58.78	68.52	40.69	1.0689	1.093
67	52.07	78.89	44.90	20.41	1.0600	0.803
68	28.52	58.45	63.63	39.13	1.0868	1.048
69	32.03	63.27	55.92	33.14	1.0976	0.968
70	43.57	72.19	55.42	27.56	1.0604	0.945
71	2.0	6.70	87.3	87.90	1.0798	0.147
72	2.0	6.85	83.1	85.45	1.0921	0.063
73	2.0	7.10	75.8	80.95	1.1144	+0.082
74	2.0	7.25	72.5	78.80	1.1253	+0.125
75	2.0	7.60	63.7	72.70	1.1570	+0.167
76	2.0	8.05	54.3	65.45	1.1941	+0.154
77	2.0	8.65	42.3	54.95	1.2444	+0.174
78	2.0	8.95	37.1	49.85	1.2686	+0.123

*Negative, unless stated otherwise.

the same time making use of the binary data. From this plot the equi-excess volume lines of Fig. 4 were interpolated. From Fig. 4 it follows that from the concentration 100 mole% acetic acid to 100 mole% chloroform there must run a curve along which the excess molar volume is zero.

Refractometric Results

Acetic Acid – Water

Table VI contains the refractive indices and molar refractions. The molar refraction calculated from those of the pure components is also given. Finally the apparent molar refraction of acetic acid has been calculated from the formula

$$[4] \qquad \phi R = \frac{R_{\text{exptl}} - x_1 R_1^0}{x_2},$$

where x_1, R_1^0 are the mole fraction and molar refraction of pure water and x_2 the mole fraction of acetic acid.

Acetic Acid – Chloroform

Table VII contains the identical data for this system as is given in Table VI for acetic acid – water.

Can. J. Chem. Downloaded from www.nrcresearchpress.com by 210.87.254.105 on 09/05/12
For personal use only.

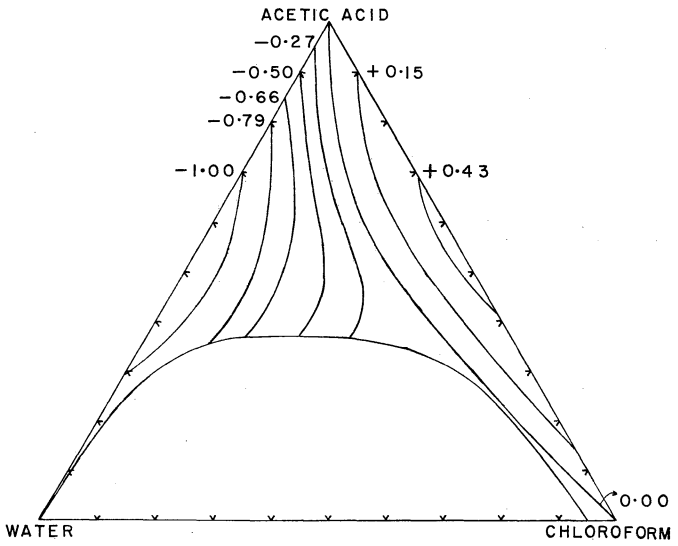

FIG. 4. The excess volume functions in the system acetic acid – chloroform – water at 25° C.

TABLE VI

Refractive properties of the system water – acetic acid

Wt% HAc	Mole% HAc	$n_D^{25.03}$	R_{expt1}	R_{calc}	ϕR HAc
0.00	0.00	1.3328	—	3.715	—
9.45	3.04	1.3395	3.999	3.998	13.06
18.60	6.42	1.3458	4.315	4.312	13.07
21.65	7.66	1.3480	4.433	4.427	13.09
27.07	10.02	1.3514	4.651	4.647	13.05
37.89	15.47	1.3585	5.165	5.154	13.09
45.89	20.29	1.3623	5.609	5.602	13.05
54.91	26.76	1.3668	6.214	6.203	13.05
62.53	33.37	1.3699	6.828	6.818	13.05
66.82	37.67	1.3718	7.235	7.218	13.06
70.21	41.42	1.3729	7.584	7.566	13.06
82.41	58.53	1.3759	9.175	9.148	13.06
84.69	62.40	1.3759	9.541	9.518	13.05
84.70	62.42	1.3761	9.547	9.519	13.06
87.06	66.87	1.3761	9.961	9.933	13.06
88.65	70.09	1.3757	10.253	10.233	13.04
90.90	74.98	1.3756	10.713	10.687	13.05
94.94	84.92	1.3743	11.633	11.612	13.04
96.94	90.48	1.3732	12.147	12.129	13.03
100.00	100.00	1.3702	—	13.014	13.01

Acetic Acid – Chloroform – Water

Table VIII contains the refractive indices as a function of composition. When these are plotted on a composition triangle, lines of equal refractive index are obtained.

VAPOR–LIQUID EQUILIBRIA

Acetic Acid – Water

Table IX gives total pressure versus concentration of acetic acid in liquid, in weight percent, and the results of isothermal distillation (equilibrium liquid and vapor composition expressed as weight percent acetic acid).

Can. J. Chem. Downloaded from www.nrcresearchpress.com by 210.87.254.105 on 09/05/12
For personal use only.

TABLE VII

Refractive properties of the system acetic acid – chloroform

Wt% $CHCl_3$	Mole% $CHCl_3$	$n_D^{25.03}$	R_{exptl}	R_{calc}	ϕR HAc
0.00	0.00	1.3702	—	13.014	13.01
3.63	1.86	1.3720	13.182	13.170	13.03
10.67	5.67	1.3753	13.508	13.489	13.03
12.98	6.98	1.3763	13.615	13.599	13.03
15.18	8.26	1.3772	13.719	13.760	13.03
28.69	16.83	1.3845	14.442	14.424	13.04
31.79	18.99	1.3865	14.638	14.605	13.06
38.97	24.31	1.3901	15.069	15.050	13.04
45.08	29.22	1.3942	15.497	15.461	13.06
45.32	29.42	1.3945	15.519	15.478	13.07
49.57	33.08	1.3970	15.820	15.785	13.07
49.70	33.20	1.3972	15.835	15.795	13.07
52.83	36.03	1.3993	16.069	16.032	13.07
71.18	55.40	1.4139	17.701	17.654	13.12
79.10	65.56	1.4210	18.554	18.505	13.16
87.31	77.58	1.4294	19.576	19.512	13.30
90.83	83.28	1.4329	20.035	19.990	13.28
100.00	100.00	1.4433	—	21.390	—

TABLE VIII

Refractive properties of the system water – acetic acid – chloroform

Wt% H_2O	Wt% HAc	$n_D^{25.03}$	Wt% H_2O	Wt% HAc	$n_D^{25.03}$
29.72	62.23	1.3758	40.82	48.89	1.3718
42.39	54.41	1.3688	20.57	68.15	1.3797
15.09	56.34	1.3882	24.33	61.11	1.3798
9.73	50.63	1.3943	26.85	64.41	1.3769
4.52	39.54	1.4042	32.09	60.50	1.3747
23.69	68.49	1.3778	49.44	47.45	1.3653
7.69	81.09	1.3800	12.32	59.70	1.3894
12.10	76.56	1.3809	10.75	62.80	1.3874
2.80	75.59	1.3831	16.93	59.96	1.3852
3.33	66.58	1.3877	16.72	50.26	1.3898
4.32	63.62	1.3893	24.21	51.73	1.3841
5.20	57.05	1.3928	9.11	63.43	1.3879
4.89	52.59	1.3954	15.54	75.77	1.3794
11.45	62.86	1.3872	25.21	51.23	1.3831
20.70	65.58	1.3808	3.14	61.43	1.3907
29.27	59.10	1.3770	16.67	69.31	1.3814
24.63	59.33	1.3802	14.42	63.90	1.3850
29.28	55.90	1.3781	28.99	52.89	1.3794
31.45	52.11	1.3780	6.65	73.86	1.3833
18.18	68.34	1.3812	12.69	74.32	1.3814
18.86	71.91	1.3793	14.37	65.14	1.3844
22.92	66.78	1.3789	9.85	85.06	1.3778
23.04	70.38	1.3774	19.86	60.08	1.3831
2.89	68.01	1.3870	8.70	71.00	1.3842
0.91	18.34	1.4230	6.65	66.86	1.3870
4.22	63.61	1.3892	16.89	51.37	1.3892
3.49	42.19	1.4023	15.34	77.21	1.3789
9.32	65.80	1.3866	13.47	51.99	1.3913
11.78	50.71	1.3932	5.29	48.01	1.3980
10.27	53.37	1.3926	7.33	61.54	1.3898
4.32	73.51	1.3842	8.67	44.29	1.3987
11.56	59.87	1.3886	8.19	62.14	1.3889
8.41	50.88	1.3950	8.40	58.30	1.3909

We have made use of the Gibbs–Duhem–Margules equation to prove the consistency of the results obtained. For this purpose it is necessary to obtain information on the

Can. J. Chem. Downloaded from www.nrcresearchpress.com by 210.87.254.105 on 09/05/12
For personal use only.

TABLE IX

Total vapor pressures in the system water – acetic acid at 25° C

Liquid	Vapor		Liquid	Vapor	
Wt% HAc	Wt% HAc	P, mm Hg	Wt% HAc	Wt% HAc	P, mm Hg
100.0	—	15.7	73.4	66.1	—
98.3	96.0	—	69.1	—	21.9
97.8	—	18.1	57.8	50.0	—
95.6	89.6	—	57.3	—	22.7
95.0	—	19.3	55.2	47.4	—
94.4	90.1	—	33.2	—	23.5
91.1	86.7	—	27.6	—	23.6
88.7	82.8	—	25.2	17.9	—
85.3	79.2	—	18.9	—	23.8
81.6	76.0	—	18.3	12.4	—
80.8	—	21.2	0.0	—	23.8

molecular state of the acetic acid in the vapor phase. This can be done by means of a formula due to Gibbs (18) which gives the relation between vapor density, pressure, and temperature:

$$[5] \qquad \log_{10}\frac{1000(\Delta-1)}{(2-\Delta)^2} = \frac{3520}{T}+\log_{10}P-8.349,$$

where

$\Delta = D/D_1$,

D = experimental vapor density, and

D_1 = 2.073 (ideal density; air = 1.0, i.e. vapor density of monomer).

Wrewsky *et al.* (6) tested this formula on the system acetic acid – water at 42° and 60° C and found that it reproduced their results over the complete concentration range.

Using the above formula it is possible to calculate the molecular weight of the acetic acid in the vapor phase by successive approximations. Complete dimerization is first assumed. From this and the vapor composition data the mole fraction of acetic acid in the vapor is calculated and from this the partial pressure of acetic acid. When this is introduced into the above equation D is obtained and hence an approximate mean molecular weight. This procedure is repeated until no change in the average molecular weight is found. It is thus possible to construct the vapor pressure curves as a function of true mole fraction.

Once the true molecular weight of the acetic acid in the vapor phase is known the percentage dimerization can be calculated and from this again the partial pressures of single and dimerized molecules, respectively, can be obtained. Lambert (19) points out that the plot of log K (K = dimerization constant) vs. $1/T$ does in actual fact yield a linear plot from which the heats and entropies of dimerization can be obtained. Entropies of dimerization usually lie between 20 and 27 cal/deg mole, but Lambert finds from MacDougall's data (20) $\Delta H = -16$ kcal/mole and $\Delta S = +54$ cal/deg mole. Thus the entropy is about twice the maximum hitherto observed for dimerization. More recently, Levy and Davis (21) have investigated this question of the dimerization of acetic acid in the presence of water. They find that a possible equilibrium between acetic acid dimer and acetic anhydride is in fact negligible, the equilibrium being between dimer and monomer molecules. They find a somewhat smaller heat of dissociation, $\Delta H = -14.4$ kcal/mole, with the

Can. J. Chem. Downloaded from www.nrcresearchpress.com by 210.87.254.105 on 09/05/12
For personal use only.

corresponding ΔS (at the normal boiling point) of +36.8 cal/deg mole. The high entropy of dimerization is ascribed to the dimers being held together by strong hydrogen bonds.

The equilibrium liquid and vapor compositions expressed in weight percent acetic acid are plotted graphically in Fig. 5. The data of Table IX have been treated by the method outlined above and the results are given in Table X. The corresponding vapor and liquid

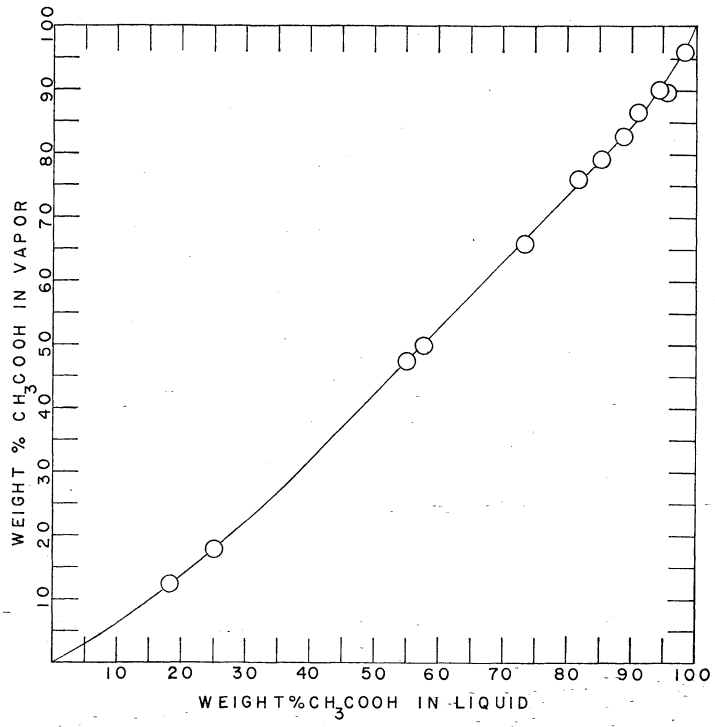

FIG. 5. Liquid–vapor composition equilibrium curve for the system acetic acid – water at 25° C.

TABLE X

Dimerization data for the system water – acetic acid

Liquid		Vapor									
Wt% HAc	Mole% HAc	Wt% HAc	Mole% HAc	M	% dimer	P_{total}*	P_{H_2O}	P_{HAc}	P''	P'	K
100.0	100.0	100.0	100.0	—	—	15.7	—	15.7	—	—	2.89
97.8	87.6	95.5	77.4	111.4	85.5	18.1	4.1	14.0	12.0	2.0	3.00
95.0	75.4	90.9	61.9	110.7	84.3	19.3	7.3	12.0	10.1	1.9	2.81
80.8	41.3	74.5	32.7	108.1	80.1	21.2	14.3	6.9	5.5	1.4	2.81
69.1	27.9	62.2	22.1	104.2	73.6	21.9	17.0	4.9	3.6	1.3	2.13
57.3	18.9	49.9	14.7	103.6	72.6	22.7	19.4	3.3	2.4	0.9	2.96
33.2	8.4	25.4	5.9	97.1	61.8	23.5	22.1	1.4	0.85	0.55	2.83
27.6	6.8	20.2	4.6	94.6	57.6	23.6	22.5	1.1	0.6	0.5	2.40
18.9	4.4	12.8	2.9	90.2	50.3	23.8	23.1	0.7	0.35	0.35	2.86
										Average K	2.8

*Pressures in mm Hg.

compositions are found graphically from Fig. 5. Table X gives the composition of the liquid in weight and mole percent, the latter being based on the average molecular weight

Can. J. Chem. Downloaded from www.nrcresearchpress.com by 210.87.254.105 on 09/05/12
For personal use only.

of the acetic acid in the vapor phase.* The composition, in weight and mole percent, of coexisting vapor is also reported, as are the average molecular weight of acetic acid in the vapor phase, percentage dimer of acetic acid in the vapor phase, total vapor pressure, partial vapor pressures of water and of acetic acid, partial vapor pressure due to acetic acid dimer P'', partial vapor pressure of monomer P', and the dimerization constant K.

$$[6] \qquad K = \frac{P''}{(P')^2}$$

von Zawidzki (22) applied the Gibbs–Duhem–Margules equation to vapor pressure relations of binary systems. He makes use of the exponential solutions in a modified form, which were found for this equation by Margules (23).

$$[7] \qquad P_1 = Px_1 \exp\left(\frac{\alpha_2}{2}x_2^{\,2} + \frac{\alpha_3}{3}x_2^{\,3}\right)$$

$$[8] \qquad P_2 = Px_2 \exp\left(\frac{\beta_2}{2}x_1^{\,2} + \frac{\beta_3}{3}x_1^{\,3}\right),$$

where $\beta_2 = \alpha_2 + \alpha_3$ and $\beta_3 = -\alpha_3$. For the determination of the constants α_2 and α_3 one of the experimental partial pressure curves is used. The data of Table X were treated by the above method using approximations and smoothed total pressure data. The constants $\alpha_2/2 = 0.41$ and $\alpha_3/3 = -0.30$ are obtained for acetic acid, so that it follows for water that $\beta_2/2 = -0.04$ and $\beta_3/3 = +0.30$. The results are expressed in Table XI, which shows measured and calculated partial pressures.

TABLE XI

Partial pressures obtained with von Zawidzki treatment in the system water – acetic acid at 25° C

Acetic acid		Water	
P_{meas}	P_{calc}	P_{meas}	P_{calc}
15.7	15.8	0	0
14.0	13.9	4.1	3.6
12.0	12.2	7.3	6.6
6.9	7.1	14.3	14.2
4.9	4.9	17.0	17.2
3.3	3.3	19.4	19.3
1.4	1.5	22.1	22.0
1.1	1.2	22.5	22.2
0.7	0.8	23.1	22.8

**The use of the average molecular weight of the acetic acid in the vapor phase for the calculation of the liquid mole fraction calls for some justification. It is realized by the authors that this "mole fraction" has no actual physical meaning, because in the liquid phase there will be a different degree of association and therefore a different average molecular weight.*

In this study, however, the attempt is made to prove the consistency of the data obtained by means of the Gibbs–Duhem–Margules equation. von Zawidzki (22) points out that in the derivation of the Gibbs–Duhem equation no surface work has been taken into account, but only work of dilution. Because of this, the mole fractions of the components in the liquid phase have to be referred to the molecular weight in the vapor phase. When, therefore, a component shows dimerization in the vapor phase, the calculations must be based on the molecular weight of the dimerizing component. von Zawidzki shows that there are two Gibbs–Duhem equations, one for the monomer and one for the dimer. He also shows that the total partial pressure of the dimerizing component follows a third Gibbs–Duhem equation in which the mole fraction in the liquid phase is calculated by means of the average molecular weight of the dimerizing component in the vapor phase. In the present work, we use the latter equation.

Can. J. Chem. Downloaded from www.nrcresearchpress.com by 210.87.254.105 on 09/05/12
For personal use only.

Kamke (24) makes use of the Gibbs–Duhem–Margules differential equation in the following form,

$$[9] \qquad \frac{x d \ln P_1}{dx} + (1-x)\frac{d \ln P_2}{dx} = 0,$$

where x is the mole fraction in the *liquid phase* of the component with the lower boiling point. This leads to the differential equation

$$[10] \qquad \frac{1}{P}\frac{dP}{dx} = -\frac{x-y}{y(1-y)}\frac{dy}{dx},$$

where y = mole fraction in the vapor phase of the component with the lower boiling point.

Kamke now writes

$$[11] \qquad f(y) = \frac{x-y}{y(1-y)}$$

and makes use of this to obtain the curve of excess free energy for a binary system. Defining the molecular free energy of mixing as

$$[12] \qquad \Delta G^{E} = RT(x_1 \ln \gamma_1 + x_2 \ln \gamma_2),$$

where γ_1 and γ_2 are the appropriate activity coefficients, he obtains

$$[13] \qquad \frac{\Delta G^{E}}{RT} = x \ln \frac{Py}{P_1^{0}x} + (1-x) \ln \frac{P(1-y)}{P_2^{0}(1-x)},$$

which leads to

$$[14] \qquad \frac{1}{RT}\frac{d\Delta G^{E}}{dx} = \ln \frac{P_2^{0}}{P_1^{0}}\frac{y(1-x)}{x(1-y)} = \ln \frac{P_2^{0}}{P_1^{0}}\theta,$$

where

$$[15] \qquad \theta = \frac{y(1-x)}{x(1-y)}$$

is the relative volatility and

$$[16] \qquad \frac{1}{RT}\frac{d^2\Delta G^{E}}{dx^2} = \frac{1}{y(1-y)}\left[\frac{1}{1+(1-2y)f(y)+y(1-y)\{df(y)/dy\}} - \frac{1}{1+(1-2y)f(y)+y(1-y)\{-f^2(y)\}}\right].$$

The data of Table X have been used to calculate $f(y)$ as defined by equation [11], and the relative volatility (equation [15]). These results are reported in Table XII together with the quantity

$$P_2^{0}/P_1^{0}\,\theta = 0.664\theta.$$

In Fig. 6, $f(y)$ is given as a function of the mole fraction of water in the vapor phase (y). The ideal curve $f_{\text{ideal}}(y)$ is calculated according to the formula

$$f_{\text{ideal}}(y) = -\frac{1}{a-y},$$

where $a = P_1^{0}/(P_1^{0}-P_2^{0}) = 23.8/(23.8-15.8) = 2.98$. Hence

$$f_{\text{ideal}}(y) = -\frac{1}{2.98-y}.$$

Can. J. Chem. Downloaded from www.nrcresearchpress.com by 210.87.254.105 on 09/05/12
For personal use only.

TABLE XII

$f(y)$ and relative volatility data for the system water – acetic acid at 25° C

x^*	y	$f(y)$ (negative)	0.664θ
0.124	0.226	0.583	1.370
0.246	0.381	0.572	1.253
0.587	0.673	0.391	0.961
0.721	0.779	0.337	0.906
0.811	0.853	0.336	0.898
0.916	0.941	0.450	0.971
0.932	0.954	0.729	1.005
0.956	0.971	0.541	1.023

*x = mole fraction H_2O in liquid; y = mole fraction H_2O in vapor.

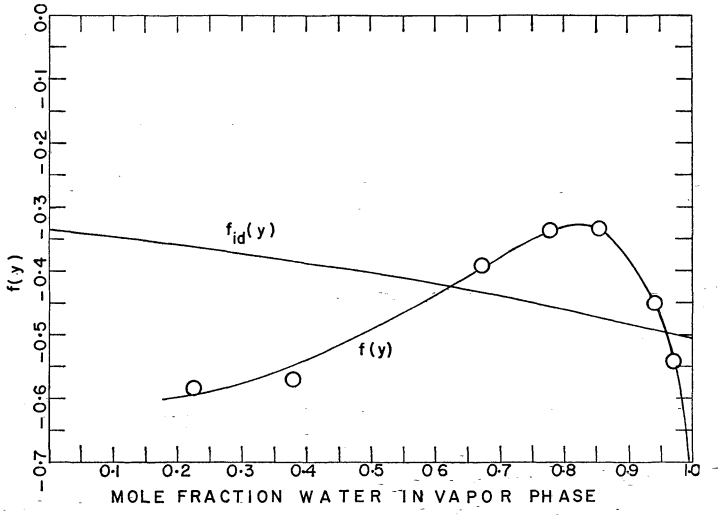

FIG. 6. $f(y)$ for the system acetic acid – water at 25° C.

Chloroform – Acetic Acid

The total vapor pressures and vapor compositions are given in Table XIII: the figures in parentheses are the number of determinations from which the average is obtained. The data of Table XIII have been treated for dimerization of the acetic acid in the vapor phase in the same way as for the water – acetic acid system. The results are reported in Table XIV. The calculation of mole fraction in the liquid is again based on the average molecular

TABLE XIII

Total vapor pressures in the system acetic acid – chloroform

Liquid	Vapor	P,	Liquid	Vapor	P,
Wt% $CHCl_3$	Wt% $CHCl_3$	mm Hg	Wt% $CHCl_3$	Wt% $CHCl_3$	mm Hg
9.3 (2)	56.3	—	41.6 (3)	89.7	—
15.6	—	46.4	43.8	—	93.5
19.2	—	51.3	47.6	—	101.7
23.5	—	58.6	53.1 (4)	93.2	—
25.8 (3)	81.4	—	61.9 (1)	94.4	—
30.1 (1)	85.4	—	68.8	—	141.1
32.5 (3)	88.2	—	85.4	—	173.5
34.3	—	77.4			

Can. J. Chem. Downloaded from www.nrcresearchpress.com by 210.87.254.105 on 09/05/12
For personal use only.

weight of acetic acid in the vapor phase. The data of Table XIII have also been treated

TABLE XIV

Dimerization data for the system acetic acid – chloroform

	Liquid		Vapor									
No.	Wt% $CHCl_3$	Mole% $CHCl_3$	Wt% $CHCl_3$	Mole% $CHCl_3$	M	% dimer	P_{total}*	P_{CHCl_3}	P_{HAc}	P''	P'	K
1	0.0	0.0	0.0	0.0	—	—	15.8	0.0	15.8	—	—	2.89
2	15.6	14.8	68.6	67.2	111.7	86.0	46.4	31.2	15.2	13.1	2.1	2.97
3	19.2	18.2	73.9	72.5	111.2	85.2	51.3	37.2	14.1	12.0	2.1	2.72
4	23.5	22.2	79.0	77.8	111.1	85.0	58.6	45.6	13.0	11.0	2.0	2.75
5	34.3	32.5	87.1	86.2	110.3	83.6	77.4	66.7	10.7	8.9	1.8	2.75
6	43.8	41.7	90.5	89.8	109.7	82.8	93.5	83.9	9.6	7.9	1.7	2.75
7	47.6	45.5	91.6	90.9	109.6	82.5	101.7	92.5	9.2	7.6	1.6	2.91
8	68.8	66.4	96.2	95.8	107.3	78.7	141.1	135.2	5.9	4.7	1.3	2.78
9	85.4	83.5	98.5	98.3	103.0	71.6	173.5	170.5	3.0	2.2	0.9	2.72
10	100.0	100.0	100.0	100.0	—	—	199.1	199.1	0.0	—	—	—
											Average K	2.75

*Pressures in mm Hg.

according to the formulae [7] and [8]. Using smoothed data for chloroform, the constants $\alpha_2/2 = 0.155$ and $\alpha_3/3 = -0.16$ are obtained. This gives for acetic acid the constants $\beta_2/2 = -0.085$ and $\beta_3/3 = +0.16$. The final results are reported in Table XV.

TABLE XV

Partial pressures obtained with von Zawidzki treatment in the system acetic acid – chloroform

	Chloroform		Acetic acid	
No.	P_{meas}	P_{calc}	P_{meas}	P_{calc}
2	31.2	29.8	15.2	13.4
3	37.2	36.7	14.1	12.9
4	45.6	45.0	13.0	12.3
5	66.7	66.2	10.7	10.6
6	83.9	84.9	9.6	9.2
7	92.5	92.5	9.2	8.4
8	135.2	134.0	5.9	5.4
9	170.5	167.0	3.0	2.7

The data of Table XIII have been used to calculate $f(y)$ and the relative volatility. This quantity is tabulated in Table XVI as $(P_2^0/P_1^0)\theta = 0.0794\theta$.

TABLE XVI

$f(y)$ and relative volatility data for the system acetic acid – chloroform

x*	y	$f(y)$ (negative)	0.079θ
0.148	0.672	2.375	1.062
0.182	0.725	2.371	0.941
0.222	0.778	3.214	0.975
0.325	0.862	4.505	1.030
0.417	0.898	5.004	0.977
0.455	0.909	5.506	0.950
0.664	0.958	7.280	0.916
0.835	0.983	8.657	0.907

*x = mole fraction $CHCl_3$ in liquid; y = mole fraction $CHCl_3$ in vapor.

Can. J. Chem. Downloaded from www.nrcresearchpress.com by 210.87.254.105 on 09/05/12
For personal use only.

Acetic Acid – Chloroform – Water

The total vapor pressures as functions of composition of liquid phase are given in Table XVII and the compositions of vapor phase in Table XVIII. As before, the figures in

TABLE XVII

Total vapor pressures in the system acetic acid – chloroform – water at 25° C

No.	Liquid composition Wt% HAc	Wt% $CHCl_3$	P mm Hg
1	67.7	21.9	94.7
2	53.0	39.3	145.7
3	58.8	32.0	129.3
4	60.4	12.6	129.9
5	65.8	4.3	73.6
6	61.9	20.0	121.6
7	43.4	44.6	171.3
8	49.0	36.9	161.6
9	74.1	16.2	76.3
10	71.4	20.2	85.5
11	—	(50)	210.5
12(*a*)	28.9	1.5	167.5
(*b*)	8.2	90.6	—

TABLE XVIII

Vapor–liquid equilibrium compositions in the system acetic acid – chloroform – water at 25° C

No.	Liquid composition		Vapor composition		Total pressure*
1	55.0 wt% HAc 28.6 wt% $CHCl_3$ 16.4 wt% H_2O	(2)	3.5 wt% HAc 95.5 wt% $CHCl_3$ 1.0 wt% H_2O	(3)	146
2	56.0 wt% HAc 13.3 wt% $CHCl_3$ 30.7 wt% H_2O	(3)	2.9 wt% HAc 96.0 wt% $CHCl_3$ 1.1 wt% H_2O	(6)	143
3	83.9 wt% HAc 5.1 wt% $CHCl_3$ 11.0 wt% H_2O	(2)	27.7 wt% HAc 66.8 wt% $CHCl_3$ 5.6 wt% H_2O	(4)	39
4	65.7 wt% HAc 4.8 wt% $CHCl_3$ 29.6 wt% H_2O	(2)	7.9 wt% HAc 89.5 wt% $CHCl_3$ 2.6 wt% H_2O	(3)	74
5	65.0 wt% HAc 24.0 wt% $CHCl_3$ 11.0 wt% H_2O	(3)	7.0 wt% HAc 91.6 wt% $CHCl_3$ 1.4 wt% H_2O	(3)	106

*In mm Hg.

parentheses indicate the number of determinations from which the average is obtained. The last column of Table XVIII contains the corresponding total vapor pressures, interpolated from Table XVII. The accuracy of the data is about ±3 mm. Table XIX contains the dimerization data, the mole fraction being again calculated on a dimerized basis.

DISCUSSION OF RESULTS

The System Water – Acetic Acid

When water and acetic acid are mixed there is a contraction in volume. This means that there is a negative excess molar volume function as shown in Fig. 7, in which the

Can. J. Chem. Downloaded from www.nrcresearchpress.com by 210.87.254.105 on 09/05/12
For personal use only.

Can. J. Chem. Downloaded from www.nrcresearchpress.com by 210.87.254.105 on 09/05/12
For personal use only.

TABLE XIX

Dimerization data for the system acetic acid – chloroform – water at 25° C

No.		Liquid		Vapor		M	% dimer	P_{total}*	P_{H_2O}	P_{CHCl_3}	P_{HAc}	P''	P'	K
		Wt%	Mole%	Wt%	Mole%									
	HAc	55.0	31.0	3.5	6.2									
1	$CHCl_3$	28.6	14.4	95.5	90.1	106.7	77.7	146	9.1	131.5	5.4	4.2	1.2	2.9
	H_2O	16.4	54.6	1.0	3.7									
	HAc	56.0	22.6	2.9	3.1									
2	$CHCl_3$	13.3	4.8	96.0	90.1	105.5	75.7	143	9.7	128.8	4.4	3.3	1.1	2.9
	H_2O	30.7	72.6	1.1	6.8									
	HAc	83.9	54.0	27.7	22.6									
3	$CHCl_3$	5.1	3.0	66.8	49.8	109.3	82.1	39	10.8	19.4	8.8	7.2	2.5	2.9
	H_2O	11.0	43.0	5.6	27.7									
	HAc	65.7	26.7	7.9	7.6									
4	$CHCl_3$	4.8	1.8	89.5	77.5	107.0	78.2	74	11.0	57.3	5.6	4.4	1.2	2.9
	H_2O	29.6	71.5	2.6	14.9									
	HAc	65.0	42.4	7.0	7.2									
5	$CHCl_3$	24.0	14.3	91.6	86.2	108.7	81.0	106	6.9	91.4	7.7	6.2	1.5	2.9
	H_2O	11.0	43.3	1.4	6.6								Average K	2.9

*In mm Hg.

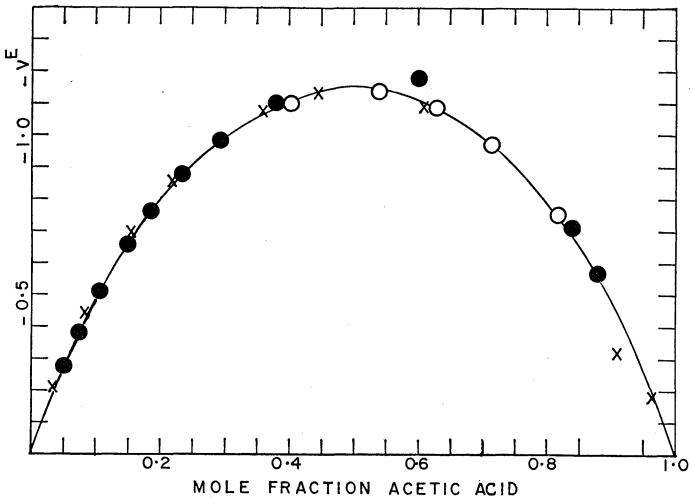

FIG. 7. The excess volume function for the system acetic acid – water at 25° C. ×, Kohner and Gressmann; ●, Woodman; ○, this research.

excess volume function is plotted against mole fraction of acetic acid. The minimum negative value, larger than 1 ml mole^{-1} of mixture, occurs at a concentration of 50 mole%. In general, dipole–dipole mixtures show a similar behavior, probably because the dipole–dipole associations of the pure liquids are partially broken up to form mixed associations and this causes the volume to decrease. We suggest that in the present case a mixed association of one molecule of acetic acid and one molecule of water may occur, due to hydrogen bonding, thus:

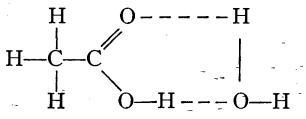

When the data of Table II are plotted, the partial molal excess volumes are perfectly symmetrical with respect to composition both for water and for acetic acid and this agrees with the above view. This symmetry implies that the changes in liquid structure on addition of water to pure acetic acid and of acetic acid to pure water have similar effects on the structure of the liquid. This is quite contrary to the behavior of the system water – ethyl alcohol, studied by Mitchell and Wynne-Jones (25), where hydrogen bonding is also involved. The viscosities of the water – acetic acid system, as reported by Campbell and Kartzmark (9), also show perfect symmetry, with the maximum at 50 mole%.

From the data on molar refractions (Table VI) it follows that the influence of the mixing process on the true volumes of acetic acid and water is very small. The slight deviations are positive but, as an approximation, it could be said that the true volumes are additive. This is confirmed by the constancy of the apparent molar refraction of the acetic acid.

Table X shows that the dimerization treatment is justified, since, within the experimental error, the "dimerization constant" retains a constant value over the entire concentration range. The amount of dimerization decreases with addition of water.

The partial pressures, calculated from the amount of dimerization by the method of

Can. J. Chem. Downloaded from www.nrcresearchpress.com by 210.87.254.105 on 09/05/12
For personal use only.

von Zawidzki (Table XI), agree with the measured values fairly well, as required by the Gibbs–Duhem–Margules equation.

Figure 8 shows that this system exhibits positive deviation from Raoult's law, and that therefore the excess free energy of mixing, ΔG^E, is greater than zero. There is no maximum

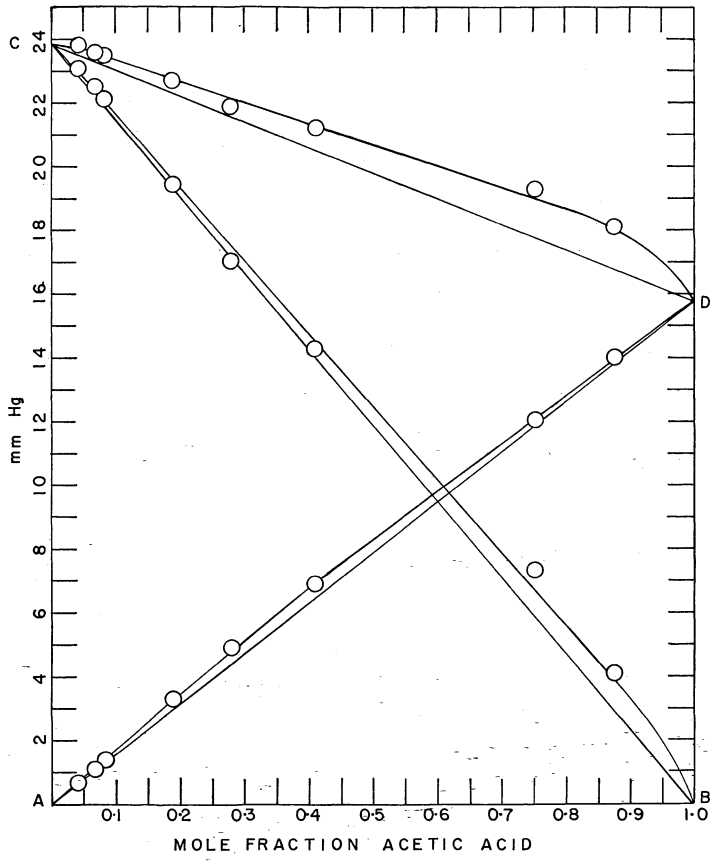

FIG. 8. Total and partial vapor pressure curves on a dimerized basis for the system acetic acid – water at 25° C. CD, total pressure curves; AD, partial pressures of acetic acid; BC, partial pressures of water (the straight lines are the "ideal" curves).

on the vapor pressure curve. Figure 5 also suggests the absence of an azeotropic point, at which the compositions of liquid and coexisting vapor would be the same. Complete separation of the components is therefore possible by an isothermal fractional distillation.

A study of the graph for $f(y)$ (Fig. 6) leads to the conclusion that the second derivative of the excess Gibbs free energy with respect to concentration $d^2\Delta G^E/dx^2$ (equation [16]) is equal to zero somewhere in the concentration region. This means that the $\Delta G^E(x)$ curve will show a point of inflection. The approximate positions of both the maximum and the point of inflection in the $\Delta G^E(x)$ curve are found from the curve in Fig. 9. When 0.664θ becomes equal to unity, the corresponding concentrations are those of the maximum and of the point of inflection. On a non-dimerized basis, the concentrations are 0.7 and 0.1 mole fraction of acetic acid in the liquid phase.

The heats of mixing as reported in the "International critical tables" are positive (heat absorbed) between 15 and 95 mole% acetic acid and for other concentrations negative.

Can. J. Chem. Downloaded from www.nrcresearchpress.com by 210.87.254.105 on 09/05/12
For personal use only.

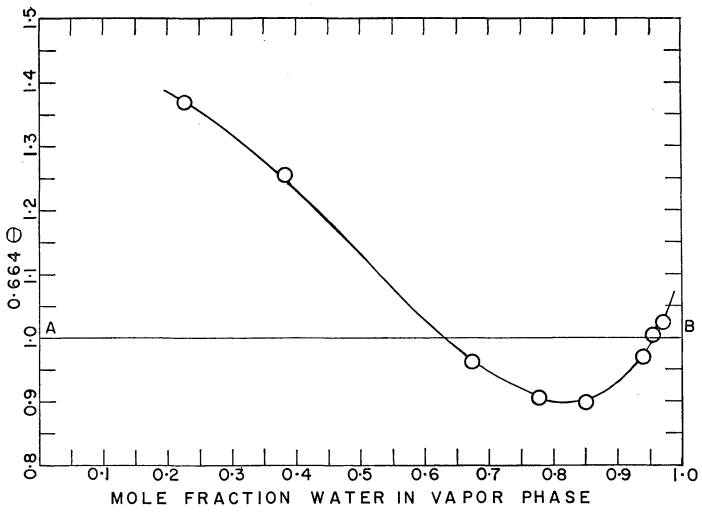

FIG. 9. The relative volatility function in the system acetic acid – water at 25° C. AB, ideal behavior.

From the relation between the excess entropy of mixing and the excess free energy of mixing $\Delta G^E + T\Delta S^E = \Delta H$ (T = constant) it follows that ΔS^E most probably has a negative sign. This seems also to be indicated by the volume contraction which occurs upon mixing. A negative ΔS^E may explain the point of inflection which occurs around 10 mole% acetic acid.

When there is a contraction in volume in dipole–dipole liquids, a negative heat of mixing is to be expected. The fact that, in the system acetic acid – water, the heat of mixing is positive over a large concentration range can be explained in accordance with the ideas of Joerges and Nikuradse (26). Energy is required to break up the individual associations of water and of acetic acid but energy is set free by the new association between the water and acetic acid. The "dissociation" energies may be large. Lambert (19) finds from MacDougall's data (20) that $\Delta H = -16$ kcal/mole. This is due to the fact that a double hydrogen bond is involved. This energy is certainly larger than that required to break up the water association. The number of mixed associations cannot be larger, and is usually smaller, than the total number of dissociations. This means that even the case where

$$[\Delta H_{\text{diss}}]_{\text{I}} + [\Delta H_{\text{diss}}]_{\text{II}} < \Delta H_{\text{ass}}$$

$$(\text{HAc})_2 + \text{H}_2\text{O}_{\text{ass}} \rightleftarrows \text{H}_2\text{O–HAc},$$

a positive ΔH of mixing can result, i.e. the energy required to break up the associations is larger than the energy set free by the mixed association.

The exact determination of the magnitude of ΔG^E from the vapor pressure data is not possible because when there is association in the vapor phase extra terms in addition to those of equation [13] have to be used. These extra terms involve the second virial coefficients, which become more complicated in systems where association occurs in the vapor phase, as has been shown by Lambert (19).

We plan an experimental investigation of the heats of mixing at 25° C and a possible application of statistical thermodynamics in order to obtain a better understanding of ΔG^E function.

Can. J. Chem. Downloaded from www.nrcresearchpress.com by 210.87.254.105 on 09/05/12
For personal use only.

It is hoped that a study of the dielectric behavior of the system will throw some light on the problem of the sign of the ΔS^E function.

The data obtained indicate that the excess free energy function ΔG^E is larger than zero and shows a point of inflection. The heat of mixing, ΔH, has both positive and negative values and shows a point of inflection. The excess entropy of mixing function $T\Delta S^E$ presumably has a negative sign and possibly exhibits a point of inflection. With the aid of these data the system acetic acid – water at 25° C can be classified according to the rules proposed by Kamke (24).

The System Acetic Acid – Chloroform

This system shows an increase of volume on mixing. Although this system is a dipole–dipole mixture, the excess volume is not negative. This indicates a tendency for the original associations to retain their identity rather than to form mixed associations between acetic acid and chloroform molecules. The maximum value of ΔV^E occurs at 45 mole% chloroform and the excess partial molal volume curves do not show a symmetry, unlike the system water – acetic acid. The data for molar refraction of mixtures (Table VII) show that the molar refractions are approximately additive and hence that the true molecular volumes remain practically unchanged on mixing.

Table XIII shows that the dimerization treatment is justified because of the constancy within the experimental error of the "dimerization constant".

The variation in the amount of dimerization of the acetic acid in the vapor phase with concentration follows the same pattern as in the system acetic acid – water. Treatment of the partial pressures calculated on the dimerized basis, according to the method of von Zawidzki shows that with reasonable approximations the Gibbs–Duhem–Margules equation is satisfied, although the values calculated for acetic acid are somewhat on the low side.

From Fig. 10 it follows that the behavior of the system is practically ideal in terms of Raoult's law; there is a very slight tendency to positive deviation. If the pressure is plotted against mole fraction on a non-dimerized basis, the apparent deviation from Raoult's law is very large. From Fig. 10 it follows that the two components can be separated completely by means of isothermal fractional distillation.

A study of Figs. 11 and 12 provides further evidence that the behavior of the system is nearly ideal. In an ideal system the function 0.079θ will be equal to unity for all concentrations. The distribution of the points around the "ideal line" shows that the apparent deviation from ideality is probably due to experimental error.

According to the "International critical tables" the heat of mixing is positive but only data for extreme dilution at both ends of the concentration region are available. Because the excess free energy function ΔG^E is only slightly positive a negative excess entropy can be expected but a definite conclusion with respect to the sign of the excess entropy should be left in abeyance until we have made a more detailed experimental study of the heats of mixing. For this reason classification according to the rules of Kamke is as yet impossible.

The System Acid – Water – Chloroform

Figure 4 shows a line running from pure acetic acid to pure chloroform along which the excess volume ΔV^E is equal to zero. This might seem to indicate that mixtures along this curve behave ideally but, as follows from the pressure data, this pseudo-ideality is merely a result of compensating deviations. Figure 4 also shows that the excess volume in the system water–chloroform is negative over the whole region of concentration.

Can. J. Chem. Downloaded from www.nrcresearchpress.com by 210.87.254.105 on 09/05/12
For personal use only.

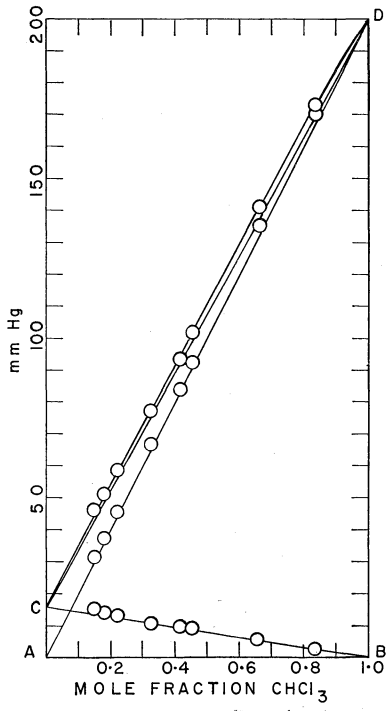

FIG. 10. Total and partial vapor pressure curves on a dimerized basis for the system acetic acid – chloroform at 25° C. CD, total pressure curves; AD, partial pressures of chloroform; BC, partial pressures of acetic acid (the straight lines are the "ideal" curves).

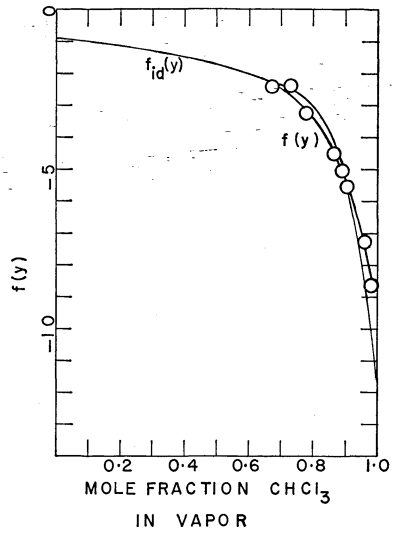

FIG. 11. $f(y)$ for the system acetic acid – chloroform at 25° C.

The results presented in Table XVII show that, in the ternary system, large positive deviations from ideality occur. These large deviations are due to the presence of water and chloroform molecules, which are almost completely immiscible in the binary system. The total vapor pressure of this system is also larger than the sum of those of the two pure

Can. J. Chem. Downloaded from www.nrcresearchpress.com by 210.87.254.105 on 09/05/12
For personal use only.

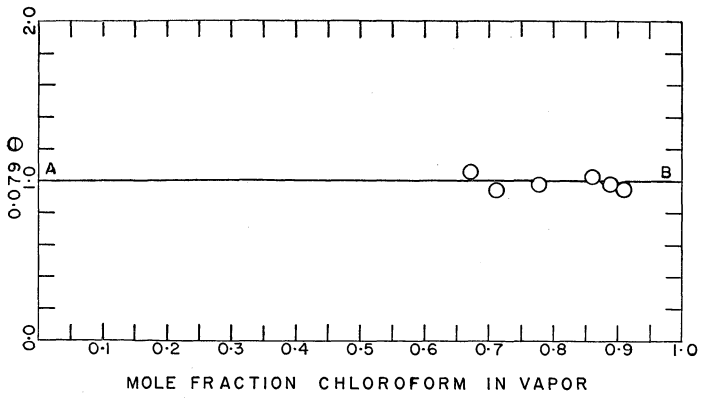

FIG. 12. The relative volatility function for the system acetic acid – chloroform at 25° C. AB, ideal behavior.

components, in the heterogeneous region. This indicates a large positive value for the excess Gibbs free energy ΔG^E. If the concentrations are expressed in mole percent, only a small part of the concentration region is covered, and for this reason it is difficult to show that for concentrations where excess molal volumes is zero, the vapor pressure behavior is not also pseudo-ideal, but, from the general behavior of the vapor pressures, ideality is not to be expected. The heats of mixing, as given in the literature, for the three binary systems also suggest a positive value over the complete concentration region of the ternary system but this has still to be shown experimentally.

From the above discussion it seems probable that the ΔG^E function is positive for all concentrations but more experimental information is necessary to determine the heats and entropies of mixing. A study of the dielectric properties of the system may also throw some light on the latter question. It is therefore not as yet possible to classify this system on the basis of the functions ΔG^E, ΔH, and $T\Delta S^E$ as proposed by Kamke and Kummerle (24).

REFERENCES

1. R. M. WOODMAN. Chem. News, **134**, 36 (1927).
2. H. KOHNER and M. L. GRESSMANN. Z. Physik. Chem. A, **144**, 137 (1929).
3. D. REDLICH and L. E. NIELSEN. J. Am. Chem. Soc. **64**, 761 (1942).
4. G. ARICH and G. TAGLIAVINI. Ric. Sci. **28**, 2493 (1958).
5. N. V. CHALOV and O. A. ALEKSANDROVA. Gidroliz n. i Lesokhim. Prom. **10**, No. 1, 14 (1957).
6. M. S. WREWSKY, K. P. MISENKO, and B. A. MURONZEW. Z. physik. Chem. **133**, 362 (1934).
7. K. FREDENHAGEN and H. LIEBSTER. Z. Physik. Chem. A, **162**, 449 (1932).
8. A. GIACALONE, F. ACCASCINA, and G. CARNESI. Gazz. Chim. Ital. **72**, 109 (1942).
9. A. N. CAMPBELL and E. M. KARTZMARK. Can. J. Res. B, **28**, 161 (1950).
10. A. B. BRANCKER, T. G. HUNTER, and A. W. NASH. J. Phys. Chem. **44**, 683 (1940).
11. W. REINDERS and C. H. DEMINJER. Rec. Trav. Chim. **66**, 573 (1947).
12. C. R. A. WRIGHT, C. THOMPSON, and J. T. LEON. Proc. Roy. Soc. (London), **49**, 174 (1891).
13. D. N. TARASENKOV. J. Gen. Chem. USSR (Eng. Transl.), **16**, 1583 (1946).
14. D. B. HAND. J. Phys. Chem. **34**, 1961 (1930).
15. J. N. PEARCE and R. D. SNOW. J. Phys. Chem. **31**, 231 (1927).
16. G. S. PARKS and C. S. CHAFFEE. J. Phys. Chem. **31**, 439 (1927).
17. F. R. VON BICHOWSKI and H. STORCH. J. Am. Chem. Soc. **37**, 2695 (1915).
18. W. GIBBS. Am. J. Sci. **18**, 277, 372 (1879).
19. J. D. LAMBERT. Discussions Faraday Soc. **15**, 226 (1953).
20. F. H. MACDOUGALL. J. Am. Chem. Soc. **58**, 2585 (1936).
21. B. LEVY and T. W. DAVIS. J. Am. Chem. Soc. **76**, 3268 (1954).
22. J. VON ZAWIDZKI. Z. Physik. Chem. **35**, 129 (1900).
23. M. MARGULES. Sitzber. Akad. Wiss. Wien. Abt II, **104**, 1243 (1895).
24. D. KAMKE and K. KUMMERLE. Z. Physik. Chem. (Frankfurt), **16**, 85 (1958).
25. A. G. MITCHELL and W. F. K. WYNNE-JONES. Discussions Faraday Soc. **15**, 161 (1953).
26. M. JOERGES and A. NIKURADSE. Z. Naturforsch. **59**, 259 (1950).

Can. J. Chem. Downloaded from www.nrcresearchpress.com by 210.87.254.105 on 09/05/12
For personal use only.

SOLVENT SHIFT OF THE CHLOROFORM NUCLEAR MAGNETIC RESONANCE LINE

REINHOLD KAISER
Departments of Chemistry and Physics, University of New Brunswick, Fredericton, New Brunswick
Received July 26, 1962

Can. J. Chem. Downloaded from www.nrcresearchpress.com by 210.87.254.40 on 09/05/12
For personal use only.

ABSTRACT

The chloroform and dioxane proton magnetic resonance line positions have been measured relative to an internal tetramethylsilane reference signal as a function of concentration in binary chloroform – 1,4-dioxane mixtures at 28° C. Corrections have been applied to eliminate the effects of the chloroform self-association and of the non-specific interactions of the chloroform dipole. Analysis of the remaining nuclear magnetic resonance line shift in terms of an equilibrium between free chloroform and 1:1 and 2:1 chloroform–dioxane complexes gives the position of the signal from chloroform in the 1:1 complex at −1.20 p.p.m. and in the 2:1 complex at −0.85 p.p.m. relative to the position of the signal from chloroform at infinite dilution in cyclohexane. Data on other binary chloroform systems have been collected from the literature and have been similarly corrected. The results support the hypothesis of a monotonic relation between the proton magnetic resonance line shift and the energy of the hydrogen bonds which are believed to cause the formation of complexes in these systems. The accuracy of the data is not sufficient to give conclusive evidence regarding the linearity of this relation or the structure of the 2:1 chloroform–dioxane complex.

INTRODUCTION

The study of the high-resolution proton magnetic resonance spectrum of a given solute in a variety of solvents has shown that the spectrum depends on the solvent used. The following mechanisms have been found (1–4) to cause this dependence in liquid solutions:

(*a*) The magnetic field inside the solution differs from the external field by an amount which depends on the volume susceptibility of the solution and on the shape of the sample. The susceptibility is different for different solvents and also varies with the solute concentration.

(*b*) The diamagnetic circulation of electric charge which is induced in a solvent molecule by the magnetic field will, in general, depend on the orientation of the molecule relative to the field direction. The molecular susceptibility, which relates the magnetic moment produced by this circulation to the applied field, is represented by a tensor. While the solvent volume susceptibility is determined by the trace of this tensor, the average field experienced by a solute molecule at the surface of the solvent molecule depends on the anisotropy of the tensor and on the shape of the solvent molecule. This "solvent anisotropy effect" is particularly strong in solvents composed of rod- or disk-shaped molecules, for example in carbon disulphide or benzene.

(*c*) Intermolecular forces of the van der Waals type distort the electronic structure of the molecules involved. This distortion affects the diamagnetic electronic circulation and thereby changes the nuclear shielding. Although these interactions are certainly different for different solutes and solvents, their effect on the nuclear magnetic resonance (n.m.r.) spectrum appears to be small (4).

(*d*) A solute molecule carrying a permanent electric dipole polarizes the surrounding medium. The resulting electric reaction field at the solute molecule can be calculated (5) from a knowledge of the electric and geometric characteristics of the solute and medium. The reaction field hinders the diamagnetic electronic circulation and thus affects the nuclear screening.

(*e*) Specific chemical interactions between two or more solute molecules or between solute and solvent molecules may lead to the formation of complexes. The relative position and orientation of two or more molecules is thereby fixed, and the contributions of mechanisms (*b*), (*c*), and (*d*) to the nuclear screening are modified. The interaction frequently occurs through formation of a hydrogen bond, and the magnetic resonance signal from the hydrogen atom forming the bond is then strongly affected. High-resolution proton magnetic resonance spectroscopy is one of the most sensitive tools for the investigation of hydrogen bonds.

The properties of a hydrogen bond can in principle be determined by the methods of quantum chemistry, but the calculations are difficult and give results of only moderate accuracy. A brief survey of recent work is given by Gränacher (6). Models have been devised that qualitatively exhibit the essential characteristics of a hydrogen bond. In the simplest model the electron donor Y and acceptor X—H are considered to be held together by purely electrostatic forces between localized point charges or dipoles (7). The hydrogen atom forming the bond is then situated in a strong electric field which, for linear hydrogen bonds, is directed along the X—H bond axis. Buckingham (8) has published an approximate calculation to determine the change of the proton shielding caused by the application of an electric field E to a covalently bonded hydrogen atom. His result has been experimentally confirmed for weak fields (where the E-term is dominant) by a study of the chemical shifts in carbonium ions (9), and for strong fields (where the E^2-term is dominant) by providing an explanation for the large chemical shifts of the ions OH^- and OH_3^+ (10). Buckingham's calculation, together with the electrostatic hydrogen bond model, predicts a deshielding of the proton involved in the hydrogen bond, i.e. the magnetic resonance line from the hydrogen bonded complex should always occur at a lower magnetic field than the line from the non-associated acceptor molecule. A shift to lower magnetic field is indeed observed for all hydrogen bonds between molecules with negligible magnetic anisotropy. When the anisotropy is not negligible, effect (*b*) adds a contribution to the normal low-field hydrogen bond shift. This additional shift may be to high or low field, depending on the relative orientation of the hydrogen bond and the anisotropy ellipsoid. For example, benzene can act as donor to form a weak hydrogen bond with the bonding proton located on the sixfold axis of the benzene ring (4). The aromatic ring current produces a large diamagnetic effect at this position, and this apparently overcompensates the paramagnetic effect of the electric field in the hydrogen bond, since the observed net shift is to high field. The diamagnetic effect of association with aromatic solvents is clearly demonstrated by the work of Hatton and Richards (11). Similar effects caused by the anisotropy of triple bonds have been observed with substituted acetylenes and nitriles (2).

The great sensitivity of the n.m.r. spectrum for the detection of hydrogen bonds makes it tempting to try and establish a relation between the n.m.r. line shift and other characteristics of the hydrogen bond. A linear relation with the shift of the infrared absorption frequency of the X—H stretching mode has been established for intramolecular hydrogen bonds in aromatic systems (12), and a correlation with bond length parameters has been reported (6) for intermolecular bonds. From a quantum chemical viewpoint the most important characteristic of the hydrogen bond is its bond energy. It has already been presumed (13–15) that the n.m.r. line shift is a monotonic function of the bond energy. It is the purpose of this report to present experimental data for this function in the range of relatively weak hydrogen bonds.

Can. J. Chem. Downloaded from www.nrcresearchpress.com by 210.87.254.40 on 09/05/12
For personal use only.

Can. J. Chem. Downloaded from www.nrcresearchpress.com by 210.87.254.40 on 09/05/12
For personal use only.

EXPERIMENTAL

A correlation between n.m.r. line shift and hydrogen bond energy can be expected through effect (*e*), which acts by application of mechanisms (*b*), (*c*), and (*d*) to the specific chemical association. Effect (*a*) and the non-specific parts of (*b*), (*c*), and (*d*) also contribute to the observed line shift, and, to isolate the contribution of (*e*), they must be held negligible or else be eliminated by correction of the measured data. Such considerations led to the rejection of hydrogen bonding systems involving aromatic molecules or molecules with triple bonds near the bonding site, to avoid corrections for the specific part of effect (*b*). Secondly, the hydroxyl group can act as donor and acceptor in forming hydrogen bonds. Alcohols, phenols, carboxylic acids, and water can therefore form open dimers with one hydrogen bond, cyclic dimers with two hydrogen bonds, or polymers with open or closed ends. This causes difficulties in the interpretation of the measurements (16) and such compounds were therefore also excluded from this study. Thirdly, measurements of the bond energy were not made in this investigation, but systems were chosen for which this parameter and the association equilibrium constant are known.

A single acceptor, chloroform, was finally chosen and was studied in several donor solvents: 1,4-dioxane, acetone, triethylamine, and diethyl ether. Nuclear magnetic resonance measurements on the dioxane system are here reported for the first time, while data on the other systems were taken from previous work (14, 17). Except for the chloroform dilution shift data determined by Schneider *et al.* (14, 18) all n.m.r. shifts have been measured with reference to the resonance line from an internal reference compound. Abraham (4) has shown that this procedure compensates for effect (*a*) and the non-specific parts of (*b*) and (*c*) even when the reference molecules differ in size or shape from the molecules of the solvent or solute. Schneider *et al.* have applied volume susceptibility corrections to eliminate the contribution of (*a*), while a correction for the non-specific contributions of (*b*) and (*c*) is probably not necessary for the system chloroform–cyclohexane (4). The non-specific contribution of mechanism (*d*) will be discussed in connection with the chloroform dilution shift.

Chloroform Dilution Shift

Several investigators (14, 18, 19, 20) have found a gradual shift of the chloroform n.m.r. line to high field with decreasing concentration of chloroform in inert solvents. The total shift, extrapolated to infinite dilution, is very nearly the same in cyclohexane, *n*-hexane, cyclopentane, and carbon tetrachloride, but uncertainty exists about its magnitude. Values from 0.17 p.p.m. to 0.29 p.p.m. have been reported. This uncertainty may have been caused by insufficient purification of the "reagent" grade chloroform, which usually contains a few percent ethanol to prevent decomposition. Schneider's data (14, 18) have been accepted for this work and are reproduced as curve *c* in Fig. 1. The total dilution shift of 0.29 p.p.m. contains contributions from effects (*d*) and (*e*), and these are discussed in the following.

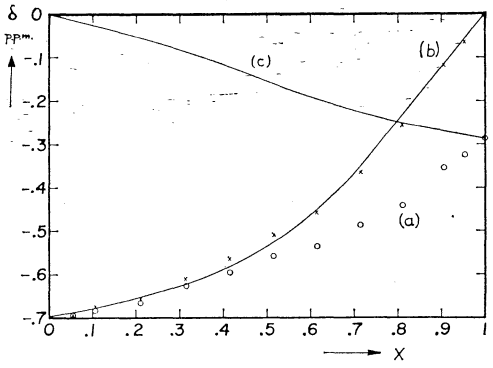

FIG. 1. Shift of chloroform proton magnetic resonance signal vs. chloroform mole fraction X: (*a*) measured in chloroform–dioxane solutions, (*b*) same as *a* but corrected for chloroform dilution shift, (*c*) measured by Schneider *et al.* in chloroform–hydrocarbon solutions. Curve *b* is not equal to the difference between *a* and *c* except at $X = \xi_a = 0$ and at $X = \xi_a = 1$.

The shift in p.p.m. caused by mechanism (*d*) at infinite dilution is given by (4, 5)

$$[1] \qquad \delta = -9.6\times10^{-6}\frac{\mu}{a\cdot b\cdot c}\eta_a[1+(n^2-1)\eta_a]\frac{\epsilon-1}{\epsilon+\beta}.$$

The symbols are explained below, where the numerical values are given for chloroform:

μ	dipole moment of solute molecule	1.02×10^{-18} e.s.u.
a, b, c	semiaxes of solute molecule ellipsoid	2.4 Å, 3.3 Å, 3.3 Å

η_a	shape factor of solute molecule (21)	0.415
n	refractive index of solute	1.44
ϵ	dielectric constant of solvent	4.81
β	$= n^2\eta_a/(1-\eta_a)$	1.53

When the neat chloroform liquid is considered to be a solution of chloroform in chloroform at infinite dilution, the contribution of effect (d) to the total chloroform dilution shift in a solvent of dielectric constant ϵ is given by

[2] $$\delta = -0.23\left(0.60 - \frac{\epsilon-1}{\epsilon+1.53}\right) \text{ p.p.m.}$$

Numerical results are listed in the third column of Table I.

TABLE I

Total dilution shift of chloroform in various solvents

	ϵ	Total shift (d), 10^{-2} p.p.m.	Total shift (e), p.p.m.	Total dilution shift, p.p.m.
n-Hexane	1.89	−7.8	−0.21	
Cyclopentane	1.97	−7.4	−0.22	−0.29
Cyclohexane	2.02	−7.1	−0.22	
CCl_4	2.24	−6.2	−0.23	
Dioxane	2.21	−6.4	−0.22	−0.28
Triethylamine	2.42	−5.5	−0.22	−0.28
Diethyl ether	4.34	−0.7	−0.22	−0.23
Acetone	20.7	+6.6	−0.22	−0.15

Subtraction of shift (d) from the total dilution shift measured in inert solvents gives the values attributed to shift (e) in the first four lines of Table I. Shift (e) is probably caused by self-association of chloroform. Reeves and Schneider (18) have observed a temperature dependence of the total chloroform dilution shift in excess of what might be expected from the temperature variation of the dielectric constants, and this supports the hypothesis of a chemical equilibrium in neat chloroform between species with different n.m.r. line positions. Nikuradse and Ulbrich (22) have reviewed other evidence in favor of this hypothesis. Shift (e) is then determined by the concentrations of the various chloroform species (monomers, dimers, etc.), and in chemical equilibrium these concentrations depend only on the equilibrium constants and on the concentration of chloroform that is not involved in a complex with the solvent. The total shift (e) will therefore be the same in all solvents that give the same equilibrium constants. The solvents listed in Table I have been assumed to satisfy this condition, and the total dilution shift in the last four lines has been determined by adding the calculated total shift (d) to the average of the total shifts (e) in the first four lines.

Chloroform–Dioxane Solutions

These solutions were prepared from "reagent" grade chloroform and "purified" grade dioxane. Both chemicals were purified shortly before the measurements by application of the second of the alternative procedures given by Vogel (23). A number of 10 cm³ samples of different chloroform concentrations was prepared volumetrically. A few drops of tetramethylsilane were added to each sample and approximately ½ cm³ was transferred into the 5-mm n.m.r. sample tubes. Air was not excluded in this sample preparation method but the reproducibility of the results was good, provided that the chloroform and dioxane were freshly purified. Measurements were taken on a Varian V 4302 spectrometer at 56.4 Mc/sec. Chemical shifts of lines from the tetramethylsilane reference line were measured by the usual side band technique. The frequency of the audio oscillator for the generation of side bands was spot-calibrated with the 60 cycle/sec mains' frequency as a standard. The sample temperature was 28±1° C. Points a in Fig. 1 give the measured position of the chloroform resonance line in binary chloroform–dioxane mixtures of various stoichiometric chloroform concentrations, and points a in Fig. 2 represent the analogous results for the dioxane resonance line. The concentrations are given in mole fraction units and the scales for the n.m.r. shift increase towards positive values with increasing magnetic field. Their origins have been shifted from the tetramethylsilane line position by an amount $\delta_a(0)$ and $\Delta_b(0)$ respectively as is explained in the Appendix. At no concentration was any broadening or splitting of the dioxane or chloroform signal noticeable. The mean lifetime of the bonded species must therefore be considerably less than 10^{-3} sec.

A total dilution shift for dioxane of 0.043 p.p.m. was found in dioxane–cyclohexane solutions, as shown by curve c in Fig. 2. These measurements were also made with a tetramethylsilane internal reference, and the cyclohexane line position was not affected by variation of the dioxane concentration.

The measured values a in Fig. 1 were then corrected for the dilution shift to obtain the shift caused by

Can. J. Chem. Downloaded from www.nrcresearchpress.com by 210.87.254.40 on 09/05/12
For personal use only.

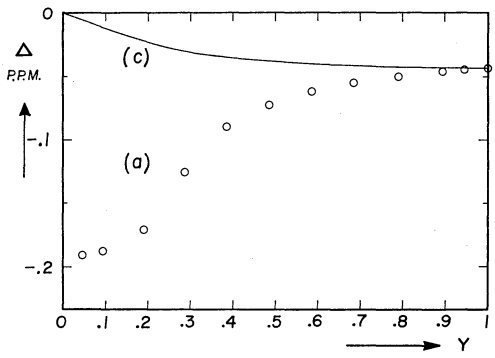

FIG. 2. Shift of dioxane proton magnetic resonance signal vs. dioxane mole fraction Y: (*a*) measured in dioxane–chloroform solutions, (*c*) measured in dioxane–cyclohexane solutions.

dioxane–chloroform hydrogen bonds. It has been assumed for this purpose that the dilution shift of chloroform in dioxane at a non-bonded chloroform concentration ξ_a is equal to the dilution shift of chloroform in cyclohexane at the stoichiometric chloroform concentration $x = \xi_a$. Contribution (*e*) satisfies this assumption if it is caused by self-association with approximately equal equilibrium constants in the two solvents, but an approximation may be involved for contribution (*d*). This approximation will not be serious, however, because Table I shows that the total shift (*d*) in dioxane is not very different from the total shift (*d*) in cyclohexane, and in either case it is only a minor contribution to the total dilution shift. The correction has been carried out on this basis as is explained in greater detail in the Appendix, and points *b* in Fig. 1 have thus been obtained.

McGlashan and Rastogi (24) have deduced from vapor pressure measurements on the chloroform–dioxane system that there exists a 2:1 complex $(CHCl_3)_2 \ldots OC_4H_8O$ in addition to the 1:1 complex $CHCl_3 \ldots OC_4H_8O$. They deduce the bond energies $\Delta H_{1:1} = -8.4$ kj/mole and $\Delta H_{2:1} = -15.1$ kj/mole and also give values for the association equilibrium constants at 50° C. They do not give the probable error for these results, but it can be estimated to be less than 10%. When the bond energy values are used in the van't Hoff equation to convert the equilibrium constants to 28° C, the results are $K_{1:1} = 1.39$ and $K_{2:1} = 1.87$ mole fraction units. A least-squares analysis was carried out with these values to fit a curve to points *b* in Fig. 1, as is described in the Appendix, and this analysis gives the following results:

$$\begin{aligned}
\text{Position of line from chloroform at infinite dilution in cyclohexane } \delta_a(0) &= -6.95_0 \text{ p.p.m. rel. TMS,}\\
\text{H-bond shift in 1:1 complex } \delta_c - \delta_a(0) &= -1.20 \pm 0.01 \text{ p.p.m,}\\
\text{Average H-bond shift in 2:1 complex } \delta_d - \delta_a(0) &= -0.85 \pm 0.02 \text{ p.p.m.,}\\
\text{Position of line from dioxane at infinite dilution in cyclohexane } \Delta_b(0) &= -3.50 \text{ p.p.m. rel. TMS.}
\end{aligned}$$

The mean error of a single measurement is ±0.01 p.p.m. This and the probable errors stated with the results above are a consequence of the limited accuracy of the n.m.r. measurements and sample preparation; they do not take into account any inaccuracy in the values for the equilibrium constants nor the approximations involved in the assumptions made above. The curve calculated with the above values from eq. [A-13] is marked *b* in Fig. 1.

Analysis of points *a* of Fig. 1 in terms of an equilibrium with only a 1:1 complex has been attempted but did not lead to satisfactory results. Measurements on the heat of mixing (25) of chloroform in dioxane also support the existence of the 2:1 complex.

Chloroform–Acetone

The position of the chloroform line relative to the line from an internal reference compound as a function of concentration in chloroform–acetone mixtures has been measured by Huggins *et al.* (17) at 28° C and at −23° C. The authors have analyzed their data in terms of an equilibrium with only a 1:1 complex and without correction for the chloroform dilution shift. They obtain for the bond energy $\Delta H = -10.5$ kj/mole, and for the association equilibrium constant $K = 1.8 \pm 0.6$ mole fraction units.

Kearns (26) has found evidence in the chloroform–acetone system of a 2:1 complex in addition to the 1:1 complex. He has determined the bond energies and equilibrium constants for both complexes. But the freezing point diagram (14) does not support the existence of a 2:1 complex, at least not in the solid phase. Since the n.m.r. data have been satisfactorily explained without postulation of a 2:1 complex, the possibility of the existence of this complex in the liquid phase has been neglected here, and for the 1:1 complex

Can. J. Chem. Downloaded from www.nrcresearchpress.com by 210.87.254.40 on 09/05/12
For personal use only.

the bond energy $\Delta H = -11.3 \pm 2$ kj/mole and the equilibrium constant $K_1 = 1.8 \pm 0.6$ mole fraction units have been accepted.

To find the hydrogen bond n.m.r. shift, Huggins' data must be corrected for the chloroform dilution shift in acetone. This was accomplished by application of eq. [A-13], which yields for $\xi_a = 0$:

$$[3] \qquad \delta_c - \delta_a(0) = \left(1 + \frac{1}{K_1}\right)[\delta(0) - \delta_a(0)] = \left(1 + \frac{1}{K_1}\right)[\delta(0) - \delta(1) + \delta_a'(1)]$$

with $\delta_a(0) = \delta_a(1) - \delta_a'(1) = \delta(1) - \delta_a'(1)$. The symbols are explained in the Appendix. Equation [3] is independent of whether or not a 2:1 complex exists as long as K_1 refers to the formation of only the 1:1 complex. The values $\delta(0) - \delta(1) = -0.68$ p.p.m. from Huggins *et al.* (17) and $\delta_a'(1) = -0.15$ from Table I then give $\delta_c - \delta_a(0) = -1.18$ to -1.52 p.p.m. with the probable value -1.29 p.p.m. for the shift caused by the hydrogen bond in the chloroform–acetone complex. The error range corresponds to the probable error in K_1.

Chloroform–Triethylamine

The n.m.r. shift in the system chloroform–triethylamine has been studied by the same investigators (17) in the same manner as the chloroform–acetone system. The results are $\Delta H = -16.7 \pm 8$ kj/mole, $K = 3.0 \pm 1$ mole fraction units at 28° C, and $\delta(0) - \delta(1) = -1.13$ p.p.m. The chloroform dilution shift in triethylamine was taken from Table I and applied as above to give the shift caused by the hydrogen bond in the chloroform–triethylamine complex $\delta_c - \delta_a(0) = -1.76$ to -2.12 with the probable value -1.88 p.p.m. The uncertainty again reflects the probable error in K.

Chloroform–Diethyl Ether

Evidence for the formation of a 1:1 complex in solutions of chloroform in diethyl ether has been found by McLeod and Wilson (27), who give the bond energy $\Delta H = -25.4$ kj/mole. Earp and Glasstone (28) deduce the value of the association equilibrium constant $K = 0.50$ mole fraction units at 20° C from measurements of the dielectric polarization in this system and, combining this with the measured heat of solution, they find $\Delta H = -29.9$ kj/mole. The average value $\Delta H = -27.7 \pm 2.5$ kj/mole has been accepted for this work and used in the van't Hoff equation to obtain the equilibrium constant $K = 0.36 \pm 0.04$ mole fraction units at 28° C.

The n.m.r. line shift has been measured by Korinek and Schneider (14). They used an external reference compound but applied a correction for effect (*a*) to obtain $\delta(0) - \delta(1) = -0.48$ p.p.m. With the chloroform dilution shift in diethyl ether taken from Table I, there results for the shift caused by the hydrogen bond in the chloroform–diethyl ether complex $\delta_c - \delta_a(0) = -2.68 \pm 0.22$ p.p.m. The uncertainty results from the probable error in K.

Correlation N.M.R. Shift – Hydrogen Bond Energy

The hydrogen bond n.m.r. shift in complexes of chloroform with dioxane (1:1 and 2:1 complexes), acetone, triethylamine, and diethyl ether has been plotted versus the respective bond energy in Fig. 3. The probable

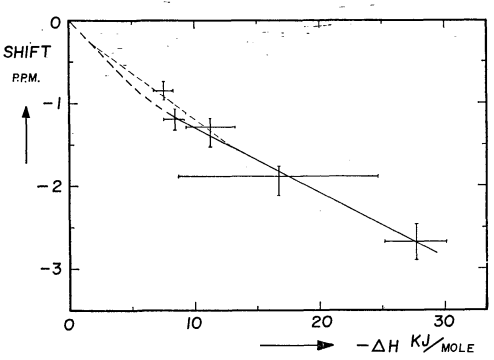

FIG. 3. Nuclear magnetic resonance shift vs. bond energy in complexes of chloroform with dioxane (2:1 and 1:1), acetone, triethylamine, and diethyl ether (in this order from left to right).

errors are indicated by the vertical and horizontal lines at each measured point. The dioxane 2:1 complex involves two hydrogen bonds and the point for this system represents the average n.m.r. shift versus the average energy per bond.

A straight line has been fitted by the method of least squares to the measured points excepting the dioxane 2:1 complex. This line intercepts the ordinate at -0.51 p.p.m. and its slope is -7.86×10^{-2} p.p.m./kj $\times$ mole^{-1}.

Can. J. Chem. Downloaded from www.nrcresearchpress.com by 210.87.254.40 on 09/05/12
For personal use only.

Can. J. Chem. Downloaded from www.nrcresearchpress.com by 210.87.254.40 on 09/05/12
For personal use only.

DISCUSSION

The intercept of −0.51 p.p.m. of the straight line in Fig. 3 is unsatisfactory since zero n.m.r. shift should be expected for zero bond energy. Three explanations may be offered:

(i) The point for the dioxane 1:1 complex and, to a lesser degree, also that for the ether complex is incorrect.

(ii) The intercept is caused by an interaction that has not been considered. Aside from the objection that this argument is more an excuse than an explanation, it fails to account for the location of the dioxane 2:1 point in Fig. 3.

(iii) The relation between n.m.r. shift and hydrogen bond energy is non-linear for energies less than approximately 9 kj/mole. I know of no reason why this relation ought to be linear, and therefore wish to interpret the data concerning the dioxane 2:1 complex with the assumption of this hypothesis:

When the line in Fig. 3 is extrapolated to low energies so as to pass through the origin, it forms a curve with the dioxane 2:1 point on its concave side. This point should lie at the midpoint of a chord to the curve since it represents the linear average of the shifts and energies of the two bonds occurring in the 2:1 complex. The end points of the chord represent the actual shifts and energies of the two bonds, and the construction in Fig. 3 indicates that one bond is considerably stronger than the other. Two conceivable structures for the 2:1 complex are shown below, and structure I is hereby disfavored because its symmetry would require the two bonds to be of equal strength. In structure II, however, the bond to dioxane can be expected to be stronger than the bond between the two chloroform molecules. It is even stronger than the bond in the 1:1 complex if the construction in Fig. 3 is correct, and this may be explained by consideration of the polarization of the middle chloroform molecule in structure II.

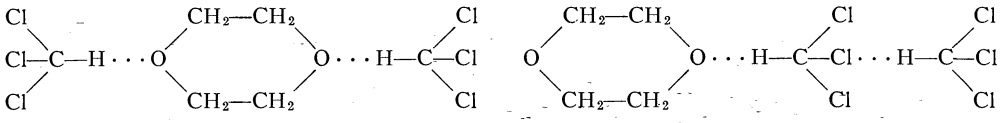

I II

Another comment may be made regarding the interpretation of the measurements presented in Fig. 2. The lack of reliable data on the dilution shift curve for dioxane in chloroform hinders a quantitative analysis. If the assumption is made that the dilution shift in chloroform is identical with that in cyclohexane (curve *c* in Fig. 2), then a least-squares analysis analogous to that made for Fig. 1 gives 0.00±0.02 p.p.m. for the shift of the signal from the eight hydrogen atoms of dioxane upon formation of the 1:1 complex, and −0.46±0.02 p.p.m. for the 2:1 complex. Although a good fit to the measured points is obtained with these values, it is unlikely that they have physical significance because the above assumption is probably a poor one. The dioxane molecule carries an electric quadrupole and the theory of Diehl and Freeman (5) is therefore not directly applicable. But when the quadrupole is approximated by two dipoles, this theory indicates that much of the shift represented by points *a* in Fig. 2 may well be caused by effect (*d*), so that very little would remain as evidence of an influence of the hydrogen bond on the shielding of the dioxane hydrogen atoms. Effect (*d*) causes a dilution shift to higher field in cyclohexane and to lower field in chloroform because the dielectric constant of dioxane is intermediate between the dielectric constants of cyclohexane and chloroform.

It is hoped that these speculations will stimulate further investigations and that this work will thereby contribute to our understanding of the hydrogen bond.

ACKNOWLEDGMENTS

I wish to thank Mr. H. R. Andrews for technical assistance and the National Research Council of Canada for financial support of this investigation. I am much obliged to the referee for his comments on an earlier version of this report.

REFERENCES

1. A. D. Buckingham, T. Schaefer, and W. G. Schneider. J. Chem. Phys. **32**, 1227 (1960).
2. J. V. Hatton and R. E. Richards. Trans. Faraday Soc. **57**, 28 (1961).
3. W. G. Schneider, H. J. Bernstein, and J. A. Pople. J. Chem. Phys. **28**, 601 (1958).
4. R. J. Abraham. Mol. Phys. **4**, 369 (1961).
5. P. Diehl and R. Freeman. Mol. Phys. **4**, 39 (1961).
6. I. Gränacher. Helv. Phys. Acta, **34**, 271 (1961).
7. P. C. McKinney and G. M. Barrow. J. Chem. Phys. **31**, 294 (1959).
8. A. D. Buckingham. Can. J. Chem. **38**, 300 (1960).
9. C. MacLean and E. L. Mackor. Mol. Phys. **4**, 241 (1961).
10. J. I. Musher. J. Chem. Phys. **35**, 1989 (1961).
11. J. V. Hatton and R. E. Richards. Mol. Phys. **3**, 253 (1960); **5**, 139, 153 (1962).
12. E. A. Allan and L. W. Reeves. J. Phys. Chem. **66**, 613 (1962).
13. C. M. Huggins, G. C. Pimentel, and J. N. Shoolery. J. Phys. Chem. **60**, 1311 (1956).
14. G. J. Korinek and W. G. Schneider. Can. J. Chem. **35**, 1157 (1957).
15. T. M. Connor and C. Reid. J. Mol. Spectry. **7**, 32 (1961).
16. J. C. Davis, K. S. Pitzer, and C. N. R. Rao. J. Phys. Chem. **64**, 1744 (1961).
17. C. M. Huggins, G. C. Pimentel, and J. N. Shoolery. J. Chem. Phys. **23**, 1244 (1955).
18. L. W. Reeves and W. G. Schneider. Can. J. Chem. **35**, 251 (1957).
19. C. M. Huggins and D. R. Carpenter. J. Phys. Chem. **63**, 238 (1959).
20. C. F. Jumper, M. T. Emerson, and B. B. Howard. J. Chem. Phys. **35**, 1911 (1961).
21. I. G. Ross and R. A. Sack. Proc. Phys. Soc. (London), Sect. B, **63**, 893 (1950).
22. A. Nikuradse and R. Ulbrich. Z. Physik. Chem. (Frankfurt), **2**, 9 (1954).
23. A. I. Vogel. Practical organic chemistry. 2nd ed. Longmans, Green and Co., London. 1951. p. 175.
24. M. L. McGlashan and R. P. Rastogi. Trans. Faraday Soc. **54**, 496 (1958).
25. S. Searles and M. Tamres. J. Am. Chem. Soc. **73**, 3704 (1951).
26. E. R. Kearns. J. Phys. Chem. **65**, 314 (1961).
27. D. B. McLeod and F. J. Wilson. Trans. Faraday Soc. **31**, 596 (1935).
28. D. P. Earp and S. Glasstone. J. Chem. Soc. 1709 (1935).

APPENDIX

Consider a solution which has been prepared by mixing A moles of chloroform with B moles of dioxane. The stoichiometric mole fractions are:

[A-1]
$$X = \frac{A}{A+B} \qquad \text{for chloroform,}$$
$$Y = \frac{B}{A+B} = 1-X \qquad \text{for dioxane.}$$

Because of the equilibria

$$CHCl_3 + C_4H_8O_2 \rightleftharpoons CCl_3H \ldots OC_4H_8O,$$

and

$$2CHCl_3 + C_4H_8O_2 \rightleftharpoons (CCl_3H)_2 \ldots OC_4H_8O,$$

there are in the solution

a moles of chloroform not hydrogen bonded to dioxane,
b moles of non-associated dioxane,
c moles of the 1:1 complex,
d moles of the 2:1 complex,

where

[A-2]
$$a+c+2d = A.$$
$$b+c+d = B.$$

Can. J. Chem. Downloaded from www.nrcresearchpress.com by 210.87.254.40 on 09/05/12
For personal use only.

The true mole fractions in the solution are:

$$\xi_a = \frac{a}{a+b+c+d} \qquad \text{for chloroform not hydrogen bonded to dioxane,}$$

$$\xi_b = \frac{b}{a+b+c+d} \qquad \text{for non-associated dioxane,}$$

[A-3]

$$\xi_c = \frac{c}{a+b+c+d} \qquad \text{for the 1:1 complex,}$$

$$\xi_d = \frac{d}{a+b+c+d} \qquad \text{for the 2:1 complex,}$$

with

[A-4] $$\xi_a+\xi_b+\xi_c+\xi_d = 1.$$

Substitution of [A-2] in [A-1] gives with the use of [A-3] and [A-4]

[A-5] $$X = \frac{\xi_a+\xi_c+2\xi_d}{1+\xi_c+2\xi_d}.$$

The equilibrium constants in mole fraction units are

[A-6] $$K_1 = \frac{\xi_c}{\xi_a \times \xi_b} \qquad \text{for formation of the 1:1 complex,}$$

[A-7] $$K_2 = \frac{\xi_d}{\xi_a^2 \times \xi_b} \qquad \text{for formation of the 2:1 complex.}$$

The independent equations [A-4], [A-6], and [A-7] relate the four quantities ξ_a, ξ_b, ξ_c, ξ_d to one another. They can be solved to express three of these quantities in terms of the fourth. Let ξ_a be the independent variable, then the solutions are

[A-8] $$\xi_b = \frac{1-\xi_a}{1+K_1\xi_a+K_2\xi_a^2},$$

[A-9] $$\xi_c = \frac{K_1\xi_a(1-\xi_a)}{1+K_1\xi_a+K_2\xi_a^2},$$

[A-10] $$\xi_d = \frac{K_2\xi_a^2(1-\xi_a)}{1+K_1\xi_a+K_2\xi_a^2}.$$

Substitution of [A-9] and [A-10] in [A-5] gives X as a function of ξ_a in the form

[A-11] $$X = \xi_a \frac{1+K_1+K_2\xi_a(2-\xi_a)}{1+K_1\xi_a(2-\xi_a)+K_2\xi_a^2(3-2\xi_a)}.$$

With the assumption of fast reaction rates for the equilibria considered above, the hydrogen resonance signal of chloroform in mixtures with dioxane appears at a chemical shift δ equal to the weighted average of the signal positions for chloroform molecules not hydrogen bonded to dioxane (δ_a), for chloroform molecules in the 1:1 complex (δ_c), and for chloroform molecules in the 2:1 complex (δ_d):

$$\delta = \frac{a}{A}\delta_a + \frac{c}{A}\delta_c + 2\frac{d}{A}\delta_d.$$

Can. J. Chem. Downloaded from www.nrcresearchpress.com by 210.87.254.40 on 09/05/12
For personal use only.

When this equation is written in the form

$$\delta-\delta_a = \frac{1}{A}\,[c(\delta_c-\delta_a)+2d(\delta_d-\delta_a)],$$

the following relation can be obtained by the use of [A-2], [A-3], [A-9], and [A-10]:

[A-12] $$\delta-\delta_a = \frac{1-\xi_a}{1+K_1+K_2\xi_a(2-\xi_a)}\,[K_1(\delta_c-\delta_a)+2K_2\xi_a(\delta_d-\delta_a)].$$

This relation together with [A-11] gives a representation of a function $\delta(X)$ through the parameter ξ_a.

It has been mentioned above that the chloroform dilution shift causes the position δ_a to depend on the chloroform concentration ξ_a. The function $\delta_a(\xi_a)$ was taken directly from Schneider's measurements (14, 18), whereby the stoichiometric mole fraction of chloroform in inert hydrocarbons has been put equal to the mole fraction ξ_a in dioxane. Introduction of $\delta_a(\xi_a)$ into eq. [A-12] gives finally

[A-13] $$\delta-\delta_a(0)-\delta_a'(\xi_a)[1-F(K_1+2K_2\xi_a)] = F[K_1(\delta_c-\delta_a(0))+2K_2\xi_a(\delta_d-\delta_a(0))],$$

where $\delta_a'(\xi_a) = \delta_a(\xi_a)-\delta_a(0)$ is the chloroform dilution shift (curve c in Fig. 1), and F is an abbreviation defined by

$$F = \frac{1-\xi_a}{1+K_1+K_2\xi_a(2-\xi_a)}\,.$$

In Fig. 1, the points labelled a represent the direct measurements of $\delta-\delta_a(0)$ plotted vs. the stoichiometric chloroform mole fraction X. Points b represent the left-hand side of eq. [A-13] with ξ_a and X related by eq. [A-11]. The values of $\delta_c-\delta_a(0)$, $\delta_d-\delta_a(0)$, and $\delta_a(0)$ were then determined so as to minimize the mean-square deviation of the r.h.s. from the l.h.s. of eq. [A-13], and this gave the results listed in the text. Curve b is a graph of the r.h.s. of eq. [A-13].

Can. J. Chem. Downloaded from www.nrcresearchpress.com by 210.87.254.40 on 09/05/12
For personal use only.

PHOTOCHEMICAL SYNTHESES

6. THE FORMATION OF HEPTANDIONES FROM ACETYLACETONE AND ALKENES[1]

P. DE MAYO AND H. TAKESHITA
Department of Chemistry, University of Western Ontario, London, Ontario
Received September 27, 1962

ABSTRACT

The irradiation of acetylacetone in the presence of oct-1-ene, cyclopentene, cyclohexene, and 1-methylcyclohexene gives substituted heptandiones. These diketones may then be cyclized with acid or base. Irradiation of isopropenyl acetate and acetylacetone gives, after cyclization, *m*-5-xylenol. The mechanism of the reaction is discussed: it represents the first cycloaddition to an isolated ethylenic linkage.

Can. J. Chem. Downloaded from www.nrcresearchpress.com by 210.87.254.105 on 09/05/12
For personal use only.

Saturated ketones have absorption bands in the ultraviolet at about 280 mμ. This band is associated with an $n \rightarrow \pi^*$ transition of a non-bonded electron on the oxygen atom into an anti-bonding π-orbital (2): α,β-unsaturated ketones have a similar band at somewhat longer wavelength. Such excitation of saturated ketones in condensed phases leads to a number of transformations which follow on the formation of the original excited species. Amongst these are cyclobutanol formation and fission between the α- and β-carbon atoms: both these processes are initiated by γ-hydrogen abstraction by the electron-deficient oxygen atom.[2]

In the presence of substrates which may give stabilized radicals by hydrogen abstraction another course may be followed, particularly when there is no such γ-hydrogen available for intramolecular abstraction. The activated ketone, most probably as the triplet (4, and references cited therein), is converted into the ketyl, which then, in turn, may react with another ketyl or with some other radical derived from the substrate (see, for instance, refs. 5, 6, 7).

The irradiation of acyclic α-diketones also appears to conform to this general pattern. In the absence of a reactive substrate cyclobutanol formation proceeds in high yield (8), whilst in the presence of benzylic (9) or allylic hydrogen (10) alkylation is observed.

The irradiation of β-diketones, on the other hand, does not appear to have been studied up to the present. Acetylacetone, the simplest readily available acyclic β-diketone, exists in solution in hydrocarbons largely in the enolic form (I) (11). In this system γ-hydrogen abstraction is, presumably, strongly favored following $n \rightarrow \pi^*$ excitation, because of the proximity of that hydrogen atom. However, in this special case the ketyl so formed is readily transformed into (II), the tautomer of (I), and differing from it at most in small internuclear distances.[3] Hydrogen abstraction from the solvent may thus be expected to be slow and might not occur provided some other mode of chemical behavior were available to the excited diketone molecule.

Irradiation of acetylacetone in cyclohexene induced a reaction which could be followed by the disappearance of the enol bands at about 6.3 μ. The product, obtained in high yield, appeared homogeneous to gas–liquid chromatographic (g.l.c.) analysis and, significantly, no trace of bicyclohexenyl could be detected. The latter is an inevitable

[1] *Part of the material contained herein formed a preliminary communication (1).*
[2] *For a review of these and other transformations following $n \rightarrow \pi^*$ excitation see reference 3.*
[3] *In the present instance the tautomers are identical, but with other unsymmetrical β-diketones capable of chelation the more general statement applies.*

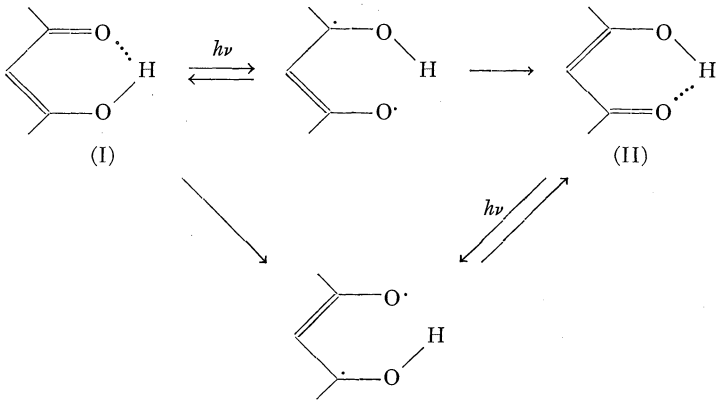

(I) (II)

by-product of radical reactions in cyclohexene and in these circumstances its absence could be taken as an encouraging indication of the absence of such processes.

That an $n \rightarrow \pi^*$ excitation was most probably responsible for the observed transformation was established by repeating the irradiation using a pyrex filter. This resulted in a decrease in yield of only one third, whilst under these conditions essentially all the light responsible for $\pi \rightarrow \pi^*$ excitation was cut out.

The product analyzed for a 1:1 adduct of cyclohexene and acetylacetone. It showed no high-intensity absorption in the ultraviolet, had a band in the infrared at 1717 cm^{-1} compatible with saturated ketones, and gave a crystalline dioxime. The n.m.r. spectrum showed the presence of a singlet (6 H) at τ 8.0, suggesting (ref. 12, p. 57) the presence of two acetyl groups, and there was no indication of vinyl hydrogen. Treatment of the diketone with acid led, with the loss of one molecule of water, to the formation of two isomeric unsaturated ketones, characterized as the 2:4-dinitrophenylhydrazones.

Both unsaturated ketones showed, in the n.m.r. spectra, the presence of allylic methyl (singlet, 3 H, τ 8.09) and of one vinyl hydrogen (at τ 4.30, singlet). The infrared spectra (bands at 1674 and 1675 cm^{-5} respectively) suggested the presence of cyclohexenones and hence the formulation of (III), (IV), and (V) for the diketone and the unsaturated ketones respectively.

A distinction between (IV) and (V) was also possible from the infrared spectra. That assigned the structure (V) showed a band at 1415 cm^{-1} attributed to the deformation vibrations of methylene α to the carbonyl (ref. 13, p. 22) whilst that assigned the structure (IV) showed a band at somewhat higher wave numbers (1423 cm^{-1}) attributed to the

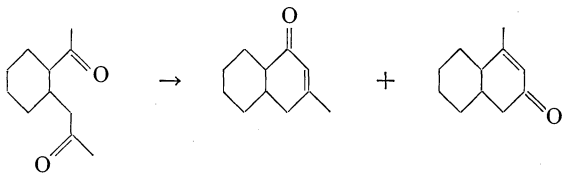

(III) (IV) (V)

allylic methylene group (ref. 13, p. 23). The assignments were confirmed in the present instance[4] by reduction of the ketones with sodium borohydride followed by dehydrogena-

[4]*The formation of (IV) had been previously reported by Barrett, Cook, and Linstead (14) as being formed by the condensation of acetylcyclohexene and sodioacetoacetate. Repetition of the preparation showed, however, that here also the product was a mixture of (IV) and (V).*

Can. J. Chem. Downloaded from www.nrcresearchpress.com by 210.87.254.105 on 09/05/12
For personal use only.

tion over palladized charcoal. This treatment gave β- and α-methylnaphthalene respectively, which were characterized as the picrates and compared with authentic specimens.

The formation of (III) most probably proceeds through the cyclobutane derivative (VI). The formation of cyclobutane derivatives by the dimerization of unsaturated ketones is well known (15) and the intramolecular addition of an ethylenic linkage to an unsaturated ketone has already been observed (16).[5] The present reaction constitutes the first intermolecular addition to an isolated ethylenic linkage. In support of this view the infrared spectrum of the crude irradiation product showed strong hydroxyl absorption which disappeared on slight warming. These conditions define the stability

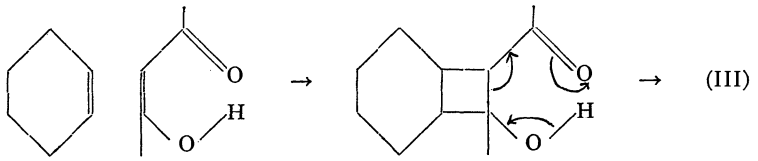

(VI) (III)

of the β-hydroxyketone since the dealdolization may be a purely thermal process (VI, see arrows).

If the mechanism proposed is correct the diketone (III) as originally formed should be cis. Although trans fusions of six- and four-membered rings do occur, and have been prepared recently in the ring D norsteroids (18(*a*)), it seems probable though not mandatory that the lower-energy pathway should be selected here (18(*b*)). However, since the stable configuration of the diketone is trans (both substituents equatorial) it is not impossible that complete or partial inversion may have occurred during distillation. Further equilibration was not attempted since, in general, such conditions are those that lead to cyclization.

Cyclization, irrespective of the stereochemical homogeneity of the starting material, could lead to both cis and trans isomers. The two ketones obtained, (IV) and (V), appeared homogeneous to g.l.c. on several columns, but this criterion must be accepted with reserve since the same was true of a derivative from 1-methylcyclohexene (see below), and this was shown to be a mixture.

Similar irradiation of acetylacetone with cyclopentene gave the expected diketone (VII), characterized as the dioxime. Cyclization with base then gave the ketones (VIII) and (IX), characterized as the 2:4-dinitrophenylhydrazones. The assignment of structure was made on the basis of the methylene deformation frequencies which occurred at the same position as in the cyclohexene series.

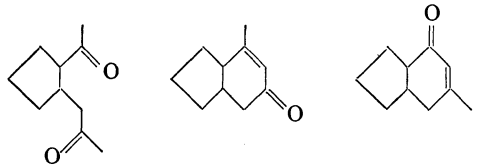

(VII) (VIII) (IX)

In those natural products in the alicyclic series in which this present approach might be of synthetic utility a common structural feature is that of an angular methyl group.

[5]*The intermolecular addition of alkenes to unsaturated acids has been observed in these laboratories and will be reported shortly (17). The addition of cyclopentenone to cyclopentene has since been reported by Eaton (27).*

Can. J. Chem. Downloaded from www.nrcresearchpress.com by 210.87.254.105 on 09/05/12
For personal use only.

Can. J. Chem. Downloaded from www.nrcresearchpress.com by 210.87.254.105 on 09/05/12
For personal use only.

Although the introduction of this feature might be achieved by methylation, an alternative route could be the use of methylcyclohexene as a substrate. Addition of acetylacetone to such an unsymmetrically substituted ethylenic linkage could proceed to give either of the two compounds (X) or (XI). Assuming that the addition is not entirely concerted,[6] then the addition should proceed to give the more stable intermediate biradical. This appears to be the case, for instance, in the related addition of carbonyl groups to methylbut-2-ene to give oxetanes (20; 28; 3, p. 379). In that instance it is the oxygen atom (which is electron deficient because of electron promotion) which attacks the π-bond. In the present case if the α-carbon be presumed to be electron deficient the predicted more stable diradical[7] would be (XII) rather than (XIII). Little analogy can be made with the dimerization of unsaturated ketones (in which, presumably, one molecule of the forming dimer is activated) because of the influence of the phase in which the irradiation is done, and the uncertainty as to whether $n \rightarrow \pi^*$ or $\pi \rightarrow \pi^*$ excitation is involved in any particular example.[8]

To form the second carbon–carbon bond two opposed steric interactions (methylene and methyl vis-à-vis methyl and hydroxyl) must be overcome. Since, until this final bond formation, the processes are reversible this interaction might be a factor which could depress the rate of (XI) formation as against that of (X). In addition, with sufficient suppression or if the charge separation is small it is conceivable that the radical (XIV), which is more stable still, may be involved, although XIV would be formed from attack of the carbon β to the carbonyl, which may be unfavorable.

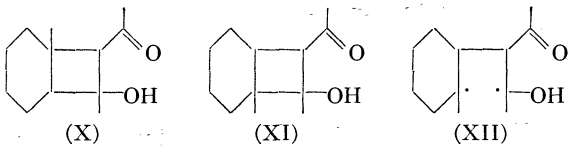

(X)

(XI)

(XII)

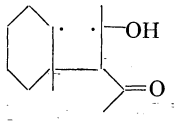

(XIII)

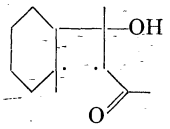

(XIV)

Irradiation of methylcyclohexene and acetylacetone led, in this event, to the formation of more than one product, as indicated by g.l.c. analysis, but at the temperature required for preparative separation extensive decomposition occurred together with the formation of cyclized products. The major component (50%) could, however, be isolated by fractional distillation. The remainder appeared to consist of three products one of which accounted for 20–30% of the original material. Its infrared spectrum indicated that it was a diketone but the best specimens were always contaminated with small amounts of cyclized products.

The major product was assigned the structure (XV) for the following reasons. It analyzes correctly, gave a crystalline dioxime, and showed a band in the infrared at 1709 cm^{-1}. Cyclization of (XV) with base gave two unsaturated ketones in the ratio

[6]*The formation of other four-membered rings has also been suggested to be non-concerted (e.g. ref. 19). Recently, results on the dimerization of cyclopentenone have been interpreted (27) to imply either concertion or the lack of effect of stabilizing factors on intermediate species, presumably because of their high energy.*

[7]*Even if the addition has ionic character the same consequence follows since attack of ethylenes is electrophilic.*

[8]*Thus benzalacetophenone in solution gives head-to-tail union (21), whilst cholestenone gives head-to-tail (22). In coumarin (21) it is more probable that $\pi \rightarrow \pi^*$ activation is involved.*

of 4:1 separable by g.l.c. The major product, (XVI), and the minor product, (XVII), both showed singlets (3 H) for the allylic methyl groups (at τ 8.16 and 8.02) (ref. 12, p. 58) and singlets at (τ 4.31 and 4.34) for one vinyl hydrogen, respectively. The compounds showed, again, the appropriate methylene deformation bands in the infrared. From this evidence it was not possible to distinguish between (XVI) and (XVII) on the one hand and the other two isomers bearing the angular methyl group at the alternative quaternary position on the other.

The unsaturated ketones were, therefore, ozonized to the keto acids, which were converted directly to the esters with diazomethane. The keto ester from (XVI) on g.l.c. was separable into two components characterized as the 2:4-dinitrophenylhydrazones. One, giving a dinitrophenylhydrazone, of m.p. 123–124°, showed a non-equivalent quartet (from the methylene group adjacent to the ketone) at 7.43 and 7.84 ($J \sim 15$ c.p.s.) (see ref. 12, p. 85). The other, giving a dinitrophenylhydrazone of m.p. 118 – ca. 119°, showed a singlet (2 H) at τ 7.44. These keto esters are, therefore, the stereoisomers of (XVIII). The presence of a hydrogen atom at the bridgehead adjacent to the methylene group discussed above would, of course, have led to more complex splitting.

The same observations were made on the 2:4-dinitrophenylhydrazones, that of m.p. 123–124° showing a singlet (2 H) at τ 7.31, the other showing a non-equivalent quartet at τ 7.31, 7.47 ($J \sim 15$ c.p.s.).

The keto ester from (XVII) was homogeneous and also showed a non-equivalent quartet (at ca. τ 7.35, 7.95), in this case partly obscured by a multiplet (see below), again requiring that there be no hydrogen vicinal to the methylene group. In addition, all keto esters showed a multiplet at ca. τ 7.3–7.4 to be attributed to the methine hydrogen next to carbonyl. Other features of the n.m.r. spectrum were in accord with expectation.

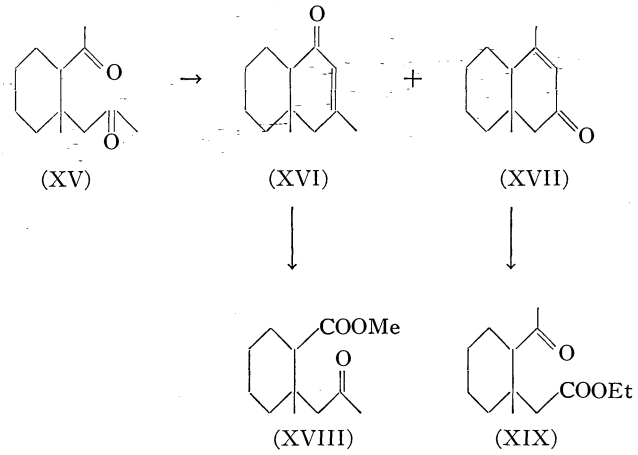

(XV) (XVI) (XVII)

(XVIII) (XIX)

The obtention of two keto esters from (XVI) may indicate that although no resolution could be obtained on the columns available (XVI) is a mixture of cis and trans forms. These may differ only slightly in energy (as do certain related decalones (24)). The same may be true of (XVII) also, but epimerization α to the ketone may have taken place after ozonolysis. Such epimerization is, of course, more likely to occur than that α to an ester.

The nature of the other irradiation products can only be inferred since they were

Can. J. Chem. Downloaded from www.nrcresearchpress.com by 210.87.254.105 on 09/05/12
For personal use only.

Can. J. Chem. Downloaded from www.nrcresearchpress.com by 210.87.254.105 on 09/05/12
For personal use only.

not obtained pure, but it seems reasonable, on the basis of the spectral data, to assume that the minor product was, as in the case of oct-1-ene (see below), the isomeric diketone. The formation of *both* diketones is consonant with the concept that steric and electronic factors were opposed, and, indeed, the introduction of the extra methyl group slowed the photochemical addition considerably over that to the simple cycloalkene. Alternative interpretations (see, for instance ref. 27) are, however, presently possible and are under investigation. However, it appears that if a two-step mechanism is involved more than one of the diradicals (XII), (XIII), or (XIV) is concerned, and to a significant extent.

A similar situation with regards asymmetry obtains in oct-1-ene. Irradiation again led to the formation of the two possible diketones. Separation by g.l.c. was difficult because of condensation and decomposition, but pure specimens were obtained by the removal of unsaturated impurities from the chromatographed products by ozonolysis. The structures (XX; R = H, R′ = C_6H_{13}) and (XX, R = C_6H_{13}, R′ = H) were allocated by means of the n.m.r. spectrum. The latter showed a single peak (6 H) at τ 7.94 for the two acetyl groups since they are identically situated, whereas the former showed two closely placed singlets at τ 7.95 and 7.96.

The unsaturated ketonic products from these cyclizations are one double-bond equivalent distant from phenols. The incorporation of a potential double-bond equivalent into the substrate seemed possible using a suitably substituted double bond. This was attempted using isopropenyl acetate.

The irradiation of isopropenyl acetate with acetylacetone in cyclohexane gave a mixture of ketones the separation of which was not attempted. Direct cyclization of the mixture with base and isolation of the acidic material gave *m*-5-xylenol (XXI), through (XXII), identified by melting point, comparison of the infrared spectrum with that published (25), and conversion into the known tribromide (26).

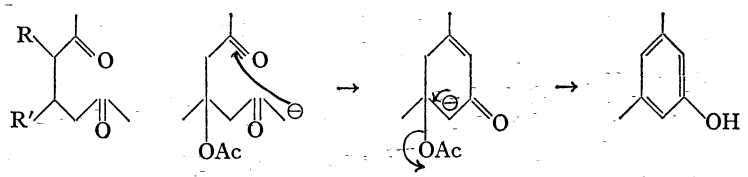

(XX) (XXII) (XXI)

The nature of the products obtained in these irradiations, together with the absence of bicyclohexenyl, appears to indicate that the only reaction is the addition to the ethylenic linkage of the enol. In agreement with the foregoing discussion with regards activation and γ-hydrogen transfer, preliminary results in these laboratories indicate that β-keto esters and cyclic β-diketones behave differently.

EXPERIMENTAL

Materials were reagent grade and were dried over magnesium sulphate and distilled before use. Cyclohexene and cyclopentene were purified by shaking with aqueous ferrous sulphate, dried, and distilled, Oct-1-ene and 1-methylcyclohexene were refluxed over sodium wire and distilled. Before use the hydrocarbons, which were homogeneous to g.l.c. analysis, were filtered through a column of alumina. Nuclear magnetic resonance spectra were recorded on a Varian D.P. 60 instrument. Liquids were run in CCl_4 solution, solids in $CDCl_3$. Irradiations were performed under nitrogen in a water-cooled immersion apparatus using the power of lamp specified. Yields are based on acetylacetone and are not maximal. Ultraviolet spectra were determined in methanolic solution.

The Irradiation of Acetylacetone with Cyclohexene (with A. B. M. A. Sattar)

A solution of the diketone (15.02 g) in cyclohexene (135 ml) was irradiated with an 80-w lamp for 45 hours. After removal of the solvent the product was fractionated on a 40-in. spinning band column to give

the adduct, b.p. 89° at 1.7 mm, n_D^{25} 1.4691 (20.2 g; 78%). Calc. for $C_{11}H_{18}O_2$: C, 72.49; H, 9.91%. Found: C, 72.13; H, 9.62%.

The oxime (hydroxylamine hydrochloride – pyridine at room temperature), crystallized from methanol, had m.p. 165.5–167.5°. Calc. for $C_{11}H_{20}O_2N_2$: C, 62.23; H, 9.50; N, 13.20%. Found: C, 62.45; H, 9.34; 12.90%.

Acid-catalyzed Cyclization of the Cyclohexene Adduct (with A. B. M. A. Sattar)

A solution of the adduct (4.5 g) in ethanol (45 ml) was heated at 80° for 80 minutes with conc. hydrochloric acid (2 ml). After removal of the solvent the product was isolated with chloroform, the chloroform solution washed and dried (Na_2SO_4), and the solvent evaporated. Distillation (b.p. 173–175 at 1.5 mm) gave a mixture (5:3) of two unsaturated ketones (4.04 g; 95%). These were separated by chromatography over a 5-ft silicone SE 30 column at 200°, the separated fractions then being distilled at 180° (bath temp.) at 35 mm to give the following ketones.

(*a*) The unsaturated ketone (IV), n_D^{25} 1.5091, λ_{max} 231 mμ (ε, 19,400), ν_{max} 1675, 1637, 1423 cm^{-1}. Calc. for $C_{11}H_{16}O$: C, 80.18; H, 9.73%. The 2:4-dinitrophenylhydrazone, crystallized from ethyl acetate, had m.p. 201–202°, λ_{max} 380 mμ (ε, 24,000). Calc. for $C_{17}H_{20}O_4N_4$: C, 59.29; H, 5.85; N, 16.27%. Found: C, 59.29; H, 5.82; N, 16.31%.

(*b*) The unsaturated ketone (V), n_D^{25} 1.5160, λ_{max} 237 mμ (ε, 18,500), ν_{max} 1674, 1623, 1415 cm^{-1}. Calc. for $C_{11}H_{16}O$: C, 80.44; H, 9.83%. Found: C, 80.30; H, 9.75%. The 2:4-dinitrophenylhydrazone, crystallized from ethyl acetate, had m.p. 157–158°, λ_{max} 380 mμ (ε, 27,100). Calc. for $C_{17}H_{20}O_4N_4$: C, 59.29; H, 5.85; N, 16.27%. Found: C, 59.57; H, 5.85; N, 16.40%.

Dehydrogenation of Ketone (IV)

The ketone (200 mg) in methanol (10 ml) was added to a solution of sodium borohydride (55 mg) in methanol (3 ml) and water (2 ml) containing a trace of sodium hydroxide (1.0 *N*; 0.02 ml), and the mixture allowed to stand overnight. After acidification with acetic acid the product was isolated with ether and heated at 310° for 12 hours under nitrogen with palladized charcoal (10%; 200 mg). After cooling the charcoal was extracted with ether, and the residue obtained after evaporation of the solvent was treated with saturated alcoholic picric acid (1.5 ml). The picrate (85 mg, m.p. 108–110°) was recrystallized from ethanol to give β-methylnaphthalene picrate, m.p. 114–115° undepressed on admixture with an authentic specimen of the same melting point. The hydrocarbon obtained on regeneration from the picrate had m.p. 31–32° and was undepressed on admixture with an authentic specimen of β-methylnaphthalene of the same melting point. The infrared spectra were identical both in CS_2 and CCl_4 solution.

Dehydrogenation of Ketone (V)

The ketone (200 mg) was reduced in a manner identical with that described above for ketone (IV). Dehydrogenation with palladized charcoal in like manner and treatment of the product with saturated ethanolic picric acid gave the picrate (115 mg), which on crystallization from ethanol had m.p. 139°, undepressed on admixture with an authentic specimen of α-methylnaphthalene of the same melting point. The infrared spectrum of regenerated hydrocarbon was identical with that of an authentic specimen of α-methylnaphthalene in CS_2 and CCl_4 solution.

The Synthesis of Ketones (IV) and (V)

An ethanolic solution of sodioethylacetoacetate (from ethylacetoacetate (2.7 g) and sodium (0.25 g)) and acetylcyclohexene (25 g) was heated on a steam bath at 95° for 6 hours. After dilution with water the product was isolated with benzene. The distillation (149–158° at 3 mm) residue gave the ester mixture (890 mg); no trace of decarboxylated product could be detected by g.l.c. The keto ester (890 mg) was hydrolyzed by refluxing in ethanol (1.5 ml) containing sodium hydroxide (50 mg) and water (0.4 ml) for 3 hours. Extraction of the mixture with ether after dilution with water gave a yellow oil (790 mg). Separation of this by g.l.c. on a silicone Se 30 column at 200° gave ketones (IV) and (V) (1:4) identical in retention times and infrared spectra with the previously described specimens.

Further Irradiations of Cyclohexene and Acetylacetone

(*a*) Cyclohexene (2.4 g) and acetylacetone (11.0 g) in cyclohexane (190 ml) were irradiated with a 350-w lamp for 14 hours. Isolation of the product as described previously gave 2.4 g of material identical in infrared spectra and g.l.c. behavior (diethylene glycol succinate ≡ DEGS column) with that prepared under non-diluted conditions.

(*b*) Cyclohexene (0.82 g) and acetylacetone (1.0 g) were diluted to 190 ml with cyclohexane and irradiated with a 350-w lamp for 5 hours. Material, 1.35 g, identical with the above was obtained.

(*c*) Acetylacetone (20 g) in cyclohexene (135 ml) was irradiated with an 80-w lamp for 15 hours. Gas–liquid chromatographic analysis indicated that 12.3 g (33.2%) of adduct was formed. In an otherwise identical experiment using a pyrex jacket for the lamp 7.09 g (19.2%) of product was obtained identical in infrared spectrum and g.l.c. retention time with the product from unfiltered light.

Irradiation of Cyclopentene and Acetylacetone

A mixture of cyclopentene (130 g) and acetylacetone (15 g) was irradiated with an 80-w lamp for 95

Can. J. Chem. Downloaded from www.nrcresearchpress.com by 210.87.254.105 on 09/05/12
For personal use only.

hours. Removal of the excess cyclopentene by distillation gave a residue of 26 g. This was fractionated by distillation through a 40-in. spinning band column to give the diketone (VII) (17 g), b.p. 129° at 22 mm, n_D^{25} 1.4647, ν_{max} 1712 cm^{-1}. Calc. for $C_{10}H_{16}O_2$: C, 71.39; H, 9.59%. Found: C, 71.76; H, 9.86%.

The oxime (hydroxylamine hydrochloride – pyridine at room temperature), crystallized from ethanol, had m.p. 138–139°. Calc. for $C_{10}H_{18}O_2N_2$: C, 60.58; H, 9.15; N, 14.13%. Found: C, 60.90; H, 9.21; N, 14.09%.

Base-catalyzed Cyclization of Cyclopentene Adduct

A solution of the diketone (VII) in methanol (100 ml) containing sodium hydroxide (50 mg; 1.2 ml water) was refluxed for 1 hour. The mixture was then neutralized with carbon dioxide, concentrated to about one-third volume under reduced pressure, and the product isolated with benzene. Distillation of the residue after evaporation of the benzene at 125° (bath temp.) at 0.4 mm gave an oil (0.76 g) consisting of two components in the ratio 3:2. These could be separated by g.l.c. on a 10-ft DEGS column at 175° to give the following ketones.

(*a*) The unsaturated ketone (VIII), n_D^{25} 1.5140, λ_{max} 236 mμ (ϵ, 19,100), ν_{max} 1673, 1636, 1418 cm^{-1}. Calc. for $C_{10}H_{14}O$: C, 79.95; H, 9.39%. Found: C, 79.57; H, 9.12%. The 2:4-dinitrophenylhydrazone, crystallized from methanol, had m.p. 174–175°, λ_{max} 382 mμ (ϵ, 25,000). Calc. for $C_{16}H_{18}O_4N_4$: C, 58.17; H, 5.49; N, 16.96%. Found: C, 58.24; H, 5.36; N, 17.25%.

(*b*) The unsaturated ketone (IX), n_D^{25} 1.5153, λ_{max} 233 mμ (ϵ, 16,100), ν_{max} 1669, 1640, 1425 cm^{-1}. Calc. for $C_{10}H_{14}O$: C, 79.95; H, 9.39%. Found: C, 79.02; H, 8.99%. The 2:4-dinitrophenylhydrazone, crystallized from methanol, had m.p. 146–147°, λ_{max} 380 mμ (ϵ, 23,000). Calc. for $C_{16}H_{18}O_4N_4$: C, 58.17; H, 5.49; N, 16.76%. Found: C, 57.90; H, 5.50; N, 16.57%.

Irradiation of 1-Octene and Acetylacetone

A mixture of oct-1-ene (135 g) and acetylacetone (15.0 g) was irradiated with a 350-w lamp for 57 hours. After removal of the excess octene the residue was distilled to give a low-boiling fraction (87–107° at 0.1 mm) (21 g) and a higher fraction (7 g). Redistillation of the main fraction through a spinning band column gave material, b.p. 90° at 0.1 mm, n_D^{25} 1.4455 (16.6 g), which consisted of two components in the ratio of approximately 3:2 as indicated by g.l.c. analysis on an SE 30 at 207°. Separation preparatively by this means was not possible because of the instability of the diketones at that temperature and decomposition rendered difficult the determination of the exact ratio of products even on the analytical column. The separated fractions were ozonized in chloroform solution cooled in CO_2–acetone (to remove cyclized contaminants), the ozonide decomposed with water, the organic layer extracted with sodium hydrogen carbonate, and the residual oil distilled (ca. 140° at 0.3 mm).

The first peak gave 5-acetylundecan-2-one, n_D^{25} 1.4500, ν_{max} 1719 cm^{-1}. Calc. for $C_{13}H_{24}O_2$: C, 73.53; H, 11.39%. Found: C, 73.54; H, 11.36%.

The second peak gave 4-acetonyldecan-2-one, n_D^{25} 1.4466, ν_{max} 1718 cm^{-1}. Calc. for $C_{13}H_{24}O_2$: C, 73.53; H, 11.39%. Found: C, 73.50; H, 11.25%.

Irradiation of Isopropenyl Acetate and Acetylacetone

A mixture of isopropenyl acetate (35 g), acetylacetone (15 g), and cyclohexane (160 ml) was irradiated with an 80-w lamp for 186 hours. After removal of the cyclohexane the residual oil was taken up in chloroform and the chloroform washed with sodium hydrogen carbonate. Evaporation of the chloroform gave the crude adduct (6.7 g).

The adduct (4 g) in methanol (150 ml) containing sodium hydroxide (2 N; 5 ml) was refluxed for 1 hour. The mixture was neutralized with carbon dioxide, evaporated, water added, and the mixture extracted with methylene dichloride. The organic phase was then extracted with sodium hydroxide (2 *N*; 4×20 ml), the aqueous extract acidified with sulphuric acid, and the phenolic material (1.04 g) extracted with carbon tetrachloride and distilled *in vacuo*.

The phenol (XXI) had an infrared spectrum (CCl_4) identical with that reported in the literature (25) and on bromination (26) in acetic acid gave tribromo-*m*-xylenol, m.p. (from cyclohexane) 162–163° (Anselmino gives 166–167°). Evaporation of the methylene dichloride layer gave 1.57 g of neutral material, probably unsaturated ketones, which was not further investigated.

Attempted separation of the uncyclized ketones by g.l.c. on DEGS (prep.) led to condensation reactions and decomposition.

Irradiation of 1-Methylcyclohexene and Acetylacetone

(*a*) Acetylacetone (20 g) in 1-methylcyclohexene (180 ml) was irradiated with a 350-w lamp for 56 hours. After removal of the excess hydrocarbon the residual oil was distilled (80–88° at 0.1 mm) to give the crude adduct (25 g).

(*b*) A mixture of acetylacetone (20 g), methylcyclohexene (130 ml), and cyclohexane (40 ml) was irradiated for 90 hours. Isolation of the product and distillation (78–90° at 0.15 mm) gave the crude mixture of ketones (28.5 g). This contained three main components but separation by g.l.c. preparatively was not possible because of condensation reaction induced by the high temperature required. Fractional distillation through a spinning band column gave the main product, (XV), in about 50% yield, b.p. 77° at 0.4 mm, n_D^{25} 1.4739. Calc. for $C_{12}H_{20}O_2$: C, 73.43; H, 10.27%. Found: C, 72.85; H, 9.86%.

Can. J. Chem. Downloaded from www.nrcresearchpress.com by 210.87.254.105 on 09/05/12
For personal use only.

The dioxime (hydroxylamine hydrochloride – pyridine at room temperature), crystallized from methanol, had m.p. 175–175.5°. Calc. for $C_{12}H_{22}O_2N_2$: C, 63.68; H, 9.80; N, 12.38%. Found: C, 63.78; H, 9.76; N, 12.09%.

Base-catalyzed Cyclization of Diketone (XV)

A solution of the diketone (XV) (7.0 g) in methanol (150 ml) containing sodium hydroxide (50 mg) was refluxed for 1 hour. The mixture was then neutralized with carbon dioxide, evaporated, diluted with water, and extracted with carbon tetrachloride. The crude material obtained on evaporation (5.8 g) consisted of two products in the ratio of 4:1 separable by g.l.c. on a preparative 10-ft DEGS column at 175°.

The main product, (XVI), had n_D^{25} 1.5154, λ_{max} 237 mμ (ϵ, 16,400), ν_{max} 1668, 1637, 1421 cm^{-1}. Calc. for $C_{12}H_{18}O$: C, 80.55; H, 10.18%. Found: C, 80.43; H, 10.14%. The 2:4-dinitrophenylhydrazone, crystallized from methanol, had m.p. 189–190°, λ_{max} 372 mμ (ϵ, 24,500). Calc. for $C_{18}H_{22}O_4N_4$: C, 60.32; H, 6.19; N, 15.63. Found: C, 60.78; H, 6.21; N, 15.52%.

The minor product (XVII) had n_D^{25} 1.5121, λ_{max} 240 mμ (ϵ, 17,000), ν_{max} 1670, 1637, 1415 cm^{-1}. Calc. for $C_{12}H_{18}O$: C, 80.85; H, 10.18%. Found: C, 80.14; H, 9.92%.

The 2:4-dinitrophenylhydrazone, crystallized from methanol, had m.p. 146–147°, λ_{max} 386 mμ (ϵ, 25,700). Calc. for $C_{18}H_{22}O_4N_4$: C, 60.32; H, 6.19; N, 15.63%. Found: C, 60.54; H, 6.19; N, 15.37%.

Ozonolysis of the Ketone (XVI)

The unsaturated ketone (XVI) (800 mg) was dissolved in methylene chloride (20 ml), immersed in an acetone–CO_2 bath, and a stream of ozone was passed for 1 hour. Hydrogen peroxide (30%; 2 ml) and aqueous sodium hydroxide (2 *N*; 5 ml) were added and the mixture stirred at room temperature for 5 hours. The mixture was extracted with methylene chloride, the aqueous phase acidified with sulphuric acid (3 *N*), and the acidic material isolated with carbon tetrachloride. Treatment of the crude acid with ethereal diazomethane gave the keto ester mixture (710 mg), which was separated by g.l.c. on a DEGS preparative column at 180° into two isomers in approximately equal amounts.

The keto-ester-I (XVIII) had n_D^{25} 1.4713. Calc. for $C_{12}H_{20}O_3$: C, 67.89; H, 9.50%. Found: C, 68.11; H, 9.33%. The 2:4-dinitrophenylhydrazone, crystallized from methanol, had m.p. 118–119°, λ_{max} 363 mμ (ϵ, 22,500). Calc. for $C_{18}H_{24}O_6N_4$: C, 55.09; H, 6.17; N, 14.28%. Found: C, 55.34; H, 6.22; N, 14.21%.

The keto-ester-II (XVIII) had n_D^{25} 1.4697. Calc. for $C_{12}H_{20}O_3$: C, 67.89; H, 9.50%. Found: C, 67.62; H, 9.18%. The 2:4-dinitrophenylhydrazone, crystallized from methanol, had m.p. 123–124°, λ_{max} 361 mμ (ϵ, 20,500). Calc. for $C_{18}H_{24}O_6N_4$: C, 55.09; H, 6.17; N, 14.28%. Found: C, 55.51; H, 6.34; N, 14.14%. The 2:4-dinitrophenylhydrazone did not show a mixed melting point depression on admixture with that from (XVIII), but showed different infrared and n.m.r. spectra.

Ozonolysis of the Ketone (XVII)

The unsaturated ketone (100 mg) was dissolved in methylene dichloride (30 ml), cooled in an acetone–CO_2 bath, and ozone was passed for 40 minutes. Hydrogen peroxide (30%; 2 ml) and aqueous sodium hydroxide (5 *N*; 5 ml) were added and the mixture stirred at room temperature for 5 hours. After removal of the neutral material by extraction the mixture was acidified with sulphuric acid (3 *N*), the acid extracted with carbon tetrachloride and esterified with diazomethane. The oil (80 mg) appeared homogeneous to g.l.c. on a DEGS column. Distillation (bath temp. 180° at ca. 0.6 mm) gave an oil, n_D^{25} 1.4689. Calc. for $C_{12}H_{18}O_3$: C, 67.89; H, 9.50%. Found: C, 67.59; H, 9.94%. The 2:4-dinitrophenylhydrazone, crystallized from methanol, had m.p. 153–154°, λ_{max} 361 mμ (ϵ, 21,600). Calc. for $C_{18}H_{24}O_6N_6$: C, 55.09; H, 6.17; N, 14.28%. Found: C, 55.29; H, 6.13; N, 14.22%.

ACKNOWLEDGMENTS

The authors wish to thank Mr. A. B. M. A. Sattar for the experiments indicated, and Mr. R. E. Klinck for the determination of the n.m.r. spectra. This work was supported by the U.S.A.F. under grant AF-AFOSR-61-6.

REFERENCES

1. P. de Mayo, H. Takeshita, and A. B. M. A. Sattar. Proc. Chem. Soc. 119 (1962).
3. G. W. Wheland. Resonance in organic chemistry. John Wiley. 1955. p. 279 *et seq.*
3. P. de Mayo. The ultraviolet photochemistry of simple unsaturated systems. Advances in organic chemistry. Vol. 2. 1950. p. 367.
4. W. M. Moore, G. S. Hammond, and R. P. Foss. J. Am. Chem. Soc. **83**, 1 (1961).
5. P. de Mayo, J. B. Stothers, and W. Templeton. Can. J. Chem. **39**, 488 (1961).
6. N. C. Yang and D-D. Yang. J. Am. Chem. Soc. **80**, 2913 (1958).
7. A. Schönberg and A. Mustafa. Chem. Rev. **40**, 181 (1947).
8. W. H. Urry and D. J. Trecker. J. Am. Chem. Soc. **84**, 119 (1962).
9. P. de Mayo and A. Stoessl. Can. J. Chem. **40**, 57 (1962).
10. P. de Mayo and P. Jolly. Unpublished observations.
11. P. Grossmann. Z. Physik. Chem. **109**, 305 (1924).

Can. J. Chem. Downloaded from www.nrcresearchpress.com by 210.87.254.105 on 09/05/12
For personal use only.

12. L. M. JACKMAN. Applications of nuclear magnetic resonance spectroscopy in organic chemistry. Pergamon Press. 1959.
13. L. J. BELLAMY. The infrared spectra of complex molecules. Methuen. 1958.
14. J. W. BARRETT, A. H. COOK, and R. P. LINSTEAD. J. Chem. Soc. 1065 (1935).
15. A. MUSTAFA. Chem. Rev. **51**, 1 (1952).
16. G. BÜCHI and I. M. GOLDMAN. J. Am. Chem. Soc. **79**, 4741 (1957).
17. P. DE MAYO and R. W. YIP. Unpublished observations.
18. (*a*) M. P. CAVA and E. MOROZ. J. Am. Chem. Soc. **84**, 115 (1962). J. MEINWALD, G. G. CURTIS, and P. G. GASSMAN. J. Am. Chem. Soc. **84**, 116 (1962).
(*b*) N. L. ALLINGER, M. NAKAZAKI, and V. ZALKOW. J. Am. Chem. Soc. **81**, 4074 (1959).
19. N. C. YANG and D-D. H. YANG. Tetrahedron Letters, No. 4, 10 (1960).
20. G. BÜCHI, C. G. INMAN, and E. S. LIPINSKY. J. Am. Chem. Soc. **76**, 4327 (1954).
21. H. STOBBE and K. BREMER. J. Prakt. Chem. **123**, (1929). H. STOBBE and A. HENSEL. Ber. **59**, 2260 (1926).
22. A. BUTENANDT *et al.* Ann. **575**, 123 (1952).
23. R. ANET. Can. J. Chem. **40**, 1249 (1962).
24. G. STORK and J. W. SCHULENBERG. J. Am. Chem. Soc. **84**, 284 (1962).
25. R. A. FRIEDEL. J. Am. Chem. Soc. **73**, 2881 (1951).
26. O. ANSELMINO. Ber. **35**, 144 (1902).
27. P. E. EATON. J. Am. Chem. Soc. **84**, 2454 (1962).
28. J. F. HARRIS and D. D. COFFMAN. J. Am. Chem. Soc. **84**, 1553 (1962).

Can. J. Chem. Downloaded from www.nrcresearchpress.com by 210.87.254.105 on 09/05/12
For personal use only.

THE SULPHURIC ACID SOLVENT SYSTEM

PART IV. SULPHATOCOMPOUNDS OF ARSENIC (III)

R. J. GILLESPIE AND E. A. ROBINSON

Departments of Chemistry, McMaster University, Hamilton, Ontario, and University College, London, England

Received August 31, 1962

ABSTRACT

The cryoscopic and conductimetric behavior of arsenic (III) oxide in 100% sulphuric acid and in dilute oleum have been investigated. It is concluded that in very dilute solutions in 100% sulphuric acid, arsenic (III) oxide forms arsonyl (III) hydrogen sulphate, $AsO.HSO_4$, which is partly ionized to give the AsO^+ cation. Both these species probably exist mainly in solvated forms, e.g., $As(OH)(SO_4H)_2$, and $As(OH)(SO_4H)^+$ respectively. At higher concentrations polymeric species such as $HO.As(HSO_4)OAs(HSO_4)_2$ are present in increasing amounts and eventually the insoluble polymeric compound $[(AsO)_2SO_4]_n$ separates from solution. In oleum the more sulphated species $As(HSO_4)_3$, $[(HSO_4)_2As]_2O$, and $[(HSO_4)_2As]_2SO_4$ are formed. Related structures are proposed for some previously prepared compounds of arsenic (III) oxide and sulphur trioxide.

Can. J. Chem. Downloaded from www.nrcresearchpress.com by 210.87.254.42 on 09/05/12
For personal use only.

Sulphuric acid has proved to be a useful reagent for the production of oxycations such as NO^+ and NO_2^+ (1) and other cations such as the triphenylcarbonium ion $(C_6H_5)_3C^+$ and the mesitoyl ion $(CH_3)_3C_6H_2CO^+$ (2). It is also a convenient solvent for these ions, which are very strong Lewis acids, and are unstable in more basic media such as water. The present work is concerned with the possible formation of the ion AsO^+ and it was undertaken as part of a more general study of the formation and stability of other inorganic oxycations in the solvent sulphuric acid.

RESULTS AND DISCUSSION

Solutions of As_2O_3 in 100% Sulphuric Acid

The freezing points and conductivities of solutions of arsenic (III) oxide in 100% sulphuric acid are shown in Tables I and II. As arsenic (III) oxide is only sparingly

TABLE I

Freezing points of solutions of As_2O_3 in 100% H_2SO_4

$m\times10^2$	F.p. (°C)	$m\times10^2$	F.p. (°C)
0.000	10.365	0.000	10.365
0.460	10.266	0.530	10.241
1.843	9.898	1.382	10.001
2.501	9.724	2.469	9.699
3.812	9.369	3.613	9.430
4.681	9.168	4.565	9.229
		5.675	8.874
		6.515	8.676

soluble in 100% sulphuric acid it was not possible to study solutions more concentrated than approximately 0.1 molal. A white precipitate formed slowly in the more concentrated solutions; somewhat more rapidly at 10° than at 25°. Analysis of the precipitate showed that it had a composition close to $As_2O_3.SO_3$.

The number of moles of hydrogen sulphate ions, γ, formed by the ionization of 1 mole of arsenic (III) oxide was found by comparison of the concentrations of arsenic (III) oxide and of water having the same specific conductance (3) and the number of moles of

TABLE II

Electrical conductivities of solutions of As_2O_3 in 100% H_2SO_4 at 25° C

$\omega \times 10^2$*	$\kappa \times 10^2$	$\omega \times 10^2$	$\kappa \times 10^2$
0.000	1.044	0.000	1.044
0.808	1.123	0.249	1.049
1.540	1.295	0.817	1.124
2.236	1.482	1.494	1.277
2.843	1.652	2.206	1.488
4.136	2.007	3.384	1.806
		4.643	2.144

*$\omega \equiv$ moles of As_2O_3 per kilogram of solution.

particles, ν, formed from 1 mole of arsenic (III) oxide was calculated from the cryoscopic results. The results of these calculations are shown in Table III.

TABLE III

Values of ν, γ, and K_b for solutions of As_2O_3 in 100% H_2SO_4

$m_{As_2O_3}$	γ	F.p. (° C)	θ	m_d/m_s	x*	ν	$(\nu-\gamma)$	K_b†$\times 10^2$
0.000	—	10.365	0.250	—	—	—	—	—
0.010	2.60	10.111	0.504	2.04	8.03	5.99	3.39	—
0.015	2.47	9.980	0.635	1.03	6.89	5.86	3.37	11.7
0.020	2.38	9.850	0.765	0.64	6.25	5.61	3.23	11.5
0.025	2.32	9.724	0.891	0.41	5.83	5.42	3.10	12.0
0.030	2.26	9.594	1.021	0.28	5.57	5.29	3.03	12.1
0.040	2.17	9.336	1.279	0.16	5.24	5.08	2.91	11.0
0.050	2.13	9.077	1.538	0.10	5.04	4.94	2.81	12.5
0.060	2.11	8.813	1.802	0.07	4.93	4.86	2.75	13.0
0.070	2.11	8.550	2.065	0.05	4.84	4.79	2.68	—
								12.0 moles kg^{-1}

*$x = \theta(1+0.002\theta)/6.12m_{As_2O_3}$.
†$K_b = [AsO^+][HSO_4^-]/[AsO.HSO_4] = (\gamma-1)[HSO_4^-]/(3-\gamma)$.

If arsenic (III) oxide behaved like N_2O_3 (4), it would ionize according to the equation

$$As_2O_3 + 3H_2SO_4 = 2AsO^+ + H_3O^+ + 3HSO_4^-, \quad [1]$$

for which, if water were fully ionized, $\nu = 6$ and $\gamma = 3$. At the lowest concentration given in Table III the observed values are $\nu = 5.9$ and $\gamma = 2.6$, which agree moderately well with the expected values. However, both ν and γ decrease considerably with increasing concentration. The simplest explanation of this is to assume that $AsO.HSO_4$ is incompletely ionized. The ν and γ factors would then be expected to decrease towards the values of 4 and 1, respectively, which would correspond to the formation of unionized $AsO.HSO_4$ according to the equation

$$As_2O_3 + 3H_2SO_4 = 2AsO.HSO_4 + H_3O^+ + HSO_4^-. \quad [2]$$

The experimental observations are reasonably consistent with this mode of reaction and an approximately constant value of the dissociation constant of $AsO.HSO_4$ may be calculated from the observed γ values, as is shown in Table III. The only remaining inconsistency is that the decrease in the value of ν is more rapid than that for γ and thus $\nu-\gamma$, which should have a constant value of 3, decreases from 3.4 to 2.7. The initially high value of $\nu-\gamma$ is discussed later; the decrease to values of less than 3 could be accounted

Can. J. Chem. Downloaded from www.nrcresearchpress.com by 210.87.254.42 on 09/05/12
For personal use only.

for by polymerization of $AsO.HSO_4$, for example, by the formation of a dimer:

$$As_2O_3 + 3H_2SO_4 = (AsO.HSO_4)_2 + H_3O^+ + HSO_4^-, \qquad [3]$$

$\nu = 3$, $\gamma = 1$, and $\nu - \gamma = 2$. The ready formation of a precipitate even from quite dilute solutions of As_2O_3 is also consistent with the formation of polymers, for which structures I or II seem reasonable:

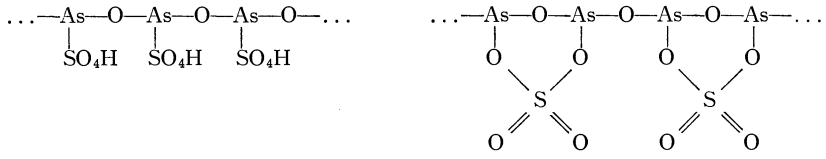

I II

An additional sulphuric molecule is needed to terminate such a chain, giving an —OH group on one end and a hydrogen sulphate group on the other:

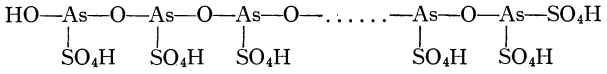

III

The first two members of this series of polymers then represent solvated forms of $AsO.HSO_4$ and $(AsO.HSO_4)_2$, respectively, i.e.,

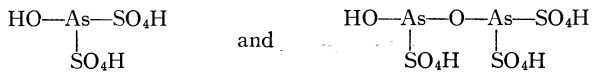

IV and V

Similarly the species written above as AsO^+ is probably more correctly written in one of the solvated forms VI and VII which can be derived from IV by loss of HSO_4^- or by proton addition. Similar dimeric ions VIII and IX are also possible.

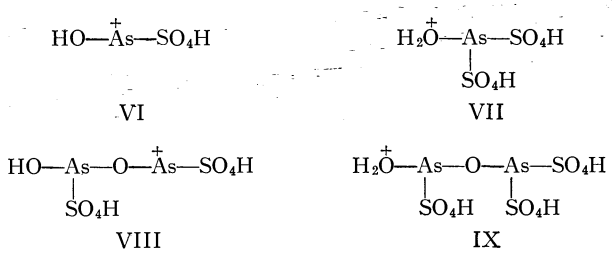

VI VII

VIII IX

The insoluble precipitate of composition $As_2O_3.SO_3$ obtained from the more concentrated solution of As_2O_3 in sulphuric acid may be formulated as $[(AsO)_2SO_4]_n$ with the structure II.

The values of ν would not be expected to be as high as 6.0 even in the most dilute solutions because of the incomplete ionization of the water formed (6). The fact that the observed values are very close to 6.0, and the initial values of $\nu - \gamma$ are higher than the expected value of 3.0, at very low concentrations, can probably be attributed to the formation, under these conditions, of small amounts of $As(HSO_4)_3$, according to equation (v) of Table IV for which $\nu = 8$ and $\gamma = 3$. Evidence for the formation of this and related species in oleum solutions is presented in the following section. Possible modes of ionization, including some which are not consistent with the experimental results, are summarized in Table IV.

Can. J. Chem. Downloaded from www.nrcresearchpress.com by 210.87.254.42 on 09/05/12
For personal use only.

TABLE IV

Equations for some possible modes of ionization of As_2O_3 in H_2SO_4

	ν	γ
(i) $As_2O_3 + 3H_2SO_4 = 2AsO^+ + H_3O^+ + 3HSO_4^-$	6	3
(ii) $As_2O_3 + 3H_2SO_4 = 2AsO.HSO_4 + H_3O^+ + HSO_4^-$	4	1
(iii) $As_2O_3 + 6H_2SO_4 = [As(HSO_4)_2]_2O + 2H_3O^+ + 2HSO_4^-$	5	2
(iv) $As_2O_3 + 8H_2SO_4 = [As(HSO_4)_2]_2SO_4 + 3H_3O^+ + 3HSO_4^-$	7	3
(v) $As_2O_3 + 9H_2SO_4 = 2As(HSO_4)_3 + 3H_3O^+ + 3HSO_4^-$	8	3
(vi) $As_2O_3 + 9H_2SO_4 = 2As(HSO_4)_4^- + 3H_3O^+ + HSO_4^-$	6	1
(vii) $As_2O_3 + 9H_2SO_4 = 2As^{3+} + 3H_3O^+ + 9HSO_4^-$	14	9

It is unfortunate that the present measurements do not enable one to distinguish between the AsO^+ ion and the solvated forms VI and VII or between the undissociated molecule $AsO.HSO_4$ and its solvated form IV. The method that was originally used to establish that NO^+ and NO_2^+ exist in solution in sulphuric acid in the unsolvated form as simple diatomic and linear triatomic ions respectively, namely Raman spectroscopy (5), could not be applied in the present case because the solutions that could be obtained were too dilute to give satisfactory Raman spectra of the dissolved species. However, the tendency for the formation of polymeric species in these solutions may well be a consequence of the inability, or at least the reluctance, of arsenic (III) to form multiple bonds. We recall that silicon compounds of the type R_2SiO, which could in principle contain a silicon–oxygen double bond, are, in fact, polymeric. Double bonds are formed only be elements of high electronegativity and on the Pauling scale arsenic has the same electronegativity as boron, namely 2.0, and boron does not form double bonds to oxygen in stable molecules. There are reasons, therefore, for thinking that the free AsO^+ ion may not exist in appreciable concentrations because of a strong tendency to eliminate its double bond by solvation and polymerization. For simplicity, however, we will generally represent IV by the formula $AsO.HSO_4$ and II and VII by the formula of the unsolvated species AsO^+.

Solutions of As_2O_3 in Dilute Oleum

The results of cryoscopic and conductimetric measurements on solutions of As_2O_3 in dilute oleum are given in Tables V and VI and Fig. 1. Addition of arsenic (III) oxide to a

TABLE V

Freezing points of solutions of As_2O_3 in oleum

$n_{As_2O_3}\times10^2$	$n_{As_2O_3}/n^i_{H_2S_2O_7}$	$g_{H_2SO_4}$	$m_{As_2O_3}\times10^2$	F.p. (° C)
	$n^i_{H_2S_2O_7} = 5.144\times10^{-2}$ mole			
0.000	0.000	122.69	0.000	7.085
0.082	0.016	124.59	0.659	7.212
0.256	0.050	128.62	1.993	7.437
0.437	0.085	132.81	3.287	7.686
0.704	0.137	139.00	5.065	7.977
0.871	0.169	143.02	6.088	8.158
	$n^i_{H_2S_2O_7} = 2.072\times10^{-2}$ mole			
0.000	0.000	122.67	0.000	9.270
0.099	0.038	124.95	0.789	9.365
0.213	0.103	127.61	1.673	9.475
0.419	0.202	132.37	3.165	9.635
0.535	0.258	135.06	3.959	9.727
0.599	0.289	137.07	4.369	9.743
0.726	0.350	141.05	5.144	9.834
0.926	0.447	147.29	6.284	9.823

Can. J. Chem. Downloaded from www.nrcresearchpress.com by 210.87.254.42 on 09/05/12
For personal use only.

TABLE VI

Electrical conductivity measurements on solutions of As_2O_3 in oleum at 25° C

$n_{As_2O_3}\times10^2$	$\frac{n_{As_2O_3}}{n^i_{H_2S_2O_7}}$	κ (10^{-2} ohm^{-1} cm^{-1})	$n_{As_2O_3}\times10^2$	$\frac{n_{As_2O_3}}{n^i_{H_2S_2O_7}}$	κ (10^{-2} ohm^{-1} cm^{-1})
$n^i_{H_2S_2O_7} = 2.125\times10^{-2}$ mole			$n^i_{H_2S_2O_7} = 7.361\times10^{-2}$ mole		
0.000	0.000	1.675	0.000	0.000	2.603
0.060	0.028	1.615	0.044	0.006	2.509
0.261	0.122	1.422	0.283	0.038	2.396
0.380	0.179	1.312	0.534	0.073	2.220
0.468	0.220	1.236	0.779	0.106	2.056
0.662	0.311	1.099	1.053	0.143	1.878
0.799	0.376	1.044	1.245	0.169	1.759
0.924	0.435	1.039	1.526	0.207	1.588
1.062	0.499	1.091	1.819	0.247	1.432
1.238	0.582	1.225	2.176	0.296	1.262
1.447	0.681	1.433	2.460	0.334	1.151
1.688	0.794	1.678	2.851	0.387	1.036
$n^i_{H_2S_2O_7} = 0.584\times10^{-2}$ mole			$n^i_{H_2S_2O_7} = 8.125\times10^{-2}$ mole		
0.000	0.000	1.200	0.000	0.000	2.237
0.247	0.423	1.042	0.414	0.051	1.957
0.327	0.560	1.071	1.040	0.128	1.563
0.450	0.771	1.179	2.697	0.332	1.136
0.761	1.303	1.564	3.468	0.415	1.037
0.900	1.542	1.704	5.363	0.660	1.563

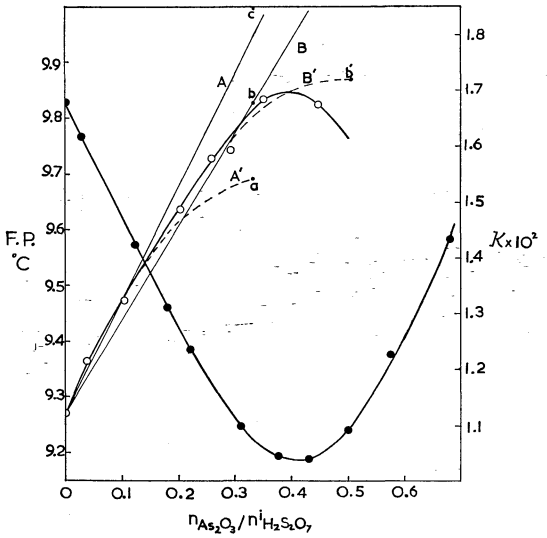

FIG. 1. Freezing points and electrical conductivities of solutions of As_2O_3 in dilute oleum. ○, freezing points; ●, conductivities. A, B, *a*, *b*, *b'*, and *c* are explained in the text and in Table VII.

dilute oleum results in a decrease of the conductivity until a minimum is reached and the conductivity then increases again. The conductivity minimum is reached when $r = n_{As_2O_3}/n^i_{H_2S_2O_7} = 0.42$, where $n_{As_2O_3}$ is the number of moles of As_2O_3 added to $n^i_{H_2S_2O_7}$ moles of $H_2S_2O_7$. The freezing point increases on addition of As_2O_3 to oleum and reaches a maximum at $r = n_{As_2O_3}/n^i_{H_2S_2O_7} \simeq 0.38$.

Since arsenic (III) oxide forms $AsO.HSO_4$ in sulphuric acid its ionization in oleum might be expected to be represented by

$$As_2O_3 + H_2S_2O_7 \rightarrow 2AsO.HSO_4 \rightleftharpoons 2AsO^+ + 2HSO_4^-. \qquad [4]$$

If $AsO.HSO_4$ behaved as a non-electrolyte the conductivity minimum in a titration of

Can. J. Chem. Downloaded from www.nrcresearchpress.com by 210.87.254.42 on 09/05/12
For personal use only.

oleum would occur at $r = 1.0$, and the freezing point of the solution would decrease since each mole of $H_2S_2O_7$* would be replaced by 2 moles of $AsO.HSO_4$ (i.e. $\Delta\nu = 2.00-1.33 = 0.67$).

For the titration of $H_2S_2O_7$ with a base B the position of minimum conductivity is given by

$$n_B/n^1_{H_2S_2O_7} = 0.56(1+0.018/K_b)$$

where n_B is the number of moles of base added to a solution containing $n^1_{H_2S_2O_7}$ moles of disulphuric acid initially, and K_b is the dissociation constant of the base (7).

If $AsO.HSO_4$ behaved as a strong base the conductivity minimum would be predicted at $n_{AsO.HSO_4}/n^1_{H_2S_2O_7} = 0.56$, (7), and therefore for the reaction

$$As_2O_3 + H_2S_2O_7 = 2AsO^+ + 2HSO_4^- \quad [5]$$

the conductivity minimum would occur at $r = 0.22$. The freezing point of the solution would remain approximately constant since the overall reaction up to the conductivity minimum would be

$$As_2O_3 + 3H_2S_2O_7 = 2AsO^+ + 2HS_2O_7^- + 2H_2SO_4, \quad [6]$$

i.e. $\Delta\nu = (3\times1.33)-4.00 = 0$.*

For $AsO.HSO_4$ reacting as a weak base a value of $K_b = 0.011$ mole kg^{-1} may be calculated from the observed composition at the minimum conductivity, in poor agreement with the value of $K_b = 0.12$ mole kg^{-1} obtained above. On the basis of this latter value the conductivity minimum would be expected to occur at $r = 0.24$. It is evident that this scheme of ionization is not consistent with the experimental results.

The experimental results can, however, be accounted for if it is assumed that $As(OH)(HSO_4)_2$ and its dimer, which are formed in 100% sulphuric acid, are further sulphated in oleum according to the equations

$$HO.As(HSO_4)_2 \xrightarrow{SO_3} As(HSO_4)_3 \quad [7]$$

$$HO.As(HSO_4).O.As(SO_4H)_2 \xrightarrow{SO_3} [(SO_4H)_2As]_2O$$

$$\xrightarrow{SO_3} [(HSO_4)_2As]_2SO_4. \quad [8]$$

The corresponding reactions when As_2O_3 is added to oleum would then be

$$As_2O_3 + 3H_2S_2O_7 = 2As(HSO_4)_3 \quad [9]$$

$$As_2O_3 + 2H_2S_2O_7 \rightarrow [(HSO_4)_2As]_2O \quad [10]$$

$$As_2O_3 + 3H_2S_2O_7 \rightarrow [(HSO_4)_2As]_2SO_4 + H_2SO_4. \quad [11]$$

Each of these reactions would lead to an increase in the freezing point of the solution. The corresponding values of $\Delta\nu$ are given in Table VII, which also includes values of ν at the compositions $r = 0.33$ and $r = 0.5$ and the corresponding freezing-point curves are shown in Fig. 1 (curves A and B). The observed freezing points are initially in good agreement with the formation of $As(HSO_4)_3$. The removal of $H_2S_2O_7$, which represses the self-ionization of the solvent, and its replacement by a non-electrolyte will cause the slopes of the freezing-point curves to decrease (A′ and B′ in Fig. 1). At $r = 0.33$ the observed freezing point of the solution agrees well with that expected for reaction [10]. It is certainly much higher than would be expected for the formation of $As(HSO_4)_3$ alone and we conclude that when As_2O_3 is added to oleum, $As(HSO_4)_3$ is formed initially but is gradually

**In dilute solution in sulphuric acid each molecule of* $H_2S_2O_7$ *behaves as approximately* $1\frac{1}{3}$ *particles (6), as a result of the ionization*

$$H_2S_2O_7 + H_2SO_4 \leftrightharpoons H_3SO_4^+ + HS_2O_7^-.$$

Can. J. Chem. Downloaded from www.nrcresearchpress.com by 210.87.254.42 on 09/05/12
For personal use only.

TABLE VII

Predicted values of ν for solutions of As_2O_3 in oleum

Reaction	Initial slope $\Delta\nu$	$r = 0.33$		$r = 0.5$	
		ν	F.p.	ν	F.p.
[9]	−2.00 (A)	2.0	9.69 (*a*)	—	—
[10]	−1.67 (B)	2.3	9.83 (*b*)	1	9.87 (*b'*)
[11]	−2.00 (A)	1.0	10.02 (*c*)	—	—
Observed	−2.00	—	9.84	—	9.77

NOTE: A, B, *a*, *b*, *b'*, and *c* refer to curves and points in Fig. 1.

replaced by $[As(HSO_4)_2]_2O$. However, the conductivity at $r = 0.33$ is not much greater than at the conductivity minimum and is considerably smaller than would be expected if one third of the original $H_2S_2O_7$ remained unreacted. It seems necessary therefore to assume that $As(HSO_4)_3$ and the fully sulphated dimer $[(HSO_4)_2As]_2SO_4$ are also present. Complete reaction according to equation [11] would give the freezing point indicated by *c* in Fig. 1.

In a previous paper on conductivity measurements on solutions of acids of the sulphuric acid solvent system (8), it was assumed that the conductivity at the composition $r = 0.33$ was due to the acid behavior of $As(HSO_4)_3$,

$$As(HSO_4)_3 + 2H_2SO_4 = H_3SO_4^+ + As(HSO_4)_4^-,$$

and a dissociation constant for the acid $HAs(HSO_4)_4$ of $K_a = 0.015$ was calculated from the conductimetric results. However, it seems clear that much of the arsenic must be present in the solution in the form of the dimer $[(HSO_4)_2As]_2O$ and a corresponding amount of $H_2S_2O_7$ must also be present. Thus at least part of the observed conductivity at this composition must be due to $H_2S_2O_7$, and the dissociation constant for $HAs(HSO)_4$ quoted above can only be regarded as a maximum value; indeed, it cannot be concluded with certainty that $As(HSO_4)_3$ exhibits any acid properties at all. Figure 2 shows the results

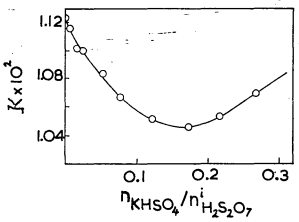

FIG. 2. Electrical conductivities obtained by adding $KHSO_4$ to a solution of As_2O_3 in oleum having the composition $n_{As_2O_3}/n^i_{H_2S_2O_7} = 0.33$.

of an experiment in which $KHSO_4$ was added to a solution of composition $r = 0.33$. The observed decrease in the conductivity may be attributed to the titration of the $H_2S_2O_7$ and perhaps to some extent also to the titration of $HAs(HSO_4)_4$.

From $r = 0.33$ to the maximum freezing point there is only a very small increase of 0.04° in the observed freezing point. This must be attributed to the simultaneous occurrence of the following reactions:

$$4As(HSO_4)_3 + As_2O_3 \rightarrow 3[As(HSO_4)_2]_2O$$
$$2[As(HSO_4)_2]_2SO_4 + As_2O_3 \rightarrow 3[As(HSO_4)_2]_2O.$$

Can. J. Chem. Downloaded from www.nrcresearchpress.com by 210.87.254.42 on 09/05/12
For personal use only.

If equal amounts of As_2O_3 reacted by each of these reactions there would be no change in the number of particles in solution, and hence no change in the freezing point.

At $r = 0.5$ the formation of $[As(HSO_4)_2]_2O$ would be complete and the solution would be expected to have a maximum freezing point (b' in Fig. 1). The observed freezing point is lower than this. It begins to decrease before $r = 0.5$, presumably because with diminishing $H_2S_2O_7$ concentration in the system some dissociation occurs according to the equation

$$[As(HSO_4)_2]_2O + 2H_2SO_4 \rightarrow 2HO.As(HSO_4)_2 + H_2S_2O_7.$$

Unfortunately these systems appear to be too complicated to be able to obtain any quantitative information from the available experimental data on the amounts of the various species present. However, the following qualitative conclusions seem reasonably well established: When As_2O_3 is first added to oleum it is largely converted to $As(HSO_4)_3$ but with increasing concentration it polymerizes and, in particular, the dimers $[As(HSO_4)_2]_2SO_4$ and $[As(HSO_4)_2]_2O$ are present in increasing amounts. At the composition $r = 0.33$, which corresponds to the stoichiometric composition $As(HSO_4)_3$, all three species appear to be present in equilibrium with some unreacted $H_2S_2O_7$. At $r = 0.5$ the species present are $[As(HSO_4)_2]_2O$ together with some $HOAs(HSO_4)_2$ and $H_2S_2O_7$.

Previous Work

Early workers reported the preparation of several sulphato compounds of trivalent arsenic by dissolving arsenic (III) oxide in sulphuric acid of various strengths, and by reactions between As_2O_3 and sulphur trioxide. Adie (69) obtained a compound corresponding to the composition $As_2O_3.SO_3$ by dissolving arsenic (III) oxide in sulphuric acid of the composition $H_2SO_4.H_2O$, and the compound $As_2O_3.8SO_3$ by dissolving As_2O_3 in hot sulphur trioxide. Several workers have analyzed the sulphato compounds of arsenic obtained from the flues of pyrites burners and all agree that the compositions of the compounds correspond closely to that expected for the compound $As_2O_3.SO_3$ (10). Stavenhagen (11) obtained the same compound by recrystallizing arsenious oxide from sulphuric acid having a composition between $H_2SO_4.H_2O$ and $2H_2SO_4.9H_2O$. However, he obtained the compound $As_2O_3.2SO_3$ from a solution of As_2O_3 in 98% H_2SO_4. Other arsenic (III) oxide – sulphur trioxide complexes which have been reported are $As_2O_3.3SO_3$, $As_2O_3.4SO_3$, and $As_2O_3.6SO_3$ (10). Complex sulphates of arsenic (III) have also been reported, e.g., $2K_2O.As_2O_3.4SO_3$, $CuO.As_2O_3.3SO_3$, $PbO.As_2O_3.2SO_3$ (10).

The compounds $As_2O_3.SO_3$, $As_2O_3.2SO_3$, and $As_2O_3.3SO_3$ are probably closely related to the species that we have found to occur in 100% H_2SO_4 and in oleum, i.e.

$$\begin{aligned} As_2O_3.SO_3 + H_2SO_4 &\rightarrow 2AsO.HSO_4 \\ As_2O_3.2SO_3 + 2H_2SO_4 &\rightarrow [As(HSO_4)_2]_2O \\ As_2O_3.3SO_3 + 3H_2SO_4 &\rightarrow 2As(HSO_4)_3 \\ As_2O_3.3SO_3 + 2H_2SO_4 &\rightarrow [As(HSO_4)_2]_2SO_4. \end{aligned}$$

Possible Structures for Sulphatoarsenic (III) Compounds

Recently we have discussed the structures of complex sulphatoboron compounds (12) and have shown that they may be satisfactorily formulated as derivatives of the six-membered ring X, which is closely related to the similar ring XI found in many polyborates. It seems likely that the preference for ring structures is partly a consequence of the inability of boron to form double bonds with oxygen. Since arsenic has the same electronegativity as boron it is reasonable to expect it to show a similar inability to form double bonds and a similar preference for six-membered ring structures.

In general, oxygen compounds of arsenic (III) are found to have only single bonds to oxygen and As_4O_6 contains the six-membered ring XII.

Can. J. Chem. Downloaded from www.nrcresearchpress.com by 210.87.254.42 on 09/05/12
For personal use only.

Therefore, we postulate that in the case of sulphatoarsenic compounds the ring XIII is an important structural unit. On this basis $As_2O_3.SO_3$ and $As_2O_3.2SO_3$, for example, may be formulated as in II and XIV.

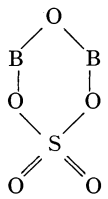

X

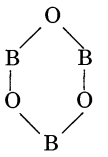

XI

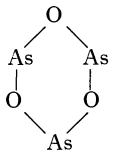

XII

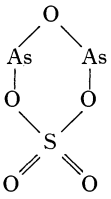

XIII

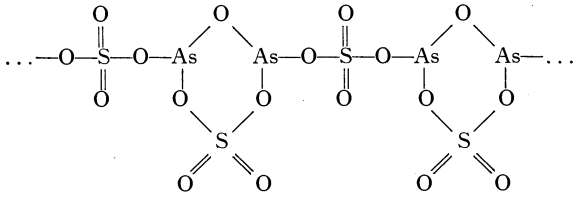

XIV

The complex sulphatoarsenites mentioned above may also be formulated similarly.

CONCLUSIONS

In very dilute solutions in 100% sulphuric acid, arsenic (III) oxide forms arsonyl (III) hydrogen sulphate, $AsO.HSO_4$, which is partly ionized to give the AsO^+ cation. Both these species probably exist in solvated forms, e.g. $As(OH)(SO_4H)_2$ and $As(OH)SO_4H^+$ respectively, and no conclusive evidence was obtained for the existence of the unsolvated form AsO^+ analogous to the well-known nitrosyl cation NO^+. At higher concentrations polymerized species such as $HO.As(HSO_4)OAs(HSO_4)_2$ are present in increasing amounts and eventually the insoluble polymeric compound $[(AsO)_2SO_4]_n$ separates from solution. In oleum the more sulphated species $As(HSO_4)_3$, $[(HSO_4)_2As]_2O$, and $[(HSO_4)_2As]_2SO_4$ are formed.

EXPERIMENTAL

The apparatus and general procedure for making the cryoscopic and conductimetric measurements has been described elsewhere (13, 14). The cryoscopic ν factors were obtained from the equation

$$\nu = \theta(1+0.002\theta)/6.12m-(m_d/m),$$

where θ is the freezing point depression calculated from the freezing point (10.625°) of hypothetically undissociated sulphuric acid, m is the concentration of arsenious oxide, m_d is the concentration of unrepressed self-dissociation products, and 6.12 is the cryoscopic constant (15). The correction m_d/m for unrepressed self-dissociation was made using the conductimetric γ factors to obtain the concentration of HSO_4^- and assuming that each molecule of arsenious oxide ionizes to give one hydronium ion. The conductimetric γ factors were calculated by comparison with the conductivities of solutions of water in sulphuric acid, as has been described previously (9). The conductimetric titrations were also carried out as previously described (3). The initial concentrations of oleum, in these titrations, were obtained from the specific conductance measurements.

Analytical grade arsenious oxide was dried at 100°.

ACKNOWLEDGMENT

We thank the National Research Council of Canada for generous financial support.

Can. J. Chem. Downloaded from www.nrcresearchpress.com by 210.87.254.42 on 09/05/12
For personal use only.

REFERENCES

1. R. J. GILLESPIE and E. A. ROBINSON. Advan. Inorg. Chem. Radiochem. **1**, 385 (1959).
2. R. J. GILLESPIE and J. A. LEISTEN. Quart. Rev. (London), **8**, 40 (1954).
3. R. J. GILLESPIE and C. SOLOMONS. J. Chem. Soc. 1796 (1957).
4. R. J. GILLESPIE, J. GRAHAM, E. D. HUGHES, C. K. INGOLD, and E. R. A. PEELING. J. Chem. Soc. 2504 (1950).
5. D. J. MILLEN. J. Chem. Soc. 2600 (1950).
6. R. J. GILLESPIE. J. Chem. Soc. 2493 (1950).
7. R. H. FLOWERS, R. J. GILLESPIE, and E. A. ROBINSON. Can. J. Chem. **38**, 1363 (1961).
8. J. BARR, R. J. GILLESPIE, and E. A. ROBINSON. Can. J. Chem. **39**, 1266 (1961).
9. R. H. ADIE. J. Chem. Soc. **57**, 540 (1890).
10. J. W. MELLOR. A comprehensive treatise on inorganic and theoretical chemistry. Vol. IX. Longmans Green, London. 1922. p. 332.
11. A. STAVENHAGEN. Z. Angew. Chem. **6**, 284 (1893).
12. R. J. GILLESPIE and E. A. ROBINSON. Can. J. Chem. **40**, 1009 (1962).
13. R. J. GILLESPIE, E. D. HUGHES, and C. K. INGOLD. J. Chem. Soc. 2473 (1950).
14. R. J. GILLESPIE, J. V. OUBRIDGE, and C. SOLOMONS. J. Chem. Soc. 1804 (1957).
15. R. J. GILLESPIE. J. Chem. Soc. 1851 (1954).

Can. J. Chem. Downloaded from www.nrcresearchpress.com by 210.87.254.42 on 09/05/12
For personal use only.

STEREOCHEMISTRY OF ARSENIC

VIII. CYANODIMETHYLARSINE (CACODYL CYANIDE)

N. CAMERMAN AND J. TROTTER

Department of Chemistry, University of British Columbia, Vancouver, British Columbia

Received September 28, 1962

ABSTRACT

Crystals of cyanodimethylarsine, $(CH_3)_2AsCN$, are triclinic with two molecules in a unit cell of dimensions $a = 6.31$, $b = 8.02$, $c = 6.27$ Å, $\alpha = 110°00'$, $\beta = 119°45'$, $\gamma = 81°47'$, space group $P\bar{1}$. The structure has been determined from projections along the three crystallographic axes, and the mean values of the bond lengths and valency angles (with estimated standard deviations) are: As—C = 1.96±0.03 Å, C—N = 1.16±0.07 Å, ∠ Me—As—Me = 105±2°, ∠Me—As—CN = 91±1½°, ∠ As—C—N = 180±4°. There is an unusually short As....N intermolecular separation, which is indicative of charge-transfer bonding involving donation of nitrogen lone pair electrons to vacant arsenic 4*d* orbitals; the other intermolecular approaches correspond to normal van der Waals interactions.

INTRODUCTION

Previous papers in this series have described the structures of halogenodiphenylarsines. The C—As—C angles are 105°, considerably larger than the value assumed in an electron-diffraction investigation of the corresponding dimethyl derivatives, so that we felt it would be useful to investigate the structure of a compound of this latter type. The halogenodimethylarsines are all liquids at room temperature, but cyanodimethylarsine (cacodyl cyanide), whose structure is described in this present communication, is a solid, m.p. 30°. This is in itself an interesting fact, and suggests that there might be some type of intermolecular interaction.

EXPERIMENTAL

Colorless needle-shaped crystals of cyanodimethylarsine were prepared by the reaction of iododimethylarsine with silver cyanide *in vacuo*, the desired product being purified by sublimation. The compound is very volatile and extremely toxic, and crystals were sealed in thin-walled Lindemann-glass capillaries. The unit cell dimensions and space group were determined from rotation and oscillation photographs about the *a*-axis, and 0*kl* and 1*kl* Weissenberg and *h*0*l* and *hk*0 precession films.

Crystal Data

Cyanodimethylarsine, $(CH_3)_2AsCN$; M, 131.0; m.p. 30° C

Triclinic, $a = 6.31$, $b = 8.02$, $c = 6.27$ Å, $\alpha = 110°00'$, $\beta = 119°45'$, $\gamma = 81°47'$

Volume of the unit cell = 258.7 Å^3

D_{calc} (with $Z = 2$) = 1.68 g cm^{-3}

Absorption coefficients for X rays, $\lambda = 1.542$ Å, $\mu = 76.8$ cm^{-1}; $\lambda = 0.7107$ Å, $\mu = 67.2$ cm^{-1}.

$F(000) = 128$

Space group is $P1$ or $P\bar{1}$. Analysis has proceeded satisfactorily on the basis of $P\bar{1}$.

Due to the extreme volatility and toxicity of the crystals, we made no effort to measure the density, but since it seemed unlikely that it was as low as 0.8 or as high as 3.4 g cm^{-3}, $Z = 2$ was assumed. This was confirmed by the subsequent analysis of the structure.

The intensities of the 0*kl* reflections were recorded on Weissenberg films (Cu $K\alpha$) and of the *h*0*l* and *hk*0 reflections on precession films (Mo $K\alpha$). The estimates were made visually, and the structure amplitudes derived as usual, the absolute scale being established later by correlation with the calculated structure factors. The crystal used had cross section 0.1×0.1 mm and no absorption corrections were considered necessary. Eighty-four independent 0*kl*, forty-eight *h*0*l*, and seventy-seven *hk*0 reflections were observed.

Structure Analysis

The position of the arsenic atom was determined from the three Patterson projections, and the other atoms were then located on electron-density maps computed with signs based on the arsenic contributions alone. Structure factors were then calculated for all three zones, using the scattering factors of Berghuis

Can. J. Chem. Downloaded from www.nrcresearchpress.com by 210.87.254.5 on 09/05/12
For personal use only.

et al. (1), with an overall temperature factor $B = 5.1$ Å^2, determined from plots of ln $(|F_c|/|F_o|)$ against $\sin^2\theta/\lambda^2$. Refinement was completed by computing successive Fourier and difference syntheses. The final electron-density projections are shown in Figs. 1 and 2, and measured and calculated structure factors are listed in Table I. The discrepancy factors for the observed planes are: $R(0kl) = 14.7\%$; $R(h0l) = 17.3\%$; $R(hk0) = 14.0\%$.

TABLE I

Measured and calculated structure factors

h	k	l	F_o	F_c	h	k	l	F_o	F_c	h	k	l	F_o	F_c	h	k	l	F_o	F_c
0	0	1	37	−36	0	4	$\bar{6}$	6	− 5	2	0	$\bar{5}$	7	+ 1	2	$\bar{5}$	0	8	−10
		2	34	−34			$\bar{5}$	12	+10			$\bar{4}$	29	+19		$\bar{4}$		12	+15
		3	34	+34			$\bar{4}$	2	− 5			$\bar{3}$	37	−34		$\bar{3}$		35	+36
		4	12	−11			$\bar{3}$	18	−18			$\bar{2}$	<4	+ 8		$\bar{2}$		20	+23
		5	7	− 6			$\bar{2}$	28	−36			$\bar{1}$	58	+51		$\bar{1}$		6	−11
		6	7	+ 7			$\bar{1}$	4	− 8			1	<4	− 4		1		33	−35
0	1	0	37	+38			1	34	+25			2	19	+20		2		9	+ 1
	2		34	−38			2	11	− 7			$\bar{3}$	8	−13		3		13	+18
	3		40	−40			3	12	−10	3	0	$\bar{6}$	<5	− 5		4		22	+21
	4		30	−26			4	9	+ 9			$\bar{5}$	14	+12		5		9	+11
	5		<3	− 1			$\bar{5}$	3	− 1			$\bar{4}$	6	−11		6		<4	− 5
	6		17	+15	0	5	$\bar{5}$	11	+10			$\bar{3}$	17	−11		7	0	9	− 9
	7		12	+11			$\bar{4}$	11	−16			$\bar{2}$	38	+38		$\bar{8}$		7	− 3
	8		4	+ 2			$\bar{3}$	<2	+ 3			$\bar{1}$	9	−17	3	$\bar{8}$	0	5	− 5
	9		3	− 3			$\bar{2}$	20	+24			1	19	+22		$\bar{7}$		5	− 6
1	0	0	18	+18			$\bar{1}$	26	−30			2	3	− 7		$\bar{6}$		4	− 2
2			43	−43			1	23	+20			3	7	− 6		$\bar{5}$		10	+13
3			24	−20			2	12	−11	4	0	$\bar{6}$	<5	+ 3		$\bar{4}$		20	+22
4			9	+ 6	0	6	$\bar{6}$	5	+ 5			$\bar{5}$	6	+ 8		$\bar{3}$		9	+ 4
5			11	+ 9			$\bar{5}$	3	+ 1			$\bar{4}$	19	+18		$\bar{2}$		12	−19
							$\bar{4}$	12	−11			$\bar{3}$	7	+12		$\bar{1}$		23	−24
0	1	$\bar{6}$	4	+ 4			$\bar{3}$	11	+11			$\bar{2}$	12	+17		1		<3	+ 3
		$\bar{5}$	11	−14			$\bar{2}$	<2	− 1			$\bar{1}$	25	−27		2		24	+25
		$\bar{4}$	3	+ 7			$\bar{1}$	16	−15			1	6	+ 9		3		23	+20
		$\bar{3}$	22	+25			1	<2	+ 1			2	6	− 9		4		3	+ 3
		$\bar{2}$	39	−45			2	11	− 8	5	0	$\bar{6}$	6	+ 4		5		9	− 9
		$\bar{1}$	23	+29			3	<2	+ 4			$\bar{5}$	<5	− 8		6		11	−11
		1	74	−77			$\bar{4}$	3	− 1			$\bar{4}$	<5	+ 3		7		4	− 3
		2	16	+16	0	7	$\bar{6}$	4	+ 4			$\bar{3}$	13	+12	4	$\bar{5}$	0	8	+10
		3	17	+17			$\bar{5}$	6	− 6			$\bar{2}$	8	−14		$\bar{4}$		<3	+ 1
		4	19	−15			$\bar{4}$	3	− 1			$\bar{1}$	5	− 2		$\bar{3}$		10	−13
		5	3	+ 5			$\bar{3}$	12	+11	6	0	$\bar{5}$	7	− 6		$\bar{2}$		16	−15
		6	<2	+ 3			$\bar{2}$	7	−10			$\bar{4}$	6	+ 8		$\bar{1}$		9	− 8
0	2	$\bar{6}$	2	− 4			$\bar{1}$	<2	− 1			$\bar{3}$	<5	− 2		1		25	+23
		$\bar{5}$	10	− 7			1	11	− 9			$\bar{2}$	7	−10		2		23	+15
		$\bar{4}$	20	+26	0	8	$\bar{5}$	4	− 4			$\bar{1}$	7	+ 8		3		4	− 6
		$\bar{3}$	8	−15			$\bar{4}$	4	+ 5							4		10	−12
		$\bar{2}$	34	−32			$\bar{3}$	4	+ 3	1	$\bar{9}$	0	4	+ 4		5		9	− 7
		$\bar{1}$	54	+61			$\bar{2}$	8	− 8		$\bar{8}$		6	+ 6		6		<4	− 1
		1	38	−30			$\bar{1}$	4	+ 4		$\bar{7}$		4	+ 3		$\bar{7}$		4	+ 3
		2	49	+45	0	9	$\bar{4}$	4	+ 4		$\bar{6}$		5	− 7	5	$\bar{4}$	0	7	− 8
		3	10	− 9			$\bar{3}$	<2	− 4		$\bar{5}$		17	−20		$\bar{3}$		5	− 5
		4	12	−11			$\bar{2}$	3	− 2		$\bar{4}$		15	−16		$\bar{2}$		<4	+ 3
		5	<2	+ 8			$\bar{1}$	4	+ 5		$\bar{3}$		<3	+ 3		$\bar{1}$		6	+ 7
		6	1	− 2			1	3	− 1		$\bar{2}$		25	+26		1		5	+ 4
0	3	$\bar{6}$	7	− 7							$\bar{1}$		54	+49		2		5	− 6
		$\bar{5}$	<2	+ 3	1	0	$\bar{5}$	11	−10		1		32	−32		3		8	− 8
		$\bar{4}$	19	+17			$\bar{4}$	10	+ 8		2		30	−31		4		7	− 3
		$\bar{3}$	30	−37			$\bar{3}$	5	+ 4		3		22	−22		5		<4	0
		$\bar{2}$	<2	+ 5			$\bar{2}$	27	−25		4		<3	+ 2		6		5	+ 2
		$\bar{1}$	39	+42			$\bar{1}$	36	+30		5		14	+19	6	$\bar{5}$	0	3	− 3
		1	10	+ 9			1	31	−33		6		15	+18		$\bar{4}$		4	− 3
		2	20	+20			2	11	+13		7		<4	+ 1		$\bar{3}$		<4	+ 2
		3	20	−18			3	4	+ 4		8		5	− 6		$\bar{2}$		10	+ 7
		4	<2	+ 2			$\bar{4}$	7	−10		$\bar{9}$		5	− 4		$\bar{1}$		6	+ 6
		5	3	+ 4	2	0	$\bar{6}$	11	− 9	2	$\bar{7}$	0	5	− 6		1		8	− 6
											$\bar{6}$		11	−13		2		8	− 6

Can. J. Chem. Downloaded from www.nrcresearchpress.com by 210.87.254.5 on 09/05/12
For personal use only.

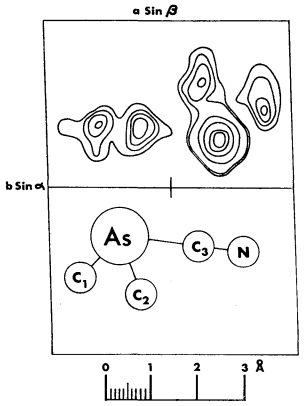

FIG. 1. Electron-density projection along the *c*-axis, with contours at intervals of 2 electrons about C and N, and at intervals of 5, 10, 20, 30 about As, and projection of the structure along *c*.

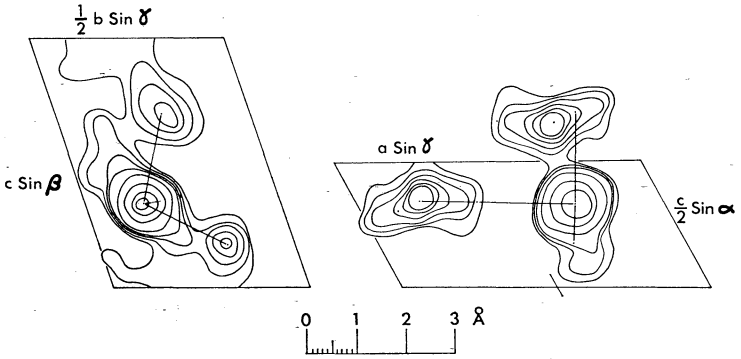

FIG. 2. Electron-density projections along the *a*- and *b*-axes.

Coordinates and Molecular Dimensions

The final positional parameters of the As, C, and N atoms are listed in Table II, *x*, *y*, and *z* being referred

TABLE II

Final positional parameters

Atom	*x*	*y*	*z*	*X'*	*Y'*	*Z'*
As	0.2115	0.1468	0.3316	0.381	0.657	1.713
C_1	0.378	0.272	0.698	0.382	1.026	3.606
C_2	0.134	0.329	0.169	0.358	2.397	0.873
C_3	−0.106	0.174	0.339	−1.623	0.573	1.751
N	−0.290	0.191	0.344	−2.786	0.533	1.777

to the triclinic crystal axes and expressed as fractions of the unit cell edges, and *X'*, *Y'*, *Z'* coordinates in Å units referred to orthogonal axis *a'* (= *a*.sin γ), *b*, and *c'* (normal to *a'* and *b*).

The bond distances and valency angles in the molecule are shown in Fig. 3.

Standard Deviations

The standard deviations of the atomic positions, calculated from Cruickshank's (2) formulae, are $\sigma(x) = \sigma(y) = \sigma(z) = 0.005$ Å for As and 0.047 Å for C and N. These values are probably optimistic, especially for the C and N atoms, because two of the projections are poorly resolved.

Can. J. Chem. Downloaded from www.nrcresearchpress.com by 210.87.254.5 on 09/05/12
For personal use only.

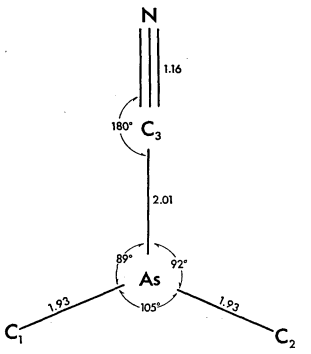

FIG. 3. Measured bond lengths and valency angles.

DISCUSSION

On the basis of the estimated standard deviations, the observed differences between As—CH_3 and As—CN bond lengths are not significant. The mean values of the bond lengths and angles, with standard deviations are:

As—C	= 1.96±0.03 Å
C—N	= 1.16±0.07 Å
∠ Me—As—Me	= 105±2°
∠ Me—As—CN	= 91±1.5°
∠ As—C—N	= 180±4°

The valency angles differ somewhat from those reported for the halogenodimethylarsines, which were determined by electron diffraction (3). The Me—As—Me angle in these halides was assumed to be 96°, the same as in trimethylarsine (4), and this is significantly smaller than the Me—As—Me angle of 105° now measured for the cyano derivative, which is similar to the angle in bromodiphenylarsine, 105° (5), and in chlorodiphenylarsine, 105° (6). The Me—As—CN angles are slightly less than those reported for Me_2AsBr (96°). The As—C and C≡N distances are normal (7).

The shortest intermolecular contact is an As---N separation of 3.18 Å (Fig. 4); this

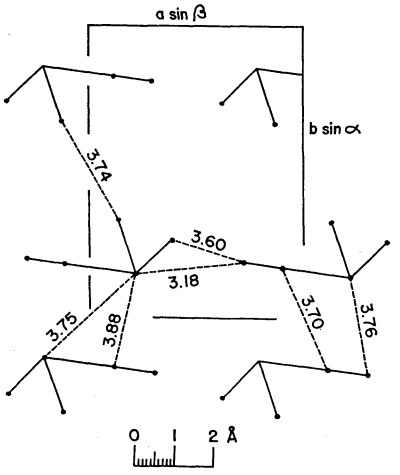

FIG. 4. Projection of the structure along [001], showing the shorter intermolecular contacts.

Can. J. Chem. Downloaded from www.nrcresearchpress.com by 210.87.254.5 on 09/05/12
For personal use only.

is considerably less than the sum of the van der Waals radii (3.5 Å) and suggests a charge-transfer bond involving donation of nitrogen lone pair electrons to the vacant arsenic 4*d* orbitals. The C≡N. . . . As angle is 168°, so that the nitrogen lone pair, which is expected to be collinear with the C≡N bond, is directed towards the arsenic atom. Figure 4 shows that, in addition, the arsenic lone pair (assuming that it makes approximately equal angles with the As—C bonds) is directed away from the nitrogen atom, so that the intermolecular bonding would be little hindered by lone-pair repulsions. Cyanodimethylarsine is a solid at room temperature, probably as a result of this intermolecular bonding, while the corresponding halogen derivatives are liquids. The cyanide melting point is 65° higher than that of the iodide, while in other series such as methyl iodide and cyanide and the corresponding ethyl, propyl, and phenyl derivatives this difference is never greater than 20°. Comparison of these differences with the increases in melting point which usually result from hydrogen bonding suggests that the energy of the charge-transfer bonds is only of the order of one or two kilocalories per mole.

The donor properties of the tripositive state of the Group V*b* elements diminish with increase in atomic number, and are pronounced only for nitrogen; the other members of the group can act as electron acceptors. For arsenic this is illustrated by the formation of complexes between $AsCl_3$ and various aromatic amines, which, although their structures have not been determined, probably involve intermolecular bonds similar to those in cyanodimethylarsine; and by the formation of complex ions such as $AsCl_4^-$.

All the other intermolecular distances in cyanodimethylarsine correspond to normal van der Waals interactions.

The authors are indebted to the National Research Council of Canada for financial support and for the award of a research bursary (to N. C.), and to Dr. W. R. Cullen for suggesting the problem, for some crystal samples and assistance with the preparation of others, and for much helpful discussion.

REFERENCES

1. J. Berghuis, Ij. M. Haanappel, M. Potters, B. O. Loopstra, C. H. MacGillavry, and A. L. Veenendaal. Acta Cryst. **8**, 478 (1955).
2. D. W. J. Cruickshank. Acta Cryst. **2**, 65 (1949).
3. H. A. Skinner and L. E. Sutton. Trans. Faraday Soc. **40**, 164 (1944).
4. H. D. Springall and L. O. Brockway. J. Am. Chem. Soc. **60**, 996 (1938).
5. J. Trotter. J. Chem. Soc. 2567 (1962).
6. J. Trotter. Can. J. Chem. **40**, 1590 (1962).
7. L. E. Sutton. Tables of interatomic distances. Chem. Soc. Special Publ. No. 11. 1958.

Can. J. Chem. Downloaded from www.nrcresearchpress.com by 210.87.254.5 on 09/05/12
For personal use only.

THE QUENCHING OF MERCURY RESONANCE RADIATION BY HYDROCARBONS: THE EFFECT OF DEUTERIUM SUBSTITUTION

YVES ROUSSEAU AND HARRY E. GUNNING
Department of Chemistry, University of Alberta, Edmonton, Alberta
Received September 19, 1962

ABSTRACT

The effect of deuteration on the quenching cross section (σ_Q^2) has been determined for propane, cyclopropane, isobutane, and propylene. The results were as follows, with the σ_Q^2 values, in Å^2, in parentheses: C_3H_8 (1.2); $CH_3CD_2CH_3$ (0.17); $CD_3CH_2CD_3$ (1.0); C_3D_8 (0.09); cyclo-C_3D_6 (0.29); $(CH_3)_3CH$ (4.8); $(CH_3)_3CD$ (0.44); C_3H_6 (29.8); and C_3D_6 (28.7). The deuterium isotope effect is most pronounced in the secondary C—H bonds of propane, and the tertiary C—H bond of isobutane. In the latter case, the isotope effect is estimated to be 15–16. For propylene, perdeuteration has little, if any, effect on σ_Q^2, indicating that C—H bonds are not involved in quenching. Further implications of the results with respect to the quenching process are discussed.

In recent studies (1, 2) in this laboratory, on the relative initial rates of *n*-propyl and *i*-propyl radical formation in the reaction of Hg $6(^3P_1)$ atoms with propane and the deuterated propanes, unusually large deuterium isotope effects were encountered in the chemical quenching reactions. Furthermore, deuteration, especially of the secondary C—H positions in propane, has been found (3) to change markedly the relative rates of product formation in reaction with Hg $6(^3P_1)$ atoms. In order to assess the overall effects of deuterium substitution in the mercury-photosensitized reactions of hydrocarbons, a knowledge of the quenching cross sections (σ_Q^2) for the deuterated species is clearly necessary. In the present study, the effects of partial and total deuteration on σ_Q^2 for a number of hydrocarbons of current interest in this laboratory have been determined. For the measurements, the very convenient nitrous oxide method developed by Cvetanović *et al.* (4, 5) has been employed. The results of the investigation follow.

EXPERIMENTAL

The light hydrocarbons (Phillips, research grade) and the deuterated hydrocarbons (Merck Sharp and Dohme of Canada) used were all further refined by peak-isolation methods in gas–liquid chromatography. The separations were made with a Burrell, Model K–4 chromatograph on a silica gel column, with helium as the carrier gas. Traces of nitric oxide were removed from the nitrous oxide used, by slow distillation from a trap immersed in liquid oxygen. Further distillation of the nitrous oxide at −131° (*n*-pentane slush) eliminated the remaining contaminants.

For each deuterated hydrocarbon, the isotopic purity was determined by mass spectrometry. The results of the analyses follow, with the composition indicated in parentheses: cyclo-C_3D_6 (92.8%; cyclo-C_3D_5H, 7.2%); $(CH_3)_3CD$ (97.8%; $(CH_3)_3CH$, 2.2%); $CH_3CD_2CH_3$ (98.2; C_3H_8, 1.8%); C_3D_8 (98.8%, C_3D_7H, 1.2%); $CD_3CH_2CD_3$ (100%); C_3D_6 (94.9%; C_3D_5H, 5.1%).

Since the general method employed has been previously described (4), only details specific for our adaptation of the procedure will be given. The mixtures of hydrocarbon and nitrous oxide were exposed under static conditions in a cylindrical quartz cell, 5 cm in diameter, and 5 cm in length. The total pressure was maintained constant throughout at 300 mm. Exposures were 5 minutes in duration, following a period of 3 hours for mercury vapor–liquid equilibration. The temperature for the runs was 25±2°. In the case of the d_6–cyclopropane, the exposure duration was reduced to 2 minutes in order to eliminate polymer deposition on the incident face of the reaction cell.

After each run, the gases were directed into a series of traps at −196°. The non-condensable portion was recovered with a Toepler pump, and analyzed by mass spectrometry.

The absorbed light intensity (I_a) at 2537 Å was determined using the light propane – Hg $6(^3P_1)$ reaction as actinometer (6, 7), with the substrate pressure at 270 mm.

Can. J. Chem. Downloaded from www.nrcresearchpress.com by 210.87.254.42 on 09/05/12
For personal use only.

Can. J. Chem. Downloaded from www.nrcresearchpress.com by 210.87.254.42 on 09/05/12
For personal use only.

RESULTS AND DISCUSSION

Cvetanović (4) has shown that a linear relation obtains between $1/\Phi(N_2)$ and $(RH)/(N_2O)$, where $\Phi(N_2)$ represents the quantum yield of nitrogen, and $(RH)/(N_2O)$, the molar ratio of hydrocarbon to nitrous oxide in the mixtures. From the propane actinometry, I_a was taken to be 5.50 μeinstein/min, assuming the quantum yield of hydrogen formation to be 0.44 mole/einstein for propane in the constant-rate region—a value consistent with recent work in this laboratory (3) on the variation of $\Phi(H_2)$ with substrate pressure and I_a in this reaction. Under such conditions, $\Phi(N_2)$ becomes unity for pure N_2O, at the pressure of 300 mm used in this study, in accordance with recent conclusions concerning this reaction (5).

The $1/\Phi(N_2)$ vs. $(RH)/(N_2O)$ plots are displayed as follows: the results for the four propanes, C_3H_8, $CH_3CD_2CH_3$, $CD_3CH_2CD_3$, and C_3D_8, are given in Fig. 1; $(CH_3)_3CH$, $(CH_3)_3CD$, n-C_4H_{10}, and cyclo-C_3D_6 in Fig. 2; and the two propylenes, C_3H_6 and C_3D_6, in Fig. 3. For each compound, the best straight line for its $1/\Phi(N_2)$ vs. $(RH)/(N_2O)$ plot

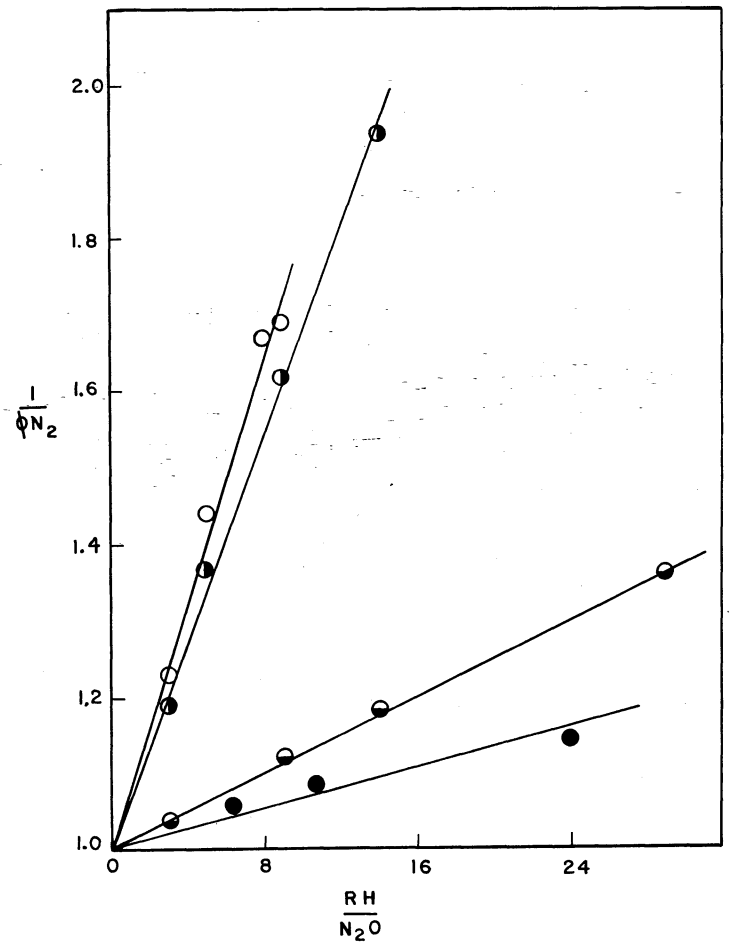

FIG. 1. Plots of $1/\phi(N_2)$ as a function of $(RH)/(N_2O)$ for C_3H_8 (○), $CD_3CH_2CD_3$ (◑), $CH_3CD_2CH_3$ (◒), and C_3D_8 (●).

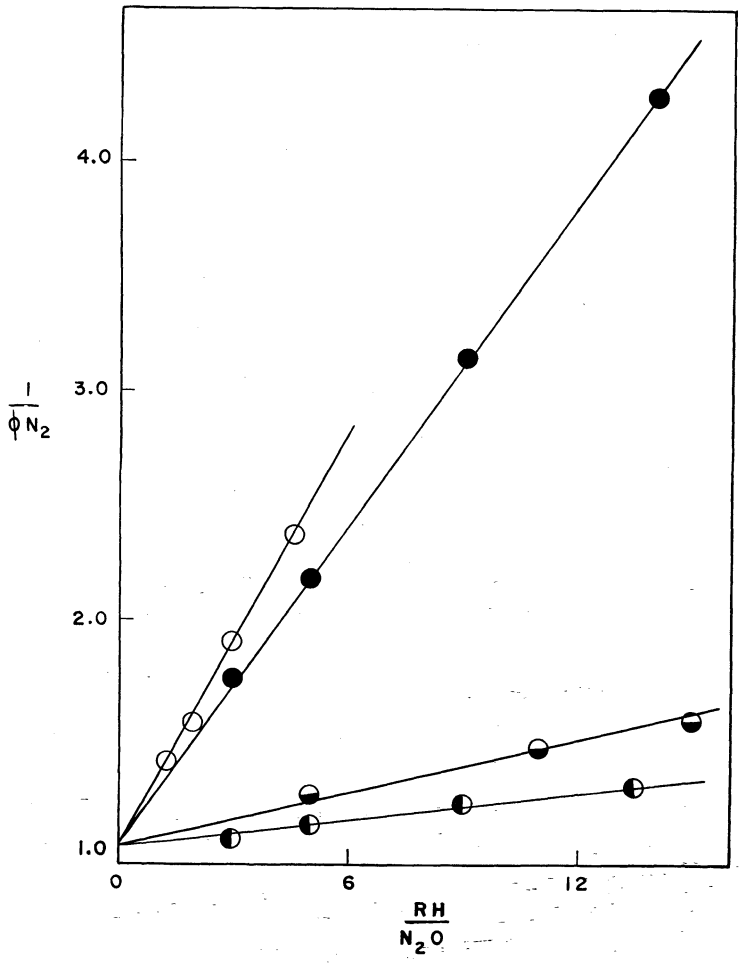

FIG. 2. Plots of $1/\phi(N_2)$ as a function of $(RH)/(N_2O)$ for $(CH_3)_3CH$ (○), $CH_3CH_2CH_2CH_3$ (●), $(CH_3)_3CD$ (◒), and cyclo-C_3D_6 (◐).

was determined by the method of least squares. It will be noted from the figures that each line extrapolates to unity at $(RH)/(N_2O) = 0$. Taking $\sigma_Q^2 = 3.6$ Å^2 for *n*-butane (4), the σ_Q^2 values for the nine hydrocarbons can be calculated from the best slope (S) for each compound and that found (S_{nb}) for the reference standard, *n*-butane, by the relation:

$$3.6/\sigma_Q^2 = (S_{nb}/S)[(1+M(\mathrm{Hg})/M)/(1+M(\mathrm{Hg})/M_{nb})]^{1/2},$$

where M, M_{nb}, and $M(\mathrm{Hg})$ are the molecular weights for the hydrocarbon being studied, *n*-butane, and mercury respectively. The results are summarized in Table I. It is estimated that the overall experimental error in the σ_Q^2 values should not exceed 10%.

From Table I, it is apparent from the results obtained for the four propanes that deuteration of the secondary C—H positions leads to a drastic reduction in the quenching cross section, from 1.2 to 0.17 Å^2. When $CH_3CD_2CH_3$ is now perdeuterated to C_3D_8, σ_Q^2 again decreases from 0.17 to 0.09 Å^2. On the other hand, deuteration of the primary positions only, in propane, to form $CD_3CH_2CD_3$ only reduces σ_Q^2 from 1.2 to 1.0 Å^2. It

Can. J. Chem. Downloaded from www.nrcresearchpress.com by 210.87.254.42 on 09/05/12
For personal use only.

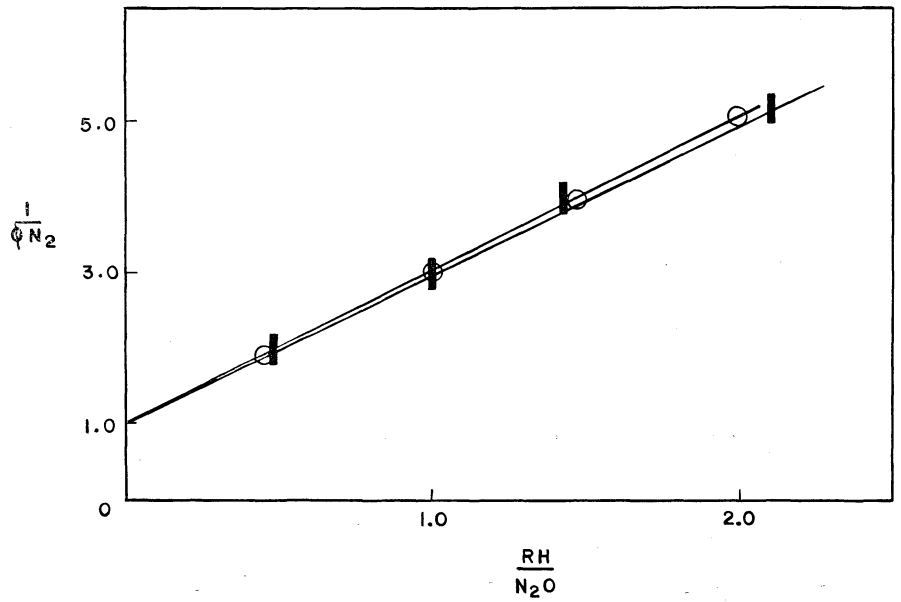

FIG. 3. Plots of $1/\phi(N_2)$ as a function of $(RH)/(N_2O)$ for C_3H_6 (○) and C_3D_6 (●).

TABLE I

The effect of deuteration on the quenching cross section (σ_Q^2)

Compound	σ_Q^2 (Å²) This study	Literature
$CH_3CH_2CH_2CH_3$	3.6*	3.0,† 4.1,‡ 3.6§
$CH_3CH_2CH_3$	1.2	1.3,† 1.6‡
$CH_3CD_2CH_3$	0.17	
$CD_3CH_2CD_3$	1.0	
$CD_3CD_2CD_3$	0.09	
Cyclo-C_3D_6	0.29	
$(CH_3)_3CH$	4.8	4.9†
$(CH_3)_3CD$	0.44	
$CH_2{:}CHCH_3$	29.8	31‖
$CD_2{:}CDCD_3$	28.7	

*Reference standard for this study.
†B. deB. Darwent. J. Chem. Phys. **18**, 1532 (1950).
‡J. R. Bates. J. Am. Chem. Soc. **52**, 3925 (1930); **54**, 569 (1932).
§Reference 4.
‖B. deB. Darwent, M. K. Phibbs, and F. G. Hurtubise. J. Chem. Phys. **22**, 859 (1954).

would thus appear that the initial interaction between Hg $6(^3P_1)$ atoms and C_3H_8 occurs almost exclusively at the secondary C—H bonds. That this first interaction does not lead directly to secondary C—H bond cleavage is indicated by the fact (1) that at least 42% of the initially formed propyl radicals is normal. In isobutane (Table I) the deuterium isotope effect on σ_Q^2 is seen to be even more marked than in propane. Thus by substituting D for H, in the tertiary position only, σ_Q^2 is reduced by more than 90%, from 4.8 to 0.44 Å². On the other hand, the complete deuteration of cyclopropane reduces σ_Q^2 from 1.1 (8) to 0.29 Å² (Table I)—a somewhat lower deuterium isotope effect than found for propane and isobutane. In short, the deuterium isotope effect on σ_Q^2 for saturated hydrocarbons

Can. J. Chem. Downloaded from www.nrcresearchpress.com by 210.87.254.42 on 09/05/12
For personal use only.

appears to be greater for hydrocarbons containing at least two types of C—H bonds. Clearly a larger number of saturated hydrocarbons must be examined before generalizations can be made with confidence.

Again from Table I, the effect of deuteration on σ_Q^2 for the typical olefin, propylene, can be seen. Perdeuteration decreases σ_Q^2 by ca. 4% from 29.8 to 28.7 Å^2—a change only slightly exceeding the overall experimental error in the σ_Q^2 values. Thus the initial quenching interaction does not appear to involve the C—H bonds—a conclusion consistent with the formation of a triplet-excited species in the primary process (9).

The overall deuterium isotope effect on the chemical quenching reaction has been discussed elsewhere (2). For isobutane, we can estimate the effect of deuteration of the tertiary (*t*) C—H bond on σ_Q^2 as follows: Taking $\sigma_Q^2(CH_3) = 0.05$ Å^2, from the fact that $\sigma_Q^2(C_2H_6) = 0.10$ Å^2 (4), it follows that $\sigma_Q^2(t\text{-C—H}) = 4.6_5$ Å^2, and $\sigma_Q^2(t\text{-C—D}) = 0.3$ Å^2. Defining the isotope effect as $\sigma_Q^2(t\text{-C—H})/\sigma_Q^2(t\text{-C—D})$, a value of ca. 15–16 is obtained. Since deuteration of the secondary positions in propane was found to increase the relative importance of initial C—H rupture in the CH_3 groups (1), a similar shift toward enhanced methyl C—H cleavage is likely upon deuteration of *t*-C—H in isobutane. Hence the overall deuterium isotope effect on *t*-C—H for the chemical quenching reaction is probably much larger than 15–16.

For saturated hydrocarbons, the quenching cross section is probably determined by the interaction of the *p*-orbital of the Hg $6(^3P_1)$ atom with the sigma bonds of the hydrocarbon. The large deuterium isotope effect found for this interaction should provide insight into the nature of the quenching reaction. This problem is currently under investigation in this laboratory (10).

ACKNOWLEDGMENTS

The authors would like to thank Dr. O. P. Strausz of this laboratory for many helpful discussions. The support of the National Research Council under grant No. T-142 is also gratefully acknowledged.

REFERENCES

1. G. N. C. Woodall and H. E. Gunning. Bull. Soc. Chim. Belges. In press.
2. Y. Rousseau, G. N. C. Woodall, and H. E. Gunning. J. Chem. Phys. **37**, 2722 (1962).
3. Y. Rousseau and H. E. Gunning. To be published.
4. R. J. Cvetanović. J. Chem. Phys. **23**, 1208 (1955).
5. R. J. Cvetanović, W. E. Malconer, and K. R. Jennings. J. Chem. Phys. **35**, 1225 (1961).
6. S. Bywater and E. W. R. Steacie. J. Chem. Phys. **19**, 326 (1951).
7. R. A. Back. Can. J. Chem. **37**, 1834 (1959).
8. B. DeB. Darwent and M. K. Phibbs. J. Chem. Phys. **22**, 110 (1954).
9. H. E. Gunning and E. W. R. Steacie. J. Chem. Phys. **14**, 57 (1946); **16**, 926 (1948).
10. Otto P. Strausz and H. E. Gunning. To be published.

Can. J. Chem. Downloaded from www.nrcresearchpress.com by 210.87.254.42 on 09/05/12
For personal use only.

TOTAL SYNTHESIS OF STEROIDAL DERIVATIVES

II. SYNTHESIS OF HYDROCHRYSENE ANALOGUES AND RELATED COMPOUNDS[1]

JAMES P. KUTNEY, JOHN WINTER,[2] WM. MCCRAE,[3] AND ARNOLD BY
Department of Chemistry, University of British Columbia, Vancouver, British Columbia
Received July 23, 1962

ABSTRACT

A synthetic sequence leading to the total synthesis of hydrochrysene derivatives possessing the trans–anti–trans backbone is described. The introduction of a ketonic function into ring C of these compounds is also given. It is noted that these substances allow entry into the synthesis of intermediates which have an open ring C.

Can. J. Chem. Downloaded from www.nrcresearchpress.com by 210.87.254.5 on 09/05/12
For personal use only.

Recently we reported in the first paper of this series (1), a synthetic sequence leading to the total synthesis of various hydrochrysene analogues. We also indicated that these compounds could serve as effective intermediates for the synthesis of a variety of steroidal derivatives which are not readily accessible from the naturally occurring steroidal compounds. We would now like to present further studies which allow entry into the trans–anti–trans series of hydrochrysene analogues. This series, of course, provides the stereochemical backbone which correlates with that of the natural steroid.

In our previous paper we were able to show that the ketol, I, besides providing entry into the cis–syn–cis hydrochrysene series, can also be converted into the tetracyclic ketone, II. It is obvious that the appropriate reductions of the styrene double bond and the unsaturated carbonyl group in II lead to the generation of new asymmetric centers at the ring junctures. Consequently stereospecific reductions of this ketone would lead to a product with well-defined stereochemistry at the asymmetric carbon atoms. Of the various methods which were available, the Birch reduction was of distinct advantage since the stereochemistry of this method, when applied to the hydrochrysene analogues, has been studied in considerable detail in the fine researches of Johnson and his co-workers (2). We therefore subjected the ketone, II, to the action of sodium (or lithium) in liquid ammonia in the presence of anhydrous ethanol—reaction conditions which were very successful in a related series (2). The expected alcohol, III, which now possessed four new asymmetric centers, could only be isolated in a very poor yield and even then only after considerable difficulty in separation from the undesirable side products. The side products indicated that the aromatic ring was being reduced and it was therefore apparent that the reduction of the olefinic bond of the *p*-methoxystyrene chromophore presented a somewhat different problem to that experienced by Johnson in the *m*-methoxystyrene series. We therefore spent a considerable amount of time in attempting to develop optimum conditions for this reduction. We initially concentrated our efforts on varying the amount of alkali metal (sodium or lithium) relative to the amount of ketone used, and on varying the length of time for the reduction. In all these cases, we were not able to show any substantial improvement to the original yield of the alcohol. We then turned our attention to the use of solutions of alkali metals in amine solvents and found an excellent improvement in the yield of the reduction. When a solution of the ketone in tetrahydrofuran was

[1]*Presented, in part, at the Chemical Institute of Canada, Edmonton Conference, May 27–30, 1962.*
[2]*National Institutes of Health Postdoctoral Fellow, 1961–1962.*
[3]*National Research Council of Canada Postdoctoral Fellow, 1960–1961.*

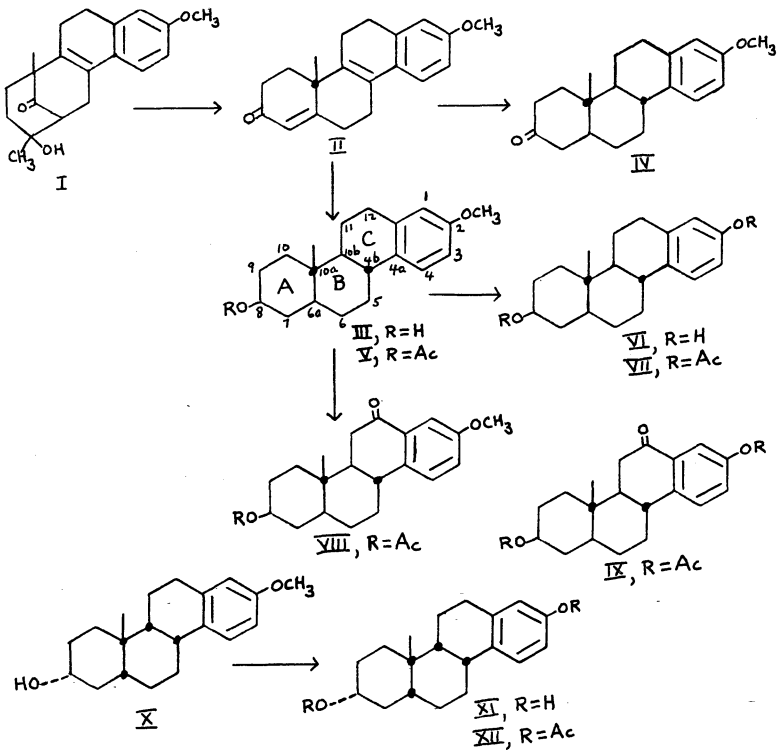

treated with sodium in liquid ammonia in the presence of aniline,* a good yield of a reduction product was obtained. The reduction product in this case, however, was not the alcohol, III, but a compound which possessed a strong carbonyl absorption in the infrared spectrum (5.88 μ). Consideration of the ultraviolet spectrum, with absorption maxima at 277 and 286 mμ characteristic of the 1,2,3,4-tetrahydro-6-methoxynaphthalene system (1), indicated that reduction of both olefinic bonds had occurred. It was therefore obvious that the correct structure of the reduction product was IV. The stereochemistry as depicted in IV is well supported by the previous work of Johnson (2) and very recently a complete confirmation has been provided by Nagata and co-workers (3). These Japanese workers have reported the conversion of the ketone, II, to racemic pregnane and androstane derivatives by a sequence which involves an alkali metal in liquid ammonia reduction of II as an integral step.

The relationship of the saturated ketone, IV, to the alcohol, III, could be readily established by reducing the ketone to the alcohol by means of hydride reagents. The reduction was, in fact, carried out with both lithium aluminum hydride and sodium borohydride in order to determine whether there was any difference in the amount of equatorial alcohol obtained. In both instances the reduction proceeded in very high yield to provide a crystalline product. Chromatographic purification indicated that less than 5% of an epimeric alcohol was present and on the basis of previous work, the predominant alcohol can be assigned the equatorial conformation.

Now that the trans–anti–trans series of hydrochrysene analogues could be obtained in

*We are very grateful to G. Douglas, G. A. Hughes, and H. Smith of the University of Manchester for information regarding this method.

Can. J. Chem. Downloaded from www.nrcresearchpress.com by 210.87.254.5 on 09/05/12
For personal use only.

high yield, we considered the introduction of a functional group into ring C of the hydrochrysene skeleton (see III) in order to provide an entry into synthetic intermediates where ring C has been opened. A possible approach to this problem was available from the work of Johnson and collaborators (4) wherein an acetate function was introduced into the C ring (C_{12}) of their hydrochrysene analogue by means of lead tetraacetate. However, it was recognized at the outset that the methoxyl function in III, by virtue of its para relationship to the carbon atom designated as 4*b* (see III), could seriously affect the success of this approach. It was felt, however, that the activation by this methoxyl function which could favor the introduction of substituents at 4*b* instead of the desired position, C_{12}, may be overcome by the ease of reaction at the secondary carbon (C_{12}) relative to the tertiary center (4*b*). Although lead tetraacetate is not the best reagent to evaluate this consideration, we felt that it should be tried first since comparable reactions were already available in the literature. When the acetate, V, of the alcohol was subjected to a reaction with lead tetraacetate, a gummy product was obtained. The ultraviolet spectrum of this material clearly indicated a naphthalenic chromophore and it was therefore apparent that aromatization of ring C had taken place. A number of experiments under varying reaction conditions were attempted but the aromatization reaction was the predominant one in each case and no further characterization of these gummy products was carried out at this stage.

Our next consideration in this direction was N-bromosuccinimide, a reagent which has been shown to react more rapidly at secondary than at tertiary carbon atoms in the mono- and poly-cyclic aromatic series (5). However when we reacted the acetate, V, with this reagent, under a variety of reaction conditions, the results were likewise very discouraging. In all instances it was apparent that the aromatization of ring C was the main reaction which was taking place, presumably via benzylic bromination followed by the elimination of the elements of hydrogen bromide. It was therefore obvious that the introduction of substituents into ring C was seriously hindered by the great tendency of our compounds toward aromatization.

We felt that if the activation of the methoxyl group was, at least in part, to blame for our failures, that we could eliminate this factor by replacing this function by an acetyl group. We therefore subjected the alcohol, III, to a demethylation procedure utilizing methylmagnesium iodide at 175° (6, 7, 8). The product obtained, in excellent yield, was the expected phenolic alcohol, VI. The spectral data for this substance was in complete agreement with the assigned structure. In particular, the ultraviolet spectrum, with its maximum absorption at 282 mμ in neutral solution, showed a bathochromic shift to 300 mμ when taken in alkaline solution. This shift, which is typical of phenolic substances of this type, was an excellent confirmation for the success of the demethylation procedure. Acetylation of this phenolic alcohol provided a good yield of the diacetate, VII. It was now possible to establish whether the diacetate was more suitable for our work. When VII was subjected to the action of N-bromosuccinimide, the isolated product indicated a naphthalenic type of absorption in the ultraviolet spectrum and it was again apparent that the undesirable aromatization reaction was the prevalent reaction which was occurring. In spite of numerous attempts to correct this we were not able to obtain any successful results.

Since the introduction of substitutents into position 12 had failed in our attempts indicated above, it became necessary to consider another approach to this problem. It appeared to us that a direct oxidation of this benzylic position may prove feasible especially since Wintersteiner and co-workers had been successful in preparing 6-keto-estradiol diacetate in this manner (9). Consequently we reacted the diacetate, VII, with

Can. J. Chem. Downloaded from www.nrcresearchpress.com by 210.87.254.5 on 09/05/12
For personal use only.

an aqueous acetic acid solution of chromium trioxide and were able to obtain from the neutral portion of the reaction product, a ketonic substance which indicated absorption at 5.68 μ, 5.80 μ, and 5.97 μ in the infrared spectrum, in complete accordance with expectation for structure IX. The ultraviolet spectrum of this product was also in good agreement with that of 6-ketoestradiol diacetate (9) and this served to establish the chromophoric group depicted in IX. The success of this approach encouraged us to extend this reaction to the methoxy acetate, V. However, it was realized that the methoxyl group may again provide for a preferential attack at the 4*b* position and for this reason the oxidation was carried out under milder conditions. Treatment of V with chromium trioxide in acetic anhydride at 0° provided the desired ketonic product VIII, although the yield was very low. Again the spectral data were in agreement with the assigned structure. The infrared spectrum with bands at 5.84 μ and 5.98 μ and the ultraviolet spectrum with absorption at 222 mμ, 254 mμ, and 322 mμ presented strong evidence for VIII. It was obvious, however, that if the oxidation was to be used in our sequence, it was necessary to improve the yield in this reaction. With this in mind, we felt that any oxidation at the tertiary carbon 4*b* could presumably be eliminated if a sterically large oxidant was used. For this reason, the methoxy-acetate was oxidized with *t*-butyl chromate and indeed a substantial improvement in the yield of VIII was realized. With these results in hand, it was apparent that the desired synthetic intermediates for further study at ring C were now available.

Finally in order to provide some information as to the reactivities at positions 4*b* and 12 in the cis–syn–cis series, we carried out some demethylation experiments on the compound represented by structure X. Reaction of X with methylmagnesium iodide as already indicated for III led in good yield to the phenolic alcohol XI. Acetylation of this compound by the use of isopropenyl acetate and a catalytic amount of *p*-toluenesulphonic acid provided the diacetate, XII.

Now that synthetic pathways have been developed to both the cis–syn–cis and the trans–anti–trans series of these hydrochrysene analogues, further investigations are being conducted to examine the versatility of these intermediates.

EXPERIMENTAL

All melting points were determined on a Fischer–Johns apparatus and are uncorrected. The ultraviolet spectra were recorded in 95% ethanol on a Cary 14 recording spectrophotometer. Infrared spectra were taken on a Perkin–Elmer Model 21 spectrophotometer. The n.m.r. spectra were taken at 60 megacycles on a Varian A 60 instrument. In all cases tetramethylsilane was the standard set at 10.0 τ units and the positions of the signals are given in the Tiers τ scale. In all cases integration of areas under the signals was carried out and the number of protons corresponding to each signal is indicated in parentheses. The analyses were performed by Dr. A. Bernhardt and his associates, Mulheim (Ruhr) Germany, and by Mrs. Aldridge, University of British Columbia.

Reduction of 2-Methoxy-8-keto-10a-methyl-5,6,8,9,10,10a,11,12-octahydrochrysene

(a) With Sodium in Liquid Ammonia in Presence of Ethanol

Only one typical experiment is recorded here although a number of different experiments were actually done. However, they all provided very similar results.

A solution of the tetracyclic ketone, II (5.0 g), in anhydrous dimethyl cellosolve (150 ml) was added to anhydrous liquid ammonia (700 ml). Anhydrous ethanol (90 ml) was then added and sodium (2.34 g) was added in small pieces, each piece being allowed to dissolve before addition of the next (about 35 minutes). After the sodium had reacted, ammonium chloride (5.5 g) and water were added and the ammonia was allowed to evaporate. The residue was extracted with ether and the ethereal extract was dried over anhydrous magnesium sulphate. Evaporation of the solvent left a brown gummy material. This gummy material was taken up in benzene and chromatographed on alumina (250 g). Elution with a mixture of benzene – ethyl ether (9:1) provided, in the initial fractions, 0.61 g of the saturated tetracyclic ketone, IV, and, in the latter fractions, eluted with benzene – ethyl ether (1:1), 3.19 g of a gummy mixture of alcoholic materials.

These gummy materials were acetylated by refluxing overnight in an excess of acetic anhydride containing several drops of pyridine. The mixture was poured onto cracked ice and allowed to stand for 30 minutes. The resulting oil was extracted with ether and the ether extract was washed successively with aqueous

Can. J. Chem. Downloaded from www.nrcresearchpress.com by 210.87.254.5 on 09/05/12
For personal use only.

sodium bicarbonate and water. After it was dried over anhydrous magnesium sulphate, the solvent was removed and the remaining product was taken up in benzene – petroleum ether and chromatographed on alumina (200 g). Elution with a mixture of benzene – petroleum ether (2:3) provided first a small amount (388 mg) of a solid material which on recrystallization from a mixture of benzene – petroleum ether gave a crystalline substance (261 mg), m.p. 140–141°. Further recrystallization provided an analytical sample, m.p. 142–142.5°; infrared in KBr: 5.78 μ, 8.0 μ; Found: C, 77.06; H, 8.55; O, 14.15. Calc. for $C_{22}H_{30}O_3$: C, 77.15; H, 8.83; O, 14.02. Although the structure of this minor product has not been completely established, it is almost certainly a stereoisomer of the desired acetate, V.

Further elution with benzene–petroleum ether (1:1) and benzene – petroleum ether (3:1) provided the major fraction (1.468 g), which on recrystallization from ethanol gave an analytical sample of the desired trans–anti–trans-2-methoxy-8β-acetoxy-10a-methyl-4b,5,6,6a,7,8,9,10,10a,10b,11,12-dodecahydrochrysene (V), m.p. 101–102°; infrared in KBr: 5.80 μ, 8.03 μ; ultraviolet: λ_{max} 278 mμ (log ϵ 3.08); n.m.r. signals ($CDCl_3$): 9.12 τ (angular methyl, area = 3H), 7.93 τ (CH_3CO, area = 3H), 6.21 τ (CH_3O, area = 3H), 5.28 τ (broad, —C(H)—OAc, area = 1H), multiplet centered at 2.92 τ (aromatic H, area = 3H); Found: C, 76.74; H, 8.67; O, 14.51. Calc. for $C_{22}H_{30}O_3$: C, 77.15; H, 8.83; O, 14.02.

(b) With Sodium in Liquid Ammonia in Presence of Aniline

To a stirred mixture of anhydrous liquid ammonia (300 ml) and aniline (50 ml), sodium (5.0 g) was added in small pieces. A solution of the tetracyclic ketone, II (5.0 g), in anhydrous tetrahydrofuran (100 ml) was added to the blue ammonia solution over a period of 10 minutes. The mixture was stirred for a further 20 minutes, after which time ammonium chloride (12 g) was added in portions. The ammonia was allowed to evaporate and the resulting residue was treated with water and then extracted with ether. The ether layer was washed with dilute hydrochloric acid, aqueous sodium carbonate, and finally with water. After the solution was dried over anhydrous magnesium sulphate, the solvent was removed to yield a crystalline product (3.51 g). This material was recrystallized several times from ethanol to provide the pure trans–anti–trans-2-methoxy-8-keto-10a-methyl-4b,5,6,6a,7,8,9,10,10a,10b,11,12-dodecahydrochrysene (IV), m.p. 141.5–142° and 145–146°; infrared in CS_2: 5.88 μ; ultraviolet: λ_{max} 277 mμ (log ϵ 3.20), λ_{max} 286 mμ (log ϵ 3.17); n.m.r. signals ($CDCl_3$): 9.06 τ (angular methyl, area = 3H), 6.33 τ (CH_3O, area = 3H), multiplet centered at 3.1 τ (aromatic H, area = 3H). Found: C, 80.77; H, 8.56; O, 10.93. Calc. for $C_{20}H_{26}O_2$: C, 80.49; H, 8.78; O, 10.72.

Synthesis of trans–anti–trans-2-Methoxy-8β-hydroxy-10a-methyl-4b,5,6,6a,7,8,9,10,10a,10b,11,12-dodecahydrochrysene (III)

(a) Reduction with Lithium Aluminum Hydride

A solution of the saturated ketone, IV (0.5 g), in warm, anhydrous ether (50 ml), was added to lithium aluminum hydride (0.395 g). The mixture was stirred at room temperature for 1 hour, after which time it was cooled in ice and decomposed with 20% sulphuric acid. The ether layer was separated, washed with water, and then dried over anhydrous magnesium sulphate. The solvent was removed to provide a crystalline product (496 mg) which had a crude melting point of 154–157°. This material was chromatographed on alumina (30 g). Elution with benzene and benzene – ethyl ether mixtures indicated that less than 5% of the epimeric alcohol was present. The product obtained here is completely identical with the product of the sodium borohydride reduction and the appropriate constants are given below.

(b) Reduction with Sodium Borohydride

A solution of the saturated ketone, IV (0.5 g), in hot methanol (20 ml) and water (5 ml), was treated with a solution of sodium borohydride (0.26 g) in methanol (20 ml) and water (5 ml), and the mixture was refluxed for 3 hours. The mixture was then treated with concentrated hydrochloric acid (5 ml) and refluxing was continued for a further hour. The solution was then concentrated *in vacuo* to a volume of 10 ml, water and ether were added, and the ether layer was separated. The ether layer was washed with water and then dried over anhydrous magnesium sulphate. Removal of the solvent provided a crystalline product (497 mg). This material was taken up in benzene and chromatographed on alumina (30 g). Elution with benzene – ethyl ether (8:5:1.5) provided essentially a quantitative recovery of the solid product and it was again possible to show that less than 4% of the epimeric alcohol was present. This solid, on recrystallization from ethyl ether, provided a pure sample of the alcohol, III, m.p. 160–161°; infrared in KBr: 2.89 μ; ultraviolet: λ_{max} 277 mμ (log ϵ 3.20), λ_{max} 286 mμ (log ϵ 3.17); n.m.r. signals ($CDCl_3$): 9.20 τ (angular methyl, area = 3H), 6.18 τ (CH_3O, area = 3H), multiplet centered at 3.0 τ (aromatic H, area = 3H). Found: C, 80.32; H, 9.08. Calc. for $C_{20}H_{28}O_2$: C, 79.95; H, 9.39.

A small sample of this alcohol was acetylated as given above and gave an acetate which was completely identical with V.

Synthesis of trans–anti–trans-2,8β-Dihydroxy-10a-methyl-4b,5,6,6a,7,8,9,10,10a,10b,11,12-dodecahydrochrysene (VI)

The tetracyclic alcohol, III (0.1 g), was added in portions to the Grignard reagent prepared in the usual manner from magnesium (1.17 g) and methyl iodide (3.07 ml) in ether. Most of the ether was removed by warming in a stream of nitrogen and finally the last traces were removed *in vacuo*. The residual mixture

Can. J. Chem. Downloaded from www.nrcresearchpress.com by 210.87.254.5 on 09/05/12
For personal use only.

was heated to 175° over the course of 1 hour and then kept at 175–180° for a further hour. The reaction mixture was then cooled in ice, petroleum ether and ethyl acetate were added carefully to decompose the excess Grignard reagent, and the whole mixture was then shaken with dilute sulphuric acid and ethyl acetate. The ethyl acetate layer was separated, washed with water, and finally dried over anhydrous magnesium sulphate. Removal of the solvents provided the phenolic alcohol as a solid powder. This powder was acetylated directly by allowing it to stand in acetic anhydride and pyridine at room temperature for 8 hours. The usual work-up provided an excellent yield (1.15 g) of the expected diacetate. Several recrystallizations from benzene – petroleum ether provided the pure trans–anti–trans-2,8β-diacetoxy-10*a*-methyl-4*b*,5,6,6*a*,7,8,9,10,10*a*,10*b*,11,12-dodecahydrochrysene (VII), m.p. 152–153° and 160–161°; infrared in KBr: 5.67 μ, 5.78 μ, 8.06 μ, 8.33 μ; ultraviolet: λ_{max} 268 mμ (log ε 2.89), λ_{max} 276 mμ (log ε 2.89); n.m.r. signals ($CDCl_3$): 9.23 τ (angular methyl), 7.83 τ, 8.07 τ (CH_3—C(=O)—), 5.38 τ (—CH(OAc)—, area = 1H), multiplet centered at 3.1 τ (aromatic H, area = 3H); Found: C, 74.35, 74.88; H, 7.96, 8.04; O, 17.68. Calc. for $C_{23}H_{30}O_4$: C, 74.56; H, 8.16; O, 17.28.

A sample of the phenolic alcohol was prepared separately from another experiment. On several recrystallizations from benzene – ethyl acetate the substance melted at 234–237°. It was sublimed to provide a pure sample, m.p. 235–238°; infrared in Nujol mull: 2.94 μ, 3.18 μ; ultraviolet: in neutral solution, λ_{max} 282 mμ (log ε 3.36), in alkaline solution, λ_{max} 300 mμ (log ε 3.46).

Synthesis of trans–anti–trans-2-Methoxy-8β-acetoxy-12-keto-10a-methyl-4b,5,6,6a,7,8,9,10,10a,10b,11,12-dodecahydrochrysene (VIII)

(a) By Oxidation with Chromium Trioxide

The methoxy-acetate, V (504 mg), was dissolved in acetic anhydride (15 ml) and the resulting solution was cooled to 0°. An ice-cold solution of chromium trioxide (225 mg) in acetic anhydride (60 ml) was then added in portions over a period of 2 hours. The reaction mixture was maintained in ice during the course of the addition and for a further 12 hours after addition was complete. The excess oxidant was reduced by the addition of ethanol (10 ml) and the reaction mixture was treated cautiously with ice to hydrolyze the acetic anhydride. The mixture was then neutralized by the addition of potassium hydroxide and the resulting solution was extracted with ethyl ether and ethyl acetate. The combined organic layer was washed with aqueous sodium bicarbonate to remove any residual acetic acid and finally washed with a 1:1 mixture of a saturated aqueous sodium bicarbonate and 1 *N* potassium carbonate solution. This carbonate wash was acidified with hydrochloric acid and extracted with ethyl acetate to yield 73 mg of an acidic fraction.

The original organic layer containing the neutral fraction was dried over anhydrous magnesium sulphate and, after removal of the solvent, provided 452 mg of a crude neutral product. The material was purified by chromatography on alumina (30 g, approx. activity II–III). Elution with benzene provided starting material (155 mg) and further elution with benzene – ethyl ether yielded the desired ketone, VIII (86 mg). This ketone seemed to exist in polymorphic forms and had several melting points, 128°, 145–147°, and 159–161°; infrared in KBr: 5.84 μ, 5.98 μ; ultraviolet: λ_{max} 222 mμ (log ε 4.08), λ_{max} 254 mμ (log ε 3.68), λ_{max} 322 mμ (log ε 3.14); n.m.r. signals ($CDCl_3$): 9.08 τ (angular methyl, area = 3H), 7.99 τ (CH_3CO—, area = 3H), 6.18 τ (CH_3O—, area = 3H), 5.20 τ (—CH(OAc)—, area = 1H), multiplet centered at 2.66 τ (aromatic H, area = 3H). Found: C, 74.10; H, 7.76. Calc. for $C_{22}H_{28}O_4$: C, 74.13; H, 7.92.

(b) By Oxidation with t-Butyl Chromate

A solution of *t*-butyl chromate in carbon tetrachloride was prepared according to the procedure of Heusler and Wettstein (10) and aliquots of this solution were then used for the various experiments.

The methoxy-acetate (1.86 g) was dissolved in carbon tetrachloride (50 ml) and the *t*-butyl chromate solution (50 ml) mixed with acetic anhydride (25 ml) was added. The mixture was stirred under reflux for 3 hours and the excess oxidant was then destroyed by stirring with a solution of oxalic acid (15 g) in water (100 ml) for 2 hours. The carbon tetrachloride layer was separated and the solvent was removed *in vacuo*. The residue was taken up in ether and the ether solution was worked up exactly as given in part (*a*) above to give acidic (56 mg) and neutral (1.72 g) materials. The neutral material upon chromatography on alumina (90 g, approx. activity II–III) yielded some starting material (731 mg) and the desired ketone VIII (400 mg).

Synthesis of trans–anti–trans-2,8β-Diacetoxy-12-keto-10a-methyl-4b,5,6,6a,7,8,9,10,10a,10b,11,12-dodecahydrochrysene (IX)

The diacetate, VII (500 mg), was partly dissolved in glacial acetic acid (1.75 ml) and a solution of chromium trioxide (425 mg) in a mixture of water (0.35 ml) and glacial acetic acid (2.5 ml) was then added. Any evolution of heat was controlled by cooling the flask in a cold water bath. The whole mixture was then stirred at room temperature for 5 hours and then allowed to stand for a further 19 hours. Ethanol (1 ml) was then added to reduce the excess chromium trioxide and the whole mixture was poured into water and extracted with ether. The ether layer was washed with portions of aqueous sodium bicarbonate to remove most of the acetic acid and then washed with a 1:1 mixture of saturated sodium bicarbonate solution and 1 *N* sodium carbonate solution.

Can. J. Chem. Downloaded from www.nrcresearchpress.com by 210.87.254.5 on 09/05/12
For personal use only.

The ether layer, now containing only the neutral fraction, was dried over anhydrous magnesium sulphate, and after the solvent was removed, provided 384 mg of a solid residue. This material was taken up in benzene – petroleum ether and chromatographed on Florisil (60 g). Elution with benzene – petroleum ether yielded 165 mg of starting material while further elution with benzene – ethyl ether (10:1) provided the desired keto-diacetate, IX (95 mg), which melted at 243–246° (with some decomposition) after recrystallization from a mixture of petroleum ether and benzene; infrared in KBr: 5.68 μ, 5.80 μ, 5.97 μ; ultraviolet: λ_{max} 218 mμ (log ϵ 4.08), λ_{max} 247 mμ (log ϵ 3.99), λ_{max} 300 mμ (log ϵ 3.36); n.m.r. signals ($CDCl_3$): 9.09 τ (angular methyl), 7.73 τ, 8.01 τ (acetate methyl groups), 5.39 τ (—C(H)—OAc), multiplet centered at 2.60 τ (aromatic H). Found: C, 72.08; H, 7.63; O, 20.80. Calc. for $C_{23}H_{28}O_5$: C, 71.85; H, 7.34; O, 20.81.

Synthesis of cis–syn–cis-2,8α-Dihydroxy-10a-methyl-4b,5,6,6a,7,8,9,10,10a,10b,11,12-dodecahydrochrysene (XI)

The cis–syn–cis alcohol, X (0.924 g), was added to an ethereal solution (5 ml) of methylmagnesium iodide prepared in the usual manner from magnesium turnings (0.264 g) and methyl iodide (0.68 ml). This mixture was allowed to stand at room temperature for 1 hour, after which time the ether was removed by being warmed in a stream of nitrogen and finally *in vacuo*. The residual solid reaction mixture was plunged into a bath at 175° and kept at this temperature for 1 hour. An atmosphere of nitrogen was kept over the reaction mixture during this heating period. The mixture was then cooled to room temperature and water was added cautiously to decompose the excess Grignard reagent. The reaction mixture was then treated with ether and dilute sulphuric acid. The organic phase was separated and the aqueous phase was washed with several portions of ether. The combined ether extract was dried over anhydrous magnesium sulphate and the solvent was removed to yield 700 mg of a solid material. Recrystallization of this material from acetone provided the pure phenolic alcohol, XI, m.p. 254–255° (with some decomposition); infrared in KBr: 2.92 μ, 3.18 μ; ultraviolet: λ_{max} 281 mμ (log ϵ 3.36), shoulder at 287 mμ (log ϵ 3.32); n.m.r. signals (pyridine): 9.63 τ (angular methyl, area = 3H), no OCH_3 absorption. Found: C, 79.75; H, 9.23; O, 11.32. Calc. for $C_{21}H_{28}O_3$: C, 79.68; H, 9.15; O, 11.17.

Synthesis of cis–syn–cis-2,8α-Diacetoxy-10a-methyl-4b,5,6,6a,7,8,9,10,10a,10b,11,12-dodecahydrochrysene (XII)

The phenolic alcohol, XI (0.579 g), was treated with isopropenyl acetate (4.5 ml) and *p*-toluenesulphonic acid monohydrate (30 mg) and the whole mixture was heated on a steam bath for 15 minutes. The volume of the reaction mixture was slowly reduced to about one-half the original by a slow distillation (about 15 minutes) and the remainder of the volatile materials was removed *in vacuo*. The residue was then treated with benzene and the benzene extract was washed successively with a saturated solution of sodium bicarbonate and water. The benzene extract was dried over anhydrous magnesium sulphate and the solvent was then removed to provide a yellow gum. This gum was taken up in a mixture of petroleum ether – benzene (9:1) and chromatographed on silica gel (20 g). Elution with benzene yielded the diacetate as a yellow glass. Distillation of this substance at a bath temperature of 190–200° at 0.01 mm provided the pure diacetate, XII, as a light yellow solid glass (280 mg); infrared in KBr: 5.69 μ, 5.81 μ; ultraviolet: λ_{max} 268 mμ (log ϵ 3.28), λ_{max} 275 mμ (log ϵ 3.29); n.m.r. signals ($CDCl_3$): 8.87 τ (angular methyl), 7.97 τ, 7.70 τ (acetate methyl groups), 5.27 τ (—C(H)—OAc), multiplet centered at 2.95 τ (aromatic H). Found: C, 74.83; H, 8.09; O, 17.12. Calc. for $C_{23}H_{30}O_4$: C, 74.56; H, 8.16; O, 17.28.

ACKNOWLEDGMENTS

Financial aid from the National Research Council of Canada and from the National Cancer Institute of the National Institutes of Health, U.S. Public Health Service, grant No. CY–5037, is very gratefully acknowledged.

REFERENCES

1. J. P. KUTNEY, W. MCCRAE, and A. BY. Can. J. Chem. **40**, 982 (1962).
2. W. S. JOHNSON, E. R. ROGIER, J. SZMUSZKOVICZ, H. I. HADLER, J. ACKERMAN, B. K. BHATTACHARYYA, B. M. BLOOM, L. STALMANN, R. A. CLEMENT, B. BANNISTER, and H. WYNBERG. J. Am. Chem. Soc. **78**, 6289 (1956).
3. W. NAGATA, T. TERASAWA, S. HIRAI, and K. TAKEDA. Tetrahedron Letters, No. 17, 27 (1960); Chem. Pharm. Bull. (Japan), **9**, 770 (1961).
4. W. S. JOHNSON, A. D. KEMP, R. PAPPO, J. ACKERMAN, and W. F. JOHNS. J. Am. Chem. Soc. **78**, 6312 (1956).
5. L. HORNER and E. H. WINKLEMANN. New methods of preparative organic chemistry. Vol. 3. Verlag Chemie, Weinheim/Bergstr. 1961. p. 98.
6. E. SPATH. Monatsh. **35**, 319 (1914).
7. A. L. WILDS and W. B. MCCORMACK. J. Am. Chem. Soc. **70**, 4127 (1948).
8. W. S. JOHNSON, E. R. ROGIER, and J. ACKERMAN. J. Am. Chem. Soc. **78**, 6322 (1956).
9. B. LONGWELL and O. WINTERSTEINER. J. Biol Chem. **133**, 219 (1940).
10. K. HEUSLER and A. WETTSTEIN. Helv. Chim. Acta, **35**, 284 (1952).

Can. J. Chem. Downloaded from www.nrcresearchpress.com by 210.87.254.5 on 09/05/12
For personal use only.

THE ALKALOIDS OF DELPHINIUM BROWNII RYDB.

THE STRUCTURE OF BROWNIINE[1]

M. H. BENN,[2] M. A. M. CAMERON,[2] AND O. E. EDWARDS
Division of Pure Chemistry, National Research Council, Ottawa, Canada

Received October 10, 1962

ABSTRACT

Methyllycaconitine and browniine have been observed to be major alkaloids of *Delphinium brownii*. The latter was proved to have the same skeleton, oxygen location, and stereochemistry as lycoctonine, but a different pattern of O-methylation.

Can. J. Chem. Downloaded from www.nrcresearchpress.com by 210.87.254.6 on 09/05/12
For personal use only.

Delphinium brownii is native to the foothills of Alberta. Its alkaloids were examined by Manske (1), who provided evidence that one of them was methyllycaconitine since on hydrolysis the amorphous base gave *l*-methylsuccinic acid, anthranilic acid, and a base resembling lycoctonine. The identity of the latter was subsequently confirmed by Marion (2). We have used the aerial portions of the plant as a source of lycoctonine and have identified the parent alkaloid as methyllycaconitine by comparison with authentic material.[3] In addition we found a new major alkaloid in the plant, which was readily separated from the other alkaloids by virtue of its weaker adsorption on alumina. It was amorphous, but formed a crystalline perchlorate, m.p. 212°, $[\alpha]_D$ +25°.

The new base, which we have named browniine, analyzed correctly for $C_{25}H_{41}O_7N$ and is thus an isomer of lycoctonine. Its infrared spectrum had the same general shape as that of lycoctonine, hydroxyl and ether bands being the most obvious features. We hence proceeded under the assumption that its chemistry would resemble that of lycoctonine, and subjected it to operations that had proved fruitful in defining the functional groups of this alkaloid and related *Delphinium* alkaloids (3, 4). The transformations will be illustrated in terms of the structure deduced below.

Oxidation of browniine (I) with chromium trioxide in pyridine produced a keto lactam (II) (dehydrooxobrowniine) with ν_{max} 1750 cm^{-1} (cyclopentanone) and 1643 cm^{-1} (six-membered lactam). Sodium borohydride reduction of this ketone gave mainly a compound with the original hydroxyl configuration. This was proved by the identity of the reduction product with the hydroxy lactam III produced by oxidation of browniine monoacetate and subsequent hydrolysis. Both oxobrowniine and dehydrooxobrowniine rapidly consumed 1 mole of lead tetraacetate, after which a very slow uptake ensued. The products of the initial reaction were a *seco*diketone ($\nu_{max}^{CHCl_3}$ 1770, 1710, 1650 cm^{-1}) and a *seco*triketone (IV) ($\nu_{max}^{CHCl_3}$ 1750, 1700, 1640 cm^{-1}). The latter pyrolyzed smoothly at 210°, eliminating methanol to give the α,β-unsaturated ketone V ($\nu_{max}^{CHCl_3}$ 1770, 1680, 1646 cm^{-1}). These reactions and spectra corresponded well with those in the lycoctonine series (3) and indicate the presence of two vicinal tertiary hydroxyl groups.

The fact that the triketone and V were colorless excluded position 6 for the secondary hydroxyl of browniine, since the analogues in delpheline chemistry are yellow and red respectively and have distinctive spectra (5). This hydroxyl thus had to be on ring C if the alkaloid had the lycoctonine skeleton. Since the three hydroxyls of browniine were

[1]*Issued as N.R.C. No. 7095.*
[2]*National Research Council Postdoctoral Fellow.*
[3]*We are grateful to Professor R. C. Cookson for a reference sample of the hydriodide of this base.*

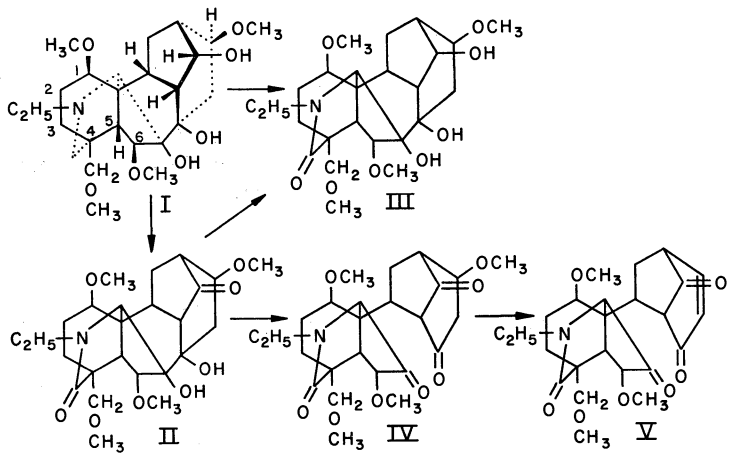

accounted for, the primary hydroxyl which is present in lycoctonine was either missing or converted to a methoxyl. A reasonable postulate for the structure of browniine was hence I. If this were correct, correlation with lycoctonine through compound VII should be possible and this was attempted.

Oxobrowniine (III) when heated with 0.2% (v/v) sulphuric acid in acetic acid was converted to the product of pinacolic dehydration, anhydrooxobrowniine (VI). Methylation of VI gave the hydroxyl-free compound VII, which proved identical with the methyl ether of anhydrolycoctonam, which had been prepared by Dr. V. Skaric.[4] Thus browniine has structure I, and merely represents a variation in methylation of a common polyhydroxy precursor of it and lycoctonine.[5] It seems likely that the O-methylation is the last stage of the biosynthesis of these alkaloids.

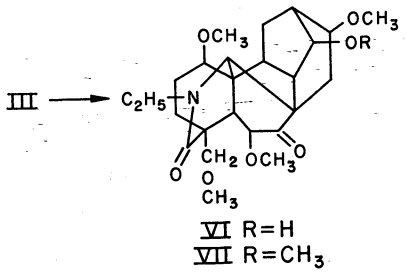

The infrared spectrum of the α,β-unsaturated triketone V is a remarkable example of trans-spatial interaction of unsaturated functions (6). The normal absorption band for cyclopentanones (ν_{max} ca. 1740 cm^{-1}) was displaced to 1770 cm^{-1} in the mull spectrum of V.

The predominant formation of the compound with an axial hydroxyl in the reduction of the ketone carbonyl of II appears to be the result of shielding of one face of the carbonyl by the nearby axial methoxyl group.

An unusual acid-catalyzed reaction of the *seco*triketone IV was observed. Hot 6 *N* sulphuric acid converted it nearly quantitatively to a mixture of acids, about 25% of

[4]*Unpublished work by L. Marion and V. Skaric, to whom we are grateful for a reference sample.*

[5]*The 6-methoxyl group in the anhydro compounds appears to retain the original configuration under the conditions of the pinacolic dehydration (3).*

Can. J. Chem. Downloaded from www.nrcresearchpress.com by 210.87.254.6 on 09/05/12
For personal use only.

which crystallized readily. The crystalline acid analyzed for $C_{24}H_{33}O_8N$, and contained only three methoxyl groups. An infrared spectrum of its sodium salt showed the presence of a six-membered or larger-ring ketone (ν_{max} 1698 cm^{-1}) and the lactam carbonyl (ν_{max} 1640 cm^{-1}). Its ultraviolet absorption spectrum had a peak at 213 mμ with ϵ 13,850, corresponding to the absorption of an α,β-unsaturated acid function, superimposed on end absorption due to the lactam function.

The same acid was produced by the action of 6 *N* sulphuric acid on the desmethanol-*seco*triketone V, thus locating the methoxyl which had been eliminated and indicating the origin of the double bond.

The acid decarboxylated smoothly at its melting point to give a non-crystalline hydroxy keto lactam which analyzed for simple loss of carbon dioxide. This had only end absorption in the ultraviolet region, but in the presence of dilute alkali an absorption maximum at 222 mμ rapidly developed. These observations are all consistent with structure VIII for the acid, the product of reverse Claisen reaction on IV followed by internal aldol condensation and elimination of methanol. The decarboxylation product would then be the β,γ-unsaturated ketone IX, rearranging in alkali to the α-β-unsaturated ketone.

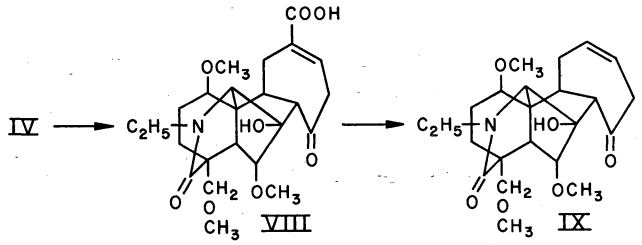

Mild treatment of the *seco*triketone with base gave an acid mixture with infrared spectrum nearly identical with that from the product of the acid-catalyzed reaction. However, no crystalline VIII was obtained from it.

Browniine seems potentially valuable for establishing the structure of alkaloids such as delcosine which appear to have a secondary hydroxyl group in the same location.

EXPERIMENTAL

Unless otherwise stated, rotations are of ethanol solutions with $c \simeq 1$, ultraviolet spectra are of solutions in 95% alcohol, and infrared spectra are of nujol mulls.

Isolation of the Alkaloids

(*a*) The aerial portion (upper stems and leaves) of *Delphinium brownii* was collected just before the flowering period in the foothills of the Rocky Mountains in Alberta. The air-dried material was ground and percolated with methanol until a test with Mayer's reagent was faint. The methanol extract was concentrated to a syrup under reduced pressure, the residue taken up in 2 *N* sulphuric acid, and the suspension extracted with ether. The ether layers were back-extracted with 2 *N* sulphuric acid. The combined aqueous layers were adjusted to pH 8 using sodium carbonate, and the weak bases extracted into chloroform. The aqueous solution was then made strongly alkaline and the 'strong' bases extracted into chloroform. The strong bases were recycled through the strong base – weak base separation. Thirty-one pounds of dry plant material yielded 157 g of 'weak' base, 3 g of 'strong' base, and 34 g of ether-soluble neutral and acid substances.

The weak base was hydrolyzed by refluxing in aqueous methanol solution containing 16 g of sodium hydroxide for 1.5 hours. The solvent was removed under reduced pressure, water was added, and the bases extracted into chloroform (yield 130 g). The aqueous layer yielded 4.85 g of amphoteric acids (extracted at pH 5) and 9.5 g of acids.

The hydrolyzed base was dissolved in benzene and adsorbed on alumina, activity IV. Benzene eluted 58 g of base which would not crystallize but which gave a perchlorate (browniine perchlorate) which crystallized from methanol – ethyl acetate mixture. The base eluted with benzene–ether mixtures and

Can. J. Chem. Downloaded from www.nrcresearchpress.com by 210.87.254.6 on 09/05/12
For personal use only.

with ether crystallized from aqueous methanol, giving 38 g of lycoctonine. The more strongly adsorbed bases would not crystallize or give crystalline salts, and were not further examined.

(*b*) A 56-lb quantity of dried plant collected during flowering gave 37 g of 'weak' base and 16 g of 'strong' base. A quantity of weak base (13.5 g) was distributed between benzene and buffer of pH 4 in a Craig countercurrent distribution machine with 10 ml in each phase. After 107 transfers the contents of the tubes were recovered. Tubes 1–26 contained 6.7 g of alkaloid with no carbonyl band in its infrared absorption spectrum. It gave 2.0 g of browniine perchlorate. Tubes 27–34 contained mixtures. Tubes 35–42 contained 1.37 g of base with strong carbonyl absorption in the infrared. It gave a crystalline hydriodide (0.8 g) which was proved by mixed melting point and comparison of infrared spectra with an authentic sample[3] to be methyllycaconitine hydriodide.

Browniine

The perchlorate of the base which was readily eluted from alumina was recrystallized from methanol – ethyl acetate mixtures. It melted at 212° and had $[\alpha]_D^{26}$ +25°. It appeared homogeneous by paper chromatography (on Whatman 1 paper with isoamyl alcohol:acetic acid:water:heptane in the ratio 3:3:2:1 as developing solvent[6] and Dragendorff's reagent for location of the spots; R_f 0.59). Its infrared spectrum had peaks at 3400 cm^{-1} (OH), 2840 and 1090 cm^{-1} (OCH_3). Found: C, 52.97; 52.95; H, 7.06, 7.23; N, 2.25; OCH_3, 21.45. Calc. for $C_{25}H_{42}O_{11}NCl$: C, 52.86; H, 7.45; N, 2.47; $4OCH_3$, 21.85. The base liberated from the perchlorate was amorphous. It had $\nu_{max}^{CHCl_3}$ 3460 cm^{-1} (OH) and 1090 cm^{-1} (OCH_3). This was converted to the hydriodide, which crystallized with difficulty from acetone – ethyl acetate. The microcrystalline solid melted at 193–196°. Found: C, 50.75; H, 6.95. Calc. for $C_{25}H_{42}O_7NI$: C, 50.42; H, 7.11.

Browniine Monoacetate

The alkaloid was only slowly acetylated by 1:1 acetic anhydride – pyridine mixture at room temperature. After 36 hours in 40 ml of the mixture, 456 mg of browniine yielded 385 mg of basic acetate and considerable neutral or very weakly basic product. The basic acetate after repeated chromatography on alumina yielded 150 mg of nearly pure crystalline monoacetate (eluted from a 30-fold ratio of neutral alumina, activity III, by benzene and 10% and 20% chloroform in benzene). More strongly adsorbed products contained a contaminant with $\nu_{max}^{CHCl_3}$ 1730 and 1640 cm^{-1}. The crystalline product when recrystallized from hexane separated as needles, m.p. 123–124°. Found: C, 63.72; H, 8.35; OCH_3, 24.08. Calc. for $C_{27}H_{43}O_8N$: C, 63.63; H, 8.51; OCH_3, 24.36. It had ν_{max} 1730 cm^{-1} in chloroform.

Dehydrooxobrowniine (II)

A solution of 1.2 g of browniine in 11 ml of pyridine was added to 2.0 g of chromium trioxide in 15 ml of dry pyridine. The mixture was shaken at room temperature for 18 hours. The bulk of the pyridine was removed below 50° under reduced pressure. To the residue was added 20 g of crushed ice, 30 ml of 3 *N* sulphuric acid, and 20 ml of chloroform. Sulphur dioxide was bubbled into the mixture until a clear green color resulted. The chloroform layer and four subsequent 20-ml chloroform extracts of the aqueous layer were washed with water and saturated sodium bicarbonate solution, combined, dried, and distilled. The 888 mg of pale yellow froth was adsorbed from benzene onto 20 g of alumina of activity IV. Forty milliliters of benzene and 20 ml of 2:1 benzene–chloroform eluted 38 mg of amorphous material. Twenty-five milliliters of 2:1, 50 ml of 1:1, and 25 ml of 1:2 benzene–chloroform mixtures eluted 830 mg of product which crystallized from ether. Yield, 630 mg, m.p. 155–162°. Two recrystallizations from acetone–hexane gave rectangular plates, m.p. 110°, resolidifying, and melting at 170°. From ether–hexane the compound separated as needles, m.p. 169.5–171°, $[\alpha]_D^{24}$ +32°; ν_{max} 1750, 1643 cm^{-1}; λ_{max} 290 mμ, ϵ 27. Found: C, 62.68; H, 7.48. Calc. for $C_{25}H_{37}O_8N$: C, 62.61; H, 7.78.

Oxobrowniine (III)

(*a*) Dehydrooxobrowniine (II) (502 mg) was dissolved in 8 ml of methanol, and 500 mg of sodium borohydride added portionwise over 20 minutes. After a further 20 minutes the reaction mixture was diluted with 30 ml of 4 *N* sulphuric acid and the product extracted into chloroform. The 505 mg of product crystallized with some difficulty when triturated with moist ether; m.p. 75–88° (capillary). After chromatography on alumina (20-fold, activity III), the fractions eluted with benzene–chloroform mixtures and chloroform crystallized from wet ether, m.p. 90–93°, $[\alpha]_D$ +40°. Later an anhydrous form was obtained[7] from ether–pentane mixtures, which melted at 164–169°. Found: C, 62.50; H, 8.20; Calc. for $C_{25}H_{39}O_8N$: C, 62.35; H, 8.16.

(*b*) Browniine monoacetate (97 mg) was dissolved in 5 ml of acetone containing 0.2 ml of water and 0.2 ml of acetic acid. Powdered potassium permanganate was added in small portions until a small excess persisted for 1 hour. Sodium bisulphite solution was added to reduce excess reagent, the suspension filtered, and the filtrate taken to dryness under reduced pressure. The residue was extracted with methylene chloride, and the solution washed with 3 *N* sulphuric acid, 3 *N* sodium carbonate solution, and water. The 68 mg of neutral product was clearly a mixture, with amide bands at 1640 and 1660 cm^{-1}. It was chromatographed

[6]*We are grateful to Dr. K. H. Palmer for suggesting this solvent system.*
[7]*We are indebted to Dr. Z. Stojanac for this observation.*

Can. J. Chem. Downloaded from www.nrcresearchpress.com by 210.87.254.6 on 09/05/12
For personal use only.

on 1.7 g of alumina, activity III. Benzene and 10% chloroform in benzene eluted 3 mg of oil, which was discarded. Twenty-five milliliters of 30% chloroform in benzene and 50 ml of 1:1 benzene–chloroform eluted 36 mg of the desired lactam acetate with $\nu_{max}^{CHCl_3}$ 1730 and 1640 cm^{-1}. Later eluates contained a mixture of this compound with what was probably the N-acetyl compound with ν_{max} 1730 and 1660 cm^{-1}.

The lactam acetate was hydrolyzed by 2 hours on the steam bath with 1 ml of 20% potassium hydroxide and sufficient ethanol to complete solution in the hot mixture. A white froth (37 mg) was produced which had an intense maximum at 1640 cm^{-1} ($CHCl_3$). It was purified by chromatography on 700 mg of alumina, after which it crystallized when hexane was added to a very concentrated solution of the compound in wet methanol. The crystals melted at 89–93° and had $[\alpha]_D$ +41°; ν_{max} 3470, 1640, and 1090 cm^{-1}. The product could also be crystallized from dry ether in an anhydrous form, m.p. 170–171.5°, which proved identical (infrared, mixed m.p., thin layer chromatography, and X-ray powder pattern) with the product described in (*a*).

Secodiketone

Oxobrowniine (54 mg) was dissolved in 20 ml of a saturated solution of lead tetraacetate in acetic acid. After 1 hour 0.97 mole of reagent had been consumed. The excess lead tetraacetate was reduced with sodium bisulphite solution, and aqueous sodium sulphate added to complete precipitation of the lead. The solid was removed by centrifuging, and washed once with methanol. The combined solutions were taken to dryness under reduced pressure and the residue dissolved in methylene chloride. The solution was washed with dilute sulphuric acid, sodium bicarbonate solution, and finally water. It was then dried and the solvent evaporated. The 46 mg of product did not crystallize. It had $\nu_{max}^{CHCl_3}$ 1770, 1710, and 1650 cm^{-1}.

Secotriketone (IV)

A solution of 107 mg of dehydrooxobrowniine (II) in 50 ml of a saturated acetic acid solution of lead tetraacetate was prepared. One-milliliter aliquots were titrated at intervals. After 1.5 hours the molar uptake of reagent was 1.06, after 5 hours, 1.12, and after 21 hours, 1.20.

In a preparative run 560 mg of II was dissolved in 100 ml of saturated lead tetraacetate solution and left at room temperature for 75 minutes. The product was worked up as described for the *seco*diketone. The 543 mg of foam crystallized readily when ether was added. Crop 1 weighed 172 mg and melted at 184–190°. Two further crops totalling 216 mg melted between 150 and 190°. After two recrystallizations from ether the *seco*triketone separated as colorless needles melting at 194–197°; $[\alpha]_D$ 62°; ν_{max} 1763, 1702, and 1650 cm^{-1}. Found: C, 62.49; H, 7.26; OCH_3, 25.67. Calc. for $C_{25}H_{35}O_8N$: C, 62.87; H, 7.39; $4OCH_3$, 25.98. It had $\nu_{max}^{CHCl_3}$ 1750, 1700, and 1640 cm^{-1}.

Desmethanolsecotriketone (V)

Thirty milligrams of the above *seco*triketone was heated at 210° under 5×10^{-4} mm pressure for 5 minutes. It was then allowed to distill over a short path under the same conditions. The distillate yield was nearly quantitative in this run but in others considerable brown residue remained. The distillate crystallized readily from ether, m.p. 150–170°. After several recrystallizations from ether the melting point was 172–175°; $\nu_{max}^{CHCl_3}$ 1770, 1680, and 1646 cm^{-1}. Found: C, 64.56; H, 6.82; OCH_3, 20.96. Calc. for $C_{24}H_{31}O_7N$: C, 64.70; H, 7.01; $3OCH_3$, 20.90.

Anhydrooxobrowniine (VI)

A solution of 500 mg of oxobrowniine (III) in 12 ml of a 0.2% (v/v) sulphuric acid in acetic acid mixture was heated at 83° for 90 minutes. Anhydrous sodium carbonate (0.3 g) was added to the reaction mixture, which was then taken to near dryness under reduced pressure. Water was added, the mixture made alkaline with conc. ammonia, and the product extracted into chloroform. The 544 mg of froth recovered from the chloroform was hydrolyzed by refluxing for 2 hours in a solution of KOH (10%) in 20% aqueous methanol. The methanol was removed under reduced pressure, water added, and the product extracted into chloroform. The 508 mg of hydrolyzate was adsorbed from benzene onto 10 g of neutral alumina, Grade II. Benzene (70 ml) and 3:1 benzene–chloroform (40 ml) eluted 19 mg of oily material, which was discarded. Forty milliliters of 2:1 and 40 ml of 1:1 benzene–chloroform eluted 219 mg of material which crystallized from ether. The more strongly adsorbed material did not crystallize.

The crystalline material was recrystallized from acetone–hexane combination, giving 173 mg of anhydrooxobrowniine, m.p. 192–195°. A further recrystallization raised the melting point to 195–197°. ν_{max} 3600, 1725, 1640 cm^{-1}. Found (sublimed sample): C, 64.97; H, 8.13. Calc. for $C_{25}H_{37}NO_7$: C, 64.77; H, 8.05.

O-Methylanhydrooxobrowniine (VII)

Anhydrooxobrowniine (170 mg) was added to a mixture of 170 mg of sodium hydride and 10 ml of dry dioxane. This was refluxed for 30 minutes after which 2 ml of methyl iodide was cautiously added. After 5 hours' refluxing the mixture was cooled, filtered and the filtrate taken to near dryness under reduced pressure. Water was added and the product extracted into chloroform. The 152 mg of oil recovered from the chloroform slowly crystallized from concentrated ether solution. It was purified by adsorption from benzene onto 3 g of neutral alumina, Grade II. Benzene (20 ml) eluted 115 mg of colorless oil which crystallized readily from ether–pentane mixture. A further 10 ml of benzene eluted 22 mg of less pure material.

Can. J. Chem. Downloaded from www.nrcresearchpress.com by 210.87.254.6 on 09/05/12
For personal use only.

The early eluate after three recrystallizations from ether–pentane melted at 120–124°. It had $[\alpha]_D$ 10° (*c*, 1.14 in $CHCl_3$). Found: C, 65.44; H, 8.28. Calc. for $C_{26}H_{39}NO_4$: C, 65.38; H, 8.23. Mixed melting point with a sample of O-methylanhydrolycoctonam (m.p. 119°) was 117–119°. An X-ray powder pattern comparison of the two compounds proved their identity.

Keto Acid VIII

(*a*) When 172 mg of *seco*triketone was dissolved in 10 ml of 6 *N* sulphuric acid on the steam bath, and heating continued for 45 minutes, 175 mg of acid was produced (extracted from chloroform by sodium hydrogen carbonate solution). This crystallized from ethyl acetate – hexane mixtures, giving 57 mg, m.p. 160–178°. After three recrystallizations from the same solvents and one recrystallization from ethyl acetate it melted at 185–188° (decomp.)[8] and had $[\alpha]_D$ 124°. $\nu_{max}^{CHCl_3}$ 3500, 1690, and 1635 cm^{-1}. Equivalent weight 467, pK_a' 5.5 (in 50% aqueous ethanol). Found: C, 62.45; H, 7.38; OCH_3, 19.46. Calc. for $C_{24}H_{33}O_8N$: C, 62.19; H, 7.18; $3OCH_3$, 20.08. Equivalent weight, 463.5. Its sodium salt had ν_{max} at 1698 cm^{-1} (ketone), 1640 cm^{-1} (lactam), 1565 cm^{-1} (COO^-).

(*b*) Desmethanol*seco*triketone (V) (12 mg) was treated as in (*a*) with 1 ml of 6 *N* sulphuric acid. The product was separated into neutral and acidic fractions. The acids crystallized from ethyl acetate, giving 6 mg of crystals, m.p. 174–180° (decomp.), which did not depress the melting point of the product from (*a*).

(*c*) The *seco*triketone was nearly completely converted to acids in 45 minutes in 0.15 *N* sodium hydroxide in aqueous ethanol. No crystalline acid was obtained, however, even after chromatography on silica gel.

Decarboxylation of VIII

The acid (VIII) decarboxylated rapidly at 195° in an evacuated tube. If the pressure was below 10^{-2} mm the product distilled at once. Attempts to induce crystallization from anhydrous solvents and aqueous methanol failed. The material was distilled at 175°, 1×10^{-3} mm. It had $[\alpha]_D$ 150°; ν_{max} 3460, 1690, and 1640 cm^{-1}; end absorption in the ultraviolet. Found: C, 66.42; H, 7.84. Calc. for $C_{23}H_{33}NO_6$: C, 65.85; H, 7.93.

A solution of the decarboxylation product in ethanol containing potassium hydroxide (80 mg in 20 ml) rapidly developed an ultraviolet absorption maximum at 222 mμ, which reached maximum intensity after 2 hours. In a preparative run under the same conditions, however, no α,β-unsaturated ketone could be isolated.

ACKNOWLEDGMENTS

We thank Mr. M. Lesage and Mr. A. Knoll for the isolation of the alkaloids, Mr. H. Seguin for the analysis, and Mr. R. Lauzon for the infrared spectra. We are grateful to Dr. E. H. Moss, Botany Department, University of Alberta, for a generous supply of plant material.

REFERENCES

1. R. H. F. Manske. Can. J. Res. Sect. B, **16**, 57 (1938).
2. L. Marion and R. H. F. Manske. Can. J. Res. Sect. B, **24**, 1 (1946).
3. O. E. Edwards, L. Marion, and D. K. R. Stewart. Can. J. Chem. **34**, 1315 (1956).
4. F. Sparatore, R. Greenhalgh, and L. Marion. Tetrahedron, **4**, 157 (1958).
5. R. C. Cookson and M. E. Trevitt. J. Chem. Soc. 3864 (1956).
6. R. N. Jones, P. Humphries, F. Herling, and K. Dobriner. J. Am. Chem. Soc. **74**, 2820 (1952).

[8]*We are grateful to Dr. Z. Stojanac for final purification of this acid and performing experiment (c).*

Can. J. Chem. Downloaded from www.nrcresearchpress.com by 210.87.254.6 on 09/05/12
For personal use only.

OXIDATION–REDUCTION POLYMERS

II. STANDARD OXIDATION POTENTIALS OF REDOX HOMOPOLYMERS AND THEIR MONOMERIC MODELS[1]

I. H. SPINNER, W. D. RAPER,[2] AND W. METANOMSKI
Department of Chemical Engineering and Applied Chemistry, University of Toronto, Toronto, Ontario
Received August 15, 1962

ABSTRACT

A new monomer, 2,5-bis-(2-tetrahydropyranyloxy)-4-methyl-4′-vinyldiphenyl sulphone, has been prepared. The standard oxidation potentials of two linear redox homopolymers, derived from this monomer and the one previously reported (1), and of their intermediate and model compounds, have been measured using continuous and discontinuous titration techniques.

Can. J. Chem. Downloaded from www.nrcresearchpress.com by 210.87.254.6 on 09/05/12
For personal use only.

In Part I (1) we reviewed briefly the literature on redox monomers and polymers, especially those containing hydroquinone units. Since then further contributions in this field have been published.

Cassidy and co-workers (2, 3) have investigated the properties and reactions of methyl-substituted hydroquinones and vinylhydroquinones in their search for redox polymers of improved stability. Manecke and Storck (4) have reported the synthesis of 1- and 2-vinylanthraquinones.

Further condensation-type polymers have been prepared: hydroquinone–resorcinol–formaldehyde (5), pyrogallol–formaldehyde (6), dichlorohydroquinone–trioxane (7), and dimethylhydroquinone–formaldehyde (7). In order to study the redox behavior of these polymers, which in their idealized form would consist of repeating hydroquinone units linked by methylene bridges, model segmers have been synthesized (8, 9) and their standard oxidation potentials measured.

Izoret (10) continued his work on anthraquinone polymers. A new polymer containing hydroquinone units has been prepared by the reaction of a polymeric amine with 2,5-dihydroxyhydrocinnamic acid lactone (11). The reaction of diamines with *p*-benzoquinone led to the synthesis of various aminoquinones (12).

Practical applications of redox polymers in batteries and dielectric compositions have been reported (13–15).

We have continued our investigations of polymers containing repeating hydroquinone units joined through a sulphone bridge to a polystyrene chain. Monomers and model compounds of increased stability were sought.

The organic syntheses are shown schematically below. Isopropylbenzene was chlorosulphonated and then reduced by alkaline sodium sulphite to give *p*-isopropylbenzenesulphinic acid (II). The sulphinic acid was reacted with *p*-benzoquinone to give diphenyl sulphone III, which was used subsequently as a model segmer of polymer X.

A new monomer, 2,5-bis-(2-tetrahydropyranyloxy)-4-methyl-4′-vinyldiphenyl sulphone (VII) was synthesized. The structure of sulphone V has not been positively established regarding the relative position of the $—SO_2Ar$ and $—CH_3$ groups on the hydroquinone

[1]*Taken in part from the thesis submitted by W. D. Raper to the School of Graduate Studies, University of Toronto, Toronto, in partial fulfillment of the requirements for the degree of Master of Applied Science in July, 1962.*
[2]*Present address: Airesearch Manufacturing Co., 9851 Sepulvede Blvd., Los Angeles 45, Calif., U.S.A.*

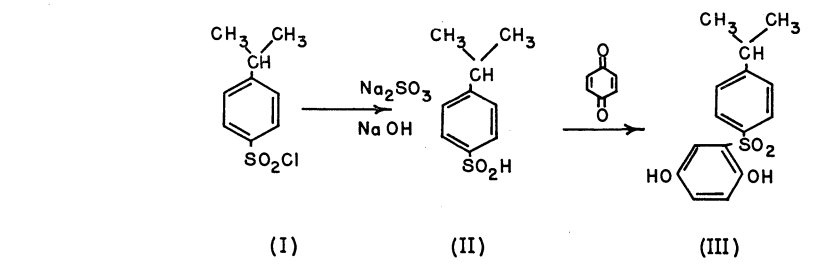

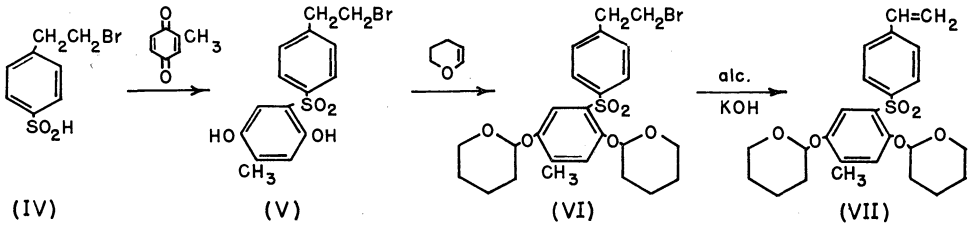

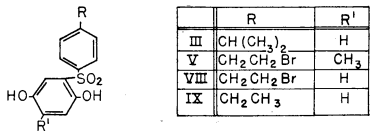

	R	R'
III	$CH(CH_3)_2$	H
V	CH_2CH_2Br	CH_3
VIII	CH_2CH_2Br	H
IX	CH_2CH_3	H

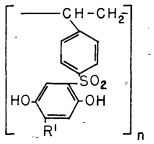

	R'
X	H
XI	CH_3

nucleus. The electron demand of the carbonyl oxygens and the low electron affinity of the $-CH_3$ group create a marked deficit at the carbon atom para to the $-CH_3$ group (16); therefore the 4-methyl isomer should be obtained in highest yield. If some 3-isomer is obtained, it should be difficult to pyranylate both phenolic groups since one of the phenolic groups would be sterically hindered. The product obtained experimentally consisted essentially of one isomer which could be fully pyranylated. A very small amount of another isomer which could not be fully pyranylated was also obtained. It is therefore suggested that the isomer used in this work is the 4-methyl isomer.

An additional model segmer (IX) with an ethyl group was synthesized by reducing the bromoethyl side chain of the sulphone VIII.

The intermediate and model compounds were characterized by analysis, infrared spectra, and their standard oxidation potentials.

The monomers were polymerized using α,α'-azodiisobutyronitrile as an initiator. After treatment with acid to expose the phenolic groups, the linear homopolymers (X and XI) were characterized by their standard oxidation potentials. Potentiometric techniques have been used with redox polymers by other investigators (5, 6, 17–19). The sulphur analyses on the polymers X and XI are lower than the theoretical and might suggest that depyranylation was incomplete. On the other hand, all phenolic groups

Can. J. Chem. Downloaded from www.nrcresearchpress.com by 210.87.254.6 on 09/05/12
For personal use only.

would be exposed during titration in strong acids. Since the titration curves of the polymers were comparatively flat, any error in estimating E_0 through an incorrect assumption of the equivalent weight of the polymers would be within the experimental limits indicated in Table II.

A simplified form of the Nernst's equation was used to calculate the standard oxidation potential (E_0) for the quinone–hydroquinone redox systems:

$$E_h = E_0 + \frac{RT}{2F} \ln \frac{[Ox]}{[Red]} + \frac{RT}{F} \ln [H^+]^*$$

where E_h is the cell potential referred to a standard hydrogen electrode. The difference between the cell potential at 50% and that at 25% oxidation, taken from the titration curve, is called the index potential (E_i) and is theoretically equal to 14.1 mv at 25° C for a simple bivalent redox reaction.

It was realized early in this work that all compounds containing the non-substituted quinone group were unstable under certain titration conditions. In cases where instability was encountered, a discontinuous titration method (20–22) was used. Briefly, predetermined amounts of the oxidant were added to known amounts of the samples to be oxidized and the change of potential with time was recorded. In all cases this change was linear and the cell potential at each stage of oxidation was obtained by extrapolation to zero time, as illustrated in Fig. 1. The value of E_0 reported for all titrations was obtained

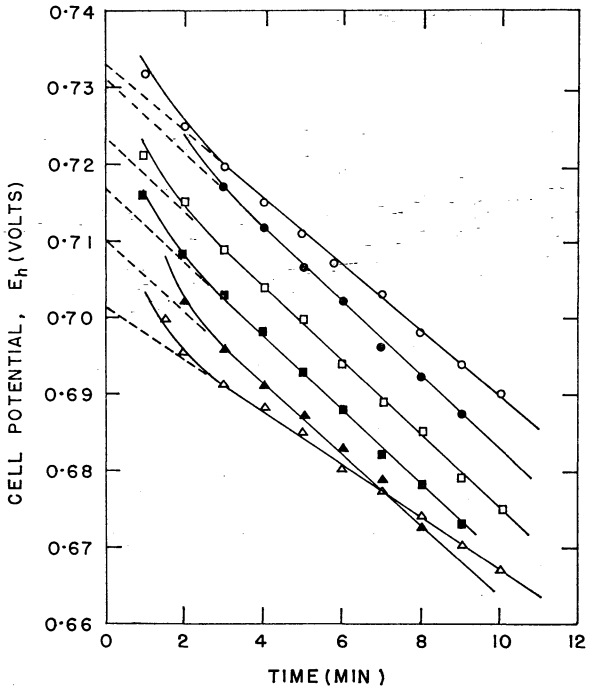

FIG. 1. Discontinuous titration of the sulphone VIII (No. 3, Table II): △ 12.2; ▲ 24.4; ■ 36.7; □ 49.0; ● 61.2; ○ 73.4% oxidation. Points were taken from recorder results.

**This simplified treatment makes the usual assumptions for a weak dibasic acid in strongly acid solution and neglects semiquinone formation, activity coefficients, and liquid junction potential. The term E_0 combines $(RT/2F) \ln K_1K_2$ with E^0, the conventional standard potential.*

Can. J. Chem. Downloaded from www.nrcresearchpress.com by 210.87.254.6 on 09/05/12
For personal use only.

by averaging the values calculated from each individual addition of oxidant as illustrated in Table I. The potential decay is a useful index of the instability of the oxidized form of

TABLE I

Discontinuous titration of sulphone VIII (No. 3, Table II), 112 mg (0.628 meq) in 250 ml acetic – sulphuric acid, pH 0.5, 24° C

0.0768 N $Ce(SO_4)_2$ (ml)	% oxidation	Initial potential E_h (v)	E_0 (v)	Potential decay (mv/min)
1.00	12.2	0.701	0.756	3.4
2.00	24.4	0.710	0.749	4.7
3.00	36.7	0.717	0.751	4.9
4.00	49.0	0.723	0.750	4.8
5.00	61.2	0.731	0.752	4.8
6.00	73.4	0.733	0.746	4.3
		Average	0.751 ±0.005	4.5±0.4

the compound. A composite curve of the cell potential at zero time versus percentage oxidation leads to the familiar potentiometric titration curve illustrated in Fig. 2.

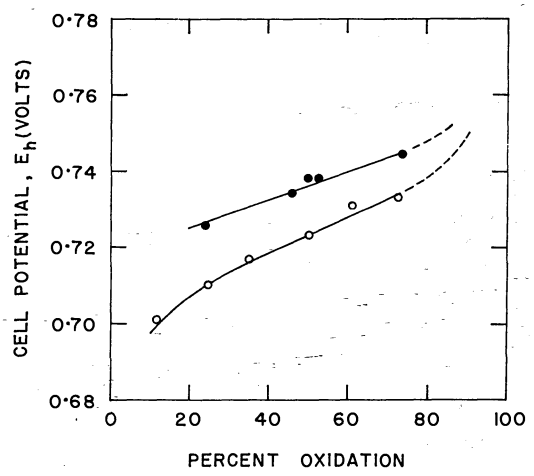

FIG. 2. Discontinuous titration (composite curve) of the sulphone VIII and polymer X (Nos. 3 and 11, Table II): ○ sulphone (pH 0.5); ● polymer (pH 0.3).

Representative examples of continuous and discontinuous titrations are shown in Table II. Hydroquinone and toluhydroquinone were titrated to check the apparatus and various techniques. The mean value of two platinum electrodes has been reported. These electrodes agreed within less than 1 mv for the model compounds and showed a maximum discrepancy of 7 mv for the polymers.

As previously mentioned the oxidized form of sulphone VIII was unstable. Therefore, a discontinuous titration was required for determination of the standard oxidation potential of this sulphone. Titration in various solvents, at different pH and using two oxidants, yielded the same values of E_0 within the experimental error. It was generally found that the decomposition of the oxidized form was much slower in solutions of lower water concentration and of lower acidity. In the case of bromine titrations it might be

Can. J. Chem. Downloaded from www.nrcresearchpress.com by 210.87.254.6 on 09/05/12
For personal use only.

Can. J. Chem. Downloaded from www.nrcresearchpress.com by 210.87.254.6 on 09/05/12
For personal use only.

TABLE II

Potentiometric titrations

No.	Compound	Solvent	Oxidant	pH	Temp. (° C)	E_0 (v)	E_i (mv)	Potential decay (mv/min)	Method
1	Hydroquinone	Acetic – sulphuric acid (*a*)	0.0764 *N* $Ce(SO_4)_2$	0.7	24	0.696±0.004 (*b*)	15	—	Continuous
2	Toluhydroquinone	50% acetic acid (*c*)	0.1060 *N* Br_2 in 50% acetic acid	1.2	22	0.639±0.004 (*d*)	14	—	Continuous
3	Sulphone VIII	Acetic – sulphuric acid (*a*)	0.0768 *N* $Ce(SO_4)_2$	0.5	24	0.751±0.005	12	4.5	Discontinuous
4	Sulphone VIII	50% acetic acid (*c*)	0.1060 *N* Br_2 in 50% acetic acid	1.4	22	0.756±0.009	10	5.1	Discontinuous
5	Sulphone VIII	50% acetic acid + Na acetate (*e*)	0.0772 *N* Br_2 in 50% acetic acid	3.7	22	0.753±0.005	20	0.7	Discontinuous
6	Sulphone VIII	80% acetic acid (*c*)	0.0482 *N* Br_2 in 80% acetic acid	0.3	25	0.748±0.004	13	1.3	Discontinuous
7	Sulphone III (isopropyl model)	Acetic – sulphuric acid (*a*)	0.0768 *N* $Ce(SO_4)_2$	0.6	22	0.740±0.003		5.9	Discontinuous
8	Sulphone IX (ethyl model)	50% acetic acid + Na acetate (*e*)	0.0772 *N* Br_2 in 50% acetic acid	3.6	22	0.762±0.005	20	1.1	Discontinuous
9	Sulphone V (methyl-substituted)	Acetic – sulphuric acid (*a*)	0.0775 *N* $Ce(SO_4)_2$	0.6	24	0.716±0.005	11	0.5	Discontinuous
10	Sulphone V (methyl-substituted)	80% acetic acid (*c*)	0.1400 *N* Br_2 in 80% acetic acid	0.25	23	0.727±0.005	15	—	Continuous
11	Polymer X	80% acetic acid (*c*)	0.0495 *N* Br_2 in 80% acetic acid	0.30	25	0.753±0.005	8	0.3	Discontinuous
12	Polymer XI (methyl-substituted)	80% acetic acid (*c*)	0.0390 *N* Br_2 in 80% acetic acid	0.30	25	0.721±0.005	12	Nil	Discontinuous
13	Polymer XI (methyl-substituted)	80% acetic acid (*c*)	0.0540 *N* Br_2 in 80% acetic acid	0.35	26	0.718±0.008	5	—	Continuous

NOTE: (*a*) Prepared by mixing equal volumes of 0.085 *N* sulphuric acid and glacial acetic acid.
(*b*) Literature value: 0.696 v at 25° C in 50% acetic acid (23).
(*c*) Percentage by volume.
(*d*) Literature value: 0.643 v at 25° C (24).
(*e*) 0.07 g of sodium acetate added per ml of solvent.

suspected that drifting potentials were due to bromination. However, this is not likely, since the redox groups are very sensitive to oxidation and the bromine concentration was less than 0.005 *N*. In any case, if bromination of the quinonoid ring did take place, the potential would have risen rather than fallen during the course of titration. It was also found that the potential decay was about the same for both ceric sulphate and bromine titrations. The secondary reaction of the quinone was first order with respect to the quinone and it is possible that an addition of water, similar to the formation of hydroxynaphthahydroquinone (21) or hydroxyhydroquinone (25), is involved.

The oxidized form of the methyl-substituted sulphone V decomposed very slowly in 50% acetic acid and was completely stable in 80% acetic acid so that redox titration of this compound and its analogous polymer could also be carried out by the continuous method (Fig. 3). The observation that the methyl-substituted polymer was more stable

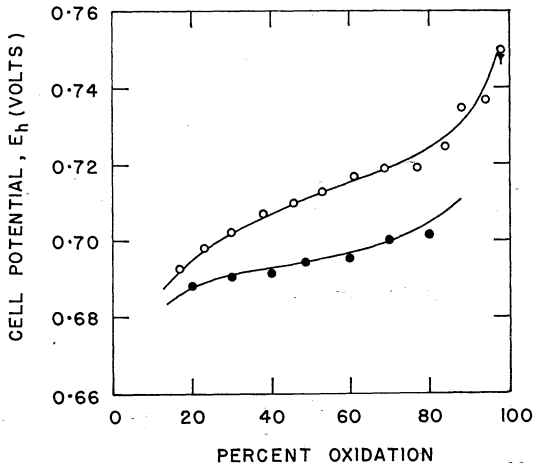

FIG. 3. Continuous titration of the methyl-substituted sulphone V and polymer XI (Nos. 10 and 13, Table II): ○ sulphone (pH 0.25); ● polymer (pH 0.35).

than the unsubstituted polymer agreed with the results of Kun and Cassidy (2).

In addition to the instability mentioned above, all compounds and polymers could not be accurately titrated past about 90% oxidation because of a downward drifting potential.

TABLE III

Standard oxidation potentials

Compound	E_0 (v)	ΔE_0* (mv)
Hydroquinone	0.696	
Sulphone VIII	0.748–0.756	52–60
Sulphone III	0.740	44
Sulphone IX	0.762	66
Polymer X	0.753	57
Toluhydroquinone	0.639	
Sulphone V	0.716–0.727	77–88
Polymer XI	0.718–0.721	79–82

*The difference between E_0 of the compound and that of the parent hydroquinone.

Can. J. Chem. Downloaded from www.nrcresearchpress.com by 210.87.254.6 on 09/05/12
For personal use only.

Table III shows that the group R on the non-oxidizable benzenoid ring did not appear to influence the E_0 of the compound to any great extent. However, the nature of the substituent R′ on the quinonoid ring influences the oxidation potential of the compound. Carter in an unpublished contribution quoted by Evans and De Heer (26) stated that there is a linear relationship between the E_0 of many substituted quinones and Hammett's substituent constant (σ_p). We have examined the literature on this point and found such a relationship exists. Data on the derivatives reported here and on other derivatives being examined indicate that a similar relationship may apply for substituted 2,5-dihydroxydiphenyl sulphones.

The addition of the $—SO_2C_6H_4R$ group to the quinones caused an increase in potential over the parent quinone in all cases. This increase ranged from 44 to 66 mv for the hydroquinone derivatives and from 77 to 88 mv for the toluhydroquinone derivatives. The increase in potential is in agreement with the expected effect of the strongly electron withdrawing $—SO_2Ar$ group. Fieser and Fieser (27) reported an increase of 121 mv for 1,4-naphthaquinone with a $—SO_2C_6H_4CH_3$ substituent. The above data and information on other derivatives now being examined indicate that there may be a linear relation between the change in E_0 (after addition of the $—SO_2C_6H_4R$ group) and Hammett's σ_p constant for the original substituent on the quinonoid nucleus.

The polymers were titrated in 80% acetic acid only, because of their limited solubility in other solvents. The oxidized polymer precipitated with the first addition of the oxidant, but seemed to remain well dispersed. The manner in which the measurements on the polymers were taken is illustrated in Fig. 4 and 5. The non-substituted polymer X (Fig. 4) appeared to be considerably more stable than its monomeric analogues (0.3 mv/minute potential decay, as compared to 1.3 mv/minute). The hydroquinone groups seemed to

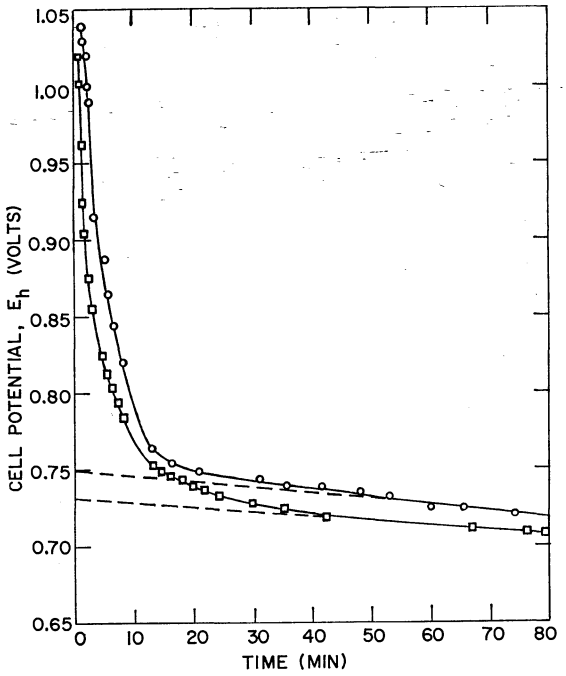

FIG. 4. Discontinuous titration of the polymer X (No. 11, Table II): □ 58.7; ○ 70.6% oxidation.

Can. J. Chem. Downloaded from www.nrcresearchpress.com by 210.87.254.6 on 09/05/12
For personal use only.

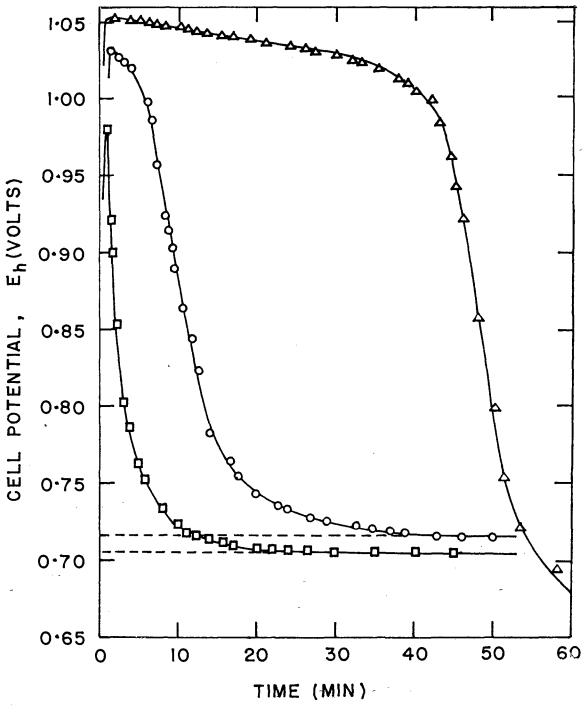

FIG. 5. Discontinuous titration of the polymer XI (No. 12, Table II): □ 51.5; ○ 77.3; △ 109.9% oxidation.

be readily accessible to oxidant, although equilibrium was attained slowly (Fig. 5), as has been noted by other investigators (18, 19). Stable equilibrium potentials were obtained for methyl-substituted polymer XI up to 80% oxidation. A downward drift of potential was obtained at higher percentage oxidation. Figure 5 also illustrates the instability of these materials when an excess of oxidant is used.

A suspension of polymer XI (80% oxidized) was reduced with hydrogen in the presence of a Pd catalyst. This stable polymer could not be completely reduced, probably because of the insoluble nature of the oxidized form. The partially reduced polymer was re-oxidized and for the same degree of oxidation the titration curve compared well with the original titration curve.

It was found that the difference between the E_0's of the polymers and those of the corresponding intermediate and model compounds was small (-13 to $+9$ mv). These results are to be contrasted with those of Robinson, Fernandez-Refojo, and Cassidy (18) and Manecke (19), who reported E_0 values for polymers up to 100 mv higher than those of the model segmers. It is probable that our results are different, because the "substitution" due to polymer growth is far removed from the redox centers. However, the possible influence of polymeric structure on E_0 cannot be overlooked.

Robinson *et al.* (18) have stated that the variation of E_0 with the ratio of the oxidized to reduced form* of their polymers was due to nearest neighbor interactions. Manecke (19) made a similar statement with regard to his data on condensation redox polymers. It

**From the experimental point of view this can be alternatively considered as a deviation of the index potential (E_i) from that expected for the simple bivalent redox reaction.*

Can. J. Chem. Downloaded from www.nrcresearchpress.com by 210.87.254.6 on 09/05/12
For personal use only.

should be pointed out that, if titrations are carried out in extremely dilute solutions, these interactions would be mainly between groups on the same chain. Examination of our results indicate that the index potentials of our polymers are closer to the theoretical value for a simple bivalent redox reaction than those of other investigators (18, 19). It thus appears that separation of the redox groups from the backbone chain by the benzene ring has considerably decreased the interaction of adjacent redox groups, as was suggested in Part I (1).

Investigation of more stable monomers and polymers is now in progress.

EXPERIMENTAL*

p-Isopropylbenzenesulphonyl Chloride (I)

This compound has been previously prepared (28, 29), but it was not isolated in a pure form.

Isopropylbenzene (cumene) (50 g, 0.416 mole) was added dropwise to chlorosulphonic acid (447 g, 3.83 mole), the temperature being maintained below 5°. The reaction mixture was poured onto crushed ice and an oil settled. This oil was separated, washed with water, and dried over anhydrous sodium sulphate. Distillation under reduced pressure gave 60 g (66%) of a colorless oil, b.p. 142–143°/12 mm, d_4^{25} 1.225, n_D^{25} 1.5350. Anal. Calc. for $C_9H_{11}ClO_2S$ (218.70): C, 49.42; H, 5.07; Cl, 16.22; S, 14.66. Found: C, 49.44; H, 5.45; Cl, 16.04; S, 14.79%. —SO_2Cl: Calc. 45.5. Found by the method of Barker *et al.* (30) 45.9%.

A derivative, *p*-isopropylbenzenesulphonamide, was prepared by reacting the sulphonyl chloride I with concentrated ammonium hydroxide. Crystallization from 60% ethanol gave white plates melting at 107–107.5° (previously reported 107–108° (31)). Anal. Calc. for $C_9H_{13}NO_2S$ (199.27): C, 54.24; H, 6.58; N, 7.03; S, 16.09. Found: C, 54.27; H, 6.60; N, 6.93; S, 15.94%.

p-Isopropylbenzenesulphinic Acid (II)

The sodium salt of this acid has been prepared by Gilman and Cason (32), but free sulphinic acid has not been reported.

The sulphonyl chloride I (20 g, 0.091 mole) was suspended in a solution of 150 g of sodium sulphite and 10 g of sodium hydroxide in 500 ml of water. The mixture was heated to 70°, stirred for 1 hour, allowed to cool to room temperature, and acidified with concentrated hydrochloric acid. A yellowish oil separated overnight. It was dissolved in 150 ml of diethyl ether and washed repeatedly with water. Evaporation of the solvent left 6.7 g (40%) of a yellowish viscous oil. The crude material gave a strong positive Smiles' test for aromatic sulphinic acids (33). It was used without further purification for the next step.

2,5-Dihydroxy-4′-isopropyldiphenyl Sulphone (III)

A suspension of *p*-benzoquinone (3.9 g, 0.036 mole) in 20% ethanol (150 ml) was added slowly to a suspension of the sulphinic acid II (6.7 g, 0.036 mole) in 20% ethanol (500 ml). The product settled overnight and crystallization from 25% ethanol gave fine, sandy crystals (4.4 g, 42%) melting at 147.5–148°. Anal. Calc. for $C_{15}H_{16}O_4S$ (292.34): C, 61.62; H, 5.52; S, 10.97. Found: C, 61.30; H, 5.66; S, 11.06%. Infrared spectrum: 1156 (s) and 1307 (s) (—SO_2—) (34), 3390 (s) (—OH) (1) cm^{-1}.

A derivative, 2,5-diacetoxy-4′-isopropyldiphenyl sulphone, was prepared by reacting the dihydroxy sulphone III with acetic anhydride and a drop of concentrated sulphuric acid as a catalyst. Crystallization from 30% ethanol gave white plates melting at 139.5–140°. Anal. Calc. for $C_{19}H_{20}O_6S$ (376.41): C, 60.62; H, 5.36; S, 8.52. Found: C, 60.53; H, 5.22; S, 8.43%.

p-(β-Bromoethyl)benzenesulphinic Acid (IV)

The preparation of this compound has been reported in Part I (1). The reduction of the corresponding sulphonyl chloride was carried out in an acid medium, instead of a more conventional reduction by alkaline sodium sulphite, because of the instability of the bromoethyl side chain in alkaline medium. Therefore in every run a large quantity (15–20%) of a by-product, *p*-(β-bromoethyl)phenyl *p*-(β-bromoethyl)benzenethiosulphonate, resulting from the disproportionation of the sulphinic acid, was obtained. This by-product was recrystallized once from 50% ethanol, and then twice from *n*-hexane, yielding white crystals, m.p. 78.5–79°. Anal. Calc. for $C_{16}H_{16}Br_2O_2S_2$ (464.24): C, 41.39; H, 3.47; Br, 34.43; S, 13.82. Found: C, 41.29; H, 3.73; Br, 34.61; S, 13.61%.

The same thiosulphonate was obtained by refluxing freshly recrystallized sulphinic acid IV for 2.5 hours in glacial acetic acid containing 4% of 1:1 sulphuric acid. The reaction mixture was diluted with water and cooled. The precipitate was filtered and recrystallized once from 50% ethanol and twice from *n*-hexane, yielding white crystals, m.p. 78.5–79°. This product gave no depression in mixed melting point with the analyzed sample.

**Melting points are corrected. All ethanol solutions are reported on a percentage by volume basis. Microanalyses were done by Galbraith Laboratories, Inc., Knoxville, Tenn.*

Can. J. Chem. Downloaded from www.nrcresearchpress.com by 210.87.254.6 on 09/05/12
For personal use only.

2,5-Dihydroxy-4-methyl-4′-(β-bromoethyl)diphenyl Sulphone (V)

A solution of toluquinone (12.7 g, 0.104 mole) in absolute ethanol (125 ml) was added dropwise to a suspension of the sulphinic acid IV (26 g, 0.104 mole) in 30% ethanol (1 liter). Stirring was continued for 1 hour, the mixture was diluted with 1125 ml of water and chilled for several hours in an ice bath. The precipitate was recrystallized from 25% ethanol, yielding 21 g (55%) of a white product melting at 121–122°. Anal. Calc. for $C_{15}H_{15}BrO_4S$ (371.25): C, 48.53; H, 4.07; Br, 21.53; S, 8.63. Found: C, 48.73; H, 4.14; Br, 21.51; S, 8.74%. Infrared spectrum: 1142 (s) and 1308 (s) (—SO_2—) (34), 3390 (s) (—OH) (1) cm^{-1}.

A derivative, 2,5-diacetoxy-4-methyl-4′-(β-bromoethyl)diphenyl sulphone, was prepared. Crystallization from 25% ethanol gave a white product melting at 59–60°. Anal. Calc. for $C_{19}H_{19}BrO_6S$ (455.33): C, 50.10; H, 4.20; Br, 17.55; S, 7.04. Found: C, 50.16; H, 4.26; Br, 17.46; S, 7.23%.

In certain runs, small amounts of a material of much higher melting point, having all the characteristics of a dihydroxydiphenyl sulphone, were isolated. This was probably 2,5-dihydroxy-3-methyl-4′-(β-bromoethyl)diphenyl sulphone. Repeated recrystallizations from 20% ethanol and mixtures of benzene and petroleum ether yielded a white product melting at 146–147°. Anal. Calc. for $C_{15}H_{15}BrO_4S$ (371.25): C, 48.53; H, 4.07; Br, 21.53; S, 8.63. Found: C, 48.88; H, 4.20; Br, 23.46; S, 9.15%. Infrared spectrum: 1147 (s) and 1302 (s) (—SO_2—) (34), 3390 (s) (—OH) (1) cm^{-1}.

Attempts to pyranylate this material fully under a variety of conditions failed. Only a monopyranylated derivative, 2-hydroxy-3-methyl-5-(2-tetrahydropyranyloxy)-4′-(β-bromoethyl)diphenyl sulphone, melting at 112–113°, was obtained. Anal. Calc. for $C_{20}H_{23}BrO_5S$ (455.39): C, 52.75; H, 5.09; Br, 17.55; S, 7.04. Found: C, 52.86; H, 5.05; Br, 17.29; S, 7.03%.

The monopyranylated sulphone was easily decomposed by treatment with hydrochloric acid, yielding the dihydroxy sulphone (3-methyl isomer).

2,5-Bis-(2-tetrahydropyranyloxy)-4-methyl-4′-(β-bromoethyl)diphenyl Sulphone (VI)

This preparation was similar to that previously reported for a non-substituted hydroquinone derivative (1). One modification included the precipitation of the final product from an absolute ethanol solution of the crude product by *n*-hexane. The pale yellow solid obtained (4.5 g, 77%) melted at 51–53°. Anal. Calc. for $C_{25}H_{31}BrO_6S$ (539.48): C, 55.65; H, 5.79; Br, 14.81; S, 5.94. Found: C, 55.37; H, 5.50; Br, 14.61; S, 6.29%.

Repeated recrystallizations did not improve the melting point range. This product is believed to be a mixture of stereoisomers of the type discussed previously (1).

2,5-Bis-(2-tetrahydropyranyloxy)-4-methyl-4′-vinyldiphenyl Sulphone (VII)

The procedure was similar to that previously reported for a non-substituted monomer (1). Potassium bromide precipitated during the course of the reaction. A pale yellow liquid (4.1 g, 87%), which gave a negative test for halogen, was obtained. It was insoluble in dilute sodium hydroxide solution, which indicated that the hydroxy groups remained protected. Attempts to purify the monomer VII by distillation were unsuccessful because of its high boiling point and instability at high temperatures.

2,5-Dihydroxy-4′-ethyldiphenyl Sulphone (IX)

2,5-Dihydroxy-4′-(β-bromoethyl)diphenyl sulphone (VIII) (1) (8.5 g, 0.024 mole) was dissolved in a hot solution of 300 ml of water, 70 ml of concentrated sulphuric acid, and 120 ml of glacial acetic acid, to which 0.5 g of zinc had been added. The solution was refluxed for 7 hours during which an additional 4.5 g of zinc was added in small portions. When the solution was diluted with 200 ml of water and cooled, a fluffy white precipitate settled. The crude product was purified by dissolution in 5% sodium hydroxide solution containing a trace of sodium hydrosulphite and precipitation with 25% acetic acid. A white product (3.8 g, 58%) melted at 181.5–182°. Anal. Calc. for $C_{14}H_{14}O_4S$ (278.31): C, 60.42; H, 5.07; S, 11.52. Found: C, 60.15; H, 5.30; S, 11.29%.

A derivative, 2,5-diacetoxy-4′-ethyldiphenyl sulphone, was prepared. Crystallization from 25% ethanol gave white plates melting at 144–144.5°. Anal. Calc. for $C_{18}H_{18}O_6S$ (362.39): C, 59.65; H, 5.01; S, 8.85. Found: C, 59.32; H, 4.81; S, 8.78%.

Poly(2,5-dihydroxy-4′-vinyldiphenyl Sulphone) (X)

2,5-Bis-(2-tetrahydropyranyloxy)-4′-vinyldiphenyl sulphone (1) (3.006 g, 0.0068 mole) and α,α′-azodiisobutyronitrile (30 mg) were dissolved in 15 ml of toluene and heated in a sealed tube at 95–96° for 72 hours. Precipitation with methanol and reprecipitation with petroleum ether (80–100°) from a toluene solution yielded a white fluffy product (1.91 g, 63%), insoluble in 5% sodium hydroxide solution, with a softening range of 165–185°. Anal. Calc. for $(C_{24}H_{28}O_6S)_n$ (444.52): S, 7.21. Found: S, 6.85%.

The polymer was treated with 50% hot acetic acid to remove the tetrahydropyranyl groups, dissolved in dioxane, and precipitated by petroleum ether. A light tan product, soluble in 5% sodium hydroxide (yellow solution), softened at 200–210°. Anal. Calc. for $(C_{14}H_{12}O_4S)_n$ (276.30): S, 11.60. Found: S, 9.79%.

Poly(2,5-dihydroxy-4-methyl-4′-vinyldiphenyl Sulphone) (XI)

The crude monomer VII (2.298, 0.0050 mole) and α,α′-azodiisobutyronitrile (28.3 mg) were heated in a sealed tube at 95° for 24 hours. The very viscous pale amber polymerization product was dissolved in 15 ml of chloroform and precipitation by petroleum ether (80–120°) yielded a white product (1.36 g, 55%),

Can. J. Chem. Downloaded from www.nrcresearchpress.com by 210.87.254.6 on 09/05/12
For personal use only.

insoluble in absolute ethanol and 5% sodium hydroxide solution, sparingly soluble in benzene and toluene, with a softening range of 170–185°. Anal. Calc. for $(C_{25}H_{30}O_6S)_n$ (458.56): S, 6.99. Found: S, 8.66%.

Treatment with 50% acetic acid and precipitation from dioxane solution by petroleum ether gave a white product, soluble in 5% sodium hydroxide solution (yellow solution), with a softening range of 175–185°. Anal. Calc. for $(C_{15}H_{14}O_4S)_n$ (290.33): S, 11.05. Found: S, 10.01%.

Potentiometric Titrations

(a) Apparatus

The assembly consisted of a saturated calomel electrode connected by a saturated potassium chloride bridge* to the titration vessel equipped with two bright platinum electrodes, a glass electrode, and a magnetic stirrer. The cell potentials were measured using a precision differential d-c. voltmeter (Model 801H, John Fluke Mfg. Co.). The change of potential with time was measured using a potential recorder (Model A-70, John Fluke Mfg. Co.). Nitrogen was purified by passage through Fieser's solution (36) and lead acetate solution.

(b) Continuous Titration

These titrations were performed in a conventional manner (35). Some of the experimental runs are listed in Table II. Between 0.685 and 1.01 meq of the compound to be titrated in 80 ml of solvent was used in each titration.

(c) Discontinuous Titration

A typical titration (No. 3 in Table II) is described. A stock solution of the sulphone VIII (equiv. wt. 178.61), containing 2.8010 g (0.0157 equiv.) in 250 ml of 90% acetic acid, was prepared. Ten milliliters of this solution (112.0 mg, 0.628 meq) was added to 240 ml of the acetic–sulphuric acid in the titration vessel. Nitrogen was bubbled through the solution and the solution stirred for 1/2 hour. One milliliter of the oxidizing agent, 0.0768 *N* ceric sulphate (corresponding to 12.2% oxidation), was added rapidly and the cell potential recorded using a potential recorder. The potential at zero time was obtained by extrapolation of the potential–time curve (Fig. 1). The same procedure was repeated by taking another 10 ml of the stock solution, adding 2.0 ml of the oxidant (corresponding to 24.4% oxidation), and recording the change of potential with time again. A third curve was obtained when 3.0 ml of the oxidant (36.7% oxidation) was added to another 10 ml sample, and so on. A composite titration curve was then constructed from the initial (zero time) potentials (Fig. 2). The standard oxidation potential (E_0) was calculated, as shown in Table I.

ACKNOWLEDGMENTS

The financial assistance of the National Research Council of Canada and the Advisory Committee on Scientific Research, University of Toronto (to W. D. R.), and of the Ontario Research Foundation (to W. M.) is gratefully acknowledged.

REFERENCES

1. I. H. Spinner, J. Yannopoulos, and W. Metanomski. Can. J. Chem. **39**, 2529 (1961).
2. K. A. Kun and H. G. Cassidy. J. Polymer Sci. **56**, 83 (1962).
3. Y-H. C. Giza, K. A. Kun, and H. G. Cassidy. J. Org. Chem. **27**, 679 (1962).
4. G. Manecke and W. Storck. Chem. Ber. **94**, 3239 (1961).
5. A. V. Gordievskiĭ, E. V. Renard, and M. N. Voronovskaya. Plasticheskie Massy, **3**, 20 (1961).
6. H. P. Gregor and M. Beltzer. J. Polymer Sci. **53**, 125 (1961).
7. R. K. Quisenberry. Ph.D. Thesis, Universiy of Utah, Salt Lake City, Utah, 1961; Dissertation Abstr. **22**, 76 (1961).
8. S. E. Hunt and A. S. Lindsey. Chem. Ind. (London), 1272 (1961). M. E. Peover and A. S. Lindsey. Chem. Ind. (London), 1273 (1961).
9. G. Manecke and H.-J. Förster. Makromol. Chem. **52**, 147 (1962).
10. G. Izoret. Compt. Rend. **253**, 274 (1961); **254**, 671 (1962).
11. L. D. Taylor. J. Appl. Polymer Sci. **6**, S13 (1962).
12. A. A. Berlin and N. G. Matveeva. Vysokomolekul. Soedin. **1**, 1643 (1959). V. P. Parini, Z. S. Kazakova, M. N. Okorokova, and A. A. Berlin. Vysokomolekul. Soedin. **3**, 402 (1961).
13. M. S. Harding. U.S. Patent No. 2,831,045 (April, 1958).
14. S. D. Ross. U.S. Patent No. 2,916,680 (December, 1959).
15. P. Faber. German Patent No. 1,035,227 (July, 1958); Chem. Abstr. **54**, 15028 (1960).
16. H. G. H. Erdtman. Proc. Roy. Soc. (London), Ser. A, **143**, 177 (1933).
17. L. Luttinger and H. G. Cassidy. J. Polymer Sci. **22**, 271 (1956).
18. I. D. Robinson, M. Fernandez-Refojo, and H. G. Cassidy. J. Polymer Sci. **39**, 47 (1959).
19. G. Manecke. Z. Elektrochem. **58**, 369 (1954). G. Manecke and Ch. Bahr. Z. Elektrochem. **62**, 311 (1958).
20. L. F. Fieser. J. Am. Chem. Soc. **52**, 4915 (1930).

**Before titration the saturated* KCl *bridge was conditioned several hours in the solvent to be used to ensure stability of junction potential (35).*

Can. J. Chem. Downloaded from www.nrcresearchpress.com by 210.87.254.6 on 09/05/12
For personal use only.

21. L. F. FIESER and M. A. PETERS. J. Am. Chem. Soc. **53**, 793 (1931).
22. A. E. CAMERON. J. Phys. Chem. **42**, 1217 (1938).
23. K. WALLENFELS and W. MÖHLE. Ber. Sect. B, **76**, 924 (1943).
24. J. B. CONANT and L. F. FIESER. J. Am. Chem. Soc. **45**, 2194 (1923).
25. J. E. LUVALLE *et al.* The chemistry of quinones. U.S. Department of Commerce. Office of Technical Services. PB Report No. 137874. Washington. 1958.
26. M. G. EVANS and J. DE HEER. Quart. Rev. (London), **4**, 94 (1950).
27. L. F. FIESER and M. FIESER. J. Am. Chem. Soc. **57**, 491 (1935).
28. E. H. HUNTRESS and J. S. AUTENRIETH. J. Am. Chem. Soc. **63**, 3446 (1941).
29. H. GILMAN and H. S. BROADBENT. J. Am. Chem. Soc. **69**, 2053 (1947).
30. J. E. BARKER, C. M. PAYNE, and J. MAULDING. Anal. Chem. **32**, 831 (1960).
31. R. MEYER. Ann. **219**, 234 (1883).
32. H. GILMAN and L. F. CASON. J. Am. Chem. Soc. **72**, 3469 (1950).
33. A. I. VOGEL. Textbook of practical organic chemistry. 3rd ed. Longmans, Green and Co., Ltd. London. 1959. p. 1078.
34. K. C. SCHREIBER. Anal. Chem. **21**, 1168 (1949).
35. A. WEISSBERGER (*Editor*). Physical methods of organic chemistry. Vol. I. Part IV. 3rd ed. Interscience Publishers, Inc. New York. 1960. p. 2986.
36. L. F. FIESER. J. Am. Chem. Soc. **46**, 2639 (1924).

Can. J. Chem. Downloaded from www.nrcresearchpress.com by 210.87.254.6 on 09/05/12
For personal use only.

GALVANIC STRESS POTENTIALS OF METALS

S. TAN AND KEN NOBE

Department of Engineering, University of California, Los Angeles, California

Received October 22, 1962

ABSTRACT

The electrode potential of silver, brass, and steel wires under tensile stress have been measured in aqueous solutions of silver nitrate, copper sulphate, and ferrous sulphate, respectively. The stress potentials were continuously measured with a stabilized d-c. microvolt amplifier which made possible the study of the transient and the steady-state period during loading and unloading. The stressed silver and steel electrodes were cathodic with respect to the reference electrode, and the e.m.f. was approximately a linear function of the stress. The slope of the e.m.f.–stress curve for silver increased with decrease in electrolyte concentration. The stressed brass electrode was anodic with respect to the reference electrode and the e.m.f. varied linearly with stress only for 1 *N* $CuSO_4$.

Can. J. Chem. Downloaded from www.nrcresearchpress.com by 210.87.254.105 on 09/05/12
For personal use only.

INTRODUCTION

The electrode potentials of silver, brass, and steel wires mechanically stressed in the elastic region have been measured in air-saturated aqueous solutions of silver nitrate, copper sulphate, and ferrous sulphate, respectively. A theoretical analysis of the effect of stress on the electrode potential of metals has been made by Flood (1). Some previous investigations have been reviewed by Fryxell and Nachtrieb (2), and it is evident that there is considerable disagreement among the investigators concerning the sign of the electrode potential of the stressed metal electrodes. In the investigation reported here, the stress potentials were observed with instrumentation which made possible a continuous measurement of the e.m.f. during the loading and the unloading process. Thus, the behavior of these stressed electrodes in the transient as well as in the steady-state region could be observed. In addition, the effects of electrolyte concentration on the stress potentials were studied.

EXPERIMENTAL

The galvanic cell consisted of the metal wire as the test electrode aligned along the axis of a cylindrical tube of the same metal. The metal wire was coated with a thin coat of lucite to eliminate the erratic behavior of the electrode potential caused by reactions occurring at the air–solution interface. Further details and a schematic drawing of the cell are given elsewhere (3).

The e.m.f. of the cell was measured with a Leeds and Northrup d-c. microvolt amplifier. The input impedance of the amplifier was greater than 10^7 ohms. A continuous trace of the amplifier output was obtained with a Leeds and Northrup Speedomax recorder.

The metal wires used in this investigation were silver, gauge B. & S. No. 20, C.P. grade 99.9% pure; brass, gauge B. & S. No. 22 (70% Cu, 30% Zn); black annealed steel, gauge B. & S. No. 20 (99.8% Fe).

The wires were cleaned with abrasive powder and etched in dilute nitric acid, rinsed several times with double-distilled water, and coated with a lucite film. A portion of the lucite film, 1 cm in height, was removed to allow the metal surface to come in contact with the solution.

Since the no-load e.m.f. of the galvanic cell was usually greater than 1 mv and the stress potentials were often considerably smaller, a bucking potential was introduced to mask out the initial potential. The e.m.f. of the cell stabilized 1 to 2 hours after the solution was introduced into the cell. A fresh cell was used for each run, and measurements were taken at room temperature.

For each value of tensile stress, the load was added and removed several times. Special care was taken not to exceed the elastic limit of the metal during each run by taking stress–strain measurements simultaneously.

RESULTS AND DISCUSSIONS

The e.m.f. measurements of the silver cell were made in the tensile stress range 0 to 6700 g/mm^2. These measurements were made in 1 *N*, 0.1 *N*, 0.01 *N*, and 0.001 *N* silver

nitrate solutions. No attempt was made to control the oxygen content other than to air-saturate the solutions since Fryxell and Nachtrieb (2) observed that the exclusion of oxygen did not appreciably affect the e.m.f.

In each run the stress potentials were both reproducible and reversible. With the application of the load, the potential of the test electrode became more positive with respect to the unstressed reference electrode (the Gibbs–Stockholm convention for the sign of the electrode potential is adopted in this paper). The e.m.f.–time response which is shown in the inset of Fig. 1 indicated that the electrode potential of the stressed wire

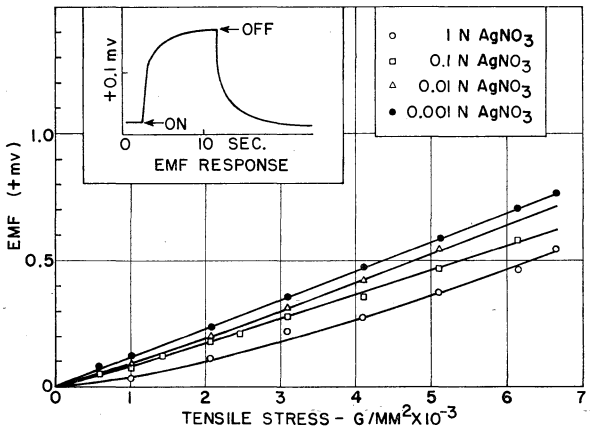

FIG. 1. Electromotive force of stressed silver electrodes.

increased monotonically with time and approached a steady-state value asymptotically (i.e., became more noble). With the removal of the load the electrode potential returned to the original no-load value in the same manner, but in the opposite sign direction to the loading process.

The experimental results of the silver – silver nitrate cells are shown in Fig. 1. For each concentration the e.m.f. values were approximately a linear function of the tensile stress. The slope of the e.m.f.–stress curve increased with decrease in concentration.

The effects of electrolyte concentration on the potentials induced by stress of silver electrodes were similar to those recently reported for copper and zinc-plated copper (3). The similarity lies between the steady-state potential of silver and the maximum amplitude of the potential response of copper. The maximum amplitude of the potential response was not the steady-state potential for copper as it was for silver. For copper, the maximum potential response attained during the transient period was explained by theoretical considerations of the electrical double-layer. The following equation was derived for the maximum transient potential, $\Delta E = -1(1-\mu)E_{0\epsilon}$ where μ is Poisson's ratio for the metal electrode, ϵ is the strain, and E_0 is the electrical potential across the double-layer at no-load. Since E_0 is a function of concentration and determined from the Nernst relation, ΔE is expressed as a function of strain and electrolyte concentration.

Fryxell and Nachtrieb (2) investigated silver electrodes (99.98% pure) in 0.1 M silver nitrate solutions. They observed that the e.m.f. was stable and reproducible for silver stressed in elastic tension and compression. Their e.m.f. measurements were taken with a Leeds and Northrup K2 potentiometer and, as a consequence, they were not able to record a continuous e.m.f.–time response. They did not observe any e.m.f. dependence

Can. J. Chem. Downloaded from www.nrcresearchpress.com by 210.87.254.105 on 09/05/12
For personal use only.

on concentration. Their results indicated that the e.m.f. of the silver electrodes was linear with stress up to 10,000 p.s.i. with a slope of 0.078±.021 mv per 1000 p.s.i. The slope of the e.m.f.–stress curve obtained in this investigation for silver in 0.1 *M* silver nitrate solution was 0.067 mv per 1000 p.s.i., which is in good agreement with the results of Fryxell and Nachtrieb.

The e.m.f.–time response and the e.m.f.–tensile stress results for the brass – copper sulphate cells* are shown in Fig. 2. The e.m.f. induced by stress was measured in the

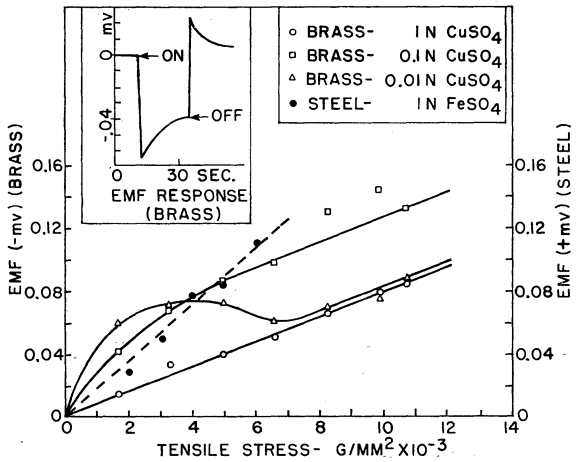

FIG. 2. Electromotive force of stressed steel and brass electrodes.

tensile stress range from 0 to 10,800 g/mm². The electrolyte concentrations were 1 *N*, 0.1-*N*, and 0.01-*N* copper sulphate solutions. On loading, the test electrode shifted to a more negative potential with respect to the reference electrode. During the transient period, the e.m.f. attained a maximum value almost instantaneously and decayed exponentially to a steady-state value. The removal of the load resulted in a mirror image of the e.m.f.–time curves for the loading process. The e.m.f.–time responses were similar to those reported for copper (3). The steady-state potentials for the brass were considerably different from the no-load value. The potentials of the copper, however, approached asymptotically the no-load potential.

E.m.f.–stress data for the steel cell were obtained only for the 1 *N* ferrous sulphate solution and are shown in Fig. 2. The e.m.f.–time reponse curve is not shown since it was similar to the silver – silver nitrate cell. However, the relaxation time for steel was somewhat less than for silver. The e.m.f.–time responses were both reproducible and reversible as the silver and brass cells. The stressed electrode shifted to a more positive potential with respect to the unstressed electrode. Runs with lower concentrations of ferrous sulphate were attempted, but the data were not reproducible within each run since steady-state conditions were difficult to attain at those concentrations.

Giulotto (4) observed for iron in 0.05 *N* $FeSO_4$ that the stressed electrode assumed more positive potentials than the unstressed electrode. His results indicated a linear relationship between e.m.f. and tensile stress with a slope of 80 microvolts per 10,000 p.s.i. The data obtained in this investigation of mild steel (99.8% Fe) in 1 *N* $FeSO_4$ resulted in an e.m.f.–stress slope of 129 microvolts per 10,000 p.s.i. and compares reasonably well with Giulotto's results for iron.

**Flood's analysis does not apply to brass–*$CuSO_4$ cells.*

Can. J. Chem. Downloaded from www.nrcresearchpress.com by 210.87.254.105 on 09/05/12
For personal use only.

ACKNOWLEDGMENT

This work was supported by funds from the University of California's Sea Water Demineralization Program.

REFERENCES

1. E. A. FLOOD. Can. J. Chem. **36**, 1332 (1958).
2. R. E. FRYXELL and N. H. NACHTRIEB. J. Electrochem. Soc. **99**, 495 (1952).
3. K. NOBE, E. BAUM, and W. F. SEYER. J. Electrochem. Soc. **108**, 97 (1961).
4. L. GIULOTTO. Nuovo Cimento, **13**, 220 (1936).

Can. J. Chem. Downloaded from www.nrcresearchpress.com by 210.87.254.105 on 09/05/12
For personal use only.

WALLACH REARRANGEMENT OF UNSYMMETRICALLY SUBSTITUTED AZOXYBENZENES AND OXIDATION OF AZO DERIVATIVES[1]

JOGINDER SINGH,[2] PRITAM SINGH, J. L. BOIVIN, AND PAUL E. GAGNON
Department of Chemistry, Laval University, Quebec, Que.
Received August 22, 1962

ABSTRACT

The Wallach rearrangement of 3-chloro-3′-methyl- and 3-methyl-3′-nitro-azoxybenzene gave rise to the corresponding 4′-hydroxyazo derivatives with the hydroxyl group attached to the benzene ring adjacent to the trivalent nitrogen bridge, while 2,2′,5,5′-tetrachloro-4′-nitro- and 2′-nitro-4,4′,5,5′-tetrachloro-azoxybenzene were hydroxylated in the ortho and para positions respectively on the ring adjacent to the pentavalent nitrogen bridge.

Oxidation of 3-methyl-3′-nitro- and 3-chloro-3′-methyl-azobenzene gave rise to the corresponding α-isomers, which was proved by the bromination and reduction products.

The ultraviolet and visible absorption spectra of the unsymmetrically and symmetrically substituted azo- and azoxy-benzenes prepared have been recorded and briefly discussed.

INTRODUCTION

In a previous paper (1), the nitration and reduction of some symmetrically substituted azo- and azoxy-benzenes were reported. It was thought of interest to apply the Wallach rearrangement to unsymmetrically substituted azoxybenzenes and also to study the oxidation of azo derivatives, and to correlate the ultraviolet and visible absorption spectra of unsymmetrically and symmetrically substituted azo- and azoxy-benzenes prepared to their degree of conjugation.

DISCUSSION OF RESULTS

Wallach Rearrangement

The Wallach rearrangement or the isomerization of azoxybenzenes to the corresponding *p*-hydroxyazobenzenes has been extensively studied. However, the reaction mechanism is controversial. There is one belief that the isomerization proceeds through a cyclic oxide intermediate as evidenced by the use of N^{15} and O^{18} (2, 3). There is another postulated mechanism in favor of ionic intermediates (4) which give rise to *p*-hydroxyazo compounds by nucleophilic attack of OSO_3H^- or OSO_2Cl^- and subsequent hydrolysis.

In this paper, the Wallach rearrangement was applied to some unsymmetrically substituted azoxybenzenes. The formation of only one corresponding hydroxyazo compound in the case of 3-methyl-3′-nitro- and 3-chloro-3′-methyl-azoxybenzene during Wallach rearrangement with chlorosulphonic acid and concentrated sulphuric acid indicates that the rearrangement proceeded through the same type of intermediate in both cases and is independent of the nature of the reagent used, the hydroxyl group being in the para position of the ring adjacent to the trivalent nitrogen bridge. The reaction mechanism might be shown by the following scheme involving monocation formation:

[1]*This paper constitutes part of a thesis submitted to the Graduate School, Laval University, by Joginder Singh, in partial fulfillment of the requirements for the degree of Doctor of Science.*
This work was supported in part by a grant from the Defence Research Board of Canada (1959).
[2]*Graduate Student, holder of scholarships from Canadian Industries Limited (1960) and Shell Oil Company of Canada (1961).*

Can. J. Chem. Downloaded from www.nrcresearchpress.com by 210.87.254.105 on 09/05/12
For personal use only.

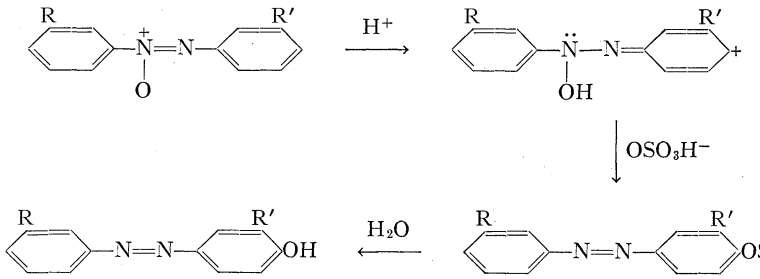

The Wallach transformation of the α-isomer 2,2′,5,5′-tetrachloro-4′-nitroazoxybenzene (1) gave the *p*-hydroxyazo compound, the hydroxyl group entering the benzene ring attached to the pentavalent nitrogen. Also in the case of the α-isomer 2′-nitro-4,4′,5,5′-tetrachloroazoxybenzene (1), the hydroxyl group entered the ring not containing the nitro group.

Oxidation

3-Methyl-3′-nitro- and 3-chloro-3′-methyl-azobenzene were oxidized with hydrogen peroxide in acetic acid at 85–90° C to give the corresponding azoxybenzenes. To ascertain the structure of the azoxy compounds, they were brominated and the bromo derivatives reduced to the corresponding amines. In the case of 3-methyl-3′-nitroazobenzene, the oxygen of the azoxy group proved to be adjacent to the benzene ring carrying the methyl group. The electron-repelling nature of the methyl group increases the availability of lone pairs of electrons of the nitrogen atom attached to the ring, while the electron-attracting effect of the nitro group on the other ring deactivates its adjacent nitrogen to the attack of electrophilic oxygen of peracetic acid (5).

3-Chloro-3′-methylazobenzene was also oxidized into the α-isomer of 3-chloro-3′-methylazoxybenzene. In this case, the attacking electrophilic oxygen went on the nitrogen adjacent to the benzene ring carrying the chlorine, as was shown by the bromination and reduction products isolated.

Ultraviolet and Visible Absorption Spectra

The absorption spectra of the symmetrically (1) and unsymmetrically substituted azo- and azoxy-benzenes synthesized have been determined in the ultraviolet and visible and the results are given in Tables I and II.

As usually observed with the azo- and azoxy compounds, three regions of absorption were exhibited; there were absorption bands in the regions 2100 to 2900 Å, 3000 to 3800 Å, and 4100 to 4300 Å.

In this work all the tetra-, penta-, or hexa-substituted azo- and azoxy-benzenes gave absorption bands in three main regions I, IA, and II. Region I showed a single peak of high intensity at about 2400 Å which is attributed to the substituted benzene rings (6). Region IA exhibited one band at about 2600 Å which is ascribed to the azophenyl group (6). Region II had, usually, a broad band of high intensity at 3000 to 4000 Å, which is explained by the conjugation of the azo linkage and the aromatic rings (6). On substitution of a nitro group at the 4′-position in tetrasubstituted azo- and azoxy-benzene and of bromine in disubstituted compounds, a pronounced bathochromic shift was observed. The transformation of 2,2′-disubstituted azo compounds to the corresponding azoxy compounds resulted in an hypsochromic shift (7).

2,2′-Dimethyl-3,3′-dichloroazo- and azoxy-benzene and their nitro derivatives showed

Can. J. Chem. Downloaded from www.nrcresearchpress.com by 210.87.254.105 on 09/05/12
For personal use only.

TABLE I

Absorption spectra of azo- and azoxy-benzenes

Compound	Solvent	Region I		Region II	
		Å	(ϵ_m)	Å	(ϵ_m)
2,2′-Dimethyl-5,5′-dichloroazobenzene	Ether	2,380	(11,800)	3,220	(11,300)
2,2′-Dimethyl-5,5′-dichloroazoxybenzene	Ethanol	2,340	(10,800)	3,080	(9,290)
2,2′-Dimethyl-4-hydroxy-5,5′-dichloroazobenzene	"	2,480	(14,400)	3,700 4,350	(30,100) (29,800)
2,2′-Dimethyl-4-nitro-5,5′-dichloroazobenzene	Ether			3,320	(15,400)
2,2′-Dimethyl-4,4′-dinitro-5,5′-dichloroazobenzene	"			3,330	(19,000)
2,2′-Dimethyl-4′-nitro-5,5′-dichloroazoxybenzene	Ethanol			3,080	(11,800)
2,2′-Dimethyl-5,5′-dichlorohydrazobenzene	"	2,490	(22,800)	2,920	(5,340)
2,2′-Dimethyl-4,4′-diacetylamino-5,5′-dichloroazobenzene	Dioxane	2,680	(19,900)	3,860	(18,600)
2,2′-Dimethoxy-4′-nitro-5,5′-dichloroazoxybenzene	Ethanol	2,220	(21,000)	2,910	(6,350)
2,2′-Dimethyl-3,3′-dichloroazoxybenzene	"	2,340	(11,000)	3,080	(9,300)
2,2′-Dimethyl-3,3′-dichloro-4,4′-dinitroazobenzene	Ether			3,320	(17,200)
2,2′-Dimethyl-3,3′-dichloro-4,4′-dinitroazobenzene	Chloroform			3,350	(20,900)
2,2′-Dimethyl-3,3′-dichloro-4,4′-diaminoazobenzene	Ethanol	2,690	(4,960)	4,120	(3,030)
2,2′-Dimethyl-3,3′-dichloro-4,4′-diaminoazoxybenzene	"	2,400	(9,330)	4,270	(27,700)
2,2′-Dimethyl-3,3′-dichloro-4,4′-diacetylaminoazobenzene	N,N-Dimethylformamide	2,670	(17,000)	3,780	(14,700)
2,2′,5,5′-Tetramethylazobenzene	Ethanol			3,400	(12,600)
2,2′,5,5′-Tetramethylazoxybenzene	"	2,360	(10,400)	3,120	(7,800)
2,2′,5,5′-Tetramethyl-4,4′-dinitroazobenzene	"	2,470	(16,000)	3,350	(20,400)
2,2′,5,5′-Tetramethyl-4,4′-dinitrohydrazobenzene	"	2,300	(11,100)	3,760	(26,900)
2,2′,5,5′-Tetramethyl-4,4′-diacetylaminoazobenzene	Dioxane	2,520	(9,720)	3,760	(9,560)
2,2′,5,5′-Tetrachloro-4-nitroazobenzene	Ethanol	2,800	(10,100)	4,180	(20,700)
2,2′,5,5′-Tetrachloro-4′-nitroazoxybenzene	Ether	2,980	(11,000)		
2,2′,5,5′-Tetrachloro-4-hydroxy-4′-nitroazobenzene	Ethanol	2,940	(9,430)	4,250	(32,000)
2′-Nitro-4,4′,5,5′-tetrachloroazoxybenzene	"	2,710	(19,700)		
2-Hydroxy-2′-nitro-4,4′,5,5′-tetrachloroazobenzene	"	2,440	(18,100)	3,360	(20,600)
3,3′,4,4′-Tetrachloro-5′-nitroazoxybenzene	"	2,390	(12,500)	3,400	(20,700)

TABLE II

Absorption spectra of azo- and azoxy-benzenes

Compound	Solvent	Region I		Region IA		Region II	
		Å	(ϵ_m)	Å	(ϵ_m)	Å	(ϵ_m)
3-Methyl-3′-nitroazobenzene	Ethanol	2,330	(17,600)	2,680	(13,300)	3,170	(23,100)
3-Methyl-3′-nitroazoxybenzene	"			2,670	(12,500)	3,120	(14,100)
3-Chloro-3′-methyl-4′-bromoazoxybenzene	"			2,580	(8,970)	3,360	(7,760)
3-Methyl-3′-nitro-4-bromoazoxybenzene	"	2,420	(33,600)			3,360	(33,600)
3-Methyl-3′-nitro-4′-hydroxyazobenzene	"			2,530	(20,600)	3,580	(26,800)
3-Chloro-3′-methylazobenzene	"	2,330	(13,000)			3,200	(18,400)
3-Chloro-3′-methylazoxybenzene	"	2,340	(18,500)	2,600	(13,000)	3,280	(26,700)
3-Chloro-3′-methyl-4′-hydroxyazobenzene	"	2,470	(18,300)			3,600	(31,000)

Can. J. Chem. Downloaded from www.nrcresearchpress.com by 210.87.254.105 on 09/05/12
For personal use only.

absorption bands at the same wavelength as 2,2′-dimethyl-5,5′-dichloro-azo- and -azoxybenzene and their nitro derivatives, but with different intensities. This effect was probably due to the chlorine atoms which are in meta position to the azo and azoxy groups.

However, the 4,4′-diacetylamino derivatives of 2,2′-dimethyl-3,3′-dichloro- and 2,2′-dimethyl-5,5′-dichloro-azoxybenzene showed different absorption bands in region II. This difference could be ascribed to the effect of different dielectric constants of the solvents used such as dioxane or N,N-dimethylformamide. The same effect was also noticed with 2,2′-dimethyl-3,3′-dichloro-4,4′-dinitroazobenzene and 2,2′-dimethyl-4,4′-dinitro-5,5′-dichloroazobenzene with ether and chloroform as solvents.

EXPERIMENTAL

3-Methyl-3′-nitroazobenzene

A solution of *m*-nitrosotoluene (5.0 g, 0.041 mole) in ethanol and acetic acid (50 ml, 1:1 by volume) was warmed to 50° C and poured quickly into a warm solution of *m*-nitroaniline (5.0 g, 0.036 mole) in glacial acetic acid (50 ml). After thorough mixing, the reaction was allowed to proceed at room temperature for 12 hours. The mixture was diluted with water and extracted with ether. The ethereal extract was washed first with a 10% solution of sodium hydroxide, then with dilute HCl, and finally with distilled water. The process was repeated until the aqueous layer in each case was colorless. The ether was evaporated and the residue was crystallized from ethanol, m.p. 80–81° C. Yield, 1.7 g (18.4%). Calc. for $C_{13}H_{11}N_3O_2$: N, 17.4%. Found: N, 17.6%.

3-Chloro-3′-methylazobenzene

m-Nitrosotoluene and *m*-chloroaniline reacted as above gave the azo compound in 48% yield, m.p. 65° C. Calc. for $C_{13}H_{11}N_2Cl$: Cl, 15.4%. Found: Cl, 15.3%.

Wallach Rearrangement

3-Chloro-3′-methyl-4′-hydroxyazobenzene

3-Chloro-3′-methylazoxybenzene (1.0 g, 0.004 mole) was dissolved in sulphuric acid (*d*, 1.84, 20 ml) and kept at room temperature for 1 hour. The mixture was diluted with water and the precipitate filtered. The solid was dissolved in aqueous sodium hydroxide (5%) and precipitated with dilute hydrochloric acid. Crystallization from petroleum ether (b.p. 65–110° C) gave red crystals, m.p. 128–130° C. Yield, 0.4 g (40%). Calc. for $C_{13}H_{11}N_2OCl$: Cl, 14.4; N, 11.3%. Found: Cl, 14.2; N, 11.4%. Reduction with Sn and HCl gave 2-hydroxy-5-aminotoluene, which was identified as the dibenzoyl derivative, m.p. 194° C (lit. 194° C) (13). When sulphuric acid was replaced by chlorosulphonic acid at −8° C, the same results were obtained (13).

The other hydroxyazo compounds were prepared by the same method as above from the corresponding azoxy derivatives (1) and identified by the isolation of the reduction products as indicated in Table III.

Oxidations

3-Chloro-3′-methylazoxybenzene

3-Chloro-3′-methylazobenzene (2.3 g, 0.0099 mole) was dissolved in a mixture of glacial acetic acid (80 ml) and hydrogen peroxide (30%, 20 ml) and the solution stirred on a water bath for 6 hours. After dilution with water, the solid was filtered and crystallized from petroleum ether (30–65° C), m.p. 57–58° C. Yield, 2.4 g (99%). Calc. for $C_{13}H_{11}N_2OCl$: Cl, 14.4%. Found: Cl, 14.3%.

Bromination of 3-Chloro-3′-methylazoxybenzene

3-Chloro-3′-methylazoxybenzene (2.0 g, 0.0081 mole) was dissolved in glacial acetic acid (15 ml) and treated with an acetic acid solution of bromine (30%, 15 ml). A tiny crystal of iodine was added and the mixture heated on a water bath. After 1 hour, the reaction mixture was diluted with water and the excess bromine destroyed with sodium sulphite. Extraction with ether and crystallization from hot ethanol gave a bromo compound, m.p. 124° C. Yield, 1.1 g (33.5%). Calc. for $C_{13}H_9N_2OBr_2Cl$: BrCl, 48.8%. Found: BrCl, 46.9%. This compound gave a positive fluorescein paper test (14) for bromine. On reduction with Sn and HCl and subsequent benzoylation, a benzoyl derivative was prepared. Purification by chromatography on alumina (activity 3) and elution with petroleum ether (b.p. 65–110° C) gave a crystalline compound of m.p. 120° C in the first fraction. This compound did not depress the melting point of the benzoyl derivative prepared from *m*-chloroaniline. The second fraction came down as an oil which could not be crystallized. However, the positive fluorescein paper test showed the presence of bromine.

3-Methyl-3′-nitroazoxybenzene was obtained by the above method, m.p. 102–103° C. Calc. for $C_{13}H_{11}N_3O_3$: N, 16.3%. Found: N, 16.5%. It was brominated to give a compound melting at 111–112° C. Calc. for $C_{13}H_{10}N_3O_3Br$: Br, 23.8%. Found: Br, 24.0%. This bromo derivative was reduced and benzoylated as above to yield the dibenzoyl derivative of 1,3-diamino-4-bromobenzene, m.p. 186° C, and the monobenzoyl derivative of *m*-toluidine, m.p. 124° C.

Can. J. Chem. Downloaded from www.nrcresearchpress.com by 210.87.254.105 on 09/05/12
For personal use only.

Can. J. Chem. Downloaded from www.nrcresearchpress.com by 210.87.254.105 on 09/05/12
For personal use only.

TABLE III

Wallach Rearrangement

Hydroxyazobenzene derivatives	Reagent*	Temp. (°C)	Time (min)	M.p. (°C)	Yield (%)	Cryst. solvent	Analyses: Formula	Analyses: Calc. (%)	Analyses: Found (%)
3-Chloro-3′-methyl-4-hydroxyazobenzene	A	25	60	128–130	40	Pet. ether 65–110°	$C_{13}H_{11}N_2OCl$	N 11.3 Cl 14.4	N 11.4 Cl 14.2
	B	−8	”	”	45	”			
3-Methyl-3′-nitro-4′-hydroxyazobenzene†	A	98	10	137–138	75	Pet. ether 30–60°	$C_{13}H_{11}N_3O_3$	N 16.3	N 16.6
	B	−8	60	”	40	”			
2,2′-Dimethyl-4′-hydroxy-5,5′-dichloroazobenzene‡	B	−8	”	182–183	30	Pet. ether 65–110°	$C_{14}H_{12}N_2OCl_2$	Cl 24.0	Cl 24.1
	A	23	30	”	20	”			
2,2′,5,5′-Tetrachloro-4-hydroxy-4′-nitroazobenzene§		65	30	224	68	Acetone	$C_{12}H_5N_3O_3Cl_4$	C 37.8 H 1.54	C 38.1 H 1.51
	A	85	”	”	”	”			
		100	”	”	”	”			
2-Hydroxy-2′-nitro-4,4′,5,5′-tetrachloroazobenzene‖	A	90	15	162–163	50	Benzene Ethanol	$C_{12}H_5N_3O_3Cl_4$	Cl 37.5	Cl 37.3

*A: concentrated sulphuric acid (*d* 1.84); B: chlorosulphonic acid.
†Identified by reduction with Sn and HCl and preparation of the tribenzoyl derivative of 2,4-diaminophenol, m.p. 242° C (8).
‡Identified by reduction with Sn and HCl and preparation of the dibenzoyl derivative of 4-chloro-3-hydroxy-6-aminotoluene, m.p. 222° C (9).
§Reduced by Sn and HCl into 2,5-dichloro-1,4-diaminobenzene, m.p. 167° C (10), and 2,5-dichloro-4-aminophenol, m.p. 178° C (11).
‖Reduced by Sn and HCl into 3,4-dichloro-1,6-diaminobenzene, m.p. 160° C (12), while the other amino compound was oxidized and could not be isolated.

Ultraviolet and Visible Absorption Spectra Determinations

The ultraviolet and visible absorption spectra of azo- and azoxy-benzenes and related compounds described in an earlier paper (1) and the present one were determined on a Beckman DK1-A spectrophotometer. The results obtained in various solvents are given in Tables I and II.

REFERENCES

1. J. Singh, P. Singh, J. L. Boivin, and P. E. Gagnon. Can. J. Chem. **40**, 1921 (1962).
2. M. M. Shemyakin, C. E. Agadzhanian, V. I. Maimind, and R. V. Kudriavcev. Dokl. Akad. Nauk SSSR, **135**, 346 (1960).
3. M. M. Shemyakin, V. J. Maimind, and B. K. Vaichunaite. Chem. Ind. (London), 755 (1958).
4. P. H. Gore. Chem. Ind. (London), 191 (1959).
5. A. Angeli and B. Valori. Atti. Accad. Lincei. Ser. I, **21**, 729 (1912).
6. A. Burawoy. J. Chem. Soc. 1177 (1939).
7. G. M. Badger and R. G. Buttery. J. Chem. Soc. 2156 (1953).
8. R. Meldola and W. F. Hollely. J. Chem. Soc. **101**, 931 (1912).
9. L. C. Raiford. J. Am. Chem. Soc. **36**, 674 (1914).
10. D. Vorländer and M. Schröder. Ber. **34**, 1651 (1901).
11. G. Bargellini and L. Monti. Gazz. Chim. Ital. **59**, 30 (1929).
12. D. W. Wooley, E. A. Singer, and N. Smith. J. Biol. Chem. **194**, 729 (1952).
13. V. O. Lukashviech and T. N. Ku-Yomova. Zh. Obshch. Khim. **18**, 1963 (1948).
14. A. I. Vogel. Practical organic chemistry. 3rd ed. Longmans, Green. 1956. p. 1042.

Can. J. Chem. Downloaded from www.nrcresearchpress.com by 210.87.254.105 on 09/05/12
For personal use only.

PROTONATED γ-PYRONES*†

DENYS COOK
Exploratory Research Laboratory, Dow Chemical of Canada, Limited, Sarnia, Ontario
Received October 3, 1962

ABSTRACT

The vibrational spectra of several salts of 4-pyrone and 2,6-dimethyl-4-pyrone have been measured in the solid state. Deuterium replacement has been used to identify motions of the hydrogen atom which is located on the carbonyl oxygen atom and forms a hydrogen bond with the anion.

Bands due to OH stretching vibrations have been observed from 2086 cm^{-1} in the HCl salt to 3310 cm^{-1} in the hexachloroantimonate of 2,6-dimethyl-4-pyrone. In-plane hydrogen-deformation modes of the OH group have been found near 1300 cm^{-1} with a much smaller range in the different salts than the stretching vibration. For the 4-pyrone salts the OH stretching vibrations were at similar frequencies, and the in-plane hydrogen-deformation frequencies were close to 1340 cm^{-1}. Bands due to the out-of-plane deformation were not observed.

Aqueous solutions of 2,6-dimethyl-4-pyrone hydrochloride at various concentrations showed the presence of both protonated and neutral molecules.

INTRODUCTION

A comparison of the vibrational spectra of several Lewis acid complexes of 2,6-dimethyl-4-pyrone with that of the pyrone hydrobromide has clarified the assignments of γ-pyrones and also shown that the carbonyl oxygen atom was the basic site and not the heterocyclic oxygen atom (1).

These results are part of a general emerging pattern which shows, contrary to previous views, that carbonyl oxygen atoms can often be more basic than ether oxygen atoms. The circumstances leading to enhanced basicity in carbonyl groups have been discussed in detail (2, 3). The γ-pyrones satisfy most of the required conditions.

The basic nature of the γ-pyrones has been known for over 50 years since the pioneering work of Collie and co-workers (4). The structural details, however, were clouded by new conceptions on the quadrivalence of oxygen, based on ultraviolet absorption spectra (5), then a newly emerging art. Thus the heterocyclic oxygen atom was regarded as the basic site, partly by analogy with the alleged salt of dimethyl ether with HCl, which showed up as a dystectic point in an equimolar mixture of the two components (6). The concept of the hydrogen bond was not, of course, known at that time.

With the advance of modern spectroscopic methods, coupled with a fund of knowledge of spectroscopic behavior of many compounds, came a re-evaluation of the situation. Wolkenstein and Syrkin (7) examined the Raman spectrum of 2,6-dimethyl-4-pyrone hydrochloride in aqueous solution, and after noting little difference between the salt and the pyrone pronounced the carbonyl group as the protonation site. Similar conclusions were reached by Kahovec and Kohlrausch (8). The infrared spectra of several thiapyrones were recorded by Tarbell and Hoffman (9), who favored protonation of the carbonyl group in salts of such compounds. Phillips (10) deduced from the Raman spectrum of an aqueous solution of 4-pyrone hydrochloride that protonation was most likely to occur at the carbonyl oxygen atom. Tsubomura (11) also commented on some

Contribution No. 50.
†*This paper was presented, in part, at the 45th Canadian Chemical Conference, Edmonton, Alberta, May 29, 1962.*

Can. J. Chem. Downloaded from www.nrcresearchpress.com by 210.87.254.6 on 09/05/12
For personal use only.

similar compounds. Crystallographic data for the hydrobromide (12) revealed a monoclinic crystal with the following parameters: $a = 6.89$ Å; $b = 15.52$ Å; $c = 15.51$ Å; $\beta = 94.9°$. There were eight molecules per unit cell.

In order to make confident assignments for the vibrations involving the proton a series of γ-pyrones salts has been prepared, along with some deuterated analogues, and their infrared spectra recorded with a prism-grating spectrometer.

RESULTS AND DISCUSSION

2,6-Dimethyl-4-pyrone Salts

The infrared absorption bands in the various recorded spectra are collected in Table I. As shown previously (1) the bands near 1490 cm^{-1} are due to carbonyl stretching vibrations (II), the 1645 cm^{-1} bands being the C=C stretching mode, or a ring vibration having these characteristics, as in I. The strong band near 1555 cm^{-1} must also be due to a ring mode (III) involving stretching of C=C bonds (see below).

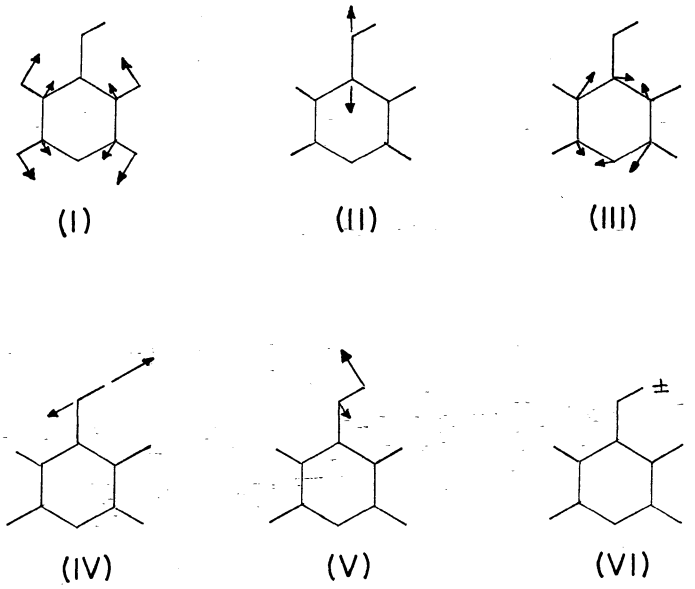

The prominent feature in the spectrum of the hydrochloride at 2086 cm^{-1}, with several subbands on either side, can only be due to the motion of a hydrogen atom attached to the carbonyl oxygen atom (IV). Its breadth, intensity, and position are all consistent with a strong interaction between the hydrogen atom and the halide ion. The frequencies and approximate half-widths of these bands for different anions are collected in Table II.

The behavior on deuteration has been observed for many of the salts studied and is quite characteristic of hydrogen bond formation. The OH bands move to lower frequencies, as shown in Table II, with a ratio of ν_{OH}/ν_{OD} close to 1.3. This is in keeping with a fairly pure hydrogen stretching motion.

The behavior of a protonated molecule forming a hydrogen bond with an anion had been discussed previously for pyridinium salts (13 and references therein to other systems). The pyrone salts presently considered exhibit a very similar behavior to the pyridinium series. As the size of the anion increases and the force field weakens the band attributed to the OH stretching vibration recedes to higher frequency. However, there is not a

Can. J. Chem. Downloaded from www.nrcresearchpress.com by 210.87.254.6 on 09/05/12
For personal use only.

great deal of evidence of significant sharpening of the bands, as some half-widths in Table II show. Nor is there any gross change in the intensity of the band in its passage to higher frequencies. While these measurements of intensity and half-width can be at best only a rough guide, they should be internally consistent. The half-widths in the deuterated compounds, however, do show a significant decrease.

The in-plane hydrogen-deformation mode (V) has been assigned to a medium-strong band which occurs near 1300 cm^{-1} in most of the compounds. On deuteration this moves to about 1000 cm^{-1}, the ratio δ_{OH}/δ_{OD} being, again, about 1.3, showing that the vibration is a reasonably pure one with little coupling with other modes (see Table III). The other vibration with which the in-plane hydrogen-deformation mode might be expected to couple is the carbonyl vibration which is at about 1490 cm^{-1}. In alcohols, and probably phenols, coupling between ν_{CO} and δ_{OH} is likely, since both have similar force constants and frequencies. In the present case, however, a separation of about 190 cm^{-1} is sufficient to preclude serious interaction, as is shown by the negligible change in ν_{CO} on deuteration.

It has been asserted that strong hydrogen bonds are associated with low stretching frequency and high bending frequency of the XH bond. In the series of pyridinium salts recently described (13) only a very rough relation was found between ν_{NH} and δ_{NH}. In the present case similar behavior was observed. A plot of ν_{OH} against δ_{OH} revealed a general trend with an inverse proportionality but with a wide scattering of points.

Accompanying the 1300 cm^{-1} band a weaker absorption near 1240 cm^{-1} was always present. This band moved to lower frequency on deuteration, to near 945 cm^{-1}, the ratio being about 1.3, showing a fairly pure vibration. The possibility that this could be an overtone of a strong band near 600 cm^{-1}, perhaps due to a torsional OH (or out-of-plane) motion, was discounted since no strong band in this region was found when a spectrum was recorded on an instrument without the limitations of NaCl optics. The assignment to a CD bending mode was also rejected since no stretching vibration was visible, and there is evidence that the hydrogens in the 3-position in 2,6-dimethyl-4-pyrone do not readily exchange (10). Coupling of the deformation mode in the unit cell seems the most likely cause of the splitting of this band, especially since the unit cell of the HBr salt is known to contain eight molecules (12).

The in-plane hydrogen-deformation mode being reasonably well assigned, an out-of-plane bending mode would be expected. No band has been found, however, in the appropriate place and with the right shift on deuteration. It must be concluded that this band is too low in frequency to be observed on a spectrometer equipped with sodium chloride optics.

Several other assignments are suggested in Table I, based on previous experience (1) and by comparison with similar molecules (10).

Aqueous Solutions of 2,6-Dimethyl-4-pyrone Hydrochloride

Previous studies of the Raman spectra of aqueous solutions of γ-pyrone salts (7, 8, 10) revealed very small differences between the spectra of the neutral pyrone and the salts. These small differences resulted in the assignment of the carbonyl oxygen atom as the probable protonation site. In view of the obvious differences between the infrared spectra of the neutral molecule and the salts, the aqueous solution spectra were required to explain these conflicting views. The bands in the spectra of aqueous solutions are shown in Table IV.

The spectrum of 2,6-dimethyl-4-pyrone in aqueous solution shows clearly two main strong bands at 1660 and 1582 cm^{-1}. These are assigned respectively to the ring mode I and the carbonyl vibration. The lower value of ν_{CO} in aqueous solution must be due

Can. J. Chem. Downloaded from www.nrcresearchpress.com by 210.87.254.6 on 09/05/12
For personal use only.

TABLE

	4-Pyrone									
	Cl^-		Br^-		Cl^-		Br^-		I^-	
	H	D	H	D	H	D	H	D	H	D
	3125w		3130w							
νCH	3070m		3067m		3070w	3075w			3052m	3050w
νCH	3050m, sh		3055w, sh		3044w	3050w	3040w	3040w	3040w	3020w
νCH_3					2993w	2998w	2990w	2990w	2988w	2987w
νCH_3					2913w	2913w	2910w	2910w		
			2658w				2655w	2025w		
			2608w							
			2572w	2070m			2550m	1970m	2850m	
			2518m	2002m			2438m	1911m	2745s, sh	2175w
			2435m	1939w	2149m, b		2404s	1870s, b	2720s, sh	2121m
νOH	2128s, b		2380m	1880s	2086m, b		2380s, b	1860s, b	2695vs, b	2079s
	2108s, b		2250w	1780w					2558s	1980m
	2040m			1756w	2050m, b				2491s	1920m
	1954m				1975m				2467s	1872m
	1838m, sh				1860m				2411m	
	1813m									
	1780m, sh									
	1765s				1788s					
			1630s, sh	1630s, sh	1655w, sh	1655m, sh	1658m, sh	1658m, sh	1655m, sh	1655m, sh
	1627s	1625s	1623s, sh	1623s, sh	1623s, sh	1637vs	1639vs	1639vs	1649s, sh	1650s, sh
νCC	1610s	1612s	1619s	1619s	1630vs	1633vs	1633vs	1630vs	1640vs	1639s
										1630s, sh
	1596s, sh	1595m, sh				1562w	1562w	1562w	1560m, sh	
νCC	1547m		1548m	1548m	1550s	1548s	1548s	1546s	1547s	1548s
		1528w		1530m	1540m, sh		1542s	1542s	1540s, sh	1542s
	1510m, sh	1510s, sh	1508m, sh							
	1500s, sh	1499vs								1490s, sh
νCO	1492vs	1495s, sh	1494s	1494s	1490s	1484s	1484s	1488s	1480s	1480s
	1485s, sh	1488s, sh	1490s, sh	1490s, sh					1470s, sh	1473s, sh
δCH_3					1416m	1412m	1417w	1420w	1411w	1409m
	1350s	1357m	1344m	1344m	1382m	1386w	1383w	1382w	1382w	1380w
					1360w	1362w	1359w	1355w	1359w	1357w
δCH_3					1326s	1320s	1329m	1329m	1329m	1328s
								1307w		
δOH	1343s, sh	1003s	1339m	988m	1316s	1010m	1307w	1002m	1290m	996m
		1320m		1318m						
δCH	1298s	1301m	1290s	1288s						
		1229m		1226m		1232m		1235w	1255w	
δOH	1209m	1058m	1203m	1052w	1210w		1209m	948m	1203m	939m
									1188w	1185w
δCH	1185s	1188s	1185s	1183s	1179s	1180s	1176s	1175s	1172s	1172s
					1072w		1074w	1070w		
					1046w	1048m	1046w	1046w	1044w	
νCC	1030w	1032m	1029w	1030m	1031m	1034m	1031m	1030m	1030m	
					973m	972m	976m	972m	978m	974m
δCC	941s	943vs	944s	943s	956m	956m	966w	948m	966w	
					921m	924m	921m	920m	920m	918m
			870m	883m	903m	904m	903m	896m	889m	888m
	861s	864s	858s	860s	895m	898m				885m, sh
δCC	848s	840m	847s	846s	866m	872m	854m			
			834m	840m						
				731w						
	658w	658w		660w		685m				

Can. J. Chem. Downloaded from www.nrcresearchpress.com by 210.87.254.6 on 09/05/12
For personal use only.

I

2,6-Dimethyl-4-pyrone

$HgCl_3^-$		ClO_4^-		$TiCl_6^=$	$ZrCl_6^=$	$SnBr_6^=$		$SnCl_6^=$	$PtCl_6^=$		$SbCl_6^-$
H	D	H	D	H	H	H	D	H	H	D	H
		3084m	3082m	3072m	3080s	3074s	3069m	3078s	3065m	3069m	3077w
3055w	3056w								3057m	3058m	
2895m, b	2200w, b										
2810m, b	2153m, b	2962m, b	2230m, b	3050s, b	3100s, b	3100s, b	2320mb	3100s, vb	3152s, vb	2350s, b	3310s, b
2740m, b	2120m	2940m, b		2602w							
2608m	1995w	2840w, b		2510w							
2515m	1938w										
									1655s, sh	1656s, sh	
1654s, sh	1655s, sh		1655vs	1653vs	1656vs	1658s, sh	1655m, sh	1654vs	1650vs	1650vs	1653vs
1646vs	1648vs	1655vs	1648vs	1650vs	1650vs	1651vs	1648vs	1650vs	1644vs	1644vs	1648vs
1640s, sh						1645vs	1642vs	1638m, sh	1638m, sh	1638s, sh	
1560m, sh	1560m, sh	1560s, sh	1560m, sh	1560s	1563s	1565s	1560m, sh	1562s	1561s	1561s, sh	1560s
1548m, sh	1548m	1550s, sh	1547s	1558s	1548s	1548s, sh	1551s	1559s		1552s	1555s
1538m	1540m, sh	1540s	1539s	1542m			1540s, sh	1542m	1542s	1547s	1540s
					1510w	1490s, sh	1490s, sh		1490m, sh	1490m, sh	1491s
1483s	1487s	1481s	1487s	1488m	1490s	1486s	1480s	1489s	1482s	1481s	1488s
1475s, sh					1477m, sh	1475m, sh	1475m, sh	1475m, sh	1475s, sh	1472s, sh	
1410w	1408w	1416m	1410m	1406w	1412m	1412w	1408w	1412w	1412w	1410w	1406w
1380vw	1380w	1360w	1360w		1380w	1380w	1378w	1379w	1380w	1380w	
					1362w	1365vw	1365vw	1362w	1365w	1364w	
1330s	1329m	1331m	1329s	1324m	1327s	1325s	1325s	1324s	1329s	1329m	1327m
								1310m, sh			
1308s	1002m	1300m	992m	1292m	1300m	1296m	992m	1290m, sh	1303m	1000m	1280m
		1252w	1232w								
1209w	945m	1209w	938m	1210w	1206w	1202m	935m	1210m	1213w	945m	1194w
				1204w				1205m, sh	1205w		
1178s		1180s	1178s	1175s	1166s	1174s	1174s	1174s	1176vs	1176m	1170s
1039m	1039m	1046s	1040s	1038w	1040m	1038m	1038m	1040m	1041m	1041m	1037m
1030m	1030m	1024s	1020s	1030w	1030m, sh	1030m	1028m	1030m, sh			1030m
979m	976m	980s	973s	978m	986m	978m	973m	979m	980m	977m	978m
963w		962m		962m	963w	962m		963w	965m	945m	963m
916m	913m	918m, sh	915s	910m	911s	910s	909m	911s	912m	912m	912m
876s	875m		890m	880m	880s	878s	876m	882s	887m	887m	865s
	859m	868m	862s	869m	868s	868s	864s	870s	878m	875m	856m
818m		800w, b					762w				
					707w						
					695w	682m					

Can. J. Chem. Downloaded from www.nrcresearchpress.com by 210.87.254.6 on 09/05/12
For personal use only.

TABLE II

OH and OD stretching frequencies in pyrone salts

	ν_{OH}	$\Delta\nu_{1/2}$*	ν_{OD}	$\Delta\nu_{1/2}$	ν_{OH}/ν_{OD}
		2,6-Dimethyl-4-pyrone salts			
Cl^-	2086	140	~1609		~1.30
Br^-	2364	172	1859	75	1.27
I^-	2695	200	2079	80	1.29
$HgCl_3^-$	2810		2153		1.31
ClO_4^-	2962		2230	160	1.33
$TiCl_6^=$	3050	215			
$ZrCl_6^=$	3100	180			
$SnBr_6^=$	3100	235	2320	110	1.34
$SnCl_6^=$	3100	200			
$PtCl_6^=$	3152	212	2350	112	1.34
$SbCl_6^-$	3310	170			
		4-Pyrone salts			
Cl^-	2128	190			
Br^-	2380	200	1880	110	1.27

*Approximate band half-widths: where none is given it could not be estimated because of overlapping of multiple bands.

TABLE III

OH and OD bending frequencies in pyrone salts

	δ_{OH}	δ_{OD}	Ratio	δ_{OH}	δ_{OD}	Ratio
			2,6-Dimethyl-4-pyrone salts			
Cl^-	1316	1010	1.30	1210		
Br^-	1307	1002	1.30	1209	948	1.28
I^-	1290	996	1.30	1203	939	1.28
$HgCl_3^-$	1308	1002	1.30	1209	945	1.28
ClO_4^-	1300	992	1.31	1209	938	1.29
$TiCl_6^=$	1294			1210		
$ZrCl_6^=$	1300			1206		
$SnBr_6^=$	1296	992	1.31	1202	935	1.29
$SnCl_6^=$	1290			1210		
$PtCl_6^=$	1303	1000	1.30	1213	945	1.28
$SbCl_6^-$	1280			1194		
			4-Pyrone salts			
Cl^-	1343	1003	1.34	1209	1058	1.14
Br^-	1339	988	1.35	1203	1052	1.14

to a hydrogen-bonded species CO···H—OH. These values of ν_{CC} and ν_{CO} fall reasonably well on a curve constructed from the values previously quoted in 2,6-dimethyl-4-pyrone complexes (1).

In the spectra of aqueous solutions of 2,6-dimethyl-4-pyrone hydrochloride, a band near 1490 cm^{-1} due to the carbonyl vibration of the protonated molecule should be observed. In aqueous solution the carbonyl proton may be hydrogen bonded, not to the Cl^- ion, as in the solid, but to the oxygen atom of a water molecule, and it would therefore be reasonable to assume a change in ν_{OH}. Such an interaction would not be expected to cause much alteration in ν_{CO} (for example, in $CHCl_3$ solution the hydrochloride has a carbonyl frequency at 1490 cm^{-1}, in almost exactly the same place as in the solid phase).

The spectra of the aqueous solutions do show the 1490 cm^{-1} band, indicating the presence of the protonated species, and this band gets more intense relative to other

Can. J. Chem. Downloaded from www.nrcresearchpress.com by 210.87.254.6 on 09/05/12
For personal use only.

TABLE IV

Bands in spectra of aqueous solutions of 2,6-dimethyl-4-pyrone and its hydrochloride

	2,6-Dimethyl-4-pyrone		2,6-Dimethyl-4-pyrone hydrochloride			
		H_2O sol.		H_2O sol.		
	Solid	2.5 *M*	Solid	1.0 *M*	2.5 *M*	5.0 *M*
ν_{CC} (H_2O)	1670vs	1660vs		1660vs	1658s	1660s
ν_{CC} (HCl)			1630vs	1645s	1642s	1642vs
ν_{CO} (H_2O)	1612vs	1582vs		1583s	1580m	1580m
ν_{CO} (HCl)			1490s	1498w	1490m	1492s
ν_{CC}	1600vs	1592s, sh				
ν_{CC}			1550s	1555m	1555s	1565s
	1432m	1430m		1430vw	1430w	1430w
δ_{CH_3}	1396s	1402s	1416m	1409w	1408m	1408m
	1372s		1382m	1375w	1370w	
δ_{CH_3}	1342m	1329m	1326s	1335m	1332m	1334m
δ_{OH}			1316s			
		1270w				
			1210w			
δ_{CH}	1200m	1194m	1179s	1192m	1190s	1190s
	1161s	1163m		1168w	1170m, sh	1166m
		1085w	1070w			
			1046w			
			973m	978w	975w	975w
	958m	948m	956m	948w	949w	950w
γ_{CH}	928m		921m			
	900s	904m	903m	908w	911m	912m
			895m			
γ_{CH}		872m	866m	872w	872m	876m

bands as the solution gets stronger. All the solutions gave spectra containing two doublets, at about 1660 and 1642 cm^{-1} and at about 1582 and 1555 cm^{-1}. Their intensities vary with the concentration. The low-frequency component of each doublet increases in intensity relative to the high-frequency one with increasing solution strength. Both these doublets are broad. The higher-frequency pair of bands is due to a C=C vibration (I) and indicates a proportion of both neutral and protonated species. The lower-frequency pair is not related, the 1582 cm^{-1} band being ν_{CO} interacting with H_2O, the 1555 cm^{-1} band being another ring mode (III). (See Table I.) This band was not confidently assigned previously (1) as in many of the complexes it was obscured by other bands.* The intensities again, though, indicate the presence of both species. The two sets of bands, together with the 1490 cm^{-1} band, show that the more dilute the solution the less the proportion of protonated material. Bands lower in frequency than 1400 cm^{-1} appear at about the same frequency in both materials.

It appears possible therefore to offer an explanation of the statement made previously that the Raman shifts in protonated and neutral molecules, *in aqueous solution*, are so similar (7, 8). In the Raman effect the OH stretching vibration produces only weak bands. The perturbed carbonyl vibration may also be expected to give rise to a weak band, since the protonated species has only C_s symmetry. For these reasons, therefore, the 2086 and 1490 cm^{-1} shifts were overlooked and the 1642 and 1555 cm^{-1} shifts regarded as due to the same vibration as in the neutral molecule. The broadness of the bands and the difficulty of exactly measuring the center also added complications.

**The spectrum of 2,6-dimethyl-4-thiopyrone contains two strong bands at 1640 and 1559 cm^{-1}. Since the* CS *stretching vibration is well removed from this region these two bands can be attributed to vibrations of type I and III respectively. In the* HBr *salt, these two bands are little changed in position at 1632 and 1528 cm^{-1}.*

Can. J. Chem. Downloaded from www.nrcresearchpress.com by 210.87.254.6 on 09/05/12
For personal use only.

It is significant that Wolkenstein and Syrkin (7) quoted a medium line at 1494 cm^{-1} in the aqueous solution of 2,6-dimethyl-4-pyrone hydrochloride, while the neutral molecule in aqueous solution had a very weak line at 1493 cm^{-1}. Kahovec and Kohlrausch (8) did not observe this line. The former authors used a solution approximately 2.3 *M* in the salt whereas the German authors used a solution of about 0.4 *M* (2 g hydrochloride in 5 ml H_2O).

4-Pyrone Salts

The bands in the spectra of 4-pyrone salts are shown in Table I; the OH stretching vibrations occur in positions similar to those of the 2,6-dimethyl-4-pyrone salts and show similar movements on deuteration (see also Table II). The in-plane hydrogen-deformation frequencies are close to 1340 cm^{-1} and, as for the 2,6-dimethyl-4-pyrone salts, are accompanied by a lower-frequency band near 1200 cm^{-1} (see Table III). On deuteration both bands disappear to be replaced by two new bands near 1050 and 1000 cm^{-1}. The ratios 1340/1050 = 1.28 and 1200/1000 = 1.20 indicate that mechanical effects may have some role in the value of the lower frequency. If the alternative ratios are considered, 1340/1000 = 1.34 and 1200/1050 = 1.14, then the higher-frequency band behaves normally, but the low ratio for the 1200 cm^{-1} band is difficult to understand.

The carbonyl vibration in the 4-pyrone salts also comes close to 1490 cm^{-1} and the C=C stretching vibration (I) moves to lower values in the salts, 1610 cm^{-1} compared with 1660 cm^{-1} in the neutral pyrone. The existence of some mechanical interaction between these two vibrations in the neutral pyrone, as proposed by Phillips (10), is therefore confirmed. These similarities between 4-pyrone and 2,6-dimethyl-4-pyrone are reasonable, and to be expected, as the replacement of a hydrogen atom by a methyl group is not expected to result in large changes in the properties of the carbonyl group, or its ability to protonate.

A few weak bands have been noticed in the 4-pyrone deuterated salts that have no analogue in the normal salts. These were at 1528, 1320, and 1229 cm^{-1} in the DCl salt, and at 1530, 1318, and 1226 cm^{-1} in the DBr salt. These must be attributed to combination tones or overtones of some band or bands associated with a low-frequency vibration involving the OD group. Strong bands in the 4-pyrone salts at 1185, 941, and 848 cm^{-1} could be combined with low-frequency vibrations at about 368 and 290 cm^{-1}, giving the following possible summation tones: 1185+368 = 1553 (1530); 941+368 = 1309 (1320); 941+290 = 1231 (1230); 848+368 = 1216 (1230). In the absence of a study of the deuterated molecules in the low-frequency region little progress can be made with these assignments. The possibility that exchange occurred between the ring protons and the deuterium in the acid is present, but is considered small since no indication of CD stretching absorption bands was noted.

In support of the assignments made for γ-pyrone salts the spectra of many 4-pyridone salts show almost identical features (14). The proton stretching bands occur in the same region and move to higher frequencies as the anion gets larger. The in-plane hydrogen-deformation vibration is near 1300 cm^{-1} (and is also doubled), moving close to 1000 cm^{-1} on deuteration. This is so similar to the 4-pyrone series that a similar structure, i.e. protonated at the carbonyl group, is suggested. Nuclear magnetic resonance experiments have been interpreted as being consistent with this view (15). N-Protonation can be rejected on a further count; such a structure would be similar to tertiary amine salts, which have bending modes near 1400 cm^{-1}, for example, trimethylamine salts,

Can. J. Chem. Downloaded from www.nrcresearchpress.com by 210.87.254.6 on 09/05/12
For personal use only.

1420 cm^{-1} (16, 17); N-alkylpiperidine salts, 1400 cm^{-1} (14); triphenylamine salts, 1390 cm^{-1} (17). The absence of a band near 1400 cm^{-1} with the appropriate shift on deuteration is strong evidence against N-protonation.

EXPERIMENTAL

The Spectra

A Perkin–Elmer model 221 prism-grating spectrometer was used to record the spectra. Solid-state spectra were of emulsions of the finely ground solid in nujol and fluorolube. Aqueous solution spectra were of thin films trapped between Irtran plates. Difference spectra were obtained by inserting a thin film of water between Irtran plates in the reference beam. A trial and error method of exact compensation was used by varying the pressure on the plates. While small differences in intensity were noted in various spectra no shifts in position in bands below about 1700 cm^{-1} were observed. The water bands in the 3-μ region varied considerably, but have not been used for diagnostic purposes.

2,6-Dimethyl-4-pyrone Salts

2,6-Dimethyl-4-pyrone was prepared from dehydroacetic acid by boiling with concentrated HCl followed by evaporation of the liquid to give the hydrated HCl salt. This was then recrystallized from pyridine to give the pyrone, which was then recrystallized from methanol. M.p. 131–133°.

Hydrochloride.—1 g 2,6-dimethyl-4-pyrone in 10 ml $CHCl_3$ and 50 ml ether when treated with anhydrous HCl gave a copious precipitate of the salt. M.p. 153–155°. This was used without further treatment. Due to its hygroscopic nature and ready hydration to the dihydrate it was handled in a dry box. To prepare the DCl salt a CCl_4 solution of the anhydrous pyrone was treated with excess DCl in a vacuum system. The excess DCl and all solvent were removed by evacuation, the solid being subsequently handled in a dry box.

Hydrobromide.—Exactly the same techniques as for the HCl salt were used. M.p. 192–193°. DBr was used to make the deuterated salt.

Hexabromostannate.—The hydrobromide was prepared as above, and redissolved in $CHCl_3$. Excess $SnBr_4$ then precipitated a white deposit of the hexabromostannate. M.p. 195–197°.

Hexachlorostannate.—Same procedure using $SnCl_4$. M.p. 210–213°.

Hexachlorotitanate.—Same procedure using $TiCl_4$. Dry box handling was necessary.

Hexachloroplatinate.—1.24 g 2,6-dimethyl-4-pyrone was dissolved in 20 g 10% aqueous $H_2PtCl_6 . 6H_2O$. After 4 days light brown crystals started forming. M.p. 188–190°. The deuterated material was made by twice exchanging with a 100-fold excess of D_2O and removing the excess D_2O *in vacuo*.

Hexachloroantimonate.—The procedure for the hexabromostannate was followed but with HCl and $SbCl_5$. M.p. 92–94°.

Hydroiodide.—Aqueous HI was shaken with ether, the ethereal layer after separation being added to a solution of the pyrone in a little $CHCl_3$ and excess ether. The pale yellow solid so formed was used without further purification. M.p. 176–179°.

Perchlorate.—1.68 g aqueous 70% perchloric acid was added to 1.24 g pyrone in 3 ml H_2O, and excess H_2O removed *in vacuo*. M.p. 78–80°.

Trichloromercurate.—An acetone solution of the pyrone:$HgCl_2$ complex was treated with dry HCl gas, and a deposit of the solid was found when the excess solvent was removed on a vacuum line. M.p. 118–120°.

Hexachlorozirconate.—A solution of the pyrone.HCl in $CHCl_3$ was added to a $CHCl_3$ solution of $ZrCl_4$, giving a white precipitate of the complex salt. M.p. 257–259°.

Aqueous Solutions

Aqueous solutions of 2,6-dimethyl-4-pyrone hydrochloride were prepared from the dihydrate. Solutions 1.0, 2.5, and 5.0 *M* were used. The solution of the pyrone in water was 2.5 *M*.

4-Pyrone Salts

4-Pyrone was prepared by the decarboxylation of chelidonic acid by heating with copper powder to about 300° C.

Hydrochloride.—Dry HCl gas was passed into a solution of pyrone in $CHCl_3$ and ether. The white solid so formed, m.p. 132–134°, was used without further treatment, and due to its hygroscopic nature, handled in a dry box. The deuterated salt was prepared from a CCl_4 solution of the pyrone and DCl using a high-vacuum apparatus. The excess fluid was decanted, leaving a white solid which was subsequently handled in a dry box. Attempts to remove solvent by evacuation resulted in decomposition of the solid.

Hydrobromide.—The pyrone in a little $CHCl_3$ and excess ether when treated with HBr gas gave a white solid. An indeterminate melting point was observed with charring between 150° and 180°. The DBr salt was obtained from a benzene solution of the pyrone though not with complete isotopic exchange. All deuterated salts were made by exchange with excess D_2O unless otherwise stated. Melting points were taken in sealed capillary tubes and are uncorrected.

Can. J. Chem. Downloaded from www.nrcresearchpress.com by 210.87.254.6 on 09/05/12
For personal use only.

ACKNOWLEDGMENT

The assistance of Miss C. D. Anderson in preparing some of the compounds and recording their spectra is gratefully acknowledged.

REFERENCES

1. D. Cook. Can. J. Chem. **39**, 1184 (1961).
2. D. Cook. J. Am. Chem. Soc. **80**, 49 (1958).
3. D. Cook. Can. J. Chem. **39**, 31 (1961).
4. J. N. Collie and T. Tickle. J. Chem. Soc. **75**, 710 (1899).
5. E. C. C. Baly, J. N. Collie, and H. E. Watson. J. Chem. Soc. **95**, 144 (1909).
6. O. Maass and D. McIntosh. J. Am. Chem. Soc. **34**, 1273 (1912).
7. M. W. Wolkenstein and J. K. Syrkin. Acta Physicochim. URSS, **10**, 677 (1939).
8. L. Kahovec and K. W. F. Kohlrausch. Ber. Sect. B, **75**, 627 (1942).
9. D. S. Tarbell and P. Hoffman. J. Am. Chem. Soc. **76**, 2451 (1954).
10. W. D. Phillips. Ph.D. Thesis, Massachusetts Institute of Technology, Cambridge, Mass., U.S.A. 1951.
11. H. Tsubomura. J. Chem. Phys. **28**, 355 (1958).
12. H. Hope. Acta Chem. Scand. **14**, 765 (1960).
13. D. Cook. Can. J. Chem. **39**, 2009 (1961).
14. D. Cook. Unpublished results.
15. A. R. Katritzky and R. A. Y. Jones. Proc. Chem. Soc. 313 (1960).
16. E. A. V. Ebsworth and N. Sheppard. Spectrochim. Acta, **13**, 261 (1959).
17. R. H. Nuttall, D. W. A. Sharp, and T. C. Waddington. J. Chem. Soc. 4965 (1960).

Can. J. Chem. Downloaded from www.nrcresearchpress.com by 210.87.254.6 on 09/05/12
For personal use only.

INFRARED SPECTRA OF COMPLEXES OF 4-PYRIDONES*†

DENYS COOK

Exploratory Research Laboratory, Dow Chemical of Canada, Limited, Sarnia, Ontario

Received October 19, 1962

ABSTRACT

The infrared spectra of many complexes of Lewis acids with some 4-pyridones have been recorded. Large shifts to lower frequencies of about 100 cm^{-1} have been observed in a band near 1560 cm^{-1} as the Lewis acid strength increased. Much smaller shifts of about 5 to 10 cm^{-1} in a band near 1640 cm^{-1} were noted. The former band has therefore been designated as the carbonyl frequency, and the latter as a ring mode involving CC stretching.

The donor site of 4-pyridones is therefore the carbonyl group, and not the nitrogen atom. Protonated 4-pyridones have similar spectra, and are consistent with O-, not N-protonation.

INTRODUCTION

In a recent paper (1) it was shown how the carbonyl frequency in 4-pyrones could be correctly identified by forming Lewis acid complexes of the pyrones and observing a very large shift to lower frequency for the carbonyl vibration, but a much smaller one for the other ring modes. A further point became clear in that 4-pyrones protonate at the carbonyl oxygen atom, and not at the heterocyclic oxygen atom (2).

In the 4-pyridones a situation similar to that in the 4-pyrones exists, namely, that a higher-frequency band at 1640 cm^{-1} (chloroform solution) and a lower-frequency band at 1560 cm^{-1} have not been clearly assigned. At first sight the 1640 cm^{-1} band would be assigned to ν_{CO} and the 1560 cm^{-1} band to ν_{CC}, a ring mode, probably similar to ν_8 in benzene. In 2,6-dimethyl-4-pyrone the carbonyl frequency in its unperturbed state (some slight interaction with the ring mode was observed) was found close to 1645 cm^{-1}. It would therefore be a little surprising to find a carbonyl frequency near 1640 cm^{-1} for the 4-pyridones. In 4-pyrones the degree of participation of the lone-pair electrons on the heterocyclic oxygen atom in ring conjugation was assumed to be small. In pyridones there is good reason for believing the N—R bond to be coplanar with the ring, with the nitrogen lone pair electrons in a $p\pi$-type orbital which can participate in an extended molecular orbital over all the heavy atoms. A lower bond order, and therefore frequency, should be expected for the carbonyl group in 4-pyridones than in 4-pyrones. The same sort of arguments have been used by Bellamy and Rogasch (3) in their paper on solvent shifts of polar bands in 1-methyl-4-pyridones.

A further objective of the present work was to investigate the ability of the ring nitrogen atom in 4-pyridones to coordinate Lewis acids or protons. It has been suggested that the 4-pyridone cation contains a quaternary nitrogen atom (4, 5), though some recent n.m.r. experiments have discounted this suggestion (6). It should be said that the present work is consistent with protonation at the oxygen atom and not at the nitrogen atom.

RESULTS

Table I shows the bands in the various spectra of 1,2,6-trimethyl-4-pyridone complexes. The band at 1635 cm^{-1} in the pure solid varies by only a few reciprocal centimeters

*Contribution No. 53.

†*This work was presented, in part, at the Eighth Ottawa Symposium on Applied Spectroscopy, September 20, 1961.*

Can. J. Chem. Downloaded from www.nrcresearchpress.com by 210.87.254.105 on 09/05/12
For personal use only.

Can. J. Chem. Downloaded from www.nrcresearchpress.com by 210.87.254.105 on 09/05/12
For personal use only.

TABLE I

Infrared bands in spectra of 1,2,6-trimethyl-4-pyridone complexes

	Nujol	$CHCl_3$	$CdCl_2$	$CaCl_2$	$SnBr_4$	$HgCl_2$	$ZnCl_2$	HCl
ν_{OH}								2410s, b
		1640s	1639m, sh	1635s, sh	1637s, sh	1639m, sh	1639w, sh	1636s
ν_{CC}	1635s	1630s, sh	1628s	1630s	1629s	1624s	1624s	1630s
			1620m, sh			1620s, sh	1620s, sh	1620w, sh
ν_{CO}	1560s	1561s	1502s	1497s	1495s	1492s	1492s	1480s
ν_{CC}	1549m	1551s, sh	1552m	1560m, sh	1570m	1548m	1562m	1586m
		1542s, sh	1542m	1552s	1560m	1542m, sh	1556m, sh	
							1542m, sh	1522w
			1510s, sh	1505s, sh	1504s, sh	1498s, sh	1498s, sh	
			1492s, sh		1482s, sh		1490s, sh	
	1472w	1480w	1472w, sh			1472m, sh	1474s, sh	
δ_{CH}	1446w	1443w	1436m	1436m	1430m	1440m	1443s	1440w
	1412m	1419m	1423m	1415m				1402w
	1380w		1368vw	1374m	1385m	1380w	1380w	1361w
δ_{CH}	1354s	1351s	1342s	1342s	1342s	1346s	1340s	1325s
δ_{OH}								1275m
δ_{OH}								1230m
			1195m	1200m	1181s	1192m	1190s	1180m
δ_{CH}	1182m	1188m	1182s	1180s	1176s, sh	1179s	1170s	1168s
	1100vw			1115vw				
	1041m	1050w			1040m			1046m
ν_{CC}	1031w	1030w	1027w	1028m		1032w	1032w	1036m
				962vw				980vw
	956w	953w						
	935vw	930w		936vw	942vw			936vw
γ_{CH}	887m	868s	881s	880s	880m	858m	865s	878s
				845vw		847w	860m, sh	858vw
				787vw				785vw
	748w		760m	759m		753w	747m	761m
	713m			720m	730w			

in the complexes and in a random manner. The band at 1560 cm^{-1} in the pure 4-pyridone shows a trend to lower frequencies as the Lewis acid gets stronger.

This behavior is closely duplicated by the 1-ethyl-2,6-dimethyl-4-pyridone complexes. Table II shows the bands abstracted from the spectra. The absorption band at about 1638 cm^{-1} does not move consistently in any direction but is scattered around a central value of about 1638 cm^{-1}. This, and the other band at about 1550 cm^{-1}, are assigned to ring vibrations. The band at 1566 cm^{-1} moving progressively to 1461 cm^{-1} is the carbonyl stretching vibration. All other bands are in approximately constant position.

The hydrochloride of each pyridone has also been prepared and the bands are listed in the tables for comparison.

DISCUSSION

These new values for carbonyl frequencies of 4-pyridones shown in the tables appear much more reasonable when compared with other carbonyl frequencies, as was noted by Bellamy and Rogasch (3). Furthermore, they introduce additional support for the contention previously advanced that the heterocyclic oxygen atom in 4-pyrones does not participate, or at least, to a very small extent, in conjugation with the ring. In this connection the data in Table III are of interest. In the compounds in series II there is no change in carbonyl frequency when CH_2 (II*a*) is replaced by O (II*b*). Since little difference in geometry is expected in the two compounds, and inductive effects should be of secondary importance, the degree of interaction of the oxygen lone pair electrons with other π-electrons is inferred to be small. (A similar small degree of interaction has also been suggested for the alkoxy oxygen atom in phenyl acetate (7).) On NH-substitution, there is a significant drop in frequency in both series, I*c* and II*c*, a certain amount of which is due to hydrogen bonding. When the opportunity for this is removed by alkyl substitution (I*d*), the compound still has a lower frequency than the oxygen compound (I*b*), and all other things being equal, must be due to a lower bond order in the CO group. Furthermore, while anthrone (II*a*) and xanthone (II*b*) are both nearly colorless, acridone (II*c*) has a pronounced yellow color.

The carbonyl frequency shifts observed on complex formation seem a little smaller than the corresponding shifts in the 4-pyrone series. In the present series the largest one is about 100 cm^{-1}, while in the 4-pyrone series it was about 150 cm^{-1}. These figures are not strictly comparable since the same Lewis acids were not used in each series. One would have expected larger shifts for the 4-pyridones than for the 4-pyrones, on the assumption that the former are better donors than the latter. (Susz has recently summarized (8) the results of carbonyl shifts in various complexes of ketones with Lewis acids, and found that the shift, $\Delta\nu$, for the same Lewis acid increased in the series acetone < 4-heptanone < acetophenone < benzophenone. This is in the order of decreasing carbonyl frequency, ionization potential, and therefore increasing donor ability (7, 9).) There are a few irregularities in the shifts that one particular Lewis acid generates with different donors. In some unpublished work on xanthone complexes the BBr_3 complex gives next to the BI_3 complex the largest shift, whereas in the 4-pyridones $TiCl_4$ and $SbCl_5$ give larger shifts. The xanthone complex shifts have been compared with the ethyl acetate shifts measured by Lappert (10), and though the general orders are similar there are some anomalies.

It should be emphasized at this point that in the complexes little variation occurs in the position of any band with the exception of that due to the carbonyl stretching vibration, which is perturbed to lower frequency, and is an acceptable criterion of complex

Can. J. Chem. Downloaded from www.nrcresearchpress.com by 210.87.254.105 on 09/05/12
For personal use only.

Can. J. Chem. Downloaded from www.nrcresearchpress.com by 210.87.254.105 on 09/05/12
For personal use only.

TABLE II

Infrared bands from the spectra of 1-ethyl-2,6-dimethyl-4-pyridone complexes

	Nujol	$CoCl_2$	$CdCl_2$	$HgCl_2$	$ZnCl_2$	$SnBr_4$	BBr_3	$TiCl_4$	$SbCl_5$	HCl
ν_{OH}										2498
		1638m, sh								1640s, sh
		1625s, sh								
ν_{CC}	1638s	1619s	1623s	1628s	1623s	1616s	1628s	1619s	1618s	1632s
	1632s, sh			1620s, sh						
ν_{CC}	1547m	1546m	1551m	1548m	1554m	1549m			1548m	1584s
ν_{CO}	1566s	1510s	1510s	1493s	1477s	1470s	1470s	1464s	1461s	1478s
		1502s, sh		1502s	1502m		1498m	1493m	1494s	1512m
	1474w	1484s	1482m			1495s				1502m
	1444m							1440m, sh	1458s, sh	1460m
δ_{CH}	1412m	1419m	1420w	1418w	1422w		1422w	1410m	1432m, sh	1440m
	1382vw	1383m, sh		1380w, sh				1380w	1365w, sh	1363m
δ_{CH}	1368m	1367s	1365m	1368s	1362s	1357s	1353s	1353s	1350m	1347m
	1340s	1348s	1328s	1334s	1326s	1318s	1312s	1311s	1310s	1327s
		1324s								
δ_{OH}										1309s
		1250w	1250w				1254m	1258m	1258m, sh	
δ_{OH}										1233m
	1216w	1220w			1225vw	1216w	1224w		1225w, sh	
	1192w	1191s	1192m	1194m	1189m	1180m, sh	1180m	1176s		1182m
δ_{CH}	1178s	1170s	1173s	1174s	1165s	1167s	1156s	1153s	1155s	1164s
					1150m, sh	1160s, sh				
	1110w	1116w								1123w
	1054w	1080m	1077w	1076w	1077w	1077m	1080m, sh	1080m	1082m	1090m
	1040w	1039m						1042m	1040m	1052m
ν_{CC}	1035w	1030m	1028w	1030w	1030w	1026m	1027w	1028m	1030m	1030w
	950w	967w		965vw	980w	980w		988m	987m	968w
	892w							880m	880m	895m
γ_{CH}	880w	883s	878m	870m	870m	867m	864s	878m	873m, sh	878s
	874w	865m		857m	862m					862s
		861m			842w					
		800w	798w		800vw		797m	794vw		805w
										788w
										764w
		732m	730m		730m	732m	730m, sh	734s	740m	
	720w	720m	720m		720m	720w	720m	722m, sh	722m	720w
								702w		

TABLE III

Carbonyl frequencies in pyridones and related molecules

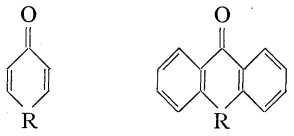

I II

	R	I	II
a	CH_2		1669 (CCl_4)
b	O	1639 (CCl_4)	1669 (CCl_4)
c	NH	1550 ($CHCl_3$)	1558 ($CHCl_3$)
d	NCH_3	1598 (C_6H_6)	1604 ($CHCl_3$)

formation at the carbonyl oxygen atom. Additional evidence is now available which helps to confirm this view. The evidence is derived from studies of complexes of Lewis acids with heterocyclic molecules, in which the donor atom is the ring heterocyclic atom. Pyridine complexes have been exhaustively studied (11–17) and experiments are in progress in this laboratory with complexes of benzothiazole, benzoxazole, and similar compounds. The conclusion being formed is that these complexes reveal spectra quite different from the parent heterocycle, but that over the whole range of Lewis acids the spectra remain remarkably similar to each other, with but minor changes in frequency in some bands. In the pyridine complexes it has been noted that there seems to be a trend towards higher frequency in a band near 1000 cm^{-1} due to the breathing mode as the Lewis acid gets stronger (16). This is only about 20 cm^{-1}, however, and even this figure may be somewhat high as there was some discrepancy in the frequency of the compound at the head of the list, as determined in two laboratories. In benzothiazole and benzoxazole complexes the similarity of the spectra for different Lewis acids has been noted, but detailed analysis is not sufficiently advanced to be able to see if the trend as shown by the pyridine series is duplicated. The conclusion to be drawn is that a very useful method of distinguishing between complex formation at ring donor atoms, or at exocyclic donor atoms, is possible. The former give practically no change, or, at most, a slight increase in frequency in the breathing mode, while the latter give spectra having one band which shows a large, progressive decrease in frequency as the Lewis acid strength in the complex increases.

4-Pyridones protonate readily. The spectra of the protonated materials are very similar to those of the complexes, with additional bands due to the hydrogen vibrations. It has been suggested (3, 4) that the nitrogen atom was the protonation site, but n.m.r. studies have been interpreted as supporting protonation at the carbonyl oxygen atom (6). The results of the present work are in better agreement with the latter view. In the first place the carbonyl frequency is displaced to about 1480 cm^{-1}. Protonation at the nitrogen atom would have a minor effect on the carbonyl frequency, and would result in a shift to a higher frequency if anything, because of the inductive effect of the formal positive charge on the nitrogen atom. Secondly, protonation at the nitrogen atom would result in a structure similar to that of a tertiary amine salt.* These have bending frequencies at about 1400 cm^{-1}: trimethylamine salts, 1420 cm^{-1} (18); N-alkylpiperidine

**Although* HN^+ *stretching modes are analytically of little value, the* HN^+ *bending mode shows promise of being an excellent group frequency, and diagnostically very useful in determining the type of nitrogen atom.*

Can. J. Chem. Downloaded from www.nrcresearchpress.com by 210.87.254.105 on 09/05/12
For personal use only.

salts, 1400 cm^{-1} (17); triarylamine salts, 1390 cm^{-1} (19). The pyridone salts have bands due to in-plane hydrogen deformations at about 1290 cm^{-1}, close to values for a hydrogen atom attached to a trigonal nitrogen or oxygen atom, for example, pyridinium salts, 1240 cm^{-1} (20); benzothiazolium salts, 1210 cm^{-1} (17); 4-pyrone salts, 1340 cm^{-1} (2); 2,6-dimethyl-4-pyrone salts, 1300 cm^{-1} (2); N,N-dicyclohexylacetamide salts, 1300 cm^{-1} (21). It is hoped to publish more details of the 4-pyridone salts shortly.

EXPERIMENTAL

The Spectra

A Perkin–Elmer model 221G prism-grating spectrometer was used to record the spectra. Those of solids were obtained as emulsions in nujol and fluorolube.

Materials

The compounds and complexes were prepared as follows.

1,2,6-Trimethyl-4-pyridone and Complexes

1,2,6-Trimethyl-4-pyridone was prepared from 2,6-dimethyl-4-pyrone by the reaction with methylamine. M.p. 241–243°. Hydrate 110–111°.

$CdCl_2$ complex was prepared from equimolar ethanolic solutions of each component. It was recrystallized from ethanol. M.p. over 300° C.

$HgCl_2$ complex was prepared by mixing hot acetone solutions of equivalents of each compound. The resulting white precipitate was recrystallized from acetone/methanol and melted at 191–193°. Found: C, 23.62%; H, 2.96%; N, 3.36%. Calc. for $C_8H_{11}NO.HgCl_2$: C, 23.5%; H, 2.70%; N, 3.43%.

$ZnCl_2$ complex was prepared in the same way as for the $HgCl_2$ complex. M.p. over 300°. Found: C, 35.77%; H, 3.94%; N, 5.09%. Calc. for $C_8H_{11}NO.ZnCl_2$: C, 35.2%; H, 3.94%; N, 5.09%.

$CaCl_2$ complex was prepared from acetone/ethanol solutions of equivalents, giving a white solid. M.p. over 300°.

$SnBr_4$ complex was obtained by adding 1 equiv of $SnBr_4$ to a $CHCl_3/CCl_4$ solution of 2 equiv of the pyridone. The precipitate was used without further treatment after filtering in a dry box. M.p. 284–286°

HCl salt was made from a solution of the pyridone in a little absolute ethanol and excess ether by saturating with HCl gas. The solid hydrochloride melted at 260–261°. Found: HCl, 22.2%. Theory: HCl, 22.36%.

1-Ethyl-2,6-dimethyl-4-pyridone and Complexes

The pyridone was prepared by the reaction of 2,6-dimethyl-4-pyrone and ethylamine. M.p. 158–161°. Hydrate 72–74°.

HCl salt was precipitated from a solution of the pyridone in a little dry ethanol and excess ether with HCl gas. M.p. 242–244°. Found: HCl, 19.2%. Theory: HCl, 19.44%.

$CoCl_2$ complex was prepared by mixing equivalents of hot ethanolic solutions of the two components, giving a deep blue solid on cooling. M.p. 267–269°. Found: C, 49.84%; H, 5.41%; N, 6.29%. Calc. for $(C_9H_{13}NO)_2.CoCl_2$: C, 50.0%; H, 6.02%; N, 6.48%.

$CdCl_2$ complex was prepared in the same way. M.p. 258–261°. Found: C, 31.65%; H, 3.74%; N, 4.00%. Calc. for $C_9H_{13}NO.CdCl_2$: C, 32.3%; H, 3.89%; N, 4.19%.

$HgCl_2$ complex precipitated when hot acetone solutions of equivalents were mixed and cooled. M.p. 165–167°. Found: C, 25.60%; H, 3.32%; N, 3.25%. Calc. for $C_9H_{13}NO.HgCl_2$: C, 25.6%; H, 3.08%; N, 3.32%.

$ZnCl_2$ complex crystallized when warm solutions of an equivalent of each component in acetone were mixed and allowed to cool. M.p. 257–262°. Found: N, 4.89%. Calc. for $C_9H_{13}NO.ZnCl_2$: N, 4.88%.

$SnBr_4$ complex was precipitated when 1 equiv of $SnBr_4$ in CCl_4 was added to 2 equiv of the pyridone in a little $CHCl_3$ and excess CCl_4. M.p. 110–114°.

BBr_3 complex was made by mixing CH_2Cl_2 solutions of equivalents in a small pyrex cell and removing excess CH_2Cl_2 on a vacuum line.

$TiCl_4$ complex was prepared in the same way. Found: C, 30.8%; H, 4.06%. Calc. for $C_9H_{13}NO.TiCl_4$: C, 31.6%; H, 3.81%.

$SbCl_5$ complex was prepared by the addition of $SbCl_5$ to a $CHCl_3/CCl_4$ solution of the pyridone. M.p. 160–165°. Found: C, 24.18%; H, 3.42%; N, 2.94%. Calc. for $C_9H_{13}NO.SbCl_5$: C, 24.0%; H, 2.89%; N, 3.11%.

The preparations listed after the $ZnCl_2$ complex were performed throughout in the dry box. All melting points were determined in sealed capillary tubes and were uncorrected.

ACKNOWLEDGMENT

The technical assistance of Miss C. D. Anderson is gratefully acknowledged.

REFERENCES

1. D. Cook. Can. J. Chem. **39**, 1184 (1961).
2. D. Cook. Can. J. Chem. **41**, 505 (1963).

Can. J. Chem. Downloaded from www.nrcresearchpress.com by 210.87.254.105 on 09/05/12
For personal use only.

3. L. J. BELLAMY and P. E. ROGASCH. Spectrochim. Acta, **16**, 30 (1960).
4. E. SPINNER. J. Chem. Soc. 1226 (1960).
5. E. SPINNER. J. Chem. Soc. 1232 (1960).
6. A. R. KATRIZKY and R. A. Y. JONES. Proc. Chem. Soc. 313 (1960).
7. D. COOK. J. Am. Chem. Soc. **80**, 49 (1958).
8. B. P. SUSZ. Compt. Rend. **248**, 2569 (1959).
9. D. COOK. Can. J. Chem. **39**, 31 (1961).
10. M. F. LAPPERT. J. Chem. Soc. 542 (1961).
11. A. R. KATRITZKY. J. Chem. Soc. 2049 (1959).
12. N. N. GREENWOOD and K. WADE. J. Chem. Soc. 1130 (1960).
13. N. S. GILL, R. H. NUTTALL, D. E. SCAIFE, and D. W. A. SHARP. J. Inorg. Nucl. Chem. **18**, 79 (1961).
14. A. N. TERENIN, V. N. FILIMONOV, and D. S. BYSTROV. Z. Elektrochem. **62**, 180 (1958).
15. G. S. RAO. Z. Anorg. Allgem. Chem. **304**, 176 (1960).
16. V. N. FILIMONOV and D. S. BYSTROV. Opt. i Spektroskopiya, **12**, 66 (1962).
17. D. COOK. Unpublished results.
18. E. A. V. EBSWORTH and N. SHEPPARD. Spectrochim. Acta, **13**, 261 (1959).
19. R. H. NUTTALL, D. W. A. SHARP, and T. C. WADDINGTON. J. Chem. Soc. 4965 (1960).
20. D. COOK. Can. J. Chem. **39**, 2009 (1961).
21. D. COOK. Can. J. Chem. **40**, 2362 (1962).

Can. J. Chem. Downloaded from www.nrcresearchpress.com by 210.87.254.105 on 09/05/12
For personal use only.

INFRARED SPECTRA OF XANTHONE:LEWIS ACID COMPLEXES*†

DENYS COOK
Exploratory Research Laboratory, Dow Chemical of Canada, Limited, Sarnia, Ontario
Received October 19, 1962

ABSTRACT

Xanthone, a member of the γ-pyrone species, which have basic carbonyl groups, forms an excellent series of solid complexes with Lewis acids. In these complexes the carbonyl oxygen atom is the donor site, and the carbonyl stretching vibration moves to progressively lower frequency as the Lewis acid strength increases. The carbonyl frequency in the BI_3 complex, 1400 cm^{-1}, is one of the lowest encountered in complexes of this type.

The wide range of Lewis acids used to form these complexes has enabled a quantitative estimate of the Lewis acid strength to be made, which compares reasonably well with previous estimates.

INTRODUCTION

The γ-pyrones have basic carbonyl groups and form salts with mineral and organic acids (1). They also form stable complexes with Lewis acids (2). The perturbation of the carbonyl stretching frequency in Lewis acid complexes of 2,6-dimethyl-4-pyrone was used recently to identify the carbonyl vibration in such pyrones, and to prove the site of protonation as the carbonyl oxygen atom. Later, all the vibrations due to motions of the proton were identified by the study of several salts and their deuterated analogues (3).

In the 2,6-dimethyl-4-pyrone complexes only a small range of Lewis acids was used. This was due in part to the ease with which the Lewis acid, MX_n, could be hydrolyzed (unless scrupulous precautions against adventitous moisture were taken) to produce halogen acids HX, which either protonated the pyrone directly, or in combination with the Lewis acid as $H^+MX_{n+1}^-$. Fortunately, xanthone is free from this limitation, as it forms solid protonated salts only with difficulty (4, 5). Thus a wide range of Lewis acids, including those susceptible to hydrolysis could be used without fear of protonation of the base.

The solid complexes so formed have been examined from the point of view of the Lewis acid's ability to coordinate the free electron pair of the carbonyl oxygen atom, for which the term Lewis acidity, or Lewis acid strength is used. A satisfactory criterion and comparison of Lewis acid strength is the free energy of formation of a complex having a coordinate bond between Lewis acids and a constant donor, in the absence of constraints due to steric factors. The technique of measuring such properties involving precise measurements of equilibrium constants and heats of mixing is painstaking and time consuming. In principle, the relative perturbation of the stretching frequency of a carbonyl group with different Lewis acids should give similar information (6). This criterion will be examined for the complexes discussed in this paper.

RESULTS AND DISCUSSION

Consideration of the spectra of the 2,6-dimethyl-4-pyrone complexes (2) led to the conclusion that the carbonyl stretching vibration and the double-bond stretching vibration (ring mode of A_1 species) were reversed in position, the CO vibration being at lower frequency but with a slight interaction between them. The unperturbed value

Contribution No. 81.
†*Presented, in part, at the Ninth Ottawa Symposium on Applied Spectroscopy, September 19, 1962.*

Can. J. Chem. Downloaded from www.nrcresearchpress.com by 210.87.254.105 on 09/05/12
For personal use only.

was estimated to be at about 1645 cm^{-1}. The value of ν_{CO} in xanthone, 1663 cm^{-1}, is an acceptable one, and is not subject to the same confusion as in 2,6-dimethyl-4-pyrone. Alteration of the character of the double-bond vibration at 1607 cm^{-1} in xanthone is doubtless part of the cause of this.

The infrared spectra of the xanthone complexes show that most of the absorption bands are hardly shifted in frequency, though minor alterations in intensity occur. The band attributed to the carbonyl stretching vibration at 1663 cm^{-1} in the free pyrone (CCl_4 solution) moves progressively to lower frequency in the Lewis acid complexes (Table I shows the frequencies attributed to this vibration). This has come to be regarded

TABLE I

	Xanthone		Ethyl acetate*	2,6-Dimethyl-4-pyrone†	1-Ethyl-2,6-dimethyl-4-pyridone‡
	νCO	$\Delta\nu$CO	$\Delta\nu$CO	$\Delta\nu$CO	$\Delta\nu$CO
CCl_4	1663				
$CdCl_2$	1629	34			56
$CaCl_2$	1616	47			
$CoCl_2$	1613	50			
$CaBr_2$	1611	52			
$HgCl_2$	1611	52		68	53
$HgBr_2$	1609	54			
$ZnCl_2$	1606	57		109	54
$BiCl_3$	1604	59			
$InCl_3$	1604	59	113		
$SnCl_4$	1530	133			
$SnBr_4$	1527	136	128		95
BF_3	1525	138	119	121	
$FeCl_3$	1522	141			
$FeBr_3$	1509	154			
$AlCl_3$			117		
$AlBr_3$	1500	163	138		
PF_5	1497	166			
$ZrCl_4$	1496	167	104		
$TiCl_4$	1488	175	128		102
$TiBr_4$	1482	181	128		
BCl_3	1434	229	176		
SbF_5	1420	243			
$SbCl_5$	1411	252		143	105
BBr_3	1410	253	191		96
BI_3	1400	263			

*Reference 6.
†Reference 2.
‡Reference 7.

as a satisfactory criterion of complex formation at a carbonyl group. The only other possible donor site in xanthone is the heterocyclic oxygen atom. A growing body of evidence (7) suggests that the Lewis acid complexes formed at a heterocyclic atom give spectra that are different from the parent heterocycle but are similar amongst themselves. A small trend, about 20 cm^{-1}, in the breathing mode, ν_1, in pyridine complexes was noted as the Lewis acid was altered (8).

The absorption band due to the carbonyl stretching vibration in the complexes is not difficult to recognize as it is usually the strongest band in the spectrum. Occasionally, when the perturbed frequency is close to another band, such as the 1607 cm^{-1} band, a little difficulty was observed, though the intensity criterion usually permitted a good choice. Some slight interaction may be present, too, to shift the ring modes somewhat. The perturbation of the carbonyl frequency is very large for some of the stronger Lewis

Can. J. Chem. Downloaded from www.nrcresearchpress.com by 210.87.254.105 on 09/05/12
For personal use only.

acids; $\Delta\nu_{CO}$ for the BI_3 complex is 263 cm^{-1}, the carbonyl frequency being 1400 cm^{-1}. This is a good deal larger than the largest previously reported, which is 191 cm^{-1} in the BBr_3 complex of ethyl acetate (6). This may be connected with the fact that the carbonyl group in xanthone is more polarizable than that in ethyl acetate.

Electron deficiency in Lewis acids and the lack of quantitative data on the acid strength has been discussed by Lappert (6). The basis for his scale of relative acid strength was the shift in ν_{CO} in the Lewis acid complexes of ethyl acetate. These measurements are compared with the present ones in Table I, along with some from other Lewis acid complexes. In Table II the xanthone measurements are compared with results on relative

TABLE II

Xanthone	I*	II†	III‡	IV§
$CdCl_2$				
$CaCl_2$				
$CoCl_2$				
$CaBr_2$				$(ZrCl_4)$
$HgCl_2$	$HgCl_2$			$(TiCl_4)$
$HgBr_2$	$(CdCl_2)$‖			$(SnCl_4)$
$ZnCl_2$	$ZnCl_2$	$ZnCl_2$	$ZnCl_2$	$ZnCl_2$
$BiCl_3$	$BiCl_3$	$BiCl_3$	(BF_3)	
$InCl_3$	$(SbCl_5)$	$(TiCl_4)$		
$SnCl_4$	$SnCl_4$	$SnCl_4$	$SnCl_4$	
$SnBr_4$				
BF_3				
$FeCl_3$	$FeCl_3$	$FeCl_3$	$FeCl_3$	$FeCl_3$
$FeBr_3$	$(AlCl_3)$	$(SbCl_5)$		
$AlBr_3$	$AlBr_3$			
$AlCl_3$		$AlCl_3$	$AlCl_3$	$AlCl_3$
PF_5				
$ZrCl_4$				
$TiCl_4$				
$TiBr_4$				
BCl_3				
SbF_5				
$SbCl_5$				
BBr_3				
BI_3				

*Reference 9.
†Reference 10.
‡Reference 11.
§Reference 12.
‖Relative acid strength increases down each column. Values in parentheses are misplaced compared with the xanthone values.

Lewis acid strengths derived from colorimetric studies (9), acylation rates (10), and general Friedel–Crafts activity (11, 12). There are many discrepancies. Since the reaction mechanisms in the substitution reactions are not known, the precise significance of the rate measurements is in doubt. If the same mechanism operated in all cases this would simplify the issue, but at least two plausible mechanisms have been suggested (13).

It would be surprising, however, if better agreement were obtained between the spectroscopic measurements, because several factors can influence the interaction. There is first of all the question of the physical state of the complex. In principle, perturbations in gas phase complexes would give the most faithful indication of the Lewis acid strength, but it is almost certain that such measurements are impracticable. It is therefore important to compare measurements made on the same phase, so that lattice effects etc. may be comparable.* Secondly, and more important, is the effect of steric factors. Lappert has

*There is a small possibility, too, in open-chain compounds, for example, esters, that the angle C—C—O may be different in the complexes than in the free ester, due to lattice effects. These angular changes may have a mechanical effect on ν_{CO} (14) and may introduce some uncertainty. Such angular alterations would be expected to be negligible in heterocyclic compounds.

Can. J. Chem. Downloaded from www.nrcresearchpress.com by 210.87.254.105 on 09/05/12
For personal use only.

argued, without quoting supporting evidence, that steric limitations in ethyl acetate complexes are small. This view, in fact, is open to question, since it has recently been suggested that in some BF_3 complexes of carbonyl compounds even an α-methyl group results in some hindrance. Bulkier groups, therefore, would furnish even larger hindering agencies (15).

The effect of such hindrance is to prevent the closest approach of the Lewis acid to the carbonyl oxygen atom that would be demanded by purely electronic considerations. The perturbation of ν_{CO} would then be underestimated, and the Lewis acid would be apparently weaker than it should be. These effects would tend to be larger for Lewis acids with large central atoms of high valency bound to the larger halogen atoms.

This hindrance, of course, exists in xanthone complexes, and it may be even greater than that in the ethyl acetate complexes since the portion of the fused ring in xanthone next to the carbonyl group resembles an ethyl group. No quantitative estimate can be made in the absence of a knowledge of the dimensions of the molecule.

The conclusion to be drawn from the existing data seems to be that when the strength of a Lewis acid is quoted it is necessary to stipulate the base, or donor, against which this was measured. Efforts are being made to find donors which are free from undesirable properties. The principle requirements are:

(1) adequate donor ability to form stable, nonhygroscopic complexes;
(2) inability to form protonated salts;
(3) absence of bulky groups which cause hindrance;
(4) large polarizability of the functional group so that weak complex formation produces a large effect;
(5) absence of mechanical effects on the perturbed group.

None of the donors considered hitherto have satisfied all these requirements, and it may be that they are mutually exclusive. One compound which satisfies the first four, and possibly the fifth, is benzaldehyde, and complexes of Lewis acids with this donor are currently being studied.

Comments on the relative positions of the different Lewis acids will be deferred until more data become available with different donors.

EXPERIMENTAL

Materials

The complexes were prepared by familiar methods. The Lewis acid, if gaseous (BF_3, PF_5, BCl_3), was passed into a $CHCl_3$ solution of xanthone, diluted with excess Freon 113; if liquid ($SnCl_4$, $SnBr_4$, $TiCl_4$, $TiBr_4$, SbF_5, $SbCl_5$, BBr_3), it was added, in an inert atmosphere, to a $CHCl_3$ solution of xanthone; if solid, a solution of the Lewis acid ($CoCl_2$, $CaBr_2$, $HgCl_2$, $HgBr_2$, $ZnCl_2$, $BiCl_3$, $InCl_3$, $FeCl_3$, $FeBr_3$, $ZrCl_4$ in acetone, $CaCl_2$, $CdCl_2$ in ethanol, $AlBr_3$ in benzene, $AlCl_3$ in ether, BI_3 in carbon tetrachloride) was added to a solution of xanthone in the same solvent. Occasionally, if no solid phase was precipitated by these operations, evaporation of the solvent ($HgBr_2$, $ZnCl_2$, $BiCl_3$) or removal *in vacuo* ($InCl_3$, $FeCl_3$, $FeBr_3$, $ZrCl_4$) gave the required solid complex.

Analysis of the complexes (microanalytical methods for carbon and hydrogen, X-ray fluorescence spectroscopy for metal and halogen) revealed in all cases that could be determined (some complexes were too hygroscopic) a 1:1 stoichiometry, except 2-xanthone:3$CoCl_2$, 2-xanthone:$SnBr_4$. It is assumed that those compounds that were too sensitive for analysis were 1:1 compounds for Lewis acid types MX_2, MX_3, and MX_5, and 2:1 for the type MX_4. The spectra of all the compounds studied substantiated the formulation of the complexes as indicated.

Spectra

The spectra of the finely ground solids in emulsion in nujol and fluorolube were recorded on a Perkin–Elmer model 221 prism-grating spectrometer. For the complexes which were sensitive to atmospheric moisture all operations were carried out in a dry box.

Can. J. Chem. Downloaded from www.nrcresearchpress.com by 210.87.254.105 on 09/05/12
For personal use only.

ACKNOWLEDGMENTS

The assistance of Miss C. D. Anderson in preparing some of the complexes and recording their spectra and of Mr. D. G. Barnes (Analytical Laboratory, Dow Chemical of Canada, Limited) in obtaining some of the analytical data is gratefully acknowledged.

REFERENCES

1. J. N. Collie and T. Tickle. J. Chem. Soc. **75**, 710 (1899).
2. D. Cook. Can. J. Chem. **39**, 1184 (1961).
3. D. Cook. Can. J. Chem. **41**, 505 (1963).
4. K. A. Hofmann, A. Metzler, and H. Lecher. Ber. **43**, 178 (1910).
5. M. Gomberg and L. H. Cone. Ann. **376**, 183 (1910).
6. M. F. Lappert. J. Chem. Soc. 542 (1961).
7. D. Cook. Can. J. Chem. **41**, 515 (1963).
8. V. N. Filimonov and D. S. Bystrov. Opt. i Spektroskopiya, **12**, 66 (1962).
9. D. L. Hawke and J. Steigman. Anal. Chem. **26**, 1989 (1954).
10. O. C. Dermer, D. M. Wilson, F. M. Johnson, and V. H. Dermer. J. Am. Chem. Soc. **63**, 2881 (1941).
11. L. Fieser and M. Fieser. Organic chemistry. D. C. Heath and Co. Boston, Mass. 1944. p. 573.
12. N. O. Calloway. Chem. Rev. **17**, 327 (1935).
13. D. Cook. Can. J. Chem. **37**, 48 (1959).
14. D. Cook. Can. J. Chem. **39**, 31 (1961).
15. D. Cook. Proceedings of the International Conference on Spectroscopy, 1962. Spartan Press, Washington, D.C. 1962.

Can. J. Chem. Downloaded from www.nrcresearchpress.com by 210.87.254.105 on 09/05/12
For personal use only.

PHASE EQUILIBRIUM STUDIES FOR THE TERNARY SYSTEM URANYL NITRATE – NITRIC ACID – WATER

J. GAUNT, I. J. BASTIEN, AND M. ADELMAN
Department of Chemistry, Essex College, Assumption University of Windsor, Windsor, Ontario
Received June 5, 1962

ABSTRACT

Phase equilibrium studies were carried out on the system $UO_2(NO_3)_2$–HNO_3–H_2O between the temperatures of −10° C and +49.1° C over a wide concentration range of both $UO_2(NO_3)_2$ and HNO_3. No phase separation occurred above 49.1° C for the concentrations studied. The three hydrates of $UO_2(NO_3)_2$ were identified in the solid phase, and a new complex of $UO_2(NO_3)_2$, possibly $UO_2(NO_3)_2.3HNO_3$, was separated as the solid phase at higher nitric acid concentrations.

Can. J. Chem. Downloaded from www.nrcresearchpress.com by 210.87.254.5 on 09/05/12
For personal use only.

Studies on the hydrates of uranyl nitrate (1–8) have been carried out by several investigators as have solubility studies of aqueous solutions (9, 11) and crystallization temperatures (12).

Investigation of the three-component system $UO_2(NO_3)_2$–HNO_3–H_2O has, however, been confined to two limited studies, that of Coloni (12) on solubility at 25°, and that of Hart and Morris (13) on the crystallization temperatures of solutions of varying concentration.

In view of the increasing importance of more detailed data for the effective processing of uranyl nitrate solutions, this investigation was undertaken to obtain the phase diagrams for the three-component system over a wider range of temperature and concentration than was previously available from existing data. The system was studied at 49.1, 30.2, 0.0, and −10° C, and nitric acid concentrations up to 80%.

Uranyl nitrate hexahydrate, trihydrate, and dihydrate were found in the solid phase at nitric acid concentrations below 75%. In the regions of higher nitric acid concentration a fine crystalline solid was obtained whose composition, as suggested by the "method of wet residues" was $UO_2(NO_3)_2.3HNO_3$.

EXPERIMENTAL

The uranyl nitrate solutions were prepared by dissolving the uranyl nitrate hexahydrate in varying concentrations of nitric acid. In the regions of high nitric acid concentration, the hexahydrate was dissolved in more concentrated acid and the crystals obtained were redissolved in increasing concentrations of nitric acid and red fuming nitric, s.g. 1.59.

Each sample was saturated at a temperature above that at which the determinations were made and transferred to glass-stoppered bottles. The samples were then placed in constant-temperature baths regulated to give an accuracy of ±0.2° C. A minimum period of 48 hours was allowed to bring the samples to equilibrium.

Weighed samples of the liquid phases and residues were taken and diluted to appropriate volumes for analysis. The total uranium content was determined by titrating the reduced form with ceric sulphate (14), standardized against electrolytic iron. The nitric acid was determined by the direct titration method of Brothers *et al.* (15). All solid phases were analyzed by the "method of wet residues".

RESULTS

The compositions of the liquid phases are reported (Table I) in weight percent of uranyl nitrate and nitric acid. The percentage of water may be obtained by difference.

TABLE I

Composition of solutions in weight percent

Liquid phase			Liquid phase		
$UO_2(NO_3)_2$	HNO_3	Nature of solid phase	$UO_2(NO_3)_2$	HNO_3	Nature of solid phase
		For system studied at 49.1° C			
62.0	5.1	A $UO_2(NO_3)_2.6H_2O$	45.9	33.4	B
63.1	3.2	A	45.6	34.1	B
62.5	5.4	A	44.4	35.8	B
59.0	11.3	A	45.7	36.3	B + C
61.4	10.7	A	41.4	37.9	C $UO_2(NO_3)_2.2H_2O$
56.8	10.9	A	40.7	40.6	C
60.9	12.4	B $UO_2(NO_3)_2.3H_2O$	36.5	48.6	C
60.8	13.1	B	35.9	49.5	C
54.6	19.7	B	35.0	52.3	C
55.4	19.7	B	26.0	63.5	
49.5	25.5	B	12.2	80.2	D $UO_2(NO_3)_2.3HNO_3$
48.2	27.2	B	12.7	80.7	D
47.8	28.2	B	10.3	83.0	D
46.3	30.8	B	8.83	85.5	D
46.4	30.0	B			
		For system studied at 30.2° C			
55.6	2.82	A	37.2	34.1	B
49.6	7.12	A	35.8	34.2	B
46.7	11.7	A	33.4	39.4	B
40.3	18.3	A	32.6	43.2	B
38.8	23.8	A	32.0	44.1	B
42.5	24.2	A	30.3	46.1	B
42.6	25.4	A	30.0	49.1	B
40.1	25.7	A	29.4	53.7	C
43.1	26.2	A + B	28.5	56.9	C
39.7	30.4	B	22.9	64.5	C
39.0	30.8	B	13.0	77.2	D
39.2	31.3	B	10.9	79.4	D
37.8	33.7	B			
		For system studied at 0.0° C			
45.2	2.72	A	17.4	49.5	B
34.8	11.3	A	17.5	49.6	B
22.9	21.3	A	17.1	52.1	B
14.3	30.9	A	15.7	53.5	B
11.1	42.7	A	15.1	58.1	B
11.5	42.7	A	14.8	59.1	B
13.4	44.7	A	14.9	59.2	B
13.3	44.3	A	15.0	59.9	B
19.9	46.1	A	15.2	60.7	B
18.6	46.2	A	15.6	62.1	B
22.2	46.1	A	17.0	62.1	B
20.0	46.5	A	18.1	61.7	B + C
18.6	46.8	A	18.4	62.0	C
20.5	46.8	B	19.5	65.4	C
18.5	48.2	B	5.81	84.4	*
		For system studied at −10.0° C			
30.0	12.0	A	11.7	63.5	B
8.46	33.6	A	11.8	63.7	B
4.65	46.2	A	14.4	65.8	B
10.0	52.0	A	15.6	63.7	B
13.7	52.2	B	18.2	66.7	C
12.1	62.1	B	6.8	82.9	D
11.4	61.1	B			

*Analysis of solid phase after filtration gave 83.5% $UO_2(NO_3)_2$ and 11.5% HNO_3.

The data, at −10°, given in Table II were communicated to the authors by A.E.C.L. and were incorporated in the phase diagram at −10° C.

Can. J. Chem. Downloaded from www.nrcresearchpress.com by 210.87.254.5 on 09/05/12
For personal use only.

TABLE II

Liquid phase			Liquid phase		
$UO_2(NO_3)_2$	HNO_3	Nature of solid phase	$UO_2(NO_3)_2$	HNO_3	Nature of solid phase
35.4	1.1	E H_2O (S)	38.4	5.7	A
30.7	2.6	E	34.0	8.4	A
25.5	4.9	E	29.1	12.8	A
19.9	7.6	E	23.9	16.9	A
13.9	9.5	E	18.4	21.9	A
42.7	2.6	A	12.4	29.6	A

DISCUSSION

In studying the ternary system, the invariant points were not always obtainable; however, the general behavior of the system as shown in Fig. 1 is quite evident. Only in the

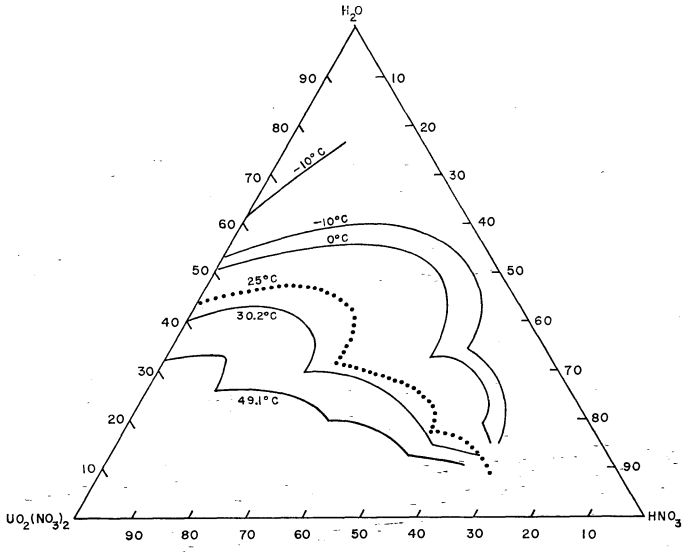

FIG. 1. Ternary system $UO_2(NO_3)_2$–H_2O–HNO_3: —solutions examined in the study; ... solubility data (12).

regions of high nitric acid concentration is the behavior of the system remarkable. It should, nevertheless, be pointed out that in order to obtain these concentrations of nitric acid, it was necessary to use red fuming nitric acid. Experimental difficulties make it improbable that a solid free of nitrogen dioxide may be obtained by equilibration at the temperatures indicated. It is assumed in this study that $UO_2(NO_3)_2.3HNO_3$ existed in the free state or a reaction occurred in the system. If the latter is feasible, other nitrogen oxide addition products may have formed. It would, therefore, be of interest to investigate this region more fully. The existence of uranyl nitrate complexes with oxides of nitrogen has been previously reported (16, 17).

At temperatures above 49.1° C, no phase separation was evident in the concentration range studied.

ACKNOWLEDGMENT

The authors wish to thank Atomic Energy of Canada Limited for financial support and encouragement, as well as for the uranyl nitrate used in these studies.

Can. J. Chem. Downloaded from www.nrcresearchpress.com by 210.87.254.5 on 09/05/12
For personal use only.

REFERENCES

1. A. M. VASILIEV. J. Russ. Phys. Chem. Soc. **42**, 570 (1910).
2. P. LEBEAU. Bull. Soc. Chim. France, Ser. 4, **9**, 298 (1911).
3. R. DE FORCRAND. Ann. Chim. (Paris), **3**, 5 (1915).
4. F. E. E. GERMANN. Phys. Rev. **11**, 245 (1918).
5. F. E. E. GERMANN. J. Am. Chem. Soc. **44**, 1466 (1922).
6. F. E. E. GERMANN and P. R. FREY. J. Colo. Wyo. Acad. Sci. **1**, No. 1, 54 (1929).
7. A. J. KING, R. PFEIFFER, and WM. ZEEK. Contract AT(30-1)-1490 (SUR I-Chem-242-578F) 4:80, OTS. August 1, 1957.
8. F. E. E. GERMANN. Phys. Rev. **19**, 623 (1922).
9. A. BENRATH. Z. Anorg. Allgem. Chem. **249**, 245 (1942).
10. W. L. MARSHALL, JR., J. S. GILL, and C. H. SECOY. J. Am. Chem. Soc. **73**, 8167 (1951).
11. B. ELLIOT (*Editor*). Progress Development Quarterly Report Part I Contract W-14108-eng.-8. OTS. MCW-1412. April 1, 1958.
12. A. COLONI. Bull. Soc. Chim. France, **39** (4), 1243 (1926).
13. R. G. HART and G. O. MORRIS. Progr. Nucl. Energy, Ser. III. **2**, 544 (1958).
14. R. R. FRASER. Volumetric methods for the determination of uranium. Atomic Energy of Canada Ltd., Chalk River, Ont. 1952.
15. J. A. BROTHERS and W. J. OLMSTEAD. Atomic Energy of Canada Ltd. Report CLE-112. November 25, 1955.
16. E. SPAITH. Monatsh. **33**, 853 (1912).
17. G. GIBSON and J. J. KATZ. J. Am. Chem. Soc. **73**, 5436 (1951).

Can. J. Chem. Downloaded from www.nrcresearchpress.com by 210.87.254.5 on 09/05/12
For personal use only.

PHASE EQUILIBRIUM STUDIES FOR THE QUATERNARY SYSTEM URANYL NITRATE – ALUMINUM NITRATE – NITRIC ACID – WATER

ROBERT D. THIBODEAU AND M. ADELMAN
Department of Chemistry, Essex College, Assumption University of Windsor, Windsor, Ontario
Received June 5, 1962

ABSTRACT

The quaternary system $UO_2(NO_3)_2$–$Al(NO_3)_3$–HNO_3–H_2O was studied in the temperature range 0–20° C, and the concentration range of 0–1.5 *M* $Al(NO_3)_3$ and 0–10 *N* HNO_3. From the data, phase diagrams were prepared. No phase separation was evident at 30° C and above, for the concentrations studied.

Can. J. Chem. Downloaded from www.nrcresearchpress.com by 210.87.254.105 on 09/05/12
For personal use only.

A knowledge of the phase behavior for the system $UO_2(NO_3)_2$–$Al(NO_3)_3$–HNO_3–H_2O is of value in connection with the recovery of spent reactor rods. Dissolution in nitric acid of the heterogeneous uranium rods encased in aluminum jackets is the initial step in aqueous processes for the recovery of fissionable materials.

The ternary system $UO_2(NO_3)_2$–HNO_3–H_2O was investigated initially by Coloni (1). Extension of this work has been done by Gaunt (2) and Bastien (3). The salting out effect at 25° C of NH_4NO_3, $Ca(NO_3)_2$, $Mg(NO_3)_2$, and $Zn(NO_3)_2$ on the system $UO_2(NO_3)_2$ – 1.5 *N* HNO_3 – H_2O was studied by Kurnakova and Nikolaev (4). However, the only published information on the system $UO_2(NO_3)_2$–$Al(NO_3)_3$–HNO_3–H_2O is the freezing point study for concentrations of 0.20 *M* $UO_2(NO_3)_2$, 0–0.6 *M* nitric acid, and 0–2.0 *M* $Al(NO_3)_3$ by Slansky (5). This study was carried out at temperatures of 0, 10, and 20° C over a limited range of aluminum nitrate concentration corresponding to that resulting from the dissolution of the reactor rod aluminum casement.

EXPERIMENTAL APPARATUS AND METHODS

Thirty-three solutions were made up ranging from 0 to 10 *M* HNO_3 inclusive and 0.5 *M*, 1.0 *M*, and 1.5 *M* $Al(NO_3)_3$. Ten milliliters of each of these solutions was pipetted into a glass bottle containing sufficient uranyl nitrate hexahydrate (approximately 25 g) to saturate the solutions. The bottles were sealed with polyethylene tops, heated to effect complete dissolution, then suspended in a constant-temperature (±0.1° C) circulating water bath for 48 hours. It was established by repeated analysis that equilibration was attained within 12 hours.

Samples of the liquid phase were extracted through a filter pipette, weighed, and diluted to 100 ml. Aliquots were analyzed for uranium by titrating the reduced form with ceric sulphate. The nitric acid content was determined by a procedure based on the method of Brothers and Olmstead (6) by which the aluminum was precipitated as the double salt by potassium fluoride, according to the reaction

$$Al^{+++} + 6KF \rightarrow K_3AlF_6 + 3K^+. \quad [1]$$

The uranium was precipitated according to the reaction

$$UO_2^{++} + 4KF \rightarrow K_2UO_2F_4 + 2K^+. \quad [2]$$

The free nitric acid was titrated with standardized sodium hydroxide to a phenolphthalein end point.

The aluminum was separated from the uranium by the addition of ammonium bicarbonate solution. The $Al(OH)_3$ formed was separated by centrifuging and decanting, then it was dissolved in hot H_2SO_4 and analyzed by the volumetric oxine method (7).

All methods of analyses were developed to an accuracy of 1% as determined on standard substances. All analyses were performed in duplicate.

The choice of axes and the general method of graphical representation was selected to best indicate the physical phenomena involved with increasing concentration of aluminum nitrate.

EXPERIMENTAL RESULTS

A typical set of experimental results representing the composition of saturated solutions made from 0.5 *M*, 1.0 *M*, and 1.5 *M* aluminum nitrate is given in Table I and shown graphically on Fig. 1. Results for the systems at 10 and 20° C are summarized in Tables II and III and shown graphically on Figs. 2 and 3. Figure 4 gives the composite phase

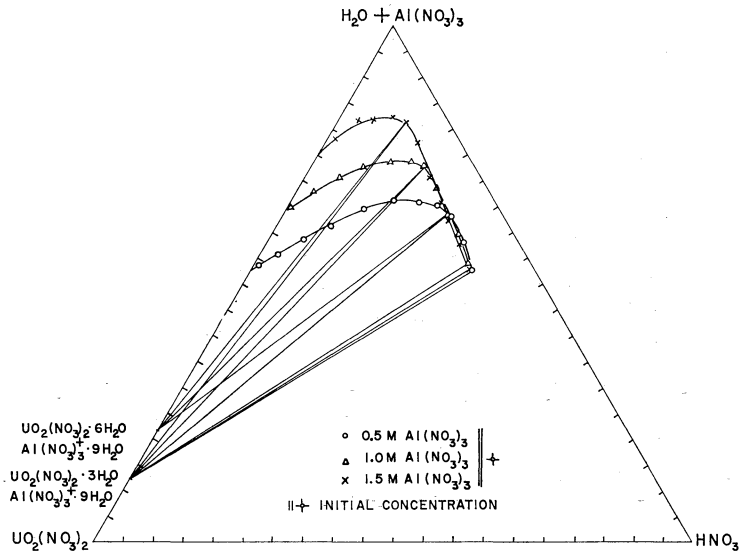

FIG. 1. The system at 0° C.

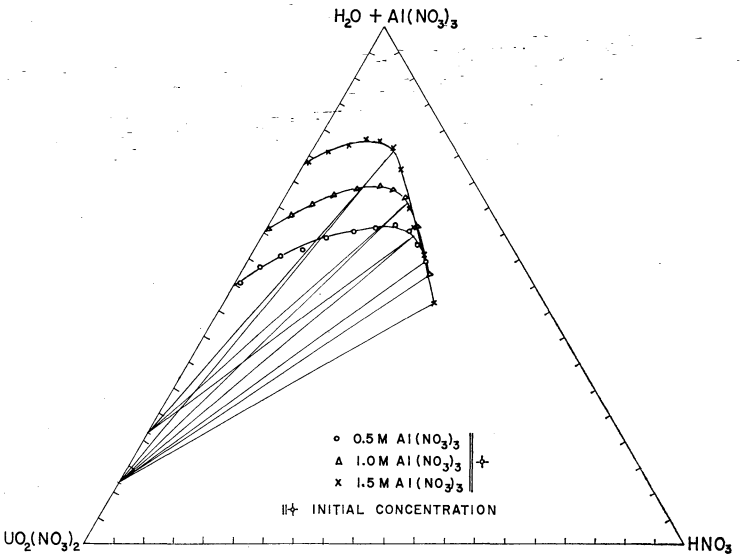

FIG. 2. The system at 10° C.

diagram for the system at the three temperatures studied. In solutions of low concentration of nitric acid and saturated with uranyl nitrate and aluminum nitrate, the solid

Can. J. Chem. Downloaded from www.nrcresearchpress.com by 210.87.254.105 on 09/05/12
For personal use only.

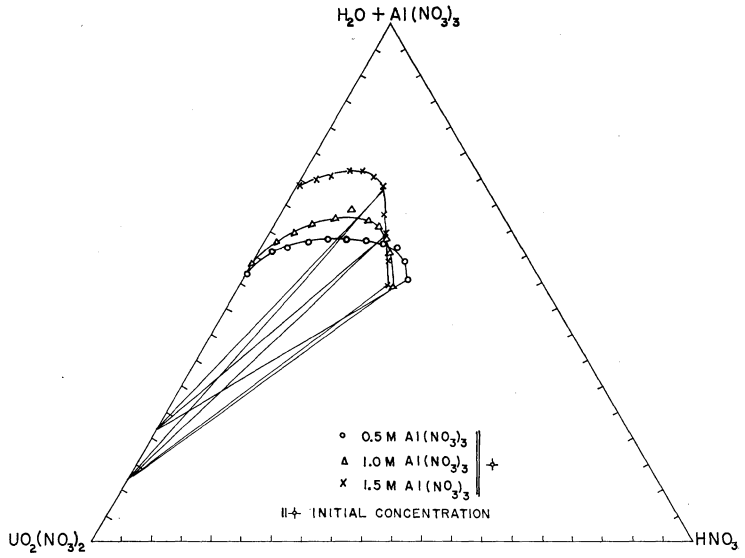

FIG. 3. The system at 20° C.

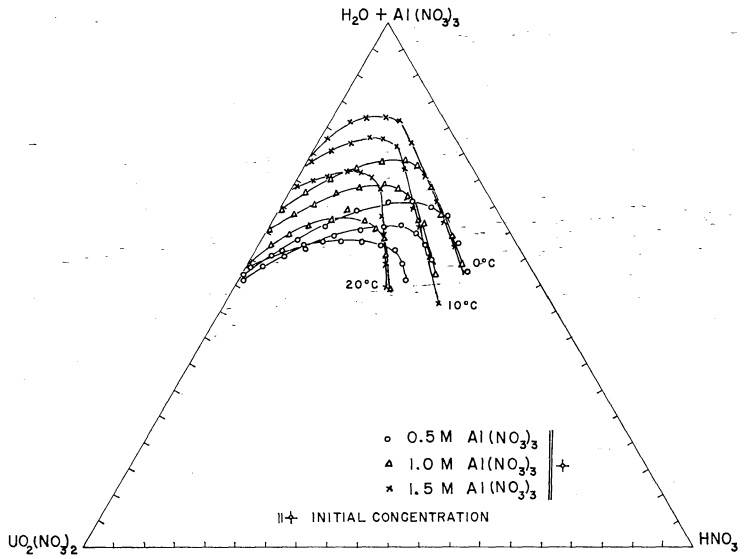

FIG. 4. Composite phase diagram for the system at 0, 10, and 20° C.

phase is $UO_2(NO_3)_2.6H_2O$ and $Al(NO_3)_3.9H_2O$. In solutions of high nitric acid concentration the solid phase consisted of $UO_2(NO_3)_2.3H_2O$ and $Al(NO_3)_3.9H_2O$. The exact position of the invariant point where the solid was composed of the hexahydrate and trihydrate of uranyl nitrate and the enneahydrate of aluminum nitrate was not determined.

At temperatures of 30° C and above, no phase separation was evident, for all the concentrations studied at the lower temperatures.

Can. J. Chem. Downloaded from www.nrcresearchpress.com by 210.87.254.105 on 09/05/12
For personal use only.

Can. J. Chem. Downloaded from www.nrcresearchpress.com by 210.87.254.105 on 09/05/12
For personal use only.

TABLE I

The system $UO_2(NO_3)_2$–$Al(NO_3)_3$–HNO_3–H_2O at 0° C

0.5 *M* $Al(NO_3)_3$				1.0 *M* $Al(NO_3)_3$				1.5 *M* $Al(NO_3)_3$			
$UO_2(NO_3)_2$*	$Al(NO_3)_3$	HNO_3	Solid phase	$UO_2(NO_3)_2$	$Al(NO_3)_3$	HNO_3	Solid phase	$UO_2(NO_3)_2$	$Al(NO_3)_3$	HNO_3	Solid phase
45.8	5.7	0.7	A + B	34.6	8.2	0.7	A + B	20.9	9.1	1.1	A + B
41.5	6.1	2.9	A + B	29.3	8.9	2.9	A + B	15.2	10.1	3.3	A + B
35.7	6.5	5.6	A + B	23.8	8.9	5.9	A + B	12.4	10.7	5.9	A + B
29.9	6.8	9.1	A + B	18.7	9.9	8.9	A + B	9.1	11.8	8.8	A + B
22.9	6.7	12.8	A + B	13.8	10.9	12.5	A + B	7.3	12.4	11.2	A + B
17.1	7.3	17.1	A + B	10.1	12.1	16.1	A + B	7.5	13.1	15.2	B + C
13.0	7.2	21.4	A + B	8.5	12.9	18.5	A + B	8.6	12.1	20.9	B + C
10.2	7.3	24.8	A + B	8.4	11.5	22.8	B + C	9.1	9.2	25.1	B + C
8.9	7.2	28.1	B + C	9.2	7.8	27.5	B + C	9.7	5.5	28.0	B + C
9.3	5.2	32.7	B + C	9.7	4.8	31.1	B + C	10.2	3.7	32.2	B + C
10.5	2.2	36.9	B + C	10.3	2.6	35.7	B + C	10.6	2.6	36.6	B + C

NOTE: A will designate $UO_2(NO_3)_2.6H_2O$; B will designate $Al(NO_3)_2.9H_2O$; C will designate $UO_2(NO_3)_2.3H_2O$.
*Units used are grams per 100 grams saturated solution.

TABLE II

The system $UO_2(NO_3)_2$–$Al(NO_3)_3$–HNO_3–H_2O at 10° C

0.5 *M* $Al(NO_3)_3$				1.0 *M* $Al(NO_3)_3$				1.5 *M* $Al(NO_3)_3$			
$UO_2(NO_3)_2$	$Al(NO_3)_3$	HNO_3	Solid phase	$UO_2(NO_3)_2$	$Al(NO_3)_3$	HNO_3	Solid phase	$UO_2(NO_3)_2$	$Al(NO_3)_3$	HNO_3	Solid phase
48.5	4.2	0.6	A + B	38.9	3.9	0.4	A + B	25.8	8.3	0.6	A + B
44.0	4.8	2.5	A + B	33.8	5.0	2.8	A + B	21.4	8.5	2.8	A + B
39.5	5.0	5.0	A + B	29.3	5.7	5.3	A + B	17.6	9.0	5.5	A + B
35.0	4.6	7.9	A + B	24.7	5.7	8.0	A + B	14.1	9.3	8.0	A + B
29.6	5.6	11.2	A + B	20.2	6.1	11.5	A + B	11.9	9.3	10.6	A + B
24.5	5.8	15.3	A + B	16.2	6.4	15.0	A + B	10.6	10.1	13.2	A + B
20.3	7.3	18.7	A + B	14.4	8.0	17.3	A + B	11.0	8.5	16.8	B + C
17.1	7.3	21.8	A + B	13.2	9.4	20.0	A + B	13.5	11.4	21.7	B + C
15.4	7.6	24.7	A + B	14.0	9.3	24.3	B + C	14.0	8.8	24.8	B + C
15.2	6.1	27.2	B + C	13.7	6.3	24.8	B + C	15.3	5.2	28.9	B + C
15.9	5.6	29.5	B + C	16.6	5.1	31.6	B + C	18.2	4.2	35.1	B + C

Can. J. Chem. Downloaded from www.nrcresearchpress.com by 210.87.254.105 on 09/05/12
For personal use only.

TABLE III

The system $UO_2(NO_3)_2$–$Al(NO_3)_3$–HNO_3–H_2O at 20° C

0.5 *M* $Al(NO_3)_3$							1.0 *M* $Al(NO_3)_3$				1.5 *M* $Al(NO_3)_3$			
$UO_2(NO_3)_2$		$Al(NO_3)_3$		HNO_3		Solid phase	$UO_2(NO_3)_2$	$Al(NO_3)_3$	HNO_3	Solid phase	$UO_2(NO_3)_2$	$Al(NO_3)_3$	HNO_3	Solid phase
Liquid	Solid	Liquid	Solid	Liquid	Solid									
48.2	68.7	6.4	—	0.0	0.0	A	46.4	9.7	0.0	A + B	30.9	8.7	0.5	A + B
42.0	64.8	6.2	—	2.1	0.7	A	40.2	10.0	2.0	A + B	27.8	9.2	2.5	A + B
39.0	65.3	6.7	—	4.4	1.4	A	36.4	10.6	4.0	A + B	25.0	9.7	4.8	A + B
35.1	64.2	6.9	—	7.2	2.2	A	32.3	10.9	6.3	A + B	21.2	10.2	7.3	A + B
31.4	64.3	7.2	—	10.2	3.1	A	28.1	11.2	9.6	A + B	19.1	9.4	9.7	A + B
28.6	66.2	7.8	—	13.3	3.2	A	24.6	11.4	11.6	A + B	17.8	9.5	12.0	A + B
25.2	64.9	8.0	—	16.9	4.0	A	23.0	11.9	15.2	A + B	17.2	10.9	14.6	B + C
22.8	63.4	7.7	—	20.0	5.1	A	21.8	11.9	17.7	A + B	19.6	10.4	17.4	B + C
20.9	64.6	7.5	—	22.6	5.4	A	21.6	10.5	20.0	B + C	21.2	10.1	19.4	B + C
21.0	64.8	7.3	—	25.1	5.8	A	22.7	10.3	21.9	B + C	23.5	8.7	22.6	B + C
22.2	64.5	7.1	—	27.3	6.7	A	25.3	5.7	25.6	B + C	25.6	6.1	25.0	B + C

ACKNOWLEDGMENT

The authors are grateful to Atomic Energy of Canada Limited for their financial support and encouragement.

REFERENCES

1. A. COLONI. Bull. Soc. Chim. France, Ser. 4, **39**, 1243 (1926).
2. J. GAUNT. B.Sc. Thesis, Essex College, Assumption University of Windsor, Windsor, Ontario. 1959.
3. I. J. BASTIEN. B.Sc. Thesis, Essex College, Assumption University of Windsor, Windsor, Ontario. 1959.
4. A. G. KURNAKOVA and A. V. NIKOLAEV. Zh. Neorgan. Khim. **3**, 1028 (1958).
5. C. M. SLANSKY. Progr. Nucl. Energy, Ser. III, **2**, 536 (1958).
6. J. A. BROTHERS and W. J. OLMSTEAD. Determination of free mineral acid in the presence of thorium, uranium, aluminum, plutonium, and iron. Unpublished communication, A.E.C.L. Chalk River, Ontario. 1955.
7. G. E. F. LUNDELL and H. B. KNOWLES. Bur. Std. J. Res. **3**, 91 (1929).

Can. J. Chem. Downloaded from www.nrcresearchpress.com by 210.87.254.105 on 09/05/12
For personal use only.

Can. J. Chem. Downloaded from www.nrcresearchpress.com by 210.87.254.6 on 09/05/12
For personal use only.

INCREASE IN THE ANODIC OVERPOTENTIAL OF ELECTROPOLISHED ALUMINUM ON EXPOSURE TO DRY AIR AT 25° C—A FILM THICKNESS OR SPECIFIC IONIC CONDUCTANCE EFFECT

M. J. DIGNAM[1]

Anode potential measurements of the type indicated in the title were made by Hart (1), who interpreted them in terms of an oxide film whose thickness increased in accordance with the Mott–Cabrera theory of metal oxidation (2). The present data cast considerable doubt on this interpretation, suggesting instead a mechanism involving a change in the specific ionic conductance of the film.

Specimens of superpurity aluminum were electropolished in an ethanolic perchloric acid solution, rinsed, dried, and stored at 25° C over activated alumina (3). Anode potentials were measured, using a method previously reported (3), at a current density of 3×10^{-6} amp/cm^2 in aqueous boric acid adjusted to pH = 6.0 with ammonia. The potentials, measured against a large-area platinum cathode (3), were reproducible to ±0.02 v. Later, several of the measurements were repeated employing a standard calomel reference electrode. Using the information so obtained and assigning the potential 1.42 v (3) to the reaction $2Al + 3H_2O \rightarrow Al_2O_3 + 3H_2$ at 1 atm of H_2 and 30° C, an additive correction of 2.43 v was calculated and applied to the original potential measurements to convert them to true anodic overpotentials (i.e. potentials against the hypothetical reversible electrode, Al, Al_2O_3/OH^-).

Figure 1 illustrates the present data, and Hart's data, from which 0.33 v has been

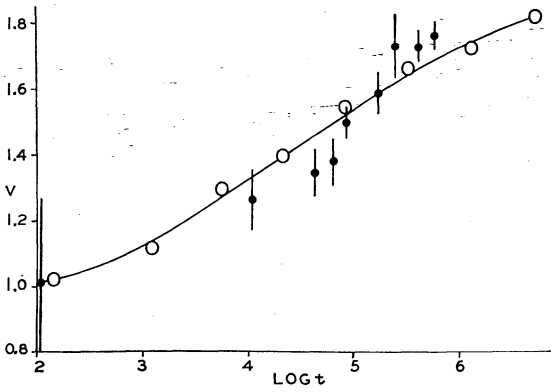

FIG. 1. Anodic overpotential for aluminum versus the logarithm of the time elapsed since electropolishing (present data open circles, Hart's data vertical lines; V in volts, t in seconds).

subtracted to facilitate comparison of potential changes. Comparison of absolute potentials cannot be made since Hart's potentials were measured against a working aluminum cathode of unknown electrochemical behavior. The two sets of data show changes in the anodic potential in agreement to within the sum of their deviations.

[1]*Present address: Department of Chemistry, University of Toronto, Toronto, Ontario.*

Can. J. Chem. Downloaded from www.nrcresearchpress.com by 210.87.254.6 on 09/05/12
For personal use only.

DISCUSSION

According to Hart's interpretation, the overpotential, V, should vary with the exposure time, t, in the manner $1/V = -C\log(t+\tau)+C'$, C, τ, and C' being constants for fixed temperature, C and τ positive. This equation predicts the slope, $dV/d\log t$, to be an increasing function of $\log t$ (or V), whereas it is seen to decrease appreciably for large values of t. Also, the oxidation parameters calculated by Hart differ considerably from those calculated from oxidation studies in oxygen between 250 and 450° C (4), and from anodic oxidation studies (5).

Interpreting the results in accordance with the oxidation law reported by Eley and Wilkinson (6), the curve is of the correct shape, but the predicted slope, $dV/d\log t$, is larger by a factor of 10^2 than that observed.

The increase in the overpotential is undoubtedly due to an increase in the oxide film resistance brought about by an increase in film thickness, a decrease in specific ionic conductance, or perhaps by a combination of both these processes. Since the first of these possibilities is in conflict with the facts, the second will be investigated.

As will be shown, the results are quite consistent with a mechanism involving a second-order decay of ionic current carriers according to the model proposed by Bean, Fisher, and Vermilyea (7). Their equations, describing high-field ionic conduction processes, can be written (8, 3, 9):

$$I = 2qa\nu n \exp -(U-Eaq)/kT \qquad [1]$$

$$dn/dt = A-Bnm, \qquad [2]$$

where $A = N\nu \exp -[W-E\lambda q]/kT$; and $B = 2a\nu\sigma \exp -[U-Eaq]/kT$. I and E are the current density and electric field strength in the oxide, n the carrier concentration (interstitial cations) of charge q and vibrational frequency ν, U and a the activation energy at zero field and activation distance for interstitial cation transport, m the concentration of trapping sites (cation vacancies) with capture cross-sectional area σ, N the concentration of sites at which Frenkel defects may form, and W and λ the activation energy at zero field and activation distance for formation of a Frenkel defect.

The films under discussion are assumed to be of constant thickness and to have been formed during electropolishing at the high current density of 0.5 amp/cm^2. Immediately following electropolishing, n should therefore be high, decreasing subsequently with time in accordance with equation [2]. Initially, then, $Bnm \gg A$, and in fact the present results are only consistent with the assertion that this inequality applies over the entire time period investigated. Accordingly, integration of equation [2] gives:

$$1/n = (B/\alpha)[1-(1-\alpha/Bn_0) \exp -\alpha t], \qquad [3]$$

where $\alpha = B(n_0-m_0)$, n_0 and m_0 being the values of n and m at $t = 0$. The overpotential, V, is obtained from equation [1] on setting $E = V/\delta$, δ being the film thickness, and substituting for n the expression given in equation [3]. Thus:

$$V+Y = K\log(t+t_0)+K', \qquad [4]$$

where $K = 2.303kT/qa$; $K' = K\log(I\sigma/q)+V'$; $t_0 = 1/Bn_0$; $Y = K\log[\alpha t(1-1/Bn_0t)]/[1-(1-\alpha/Bn_0)\exp -\alpha t] \simeq K\log[\alpha t/(1-\exp -\alpha t)]$ for $n_0 \gg (n_0-m_0)$; and V' is the electrical potential across the film that arises from chemisorption of oxygen on the alumina in accordance with the Mott–Cabrera theory (2, 10), during exposure of the metal to air.

The data are plotted in Fig. 2 according to equation [4], the values for the parameters being: $K = 0.21_0$ v; $K' = 0.49$ v; $t_0 = 220$ seconds; and $\alpha = 4.5\times10^{-7}$ sec^{-1}. The

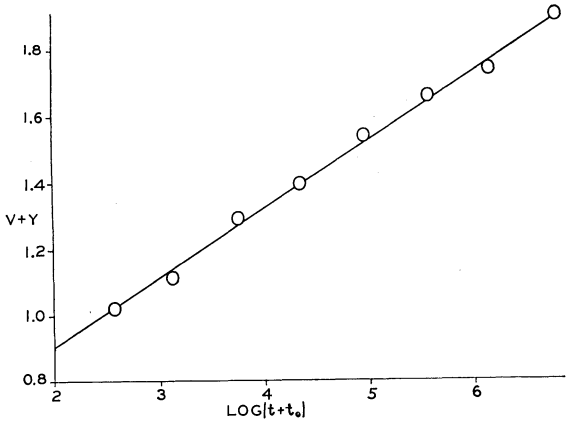

FIG. 2. Anodic overpotential data for aluminum plotted according to equation [4] (V and Y in volts, t and t_0 in seconds).

average deviation of the points from the straight line is ±0.015 v, which is within the experimental scatter.

To check further the credibility of this proposed mechanism, secondary calculations were made using the following values for the parameters: $kT = 0.0252$ ev; $q = 3\times$ (charge on electron); $a = 1.2_4\times10^{-8}$ cm, and $\sigma = 5\times10^{-15}$ cm^2 (both values reported in a recent publication (9)); $I = 3\times10^{-6}$ amp/cm^2; $V' = 0.73$ v (a value deduced from oxidation studies in the temperature range 250 to 450° C (4)); and $\nu = 2\times10^{12}$ sec^{-1}.

From K, the result $\delta = 13.0$ Å is obtained. This value is somewhat greater than the 10 Å found to form on aluminum when it is exposed to dry oxygen for 2 hours at 25° C (11), in agreement with expectations if the proposed mechanism is accepted.

From α and t_0, $(n_0-m_0)/n_0 = 10^{-4}$, indicating a slight excess of metal in the film following electropolishing. This conclusion is consistent with the expectation that aluminum forms a metal excess oxide.

From the relation $1/t_0 = 2a\nu\sigma n_0 10^{V'/K} \exp -U/kT$ and the inequality $n_0 \ll$ the concentration of lattice cations, 4×10^{22} cm^{-3}, the result $U < 1.1$ ev is obtained. Once again this result is reasonable, comparing favorably with estimates of U for tantala films (12).

Finally, K' may be calculated as 0.41 v, which is in excellent agreement with the observed value 0.49 v. Such good agreement must be considered largely fortuitous as the estimated errors in the experimental and calculated values are 0.05 v and 0.1 v respectively.

It remains now to check the consistency of the initial assumption that δ is constant. The rate of growth of the film is given by equation [1] with E replaced by V'/δ and n replaced by the expression given in equation [3]. Integration of this rate expression assuming the change in δ, $\Delta\delta$, small compared with δ gives:

$$[5] \qquad \Delta\delta = (\Omega/\sigma) \ln [(\exp \alpha t - 1 + \alpha t_0)/\alpha t_0],$$

where Ω is the volume per metal atom in the oxide and is 2.5×10^{-23} cm^3 for alumina. For $t = 5.72\times10^6$ seconds, the longest time period, $\Delta\delta = 5.8$ Å, which would correspond to an increase of about 0.4 v (5) in the overpotential if the specific conductivity remained

Can. J. Chem. Downloaded from www.nrcresearchpress.com by 210.87.254.6 on 09/05/12
For personal use only.

constant. The value of σ used for this calculation was measured at a field strength about double that present during the supposed film growth. Since σ would be expected to increase substantially with decreasing field, this value for $\Delta\delta$ should be regarded as an upper limit.

In summary, the proposed mechanism is consistent with the data and with other available information. It is very unlikely that changes in film thickness alone are responsible for the overpotential changes, although it seems probable that the processes involved are somewhat more complex than those outlined herein.

1. R. K. Hart. Proc. Roy. Soc. (London), Ser. A, **236**, 68 (1956).
2. N. Cabrera and N. F. Mott. Rept. Progr. Phys. **12**, 163 (1949).
3. M. J. Dignam. J. Electrochem. Soc. **109**, 184 (1962).
4. M. J. Dignam. J. Electrochem. Soc. **109**, 192 (1962).
5. W. J. Bernard and J. W. Cook. J. Electrochem. Soc. **106**, 643 (1959).
6. D. D. Eley and P. R. Wilkinson. Proc. Roy. Soc. (London), Ser. A, **254**, 327 (1960).
7. C. P. Bean, J. C. Fisher, and D. A. Vermilyea. Phys. Rev. **101**, 551 (1956).
8. J. F. Dewald. J. Phys. Chem. Solids, **2**, 55 (1957).
9. P. J. Ryan and M. J. Dignam. Can. J. Chem. **40**, 1875 (1962).
10. T. B. Grimley. Discussions Faraday Soc. **28**, 223 (1959).
11. G. Hass. Z. Anorg. Chem. **254**, 96 (1947).
12. D. A. Vermilyea. J. Electrochem. Soc. **104**, 427 (1957).

Received July 10, 1962.
Aluminum Laboratories Ltd.,
Kingston, Ontario,
and
Department of Chemistry,
University of Toronto,
Toronto, Ontario.

Can. J. Chem. Downloaded from www.nrcresearchpress.com by 210.87.254.6 on 09/05/12
For personal use only.

EXCHANGE RATE AND ACTIVATION ENERGY OF EXCHANGE FOR N,N-DIMETHYLANILINE IN TRIFLUORACETIC ACID

W. F. Reynolds* and T. Schaefer

The exchange rate of N,N-dimethylaniline in trifluoracetic acid has been determined by n.m.r. techniques. The rate of change of the lifetime of the protonated aniline has been used to calculate a value for the activation energy of proton exchange.

Under conditions of slow exchange, a doublet is observed for the N,N-dimethyl group. The doublet separation is equal to the H^+—H_3C coupling constant. As the exchange rate increases the doublet collapses into a single, averaged peak. In the region of intermediate lifetime, an equation similar to that proposed by Gutowsky and Holm (1) may be used to calculate the lifetime of protonated N,N-dimethylaniline:

$$\text{(I)} \qquad \frac{\text{separation of peaks}}{\text{separation of peaks at large } \tau} = \left[1-\frac{1}{2\pi^2\tau^2[J_{(H^+-H_3C)}]^2}\right]^{1/2}.$$

τ = lifetime of protonated species in seconds, $J_{(H^+-H_3C)}$ = coupling constant in cycles/sec. The original equation was intended for exchange between two chemically non-equivalent positions, in which case [coupling constant] is replaced by [chemical shift]. The estimation of lifetime is more difficult for high and low exchange rates and involves a study of line

Holder of an N.R.C. Studentship 1961–62.

constant. The value of σ used for this calculation was measured at a field strength about double that present during the supposed film growth. Since σ would be expected to increase substantially with decreasing field, this value for $\Delta\delta$ should be regarded as an upper limit.

In summary, the proposed mechanism is consistent with the data and with other available information. It is very unlikely that changes in film thickness alone are responsible for the overpotential changes, although it seems probable that the processes involved are somewhat more complex than those outlined herein.

1. R. K. HART. Proc. Roy. Soc. (London), Ser. A, **236**, 68 (1956).
2. N. CABRERA and N. F. MOTT. Rept. Progr. Phys. **12**, 163 (1949).
3. M. J. DIGNAM. J. Electrochem. Soc. **109**, 184 (1962).
4. M. J. DIGNAM. J. Electrochem. Soc. **109**, 192 (1962).
5. W. J. BERNARD and J. W. COOK. J. Electrochem. Soc. **106**, 643 (1959).
6. D. D. ELEY and P. R. WILKINSON. Proc. Roy. Soc. (London), Ser. A, **254**, 327 (1960).
7. C. P. BEAN, J. C. FISHER, and D. A. VERMILYEA. Phys. Rev. **101**, 551 (1956).
8. J. F. DEWALD. J. Phys. Chem. Solids, **2**, 55 (1957).
9. P. J. RYAN and M. J. DIGNAM. Can. J. Chem. **40**, 1875 (1962).
10. T. B. GRIMLEY. Discussions Faraday Soc. **28**, 223 (1959).
11. G. HASS. Z. Anorg. Chem. **254**, 96 (1947).
12. D. A. VERMILYEA. J. Electrochem. Soc. **104**, 427 (1957).

RECEIVED JULY 10, 1962.
ALUMINUM LABORATORIES LTD.,
KINGSTON, ONTARIO,
AND
DEPARTMENT OF CHEMISTRY,
UNIVERSITY OF TORONTO,
TORONTO, ONTARIO.

Can. J. Chem. Downloaded from www.nrcresearchpress.com by 210.87.254.40 on 09/05/12
For personal use only.

EXCHANGE RATE AND ACTIVATION ENERGY OF EXCHANGE FOR N,N-DIMETHYLANILINE IN TRIFLUORACETIC ACID

W. F. REYNOLDS* AND T. SCHAEFER

The exchange rate of N,N-dimethylaniline in trifluoracetic acid has been determined by n.m.r. techniques. The rate of change of the lifetime of the protonated aniline has been used to calculate a value for the activation energy of proton exchange.

Under conditions of slow exchange, a doublet is observed for the N,N-dimethyl group. The doublet separation is equal to the H^+—H_3C coupling constant. As the exchange rate increases the doublet collapses into a single, averaged peak. In the region of intermediate lifetime, an equation similar to that proposed by Gutowsky and Holm (1) may be used to calculate the lifetime of protonated N,N-dimethylaniline:

$$\text{(I)} \qquad \frac{\text{separation of peaks}}{\text{separation of peaks at large } \tau} = \left[1-\frac{1}{2\pi^2\tau^2[J_{(H^+-H_3C)}]^2}\right]^{1/2}.$$

τ = lifetime of protonated species in seconds, $J_{(H^+-H_3C)}$ = coupling constant in cycles/sec. The original equation was intended for exchange between two chemically non-equivalent positions, in which case [coupling constant] is replaced by [chemical shift]. The estimation of lifetime is more difficult for high and low exchange rates and involves a study of line

Holder of an N.R.C. Studentship 1961–62.

widths (1). The calculated values of τ at different temperatures may be used to obtain an activation energy for proton exchange, using the following equation (1):

$$\text{(II)} \qquad \log_{10}\left[\frac{1}{2\pi\tau J_{(H^+-H_3C)}}\right] = \log_{10}\left[\frac{k_0}{\pi J_{(H^+-H_3C)}}\right] - \frac{E_A}{2.303RT}.$$

E_A = activation energy, k_0 = frequency factor. This equation is in the standard slope plus intercept form and a plot of $\log_{10}[1/(2\pi\tau J)]$ vs. $1/T$ should give a value for the activation energy from the slope.

EXPERIMENTAL

The sample solution contained 10.0 mole% N,N-dimethylaniline in CF_3COOH. Both chemicals were Eastman Grade as supplied by Distillation Products Ind. and were used without further purification. The sample was degassed and sealed in an evacuated 5 mm O.D. sample tube.

Spectra were run on a Varian dual purpose 60 Mc spectrometer. Temperature control was provided by a temperature device constructed at the National Research Council (2). Temperature was measured by an iron–constantan thermocouple attached to a Minneapolis-Honeywell Brown recording potentiometer. The temperature was kept constant and measured within 0.2° C.

The separation of the doublet peaks was measured by placing side bands of the doublet on both sides of itself, approximately 20 cycles/sec away. Each spectrum was repeated 10 times forward and reverse. Side-band frequencies were measured by a Hewlett–Packard Model 521 C electronic counter.

RESULTS

Measured values of doublet separations, as well as root mean square deviation in these values, are given in Table I. The temperature range was chosen so that the exchange rate

TABLE I

The values of proton exchange rates as calculated from measured doublet separations

Temperature (°C)	Doublet separation (cycles/sec)	Lifetime of protonated molecule (sec)	Exchange rate (sec^{-1})
17.6±0.2	5.26±0.03	—	—
26.8 "	5.26±0.03	—	—
46.8 "	5.11±0.04	0.189±0.029	5.3±0.9
50.6 "	5.02±0.03	0.143±0.010	7.0±0.5
52.8 "	4.90±0.06	0.118±0.010	8.5±0.8
55.5 "	4.67±0.04	0.093±0.003	10.8±0.4
57.0 "	4.52±0.03	0.084±0.002	11.9±0.3
58.9 "	4.11±0.05	0.069±0.001	14.6±0.3
60.6 "	3.65±0.10	0.060±0.001	16.8±0.4

could be calculated, using equation (I). At higher temperatures, where the two peaks were broad and almost coalesced, the error in measuring the separation was very large. At lower temperatures, small differences in the measured separations result in large errors in the calculated exchange rates.

The constancy of the measured separation at the two lowest temperatures would indicate that the condition of slow exchange is fulfilled at these temperatures. Therefore, the coupling constant should be the same as the measured separation.

The limits of error in measurements of temperature and τ are shown in Fig. 1 by the rectangular boxes. The solid line gives the least-squares plot for the last six measurements. The measured value for 46.8° C was not included in the least-squares plot due to the

Can. J. Chem. Downloaded from www.nrcresearchpress.com by 210.87.254.40 on 09/05/12
For personal use only.

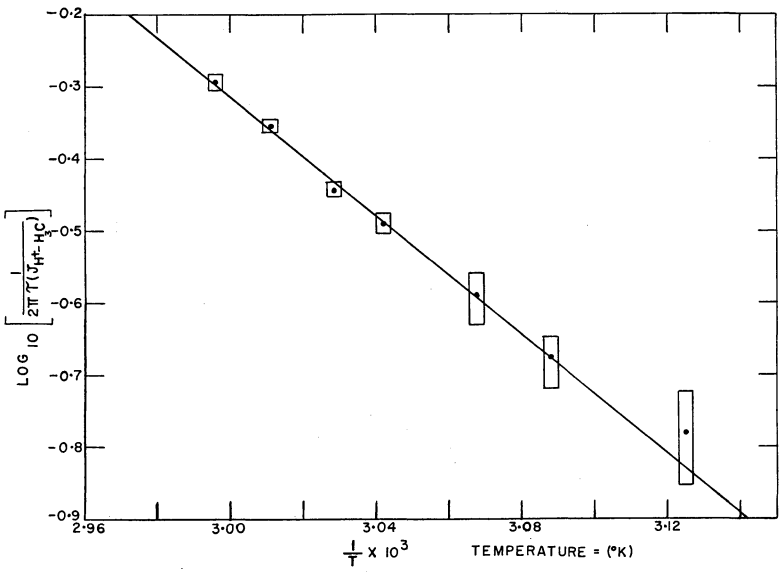

FIG. 1. Temperature dependence of the amino proton exchange rate of N,N-dimethylaniline in trifluoracetic acid.

large possible error. The slope of the line was $-4.11\times10^{3°}$ K. The most extreme values of slope which could be obtained for lines passing through the limits of experimental error were $-3.64\times10^{3°}$ K and $-4.55\times10^{3°}$ K. A further uncertainty of $0.25\times10^{3°}$ K is introduced due to possible error in the value of the coupling constant. By multiplying by the constant $2.303R$, the value of 18.8 ± 3.2 kcal/mole was obtained for the activation energy of proton exchange.

The value of k_0, the frequency factor, was calculated from equation (II). The calculated value was 1.7×10^{13} sec^{-1} with a possible range of 6×10^{11} to 4×10^{14} sec^{-1}. The frequency factor represents the internal vibration frequency of the protonated molecule. The value obtained is considerably higher than those obtained elsewhere, by n.m.r., for different molecules (1). However, its magnitude is in agreement with the classical theory of unimolecular reactions, in which the frequency factor should lie in the range 10^{12} to 10^{14} sec^{-1} (3).

Complete collapse of the doublet should occur when the exchange rate exceeds the value $2\pi J_{(H^+-H_3C)}$. By extrapolation from the graph, the temperature at which this exchange rate would be exceeded is 69° C. As expected, the doublet collapse occurs over a range of temperature, starting at about 65° C. It is impossible to determine the exact temperature at which the peaks overlap.

The exchange rate is strongly a function of concentration. A 5 mole% solution of N,N-dimethylaniline in acid showed no appreciable change in doublet separation up to 150° C. Higher temperatures could not be obtained due to the high vapor pressure of the solvent.

It is planned to study the effect of base concentration and pH upon the exchange rate for N,N-dimethylaniline and similar substituted anilines. A series of ring-substituted N-alkyl anilines will be investigated to determine the effect of substituent groups upon exchange rates and activation energies. Non-aqueous acids with a larger liquid range will also be used.

Can. J. Chem. Downloaded from www.nrcresearchpress.com by 210.87.254.40 on 09/05/12
For personal use only.

ACKNOWLEDGMENTS

We thank Mr. G. Ensell for the construction of the variable-temperature assembly. The work was supported by the National Research Council and the Research Corporation.

1. H. S. GUTOWSKY and C. H. HOLM. J. Chem. Phys. **25**, 1228 (1956).
2. J. A. POPLE, W. G. SCHNEIDER, and H. J. BERNSTEIN. High resolution nuclear magnetic resonance. McGraw-Hill Book Co., Inc., New York, N.Y. 1959. p. 73.
3. S. W. BENSON. The foundations of chemical kinetics. McGraw-Hill Book Co., Inc., New York, N.Y. 1960. p. 250.

RECEIVED SEPTEMBER 21, 1962.
DEPARTMENT OF CHEMISTRY,
UNIVERSITY OF MANITOBA,
WINNIPEG, MANITOBA.

Can. J. Chem. Downloaded from www.nrcresearchpress.com by 210.87.254.40 on 09/05/12
For personal use only.

THE PREPARATION OF SOME NEW 1-PHENYL-2-NITROETHANOL DERIVATIVES

R. A. HEACOCK AND O. HUTZINGER

An improved method for the synthesis of 1-phenyl-2-nitroethanol derivatives, substituted in the 3- and 4-positions of the benzene ring (of the general type shown in formula III), has recently been described (1). The preparative procedure involved condensation of a suitable aldehyde (I) with excess nitromethane (II: $R_5 = H$) at about 5°, in the presence of sodium hydroxide in aqueous alcoholic solution, using a very short reaction time ($\gtrsim$60 seconds).

This communication describes the preparation of eight further examples of this class of compound containing two, three, or four substituents in the benzene ring. (In all cases, the substituents in the 3- and 4-positions of the aromatic ring were either methoxy or benzyloxy groups.) Uusally, no particular difficulties were encountered when the condensation was carried out with nitroethane (II: $R_5 = CH_3$) instead of nitromethane (II: $R_5 = H$). However, 4-benzyloxy-3,5-dimethoxybenzaldehyde, which condensed readily with nitromethane under the conditions described above, could not be induced to condense with nitroethane by this technique. The following new 1-phenyl-2-nitroethanol derivatives have been prepared: 4-benzyloxy-3,5-dimethoxy-α-nitromethylbenzyl

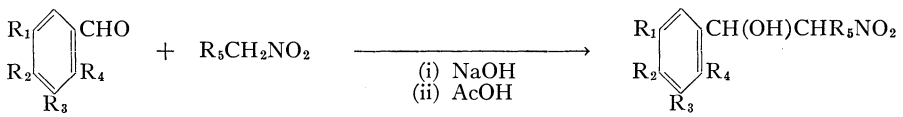

I II III

alcohol (III: $R_1 = R_3 = OCH_3$; $R_2 = OCH_2C_6H_5$; $R_4 = R_5 = H$); 3,4,5-trimethoxy-α-(1-nitroethyl)-benzyl alcohol (III: $R_1 = R_2 = R_3 = OCH_3$; $R_4 = H$; $R_5 = CH_3$); 3,4-dimethoxy-6-nitro-α-nitromethylbenzyl alcohol (III: $R_1 = R_2 = OCH_3$; $R_3 = R_5 = H$; $R_4 = NO_2$); 3,4-dimethoxy-6-nitro-α-(1-nitroethyl)-benzyl alcohol (III: $R_1 = R_2 = OCH_3$; $R_3 = H$; $R_4 = NO_2$; $R_5 = CH_3$); 5-iodo-3,4-dimethoxy-α-nitromethylbenzyl alcohol (III: $R_1 = R_2 = OCH_3$; $R_3 = I$; $R_4 = R_5 = H$); 5-iodo-3,4-dimethoxy-α-(1-nitroethyl)-benzyl alcohol (III: $R_1 = R_2 = OCH_3$; $R_3 = I$; $R_4 = H$; $R_5 = CH_3$);

ACKNOWLEDGMENTS

We thank Mr. G. Ensell for the construction of the variable-temperature assembly. The work was supported by the National Research Council and the Research Corporation.

1. H. S. GUTOWSKY and C. H. HOLM. J. Chem. Phys. **25**, 1228 (1956).
2. J. A. POPLE, W. G. SCHNEIDER, and H. J. BERNSTEIN. High resolution nuclear magnetic resonance. McGraw-Hill Book Co., Inc., New York, N.Y. 1959. p. 73.
3. S. W. BENSON. The foundations of chemical kinetics. McGraw-Hill Book Co., Inc., New York, N.Y. 1960. p. 250.

RECEIVED SEPTEMBER 21, 1962.
DEPARTMENT OF CHEMISTRY,
UNIVERSITY OF MANITOBA,
WINNIPEG, MANITOBA.

Can. J. Chem. Downloaded from www.nrcresearchpress.com by 210.87.254.42 on 09/05/12
For personal use only.

THE PREPARATION OF SOME NEW 1-PHENYL-2-NITROETHANOL DERIVATIVES

R. A. HEACOCK AND O. HUTZINGER

An improved method for the synthesis of 1-phenyl-2-nitroethanol derivatives, substituted in the 3- and 4-positions of the benzene ring (of the general type shown in formula III), has recently been described (1). The preparative procedure involved condensation of a suitable aldehyde (I) with excess nitromethane (II: $R_5 = H$) at about 5°, in the presence of sodium hydroxide in aqueous alcoholic solution, using a very short reaction time (≥ 60 seconds).

This communication describes the preparation of eight further examples of this class of compound containing two, three, or four substituents in the benzene ring. (In all cases, the substituents in the 3- and 4-positions of the aromatic ring were either methoxy or benzyloxy groups.) Uusally, no particular difficulties were encountered when the condensation was carried out with nitroethane (II: $R_5 = CH_3$) instead of nitromethane (II: $R_5 = H$). However, 4-benzyloxy-3,5-dimethoxybenzaldehyde, which condensed readily with nitromethane under the conditions described above, could not be induced to condense with nitroethane by this technique. The following new 1-phenyl-2-nitroethanol derivatives have been prepared: 4-benzyloxy-3,5-dimethoxy-α-nitromethylbenzyl

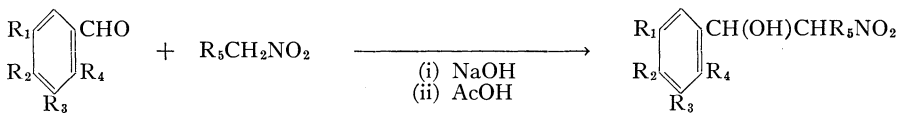

I II III

alcohol (III: $R_1 = R_3 = OCH_3$; $R_2 = OCH_2C_6H_5$; $R_4 = R_5 = H$); 3,4,5-trimethoxy-α-(1-nitroethyl)-benzyl alcohol (III: $R_1 = R_2 = R_3 = OCH_3$; $R_4 = H$; $R_5 = CH_3$); 3,4-dimethoxy-6-nitro-α-nitromethylbenzyl alcohol (III: $R_1 = R_2 = OCH_3$; $R_3 = R_5 = H$; $R_4 = NO_2$); 3,4-dimethoxy-6-nitro-α-(1-nitroethyl)-benzyl alcohol (III: $R_1 = R_2 = OCH_3$; $R_3 = H$; $R_4 = NO_2$; $R_5 = CH_3$); 5-iodo-3,4-dimethoxy-α-nitromethylbenzyl alcohol (III: $R_1 = R_2 = OCH_3$; $R_3 = I$; $R_4 = R_5 = H$); 5-iodo-3,4-dimethoxy-α-(1-nitroethyl)-benzyl alcohol (III: $R_1 = R_2 = OCH_3$; $R_3 = I$; $R_4 = H$; $R_5 = CH_3$);

TABLE

Preparation of nitroalcohols

Nitroalcohol prepared					Reagents used and reaction conditions						Yield of purified product	
R_1	R_2	R_3	R_4	R_5	Aldehyde (g)	CH_3NO_2 (ml)	$C_2H_5NO_2$ (ml)	Solvent	10% NaOH (ml)	2% AcOH (ml)	(g)	(%)
CH_3O	$C_6H_5CH_2O$	CH_3O	H	H	1.0	0.7	—	95% ethanol (20 ml)	1.3	11.5	0.9	74
CH_3O	CH_3O	CH_3O	H	CH_3	1.0	—	1.2	95% ethanol (20 ml)	1.84	16.0	0.4	29
CH_3O	CH_3O	H	NO_2	H	1.0	0.7	—	Ethanol (40 ml) +dioxane (5 ml)	1.72	14.2	0.9	70
CH_3O	CH_3O	H	NO_2	CH_3	1.0	—	1.0	Ethanol (40 ml) +dioxane (5 ml)	1.72	14.2	0.6	44.5
CH_3O	CH_3O	I	H	H	0.5	0.35	—	Ethanol (10 ml) +dioxane (2 ml)	0.6	5.5	0.4	66
CH_3O	CH_3O	I	H	CH_3	1.0	—	1.0	Ethanol (20 ml) +dioxane (5 ml)	1.2	11.0	0.8	63.5
CH_3O	CH_3O	I	NO_2	H	0.5	0.35	—	Ethanol (7 ml) +dioxane (7 ml)	0.55	4.6	0.4	68
CH_3O	CH_3O	I	NO_2	CH_3	0.2	—	0.18	Ethanol (2 ml) +dioxane (2 ml)	0.22	1.8	0.17	69.5

*The crude product, an oil, was stirred with concentrated sodium bisulphite solution for 20 minutes before recrystallization from benzene.
†LP = light petroleum (b.p. 60–80°); B.D.H. AnalaR grade.

5-iodo-3,4-dimethoxy-6-nitro-α-nitromethylbenzyl alcohol (III: $R_1 = R_2 = OCH_3$; $R_3 = I$; $R_4 = NO_2$; $R_5 = H$); 5-iodo-3,4-dimethoxy-6-nitro-α-(1-nitroethyl)-benzyl alcohol (III: $R_1 = R_2 = OCH_3$; $R_3 = I$; $R_4 = NO_2$; $R_5 = CH_3$).

Unsuccessful attempts were made to condense 3-benzyloxy-4-methoxybenzaldehyde and 3,4-dibenzyloxybenzaldehyde with nitromethane using this procedure; in both cases the starting material was essentially recovered unchanged, even when considerably longer reaction times were employed. The failure of these two aldehydes to condense with nitromethane under the conditions employed is not altogether surprising in view of the fact that veratraldehyde would not condense with nitroalkanes in similar circumstances (cf. ref. 1).

EXPERIMENTAL

Aldehydes

4-Benzyloxy-3,5-dimethoxybenzaldehyde.—A solution of 4-hydroxy-3,5-dimethoxybenzaldehyde (12.0 g), potassium hydroxide (4 g), and benzyl chloride (9.0 g) in ethanol (60 ml) was boiled under reflux for 4 hours. The product was poured into water, and the aqueous reaction mixture repeatedly extracted with ether. The ethereal extract was washed with aqueous potassium hydroxide and water, dried (Na_2SO_4), and on evaporation to dryness, afforded a pale yellow oil, which on purification by distillation in vacuum (b.p. 190° at 0.5–1.0 mm) and recrystallization first from 95% ethanol and finally from benzene/light petroleum (b.p. 80–100°) afforded 4-benzyloxy-3,5-dimethoxybenzaldehyde as colorless prisms, m.p. 63°. Kratzl *et al.* prepared this compound by a somewhat different procedure but report the same melting point (2).

3,4,5-Trimethoxybenzaldehyde and 6-nitroveratraldehyde.—These compounds were obtained from the Aldrich Chemical Company.

5-Iodoveratraldehyde.—This compound was prepared by the methylation of 5-iodovanillin by the method of Dominguez *et al.* (3).

Can. J. Chem. Downloaded from www.nrcresearchpress.com by 210.87.254.42 on 09/05/12
For personal use only.

I

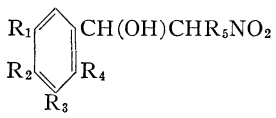

Properties of products			Analyses							
			Found				Calculated			
Crystalline form	M.p. (°C)	Empirical formula	C	H	N	I	C	H	N	I
Colorless prisms from benzene	108	$C_{17}H_{19}O_6N$	61.09	5.56	4.10	—	61.25	5.75	4.20	—
Colorless prisms* from benzene	135	$C_{12}H_{17}O_6N$	53.20	6.46	5.08	—	53.13	6.32	5.16	—
Pale yellow needles from benzene (darken in light)	142	$C_{10}H_{12}O_7N_2$	44.25	4.54	10.31	—	44.12	4.44	10.29	—
Colorless needles (yellow in light) from benzene	141–142	$C_{11}H_{14}O_7N_2$	46.26	5.06	9.80	—	46.15	4.93	9.79	—
Colorless needles from benzene/LP†	120	$C_{10}H_{12}O_6NI$	34.09	3.40	3.71	35.86	34.01	3.42	3.96	35.94
Colorless prisms from aqueous ethanol	135	$C_{11}H_{14}O_6NI$	35.91	3.97	3.73	34.40	35.98	3.85	3.82	34.57
Pale yellow prisms from benzene/LP†	126–127	$C_{10}H_{11}O_7N_2I$	30.15	2.84	7.01	31.96	30.16	2.78	7.04	31.88
Pale yellow prisms from benzene/LP†	162	$C_{11}H_{13}O_7N_2I$	32.36	3.30	6.80	30.84	32.05	3.18	6.79	30.79

5-Iodo-6-nitroveratraldehyde.—This compound was prepared by the nitration of 5-iodoveratraldehyde, the nitroaldehyde being purified via its bisulphite derivative (4).

1-Phenyl-2-nitroethanol Derivatives (General Procedure) (cf. Ref. 1)*

Aqueous sodium hydroxide (10%; 1.05 mole) was added with stirring to a mixture of the aldehyde and nitromethane (2–3 mole) dissolved in a suitable solvent (see Table I) at ca. 5°; the product was vigorously stirred for a further 30–45 seconds. Aqueous acetic acid (2%) was then added to halt the reaction and decompose the sodium derivative of the nitroalcohol; the crude product separated out as a yellow to colorless solid or oil. After being allowed to stand at 4° for 1 hour, the crude product was filtered and purified by repeated recrystallization from a suitable solvent.

In the previous note on this subject (1), it was reported that 95% alcohol was invariably used as a solvent for this type of reaction mixture. However, in several of the cases described above, the solubility of the aldehyde in 95% ethanol was quite low, and it was necessary to use mixtures of absolute alcohol and dioxane to ensure complete solution of all the reactants.

This investigation was supported by grants from the Department of National Health and Welfare (Ottawa) and the Government of Saskatchewan (Department of Public Health).

1. R. A. Heacock, O. Hutzinger, and C. Nerenberg. Can. J. Chem. **39**, 1143 (1961).
2. K. Kratzl, T. Horejschi, and G. Billek. Monatsh. **85**, 1154 (1954).
3. X. A. Dominguez, G. L. Diaz, and F. V. Gonzalez. Ciencia (Mex.), **15**, 208 (1955); Chem. Abstr. **50**, 12886 (1956).
4. R. A. Heacock and O. Hutzinger. In preparation.

Received September 17, 1962.
Psychiatric Research Unit,
University Hospital,
Saskatoon, Saskatchewan.

**The specific quantities of reagents used are given in Table I.*

Can. J. Chem. Downloaded from www.nrcresearchpress.com by 210.87.254.42 on 09/05/12
For personal use only.

PRESSURE EFFECT AND MECHANISM IN ACID CATALYSIS XII. RACEMIZATION OF *sec*-BUTANOL[1]

R. J. WITHEY[2] AND E. WHALLEY

1. INTRODUCTION

The acid-catalyzed racemization of *sec*-butanol (1, 2), which is usually assumed to go via a pre-equilibrium proton transfer, is about twice as fast as the acid-catalyzed exchange of oxygen between *sec*-butanol and the solvent, so that inversion occurs at each substitution. The rates of both processes are approximately proportional to the acidity function h_0 and it was concluded (1), because of this, that the slow step is unimolecular

$$C_2H_5.CH_3CHOH_2^+ \rightleftharpoons C_2H_5.CH_3CH^+ + H_2O.$$

The Zucker–Hammett hypothesis (3) on which this conclusion is based has since been shown to be invalid (4, 5), and so there was no evidence about the mechanism. In fact the occurrence of inversion at every exchange can be interpreted to favor a bimolecular slow step, and Bunnett (6), who has reinterpreted the rates in concentrated acids, concludes that they show that the slow step is bimolecular. We have therefore attempted to learn more about the mechanism by measuring the volume of activation (see ref. 7 and later papers) for the racemization.

2. EXPERIMENTAL METHODS AND RESULTS

sec-Butanol was resolved via the brucine salt of its hydrogen phthalate ester by the method of Kantor and Hauser (8). The alcohol, b.p. 98–99° C, $[\alpha]_D^{20°} = +13.28°$, was obtained by hydrolyzing the resolved ester. The highest specific rotation reported (9) is 13.52°, so the alcohol appeared to be at least 98% optically pure.

Reagent grade perchloric acid (1.012 *M*) was used as catalyst. About 1.3 g of *sec*-butanol in 50 cm³ of acid solution was used for each run, resulting in an initial optical rotation of about 1°.

The rotation was measured with a Rudolph model 70 polarimeter which was modified to allow changes of rotation of 0.001° to be measured. The front cover was removed and a rigid brass beam was bolted to the graduated circle. A ball bearing pressed into the end of the beam rested on the head of a micrometer graduated in 0.0001 in. The reproducibility was better than ±0.0001 in., which corresponded to about ±0.001°. Since the rotation during a run changed by only ½–1°, direct readings of the micrometer were used to calculate the first-order rate constants. A 4-dm micropolarimeter tube of volume ~5 cm³ was used and at least 10 readings of the rotation were taken for each sample. Infinity readings were determined by keeping samples of the reaction solution in sealed ampoules at 100.3° C for at least 10 half-lives. The rotation was always zero within the experimental error.

The pressure system was similar to that described previously (10). About eight samples were taken during each run.

Formation of olefin during the reaction at ordinary pressure was tested for by the method used by Bunton, Konasiewicz, and Llewellyn (1). In 24 hours, less than 0.4% of the alcohol was converted to olefin, and so any conversion can be ignored.

The first-order rate constants k_1, which are accurate to about ½%, and second-order rate constants k_a ($= k_1/c_{HClO_4}$, where c_{HClO_4} is the concentration of perchloric acid at the temperature and pressure (11) of the experiment) are listed in Table I. They agree well with previous measurements (1) at 99.8° when allowance is made for the small difference in temperature. The volume of activation defined as

$$\Delta V^{\ddagger} = -RT\partial \ln k_a/\partial p$$

is $-0.7 \pm \sim 0.5$ cm³ mole^{-1}. In fact, the racemization is more nearly first order in h_0 than in concentration of hydrogen ion (1, 2), and so the increase in rate due to compression of the acid may be somewhat greater than the increase in density. This would make the real volume of activation, calculated from the pseudo

[1]*Issued as N.R.C. No. 7106.*
[2]*N.R.C. Postdoctoral Fellow 1960–1962.*

Can. J. Chem. Downloaded from www.nrcresearchpress.com by 210.87.254.6 on 09/05/12
For personal use only.

TABLE I

Rate constants for the acid-catalyzed racemization of *sec*-butanol at 100.3° C in 1.012 *M* (at room temperature and pressure) perchloric acid

p/bar	$10^6 k_1$/sec^{-1}	$10^6 k_a$/l. mole^{-1} sec^{-1}
1	241	249
100	243	249
1000	256	253
1000	257	254
2000	270	259
2000	270	259
3000	283	264

second-order rate constant k_1/h_0, less negative than the above value. This would have no effect on the conclusions drawn in the next section.

3. DISCUSSION

A bimolecular mechanism

$$H_2O + d\text{-}sec\text{-}C_4H_9OH_2^+ \rightarrow l\text{-}sec\text{-}C_4H_9OH_2^+ + H_2O$$

would have a volume of activation of around -8 or -10 cm^3 mole^{-1} (7). A unimolecular mechanism

$$d\text{-}sec\text{-}C_4H_9OH_2^+ \underset{k_2}{\overset{k_1}{\rightleftharpoons}} sec\text{-}C_4H_9^+ + H_2O$$

$$sec\text{-}C_4H_9^+ + H_2O' \xrightarrow{k_3} l\text{-}sec\text{-}C_4H_9O'H_2^+,$$

where H_2O' is a different water molecule from that formed from the alcohol and which presumably attacks from the opposite side of the *sec*-butyl ion, would give a volume of activation of about zero or slightly positive whatever the relative magnitudes of k_2 and k_3. The measured volume of activation of $-0.7 \pm \sim 0.5$ cm^3 mole^{-1} clearly shows that the mechanism is unimolecular. The entropy of activation, which is about 12 cal mole^{-1} deg^{-1} (2), in consistent with this mechanism, but does not support it except on purely empirical grounds (7).

The modification of the Zucker–Hammett relation proposed by Bunnett (6) indicates that the mechanism is bimolecular, and it is therefore not valid for the racemization of *sec*-butanol.

1. C. A. Bunton, A. Konasiewicz, and D. R. Llewellyn. J. Chem. Soc. 604 (1955).
2. C. A. Bunton and D. R. Llewellyn. J. Chem. Soc. 3402 (1957).
3. L. M. Zucker and L. P. Hammett. J. Am. Chem. Soc. **61**, 2791 (1939).
4. J. Koskikallio and E. Whalley. Trans. Faraday Soc. **55**, 815 (1959).
5. J. Koskikallio and E. Whalley. Can. J. Chem. **37**, 788 (1959).
6. J. F. Bunnett. J. Am. Chem. Soc. **83**, 4956 etc. (1961).
7. E. Whalley. Trans. Faraday Soc. **55**, 798 (1959).
8. S. W. Kantor and C. R. Hauser. J. Am. Chem. Soc. **75**, 1744 (1953).
9. J. Timmermans and F. Martin. J. Chim. Phys. **25**, 431 (1928).
10. J. Koskikallio and E. Whalley. Trans. Faraday Soc. **55**, 809 (1959). A. R. Osborn and E. Whalley. Can. J. Chem. **39**, 1094 (1961).
11. P. W. Bridgman. Proc. Am. Acad. Arts Sci. **66**, 185 (1931).

Received September 25, 1962.
Division of Applied Chemistry,
National Research Council,
Ottawa, Canada.

Can. J. Chem. Downloaded from www.nrcresearchpress.com by 210.87.254.6 on 09/05/12
For personal use only.

GAS CHROMATOGRAPHIC SEPARATION OF HYDROGEN ISOTOPES ON ACTIVATED ALUMINA*

M. VENUGOPALAN† AND K. O. KUTSCHKE

Can. J. Chem. Downloaded from www.nrcresearchpress.com by 210.87.254.105 on 09/05/12
For personal use only.

The quantitative separation of hydrogen, hydrogen deuteride, and deuterium using a chromia–alumina column operated at 77° K with neon as the carrier gas was reported by Smith and Hunt (1, 2). Subsequently Moore and Ward (3), Shipman (4), and Furuyama and Kwan (5) have shown that good isotopic separation results with helium as the carrier gas on columns of alumina "coated" with ferric oxide. It was observed by Moore and Ward (3) that columns of strongly activated (480° C, 8 hours) reagent-grade alumina (apparently iron-free) also lead to ortho–para equilibration. We have confirmed this observation and applied this method successfully to the quantitative analysis of micromole quantities of the hydrogen isotopes.

Pyrex columns packed with alumina were activated at 450° for 1 week in flowing helium and operated at 77° K. Detection was by means of a katharometer (Gow-Mac Model 9285) with prior oxidation over hot CuO (3, 4). Two grades of alumina (activated alumina, Aluminum Company of America; alumina for adsorption, Fisher Scientific Company) showed similar chromatographic behavior for the same particle size.

Commercial hydrogen and deuterium were passed through a palladium thimble and stored in 1-liter bulbs at 110 mm pressure. Hydrogen deuteride was prepared by slowly passing the vapors from well-outgassed heavy water over lithium aluminum hydride deposited on glass wool. Several first samples of the HD generated were analyzed mass spectrometrically. A purity of 95% was observed, the remainder being H_2 and D_2. A chromatographic analysis of the same HD, run at maximum sensitivity, showed no peak for H_2 and D_2; for these conditions an amount of H_2 equal to 1% of the HD taken could have been detected readily. It seems probable that much of the 5% H_2 and D_2, indicated as an impurity by mass spectrometric analysis, arose from partial equilibration of the HD in the ion source of the instrument. After storage for 6 months, small amounts (<3% each) of H_2 and D_2 could be detected in the HD by the gas chromatograph. Mass spectrometric analysis at this time indicated the presence of about 5% each of H_2 and D_2.

Each of the three storage bulbs was attached to the vacuum system with two capillary stopcocks; the volume between the stopcocks was chosen to contain approximately one micromole of gas, which could be transferred quantitatively to a gas burette for measurement. A sample could be removed from the gas burette and sealed, behind a thread of solid mercury, into a length of 3 mm o.d. tubing; such sample tubes were crushed in the stream of carrier gas. Mixtures of the isotopes could be prepared in analogous fashion.

A typical chromatogram of micromole quantities of the hydrogen isotope mixture is shown in Fig. 1. The H_2, HD, and D_2 peaks appeared at 13.5, 17.9, and 28.2 minutes respectively for the column and flow conditions specified in the caption.

Preliminary calibration curves of peak areas for H_2, HD, and D_2 were linear in the range 0.5 to 4 μmoles of the isotopes; for smaller quantities some curvature was noted in each plot. The slopes of the straight-line portions of these plots were 0.254, 0.267, and 0.238 (arbitrary units) for H_2, HD, and D_2 respectively. Work is in progress to establish the precise shape of the calibration curve in the region of 10^{-7} moles.

*Issued as N.R.C. No. 7096.
†*National Research Council Postdoctoral Fellow 1961–1962.*

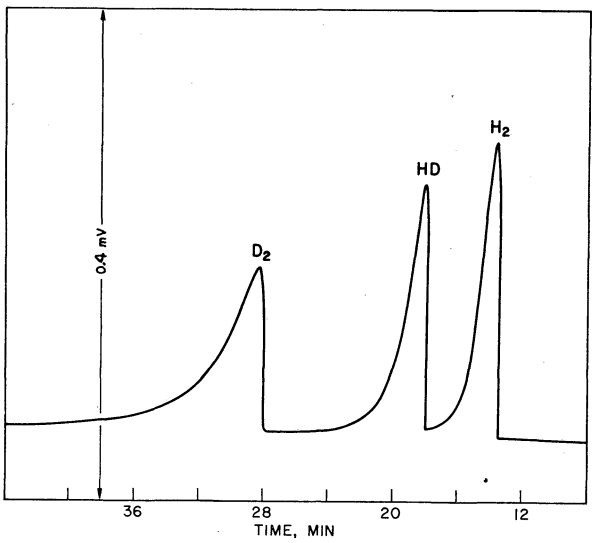

FIG. 1. Separation of a mixture of 1.073 μmoles of H_2, 1.106 μmoles of HD, and 1.341 μmoles of D_2 on a 80–100 mesh, strongly activated, 0.4-cm×6-ft alumina (Fisher) column. Column temperature, −196° C; helium flow rate, 100 cc/min at column exit; combustion temperature, 416° C; bridge current, 302 ma. Peak areas in arbitrary units are 0.264, 0.265, 0.339 for H_2, HD, and D_2 respectively.

ACKNOWLEDGMENT

The authors wish to thank Mr. R. J. Pilon for his assistance in the early trials of this technique.

1. H. A. SMITH and P. P. HUNT. J. Phys. Chem. **64**, 383 (1960).
2. P. P. HUNT and H. A. SMITH. J. Phys. Chem. **65**, 87 (1961).
3. W. R. MOORE and H. R. WARD. J. Phys. Chem. **64**, 832 (1960).
4. G. F. SHIPMAN. Anal. Chem. **34**, 877 (1962).
5. S. FURUYAMA and T. KWAN. J. Phys. Chem. **65**, 190 (1961).

RECEIVED SEPTEMBER 20, 1962.
DIVISION OF PURE CHEMISTRY,
NATIONAL RESEARCH COUNCIL,
OTTAWA, CANADA.

SYNTHESIS OF ALKYLETHYNYL COMPOUNDS OF MERCURY[1]

M. KRAUT AND L. C. LEITCH

Alkylethynyl and arylethynyl compounds of germanium (4), antimony (2), and bismuth (3) have recently been reported for the first time. The synthesis of the corresponding mercury compounds with the formula $RHgC{\equiv}CH$ where R is CH_3, C_2H_5, *n*-C_3H_7, *i*-C_3H_7, *i*-C_4H_9, and *tert*-C_4H_9 is now reported. These new organic mercurials were prepared from alkyl mercuric halides and ethynyl magnesium bromide as described in the experimental part. Methylethynyl mercury and ethylethynyl mercury are solids melting at 117–118° and 71–72° respectively while the higher members are liquids of

[1]*Issued as N.R.C. No. 7137.*

Can. J. Chem. Downloaded from www.nrcresearchpress.com by 210.87.254.105 on 09/05/12
For personal use only.

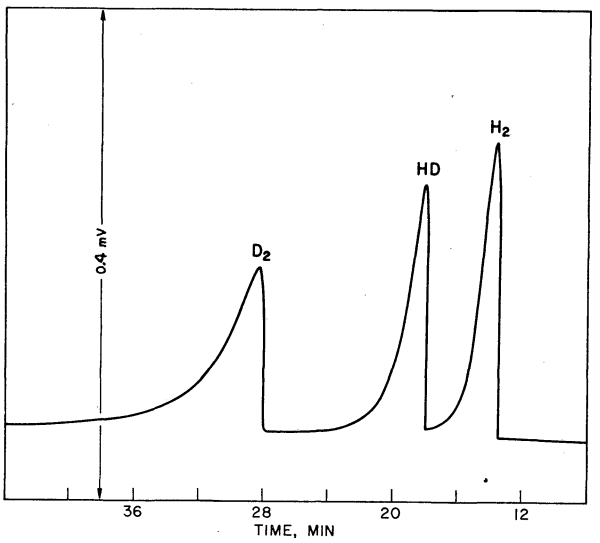

FIG. 1. Separation of a mixture of 1.073 μmoles of H_2, 1.106 μmoles of HD, and 1.341 μmoles of D_2 on a 80–100 mesh, strongly activated, 0.4-cm×6-ft alumina (Fisher) column. Column temperature, −196° C; helium flow rate, 100 cc/min at column exit; combustion temperature, 416° C; bridge current, 302 ma. Peak areas in arbitrary units are 0.264, 0.265, 0.339 for H_2, HD, and D_2 respectively.

ACKNOWLEDGMENT

The authors wish to thank Mr. R. J. Pilon for his assistance in the early trials of this technique.

1. H. A. SMITH and P. P. HUNT. J. Phys. Chem. **64**, 383 (1960).
2. P. P. HUNT and H. A. SMITH. J. Phys. Chem. **65**, 87 (1961).
3. W. R. MOORE and H. R. WARD. J. Phys. Chem. **64**, 832 (1960).
4. G. F. SHIPMAN. Anal. Chem. **34**, 877 (1962).
5. S. FURUYAMA and T. KWAN. J. Phys. Chem. **65**, 190 (1961).

RECEIVED SEPTEMBER 20, 1962.
DIVISION OF PURE CHEMISTRY,
NATIONAL RESEARCH COUNCIL,
OTTAWA, CANADA.

SYNTHESIS OF ALKYLETHYNYL COMPOUNDS OF MERCURY[1]

M. KRAUT AND L. C. LEITCH

Alkylethynyl and arylethynyl compounds of germanium (4), antimony (2), and bismuth (3) have recently been reported for the first time. The synthesis of the corresponding mercury compounds with the formula $RHgC{\equiv}CH$ where R is CH_3, C_2H_5, *n*-C_3H_7, *i*-C_3H_7, *i*-C_4H_9, and *tert*-C_4H_9 is now reported. These new organic mercurials were prepared from alkyl mercuric halides and ethynyl magnesium bromide as described in the experimental part. Methylethynyl mercury and ethylethynyl mercury are solids melting at 117–118° and 71–72° respectively while the higher members are liquids of

[1]*Issued as N.R.C. No. 7137.*

Can. J. Chem. Downloaded from www.nrcresearchpress.com by 210.87.254.40 on 09/05/12
For personal use only.

low volatility. They have been characterized by their mass spectra, which give a peak corresponding to the fragment $^{+}HgC{\equiv}CH$. Further work on these interesting new compounds is in active progress and will be reported in detail later.

EXPERIMENTAL

Ethylethynyl Mercury, $C_2H_5HgC{\equiv}CH$

A magnetically stirred solution of ethynylmagnesium bromide, freshly prepared by the method given in reference 5 from 2.07 g (0.086 atoms) of magnesium in 125 ml of tetrahydrofuran, was cooled in ice–water, while there was added dropwise, over a period of 50 minutes, a solution of 8.75 g (0.0247 mole) of ethyl mercuric iodide (1) in 50 ml of tetrahydrofuran. A slow current of dry nitrogen was passed through the apparatus all the while. After addition of the solution had been completed the reaction mixture was stirred for 17 hours at room temperature. It was then cooled to +5° and added slowly to a stirred ice-cold mixture of 450 ml of 6.6% aqueous ammonium nitrate and 190 ml of ether. The lower aqueous layer was separated and extracted twice with two 100-ml portions of ether. The combined ether extracts were washed with two 200-ml portions of water and dried over anhydrous magnesium sulphate. After evaporation of solvent under reduced pressure 5.37 g of yellow crystalline product with a characteristic bad odor remained. Sublimation of the crude material at room temperature under a pressure of 1 mm gave 4.6 g of white crystalline sublimate, m.p. 71–72°. Yield: 73.4%.

The mass analysis of the compound showed peaks at 254, 255, and 256 corresponding to $C_2H_5Hg^{200}C_2H$, $C_2H_5Hg^{201}C_2H$, and $C_2H_5Hg^{202}C_2H$ and also peaks at 225, 226, and 227, which in turn corresponded to $Hg^{200}C{\equiv}CH$, $Hg^{201}C{\equiv}H$, and $Hg^{202}C{\equiv}CH$.

The authors are indebted to Dr. F. P. Lossing of these laboratories for the mass analysis of the compound.

1. A. A. Baldoni and J. J. Miyashiro. To Morton Chem. Co. U.S. Patent No. 2,914,451 (Nov. 24, 1959); Chem. Abstr. **54**, 5467*e*.
2. H. Hartmann and G. Z. Kühl. Z. Anorg. Allgem. Chem. **312**, 186 (1961).
3. H. Hartmann, G. Habenicht, and W. Reiss. Z. Anorg. Allgem. Chem. **317**, 54 (1962).
4. P. Mazerolles. Bull. Soc. Chim. France, 1911 (1961).
5. L. Skatterbøl, E. R. H. Jones, and M. C. Whiting. Organic syntheses. Vol. 39. John Wiley and Sons, New York. 1959. p. 56.

Received October 25, 1962.
Division of Pure Chemistry,
National Research Council,
Ottawa, Canada.

THE PREPARATION OF 2,3-DICYANO-5,6-DICHLOROQUINONE (D.D.Q.)

P. W. D. Mitchell

An intensive program of work on hydrogen-transfer reactions started by Linstead and Braude in 1951 (1) led to many interesting observations of the value of quinones as dehydrogenating agents. D.D.Q. was found by these authors to be of particular interest in this respect. Thus it was shown (2, 3) that D.D.Q. was capable of converting tetralin almost quantitatively into naphthalene in 2 hours at 80°. Recently, D.D.Q. has been used successfully in steroid chemistry to oxidize allylic alcohols into the corresponding α,β-unsaturated ketones (4), and to effect the conversion of Δ^4- and $\Delta^{4,6}$-steroidal 3-ketones into the corresponding $\Delta^{1,4}$- and $\Delta^{1,4,6}$-ketones in excellent yields (5). It is evident from the examples given by Petrow (4, 5) that D.D.Q. is a valuable reagent.

The quinone was prepared previously by Linstead and co-workers (2, 8), who improved the original method of Thiele and Günther (6, 7). This still involved a five-step sequence

Can. J. Chem. Downloaded from www.nrcresearchpress.com by 210.87.254.40 on 09/05/12
For personal use only.

low volatility. They have been characterized by their mass spectra, which give a peak corresponding to the fragment $^{+}HgC{\equiv}CH$. Further work on these interesting new compounds is in active progress and will be reported in detail later.

EXPERIMENTAL

Ethylethynyl Mercury, $C_2H_5HgC{\equiv}CH$

A magnetically stirred solution of ethynylmagnesium bromide, freshly prepared by the method given in reference 5 from 2.07 g (0.086 atoms) of magnesium in 125 ml of tetrahydrofuran, was cooled in ice–water, while there was added dropwise, over a period of 50 minutes, a solution of 8.75 g (0.0247 mole) of ethyl mercuric iodide (1) in 50 ml of tetrahydrofuran. A slow current of dry nitrogen was passed through the apparatus all the while. After addition of the solution had been completed the reaction mixture was stirred for 17 hours at room temperature. It was then cooled to +5° and added slowly to a stirred ice-cold mixture of 450 ml of 6.6% aqueous ammonium nitrate and 190 ml of ether. The lower aqueous layer was separated and extracted twice with two 100-ml portions of ether. The combined ether extracts were washed with two 200-ml portions of water and dried over anhydrous magnesium sulphate. After evaporation of solvent under reduced pressure 5.37 g of yellow crystalline product with a characteristic bad odor remained. Sublimation of the crude material at room temperature under a pressure of 1 mm gave 4.6 g of white crystalline sublimate, m.p. 71–72°. Yield: 73.4%.

The mass analysis of the compound showed peaks at 254, 255, and 256 corresponding to $C_2H_5Hg^{200}C_2H$, $C_2H_5Hg^{201}C_2H$, and $C_2H_5Hg^{202}C_2H$ and also peaks at 225, 226, and 227, which in turn corresponded to $Hg^{200}C{\equiv}CH$, $Hg^{201}C{\equiv}H$, and $Hg^{202}C{\equiv}CH$.

The authors are indebted to Dr. F. P. Lossing of these laboratories for the mass analysis of the compound.

1. A. A. Baldoni and J. J. Miyashiro. To Morton Chem. Co. U.S. Patent No. 2,914,451 (Nov. 24, 1959); Chem. Abstr. **54**, 5467*e*.
2. H. Hartmann and G. Z. Kühl. Z. Anorg. Allgem. Chem. **312**, 186 (1961).
3. H. Hartmann, G. Habenicht, and W. Reiss. Z. Anorg. Allgem. Chem. **317**, 54 (1962).
4. P. Mazerolles. Bull. Soc. Chim. France, 1911 (1961).
5. L. Skatterbøl, E. R. H. Jones, and M. C. Whiting. Organic syntheses. Vol. 39. John Wiley and Sons, New York. 1959. p. 56.

Received October 25, 1962.
Division of Pure Chemistry,
National Research Council,
Ottawa, Canada.

THE PREPARATION OF 2,3-DICYANO-5,6-DICHLOROQUINONE (D.D.Q.)

P. W. D. Mitchell

An intensive program of work on hydrogen-transfer reactions started by Linstead and Braude in 1951 (1) led to many interesting observations of the value of quinones as dehydrogenating agents. D.D.Q. was found by these authors to be of particular interest in this respect. Thus it was shown (2, 3) that D.D.Q. was capable of converting tetralin almost quantitatively into naphthalene in 2 hours at 80°. Recently, D.D.Q. has been used successfully in steroid chemistry to oxidize allylic alcohols into the corresponding α,β-unsaturated ketones (4), and to effect the conversion of Δ^4- and $\Delta^{4,6}$-steroidal 3-ketones into the corresponding $\Delta^{1,4}$- and $\Delta^{1,4,6}$-ketones in excellent yields (5). It is evident from the examples given by Petrow (4, 5) that D.D.Q. is a valuable reagent.

The quinone was prepared previously by Linstead and co-workers (2, 8), who improved the original method of Thiele and Günther (6, 7). This still involved a five-step sequence

Can. J. Chem. Downloaded from www.nrcresearchpress.com by 210.87.254.42 on 09/05/12
For personal use only.

from 2,3-dicyanohydroquinone involving oxidation to the quinone, addition of hydrogen chloride, the repetition of these steps, and a final oxidation of the dichlorodicyanohydroquinone.

It has now been found that chlorination of 2,3-dicyanohydroquinone in refluxing acetic acid (a procedure based on that for preparation of 2,3-dichloroquinone (9, 10)) gives a crystalline compound (3–4 molecular equivalents of Cl_2) which redissolves after the introduction of a total of 7 molecular equivalents of Cl_2. The crystalline compound proved to be 2,3-dicyano-5,6-dichlorohydroquinone (40–50% yield); thus four steps of the older method of preparation are eliminated.

The solution from the prolonged chlorination was taken to dryness. The crystalline residue contained four chlorine atoms and one or more carbonyls (λ_{max} 1733 cm^{-1}). It appeared to oxidize activated charcoal, giving hydrogen chloride and a 70% yield of D.D.Q. These facts and analogy to the hexachlorocyclohexenedione (V) prepared by Zincke (11) and the tetrachlorocyclohexadione of Clark (12) suggest structures IV*a* or IV*b* for this compound. It is presumed that D.D.Q. is an intermediate in the formation of IV since it can be converted into IV by chlorine.

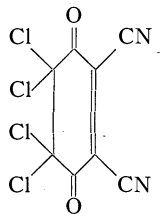

IV*a*

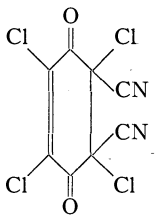

IV*b*

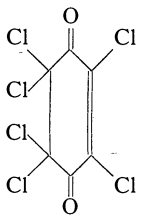

V

A greatly improved procedure for the oxidation of the hydroquinone to D.D.Q. by vigorous shaking of a slurry of the compound in aqueous ethanol containing 5% hydrochloric acid with benzene and lead dioxide was developed. An 80% yield of the quinone concentrated in the benzene phase. No D.D.Q. was formed in the absence of hydrochloric acid.

The following scheme summarizes the reactions described above for the preparation of D.D.Q.

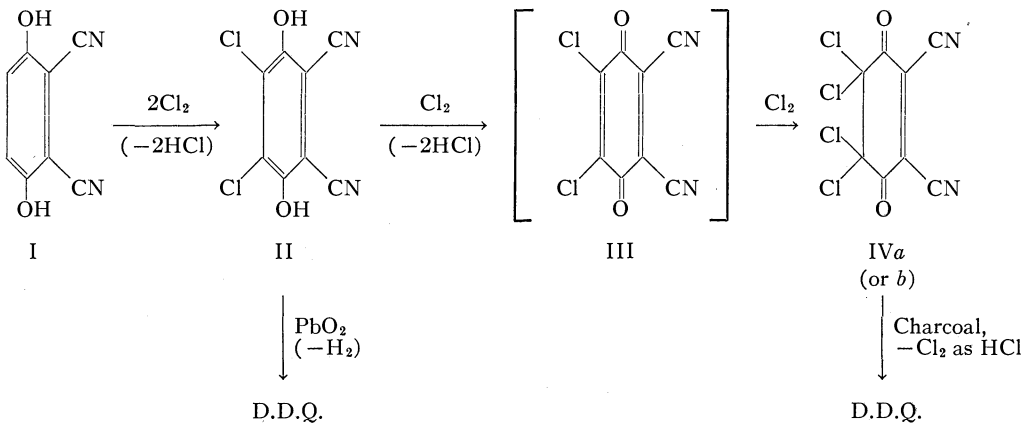

Can. J. Chem. Downloaded from www.nrcresearchpress.com by 210.87.254.42 on 09/05/12
For personal use only.

Can. J. Chem. Downloaded from www.nrcresearchpress.com by 210.87.254.42 on 09/05/12
For personal use only.

EXPERIMENTAL

2,3-Dicyano-5,6-dichlorohydroquinone

2,3-Dicyanohydroquinone (10 g) and glacial acetic acid (100 ml) were heated to gentle reflux in a three-necked flask fitted with a stirrer, condenser, and gas inlet tube. Dry chlorine was then passed into the clear solution at a rate of about 0.2 g per minute and after 1 hour a crystalline solid began to separate from the refluxing solution. After a further 30 minutes, chlorination was stopped, the contents of the flask cooled to room temperature, and the solid separated by filtration. It was washed with chloroform (50 ml) and dried. The yield of chunky white crystals was 6.4 g (44%). The product was practically insoluble in hot water and could be crystallized from aqueous ethanol as needles, unchanged on heating to 300° (lit. (6), blackens at 265°).

2,3-Dicyano-5,6-dichlorobenzoquinone

2,3-Dicyano-5,6-dichlorohydroquinone (10 g) was suspended in a solution of ethanol (40 ml) and 5% hydrochloric acid (110 ml)[1] contained in a stoppered Erlenmeyer flask. Benzene (220 ml) was added, followed by lead dioxide (44 g), and the contents of the flask shaken vigorously by hand for 5 minutes. The emulsion was then filtered through a Büchner funnel containing a layer of celite, and the residue washed with benzene. The combined filtrates were transferred to a separating funnel, the aqueous layer removed, and the organic phase washed twice with a small quantity of water. Concentration of the dried benzene solution yielded red crystals of the quinone, and precipitation was completed by the addition of light petroleum (30–60°). The solid was separated by filtration and washed with a little petrol. When dry the quinone was yellow and melted at 206–209° (lit. (6) m.p. 203°). The yield was 8.3 g (83%).

The Tetrachlorodicyano Derivative

2,3-Dicyanohydroquinone (20 g) was dissolved in refluxing acetic acid (200 ml), and chlorine passed into the stirred solution at a rate of about 0.2 g per minute. Chlorination was continued until the crystalline precipitate of dicyanodichlorohydroquinone had redissolved. This occurred when about 7 molar equivalents of chlorine had been introduced. Chloroform (100 ml) was added to the cooled solution and a small quantity of dicyanodichlorohydroquinone (3.26 g) removed by filtration. The filtrate was evaporated *in vacuo* and the semicrystalline residue triturated with a mixture of benzene and *n*-hexane. A pale yellow solid (20 g) was obtained. It crystallized from *n*-hexane in needles, m.p. 130–132°, and was readily soluble in ether, benzene, ethanol, and chloroform. The compound was unstable in aqueous ethanol. It sublimed readily at 100° and 0.1 mm. The sublimate was colorless and melted at 130–131°.

Calc. for $C_8O_2N_2Cl_4$: C, 32.25; N, 9.41; Cl, 47.61. Found: C, 32.45; N, 9.51; Cl, 47.06, 47.22.

Infrared (CS_2): carbonyl absorption at 1733 cm^{-1}, C≡N at 2260 cm^{-1}, C–Cl at 790 and 765 cm^{-1}, strong band at 1137 cm^{-1}, weak C=C at 1558 cm^{-1} ($CHCl_3$).

Ultraviolet: no maxima in range 220 to 350 mμ (ϵ at 220 mμ = 14,500).

Preparation of D.D.Q. from the "Tetrachloro Compound"

The above compound (1 g), m.p. 130–131°, was dissolved in benzene (20 ml) and the solution refluxed for 40 minutes with charcoal (1 g). The solution was filtered and the orange-red-colored filtrate concentrated to about 10 ml, when red crystals separated. These were removed and washed with a little *n*-hexane. The dried material weighed 0.55 g (73%) and had m.p. 210–213°. It crystallized in long amber-colored needles from chloroform, m.p. 215–217°.

Calc. for $C_8N_2O_2Cl_2$: Cl, 31.25; N, 12.34. Found: Cl, 31.71, 31.88; N, 11.88, 11.81.

Infrared ($CHCl_3$): C=O at 1696 cm^{-1}, C=C at 1560 cm^{-1}, strong band at 1175 cm^{-1}, C≡N at 2240 cm^{-1}.

Ultraviolet: λ_{max} at 238 mμ (ϵ 11,950); 257 mμ (ϵ 10,700); 290 mμ (ϵ 8,900); 345 mμ (ϵ 1,360); 482 mμ (ϵ 870).

Measurement of the Acid Liberated during the Treatment of the Tetrachloro Compound with Charcoal

The compound (151 mg) was refluxed in benzene (10 ml) containing charcoal (0.5 g). A slow stream of nitrogen was passed through the solution and then into *N*/10 sodium hydroxide solution. After 2 hours a total of 4.65 ml of alkali had been neutralized. If two molecules of hydrochloric acid were obtained from the *tetrachloro* compound, the alkali equivalent would be 10 ml. Since the compound is believed to be hydrogen free, it is assumed that the source of the hydrogen is the charcoal.

Preparation of the Tetrachloro Compound by Chlorination of a Mixture of Chlorinated Dicyanoquinones

The mixture (15 g) was obtained by the lead dioxide oxidation of an incompletely chlorinated sample of dicyanodichlorohydroquinone and contained 2,3-dicyanoquinone, 5-chloro-2,3-dicyanoquinone, and D.D.Q. It was dissolved in acetic acid (50 ml) and chlorinated at reflux temperature for 30 minutes. A small quantity of solid (1.7 g), identified as dicyanodichlorohydroquinone, was separated from the cooled solution, which was then evaporated *in vacuo*. The residue was crystallized from benzene and gave 7.5 g of the *tetrachloro*

[1]*When the concentration of hydrochloric acid was reduced to 2%, the yield of quinone was lower, and with 1% hydrochloric acid no quinone was obtained.*

compound, m.p. 130–132°. The filtrate was diluted with benzene (50 ml) and refluxed with charcoal (5 g) for 30 minutes. The resulting orange solution, after filtration and evaporation, yielded 4.5 g of D.D.Q., m.p. 213–215°.

Thanks are due to Mr. Robert Guthrie for technical assistance and to Ayerst, McKenna & Harrison Ltd. for permission to publish.

1. R. P. Linstead, E. A. Braude, P. W. D. Mitchell, K. R. H. Wooldridge, and L. M. Jackman. Nature, **169**, 100 (1952).
2. E. A. Braude, A. G. Brook, and R. P. Linstead. J. Chem. Soc. 3569 (1954).
3. R. P. Linstead, E. A. Braude, L. M. Jackman, and A. N. Beames. Chem. Ind. (London), 1174 (1954).
4. D. Burn, V. Petrow, and G. O. Weston. Tetrahedron Letters, **9**, 14 (1960).
5. D. Burn, D. N. Kirk, and V. Petrow. Proc. Chem. Soc. 14 (1960).
6. J. Thiele and F. Günther. Ann. **349**, 45 (1906).
7. B. Helferich and H. G. Bodenbender. Ber. B, **56**, 1112 (1923).
8. A. G. Brook. J. Chem. Soc. 5040 (1952).
9. A. Eckert and R. Endler. J. Prakt. Chem. [2], **104**, 81 (1922).
10. J. B. Conant and L. F. Fieser. J. Am. Chem. Soc. **45**, 2194 (1923).
11. Th. Zincke and O. Fuchs. Ann. **267**, 15 (1892). F. K. Beilstein. Handbuch der organischen Chemie. Vol. 7. 4th ed. Springer, Berlin. pp. 574, 638.
12. T. H. Clark. Am. Chem. J. **14**, 553 (1892). F. K. Beilstein. Handbuch der organischen Chemie. Vol. 7. 4th ed. Springer, Berlin. p. 612.

Received June 21, 1961.
Research Laboratories,
Ayerst, McKenna & Harrison Limited,
Montreal, Que.

Can. J. Chem. Downloaded from www.nrcresearchpress.com by 210.87.254.42 on 09/05/12
For personal use only.

Canadian Journal of Chemistry

Issued by THE NATIONAL RESEARCH COUNCIL OF CANADA

VOLUME 41 MARCH 1963 NUMBER 3

METHANOLYSIS OF CARBOHYDRATE ORTHOACETATES[1]

A. S. PERLIN

Prairie Regional Laboratory, National Research Council, Saskatoon, Saskatchewan

Received November 5, 1962

ABSTRACT

Acid methanolysis of D-mannose 1,2-(methyl orthoacetate) 3,4,6-triacetate (I) yields mainly 3,4,6-tri-*O*-acetyl-D-mannose (II). D-Glucose 1,2-(ethyl orthoacetate) 3,4,6-triacetate (VIII) yields 3,4,6-tri-*O*-acetyl-D-glucose and methyl 3,4,6-tri-*O*-acetyl-β-D-glucopyranoside. The rate of methanolysis of II differs little from that of VIII, in marked contrast to the relative rates of hydrolysis of these compounds in aqueous acid. Several concurrent reactions appear to take place in methanol initiated by protonation at different positions on the orthoester ring.

During isolation, II is converted partially to 2,4,6-tri-*O*-acetyl-D-mannose (VI), a novel instance of acyl migration in the sugar series. Structural assignments for these two triacetates are based on chemical and proton magnetic resonance spectral data. The 2-acetate group of VI migrates during methylation, both II and VI yielding the same 2-*O*-methyl ether.

Orthoacetates undergo a rapid optical rotatory change in cold dilute methanolic hydrogen chloride. Dale (1), who first reported this property, obtained a small yield of methyl 2,3,4,6-tetra-*O*-acetyl-β-D-mannoside as the only identifiable product formed by methanolysis of β-D-mannose-1,2-(methyl orthoacetate) 3,4,6-triacetate (I). However, a related disaccharide orthoester [4-*O*-β-D-glucopyranosyl-β-D-mannose 1-2-(methyl orthoacetate) hexaacetate] was shown by Isbell (2) to furnish a hexaacetate of the disaccharide. Both types of products were isolated from the methanolysate of β-L-rhamnose 1,2-(methyl orthoacetate) 3,4-diacetate, i.e., the β-L-rhamnoside triacetate and a syrupy fraction that contained 3,4-di-*O*-acetyl-L-rhamnose (3). Pacsu has suggested (4) that transesterification occurs in these reactions between the orthoester group and the solvent, affording a derivative in which carbons-1 and -2 are unsubstituted. Intermediate formation of some 1,2-*trans* acyl chloride appeared to be the most likely source of the 1,2-*cis*-glycoside.

The methanolysis reaction has now been examined further as a route to some partially acylated sugars and as a means for characterizing complex orthoesters (5). The early experiment of Dale on the D-mannose orthoacetate (I) has been repeated and found chromatographically to yield mainly a partially acetylated D-mannose (II) and a small proportion of each of the anomeric glycosides.* When treated with lead tetraacetate in acetic acid the mixture of products rapidly consumed about 0.8 mole of oxidant per mole and, in place of II, the chromatogram now showed the presence of a pentose derivative (III). Hence II appeared to be 3,4,6-tri-*O*-acetyl-D-mannose, the product expected on the basis of Pacsu's proposed mechanism, and it thus amounted to about 80% of the total

[1]*Issued as N.R.C. No. 7165.*

Presented to the Organic Chemistry Division, 45th Annual Conference of the Chemical Institute of Canada in Edmonton, Alberta, June, 1962.

**The methanolysis conditions are critical in that prolonged treatment yields products that correspond to di- and mono-acetates, as well as free mannose (cf. ref. 6).*

Can. J. Chem. Downloaded from www.nrcresearchpress.com by 210.87.254.6 on 09/05/12
For personal use only.

product. By column chromatography on silicic acid using chloroform–ether as eluant, or by countercurrent distribution between chloroform and water, II was readily isolated in a chromatographically pure condition. In the course of several preparations three different crystalline modifications of this product were obtained. One of these appeared to be hydrated and had m.p. 59° C; the other two were polymorphic forms of the anhydrous triacetate and had m.p. 98° or 108° C. All rapidly consumed 1 mole of lead tetraacetate and, from their optical rotatory properties, appeared to be α-anomers.

The product formed in the lead tetraacetate oxidation of II was a crystalline pentose derivative to which is assigned the structure 2,3,5-tri-*O*-acetyl-4-*O*-formyl-*aldehydo*-D-arabinose (III). Treatment of II with methyl iodide – silver oxide afforded methyl 3,4,6-tri-*O*-acetyl-2-*O*-methyl-β-D-mannopyranoside (IV) (7). When II was benzoylated, the acetate–benzoate treated with hydrogen bromide followed by methanol in the presence of silver carbonate, and the product deacetylated, β-D-mannose 1,2-(methyl orthobenzoate) (V) (8) was obtained. Assuming that no acetyl migration occurred during each of the treatments, these findings establish that II is 3,4,6-tri-*O*-acetyl-D-mannose. Additional evidence for this assignment is given below.

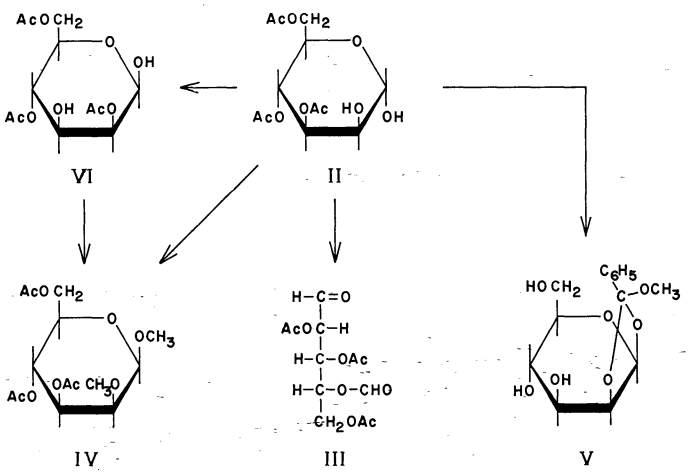

During isolation, II was converted in part to a triacetate (m.p. 170° C) (VI) which did not consume lead tetraacetate, was poorly soluble in organic media, and appeared from optical rotatory data to be a β-anomer. The compound dissolved readily in water and was recovered from the mutarotated solution, which thus showed that position 1 was unsubstituted. Therefore, the resistance to glycol cleavage meant that position 2 must have been acetylated. Because of the favorable orientation of the 2- and 3-hydroxyl groups of D-mannose, it appeared that VI could have been formed from II by migration of an acetyl group from position 3 to 2. Perhaps less likely was the alternative of successive migrations from position 6 to 1 to 2. Hence two feasible structures for VI were those of the 2,4,6- or the 2,3,4-triacetate.

A choice between these possibilities was readily provided by proton magnetic resonance spectroscopy. The spectra for several D-mannose derivatives,* including II, showed that when the primary group is not acetylated the signal for the two C_6 protons is close to

**The reference compounds were D-mannose, its 2-acetate (9), its α- and β-hexaacetates, 2,3,4,6-tetraacetate, and αβ-1,2,3,4-tetraacetate (8), and methyl α-D-mannoside. For some, the solvent was chloroform and for others, deuterium oxide; according to R. U. Lemieux (private communication) the chemical shift for a given proton generally appears at about the same frequency with each of these solvents.*

Can. J. Chem. Downloaded from www.nrcresearchpress.com by 210.87.254.6 on 09/05/12
For personal use only.

3.9 p.p.m. When acetylated, however, the typical paramagnetic shift (see ref. 10) of 0.3–0.4 p.p.m. is observed and the proton frequencies are about 4.2 p.p.m. Aside from the signals of the acetoxy protons, all signals in the spectrum of VI were at frequencies lower than 4.2 p.p.m., clearly indicative of an acetoxyl group at C_6. The spectrum of VI was similar to that of the 3,4,6-triacetate (II), which is to be expected because chemical shifts for the 2-, 3-, and 4-protons of D-mannose acetates are approximately the same (11). However, neither spectrum was well resolved. In each, signals for three protons were grouped closely together in the region 5.1–5.4 p.p.m., and signals for four protons in the region 4.2–4.4 p.p.m. Presumably, the relative positions for the H_2 and H_3 signals in the spectra of II and VI were interchanged, that is, the H_2 signal of II (or the H_3 signal of VI) was included in the broad band at higher field, whereas the H_3 signal of II (or the H_2 signal of VI) was included in the band at lower field. The absence of proton signals at frequencies of 5.9 to 6.1 p.p.m. confirmed that the anomeric hydroxyl group of each isomer was not acetylated (11). All of the acetoxy protons of II were closely equivalent, in agreement with the all-equatorial orientation assigned above, but the acetoxy-proton signals of VI were resolved into a major component at 2.22 p.p.m. and a minor component at 2.30 p.p.m., the latter perhaps corresponding to the presence of an axial acetate group at C_2 (11). These data, therefore, support the designation of VI as 2,4,6-tri-*O*-acetyl-D-mannose and of II as 3,4,6-tri-*O*-acetyl-D-mannose.

Most instances of acyl migration in the sugar series occur in the direction *away from* the anomeric center (12, 13), although the hydrolysis of acylated glycosyl halides may involve migration from C_2 to C_1 (e.g. ref. 14). Hence the formation of triacetate VI from triacetate III appears to be a novel type of rearrangement in that the direction is *towards* the anomeric center but does not actually involve C_1. This rearrangement takes place under the seemingly mild conditions to which II is subjected during isolation, although the compound is stable in water, dry or moist pyridine, or acetic acid. Triacetate VI is also stable in these solvents, but when treated with methyl iodide and silver oxide yielded the 2-*O*-methyl β-D-glycoside (IV), the same product as was formed on methylation of II. In the latter instance, therefore, the migration conforms to that generally observed in the methylation of partially acylated sugar derivatives (12, 13), the 2-acetate group migrating back to position 3.

Acid methanolysis of α-D-glucose 1,2-(ethyl orthoacetate) 3,4,6-triacetate (VII) (15) afforded two products in about equal proportion. These products were readily separated by countercurrent distribution between chloroform and water. One (VIII) was a syrupy triacetate which consumed 1 mole of lead tetraacetate and yielded pentose derivative III, and hence undoubtedly was 3,4,6-tri-*O*-acetyl-D-glucose; the other was methyl 3,4,6-tri-*O*-acetyl-β-D-glucoside (IX). Both of these products have been prepared from 1,2-anhydro-D-glucose triacetate (16, 17).

From the studies referred to at the outset and the current findings it is seen that the predominant type of product formed by acid methanolysis of 1,2-orthoacetates is that represented by 3,4,6-tri-*O*-acetyl-D-mannose (II) and -glucose (VIII). As visualized by Pacsu (4), its formation likely involves transesterification between the orthoester and the hydroxylic solvent. Thus, protonation of the orthoacetate (X) can lead successively to XI and the rearranged ion XII, and solvent attack can then give (protonated) orthoester XIII. By a similar sequence involving protonation of the C_2-oxygen of XIII, the acyclic orthoester group can be removed as methyl orthoacetate, and a 3,4,6-triacetate (XIV) thus liberated. The overall result should be the same if the reaction is initiated by protonation of the C_2-oxygen of X, except that in the intermediates corresponding to XII and XIII carbon-1, rather than -2, would be substituted.

Can. J. Chem. Downloaded from www.nrcresearchpress.com by 210.87.254.6 on 09/05/12
For personal use only.

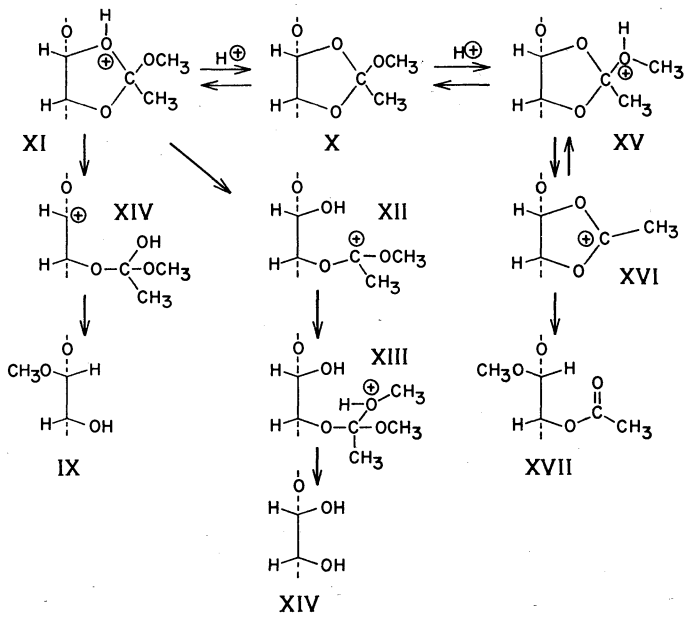

If rearrangement of XI occurs with opening of the C_1-oxygen bond, the orthoacid ion XIV would be formed. Solvent attack on the latter and transesterification of the orthoacid group could then yield a 3,4,6-triacetate of the methyl glycoside (i.e., IX). Because of the 1,2-*cis* orientation of XI and the 1,2-*trans* arrangement in the derived glycoside, ion XIV may be regarded as analogous to the ionic intermediate associated with nucleophilic substitution of 1,2-*cis* acyl halides (18). Protonation of the *O*-methyl group (as in XV) can give cyclic ion XVI, which, by rearward solvent attack, yields the 1,2-*trans* acyl glycoside (XVII, e.g., the α-D-mannoside). As pointed out by Pacsu (4), the 1,2-*cis* acyl glycoside could be formed via the 1,2-*trans* acyl chloride.

Methanolysis rates for the D-mannose- and D-glucose orthoacetate (I and VIII) differ by less than a factor of two (0.056 and 0.10 minutes^{-1}, respectively). In marked contrast, the D-glucose isomer is hydrolyzed by aqueous acid 19 times as fast as the D-mannose orthoester (19), this large difference being attributed to differences in stability of the transient cyclic ions (corresponding to XVI) involved in the hydrolyses. With a change of solvent from water to methanol, however, the course of reaction is altered and other types of pathways become more important. Presumably, also, the steric influence of the epimeric sugars on the relative stability of the cyclic carbonium ions (and hence on the hydrolysis rates (19)) is less of a factor with acyclic ions of the type visualized as intermediates in the methanolysis reactions.

EXPERIMENTAL

Melting points are corrected. Optical rotations were measured at 25±2°. Solutions were concentrated *in vacuo* at 40–45° C.

Nuclear magnetic resonance spectra were prepared with a Varian A60 spectrometer, chloroform or deuterium oxide being used as solvents and tetramethylsilane as the reference compound.

Methanolysis of β-D-Mannose 1,2-(Methyl orthoacetate)-3,4,6-triacetate (I)

To a solution of the crystalline orthoester (I) in methanol (350 mg in 4 ml; α_D −1.08°) was added a solution of hydrogen chloride in methanol (70 mg in 5 ml); the observed rotation changed to 0.30° within 1 minute, remaining constant during the next 10 minutes. Excess silver carbonate was then added and the

Can. J. Chem. Downloaded from www.nrcresearchpress.com by 210.87.254.6 on 09/05/12
For personal use only.

solution concentrated to a syrup (wt., 280 mg). Paper chromatographic examination of the syrup showed the presence of a major product ($R_{mannose}$ 4.3) and a minor product ($R_{mannose}$ 3.2); after deacetylation, the syrup contained mainly mannose, and methyl α- and β-D-mannoside as minor constituents. With longer methanolysis periods the proportion of product $R_{mannose}$ 3.2 increased, and a third material ($R_{mannose}$ 2.2) as well as free mannose were then detected.

The syrup (14.7 mg) in acetic acid (1 ml), when treated with lead tetraacetate solution (50 mg in 3 ml acetic acid), consumed (moles/mole (minute)): 0.80 (5); 0.85 (10); 0.85 (20), based on (approximate) m.w. of 306. Chromatographic examination of the oxidation product showed the presence mainly of material giving typical color reactions for pentose.

When the orthoester (I) in methanol was first deacetylated with sodium methoxide and the solution then acidified with methanolic hydrogen chloride, mannose was found chromatographically as the major product.

3,4,6-Tri-O-acetyl-α-D-mannose (II)

(*a*) The syrupy reaction product (2.80 g) obtained as above (methanolysis period, 5 minutes) was taken up in chloroform and added to a column of silicic acid (2×15 cm). First, the column was developed with chloroform (1000 ml), and then with chloroform:ether (95:5). Fractions of the eluate (100 ml) were collected and each examined by paper chromatography before and after deacetylation with sodium methoxide. Fractions 3–17 contained a mixture of the acetylated anomeric glycosides and tetraacetyl mannose (0.83 g); fractions 18–56 contained syrupy product II (1.35 g) which, on extraction into ether, afforded crystalline material (0.9 g), m.p. 108–109° C; $[\alpha]_D$ 51° → 39° (72 hours) (*c*, 1.4 chloroform); $[\alpha]_D$ 23° → 8° (eqm.) (*c*, 0.9 water). Calculated for $C_{12}H_{18}O_9$: C, 47.06%; H, 5.92%. Found: C, 47.01%; H, 5.82%.

The crystalline product obtained in this way in another experiment had m.p. 96–98° C, $[\alpha]_D$ 22° → 7° (eqm.) (*c*, 2.3 water); when recrystallized from ether by seeding with the higher-melting form, the m.p. was 106–109° C. Calculated for $C_{12}H_{18}O_9$: C, 47.06%; H, 5.92%; acetyl, 42.16%. Found: C, 47.01%; H, 5.86%; acetyl, 42.1%.

(*b*) The crude methanolysis product (650 mg) in chloroform (10 ml) was subjected to countercurrent extraction (four stages) against water (10-ml portions). By paper chromatography, water layers 1 and 2 were found to contain most of II (350 mg and 50 mg, respectively) whereas chloroform layer 4 contained most of the glycoside fraction (90 mg). Extraction of syrupy II with ether gave crystalline material of m.p. 95–97° C.

Material isolated from the aqueous phase in a second experiment had m.p. 57–59° C, $[\alpha]_D$ 12° → 8° (*c*, 1.1 water). This product rapidly consumed approximately 1 mole of lead tetraacetate per mole. Calculated for $C_{12}H_{18}O_9 \cdot H_2O$: C, 44.44%; H, 6.22%. Found: C, 45.02%; H, 6.24%.

2,3,5-Tri-O-acetyl-4-O-formyl-aldehydo-D-arabinose (III)

Triacetate II (m.p. 108–109° C; 0.20 g) in acetic acid (25 ml) was treated with a solution of lead tetraacetate in acetic acid (0.28 g in 12.5 ml). After 20 minutes the solvent was evaporated off, the residue was triturated several times with ether, and the ether extract was concentrated, affording a product of m.p. 84.5–85° C, $[\alpha]_D$ +88° (*c*, 1.4 benzene), λ_{max} 293 mμ (in ether). Calculated for $C_{12}H_{16}O_9$: C, 47.37%; H, 5.30%; neut. equiv., 76.0. Found: C, 47.42%; H, 5.34%; neut. equiv., 76.5 (by cold alkaline saponification). The saponification mixture was acidified and distilled, the distillate giving a positive mercuric chloride test for formic acid.

Methyl 3,4,6-Tri-O-acetyl-2-O-methyl-β-D-mannoside (IV) from II

Triacetate II (m.p. 96–98°; 0.63 g) was suspended in methyl iodide (15 ml); anhydrous calcium sulphate (6.0 g) and silver oxide (4.0 g) were added; and the mixture was heated under reflux for 7 hours. The solids were filtered off and washed with ether, the combined filtrates on concentration yielding a partially crystalline residue (0.65 g). The latter was triturated with ether, and the solids were recrystallized from ethanol–ether; m.p. 148–149° C, $[\alpha]_D$ −65° (*c*, 1.7 chloroform) (lit. (7): m.p. 146° C, $[\alpha]_D$ −46°). Calculated for $C_{14}H_{22}O_9$: C, 50.29%; H, 6.63%. Found: C, 50.21%; H, 6.68%.

The deacetylated product consumed 1.0 mole of lead tetraacetate per mole (in glacial acetic acid containing potassium acetate (20)). Hydrolysis of the deacetylated glycoside with 0.5 *N* sulphuric acid yielded a reducing sugar ($R_{rhamnose}$ 1.0) which was attacked very slowly by lead tetraacetate; in the presence of potassium acetate, the sugar was oxidized readily yielding formaldehyde. These oxidation properties are characteristic of a 2-substituted hexose (21).

The ether-soluble fraction (0.25 g) ($[\alpha]_D$ 0°) appeared, from chromatographic examination after deacetylation, to contain more of IV, as well as a high proportion of methyl β-D-mannoside and a trace of the α-D-glycoside.

β-D-Mannose 1,2-(Methyl orthobenzoate) (V)

Triacetate II (m.p. 96–98° C; 0.20 g) in pyridine (10 ml) was treated with benzoyl chloride (2 ml) at 3° C for 18 hours. The product was extracted into chloroform, the extract was washed successively with sodium bicarbonate solution, tartaric acid solution, and water, then dried, and saturated with hydrogen bromide. After 6 hours the extract was again washed with bicarbonate solution and water, and concentrated. The

Can. J. Chem. Downloaded from www.nrcresearchpress.com by 210.87.254.6 on 09/05/12
For personal use only.

syrup residue, in benzene (1 ml), was added to methanol (10 ml) containing silver carbonate (1 g), the suspension was shaken for 2 hours, filtered, and the filtrate concentrated (yield, 0.20 g; $[\alpha]_D$ −61°, *c*. 5.7 methanol). Excess barium methoxide was added to a solution of the syrup in methanol, the solution was neutralized with carbon dioxide after 2 hours, filtered, and evaporated. The infrared absorption spectrum and paper chromatographic mobility of the syrupy product were indistinguishable from those of syrupy β-D-mannose 1,2-(methyl orthobenzoate) (8).

2,4,6-Tri-O-acetyl-β-D-mannose (VI)

After elution of II from the silicic acid by chloroform:ether (as described above), additional material (0.66 g from 2.8 g of the crude methanolysate) was obtained by washing the adsorbent with acetone. When triturated with ether, the product solidified; m.p. 163–167° C, $[\alpha]_D$ −38° → 18° (eqm.) (*c*, 1.1 water); $[\alpha]_D$ −70° → 4° (18 hours) (*c*, 1 pyridine). Treated with lead tetraacetate in acetic acid for 20 minutes, the compound consumed only a trace of oxidant; little oxidation occurred also when pyridine was the solvent, the compound being tested both before and after mutarotation had occurred. Calculated for $C_{12}H_{18}O_9$: C, 47.06%; H, 5.92%; acetyl, 42.16%; mol. wt., 306. Found: C, 47.09%; H, 5.95%; acetyl, 41.9%; mol. wt., 271 (in water at 37°, by vapor pressure thermometry).

An aqueous solution of VI, after mutarotation had occurred, was concentrated and stored at 3° C, affording crystals of m.p. 170–171°, which were shown by X-ray diffraction to be unchanged starting material. Calculated for $C_{12}H_{18}O_9$: C, 47.06%; H, 5.92%. Found: C, 46.82%; H, 5.92%.

Triacetate VI also was obtained following countercurrent extraction of the methanolysate (as described above), in admixture with II, the latter being removed by washing with ether.

Methyl 3,4,6-Tri-O-acetyl-2-O-methyl-β-D-mannoside (IV) from VI

Triacetate VI (0.30 g) was suspended in methyl iodide (10 ml); anhydrous calcium sulphate (3.0 g) and silver oxide (2.0 g) were added; the mixture was heated under reflux for 18 hours and then extracted with chloroform. The extract was concentrated and the residue was remethylated, giving 0.23 of a partially crystalline product. The solid portion was separated out in ether and, on recrystallization from ethanol–ether, had m.p. 148–149° C; the X-ray powder diagram was indistinguishable from that of IV. The ether extract (0.10 g), $[\alpha]_D$ −10° (*c*, 2 chloroform), appeared, from chromatographic examination after deacetylation, to consist of IV and a second component of slightly greater R_f, in about equal proportions. On treatment with lead tetraacetate – potassium acetate in acetic acid the deacetylated glycoside mixture consumed 0.6 mole of oxidant per mole, indicating the presence of the 3-*O*-methyl ether as a minor component.

Methanolysis of α-D-Glucose 1,2-(Ethyl orthoacetate) 3,4,6-triacetate

The orthoester (15) (0.10 g) in methanol (2 ml) (α_D 2.14°) was treated with methanolic hydrogen chloride (0.2 ml, 2%); in 2 minutes the observed rotation was α_D 3.53°, and at 5 minutes 3.30°. Excess of ethereal diazomethane was added and the solution concentrated to a syrup (0.08 g). Chromatographic examination of the product showed the presence of a major component travelling slightly slower than II; after deacetylation, glucose and methyl glucoside were detected in about equal proportion. On treatment with lead tetraacetate in acetic acid the observed uptake of oxidant (moles/mole (minute)) by the syrup was 0.25 (15), 0.37 (30), 0.48 (85), 0.50 (270).

3,4,6-Tri-O-acetyl-D-glucose (VII)

To the orthoester (1.0 g) in methanol (20 ml) was added methanolic hydrogen chloride (2 ml, 2%) and after 2 minutes the solution was neutralized with silver carbonate. The filtrate was acidified slightly with acetic acid, concentrated, and the syrupy residue (0.79 g) was subjected to a four-stage countercurrent extraction between chloroform (25-ml portions) and water (15-ml portions). Water layers 1 and 2 and chloroform layers 1 and 2 were combined and concentrated to yield a syrup (0.38 g). Calculated for $C_{12}H_{18}O_9$: C, 47.06%; H, 5.92%; acetyl, 42.16%. Found: C, 46.93%; H, 6.04%; acetyl, 40.9%.

The syrup (0.10 g) in acetic acid (20 ml) was treated with lead tetraacetate (0.13 g) and, when a negative starch–iodide test was obtained, the reaction mixture was worked up as in the oxidation of II, the ether extract affording crystals (0.06 g) having m.p. 83–85°, undepressed by admixture with III.

Methyl 3,4,6-Tri-O-acetyl-β-D-glucoside (VIII)

The material contained in chloroform layers 3 and 4 afforded a crystalline product (0.23 g) from ethanol–ether–hexane; m.p. 97–99° C, $[\alpha]_D$ 18.5° (*c*, 1.1 chloroform) (lit. (16): m.p. 95° C, $[\alpha]_D$ 19°). Calculated for $C_{13}H_{20}O_9$: C, 48.75%; H, 6.29%; acetyl, 40.25%. Found: C, 48.57%; H, 6.17%; acetyl, 40.0%.

When fully acetylated the product afforded methyl 2,3,4,6-tetra-*O*-acetyl-β-D-glucoside, m.p. 104–106° C, the X-ray powder diagram of which was indistinguishable from that of an authentic specimen.

Rates of Methanolysis of Orthoesters

β-D-Mannose 1,2-(methyl orthoacetate) 3,4,6-triacetate (15.3 mg) or α-D-glucose 1,2-(ethyl orthoacetate) 3,4,6-triacetate (16.2 mg), in methanol (1 ml), was treated with 0.25 *N* methanolic hydrogen chloride (0.005 ml). From the observed changes in optical rotation of the solutions, first-order rate constants were calculated:

Can. J. Chem. Downloaded from www.nrcresearchpress.com by 210.87.254.6 on 09/05/12
For personal use only.

D-*manno*-			D-*gluco*-		
Time (min)	α_D	k_{25} (min^{-1})	Time (min)	α_D	k_{25} (min^{-1})
0	−0.15	—	0	1.25	—
3	−0.00	0.066	2	1.35	0.100
5	0.05	0.057	5	1.48	0.105
7	0.12	0.058	7	1.54	0.105
13	0.28	0.056	10	1.60	0.100
eqm.	0.67	—	eqm.	1.80	—

ACKNOWLEDGMENTS

The author gratefully acknowledges the able technical assistance of Mrs. J. Nuttall. Proton magnetic resonance spectra were prepared by Mr. M. Mazurek and Mr. W. Haid at the University of Saskatchewan through the kind cooperation of Prof. K. J. McCallum.

REFERENCES

1. J. K. Dale. J. Am. Chem. Soc. **46**, 1046 (1924).
2. H. S. Isbell. J. Res. Natl. Bur. Std. **7**, 1115 (1931).
3. H. B. McPhillamy and R. C. Elderfield. J. Org. Chem. **4**, 150 (1939).
4. E. Pacsu. Advanc. Carbohydrate Chem. **1**, 77 (1945).
5. H. R. Goldschmid and A. S. Perlin. Can. J. Chem. **39**, 2025 (1961).
6. P. A. Levene and M. L. Wolfrom. J. Biol. Chem. **78**, 525 (1928).
7. F. Micheel, A. Klemer, and R. Flitsch. Ber. **91**, 663 (1958).
8. P. A. J. Gorin and A. S. Perlin. Can. J. Chem. **39**, 2474 (1961).
9. A. S. Perlin. Can. J. Chem. **41**, 399 (1963).
10. L. M. Jackman. Applications of nuclear magnetic resonance spectroscopy in organic chemistry. Pergamon Press. 1959. p. 55.
11. R. U. Lemieux, R. K. Kullnig, H. J. Bernstein, and W. G. Schneider. J. Am. Chem. Soc. **80**, 6098 (1958).
12. F. Brown, L. Hough, and J. K. N. Jones. J. Chem. Soc. 1125 (1950).
13. W. A. Bonner. J. Org. Chem. **24**, 1388 (1959).
14. N. K. Richtmyer and C. S. Hudson. J. Am. Chem. Soc. **58**, 2534 (1936).
15. R. U. Lemieux and J. D. T. Cipera. Can. J. Chem. **34**, 906 (1956).
16. W. J. Hickinbottom. J. Chem. Soc. 3140 (1928).
17. P. Brigl and R. Schinle. Ber. **62**, 1719 (1929).
18. R. U. Lemieux. Advan. Carbohydrate Chem. **9**, 1 (1954).
19. R. U. Lemieux and C. Brice. Can. J. Chem. **33**, 109 (1955).
20. A. S. Perlin. J. Am. Chem. Soc. **76**, 5505 (1954).
21. A. J. Charlson and A. S. Perlin. Can. J. Chem. **34**, 1200 (1956).

Can. J. Chem. Downloaded from www.nrcresearchpress.com by 210.87.254.6 on 09/05/12
For personal use only.

THE THERMAL DECOMPOSITION OF AZOMETHANE

I. EFFECT OF ADDED OLEFIN AND NITRIC OXIDE[1, 2]

W. FORST
Department of Chemistry, Laval University, Quebec, Que.

AND

O. K. RICE
Department of Chemistry, University of North Carolina, Chapel Hill, North Carolina

Received October 12, 1962

ABSTRACT

The addition of ethylene and propylene reduces the rate of azomethane decomposition as measured by the rate of nitrogen production, and also reduces the ratio CH_4/N_2 in the products, but the reduction in the value of both quantities is different for each of the two olefins. In 100% decomposition, ethylene and propylene both increase somewhat the ratio (nitrogen recovered)/(azomethane decomposed). These results are interpreted to mean that there is in fact a short chain in the pyrolysis, but that ethylene and propylene are unsuitable inhibitors.

The addition of a few millimeters of NO reduces the rate to a minimum which is lower than that with added propylene or ethylene (apparent chain length 2 to 3), but further addition of NO increases the rate again. Identical result is obtained in a packed vessel. The yield of methane, ethane, and ethylene is reduced to almost zero with a sufficient amount of NO. The ratio (NO consumed)/(nitrogen produced) reaches the value of two in the neighborhood of the rate minimum. It is concluded that the net inhibited rate, i.e. rate corrected for the stimulatory effect of NO, refers to the initial unimolecular process $CH_3N_2CH_3 \rightarrow 2CH_3 + N_2$. The rate as well as the activation energy of this process is found to be pressure dependent.

It is shown by the use of the isotopic nitric oxide ^{15}NO that about one-half of the rate increase at higher NO pressures is due to nitrogen produced from NO. The remainder of the rate increase is accounted for by a NO-induced decomposition of azomethane.

INTRODUCTION

Azomethane has long been believed to represent a good example of a unimolecular reaction. All earlier studies were done by the manometric method (1), but when the products were analyzed and found complex (2) doubts arose about the significance of manometric results, and about the unimolecularity of the reaction. Later, the reaction was studied by the toluene-carrier technique and followed by the rate of appearance of nitrogen (3), and the new results were still consistent with the old. Recently, however, the toluene-carrier results were disavowed (4). New work by the static method by Steel and Trotman-Dickenson (4), in which the reaction was followed by analyzing for nitrogen, revealed that propylene inhibited the reaction at higher pressures of azomethane, but accelerated it at lower pressures of azomethane; at a sufficiently high pressure of propylene the rate became independent of initial azomethane pressure. These results were interpreted by the authors to mean that the effect of propylene was twofold: increase in the rate of reaction due to an increased rate of energization, and inhibition of a short chain in azomethane. The presence of surface effects was cited by the authors as further proof for the presence of a chain in the decomposition.

In the presence of toluene, however, no inhibition was observed, at least in the range of azomethane pressures studied by the authors, and the limiting rate reached at high toluene pressure was below the limiting rate at high propylene pressure.

[1]*Experimental work done at the University of North Carolina under a grant from the National Science Foundation.*

[2]*Based in part on a paper presented before the Division of Physical Chemistry, 139th Meeting of the American Chemical Society, St. Louis, Mo., March 1961.*

Can. J. Chem. Downloaded from www.nrcresearchpress.com by 210.87.254.105 on 09/05/12
For personal use only.

Thus, while these results do indicate the probable existence of a reaction chain in azomethane, the exact chain length, as well as the amount of inhibition, if any, obtainable with toluene or propylene, remains in doubt. It was therefore decided that further investigation of the inhibition of azomethane was warranted.

EXPERIMENTAL

I. Azomethane

Azomethane was prepared by the method of Renaud and Leitch (5): *sym*-dimethyl hydrazine hydrochloride (purchased from the K & K Laboratories, Jamaica, N.Y.) was treated with excess alkali to liberate the free base. This alkaline mixture was then added, under constant stirring, to a suspension of yellow mercuric oxide in water. When the pressure was reduced, azomethane escaped and was collected in a liquid nitrogen trap, from which it was distilled by three trap-to-trap distillations through two 1-m lengths of 20 mm I.D. tubing packed with KOH and P_2O_5, respectively, and then into a blackened storage flask.

An attempt to purify azomethane by gas chromatography was unsuccessful. Azomethane cuts obtained from crushed firebrick columns with a variety of partitioning liquids (Octoil-S, dioctyl phthalate, dimethyl formamide, cuprous chloride in benzonitrile, polyethylene glycol 400) and examined by infrared spectroscopy generally revealed the presence of numerous impurities not present in the sample before "purification". Purification, when required, was therefore done by orthodox means. The spectrum of fresh azomethane was generally identical with the published datum (6); impurities, when present, turned out to be an assortment of the various chlorinated methanes.* Azomethane containing any absorption at or above 13 μ (methyl chloride, methylene chloride, chloroform) was discarded; azomethane with traces of carbon tetrachloride (absorption at 12.6 μ) was purified by distillation at dry ice temperature. To facilitate this operation, and to keep the decomposition of azomethane at a minimum, the gas was kept in dry ice at all times, and when required, samples withdrawn by a distillation into a trap immersed in liquid nitrogen. During manipulations, azomethane gas was shielded from daylight by painting all connecting tubing black and by working in subdued daylight when necessary; its exposure to room temperature was kept to a minimum. With this procedure, different batches of azomethane gave identical rates of decomposition within experimental error.

II. Other Materials

Propylene, ethylene, and nitric oxide were "C.P." grade gases obtained from the Matheson Co. The hexafluoroethane was a gift from the DuPont Co. The olefins and the C_2F_6 were purified by three bulb-to-bulb distillations and dried by passage through KOH and P_2O_5 tubes. These gases contained less than 0.1% of impurity as determined by gas chromatography.

Nitric oxide was purified as described by Calvert, Thomas, and Hanst (7), followed by three trap-to-trap distillations and drying by passage through KOH and P_2O_5 tubes. The nitric oxide so obtained had about 0.4% of nitrous oxide, as determined by gas chromatography. This impurity was removed by subliming the NO from a trap immersed in liquid oxygen to a trap immersed in liquid nitrogen. This procedure, though tedious, is very effective: The N_2O content was thus reduced to 0.06%, as determined by gas chromatography.

The isotopic nitric oxide, ^{15}NO, stated to contain 97.7 ± 0.3 atom% ^{15}N (this quantity includes nitrogenous impurities), was purchased from the Isomet Corp., Newark, N.J. This NO, as received, contained about 0.3% of nitrous oxide. Sublimation, described above, reduced this content to 0.02%. Assuming, as seems reasonable, that the isotopic composition of the N_2O was roughly the same as that of the bulk NO, the purification process did not change the isotopic composition of NO.

III. Apparatus

A conventional static system was employed. The reaction vessel was placed inside a furnace with a heavy iron core and thick insulation of glass wool all around. The temperature of this furnace was controlled by a platinum wire winding wound between the heater windings in the manner described by Schneider and Hollies (8). This platinum winding was part of a resistance bridge, the output of which was fed to a mirror galvanometer, which, in turn, actuated a photoelectric relay by means of an optical lever. This arrangement was capable of maintaining the temperature inside the reaction vessel (as determined at the location of the thermocouple) within $\pm 0.02°$ C.

The temperature was measured with an iron–constantan thermocouple calibrated at the melting point of tin (231.9° C), cadmium (320.9° C), and zinc (419.5° C). Readings were taken with a Leeds & Northrup Type K potentiometer.

The majority of runs were done in a spherical reaction vessel fabricated from a 250-ml spherical Pyrex flask and provided with a radial thermocouple well. The surface-to-volume ratio of this vessel was about 0.75 cm^{-1}. Packed runs were done in a similar vessel made from a 1000-ml spherical Pyrex flask packed with 217 pieces of 7 mm O.D. Pyrex tubing, each about 4 cm long, with fire-polished ends. The surface-to-volume ratio of this flask was about 5.7 cm^{-1}. Prior to use each flask was carefully cleaned with fuming sulphuric acid. Vessels so cleaned gave reproducible results from the very start, the rate of the second run

*The authors are indebted to Mr. G. Beaudoin for help in the determination of impurities.

Can. J. Chem. Downloaded from www.nrcresearchpress.com by 210.87.254.105 on 09/05/12
For personal use only.

generally corresponding to the constant reproducible value. Upon removal, the inside of such a vessel showed a thin uniform carbonaceous film resembling a photographic neutral density filter.

The gas chromatograph used consisted of a Perkin–Elmer Model 154-B thermistor detector placed inside an insulated box. The temperature inside this box was regulated at 40.25±0.05° C by means of a mercury regulator and relay. The detector circuit was in all essentials similar to that of the Perkin–Elmer. The output signal was displayed by a Brown "Elektronik" recorder Model 153.

Helium (purchased from the Southern Oxygen Co., Charlotte) was used as carrier gas; it was purified by passage through a charcoal trap immersed in liquid nitrogen. The helium flow was maintained at about 40 ml/min, as determined by a capillary flowmeter calibrated by a wet gas meter.

Gases for analysis by gas chromatography were collected, measured, and injected in the column by the simple apparatus shown in Fig. 1. It functions as follows: By pumping with the Toepler pump, the gas to

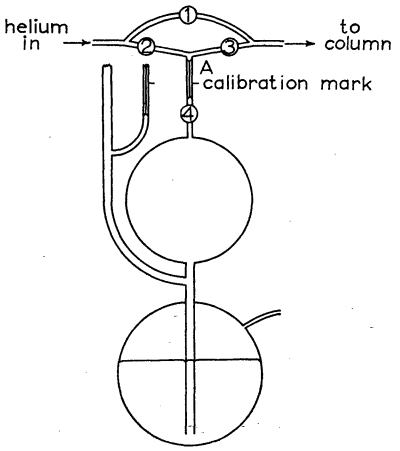

FIG. 1. Combination Toepler pump and sample injection device.

be analyzed is collected in the Y-shaped calibrated volume A enclosed by the calibration mark and by stopcocks 2 and 3. While pumping is in progress, carrier gas is routed through a bypass (stopcock 1 open, stopcocks 2 and 3 closed, stopcock 4 closed between pump strokes). When pumping is complete, mercury is brought to the calibration mark, and the pressure inside A is read on a scale attached to the manometer arm of the Toepler pump. Stopcock 4 is then closed, and stopcocks 2 and 3 opened, in that order, and stopcock 1 closed. The sample has now been injected into the carrier gas stream.

IV. Procedure

In a typical experiment, a mixture of azomethane with foreign gas was prepared by measuring out the requisite amounts of each gas in a gas buret. Prior to expansion in the reaction vessel, the gases were thoroughly mixed by raising and lowering mercury in a 500-ml flask 30 times. The reaction was allowed to proceed to no more than 5% conversion in every case. At the end of the selected reaction time, the reaction was quenched by expanding the gases into a trap immersed in liquid nitrogen. After 5 minutes, non-condensable gases were pumped out by means of a Toepler pump, measured, and injected in the gas-chromatographic column in the manner described under Section III. When nitric oxide was present as foreign gas, the non-condensable fraction, in addition to nitrogen and a trace of methane, contained also nitric oxide, owing to the appreciable vapor pressure of nitric oxide at liquid nitrogen temperature (about 0.1 mm at −196° C).

In experiments with the isotopic nitric oxide, ^{15}NO, it was necessary to remove the nitric oxide from the non-condensable fraction because of possible interference in a subsequent mass-spectrometric analysis. The non-condensable fraction (including ^{15}NO) was collected as above; a small aliquot was then analyzed by gas chromatography to determine roughly its content in nitric oxide. A slight excess of pure oxygen (Air Reduction Co. "Assayed Reagent Oxygen") was then added, and the NO_2 removed by passing the gas five times through a U trap immersed in liquid nitrogen. Next another aliquot was taken for analysis to make sure that all the nitric oxide has been removed. The sample was then sealed in a break-seal bulb for analysis on a mass spectrometer. In these experiments the extent of decomposition of azomethane was 8% in order to increase the amount of nitrogen for analysis.

In runs in which the consumption of nitric oxide was measured, the non-condensable fraction was first pumped off at −196° C, the trap containing the reaction products placed in liquid oxygen, and the nitric oxide then pumped off and measured (vapor pressure of NO at −183° C is about 4 mm). Total nitric oxide recovered was the sum of NO pumped off at −196 and −183° C.

Can. J. Chem. Downloaded from www.nrcresearchpress.com by 210.87.254.105 on 09/05/12
For personal use only.

When analysis was made for C_2 and C_3 hydrocarbons, nitrogen and methane were first removed at −196° as above. The trap containing the reaction products was then placed in a pentane slurry (−130°), left standing for 5 minutes, and the C_2+C_3 fraction pumped off with a Toepler pump, measured, and injected in a column for analysis. If nitric oxide was present, it had to be removed first, either with oxygen or by pumping at −183° C. The former procedure was preferred in runs in which the NO consumption was not measured. The latter procedure resulted in the presence of some NO in the C_2+C_3 fraction, but this caused no interference. NO also caused the presence of N_2O in the C_2+C_3 fraction. A small part of the N_2O found was originally present in the NO as an impurity (see Section II), but most of it was produced in the reaction. The N_2O figures reported under Results have been corrected for the N_2O impurity in NO.

V. Analysis

All analyses were done by quantitative gas chromatography. The non-condensable fraction was analyzed on a 3-m ¼-in. copper column filled with 40–60 mesh high-activity charcoal (Burrell, cat. No. 341–10). The column was capable of separating nitrogen, nitric oxide, carbon monoxide, and methane. The separation of CO from NO was incomplete if an excess of NO was present, but the CO could still be detected as a small peak in the NO tail.* None of the reaction mixtures analyzed, however, showed the presence of even a trace of CO.

The column was calibrated for nitrogen and methane by injecting a known amount of each gas on the column and measuring the corresponding peak area on the chromatogram. The calibration was then checked on synthetic nitrogen–methane and nitrogen – nitric oxide mixtures. About 20 calibration points each were obtained for nitrogen and methane, spaced over the range 0–20 μmole. Peak areas were measured with a polar planimeter, in duplicate determination, and also by multiplying peak height by width at half-height. It turned out that the latter method offered a precision at least as great as duplicate planimetering, and was considerably faster; it was therefore adopted. A similar conclusion was reached by Janák (9). Weighing of cut-out chromatograms was not feasible because of great seasonal variations in ambient humidity.

The calibration was linear over the entire range, and the calibration factor, determined by the method of least squares, showed a standard deviation of ±0.8% for nitrogen and ±1.6% for methane. The ratio of calibration factors (= ratio of sensitivities) for nitrogen and methane was 1.14, in agreement with the figure 1.17 determined by Messner *et al.* (10). First-order rate constants were calculated from the amount of nitrogen found, assuming ideal gas behavior.

The presence of nitric oxide affected the quantitative results for nitrogen to some extent when the amount of NO relative to nitrogen was large. It was found that nitric oxide produced an enhancement of the nitrogen peak. That this was not due to the presence of nitrogen in the NO was established by numerous purification experiments. This "nitrogen shadow" increased linearly with the amount of NO, corresponding to 1.2% of the NO present in the sample injected in the column. An appropriate correction was applied to the nitrogen peak in cases where the amount of NO present was large enough to make this correction significant. It is interesting to note that a similar enhancement of the nitrogen peak due to NO was observed by Smith *et al.* (11), although these authors used a very different column and obtained NO by difference.

Several calibration runs were done with nitric oxide, but it soon became apparent that an accuracy comparable with that for nitrogen was attainable only under special precautions. The amount of nitric oxide was therefore obtained by difference in cases where this information was desired.

The C_2+C_3 fraction was analyzed on a 3-m, ¼-in. copper column filled with activated alumina (Burrell, cat. No. 341–35). This column was capable of separating nitrogen and methane, but not N_2–NO or NO–CH_4 mixtures, which were eluted as one peak. Ethane, nitrous oxide, ethylene, propane, and propylene were well separated. The column was calibrated for ethane, nitrous oxide, ethylene, and propane in the manner described above for the non-condensable fraction. The ratios of sensitivities ethane to ethylene and ethane to propane were 1.03 and 0.84, respectively, compared with 1.06 and 0.79 determined by Messner *et al.* (10). This column was also used for checking nitric oxide for nitrous oxide impurity.

RESULTS

I. Inhibition by Olefin

The results of inhibition experiments with ethylene and propylene at 275.9° C are shown in Fig. 2. The initial azomethane pressure was kept constant at 22.2 mm in each case. The limiting inhibited rate in the presence of propylene, about 2.25×10^{-5} sec^{-1}, is in agreement with the results of Steel and Trotman-Dickenson (4), who found a limiting rate of about 2.2×10^{-5} sec^{-1} at 276.3° C and 19.7 mm of azomethane.

Table I gives results of runs carried to completion, i.e. 100% conversion. The theoretical reaction time for 99.9% reaction was calculated from rate constants read off the graph

**The separation of O_2 and N_2 was likewise incomplete, but it was good enough to permit the detection of a small amount of one gas in the presence of a large amount of the other.*

Can. J. Chem. Downloaded from www.nrcresearchpress.com by 210.87.254.105 on 09/05/12
For personal use only.

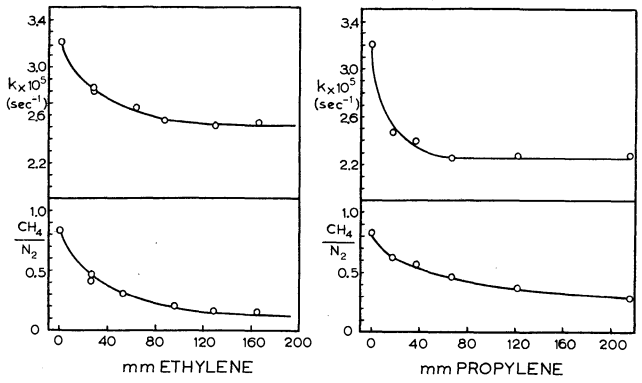

FIG. 2. Olefin inhibition at 275.9° C. Azomethane initial pressure $(A)_0$ constant at 22.2 mm.

TABLE I

Total decomposition runs at 275.9° C

	Azomethane only	Ethylene present	Propylene present
Initial pressure of azomethane (mm)	22.2	22.2	22.2
Initial pressure of foreign gas (mm)	—	168.5	167.0
Reaction time (hr)	89	82	82
Theoretical reaction time for 99.9% decomposition (hr)	60	75	84
Nitrogen recovery (%)	78.5	86.0	82.0
CH_4/N_2 ratio in non-condensables	1.0	0.46	0.44

in Fig. 2 for the appropriate olefin pressure. These results are the average of at least two runs in each case. Nitrogen recovery is defined as (nitrogen found)/(nitrogen input), the nitrogen input being equal to 100% azomethane decomposed. The results for unadulterated azomethane are essentially identical with those reported by Riblett and Rubin (2).

II. Inhibition by Nitric Oxide

Typical results of inhibition experiments with nitric oxide in an ordinary and packed vessel are shown in Fig. 3 for an initial azomethane pressure of 40 mm. The figure does not show results of propane analyses since no propane was found even at the lowest nitric oxide pressure, although in the absence of nitric oxide propane was formed in amounts comparable with ethylene yields. On the other hand, the quantities of CH_4, C_2H_6, and C_2H_4 found in the presence of more than 20 or 30 mm NO, though small, were not zero. It is seen that in the presence of NO packed runs actually gave rates closer to unpacked values than in the absence of NO. All previous investigators (12, 13, 14) agree that packing has little influence on the rate. In addition, nitric oxide showed no residual effect of the sort reported by Szabó and Márta (15) in the case of the NO-inhibited decomposition of propionic aldehyde, since unadulterated azomethane decomposed at the usual higher rate when introduced in the reaction vessel immediately after a series of experiments with NO.

The ascending portion of the rate constant vs. NO pressure plot is linear within experimental error. The broken line represents an extrapolation of the linear part back to zero NO pressure, calculated by the method of least squares. This extrapolated rate will be called the "net inhibited rate", k_0.

Some of the runs shown in Fig. 3 were repeated using the isotopic nitric oxide ^{15}NO

Can. J. Chem. Downloaded from www.nrcresearchpress.com by 210.87.254.105 on 09/05/12
For personal use only.

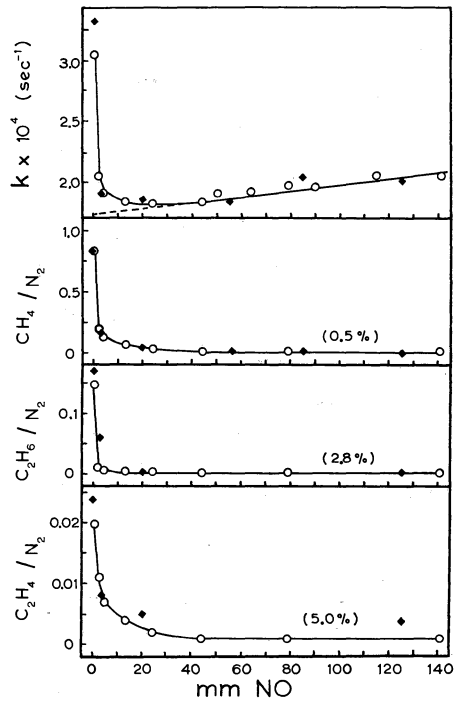

FIG. 3. Nitric oxide inhibition at 303° C. Azomethane initial pressure $(A)_0$ constant at 40 mm. ○, 250-ml spherical vessel, S:V ~ 0.75 cm^{-1}; ◆, packed vessel, S:V ~ 5.7 cm^{-1}. Numbers in parentheses indicate amount of product formed at high NO pressure (>100 mm), in percentage of the amount formed in the absence of NO. Broken line shows extrapolation of rate constant to zero NO pressure. Common NO scale.

(97.7% ^{15}NO, 2.3% ^{14}NO). The results of the nitrogen analyses of these runs are shown in Table II. P_{28}, P_{29}, and P_{30} are parent peaks corresponding to the molecules $^{14}N_2$, $^{14}N^{15}N$, and $^{15}N_2$, respectively. The natural abundance of $^{14}N^{15}N$ in ordinary nitrogen is

TABLE II

Mass-spectrometric analysis of runs with ^{15}NO at 303° C
(Azomethane initial pressure constant at 40 mm in all cases)

Initial pressure of NO (mm)	Analysis of nitrogen formed. Peak heights at various mass:charge ratios (in arbitrary units)						
	P_{28}	P_{29}	P_{30}	ΔP_{29}*	$f_{N_2}^{azo}$	$f_{N_2}^{NO}$	k_{corr} $\times 10^4$ (sec^{-1})
2.20	2017	19.6	2.7	4.8	0.9964	0.0014	2.05
4.0	1596	15.6	2.9	3.8	0.9960	0.0019	1.90
25.0	2022	19.6	11.8	4.3	0.9920	0.0060	1.78
44.8	1800	18.3	23.2	4.1	0.9845	0.0132	1.84
79.7	2067	23.4	70.2	4.9	0.9636	0.0341	1.89
140.2	1460	20.9	135.5	3.7	0.9100	0.0878	1.92

*$\Delta P_{29} = P_{29} - 0.00735P_{28} - 0.048P_{30}$.

0.73 mole% (16), so that the contribution from this source is equal to $0.00735P_{28}$, and the fraction of nitrogen, of natural isotopic composition, from azomethane, $f_{N_2}^{azo}$, is then:

$$f_{N_2}^{azo} = \frac{1.00735P_{28}}{P_{28}+P_{29}+P_{30}}.$$

Can. J. Chem. Downloaded from www.nrcresearchpress.com by 210.87.254.105 on 09/05/12
For personal use only.

The rate constant calculated on the basis of ordinary nitrogen, i.e. corrected for the nitrogen *not* formed from azomethane, is given in the last column of Table II under "k_{corr}". The natural abundance of the isotopic species $^{15}N_2$ was ignored, since the amount is only 0.0014 mole% (17).

The amount of NO decomposed to nitrogen can be calculated by observing that of 100 molecules of NO that have reacted, 97.7 will be ^{15}NO and 2.3 ^{14}NO. Since it obviously requires 2 molecules of NO to form N_2, the composition of the reaction products will be very nearly 2.3 molecules $^{14}N^{15}N$ and 47.7 molecules $^{15}N_2$ per 100 molecules NO, or $P_{29} = 0.048P_{30}$. This neglects the chance of two molecules of ^{14}NO reacting to form $^{14}N_2$. The fraction of nitrogen originating from NO, $f_{N_2}^{NO}$, is then:

$$f_{N_2}^{NO} = \frac{1.048P_{30}}{P_{28}+P_{29}+P_{30}}.$$

ΔP_{29}, defined as $P_{29}-0.00735P_{28}-0.048P_{30}$, is the remainder of the 29 peak that cannot be accounted for by the isotopic composition of nitrogen in the reactants. It remains fairly constant throughout the range of NO pressures, which would suggest either an experimental error in the isotopic analysis, or perhaps a slight fractionation of nitrogen in the course of the azomethane synthesis. In Fig. 4 k_{corr} is plotted, where the solid line

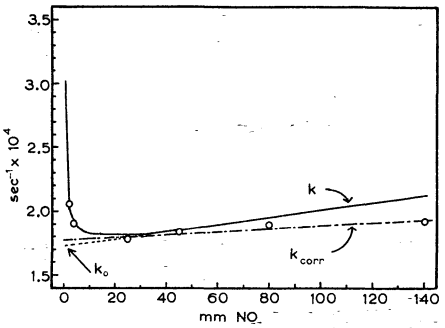

FIG. 4. Extrapolation for "net inhibited rate" k_0. Full line is k from Fig. 3; circles are k_{corr} from Table II. $(A)_0 = 40$ mm; 303° C.

represents k from Fig. 3. and the circles are values of k_{corr} from Table II. It is seen that the plot of k_{corr} vs. NO pressure is of the same type as the plot of k, i.e. a rapid initial drop followed by a slow linear increase. The dot–dash line in Fig. 4 is a least-squares straight line calculated for the linear ascending portion of k_{corr}. The "net inhibited rate" extrapolated from k is 1.73×10^{-4} sec^{-1}, while that extrapolated from k_{corr} is 1.78×10^{-4} sec^{-1}. The discrepancy between the two is probably somewhat less than the estimated experimental error, so that it may be concluded that both k and k_{corr} extrapolate essentially to the same "net inhibited rate".

Figure 5 shows results of inhibition experiments at 5 mm azomethane initial pressure. In this case, in addition to analyses for CH_4, C_2H_6, C_2H_4, and N_2O, the consumption of NO was also measured. The dependence of the various product yields on initial NO pressure is quite analogous to the pattern shown in Fig. 3. Analyses for propane are not reported since no propane was found even at the lowest NO pressure.

It was not possible to measure NO consumption at higher azomethane pressures because the linear part of the ascending portion of the rate curve then shifts to higher NO pressures. The NO consumed, a small number, is then given by the difference between two large numbers, NO (initial) — NO (final), which results in poor accuracy.

Can. J. Chem. Downloaded from www.nrcresearchpress.com by 210.87.254.105 on 09/05/12
For personal use only.

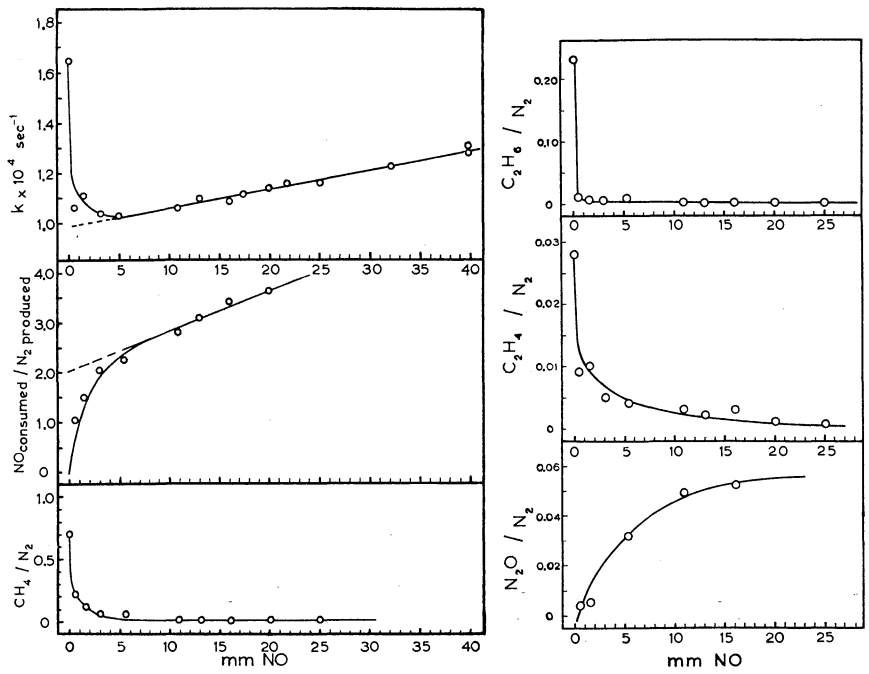

FIG. 5. Nitric oxide inhibition at 303° C. Azomethane initial pressure $(A)_0$ constant at 5 mm. Broken lines are extrapolations to zero NO pressure. Common NO scale.

Figure 6 shows the results of nitric oxide inhibition at 275.9° C and at three different initial azomethane pressures, covering an almost 200-fold pressure range. The results of

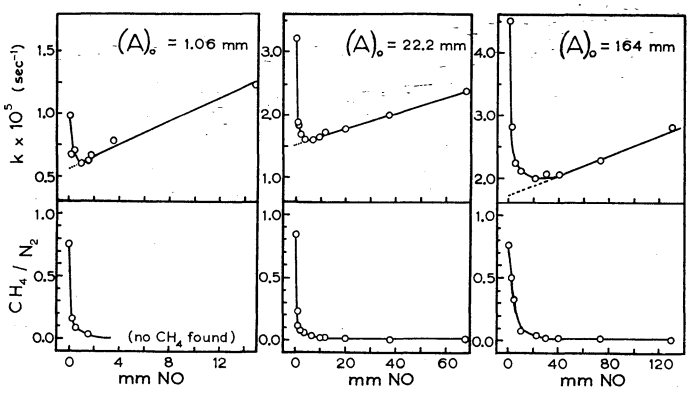

FIG. 6. Nitric oxide inhibition at 275.9° C and at three different initial pressures $(A)_0$ of azomethane. Dotted line indicates extrapolation for "net inhibited rate".

analyses for methane, the other major product after nitrogen, are also given. It is seen that at each azomethane pressure the general pattern is identical with results shown in Figs. 3 and 5. Only linear portions of the ascending parts of the rate curves are shown. At $(A)_0 = 22.2$ and 163.5 mm, linearity ceases above about 120 mm NO, and at $(A)_0 = 1.06$ mm above approximately 20 mm NO.

Can. J. Chem. Downloaded from www.nrcresearchpress.com by 210.87.254.105 on 09/05/12
For personal use only.

The "net inhibited rate", k_0, has been determined by means of the above extrapolation procedure at two additional temperatures for each of the three azomethane pressures. From these the activation energy and the pre-exponential factor, together with the corresponding standard deviation, were calculated for each pressure. The complete results, including those plotted in Fig. 6, are shown in Table III.

DISCUSSION

No discussion of these results is possible without making first some assumption about the mechanism of azomethane decomposition in the absence of inhibitor. It is generally agreed that the first step in the decomposition is the process

$$CH_3N{=}NCH_3 \rightarrow CH_3 + CH_3N{=}N.$$

Thermochemical arguments have been advanced (3) to show that the $CH_3N{=}N$ fragment is highly unstable and will rapidly, if not immediately, decompose according to

$$CH_3N{=}N \rightarrow CH_3 + N_2.$$

Consideration of the potential energy surface involved shows that the simultaneous splitting of the two methyls,

$$CH_3N{=}NCH_3 \rightarrow 2CH_3 + N_2, \qquad [1]$$

affords a reaction path of lowest energy (8). In any event, it is very likely that there is one nitrogen formed per C—N bond broken, the rate of this bond rupture being the information desired.

There exist numerous proofs for the presence of methyl radicals in the system (19), the most recent of which (20) is the demonstration that in the gas phase photolysis of azomethane in the presence of 1,4-cyclohexadiene almost all of the carbon ends up as methane.

At low conversion, provided the fragment $CH_3N{=}N$ has no appreciable lifetime, the main secondary reaction is likely to be

$$CH_3 + CH_3N{=}NCH_3 \rightarrow CH_4 + CH_2N{=}NCH_3. \qquad [A]$$

Since the rate of the azomethane decomposition is followed by the rate of formation of nitrogen, the above reaction will affect the rate only if the ultimate fate of the $CH_2N_2CH_3$ radical is the formation of nitrogen. If it does form nitrogen, then a methyl radical scavenger should decrease the rate as measured by the rate of formation of nitrogen. If, on the other hand, the fragment $CH_3N{=}N$ is relatively long lived, the possible complications are numerous, the most obvious of which is that in the presence of a radical scavenger there could be fewer than one nitrogen formed per C—N bond broken. A simple test (see below) shows that this is not the case.

I. Inhibition by Olefin

If the fragment $CH_3N{=}N$ is relatively long lived, the following possibility arises: ethylene (21) and propylene (22) are known to polymerize under the influence of methyl radicals from azomethane. If this polymer were to scavenge some of the $CH_3N{=}N$ fragments, the nitrogen yield (i.e. the rate) could be reduced, even if the $CH_2N{=}NCH_3$ radical yielded ultimately no nitrogen, that is, even if there were no chain.

Experiments summarized in Table I were designed to test this possibility. A scavenging of the fragments $CH_3N{=}N$ by propylene or ethylene would manifest itself in the reduction of the ratio (N_2 found)/(azomethane decomposed) relative to unadulterated azomethane. Such is not the case, which means that $CH_3N{=}N$ is very short lived, or that no scavenging

Can. J. Chem. Downloaded from www.nrcresearchpress.com by 210.87.254.105 on 09/05/12
For personal use only.

Can. J. Chem. Downloaded from www.nrcresearchpress.com by 210.87.254.105 on 09/05/12
For personal use only.

TABLE III

Summary of inhibition experiments with NO at various initial pressures of azomethane ($(A)_0$)

	$(A)_0$ = 1.06 mm			$(A)_0$ = 22.2 mm			$(A)_0$ = 163.5 mm		
Temperature (°C):	275.9	293.5	315.7	254.1	275.9	303.0	254.1	275.9	294.0
$k_0 \times 10^6$ (sec^{-1})	6.0	27.2	127	1.77	15.1	162	1.96	16.8	82.1
Chain length	1.65	1.47	1.44	2.38	2.13	1.77	3.35	2.71	2.41
CH_4/N_2	0.000	0.000	0.000	0.000	0.002	0.005	0.002	0.004	0.010
NO pressure range (mm)	1.6–15	3–9	3–9	19–123	7–120	20–120	60–140	40–130	80–140
$\log_{10}$ (A)		14.45±0.65			17.24±0.19			17.28±0.23	
$E_{activation}$ (kcal/mole)		49.4±1.7			55.5±0.5			55.4±0.6	

NOTE: "Chain length" is defined as the uninhibited rate divided by k_0. "CH_4/N_2" means the value of this ratio at the high end of the "NO pressure range"; the latter indicates the range of NO pressures over which the rate increases linearly.

of this fragment takes place. The fact that the ratio actually increases in the presence of ethylene and propylene does not necessarily mean, however, that reaction [A] starts a chain in azomethane, since ethylene and propylene could merely prevent methyl radicals from adding to azomethane (to form hydrazines) and might thus increase the amount of azomethane available for formation of nitrogen.

Results shown in Fig. 2, which refer to less than 5% decomposition, show that both ethylene and propylene reduce the rate, i.e. inhibit the formation of nitrogen. The possibility of a reaction of the fragment $CH_3N{=}N$ with olefin having been eliminated, it must be concluded that some nitrogen is prevented from being formed via reaction [A], that is, that the radical $CH_2N{=}NCH_3$ ultimately yields nitrogen.

The answer to the question of how propylene or ethylene interferes with the formation of nitrogen depends on the assumed mode of action of olefin as inhibitor. A theory has been suggested by Laidler and Wojciechowski (23) according to which the inhibiting action of propylene is due to a special type of chain mechanism initiated via hydrogen abstraction by the allyl radical formed from propylene by thermal cracking. The latter reaction has an activation energy of 78 kcal/mole (23), and thus its rate would be negligible around 300° C (about 10^{11} times smaller than the rate at 600° C, where the pyrolysis of propylene proceeds at a convenient rate). However, allyl could still be formed by hydrogen abstraction from propylene by methyl radicals, a reaction that has a low activation energy (24, p. 296). There is evidence (25) that the allyl radical is relatively stable at low temperatures and does not abstract hydrogen until about 500° C. It would thus appear that at low temperatures, such as those encountered in the present work, propylene acts solely as a radical remover, i.e. the mechanism suggested by Laidler and Wojciechowski does not apply here, as in fact it would not apply in any propylene inhibition below 500° C.

It is seen (Fig. 2) that propylene and ethylene each inhibit the nitrogen production to a different extent. The yield of methane, the next major product after nitrogen, is also reduced by ethylene and propylene, but again to a different extent by each. If propylene, and presumably also ethylene, act only as radical removers, selective removal of the $CH_2N{=}NCH_3$ radical by simple addition would reduce the yield of nitrogen but not the yield of methane. Hydrogen abstraction by this radical from propylene, for example, would reduce the yield of nitrogen and leave the yield of methane unaffected. Neither of these two possibilities is evidently the predominant factor (Fig. 2). The complete removal of methyl radicals by simple addition to ethylene or propylene (to form a C_3 and C_4 radical, respectively) would reduce the rate to the same limiting value for both inhibitors and stop the formation of methane altogether. Clearly, such is not the case, so that if methyl radical addition occurs, it is not an efficient process. Another argument against such an addition is the low stability of radicals formed by addition (26). It should be noted that there is found less methane in the presence of ethylene than in the presence of propylene. This is what might be expected from the fact that propylene is more readily attacked by methyl radicals to form methane (24, p. 296). Hence it would seem that at least some methyl radicals are removed by hydrogen abstraction from olefin.

It must be concluded that of the four possible processes, hydrogen abstraction or addition by CH_3 and $CH_2N{=}NCH_3$, the experimental results on methane formation do not point to any one process as the dominant one. It is probable that all four processes occur simultaneously in the presence of ethylene and propylene, the relative importance of each process depending on the olefin. It is interesting to note that toluene seems to have no inhibiting effect at all (4) and this despite the fact that toluene should react with methyl radicals (to form CH_4) at about the same rate as propylene (24, p. 296). The

Can. J. Chem. Downloaded from www.nrcresearchpress.com by 210.87.254.105 on 09/05/12
For personal use only.

picture is further complicated by the circumstance that below about 100 mm of azomethane the decomposition is in the pressure-sensitive region, so that the addition of a fairly complex molecule, such as propylene or toluene, tends to increase the rate of the unimolecular part of the decomposition. This effect can be clearly seen in the observation (4) that at 0.9 mm of azomethane, propylene and toluene both actually *increased* rate.

The inhibition by olefin thus appears to be a fairly complex process and while it leaves little doubt that there is in fact a chain in the decomposition, experimental results offer no clear-cut evidence that any of the three olefins mentioned is capable of completely stopping the chain in azomethane. In short, ethylene, propylene, or toluene are not "good" chain suppressors in the azomethane decomposition.

II. Inhibition by Nitric Oxide

A. Comparison with Other Work

Nitric oxide, being a simple molecule, can be reasonably expected to add little to collisional activation in the pressure-sensitive region of the azomethane decomposition, so that, from this point of view at least, it is more a desirable inhibitor than olefins.

First experiments with NO were reported by Davis, Jahn, and Burton (27), who photolyzed (for an unspecified time) mixtures of about 100 mm azomethane and 10 mm NO between 20 and 222° C. Nitric oxide reduced the yields of methane and ethane to very small values, particularly at the higher temperatures. Calvert *et al.* (7) found nitrogen and nitrosomethane as the only products of flash photolysis of azomethane–NO mixtures at 25° C. Jahn and Taylor (28) pyrolyzed, around 300° C, mixtures of about 100 mm azomethane and 200 mm NO; the extent of decomposition was usually around 50%. Only insignificant quantities of hydrocarbon were found in the products, and the rate decreased by a factor of about two relative to the rate in absence of NO.

Neither of these studies is directly comparable with the present work, the first two because they are low-temperature photolyses, and the third on account of the large extent of decomposition. A high extent of decomposition may lead to misleading results, as shown by the experiments of Steacie and Folkins (29), who found in the case of the NO-inhibited decomposition of butane that after the reaction had progressed to 25 or 50% of completion the rate increased again. Nevertheless, the present work (Fig. 3) confirms the general feature of these studies. The novel feature is the accelerating effect of NO at higher NO pressures, a pattern that—unlike the case of propylene inhibition (4)—is seen to persist over an almost 200-fold range of initial azomethane pressures (Fig. 6) and over the entire temperature range investigated (Table III). It is understandable that Jahn and Taylor should have missed this effect since they did not study the rate as a function of NO pressure.

It will be noticed that the amount of NO required to reduce the rate to a minimum is appreciable, of the order of several millimeters of mercury, in contrast with traces of NO sufficient to inhibit the decompositions of hydrocarbons (26). The effect of NO on azomethane thus resembles somewhat the acetone pyrolysis in the presence of NO (30), which is not too surprising in view of certain similarities between the structures of the two molecules. Unfortunately, the acetone inhibition results refer to 50% reaction, so that they are not as reliable as might be desired. The chain length in both cases is quite small (acetone: < 1 (30), azomethane: 1.7 to 3.1 (Table III)), which is the reason why appreciable pressures of NO are required to produce noticeable inhibition: the small chain length indicates that many chains are broken even in the absence of NO; if NO is to have a noticeable effect, it must break many more chains, which will not happen unless NO pressure is appreciable.

Can. J. Chem. Downloaded from www.nrcresearchpress.com by 210.87.254.105 on 09/05/12
For personal use only.

There is, however, one effect in which the NO-inhibited decomposition of acetone and azomethane differ: in the former case it is found by extrapolation that both NO and propylene reduce the rate to the same minimum value, while in the present case the minimum rate with NO is lower than the minimum rate in the presence of propylene (cf. Figs. 2 and 6). This difference between acetone and azomethane, if it does not represent a complication due to the high extent of decomposition in the acetone work, can be accounted for by different behavior of propylene at low and high temperatures discussed above in connection with olefin inhibition, considering that the acetone inhibition was studied at 570° C. Calculations have been made (26) to show that if methyl radicals disappear in the presence of propylene and NO by the processes

$$CH_3 + C_3H_6 \rightarrow CH_4 + C_3H_5$$

$$CH_3 + NO \rightarrow \text{products},$$

respectively, propylene should be several hundred times less effective than NO as inhibitor. The present data, while offering no direct support for this conclusion, at least do not contradict it. Although the rate curve in the presence of propylene (Fig. 2) appears to reach a limiting value at one hundred millimeters propylene or so, it could actually have a small downward slope and it is not impossible that at a pressure of a few atmospheres of propylene the rate could decrease to the NO value.

It should be noted that also in all other cases where propylene and NO reduce the rate to the same limiting value: propionaldehyde (31), diethyl ether (32), and *n*-pentane (33), the pyrolyses were studied above 500° C. The inhibition of acetaldehyde at 525° C (34), where propylene is more effective than NO, is an exception. In all these cases, and in many olefin decompositions as well (35), NO at higher concentrations increases the rate again, so that the stimulatory effect of NO seems to be the rule.

B. The Nature of the Inhibited Reaction

Arguments presented in Section I show that there is a chain in azomethane, due probably to the formation and subsequent decomposition of the $CH_2N{=}NCH_3$ radical. The observed inhibition with NO (Figs. 3 and 5) is consistent with such an interpretation. A reduction in rate implies the removal of $CH_2N{=}NCH_3$, or of its precursor, the methyl radical. Since the bulk of hydrocarbons must be due to subsequent reactions of methyl radicals, the drastic reduction by NO of the yield of hydrocarbons (Fig. 3) indicates the removal of methyl radicals rather than removal of $CH_2N{=}NCH_3$. It could be objected to this line of argument that since no analyses were made for C_4 and higher hydrocarbons, NO could conceivably catalyze methyl radical reactions in such a fashion as to favor the formation of higher hydrocarbons. It seems, however, extremely unlikely that there should exist a pathway permitting the synthesis of higher hydrocarbons from methyl radicals in such a way as to leave not more than a trace of CH_4 and C_2H_6 and no propane or propylene at all. Thus the absence of lower hydrocarbons necessarily means also the absence of higher hydrocarbons.

From Fig. 3, which refers to 40 mm azomethane, it is seen that while in the absence of NO there are about 9 methane and 1 ethane molecules formed per 10 nitrogen molecules produced, at 141 mm NO the production amounts only to 4 methane and 4 ethane molecules per 1000 molecules N_2, which is very small indeed, and amounts to 0.48% of the methane and 2.8% of the ethane produced in the absence of NO. The drop-off is less rapid in methane than in ethane production. At 5 mm of azomethane (Fig. 5) conditions are quite analogous. Evidently the ethane production is more sensitive to a reduction in

Can. J. Chem. Downloaded from www.nrcresearchpress.com by 210.87.254.105 on 09/05/12
For personal use only.

methyl radical concentration than is the methane production, which is to be expected because the rate of ethane production is second order in $[CH_3]$, while methane production is first order in $[CH_3]$.

If the scheme for the decomposition of unadulterated azomethane given at the beginning of the Discussion is correct, a methyl radical will have a choice of recombining to form ethane, or to react further and continue a chain, forming methane in the process. Absence of ethane and methane then would mean that the methyl radical does neither, i.e. reacts preferentially in some other way, so that the chain is stopped short. There seems to be little doubt now that methyl radicals are removed (7) by the process

$$CH_3 + NO \rightarrow CH_3NO, \qquad [2]$$

although it is generally appreciated that the nitrosomethane might decompose further at higher temperatures. If the methyl radicals are removed by the overall process

$$CH_3 + NO \rightarrow \text{products other than } N_2 \text{ or hydrocarbon} \qquad [B]$$

then one nitric oxide molecule must be consumed per methyl, and since two methyls are formed per nitrogen molecule produced, a complete, or almost complete removal of methyl radicals by NO according to [B] should lead to the consumption of two molecules of NO per nitrogen molecule produced. The consumption of NO is shown in Fig. 5. The ratio (NO consumed)/(N_2 produced) rises quickly with increasing NO pressure and reaches the vicinity of 2 just about at the same time as the ratios CH_4/N_2 and C_2H_6/N_2 become very small. Beyond this point the amount of NO consumed continues to rise at a smaller rate, probably due to a secondary reaction with azomethane. This complicating factor can be roughly corrected for by extrapolation to zero NO pressure (broken line in Fig. 5); the extrapolated value of (NO consumed)/(N_2 produced) is still around 2. These results are similar to those obtained by Hoare (36) in the photolysis of acetone + NO mixtures at 200° C. At low pressures of NO there is one NO molecule consumed per 2.2 to 2.3 methyl radicals, while at high NO pressures the consumption exceeds one NO molecule per methyl radical.

The reduction in the yield of hydrocarbon and the amount of NO consumed thus both support the conclusion that at NO pressures corresponding roughly to the minimum in the rate curve, and beyond, nearly all radicals are removed from the system by a process of the type represented by [B]. This means that under these conditions the chain reaction in azomethane is for all practical purposes completely stopped. The very small amount of hydrocarbon formed, even at the highest NO pressures (except at 1 mm azomethane where the amount was too small to be detected), can be due either to a small portion of the methyl radicals remaining unscavenged, or to a small dissociation of CH_3NO. It remains now to elucidate the nature of the residual, fully inhibited reaction. The fact that the rate, after reaching a minimum, slowly rises again (Figs. 3, 5, and 6) while the amount of hydrocarbon produced remains very low, or actually keeps decreasing, indicates a complicating process, not connected with the radical scavenging just described. For the purpose of discussion, this complication can be ignored for NO pressures not too much beyond the minimum rate.

The school of Hinshelwood believes that the reaction fully inhibited by NO is molecular, at least in part. In the case of azomethane, the molecular reaction would give nitrogen and ethane in one step, so that C_2H_6/N_2 should approach unity at some sufficiently high NO pressure. This is not the case, so that the residual reaction is not molecular to any significant degree. However, even if it were assumed that the value $C_2H_6/N_2 = 0.004$

Can. J. Chem. Downloaded from www.nrcresearchpress.com by 210.87.254.105 on 09/05/12
For personal use only.

found at high NO pressures represents the extent of molecular reaction, it would be difficult to explain why under those conditions CH_4/N_2 is equal to 0.004 and not to zero, for the presence of methane implies the presence of methyl radicals.

It seems equally unlikely that the residual reaction is a surface reaction since the azomethane decomposition is rather insensitive to surface effects (see Experimental), and the rate in the presence of NO is not affected by a change in the surface-to-volume ratio. Furthermore, the activation energy of the residual reaction, which is about 55 kcal/mole (Table III), is certainly much too high for a surface reaction. The residual reaction could, however, be of the kind where chains are started and terminated at the walls, which would be insensitive to a change in the S/V ratio; in addition, the rate of nitrogen formation need not involve the rate of the surface initiation or termination, so that the activation energy criterion would no longer apply. It will be shown in more detail in a forthcoming publication that the residual reaction behaves like a typical unimolecular reaction, including rate increase by inert gas (C_2F_6). If the accelerating effect of inert gas is merely a diffusion effect, it would mean that the species responsible for chain initiation and termination at the wall are different, and that their diffusion coefficients in C_2F_6 are also different, with the net result that the average chain length is increased. Now the rate of a diffusion-controlled process in a spherical vessel is given (37) by

$$\text{rate} = 2\pi^2 D/3d,$$

where D = diffusion coefficient of the species under consideration, d = diameter of the vessel. Since the diameter is inversely proportional to the S/V ratio, packing the vessel in the absence of C_2F_6 should have an effect on rate. This does not happen, and hence the effect of inert gas is not attributable to a surface reaction.

It has been suggested that the fully inhibited reaction might be a new kind of chain reaction (26). The consensus of opinion at the present time (35, 38, 39) seems to favor a chain reaction initiated by a hydrogen abstraction by NO to form HNO and a radical. The question in the case of azomethane is whether at the point where the rate goes through a minimum, and where very little hydrocarbon is produced, an important part of the nitrogen is produced from azomethane by a NO-induced reaction. (It is shown in the following section that at this point practically all the nitrogen comes from azomethane.) By implication, this means that the rate of the process [1] should be at least an order of magnitude slower than the NO-induced process, which might be

$$CH_3N_2CH_3 + NO \rightarrow HNO + CH_2N_2CH_3, \qquad [C]$$

the $CH_2N_2CH_3$ radical then giving nitrogen. One important feature of nitrogen production via such a reaction is of course that no nitrogen is produced when there is no nitric oxide. In other words, if this reaction were important at relatively low pressures of NO, the rate vs. NO pressure curve should extrapolate to zero rate at zero NO pressure without too much strain on the imagination. A glance at k_{corr} in Fig. 4 shows that such an extrapolation would be an exercise in gamesmanship. A similar argument would lead to the rejection of the alternative reaction

$$CH_3N_2CH_3 + 2NO \rightarrow 2CH_3NO + N_2. \qquad [D]$$

There are other difficulties. With reaction [C] or [D] as the important source of nitrogen [1] must be very slow. To account for the high rate in the absence of NO, one would have to suppose a chain of considerable length. Rate supported by a long chain should then show appreciable inhibition by very small amounts of NO, which is not observed. Also,

Can. J. Chem. Downloaded from www.nrcresearchpress.com by 210.87.254.105 on 09/05/12
For personal use only.

the amount of inhibition by propylene and ethylene might be expected to be higher than it is. Moreover, a long chain would imply high rate for the decomposition

$$CH_2N_2CH_3 \rightarrow N_2 + \text{other products.}$$

Now the radical $CH_2N_2CH_3$ can be expected to resonate between two structures

$$\cdot CH_2—N{=}N—CH_3 \text{ and } CH_2{=}N—\dot{N}—CH_3.$$

Thermochemical data on azo compounds are too scanty to permit even an estimate of the resonance energy involved, but some resonance stabilization can be reasonably expected. As a result, the radical $CH_2N_2CH_3$ is very likely to react rather sluggishly, making a long chain in azomethane improbable. The odds are thus against an important NO-induced reaction in the neighborhood of minimum rate.

The remaining possibility for the residual (fully inhibited) reaction is that it represents the primary process of the chain, i.e. the unimolecular fission of the C—N bond,

$$CH_3N{=}NCH_3 \rightarrow 2CH_3 + N_2. \qquad [1]$$

This reaction is free of all the qualitative objections raised against the other possibilities, and so it permits a simple explanation of the inhibition phenomenon. It is unfortunate that the inhibited reaction is complicated by a NO-induced reaction, so that the rate of [1] can be obtained only after a correction for the NO-induced process has been made. However, the short extrapolation necessary to obtain this "net inhibited rate" (Fig. 4) is unlikely to lead to a very large discrepancy from the actual value.

The important quantitative parameters of the residual reaction [1], based on the "net inhibited rate", are summarized in Table III. The pressure-dependent activation energy (55.5 kcal at 22 mm) is higher than that determined by Steel and Trotman-Dickenson (4) (51.6 kcal around 20 mm), which refers to the activation energy of unadulterated azomethane, i.e. the chain process. This rise in activation energy is easily understood in terms of chain inhibition, since in blocking a chain path of lower activation energy inhibition makes the rate entirely dependent on the initial step with the highest activation energy of the sequence. The concomitant rise in the pre-exponential factor is less easily understood in elementary terms. However, it will be shown in a forthcoming publication that the residual reaction has all the features of a typical unimolecular reaction, and that the high pre-exponential factor can be satisfactorily accounted for from the entropy change in the activated state. Thus the assumption that the fully inhibited reaction corresponds to process [1] leads to consequences that are self-consistent.

C. The NO-induced Reaction

Since both azomethane and NO contain nitrogen, and the rate of azomethane decomposition is measured by the rate of formation of nitrogen, the accelerating effect of NO is ambiguous, that is, the rate increase at high NO pressures could be due to the production of nitrogen either from azomethane or from NO. Experiments with the isotopic nitric oxide, ^{15}NO, summarized in Table II, were designed to permit a distinction between the two possible sources of nitrogen. Column 4 of Table II shows that there is in fact formation of molecules $^{15}N_2$, i.e. part of the rate rise is only apparent, being due to nitrogen formed by the decomposition of NO. Quantitatively these results will not have much meaning unless isotopic exchange reactions involving nitrogen are slow at the temperature of the experiment.

Johnston and Anstett (40) measured the rate of approach to thermal equilibrium in mixtures of $^{14}N_2$, $^{15}N_2$, and $^{14}N^{15}N$. They found that no thermal exchange took place in

Can. J. Chem. Downloaded from www.nrcresearchpress.com by 210.87.254.105 on 09/05/12
For personal use only.

1 month at room temperature or in 19 hours at 850° C. Another possible exchange reaction is

$$^{14}N_2 + {}^{15}NO \rightarrow {}^{14}NO + {}^{14}N{}^{15}N,$$

the rate of which does not appear to have been measured. It can be roughly calculated from statistical mechanics, by considering only the symmetry numbers of the corresponding partition functions, that the equilibrium constant of this reaction, K, is given by

$$K = \frac{[^{14}N^{15}N][^{14}NO]}{[^{14}N_2][^{15}NO]} \sim 2.$$

If, as seems reasonable for a short azomethane run, ^{14}NO remains at 2.3% of total NO (no change in initial isotopic composition), we have $[^{14}NO]/[^{15}NO] = 0.0235$, so that, with reference to Table II, there should be $P_{29}/P_{28} \sim 2/0.0235 = 85$. The experimental results are not anywhere near this figure, which would mean that equilibrium is approached very slowly. Presumably any exchange reaction involving molecular nitrogen would be slow. The fact that ΔP_{29} (Table II) is independent of NO pressure can also be cited as evidence against any important exchange.

The values of k_{corr} in the last column of Table II were calculated on the assumption that no $^{14}N_2$ was lost by exchange. However, even if it were assumed that the entire 29-peak was the result of exchange, the values of k_{corr} would be affected to not more than 1%, which is less than the experimental error in the rate constant. It can therefore be concluded, with reference to Fig. 4, that about one-half of the upward slope in the positive catalysis region of the rate curve is due to the decomposition of azomethane.

The fraction of the N_2 arising from the decomposition of NO is given in Table II under $f^{NO}_{N_2}$. This decomposition is quite small, at 140 mm NO only 8.8% of the total nitrogen formed comes from NO (Table II), which, at 8% decomposition of 40 mm azomethane present initially represents 8.8% of 3.2 mm = 0.28 mm N_2 originating from NO, i.e. 0.56 mm NO decomposed out of 140 mm, which amounts to 0.4% decomposition of NO. This amount, even though it is the largest recorded in Table II, is small enough to make it appear possible that this nitrogen might arise by a slight thermal decomposition of NO at the temperature of the experiment. However, Wise and Frech (41) have studied the thermal decomposition of NO and found it to be heterogeneous and second order in NO below 1000° K, with the rate constant given by

$$k_{het} = 1.4 \times 10^4 \exp(-21{,}400/RT) \text{ cc/mole-sec.}$$

It can be calculated from this information that at 303° C and 140 mm NO the time required for 1% thermal decomposition is over 7000 hours, so that the amount of NO decomposed thermally at this temperature in the course of a typical run of a few minutes is negligible. The conclusion is then that azomethane, or its decomposition products, provokes slight decomposition of nitric oxide to form N_2.

The first-order rate constant for the formation of nitrogen from nitric oxide, defined as

$$k^{NO}_{N_2} = \frac{1}{NO}\frac{d(N_2^{NO})}{dt},$$

is plotted against NO pressure in Fig. 7; initial azomethane pressure is constant at 40 mm. The rate constant depends linearly on NO pressure, which means that nitrogen is formed from NO in a reaction second order in NO. The plot, however, does not extrapolate to $k^{NO}_{N_2} = 0$ at zero pressure of NO, which might suggest that the reaction has a first-order

Can. J. Chem. Downloaded from www.nrcresearchpress.com by 210.87.254.105 on 09/05/12
For personal use only.

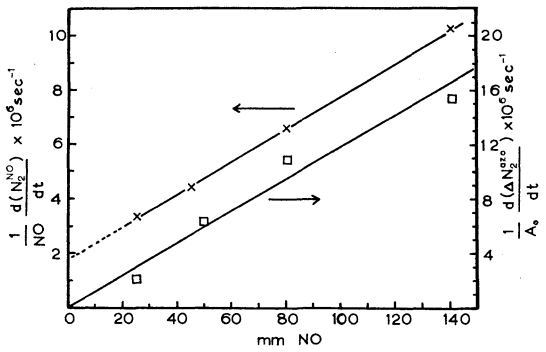

FIG. 7. Plot vs. NO pressure of the first-order rate constant for nitrogen formation from NO (×, left scale), and of the first-order rate constant for the NO-induced formation of nitrogen from azomethane (□, right scale).

heterogeneous component amounting to about 2×10^{-6} sec^{-1}. This is about one-hundredth of the rate of the initial step [1] so that the latter is not appreciably affected.

The formation of nitrogen from nitric oxide has been postulated by several workers as due to a reaction with nitrosomethane. Yakubovich *et al.* (42) observed that NO reacts very easily with CF_3NO at room temperature. The mixture turns immediately brown from N_2O_4, and after several weeks there accumulates some trifluoronitromethane and *N,N*-bis(trifluoromethyl)hydroxylamine nitrite. No other experimental details are given. The mechanism postulated is

$$CF_3NO + 2NO \rightarrow CF_3N(NO)ONO \xrightarrow{+NO} CF_3\cdot + N_2 + 2NO_2,$$

followed by further reactions of $CF_3\cdot$, NO, and CF_3NO to give the nitromethane and hydroxylamine derivative. A rapid reaction, however, seems to be incompatible with the postulated third-order kinetics. Levy (43) heated nitrosomethane in the presence of NO and found nitromethane by infrared analysis. Batt and Gowenlock (44) studied the decomposition of nitrosomethane monomer at 250–525° C and found that the disappearance of CH_3NO was first order and was accelerated by NO, which was itself consumed; a non-condensable gas was produced which they thought was nitrogen. They suggested elimination of nitrogen via methyl diazonium nitrate, which then decomposes into methyl nitrate ester and nitrogen:

$$CH_3NO + 2NO \rightarrow CH_3N_2^+NO_3^- \rightarrow CH_3ONO_2 + N_2.$$

This scheme is not necessarily at variance with the previous observations on the formation of nitromethane, since the nitrate ester would decompose above 200° C, and it has been shown that ethyl nitrate, for example (45), produces nitromethane as one of the decomposition products. Christie (46) found that CH_3NO and NO react at toom temperature to form an unidentified product Y in a third-order process

$$CH_3NO + 2NO \rightarrow Y,$$

with a minimum value of 0.1 liter^2 mole^{-2}sec^{-1} for the third-order rate constant.

Since the presence of some CH_3NO can be reasonably expected in the mixture of decomposing azomethane and NO, the present results on the formation of nitrogen from NO lend some support to the previous work just cited. The heterogeneous component found in this work finds an analogue in surface effects which plagued the study of CH_3NO decomposition (44). As for the homogeneous part of the reaction, it is convenient to

Can. J. Chem. Downloaded from www.nrcresearchpress.com by 210.87.254.105 on 09/05/12
For personal use only.

consider the reaction scheme given in the Appendix. It is assumed there that every methyl radical ends up as CH_3NO (Section IIB), and that CH_3NO decomposes only in a third-order reaction with NO to yield nitrogen, or in a first-order reaction to yield some other product (44). It turns out that the kinetics depends on the relative magnitudes of k_4 and $k_3(NO)_0^2$, where k_4 is the first-order rate constant for the decomposition of CH_3NO (believed to yield the oxime $CH_2{=}NOH$ as the first step (44)), k_3 is the third-order rate constant for the process

$$CH_3NO + 2NO \rightarrow N_2^{NO} + \text{products},$$

and $(NO)_0$ = initial concentration of nitric oxide.

A crude estimate of E_4 has been made by Gowenlock, Trotman, and Batt (47), who proposed the value of 40 kcal/mole. Assuming a "normal" pre-exponential factor of 10^{13} sec^{-1}, this gives $k_4 = 7\times10^{-3}$ sec^{-1} at 303° C. Since most unimolecular reactions seem to have an "abnormal" pre-exponential factor (18), the possibility of an "abnormal" value for the CH_3NO decomposition must be considered. Assuming for this factor a maximum value of 10^{17} sec^{-1}, the value of k_4 at 303° C will be below 10^{-2} sec^{-1} only if $E_4 > 50$ kcal/mole. Now since the above authors estimate the dissociation energy $D(CH_3{-}NO) = 57\pm4$ kcal/mole, regeneration of radicals will be prevented as long as $E_4 < 57$ kcal/mole, so that inhibition by NO is still consistent with a value of E_4 around 50 kcal/mole or so. It seems that $k_4 \sim 7\times10^{-3}$ sec^{-1} is not an unreasonable value for k_4; however, in view of what has been said above, it is manifest that this value is subject to a considerable uncertainty, perhaps a factor of several powers of 10. The upper limit for k_3 can be taken as 10 $liter^2$ $mole^{-2}sec^{-1}$, a value somewhat higher than the usual value of third-order rate constants involving nitric oxide (24, p. 310), and $(NO)_0^2$, for the highest pressure used, is 1.5×10^{-5} $mole^2$ $liter^{-2}$, so that the maximum value of $k_3(NO)_0^2$ works out to 1.5×10^{-4} sec^{-1}. Finally, t, the experimental reaction time, is of the order of 500 seconds. Owing to the large uncertainty in k_4 it is best to consider three possible values of k_4.

(*i*) $k_4 \ll 10^{-4}$ sec^{-1}.—This leads to $k_4 \ll k_3(NO)_0^2$ for the range of NO pressures of interest, and from the Appendix, Case II, it is seen that $d(N_2^{NO})/dt$ becomes independent of NO, contrary to experiment (Fig. 7). If $k_4 \sim k_3(NO)_0^2$ (i.e. if k_4 is close to 10^{-4} sec^{-1}), the plot of

$$\frac{1}{(NO)_0}\frac{d(N_2^{NO})}{dt} \equiv k_{N_2}^{NO}$$

versus $(NO)_0$ should show a distinct curvature, likewise contrary to experiment. Obviously, then, under these conditions CH_3NO cannot reach a steady state. For Case I (Appendix), we note that the exponent in the exponential becomes smaller than unity (for $t = 500$ seconds), so that we can write, by expanding the exponential and keeping only the first two terms,

$$1 - \exp\left[-\{k_4+k_3(NO)_0^2\}t\right] \sim \{k_4+k_3(NO)_0^2\}t$$

and

$$(CH_3NO) \sim 2k_1(A)_0t,$$

so that

$$d(N_2^{NO})/dt \sim 2k_1k_3(A)_0(NO)_0^2t.$$

This expression can be integrated:

$$\int_0^x d(N_2^{NO}) = 2k_1k_3(A)_0(NO)_0^2\int_0^{t_x} tdt,$$

Can. J. Chem. Downloaded from www.nrcresearchpress.com by 210.87.254.105 on 09/05/12
For personal use only.

where x is the amount of nitrogen formed from NO in the time interval t_x. Integration gives

$$x = k_1k_3(A)_0(NO)_0^2t_x^2,$$

where x and t_x are experimental quantities. Under these conditions, then, experiment should satisfy the relation (for $(A)_0$ = const.)

$$x/(NO)_0^2t_x^2 = \text{const.}$$

(ii) $k_4 \sim 10^{-1}$ *to* 10^{-3} *sec*$^{-1}$.—Here we have roughly $k_4 \gg k_3(NO)_0^2$ (except, perhaps, at the highest NO pressure used), so that Case II in the Appendix yields

$$d(N_2^{NO})/dt = 2k_1k_3(A)_0(NO)_0^2/k_4,$$

a relation that satisfies the linear dependence shown in Fig. 7. Integrating

$$\int_0^x d(N_2^{NO}) = \frac{2k_1k_3}{k_4}(A)_0(NO)_0^2\int_0^{t_x} dt$$

we get

$$x = 2k_1k_3(A)_0(NO)_0^2t_x/k_4,$$

where x and t_x have the same significance as before. Under these conditions CH_3NO can reach a steady state and theory predicts that, for $(A)_0$ = const.,

$$x/(NO)_0^2t_x = \text{const.}$$

As for Case I in the Appendix, provided $k_4 < 2\times10^{-3}$ sec^{-1}, we still have an exponent smaller than unity in the exponential, and Case I thus leads to the same relation as under (i). For $k_4 > 2\times10^{-3}$ sec^{-1}, Case I gives the relation shown below under (iii).

(iii) $k_4 \gg 10^{-3}$ *sec*$^{-1}$.—This value of k_4 leads to $k_4 \gg k_3(NO)_0^2$, so that Case II in the Appendix yields the same relation as under (ii) above. In Case I, we observe that, for t = 500 seconds, under these conditions

$$\exp[-\{k_4+k_3(NO)_0^2\}t] \ll 1,$$

so that

$$(CH_3NO) = 2k_1(A)_0/k_4,$$

and

$$d(N_2^{NO})/dt = 2k_1k_3(A)_0(NO)_0^2/k_4,$$

which is the expression obtained under Case II. In other words, with $k_4 \gg 10^{-3}$ sec^{-1} CH_3NO cannot accumulate in the system.

These considerations show that some choice between the various possibilities can be made by observing the value of the ratios $x/(NO)_0^2t_x^2$ and $x/(NO)_0^2t_x$. The pertinent data are summarized in Table IV. Although the evidence is not overwhelming (a larger

TABLE IV

$(NO)_0$ (mm)	t_x (sec)	x (mm)	$x/(NO)_0^2t_x$ $\times10^8$	$x/(NO)_0^2t_x^2$ $\times10^{11}$
137.0	420	0.242	3.07	7.31
77.9	480	0.085	2.92	6.08
43.8	482	0.0238	2.58	5.35
24.4	480	0.0082	2.85	5.93

NOTE: x has been corrected for the heterogeneous contribution to $k_{N_2}^{NO}$.

Can. J. Chem. Downloaded from www.nrcresearchpress.com by 210.87.254.105 on 09/05/12
For personal use only.

variation in t_x would have been desirable), it can nevertheless be seen that $x/(NO)_0^2t_x$ is reasonably constant, while $x/(NO)_0^2t_x^2$ is not, as might have been expected merely from looking at Fig. 7. This result means that

(*a*) k_4 is of the order of 10^{-3} sec^{-1} or larger;
(*b*) CH_3NO reaches a steady state.

It is now possible to set a lower limit on the value of k_3, where

$$k_3 = xk_4/2k_1(A)_0(NO)_0^2t_x.$$

Taking $x/(NO)_0^2t_x = 3\times10^{-8}$ $mm^{-1}sec^{-1} = 10.8\times10^{-4}$ liter $mole^{-1}sec^{-1}$, and the value of $2k_1(A)_0$ being 4.3×10^{-7} mole $liter^{-1}sec^{-1}$ for the conditions of the experiment, we get

$$k_3 \geqslant 2.5 \text{ liter}^2 \text{ mole}^{-2}\text{sec}^{-1}.$$

This is a reasonable value for a third-order rate constant involving nitric oxide (24, p. 310), which would suggest that the proposed mechanism for the formation of nitrogen from nitrosomethane is entirely feasible.

The amount of nitrogen produced from azomethane ($(A)_0 = 40$ mm) by the NO-induced reaction, ΔN_2^{azo}, can be obtained by subtracting from the total amount of nitrogen produced from azomethane ($f_{N_2}^{azo}$, Table II), the amount of nitrogen corresponding to the "net inhibited rate" ($k_0 = 1.78\times10^{-4}$ sec^{-1}, the extrapolated value of k_{corr} from Fig. 4), which represents nitrogen formed in the initial step of the decomposition (Section IIB). The first-order rate constant for nitrogen formation by the NO-induced reaction, defined as

$$k_{N_2}^{azo} = \frac{1}{A_0}\frac{d(\Delta N_2^{azo})}{dt},$$

is shown plotted against NO pressure in Fig. 7. Plotting against $NO^{1/2}$, $NO^{3/2}$, or NO^2 results in distinctly curved plots, so that despite the rather poor straight line it must be concluded that the plot is linear with respect to NO, i.e. the reaction is first order in NO. Not much more can be deduced about the NO-induced decomposition of azomethane from the present results. The presence of N_2O (Fig. 5), if it is due to the oft-postulated reaction (without much evidence, cf. refs. 48, 49)

$$2HNO \rightarrow N_2O + H_2O,$$

would suggest the presence of HNO, which might lend some credence to hydrogen abstraction by NO. N_2O was also found in the products when NO was added to decomposing 2,2′-azoisobutane (50).

The information that the formation of ΔN_2^{azo} is first order in NO means that very likely one molecule of NO is used up for each molecule of ΔN_2^{azo} formed. It was shown above that quite probably for each molecule of N_2^{NO} formed two molecules of NO are used up. The amount of NO consumed shown in Fig. 5 can now be used to attempt a sort of crude nitric oxide balance. The "net inhibited rate" at $(A)_0$ is 5 mm is 9.8×10^{-5} sec^{-1}, assuming that for each nitrogen formed at this rate 2 molecules of NO are consumed (1 for each methyl), and that every nitrogen produced in excess of this "net inhibited rate" is due to a secondary reaction; then to account for the observed ratio of (NO consumed)/(N_2 produced) = 3.64 at 20 mm NO, there must be 13.8 molecules of NO consumed for every molecule of ($\Delta N_2^{azo} + N_2^{NO}$) formed. The latter process can reasonably lead to the consumption of not more than three molecules of NO; clearly, then, the bulk of NO at NO pressure above the minimum rate takes part in reactions that do not yield nitrogen.

Can. J. Chem. Downloaded from www.nrcresearchpress.com by 210.87.254.105 on 09/05/12
For personal use only.

While the present study accounts for most of the NO used up around minimum rate, it offers no information about the fate of the portion of NO molecules consumed at higher NO pressures.

ACKNOWLEDGMENTS

The authors are greatly indebted to Mr. L. Landau and Dr. J. S. Drury of the Oak Ridge National Laboratory, Oak Ridge, Tenn., for the mass spectrometric analyses reported in this work.

APPENDIX

Assume that the formation of N_2^{NO} is described by the following sequence of reactions:

$$CH_3N_2CH_3 \rightarrow 2CH_3 + N_2^{azo} \qquad k_1$$

$$CH_3 + NO \rightarrow CH_3NO \qquad k_2$$

$$CH_3NO + 2NO \rightarrow N_2^{NO} + \text{products} \qquad k_3$$

$$CH_3NO \rightarrow \text{products} \qquad k_4$$

The stationary concentration of CH_3 is:

$$(CH_3) = 2k_1(A)/k_2(NO),$$

where (A) stands for the concentration of azomethane. Hence,

$$\begin{aligned} d(CH_3NO)/dt &= k_2(CH_3)(NO) - k_3(CH_3NO)(NO)^2 - k_4(CH_3NO) \\ &= 2k_1(A) - \{k_4 + k_3(NO)^2\}(CH_3NO). \end{aligned} \qquad \text{(I)}$$

Case I. CH_3NO Accumulates in the System

Equation (I) can be integrated, assuming $(A) = (A)_0$, $(NO) = (NO)_0$, where the subscript indicates initial conditions; this approximation is justified by the low conversion used in this work. We get

$$\int_0^{(CH_3NO)} \frac{d(CH_3NO)}{2k_1(A)_0 - \{k_4 + k_3(NO)_0^2\}(CH_3NO)} = \int_0^t dt.$$

The result of the integration, after some rearranging, is

$$(CH_3NO) = \frac{2k_1(A)_0}{k_4 + k_3(NO)_0^2}\,[1 - \exp\,(-\{k_4 + k_3(NO)_0^2\}t)],$$

so that

$$\begin{aligned} d(N_2^{NO})/dt &= k_3(CH_3NO)(NO)^2 \\ &= \frac{2k_1k_3(A)_0(NO)_0^2}{k_4 + k_3(NO)_0^2}\,[1 - \exp\,(-\{k_4 + k_3(NO)_0^2\}t)]. \end{aligned}$$

Case II. CH_3NO Reaches a Steady State

In this case, $d(CH_3NO)/dt = 0$, and

$$(CH_3NO) = \frac{2k_1(A)}{k_4 + k_3(NO)^2} = \frac{2k_1(A)_0}{k_4 + k_3(NO)_0^2}$$

$$d(N_2^{NO})/dt = \frac{2k_1k_3(A)_0(NO)_0^2}{k_4 + k_3(NO)_0^2}.$$

Can. J. Chem. Downloaded from www.nrcresearchpress.com by 210.87.254.105 on 09/05/12
For personal use only.

RÉSUMÉ

L'éthylène et le propylène diminuent la vitesse de décomposition de l'azométhane, vitesse mesurée par la vitesse de formation de l'azote. Ils diminuent aussi le rapport CH_4/N_2 dans les produits, mais la diminution dans la valeur des deux quantités est différente pour chacune des deux oléfines. Dans la décomposition à 100%, l'éthylène et le propylène augmentent un peu le rapport (azote récupéré)/(azométhane décomposé). L'interprétation de ces résultats indique la présence d'une courte chaîne dans la pyrolyse, et aussi que l'éthylène et le propylène ne sont pas convenables comme inhibiteurs.

Lorsqu'on ajoute quelques millimètres de NO, la vitesse de la réaction diminue pour atteindre un minimum, qui est inférieur à celui obtenu avec le propylène ou l'éthylène (longueur de chaîne apparente: 2 à 3). La vitesse de réaction augmente ensuite en fonction de la pression de NO. Un résultat identique peut être obtenu dans un récipient garni de tubes de verre. Le rendement en méthane, en éthane et en éthylène est réduit presqu'à zéro par une pression suffisante de NO. Le rapport (NO détruit)/(azote formé) atteint la valeur de deux aux environs du minimum de la vitesse de réaction. On peut conclure que la vitesse inhibée nette, c.-à-d. corrigée de l'effet stimulant du NO, est celle du processus monomoléculaire initial $CH_3N_2CH_3 \rightarrow 2CH_3 + N_2$. La vitesse ainsi que l'énergie d'activation de ce processus s'avèrent dépendantes de la pression.

On a prouvé au moyen de l'oxyde nitrique isotopique ^{15}NO qu'à peu près une moitié de l'acroissement de la vitesse de réaction aux pressions élévées de NO est dûe à l'azote formé à partir de NO. L'autre moitié est attribuée à une décomposition de l'azométhane déclenchée par NO.

REFERENCES

1. H. J. SCHUMACHER. Chemische Gasreaktionen. Steinkopf, Dresden. 1939. pp. 223–228.
2. E. W. RIBLETT and L. C. RUBIN. J. Am. Chem. Soc. **59**, 1537 (1937).
3. M. PAGE, H. O. PRITCHARD, and A. F. TROTMAN-DICKENSON. J. Chem. Soc. 3878 (1953).
4. C. STEEL and A. F. TROTMAN-DICKENSON. J. Chem. Soc. 975 (1959).
5. R. RENAUD and L. C. LEITCH. Can. J. Chem. **32**, 545 (1954).
6. R. H. PIERSON, A. N. FLETCHER, and E. ST. CLAIR GANTZ. Anal. Chem. **28**, 1218 (1956).
7. J. G. CALVERT, S. S. THOMAS, and P. L. HANST. J. Am. Chem. Soc. **82**, 1 (1960).
8. W. G. SCHNEIDER and N. R. S. HOLLIES. Rev. Sci. Instr. **21**, 94 (1950).
9. J. JANÁK. J. Chromatog. **3**, 308 (1960).
10. A. E. MESSNER, D. M. ROSIE, and P. A. ARGABRIGHT. Anal. Chem. **31**, 230 (1959).
11. R. N. SMITH, J. SWINEHEART, and D. G. LESMINI. Anal. Chem. **30**, 1217 (1958).
12. H. C. RAMSPERGER. J. Am. Chem. Soc. **49**, 914, 1498 (1927).
13. O. K. RICE and D. V. SICKMAN. J. Chem. Phys. **4**, 242 (1936).
14. R. D. MCCOY. Ph.D. Thesis, University of Oregon, Eugene, Oregon. 1956.
15. Z. G. SZABÓ and F. MÁRTA. J. Am. Chem. Soc. **83**, 768 (1961).
16. MASS SPECTRAL DATA. American Petroleum Institute Research Project 44. Carnegie Institute of Technology, Pittsburgh. No. 1595. 1959.
17. K. CLUSIUS. Helv. Chim. Acta, **33**, 2134 (1950).
18. C. STEEL and K. J. LAIDLER. J. Chem. Phys. **34**, 1827 (1961).
19. A. F. TROTMAN-Dickenson. Gas kinetics. Butterworths, London. 1955. p. 70.
20. L. HERK, M. FELD, and M. SZWARC. J. Am. Chem. Soc. **83**, 2998 (1961).
21. O. K. RICE and D. V. SICKMAN. J. Am. Chem. Soc. **57**, 1384 (1935).
22. D. V. SICKMAN and O. K. RICE. J. Chem. Phys. **4**, 608 (1936).
23. K. J. LAIDLER and B. W. WOJCIECHOWSKI. Proc. Roy. Soc. (London), Ser. A, **259**, 257 (1960).
24. S. W. BENSON. The foundations of chemical kinetics. McGraw-Hill Book Co., New York. 1960.
25. D. J. RUZICKA and W. A. BRYCE. Can. J. Chem. **38**, 827 (1960).
26. A. F. TROTMAN-DICKENSON. Gas kinetics. Butterworths, London. 1955. p. 152.
27. T. W. DAVIS, F. P. JAHN, and M. BURTON. J. Am. Chem. Soc. **60**, 10 (1938).
28. F. P. JAHN and H. A. TAYLOR. J. Chem. Phys. **7**, 474 (1939).
29. E. R. W. STEACIE and H. O. FOLKINS. Can. J. Res. Sect. B, **18**, 1 (1940).
30. J. R. E. SMITH and C. HINSHELWOOD. Proc. Roy. Soc. (London), Ser. A, **183**, 33 (1944).
31. J. R. E. SMITH and C. HINSHELWOOD. Proc. Roy. Soc. (London), Ser. A, **180**, 237 (1942).
32. G. R. FREEMAN. Proc. Roy. Soc. (London), Ser. A, **245**, 49 (1958).
33. D. R. BLACKMORE and C. HINSHELWOOD. Proc. Roy. Soc. (London), Ser. A, **268**, 21 (1962).
34. G. R. FREEMAN, C. J. DANBY, and C. HINSHELWOOD. Proc. Roy. Soc. (London), Ser. A, **245**, 456 (1958).

Can. J. Chem. Downloaded from www.nrcresearchpress.com by 210.87.254.105 on 09/05/12
For personal use only.

35. M. TANIEWSKI. Proc. Roy. Soc. (London), Ser. A, **266**, 519 (1962).
36. D. E. HOARE. Paper presented at the XVIIIth International Congress of Pure and Applied Chemistry, Montreal, August, 1961.
37. D. A. FRANK-KAMENETSKII. Diffusion and heat exchange in chemical kinetics. Princeton University Press, Princeton, N.J. 1955. p. 77.
38. C. HINSHELWOOD. Chem. Soc. (London), Spec. Publ. **10**, 75 (1957).
39. B. W. WOJCIECHOWSKI and K. J. LAIDLER. Can. J. Chem. **38**, 1027 (1960).
40. W. H. JOHNSTON and R. M. ANSTETT. J. Chem. Phys. **22**, 146 (1954).
41. H. WISE and M. F. FRECH. J. Chem. Phys. **20**, 22 (1952).
42. A. Y. YAKUBOVICH, S. P. MAKAROV, V. A. GINSBURG, N. G. PRIVEZENTZEVA, and L. L. MARTINOVA. Dokl. Akad. Nauk SSSR, **141**, 125 (1961).
43. J. B. LEVY. Ind. Eng. Chem. **48**, 762 (1956).
44. L. BATT and B. G. GOWENLOCK. Trans. Faraday Soc. **56**, 682 (1960).
45. J. B. LEVY. J. Am. Chem. Soc. **76**, 3254 (1954).
46. M. I. CHRISTIE. Proc. Roy. Soc. (London), Ser. A, **249**, 258 (1959).
47. B. G. GOWENLOCK, J. TROTMAN, and L. BATT. Chem. Soc. (London), Spec. Publ. **10**, 75 (1957).
48. J. A. GRAY and D. W. G. STYLE. Trans. Faraday Soc. **48**, 1137 (1952).
49. J. B. LEVY. J. Am. Chem. Soc. **78**, 1780 (1956).
50. J. B. LEVY and B. K. W. COPELAND. J. Am. Chem. Soc. **82**, 5314 (1960).

Can. J. Chem. Downloaded from www.nrcresearchpress.com by 210.87.254.105 on 09/05/12
For personal use only.

THE ELECTRON DENSITY DISTRIBUTIONS IN HYDRIDE MOLECULES

I. THE WATER MOLECULE[1]

R. F. W. Bader and G. A. Jones[2]
Department of Chemistry, University of Ottawa, Ottawa, Canada
Received October 18, 1962

ABSTRACT

The electron density distribution for the water molecule in its equilibrium configuration is determined by requiring that the forces exerted on the nuclei by this distribution (as calculated by the Hellmann–Feynman theorem) balance the nuclear forces of repulsion. The density distribution is expressed in terms of equivalent orbitals, and to achieve electrostatic equilibrium it is found necessary to have an angle between the bonding orbitals which is less than the structural bond angle (bent bonds), to delocalize the equivalent orbitals and to place the lone pair electrons in sp hybrid orbitals. Further, a discussion of the forces operative in XH_2 and XH_3 molecules (X = C, N, O) leads to an explanation of the observed bond angles and to general conclusions regarding the hybridization to be expected in such molecules.

Can. J. Chem. Downloaded from www.nrcresearchpress.com by 210.87.254.6 on 09/05/12
For personal use only.

INTRODUCTION

The electron density distributions for molecules which contain lone pair electrons are of considerable interest to chemists. The work of Lennard-Jones, Pople, and Coulson (1–4) has stressed the important role that lone pairs of electrons can play in the determination of molecular geometries and dipole moments. The effects are, of course, most prominent when the lone pair electrons are found in orbitals with a large amount of directional character (i.e., p atomic orbital character) such that the orbitals project out from the nucleus. With these results in mind Pople (2) and Pople and Duncan (3) have performed calculations for the water and ammonia molecules which indicate that the hybridization in these molecules is indeed close to sp^3. This implies that the lone pair electrons in these molecules possess their maximal directional character and hence they are predicted to exert prominent effects in determining the dipole moment and bond angle.

In this paper we propose to determine the electron density distribution for the water molecule through a consideration of the *forces* exerted on the nuclei by the distribution. There are a number of reasons for adopting this approach, two of them being the great sensitivity of the forces to the degree of hybridization and to the molecular geometry. It should be remembered that the very existence of the electronic forces is a direct result of molecule formation. Another advantage stems from the obvious fact that when the molecule is in its equilibrium configuration the resultant force acting on any nucleus in the molecule must be zero. Given a nuclear framework with the observed equilibrium bond lengths and bond angles it is a simple matter to calculate the forces of repulsion acting on a nucleus due to presence of the other nuclei. The forces of attraction exerted by the electron density distribution are thus also known since they must be equal and opposite to the nuclear forces of repulsion for the attainment of electrostatic equilibrium. It is well known that the Hellmann–Feynman theorem allows one to calculate the forces acting on a nucleus in a molecule if the electron density function is known. Alternatively,

[1]*Abstracted from the thesis submitted by G. A. Jones in partial fulfillment of the requirements for the degree of Doctor of Philosophy.*
[2]*Recipient of a Commonwealth Scholarship.*

knowing the forces as we do at electrostatic equilibrium, we may reverse this procedure and calculate the equilibrium electron density from our knowledge of the forces. Thus the requirement of zero resultant forces provides one with a number of constraints which, through the use of the Hellmann–Feynman theorem, any proposed density function must fulfill. These constraints may be used to fix a corresponding number of parameters in the density function. For example, in the water molecule three parameters in the density function may be determined by observing the requirement that the resulting forces exerted on the oxygen nucleus along the symmetry axis and on the hydrogen nuclei along the bonds and perpendicular to the bond axes must be zero. The remaining force components give trivial conditions as they are zero by symmetry alone. Therefore, the criteria of zero resultant forces may be used to fit a relatively sophisticated density function to any nuclear framework.

The Determination of the Density Distribution

We shall determine the electron density distribution for the water molecule within the framework of the single-configuration L.C.A.O. molecular orbital theory. The equivalent orbital representation is used so as to retain the concepts of lone pair and bonding electrons. Slater atomic orbitals with suitable screening constants are employed to approximate the atomic orbitals. The $2s$ function on oxygen is made orthogonal to the $1s$ orbital on the same atom. All the calculations are carried out for a bond length of 1.81 a.u. and a bond angle of 104.45° (5).

We assume that the inner pair of electrons on the oxygen atom are in a pure $1s$ orbital (a point we shall reconsider later in the paper) and that the $1s$ atomic orbital does not contribute to any of the valence orbitals. Then the most general orbitals that can be written for the water molecule are, for the bonding orbitals,

$$\phi_{b1} = \lambda[\cos \epsilon_b\, 2s + \sin \epsilon_b\, 2p_1] + \mu[s_1 - \delta s_2]$$
$$\phi_{b2} = \lambda[\cos \epsilon_b\, 2s + \sin \epsilon_b\, 2p_2] + \mu[s_2 - \delta s_1],$$

and for the lone pair orbitals,

$$\phi_{l1} = \cos \epsilon_l\, 2s + \sin \epsilon_l\, 2p_3$$
$$\phi_{l2} = \cos \epsilon_l\, 2s + \sin \epsilon_l\, 2p_4.$$

The s_1 and s_2 denote $1s$ orbitals on $H_{(1)}$ and $H_{(2)}$ respectively and $2s$ and $2p_i$ are atomic orbitals centered on the oxygen nucleus. The directions of p_1 and p_2 are shown in Fig. 1 (note that they do not necessarily coincide with the bond axes) and p_3 and p_4 determine the directions of the lone pair orbitals.

These orbitals embody five parameters:

(i) ϵ_b and ϵ_l, the hybridization parameters of the bonding and lone pair orbitals;

(ii) λ/μ, the polarity factor for the bonding orbitals;

(iii) α, the angle between the p functions of the bonding orbitals; it is termed the orbital angle as opposed to the bond angle $\mathscr{E}$, and when $\alpha \neq \mathscr{E}$ the bonds are termed "bent";

(iv) δ, the parameter which determines the extent of delocalization of the equivalent orbitals.

The requirement that all four of the molecular orbitals be mutually orthogonal gives rise to three conditions which determine the hybridization parameters ϵ_b and ϵ_l and the angle between the lone pair orbitals. These three conditions, together with the one determining the relative values of λ and μ once their ratio is known, are given in the Appendix.

Can. J. Chem. Downloaded from www.nrcresearchpress.com by 210.87.254.6 on 09/05/12
For personal use only.

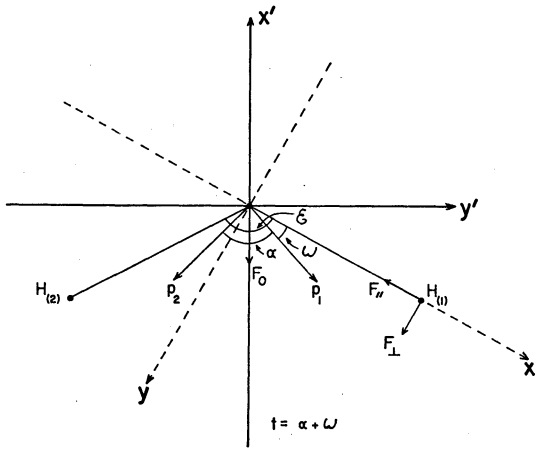

FIG. 1. The coordinate system used in the calculations. The arrows indicate the direction of a positive force. R is the distance between the hydrogen nuclei and d is the bond length.

The requirement of zero resultant forces may be employed to fix the remaining three parameters, λ/μ, α, and δ. The three electronic forces (those due to the electron density distribution) to be determined are shown in Fig. 1. $F_\perp$ is the force on $H_{(1)}$ perpendicular to the O—H bond axis, $F_\parallel$ is the force on $H_{(1)}$ along the O—H bond axis, and F_O is the force on the oxygen atom along the x' axis. The Hellmann–Feynman theorem states that the total force acting on any nucleus in a molecule is simply the sum of the classical electrostatic forces due to the other nuclei and to the three-dimensional electron density distribution.* We have previously demonstrated the capabilities of the Hellmann–Feynman theorem in predicting reasonable magnitudes for the forces found in simple molecules (6). Moreover, its application gives a readily understandable interpretation of the forces operative in a molecule (7).

Since the orbitals we are to employ are mutually orthogonal and doubly occupied, the electron density is

$$\rho = 2(\phi_{b1}^2+\phi_{b2}^2+\phi_{11}^2+\phi_{12}^2+\phi_o^2),$$

where ϕ_o is the innermost orbital of the oxygen atom. As previously explained (5, 6) the force exerted on a nucleus by the electron density distribution is simply the sum of the forces exerted by the density obtained from each of the orbitals. The three conditions for electrostatic equilibrium are given below, where $F_\perp$, $F_\parallel$, and F_O will refer to the magnitudes of the electronic forces:

$$F_\perp = F_\perp(\phi_{b1}^2)+F_\perp(\phi_{b2}^2)+2F_\perp(\phi_1^2) = (1/R^2)\cos(\mathscr{E}/2)$$

$$F_\parallel = F_\parallel(\phi_{b1}^2)+F_\parallel(\phi_{b2}^2)+2F_\parallel(\phi_1^2)+F_\parallel(\phi_o^2)$$

$$= (8/d^2)+(1/R^2)\sin(\mathscr{E}/2)$$

$$F_O = 2F_O(\phi_b^2)+2F_O(\phi_1^2) = (2/d^2)\cos(\mathscr{E}/2).\dagger$$

We may thus discuss separately the forces exerted by the bonding and the lone pair

*A discussion of the application of this theorem to molecular problems may be found in references 6, 7, and 8.

†Where no distinction is made between the forces exerted by ϕ_{b1} and ϕ_{b2} or ϕ_{11} and ϕ_{12}, the two forces are equal. A common factor of eight, the nuclear charge on the oxygen atom, has been removed from the nuclear and electronic force on oxygen.

Can. J. Chem. Downloaded from www.nrcresearchpress.com by 210.87.254.6 on 09/05/12
For personal use only.

electron densities. Explicit expressions for all of the forces are given in the Appendix together with all the details of the calculation. During the discussion of these forces we shall be most interested in the relative magnitudes of the various orbital contributions. Three sets of density functions will be considered, from the simplest embodying only ϵ_b, ϵ_l, and λ/μ to one including all five parameters. Each distribution will be regarded in the light of whether or not it can simultaneously satisfy all three of the zero force conditions. In addition we shall require that the distribution give the correct dipole moment, of magnitude 0.724 a.u.

Case I. Equivalent Localized Orbitals Directed Along the O—H Bonds

The set of orbitals with $\alpha = \mathscr{E}$ (bonds pointing at the hydrogen atoms) and $\delta = 0$ (the equivalent orbitals are completely localized) is the simplest that one can construct for the water molecule. Of the three remaining parameters, ϵ_b and ϵ_l are determined by the orthogonality conditions, leaving only λ/μ to be determined by any of the force conditions or the dipole moment. This was the set of orbitals employed by Pople and Duncan (2, 3) in their determination of the electron density distribution in the water molecule. They fixed the polarity parameter λ/μ by requiring that the density function give the observed dipole moment. We shall reinvestigate this same density function in terms of the forces it exerts on the hydrogen and oxygen nuclei.

First a word about the density function. Disregarding the overlap with the hydrogens for the moment, an orbital angle of 104.45° on the oxygen atom gives orbitals very close to sp^3 which occur at an orbital angle of 109°28′ ($\epsilon_b = \epsilon_l = 60°$). The decrease from the tetrahedral angle to 104.45° slightly increases the amount of p character in the bonding orbitals and increases slightly the $2s$ character of the lone pair orbitals. Anticipating bent bonds, in the limit of an orbital angle of 90°, the bonding orbitals become pure p ($\epsilon_b = 90°$) and the lone pair orbitals become sp hybrids ($\epsilon_l = 45°$). Because of the overlap with the hydrogen $1s$ orbitals the amount of p character in the bonding orbitals at any value of the orbital angle is increased over what it would be if the overlap were zero. Similarly the amount of $2s$ in the lone pair orbitals is slightly decreased by the presence of the hydrogen atoms.

Since the bond orbitals in case I are directed at the hydrogen atoms, the order of hybridization is automatically fixed. A variation of λ/μ, the only remaining parameter, brings about only small variations in ϵ_b and ϵ_l, ϵ_b changing from 79° to 73° and ϵ_l from 56.0° to 56.5° for a change in λ/μ from 1.0 to 1.5. Thus the lone pairs are always dominant in this case, as ϵ_l is fixed close to 60°, the value for sp^3 orbitals. The correct dipole moment is obtained at a $\lambda/\mu = 1.07$ with $\epsilon_b = 77.8°$ and $\epsilon_l = 56.0°$.* Since all the factors vary so little with λ/μ in this case, it will be sufficient to consider the forces† obtained for this one point, and they are given in Table I. Consider first the electronic force exerted on the hydrogen nucleus at right angles to the bond, $F_\perp$. Since the electron distribution in ϕ_{b1} possesses axial symmetry along the O—$H_{(1)}$ bond, $F_\perp(\phi_{b1}^2)$ is zero. The density in ϕ_{b2} attracts $H_{(1)}$ but the lone pairs exert a force in the opposite direction, tending to open up the bond angle, which almost cancels the attractive force of ϕ_{b2}. The resultant electronic attractive force $F_\perp$ is thus very much less than the nuclear force of repulsion. The electronic forces on $H_{(1)}$ along the bond are also insufficient to overcome the repulsive force. The case of the forces operative on the oxygen nucleus is very similar to that for $F_\perp$. The lone pairs exert a force which is almost equal and opposite to the attractive

*These values for λ/μ, ϵ_b, and ϵ_l are slightly different than those obtained by Duncan and Pople (1.06, 85°, and 55° respectively) as we have used a different value for the effective nuclear charge in the hydrogen 1s orbital.

†All forces in this paper are given in atomic units: 1 a.u. = $e^2/a_o^2 = 8.2377 \times 10^{-3}$ dynes.

Can. J. Chem. Downloaded from www.nrcresearchpress.com by 210.87.254.6 on 09/05/12
For personal use only.

TABLE I

The forces for case I

	$F(\phi_{b1}^2)$	$F(\phi_{b2}^2)$	$2F(\phi_1^2)$	$F(\phi_o^2)$	Total electronic force	Nuclear repulsion
$F_\perp$	0.0000	0.1206	−0.1046	0.0000	0.0160	−0.0748
$F_\parallel$	0.6812	0.3058	0.8120	0.6105	2.4095	−2.5384
F_O	0.4845	0.4845	−0.9446	0.0000	0.0244	−0.3740

forces of the bonding electrons. The net result is a large negative force acting on the oxygen nucleus almost equal to the total nuclear force of repulsion.

This simple density distribution does not come close to satisfying the conditions of zero resultant forces. The reasons for this are clear. The projection of the lone pair electron density out to the back of the molecule in approximately sp^3 orbitals results in unreasonably large forces tending to pull the oxygen atom back and to open up the bond angle. While such a simple distribution function can duplicate the observed dipole moment it does so only through the presence of prominent lone pairs of electrons and at the expense of a low polarity factor λ/μ for the bond orbitals. (The atomic dipole moment for the lone pair electrons in this case is 1.24 a.u. where the total dipole moment in these same units is 0.72.) It is clear that the equilibrium forces will be attained only by greatly reducing the prominence of the lone pair electrons.

Case II. Localized Equivalent Orbitals with Bent Bonds

The above requirement may be attained by allowing the bonds to bend. By relaxing the restraint that the orbital angle α must equal the bond angle $\mathscr{E}$ we may allow the bonding orbitals to attain more p character and at the same time increase the s character of the lone pair electrons. Increasing the s character in the lone pair orbitals can increase the angle β between the lone pair orbitals from 109°28′ (sp^3 hybrids) to a limiting value of 180° (sp hybrids). In the limit of sp hybridization the lone pair orbitals project out above and below the plane of the molecule at right angles to the O—H bonds. In this limit they will neither exert a force on the oxygen nucleus or on the hydrogen nuclei in the perpendicular direction, nor will they contribute an atomic dipole moment.

The parameters ϵ_b and ϵ_1 may again be determined by the orthogonality conditions [1] and [2] for various assumed values of α and λ/μ. We may then examine the forces predicted by the various density distributions so obtained, which give the correct dipole moment. The smallest value which the angle α may attain is determined by the requirement that the two orthogonality conditions [1] and [2] possess real solutions for ϵ_b and ϵ_1. It is found that the limiting value of α, approximately 87°, is almost independent of the ratio of λ/μ. This value of α gives an ϵ_b of 107.61° and an ϵ_1 of 45.06°, which implies sp hybridization for the lone pair orbitals. If the hydrogens were absent this would of course occur at an angle of 90° between the two bonding orbitals, which would now be pure p bonds. However, because of the overlap with the hydrogens the orbital angle necessary to decrease the p character in the lone pair to that of sp must now be less than 90° (i.e., 87°) and correspondingly the bonding orbitals must now contain negative $2s$ character (the cos ϵ_b is now negative) to the extent of about 9%. Thus depressing the p character of the lone pair orbitals to values close to that found in sp hybrids is obtained only at the expense of introducing negative $2s$ character into the bonding orbitals.

The nature of the results for bent bonds is as follows. As α is decreased the lone pairs become less prominent, and the dipole moment can be met only by increasing the polarity

Can. J. Chem. Downloaded from www.nrcresearchpress.com by 210.87.254.6 on 09/05/12
For personal use only.

of the OH bond. Thus, while for an $\alpha = 104.45°$ the correct dipole moment is found to occur at a $\lambda/\mu = 1.07$, at $\alpha = 87°$, the value of λ/μ must be increased to 1.45 to attain the same moment. The forces vary in a regular manner with α. In Fig. 2 we show the

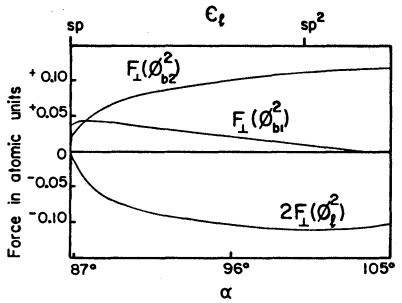

FIG. 2. The orbital contributions to $F_\perp$. The scale for ϵ_l given at the top of the figure is not a linear one.

variation with α of the orbital components to the perpendicular force on the hydrogen atom, $F_\perp$, for a λ/μ of 1.45. We choose this value of λ/μ since it contains (at $\alpha = 87°$) the best forces so far obtained, gives the correct dipole moment, and illustrates the general behavior for all the λ/μ values. From Fig. 2 we note that both $F_\perp(\phi_{b2}^2)$ and $-F_\perp(\phi_l^2)$ decrease with decreasing α, $F_\perp(\phi_{b2}^2)$ because of the decreasing amount of $2s$ character in ϕ_b and $F_\perp(\phi_l^2)$ because of the increasing $2s$ character in ϕ_l, which pulls the lone pair orbitals from behind the molecule onto the z axis. The contributions from ϕ_{b2} and the two lone pair orbitals are almost symmetrically placed about the zero force line and their contributions thus largely cancel. This leaves only the force from ϕ_{b1} to counteract the nuclear repulsion. $F_\perp(\phi_{b1}^2)$ increases as α decreases since charge is moved off the O—$H_{(1)}$ bond axis and placed alongside the bond, where it exerts a perpendicular force of attraction on $H_{(1)}$. However, $F_\perp(\phi_{b1}^2)$ never attains a value great enough to overcome the nuclear repulsive forces. The maximum attractive force of magnitude 0.04814 a.u. is attained at $\alpha = 87°$ and is insufficient to balance the nuclear repulsion of -0.07482 a.u.

The forces exerted on the oxygen nucleus present a similar picture. The large negative force due to the lone pair electrons can be reduced by bending the bonds. However, as these low values of α (and thus of $F_O(\phi_l^2)$) are obtained only by introducing negative $2s$ character into the bonding orbitals, the decrease in force exerted by the lone pair electrons is obtained only at the expense of a decrease in the positive forces exerted by the bonding electron density. The best result is again attained at $\alpha = 87°$, where the values of $2F_O(\phi_l^2)$ and $2F_O(\phi_b^2)$ are -0.02926 and 0.2844 a.u. respectively. This gives a final net force of -0.1188 a.u., which while it represents an improvement by a factor of three over the value obtained with $\alpha = \mathscr{E}$ is still far from a zero force. The electronic force exerted on $H_{(1)}$ along the bond is increased to 2.518 a.u. This is a great improvement over that obtained in case I and the net force is now decreased to only -0.020 a.u.*

The introduction of bent bonds has reduced the error in the perpendicular force on hydrogen by one-half, in the force on oxygen by one-third, and has come close to predicting a zero force on hydrogen along the bond. However, no combination of ϵ_b, ϵ_l, λ/μ, and α is capable of giving a density function which results in values of $F_\perp$ and F_O

The forces F_O and $F_\parallel$ will be discussed in greater detail in a following section.

Can. J. Chem. Downloaded from www.nrcresearchpress.com by 210.87.254.6 on 09/05/12
For personal use only.

large enough to even approach small net forces. To better the forces it is necessary to "bend" the bonds more than is possible in case II. Furthermore, it is necessary to ensure that a smaller amount of negative $2s$ character is introduced into the bonding orbitals when the lone pairs are forced towards sp hybridization. Both of these conditions may be met by delocalizing the bonding orbitals.

Case III. Delocalized Equivalent Orbitals with Bent Bonds

It is well known (2, 4) that the exact transformation of a set of molecular orbitals into the corresponding set of equivalent orbitals will not in general result in completely localized bonding orbitals. Although it was at one time hoped that the amount of delocalization or mixing of the components of different bond orbitals would be negligibly small this has not proved true in known cases. We wish to show that it is of crucial importance in the description of the water molecule. The delocalization in this case requires the introduction of the $1s$ orbital of $H_{(2)}$ into ϕ_{b1} and of the $1s$ orbital of $H_{(1)}$ into ϕ_{b2}. The amount of delocalization will be designated by δ, as shown in the general expressions for ϕ_{b1} and ϕ_{b2}.

Introduction of delocalization into the bonding orbitals has a very pronounced effect upon the electron density distribution. The reasons for this are easy to understand. By subtracting some $H_{(2)}(1s)$ from the $H_{(1)}(1s)$ function and vice versa we effectively reduce the overlap between the two hydrogen atoms and between the hydrogens and the oxygen $2s$ and $2p$ orbitals as well.* The immediate result of this reduced overlap between the hydrogens is that the bonding orbitals may now approach much more closely than was previously possible, thus allowing the bonds to bend to a much greater degree. It should be recalled that the requirement of orthogonality between orbitals is simply the way in which the Pauli exclusion principle is satisfied. By placing electrons with the same spin functions in orbitals which overlap we obviously violate the Pauli exclusion principle. Thus the requirement of orthogonality between two orbitals made up of components with finite overlap places a definite limitation on their possible proximity in space. The reduced overlap of the hydrogens not only allows for a greater degree of bending of the bonds but does so at smaller values of ϵ_b. Thus whereas with $\delta = 0$, an $\alpha = 87°$ was obtained with an $\epsilon_b = 108°$, the same value of α with $\delta = 0.355$ may be attained at an ϵ_b of approximately 60°, thus avoiding, or at smaller values of α, greatly reducing, the introduction of negative $2s$ character in the bonding orbitals. In addition the introduction of delocalization, again because of the decreased hydrogen overlap integrals, gives smaller values of ϵ_l for a given value of ϵ_b. Thus delocalization corrects just those deficiencies which were noted in consideration of the case II densities.

In Table II we show the effect which the introduction of δ has on the electronic forces. All of the forces listed below are calculated from density distributions which have the

TABLE II

The forces for case III

δ	$F_\perp$	$F_\parallel$	F_O	α	λ/μ	ϵ_b	ϵ_l
0.40	0.0676	2.516	0.316	63.75°	1.479	100.59°	45.00°
0.45	0.0690	2.512	0.322	61.30°	1.495	99.58°	45.00°
0.50	0.0704	2.510	0.326	59.00°	1.514	98.55°	45.00°
0.60	0.0720	2.506	0.332	54.95°	1.563	96.44°	45.00°
*	−0.0748	−2.538	−0.374	—	—	—	—

*The final line lists the values of the nuclear repulsions opposing each of the electronic forces.

**The overlap integrals which were initially S_1, S_2, and S_3 for the hydrogen–hydrogen, hydrogen–2s, and hydrogen–2p overlaps respectively now become $[S_1(1+\delta^2)-2\delta]$, $S_2(1-\delta)$, and $S_3(1-\delta\cos\theta)$.*

Can. J. Chem. Downloaded from www.nrcresearchpress.com by 210.87.254.6 on 09/05/12
For personal use only.

correct dipole moment. The introduction of delocalization increases $F_\perp$ and F_O very markedly, giving electron density distributions which have the correct dipole moment and yield close to the correct values for the electronic forces. The forces $F_\perp$ and F_O increase with increasing values of δ. $F_\parallel$ passes through a maximum in the region $0.35 < \delta < 0.40$ and, therefore, it is not possible to satisfy all of the forces simultaneously. However, special considerations arise in the case of the forces operative on the oxygen atom.

The value of F_O reported in Table II is the contribution of the valence electrons only. Up to this point the inner shell electrons on the oxygen atom have been assumed to be in a spherically symmetrical distribution on the oxygen nucleus. However, it is a known fact that a spherical charge distribution, when in the presence of an electric field, will polarize to the extent necessary to overcome the force exerted by the field.* It is also known that variational calculations predict slight polarizations of the inner shell orbital through the introduction of $2p$ character (10). The same slight polarization of the oxygen inner shell electrons in the present case can readily account for the final discrepancy of 0.04 a.u. in F_O. We can fix this additional parameter, the amount of $2p$ introduced into the inner shell orbital ϕ_o, by using the observed dipole moment as another constraint which the density function must fulfill. We then have six conditions to fix the six parameters. Taking

$$\phi_o = N(1s_o - k2p_{x'})$$

($2p_{x'}$ is directed along the x' axis of Fig. 1, i.e., away from the hydrogens) a value of $k = 0.0044$ is sufficient to balance the total calculated electronic force with the nuclear repulsive force exerted on the oxygen atom. This small amount of polarization is realistic and does not change the reported values of $F_\parallel$, $F_\perp$, or the dipole moment. Nor does the introduction of polarization seriously upset the orthogonality conditions. The non-orthogonality of the orbital ϕ_o with the bonding orbitals is 0.003 and with the lone pair orbitals is only 7×10^{-6}. This can be corrected for by reorthogonalization, which changes the final force on oxygen by only 2×10^{-4} a.u. Both the introduction of $2p_{x'}$ into ϕ_o and the subsequent reorthogonalization change the forces on hydrogen by the same small amount.

Undoubtedly, part of the remaining discrepancy in the forces on hydrogen could be removed by allowing for polarization of the hydrogen atoms as well. However, the forces are not nearly as sensitive to polarization of the hydrogens as they are to inner shell polarizations. Polarization of inner shell electrons displaces charge density very close to the nucleus and hence gives rise to a large atomic force term. Since the density around the hydrogen nuclei is not contracted to this same extent the relevant force integral is much smaller. For example, an amount of polarization of the hydrogen density comparable to that suggested for the inner shell on oxygen increases $F_\parallel$ by only 0.003 a.u. compared to a total electronic force of $\sim$2.5 a.u.

We have arrived at an expression for the electron density distribution for the water molecule which gives the correct dipole moment, satisfies the requirement of zero resultant forces for the oxygen nucleus, and comes close to satisfying this same condition for the hydrogen nuclei as well. The remaining forces on hydrogen are reasonably small and correspond to those encountered in an O—H bond compression of two one-hundredths of an Angstrom and to a change in the bond angle of 1.5°. The essential features of the

*The question of inner shell polarization has been discussed by Salem and Wilson (9) from the standpoint of the Hellmann–Feynman theorem. These authors point out that the problem of treating the inner shell electrons is simplest when there is no appreciable overlap with other orbitals. This is true in the present case as the overlap of ϕ_o with the 1s orbitals on hydrogen is so small that it can be ignored.

Can. J. Chem. Downloaded from www.nrcresearchpress.com by 210.87.254.6 on 09/05/12
For personal use only.

distribution vary only slightly with δ. Thus even though our inability to achieve final electrostatic equilibrium makes it difficult to decide on a final value of δ (a value close to 0.5 is indicated) we can specify the values of the remaining parameters within small bounds. The value of ϵ_b will be within a few degrees of 98°. This gives bonding orbitals which are 98% $2p$ in character and contain a very small amount of negative $2s$ character. The bonding orbitals from oxygen are thus essentially pure p bonds. The value of ϵ_l is always within one-hundredth of a degree from the value of 45°, which corresponds to sp hybrids directed above and below the molecular plane, with no component projected out the back of the molecule. This orbital picture is close to that obtained from a qualitative use of valence bond theory with the exception of course that this distribution is for a bond angle of 104.45° and not the 90° molecule predicted by valence bond theory. The bonds are, therefore, necessarily strongly bent with an orbital angle of approximately 59°. This gives ω (the angle between the bond direction and the orbital direction) a value of approximately 22°. It is also found that the bonding orbitals are quite polar with a λ/μ of approximately 1.5. An electron density contour map for the distribution with $\delta = 0.5$ is given in Fig. 3 and the expressions for the orbitals are

$$\phi_{b1} = 0.486474(s_1) - 0.243237(s_2) - 0.109490(2s) - 0.633912(2p_{x'}) + 0.358651(2p_{y'})$$
$$\phi_{l1} = 0.707105(2s) + 0.707107(2p_{z'}) + 0.001814(2p_{x'}).$$

The most radical difference between this electron density distribution and that proposed by Pople (and widely quoted, for example by Coulson (4) in his book "Valence") is the decrease in the prominence of the lone pair electrons. The lone pair orbitals according to Pople are sp^3 in character, projected out the back of the molecule, as opposed to the sp hybrids found in this work. The lone pair electrons in the present density distribution do not make a significant contribution to the dipole moment as opposed to Pople's case where they were predicted to make up almost the complete electronic contribution. Consequently, the present distribution predicts a much greater polarity for the O—H bonds than found by Pople. Again the present results agree with earlier views, that the dipole moment of the water molecule is due largely to the polarity of the bonds.* Pople (2) states that his calculations probably do overestimate the p character of the lone pair electrons. He stressed that the most important single factor in determining the bond angle of water was the repulsion between the lone pairs and that the angle between the lone pair orbitals should thus be as large as possible. By not allowing for bent bonds or delocalization the minimum angle they could obtain was close to 109° as determined by the molecular geometry. By allowing the bonds to bend, this lone pair repulsion can be reduced to its minimum, which occurs when they occupy sp hybrid orbitals.

The danger of believing hybridization to be determined by molecular geometry has of course been pointed out before, specifically for the water molecule by Shull and Ellison (10), who have carried out a S.C.F. L.C.A.O. M.O. treatment for the water molecule. Their results predict an equilibrium bond angle of 120°, a dipole moment which is too low by 0.3 D, and a binding energy 77% of the observed value at the correct bond angle. It is of interest to compare the orbitals obtained by them at 105° (not their equilibrium angle) with the present results. They too predict p bonds to the hydrogen atoms with a very small amount of negative $2s$ character. Their orbital angle is 69° as opposed to the 59° obtained here. They also arrive at lone pair orbitals which are closer to sp than sp^3. Their value for ϵ_l is in fact 47° (53% $2p$ character), as compared to 45°

**The fact that the bonds are bent in the present case lowers the value λ/μ required to meet the observed dipole moment.*

Can. J. Chem. Downloaded from www.nrcresearchpress.com by 210.87.254.6 on 09/05/12
For personal use only.

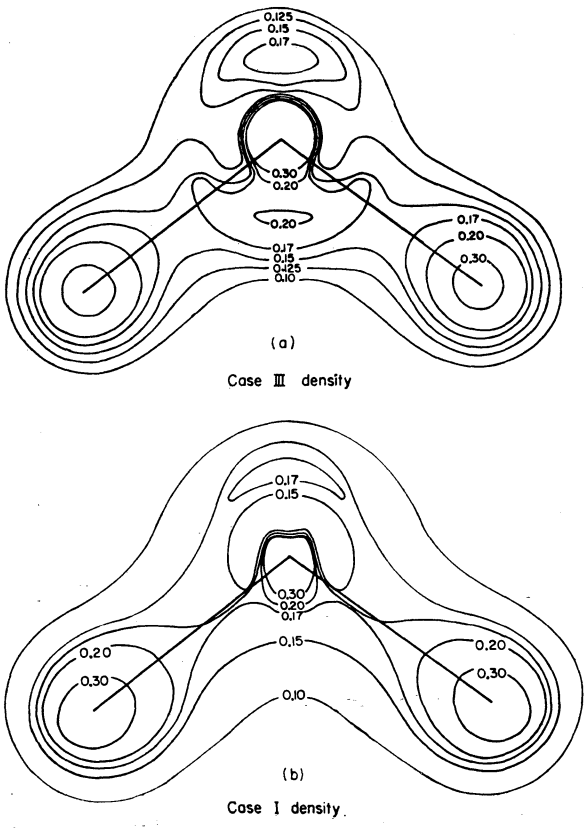

FIG. 3. Electron density contour maps for the density due to the valence electrons in the plane of the water molecule. Map (*a*) is for case III with $\delta = 0.5$, the best approximation to the density we have obtained. Map (*b*) is for the Pople-like distribution described in case I with prominent lone pairs. Map (*b*) is included for comparison to illustrate the effect of bent bonds and delocalization on the electron density. In distribution (*b*) there is a large bulge of density, due to the prominent lone pairs, projected out behind the oxygen nucleus which is responsible for the large imbalance in the forces on oxygen and on the hydrogens. In distribution (*a*) this same charge is more symmetrically placed with respect to the oxygen atom. Distribution (*a*) gives an accumulation of charge just below the oxygen atom which exerts an attractive force on all three nuclei. There is a valley in the (*b*) distribution along this same line. Distribution (*a*) clearly accumulates more charge in the binding regions between the nuclei than does distribution (*b*).

(50% $2p$ character) in the present case. It should be emphasized that with this value of ϵ_1 Shull and Ellison were not able to achieve an energy minimum at this angle.

To illustrate that results obtained by the present electrostatic method will not be radically different from those obtained by variational calculations we have used the orbitals determined by Shull and Ellison at the predicted equilibrium angle of 120° to calculate $F_\perp$. The component of the nuclear repulsion at this angle is 0.0508 a.u. and $F_\perp$ is found to be 0.0548 a.u., i.e., a force slightly larger than that required to balance the repulsive forces. This agreement is as good as can be expected as Shull and Ellison did not do a sufficient number of calculations to determine the energy minimum to an accuracy greater than approximately ±5°. This result would indicate that their true calculated minimum comes at an angle slightly less than 120°. Shull and Ellison (10) point out that the total electronic energy calculated for the water molecule by the variational method changes by only 0.13% as the bond angle is varied from 90° to

Can. J. Chem. Downloaded from www.nrcresearchpress.com by 210.87.254.6 on 09/05/12
For personal use only.

180°. As stated in the introduction, a force calculation is free from this defect and thus provides a method for determining densities which is more sensitive and more immediate than one based on a consideration of the energies.

The Electron Density Distributions and Geometries of the Hydride Molecules XH_2 and XH_3

The electron density distribution we have derived for the water molecule has two distinctive features: the lone pair electrons are in orbitals with the maximum amount of $2s$ character and the bonding electrons are in orbitals of almost pure $2p$ character. We wish now to illustrate, through the use of some general force curves to be given below, that an electron distribution of this type is to be expected for all hydride molecules which contain lone pair electrons, i.e., *in hydride molecules which possess at least one lone pair of electrons the bond orbitals will be primarily of p character and the lone pair orbitals will contain close to the maximum possible amount of s character.*

To see clearly what effects hybridization has on the forces exerted by the lone pair and bonding electrons we consider a simple diatomic hydride molecule X—H. The general expression for the normalized bond orbital due to the overlap of some hybrid of s and p orbitals on X with a $1s$ orbital on H is

$$\phi_b = \lambda[\cos \epsilon_b\, 2s + \sin \epsilon_b\, 2p] + \mu 1s,$$

and for a lone pair orbital directed out the back of the X atom along the bond axis,*

$$\phi_l' = \cos \epsilon_l'\, 2s - \sin \epsilon_l'\, 2p.$$

The forces exerted on the X atom along the bond axis by the electron density distribution are, for the bonding orbital,

$$F_{bx} = \lambda^2[4 \cos \epsilon_b \sin \epsilon_b\, A_x(2s,2p)] + \mu^2[2P_x(1s,1s)] + 4\lambda\mu[\cos \epsilon_b\, O_x(2s,1s) + \sin \epsilon_b\, O_x(2p,1s)],$$

and for the lone pair orbital (the direction of this force is opposite to that for F_{bx}),

$$F_{lx} = -4 \cos \epsilon_l' \sin \epsilon_l'\, A_x(2s,2p).$$

These expressions illustrate the three kinds of force expressions encountered in an atomic orbital description of an electron density:

$A_x(2s,2p)$—the force exerted on the X nucleus due to the s–p hybridization of the density on that nucleus. The same term in the electron density expression gives rise to the so-called atomic dipole.

$P_x(1s,1s)$—the force exerted on the X nucleus by the charge density situated at the hydrogen nucleus. Integrals of this type (i.e., the force on one atom due to the density situated entirely on another atom) are termed penetration integrals as their value is determined by the extent to which nucleus X penetrates the charge density on the other atom. The integral thus determines the extent to which the one nucleus is shielded from the other.

$O_x(2s,1s)$; $O_x(2p,1s)$—the force exerted on the X nucleus due to the charge density contained in the overlap regions of the $2s$ and $2p$ orbitals with the $1s$ orbital.

In Fig. 4 we have plotted F_{bx} and F_{lx} versus their hybridization parameters for orbitals corresponding to an O—H bond. The forms of these curves are the same for any X—H molecule. The force F_{bx} is shown for a λ/μ value of 1.00. In the limit of

*The lone pair hybridization parameter is primed in this case so that it will not be confused with ϵ_l, the one used to denote the hybridization of two equivalent lone pairs.

Can. J. Chem. Downloaded from www.nrcresearchpress.com by 210.87.254.6 on 09/05/12
For personal use only.

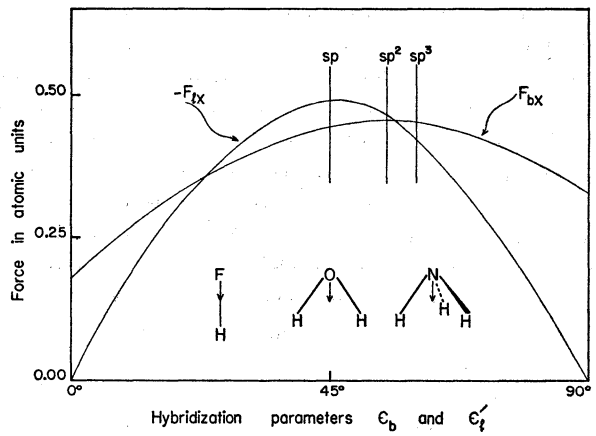

FIG. 4. The forces exerted on the X nucleus in HX by the lone pair and bonding electron densities as a function of their respective hybridization parameters ϵ_l' and ϵ_b.

$\lambda/\mu = \infty$, F_{bX} will of course equal $-F_{lX}$. For values of λ/μ only slightly greater than unity ($\sim$1.4) the two end points of F_{bX} drop slightly and the maximum in the curve is slightly increased. We assume that any other electron pairs present on the X nucleus are in s or p_π orbitals and thus they exert no force on the X nucleus since their density is symmetrically placed around X. The force exerted on X by the lone pair is zero for pure s or pure p orbitals but increases rapidly with hybridization to a maximum corresponding to an sp hybrid. This force is due entirely to the atomic force term $A_X(2s,2p)$. The force due to the bonding pair of electrons is of some interest. It gives the order of the forces exerted on X versus hybridization as

$$sp^2 \sim sp \sim sp^3 > p > s.$$

The hybrid orbitals exert the greatest force on X, and the force due to a pure p orbital on X is considerably greater than that due to a pure s orbital on X when forming a bond with hydrogen. This increased force of a $2p$ bond over an $2s$ bond with hydrogen is due almost entirely to a much greater value of $O_X(2p,1s)$ as compared to $O_X(2s,1s)$ (a factor of almost three for O—H bonds). This is to be expected as the overlap of a p bond with a $1s$ orbital on H places most of the overlap charge density along the bond axis, where it exerts a maximum force. The increase in the forces encountered in the s–p hybridizations is due to the presence of the atomic force term $A_X(2s,2p)$ which results from the polarized charge density relatively close to the X nucleus.

We can employ Fig. 4 in a qualitative application of the proposed rule to all 3 of the 10 electron hydrides, NH_3, H_2O, and HF. For each of these molecules we are interested in considering the resultant force on the N, O, and F nuclei as indicated for each case in Fig. 4. Each of these molecules, as it turns out, has but one lone pair of electrons which can exert a force on the heavy nucleus. The ammonia molecule has one lone pair orbital and it is directed along the force axis, in the negative direction. Its hybridization can vary from pure s to approximately sp^3. The two equivalent lone pair orbitals of the water molecule which can vary from sp to approximately sp^3 may be considered equally well as a single p_π orbital perpendicular to the plane of the molecule (which exerts no force on the oxygen atom) and a second orbital in the plane directed along the force axis which can vary from pure s to approximately sp^2. Linear combinations of these

Can. J. Chem. Downloaded from www.nrcresearchpress.com by 210.87.254.6 on 09/05/12
For personal use only.

two orbitals give back the two equivalent lone pair orbitals.* The three lone pairs of electrons in hydrogen fluoride occupy two p_π orbitals which exert no force on the fluorine nucleus and a hybrid orbital along the bond axis which may vary from pure s to pure p. F_{1X} thus applies directly to all three of these molecules, as does F_{bX} for HF. For H_2O and NH_3 components of F_{bX} for each bond must of course be taken along the indicated force axis. The components are such that the two O—H bonds in H_2O and the three N—H bonds in NH_3 add up very close to that of a single O—H and N—H bond respectively along the direction of the force. In actual fact new force components appear in F_{bX} for H_2O and NH_3 ($O_X(2s,2p_\pi)$ for example) at the expense of those indicated. It will be apparent that these effects do not alter the nature of the general results we wish to obtain here. This may be seen by comparing F_{bX} with the exact force expression for $F_O(\phi_b^2)$ given in the Appendix.

It is obvious from Fig. 4 that the lone pair of electrons in any of these three molecules cannot be placed in an orbital which is strongly s–p hybridized if electrostatic equilibrium is to be attained. Large hybridization of the lone pair results in a negative force on the X atom which is greater than or only slightly less than the attractive force exerted by the bonding electrons, and an insufficient amount of attractive force would remain to compensate for the nuclear repulsion. The force due to the lone pair electrons can be decreased either by placing them in an almost pure $2p$ or pure $2s$ orbital. The direction taken is determined by which of the two alternatives gives the best bonding force, as the hybridization parameters ϵ_b and ϵ_1' are, of course, not independent. If the lone pair is pushed towards pure $2p$ bonds the bonding orbital approaches pure $2s$, which as we have seen is not as effective as a pure p bonding orbital in the force it exerts on the X nucleus. Thus by placing the lone pair electrons in an almost pure $2s$ orbital and the bonding electrons in an orbital largely $2p$ in character the negative force of the lone pair electrons can be reduced at the expense of only a small decrease in the force exerted by the bonding electrons. In HF this is achieved simply by making the bonding orbital largely $2p$ in character and the lone pair thus becomes mostly $2s$. In H_2O and NH_3 the same result is achieved by bending the bonds. Since the hybridization in these molecules, if determined by the molecular geometry, would place the lone pair in either an sp^2 or sp^3 orbital for H_2O and NH_3, respectively, bent bonds are an absolute necessity in order to remove the great imbalance in forces created by the lone pair electrons. It should be recalled that delocalization of the bonding orbitals in H_2O also operated so as to increase the amount of s character in the lone pair orbitals for a given amount of s–p hybridization (and hence a larger force) in the bonding orbitals. This is the principal reason for the delocalization in molecules such as H_2O and NH_3.

A consideration of the forces exerted on the hydrogen atom by the same two orbitals in HX leads to an identical conclusion, i.e., that in these molecules the lone pairs will be largely $2s$ and the bonding orbitals largely $2p$. A consideration of the forces exerted on the hydrogen nucleus in this model are also of use in understanding why certain hydride molecules are bent as opposed to being linear, or pyramidal as opposed to being planar. The expressions for these forces are

$$\begin{aligned} F_{bH} = {} & 2\lambda^2[\cos^2\epsilon_b\, P_H(2s,2s) + \sin^2\epsilon_b\, P_H(2p,2p) \\ & +2\cos\epsilon_b \sin\epsilon_b\, P_H(2s,2p)] \\ & +4\lambda\mu[\cos\epsilon_b\, O_H(1s,2s) + \sin\epsilon_b\, O_H(1s,2p)]; \end{aligned}$$

*ϵ_1 *gives the hybridization in water for two equivalent lone pairs and* ϵ_1' *gives the hybridization of a single lone pair in water when the second pair is placed in a* p_π *orbital. When* ϵ_1' *gives pure* s, ϵ_1 *gives* sp *and when* ϵ_1' *gives* sp^2, ϵ_1 *gives* sp^3.

Can. J. Chem. Downloaded from www.nrcresearchpress.com by 210.87.254.6 on 09/05/12
For personal use only.

$$F_{1H} = 2[\cos^2 \epsilon_1' P_H(2s,2s) + \sin^2 \epsilon_1' P_H(2p,2p) - 2 \sin \epsilon_1' \cos \epsilon_1' P_H(2p,2s)].$$

The lone pair and bond densities both exert an attractive force on the hydrogen nucleus. Hybridization increases the force due to the bonding electrons on the hydrogen nucleus and as can be seen from Fig. 5, the order of the forces as determined by the hybridization on X is

$$sp^3 \sim sp^2 \sim sp > p > s.$$

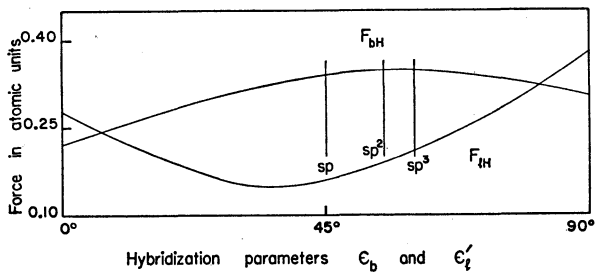

FIG. 5. The forces exerted on the H nucleus in HX by the lone pair and bonding electron densities as a function of their respective hybridization parameters ϵ_l' and ϵ_b.

Aside from a slight reordering of the forces for large hybridizations the results are the same as for the forces on the X atom, with a $2p$ bond exerting a much stronger force than that of a bond formed by a $2s$ orbital from the X atom. The force exerted by the lone pair, F_{1H}, undergoes a great decrease when hybridization on X is extreme. The contributions to F_{1H} are all of the penetration type. Hybridization results in charge being removed from the hydrogen side of X and being placed on the side remote from hydrogen. This explains the great decrease in shielding (i.e., decrease in the value of F_{1H}) as hybridization on X becomes important. Thus large hybridization results in a great increase in the repulsive force on hydrogen as the lone pair no longer effectively shields its part of the nuclear charge on X. Again, of the two possibilities the greatest possible force is achieved by making the bonds largely p in character and the lone pair largely s.

With these general curves for the variation of the forces on hydrogen versus hybridization in mind, we may go on to consider the question of bond angles. Consider the general expression for the electronic force exerted on the hydrogen nucleus along the O—H bond axis in H_2O. For a linear or bent molecule this can be written as

$$F_\parallel = F_{b1}+F_{b2}+F_{l1}+F_{l2}+F_{1s},$$

where F_{b1} designates the force on $H_{(1)}$ due to its bonding orbital, F_{b2} the force on $H_{(1)}$ due to second bonding orbital, F_{l1}, F_{l2}, and F_{1s} the forces due to the two lone pairs and the inner shell electrons.

The total nuclear repulsion between the O and H nuclei can be written as $4(-2/d^2)$ where d is the O—H bond length. Then the four pairs of electrons contained in ϕ_{b1}, ϕ_{l1}, ϕ_{l2}, and ϕ_{1s} can each be considered as exerting a force opposed to a nuclear contribution of $-2/d^2$. In the same way the pair of electrons in ϕ_{b2} must balance the force of $1/R^2 \cdot (\sin \mathscr{E}/2)$, where R is the H—H separation. This is a useful device for the following reason. Consider the pair of electrons in ϕ_{1s}. They are tightly held around the oxygen nucleus and at the bond distance d the hydrogen nucleus has not effectively penetrated

Can. J. Chem. Downloaded from www.nrcresearchpress.com by 210.87.254.6 on 09/05/12
For personal use only.

this charge distribution. Thus this pair of electrons should effectively shield a nuclear charge of two units. This is precisely what is found, as F_{1s} equals $2/d^2$, i.e. $P_H(1s_o,1s_o)$ equals simply $1/d^2$ and for two electrons we obtain an exact screening of two units of nuclear charge. In a linear H_2O molecule, ϕ_{11} and ϕ_{12} are both p_π orbitals. For very large values of d, the value of any penetration integral is simply $1/d^2$ as there is no penetration of the charge density. However, for values of d corresponding to those observed in stable molecules the value of $P_H(2p_\pi,2p_\pi)$ is much less than $1/d^2$ as π orbitals place charge above and below the bond axis and poor shielding results. Thus electrons in p_π orbitals do not effectively shield their share of the nuclear charge. The force exerted by a pair of electrons in a bonding orbital is generally greater than $2/d^2$ as charge is actually moved off the nuclei and concentrated between them, leading to an increase in the effectiveness of the electron density in attracting the nuclei. We thus have non-bonding or inner shell electrons whose presence leads to a zero net force; we have lone pair electrons in p_π orbitals whose presence leads to a net force of repulsion; and bonding electrons which lead to a net attractive force. We now consider what happens to these various contributions as the bond angle is decreased from 180°.

(i) F_{b1} decreases in value as the molecule is bent since the hybridization changes from approximately sp to almost pure p. F_{b2} increases markedly on bending the molecule as the density contained in ϕ_{b2} is now moved closer to $H_{(1)}$. The nuclear repulsion also increases as the hydrogens approach one another but F_{b2} (which is always greater than $\sin(\mathscr{E}/2)\ (1/R^2)$) increases much more rapidly. The net result of decreasing the bond angle is an almost constant or at most a slightly decreasing contribution to the force on $H_{(1)}$ due to the bonding electrons.

(ii) As the bond angle is decreased from 180° one of the lone pair orbitals takes on an increasing amount of $2s$ character and in the limit becomes a pure $2s$ orbital. A $2s$ orbital is much more effective at screening a nucleus that is a $2p_\pi$ orbital. Furthermore, the remaining p character of this same orbital now assumes p_σ character with respect to $H_{(1)}$ as the molecule is bent. The penetration integral for p_σ actually exceeds $1/d^2$. Thus the effect of bending the molecule is to obtain a much greater screening of the oxygen nucleus and hence a large increase in the force of attraction due to one of the lone pairs. The force due to the second lone pair orbital is independent of bond angle as it remains a p_π orbital.

This is the reason for a bond angle of less than 180° for the water molecule. In decreasing the bond angle the attractive force of the bonding electrons remains almost constant but the attractive force of the lone pair electrons increases greatly as the p_π orbital assumes $2s$ character, resulting in a much greater shielding of the oxygen nucleus.

Precisely the same reasoning holds for the pyramidal form of NH_3 being more stable than the planar form. In bending the hydrogens out of plane the forces due to the bonding electrons decrease only slightly for the same reasons given for water. The lone pair orbital, however, changes from a p_π orbital to a $2s$ orbital in the limit. Thus again by bending the hydrogens out of the plane the shielding of the nitrogen nucleus is greatly increased, leading to a greater force of attraction on the hydrogens and a more stable molecule. The planarity of CH_3^+ and BH_3 and the pyramidal shape of CH_3^- are easily explained on the same basis. In CH_3^+ and BH_3 there are no lone pair electrons. The molecules thus gain nothing by bending. They would in fact undergo a slight decrease in force, as the bonding orbitals would change from approximately sp^2 in the planar form to some hybrid approaching pure p, and Fig. 5 illustrates that this is unfavorable. The CH_3^- ion on the other hand is isoelectronic with NH_3 and again can reach a more

Can. J. Chem. Downloaded from www.nrcresearchpress.com by 210.87.254.6 on 09/05/12
For personal use only.

stable configuration by assuming a pyramidal shape and thereby can increase the shielding of the carbon nucleus. The methyl radical CH_3 with but one electron in the p_π orbital in its planar form will obviously be a borderline case and a firm prediction could be made only by a complete calculation. However, a comparison of the values of $P_H(2p_\pi,2p_\pi)$ and $P_H(2s,2s)$ would suggest that the difference between these two penetration integrals for an occupation by only one electron might not be sufficient to cause the molecule to bend.

In summary, one concludes from a consideration of the electronic forces exerted on the hydrogen nuclei in XH_2 and XH_3 molecules that the main factor determining their most stable configuration is the presence or absence of at least one lone pair of electrons in a single orbital. XH_2 and XH_3 molecules which do not possess an unshared pair of electrons obtain their maximum force on the hydrogen nuclei in their linear and planar forms respectively.* For XH_2 and XH_3 molecules with lone pair electrons the largest electronic force on hydrogen is attained by decreasing the bond angle. This converts one lone pair $2p_\pi$ orbital into a $2s$ orbital, which screens the X nucleus much more effectively than does a $2p_\pi$ orbital. To attain this limiting form for the lone pair orbital it is not necessary to decrease the bond angle to 90°. By bending the bonds as discussed in detail for H_2O it is possible to attain this limiting form at intermediate angles. In fact the extent to which it is possible to bend the bonds to reach this limiting case will determine the final bond angle. The discussion regarding the hybridization in the bent or non-planar forms of the hydride molecules also demonstrated that the bonds must be bent at these intermediate angles if the X nucleus is to achieve electrostatic equilibrium.

It is only in hydride molecules such as CH_3^+ or CH_4 which do not possess lone pairs of electrons that the full benefit of the large attractive forces associated with sp^2 or sp^3 hybridization can be realized. In methane the density distribution of every projected orbital is directed to a hydrogen nucleus and thus no large imbalance occurs in the forces exerted on the carbon atom. The conclusions we have reached in this paper concerning the factors governing the shapes of XH_2 and XH_3 molecules are the same as the empirically based rules advanced by Walsh (11). Our method of arriving at these conclusions and our interpretations of them are entirely different from his.

It should not be assumed that the density distribution advanced for the water molecule in this work is inconsistent with an almost tetrahedral structure for ice. The bonds in the water molecule have been predicted to be quite polar. Thus the proximity of hydrogen nuclei belonging to neighboring water molecules can easily bring about an increase in the p character of the lone pair orbitals and a corresponding decrease in the angle β between these orbitals. The presence of the partially unshielded hydrogen nuclei would now balance the large forces which the lone pairs exert in this position on the oxygen nucleus and on the hydrogens, tending to open up the bond angle. A familiarity with the sensitivity of electronic forces to hybridization and external centers of force would lead us to predict a substantial change in the electron density distribution upon hydrogen bonding. An increase in the orbital angle with a corresponding increase in the amount of s–p hybridization in the bonding orbitals would accompany the increased hybridization of the lone pairs. Thus the lone pair orbitals can approach sp^3 hybridization when hydrogen bonded for the same reasons that such hybridization is possible in the methane

**The molecules BH_2 with one unshared p_π electron and CH_2 with two unshared electrons in two distinct p_π orbitals (in their linear forms) are borderline cases as is CH_3. The singlet state of CH_2 with both unshared electrons in a single orbital should be bent.*

Can. J. Chem. Downloaded from www.nrcresearchpress.com by 210.87.254.6 on 09/05/12
For personal use only.

molecule. It is this favorable methane-like distribution which the water molecule can approach when hydrogen bonded in ice.

ACKNOWLEDGMENTS

We wish to thank the staff of the computing center at the University of Ottawa for their generous assistance with these calculations. Special thanks are due to Miss O. Boshko for writing the program to calculate the three-center integrals, and to Mr. P. Sefton for help with the general program. We also acknowledge the assistance of Miss V. Zahradnitzky and Mr. D. Hill in checking the numerical work.

Can. J. Chem. Downloaded from www.nrcresearchpress.com by 210.87.254.6 on 09/05/12
For personal use only.

APPENDIX

The Atomic Orbitals and Orthogonality Conditions

The atomic orbital functions employed in the calculation are of the Slater type. It is a well-recognized fact that variational calculations indicate a substantial increase in the hydrogen 1*s* orbital exponent over the free atom value when the hydrogen is involved in bond formation. Some recent calculations by Ransil illustrate this point (15). We have employed a value of 1.32 (as opposed to 1.00, the free atom value, employed by Pople and Duncan (3) and Shull and Ellison (10)) which was obtained by the use of a formula previously discussed (6). This formula relates the orbital exponents to the free atom and united atom (in this case neon) limits through a correlation of the molecular orbitals. That the method is reliable is illustrated by the calculation of the orbital exponent for hydrogen in HF. This exponent has been determined by Ransil in a variation calculation (15) and the best value is found to be 1.32. An application of the formula gives a value of 1.34. Both the formula and the results of variational calculations predict only small changes in the exponents of the 1*s* inner shell and 2*s* and 2*p* orbitals on the atoms bonded to hydrogen. We have repeated a large number of the calculations using these slightly different values and find no significant changes in our results. We have, therefore, employed the free atom values of the orbital exponents for the $1s_o$, 2*s*, and 2*p* orbitals on oxygen. These values are 7.700 for $1s_o$ and 2.275 for 2*s* and 2*p*.

It is most important in force calculations that all the important orthogonality conditions be met. Particularly important is the condition of orthogonality between the 2*s* and 1*s* orbitals on the same atom. Thus the oxygen 2*s* orbital indicated in all the formulae is the orthogonalized one

$$2s = (1-S_o^2)^{-\frac{1}{2}}(2s'-S_o 1s_o),$$

where 2*s*′ is the nodeless Slater orbital, and S_o is the overlap integral between 2*s*′ and $1s_o$. The only orthogonality neglected in the present calculations is that between the 1*s* orbital on oxygen, $1s_o$, and the hydrogen 1*s* orbital. The overlap between $1s_o$ and $1s_H$ is very slight and consequently the magnitudes of the force integrals due to this overlap are so small that they can be neglected without incurring any error to the accuracy employed in the present calculations.

In the following formulae we denote the overlap integrals between the oxygen 2*s* and 2*p* orbitals with a hydrogen 1*s* orbital as S_2 and S_3 respectively and that between the two hydrogen 1*s* orbitals as S_1.

When the two lone pair orbitals are expressed in their equivalent form, the $2p_z$ orbital makes a constant contribution of $1/\sqrt{2}$. Since this $2p_z$ orbital makes no contribution

to F_O or $F_\perp$ and a constant contribution to $F_\parallel$ it greatly simplifies all of the calculations if the lone pair orbitals are taken instead as the orthogonal set:

$$\phi'_{11} = \cos \epsilon'_1\, 2s + \sin \epsilon'_1\, 2p'_3$$
$$\phi'_{12} = 2p_z,$$

where p_3' is directed in the plane of the molecule along the x' axis. This is the alternative form of the lone pair orbitals discussed earlier in the paper. The hybridization parameters ϵ_1 and ϵ_1' are easily related: $\cos \epsilon_1 = (1/\sqrt{2}) \cos \epsilon_1'$, $\sin \epsilon_1 = (1/\sqrt{2}) \sin \epsilon_1'/\cos (\beta/2)$, where β is the angle between the lone pair orbitals. The requirement that the equivalent lone pair orbitals be orthogonal gives $\cos \beta = -\cot^2 \epsilon_1$.

The following equations [1] and [2] are the relationships obtained by requiring the orbitals to be mutually orthogonal. For orthogonality between the bonding orbitals we obtain:

$$[1] \quad \lambda^2[\cos^2 \epsilon_b + \sin^2 \epsilon_b \cos \alpha] + \mu^2[S_1(1+\delta^2) - 2\delta] + 2\lambda\mu[S_2 \cos \epsilon_b\, (1-\delta) + S_3 \sin \epsilon_b\, (\cos t - \delta \cos \omega)] = 0$$

and for orthogonality between the bonding and lone pair orbitals

$$[2] \quad \tan \epsilon_1' = \frac{S_2(1-\delta) + (\lambda/\mu) \cos \epsilon_b}{S_3 \cos (\mathscr{E}/2)\, (1-\delta) + (\lambda/\mu) \sin \epsilon_b \cos (\alpha/2)} = \tan \epsilon_1 \cos (\beta/2).$$

A third condition obtained from the normalization of the bonding orbitals allows one to determine the absolute values of λ and μ once their ratio is known. This condition is

$$[3] \quad \lambda^2 + \mu^2[1+\delta^2-2\delta S_1] + 2\lambda\mu[S_2 \cos \epsilon_b\, (1-\delta) + S_3 \sin \epsilon_b\, (\cos \omega - \delta \cos t)] = 1.$$

When it was realized that a total of five parameters would be required to describe the density distribution of the water molecule the calculations were programmed for machine computation on an IBM 650. The sequence of steps employed in the program are as follows. For a particular choice of λ/μ, δ, and α, the parameter ϵ_b is obtained from equation [1]. Equation [1] as written can be solved only by a trial and error method. However, since ϵ_b is $(90 \pm m)$ where m is less than 15°, $\cos \epsilon_b$ and $\sin \epsilon_b$ can be expanded in terms of m. Retaining terms to the order of m^2 converts equation [1] into a quadratic expression in m. This method and equation [1] as it stands give identical results well within the accuracy required. As an example, for $\delta = 0.3$, $\lambda/\mu = 1.4$, and $\alpha = 70.00°$, both methods give $\epsilon_b = 95.87°$. Equation [2] was then used to obtain ϵ_1' and equation [3] to obtain λ and μ. In the program this was followed by a calculation of $F_\perp$, $F_\parallel$, F_O, and the dipole moment.

The Calculation of the Forces

All of the force integrals are of the form

$$\int \mathscr{D}_{\alpha x} \phi_i \phi_j d\tau,$$

where $\mathscr{D}_{\alpha x}$ is the expression for the x-component of the electric field due to nucleus α, and ϕ_i and ϕ_j are atomic orbitals (7). The positions of ϕ_i and ϕ_j with respect to atom α generate either $A_\alpha(\phi_i,\phi_j)$, $P_\alpha(\phi_i,\phi_j)$, or $O_\alpha(\phi_i,\phi_j)$ integrals as explained earlier in the text. General formulae for all the penetration integrals (two- and three-center forms) have been given previously (12) and the formulae for the O_α integrals may be obtained from tables published by Coulson (13). All the force expressions are for double occupation

Can. J. Chem. Downloaded from www.nrcresearchpress.com by 210.87.254.6 on 09/05/12
For personal use only.

of the orbitals and $2p_x$, $2p_y$, and $2p_z$ refer to the $2p$ atomic orbitals directed along the x, y, and z axes of Fig. 1.

The Forces on Hydrogen

All the forces calculated for hydrogen refer to the hydrogen atom labelled $H_{(1)}$. The component of the electric field $\mathscr{D}_{\perp H}$, which appears in the integrals for the perpendicular forces on hydrogen, is in the direction indicated for $F_\perp$ in Fig. 1, except for the integrals $P_H(1s_2,1s_2)$ and $O_H(1s_1,1s_2)$. In these two latter integrals the field component was taken along the line joining the two hydrogens, and the proper component of the resulting force (cos ($\mathscr{E}$/2)) was then taken along the direction of $F_\perp$. These two integrals are primed for this reason.

$$\begin{aligned}
F_\perp(\phi_{b1}^2) = {} & 2\lambda^2[2\cos\epsilon_b \sin\epsilon_b \sin\omega\, P_H(2s,2p_y)+2\sin^2\epsilon_b\cos\omega\times \\
& \sin\omega\, P_H(2p_x,2p_y)] +2\mu^2[\delta^2 P'_H(1s_2,1s_2)-2\delta O'_H(1s_1,1s_2)] \\
& + 4\lambda\mu[\sin\epsilon_b \sin\omega\, O_H(1s_1,2p_y)-\delta\{\cos\epsilon_b\, P_H(2s,1s_2) \\
& + \sin\epsilon_b\cos\omega\, P_H(2p_x,1s_2) + \sin\omega\sin\epsilon_b\, P_H(2p_y,1s_2)\}] \\
F_\perp(\phi_{b2}^2) = {} & 4\lambda^2[\cos\epsilon_b \sin\epsilon_b \sin t\, P_H(2s,2p_y) + \sin^2\epsilon_b\cos t\sin t\times \\
& P_H(2p_x,2p_y)] + 2\mu^2[P'_H(1s_2,1s_2)-2\delta O'_H(1s_1,1s_2)] \\
& + 4\lambda\mu[\cos\epsilon_b\, P_H(2s,1s_2) + \sin\epsilon_b\{\cos t\, P_H(2p_x,1s_2) \\
& + \sin t\, P_H(2p_y,1s_2) - \delta\sin t\, O_H(1s_1,2p_y)\}] \\
2F_\perp(\phi_1^2) = {} & 4[\sin^2\epsilon'_1 \sin(\mathscr{E}/2)\cos(\mathscr{E}/2)\, P_H(2p_x,2p_y) \\
& - \sin\epsilon'_1\cos\epsilon_1'\sin(\mathscr{E}/2)\, P_H(2s,2p_y)]
\end{aligned}$$

The component of the electric field $\mathscr{D}_{\parallel H}$ for the forces on hydrogen along the bond has the direction indicated by $F_\parallel$. This $\mathscr{D}_{\parallel H}$ was employed in all the integrals but $P_H(1s_2,1s_2)$ and $O_H(1s_1,1s_2)$, which were calculated as in $F_\perp$ but multiplied by sin ($\mathscr{E}$/2) to obtain the proper component for $F_\parallel$.

$$\begin{aligned}
F_\parallel(\phi_{b1}^2) = {} & 2\lambda^2[\cos^2\epsilon_b\, P_H(2s,2s) + \sin^2\epsilon_b\{\cos^2\omega\, P_H(2p_x,2p_x) \\
& + \sin^2\omega\, P_H(2p_y,2p_y)\} + 2\cos\epsilon_b\sin\epsilon_b\cos\omega\, P_H(2s,2p_x)] \\
& + 2\mu^2[\delta^2 P''_H(1s_2,1s_2)-2\delta O''_H(1s_1,1s_2)] \\
& + 4\lambda\mu[\cos\epsilon_b\, O_H(1s_1,2s) + \sin\epsilon_b\cos\omega\, O_H(1s_1,2p_x) \\
& - \delta\{\cos\epsilon_b\, P_H(2s,1s_2) + \sin\epsilon_b\cos\omega\, P_H(2p_x,1s_2) \\
& + \sin\epsilon_b\sin\omega\, P_H(2p_y,1s_2)\}] \\
F_\parallel(\phi_{b2}^2) = {} & 2\lambda^2[\cos^2\epsilon_b\, P_H(2s,2s) + \sin^2\epsilon_b\{\cos^2 t\, P_H(2p_x,2p_x) \\
& + \sin^2 t\, P_H(2p_y,2p_y)\} + 2\cos\epsilon_b\sin\epsilon_b\cos t\, P_H(2s,2p_x)] \\
& + 2\mu^2[P''_H(1s_2,1s_2)-2\delta O''_H(1s_1,1s_2)] \\
& + 4\lambda\mu[\cos\epsilon_b\, P_H(2s,1s_2) + \sin\epsilon_b\cos t\, P_H(2p_x,1s_2) \\
& + \sin\epsilon_b\sin t\, P_H(2p_y,1s_2) - \delta\cos\epsilon_b\, O_H(1s_1,2s) \\
& - \delta\sin\epsilon_b\cos t\, O_H(1s_1,2p_x)] \\
2F_\parallel(\phi_1^2) = {} & 2[\cos^2\epsilon'_1\, P_H(2s,2s) + \sin^2\epsilon'_1\{\cos^2(\mathscr{E}/2)\, P_H(2p_x,2p_x) \\
& + \sin^2(\mathscr{E}/2)\, P_H(2p_y,2p_y)\} - 2\cos\epsilon'_1\sin\epsilon'_1\cos(\mathscr{E}/2)\times \\
& P_H(2s,2p_x) + P_H(2p_z,2p_z)] \\
F_\parallel(\phi_o^2) = {} & 2P_H(1s_o,1s_o)
\end{aligned}$$

Can. J. Chem. Downloaded from www.nrcresearchpress.com by 210.87.254.6 on 09/05/12
For personal use only.

The Forces on Oxygen

It is most convenient in the calculation of the orbital contribution to F_O to employ a number of different field components for $\mathscr{D}_o$ in the calculation of the integrals. For those integrals which contain a $2p$ orbital $\mathscr{D}_o$ was directed along the $2p$ orbital in question and the proper component along F_O then taken. For those involving the $1s$ and $2s$ orbitals $\mathscr{D}_o$ was directed along the bond axis and the proper component again taken along F_O. As stated in the introduction a common factor of eight, the nulcear charge on oxygen, has been omitted from the expressions for F_O and the nuclear repulsion.

$$\begin{aligned} F_O(\phi_b^2) = {} & 2\lambda^2[2\cos\epsilon_b \sin\epsilon_b \cos(\alpha/2)\, A_o(2s,2p_1)] \\ & + 2\mu^2[\cos(\mathscr{E}/2)\,(1+\delta^2)P_o(1s_1,1s_1) - 2\delta P_o(1s_1,1s_2)] \\ & + 4\lambda\mu[\cos(\mathscr{E}/2)\cos\epsilon_b\,(1-\delta)O_o(2s,1s) \\ & + \sin\epsilon_b \cos(\mathscr{E}/2)\, O_o(2p_x,1s)(\cos\omega - \delta\cos t) \\ & + \sin\epsilon_b \sin(\mathscr{E}/2)\, O_o(2p_y,1s)(\sin\omega - \delta\sin t)] \end{aligned}$$

$$2F_O(\phi_1^2) = -4\cos\epsilon_1' \sin\epsilon_1' A_o(2s,2p_{x'})$$

$$F_O(\phi_o^2) = 4N^2 k A_o(1s_o,2p_{x'}),$$

where $p_{x'}$ is directed along the x′ axis. The expression for $F_O(\phi_o{}^2)$ applies when ϕ_o contains $2p_{x'}$ character with coefficient k.

A number of three-center integrals occur in these calculations. For the forces on hydrogen they are $P_H(2s,1s_2)$, $P_H(2p_x,1s_2)$, and $P_H(2p_y,1s_2)$ for both the parallel and perpendicular cases. The integrals represent the forces exerted on $H_{(1)}$ in the direction of $F_\perp$ (with $\mathscr{D}_{\perp H}$) or $F_\parallel$ (with $\mathscr{D}_{\parallel H}$) due to the overlap charge density between the $2s$ and $2p$ orbitals on oxygen with the $1s$ orbital on $H_{(2)}$. We have recently published an account of a method for evaluating these integrals (12). The method employs a series expansion centered on the oxygen atom for $\mathscr{D}_{\perp H}$ and $\mathscr{D}_{\parallel H}$ in terms of Gegenbauer polynomials coupled with the method of Coulson and Barnett (14) for the expansion of the $1s$ orbital of $H_{(2)}$ on the same center. Since six such integrals had to be evaluated at a number of bond angles a numerical method employing an IBM 650 computer was also developed for their evaluation. The two methods gave good agreement. For example, $P_H(2p_y,1s_2)$ for the perpendicular case when evaluated by the expansion method was found to be equal to 0.050331 a.u. and by the machine method to equal 0.049962 a.u.

There is one three-center integral involved in the calculation of F_O. It is $P_o(1s_1,1s_2)$, i.e., the force on oxygen due to the overlap charge density between the two hydrogen atoms. This integral is expected to be small in magnitude and it occurs in F_O with a small coefficient. For these reasons the charge density $\rho(1s_1,1s_2)$ was approximated by

$$\rho(1s_1,1s_2) = \tfrac{1}{2}S_1(1s_1^2+1s_2^2).$$

When integrated over all space the correct charge density and the approximate expression both yield S_1. Thus the approximate density expression represents the same total amount of charge and places it in approximately the proper position. With this approximation

$$P_o(1s_1,1s_2) = S_1 P_o(1s_1,1s_1)\cos(\mathscr{E}/2).$$

Numerical Values of the Overlap and Force Integrals

In the following, the symbol $2s'$ refers to the nodeless Slater $2s$ orbital for oxygen and $2s$ to the orthogonal form $2s = 1.02841(2s' - 0.2334501s_o)$.

Can. J. Chem. Downloaded from www.nrcresearchpress.com by 210.87.254.6 on 09/05/12
For personal use only.

$S_1 = S(1s_1,1s_2) = 0.218210$ $S_2 = S(2s,1s) = 0.457449$
$S_3 = S(2p_x,1s) = 0.394475$ $S_o = S(2s',1s_o) = 0.233450$
$S(1s_o,1s) = 0.0524706$

$F_\perp$ integrals

$P'_H(1s_2,1s_2) = 0.0733651$ $P_H(2p_x,2p_y) = 0.0683187$ $O'_H(1s_1,1s_2) = 0.0327957$
$P_H(2s,1s_2) = 0.030064$ $P_H(2s,2p_y) = 0.100790$ $O_H(1s_1,2p_y) = 0.109553$
$P_H(2p_x,1s_2) = 0.012473$ $P_H(2s',2p_y) = 0.100133$
$P_H(2p_y,1s_2) = 0.049962$ $P_H(1s_o,2p_y) = 0.00911452$

$F_\parallel$ integrals

$P''_H(1s_2,1s_2) = 0.0946676$ $P_H(2p_x,2p_x) = 0.380564$ $O''_H(1s_1,1s_2) = 0.0423183$
$P_H(2s,1s_2) = 0.085669$ $P_H(2p_y,2p_y) = 0.227782$ $O_H(1s_1,2p_x) = 0.234244$
$P_H(2p_x,1s_2) = 0.025084$ $P_H(2s,2s) = 0.271943$ $O_H(1s_1,2s) = 0.184087$
$P_H(2p_y,1s_2) = 0.055147$ $P_H(2s,2p_x) = 0.166433$ $O_H(1s_1,2s') = 0.183329$
$P_H(2s',2s') = 0.278709$ $O_H(1s_1,1s_o) = 0.0185325$
$P_H(1s_o,1s_o) = 0.305241$
$P_H(2s',2p_x) = 0.166090$
$P_H(1s_o,2p_x) = 0.0182272$
$P_H(1s_o,2s') = 0.0712566$

F_O integrals

$P_o(1s_1,1s_1) = 0.261103$ $A_o(2s,2p) = 0.487736$ $O_o(2p_x,1s) = 0.336497$
$P_o(1s_1,1s_2) = 0.0349009$ $A_o(2s',2p) = 0.996051$ $O_o(2p_y,1s) = 0.141007$
$A_0(1s_o,2p) = 2.23513$ $O_o(2s,1s) = 0.134039$
$O_o(2s',1s) = 0.151302$
$O_o(1s_o,1s) = 0.089808$

REFERENCES

1. J. Lennard-Jones and J. A. Pople. Proc. Roy. Soc. (London), Ser. A, **202**, 166 (1950).
2. J. A. Pople. Proc. Roy. Soc. (London), Ser. A, **202**, 323 (1950).
3. A. B. F. Duncan and J. A. Pople. Trans. Faraday Soc. **49**, 217 (1953).
4. C. A. Coulson. Valence. 2nd ed. Oxford University Press. 1961.
5. L. Sutton. Chem. Soc. (London), Spec. Publ. No. 11. (1958).
6. R. F. W. Bader. Can. J. Chem. **38**, 2117 (1960).
7. R. F. W. Bader and G. A. Jones. Can. J. Chem. **39**, 1253 (1961).
8. A. C. Hurley. Proc. Roy. Soc. (London), Ser. A, **226**, 170, 179, 193 (1954); **235**, 224 (1956).
9. L. Salem and E. B. Wilson, Jr. J. Chem. Phys. **36**, 3421 (1962).
10. H. Shull and F. O. Ellison. J. Chem. Phys. **23**, 2348 (1955).
11. A. D. Walsh. J. Chem. Soc. 2260, 2296 (1953).
12. R. F. W. Bader. Can. J. Chem. **40**, 2140 (1962).
13. C. A. Coulson. Proc. Cambridge Phil. Soc. **38**, 210 (1942).
14. C. A. Coulson and M. P. Barnett. Phil. Trans. Roy. Soc. (London), Ser. A, **243**, 221 (1951).
15. B. J. Ransil. Rev. Mod. Phys. **32**, 245 (1960).

Can. J. Chem. Downloaded from www.nrcresearchpress.com by 210.87.254.6 on 09/05/12
For personal use only.

BIOSYNTHESIS OF PLANT CONSTITUENTS

I. THE COMPLETE DEGRADATION OF 2-DEOXY-D-RIBOSE AND SOME 2-DEOXY-D-HEXOSES[1]

A. M. UNRAU AND D. T. CANVIN
Department of Plant Science, University of Manitoba, Winnipeg, Manitoba

Received September 28, 1962

ABSTRACT

A simple procedure is described whereby the complete stepwise degradation of 2-deoxy-D-ribose was achieved. Yields as high as 90% or better of the available carbon was obtained. The 2-deoxy pentose was reduced (KBH_4) to the corresponding polyol and the latter oxidatively cleaved with periodate. Formic acid (C_4) was converted to CO_2 quantitatively by oxidation with HgO. Formaldehyde and β-hydroxypropionaldehyde were oxidized with bromine. Formic acid (C_5) thus formed was converted to CO_2 in quantitative yields and the hydroxy acid decarboxylated with permanganate; thusly C_3 was obtained. The acetic acid (from C_1 and C_2) was extracted with ether and subsequently degraded by the Schmidt–Phares procedure. The procedure was further used to degrade some 2-deoxy hexoses.

Can. J. Chem. Downloaded from www.nrcresearchpress.com by 210.87.254.40 on 09/05/12
For personal use only.

DISCUSSION

It has been suggested that 2-deoxy-D-ribose is formed by either of two pathways in animal and bacterial systems, namely an aldol-type condensation of acetaldehyde and D-glyceraldehyde-3-phosphate to yield 2-deoxy-D-ribose-5-phosphate (1), or a pathway involving the direct reduction of the riboside or ribotide to the 2-deoxy pentose (2). High deoxyribose-5-phosphate aldolase activity has been found in tumor extracts (3); however, investigations on *Escherichia coli* (4) and mammalian tissue (5) have indicated that a ribose compound is a precursor of deoxyribose or that both appear to have a common precursor. Purified aldolase from *Lactobacillus plantarum* was found to be specific for acetaldehyde, L-glyceraldehyde-3-phosphate, and a number of other aldoses but not for D-glyceraldehyde-3-phosphate (6). Studies on bacteriophage-infected *E. coli* indicated that about 60% of the sugar was elaborated via an oxidative pathway involving 6-phosphogluconate and no evidence for a C_2+C_3 condensation mechanism was found (7). Further evidence for reduction of ribose to deoxyribose has appeared (8). The above routes for the elaboration of 2-deoxy-D-ribose in animals and bacteria may be extended to higher plants. This aspect is under investigation by the authors. In either case, when C^{14}-labelled possible precursors are considered or used to determine the biosynthetic pathway, a procedure whereby the products may be degraded in some detail is essential. Recently, Jones and associates have reported on the biosynthesis of rhamnose and a heptose in a bacterial species in which they describe in some detail the degradation of these particular sugars (9).

In this communication, a relatively simple procedure is described whereby each of the five carbons of 2-deoxy-D-ribose may eventually be isolated as barium carbonate, and their radioactivity, if any, might then be determined. Reduction of the dexoy pentose with sodium or potassium borohydride (10) gave the corresponding polyol, which upon periodate oxidation liberated the required amount of formaldehyde (11). Three easily differentiable products are obtained in this oxidation, namely formic acid, β-hydroxypropionaldehyde, and formaldehyde. Formic acid, from C_4, was quantitatively oxidized to carbon dioxide using mercuric oxide (12). The two aldehydes were then oxidized with

[1]*Contribution No. 66.*

bromine to the corresponding acids. Formic acid thus generated from formaldehyde was oxidized to carbon dioxide as described and, thusly, C_5 was obtained quantitatively.

β-Hydroxypropionic acid was quantitatively decarboxylated with alkaline permanganate (12), and carbon dioxide, which constitutes C_3, was collected as barium carbonate. The remaining two-carbon fragment, which constitutes C_1 and C_2 of the original propionic acid derivative, was oxidized with acid permanganate to give acetic acid. The latter was extracted with ether and converted to the sodium salt. The salt was heated in an oven at 100° C for 4 to 6 hours, or overnight, after which time the residue was treated with the Schmidt–Phares reagents (12). A good yield of carbon dioxide, constituting C_1, was obtained upon treatment with sodium azide. The methyl amine was oxidized to carbon dioxide using alkaline permanganate. This last step thus yielded C_2. The steps yielding C_5, C_4, and C_3 of the 2-deoxy pentose were quantitative. A small loss of carbon was usually encountered in the Schmidt–Phares degradation of acetic acid. However, in the two steps of this reaction sequence essentially equal quantities of carbon dioxide were obtained.

The utility of the described procedure was established using suitable model compounds. For this purpose, standard formic acid, formaldehyde, and β-hydroxypropionic acid solutions were used. In this manner, quantitative recoveries were obtained for formic acid alone and when mixed with the other two compounds. It was also shown that formaldehyde, in admixture with the two acids, was transformed to the corresponding acid upon bromine oxidation, and the generated formic acid was again recovered quantitatively as carbon dioxide. β-Hydroxypropionic acid was obtained by hydrolysis of β-propiolactone with concentrated barium hydroxide. Excess barium hydroxide was converted to the water-insoluble carbonate and the solution of barium β-hydroxypropionate standardized by determining barium as barium sulphate. The acid was quantitatively decarboxylated with alkaline permanganate either by itself or in admixture with formic acid and formaldehyde, from which the latter two had been removed as carbon dioxide by the previously described reactions.

Controlled reaction conditions, i.e. pH, temperature, were found necessary for best results. In the mercuric oxide oxidations of formic acid, a pH of 5.0 to 5.5 was most desirable. This was particularly important after bromine oxidation of formaldehyde to formic acid. A bath temperature of 75–80° C was found sufficiently high. The combination of greater acidity and higher temperatures greatly reduced the yield of carbon dioxide from the propionic acid derivative. This is believed to be due to the tendency of β-hydroxy carboxylic acids to lose water at high temperatures. The resulting acrylic acids under these conditions would then proceed to form acrylate polymers. Very high alkalinity in the permanganate oxidation of the β-hydroxypropionic acid resulted in overoxidation whereas very weakly alkaline conditions gave much less than expected yields of carbon dioxide. It was found that the addition of 2 to 3 ml of 0.5 *N* sodium hydroxide to the neutral solution containing an excess of permanganate gave quantitative yields. The reaction mixture, after acidification, could be aerated at length without further carbon dioxide liberation. Persulphate oxidation (12) of the residue remaining after the above reactions indicated that the expected two-carbon fragment was present.

The acidified reaction mixtures containing permanganate were left at room temperature for about 16 hours to convert the two-carbon fragment to acetic acid. Ether extraction of the mixture followed by neutralization of the extract, evaporation to dryness, and persulphate oxidation of the residue gave almost theoretical yields of carbon dioxide. It was therefore apparent that the ethanol formed in the alkaline permanganate decarboxylation of β-hydroxypropionic acid was effectively oxidized to acetic acid. As indicated

Can. J. Chem. Downloaded from www.nrcresearchpress.com by 210.87.254.40 on 09/05/12
For personal use only.

previously, somewhat less than the expected amount of carbon dioxide was obtained in the Schmidt–Phares oxidation of acetate.

The procedure was extended for the complete carbon degradation of some 2-deoxy hexoses, namely 2-deoxy-D-galactose and 2-deoxy-D-glucose. In these instances, C_4 and C_5 both yield formic acid upon periodate oxidation of the corresponding polyols and therefore cannot be differentiated in this degradative procedure.

EXPERIMENTAL

Preparation and Degradation of Barium β-Hydroxypropionate

To β-propiolactone, 1.608 g, was added a concentrated solution of barium hydroxide (about 50% excess) and the solution heated to 60° C for 30 minutes. Excess barium hydroxide was converted to the insoluble carbonate by bubbling a stream of CO_2 through the solution. The precipitate was removed and the solution brought to 250 ml. The amount of barium salt per milliliter of solution was determined by acidification of 2-ml aliquots with 2 *N* sulphuric acid (5 ml) and weighing the dry precipitate ($BaSO_4$). To remove other possible organic impurities, the solution was evaporated to a small volume (30 ml) and added, with vigorous stirring, to 200 ml acetone. The gummy precipitate was redissolved in water (50 ml) and the solution heated (85–90°) to remove acetone, the volume again adjusted to 250 ml, and the solution standardized:

$BaSO_4$ from 2 ml before purification	17.3 mg
$BaSO_4$ from 2 ml after purification	17.2 mg

Decarboxylation with $KMnO_4$

To 3 ml of the above solution in a 50-ml distillation flask was added alkaline permanganate solution (1.5 ml) (oxidant solution consisted of 0.1 *M* NaOH, 0.2 *M* $KMnO_4$, and 0.02 *M* $MnSO_4$). The flask was fitted to an aeration train and the contents held at room temperature for about 45 minutes. Before acidifying the solution, the train was swept with nitrogen for 10 to 15 minutes. The solution was acidified (2 *N* H_2SO_4, 1 ml) and the CO_2 swept into a $Ba(OH)_2$ trap. The precipitate ($BaCO_3$) was collected on tared porcelain planchets, dried, and weighed. These results and those obtained from the decarboxylation of malic acid, made as a further check of the reaction, are given in Table I.

TABLE I

Weight of $BaCO_3$ (mg)			
β-Hydroxypropionate		Malic acid	
Expected	Obtained	Expected	Obtained
21.5	20.6	39.9	39.4
21.5	22.0	40.3	39.4
29.5	31.3		
24.5	24.0		

Degradation of Remaining Two-carbon Fragment From β-Hydroxypropionate

The acidified solution was left at room temperature overnight to facilitate oxidation of the initial product, ethanol, to acetic acid. The solution was thereupon thoroughly extracted with ether and the moist ether solution evaporated almost to dryness. The residue was made alkaline by addition of a few drops of 0.5 *N* NaOH and the solution evaporated to dryness followed by overnight drying at 100° C. The residue was then treated with reagents according to the Schmidt–Phares (12) procedure and the CO_2 from the carboxyl group and subsequently from methylamine collected as $BaCO_3$. The results are summarized in Table II.

TABLE II

Weight of $BaCO_3$ (mg)			
—COOH		CH_3NH_2	
Expected	Obtained	Expected	Obtained
21.5	19.8	21.5	18.9
21.5	20.8	21.5	19.2
29.5	28.2	29.5	27.6
24.5	23.7	24.5	22.2

Can. J. Chem. Downloaded from www.nrcresearchpress.com by 210.87.254.40 on 09/05/12
For personal use only.

Persulphate Oxidation of the Two-carbon Fragment from β-Hydroxypropionate

Several samples of β-hydroxypropionate were decarboxylated as described previously and the residual mixtures left overnight at room temperature. The residue was oxidized with persulphate according to a prescribed procedure (12). The results are summarized in Table III.

TABLE III

Weight of $BaCO_3$ (mg)			
$KMnO_4$ decarboxylation		Persulphate oxidation	
Expected	Obtained	Expected	Obtained
26.5	25.3	53.0	53.6
38.1	36.9	76.2	75.7
19.7	19.8	39.4	38.8

The Schmidt–Phares degradation of the two-carbon fragment left after permanganate decarboxylation of malic acid and of fused, reagent grade sodium acetate gave the results shown in Table IV.

TABLE IV

Weight of $BaCO_3$ (mg)			
—COOH		CH_3NH_2	
Expected	Obtained	Expected	Obtained
Malic acid			
39.9	38.3	39.9	37.1
40.3	39.2	40.3	38.4
Sodium acetate			
62.0	59.0	62.0	57.5
20.4	18.5	20.4	17.1

Sequential Degradation of a Mixture of Formic Acid, Formaldehyde, and β-Hydroxypropionate

For this series of reactions, a mixture of the above three compounds containing known quantities of each was treated in the following manner: Formic acid was converted to CO_2 by oxidation with mercuric oxide in the usual manner (11). The train was fitted with a cold-water condenser to prevent the escape of formaldehyde. After all the CO_2 had been swept into the $Ba(OH)_2$ trap, the flask containing the reaction mixture was removed, wrapped with aluminum foil, and 4 to 5 drops of bromine added. The contents were swirled vigorously, and after 30 minutes, excess bromine removed by aeration, the pH of the solution adjusted to 4.5–5.0, more HgO added, and the evolved CO_2 collected as usual. The solution was then made alkaline (pH about 11–12), $KMnO_4$ reagent added (3 ml), and after 30 to 40 minutes, the solution again acidified and the CO_2 collected as $BaCO_3$. The oxidation mixture containing the two-carbon fragment was left overnight and thence treated with the Schmidt–Phares reagents as described previously. The results are summarized in Table V.

TABLE V

Weight of $BaCO_3$ (mg)							
HCOOH		CH_2O		β-Hydroxypropionate			
Expected	Obtained	Expected	Obtained	C_1	C_2	C_3	Expected
24.1	23.4	30.9	30.0	26.5	20.1	22.5	26.4
34.0	27.5	16.8	17.5	15.1	12.0	12.9	16.0
24.1	22.2	15.7	15.9	16.9	14.2	15.0	16.2

Total Degradation of 2-Deoxy-D-ribose

To a small quantity (16.2 mg) of this sugar in water (2 ml) was added potassium borohydride (about 15 mg) and the mixture left overnight at room temperature. The solution was acidified (H_2SO_4) to about

Can. J. Chem. Downloaded from www.nrcresearchpress.com by 210.87.254.40 on 09/05/12
For personal use only.

pH 5 and sodium metaperiodate (7.5 mg) added. After standing the solution for 20 minutes, sodium arsenite (about 15 mg) was added and the pH again adjusted to about 5. The formic acid formed was oxidized to CO_2 as described. Formaldehyde and β-hydroxypropionaldehyde were simultaneously oxidized to the corresponding acids with bromine. The degradation sequence described previously was thereupon followed. In this manner, several samples of the 2-deoxy pentose were degraded. The results are given in Table VI.

TABLE VI

	Weight of $BaCO_3$ (mg)					
				β-Hydroxypropionate		
	Expected	HCOOH	CH_2O	C_1	C_2	C_3
(16.2 mg)	23.8	20.0	21.0	19.5	18.0	18.8
(13.7 mg)	20.1	19.0	20.2	18.3	17.0	21.0
(10.4 mg)	15.3	14.5	14.7	15.0	13.0	13.9
(8.8 mg)	12.9	12.6	13.2	12.0	10.6	11.2

Degradation of Some 2-Deoxy-D-hexoses

The above procedure was applied to the degradation of 2-deoxy-D-glucose and 2-deoxy-D-galactose. In this case, two molar proportions of formic acid would be produced from the corresponding alditols (C_4 and C_5). The results are summarized in Table VII.

TABLE VII

	Weight of $BaCO_3$ (mg)				
			β-Hydroxypropionate		
Expected	HCOOH*	CH_2O	C_1	C_2	C_3
2-Deoxyglucose					
27.8	53.0	30.0	25.0	21.9	23.8
20.1	38.0	20.2	17.8	17.0	21.0
19.3	39.9	18.1	18.0	18.9	20.2
2-Deoxygalactose					
16.3	30.8	15.0	14.8	13.3	14.2
14.5	29.2	14.1	14.3	12.2	13.9

*Values for this column should be twice those of corresponding values in the first column since both C_4 and C_5 are obtained here.

Formaldehyde Production upon Periodate Oxidation of Polyols

Small quantities of 2-deoxy-D-ribose and 2-deoxy-D-hexoses were reduced with potassium borohydride in the usual manner. The generated polyols were oxidized with periodic acid, and the formaldehyde evolved was periodically estimated by a described procedure (11, 13). The results are summarized in Table VIII.

TABLE VIII

	Formaldehyde produced (mg)				
		Obtained			
	Expected	20 min	40 min	80 min	160 min
2-Deoxyribose					
(6.3 mg)	1.389	1.375	1.379	1.385	1.386
(6.9 mg)	1.522	1.511	1.519	1.519	1.520
2-Deoxyglucose					
(15.2 mg)	2.745	2.741	2.747	2.742	2.750
(17.1 mg)	3.090	3.080	3.091	3.089	3.085
2-Deoxygalactose					
(5.3 mg)	0.957	0.950	0.956	0.953	0.959
(7.1 mg)	1.283	1.272	1.279	1.285	1.279

Can. J. Chem. Downloaded from www.nrcresearchpress.com by 210.87.254.40 on 09/05/12
For personal use only.

ACKNOWLEDGMENT

Financial support from the National Research Council, Canada, is gratefully acknowledged.

REFERENCES

1. E. RACKER. J. Biol. Chem. **196**, 347 (1952).
2. J. A. ROSE and B. S. SCHWEIGERT. J. Biol. Chem. **202**, 635 (1953).
3. G. E. BOXER and C. E. SHANK. J. Biol. Chem. **233**, 535 (1958).
4. F. K. BAGATELLI, E. M. WRIGHT, and H. Z. SABLE. J. Biol. Chem. **234**, 1369 (1959).
5. B. L. HORECKER, G. DOMAGK, and H. H. HIAT. Arch. Biochem. Biophys. **78**, 510 (1958).
6. W. E. PRICE and B. L. HORECKER. J. Biol. Chem. **235**, 1292 (1960).
7. E. M. WRIGHT, H. Z. SABLE, and J. L. BAILY. J. Bacteriol. **81**, 845 (1961).
8. S. S. COHEN, H. D. BARNER, and J. LICHTENSTEIN. J. Biol. Chem. **236**, 1448 (1961).
9. J. K. N. JONES, M. B. PERRY, and R. J. STOODLEY. Can. J. Chem. **40**, 856, 1798 (1962).
10. M. ABDEL-AKHER, J. K. HAMILTON, and F. SMITH. J. Am. Chem. Soc. **73**, 4691 (1951).
11. A. M. UNRAU and F. SMITH. Chem. Ind. (London), 330 (1957).
12. S. ARONOFF. Techniques of radiobiochemistry. The Iowa State College Press, Ames, Iowa, U.S.A. 1956.
13. M. LAMBERT and A. C. NEISH. Can. J. Res. Sect. B, **28**, 83 (1950).

Can. J. Chem. Downloaded from www.nrcresearchpress.com by 210.87.254.40 on 09/05/12
For personal use only.

AZA STEROIDS

II. SYNTHESIS OF 6-AZA STEROIDS—A NOVEL CLASS OF AZAANDROSTANE ANALOGUES

JAMES P. KUTNEY, ROY A. JOHNSON, AND I. VLATTAS
Department of Chemistry, University of British Columbia, Vancouver, British Columbia
Received July 23, 1962

ABSTRACT

A synthesis of N-benzyl-6-azacholestane is described and the generality of the approach is exemplified by the successful synthesis of 17β-hydroxy-N-benzyl-6-azaandrostane. This represents the first synthesis of a 6-aza derivative in the androstane series.

Can. J. Chem. Downloaded from www.nrcresearchpress.com by 210.87.254.40 on 09/05/12
For personal use only.

In recent years there have been numerous investigations concerned with the effect of substituents attached to the normal steroid skeleton on the biological properties of these important substances. These investigations have brought forth the realization that very dramatic alterations in these properties are indeed encountered when such substituents as halogen, particularly fluorine, hydroxyl, and methyl are placed at rather specific positions in the molecule (1–3). These steroidal derivatives still possess the basic steroid skeleton so that the nature of the molecule is not altered to a very significant extent. In this connection, it appeared of interest to us to consider a more substantial alteration in the chemical nature of steroidal substances in order to determine whether any appreciable differences in the biological activity of these molecules are associated with this change. We therefore considered the replacement of one or more carbon atoms of the cyclopentanoperhydrophenanthrene system by a hetero atom.

The introduction of a nitrogen atom into the steroid nucleus has attracted the interests of chemists for some time. However, inspection of the older literature reveals that most of the aza steroids represent analogues in which one of the rings of the skeleton has been expanded from a 6- to a 7-membered ring or in the case of ring D from a 5- to a 6-membered cycle. Very recently some successful syntheses of 4-aza steroids possessing the true steroid skeleton have been reported (4) and some interesting biological properties of these compounds have been described (5).

Our interest in the chemistry and biological properties of aza steroids led us to initiate studies in this area. Our initial considerations were directed toward the synthesis of ring B aza steroids since we felt that the introduction of a nitrogen atom in this ring would allow the retention of a Δ^4-3-keto moiety in ring A—a structural feature present in most of the active steroidal hormones. At the time that our work was initiated, there were no ring B aza steroids known although, since that time, two laboratories have independently reported some work on 6-aza cholestane derivatives (6, 7). Our own work in this area has been briefly described, in part, in a preliminary communication (8). This paper outlines, in detail, a general approach to the synthesis of 6-aza steroids and describes the first synthesis of a 6-aza derivative in the androstane series.

In considering a synthetic approach to this class of compounds, it became apparent that investigations in the cholesterol series would be of distinct advantage since larger quantities of the appropriate starting materials were obviously available. In this regard, a particularly attractive sequence involved the utilization of intermediates in which ring B had been opened since it was clear that the appropriate cyclization of such compounds

would lead to substances possessing the nitrogen atom in the ring system. This type of cyclization had been observed in ring A in the elegant researches of Woodward and co-workers on the total synthesis of steroids (9) and more recently by Uskokovic and Gut (4). The application of this reaction to ring B has been independently completed by Jacobs and Brownfield (6) and by the present authors (8).

Of a number of alternatives which could be used to open ring B, the ozonization of the appropriate α,β-unsaturated ketone system appeared most attractive since the ozonization of such systems had been studied in ring A (10) and, in one instance, in ring B (11).

Oxidative ring opening of 7-oxocholesteryl acetate to 5-oxo-5,7-seco-6-nor-3-cholesten-7-oic acid (I) was initially conducted by ozonolysis in glacial acetic acid followed by oxidative hydrolysis of the intermediate ozonide with aqueous hydrogen peroxide and treatment of the reaction mixture with sodium hydroxide in order to separate the desired acidic components from any neutral products. The initial intermediate, 3β-acetoxy-5-oxo-5,7-seco-6-norcholestan-7-oic acid (VI), readily lost the elements of acetic acid to provide I, a result also obtained by the American workers (6). The conjugated carbonyl chromophore present in I was reflected in its spectral data (226 mμ, 5.97 μ), and other evidence cited below served to establish the chemical structure. Since the ozonization product was an attractive intermediate for the preparation of 6-aza steroids it became necessary to obtain significant yields in this reaction. Under the reaction conditions mentioned above, the yield of I was low (22%) and in spite of numerous experiments wherein such reaction conditions as temperature and quantity of ozone used were varied, we were not able to raise the yield of acidic material. This difficulty was subsequently overcome by conducting the ozonolysis reaction under conditions where the ester was generated directly and is discussed in the later portion of this paper.

The conversion of the unsaturated keto acid to the saturated keto acid (II) was readily accomplished by catalytic hydrogenation and this provided us with the necessary intermediate for investigating the appropriate cyclization reactions to generate 6-aza steroidal analogues. As anticipated, the mild reaction conditions of Uskokovic and Gut (4) wherein anhydrous ammonia at room temperature is utilized were unsuccessful with our keto acid, II. However, when II was treated with refluxing benzylamine for 18 hours (9), an excellent yield of the expected enol lactam (III) was obtained. This material possessed the characteristic infrared absorption and, in particular, had an ultraviolet spectrum typical of these types of lactams (4, 6). The enol lactam was readily reduced to give an excellent yield of the expected product, N-benzyl-6-aza-5ξ-cholestan-7-one (IV), which possessed no absorption in the ultraviolet but still retained the lactam absorption in its infrared spectrum. Finally, reduction of IV with lithium aluminum hydride afforded the desired N-benzyl-6-aza-5ξ-cholestane (V).

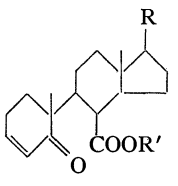

I, R′ = H
VII, R′ = CH_3
IX, R′ = H

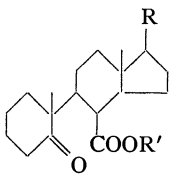

II, R′ = H
VIII, R′ = CH_3
X, R′ = H

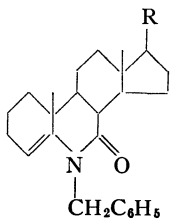

III, XI

Can. J. Chem. Downloaded from www.nrcresearchpress.com by 210.87.254.40 on 09/05/12
For personal use only.

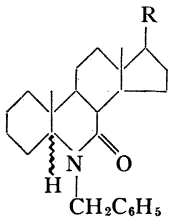

IV, XII

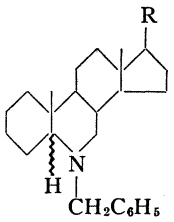

V, XIII
I–VIII, R = C_8H_{17}
IX–XIII, R = OH

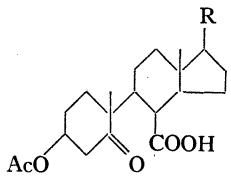

VI

It is pertinent to point out that in contrast to the American workers (6), who have devoted most of their attention to the parent 6-aza cholestane, we have concentrated our efforts on the N-benzyl-6-aza analogues. We feel that the presence of a tertiary nitrogen atom, as in the N-benzyl series provides more suitable intermediates for the reintroduction of an oxygen function at C_3 since undesirable double-bond migrations might be expected when a secondary nitrogen atom is present. Indeed, Jacobs and co-workers (6) have already suggested a migration of the C_4–C_5 double bond in their isolation of 6-aza-5-cholestene, a situation quite unlikely to occur in the N-benzyl series.

We would now like to exemplify the generality of the above approach by presenting the first synthesis of a 6-aza derivative in the androstane series.

The appropriate starting material 3β,17β-diacetoxy-5-androsten-7-one was readily converted to 17β-hydroxy-5-oxo-5,7-seco-6-nor-3-androsten-7-oic acid (IX) by ozonolysis and hydrolysis of the ozonide, as indicated above. As in the cholestane series, the yield of the desired product was quite low when the reaction was conducted under various conditions in acetic acid as solvent. The spectral data were again consistent with the structural assignment. Catalytic reduction of IX proceeded smoothly at room temperature to yield 17β-hydroxy-5-oxo-5,7-seco-6-norandrostan-7-oic acid (X), which, on treatment with refluxing benzylamine, provided an excellent yield of the desired enol lactam (XI). The unsaturated lactam on reduction with Adams catalyst in glacial acetic acid yielded 17β-hydroxy-N-benzyl-6-aza-5ξ-androstan-7-one (XII). As expected, the characteristic absorption of the enol lactam was no longer present in the ultraviolet spectrum of the reduction product but the typical lactam absorption was still evident in the infrared spectrum. This substance was finally reduced with lithium aluminum hydride to the desired 6-aza compound, 17β-hydroxy-N-benzyl-6-aza-5ξ-androstane (XIII).

The success of this last sequence allows entry into a novel class of androstane analogues and it should be of interest to determine whether any significant modifications in biological properties are associated with these compounds. It is clear that since the necessary starting substances are readily available in the progesterone series, the corresponding 6-aza derivatives should also be easily obtained in this series and, in turn, in the adrenocortical hormone series.

It was evident to us that although the above approach was of considerable applicability, it suffered from the fact that the ozonolysis reaction provided the desired product in low yield. Consequently, a considerable amount of experimentation was done to find optimum conditions for this reaction. Although we have not been able to obtain the corresponding acidic products in substantially higher yields, we have been able to overcome the difficulty by preparing the neutral esters directly from the ozonization. It appeared to us that it

Can. J. Chem. Downloaded from www.nrcresearchpress.com by 210.87.254.40 on 09/05/12
For personal use only.

may be of advantage to conduct the ozonolysis in non-acidic solvents and in particular in the presence of an alcohol so that the direct conversion of the ozonide to an ester would be possible. Indeed when we carried out this reaction in a solvent mixture of methylene chloride – methanol at −78°, we obtained the unsaturated keto ester (VII) from the neutral portion of the reaction product. In addition, the acidic portion contained a significant amount of unsaturated keto acid (I) so that the actual yield of starting material has been substantially increased.

It became necessary to confirm our suspicions that the unsaturated keto ester (VII) could be used effectively as a starting material. For this reason, we subjected VII to catalytic reduction and obtained the expected keto ester (VIII) as a beautifully crystalline substance. The structure of VIII was finally confirmed when the reduction product was treated with benzylamine, and the enol lactam which resulted was shown to be identical in every respect with N-benzyl-6-aza-4-cholesten-7-one (III). In this manner, the overall yield of the enol lactam from 7-oxocholesteryl acetate was raised to 40%. This marked improvement now makes the above approach a very attractive one indeed. It was not necessary to extend our studies to the androstane series since at the time that our investigations in the cholesterol series were being conducted Atwater, in his paper on 6-oxa-androstane derivatives (12), indicated that the analogous ozonolysis reaction provided the corresponding B-nor seco ester in yields up to 73%. It is now clear that the extension to the androstane series is valid.

EXPERIMENTAL

All melting points were determined on a Fischer–Johns apparatus and are uncorrected. The ultraviolet spectra were recorded in 95% ethanol on a Cary 14 recording spectrophotometer and the rotations were taken in 1% chloroform solutions. The n.m.r. spectra were taken at 60 Mc on a Varian A60 instrument. The values are given in the Tiers τ scale with the signal of tetramethylsilane, which was used as the internal standard, set at 10.0 τ units. Analyses were performed by A. Bernhardt, Mulheim (Ruhr), Germany, and by Mrs. Aldridge, University of British Columbia.

5-Oxo-5,7-seco-6-nor-3-cholesten-7-oic Acid (I)

Solutions of 7-oxocholesteryl acetate (25.0 g) in glacial acetic acid (100 ml) were ozonized in 5-g portions at 25° over a period of 20 minutes at a rate of 0.1 mole per hour. The solution attained a bright yellow color during the course of the ozonization but this color slowly disappeared when the ozonide was treated with 30% hydrogen peroxide (19 ml) and water (50 ml, for each 5-g portion). After the solution had been allowed to stand for 15 hours at room temperature, the solvent was removed under reduced pressure and the residue was taken up in ether. The ether solution was washed with water and then extracted with 5% aqueous sodium hydroxide to remove all acidic components. The basic extract was acidified with dilute hydrochloric acid and this acid layer was extracted with ether. The ether extract was dried over anhydrous magnesium sulphate, the solvent was evaporated to yield 20.3 g of a viscous oil. Chromatography of this oil on silica gel (500 g) gave the keto acid (I) as an oil when elution with chloroform was carried out. Crystallization from hexane gave 4.86 g (22%) of virtually pure, crystalline keto acid, m.p. 179–183°. Three recrystallizations from hexane gave analytically pure acid (I) as colorless needles, m.p. 183–184°; $[\alpha]_D$+79°; λ_{max} 226 mμ (log ϵ 3.93); infrared in chloroform: 5.86 μ, 5.97 μ; lit. (6). Found: C, 77.82; H, 10.46; O, 12.09; neutralization equivalent, 394; mol. wt. (Rast), 402. Calc. for $C_{26}H_{42}O_3$: C, 77.56; H, 10.51; O, 11.92; mol. wt., 402.

When the ozonization was carried out as above with the exception that the acidic materials were extracted from the reaction mixture with dilute potassium carbonate instead of sodium hydroxide, another acidic oil was obtained from the carbonate layer after acidification and ether extraction. This oil (3.51 g from 5.0 g of starting material) on chromatography on silica gel and elution with chloroform yielded a fraction (3.5 g) which crystallized from ether – petroleum ether, m.p. 171–177°. Although not pure, this material is beyond doubt predominantly 3β-acetoxy-5-oxo-5,6-seco-6-norcholestan-7-oic acid (VI) as evidenced by no absorption in the ultraviolet and its infrared spectrum in (KBr): 5.75 μ, 5.78 μ, 5.83 μ, 5.88 μ, 8.03μ.

This was further confirmed when the above material was converted, in essentially quantitative yield, to the unsaturated keto-acid (I) by merely shaking an ether solution of this substance with 5% aqueous sodium hydroxide, acidifying the alkaline layer, and extracting again with ether.

5-Oxo-5,7-seco-6-norcholestan-7-oic Acid (II)

The unsaturated keto-acid (I) (0.398 g) was reduced over 10% palladium on charcoal (0.4 g) in ethanol (30 ml) at room temperature and atmospheric pressure. The hydrogen uptake was virtually complete in 15

Can. J. Chem. Downloaded from www.nrcresearchpress.com by 210.87.254.40 on 09/05/12
For personal use only.

minutes, after which time the catalyst was filtered off and the solvent removed under reduced pressure. The remaining white solid crystallized from hexane yielding 0.237 g of the saturated keto-acid (II), m.p. 188–193°. Three additional recrystallizations from hexane gave an analytical sample, m.p. 192–194°; $[\alpha]_D$+91°; infrared in KBr: 5.83 μ, 5.89 μ; lit. (6). Found: C, 76.80; H, 10.84; O, 12.11. Calc. for $C_{26}H_{44}O_3$: C, 77.17; H, 10.98; O, 11.86.

N-Benzyl-6-aza-4-cholesten-7-one (III)

The saturated keto-acid (II) (4.0 g) was dissolved in benzylamine (19 ml) and refluxed for 18 hours in a nitrogen atmosphere. The cooled yellow reaction mixture was taken up in ether and extracted with aqueous hydrochloric acid until the extract was acidic to litmus. The ether layer was then washed once with 5% aqueous sodium hydroxide and once with a saturated salt solution and then dried over anhydrous magnesium sulphate. Evaporation of the solvent, after removal of the drying agent by filtration, yielded a light yellow oil. Crystallization from methanol afforded 3.93 g (84%) of colorless crystals, m.p. 135–140°. Three recrystallizations from methanol gave pure N-benzyl-6-aza-4-cholesten-7-one (III) as long, flat crystals, m.p. 139–141°; $[\alpha]_D$ +93°; λ_{max} 237 mμ (log ϵ 4.05); infrared in KBr: 6.10 μ, 6.02 μ; lit. (6). Found: C, 82.92; H, 10.33; N, 3.01; O, 3.48. Calc. for $C_{33}H_{49}NO$: C, 83.31; H, 10.38; N, 2.94; O, 3.36.

N-Benzyl-6-aza-5ξ-cholestan-7-one (IV)

The enol lactam (III) (0.50 g) was hydrogenated in acetic acid (40 ml) over 0.05 g of platinum oxide at room temperature and atmospheric pressure. The uptake of hydrogen stopped after 1 hour, and the catalyst was filtered off. The solvent was removed *in vacuo* and the remaining oil was placed in a vacuum desiccator and allowed to stand, over solid potassium hydroxide, for several hours. The oil (0.487 g, 90%) crystallized from ether–methanol and melted at 141–145°. Three recrystallizations from ether–methanol provided an analytical sample of the lactam (IV), m.p. 143–145°; $[\alpha]_D$+63°; infrared in Nujol: 6.08 μ. Found: C, 83.19; H, 10.53; N, 3.19; O, 3.50. Calc. for $C_{33}H_{51}NO$: C, 82.96; H, 10.76; N, 2.93; O, 3.35.

N-Benzyl-6-aza-5ξ-cholestane (V)

N-Benzyl-6-aza-5ξ-cholestan-7-one (0.50 g) was dissolved in anhydrous ether (100 ml) and refluxed for 24 hours with lithium aluminum hydride (0.6 g), which was initially placed in a Soxhlet extractor and gradually brought into the vessel by the refluxing ether. The excess hydride was decomposed by cautious addition of moist ether and water, followed by refluxing for 0.5 hours. The inorganic solids were filtered off and the ether solution was dried over anhydrous magnesium sulphate. Removal of the solvent yielded 0.423 g (87%) of a light yellow oil which crystallized from ether–methanol (0.410 g), m.p. 65–68°. Two further recrystallizations from ether–methanol yielded N-benzyl-6-aza-5ξ-cholestane, m.p. 68–69°; $[\alpha]_D$+71°. Found: C, 85.42; H, 11.27; N, 3.30. Calc. for $C_{33}H_{53}N$: C, 85.46; H, 11.52; N, 3.02.

17β-Hydroxy-5-oxo-5,7-seco-6-nor-3-androsten-7-oic Acid (IX)

A solution of 3β,17β-diacetoxy-5-androsten-7-one (3.42 g) in glacial acetic acid (125 ml) was treated with ozone for 15 minutes at room temperature at a rate of 0.1 mole per hour. The resulting yellow solution was treated with dilute hydrogen peroxide (3 ml) and water (15 ml) after 20 minutes and then allowed to stand at room temperature for 20 hours. During this time, the solution lost its yellow color. The excess acetic acid was then removed *in vacuo* and the oily residue was taken up in ether. The ether solution was washed with 5% aqueous sodium hydroxide and water to remove acidic components. The alkaline extracts were made acidic by the addition of dilute hydrochloric acid and this acidic material was then extracted with ether. The ether extract was dried over anhydrous magnesium sulphate, the drying agent removed by filtration, and the solvent evaporated to yield 1.6 g of a glassy acidic material. This material was chromatographed on silica gel (100 g) and elution with chloroform – 2½% methanol yielded a glassy material (0.96 g, 36%) which crystallized from ether – petroleum ether (0.92 g), m.p. 142–148°. Two further recrystallizations from ether – petroleum ether gave shiny crystals which appeared to have a double melting point, 145–150° and 195–200°, probably due to strong solvation. However, after the crystals had dried at 100°/0.1 mm for several hours, the melting point was greatly improved and a pure sample melted at 203–204°; $[\alpha]_D$+88°; λ_{max} 227 mμ (log ϵ 3.98); infrared in KBr: 2.94 μ, 5.81 μ, 6.04 μ. Found: C, 70.65; H, 8.52; O, 21.14. Calc. for $C_{18}H_{26}O_4$: C, 70.56; H, 8.55; O, 20.89.

17β-Hydroxy-5-oxo-5,7-seco-6-norandrostan-7-oic Acid (X)

A solution of the unsaturated keto-acid (IX) (0.896 g) in 95% ethanol (50 ml) was hydrogenated over 0.54 g of 10% palladium on charcoal at room temperature and atmospheric pressure. After the uptake of hydrogen was complete (20 minutes), the catalyst was filtered off and the solvent removed *in vacuo* to yield an oily product (0.75 g). Chromatography of this oil on silica gel (50 g) gave the product as an oil by elution with chloroform – 2½% methanol. This oil (0.70 g) slowly crystallized when it was left standing and after two recrystallizations from hexane gave pure 17β-hydroxy-5-oxo-5,7-seco-6-norandrostan-7-oic acid (0.65 g), m.p. 228–229; $[\alpha]_D$+96°; infrared in KBr: 2.90 μ, 5.81 μ, 5.93 μ. Found: C, 69.67; H, 9.01; O, 21.23. Calc. for $C_{18}H_{28}O_4$: C, 70.09; H, 9.15; O, 20.76.

17β-Hydroxy-N-benzyl-6-aza-4-androsten-7-one (XI)

A solution of the saturated keto-acid (X) (0.553 g) in benzylamine (10 ml) was refluxed gently for 15

Can. J. Chem. Downloaded from www.nrcresearchpress.com by 210.87.254.40 on 09/05/12
For personal use only.

hours in a nitrogen atmosphere. The cooled, yellow solution was taken up in ether and washed with dilute hydrochloric acid until the aqueous layer was acidic. The ether solution was then washed once with 5% aqueous sodium hydroxide followed by water and finally dried over anhydrous magnesium sulphate. The drying agent was filtered off and the ether evaporated to yield a light yellow oil (0.56 g). Chromatography of this oil on silica gel (50 g) gave 0.46 g (68%) of an oil when the column was eluted with benzene–chloroform (1:1). This oil crystallized from ether–hexane as colorless needles, m.p. 105–109°. Three further recrystallizations gave an analytical sample, m.p. 109–110°; $[\alpha]_D$+102; λ_{max} 237 mμ (log ϵ 4.02); infrared in KBr: 6.11 μ, 6.02 μ. Found: C, 79.49; H, 8.82; N, 3.72; O, 8.30. Calc. for $C_{25}H_{33}NO_2$: C, 79.11; H, 8.76; N, 3.69; O, 8.43.

17β-Hydroxy-N-benzyl-6-aza-5ξ-androstan-7-one (XII)

A solution of the enol lactam (0.185 g) in glacial acetic acid (30 ml) was hydrogenated over platinum oxide (0.050 g) at room temperature and atmospheric pressure for 2 hours. The catalyst was filtered off and the acetic acid was removed *in vacuo* to yield 0.168 g (90%) of an oil. The oil was chromatographed on silica gel (19 g) and the oily product was eluted with benzene–chloroform (1:1). This oil crystallized upon standing and was recrystallized from acetone – petroleum ether as colorless needles, m.p. 134–136°; $[\alpha]_D$−1°; infrared in KBr: 2.93 μ, 6.13 μ. Found: C, 78.73; H, 9.61; N, 3.90; O, 8.66; active H, 0.27. Calc. for $C_{25}H_{35}NO_2$: C, 78.69; H, 9.25; N, 3.67; O, 8.38; active H, 0.264.

17β-Hydroxy-N-benzyl-6-aza-5ξ-androstane (XIII)

The saturated lactam (XII) (0.90 g) was dissolved in anhydrous ether (100 ml) and refluxed for 24 hours with lithium aluminum hydride (1.0 g), which was initially placed in a Soxhlet extractor and gradually brought into the reaction vessel by the refluxing ether. The reaction mixture was then allowed to stand for a further 56 hours at room temperature. The excess hydride was decomposed by the dropwise addition of an ether–acetone solution. Water (1 ml) was then added cautiously and the reaction mixture was warmed on a steam bath for 0.5 hour. The inorganic salts were filtered off and washed with ether and the combined ether solutions were dried over anhydrous magnesium sulphate. Filtration and evaporation of the solvent gave a colorless oil which slowly crystallized. The yield of solid crystalline product was 0.843 g (97%). Recrystallization of the solid from petroleum ether gave needles, melting point 109–111°, which, after two more recrystallizations from the same solvent, provided a pure sample of the aza steroid, m.p. 111–112°; $[\alpha]_D$ +67°. Found: C, 81.57; H, 10.34; N, 4.14; O, 4.51. Calc. for $C_{25}H_{37}NO$: C, 81.69; H, 10.15; N, 3.81; O, 4.35.

Methyl 5-Oxo-5,7-seco-6-nor-3-cholesten-7-oate (VII)

A solution of 7-oxocholesteryl acetate (5.0 g) in dichloromethane (75 ml) and absolute methanol (25 ml) was ozonized at −78° until the solution had attained a blue color (about 20 minutes at a rate of 0.1 mole per hour). The solution was allowed to warm to room temperature, 30% aqueous hydrogen peroxide (0.7 ml) and water (1.7 ml) were added, and the mixture was then allowed to stand at room temperature for 16 hours. The organic phase was separated and the aqueous phase was extracted several times with dichloromethane. The organic extracts were combined, washed with water, and then dried over anhydrous magnesium sulphate. Evaporation of the solvent after removal of the drying agent by filtration provided a viscous clear oil. This oil was taken up in ether and the ethereal solution was washed with 5% aqueous sodium hydroxide to remove any acidic materials. The workup of this aqueous layer is given below.

The ether layer was washed with water and dried over anhydrous magnesium sulphate, and the solvent was removed to provide a viscous, neutral oil (3.3 g). This neutral oil was taken up in dioxane, treated with 5% aqueous sodium hydroxide (30 ml), and the whole mixture was stirred for 30 minutes. This mixture was then treated with 1.5 liters of water and extracted exhaustively with ether in a continuous extraction apparatus. The resulting ether extract was washed with water, and dried over anhydrous magnesium sulphate. The solvent was removed to yield a viscous oil (2.25 g). This oil was taken up in benzene and chromatographed on silica gel (80 g). The desired unsaturated keto ester was eluted with benzene as a clear viscous oil (1.76 g) and, in spite of numerous attempts, it resisted all efforts to obtain it in crystalline form. Infrared in CCl_4: 5.98 μ, 5.81 μ; λ_{max} 227 mμ (log ϵ 3.84); $[\alpha]_D$ +83; n.m.r. signals (CCl_4): sharp signal at

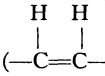

6.5 τ (−$COOCH_3$), multiplets at 4.25 τ and 3.8 τ (—C=C—C=O). Found: C, 77.52; H, 10.31. Calc. for $C_{27}H_{44}O_3$: C, 77.83; H, 10.65.

The aqueous alkaline layer from the potassium hydroxide in dioxane treatment was acidified with hydrochloric acid and the resulting mixture was extracted with ether. The ethereal extract was washed with water, then dried over anhydrous magnesium sulphate. Removal of the solvent yielded an acidic material (0.7 g).

This acidic material (0.7 g) was reduced over 10% palladium on charcoal (0.4 g) in ethanol at room temperature and atmospheric pressure. The catalyst was filtered off and the solvent was removed under reduced pressure. This crude reduction product was chromatographed on silica gel (16 g) and a solid material (200 mg) which was obtained upon elution with benzene–chloroform turned out to be 5-oxo-5,7-seco-6-norcholestan-7-oic acid (II). This was identified by infrared comparison and mixed melting point with an authentic sample.

The original aqueous alkaline extract of the product resulting directly from the ozonization was acidified with hydrochloric acid and this acidic mixture was then extracted with ether. The ether extract was washed

Can. J. Chem. Downloaded from www.nrcresearchpress.com by 210.87.254.40 on 09/05/12
For personal use only.

with water, and dried over anhydrous magnesium sulphate. Removal of the solvent yielded an acidic material (1.94 g).

Methyl 5-Oxo-5,7-seco-6-norcholestan-7-oate (VIII)

The unsaturated keto ester, VII (1.65 g), was hydrogenated over 10% palladium on charcoal (1 g) in ethanol at room temperature and atmospheric pressure. The catalyst was removed by filtration and the solvent evaporated to yield a white solid. This solid was taken up in benzene and chromatographed on silica gel (60 g). Elution with benzene provided a white crystalline material (1.5 g) which on several recrystallizations from benzene yielded an analytical sample, m.p. 81–83°; $[\alpha]_D^{28}$ +97°; infrared in KBr: 5.90 μ, 5.80 μ; lit. (6). Found: C, 77.30; H, 10.96. Calc. for $C_{27}H_{46}O_3$: C, 77.46; H, 11.08.

N-Benzyl-6-aza-4-cholesten-7-one from VIII

The saturated keto ester, VIII (1 g), was refluxed in benzylamine (2.5 ml) for 20 hours in a nitrogen atmosphere. The resulting reaction mixture was taken up in ether and the ethereal solution was washed with dilute hydrochloric acid to remove any benzylamine. This solution was then washed with 5% aqueous sodium hydroxide, water, and finally dried over anhydrous magnesium sulphate. Removal of the solvent gave a white solid (1.1 g) which, upon recrystallization from ethanol, provided a pure sample of the enol lactam, III (0.95 g).

ACKNOWLEDGMENT

The authors are very grateful to Professor Jacobs and Dr. Brownfield for providing them with several comparison samples. Financial aid from the National Research Council of Canada and from the National Cancer Institute of the National Institutes of Health, U.S. Public Health Service, grant No. CY-5037, is very gratefully acknowledged.

REFERENCES

1. J. FRIED and A. BORMAN. Vitamins Hormones, **16**, 303 (1958).
2. V. A. DRILL and B. RIEGEL. Recent Progr. Hormone Res. **14**, 29 (1958).
3. R. HIRSCHMANN, G. A. BAILEY, R. WALKER, and J. M. CHEMERDA. J. Am. Chem. Soc. **81**, 2822 (1959).
4. M. USKOKOVIC and M. GUT. Helv. Chim. Acta, **42**, 2258 (1959). See also reference 6 for numerous related references cited therein.
5. R. I. DORFMAN, M. USKOKOVIC, and M. GUT. 137th Meeting of the American Chemical Society. 1960. p. 19 N.
6. T. L. JACOBS and R. B. BROWNFIELD. J. Am. Chem. Soc. **82**, 4033 (1960).
7. H. LETTRE and L. KNOF. Ber. **93**, 2860 (1960).
8. J. P. KUTNEY and R. A. JOHNSON. Chem. Ind. (London), 1713 (1961).
9. R. B. WOODWARD, F. SONDHEIMER, D. TAUB, K. HEUSLER, and W. M. MCLAMORE. J. Am. Chem. Soc. **74**, 4223 (1952).
10. C. C. BOLT. Rec. Trav. Chim. **57**, 906 (1938). R. B. TURNER. J. Am. Chem. Soc. **69**, 726 (1947); **72**, 579 (1950).
11. W. G. DAUBEN and K. H. TAKEMURA. J. Am. Chem. Soc. **75**, 6302 (1953).
12. N. W. ATWATER. J. Am. Chem. Soc. **83**, 3071 (1961).

Can. J. Chem. Downloaded from www.nrcresearchpress.com by 210.87.254.40 on 09/05/12
For personal use only.

REARRANGEMENT STUDIES WITH C^{14}

XIV. THE REACTION OF 2-*p*-ANISYLETHANOL-1-C^{14} WITH THIONYL CHLORIDE[1]

C. C. LEE, DONNA NEWMAN, AND D. P. THORNHILL[2]

Department of Chemistry, University of Saskatchewan, Saskatoon, Saskatchewan

Received October 12, 1962

ABSTRACT

Reaction between 2-*p*-anisylethanol-1-C^{14} and thionyl chloride was carried out with pyridine, *n*-hexane, toluene, dioxane, or excess thionyl chloride as solvent. The 2-*p*-anisylethyl chloride obtained showed rearrangement of the C^{14} label from the C-1 to C-2 positions ranging from about 0.5% for the reaction in pyridine to about 46% for the reaction in excess thionyl chloride. The results can be explained on the basis of varying degrees of involvement of the ethylene-*p*-methoxyphenonium chlorosulphite ion pair, thus supporting the suggestion that thermal decomposition of alkyl chlorosulphites to give chlorides may be considerably ionic in character.

Can. J. Chem. Downloaded from www.nrcresearchpress.com by 210.87.254.42 on 09/05/12
For personal use only.

INTRODUCTION

It is generally agreed that the reaction of thionyl chloride with an aliphatic alcohol involves the formation of an alkyl chlorosulphite which is thermally decomposed to give the alkyl chloride (1). Since the suggestion that the decomposition of the chlorosulphite has considerable ionic character (2), and that the S_Ni reaction is quite similar to the S_N1 reaction in that both involve ion pairs (3), a number of studies on the ionic nature of this reaction have been reported (1, 4–8). Among these were investigations on isotope position rearrangements in the thermal decomposition, in a number of solvents, of allyl-1-C^{14} chlorosulphite (4) and of 2-butyl-1-C^{14} chlorosulphite (8). The present paper reports the extents of rearrangement of the C^{14} label, and discusses the mechanistic implications of these rearrangements, in the reaction between 2-*p*-anisylethanol-1-C^{14} and thionyl chloride, with pyridine, *n*-hexane, toluene, dioxane, or excess thionyl chloride as solvent.

RESULTS AND DISCUSSION

2-*p*-Anisylethanol-1-C^{14} (I) has been synthesized by Jenny and Winstein (9) from reaction of *p*-methoxybenzyl chloride with sodium cyanide-C^{14}, followed by hydrolysis and treatment of the resulting *p*-anisylacetic acid-1-C^{14} (II) with lithium aluminum hydride. In the present work, II was obtained from reaction of carbon dioxide-C^{14} with *p*-methoxybenzylmagnesium chloride. This route to II is less time consuming and permits the use of carbonate instead of the more costly cyanide as the source of C^{14}. The preparation of the Grignard reagent requires special conditions of high dilution and use of amalgamated magnesium (10, 11); otherwise, the coupling product, *p*,*p*′-dimethoxydibenzyl, will result. The reduction of II to I was effected with lithium aluminum hydride (9). That all the C^{14}-label was located in the C-1 position of I was shown by the oxidation of I to essentially inactive *p*-anisic acid.

Reaction of I with thionyl chloride was carried out in pyridine, *n*-hexane, toluene, dioxane, or excess thionyl chloride as solvent. 2-*p*-Anisylethyl-*x*-C^{14} chloride (III) was obtained in yields ranging from 23 to 67% for the different runs in the different solvents. From the reaction carried out in *n*-hexane, besides the chloride III, some di-2-*p*-anisylethyl sulphite (IV) was recovered. Similarly, when the reaction of I with thionyl chloride was

[1]*For paper XIII, see reference 8.*

[2]*Commonwealth Scholar from the Federation of Rhodesia and Nyasaland, 1961–1963.*

tried in diethyl ether, with or without the presence of pyridine, the only product isolated was sulphite IV. It is known that reaction of an excess of alcohol with thionyl chloride in ether and pyridine will give dialkyl sulphite (5). In the current experiments, the general procedure involves allowing the alcohol and a small excess of thionyl chloride to stand at room temperature overnight followed by several hours of refluxing. In the cases where IV was isolated as a product, namely in reactions with *n*-hexane or with ether as solvent, possibly the decomposition of the chlorosulphite to chloride is quite slow because of the relatively low temperature of reflux and because of the nonionizing nature of these solvents. Consequently, if the conversion of alcohol I to chlorosulphite is not 100% complete, the chlorosulphite formed could react with the remaining alcohol to give sulphite IV rather than decompose to give chloride III.

For the degradation of III, it was first converted, through the Grignard reagent and reaction with carbon dioxide, to a solid derivative, 3-*p*-anisylpropanoic acid-*x*-C^{14} (V). Oxidation of V with alkaline permanganate yielded *p*-anisic acid (VI) whose radioactivity would correspond to the amount of C^{14} in the C-2 position of III. The activity of VI, expressed as a percentage of the activity of V, is, therefore, a measure of the percentage rearrangement of the C^{14} label from the C-1 to C-2 positions in the reaction of 2-*p*-anisylethanol-1-C^{14} (I) with thionyl chloride to give 2-*p*-anisylethyl-*x*-C^{14} chloride (III). The results from degradation of III, obtained from reactions in the various solvents, are summarized in Table I.

TABLE I

Rearrangement in the reaction between 2-*p*-anisylethanol-1-C^{14} (I) and thionyl chloride

Reaction solvent	Specific activity* of *p*-anisic acid (c.p.m./mmole)		% rearrangement†	
	Run 1	Run 2	Run 1	Run 2
(Oxidation of I)	60		0.03	
Pyridine	1,105	950	0.5	0.4
n-Hexane	8,764	9,722	3.8	4.2
Toluene	36,730	33,560	16.0	14.6
Dioxane	103,100	101,900	44.8	44.3
Thionyl chloride	107,700	105,000	46.8	45.6

*Radioactivity was measured in a liquid scintillation counter. Each sample, weighing about 10 mg, was dissolved in 20 ml of toluene containing 4 g/l. of DPO and 100 mg/l. of POPOP and then counted for a sufficient length of time to give at least 10,000 counts. Under these conditions, use of toluene-C^{14} as internal standard showed a slight degree (about 1%) of quenching for both *p*-anisic acid and 3-*p*-anisylpropanoic acid, which would not significantly alter the calculated % rearrangement.

†All reactions were carried out using the same stock of alcohol I whose specific activity, assayed as 3-*p*-anisylpropanoic acid (V), was 230,200 c.p.m./mmole. Individual samples of V derived from various runs agree with this value within ±1%. Therefore, % rearrangement = (specific activity of *p*-anisic acid/230,200) × 100.

The rearrangements recorded in Table I may be best accommodated by assuming the involvement of ion pair VII, or its equivalent, in the decomposition of 2-*p*-anisylethyl-1-C^{14} chlorosulphite. The structure of the carbonium ion moiety of VII, the ethylene-*p*-methoxyphenonium ion, is the same as that suggested by Jenny and Winstein (9) as intermediate in the solvolysis of 2-*p*-anisylethyl-1-C^{14} *p*-toluenesulphonate. The collapse of VII to give final products (3) would result in the formation of 2-*p*-anisylethyl-1-C^{14} chloride and 2-*p*-anisylethyl-2-C^{14} chloride.

For the reaction in pyridine, the extent of rearrangement observed is very small. This is in agreement with expectation that the process is almost completely S_N2 in character

Can. J. Chem. Downloaded from www.nrcresearchpress.com by 210.87.254.42 on 09/05/12
For personal use only.

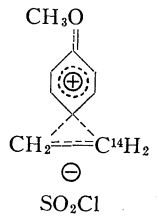

VII

(12, 13). Exclusive S_N2 reaction would lead to no rearrangement as was noted in the decomposition of 2-butyl-1-C^{14} chlorosulphite in pyridine (8). For the present system, the 0.4–0.5% rearrangement observed in pyridine is beyond experimental error, indicating some contribution from VII even in pyridine. Mixture of chlorides resulting from rearrangement has been reported for the reaction between α- or γ-methylallyl alcohol and thionyl chloride in pyridine; the findings were explained on the basis of the S_N2 mechanism along with some contribution from the S_Ni ion-pair mechanism (5).

From the reactions of I with thionyl chloride in solvents other than pyridine (Table I), the extents of rearrangement appear to follow the capability of the medium in supporting ionization. The least ionizing solvent, *n*-hexane, gave the least rearrangement, while reaction in excess thionyl chloride, the most ionizing solvent employed, resulted in the largest observed rearrangement. These effects of changes in medium on the extent of rearrangement further support the suggestion that the observed results arise from intervention of ionic intermediates such as VII, and not from an S_Ni' mechanism (equation [1]) which maintains a large degree of covalent character (4–6).

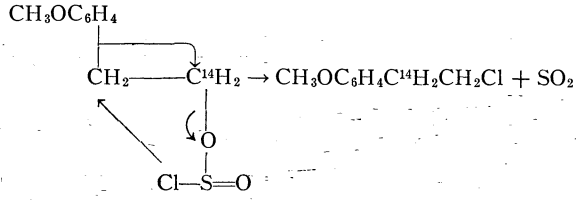

[1]

It may be worth noting that of the two hydrocarbon solvents studied, reaction in toluene resulted in more rearrangement than reaction in *n*-hexane (Table I). In line with the idea that more rearrangement would result from reaction in a medium that can better support ion-pair formation, it may be pointed out that toluene has a higher dielectric constant than *n*-hexane (14) and that 2-butyl chlorosulphite has been found to decompose faster in toluene than in an aliphatic hydrocarbon such as isooctane (1).

Decomposition of chlorosulphites in dioxane is of special interest. Boozer and Lewis (1) have reported that this solvent is particularly effective in promoting retention of configuration in the decomposition of a number of optically active *s*-alkyl chlorosulphites. It was suggested that dioxane may solvate the carbonium ion as the chlorosulphite ion is displaced. A subsequent displacement of the dioxane by chloride ion would lead to overall retention (1). Relatively low degrees of rearrangement, attributable to the special solvent effect of dioxane, were reported for the decomposition in dioxane of allyl-1-C^{14} chlorosulphite (4) and of 2-butyl-1-C^{14} chlorosulphite (8). In the case of the 2-butyl-1-C^{14} system, the relative inability of neighboring hydrogen to participate and displace dioxane from the solvated cation was suggested as a possible explanation for the relatively small

Can. J. Chem. Downloaded from www.nrcresearchpress.com by 210.87.254.42 on 09/05/12
For personal use only.

rearrangement observed (8). In the 2-*p*-anisylethyl-1-C^{14} system, the rearrangement obtained for reaction in dioxane is almost as large as that found in the reaction in excess thionyl chloride (Table I). This finding is likely due to the fact that the bridged carbonium ion of ion pair VII is of considerable stability (9). One might visualize the neighboring *p*-anisyl group as much more effective than the neighboring hydrogen of the 2-butyl system in displacing dioxane from solvating a carbonium ion with classical structure. Participation of the *p*-anisyl group may be regarded as well developed before solvation and dioxane will solvate the cation with nonclassical structure as in VII, giving rise to a large degree of isotope position rearrangement in the final product. In line with these views are the results reported by Cram (3). For example, with optically active *threo*-isomer of 3-phenyl-2-butanol, reaction with thionyl chloride in dioxane and in excess thionyl chloride gave, respectively, 95% and 97% racemization, indicating a large degree of phenyl participation when the reaction was carried out with either dioxane or excess thionyl chloride as solvent.

EXPERIMENTAL

p-Anisylacetic Acid-1-C^{14} (II)

Amalgamated magnesium was prepared by stirring for a few minutes 10 g of magnesium turning in 100 ml of water containing about 200 mg of mercuric chloride. Upon this treatment, the metal lost its luster and assumed a dull grey appearance. It was rinsed with water until the washing was clear, and then rinsed with acetone and dried in a vacuum desiccator. The Grignard reagent was prepared, under nitrogen, by dropwise addition of a solution of 1.0 ml (7.4 mmoles) of *p*-methoxybenzyl chloride in 30 ml of anhydrous ether, over a period of 30 minutes, to a vigorously stirred mixture of 2.0 g of amalgamated magnesium in 20 ml of anhydrous ether. After refluxing for an additional 30 minutes, the Grignard solution was decanted, under nitrogen, from the excess magnesium and placed in a vacuum line for carbonation. Each run was carried out with carbon dioxide-C^{14} generated from roasting a mixture of barium carbonate-C^{14} (500–600 mg, 2.8–3.0 mmoles) and lead chloride (1.0–1.2 g). Overall yields of *p*-anisylacetic acid were of the order of 75–80% based on the barium carbonate.

Under conditions of higher reactant concentration and using magnesium powder, the chief product was *p,p'*-dimethoxydibenzyl. A sample trial is given below.

Under nitrogen, a solution of 5.0 ml (37 mmoles) of *p*-methoxybenzyl chloride in 100 ml of anhydrous ether was added dropwise, over a period of 45 minutes, to a stirred mixture of 2.7 g (111 mmoles) of magnesium powder in 40 ml of anhydrous ether. After refluxing for an additional 30 minutes, the mixture was treated with excess carbon dioxide, acidified, and extracted with ether. Only 0.5 g (8%) of acid II was obtained from the sodium hydroxide washing of the ether extract. Removal of most of the solvent from the sodium hydroxide washed ether solution resulted in the recovery of 3.1 g (69%) of crystalline product which recrystallized from ethanol as colorless needles, m.p. 127–128° C (lit. (15) m.p. of *p,p'*-dimethoxydibenzyl, 126–127° C).

2-p-Anisylethanol-1-C^{14} (I)

This labelled alcohol was prepared by the treatment of *p*-anisylacetic acid-1-C^{14} with lithium aluminum hydride in anhydrous ether according to the method of Jenny and Winstein (9).

Reaction of I with Thionyl Chloride

The reaction was carried out with pyridine, *n*-hexane, toluene, dioxane, or excess thionyl chloride as solvent. The general procedure adopted is described below, with minor modifications in certain cases as subsequently indicated.

2-*p*-Anisylethanol-1-C^{14} (I) (3.0 g, 19.7 mmoles) was added dropwise (10 minutes) at room temperature to a stirred solution of 3.0 ml (26 mmoles) of thionyl chloride in 50 ml of solvent (or to 25 ml of thionyl chloride only where this reagent also served as solvent). The mixture was allowed to stand at room temperature overnight, refluxed for 3 hours, poured onto ice, and then extracted with ether. The extract was washed with water, sodium bicarbonate solution, and again with water. After drying over anhydrous sodium sulphate, the ether was removed and the residue distilled under reduced pressure. The 2-*p*-anisylethyl-*x*-C^{14} chloride (III) was recovered at 86–90° at 1 mm (lit. (16) b.p. 129.5–131° C at 10 mm).

Anal. Calc. for $C_9H_{11}OCl$: C, 63.34; H, 6.50; Cl, 20.78. Found: C, 63.15; H, 6.68; Cl, 20.32 Identification of individual samples of III from the different runs was made by comparison of its infrared absorption spectrum with that of an analytically pure specimen as well as by its conversion to 3-*p*-anisylpropanoic acid.

The above procedure applies to reactions in *n*-hexane, toluene, and dioxane. For the reaction in pyridine, the mixture was worked up after standing at room temperature overnight without refluxing. The material was poured onto ice and hydrochloric acid instead of ice alone before extraction with ether. For the reaction

Can. J. Chem. Downloaded from www.nrcresearchpress.com by 210.87.254.42 on 09/05/12
For personal use only.

in excess thionyl chloride, the reaction mixture was allowed to stand at room temperature for only 2 hours and then refluxed for 1 hour before the material was worked up the usual way. A typical set of yields of chloride III is 23, 32, 66, 67, and 34%, respectively, for reactions in pyridine, *n*-hexane, toluene, dioxane, and excess thionyl chloride.

Di-2-p-anisylethyl Sulphite (IV)

From the reaction of I with thionyl chloride in *n*-hexane, a solid product was recovered after the reaction mixture was poured onto ice. It crystallized as colorless needles from ether–pentane mixture, m.p. 45–47° C. Its analysis agrees with that expected for di-2-*p*-anisylethyl sulphite (IV).

Anal. Calc. for $C_{18}H_{22}O_5S$: C, 61.70; H, 6.28; S, 9.14. Found: C, 61.81; H, 6.44; S, 9.20. For the active runs in *n*-hexane, the yields of chloride III were 32 and 44%, and of sulphite IV were 12 and 9%, respectively, for runs 1 and 2. No sulphite IV was obtained from reactions in pyridine, toluene, dioxane, or excess thionyl chloride.

When I was treated with thionyl chloride in ether according to the general procedure described in the previous section, the only product, besides unreacted alcohol I, was a 4% yield of sulphite IV. The inclusion of 5 ml of pyridine in the reaction mixture of I and thionyl chloride in ether raised the yield of sulphite IV to 39%.

Degradation of p-Anisylethyl-x-C^{14} Chloride (III)

The conversion of chloride III to the corresponding Grignard reagent followed by reaction with carbon dioxide to give 3-*p*-anisylpropanoic acid-*x*-C^{14} (V), m.p. 104–105° C (lit. (17) m.p. 104–105° C), and the subsequent oxidation of V to *p*-anisic acid (VI) were carried out in a manner analogous to the conversion of 2-phenylethyl iodide to hydrocinnamic acid and the oxidation of the latter to benzoic acid previously reported from this laboratory (18). Samples of V and VI were repeatedly crystallized and sublimed before they were assayed for radioactivity.

ACKNOWLEDGMENT

The financial support given by the National Research Council of Canada is gratefully acknowledged.

REFERENCES

1. C. E. Boozer and E. S. Lewis. J. Am. Chem. Soc. **75**, 3182 (1953).
2. E. S. Lewis and C. E. Boozer. J. Am. Chem. Soc. **74**, 308 (1952).
3. D. J. Cram. J. Am. Chem. Soc. **75**, 332 (1953).
4. S. H. Sharman, F. F. Caserio, R. F. Nystrom, J. C. Leak, and W. G. Young. J. Am. Chem. Soc. **80**, 5965 (1958).
5. W. G. Young, F. F. Caserio, Jr., and D. D. Brandon, Jr. J. Am. Chem. Soc. **82**, 6163 (1960).
6. J. A. Pegolotti and W. G. Young. J. Am. Chem. Soc. **83**, 3251 (1961).
7. C. C. Lee and A. J. Finlayson. Can. J. Chem. **39**, 260 (1961).
8. C. C. Lee, J. W. Clayton, D. G. Lee, and A. J. Finlayson. Tetrahedron, **18**, 1395 (1962).
9. E. F. Jenny and S. Winstein. Helv. Chim. Acta, **41**, 807 (1958).
10. M. S. Kharasch and O. Reinmuth. Grignard reactions of nonmetallic substances. Prentice-Hall Inc., New York. 1954. pp. 23–24.
11. M. G. VanCampeu, D. F. Meisner, and S. M. Parmerter. J. Am. Chem. Soc. **70**, 2296 (1948).
12. W. A. Cowdrey, E. D. Hughes, C. K. Ingold, S. Masterman, and A. D. Scott. J. Chem. Soc. 1267 (1937).
13. E. S. Lewis and G. M. Coppinger. J. Am. Chem. Soc. **76**, 796 (1954).
14. C. D. Hodgman (*Editor-in-chief*). Handbook of chemistry and physics. 43rd ed. Chemical Rubber Publishing Co., Cleveland, Ohio. 1961–62. pp. 2556–2557.
15. E. Spath. Monatsh. **34**, 1965 (1913).
16. H. Plimmer, W. F. Short, and P. Hill. J. Chem. Soc. 694 (1938).
17. I. Heilbron and H. J. Bunbury. Dictionary of organic compounds. Vol. 3. Eyre and Spottiswoode, London. 1953. p. 283.
18. C. C. Lee, R. Tkachuk, and G. P. Slater. Tetrahedron, **7**, 206 (1959).

Can. J. Chem. Downloaded from www.nrcresearchpress.com by 210.87.254.42 on 09/05/12
For personal use only.

THE STRUCTURE OF '3-HYDROXYPYRROLES'

R. S. Atkinson and E. Bullock
Department of Chemistry, University of Nottingham, Nottingham, England
Received October 24, 1962

ABSTRACT

Spectroscopic studies by infrared, ultraviolet, and n.m.r. methods have shown that '3-hydroxypyrroles' exist in the 4-oxo-Δ^2-pyrroline form and are not tautomeric substances.

Can. J. Chem. Downloaded from www.nrcresearchpress.com by 210.87.254.5 on 09/05/12
For personal use only.

INTRODUCTION

Several authors have discussed the possibility of tautomerism in the '3-hydroxypyrrole' system (1–4). The earlier workers assigned a hydroxypyrrole (II) structure and the later ones (3, 4) an oxo-Δ^2-pyrroline (I) form for these compounds. Treibs (4) proposed that the oxo-Δ^2-pyrroline form was best represented by a dipolar structure (IA) (i.e. a resonance hybrid of I and IA but with very marked dipolar character). Examination of

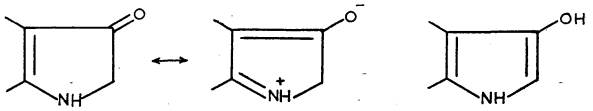

I IA II

this problem by spectroscopic methods has so far been restricted to ultraviolet and solid phase infrared spectra, due to the insolubility of the compounds in organic solvents. (The results presented here establish III as the correct formula for one type of '3-hydroxypyrrole' and the compounds will subsequently be referred to as oxo-Δ^2-pyrrolines.) The synthesis of 3-carbethoxy-4-oxo-Δ^2-pyrrolines (III) is relatively easy and our study of is this type of compound. In an attempt to obtain spectra in organic solvents the *t*-butyl, benzyl (3), and *n*-octyl esters of III were prepared, and the last was sufficiently soluble in chloroform for our purpose.

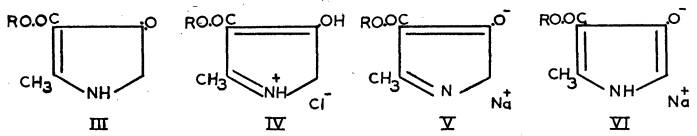

III IV V VI

EXPERIMENTAL

The esters were prepared from the appropriate acetoacetate (1). *n*-Octyl acetoacetate was synthesized by ester exchange between *n*-octanol and ethyl acetoacetate in the presence of *p*-toluenesulphonic acid. *t*-Butyl 2-methyl-4-oxo-Δ^2-pyrroline-3-carboxylate (III; R = $C(CH_3)_3$) forms white needles, m.p. 197–200° (decomp.; m.p. very dependent on rate of heating, above value is from a preheated Kofler block). Calc. for $C_{10}H_{15}O_3N$: C, 60.89; H, 7.67; N, 7.1%. Found: C, 61.00; H, 7.66; N, 6.97%. *n*-Octyl 2-methyl-4-oxo-Δ^2-pyrroline (III; R = $(CH_2)_7CH_3$) crystallized as small buff needles from ethanol, m.p. 145–147°. Calc. for $C_{14}H_{23}O_3N$: C, 66.37; H, 9.15; N, 5.53%. Found: C, 66.2; H, 9.39; N, 5.91%. Molecular weight (Rast): 214 (requires 253).

The n.m.r. spectrometer is an A.E.I. RS2 60 Mc/sec instrument. Tetramethylsilane was used as internal reference where possible and results are given on the τ scale. Spectra were calibrated by generation of side bands from appropriate peaks. Ultraviolet spectra were recorded on a Perkin–Elmer model 137 ultraviolet spectrophotometer on ethanol solutions, unless otherwise stated. Infrared spectra were measured (generally on chloroform solutions) on Unicam SP100 and SP200 instruments.

RESULTS

(a) Nuclear Magnetic Resonance Spectroscopy

(i) n-Octyl Ester (III; R = $(CH_2)_7CH_3$)

The spectrum of a saturated solution in chloroform is shown in Fig. 1. The ratio of the

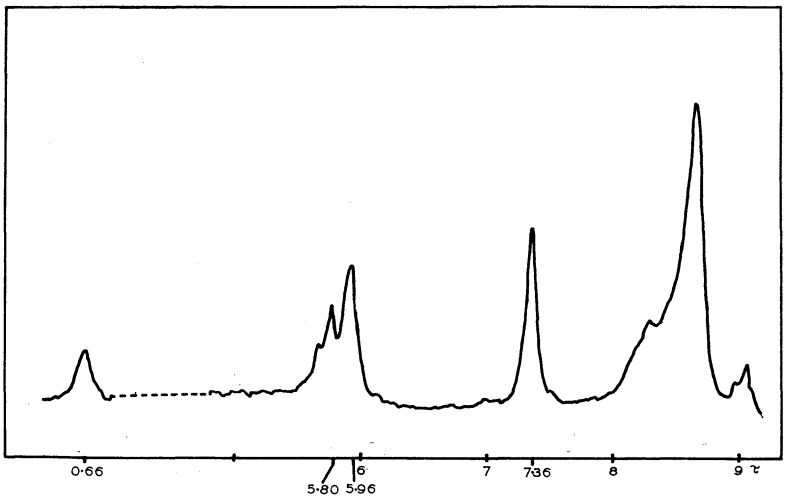

FIG. 1. Nuclear magnetic resonance spectrum of III; R = $(CH_2)_7CH_3$.

area under the combined peaks at 5.80 and 5.96 τ to that under the 7.36 τ absorption is 4:3. The NH (0.66 τ) signal is sensitive to concentration of solute and moves to high field with dilution. After shaking the solution with D_2O, the 0.66 and 5.96 τ peaks disappeared, showing the triplet nature of the 5.80 τ signal clearly.

Trifluoracetic acid was added to a chloroform solution (about 30% v/v) and caused several of the signals to shift to low field. The NH band became very broad (intensity $\equiv$ 1 proton) at -0.52 τ and the 5.96 τ signal was broadened and appeared at 5.12 τ. The ring-methyl group gave a slightly broadened signal at 7.22 τ.

(ii) Ethyl Ester (III; R = CH_2CH_3)

This ester was examined in trifluoracetic acid and the overall features were very similar to those of the acidified chloroform solution recorded above.

In alkaline solution (aqueous sodium hydroxide) the signals appeared sufficiently to high field of the solvent (solvent assumed at 5.31 τ) to facilitate a satisfactory interpretation. The absorption corresponding to the 5.96 τ signal in (i) now appears, as a poorly defined quartet, at 6.30 τ. The most striking change is in the ring-methyl signal, which is now a triplet (7.78 τ, J = 1.7 c.p.s.), clearly by long-range interaction with the pyrroline CH_2 group.

(b) Infrared Spectroscopy

Figure 2 shows the 3000 cm^{-1} region for four different samples of III, R = $(CH_2)_7CH_3$. The bands at 3162 and 3065 cm^{-1} in the solid phase spectrum (Fig. 2(*a*)) are presumably the 'immonium' bands of Treibs (4). It is clear from the subsequent solution spectra (Fig. 2(*b*, *c*, *d*)) that these are 'bonded' NH absorptions and that the free NH frequency is probably that at 3468 cm^{-1}. A second hydrogen-bonded band appears at 3252 cm^{-1} in strong solutions.

Can. J. Chem. Downloaded from www.nrcresearchpress.com by 210.87.254.5 on 09/05/12
For personal use only.

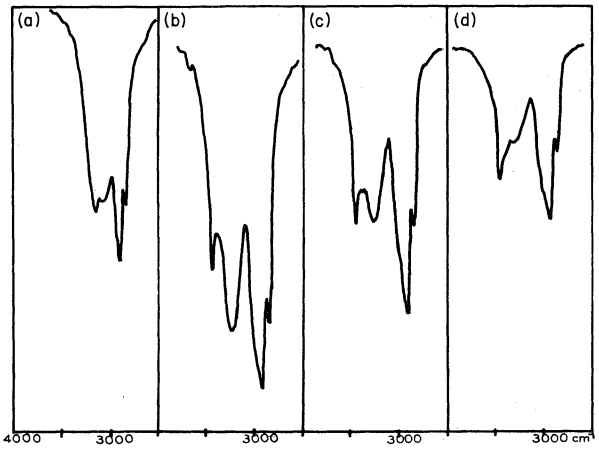

FIG. 2. Infrared spectrum of III; R = $(CH_2)_7CH_3$.

The carbonyl region is unresolved in KBr disk spectra though there appear to be two distinct absorptions at 1697 and 1722 cm^{-1} (shoulder). In chloroform solution these peaks are better resolved and appear at 1675 and 1710 cm^{-1}. The material was too insoluble in carbon tetrachloride to give satisfactory spectra.

(c) Ultraviolet Spectra

The absorption of III, R = $(CH_2)_7CH_3$, is sensitive to pH. The material is amphoteric, though both acidic and basic functions are relatively weak. In particular, addition of concentrated acid until the strength was about 3 *N* (in hydrogen chloride) was necessary to produce a marked change in spectrum. The positions and intensities of absorptions in various solutions are given in Table I.

TABLE I

Ultraviolet absorption of III, R = $(CH_2)_7CH_3$

Solution	λ_{max} (mμ)	Extinction coefficient
Neutral	241.3	14,500
	294.5	9,300
Approx. 2.2 *N* HCl	241.5	11,100
	291	8,430
Approx. 4.4 *N* HCl	223	9,950
	241 (infl.)	6,290
	282	7,680
Approx. 0.1 *N* NaOEt	254.3	17,530
	285	7,930

The absorptions in neutral and acidic solutions showed a marked isosbestic point, indicating that only protonation and not condensation (1) had occurred.

DISCUSSION

The n.m.r. spectra show that in neutral, acidic, and alkaline solutions the compounds exist as a single species and that one CH_2 group is present which can be satisfactorily ascribed only to the 5-position of a Δ^2-pyrroline.

Can. J. Chem. Downloaded from www.nrcresearchpress.com by 210.87.254.5 on 09/05/12
For personal use only.

Assessment of the contribution from a charged form (I ↔ IA) to the structure of the molecule in neutral solution is difficult. Treibs (4) quoted two main pieces of evidence: (*a*) the presence of bands in the infrared due to $\overset{+}{N}H$ and (*b*) a Rast molecular weight for III, R = CH_2CH_3, equivalent to a dimeric formula.

Point (*a*) is probably invalid. The 4-oxo-Δ^2-pyrroline formula is equivalent to the vinylogue of a γ-lactam. Certain simple γ-lactams, in the solid phase, show absorptions at 3175 and 3080 cm^{-1}, and an NH— stretching band near 3440 cm^{-1} is observed in dilute solution spectra of many secondary amides (5). These are very closely similar to the values for 4-oxo-Δ^2-pyrrolines and suggest that there are no grounds for proposing a more polar structure than is present in a simple amide, for these compounds. The anomalous molecular weight is probably due to the insolubility of the ethyl ester in camphor, since the octyl ester gave a value corresponding to a monomer.

The low-field NH band of intensity 1 and the low-field shift of the 5-proton signals in the n.m.r. spectra of acidified solutions of oxopyrrolines suggest that protonation occurs on the carbonyl oxygen atom (IV; cf. ref. 6). The protonated form is thus completely analogous to that of a simple pyrrole (7). It is surprising that the anions show no tendency to exist in the pyrrole (VI) form, but the evidence clearly supports V.

REFERENCES

1. E. Benary and B. Silbermann. Ber. **46**, 1363 (1913).
2. W. Kuster. Z. Physiol. Chem. **121**, 135 (1922).
3. J. Davoll. J. Chem. Soc. 3802 (1953).
4. A. Treibs and A. Ohorodnik. Ann. **611**, 149 (1958).
5. L. J. Bellamy. Infra-red spectra of complex molecules. Methuen, London. 1958. p. 206.
6. A. R. Katritsky and R. A. Y. Jones. Proc. Chem. Soc. 313 (1960).
7. R. J. Abraham, E. Bullock, and S. S. Mitra. Can. J. Chem. **37**, 1859 (1959).

Can. J. Chem. Downloaded from www.nrcresearchpress.com by 210.87.254.5 on 09/05/12
For personal use only.

METAL OXIDE TRIALKYLSILYLOXIDE POLYMERS (POLYTRIALKYLSILOXANOMETALLOXANES)

PART I. TITANIUM OXIDE TRIMETHYLSILYLOXIDE POLYMERS

D. C. BRADLEY AND C. PREVEDOROU-DEMAS
Department of Chemistry, The University of Western Ontario, London, Ontario

Received September 20, 1962

Can. J. Chem. Downloaded from www.nrcresearchpress.com by 210.87.254.5 on 09/05/12
For personal use only.

ABSTRACT

Tetrakis-(trimethylsilyloxy)-titanium $Ti(OSiMe_3)_4$ has been hydrolyzed under controlled conditions in dioxane. The initial products of hydrolysis undergo facile disproportionation, e.g. $3Ti_2O(OSiMe_3)_6 \rightarrow 4Ti(OSiMe_3)_4$ + polymeric $Ti_2O_3(OSiMe_3)_2$. Molecular weight determinations were made on the titanium oxide trimethylsilyloxide polymers (polytrimethylsiloxanotitanoxanes) obtained by thermal disproportionation. Structures have been suggested for the polymers on the basis of the variation of number-average degree of polymerization with the degree of hydrolysis.

INTRODUCTION

In a previous communication (1) we reported the preparation and properties of some trialkylsilyloxy derivatives of titanium, zirconium, niobium, and tantalum. It was observed that these compounds were less susceptible to hydrolysis than the metal alkoxides and it was suggested that this property was connected with the water-repellant nature of the trialkylsilyloxy group. A study of the controlled hydrolysis of tetrakis-trimethylsilyloxy-titanium was of interest because of the likely formation of titanium oxide trimethylsilyloxide polymers $[TiO_x(OSiMe_3)_{4-2x}]_n$ (also known as polytrimethylsiloxanotitanoxanes (9)). These polymers were of particular interest in connection with the structural work of Bradley and co-workers (2–8) on the metal oxide alkoxides and also because of their potentialities as thermally stable polymers and water-repellant agents.

Andrianov and co-workers (9) studied the hydrolysis of $Ti(OSiMe_3)_4$ in acetone at 50° C. They claimed that with the reactants in the molar proportions of 1 of water to 2 of $Ti(OSiMe_3)_4$ there was no reaction during 3 hours and that most of the $Ti(OSiMe_3)_4$ was recovered by distillation. However, with more than 1 g-mol of water to 1 of $Ti(OSiMe_3)_4$ in acid solution they found that polymers were formed which were soluble in organic solvents.

We now report some results on the hydrolysis of $Ti(OSiMe_3)_4$ in dioxane at room temperature. In the course of this work some interesting polymeric titanium oxide trimethylsilyloxides were isolated.

RESULTS AND DISCUSSION

In keeping with previous nomenclature (2–8) we call the molar ratio of water added to $Ti(OSiMe_3)_4$ h, but in contrast to the hydrolysis of the metal alkoxides the hydrolysis of $Ti(OSiMe_3)_4$ was incomplete and the degree of hydrolysis in the product was not h. The actual degree of hydrolysis x was determined by analysis of the polymer $[TiO_x(OSiMe_3)_{(4-2x)}]_n$, where n is the number-average degree of polymerization determined by cryoscopy in cyclohexane.

According to equation [1] hydrolysis with $h = 0.5$ should produce $Ti_2O(OSiMe_3)_6$.

$$2Ti(OSiMe_3)_4 + H_2O \rightarrow Ti_2O(OSiMe_3)_6 + 2Me_3SiOH \quad [1]$$

Aqueous dioxane (for $h = 0.5$) was added to $Ti(OSiMe_3)_6$ in dioxane (approx. 2 molal

solution) with vigorous stirring at room temperature (approx. 23° C) and after 1 hour the solvent and volatile products were evaporated off *in vacuo* at room temperature. Gas chromatographic analysis of the volatile products confirmed the presence of trimethylsilanol with some hexamethyldisiloxane and a trace of water. The non-volatile residue was a colorless liquid with the correct analysis for $Ti_2O(OSiMe_3)_6$ but it soon deposited some white precipitate. Vacuum distillation of the residue at 120° C gave a substantial recovery of $Ti(OSiMe_3)_4$ and after heating to 160° C left a non-volatile white residue corresponding in analysis to a highly hydrolyzed product (i.e. $x \sim 1.6$). This experiment demonstrated, contrary to the report of Andrianov *et al.* (9), that $Ti(OSiMe_3)_4$ is hydrolyzed at $h = 0.5$ in neutral solution and that the product of hydrolysis undergoes a ready disproportionation.

The experiment was repeated on a larger scale and again a liquid product corresponding to "$Ti_2O(OSiMe_3)_6$" was obtained and its infrared absorption spectrum suggested that no hydroxyl groups were present. The infrared spectrum also showed that the characteristic intense Ti—O—Si band at 918 cm^{-1} (10–12) of $Ti(OSiMe_3)_4$ was diminished in intensity and that a new strong band was present at 975 cm^{-1}.

A portion of the product was heated at 120° C for 1 hour and allowed to cool. Evaporation *in vacuo* at room temperature gave as condensate a small quantity of silanol, hexamethyldisiloxane, and water, and left a liquid containing a white precipitate (I). The formation of silanol, disiloxane, and water suggested that some hydroxy compounds, e.g. $Ti(OH)(OSiMe_3)_3$, $Ti(OH)_2(OSiMe_3)_2$, and (or) polymeric hydroxy compounds were present in "$Ti_2O(OSiMe_3)_6$", although no absorption due to hydroxyl was detected in the infrared. Compound I was separated by filtration and shown to be a titanium oxide trimethylsilyloxide ($x \sim 1.5$) whilst the filtrate was substantially $Ti(OSiMe_3)_4$. The remainder of the original "$Ti_2O(OSiMe_3)_6$" was kept at room temperature for 2 weeks, slowly depositing a white solid which was found to be similar in degree of hydrolysis to I, and the supernatant liquor was again substantially $Ti(OSiMe_3)_4$. Another interesting result of this experiment was the discovery from a material balance of reactants and products that the percentage hydrolysis based on equation [1] was only about 74%.

From these experiments it was concluded that at $h = 0.5$ hydrolysis is incomplete after 1 hour and that the titanium product of hydrolysis is unstable, undergoing disproportionation slowly at room temperature and rapidly at 120° C to give $Ti(OSiMe_3)_4$ and a solid approximating in composition to $Ti_2O_3(OSiMe_3)_2$ (see equation [2]). Molecular

$$3Ti_2O(OSiMe_3)_6 \rightarrow 4Ti(OSiMe_3)_4 + \frac{1}{n}[Ti_2O_3(OSiMe_3)_2]_n \qquad [2]$$

weight determinations (cryoscopic) in cyclohexane suggested that the solid I had a degree of polymerization of 12, which in comparison with titanium oxide alkoxides is very low for such a high degree of hydrolysis.

To explore the field more fully a number of hydrolyses were done over a range of h values (0.1 to 2.50) at room temperature under similar conditions. In each case the product remaining after evaporation of dioxane and volatile products was heated at 160° C *in vacuo* until no more $Ti(OSiMe_3)_4$ distilled out. The non-volatile residue was analyzed for % Ti and % Si, and its molecular weight (in cyclohexane) and infrared spectrum were determined. From the analytical data the degree of hydrolysis x was determined and from the molecular weights n was calculated. For $h > 1.5$ the non-volatile residues were sparingly soluble and molecular weights could not be obtained with sufficient accuracy. Values of h, x, and n are given in Table I together with some values for the percentage hydrolysis.

Can. J. Chem. Downloaded from www.nrcresearchpress.com by 210.87.254.5 on 09/05/12
For personal use only.

TABLE I

Degrees of polymerization of $[TiO_x(OSiMe_3)_{(4-2x)}]_n$

h	% hydrolysis	Degree of hydrolysis (x)	Degree of polymerization n_{obs}	Degree of polymerization n_{calc}
0.10	—	1.505	8.1	8.26
0.20	—	1.515	8.35	8.85
0.30	—	1.52	9.2	9.09
0.35	—	1.53	9.5	9.50
(0.60)*	—	1.535	9.9	9.80
(0.60)†	—	1.54	10.35	10.20
0.40	—	1.545	11.1	10.53
(0.60)‡	—	1.555	11.25	11.24
0.50	74.2	1.56	12.0	11.63
0.55	—	1.57	11.7	12.50
0.60	—	1.58	13.7	13.51
0.65	—	1.585	15.0	13.89
0.75	—	1.59	14.8	14.71
0.90	—	1.595	16.8	15.38
1.00	53.3	1.60	18.4	16.13
1.25	—	1.625	19.9	21.28
1.35	—	1.645	25.4	28.57
1.50	48.6	1.645	26.5	28.57
1.75	—	1.69	Sparingly soluble	
2.00	47.3	1.68	"	
2.25	—	1.68	"	
2.50	44.2	1.68	"	

*With 1 mole Me_3SiOH/mole $Ti(OSiMe_3)_4$.
†With 1.5 moles Me_3SiOH/mole $Ti(OSiMe_3)_4$.
‡With 2 moles Me_3SiOH/mole $Ti(OSiMe_3)_4$.

It is extremely interesting to note that the lowest polymer obtained (from $h = 0.1$) corresponds to $Ti_8O_{12}(OSiMe_3)_8$ (found: Ti, 29.7; Si, 17.3; M.W., 1310; $Ti_8O_{12}(OSiMe_3)_8$ requires: Ti, 29.7; Si, 17.4; M.W., 1288). This could have a large ring structure but we are inclined to favor the compact cubical structure shown in the Fig. 1. This molecule

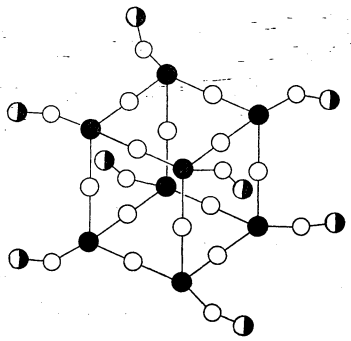

FIG. 1. $Ti_8O_{12}(OSiMe_3)_8$: ● = Ti; ○ = oxygen; ◑ = $SiMe_3$ group.

must possess considerable stability to be formed so readily at such a low value of h. The molecular weight determination showed no concentration dependence and we concluded that a single molecular species was present. A remarkable feature of the structure proposed for $Ti_8O_{12}(OSiMe_3)_8$ is the presence of 4-coordinated titanium in contrast to the titanium oxide alkoxides (2, 3), which are believed to involve 6-coordinated titanium.

Another interesting feature of the data in Table I is that as h is increased from 0.1 to 1.75 the value of x slowly increases from 1.5 to 1.7. It appears that x has a limiting value of 1.7 because increasing h to 2.5 appears not to increase x beyond ~1.7.

Can. J. Chem. Downloaded from www.nrcresearchpress.com by 210.87.254.5 on 09/05/12
For personal use only.

Also it is clear that as h is increased the percentage hydrolysis is steadily decreased. This suggested that the more highly hydrolyzed species are more resistant to hydrolysis or that the hydrolysis is reversible. To test the latter possibility more hydrolyses were made at $h = 0.6$ with the addition of trimethylsilanol in ratios Me_3SiOH:$Ti(OSiMe_3)_4$ of 1.0, 1.5, and 2.0. There are two possible consequences of the addition of trimethylsilanol: (i) to raise the value of h and hence x by addition of water caused by condensation of the unstable silanol, (ii) to lower h and x because of the reversal of the hydrolysis (e.g. in equation [1]). Attempts were made to preclude (i) by using freshly prepared silanol but the condensation of Me_3SiOH is notoriously sensitive to acid catalysis. The results in Table I show that the addition of Me_3SiOH caused a significant lowering in x although the suppression of hydrolysis did not increase in proportion to the ratio of Me_3SiOH:$Ti(OSiMe_3)_4$. This lack of quantitative correlation could be due to the condensation of silanol as already mentioned. Whilst not conclusive these experiments suggested that hydrolysis of $Ti(OSiMe_3)_4$ is reversible, thus explaining the decrease in percentage hydrolysis with increase in h.

Bradley and co-workers (1–8) have shown that metal oxide alkoxide polymers appear to conform to certain structural models determined by the stereochemistry of the metal and that each model gives a characteristic variation of the number-average degree of polymerization as a function of the degree of hydrolysis. Bradley and Holloway (8) have developed a mathematical approach to the analysis of the variation of n with x in terms of structural models for any system constituting a regular polymer series. Thus a regular polymer series built up by condensation of p-mer units ($n_0 = p$) with q linkages between adjacent units will have the following equation:

$$n^{-1} = p^{-1} - q^{-1}x. \qquad [3]$$

The data for n and x in Table I treated by the method of least squares gave the following equation: $n^{-1} = 1.028 - 0.604x$. The values of n_{calc} in Table I are those calculated from the least-squares equation assuming experimental values of x are correct. From the deviations $n_{calc} - n_{obs}$ the coefficient of variation for the 18 points was found to be $\pm 6\%$, corresponding to a most probable error of $\pm 4\%$ for any point. Bearing in mind that x calculated from the analytical data is very sensitive to analytical errors and the possibility of an error of 5% in n, the above agreement seems very satisfactory.

Putting $n^{-1} = 0$ in the least-squares equation gives a value $x_\infty = 1.70$ corresponding to an infinite polymer with $x = 1.70$. This agrees very well with our observation that the limiting value of $x = 1.7$ independent of $h > 1.75$ and that the products with $x \rightarrow 1.7$ were insoluble as would be expected for the higher polymers.

Putting $x = 0$ in the least-squares equation gives $n_0^{-1} = 1.028$, corresponding to $p = 0.97$ and suggesting that a monomer titanium unit is involved in the polymer series. However, we could not obtain polymers with $x < 1.5$ and hence the value of n_0 may have no real significance. On the other hand the least-squares equation gives $q = 1.65$ for the average number of linkages between each repeating unit in the polymer. In view of the facile formation of $Ti_8O_{12}(OSiMe_3)_8$ even at very low values of h we explored the possibility that the polymers with $x = 1.5$ to 1.7 were formed by condensation of the octamer $Ti_8O_{12}(OSiMe_3)_8$. In Fig. 2 is represented a polymer formed by condensing two $Ti_8O_{12}(OSiMe_3)_8$ units with one oxygen bridge. Continuation of such a mode of condensation leads to a regular polymer series of the general formula $Ti_{8(y+1)}O_{(13y+12)}(OSiMe_3)_{(6y+8)}$, where $y = 0$, 1, 2, etc., leading to the relationship $n^{-1} = 1.625 - x$. It was clear that such a series, which we will designate Series A, did not agree with the

Can. J. Chem. Downloaded from www.nrcresearchpress.com by 210.87.254.5 on 09/05/12
For personal use only.

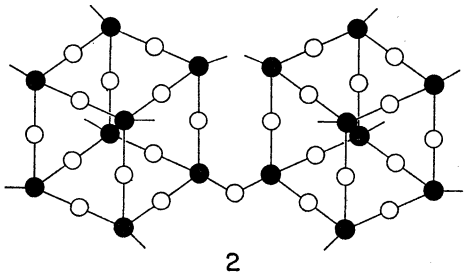

2

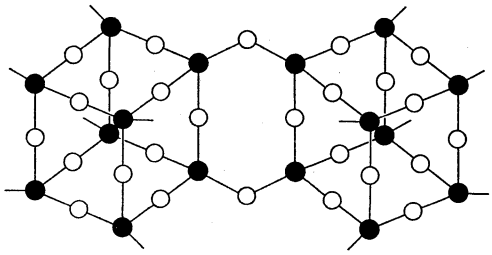

3

FIG. 2. $Ti_{16}O_{25}(OSiMe_3)_{14}$: ● = Ti; ○ = oxygen ($Me_3SiO$ groups omitted).
FIG. 3. $Ti_{16}O_{26}(OSiMe_3)_{12}$: ● = Ti; ○ = oxygen ($Me_3SiO$ groups omitted).

results in Table I. In Fig. 3 is shown another polymer formed by condensation from two $Ti_8O_{12}(OSiMe_3)_8$ units but with two oxygen bridges. This process leads to Series B with the general formula $Ti_{8y}O_{2(7y-1)}(OSiMe_3)_{4(y+1)}$, where $y = 1, 2, 3$, etc., with $n^{-1} = 0.875-0.5x$. Clearly the least-squares equation is closer to the requirements of Series B than to Series A. Finally, in view of the value of $q = 1.65$, the possibility was considered that Series A and Series B were present simultaneously. Following the theory of Bradley and Holloway (8) it is readily shown that if the proportion of titanium atoms in Series B is α and in Series A is $1-\alpha$, then

$$n^{-1} = \alpha n_B^{-1} + (1-\alpha)n_A^{-1} = \alpha(0.875-0.5x) + (1-\alpha)(1.625-x). \quad [4]$$

Hence

$$n^{-1} = 1.625-0.75\alpha-(1.00-0.5\alpha)x. \quad [5]$$

If equation [5] is to be identical with the least-squares equation $n^{-1} = 1.028-0.604x$, it follows that $1.625-0.75\alpha = 1.028$. Hence $\alpha = 0.796$. A check on the theory is provided by the fact that the slope $d(n^{-1})/dx$ of equation [5] is given by $-(1.00-0.5\alpha)$. Substitution of the value for α gives a calculated slope of -0.602, which is remarkably close to the least-squares slope of -0.604. It thus appears that the variation of n with x for the polymeric titanium oxide trimethylsilyloxides is very well explained in terms of the two series (A and B) of regular polymers based on the octamer $Ti_8O_{12}(OSiMe_3)_8$. Other regular polymer series including one involving 6-coordinated titanium were considered either singly or as mixtures but the experimental variation of n with x could not be reproduced by any of them. A remarkable feature of the structure (Fig. 1) proposed for $Ti_8O_{12}(OSiMe_3)_8$ is the presence of 4-coordinated titanium in a near-tetrahedral configuration. Thus the polymeric titanium alkoxides and titanium oxide alkoxides appear to involve 6-coordinated octahedral titanium (2, 3) while titanium dioxide certainly contains octahedral titanium. It remains to be explained how the trimethylsilyloxy groups can promote the stabilization of 4-coordinated titanium in the new polymers. It is reasonable to assume that 4-coordinated titanium attached to electronegative ligands will achieve an increase in covalency by "intramolecular coordination" involving donation of p_π electrons of the ligand to vacant d_π orbitals of the titanium. Now in the Si—O—Ti groups there will be competition between silicon and titanium for a share in the p_π electrons of the oxygen whereas in the Ti—O—Ti groups the d_π–p_π bonding is presumably shared equally between the titaniums. It may be that the compact and symmetrical structure of $Ti_8O_{12}(OSiMe_3)_8$ (Fig. 1) with linear Ti—O—Ti bonds promotes the supplementary Ti—O π-bonding thereby providing additional stabilization for the structure. It is still not obvious how the trimethylsilyloxy groups

Can. J. Chem. Downloaded from www.nrcresearchpress.com by 210.87.254.5 on 09/05/12
For personal use only.

help to bring about this structure but it is possible that in the Si—O—Ti groups, the silicon by withdrawing the oxygen's π-electrons at the expense of the titanium causes the latter to draw upon the π-electrons of the oxygens in the Ti—O—Ti groups thus promoting the π-bonding within the Ti—O—Ti framework. It is hoped that infrared absorption spectra will throw further light on this problem. Preliminary results show that the polymers contain a strong characteristic band around 973 cm^{-1} in addition to the Si—O band at 918 cm^{-1}, which is also present in $Ti(OSiMe_3)_4$ (10–12). In addition, the intense band at 755 cm^{-1} due to the $SiMe_3$ group has in the polymers shoulders at around 775 and 735 cm^{-1} which may be due to the Ti—O—Ti system (11, 13).

EXPERIMENTAL

The preparation and analysis of $Ti(OSiMe_3)_4$ were carried out using essentially the procedures already reported (1). Dioxane was carefully purified by prolonged refluxing over sodium followed by fractional distillation. Molecular weights were determined cryoscopically in cyclohexane in a Beckman apparatus suitably modified to exclude atmospheric moisture. The infrared spectra were determined in approximately 2.5% solutions in carbon disulphide in a cell fitted with KBr windows. Measurements were made using the Beckman IR-7 and IR-5A instruments.

Preparation of Polymeric Titanium Oxide Trialkylsilyloxides

All experiments were carried out under essentially the same conditions. A measured quantity of water as aqueous dioxane was added with vigorous stirring to a solution of $Ti(OSiMe_3)_4$ in dioxane at approximately 23° C. The concentration of $Ti(OSiMe_3)_4$ was in each case approximately 2 molal. Stirring was continued for 1 hour after the addition of the water, and the clear solution was then evaporated to dryness at 0.1 mm pressure. The liquid residue thus obtained was heated at 120° C at 0.1 mm to distill out the $Ti(OSiMe_3)_4$ and finally heated at 160° C at 0.1 mm until $Ti(OSiMe_3)_4$ ceased to be evolved. In the experiments at $h = 0.5$, 1.0, 1.5, 2.0, and 2.5, the weights of reactants and products were carefully determined, thus allowing calculation of the percentage hydrolysis. Analysis (Ti and Si) of the polymers $[TiO_x(OSiMe_3)_{(4-2x)}]_n$ enabled the degree of hydrolysis x to be calculated and the determination of the molecular weight gave the value of n, the number-average degree of polymerization (i.e. the number of Ti atoms per average molecule). The data are presented in Table II, where the calculated values of % Ti and % Si provide a

TABLE II

Analyses and molecular weights of $[TiO_x(OSiMe_3)_{4-2x}]_n$

	% Ti		% Si		
x	Calc.	Obs.	Calc.	Obs.	M.W.
1.505	29.8	29.7	17.4	17.4	1310
1.515	30.2	30.0	17.2	17.1	1330
1.52	30.3	30.4	17.1	17.0	1450
1.53	30.6	30.9	16.9	17.1	1472
1.535	30.8	31.0	16.85	17.0	1530
1.54	31.0	30.9	16.7	16.6	1607
1.545	31.1	31.5	16.6	16.6	1690
1.555	31.5	31.3	16.4	16.35	1725
1.56	31.7	32.0	16.3	16.5	1800
1.57	32.0	31.3	16.15	15.8	1792
1.58	32.3	32.7	16.0	16.0	2010
1.585	32.5	32.6	15.85	15.9	2200
1.59	32.6	33.7	15.7	16.2	2112
1.595	32.8	33.0	15.6	15.7	2436
1.60	33.1	33.6	15.5	15.7	2630
1.625	33.8	34.0	14.9	15.0	2784
1.645	34.8	35.1	14.5	14.65	3479
1.645	34.8	35.0	14.5	14.6	3627

check on the accuracy of x or the purity of the polymer (e.g. if a polymer is contaminated with solvent the value of x could be correct but the absolute values of % Ti and % Si would be incorrect).

Can. J. Chem. Downloaded from www.nrcresearchpress.com by 210.87.254.5 on 09/05/12
For personal use only.

ACKNOWLEDGMENTS

We are grateful to the Defence Research Board of Canada for generously supporting this research under Grant No. 7583-04.

REFERENCES

1. D. C. Bradley and I. M. Thomas. J. Chem. Soc. 3404 (1959).
2. D. C. Bradley, R. Gaze, and W. Wardlaw. J. Chem. Soc. 3977 (1955).
3. D. C. Bradley, R. Gaze, and W. Wardlaw. J. Chem. Soc. 469 (1957).
4. D. C. Bradley and D. G. Carter. Can. J. Chem. **39**, 1434 (1961).
5. D. C. Bradley and H. Holloway. Can. J. Chem. **39**, 1818 (1961).
6. D. C. Bradley and D. G. Carter. Can. J. Chem. **40**, 15 (1962).
7. D. C. Bradley and H. Holloway. Can. J. Chem. **40**, 62 (1962).
8. D. C. Bradley and H. Holloway. Can. J. Chem. **40**, 1176 (1962).
9. K. A. Andrianov, A. A. Zhdanov, N. A. Kurasheva, and V. G. Dulova. Dokl. Akad. Nauk SSSR, **112**, 1050 (1957).
10. C. G. Barraclough, D. C. Bradley, J. Lewis, and I. M. Thomas. J. Chem. Soc. 2601 (1961).
11. V. A. Zeitler and C. A. Brown. J. Phys. Chem. **61**, 1174 (1957).
12. H. Kriegsmann and K. Licht. Z. Elektrochem. **62**, 1163 (1958).
13. D. C. Bradley and A. H. Westlake. Nature, **191**, 273 (1961).

Can. J. Chem. Downloaded from www.nrcresearchpress.com by 210.87.254.5 on 09/05/12
For personal use only.

SYNTHESIS OF A SUGAR DERIVATIVE WITH NITROGEN IN THE RING

J. K. N. JONES AND W. A. SZAREK
Department of Chemistry, Queen's University, Kingston, Ontario
Received October 25, 1962

ABSTRACT

1-Acetyl-D-*gulo*(*ido*)-2,3,4,5-tetrahydroxypiperidine, a sugar derivative with nitrogen in the ring, has been synthesized from D-xylose. The synthetic route and proof of structure are described.

Very recently the first synthesis was achieved of a sugar derivative containing nitrogen as the hetero atom in the ring (1). The compound was obtained from L-arabinose and was shown to have the structure I. We now report the synthesis of the analogous compound from D-xylose. Structure II has been established for this new compound.

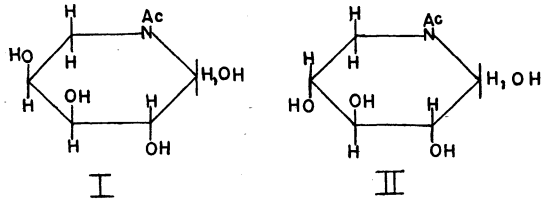

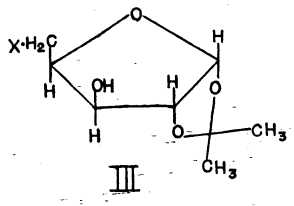

1,2-*O*-Isopropylidene-5-*O*-toluene-*p*-sulphonyl-D-xylose was prepared from D-xylose by the method of Levene and Raymond (2). Reaction with methanolic ammonia, followed by *N*-acetylation, gave 5-acetamido-5-deoxy-1,2-*O*-isopropylidene-D-xylose (III; X = NHAc). Hydrolysis of III with 20% aqueous acetic acid yielded a syrupy mixture of unchanged III and at least three other components. Cellulose column chromatography of this mixture gave in a pure state compound III and two new compounds. One of these was obtained as a brown syrup which could not be induced to crystallize; the other was obtained in crystalline form. The infrared spectrum of the syrupy compound was consistent with that of a xylofuranose. The results of periodate oxidation in unbuffered aqueous solution also indicated that the compound possessed the furanose ring form. The compound was therefore 5-acetamido-5-deoxy-D-xylofuranose. The crystalline compound, for which structure II is proposed, showed no *NH* band in its infrared spectrum. The results of periodate oxidation in unbuffered aqueous solution were consistent with the proposed structure. This compound has been named 1-acetyl-D-*gulo*(*ido*)-2,3,4,5-tetrahydroxypiperidine.

Can. J. Chem. Downloaded from www.nrcresearchpress.com by 210.87.254.42 on 09/05/12
For personal use only.

Both 5-acetamido-5-deoxy-D-xylofuranose and 1-acetyl-D-*gulo*(*ido*)-2,3,4,5-tetrahydroxypiperidine gave the same crystalline phenylosazone. Analysis indicated it to be a phenylosazone of an acetamido-deoxy pentose and the compound gave absorptions in the infrared corresponding to *OH*, *NH*, the aromatic ring, and the amide linkage. Reduction with sodium borohydride of both reducing sugars also gave the same product, probably 5-acetamido-5-deoxy-D-xylitol. These results indicate that the two compounds differ only in the position of ring closure of the terminal aldehyde group.

5-Acetamido-5-deoxy-D-xylofuranose gave with methanolic hydrogen chloride a syrupy methyl glycoside which on periodate oxidation gave results in agreement with those expected for the oxidation of a furanoside.

1-Acetyl-D-*gulo*(*ido*)-2,3,4,5-tetrahydroxypiperidine with methanolic hydrogen chloride rapidly formed a methyl glycoside which was obtained crystalline. It was named 1-acetyl-D-*ido*(*gulo*?)-2-methoxy-3,4,5-trihydroxypiperidine. The results of periodate oxidation of this glycoside indicate the presence of a six-membered ring.

Both 5-acetamido-5-deoxy-D-xylofuranose and 1-acetyl-D-*gulo*(*ido*)-2,3,4,5-tetrahydroxypiperidine are stable in neutral aqueous solution at room temperature. A mixture of the two is formed, however, when an aqueous solution of either compound is heated.

Some light was shed on the nature of the product(s) not isolated from the syrupy hydrolyzate by the observation that the syrup gave on paper chromatograms a component which reacted with a ketose spray reagent as well as with the alkaline silver nitrate and *p*-anisidine hydrochloride spray reagents (*vide infra*). A ketose could conceivably be formed from compound II via an Amadori rearrangement of II in the acid hydrolysis medium. This sequence would give rise to a compound which could be named 1-acetyl-3-keto-4,5-D-*threo*-dihydroxypiperidine. An attempt is being made to isolate the unidentified substance(s).

EXPERIMENTAL

Solutions were concentrated under reduced pressure below 40° C with a rotating vacuum-type evaporator. Melting points were determined on a Fisher–Johns melting point apparatus. Optical rotations were measured at 23±3° C with a Hilger Standard Polarimeter. Infrared spectra were measured with a Perkin–Elmer Model 21 spectrophotometer. Paper chromatography was carried out by the descending method at room temperature on Whatman No. 1 filter paper for qualitative purposes or on Whatman 3MM filter paper for preparative purposes in the following solvent systems (v/v): (A) butan-1-ol:ethanol:water, 3:1:1; (B) butan-1-ol:pyridine:water, 10:3:3. Sugars were detected on paper chromatograms by the following spray reagents: (i) alkaline silver nitrate (3); (ii) *p*-anisidine hydrochloride (4); (iii) modified ceric ammonium nitrate reagent (5); (iv) orcinol – trichloroacetic acid (ketose spray) (6). Rates of movement of the sugars on paper chromatograms are given relative to that of rhamnose (R_{rh}).

1,2-O-Isopropylidene-5-O-toluene-p-sulphonyl-D-xylose

This compound was prepared from D-xylose (33 g) by the method of Levene and Raymond (2). The crystalline product (44 g, 58%) was recrystallized from ethyl acetate and it then melted at 133–134° and had $[\alpha]_D = -12.4°$ (*c*, 2.9 in chloroform). Levene and Raymond report m.p. 133–134° and $[\alpha]_D^{20} = -13.0°$ (*c*, 2.0 in chloroform).

5-Acetamido-5-deoxy-1,2-O-isopropylidene-D-xylose

1,2-*O*-Isopropylidene-5-*O*-toluene-*p*-sulphonyl-D-xylose (26 g) was dissolved in anhydrous methanol (500 ml) and the solution was cooled to 0° and saturated with dry ammonia. The solution was then heated in an autoclave at 120° for 16 hours. After cooling, the dark reaction mixture was boiled with charcoal, filtered, and the filtrate was passed through Amberlite IRA 400 (OH form) anion exchange resin (300 ml). The eluate was evaporated to dryness under reduced pressure to yield a dark syrup (12.8 g). This material was dissolved in water (104 ml) and treated with acetic anhydride (14.5 ml). The solution was allowed to stand for 20 minutes with occasional shaking, then evaporated to dryness under reduced pressure to leave a syrup (14.9 g) which crystallized on standing. Two recrystallizations of this material from methanol–ether gave rectangular plates (7.2 g, 41%) which melted at 111–112° and had $[\alpha]_D = +31°$ (*c*, 2.29 in methanol) and R_{rh} 2.44 (solvent A, spray iii). The infrared spectrum in chloroform showed strong absorption at 3330

Can. J. Chem. Downloaded from www.nrcresearchpress.com by 210.87.254.42 on 09/05/12
For personal use only.

cm^{-1} and at 1527 cm^{-1} attributable to NH, strong absorption at 1657 cm^{-1} owing to N—Ac, and absorption at 1377 cm^{-1} attributable to CH of the isopropylidene group. Calc. for $C_{10}H_{17}NO_5$: C, 52.0; H, 7.4; N, 6.1%. Found: C, 52.3; H, 7.5; N, 6.0%.

*Hydrolysis of 5-Acetamido-5-deoxy-1,2-O-isopropylidene-*D*-xylose*

5-Acetamido-5-deoxy-1,2-*O*-isopropylidene-D-xylose (6.4 g) was dissolved in 20% aqueous acetic acid (40 ml) and the solution was heated at 90° for 1.5 hours. The dark solution was then evaporated under reduced pressure to yield a brown syrup (5.9 g) which was examined on paper chromatograms. Sprays i and ii both showed the presence of components at R_{rh} 0.66 and 1.18 (solvent A) and 0.48 and 0.99 (solvent B). An elongated spot running slightly faster than that with R_{rh} 1.18 was also detected (solvents A and B, sprays i and ii). This spot was also detected with the orcinol – trichloroacetic acid ketose spray reagent (spray iv). Spray iii showed an additional component with R_{rh} 2.44 (solvent A) which was unchanged 5-acetamido-5-deoxy-1,2-*O*-isopropylidene-D-xylose. The syrup was placed on a cellulose column (54×4.5 cm) and irrigated with butan-1-ol half-saturated with water. Three components of the hydrolyzate were obtained in a pure state:

*(a) 5-Acetamido-5-deoxy-1,2-O-isopropylidene-*D*-xylose*

This component was obtained from the eluate as a brown syrup (2.9 g) which crystallized on standing. After recrystallization from methanol–ether the compound melted at 111–112°. There was no depression of the melting point on admixture with an authentic sample of 5-acetamido-5-deoxy-1,2-*O*-isopropylidene-D-xylose. The infrared spectrum in chloroform was also identical with that of 5-acetamido-5-deoxy-1,2-*O*-isopropylidene-D-xylose.

*(b) 5-Acetamido-5-deoxy-*D*-xylofuranose*

This component was obtained from the eluate as a brown syrup (0.43 g) which could not be induced to crystallize. The compound had $[\alpha]_D$ +13.2° (*c*, 1.36 in methanol) and R_{rh} 1.18 (solvent A), 0.99 (solvent B). The infrared spectrum (smear between "IR tran 2" plates) showed strong absorption at 3300 cm^{-1} attributable to OH and NH, weak absorption at 1730 cm^{-1} attributable to the C=O stretching vibration of a small amount of the acyclic aldehyde form of the compound, strong absorption at 1630 cm^{-1} owing to N—Ac, and strong absorption at 1557 cm^{-1} owing to NH.

*(c) 1-Acetyl-*D*-gulo(ido)-2,3,4,5-tetrahydroxypiperidine*

This component was obtained from the eluate as a white crystalline solid (1.80 g). After recrystallization from methanol–ether it melted at 153–154°, and had $[\alpha]_D = -11.3°$ (*c*, 0.95 in methanol) and R_{rh} 0.66 (solvent A), 0.48 (solvent B). The infrared spectrum of this material (0.8% in KBr) showed strong absorption at 3310 cm^{-1} attributable to OH, and strong absorption at 1598 cm^{-1} owing to N—Ac, but no absorption due to NH. Calc. for $C_7H_{13}NO_5$: C, 43.97; H, 6.85; N, 7.33%. Found: C, 43.93; H, 6.87; N, 7.54%.

Preparation of Phenylosazones

*(a) From 5-Acetamido-5-deoxy-*D*-xylofuranose*

5-Acetamido-5-deoxy-D-xylofuranose (0.036 g) in 20% aqueous acetic acid (2.5 ml) was heated at 70° C for 1 hour with sodium metabisulphite (0.030 g) and freshly distilled phenylhydrazine (0.5 ml). The solution was allowed to cool in a refrigerator and the osazone that crystallized (0.053 g) was removed by filtration. Recrystallization from ethanol–water gave yellow needles which melted at 162–164° (decomp.). The infrared spectrum of this compound (0.8% in KBr) showed absorption at 3260 cm^{-1} (OH and NH), 3080 cm^{-1} (aromatic CH), 1657 cm^{-1} (amide I), 1640 cm^{-1} (amide II), and 1605, 1500, 745, 686 cm^{-1} (aromatic ring).

*(b) From 1-Acetyl-*D*-gulo(ido)-2,3,4,5-tetrahydroxypiperidine*

The phenylosazone was prepared as above and was obtained as yellow needles, m.p. 162–164° (decomp.). There was no depression of the melting point on admixture with the phenylosazone from 5-acetamido-5-deoxy-D-xylofuranose. The two preparations of the phenylosazone gave indistinguishable infrared spectra over the range 4000–650 cm^{-1} and moved at identical rates on paper chromatograms. Calc. for $C_{19}H_{23}O_3N_5.H_2O$: C, 58.9; H, 6.5%. Found: C, 58.8; H, 7.0%.

Reductions with Sodium Borohydride

*(a) 5-Acetamido-5-deoxy-*D*-xylofuranose*

5-Acetamido-5-deoxy-D-xylofuranose (0.100 g) was dissolved in distilled water (50 ml) and an excess of sodium borohydride (0.100 g) was added. The solution was allowed to stand in a refrigerator and tested from time to time with Fehling's solution. When the solution became non-reducing (10 hours) acetone was added to destroy the excess sodium borohydride. The solution was passed through a column of Amberlite IR 120 (H form) resin (10 ml) and the resin was washed with an excess of water. The eluate and washings were evaporated to dryness under reduced pressure. Boric acid was removed by repeated distillation with methanol. The residual clear colorless syrup (0.090 g) could not be induced to crystallize from a variety of solvents. Paper chromatography in solvent A showed the presence of a major component at R_{rh} 0.74 and of a minor one at R_{rh} 1.18 (spray i); the latter was probably 5-acetamido-5-deoxy-D-xylofuranose. The component

Can. J. Chem. Downloaded from www.nrcresearchpress.com by 210.87.254.42 on 09/05/12
For personal use only.

having R_{rh} 0.74 was separated by chromatography on 3 MM paper in solvent A and obtained as a clear colorless syrup which could not be induced to crystallize. The syrup had $[\alpha]_D = +21.2°$ (*c*, 0.33 in methanol).

(b) 1-Acetyl-D-gulo(ido)-2,3,4,5-tetrahydroxypiperidine

This compound (0.100 g) was reduced with sodium borohydride as above. Reduction was considerably slower in this case and required 40 hours for completion. A clear colorless syrup (0.093 g) was obtained which had R_{rh} 0.74 (solvent A, spray i) and $[\alpha]_D = +20°$ (*c*, 0.60 in methanol). The reduced product and the one described above had identical infrared spectra over the range 4000–650 cm^{-1}.

Influence of Heat on 5-Acetamido-5-deoxy-D-xylofuranose and 1-Acetyl-D-gulo(ido)-2,3,4,5-tetrahydroxypiperidine

Aqueous solutions of each compound (2%) were heated in a water bath at 80° C for 1 hour and then examined on paper chromatograms run in solvent A. Two components with R_{rh} 0.66 and 1.18 were detected by sprays i and ii in each case. No interconversion was detectable by paper chromatography when aqueous solutions of either compound were kept at room temperature for 12 hours.

Reaction of 5-Acetamido-5-deoxy-D-xylofuranose with Methanolic Hydrogen Chloride

5-Acetamido-5-deoxy-D-xylofuranose (0.042 g) was dissolved in methanolic hydrogen chloride (1.2%, 4 ml) and allowed to stand at room temperature. The optical rotation was measured at intervals:

Time (hr)	0.23	0.58	1.10	3.50
$[\alpha]_D$	+27.4	+29.2	+23.6	+22.6

The solution became deep yellow and the optical rotation could not be measured after 3.5 hours. The solution was then neutralized with silver carbonate and filtered. The filtrate was treated with hydrogen sulphide and filtered again through Celite. The clear solution was evaporated under reduced pressure to yield a brown syrup (0.040 g) which was non-reducing towards Fehling's solution. Paper chromatography in solvent A gave only one spot, R_{rh} 1.04 (spray ii). The infrared spectrum (smear between "IR tran 2" plates) showed absorption at 3320 cm^{-1} (OH and NH), 1637 cm^{-1} (N—Ac), and 1565 cm^{-1} (NH).

Reaction of 1-Acetyl-D-gulo(ido)-2,3,4,5-tetrahydroxypiperidine with Methanolic Hydrogen Chloride

Qualitative Experiment

1-Acetyl-D-*gulo*(*ido*)-2,3,4,5-tetrahydroxypiperidine (0.045 g) was dissolved in methanolic hydrogen chloride (1.2%, 4 ml) and allowed to stand at room temperature. The optical rotation was measured at intervals:

Time (hr)	0.33	0.78	1.80	3.35	6.64
$[\alpha]_D$	+14.1	+15.0	+15.9	+15.9	+15.9

The solution remained clear and colorless.

Preparative Experiment

1-Acetyl-D-*gulo*(*ido*)-2,3,4,5-tetrahydroxypiperidine (0.126 g) was dissolved in methanolic hydrogen chloride (1.2%, 11.2 ml) and allowed to stand at room temperature for 2 hours. The solution was then worked up as described above to yield a yellow syrup (0.130 g) which crystallized on standing. Paper chromatography in solvent A showed the presence of traces of starting material at R_{rh} 0.65, a major component at R_{rh} 1.15, and a minor at R_{rh} 1.48 (spray ii). The crystalline material was recrystallized first from methanol – ethyl acetate and then from methanol–ether to yield colorless rectangular crystals which were non-reducing towards Fehling's solution. The melting point of this material was 153.5–154.5°; the mixed melting point on admixture with 1-acetyl-D-*gulo*(*ido*)-2,3,4,5-tetrahydroxypiperidine was 139–150°. Paper chromatography in solvent A showed only one major component, at R_{rh} 1.15. The infrared spectrum (0.8% in KBr) showed strong hydroxyl absorption at 3400 cm^{-1} and absorption owing to N—Ac at 1625 cm^{-1} but no absorption attributable to NH. Calc. for $C_8H_{15}O_5N$: C, 46.8; H, 7.37; N, 6.8; OCH_3, 15.1%. Found: C, 46.85; H, 7.24; N, 6.8; OCH_3, 13.2%.

Periodate Oxidation

The compound under examination (10–15 mg) was dissolved in water containing 0.3 *M* sodium metaperiodate solution (1 ml). The total volume was made up to 25 ml with additional water. A blank was prepared with 0.3 *M* sodium metaperiodate (1 ml), which was made up to 25 ml with water. The solutions were stored in the dark at room temperature and 2-ml aliquots were removed at intervals from each of the two solutions for the determination of periodate uptake (7). Formic acid production was determined by addition of ethylene glycol (1 ml) to an aliquot portion (2 ml), followed by titration after 10 minutes with 0.01 *N* sodium hydroxide using methyl red screened with methylene blue as the indicator. The results are summarized in Table I. (No formaldehyde was detected in either (*a*) or (*b*) by the chromotropic acid method (8).)

Can. J. Chem. Downloaded from www.nrcresearchpress.com by 210.87.254.42 on 09/05/12
For personal use only.

TABLE I

	(*a*) 5-Acetamido-5-deoxy-D-xylofuranose						
Time (hr)	0.32	1.28	3.52	6.42	11.2	28.7	48.0
Periodate (moles/mole)	1.21	1.59	1.60	1.68	1.78	1.88	1.90
Formic acid (moles/mole)	0.78	0.91	1.16	1.24	1.36	1.63	
	(*b*) 1-Acetyl-D-*gulo*(*ido*)-2,3,4,5-tetrahydroxypiperidine						
Time (hr)	0.22	1.17	4.07	6.86	10.2	24.0	
Periodate (moles/mole)	1.45	2.54	2.70	2.75	2.80	2.88	
Formic acid (moles/mole)	0.93	1.60	1.83	2.03	2.19	2.50	
	(*c*) Methyl 5-acetamido-5-deoxy-D-xylofuranoside						
Time (hr)	0.28	1.00	3.58	6.00	17.2	22.2	
Periodate (moles/mole)	0.20	0.50	0.83	0.85	1.10	1.09	
Formic acid (moles/mole)	—	0.13	0.23	0.23	0.33	0.33	
	(*d*) 1-Acetyl-D-*ido*(*gulo*?)-2-methoxy-3,4,5-trihydroxypiperidine						
Time (hr)	0.15	0.75	4.16	10.5	23.8	54.4	
Periodate (moles/mole)	0.15	0.49	1.34	1.74	1.85	2.00	
Formic acid (moles/mole)	—	0.10	0.40	0.60	0.73	0.84	

ACKNOWLEDGMENTS

The authors wish to thank the National Research Council for the award of a scholarship (to W. A. S.) and for a grant (N.R.C. T-19) which made this work possible. They also wish to thank Dr. D. G. M. Diaper of the Royal Military College for permitting them the use of an autoclave.

REFERENCES

1. J. K. N. JONES and J. C. TURNER. J. Chem. Soc. 4699 (1962).
2. P. A. LEVENE and A. L. RAYMOND. J. Biol. Chem. **102**, 317 (1933).
3. W. E. TREVELYAN, D. P. PROCTOR, and J. S. HARRISON. Nature, **166**, 444 (1950).
4. L. HOUGH, J. K. N. JONES, and W. H. WADMAN. J. Chem. Soc. 1702 (1950).
5. J. W. BIRD. Can. J. Chem. **40**, 1716 (1962).
6. R. KLEVSTRAND and A. NORDAL. Acta. Chem. Scand. **4**, 1320 (1950).
7. G. NEÜMULLER and E. VASSEUR. Arkiv. Kemi, **5**, 235 (1953).
8. J. F. O'DEA and R. A. GIBBONS. Biochem. J. **55**, 580 (1953).

Can. J. Chem. Downloaded from www.nrcresearchpress.com by 210.87.254.42 on 09/05/12
For personal use only.

STUDIES ON THE PIGMENTS OF PENICILLIUM HERQUEI[1]

N. NARASIMHACHARI[2] AND L. C. VINING[3]

The National Research Council of Canada, Prairie Regional Laboratory, Saskatoon, Saskatchewan

Received October 9, 1962

ABSTRACT

Several minor pigments from cultures of *Penicillium herquei* are described. One of these has been identified as the naphthalic anhydride which is formed when atrovenetin is oxidized with alkaline peroxide. Evidence is presented which suggests that the characteristic green pigment found in this fungus is formed by a reaction analogous to that between ninhydrin and amino derivatives. In *P. herquei* the 1,2,3-trione is probably generated by mild oxidation of perinaphthenone pigments known to be produced by this organism.

Two red pigments, norherqueinone and its monomethyl ether, herqueinone, have been shown (1, 2) to account in a large measure for the color of the mycelium of stationary cultures of *Penicillium herquei* Bainier and Sartory. These are known (3) to be related in structure to atrovenetin [I], the yellow perinaphthenone derivative produced by *P. atrovenetum* G. Smith, since the latter compound can be obtained from norherqueinone by mild reduction. It has been suggested (3) that in herqueinone and norherqueinone the aromaticity of the perinaphthenone system is blocked by a hydroxyl function but no detailed chemical structures for the two pigments have yet been published.

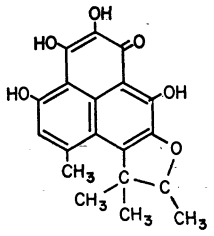

I

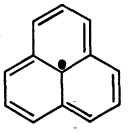

II

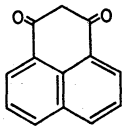

III

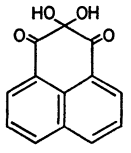

IV

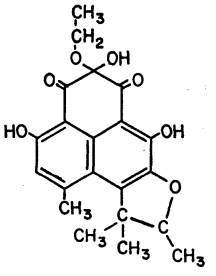

V

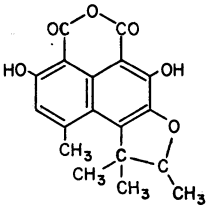

VI

In their original description of *P. herquei*, Bainier and Sartory (4) observed that yellow pigments were produced on banana, carrot, or potato extracts or Raulin's medium

[1]*Issued as N.R.C. No. 7145.*

[2]*National Research Council of Canada Postdoctoral Fellow, 1960–62. Present address: Hindustan Antibiotics Limited, Pimpri, near Poona, India.*

[3]*Present address: Atlantic Regional Laboratory, National Research Council, Halifax, N.S.*

Can. J. Chem. Downloaded from www.nrcresearchpress.com by 210.87.254.42 on 09/05/12
For personal use only.

but, in media rich in peptone, a deep blue pigment was formed. The presence of dark green pigments in *P. herquei* and *P. atrovenetum* was noted by Raistrick and co-workers (2, 5). Unlike most other green pigments occurring in fungal mycelia these could be readily extracted into chloroform. They were not isolated in a pure condition but it was suggested that the formation of quinhydrones analogous to that prepared by Koelsch and Anthes (6) from a mixture of perinaphthenone and perinaphthanone might be responsible for the deep color. In this connection it is of interest that the perinaphthyl radical [II] is relatively stable (7, 8) and displays a blue-green color; the long wavelength absorption maximum for acetoxyperinaphthyl is reported (8) to be at 613 mμ. The presence of similar green pigments in *P. herquei* and *P. atrovenetum* was considered by Raistrick and his colleagues (5) to be further evidence of the close relationship between the two species of fungi.

A green chloroform-extractable pigment in the mycelium of *P. herquei* has also been observed by Riedhart and Porter (9). These authors showed that when a viable mycelium containing the green substance was incubated in the dark, a color change to yellow occurred. Reversion to the green product took place in the light in the presence of oxygen. They prepared both the green pigment and its reduced form in a crude state and described a number of their properties.

The presence of other pigments in extracts from the mycelium of *P. herquei* was recorded by Raistrick and co-workers (2). One of these was isolated in a pure state and identified as physcion. A yellow-brown crystalline substance with antibacterial activity was obtained by Burton (10) from culture filtrates of the fungus. A number of its properties were described but no structural studies appear to have been carried out. Gopalkrishnan and Narasimhachari (11) also isolated a brownish-yellow pigment from an Indian isolate of *P. herquei* which showed similar antibiotic activity to Burton's culture. The properties of this pigment differed markedly from those of herquein, as well as from other known pigments of *P. herquei*.

In the present study two strains of *P. herquei* were employed. The first was that used by Gopalkrishnan and Narasimhachari and is here designated the Ajmer strain. The second was strain I of the organism used by Riedhart and Porter (9). It is referred to here as the Purdue strain. Attention was directed initially towards identification of the pigment produced by the Ajmer strain. However, changes in the cultural characteristics of this organism resulted in loss of the desired properties after only a small quantity of the fermentation products had been accumulated. One of these appeared to be a new compound. Work was continued with the Purdue strain in the expectation that it would also produce the new substance and provide a quantity sufficient for chemical studies. This expectation was not realized and subsequent studies were devoted to the pigments isolated from the Purdue strain when the fungus was grown in surface or submerged culture.

Ajmer Strain

Chromatographic examination of material extracted from the mycelium of stationary cultures showed it to be a mixture of two pigments. One was identified as herqueinone. The other, which will be referred to as compound A, corresponded in most of its properties to the pigment isolated by Gopalkrishnan and Narasimhachari (11). Reliable elemental analyses could not be obtained because of the shortage of material, but the molecular weight estimation of 390 is of the same order as those of the hydroxyperinaphthenone pigments of *P. herquei*. The color reaction with ferric chloride and intense yellow fluores-

Can. J. Chem. Downloaded from www.nrcresearchpress.com by 210.87.254.42 on 09/05/12
For personal use only.

cence obtained with concentrated sulphuric acid support such a structure. Reductive acetylation gave a product which, though not purified, showed some resemblance in its ultraviolet and visible absorption spectra to that of a 9-hydroxyperinaphthen-1-one (3). Compound A differed from known pigments of this type in possessing multiple carbonyl absorption peaks in the infrared spectrum. The positive reaction with 2,4-dinitrophenylhydrazine indicates that at least one of these is due to an aldehydic or ketonic function.

Purdue Strain, Surface Culture

A red pigment was obtained from the mycelium of stationary cultures grown and extracted in the manner used for the Ajmer strain. Chromatographic examination showed it to be mainly herqueinone, with smaller amounts of norherqueinone, and only traces of other pigmented and fluorescent products. One of the latter (compound B), which had an intense greenish yellow fluorescence, was obtained in a small amount as yellow crystals, m.p. 168° C. Analyses and molecular weight estimations agreed with the formula $C_{21}H_{22}O_9$. The substance showed only a single, broad absorption maximum in the carbonyl stretching region centered at 1612 cm^{-1} (cf. atrovenetin, 1620 cm^{-1}). It possessed neither ketonic nor quinonoid properties but gave, by acetylation under reducing conditions, an acetyl derivative different from that obtained by simple acetylation. Neither of these products possessed the typical ultraviolet absorption spectrum of perinaphthenone.

The ultraviolet absorption spectrum of ethanolic solutions of compound B underwent a slow change. The end product, which exhibited a blue fluorescence, had a spectrum similar in shape and the positions of the maxima to those of compound A, compound B leucoacetate, and atrovenetinone ethanolate (see later). It is suggested therefore that each of these substances contains perinaphthane-1,3-dione [III] as a common structural feature.

Purdue Strain, Submerged Culture

Prolonged Soxhlet extraction of the mycelium with ether gave atrovenetin as the major product. The isolation of this pigment, which had hitherto been found only in surface cultures of the related species *Penicillium atrovenetum* G. Smith, has already been commented upon (12). Mild oxidation of atrovenetin in ethanol with *p*-benzoquinone gave a pale yellow product, $C_{21}H_{22}O_7$. At approximately 130° C this is converted to an unstable, brownish-red compound which sublimes under high vacuum. The sublimate dissolves easily in ethanol to regenerate the initial oxidation product. Reduction of the latter with zinc in acetic acid gave a mixture of products, one of which was identified chromatographically as atrovenetin. Reductive acetylation gave atrovenetin triacetate. Methylation with diazomethane gave a derivative believed to be a dimethyl ether, but insufficient product was available for adequate characterization. Oxidation of atrovenetin yellow trimethyl ether or herqueinone with *p*-benzoquinone gave only unchanged starting material. The infrared spectrum of the oxidation product showed absorption maxima attributable to intramolecularly bonded and unbonded hydroxyl groups and at least one conjugated and hydrogen-bonded carbonyl function.

Mild oxidation of 2,3-dihydroxyperinaphthen-1-one with bromine water has been reported by Errera (13) to give perinaphthane-1,2,3-trione. This forms a stable hydrate or alcoholate, considered to have the structure [IV]. By analogy with this reaction and by considering the properties described above, the oxidation product from atrovenetin is formulated as [V]. The parent triketone has been named atrovenetinone.

Can. J. Chem. Downloaded from www.nrcresearchpress.com by 210.87.254.42 on 09/05/12
For personal use only.

From the filtrates of submerged cultures of the Purdue strain of *P. herquei*, herqueinone, norherqueinone, and atrovenetin were isolated. Traces of other pigmented and fluorescent substances were also detected; chromatographic examination showed several of these as well as a small amount of herqueinone to be present also in the mycelial extracts. One of them, distinguished by its intense blue fluorescence, was isolated in sufficient quantity for chemical study and shown to be identical with the naphthalic anhydride obtained from atrovenetin by oxidation with alkaline peroxide and shown by Barton and colleagues (14) to have the structure [VI].

After solvent fractionation and repeated chromatography on silicic acid, a small amount of a green pigment was obtained in an apparently homogeneous condition. This was an amorphous solid of no distinct melting point with a molecular weight of 1090. Insufficient material was obtained for carbon and hydrogen analyses but the molecule contained 1 atom of nitrogen. Weakly basic properties were suggested by the color shift which occurred when an ethereal solution was shaken with dilute mineral acid. An unstable violet product was formed which, if neutralized within a short time, reverted to the original green pigment. On prolonged exposure to acid, irreversible decomposition occurred to a pale yellow product, the ultraviolet absorption spectrum of which was similar to that of atrovenetinone ethanolate. The green pigment was reversibly reduced with zinc in acetic acid to a yellow substance. Reoxidation took place slowly in air and appeared to be more rapid in the light than in the dark, though no definitive tests were made. Repeated reduction and reoxidation under these conditions caused a change in the color of the oxidized form to bluer shades, with a corresponding decrease in the visible absorption maximum from 612 mμ to 604 mμ.

These properties are consistent with those described by Riedhart and Porter (9) for the green pigment which they obtained from *P. herquei*, except that these authors apparently overlooked the transient reversible change in acid. The formation of colorless crystals by evaporation of a pyridine solution of the pigment and the sublimation from the crude solid of a yellow crystalline product could not be reproduced, but may well have been due to impurities. Samples of the green pigment prepared in the manner described by Riedhart and Porter were found to be chromatographically inhomogeneous. An indication that the green pigment is a perinaphthenone derivative is provided by the position of the carbonyl absorption maximum in the infrared spectrum. The similarity between the ultraviolet absorption spectra of its leucoacetate and substituted perinaphthenones, and of the acid degradation product and atrovenetinone ethanolate, affords further evidence.

Perinaphthane-1,2,3-trione (or its hydrate) has been shown by Moubasher and Awad (15) to react, as might be expected from its structural resemblance to ninhydrin, with amino acids, ammonia, or bases to give highly colored products. In view of the molecular weight of the green pigment from *P. herquei* and the presence of nitrogen in the molecule, we suggest that it is formed in the fungus by a similar reaction. In support of this argument, conditions have been discovered under which atrovenetinone will react with ammonia or amino acids to give a product with properties very similar to those of the pigment isolated from the natural source.

Such a structure for the blue-green pigments of *P. herquei* and *P. atrovenetum* offers a plausible explanation for Bainier and Sartory's observation that nutrient media with a high peptone content cause a change in pigmentation of *P. herquei* from orange-yellow to blue. We have also observed that lowering the redox potential of the culture medium,

Can. J. Chem. Downloaded from www.nrcresearchpress.com by 210.87.254.42 on 09/05/12
For personal use only.

e.g., by the addition of sodium sulphite, prevents the appearance of blue-green pigmentation in the mycelium. That cultures of the fungus used in these studies are strongly oxidizing in character is attested to by the isolation of the anhydride [VI], which is almost certainly formed by oxidation of atrovenetin. Whether this and the postulated conversion of atrovenetin to atrovenetinone are brought about by chemical or enzymatic reactions is a matter requiring further study.

EXPERIMENTAL

Conditions of Culture

All cultures were grown in Erlenmeyer flasks (500 ml) containing a nutrient solution of the following composition: 5% sucrose, 0.3% $NaNO_3$, 0.2% corn steep liquor, 0.1% KH_2PO_4, 0.1% KCl, 0.05% $MgSO_4.7H_2O$, 0.001% $FeSO_4.7H_2O$, 0.005% $ZnSO_4.7H_2O$, and 0.3% $CaCO_3$.

For surface cultures, a young 3% vegetative inoculum and 350 ml of medium per flask were used. Cultures were left undisturbed at 25° C for 25 to 30 days, by which time a red-brown mycelial mat had developed.

Submerged cultures were prepared with a young 10% vegetative inoculum and 100 ml of nutrient per flask. They were agitated on a rotary shaker for 7 to 8 days. The mycelium became greenish yellow and finally dark green in color. The broth varied from yellow to reddish yellow but invariably had an intense greenish yellow fluorescence.

Isolation of Pigments

Ajmer Strain, Stationary Culture

The mycelial mat was separated, washed with water, pressed firmly on a Büchner funnel, and vacuum applied to remove excess moisture. It was then extracted in a Soxhlet apparatus for 24 hours with ether. Evaporation of the ethereal extract left an oily residue which could be converted to a red solid by trituration with petroleum ether. Circular paper chromatography on formamide-treated paper with benzene as mobile phase showed this to be a mixture of two pigments giving an orange zone with the same R_f value (0.82) as authentic herqueinone and a yellow zone, R_f 0.03.

A sample (49 mg), chromatographed on a column of silicic acid (10 g) developed with chloroform, separated into two fractions. A red zone was eluted first and gave, on evaporation, a partially crystalline substance (30 mg). This was recrystallized from methanol as red prisms, m.p. 224–226° C undepressed on admixture with authentic herqueinone. The ultraviolet, visible, and infrared spectra and R_f value (0.65), when examined by thin-layer chromatography on silica gel G using chloroform – acetic acid (7:3) as developing solvent, were also indistinguishable from those of herqueinone. The second zone, orange yellow in color, yielded a residue (compound A, 8 mg) which was crystallized from an acetone–petroleum ether (b.p. 60–80° C) mixture as orange-brown, boat-shaped prisms decomposing slowly above 190° C without exhibiting a distinct melting point; mol. wt. (Mechrolab Osmometer using acetone as solvent) 390; $\lambda\lambda_{max}$ (in ethanol) 257 mμ ($E^{1\%}_{1\,cm}$ = 353), 321 mμ ($E^{1\%}_{1\,cm}$ = 350), and 420 mμ (infl., $E^{1\%}_{1\,cm}$ = 26); ν_{max} (KBr disk) 3395, 1724, 1708, 1685, 1657, 1588, 840, and 802 cm^{-1}.

Compound A was insoluble in water or petroleum ether, sparingly soluble in benzene or carbon tetrachloride, but easily soluble in other common organic solvents. It dissolved slowly in 0.1 *N* $NaHCO_3$ and readily in dilute Na_2CO_3 or NaOH, giving an orange solution. In concentrated sulphuric acid it gave a yellow solution with bright yellow fluorescence but it was insoluble in dilute acids. With ferric chloride in ethanol it gave a brownish-green color and with 2,4-dinitrophenylhydrazine an orange-red precipitate. Treatment with zinc in acetic acid at room temperature rapidly reduced the orange solution to a pale greenish yellow. Prolonged shaking in air partially restored the original color. Reductive acetylation (30 minutes on a steam bath with acetic anhydride and anhydrous sodium acetate) gave a product with brilliant blue fluorescence and $\lambda\lambda_{max}$ at 230, 252 (infl.), 263, 333, 350, 367, 388 (infl.), and 435 mμ.

Purdue Strain, Stationary Culture

Mycelium.—The pigment was extracted as above with ether from the pressed mycelial mats of five flasks and gave, after trituration with petroleum ether, a red solid (500 mg). Extraction of this material with several portions of cold chloroform left a residue (64 mg) which, after two crystallizations from glacial acetic acid, gave fine red needles decomposing at 262° C on slow heating. The melting point behavior was unchanged on admixture with authentic norherqueinone. Found: C, 63.59%; H, 5.10%. Calc. for $C_{19}H_{18}O_7$: C, 63.58%; H, 5.06%. The ultraviolet, visible, and infrared spectra were also indistinguishable from those of authentic norherqueinone.

A sample (327 mg) of the chloroform-soluble fraction was chromatographed on a column (5×50 cm) of silicic acid developed initially with benzene. Three very minor zones were slowly eluted. The first contained an intensely blue fluorescent substance, $\lambda\lambda_{max}$ (in ether) 255, 355 (infl.), 360, and 378 mμ. The second and third contained yellow non-fluorescent products, $\lambda\lambda_{max}$ (in $CHCl_3$) 257, 280 (infl.), 344, 365 (infl.), 410 (infl.) mμ and $\lambda\lambda_{max}$ (in $CHCl_3$) 259.5, 344 mμ respectively. On changing the developing solvent to

Can. J. Chem. Downloaded from www.nrcresearchpress.com by 210.87.254.42 on 09/05/12
For personal use only.

chloroform a major red zone was eluted. Evaporation of the solvent left deep red needles (280 mg) which after two recrystallizations from aqueous methanol gave clusters of small red prisms, m.p. 224° C, undepressed on admixture with authentic herqueinone. Found: C, 64.3%; H, 5.3%; OCH_3, 8.3%. Calc. for $C_{20}H_{20}O_7$: C, 64.5%; H, 5.4%; 1-OCH_3, 8.35%. The ultraviolet, visible, and infrared spectra were also indistinguishable from those of authentic herqueinone.

After herqueinone a minor zone showing intense yellow fluorescence was eluted. The ultraviolet absorption spectrum showed this fraction to be contaminated with herqueinone. It was therefore rechromatographed on a second column (2.5×30 cm) of silicic acid and the product from appropriate fractions of the chloroform eluate crystallized twice from a chloroform – carbon tetrachloride mixture to give lemon yellow needles (compound B, 18 mg), m.p. 168° C. Found: C, 60.51%; H, 5.24%; CCH_3, 16.5%; mol. wt. (Mechrolab Osmometer using acetone as solvent) 403. Calc. for $C_{21}H_{22}O_9$: C, 60.28%; H, 5.30%; 3CCH_3, 19.35%; mol. wt. 418; $\lambda\lambda_{max}$ (in ethanol) 244 mμ (ϵ = 24,000), 252 mμ (infl., ϵ = 21,500), 283 mμ (ϵ = 13,080), 340 mμ (infl., ϵ = 8500), 377 mμ (infl., ϵ = 14,950), 400 mμ (ϵ = 16,500), and 420 mμ (infl., ϵ = 15,150). In less polar solvents the shape of the spectrum changed appreciably so that the long wavelength maximum occurred at 378 mμ in ether and 377 mμ in $CHCl_3$ with inflections at 382 and 410 mμ in both solvents. The spectrum in ethanol underwent a slow change giving, after approximately 24 hours in redistilled 99% ethanol, a stable chromophore with a blue fluorescence and $\lambda\lambda_{max}$ 244 mμ (ϵ = 43,800), 265 mμ (infl., ϵ = 20,750), 343 mμ (ϵ = 13,400), and 372 mμ (infl., ϵ = 5750).

The infrared spectrum (KBr disk) of compound B had maxima at 3440, 1612 (broad), 1465, 1385, 910, and 854 cm^{-1}. The pigment was very soluble in ethanol, acetone, chloroform, or acetic acid; moderately soluble in ether or carbon tetrachloride; and insoluble in petroleum ether or water. It dissolved readily in 0.1 *N* $NaHCO_3$ or NaOH to a yellow solution which slowly decolorized. This was accompanied by a change in the fluorescence of the solution from yellow to blue. It was insoluble in dilute HCl but dissolved in concentrated H_2SO_4 to a greenish yellow solution with a bright yellow fluorescence. Ferric chloride in ethanol gave a green color. Tests for ketonic and aldehydic carbonyl functions were negative.

Acetylation (30 minutes at 100° C with acetic anhydride and anhydrous sodium acetate) gave a product with weak yellow fluorescence and $\lambda\lambda_{max}$ 243, 338 (infl.), 354, and 400 mμ. Reductive acetylation, as above but with the addition of zinc dust, gave a product with intense blue fluorescence and $\lambda\lambda_{max}$ 260, 341, and 412 mμ (infl.) in ether.

Culture filtrate.—A portion (1 liter) of the filtered broth from these stationary cultures was acidified to pH 2 and extracted twice with ethyl acetate. When the extracts were combined and evaporated, a red solid (100 mg) was obtained. Chromatography on a silicic acid column gave only a single, orange-red zone from which, by evaporation of the solvent and crystallization of the residue from methanol, herqueinone (75 mg), m.p. 224–226° C, separated.

Purdue Strain, Shaken Culture

Mycelium.—Removal of the pigment was found to be very difficult if the filtered mycelial solids were dried before extraction. When the pressed filter cake (wet weight 75 g) from 10 flasks was extracted with ether in a Soxhlet apparatus for 24 hours, then drained and re-extracted with methanol for a further 12 hours, most of the pigment was removed. The ether extract deposited on the walls of the receiver a yellow solid which, after several recrystallizations, yielded yellow needles, m.p. 290° C (decomp.) with prior darkening from 270° C. Found: C, 66.8%; H, 5.6%. Calc. for $C_{19}H_{18}O_6$: C, 66.7%; H, 5.3%. The melting point showed no depression on admixture with an authentic sample of atrovenetin, and the ultraviolet, visible, and infrared spectra of the two substances were indistinguishable.

The washings and mother liquors from the purification of atrovenetin were combined with the methanolic extract of the mycelium and the deep green solution evaporated to dryness *in vacuo*. The solid was taken up in chloroform, filtered, and the soluble portion chromatographed on a column of silicic acid. Development with chloroform eluted a dark zone, collected as a series of fractions ranging in color from blue to green. On keeping, they all changed to a stable, dark green color. Evaporation of the pooled solutions gave a green amorphous solid. By thin-layer chromatography on silica gel G using benzene as solvent and paper chromatography using benzene – petroleum ether (1:1) with formamide-treated paper, this was found to be heterogeneous.

The material (110 mg) was redissolved in benzene and applied to a column (30×2.5 cm) of silicic acid. On prolonged developing with benzene the deep green band resolved into a series of zones which were eluted in succession to give (*a*) orange yellow cubes (2 mg) by slow evaporation of an ethereal solution, $\lambda\lambda_{max}$ (in ether) 255, 382, and 404 mμ, (*b*) orange yellow rods (5 mg) by slow evaporation of an ethereal solution, $\lambda\lambda_{max}$ (in ether) 293 and 409 mμ, and (*c*) a blue fluorescent substance (compound C) which was crystallized from benzene, ethanol, or carbon tetrachloride as cream-colored needles (32 mg), m.p. 256° C. Found for a sample sublimed at 140° C in high vacuum: C, 65.97%; H, 4.97%; CCH_3, 12.52%; mol. wt. (Mechrolab Osmometer using acetone as solvent) 338. Calc. for $C_{18}H_{16}O_6$: C, 65.85%; H, 4.89%; 2CCH_3, 14.14%; mol. wt. 328.2. The ultraviolet and infrared spectra were indistinguishable from those of an authentic specimen of the anhydride [VI]. The authentic sample, m.p. 257–258° C, caused no depression of melting point on admixture with compound C and had similar properties. Compound C was very soluble in chloroform; moderately soluble in acetone, ethanol, ether, and carbon tetrachloride; poorly soluble in benzene and insoluble in petroleum ether, water, dilute HCl or Na_2CO_3. It dissolved only slowly in caustic

Can. J. Chem. Downloaded from www.nrcresearchpress.com by 210.87.254.42 on 09/05/12
For personal use only.

alkali but easily in concentrated H_2SO_4 to an orange-brown solution with a weak yellow fluorescence. An intense reddish-violet color formed on addition of ferric chloride in ethanol. Acetylation (30 minutes at 100° C with acetic anhydride and anhydrous sodium acetate) afforded a product with an ultraviolet absorption spectrum similar to that given by an authentic specimen of the diacetate of [VI].

Further elution of the column gave (*d*) orange-yellow plates (15 mg) by slow evaporation from ether, $\lambda\lambda_{max}$ (in ether) 288 and 431 mμ; this fraction was contaminated with compound C; and (*e*) a deep green substance purified further by precipitating with ethanol from a solution in chloroform. It was an amorphous solid (7 mg) which decomposed slowly above 200° C. Found: N (Dumas), 1.44%; mol. wt. (Mechrolab Osmometer, using carbon tetrachloride as solvent), 1090; $\lambda\lambda_{max}$ (in ether) 260, 340 (infl.), 366, 400 (infl.), and 612 mμ; ν_{max} (KBr disk) 1610, 1458, 1385, 865, and 800 cm^{-1}.

The green pigment was very soluble in chloroform, carbon tetrachloride, and acetone; moderately soluble in ether; and poorly soluble in ethanol, methanol, acetic acid, water, dilute HCl, and NaOH. In concentrated H_2SO_4 it gave a greenish-brown solution with a bright yellow fluorescence. Ferric chloride in ethanol gave a weak orange-brown color. On treatment with zinc an acetic acid solution of the green pigment became yellow in color. The change was accompanied by loss of the peak at 612 mμ, a shift of the 366 mμ maximum to 384 mμ, and a reduction in intensity of the 260 mμ peak. When the excess zinc was removed and the solution shaken in air the green color returned and the spectrum reverted to that of the original green solution. Reductive acetylation (30 minutes at 100° C with acetic anhydride, zinc dust, and anhydrous sodium acetate) gave a yellow fluorescent product with $\lambda\lambda_{max}$ (in ether) at 370 and 402 mμ and an inflection at 425 mμ.

When a solution of the green pigment in chloroform or ether was shaken with dilute aqueous hydrochloric acid the color rapidly changed to violet and was accompanied by a shift in the visible absorption maximum at 612 mμ to 550 mμ. If the solution was neutralized at this stage the change was reversible. Prolonged contact with acid caused a slow disappearance of the 550 mμ maximum. By 3 hours the spectral changes were complete and no longer reversible. The product of the reaction showed $\lambda\lambda_{max}$ (in ether) at 250 (infl.), 259, 343, and 360 (infl.) mμ.

Culture filtrate.—From the filtered broth (800 ml) of submerged cultures, by acidification with hydrochloric acid to pH 2, and extraction with ethyl acetate, a red solid (150 mg) was obtained. This was dissolved in benzene and chromatographed on a column of silicic acid. Development with benzene eluted in succession: (*a*) a trace of blue fluorescent material identified spectrally and by thin-layer chromatography on silica gel G using chloroform – acetic acid (7:3) as the anhydride [VI] (R_f 0.89); (*b*) and (*c*) traces of non-fluorescent orange products (R_f 0.82) not further examined. Use of chloroform as developing agent eluted (*d*), a non-fluorescent orange zone from which herqueinone (50 mg) was obtained. Addition of 10% methyl ethyl ketone to the chloroform used as elutriant removed (*e*), a poorly defined, fluorescent, yellow zone from which atrovenetin (30 mg) was crystallized. Thin-layer chromatography of the mother liquor showed that, in addition to atrovenetin (R_f 0.05), compound B (R_f 0.25) was present. Finally, elution of the column with methanol removed an orange zone which, on evaporation, gave a red-brown amorphous substance (20 mg). Circular paper chromatography using formamide-treated paper and chloroform as mobile phase showed this to be mainly norherqueinone (R_f 0.64).

Oxidation of Atrovenetin with p-Benzoquinone

Atrovenetin (50 mg) suspended in ethanol (3 ml) was heated on a water bath for 15 minutes with *p*-benzoquinone (20 mg). From the resulting deep brown solution pale yellow needles of atrovenetinone ethanolate were deposited on cooling. These were separated and recrystallized from ethanol. The crystals begin to sinter and darken from 130° C, melting finally at 212–216° C. Found in a sample dried in high vacuum at room temperature: C, 65.35%; H, 5.74%; mol. wt. (Mechrolab Osmometer using acetone as solvent) 395. Calc. for $C_{21}H_{22}O_7$: C, 65.27%; H, 5.74%; mol. wt. 386; $\lambda\lambda_{max}$ (in ethanol) 251 mμ (infl., ϵ = 46,300), 259 mμ (ϵ = 70,300), 275 mμ (infl., ϵ = 8320), 339 mμ (ϵ = 23,300), and 366 mμ (infl., ϵ = 12,500); ν_{max} (KBr disk) 3440, 3000–2600, 1605–1660 (broad), 1458, 1380, 856, 815, 805, and 796 cm^{-1}; (in CCl_4) 3490, 3000–2600, 1640–1610, 1459, and 1380 cm^{-1}.

Atrovenetinone was readily soluble in acetone, ether, chloroform, carbon tetrachloride, and benzene; sparingly soluble in ethanol and methanol; and insoluble in water. Addition of zinc dust to a solution in acetic acid caused a marked increase in intensity of the yellow color. Thin-layer chromatography showed that the reaction gave a mixture of products; one of these possessed the same R_f value as atrovenetin. Reductive acetylation (30 minutes at 100° C in acetic anhydride with anhydrous sodium acetate) gave a product indistinguishable from atrovenetin triacetate.

Reaction of Atrovenetinone with Ammonia and Amino Acids

Atrovenetinone (1 mg) in acetone (1 ml) was added to 0.01 *M* solution of NH_4Cl, phenylalanine, or leucine in 1 *M* phosphate buffer of pH 7.0. On heating of the mixture for 10 minutes on a steam bath, a green precipitate formed. This, when separated and dissolved in ether, afforded a deep green solution with λ_{max} 612 mμ. The solubility, color reactions, and spectral changes of this pigment when treated with acid and alkali, or reduced with zinc and acetic acid and allowed to reoxidize in air, were identical with those of the green pigment isolated from *P. herquei*. Its infrared spectrum and content of nitrogen (0.9%)

Can. J. Chem. Downloaded from www.nrcresearchpress.com by 210.87.254.42 on 09/05/12
For personal use only.

were similar to, but not identical, with those of the natural product. Thorough purification of the product was not attempted.

No green color was obtained when ammonia or the amino acid was omitted. Pure atrovenetin, herqueinone, compounds A and B, and the anhydride [VI] did not give the reaction.

ACKNOWLEDGMENTS

The authors wish to thank Professor C. L. Porter, Purdue University, Lafayette, Indiana, for a transfer of *P. herquei*; Professor H. Raistrick, Belfairs, Sea Drive, Felpham, Bognor Regis, Sussex, Professor D. H. R. Barton, Imperial College, London, and Dr. G. A. Morrison, Department of Organic Chemistry, The University, Leeds, for providing authentic specimens of known pigments of *P. herquei* and derivatives; Dr. R. H. Haskins, Mr. L. R. Nesbitt, and Mr. E. G. Rogala of the Prairie Regional Laboratory, and Mr. K. S. Gopalkrishnan of Hindustan Antibiotics Limited, Pimpri, near Poona, India, for help with microbiological aspects of the problem. Microanalyses and infrared spectra were provided by Mr. M. Mazurek and Mr. W. C. Haid of the Prairie Regional Laboratory. Miss M. J. A. Gates gave valuable technical assistance.

REFERENCES

1. R. E. HARMAN, J. CASON, F. H. STODOLA, and A. L. ADKINS. J. Org. Chem. **20**, 1260 (1955).
2. J. A. GALARRAGA, K. G. NEILL, and H. RAISTRICK. Biochem. J. **61**, 456 (1955).
3. D. H. R. BARTON, P. DE MAYO, G. A. MORRISON, W. H. SCHAEPPI, and H. RAISTRICK. Chem. Ind. (London), 552 (1956).
4. G. BAINIER and A. SARTORY. Soc. Mycol. France, Bul. Trimest. **28**, 121 (1912).
5. K. G. NEILL and H. RAISTRICK. Biochem. J. **65**, 166 (1957).
6. C. F. KOELSCH and J. A. ANTHES. J. Org. Chem. **6**, 558 (1941).
7. D. H. REID. Chem. Ind. (London), 1504 (1956).
8. E. CLAR. *In* Aromatische Kohlenwasserstoffe. 2nd ed. Springer Verlag. 1952. p. 431.
9. J. M. RIEDHART and C. L. PORTER. Mycologia, **50**, 390 (1958).
10. H. S. BURTON. Brit. J. Exptl. Pathol. **30**, 151 (1949).
11. K. S. GOPALKRISHNAN and N. NARASIMHACHARI. *In* Antibiotics, a symposium held at the Hindustan Antibiotics (Private) Ltd., Pimpri, March 27. Council of Scientific and Industrial Research, New Delhi, India. 1958. p. 176.
12. N. NARASIMHACHARI, K. S. GOPALKRISHNAN, R. H. HASKINS, and L. C. VINING. Can. J. Microbiol. In press.
13. G. ERRERA. Gazz. Chim. Ital. **43**, I, 583 (1913); Chem. Abstr. **7**, 3756 (1913).
14. D. H. R. BARTON, P. DE MAYO, G. A. MORRISON, and H. RAISTRICK. Tetrahedron, **6**, 48 (1959).
15. R. MOUBASHER and W. I. AWAD. J. Chem. Soc. 1137 (1949).

Can. J. Chem. Downloaded from www.nrcresearchpress.com by 210.87.254.42 on 09/05/12
For personal use only.

LYCOPODIUM ALKALOIDS

V. THE BROMINATION OF LYCOPODINE AND THE STRUCTURE OF ALKALOID L.20[1]

W. A. Ayer, J. A. Berezowsky, and D. A. Law
Chemistry Department, University of Alberta, Edmonton, Alberta

Received November 13, 1962

ABSTRACT

Monobromination of lycopodine hydrobromide in chloroform yields 6α-bromolycopodine hydrobromide, which can be epimerized to 6β-bromolycopodine hydrobromide. Hydrolysis of 6α-bromolycopodine proceeds with overall retention of configuration to give 6α-hydroxylycopodine, which is identical with the *Lycopodium lucidulum* alkaloid L.20. On the basis of some of the rotatory dispersion data presented it is suggested that positively charged nitrogen has a negative specific rotativity.

Can. J. Chem. Downloaded from www.nrcresearchpress.com by 210.87.254.5 on 09/05/12
For personal use only.

In 1956 Barclay and MacLean reported (1) that the bromination of lycopodine, now known (2, 3) to have structure I, in carbon tetrachloride yielded a monobrominated product, isolated as its hydrobromide, of melting point 290–295° (decomp.). Attempts to isolate the corresponding free base were unsuccessful. In connection with structural studies on lycoclavine (4) we have had occasion to repeat and extend this work and wish at this time to report the results of this investigation.

In our hands treatment of lycopodine with an equimolar amount of bromine in either carbon tetrachloride or chloroform without added hydrogen bromide led to the isolation of a crystalline product which proved to be a mixture of lycopodine hydrobromide and bromolycopodine hydrobromide. The melting point of this mixture (285–295°) corresponds to that reported by the earlier workers (1) and differs considerably from that of pure bromolycopodine hydrobromide (see below). The composition of the crystalline product was shown in the following manner. The analytical results obtained on an extensively recrystallized sample fitted best an approximately 1:1 mixture of bromolycopodine hydrobromide and lycopodine hydrobromide. Treatment of the mixture with aqueous sodium hydroxide followed by chromatography led to the isolation of lycopodine, in about 50% yield, as well as the enolic α-diketone III. Cocrystallization of equimolar quantities of lycopodine hydrobromide and bromolycopodine hydrobromide from a small volume of solvent yielded material the melting point and infrared spectrum

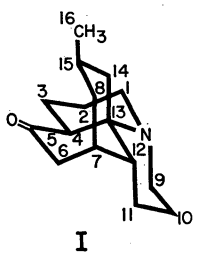

I

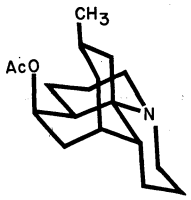

II

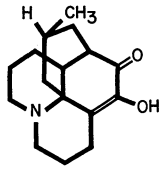

III

of which were similar to those of the recrystallized bromination product. The analytical results recorded by Barclay and MacLean suggest that their material contained approximately 80% of the bromo compound. Since bromolycopodine hydrobromide is some-

[1]*Part IV: W. A. Ayer and D. A. Law. Can. J. Chem.* **40**, *2088 (1962).*

what more soluble than lycopodine hydrobromide in the solvents used, the material obtained after several recrystallizations is actually richer in the non-brominated material. It was possible to obtain small quantities of pure bromolycopodine hydrobromide by fractional crystallization of the mother liquors. Since all of the bromine is consumed during the reaction, we attribute the incomplete bromination to competitive oxidative attack by bromine at the tertiary nitrogen. This view is supported by the observations that the preformed hydrobromide is cleanly monobrominated when treated with 1 mole of bromine (see below) and that acetyldihydrolycopodine (II) rapidly decolorizes 0.5 equivalent of bromine. In the latter reaction it was possible to recover 70% of the acetyldihydrolycopodine *as its hydrobromide*, indicating that reduction of the bromine had occurred.

Bromination of lycopodine hydrobromide in chloroform containing a slight excess of hydrogen bromide gave, in better than 90% yield, 6α-bromolycopodine hydrobromide[2] (IV·HBr), m.p. 266–269°. The position and orientation of the bromine were shown in the following way. The nuclear magnetic resonance spectrum of IV showed a one-proton signal at 5.82 τ (broadened singlet), indicating that bromination had occurred at C-6 rather than C-4. The infrared spectrum of the hydrobromide in chloroform solution showed carbonyl absorption at 1711 cm^{-1}, little shifted from that of lycopodine hydrobromide (1707 cm^{-1}) and indicative of the axial nature of the C-6 bromine (6). The ultraviolet spectrum of the bromo compound (λ_{max} 306 mμ) showed the expected (7) bathochromic shift relative to lycopodine hydrobromide (λ_{max} 280 mμ).

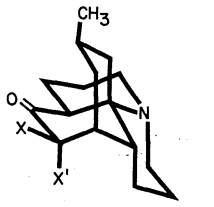

IV X = H; X' = Br
VI X = Br; X' = H
X X = H; X' = OH

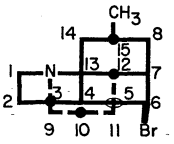

V

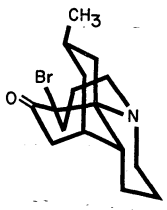

VII

With the structure of the bromo compound thus assigned, it was of interest to examine its optical rotatory dispersion curve in the light of the axial haloketone rule (8) and provide further evidence for the absolute configuration of lycopodine. The absolute configuration represented by structure I was first assigned by application of the octant rule to lycopodine itself (9). If structure IV represents the absolute configuration of 6α-bromolycopodine the axial haloketone rule predicts that it will show a positive Cotton effect whereas the enantiomer will show a negative Cotton effect. In fact, 6α-bromolycopodine hydrobromide does exhibit a *positive* Cotton effect with extrema at 332 and 280 mμ, amplitude[3] +10,650°. Lycopodine hydrobromide exhibits a negative Cotton effect with extrema at 305 and 268 mμ, amplitude −2770°. Since lycopodine itself shows a positive Cotton effect (9), amplitude +17,000°, it appears that positively charged nitrogen (which in the octant diagram (V)[4] for this system appears in the rear upper

[2]*The numbering system used is that suggested by Wiesner (5). Substituents in rings A, B, and C are referred to as α if trans to the C-7 to C-13 bridge and β if cis to the bridge.*

[3]*Amplitudes are given as the algebraic difference between molecular rotation for peak and trough.*

[4]*In the octant diagram V carbons 9, 10, and 11 lie directly behind carbons 3, 4, and 5, respectively, i.e., they they are in the horizontal plane.*

Can. J. Chem. Downloaded from www.nrcresearchpress.com by 210.87.254.5 on 09/05/12
For personal use only.

left octant) has, like fluorine, a negative specific rotativity (10). An alternate explanation, that the difference is due to a change in conformation on salt formation, seems, on the basis of the examination of molecular models (Dreiding), unlikely. Both lycopodine perchlorate and lycopodine methiodide show negative Cotton effects with amplitudes similar to that of the hydrobromide. A solution of lycopodine in acetic acid also exhibits a negative Cotton effect. In agreement with the octant rule (10) 6α-bromolycopodine shows a more strongly positive Cotton effect (amplitude +29,500°) than does lycopodine (see V).

When a solution of 6α-bromolycopodine hydrobromide (IV·HBr) in glacial acetic acid was heated for an hour on the steam bath the product, isolated in 75% yield after evaporation of the acetic acid and washing of the residue with acetone, showed carbonyl absorption (nujol) of approximately equal intensity at 1720 and 1703 cm^{-1}. By fractional crystallization from methanol it was possible to isolate the component responsible for the 1720 cm^{-1} band in about 10% overall yield. This has been assigned the structure 6β-bromolycopodine hydrobromide (VI·HBr) on the basis of its analysis and its infrared (ν_{max} 1728 cm^{-1} in $CHCl_3$) and ultraviolet (λ_{max} 276 mμ) spectra, both of which are indicative of an equatorial α-bromoketone (6, 7). The alternate formulation, 4β-bromolycopodine hydrobromide, although not excluded by this data, is considered highly unlikely, since it would force the molecule to adopt a conformation in which ring C is in a boat conformation involving a serious bowsprit–flagpole interaction (VII). The negative rotatory dispersion curve is almost plain, with a slight inflexion toward the negative side at 310 mμ. Attempts to effect the epimerization in higher yield by use of more strenuous reaction conditions resulted in extensive decomposition and much lower overall yields. When 6β-bromolycopodine hydrobromide (VI·HBr) was subjected to the epimerizing conditions noted above, the crude product did not show a detectable (by infrared) amount of the 6α-epimer, demonstrating that the product obtained from the 6α-compound is not an equilibrium mixture.

The free bromoketone IV was extremely sensitive to basic conditions. It was prepared by shaking a chloroform solution of the hydrobromide with cold dilute ammonium hydroxide or sodium bicarbonate. It decomposed on melting, with the elimination of hydrogen bromide and the formation of the unsaturated ketone VIII (see below), or on standing in methanol, as revealed by the decrease in amplitude of the optical rotatory dispersion curve with time and by the appearance of salt bands ($\overset{+}{N}H$) in the infrared spectrum of material recovered from the optical rotatory dispersion measurements. Treatment of 6α-bromolycopodine hydrobromide with aqueous sodium hydroxide at room temperature yielded a mixture of the enolic α-diketone III, previously prepared by selenium dioxide of lycopodine (4), and the unsaturated ketone VIII. The diketone III is presumably formed by aerial oxidation of the Δ^5-enolate form of the corresponding α-ketol (4), and the unsaturated ketone VIII by 1,4-elimination of HBr from the Δ^4-enol form of the bromoketone. The structure of the ketone VIII was shown in the following way. The ultraviolet spectrum showed a maximum at 244 mμ (log ε 3.9). The infrared spectrum showed peaks of almost equal intensity at 1680 and 1610 cm^{-1}, indicating (11) the cisoid nature of the α,β-unsaturated ketonic function. The n.m.r. spectrum revealed the presence of a single olefinic proton (poorly resolved triplet at 3.04 τ) located at the β-position of the unsaturated system (12). Reduction of the unsaturated ketone VIII with lithium and ammonia gave lycopodine (I), showing that no skeletal rearrangement had occurred during the dehydrobromination. The ketone VIII has recently been prepared by dehydration of flabelliformine (IX) (13).

Can. J. Chem. Downloaded from www.nrcresearchpress.com by 210.87.254.5 on 09/05/12
For personal use only.

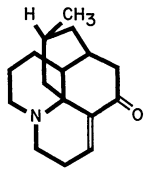

VIII

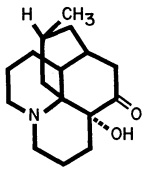

IX

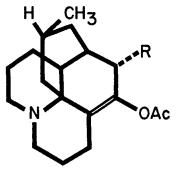

XI R = OAc
XII R = H

When sodium bicarbonate was substituted for sodium hydroxide in the hydrolysis of 6α-bromolycopodine hydrobromide a crystalline compound, $C_{16}H_{25}O_2N$, m.p. 258–259°, was obtained in high yield. The high melting point and the infrared spectrum, which showed (in nujol) an unusually broad OH stretching vibration (2400–3200 cm^{-1}) were reminiscent of alkaloid L.20, first isolated by Manske and Marion from *Lycopodium lucidulum* Michx. (14) and later in these laboratories from the same plant.[5] Direct comparison (mixed melting point, infrared spectra, optical rotatory dispersion curves) confirmed the identity of the compounds from the two sources. This finding, coupled with the evidence presented below, necessitates a revision of the molecular formula of alkaloid L.20 from $C_{17}H_{27}O_2N$ (14) to $C_{16}H_{25}O_2N$.

The infrared spectrum of alkaloid L.20 in alcohol-free chloroform showed absorption at 3620 cm^{-1} (free OH) and 1710 cm^{-1} (ketone), thus defining the nature of the two oxygen atoms. Reduction of L.20 with calcium and ammonia (15) gave lycopodine, defining the carbon–nitrogen skeleton and the position of the carbonyl. The fact that the hydroxyl group was eliminated during the reduction shows that it is α to the carbonyl and suggests that it is axially orientated (15). This orientation is confirmed by the ultraviolet spectrum, which shows carbonyl absorption at 296 mμ (16), and the infrared spectrum, which reveals a non-hydrogen-bonded hydroxyl. The secondary nature of the hydroxyl group follows from the observation that L.20 is transformed to the diketone III in aqueous sodium hydroxide in the presence of air, and from the fact that the nuclear magnetic resonance spectrum of its acetyl derivative shows a one-proton signal at 5.11 τ (C*H*OAc). Thus alkaloid L.20 is 6α-hydroxylycopodine (X) and the hydrolysis of 6α-bromolycopodine proceeds with overall retention of configuration. When alkaloid L.20 (X) was treated with sodium propoxide in *n*-propanol in an atmosphere of nitrogen it was epimerized to the known (4) 6β-hydroxylycopodine. The epimerization also occurred when L.20 was passed through a column of basic alumina. The unsaturated ketone VIII was obtained when L.20 was subjected to the action of hot 10% hydrochloric acid.

Displacement reactions of α-haloketones normally proceed with inversion of configuration (17); however, in this case attack from the backside is extremely hindered by the C-7 to C-13 bridge and displacement is likely preceded by epimerization. In agreement with this view, the 6β-bromoketone (VI) also yields alkaloid L.20 (X) when treated with aqueous bicarbonate.

Acetylation of alkaloid L.20 with pyridine – acetic anhydride at −10° yielded the expected acetyl-L.20 (X, OAc in place of OH). However, when the acetylation was carried out at room temperature a high yield of the enol acetate XI was obtained. Compound XI absorbed in the infrared at 1760 and 1680 cm^{-1} (enol acetate carbonyl and double bond, respectively) and at 1735 cm^{-1} (acetoxyl). The nuclear magnetic resonance

[5]*We wish to thank Dr. L. Marion for an authentic sample of alkaloid L.20.*

Can. J. Chem. Downloaded from www.nrcresearchpress.com by 210.87.254.5 on 09/05/12
For personal use only.

spectrum showed two acetoxyl methyls (7.98 and 8.06 τ) as well as a one-proton signal at 5.02 τ (C*H*OAc). Hydrolysis of XI with dilute acid at room temperature afforded acetyl-L.20 and hydrolysis with aqueous bicarbonate gave back alkaloid L.20 (X). The same enol acetate XI was obtained, together with the unsaturated ketone VIII, when 6α-bromolycopodine hydrobromide was refluxed with sodium acetate in acetic acid – acetic anhydride.

It is interesting to note that the enol acetylation of lycopodine (I) with acetic anhydride – *p*-toluenesulphonic acid yields the Δ^4-enol acetate XII, as shown by the lack of olefinic absorption in the n.m.r. spectrum, whereas bromination occurs via the Δ^5-enol. Provided that the direction of acid-catalyzed enol acetylation is a measure of the preferred direction of acid-catalyzed enolization in this system, the position of bromination must be due to the greater degree of steric hindrance at C-4 than at C-6.

EXPERIMENTAL

Ultraviolet absorption spectra were determined in 95% ethanol. Optical rotatory dispersion spectra were measured on a Rudolph Automatic Recording Spectropolarimeter. Nuclear magnetic resonance spectra were measured on ca. 10% w/v solutions in deuteriochloroform using a Varian Associates Model A-60 spectrometer with tetramethylsilane as an internal standard. Melting points were determined on a hot stage and are uncorrected. Alumina, unless otherwise specified, means basic alumina of activity III–IV (Brockmann scale). Skellysolve B refers to Skelly Oil Company light petroleum, b.p. 62–70°.

Bromination of Lycopodine

A solution of lycopodine (0.45 g) in chloroform (20 ml) was treated with a solution of bromine (0.30 g) in chloroform (20 ml). After standing 2 hours at room temperature the faintly yellow solution was evaporated at the pump. The solid residue was washed with a small volume of cold acetone, leaving a colorless solid (0.57 g), m.p. 280–295° (decomp.). The analytical sample, prepared by recrystallizing three times from methanol, melted at 285–295° (decomp.). Calc. for $C_{16}H_{26}ONBr \cdot C_{16}H_{25}ONBr_2$: C, 52.26; H, 6.99; Br, 32.60%. Found: C, 51.95, 52.27; H, 6.93, 6.88; Br, 32.09%. Infrared spectrum: ν_{max}^{nujol} 2540 (+NH), 1700 cm^{-1} (C=O).

By fractional crystallization of the combined mother liquors of several such brominations from methanol–acetone it was possible to isolate small quantities of relatively pure 6α-bromolycopodine hydrobromide, m.p. 260–269° (decomp.).

The recrystallized bromination product (0.30 g) was stirred overnight with 3% aqueous sodium hydroxide, then the reaction mixture adjusted to pH 7.5 and extracted with ether to give a dark brown oil (0.21 g). Chromatography of the oil over alumina (5 g) gave lycopodine (91 mg), eluted with benzene, and the enolic α-diketone III (36 mg), eluted with chloroform–methanol (99:1).

Bromination of Lycopodine Hydrobromide

A solution of bromine (0.78 g) in chloroform (15 ml) was added dropwise with stirring to a solution of lycopodine hydrobromide (1.45 g) in chloroform (30 ml) to which had been added 0.1 ml of chloroform saturated with hydrogen bromide. The mixture (a small amount of precipitate formed shortly after bromine addition was completed) was kept at room temperature overnight, then evaporated at the pump, and cold acetone (20 ml) was added to the residual off-white solid. The solid was collected and crystallized once from methanol to give almost pure 6α-bromolycopodine hydrobromide (1.64 g, 91%), m.p. 261–265° (decomp.). Two further recrystallizations from methanol furnished the analytical sample, m.p. 266–269° (decomp.). Calc. for $C_{16}H_{25}ONBr_2$: C, 47.19; H, 6.19; N, 3.50; Br, 39.25%. Found: C, 47.25, 47.45; H, 6.32, 6.43; N, 3.44; Br, 39.27%. Infrared spectrum: $\nu_{max}^{CHCl_3}$ 2470 (+NH), 1711 cm^{-1} (C=O); ν_{max}^{nujol} 2550, 1703 cm^{-1}. Ultraviolet spectrum: λ_{max} 306 mμ (log ϵ 2.19). Rotatory dispersion in methanol (*c*, 0.10): $[\phi]_{589}$ +150°, $[\phi]_{400}$ +910°, $[\phi]_{332}$ +4550°, $[\phi]_{280}$ −6100°, $[\phi]_{250}$ −2300°.

Optical Rotatory Dispersion Spectra of Lycopodine Salts

The salts were prepared by the usual methods.

Lycopodine hydrobromide, in methanol (*c* 0.12): $[\phi]_{589}$ −330°, $[\phi]_{500}$ −430°, $[\phi]_{400}$ −600°, $[\phi]_{305}$ −2340°, $[\phi]_{268}$ +430°, $[\phi]_{253}$ ±0°.

Lycopodine, in acetic acid (*c* 0.10): $[\phi]_{589}$ −230°, $[\phi]_{500}$ −345°, $[\phi]_{400}$ −545°, $[\phi]_{300}$ −2270°, $[\phi]_{263}$ +540°, $[\phi]_{255}$ +400°.

Lycopodine methiodide, in methanol (*c* 0.12): $[\phi]_{589}$ −110°, $[\phi]_{500}$ −160°, $[\phi]_{400}$ −560°, $[\phi]_{304}$ −2450°, $[\phi]_{268}$ +260°, $[\phi]_{255}$ ±0°.

Lycopodine perchlorate, in methanol (*c* 0.096): $[\phi]_{589}$ +80°, $[\phi]_{500}$ ±0°, $[\phi]_{400}$ −360°, $[\phi]_{302}$ −1600°, $[\phi]_{260}$ +280°, $[\phi]_{250}$ ±0°.

Can. J. Chem. Downloaded from www.nrcresearchpress.com by 210.87.254.5 on 09/05/12
For personal use only.

Reaction of Acetyldihydrolycopodine with Bromine

A solution of bromine (14 mg, 0.09 mmole) in chloroform (10 ml) was added all at once to a solution of acetyldihydrolycopodine (II) (55 mg, 0.18 mmole). The solution decolorized immediately and after 15 minutes was evaporated to dryness to give a light brown foam.

Crystallization from acetone–ether yielded acetyldihydrolycopodine hydrobromide (49 mg, 71%), identical with an authentic sample. The mother liquors yielded a light brown oil which rapidly darkened on standing and failed to yield further crystalline material.

6α-Bromolycopodine (IV)

A solution of 6α-bromolycopodine hydrobromide (0.156 g) in chloroform (60 ml) was shaken with cold dil. ammonium hydroxide (aqueous sodium bicarbonate gave similar results). The chloroform layer was separated, washed with water, dried ($MgSO_4$), and evaporated to give a colorless solid (0.12 g). Crystallization from ether or acetone yielded colorless spars which melted at 163–165° with partial decomposition, then resolidified and melted with decomposition at 238–240°. Calc. for $C_{16}H_{24}ONBr$: C, 58.90; H, 7.41; N, 4.29; Br, 24.49%. Found: C, 59.63; H, 7.42; N, 4.46; Br, 24.80%. Infrared spectrum: ν_{max}^{nujol} 1702 cm^{-1}; $\nu_{max}^{CCl_4}$ 1711 cm^{-1}. Ultraviolet spectrum: λ_{max} 305 mμ (log ε 2.22). Nuclear magnetic resonance spectrum: 5.82 τ (C*H*Br, broadened singlet, half-height width 3.2 c.p.s.), 9.16 τ (CH—C*H*$_3$, doublet, splitting 3.8 c.p.s.). Rotatory dispersion in methanol (*c* 0.064, freshly prepared solution): $[\phi]_{400}$ +1,070°, $[\phi]_{335}$ +8,950°, $[\phi]_{294}$ −20,550°, $[\phi]_{250}$ −4,500°. After 2½ hours the amplitude had fallen to +27,250°, and after 24 hours, to +13,900°. The material recovered from the optical rotatory dispersion measurements (24 hours) showed distinct +NH bands in the infrared. When a sample of the 6α-bromoketone was heated to 170° for 1 minute the infrared spectrum of the dark solid remaining showed peaks (1690, 1620, 2520 cm^{-1}) characteristic of the unsaturated ketone VIII as well as typical +NH stretching vibrations.

6β-Bromolycopodine Hydrobromide (VI·HBr)

A solution of 6α-bromolycopodine hydrobromide (IV·HBr, 2.24 g) in glacial acetic acid (50 ml) was heated on the steam bath for 1 hour, then cooled to room temperature and evaporated to dryness under reduced pressure. The residue was washed with cold acetone (50 ml) and filtered to give a colorless solid (1.71 g). Infrared spectrum: ν_{max}^{nujol} 2450, 1720, 1703 cm^{-1}.

Seven recrystallizations from methanol yielded pure 6β-bromolycopodine hydrobromide (VI·HBr, 0.21 g), m.p. 257–262° (decomp.). Calc. for $C_{16}H_{25}ONBr_2$: C, 47.19; H, 6.19; N, 3.44; Br, 39.25%. Found: C, 47.21, 47.22; H, 6.28, 6.32; N, 3.71; Br, 39.62, 39.94%. Infrared spectrum: $\nu_{max}^{CHCl_3}$ 2440 (+NH), 1728 cm^{-1} (>C=O); ν_{max}^{nujol} 2590, 2550 (+NH), 1718 cm^{-1}. Ultraviolet spectrum: λ_{max} 276 mμ (log ε 2.07). Rotatory dispersion in methanol (*c* 0.10): $[\phi]_{589}$ −265°, $[\phi]_{500}$ −400°, $[\phi]_{400}$ −660°, $[\phi]_{350}$ −880°, $[\phi]_{310}$ −1000°, $[\phi]_{300}$ −1290°.

Because of the low yields obtained in the epimerization no attempt was made to prepare the free base. When a solution of 6β-bromolycopodine hydrobromide in glacial acetic acid was heated on the steam bath for an hour, the infrared spectrum of the solid recovered after evaporation of the acetic acid was almost identical with that of the starting material.

Reaction of 6α-Bromolycopodine Hydrobromide with Sodium Hydroxide

6β-Bromolycopodine (0.35 g) was suspended in 3% aq. sodium hydroxide (40 ml) and stirred at room temperature for 18 hours. The dark brown solution thus obtained was adjusted to pH 7.5 with acetic acid and extracted four times with chloroform to give a brown semisolid (0.15 g). The semisolid was chromatographed over alumina (5 g). Elution with ether yielded the unsaturated ketone VIII as a pale yellow oil (0.05 g). The unsaturated ketone did not crystallize readily and was characterized as the methiodide, which after recrystallization from acetone, melted at 271–273°. Calc. for $C_{16}H_{23}ON\cdot CH_3I$: C, 52.72; H, 6.77%. Found: C, 52.71, 52.47; H, 6.74; 6,82%. Infrared spectra: methiodide: ν_{max}^{nujol} 1698, 1629 cm^{-1}; free base: $\nu_{max}^{CCl_4}$ 1686, 1614 cm^{-1}. Ultraviolet spectrum: λ_{max} 244 mμ (log ε 3.90). Nuclear magnetic resonance spectrum: 3.04 τ (olefinic H), 9.18 τ (CHC*H*$_3$, doublet, splitting 3.5 c.p.s.).

Elution of the chromatogram with chloroform–methanol (49:1) yielded a light brown solid (0.057 g) which on sublimation afforded the pure diosphenol III (41 mg), m.p. 185–186°, identical with that prepared previously (4) from lycopodine.

Lithium–Ammonia Reduction of the Unsaturated Ketone VIII

3,4-Dehydrolycopodine (VIII, 0.103 g) in ether (25 ml) was added to a stirred solution of lithium (0.2 g) in ammonia (150 ml). After 30 minutes solid ammonium chloride was added until the blue color disappeared, and the ammonia was allowed to evaporate. The residue was distributed between chloroform and water and the layers separated. The aqueous layer was washed with chloroform and the combined organic extracts washed with water. Evaporation of the chloroform left a colorless oil (0.105 g) which solidified on scratching. The solid material was dissolved in acetone and neutralized with 70% perchloric acid. The perchlorate which separated (0.115 g) was identical with authentic lycopodine perchlorate.

Can. J. Chem. Downloaded from www.nrcresearchpress.com by 210.87.254.5 on 09/05/12
For personal use only.

Alkaloid L.20

(a) From 6α-Bromolycopodine Hydrobromide

6α-Bromolycopodine hydrobromide (IV·HBr, 1.32 g) was added to a stirred solution of 5% aq. sodium bicarbonate (80 ml) at room temperature. The bromo compound slowly dissolved but a second crystalline phase began to separate before solution was complete. After 24 hours the reaction mixture was transferred to a liquid–liquid extractor and continuously extracted with ether. The ethereal extract was dried ($MgSO_4$) and evaporated to yield an off-white solid (0.78 g, 92%) whose infrared spectrum was identical with that of an authentic sample of alkaloid L.20 (see Section (*b*)). Crystallization from methanol yielded colorless needles, m.p. 258–259°, both pure and mixed with an authentic sample of alkaloid L.20. Both samples had identical rotatory dispersion curves.

(b) From L. lucidulum Michx.

Dried, finely ground *L. lucidulum* Michx. (11 kg) was Soxhlet-extracted with methanol and the extract concentrated to a thick, dark residue. The residue was digested for 24 hours with cold, dilute hydrochloric acid, filtered, and the filtrate washed with ether. The acid solution was adjusted to ca. pH 8 with ammonium hydroxide and extracted with chloroform (extract A), then the aqueous layer was made strongly basic with ammonium hydroxide and again extracted with chloroform (extract B). Extract B was concentrated at the pump and the residue (19.1 g) dissolved in methanol. After standing several days in the refrigerator the solution deposited crystals (0.31 g) which, after recrystallization from methanol or acetone, melted at 258–259°. This substance was shown to be alkaloid L.20 by comparison (infrared spectrum, mixed melting point, rotatory dispersion curve) with an authentic sample kindly furnished by Dr. L. Marion. Calc. for $C_{16}H_{25}O_2N$: C, 72.96; H, 9.57; N, 5.32%. Found: C, 72.43, 72.57; H, 9.76, 9.81; N, 5.24%. Infrared spectrum: $\nu_{max}^{CHCl_3}$ 3620 (OH), 1710 cm^{-1} (>C=O). Ultraviolet spectrum: λ_{max} 296 mμ (log ε 1.85). Rotatory dispersion in methanol (*c* 0.137): $[\phi]_{500}$ +105°, $[\phi]_{400}$ +400°, $[\phi]_{330}$ +4,300°, $[\phi]_{285}$ −10,500°, $[\phi]_{270}$ −3,000°.

Chromatography of the mother liquors obtained from extract B yielded lycopodine and lycodoline (alkaloid L.8) as the only crystalline material. Extract A was reserved for future examination.

(c) From 6β-Bromolycopodine Hydrobromide

6β-Bromolycopodine hydrobromide (VI·HBr, 84 mg) was stirred for 24 hours with 5% aq. sodium bicarbonate (20 ml). The resulting brown solution was extracted six times with chloroform. The product obtained was crystallized from acetone to give alkaloid L.20 (19 mg, 35%). Although the yield is lower than that quoted in section (*a*) we believe that this is largely due to the change in reaction conditions (w/v ratio), since the 6α-bromo compound, when treated under conditions identical with those described here, gave only a 30% yield of alkaloid L.20.

Calcium–Ammonia Reduction of Alkaloid L.20

A solution of alkaloid L.20 (X, 97 mg) in tetrahydrofuran (7 ml) was added to a blue solution of calcium (0.10 g) in liquid ammonia (150 ml). The reaction mixture was stirred for 15 minutes, then the excess calcium destroyed by addition of bromobenzene followed by water (5 ml). After most of the ammonia had evaporated more water was added and the aqueous layer was extracted several times with chloroform. Evaporation of the chloroform left a light brown oil (0.07 g) which was dissolved in dichloromethane and chromatographed over alumina (3 g). Dichloromethane eluted lycopodine (43 mg), chloroform eluted epidihydrolycopodine (20 mg) (4), and chloroform–methanol (24:1) eluted the diosphenol III (3 mg). All three products were identified by comparison with authentic samples.

When lithium–ammonia–methanol was used for the reduction only epidihydrolycopodine was obtained.

6β-Hydroxylycopodine from Alkaloid L.20

(*a*) A solution of alkaloid L.20 (X, 45 mg) in *n*-propanol (10 ml) containing sodium propoxide (80 mg) was shaken in an atmosphere of nitrogen for 40 hours, then chloroform (50 ml) and water (50 ml) were added. The chloroform layer was separated, washed with water, and evaporated. The residue was crystallized from acetone, yielding 6β-hydroxylycopodine (30 mg), m.p. 121–122°, both pure and mixed with an authentic sample (4). Both samples had identical infrared spectra ($CHCl_3$).

(*b*) A solution of alkaloid L.20 (0.13 g) was absorbed on a column of basic alumina (10 g) in ether–benzene (1:1). After 12 hours the column was eluted with ether–methanol, affording a colorless semisolid (0.12 g) which on sublimation furnished 6β-hydroxylycopodine (0.10 g), identical with an authentic sample.

Dehydration of Alkaloid L.20

A solution of alkaloid L.20 (X, 0.19 g), in 10% aq. hydrochloric acid (30 ml) was heated under reflux for 3 hours. After being cooled, the solution was neutralized with sodium bicarbonate and continuously extracted with ether. The residue (0.18 g) was triturated with Skellysolve B (in which the starting material is insoluble). The Skellysolve solution was concentrated, the residual oil dissolved in cold acetone (5 ml), and methyl iodide (1 ml) added. On standing the solution overnight in the refrigerator crystals (0.23 g) of 3,4-dehydrolycopodine methiodide (VIII·CH_3I), m.p. 270–273°, separated.

Can. J. Chem. Downloaded from www.nrcresearchpress.com by 210.87.254.5 on 09/05/12
For personal use only.

Acetylation of Alkaloid L.20

(a) At Room Temperature, Formation of Enol Acetate XI

A solution of alkaloid L.20 (X, 0.31 g) in acetic anhydride – pyridine (9 ml of 1:1) was kept at room temperature for 12 hours, then diluted with chloroform and ice-cold dil. ammonium hydroxide. The chloroform layer was separated and the aqueous layer extracted twice more with chloroform. The combined chloroform extracts were washed with water, dried ($MgSO_4$), and evaporated to give a colorless oil (0.39 g). The oil could not be induced to crystallize and was purified and characterized as the perchlorate, formed in acetone and recrystallized from acetone–ether, which melted at 258–259° (decomp.). Calc. for $C_{20}H_{29}O_4N \cdot HClO_4$: C, 53.63; H, 6.75; N, 3.11%. Found: C, 53.78; H, 6.82; N, 3.03%. Infrared spectra: perchlorate: ν_{max}^{nujol} 3060 (+NH), 1740 (2 OAc), 1690 cm^{-1} (C=C); free base: $\nu_{max}^{CCl_4}$ 1760, 1735 (2 OAc), 1680 cm^{-1} (C=C). The nuclear magnetic resonance spectrum of the free base showed signals at 5.02 τ (1H, broadened singlet, half-height width 4 c.p.s.), 7.98 and 8.06 τ (total of 6H), and 9.17 τ (3H, doublet, splitting 5.5 c.p.s.).

Hydrolysis of the enol acetate XI (0.39 g) with 8% aq. hydrochloric acid (20 ml) at room temperature for 3 hours, followed by working up in the usual manner, afforded a yellowish oil which after filtration through alumina and crystallization from Skellysolve B gave acetyl-L.20 (0.12 g), m.p. 143–144° (see below). The mother liquors (0.15 g) contained mainly starting enol acetate as judged by the infrared spectrum.

Hydrolysis of the enol acetate XI with aqueous methanolic sodium bicarbonate at room temperature afforded alkaloid L.20 in about 50% yield.

(b) At −10°, Formation of Acetyl-L.20

A solution of alkaloid L.20 (0.12 g) in acetic anhydride (5 ml) – pyridine (2 ml) was kept at −10° for 4 hours, then poured into chloroform and dil. ammonium hydroxide. The aqueous layer was separated and washed twice more with chloroform. The combined chloroform extracts, after washing with water and drying, were evaporated to give a colorless solid (0.11 g), m.p. 126–134°. Three recrystallizations from Skellysolve B gave analytically pure needles of acetyl-L.20 (58 mg), m.p. 143–144°. Calc. for $C_{18}H_{27}O_3N$: C, 70.79; H, 8.92; N, 4.59%. Found: C, 70.97, 70.66; H, 8.92, 8.82; N, 4.72. Infrared spectrum: $\nu_{max}^{CCl_4}$ 1755 (OAc), 1723 (ketone), 1230 cm^{-1} (OAc). Ultraviolet spectrum: λ_{max} 300 mμ (log ϵ 1.95). The rotatory dispersion spectrum showed a positive Cotton effect with peak at 327 mμ (+1,800°) and trough at 282 mμ (−10,900°). Details of the nuclear magnetic resonance spectrum have been published (4).

Lycopodine Enol Acetate (XII)

The method used was that of Barton *et al.* (18). A solution of lycopodine (0.5 g) and *p*-toluenesulphonic acid (0.45 g) in acetic anhydride (25 ml) was heated until the acetic anhydride slowly distilled. After 4 hours most of the acetic anhydride had been removed. The residue was diluted with ether and dil. aq. sodium hydroxide and shaken. The aqueous layer was separated and washed twice more with ether. The combined ethereal extracts were washed with water, dried ($MgSO_4$), and evaporated, leaving an off-white solid which was crystallized from acetone to give lycopodine enol acetate (0.4 g), m.p. 98–100°. The analytical sample was prepared by recrystallization from acetone, then from Skellysolve B, and melted at 100–101°. Calc. for $C_{18}H_{27}O_2N$: C, 74.70; H, 9.41; O, 11.06. Found: C, 74.30, 74.49; H, 9.24, 9.40; O, 11.49%. Infrared spectrum: $\nu_{max}^{CCl_4}$ 1755 (OAc), 1696 cm^{-1} (C=C). Nuclear magnetic resonance spectrum: 7.86 τ (3H, $OCOCH_3$), 9.12 τ (3H, $CHCH_3$, doublet, splitting 6 c.p.s.).

ACKNOWLEDGMENTS

We wish to thank Drs. K. Wiesner and Z. Valenta for valuable correspondence in connection with the rotatory dispersion data, Mr. M. A. Stillwell for the collection and identification of the plant material, Mr. R. N. Swindlehurst and Mrs. G. B. Conway for most of the infrared, nuclear magnetic resonance, and optical rotatory dispersion measurements, and the National Research Council of Canada for financial support.

REFERENCES

1. L. R. C. Barclay and D. B. MacLean. Can. J. Chem. **34**, 1519 (1956).
2. W. A. Harrison and D. B. MacLean. Chem. Ind. (London), 261 (1960). W. A. Harrison, M. Curcumelli-Rodostamo, D. F. Carson, L. R. C. Barclay, and D. B. MacLean. Can. J. Chem. **39**, 2086 (1961).
3. F. A. L. Anet. Tetrahedron Letters, No. 20, 13 (1960).
4. W. A. Ayer and D. A. Law. Can. J. Chem. **40**, 2088 (1962).
5. K. Wiesner. Sci. Rept. 1st Super. Sanita, **1**, 560 (1961).
6. R. M. Jones, D. A. Ramsey, F. Herling, and K. Dobriner. J. Am. Chem. Soc. **74**, 2828 (1952).
7. R. C. Cookson. J. Chem. Soc. 282 (1954).
8. C. Djerassi. Optical rotatory dispersion. McGraw-Hill Book Co., New York. 1960. p. 115.
9. K. Wiesner, J. E. Francis, J. A. Findlay, and Z. Valenta. Tetrahedron Letters, No. 5, 187 (1961).

Can. J. Chem. Downloaded from www.nrcresearchpress.com by 210.87.254.5 on 09/05/12
For personal use only.

10. W. MOFFIT, R. B. WOODWARD, A. MOSCOWITZ, W. KLYNE, and C. DJERASSI. J. Am. Chem. Soc. **83**, 4013 (1961).
11. R. L. ERSKINE and E. S. WAIGHT. J. Chem. Soc. 3425 (1960).
12. W. VON E. DOERING, M. R. WILLCOTT, III, and M. JONES, JR. J. Am. Chem. Soc. **84**, 1224 (1962).
13. M. CURCUMELLI-RODOSTAMO and D. B. MACLEAN. Can. J. Chem. **40**, 1068 (1962).
14. R. H. F. MANSKE and L. MARION. Can. J. Res. Sect. B, **24**, 57 (1946).
15. J. H. CHAPMAN, J. ELKS, G. H. PHILLIPS, and L. J. WYMAN. J. Chem. Soc. 4344 (1956).
16. R. C. COOKSON and S. H. DANDEGAENKER. J. Chem. Soc. 352 (1955).
17. E. L. ELIEL. *In* Steric effects in organic chemistry. *Edited by* M. S. Newman. John Wiley and Sons, New York. 1956. p. 103.
18. D. H. R. BARTON, R. M. EVANS, J. C. HAMLET, P. G. JONES, and T. WALKER. J. Chem. Soc. 747 (1954).

Can. J. Chem. Downloaded from www.nrcresearchpress.com by 210.87.254.5 on 09/05/12
For personal use only.

STERIC EFFECTS IN THE SYNERGIC EXTRACTION OF THE LANTHANIDES, YTTRIUM, AND SCANDIUM[1]

P. G. MANNING[2]

Mineral Sciences Division, Department of Mines and Technical Surveys, Ottawa, Canada

Received August 27, 1962

ABSTRACT

From a study of the partitioning of the carrier-free radioisotopes Tm^{170}, Ce^{144}, $Eu^{152/154}$, Tb^{160}, Lu^{177}, and Y^{91} between nitric acid and organic solutions containing various proportions of thenoyltrifluoroacetone (HTTA) and dialkyl alkyl phosphonates (S) in odorless kerosene, concentration equilibrium constants (k_2) have been computed for the reaction

$$M^{3+}_w + 3HTTA_o + 2S_o = M(TTA)_3S_{2o} + 3H^+_w,$$

where M represents a metal ion, and "w" and "o" are aqueous and organic species respectively.

When used in conjunction with the data of Bronaugh and Suttle, the equilibrium constants determined in this study yielded comparative equilibrium constants (k_3) for the solvation process

$$M(TTA)_{3o} + 2S_o = M(TTA)_3S_{2o}$$

for the rare-earth metals listed.

In the extraction of Sc^{46}, however, the species extracted is dependent on the alkyl groups of the phosphonates, the butyl and 2-ethylhexyl derivatives giving mono- and di-solvates respectively.

It is concluded that steric effects are dominant in these synergic systems.

INTRODUCTION

That steric effects can influence the formation and the stabilities of higher complexes of the lanthanide, Y, and Sc metals has been demonstrated by a number of workers, and much of this work has been summarized in a recent publication by Warren (2). The synergic extraction of Pm, Eu, and Tm by mixtures of thenoyltrifluoroacetone (HTTA) and tributyl phosphate (TBP) has been shown to proceed via the formation of the complex $M(TTA)_3(TBP)_2$ (3, 4), where M is the metal ion, and it is conceivable that steric hindrance could operate in such systems. Since the lanthanides, yttrium, and scandium possess almost identical chemical properties, variations in the ionic radii would then be expected to induce similar trends in the magnitude of the synergic enhancement.

Two systems have been chosen for study, namely (*a*) the metal – nitric acid – HTTA – dibutyl butyl phosphonate (DBBP) – kerosene and (*b*) the metal – nitric acid – HTTA – bis-2-ethylhexyl 2-ethylhexyl phosphonate (DEEP) – kerosene systems. Any steric effects may, therefore, be studied from two angles, that of varying cation radius and that of varying bulkiness of the alkyl group of the phosphonate.

Experiments were conducted at trace metal concentration ($<10^{-5}$ *M*) using radioisotopes; this ensured that there was no change in the effective concentrations of the extractants.

EXPERIMENTAL

DEEP, of approximately 0.3% acidic content, was purchased from the Virginia-Carolina Chemical Corporation and was used without further purification, previous experiments having shown that the acidic impurity had a negligible effect on the metal distribution coefficients. HTTA, obtained from the Fisher

[1]*Presented before the 45th Annual Conference of the Chemical Institute of Canada, Edmonton, Alberta, May 1962.*

[2]*National Research Council Postdoctoral Fellow.*

Can. J. Chem. Downloaded from www.nrcresearchpress.com by 210.87.254.105 on 09/05/12
For personal use only.

Scientific Company, was purified either by recrystallization from hexane or by a 3-hour stay in a vacuum desiccator at a pressure of 3 mm. Both methods gave identical metal distribution coefficients. All other reagents were as described in a previous publication (5).

The radioisotopes Ce^{144}, $Eu^{152/154}$, Tb^{160}, Tm^{170}, Lu^{177}, and Y^{91} were obtained from the Radiochemical Centre, Amersham, England, and Sc^{46} from Atomic Energy of Canada Ltd., Chalk River, Ontario. The radioactive content of the equilibrated aqueous and organic phases was determined using a NaI(Tl) scintillation counter in the $Eu^{152/154}$, Tb^{160}, and Sc^{46} measurements, and a Geiger–Müller counter for the other β-emitting isotopes.

Equal volumes (10.00 ml) of both aqueous and organic phases were shaken for 3 hours in ground-glass stoppered Erlenmeyer flasks fitted with polytetrafluoroethylene (PTFE) sleeves. All organic phases were pre-equilibrated. The temperature was 28±3° C.

The distribution coefficient of a given nuclide is defined as

$$K = \frac{\text{concentration of nuclide in organic phase}}{\text{concentration of nuclide in aqueous phase}}.$$

RESULTS

Metal – Nitric Acid – HTTA – DBBP – Kerosene System

For a general reaction

$$M^{n+} + x\text{Cl}^- + (n-x)\text{HX} + m\text{S} = \text{MCl}_x\text{X}_{n-x}\text{S}_m + (n-x)\text{H}^+,$$

where HX and S represent acidic and neutral extractants, the equilibrium constant is

[1] $$k_2 = \frac{[\text{MCl}_x\text{X}_{n-x}\text{S}_m][\text{H}^+]^{n-x}}{[\text{M}^{n+}][\text{Cl}]^x[\text{HX}]^{n-x}[\text{S}]^m} = \frac{K[\text{H}^+]^{n-x}}{[\text{Cl}]^x[\text{HX}]^{n-x}[\text{S}]^m},$$

whence

$$K = \frac{k_2[\text{Cl}]^x[\text{HX}]^{n-x}[\text{S}]^m}{[\text{H}^+]^{n-x}}.$$

A log–log plot of K against [S], with [H^+] and [HX] kept constant, has a slope of m. Similarly, log–log plots of K against [H^+] and K against [HX], with the other parameters constant, possess slopes of $-(n-x)$ and $+(n-x)$ respectively. These latter plots should, therefore, complement one another, provided that HTTA functions only as a bidentate chelating agent, i.e., the ability of undissociated HTTA to function as coordinated S molecules is negligible.

The metal extraction dependencies upon aqueous acidity, organic phosphonate concentration, and organic HTTA concentration are presented in Figs. 1, 2, and 3. Ignoring Sc for the time being, the plots possess slopes of −3.0, 2.0, and 3.0. This means that $n-x = n = 3$, $x = 0$, and $m = 2$, and the extraction mechanism is

$$M^{3+}_w + 3\text{HTTA}_o + 2\text{DBBP}_o = \text{M(TTA)}_3(\text{DBBP})_{2o} + 3\text{H}^+_w,$$

where "w" and "o" designate aqueous and organic species respectively.

The slopes of all plots have been calculated to within 0.05, and the estimated error in k_2 is ±3%.

The possibility exists that the mechanism of extraction at the higher phosphonate concentrations employed in the evaluation of $n-x$ (Figs. 1 and 4) differs from that at the lower phosphonate concentrations employed in the remainder of this work. Since the formation of the extractable species MX_3 and $M(NO_3)_3S_3$ may be ignored (1, 5), and since MX_3S_2 is the extractable complex at the lower phosphonate concentrations, then the formation of such molecules as $MX_3S_2.HX$ or MX_3S_3 would have to be considered were the mechanism concentration dependent. Both $MX_3S_2.HX$ and MX_3S_3 require a central metal ion coordination number of 9, which renders their formation unlikely.

Can. J. Chem. Downloaded from www.nrcresearchpress.com by 210.87.254.105 on 09/05/12
For personal use only.

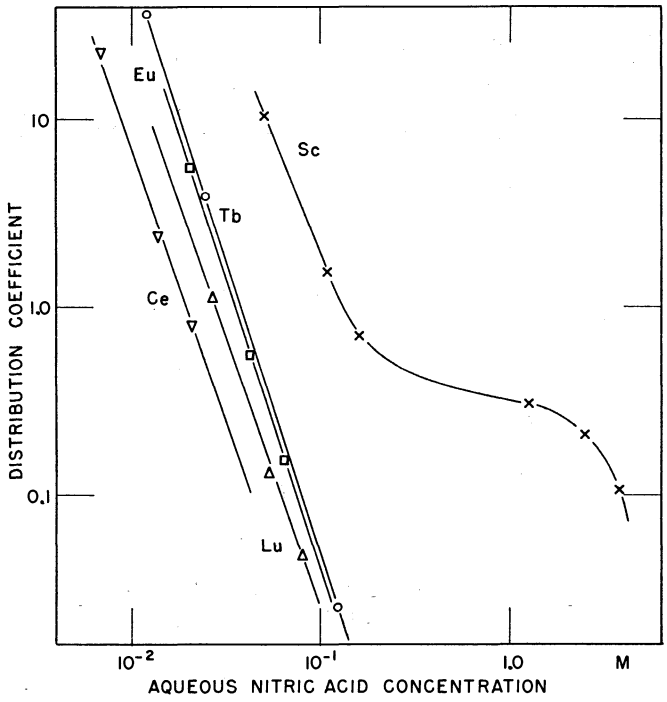

FIG. 1. Metal distribution coefficients as a function of the aqueous nitric acid concentration. 0.020 *M* HTTA, 0.379 *M* DBBP.

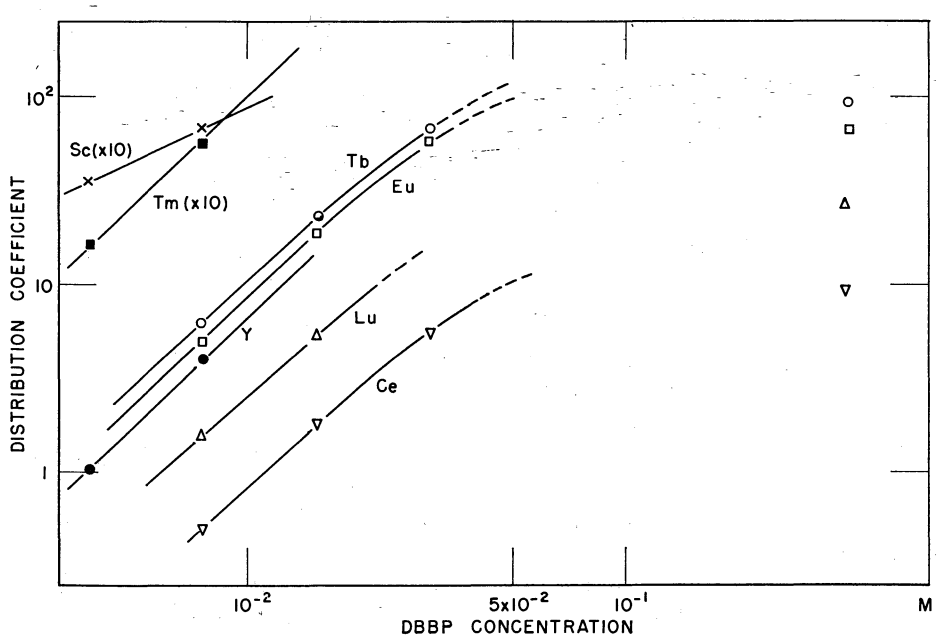

FIG. 2. Metal distribution coefficients as a function of DBBP concentration. 0.020 *M* HTTA, 0.0095 *M* HNO_3; for Sc, 0.0316 *M* HNO_3.

Can. J. Chem. Downloaded from www.nrcresearchpress.com by 210.87.254.105 on 09/05/12
For personal use only.

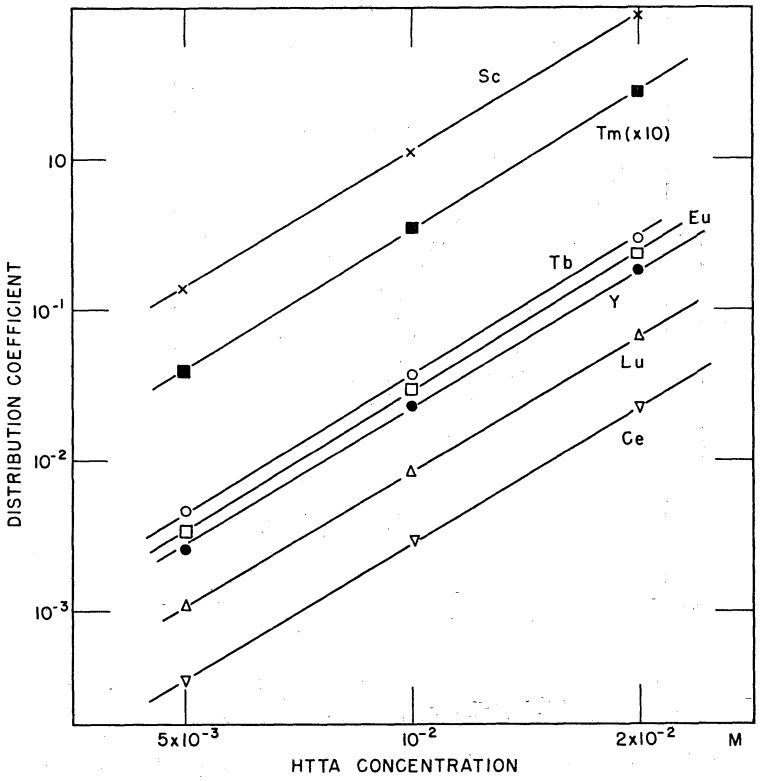

FIG. 3. Variation in K with HTTA concentration. 0.010 *M* DBBP, 0.0316 *M* HNO_3.

Moreover, Healy (6) has investigated similar synergic systems at extractant concentrations as high as those employed in the present work, and his results show that MX_3S_2 is the sole extractable complex.

The results of Peppard *et al.* (7) for the partitioning of Sc between nitric acid and TBP phases would suggest that the non-linearity of the Sc plot in Fig. 1 is due to extraction of the metal according to the reaction

$$Sc^{3+}_w + 3NO^-_{3w} + x\text{DBBP}_o = Sc(NO_3)_3(\text{DBBP})_{x_o}.$$

The limiting slope at lower acidities is, however, −3, and, since Sc obeys a first-power dependency upon DBBP concentration (Fig. 2) and a third-power dependency upon HTTA concentration (Fig. 3), the extraction process is

$$Sc^{3+}_w + 3\text{HTTA}_o + \text{DBBP}_o = Sc(\text{TTA})_3(\text{DBBP})_{1_o} + 3H^+_w.$$

The corresponding equilibrium constants have been calculated by substituting the following data in equation [1]:

[HTTA] = 0.0200 *M*	$n-x$ = 3.0
[DBBP] = 0.0100 *M*	m = 2.0 (metals other than Sc)
$[H^+]$ = 0.0316 *M*	m = 1.0 (Sc only)

These constants are tabulated in Table I.

Can. J. Chem. Downloaded from www.nrcresearchpress.com by 210.87.254.105 on 09/05/12
For personal use only.

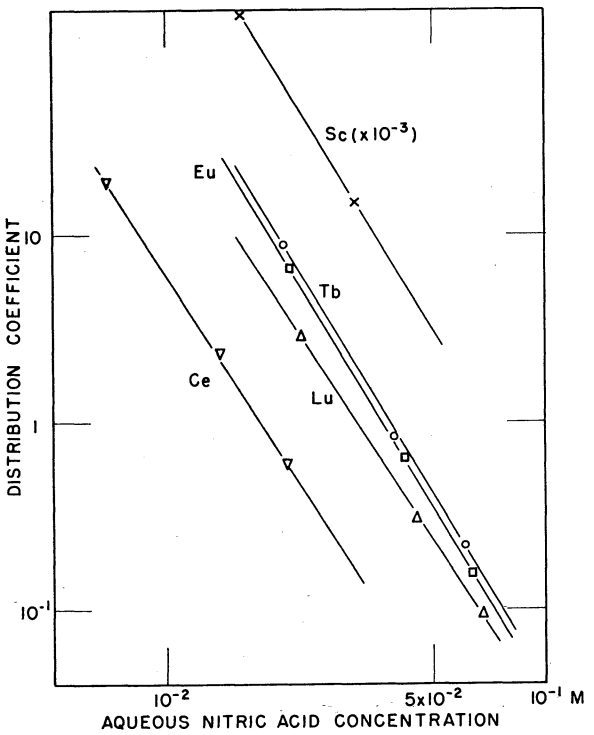

FIG. 4. Metal distribution coefficients against aqueous acidity. 0.020 *M* HTTA, 0.217 *M* DEEP.

TABLE I

k_2 values for the metal–HTTA–DBBP system

Metal	Ce	Eu	Tb	Tm	Lu	Y	Sc*
$10^{-3}k_2$	0.86	9.1	11	11	2.7	6.1	3.5

*Calculated from $k_2 = \{[M(TTA)_3(DBBP)_1][H^+]^3\}/\{[M^{3+}][HTTA]^3[DBBP]\}$.

Metal – Nitric Acid – HTTA – DEEP – Kerosene System

Plots of the distribution coefficients of Ce, Eu, Tb, Lu, and Sc against aqueous nitric acid concentration, organic phosphonate concentration, and organic HTTA concentration are presented in Figs. 4, 5, and 6. The limiting slopes are −3.0, 2.0, and 3.0; the metals, therefore, extract as trischelates disolvates, $M(TTA)_3(DEEP)_2$.

In Table II are listed equilibrium constants calculated from the data

$$[HTTA] = 0.0200\ M \qquad n-x = 3.0$$
$$[DEEP] = 0.0100\ M \qquad m = 2.0$$
$$[H^+] = 0.0316\ M$$

TABLE II

k_2 values for the metal–HTTA–DEEP system

Metal	Ce	Eu	Tb	Lu	Sc
$10^{-3}k_2$	0.15	1.7	2.1	1.1	4100

Can. J. Chem. Downloaded from www.nrcresearchpress.com by 210.87.254.105 on 09/05/12
For personal use only.

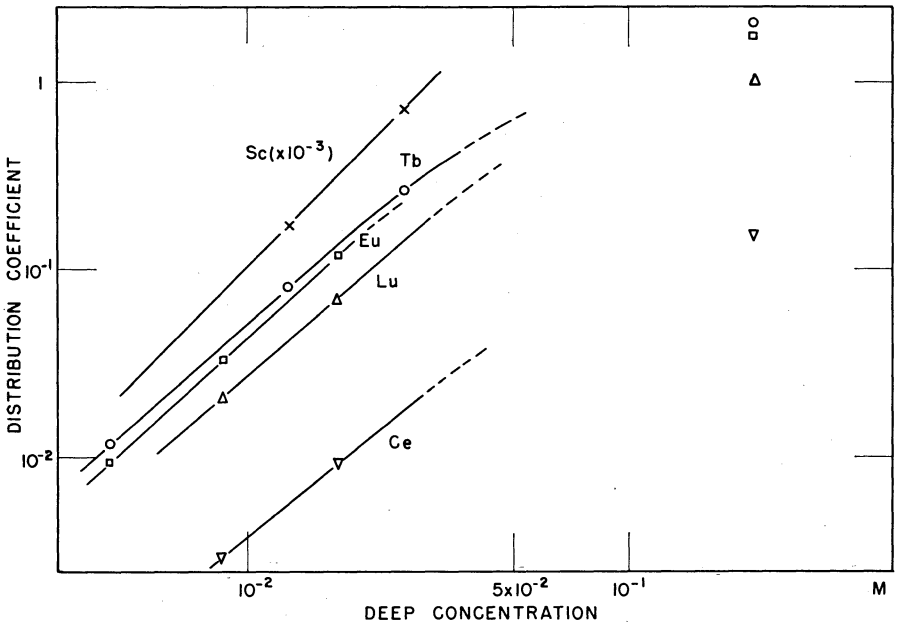

FIG. 5. Variation in K with DEEP concentration. 0.020 M HTTA, 0.0316 M HNO_3.

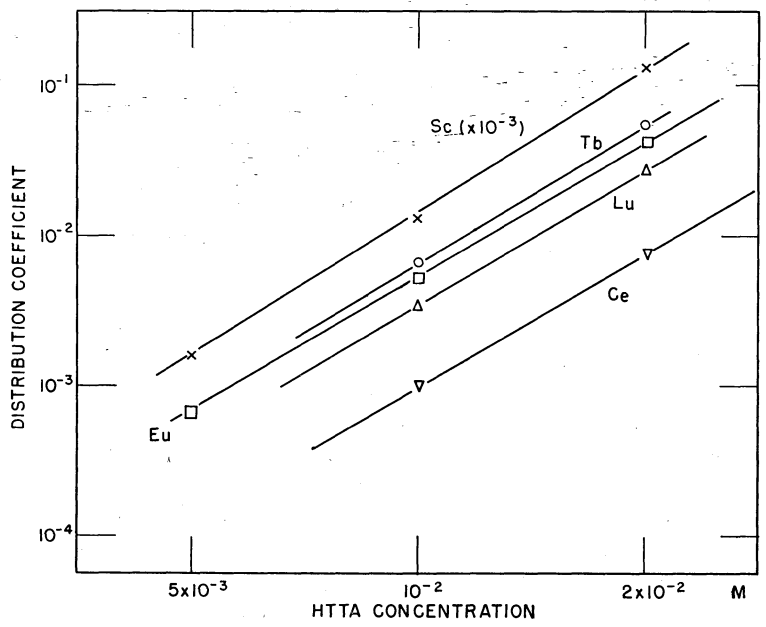

FIG. 6. Variation in K with HTTA concentration. 0.0100 M DEEP, 0.0316 M HNO_3.

Can. J. Chem. Downloaded from www.nrcresearchpress.com by 210.87.254.105 on 09/05/12
For personal use only.

DISCUSSION

That all the metals studied exhibit synergism is apparent from a comparison of the values of k_2, measured in both the DBBP and DEEP systems (Tables I and II), with those of k_1 (Table III) determined by Bronaugh and Suttle (1) for the extraction process

$$M_w^{3+} + 3HTTA_o = M(TTA)_{3o} + 3H_w^+,$$

whence

$$[2] \qquad k_1 = \frac{[M(TTA)_3]_o[H^+]_w^3}{[M^{3+}]_w[HTTA]_o^3}.$$

TABLE III

k_3 values for metal–HTTA–DBBP/DEEP systems

Metal	k_1	k_3(DBBP)	k_3(DEEP)	Ionic radius (9) (Å)
Ce	1.53×10^{-9}	5.6×10^{11}	1.0×10^{11}	1.03
Eu	9.2×10^{-8}	9.9×10^{10}	1.8×10^{10}	0.95
Tb	1.29×10^{-7}	8.5×10^{10}	1.6×10^{10}	0.92
Y	1.68×10^{-7}	3.6×10^{10}		0.90
Tm	4.6×10^{-7}	2.4×10^{10}		0.87
Lu	6.8×10^{-7}	4.0×10^{9}	1.6×10^{9}	0.85
Sc	0.69	5.1×10^{3} *	5.9×10^{6}	0.78

*For the reaction $Sc(TTA)_3 + DBBP = Sc(TTA)_3(DBBP)_1$.

These workers employed a 0.2 *M* solution of HTTA in benzene in extracting the lanthanides from chloride media.

Although the experimental conditions used by Bronaugh and Suttle (1) differ in some respects from those employed in the present investigation, e.g., different diluent, supporting anion, and HTTA concentration, we feel that k_1 and k_2 may still be compared for the following reasons:

(*a*) Cl^- and NO_3^-, anions of strong acids, take no part in the extraction reaction;

(*b*) at [HTTA] = 0.200 *M* (conditions employed by Bronaugh and Suttle) the organic phase may not be ideal, but Figs. 2 and 4 indicate that deviations from ideality are similar for all metals;

(*c*) from the data of Healy (6) for the extraction of Am, Cm, Pm, and Tm by 0.18 *M* HTTA and 0.1 *M* TBP, changes in diluent produce proportional changes in metal distribution coefficients, and, provided that the extracted species are of the same molecular composition, the ratios $K_{Am}:K_{Cm}:K_{Pm}:K_{Tm}$ remain constant for both benzene and cyclohexane.

The magnitude of the synergic enhancement, which we may define as $k_3 = k_2/k_1$, and values of which are tabulated in Table III, varies from metal to metal and is seen to be largest for Ce. The magnitude of k_3 decreases with decreasing ionic radius, and for Lu, whose ionic radius of 0.85 Å compares with that of 1.03 Å for Ce, the synergic enhancement has decreased by factors of 140 and 170, using DBBP and DEEP respectively. For Sc, using the latter reagent, the corresponding figure is 1.7×10^4. This correlation of k_3 with ionic radius holds for all the metals studied, including Y, and may be attributed to steric crowding, the geometrical obstruction to the addition of phosphonate molecules to the metal chelate increasing with decreasing central ion radius.

The fact that the Sc chelate forms a monosolvate with DBBP is also indicative of steric hindrance, but the species extracted, $Sc(TTA)_3(DBBP)_1$, presupposes a coordination number of seven. Similarly, the disolvates formed by the other trivalent metals

Can. J. Chem. Downloaded from www.nrcresearchpress.com by 210.87.254.105 on 09/05/12
For personal use only.

indicate coordination numbers of eight. It is possible, therefore, that the Sc species is a monohydrate, and that the actual solvation process is one involving replacement of water molecules by phosphonates (S), i.e.

$$M(TTA)_3.2H_2O + xS = M(TTA)_3.S_x.H_2O_{(2-x)} + xH_2O.$$

For all the metals studied, k_2 and k_3 values measured in the DBBP investigations exceeded those of the DEEP system by factors of 3–6. These figures indicate that the alkyl groups of the phosphonate also offer steric obstruction.

The value of k_3 for Y, when compared with those of the lanthanides (Table III), is in keeping with its ionic radius, and Y behaves as a lanthanide of atomic number 65–69.

In Fig. 7 are plotted metal distribution coefficients against atomic number. For the

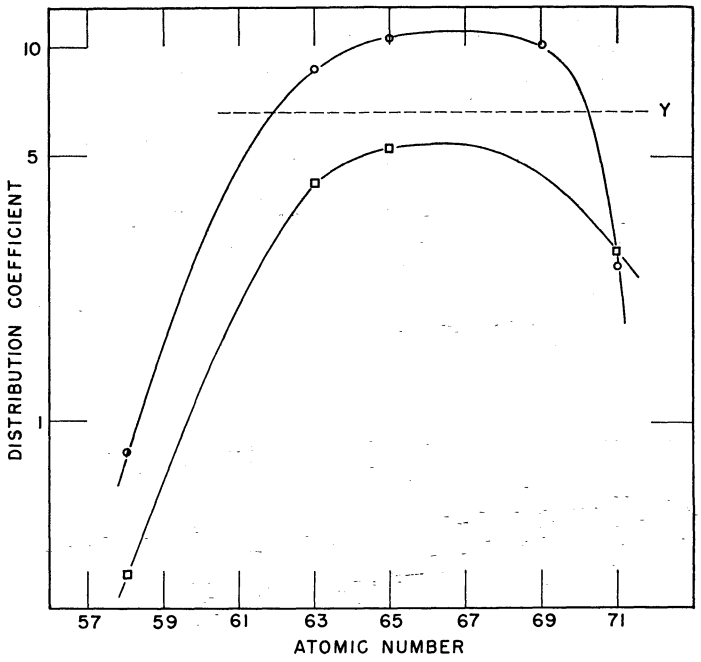

FIG. 7. Lanthanide and Y distribution coefficients against atomic number: ○ 0.020 *M* HNO_3, 0.020 *M* HTTA, 0.379 *M* DBBP; □ 0.024 *M* HNO_3, 0.020 *M* HTTA, 0.217 *M* DEEP.

middle members of the rare-earth series, increased Coulomb interaction (and therefore increased extractability) due to decreasing ionic radius is almost exactly counterbalanced by increased steric hindrance, and from $Z = 63$ to $Z = 69$ overall distribution coefficients are spread over a range of just 15%. In the overall synergic reaction, Y behaves as a rare earth of $Z = 62$ or $Z = 70$.

As a consequence of steric hindrance, separation factors between successive lanthanides (defined as K_{z+1}/K_z) are poor, and are inferior to those obtained by Cunninghame *et al.* (8) for the system Pr/Nd–HTTA–TBP–kerosene.

CONCLUSION

Both steric and synergic effects operate in the extraction of the lanthanides, yttrium, and scandium by mixtures of HTTA and coordinating organophosphorus reagents. The

Can. J. Chem. Downloaded from www.nrcresearchpress.com by 210.87.254.105 on 09/05/12
For personal use only.

former effects lead to poor separation factors, and synergic systems generally would seem to possess little practical application to the improved separation of the metals. An exception might be in cases where the lower lanthanide chelates form disolvates and the higher, monosolvates.

Further studies are being pursued in other potentially synergic systems.

ACKNOWLEDGMENT

The author is indebted to the National Research Council of Canada for the award of a Fellowship.

REFERENCES

1. H. J. BRONAUGH and J. F. SUTTLE. Chelation of the rare earth elements as a function of pH using thenoyltrifluoroacetone. USAEC Document LA-1561. 1951.
2. G. G. WARREN. J. Inorg. Nucl. Chem. **23**, 103 (1961).
3. H. IRVING and D. N. EDGINGTON. J. Inorg. Nucl. Chem. **21**, 169 (1961).
4. T. V. HEALY. J. Inorg. Nucl. Chem. **19**, 314 (1961).
5. P. G. MANNING. Can. J. Chem. **40**, 1684 (1962).
6. T. V. HEALY. J. Inorg. Nucl. Chem. **19**, 328 (1961).
7. D. F. PEPPARD, G. W. MASON, and J. L. MEIER. J. Inorg. Nucl. Chem. **3**, 215 (1956).
8. J. G. CUNNINGHAME, P. SCARGILL, and H. M. WILLIS. The solvent-extraction of praseodymium and neodymium. UKAEA Document AERE-C/M-215. 1954.
9. D. H. TEMPLETON and C. H. DAUBEN. J. Am. Chem. Soc. **76**, 5237 (1954). W. M. ZACHARIASEN. Z. Krist. **80**, 137 (1931).

Can. J. Chem. Downloaded from www.nrcresearchpress.com by 210.87.254.105 on 09/05/12
For personal use only.

THE COLORIMETRIC DETERMINATION OF PLATINUM WITH 5-(*p*-DIMETHYLAMINOBENZYLIDENE)-RHODANINE[1]

FRANCES E. PIERCY AND D. E. RYAN
Department of Chemistry, Dalhousie University, Halifax, Nova Scotia
Received October 17, 1962

ABSTRACT

5-(*p*-Dimethylaminobenzylidene)-rhodanine is used to determine 0.5 to 6 p.p.m. of platinum colorimetrically, after reduction of platinum IV with ascorbic acid. Platinum can be determined in the presence of a 10-fold excess of palladium; low concentrations of the other platinum metals, except rhodium, do not seriously interfere.

INTRODUCTION

The colorimetric methods that have proved successful for the determination of platinum involve the use of valences lower than the usual quadrivalent state. The widely used stannous chloride method (1) contains tin, platinum, and chloride in a complex in which the platinum has a valence of zero (2). Both the *p*-nitrosodimethylaniline (3), and the N,N′-bis(3-dimethylaminopropyl)-dithiooxamide (4) procedures make use of the bivalent state, reduction of quadrivalent platinum occurring either through the action of excess reagent or by deliberate addition of a reducing agent. The colorimetric method described herein constitutes part of the results of an investigation into the use of the bivalent state in the determination of platinum.

EXPERIMENTAL

Preliminary

In preliminary studies, a large number of compounds were investigated as possible reagents for reducing platinum, at room temperature and in dilute acid solution, from the quadrivalent to the bivalent state. Since *p*-nitrosodimethylaniline gave immediate color development with bivalent platinum at room temperature, but not with quadrivalent platinum, the compound being investigated was added to platinum IV solutions containing *p*-nitrosodimethylaniline and the development of color taken as evidence of reduction. Only sodium sulphite, chromous chloride, and ascorbic acid, of the following compounds investigated, were effective for this purpose: resorcinol, hydrazine, hydroxylamine, ascorbic acid, *d*-glucose, hydrogen peroxide, chromous chloride, formic acid, methyl alcohol, sodium sulphite. Ascorbic acid, which is itself colorless and gives a colorless oxidation product, has been used by Maksimyuk (5) to reduce platinum IV to platinum II quantitatively, and was therefore used throughout the remainder of the experimental work.

5-(*p*-Dimethylaminobenzylidene)-rhodanine, of a number of reagents investigated for the determination of platinum in the bivalent state, appeared most promising. This reagent, which has been used for the colorimetric determination of palladium (6), reacted immediately with platinum II to give a dark red precipitate in aqueous solution but very slowly with platinum IV. The problem in using this reaction for the colorimetric determination of platinum was to find a suitable solvent or a suitable extractant for the precipitate. Difficulties in obtaining complete extraction with chloroform, petroleum ether, benzene, and carbon tetrachloride discouraged further investigation into extraction possibilities. Although water-miscible solvents, such as alcohols, acetone, and dioxane, dissolved the precipitate, the resulting solutions were unstable, with solid separating from solution or the color fading on standing. Propionic acid, however, used by Ayres and Narang in the determination of palladium, dissolved the platinum complex to give stable, red-colored solutions and proved a satisfactory solvent in the colorimetric determination.

Reagents

Standard platinum solutions.—These solutions were prepared by dissolving a known weight of Johnson Matthey, "Specpure" ammonium chloroplatinate in water containing a few drops of dilute hydrochloric acid, and diluting to volume.

[1]*This work received financial assistance from the National Research Council, and is abstracted from the M.Sc. Thesis of Frances E. Piercy.*

Can. J. Chem. Downloaded from www.nrcresearchpress.com by 210.87.254.6 on 09/05/12
For personal use only.

5-(p-Dimethylaminobenzylidene)-rhodanine.—The reagent was obtained from Eastman Kodak, and reagent solutions contained 0.04% reagent in 98% formic acid. Ninety percent formic acid was also satisfactory.

L-*Ascorbic acid.*—These solutions were prepared fresh daily to avoid possible deterioration. The solutions were 0.1 *M* ascorbic acid in water, adjusted to pH 2 with dilute hydrochloric acid.

Propionic acid.—Reagent grade was used.

Spectral Curves

The absorption curves for reagent and for a solution containing 2 p.p.m. of platinum are shown in Fig. 1. These curves were obtained using a Bausch and Lomb spectronic recording Spectrophotometer. Maximum absorption occurs at 545 mμ but, since the reagent absorbs strongly at that wavelength, all colorimetric results recorded were carried out at 590 mμ, where the reagent shows 100% transmittance.

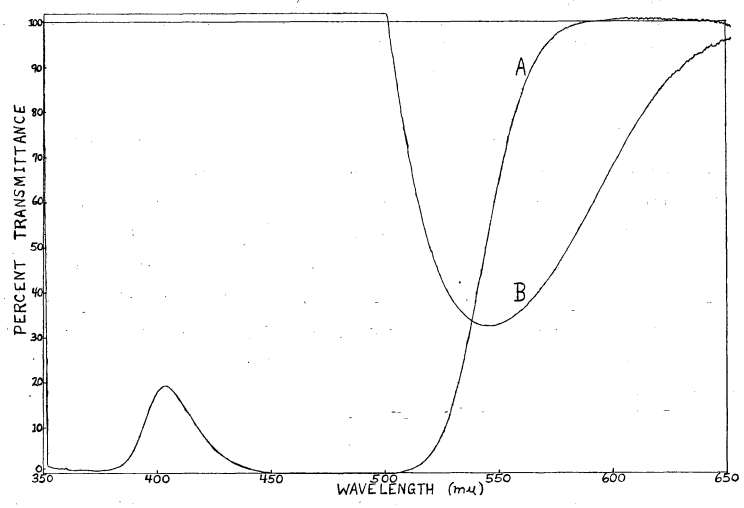

FIG. 1. Absorption spectra: A, 1 ml reagent solution (1.51×10^{-6} mole reagent) + 2 ml water + 3 drops ascorbic acid diluted to 10 ml with propionic acid; B, as A plus 2 p.p.m. of platinum.

Effect of Heating

Although immediate color development is obtained on adding reagent to platinum solutions reduced with ascorbic acid, maximum color is not attained for several hours. However, by heating the sample solutions at 65–75° C for 5 minutes, stable maximum color is obtained. For example, the optical density of a solution containing 2 p.p.m. of platinum changed from 0.158, without heating, to 0.233, after heating for 5 minutes at 70° C. In a number of experiments in which the heating was carried out by immersing the 10-ml volumetric flasks in a water bath at the desired temperature, consistent results were obtained in solutions heated for 5 to 10 minutes at temperatures between 65 and 75° C. There was some decrease in optical density if solutions were heated for a longer period; thus a reading of 0.219 was obtained after heating for 15 minutes at 70° C.

Effect of pH

For the reagent blank alone, the pH of the water solution may be varied between 2 and 6 without significant changes in the resulting spectra, and with 100% transmittance at 590 mμ; at pH 1, the reagent color is considerably faded. In samples containing 1.6 p.p.m. platinum, the optical density at 590 mμ was found to be 0.185, between pH 2 and 4. At pH 1, this falls off to 0.156; at pH 5, the reading is 0.174. From these experiments it was obvious that between pH 2 and 4, consistent results may be obtained.

Effect of Water, Ascorbic Acid, and Reagent

When optical density measurements are made at 590 mμ, the sample solution may contain from 5% to 25% water solution; if more than 2.5 ml of water per 10 ml final solution is present, the precipitate may be difficultly soluble in the propionic acid. Since the reagent does not absorb at 590 mμ, the concentration of reagent has no effect on the optical density; however, a large excess must be avoided due to the limit of its solubility in propionic acid. The volume of 0.1 *M* ascorbic acid solution added can be varied from 2 drops to 1 ml, with no effect on the resulting optical density.

Procedure

The platinum solution was adjusted to pH 2 to 4 with dilute hydrochloric acid, and a 0.5- to 2.5-ml aliquot (containing 5 to 60 μg platinum) was taken for analysis. To this aliquot, in a 10-ml volumetric

Can. J. Chem. Downloaded from www.nrcresearchpress.com by 210.87.254.6 on 09/05/12
For personal use only.

flask, was added three drops of 0.1 *M* ascorbic acid and the solution mixed. One milliliter of reagent was added and the flask placed in a water bath at 65–75° C for 5 minutes. The solution was then cooled to room temperature under cold water. Propionic acid was added, almost to volume, and the solution allowed to come to room temperature (about 15 minutes). The volume was then adjusted to 10 ml with propionic acid and the optical density read at 590 mμ against a reagent blank.

Optical densities obtained on a series of platinum samples are given in Table I. These results show that Beer's law is obeyed between 0.5 and 6 p.p.m. The color was stable for 1 hour, after which time it faded very slowly; a sample containing 2.0 p.p.m. platinum gave a constant optical density of 0.236 for 1 hour, falling to 0.233 after 90 minutes and to 0.226 after 2 hours.

TABLE I

Optical densities for varying platinum concentrations

Pt (p.p.m.)	Optical density	Pt (p.p.m.)	Optical density
0.5	0.058	4.0	0.454
1.0	0.112	5.0	0.577
2.0	0.232	6.0	0.688
3.0	0.335	7.6	0.796

Effect of Various Ions

No interference was noted when 2000 p.p.m. of the sodium, potassium, or ammonium salts of the following ions was added to 2 p.p.m. of platinum, as the chloride, and the usual colorimetric procedure carried out: Cl^-, SO_4^{-2}, NO_3^-, BO_2^-, PO_4^{-3}, CO_3^{-2}. Acetate ion, in excess of 500 p.p.m., and fluoride or bromide, beyond 100 p.p.m., interfere. Thiosulphate, sulphite, sulphide, oxalate, and iodide ions interfere by producing turbid solutions. Although sulphate in large amounts does not interfere in the determinations, the colored complex does not form in solutions that have been fumed with sulphuric acid.

Studies of the reactions of various ions, when 200 p.p.m. of the metal ions as chlorides or nitrates was added to 2 p.p.m. of platinum, showed no interference from the following ions: K^+, Na^+, NH_4^+, Ni^{+2}, Co^{+2}, Cd^{+2}, Mg^{+2}, Ca^{+2}, Sr^{+2}, Ba^{+2}, Al^{+3}, As^{+3}. Zinc and manganese interfered beyond 50 p.p.m. Antimony, tin, iron, and chromium ions interfere through precipitate formation or by giving low optical density readings.

Silver, mercury, copper, gold, palladium, and rhodium react with the reagent to give precipitates similar to that obtained with platinum. Of these, only interferences from palladium can be eliminated in the determination of platinum; 25 p.p.m. of palladium in the presence of 2 p.p.m. of platinum does not interfere if a small amount of dimethylgloxime is added. Some results obtained in the presence of other platinum group metals are given in Table II.

TABLE II

Platinum determinations in the presence of other platinum group metals

Pt taken (μg)	Pt found (μg)	Pt metal present (μg)	Remarks
20.0	20.0	21.5 Ir	Added as ammonium chloroiridate
19.0	19.2	43.0 Ir	
19.0	20.5	86.0 Ir	
57.0	57.0	107 Ir	
19.0	19.0	35.0 Pd	Two drops 0.1 *M* dimethylglyoxime
19.0	19.2	150 Pd	added
20.0	19.9	250 Pd	
19.0	18.5	300 Pd	0.5 ml dimethylgloxime added in excess
19.0	18.8	23.0 Ru	Added as ammonium chlororuthenate;
20.0	22.3	40.0 Ru	ruthenium absorbs itself at 590 mμ
19.0	18.8	108 Os	Added as ammonium chloroosmate
20.0	22.8	200 Os	
20.0	21.8	4.0 Rh	A color is developed with Rh alone
20.0	20.1	21.5 Ir, 20 Ru, 20 Os, 25 Pd	Two drops 0.1 *M* dimethylglyoxime added
30.0	30.0	21.5 Ir, 20 Ru, 20 Os, 25 Pd	

Can. J. Chem. Downloaded from www.nrcresearchpress.com by 210.87.254.6 on 09/05/12
For personal use only.

Rhodium interferes seriously and gives a color nearly as intense as that of platinum. The results show that iridium, ruthenium, and osmium, in low concentration, do not interfere and that platinum can be determined (provided dimethylglyoxime is added) in the presence of a 10-fold excess of palladium.

Stoichiometry of the Reaction

The stoichiometry of the reaction was investigated spectrophotometrically by both the mole ratio method (7) and the method of continuous variations (8); both studies showed that three molecules of reagent reacted with one atom of platinum. Attempts to support this somewhat surprising result by analysis of the precipitated product were unsuccessful because of the inability to obtain a pure product.

REFERENCES

1. E. B. SANDELL. Colorimetric determination of traces of metals. Interscience Publishers, Inc., New York, N.Y. 1944.
2. G. H. AYRES and A. S. MEYER. J. Am. Chem. Soc. **77**, 2671 (1955).
3. J. J. KIRKLAND and J. H. YOE. Anal. Chem. **26**, 1340 (1954).
4. W. D. JACOBS. Anal. Chem. **33**, 1279 (1961).
5. E. A. MAKSIMYUK. Izv. Sektora Platiny i Drug. Blagorodn. Metal., Inst. Obshch. i Neorgan. Khim., Akad. Nauk SSSR, **30**, 180 (1955).
6. G. H. AYRES and B. D. NARANG. Anal. Chim. Acta, **24**, 241 (1961).
7. J. H. YOE and A. L. JONES. Ind. Eng. Chem., Anal. Ed. **16**, 111 (1944).
8. P. JOB. Ann. Chim. Ser. 10, **9**, 113 (1928).

Can. J. Chem. Downloaded from www.nrcresearchpress.com by 210.87.254.6 on 09/05/12
For personal use only.

AN INVESTIGATION OF THE ALUMINUM–OXYGEN–CARBON SYSTEM

J. H. Cox and L. M. Pidgeon

Department of Metallurgical Engineering, University of Toronto, Toronto, Ontario

Received November 13, 1962

ABSTRACT

A differential thermal analysis technique was used to study the carbothermic reduction of aluminum oxide at reduced pressures in the temperature range 1700–2200° K. The reduction was found to proceed through the intermediate oxycarbide Al_4O_4C, identified by previous workers, to the aluminum carbide. The Al_4O_4C and another oxycarbide, Al_2OC, were formed by a direct solid–solid reaction, rather than by formation of a gaseous aluminum suboxide and subsequent reaction with carbon as has been postulated.

The carbon monoxide pressures over the following reactions were measured:

$$Al_2O_3 + 3C = Al_2OC + 2CO$$

$$2Al_2O_3 + 3C = Al_4O_4C + 2CO$$

$$Al_4O_4C + 6C = Al_4C_3 + 4CO.$$

Heats and free energies of reaction were found and standard heats and free energies of formation were calculated for Al_2OC, Al_4O_4C, and Al_4C_3. The values for Al_4C_3 agreed with previously published results.

The direct reaction

$$Al_2O_3 + 3C = 2Al + 3CO$$

did not occur. To account for the aluminum produced at high temperatures, the reaction below was postulated:

$$Al_4O_4C + Al_4C_3 = 8Al + 4CO.$$

The calculated equilibrium pressure above this reaction agreed with experimental observations.

INTRODUCTION

In the past few years, there has been a revival of interest in the production of aluminum by direct reduction (1, 2). Since a carbothermic reduction of aluminum oxide is involved in these processes, the present work was carried out to investigate the details of this reaction.

Despite the industrial supremacy of the Hall–Heroult electrolytic process, there has been a sustained experimental interest in the aluminum–oxygen–carbon* system. Previous experiments on the system may be divided into two main groups. The first of these involved studies of the gas pressures existing above the system and paralleled the present investigation. The second, and more recent group, was a study of the compounds and phase relations occurring in the system, as determined by analyses of solidified melts of varying composition. In the latter group, a large number of compounds have been postulated by various workers (3, 4), but the existence of many of these has been disproved at a later date. Foster, Long, and Hunter (5) have subjected the system to an extensive analysis in which two oxycarbides, Al_2OC and Al_4O_4C, were found, as well as the known carbide, Al_4C_3. The existence of the two oxycarbides has been confirmed by Filonenko *et al.* (6, 7).

**In the text, the words graphite and carbon are used interchangeably.*

Can. J. Chem. Downloaded from www.nrcresearchpress.com by 210.87.254.40 on 09/05/12
For personal use only.

From the earlier work on reaction pressures, various reactions have been postulated as follows:

$$2Al_2O_3 + 9C = Al_4C_3 + 6CO \quad [1]$$

$$Al_2O_3 + 3C = 2Al + 3CO \quad [2]$$

$$Al_2O_3 + Al_4C_3 = 6Al + 3CO \quad [3]$$

$$Al_4C_3 = 4Al + 3C. \quad [4]$$

Since the gas pressures for reactions [1]–[3], as determined by previous workers (8, 9, 10), were of the same order of magnitude, it was thought that a pressure attributed to one reaction by one experimenter could easily have been linked with another reaction by a later worker. The major source of error in this case would be improper or inadequate analysis of the reaction products, and Foster *et al.* (5) have shown that this has occurred repeatedly in the phase diagram studies. Another source of error could be the methods of pressure measurement used. In the pseudostatic (8), static (9), and modified transportation (10) techniques, an "integrated" pressure measurement can be obtained at a specific temperature if two or more simultaneous reactions occur with nearly the same equilibrium pressure. A pressure-measuring method was required which could differentiate between the various reactions.

EXPERIMENTAL

(1) Pressure Measurement

The experimental methods (11, pp. 140–171; 12) which measure the gas pressure exerted at various temperatures will require excessive resolving power to separate the initial pressure contribution of a second reaction. It would be preferable to measure some other effect of the new reaction. One method involves measurement of the weight change produced by reactions which form volatile components. At the onset of a new reaction, the rate of change of weight will alter, and the corresponding pressure and temperature may be obtained by extrapolation. Such a method was used by Ruff (13). In this technique, a crucible containing the reactants was suspended from a spring balance inside a furnace. An inert gas at a predetermined pressure was added to the system and the temperature was increased at a constant rate while the change of weight was recorded. The position at which there was a change in the rate of weight loss was taken as the equilibrium point. The method is a dynamic or "boiling point" measuring technique. In a variation of this method, Fischer and Rahlfs (14) maintained a constant temperature and decreased the pressure. The change in rate was found to be more pronounced, and consequently the boiling point determination was more precise. Ruff's original procedure has recently been used by Chapman, Foster, and Shevlin (15) in a study of the silicon–oxygen–carbon system.

Theoretically, either of the procedures above would be suitable for the Al–O–C system, since the rate of weight loss would change with each successive reaction. In practice, however, the major disadvantage is the gradual change in weight loss which sometimes occurs near the reaction point. This causes uncertainties in the extrapolation to determine the equilibrium point. Other disadvantages are the relatively small size of the sample and container, and the possibility that the crucible might move in the furnace, thus causing a variation in heating conditions or a change in temperature of the sample.

The method adopted in this work measures the heat change which results from the onset of a new reaction, and is an adaptation of differential thermal analysis (D.T.A.). The measurement of the heat effect of a reaction is more sensitive than the change of weight, and the uncertainties of extrapolation were avoided. The method has been used in mineralogy to study a wide range of decomposition reactions at low temperatures. For example, Stone (16) studied the decomposition characteristics of various kaolin group minerals under an atmosphere of water vapor, and Haul and Heystek (17) investigated the decomposition of dolomite under varying carbon dioxide pressures.

In the experiments, the reactants and an inert reference sample were placed in the separate compartments of a divided reaction crucible, each compartment having a tight-fitting cap pierced by an aperture small enough to restrict diffusion, but large enough to permit flow when a small pressure differential was established. The crucible, with its differential thermocouple assembly, was placed in a furnace, and after preliminary outgassing and heating of the apparatus an atmosphere was added at a predetermined pressure. The reference and experimental sample were then heated at a constant rate, while readings of absolute and differential temperature against time were recorded. At the equilibrium point, the vapor pressure over the sample was just equal to the external pressure. At a slightly higher temperature, the reaction

Can. J. Chem. Downloaded from www.nrcresearchpress.com by 210.87.254.40 on 09/05/12
For personal use only.

proceeded and there was a quantity of heat evolved or absorbed. This produced a discontinuity in the differential trace, generally in the form of a reaction peak.

The method retains all the good points of the weight loss techniques and possesses some additional features. Unlike the thermobalance procedures, the reaction crucible is always stationary in the furnace and, therefore, it is easier to achieve uniform temperatures. The sample size may be increased considerably, the limit being governed by the need for temperature uniformity. The difficulty inherent in maintaining constant temperatures at high temperatures for long periods of time is bypassed. The D.T.A. is sensitive to all reactions which involve heat effects in the system.

Theoretically, the method can approach equilibrium from both sides. If the reaction is progressing at some temperature higher than the equilibrium, there will be a temperature effect on the differential trace. If the temperature is decreased linearly, a point will be reached where the reaction and the heat effect on the differential trace both cease. If the pressures are equal during the measurements from above and below, the equilibrium temperatures found should be the same. Since there is a ΔT effect for both determinations, they would differ by $2\Delta T$. This difference is an indication of the accuracy of the results. If small, the reaction point determinations can be treated as the correct equilibrium points, excluding errors in temperature and pressure measurement.

The method is similar to other high-temperature techniques in that the design of the apparatus and the establishment of suitable experimental conditions vary from reaction system to reaction system, and must be found empirically.

(2) Apparatus

The furnace used in the experiment is shown in Fig. 1. It consisted of a vacuum-tight water-cooled shell (volume 150±10 liters) which could be isolated from the pumps by either a baffle or a sliding valve (not shown). The pumping system consisted of a 4-in., three-stage, oil diffusion pump and a two-stage, air-ballasted, rotary mechanical pump. Points A, B, and C were Pirani-type thermocouple gauges and point D was a cold cathode gauge. For measurement of inert gas pressures, a mercury manometer was located at a point just ahead of the baffle valve. The mercury levels were determined with a cathetometer.

The furnace element shown in Fig. 1 was a tubular split graphite resistor. The power source was a 15.6 K.V.A. variable transformer connected in a series with 20:1 step-down transformer giving maximum power across the resistor at 12.5 v and 1300 amp, offering the furnace a maximum temperature of 2000° C. The furnace temperature was increased linearly by means of a motor-driven winch which drove the variable transformer. The rate of temperature increase could be varied by changing the motor reduction ratio. After experimenting with various rates of temperature increase, a rate of rise of 3.5° C per minute was selected.

Figure 2 is a diagram of one of the graphite reaction systems used for runs in which temperatures were measured optically. The disappearing filament-type pyrometer was sighted into the sight hole in the two-compartment reaction crucible by means of a quartz prism. Since temperature measurement at high temperatures was a possible major point of error, temperatures were also measured by a W-W 26% Re thermocouple. Both optical pyrometer and thermocouple were calibrated *in situ* against the melting points of analytical grade copper and nickel and nuclear grade zirconium. The accuracy of the temperature-measuring devices was ±10° C at 1850° C and ±3° C at 1083° C. When the thermocouple was used as a means of measuring absolute temperature, the graphite reaction assembly was modified slightly from that shown in Fig. 2 in that a thermocouple well extended up through the bottom of the reaction assembly to within $\frac{1}{8}$ in. of the bottom of the crucible compartments.

Because graphite was one of the reaction components, an all-alumina system was also used to ensure that the graphite assemblies did not interfere with the equilibrium point determinations. The alumina assembly consisted of a recrystallized alumina tube which extended through the top plate of the furnace of Fig. 1 and was connected to the inert gas pressure-controlling systems by a separate line so that the carbonaceous atmosphere surrounding the graphite resistor would not affect the reaction point determinations. Molybdenum baffles and spacers were used in this assembly.

The differential thermocouple was separated from the absolute temperature measuring devices and consisted of a tungsten–graphite–tungsten couple. This thermoelement was similar to that originally developed by Watson and Abrams (18), but was much smaller in size. In the graphite crucibles, the crucible bottom served as the common joining the two 0.010-in. tungsten wires. In an alumina crucible, a $\frac{1}{4}$-in. graphite rod was used as a common. The tungsten wires were forced into holes bored in the ends of 0.057-in. graphite rods, of $\frac{3}{4}$-in. length, and the free ends of the rods were inserted into holes bored in the graphite common. Figure 2 shows the graphite thermocouple pegs in position in the crucible. The tungsten wires, protected by alumina "spaghetti" tubing, were led out through the top plate of the furnace and connected to a precision potentiometer.

(3) Sample Preparation

In the examination of the alumina–carbon system, mixtures of alumina and graphite were prepared in the stoichiometric ratios $2Al_2O_3$:3C, $2Al_2O_3$:6C, and $2Al_2O_3$:9C. The aluminum oxide was analytical grade reagent and the graphite was National Carbon A.G.S.R. grade* (−100 mesh).

**Reaction assemblies and crucibles were also made from this graphite.*

Can. J. Chem. Downloaded from www.nrcresearchpress.com by 210.87.254.40 on 09/05/12
For personal use only.

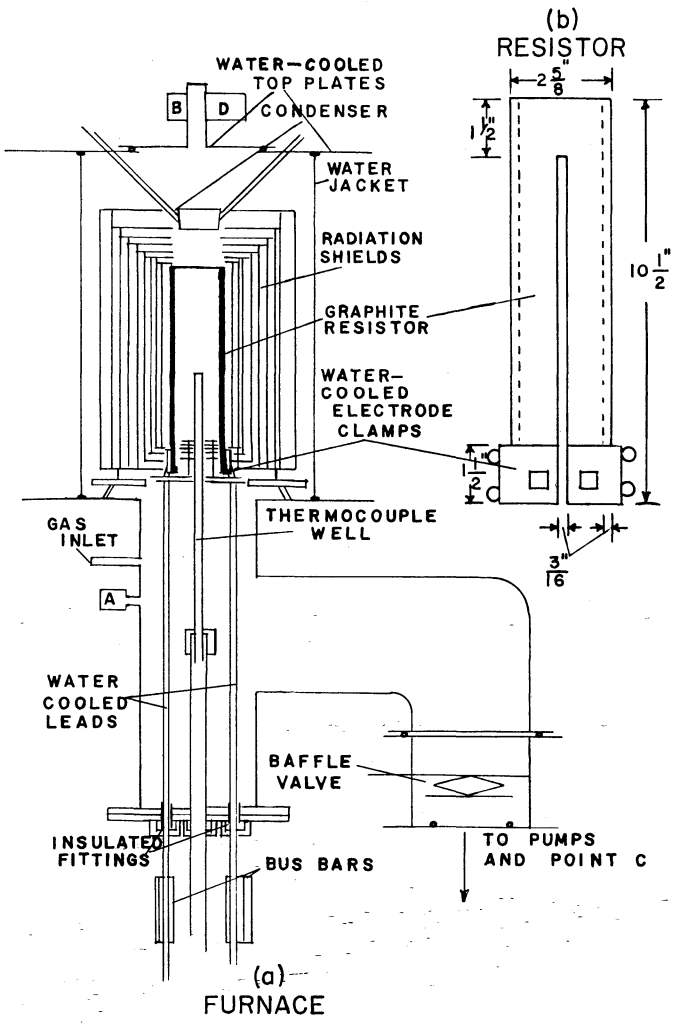

FIG. 1. Furnace (*a*) and resistor (*b*).

The mixtures were briquetted in a 1-in. steel die under 40,000 p.s.i. supplied by using a 3-in. hydraulic press. The pellets were then broken up and screened. Particles in the range −6, +20 mesh were retained. Blanks consisting only of alumina* were made in the same manner.

(4) Experimental Run

The differential thermocouple was assembled in the reaction crucible and the reference and sample were added to their respective compartments. The caps were placed on the crucible, followed by the alumina insulators. The assembly was lowered into the furnace by rods screwed into the tapped holes of the crucibles. The rods were removed, the various baffles and the condenser sleeve were added, and the tungsten wires were led out through the insulator in the top plate. The thermocouple outlet was sealed, and the leads connected to a potentiometer.

The system was evacuated at room temperature for 6 hours, after which a timing switch started the winch, and over a period of 4½ hours the temperature was increased from ambient to 1150° C. The furnace was degassed at this temperature for a further 3 hours prior to starting the differential thermal analysis. At the end of this degassing sequence, the baffle valve was closed and the pumps were isolated from the furnace. Purified argon was passed through the "cartesian diver" type controller and into the furnace.

**Reference samples of alumina were suitable only in the lower and intermediate temperature ranges. At higher temperatures, the carbon monoxide produced in the reactions reacted to some extent with the alumina in the reference compartment. The alumina was subsequently replaced with −6, +20 mesh graphite particles.*

Can. J. Chem. Downloaded from www.nrcresearchpress.com by 210.87.254.40 on 09/05/12
For personal use only.

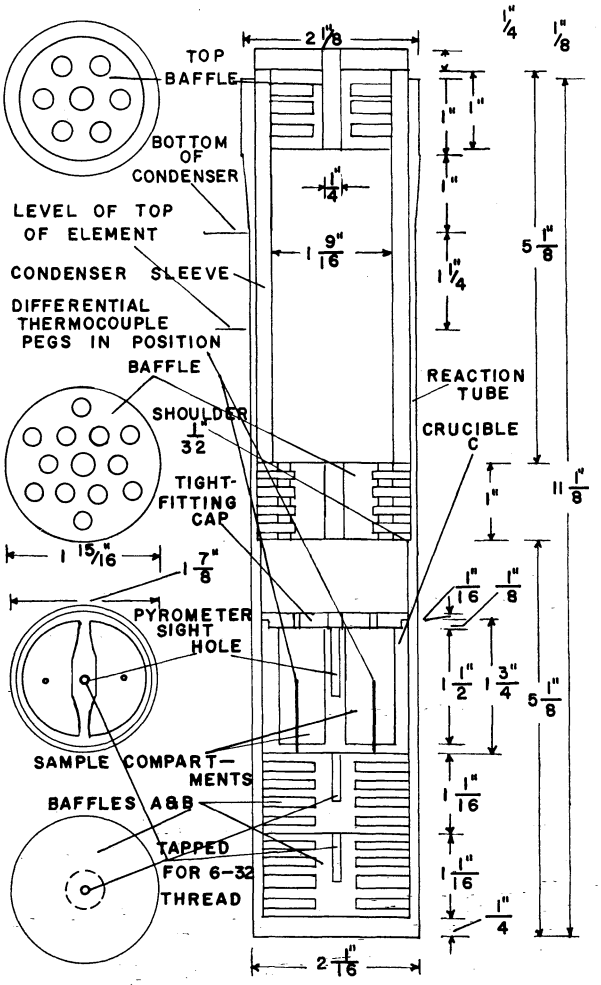

FIG. 2. Graphite reaction tube.

As the temperature of the furnace was increased linearly, readings of differential and absolute temperature were taken every 100 seconds, and the pressure, as indicated by the mercury manometer, was read every 10 minutes using the cathetometer.

After the completion of the run, the furnace was cooled and the crucible contents examined. Owing to the extreme fragility of tungsten after heating, excessive care was required to remove the differential thermocouple without damage. Therefore, the thermocouple was broken on removal from the furnace and a fresh couple was inserted for each run. This did not interfere with the results, as the readings of the differential thermocouple were only relative with respect to the reference compartment.

RESULTS

(1) Differential Traces

The differential traces obtained using the W-C-W thermocouple did not resemble the standard type of trace in which a discrete peak is formed for several reasons. In most of the standard forms (17) of D.T.A., extremely small samples are used and the reaction proceeds to completion in a short time, after which the differential trace returns to some value near its original. During the present work, the experimental samples were much

Can. J. Chem. Downloaded from www.nrcresearchpress.com by 210.87.254.40 on 09/05/12
For personal use only.

larger and the trace did not return to a near "normal" value and form a peak. The abnormal behavior was also due to the rate of reaction and will be discussed with reference to Figs. 3*a* and 3*b*. The figures are plots of the differential e.m.f. versus absolute tem-

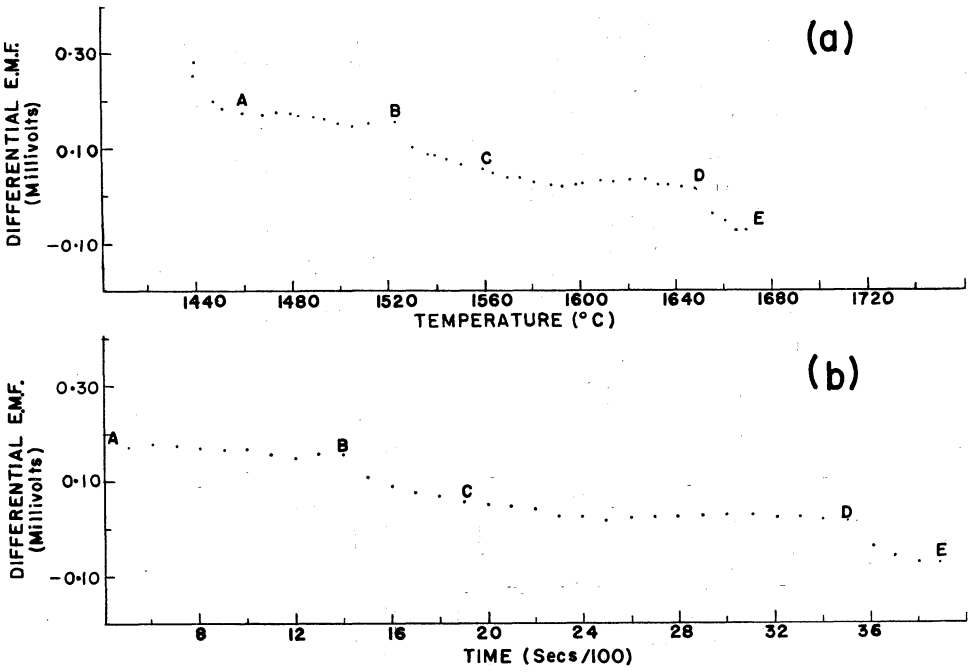

FIG. 3. (*a*) Differential e.m.f. vs. temperature (run 62). (*b*) Differential e.m.f. vs. time (run 62).

perature and time. Equivalent points on the curves are indicated by letter. Along AB, the rate of heating and the differential e.m.f. were constant. At B, the pressure of vapor product in the reaction crucible was equal to that of the argon in the system. As the temperature increased, the reaction proceeded to the right and there was a considerable change in the slope of the curve. After the initial rapid change (BC) the slope of the curve approached a steady-state condition once more. At D, a second reaction occurred and a curve similar to BCD was obtained (DE).

There was no "normal" differential peak after BC because the reaction was still proceeding up to D, where the second reaction started. Therefore, a distinct peak did not appear in the trace because, in the alumina–carbon system, the rate of reaction was a controlling factor and the mixture continued to react as the temperature was increased over the interval CD.

At D, because of the construction of the reaction tube, the original atmosphere of argon had been displaced in the space above the reaction crucible by the carbon monoxide generated by the reaction at B, over the time interval BD. Since the total pressure above the crucible was unchanged, this did not affect the reaction point determinations. The equilibrium points were taken as B and D for the two reactions.

The form of the D.T.A. curves made the task of obtaining equilibrium points for the back reactions somewhat easier. The curves were similar to those already described; the sole difference in method was that the equilibrium position was taken as the point at

Can. J. Chem. Downloaded from www.nrcresearchpress.com by 210.87.254.40 on 09/05/12
For personal use only.

which the differential trace returned to a constant or near-constant value after the change in slope caused by the reaction. Since the argon had been displaced from the reaction tube, the back reaction was measured under a carbon monoxide atmosphere.

(2) Reactions Present in the System

All the stoichiometric ratios showed the same reactions occurring. The pressure–temperature relationship for three of these reactions could be measured and a fourth was observed. Figure 4 shows these relationships. The first three reactions occurred at

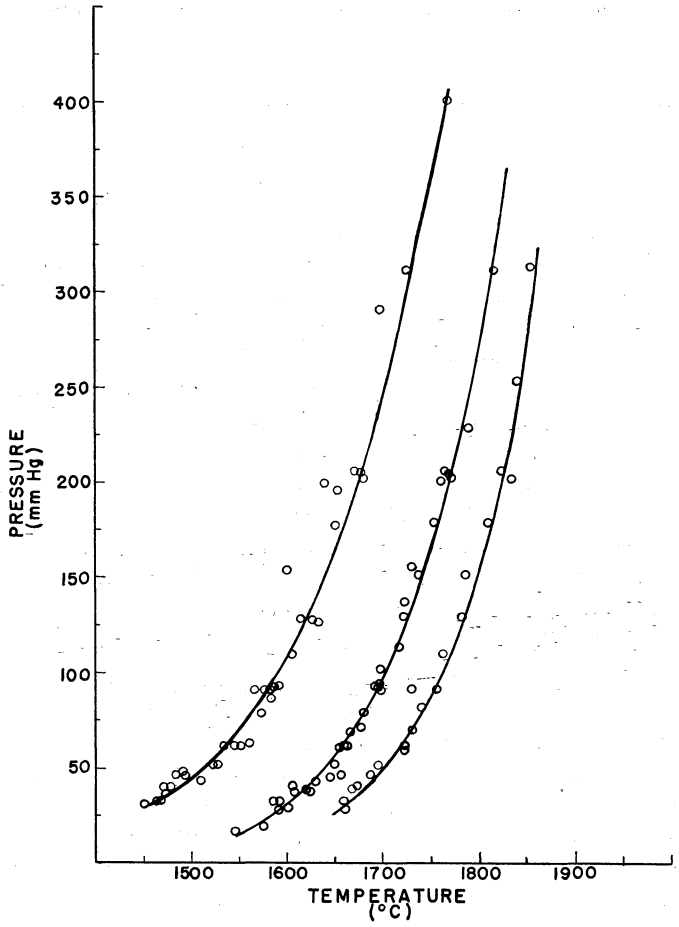

FIG. 4. Pressure vs. temperature for the reactions measured.

greatly different temperatures (at constant pressure), and gave a curve of the general form of Fig. 3. However, the fourth reaction occurred at almost the same temperature as reaction [3], and since the differential e.m.f. was still changing rapidly, the point for reaction [4] was obscured. For the first three reactions, the gaseous product was carbon monoxide. The product from the fourth reaction was a condensable vapor, and this condensed product was found to be a mixture of Al_4C_3, Al, C, and Al_2O_3, with some minor constituents.

Can. J. Chem. Downloaded from www.nrcresearchpress.com by 210.87.254.40 on 09/05/12
For personal use only.

A high-angle X-ray diffractometer using a copper target and nickel filter was employed to identify the respective reactions. A sample mixture was placed in the furnace heated to the reaction point, as determined from the differential traces, and held there for varying lengths of time. The furnace was then cooled, a portion of the sample was removed for X-ray analysis, and the remainder was returned to the furnace. The process was repeated at 10° C intervals over the range of interest of the system. The patterns were compared with those in the ASTM files (19). The first reaction was found to be:

$$Al_2O_3 + 3C = Al_2OC + 2CO. \quad [5]$$

The second was the analogous reaction to form the second oxycarbide:

$$2Al_2O_3 + 3C = Al_4O_4C + 2CO. \quad [6]$$

The third was the reaction of the oxycarbide of reaction [6] with graphite to form the carbide Al_4C_3:

$$Al_4O_4C + 6C = Al_4C_3 + 4CO. \quad [7]$$

Reaction [5] had a relatively slow rate of reaction and produced only small amounts of the oxycarbide Al_2OC. However, reaction [6] proceeded rapidly and after a short period of time all the free alumina in the system was converted to Al_4O_4C.

Since Al_2OC was present in only minor amounts, and since there was no Al_2O_3 present, the reaction to produce the carbide must be reaction [7].

The fourth reaction could not be determined directly because of the condensable vapor product which appeared in the colder sections of the apparatus. It is likely that this fourth reaction yielded aluminum vapor as one of the gaseous products. This metal vapor then back-reacted in the cooler portions of the apparatus with either graphite or carbon monoxide to form the Al_4C_3, C, Al, Al_2O_3 mixture which was found. Since there was no alumina present in the system at this temperature, neither reactions [2] nor [3] could take place. The amount of Al vapor produced was too great for [4] to be the reaction occurring. However, aluminum may be produced by a reaction with the oxycarbide analogous to [3]:

$$Al_4O_4C + Al_4C_3 = 8Al + 4CO. \quad [8]$$

The reason why reactions [1], [2], and [3] were postulated by early workers would probably be in their methods of analysis. In the early work, the substances analyzed were the back-reaction products and the previous reactions were deduced from these products. Since these products were generally formed under non-equilibrium conditions, the wrong reactions were postulated. Reaction [1], measured by Prescott (8), is simply the sum of the reactions [6] and [7] measured in this work. Reaction [2], measured by Brunner (9) and Treadwell and Gyger (10), did not occur directly. Reaction [3], postulated by Brunner (9), would not take place because of the absence of alumina at this stage of the carbothermic reduction.

In the present work, the order of appearance of the oxycarbides was also unexpected. With respect to increasing percentages of carbon, the series is: $2Al_2O_3$–Al_4O_4C–$2Al_2OC$–Al_4C_3.

The appearance of Al_2OC at lower temperatures than the Al_4O_4C was probably due to the similarity in size between the Al_2OC and Al_2O_3 molecules. In this case, more energy would be required to form the larger Al_4O_4C molecule than the smaller and less complex molecule of Al_2OC.

Can. J. Chem. Downloaded from www.nrcresearchpress.com by 210.87.254.40 on 09/05/12
For personal use only.

It has been suggested (20) that the distillation of material was caused by the reduction of alumina to a suboxide, either AlO or Al_2O, and then a subsequent reaction with carbon occurred to form the oxycarbides. Possible reactions for this process would be:

$$Al_2O_3 + C = 2AlO + CO \quad [9]$$

$$Al_2O_3 + 2C = Al_2O + 2CO \quad [10]$$

followed by:

$$Al_2O + C = Al_2OC \quad [11]$$

or

$$4AlO + C = Al_4O_4C. \quad [12]$$

Using the data from Lewis and Randall (21), the free energies of reaction for [9] and [10] were calculated. The equilibrium pressure above the system was found by using the relation

$$\Delta F^0_T = -RT \ln K_p.$$

For [9]:

$$\Delta F^0_{2000} = 125{,}000 \text{ cal} = -2000R \ln P^3_{AlO/2}$$
$$(P_{AlO} = 4.3 \times 10^{-2} \text{ mm Hg})$$

For [10]:

$$\Delta F^0_{2000} = 47{,}700 \text{ cal} = -2000R \ln 4P^3_{Al_2O}$$
$$(P_{Al_2O} = 3.5 \text{ mm Hg}).$$

As seen in Fig. 4, the measured pressures at 2000° K were greater than the calculated pressures by one to two orders of magnitude. Therefore, neither [9] nor [10] were the reactions measured during the experiment.

(3) Validity of the Measurements

Two series of tests were carried out with the D.T.A. apparatus, to establish whether the true equilibrium points were being measured. In one case, the equilibrium was approached from both sides. The second method was an attempt to check the apparatus by examining an established, simpler system. (The alumina–carbon system is one of the most complex of the oxide–carbide systems, and aluminum oxide is second only to thoria in its high-temperature stability with respect to carbon.) The zirconium doixide – carbon binary is such a system.

It has been examined by both Prescott (22) and Kutsev *et al.* (23). They measured the carbon monoxide pressures above this system using a pseudostatic method in which equilibrium could be approached from both above and below. In the present method, the values obtained on runs approaching equilibrium from below fell between those of the two earlier workers in the temperature range covered (1790–1900° K).

When points were measured from above using the alumina–carbon system, the values obtained were equal to those obtained from below at the same pressure within the limits of experimental error (±10° C). Values could only be obtained for reactions [5] and [6] in the lower-temperature ranges because of the rapid distillation of materials out of the crucible by means of reaction [8] at higher temperature. This was not a drawback because Kutsev (23) has found that in the case of refractory oxide–carbon systems, errors that might occur in determinations from both sides were much greater at lower temperatures and were negligible at higher temperatures. Therefore, both checks indicated that equilibrium had been measured in the present work.

Can. J. Chem. Downloaded from www.nrcresearchpress.com by 210.87.254.40 on 09/05/12
For personal use only.

(4) Reproducibility of Results

Figure 5 shows the van't Hoff relation obtained for reaction [6]. The outer limits are the two-sigma limits and correspond to an uncertainty of ±1.2 mm Hg in the results.

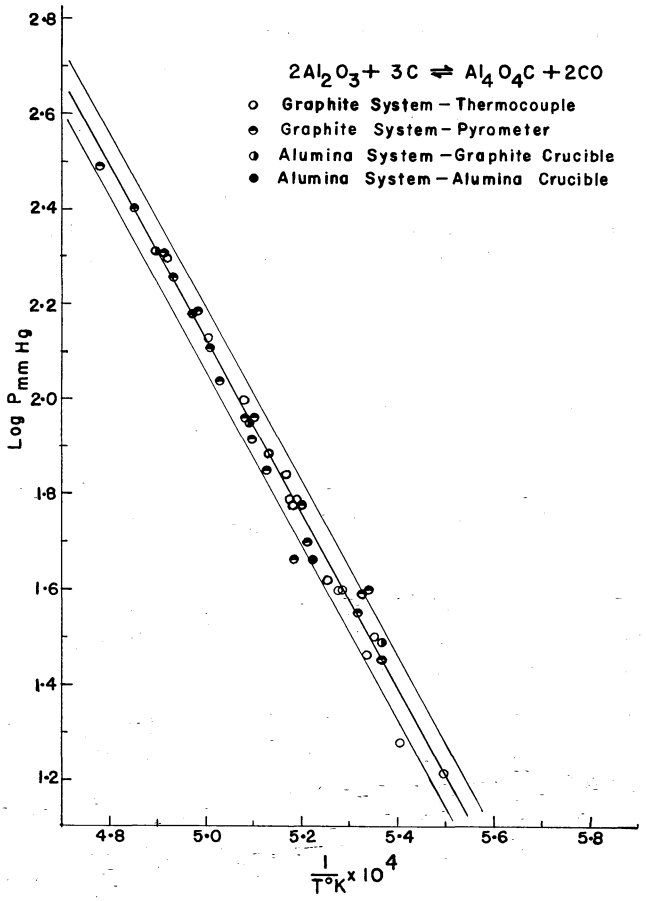

FIG. 5. Log $P_{mm\ Hg}$ vs. $(1/T)\times 10^4$.

The values for reactions [5] and [7] were ±1.3 and ±1.2 mm Hg respectively. These values were within the sensitivity limits of the instruments used for controlling the pressure of argon in the system.

It is apparent from Fig. 5 that there was no statistical difference between the results obtained using either the optical pyrometer or thermocouple, or the results obtained using either an alumina or a graphite system. (In these runs, the holes in the caps of the reaction crucible were also varied from 0.080 in. to 0.120 in. with no significant difference in the results obtained.)

(5) Thermodynamic Calculations

Because of the lack of heat capacity data for the aluminum oxycarbides, it was necessary to estimate values for these compounds. This, in turn, made it advisable to use "a third law" method of calculating the heats of reaction for reactions [5], [6], and [7]. For each equilibrium measurement, a value of $\Delta F^0_T/T$ was found, and by using the relation

$$\Delta H^0_{298} = T(\Delta F^0_T/T - \Delta(F^0_T - H^0_{298})/T)$$

Can. J. Chem. Downloaded from www.nrcresearchpress.com by 210.87.254.40 on 09/05/12
For personal use only.

a standard heat of reaction was obtained. Ideally, if there is no temperature-dependent error, and if the $(F_T^0-H_{298}^0)/T$ values are correct, the ΔH_{298}^0 values obtained are constant. In the case of a temperature-dependent error, or erroneous free energy functions, there is a drift in the ΔH_{298}^0 values obtained, but a fairly accurate (24) value of the standard heat may be obtained by taking an average value.

Kelley (25) has given a relation for the heat capacity of alumina in the range 298–1800° K. This relation was used over the temperature range 298–2200° K, with some unavoidable loss in accuracy.

Kubaschewski's (26) listed value of the heat capacity of the carbide was used. This molal heat capacity was recalculated to give the more usual three-term relation.

$$\text{For } Al_2O_3\text{: } C_p = 27.49+2.82\times10^{-3}T-8.38\times10^{5}T^{-2}$$

$$\text{For } Al_4C_3\text{: } C_p = 44.30+3.19\times10^{-3}T-12.39\times10^{5}T^{-2}.$$

Heat capacities for Al_4O_4C and Al_2OC were estimated using Kopp's rule and treating the oxycarbides as mixtures of Al_2O_3 and Al_4C_3.

$$\text{For } Al_2OC\text{: } C_p = \frac{C_p(Al_2O_3)+C_p(Al_4C_3)}{3}$$

$$C_p = 23.93+2.00\times10^{-3}T-6.92\times10^{5}T^{-2}$$

$$\text{For } Al_4O_4C\text{: } C_p = \frac{4C_p(Al_2O_3)+C_p(Al_4C_3)}{3}$$

$$C_p = 51.42+4.82\times10^{-3}T-15.30\times10^{5}T^{-2}$$

The absolute entropy of alumina at 298° K, S_{298}^0, was obtained from Kelley (27), that of the carbide from Circular 500 (28), and from these values, S_{298}^0 for Al_4O_4C was calculated according to the recommendation of Kubaschewski (11, p. 194). The value used for Al_2OC was estimated in a different manner and will be explained below:

For Al_2O_3, $S_{298}^0 = 12.5$ e.u. For Al_4C_3, $S_{298}^0 = 25$ e.u.

For Al_4O_4C, $S_{298}^0 = 25$ e.u. For Al_2OC, $S_{298}^0 = 6.5$ e.u.

From these values, the free energy functions were calculated and from these the heats and free energies of reaction were found. Using the values for alumina and carbon monoxide from Elliott and Gleiser (29), the standard heats and free energies of formation for the compounds were found and are given in Table I below.

TABLE I

Thermodynamic functions

Compound	ΔH_{298}^0 (kcal)	ΔF_{298}^0 (kcal)	Limits (kcal)
Al_2OC	−171.4	−158.9	±10
Al_4O_4C	−543.1	−511.7	± 8
Al_4C_3	− 35.9	− 28.4	± 8

The experimental heats and free energies of formation for the carbide could be compared with the values obtained by other workers using calorimetric and equilibrium pressure measurements. The standard heat of formation agreed favorably with the 40±3 kcal obtained by Roth (30). Meschi and Searcy (31) found 50±10 kcal and Elliott and

Can. J. Chem. Downloaded from www.nrcresearchpress.com by 210.87.254.40 on 09/05/12
For personal use only.

Gleiser (29) list -35.9 ± 3 kcal from the work of C. S. Campbell. The free energy of formation was reported as -38.1 kcal by Roth (30), -35.9 kcal by Elliott and Gleiser, and -28.4 kcal in the present work.

The estimated and experimental values for the oxycarbide Al_4O_4C could be treated with confidence since these values were used to calculate the thermodynamic functions for Al_4C_3, and the carbide values were similar to those obtained in calorimetric measurements.

The situation was somewhat less satisfactory for the other oxycarbide Al_2OC. Initially an estimated value of $S^0_{298} = 12.5$ e.u. was used to calculate the free energy functions. From the experimental values for the heats and free energies of formation, a value of $S^0_{298} = 1.0$ e.u. was obtained. The magnitude of $\Delta H^0_{298}-\Delta F^0_{298}$ was great enough so that the results were not affected unduly. Since the difference between the estimated and calculated values was so large, and since ΔS^0_{298} did not change very rapidly with the absolute values of ΔH^0_{298} and ΔF^0_{298}, a corrected value of S^0_{298} was obtained by averaging the calculated and estimated values in the first approximation. A value of $S^0_{298} = 6.5$ e.u. was therefore used. A second low treatment of the data also yielded a value approximately equal to this.

It was possible to calculate the total equilibrium pressure above reaction [8] using the experimentally derived free energies for the oxycarbide Al_4O_4C and the carbide Al_4C_3.

Volume 41, 1963

Page 682. The author has submitted the following regarding an error in lines 18–33:

"This has been pointed out to me by K. Motzfeldt, of the Norwegian Technical University, Trondheim, Norway, and involves the calculated pressure above the reaction

$$Al_4O_4C + Al_4C_3 \rightleftharpoons 8Al + 4CO. \qquad [8]$$

The correct total pressure above the reaction is 38.4 mm Hg and therefore [8] alone would not be the reaction observed in which volatile products were evolved. These products would occur by a combination of [8], and, possibly, the reactions given below,

$$Al_4O_4C + C \rightleftharpoons 2Al_2O + 2CO,$$

$$Al_4O_4C \rightleftharpoons 4AlO + C.$$

Because of this, the conclusion given in paragraph 3, page 683, is wrong."

) mm
'co is
) mm
ction
and
lated
The

calculated pressure of reaction [8] theoretically should be less than that of [7] but the difference noted was due to the errors in the experimentally determined thermodynamic functions (±8 kcal).

CONCLUSIONS

The method of determining vapor pressures produced results which were reproducible when equilibrium was approached from temperatures above and below the equilibrium value. The reproducibility was within $\pm1.5\%$, which was considerably better than that of static methods of measurement on similar systems.

The oxycarbides, Al_4O_4C and Al_2OC, were formed by a solid–solid reaction; the formation of aluminum suboxides as an intermediate step in the oxycarbide formation is unlikely. The carbothermic reduction to the carbide, Al_4C_3, proceeded through Al_4O_4C. There was no Al_2OC step in this reduction; it was formed only in small quantities and its formation was considered to be a side reaction in the process.

The equilibrium pressures above three reactions were measured in the system. These were:

$$Al_2O_3 + 3C = Al_2OC + 2CO$$

Can. J. Chem. Downloaded from www.nrcresearchpress.com by 210.87.254.40 on 09/05/12
For personal use only.

$$2Al_2O_3 + 3C = Al_4O_4C + 2CO$$
$$Al_4O_4C + 6C = Al_4C_3 + 4CO.$$

The reactions occurred at progressively higher temperatures in the order listed. From the experimental results, the heats and free energies of formation for Al_2OC, Al_4O_4C, and Al_4C_3 were calculated.

In the experiment, alumina was completely converted to the oxycarbide before the carbide was formed. Therefore, the direct reaction

$$Al_2O_3 + 3C = 2Al + 3CO$$

did not occur. To account for the large amounts of back-reaction products produced, the reaction below was postulated:

$$Al_4O_4C + Al_4C_3 = 8Al + 4CO.$$

The calculated equilibrium pressure above this reaction agreed with experimental observations.

ACKNOWLEDGMENT

The authors gratefully acknowledge financial support from the Advisory Committee on Scientific Research of the University of Toronto.

REFERENCES

1. P. Gross. Symposium on the refining of non-ferrous metals. The Institute of Mining and Metallurgy, London. 1950. pp. 461–70.
2. Rev. Aluminium, **38**, No. 283, 58 (1961).
3. E. Bauer and R. Brunner. Z. Elektrochem. **40**, 154 (1934).
4. E. J. Kohlmeyer and S. Lundquist. Z. Anorg. Chem. **260**, 208 (1949).
5. L. M. Foster, G. Long, and M. S. Hunter. J. Am. Ceram. Soc. **39**, 1 (1956).
6. N. E. Filonenko, I. V. Lavrov, and G. V. Andreyeva. Dokl. Akad. Nauk SSSR, **134**, 155 (1959).
7. N. E. Filonenko, I. V. Lavrov, G. V. Andreyeva, and R. L. Pevzner. Dokl. Akad. Nauk SSSR, **115**, 583 (1957).
8. C. H. Prescott, Jr. and W. B. Hincke. J. Am. Chem. Soc. **49**, 2753 (1927).
9. R. Brunner. Z. Elektrochem. **38**, 55 (1932).
10. W. D. Treadwell and A. Gyger. Helv. Chim. Acta, **16**, 1214 (1933).
11. O. Kubaschewski and E. U. Evans. Metallurgical thermochemistry. Pergamon Press Ltd., London. 1955.
12. W. D. Kingery. Property measurements at high temperatures. John Wiley and Sons Inc., New York. 1959. pp. 315–327.
13. O. Ruff and D. Bergdahl. Z. Anorg. Chem. **106**, 76 (1919).
14. W. Fischer and O. Rahlfs. Z. Anorg. Chem. **205**, 1 (1932).
15. A. T. Chapman, Jr., W. R. Foster, and T. S. Shevlin. Ohio State Univ. Eng. Expt. Sta. Bull. No. 185.
16. R. L. Stone. J. Am. Ceram. Soc. **35**, 91 (1952).
17. R. A. W. Haul and H. Heystak. Am. Mineralogist, **37**, 166 (1952).
18. H. R. Watson and H. Abrams. Trans. Am. Electrochem. Soc. **54**, 19 (1928).
19. ASTM. X-Ray powder data.
20. A. Schneider and O. Hilmer. Metall. **14**, 186 (1920).
21. G. N. Lewis and M. Randall. Thermodynamics. 2nd ed. *Revised by* H. S. Pitzer and L. Brewer. McGraw-Hill Book Co. Inc., New York. 1961. pp. 685.
22. C. H. Prescott, Jr. J. Am. Chem. Soc. **48**, 2534 (1926).
23. V. S. Kutsev, B. F. Ormont, and V. A. Epel'Baum. Dokl. Akad. Nauk, SSSR, **104**, 567 (1955).
24. G. N. Lewis and M. Randall. Dokl. Akad. Nauk SSSR, **104**, 178 (1955).
25. K. K. Kelley. Contributions to the data on theoretical metallurgy xiii. U.S. Bur. Mines. Bull. 584.
26. O. Kubaschewski and E. U. Evans. Metallurgical thermochemistry. Pergamon Press Ltd., London. 1958.
27. K. K. Kelley. Contributions to the data on theoretical metallurgy XI. U.S. Bur. Mines. Bull. 477.
28. F. D. Rossini, D. D. Wagman, W. H. Evans, S. Levine, and L. Jaffe. Selected values of chemical thermodynamic properties. Natl. Bur. Std. Circ. 500.
29. J. F. Elliott and M. Gleiser. Thermochemistry for steelmaking. Vol. 1. Addison-Wesley Publishing Co. Inc., Reading, Mass. 1960.
30. W. A. Roth. Z. Elektrochem. **48**, 267 (1942).
31. D. J. Meschi and A. W. Searcy. J. Phys. Chem. **63**, 1175 (1959).

Can. J. Chem. Downloaded from www.nrcresearchpress.com by 210.87.254.40 on 09/05/12
For personal use only.

PROTON COUPLING CONSTANTS IN SUBSTITUTED CYCLOPROPANES

H. M. HUTTON AND T. SCHAEFER
Department of Chemistry, University of Manitoba, Winnipeg, Manitoba
Received September 5, 1962

ABSTRACT

Coupling constants between geminal protons are reported for a number of cyclopropane derivatives. They are compared with results from previous work and other values in the literature. It is suggested that the geminal couplings are of opposite sign to the vicinal couplings and therefore negative. Comparison of the H—C—H angles with the former are therefore no longer valid. It is also suggested that the geminal couplings are zero in ethylene sulphides and positive in epoxides and that there is a change in sign in going from carbon through sulphur to oxygen as the third atom in the ring. The vicinal coupling constants depend on the dihedral angle as predicted by theory but the substituent effects do not appear to follow a simple dependence on the electronegativity as they do in substituted ethanes.

INTRODUCTION

We recently determined fairly certainly that the cis proton coupling constant in the cyclopropane ring is larger than the trans coupling constant (1). The magnitudes are in reasonable agreement with the $\cos^2 \phi$ relationship between the coupling constant and the dihedral angle ϕ as predicted by Karplus (2). There had been some disagreement in the literature about the relative magnitudes of these constants (1, 3). We have now measured the geminal coupling constant between protons for a number of cyclopropane derivatives. In the meantime coupling constants for the cyclopropane ring have been measured by others, and these are compared with our results (4–7). As in our previous work we have again measured relative amounts of cis and trans isomers for one derivative. Some relative chemical shifts are also discussed.

EXPERIMENTAL

The proton resonance spectra were obtained on a Varian V4302 DP 60 Mc/s spectrometer at room temperature. Peak separations were measured by the side-band technique, using a frequency counter. The analyses were the averages of a minimum of 10 spectra and were repeated on a separate occasion to verify the findings.

The compounds were a gift from Dr. Layton L. McCoy. Their physical constants are given in his paper (26*b*) and were certainly of sufficient purity for our purposes since a weak impurity peak was found in only one case. Solvents were used which preferentially shifted the ring proton peaks so that they were not obscured by other peaks. For reasons of solubility a mixed solvent of acetone and benzene was used for the dicarboxylic acids. For these reasons chemical shift comparisons are of doubtful value. Tetramethylsilane was the internal reference.

RESULTS

Coupling between ring protons and substituents like methyl groups was not observable and must thus be less than 0.4 c.p.s. Therefore the ring proton spectra were of the four-peak AB type and were analyzed as such. Table I gives the chemical shifts relative to internal tetramethylsilane as well as the coupling constants. The assignment for the ring protons could conceivably be interchanged. It has been made on the basis of the assignment for cyclopropane-1,1,2-tricarboxylic acid given by Graham and Rogers (4). The carboxyl protons are not included in Table I. They occurred at approximately 600 c.p.s. from the reference and will be omitted from the discussion.

Figure 1 shows the proton resonance spectrum of a mixture of *cis*- and *trans*-1-chloro-2-methyl-2-cyanocylopropane carboxylates and is discussed below.

Can. J. Chem. Downloaded from www.nrcresearchpress.com by 210.87.254.5 on 09/05/12
For personal use only.

TABLE I

Proton chemical shifts and coupling constants of some substituted cyclopropanes

Compound (numbered as in Table II)	State	Chemical shifts*				Coupling constant
		H_A	H_B	CH_3	$COOCH_3$	$J_{AB} = J_{gem}$ (c.p.s.)
2	Sat'd. in 1:8 acetone/benzene	126.4	108.0	90.3	—	6.44±0.12†
2	Sat'd. in 1:10 acetone/benzene	128.2	108.6	91.0	—	6.37±0.09
3	Sat'd. in 1:1 acetone/benzene	136.4	72.7	94.1	—	6.39±0.05
3	Sat'd. in formic acid	145.2	91.5	100.3	—	6.97±0.18
4	Diluted 1:3 in benzene	134.0	59.5	85.6	203.9, 206.0	6.52±0.12
5	Diluted 1:3 in benzene	125.7	53.5	74.5	210.3	7.02±0.11
6	Diluted 1:3 in benzene	98.5	87.0	67.5	206.1	7.06±0.13

*In c.p.s. at 60 Mc/s from internal tetramethylsilane.
†Standard deviations.

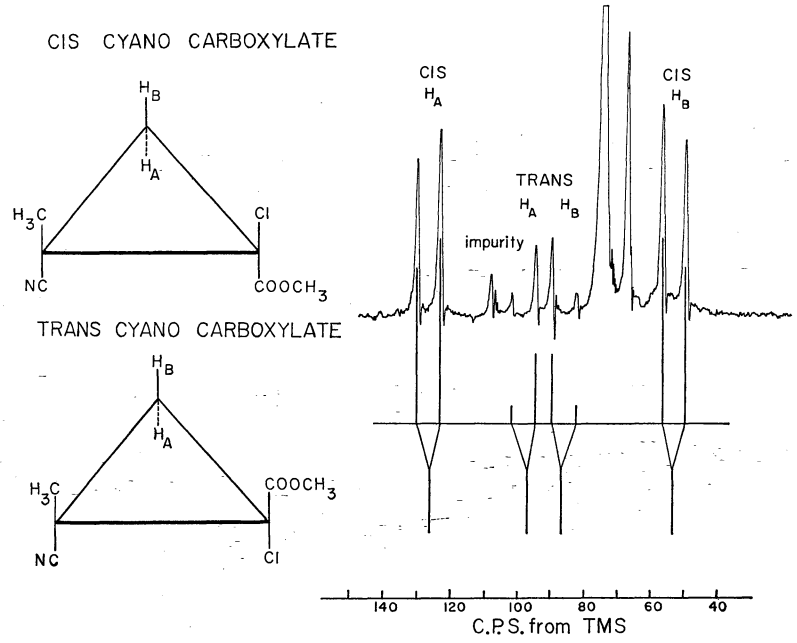

FIG. 1. The proton magnetic resonance spectrum of a mixture of *cis*- and *trans*-1-chloro-2-methyl-2-cyanocyclopropane carboxylates in benzene solution at 60 Mc/s. The internal reference is tetramethylsilane and occurs at high field.

DISCUSSION

Coupling Constants

The values of the three types of coupling constants for cyclopropane derivatives which are known fairly accurately are given in Table II. We examine them as to magnitude and sign.

(a) Vicinal Couplings

The average values of J_{cis} and J_{trans} in Table II are 8.67 and 5.71 c.p.s., respectively. The most recent determination of the cyclopropane geometry gives 113.8±2° for the H—C—H angle (8), compared to a previous value of 118° (9). The smaller angle improves the agreement between J_{trans} and the predicted value. For an H—C—H angle of 118°

Can. J. Chem. Downloaded from www.nrcresearchpress.com by 210.87.254.5 on 09/05/12
For personal use only.

Can. J. Chem. Downloaded from www.nrcresearchpress.com by 210.87.254.5 on 09/05/12
For personal use only.

TABLE II

Coupling constants in substituted cyclopropanes in c.p.s.

Compound	R	R′	S	S′	T	T′	J_{cis}	J_{trans}	J_{gem} *	Reference
1	H	H	H	COOH	H	H	ST = 8.0 TR = 10.5 T′R′ = 11.0	ST′ = 4.6 TR′ = 7.5	−4.3	6
2	COOH	Cl	CH_3	COOH	H	H			6.44	This paper
3	Cl	COOH	CH_3	COOH	H	H			6.39 (6.97)	This paper
4	Cl	$COOCH_3$	CH_3	$COOCH_3$	H	H			6.52	This paper
5	CH_3	CN	Cl	$COOCH_3$	H	H			7.02	This paper
6	CH_3	CN	$COOCH_3$	Cl	H	H			7.06	This paper
7	OCH_3	H	Cl	Cl	H	H	7.90	5.28	8.38	4
8	OCH_2CH_3	H	Cl	Cl	H	H	8.25	5.27	8.09	4
9	COOH	H	COOH	COOH	H	H	9.33	6.55	4.80	4
10	CH_3	C_6H_5	Cl	Cl	H	H			7.10	4
11	H	C_6H_5	Cl	Cl	H	CH_3	8.28			4
12	H	COC_6H_5	COC_6H_5	H	H	COC_6H_5		5.61 (6.0)		4 (3)
13	COOH	CH_3	C_6H_5	C_6H_5	H	H			4.65	5
14	COOH	H	C_6H_5	C_6H_5	H	H	7.70	5.85	−4.37	5
15	NO_2	O=C	—H—	C=O	H	H	9.0	6.0	6.7	14
16	COOH	H	$CH{=}C(CH_3)_2$	H	CH_3	CH_3	8.7			1
17	H	COOH	$CH{=}C(CH_3)_2$	H	CH_3	CH_3		5.4		1
18	CH_3	CH_3	H	S—C_6H_5	H	H	8.5	5	5	7

*See text for discussion of the sign of the geminal coupling.

the dihedral angle is very nearly 147°, giving a predicted value of 6.4 c.p.s., while for 114° the dihedral angle is about 144°, giving a predicted value of 5.9 c.p.s.

However, apart from the fact that the theory assumes sp^3 hybridization and is, furthermore, one which is to be used as a rough guide only, substituent effects may be of some importance. Glick and Bothner-By (10) some time ago suggested that in ethyl compounds the average vicinal coupling constant was a linear function of the electronegativity: J (c.p.s.) $= 8.4-0.4E$, where E is the Huggins electronegativity of the substituent. A slightly different relation, based on more extensive data, has been recently given by Banwell and Sheppard (11). They have found it to be valid for more heavily substituted ethanes. In both relations the dependence on electronegativity is about 10 times smaller than that in vinyl compounds (12, 13).

Although there is a variation of vicinal coupling constants with the substituent for the cyclopropanes, it does not clearly depend on the electronegativity of the substituent. Thus, for compounds 9 and 14 the substituent is the carboxyl group and $J_{cis}+J_{trans} =$ 15.88 and 13.55 c.p.s., respectively. The neighbor groups are carboxyl groups in one case and phenyl groups in the other. In compound 15 we have $J_{cis}+J_{trans} = 15.0$ c.p.s. and the trend is in the opposite direction to that expected from the behavior of ethanes. In the latter compound there may be a certain amount of distortion of the molecule. One suspects that for all these compounds the high degree of substitution involves enough distortion of the molecule to obscure any small linear dependence of the couplings on the electronegativity of the substituent. This point can only be settled by a systematic study of a series of cyclopropanes. Compound 1, the only monosubstituted molecule in Table II, does show a substituent effect on vicinal couplings which appears to be appreciable and in the right direction.*

It has been suggested that the cyclopropane ring has some π-electron character (15(*b*)), but it appears that, if present, it does not contribute noticeably to the coupling. Otherwise, we should see a large substituent electronegativity effect as in ethylenic compounds (12, 13). Also, one might expect appreciable coupling to the methyl substituents through four bonds as is usually observed when the C—C bond has appreciably π character (15(*a*)).

(b) Geminal Couplings

In the two cases in Table II where it has been determined J_{gem} is of opposite sign to the vicinal couplings.† In almost all cases, with the exception of certain ethylenes and epoxide groupings, this is true also in other systems (16–20). The agreement between theory and experiment for vicinal couplings through three bonds leads to the conclusion that these are positive as required by theory. Then geminal couplings through two bonds are negative, at least in sp^3 systems. We suggest that all geminal coupling constants in Table II are negative, as predicted by the Dirac vector model (21).

The magnitudes are smaller than those found in tetrahedral systems but similar to the one found in propylene oxide, although it is zero in propylene sulphide (22). J_{gem} appears to be of the same sign as the vicinal coupling constants in a series of epoxides, with an average value of 5.7 c.p.s. (23). We suggest that J_{gem} therefore goes through about zero for the heterocyclic sulphides and becomes negative for the cyclopropanes. The

**In benzene solution the proton spectrum is nicely separated into three groups of lines (ignoring the carboyxl group) and we are analyzing the spectrum at both 60 Mc/s and 100 Mc/s as a check.*

There appears to be a definite solvent effect on the geminal coupling constant of compound 3 in Table II (see Table I). A similar situation exists for compound 12 where two different values for J_{trans} have been reported in different solvents (3, 4). This needs investigation.

†Preliminary spin decoupling experiments on a cyclopropane derivative in this laboratory indicate a third case of opposite signs for J_{gem} and J_{vic}.

Can. J. Chem. Downloaded from www.nrcresearchpress.com by 210.87.254.5 on 09/05/12
For personal use only.

H—C—H angles in both ethylene oxide and ethylene sulphide are almost equal (24) and the relation between J_{gem} and this angle is no longer justified (25), especially since J_{gem} is almost certainly negative in sp^3 systems. The reason for the change in sign of J_{gem} on going from the oxide to cyclopropane remains to be explained.

For compounds 7, 8, 9, and 15 the sum of the three coupling constants is fairly constant, as noted by Graham and Rogers (4). But if J_{gem} is negative for these compounds, as we suggest, then the sum varies between 4.8 and 11.1 c.p.s. and this regularity no longer holds.

Chemical Shifts

These were determined either for pure compounds or in solvents which would have large solvent effects. Detailed discussion is therefore not in order. Some instructive points may, however, be made about the mixture of *cis*- and *trans*-1-chloro-2-methyl-2-cyanocyclopropane carboxylates. An analysis by gas chromatography of this mixture gave approximately 20% trans ester (26(*a*)). From peak heights we find 20.5±0.8% for the less abundant component, which we therefore assume to be the trans isomer.

We can then argue as follows. Graham and Rogers find the proton trans to the two carboxyl groups in cyclopropane-1,1,2-tricarboxylic acid to be more shielded than the cis proton. On that basis we can assign the proton trans to the two carboxymethyl groups (proton B) in our cis ester to the peaks centered at 53.5 c.p.s. in Fig. 1. The shielding difference is presumably due to magnetic anisotropy effects since electronegativity effects should be the same for both protons. On interchanging the chlorine and carboxymethyl group proton A is shifted to high field by 27.2 c.p.s. and proton B to low field by 33.5 c.p.s. The difference between these values could then be attributed to the anisotropy of the chlorine.

Two weaknesses in this argument are clear. First, although the dielectric constant of benzene is low, field effects arising from the difference in dipole moment of the two isomers could be appreciable (27). Second, the solvent effect due to the magnetic anisotropy of the benzene molecules may be large (28). If the benzene molecules pack around the solute molecules in such a way as to avoid electron-rich centers (29) and if one considers that volume effects are also important, then proton B in the cis isomer should experience the highest solvent shift to high field. The size of this shift is possibly as large as 0.5 p.p.m. or even more (28).

The conclusion is, of course, that before any definite statements about substituent effects can be made systematic studies must be carried out in a number of well-chosen solvents. Dipole moments of the solutes are also needed. Due to the limited solubility of carboxyl-substituted cyclopropanes in electrically and magnetically inert solvents, the synthesis of a series of cyclopropane derivatives with other groups is indicated. That appreciable substituent effects are present is seen from the 13.2 c.p.s. shift of cyclopropane itself from tetramethylsilane (30).

ACKNOWLEDGMENTS

We are indebted to Dr. Layton L. McCoy for his generous gift of compounds. We are also in debt to Dr. N. Sheppard, who let us see some of his results prior to publication. One of us (H. M. H.) would like to thank Canadian Industries Limited for fellowship support. This work was aided by the National Research Council and the Research Corporation.

Can. J. Chem. Downloaded from www.nrcresearchpress.com by 210.87.254.5 on 09/05/12
For personal use only.

REFERENCES

1. H. M. HUTTON and T. SCHAEFER. Can. J. Chem. **40**, 875 (1962).
2. M. KARPLUS. J. Chem. Phys. **30**, 13 (1959).
3. G. L. CLOSS and L. E. CLOSS. J. Am. Chem. Soc. **82**, 5723 (1960).
4. J. D. GRAHAM and M. T. ROGERS. J. Am. Chem. Soc. **84**, 2249 (1962).
5. J. I. MUSHER. Private communication.
6. K. WIBERG. Private communication.
7. U. SCHÖLLKOPF and G. J. LEHMANN. Tetrahedron Letters, 165 (1962).
8. O. BASTIANSEN and M. TRAETTEBERG. Tetrahedron, **17**, 147 (1962).
9. O. HASSEL and J. H. VIERVOLL. Acta Chem. Scand. **1**, 149 (1947).
10. R. E. GLICK and A. A. BOTHNER-BY. J. Chem. Phys. **25**, 362 (1956).
11. N. SHEPPARD. Private communication.
12. T. SCHAEFER. Can. J. Chem. **40**, 1 (1962).
13. S. CASTELLANO and J. S. WAUGH. J. Chem. Phys. **35**, 1900 (1961).
14. J. SMIDT and TH. J. DE BOER. Rec. Trav. Chim. **79**, 1235 (1960).
15. (*a*) M. KARPLUS. J. Chem. Phys. **33**, 1842 (1960).
    (*b*) A. D. WALSH. Trans. Faraday Soc. **45**, 179 (1949).
16. K. A. MCLAUCHLAN and D. H. WHIFFEN. Proc. Chem. Soc. 144 (1962).
17. F. KAPLAN and J. D. ROBERTS. J. Am. Chem. Soc. **83**, 4666 (1961).
18. R. R. FRASER, R. U. LEMIEUX, and J. D. STEVENS. J. Am. Chem. Soc. **83**, 3901 (1961).
19. C. A. REILLY and J. D. SWALEN. J. Chem. Phys. **35**, 1522 (1961).
20. H. FINEGOLD. Proc. Chem. Soc. 213 (1962).
21. H. M. MCCONNELL. J. Chem. Phys. **23**, 2454 (1955).
22. J. I. MUSHER and R. G. GORDON. J. Chem. Phys. **36**, 3097 (1962).
23. C. A. REILLY and J. D. SWALEN. J. Chem. Phys. **34**, 980 (1961).
24. F. S. MORTIMER. J. Mol. Spectry. **5**, 109 (1960).
25. H. S. GUTOWSKY, M. KARPLUS, and D. M. GRANT. J. Chem. Phys. **31**, 1278 (1959).
26. (*a*) L. L. MCCOY. Private communication.
    (*b*) L. L. MCCOY. J. Org. Chem. **25**, 2078 (1960).
27. A. D. BUCKINGHAM. Can. J. Chem. **38**, 300 (1960).
28. T. SCHAEFER and W. G. SCHNEIDER. J. Chem. Phys. **32**, 1218 (1960).
29. T. SCHAEFER. Can. J. Chem. **39**, 1864 (1961).
30. L. M. JACKMAN. Applications of NMR spectroscopy in organic chemistry. Pergamon Press, New York. 1959. p. 52.

Can. J. Chem. Downloaded from www.nrcresearchpress.com by 210.87.254.5 on 09/05/12
For personal use only.

KINETICS OF THE REACTION $H + C_3H_8 = H_2 + C_3H_7$

H. A. KAZMI,[1] R. J. DIEFENDORF,[2] AND D. J. LE ROY
Department of Chemistry, University of Toronto, Toronto, Ontario
Received October 30, 1962

ABSTRACT

The kinetics of the reaction $H + C_3H_8 = H_2 + C_3H_7$ have been studied in the range 95 to 170° C by a method permitting the evaluation of the absolute value of the rate constant. This was found to be $2.2\times10^{-10} \exp(-8.2\times10^3/RT)$ cm^3 molecule^{-1}sec^{-1}.

Can. J. Chem. Downloaded from www.nrcresearchpress.com by 210.87.254.42 on 09/05/12
For personal use only.

Some years ago we reported (1, 2, 3) the results of experiments designed to determine the rate constants and other kinetic parameters for elementary reactions of the type

$$H + RH = H_2 + R. \qquad [1]$$

The method involved the production of atomic hydrogen at a concentration of the order of 1% by the dissociation of hydrogen on a tungsten filament and the use of a detector to measure H atom consumption as a function of distance along a cylindrical reactor. The detector (3) consisted of a flat spiral of tungsten or platinum on which H atoms combined; operated as an isothermal calorimeter, it measured the number of H atoms combining on it in unit time in terms of W_H, the rate of liberation of the heat of combination in watts. Schulz and Le Roy (4) have recently modified the theory of the method to take into account diffusion effects. In the present paper the new theory is applied to the results of experiments on the reaction between atomic hydrogen and propane.

We have shown (4) that under suitable conditions the slope of a plot of $-\ln W_H$ vs. x_0, the distance between the detector and the point of admission of the RH, is equal to β_1, where β_1 is related to the first-order rate constant for H atom consumption, k, the flow rate, f, and the diffusion coefficient of atomic hydrogen, D, by the expression

$$\beta_1 = \frac{f}{2D}\left\{\left(1 + \frac{4kD}{f^2}\right)^{1/2} - 1\right\}. \qquad [i]$$

The values of D were taken from Amdur (5). In the absence of RH the rate constant k will be equal to k_b, the first-order rate constant for the consumption of H atoms on the walls of the reactor; in the presence of RH it will be equal to $k_b+\alpha k_1(RH)$, where k_1 is the rate constant for reaction [1] and α is equal to the number of H atoms consumed (other than by combination on the walls) for every RH molecule consumed in reaction [1].

If all R radicals are eventually converted to methane, and if this is formed by CH_3+H (+ M), rather than by CH_3+H_2 (3), then the theoretical value of α follows from stoichiometry. Thus, α would be equal to 4 if RH = C_2H_6, equal to 6 if RH = C_3H_8. If there should be any radical–radical combination or any combination of radicals (other than methyl) with atomic hydrogen α would have less than the theoretical value. The concentration of RH used in the expression $k = k_b+\alpha k_1(RH)$ should be that obtaining at the particular value of x_0 at which the slope of the plot of $-\ln W_H$ vs. x_0 is taken. In the first of two series of experiments the conditions were such that the change in RH concentration was small, and we used, as a first approximation, the initial value, $(RH)_0$. The

[1]*Present address: Department of Chemistry, University of Peshawar, Peshawar, Pakistan.*
[2]*Present address: General Electric Company, Schenectady, New York.*

second approximation was to use the average concentration, $(\overline{RH})$, estimated as described below. The condition required to ensure a small fractional change in (RH) is to start with a relatively high ratio of (RH) to (H). This also ensures a large fractional change in (H), a practically constant slope for the $-\ln W_H$ vs. x_0 plot, and greater accuracy in the evaluation of αk_1 from measurements of β_1 made in the presence and in the absence of RH.

In order to evaluate α and to calculate k_1 from the actual change in (RH) the RH concentrations used in the second series of experiments were, in all but one instance, made relatively small compared to the H atom concentrations. If RH is consumed only by reaction [1] and is not re-formed then

$$\ln \frac{(RH)_0}{(RH)_{x_0}} = \frac{k_1}{f} \int_0^{x_0} (H)dx. \qquad [ii]$$

As shown previously (4),

$$(H) = (H)_0 \frac{e^{\beta_1(x_0-x)} - e^{-\beta_2(x_0-x)}}{e^{\beta_1 x_0} - e^{-\beta_2 x_0}} \qquad [iii]$$

and

$$(H)_0 = \frac{W_H N}{4.184 \Delta H D A} \cdot \frac{1-e^{-(\beta_1+\beta_2)x_0}}{(\beta_1+\beta_2)e^{-\beta_1 x_0}}, \qquad [iv]$$

where $\beta_2 = \beta_1 + f/D$, ΔH is the standard enthalpy of formation of atomic hydrogen, A is the cross-sectional area of the reaction vessel (3.93 cm^2), and N is Avogadro's number. It follows that

$$\ln \frac{(RH)_0}{(RH)_{x_0}} = \frac{k_1 W_H N}{4.184 \Delta H D A f(\beta_1+\beta_2)} \left\{ \frac{e^{\beta_1 x_0}-1}{\beta_1} - \frac{1-e^{-\beta_2 x_0}}{\beta_2} \right\}. \qquad [v]$$

In order to obtain adequate accuracy in the determination of $(RH)_0/(RH)_{x_0}$ carbon dioxide was used as an inert reference substance. The condensable gases were trapped out downstream from the detector (beyond which there was presumed to be no further reaction) and analyzed by gas chromatography, using helium as the carrier gas and silica gel as the column material. Since the sensitivity factors for propane and carbon dioxide cancel, $(RH)_0/(RH)_{x_0}$ was obtained by substituting peak areas for concentrations in the expression

$$\frac{(RH)_0}{(RH)_{x_0}} = \frac{[(RH)/(CO_2)]_0}{[(RH)/(CO_2)]_{x_0}}. \qquad [vi]$$

In Table I the upper and lower values of β_1 for any particular experiment are the slopes of $-\ln W_H$ vs. x_0 plots corresponding to the absence and to the presence of RH, respectively. The corresponding values of k were derived from equation [i] expressed in the form

$$k = \beta_1 f(1+\beta_1 D/f). \qquad [vii]$$

(In our previous work we equated the slope of the $-\ln W_H$ vs. x_0/f plot to k; the present theory (4) introduces the factor $(1+\beta_1 D/f)$.) The quantity $\alpha k_1(\overline{RH})$ is simply the difference between the two values of k. The values of $(\overline{RH})$ were obtained by applying equation (v) and assuming that α was equal to 6 (see below). The decrease in RH concentration

Can. J. Chem. Downloaded from www.nrcresearchpress.com by 210.87.254.42 on 09/05/12
For personal use only.

Can. J. Chem. Downloaded from www.nrcresearchpress.com by 210.87.254.42 on 09/05/12
For personal use only.

TABLE I

Determination of αk_1 from values of β_1 obtained with and without RH

Expt.	Temp. (°C)	Press. (mm)	f (cm sec^{-1})	$(RH)_0$ $\times 10^{-14}$	$(H)_0$ $\times 10^{-14}$	D (cm^2 sec^{-1})	β_1 (cm^{-1})	k (sec^{-1})	$\alpha k_1(\overline{RH})$ (sec^{-1})	$(\overline{RH})$ $\times 10^{-14}$	αk_1 $\times 10^{14}$
17	95.1	3.44	195	3.22	3.78	551	0.0248	5.18	4.98	3.13	1.59
							0.0461	10.16			
18	94.5	3.44	194	4.42	7.64	549	0.0476	10.49	8.15	4.21	1.94
							0.0786	18.64			
28	122.8	3.45	210	3.02	3.48	608	0.0190	4.21	10.32	2.92	3.53
							0.0591	14.53			
29	123.5	3.48	213	3.07	2.31	612	0.0271	6.22	8.68	3.02	2.87
							0.0597	14.90			
22	149.4	3.65	233	2.68	1.27	645	0.0508	13.49	17.66	2.64	6.69
							0.1038	31.15			
24	149.4	3.65	236	2.62	1.61	645	0.0415	10.90	17.56	2.55	6.89
							0.0956	28.46			
31	172.1	3.47	243	1.38	1.92	736	0.0462	12.82	15.77	1.33	11.86
							0.0920	28.59			
32	172.4	3.47	240	1.59	1.73	737	0.0470	12.92	19.88	1.53	12.99
							0.1037	32.80			

NOTE: Concentrations are given in molecules cm^{-3}.

TABLE II

Determination of k_1 from RH consumption

Expt.	Temp. (°C)	Press. (mm)	f (cm sec^{-1})	(RH_0) $\times 10^{-14}$	$(H)_0$ $\times 10^{-14}$	D (cm^2 sec^{-1})	β_1 (cm^{-1})	x_0 (cm)	$\frac{(RH)_0}{(RH)x_0}$	$(W_H)_{x_0}$	k_1 $\times 10^{14}$
5	94.3	3.66	214	5.31	4.10	516	0.0345	29.4	1.18	0.0617	0.412
7	94.3	3.60	208	0.71	11.51	525	0.0303	30.0	1.319	0.1540	0.269
8	123.1	3.58	223	0.66	13.69	594	0.0322	30.0	1.810	0.1950	0.517
9	123.3	3.54	219	1.43	10.82	602	0.0532	30.0	1.534	0.0468	0.598
12	167.3	3.54	239	0.56	6.96	710	0.0849	29.8	1.907	0.0224	2.601
13	170.4	3.52	246	0.55	6.87	722	0.0150	29.4	2.610	0.1445	1.798

NOTE: Concentrations are given in molecules cm^{-3}.

in this series is seen to be small and the error that would have been introduced if $(RH)_0$ rather than $(\overline{RH})$ had been used would have been almost negligible.

The lower curve of Fig. 1 shows an Arrhenius plot for the values of αk_1. The least-

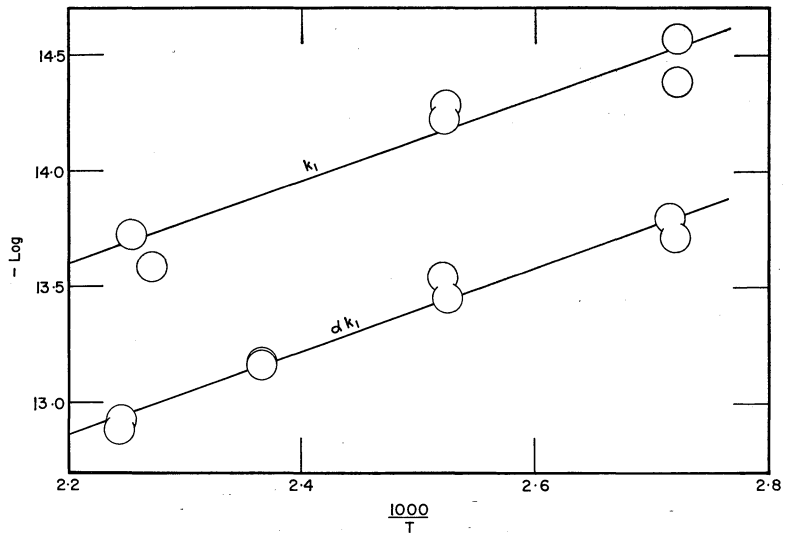

FIG. 1. Arrhenius plots for αk_1 and k_1.

squares line corresponds to $\alpha k_1 = 1.3_0 \times 10^{-9} \exp(-8.2_6 \times 10^3/RT)$. The values of k_1 given in Table II were obtained through the application of equation [v]. From the corresponding least-squares plot shown in Fig. 1 $k_1 = 2.2 \times 10^{-10} \exp(-8.2 \times 10^3/RT)$. The ratio of the pre-exponential factors for αk_1 and k_1 (13.0/2.2 = 5.8) affords some justification for the assumption that α is equal to 6. In the ordinary experiments, such as those referred to in Tables I and II, we could obtain no evidence for any products other than methane. However, by using much higher ratios of (RH) to (H) and placing the detector fairly close to the inlet we were able to detect a small amount of 2,3-dimethylbutane.

DISCUSSION

The determination of absolute, as opposed to relative, values of the rate constants of elementary reactions of atoms or free radicals is fraught with many difficulties, and the present work was not exceptional in this regard. Assuming that the combination of H atoms in the absence of RH is indeed first order, the accuracy of the values of αk_1 should be independent of the efficiency of the detector provided the slope of $-\ln W_H$ vs. x_0 is constant (4, 6). However, the constancy of the slope and its most accurate determination can only be achieved for relatively high values of (RH)/(H), a condition which decreases the accuracy with which RH consumption can be measured. On the other hand, the accurate determination of k_1 from RH consumption demands relatively small (RH)/(H) ratios, and one must be prepared to put up with some curvature in the $-\ln W_H$ vs. x_0 plots and hence some degree of uncertainty in β_1. This curvature arises, not because of failure of the theory (4), but because of the decrease in k $(=k_b+\alpha k_1(RH))$ as RH is used up in the reaction. The determination of k_1 from RH consumption also involves the assumption that the efficiency of the detector in removing H atoms is 100%. The experimental conditions used in the present work were chosen in the hope of minimizing the errors.

Can. J. Chem. Downloaded from www.nrcresearchpress.com by 210.87.254.42 on 09/05/12
For personal use only.

The most recent measurements on the kinetics of the reaction $H+C_3H_8 = H_2+C_3H_7$ with which the present results can be compared are those of Gorban and Nalbandyan (7), which have been discussed at some length by Voevodsky and Kondratiev (8). Their method was based on the effect of propane on the first explosion limit of stoichiometric mixtures of hydrogen and oxygen, and involved the use of kinetic data for the reaction of atomic hydrogen with O_2. Their values of A and E (8) were 7.8×10^{-10} liters mole^{-1}sec^{-1} (1.3×10^{-10} cm^3 molecule^{-1}sec^{-1}) and 9.6 kcal, compared to our present values of 2.2×10^{-10} cm^3 molecule^{-1}sec^{-1} and 8.2 kcal. It is interesting to note that at 480° C, in the range of their experimental conditions, their values of A and E correspond to $k_1 = 2.2\times10^{-13}$, while ours predict a value of 9.2×10^{-13}.

ACKNOWLEDGMENTS

We are indebted to the National Research Council for continued financial support and to the Senate of the University of Toronto for the L. V. Redman Fellowship and the Special Open Fellowship awarded to one of us (H. A. K.).

REFERENCES

1. E. L. Tollefson and D. J. Le Roy. J. Chem. Phys. **16**, 1057 (1948).
2. J. R. Dingle and D. J. Le Roy. J. Chem. Phys. **18**, 1632 (1950).
3. M. R. Berlie and D. J. Le Roy. Discussions Faraday Soc. **14**, 50 (1953).
4. W. R. Schulz and D. J. Le Roy. Can. J. Chem. **40**, 2413 (1962).
5. I. Amdur. J. Chem. Phys. **4**, 339 (1936).
6. P. G. Dickens, R. D. Gould, J. W. Linnett, and A. Richmond. Nature, **187**, 686 (1960).
7. H. I. Gorban and A. B. Nalbandyan. Dokl. Akad. Nauk SSSR, **132**, 1335 (1960).
8. V. V. Voevodsky and V. N. Kondratiev. *In* Progress in reaction kinetics. Vol. I. *Edited by* G. Porter. Pergamon Press Ltd., Oxford. 1961.

Can. J. Chem. Downloaded from www.nrcresearchpress.com by 210.87.254.42 on 09/05/12
For personal use only.

SYNTHESIS IN THE PYRIDINE SERIES

III. THE SYNTHESIS OF NEW 3,5-DIMETHYL-4-SUBSTITUTED PYRIDINES. STERIC EFFECTS AS AN AID TO SYNTHESIS

JAMES P. KUTNEY AND T. TABATA

Department of Chemistry, University of British Columbia, Vancouver, British Columbia

Received July 23, 1962

ABSTRACT

A synthetic sequence leading to 3,5-dimethyl-4-substituted pyridines is described. The sequence takes advantage of the steric influence exerted by substituents attached to the pyridine nucleus at the 3- and 5-positions on functional groups at the 4-position. In this manner a number of new trialkylated pyridines become available.

Some time ago we became involved in the synthesis of 3,4,5-trialkylated pyridines since these substances were necessary for other studies in our laboratory. In two previous papers in this series (1, 2) we described a general synthetic approach to virtually any type of trialkylated pyridine of this type and indicated that these previously inaccessible substances can now be made readily available by rather simple modifications in our sequence. In related studies we had occasion to consider the preparation of 3,5-dimethyl-4-ethylpyridine and it appeared that an extension of the method of Wibaut and Arens seemed attractive. This method has been used rather effectively for the introduction of alkyl substitutents into the γ position of the pyridine ring (3–6). However, when we reacted 3,5-lutidine with acetic anhydride and zinc under the specified reaction conditions we did not isolate the expected 3,5-dimethyl-4-ethylpyridine but a compound which exhibited a strong carbonyl absorption in its infrared spectrum (5.83 μ). The ultraviolet spectrum indicated that the normal pyridine absorption was still present and it became obvious that we had most probably obtained the intermediate ketone, 3,5-dimethyl-4-acetylpyridine (I). Our suspicions were confirmed when we obtained a nuclear magnetic resonance (n.m.r.) spectrum of this substance. The n.m.r. spectrum indicated a sharp signal at 7.62 τ which served to establish the presence of the acetyl group. In addition, a very intense signal at 7.83 τ, characteristic of methyl groups attached at the β positions of the pyridine nucleus, and a signal at 1.82 τ attributable to α protons (1, 2), served to establish the assigned structure. It was thus clear that the steric influence of the two neighboring methyl groups had been sufficient to allow us to isolate the intermediate in this reaction.

The reduction of 3,5-dimethyl-4-acetylpyridine to the known 3,5-dimethyl-4-ethylpyridine could be accomplished by the use of zinc and acetic acid but only under much more drastic conditions. This conversion served to confirm further the structure of the acetylpyridine.

It became apparent to us that the steric effect of the methyl groups at the β positions could be used to advantage in synthesizing new 3,4,5-trialkylated pyridines since the 4-acetylpyridine derivative is a versatile synthetic intermediate. Consequently we have performed numerous experiments to obtain optimum reaction conditions for the preparation of 3,5-dimethyl-4-acetylpyridine and have been able to obtain this substance in high yield (70%).

In order to provide entry into pyridine derivatives possessing branched alkyl chains at the γ position, we first considered the possibility of reacting I with organometallic

reagents although it could be anticipated that the steric factor may prevent a successful reaction. Reaction of the acetylpyridine with methylmagnesium iodide or bromide under various reaction conditions met with failure, a large proportion of the starting ketone was recovered in each case. It should be pointed out that we have used very drastic conditions in an attempt to obtain reaction and such high boiling solvents as diglyme or dibutyl carbitol were used on various occasions. In the latter instance a trace of an alcoholic component was obtained but the extremely low yield discouraged any further characterization. Similar unsuccessful attempts were made with methyllithium. It thus became apparent that the steric hindrance of the carbonyl group was so effective as to make this function completely unreactive to the action of organometallic reagents.

Our next consideration was to attempt reduction of the carbonyl function to an alcohol group since this substance could lend itself to a variety of interesting reactions. When 3,5-dimethyl-4-acetylpyridine was treated with lithium aluminum hydride the expected alcohol (II) was obtained as a crystalline material. The spectral properties of this product were in complete accord with the assigned structure. The presence of the hydroxyethyl group was clearly shown by the n.m.r. spectrum—a doublet centered at 8.62 τ as would be expected for the methyl group and a quartet centered at 4.88 τ for the tertiary proton on the oxygen-bearing carbon. Having obtained the desired alcohol, we considered its conversion to other analogues in this series. In our previous work in this series (1, 2) we had studied in some detail the reductive removal of a hydroxyl function by the use of hydriodic acid in the presence of red phosphorus. In these studies we obtained the intermediate olefinic substances which undoubtedly arise from an acid-catalyzed elimination reaction. It therefore appeared of some interest to see whether the steric environment of our alcohol, II, would lend itself to a reaction of this type. We chose to utilize hydrobromic acid for this purpose since under these conditions, the olefinic intermediate would readily enter into an addition reaction and thus it may be possible to obtain some relevant information about elimination and (or) substitution and addition in this series. When the alcohol, II, was treated with concentrated hydrobromic acid, under drastic conditions, we obtained a crystalline hydrobromide. The analytical data indicated that the hydroxyl function had been lost and that a bromine atom had entered into the molecule. At the outset, it could be argued that a simple displacement of the hydroxyl function had occurred and that the structure of the reaction product was VI. This argument was quickly dismissed when we considered the n.m.r. spectrum of this material. An obvious feature which was absent in the spectrum was a signal for the methyl group attached to the carbon atom bearing the bromine as would be expected if the structure VI was the correct one. Furthermore this signal would be expected to be split into a doublet by the tertiary hydrogen on the adjacent carbon atom. The highest signal which was observed in the spectrum was at 7.32 τ and its position as well as the high intensity indicated beyond any doubt that it was due to the two methyl groups at the β positions of the ring. The remaining signals were at lower fields and it was therefore clear that the structure of the hydrobromide was not VI. On the other hand, consideration of the nature of the entire spectrum and the integrated areas revealed that the alternative structure, III, was the correct one. A more detailed description of the n.m.r. results is given in the experimental portion.

In order to eliminate any doubt about the actual chemical shift that a methyl group of the type depicted in VI should exhibit, we decided to synthesize, unambiguously, an analogous structure and then consider its n.m.r. spectrum. The most direct approach to this problem involved the reaction of 4-ethylpyridine with N-bromosuccinimide, a

reagent which might be expected to introduce a bromine atom at the methylenic carbon (7). Indeed when this reaction was carried out and the reaction product treated with hydrogen bromide, a crystalline hydrobromide was obtained. The analytical data and the spectral properties were in complete accord with the expected structure VII. The n.m.r. spectrum was of particular significance and served to confirm our assignments in the n.m.r. spectrum of III. The presence of the 1-bromoethyl group in VII was established by a doublet at 7.89 τ, as would be expected for the methyl group attached to the halogen bearing carbon, and a quartet at 4.66 τ for the tertiary hydrogen atom.

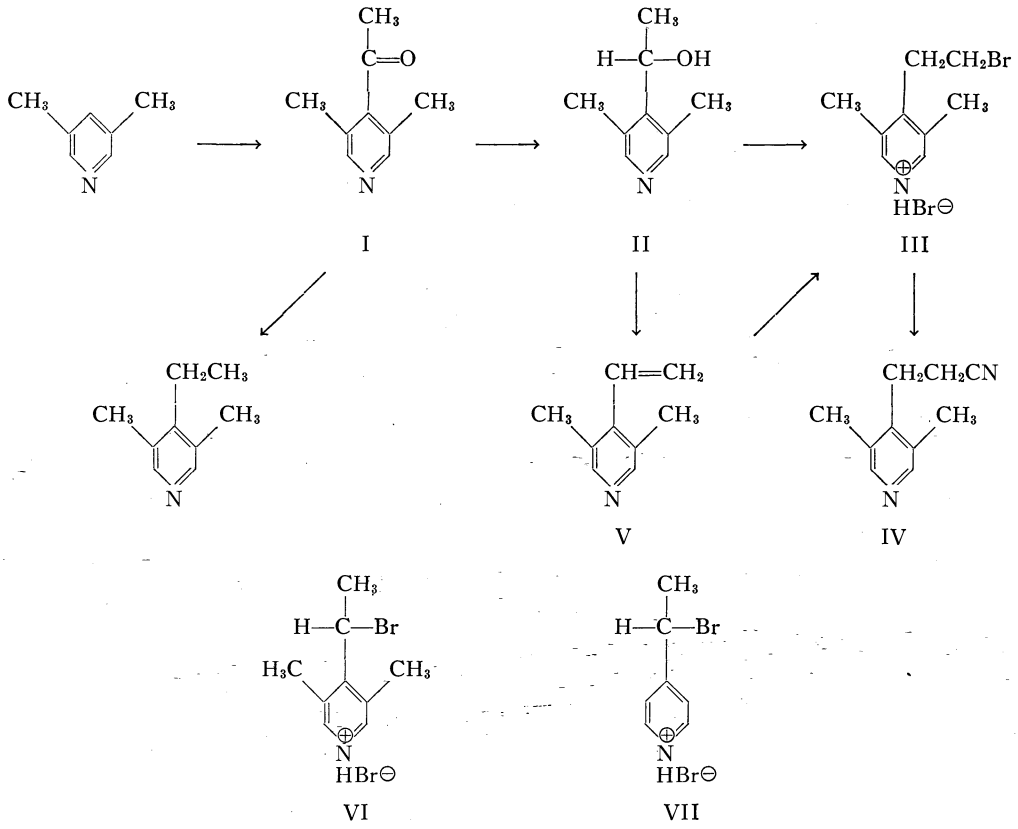

The isolation of III is of some theoretical interest since it is apparent that a simple substitution of the hydroxyl group by the halogen atom has not taken place. Since the reaction conditions utilized in the preparation of III are similar to the conditions normally employed in the synthesis of the side chain halopyridines from hydroxyalkylpyridines (8, p. 360), and since this type of reaction normally proceeds through a S_N1 mechanistic pathway, it is necessary to comment on our present results. It is reasonable to postulate that the initial step leads to the carbonium ion, VIII, which can either react with bromide ion to provide VI*a* or eliminate a proton to yield V. In the instances where the carbonium ion is sterically unhindered, it reacts according to the S_N1 pathway to provide halopyridines. However, it is clear that in VIII, the steric shielding by the neighboring methyl groups will tend to make the S_N1 reaction less favorable and therefore proton elimination occurs to yield 3,5-dimethyl-4-vinylpyridine (V). The subsequent addition of hydrobromic acid to the olefinic bond provides the actual isolated product.

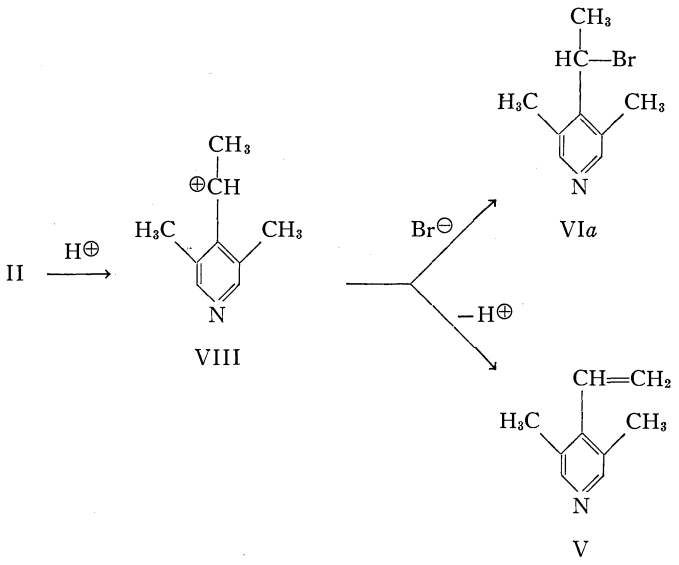

The mode of electrophilic addition to the double bond of alkenylpyridines has not been studied in great detail and, in particular, little is known about the addition of hydrogen halide to these types of compounds (8, p. 364). Although products resulting from the addition of hydrogen halide to vinylpyridines have been reported (9, 10), there is no conclusive evidence regarding the correct structures of these substances. It has been suggested (8, p. 364) that the halogen would enter at the carbon atom adjacent to the pyridine nucleus. Our present studies do not bear out this statement and, indeed, this statement does not agree with the expected addition based on theoretical arguments. Theoretical consideration of the electronic interaction of the pyridine nucleus with a conjugated double bond leads to the conclusion that 4-vinylpyridine should react according to the resonance structure IX. It would, therefore, be expected that, under acidic

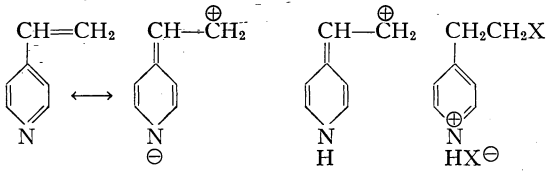

conditions, the important species in the reaction would be IX*a* and that, in fact, the product resulting from the addition of such reagents as hydrogen halide would be X. An extension of this argument to 3,5-dimethyl-4-vinylpyridine (V) leads to the prediction that III would be the actual product formed in the reaction with hydrobromic acid. It is also pertinent to note that the addition of hydrazoic acid to 2-vinylpyridine has been shown to provide 2-(β-azideoethyl)-pyridine (11, 12). This work provides considerable strength to our argument.

Our rationalization for the formation of the bromide, III, from the alcohol, II, involves the possible formation of the intermediate olefinic substance, 3,5-dimethyl-4-vinylpyridine. In order to provide some support for this proposal we felt that we should investigate the reaction of the vinylpyridine with hydrobromic acid. For this reason, we reacted

the alcohol, II, with phosphorus pentoxide and obtained the expected 3,5-dimethyl-4-vinylpyridine (V). The spectral data was in complete agreement with this assignment. In particular, the n.m.r. spectrum exhibited multiplets at 4.27 τ and 3.62 τ to provide strong evidence for the presence of a vinyl group. When the vinylpyridine was subjected to the action of concentrated hydrobromic acid under conditions identical with those used for the alcohol, we obtained an excellent yield of a crystalline hydrobromide. This salt proved to be identical in every respect with the hydrobromide, III. This sequence of reactions therefore showed that the vinylpyridine could be an intermediate in the conversion II $\rightarrow$ III.

Finally we considered the possibility of converting the bromide, III, into a pyridine derivative which was somewhat more stable and where one could actually consider the n.m.r. spectrum of the parent base. It should be noted that the halopyridines of the type described above can only be isolated as salt derivatives since the parent bases decompose rapidly.

An attractive analogue appeared to be the corresponding nitrile since in addition to being somewhat more stable, it would provide a versatile synthetic intermediate for a variety of 4-substituted pyridines. Upon reaction of the bromide, III, with an aqueous alcoholic solution of potassium cyanide, an excellent yield of 3,5-dimethyl-4-(2-cyanoethyl)-pyridine (IV) was obtained. The substance which could be conveniently isolated as the parent base had an n.m.r. spectrum which was quite instructive and in accord with the structural assignment. The spectrum indicated an intense signal at 7.61 τ due to the methyl groups attached to the pyridine nucleus. The four protons of the cyanoethyl group were evident from two sets of multiplets centered at 6.94 τ and 7.34 τ and finally a signal at low field (1.67 τ) accounted for the α protons on the pyridine ring. The relative areas under the signals served to finally establish the structure, IV, for the nitrile. Since numerous modifications of the cyano group are possible, this material may be utilized to prepare new types of 4-substituted pyridine analogues.

It is therefore apparent that the steric hindrance created by substituents attached to the β positions of the pyridine nucleus can be used to considerable advantage in the synthesis of new and otherwise inaccessible 3,4,5-trisubstituted pyridines.

EXPERIMENTAL

All melting points were determined on a Fischer–Johns apparatus and are uncorrected. The ultraviolet spectra were recorded in 95% ethyl alcohol on a Cary 14 recording spectrophotometer. Infrared spectra were recorded on a Perkin–Elmer model 21 spectrophotometer. The n.m.r. spectra were done at 60 Mc on a Varian A60 instrument. The values are given in the Tiers τ scale, with the signal of tetramethylsilane, which was used as the internal standard, set at 10.0 τ units. Integration of areas under the signals was carried out in all cases and the number of protons is indicated in parentheses. The solvents used were carbon tetrachloride or deuteriochloroform. The analyses were performed by Dr. A. Bernhardt and his associates, Mulheim (Ruhr), Germany, and by Mrs. A. Aldridge, University of British Columbia.

3,5-Dimethyl-4-acetylpyridine (I)

The zinc which was used in this experiment was activated as follows. Zinc dust (208 g) was stirred in 10% aqueous hydrochloric acid (75 ml) for 2–3 minutes. It was then filtered, washed with distilled water (150 ml), acetone (100 ml), anhydrous ether (50 ml), and dried *in vacuo*. It was then ready for use.

A 1-liter three-necked flask was fitted with a mechanical stirrer and acetic anhydride (250 ml) and 3,5-lutidine (136 g, dried over calcium oxide and freshly distilled *in vacuo*) were then added to the flask. This stirred mixture was then treated with small portions of zinc until a total of 100 g had been added. The addition required about $\frac{1}{2}$ hour during which time the temperature of the reaction rose to 70° and the mixture developed a light green color. Glacial acetic acid (100 ml) and activated zinc (40 g) were added and the reaction mixture was refluxed for 15 minutes. After allowing to stand overnight at room temperature the mixture was cooled in ice and treated cautiously with 40% aqueous sodium hydroxide (700 ml). The resulting brown oil which formed as a layer at the top was extracted with ether. The ethereal extract was

dried over anhydrous magnesium sulphate, and the solvent evaporated to leave a brown viscous liquid (172 g). This liquid was fractionally distilled to yield an initial fraction (57.2 g, distilling up to 189°) of unreacted 3,5-lutidine. The second fraction (24.9 g) distilling in the range of 190–220° contained some 3,5-lutidine and some of the desired acetylpyridine whereas the last fraction (61.6 g), collected at 220–295°, was the desired 3,5-dimethyl-4-acetylpyridine. A second distillation of the last fraction at 167–169° at 100 mm provided the pure product (55.8 g). An analytical sample could also be conveniently obtained on purification by vapor phase chromatography on the Megachrome, operating at 240° with a column of Apiezon J and using helium as the carrier gas. The retention time was 10.2 minutes.

The product after this purification still distilled at 167–169° at 100 mm or 252–254°; n_D^{25} 1.5152; infrared: 5.90 μ; ultraviolet: λ_{max} 270 mμ (log ϵ 3.42), λ_{min} 234 mμ (log ϵ 2.54); n.m.r. signals (CCl_4): intense signal at 7.83 τ (methyls attached to ring, area = 6 H), signal at 7.62 τ (CH_3—$\overset{O}{\overset{\|}{C}}$—, area = 3 H), 1.82 τ (α H, area = 2 H). Found: C, 72.10; H, 7.48; O, 10.71; N, 9.32. Calc. for $C_9H_{11}NO$: C, 72.45; H, 7.43; O, 10.72; N, 9.37.

A picrate was prepared and after several recrystallizations from alcohol melted at 181–183°. Found: C, 47.81; H, 3.76; O, 33.37; N, 14.71. Calc. for $C_{15}H_{14}O_8N_4$: C, 47.62; H, 3.73; O, 33.84; N, 14.81.

It is pertinent to note that it was found imperative to carry out the initial fractional distillation of the crude reaction product at atmospheric pressure. In this way, the high temperature ensures that the intermediates are decomposed to the desired product. If the distillation is carried out at lower temperatures under reduced pressure, the intermediates are actually distilled over and it becomes necessary to heat these to a higher temperature to convert them to I.

3,5-Dimethyl-4-(1-hydroxyethyl)-pyridine (II)

A 50-ml three-necked flask was fitted with a dropping funnel, a reflux condenser, and a magnetic stirrer, and charged with a solution of lithium aluminum hydride (0.819 g) in anhydrous ethyl ether (12 ml). To this was added cautiously, from the dropping funnel, a solution of 3,5-dimethyl-4-acetylpyridine (3.22 g) in anhydrous ether (11 ml), over a period of 20 minutes. After the addition was complete, the reaction mixture was stirred at room temperature for ½ hour and then water (20 ml) was added slowly to destroy the excess hydride. The reaction mixture was filtered, the solid which remained on the filter paper was washed thoroughly with methanol, and the methanol washings were combined with the ethereal filtrate. The filtrate was then concentrated and the soluble organic materials were extracted with chloroform. After drying the chloroform extract over anhydrous magnesium sulphate and removing the solvent, the residual product was distilled. The initial fraction (220 mg) distilling up to a temperature of 130° (bath temperature) at 0.5 mm proved to be unreacted acetylpyridine. The second fraction (2.3 g) which came over at 145–210° (bath temp.) at 0.1 mm was the desired alcohol, II. An analytical sample was prepared by several recrystallizations from a chloroform – petroleum ether mixture, and melted at 85–86°; infrared: 3.09 μ; ultraviolet: λ_{max} 2.67 mμ (log ϵ 3.40), shoulder at 274 mμ (log ϵ 3.35), λ_{min} 231 mμ (log ϵ 2.69); n.m.r. signals (CCl_4): doublet centered at 8.62 τ (CH_3—$\overset{H}{\overset{|}{C}}$—OH, area = 3 H), intense signal at 7.75 τ (methyls attached to ring, area = 6 H), quartet centered at 4.88 τ (tertiary proton of CH_3—$\overset{H}{\overset{|}{C}}$—OH, area = 1 H), signal at 2.28 τ (α H, area = 2 H). Found: C, 71.57; H, 8.70; O, 10.76; N, 9.07. Calc. for $C_9H_{13}ON$: C, 71.49; H, 8.67; O, 10.58; N, 9.26.

A picrate, m.p. 148–148.5°, was prepared in ethanol and recrystallized from the same solvent. Found: C, 47.88; H, 4.29; N, 14.48. Calc. for $C_{15}H_{16}O_8N_4$: C, 47.37; H, 4.24; N, 14.73.

3,5-Dimethyl-4-(2-bromoethyl)-pyridine Hydrobromide (III)

A mixture of 3,5-dimethyl-4-(1-hydroxyethyl)-pyridine (196 mg) and concentrated hydrobromic acid (171 ml, 48%) was heated at 160° in a sealed tube for 24 hours. After cooling, the contents of the tube were evaporated to dryness *in vacuo*. The residual material was taken up in ethyl alcohol and recrystallized from a mixture of alcohol–chloroform to yield a first crop of crystals (235 mg). An additional 66 mg (total 301 mg) was obtained when the mother liquor was diluted with petroleum. Several recrystallizations of this product from ethanol – petroleum ether provided an analytical sample, m.p. 208–209°; infrared: absence of hydroxyl absorption; ultraviolet: λ_{max} 266 mμ (log ϵ 3.76), λ_{min} 245 mμ (log ϵ 3.62); n.m.r. signals ($CDCl_3$): intense signal at 7.32 τ (methyls attached to ring, area = 6 H), multiplet centered at 6.40 τ (CH_2CH_2Br, area = 4 H), 1.32 τ (α H, area = 2 H). Found: C, 36.43; H, 4.31; N, 4.62; Br, 54.22. Calc. for $C_9H_{13}NBr_2$: C, 36.64; H, 4.41; N, 4.74; Br, 54.44.

3,5-Dimethyl-4-(2-cyanoethyl)-pyridine (IV)

The pyridine hydrobromide, III (206 mg), was added to a solution of potassium cyanide (610 mg) in water (4.6 ml) and methanol (11 ml) and the mixture was refluxed for 2 hours. After the mixture had cooled, water (10 ml) was added and the reaction mixture was then made alkaline by the addition of sodium bicar-

bonate. This reaction mixture was extracted exhaustively with ethyl acetate. The ethyl acetate extract was dried over anhydrous magnesium sulphate and the solvent was removed to yield a viscous liquid. This liquid was distilled at 100–150° (bath temperature) at 0.1 mm to yield 106 mg of a viscous liquid which solidified partially on short standing. Crystallization from a mixture of benzene – petroleum ether – acetone provided a crystalline material, m.p. 74–75°. Infrared: 4.46 μ; ultraviolet: λ_{max} 266 mμ (log ϵ 3.31), λ_{min} 230 mμ (log ϵ 2.78); n.m.r. signals ($CDCl_3$): intense signal at 7.61 τ (methyls attached to ring, area = 6 H) two sets of multiplets centered at 7.34 τ and 6.94 τ (—CH_2CH_2—CN, area = 4 H), 1.67 τ (α H, area = 2 H).

A picrate of this material was readily prepared and upon several recrystallizations from alcohol an analytical sample was obtained, m.p. 177–178.5°. Found: C, 49.01; H, 4.08; N, 17.78. Calc. for $C_{16}H_{15}N_5O_7$: C, 49.36; H, 3.88; N, 17.99.

3,5-Dimethyl-4-vinylpyridine (V)

A solution of 3,5-dimethyl-4-(1-hydroxyethyl)-pyridine (991 mg) in anhydrous xylene (30 ml) was treated with phosphorus pentoxide (7.73 g) and the mixture was refluxed for 3 hours. After it had been cooled, the reaction mixture was treated cautiously with water (20 ml) to destroy the excess phosphorus pentoxide and the resulting solution was separated into the respective organic and aqueous portions. The acidic aqueous layer was neutralized, then made alkaline by the addition of potassium hydroxide pellets, and this mixture was extracted with ether. The ethereal extract was dried over anhydrous magnesium sulphate and the solvent evaporated to yield a mobile liquid. Distillation of this liquid provided the desired vinylpyridine (475 mg, b.p. 146–147° at 90 mm); n_D^{27} 1.5333; infrared: 6.11 μ; ultraviolet: λ_{max} 273 mμ (log ϵ 3.39), λ_{min} 261 mμ (log ϵ 3.32), λ_{max} 234 mμ (log ϵ 3.77), λ_{min} 223 mμ (log ϵ 3.71); n.m.r. signals (CCl_4): intense signal at 8.02 τ (methyls attached to ring, area = 6 H), multiplet centered at 4.72 τ (—C=CH_2, area = 2 H), quartet

centered at 3.62 τ (—C=C, area = 1 H), 2.10 τ (α H, area = 2 H). Found: C, 80.86; H, 8.34; N, 10.31. Calc. for $C_9H_{11}N$: C, 81.16; H, 8.33; N, 10.52.

A picrate, m.p. 155–156°, was prepared in ethanol and recrystallized from the same solvent. Found: C, 49.75; H, 3.90; O, 30.45; N, 15.41. Calc. for $C_{15}H_{14}N_4O_7$: C, 49.73; H, 3.84; O, 30.52; N, 15.20.

3,5-Dimethyl-4-(2-bromoethyl)-pyridine Hydrobromide (III) from 3,4-Dimethyl-4-vinylpyridine

A mixture of 3,5-dimethyl-4-vinylpyridine (188 mg) and concentrated hydrobromic acid (16 ml, 48%) was heated for 24 hours in a sealed tube at 160°. When the reaction mixture was worked up in exactly the same manner as given above for the alcohol, a crystalline hydrobromide (348 mg) was obtained. This was shown to be III by mixed melting point, infrared, ultraviolet, and n.m.r. comparison.

3,5-Dimethyl-4-ethylpyridine

A stirred solution of 3,5-dimethyl-4-acetylpyridine (19 g) in glacial acid (200 ml) was cautiously treated with activated zinc (10 g) and the whole mixture was then refluxed for 1 hour. An additional 18 g of activated zinc was added and refluxing was continued for a further 15 hours, by which time the reaction mixture had become intensely yellow in color. After it had been cooled, the mixture was made alkaline by the addition of 40% aqueous sodium hydroxide (400 ml) and the resulting mixture was steam-distilled until the distillate was clear. The distillate was then extracted exhaustively with ether and the ethereal extract dried over anhydrous magnesium sulphate. Evaporation of the solvent left a brown residual liquid (17.7 g) which, upon distillation (b.p. 218–219°), yielded 12.7 g of 3,5-dimethyl-4-ethylpyridine. Infrared: complete disappearance of carbonyl band; ultraviolet: λ_{max} 263 mμ (log ϵ 3.45), λ_{min} 231 mμ (log ϵ 2.87); n.m.r. signals (CCl_4): triplet centered at 8.94 τ (methyl of ethyl group, area = 3 H), intense signal 7.80 τ (methyls attached to ring, area = 6 H), quartet centered at 7.42 τ (methylene of ethyl group, area = 2 H), 1.96 τ (α H, area = 2 H). A picrate of this compound was readily prepared and the analytical sample melted at 156.5–157°. Found: C, 49.49; H, 4.17; N, 15.36. Calc. for $C_{15}H_{16}N_{14}O_7$: C, 49.45; H, 4.43; N, 15.38.

The literature values (13, 14) are b.p. 216–217°, 219–220° for the base, and m.p. 155–156° for the picrate.

4-(1-Bromoethyl)-pyridine Hydrobromide (VII)

A solution of 4-ethylpyridine (6.41 g) in anhydrous carbon tetrachloride (200 ml) was treated with N-bromosuccinimide (10.7 g) and benzoyl peroxide (0.91 g) and the whole mixture was refluxed for 3 hours. The slightly brown reaction mixture was filtered to remove the solid suspension and the filtrate was washed successively with 4% aqueous sodium hydroxide (100 ml), water (100 ml), 2% aqueous hydrobromic acid (100 ml), and finally dried over anhydrous magnesium sulphate. This dried carbon tetrachloride extract was then saturated with hydrogen bromide and finally the solvent was removed to furnish a residual gum (7.4 g). The latter was taken up in ethanol and then crystallized from a solvent mixture of ethanol – ethyl ether to afford 3.25 g of a crystalline hydrobromide, m.p. 151–151.5°; ultraviolet: λ_{max} 260 mμ (log ϵ 3.50),

λ_{min} 325 mμ (log ϵ 3.30); n.m.r. signals ($CDCl_3$): doublet centered at 7.89 τ (CH_3—C—Br, area = 3 H),

quartet centered at 4.66 τ (tertiary hydrogen of $CH_3—\underset{\displaystyle Br}{\overset{\displaystyle |}{\underset{|}{C}}}—H$, area = 1 H), doublet centered at 1.85 τ (β H, area = 2 H), doublet centered at 0.83 τ (α H, area = 2 H). Found: C, 31.56; H, 3.39; N, 5.40; Br, 59.87. Calc. for $C_7H_9NBr_2$: C, 31.47; H, 3.40; N, 5.25; Br, 59.88.

ACKNOWLEDGMENT

Financial aid from the National Research Council of Canada and Eli Lilly and Company is very gratefully acknowledged.

REFERENCES

1. J. P. KUTNEY and R. C. SELBY. J. Org. Chem. **26**, 2733 (1961).
2. J. P. KUTNEY and T. TABATA. Can. J. Chem. **40**, 1140 (1962).
3. J. F. ARENS and J. P. WIBAUT. Rec. Trav. Chim. **61**, 59 (1942).
4. R. L. FRANK and P. V. SMITH. Org. Syn. **27**, 38 (1947).
5. J. P. WIBAUT and S. VROMEN. Rec. Trav. Chim. **67**, 545 (1947).
6. S. WAWZONEK, M. F. NELSON, and P. J. THELEN. J. Am. Chem. Soc. **74**, 2894 (1952).
7. J. HURST and D. G. WIBBERLEY. J. Chem. Soc. 119 (1962).
8. E. KLINGSBERG. Heterocyclic compounds, pyridine and its derivatives. Part 2. Interscience Publishers Inc., New York. 1961.
9. G. H. LENART. Ann. **410**, 95 (1915).
10. H. BACH. Ber. **34**, 2223 (1901).
11. J. H. BOYER. J. Am. Chem. Soc. **73**, 5248 (1951).
12. R. D. WESTLAND and W. E. MCEWEN. J. Am. Chem. Soc. **74**, 6141 (1952).
13. I. HEILBRON and H. M. BUNBURY. Dictionary of organic compounds. Vol. I. 1946. p. 913.
14. BEILSTEIN'S Handbuch der Organischen Chemie. Vol. 20. 1935. p. 254; Vol. II. 1953. p. 166.

STEROIDS AND RELATED PRODUCTS

XXI. THE SYNTHESIS OF 17α-BROMO-6α-METHYLPROGESTERONE[1, 2]

S. RAKHIT, R. DEGHENGHI, AND CH. R. ENGEL[3]
Department of Chemistry, Laval University, Quebec, Que.
Received October 17, 1962

ABSTRACT

The synthesis fo 17α-bromo-6α-methylprogesterone, from pregnenolone acetate, is reported. The product is a potent luteoid with marked oral activity. In the course of this investigation, a useful variation of the synthesis of 6α-methylprogesterone, from pregnenolone, was devised. The rearrangement of a 5β,6β-epoxide to a 6-ketone, upon chromatography on aluminum oxide "Woelm", was observed.

Can. J. Chem. Downloaded from www.nrcresearchpress.com by 210.87.254.6 on 09/05/12
For personal use only.

A few years ago, this group reported the synthesis and marked progestational activity of 17α-bromoprogesterone (2). As we exposed recently (3), we considered that it would be useful to establish whether or not the enhancing effect on progestational activity of the 17α-bromine substituent is an isolated phenomenon in the case of 17α-bromoprogesterone, particularly in view of our thesis that bulky 17α-substituents increase, in general, the luteoid activity of 20-keto steroids of the progesterone type (cf. ref. 4). The investigation of 6α-substituted 17α-bromoprogesterones seemed attractive since it was known that the introduction of various 6α-substituents might lead to potentiation of the progestational activity, in particular of the oral progestational activity (cf. refs. 4–10 and 13, 14 of the article quoted as ref. 3). In a first paper (3), we reported the synthesis and considerable luteoid activity of 6α-fluoro-17α-bromoprogesterone (cf. also refs. 4 and 5[4]); in the present paper, we record the synthesis and high progestational activity of 17α-bromo-6α-methylprogesterone (XII). The introduction of a methyl substituent in position 6α appeared of particular interest in view of the observation that this group exerted, in a number of instances, a drastic potentiating effect on the *oral* progestational activity (cf. refs. 7–11).[5]

Pregnenolone acetate (I) served as starting material. It was transformed, in high yield, to the 20-ethylene ketal (II) (14) by slow evaporation of its solution in ethylene glycol in the presence of *p*-toluenesulphonic acid, according to the procedure of Allen *et al.* (15). The use of the classical method which was employed by Gut (14) and which consists in refluxing the benzene solution of the ketone with ethylene glycol in the presence of *p*-toluenesulphonic acid, with periodic removal of water, gives less satisfactory yields of the desired ketal.[6] Epoxidation of the unsaturated acetoxy ketal II*a* with monoperphtalic acid in chloroform afforded predominantly the α-epoxide III, as expected. The product gave no tetranitromethane reaction and the analytical data and spectral characteristics were in accord with structure III. The α-configuration was not only assigned in analogy with data from the literature (cf., e.g., refs. 16–19; also refs. 20 and 21) but was also

[1]*The main results of this paper were the subject of a communication presented before the 43rd Annual Conference of the Chemical Institute of Canada, June 1960.*
[2]*For the previous paper in this series, see ref. 1.*
[3]*Correspondence should be addressed to this author.*
[4]*Subsequent to our publication, Mills, Candiani, and Djerassi (6) also published a synthesis of 6α-fluoro-17α-bromoprogesterone, without indicating the progestational activity of the product.*
[5]*In this respect it may be mentioned that after completion of this work one of us (R. D.) established, in collaboration with R. Gaudry, that the addition of a 6α-methyl substituent transformed the parenterally potent but orally almost inactive 17α-methylprogesterone (12) to an orally active progestin (13).*
[6]*Unpublished results from our laboratory by R.-M. Hoegerle and Ch. R. Engel.*

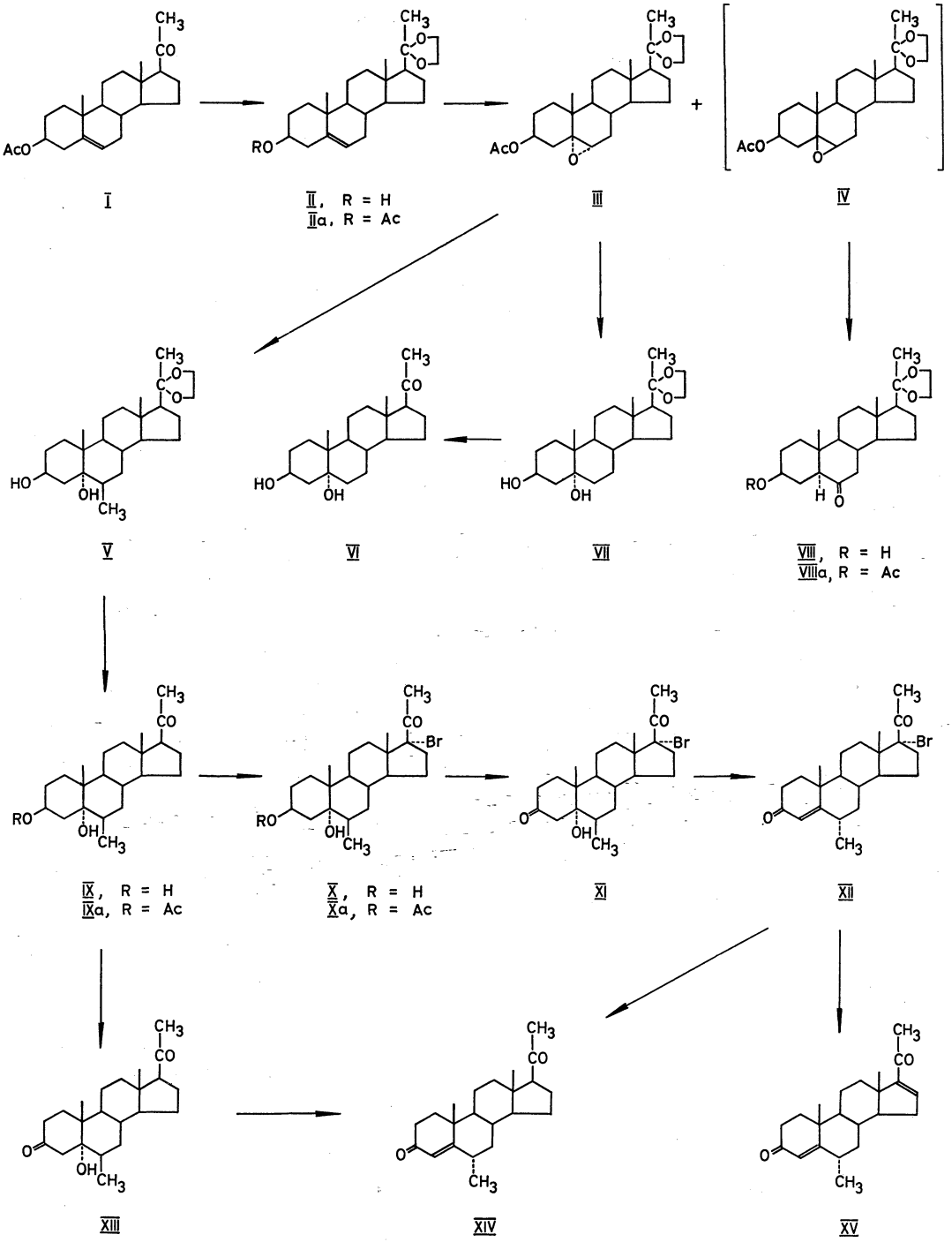

proved by the conversion of the epoxide III, with lithium aluminum hydride, to the 3β,5α-dihydroxy ketal VII, and hence, by an exchange reaction with acetone in the presence of *p*-toluenesulphonic acid (22), to the known (23) 3β,5α-dihydroxypregnan-20-one (VI).

Can. J. Chem. Downloaded from www.nrcresearchpress.com by 210.87.254.6 on 09/05/12
For personal use only.

Can. J. Chem. Downloaded from www.nrcresearchpress.com by 210.87.254.6 on 09/05/12
For personal use only.

In an attempt to isolate, out of the crude epoxidation product, the isomeric 5β,6β-epoxide IV—the formation of which was to be expected (cf. refs. 17, 18, and 20)—we subjected the mother liquors which remained after the separation of the α-epoxide III and of intermediate fractions to chromatography on non-alkaline aluminum oxide "Woelm". Apart from small quantities of the α-epoxide III, the only product which could be isolated in the pure state (by recrystallization of the less-polar chromatogram fractions) was an isomer of the oxide III, to which we assign the structure of 3β-acetoxy-20-ethylenedioxy-5α-pregnan-6-one (VIII*a*) since its infrared spectrum shows the band of a 6-membered-ring ketone. (The retention of the ketal function in position 20 was evident from the infrared spectrum and the analytical data.) Also, upon saponification with methanolic sodium hydroxide, there remains only a single ketonic carbonyl band, attributable to the 6-keto function (ν_{max}^{KBr} 1715 cm^{-1}) (cf. VIII), and reacetylation of the saponified product leads back to the acetoxy ketone VIII*a*, which has two distinct carbonyl-absorption bands (ν_{max}^{KBr} 1741 and 1713 cm^{-1}). Since the crude epoxidation product shows practically no carbonyl absorption in the infrared, we assume that the 5β,6β-epoxide, originally formed as the minor epoxidation product, was isomerized in the course of chromatography on the particular brand of aluminum oxide used (Woelm) to the 6-ketone. Such rearrangements are known to occur under the influence of Lewis acids (24, 25) and can be rationalized readily by assuming that, initially, the C—O bond is ionized at the most substituted carbon atom and that, subsequently, a cis hydrogen shift occurs. We thus suggest the 5α-configuration for the ketones VIII and VIII*a*. The assumption that the ketone arises from the 5β,6β-epoxide and not from the α-epoxide was substantiated by the fact that chromatography (on the same brand of aluminum oxide) of the α-epoxide III resulted in the quantitative recovery of unchanged α-epoxide. Henbest and Wrigley have already shown (24) that 5β,6β-epoxides are more prone to rearrangement to 6-ketones than the corresponding 5α,6α-epoxides.

Treatment of the acetoxy ethylenedioxy α-epoxide III with an excess of methyl magnesium bromide gave the 3β,5α-dihydroxy 6β-methyl ketal V in 50% yield. Deketalization with acetone and *p*-toluenesulphonic acid (22) afforded 3β,5α-dihydroxy-6β-methylpregnan-20-one (IX), which was converted directly to the acetate IX*a*. The structure of the intermediates V, IX, and IX*a* was confirmed by oxidation, with chromic acid and sulphuric acid in acetone (26, 27), of the dihydroxy ketone IX to the known (28, 29) 5α-hydroxy-6β-methylpregnane-3,20-dione (XIII). Since this diketone XIII is readily converted to 6α-methylprogesterone (XIV) (and also to its 6β-epimer) (28, 29, cf. also Experimental), the sequence of reactions described above represents a new and useful variation of the synthesis of 6-methylated progesterones from pregnenolone or pregnenolone acetate. In our syntheis, we protect the 20-keto function against the action of the Grignard reagent by the formation of a 20-ketal, while the British authors (29) reduce the 20-ketone to a mixture of epimeric 20-alcohols, which they acetylate prior to the Grignard reaction; the authors from Mexico (28) use a homogeneous, but less readily available, 3β,20β-diacetoxy derivative as starting material.

In pursuance of our main objective, we brominated 3β-acetoxy-5α-hydroxy-6β-methylpregnan-20-one (IX*a*) with N-bromosuccinimide under illumination (cf. refs. 30 and 3) and thus obtained the 17α-bromo adduct X*a*. Particularly rewarding results were achieved when a small amount of a tertiary base, such as pyridine, was added to the reaction mixture (cf. ref. 5). Since the acetoxy bromide X*a* is not readily purified, it was hydrolyzed directly to 17α-bromo-3β,5α-dihydroxy-6β-methylpregnan-20-one (X) with perchloric acid in methanol (2, 31). The resulting hydroxy bromide X was purified by chromatography

and recrystallization; the yield of pure bromide X from the acetoxy hydroxy ketone IX*a* amounted to 57%. Upon bromination in position 17α, the typical levorotatory shift (2, 3, 12, 32) was observed. The location of the bromine substituent could be anticipated from analogous reactions (cf. refs. 2, 3, and 30) and was proved by the conversion of the final product, 17α-bromo-6α-methylprogesterone (XII), to 16-dehydro-6α-methylprogesterone (XV), as described below. The α-configuration of the 17-halogen substituent follows from the fact that a free-radical bromination of a 20-ketone affords the same stereoisomer as an acid-catalyzed bromination (cf., e.g., refs. 32 and 33), which leads exclusively to the 17α-bromo derivative (34).

The hydroxy keto bromide X was oxidized, in high yield, with chromic acid and sulphuric acid in acetone (26, 27) to 17α-bromo-5α-hydroxy-6β-methylpregnane-3,20-dione (XI). Dehydration with concomitant epimerization in position 6, leading to the desired 17α-bromo-6α-methylprogesterone (XII), was achieved in good yield by treatment with hydrogen chloride in acetic acid (cf. refs. 3 and 19). The structure and the stereochemistry of the skeleton were proved by reduction of the progesterone derivative XII, with zinc and acetic acid, to 6α-methylprogesterone (XIV) (28, 29)[7] and was further confirmed by dehydrobromination with dimethylformamide and lithium chloride (cf. ref. 35) to the known (29) 16-dehydro-6α-methylprogesterone (XV). This last reaction also constitutes a proof of the location of the bromine substituent.

According to preliminary biological tests—for which we are indebted to Dr. E. G. Shipley of the Endocrine Laboratories of Madison, Inc., Madison, Wisc., and to Drs. J. Tripod and P. Desaulles of Ciba Ltd., Basle, Switzerland—17α-bromo-6α-methylprogesterone is a potent progestin which considerably exceeds in activity not only the natural hormone of the *corpus luteum* but also 17α-bromoprogesterone, both upon parenteral and oral administration.[8] The enhancing effect of the bulky 17α-bromine substituent on progestational activity (cf. refs. 2–4) is thus further substantiated. The implications of the establishment of high progestational activity of 17α-brominated progestins on activity–structure relationships will be discussed elsewhere on a broader basis.

EXPERIMENTAL[9, 10, 11]

Δ^5-3β-Acetoxy-20-ethylenedioxypregnene (IIa) (14)

Following the procedure of Allen *et al.* (15), 20 g of Δ^5-3β-acetoxypregnen-20-one (I) was ketalized with ethylene glycol in the presence of *p*-toluenesulphonic acid, by slow distillation of ethylene glycol, at 72–75° and 2 mm Hg pressure. The infrared spectrum of the reaction product revealed that hydrolysis in position 3 had occurred. The usual acetylation with acetic anhydride in pyridine at room temperature afforded 20.6 g of semicrystalline acetoxy ketal II*a*, which gave, upon crystallization from ether–methanol, 18.01 g of pure ketal II*a*, m.p. 156–158°, and a second batch of 600 mg, melting between 152 and 154° (yield of pure product 83%). A sample was recrystallized once from methanol for analysis; colorless scales; m.p. 159–161°; $[\alpha]_D^{24}$ −41.5° (*c*, 1.000 in $CHCl_3$); ν_{max}^{KBr} 1740 and 1250 cm^{-1} (acetate), 1042 cm^{-1} (20-ketal). Anal. Calc. for $C_{25}H_{38}O_4$: C, 74.59; H, 9.52. Found: C, 74.30; H, 9.35.

5α,6α-Epoxy-3β-acetoxy-20-ethylenedioxypregnane (III) and 3β-Acetoxy-20-ethylenedioxy-5α-pregnan-6-one (VIIIa)

To a solution of 38.5 g of Δ^5-3β-acetoxy-20-ethylenedioxypregnene (II*a*), m.p. 156–158°, in 1.9 liters of chloroform, there was added, at −80°, over a period of 20 minutes, 520 cc of a 0.4 *N* ethereal monoperphtalic

[7]*We sincerely thank Dr. V. Petrow for an authentic sample of 6α-methylprogesterone.*
[8]*A detailed report on the biological effects of 17α-bromo-6α-methylprogesterone will appear elsewhere.*
[9]*The melting points were taken in evacuated capillaries and the temperatures were corrected.*
[10]*If not otherwise stated, Woelm's non-alkaline aluminum oxide and Davison's silica gel No. 923 were used for chromatography.*
[11]*The microanalyses were performed by Dr. O. Schwarzkopf, New York, N.Y.; Dr. C. Daesslé, Montreal, Quebec; Mr. J. F. Alicino, Metuchen, N.J.; and Mr. A. Bernhardt, Mülheim (Ruhr), Germany, and their associates, to whom we express our sincere appreciation.*

Can. J. Chem. Downloaded from www.nrcresearchpress.com by 210.87.254.6 on 09/05/12
For personal use only.

acid solution. The mixture was kept at −80° for 2 hours, and between 0 and 5° for another 16 hours. Subsequently, the solution was washed with a cold 5% sodium carbonate solution and with water and was dried over sodium sulphate. Removal of the solvent gave 41.2 g of crude crystalline material which yielded, upon recrystallization from ether–methanol containing a few drops of pyridine, 27.06 g (67.6%) of pure *5α,6α-epoxy-3β-acetoxy-20-ethylenedioxypregnane (III)*, m.p. 183–185°. The infrared spectrum revealed no significant carbonyl absorption. A portion of this product was recrystallized once from ether–methanol for analysis; colorless needles; m.p. 184–186°; $[\alpha]_D^{25}$ −50° (*c*, 1.000 in $CHCl_3$); ν_{max}^{KBr} 1740 and 1250 cm^{-1} (acetate), 1042 cm^{-1} (ketal). Anal. Calc. for $C_{25}H_{38}O_5$: C, 71.74; H, 9.15. Found: C, 71.54; H, 9.02.

From the mother liquors of the first crystallization two further batches of crystals were isolated: a first crop of 1.457 g, m.p. 154–161°, $[\alpha]_D^{24}$ −33.3° (*c*, 1.000 in $CHCl_3$), and a second crop of 1.04 g, m.p. 104–108°, $[\alpha]_D^{24}$ −5.9° (*c*, 1.000 in $CHCl_3$). The remaining mother liquors (10.1 g) were absorbed on 300 g of aluminum oxide Woelm, activity III, pH 7.5–8. Elutions with petroleum ether – benzene (4:1) afforded 5.199 g of crystals, m.p. 109–112°, $[\alpha]_D^{23}$ −5°; petroleum ether – benzene (1:1) eluted at first 2.316 g of crystals melting between 104 and 115°, $[\alpha]_D^{23}$ −6°, and subsequently 2.285 g of a crystalline product, representing a crude mixture and melting between 130 and 173°, with specific rotations ranging from −20.5 to −35°. The last petroleum ether – benzene (1:1) eluates represented 265 mg (0.66%) of pure α-epoxide III, m.p. 181–184°, $[\alpha]_D^{24}$ −46°, identified by mixed melting point and infrared analysis. The fractions with a specific rotation of −5 to −6° (7.5 g) showed in the infrared a ketonic carbonyl absorption and represented crude *3β-acetoxy-20-ethylenedioxy-5α-pregnan-6-one (VIIIa)*. They were recrystallized four times from ether for analysis; colorless plates; m.p. 141–143°; $[\alpha]_D^{24}$ −12.5° (*c*, 1.000 in $CHCl_3$); ν_{max}^{KBr} 1741 cm^{-1} (acetate), 1713 cm^{-1} (6-ketone), 1250 cm^{-1} (acetate), 1040 cm^{-1} (ketal). Anal. Calc. for $C_{25}H_{38}O_5$: C, 71.74; H, 9.15. Found: C, 72.00; H, 9.07.

Saponification and Reacetylation

To a solution of 110 mg of the above-described 6-ketone VIII*a*, m.p. 140–142°, in 50 cc of methanol was added 2 cc of a 2 *N* sodium hydroxide solution. The mixture was refluxed for 7.5 hours and subsequently the volume of the solution was reduced, *in vacuo*, to 10 cc. The product was poured into cold water and the precipitate was extracted with ether. The ethereal solution was washed with water and was dried over sodium sulphate. Removal of the solvent afforded 100 mg of an amorphous product representing crude *hydroxy keto ketal VIII*, ν_{max}^{KBr} 1715 cm^{-1} (6-ketone), 1050 cm^{-1} (ketal). Upon reacetylation with 0.5 cc of acetic anhydride in 1 cc of pyridine, at room temperature, over a period of 16 hours, there was obtained 108 mg of crystalline ketone VIII*a*, which melted after one recrystallization from ether at 140–142°. The identity with the product isolated from the epoxidation mixture was established by a mixed melting point determination and infrared analysis.

Chromatography of Epoxide III

A quantity of 1 g of 5α,6α-epoxide III, m.p. 181–183°, was chromatographed on 40 g of non-alkaline aluminum oxide Woelm, activity III. Petroleum ether – benzene mixtures (4:1, 1:1, and 1:4) eluted 1 g of the 5α,6α-epoxide III; the melting points of the various fractions ranged from 180 to 184°. The product was in every respect identical with the starting material.

In other runs, there were obtained 10 g of α-epoxide III, m.p. 183–184°, from 14.05 g of ketal II*a* (68.4% yield) and 7.945 g of epoxide III, m.p. 178–184°, from 10 g of ketal II*a* (76.4% yield).

3β,5α-Dihydroxypregnan-20-one (VI)

A solution of 200 mg of 5α,6α-epoxy-3β-acetoxy-20-ethylenedioxypregnane (III), m.p. 181–183°, in 20 cc of absolute tetrahydrofuran was added, with stirring, to a slurry of 200 mg of lithium aluminum hydride in 100 cc of tetrahydrofuran. The mixture was refluxed for 1 hour with exclusion of moisture and was left for another 16 hours at room remperature. The excess reagent was decomposed by careful addition of moist ethyl acetate. Ice water was added and the mixture was extracted with ether. The organic layer was washed with iced dilute sulphuric acid, cold sodium bicarbonate solution, and with water and was dried over sodium sulphate. Removal of the solvent afforded 175 mg of a product representing crude *3β,5α-dihydroxy-20-ethylenedioxypregnane (VII)*; m.p. 217–222°; ν_{max}^{KBr} 3400 cm^{-1} (3β-hydroxyl), 3280 cm^{-1} (5α-hydroxyl), 1046 cm^{-1} (ketal). The product was dissolved without further purification in 10 cc of methanol and was treated for 1 hour, at reflux temperature, with 2 cc of an 8% sulphuric acid solution. The mixture was cooled and poured into a sodium bicarbonate solution. The precipitate was extracted with ether, the ethereal solution was washed with water and was dried over sodium sulphate. Removal of the solvent afforded 130 mg of 3β,5α-dihydroxypregnan-20-one (VI), m.p. 222–226°. A sample was recrystallized once from ethyl acetate – methanol and once from methanol, and was finally sublimed at 175° for analysis; prisms; m.p. 232–234°; $[\alpha]_D^{24}$ +105° (*c*, 1.000 in $CHCl_3$); ν_{max}^{KBr} 3480 cm^{-1} (3β-hydroxyl), 3450 cm^{-1} (partly associated 5α-hydroxyl), 1690 cm^{-1} (20-ketone). Anal. Calc. for $C_{21}H_{34}O_3$: C, 75.40; H, 10.25. Found: C, 75.14; H, 10.00.

3β,5α-Dihydroxy-20-ethylenedioxy-6β-methylpregnane (V)

To an ethereal Grignard solution prepared from 1.5 g of magnesium and a slight excess of methyl bromide there was added a solution of 3 g of 5α,6α-epoxy-3β-acetoxy-20-ethylenedioxypregnane (III), m.p. 183–185°, in 450 cc of absolute benzene. The reaction mixture was refluxed for 4 hours, and, after cooling, the excess

Can. J. Chem. Downloaded from www.nrcresearchpress.com by 210.87.254.6 on 09/05/12
For personal use only.

reagent was decomposed with an aqueous solution of ammonium chloride. The organic layer was washed with an aqueous ammonium chloride solution and with water and was dried over sodium sulphate. Removal of the solvent afforded 2.9 g of a solid which was chromatographed on 80 g of aluminum oxide, activity III, pH 7.5. Elutions with benzene–ether mixtures (4:1 and 1:1) and with pure ether afforded 1.4 g (50%) of 3β,5α-dihydroxy-20-ethylenedioxy-6β-methylpregnane (V), m.p. 162–164°. A sample was recrystallized twice, from ether, for analysis; fine needles; m.p. 168.5–169.5°; $[\alpha]_D^{25}$ −32° (*c*, 0.900 in $CHCl_3$); ν_{max}^{KBr} 3450 cm^{-1} (3β-hydroxyl), 3380 cm^{-1} (5α-hydroxyl), 1045 cm^{-1} (20-ketal). Anal. Calc. for $C_{24}H_{40}O_4$: C, 73.42; H, 10.27. Found: C, 73.63; H, 9.91.

3β-Acetoxy-5α-hydroxy-6β-methylpregnan-20-one (IXa)

A solution of 1.3 g of 3β,5α-dihydroxy-20-ethylenedioxy-6β-methylpregnane (V), m.p. 162–164°, and of 175 mg of *p*-toluenesulphonic acid in 100 cc of absolute acetone was refluxed for 1 hour. The volume of the solution was reduced *in vacuo* to approximately 25 cc and the product was poured into an iced sodium bicarbonate solution. The precipitate was extracted with dichloromethane, the organic solution was washed with water and was dried over sodium sulphate. Removal of the solvent afforded 1.2 g of crude *3β,5α-dihydroxy-6β-methylpregnan-20-one (IX)*, which was acetylated in the usual fashion with 1 cc of acetic anhydride in 4 cc of pyridine at room temperature, for a period of 16 hours. The usual working up afforded 1.15 g of a solid which, upon recrystallization from acetone–ether, gave 800 mg of pure *3β-acetoxy-5α-hydroxy-6β-methylpregnan-20-one (IXa)*, m.p. 195–197°. Chromatography of the mother liquors on aluminum oxide gave another 240 mg of the same product (total yield 80%). A sample was recrystallized once from acetone–ether for analysis; prisms; m.p. 198–200°; $[\alpha]_D^{24}$ +29.6° (*c*, 0.950 in $CHCl_3$); ν_{max}^{KBr} 3500 cm^{-1} (5α-hydroxyl), 1745 cm^{-1} (acetate), 1705 cm^{-1} (20-ketone), 1250 cm^{-1} (acetate). Anal. Calc. for $C_{24}H_{38}O_4$: C, 73.81; H, 9.81. Found: C, 73.69, 73.83; H, 9.60, 9.77.

In another run, 14.91 g of ketal V was transformed in a similar manner to 12.2 g of acetoxy ketone IX*a*, m.p. 192–193° (82% yield).

3β,5α-Dihydroxy-6β-methylpregnan-20-one (IX)

A solution of 100 mg of 3β-acetoxy-5α-hydroxy-6β-methylpregnan-20-one (IX*a*) in 15 cc of methanol and 0.75 cc of 70% perchloric acid was kept at room temperature for 20 hours. The product was poured into an iced sodium bicarbonate solution and the precipitate was extracted with dichloromethane. The organic solution was washed until neutral, dried over sodium sulphate, and taken to dryness. The resulting product (90 mg), representing *3β,5α-dihydroxy-6β-methylpregnan-20-one (IX)*, crystallized from ether; m.p. 186–187°; ν_{max}^{KBr} 3450 cm^{-1} (broad 3β,5α-dihydroxy band), 1707 cm^{-1} (20-ketone).

In another run, 4 g of acetate IX*a* was hydrolyzed in a similar manner to yield 3.2 g of purified dihydroxy ketone IX, m.p. 186–187°. The material was not further purified and was used directly in the following reaction.

5α-Hydroxy-6β-methylpregnane-3,20-dione (XIII) (cf. refs. 28 and 29)

To a solution of 160 mg of the dihydroxy ketone IX in 10 cc of absolute acetone there was added, dropwise and with stirring, at 0–5°, an oxidizing solution prepared by dissolving 267 mg of chromic acid in 230 cc of concentrated sulphuric acid and 770 cc of water. The addition was continued until the solution remained light brown. The mixture was stirred for another 3 minutes and was poured subsequently into ice water. The precipitate was collected, washed, and dried. The resulting 150 mg of crude material was absorbed on 5 g of aluminum oxide, Merck, activity II–III, pH 7.0, prepared as described under footnote 31 of reference 36. Methylene chloride and methylene chloride – acetone (4:1) eluted 55 mg of crystalline hydroxy diketone XIII. The product was recrystallized once from acetone–ether for analysis; needles; m.p. 250–252°; ν_{max}^{KBr} 3400 cm^{-1} (5α-hydroxyl), 1710 cm^{-1} (broad 3,20-diketo band). Anal. Calc. for $C_{22}H_{34}O_3$: C, 76.25; H, 9.85. Found: C, 76.20; H, 9.70.

In another run, 3.2 g of the dihydroxy ketone IX was oxidized in a similar fashion and gave 2.811 g of crude crystalline hydroxy diketone XIII, m.p. 230–235°, contaminated with some dehydrated product. This material was transformed directly to 6α-methylprogesterone (XIV) (cf. below).

17α-Bromo-3β,5α-dihydroxy-6β-methylpregnan-20-one (X)

A solution of 1.0 g of 3β-acetoxy-5α-hydroxy-6β-methylpregnan-20-one (IX*a*) in 80 cc of absolute carbon tetrachloride was refluxed for 10 minutes with 456 mg of N-bromosuccinimide and 0.2 cc of pyridine, over a photoflood lamp. The mixture was cooled and filtered through sodium sulphate, the sodium sulphate was washed with carbon tetrachloride, and the original solution and the washings were combined. The resulting solution was washed with iced 10% sodium bisulphite solution, iced bicarbonate solution, and with water and was dried over sodium sulphate. Removal of the solvent *in vacuo* afforded 1.21 g of a yellow foam which did not crystallize readily and which represented crude *17α-bromo-3β-acetoxy-5α-hydroxy-6β-methylpregnan-20-one (Xa)*. The product was not further purified and was hydrolyzed as follows.

A quantity of 1.2 g of the above-described crude acetoxy bromide X*a* was subjected, for 22 hours, to the action of 7.5 cc of 70% perchloric acid in 180 cc of methanol. Subsequently, the solution was poured into an iced sodium bicarbonate solution and the precipitate was extracted with methylene chloride. The organic layer was washed with water and was dried over sodium sulphate. Removal of the solvent *in vacuo* afforded

Can. J. Chem. Downloaded from www.nrcresearchpress.com by 210.87.254.6 on 09/05/12
For personal use only.

1.05 g of an amorphous product. The material was dissolved in a small quantity of benzene and absorbed on 100 g of silica gel. Elutions with benzene – ethyl acetate (4:1) afforded 620 mg (56.6% yield from ketone IX*a*) of crystalline *17α-bromo-3β,5α-dihydroxy-6β-methylpregnan-20-one (X)*, m.p. 151–153° decomp. A sample was recrystallized three times from ether–hexane for analysis; small needles; m.p. 155–156° decomp.; $[\alpha]_D^{26}$ −68.0° (*c*, 0.750 in $CHCl_3$); ν_{max}^{KBr} 3450 cm^{-1} (3β-hydroxyl), 3350 cm^{-1} (5α-hydroxyl), 1709 cm^{-1} (20-ketone). Anal. Calc. for $C_{22}H_{35}O_3Br$: C, 61.82; H, 8.25; Br, 18.70. Found: C, 61.70, 61.66; H, 8.00, 8.56; Br, 18.48, 18.99.

17α-Bromo-5α-hydroxy-6β-methylpregnane-3,20-dione (XI)

To a solution of 600 mg of 17α-bromo-3β,5α-dihydroxy-6β-methylpregnan-20-one (X), m.p. 151–153° decomp., in 40 cc of absolute acetone there was added, at 0–5°, 0.9 cc of the previously described chromic acid solution in dilute sulphuric acid. The mixture was stirred for 3 minutes and was poured into an iced sodium bicarbonate solution. The precipitate was extracted with dichloromethane and the organic layer was washed with water and was dried over sodium sulphate. Removal of the solvent *in vacuo* afforded 580 mg of a semicrystalline solid which, upon crystallization from acetone–ether, gave 400 mg of 17α-bromo-5α-hydroxy-6β-methylpregnane-3,20-dione (XI), m.p. 168–170° decomp. The mother liquors were chromatographed on 18 g of silica gel. Elutions with benzene – ethyl acetate (96:4) gave another 150 mg of the bromo diketone XI, m.p. 168–170° decomp. (total yield 92%). A sample was recrystallized once from ether–acetone for analysis; fine needles; m.p. 170–171° decomp.; $[\alpha]_D^{26}$ −49.9° (*c*, 0.850 in $CHCl_3$); ν_{max}^{KBr} 3450 cm^{-1} (5α-hydroxyl), 1707 cm^{-1} (broad 3,20-diketo band). Anal. Calc. for $C_{22}H_{33}O_3Br$: C, 62.11; H, 7.82; Br, 18.78. Found: C, 62.36, 61.95; H, 8.01, 7.84; Br, 19.00, 19.08.

Δ^4-17α-Bromo-6α-methylpregnene-3,20-dione (17α-Bromo-6α-methylprogesterone) (XII)

Through a solution of 500 mg of 17α-bromo-5α-hydroxy-6β-methylpregnane-3,20-dione (XI), m.p. 168–170° decomp., in 100 cc of acetic acid, there was passed, at 10° and for 2 hours, a stream of dry hydrogen chloride. Subsequently, the solution was kept for 16 hours at 0–5° and was then poured into an iced sodium chloride solution. The precipitate was extracted with ether, the ethereal solution was washed with ice water, with iced sodium bicarbonate solution, and with water and was dried over sodium sulphate. Upon removal of the solvent *in vacuo* 450 mg of a semicrystalline material was obtained. The product was absorbed on 45 g of silica gel. Elutions with benzene – ethyl acetate (97:3) gave 280 mg (58.5% yield) of 17α-bromo-6α-methylprogesterone (XII), m.p. 149–151° decomp. A sample was recrystallized four times from ether–hexane for analysis; colorless prisms; m.p. 153–154° decomp.; $[\alpha]_D^{24}$ +10.2° (*c*, 1.580 in $CHCl_3$); λ_{max}^{EtOH} 237 mμ (log ε 4.19); ν_{max}^{KBr} 1703 cm^{-1} (20-ketone), 1672 and 1610 cm^{-1} (Δ^4-3-keto doublet). Anal. Calc. for $C_{22}H_{31}O_2Br$: C, 64.86; H, 7.67; Br, 19.62. Found: C, 64.97, 64.62; H, 7.80, 7.72; Br, 19.89, 19.77.

Δ^4-6α-Methylpregnene-3,20-dione (6α-Methylprogesterone) (XIV) (cf. refs. 28 and 29)

(a) From 5α-Hydroxy-6β-methylpregnane-3,20-dione (XIII)

Through a solution of 2.5 g of crude, partly dehydrated 5α-hydroxy-6β-methylpregnane-3,20-dione (XIII), obtained by oxidation of the dihydroxy ketone IX (see above), in 100 cc of acetic acid, there was passed, at 10–15°, for 2 hours, a stream of dry hydrogen chloride. The product was further treated and worked up as described for the preparation of 17α-bromo-6α-methylprogesterone (XII) (see above). Thus, 2 g of crude 6α-methylprogesterone (XIV), λ_{max}^{EtOH} 241 mμ (log ε 4.08), was obtained. Chromatography on 60 g of aluminum oxide, activity III, afforded 1.6 g (67.5% yield) of 6α-methylprogesterone (XIV), m.p. 119–122°, $[\alpha]_D^{23}$ +172° (*c*, 0.850 in $CHCl_3$). The infrared spectrum of the product was identical with that of an authentic sample of 6α-methylprogesterone, kindly supplied by Dr. V. Petrow,[7] and no depression of melting point was observed upon mixture of the two samples.

(b) From 17α-Bromo-6α-methylprogesterone (XII)

To a solution of 30 mg of 17α-bromo-6α-methylprogesterone (XII) in 10 cc of acetic acid there was added, at 80°, portionwise and with shaking, 500 mg of zinc dust. The mixture was heated with intermittent shaking for another 2 hours on a boiling water bath. The reaction mixture was cooled, diluted with ether, and filtered. The filtrate was further diluted with ether and the ethereal solution was washed with dilute hydrochloric acid, water, sodium bicarbonate solution, and with water and was dried over sodium sulphate. Evaporation of the solvent afforded 20 mg of an amorphous product which crystallized from acetone–hexane. Thus, 14 mg of 6α-methylprogesterone (XIV), m.p. 121–123°, $[\alpha]_D^{25}$ +176° (*c*, 0.600 in $CHCl_3$), λ_{max}^{EtOH} 241 mμ (log ε 4.19), was obtained. The identity of this product with authentic 6α-methylprogesterone[7] was established by a mixed melting point and by the comparison of the infrared spectra.

$\Delta^{4,16}$-6α-Methylpregnadiene-3,20-dione (6α-Methyl-16-dehydroprogesterone) (XV) (29)

A solution of 60 mg of 17α-bromo-6α-methylprogesterone (XII), m.p. 150–152° decomp., in 15 cc of dimethylformamide was refluxed, in a nitrogen atmosphere, with 12 mg of lithium chloride, for 1 hour. Subsequently, the mixture was cooled and extracted with ether. The ethereal solution was washed with dilute hydrochloric acid, water, sodium bicarbonate solution, and again with water and was dried over sodium sulphate. Removal of the solvent afforded 45 mg (93.6% yield) of crude, crystalline 6α-methyl-16-dehydroprogesterone (XV), m.p. 172–175°. The product was absorbed on a column of 2 g of silica gel and

Can. J. Chem. Downloaded from www.nrcresearchpress.com by 210.87.254.6 on 09/05/12
For personal use only.

eluted with benzene – ethyl acetate (97:3). Thus, 30 mg (62.4%) of colorless crystals, m.p. 174–176°, were obtained. The product was recrystallized twice from ether for analysis; prisms; m.p. 180–182°; $[\alpha]_D^{24}$ +153° (*c*, 0.650 in $CHCl_3$); λ_{max}^{EtOH} 240 mμ (log ε 4.46); ν_{max}^{KBr} 1670 and 1610 cm^{-1} (Δ^4-3-keto doublet), 1661 cm^{-1} (shoulder), 1590 cm^{-1} (Δ^{16}-20-keto doublet). Anal. Calc. for $C_{22}H_{30}O_2$: C, 80.93; H, 9.26. Found: C, 80.54; H, 9.22.

ACKNOWLEDGMENTS

We sincerely thank Mrs. J. Capitaine and Mr. D. Capitaine for their most competent assistance in our experiments. We are greatly indebted to Dr. E. Shipley, Endocrine Laboratories of Madison Inc., Madison, Wisc., and to Dr. J. Tripod and Dr. P. Desaulles, Ciba Ltd., Basle, Switzerland, for the biological tests briefly mentioned in this paper. Sincere thanks are also due to Dr. M. Eisler and Dr. P. Perlman, Schering Corporation, Bloomfield, N.J., and to Dr. H. A. Salhanick, University of Nebraska, Omaha, Nebraska, for preliminary biological investigations. Generous financial support from the National Research Council of Canada, the Schering Corporation, Bloomfield, N.J., and the Schering Corporation Ltd., Montreal, Quebec, is gratefully acknowledged.

REFERENCES

1. S. Rakhit and Ch. R. Engel. Can. J. Chem. **40**, 2163 (1962).
2. Ch. R. Engel and H. Jahnke. Can. J. Biochem. Physiol. **35**, 1047 (1957).
3. Ch. R. Engel and R. Deghenghi. Can. J. Chem. **38**, 452 (1960).
4. Ch. R. Engel. Abstracts, 1st International Congress of Endocrinology, Copenhagen. 1960. p. 913.
5. D. J. Marshall and R. Gaudry. Can. J. Chem. **38**, 1495 (1960).
6. J. S. Mills, O. Candiani, and C. Djerassi. J. Org. Chem. **25**, 1056 (1960).
7. A. David, F. Hartley, D. R. Millson, and V. Petrow. J. Pharm. Pharmacol. **9**, 929 (1957).
8. J. A. Campbell, J. C. Babcock, and J. A. Hogg. J. Am. Chem. Soc. **80**, 4717 (1958).
9. J. C. Babcock, E. S. Gutsell, M. E. Herr, J. A. Hogg, J. C. Stucki, L. E. Barnes, and W. E. Dulin. J. Am. Chem. Soc. **80**, 2904 (1958).
10. H. J. Ringold, J. P. Ruelas, E. Batres, and C. Djerassi. J. Am. Chem. Soc. **81**, 3712 (1959).
11. P. B. Sollman, R. L. Elton, and R. M. Dodson. J. Am. Chem. Soc. **81**, 4435 (1959).
12. H. Heusser, Ch. R. Engel, P. Th. Herzig, and Pl. A. Plattner. Helv. Chim. Acta, **33**, 2229 (1950).
13. R. Deghenghi and R. Gaudry. J. Am. Chem. Soc. **83**, 4668 (1961).
14. M. Gut. J. Org. Chem. **21**, 1327 (1956).
15. W. S. Allen, S. Bernstein, and R. Littell. J. Am. Chem. Soc. **76**, 6116 (1954).
16. L. Ruzicka and W. Bosshard. Helv. Chim. Acta, **20**, 244 (1937).
17. Pl. A. Plattner, Th. Petrzilka, and W. Lang. Helv. Chim. Acta, **27**, 513 (1944).
18. L. Ruzicka and A. C. Muhr. Helv. Chim. Acta, **27**, 503 (1944).
19. A. Bowers and H. J. Ringold. Tetrahedron, **3**, 14 (1958).
20. M. Ehrenstein. J. Org. Chem. **6**, 626 (1941).
21. M. Ehrenstein and Th. O. Stevens. J. Org. Chem. **6**, 908 (1941).
22. H. Schinz and G. Schäppi. Helv. Chim. Acta, **30**, 1483 (1947).
23. S. Julia. Ann. Chim. France, **8**, 410 (1953).
24. H. B. Henbest and T. I. Wrigley. J. Chem. Soc. 4596 (1957).
25. H. B. Henbest and T. I. Wrigley. J. Chem. Soc. 4765 (1957).
26. K. Bowden, J. M. Heilbron, E. R. H. Jones, and B. C. L. Weedon. J. Chem. Soc. 39 (1946).
27. C. Djerassi, R. R. Engle, and A. Bowers. J. Org. Chem. **21**, 1547 (1956).
28. H. J. Ringold, E. Batres, and G. Rosenkranz. J. Org. Chem. **22**, 99 (1957).
29. D. Burn, B. Ellis, V. Petrow, I. A. Stuart-Webb, and D. M. Williamson. J. Chem. Soc. 4092 (1957).
30. R. U. Shock and W. J. Karpel. U.S. Patent No. 2,684,963 (1954).
31. J. Fried and F. Sabo. J. Am. Chem. Soc. **79**, 1130 (1957).
32. R. Deghenghi and Ch. R. Engel. J. Am. Chem. Soc. **82**, 3201 (1960).
33. Ch. R. Engel, G. Just, and R. Buttery. Can. J. Chem. **39**, 1805 (1961).
34. N. L. Wendler, R. P. Graber, and G. G. Hazen. Tetrahedron, **3**, 144 (1958).
35. R. P. Holysz. J. Am. Chem. Soc. **75**, 4432 (1953).
36. Ch. R. Engel and G. Just. J. Am. Chem. Soc. **76**, 4909 (1954).

Can. J. Chem. Downloaded from www.nrcresearchpress.com by 210.87.254.6 on 09/05/12
For personal use only.

NUCLEAR MAGNETIC RESONANCE SPECTRA OF DURENE AND MESITYLENE DERIVATIVES

E. BULLOCK
Department of Chemistry, The University, Nottingham, England
Received October 24, 1962

ABSTRACT

The nuclear methyl groups and ring protons in nitro- and dimethylamino-durenes and -mesitylenes show considerable chemical shifts relative to the parent hydrocarbons. The shifts are generally in the direction expected from a mesomeric effect, despite the lack of coplanarity between the aromatic ring and the substituent.

Can. J. Chem. Downloaded from www.nrcresearchpress.com by 210.87.254.5 on 09/05/12
For personal use only.

INTRODUCTION

The n.m.r. spectra of a considerable number of 1-substituted 2,6-dimethylbenzene derivatives have been studied and an attempt made to relate the observed chemical shifts of the ring protons to steric effects of the substituents and Hammett sigma values (1). Since the degree of interaction of various substituents with adjacent methyl substituents is not generally known with any accuracy it seemed worthwhile to make a further study of very large substituents in which deviations from coplanarity are well known to be great and hence mesomeric effects will be very markedly reduced. Nitro and dimethylamino groups are particularly valuable in this respect since a recent study has given accurate chemical shift data for the benzene derivatives (2) and, also, they provide examples of the two opposite types of mesomeric effect. Nitromesitylene and nitrodurene have been studied extensively by X-ray and spectroscopic methods (3, 4) which provide ample evidence of the lack of coplanarity between the substituent and the aromatic ring. Ortho-substituted dimethylanilines are even more sterically hindered, one substituent being sufficient to inhibit mesomeric interaction (5).

Materials

Mesitylene was distilled commercial (B.D.H.) material. The three nitromesitylenes were prepared by standard methods (6) by Mr. C. E. Loader of this university. The dimethylamino derivatives were prepared from these by catalytic (PtO) reduction at room temperature and atmospheric pressure and methylation with dimethyl sulphate (7). Durene was also commercial material (B.D.H.) and the nitro compounds were prepared by literature methods (8). The dimethylamino compounds were prepared as above.

EXPERIMENTAL

The n.m.r. spectrometer is an A.E.I. RS2 instrument operating at 60 Mc/sec. A standard sweep rate of about 90 c.p.s./min was used. The samples were examined as very dilute solutions in carbon tetrachloride containing 2% tetramethylsilane, the concentration in all cases being just sufficient to permit reasonable recording of the spectra. The spectra were calibrated by generation of side bands from the tetramethylsilane absorption.

RESULTS

The results are expressed on the τ scale in Table I. The values were reproducible to about ± 0.01 p.p.m. over at least five runs. The table also includes the chemical shifts of methyl groups in the three N,N-dimethyltoluidines. The figures in the last two columns show the shift of signals, other than those which are affected by an ortho substituent,

TABLE I

Chemical shifts of nitro and dimethylamino derivatives

Compound	Methyl	Ring proton	NMe_2	ΔH	ΔCH_3
Mesitylene	7.73	3.29	—	—	—
Nitro-	7.71 (2), 7.65 (1)*	3.09	—	*m*, −0.20	*p*, −0.08
Dinitro-	7.74 (1), 7.64 (2)*	2.88	—	*m*, −0.41	—
Trinitro-	7.66	—	—	—	—
Dimethylamino-	7.77	3.31	7.20	*m*, +0.02	*p*, +0.04
Di(dimethylamino)-	7.82	3.34	7.19	*m*, +0.05	—
Durene	7.83	3.19	—	—	—
Nitro-	7.84 (1), 7.69 (1)*	3.00	—	*p*, −0.19	*m*, −0.14
Dinitro-	7.73	—	—	—	—
Dimethylamino-	7.81 (1), 7.83 (1)*	3.35	7.13	*p*, +0.16	*m*, +0.02
Toluene (9)	7.66	2.83	—	—	—
o-Dimethylamino-	7.69	—	7.30	—	+0.03
m-Dimethylamino-	7.69	—	7.07	—	+0.03
p-Dimethylamino-	7.74	—	7.11	—	+0.08

*Figures in parenthesis show relative intensities of the peaks.

relative to the corresponding parent hydrocarbon. It is clear that a methyl group with an ortho non-coplanar nitro group appears to *high* field of one with the corresponding meta or para relationship (cf. *o*-nitrotoluene and its isomers (9)).

DISCUSSION

In any attempt to relate the observed effects to simpler substituted benzenes, several factors must be considered. Diehl (10) has shown that substituent effects on aromatic systems are often additive, but the additivity rules may break down with polysubstituted (especially vicinal halogeno) compounds. Apart from inductive and resonance effects, field (11), anisotropy, and solvent effects and perhaps deviations of the aromatic ring from the regular hexagon form on substitution (2) may be important. The last effect can probably be neglected since meta-disubstituted benzenes show additive chemical shift relationships, even for the proton between the substituents (10) and yet there are often very large distortions of the ring (12) in such cases. Furthermore, the present study indicates that substituent effects on mesitylenes are additive for both nitro and dimethylamino substitution. The "substituent-shifts" are calculated using the parent hydrocarbon as a standard, rather than by reference to benzene (cf. ref. 1), and the values of Fraser (1) can be recalculated on the same basis (using chemical shift values for 1-*d*-2,6-dimethylbenzene) to give comparable results. Whilst many of the shifts are very small and cannot therefore be used for quantitative comparison, there is an unmistakable trend which suggests that despite lack of coplanarity the chemical shifts produced by substituents are in the same direction as would be expected from mesomeric effects. This is particularly interesting in the dimethylamino compounds since the inductive effect of this group is presumed to be in the opposite sense to the mesomeric effect and might be expected to be the main electronic effect in the hindered systems.

Nitro Compounds

The chemical shifts of ring protons of nitrobenzene (relative to benzene) are *o*, −0.95; *m*, −0.21; and *p*, −0.33 p.p.m. (2). The shifts of methyl groups in nitrotoluenes (relative to toluene) are *o*, −0.19; *m*, −0.08; and *p*, −0.09 p.p.m. (9). Comparison with Table I suggests that an "out-of-plane" nitro group produces shifts of (*a*) a meta proton and (*b*) a para-methyl group as large as does a coplanar nitro substituent. The values for

Can. J. Chem. Downloaded from www.nrcresearchpress.com by 210.87.254.5 on 09/05/12
For personal use only.

nitrodurene are less clear-cut but still show marked low-field shifts for meta methyl and para proton.

Fraser's values (1) when calculated on the same basis give a meta-proton shift of −0.21 p.p.m. and a para-proton shift of −0.16 p.p.m., in good agreement with the present values.

Dimethylamino Compounds

The ring-proton shifts in dimethylaniline are +0.60, +0.10, and +0.62 for ortho, meta, and para positions respectively (2). The methyl shifts for dimethylaminotoluenes are included in Table I. The values are comparable in magnitude with those of the nitro compounds but all in the high-field direction. The ring-methyl resonances are not resolved in the dimethylaminomesitylenes.

The results of this and the earlier studies suggest that for the meta proton in nitrobenzene and the hindered ortho-substituted compounds there is no mesomeric contribution at all, although there is clearly some considerable para effect (cf. ref. 2). An analogous effect has been postulated to account for fluorine chemical shifts of meta-fluoro-substituted benzene derivatives (13).

Ortho-methyl Groups

The relative intensities of the resonances of the nuclear methyl substituents in the nitromesitylenes show that the ortho-methyl peaks are scarcely shifted from the value for the parent hydrocarbon. This can be understood if there is a magnetically induced circulation of the π electrons in the nitro group which produces a region of positive shielding above and below the plane containing the atoms of the group, thus neutralizing any electronic effects of the substituent (cf. ref. 14).

REFERENCES

1. R. R. Fraser. Can. J. Chem. **38**, 2226 (1960).
2. H. Spiesecke and W. G. Schneider. J. Chem. Phys. **35**, 731 (1961).
3. W. A. Brown and H. Reagan. J. Am. Chem. Soc. **69**, 1032 (1947).
4. J. Trotter. Can. J. Chem. **37**, 1487 (1959).
5. J. Burgers, M. A. Hoefnagel, P. E. Verkadi, H. Visser, and B. M. Wepster. Rev. Trav. Chim. **77**, 491 (1958).
6. A. H. Blatt (*Editor*). Organic syntheses. Coll. Vol. 2. Wiley. 1943. p. 449. G. Dyson and R. F. Hunter. J. Soc. Chem. Ind. **45**, 847 (1926). M. P. de Lange. Rec. Trav. Chim. **45**, 47 (1926).
7. C. E. Ingham and G. C. Hampson. J. Chem. Soc. 981 (1939).
8. G. Illuminati. J. Am. Chem. Soc. **74**, 4951 (1952). G. Illuminati and M. P. Illuminati. J. Am. Chem. Soc. **75**, 2159 (1953).
9. L. M. Jackmann. Applications of N.M.R. spectroscopy. Pergamon Press. 1959. p. 63.
10. P. Diehl. Helv. Chim. Acta, **44**, 829 (1961).
11. A. D. Buckingham. Can. J. Chem. **38**, 300 (1960).
12. J. Trotter. Can. J. Chem. **39**, 1638 (1961).
13. R. W. Taft, Jr. J. Am. Chem. Soc. **79**, 1045 (1957).
14. A. C. Huitric and W. F. Trager. J. Org. Chem. **27**, 1926 (1962).

Can. J. Chem. Downloaded from www.nrcresearchpress.com by 210.87.254.5 on 09/05/12
For personal use only.

EXCHANGE BROADENING OF SPIN–SPIN TRIPLETS IN NUCLEAR MAGNETIC RESONANCE SPECTRA. APPLICATION TO THE SYSTEM ETHANOL–WATER

W. G. PATERSON

Department of Chemistry, University of Alberta, Edmonton, Alberta

Received July 13, 1962

ABSTRACT

Using an extension of the method of McConnell (1), an expression is derived for the nuclear magnetic resonance spectrum of a hydroxyl proton in a —CH_2OH group which is undergoing intermolecular exchange. A graphical method is presented which enables a rapid evaluation of τ, the average lifetime of a hydroxyl proton between exchange events. Measurements of line widths and multiplet spacings in the n.m.r. spectra of ethanol–water solutions are interpreted in terms of the proton exchange reaction

$$C_2H_5OH + HOH^* \rightleftarrows C_2H_5OH^* + HOH,$$

for which a value of 2.7 l. mole^{-1} sec^{-1} at 42±1° C is suggested as an upper limit to the rate constant.

THEORETICAL

The quantitative description of exchange processes which modify the nuclear magnetic resonance spectrum of a system follows most easily from an appropriate modification of the Bloch phenomenological equations (1–26). This approach, first used by Gutowsky, McCall, and Slichter (5), has been presented in a simplified form by McConnell (1). The modification (2) of McConnell's (1) original treatment for nuclear exchange between two sites to include the movement of individual nuclei among n sites in a random statistical manner gives

$$\frac{dG_j}{dt} + \alpha_j G_j = -i\gamma H_1 M_0 p_j + \sum_k \left(\frac{G_k}{\tau_{kj}} - \frac{G_j}{\tau_{jk}}\right), \qquad [1]$$

where G is the complex moment $u+iv$ in the xy plane; u and v are the transverse components of the macroscopic nuclear magnetic moment M along and perpendicular to the rotating magnetic field H_1; γ is the nuclear magnetogyric ratio; M_0 is the equilibrium value of M; p_j is the fractional population of the j sites ($j = 1, 2, \ldots, n$); τ_{kj}^{-1} is the probability per unit time of a nucleus on a k site making a jump to a j site, and analogously for τ_{jk}^{-1}; and α_j is given by

$$\alpha_j = \frac{1}{T_{2j}} - i(\omega_j - \omega),$$

where T_{2j} and ω_j are the transverse relaxation time T_2 and the Larmor frequency, respectively, of a nucleus on a j site, and ω is the angular rotation frequency of H_1. Thus $\sum_k \tau_{kj}^{-1} G_k$ in equation [1] represents the rate of increase of G_j due to transfer of magnetization from k to j sites and $\sum_k \tau_{jk}^{-1} G_j$ represents the corresponding rate of loss. Since jumps between two sites of the same types have no effect on the spectrum (1, 2), τ_{jk}^{-1} and τ_{kj}^{-1} are zero if $j = k$.

Equation [1] may be applied to the n.m.r. spectra of alcohols containing the —CH_2OH group. The hydroxyl protons of such compounds show a triplet spectrum (due to coupling

Can. J. Chem. Downloaded from www.nrcresearchpress.com by 210.87.254.5 on 09/05/12
For personal use only.

with the methylene protons) in the absence of hydroxyl proton exchange, but the triplet structure collapses if the exchange rate is increased (10). The methylene group can have any one of four equally probable spin states, and in an exchange event, a hydroxyl proton is equally likely to become attached to a molecule with any of the four configurations. For the hydroxyl proton of a —CH_2OH group, all τ_{kj}^{-1} and τ_{jk}^{-1} are equal, all p_j are 1/4, and equation [1] becomes

$$\frac{dG_j}{dt} + \alpha_j G_j = -\frac{1}{4} i\gamma H_1 M_0 - \frac{3G_j}{\tau_{jk}} + \frac{1}{\tau_{kj}} \sum_{k \neq j} G_k. \qquad [2]$$

To a good approximation, the two inner frequencies of the triplet are coincident if the chemical shift between the methylene and hydroxyl protons is much larger than the spin coupling constant between them (2). Since in a symmetrical triplet a hydroxyl proton on a j site has a choice of only two other different sites in an exchange event, and since two protons are involved in each exchange event, the average lifetime τ of a hydroxyl proton before exchange is given by $\tau = \tau_{jk}/4$, and equation [2] becomes

$$\frac{dG_j}{dt} + \alpha_j G_j = -\frac{1}{4}\gamma H_1 M_0 - \frac{3}{4\tau} G_j + \frac{1}{4\tau} \sum_{k \neq j} G_k. \qquad [3]$$

In the case of a symmetric —OH triplet, there are only three different values of α_j, namely,

$$\alpha_j = \frac{1}{T_{2j}} - i(\Delta\omega + m\delta\omega), \qquad [4]$$

where $\Delta\omega$ is the angular frequency of the applied field, the center of the multiplet being taken as zero; $\delta\omega$ is half the multiplet spacing between adjacent lines; and $m = 2$, 0, or -2 depending on which triplet component is under consideration. The steady-state solution of equation [3] follows (1, 2) by setting dG_j/dt equal to zero, and solving the resulting set of linear equations for $G = \sum_j G_j$, which yields

$$G = \frac{\dfrac{-i\gamma H_1 M_0}{\delta\omega}\left\{t\left[\left(\dfrac{1}{t} + \dfrac{1}{Q} - iZ\right)^2 + 2\right]\right\}}{t\left(\dfrac{1}{t} + \dfrac{1}{Q} - iZ\right)\left[\left(\dfrac{1}{t} + \dfrac{1}{Q} - iZ\right)^2 + 4\right] - \left(\dfrac{1}{t} + \dfrac{1}{Q} - iZ\right)^2 - 2}, \qquad [5]$$

where, for convenience (22), $Q = T_2\delta\omega$, $t = \tau\delta\omega$, and $Z = \Delta\omega/\delta\omega$. Equation [5] has been derived by Meiboom *et al.* (17) using the more elegant and complicated argument of Gutowsky, McCall, and Slichter (5). A comparison of equation [5] and the equation $G = u + iv$ shows that the intensity of the absorption mode v is proportional to the imaginary part of equation [5]. Rationalization of the latter yields

$$v = \frac{-\dfrac{\gamma H_1 M_0}{\delta\omega}\{Z^4 + 2Z^2(x^2 + Qx - 2) + (x^2+2)(x^2+2Qx+2)\}}{\left\{QZ^6 + Z^4\left(2Qx^2 + \dfrac{1}{Q} - 8Q\right) + Z^2\left(Qx^4 + \dfrac{2}{Q}x^2 + \dfrac{4}{t} + 16Q\right) + \dfrac{1}{Q}(x^2+2Qx+2)^2\right\}}, \qquad [6]$$

where $x = (1/t) + (1/Q)$. When both τ and T_2 are large, this expression predicts three lines of intensity distribution 1:2:1, separated by a frequency interval $2\delta\omega$. For much smaller values of τ and T_2, the behavior of equation [6] is such that for some values three peaks are produced, and for others only a single peak is to be expected. Values

Can. J. Chem. Downloaded from www.nrcresearchpress.com by 210.87.254.5 on 09/05/12
For personal use only.

of τ may be obtained from experimental data by computing line shapes for all probable values of Q, Z, and t and comparing with the observed line shape (17). This method is convenient only for triplets with symmetric intensity distribution. In an alternative method described below, which is applicable under conditions of slow hydroxyl proton exchange, the derivative of v with respect to applied frequency $\Delta\omega$ is set equal to zero, and the resulting equation in Z is solved for the location of the maxima. This procedure has been used previously (22, 27) for spin–spin doublets. In cases where the triplet has a slightly asymmetric intensity distribution, the average observed line separation may be used. The result obtained is

$$\frac{dv}{dZ} = 0 = Z^9+4Z^7\{x^2+Qx-2\} +2Z^5\left\{3(x^2-1)^2+5Qx^3-\left(2Q+\frac{1}{Q}\right)x+11\right\} +4Z^3\left\{(x^2+2Qx+2)\left(x^4-2x^2-\frac{x}{Q}-8\right)\right\} +2Z\left\{(x^2+2Qx+2)\left(\frac{x^6}{2}+x^4-\frac{x^3}{Q}+6x^2+\frac{6x}{Q}+16\right)\right\}. \quad [7]$$

The roots of this equation must correspond to the maxima and minima of the triplet signal. One solution is obviously $Z = 0$; evaluation of $(d^2v/dZ^2)_{Z=0}$ shows that this is always a maximum. The roots of equation [7] which correspond to the outer maxima $Z_{max} = \Delta\omega_{max}/\delta\omega$ were obtained from a program written for the IBM 1620 computer. Some values of Z_{max}, calculated for a range of values of Q and t, are summarized in Table I and plotted in Fig. 1.[1] With the aid of such a graph, a measurement of T_2, $\delta\omega$,

TABLE I

Calculated values of Z_{max} for various values of Q and t

	1/Q:					
t	A 0.02	B 0.10	C 0.15	D 0.20	E 0.25	F 0.30
10.00	1.996	1.994	1.992	1.989	1.986	1.982
8.00	1.994	1.991	1.988	1.985	1.982	1.977
6.00	1.990	1.985	1.982	1.978	1.973	1.968
5.00	1.986	1.980	1.976	1.971	1.965	1.959
4.00	1.978	1.971	1.965	1.959	1.952	1.943
3.50	1.972	1.963	1.957	1.949	1.940	1.930
3.00	1.962	1.951	1.943	1.934	1.923	1.910
2.50	1.944	1.930	1.920	1.908	1.893	1.876
2.00	1.911	1.891	1.876	1.857	1.836	1.809
1.75	1.881	1.855	1.834	1.810	1.780	1.742
1.50	1.830	1.792	1.762	1.723	1.669	1.574

NOTE: The letters A–F correspond to curves in Fig. 1.

and the maxima separation in the n.m.r. spectrum permits a rapid evaluation of τ, the average lifetime of the hydroxyl proton before exchange.

APPLICATION TO THE SYSTEM ETHANOL–WATER

Proton exchange in ethanol and in ethanol–water solutions has been investigated several times (10, 21, 28–32), with widely varying results being reported, but only once

[1]*Other values may be obtained from the author.*

Can. J. Chem. Downloaded from www.nrcresearchpress.com by 210.87.254.5 on 09/05/12
For personal use only.

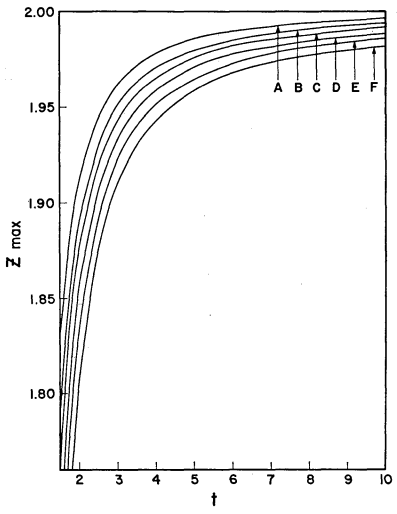

FIG. 1. Plot of Z_{max} vs. t for various values of $1/Q$. The lettering of curves corresponds to the values of $1/Q$ listed in Table I.

has the work been on a quantitative kinetic basis. In the latter (21), rates of acid- and base-catalyzed protolysis of ethanol in aqueous solution were found, and the rate constant of reaction [8] was obtained by inference as $k = 0.8$ l. mole^{-1} sec^{-1} at 22±2° C. In the

$$C_2H_5OH + HOH^* \rightleftarrows C_2H_5OH^* + HOH \qquad [8]$$

present paper, a direct measurement of the rate of reaction [8] is reported, utilizing the method described in the preceding section.

EXPERIMENTAL

The n.m.r. spectra were measured on a Varian A-60 Analytical n.m.r. spectrometer operating at 60 Mc/s. Using a copper–constantan thermocouple, the temperature of the solutions when in the spectrometer probe was measured as 42±1° C. Calibration of the instrument was achieved by the customary side-band technique (33), using a Hewlett–Packard Model 200 AB audio-oscillator and a Hewlett–Packard Model 521C frequency counter. The precision in measurement was generally better than 0.1 c.p.s. All measurements were an average of at least five determinations. Transverse relaxation times (T_2) were considered to be governed chiefly by magnetic field inhomogeneities (34), and were estimated from the line width of a degassed spectrograde cyclohexane or purified water sample, by means of the relation $T_2 = 1/\pi\Delta\nu_{1/2}$, where $\Delta\nu_{1/2}$ is the full width of the signal at half-maximum amplitude. These two substances gave identical T_2 values within experimental error. The degree of resolution of the n.m.r. spectrometer was deliberately set at a lower value than would be generally used in order that the assumption made above concerning field inhomogeneities would be valid.

All glassware which was used either in the purification of materials or in the rate measurements was cleaned with the following substances in the order written, and then heated for several hours at 120°: Fisher "Sparkleen" detergent, distilled water, ~3 N HCl, distilled water, ~3 N NH_4OH, distilled water. The rinsings with distilled water were done 10–20 times. In the early experiments, no significant differences were observed in exchange rates when measurements were made using pyrex or quartz[2] sample tubes. All the results quoted in this paper are from measurements made with standard Varian pyrex sample tubes.

Anhydrous ethanol was prepared by Fieser's method (35). A 30-in. Vigreux fractionating column and a Kjeldahl spray trap were used in the distillation, and air was excluded from the apparatus by passing a slow stream of dried, carbon-dioxide-free nitrogen through it. A middle fraction was collected ($n_D^{26} = 1.358_5$; this slightly high value is possibly due to small amounts of benzene). The triplet spacing of the —OH signal in "pure" ethanol varied from 5.05±0.06 to 4.97±0.04 c.p.s. depending on the degree of purification and the resolution of the n.m.r. spectrometer. These variations should have a small effect on the results quoted

[2]*Baumbach Bros., Thundersley, Essex, England.*

Can. J. Chem. Downloaded from www.nrcresearchpress.com by 210.87.254.5 on 09/05/12
For personal use only.

since any set of measurements on ethanol–water solutions was compared to the "pure" ethanol prepared for that set. Pure water ($n_D^{28} = 1.332_3$) was prepared in two different ways: (1) by refluxing distilled water from the tap over alkaline $KMnO_4$ and distilling in the apparatus described above, and (2) by passing distilled water from the tap through a Barnstead "Bantam Demineralizer" ion-exchange column followed by a bubbling treatment with carbon-dioxide-free nitrogen. The pH of water thus prepared was usually 6.7, corresponding to $[H^+] = 2\times10^{-7}$ mole/l. or less. A 40% v/v ethanol–water solution gave a similar pH reading. pH measurements were made with a Radiometer pH meter calibrated with a standard phthalate buffer.

All flasks and n.m.r. tubes which were used in sample preparation were flushed with dried, carbon-dioxide-free nitrogen before use. Since the solutions slowly leach impurities from glass, it was found necessary to do a given set of n.m.r. measurements on the same day that the materials were distilled.

RESULTS AND DISCUSSION

In the kinetic analysis, it is assumed that the only exchange reaction of significance is reaction [8]. Since ionic concentrations in neutral alcohol–water solutions are extremely small (21, 36), proton transfer reactions other than [8] should be relatively unimportant. The pH measurements quoted in the experimental section suggest that the solutions used were approximately neutral. Separate experiments proved the absence of significant proton exchange in pure ethanol.

It follows that

$$\pm\frac{d[C_2H_5OH]}{dt} = k[C_2H_5OH][HOH].$$

The average lifetime $\tau_{C_2H_5OH}$ of a hydroxyl proton on a molecule of C_2H_5OH before exchange with a proton on a different site will be

$$\tau_{C_2H_5OH} = \frac{[C_2H_5OH]}{d[C_2H_5OH]/dt} = \frac{1}{k[HOH]}$$

or

$$\frac{1}{\tau_{C_2H_5OH}} = k[HOH].$$

Thus a plot of $1/\tau_{C_2H_5OH}$ vs. [HOH] should be a straight line with slope k passing through the origin. Figure 2 indicates that this is approximately true. The wide scatter of points

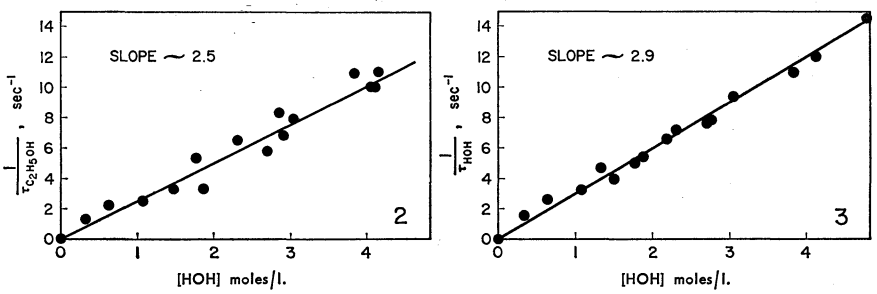

FIG. 2. Variation of $1/\tau_{C_2H_5OH}$ with [HOH].
FIG. 3. Variation of $1/\tau_{HOH}$ with [HOH].

is due to a number of factors. The rate of proton exchange is very susceptible to catalysis (21) and trace impurities (10, 27). Further errors are due to inaccurate T_2 values, but fortunately τ is relatively insensitive to the value of T_2. The identification of k as the rate constant for reaction [8] is valid only if it is the sole exchange reaction.

Since $\tau_{C_2H_5OH} = \tau_{HOH}$ for reaction [8], where τ_{HOH} is the average lifetime of a proton on a water molecule before exchange with a proton on ethanol, a plot of $1/\tau_{HOH}$ vs. [HOH]

Can. J. Chem. Downloaded from www.nrcresearchpress.com by 210.87.254.5 on 09/05/12
For personal use only.

should also be a straight line with slope k passing through the origin. Figure 3 suggests that this is approximately the case.

The values of $1/\tau_{C_2H_5OH}$ were obtained from the transverse relaxation time, T_2, the triplet spacing in pure ethanol, and the maxima separations in the partially collapsed —OH triplet, using the method outlined in the theoretical section. The values of $1/\tau_{HOH}$ were obtained from the relation (1, 5, 21)

$$\frac{1}{\tau_{HOH}} = \pi\Delta\nu_{\frac{1}{2}} - \frac{1}{T_2},$$

where $\Delta\nu_{\frac{1}{2}}$ is the full width of the water signal of half-maximum amplitude. Typical —OH and HOH signals are shown in Fig. 4.

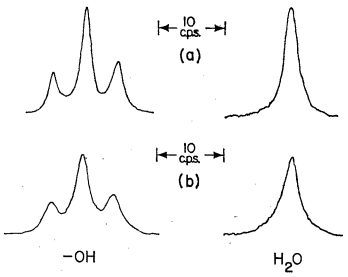

FIG. 4. Typical —OH and HOH signals. (*a*) [HOH] = 2.18 moles/l.; (*b*) [HOH] = 2.76 moles/l. The —OH and HOH signals were recorded at different gain settings.

The average of the slopes of Figs. 2 and 3, obtained by a least-squares treatment (37), yields a rate constant k for reaction [8] approximately equal to 2.7 l. mole^{-1}sec^{-1} at 42±1° C. This compares with the value 0.8 l. mole^{-1}sec^{-1} at 22±2° C reported by Meiboom and coauthors (21). These two rate constants yield a crude estimate of 10 kcal/mole for the activation energy for proton transfer between ethanol and water. An approximate value of 7.6 kcal/mole has been suggested by Schneider and Reeves (31).

It is quite possible that the rate constant quoted in the present work is too high due to the presence of trace acidic impurities. Inclusion even to a limited extent of reactions such as

$$C_2H_5OH + H_3O^+ \rightleftharpoons C_2H_5OH_2^+ + H_2O$$
$$C_2H_5OH + C_2H_5OH_2^+ \rightleftharpoons C_2H_5OH_2^+ + C_2H_5OH$$
$$C_2H_5OH + H_2O + C_2H_5OH_2^+ \rightleftharpoons C_2H_5OH_2^+ + H_2O + C_2H_5OH,$$

the first two of which have rate constants of 2.8×10^6 and 1.1×10^8 l. mole^{-1}sec^{-1} at 22±2° C, respectively, could result in a high value for the rate constant quoted here.

A possible formulation of the mechanism of reaction [8] is

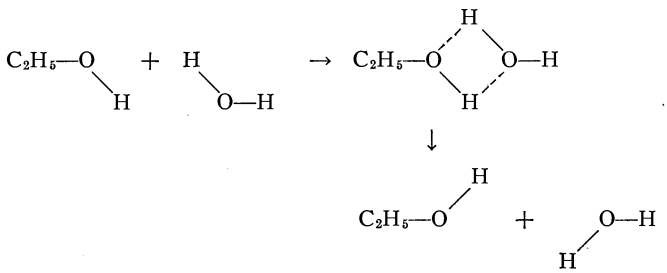

Can. J. Chem. Downloaded from www.nrcresearchpress.com by 210.87.254.5 on 09/05/12
For personal use only.

ACKNOWLEDGMENTS

This work was supported in part by the National Research Council of Canada, whose financial assistance is greatly appreciated. The author is very much indebted to Mr. D. D. Simpson of the University of Alberta Computing Center for the numerical solution of equation [7]. Several helpful discussions with Dr. D. Darwish and Dr. H. Spedding are also acknowledged.

REFERENCES

1. H. M. McConnell. J. Chem. Phys. **28**, 430 (1958).
2. J. A. Pople, W. G. Schneider, and H. J. Bernstein. High resolution nuclear magnetic resonance. McGraw-Hill Book Co., Inc., New York. 1959. Chap. 10.
3. F. Bloch. Phys. Rev. **70**, 460 (1946); **102**, 104 (1956).
4. R. K. Wangsness and F. Bloch. Phys. Rev. **89**, 728 (1953).
5. H. S. Gutowsky, D. W. McCall, and C. P. Slichter. J. Chem. Phys. **21**, 279 (1953).
6. H. S. Gutowsky and A. Saika. J. Chem. Phys. **21**, 1688 (1953).
7. P. W. Anderson. J. Phys. Soc. Japan, **9**, 316 (1954).
8. R. Kubo. J. Phys. Soc. Japan, **9**, 935 (1954).
9. I. Solomon and N. Bloembergen. J. Chem. Phys. **25**, 261 (1956).
10. J. T. Arnold. Phys. Rev. **102**, 136 (1956).
11. H. S. Gutowsky and C. H. Holm. J. Chem. Phys. **25**, 1228 (1956).
12. G. A. Williams and H. S. Gutowsky. Phys. Rev. **104**, 278 (1956).
13. H. M. McConnell and S. B. Berger. J. Chem. Phys. **27**, 230 (1957).
14. E. Grunwald, A. Loewenstein, and S. Meiboom. J. Chem. Phys. **27**, 630 (1957).
15. A. Loewenstein and S. Meiboom. J. Chem. Phys. **27**, 1067 (1957).
16. S. Meiboom, Z. Luz, and D. Gill. J. Chem. Phys. **27**, 1411 (1957).
17. S. Meiboom *et al.* Tables of exchange broadened NMR multiplets. The Weizmann Institute of Science, Rehovot, Israel.
18. J. I. Kaplan. J. Chem. Phys. **28**, 278 (1958).
19. R. A. Sack. Mol. Phys. **1**, 163 (1958).
20. P. Diehl. Helv. Phys. Acta, **31**, 685 (1958).
21. Z. Luz, D. Gill, and S. Meiboom. J. Chem. Phys. **30**, 1540 (1959).
22. M. Takeda and E. O. Stejskal. J. Am. Chem. Soc. **82**, 25 (1960).
23. R. G. Pearson, J. Palmer, M. M. Anderson, and A. L. Allred. Z. Elektrochem. **64**, 110 (1960).
24. H. G. Hertz. Z. Elektrochem. **65**, 36 (1961).
25. H. B. Charman, D. R. Vinard, and M. M. Kreevoy. J. Am. Chem. Soc. **84**, 347 (1962).
26. M. T. Rogers and J. C. Woodbrey. J. Phys. Chem. **66**, 540 (1962).
27. W. G. Paterson and R. E. Richards. Trans. Faraday Soc. In press (1963).
28. I. Weinberg and J. R. Zimmerman. J. Chem. Phys. **23**, 748 (1955).
29. W. A. Anderson and J. T. Arnold. Discussions Faraday Soc. **19**, 226 (1955).
30. J. B. Leane. D. Phil. Thesis, Oxford University, Oxford, England. 1958.
31. W. G. Schneider and L. W. Reeves. Ann. N.Y. Acad. Sci. **70**, 806 (1958).
32. G. Mavel. Compt. Rend. **250**, 1477 (1960).
33. J. T. Arnold and M. E. Packard. J. Chem. Phys. **19**, 1608 (1951).
34. Varian Associates and Staff. NMR–EPR spectroscopy. Pergamon Press. 1960. Chap. 9.
35. L. F. Fieser. Experiments in organic chemistry. D. C. Heath, Boston. 1957. p. 285.
36. L. P. Hammett. Physical organic chemistry. McGraw-Hill, New York. 1940. pp. 256, 262.
37. F. Daniels, J. H. Mathews, J. W. Williams, P. Bender, and R. A. Alberty. Experimental physical chemistry. McGraw-Hill, New York. 1956. p. 339.

Can. J. Chem. Downloaded from www.nrcresearchpress.com by 210.87.254.5 on 09/05/12
For personal use only.

IONIZATION OF ORGANIC COMPOUNDS

V. THIOLACTAMS IN SULPHURIC ACID

J. T. EDWARD AND H. STOLLAR
Department of Chemistry, McGill University, Montreal, Que.

Received November 19, 1962

ABSTRACT

The ionization in aqueous sulphuric acid of thiolactams consisting of five-, six-, and seven-membered rings has been studied. With increasing concentration of acid the ionization ratio increases more rapidly than h_0. A possible explanation involving the hydration of the thiolactam is given. Changes in the basicity of thiolactams with ring size parallel changes previously found for lactams.

Can. J. Chem. Downloaded from www.nrcresearchpress.com by 210.87.254.42 on 09/05/12
For personal use only.

By analogy with the resonance structures of simple amides (1), the structure of lactams (I; X = O) would be expected to be made up by a 60% contribution from structure I*a* (X = O) and 40% contribution from structure I*b* (X = O), although the relative weights of the contributions could be altered somewhat by ring strain (2). Thiolactams (I; X = S) have higher dipole moments (3), and so should be represented to a preponderant extent by the dipolar form I*b* (X = S). The high polarity of the thiolactams (I; X = S, n = 3, 4, and 5) may in part account for the fact that they are solids at room temperature while the corresponding lactams (I; X = O, n = 3, 4, and 5) are liquid, and that (as postulated later in this paper) they appear to be more extensively hydrated in aqueous solution than are the lactams.

It is probable that lactams and thiolactams in strong acid are protonated on the oxygen or sulphur atom to give the conjugate acids (II; X = O or S) (4). Consequently it became of interest to compare the basicities of the two classes of compounds. It seemed

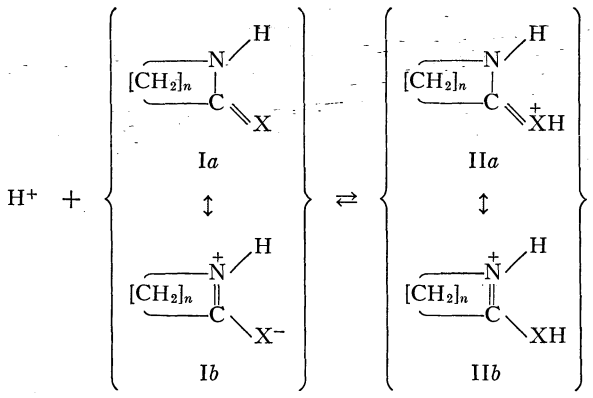

possible that in spite of the greater intrinsic basicity of oxygen as compared with sulphur (cf. OH^- and SH^-), the greater negative charge on the sulphur of thiolactams would cause them to be more basic than lactams. We have accordingly determined the protonation constants of the thiolactams (I; X = S, n = 3, 4, and 5) for comparison with the protonation constants reported for the lactams (I; X = O, n = 3, 4, and 5) (2).

EXPERIMENTAL

Materials

Piperidone (I; X = O, $n = 4$) and caprolactam (I; X = O, $n = 5$) were prepared in 38% and 67% yields, respectively, by Cornforth, Hunter, and Popjak's modification (5) of the Schmidt reaction. Pyrrolidone (I; X = O, $n = 3$) was a commercial product. Thiolactams were prepared from these lactams by treatment with phosphorus pentasulphide following the procedure of Tafel and Lawaczeck (6), and recrystallized to constant (though not necessarily sharp) melting point: thiopyrrolidone from water, m.p. 110–114° (lit. m.p. 116° (6)); thiopiperidone from aqueous ethanol, m.p. 94–95° (lit. m.p. 93–94° (7)); and thiocaprolactam from aqueous ethanol, m.p. 105–107° (lit. m.p. 105–105.5° (7)).

Sulphuric acid solutions were prepared and standardized as described previously (8).

Procedure

Apparatus and procedure were essentially as described before (9), except that thiocaprolactam, because of its insolubility in water, was dissolved in ethanol to make up a stock solution. Aliquots (1.00 ml) of this stock solution were diluted with aqueous sulphuric acid to 50.0 ml, so that the thiocaprolactam solutions contained about 2% (v/v) ethanol. No account was taken of this content of the ethanol in calculations of the H_0 values of the solutions; this seems reasonable from data in the literature (10).

RESULTS AND DISCUSSION

The absorption spectra of thiolactams in aqueous solution (Table I) show a strong peak at about 260 mμ due to a $n \rightarrow \sigma^*$ transition (11), and a second peak at about

TABLE I

Absorption peaks of thiolactams

	In water		In sulphuric acid		
Compound	λ_{max} (mμ)	ϵ_{max}	Concn. (%)	λ_{max} (mμ)	ϵ_{max}
Thiopyrrolidone	211	5,860	78.8	234	10,200
	260	14,400			
Thiopiperidone	212	5,620	69.4	239.5	9,400
	269	13,000			
Thiocaprolactam*	210	5,410	87.0	243	10,500
	271	15,100			

*Solutions contained about 2% (v/v) ethanol.

210 mμ which may be due to a $\pi \rightarrow \pi^*$ transition, although the assignment is uncertain (11). In strong sulphuric acid these are replaced by a single peak at about 240 mμ (Table I) which may be the $\pi \rightarrow \pi^*$ peak shifted to longer wavelengths by protonation (12), the blue shift of the $n \rightarrow \sigma^*$ peak (11) caused by protonation having taken it out of the observable region of the spectrum. These spectral changes are very similar to those already observed for thioacetamide (11, 13).

In keeping with the conception that the spectra of the thiolactams in strong acid are due to the monoprotonated species (II), the curves obtained in intermediate concentrations of acid are intermediate in character, and pass through an isobestic point at about 250 mμ and almost through a second isobestic point at about 220 mμ. This is shown for thiopiperidone in Fig. 1. The failure of the curves to pass through the second isobestic point indicates that the peak at lower wavelengths is being shifted by changing acid concentration through a "medium effect" (14).

Plots of the molar extinction coefficients of the thiolactams at a given wavelength against the H_0 values of the acid solutions give sigmoid waves whose inflection points indicate protonation constants (pK_{BH^+}) of −2.0 for thiopyrrolidone, −1.4 for thiopiperidone, and −1.6 for thiocaprolactam. However, as shown in Fig. 2, the curves drawn

Can. J. Chem. Downloaded from www.nrcresearchpress.com by 210.87.254.42 on 09/05/12
For personal use only.

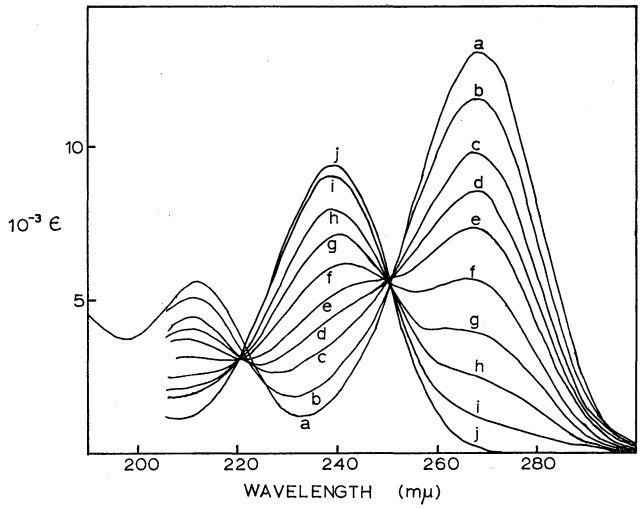

FIG. 1. Ultraviolet absorption of thiopiperidone in the following concentrations of sulphuric acid: *a*, 0; *b*, 15.0; *c*, 20.3; *d*, 23.0; *e*, 25.0; *f*, 27.8; *g*, 30.5; *h*, 33.0; *i*, 38.3; *j*, 69.4%.

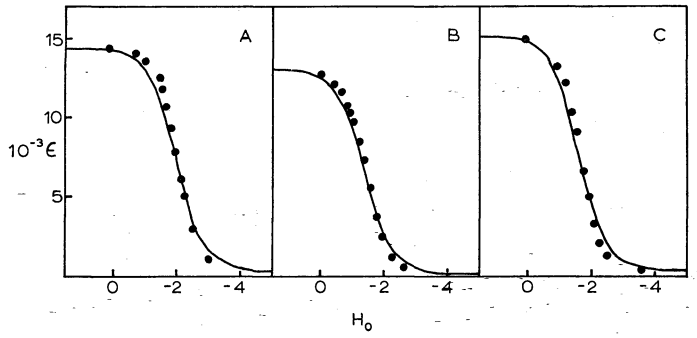

FIG. 2. Ionization of thiolactams in sulphuric acid. Points: experimental values of ε for wavelengths (λ) indicated below; curves: calculated from equation [1] using parameters indicated below. (A) Thiopyrrolidone: λ 260 mμ; pK_{BH^+} −2.0; ϵ_B 14,400; ϵ_{BH^+} 360. (B) Thiopiperidone: λ 269 mμ; pK_{BH^+} −1.4; ϵ_B 13,050; ϵ_{BH^+} 150. (C) Thiocaprolactam: λ 271 mμ; pK_{BH^+} −1.6; ϵ_B 15,100; ϵ_{BH^+} 400.

through the experimental points are all slightly steeper in the region of half-ionization than the curves theoretically required by the equation

$$pK_{BH^+} = H_0 - \log\{(\epsilon_{BH^+} - \epsilon)/(\epsilon - \epsilon_B)\}, \qquad [1]$$

ϵ_B, ϵ_{BH^+}, and ϵ being the molar extinction coefficients of the unprotonated base, the protonated base, and the mixture of protonated and unprotonated molecules in a solution of acidity function H_0, respectively.

Systematic deviation of experimental points from such a theoretical curve has often been attributed to the medium effect (14). However, in the present instance medium effects seem to be absent in the spectral region 240–270 mμ as shown by the behavior of the curves in passing through an isobestic point. It seems more probable that we are encountering another class of compounds whose protonation in acid solution does

Can. J. Chem. Downloaded from www.nrcresearchpress.com by 210.87.254.42 on 09/05/12
For personal use only.

not follow exactly the Hammett H_0 function. It has been shown already that the protonation of amides does not follow this function (9). However, the behavior of amides contrasts with that of thiolactams, in that plots of ϵ against H_0 for the former compounds are *less* steep in the region of half-ionization than required by equation [1].

The contrasting behavior of amides (A) and thiolactams (T) may be explained by postulating that their protonation equilibria (equations [2] and [3]) involve numbers of water molecules (m and p) differing from each other and from the number (n) involved in the protonation of the indicator (In) (equation [4]) used by Hammett (15) for establishing this range of the H_0 scale:

$$AH^+ + mH_2O \rightleftarrows A + H^+ \quad [2]$$

$$TH^+ + pH_2O \rightleftarrows T + H^+ \quad [3]$$

$$InH^+ + nH_2O \rightleftarrows In + H^+. \quad [4]$$

(The formulae in these equations represent hydrated ions or molecules.) If $p > n$, it can be shown (9) that this requires that the ionization ratio ($[TH^+]/[T]$) increase with acid concentration more rapidly than h_0, and hence that the curve of ϵ against H_0 should be steeper than required by equation [1] at half-neutralization, as was found for thiolactams. On the other hand, if $n > m$, the ionization ratio ($[AH^+]/[A]$) must increase less rapidly than h_0, and hence the curve of ϵ against H_0 must be less steep than required by equation [1], as was found for amides.

While at the moment it would be difficult to predict that $p > n > m$, it seems reasonable to expect $p > m$, because the very polar T should be expected to be more heavily hydrated than the less polar A (1). (AH^+ and TH^+, having very similar structures, are expected to be hydrated to approximately the same extent.) Similar considerations probably apply to the hydration of some thioureas, whose ultraviolet absorption changes with acidity in a fashion similar to that shown in Fig. 2 (16).

Thiolactams thus prove to be considerably weaker bases than the corresponding lactams (2), the greater intrinsic basicity of the oxygen atom evidently being more important than the greater negative charge on the sulphur atom. The change in basicity of thiolactams with ring size parallels the charge in basicity of lactams with ring size, as shown in Fig. 3. (In this figure pK_{BH^+} values of lactams (2) obtained by the indicator

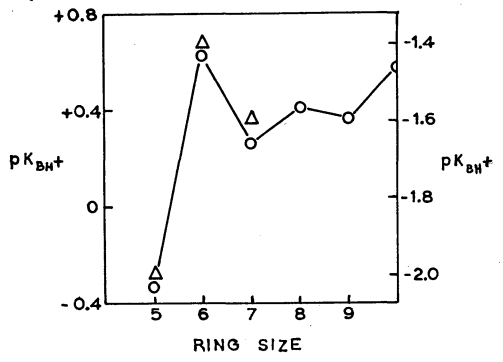

FIG. 3. Relation of protonation constants of lactams (○, left-hand scale) and of thiolactams (△, right-hand scale) to ring size.

method of Lemaire and Lucas (17) are used.) It is accordingly possible that the reasons given by Huisgen and his co-workers (2) for the variation in basicity of lactams with

Can. J. Chem. Downloaded from www.nrcresearchpress.com by 210.87.254.42 on 09/05/12
For personal use only.

ring size apply also to thiolactams. For the very limited data available the basicities of thiolactams are given with fair precision by the equation

$$pK_{BH^+}\text{ (thiolactam)} = 0.62pK_{BH^+}\text{ (lactam)} - 1.8. \quad [5]$$

No simple relationship is discernible between the dipole moments of lactams (18) or thiolactams (3) and their basicities.

ACKNOWLEDGMENTS

We are grateful to Professor G. C. B. Cave for the loan of equipment, and to the National Research Council for financial support.

REFERENCES

1. L. Pauling. The nature of the chemical bond. 3rd ed. Cornell University Press, Ithaca, N.Y. 1960. p. 281.
2. R. Huisgen, H. Brade, H. Walz, and I. Glogger. Chem. Ber. **90**, 1437 (1957).
3. C. M. Lee and W. D. Kumler. J. Org. Chem. **27**, 2052 (1962).
4. A. R. Katritzky and R. A. Y. Jones. Chem. Ind. (London), 722 (1961).
5. J. W. Cornforth, G. D. Hunter, and G. Popjak. Biochem. J. **54**, 590 (1953).
6. J. Tafel and P. Lawaczeck. Ber. **40**, 2842 (1907).
7. J. Prochazka. Chem. Tech. (Berlin), **7**, 19 (1955); Chem. Abstr. **50**, 4160 (1956).
8. H. J. Cambpell and J. T. Edward. Can. J. Chem. **38**, 2109 (1960).
9. J. T. Edward and I. C. Wang. Can. J. Chem. **40**, 966 (1962).
10. S. J. Yeh and H. H. Jaffe. J. Am. Chem. Soc. **81**, 3274 (1959).
11. M. J. Janssen. Rec. Trav. Chim. **79**, 454, 464, 1066 (1960).
12. S. Nagakura, A. Minegishi, and K. Stanfield. J. Am. Chem. Soc. **79**, 1033 (1957).
13. D. Rosenthal and T. I. Taylor. J. Am. Chem. Soc. **79**, 2684 (1957).
14. L. A. Flexser, L. P. Hammett, and A. Dingwall. J. Am. Chem. Soc. **57**, 2103 (1935).
15. L. P. Hammett and A. J. Deyrup. J. Am. Chem. Soc. **54**, 2721 (1932).
16. J. T. Edward and I. C. Wang. Unpublished researches.
17. H. Lemaire and H. J. Lucas. J. Am. Chem. Soc. **73**, 5198 (1951).
18. R. Huisgen and H. Walz. Chem. Ber. **89**, 2616 (1956).

Can. J. Chem. Downloaded from www.nrcresearchpress.com by 210.87.254.42 on 09/05/12
For personal use only.

PYRAZOLINES

PART III. THE PREPARATION AND PYROLYSIS OF 4,5-DIMETHYL-3-CARBOMETHOXY-Δ^2-PYRAZOLINE AND 3,5-DIMETHYL-3-CARBOMETHOXY-Δ^1-PYRAZOLINE

DONALD E. MCGREER, PETER MORRIS, AND GEORGE CARMICHAEL
Department of Chemistry, University of British Columbia, Vancouver, British Columbia
Received November 1, 1962

ABSTRACT

4,5-Dimethyl-3-carbomethoxy-Δ^2-pyrazoline and 3,5-dimethyl-3-carbomethoxy-Δ^1-pyrazoline have been synthesized and pyrolized neat and in the vapor phase. The product analysis from these and a related dimethyl-3-carbomethoxypyrazoline indicate that substituent effects of methyls in the ring are cumulative.

Can. J. Chem. Downloaded from www.nrcresearchpress.com by 210.87.254.105 on 09/05/12
For personal use only.

In an earlier study (1) it has been shown that of the methyl 3-carbomethoxypyrazolines studied the compound with methyl substitution at 3 gives a higher proportion of cyclopropane derivative in the product than was obtained from 3-carbomethoxy-Δ^2-pyrazoline. However, substitution by methyl at position 5 has little effect on the proportion of cyclopropane derivative and substitution at position 4 gives a reduced proportion of cyclopropane product. It is of interest to see if these effects are cumulative and for this reason we have investigated the pyrolysis of the dimethyl-substituted 3-carbomethoxypyrazolines I and II.

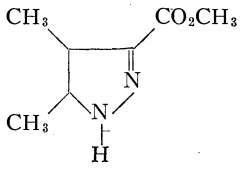

I

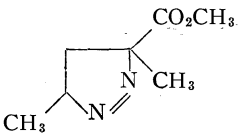

II

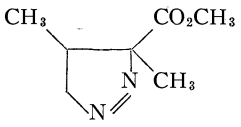

III

4,5-Dimethyl-3-carbomethoxy-Δ^2-pyrazoline (I) was prepared by the addition of diazoethane to methyl *trans*-crotonate. The stereochemistry in the pyrazoline was not determined but would be expected to be mainly with the methyls trans since these groups would be in close proximity in the transition state leading to the pyrazoline.

Pyrolysis of I (the pyrolysis of I has been reported (2) to give methyl 3-methyl-3-pentenoate as the sole product) gave the products indicated in Chart I in the proportions listed in Table I. These products were isolated by vapor chromatography and identified on the basis of their physical and chemical properties. The cyclopropane derivatives having methyls cis and trans (IX and VIII) were characterized through a comparison with the physical properties and infrared spectra reported for these compounds by Doering (3). The unsaturated esters were readily identified from their n.m.r. and infrared spectra.

The α,β-unsaturated esters (IV and V) showed carbonyl absorption at 1702 cm^{-1} and carbon–carbon double-bond absorption near 1645 cm^{-1}, and the n.m.r. spectra were in agreement with the structural assignments given by Wagner and Moore (4).

The β,γ-unsaturated esters (VI and VII) showed carbonyl absorption at 1725 cm^{-1} and weak carbon–carbon double-bond absorption at 1665 cm^{-1}. The n.m.r. spectra were

as expected for the isomeric methyl 3-methyl-3-pentenoates and excluded the possibility that one of these isomers was methyl 3-ethyl-3-butenoate. The stereochemistry of the β,γ-isomers was determined by the following sequence of steps.

Bromination of tiglic acid (methyl groups cis) under conditions to give trans bromination gave 2-methyl-2,3-dibromobutanoic acid. This acid was converted with thionyl chloride to the acid chloride and then by treatment with diazomethane to the diazoketone. Treatment of the dibromodiazoketone with silver oxide in methanol gave a mixture of brominated products. Reaction of this mixture with zinc gave a debrominated product from which was isolated methyl tiglate and the isomeric methyl 3-methyl-3-pentenoates in the ratio of 1:10. The major isomer was assigned the trans structure on the basis of earlier demonstrations of trans stereochemistry in the zinc debromination of 2,3-dibromobutane (5).

All of the unsaturated esters found in the product from the pyrazoline pyrolysis were also formed in the dehydration of methyl 3-methyl-3-hydroxypentanoate with phosphorus pentoxide by the procedure of Kon and Nargund (6). Under these conditions the β,γ-unsaturated esters formed 72% of the product (ref. 4 reports 61%). From the dehydration product there was isolated, in addition to the four unsaturated esters described above, a compound with infrared bands at 1725 and 1650 cm^{-1} believed to be methyl 3-ethyl-3-butenoate.

3,5-Dimethyl-3-carbomethoxy-Δ^1-pyrazoline (II) was prepared by the addition of diazoethane to methyl methacrylate. The n.m.r. of this pyrazoline showed it to be a 60:40 mixture of the two possible isomers; however, it was not possible to determine which was present to the greater extent.

Pyrolysis of II gave the products indicated in Chart I in the proportions listed in Table I. These products were isolated and identified on the basis of their physical constants. The low yield of the unsaturated esters prevented complete identification of these esters and thus the structural assignments are tentative. The cyclopropane derivatives having the methyls cis and trans (XIV and XIII) were characterized by comparison of their physical properties with those obtained by van Auken and Rinehart (7, 8).

The major unsaturated ester product showed infrared bands at 1700 and 1645 cm^{-1} indicative of an α,β-unsaturated ester. The n.m.r. was consistent with the structure methyl 2-methyl-*trans*-2-pentenoate (X) since the methyl hydrogens at C_4 gave a value of 7.94 τ (compare 7.73 τ for methylene hydrogens trans to the carbomethoxy group in methyl *trans*-3-methyl-2-pentenoate and 7.45 τ for methylene hydrogens cis to the carbomethoxy group in methyl *cis*-3-methyl-2-pentenoate).

A second unsaturated ester which was isolated (infrared bands at 1705 and 1641 cm^{-1}) was tentatively assigned the structure methyl 2-methyl-*cis*-2-pentenoate (XI). Insufficient sample was obtained for an n.m.r. spectrum.

A final sample (infrared bands at 1725 and 967 cm^{-1}) was isolated but could not be completely characterized. However, the infrared spectrum suggests that it is methyl *trans*-2-methyl-3-pentenoate (XII).

The product analyses reported in Table I when compared to the analyses of the products from the monomethyl pyrazolines (1) suggests that indeed the effects of methyl substitution are cumulative, although I yielded a higher proportion of cyclopropanes than might have been predicted. The product composition from a pyrolysis is somewhat influenced by the stereochemistry of the pyrazoline (see the results of van Auken and Rinehart given in Table I); however, in general it should now be possible to predict the usefulness of the pyrazoline method for synthesizing cyclopropane derivatives with a

Can. J. Chem. Downloaded from www.nrcresearchpress.com by 210.87.254.105 on 09/05/12
For personal use only.

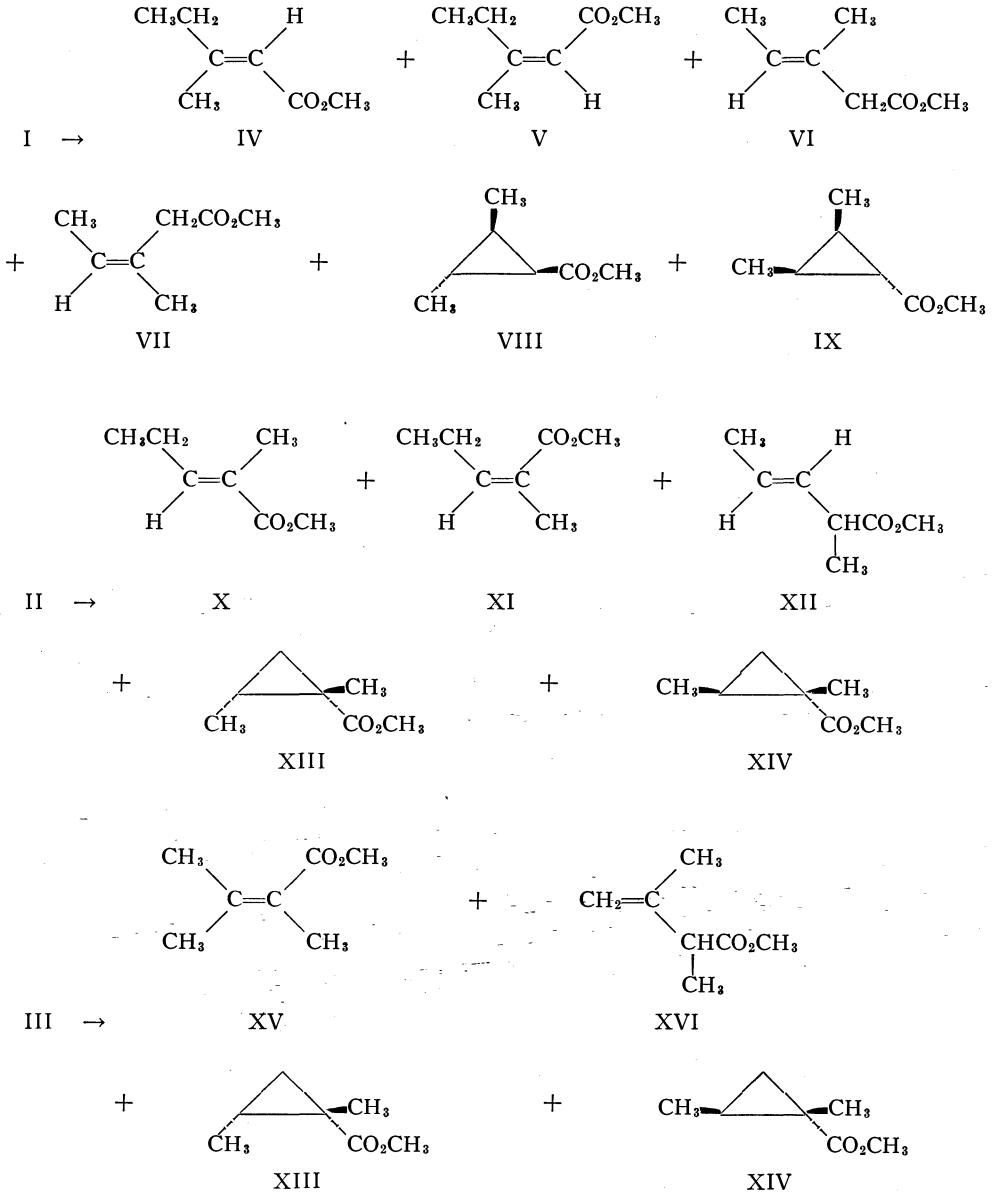

CHART I

variety of alkyl substituents. A number of examples in the literature (9–14) fit in well with the general trends found in this work.

Vapor phase pyrolysis of I and II yielded a higher proportion of cyclopropane derivative than was obtained in the liquid phase, proving again that this is a useful modification of the pyrolysis procedure. It has been found that 20-mesh firebrick makes an excellent column packing for the pyrolysis of Δ^2-pyrazolines in the vapor phase. Presumably there are sufficient acid sites on the firebrick to catalyze the tautomerism of the Δ^2-pyrazoline into the pyrolizable Δ^1-form.

Can. J. Chem. Downloaded from www.nrcresearchpress.com by 210.87.254.105 on 09/05/12
For personal use only.

TABLE I

Product compositions for the pyrolysis of dimethyl-3-carbomethoxypyrazolines

Pyrazoline	Phase	Unsaturated esters α,β		Unsaturated esters β,γ		Cyclopropanes	
		IV	V	VI	VII	VIII	IX
I	Liquid	25	26	2	3	27	16
	Vapor	15	14	2	2	43	24
		X	XI	XII		XIII	XIV
II	Liquid	15	10	3		27	45
	Vapor	2	3	1		42	53
		XV		XVI		XIII	XIV
III (methyls cis)*	Liquid	66		4		12	18
III (methyls trans)*	Liquid	33		4		35	28

*Reference 8.

EXPERIMENTAL

Melting points and boiling points are uncorrected. Most boiling points were determined by the micro inverted capillary method. Infrared spectra were measured with a Perkin–Elmer Model 21 spectrometer using sodium chloride optics. The n.m.r. spectra were recorded on a 40 Mc/s Varian spectrophotometer with field stabilizer VK 3506, and the methylene chloride used as an external standard was observed to have a value of 4.60 τ. The vapor chromatography unit was an Aerograph A-100-C.

4,5-Dimethyl-3-carbomethoxy-Δ^2-pyrazoline

Methyl crotonate was reacted with diazoethane in ether prepared from ethyl nitrosourea. After distillation of the ether the product was distilled to give a yellow solid, m.p. 46–47° and b.p. 101–102° at 1.8 mm (lit. (15) b.p. 139–140 at 14 mm). The infrared spectrum showed bands at 3400, 1710, and 1557 cm^{-1} characteristic of a 3-carbomethoxy-Δ^2-pyrazoline (1, 16).

Pyrolysis of 4,5-Dimethyl-3-carbomethoxy-Δ^2-pyrazoline

Pyrolyses in the liquid and vapor phase were carried out as reported earlier except that 20-mesh firebrick was used as the packing material in the vapor phase pyrolysis apparatus. The product compositions are reported in Table I. The product from the liquid phase pyrolysis (12 g, b.p. 140–165°, from 17 g of pyrazoline) was separated into five components using a dinonyl phthalate column, and one of these fractions was further separated into two components with a Ucon Polar column. The components were identified as indicated below, where boiling point, refractive index, retention time in the vapor chromatogram using a 10-ft dinonyl phthalate column of 0.25-in. diameter at 116° with a helium flow rate of 67 cc/min, and infrared bands for 5% solutions in chloroform are given.

Methyl *trans*-3-methyl-2-pentenoate: b.p. 160°, n_D^{25} 1.4424 (lit. (4) b.p. 79° at 50 mm, n_D^{20} 1.4446), 44.8 minutes, 1702 and 1647 cm^{-1}. The n.m.r. spectrum (0.5 ml per ml of carbon tetrachloride) showed vinyl hydrogen signals at 4.55 τ (singlet), ester methyl hydrogens at 6.36 τ (singlet), methylene hydrogens at 7.73 τ (quartet with $J \simeq 7$ c.p.s.), and alkyl methyl hydrogens at 7.70 τ (singlet) and 8.66 τ (triplet with $J \simeq 7$ c.p.s.).

Methyl *cis*-3-methyl-2-pentenoate: b.p. 151°, n_D^{23} 1.4409 (lit. (4) b.p. 74° at 50 mm, n_D^{20} 1.4420), 36.8 minutes (67.2 minutes on a 10-ft Ucon Polar column at 112° and a flow rate of 45 cc/min), 1702 and 1645 cm^{-1}. The n.m.r. spectrum (0.30 ml per ml of carbon tetrachloride) showed a vinyl hydrogen signal at 4.51 τ (singlet) and peaks for the ester methyl hydrogens at 6.46 τ (singlet), methylene hydrogens at 7.45 τ (quartet with $J \simeq 6.9$ c,p.s.), and alkyl methyl hydrogens at 8.22 τ (singlet) and 8.19 τ (triplet with $J \simeq 7$ c.p.s.).

Methyl *cis*-3-methyl-3-pentenoate: b.p. 148°, n_D^{20} 1.4321, 29.6 minutes, 1725 and 1665 (weak) cm^{-1}. Calc. for $C_7H_{12}O_2$: C, 65.49; H, 9.45. Found: C, 65.65; H, 9.41. The n.m.r. spectrum (0.33 ml per ml of carbon tetrachloride) showed vinyl hydrogen signals at 4.70 τ (multiplet), ester methyl hydrogens at 6.40 τ (singlet), methylene hydrogens at 7.07 τ (singlet), and methyl hydrogens at 8.29 τ (singlet) and 8.43 τ (doublet with $J \simeq 6.8$ c.p.s.). This ester was assigned the cis structure on the basis of the synthesis of the trans ester described below.

Methyl *trans*-3-methyl-3-pentenoate: b.p. 150°, n_D^{21} 1.4323, (lit. (17) b.p. 74° at 50 mm, n_D^{20} 1.4306), 33.6 minutes, 1725 and 1665 (weak) cm^{-1}. Calc. for $C_7H_{12}O_2$: C, 65.49; H, 9.45. Found: C, 65.43; H, 9.51. The n.m.r. spectrum (0.50 ml per ml of carbon tetrachloride) showed vinyl hydrogen signals at 4.67 τ (multiplet), ester methyl hydrogens at 6.41 τ (singlet), methylene hydrogens at 7.14 τ (singlet), and methyl hydrogens at 8.33 τ (singlet) and 8.42 τ (doublet with $J \simeq 7$ c.p.s.). The trans geometry of this ester was assigned on the basis of its synthesis from tiglic acid (see below).

Methyl *trans*-1,2-cyclopropane-3-carboxylate: b.p. 143°, n_D^{25} 1.4241 (lit. (3) b.p. 40–50 at 20 mm, n_D^{20}

Can. J. Chem. Downloaded from www.nrcresearchpress.com by 210.87.254.105 on 09/05/12
For personal use only.

1.4252), 26.0 minutes; infrared bands found at 1365, 1302, 1165, 1095, and 1055 cm^{-1} are not found in the spectra of the other cyclopropane isomer (lit. (18) reports bands at 1363, 1302, 1164, 1093, and 1055 cm^{-1} for this isomer). The n.m.r. spectrum (0.50 ml per ml of carbon tetrachloride) showed signals assigned to the ester methyl hydrogens at 6.49 τ (singlet) and the remaining hydrogens in a group at 9.05 τ.

Methyl *cis*-1,2-dimethyl-3-*trans*-carboxylate: b.p. 150° at 759 mm, n_D^{18} 1.4330 (lit. (3) n_D^{20} 1.4306), 36.8 minutes (70.8 minutes on a 10-ft Ucon Polar column at 112° and a flow rate of 45 cc/min); infrared bands found at 1325, 1125, 1085, and 1040 cm^{-1} are not found in the spectra of the other cyclopropane isomer (lit. (18) reports bands at 1322, 1128, 1089, and 1040 cm^{-1} for this isomer and 1378, 1158, 1115, 1093, and 1026 cm^{-1} for methyl *cis*-1,2-dimethyl-3-*cis*-carboxylate). The n.m.r. spectrum (0.20 ml per ml of carbon tetrachloride) showed signals assigned to the ester methyl hydrogens at 6.42 τ (singlet) and the remaining hydrogens in a group at 8.9 τ.

Methyl trans-3-Methyl-3-pentenoate

Tiglic acid (30 g, 0.3 mole) in carbon tetrachloride was brominated with 48 g of bromine (0.3 mole) by the procedure of Buckles and Mock (19) to give 63 g (83%) of 2,3-dibromo-2-methylbutanoic acid, m.p. 85–88° (lit. (19) m.p. 82–88°).

2,3-Dibromo-2-methylbutanoyl chloride (62 g, 86%), b.p. 73–74° at 14 mm, was prepared by refluxing 39 g of thionyl chloride with 63 g of the acid. Calc. for $C_5H_7OBr_2Cl$: C, 21.54; H, 2.51. Found: C, 21.69; H, 2.38.

Methyl 2,3-dibromo-3-methylpentanoate.—2,3-Dibromo-2-methylbutanoyl chloride (36 g, 0.12 mole) was reacted with an ether solution containing 13 g of diazomethane at 0–5°. The solution was let stand for 12 hours and the ether distilled. Anhydrous methanol (200 ml) was added to the oily diazoketone and the solution stirred and warmed on a water bath. Silver oxide (50 g as a slurry in anhydrous methanol) was added in portions to the hot methanolic solution. After it was cooled the methanol solution was decanted from the silver residues, filtered through alumina to remove colloidal silver and silver salts, and distilled to give 13.6 g of a product, b.p. 62–64° at 2 mm. The n.m.r. spectra, the analysis, and the debromination results showed this to be a mixture of brominated esters. Calc. for $C_7H_{12}O_2Br_2$: C, 29.18; H, 4.20. Found: C, 36.39; H, 5.10. Further purification by V.P.C. was found not practical.

Methyl trans-3-methyl-3-pentenoate.—A mixture of 7 g of the brominated esters, 10 g of 20-mesh zinc, and 30 ml of water was stirred in the dark according to the procedure of Schubert *et al.* (5) for 20 hours. The product was extracted with ether and filtered. The ether solution was washed with water, dried over sodium sulphate, filtered, and distilled to give 2 g of product, b.p. 38–49° at 40 mm. Vapor chromatography of the product showed the presence of three components in the ratio of 11:1:10. The first component was identified as methyl tiglate, n_D^{28} 1.4346, b.p. 141° (lit. (20) b.p. 139.4–139.6°, n_D^{20} 1.4370). The infrared spectrum was identical with that of an authentic sample. The second component was shown by its V.P.C. retention time and infrared spectrum to be identical with the lower-boiling methyl 3-methyl-3-pentenoate. The third component, n_D^{25} 1.4308, b.p. 152°, had a V.P.C. retention time and infrared spectrum identical with those of the higher-boiling methyl 3-methyl-3-pentenoate. Because of the absence of methyl angelate in the debromination and the known stereochemical requirements of the debromination reaction (5), the higher-boiling isomer of methyl 3-methyl-3-pentenoate was assigned the trans structure. The cis and trans esters show some differences in the fingerprint region of their infrared spectra. Particularly, there is a band at 1380 cm^{-1} for the trans ester which is much stronger than any band near this region for the cis ester. For the trans ester below 1500 cm^{-1} bands are found at 1433 (s), 1510 (w), 1380 (m), 1330 (m), 1296 (m), 1255 (s), 1220 (m), 1188 (m), 1150 (s), 1112 (vw), 1090 (w), 1035 (m), 1002 (m), and 957 (w) cm^{-1} and for the cis ester at 1432 (s), 1420 (sh), 1372 (w), 1350 (vw), 1315 (m), 1285 (m), 1245 (s), 1192 (m), 1150 (s), 1175 (m), 1035 (w), and 1005 (m).

Methyl 3-Methyl-2- and -3-pentenoates from Methyl 3-Methyl-3-hydroxypentanoate

Methyl 3-methyl-3-hydroxypentanoate (28 g, 0.19 mole) prepared by the procedure of Kuhn *et al.* (21) was refluxed in 125 ml of benzene with 3 g of phosphorus pentoxide for 5 hours (6). Distillation gave 17 g (70%) of a methyl 3-methylpentenoate mixture, b.p. 145–160°.

Separation of the mixture by vapor chromatography on a dinonyl phthalate column gave:

Methyl *trans*-3-methyl-2-pentenoate: b.p. 160°, n_D^{25} 1.4425, 19%
Methyl *cis*-3-methyl-2-pentenoate: b.p. 150°, n_D^{17} 1.4431, 9%
Methyl *cis*-3-methyl-3-pentenoate: b.p. 148°, n_D^{25} 1.4307, 26%
Methyl *trans*-3-methyl-3-pentenoate: b.p. 150°, n_D^{25} 1.4302, 38%

Methyl 3-ethyl-3-butenoate (?): b.p. 146°, n_D^{23} 1.4261. Infrared bands at 1725, 1650, 1420, and 897 cm^{-1} indicate this to be a β,γ-unsaturated ester with a terminal double bond; however, insufficient sample was obtained for analysis.

3,5-Dimethyl-3-carbomethoxy-Δ^1-pyrazoline

Methyl methacrylate was reacted with diazoethane in ether and the product distilled to give a colorless liquid, b.p. 54° at 0.5 mm. Calc. for $C_7H_{12}N_2O_2$: C, 53.83; H, 7.74; N, 17.94. Found: C, 53.75; H, 7.91;

Can. J. Chem. Downloaded from www.nrcresearchpress.com by 210.87.254.105 on 09/05/12
For personal use only.

N, 18.11. The n.m.r. spectrum showed this to be a mixture of the two possible isomers (C_5-methyl cis or trans to the carbomethoxy group) with peaks at 4.28, 4.34 τ (ester methyl), 8.53, 8.51 τ (doublet for C_5-methyl), 8.64, 8.39 τ (C_3-methyl), and 5.45 τ (multiplet), 7.69 τ (multiplet), and 9.26 τ (multiplet) for the various ring protons. The proportion of these isomers was 3:2 as determined by integration of the peaks. Where two signals are reported the larger signal is given first. It is felt that this data is not sufficient to permit designation of the isomer present in the larger amount as cis or trans.

Pyrolysis of 3,5-Dimethyl-3-carbomethoxy Δ^1-pyrazoline

Pyrolysis in the liquid phase was vigorous at 120°. In the gas phase the pyrolysis was carried out using a packing of glass beads and a pressure of 5 mm (1). The product compositions are reported in Table I. The product from the liquid phase pyrolysis (8 g from 11 g of pyrazoline) was separated into five components using a dinonyl phthalate column. The components were identified or partially identified as indicated below, where boiling point, refractive index, retention time in the vapor chromatogram using a 10-ft dinonyl phthalate column of 0.25-in. diameter at 98° with a helium flow rate of 55 cc/min, and infrared bands for 5% solutions in chloroform are given.

Methyl *trans*(?)-2-methyl-2-pentenoate: b.p. 156°, n_D^{24} 1.4394, 58 minutes, 1700 and 1645 cm^{-1}. Calc. for $C_7H_{12}O_2$: C, 65.49; H, 9.45. Found: C, 65.27; H, 9.45. The n.m.r. spectrum (0.05 ml per ml of carbon tetrachloride) had a triplet signal in the olefin region at 3.48 τ with $J \simeq 7.5$ c.p.s. Other peaks were due to ester methyl hydrogens at 6.41 τ (singlet), methylene hydrogens at 7.94 τ (multiplet), and alkyl methyl hydrogens at 8.26 τ (singlet) and 9.04 τ (triplet with $J \simeq 7.2$ c.p.s.).

Methyl *cis*(?)-2-methyl-2-pentenoate: b.p. 143°, n_D^{24} 1.4351, 36 minutes, 1705 and 1641 cm^{-1}. Calc. for $C_7H_{12}O_2$: C, 65.49; H, 9.45. Found: C, 65.23; H, 9.46.

In addition there was a minor component at 31.6 minutes with b.p. 139°, n_D^{23} 1.4229, and infrared bands at 1725 and 967 cm^{-1}. The position of the carbonyl band and the absence of carbon–carbon double-bond stretch indicate that this is a symmetric non-conjugated unsaturated ester. The presence of the characteristic band at 967 cm^{-1} for trans olefins suggests that this is methyl *trans*-2-methyl-3-pentenoate.

Methyl *cis*-1,2-dimethyl cyclopropane-1-carboxylate: b.p. 145°, n_D^{20} 1.4314 (lit. (7) n_D^{25} 1.4289), 39.6 minutes, 1720 cm^{-1}. The infrared and n.m.r. spectra were identical with those obtained by Rinehart and van Auken (8).

Methyl *trans*-1,2-dimethylcyclopropane-1-carboxylate: b.p. 136°, n_D^{27} 1.4220 (lit. (7) n_D^{25} 1.4218), 26.4 minutes, 1720 cm^{-1}. The infrared and n.m.r. spectra were identical with those obtained by Rinehart and van Auken (8).

ACKNOWLEDGMENTS

The authors gratefully appreciate the support received for this work from the National Research Council of Canada and from the President's Committee on Research of the University of British Columbia.

Thanks are also extended to Mrs. M. Zell for determining the infrared spectra and to Mrs. A. Aldridge for carrying out some of the microanalyses.

REFERENCES

1. D. E. McGreer, W. Wai, and G. Carmichael. Can. J. Chem. **38**, 2410 (1960).
2. K. von Auwers and F. Konig. Ann. **496**, 252 (1932).
3. W. von E. Doering and T. Mole. Tetrahedron, **10**, 65 (1960).
4. R. B. Wagner and J. A. Moore. J. Am. Chem. Soc. **72**, 974 (1950).
5. W. M. Schubert, B. S. Rabinovitch, W. R. Larson, and V. A. Sims. J. Am. Chem. Soc. **74**, 4590 (1952). H. O. House and R. S. Ro. J. Am. Chem. Soc. **80**, 182 (1958).
6. G. A. R. Kon and K. S. Nargund. J. Chem. Soc. 2461 (1932).
7. K. L. Rinehart, Jr. and T. V. van Auken. J. Am. Chem. Soc. **82**, 5251 (1960).
8. K. L. Rinehart, Jr. and T. V. van Auken. Personal communication.
9. D. Gotkis and J. B. Cloke. J. Am. Chem. Soc. **56**, 2710 (1934).
10. W. G. Young, L. J. Andrews, S. L. Lindenbaum, and S. J. Cristol. J. Am. Chem. Soc. **66**, 810 (1944).
11. P. C. Guha and D. K. Sankaran. Ber. **71**, 2673 (1938).
12. H. L. Slates and N. L. Wender. J. Am. Chem. Soc. **81**, 5472 (1959).
13. K. Kocsis, P. G. Ferrini, D. Arigoni, and O. Jeger. Helv. Chim Acta, **43**, 2178 (1960).
14. G. Nomine and D. Bertin. Bull. Soc. Chim. France, **82**, 550 (1960).
15. K. von Auwers and E. Caver. Ann. **470**, 284 (1929).
16. J. A. Moore. J. Org. Chem. **20**, 1607 (1955).
17. R. B. Wagner and J. A. Moore. J. Am. Chem. Soc. **71**, 3214 (1949).
18. W. von E. Doering and T. Mole. Personal communication.
19. R. E. Buckles and G. V. Mock. J. Org. Chem. **15**, 680 (1950).
20. M. Naster and A. Gavriloff. Bull. Soc. Chim. Belges, **42**, 519 (1933).
21. R. Kuhn, F. Kohler, and L. Kohler. J. Physiol. Chem. **247**, 197 (1937).

Can. J. Chem. Downloaded from www.nrcresearchpress.com by 210.87.254.105 on 09/05/12
For personal use only.

THE CHEMILUMINESCENT REACTION OF ACTIVE NITROGEN WITH THALLOUS HALIDES[1]

L. F. PHILLIPS
Chemistry Department, University of Canterbury, Christchurch, New Zealand
Received October 22, 1962

ABSTRACT

Energy transfer from active nitrogen to gaseous thallous halides leads to dissociation of the halide molecules with simultaneous production of excited thallium atoms. Thallium emission lines have been observed to correspond to the transfer of up to 221 kcal/mole to the TlX molecule. The process is kinetically third order but the high overall efficiency of light emission and thallous halide destruction requires a mechanism which involves a bimolecular reaction of TlX with an excited N_2 formed during N-atom recombination.

INTRODUCTION

Photodissociation of gaseous metallic iodides by ultraviolet radiation has been used as a means of producing excited metal atoms for quenching measurements (1, 2). The present work is concerned with the analogous process in which energy from the recombination of atomic nitrogen takes the place of the ultraviolet radiation. Such a process may be visualized as occurring either through a single termolecular step,

$$TlX + N + N \rightarrow Tl^* + N_2 + X, \qquad [1]$$

or by a bimolecular reaction of TlX with an excited nitrogen molecule formed during N-atom recombination,

$$N + N + M \rightarrow N_2^* + M \qquad [2]$$

$$N_2^* + TlX \rightarrow N_2 + Tl^* + X. \qquad [3]$$

Here M signifies a third body, which will usually be N_2 or the wall of the reaction vessel.

Both of these mechanisms lead to overall third-order kinetics, provided the N_2^* molecule is not too long lived, but at low concentrations of TlX the second mechanism can lead to a faster rate than the first because of the high concentration of M relative to that of TlX. Reaction [1] cannot have a rate constant greater than about 10^{-31} cm^6 molecule^{-2}sec^{-1} (3), and, because the present observations will be shown to require a much higher value than this for the third-order rate constant, the first mechanism may be excluded. An alternative scheme, involving the formation of an intermediate NTlX complex, is regarded as equivalent to equation [1] in the present discussion.

In the case of the second mechanism the excited states of N_2 are sufficiently well known for it to be possible, in principle, to decide which excited state is taking part in the reaction by observing which energy levels of thallium are able to be produced from halides of various dissociation energies. The relevant dissociation energies of thallous halides (4), thallium energy levels (5), and excited states of N_2 (6, 7, 8) are summarized in Table I.

[1]*Financial support for this work was provided by the New Zealand University Research Grants Committee.*

Can. J. Chem. Downloaded from www.nrcresearchpress.com by 210.87.254.5 on 09/05/12
For personal use only.

TABLE I

Halide	D^0, kcal	Tl term	E, kcal	Allowed transitions	λ, Å	N_2 state	E (v=0), kcal
TlF	110	$6.^2P_{\frac{1}{2}}$	0	$7.^2S_{\frac{1}{2}}$–$6.^2P_{1\frac{1}{2}}$	5350	$X^1\Sigma_g^+$	0
TlCl	89	$6.^2P_{1\frac{1}{2}}$	22.3	$7.^2S_{\frac{1}{2}}$–$6.^2P_{\frac{1}{2}}$	3776	$A^3\Sigma_u^+$	142
TlBr	77	$7.^2S_{\frac{1}{2}}$	75.5	$6.^2D_{1\frac{1}{2}}$–$6.^2P_{1\frac{1}{2}}$	3530	$^3\Delta_u$	<171
TlI	68	$6.^2D_{1\frac{1}{2}}$	103.4	$6.^2D_{2\frac{1}{2}}$–$6.^2P_{1\frac{1}{2}}$	3519	$B^3\Pi_g$	171
		$6.^2D_{2\frac{1}{2}}$	103.7	$8.^2S_{\frac{1}{2}}$–$6.^2P_{1\frac{1}{2}}$	3230	$^5\Sigma_g^+$	222
		$8.^2S_{\frac{1}{2}}$	111.0	$6.^2D_{1\frac{1}{2}}$–$6.^2P_{\frac{1}{2}}$	2765	$N + N(^4S_{1\frac{1}{2}})$	225
				$8.^2S_{\frac{1}{2}}$–$6.^2P_{\frac{1}{2}}$	2580	$C^3\Pi_u$	255

EXPERIMENTAL

A diagram of the reaction vessel used for these experiments is given in Fig. 1. It consists of a 25-cm length of 34 mm o.d. quartz tubing with three quartz windows at one end. One window looks along the length of

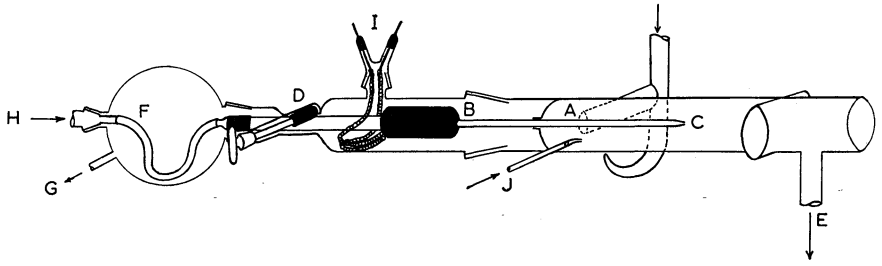

FIG. 1. Reaction vessel, heating jacket not shown. A, active nitrogen inlet; B, thallous halide oven; C, moveable inlet jet; D, rubber-covered rod, the rotation of which causes the thallous halide oven and inlet jet to move along the axis of the reaction tube; E, main pumping lead; F, flexible plastic tubing; G, subsidiary pumping lead; H, argon inlet; I, electrical leads for oven; J, fixed reactant inlet. Not drawn exactly to scale.

the tube and has been used for photographing spectra. Two parallel windows enable observations to be made at right angles to the gas stream. The tube is heated electrically to 400° C. Partially dissociated nitrogen from a microwave discharge passes a light trap and enters the reaction vessel at A. Thallous halide is carried by a slow stream of argon from the independently heated oven B through a 3-mm quartz tube to the inlet jet C, which can be moved along the axis of the reaction tube by rotating the rubber-covered rod D. A fixed jet J is provided for the addition of a third reactant such as nitric oxide. Reaction products are pumped away at E. Temperatures are measured by means of thermocouples in the heating jacket, gas stream, and thallous halide oven. Gas flows are controlled by needle valves and measured with capillary flowmeters.

Nitrogen-atom concentrations, as determined by visual titration with nitric oxide (9), vary from 0.02 to 0.05 mm for N_2 pressures of 1.5 to 6 mm Hg. The thallous halide concentration is calculated from the vapor pressure (10) at the known oven temperature, the argon flow, and the pressure drop across the inlet jet, and is generally about 10^{-4} mm Hg.

Emission spectra are photographed using a Hilger medium quartz spectrograph with Ilford Astra III plates. Exposures usually last 8 hours. The intensity of the thallium green line is measured using a 5350 Å interference filter and a 1P28 photomultiplier connected through a cathode follower to a 0–250 μamp meter.

Nitrogen is purified by being passed over hot, activated copper wool and through a liquid nitrogen trap. Nitric oxide is purified by distillation from KOH pellets at −80° C. Commercial 99.9% argon is used. Thallous chloride, bromide, and iodide are precipitated from hot solutions of recrystallized thallous sulphate by addition of the "Analar" brand potassium halides. Thallous fluoride is prepared by reacting excess thallium with "Analar" hydrofluoric acid in a platinum vessel, solid TlF being precipitated from the filtered solution by addition of ethanol.

Solid deposits are removed from the walls of the reaction vessel periodically by rinsing with 10% hydrofluoric acid.

RESULTS

With the discharge activated at low thallous halide flows the tip of the mobile jet was followed by an approximately spherical, bright green reaction flame. The yellow

Can. J. Chem. Downloaded from www.nrcresearchpress.com by 210.87.254.5 on 09/05/12
For personal use only.

nitrogen afterglow persisted in the region which followed the flame, so it is apparent that under these conditions thallium itself is not readily excited by active nitrogen. This is in contrast to previous experiments in which the metal was present in the discharge (11). At high thallous halide flows the green flame filled the reaction vessel.

In the cool part of the apparatus immediately beyond the reaction vessel a dark, lustrous solid was deposited. Microanalysis (carried out by Dr. A. D. Campbell of Otago University) of the solid formed during the thallous iodide reaction showed that 30.64% of iodine and 2.00% of nitrogen were present, corresponding to the formula $Tl_{3.0}I_{2.2}N_{1.3}$. A similar product from the reaction of active nitrogen with germane (12) consisted of amorphous Ge_2N_3. However, no nitride of thallium is known, and in the present case an X-ray powder photograph[2] indicated that the solid contained crystalline thallous halide and thallium metal. It seems likely, therefore, that the nitrogen in the material may be held physically rather than chemically.

In Fig. 2 is shown the dependence of the intensity of the 5350 Å line on the concentrations of thallous halide and atomic nitrogen. The results for thallous iodide (in Fig.

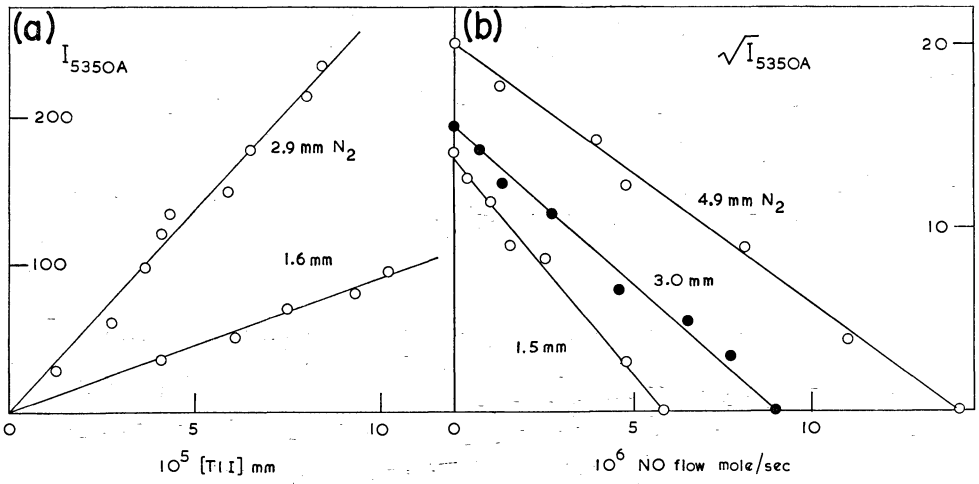

FIG. 2. Dependence of intensity of emission at 5350 Å on (*a*) thallous iodide concentration, and (*b*) N-atom concentration.

2*a*) show that the intensity is proportional to the first power of the halide concentration. Figure 2*b* shows the effect of reducing the N-atom concentration by adding various amounts of nitric oxide before the TlI inlet. Nitric oxide removes atomic nitrogen quantitatively (13) by reaction [4]. Graphs of the square root of intensity versus NO flow rate

$$N + NO \rightarrow N_2 + O \qquad [4]$$

are linear, showing that the intensity is proportional to the square of the N-atom concentration. Points for zero intensity are the NO flows which were found, in absence of TlI, to correspond exactly to removal of all N-atoms by reaction [4]. Preliminary experiments showed that no luminescent reaction occurred with thallous iodide and atomic oxygen (or hydrogen). During the addition of nitric oxide the photomultiplier was arranged to observe the reaction flame at a point sufficiently close to the TlI inlet for the results to be unaffected by variation in the amount of TlI consumed before the point of observation.

[2]*The author is indebted to Dr. B. R. Penfold of this department for the use of X-ray diffraction equipment.*

Can. J. Chem. Downloaded from www.nrcresearchpress.com by 210.87.254.5 on 09/05/12
For personal use only.

In order to determine the efficiency of the light-emitting process, the intensity at 400° C of the 5350 Å line at known TlI and N-atom concentrations was compared with the intensity at room temperature of the NO–O continuum (14) obtained by the addition of a known excess of nitric oxide to a stream of discharged nitrogen. The same filter was used for both intensity measurements. The fraction of the continuum passed by the filter was calculated from the wavelength variation of intensity in the continuum (15) and the transmission curve of the filter. The rate constant for emission of the continuum is 3×10^{-17} quanta $cm^3 molecule^{-1} sec^{-1}$ (16). The result obtained, expressed as

$$d[Tl(7.^2S_{\frac{1}{2}})]/dt = k_1[TlI][N]^2 - 7.2\times10^7[Tl(7.^2S_{\frac{1}{2}})], \quad [5]$$

was $k_1 = 1\times10^{-29}\ cm^6 molecule^{-2} sec^{-1}$. This is probably correct to within a factor of two. Allowance has been made for radiation emitted at 3776 Å (17). Quenching of $Tl(7.^2S_{\frac{1}{2}})$ is negligible at the pressures used in this work (1). At the steady state the left-hand side of equation [5] is zero. The total rate of production of excited thallium atoms will be several times greater than that given by the above value of k_1 because emission from $6.^2D_{1\frac{1}{2}}$, $6.^2D_{2\frac{1}{2}}$, and $8.^2S_{\frac{1}{2}}$ levels also occurs. Radiative transitions among these levels are forbidden.

A second estimate of k_1 is based on a measurement of the rate of consumption of TlI in the reaction, as indicated by the decrease of intensity of the reaction flame with distance from the TlI inlet. Since the N-atom concentration is invariably much greater than that of TlI it should be a good approximation to treat the intensity decay as first order, with a rate constant equal to $k_1[N]^2$. Logarithmic plots of intensity versus time from the TlI inlet are in fact linear, as is shown in Fig. 3. This linearity indicates that the species which reacts with TlI is either present in excess or is being produced continuously during the reaction. There is no obvious dependence of the slopes in Fig. 3 on N-atom or N_2 concentration. This is attributed to differences in the nature of the wall surface of the reaction vessel during the different sets of measurements. From a typical result of Fig. 3, namely that the slope of the log plot equals -28 for an N-atom concentration of 0.036 mm, the value of k_1 is $4\times10^{-29}\ cm^6 molecule^{-2} sec^{-1}$, in good agreement with the result of the intensity measurement. These values are too high for a termolecular reaction, and further discussion must be in terms of a bimolecular reaction of TlX with excited N_2.

Emission spectra of nitrogen afterglows and of the flames with thallium halides were photographed in order to determine how much energy was available to the excited species which reacted with the halide. If a number of different excited states are able to take part in the reaction then this approach will yield information only about the most energetic of them. Previous work in this field has shown that reactions with excited molecules in active nitrogen are likely to be quite specific with regard to the nature of the excited species involved (18). It will be assumed for the present that only one state of N_2 is important in the reaction with thallous halide.

The ordinary nitrogen afterglow consists largely of N_2 first positive system bands, arising from the $B(^3\Pi_g)$ level, with weak second positive system bands arising from the $C(^3\Pi_u)$ level (7). It was observed that the $(0,v'')$ progression of the latter system appeared strongly when the nitrogen was moist. In addition it was possible, with dry nitrogen, to produce the very energetic "pink afterglow" inside the reaction vessel, with enhanced first positive system emission and intense bands of N_2^+ (19).

All of the reaction flames showed the same features, namely the quenching of nitrogen afterglow emission and the appearance of strong lines of thallium at 5350, 3776, 3530,

Can. J. Chem. Downloaded from www.nrcresearchpress.com by 210.87.254.5 on 09/05/12
For personal use only.

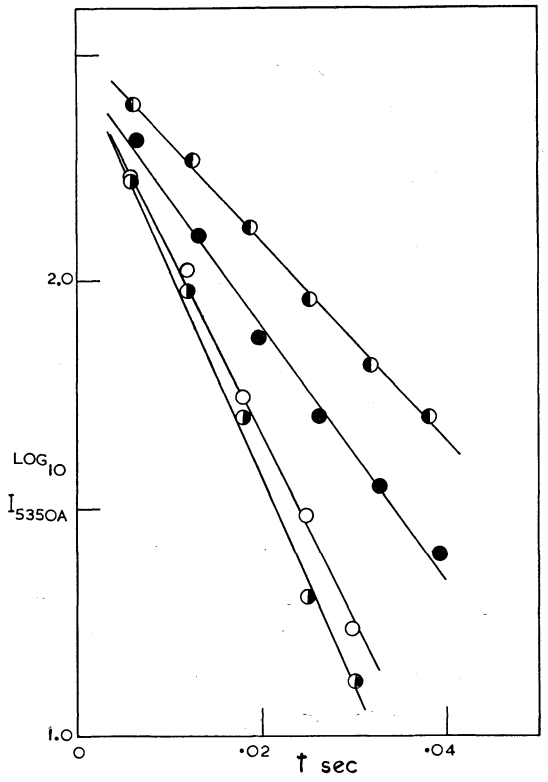

FIG. 3. Exponential decay of intensity of the 5350 Å line with time from the thallous iodide inlet. Points: ◑, 4.8 mm N_2, 0.045 mm N; ○, 2.0 mm N_2, 0.30 mm N; ●, 2.8 mm N_2, 0.036 mm N; ◐, 4.3 mm N_2, 0.052 mm N.

and 3519 Å, with a weaker line at 3230 Å. The resonance lines at 2765 and 2580 Å were too faint to be detected. With the "pink afterglow" the thallium emission was much more intense than usual, but no new lines appeared. Precise intensity comparisons among the various lines await the arrival of a photomultiplier carriage for the spectrograph.

Winkler and co-workers (18) have found that ammonia appears to react selectively with the $A(^3\Sigma_u^+)$ state of nitrogen, so that if the A state were taking part in the present reaction the addition of ammonia should bring about a reduction in the intensity of the thallium emission. In fact the addition of ammonia has been found to produce an increase in intensity for all of the emission lines, an effect which probably results from its action as a wall poison (18).

DISCUSSION

Inspection of Table I reveals that in order to produce thallium in the $8.^2S_{\frac{1}{2}}$ level from thallous fluoride the excited N_2^* molecule has to be able to provide at least 221 kcal/mole of energy. This eliminates the $A(^3\Sigma_u^+)$ state from consideration. Kenty (8) has presented evidence for the presence in discharged nitrogen of a metastable $^3\Delta_u$ state of N_2 having an energy of between 180 and 200 kcal/mole. This amount of energy would place it above the $B^3\Pi_g$ state and it would not be metastable, so in Table I the energy of the zeroth vibrational level of this state has been listed as less than 171 kcal. Only

Can. J. Chem. Downloaded from www.nrcresearchpress.com by 210.87.254.5 on 09/05/12
For personal use only.

the lowest vibrational levels would be sufficiently long lived to react with TlX, and these levels would not possess the 221 kcal/mole that is necessary to explain the observed reaction. Both the $B(^3\Pi_g)$ and the $^5\Sigma_g^+$ states are capable of providing this energy, the former because many molecules are produced in this state with 10, 11, or 12 vibrational quanta as a result of collision-induced radiationless transitions from the $^5\Sigma_g^+$ state (20, 7). Reaction of TlX with either of these states would explain the observed quenching of the afterglow in the region of the reaction flame. However, in the case of the B state the transfer of energy to the thallium halide would have to compete with an allowed radiative transition to the A state, whereas with the $^5\Sigma_g^+$ state the competition would be between reaction with TlX and two other collision-induced processes, namely dissociation to ground-state N-atoms and non-radiative transition to the B or lower state. The best value for the radiative lifetime of the B state (in the zeroth vibrational level) is 1.2×10^{-6} sec (21), so that at the halide concentrations used here the emission of radiation from the B state should have been at least two orders of magnitude more probable than collision with TlX. Wright and Winkler (22) have recently obtained evidence that the radiative lifetime of the $^5\Sigma_g^+$ state is about 0.02 sec. These considerations favor the choice of the $^5\Sigma_g^+$ state, and on this basis the mechanism of the reaction is:

$$N + N + M \xrightarrow{k_6} N_2(^5\Sigma_g^+) + M \quad [6]$$

$$N_2(^5\Sigma_g^+) + M' \xrightarrow{k_7} N + N + M' \quad [7]$$

$$N_2(^5\Sigma_g^+) + M'' \xrightarrow{k_8} N_2 + M'' \quad [8]$$

$$N_2(^5\Sigma_g^+) + TlX \xrightarrow{k_9} N_2 + Tl^* + X; \quad [9]$$

whence

$$-d[TlX]/dt = k_6.k_9.[M][N]^2[TlX]/(k_7[M']+k_8[M'']) \quad [10]$$

at low TlX concentrations. When quenching of excited thallium is ignored this is equal to

$$d[Tl^*]/dt + \sum_\lambda A_\lambda[Tl^*], \quad [11]$$

where A_λ is the Einstein transition probability for emission of radiation at wavelength λ, and $d(Tl^*)/dt$ is zero in the steady state. From equations [10] and [11] and the value found for k_1, it follows that if the above mechanism is correct,

$$k_9[M] > 10^2(k_7[M']+k_8[M'']), \quad [12]$$

since k^9 is a normal termolecular rate constant. This implies that the kinetic lifetime of a $^5\Sigma_g^+$ molecule in nitrogen at 2 mm pressure is greater than 10^{-5} sec.

In these expressions the effects of processes occurring on the walls are included in the various M terms. It is to be expected that variation in the nature of the wall surface, as a result of a deposition of solid material consisting largely of metallic thallium, will not affect each term to the same extent, and this expectation is borne out by the unsystematic variation of the slopes of the lines in Fig. 3.

REFERENCES

1. P. PRINGSHEIM. Fluorescence and phosphorescence. Interscience, New York. 1949.
2. D. J. DOWLING and E. WARHURST. Trans. Faraday Soc. **55**, 532 (1959).
3. J. C. POLANYI and C. M. SADOWSKI. J. Chem. Phys. **36**, 2239 (1962).

Can. J. Chem. Downloaded from www.nrcresearchpress.com by 210.87.254.5 on 09/05/12
For personal use only.

4. E. M. BULEWICZ, L. F. PHILLIPS, and T. M. SUGDEN. Trans. Faraday Soc. **57**, 921 (1962).
5. C. E. MOORE. N.B.S. circular 467. Vol. III. Washington. 1958.
6. G. HERZBERG. Spectra of diatomic molecules. 2nd ed. Van Nostrand, New York. 1950.
7. K. R. JENNINGS and J. W. LINNETT. Quart. Rev. (London), **12**, 116 (1958).
8. C. KENTY. J. Chem. Phys. **35**, 2267 (1961).
9. K. KAUFMAN and J. R. KELSO. J. Chem. Phys. **27**, 1209 (1957).
10. HANDBOOK OF CHEMISTRY AND PHYSICS. Chemical Rubber Publishing Co., Cleveland, Ohio. 1960.
11. C. KENTY. J. Chem. Phys. **23**, 1555 (1955).
12. R. STORR, A. N. WRIGHT, and C. A. WINKLER. Can. J. Chem. **40**, 1296 (1962).
13. G. B. KISTIAKOWSKY and G. G. VOLPI. J. Chem. Phys. **27**, 1141 (1957).
14. F. KAUFMAN. Progress in reaction kinetics. Vol. I. Pergamon Press, New York. 1961.
15. E. M. BULEWICZ. Ph.D. Dissertation, University of Cambridge, Cambridge, England. 1957.
16. A. FONTIJN and H. I. SCHIFF. International Symposium on the Chemistry of the Upper and Lower Atmosphere, San Francisco. April, 1961.
17. A. C. G. MITCHELL and M. W. ZEMANSKY. Resonance radiation and excited atoms. Cambridge University Press. 1934.
18. A. N. WRIGHT, R. L. NELSON, and C. A. WINKLER. Can. J. Chem. **40**, 1082 (1962).
19. G. E. BEALE and H. P. BROIDA. J. Chem. Phys. **31**, 1030 (1959).
20. G. B. KISTIAKOWSKY and P. WARNECK. J. Chem. Phys. **27**, 1417 (1957).
21. N. P. CARLETON and O. OLDENBERG. J. Chem. Phys. **36**, 3460 (1962).
22. A. N. WRIGHT and C. A. WINKLER. J. Chem. Phys. In press. 1963.

Can. J. Chem. Downloaded from www.nrcresearchpress.com by 210.87.254.5 on 09/05/12
For personal use only.

THE ALUMINUM REDUCTION OF MAGNESIUM COMPOUNDS

III. THE VAPOR PRESSURE OF MAGNESIUM OVER THE SYSTEM Al–Mg_2SiO_4 (OLIVINE)

K. GRJOTHEIM, O. HERSTAD, R. SKARBÖ, AND J. M. TOGURI[1]

Institute of Inorganic Chemistry, The Technical University of Norway, Trondheim, Norway

Received July 26, 1962

ABSTRACT

The equilibrium vapor pressure of magnesium over the reaction between olivine (Mg_2SiO_4) and aluminum was measured by means of the transportation method in the temperature range 943–1150° C.

It was concluded that olivine and aluminum form an unstable system which reacts completely according to the equation

$$3Mg_2SiO_{4(s)} + 4Al_{(l)} \rightarrow 2MgAl_2O_{4(s)} + 4MgO_{(s)} + 3Si_{(s)}.$$

However, in the presence of excess aluminum, an Al–Si alloy results. This alloy in turn reacts with magnesium oxide according to the equilibrium

$$4MgO_{(s)} + 2AlSi_{(l)} = MgAl_2O_{4(s)} + 3Mg_{(g)} + 2Si_{(s)}.$$

The vapor pressure of magnesium over this equilibrium system was found to obey the equation

$$\log P_{\text{mm of Hg}} = -\frac{7643}{T} + 7.06.$$

The aluminum activity of the Al–Si alloy along the liquidus line of the silicon side of the phase diagram has been calculated. Within the temperature range 943–1150° C this activity can be represented by the equation

$$\log a_{Al} = \frac{2455}{T} - 2.40.$$

INTRODUCTION

In the present investigation, the reduction of olivine with aluminum was examined. The reactions involved in this system are between condensed states, with the formation of a gaseous phase. The equilibrium vapor pressure of magnesium was therefore determined and the end products of the reaction were identified to establish the reaction scheme.

EXPERIMENTAL

Preliminary experiments indicated that the vapor pressure of magnesium over olivine and aluminum was about 11 mm of Hg at 1000° C. The well-established transportation method was therefore employed. The apparatus and procedures adopted have been fully described previously (1).

Argon (99.94%) was used as a carrier gas. The impurities CO_2 and H_2O were removed by passing the gas through ascarite and dehydrite towers respectively.

The aluminum powder (99.4%) was obtained from Merck, Germany. The olivine was obtained from A/S Olivin (Norway), with the following analysis, in weight percent: 48.0% MgO, 40.0% SiO_2, 7–8% FeO, 0.2–0.3% Cr_2O_3, 0.2% NiO, 0.1% Al_2O_3, 0.1% MnO, and 1.0% H_2O.

Since the reaction between iron oxide and aluminum is exothermic, it is reasonable that the iron oxide is readily reduced to form an aluminum–iron alloy. However, when a few experiments were performed with synthetic forsterite instead of olivine, the equilibrium vapor pressure of magnesium was identical with that over olivine and aluminum. The content of iron in the olivine therefore appears to have negligible influence on the equilibrium.

The olivine powder (−100 mesh) was dried at 1000° C for 1 hour, then mixed with aluminum in the required mole ratio, and ground in a ball mill for 12 hours. Finally, the mixture was pressed into briquettes, 2.0 cm in diameter by 1.0 cm in height, at a pressure of 500 kg/cm², then broken into pieces of approximately 5-mm size. Each charge contained about 150 g of such broken briquettes.

[1]*Presently associated with Noranda Research Centre, Pointe Claire, Quebec.*

Can. J. Chem. Downloaded from www.nrcresearchpress.com by 210.87.254.105 on 09/05/12
For personal use only.

Can. J. Chem. Downloaded from www.nrcresearchpress.com by 210.87.254.105 on 09/05/12
For personal use only.

RESULTS

(a) Vapor Pressure Measurements

The vapor pressure of magnesium was found to vary with the ratio of aluminum to olivine in the reaction mixture. Below a mole ratio of 4:3 (aluminum:olivine), no magnesium was obtained even at 1000° C. However, at a ratio of 2:1 and higher, the vapor pressure of magnesium was constant and a function of temperature only. Consequently, a ratio of 2:1 (aluminum:olivine) has been selected for the present investigation.

Below a temperature of 943° C consistent results could not be obtained, while above 1150° C the iron reaction tube was seriously attacked by the aluminum. The measurements were therefore confined within this temperature range.

The results of the vapor pressure measurements over olivine and aluminum are summarized in Table I. In Fig. 1 log P is plotted against the reciprocal of the absolute

TABLE I

Experimental vapor pressure of magnesium

T (°C)	P (mm of Hg)	T (°C)	P (mm of Hg)
943	6.01	1046	18.46
949	6.38	1100	30.95
953	6.67	1150	48.86
999	10.94		

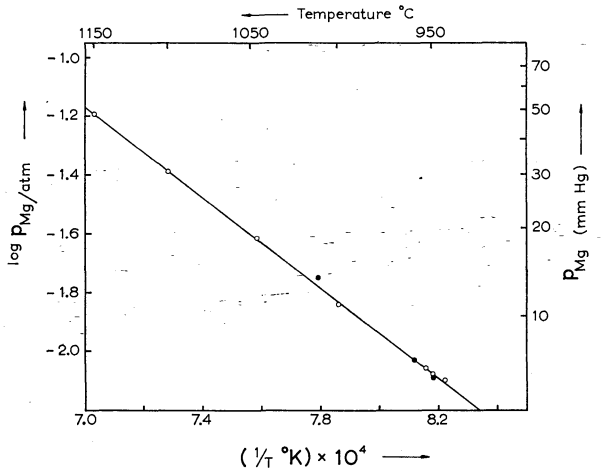

FIG. 1. Log(P_{atm}) of Mg versus $1/T$ (° K)×10^4: ○ Mg_2SiO_4 + Al; ● MgO + AlSiFe (Al: 0.38, Si: 0.54, Fe: 0.08 mole fraction).

temperature. The value of the equilibrium vapor pressure at each temperature is the result of a number of experiments at different flow rates. A least-square analysis of the results leads to a linear equation

$$\log P_{\text{mm of Hg}} = -\frac{7643}{T} + 7.06,$$

where P is pressure in mm of Hg and T is the absolute temperature.

(b) Analysis of the Reaction Products

X-Ray diffraction analysis was carried out on the solid residue. When the mole

ratio of aluminum to olivine was 4:3, large amounts of $MgAl_2O_4$, MgO, and Si and traces of metallic aluminum and olivine were present. As the aluminum was increased to the ratio 2:1, $MgAl_2O_4$, MgO, and Al–Si alloy were the only phases present.

DISCUSSION

To account for the present observations, a number of reactions can be formulated. One possible reaction to consider is reaction [I].

$$Mg_2SiO_{4(s)} + 2Al_{(l)} = MgAl_2O_{4(s)} + Si_{(s)} + Mg_{(g)} \quad [I]$$

From the available thermodynamic data (2), the ΔG^0 value at 1000° C is calculated to be −5 kcal. However, this would lead to an extremely large magnesium pressure and, further, would not explain the presence of magnesium oxide.

Reaction [II], on the other hand, will account for the observed magnesium oxide as well as the spinel and silicon.

$$Mg_2SiO_{4(s)} + 4/3\ Al_{(l)} = 2/3\ MgAl_2O_{4(s)} + 4/3\ MgO_{(s)} + Si_{(s)} \quad [II]$$

The value of the standard free energy change calculated for reaction [II] at 1000° C is −28 kcal. The reaction will therefore proceed completely to the right in agreement with the observed rapid reaction between olivine and aluminum. Reaction [II] also accounts for the absence of magnesium when the mole ratio Al:Mg_2SiO_4 is less than 4:3.

When larger amounts of aluminum than that required by reaction [II] are used, it appears reasonable that the excess aluminum forms an alloy with silicon. This alloy then reacts with magnesium oxide according to equation [III].

$$4MgO_{(s)} + 2AlSi_{(l)} = MgAl_2O_{4(s)} + 3Mg_{(g)} + 2Si_{(s)} \quad [III]$$

The measured vapor pressure of magnesium is therefore over the above equilibrium (equation [III]).

This was confirmed by determining the equilibrium between magnesium oxide and an aluminum–silicon alloy (Al: 0.38, Si: 0.54, Fe: 0.08). The measured vapor pressure of magnesium over this system, within the temperature range of the investigation, is identical with that over the present olivine and aluminum system. These results are shown in Fig. 1.

Using a mole ratio of Al:Mg_2SiO_4 of 2:1 should lead to an alloy containing Al:Si in a mole ratio 2:3. In the case of olivine the formed alloy also contains about 8 mole% iron, which together with silicon acts as a solute in aluminum. The phase diagram of the Al:Si:Fe system (3) shows that a liquid alloy of this composition is saturated with silicon at temperatures below 1200° C. On the basis that the measured pressure was found to be only a function of the temperature, the corresponding composition of the liquid alloy at each temperature is simply given by the liquidus line of the phase diagram.

At a constant temperature the phase diagram indicates that as the aluminum is consumed in reaction [III] silicon will also precipitate out from the liquid alloy in a manner such that the composition of the liquid alloy remains constant. It is therefore possible to use the Gibbs–Duhem relationship to calculate an approximate value for the activity of aluminum in the liquid alloy from the phase diagram combined with the knowledge of the heat of fusion of silicon.

However, a direct value of the activity of aluminum along the liquidus line on the silicon side of the phase diagram is obtainable, if the present vapor pressure measurements are combined with the previously reported magnesium pressure determinations

Can. J. Chem. Downloaded from www.nrcresearchpress.com by 210.87.254.105 on 09/05/12
For personal use only.

over the equilibrium system MgO–Al (1). The activity of aluminum along the liquidus is given by the expression

$$a_{Al} = \left(\frac{P_1}{P_0}\right)^{3/2},$$

where P_1 is the equilibrium magnesium pressure over reaction [III], and P_0 the equilibrium magnesium pressure over the system MgO–Al.

Substituting for the values of P, the activity of aluminum along the liquidus in the temperature range 943–1150° C is given by

$$\log a_{Al} = \frac{2455}{T} - 2.40.$$

Thus, at 950° C, $N_{Al} = 0.55$ and $a_{Al} = 0.41$ and similarly at 1150° C, $N_{Al} = 0.36$ and $a_{Al} = 0.21$.

CONCLUSION

Olivine and aluminum form an unstable system which in the presence of excess aluminum reacts completely according to the equation

$$3Mg_2SiO_{4(s)} + 6Al_{(l)} \rightarrow 2MgAl_2O_{4(s)} + 4MgO_{(s)} + 2AlSi_{(l)} + Si_{(s)}.$$

The products of this reaction form the equilibrium system

$$4MgO_{(s)} + 2AlSi_{(l)} = MgAl_2O_{4(s)} + 3Mg_{(g)} + 2Si_{(s)}.$$

In the temperature range 943–1150° C the equilibrium vapor pressure of magnesium is given by the equation

$$\log P_{\text{mm of Hg}} = -\frac{7643}{T} + 7.06.$$

The present results also permit an evaluation of the aluminum activities in the liquid Al–Si alloy at compositions along the liquidus line on the silicon side of the phase diagram. Within the temperature range 943–1150° C the activity is given by

$$\log a_{Al} = \frac{2455}{T} - 2.40.$$

ACKNOWLEDGMENTS

This investigation has been sponsored by the Norsk Metallurgisk Komité, to whom the authors are grateful.

REFERENCES

1. K. Grjotheim, O. Herstad, and J. M. Toguri. Can. J. Chem. **39**, 443 (1961).
2. O. Kubaschewski and E. L. Evans. Metallurgical thermochemistry. Pergamon Press Ltd., London. 1958.
3. S. Takeda and K. Mutuzaki. Tetsu To Hagane, **26**, 335 (1940).

Can. J. Chem. Downloaded from www.nrcresearchpress.com by 210.87.254.105 on 09/05/12
For personal use only.

THE SYSTEM ALUMINUM–ANTIMONY–BISMUTH

A. N. CAMPBELL AND J. WINKLER
Department of Chemistry, University of Manitoba, Winnipeg, Manitoba
Received September 12, 1962

ABSTRACT

A complete study, by the methods of thermal and isothermal analysis and of X-ray powder photography, has been made of the equilibrium diagram of the system aluminum–antimony–bismuth. The critical solution temperature and composition of the congruent liquids in the system aluminum–bismuth have been determined as have also the compositions of congruent liquids in the ternary system. The only compound occurring in this system is AlSb and the solid model is largely occupied by the equilibrium surface of this compound.

An explanation of the anomalous form of the solidus in the antimony–bismuth system is given.

Can. J. Chem. Downloaded from www.nrcresearchpress.com by 210.87.254.42 on 09/05/12
For personal use only.

The ternary alloy described by the title is based on the three binary systems aluminum–antimony, aluminum–bismuth, and antimony–bismuth. These systems are described briefly in what follows: complete bibliographies are given under References.

In the system aluminum–antimony, the compound AlSb, melting congruently at 1060° C, is formed. This compound decomposes rapidly in moist air, forming $Al(OH)_3$ and hydrogen. The two eutectics lie very close to pure aluminum and pure antimony respectively, and the solid solubilities of aluminum in antimony and of antimony in aluminum are exceedingly small. The crystal structure of AlSb is face-centered cubic. The literature on the system is extensive (1).

The system aluminum–bismuth forms two liquid layers at all temperatures hitherto investigated (2). Kempf and van Horn give the monotectic temperature (equilibrium of liquid 1, liquid 2, and solid aluminum) as 657.1°. The solubility of bismuth in solid aluminum does not exceed 0.2%. In view of the close chemical similarity of bismuth and antimony it is perhaps surprising that aluminum and bismuth do not form a compound analogous to AlSb, but there is no evidence for the existence of such a compound.

The equilibrium diagram of the system antimony–bismuth has presented difficulties (3). Alternative diagrams are shown in Fig. 1. There is no doubt that the liquidus is continuous

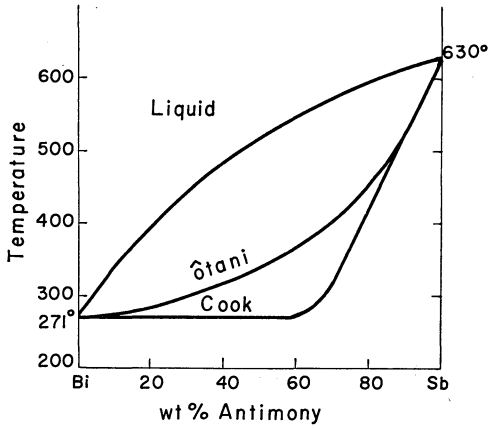

FIG. 1.

and therefore one would expect that the solidus would also be so. Thermal analysis, however, as applied for instance by Cook, results in a solidus as shown in Fig. 1, that is, unbroken but horizontal up to 60% antimony. Otani, however, using the method of electrical resistance, obtains a solidus which may be described as normal, i.e. temperature rises continuously with increasing antimony content. X-Ray analysis shows that the (solid) system antimony–bismuth consists of one phase only, corresponding to a complete series of solid solutions. An explanation is offered in the present work of the apparently abnormal form of the solidus, which results from thermal analysis on cooling.

The ternary system aluminum–antimony–bismuth has received little attention (4). Some preliminary work by Wright yielded nothing of importance. Some experiments were done by Kasten and these were offered, in an idealized form, as a practical illustration in a paper by Ritzau on the representation of quaternary systems.

EXPERIMENTAL

Aluminum was obtained from the Department of Mines and Technical Surveys, Mines Branch, Ottawa, and was stated to have the following composition: Al, 99.9945; Fe, 0.0019; Si, 0.0018; Cu, 0.0018%. The antimony used was Fisher Certified Reagent, the analysis being: Sb, 99.8; As, 0.0004; Cu, 0.001; Pb, 0.04; Fe, 0.0025%. The bismuth was also Fisher Certified Reagent with impurities given as: As, 0.0001; Cu, 0.002; Fe, 0.002; Pb, 0.005; Sb, 0.005%.

For the lower-temperature work, iron–constantan thermocouples were used, standardized by the freezing points of pure tin and pure cadmium. For the high-temperature work, thermocouples of platinum – platinum rhodium (10% Rh) were used. They were standardized from the freezing points of tin, cadmium, zinc, antimony, and silver, the last metal being allowed to freeze under a stream of hydrogen.

For thermal analysis, a Honeywell Brown single-pen recorder was used. The thermocouple was connected in parallel with the recorder and a vernier precision potentiometer, by means of a six-point switch, so that the temperatures corresponding to points of interest on the recorder diagram could be determined. The potentiometer had a sensitivity of ± 0.001 mv, corresponding to a temperature uncertainty of $\pm 0.05°$ C with the iron–constantan thermocouple and of $\pm 0.1°$ with the less sensitive platinum – platinum rhodium thermocouple. The accuracy of reading does not, of course, represent the accuracy of measurement, since all thermal analysis measurements suffer from supercooling effects, the amount of which it is difficult to estimate. Our results were, at least, all reproducible and we feel that they are accurate to within $\pm 1°$. A Hoskins combustion furnace (resistance type) was used for thermal and isothermal analysis but the alloys for investigation were prepared by melting appropriate weights of the pure metals, either under vacuum or in a current of argon, in an Ajax–Northrup high-frequency induction furnace.

For isothermal work, the resistance furnace was kept at constant temperature by means of a photocell, as described by Campbell and Kartzmark (5).

Thermal analysis was used only for the determination of the surface of primary crystallization of the compound AlSb. The alundum crucibles, in which the melts were contained, invariably ruptured on solidification of the alloy, because of the well-known expansion on solidification of bismuth and antimony. It was, therefore, not possible to repeat determinations with the identical alloy. As the compound AlSb forms from its components only very slowly at temperatures below the melting point of the compound, the procedure adopted was to add the compound itself to a mixture of aluminum and bismuth or of bismuth and antimony. For example, the composition of alloy No. 3, on the AlSb surface, was 20.0% Al, 50.0% Sb, and 30.0% Bi: the 80-g specimen therefore contained 16.0 g Al, 40.0 g Sb, and 24.0 g Bi. This composition was attained by using 48.9 g AlSb, 7.1 g Al, and 24.0 g Bi. The compound itself was readily prepared by melting stoichiometric quantities of aluminum and antimony in the induction furnace under argon atmosphere, at a temperature of 1200° C. It was necessary to keep the preparation in a vacuum desiccator, out of contact with moist air.

The determination of the eutectic temperatures, namely those of the eutectic Al–Bi, of the pseudobinary system AlSb–Bi, and of the ternary eutectic, was carried out by means of a differential thermocouple, similar to that described by Desch (6, p. 95). The reference body was pure bismuth, of the same weight as the alloy.

Because of the existence of (liquid) miscibility gaps in both ternary and in one of the binary systems, most of the work was isothermal. The alloys were kept at constant temperatures until equilibrium was attained, when both liquid layers were sampled for analysis. For work on the binary miscibility gap, equal volumes (78.4 g Bi, 21.6 g Al) were melted in the induction furnace: the stirring action of the eddy currents in this type of furnace is advantageous in attaining equilibrium. The melt was then transferred to the Hoskins furnace, already under control at the desired equilibrium temperature, and, after 1 hour, both layers were sampled by withdrawing through narrow (1.7-mm i.d.) alundum tubing. The variation of

Can. J. Chem. Downloaded from www.nrcresearchpress.com by 210.87.254.42 on 09/05/12
For personal use only.

temperature in the furnace was about ±1°. The method was used successfully up to 1180° but above this temperature the alundum tubing always broke. This temperature then, 1180°, represents the upper limit of our work, so that direct determinations of critical solution temperature and composition were not possible. The samples withdrawn as described above were weighed, dissolved in concentrated nitric acid, diluted to volume, and analyzed.

Essentially the same method was used for the investigation of congruent solutions in the ternary system, except that here more than one alloy had to be prepared, at each temperature, to obtain suitable variation in the tie lines.

Standard methods were used for the analysis of the alloys. In the bismuth-rich layer of the system aluminum–bismuth, the bismuth was determined by direct titration with EDTA (ethylenediaminetetracetic acid) using xylenol orange indicator (7). The aluminum was determined with 8-hydroxyquinoline. In the aluminum-rich layer only, bismuth was determined as BiOCl (8). Alloys containing all three metals were analyzed as follows: The antimony and bismuth were precipitated with H_2S and the antimony separated with ammonium sulphide. The bismuth was then titrated with EDTA and the antimony determined by titration with potassium bromate. Small quantities of aluminum were determined directly with 8-hydroxyquinoline but large amounts of aluminum were obtained by difference.

X-Ray powder photography was carried out in the usual way, using collodion rollings.

EXPERIMENTAL RESULTS

TABLE I

Equilibrium composition of the two congruent liquids in the system aluminum–bismuth

Temperature (° C)	Wt% Bi			Temperature (° C)	Wt% Bi		
	Liquid 1	Liquid 2	Mean		Liquid 1	Liquid 2	Mean
678	4.1	98.3	51.25	1018	25.1	96.1	60.6
720	5.8	97.9	51.85	1098	32.0	94.6	63.3
796	10.2	97.8	54.0	1183	41.2	89.7	65.45
903	16.8	97.2	57.0				

When the data of Table I are plotted, it appears that the miscibility gap will close at about 1300° C. The critical composition is then obtained by application of the law of the rectilinear diameter, as about 68% bismuth.

Eutectic Points

(a) Binary Eutectic in System Aluminum–Bismuth

The maximum decrease in the freezing temperature of bismuth was found to be 1.8°, produced by the addition of 0.30% Al. The effects of progressive additions of aluminum are shown in Table II, sample Nos. B1–B7.

(b) The Eutectic in the Pseudobinary System Bi–AlSb

The maximum decrease in the freezing temperature of bismuth was found to be 2.30° C, caused by the addition of 0.50% AlSb. The experimental results are given in Table II, Nos. C1–C4.

(c) The Ternary Eutectic

The addition of 0.20% Al to an alloy of the composition of the pseudobinary eutectic alloy caused a further decrease of 0.20° C. Hence we conclude that the eutectic temperature in the ternary system Al–Sb–Bi is 268.8° C, at a composition of 99.3% Bi, 0.40% Sb, and 0.30% Al. The experimental data are given in Table II, Nos. T1–T4. The solid phases are Al, AlSb, and solid solution of antimony in bismuth. Since antimony and bismuth form a continuous series of solid solutions, there is only one ternary eutectic in this system.

Thermal Analysis on Cooling

Since the equilibrium solid model is largely occupied by the AlSb surface, it was

Can. J. Chem. Downloaded from www.nrcresearchpress.com by 210.87.254.42 on 09/05/12
For personal use only.

TABLE II

Eutectic data: decrease in temperature and eutectic compositions

Sample No.	Addition wt%	ΔT (° C)	Sample No.	Addition wt%	ΔT (° C)
B1	0.05 Al	0.5	C2	0.50 AlSb	2.30
B2	0.10 Al	0.9	C3	0.75 AlSb	1.94
B3	0.20 Al	1.2	C4	1.00 AlSb	1.96
B4	0.30 Al	1.8	T1	0.1 Al	2.32
B5	0.40 Al	1.6	T2	0.2 Al	2.50
B6	0.50 Al	1.7	T3	0.3 Al	2.46
B7	1.5 Al	1.7	T4	0.5 Al	2.38
C1	0.25 AlSb	1.63			

necessary to determine the temperatures of primary separation of AlSb from different melts. The results are contained in Table III.

TABLE III

Three-component system: computed compositions and temperatures of primary crystallization (AlSb)

Point No.	Wt% Sb	Wt% Bi	Temp. (° C)	Point No.	Wt% Sb	Wt% Bi	Temp. (° C)
1	45.0	20.0	910	5	33.3	12.6	894
2	45.0	10.0	934	6	22.0	75.0	785
3	50.0	30.0	972	7	18.0	75.0	850
4	35.0	60.0	768				

Thermal Analysis on Heating

Because of the uncertainty as to the true form of the solidus in the antimony–bismuth system two alloys were prepared, annealed for 120 hours at 280° C, and then heated uniformly. Hysteresis effects are usually less marked on heating than on cooling. The results are given in Table IV.

TABLE IV

Thermal analysis on heating

Composition of alloy	Temperature of inflection on heating curve (° C)
63 wt% Bi (50 atomic%)	350
50.4 wt% Bi (40 atomic%)	368

Conjugate Liquids in Ternary System

TABLE V

Three-component system: composition of the two conjugate liquids in isothermal sections

Equilibrium temperature (° C)	Al-rich layer		Bi-rich layer	
	Wt% Sb	Wt% Bi	Wt% Sb	Wt% Bi
704	7.5	19.2	3.9	91.7
	14.9	41.3	11.2	76.9
800	7.2	28.5	2.1	93.3
	11.1	41.0	3.7	91.5
897	4.0	27.9	0.9	95.2
	4.5	30.8	1.8	93.0

Can. J. Chem. Downloaded from www.nrcresearchpress.com by 210.87.254.42 on 09/05/12
For personal use only.

From the totality of the preceding data, the solid model, of which Fig. 2 is a projection, can be constructed. This figure gives a complete picture of all equilibria.

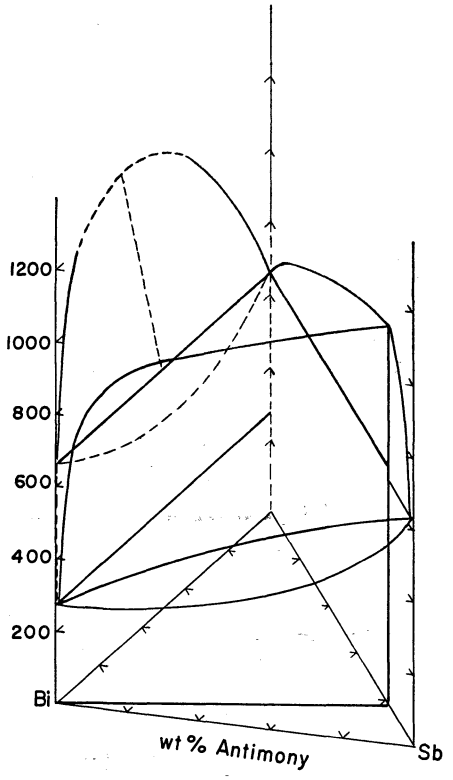

FIG. 2.

DISCUSSION OF RESULTS

The system as a whole is simple: it presents no features of unusual interest. The alloys of the system, however, have recently become of considerable commercial interest. The point of chief importance lies in the binary system antimony–bismuth, and is concerned with the true form of the solidus curve.

Our X-ray work, details of which we do not give, since it was merely a repetition of previous work, was directed to an examination of the question of the existence, or otherwise, of an unbroken series of mix-crystals between antimony and bismuth. We confirmed the results of previous workers: no lines indicative of the presence of a second solid phase ever occur on the X-ray powder photographs. Using annealed specimens, we found also that the lattice dimensions vary linearly with composition, especially if composition be expressed in atomic percent.

On the other hand, the X-ray photographs of the unannealed specimens showed a characteristic structure. The appearance was not that of a mechanical mixture, in which the lines both of bismuth and of antimony would have appeared sharply defined, but rather an indefinite spread of the blackening between the lines. The back-reflection of the unannealed specimens was almost completely extinguished. With increasing annealing time (24 → 280 hours) the sharpness of the diffraction lines improved greatly and the lines of the back-reflection reappeared. It is evident that an irregular lattice distortion

Can. J. Chem. Downloaded from www.nrcresearchpress.com by 210.87.254.42 on 09/05/12
For personal use only.

takes place, when bismuth is added to antimony and that this is arrested by too rapid cooling. On annealing, a superstructure is formed, corresponding to the composition of the solid solution.

The conclusion seems inescapable that bismuth and antimony form a continuous series of solid solutions and that therefore the solidus should be continuous. The problem remains of why the solidus determined by the ordinary method of thermal analysis on cooling should exhibit an apparently horizontal portion, while the solidus determined by the method of electrical resistance, on annealed specimens, should be normal in form. For the sake of convenience, we describe the abnormal form of the solidus as "Cook's solidus" and the other one as "Otani's solidus". We think we have an explanation for the discrepancy as follows:

It was observed throughout the present investigation that all alloys containing an appreciable amount of bismuth release or press out drops or globules of alloy on solidification, an evident consequence of the well-known expansion of bismuth on solidification. Alloys containing less than 30 atomic% of bismuth showed no tendency to squeeze out alloy. Beginning with 30 atomic% increasing quantities of metal appear on the surface of the ingot as the concentration of bismuth is increased (Fig. 3). The crystallization of alloys (of isomorphous metals) whose freezing points all lie between those of the pure metals is discussed by Desch (6, p. 26), who shows how the solidus may undergo an apparent lowering owing to slow diffusion within the solid solution but the existence of a horizontal solidus cannot be explained by slow diffusion only. We think, however, that the existence of extruded globules from the solidified alloy offers an explanation.

Consider an alloy of composition X in Fig. 4. On cooling, the first crystals will appear at a temperature T_1, with composition x'. If the behavior is ideal, on further lowering of temperature the composition of the liquid will change along the liquidus and that of the equilibrium solid along the solidus. At temperature T_2, the last infinitesimal amount of melt has the composition x''. In the system containing antimony and bismuth, however, this last portion of the melt is squeezed out of the solidified ingot and, since it is no longer in equilibrium with the rest of the alloy, constitutes a new system. The final solidification temperature will be some such temperature as T_3. Following this reasoning, the curve Bi–T_3–Sb has been constructed for concentrations varying from 20 to 60% antimony, as shown in Fig. 4. The curve so obtained has a surprising similarity to Cook's solidus. Moreover, bearing in mind that solid diffusion in antimony–bismuth alloys is slow, it can be seen that the experimentally determined solidus will be still lower.

The conditions for the expulsion of the last melt are twofold. First, cooling must progress at a rate too great for the establishment of equilibrium, and this is nearly always true in thermal analysis, where the rate of cooling has to be great enough for inflections to show up. Secondly, the specimens must have a compact form, as with the ingots shown in Fig. 3. The specimens used by Otani were round bars of dimensions 5×90 mm. Here the expansion takes place mainly in one dimension without expulsion of liquid. This is why Otani finds higher temperatures for his solidus, even without annealing.

The last melt is squeezed out at the mechanically weakest point of the ingot and any temperature-measuring device introduced into the melt constitutes such a weak point, so that the last melt is squeezed out around the thermometer and the (erroneous) temperature T_3 recorded.

As mentioned under Experimental Results, two experiments were conducted in an endeavor to obtain the true solidus temperature by thermal analysis, using rising temperature. Two ingots of different composition were annealed for 120 hours at 280° C,

Can. J. Chem. Downloaded from www.nrcresearchpress.com by 210.87.254.42 on 09/05/12
For personal use only.

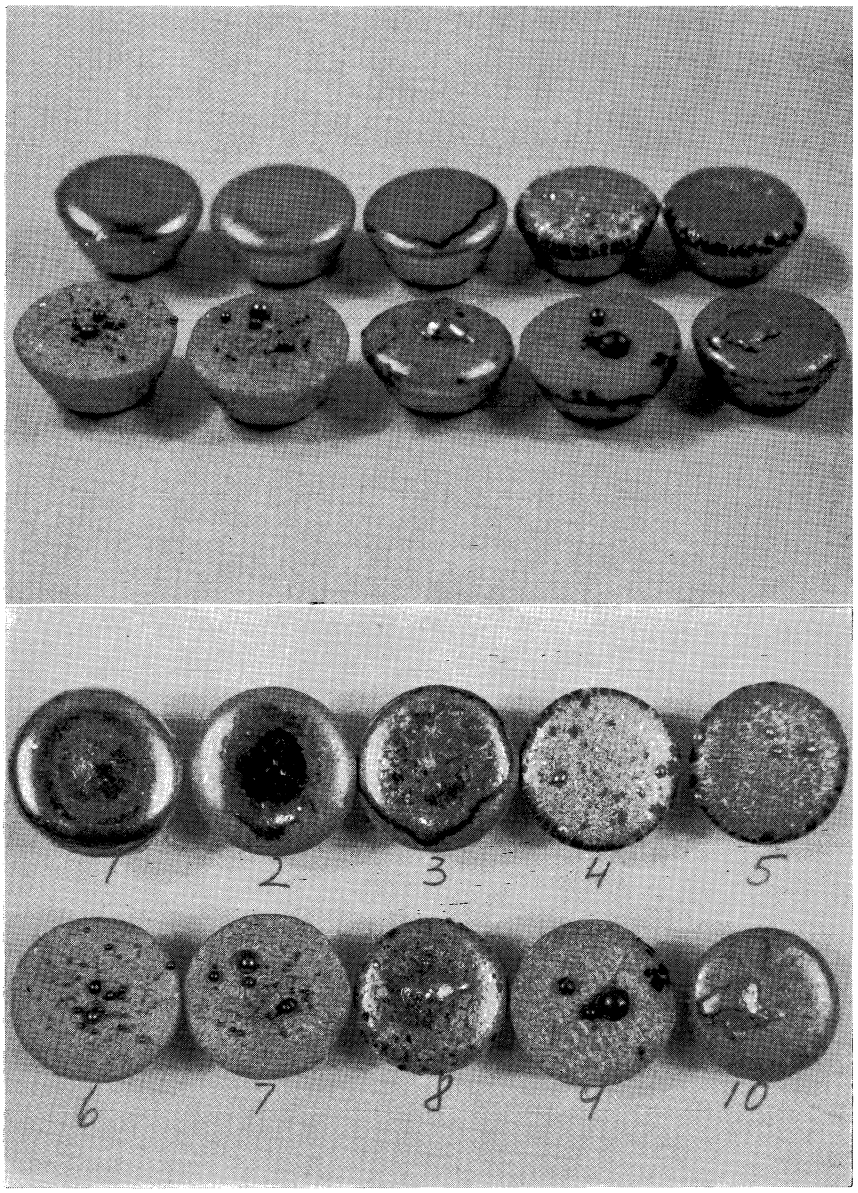

FIG. 3.

Can. J. Chem. Downloaded from www.nrcresearchpress.com by 210.87.254.42 on 09/05/12
For personal use only.

Can. J. Chem. Downloaded from www.nrcresearchpress.com by 210.87.254.42 on 09/05/12
For personal use only.

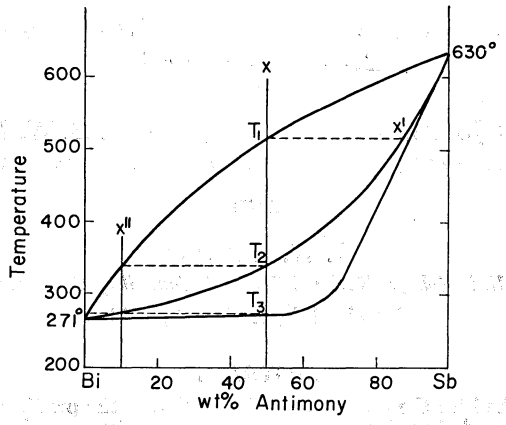

FIG. 4.

when it was observed that the (solidified) globules were incorporated again in the ingots. A 30-gauge iron–constantan thermocouple in a thin alundum tube was introduced into the center of the ingot and the heating curve recorded. The beginning of melting was found to lie at temperatures which, while they do not lie exactly on Otani's curve, are evidently higher than the temperatures of Cook's solidus.

REFERENCES

1. C. R. A. WRIGHT. J. Soc. Chem. Ind. **11**, 492 (1892). D. A. ROCHE. Moniteur Scientifique, **7** (4), 269 (1893). H. GAUTIER. Bull. Soc. d'Encour. Ind. Nat. **1** (5), 1315 (1896); Contribution l'Etude des Alliages. Paris. 1901. pp. 93, 112. W. CAMPBELL and J. A. MATHEWS. J. Am. Chem. Soc. **24**, 259 (1902). G. TAMMANN. Z. Anorg. Chem. **48**, 54 (1906). G. TAMMANN. Lehrbuch der heterogenen Gleichgewichte. Braunschweig. 1924. K. BORNEMANN. Metallurgie, **7**, 573 (1910). M. VON SCHWARZ. Metall -und Legierungskunde, 78 (1929). F. SAUERWALD. Z. Metallkunde, **14**, 458 (1922). W. GUERTLER and A. BERGMANN. Z. Metallkunde, **25**, 82 (1933). E. LOOFS-RASSOW. Aluminium, **3**, 20 (1931). E. H. DIX, F. KELLER, and L. A. WILLEY. Trans. AIME, Metals Div. **93**, 396 (1931). J. VESZELKA. Mitt. berg.-huttenmann. Abt. ungar. Hochschule Berg-Forstw. Sopron. **3**, 193 (1931). METALS HANDBOOK. American Society for Metals. 1948. E. H. WRIGHT and L. A. WILLEY. ALCOA Technical Paper No. 15. 1960. G. G. URAZOV. J. Russ. Phys.-Chem. Soc. **51**, 461 (1919). E. A. OWEN and G. D. PRESTON. Proc. Phys. Soc. (London), **36**, 341 (1924). R. F. BLUNT, H. P. R. FREDERIKSE, J. H. BECKER, and W. R. HOSLER. Phys. Rev. **96**, 578 (1954). H. WELKER. Z. Naturforsch. **7a**, 744 (1952); **8a**, 248 (1953).
2. C. R. A. WRIGHT. J. Soc. Chem. Ind. **11**, 492 (1892). C. T. HEYCOCK and F. H. NEVILLE. J. Chem. Soc. **61**, 893 (1892). W. CAMPBELL and J. A. MATHEWS. J. Am. Chem. Soc. **24**, 259 (1902). PECHEUX. Compt. Rend. **138** (2), 1501 (1904). A. G. C. GWYER. Z. Anorg. Chem. **49**, 311 (1906). M. HANSEN and B. BLUMENTHAL. Metallwirtschaft, **10**, 925 (1931). L. W. KEMPF and K. R. VAN HORN. Trans. AIME, Inst. Metals Div. **133**, 81 (1939).
3. K. HUTTNER and G. TAMMANN. Z. Anorg. Chem. **44**, 138 (1905). H. GAUTIER. Contribution a l'Etude des Alliages. Paris. 1901. p. 114. M. COOK. J. Inst. Metals, **28**, 421 (1922). B. OTANI. Sci. Repts. Tohoku Imp. Univ. **13**, 293 (1925). CHU-PHAY YAP. Trans. AIME, **93**, 185 (1931). E. G. BOWEN and W. M. JONES. Phil. Mag. **13**, 1029 (1932). W. F. EHRET and M. B. ABRAMSON. J. Am. Chem. Soc. **56**, 385 (1934). E. SCHEIL. Z. Elektrochem. **49**, 242 (1943). G. MASING, P. RAHLFS, and W. SCHAARWACHTER. Z. Metallkunde, **40**, 333 (1949). T. HEUMANN. Z. Naturforsch. **5a**, 216 (1950); Z. Metallkunde, **42**, 182 (1951). C. A. ZAPFFE. Z. Metallkunde, **44**, 397 (1953). P. W. BRIDGMAN. Proc. Am. Acad. Arts Sci. **84**, 43.
4. C. R. A. WRIGHT. Proc. Roy. Soc. (London), **55**, 137 (1894). GÖTZ-WERNER KASTEN. Wiss. Veröffentl. Siemens-Werken, Werkstoff Sonderheft, 53 (1940); G. Ritzau. Wiss. Veröffentl. Siemens-Werken, Werkstoff Sonderheft, 44 (1940).
5. A. N. CAMPBELL and R. KARTZMARK. Can. J. Chem. **34**, 1431 (1956).
6. C. H. DESCH. Metallography. 5th ed. 1942.
7. F. J. WELCHER. The analytical uses of ethylenediamine tetracetic acid. p. 207.
8. W. W. SCOTT. Standard methods of chemical analysis. 5th ed. p. 153.

Can. J. Chem. Downloaded from www.nrcresearchpress.com by 210.87.254.42 on 09/05/12
For personal use only.

A STATISTICAL APPROACH TO THE ANALYSIS OF INFRARED BAND PROFILES[1]

R. NORMAN JONES, K. S. SESHADRI,[2] AND N. B. W. JONATHAN[2]
Division of Pure Chemistry, National Research Council of Canada, Ottawa, Canada

AND

J. W. HOPKINS
Division of Applied Biology, National Research Council of Canada, Ottawa, Canada

Received September 12, 1962

Can. J. Chem. Downloaded from www.nrcresearchpress.com by 210.87.254.6 on 09/05/12
For personal use only.

ABSTRACT

A method is described for the quantitative description of the profile and asymmetry of an infrared absorption band, based on the computation of the second and third incomplete moments of the absorbance curve. Provision is included for differentiation between the intrinsic band asymmetry and that induced by instrumental factors dependent on the direction of scan. A program has been prepared for an I.B.M. 1620 computer to facilitate the calculation of the moments. This program also yields the incomplete fourth moments, the statistical kurtosis parameter ($\sqrt{\beta_2}$), and the Gauss–Cauchy index, though these quantities are not employed in the present investigation. Examples are given of the application of these computations to the analysis of the effect of the spectral slit width on the profiles of bands at 812.7 and 726.6 cm^{-1} respectively in the spectra of carbon disulphide solutions of perylene and anthracene, and of the effect of the amplifier time constant on the asymmetry of the band at 2234.4 cm^{-1} in the spectrum of *p*-chlorobenzonitrile in tetrachloroethylene solution.

INTRODUCTION

The current availability of commercially manufactured grating infrared spectrophotometers adds interest to the quantitative description of the profiles of infrared absorption bands, particularly for bands measured on liquids and solutions. With increasing resolution, the shape of the band provides progressively more information about the physical state of the absorbing system. A quantitative treatment of the band profile, and particularly of its asymmetry, would be valuable, the more so if the treatment could be made precise enough to quantify the small changes in band contour that result from changes in temperature, solvent, and other experimental variables. A quantitative description of the band shape is also desirable to facilitate the transfer of data between different spectrophotometers, and to place the analysis of instrumental distortion on a quantitative basis.

It is customary to describe infrared absorption bands of materials in the liquid phase in terms of the wavenumber at the band maximum (ν_0), the band width in cm^{-1} at half the maximal molecular extinction coefficient or absorbance ($\Delta\nu_{1/2}$), and the area beneath the absorption curve. For solutions, the extinction coefficient is expressed as

$$[1] \qquad \epsilon_\nu = \frac{1}{bc}\log_{10}\left(\frac{I_0}{I}\right)_\nu,$$

where b is the path length in cm and c the concentration in moles per liter of solution. In

[1]*Issued as N.R.C. No. 7170.*
Presented, in part, at the Symposium on Molecular Structure and Spectroscopy, The Ohio State University, Columbus, Ohio, U.S.A., June 14th, 1962.
[2]*National Research Council Postdoctoral Fellow.*

purely experimental work, the band area can be conveniently described by the I.U.P.A.C. "practical unit" (1),

$$[2] \qquad E_{\nu_1}^{\nu_2} = \int_{\nu_1}^{\nu_2} \epsilon_\nu d\nu,$$

with ν measured in cm^{-1}, though alternative expressions, differing dimensionally, or in the magnitude of the concentration units are also employed, particularly where it is desired to relate the measured band area to polar properties of the associated normal vibration. The relationships among these units have been summarized (2).

When dealing solely with the characteristics of the measured band profile, it is preferable to use either the absorbance ($\log_{10} (I_0/I)_\nu$), or the equivalent expression in terms of natural logarithms, for the ordinate scale. In the conversion to molecular extinction coefficients it is necessary to assume that the system obeys the Beer–Lambert law, and this involves physical considerations that are external to the analysis of the observed band profile. For analyses of instrumental distortion per se an ordinate scale of fractional absorption ($1-(I/I_0)_\nu$) should preferably be employed, but this considerably complicates the mathematical treatment. The statistical analysis of the band profiles developed in this article is based on the absorbance ordinate scale, though attempts are now in progress to extend this type of profile analysis to the fractional absorption curves.

If the band contour can be specified by a Lorentz or Gauss function, the three constants ν_0, $\log_{10} (I_0/I)_{\nu_0}$, and $\Delta\nu_{1/2}$ serve to define the location of the band and its profile at all points. These functions can be expressed

$$[3] \qquad \log_{10}\left(\frac{I_0}{I}\right)_\nu = \frac{a}{(\nu-\nu_0)^2+b^2}$$

for the Lorentz curve,* and

$$[4] \qquad \log_{10}\left(\frac{I_0}{I}\right)_\nu = \frac{a}{b^2}\cdot e^{-[(\nu-\nu_0)^2(\ln 2)]/b^2}$$

for the Gauss curve, where $a/b^2 = \log_{10} (I_0/I)_{\nu_0}$ and $2b = \Delta\nu_{1/2}$.

Unfortunately, band profiles conforming to equations [3] or [4] will rarely be encountered in practice. The observed profile will be perturbed by various physical factors affecting the true band shape, and also by instrumental distortion associated principally with the use of finite spectral slit widths and finite time constants in the electronic system of the recorder. As these perturbing factors have been recently reviewed (2) we need not discuss them further here.

If instrumental distortion is present, or if the true band profile departs significantly from the idealized forms discussed above, mathematical analysis in terms of the peak height and half-width parameters will not suffice. The curve form may become very complex, and at best, be resolvable into a convolution of several contributing functions which may contain asymmetric elements (2). It is therefore desirable to develop a calculus that will permit a quantitative description of the shape of an infrared absorption band based on purely empirical considerations. Such a technique should take account of the

**The expression "Lorentz curve" will subsequently be retained for the description of band contours that result from the Lorentz broadening effect. Equation [3] is, mathematically, a particular example of the more general Cauchy function. It is preferable to use this expression in dealing with the mathematical analysis of this type of curve profile, since the analysis is also applicable to the description of Cauchy type distribution functions arising from other causes, as for example, the natural width of a spectroscopic line, determined by the Heisenberg uncertainty principle, and other statistical applications outside the field of spectroscopy.*

Can. J. Chem. Downloaded from www.nrcresearchpress.com by 210.87.254.6 on 09/05/12
For personal use only.

fact that it is not usually practical to measure the band out into the wings to a point where the absorbance becomes negligible. Overlap with neighboring bands is almost invariably present, and it is therefore desirable to deal quantitatively with sections of the band envelope truncated at predetermined distances from the center.

These requirements can be met by statistical methods of analysis that involve no assumptions about the nature of the physical processes involved in the absorption. The technique of moment analysis, developed by Pearson (4, 5), has been applied extensively in the fields of biometrics and actuarial statistics. In these instances the applications have been concerned predominantly with Gaussian and near-Gaussian distribution curves. With the modifications described below, however, related procedures can be applied to truncated band profiles of Cauchy or Gauss form.

DEFINITION OF THE BAND MOMENTS

The general moments of the function $\log_{10}(I_0/I)_\nu = f(\nu)$ about the point $\nu = k$ are defined by the equation

$$[5] \qquad \mu_r' = \frac{\int_{-\infty}^{+\infty} (\nu-k)^r f(\nu)d\nu}{\int_{-\infty}^{+\infty} f(\nu)d\nu},$$

where r is a positive integer or zero.

It is necessary to specify the point about which the moments are taken. In principle, moments may be taken about any abscissal value, but in this article we shall be concerned only with absorption profiles having a single maximum, and with moments taken about this maximal ordinate at abscissa ν_0. Under these conditions equation [5] becomes

$$[6] \qquad \mu_r = \frac{\int_{-\infty}^{+\infty} (\nu-\nu_0)^r f(\nu)d\nu}{\int_{-\infty}^{+\infty} f(\nu)d\nu}.$$

It is important to note that ν_0 is not to be confused with the mean abscissal value of the curve, and will not coincide with this unless the function is symmetric. Likewise the μ_r should not be confused with the *central moments* which are those taken about the mean, i.e. centroid of the ν_0.

The Incomplete (Truncated) Moments of the Cauchy Curve ($\mu_r^C(j)$)

As the band profiles with which we shall be dealing can in many cases be approximated by Cauchy functions, it will be convenient to deal first with the analytic expressions for the moments of the Cauchy curve. These can be obtained by substituting equation [3] into equation [6] and integrating where it is feasible to do so.

Since the Cauchy function is symmetric about ν_0, all its odd central moments are zero, and except for μ_0 its even moments are all infinite.* Therefore the moments as defined by equation [6] do not give any useful information about this distribution.

In this instance, however, the numerators of equation [6] can be conveniently integrated within definite limits, and the resulting definite integrals evaluated numerically. These may then be used to compute incomplete moments of degree r for progressively increasing

*This follows from the fact that the even moments are functions of $\tan^{-1}((\nu-\nu_0)/b)$ (cf. equations [9], [10]) which become meaningless when $(\nu-\nu_0) \rightarrow \pm\infty$.

Can. J. Chem. Downloaded from www.nrcresearchpress.com by 210.87.254.6 on 09/05/12
For personal use only.

$(\nu-\nu_0)$, and such incomplete moments will be quantitative characteristics of the curve profile.

When scaled in units of j, the semi-half-band width (Fig. 1), so that

$$[7] \qquad j = \frac{(\nu-\nu_0)}{b},$$

the incomplete moments

$$[8] \qquad \mu_r(j) = \frac{1}{b^r} \frac{\int_{-j}^{+j} (\nu-\nu_0)^r f(\nu)d\nu}{\int_{-j}^{+j} f(\nu)d\nu}$$

become dimensionless numbers, and may be regarded as pure shape parameters appropriate to comparisons of band profiles differing in band width. For quantification of instrumental distortion of a single profile, on the other hand, moments $\mu_r(\nu-\nu_0)$ in the scale of ν, in which instrumental factors actually interact, may be more appropriate. For comparisons the latter can readily be scaled to the dimensionless ratio $\mu_r(\nu-\nu_0)/\mu_2(\nu-\nu_0)^{r/2}$.*

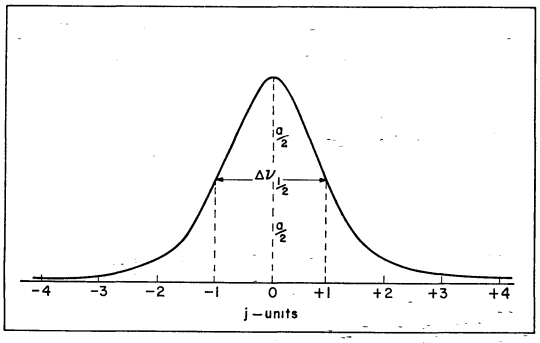

FIG. 1. Diagram illustrating the truncation of an infrared absorption band in units of j.

Making the appropriate substitutions, the expressions given in equations [9] and [10] are obtained for the second and fourth incomplete moments of the Cauchy curve in units of the semi-half-band width,

$$[9] \qquad \mu_2{}^C(j) = \left[\frac{j}{\tan^{-1} j} - 1\right]$$

$$[10] \qquad \mu_4{}^C(j) = \left[\frac{j(j^2-3)}{3\tan^{-1} j} + 1\right].$$

These are listed in Table I for the range $j = 0.2$ to $j = 4$ at intervals of 0.2.

The Incomplete Moments of the Gauss Curve ($\mu_r{}^G(j)$)

Comparable analytic expressions are not easily derived for the second and fourth incomplete moments of the Gauss curve, but by appropriate scaling the numerical values can be approximated from tables published by Pearson (6).†

*Specifically $\beta_1(\nu-\nu_0) = \mu_3(\nu-\nu_0)/\mu_2(\nu-\nu_0)^{3/2}$ is directly analogous to the statistically familiar $\beta_1 = \mu_3/\mu_2{}^{3/2}$ computed from complete moments.

†Pearson's tables are normalized with respect to the complete and not the incomplete zeroth moment, and his integration ranges are in units of the standard deviation ($\sigma = b\ (2\ \ln\ 2)^{-1/2}$) not of the semi-half-band width b.

Can. J. Chem. Downloaded from www.nrcresearchpress.com by 210.87.254.6 on 09/05/12
For personal use only.

TABLE I

Incomplete second and fourth moments of the Cauchy, Gauss, and triangular functions in units of j (the semi-half-band width)

	Second moment			Fourth moment		
j	Cauchy	Gauss	Triang.	Cauchy	Gauss	Triang.
0.2	0.0132	0.0149	0.0130	0.0003	0.0005	0.0003
0.4	0.0512	0.0530	0.0504	0.0048	0.0053	0.0047
0.6	0.1102	0.1125	0.1094	0.0230	0.0238	0.0229
0.8	0.1856	0.1899	0.1867	0.0673	0.0702	0.0683
1.0	0.2732	0.2763	0.2778	0.1512	0.1532	0.1556
1.2	0.3698	0.3655	0.3771	0.2877	0.2792	0.2962
1.4	0.4728	0.4504	0.4774	0.4894	0.4454	0.4925
1.6	0.5807	0.5256	0.5689	0.7682	0.6376	0.7282
1.8	0.6922	0.5874	0.6382	1.1354	0.8385	0.9543
2.0	0.8064	0.6346	0.6667	1.6021	1.0284	1.0667
2.2	0.9228	0.6686		2.1793	1.1927	
2.4	1.0408	0.6910		2.8775	1.3215	
2.6	1.1601	0.7049		3.7074	1.4149	
2.8	1.2805	0.7130		4.6793	1.4781	
3.0	1.4018	0.7173		5.8037	1.5164	
3.2	1.5238	0.7195		7.0908	1.5386	
3.4	1.6464	0.7205		8.5512	1.5506	
3.6	1.7696	0.7210		10.1949	1.5564	
3.8	1.8931	0.7212		12.0323	1.5591	
4.0	2.0170	0.7213		14.0737	1.5603	

Pearson's data have been transposed into the semi-half-band width used above for the Cauchy moments and are also listed in Table I for specified values of j. The second and fourth incomplete moments of the Cauchy and Gauss curves are compared in Figs. 2 and 3. It will be seen that the incomplete second moment of the Gauss curve rapidly

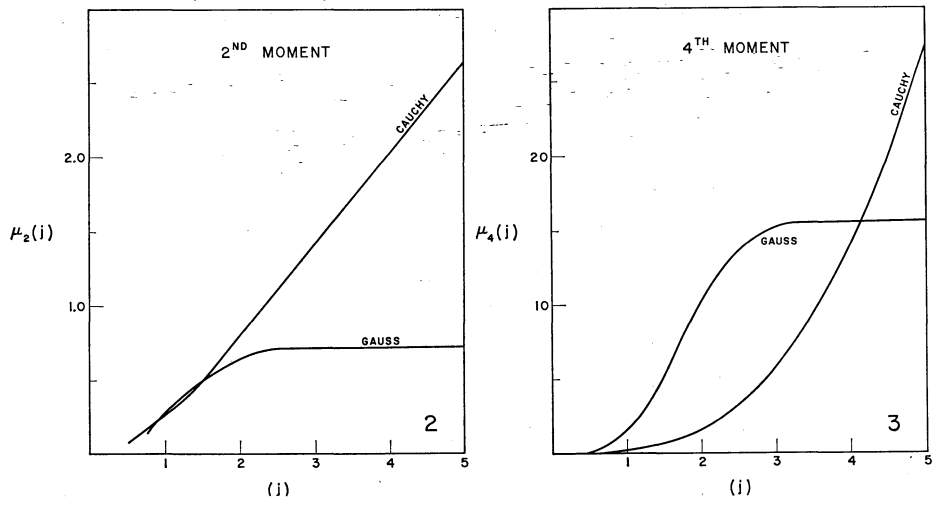

FIG. 2. Comparison of the incomplete second moments of Gauss and Cauchy curves.
FIG. 3. Comparison of the incomplete fourth moments of Gauss and Cauchy curves.

converges to a limiting value of 0.721 with increasing j, whereas the incomplete second moment of the Cauchy curve increases continuously with j in an approximately linear fashion. The incomplete fourth moments behave qualitatively in a similar fashion to the

Can. J. Chem. Downloaded from www.nrcresearchpress.com by 210.87.254.6 on 09/05/12
For personal use only.

second moments, though the fourth moments versus j plots for both functions are significantly non-linear over the calculated range.

Incomplete Moments of the Triangular Function ($\mu_r^{\triangle}(j)$)

Since triangular functions are encountered in the analysis of spectral slit widths, it is convenient to record here that the second and fourth truncated moments of the triangular function with apex at ν_0 and half width $2b$ are given by the expressions

$$\mu_2^{\triangle}(j) = \frac{j^2\left[\frac{1}{3} - \frac{j}{8}\right]}{\left[1 - \frac{j}{4}\right]} \qquad [11]$$

$$\mu_4^{\triangle}(j) = \frac{j^4\left[\frac{1}{5} - \frac{j}{12}\right]}{\left[1 - \frac{j}{4}\right]} \qquad [12]$$

The values are listed in Table I. They have no physical significance beyond $j = 2$.

Moments About Ordinates Displaced Slightly From the Band Maximum

There will inevitably be some error in evaluating the abscissal location of the maximum ordinate of an absorbance curve, and it is therefore important to assess the sensitivity of the incomplete moments to small displacements of the maximum. If the abscissal displacement is $\Delta\nu$, it can be shown that for the Cauchy distribution

$$\mu_2^{\leftrightarrow}(j) = \left[\frac{j'^{\,1/2}}{\tan^{-1} j'^{1/2}}\right] + \alpha^2 - 1 \qquad [13]$$

$$\mu_3^{\leftrightarrow}(j) = 3\alpha\left[\frac{j'^{\,1/2}}{\tan^{-1} j'^{\,1/2}} - 1\right] + \alpha^3 \qquad [14]$$

$$\mu_4^{\leftrightarrow}(j) = \left[\frac{j'^{\,1/2}(n-4+n\alpha^2)}{3\tan^{-1} j'^{\,1/2}} + 1\right] + 6\alpha^2\left[\frac{j'^{\,1/2}}{\tan^{-1} j'^{\,1/2}}\right] + \alpha^4, \qquad [15]$$

where $\alpha = 2\Delta\nu/\Delta\nu_{1/2}$, $n = j^2+1$, and $j' = n(\alpha^2+1)-1$.

When $\alpha = 0$, $\mu_3^{\leftrightarrow}(j) = 0$ and the equations [13] and [15] reduce to [9] and [10] respectively. Taking $\alpha = 0.1$, the values obtained for Cauchy $\mu_2^{\leftrightarrow}(j)$ are compared in Table II

TABLE II

Effect of abscissal displacement on the incomplete second moment of the Cauchy function ($\alpha = 0.10$)

j	$\mu_2(j)$	$\mu_2^{\leftrightarrow}(j)$
1.0	0.2732	0.2879
2.0	0.8064	0.8236
3.0	1.4018	1.4220
4.0	2.0170	2.0501

with those for the Cauchy distribution about ν_0. The differences are seen to be small: $\mu_2(1)$ is overestimated by about $1\frac{1}{4}\%$ and μ_2 (4.0) by about 5%. Measurements on a variety of absorption band profiles (7) indicate that the average uncertainty in the measurement of ν_0 is ± 0.3 cm^{-1}. Under these conditions a value of $\alpha \gtrsim 0.1$ would be

Can. J. Chem. Downloaded from www.nrcresearchpress.com by 210.87.254.6 on 09/05/12
For personal use only.

obtained for bands having $\Delta\nu_{1/2} \lesssim 6$ cm^{-1}. It does not necessarily follow that α will increase at narrower half-band width since the precision in the measurement of ν_0 improves. Thus for the very narrow perylene band for which $\Delta\nu_{1/2} = 2.16$ the estimated uncertainty in ν_0 is ± 0.1 cm^{-1} corresponding to $\alpha = 0.09$.

The Effect on the Moments of a Uniform Displacement of the Base Line

The effect of a small ordinate displacement of the base of the curve on the incomplete moments of the Cauchy function has been examined to determine the sensitivity to errors resulting from drift of the 100%-transmission line. For a displacement α times the maximum ordinate height, the following expressions are obtained for the second and fourth incomplete moments:

[16] $$\mu_2^{\updownarrow}(j) = \frac{\left[j - d^{1/2}\tan^{-1}\left(\frac{j}{d^{1/2}}\right) - \frac{\alpha j^3}{3d}\right]}{\left[\frac{1}{d^{1/2}}\tan^{-1}\left(\frac{j}{d^{1/2}}\right) - \frac{\alpha j}{d}\right]}$$

[17] $$\mu_4^{\updownarrow}(j) = \frac{\left[d^{3/2}\left\{\frac{j^3}{3d^{3/2}} - \frac{j}{d^{1/2}} + \tan^{-1}\left(\frac{j}{d^{1/2}}\right)\right\} - \frac{\alpha j^5}{5d}\right]}{\left[\frac{1}{d^{1/2}}\tan^{-1}\left(\frac{j}{d^{1/2}}\right) - \frac{\alpha j}{d}\right]},$$

where $d = (1+\alpha)/(1-\alpha)$.

When $\alpha = 0$, giving $d = 1$, expressions [16] and [17] reduce to [9] and [10] respectively. Taking $\alpha = 0.01$, the second moments of the new distribution are compared with the true Cauchy moments in Table III, from which it will be evident that an error of 1% in

TABLE III

Effect of ordinate displacement of the base line on the incomplete second moment of the Cauchy function ($\alpha = 0.01$)

j	$\mu_2(j)$	$\mu_2^{\updownarrow}(j)$
1.0	0.2732	0.2782
2.0	0.8064	0.8112
3.0	1.4018	1.3870
4.0	2.0170	1.9521

the location of the base line would not greatly affect computation of the second moments of a Cauchy distribution, or, by inference, the second moments of an experimentally observed absorbance curve of near-Lorentzian contour.

EXPERIMENTAL

The experimental work described in this section was undertaken as a preliminary exploration of the use of the moment method for characterizing band shapes. These experiments are intended to be illustrative only, and a considerably more extended series of measurements, performed under more carefully controlled conditions, preferably on a double-beam spectrophotometer, will be necessary before significant conclusions can be drawn concerning the physical implications of the results.

Well-isolated bands in the spectra of solutions of perylene at 812.7 cm^{-1} and of anthracene at 726.6 cm^{-1} in carbon disulphide solution and of *p*-chlorobenzonitrile at 2234.4 cm^{-1} in tetrachloroethylene have been used in this investigation. The perylene was crystallized from toluene and further purified by vacuum distillation; the anthracene was zone refined and the *p*-chlorobenzonitrile was repeatedly recrystallized from *n*-pentane.*

**In a new series of experiments now in progress, perylene, anthracene, and p-chlorobenzonitrile have all been purified by repeated zone refining, and this method is preferable to those described above.*

Can. J. Chem. Downloaded from www.nrcresearchpress.com by 210.87.254.6 on 09/05/12
For personal use only.

The spectra were measured on a Perkin–Elmer Model 112G single-beam double-passed grating spectrometer. The main features of the bands and the experimental conditions of measurement are listed in Table IV; a typical instrumental chart record is reproduced in Fig. 4. The solvent base line and the experi-

TABLE IV

Experimental conditions of band measurement

	Perylene band	Anthracene band	*p*-Chlorobenzonitrile band
Position of band maximum (cm^{-1})	812.7	726.6	2234.4
Half-band width extrapolated to zero slit width ($\Delta\nu_{1/2}{}^t$) (cm^{-1})	2.16	2.5	5.0
Solvent	CS_2	CS_2	C_2Cl_4
Concentration (M)	5.33×10^{-3}	5.87×10^{-3}	52.6×10^{-3}
Cell thickness (mm)	1.0	1.0	1.0
Range of scan (cm^{-1})	820–805	735–715	2260–2210
Scanning rate ($cm^{-1}min^{-1}$)	1.5	1.25	7.5
Chart speed (cm min^{-1})	5	5	10
Recorder response setting*	2	2	2/3/4
Mechanical slit width (mm)	0.5–1.5	0.5–1.75	0.3
Nominal spectral slit width† (S) (cm^{-1})	0.83–2.2	0.65–2.0	1.25
$S/\Delta\nu_{1/2}{}^t$	0.38–1.0	0.26–0.8	0.25

*Response 2 corresponds to 5 seconds for 95% throw; Response 3 corresponds to 11 seconds for 95% throw; response 4 corresponds to 18 seconds for 95% throw.
†For method of computation see pp. 32–35 of reference 2.

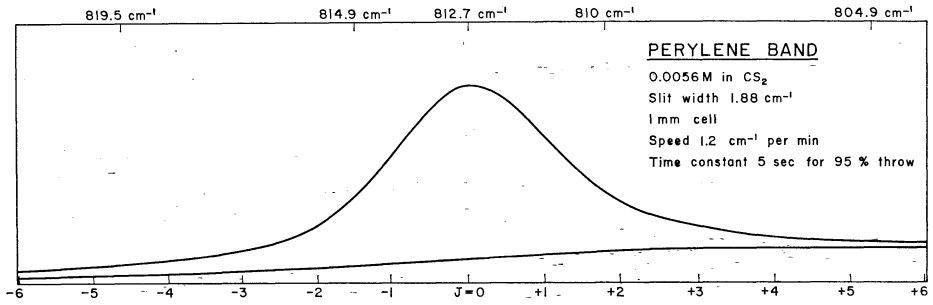

FIG. 4. A representative instrumental chart record from the 112G grating spectrometer under the scanning conditions used in these measurements.

mental curve were run consecutively using the same cell. The 100%-absorption line was recorded before and after the completion of the solvent and solute measurements. The instrumental stray light was less than 1% as measured by the method described in reference 2. The gain was adjusted so that the pen throw for 100%-transmission remained approximately the same through each series of measurements. In one set of experiments the effect of change of spectral slit width at a fixed amplifier time constant was investigated, while in a second series the time constant was varied while maintaining a fixed slit width. The spectral slit width was computed from the mechanical slit width as described in reference 2, and did not vary significantly over the scanning range of a band.

For each experimental curve, I and I_0 were read at intervals across the curve. Between 15 and 20 absorbance ordinates were determined; the readings were taken at close abscissal intervals in the neighborhood of the maximum and at increasing intervals out into the wings. The position of the maximum was estimated visually (ν_0'), and the half-band width with respect to this estimated maximum ordinate was determined ($\Delta\nu_{1/2}'$). Four points on the curve were next selected on either side of ν_0', within an abscissal range not exceeding $\frac{1}{2}\Delta\nu_{1/2}'$. The Part I program for the I.B.M. 1620 computer (8) was then used to pass second, third, and fourth degree polynomial curves through the selected points by a least squares approximation and the displacement ($\nu_0'-\nu_0$) was evaluated to give the corrected band maximum ν_0 (7).

Next the measured absorbance values were plotted against ($\nu-\nu_0$) for the complete band on a large sheet of graph paper, and a smooth curve passed through the points. The peak height was read from this curve, and the abscissal distances in cm^{-1} corresponding to half the peak height were obtained for both the negative and positive halves of the curve. For the perylene and anthracene bands, which are nearly symmetric, these

Can. J. Chem. Downloaded from www.nrcresearchpress.com by 210.87.254.6 on 09/05/12
For personal use only.

values are almost identical, but for the more pronouncedly asymmetric *p*-chlorobenzonitrile band they differ appreciably. By convention, the averaged value of the two measurements was accepted as the semi-half-band width b.*

The abscissal scale unit j was next obtained, and the abscissal values (in cm^{-1}) tabulated with their corresponding absorbance ordinates at intervals of $0.1j$ for the complete curve, in a sequence of diminishing wavenumber. An equal number of measurements were taken on either side of the maximum which was included in the series. These data were then transferred to I.B.M. cards and processed through the Part II program of the I.B.M. 1620 computer, which is designed to evaluate the incomplete moments (8). The computer prints out the values of $\mu_2(j)$, $\mu_3(j)\cdot b^3 = \mu_3(\nu-\nu_0)$, $\mu_4(j)$, $\sqrt{[\beta_2(j)]}$, and the Gauss–Cauchy index at intervals of $0.4j$.

In the following discussion we shall consider only $\mu_2(j)$ and $\mu_3(\nu-\nu_0)$. The Gauss–Cauchy index is defined as

$$\frac{\mu_2(j)-\mu_2{}^{G}(j)}{\mu_2{}^{C}(j)-\mu_2{}^{G}(j)} \qquad [18]$$

and $\beta_2(j) = \mu_4(j)/\mu_2(j)^2$. The evaluation of these quantities, as well as of $\mu_4(j)$, has been incorporated into the Part II program in anticipation that they will provide additional information about the band profile that may be useful at a later date.

RESULTS

Effect of the Spectral Slit Width on the Perylene and Anthracene Band Profiles

The perylene and anthracene spectra were measured under instrumental conditions where the effect of the amplifier time constant on the asymmetry of the band profile should be negligible. The spectra were obtained over a range of spectral slit widths, and the values of the second moments are listed in Table V and illustrated graphically in Fig. 5. The corresponding values for the Cauchy and Gauss distributions are also included

TABLE V

Incomplete second moments of the perylene and anthracene bands as obtained under the experimental conditions listed in Table IV

	Perylene band			Anthracene band		
	Mechanical slit width (mm):			Mechanical slit width (mm):		
	0.50	1.00	1.50	0.50	1.00	1.75
	Spectral slit width (cm^{-1}):			Spectral slit width (cm^{-1}):		
j	0.83	1.52	2.20	0.65	1.20	2.00
0.4	0.0507	0.0509	0.0510	0.0502	0.0510	0.0510
0.8	0.1852	0.1854	0.1861	0.1845	0.1846	0.1852
1.2	0.3720	0.3690	0.3676	0.3765	0.3705	0.3691
1.6	0.5758	0.5651	0.5591	0.5970	0.5794	0.5703
2.0	0.7765	0.7620	0.7457	0.8264	0.7919	0.7706
2.4	0.9882	0.9539	0.9302	1.0576	1.0064	0.9603
2.8	1.1923	1.1485	1.1041	1.2830	1.2173	1.1431
3.2	1.4036	1.3420	1.2693	1.5059	1.4263	1.3165
3.6	1.6209	1.5344	1.4351	1.7318	1.6361	1.4755
4.0	1.8441	1.7273	1.6007	1.9685	1.8446	1.6273

in the diagram. It will be clear that the results conform closely with the expectations for the Cauchy curve over the central region, but begin to depart beyond $j = 1.5$, and the

**In preliminary investigations the maximum ordinate was normalized to unity, but this was later discontinued. It is unnecessary because the moments are effectively normalized by virtue of the presence of $\int f(\nu)d\nu$ in the denominator of equation [8].*

Can. J. Chem. Downloaded from www.nrcresearchpress.com by 210.87.254.6 on 09/05/12
For personal use only.

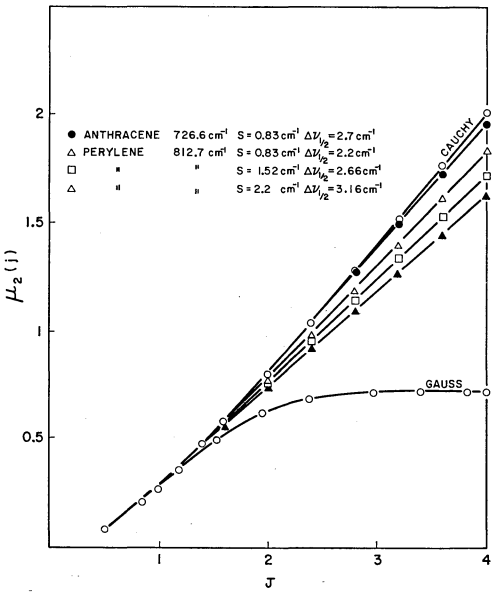

FIG. 5. The 812.7 cm^{-1} perylene band. The effect of the spectral slit width on the incomplete second moment. The moment for the 726.6 cm^{-1} band of anthracene, as measured at the narrowest slit width, is also included.

difference increases progressively into the wings. As the slit becomes wider, the departure from Cauchy towards Gauss values becomes more pronounced. These results are consistent with the hypothesis that the observed band profiles are intermediate between Cauchy and Gauss distributions, and might be represented in good approximation by convolutions of Gauss and Cauchy functions, viz. by Voigt functions (2). This aspect of the curve analysis will be considered in more detail in a later publication; it is in accord with recent work of Abramowitz and Bauman (9) on other absorption bands. It is not, however, legitimate to conclude that the slit function itself is necessarily Gaussian. It must be remembered that, physically, it is the fractional absorption curve and not the absorbance curve that is convoluted with the slit function. This point is currently being studied in greater detail, and preliminary computations, based on an approximate deconvolution of the fractional absorbance curves of the perylene band with Gaussian and triangular slit functions, suggest that the best approximation may perhaps be a function intermediate between these two; if it be assumed that the absorbance band is truly Lorentzian, deconvolution with a triangular slit function appears to overcorrect, and to displace the $\mu_2(j)$ versus j plot above the Cauchy line, whereas a Gaussian slit function does not raise it sufficiently. A more complete analysis may modify these provisional conclusions.

The $\mu_2(j)$ versus j plots for the anthracene bands are qualitatively similar to the perylene band plots, but the band is intrinsically wider, having $\Delta\nu_{1/2}{}^t = 2.5$ cm^{-1} compared with 2.16 cm^{-1} for the perylene band ($\Delta\nu_{1/2}{}^t$ is the extrapolated value of $\Delta\nu_{1/2}$ at zero spectral slit width). This could explain why measurements at the narrowest slit width suggest more nearly Lorentzian $\mu_2(j)$ characteristics for the anthracene than for the perylene band. The anthracene plot for the narrowest slit width is included in Fig. 5.

Can. J. Chem. Downloaded from www.nrcresearchpress.com by 210.87.254.6 on 09/05/12
For personal use only.

Measurement of the Band Asymmetry—The Effect of the Amplifier Time Constant on the Profile of the p-Chlorobenzonitrile Band

In the initial study of the second moments described above, it was considered desirable to work with bands of high symmetry, and the perylene and anthracene bands were chosen for this reason. A preliminary study of the third moment, as a means to quantify instrumental effects on band asymmetry, is more conveniently carried out with a band that has appreciable intrinsic skewness, and the —C≡N stretching band of *p*-chlorobenzonitrile was selected for this purpose.* The spectra were measured in tetrachloroethylene solution, and the data were processed exactly as described for the perylene and anthracene bands.

In these measurements the slit width was maintained unaltered, but the amplifier time constant was varied. Whereas the instrumental distortion introduced by the finite slit width is approximately symmetrical, that introduced by the finite amplifier time constant contains a strongly asymmetric second order component (10), so that the asymmetry of the experimentally observed band will change as the time constant is altered, and this should be reflected in the third moment measurements.

In fact, the lag in the amplifier response caused by the finite time constant extends the band in the direction of scan, and this effect on the band shape will invert in sign when the direction of scanning is reversed. It is therefore possible to separate the intrinsic band asymmetry from that associated with the scanning process by scanning the band in both the forward and reverse directions, and observing the differences in the resulting third moments. Reversal of the scanning direction will also displace the location of the maximum, but this will not affect the third moment computations if ν_0 is obtained separately for the forward and reverse runs as described above.†

It is convenient to define the two distinct third moment parameters

$$\mu_3^{F}(\nu-\nu_0) = \mu_3^{F}(j)\cdot b_F^3 \quad [19]$$

and

$$\mu_3^{R}(\nu-\nu_0) = \mu_3^{R}(j)\cdot b_R^3 \quad [20]$$

for the dimensional moments measured in the forward (F) and reverse (R) directions (by convention the forward direction is that associated with increasing wavenumber).

We also define $\mu_3^{a}(\nu-\nu_0)$ and $\mu_3^{i}(\nu-\nu_0)$ as parameters associated respectively with the directional insensitive (largely intrinsic) band asymmetry and with the directionally sensitive, instrumentally induced asymmetry, such that

$$\mu_3^{a}(\nu-\nu_0) = \tfrac{1}{2}[\mu_3^{F}(\nu-\nu_0)+\mu_3^{R}(\nu-\nu_0)] \quad [21]$$

and

$$\mu_3^{i}(\nu-\nu_0) = \tfrac{1}{2}[\mu_3^{F}(\nu-\nu_0)-\mu_3^{R}(\nu-\nu_0)]. \quad [22]$$

The values obtained for $\mu_3^{a}(\nu-\nu_0)$ and $\mu_3^{i}(\nu-\nu_0)$ for the *p*-chlorobenzonitrile band measured at three different amplifier response settings are shown in Figs. 6 and 7 in relation to $j = (\nu-\nu_0)/b$. These effectively illustrate the separation of the intrinsic from

*The corresponding —C≡N stretching bands of several other substituted benzonitriles were also surveyed, but most of these are unsuitable because the wing contours are distorted by overlap with other weak bands. The p-chloro derivative is singularly favorable in this respect.

†There will be a real displacement of the maximum due to the first order effect of the electronic filter system, and also an apparent displacement due to scale shift associated with the backlash in the gears of the wavenumber drive.

Can. J. Chem. Downloaded from www.nrcresearchpress.com by 210.87.254.6 on 09/05/12
For personal use only.

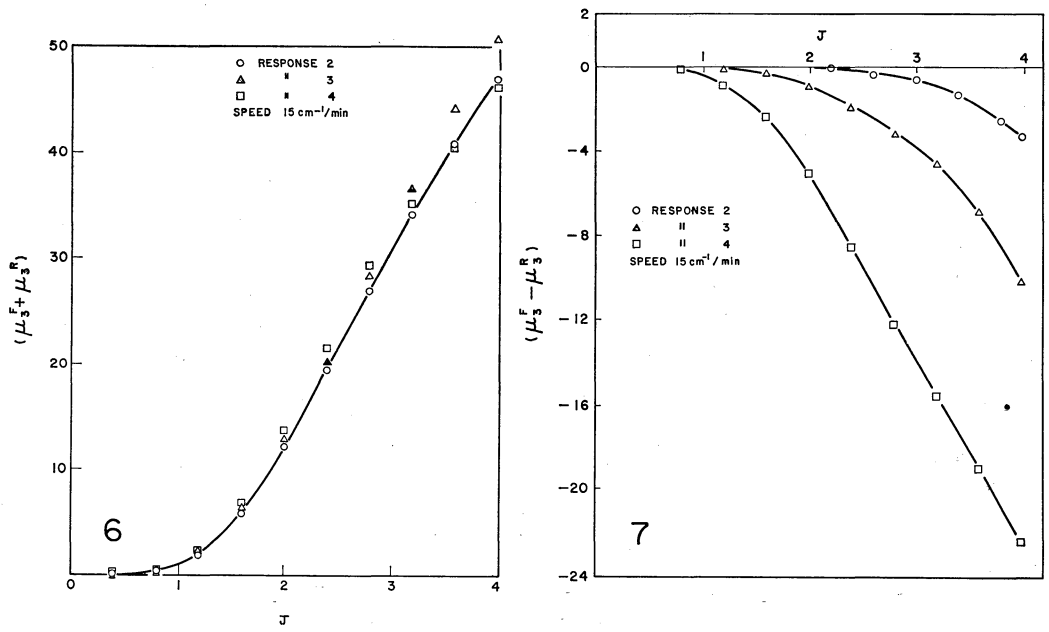

FIG. 6. The 2234.4 cm^{-1} band of *p*-chlorobenzonitrile. The effect of the amplifier response setting on $\mu_3{}^a(\nu-\nu_0)$.

FIG. 7. The 2234.4 cm^{-1} band of *p*-chlorobenzonitrile. The effect of the amplifier response setting on $\mu_3{}^i(\nu-\nu_0)$.

the instrumentally induced, directionally sensitive asymmetry. By repeating the measurements at different scanning rates it is possible to select, and to objectively describe, the optimum scanning conditions for a given instrument. More detailed analysis of these $\mu_3{}^a(\nu-\nu_0)$ versus j and $\mu_3{}^i(\nu-\nu_0)$ versus j plots should help in the quantitative treatment of electronic filter distortion. Brodersen (10) has emphasized the difficulties of dealing with this problem, even for simple RC-networks, and it will become increasingly more so as the electronic systems of infrared spectrophotometers become more complex with the increasing sophistication of the servo-operated response control circuits.

CONCLUDING REMARKS

The experimental work described in this paper is purely of an illustrative character, and the extent to which this treatment of band profiles can contribute to a better understanding of the spectra remains to be established. In making available a computer program to obtain the incomplete moments without undue tedium, we hope that we can encourage other investigators to apply these techniques to a variety of spectroscopic problems involving band shape and band intensity analysis. The necessity of separating the computation into Parts I and II, with the intermediary graphing of the absorbance curve, can probably be avoided if the number of data points is sufficiently large. This would probably necessitate the use of a spectrophotometer equipped with direct digital read-out, and would limit the application to the comparatively few laboratories that are so equipped. The method as described here can be applied to any laboratory possessing a good infrared spectrophotometer and access to comparatively modest computer facilities.

Can. J. Chem. Downloaded from www.nrcresearchpress.com by 210.87.254.6 on 09/05/12
For personal use only.

ACKNOWLEDGMENTS

We wish to thank Dr. S. D. Baxter, Dr. A. Croteau, and Dr. B. W. Attfield of the Mathematical Analysis Laboratory of the National Research Council for their technical help in providing the computational facilities and for advice and assistance with the development of the computer program.

REFERENCES

1. INTERNATIONAL UNION OF PURE AND APPLIED CHEMISTRY. Compt. Rend. Vingtième Conférence, Munich. 1959. Butterworth, London. p. 187.
2. K. S. SESHADRI and R. N. JONES. Spectrochim. Acta. In press.
3. S. G. RAUTIAN. Usp. Fiz. Nauk, **66**, 475 (1958); English Transl. Soviet Phys.-Usp, **1**, 245 (1958).
4. K. PEARSON. Biometrika, **1**, 265 (1902); **2**, 1 (1903).
5. W. P. ELDERTON. Frequency curves and correlation. 4th ed. Cambridge University Press. 1953.
6. K. PEARSON. Tables for statisticians and biometricians. Part I. 2nd ed. Cambridge University Press. 1924.
7. R. N. JONES, K. S. SESHADRI, and J. W. HOPKINS. Can. J. Chem. **40**, 334 (1962).
8. R. N. JONES, K. S. SESHADRI, and J. W. HOPKINS. Natl. Res. Council Can. Bull. No. 9, (1962).
9. S. ABRAMOWITZ and R. P. BAUMAN. Abstracts of symposium on molecular structure and spectroscopy. The Ohio State University, Columbus, Ohio. June, 1962.
10. S. BRODERSEN. J. Opt. Soc. Am. **43**, 1216 (1953).

Can. J. Chem. Downloaded from www.nrcresearchpress.com by 210.87.254.6 on 09/05/12
For personal use only.

THE REACTION OF ISOPROPANOL VAPOR WITH Hg 6($^3P_1$) ATOMS

PART II. REACTION IN THE PRESENCE OF NITRIC OXIDE

ARTHUR R. KNIGHT AND HARRY E. GUNNING
Department of Chemistry, University of Alberta, Edmonton, Alberta
Received October 29, 1962

Can. J. Chem. Downloaded from www.nrcresearchpress.com by 210.87.254.6 on 09/05/12
For personal use only.

ABSTRACT

The reaction of isopropanol vapor with Hg 6($^3P_1$) atoms in the presence of nitric oxide has been investigated in a static system at room temperature as a function of exposure time. In addition to the major products hydrogen, pinacol, and acetone found in the pure substrate reaction, the new products isopropyl nitrite, nitrous oxide, and nitrogen were observed. The effect on the reaction of the inert gas carbon tetrafluoride was also studied.

Evidence is adduced for the production of excited isopropoxy radicals in the primary process, and the rise in the nitrite and acetone yields, observed upon increasing the added inert gas pressure, is ascribed to quenching of these excited species.

The nitrite produced in the decomposition of Me_2CDOH was found to be ca. 98% Me_2CDONO, dictating its formation from the isopropoxy radical and not from Me_2COH.

A nitrite-producing dark reaction was observed when high pressures of CF_4 were added and the reaction could be prevented only by measures designed to exclude trace quantities of NO_2 from the reaction vessel.

INTRODUCTION

In Part I (1) of this series the reaction of pure isopropanol vapor with Hg 6($^3P_1$) atoms was shown to produce H_2, pinacol, and acetone as major products of the reaction, in addition to smaller quantities of CH_3CHO, CO, C_2H_6, and CH_4. Under conditions of continuous illumination quantum yield values for hydrogen and acetone were 0.72 and 0.25 respectively. For intermittent illumination, where the light period, t_L, was less than 0.45 millisecond, $\Phi(H_2)$ was unity within experimental error.

Nitric oxide has been used previously in this laboratory, in studies (2–4) of the reactions of alcohol vapors with Hg 6($^3P_1$) atoms, to detect alkoxy radicals through the formation of the corresponding nitrite. Thus, on continuous illumination of 50 mm MeOH + 5.5 mm NO and 40 mm EtOH + 10 mm NO, initial quantum yields of 0.15 and 0.25 were found for methyl and ethyl nitrite respectively. These yields are lower than expected in view of the higher initial hydrogen quantum yields observed and the fact that the general features of the reactions indicate a primary scission into alkoxy radicals and H atoms. Now the energy of the Hg 6($^3P_1$) atom, 112 kcal/mole, is ca. 10 kcal/mole higher than D(RO—H) for the alcohols (5). Hence the alkoxy radicals initially formed may possess excess energy up to ca. 10 kcal/mole, thereby leading to a strong third-body restriction on the nitrite-forming step in these systems. Pertinently McMillan (6–8) has recently reported the formation of excited alkoxy radicals in the photolysis of dialkyl peroxides, attributable to the energy difference between D(RO—OR) and that of the exciting quanta. To investigate the importance of excited isopropoxy radicals in the present system, the effect of increasing pressure of inert gas on the nitrite yield has been examined.

Bäckstrom *et al.* (9) have investigated the reactions of liquid isopropanol in the presence of nitric oxide, using benzophenone as sensitizer. One mole each of N_2, N_2O, and Me_2CO and two moles of isopropyl nitrite were found for each six moles of NO taken up by the system. Since these authors assumed the production of $Me_2\dot{C}OH$ radicals in the initial interaction between sensitizer and substrate, the nitrite must then arise by combination

of $(Me)_2\dot{C}OH$ and NO, followed by isomerization. In view of these conclusions the deuterium content of the nitrite produced in the decomposition of Me_2CDOH in the presence of NO was investigated.

The present investigation extends the work on the pure substrate, as described previously (1), to include the Hg $6(^3P_1)$-sensitized decomposition of Me_2CHOH and Me_2CDOH in the presence of small amounts of nitric oxide, and in addition includes a study of the effect of added inert gas on the reaction.

EXPERIMENTAL

The apparatus and procedures have been partially described in Part I (1) of this series.

Matheson nitric oxide was purified by successive passes through a small Hg-diffusion pump, distillation from liquid oxygen temperature, and a final degassing at liquid nitrogen temperature. Matheson carbon tetrafluoride was purified by a preliminary distillation from −130° C (*n*-pentane slush), followed by three trap-to-trap distillations at −160° C isopentane slush), and finally a thorough degassing from liquid nitrogen.

Isopropanol (Nicholls, Reagent grade) was twice fractionally distilled, a small constant-boiling fraction being retained, which was admitted to the vacuum system, degassed, and trap-to-trap distilled, with rejection of large head and tail fractions. Me_2CDOH (Merck, Montreal) was chemically purified by preparative-scale gas chromatography, followed by thorough degassing on the line. Mass spectrometric analysis showed the presence of 1.3% Me_2CDOD, while an infrared spectrum of the sample revealed that the material contained a maximum of ca. 1% ROD alcohol. The isotopic purity of the refined material was therefore 98.7%.

Analytical procedures, as well as the determination of and values for the light intensity, have been given previously (1).

Preliminary experiments showed that while no nitrite formation could be detected when a mixture of 40 mm isopropanol and 10 mm nitric oxide was carried through all stages of the procedure except irradiation, a nitrite-producing dark reaction did occur when high pressures of CF_4 were added to the reaction cell. The possibility that trace quantities of oxygen, not removable from CF_4 by degassing, were responsible for the dark reaction was investigated. Levy (10), in the analysis of the products from the pyrolysis of ethyl nitrate, found that the alcohol present was converted quantitatively to ethyl nitrite when air was admitted to the analysis cell containing the alcohol and nitric oxide. The reaction was ascribed to the formation of NO_2 by air oxidation of NO, followed by reaction of NO_2 with ethanol. Since, in the present system, CF_4 appeared to be necessary for the occurrence of the dark reaction and since mass spectrometric analysis showed the material to be free from detectable impurities, it appeared likely that an analogous mechanism was operative here. To prevent the interaction of any NO_2 with the alcohol, the following procedure was adopted. NO and CF_4 were measured in the reaction cell and stored overnight in a side trap at room temperature. The mixture was then distilled into a cell containing the alcohol with the side trap cooled to −160° C. In this way any NO_2 formed during the storage period was excluded from the reaction vessel. Blank runs performed over the entire range of CF_4 pressures used in the reported runs showed that this method of reagent introduction resulted in the complete elimination of the dark reaction.

RESULTS

The reaction in the presence of nitric oxide resulted in the formation of the same products as in the case of pure substrate, although several were markedly reduced in yield, and in addition the products isopropyl nitrite, nitrous oxide, and nitrogen were observed. A careful search of the reaction products was made for any compound which might have arisen from the reaction of NO with hydroxy isopropyl radicals. Mixtures of 35 mm isopropanol and 3 mm nitric oxide were exposed for 60 minutes and the reaction products frozen in isopentane slush (−160° C), and non-condensable gases pumped off. Fractions were then removed at −130, −98, and −45° C, and infrared spectra taken of these fractions and the residue in the reaction cell. These analyses showed that a large yield of pinacol was formed even though NO was present and that no products were present other than those found previously by mass spectrometric examination of the various compounds eluted on the G.L.C. columns.

The results of a series of experiments designed to study the effect of exposure duration on the quantum yields (Φ) for a mixture of 40 mm isopropanol and 10 mm nitric oxide are displayed as follows: Fig. 1, $\Phi(Me_2CHONO)$, and Fig. 2, $\Phi(Me_2CO)$, $\Phi(H_2)$, and

Can. J. Chem. Downloaded from www.nrcresearchpress.com by 210.87.254.6 on 09/05/12
For personal use only.

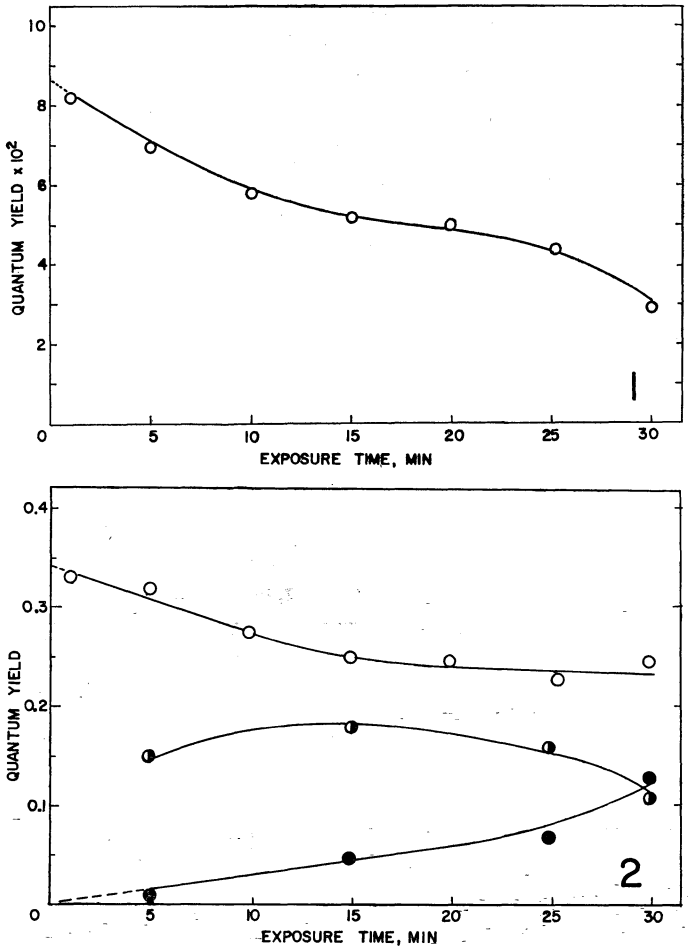

FIG. 1. Quantum yield of isopropyl nitrite as a function of exposure time for a mixture of 10 mm nitric oxide and 40 mm isopropanol.

FIG. 2. Quantum yield of acetone, ○; hydrogen, ◑; and carbon monoxide, ●, as a function of exposure time for a mixture of 10 mm nitric oxide and 40 mm isopropanol.

Φ(CO). In all figures the yields of products have been corrected for competitive quenching by nitric oxide assuming a quenching cross section (σ^2) of 12 Å^2 for isopropanol. The resulting correction factor was 1.7. Nitrous oxide and nitrogen were not determined as a function of exposure time (t), except at t = 30 minutes, where the values were $\Phi(N_2O)$ = 0.361 and $\Phi(N_2)$ = 0.071. The yields of MeCHO and CH_4 are not shown in the figures. Both these products appeared to remain constant within experimental error in the investigated range. The observed values were $\Phi(MeCHO) = 1.1\times10^{-2}$ (t = 10 to 30 minutes) and $\Phi(CH_4) = 5\times10^{-2}$ (t = 15 to 25 minutes).

Two experiments were performed with Me_2CDOH, at a pressure of 40 mm, and nitric oxide pressure of 10 mm. The condensable products of the reaction were analyzed in the usual manner and the nitrite trapped from the G.L.C. effluent and analyzed on the mass spectrometer. For 20 minutes of reaction, the nitrite was found to be 97.6% Me_2CDONO, with 2.4% Me_2CHONO present, while after 10 minutes of exposure, the heavy nitrite amounted to 97.4% of the total.

Can. J. Chem. Downloaded from www.nrcresearchpress.com by 210.87.254.6 on 09/05/12
For personal use only.

The data in Figs. 3 and 4 give respectively the yields of isopropyl nitrite and acetone as a function of pressure of added carbon tetrafluoride. This series of runs was performed with 40 mm isopropanol and 10 mm nitric oxide for an exposure time of 3.00 minutes.

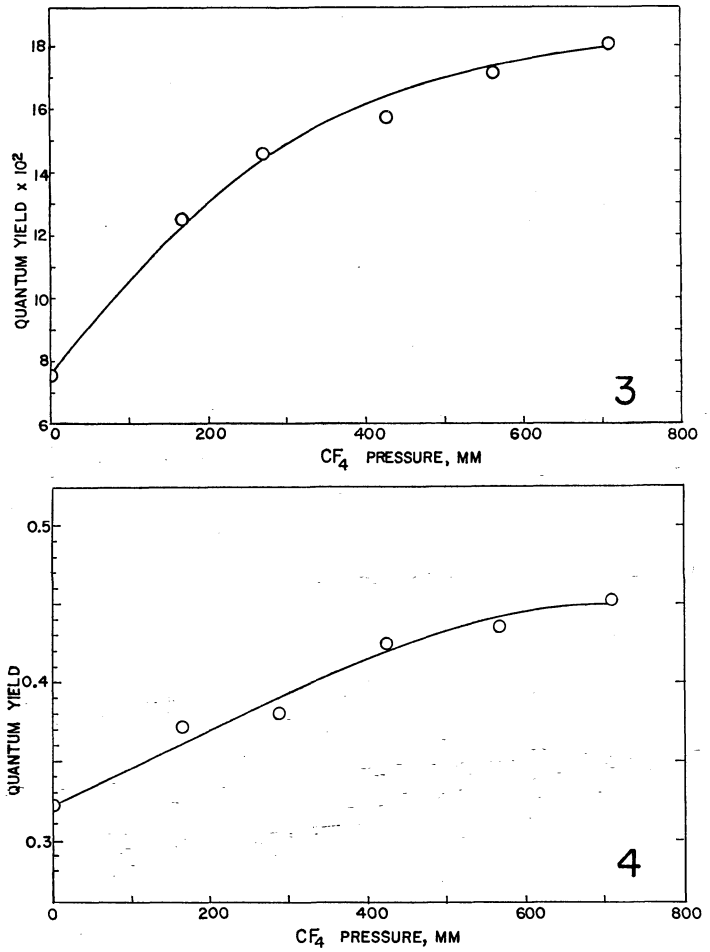

FIG. 3. Quantum yield of isopropyl nitrite as a function of pressure of carbon tetrafluoride for a mixture of 40 mm isopropanol and 10 mm nitric oxide at an exposure time of 3.00 minutes.

FIG. 4. Quantum yield of acetone as a function of pressure of carbon tetrafluoride for a mixture of 40 mm isopropanol and 10 mm nitric oxide.

DISCUSSION

The appearance of isopropyl nitrite as a reaction product suggests the presence of isopropoxy radicals in the system. The possibility that the nitrite arises by some mechanism other than the combination of $Me_2CH\dot{O}$ and NO must not be excluded immediately, however, particularly in view of the results of Bäckstrom *et al.* (9). If the $Me_2\dot{C}OH$ radical, produced in either a second primary process or by the abstractive attack of the primary fragments on the substrate, were the source of isopropyl nitrite through the sequence

$$Me_2\dot{C}OH + NO \rightarrow Me_2C(NO)OH \rightarrow Me_2CHONO, \qquad [1]$$

Can. J. Chem. Downloaded from www.nrcresearchpress.com by 210.87.254.6 on 09/05/12
For personal use only.

Can. J. Chem. Downloaded from www.nrcresearchpress.com by 210.87.254.6 on 09/05/12
For personal use only.

then the nitrite obtained from the decomposition of Me_2CDOH would contain no deuterium. The observed result that Me_2CDONO accounts for ca. 98% of the nitrite formed shows that reaction [1] does not occur to a significant extent in the present system. The observed nitrite formation in the liquid phase (9), rather than arising from photochemically produced $Me_2\dot{C}OH$ radicals, may in fact be linked with the occurrence of a dark reaction in that system between the alcohol and NO_2. (Bäckstrom *et al.* (9) reported a yellow discoloration of the solutions possibly due to NO_2 formation.) The formation of NO_2 by air contamination is rendered the more probable by the fact that the solutions were allowed to stand for 2 to 6 months before analysis for the nitrite was performed (9).

In the present system, the observation that no detectable products arise from the reaction of NO and hydroxy isopropyl radicals suggests either that this reaction is very inefficient or that the addition product is unstable or both. A possible route for the interaction would be

$$Me_2\dot{C}OH + NO \rightarrow Me_2C(NO)OH \rightarrow Me_2CO + HNO. \qquad [1']$$

The assumption made in Part I (1) that H-atoms are produced in the primary step is supported by the observed yields of N_2, N_2O, and water, which arise from the HNO formed by the scavenging of H-atoms by nitric oxide (*vide infra*).

The following mechanism is proposed to account for the observed results of the decomposition in the presence of nitric oxide:

$$Me_2CHOH + Hg\ 6(^3P_1) \rightarrow Me_2CH\dot{O} + H + Hg\ 6(^1S_0) \qquad [2]$$

$$H + Me_2CHOH \rightarrow H_2 + Me_2\dot{C}OH \qquad [3]$$

$$Me_2CH\dot{O} + Me_2CHOH \rightarrow Me_2CHOH + Me_2\dot{C}OH \qquad [4]$$

$$Me_2CH\dot{O} + NO \rightarrow Me_2CHONO \qquad [5]$$

$$H + NO + M \rightarrow HNO + M \qquad [6]$$

$$2HNO \rightarrow N_2O + H_2O \qquad [7]$$

$$HNO + 2NO \rightarrow N_2 + HNO_3 \qquad [8]$$

$$H + HNO \rightarrow H_2 + NO \qquad [9]$$

$$H + \dot{A} \rightarrow Me_2CHOH \qquad [10]$$

$$\dot{A} + Me_2CHONO \rightarrow Me_2CHOH + Me_2CO + NO \qquad [11]$$

$$2\dot{A} \rightarrow Me_2CO + Me_2CHOH \qquad [12]$$

$$2Me_2\dot{C}OH \rightarrow \text{pinacol}, \qquad [13]$$

where $\dot{A}$ represents either the $Me_2CH\dot{O}$ or the $Me_2\dot{C}OH$ radical.

Our findings can be explained through a single primary process, [2], involving O—H scission, as in the studies on methanol and ethanol (2–4). However, since the $\Phi(Me_2CHONO)$ values are considerably lower than $\Phi(H_2)$ in the uninhibited reaction (1), primary C—H cleavage cannot be excluded.

In the presence of NO, $\Phi(H_2)$ is reduced (Fig. 2). Thus at $t = 15$ minutes we find $\Phi(H_2) = 0.18$; whereas for the uninhibited reaction under the same conditions the value is 0.56 (1). Owing to the third-body restriction on [6], the primary H-atoms are probably not efficiently scavenged by NO, and abstraction from the substrate through [3] would still be operative.

The formation of the nitrite by step [5] has been observed in several systems containing isopropoxy radicals and NO (5, 6). Our finding that Me_2CDONO forms in the MeCDOH + NO system confirms this reaction. Extensive evidence is available for the occurrence of [6] and [7] to explain N_2O and H_2O formation from H atoms and NO (10–18). In

addition, in the H+NO system, it has been recently demonstrated that N_2 is a significant product (19). Reaction [8] has been postulated (19) to explain the formation of N_2, found also in this study. The formation of hydrogen through [9] has been shown by Clyne and Thrush (20), and this reaction could account for part of the hydrogen formed in the present inhibited system.

Since [6] is inefficient, there will be a finite concentration of H atoms in the system, and therefore back reaction through [10] can occur. In this step, Ȧ will likely be $Me_2\dot{C}OH$, since isopropoxy radicals can react with the substrate via [3], and be fixed as the nitrite in [5]. Furthermore, our observation that pinacol, which clearly forms via [13], is an important product even at the high NO concentrations used in this study indicates that the $Me_2\dot{C}OH$ radicals show low reactivity to NO, thereby suggesting high steady-state levels for these species.

The decrease in $\Phi(Me_2CHONO)$ with t (Fig. 1) can be explained by [11], first proposed by Steacie and Shaw (21), for Ȧ as $Me_2CH\dot{O}$. Alternately, or in addition, the nitrite can suffer photolysis and mercury photosensitization with increasing duration of exposure. This secondary photodecomposition readily accounts for the decay of $\Phi(Me_2CO)$ with exposure time (Fig. 2), with the concomitant rise in $\Phi(CO)$ (Fig. 2). As in the study of the uninhibited reaction (1), primary acetone formation is attributed to [12].

The low yield of isopropyl nitrite (Fig. 1) in the absence of inert gas requires that [2] account for only a small fraction of the primary reaction, or that [4] is very fast. A rough estimate of the activation energy of [4] can be made from the facts that abstraction by CH_3 from isopropanol has an activation energy of 7.3 kcal/mole (22), and that the value for $Et\dot{O}$ radicals abstracting from ethyl propionate (23) is 5.5 kcal/mole. Since [4] involves abstractive attack on a secondary hydrogen, E[4] would probably not exceed 5 kcal/mole. Now if we assume [2] to describe at least the predominant primary process, the resulting isopropoxy radicals would be expected to be scavenged by NO in [5], since E[5] should be near zero and the NO concentration is 20 mole% in the present system. Reaction [4] could only be significant if the primary radicals possess excess energy.

Compelling evidence for energy-rich species in the present system is seen in the effect of the inert gas, CF_4, on $\Phi(Me_2CHONO)$ in Fig. 3, and on $\Phi(Me_2CO)$ in Fig. 4. Thus with increasing CF_4 pressure, $\Phi(Me_2CHONO)$ rises steadily so that at $P(CF_4) = 710$ mm, the highest inert gas pressure used, the value is 2.4 times higher than that without added inert gas (Fig. 3). Similarly, $\Phi(Me_2CO)$ increases from 0.32 at $P(CF_4) = 0$ to 0.45 at $P(CF_4) = 710$ mm (Fig. 4). Now it has been pointed out that the initially formed $Me_2CH\dot{O}$ radicals could acquire up to 10 kcal/mole of excess energy in their formation in [2]. In short the isopropoxy radicals may possess more than the approximately 5 kcal/mole of energy required for reaction via [4]. And it should be noted that the substrate molecules will have the highest probability of first encountering these energized isopropoxy radicals. Now here CF_4 should function to deactivate the excited $Me_2CH\dot{O}$ radicals, and thereby the rate of [4] would be markedly reduced, with a concomitant rise in the concentration of thermalized $Me_2CH\dot{O}$ species. Since both the nitrite yield via [5] and the acetone yield via [12] will be directly dependent on $(Me_2CH\dot{O})$, the increase in these yields with increasing $P(CF_4)$ is readily explicable. It should further be noted that the almost first-order dependence of $\Phi(Me_2CO)$ on $P(CF_4)$ suggests that [12] involves $Me_2CH\dot{O}$ radicals interacting with excess $Me_2\dot{C}OH$ radicals:

$$Me_2CH\dot{O} + Me_2\dot{C}OH \rightarrow Me_2CO + Me_2CHOH. \qquad [14]$$

Can. J. Chem. Downloaded from www.nrcresearchpress.com by 210.87.254.6 on 09/05/12
For personal use only.

Further evidence for the presence of excited isopropoxy radicals in the system is provided by the fact that acetaldehyde is formed in the reaction, and that its yield is only slightly decreased by the presence of NO. This product evidently arises from the unimolecular decomposition of excited isopropoxy radicals, since in both the inhibited and NO-free systems its yield is almost invariant in exposure duration, with values of 1.1×10^{-2} and 1.5×10^{-2} respectively. The activation energy for the unimolecular reaction

$$Me_2CH\dot{O} \rightarrow MeCHO + CH_3 \qquad [15]$$

would be expected to be slightly higher than that for *t*-butoxy, for which a value of 13 kcal/mole has been found (5).

CONCLUSIONS

The present study has provided evidence that the reaction of isopropanol vapor with Hg $6(^3P_1)$ atoms proceeds through the formation of energy-rich isopropoxy radicals and H-atoms. Primary C—H scission may also occur, although no direct evidence for this mode of decomposition has been found. From the present study, and earlier work on the simple alcohols (1–4), primary alkoxy radical formation appears to be a general characteristic of the reactions of these molecules with Hg $6(^2P_1)$ atoms.

ACKNOWLEDGMENTS

This investigation was supported in part by the National Research Council under N.R.C. Grant No. T-162. This assistance is gratefully acknowledged by the author.

REFERENCES

1. A. R. KNIGHT and H. E. GUNNING. Can. J. Chem. **40**, 1134 (1962).
2. A. R. KNIGHT and H. E. GUNNING. Can. J. Chem. **39**, 1231 (1961).
3. A. R. KNIGHT and H. E. GUNNING. Can. J. Chem. **39**, 2251 (1961).
4. A. R. KNIGHT and H. E. GUNNING. Can. J. Chem. **39**, 2466 (1961).
5. P. GRAY and A. WILLIAMS. Chem. Rev. **59**, 240 (1959).
6. G. R. MCMILLAN. J. Am. Chem. Soc. **83**, 3018 (1961).
7. G. R. MCMILLAN. J. Am. Chem. Soc. **84**, 2514 (1962).
8. G. R. MCMILLAN. 142nd Meeting, American Chemical Society, Atlantic City. 1962.
9. H. L. J. BÄCKSTROM, A. STRENERYR, and P. PERLMANN. Acta Chem. Scand. **12**, 8 (1958).
10. J. B. LEVY. J. Am. Chem. Soc. **78**, 1780 (1956).
11. J. A. GRAY and D. W. G. STYLE. Trans. Faraday Soc. **48**, 1137 (1952).
12. R. L. HUANG and S. S. SING. Proc. Chem. Soc. 354 (1957).
13. J. K. CASHION and J. C. POLANYI. J. Chem. Phys. **30**, 317 (1959).
14. M. J. Y. CLEMENT and D. A. RAMSAY. Can. J. Phys. **39**, 205 (1961).
15. E. ARDEN and J. ROWLING. Combust. Flame, **2**, 55 (1958).
16. A. G. CARTER and M. W. TRAVERS. Proc. Roy. Soc. (London), Ser. A, **158**, 455 (1937).
17. G. I. SHAW and A. F. TROTMAN-DICKENSON. J. Chem. Soc. 3210 (1959).
18. A. SKITA and W. FUAST. Ber. **64**, 2878 (1931).
19. O. P. STRAUSZ and H. E. GUNNING. To be published.
20. M. A. H. CLYNE and B. A. THRUSH. Trans. Faraday Soc. **57**, 1305 (1961).
21. E. W. R. STEACIE and G. T. SHAW. Proc. Roy. Soc. (London), Ser. A, **151**, 685 (1935).
22. A. F. TROTMAN-DICKENSON and E. W. R. STEACIE. J. Chem. Phys. **19**, 329 (1951).
23. M. H. J. WIJNEN. J. Am. Chem. Soc. **82**, 3034 (1960).

Can. J. Chem. Downloaded from www.nrcresearchpress.com by 210.87.254.6 on 09/05/12
For personal use only.

Can. J. Chem. Downloaded from www.nrcresearchpress.com by 210.87.254.42 on 09/05/12
For personal use only.

PENTAERYTHRITOL DERIVATIVES

I. MECHANISM OF FORMATION OF DIPENTAERYTHRITOL[1]

L. W. TREVOY AND M. E. MYERS
Research Department, Canadian Chemical Company, Limited, Edmonton, Alberta

Received October 30, 1962

ABSTRACT

Dipentaerythritol, $(CH_2OH)_3CCH_2OCH_2C(CH_2OH)_3$, is a product of the base-catalyzed Tollens condensation of acetaldehyde with formaldehyde. The mechanism for formation of dipentaerythritol has not been hitherto established.

Three types of experimental evidence support the conclusion that monopentaerythritol, $C(CH_2OH)_4$, is an intermediate in the sequence of reactions leading to dipentaerythritol: (1) the isolation of radioactive dipentaerythritol from a Tollens condensation in which monopentaerythritol-C^{14} was present, (2) comparison of the radioactivity levels of mono- and di-pentaerythritol prepared by reaction of formaldehyde-C^{14} with inactive monopentaerythritol and inactive acetaldehyde, and (3) the observed dependence of the yield of dipentaerythritol on the concentration of monopentaerythritol present in the condensation reaction mixture.

Dipentaerythritol is a by-product (1) of the base-catalyzed condensation of acetaldehyde with formaldehyde. A number of different reaction mechanisms have been postulated to explain the formation of dipentaerythritol (II) from smaller building blocks in the Tollens hydroxymethylation reaction. Wawzonek and Rees (2) suggested a mechanism in which β-hydroxypropionaldehyde, from the condensation of formaldehyde with acetaldehyde, was considered to react with acrolein to form a dialdehyde (I). Further reaction of I with formaldehyde by consecutive condensation and Cannizzaro reactions

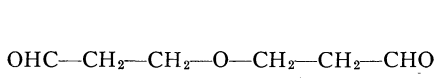

I

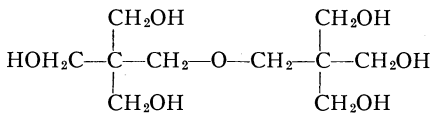

II

was considered to lead to dipentaerythritol (II). Wawzonek and Rees reached the conclusion that monopentaerythritol was not necessary for the formation of II.

A rather different reaction sequence was favored by Barth *et al.* (3). The hydrated dimer of formaldehyde (III) was thought to be capable of condensing with 2 moles of acetaldehyde, thus resulting in the generation of I, the precursor of the dimeric ether of monopentaerythritol (II).

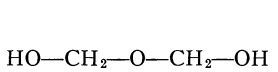

III

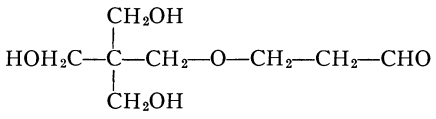

IV

An alternate mechanism not heretofore considered seriously is the one in which monopentaerythritol is postulated as an intermediate which is converted by reaction with acetaldehyde and formaldehyde into the pentaerythrityl ether of β-hydroxypropionaldehyde (IV), which could readily be transformed into dipentaerythritol by further reaction with formaldehyde.

[1]*Presented at the Annual Meeting of the Chemical Institute of Canada in Montreal, August, 1961.*

Formation of ethers in the pentaerythritol reaction has also been observed when the reaction was conducted with alcohols as solvents (2, 4). Thus Wawzonek and Rees isolated both the monomethyl and dimethyl pentaerythrityl ethers as products of reaction in methanolic solution. They explained this ether formation by the addition of the alcohol to the olefinic linkage of acrolein; the base-catalyzed addition of alcohols to α,β-unsaturated aldehydes is a well-established reaction. Wawzonek and Rees considered that acrolein may be an intermediate in both the formation of methyl pentaerythrityl ethers and in the formation of dipentaerythritol.

By using a tracer technique it should be possible to distinguish between the mechanisms of Wawzonek and Barth on the one hand, in which dipentaerythritol is built up directly from acetaldehyde and formaldehyde, and the distinctly different mechanism in which a 5-carbon unit such as monopentaerythritol or pentaerythrose is first synthesized and reacts in further steps with acetaldehyde and formaldehyde to form dipentaerythritol. Thus, by introducing monopentaerythritol-C^{14} in the reaction medium and by examination of the dipentaerythritol produced for radioactivity, it should be possible to determine whether or not monopentaerythritol is a precursor of dipentaerythritol.

EXPERIMENTAL

Radioactivity Measurements

Relative activities of mono- and di-pentaerythritol preparations were determined by counting solid samples under standard conditions. "Infinitely thick" samples were prepared by pelletizing 0.5 g of material into disks approximately 1.2 cm in diameter. The counting chamber was a CFlS-2 gas-flow counter purchased from Atomic Energy of Canada, Chalk River, Ontario, and Tracerlab G-1 Geiger Gas was used. Samples were counted for 10,000 counts in order to reduce the counting error to the 1% level. Correction was made for background count and the stability of the counter was checked periodically using a standard sample.

(1) Synthesis of Monopentaerythritol-C^{14}

Monopentaerythritol-C^{14} was synthesized by the sodium hydroxide catalyzed reaction of formaldehyde-C^{14} with inactive acetaldehyde. The preparation was conducted on a 0.4-mole scale, using formaldehyde (20% aqueous solution, sodium hydroxide (20% aqueous solution), and acetaldehyde in the mole ratio of 4.6:1.1:1.0. The initial reaction temperature was 25° C and the Cannizzaro reaction was completed at 50° C. Total radioactivity used was 0.1 mc and the monopentaerythritol which was isolated possessed an activity of approximately 0.12 μc/mmole. After neutralizing the reaction mixture with acetic acid, excess formaldehyde was removed by distillation and the crude pentaerythritol crystallized upon cooling the residual solution.

The monopentaerythritol-C^{14} was purified by conversion to the tetraacetate ester with acetic anhydride followed by fractional distillation to remove the dipentaerythritol hexaacetate. Methanolysis of the monopentaerythritol tetraacetate, b.p. 145–165° C at 0.4 mm, with methanolic hydrogen chloride regenerated the monopentaerythritol-C^{14}, which was further purified by recrystallization from water.

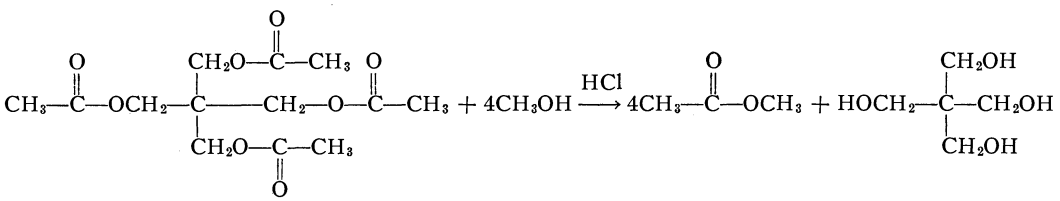

(2) Synthesis of Pentaerythritol in the Presence of Monopentaerythritol-C^{14}

A pentaerythritol synthesis was conducted in aqueous medium, in which, in addition to the acetaldehyde, formaldehyde, and sodium hydroxide which are required for the condensation reaction, monopentaerythritol-C^{14} was also present.

The monopentaerythritol-C^{14} (0.5 mole, radioactivity 817 c.p.m.) was dissolved in water and placed in a stirred reactor. After cooling the mixture to 16° C, a formaldehyde solution (75 g of 20% aqueous solution) and a sodium hydroxide solution (2 g in 8 g water) were added. Acetaldehyde (0.5 mole) was then added to the reactor and the temperature was held at 16° C for an additional 20 minutes. More formaldehyde (262 g of 20% aqueous solution) and sodium hydroxide (100 g of 20% aqueous solution) were added in succession. The reactor temperature was subsequently raised to 50° C for 90 minutes in order to complete the Cannizzaro

Can. J. Chem. Downloaded from www.nrcresearchpress.com by 210.87.254.42 on 09/05/12
For personal use only.

reaction. After concentration of the solution and removal of the excess formaldehyde by distillation, the crude product crystallized upon cooling the solution and was collected by filtration.

The monopentaerythritol and dipentaerythritol were separated by conversion to the acetate esters, fractional distillation at reduced pressure (1 mm), and alcoholysis of the individual ester fractions. The recovered monopentaerythritol (68 g) and dipentaerythritol (7.7 g) were purified by recrystallization from water; purity was established by hydroxyl value determination (5), and the radioactivity levels of both monopentaerythritol and dipentaerythritol were determined. The final purified monopentaerythritol possessed an activity of 392 c.p.m. and hydroxyl value of 49.4 (calcd. for monopentaerythritol, 50.0); the purified dipentaerythritol had an activity of 316 c.p.m. and hydroxyl value of 39.0 (calcd. for dipentaerythritol, 40.0).

(3) Synthesis of Pentaerythritol in the Presence of Formaldehyde-C^{14}

Formaldehyde-C^{14} (0.1 mc) was diluted with inactive formaldehyde and was used with inactive monopentaerythritol (0.25 mole) and inactive acetaldehyde (0.5 mole) in the synthesis of pentaerythritol. The procedure was similar to that used in Section (2). Based on pentaerythritol recovered and the pentaerythritol present in the mother liquor, the conversion of acetaldehyde to pentaerythritols was calculated to be 70%.

An efficient separation of the acetates was achieved by distillation at 10^{-4} to 10^{-5} mm Hg pressure, and monopentaerythritol tetraacetate, dipentaerythritol hexaacetate, and tripentaerythritol octaacetate were recovered. Methanolysis of the esters yielded monopentaerythritol (31 g), dipentaerythritol (9.5 g), and tripentaerythritol (1 g). Radioactivities of the purified monopentaerythritol and dipentaerythritol, respectively, were found to be 1070 c.p.m. and 1255 c.p.m.

(4) Effect of Mole Ratio of Monopentaerythritol to Acetaldehyde on Product Composition

Using constant mole ratios of formaldehyde, acetaldehyde, and sodium hydroxide (4.5:1.0:1.1) the quantity of monopentaerythritol added prior to the condensation reaction was varied from 0 to 2.5 moles per mole of acetaldehyde. The product from each reaction was isolated, was recrystallized from aqueous solution after boiling the solution with dilute sulphuric acid in order to hydrolyze formals, and the hydroxyl value of the product was determined. The experimental data are presented in Table I and in Fig. 3A.

TABLE I

The effect of monopentaerythritol concentration on formation of dipentaerythritol

Experiment No.	Mole ratio of initial monopentaerythritol to acetaldehyde	Pentaerythritol recovered* (g)	Hydroxyl value (%)	Dipentaerythritol (mole)
1	0	86.6	47.8	0.087
2	0.25	98.4	46.8	0.124
3	0.5	137.5	46.7	0.163
4	0.7	156.5	46.3	0.231
5	1.0	188.0	46.5	0.255
6	1.4	220.3	46.4	0.313
7	1.6	245.5	46.7	0.318
8	2.0	288.6	47.2	0.318
9	2.4	335.0	47.1	0.382

*Based on the reaction of 1 mole of acetaldehyde.

DISCUSSION OF RESULTS

In the initial experiment in which monopentaerythritol-C^{14} was used, the recovered monopentaerythritol had approximately one-half the original activity because of dilution with a similar quantity of inactive monopentaerythritol which had been synthesized in the reaction from acetaldehyde and formaldehyde. The dipentaerythritol was found to be radioactive, which was a definite indication that monopentaerythritol had been a building block in the formation of dipentaerythritol.

By analysis of the data obtained from this tracer experiment it is possible to conclude that all of the dipentaerythritol formed was built up from monopentaerythritol as starting material. The reactions by which mono- and di-pentaerythritol are formed are competing reactions and occur simultaneously. For the reaction

$$\text{mono-PE-C}^{14} + CH_3CHO + 4CH_2O + OH^- \rightarrow \text{di-PE-C}^{14} + HCOO^-$$

Can. J. Chem. Downloaded from www.nrcresearchpress.com by 210.87.254.42 on 09/05/12
For personal use only.

with an initial monopentaerythritol activity of 817 c.p.m. the initial dipentaerythritol activity would be $817\times(136/254) = 437$ c.p.m. Similarly for a final measured monopentaerythritol activity of 392 c.p.m. the final dipentaerythritol formed would have an activity of $392\times(136/254) = 210$ c.p.m. Since dipentaerythritol is formed in parallel with monopentaerythritol via a competing reaction then the average monopentaerythritol activity of 604 c.p.m. should lead to an average dipentaerythritol activity of 323 c.p.m. Figure 1 presents the data for the reaction in which monopentaerythritol and

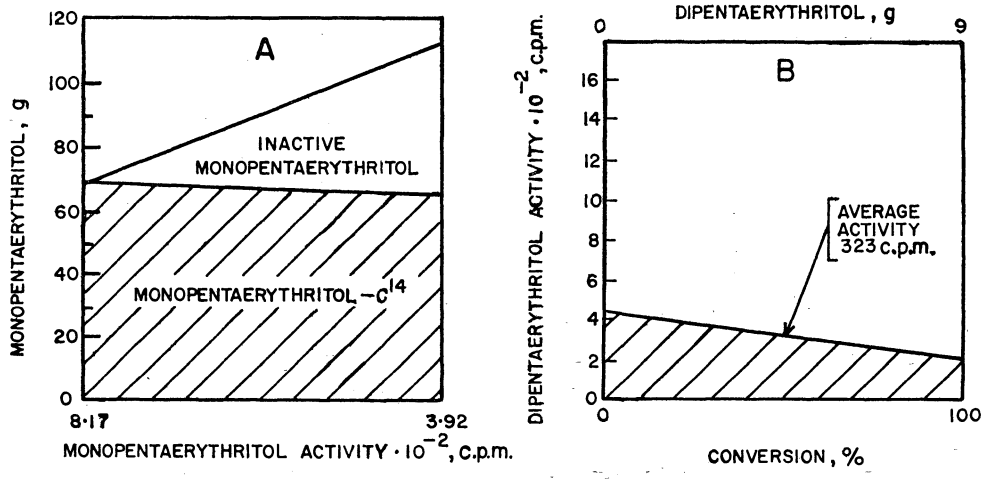

FIG. 1. Synthesis of pentaerythritol using monopentaerythritol-C^{14}. A. Dilution of monopentaerythritol during the condensation reaction. B. Dependence of dipentaerythritol activity on monopentaerythritol activity.

dipentaerythritol were formed in the presence of pentaerythritol-C^{14}. The experimentally determined activity of 316 c.p.m. for dipentaerythritol is the same as that calculated within experimental error and indicates that all of the dipentaerythritol synthesized was formed via the monopentaerythritol route.

In the tracer experiment in which C^{14}-formaldehyde was used in the synthesis of mono- and di-pentaerythritol, the data obtained are also in accord with a mechanism involving monopentaerythritol as an intermediate in dipentaerythritol formation. From the final observed activity of monopentaerythritol, and taking into account the 0.25 mole of inactive monopentaerythritol initially present, the activity of monopentaerythritol synthesized in the reaction may be calculated to be $1070\times[0.60/(0.60-0.25)] = 1835$ c.p.m. If all of the dipentaerythritol were formed directly from acetaldehyde and formaldehyde-C^{14} then the dipentaerythritol activity would be $1835\times(272/254) = 1964$ c.p.m. But since the dipentaerythritol activity was found to be 1255 c.p.m. then this is evidence against direct formation of dipentaerythritol from acetaldehyde and formaldehyde, and it is apparent that inactive monopentaerythritol initially present must also have been incorporated into the dipentaerythritol during synthesis. By comparing the calculated activity of 1964 c.p.m. with the observed activity of 1255 c.p.m. we may conclude that 64% of the monopentaerythritol units incorporated in the final dipentaerythritol were active and 36% were inactive. It follows that 72% of the dipentaerythritol was of the mixed variety, synthesized by reaction of inactive monopentaerythritol with inactive acetaldehyde and radioactive formaldehyde, while 28% was fully labelled dipentaerythritol, synthesized from radioactive monopentaerythritol or pentaerythrose formed

Can. J. Chem. Downloaded from www.nrcresearchpress.com by 210.87.254.42 on 09/05/12
For personal use only.

during the reaction which had entered into further reaction with radioactive formaldehyde. Assuming that the dipentaerythritol is formed in parallel with the monopentaerythritol, we may again calculate the dipentaerythritol activity based on an average monopentaerythritol activity during the reaction. By reacting monopentaerythritol, average activity 535 c.p.m., with inactive acetaldehyde and labelled formaldehyde-C^{14}, the calculated activity of dipentaerythritol formed = $[(535+1835)/2]\times[272/254] = 1268$ c.p.m., which is in good agreement with the observed activity of 1255 c.p.m. (see Fig. 2).

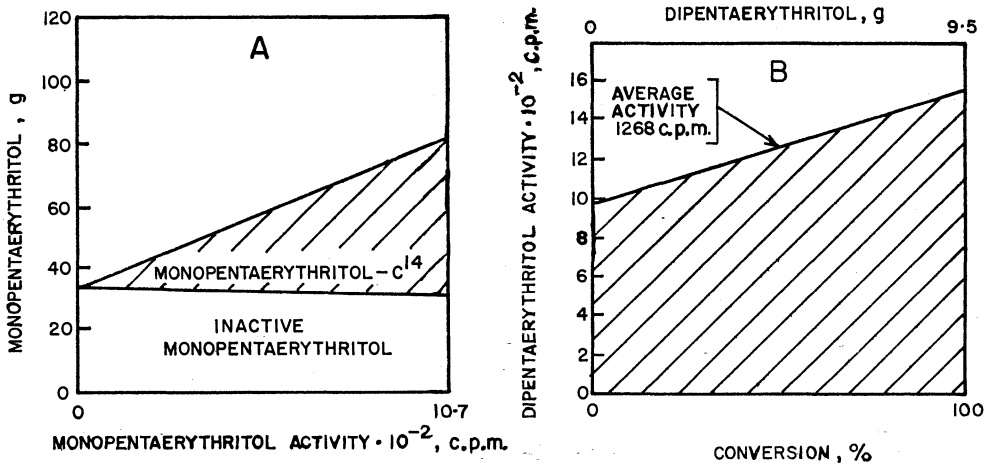

FIG. 2. Synthesis of pentaerythritol using formaldehyde-C^{14}. A. Change in monopentaerythritol activity during the synthesis. B. Dependence of dipentaerythritol activity on monopentaerythritol activity.

It may be concluded that some inactive monopentaerythritol which was originally present in the reaction mixture was used for synthesis of dipentaerythritol.

The experimental data presented in Fig. 3A show the effect of increasing monopentaerythritol concentration in the reaction mixture on the quantity of dipentaerythritol formed. The mass action effect of the increasing monopentaerythritol concentration is responsible for the substantial reduction of the hydroxyl value of the isolated reaction product, indicating an increase in the quantity of dipentaerythritol formed. With monopentaerythritol to acetaldehyde ratios greater than 1 the effect in Fig. 3A is obscured by the large quantities of monopentaerythritol present. From the experimentally determined hydroxyl values the quantity of dipentaerythritol produced in each experiment may be calculated and in Fig. 3B the dipentaerythritol formed is observed to increase as the concentration of monopentaerythritol in the original reaction was increased from 0 to 2.4 moles per mole of acetaldehyde. It may be noted that when the ratio of monopentaerythritol to acetaldehyde was increased to 2.4 then approximately 40% of the acetaldehyde was converted to dipentaerythritol in the course of the condensation reaction. The fact that the addition of monopentaerythritol to the pentaerythritol reaction mixture resulted in the formation of increased amounts of dipentaerythritol provides additional evidence in support of the conclusion that monopentaerythritol is an intermediate in the reaction sequence leading to dipentaerythritol.

The evidence presented here supports a reaction mechanism for dipentaerythritol formation in which a 5-carbon unit, monopentaerythritol, reacts with a 3-carbon unit (formed from acetaldehyde and formaldehyde) to generate an 8-carbon unit which in

Can. J. Chem. Downloaded from www.nrcresearchpress.com by 210.87.254.42 on 09/05/12
For personal use only.

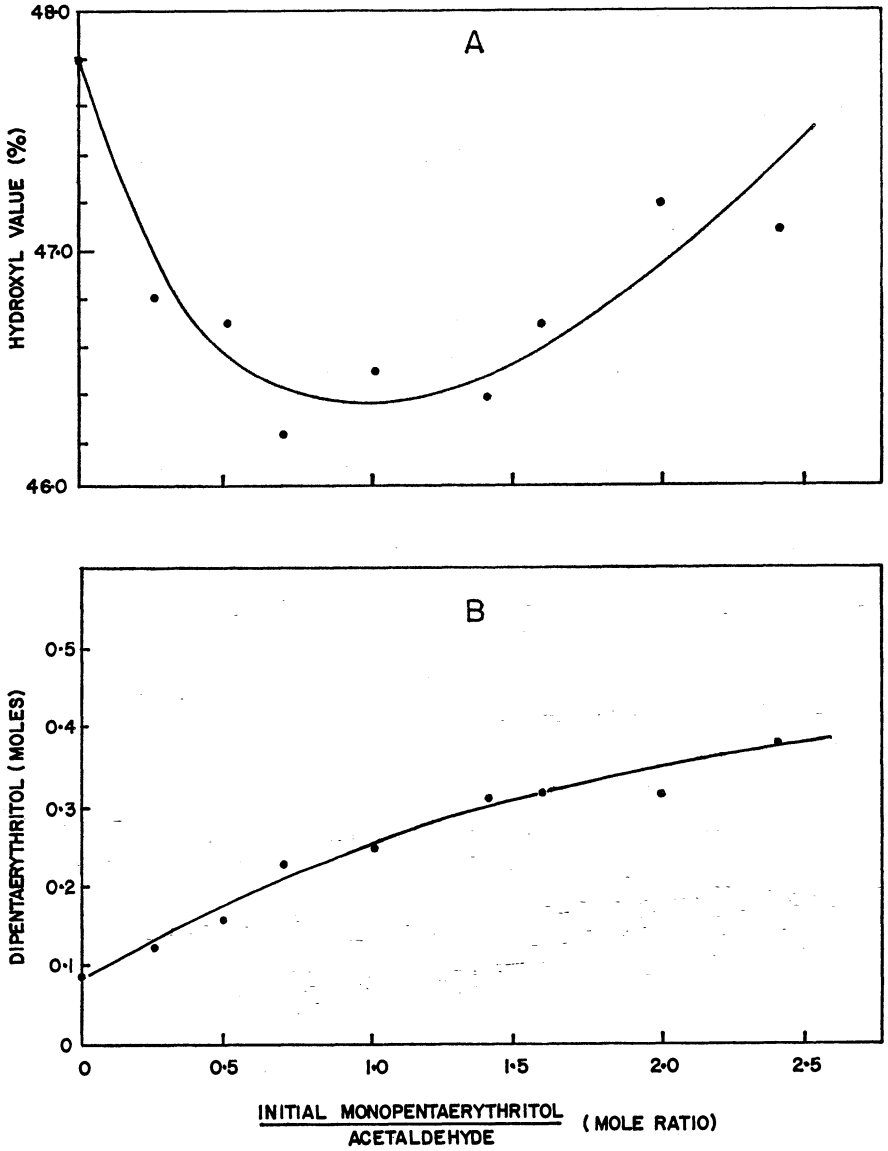

FIG. 3. The effect of monopentaerythritol concentration on the formation of dipentaerythritol in the condensation reaction. A. The effect of mole ratio of monopentaerythritol to acetaldehyde on the hydroxyl value of the isolated product. B. The relationship between dipentaerythritol formed and monopentaerythritol present in the condensation reaction.

turn reacts in the final stage with two single-carbon formaldehyde units. The results obtained in this investigation are contrary to the previously suggested mechanisms in which either a dimeric formaldehyde unit or 4-oxa-1,7-heptanedial was assumed to provide the ether linkage which was eventually converted to dipentaerythritol.

The present work has established that monopentaerythritol is an intermediate in the formation of dipentaerythritol and this conclusion is based on three different types of experimental evidence: (1) the isolation of labelled dipentaerythritol from a pentaerythritol reaction in which monopentaerythritol-C^{14} was used, (2) a comparison of the

Can. J. Chem. Downloaded from www.nrcresearchpress.com by 210.87.254.42 on 09/05/12
For personal use only.

radioactivity levels of monopentaerythritol and dipentaerythritol produced from formaldehyde-C^{14} and inactive monopentaerythritol and acetaldehyde, and (3) the dependence of the yield of dipentaerythritol upon the concentration of monopentaerythritol in the reaction mixture.

ACKNOWLEDGMENT

The authors wish to acknowledge helpful discussions with Dr. J. W. T. Spinks, University of Saskatchewan.

REFERENCES

1. W. FRIEDERICK and W. BRUN. Ber. **63**, 2681 (1930).
2. S. WAWZONEK and D. A. REES. J. Am. Chem. Soc. **70**, 2433 (1948).
3. R. H. BARTH, J. E. SNOW, and E. H. WOOD. Paper presented before North Jersey Section, American Chemical Society, January, 1951. E. BERLOW, R. H. BARTH, and J. E. SNOW. The pentaerythritols. Reinhold Publishing Corp., New York. 1958. pp. 5–6.
4. R. H. BARTH. U.S. Patent No. 2,644,013 (June 30, 1953).
5. H. N. WILSON and W. C. HUGHES. J. Soc. Chem. Ind. **58**, 74 (1939).

Can. J. Chem. Downloaded from www.nrcresearchpress.com by 210.87.254.42 on 09/05/12
For personal use only.

PROTON MAGNETIC RESONANCE SPECTROSCOPY AND THE SULPHATION OF LINEAR AND BRANCHED DEXTRAN[1]

W. M. Pasika and L. H. Cragg
Department of Chemistry, University of Alberta, Edmonton, Alberta
Received November 22, 1962

ABSTRACT

The introduction of sulphate groups into dextran produces characteristic changes in its proton magnetic resonance spectrum. With linear dextran a new signal appears which can be attributed solely to an effect of sulphate groups; with branched dextran this signal coincides with that due to the branching. From a comparison of peak areas in these spectra with peak areas in the spectra of the unsulphated linear and branched dextrans it is concluded that during sulphation no appreciable degradation occurred, whether by chain scission or branch hydrolysis.

The proton magnetic resonance spectra also provide evidence for preferential substitution of sulphate at carbon 2 in the anhydroglucose unit.

Can. J. Chem. Downloaded from www.nrcresearchpress.com by 210.87.254.5 on 09/05/12
For personal use only.

Recently we have been comparing (1) the viscosity behavior of branched and linear dextran sulphates prepared from samples of branched dextran and linear dextran of known structure. Although the sulphations were performed under mild conditions—with chlorosulphonic acid in formamide at 0° C—in order to minimize degradation (chain scission and branch hydrolysis) of the dextrans, it was clearly desirable to determine to what extent, if any, such degradation had occurred during sulphation.

Proton magnetic resonance spectroscopy, which we have already shown to be useful in detecting and estimating branching in dextran (2), proved to be a valuable means of obtaining this information about degradation. In addition, it yielded evidence for preferential sulphation at the C_2 position.

RESULTS AND DISCUSSION

Proton magnetic resonance spectra were obtained (see Experimental) for the linear dextran and the branched dextran and for the sulphated dextrans prepared from them. These spectra are reproduced in Fig. 1: (*a*) linear dextran, (*b*) branched dextran, (*c*) linear dextran sulphate, and (*d*) branched dextran sulphate. The peaks are numbered as in the earlier paper (2) (with one exception, peak 8, which will be discussed later). Peak 4 at −4.7 p.p.m. is due to the proton of deuterium hydroxide. Peaks 1 and 2 in the dextran sulphate spectra occur at the same positions as the corresponding peaks in the dextran spectra (see Table I); they may therefore be attributed to the C_5 and C_6 protons and the C_2, C_3, and C_4 protons respectively (2) (see Fig. 2). Similarly peak 5 occurs at the same position in the dextran sulphate spectra as in the dextran spectra (Table I); in all spectra it is due to anomeric (C_1) protons involved in 1,6-linkages.

Comparison of spectrum 1(*c*) with 1(*a*) and 1(*b*) reveals that there is a new peak, 8, in the linear dextran sulphate spectrum that is not present in the spectrum of the unsulphated linear dextran, and that this peak occurs, unfortunately, at just the same position as does the branching peak (peak 7) in the spectrum of branched dextran, namely at −5.4 p.p.m. In the spectrum of linear dextran sulphate this peak cannot be due to branching. Rather, it must be due in some way to the sulphate groups, the feature that distinguishes the dextran sulphate from the parent dextran.

[1]*Based on research done by W. M. Pasika for the degree Ph.D.*

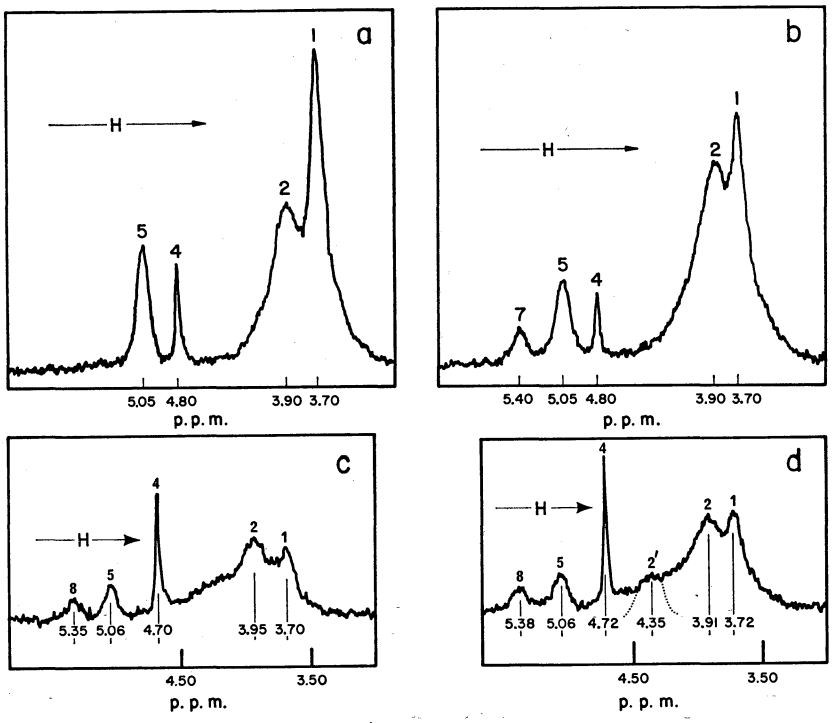

FIG. 1. Proton magnetic resonance spectra. (*a*) Linear dextran; (*b*) branched dextran; (*c*) linear dextran sulphate; (*d*) branched dextran sulphate.

TABLE I

Peak positions and assignments for dextrans and dextran sulphates

Spectrum	Peak	Protons responsible	Chemical shift (p.p.m.)*
B-512 dextran	1	C_5, C_6	−3.70
B-512 dextran sulphate	1		−3.70
B-742 dextran	1		−3.70
B-742 dextran sulphate	1		−3.72
B-512 dextran	2	C_2, C_3, C_4	−3.90
B-512 dextran sulphate	2		−3.95
B-742 dextran	2		−3.90
B-742 dextran sulphate	2		−3.91
B-512 dextran	5	C_1 (1,6-linkage)	−5.05
B-512 dextran sulphate	5		−5.06
B-742 dextran	5		−5.05
B-742 dextran sulphate	5		−5.06
B-512 dextran sulphate	8	C_1 (1,6-linkage)†	−5.35
B-742 dextran	7	C_1 (non-1,6-linkage)	−5.40
B-742 dextran sulphate	8	C_1 (1,6-linkage)† C_1 (non-1,6-linkage)	−5.38

*External standard was tetramethylsilane.
†C_1 carbon bonded to sulphate-bearing C_2 carbon.

The corresponding peak occurs in 1(*d*), the spectrum of branched dextran sulphate, and again it occurs at −5.4 p.p.m. where peak 7 occurs in the spectrum of branched dextran, 1(*b*). In this spectrum, then, peak 8 must be due to both sulphate and to branching (non-1,6-linkages).

Can. J. Chem. Downloaded from www.nrcresearchpress.com by 210.87.254.5 on 09/05/12
For personal use only.

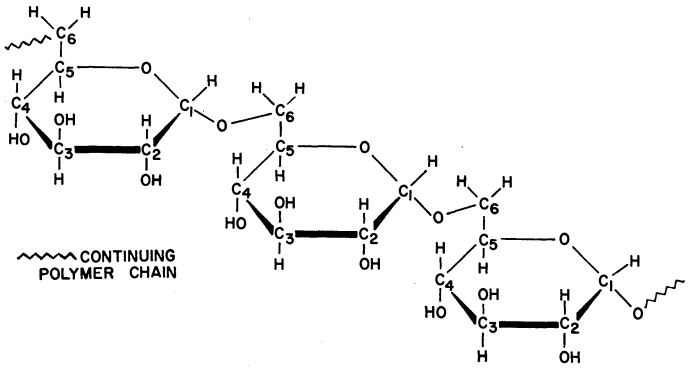

FIG. 2. Structural diagram of linear dextran.

Careful comparison also reveals the existence of a new feature in both the dextran sulphate spectra, a broad shoulder or "tail" between −4.0 and −4.5 p.p.m. For this, too, the sulphate groups must in some way be responsible. (In the branched dextran sulphate spectrum there is, moreover, a semblance of a peak, designated 2′ in Fig. 1(*d*), on this tail.) The presence of this "tail" in the sulphate spectra made impractical any attempt to measure the area of the combined peaks 1 and 2 or the area of peak 2′. Area measurements were therefore made only on peaks 5 and 8.

Peak Assignments

In the linear dextran sulphate, the sulphate groups will be attached to carbons 2, 3, and 4 of the anhydroglucose units (Fig. 2). The presence of these electronegative groups should reduce the electron density around the protons attached to these carbons and hence produce a shift downfield from −3.95 p.p.m. Since our samples are only partially sulphated, peak 2 would not disappear but would be diminished in area, with a new signal appearing at its expense.

The sulphate groups might also affect the C_1 protons (those associated with the 1,6-linkages), but if so only the sulphate groups on the adjacent carbon, C_2, would be expected to cause a shift large enough to produce a separate peak (3). Again, the effect would be an increased chemical shift from −5.05 p.p.m.; peak 5 would be diminished in favor of a new peak somewhere to its left on the spectrum as drawn.

On this basis, it is reasonable to assign peak 8 to anomeric protons attached to C_1 carbons that are bonded to sulphate-bearing C_2 carbons, and to assign the shoulder between −4 and −4.5 p.p.m. to protons on sulphate-bearing C_2, C_3, and C_4 carbons. Peak 8, then, would be formed at the expense of peak 5. The alternative would *not* be reasonable, for assignment of peak 8 to protons on the sulphate-bearing C_2, C_3, and C_4 carbons would imply a very large negative shift from −3.9 to −5.4 p.p.m., and the consequent assignment of the "shoulder" to the anomeric protons would imply a most unlikely *positive* shift from −5.05 to −4.5 p.p.m. Furthermore, the effect of sulphate groups on anomeric protons should be manifested as a sharp peak rather than as a broad shoulder, for only the groups on the C_2 carbons should contribute to the effect; the effects of sulphate groups attached to the C_2, C_3, and C_4 carbons on the protons on these carbons would be of various strengths and therefore might be expected to result in a number of closely spaced peaks merging into a shoulder. (The peak at 2′, found only in the branched dextran sulphate spectrum, may be attributed to C_6 protons affected by

Can. J. Chem. Downloaded from www.nrcresearchpress.com by 210.87.254.5 on 09/05/12
For personal use only.

sulphate groups on the same C_6 carbons; the branched dextran contains many primary alcohol groups at the branch ends and these would be preferentially substituted.)

Evidence for or against degradation was obtained from comparison of peak areas in different spectra. In order to do this, we obtained proton magnetic resonance spectra at several different concentrations, under otherwise identical conditions, for the dextrans and dextran sulphates, and measured the areas of peaks 5, 7, and 8 in the same area units.

In Fig. 3 are plotted, against concentration: A, the area of peak 5 for the linear dextran; B, the area of peak 5 for the branched dextran; and C, the area of peak 7 for the

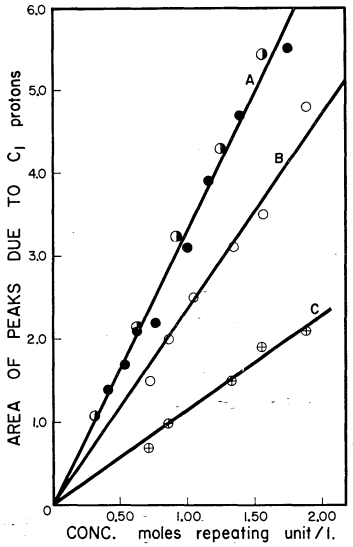

FIG. 3. Peak areas as a function of grundmolar concentration—linear and branched dextrans: ○, B, area peak 5 (branched dextran); ⊕, C, area peak 7 (branched dextran); ◑, A, sum of areas of peaks 5 and 7 (branched dextran); ●, A, area of peak 5 (linear dextran).

branched dextran. Points representing the sum of the areas of peaks 5 and 7 for branched dextran fall, as expected, on line A; for the same number (or number of moles) of anhydroglucose units, the number of 1,6-linkages and non-1,6-linkages, taken together, in branched dextran should equal the number of 1,6-linkages in linear dextran.

In Fig. 4 are plotted against concentration for linear dextran sulphate: B, the area of peak 5; C, the area of peak 8; and Σ, the sum of these areas (as taken from the lines B and C). If there is no degradation (scission of 1,6-linkages) the number of 1,6-linkages per given number of moles of the repeating unit will be the same in linear dextran sulphate as in the parent linear dextran, and hence the combined intensity of the two signals (5 and 8) due to anomeric (1,6-linkage) protons in the sulphated dextran should equal the intensity of the one signal, 5, due to anomeric (1,6-linkage) protons in the parent dextran. On the other hand, if degradation had occurred during sulphation, 1,6-linkages would have been broken and the combined areas of peaks 5 and 8 for sulphated dextran would be less than the area of peak 5 for the parent dextran (the percentage decrease being equal to the percentage of linkages broken). In Fig. 4, line Σ should coincide with line A (which is the same as line A of Fig. 3) if there is no degradation, or lie *below* it if there *is* degradation. Actually, it lies somewhat above it. We may conclude, then, that there has been no appreciable degradation of the dextran during the sulphation.

Can. J. Chem. Downloaded from www.nrcresearchpress.com by 210.87.254.5 on 09/05/12
For personal use only.

This conclusion is strengthened by a similar consideration of peak areas of the spectra of branched dextran and branched dextran sulphate. In Fig. 5, line A is the same as

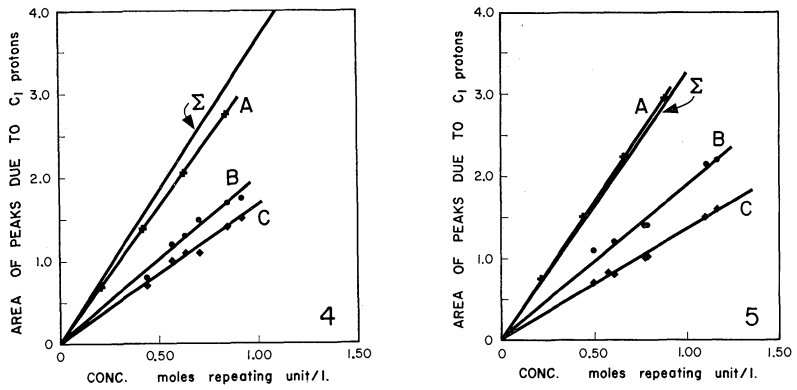

FIG. 4. Peak areas as a function of grundmolar concentration—linear sodium dextran sulphate and linear dextran (for comparison): B, peak 5 area; C, peak 8 area; Σ, sum of areas of peaks 5 and 8; A, peak 5 area (linear dextran).

FIG. 5. Peak areas as a function of grundmolar concentration—branched sodium dextran sulphate and branched dextran (for comparison): B, peak 5 area; C, peak 8 area; Σ, sum of areas of peaks 5 and 8; A, sum of peaks 5 and 7 (branched dextran).

line A of Fig. 3. Here it may be taken as a plot against concentration (in moles of repeating units—grundmoles—per liter) of the combined areas of peaks 5 and 7 of the branched dextran, i.e. of the total intensity of signals due to anomeric protons (1,6-linkages *and* non-1,6-linkages). Since line Σ is, for the branched dextran sulphate, a plot of the comparable measure of the total intensity of signals due to anomeric protons (1,6- and non-1,6-linkages), and since the abscissa for both plots is concentration in moles of repeating units per liter, line Σ should coincide with line A if there has been no chain scission (breaking of 1,6-linkages) and no branch hydrolysis (breaking of non-1,6-linkages) and it should lie *below* line A if there has been an appreciable amount of either branch hydrolysis or chain scission. Considering the imprecision of peak-area measurements, the two lines may be said to coincide within experimental error. (The experimental error should not be more than 10% and with cancellation of errors considerably less.)

We conclude, therefore, that during sulphation there has been no appreciable degradation of the dextran, and that the extent of branching in the branched dextran sulphate remains essentially the same as it was in the parent branched dextran.

Preferential Sulphation

Analysis of the spectrum of linear dextran sulphate also yields information regarding the carbon of the anhydroglucose unit on which sulphation preferentially occurs.

Our sample of linear dextran sulphate contained 9.96% sulphur* or 0.74 sulphate group per anhydroglucose unit (repeating unit). The signal at −5.35 p.p.m., peak 8, is due to anomeric (1,6-linkage) protons attached to C_1 carbons bonded to sulphate-bearing C_2 carbons, and the signal at −5.06 p.p.m., peak 5, is due to protons on 1,6-linked C_1 carbons linked to C_2 carbons which are not sulphated.

If the sulphate groups were equally distributed among the C_2, C_3, and C_4 carbons, only one-third of them would be effective in causing the shift from −5.06 to −5.35 p.p.m.,

**Commercial analysis.*

Can. J. Chem. Downloaded from www.nrcresearchpress.com by 210.87.254.5 on 09/05/12
For personal use only.

i.e. in producing peak 8 and reducing peak 5. The ratio of the area of peak 5 to the area of peak 8 then would be equal to the ratio

$$\frac{(\text{number of moles sulphate})\times 1/3}{(\text{number of moles of repeating unit}-\text{number of moles sulphate})\times 1/3} = \frac{0.74/3}{(1-0.74)/3} = 0.33.$$

The measured value of the peak ratio is 0.84. This means that sulphate groups have concentrated on C_2 carbons; in fact back calculation indicates that approximately 62% of the sulphate groups are in this position.

This evidence for preferential sulphation at the C_2 position is in qualitative agreement with earlier chemical evidence that, of the three secondary hydroxyls in polysaccharides, the one on carbon 2 is the most reactive. (See, for example, Mahoney and Purves (4) or, for a review, Sugihara (5).)

EXPERIMENTAL

Materials and Methods

The samples of linear dextran and branched dextran were those used earlier (2). They were sulphated by a procedure previously described (1) to produce the sulphated dextrans used in this investigation: linear dextran sulphate: 9.96% sulphur, 0.74 sulphate groups per anhydroglucose unit; branched dextran sulphate: 9.26% sulphur, 0.54 sulphate groups per anhydroglucose unit.

The sodium salts of these sulphated dextrans were used because of their greater solubility. They were prepared by passing the dextran sulphate solutions through columns of sodium-charged Dowex 50 cation exchange resin, and freeze-drying.

Prior to the determination of spectra, the dextran and dextran sulphate samples were treated, to exchange labile protons of the hydroxyl groups with deuterons, by thrice repeated dissolution in deuterium oxide and freeze-drying. (The deuterium oxide was the same as that used earlier (2).)

Spectra were obtained on a Varian A-60 analytical proton magnetic resonance spectrophotometer which operated at 60 Mc/s. The solvent in all instances was deuterium oxide, and all spectra were obtained at identical machine settings. The external standard was tetramethylsilane.

Peak areas were measured, as before, with a planimeter.

ACKNOWLEDGMENTS

We are grateful to Dr. R. K. Brown for helpful discussions and to the Defence Research Board of Canada for a grant (DRB 9530-09) in aid of the research.

REFERENCES

1. W. M. Pasika and L. H. Cragg. J. Polymer Sci. **57**, 301 (1962).
2. W. M. Pasika and L. H. Cragg. Can. J. Chem. **41**, 293 (1963).
3. J. A. Pople, W. G. Schneider, and J. H. Bernstein. High-resolution nuclear magnetic resonance. McGraw-Hill, Toronto. 1959. p. 277.
4. J. F. Mahoney and C. B. Purvis. J. Am. Chem. Soc. **64**, 9 (1942).
5. J. M. Sugihara. *In* Advances in carbohydrate chemistry. Vol. 8. Academic Press, New York. 1953. pp. 1–44.

Can. J. Chem. Downloaded from www.nrcresearchpress.com by 210.87.254.5 on 09/05/12
For personal use only.

THE BIOSYNTHESIS OF HYDRASTINE AND BERBERINE[1]

J. R. GEAR AND IAN D. SPENSER
Department of Chemistry, McMaster University, Hamilton, Ontario
Received September 17, 1962

ABSTRACT

The biosynthesis of hydrastine and of berberine was investigated by administering radioactive glucose, phenylalanine, tyrosine, and dopamine to *Hydrastis canadensis* L. Both hydrastine and berberine were found to be specifically derived from two molecules of tyrosine. The ratio of incorporation of the two molecules of radiotyrosine into hydrastine was not unity, and varied with time. Dopamine was also incorporated into hydrastine without randomization, but only one molecule was utilized. These results, which are consistent with the classical hypothesis and disprove the prephenic acid hypothesis of biogenesis, provide direct evidence for some of the steps in the biosynthetic pathway by which hydrastine and berberine are formed in the plant.

Can. J. Chem. Downloaded from www.nrcresearchpress.com by 210.87.254.40 on 09/05/12
For personal use only.

INTRODUCTION

Two major hypotheses have been advanced concerning the biogenesis of alkaloids containing the isoquinoline ring system.

The classical hypothesis, put forward in 1910 by Winterstein and Trier (4), elaborated by Robinson (5), and refined and extended by Robinson (6) and others (e.g. ref. 7), looked upon the aromatic amino acids tyrosine (I) and, more particularly, dihydroxyphenylalanine (dopa) (II) as the progenitors of this group of alkaloids. By decarboxylation dopa was thought to give rise to the corresponding arylethylamine, dopamine (III), which may undergo condensation, in a Mannich reaction, with carbonyl compounds, derivable from amino acids by oxidative deamination. Such a condensation of dopamine with the arylpyruvate (IV) or arylacetaldehyde derived from dopa would yield norlaudanosoline (V). This compound contains a ring skeleton from which a large number of the structural variants of the isoquinoline alkaloids may be formally derived by such comparatively simple processes as methylation, aromatization, and intra- and intermolecular oxidative coupling. It was believed that a second Mannich reaction of norlaudanosoline with formaldehyde could lead, by introduction of the so-called 'berberine bridge', to a tetracyclic system (VI) from which, by various oxidative modifications, the skeletons of further alkaloids could be obtained. This well-known hypothesis, different aspects of which have been repeatedly discussed (8–14), encompasses the biogenesis of the great majority of known naturally occurring isoquinolines, and has received circumstantial support from model syntheses under chemical (e.g. 15, 16) and "pseudophysiological" (8, 17–21) conditions.

Recently an alternative hypothesis, based on current knowledge of the role of prephenic acid in the biosynthesis of the aromatic amino acids (22, 23), has been put forward by Wenkert (24). He advanced the view that it was not tyrosine but its biochemical precursor, prephenic acid, which served directly as the progenitor of the arylethylamine (III) and the arylpyruvate (IV) whose condensation would yield norlaudanosoline (V). 'Berberine-bridged' structures were thought to arise not by introduction of a one-carbon unit into norlaudanosoline but by interaction of two prephenate-derived precursors, one of which contained the one-carbon unit prior to condensation.

[1]*Parts of this work have been reported in preliminary communications (1, 2, 3).*

The differences between the amino acid and the prephenic acid hypotheses of biogenesis may be summarized as follows:

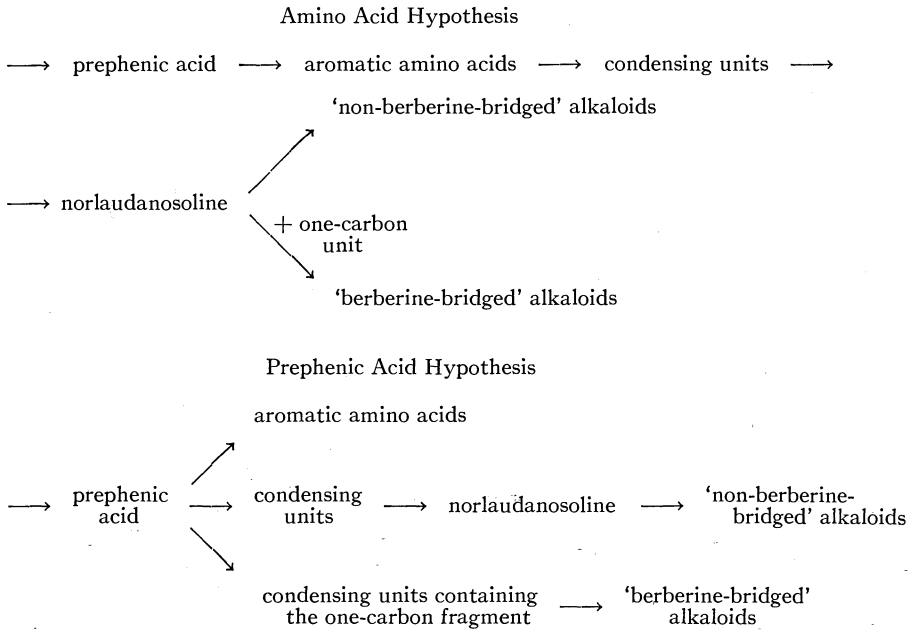

No experiments have yet been carried out which can differentiate between these two rival hypotheses. The general validity of the biogenetic approach has been established however. Two alkaloids which may be biogenetically derived from norlaudanosoline, papaverine (25) and morphine (26), have been the objects of unequivocal biosynthetic investigation. In both cases it was shown by unambiguous degradation of the labelled alkaloids, obtained from DL-[2-^{14}C]-tyrosine in *Papaver somniferum* L., that two units of precursor were incorporated without scrambling of radioactivity, in the manner predicted by the classical hypothesis. It was shown further that norlaudanosoline itself was also incorporated into both alkaloids without randomization (27).

Since these findings can also be reconciled with the prephenic acid hypothesis, however, the results of these investigations cannot serve to differentiate between the two biogenetic proposals. Both hypotheses predict that the two alkaloids are derived from norlaudanosoline, which arises by condensation of an hydroxylated phenylethylamine with an hydroxylated phenylpyruvic acid unit. The question at issue is therefore whether these two intermediates are *normally* derived from tyrosine or whether they are *normally* derived directly from prephenic acid.

It is difficult to design a critical experiment capable of giving an unequivocal answer to this question. In most cases the 'Wenkert precursor' would be predicted to yield the 'classical precursor' by known metabolic steps. Biosynthetic incorporation into an alkaloid of the labelled 'Wenkert precursor' would thus not invalidate the classical hypothesis. Also, the biogenetic condensing units (e.g., III and IV) could arise in most cases either from tyrosine or directly from prephenic acid, by unexceptional metabolic steps. It is conceivable that both of these pathways may be available simultaneously, one as the major route, the other as an alternative route of minor quantitative importance. Incorporation into an alkaloid of a labelled 'classical precursor' may thus represent the

Can. J. Chem. Downloaded from www.nrcresearchpress.com by 210.87.254.40 on 09/05/12
For personal use only.

minor pathway and does not therefore disprove the prephenic acid hypothesis. It is for this reason that the investigations on papaverine (25) and morphine (26) do not distinguish between the two hypotheses.

The work to be described deals with one of the few instances where different pairs of biogenetic condensing units are postulated by the classical and by Wenkert's hypothesis so that clear-cut differentiation of the two hypotheses is possible. The results unequivocally disprove the prephenic acid hypothesis.

RESULTS

The plant chosen for experiment was the Canadian Goldenseal, *Hydrastis canadensis* L., which elaborates three alkaloids, berberine (VIII), hydrastine (IX), and canadine (VII). In a series of feeding experiments D-[U-^{14}C]-glucose, DL-[2-^{14}C]-phenylalanine, DL-[2-^{14}C]-tyrosine, DL-[3-^{14}C]-tyrosine, and [1-^{14}C]-dopamine were administered, either by way of the root or by infusion into the stem (expts. 1–10, Table I). In each experiment

TABLE I

^{14}C-Labelled compounds administered to *Hydrastis canadensis* L.

Expt.	Compound fed	Weight fed (mg)	Specific activity (counts/min mmole) $\times 10^{-8}$	Total activity fed (counts/min) $\times 10^{-7}$	Number of plants	Period of growth in contact with tracer (days)
			Root-fed plants			
1	U-^{14}C-Glucose	18.0	8.75	8.77	9	17
2	2-^{14}C-Phenylalanine	35.0	4.18	8.87	9	8
3	2-^{14}C-Tyrosine	30.5	6.55	11.0	9	8
4	2-^{14}C-Tyrosine	30.5	5.15	8.68	9	17
5	3-^{14}C-Tyrosine	2.8	7.23	1.12	6	3
6	3-^{14}C-Tyrosine	2.8	6.96	1.08	6	6
7	3-^{14}C-Tyrosine	5.6	6.75	2.10	9	9
8	3-^{14}C-Tyrosine	2.8	6.58	1.03	6	24
			Wick-fed plants			
9	3-^{14}C-Tyrosine	2.8	6.95	1.07*	4	9
10	1-^{14}C-Dopamine hydrobromide	13.0	6.12	2.16†	6	10

*The wicks used in this experiment contained negligible residual activity at the end of the feeding period.
†The solution initially fed in this experiment had a total activity of 3.40×10^7 counts/min. Extraction of the wicks at the time of harvesting yielded a total activity of 1.24×10^7 counts/min, which was shown to be due to unchanged dopamine by chromatography in *n*-propanol – water (7:3) and by radioassay of the chromatogram. The total activity of dopamine taken up by the plant was thus 2.16×10^7 counts/min.

berberine and hydrastine were extracted from the roots and rhizomes of the plants, and in one case (expt. 4L) also from stems and leaves.

The alkaloids were assayed for radioactivity (Table II) and those derived from selected experiments were systematically degraded to ascertain the precise location of radiocarbon.

Of the compounds tested, tyrosine was found to be the most efficient precursor of the alkaloids (Table III). In experiments of the same duration, administration by infusion resulted in higher incorporation of radioactivity than administration by way of the root (expts. 7 and 9, Table IV). Stems and leaves contained only small amounts of alkaloids, and the specific activity of the alkaloids isolated from the aerial parts of the plant was much lower than that of the alkaloids isolated from roots and rhizomes of the same plant (expts. 4 and 4L). Dopamine was almost as good a precursor of berberine as was tyrosine, but appeared to be less efficient as a precursor of hydrastine. Glucose was a much less efficient precursor of the alkaloids, and phenylalanine incorporation was almost

Can. J. Chem. Downloaded from www.nrcresearchpress.com by 210.87.254.40 on 09/05/12
For personal use only.

TABLE II

Chemical and radioactive yield of alkaloids

Expt.	Weight of dry plant material (g)	Hydrastine Weight (mg)	Hydrastine % yield	Hydrastine Specific activity (counts/min mmole) $\times 10^{-4}$	Berberine hydrochloride Weight (mg)	Berberine hydrochloride % yield	Berberine hydrochloride Specific activity (counts/min mmole) $\times 10^{-4}$
1	36.7	553	1.5	0.35	679	1.9	1.0
2	25.7	463	1.8	0.06	511	2.0	0.07
3	9.3	173	1.9	4.48	205	2.2	6.54
4	14.5	205	1.4	5.17	380	2.6	10.50
4L	5.0	22	0.4	0.49	16	0.3	3.92
5	14.2	238	1.7	1.19	389	2.7	2.53
6	15.4	273	1.8	1.42	359	2.3	3.07
7	15.2	240	1.6	4.96	415	2.7	7.32
8	12.0	219	1.8	1.36	355	3.0	1.83
9	35.6	424	1.2	5.76	818	2.3	8.90
10	36.0	555	1.5	0.87	825	2.5	4.50

TABLE III

Efficiency of incorporation of radioactive precursors

Expt.	Precursor	Specific radiochemical yield* $\times 10^4$ Hydrastine	Berberine
1	U-^{14}C-Glucose	4.0	11.0
2	2-^{14}C-Phenylalanine	1.4	1.7
3	2-^{14}C-Tyrosine	68.0	100.0
4	"	100.0	240.0
4L	"	9.5	76.0
5	3-^{14}C-Tyrosine	16.5	35.0
6	"	20.0	44.0
7	"	73.0	108.0
8	"	21.0	36.0
9	"	83.0	128.0
10	1-^{14}C-Dopamine HBr	14.0	74.0

*Specific radiochemical yield $= \frac{\text{specific activity of product}}{\text{specific activity of precursor}} \times 100$.

TABLE IV

Incorporation of [3-^{14}C]-tyrosine into the alkaloids using different modes of administration

Expt.	Mode of administration	Total activity of hydrastine (counts/min) $\times 10^{-4}$	Total activity of berberine (counts/min) $\times 10^{-4}$
7	Root	1.55	3.60
9	Wick	6.38	17.9

negligible. Without exception berberine isolated from a particular experiment had a higher specific activity than hydrastine obtained from the same experiment, even though the quantity of berberine isolated always exceeded that of hydrastine. The specific radiochemical yields obtained in each of the experiments are shown in Table III.

Degradation of hydrastine (IX) derived from DL-[2-^{14}C]-tyrosine (expt. 4) showed that activity was located exclusively at carbon atoms 1 and 3 of the hydrastine skeleton. This establishes tyrosine as a specific precursor of hydrastine, and demonstrates that two molecules of tyrosine are utilized in the biosynthesis of each molecule of hydrastine. However,

Can. J. Chem. Downloaded from www.nrcresearchpress.com by 210.87.254.40 on 09/05/12
For personal use only.

the ratio (radioactivity in C_1/radioactivity in C_3) was not 1:1 but 2:3. To investigate whether this ratio was affected by the period of growth of the plants in contact with tracer, hydrastine obtained from experiments 5–8, in which plants had been exposed to DL-[3-^{14}C]-tyrosine for varying periods of time, was partially degraded.[2] The results are shown in Table V but no simple trend is apparent.

TABLE V

	Hydrastine		Hydrastinine		Opianic acid	
Expt.	Specific activity (counts/min mmole) $\times 10^{-4}$	Relative specific activity	Specific activity (counts/min mmole) $\times 10^{-4}$	Relative specific activity	Specific activity (counts/min mmole) $\times 10^{-4}$	Relative specific activity
5	1.19	100	0.50	42.0	0.65	54.5
6	1.42	100	0.70	49.0	0.69	49.0
7	4.96	100	2.44	49.0	2.46	49.5
8	1.36	100	0.60	44.0	0.74	54.0
9	5.76	100	3.28	57.0	2.46	42.7

Degradation of the hydrastine isolated from plants to which [1-^{14}C]-dihydroxyphenylethylamine had been administered (expt. 10) showed that activity was located exclusively at carbon atom 3. Thus dopamine was a specific precursor of hydrastine but only one molecule of dopamine was used in the biosynthesis of the alkaloid.

Degradation of the berberine obtained in experiment 4 showed that activity was confined to carbon atoms 1 and 3 of berberine (VIII). Tyrosine was therefore a specific precursor of berberine and two tyrosine units had been incorporated into the alkaloid. The ratio (radioactivity in C_1/radioactivity in C_3) in this case was found to be unity.

DISCUSSION

According to classical hypothesis the major steps in the biogenesis of hydrastine (IX) are (i) the condensation of dopamine (III) and dihydroxyphenylpyruvic acid (IV), both derived from tyrosine (I), to yield norlaudanosoline (V), (ii) the introduction of a one-carbon unit into norlaudanosoline, giving a tetrahydroberberine ring system (VI), and (iii) oxidative modification of the latter to yield the alkaloid.

The hypothesis demands that, in a biosynthetic experiment, radioactivity from [2-^{14}C]-tyrosine should enter hydrastine at two sites and should be confined to carbon atoms 1 and 3 (Fig. 1).

Wenkert's prephenic acid hypothesis, on the other hand, postulates that the skeleton of hydrastine is derived without the intervention of norlaudanosoline, by combination of two fragments thought to arise directly from prephenic acid (X), an arylethylamine (III) and an *o*-carboxyarylpyruvic acid (XII) (Fig. 2). The latter precursor retains carbon atom 7 of prephenic acid as an aromatic carboxyl group, from which the 'one-carbon bridge' of hydrastine is formed. Whereas the amine (III), derived according to Wenkert from prephenate, could also be derived from tyrosine by a sequence of enzymic reactions for which there is ample precedent (28), *there is no known metabolic process whereby the second fragment* (XII), also derivable from prephenate, *can originate directly from tyrosine*, since the enzymic conversion of prephenate to tyrosine has been shown to be irreversible (29).

[2]*Since incorporation of two molecules of tyrosine into hydrastine had already been proved, it was sufficient in these experiments to separate the two labelled carbon atoms (4 and 7') from one another, and unnecessary to isolate them completely.*

Can. J. Chem. Downloaded from www.nrcresearchpress.com by 210.87.254.40 on 09/05/12
For personal use only.

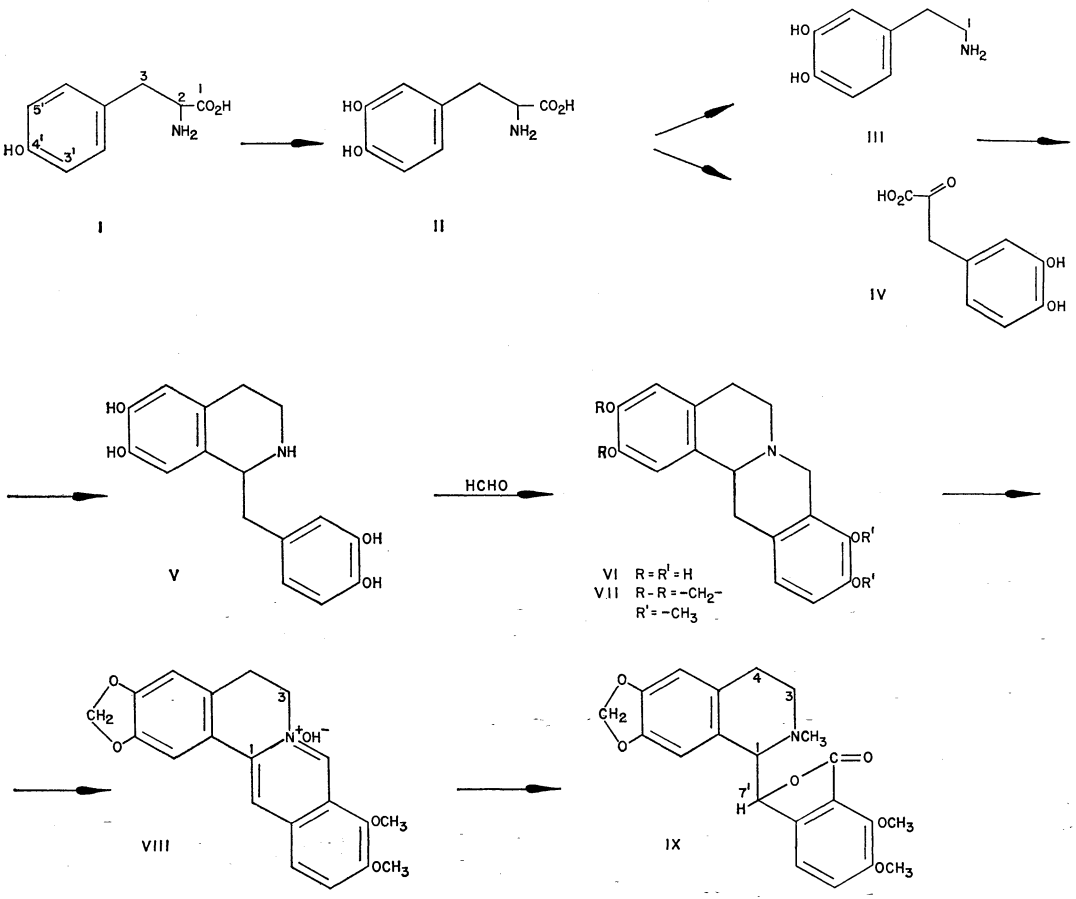

FIG. 1. Classical hypothesis of biogenesis of hydrastine and berberine.
Hydrastine (IX) could also be derived directly from V or VI and not by further oxidation of berberine (VIII). Experiments to establish the metabolic interrelationships of the two alkaloids are in progress.

Wenkert's hypothesis thus requires that if radioactivity from [2-^{14}C]-tyrosine were incorporated into hydrastine without randomization, it should be confined to carbon atom 3 of the molecule.[3]

[3]*Conversion of [2-^{14}C]-tyrosine to glucose (30) and of [U-^{14}C]-tyrosine to carbohydrates (31) has been reported to take place in plants. The steps of this pathway have not been investigated. If the metabolic breakdown of tyrosine in plants is analogous to that in microorganisms and in rats, as seems likely (31), then activity from [2-^{14}C]-tyrosine should appear at carbon atoms 3 and 4 of glucose, by way of [1-^{14}C]-acetoacetate, [1-^{14}C]-acetyl-CoA, [1-^{14}C]-citrate, [1,4-^{14}C]-oxalacetate, [1-^{14}C]-pyruvate, followed by reversal of glycolysis. If, furthermore, shikimic and prephenic acid biosynthesis in plants parallels that in microorganisms, and evidence for this view is accumulating (32), then activity from [3,4-^{14}C]-glucose or any of the intermediates between [2-^{14}C]-tyrosine and [3,4-^{14}C]-glucose would appear in carbon atoms 7, 3, and 4 of shikimic acid (23) and, after assimilation of a [1-^{14}C]-pyruvate moiety, in carbon atoms 3 and/or 5, 4, 7, and 10 of prephenic acid. If this prephenic acid then served as a precursor of hydrastine, according to Wenkert's scheme, activity in the alkaloid would be randomized over carbon atoms 6 and/or 8, 7, 2' and/or 4', 3' and 10'. If the above assumptions are valid, demonstration of such randomization of activity in hydrastine derived from [2-^{14}C]-tyrosine would favor Wenkert's hypothesis, but would not prove its validity conclusively, for if the process leading from [2-^{14}C]-tyrosine to [3,(5),4,7,10-^{14}C]-prephenic acid were rapid, the latter would yield [1,3',4',5'-^{14}C]-tyrosine, incorporation of which into hydrastine, as predicted by the classical hypothesis, would also yield multiply labelled alkaloid, which in addition to ^{14}C at carbon atoms 6, 7, 8, 3', 4', and 5' would also show activity at carbon atoms 1 and 3, from the original [2-^{14}C]-tyrosine. In either case carbon atoms 11, 12, 8', and 9' and in the latter case carbon atom 10' of hydrastine may also show radioactivity derived from the one-carbon fragment split off as carbon dioxide from carbon atom 7 of prephenic acid.*

Can. J. Chem. Downloaded from www.nrcresearchpress.com by 210.87.254.40 on 09/05/12
For personal use only.

Can. J. Chem. Downloaded from www.nrcresearchpress.com by 210.87.254.40 on 09/05/12
For personal use only.

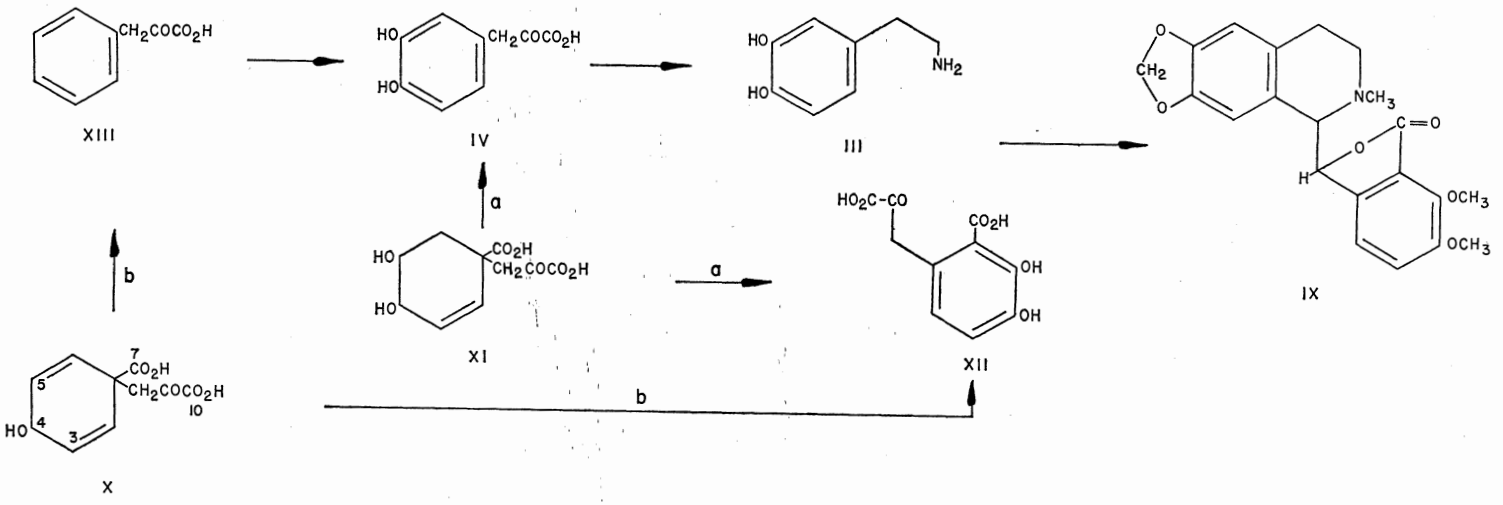

FIG. 2. Prephenic acid hypothesis of biogenesis of hydrastine. Original scheme (*a*) based on hydrated prephenic acid (XI) and revised scheme (*b*) based on prephenic acid (X).

Demonstration of specific incorporation of one tyrosine unit into the isoquinoline segment of hydrastine would clearly confirm Wenkert's hypothesis and invalidate the classical hypothesis. Demonstration of specific incorporation of two tyrosine units into hydrastine, on the other hand, would establish the validity of the classical hypothesis and unequivocally disprove Wenkert's scheme for the biogenesis of hydrastine.

The results of the present feeding and degradation experiments show that tyrosine is a direct precursor of hydrastine and that two molecules of tyrosine are used in the biosynthesis of hydrastine. It follows that Wenkert's scheme for the biogenesis of the phthalideisoquinoline alkaloids (Fig. 2) is not valid for hydrastine, a member of this group. The results are in agreement with the classical hypothesis (Fig. 1).

The significance of the unequal incorporation of radioactivity from DL-[2-^{14}C]-tyrosine into carbon 1 and carbon 3 of hydrastine, which was regarded as evidence for a split biosynthetic pathway, has been discussed elsewhere (1).

A study of the variation with time of the ratio (radioactivity in C_1/radioactivity in C_3) (Table VI) did not indicate a simple trend. Further experiments are required before a

TABLE VI

Variation of ratio C_1/C_3 or C_7'/C_4 of hydrastine with time

Expt.	Precursors fed to plants	Mode of administration	Duration of feeding (days)	Ratio of C_1 to C_3 or C_7' to C_4
5	3-^{14}C-Tyrosine	Root	3	1.30
6	"	"	6	1.00
7	"	"	9	1.01
9	"	Wick*	(9)	(0.75)
4	2-^{14}C-Tyrosine	Root	17	0.61
8	3-^{14}C-Tyrosine	"	24	1.23

*Since experiment 9 was a wick-feeding experiment whereas all others were root-feeding experiments, the ratio of 0.75 obtained from it is not directly comparable with the other ratios. At the same time it is interesting to see that the value of 0.75 lies between the values of 1.01 for experiment 7 and 0.61 for experiment 4. This would appear to indicate that wick-feeding causes faster uptake of precursor, and that a 9-day wick-feeding experiment is equivalent to a root-feeding experiment of greater than 9 but less than 17 days' duration.

meaningful interpretation of this variation can be attempted.

Dopamine was found to be a specific precursor of hydrastine. Since radioactivity from [1-^{14}C]-dopamine was confined to carbon 3 of hydrastine, only one dopamine unit was incorporated into the alkaloid molecule. This finding, which provides confirmation of the 'split biosynthetic pathway' and establishes the association of dopamine with one of the branches of the biosynthetic route to hydrastine, has already been reported (2). Present knowledge of the biosynthesis of hydrastine may be summarized as shown in Fig. 3.

The test which was applied to establish the validity of one or the other of the classical or the prephenate hypotheses in the case of hydrastine is not applicable in the case of berberine, another alkaloid of *H. canadensis* L. It was found that two tyrosine units were specifically incorporated into berberine, radioactivity from DL-[2-^{14}C]-tyrosine being located exclusively at carbon atoms 1 and 3 of the alkaloid. In this instance, however, specific incorporation of radiotyrosine is not of diagnostic value in differentiating between the two hypotheses, since *both* of the prephenate-derived 'Wenkert precursors' (IV and III*a*) (Fig. 4) *could* also arise by feasible metabolic routes from tyrosine.

A second line of evidence is available, however, which not only substantiates the conclusions reached with respect to Wenkert's scheme for hydrastine biogenesis, but also serves to invalidate his prephenic acid hypothesis in the case of berberine. In its original form (24) the prephenic acid hypothesis postulated that each of the two fragments, whose

Can. J. Chem. Downloaded from www.nrcresearchpress.com by 210.87.254.40 on 09/05/12
For personal use only.

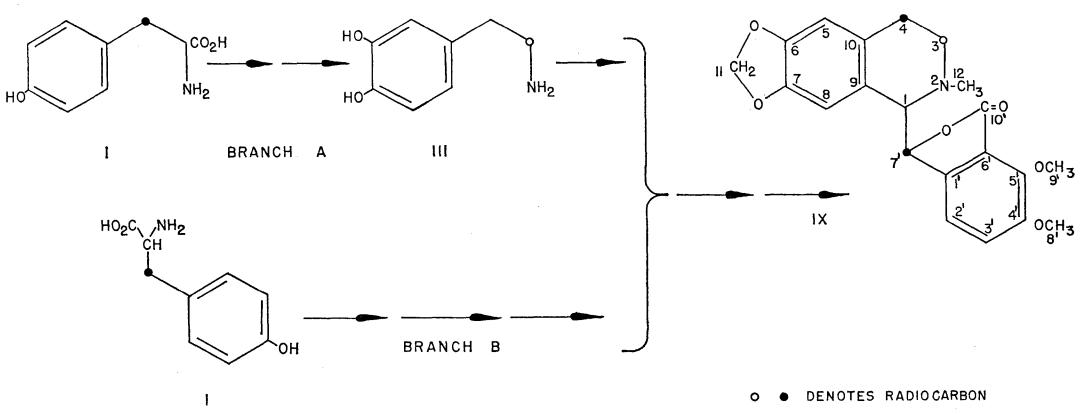

FIG. 3. Biosynthesis of hydrastine.

union yields the skeleton of the isoquinoline alkaloids, was derived from a hydrated prephenic acid moiety (XI). When it was demonstrated that the enzymic conversion of shikimate to prephenate proceeds without the intervention of such a hydrated form (33, 23), the hypothesis was modified (34) to accommodate this fact. According to the modified hypothesis the hydroxylated arylethylamine and arylpyruvate units required in the biogenesis of the isoquinoline alkaloids are derived from prephenate by way of phenylpyruvic acid (XIII). Phenylpyruvic acid is thus regarded as an intermediate in the hypothetical pathway. Since phenylpyruvate would be expected to arise from phenylalanine by transamination, and since transamination of phenylalanine is known to occur in plants (35), it can be predicted that, if this hypothesis were valid, phenylalanine would serve as an efficient precursor of the isoquinoline alkaloids. Incorporation of radiophenylalanine into hydrastine and berberine has now been shown to be almost negligible however, at a time of development of the plants when tyrosine was actively incorporated into the alkaloids. That this low level of incorporation of phenylalanine was not due to endogenous dilution is shown by the finding that the incorporation of radioglucose into hydrastine and berberine, at the same stage of development of the plants, was far more efficient than incorporation of phenylalanine. Nor is it likely that the low level of phenylalanine incorporation was due to lack of absorption of the precursor by the plant. Phenylalanine was found to disappear from the nutrient solution as rapidly as tyrosine and glucose. Assuming the biochemical equivalence of phenylalanine and phenylpyruvic acid in *H. canadensis*, the prephenate hypothesis is thus shown to be invalid in the case of berberine as well as in the case of hydrastine.

The present results provide strong evidence against the prephenic acid hypothesis only in the instances of hydrastine and berberine. A review of recent work on the biosynthesis of alkaloids (36) however shows that alkaloids of the same group, differing only in oxidation state and extra-skeletal substituents, are often derived from the same precursors. Since both hydrastine and berberine are representative of a much larger class of naturally occurring compounds of common and related skeletal structure, the present findings cast doubt on the validity of the prephenic acid hypothesis of biogenesis of the isoquinoline alkaloids in general.

The classical hypothesis of biogenesis, however, is supported by all available biosynthetic data (36). At the time this hypothesis was conceived half a century ago, experimental methods capable of eliciting supporting evidence were lacking. Despite this lack

Can. J. Chem. Downloaded from www.nrcresearchpress.com by 210.87.254.40 on 09/05/12
For personal use only.

Can. J. Chem. Downloaded from www.nrcresearchpress.com by 210.87.254.40 on 09/05/12
For personal use only.

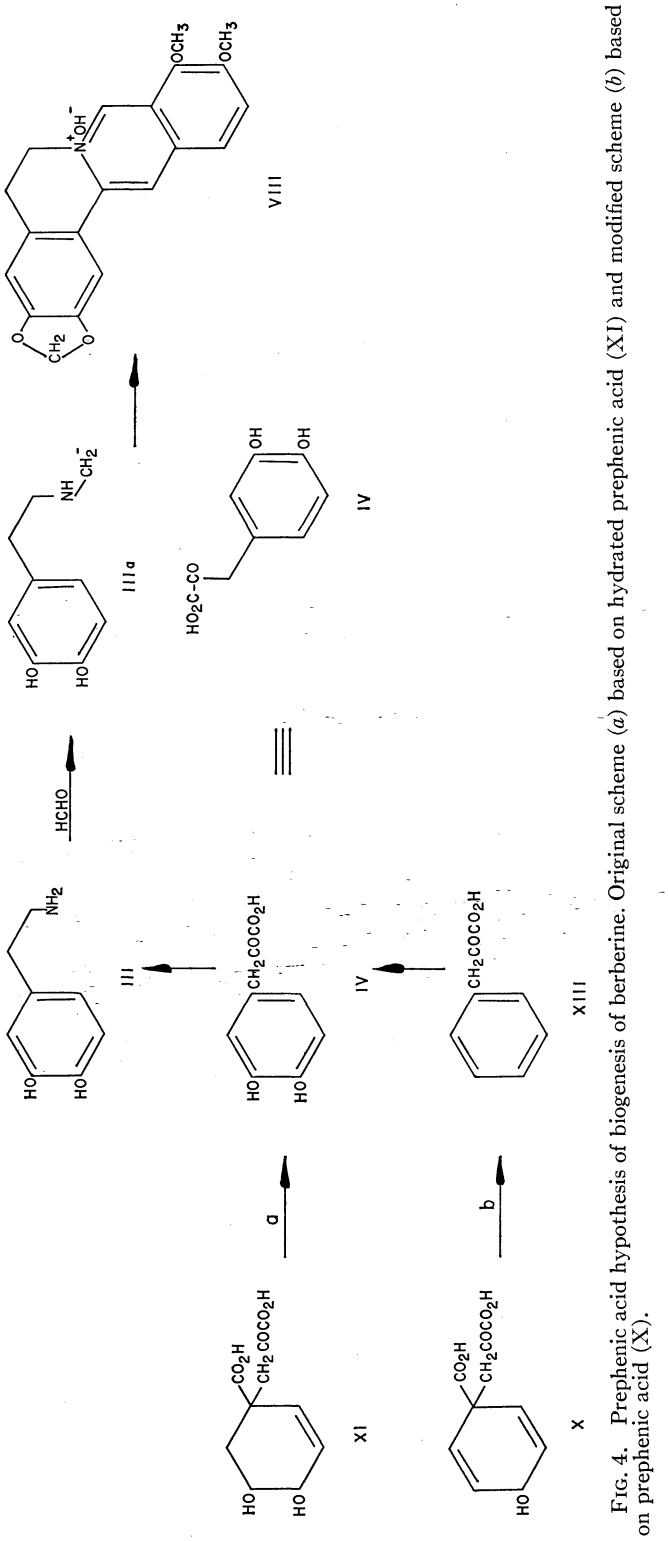

FIG. 4. Prephenic acid hypothesis of biogenesis of berberine. Original scheme (*a*) based on hydrated prephenic acid (XI) and modified scheme (*b*) based on prephenic acid (X).

of experimental proof, the importance of the hypothesis in giving direction to the use of the experimental tools, when these became available, is self-evident. Now that these tools are commonly used, there seems little to justify the publication of biogenetic speculations unsupported by direct experiment.

DEGRADATION SEQUENCES

Hydrastine

Specific incorporation of [2-^{14}C]-tyrosine was expected to yield hydrastine labelled at C_1 and/or C_3. A degradation, permitting the isolation of these two atoms, was therefore devised (Fig. 5).

Oxidation of hydrastine (IX) gave opianic acid (XIV) and hydrastinine (XV), the latter containing both C_1 and C_3 of hydrastine.

To remove the nitrogen atom and *N*-methyl group, hydrastinine was subjected to exhaustive methylation. Attempts to effect this reaction in two stages by way of the quaternary methiodide (37) gave low yields. Hofmann degradation in one step in a heterogeneous system (benzene–water), however, gave hydrastal (XVI) in high yield. Hydrastal was oxidized by silver oxide to 6-vinylpiperonylic acid (XVII), which still contained C_1 and C_3. C_1 of hydrastine was isolated by bromo-decarboxylation of the acid XVII. Jones and Robinson (38) had used this reaction for the removal of the carboxyl group from piperonylic acid, using bromine–water in dilute sodium carbonate. Since, in the degradation of radioactive material, the carbon dioxide from C_1 was to be collected and assayed for activity, these conditions were not applicable to the present problem. Attempts to carry out the reaction with bromine–water in acetone or carbon disulphide did not lead to decarboxylation. Bromination of XVII in carbon disulphide gave the dibromo derivative XVIII, which on recrystallization from acetone–water underwent spontaneous hydrolysis (cf. ref. 46) and lactonization to yield the lactone XIX. The same lactone was isolated directly when XVII was brominated in acetone solution.

Bromo-decarboxylation of the acid XVII by bromine–water in a solution of disodium hydrogen phosphate, however, gave the bromohydrin XX in good yield. The carbon dioxide (C_1 of hydrastine) was collected as barium carbonate, which, for radioassay,[4] was converted to benzoic acid XXI.

It remained to separate C_3 of hydrastine from the rest of the molecule. The bromohydrin XX did not undergo the haloform reaction, but oxidation with potassium permanganate in pyridine–water gave 6-bromopiperonal XXII. The other fragment was not isolated, but since only C_3 of hydrastine was lost its activity could be found by difference. 6-Bromopiperonal (XXII) was difficult to purify and was therefore converted into a derivative. Oxidation with silver oxide gave 6-bromopiperonylic acid (XXIII) in good yield, while condensation with acetone gave 6-bromopiperonylidene acetone (XXIV).

Berberine

In the degradation of berberine a series of reactions was used which had been originated by Freund and Fleischer (39) (Fig. 6). Berberine hydrochloride (VIII) was reacted with benzylmagnesium bromide to give benzyldihydroberberine (XXV) in good yield.

Reduction of this compound with tin and hydrochloric acid (39) could not be repeated. Sodium borohydride, however, converted XXV rapidly to benzyltetrahydroberberine (XXVI) in almost quantitative yield. The latter was converted into the methiodide

[4]*The carbon dioxide was converted into an organic compound in order that its radioactivity could be assayed under the conditions which were used for all other compounds of the degradation sequence, thus making direct comparison of count rates possible.*

Can. J. Chem. Downloaded from www.nrcresearchpress.com by 210.87.254.40 on 09/05/12
For personal use only.

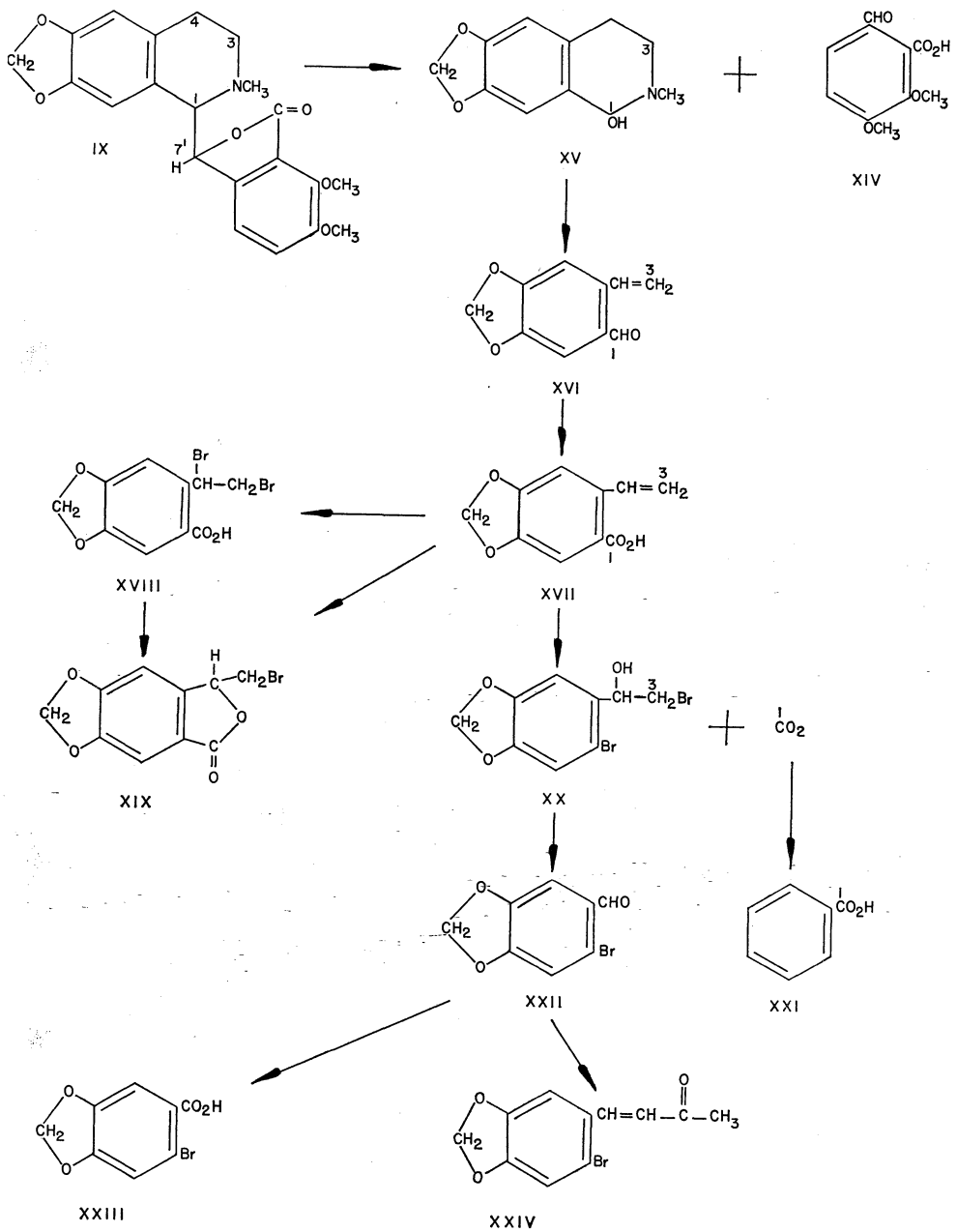

FIG. 5. Degradation of hydrastine.

(XXVII), which was then allowed to undergo Hofmann degradation. Silver oxide and solid sodium hydroxide (39) gave poor yields of product. Good yields of des-*N*-methyl-styryltetrahydroberberine (XXVIII) were obtained using methanolic potassium hydroxide.

Oxidation of XXVIII with sodium dichromate in acetic acid gave hydrastinine (XV) and 3,4-dimethoxy-2-styrylbenzaldehyde (XXIX). The hydrastinine, containing both

Can. J. Chem. Downloaded from www.nrcresearchpress.com by 210.87.254.40 on 09/05/12
For personal use only.

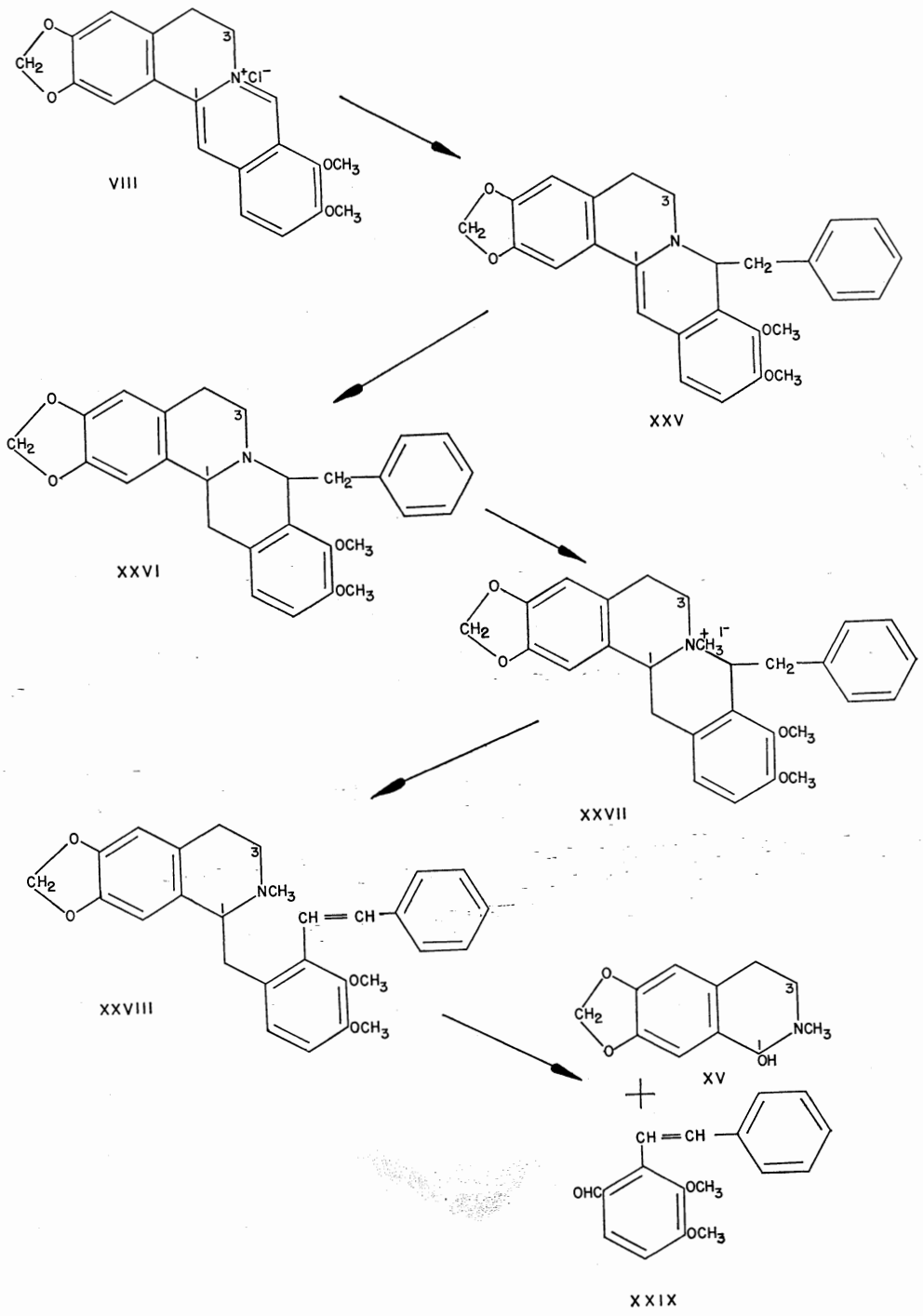

FIG. 6. Degradation of berberine.

predicted sites of radioactive carbon (C_1 and C_3 of berberine), was degraded in the manner already described.

Can. J. Chem. Downloaded from www.nrcresearchpress.com by 210.87.254.40 on 09/05/12
For personal use only.

Can. J. Chem. Downloaded from www.nrcresearchpress.com by 210.87.254.40 on 09/05/12
For personal use only.

EXPERIMENTAL

Administration of ^{14}C-Labelled Compounds to Hydrastis canadensis L. Plants

For root-feeding experiments small 2- and 3-year-old plants were used, which had wintered in the open and had grown in soil during spring and early summer. For each experiment a number of plants were placed under hydroponic culture. Soil was removed from the roots by soaking in distilled water. The plants were inserted through holes in a wooden box, their stems supported by glass wool plugs, and their roots dipping into nutrient solution (40) in a glass dish which was left in the dark. Filtered air was bubbled through the solution continuously. The plants were kept in 75% shade. Each group of plants was allowed to grow under these conditions for 1 week, by which time they had recovered from transplanting, and fresh root growth was apparent. The nutrient solution was replaced by fresh nutrient solution (1500 ml), containing the labelled compound, and the plants were allowed to grow in this system for the required time. During this period the radioactivity of the nutrient solution and of specimens of leaf was assayed daily. In all cases 95% of the activity had disappeared from the nutrient solution within 40 hours.

The roots and rhizomes were separated from the leaves and stems, dried to constant weight in a vacuum desiccator over NaOH, and stored.

Wick-feeding experiments were carried out with large 3- and 4-year-old plants which were allowed to grow in soil under 75% shade. Wicks of unmercerized cotton were passed through the stem of each plant. The ends were allowed to dip into an aqueous solution[5] of the ^{14}C-labelled compound in a small container (capacity 1 ml) which was repeatedly refilled with distilled water after the original solution had been absorbed. After the required time in contact with tracer, the plants were harvested and stored in the same manner as the root-fed plants. The cotton wicks were extracted with methanol and with water, and the extracts were assayed for residual activity.

Eight root-feeding experiments (expts. 1–8) and two wick-feeding experiments (expts. 9, 10) were carried out. The details of these are summarized in Table I.

Extraction of Alkaloids from the Plants

Hydrastine and berberine were extracted by standard methods (41). A typical experiment (expt. 3) is described.

The roots and rhizomes of well-dried *H. canadensis* L. plants (9.3 g) were ground to a fine powder in a mortar. To extract hydrastine the powder was thoroughly moistened with 3 *M* ammonium hydroxide (10 ml), allowed to stand for 30 minutes, transferred to a Soxhlet thimble (Whatman, 35×80 mm), and extracted continuously with ether (125 ml) for 26 hours. The ether extract was transferred to a separatory funnel and washed, first with 3 *M* ammonium hydroxide (30 ml), and then with water (30 ml). The washings were rejected. The washed ether solution was extracted with 10% hydrochloric acid (4×25 ml), and the combined acid portions were made strongly basic with 15 *M* ammonium hydroxide. This ammoniacal solution was extracted with ether (4×50 ml), the combined ether extracts were evaporated to dryness, and the residue was dissolved in a very small amount of hot ethanol. Hydrastine (173 mg, 1.9%) crystallized on cooling.

To obtain berberine the material remaining in the thimble was extracted continuously with 95% ethanol (125 ml) for 24 hours. The ethanolic extract was evaporated to dryness, water (30 ml) was added to the residue, and the mixture was heated on the steam bath and filtered. The filtrate was made strongly acidic with concentrated hydrochloric acid and allowed to stand overnight, when berberine hydrochloride (205 mg, 2.2%) crystallized.

In this way hydrastine and berberine were isolated from roots and rhizomes of the plants from each of the 10 experiments. In one case the alkaloids were also isolated from the leaves and stems by the same procedure (expt. 4L). Chemical and radioactive yields from all experiments are shown in Table II.

Degradation of Hydrastine

Conversion of Hydrastine to Hydrastinine and Opianic Acid (Cf. Ref. 42)

Nitric acid (2.5 ml, 20%) was added to hydrastine (136 mg) and the mixture was kept at 41° for 8.5 hours. The solution was cooled in an ice bath, and concentrated aqueous sodium hydroxide was added at a rate such that room temperature was not exceeded. A gummy mass separated, which on vigorous stirring first solidified and then broke up into finer particles which were filtered off to give hydrastinine (65 mg, 88%) melting at 110–113°. One crystallization from ethyl acetate raised the melting point to 116–117°; reported melting point 116–117° (43). The filtrate remaining after hydrastinine had been removed was made strongly acidic with concentrated hydrochloric acid and stored in the freezer overnight. The solid which separated when the frozen mixture was restored to room temperature was filtered off to give opianic acid (38 mg, 51%) melting at 141–144°. One crystallization from water raised the melting point to 144–145°; reported melting point 146° (42).

Conversion of Hydrastinine to Hydrastal (Cf. Ref. 44)

Benzene (10 ml), 20% aqueous sodium hydroxide (10 ml), and methyl iodide (5 ml) were added to hydrastinine (101 mg). The mixture was shaken for 24 hours. Water (10 ml) was added, a downward condenser

[5]*A drop of hydrochloric acid was added to the aqueous solution in order to dissolve tyrosine.*

was fitted, and the flask was heated on a steam bath for 30 minutes. Benzene and excess methyl iodide distilled off, leaving an aqueous basic solution, from which hydrastal separated as an oil which solidified on cooling. After standing for 3 hours this solid was filtered off to give hydrastal (75 mg, 87%) melting at 75–78°. One crystallization from ethyl acetate raised the melting point to 78–79°; reported melting point 78–79° (45).

Conversion of Hydrastal to 6-Vinylpiperonylic Acid (Cf. Ref. 44)

Hydrastal (106 mg) was suspended in a solution of potassium hydroxide (425 mg) in water (4.25 ml), and a solution of silver nitrate (650 mg) in 50% ethanol (8 ml) was added. After 5 minutes the mixture was heated at 80° on a water bath for 15 minutes, was allowed to cool for 2.5 hours with occasional swirling, and was filtered. The pH of the filtrate was adjusted to pH 1 by means of 50% nitric acid, and the mixture was then heated on a steam bath (with the addition of a little ethanol if necessary) until a clear solution was obtained. The solution was allowed to cool, and the solid was filtered off to give *6-vinylpiperonylic acid* (95 mg, 82%) melting at 166–168°. One crystallization from aqueous ethanol raised the melting point to 168°. (Found: C, 62.4; H, 4.5. $C_{10}H_8O_4$ requires: C, 62.5; H, 4.2%.)

Conversion of 6-Vinylpiperonylic Acid to 6-Bromo-α-hydroxyhomopiperonyl Bromide

6-Vinylpiperonylic acid (59 mg) was dissolved in 3% disodium hydrogen phosphate (15 ml) by swirling for 1 minute, and the solution was cooled in an ice bath for 10 minutes. Saturated bromine–water (10 ml) was added dropwise over a period of 2 minutes, and the mixture was allowed to stand for 3 minutes. It was then filtered quickly under moderately reduced pressure, and the wet precipitate (A) was set aside. The filtrate was immediately transferred to a 50-ml round-bottomed flask which was attached to a gas line. Nitrogen, which had been purified by passage through saturated barium hydroxide solution and through concentrated sulphuric acid, was bubbled through the solution. The exit gases were passed through 1 *M* aqueous sodium hydroxide (15 ml), which was protected from the atmosphere by a trap containing saturated barium hydroxide solution. Through a small dropping funnel in a side arm concentrated hydrochloric acid (3 ml) was added to the flask containing the reaction filtrate. The liberated carbon dioxide was swept into the sodium hydroxide trap by a stream of nitrogen. After 1 hour 17% barium chloride solution (3 ml) was added to the solution in the trap. The precipitate of barium carbonate (44 mg, 61%) was filtered off.[6] Meanwhile the wet precipitate (A) was dissolved in warm methanol, the mixture was filtered, and the filtrate was evaporated to dryness at the water pump. The residue was 6-bromo-α-hydroxyhomopiperonyl bromide (79 mg, 79%) melting at 148–153°. Two crystallizations from aqueous methanol raised the melting point to 157–158°; reported melting point 158° (46), 157–158° (47).

Conversion of 6-Bromo-α-hydroxyhomopiperonyl Bromide to 6-Bromopiperonal

6-Bromo-α-hydroxyhomopiperonyl bromide (65 mg) was dissolved in pyridine (6 ml) in a 2-necked flask. A small reflux condenser and a small dropping funnel were fitted. Powdered potassium permanganate (65 mg) was dissolved in water (4 ml) by warming on a steam bath, and a pellet of potassium hydroxide was added. The solution was poured into the dropping funnel and the last drops washed in with water (2 ml). The flask was warmed on a heating mantle until the contents boiled gently. The permanganate solution was then added dropwise, and washed in with water (2 ml). After boiling for a further 10 minutes the mixture was allowed to cool, and a few drops of ethanol were added to destroy any unreacted potassium permanganate. When quite cold the mixture was filtered. The filtrate was made strongly acidic with concentrated hydrochloric acid and then extracted with ether (4×25 ml). The combined ether extracts were evaporated to dryness, leaving a residue of 6-bromopiperonal (28 mg, 61%) melting at 105–110°. Recrystallization from aqueous ethanol gave a purer sample of 6-bromopiperonal (*vide infra*), but it was found that the best way to purify this compound for the purposes of this experiment was to convert it either to 6-bromopiperonylic acid or to 6-bromopiperonylidene acetone.

Conversion of 6-Bromopiperonal to 6-Bromopiperonylic Acid (Cf. Refs. 48, 49)

A solution of potassium hydroxide (500 mg) in water (5 ml) was added to 6-bromopiperonal (28 mg). A solution of silver nitrate (750 mg) in 50% ethanol (10 ml) was added to this mixture, which, after standing for 5 minutes, was heated on a water bath at 85° for 30 minutes. The mixture was then allowed to stand for 2.5 hours and filtered. The filtrate was acidified with concentrated hydrochloric acid and then extracted with ether (3×30 ml). The combined ether extracts were evaporated to dryness and the residue dissolved in hot water (30 ml). The solution was filtered and allowed to cool. The solid was filtered off to give 6-bromopiperonylic acid (25 mg, 83%) melting at 200–202°. One crystallization from water raised the melting point to 204–205°; reported melting point 200–204° (48), 201–202° (47).

Conversion of 6-Bromopiperonal to 6-Bromopiperonylidene Acetone (50)

6-Bromopiperonal (28 mg) was dissolved in acetone (3 ml). Aqueous sodium hydroxide (2 ml, 3%) was added, and the solution was heated on a steam bath until a precipitate had formed and the excess acetone had evaporated. The solid was filtered off to give 6-bromopiperonylidene acetone (25 mg, 81%) melting at

[6]*It was found by several control experiments that if this procedure were followed exactly, 3 mg of the barium carbonate so obtained came from extraneous sources, and would thus act as an inactive impurity if the barium carbonate derived from the reaction contained* ^{14}C. *A correction factor to account for this must be incorporated into any calculations which derive results from the count rate of this barium carbonate or of its derivatives.*

Can. J. Chem. Downloaded from www.nrcresearchpress.com by 210.87.254.40 on 09/05/12
For personal use only.

148–151°. One crystallization from methanol raised the melting point to 152–154°; reported melting point 152–154° (50).

Conversion of Piperonal to 6-Bromopiperonylidene Acetone (50, Cf. Ref. 49)

Piperonal (1.38 g) was dissolved in 95% ethanol (20 ml), and bromine–water was added until a brown oil and some crystals separated. The crystals were filtered off, washed well with water, and recrystallized from aqueous ethanol to give 6-bromopiperonal (390 mg, 19%) melting at 126–127°; reported melting point 129–130° (50). A portion of this 6-bromopiperonal was converted, in the manner just described, to 6-bromopiperonylidene acetone melting at 152–154°, identical in melting point, mixed melting point, and infrared absorption with 6-bromopiperonylidene acetone derived from the degradation of hydrastine.

Conversion of Barium Carbonate to Benzoic Acid

The apparatus used (cf. ref. 51), is illustrated in Fig. 7. All ground-glass joints were greased with Apiezon

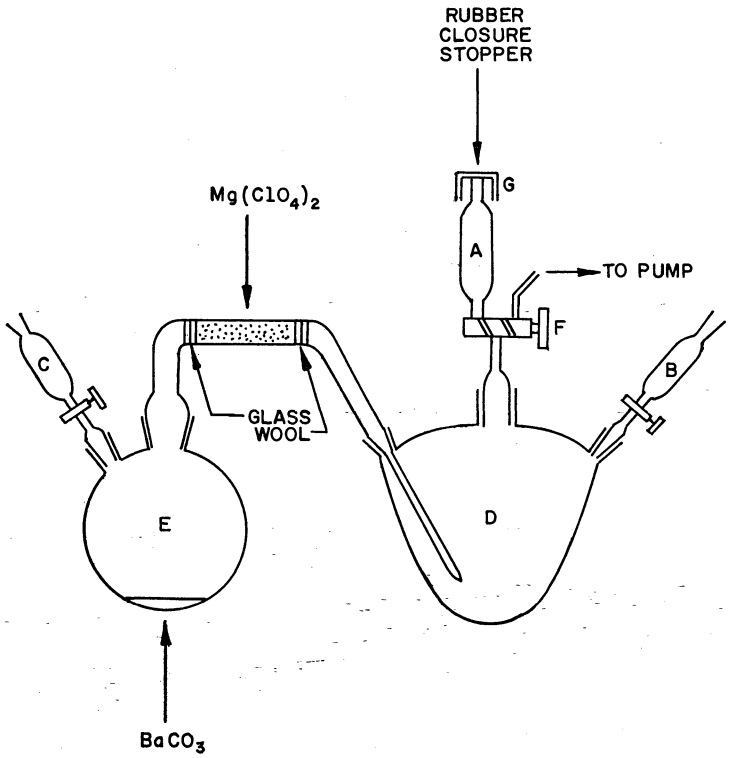

FIG. 7. Apparatus.

except F, which was greased with Dow-Corning high-vacuum grease. Barium carbonate (64 mg) was placed in flask E. The apparatus was assembled and evacuated (including funnel A) by a water pump to as low a pressure as possible. Hydrochloric acid (20%) was placed in funnels B and C. Using an all-glass hypodermic syringe with a 3-inch needle, phenylmagnesium bromide solution (8 ml, approximately 0.25 *M* (in dry ether), which had been stored at 10° in a flask with a rubber closure stopper) was withdrawn from the stock flask and inserted through the rubber closure stopper G into funnel A. The bottom of flask D was immersed in liquid air and a little hydrochloric acid was run into flask E from funnel C. The carbon dioxide which was liberated solidified at the bottom of flask D. A little of the phenylmagnesium bromide solution was then run into flask D. This at first vaporized the carbon dioxide, and then both froze as an intimate mixture. This procedure was repeated until all carbon dioxide and all of the phenylmagnesium bromide were frozen together in D. The liquid air was then replaced by an ice-water bath until the contents of D had melted. After 5 minutes the mixture was refrozen, and was then allowed to melt again. The ice bath was removed and hydrochloric acid was added from B until the vigorous reaction ceased, showing that excess phenylmagnesium bromide had been destroyed. The system was evacuated again to remove any unreacted carbon dioxide, and then allowed to reach atmospheric pressure. The contents of D were rinsed out with ether into a separatory funnel and the water layer was extracted with ether (3×20 ml). The combined ether

Can. J. Chem. Downloaded from www.nrcresearchpress.com by 210.87.254.40 on 09/05/12
For personal use only.

extracts were evaporated to dryness and the residue was dissolved in hot water, filtered, and cooled. The solid was filtered off to give benzoic acid (17 mg, 43%) melting at 119–121°. One crystallization from water raised the melting point to 122°.

Conversion of 6-Vinylpiperonylic Acid to 6-(β-Bromo-α-hydroxyethyl)-piperonylic Acid Lactone

6-Vinylpiperonylic acid (150 mg) was dissolved in acetone (10 ml). Saturated bromine–water (15 ml) was added dropwise to the solution over a period of 30 minutes, followed by water (10 ml) over a period of 5 minutes. The solid was filtered off to give *6-(β-bromo-α-hydroxyethyl)-piperonylic acid lactone* (190 mg, 90%) melting at 134–134.5°. Recrystallization did not raise the melting point. (Found: C, 44.5; H, 2.7; Br, 29.5. $C_{10}H_7BrO_4$ requires: C, 44.6; H, 2.6; Br, 29.5%.)

The lactone was also obtained in the following manner. 6-Vinylpiperonylic acid (54 mg) was dissolved in carbon disulphide (5 ml), excess bromine in carbon disulphide was added, and the mixture was allowed to stand overnight. Excess petroleum ether was added and the product, presumably 6-(α,β-dibromoethyl)-piperonylic acid (87 mg, 88%), melting at 158°, was filtered off. When this compound (70 mg) was recrystallized from aqueous acetone, 6-(β-bromo-α-hydroxyethyl)-piperonylic acid lactone (40 mg, 74%) was obtained which melted at 134–134.5°. A mixed melting point of samples of the lactone prepared by the two different procedures showed no depression.

Degradation of Berberine (39)

Conversion of Berberine Hydrochloride to Benzyldihydroberberine (52)

Magnesium turnings (720 mg), which had been ground in a mortar, and a crystal of iodine were introduced into a flask. A solution of freshly distilled benzyl chloride (3.25 g) in sodium-dried ether (36 ml) was added, a condenser was fitted to the flask, and after the vigorous reaction had ceased the mixture was heated under reflux for 2 hours. The solution was then slowly added to berberine hydrochloride (800 mg) in sodium-dried ether (10 ml) in a 100-ml round-bottomed flask. When the initial reaction had subsided the mixture was heated under reflux for 2.75 hours. The contents of the flask were then extracted with 6 *M* hydrochloric acid (50 ml) in a separatory funnel and the aqueous layer was transferred to a 400-ml beaker. This solution was cooled in an ice bath, and 15 *M* ammonium hydroxide was added at a rate such that the temperature did not rise above room temperature. A gummy mass separated, which, when the cold solution was stirred vigorously, first solidified and then broke up into finer particles, which were filtered off to give benzyldihydroberberine (770 mg, 92%) melting at 131–134°. One crystallization from methanol–acetone raised the melting point to 135–137°. Further recrystallization did not raise the melting point again, and at no time was benzyldihydroberberine obtained which had the reported melting point of 161–162° (52).

Conversion of Benzyldihydroberberine to Benzyltetrahydroberberine (Cf. Ref. 39)

Benzyldihydroberberine (768 mg) was suspended in methanol (100 ml) and sodium borohydride (2.0 g) was added carefully in small portions. A reflux condenser was fitted to the flask, and when the vigorous reaction had ceased the solution was heated under reflux for 15 minutes. The solution was allowed to cool, and was acidified with 6 *M* hydrochloric acid while being stirred with a magnetic stirrer. The contents of the flask were then made basic with 15 *M* ammonium hydroxide and allowed to cool. The solid was filtered off to give benzyltetrahydroberberine (716 mg, 93%) melting at 162–165°. One crystallization from methanol–acetone raised the melting point to 165°; reported melting point 163–165° (39).

Conversion of Benzyltetrahydroberberine to Benzyltetrahydroberberine Methiodide (39)

Benzyltetrahydroberberine (715 mg) was introduced into a heavy-walled hard-glass tube (7 mm×600 mm which had been sealed at one end), and washed in with methyl iodide (8 ml). The tube was cooled in ice and the open end was sealed. It was then kept at 100–105° for 5 hours. After cooling in ice the tube was opened, and the solid in it was filtered off to give benzyltetrahydroberberine methiodide (798 mg, 84%) melting at 203–208°. One crystallization from methanol which contained a little sodium hydroxide raised the melting point to 220° (decomp.); reported melting point 224° (decomp.) (39).

Conversion of Benzyltetrahydroberberine Methiodide to Des-N-methylstyryltetrahydroberberine (Cf. Ref. 39)

Benzyltetrahydroberberine methiodide (795 mg) was suspended in methanol (2 ml). A solution of potassium hydroxide (2.0 g) in methanol (11 ml) was added, a condenser was fitted, and the mixture was heated under reflux for 1 hour. It was stored at 10° for 2 hours and the liquid layer was removed by decantation. The residue was dissolved in a minimum of hot methanol and stored in the freezer for several hours. The solid was filtered off to give des-*N*-methylstyryltetrahydroberberine (392 mg, 64%) melting at 121–123°. One crystallization from methanol raised the melting point to 123–124°; reported melting point 121–122.5° (39).

Conversion of Des-N-methylstyryltetrahydroberberine to Hydrastinine and 2-Styryl-3,4-dimethoxybenzaldehyde (39)

Des-*N*-methylstyryltetrahydroberberine (350 mg) was dissolved in glacial acetic acid (1 ml). A solution of sodium dichromate (271 mg) in 50% acetic acid (3 ml) was added, a condenser was fitted, and the solution was heated on a steam bath for 3.25 hours. The solution was cooled in an ice bath and water (4 ml) was added. After being stored at 10° for 3 hours the solution was decanted into a beaker, leaving an oily solid (A), which was set aside. The solution in the beaker was saturated with sodium carbonate, decanted from an oily residue into a separatory funnel, made strongly basic with concentrated sodium hydroxide, and

Can. J. Chem. Downloaded from www.nrcresearchpress.com by 210.87.254.40 on 09/05/12
For personal use only.

extracted with ether (2×20 ml). The combined ether extracts were evaporated to dryness and the residue was suspended in water, and filtered off to give hydrastinine (105 mg, 64%) melting at 100–105°. One crystallization from ethyl acetate raised the melting point to 116–117°. Meanwhile, the oily solid (A) was dissolved in a minimum of hot methanol, filtered, and stored in the freezer overnight. The solid was filtered off to give 2-styryl-3,4-dimethoxybenzaldehyde (66 mg, 31%) melting at 64–67°. One crystallization from methanol raised the melting point to 68–70°; reported melting point 71–74° (39).

Degradation of Radioactive Alkaloids

Hydrastine from Experiment 3

Hydrastine (115 mg; specific activity 4.48×10^4 counts/min mmole) from this experiment was oxidized with nitric acid to give hydrastinine (50 mg, 81%; specific activity 4.10×10^4 counts/min mmole) and opianic acid (15 mg, 22%; specific activity 0.06×10^4 counts/min mmole). In order to have sufficient hydrastinine for further degradation, the active hydrastinine (44.85 mg; specific activity 4.10×10^4 counts/min mmole) was mixed with an equal weight of inactive hydrastinine.[7]

Hydrastinine (89.7 mg; specific activity 4.10×10^4 counts/min mmole*) underwent a Hofmann reaction to give hydrastal (62 mg, 82%; specific activity 4.51×10^4 counts/min mmole).

Hydrastal (55 mg; specific activity 4.51×10^4 counts/min mmole) was oxidized with silver oxide to give 6-vinylpiperonylic acid. However, when the reaction mixture was acidified, excess nitric acid was inadvertently added. This caused oxidation and subsequent loss of product when the solution was heated.

Hydrastine from Experiment 4

Hydrastine (144 mg; specific activity 5.17×10^4 counts/min mmole) from this experiment was oxidized with nitric acid to give hydrastinine (63 mg, 81%; specific activity 5.10×10^4 counts/min mmole) and opianic acid (40 mg, 51%; specific activity 0.04×10^4 counts/min mmole). In order to have sufficient hydrastinine to continue the degradation sequence the active hydrastinine (57.5 mg; specific activity 5.10×10^4 counts/min mmole) was mixed with an equal weight of inactive hydrastinine.

Hydrastinine (115 mg; specific activity 5.10×10^4 counts/min mmole*) underwent a Hofmann reaction to give hydrastal (79 mg, 81%; specific activity 5.16×10^4 counts/min mmole).

Hydrastal (72 mg; specific activity 5.16×10^4 counts/min mmole) was oxidized by silver oxide to give 6-vinylpiperonylic acid (67 mg, 86%; specific activity 5.02×10^4 counts/min mmole).

6-Vinylpiperonylic acid (59 mg; specific activity 5.02×10^4 counts/min mmole) was bromodecarboxylated to give barium carbonate (43 mg, 61%) and 6-bromo-α-hydroxyhomopiperonyl bromide (76 mg, 76%; specific activity 3.20×10^4 counts/min mmole). Active barium carbonate (22 mg) was diluted to 64 mg with inactive barium carbonate, and the mixture was converted to benzoic acid (17 mg, 43%; specific activity 2.00×10^4 counts/min mmole*).

6-Bromo-α-hydroxyhomopiperonyl bromide (65 mg; specific activity 3.20×10^4 counts/min mmole) was oxidized by potassium permanganate to 6-bromopiperonal, which was further oxidized by silver oxide to give 6-bromopiperonylic acid (23 mg, 47%; specific activity 0.14×10^4 counts/min mmole).

The results of the degradation of hydrastine samples from experiments 3 and 4 are summarized in Table VII.

Hydrastine from Experiment 5

Hydrastine (180 mg; specific activity 1.19×10^4 counts/min mmole) from this experiment was oxidized by nitric acid to give hydrastinine (84 mg, 86%; specific activity 0.50×10^4 counts/min mmole) and opianic acid (45 mg, 46%; specific activity 0.65×10^4 counts/min mmole).

Hydrastine from Experiment 6

Hydrastine (181 mg; specific activity 1.42×10^4 counts/min mmole) from this experiment was oxidized by nitric acid to give hydrastinine (87 mg, 89%; specific activity 0.70×10^4 counts/min mmole) and opianic acid (47 mg, 48%; specific activity 0.69×10^4 counts/min mmole).

Hydrastine from Experiment 7

Hydrastine (178 mg; specific activity 4.96×10^4 counts/min mmole) from this experiment was oxidized by nitric acid to give hydrastinine (83 mg, 86%; specific activity 2.44×10^4 counts/min mmole) and opianic acid (44 mg, 45%; specific activity 2.46×10^4 counts/min mmole).

Hydrastine from Experiment 8

Hydrastine (150 mg; specific activity 1.36×10^4 counts/min mmole) from this experiment was oxidized by nitric acid to give hydrastinine (73 mg, 90%; specific activity 0.60×10^4 counts/min mmole) and opianic acid (39 mg, 48%; specific activity 0.74×10^4 counts/min mmole).

Hydrastine from Experiment 9

Hydrastine (350 mg; specific activity 5.76×10^4 counts/min mmole) from this experiment was oxidized by nitric acid to give hydrastinine (166 mg, 88%; specific activity 3.28×10^4 counts/min mmole) and opianic acid (95 mg, 50%; specific activity 2.46×10^4 counts/min mmole).

[7]*This gave a total of 89.7 mg, with a specific activity half that of the original hydrastinine. The specific activity of all further degradation products was decreased correspondingly. In order to avoid confusion, however, the reported specific activities of further degradation products take into account this dilution factor, so that the figures quoted are directly comparable to the specific activity of the initial alkaloid. Wherever such a dilution was carried out, the specific activities are marked by an asterisk.*

Can. J. Chem. Downloaded from www.nrcresearchpress.com by 210.87.254.40 on 09/05/12
For personal use only.

TABLE VII

Degradation of hydrastine derived from DL-[2-^{14}C]-tyrosine

Compound	Specific activity (counts/min mmole) $\times 10^{-4}$	Relative specific activity (hydrastine = 100)
	Experiment 3	
Hydrastine	4.48	100
Hydrastinine	4.10	92
Opianic acid	0.06	1
Hydrastal	4.51	100
	Experiment 4	
Hydrastine	5.17	100
Hydrastinine	5.10	99
Opianic acid	0.04	1
Hydrastal	5.16	100
6-Vinylpiperonylic acid	5.02	97
6-Bromo-α-hydroxy-homopiperonyl bromide	3.20	62
Benzoic acid	2.00	39
6-Bromopiperonylic acid	0.14	3

The results of the degradation of hydrastine samples from Experiments 5–9 are summarized in Table V.

Hydrastine from Experiment 10

Hydrastine (450 mg; specific activity 0.87×10^4 counts/min mmole) from this experiment was oxidized by nitric acid to give hydrastinine (215 mg, 89%; specific activity 0.87×10^4 counts/min mmole) and opianic acid (96 mg, 35%; specific activity 0.0084×10^4 counts/min mmole).

Hydrastinine (197 mg; specific activity 0.87×10^4 counts/min mmole) underwent a Hofmann reaction to give hydrastal (148 mg, 89%; specific activity 0.83×10^4 counts/min mmole).

Hydrastal (126 mg; specific activity 0.83×10^4 counts/min mmole) was oxidized by silver oxide to give 6-vinylpiperonylic acid (112 mg, 82%; specific activity 0.87×10^4 counts/min mmole).

6-Vinylpiperonylic acid (97 mg; specific activity 0.87×10^4 counts/min mmole) was bromodecarboxylated to give barium carbonate (83 mg, 83%) and 6-bromo-α-hydroxyhomopiperonyl bromide (125 mg, 76%; specific activity 0.89×10^4 counts/min mmole). Barium carbonate (82 mg) was converted to inactive benzoic acid (20 mg, 40%; specific activity nil).

6-Bromo-α-hydroxyhomopiperonyl bromide (51 mg; specific activity 0.89×10^4 counts/min mmole) was oxidized by potassium permanganate to 6-bromopiperonal. This was reacted with acetone to give 6-bromopiperonylidene acetone (30 mg, 71%; specific activity 0.015×10^4 counts/min mmole).

The results of the degradation of hydrastine from Experiment 10 are summarized in Table VIII.

TABLE VIII

Degradation of hydrastine derived from [1-^{14}C]-dopamine (expt. 10)

Compound	Specific activity (counts/min mmole) $\times 10^{-4}$	Relative specific activity (hydrastine = 100)
Hydrastine	0.87	100
Hydrastinine	0.87	100
Opianic acid	0.0084	1
Hydrastal	0.83	96
6-Vinylpiperonylic acid	0.87	100
6-Bromo-α-hydroxyhomo-piperonyl bromide	0.89	102
Benzoic acid	0	0
6-Bromopiperonylidene acetone	0.015	2

Berberine from Experiment 4

In order to have sufficient alkaloid to complete the degradation sequence active berberine hydrochloride (319.6 mg; specific activity 10.50×10^4 counts/min mmole) was mixed with inactive berberine hydrochloride (639.2 mg) and recrystallized to give berberine hydrochloride (935 mg; specific activity 3.50×10^4 counts/min

Can. J. Chem. Downloaded from www.nrcresearchpress.com by 210.87.254.40 on 09/05/12
For personal use only.

mmole). Berberine hydrochloride (894 mg; specific activity 3.50×10^4 counts/min mmole) then underwent a Grignard reaction with benzyl chloride and magnesium to give benzyldihydroberberine (876 mg, 94%).

This benzyldihydroberberine (876 mg) was reduced by sodium borohydride in methanol to give benzyltetrahydroberberine (637 mg, 72%; specific activity 3.60×10^4 counts/min mmole).

Benzyltetrahydroberberine (632 mg; specific activity 3.60×10^4 counts/min mmole) was converted by methyl iodide to benzyltetrahydroberberine methiodide (677 mg, 81%).

This benzyltetrahydroberberine methiodide (677 mg) underwent a Hofmann reaction to give des-*N*-methylstyryltetrahydroberberine (320 mg; specific activity 3.65×10^4 counts/min mmole), which was oxidized by sodium dichromate in acetic acid to give hydrastinine (114 mg, 76%; specific activity 3.40×10^4 counts/min mmole), and 2-styryl-3,4-dimethoxybenzaldehyde (69 mg, 36%; specific activity 0.03×10^4 counts/min mmole).

Hydrastinine (110 mg; specific activity 3.40×10^4 counts/min mmole) underwent a Hofmann reaction to give hydrastal (79 mg, 85%).

This hydrastal (79 mg) was oxidized by silver oxide to give 6-vinylpiperonylic acid (44 mg, 51%). In order to have sufficient 6-vinylpiperonylic acid to continue the degradation sequence, the active 6-vinylpiperonylic acid (32.3 mg) was mixed with an equal weight of inactive 6-vinylpiperonylic acid.

6-Vinylpiperonylic acid (64.6 mg) was bromodecarboxylated to give barium carbonate (59 mg, 89%) and 6-bromo-α-hydroxyhomopiperonyl bromide (91 mg, 83%; specific activity 1.72×10^4 counts/min mmole*).

Active barium carbonate (59 mg) was converted into benzoic acid (12 mg, 33%; specific activity 1.75×10^4 counts/min mmole*).

6-Bromo-α-hydroxyhomopiperonyl bromide (72 mg; specific activity 1.72×10^4 counts/min mmole) was oxidized by potassium permanganate to 6-bromopiperonal. This was reacted with acetone to give 6-bromopiperonylidene acetone (31 mg, 52%; specific activity 0.07×10^4 counts/min mmole).

The results of the degradation of berberine from experiment 4 are summarized in Table IX.

TABLE IX

Degradation of berberine derived from DL-[2-^{14}C]-tyrosine (expt. 4)

Compound	Specific activity (counts/min mmole) $\times10^{-4}$	Relative specific activity (berberine = 100)
Berberine hydrochloride	3.50	100
Benzyltetrahydroberberine	3.60	103
Des-*N*-methylstyryltetrahydroberberine	3.65	104
Hydrastinine	3.40	97
2-Styryl-3,4-dimethoxybenzaldehyde	0.03	1
6-Bromo-α-hydroxyhomopiperonyl bromide	1.72	49
Benzoic acid	1.75	50
6-Bromopiperonylidene acetone	0.07	2

Assay of Activity

Radioactivity was assayed on samples of finite thickness on aluminum planchettes, using a Model D47 gas flow counter with "micromil" window (Nuclear Chicago Co.) in a low-background automatic sample changer (Nuclear Chicago Co., Model C 115). Counts were recorded either on a scaler (Nuclear Chicago Co., Model 161A), or on an electronic counter (Beckman-Berkeley, Model 7060).

ACKNOWLEDGMENTS

We are greatly indebted to Mr. L. Laking, Director, and Mr. R. E. Halward, Propagator, of the Royal Botanical Gardens, Hamilton, without whose generous advice and help in the cultivation of *Hydrastis canadensis* L. this investigation could not have been undertaken.

Financial assistance by the National Research Council of Canada and by the Ontario Research Foundation is gratefully acknowledged. This work was carried out during the tenure (by J. R. G.) of a National Research Council of Canada Studentship.

Can. J. Chem. Downloaded from www.nrcresearchpress.com by 210.87.254.40 on 09/05/12
For personal use only.

Can. J. Chem. Downloaded from www.nrcresearchpress.com by 210.87.254.40 on 09/05/12
For personal use only.

REFERENCES

1. J. R. GEAR and I. D. SPENSER. Nature, **191**, 1393 (1961).
2. I. D. SPENSER and J. R. GEAR. J. Am. Chem. Soc. **84**, 1059 (1962).
3. I. D. SPENSER and J. R. GEAR. Proc. Chem. Soc. 228 (1962).
4. E. WINTERSTEIN and G. TRIER. Die Alkaloide. Borntraeger, Berlin. 1910. p. 307.
5. R. ROBINSON. J. Chem. Soc. **111**, 876 (1917).
6. R. ROBINSON. Proc. Univ. Durham Phil. Soc. **8**, 14 (1927–8); IX Congres Internacional de Quimica Pura y Aplicada, Madrid. Conferencias de Introduccion, 153 (1934); J. Chem. Soc. 1079 (1936); J. Royal Soc. Arts, **96**, 795 (1948); Nature, **162**, 524 (1948); The structural relations of natural products. Clarendon Press, Oxford. 1955. p. 78.
7. G. BARGER. IX Congreso Internacional de Quimica Pura y Aplicada, Madrid. Conferencias de Introduccion, 177 (1934).
8. C. SCHÖPF. Angew. Chem. **50**, 779, 797 (1937).
9. L. RETI. Fortschr. Chem. Org. Naturstoffe, **6**, 242 (1950).
10. G. K. HUGHES and E. RITCHIE. Rev. Pure Appl. Chem. **2**, 125 (1952).
11. R. B. TURNER and R. B. WOODWARD. *In* The alkaloids. Vol. 3. *Edited by* R. H. F. Manske and H. L. Holmes. Academic Press, New York. 1953. p. 54.
12. E. WENKERT. Experientia, **10**, 346 (1954).
13. R. H. F. MANSKE. J. Chem. Soc. 2987 (1954).
14. R. H. F. MANSKE. *In* The alkaloids. Vol. 4. *Edited by* R. H. F. Manske and H. L. Holmes. Academic Press, New York. 1954. p. 1.
15. E. SPÄTH and F. BERGER. Ber. **63**, 2098 (1930).
16. E. SPÄTH, F. KUFFNER, and F. KESZTLER. Ber. **70**, 1017 (1937).
17. C. SCHÖPF and H. BAYERLE. Ann. **513**, 190 (1934).
18. G. HAHN and O. SCHALES. Ber. **68**, 24 (1935); **69**, 622 (1936); c.f. E. SPÄTH, F. KUFFNER, and F. KESZTLER. Ber. **69**, 378 (1936).
19. G. HAHN and K. STIEHL. Ber. **69**, 2627 (1936).
20. G. HAHN and H. J. SCHULS. Ber. **71**, 2135 (1938).
21. G. HAHN and F. RUMPF. Ber. **71**, 2141 (1938).
22. B. D. DAVIS. Advan. Enzymol. **16**, 247 (1955).
23. D. B. SPRINSON. Advan. Carbohydrate Chem. **15**, 235 (1960).
24. E. WENKERT and N. V. BRINGI. J. Am. Chem. Soc. **81**, 1474 (1959). E. WENKERT. Experientia, **15**, 165 (1959).
25. A. R. BATTERSBY and B. J. T. HARPER. Proc. Chem. Soc. 152 (1959).
26. A. R. BATTERSBY and B. J. T. HARPER. Chem. Ind. (London), 364 (1958). A. R. BATTERSBY, R. BINKS, and D. J. LECOUNT. Proc. Chem. Soc. 287 (1960); E. LEETE. Chem. Ind. (London), 977 (1958); J. Am. Chem. Soc. **81**, 3948 (1959).
27. A. R. BATTERSBY, R. BINKS, and G. V. PARRY. Unpublished work, quoted in Reference 36.
28. S. UDENFRIEND and J. B. WYNGAARDEN. Biochim. Biophys. Acta, **20**, 48 (1956). McC. GOODALL and N. KIRSHNER. J. Biol. Chem. **226**, 213 (1957).
29. I. SCHWINK and E. ADAMS. Biochim. Biophys. Acta, **36**, 102 (1959).
30. I. IMASEKI, R. ONEYAMA, and M. TAJIMA. J. Pharm. Soc. Japan, **80**, 1802 (1960).
31. R. K. IBRAHIM, S. G. LAWSON, and G. H. N. TOWERS. Can. J. Biochem. Physiol. **39**, 873 (1961).
32. S. MITSUHASHI and B. D. DAVIS. Biochim. Biophys. Acta, **15**, 54 (1954). T. HIGUCHI. Proc. Intern. Congr. Biochem. 4th Vienna. **2**, 161 (1958). A. C. NEISH. Ann. Rev. Plant Physiol. **11**, 55 (1960).
33. J. G. LEVIN and D. B. SPRINSON. Biochem. Biophys. Res. Commun. **3**, 157 (1960).
34. E. WENKERT. J. Am. Chem. Soc. **84**, 98 (1962).
35. D. G. WILSON, K. W. KING, and R. H. BURRIS. J. Biol. Chem. **208**, 863 (1954). V. L. KRETOVICH and Z. V. USPENSKAYA. Biokhimiya, **23**, 248 (1958); **24**, 116 (1959).
36. A. R. BATTERSBY. Quart. Rev. (London), **15**, 259 (1961).
37. J. T. BROWN and G. T. NEWBOLD. J. Chem. Soc. 4397 (1952).
38. T. G. H. JONES and R. ROBINSON. J. Chem. Soc. **111**, 909 (1917).
39. M. FREUND and K. FLEISCHER. Ann. **397**, 30 (1913).
40. E. LEETE, L. MARION, and I. D. SPENSER. Can. J. Chem. **32**, 1116 (1954).
41. B. T. CROMWELL. *In* Modern methods of plant analysis. Vol. 4. *Edited by* K. Paech and M. V. Tracey. Springer-Verlag, Berlin. 1955. p. 382.
42. M. FREUND and W. WILL. Ber. **19**, 2797 (1886).
43. M. FREUND and W. WILL. Ber. **20**, 88 (1887).
44. W. J. GENSLER, E. M. HEALY, I. ONSHUUS, and H. L. BLUHM. J. Am. Chem. Soc. **78**, 1713 (1956).
45. M. FREUND. Ber. **22**, 2329 (1889).
46. G. BARGER and H. A. D. JOWETT. J. Chem. Soc. **87**, 967 (1905).
47. K. BÖTTCHER. Ber. **42**, 253 (1909).
48. H. M. FALES, E. W. WARNHOFF, and W. C. WILDMAN. J. Am. Chem. Soc. **77**, 5885 (1955).
49. E. OERTLY and A. PICTET. Ber. **43**, 1336 (1910).
50. A. OELKER. Ber. **24**, 2592 (1891).
51. J. T. VAN BRUGGEN, C. K. CLAYCOMB, and T. T. HUTCHENS. Nucleonics, **7** (3), 45 (1950).
52. M. FREUND and H. BECK. Ber. **37**, 4673 (1904).

Can. J. Chem. Downloaded from www.nrcresearchpress.com by 210.87.254.5 on 09/05/12
For personal use only.

NOTES

THE SYNTHESIS OF CYCLIC ANALOGUES OF TOLBUTAMIDE

D. L. Simmons, J. M. Dodsworth, and Francis L. Chubb

Since the original synthesis of 3-oxo-3,4-dihydro-1,2,4-benzothiadiazine (1) relatively few derivatives of this compound have been reported (2, 3). More recently sulphamyl substituted 3-oxo-3,4-dihydro-1,2,4-benzothiadiazine-1,1-dioxides have been synthesized as potential diuretics (4, 5) and as intermediates in the synthesis of diuretics (6, 7). These compounds are cyclic sulphonylureas, since they contain the —$SO_2NHCONH$— group in the heterocyclic ring. In this communication we wish to report the synthesis of a series of substituted 3-oxo-3,4-dihydro-1,2,4-benzothiadiazine-1,1-dioxides (I) which may be considered as cyclic analogues of the hypoglycemic sulphonylureas such as tolbutamide (II).

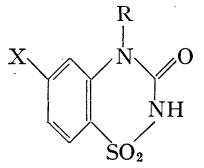

I

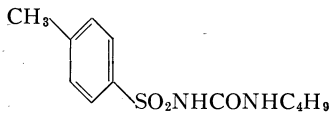

II

a: X = CH_3, R = H
b: X = Cl, R = H
c: X = CF_3, R = H

d: X = CH_3, R = *n*-C_4H_9
e: X = Cl, R = *n*-C_4H_9
f: X = CF_3, R = *n*-C_4H_9

These compounds were obtained from the corresponding 2-sulphamylanilines by treatment with phosgene (7). In the case of the 2-sulphamylanilines (III) with no substituent on the aniline nitrogen, treatment with phosgene yielded the final products directly. However, when the N-butyl-2-sulphamylanilines (IV) were treated with phosgene, the intermediate N-carbonyl chlorides (V) were isolated. Treatment with base effected ring closure to yield I. The N-butyl-2-sulphamylanilines were obtained by acylation of the corresponding anilines (4) with *n*-butyryl chloride followed by reduction with lithium aluminum hydride. The anilines were obtained from the appropriate 2-chloronitrobenzene according to the procedure of Topliss, Sperber, and Rubin (8). The pharmacology of these compounds will be reported elsewhere.

EXPERIMENTAL

Melting points are uncorrected. Microanalyses were carried out at the microanalytical laboratory of C. Daesslé, 5757 Decelles Avenue, Montreal, Quebec. Infrared spectra were obtained on a Perkin–Elmer spectrophotometer Model 237. Ultraviolet spectra were obtained on a Beckman DK2 spectrophotometer.

5-Methyl-2-sulphamylaniline

5-Methyl-2-sulphamylaniline was prepared in 15% overall yield from 2-chloro-5-methylnitrobenzene according to the procedure of Topliss, Sperber, and Rubin (8). It crystallized from benzene and melted at 125–126°. λ_{max}^{MeOH} 246 mμ (7800), 304 mμ (3630). Anal. Calculated for $C_7H_{10}N_2O_2S$: C, 45.14; H, 5.41; N, 15.04; S, 17.21. Found: C, 45.14; H, 5.38; N, 15.58; S, 17.60.

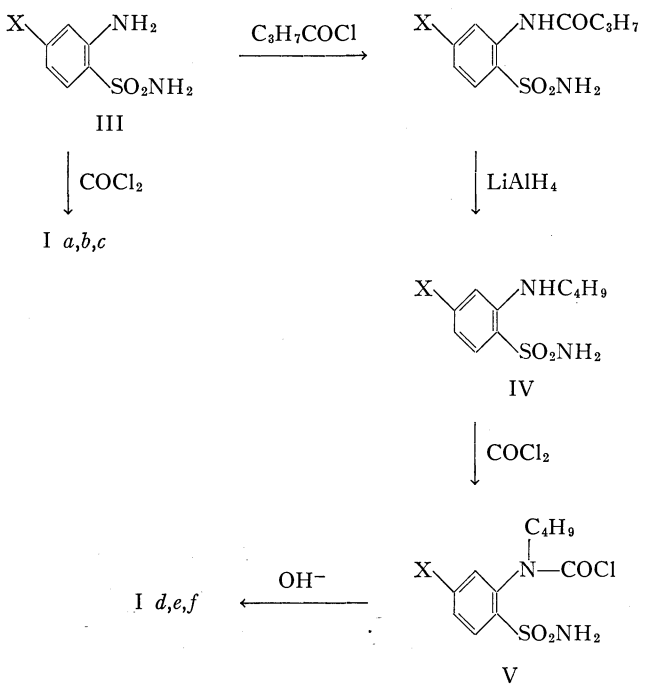

5-Chloro-2-sulphamylaniline

5-Chloro-2-sulphamylaniline was obtained from 2,5-dichloronitrobenzene by the above procedure in 22% yield, and melted at 143–145° (reported 144–146°) (9).

3-Oxo-6-trifluoromethyl-3,4-dihydro-1,2,4-benzothiadiazine-1,1-dioxide

3-Oxo-6-trifluoromethyl-3,4-dihydro-1,2,4-benzothiadiazine-1,1-dioxide was prepared by the action of phosgene on 5-trifluoro-2-sulphamylaniline (4) according to the procedure of Close, Swett, and Nordeen (7) and was isolated in 89% yield. It crystallized from ether – petroleum ether and melted at 227°. λ_{max}^{MeOH} 244 mμ (10,800), 295 mμ (2,320); ν_{max}^{Nujol} 3550 cm^{-1}, 3510 cm^{-1}, 1748 cm^{-1} (strong), 1648 cm^{-1} (weak). Anal. Calculated for $C_8H_5N_2SO_3F_3$: C, 36.09; H, 1.89; N, 10.53; S, 12.04. Found: C, 36.02; H, 1.98; N, 10.40; S, 12.60.

6-Methyl-3-oxo-3,4-dihydro-1,2,4-benzothiadiazine-1,1-dioxide

6-Methyl-3-oxo-3,4-dihydro-1,2,4-benzothiadiazine-1,1-dioxide was obtained in 89% yield by the action of phosgene on 5-methyl-2-sulphamylaniline. It crystallized from alcohol–water and melted at 298–300°. λ_{max}^{MeOH} 243 mμ (11,600), 287 mμ (1,740); ν_{max}^{Nujol} 3208 cm^{-1}, 1716 cm^{-1}. Anal. Calculated for $C_8H_8N_2SO_3$: C, 45.27; H, 3.80; N, 13.20; S, 15.11. Found: C, 45.39; H, 3.83; N, 13.45; S, 15.03.

6-Chloro-3-oxo-3,4-dihydro-1,2,4-benzothiadiazine-1,1-dioxide

6-Chloro-3-oxo-3,4-dihydro-1,2,4-benzothiadiazine-1,1-dioxide was prepared by the action of phosgene on 5-chloro-2-sulphamylaniline in 88% yield. It crystallized from alcohol and melted at 300° decomp. λ_{max}^{MeOH} 245 mμ (10,000), 292.5 mμ (2,000); ν_{max}^{Nujol} 3290 cm^{-1}, 1685 cm^{-1}. Anal. Calculated for $C_7H_5N_2ClSO_3$: C, 36.14; H, 2.17; N, 12.04; S, 13.78. Found: C, 35.87; H, 2.26; N, 12.47; S, 13.95.

N-Butyryl-2-sulphamyl-5-trifluoromethylaniline

N-Butyryl-2-sulphamyl-5-trifluoromethylaniline was prepared from 2-sulphamyl-5-trifluoromethylaniline (4) by treatment with *n*-butyryl chloride in dioxane according to the procedure of Novello *et al.* (4). It separated from benzene as needles and melted at 135–136°. λ_{max}^{MeOH} 247 mμ (13,500), 292 mμ (3,800). Anal. Calculated for $C_{11}H_{13}N_2O_3SF_3$: C, 42.59; H, 4.19; N, 9.03. Found: C, 42.79; H, 3.98; N, 9.33.

N-Butyryl-5-methyl-2-sulphamylaniline

N-Butyryl-5-methyl-2-sulphamylaniline was prepared in 90% yield by the action of *n*-butyryl chloride on 5-methyl-2-sulphamylaniline as described above. It crystallized from alcohol as prisms and melted at 135–137°. λ_{max}^{MeOH} 247.5 mμ (12,900), shoulder 283 mμ (2,560), shoulder 288 mμ (2,480). Anal. Calculated for $C_{11}H_{16}N_2O_3S$: C, 51.54; H, 6.29; N, 10.93; S, 12.51. Found: C, 51.65; H, 6.67; N, 11.08; S, 12.24.

Can. J. Chem. Downloaded from www.nrcresearchpress.com by 210.87.254.5 on 09/05/12
For personal use only.

N-Butyryl-5-chloro-2-sulphamylaniline

N-Butyryl-5-chloro-2-sulphamylaniline was prepared in 87% yield by the action of *n*-butyryl chloride on 5-chloro-2-sulphamylaniline as described above. It crystallized from benzene as prisms and melted at 141–142°. λ_{max}^{MeOH} 248.5 mμ (15,200), shoulder 286.5 mμ (2,500), shoulder 292 mμ (2,450). Anal. Calculated for $C_{10}H_{13}N_2O_3SCl$: C, 43.40; H, 4.73; N, 10.13; Cl, 12.81. Found: C, 43.63; H, 4.79; N, 10.27; Cl, 12.84.

N-Butyl-2-sulphamyl-5-trifluoromethylaniline

N-Butyryl-2-sulphamyl-5-trifluoromethylaniline (2.23 g) was added portionwise and with stirring to a suspension of lithium aluminum hydride (0.7 g) in hydride-stable tetrahydrofuran (50 cc). After the addition was complete, the contents were gently refluxed for 3 hours. The excess hydride was destroyed by careful addition of ethyl acetate and water, and the contents then concentrated *in vacuo*. Water (100 ml) was added and the solution made acidic with concentrated phosphoric acid and extracted with ether. Evaporation of the dried ethereal extracts *in vacuo* provided a white solid (2.0 g) which crystallized from ether – petroleum ether as fine needles, m.p. 140–141°. λ_{max}^{MeOH} 254 mμ (20,000), 330 mμ (10,000). Anal. Calculated for $C_{11}H_{15}N_2O_2SF_3$: C, 44.59; H, 5.07; N, 9.46. Found: C, 44.80; H, 5.51; N, 9.69.

N-Butyl-5-methyl-2-sulphamylaniline

N-Butyl-5-methyl-2-sulphamylaniline was prepared in 75% yield from the N-butyryl derivative according to the procedure described above. It crystallized from ether – petroleum ether as needles and melted at 112°. λ_{max}^{MeOH} 253 mμ (18,000), 315 mμ (9,700). Anal. Calculated for $C_{11}H_{18}N_2O_2S$: C, 54.52; H, 7.49; N, 11.56; S, 13.23. Found: C, 54.66; H, 7.51; N, 11.75; S, 13.29.

N-Butyl-5-chloro-2-sulphamylaniline

N-Butyl-5-chloro-2-sulphamylaniline was obtained in 79% yield from the N-butyryl derivative by the above procedure. It crystallized from ether – petroleum ether as needles and melted at 119°. λ_{max}^{MeOH} 255.5 mμ (19,460), 320 mμ (10,000). Anal. Calculated for $C_{10}H_{15}N_2SO_2Cl$: C, 45.71; H, 5.75; N, 10.66; S, 12.20. Found: C, 45.98; H, 5.94; N, 10.77; S, 12.22.

N-Butyl-N-chlorocarbonyl-5-methyl-2-sulphamylaniline

N-Butyl-N-chlorocarbonyl-5-methyl-2-sulphamylaniline was prepared by the same procedure used in the preparation of the 3-oxo-benzothiadiazines (7) and was isolated in 92% yield. It crystallized from ether – petroleum ether and melted at 98°. $\nu_{max}^{CHCl_3}$ 3500 cm^{-1}, 3450 cm^{-1}, 3275 cm^{-1}, 1745 cm^{-1}, 1718 cm^{-1}. Anal. Calculated for $C_{12}H_{17}N_2SO_3Cl$: C, 47.28; H, 5.62; N, 9.19; S, 10.52; Cl, 11.63. Found: C, 47.05; H, 5.48; N, 9.36; S, 10.68; Cl, 11.58.

The corresponding 5-chloro- and 5-trifluoro-methyl analogues failed to crystallize and were employed in the following reactions without further purification. Infrared spectroscopy of these products revealed the characteristic doublet of carbonyl chlorides in the 1715–1750 cm^{-1} region.

4-Butyl-6-methyl-3-oxo-3,4-dihydro-1,2,4-benzothiadiazine-1,1-dioxide

The N-carbonyl chloride derivative (0.69 g) was gently refluxed with 5% methanolic potassium hydroxide (20 ml) for 1 hour. The reaction mixture was then cooled, diluted with water, and extracted with ether. The aqueous extract was acidified with concentrated hydrochloric acid and extracted with ether. Evaporation of the dried ethereal extracts (acidic) provided a white solid (0.65 g) which crystallized from methylene chloride – petroleum ether and melted at 173–174°. λ_{max}^{MeOH} 250 mμ (11,100), 290 mμ (1,960); $\nu_{max}^{CHCl_3}$ 3350 cm^{-1}, 1700 cm^{-1}. Anal. Calculated for $C_{12}H_{16}N_2O_3S$: C, 53.71; H, 6.01; N, 10.44; S, 11.95. Found: C, 53.96; H, 5.78; N, 10.75; S, 11.99.

4-Butyl-3-oxo-6-trifluoromethyl-3,4-dihydro-1,2,4-benzothiadiazine-1,1-dioxide

N-Butyl-3-oxo-6-trifluoromethyl-3,4-dihydro-1,2,4-benzothiadiazine-1,1-dioxide was prepared in 90% yield from the oily N-carbonyl chloride derivative by the above procedure. It crystallized from ether – petroleum ether and melted at 144°. λ_{max}^{MeOH} 250.5 mμ (12,690), 298 mμ (2,660); $\nu_{max}^{CHCl_3}$ 3350 cm^{-1}, 1708 cm^{-1}. Anal. Calculated for $C_{12}H_{13}N_2SO_3F_3$: C, 44.72; H, 4.06; N, 8.69; S, 9.95. Found: C, 44.47; H, 3.81; N, 8.95; S, 10.32.

4-Butyl-6-chloro-3-oxo-3,4-dihydro-1,2,4-benzothiadiazine-1,1-dioxide

4-Butyl-6-chloro-3-oxo-3,4-dihydro-1,2,4-benzothiadiazine-1,1-dioxide was obtained in 88% yield from the oily N-carbonyl chloride derivative by the above procedure. It crystallized from ether – petroleum ether and melted at 152°. λ_{max}^{MeOH} 252.5 mμ (11,310), 295 mμ (2,170); $\nu_{max}^{CHCl_3}$ 3350 cm^{-1}, 1705 cm^{-1}. Anal. Calculated for $C_{11}H_{13}N_2SO_3Cl$: C, 45.75; H, 4.54; N, 9.70; S, 11.10. Found: C, 45.78; H, 4.59; N, 9.51; S, 11.12.

1. E. SCHRADER. J. Prakt. Chem. Ser. 2, **95**, 392 (1917).
2. D. V. PARK and R. T. WILLIAMS. J. Chem. Soc. 1760 (1950).
3. L. RAFFA. Farmaco (Pavia) Ed. Sci. **9**, 661 (1954); **12**, 41, 400, 448, 495 (1957).
4. F. C. NOVELLO, S. C. BELL, E. L. A. ABRAMS, C. ZIEGLER, and J. M. SPRAGUE. J. Org. Chem. **25**, 970 (1960).
5. H. L. YALE, K. LOSEE, and J. BERNSTEIN. J. Am. Chem. Soc. **82**, 2043 (1960).

Can. J. Chem. Downloaded from www.nrcresearchpress.com by 210.87.254.5 on 09/05/12
For personal use only.

6. W. J. CLOSE, L. R. SWETT, L. E. BRADY, J. H. SHORT, and M. VERNSTEIN. J. Am. Chem. Soc. **82**, 1132 (1960).
7. W. J. CLOSE, L. R. SWETT, and C. W. NORDEEN. J. Org. Chem. **26**, 3423 (1961).
8. J. G. TOPLISS, N. SPERBER, and A. A. RUBIN. U.S. Patent No. 2,986,573.
9. J. H. SHORT and U. BIERMACHER. J. Am. Chem. Soc. **82**, 1135 (1960).

RECEIVED OCTOBER 17, 1962.
RESEARCH LABORATORIES,
FRANK W. HORNER LIMITED,
MONTREAL, QUE.

Can. J. Chem. Downloaded from www.nrcresearchpress.com by 210.87.254.5 on 09/05/12
For personal use only.

THE VINYLTRIFLUOROBORATE ANION[1,2]

S. L. STAFFORD

Recent interest in vinyl-metallic compounds in general (1), and in particular in the extent of carbon–boron π-bonding in vinyl-boron derivatives (2), prompted the preparation of the new vinylfluoroborate anion $CH_2{=}CHBF_3^-$. The anion was desired in order to study the effect on carbon–boron π-bonding, and also as a member of a class of potentially useful compounds of which little is known, the mixed organohaloborates. Only two such anions—$(C_6H_5)_3BF^-$ (3) and $CF_3BF_3^-$ (4)—have been characterized previously.[3]

A solution of 2.59 g (27.5 mmoles) of $KF.2H_2O$ dissolved in 3 ml of water was introduced into a reaction tube and 560 cc (STP) (25 mmoles) of $CH_2{:}CHBF_2$ (prepared from $(CH_2{:}CH)_4Sn$ and BF_3 (6)) containing a small amount of BF_3 was condensed onto it. The tube was sealed and placed in an ice bath for 4 hours. Volatile products were then removed under high vacuum through traps held at −78° and −196°. The only volatile material removed other than water was 56 cc (STP) of ethylene, collected at −196°. The solid residue was extracted with boiling acetonitrile. Removal of the solvent gave 1.84 g (55% yield, based on $CH_2{:}CHBF_2$) of $K^+CH_2{:}CHBF_3^-$. Anal.: Required for $C_2H_3F_3BK$: C, 17.9; H, 2.24; F, 42.5; B, 8.2%. Found: C, 17.6; H, 2.46; F, 44.6; B, 7.7%.

The infrared spectrum (KBr disk) of the compound shows absorptions at 3067, 2967 (C—H stretch); 1623 (C=C stretch); 1422, 1294 (CH_2 and CH in-plane deformations); 1132, 1107 (B—C stretch); 1035 (B—F asymmetric stretch); 950–920; and 694 cm^{-1}.

The F-19 nuclear magnetic resonance spectrum, in aqueous solution, consists of a quartet centered at $\delta_{CCl_3F} = 138$ p.p.m., with $J_{B^{11}-F} = 51.8$ c.p.s. After standing in the tube for several days at room temperature, the solution was re-examined. In addition to the original quartet, a peak was observed at $\delta_{CCl_3F} = 150$ p.p.m. (assignable to BF_4^-) and there appeared to be a weak, very broad quartet centered near $\delta_{CCl_3F} = 143$ p.p.m. (perhaps due to $(CH_2{:}CH)_2BF_2^-$). This apparent disproportionation has not been studied further.

As would be expected, the $CH_2{:}CHBF_3^-$ anion shows greater hydrolytic stability than does $CH_2{:}CHBF_2$. Thus, $CH_2{:}CHBF_2$ in contact with water at room temperature gives appreciable amounts of ethylene in a few hours. Solutions containing $CH_2{:}CHBF_3^-$, on the other hand, are stable to hydrolysis for at least several days.

[1]*This work was supported by the Advanced Research Projects Agency (ARPA) under Contract No. DA-30-069-ORD-2638.*

[2]*Presented in part at the Symposium on Organometallic Chemistry at the University of British Columbia, September, 1962.*

[3]*The formation of organohaloborate anions by addition of hydrogen halides to amine adducts of organoboron halides has been postulated (5).*

6. W. J. CLOSE, L. R. SWETT, L. E. BRADY, J. H. SHORT, and M. VERNSTEIN. J. Am. Chem. Soc. **82**, 1132 (1960).
7. W. J. CLOSE, L. R. SWETT, and C. W. NORDEEN. J. Org. Chem. **26**, 3423 (1961).
8. J. G. TOPLISS, N. SPERBER, and A. A. RUBIN. U.S. Patent No. 2,986,573.
9. J. H. SHORT and U. BIERMACHER. J. Am. Chem. Soc. **82**, 1135 (1960).

RECEIVED OCTOBER 17, 1962.
RESEARCH LABORATORIES,
FRANK W. HORNER LIMITED,
MONTREAL, QUE.

Can. J. Chem. Downloaded from www.nrcresearchpress.com by 210.87.254.40 on 09/05/12
For personal use only.

THE VINYLTRIFLUOROBORATE ANION[1,2]

S. L. STAFFORD

Recent interest in vinyl-metallic compounds in general (1), and in particular in the extent of carbon–boron π-bonding in vinyl-boron derivatives (2), prompted the preparation of the new vinylfluoroborate anion $CH_2{=}CHBF_3^-$. The anion was desired in order to study the effect on carbon–boron π-bonding, and also as a member of a class of potentially useful compounds of which little is known, the mixed organohaloborates. Only two such anions—$(C_6H_5)_3BF^-$ (3) and $CF_3BF_3^-$ (4)—have been characterized previously.[3]

A solution of 2.59 g (27.5 mmoles) of $KF.2H_2O$ dissolved in 3 ml of water was introduced into a reaction tube and 560 cc (STP) (25 mmoles) of $CH_2{:}CHBF_2$ (prepared from $(CH_2{:}CH)_4Sn$ and BF_3 (6)) containing a small amount of BF_3 was condensed onto it. The tube was sealed and placed in an ice bath for 4 hours. Volatile products were then removed under high vacuum through traps held at −78° and −196°. The only volatile material removed other than water was 56 cc (STP) of ethylene, collected at −196°. The solid residue was extracted with boiling acetonitrile. Removal of the solvent gave 1.84 g (55% yield, based on $CH_2{:}CHBF_2$) of $K^+CH_2{:}CHBF_3^-$. Anal.: Required for $C_2H_3F_3BK$: C, 17.9; H, 2.24; F, 42.5; B, 8.2%. Found: C, 17.6; H, 2.46; F, 44.6; B, 7.7%.

The infrared spectrum (KBr disk) of the compound shows absorptions at 3067, 2967 (C—H stretch); 1623 (C=C stretch); 1422, 1294 (CH_2 and CH in-plane deformations); 1132, 1107 (B—C stretch); 1035 (B—F asymmetric stretch); 950–920; and 694 cm^{-1}.

The F-19 nuclear magnetic resonance spectrum, in aqueous solution, consists of a quartet centered at $\delta_{CCl_3F} = 138$ p.p.m., with $J_{B^{11}-F} = 51.8$ c.p.s. After standing in the tube for several days at room temperature, the solution was re-examined. In addition to the original quartet, a peak was observed at $\delta_{CCl_3F} = 150$ p.p.m. (assignable to BF_4^-) and there appeared to be a weak, very broad quartet centered near $\delta_{CCl_3F} = 143$ p.p.m. (perhaps due to $(CH_2{:}CH)_2BF_2^-$). This apparent disproportionation has not been studied further.

As would be expected, the $CH_2{:}CHBF_3^-$ anion shows greater hydrolytic stability than does $CH_2{:}CHBF_2$. Thus, $CH_2{:}CHBF_2$ in contact with water at room temperature gives appreciable amounts of ethylene in a few hours. Solutions containing $CH_2{:}CHBF_3^-$, on the other hand, are stable to hydrolysis for at least several days.

[1]*This work was supported by the Advanced Research Projects Agency (ARPA) under Contract No. DA-30-069-ORD-2638.*

[2]*Presented in part at the Symposium on Organometallic Chemistry at the University of British Columbia, September, 1962.*

[3]*The formation of organohaloborate anions by addition of hydrogen halides to amine adducts of organoboron halides has been postulated (5).*

A sample of dry $K^+CH_2{:}CHBF_3^-$ was heated on the vacuum line. The solid did not melt below 225°, at which temperature decomposition of the salt began. Decomposition was rapid above 250°. The gas evolved was shown by its infrared spectrum to be $CH_2{:}CHBF_2$ of high purity. By way of comparison, $K^+BF_4^-$ does not dissociate appreciably below 500° (7, and references cited therein). Thus salts of organohaloborates may be an excellent means of storing and handling organohaloboranes, and of regenerating these compounds in a highly pure form.

Solutions of $K^+CH_2{=}CHBF_3^-$ were found to generate $(CH_2{=}CH)_2Hg$ rapidly when in contact with mercury, as in a sink trap. It should be stressed, therefore, that such solutions should be treated with nitric acid before attempting disposal, in order to prevent the formation of the highly toxic organomercury compounds.

The synthesis of $K^+CH_3BF_3^-$ in a similar manner is indicative of the general applicability of the reaction. Anal.: Required for CH_3BF_3K: C, 9.84; H, 2.46; F, 46.7%. Found: C, 9.43; H, 2.63; F, 46.8%. The F-19 n.m.r. spectrum in aqueous solution revealed a quartet centered at $\delta_{CCl_3F} = 132$ p.p.m., $J_{B^{11}-F} = 64$ c.p.s.

Further details of these and related studies will be reported more fully at a future date.

The author wishes to thank Mrs. N. Bolan and Dr. B. B. Stewart for their assistance in obtaining the infrared and n.m.r. spectra.

1. H. D. Kaesz and F. G. A. Stone. Organometallic compounds. *Edited by* H. Zeiss. Reinhold Publishing Co., New York, New York. 1960. Chap. 3.
2. T. D. Coyle, S. L. Stafford, and F. G. A. Stone. J. Chem. Soc. 3103 (1961).
3. D. L. Fowler and C. A. Kraus. J. Am. Chem. Soc. **62**, 1143 (1940).
4. R. D. Chambers, H. C. Clark, and C. J. Willis. J. Am. Chem. Soc. **82**, 5298 (1960).
5. F. E. Brinckman and F. G. A. Stone. Chem. Ind. (London), 254 (1955).
6. F. E. Brinckman and F. G. A. Stone. J. Am. Chem. Soc. **82**, 6218 (1960).
7. D. W. A. Sharpe. Advances in fluorine chemistry. Vol. 1. Academic Press, Inc., New York, New York. 1960.

Received October 4, 1962.
Research Laboratories,
General Chemical Division,
Allied Chemical Corporation,
Morristown, New Jersey.

THE PHOTOLYSIS OF LIQUID O_2–N_2 SOLUTIONS[1]

W. B. DeMore and Odell Raper

INTRODUCTION

Recently McNesby has found that the irradiation of liquid O_2–N_2 solutions with a low-pressure mercury arc yields O_3 and N_2O as products (1). One question which has arisen from this work concerns the origin of the N_2O. The radiation emitted by the low-pressure arc which is photochemically active in this system is at 1849 Å and 2537 Å, and the formation of O_3 must be initiated by the interaction of 1849 Å radiation with O_2. The N_2O may be formed in a process involving photolysis of O_2 at 1849 Å or may result from photolysis of the product O_3, which absorbs strongly in the ultraviolet, particularly

[1]*This paper represents the results of one phase of research carried out at the Jet Propulsion Laboratory, California Institute of Technology, under Contract No. NAS 7-100, sponsored by the National Aeronautics and Space Administration.*

Can. J. Chem. Downloaded from www.nrcresearchpress.com by 210.87.254.40 on 09/05/12
For personal use only.

A sample of dry $K^+CH_2{:}CHBF_3^-$ was heated on the vacuum line. The solid did not melt below 225°, at which temperature decomposition of the salt began. Decomposition was rapid above 250°. The gas evolved was shown by its infrared spectrum to be $CH_2{:}CHBF_2$ of high purity. By way of comparison, $K^+BF_4^-$ does not dissociate appreciably below 500° (7, and references cited therein). Thus salts of organohaloborates may be an excellent means of storing and handling organohaloboranes, and of regenerating these compounds in a highly pure form.

Solutions of $K^+CH_2{=}CHBF_3^-$ were found to generate $(CH_2{=}CH)_2Hg$ rapidly when in contact with mercury, as in a sink trap. It should be stressed, therefore, that such solutions should be treated with nitric acid before attempting disposal, in order to prevent the formation of the highly toxic organomercury compounds.

The synthesis of $K^+CH_3BF_3^-$ in a similar manner is indicative of the general applicability of the reaction. Anal.: Required for CH_3BF_3K: C, 9.84; H, 2.46; F, 46.7%. Found: C, 9.43; H, 2.63; F, 46.8%. The F-19 n.m.r. spectrum in aqueous solution revealed a quartet centered at $\delta_{CCl_3F} = 132$ p.p.m., $J_{B^{11}-F} = 64$ c.p.s.

Further details of these and related studies will be reported more fully at a future date.

The author wishes to thank Mrs. N. Bolan and Dr. B. B. Stewart for their assistance in obtaining the infrared and n.m.r. spectra.

1. H. D. Kaesz and F. G. A. Stone. Organometallic compounds. *Edited by* H. Zeiss. Reinhold Publishing Co., New York, New York. 1960. Chap. 3.
2. T. D. Coyle, S. L. Stafford, and F. G. A. Stone. J. Chem. Soc. 3103 (1961).
3. D. L. Fowler and C. A. Kraus. J. Am. Chem. Soc. **62**, 1143 (1940).
4. R. D. Chambers, H. C. Clark, and C. J. Willis. J. Am. Chem. Soc. **82**, 5298 (1960).
5. F. E. Brinckman and F. G. A. Stone. Chem. Ind. (London), 254 (1955).
6. F. E. Brinckman and F. G. A. Stone. J. Am. Chem. Soc. **82**, 6218 (1960).
7. D. W. A. Sharpe. Advances in fluorine chemistry. Vol. 1. Academic Press, Inc., New York, New York. 1960.

Received October 4, 1962.
Research Laboratories,
General Chemical Division,
Allied Chemical Corporation,
Morristown, New Jersey.

THE PHOTOLYSIS OF LIQUID O_2–N_2 SOLUTIONS[1]

W. B. DeMore and Odell Raper

INTRODUCTION

Recently McNesby has found that the irradiation of liquid O_2–N_2 solutions with a low-pressure mercury arc yields O_3 and N_2O as products (1). One question which has arisen from this work concerns the origin of the N_2O. The radiation emitted by the low-pressure arc which is photochemically active in this system is at 1849 Å and 2537 Å, and the formation of O_3 must be initiated by the interaction of 1849 Å radiation with O_2. The N_2O may be formed in a process involving photolysis of O_2 at 1849 Å or may result from photolysis of the product O_3, which absorbs strongly in the ultraviolet, particularly

[1]*This paper represents the results of one phase of research carried out at the Jet Propulsion Laboratory, California Institute of Technology, under Contract No. NAS 7-100, sponsored by the National Aeronautics and Space Administration.*

at 2537 Å (2). This report describes studies of the mechanism of N_2O formation in the O_2–N_2 system by examination of the ratio of N_2O to O_3 as a function of the quantum dosage.

EXPERIMENTAL

In order to study the N_2O/O_3 ratio at the smallest possible quantum dosages and still obtain sufficient products for accurate analysis, an apparatus was designed which rapidly removed the products while recirculating the original O_2–N_2 solution. This apparatus is shown in Fig. 1. For a run, measured amounts

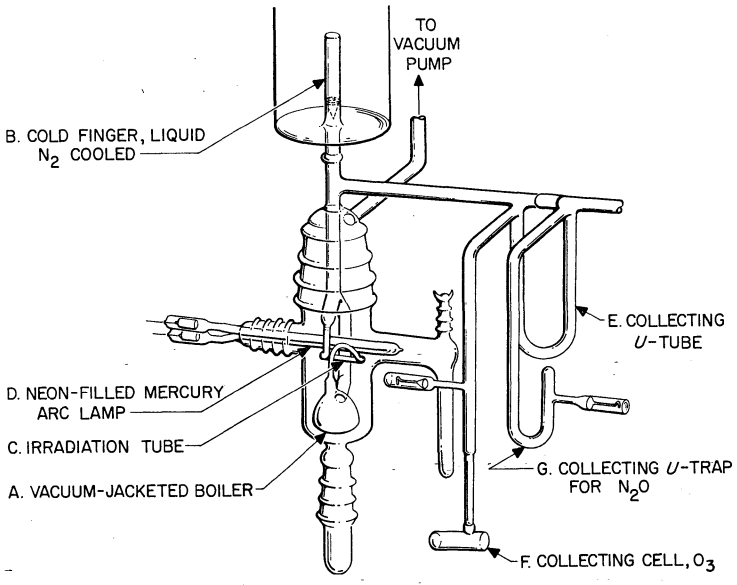

FIG. 1. Experimental apparatus.

of N_2 and O_2, purified by passage through a Drierite–Ascarite train and one distillation from the liquid, were condensed in the vacuum-jacketed boiler A, and the resultant solution boiled at a rate determined by its composition and the absorption of heat from the surroundings. The vapor was condensed in the inverted cold finger B, dripped into the quartz irradiation tube C, and was irradiated by the mercury arc D as it passed through the tube. Only the tube C was of quartz, and only that portion which was continuously filled with liquid was irradiated, all other areas being masked off. These precautions were taken to assure that no photolysis occurred in the gas phase or in the boiler. Due to fractionation the composition of the solution in the tube C was not the same as that in the boiler, so before any runs were made the true composition of the irradiated solution was determined by direct liquid sampling of the condensate in the irradiation tube over a range of liquid compositions in the boiler.

The O_3 and N_2O formed during irradiation were washed into the boiler, where they remained, while the volatile O_2 and N_2 were continuously recirculated. After a photolysis period of 4 hours, the lamp was turned off, the vacuum jacket removed from the cell, and a liquid nitrogen bath placed over the boiler. The excess O_2 and N_2 were then carefully pumped off by evacuation to a good vacuum. O_3 was separated from N_2O by placing a liquid oxygen bath over the boiler and collecting the O_3 in the U-tube E at liquid nitrogen temperature. The O_3 was then transferred to cell F and sealed off. A dry ice trap was then placed around the boiler and the N_2O was collected in the U-trap G at liquid nitrogen temperature and sealed off. The O_3 was converted to O_2 by flaming, and the O_2 and N_2O concentrations were determined by mass spectrometry. The mass 30 peak was used for N_2O analysis to avoid any possible confusion with CO_2 impurity, although blank runs showed such impurities to be small.

RESULTS AND DISCUSSION

The results of two experiments at different O_2/N_2 ratios are shown in Fig. 2. The lamp power, which was found to be linear with the 2537 Å intensity I, was varied for each run and plotted against R, the ratio of N_2O to O_3 produced. Most of the radiation absorbed

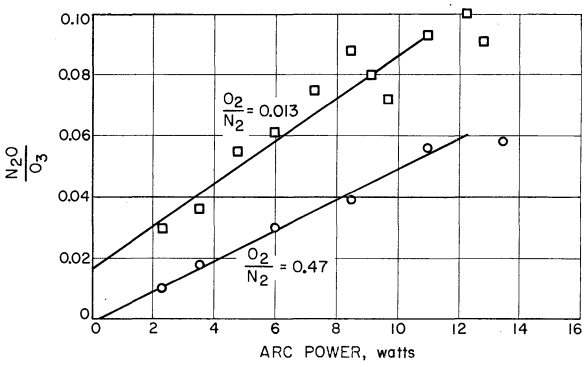

FIG. 2. N_2O/O_3 ratio as a function of arc power.

by O_3 was at 2537 Å, absorption of 1849 Å radiation by either product being negligible due to their low extinction coefficients in this region (3) and the small amount of 1849 Å light available. For a given O_2/N_2 ratio the photolysis time Δt remained constant, so the variation in lamp power represents a linear variation in the intensity of the light absorbed by O_3. If both N_2O and O_3 are formed in amounts proportional to the absorption of 1849 Å light by O_2, the ratio N_2O/O_3 should extrapolate to a non-zero intercept with decreasing quantum dosage. The results of Fig. 2 clearly indicate that N_2O is not being formed efficiently as a result of primary photolysis of O_2. In the upper curve, where N_2 is present in large excess over O_2, the intercept is small, indicating that N_2 is competing very weakly with O_2 for the primary reactive species present. At sufficiently high O_2 to N_2 ratios, as in the lower curve, initial N_2O formation can no longer be observed. A difficulty arises in attempting to place numerical values on the relative efficiencies for initial O_3 and N_2O formation in this system. Absorption of 1849 Å radiation by the O_2 molecule does not lead directly to its dissociation, producing instead O_2 in the excited $^3\Sigma_u^-$ state. In the gas phase these excited molecules may undergo predissociation to ground-state atoms (4–6), but in the liquid they may also react directly with the N_2 and O_2 present. Several mechanisms for initial product formation in this system are therefore possible and the data in the present work is insufficient to allow a choice to be made between them. By any reasonable mechanism compatible with the possible reactions in the system, however, the ratio of the efficiency of primary N_2O formation relative to that of O_3 is of the order of 10^{-4}.

The linear dependence of the N_2O/O_3 ratio on quantum dosage shown in Fig. 2 may be explained by formation of N_2O as a result of O_3 photolysis. Recent work by the authors in the ultraviolet photolysis of O_3 in liquid N_2 and N_2–O_2 solutions indicates that $O(^1D)$ is produced, which reacts with N_2 to form N_2O in a yield proportional to the light quanta absorbed by O_3, the actual quantum yield depending on the O_2/N_2 ratio (7). The average O_3 concentration in the irradiation tube was about 10^{-5} mole/liter, and therefore the amount of light absorbed by O_3 was proportional to the average O_3 concentration, since the optical density of the O_3 in the 2-mm tube was not greater than about 0.006 at 2537 Å. It then follows that the amount of N_2O produced was proportional to the product $I\Delta t[O_3]_{av}$. If the total amount of O_3 destroyed by photolysis was small, the ratio N_2O/O_3 would then be proportional to $I\Delta t$, the quantum dosage. The results of reference 7 show that at O_3 concentrations less than about 10^{-2} mole/liter the reaction $O + O_3 \rightarrow 2O_2$ can be neglected, since at such low concentrations it is not fast enough to compete with

the reaction of ^1D atomic oxygen with the N_2 and O_2. Therefore, the O_3 destroyed was equal to the N_2O produced, which, from Fig. 2, was not greater than 10% of the O_3. The conclusion is therefore drawn that the linearly increasing N_2O/O_3 ratio results from the photolysis of the product O_3 during the residence time in the irradiation tube.

Further support for the suggestion that N_2O is formed by O_3 photolysis may be obtained from the observed effect of the O_2/N_2 solution ratio on the N_2O/O_3 product ratio. If formation of N_2O by O_2 photolysis at 1849 Å is neglected, the ratio R is given by the following expression:

$$R = \frac{CI\Delta t}{1 + \dfrac{(k_{rO_2}+k_{dO_2})\,[O_2]}{(k_{rN_2}+k_{dN_2})\,[N_2]}}. \tag{A}$$

In this expression C is a constant proportional to the O_3 cross section for 2537 Å radiation, $I\Delta t$ the quantum dosage at this wavelength, and the k's are the appropriate rate constants for reaction and deactivation of $O(^1D)$ with O_2 and N_2. A value of the ratio of these rate constants was obtained from the experiment shown in Fig. 3. In this experiment, $I\Delta t$ was

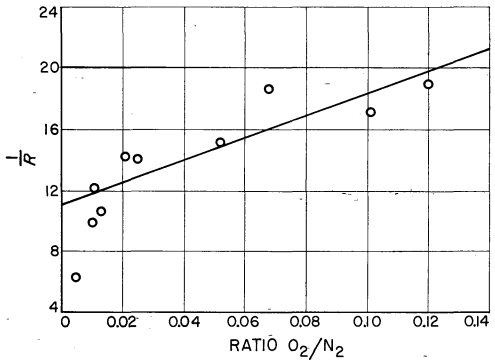

FIG. 3. O_3/N_2O ratio as a function of the ratio of O_2 to N_2.

held constant and $1/R$, or O_3/N_2O, determined as a function of the O_2/N_2 ratio. Dividing the slope by the intercept in Fig. 3 gives a value for $(k_{rO_2}+k_{dO_2})/(k_{rN_2}+k_{dN_2})$ equal to 6.5. This can be taken only as an order of magnitude value since primary N_2O formation has been neglected and also since Δt does not remain precisely constant as the O_2/N_2 ratio is varied. The value is in good agreement, however, with the value 4.5 obtained recently by the authors using a different method (7). The deviation at low O_2/N_2 ratios in Fig. 3 may be due to experimental error in preparing the dilute solutions, but is also compatible with the small contribution to R due to primary N_2O formation as determined in Fig. 2. This term becomes more significant as O_2/N_2 becomes smaller, and should cause a deviation towards zero in Fig. 3.

We conclude, therefore, that little or no N_2O formation occurs in this system as a direct result of the primary photolysis of O_2 by 1849 Å radiation, and that the N_2O yield can be attributed to the reaction between N_2 and the ^1D atomic oxygen produced in the secondary photolysis of O_3.

1. J. R. McNESBY. J. Chem. Phys. **31**, 283 (1959).
2. A. LAUCHLE. Helv. Phys. Acta, **1**, 208 (1928).
3. K. WATANABE, M. ZELIKOFF, and E. C. Y. INN. AFCRC Technical Report No. 53-23. Geophysical Research Paper No. 21. 1953.

4. P. J. FLORY. J. Chem. Phys. **4**, 23 (1936).
5. D. H. VOLMAN. J. Chem. Phys. **24**, 122 (1956).
6. D. H. VOLMAN. J. Chem. Phys. **25**, 288 (1956).
7. W. DEMORE and O. F. RAPER. J. Chem. Phys. **37**, 2048 (1962).

RECEIVED SEPTEMBER 14, 1962.
JET PROPULSION LABORATORY,
CALIFORNIA INSTITUTE OF TECHNOLOGY,
PASADENA, CALIFORNIA.

TEMPERATURE CONTROL ATTACHMENTS FOR VARIABLE AND FIXED PATH LENGTH INFRARED CELLS

M. S. SMITH AND P. A. D. DE MAINE

Quantitative studies of the temperature dependence of infrared spectra for liquids have been frustrated by the difficulties in designing adequate devices for controlling the liquid temperature in the cells. Lord *et al.* (1) have given full bibliography for cells designed before 1951.

The heating-block cells sold by the instrument manufacturers provide uncertain temperature regulation and are useful only above room temperature. The high and low temperature gas convection cells used by Bernstein and Powling (2, 3) are elaborate and lack precision because of the low thermal conductivity of dry air and nitrogen.

Maguire and West (4) used a hollow brass block to control the temperature between −17.5° C and 45° C in their study of hydrogen bonds. They reported a temperature sensitivity of 0.05° C above 0° C and 0.5° C below 0° C. We have found that the sample temperatures can be quite different from the cell casing or reservoir temperatures. Also, the measured temperature sensitivity of the sample liquid is determined by the potentiometer–thermocouple combination used. With this system the recorded "temperature of the solution" may be incorrect.

Becker (5) used a water-jacketed cell to measure spectra at temperatures between −15° C and 60° C. Vinogradov and Crawford (6) have described a demountable temperature-regulated fixed path length liquid cell sensitive to 0.1° C between 0° C and 80° C. This cell is designed specifically for the Perkin–Elmer 112G Spectrophotometer and requires modifications to the sample housing. Both the Becker and the Vinogradov–Crawford cells are primarily designed for single-beam instruments.

Here we describe an inexpensive attachment for controlling the sample temperature in ordinary infrared cells.

DESCRIPTION OF ATTACHMENTS

(a) Cooling Blocks

Two cooling blocks were machined from 1/2-inch DURAL plate and 1/4-inch brass rod, and each was attached to the front or back plate of an infrared cell. Details of construction and assembly are shown in Fig. 1. Either Dupont Duco or Dekaphane cements were used for the pressure sealant between the open face of the cooling blocks and the cell plates. A 1/16-inch flange is sufficient for a water-tight seal.

Polyethylene tubing and tubing connectors were used to couple the cells to each other and to the reservoir.

4. P. J. FLORY. J. Chem. Phys. **4**, 23 (1936).
5. D. H. VOLMAN. J. Chem. Phys. **24**, 122 (1956).
6. D. H. VOLMAN. J. Chem. Phys. **25**, 288 (1956).
7. W. DEMORE and O. F. RAPER. J. Chem. Phys. **37**, 2048 (1962).

RECEIVED SEPTEMBER 14, 1962.
JET PROPULSION LABORATORY,
CALIFORNIA INSTITUTE OF TECHNOLOGY,
PASADENA, CALIFORNIA.

Can. J. Chem. Downloaded from www.nrcresearchpress.com by 210.87.254.40 on 09/05/12
For personal use only.

TEMPERATURE CONTROL ATTACHMENTS FOR VARIABLE AND FIXED PATH LENGTH INFRARED CELLS

M. S. SMITH AND P. A. D. DE MAINE

Quantitative studies of the temperature dependence of infrared spectra for liquids have been frustrated by the difficulties in designing adequate devices for controlling the liquid temperature in the cells. Lord *et al.* (1) have given full bibliography for cells designed before 1951.

The heating-block cells sold by the instrument manufacturers provide uncertain temperature regulation and are useful only above room temperature. The high and low temperature gas convection cells used by Bernstein and Powling (2, 3) are elaborate and lack precision because of the low thermal conductivity of dry air and nitrogen.

Maguire and West (4) used a hollow brass block to control the temperature between −17.5° C and 45° C in their study of hydrogen bonds. They reported a temperature sensitivity of 0.05° C above 0° C and 0.5° C below 0° C. We have found that the sample temperatures can be quite different from the cell casing or reservoir temperatures. Also, the measured temperature sensitivity of the sample liquid is determined by the potentiometer–thermocouple combination used. With this system the recorded "temperature of the solution" may be incorrect.

Becker (5) used a water-jacketed cell to measure spectra at temperatures between −15° C and 60° C. Vinogradov and Crawford (6) have described a demountable temperature-regulated fixed path length liquid cell sensitive to 0.1° C between 0° C and 80° C. This cell is designed specifically for the Perkin–Elmer 112G Spectrophotometer and requires modifications to the sample housing. Both the Becker and the Vinogradov–Crawford cells are primarily designed for single-beam instruments.

Here we describe an inexpensive attachment for controlling the sample temperature in ordinary infrared cells.

DESCRIPTION OF ATTACHMENTS

(a) Cooling Blocks

Two cooling blocks were machined from 1/2-inch DURAL plate and 1/4-inch brass rod, and each was attached to the front or back plate of an infrared cell. Details of construction and assembly are shown in Fig. 1. Either Dupont Duco or Dekaphane cements were used for the pressure sealant between the open face of the cooling blocks and the cell plates. A 1/16-inch flange is sufficient for a water-tight seal.

Polyethylene tubing and tubing connectors were used to couple the cells to each other and to the reservoir.

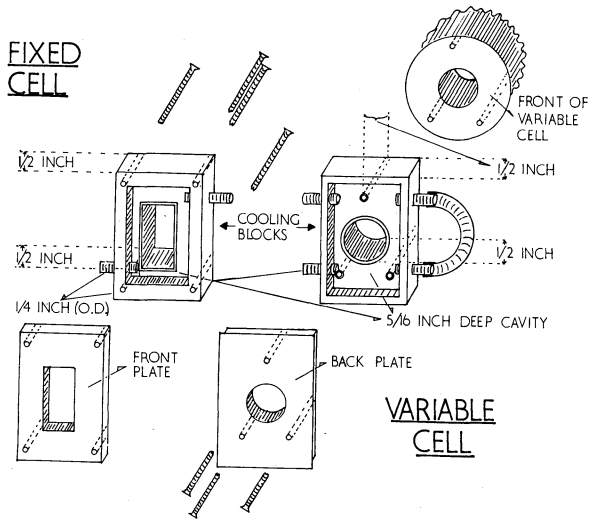

FIG. 1. Construction details and assembly of the variable and fixed path length cells.

(b) Constant-Temperature Bath

A constant-temperature bath was constructed from a 5-gal IGLOO insulated drinking water can, a 1/4- or 1/8-hp refrigerator compressor unit, a 500-watt immersion heater, and a heavy-duty double-pole relay switch (Potter and Brumfield type PRLLAY) with a Philadelphia microstat. A high-speed 1/20-hp air-cooled motor operated the stirrer for the reservoir liquid. A variable-speed pump (Fisher Scientific Company, Model B1) circulated the liquid through the cooling blocks. With the 1/4-hp compressor unit the reservoir could be varied between −30° C and 100° C.

At most temperatures the sensitivity of the reservoir controls was 0.05° C. However, below 10° C the sensitivity increased to 0.20° C. The sensitivity at all temperatures can be improved considerably with two independent mercury plunger relay switches to control the compressor and heater circuits. The uncertainty in measuring the temperatures in the cells does not justify the use of a high-precision temperature-controlled bath

CALIBRATION AND USE OF ATTACHMENTS

(a) Calibration

The equilibrium temperatures of the variable and fixed path length cells for different reservoir temperatures were measured with a Minneapolis-Honeywell Model No. 2745 potentiometer and an iron–constantan thermocouple in contact with the sample liquid. The reference thermocouple was in ice water. It was found that the equilibrium temperature in each cell does not vary with different sample liquids. The reproducibility of successive temperature measurements with either cell was within 0.15° C.

Because of the slight temperature difference between the two cells at equilibrium, calibration base lines were recorded at 5, 20, and 45° C with CCl_4 in both cells. When both cell path lengths were identical, no deviation was observed in the base line even in regions of high absorption (near 1200 cm^{-1}). Cell path lengths do not change measurably between 0° C and 50° C.

(b) Use of Attachments

At temperatures below 10° C appreciable fogging of the NaCl or KBr cell windows

Can. J. Chem. Downloaded from www.nrcresearchpress.com by 210.87.254.40 on 09/05/12
For personal use only.

occurs, even in the dry air purged cell compartment of the Beckman IR-7 spectrophotometer. To eliminate fogging at these lower temperatures two thermostated variable path length cells with IRTRAN-2 windows were used.

Once temperature equilibrium was established, both cells were flushed and filled with fresh solutions *in situ* in the cell compartment with the aid of hypodermic syringes and a glass trough. Temperature equilibrium was re-established in 2 to 3 minutes. With this technique a complete set of samples can be measured without the cells being removed from the cell compartment or uncoupled from the reservoir.

ACKNOWLEDGMENTS

Financial support for equipment and for a Research Fellowship to M. S. S. from the Directorate of Chemical Sciences, Air Force Office of Scientific Research, under Grant No. AF-AFOSR, 62–19, is gratefully acknowledged.

1. R. C. Lord, R. S. McDonald, and F. A. Miller. J. Opt. Soc. Am. **42**, 149 (1952).
2. H. J. Bernstein. J. Chem. Phys. **18**, 897 (1950).
3. J. Powling and H. J. Bernstein. J. Am. Chem. Soc. **73**, 1815 (1951).
4. M. M. Maguire and R. West. Spectrochim. Acta, **17**, 369 (1961).
5. E. D. Becker. Spectrochim. Acta, **17**, 436 (1961).
6. S. N. Vinogradov and R. J. Crawford. Spectrochim. Acta, **18**, 430 (1962).

Received November 26, 1962.
Chemistry Department,
The University of Mississippi,
University, Mississippi.

Can. J. Chem. Downloaded from www.nrcresearchpress.com by 210.87.254.40 on 09/05/12
For personal use only.

3-TRIFLUOROMETHYL AND 4-*t*-BUTYL DERIVATIVES OF TETRAPHENYLTIN

Roy G. Neville

Although in recent years many alkyl- and aryl-substituted derivatives of tetraphenyltin have been reported (1) only one trifluoromethyl derivative has been described, namely tetrakis(3-trifluoromethylphenyl)tin (2). Tetraphenyltin derivatives bearing a *t*-butyl substituent have not been reported.

In connection with other work in this laboratory certain derivatives of tetraphenyltin have been studied in which the substituents are either strongly electropositive or electronegative with respect to the phenyl–tin bond. This report describes seven derivatives of tetraphenyltin bearing 3-trifluoromethyl or 4-*t*-butyl substituents.

Four derivatives of the general formula $[(CH_3)_3C.C_6H_4]_nSn(C_6H_5)_{4-n}$, where $n = 1$–4, have been prepared. In the case of the 3-trifluoromethyl compounds, of general formula $(CF_3C_6H_4)_nSn(C_6H_5)_{4-n}$, only the derivatives for which n is 1, 3, or 4 are reported. Repeated attempts to prepare the derivative for which n is 2 were unsuccessful, the only product being an intractable oil which could not be induced to crystallize even on standing for several months. The reason for this lack of success has not been ascertained as no difficulty was encountered in obtaining the corresponding 4-*t*-butyl compound.

Both the 4-*t*-butyl and 3-trifluoromethyl derivatives were prepared using standard Grignard procedures. The products were colorless crystalline solids. As was anticipated, in the 4-*t*-butyl series melting points increased as the number of butyl substituents increased. Although tetraphenyltin melts at 225° (3), the "unsymmetrical" members

occurs, even in the dry air purged cell compartment of the Beckman IR-7 spectrophotometer. To eliminate fogging at these lower temperatures two thermostated variable path length cells with IRTRAN-2 windows were used.

Once temperature equilibrium was established, both cells were flushed and filled with fresh solutions *in situ* in the cell compartment with the aid of hypodermic syringes and a glass trough. Temperature equilibrium was re-established in 2 to 3 minutes. With this technique a complete set of samples can be measured without the cells being removed from the cell compartment or uncoupled from the reservoir.

ACKNOWLEDGMENTS

Financial support for equipment and for a Research Fellowship to M. S. S. from the Directorate of Chemical Sciences, Air Force Office of Scientific Research, under Grant No. AF-AFOSR, 62–19, is gratefully acknowledged.

1. R. C. Lord, R. S. McDonald, and F. A. Miller. J. Opt. Soc. Am. **42**, 149 (1952).
2. H. J. Bernstein. J. Chem. Phys. **18**, 897 (1950).
3. J. Powling and H. J. Bernstein. J. Am. Chem. Soc. **73**, 1815 (1951).
4. M. M. Maguire and R. West. Spectrochim. Acta, **17**, 369 (1961).
5. E. D. Becker. Spectrochim. Acta, **17**, 436 (1961).
6. S. N. Vinogradov and R. J. Crawford. Spectrochim. Acta, **18**, 430 (1962).

Received November 26, 1962.
Chemistry Department,
The University of Mississippi,
University, Mississippi.

Can. J. Chem. Downloaded from www.nrcresearchpress.com by 210.87.254.6 on 09/05/12
For personal use only.

3-TRIFLUOROMETHYL AND 4-*t*-BUTYL DERIVATIVES OF TETRAPHENYLTIN

Roy G. Neville

Although in recent years many alkyl- and aryl-substituted derivatives of tetraphenyltin have been reported (1) only one trifluoromethyl derivative has been described, namely tetrakis(3-trifluoromethylphenyl)tin (2). Tetraphenyltin derivatives bearing a *t*-butyl substituent have not been reported.

In connection with other work in this laboratory certain derivatives of tetraphenyltin have been studied in which the substituents are either strongly electropositive or electronegative with respect to the phenyl–tin bond. This report describes seven derivatives of tetraphenyltin bearing 3-trifluoromethyl or 4-*t*-butyl substituents.

Four derivatives of the general formula $[(CH_3)_3C.C_6H_4]_nSn(C_6H_5)_{4-n}$, where $n = 1$–4, have been prepared. In the case of the 3-trifluoromethyl compounds, of general formula $(CF_3C_6H_4)_nSn(C_6H_5)_{4-n}$, only the derivatives for which n is 1, 3, or 4 are reported. Repeated attempts to prepare the derivative for which n is 2 were unsuccessful, the only product being an intractable oil which could not be induced to crystallize even on standing for several months. The reason for this lack of success has not been ascertained as no difficulty was encountered in obtaining the corresponding 4-*t*-butyl compound.

Both the 4-*t*-butyl and 3-trifluoromethyl derivatives were prepared using standard Grignard procedures. The products were colorless crystalline solids. As was anticipated, in the 4-*t*-butyl series melting points increased as the number of butyl substituents increased. Although tetraphenyltin melts at 225° (3), the "unsymmetrical" members

(n = 1–3) of each series melted below this temperature despite their greater molecular weight. Tetrakis(4-*t*-butylphenyl)tin, I, on the other hand, could be heated almost to 300° before melting. The high melting point of this compound may not only be attributed to its large molecular weight but also to its overall molecular symmetry resulting from para substitution by the symmetrical *t*-butyl groups. In the case of tetrakis(3-trifluoromethylphenyl)tin, II, although the trifluoromethyl group is symmetrical (with regard to the carbon–phenyl bond), the molecule itself possesses less overall symmetry than compound I. Consequently, even though the molecular weights of I and II are comparable (651 and 699, respectively), II melts at a significantly lower temperature than I. Other factors also influence the temperature of fusion. The difference in the crystal lattice energy between a *t*-butyl- and a 3-trifluoromethyl-substituted derivative undoubtedly plays an important role in determining the melting point. However, within a given series, it was found that compounds possessing the highest degree of molecular symmetry melt at the highest temperature.

EXPERIMENTAL

Tris(4-t-butylphenyl)phenyltin

The procedure employed for the preparation of this compound is typical of that used for the other *t*-butyl derivatives.

The following reactants were placed in a 500-ml three-necked flask, fitted with reflux condenser, motor-driven stirrer, thermometer, and dropping funnel: magnesium turnings (2.7 g, 0.11 g-atom), sodium-dried diethyl ether (50 ml), and methyl iodide (0.5 ml). The flask was flushed with dry nitrogen and gently warmed on the water bath until the methylmagnesium iodide had formed. A solution of 4-bromo-*t*-butylbenzene (21.3 g, 0.1 mole) in ether (50 ml) was then added, dropwise with stirring, over a 20-minute period. The mixture was then refluxed for 1 hour. Trichlorophenyltin (10.08 g, 0.033 mole) dissolved in anhydrous (sodium dried) benzene (100 ml) was slowly added to the boiling solution and refluxing was continued for 5 hours. The flask was then cooled in an ice bath, and ice-cold water (300 ml) was run in at such a rate that the temperature of the well-stirred mixture did not exceed 20°. After filtering the mixture, the organic layer was washed three times with water (100 ml-aliquots), dried over anhydrous sodium sulphate, and the solvent removed by using a rotary evaporator. The resulting solid was recrystallized three times from a mixture of ethyl alcohol and benzene. The yield of white crystals was 25.0 g (42%), m.p. 190° (uncorr.). Analytical data are given in Table I.

TABLE I

Trifluoromethyl and *t*-butyl derivatives of tetraphenyltin

Formula	M.p.* (°C)	Yield (%)	Calcd. % C	Calcd. % H	Found % C	Found % H
$(C_6H_5)_3SnC_6H_4C(CH_3)_3$-*p*	130	96	69.60	5.84	69.31	5.46
$(C_6H_5)_2Sn(C_6H_4C(CH_3)_3$-*p*$)_2$	156	36	71.26	6.73	71.07	6.65
$C_6H_5Sn(C_6H_4C(CH_3)_3$-*p*$)_3$	190	42	72.62	7.45	72.34	7.30
$Sn(C_6H_4C(CH_3)_3$-*p*$)_4$	295	31	73.74	8.04	73.36	7.84
$(C_6H_5)_3SnC_6H_4CF_3$-*m*	108	91	60.64	3.87	60.68	3.92
$C_6H_5Sn(C_6H_4CF_3$-*m*$)_3$	109	30	51.38	2.72	50.89	2.63
$Sn(C_6H_4CF_3$-*m*$)_4$	143	16	48.10	2.31	48.36	2.25

*Melting points are uncorrected.

Tetrakis(3-trifluoromethylphenyl)tin

The synthesis of this compound in 12% yield, by the reaction of stannic chloride with 3-lithio-α,α,α-trifluorotoluene, has been reported previously (2). In the present work all trifluoromethyl compounds were prepared by the Grignard reaction.

The procedure employed for the preparation of the 3-trifluoromethylphenyltin compounds was identical with that used for the *t*-butyl derivatives. The tetrakis compound was prepared using the following reactants: magnesium turnings (2.7 g, 0.11 g-atom), 3-bromo-α,α,α-trifluorotoluene (22.5 g, 0.1 mole), and stannic chloride (6.67 g, 0.025 mole). After refluxing for 5 hours, and working up as in the previous preparation, 11.0 g (15.8%) of white crystals was obtained which melted at 143°, in excellent agreement with the literature value (2). Analytical data are given in Table I.

Can. J. Chem. Downloaded from www.nrcresearchpress.com by 210.87.254.6 on 09/05/12
For personal use only.

Infrared Spectra

Each compound reported in Table I was characterized by its infrared spectrum (4), using a Nujol mull.

In the *t*-butyl series the following bands were identified: *p*-substitution at 825 cm^{-1}, aromatic C:C at 1600 cm^{-1}, Sn—C_6H_5 at 1065 cm^{-1}, and *t*-butyl at 1365 cm^{-1}.

The following bands were observed in the trifluoromethyl series: *m*-substitution at 805 and 690 cm^{-1}, C:C at 1600 cm^{-1}, Sn—C_6H_5 at 1065 cm^{-1}, and a very strong absorption for C—F stretching at 1325, 1175, 1120, and 1105 cm^{-1}.

ACKNOWLEDGMENTS

For permission to publish this work the author thanks Dr. Harvey J. Crosby of Lockheed Missiles and Space Company, Palo Alto, Calif., where the bulk of this research was conducted. Thanks are also due to Mr. Stanley T. Peters for the infrared data.

1. R. K. Ingham, S. D. Rosenburg, and H. Gilman. Chem. Rev. **60**, 459 (1960).
2. O. Fuchs and H. W. Post. Rec. Trav. Chim. **78**, 566 (1959).
3. E. G. Rochow, D. T. Hurd, and R. N. Lewis. The chemistry of organometallic compounds. John Wiley & Sons, Inc., New York. 1957. p. 186.
4. L. J. Bellamy. The infra-red spectra of complex molecules. 2nd ed. Methuen & Co., Ltd., London.1958.

Received November 19, 1962.
Materials Sciences Laboratory,
Aerospace Corporation,
P.O. Box 95085,
Los Angeles 45, Calif.

Can. J. Chem. Downloaded from www.nrcresearchpress.com by 210.87.254.6 on 09/05/12
For personal use only.

Canadian Journal of Chemistry

Issued by THE NATIONAL RESEARCH COUNCIL OF CANADA

VOLUME 41 APRIL 1963 NUMBER 4

THE ALDOL CONDENSATION WITH 2,3-DIPHENYL-4-THIAZOLIDINONE

FRANCES C. BROWN, R. SIDNEY JONES, AND MILDRED KENT

Department of Chemistry, Duke University, Durham, North Carolina, U.S.A.

Received November 13, 1962

ABSTRACT

The aldol condensation between 2,3-diphenyl-4-thiazolidinone and aromatic aldehydes, which cannot be effected by the usual catalysts used in the analogous reactions of 2-thiono-, 2-oxo-, and 2-imino-4-thiazolidinones, was achieved by the use of ethoxide ion. The structure of the 2,3-diphenyl-5-arylidene-4-thiazolidinone was confirmed by ultraviolet spectral data.

Less information is available about the 4-thiazolidinones with hydrogen or hydrocarbon substituents in the 2-position (I) than about those 4-thiazolidinones with sulphur, oxygen, or an imino group in the same position (II) (1). For example, no aldol condensation

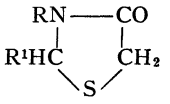

I

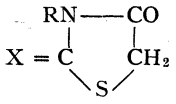

II (X = S, O, or NH)

between the methylene group of I and an aromatic aldehyde has been reported, although this reaction occurs readily with all three types of compound II. From the information available in the literature, it was uncertain whether the aldol condensation between 4-thiazolidinones (I) and aromatic aldehydes could not be effected or whether it had never been tried. Therefore, efforts were made to prepare the 5-benzylidene derivative of I.

The compound chosen for study was 2,3-diphenyl-4-thiazolidinone, which is available by the reaction of mercaptoacetic acid and the Schiff base from benzaldehyde and aniline (2). When the aldol condensation of this compound with benzaldehyde was attempted using sodium acetate and acetic acid (3), or ammonia and ammonium chloride in an aqueous ethanolic solution (4), no condensation product was obtained and in each case the starting material was recovered in 88–94% yield. With anhydrous benzene as the solvent, piperidinium acetate as the catalyst, and a water separator attached to the reaction flask to displace the equilibrium (5), the starting material was likewise recovered. After this work was completed, it was found that Baranov (6) had been unable to condense I (R = H; $R^1 = C_6H_5$) with carbonyl compounds such as *p*-dimethylaminobenzaldehyde. Presumably, he used sodium acetate in acetic acid solution to effect the condensation since these are the conditions which he had used in similar condensations.

It seemed probable that the failure of the reaction was caused by the decreased reactivity of the methylene group and that a stronger base, such as ethoxide ion, would be

Can. J. Chem. Downloaded from www.nrcresearchpress.com by 210.87.254.42 on 09/05/12
For personal use only.

able to form the anion of 2,3-diphenyl-4-thiazolidinone. The reaction was run in anhydrous benzene, and 2,3-diphenyl-4-thiazolidinone was added to sodium ethoxide, which had been prepared from sodium sand and anhydrous ethanol. The color of the solution became yellow and a small sample, withdrawn and neutralized, gave, on evaporation of the solvent, 2,3-diphenyl-4-thiazolidinone. Recovery of the starting material at this point indicated that the thiazolidinone nucleus had not been ruptured by contact with ethoxide ion. Addition of benzaldehyde, followed by refluxing for 30 minutes, yielded a pale yellow product which, after recrystallization from benzene, melted at 193–194° and which, from its analysis and spectra, is 2,3-diphenyl-5-benzylidene-4-thiazolidinone.

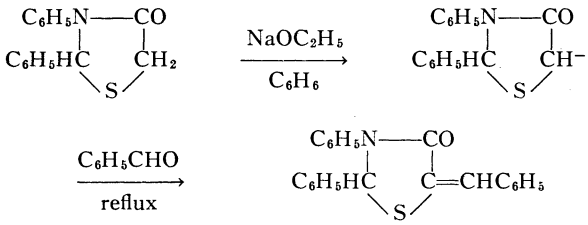

The 2,3-diphenyl-5-benzylidene-4-thiazolidinone is stable in the presence of several fairly drastic reagents and under fairly rigorous conditions. It was recovered unchanged after 1½ hours of heating with $KHSO_4$ in refluxing xylene, after 3 hours of heating with acetic anhydride, after 3 hours of heating with phosphorus oxychloride in benzene, after 4½ hours of heating at 100° in polyphosphoric acid (raising the temperature of the polyphosphoric acid solution to 200° decomposed the compound), and after 1½ hours of heating with acetyl chloride in benzene solution.

Similar condensations took place when the anion of 2,3-diphenyl-4-thiazolidinone was treated with other aromatic aldehydes. Anisaldehyde, *p*-chlorobenzaldehyde, and *p*-bromobenzaldehyde gave the corresponding 5-arylidene derivatives. The infrared spectra of these compounds are consistent with the structures assigned.

Table I gives the ultraviolet spectral data for the four compounds. 2,3-Diphenyl-4-thiazolidinone has no band present in the region 300–400 mμ. The introduction of a high-intensity band in this region into the spectra of the 5-arylidene derivatives must be attributed to conjugation of the phenyl group with the 4-thiazolidinone nucleus. Table I

TABLE I

Ultraviolet spectral data of 2,3-diphenyl-5-arylidene-4-thiazolidinones*

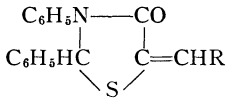

R	λ (mμ)	log ε	λ (mμ)	log ε	λ (mμ)	log ε
C_6H_5	323	4.40	335†	4.36		
p-ClC_6H_4	328	4.45	340†	4.40		
p-BrC_6H_4	328	4.43	341†	4.38		
p-$CH_3OC_6H_4$	336	4.46				
5-Benzylidene-rhodanine‡	233	3.39	271.5	3.97	376	4.54

*Measured in $CHCl_3$ solution.
†Shoulder.
‡From R. A. Potter, Ph.D. Dissertation, Duke University, Durham, N.C., 1952. This compound was measured in alcohol solution.

Can. J. Chem. Downloaded from www.nrcresearchpress.com by 210.87.254.42 on 09/05/12
For personal use only.

Can. J. Chem. Downloaded from www.nrcresearchpress.com by 210.87.254.42 on 09/05/12
For personal use only.

TABLE II

2,3-Diphenyl-5-arylidene-4-thiazolidinones

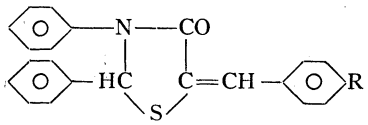

R	M.p. (°C)	Yield (%)*	Formula	Analysis							
				Calcd.				Found			
				C	H	N	S	C	H	N	S
H	193–194	51	$C_{22}H_{17}NOS$	76.94	4.99	4.08	9.33	77.12	5.04	4.18	9.26
Cl	198–199	24	$C_{22}H_{16}ClNOS$†	69.93	4.27	3.71	8.48	70.18	4.24	4.03	8.45
Br	195–196	22	$C_{22}H_{16}BrNOS$‡	62.56	3.82	3.32	7.59	62.71	3.85	3.42	7.59
CH_3O	223–224	52	$C_{23}H_{19}NO_2S$	73.99	5.09	3.75	8.58	73.97	5.13	3.82	8.40

*After one recrystallization.
†Chlorine: calcd., 9.38; found, 9.60.
‡Bromine: calcd., 18.92; found, 18.46.

includes the ultraviolet spectral data for 5-benzylidenerhodanine. The greater electron-attracting capacity of the thione group in the 2-position (II) over that of a phenyl and a hydrogen (I) causes a bathochromic shift of the *K* band from 323 to 376 mμ. The shift agrees qualitatively with that reported for compounds of the structure $[(CH_3)_2NC_6H_4]_2$-C=X (7) where X represents the groups attached to position 2 of formulas I (R^1 = H) and II.

Baranov (8) has measured the ultraviolet spectra of the 5-benzylidene derivatives of II (R = H). The location of the *K* band varies with the nature of X (X = S, 370 mμ; X = NH, 333 mμ; X = O, 329 mμ). The mobility of the hydrogen atoms of II varies in the same order, with X = S > X = NH > X = O. Since the ultraviolet spectra of 5-*p*-acetaminobenzylidenerhodanine is very similar to that of its 3-phenyl derivative (9), the spectra of our 3-phenyl derivative of 2-phenyl-5-benzylidene-4-thiazolidinone should be comparable with the series he has reported. The position of the *K* band of 2,3-diphenyl-5-benzylidene-4-thiazolidinone is in the same region as that of the 5-benzylidene derivatives of pseudothiohydantoin and 2,4-thiazolidinedione, but the intensity is greater with the former. From the ultraviolet spectra of its 5-benzylidene derivative the decreased reactivity of the hydrogens of the methylene group of 2,3-diphenyl-4-thiazolidinone would not be evident.

EXPERIMENTAL

All melting points were taken on a Fischer-Johns melting point apparatus and are uncorrected. Infrared spectra were determined with a Perkin–Elmer spectrophotometer No. 237 and ultraviolet spectra with a Cary 14 spectrophotometer.

2,3-Diphenyl-5-arylidene-4-thiazolidinones

Sodium sand (10), prepared from 1.5 g (0.065 g-atom) of sodium, was covered with 120 ml of anhydrous benzene. The flask was cooled with an ice bath and 3–4 ml of absolute ethanol (dried over magnesium methoxide) was added with stirring. After the vigorous reaction was over, 16.0 g (0.063 mole) of 2,3-diphenyl-4-thiazolidinone was added. When the thiazolidinone had dissolved, the yellow solution was allowed to warm up to room temperature, and the color deepened. The aldehyde (0.063 mole) was added slowly at room temperature, after which the solution was refluxed for 30 minutes. The solution was cooled to room temperature and any unreacted sodium destroyed by the careful addition of 50 ml of glacial acetic acid. After the addition of 50–75 ml of water, the aqueous layer was discarded. The benzene layer was concentrated by distillation at atmospheric pressure and cooled in an ice bath. The crystals were collected and purified by recrystallization from benzene. The melting points, yields, and analytical data are assembled in Table II. Strong bands in the infrared spectra are present at 1680–1690 cm^{-1} (carbonyl group), at 1610 cm^{-1} and at 1495–1510 cm^{-1} (phenyl group), and at 700–800 cm^{-1} (phenyl with one substituent), and, where *p*-substituted aldehydes were used, additional bands are present in the 800–850 cm^{-1} region.

ACKNOWLEDGMENTS

This research was supported by a grant from the Duke University Research Council. The authors are indebted to Roland Brierre, who measured the ultraviolet spectra.

REFERENCES

1. F. C. Brown. Chem. Rev. **61**, 463 (1961).
2. A. R. Surrey. J. Am. Chem. Soc. **69**, 2911 (1947).
3. P. L. Julian and B. M. Sturgis. J. Am. Chem. Soc. **57**, 1126 (1935).
4. F. C. Brown, C. K. Bradsher, S. G. McCallum, and M. Potter. J. Org. Chem. **15**, 174 (1950).
5. F. C. Brown, C. K. Bradsher, and S. W. Chilton. J. Org. Chem. **21**, 1269 (1956).
6. S. N. Baranov. Zh. Obshch. Khim. **31**, 512 (1961).
7. A. E. Gillam and E. S. Stern. An introduction to electronic absorption spectroscopy in organic chemistry. Edward Arnold, Ltd., London. 1957. p. 128.
8. S. N. Baranov. Zh. Obshch. Khim. **32**, 1230 (1962).
9. N. M. Turkevich and E. V. Vladzimirskaya. Zh. Obshch. Khim. **27**, 1348 (1957).
10. C. S. Marvel and W. B. King. Org. Syn. Coll. Vol. **I**, 252 (1941).

Can. J. Chem. Downloaded from www.nrcresearchpress.com by 210.87.254.42 on 09/05/12
For personal use only.

HYDROXYMETHYL PHOSPHORUS DERIVATIVES FROM TETRAKIS(HYDROXYMETHYL) PHOSPHONIUM CHLORIDE. REACTION WITH LEAD CARBONATE AND OXIDE

N. FILIPESCU, L. M. KINDLEY, H. E. PODALL, AND F. A. SERAFIN
Melpar, Incorporated, Research Division, Falls Church, Virginia, U.S.A.
Received November 13, 1962

ABSTRACT

A novel and convenient method has been developed for the preparation of tris(hydroxymethyl) phosphine oxide (THPO) from tetrakis(hydroxymethyl) phosphonium chloride (THPC). The method consists essentially of oxidative deformylation of THPC with lead carbonate in *n*-propyl alcohol. The reaction is facilitated by azeotropic distillation of di-*n*-propylformal and *n*-propyl alcohol.

The reaction of THPC with lead carbonate as well as with lead oxide has been studied in detail in aqueous solution and in *n*-propyl alcohol. The reaction proceeds via the initial formation of tetrakis(hydroxymethyl) phosphonium hydroxide (THPOH) followed by deformylation to tris(hydroxymethyl) phosphine (THP). THP then undergoes oxidation by air as well as by lead carbonate or oxide to THPO. If air is bubbled through the mixture at elevated temperatures, atmospheric oxidation predominates with little or no oxidation by the lead compound.

Depending upon the reaction conditions, a phosphonium hydroxide, a phosphine, or a phosphine oxide are products of the reaction of tetrakis(hydoxymethyl) phosphonium chloride with lead carbonate or oxide.

Can. J. Chem. Downloaded from www.nrcresearchpress.com by 210.87.254.42 on 09/05/12
For personal use only.

For several years this laboratory has been engaged in the synthesis of phosphorus-containing polymers in order to provide flame resistant and thermally stable end products. One of the starting materials for the introduction of phosphorus into the polymeric molecules was tetrakis(hydroxymethyl) phosphonium chloride, referred to as THPC.

Although several polymers derived from THPC have been reported (5, 6), we have found that in many instances phosphorus was not incorporated into the polymeric chains which are primarily formed by polycondensation reactions of formaldehyde resulting from the degradation of THPC. These polymers, insufficiently characterized, possessed poor hydrolytic stability and fracture strength. By use of tris(hydroxymethyl) phosphine oxide (THPO) and its monobenzoylated derivative we were able to obtain polymers containing phosphorus in the polymeric chain which possessed markedly improved hydrolytic stability, fracture strength, flame resistance, etc. (3).

A key problem which arose in the initial stages of work with THPO-derived polymers was the conversion of commercially available THPC to THPO. Methods previously described for this conversion required a number of tedious operations to isolate the product. In attempting to devise a better method for the synthesis of THPO from THPC some interesting chemistry was uncovered involving not only the preparation of THPO but also the formation of tetrakis(hydroxymethyl) phosphonium hydroxide (THPOH) and tris(hydroxymethyl) phosphine (THP). This paper is concerned with a new synthesis of THPO from THPC and with the properties and reactions of some of the intermediates.

THPC was reported (1, 2) to react with aqueous sodium hydroxide at room temperature or upon gentle heating *below* 80° C to yield THPO with the evolution of one molecule of hydrogen. On boiling, a second molecule of hydrogen is given off with the formation of the sodium salt of bis(hydroxymethyl) phosphinic acid. The same results are obtained if one uses an alkali metal carbonate instead of the hydroxide, but the reaction rate is

slower. An insoluble carbonate, such as calcium or barium carbonate, produces only THPO and one molecule of hydrogen even after prolonged boiling.

Each of these procedures yields THPO in an aqueous solution mixed with soluble inorganic chloride (sodium, barium, or calcium). Separation of THPO from the inorganic chloride is difficult because of the former's extreme solubility in water and low solubility in organic solvents. Isolation by distillation is not possible because THPO decomposes at temperatures far below its boiling point. The most successful isolation of THPO to date involves long, tedious extractions of the dry mixture of THPO and inorganic salts with relatively low molecular weight alcohols, such as isopropyl alcohol.

In our laboratory, attention was directed toward an approach which had appeal as a simple, economical reaction for converting THPC to THPO and at the same time avoiding the isolation problems encountered heretofore. The proposed method was:

$$2[(HOCH_2)_4P]^+Cl^- + PbCO_3 \xrightarrow{\text{air}} 2(HOCH_2)_3PO + PbCl_2 + 2CH_2O + H_2O + CO_2. \quad [1]$$

Experimental investigation, however, proved that the reaction of THPC with lead carbonate was considerably more complex than originally believed, and that several different organophosphorus compounds can be formed depending on the reaction conditions.

The conditions under which the reaction of THPC with lead carbonate was investigated may be summarized as follows:

(1) in water at 55–65° C,
(2) in water at temperatures from 65 to 90° C,
(3) in *n*-propyl alcohol at 60–65° C,
(4) in *n*-propyl alcohol at approximately 96° C.

Under each of these conditions the reaction time was varied over wide ranges (1 hour to several days). In the reactions conducted in water, it was observed that metallic lead precipitated if the reaction temperature exceeded about 65° C. For this reason, a series of experiments was carried out below 65° C and another series above this temperature.

In the "low" temperature experiments THPC and lead carbonate were heated in water at 55–65° C, and the solids were removed by filtration. After removal of water from the filtrate there remained a syrupy, liquid product. Removal of final traces of volatile materials, particularly water, was attempted by long periods of stirring under vacuum, azeotropic distillation with benzene, and repeated extractions with acetone. Infrared spectra of this product (still a syrupy liquid) indicated very little P → O absorption and thus very little formation of THPO. Furthermore, several qualitative reactions of the product were quite different from those of THPO. For example, the product reacted violently with oxidizing agents such as H_2O_2 and HNO_3 (indicating the presence of a strong reducing compound), it exhibited a highly exothermic reaction with α,β-unsaturated carbonyl compounds, and cured unsaturated polyester resins to elastomeric materials. Furthermore it possessed a strong odor suggestive of a phosphine.

Based on the above results and evidence obtained in later experiments it appears that the main reaction occurring between THPC and lead carbonate in water at 55–65° is:

$$2[(HOCH_2)_4P]^+Cl^- + PbCO_3 \xrightarrow{H_2O} \underset{\text{(THPOH)}}{2[(HOCH_2)_4P]^+OH^-} + PbCl_2 + 2CH_2O + CO_2. \quad [2]$$

The THPOH (tetrakis(hydroxymethyl) phosphonium hydroxide) is believed to exist in equilibrium with tris(hydroxymethyl) phosphine (THP), i.e.,

$$[(HOCH_2)_4P]^+OH^- \rightleftharpoons \underset{\text{(THP)}}{(HOCH_2)_3P} + CH_2O + H_2O. \quad [3]$$

Can. J. Chem. Downloaded from www.nrcresearchpress.com by 210.87.254.42 on 09/05/12
For personal use only.

It was found that not all of the ionic chloride was completely removed as $PbCl_2$. The main reason for this appears to be due to the fact that hydroxymethyl-phosphorus compounds, such as THPC, THPOH, etc., were found to form *soluble* complexes with $PbCl_2$ as well as with AgCl. We believe that these complexes are formed by coordination of the metal ion with the hydroxyl functions of the phosphorus compound, e.g.

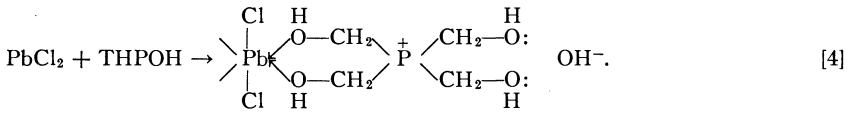

[4]

Not all of the complexes were water or alcohol soluble. The solids removed from the reaction by filtration even after repeated washing with hot water contained significant amounts of phosphorus compounds strongly adsorbed or complexed with the lead carbonate or lead chloride. These solids were similar in appearance to litharge–glycerine cements, suggestive of some polymerization.

In the second series of experiments, THPC and lead carbonate were heated in water at 65–90° C for various lengths of time. In addition to the reactions which occur at lower temperature, a redox reaction was found to occur with the formation of metallic lead. The reaction appears to be as follows:

$$(HOCH_2)_3P + PbCO_3 \rightarrow (HOCH_2)_3PO + Pb + CO_2. \qquad [5]$$

The evidence for this reaction is based upon the following facts:

(1) isolation and identification of THPO,
(2) no evidence of hydrogen formation,
(3) PbO gave similar results, and
(4) similar results were obtained in *n*-PrOH instead of water at elevated temperatures.

It was also found that when air was passed through the mixture while it was being heated, less metallic lead was produced, and the conversion of THP to THPO appeared to occur more rapidly. The predominant reaction under these conditions appears therefore to be simply the direct atmospheric oxidation of THP to THPO. The product recovered after filtration of the solids from the reaction mixture and exhaustive removal of water and other volatile materials was a partially crystallized syrupy mixture. Attempts to separate this mixture into pure individual compounds by a variety of techniques were not successful. It was, however, possible to separate two major fractions—one containing a large percentage of THPO and another consisting mostly of THP plus some THPOH.

By thoroughly drying the reaction mixture and cooling it for a long period of time, it was possible to obtain a distinct crystalline solid which could be separated from the syrupy liquid. This solid reacted with benzoyl chloride in a Schotten–Bauman reaction to give the known pure tribenzoate (5) of THPO in good yield. The presence of THP in the syrupy liquid phase was indicated by formation of the known yellow benzoquinone–THP complex (4), its "characteristic" exothermic reactions with oxidants such as H_2O_2 and HNO_3, and finally its reactions with unsaturated carbonyl compounds such as diethyl maleate, acrolein, acrylamide, etc. (The latter reactions will be the subject of another communication.)

Vacuum distillation (5 mm) of the product resulting from the reaction of THPC and lead carbonate at 65–90° C yielded a viscous colorless liquid distilling at 130–140° C. The pH of this distillate was 4 and elementary analysis indicated its composition to be as follows: THP, 51.8; CH_2O, 31.5; water, 9.4; HCl, 7.6%. The distillate gave reactions with H_2O_2, HNO_3, and unsaturated carbonyl compounds previously described as those of THP.

Can. J. Chem. Downloaded from www.nrcresearchpress.com by 210.87.254.42 on 09/05/12
For personal use only.

The residue from the distillation failed to react with any of the above-mentioned reagents. It had a pH of 6 and elementary analysis which corresponded to the following composition: THPO, 53.0; THPC, 18.0; CH_2O, 25.6; water, 3.4%.

Further verification of the composition of the distilled and residue fractions was obtained by measuring the amount of hydrogen evolved upon boiling a sample of each fraction with an excess of aqueous sodium hydroxide. The reactions of sodium hydroxide with the compounds of interest are as follows:

$$(HOCH_2)_3PO + NaOH \rightarrow (HOCH_2)_2PO(ONa) + CH_2O + H_2 \quad [6]$$

$$(HOCH_2)_3P + NaOH + H_2O \rightarrow (HOCH_2)_2PO(ONa) + CH_2O + 2H_2 \quad [7]$$

$$[(HOCH_2)_4P]^+Cl^- + 2NaOH \rightarrow (HOCH_2)_2PO(ONa) + 2CH_2O + NaCl + 2H_2. \quad [8]$$

The experimental results were as follows (based on 100 g of sample). Distillate: 20.6 l. of H_2; calc. for indicated composition (51.8% THP), 20.2 l. Residue: 12.9 l. of H_2; calc. for 53.0% THPO and 18.0% THPC, 12.7 l.

In the third series of experiments, water was present only in traces in the reaction of THPC with lead carbonate. The THPC and lead carbonate was *suspended* in *n*-propyl alcohol and the mixture was heated at 60–65° C for 6 to 8 hours. After filtration and removal of alcohol, a syrupy liquid was obtained. This product contained practically no ionic chloride and reacted exothermally with oxidizing agents and with α,β-unsaturated carbonyl compounds. Comparison of this product with samples prepared by an alternate route* strongly indicated that it was essentially THPOH containing some THP. The reaction scheme may be described as follows:

$$2[(HOCH_2)_4P]^+Cl^- + PbCO_3 + H_2O \xrightarrow{n\text{-PrOH}} 2[(HOCH_2)_4P]^+OH^- + PbCl_2 + CO_2 \quad [9]$$

$$THPOH \rightleftharpoons THP + CH_2O + H_2O. \quad [10]$$

If an excess of lead carbonate is used in the above reaction and the intermediate product is not isolated, further reaction occurs when the reaction temperature is raised to 96° C. The reactions in this step appear to be as follows:

$$[(HOCH_2)_4P]^+OH^- \rightleftharpoons (HOCH_2)_3P + CH_2O + H_2O \quad [11]$$

$$CH_2O + n\text{-PrOH} \rightarrow (n\text{-PrO})_2CH_2 + H_2O \quad [12]$$

$$THP + PbCO_3 \rightarrow THPO + Pb + CO_2. \quad [13]$$

During reaction, metallic lead precipitated and the dipropyl formal – propyl alcohol azeotrope was removed at 96° C. Removal of formaldehyde as an azeotrope evidently facilitates the formation of THP, which is immediately oxidized to THPO. The final product (THPO) was recovered as a white solid after filtration of metallic lead and removal of volatile components by vacuum distillation at about 50° C. Its identity was confirmed by formation of the tribenzoate derivative and by comparison of its infrared spectrum with an authentic sample of THPO. In a typical reaction 1 mole of THPC and 1.8 mole of $PbCO_3$ in 1500 ml *n*-propyl alcohol were stirred with heating. During the reaction (8–10 hours) the distillate was continuously removed and fresh *n*-propyl alcohol added from time to time. The reaction mixture was cooled in an ice bath and filtered. The filtrate was dried *in vacuo* to obtain crystalline THPO. The yields were in excess of 90%.

*THPOH *was prepared by reaction of* THPC *with methanolic sodium hydroxide at room temperature, filtration of* NaCl, *and vacuum removal of solvent.* THP *was prepared by passing phosphine through an alcoholic solution of* THPOH *in the presence of a platinum oxide catalyst. The* THP *was recovered as a white waxy solid after solvent removal in vacuo and identified via its benzoquinone and mercuric chloride complexes.*

Can. J. Chem. Downloaded from www.nrcresearchpress.com by 210.87.254.42 on 09/05/12
For personal use only.

A possible explanation for the difficulties encountered in separating THPO from THP and/or THPOH may be due to the high association and possible complex formation between these compounds, e.g.,

$$\mathrm{THP} + \mathrm{THPO} \rightarrow [\mathrm{THPH}]^{+}(\mathrm{HOCH_2})_2\overset{\uparrow}{\underset{\mathrm{O}}{\mathrm{P}}}\mathrm{—CH_2O^-} \qquad [14]$$

$$\mathrm{THPOH} + \mathrm{THPO} \rightarrow [(\mathrm{HOCH_2})_3\overset{+}{\mathrm{P}}\mathrm{CH_2OH} \ldots \mathrm{O—P(CH_2OH)_3}]\mathrm{OH^-}. \qquad [15]$$

In summary it has been found that:

(1) THPO can be conveniently prepared by reaction of THPC with $PbCO_3$ in *n*-PrOH at 96° while azeotropically distilling di-*n*-propyl formal and *n*-propyl alcohol;

(2) the conversion of THPC to THPO in the presence of $PbCO_3$ proceeds via THPOH and THP, respectively;

(3) $PbCO_3$ and PbO each oxidize THP to THPO;

(4) $PbCl_2$ and AgCl form two types of complexes with THPO and related compounds, viz. soluble and insoluble products.

REFERENCES

1. A. Hoffman. J. Am. Chem. Soc. **43**, 1684 (1921).
2. A. Hoffman. J. Am. Chem. Soc. **52**, 2995 (1930).
3. L. M. Kindley, H. E. Podall, and N. Filipescu. SPE Trans. **2**, 122 (1962).
4. G. M. Kosolapoff. Organophosphorus compounds. J. Wiley and Sons, Inc., New York. 1950.
5. W. A. Reeves and J. D. Guthrie. U.S.Dep. Agr., Agr. Chem. Cir. Rev. 364 (1954).
6. R. A. Wilson and J. D. Guthrie. Incl. Eng. Chem. **48**, 64 (1956).

Can. J. Chem. Downloaded from www.nrcresearchpress.com by 210.87.254.42 on 09/05/12
For personal use only.

THE PHOTOLYSIS OF ISOCYANIC ACID VAPOR[1]

J. Y. P. MUI[2] AND R. A. BACK
Division of Pure Chemistry, National Research Council of Canada, Ottawa, Canada

Received December 6, 1962

ABSTRACT

The photolysis of isocyanic acid vapor has been studied at temperatures ranging from −31 to 200° C, and pressures from about 2 to 200 mm. Products identified were CO and N_2 in a ratio which varied from 2.5 to 5, together with much smaller amounts of hydrogen. The mechanism

$$HNCO + h\nu \rightarrow NH + CO$$
$$NH + HNCO \rightarrow NH_2 + NCO$$
$$NH_2 + HNCO \rightarrow NH_3 + NCO$$
$$2NCO \rightarrow N_2 + 2CO$$
$$2NH \rightarrow N_2 + H_2$$

accounts approximately for the products of the photolysis at low HNCO pressures and low temperatures. Additional reactions of NCO radicals with HNCO are postulated to account for increased production of CO and N_2 as the temperature and HNCO pressures were increased.

The effects of adding ethylene and hydrogen to the system were briefly investigated. The results are explained in terms of reactions of NH and NCO radicals with hydrogen and ethylene.

INTRODUCTION

After some earlier controversy, it was shown conclusively in 1950 that cyanic acid in the vapor phase had the structure H—N=C=O, and should thus properly be called isocyanic acid (1). This structure is analogous to that of ketene, and similar photolytic behavior might be anticipated. Flash photolysis of isocyanic acid vapor (2, 3) has yielded strong absorption spectra of NH radicals, together with NCO and NH_2, but apart from these spectroscopic experiments, the photolysis of the vapor has apparently not been studied. It would appear to be a promising source of NH radicals, suitable for kinetic studies of their reactions.

EXPERIMENTAL

Isocyanic acid was prepared by the pyrolysis of cyanuric acid vapor in a stream of dry nitrogen at 750° C (1, 4). Repeated bulb-to-bulb distillation *in vacuo*, a large middle fraction being kept, reduced the impurities, CO_2, HCN, and C_2N_2, to less than 1%. This was estimated by gas chromatography on a 1-m column of dinonyl phthalate on firebrick at 50° C, which gave appearance times of 0.5, 2.5, 3.8, and 8.5 minutes for CO_2, HCN, C_2N_2, and HNCO, respectively, with a flow rate of 100 cc/min of helium. Treatment of the acid with silver oxide powder (4) reduced the content of HCN and C_2N_2 to about 0.2 and 0.3% respectively, and the only other impurities detectable by mass spectrometry or gas chromatography were small amounts of CO_2 and NH_3. It proved almost impossible to remove these latter compounds completely, probably because they are formed readily by hydrolysis of the isocyanic acid by traces of water. The mass spectrum of the purified HNCO vapor, which has not been previously reported, is shown in Table I.*

Isocyanic acid is a gas at room temperature (b.p. ~ 24° C), and behaves, in a vacuum system, much like ketene. It tends to trimerize slowly on standing as a vapor, forming a mixture of the two trimers, cyanuric acid and cyammelide (5, 6). This is apparently a surface recation, very slow in a clean vessel, but catalyzed by the trimers which are deposited on the surface. The trimerization was slow enough that the acid vapor could be stored in a darkened vessel at pressures below 10 cm without serious loss.

The acid vapor was photolyzed in a conventional cylindrical quartz vessel, 10 cm long and 5 cm in diameter, with plane windows at each end, which was mounted in an air thermostat. The rate of trimerization

[1]*Issued as N.R.C. No. 7227.*

[2]*Summer Research Assistant, 1962. Present address: Department of Chemistry, Massachusetts Institute of Technology, Cambridge, Mass., U.S.A.*

**The authors are grateful to Mr. R. Pilon for the determination of this mass spectrum.*

Can. J. Chem. Downloaded from www.nrcresearchpress.com by 210.87.254.5 on 09/05/12
For personal use only.

TABLE I
Mass spectrum of HNCO vapor

Mass	Relative intensity	Ion	Mass	Relative intensity	Ion
12	0.6	C^+	28	22.6	CO^+
14	1.1	N^+	29	10.1	HCO^+
15	6.6	NH^+	30	1.5	NO^+
16	0.4	O^+	42	19.0	NCO^+
26	2.0	CN^+	43	100.0	$HNCO^+$
27	4.2	CNH^+			

of the acid was considerably enhanced during the photolysis, and in a typical 30-minute experiment from 1 to 2% of the HCNO would be converted to trimer. The deposition of these compounds on the windows caused a progressive reduction in the light intensity during a series of experiments. This difficulty was circumvented by baking the reaction vessel for several hours (usually overnight) at 200° C, so that the slightly volatile trimers were sublimed out of the vessel. This technique gave an approximately constant light intensity and reproducible rates of photolysis. The trimerization was also favored by high pressures of acid, and in practice pressures greater than 200 mm were avoided.

Careful blank experiments were done at all temperatures, both with the light off, to look for possible thermal reactions of HNCO, and with the light on, but no HNCO vapor, to look for possible products of the photolysis of the trimers. No non-condensable products were found in any of these experiments; a small trace of CO_2 was the only detectable product from the photolysis of the trimers.

The light source was an unfiltered Hanovia S-500 medium-pressure mercury arc, partially collimated to fill the reaction vessel uniformly. Isocyanic acid vapor absorbs continuously at wavelengths below 2240 Å, with diffuse bands from 2570 to 2250 Å (7), so that the effective light was mostly between 2240 and 2000 Å.

Non-condensable products, CO, N_2, and H_2, were removed at −196° C, measured in a gas burette, and analyzed by combustion on copper oxide. Hydrogen was measured by difference in this technique, and to confirm that the very small yields observed in some experiments were real, samples were analyzed by mass spectrometry. The results agreed very closely with the combustion analysis, and also showed that CO, N_2, and H_2 were the only non-condensable products.

Careful analysis by low-temperature distillation and gas chromatography showed that CO_2 was not a product of the photolysis, although traces of it, probably formed by hydrolysis of HNCO, were always present. Small amounts of NH_3 and N_2H_4 have been detected in the reaction products by gas chromatography (8), but quantitative analysis of these basic compounds in the presence of a large excess of HNCO is very difficult. No other reaction products have been detected by gas chromatography on a variety of columns, or by mass spectrometry.

Ethylene (Phillips research grade) was added in some experiments, and a solid-nitrogen trap at −210° C was used to separate the non-condensable gases. Hydrogen was added in a few experiments, and was introduced into the vacuum line from a cylinder, through a hot palladium thimble.

RESULTS

The non-condensable products of the photolysis were CO and N_2 in a ratio which varied from about 2.5:1 to 5:1, together with much smaller amounts of H_2. In Fig. 1 is shown the rate of production of CO as a function of HNCO concentration, at several temperatures, with constant light intensity. In Fig. 2 are shown values of the N_2:CO ratio found in the same experiments, and in Fig. 3 are similar plots of the ratio H_2:CO multiplied by 100.

The effect of added ethylene on the products of the photolysis at 37° C and constant pressure of acid (~22 mm) is shown in Fig. 4. The hydrogen yield in the same experiments was negligibly small, even at the lowest concentration of ethylene. In Fig. 5 is shown the yield of CO from the photolysis of HNCO at several pressures and temperatures, in the presence of a high pressure (~600 mm) of ethylene. These data are directly comparable with those for the photolysis of the pure acid plotted in Fig. 1. The yields of both N_2 and H_2 in the experiments with high pressures of ethylene were close to zero.

In a few experiments, hydrogen was added to the system, and in Table II are shown

Can. J. Chem. Downloaded from www.nrcresearchpress.com by 210.87.254.5 on 09/05/12
For personal use only.

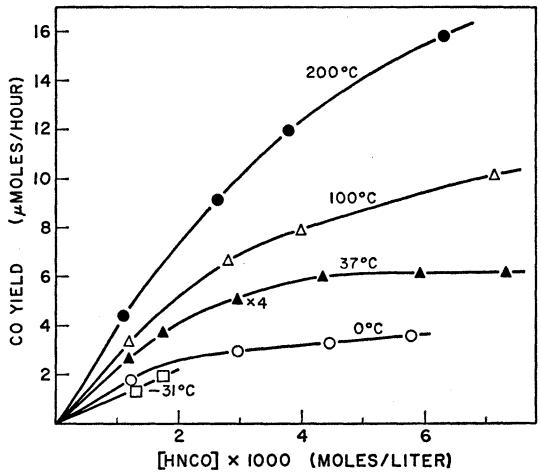

FIG. 1. The production of CO from the photolysis of HNCO. Some experimental points at low pressures of HNCO have been omitted.

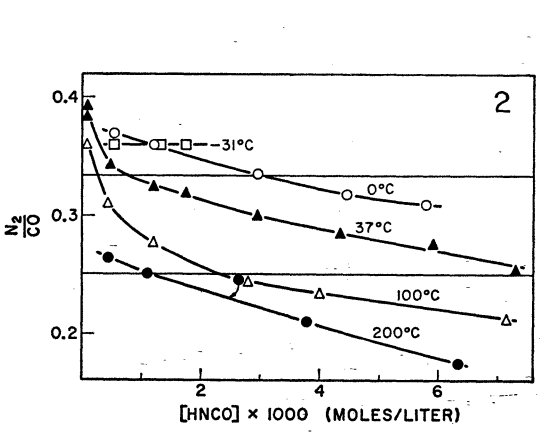

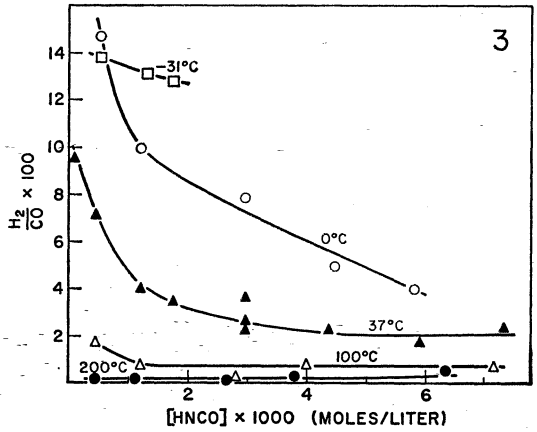

FIG. 2. The ratio of N_2 to CO produced in the photolysis of HNCO.
FIG. 3. The ratio of H_2 to CO produced in the photolysis of HNCO.

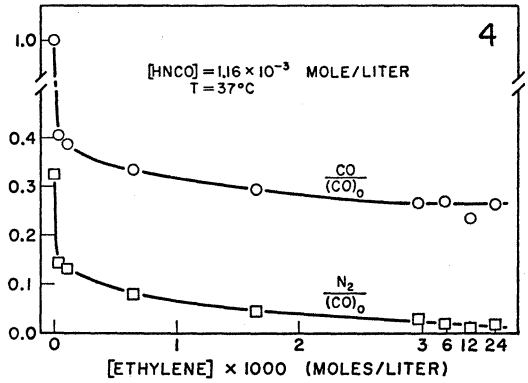

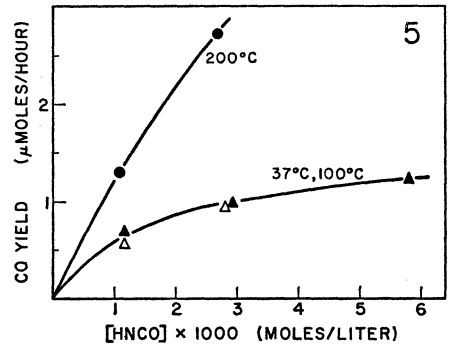

FIG. 4. The effect of added ethylene on the production of CO and N_2 from the photolysis of HNCO. $(CO)_0$ and $(N_2)_0$ are the normal yields of CO and N_2 in the absence of ethylene.
FIG. 5. The production of CO from the photolysis of HNCO in the presence of about 600 mm pressure of ethylene. △ = 37° C, ▲ = 100° C, ● = 200° C.

Can. J. Chem. Downloaded from www.nrcresearchpress.com by 210.87.254.5 on 09/05/12
For personal use only.

the results. Rates of production of CO and N_2 are expressed as yields relative to the normal yields in the pure acid. Hydrogen, of course, could not be measured in these experiments.

TABLE II

Effect of hydrogen on the photolysis of HNCO
(HNCO = 21 mm, H_2 = 52 mm)

Temperature (°C):	37	100	200
$CO/(CO)_0$	1.06	1.52	5.09
$N_2/(N_2)_0$	0.85	0.75	0.68

NOTE: $(CO)_0$ and $(N_2)_0$ are yields of CO and N_2 in the absence of hydrogen.

In all the experiments, rates of production of products were independent of irradiation time up to about 1 hour, and if care was taken to avoid the accumulation of solid materials on the windows, for much longer times. Thus a sample of HNCO could be photolyzed, removed from the vessel, and the non-condensable products taken away; if the sample of acid were then returned to the reaction vessel (thoroughly baked out in the interim) and photolyzed again, the product yields were unchanged. In fact, a single sample of acid could be reused many times, and gave results indistinguishable from those obtained with a freshly prepared sample.

As mentioned earlier, no other products, condensable or non-condensable, could be detected by low-temperature distillation, mass spectrometry, or gas chromatography. In particular, CO_2, HCN, C_2N_2, NO, N_2O, or NO_2 could have been easily detected but were unobserved. Small amounts of NH_3 and N_2H_4 have been found as products, but their quantitative estimation is difficult. Traces of CO_2 were always found, but a careful series of experiments showed that this was not produced in the photolysis.

DISCUSSION

The following simple mechanism roughly accounts for the main features of the photolysis, and while its inadequacies will become evident, it is a useful point of departure.

$$h\nu + HNCO \rightarrow NH + CO \quad [1]$$

$$NH + HNCO \rightarrow NH_2 + NCO \quad [2]$$

$$NH_2 + HNCO \rightarrow NH_3 + NCO \quad [3]$$

$$NCO + NCO \rightarrow N_2 + 2CO \quad [4]$$

The persistent production of CO, and the complete suppression of N_2 and H_2, in the presence of ethylene, strongly supports reaction [1] as the primary step, rather than the possible alternative

$$h\nu + HNCO \rightarrow H + NCO. \quad [1A]$$

The pressure dependence of the photolysis products, and the approximately constant CO production, independent of ethylene pressure above about 3×10^{-3} mole/liter (Fig. 4), indicate that any intermediate excited HNCO molecule in reaction [1] was too short lived to suffer collisional deactivation, which is not surprising in view of the high energy of the light quanta absorbed.

The observed values of N_2:CO, and the very low yields of H_2, would appear to favor reaction [2] over the alternative

$$NH + HNCO \rightarrow CO + N_2H_2 \rightarrow CO + N_2 + H_2, \quad [2A]$$

Can. J. Chem. Downloaded from www.nrcresearchpress.com by 210.87.254.5 on 09/05/12
For personal use only.

which would have led to a product ratio $CO:N_2:H_2$ of 2:1:1. It will be seen later that the persistent low yield of hydrogen at high pressures of HNCO (Fig. 3) may have arisen from reaction [2A] occurring to a very slight extent. The predominance of reaction [2] over [2A] is just the reverse of the behavior found in the photolysis of ketene, where the reaction of CH_2 with ketene to form ethylene and CO (analogous to [2A]) is much faster than the abstraction of hydrogen (9–12).

The detection of NH, NH_2, and NCO radicals by their absorption spectra in the flash photolysis of HNCO vapor (2, 3) lends some support to the occurrence of reactions [1], [2], and [3].

Reaction [4] was suggested previously to be the fate of NCO radicals in the photolysis of methyl isocyanate (13). In the absence of reaction products other than N_2 and CO, reaction [4] again seems the most reasonable possibility in the present system.

The simple mechanism comprising reactions [1], [2], [3], and [4] predicts a ratio of N_2:CO of 0.33, corresponding to the upper horizontal line in Fig. 2. At low temperatures and pressures of HNCO, N_2:CO rose somewhat above this level. With increasing temperature and HNCO pressure, N_2:CO decreased systematically to much lower values. The simple mechanism also takes no account of the production of hydrogen in the photolysis. The pressure and temperature dependence of the H_2:CO ratio (Fig. 3) strongly suggest that H_2 arose from the radical combination reaction

$$NH + NH \rightarrow N_2 + H_2. \qquad [5]$$

A simple kinetic treatment of a competition between reactions [5] and [2] yielded reasonably linear plots of $R_2/R_5^{1/2}$ against HNCO concentration for the data at 0 and 37° C and low pressures of HNCO. Values of $k_2/k_5^{1/2}$ were obtained from the slopes of these plots, and if $E_5 = 0$, a very rough estimate of $E_2 = 3.6$ kcal/mole may be made. In a simple competition between reactions [5] and [2], the H_2:CO ratio should have fallen to zero at high pressures of HNCO, but it is seen instead that the ratio reached a constant value, small but measurable, at 37 and 100° C (Fig. 3). Reaction [2A] is the most probable source of this hydrogen, which corresponded to about 6, 2, and 1% of the estimated rate of reaction [2] at 37, 100, and 200° C respectively, with the dependence on temperature presumably reflecting a slightly higher activation energy for reaction [2].

If reaction [5] is taken into account, the mechanism then predicts that the ratio $(N_2–H_2):(CO–2H_2)$ should equal 0.33, and in Fig. 6 it is seen that this modification has eliminated the high values observed at low HNCO pressure in the similar plot of N_2:CO (Fig. 2). However, the downward trend with increasing pressure of HNCO and temperature persists in Fig. 6, and only as the HNCO pressure approaches zero does the ratio

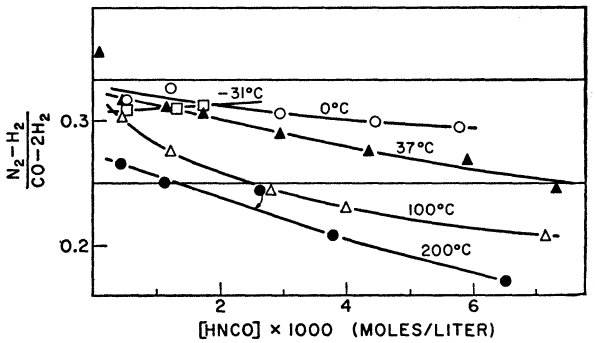

FIG. 6. Values of the ratio $(N_2–H_2):(CO–2H_2)$ in the photolysis of HNCO.

Can. J. Chem. Downloaded from www.nrcresearchpress.com by 210.87.254.5 on 09/05/12
For personal use only.

$(N_2–H_2)$:$(CO–2H_2)$ approach the predicted value of 0.33. Values as low as 0.25, the lower horizontal line in Figs. 2 and 6, could be explained if hydrazine, rather than ammonia, were a reaction product. The radical combination reactions

$$NH_2 + NH_2 \rightarrow N_2H_4 \quad [6]$$

$$NH_2 + NH \rightarrow N_2H_3, \quad [7]$$

followed by

$$N_2H_3 + HNCO \rightarrow N_2H_4 + NCO \quad [8]$$

are possible sources of hydrazine, but could not explain the decrease in N_2:CO with increasing HNCO pressure, and in fact should lead to just the reverse. The production of hydrazine would also require a reduction in the yield of CO from three to two molecules for each HNCO photolyzed by reaction [1], whereas it will be seen that the yield of CO rose much above this value. Reactions [6], [7], and [8] must thus be considered unlikely, and the variation of N_2:CO with HNCO pressure remains unexplained.

The temperature dependence of the yields of CO and N_2 is also not explained by the simple mechanism. An examination of Figs. 1 and 2 shows that there was a marked increase in the rates of production of both CO and N_2 with increasing temperature, as well as an increase in CO relative to N_2. It is seen from Fig. 5 that up to 100° C, the yield of CO in the presence of a high pressure of ethylene was independent of temperature. The most probable interpretation of these experiments is that reaction with ethylene removed NH, NH_2, and NCO radicals, thus suppressing formation of N_2 and CO by reaction [4], so that the residual CO production was a measure of reaction [1], the primary photolytic process. Thus the primary quantum yield was apparently independent of temperature between 37 and 100° C; on raising the temperature to 200° C, however, it appears to have increased sharply. This seems unlikely, on several counts, although it cannot be entirely ruled out, and it seems more probable that at the higher temperature ethylene failed to completely supress the formation of CO by secondary reactions. The nitrogen yield was close to zero in these experiments, so that a simple failure to scavenge NH or NCO completely would not suffice. The reaction

$$NCO + C_2H_4 \rightarrow CO + [NC_2H_4] \rightarrow \text{higher products}, \quad [9]$$

which would supress N_2 formation, but not CO, is one possibility, but a more thorough study of the system at 200° C is obviously needed.

If it is accepted tentatively that the extent of reaction [1] was constant at all temperatures, and is given by the yield of CO measured at 37 and 100° C in the presence of excess ethylene (Fig. 5), some values of quantum yield (yield per primary photolytic act) may be calculated, and are shown in Table III. The simple mechanism (reactions [1] to [4]) predicts quantum yields of 3 and 1 for CO and N_2 respectively; the measured yields were lower than this at low temperature, but rapidly rose to much larger values with increasing temperature and HNCO pressure. If allowance is made for the formation of H_2 and N_2 by reaction [5], then $(CO + 4H_2)$ and $(N_2 + H_2)$ should have had quantum yields of 3 and 1 respectively, and it is seen in Table III that this modification raises the yields at low temperature close to the predicted values.

The quantum yield data show a behavior very similar to that of the N_2:CO ratios. Both tend towards agreement with the simple mechanism at low temperatures and HNCO pressures, but indicate sharply increasing production of "extra" CO and N_2 as temperature and HNCO pressure were raised, and it is evident that additional reactions must be

Can. J. Chem. Downloaded from www.nrcresearchpress.com by 210.87.254.5 on 09/05/12
For personal use only.

TABLE III
Calculated quantum yields in the photolysis of HNCO

Temperature (°C)	HNCO×1000 (mole/l.)	Yield per primary photolytic act			
		CO	N_2	$CO + 4H_2$	$N_2 + H_2$
−31	1.2	1 92	0.69	2.94	0.94
0	1.2	2.62	0.94	3.67	1.21
0	2.9	2.96	0.99	3.85	1.22
37	1.2	4.05	1.32	4.74	1.49
37	2.9	5.15	1.55	5.69	1.68
100	1.2	5.11	1.42	5.27	1.46
100	2.9	6.89	1.67	7.08	1.72
200	1.2	7.26	1.81	7.32	1.82
200	2.9	10.0	2.23	10.0	2.25

occurring. Reactions of NCO radicals with HNCO would seem the most promising source of extra products. The sequence

$$NCO + HNCO \rightarrow HN_2CO + CO \quad [10]$$

$$HN_2CO \rightarrow H + N_2 + CO \quad [11]$$

$$H + HNCO \rightarrow NH_2 + CO \quad [12]$$

$$NH_2 + HNCO \rightarrow NH_3 + NCO \quad [3]$$

constitutes a chain carried by NCO radicals which yields CO, N_2, and NH_3 in the same porportion as the simple mechanism, and would be favored by increasing HNCO pressure and temperature. This could account for extra CO and N_2 in a 3:1 ratio, but the marked increase in CO:N_2 requires another reaction producing CO without N_2. This is a stoichiometric problem as well as a mechanistic one, for as long as CO and N_2 are accompanied only by NH_3, they must be formed in a 3:1 ratio. Hydrazine formation could lead to a 4:1 ratio, but also decreased quantum yields, and, as discussed earlier, seems improbable. A product deficient in CO and stable and slightly volatile at 200° C (since no involatile compounds or polymers accumulated on the vessel windows) is required. One such possible product is urazine, NH·CO·NH·NH·CO·NH, which might be formed by reaction [10] followed by stepwise reaction of HN_2CO with three more molecules of HNCO, according to the overall equation

$$4HNCO \rightarrow \text{urazine} + 2CO. \quad [13]$$

The reactions [10] to [13] suggested here to account for the deviation from the simple mechanism are obviously tentative. Analysis for NH_3, N_2H_4, urazine, and other nitrogenous products will be needed to resolve the details of the reaction mechanism, but the separation of these basic compounds from the excess of HNCO presents some difficulties.

The effect of hydrogen on the photolysis of HNCO, shown in Table II, was rather unexpected. If the reaction

$$NH + H_2 \rightarrow NH_3 \quad [14]$$

had occurred, then the yields of N_2 and CO should have been reduced in much the same way as with ethylene. On the other hand the reaction

$$NH + H_2 \rightarrow NH_2 + H \quad [15]$$

(which is about 10 kcal endothermic), followed by reactions of NH_2 and H with HNCO, would have caused no reduction in the yields of CO and N_2. From Table II, N_2 is seen to

Can. J. Chem. Downloaded from www.nrcresearchpress.com by 210.87.254.5 on 09/05/12
For personal use only.

have decreased steadily with increasing temperature, suggesting that reaction [14] did occur with rates approximately 14, 7, and 5 times slower than reaction [2] at 37, 100, and 200° C respectively. The CO yield, however, increased, slightly at 37° and much more at the higher temperatures. Again, a reaction sequence involving NCO radicals,

$$NCO + H_2 \rightarrow NH_2 + CO \quad [16]$$

$$NH_2 + HNCO \rightarrow NH_3 + NCO, \quad [3]$$

which generates CO and NH_3 without otherwise affecting the system may be tentatively suggested as the source of the extra CO.

It is interesting to compare the photolysis of HNCO with that of its analogue, ketene. The chief similarities are in the primary process, and in the formation of excess CO accompanied by reactions leading to higher products. The chief differences between the two photolyses arise from the apparent tendency of NH radicals to abstract hydrogen from HNCO (reaction [2]) in preference to reaction [2A]. In the ketene photolysis, the reaction of CH_2 radicals with ketene analogous to [2A] is very fast and predominates over the abstraction reaction (9–12). This contrasting behavior probably depends on the weaker bonding of the hydrogen atom in HNCO, and perhaps on the lower stability of N_2H_2 compared to C_2H_4, which might require the formation of N_2 and H_2 in the reaction complex, and a consequent low frequency factor. The reaction of NH with HNCO, whether by [2] or [2A], must be considerably slower than the reaction of CH_2 with ketene, since the combination reaction, [5], competed appreciably with reaction [2], while in the ketene photolysis the combination of CH_2 radicals appears to have been suppressed almost completely by their removal by reaction with ketene, even at low temperatures and high light intensity (11, 12).

The photolysis of HNCO appears to be a useful source of NH radicals for kinetic studies of their reactions. Its chief disadvantage would seem to be the complications arising from the simultaneous presence of the three radicals NH, NH_2, and NCO.

REFERENCES

1. G. Herzberg and C. Reid. Discussions Faraday Soc. **9**, 92 (1950).
2. R. Holland, D. W. G. Style, R. N. Nixon, and D. A. Ramsay. Nature, **182**, 336 (1958).
3. R. N. Nixon. Can. J. Phys. **37**, 1171 (1959).
4. M. Linhard. Z. Anorg. Chem. **236**, 200 (1938).
5. P. Karrer. Organic chemistry. 4th ed. (English). Elsevier, New York. 1950.
6. H. E. Williams. The chemistry of cyanogen compounds. Churchill, London. 1915.
7. S. Woo and T. Liu. J. Chem. Phys. **3**, 544 (1935).
8. J. Brash and R. A. Back. Unpublished results.
9. A. N. Strachan and W. A. Noyes. J. Am. Chem. Soc. **76**, 3258 (1954).
10. J. Chanmugam and M. Burton. J. Am. Chem. Soc. **78**, 509 (1956).
11. G. B. Kistiakowsky and K. Sauer. J. Am. Chem. Soc. **80**, 1066 (1958).
12. W. G. Paterson and H. Gesser. Can. J. Chem. **35**, 1137 (1957).
13. D. A. Bamford and C. H. Bamford. J. Chem. Soc. 30 (1941).

Can. J. Chem. Downloaded from www.nrcresearchpress.com by 210.87.254.5 on 09/05/12
For personal use only.

THE PREPARATION OF DEHYDROABIETANE-1-AMINE

RICHARD F. STOCKEL[1]
Department of Chemistry and Geology, Clemson College, Clemson, South Carolina, U.S.A.
Received September 18, 1962

ABSTRACT

The preparation of dehydroabietane-1-amine (II) has been achieved and characterized by base hydrolysis of the methyl carbamate (VII) via the following path: acid (I) → acid chloride (IV) → amide (V) → methyl carbamate (VII) → primary amine (II). The overall yield from acid (I) to amine (II) was approximately 50%. Other reactions leading to poor yields of the primary amine are discussed.

INTRODUCTION

The investigation of resin acids has been an active field of endeavour for a number of workers (1–8), the purpose of which was to synthesize 1-ketonordehydroabietane (X) either from dehydroabietic acid (I) or by total synthesis.

It seems remarkable that dehydroabietane-1-amine (II), the subject of this report, had not previously been characterized nor prepared in good yields, since it would be a natural precursor to the tricyclic ketone 1-ketonordehydroabietane (X).

It was reported (1) that dehydroabietane-1-isocyanate (III) upon acid hydrolysis gave a negligible amount of the primary amine (II), but no data were given. The only other report of this amine (7) gave indirect evidence of its existence via infrared analysis and by conversion to the known tertiary amine (1), N,N-dimethyldehydroabietane-1-amine (IX).

Since the Curtius reaction led to the isocyanate (1), it was decided to study the Schmidt and Hofmann reactions and some of their many modifications.

DISCUSSION

It has been found that the Schmidt reaction, on dehydroabietic acid (I), run in the conventional way, led to considerable sulphonation of the C ring (8). No doubt the sulphonation occurred in the 6- or 8-positions or both (9). This was not unusual since the C ring is formally a 1,2,4-trisubstituted aromatic ring, thus being very reactive towards electrophilic substitution. Although the carboxyl group was converted to the amine, the sulphonic acid group was resistant to hydrolysis; therefore, the desired product could not be obtained.

A modification of the Schmidt reaction on the acid (I), employing polyphosphoric acid (10, 11), gave 18.8% yield of the amine (II) along with 80.6% of unchanged acid (I). Replacement of the polyphosphoric acid by a mixture of trifluoroacetic acid and trifluoroacetic anhydride (12) gave the isocyanate (III) and unchanged acid (I), in yields of 27.3% and 63.6%, respectively. Longer reaction time resulted in little change in the ratio of these two products.

The results of these two modifications of the Schmidt reaction seem incongruous since the intermediate in this reaction is the isocyanate. Why the isocyanate is completely hydrolyzed in one method while not in the other is not at all obvious. It may be a temperature-dependent factor or it may be due to the fact that in the first case a basification is performed. This situation is not found in the second method. The formation of

[1]*Present address: Research and Development, American Cyanamid Company, Bound Brook, New Jersey.*

Can. J. Chem. Downloaded from www.nrcresearchpress.com by 210.87.254.5 on 09/05/12
For personal use only.

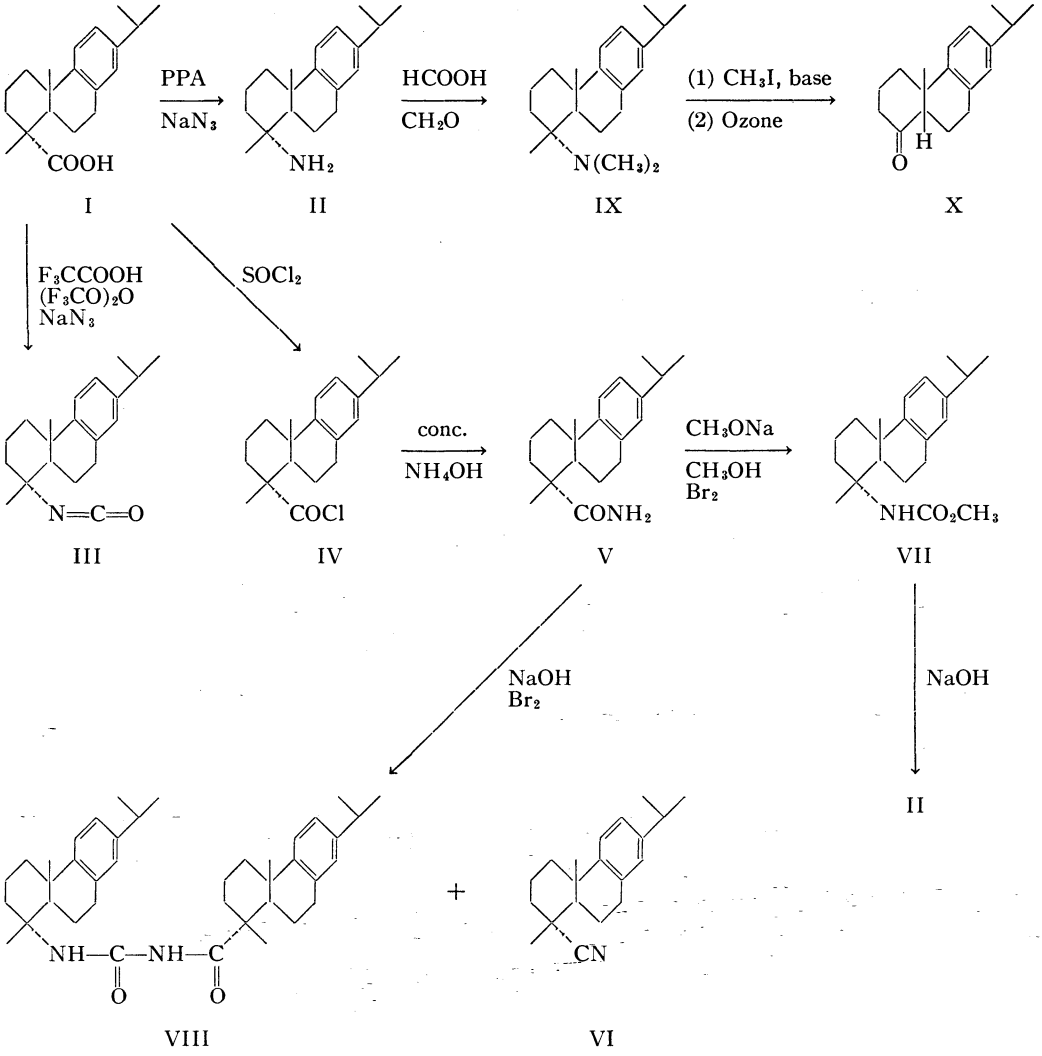

the isocyanate with trifluoroacetic acid and trifluoroacetic anhydride was compatible with the observation that 4-phenanthrenecarboxylic acid gave 4-phenanthreneisocyanate (12). Also the fact that the isocyanate (III) was not hydrolyzed by aqueous hydrochloric acid (1) may be due to the heterogeneous system.

The Hofmann reaction performed on the amide (V), made in excellent yield by treating the acid halide (IV) with concentrated ammonium hydroxide (14), gave a complex mixture. Infrared analysis revealed the presence of the nitrile (VI), the alkyl acyl urea (VIII), plus unchanged amide (V). The formation of the nitrile and urea is not unusual, since for aliphatic monoamides having more than eight carbons and also for many alicyclic monoamides these are the only products obtained (13). In view of the complex nature of the mixture and the fact that no primary amine (II) was obtained, it was decided not to pursue this procedure and attempt to characterize the products. The innovation of the Hofmann reaction using methanol and bromine (13) gave a good yield of the methylcarbamate (VII), which could then be hydrolyzed under basic conditions to the amine (II).

Can. J. Chem. Downloaded from www.nrcresearchpress.com by 210.87.254.5 on 09/05/12
For personal use only.

The greatest overall yield of amine was obtained by the sequence (I) → (IV) → (V) → (VII) → (II), as shown in the accompanying chart.

EXPERIMENTAL

Melting points were determined on a Hershberg melting point apparatus and are uncorrected. Infrared spectra were carried out as liquid films, or Nujol mulls on a Perkin–Elmer Model 317 spectrophotometer.

Preparation of Dehydroabietane-1-amine

A. Schmidt Reaction Using Polyphosphoric Acid

To 30 g of polyphosphoric acid was added 3 g (0.01 mole) of dehydroabietic acid at room temperature and the mixture stirred vigorously. Then 0.8 g of sodium azide (0.012 mole) was added over a period of 1 hour so that no temperature rise was noticed. After the reaction mixture had been stirred for 3 hours, an ice-cold aqueous solution of KOH (50%) was added until the mixture was slightly basic. The solution was extracted with ether and the ether dried over anhyrous magnesium sulphate. After removal of the solvent, 0.51 g (18.8%) of the primary amine was left. Upon acidification of the aqueous layer 2.29 g (76.3%) of unreacted acid was obtained.

In every case where the primary amine was obtained, the following characterizations were performed.

The primary amine was a white glassy substance which resisted molecular distillation at temperatures up to 200° at pressures of 0.02–0.04 mm. Purification was effected by extraction of the glassy substance with 10% aqueous hydrochloric acid. An ether extract of the neutralized aqueous solution afforded the purified amine. Its infrared spectrum (neat) gave the following peaks: 2.90 μ (N—H asymmetric stretch), 2.99 μ (N—H symmetric stretch), and 6.20 μ (N—H deformation).

The amine gave a yellow picrate from a saturated ethanolic solution of picric acid. The melting point was 222–223°. Anal. Calc. for $C_{25}H_{32}N_4O_7$: C, 59.98; H, 6.44; N, 11.19. Found: C, 59.86; H, 6.30; N, 11.20.

The primary amine was converted to the tertiary amine by the usual reductive methylation technique (8). The melting point and infrared spectrum of this tertiary amine and its picrate agreed with those for the known authentic compounds (1, 8).

B. Schmidt Reaction Using Trifluoroacetic Acid and Trifluoroacetic Anhydride

To 30 ml of trifluoroacetic acid and 30 ml of trifluoroacetic anhydride at 0° was added 2 g of dehydroabietic acid (0.0066 mole). Then 0.65 g of sodium azide (0.01 mole) was added while the solution was vigorously stirred. After the solution had been stirred for 10 minutes, it was poured into water and the resulting mixture extracted with ether. Unreacted dehydroabietic acid was extracted from the ether with 5% sodium bicarbonate to give 1.2 g (63.6%). The neutral material, a viscous yellow oil (0.6 g or 27.3%), gave an infrared spectrum (neat) with a strong peak at 4.45 μ (N=C=O stretch). The isocyanate was then treated with absolute methanol to form the methyl carbamate. This latter compound is described under Section D below.

C. Hofmann Reaction Using Sodium Hydroxide and Bromine

The dehydroabietamide (2 g, 0.0066 mole) was dissolved in 25 ml of sodium hypochlorite prepared by mixing 7 g of sodium hydroxide, 50 ml of water, and 1 ml of bromine. This was warmed on a steam bath and after 25 minutes the solution was clear. The solution was heated on a steam bath for an additional 1½ hours, then poured into water, the water extracted with ether, and the ether extract dried. When the ether was evaporated, a viscous oil (1.85 g) was obtained. The infrared spectrum (neat) gave the following peaks: 2.86, 2.95, and 6.18 μ (unreacted amide), 4.42 μ (probably the nitrile), and a series of carbonyl vibrations at 5.80, 5.85, 5.98, and 6.04 μ (probably the alkyl acyl urea). No basic material could be obtained from this reaction.

D. Hofmann Reaction Using Sodium Methoxide and Bromine

To 20 ml of absolute methanol was added 0.5 g of amide (0.00167 mole), 0.18 g of sodium methoxide (0.0034 mole), and 0.27 g of bromine (0.00167 mole). The solution was refluxed for 2 hours. Then it was taken up in ether and washed thoroughly with water. The crude yield was 0.32 g (59.2%); however, if the refluxing was continued for a period of 10 hours or longer, a crude yield of 0.39 g (70.9%) was obtained. The methyl carbamate was recrystallized from either 95% ethanol or petroleum ether – absolute ether mixture. The infrared spectrum (Nujol mull) showed the following characteristic peaks: 2.94 μ (N—H stretch) and 5.82 μ ($\diagdown$C=O vibration). The methyl carbamate was obtained as a white crystalline solid which melted at 68–69°. Anal. Calc. for $C_{21}H_{31}NO_2$: N, 4.25. Found: N, 4.01.

The ethyl carbamate was prepared by refluxing with absolute ethanol. Its infrared spectrum was similar to that of the methyl carbamate. However, it melted considerably higher, at 216–217°. Anal. Calc. for $C_{22}H_{33}NO_2$: C, 76.92; H, 9.68. Found: C, 76.96; H, 9.48.

Hydrolysis of the Methyl Carbamate

To 2 ml of water, 6 ml of 95% ethanol, and 0.5 g of sodium hydroxide was added 0.5 g of the methyl carbamate (0.0015 mole). The solution was refluxed on a steam bath for 3–5 hours. A yield of 0.36 g (88.0%) of amine was found. This compound has been described in Section A of Experimental.

Can. J. Chem. Downloaded from www.nrcresearchpress.com by 210.87.254.5 on 09/05/12
For personal use only.

Preparation of Dehydroabietamide

To 3.18 g (0.01 mole) of the acid chloride (1) in 100 ml of absolute ether was added concentrated ammonium hydroxide in excess with vigorous stirring. The stirring was continued for 10–20 minutes, then the contents were poured into ice water and the amide filtered off. The yield was 2.8 g (96.2%). The amide was recrystallized from 95% ethanol to give a white crystalline solid which melted at 165–166°. The infrared spectrum (Nujol mull) gave peaks at 2.86 μ (asymmetric N—H stretch), 2.95 μ (symmetric N—H stretch), and 6.18 μ ($\diagdown$C=O vibration). Anal. Calc. for $C_{20}H_{29}NO$: C, 80.21; H, 9.76; N, 4.67. Found: C, 80.21; H, 9.82; N, 4.60.

REFERENCES

1. H. H. Zeiss and W. B. Martin. J. Am. Chem. Soc. **75**, 5935 (1953).
2. A. Brossi, H. Gutman, and O. Jeger. Helv. Chim. Acta. **23**, 1730 (1950).
3. R. P. Jacobsen. J. Am. Chem. Soc. **75**, 4709 (1953).
4. G. Stork and A. W. Burgstahler. J. Am. Chem. Soc. **73**, 3544 (1951).
5. G. Stork and J. W. Schulenberg. J. Am. Chem. Soc. **84**, 284 (1962).
6. N. N. Saka, B. K. Ganyuly, and P. C. Dutta. J. Am. Chem. Soc. **81**, 3670 (1959).
7. J. W. Huffman and R. F. Stockel. In press.
8. R. F. Stockel. Ph.D. Thesis, Clemson College, Clemson, South Carolina.
9. L. F. Fieser and W. P. Campbell. J. Am. Chem. Soc. **60**, 159 (1938).
10. H. R. Snyder and C. T. Elston. J. Am. Chem. Soc. **76**, 3039 (1954).
11. R. T. Conley and B. E. Nowok. Chem. Ind. (London), 1161 (1956).
12. M. S. Newman and K. G. Rutherford. J. Am. Chem. Soc. **79**, 213 (1957).
13. E. S. Wallis and J. F. Lane. Organic reactions. Vol. III. John Wiley and Sons, Inc., New York. 1946. Chap. 7.
14. E. R. Littmann. U.S. Patent No. 2,201,237; Chem. Abstr. **34**, 6386[3] (1940).

Can. J. Chem. Downloaded from www.nrcresearchpress.com by 210.87.254.5 on 09/05/12
For personal use only.

KINETICS AND MECHANISMS OF THE PYROLYSIS OF *n*-BUTANE

PART I. THE UNINHIBITED DECOMPOSITION

N. H. SAGERT AND K. J. LAIDLER

Department of Chemistry, University of Ottawa, Ottawa, Canada

Received October 31, 1962

ABSTRACT

The kinetics of the pyrolysis of *n*-butane have been studied at temperatures from 520° to 590° C, and at pressures from 30 to 600 mm Hg; the rate was followed from pressure changes and by gas chromatography. The reaction was accurately of the three-halves order; the activation energy was found to be 59.9 kcal mole^{-1}, and the frequency factor 3.24×10^{15} cc$^{1/2}$ mole$^{-1/2}$ sec^{-1}. The reaction is sensitive to surface; packing the vessel and 'conditioning' it usually led to a decrease in rate and an increase in activation energy. The reaction is concluded to be largely homogeneous, and to occur almost entirely by a free-radical mechanism; the initiation reaction is considered to be the dissociation of a butane molecule into two ethyl radicals, in its first-order region, and termination is believed to be the second-order combination of ethyl radicals. The mechanism proposed is shown to account satisfactorily for the observed behavior. The surface effect is attributed to a certain amount of initiation by abstraction, by a surface atom, of a hydrogen atom from butane, and to surface catalysis of the recombination of ethyl radicals.

Can. J. Chem. Downloaded from www.nrcresearchpress.com by 210.87.254.5 on 09/05/12
For personal use only.

INTRODUCTION

Recent papers from this laboratory have dealt with the kinetics and mechanisms of the thermal decomposition of ethane (1) and propane (2). The *n*-butane decomposition presents an interesting contrast in that hydrogen atoms are no longer predominant as chain carriers; the free-radical mechanisms are therefore of a different character. A considerable amount of recent work has been done on the pyrolysis of *n*-butane, but certain features of the mechanism have still remained obscure; in particular may be mentioned the order of the initiating reaction, the nature of the main chain-ending step, and the role of the surface. A reinvestigation of the reaction was therefore considered to be worthwhile, and was carried out in conjunction with the study of the inhibited reaction described in the following paper (Part II).

The main features of the previous work on this reaction may be summarized as follows. Pease (3) and Pease and Durgan (4) established that the reaction is largely homogeneous and approximately of the first order; the overall reaction could be represented mainly by the equations

$$C_4H_{10} \rightarrow C_3H_6 + CH_4$$

$$C_4H_{10} \rightarrow C_2H_4 + C_2H_6.$$

Steacie and Puddington (5) found that the reaction products could initially be represented by the equation

$$C_4H_{10} = \tfrac{2}{3}CH_4 + \tfrac{2}{3}C_3H_6 + \tfrac{1}{3}C_2H_4 + \tfrac{1}{3}C_2H_6.$$

They reported the first-order rate constant as

$$k = 5.1\times10^{12}e^{-58{,}700/RT}\ \text{sec}^{-1}.$$

Echols and Pease (6) found that the order was closer to 3/2 than to unity.

The presence of free radicals in the reaction system was demonstrated by Rice, Johnston, and Evering (7), and Rice and Rice (8) proposed a free-radical mechanism which has been modified by Steacie (9), Semenov (10), and Benson (11). The latter proposed termination steps of the $\beta\beta$ type, leading to 3/2-order kinetics.

Purnell and Quinn have made a detailed investigation of the effect of surface on the pyrolysis of *n*-butane (12(*a*)), and in a recent paper* (12(*b*)) have described a study of the overall kinetics, in which they pay particular attention to the rate of production of the chief products. They concluded (12(*a*)) that 'conditioning' the surface, by carbon deposition, increases the rate of the heterogeneous removal of the radicals. Much of the work in their second paper (12(*b*)) was concerned with the breakdown of the ethyl radical, which they conclude to be in its pressure-dependent region. Kuppermann and Larson (13) have recently reported a first-order rate constant given by

$$k = 1.7\times10^{10}e^{-52,500/RT}\ \text{sec}^{-1}.$$

Their frequency factor and activation energy are significantly smaller than those of other investigations, including the present one. They found that packing the vessel and adding carbon dioxide had very little effect on the rate.

EXPERIMENTAL

The apparatus was essentially as described in previous papers (14, 1, 2). The reaction was carried out in vessels of approximately 200-ml capacity supported inside a large metal block the temperature of which was electrically controlled to within 0.2° C. Two quartz reaction vessels were used; one was unpacked and the other packed with quartz tubing to give a 11.6-fold increase in the surface:volume ratio. Except for runs carried out to investigate special surface effects, the results were obtained in vessels cleaned by three washings at 60° C with concentrated nitric acid, followed by rinsing with distilled water. A quartz spiral pressure gauge was used to follow pressure changes, the pressures being recorded on a Beckman photo-pen recorder; rates were determined by measuring the slopes of these records.

The *n*-butane used was research grade (99.9% pure), obtained from the Phillips Petroleum Company; it was further purified by one bulb-to-bulb distillation and was rigorously degassed.

Analyses were carried out on a Perkin–Elmer Vapor Fractometer. The C_1 to C_3 hydrocarbons and *n*-butane were analyzed using a 2-m silica gel column at 60° C; butenes were analyzed using a 3-m column containing 30% (w/w) 2,5-hexanedione on 30- to 60-mesh firebrick.

RESULTS

The pyrolysis of *n*-butane was studied in the temperature range from 520 to 590° C, and at pressures from 30 to 600 mm Hg. Figure 1 shows a typical pressure–time record.

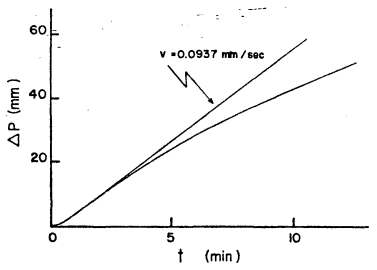

FIG. 1. A typical pressure–time curve. Temperature = 530° C, initial butane pressure = 386 mm, unpacked vessel.

There is seen to be a short induction period, and slopes were measured at the inflection point. Figure 2 shows double logarithmic plots of initial rate against pressure at various temperatures, in both packed and unpacked vessels. The order in the unpacked vessel is close to 3/2, while that in the packed vessel is slightly lower. Table I lists the 3/2-order rate constants obtained in the unpacked vessel, and Table II gives the rates at 200 mm

**This paper appeared while our paper was in course of publication.*

Can. J. Chem. Downloaded from www.nrcresearchpress.com by 210.87.254.5 on 09/05/12
For personal use only.

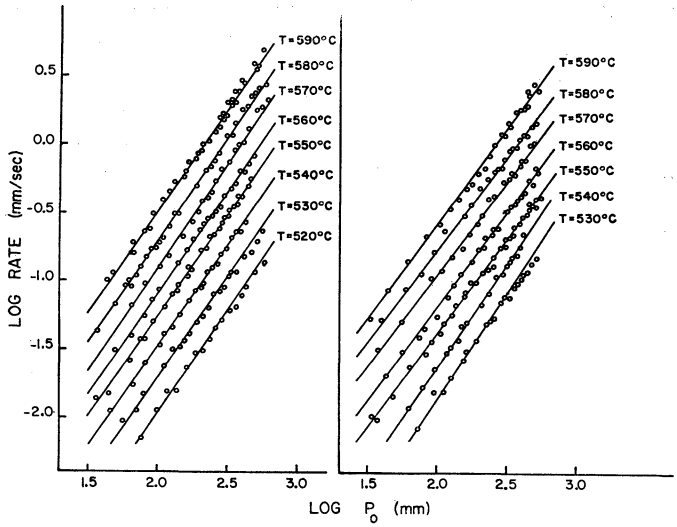

FIG. 2. Logarithmic plots of rate against pressure. The left-hand plots are for the unpacked vessel, the right-hand ones for the packed vessel.

TABLE I

Three-halves-order rate constants in the unpacked unconditioned vessel

Temperature (°C)	10^5k ($mm^{-1/2}$ sec^{-1})	Temperature (°C)	10^5k ($mm^{-1/2}$ sec^{-1})
520	1.09	560	7.92
530	1.94	570	13.0
540	3.29	580	20.4
550	5.50	590	32.5

TABLE II

Rates at 200 mm initial pressure in the packed vessel

Temperature (°C)	Rate$\times 10^2$ (mm sec^{-1})	Temperature (°C)	Rate$\times 10^2$ (mm sec^{-1})
530	4.34	570	28.1
540	7.24	580	43.7
550	11.0	590	70.5
560	16.8		

Hg in the packed vessel. Figure 3 shows a comparison of the rates in the packed and unpacked vessels at 550° C; there is seen to be a small but significant inhibition by surface, accompanied by a slight decrease in order of reaction.

Figure 4 shows an Arrhenius plot, on which the results of other workers (5, 6, 15) are included for comparison; where necessary the results were converted from first-order constants to 3/2-order ones. The activation energy is calculated to be 59.9 kcal $mole^{-1}$. Figure 5 shows that the addition of a $2\frac{1}{2}$-fold excess of carbon dioxide leads to no significant increase in the rate.

Figure 6 shows the effect of packing the reaction vessel and of conditioning it by pyrolyzing butane in it at 300 mm Hg for 48 hours. The reaction is quite sensitive to the state of the surface, and almost any change from a clean unpacked vessel tends to raise the activation energy; that in the packed vessel is 62.3 kcal $mole^{-1}$.

Can. J. Chem. Downloaded from www.nrcresearchpress.com by 210.87.254.5 on 09/05/12
For personal use only.

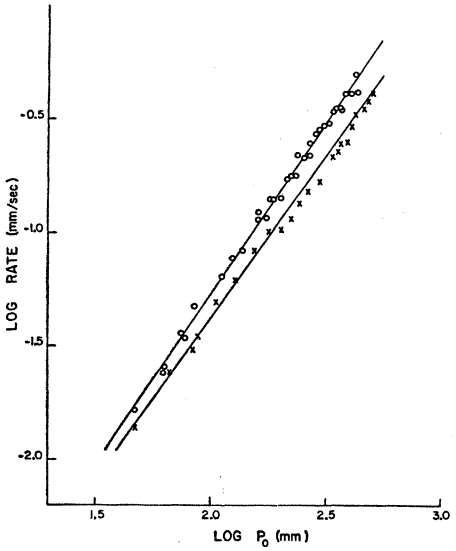

FIG. 3. Rates in the packed (×) and unpacked (○) vessel at 550° C, plotted logarithmically against the initial pressure of butane.

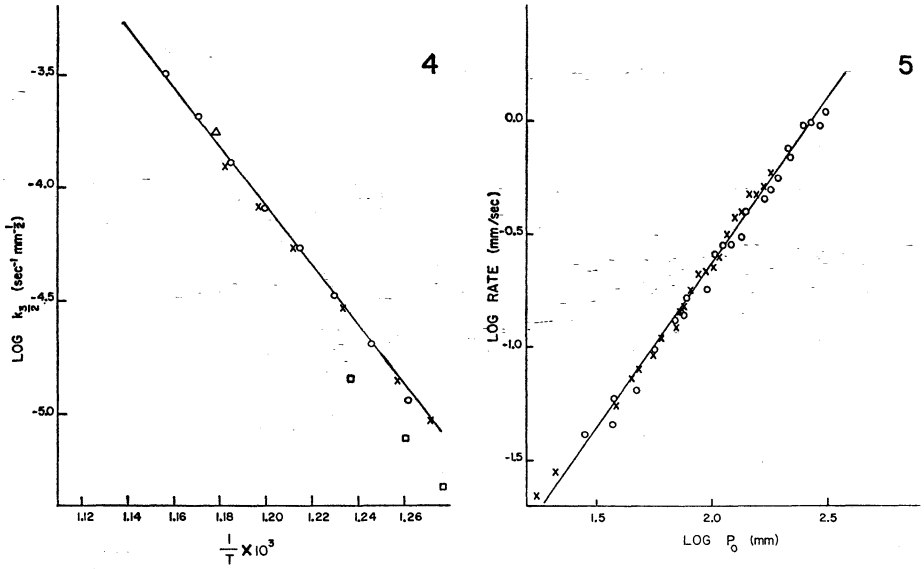

FIG. 4. Arrhenius plot for the unpacked vessel. The results of this investigation are shown as ○, those of Steacie and Puddington (5) as ×, those of Frey and Hepp (15) as △, and those of Echols and Pease (6) as □.

FIG. 5. Plot of the logarithm of the rate against the logarithm of the pressure at 580° C, showing the effect of added CO_2. ○ denotes no added CO_2, × denotes rate measured with $CO_2/C_4H_{10} \approx 2.5$.

Some of the analytical results are presented in Fig. 7. Figure 7(*a*) shows that unit decrease in butane pressure corresponds roughly to unit increase of the total pressure, while Fig. 7(*b*) represents the production of methane and ethane. Additional analytical data are shown in Table III; it gives some product ratios at three temperatures, all at 15% conversion and 200 mm Hg initial pressure.

Can. J. Chem. Downloaded from www.nrcresearchpress.com by 210.87.254.5 on 09/05/12
For personal use only.

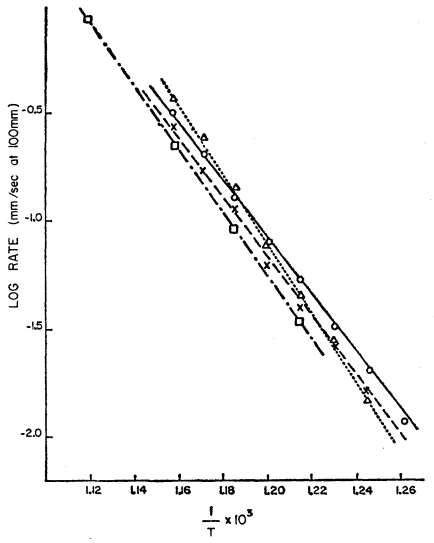

FIG. 6. Arrhenius plot showing the effect of surface. Rates measured in the clean, unpacked vessel are given by ○, in a clean packed vessel by ×, in a conditioned unpacked vessel by △, and in a conditioned packed vessel by □.

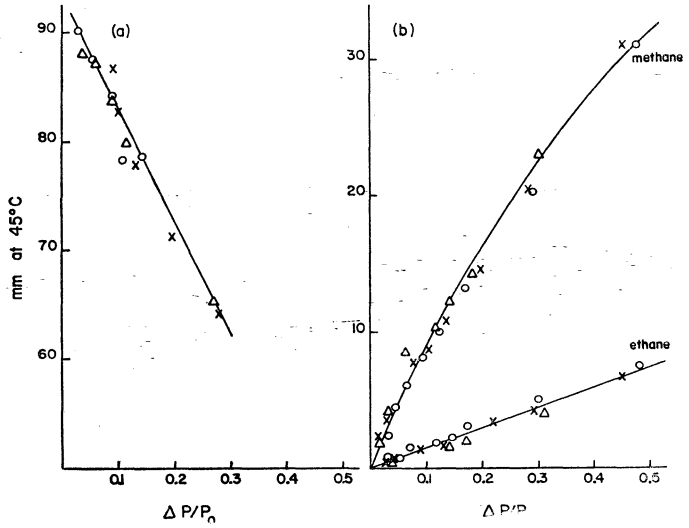

FIG. 7. Analytical results. The left-hand plot shows the correlation between the increase in total pressure and decrease in partial pressure of butane, the right-hand gives that between the increase in total pressure and appearance of methane and ethane, at 550° C (○), 570° C (×), and 590° C (△).

TABLE III

Ratios of decomposition products
(Initial pressure 202 mm Hg; 15% decomposition)

Temperature (°C)	$\frac{C_2H_6}{C_2H_4}$	$\frac{C_4 \text{ products}}{C_1, C_2, \text{ and } C_3 \text{ products}}$	$\frac{\text{Alkanes}}{\text{Alkenes}}$	$\frac{CH_4+C_3H_6}{C_2H_4+C_2H_6}$
550	0.616	0.012	1.08	1.92
570	0.523	0.014	1.03	1.81
590	0.467	0.021	1.02	1.80

Can. J. Chem. Downloaded from www.nrcresearchpress.com by 210.87.254.5 on 09/05/12
For personal use only.

On the basis of the present work the 3/2-order rate constant for the reaction is concluded to be

$$k_{3/2} = 3.24\times10^{15}e^{-59,900/RT}\ \text{cc}^{1/2}\ \text{mole}^{-1/2}\ \text{sec}^{-1}.$$

DISCUSSION

Overall Reaction Mechanism

The work of Purnell and Quinn (12(*a*)), and the results described in Part II, indicate that the molecular component of the reaction is of minor importance; this conclusion is supported by the fact that the order in a clean unpacked vessel is accurately three-halves. The following free-radical mechanism, which is very similar to that of Echols and Pease (6), is proposed to explain the facts:

$$C_4H_{10} \rightarrow 2C_2H_5 \quad [1]$$

$$C_2H_5 + C_4H_{10} \rightarrow C_2H_6 + C_4H_9 \quad [2]$$

$$C_4H_9 \rightarrow CH_3 + C_3H_6 \quad [3]$$

$$C_4H_9 \rightarrow C_2H_5 + C_2H_4 \quad [4]$$

$$CH_3 + C_4H_{10} \rightarrow CH_4 + C_4H_9 \quad [5]$$

$$C_2H_5 \rightarrow C_2H_4 + H \quad [6]$$

$$H + C_4H_{10} \rightarrow H_2 + C_4H_9 \quad [7]$$

$$C_2H_5 + C_2H_5 \rightarrow C_4H_{10} \text{ or } C_2H_6 + C_2H_4. \quad [8]$$

Table IV lists the known and estimated rate constants, activation energies, and frequency factors.

TABLE IV

Kinetic parameters for elementary reactions

Reaction	Frequency factor*	Activation energy (kcal mole^{-1})	Rate constant* at 570° C	Reference
[1]	1.0×10^{17}	80.0	1.85×10^{-4}	Trotman-Dickenson (16)
[2]	7.7×10^{11}	10.4	1.55×10^{9}	Boddy and Steacie (17)
[3]	6.5×10^{11}	24.0	3.92×10^{5}	Gruver and Calvert (18)
[4]	1.6×10^{10}	22.0	3.18×10^{5}	Kerr and Trotman-Dickenson (19)
[5]	2.7×10^{11}	9.0	1.26×10^{9}	Jones and Steacie (20)
[6]	3.0×10^{14}	39.5	1.74×10^{4}	Bywater and Steacie (21) and Trotman-Dickenson (22)
[7]	1.0×10^{14}	7.9	8.97×10^{11}	Schiff and Steacie (23)
[8]	1.6×10^{13}	0.0	1.60×10^{13}	Ivin and Steacie (24)

*In the units sec^{-1} or cc mole^{-1} sec^{-1}.

The proposed mechanism gives rise to the following expressions for the steady-state radical concentrations:

$$[H] = \frac{k_6}{k_7}\left(\frac{2k_1}{k_8}\right)^{1/2}[C_4H_{10}]^{-1/2}$$

Can. J. Chem. Downloaded from www.nrcresearchpress.com by 210.87.254.5 on 09/05/12
For personal use only.

$$[C_2H_5] = \left(\frac{2k_1}{k_8}\right)^{1/2}[C_4H_{10}]^{1/2}$$

$$[C_4H_9] = \frac{k_2}{k_4}\left(\frac{2k_1}{k_8}\right)^{1/2}[C_4H_{10}]^{3/2} + \frac{k_6}{k_4}\left(\frac{2k_1}{k_8}\right)^{1/2}[C_4H_{10}]^{1/2}.$$

With the assumption of long chains, so that the removal of butane by reaction [1] is negligible, the overall rate is found to be

$$v = \left(\frac{k_3}{k_4} + 1\right)\left\{k_2\left(\frac{2k_1}{k_8}\right)^{1/2}[C_4H_{10}]^{3/2} + k_6\left(\frac{2k_1}{k_8}\right)^{1/2}[C_4H_{10}]^{1/2}\right\}.$$

The data from Table IV indicate that k_3 and k_4 are very close to each other, although k_3 is usually slightly higher.

Experimentally it is found that the reaction is strictly of the 3/2 order over the range of conditions employed, and this requires that the second term in the rate equation be negligible compared with the first. At first sight the mechanism proposed would not seem to lead to this conclusion; thus, insertion of the values of the rate constants from Table IV leads to the result that, at 570° C and 500 mm Hg,

$$\frac{\text{term 1}}{\text{term 2}} = \frac{k_2}{k_6}[C_4H_{10}] = 0.85,$$

so that the two terms appear to be comparable in magnitude. The reason for this apparent discrepancy is presumably that, as found by Purnell and Quinn (12(*b*)), the decomposition of the ethyl radical is not in its first-order region, but in the pressure-dependent region, the apparent order of the reaction being slightly greater than unity. In view of this the rate of decomposition of the ethyl radical is less than it would be if the reaction were of the first order. The predominance of the first term in the rate equation is therefore explained.

In the scheme as written above all butyl radicals are treated as the same. In fact *s*-butyl radicals are formed slightly more easily, as shown by Kuppermann and Larson (13) and by McNesby and Gordon (25). Kuppermann and Larson (13) estimate that for abstraction reactions such as [2] and [5] the ratio of secondary to primary hydrogen atom abstraction is

$$\frac{k_p}{k_s} = 2.43e^{-2640/RT}.$$

This ratio is about 0.5 at 570° C. About one-third of the C_4H_9 produced is thus *n*-C_4H_9, and two thirds is *s*-C_4H_9. The ratio (propylene+methane)/(ethylene+ethane) should therefore be about 2, in reasonable agreement with the experimental ratios of 1.8–1.9 (Table III). According to McNesby and Gordon (25) the ratio k_p/k_s is $1.50e^{-2100/RT}$, and this leads to a $(CH_4+C_3H_6)/(C_2H_4+C_2H_6)$ ratio of 2.4. The fact that our ratios are significantly less than this may be due to the fact that there is hydrogen-atom abstraction from propylene; the resulting radical may combine with a methyl or ethyl radical, giving butene-1 in the former case. This suggestion is related to the conclusion by Dintses and co-workers (27) that the butane decomposition is inhibited by products. Some isomerization of butyl radicals is possible, but Gordon and McNesby (26) detected none at somewhat lower temperatures (up to 450° C).

The mechanism proposed does not explain the small amounts of butenes formed in the reaction. The kinetic parameters for the decomposition of either *n*-butyl or *s*-butyl

Can. J. Chem. Downloaded from www.nrcresearchpress.com by 210.87.254.5 on 09/05/12
For personal use only.

radicals into butenes and hydrogen atoms have not been determined, but the activation energy is probably (21) well above 40 kcal mole^{-1}. On this basis, assuming normal frequency factors, the amounts of butenes should be less than 0.1% of the total products; actually they are 10 to 20 times this (Table III). Possibly the butenes arise from surface dehydrogenation or from a small molecular component of the reaction. It is to be noted that the butenes are about one-quarter butadiene, the formation of which is difficult to explain by any chain mechanism.

According to the rules of Goldfinger, Letort, and Niclause (28) (cf. Table 2 of ref. 2), in order to have 3/2-order overall kinetics one must postulate one of the following possibilities:*

(1) first-order initiation, $\beta\beta$ recombination;

(2) second-order initiation, $\beta\mu$ recombination;

(3) second-order initiation, $\beta\beta$M recombination.

The first is the one that is believed to apply. The second can be eliminated since it predicts a positive inert gas effect, which was not found, and also the $\beta\mu$ termination can be shown, by the insertion of kinetic parameters, to be considerably slower than the $\beta\beta$ recombination (by ~50 times at 500 mm Hg). This termination might become important at very low pressures, when the order should change to unity (assuming initiation to remain first order). The third possibility cannot be positively eliminated on the basis of the present work, since it predicts the same kind of behavior as the first; our reasons for preferring the first possibility are considered in the next section.

In connection with the lack of inert gas effect found for this system it is to be noted that a small inert gas effect was reported by Jach and Hinshelwood (29, 30), who used mainly sulphur hexafluoride. This substance was shown in an investigation of the propane decomposition (2) to be not inert, and results with it are therefore suspect.

The Initiation and Termination Reactions

The initiating reaction has been postulated to be the breakdown of *n*-butane into two ethyl radicals, in its high-pressure first-order region. Brinton and Steacie (31) have shown that at 250° C the recombination of ethyl radicals is certainly first-order at pressures of 0.5 mm and higher, and is probably first-order at pressures as low as 0.02 mm Hg. The Kassel–Rice–Ramsperger theories predict that the transition pressure should vary with the $(s - 1/2)$th power of the temperature, where s is the number of effective degrees of vibrational freedom. If s is taken as 12 in this case the initiating reaction should be first-order down to very low pressures; even if s were as large as 19 the reaction is probably still first-order at 100 mm Hg. It therefore seems most reasonable to consider that the initiation is in its first-order region under all of the experimental conditions employed in this work, and that the termination step [8] is in the second-order region. Support for this view is provided by the fact that for the ethane decomposition the evidence strongly supports the conclusion that the ethyl radical recombination is in its second-order region (1).

Another possible initiation reaction is the split into a methyl and a propyl radical. However, Trotman-Dickenson (16) has estimated that the dissociation energy for this process is some 4 kcal mole^{-1} higher than for the split into two ethyl radicals. The frequency factor may be slightly higher and may partly compensate for this; on the whole, however, it seems likely that the split into two ethyl radicals will predominate.

**A β radical is one which undergoes second-order propagation reactions, a μ radical one that undergoes first-order reactions. In the present scheme the ethyl radical is both a β and a μ radical (reactions [2] and [6]), but is predominantly a β radical since reaction [2] is more rapid than reaction [6].*

Can. J. Chem. Downloaded from www.nrcresearchpress.com by 210.87.254.5 on 09/05/12
For personal use only.

If initiation is first order the termination step must be $\beta\beta$. The reactions

$$CH_3 + CH_3 \rightarrow C_2H_6 \quad [9]$$

and

$$CH_3 + C_2H_5 \rightarrow C_3H_8 \quad [10]$$

occur in their third-order regions (1, 2) under the conditions of these experiments; the termination must therefore be by reaction [8]. By inserting numerical values it can in fact be shown that this reaction should be the predominant one.

Surface Effects

The rates in the packed clean vessel are seen from Fig. 6 to be lower at all temperatures than those in the unpacked clean vessel. They are most depressed at lower temperatures, so that the activation energy is slightly higher in the packed vessel. It is suggested that free surface sites (S) on the quartz can abstract hydrogen atoms from the butane molecule, in a manner similar to nitric oxide. According to this view the reaction occurs in part as

$$C_4H_{10} + S \rightarrow SH + C_4H_9 \quad [1s]$$

$$C_4H_9 \rightarrow C_3H_6 + CH_3 \quad [3]$$

$$C_4H_9 \rightarrow C_2H_4 + C_2H_5 \quad [4]$$

$$C_2H_5 + C_4H_{10} \rightarrow C_2H_6 + C_4H_9 \quad [2]$$

$$CH_3 + C_4H_{10} \rightarrow CH_4 + C_4H_9 \quad [5]$$

$$SH \rightarrow S + H \quad [14s]$$

$$S + C_2H_5 \rightarrow S{-}C_2H_5 \quad [11s]$$

$$S{-}C_2H_5 \rightarrow S + C_2H_5 \quad [12s]$$

$$S{-}C_2H_5 + C_2H_5 \rightarrow C_4H_{10} + S. \quad [13s]$$

Application of the steady-state treatment leads to the following expression for the overall rate:

$$v \approx k_2 \left(\frac{k_3}{k_4}\right) \left(\frac{k_{1s}k_{12s}}{k_{11s}k_{13s}}\right)^{1/2} [C_4H_{10}]^{3/2}.$$

No reliable estimates of the individual rate constants can be made. The surface-controlled reaction should become more important as the temperature is lowered, and an increase in activation energy is to be expected.

The results in the 'conditioned' vessel are of some interest. The reaction in the conditioned unpacked vessel has a very high activation energy, and its rate at high temperatures is greater than that in the clean vessel. The effect of packing in the conditioned vessel is much more pronounced than in the clean vessel. These results confirm the conclusion that some of the initiation and termination is taking place at the vessel walls. The larger effect of packing indicates that the conditioned surface is a better inhibitor than initiator, compared with the clean surface. As graphite consists of a two-dimensional fused ring it is not surprising that atoms and small free radicals are able to recombine readily on the surface. The slight increase in rate over that in the clean vessel at the highest temperatures suggests that a small, purely heterogeneous decomposition may be taking place in addition.

Kinetic Parameters

If the reaction is assumed to be completely homogeneous the predicted activation energy is

$$E = E_3 - E_4 + E_2 + \tfrac{1}{2}(E_1 - E_8).$$

Can. J. Chem. Downloaded from www.nrcresearchpress.com by 210.87.254.5 on 09/05/12
For personal use only.

Insertion of the values in Table IV leads to 52.4 kcal mole^{-1}, to be compared with the experimental value of 59.9 kcal mole^{-1}. The calculated frequency factor is 2.5×10^{14} cc$^{1/2}$ mole$^{-1/2}$ sec^{-1}, to be compared with the experimental value of 3.2×10^{15}. The calculated absolute rate is 6.5 cc$^{1/2}$ mole$^{-1/2}$ sec^{-1} at 570° C, to be compared with the experimental value of 0.97.

The agreement is not as good as with ethane (1) and propane (2); this is probably to be attributed to the greater importance of the heterogeneous reaction. This, as seen in the previous section, tends to raise the experimental activation energy.

ACKNOWLEDGMENTS

The authors thank Drs. B. W. Wojciechowski and Margaret H. Back for helpful discussions. They are indebted to the Petroleum Research Fund (administered by the American Chemical Society) for grants in support of this work, and one of us (N. H. S.) is grateful to the National Research Council of Canada for a Studentship.

REFERENCES

1. K. J. Laidler and B. W. Wojciechowski. Proc. Roy. Soc. (London), Ser. A, **260**, 91 (1961).
2. K. J. Laidler, N. H. Sagert, and B. W. Wojciechowski. Proc. Roy. Soc. (London), Ser. A, **270**, 242 (1962).
3. R. N. Pease. J. Am. Chem. Soc. **50**, 1779 (1928).
4. R. N. Pease and E. S. Durgan. J. Am. Chem. Soc. **52**, 1262 (1930).
5. E. W. R. Steacie and I. E. Puddington. Can. J. Res. Sect. B, **16**, 176 (1938).
6. L. S. Echols and R. N. Pease. J. Am. Chem. Soc. **61**, 208 (1939).
7. F. O. Rice, W. R. Johnston, and B. L. Evering. J. Am. Chem. Soc. **54**, 3529 (1932).
8. F. O. Rice and K. K. Rice. The aliphatic free radicals. Johns Hopkins Press, Baltimore. 1935.
9. E. W. R. Steacie. Atomic and free radical reactions. Reinhold, New York. 1954.
10. N. N. Semenov. Some problems in chemical kinetics and reactivity. Vol. 1. Pergamon Press, London. 1954.
11. S. W. Benson. The foundations of chemical kinetics. McGraw-Hill, New York. 1960. pp. 343–363.
12. (*a*) J. H. Purnell and C. P. Quinn. J. Chem. Soc. 4128 (1961).
    (*b*) J. H. Purnell and C. P. Quinn. Proc. Roy. Soc. (London), Ser. A, **270**, 267 (1962).
13. A. Kuppermann and J. G. Larson. Long abstracts of papers presented at American Chemical Society meeting, Washington, D.C. 21–24 March, 1962.
14. K. J. Laidler and B. W. Wojciechowski. Proc. Roy. Soc. (London), Ser. A, **259**, 257 (1960).
15. F. E. Frey and H. J. Hepp. Ind. Eng. Chem. **25**, 441 (1933).
16. A. F. Trotman-Dickenson. Gas kinetics. Butterworth Scientific Publication, London. 1955. p. 125.
17. P. J. Boddy and E. W. R. Steacie. Can. J. Chem. **38**, 1576 (1960).
18. J. T. Gruver and J. G. Calvert. J. Am. Chem. Soc. **78**, 5208 (1956).
19. J. A. Kerr and A. F. Trotman-Dickenson. J. Chem. Soc. 1602 (1960).
20. M. H. Jones and E. W. R. Steacie. Can. J. Chem. **31**, 505 (1953).
21. S. Bywater and E. W. R. Steacie. J. Chem. Phys. **19**, 326 (1951).
22. A. F. Trotman-Dickenson. J. Chem. Phys. **21**, 211 (1953).
23. H. I. Schiff and E. W. R. Steacie. Can. J. Chem. **29**, 1 (1951).
24. K. J. Ivin and E. W. R. Steacie. Proc. Roy. Soc. (London), Ser. A, **208**, 25 (1951).
25. J. R. McNesby and A. S. Gordon. J. Am. Chem. Soc. **78**, 3570 (1956).
26. A. S. Gordon and J. R. McNesby. J. Chem. Phys. **33**, 1882 (1960).
27. A. I. Dintses, D. A. Kyvatkovskii, A. D. Stepukhovich, and A. V. Frost. J. Gen. Chem. U.S.S.R. **17**, 1564 (1937).
28. P. Goldfinger, M. Letort, and M. Niclause. Contribution à l'étude de la structure moléculaire; Volume commémoratif Victor Henri. Desoer, Liège. 1948 p. 383.
29. J. Jach and C. N. Hinshelwood. Proc. Roy. Soc. (London), Ser. A, **229**, 143 (1955).
30. J. Jach and C. N. Hinshelwood. Proc. Roy. Soc. (London), Ser. A, **231**, 145 (1955).
31. R. K. Brinton and E. W. R. Steacie. Can. J. Chem. **33**, 1840 (1955).

Can. J. Chem. Downloaded from www.nrcresearchpress.com by 210.87.254.5 on 09/05/12
For personal use only.

KINETICS AND MECHANISMS OF THE PYROLYSIS OF *n*-BUTANE

PART II. THE REACTION INHIBITED BY NITRIC OXIDE

N. H. SAGERT AND K. J. LAIDLER

Department of Chemistry, University of Ottawa, Ottawa, Canada

Received October 31, 1962

ABSTRACT

The kinetics of the pyrolysis of *n*-butane, when maximally inhibited by nitric oxide, were studied at temperatures from 540° to 610° C, and at pressures from 30 to 550 mm Hg. The reaction has a short induction period and is accurately of the three-halves order; the activation energy was 65.9 kcal mole^{-1} and the frequency factor 5.3×10^{16} cc$^{1/2}$ mole$^{-1/2}$ sec^{-1}. The reaction was somewhat less inhibited by surface than was the uninhibited reaction. Excess of carbon dioxide had no effect on the rate. The results are explained in terms of a free-radical mechanism for the maximally inhibited decomposition. It is proposed that the initiation step in the inhibited decomposition is mainly $C_4H_{10} + NO \rightarrow C_4H_9 + HNO$. This is followed by the ordinary chain-propagating reactions, and by processes such as $C_2H_5 + NO \rightarrow C_2H_5NO$. The main chain-terminating step, of the type $\beta + \beta NO$, is concluded to be $C_2H_5 + C_2H_5NO \rightarrow C_4H_{10} + NO$ or $C_2H_6 + C_2H_4 + NO$. This scheme leads to three-halves-order kinetics, and provides a satisfactory quantitative interpretation of the experimental behavior.

INTRODUCTION

Previous work from this laboratory (1–4) has led to the conclusion that reactions that are maximally inhibited by nitric oxide are not occurring by molecular mechanisms, but take place by free-radical mechanisms. General schemes for maximal inhibition have been worked out (1, 4) and have been applied in detail to the experimental results for ethane (2), propane (3), and dimethyl ether (4). In the cases of ethane and propane hydrogen atoms are chain carriers, and it is found that the species HNO plays an important role in the inhibited decompositions. Butane presents an interesting contrast in that hydrogen atoms are not important chain carriers (cf. Part I). The present paper is concerned with the detailed eludication of the free-radical mechanism for the decomposition of *n*-butane in the presence of nitric oxide.

A good deal of previous work has been done on this problem, and the main features are as follows. Following Staveley's (5) discovery that organic decompositions can be inhibited by nitric oxide Echols and Pease (6) found this effect with *n*-butane. Rice and Polly (7) studied the inhibition by propylene and proposed a free-radical mechanism that was later modified by Goldanskii (8). These mechanisms were not, however, completely satisfactory in that they could not account for the limiting inhibition.

Evidence against the hypothesis that the maximally inhibited reaction is a molecular process was obtained by Steacie and Folkins (9), who found that small amounts of ethylene oxide could sensitize the maximally inhibited reaction; at 450° C they obtained a chain length of four in the presence of nitric oxide. They also found (10) that the products of the inhibited reaction were identical with those of the uninhibited reaction; they concluded from this, in agreement with the present point of view, that the inhibited and uninhibited reactions occurred by similar mechanisms.

The maximally inhibited decomposition of *n*-butane was studied by Stubbs, Ingold, and Hinshelwood (11–14), who concluded that the reaction was of the first order; this result is in disagreement with the present work, which indicates the order to be three-halves. They found that the activation energy varied with pressure. Jach and Hinshelwood (15, 16) reported that added inert gas caused some increase in the rate, and reported that

the absolute increase was the same for the maximally inhibited reaction as for the uninhibited reaction; this fact was taken to be evidence for the molecular nature of the inhibited reaction. These results are, however, suspect, since the chief inert gas used was sulphur hexafluoride: this gas has been shown (3) to be not truly inert. It was seen in Part I that carbon dioxide has no effect on the rate of the uninhibited decomposition of butane.

Purnell and Quinn (17) have recently studied the kinetics of the propylene-inhibited decomposition of *n*-butane. They found that as the pressure was lowered there was an increase in the production of ethylene relative to ethane, and attributed this to competition between decomposition of and abstraction by the ethyl radical:

$$C_2H_5 \rightarrow C_2H_4 + H$$
$$C_2H_5 + C_4H_{10} \rightarrow C_2H_6 + C_4H_9.$$

The decomposition is favored by lower pressures and higher temperatures. Their work clearly provides some evidence that the fully inhibited reaction proceeds by a free-radical mechanism.

The fact that the maximally inhibited decomposition is not a molecular process was established by Kuppermann and Larson (18, 19) using deuterium-mixing techniques. They pyrolyzed a mixture of C_4H_{10} and C_4D_{10} and found that the ratio of CD_3H to CD_4 in the products was independent of the amount of nitric oxide. They found that whereas the ethanes and methanes are mixed, ethylenes and propylenes are essentially unmixed. This result is consistent with the view that ethylene and propylene are formed by the unimolecular decomposition of larger radicals.

EXPERIMENTAL

The work was carried out in the same apparatus, and in the same way, as that described in Part I. The *n*-butane was prepared and purified as in Part I. The nitric oxide was Matheson C.P. grade purified by passing the vapor over silica gel (to remove higher oxides) and pumping to remove nitrogen; this procedure was followed by two distillations.

RESULTS

The work was carried out in the temperature range from 540 to 610° C and at butane pressures from 30 to 550 mm Hg. A typical pressure–time record for an inhibited reaction is shown in Fig. 1. The induction period is slightly more pronounced than in the uninhibited reaction; it was lengthened by lowering the butane pressure but was not much affected by changes in the partial pressure of nitric oxide.

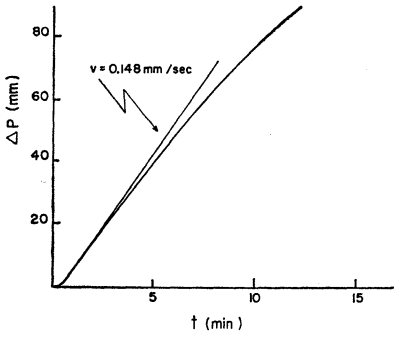

FIG. 1. A typical pressure–time curve, obtained at 570° C, with an initial butane pressure of 225 mm Hg and a nitric oxide pressure of 32 mm Hg, in an unpacked vessel.

About 12% nitric oxide gave maximal inhibition, and large amounts (over 40%) produced a slight increase in rate compared with the maximally inhibited rate. Most of the experiments were carried out with about 15% nitric oxide.

Double logarithmic plots of rate against pressure of *n*-butane are shown for the maximally inhibited reaction in Fig. 2. The reaction is seen to be accurately of the three-halves

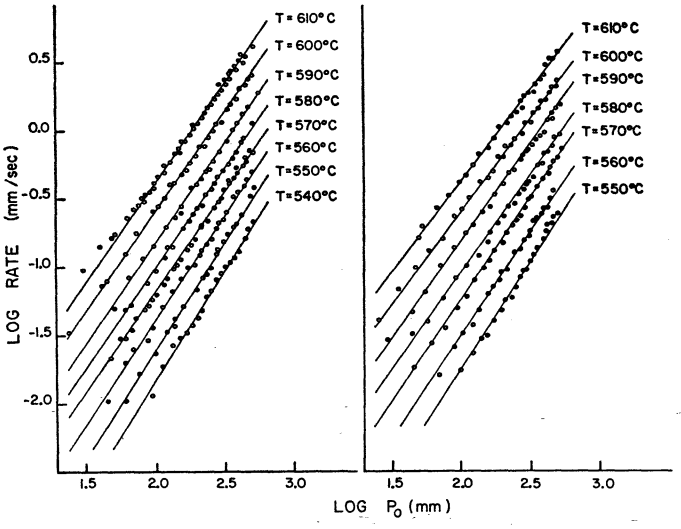

FIG. 2. Logarithmic plots of rate against pressure. The plot on the left-hand side is for the unpacked vessel, that on the right-hand side for the packed vessel.

order. Table I lists the three-halves-order rate constants obtained in the unpacked and packed vessels.

TABLE I

Three-halves-order rate constants for the inhibited decomposition of *n*-butane

Temperature (°C)	Rate constant $\times 10^5$ ($mm^{-1/2}$ sec^{-1}) Unpacked vessel	Packed vessel	Temperature (°C)	Rate constant $\times 10^5$ ($mm^{-1/2}$ sec^{-1}) Unpacked vessel	Packed vessel
540	1.46	—	580	9.55	8.32
550	2.24	1.79	590	14.38	13.17
560	3.68	3.08	600	24.45	22.4
570	6.32	5.48	610	37.6	35.6

Figure 3 shows a typical comparison of the maximally inhibited and uninhibited rates at 570° C. The orders are seen to be the same (3/2); the ratio of rates is therefore independent of pressure, in contrast to the conclusion of Stubbs and Hinshelwood (12). An Arrhenius plot is shown in Fig. 4, which includes rates obtained by other workers (10, 13). The three-halves-order rate constant for the maximally inhibited reaction may be written as

$$k_{3/2} = 4.6 \times 10^{12} e^{-65{,}100/RT} \text{ mm}^{-1/2} \text{ sec}^{-1}.$$

Figure 5 shows that there is no significant effect of adding an excess of carbon dioxide.

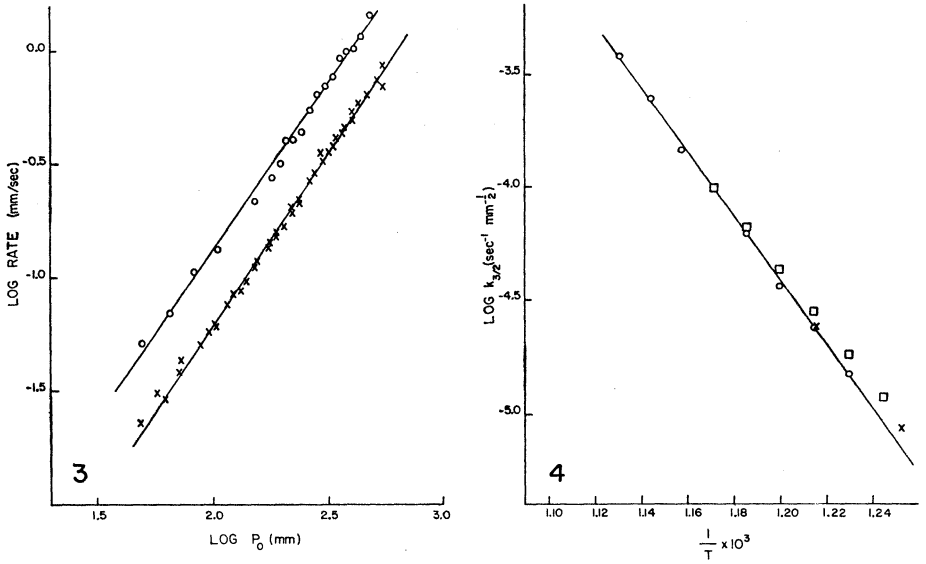

FIG. 3. Plots of the logarithm of the rate against the logarithm of the pressure for the uninhibited (×) and inhibited (○) reaction at 570° C.

FIG. 4. Arrhenius plot for the clean, unpacked vessel. The results of this investigation are shown as ○, those of Steacie and Folkins (10) as ×, and those in Ingold, Stubbs, and Hinshelwood (13) as □.

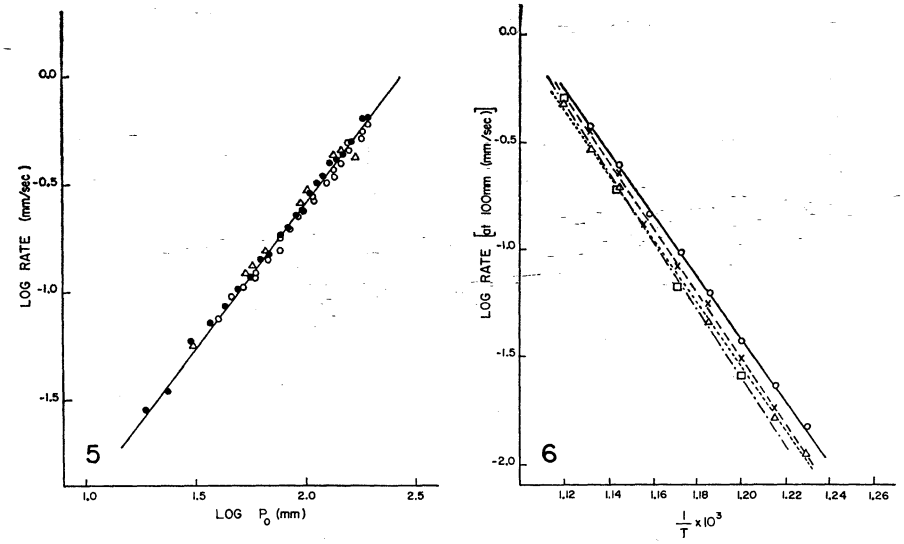

FIG. 5. Plots of the logarithm of the rate against the logarithm of the pressure, showing the effect of added carbon dioxide. ○ denotes results with no added CO_2, △ denotes rates with $CO_2/C_4H_{10} \approx 3$, and ● denotes rates with $CO_2/C_4H_{10} \approx 2.1$.

FIG. 6. Arrhenius plots showing the effect of surface. Rates measured in a clean unpacked vessel are given as ○, those in the clean packed vessel as ×, those in the conditioned unpacked vessel as △, and those in the conditioned packed vessel as □.

Figure 6 shows the effects of various surface conditions. Some of the reactions were done in a 'clean' vessel; this was washed three times with concentrated nitric acid, and then with water, before each run (a similar procedure was employed in Part I and by Purnell and Quinn (20)). The 'conditioned' vessel was prepared by pyrolyzing 300 mm Hg

of *n*-butane for 48 hours before carrying out a series of reactions. The packed vessel had a surface:volume ratio 11.6 times that of the unpacked vessel. The rates in the conditioned vessel and in the packed vessel are close to those in the unpacked vessel; they are somewhat lower at the lower temperatures, so that the activation energy is higher. The effect of surface is much smaller for the inhibited reaction than for the uninhibited.

Figure 7 summarizes the analytical results. Figure 7(*a*) relates the pressure increase

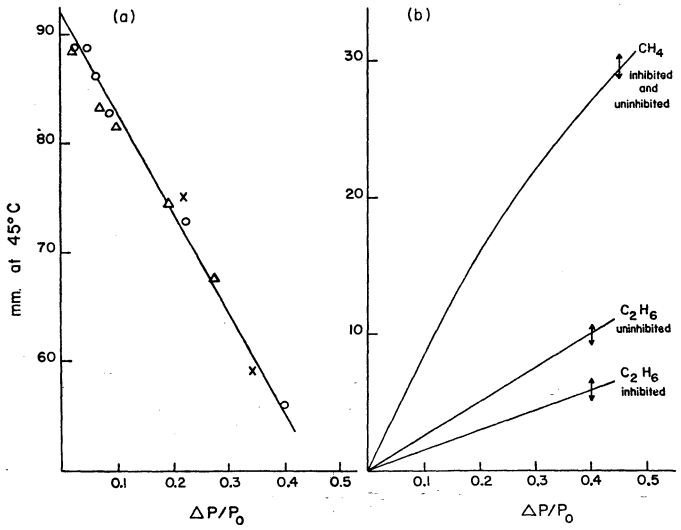

FIG. 7. Analytical results showing the partial pressure of butane (left-hand side) and of methane and ethane (right-hand side) plotted against the extent of reaction for 570° C (○), 590° C (×), and 610° C (△).

to the amount of *n*-butane used up; there is seen to be a close correspondence. Figure 7(*b*) shows the production of methane and ethane, and compares the behavior in the inhibited and uninhibited reactions. The relative rate of production of methane is seen to be unaffected by the presence of nitric oxide, whereas with nitric oxide present relatively smaller amounts of ethane are formed. Table II lists the C_2H_6/C_2H_4 ratios, as well as other

TABLE II

Ratios of reaction products
(Initial butane pressure 200 mm Hg; initial nitric oxide pressure 29 mm Hg; 15% decomposition)

Temperature (°C)	$\frac{C_2H_6}{C_2H_4}$	$\frac{\text{Alkanes}}{\text{Alkenes}}$	$\frac{C_4 \text{ products}}{C_1, C_2, \text{ and } C_3 \text{ products}}$	$\frac{CH_4+C_3H_6}{C_2H_4+C_2H_6}$
570	0.405	0.927	0.014	1.74
590	0.381	0.988	0.016	1.69
610	0.366	0.905	0.014	1.66

product ratios, at three temperatures. It is to be noted that, comparing the C_2H_6/C_2H_4 ratio at 570° C with that obtained in Part I for the uninhibited reaction, about 25% extra ethylene is produced.

On the basis of the kinetic and analytical results it is concluded that the 3/2-order rate constant for the disappearance of *n*-butane is given by

$$k_{3/2} = 5.3\times10^{16}e^{-65,900/RT} \text{ cc}^{1/2} \text{ mole}^{-1/2} \text{ sec}^{-1}.$$

DISCUSSION

The Overall Reaction Mechanism

In line with previous suggestions (1–4) it is proposed that in the maximally inhibited reaction the main initiating step is

$$C_4H_{10} + NO \rightarrow C_4H_9 + HNO. \qquad [1i]$$

The usual chain-propagating steps then occur. The species HNO will dissociate into H+NO, and other equilibria involving NO will be set up, in particular

$$C_2H_5 + NO \rightleftarrows C_2H_5NO.$$

In order for the overall kinetics to be three-halves order termination must be by steps such as

$$C_2H_5 + HNO \rightarrow C_2H_6 + NO$$
$$C_2H_5 + CH_3NO \rightarrow C_3H_8 + NO,$$

that is by processes of the type $\beta + \beta NO$. (It should be noted that, as discussed in Part I, C_2H_5 is a β radical under the conditions of these experiments.) The mechanism to which these considerations lead is

$$C_4H_{10} + NO \rightarrow C_4H_9 + HNO \qquad [1i]$$
$$C_4H_9 \rightarrow C_3H_6 + CH_3 \qquad [3]$$
$$C_4H_9 \rightarrow C_2H_4 + C_2H_5 \qquad [4]$$
$$C_2H_5 + C_4H_{10} \rightarrow C_2H_6 + C_4H_9 \qquad [2]$$
$$CH_3 + C_4H_{10} \rightarrow CH_4 + C_4H_9 \qquad [5]$$
$$C_2H_5 \rightarrow C_2H_4 + H \qquad [6]$$
$$C_2H_5 + NO \rightarrow C_2H_5NO \qquad [11]$$
$$C_2H_5NO \rightarrow C_2H_5 + NO \qquad [12]$$
$$C_2H_5NO + C_2H_5 \rightarrow C_4H_{10} + NO \text{ or } C_2H_6 + C_2H_4 + NO \qquad [13]$$
$$H + C_4H_{10} \rightarrow C_4H_9 + H_2 \qquad [7]$$
$$X + HNO \rightarrow H + NO + X \qquad [14]$$
$$C_2H_5NO \rightarrow CH_3CH_2NOH \rightarrow \text{products.} \qquad [15]$$

Values for the rate constants, activation energies, and frequency factors for these reactions are listed in Table III.

The above scheme leads to the following expressions for the radical concentrations, some small terms having been dropped:

$$[C_2H_5] = \left(\frac{k_{11}k_{12}}{k_{11}k_{13}}\right)^{1/2}[C_4H_{10}]^{1/2}$$

$$[H] = \frac{k_{11}}{k_7}[NO] + \frac{k_6}{k_7}\left(\frac{k_{11}k_{12}}{k_{11}k_{13}}\right)^{1/2}[C_4H_{10}]^{-1/2}$$

$$[CH_3] = \frac{2k_{11}k_3}{k_4k_5}[NO] + \frac{k_3k_6}{k_4k_5}\left(\frac{k_{11}k_{12}}{k_{11}k_{13}}\right)^{1/2}[C_4H_{10}]^{-1/2} + \frac{k_2k_3}{k_4k_5}\left(\frac{k_{11}k_{12}}{k_{11}k_{13}}\right)^{1/2}[C_4H_{10}]^{1/2}$$

$$[C_4H_9] = \frac{2k_{11}}{k_4}[C_4H_{10}][NO] + \frac{k_2}{k_4}\left(\frac{k_{11}k_{12}}{k_{11}k_{13}}\right)^{1/2}[C_4H_{10}]^{3/2} + \frac{k_6}{k_4}\left(\frac{k_{11}k_{12}}{k_{11}k_{13}}\right)^{1/2}[C_4H_{10}]^{1/2}$$

$$[HNO] = \frac{k_{11}}{k_{14}}[NO]$$

$$[C_2H_5NO] = \left(\frac{k_{11}k_{11}}{k_{12}k_{13}}\right)^{1/2}[C_4H_{10}]^{1/2}[NO].$$

TABLE III

Kinetic parameters for elementary reactions

Reaction	Frequency factor*	Activation energy (kcal mole^{-1})	Rate constant* at 570° C	Reference
[1i]	1.0×10^{14}	50	11.0	Estimated
[2]	7.7×10^{11}	10.4	1.55×10^{9}	Est. from Boddy and Steacie (21)
[3]	6.5×10^{11}	24.0	3.92×10^{5}	Gruver and Calvert (22)
[4]	1.6×10^{11}	22.0	3.18×10^{5}	Kerr and Trotman-Dickenson (23)
[5]	2.7×10^{11}	9.0	1.26×10^{9}	Jones and Steacie (24)
[6]	3.0×10^{14}	39.5	1.74×10^{4}	Bywater and Steacie (25)
[7]	1.0×10^{14}	7.9	8.97×10^{11}	Schiff and Steacie (26)
[11]	3.0×10^{11}	0	3.00×10^{11}	Estimated
[12]	5.0×10^{14}	59	2.56×10^{-1}	Est. from McKenney, Wojciechowski, and Laidler (4) and Gowenlock, Trotman, and Batt (27)
[13]	7.0×10^{9}	0	7.0×10^{9}	Estimated
[14]	1.9×10^{16}	48	6.90×10^{3}	Calc. from Clyne and Thrush (28) using $S = 3$

*In the units sec^{-1} or cc mole^{-1} sec^{-1}.

The overall rate of disappearance of butane is then found to be, with small terms being neglected as in Part I,

$$v = \frac{k_2k_3}{k_4}\left(\frac{k_{11}k_{12}}{k_{11}k_{13}}\right)^{1/2}[C_4H_{10}]^{3/2}.$$

The mechanism thus predicts three-halves order, in agreement with experiment.

Rates of Production of Methane, Ethane, and Ethylene

The above expression is for the rate of disappearance of butane. The rate of appearance of ethylene is

$$\begin{aligned} v_{C_2H_4} &= k_4[C_4H_9] + k_6[C_2H_5] \\ &= 2k_{11}[C_4H_{10}][NO] + k_2\left(\frac{k_{11}k_{12}}{k_{11}k_{13}}\right)^{1/2}[C_4H_{10}]^{3/2} \\ &\quad + 2k_6\left(\frac{k_{11}k_{12}}{k_{11}k_{13}}\right)^{1/2}[C_4H_{10}]^{1/2}. \end{aligned}$$

The rate of production of ethane is

$$v_{C_2H_6} = k_2\left(\frac{k_{11}k_{12}}{k_{11}k_{13}}\right)^{1/2}[C_4H_{10}]^{3/2}.$$

More ethylene than ethane is produced, largely because of reaction [6]. In addition, when enough nitric oxide is added to make reaction [1i] important a small amount of additional ethylene will be produced. The mechanism thus predicts that as nitric oxide is added the rate of production of ethylene should increase relative to that of ethane, and this is found experimentally. The mechanism also gives a quantitative interpretation of this effect; at 570° C, 500 mm Hg of butane, and 75 mm Hg of nitric oxide, introduction of the rate constants leads to the result that 18% additional ethylene should be produced; this compares satisfactorily with the experimental result that 20–25% extra ethylene is formed under these conditions.

In a similar way it can be shown that the mechanism predicts that the rates of formation of methane and of propylene should be equally increased by large amounts of nitric oxide, in agreement with experiment.

The Initiation and Termination Steps

An estimated activation energy and frequency factor for the initiation reaction [1i] are given in Table III. The activation energy is based on a value of 48.0 kcal for the HNO dissociation energy (1, 2, 3, 28), and on 96.0 for the C—H dissociation energy. Using the parameters for reactions [1] (for the uninhibited reaction) and [1i] the latter reaction is found to be significant at maximal inhibition.

In order to obtain 3/2-order kinetics the termination reaction must be of the type $\beta + \beta\text{NO}$; the β radical in this case may be H, CH_3, or C_2H_5. By using the kinetic parameters in Table III it is readily shown that reaction [13] and the analogous reaction

$$CH_3 + CH_3NO \rightarrow C_2H_6 + NO \qquad [16]$$

are much more important than any other terminating reaction. The situation is to be contrasted with that with propane (3); there hydrogen atoms are chain carriers and therefore are present in much larger amounts; HNO thus plays a role in termination in the propane decomposition, but not in the butane decomposition. Termination by reaction [16] would mean that more propylene should be produced relative to methane when nitric oxide is added, while the ratio C_2H_6/C_2H_4 should remain constant. Since in fact the amount of C_2H_4 increases relative to C_2H_6, while the CH_4/C_3H_6 ratio remains constant on adding nitric oxide, termination by reaction [13] would seem to be more important.

The rate of reaction [13] can be shown to be much more important than that of the termination step $C_2H_5+C_2H_5$ in the uninhibited reaction. Thus

$$\frac{v_{13}}{v_8} = \frac{k_{13}[C_2H_5][C_2H_5NO]}{k_8[C_2H_5][C_2H_5]}$$

$$= \frac{k_{13}k_{11}}{k_8k_{12}}[NO].$$

At 570° C and 75 mm pressure of nitric oxide this ratio $\approx$ 50. The termination by reaction [13] is therefore dominant at all pressures used.

Effect of Inert Gas

Reactions [3], [4], [6], [11], [12], and [14] are influenced by the presence of an inert gas. Reactions [11] and [12], however, form a reversible equilibrium, and all of the expressions for free-radical concentrations and for rates involve the ratio k_{11}/k_{12}, which is not affected by inert gas. The rate constant for reaction [14] does not appear in the important terms in the rate expressions, and in any case this reaction probably remains in its second-

order region under all of the experimental conditions employed. Reactions [3], [4], and [6] are probably first-order under all ordinary conditions.

Kinetic Parameters

The activation energy predicted on the basis of the proposed mechanism is

$$E = E_2+E_3-E_4+\tfrac{1}{2}(E_{11}+E_{12}-E_{11}-E_{13}).$$

Introduction of the values in Table III gives 66.9 kcal mole^{-1}, in good agreement with the experimental value of 65.9 kcal mole^{-1}. The activation energy calculated from inflection point rates extrapolated to initial conditions is 66.9 kcal mole^{-1}.

The predicted frequency factor is

$$A = \frac{A_2A_3}{A_4}\left(\frac{A_{11}A_{12}}{A_{11}A_{13}}\right)^{1/2} = 1.53\times10^{16}\ \text{cc}^{1/2}\,\text{mole}^{-1/2}\,\text{sec}^{-1},$$

in good agreement with the experimental value of 5.30×10^{16} cc$^{1/2}$ mole$^{-1/2}$ sec^{-1}. The calculated overall rate constant at 570° C is 7.02×10^{-2} cc$^{1/2}$ mole$^{-1/2}$ sec^{-1}, as compared with the experimental value of 0.44 cc$^{1/2}$ mole$^{-1/2}$ sec^{-1}.

Surface Effects

The fact that there is some inhibition by surface, and that the effect is less in the reaction maximally inhibited by nitric oxide than in the uninhibited reaction, is consistent with the mechanism proposed. The surface sites permit a new type of initiation, and of termination, to occur, as discussed in Part I.

ACKNOWLEDGMENTS

The authors thank Drs. B. W. Wojciechowski and Margaret H. Back for helpful discussions. They are indebted to the Petroleum Research Fund (administered by the American Chemical Society) for grants in support of this work, and one of us (N. H. S.) is grateful to the National Research Council of Canada for a Studentship.

REFERENCES

1. B. W. Wojciechowski and K. J. Laidler. Can. J. Chem. **38**, 1027 (1960).
2. K. J. Laidler and B. W. Wojciechowski. Proc. Roy. Soc. (London), Ser. A, **260**, 103 (1961).
3. K. J. Laidler, N. H. Sagert, and B. W. Wojciechowski. Proc. Roy. Soc. (London), Ser. A, **270**, 254 (1962).
4. D. J. McKenney, B. W. Wojciechowski, and K. J. Laidler. To be published.
5. L. A. K. Staveley. Proc. Roy. Soc. (London), Ser. A, **162**, 558 (1937).
6. L. S. Echols and R. N. Pease. J. Am. Chem. Soc. **59**, 766 (1937).
7. F. O. Rice and O. L. Polly. J. Chem. Phys. **6**, 273 (1938).
8. V. E. Goldanskii. Uspei. Khim. **15**, 63 (1946).
9. E. W. R. Steacie and H. O. Folkins. Can. J. Res. Sect. B, **17**, 105 (1939).
10. E. W. R. Steacie and H. O. Folkins. Can. J. Res. Sect. B, **18**, 1 (1940).
11. F. J. Stubbs and C. N. Hinshelwood. Proc. Roy. Soc. (London), Ser. A, **200**, 458 (1950).
12. F. J. Stubbs and C. N. Hinshelwood. Proc. Roy. Soc. (London), Ser. A, **201**, 18 (1950).
13. K. U. Ingold, F. J. Stubbs, and C. N. Hinshelwood. Proc. Roy. Soc. (London), Ser. A, **203**, 486 (1950).
14. F. J. Stubbs, K. U. Ingold, B. C. Spall, C. J. Danby, and C. N. Hinshelwood. Proc. Roy. Soc. (London), Ser. A, **214**, 20 (1952).
15. J. Jach and C. N. Hinshelwood. Proc. Roy. Soc. (London), Ser. A, **229**, 143 (1955).
16. J. Jach and C. N. Hinshelwood. Proc. Roy. Soc. (London), Ser. A, **231**, 145 (1955).
17. J. H. Purnell and C. P. Quinn. Nature, **189**, 656 (1961).
18. A. Kuppermann and L. G. Larson. J. Chem. Phys. **33**, 1264 (1960).
19. A. Kuppermann and L. G. Larson. Long abstracts of papers presented at American Chemical Society meeting, Washington, D.C. March 21–24, 1962.
20. J. H. Purnell and C. P. Quinn. J. Chem. Soc. 4128 (1961).
21. P. J. Boddy and E. W. R. Steacie. Can. J. Chem. **38**, 1576 (1960).
22. J. T. Gruver and J. G. Calvert. J. Am. Chem. Soc. **78**, 5208 (1956).
23. J. A. Kerr and A. F. Trotman-Dickenson. J. Chem. Soc. 1602 (1960).

24. M. H. JONES and E. W. R. STEACIE. Can. J. Chem. **31**, 505 (1953).
25. S. BYWATER and E. W. R. STEACIE. J. Chem. Phys. **19**, 326 (1951).
26. H. I. SCHIFF and E. W. R. STEACIE. Can. J. Chem. **29**, 1 (1951).
27. B. G. GOWENLOCK, J. TROTMAN, and L. BATT. Chem. Soc. (London), Spec. Publ. **10**, 74 (1957).
28. M. A. A. CLYNE and B. A. THRUSH. Trans. Faraday Soc. **57**, 1305 (1961).

THE CONFIGURATION OF DEOXYSTREPTAMINE[1]

R. U. LEMIEUX AND R. J. CUSHLEY
Department of Chemistry, University of Alberta, Edmonton, Alberta
Received October 29, 1962

ABSTRACT

The nuclear magnetic resonance (n.m.r.) spectrum of 5-*O*-methyl-1,3-di-*N*-methyl-4,6-di-*O*-acetyldeoxystreptamine dihydrogenperchlorate requires the all-trans configuration since the signal for the equivalent ring hydrogens at the 4- and 6-positions is in the form of a triplet with a spacing of 10 c.p.s. This spacing requires these hydrogens to be axial and coupled with axial hydrogens at the neighboring 1-, 3-, and 5-positions.

Can. J. Chem. Downloaded from www.nrcresearchpress.com by 210.87.254.42 on 09/05/12
For personal use only.

Streptamine is obtained by hydrolysis of the antibiotic streptomycin (1) and evidence has been obtained (2, 3) that the compound is 1,3-dideoxy-1,3-diaminoscylloinositol. The substance known as deoxystreptamine, first isolated from the antibiotics neomycin A (neamine), B, and C (4), was found to be a meso form of 1,3-diamino-4,5,6-trihydroxycyclohexane (4) and its name was assigned on the basis of the assumption that it was configurationally related to streptamine. Although circumstantial evidence has accumulated (5) which rendered the correctness of this assumption highly probable, the evidence cannot be considered definitive. Deoxystreptamine is also a building unit of the kanamycins A (6) and B (7) and paromomycin (8). This widespread occurrence renders a knowledge of its configuration of particular interest and especially since Hoeksema, Argoudelis, and Wiley (9) have recently isolated the 1,3-di-*N*-methyl derivative of the 2-epimer (10) of streptamine from the antibiotic actinospectacin. The compound was termed "actinamine." It could be anticipated that a direct proof of the configuration of deoxystreptamine may be available by application of n.m.r. spectroscopy along the lines described by Lemieux, Moir, and Kullnig (11). Advantage is taken of the fact that neighboring hydrogens in axial orientation are coupled to the extent of 8 or more c.p.s. and this coupling is three to four times stronger than when the hydrogens are in gauche relationship (12).

The n.m.r. spectrum of deoxystreptamine in deuterium oxide is shown in Fig. 1. The structures of the signals for the hydrogens of the methylene group require the two amino groups to be equatorially oriented. This is evident from the 12- and 13-c.p.s. spacings found in the signal for the axial hydrogen at 1.28 p.p.m. and demonstrated through the first-order analysis shown in Fig. 1. However, the spectrum provides no simply derivable information about the configurations at the other centers because of the small chemical shift between the signals for the 4-, 5-, and 6-hydrogens in the region 3.0 p.p.m. Slomp and MacKellar (10) found the equivalent axial 4- and 6-hydrogens of actinamine to produce their signal about 0.7 p.p.m. to lower field than that for the axial 5-hydrogen at 3.46. This situation is mainly due to the deshielding effect on the 4- and 6-hydrogens by the axial and opposing hydroxyl group at the 2-position (13).

The signals for the 4-, 5-, and 6-hydrogens were also bunched together in the n.m.r. spectrum for the diperchlorate salt of tri-*O*-acetyldeoxystreptamine. However, the signals for the 1- and 3-hydrogens were well separated from those at the 4-, 5-, and 6-positions. Consequently, it was evident that a solution of the configuration of deoxystreptamine through first-order analysis of the spectrum could be obtained (14) if the acetyl group

[1]*Presented at the 45th National Conference of the Chemical Institute of Canada, Edmonton, Alberta, May 28–30, 1962.*

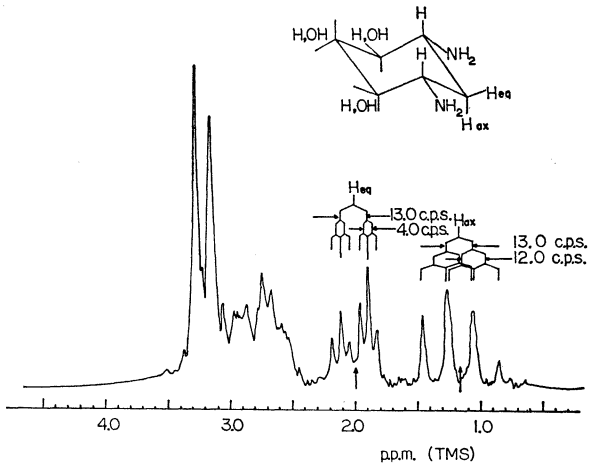

FIG. 1. The proton magnetic resonance spectrum of deoxystreptamine in deuterium oxide.

at the 5-position could be substituted in such a way as to achieve a substantial chemical shift between the signal for the 5-hydrogen and that for the neighboring 4- and 6-hydrogens. The antibiotic kanamycin A provided a convenient starting point for the preparation of such a derivative of deoxystreptamine.

Umezawa and co-workers (15) have reported the methylation of the tetra-*N*-acetyl derivative of kanamycin. Acid hydrolysis of the permethylated compound provided a substance, m.p. 207–209°, reported to be 5-*O*-methyldeoxystreptamine dihydrochloride. It has now been observed that methylation with methyl iodide and silver oxide in dimethylformamide (16) (instead of dimethyl sulphate in aqueous sodium hydroxide (15)) and acid hydrolysis produced a mono-*O*-methyl-di-*N*,*N*′-methyl derivative of deoxystreptamine dihydrochloride with a melting point, 207–210.5°, very close to that reported by Umezawa and his co-workers (15). It seems possible that the two compounds are identical.

The derivative of deoxystreptamine was converted to the dihydrogenperchlorate salt for *O*-acetylation (17). Although the product failed to crystallize, the n.m.r. spectrum (Fig. 2) and microanalyses require the substance to be virtually pure 5-*O*-methyl-1,3-di-*N*-methyl-4,6-di-*O*-acetyldeoxystreptamine dihydrogenperchlorate. It is seen that, as expected for this structure, sharp signals are present with the chemical shifts and intensities for two *O*-acetyl groups, two *N*-methyl groups, and one *O*-methyl group. The triplet of intensity two at 5.30 p.p.m. is in the region expected for the signal from hydrogens bonded to secondary carbons attached to acetoxy groups and must arise from the 4- and 6-hydrogens. The spacing of 10 c.p.s. requires these hydrogens to be axial and coupled with two neighboring axial hydrogens. Therefore, the spectrum comprises direct evidence for the all-trans configuration for deoxystreptamine and confirms the previous evidence for the points of attachment of the aminosugars to deoxystreptamine in kanamycin A (15, 18).

EXPERIMENTAL

Tetra-N-acetyl Kanamycin A

A solution of 100 g of kanamycin A* in 150 ml of water and 450 ml of methanol was cooled to 0–5°, and 100 ml of acetic anhydride was added dropwise. The temperature rose to 50°. After standing at room temperature for 1 hour, acetone (4 liters) was added with stirring. After 1 hour, the precipitate was collected by filtration and washed with acetone. The solid was dried *in vacuo* for 2 days. The crude material was

**Kindly provided by Bristol Laboratories Inc., Syracuse, N.Y.*

Can. J. Chem. Downloaded from www.nrcresearchpress.com by 210.87.254.42 on 09/05/12
For personal use only.

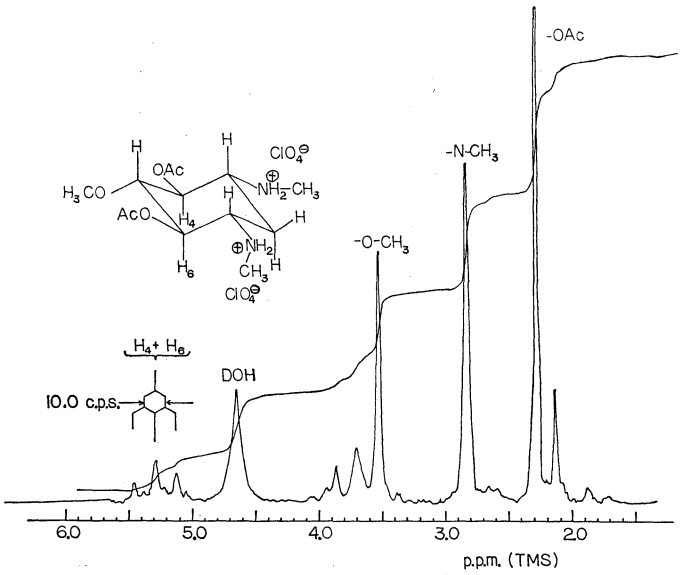

FIG. 2. The proton magnetic resonance spectrum of 4,6-di-*O*-acetyl-5-*O*-methyl-1,3-di-*N*-methyldeoxystreptamine dihydrogenperchlorate in deuterium oxide.

recrystallized from a minimum amount of water to which equal volumes of methanol and ethanol were added until crystals began to appear. The product was powdered and dried for 6 hours in a vacuum oven at 80°. The yield was 112.5 g of a product which melted at 265–266° (literature (6) m.p. 250–255° (with decomposition)), gave a negative test with ninhydrin, showed absorption at 1640 cm^{-1} characteristic of the *N*-acetyl group, and had $[\alpha]_D$ +88.3° (*c*, 5 in water). Calculated for $C_{26}H_{44}N_4O_{15}$: CH_3CO, 26.35%. Found: CH_3CO, 24.15%.

Methylation of Tetra-N-acetyl Kanamycin A

A suspension of 25.8 g of tetra-*N*-acetyl kanamycin A (39.5 mmoles) in dimethylformamide (800 ml) and methyl iodide (142 ml) was reacted with 280 g of freshly prepared silver oxide. The silver oxide was added to the rapidly stirred mixture in four 70-g portions at intervals of 20 minutes. After stirring at room temperature for 12 hours, a further 70 g of silver oxide and 50 ml of methyl iodide were added. Stirring was continued for a total of 48 hours. The silver salts were collected by filtration and washed with dimethylformamide (2×100 ml). The combined filtrate and washings were evaporated. The salts were extracted with several portions of methanol and evaporated to dryness. The amber oil was dissolved in chloroform and the solution was washed once with water. The chloroform was removed and several small portions of benzene were distilled from the residue to leave an orange amorphous solid (13.0 g, 41%); m.p. 123–125°; $[\alpha]_D$ +94.5 (*c*, 4 in chloroform). The infrared absorption indicated that the substance was free of hydroxyl groups. The product, formed on hydrolysis in refluxing 4 *N* hydrochloric acid for 20 minutes, when chromatographed on paper using 1-butanol – pyridine – acetic acid – water (6:4:3:1) showed three ninhydrin-positive (19) spots, R_f = 0.16 (brown), 0.34 (orange), 0.55 (violet), and no trace of deoxystreptamine, R_f = 0.05.

5-O-Methyl-1,3-di-N-methyldeoxystreptamine Dihydrochloride

Fully methylated kanamycin A tetra-*N*-acetate (4.80 g) was dissolved in 4 *N* hydrochloric acid (150 ml) and the solution refluxed for 1.5 hours. The solution was evaporated *in vacuo* at 50°. The solid residue was dissolved in water (20 ml) and decolorized with charcoal (0.6 g). Evaporation left 4.02 g of a solid which was dissolved in methanol (6 ml), and ether (29 ml) was then added to precipitate the 5-*O*-methyl-1,3-di-*N*-methyldeoxystreptamine dihydrochloride (2.26 g). A further similar treatment yielded 1.0 g of material which was dissolved in the developing phase (8 ml) for chromatograghy on a column of cellulose (18 cm×1.5 cm) using 1-butanol – ethanol – water (4:1:5). Three-milliliter fractions were collected and fractions 11 to 13 contained 560 mg of 5-*O*-methyl-1,3-di-*N*-methyldeoxystreptamine dihydrochloride, which was recrystallized by solution in a minimum amount of methanol and the addition of ethanol to turbidity. The yield was 510 mg of a crystalline substance; m.p. 207–210.5°. Chromatography on paper using the above solvent system showed only one spot (R_f = 0.16) using either ninhydrin (19) or periodate–permanganate (20) spray reagents. Calculated for $C_9H_{22}Cl_2N_2O_3 \cdot H_2O$: C, 36.95; H, 8.19; N, 9.49; *O*-CH_3, 10.51%. Found: C, 36.71, 37.01; H, 7.80, 8.03; N, 9.80; *O*-CH_3, 13.16%.

Can. J. Chem. Downloaded from www.nrcresearchpress.com by 210.87.254.42 on 09/05/12
For personal use only.

4,6-Di-O-acetyl-5-O-methyl-1,3-di-N-methyldeoxystreptamine Dihydrogenperchlorate

5-*O*-Methyl-1,3-di-*N*-methyldeoxystreptamine dihydrochloride (104.0 mg, 0.375 mmole) was added to 0.194 ml of 3.87 *M* perchloric acid (0.75 mmole) in acetic acid. The mixture was cooled to 0–5° and acetic anhydride (0.4 ml) was added dropwise. Solution was completed after 1 hour. After 4 hours, the reaction was complete, as indicated by a constant n.m.r. spectrum. The solution was freeze-dried to remove excess acetic anhydride and acetic acid. The residue was dissolved in water and the solution freeze-dried to leave a white amorphous solid. The substance was triturated with boiling chloroform and, after drying, dissolved in water and freeze-dried. Calculated for $C_{13}H_{26}Cl_2N_2O_{13}\cdot 2H_2O$: C, 29.74; H, 5.75; N, 5.33; *O*-CH_3, 5.90; *N*-CH_3, 5.72; CH_3CO, 16.36%. Found: C, 29.14, 29.36; H, 5.27, 5.33; N, 5.51; *O*-CH_3, 6.25; *N*-CH_3, 4.65; CH_3CO, 14.00, 15.76%.

After freeze-drying twice from deuterium oxide (2×1 ml), the material (145 mg, 88%) gave the n.m.r. spectrum shown in Fig. 2. The ratio of the intensity of the signal of the *N*-methyl groups to that of the *O*-acetyl groups was only 0.9 to 1. A further indication that the compound was not pure was the presence of the low-intensity triplet to slightly higher field in the region 5.30 p.p.m. for the 4- and 6-hydrogens.

When a paper chromatogram, using the above-mentioned conditions, was run for 60 hours, two components were separated. It seems most probable that the substance was about a 9:1 mixture of the di-*N,N'*-methyl and mono-*N*-methyl derivatives of 4,6-di-*O*-acetyl-5-*O*-methyldeoxystreptamine dihydrogenperchlorate.

Deoxystreptamine

Kanamycin A (25 g) in 4 *N* hydrochloric acid (250 ml) was refluxed for 20 minutes. The cooled solution was diluted with water (200 ml) and treated with decolorizing charcoal (40 g). The filtered solution was concentrated *in vacuo* to 50 ml and methanol (50 ml) was added. When crystals began to appear, 400 ml of ethanol was added with stirring. After 24 hours at room temperature, the crude deoxystreptamine dihydrochloride (14.4 g) was collected and dissolved in a minimum amount of boiling methanol. Ethanol was added to turbidity. The precipitate was examined by paper chromatography and found to contain traces of 6-deoxy-6-amino-D-glucose hydrochloride. The precipitate was therefore added to a Dowex 50 (H^+) ion exchange resin contained in a column (32 cm×2.5 cm) which had been washed with 4 liters of 0.7 *N* hydrochloric acid. The column was washed free of the aminosugar with 0.7 *N* hydrochloric acid. Stronger hydrochloric acid (2.5 *N*) was required to elute the deoxystreptamine dihydrochloride (21). The free base was prepared by passing the hydrochloride through an Amberlite IR-120 (OH^-) column and eluting with water.

4,5,6-Tri-O-acetyldeoxystreptamine Dihydrogenperchlorate

A solution of 25 ml of acetic acid, 2 ml of 70% perchloric acid, and 15 ml of acetic anhydride was added to 500 mg of deoxystreptamine dihydrochloride. The mixture was shaken overnight, and the hydrochloride slowly dissolved. The white gelatinous product was collected by filtration, washed with acetic acid, and dried *in vacuo*. The yield was 500 mg (67%). After two recrystallizations from water, the nicely crystalline compound possessed the following physical properties: the infrared spectrum showed a strong band at 1726 cm^{-1} characteristic of the carbonyl group of *O*-acetates but no signal in the region (about 1640 cm^{-1}) characteristic of *N*-acetates, the n.m.r. spectrum showed two bands for the *O*-acetyl groups, one at 2.22 p.p.m. which was half the intensity of that at 2.28 p.p.m. Calculated for $C_{12}H_{22}Cl_2N_2O_{14}$: C, 29.47; H, 4.53; N, 5.73; CH_3CO, 26.32%. Found: C, 29.51; H, 4.33; N, 5.79; CH_3CO, 24.80, 25.70%.

ACKNOWLEDGMENTS

This research was made possible through grants made to R. U. L. by the National Research Council of Canada (T 172) and the Bristol Laboratories Inc., Syracuse, New York.

REFERENCES

1. R. L. Peck, C. E. Hoffhine, E. W. Peel, R. P. Graber, F. W. Holly, R. Mozingo, and K. Folkers. J. Am. Chem. Soc. **68**, 776 (1946).
2. M. L. Wolfrom, S. M. Olin, and W. J. Polyglase. J. Am. Chem. Soc. **72**, 1724 (1950).
3. H. Straube-Rieke, H. A. Lardy, and L. Anderson. J. Am. Chem. Soc. **75**, 694 (1953).
4. F. A. Kuehl, M. N. Bishop, and K. Folkers. J. Am. Chem. Soc. **73**, 881 (1951).
5. H. E. Carter, J. R. Dyer, P. D. Shaw, K. L. Rinehart, Jr., and M. Hichens. J. Am. Chem. Soc. **83**, 3723 (1961).
6. M. J. Cron, D. L. Johnson, F. N. Palermiti, Y. Perron, H. D. Taylor, D. F. Whitehead, and I. R. Hooper. J. Am. Chem. Soc. **80**, 752 (1958).
7. H. Schmitz, O. B. Fardig, F. A. O'Herron, M. A. Rousche, and I. R. Hooper. J. Am. Chem. Soc. **80**, 2912 (1958).
8. T. H. Haskell, J. C. French, and Q. R. Bartz. J. Am. Chem. Soc. **81**, 3480 (1959).
9. H. Hoeksema, A. D. Argoudelis, and P. F. Wiley. J. Am. Chem. Soc. **84**, 3212 (1962).
10. G. Slomp and F. A. MacKellar. Tetrahedron Letters, No. 12, 521 (1962).
11. R. U. Lemieux, R. K. Kullnig, and R. Y. Moir. J. Am. Chem. Soc. **80**, 2237 (1958).

Can. J. Chem. Downloaded from www.nrcresearchpress.com by 210.87.254.42 on 09/05/12
For personal use only.

12. R. U. LEMIEUX, R. K. KULLNIG, H. J. BERNSTEIN, and W. G. SCHNEIDER. J. Am. Chem. Soc. **80**, 6098 (1958).
13. J. D. STEVENS and R. U. LEMIEUX. 45th National Meeting of the Chemical Institute of Canada, Edmonton, Alberta, May 28–30, 1962.
14. R. U. LEMIEUX and J. W. LOWN. Can. J. Chem. This issue.
15. S. UMEZAWA, Y. ITO, and S. FUKASU. Bull. Chem. Soc. Japan, **32**, 81 (1959).
16. R. KUHN, H. TRISCHMANN, and I. LÖW. Angew. Chem. **67**, 32 (1955).
17. R. U. LEMIEUX and N. J. CHÜ. J. Am. Chem. Soc. **80**, 4745 (1958).
18. M. J. CRON, O. B. FARDIG, D. L. JOHNSON, D. F. WHITEHEAD, I. R. HOOPER, and R. U. LEMIEUX. J. Am. Chem. Soc. **80**, 4115 (1958).
19. J. F. THOMPSON, R. M. ZACHARIUS, and F. C. STEWARD. Plant Physiol. **26**, 375, 421 (1951).
20. R. U. LEMIEUX and H. F. BAUER. Anal. Chem. **26**, 920 (1954).
21. M. J. CRON, O. B. FARDIG, D. L. JOHNSON, H. SCHMITZ, D. F. WHITEHEAD, I. R. HOOPER, and R. U. LEMIEUX. J. Am. Chem. Soc. **80**, 2342 (1958).

Can. J. Chem. Downloaded from www.nrcresearchpress.com by 210.87.254.42 on 09/05/12
For personal use only.

ELECTRICAL POLARIZATION OF TETRAMETHYLCYCLOBUTANES

F. LAUTENSCHLAEGER AND GEORGE F WRIGHT
Department of Chemistry, University of Toronto, Toronto, Ontario
Received October 31, 1962

ABSTRACT

Because the postulated non-planarity of *sym*-tetramethylcyclobutanedione is based on a small value of electrical polarization, the *cis*- and *trans*-2,2,4,4-tetramethylcyclobutane-1,3-diisocyanides have been prepared and stereospecifically rearranged to the analogous dicyanides. These substances show sufficiently large polarizations that the explanation of ring non-planarity is substantiated. Calculations in terms of the expected and observed dipole moments show that the ring deviates 20–30° from planarity. Although this non-planarity is not static, according to consideration of the cis geoisomers it would appear that one conformation is more prevalent than any others.

Can. J. Chem. Downloaded from www.nrcresearchpress.com by 210.87.254.6 on 09/05/12
For personal use only.

Although many investigators have concluded that their cyclobutanes existed in planar ring conformation (1–7) there have been others who found evidence for non-planarity on the basis of infrared and Raman absorption (8) (perfluorocyclobutane) and of electron diffraction with perfluorocyclobutane and methylcyclobutane (9) as well as with unsubstituted cyclobutane (10) and 1,3-dimethylenecyclobutane (11).

Electrical polarization studies also have indicated non-planarity. An apparent moment which was increased by higher temperature was found for 1-↑-2-↑-3-↓-4-↓-tetraphenylcyclobutane. Also the difference between the total polarization of 2,2,4,4-tetramethylcyclobutane-1,3-dione and its electronic polarization could no longer be attributed to abnormally high atom polarization, as Coop and Sutton had done (3), after the distortion polarization (P_{E+A}) of the substance was measured (12) and was found to be only 0.6 cc higher than the calculated electronic polarization. An apparent moment of 0.8 D had then to be assigned to tetramethylcyclobutanedione. Assuming the group moment of the carbonyl group to be 2.8 D the apparent deviation from ring planarity thus is calculated to be 20°, a value conforming roughly with earlier postulations (7, 9).

We have confirmed this evidence for non-planarity by preparation of the 1,3-diisocyanides and the 1,3-dicyanides of 2,2,4,4-tetramethylcyclobutane. These compounds were prepared from the geoisomeric diamines, I, which recently have been made available (13), but the reaction of Hofmann was not satisfactory for conversion of the amines to the isocyanides. However, Ugi's method (16) involving formamides with phosphorus oxychloride and pyridine gives good conversions of the *cis*- and *trans*-tetramethycyclobutane-1,3-diformamides, II, to the diisocyanides, III. Although an efficient method for separation of the geoisomeric amines has not yet been evolved the mixture obtained by formylation may easily be separated into *cis*- and *trans*-II by crystallization.

The diisocyanides III (cis and trans) are reconvertible to the corresponding formamides II by treatment with acetic acid. Also, they form cis and trans dibromides, VI. Of greater interest is the ease with which they are rearranged stereospecifically in good yield to the cis and trans cyanides, IV, by rapid heating at temperatures of about 310°. This reaction is most welcome, because any doubt about the linearity of the isocyanide group (and linearity is a necessary condition for unequivocal interpretation of the observed electrical polarization) is allayed by the well-known linearity of the cyanide group. The results of electrical polarization measurements (Table I) confirm that the isocyanide group is

Can. J. Chem. Downloaded from www.nrcresearchpress.com by 210.87.254.6 on 09/05/12
For personal use only.

TABLE I

Electrical polarization of solutions in benzene (b) or dioxane (d)

Substance	Temp. (C°)	$\frac{\delta\epsilon}{\delta\omega}$	$\frac{\delta\bar{V}}{\delta\omega}$	ϵ b or d	ϵ extrap.	$\bar{V}$ b or d	$\bar{V}$ extrap.	P_T solute	P_D	μ (D)
cis-TMCB-1,3-dicyanide*	20 b	12.6	−0.123	2.2825	2.283	1.13795	1.13780	429	46.4†	4.26
trans-TMCB-1,3-dicyanide	20 b	1.05	−0.10	2.2825	2.2822	1.13805	1.13810	82	50.2†	1.23
cis-TMCB-1,3-diisocyanide	20 b	9.45	−0.05	2.2822	2.2823	1.13805	1.13805	339	52.1†	3.68
	40 b	8.36	−0.05	2.2431	2.2430	1.16647	1.16640	317	52.1†	3.66
trans-TMCB-1,3-diisocyanide	20 b	0.88	−0.05	2.2822	2.2823	1.13805	1.13805	79.6	47.3	1.24
	35 b							76.9	47.3	1.22
	20 d	1.35	−0.14	2.2202	2.2202	0.96745	0.96735	87.5	47.3	1.38
TMCB-1-isocyanide	20 b	9.92	+0.068	2.2828	2.2824	1.13813	1.13811	303	43.0‡	3.52
1-Keto-TMCB	20 b	6.18	+0.055	2.2828	2.2845	1.13881	1.13802	203	37.0§	2.81
TMCB dione	20 b	0.22	−0.03	2.2837	2.2838	1.13768	1.13768	52.4	38.3	0.82
	30 b	0.18	−0.05	2.2625	2.2624	1.15207	1.15196	50.7	38.3	0.78
	40 b	0.13	−0.06	2.2418	2.2419	1.16686	1.16682	48.9	38.3	0.73
cis-TMCB-1,3-diol	20 d	5.04	+0.04	2.2255	2.2256	0.96770	0.96770	160	40	2.39
trans-TMCB-1,3-diol	20 d	3.72	+0.05	2.2255	2.2263	0.96770	0.96770	130	40	2.10
p-Chlorobenzonitrile	20 b	5.78	−0.30	2.2825	2.2825	1.13810	1.13811	182	33.6	2.64
	20 d	6.65	−0.13	2.2180	2.2185	0.96740	0.96748	182	33.6	2.64
p-Tolunitrile	20 b	19.25	−0.13	2.2825	2.2819	1.13814	1.13820	455	35.8	4.47
	20 d	22.90	+0.05	2.2184	2.2184	0.96742	0.96742	472	35.8	4.53
p-Diisocyanobenzene	20 b	0.62	−0.207	2.2825	2.2825	1.13812	1.13812	50.4	41.4	0.57

*TMCB refers to "2,2,4,4-tetramethylcyclobutane".
†See Table II.
‡Evaluated from $d_4^{20} = 1.428$ and $n_D^{20} = 0.821$.
§Evaluated from $d_4^{20} = 1.4143$ and $n_D^{20} = 0.824$.

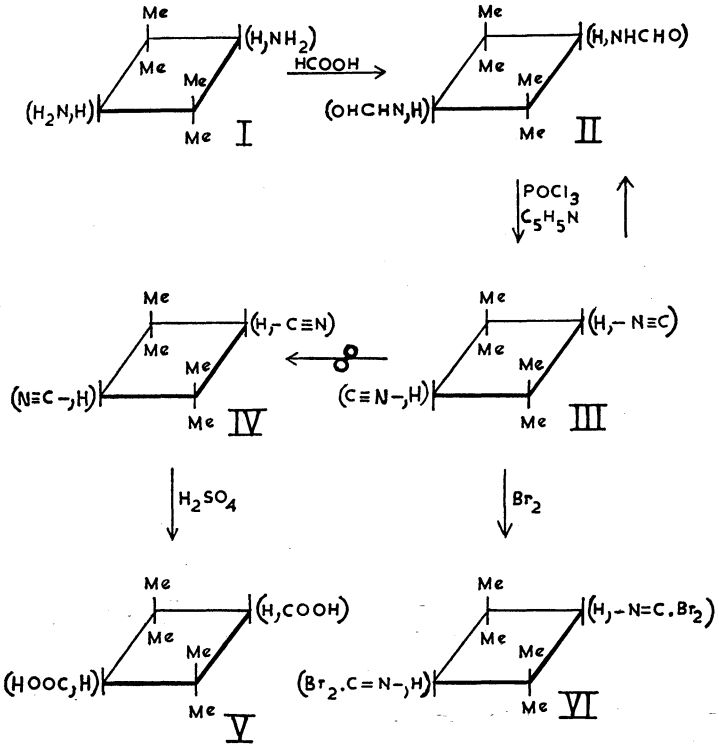

linear, at least in cyclobutanes, since the observed moments of *trans*-III and *trans*-IV are almost identical.

The rearrangement of isocyanides to cyanides at elevated temperatures has long been known (17–19). Our reactions are noteworthy only because the behavior is not in accord with that observed by Wade (20). This worker found that thoroughly dried methyl and ethyl isocyanide did not rearrange during 2 hours at 250° although the moist substances reacted rapidly below 184°. Likewise impure phenylisocyanide in his hands rearranged rapidly whereas the pure compound resinified without a trace of rearrangement.

Our reaction conditions differ from Wade's in respect of our higher temperature (310° because we found that temperatures of 220–240° for 8–10 hours led to extensive side reaction) but our rearrangements were complete within 3 minutes despite the fact that our isocyanides were dried and freed from amine at least as rigorously as were Wade's. Consequently we cannot for our reaction accept Wade's postulation that the contaminating parent amine acts as catalyst even though his suggestion would be compatible with our observation of stereospecificity:

$$\phi\text{—N}\equiv\text{C} + \text{H}_2\text{N—}\phi \rightarrow \text{H—C(=N—}\phi\text{)—NH—}\phi$$

$$\phi\text{—C}\equiv\text{N} + \text{H}_2\text{N—}\phi \leftarrow \phi\text{—C(=N—H)—NH—}\phi$$

Can. J. Chem. Downloaded from www.nrcresearchpress.com by 210.87.254.6 on 09/05/12
For personal use only.

Certainly our stereospecificity precludes the possibility that the isocyanide–cyanide rearrangement is acid catalyzed because the cyclobutane ring system is amenable to protonic isomerization. This catalyzed interconversion of stereoisomers was demonstrated for norpinic acid (21) and has also been observed during our acid hydrolysis of tetramethylcyclobutanedicyanide, IV, cis or trans, to the same equilibrium mixture of dicarboxylic acids, V.

The dipole moments of many aliphatic nitriles have been determined (22). On the other hand moment data for aliphatic isocyanides are sparse and none includes the cyclobutane ring. For this reason it seemed advisable to prepare 2,2,4,4-tetramethylcyclobutylisocyanide, XII. To this end 2,2,4,4-tetramethylcyclobutanone VII was prepared in low yield (together with 1,1,3,3-tetramethylcyclobutane) by the method of Herzog (23) and then was converted to the oxime VIII. Reduction with hydrogen and nickel gave the amine, X, but lithium aluminum hydride produced a secondary amine. This product of reductive rearrangement must evidently be 2,2,4,4-tetramethylpyrrolidine, IX. The formamide XI, which was prepared with ease from the amine X, was converted in good yield to the isocyanide, XII, by the method of Ugi and Meyr. The moment of XII, 3.5 D, is in reasonable agreement with values found for other aliphatic isocyanides (except methyl isocyanide) (22). Assuming that the C—H moment, which must be added algebraically, is directionally negative toward hydrogen (22), the group moment (in benzene) for the isocyano group is 3.8 D. Upon the same assumption (C → H), the cyano group has essentially the same moment (3.8 D).

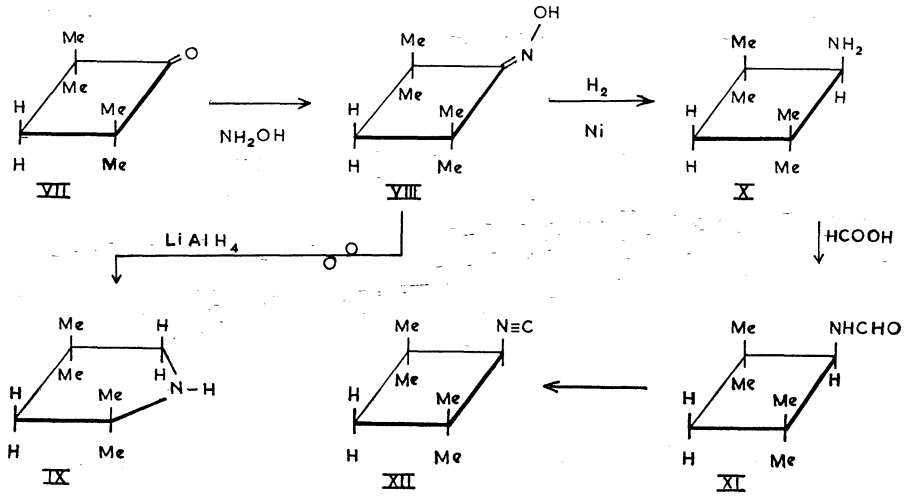

One might expect from similarity in group moment that the moments of the tetramethylcyclobutane-dicyanides and -diisocyanides would be nearly identical. As may be seen in Table I the moments of the trans isomers are the same (1.23 and 1.24 D) within experimental error. Of interest is the fact that the values are not zero; i.e., the groups do not mutually cancel one another. It is evident that the *trans*-tetramethylcyclobutanedicyanide and -diisocyanide present some asymmetry to the external electric field; they are dipolar.

The alternative interpretation (in which the excess of total polarization over that which may be assigned as electronic polarization is due to atom polarization, P_A) is unrealistic. This is apparent in view of our measurements from which the distortion polarization can

Can. J. Chem. Downloaded from www.nrcresearchpress.com by 210.87.254.6 on 09/05/12
For personal use only.

be calculated according to the method reported previously (12). These values are shown in Table II. Although a correlation between molecular geometry and atom polarization

TABLE II

Electrical polarization of pelleted solids

Substance	d_4^{20}	ϵ	P_{E+A}	MR_D*		
				Vogel c-aliphatic	Vogel c-aromatic	Eisenlohr
trans-TMCB-1,3-dicyanide†	1.067	2.48	50.2	46.4	—	46.3
cis-TMCB-1,3-dicyanide	1.060	2.31	46.4	46.4	—	46.3
trans-TMCB-1,3-diisocyanide	1.051	2.33	47.3	47.8	—	48.1
cis-TMCB-1,3-diisocyanide	1.056	2.54	52.1	47.8	—	48.1
Terephthalonitrile	1.280	2.94	39.4	35.4	35.1	31.1
p-Chlorobenzonitrile	1.511	2.75	33.6	35.7	35.5	35.1
p-Diisocyanobenzene	1.048	2.54	41.4	33.8	33.5	34.6

*Since refraction values for —N≡C are unknown a group refraction (Eisenlohr atom, 6.10 cc or Vogel bond, 5.34 cc) has been calculated from n_D^{20} and d_4^{20} of cyclohexane and tetramethylcyclobutane versus their analogous isocyanides. Similarly for —C≡N the Eisenlohr value is 5.46 cc and the Vogel value is 4.82 cc.

†TMCB refers to "2,2,4,4-tetramethylcyclobutane".

is not at present discernible it is at least apparent that P_A is not large (0–2 cc per nitrile or isonitrile group). In view of a general tendency to disregard our earlier determinations of distortion polarization which lead to assignment of orientation polarizations to benzoquinone (24), diphenylmercury (25), and tetramethylcyclobutanedione (12) it is satisfying that the high moment values for the dicyanides IV and the diisocyanides III do not depend very much on the spread of P_{E+A} values shown in Table II.

Since the measured dipole moments of the tetramethylcyclobutane-dinitrile and -diisonitrile are not zero the cyclobutane ring cannot be rigidly planar. It remains to ascertain the mode and the magnitude of this non-planarity. Evaluation of this magnitude does in general require a vectorial analysis which depends upon the angular distribution of hydrogen and cyano (or isocyano) substituents about the atom to which they are bound, but there is no fixed value for their angular distribution. Referring to Fig. 1 Friedlander

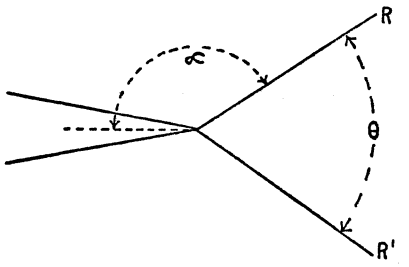

FIG. 1.

and Robertson (26) found in 2,2,4,4-tetramethylcyclobutanedione that θ was 111° while Lemaire and Livingston (7) called θ 107–112° in octofluorocyclobutane. The same authors (9) assigned to θ in methylcyclobutane a value of 100°. There is then a choice for α of 125° or 130°.

Can. J. Chem. Downloaded from www.nrcresearchpress.com by 210.87.254.6 on 09/05/12
For personal use only.

However, the vectorial analyses for the trans isomers do not involve the angle α if (as seems reasonable) the deformation from planarity is symmetrical. Reference to Fig. 2

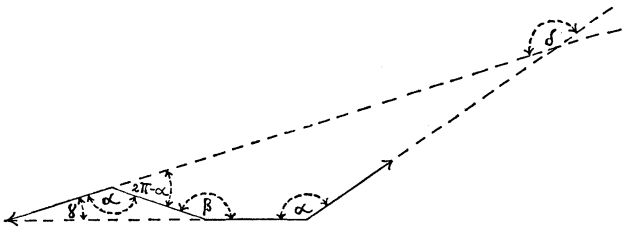

FIG. 2.

shows by consideration of the congruent triangles which include the angles $2\pi-\beta$, γ, α and the angles $2\pi-\delta$, γ, α respectively that $\delta = \beta$. Therefore, the resultant moment depends only on the group moments and the dihedral angle β, that is,

$$\mu_{res}^2 = (1.24)^2 = 2m^2+2m^2 \cos \beta,$$

where m = 3.8 Debye = group moment of cyanide or isocyanide, the moment contribution of the hydrogens being neglected.

The existence of a moment for the trans isomers of III and IV precludes the fixed planar structure XII in favor of the non-planar XIII. If XIII were fixed then β is 162°

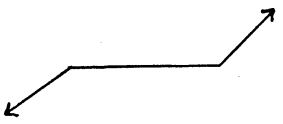

XII

XIII

for both the cyanide and the isocyanide. Alternatively one may consider an oscillating "structure" in which XII and XIII partake equally. Then the resultant (observed) moment, μ_{res}, may be used to ascertain the moment of conformer XIII:

$$\mu_{res}^2 = n_{XII}\mu_{XII}^2+n_{XIII}\mu_{XIII}^2,$$

where $n_{XII} = n_{XIII} = 1/2$;

then $2\mu_{res}^2 = \mu_{XII}^2+\mu_{XIII}^2$;

but since $\mu_{XII}^2 = 0$,

$\mu_{XIII} = \sqrt{(2\mu_{res}^2)}$.

So if μ_{res} for *trans*-III or -IV = 1.24 D then μ_{XIII} = 1.76 D. Similarly if μ_{res} for tetramethylcyclobutanedione = 0.8 D then μ for the non-planar conformer = 1.26 D.

A graph may be constructed from calculations of expected moment at various β angles for 1,3-disubstituted tetramethylcyclobutane using a group moment of 3.8 D for cyano and for isocyano in benzene. A similar graph has been constructed for cyclobutanedione using a group moment (benzene solution) of 3.1 D (2.8+0.3) for keto. For an oscillating "structure" where μ_{XIII} = 1.76 D the angle β may be interpolated, 152° for the diisocyanide III and 152° for the dicyanide IV. An oscillating "structure" for 2,2,4,4-tetramethylcyclobutanedione (μ_{obs}, 0.8 D) would have β = 156° in contrast to a β angle of 165° for a rigid non-planar structure.

Can. J. Chem. Downloaded from www.nrcresearchpress.com by 210.87.254.6 on 09/05/12
For personal use only.

We do not attach any significance to the relatively narrow range (4°) between the values derived from the β vs. moment graphs for the trans dicyanide and diisocyanide on the one hand and the diketone on the other. These values depend on the choice of group moment that is chosen for a substituent. Although the choice of 3.1 D for carbonyl in the dione is not completely arbitrary, being derived from the observed moment of 2,2,4,4-tetramethylcyclobutanone, there is no certainty that this moment is applicable. The carbonyl absorption of the monoketone in potassium bromide occurs strongly at 1770 cm^{-1}, in the same range and extent that does 3-hydroxy-2,2,4,4-tetramethylcyclobutanone (1780 cm^{-1} in chloroform) (27). These high frequencies are comparable with that found (28) for cyclobutanone. On the other hand the absorption of the dione carbonyls (potassium bromide) is split into two strong bands at 1725 and 1750 cm^{-1}, which indicates a marked difference from carbonyl in the monoketone.

It should be emphasized that the deviations from ring planarity as exemplified by angle β are not to be construed as absolute values because solvent effects will contribute to the apparent moment. A real moment may be estimated only after apparent moments have been found in a number of solvents (24). The contrast in the present study (μ = 1.24 D in benzene versus 1.38 D in dioxane for trans diisonitrile III) is not sufficiently diverse for choice of a real dipole moment.

The electrical polarization data for the trans dicyanide IV and diisocyanide III do not permit a choice of rigid versus oscillating "structure" but additional information about 2,2,4,4-tetramethylcyclobutanedione favors the oscillating "structure". The nuclear magnetic resonance spectrum of this dione ought to show a difference in methyl–hydrogen environments if the substance were rigidly non-planar. On the other hand, it would display a single hydrogen-atom absorption either if the substance were rigidly planar or alternatively if it were oscillating at a rate greater than the several hundred cycles per second which is involved in the measurement of n.m.r. Since the rigidly planar structure is excluded by the existence of a dipole moment for *trans*-III and -IV it would appear that these molecules are oscillating at a rate between 200 and 10^6 cycles/sec in view of the single peak which we have observed as the n.m.r. spectrum. The more rapid of these rate limits is favored by the low-temperature coefficient of moment (Table I) found for the diisonitriles and the dione.

Whereas the angle (α) which the cyano or isocyano group forms with the tetramethylcyclobutane ring is inconsequential in respect of trans geoisomeric configurations, it becomes crucial in consideration of cis isomers. The choice of α = 125° will be used in the following calculations.

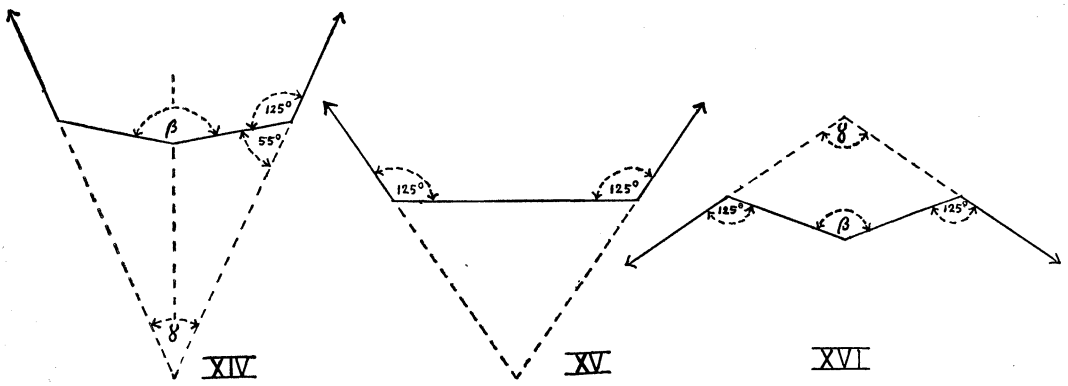

Can. J. Chem. Downloaded from www.nrcresearchpress.com by 210.87.254.6 on 09/05/12
For personal use only.

The three conformers to be considered for the cis isomers are shown as XIV, XV, and XVI. The angle of vector interaction in XV is obvious (70°) while that in XIV is

$$\gamma/2 + 55 + (180-\beta/2) = 180$$
$$\beta = \gamma+110$$

and that in XVI is

$$\gamma/2 + \beta/2 + 55 = 180$$
$$\beta = 250-\gamma.$$

A set of resultant moments using μ_{-CN} and μ_{-NC} of 3.8 D for different β values has been calculated for XIV and XVI and is shown in Fig. 3. The intersection of these two at 180° marks the calculated moment of the planar conformer XV.

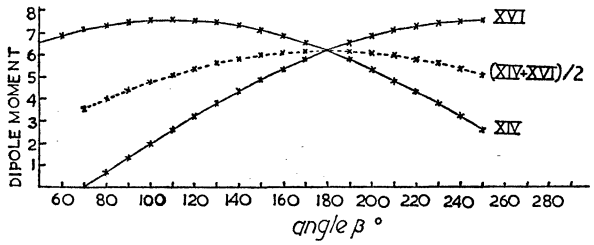

FIG. 3.

From Fig. 3 it may be concluded that conformation XV with calculated resultant moment of 6.2 D cannot alone represent the *cis*-2,2,4,4-tetramethylcyclobutane-1,3-dicyanide of observed moment 4.26 D in benzene at 20°. It may be seen that if XVI were the sole conformer then β would be 138° but that XIV would have μ = 4.26 D only if β were 222°, i.e., if it were XVI. Finally, an oscillating species comprised of XVI, XIV, and XV in proportion 1:1:2 could according to the dotted line of Fig. 3 have a resultant moment of 4.26 D only if β were 87°, which is absurd. It is evident then that XVI must be grossly preponderant in order to account for the observed moment. It may be noted that XVI is the equatorial conformer.

Exactly the same analysis for the cis diisocyanide shows that conformer XV (dotted line at 180°) would have a moment (6.2 D) much larger than that observed (3.68 D) for *cis*-III in benzene at 20°. This observed moment would be explained by conformer XVI alone if β were 129° but not by XIV alone unless β were 231°, i.e., identical with XVI. As before, a 1:1:2 oscillating mixture of XIV, XVI, and XV would lead to an absurdly small β angle. It would seem that *cis*-tetramethylcyclobutane-1,3-diisocyanide (III) also exists preponderantly as the equatorial conformer XVI.

Of course any contribution from conformer XIV would require that β were smaller than the 141° and 145° attributed to the geometry of the diisocyanide and the dicyanide of conformation XVI (Fig. 3), but this further deviation from 180° (planarity) required by a dynamic molecule should not be taken too seriously. If in the calculations outlined above for the cis isomers the angle θ (between C≡N and H at carbons 1 and 3) had been chosen as 105° rather than 110° then all of the β angles would be about 10° higher than those specified here.

Can. J. Chem. Downloaded from www.nrcresearchpress.com by 210.87.254.6 on 09/05/12
For personal use only.

EXPERIMENTAL

Melting points have been corrected against known standards.

trans-2,2,4,4-Tetramethylcyclobutane-1,3-diformamide

To an ice-cooled mixture of *cis-* and *trans*-2,2,4,4-tetramethylcyclobutane-1,3-diamine (13) (44 g, 0.33 mole) was added 60 g (1.3 mole) of 98+ % formic acid. The solid was heated until, after bubbling ceased when the pot temperature reached 260°, all water and formic acid had distilled off. The residue, m.p. 175–222°, weighed 60 g (90%) and was finely ground before it was eluted with 400 ml of boiling 95% ethanol to leave 26 g, m.p. 240–244°. Three crystallizations from dioxane raised the melting point to 257–258°, 22 g. By repetition of this procedure with the evaporated mother liquor from the initial isolation of both geoisomers an additional 6 g, m.p. 257–258°, was isolated. This total yield of the trans isomer was 47% of the 91% yield of both isomers. Calc. for $C_{10}H_{18}N_2O_2$: C, 60.5; H, 9.16; N, 14.1. Found: C, 60.3; H, 9.14; N, 14.2.

cis-2,2,4,4-Tetramethylcyclobutane-1,3-diformamide

The 400 ml of ethanolic extract mentioned above was concentrated to a volume of 100 ml and 24 g, m.p. 160–185°, crystallized out. These crystals were dissolved in 100 ml of boiling 95% ethanol, and 500 ml of ethyl acetate was added. Upon chilling, 20.5 g crystallized, m.p. 205–212°. This portion was recrystallized four times from ethanol – ethyl acetate (1:3), 15 g, m.p. 216–217°. An additional 12 g of this pure cis isomer was obtained via the repetition step used in the isolation of the additional trans isomer. The total amount of cis isomer (27 g, m.p. 216–217°) amounted to 45% of the combined yield (91%) of formamides. Calc. for $C_{10}H_{18}N_2O_2$: C, 60.6; H, 9.16; N, 14.1. Found: C, 60.5; H, 9.17; N, 14.0.

cis-2,2,4,4-Tetramethylcyclobutane-1,3-diisocyanide

A suspension of 19.8 g (0.1 mole) of *cis*-tetramethylcyclobutane-1,3-diformamide (m.p. 216–217°) in 100 ml of barium-oxide-dried pyridine and 65 ml of petroleum ether (b.p. 40–60°) was ice-cooled and stirred while 24 g (0.156 mole) of freshly distilled phosphorus oxychloride was added dropwise during 10 minutes. The suspension became cheesy and blue-green. Subsequent reflux for 30 minutes at 55° was followed by the addition of 200 ml of ice water with cooling of the system, which was then thrice extracted with a total of 200 ml of petroleum ether (b.p. 40–60°). The extract was washed with 2% hydrochloric acid, then water, and finally was dried by use of anhydrous magnesium sulphate. Vacuum evaporation left 11 g (67%) of a brown solid, m.p. 46–54°. This was sublimed at 40° (10 mm) to give 9.7 g, m.p. 57.5–58°, colorless. The substance was decomposed (5 days to an oil) by ultraviolet radiation, maximum at 360 mμ. In a potassium bromide pellet (1/400 by weight) it absorbed at the following cm^{-1}: 2970 (s); 2950 (s, shoulder); 286 (w); 2135 (s); 2040 (vw), 1465 (s), 1455 (m); 1400, 1388, 1375 (m); 1362, 1325, 1280 (m), 1215 (w), 1185 (m); 1077, 1065, 1032 (m); 975 (s); 797, 771 (m). Calc. for $C_{10}H_{14}N_2$: C, 74.0; H, 8.69; N, 17.3. Found: C, 73.9; H, 8.65; N, 16.9.

When 0.01 mole of this diisonitrile in 3 ml of acetic acid was heated to 100° for 5 minutes the vacuum-evaporated system left 98% of crude cis diformamide, m.p. 195–205°. Crystallization from dioxane yielded 80% of the crude product, m.p. 216–217°, m.m.p. not depressed.

Bromine was added to a solution of 0.162 g (0.001 mole) of the diisonitrile in 25 ml of hexane until a faint yellow color persisted. Although crystals separated, the system was concentrated under vacuum to a volume of 5 ml before 0.29 g (68% as the tetrabromide) was filtered, m.p. 128–129°. A second crop (0.21 g, 44%) was obtained by complete evaporation of solvent, m.p. 110–129°. This tetrabromide was too unstable for routine analysis. It was soluble in water but insoluble in diethyl ether.

cis-2,2,4,4-Tetramethylcyclobutane-1,3-dicyanide

When 3.42 g (0.02 mole) of the cis diisocyanide was heated in a sealed tube at 320° (electric oven) for 3 minutes and cooled the resulting crystals melted at 89–97°. Crystallization from carbon tetrachloride and from 4:6 aqueous ethanol gave 2.91 g (85%) of rearranged product, m.p. 99.5–100.5°, unreactive toward bromine. In potassium bromide pellets (1/400) it absorbed at cm^{-1} as follows: 2970 (s), 2950 (s), 2880 (w), 2240 (s); 1465 (s), 1455 (m, shoulder), 1403 (w), 1395 (w), 1385 (m); 1282 (m), 1200 (m), 1180 (s). Calc. for $C_{10}H_{14}N_2$: C, 74.0; H, 8.69; N, 17.3. Found: C, 74.2; H, 8.79; N, 17.4.

trans-2,2,4,4-Tetramethylcyclobutane-1,3-diisocyanide

A. From Trans Diformamide

A finely ground suspension of 19.8 g (0.1 mole) of *trans*-2,2,4,4-tetramethylcyclobutane-1,3-diformamide (m.p. 256–257°) in 100 ml of barium-oxide-dried pyridine and 65 ml of petroleum ether (b.p. 40–60°) was ice-cooled and strongly stirred while 24 g (0.156 mole) of freshly distilled phosphorus oxychloride was added dropwise during 10 minutes. The cheese-like green suspension was heated subsequently for 1 hour at 55° and then was chilled while 200 ml of ice water was added. The solid and the non-aqueous phases were separated. The aqueous phase was repeatedly extracted with a total of 150 ml of petroleum ether (b.p. 40–60°). This extract was combined with the solid phase and the non-aqueous phase, and the whole was evaporated. The residue was digested with 1% hydrochloric acid, then with aqueous sodium bicarbonate, and finally with water.

Can. J. Chem. Downloaded from www.nrcresearchpress.com by 210.87.254.6 on 09/05/12
For personal use only.

When this crude product was dried it weighed 13 g (80%, m.p. 136–138°) and was almost soluble in 250 ml of hot commercial hexane. This solution yielded 11.2 g (69%) of colorless trans diisocyanide, m.p. 138–139°, in several crops when it was cooled and concentrated. Calc. for $C_{10}H_{14}N_2$: C, 74.0; H, 8.69; N, 17.3. Found: C, 74.0; H, 8.92; N, 17.3. The trans diisocyanide absorbed in 2% carbon tetrachloride solution as follows: 2960 (s), 2940 (m), 2880 (w), 2140 (s), 2065 (w), 1470 (s), 1460 (m), 1455 (m), 1329 (m), 1383 (m), 1352 (m), 1240 (w), 1190 (w), 998 (m), 977 (w), 954 (w).

B. By Chromatography of a Cis–Trans Mixture

A mixture of 50 mg each of the cis and trans diisocyanides was dissolved in 5 ml of benzene plus 5 ml of commercial hexane and was washed by the same solution onto 22 cm of alumina on a column 1 cm in diameter and 20 cm long (150–170 mesh activated 10 hours at 200° C). The column was washed with 150 ml of the same solution and then was developed with a solution of commercial hexane – ethyl acetate (50:1), which gave a first fraction, m.p. 57.5–58.5° C. A second fraction, m.p. 138–139°, was developed with pure ethyl acetate.

The trans diisocyanide, m.p. 138–139°, could be reconverted to the trans diformamide if it were heated (0.005 mole) in 8 ml of acetic acid for 5 minutes at 100°. A quantitive yield was obtained by vacuum evaporation of the solvent and crystallization of the residue from boiling water. A mixture melting point with original trans diformamide was not depressed.

Like the corresponding derivative of the cis diisocyanide, the tetrabromide of the trans diisocyanide was unstable, although the two were not identical (m.m.p. depressed). An 88% yield was obtained, m.p. 129–130°, when all but 5 ml of solvent was evaporated from the system comprised of 0.198 g diisocyanide, 40 ml of petroleum ether (b.p. 40–60°), and bromine in slight excess.

By contrast to the cis diisocyanide, exposure to ultraviolet light (max. 360 mμ) during a month did not depress the melting point of the trans diisocyanide.

trans-2,2,4,4-Tetramethylcyclobutane-1,3-dicyanide

When 1.62 g (0.01 mole) of trans diisocyanide (m.p. 138–139°) was heated in a sealed tube for 4 minutes at 310° (electric oven) it was converted to the dinitrile, m.p. 153–154° after crystallization from carbon tetrachloride and 4:6 water–ethanol. The product (yield 1.34 g, 83%) did not react with bromine in carbon tetrachloride. In potassium bromide pellets (1/400) it absorbed at the following cm^{-1}: 2970 (s), 2950 (m), 2880 (w), 2250 (m), 1470 (s), 1460 (m), 1395 (s), 1385 (s); 1205, 1188, 1177 (m) with no further absorption down to 650 cm^{-1}. Calc. for $C_{10}H_{14}N_2$: C, 74.0; H, 8.69; N, 17.3. Found: C, 73.8; H, 8.62; N, 17.2.

trans-2,2,4,4-Tetramethylcyclobutane-1,3-dicarboxylic Acid

A solution either of 3 g of *cis-* or *trans*-tetramethylcyclobutanedicyanide (0.018 mole) in 15 ml of 70% (w/w) sulphuric acid was boiled for 7 minutes. The cooled system was diluted with 20 ml of water, then was continuously extracted with diethyl ether. The ether solution, water washed to remove sulphuric acid and dried by use of magnesium sulphate, was evaporated to a volume of 25 ml, whereupon 2.2 g (59%) of crude trans acid, m.p. 264–266°, separated and was filtered off. Crystallization from water raised this melting point to 270–271.5° (sample introduced at 268°). Calc. for $C_{10}H_{16}O_4$: C, 60.0; H, 8.06. Found: C, 60.0; H, 8.19. The dimethyl ester, prepared by use of diazomethane, melts at 8–10° after crystallization from petroleum ether (b.p. 40–60°). Titration of an aqueous acetone solution gave a pK_A^1 of 6.60; the pK_A^2 value could not be observed.

cis-2,2,4,4-Tetramethylcyclobutane-1,3-dicarboxylic Acid

The ether filtrate from which the trans acid was isolated according to the procedure described above was evaporated to leave 1.2 g, m.p. 233–236°. Crystallization from water raised this m.p. to 235–236°. Calc. for $C_{10}H_{16}O_4$: C, 60.0; H, 8.06. Found: C, 59.8; H, 8.12. The dimethyl ester (from diazomethane) melted at 3–6° after crystallization from petroleum ether (b.p. 40–60°). The pK_A^1 found for an aqueous acetone solution was 6.78.

2,2,4,4-Tetramethylcyclobutane

The disemicarbazone of 2,2,4,4-tetramethylcyclobutanedione was prepared in 98% yield, m.p. 213 (decomp.) (23).

Into a solution prepared from 229 g (10 atom weight) of sodium and 2800 ml of diethylene glycol at 110° was added (at 130°) 305 g (1.2 mole) of the disemicarbazone, and the temperature was raised. At 155° nitrogen evolution commenced and continued during 45 minutes after the temperature had been raised to 210° during 30 minutes. The vapors were caught in a dry ice trap. Then 2 liters of water were added to the residue and it was steam-distilled.

The non-aqueous phase of steam distillations, the ether extract of the aqueous phases, and the trap condensates from five such experiments were combined, washed with 1% hydrochloric acid, dried by use of magnesium sulphate, and distilled (760 mm) to give 8 g b.p. 75–84°, 20 g b.p. 84–85°, and 50 g b.p. 85°. After this tetramethylcyclobutane had been separated (b.p. according to Herzog 86–87° at 745 mm) subsequent fractions were distilled off: 52 g b.p. 62–87° (42–38 mm), 176 g b.p. 96° (52 mm), 40 g b.p. 96–124° (52 mm), leaving a pot residue which crystallized but was discarded.

Can. J. Chem. Downloaded from www.nrcresearchpress.com by 210.87.254.6 on 09/05/12
For personal use only.

2,2,4,4-Tetramethylcyclobutanone

The 176 portion (conforming approximately with the b.p. 90–93° at 45 mm reported by Herzog from tetramethylcyclobutane hydrazone) represents a 23% yield of this substance. A solution of 155 g (1.1 mole) in 350 ml of conc. hydrochloric acid was shaken until a sample of the non-aqueous top phase did not diminish in volume when treated with fresh conc. hydrochloric acid nor did it produce cloudiness in the test-acid phase during 5 minutes. The top layer was then separated and was augmented by ether extractions of the aqueous phase. The combination (ether solution of the non-aqueous phase) was washed acid free by means of water, then dried by use of magnesium sulphate, and was distilled at 760 mm to yield 13 g b.p. 124–130.5° and 108 g b.p. 130.5–131°. This latter fraction (77% on the basis of hydrazone used) was redistilled and the distillate was allowed to crystallize (slowly) at about 19° C. The crystalline portion (100 g) with camphor-like odor melted at 19–21°, n_D^{20} 1.41425. This ketone, which boiled like that of Herzog (128.5–129° at 745 mm), absorbed in 1.4% carbon tetrachloride at cm^{-1} as follows: 2970 (s), 2900 (m), 1770 (s), 1470 (m), 1460 (m), 1390 (m), 1370 (m), 1290 (w), 1240 (w), 1200 (w), 1160 (w), 1028 (s), 910 (m). The 2,4-dinitrophenylhydrazone of this ketone melted at 114–115°. The ketone was recovered (80%) unchanged upon attempted conversion to the amine by means of the Leuckart reaction using a nickel catalyst (29).

2,2,4,4-Tetramethylcyclobutanone Oxime

A solution of 6.3 g (0.05 mole) of ketone in 50 ml of ethanol was treated with 3.8 g (0.055 mole) of hydroxylamine hydrochloride in 4.5 ml of water and 5 ml of pyridine. After 2 hours at 60° dilution with 200 ml of water gave 6.9 g (98%) of oxime, m.p. 88.5–89.7°. Crystallization by solution of 1 g in 10 ml of water plus 8.5 ml of methanol at 70° raised the melting point to 89–90°. The oxime was quite soluble in petroleum ether (b.p. 40–60°) and in diethyl ether. Calc. for $C_8H_{15}NO$: C, 68.0; H, 10.8; N, 9.92. Found: C, 68.2; H, 10.4; N, 9.65. A 2% solution in carbon tetrachloride showed the following absorption at cm^{-1}: 3620 (m); 3240, 3140 (s); 2980, 2950, 2860 (s); 1705 (m); 1465, 1455, 1440 (s); 1380, 1370, 1345 (m); 1230, 1197, 1162 (w); 1070 (m); 980 (w); 950, 930, 920, 893 (s).

2,2,4,4-Tetramethylpyrrolidine

A solution in 800 ml of absolute diethyl ether of 63.5 g (0.45 mole) of the oxime described above was added during 30 minutes to a stirred suspension of 29.2 g (0.77 mole) of lithium aluminum hydride. The suspension was refluxed for 8 hours. The now-light-grey and thickened suspension was stirred with 12 g (0.2 mole) of acetone and, after 1 hour, with 100 ml of water. The non-aqueous layer was separated and the aqueous layer was extracted by use of 50 ml of diethyl ether. The combination of non-aqueous phases was washed with a little water, and then with 5% hydrochloric acid. The aqueous acid layer was washed with a little ether, then was basified, and continuously extracted during 1 day by use of diethyl ether. The extract, dried by use of potassium carbonate, was fractionally distilled. The main fraction, b.p. 128–132°, weighed 30 g (53%). Calc. for $C_8H_{17}N$: C, 75.6; H, 13.47; N, 11.0. Found: C, 75.3; H, 13.5; N, 11.2.

This 2,2,4,4-tetramethylpyrrolidine is strongly basic and slightly soluble in water. Reactions with nitrous acid and with benzene sulphonyl chloride show that it is a secondary amine. In carbon tetrachloride solution it shows medium absorption at 3250, 3150, and 2680 cm^{-1}. It reacts with phenylisocyanate to give N-phenylcarbamyl-2,2,4,4-tetramethylpyrrolidine, m.p. 157–157.5°, after crystallization from petroleum ether (b.p. 90–100°, 0.45 g from 10 ml); from petroleum ether (b.p. 60–70) – chloroform, 1:1; from carbon tetrachloride; and from chloroform – petroleum ether (b.p. 90–100), 1:1. Calc. for $C_{15}H_{22}N_2O$: C, 73.1; H, 9.00; N, 11.4. Found: C, 73.0; H, 8.93; N, 12.0. The amine forms a picrate, m.p. 132–133.5°, and a *p*-nitrobenzoyl derivative, m.p. 184.5–186.5°.

2,2,4,4-Tetramethylcyclobutylamine

A solution of 11.3 g of the oxime (m.p. 88–89°) in 120 ml of absolute ethanol was saturated with ammonia at +5° and reduced by hydrogen using pelleted Raney nickel (British Drug House) from which the paraffin was removed by use of petroleum ether. The reduction was first carried out at 500 p.s.i. (90°) for 45 minutes and then at 14,000 p.s.i. (90°) for 3 hours. Stirring in the stainless steel container was effected magnetically with a bar constructed by vacuum shrinkage of Corning 7052 glass onto Kovar alloy which had previously been treated with hydrogen at 1100° C. The filtered system was then distilled through a 10-in. Vigreux column at atmospheric pressure, to obtain finally 1.2 g b.p. 80–134°, 0.4 g b.p. 134–136°, and 4 g b.p. 136°. The 0.2-g and 0.4-g portions were combined with the distilled ethanol from the original hydrogenation product, acidified with formic acid, and distilled, to give finally 2.8 g of the formamide described below, b.p. 246°. The total yield may thus be calculated as 63%, of which 4 g is free amine. The absorption spectrum of the amine in 7% solution in carbon tetrachloride was found in cm^{-1} to be: 3480 (w); 3200 (w); 2970, 2870 (s); 2750 (w); 1620 (m); 1470, 1455 (m), 1450 (m, shoulder); 1390 (w, shoulder); 1380 (w, shoulder); 1360 (m); 1290 (w), 1140 (m); 1110 (m); 1010 (w); 980 (w); 965 (m); 880 (m, broad). The amine evolved nitrogen on treatment with nitrous acid, formed the carbonate salt readily in air, and was insoluble in water or 5% aqueous sodium hydroxide but was readily soluble in 5% hydrochloric acid. Calc. for $C_8H_{17}N$: C, 75.3; H, 13.6; N, 11.0. Found: C, 74.9; H, 13.1; N, 10.4. The amine formed a picrate, m.p. 207°. It was converted into the phenylthiourea derivative in 97% yield, m.p. 151–154°. After two crystallizations from petroleum ether (b.p. 90–100°) and 1:1 ethanol–water this derivative melted at 153–154°. Calc. for $C_{15}H_{22}N_2S$: C, 68.6; H, 8.45; N, 10.7. Found: C, 68.5; H, 8.33; N, 10.8.

Can. J. Chem. Downloaded from www.nrcresearchpress.com by 210.87.254.6 on 09/05/12
For personal use only.

2,2,4,4-Tetramethylcyclobutylformamide

A solution of 3.8 g (0.03 mole) of tetramethylcyclobutylamine in 1.8 g (0.04 mole) was prepared with cooling and then was heated gradually to 205° to distill off formic acid and water. The residue was distilled at 242–245°. This distillate (4.1 g, 87%), m.p. 65–67°, was crystallized from petroleum ether, first of b.p. 40–60° and then of b.p. 90–100°, by chilling to −50°. Finally the formamide was sublimed, m.p. 68–68.8°. Calc. for $C_9H_{17}NO$: C, 69.6; H, 11.0; N, 9.02. Found: C, 69.4; H, 11.2; N, 8.77. The formamide, soluble in organic solvents but insoluble in water, showed the following absorptions in 1.5% carbon tetrachloride in cm^{-1}: 3460 (m), 3920 (m), 3210 (m), 3100 (m), 2960 (s), 2870 (s), 1690 (s), 1480 (s), 1460 (s), 1380 (s), 1370 (s), 1325 (m), 1300 (m), 1250 (m), 1235 (m), 1220 (m), 1190 (m), 1135 (m), 1070, 1028, 1015, 965, 878, 555 (w).

2,2,4,4-Tetramethylcyclobutylisocyanide

A procedure identical with those described above was effected using 6 g (0.04 mole) of the formamide, from which 2.9 g (60%) of isocyanide, b.p. 160° (m.p. −25.5 to −24.5°), was obtained, n_D^{20} 1.4506. It reacted with bromine in carbon tetrachloride. In 2% solution in carbon tetrachloride it showed the following absorptions at cm^{-1}: 2960, 2860 (s, with shoulder at 2850); 2140 (s); 1460, 1450, 1445 (m); 1380, 1370 (m); 1330, 1280, 1250, 1230, 1190, 1130, 1100, 1035, 1005, 970 (w). Calc. for $C_9H_{15}N$: C, 78.8; H, 11.0; N, 10.2. Found: C, 78.9; H, 10.9; N, 10.0. When 0.2 g of the isocyanide was boiled for 10 minutes in 2 ml of acetic acid it was recovered in 91% yield as the formamide, m.p. 65–67°, m.m.p. not depressed.

Electrical Measurements

The dielectric constants of solutions were determined in the customary manner (30). The apparatus described recently (31) was used for measurement of the dielectric constants of the nitriles and isonitriles in the solid state. Because of the unexpected lack of correlation among the measured distortion polarizations of the geoisomeric nitriles and isonitriles a large number of experiments were made. These data made it possible to examine the unexplained phenomenon that the slope of the linear plot of apparent dielectric constant with respect to pellet thickness for any substance is variable from run to run. When the extrapolated dielectric constants of a series of six separate determinations of terephthalonitrile were plotted against the slopes, ϵ/thickness, a reasonably linear relationship was found which showed that change in slope from 0.5 to 2.0 would cause a change in dielectric constant from 2.945 to 2.940. Therefore it appears that an uncontrolled error is present in the determination. However, the variation in dielectric constant shows that this error is less than that inherent in the overall determination of solid dielectric constant.

ACKNOWLEDGMENTS

The authors wish to thank the National Research Council and the Defence Research Board of Canada for financial aid. They are grateful to the Tennessee Eastman Company for aid with materials and n.m.r. analyses. They acknowledge valuable technical aid from Mr. Helmut Huber.

REFERENCES

1. T. P. Wilson. J. Chem. Phys. **11**, 369 (1943).
2. S. H. Bauer and J. Y. Beach. J. Am. Chem. Soc. **64**, 1142 (1942).
3. I. E. Coop and L. E. Sutton. J. Chem. Soc. 1269 (1938).
4. W. N. Lipscombe and V. Schomaker. J. Chem. Phys. **14**, 475 (1946).
5. J. D. Dunitz. Acta Cryst. **2**, 1 (1949).
6. H. H. Claassen. J. Chem. Phys. **18**, 543 (1950).
7. H. P. Lemaire and R. L. Livingston. J. Chem. Phys. **18**, 569 (1950).
8. W. W. Edyell and D. C. Weiblein. J. Chem. Phys. **18**, 571 (1950).
9. H. P. Lemaire and R. L. Livingston. J. Am. Chem. Soc. **74**, 5732 (1952).
10. J. D. Dunitz and V. Schomaker. J. Chem. Phys. **20**, 1703 (1952).
11. J. P. McHugh. Doctoral Dissertation, California Institute of Technology, Pasadena, Calif. 1957.
12. P. Podleschka, L. Westland, and G. F Wright. Can. J. Chem. **36**, 574 (1958).
13. Tennessee Eastman Company, Kingsport, Tennessee, U.S.A.
14. A. W. Hofmann. Ann. **144**, 114 (1867).
15. A. W. Hofmann. Ann. **146**, 107 (1868).
16. I. Ugi and R. Meyr. Ber. **93**, 239 (1961).
17. A. Gautier. Ann. Chim. (Paris), Ser. 4, **17**, 233 (1869).
18. J. U. Nef. Ann. **280**, 291 (1894).
19. F. Kaufler. Ber. **34**, 1578 (1901).
20. J. Wade. J. Chem. Soc. **81**, 1596 (1902).
21. W. H. Perkin, Jr. and J. L. Simonsen. J. Chem. Soc. **95**, 1176 (1909).
22. C. P. Smyth. Dielectric behavior and structure. McGraw-Hill, New York. 1955.
23. H. L. Herzog and E. R. Buchman. J. Org. Chem. **16**, 99 (1951).
24. C. C. Meredith, L. Westland, and G. F Wright. J. Am. Chem. Soc. **79**, 2385 (1957).

Can. J. Chem. Downloaded from www.nrcresearchpress.com by 210.87.254.6 on 09/05/12
For personal use only.

25. H. SAWATZKY and G. F WRIGHT. Can. J. Chem. **36**, 1555 (1958).
26. P. FRIEDLANDER and F. M. ROBERTSON. J. Chem. Soc. 3083 (1956).
27. R. H. HASEK, E. U. ELAM, J. C. MARTIN, and R. G. NATIONS. J. Org. Chem. **26**, 700 (1961).
28. D. H. WHIFFEN and H. W. THOMPSON. J. Chem. Soc. 1005 (1946).
29. A. N. KOST and J. J. GRANDBERG. J. Gen. Chem. USSR, **25**, 1377 (1955).
30. C. C. MEREDITH and G. F WRIGHT. Can. J. Chem. **38**, 1177 (1960).
31. M. BEDARD, H. HUBER, J. L. MYERS, and G. F WRIGHT. Can. J. Chem. **40**, 2278 (1962).

Can. J. Chem. Downloaded from www.nrcresearchpress.com by 210.87.254.6 on 09/05/12
For personal use only.

COORDINATION COMPOUNDS OF HYDRAZINE

PART III. THE INTERACTION OF SILICON TETRAFLUORIDE WITH HYDRAZINE[1, 2]

R. C. AGGARWAL[3] AND M. ONYSZCHUK
Department of Chemistry, McGill University, Montreal, Que.

Received November 28, 1962

ABSTRACT

Silicon tetrafluoride and hydrazine react in a vacuum to produce a white, non-volatile, solid, 1:2 complex, $SiF_4.2N_2H_4$. This compound sublimes with decomposition above 200° and is insoluble in common organic solvents. It reacts with (*a*) 55% hydrofluoric acid, (*b*) anhydrous hydrogen chloride, (*c*) ethylenediamine, (*d*) ammonia, and (*e*) boron trifluoride, producing: (*a*) $(N_2H_5^+)_2SiF_6^{2-}$, (*b*) $N_2H_5^+Cl^-$, (*c*) $SiF_4.NH_2(CH_2)_2NH_2$, (*d*) $SiF_4.2NH_3$, and (*e*) $BF_3.N_2H_4$. A comparison of the infrared spectra of $SiF_4.2NH_3$, $SiF_4.2N_2H_4$, and $SiF_4.NH_2(CH_2)_2NH_2$ suggests that all three complexes have cis octahedral structure.

Can. J. Chem. Downloaded from www.nrcresearchpress.com by 210.87.254.42 on 09/05/12
For personal use only.

INTRODUCTION

Both nitrogen atoms in hydrazine are electron-pair donors since each is capable of coordinating with borane (BH_3) (1, 2), boron trifluoride (3), or trimethylborane (4). With the object of obtaining further information about the donor activity of hydrazine, we have examined its interaction with silicon tetrafluoride, a powerful acceptor molecule.

The behavior of silicon tetrafluoride as a strong electron-pair acceptor arises from the tendency of silicon to increase its covalency from four to six by using two of its five vacant 4*d*-orbitals in octahedral bonding through sp^3d^2 hydridization. Monofunctional nitrogen donors such as ammonia (5), trimethylamine (6), pyridine (7), dimethylanaline (8), and cyclic amines (9) form complexes of the type $SiF_4.2$ donor; trimethylamine (6) and pyridine (10, 8) also produce 1:1 complexes. Ethylenediamine functions as a bidentate ligand in forming a 1:1 complex (11). The results reported in this paper reveal that hydrazine, conceivably a bidentate ligand, behaves only as a monodentate ligand towards silicon tetrafluoride, forming $SiF_4.2N_2H_4$, some properties of which are also reported.

RESULTS AND DISCUSSION

Preparation of $SiF_4.2N_2H_4$

An exothermic reaction occurred between SiF_4 and N_2H_4 in a vacuum at 60–70°, and a finely divided white powder with composition $SiF_4.2N_2H_4$ was the only product. This product resulted no matter which reactant was taken in excess initially. Tensimetric titration of N_2H_4 by addition of successive small amounts of SiF_4 to N_2H_4 (Fig. 1A), and the reverse titration (Fig. 1B) confirmed the 1:2 composition of the compound and showed conclusively the absence of a 1:1 complex.

Properties of $SiF_4.2N_2H_4$

The new compound $SiF_4.2N_2H_4$ is a white, non-hygroscopic solid which is insoluble in common organic solvents, such as ethanol, acetone, dimethylsulphoxide, acetonitrile, benzene, chloroform, carbon tetrachloride, and ethyl acetate. Its hydrolysis yielded a turbid solution due to precipitation of colloidal hydrated silica:

$$2(SiF_4.2N_2H_4) + (2+x)H_2O \rightarrow 4N_2H_5^+ + SiF_6^{2-} + 2F^- + SiO_2.xH_2O.$$

[1]*This work was supported by a grant from The Defence Research Board of Canada (Grant number 9530-20, Project D46-95-30-20).*
[2]*Part II: Can. J. Chem.* **39**, *2324 (1961).*
[3]*On leave from the Department of Chemistry, University of Lucknow, Lucknow, India.*

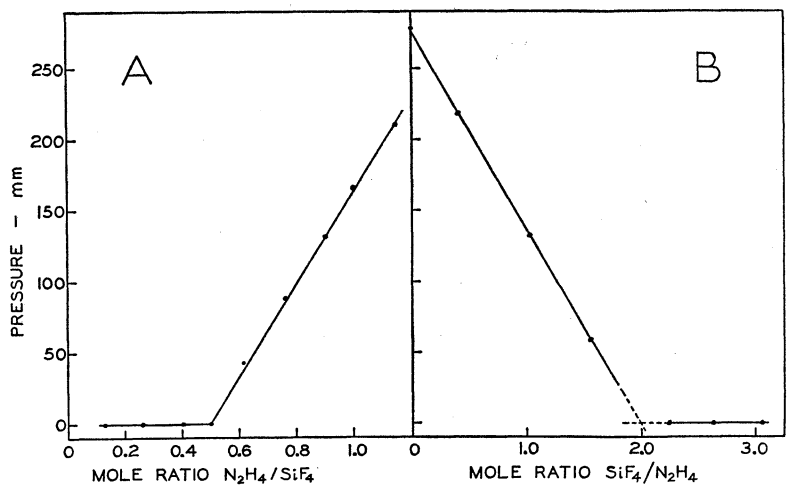

FIG. 1. Tensimetric titrations. A: SiF_4 added to N_2H_4; B: N_2H_4 added to SiF_4.

The compound $SiF_4.2N_2H_4$ sublimed slowly at 100° without measureable decomposition, and above 200° it decomposed (without melting) into nitrogen, ammonia, and an unidentified heterogeneous, non-volatile, white solid.

Hydrofluoric acid (55%) reacted almost quantitatively with $SiF_4.2N_2H_4$ according to the following stoichiometry:

$$SiF_4.2N_2H_4 + 2HF \rightarrow 2N_2H_5^+ + SiF_6^{2-}.$$

Anhydrous hydrogen chloride liberated SiF_4 almost completely from $SiF_4.2N_2H_4$, as expected in the reaction

$$SiF_4.2N_2H_4 + 2HCl \rightarrow 2N_2H_5^+ + 2Cl^- + SiF_4.$$

Ethylenediamine displaced hydrazine quantitatively from $SiF_4.2N_2H_4$:

$$SiF_4.2N_2H_4 + NH_2(CH_2)_2NH_2 \rightarrow SiF_4.NH_2(CH_2)_2NH_2 + 2N_2H_4.$$

This displacement is favored by an entropy increase due to a net increase in number of particles in going from reactants to products. Both complexes are octahedral as evident from their infrared spectra, which are discussed later. In the octahedral structure the following cis and trans arrangements of ligands are possible:

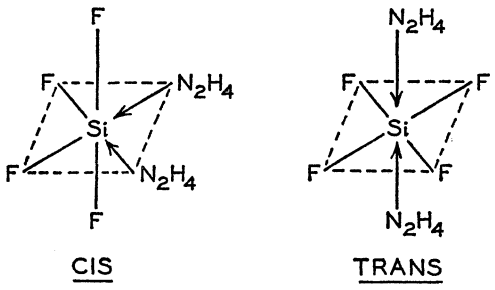

Silicon tetrafluoride – ethylenediamine must exist in the cis form because the distance between trans sites is greater than that which can be spanned by ethylenediamine. If

Can. J. Chem. Downloaded from www.nrcresearchpress.com by 210.87.254.42 on 09/05/12
For personal use only.

displacement of two hydrazines with one ethylenediamine does not occur with change of configuration, $SiF_4.2N_2H_4$ must also exist in the cis configuration.

Ammonia displaced hydrazine from $SiF_4.2N_2H_4$ to an extent of only 31%, whereas the reverse displacement, i.e. of NH_3 from $SiF_4.2NH_3$ by N_2H_4, was about 75% complete. These crude results show that the equilibrium constant at 150° in the following reaction,

$$SiF_4.2N_2H_4 + 2NH_3 \leftrightarrows SiF_4.2NH_3 + 2N_2H_4,$$

is less than unity. Silicon tetrafluoride – 2-hydrazine appears to be more stable than $SiF_4.2NH_3$. This is also indicated by the observation that $SiF_4.2NH_3$ dissociates rapidly above 80° (5), while $SiF_4.2N_2H_4$ does not dissociate or decompose appreciably below 200°.

Boron trifluoride displaced SiF_4 quantitatively from $SiF_4.2N_2H_4$ at 170°, and $BF_3.N_2H_4$ rather than $2BF_3.N_2H_4$ was formed:

$$SiF_4.2N_2H_4 + 2BF_3 \rightarrow 2(BF_3.N_2H_4) + SiF_4.$$

This suggests that BF_3 is a stronger electron-pair acceptor than SiF_4, but this will have to be verified by determination of the heats of formation of their hydrazine adducts. These measurements are now in progress.

Infrared Spectra

The infrared spectra of $SiF_4.2NH_3$, $SiF_4.2N_2H_4$, and $SiF_4.NH_2(CH_2)_2NH_2$ are shown in Fig. 2 and frequency assignments for the main bands are given in Table I together

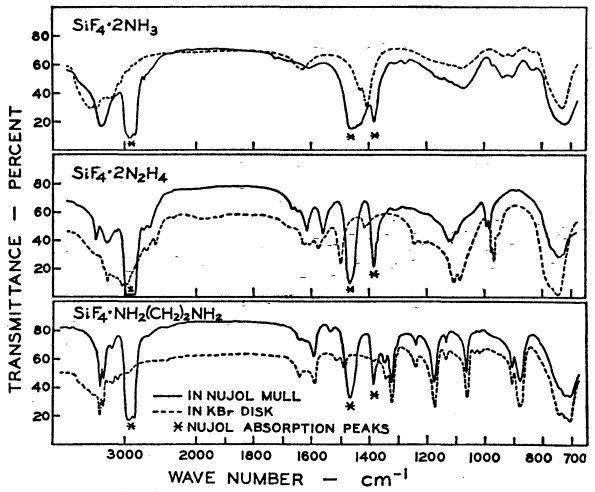

FIG. 2. Comparison of infrared spectra of $SiF_4.2NH_3$, $SiF_4.2N_2H_4$, and $SiF_4.NH_2(CH_2)_2NH_2$.

with those for gaseous ammonia (12), liquid hydrazine (13), and liquid ethylenediamine (14). There is surprisingly little difference between spectra taken in Nujol mulls and in KBr disks.

Transition metal amines show four principal absorption bands in the 4000–650 cm^{-1} range; these have been assigned to N—H stretching (3300–3200 cm^{-1}), degenerate NH_3 deformation (~1600 cm^{-1}), symmetric NH_3 deformation (~1300 cm^{-1}), and NH_3 rocking (~850 cm^{-1}) vibrations (15). In addition to a similar set of four bands, $SiF_4.2NH_3$ exhibits a strong, broad band at 725 cm^{-1}, which has been identified with stretching vibrations of Si—F bonds in octahedral positions (16). These vibrations occur 305 cm^{-1}

Can. J. Chem. Downloaded from www.nrcresearchpress.com by 210.87.254.42 on 09/05/12
For personal use only.

TABLE I

Comparison of infrared frequencies (cm^{-1}) and assignments

$SiF_4.2NH_3$	NH_3	$SiF_4.2N_2H_4$	N_2H_4	SiF_4.en	en*	Assignment
3500 to 3000 s, b	3378 3297	3395 to 2650 s, b	3350 to 3280 s, b	3335 m 3300 m 3180 w	3351 s 3277 s 3195 m	N—H stretching
				2930 w	2926 s 2857 s	C—H stretching
1610 vw	1646 1600	1667 m 1646 m 1616 s 1558 s	1628 s 1587 s	1642 w 1590 m 1533 w	1595 s	NH_2 bending
				1487 w	1456 m	CH_2 bending
1435 s 1408 vs 1387 m, sh	968 to 931	1498 s	1493 vw			NH_2 bending
				1343 m	1352 m	CH_2 twisting
				1318 s	1310 w	CH_2 wagging
			1275 w			NH_2 rocking
				1237 w 1173 s	1248 vw	NH_2 twisting
1070 m, b						Si—O impurity
		1118 s, vb 1092 m	1098 w			NH_2 rocking
				1132 w 1060 s	1095 m 1050 m	CN stretching
935 w 905 w		988 s 978 s 950 m, sh	966 s 933 s			Si—N stretching, NH_2 wagging, and N—N stretching
			850 s			N—N stretching
			780 s	903 s	902 vs	NH_2 wagging
				877 s	832 m	Unidentified
835 w						NH_3 rocking
725 s		765 s, sh 740 s		745 vs 725 vs 703 vs		Si—F cis octahedral stretching

Note: s = strong; m = medium; w = weak; b = broad; sh = shoulder; v = very.
*Represents ethylenediamine.

lower than the tetrahedral Si—F bond stretching mode in SiF_4 (17). The doublet at 935 and 905 cm^{-1} in the spectrum of $SiF_4.2NH_3$ might be due to asymmetric and symmetric Si—N stretching vibrations, respectively. A variety of compounds having Si—N bonds show bands in the 900–1000 cm^{-1} region which have been assigned to Si—N stretching vibrations (18–21). The 935 and 905 cm^{-1} doublet in $SiF_4.2NH_3$ strongly suggests that the complex has cis structure. If it were trans, only the asymmetric Si—N stretching mode would be infrared active and only one absorption band would appear. Alternatively, the observed splitting might be due to crystal lattice effects of the type described by Cotton (15, p. 372).

Except for some minor changes in position and intensity, absorption bands of hydrazine and ethylenediamine are easily recognized in their SiF_4 complexes. Like $SiF_4.2NH_3$, $SiF_4.2N_2H_4$ shows a doublet at 988 and 978 cm^{-1}, which probably results from stretching of Si—N bonds in cis positions, although this splitting might be due to crystal lattice

Can. J. Chem. Downloaded from www.nrcresearchpress.com by 210.87.254.42 on 09/05/12
For personal use only.

effects. Surprisingly, $SiF_4.NH_2(CH_2)_2NH_2$ does not show a similar doublet, unless it is masked by the bands at 903 and 877 cm^{-1} which are characteristic of ethylenediamine. Both $SiF_4.2NH_3$ and $SiF_4.2N_2H_4$ show the strong band near 740 cm^{-1} which is characteristic of Si—F octahedral bond stretching vibrations. If these complexes were trans octahedral, only one Si—F stretching mode would be infrared active and this would produce a single, presumably sharp absorption band near 725 cm^{-1}. By contrast, four Si—F stretching modes would be infrared allowed if the complexes had cis octahedral structure, and four bands would be expected in the 725 cm^{-1} region unless coupling of these vibrations occurred, in which case a broad, unresolved band would probably result. In each of the complexes in Fig. 2 the band near 725 cm^{-1} is broad and poorly resolved. A similar band appears at above 740 cm^{-1} in the spectra of SiF_4 – cyclic amine complexes reported recently by Gutmann *et al.* (9). Although the broadness and lack of detail in these bands might result from solid-state effects, at least in the case of $SiF_4.NH_2(CH)_2NH_2$, undoubtedly cis octahedral, the well-defined maxima in its broad 740 cm^{-1} band are probably associated with its cis structure. In the absence of any convincing evidence to the contrary, we believe that $SiF_4.2N_2H_4$, whose 740 cm^{-1} band shows some detail, also exists in the cis octahedral form. Additional evidence in support of the cis structure is provided by the replacement of two hydrazines by one ethylenediamine, as mentioned earlier. Unfortunately our complexes are insoluble and therefore other measurements such as dipole moment and F^{19} magnetic resonance cannot be made to test the validity of the cis structure for $SiF_4.2NH_3$ and $SiF_4.2N_2H_4$ that was suggested by our infrared data, which are not conclusive.

Muetterties (8) measured the F^{19} magnetic resonance spectra of some soluble octahedral SiF_4 complexes and found only a single resonance line in each case. This suggests trans octahedral structure because a cis configuration would give two triplets of equal intensity. This evidence is not conclusive, however, because fast ligand exchange might prevent detection of the cis form if it existed. Muetterties (22) concluded that the dimethylsulphoxide complexes $SiF_4.2(CH_3)_2SO$ and $GeF_4.2(CH_3)_2SO$ have trans octahedral structure because their infrared spectra show that the S—O stretching bands are not split into two, as they would be if the complexes were cis octahedral. He proposes that in octahedral Group IV tetrafluoride complexes the cis structure is stabilized by secondary π-bonding between acceptor and donor atoms, an effect which appears to be greater in the cis than in the trans form. Such bonding, he suggests, is not significant in SiF_4 complexes so that they are trans. This cannot be true in SiF_4 complexes with NH_3 and N_2H_4 which appear to be cis. Either hyperconjugative π-bonding is strong enough in these complexes to favor the cis form, or other factors are significant. One possibility is dipole–dipole interactions in the solid phase;* these would favor the cis form because its dipole moment is undoubtedly finite while that of the trans form is probably zero. If this effect is predominant, the preferred structure of SiF_4 complexes in the solid should be cis, but in solution they may be either cis or trans. The fact that Muetterties found some SiF_4 complexes to be trans in solution does not preclude the possibility that they might well be cis in the solid state.

Several Group IV tetrahalide complexes appear to exist in the trans form in the solid state. Titanium tetrahalide – nitrile complexes are thought by Rao (23) to be trans because their infrared spectra (as solids in Nujol mulls) do not show splitting of nitrile absorption bands. Brown and Kubota (24) have reported low-frequency infrared data which support a trans structure for solid $SnCl_4.2p\text{-}CH_3OC_6H_4CN$. X-Ray measurements

We are grateful to Dr. A. D. Westland of the University of Ottawa for this suggestion.

Can. J. Chem. Downloaded from www.nrcresearchpress.com by 210.87.254.42 on 09/05/12
For personal use only.

by Hulme *et al.* (25) reveal that the pyridine complex $GeCl_4.2NC_5H_5$ is trans octahedral, and infrared measurements (as solid deposits on NaCl plates) suggest that $SiCl_4.2NC_5H_5$ and $TiCl_4.2NC_5H_5$ are structurally similar. The reason for the preferred trans structure of these complexes in the solid phase is not obvious.

EXPERIMENTAL

The apparatus and techniques have been described in Part I of this series (3).

Anhydrous hydrazine was obtained by refluxing the 95+% material (Eastman Kodak) for several hours over sodium hydroxide pellets in an atmosphere of dry nitrogen. This was repeated three times with fresh sodium hydroxide pellets before the material was fractionally distilled. The fraction boiling in the range 111–113° was found to be 100% pure by the iodate method (26). Ethylenediamine (Eastman Kodak) was also purified by refluxing with sodium hydroxide pellets followed by fractional distillation in a vacuum; the pure fraction boiled at 117.0° (lit. (27) value 116.1°). Samples (Matheson) of SiF_4, BF_3, HCl, and NH_3 were purified by several low-temperature fractionations immediately before they were used. The purities of all volatile reagents were checked by vapor pressure (v.p.) and molecular weight (M) measurements.

Hydrazine was determined by the iodate method (26) and fluoride as lead chlorofluoride (28). Infrared spectral measurements were made in the range 4000–650 cm^{-1} using a Perkin–Elmer Model 21 spectrophotometer equipped with sodium chloride optics. Samples were examined in KBr disks or in Nujol mulls.

Preparation of $SiF_4.2N_2H_4$

(a) Using Excess SiF_4

When N_2H_4 (12.16 mmole) and SiF_4 (27.57 mmole) were condensed together in a vacuum and warmed to 70°, a vigorous exothermic reaction occurred, producing a finely divided white powder. The amount of SiF_4 (21.32 mmole), recovered by distillation of the product mixture at −130°, showed that SiF_4 (6.25 mmole) and N_2H_4 (12.16 mmole) had combined in a mole ratio of 1:1.95, corresponding to the complex $SiF_4.2N_2H_4$. (Found: N_2H_4, 37.8%; F, 45.4%. Calc. for $SiF_4.2N_2H_4$: N_2H_4, 38.11%; F, 45.18%.)

(b) Using Excess N_2H_4

Silicon tetrafluoride (26.85 mmole) and N_2H_4 (70.50 mmole) gave, on interaction in a vacuum at 70°, a white powder and unreacted hydrazine (16.70 mmole). The mole ratio of SiF_4 to N_2H_4 was 1:2.04, indicating the formation of $SiF_4.2N_2H_4$. (Found: N_2H_4, 38.3%; F, 45.0%. Calc. for $SiF_4.2N_2H_4$: N_2H_4, 38.11%; F, 45.18%.)

(c) Tensimetric Titrations

In the first series of measurements SiF_4 (25.57 mmole) was added in successive small portions to N_2H_4 (22.48 mmole); after each addition the reaction vessel was heated to 70° for 10–15 minutes before it was cooled to −78°, at which temperature pressure measurements were made. The results (Fig. 1A) show that the pressure remained zero until the mole ratio SiF_4/N_2H_4 was 0.5, corresponding to $SiF_4.2N_2H_4$; thereafter the pressure increased due to the excess SiF_4. In a second series of measurements, N_2H_4 (57.47 mmole) was added in successive small portions to SiF_4 (18.76 mmole) and pressure measurements were made as before. As shown in Fig. 1B, the pressure decreased linearly until the mole ratio SiF_4/N_2H_4 was exactly 2.0, when the pressure became zero. The pressure remained zero at higher ratios of N_2H_4/SiF_4 because the product, $SiF_4.2N_2H_4$, and excess N_2H_4 are involatile at −78°. The two titrations prove that the 1:2 complex is the only one formed by SiF_4 and N_2H_4.

Properties of $SiF_4.2N_2H_4$

(a) Thermal Decomposition

When $SiF_4.2N_2H_4$ (2.26 mmole) was heated for 20 hours at 230°, nitrogen (1.05 mmole; found: M, 27.2, calc. for N_2: M, 28.02) and ammonia (1.85 mmole; found: M, 17.2, calc. for NH_3: M, 17.05) were the only volatile products. The non-volatile residue was not homogeneous and no attempt was made to analyze it.

(b) Reaction with HF (55%)

Silicon tetrafluoride – 2-hydrazine (0.2744 g) was treated with 55% HF (3 ml) in a platinum crucible and the mixture heated to 100–110°. The residue was $(N_2H_5)_2SiF_6$ (found: N_2H_4, 30.3%; calc. for $(N_2H_5)_2SiF_6$: N_2H_4, 30.08%) in an amount (0.3405 g) which is slightly greater than expected (0.3397 g) for quantitative conversion of $SiF_4.2N_2H_4$ into $(N_2H_5)_2SiF_6$.

(c) Reaction with Anhydrous HCl

Anhydrous HCl (5.85 mmole) and $SiF_4.2N_2H_4$ (2.93 mmole) were heated together for 12 hours at 150°. The non-volatile product was N_2H_5Cl (found: N_2H_4, 46.6%, m.p. 90°, lit. m.p. (27) 89°; calc. for N_2H_5Cl: N_2H_4, 46.75%), and the volatile product (3.15 mmole; found: M, 94.3) was a mixture of SiF_4 (2.87 mmole) and HCl (0.46 mmole). These results indicate that there was a 91.8% conversion of $SiF_4.2N_2H_4$ into N_2H_5Cl.

(d) Reaction with Ethylenediamine

Anhydrous ethylenediamine (2.8636 g) and $SiF_4.2N_2H_4$ (0.4220 g) were refluxed for 24 hours, and then distilled. The amount of hydrazine (0.1603 g) in the distillate was almost exactly that expected (0.1608 g)

Can. J. Chem. Downloaded from www.nrcresearchpress.com by 210.87.254.42 on 09/05/12
For personal use only.

for quantitative displacement of N_2H_4 from $SiF_4.2N_2H_4$ by $NH_2(CH_2)_2NH_2$. The residue was $SiF_4.NH_2(CH_2)_2NH_2$. (Found: F, 46.5%. Calc. for $SiF_4.NH_2(CH_2)_2NH_2$: F, 46.35%.)

(e) Reaction with BF_3

A vigorous reaction occurred when $SiF_4.2N_2H_4$ (2.17 mmole) and BF_3 (11.28 mmole) were heated at 180° for 30 minutes. The volatile product (8.91 mmole; M, 75.7) was a mixture of SiF_4 (2.18 mmole) and BF_3 (6.73 mmole), and the residue was $BF_3.N_2H_4$ (found: N_2H_4, 31.9%, m.p. 86°, lit. m.p. (3) 87°; calc. for $BF_3.N_2H_4$: N_2H_4, 32.09%). Thus, SiF_4 was quantitatively displaced from $SiF_4.2N_2H_4$ by BF_3.

(f) Reaction with NH_3

The reaction of $SiF_4.2N_2H_4$ (2.73 mmole) with NH_3 (6.05 mmole) at 150° for 20 hours produced N_2H_4 (1.67 mmole), unreacted NH_3 (4.36 mmole), and a non-volatile, heterogeneous, white solid. Thus, 1.67 mmole of N_2H_4 was liberated by an equimolar amount (1.69 mmole) of NH_3, indicating that the displacement reaction $SiF_4.2N_2H_4 + 2NH_3 \rightarrow SiF_4.2NH_3 + 2N_2H_4$ had occurred to an extent of only 30.5%. In another experiment $SiF_4.2NH_3$ (1.85 mmole) and N_2H_4 (10.53 mmole) were heated for 20 hours at 150°, and NH_3 (2.78 mmole) was recovered from the product mixture. This indicated that the reverse displacement, i.e. of NH_3 from $SiF_4.2NH_3$ by N_2H_4, was 75.3% complete.

ACKNOWLEDGMENTS

We thank the Defence Research Board for financial assistance, and Mr. J. Guertin of this laboratory for several infrared measurements.

REFERENCES

1. H. J. Emeléus and F. G. A. Stone. J. Chem. Soc. 840 (1951).
2. M. J. Steindler and H. I. Schlesinger. J. Am. Chem. Soc. **75**, 756 (1953).
3. W. G. Paterson and M. Onyszchuk. Can. J. Chem. **39**, 986 (1961).
4. W. G. Paterson and M. Onyszchuk. Can. J. Chem. **39**, 2324 (1961).
5. D. M. Miller and H. H. Sisler. J. Am. Chem. Soc. **77**, 4998 (1955).
6. C. J. Wilkins and D. K. Grant. J. Chem. Soc. 927 (1953).
7. U. Wannagat and R. Schwarz. Z. Anorg. Allgem. Chem. **277**, 73 (1954).
8. E. L. Muetterties. J. Am. Chem. Soc. **82**, 1082 (1960).
9. V. Gutmann, P. Heilmayer, and K. Utvary. Monatsh. Chem. **92**, 322 (1961).
10. J. Goubeau and H. Grosse-Ruyken. Z. Anorg. Allgem. Chem. **264**, 240 (1951).
11. W. C. Schumb and P. S. Cook. J. Am. Chem. Soc. **75**, 5133 (1953).
12. G. Herzberg. Infrared and Raman spectra. Van Nostrand, New York. 1945. p. 295.
13. P. A. Giguère and I. D. Liu. J. Chem. Phys. **20**, 136 (1952).
14. A. Sabatini and S. Califano. Spectrochim. Acta, **16**, 677 (1960).
15. F. A. Cotton. *In* Modern coordination chemistry. *Edited by* J. Lewis and R. G. Wilkins. Interscience Publishers, Inc., New York, London. 1960. p. 362.
16. T. S. Piper and E. G. Rochow. J. Am. Chem. Soc. **76**, 4318 (1954).
17. E. A. Jones, J. S. Kirby-Smith, P. J. H. Woltz, and A. H. Nielson. J. Chem. Phys. **19**, 242 (1951).
18. E. A. V. Ebsworth, J. R. Hall, M. J. Mackillop, D. C. McKean, N. Sheppard, and L. A. Woodward. Spectrochim. Acta, **13**, 202 (1958).
19. E. A. V. Ebsworth, M. Onyszchuk, and N. Sheppard. J. Chem. Soc. 1453 (1958).
20. H. Kriegsmann and G. Engelhardt. Z. Anorg. Allgem. Chem. **310**, 320 (1961).
21. U. Wannagat and H. Niederprüm. Z. Anorg. Allgem. Chem. **308**, 337 (1961).
22. E. L. Muetterties. *In* Advances in the chemistry of the coordination compounds. *Edited by* S. Kirschner. The Macmillan Co., New York. 1961. p. 509.
23. G. S. Rao. Z. Anorg. Allgem. Chem. **304**, 351 (1960).
24. T. L. Brown and M. Kubota. J. Am. Chem. Soc. **83**, 4175 (1961).
25. R. Hulme, G. J. Leigh, and I. R. Beattie. J. Chem. Soc. 366 (1960).
26. L. F. Audrieth and B. A. Ogg. The chemistry of hydrazine. John Wiley and Sons, Inc., New York. 1951. p. 159.
27. Handbook of Physics and Chemistry. 41st ed. Chemical Rubber Publishing Co., Cleveland, Ohio. 1959.
28. R. Belcher and J. Tatlow. Analyst, **76**, 593 (1951).

Can. J. Chem. Downloaded from www.nrcresearchpress.com by 210.87.254.42 on 09/05/12
For personal use only.

THE STRUCTURE OF STRYCHNOSPERMINE EVIDENCE FROM DOUBLE IRRADIATION AND VARIABLE TEMPERATURE N.M.R.

F. A. L. ANET
Department of Chemistry, University of Ottawa, Ottawa, Ontario
Received October 26, 1962

ABSTRACT

The nuclear magnetic resonance spectrum of strychnospermine has been measured at −20°, room temperature, and at +80°. The changes observed are attributed to restricted rotation in the *N*-acetyl group. At room temperature the rate of rotation is such that the band of one aromatic proton is extremely broad and therefore almost invisible. Double irradiation has been used to determine the environment of the *C*-methyl group of the alkaloid. The n.m.r. results confirm the structure previously postulated.

In a previous paper (1) structures I and II respectively were proposed for spermostrychnine and strychnospermine, two alkaloids isolated (2) from *Strychnos psilosperma.* Although the two alkaloids were chemically related to each other and to strychnine, two features, apart from the stereochemistry, remained uncertain, namely the exact position of the cyclic ether ring, and, for strychnospermine, that of the methoxyl group. The

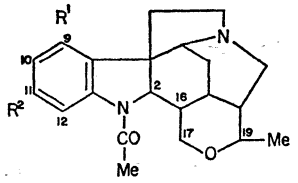

I, $R^1 = R^2 = H$
II, $R^1 = H$, $R^2 = OMe$
III, $R^1 = OMe$ $R^2 = H$

cyclic ether was placed largely on biosynthetic arguments which were not above objections. The methoxyl group of strychnospermine was found to be definitely meta to the nitrogen atom, but the choice between the two alternatives (II and III) was made solely on the basis of minor differences in the ultraviolet spectra and color reactions of the alkaloids and of model compounds of known structures.

In order to try to settle these uncertainties, the high-resolution proton magnetic resonance spectra of the alkaloids were studied. Since the coupling constants in benzenoid compounds vary (3) as follows: $J_{ortho} \sim 8$ c.p.s., $J_{meta} \sim 2$ c.p.s., $J_{para} \sim 0$ c.p.s., the determination of the substitution pattern (II or III) in strychnospermine should be straightforward, provided there is sufficient chemical shift between the aromatic protons that the coupling constants can be measured.

The n.m.r. spectrum of strychnospermine in deuterated chloroform at room temperature is shown in Fig. 1. The doublet at 8.83 τ confirms the presence of a single methyl group, and shows that the adjacent carbon atom bears a single hydrogen atom. Certain features of this band will be discussed later in this paper. The acetyl methyl and the *O*-methyl groups appear as sharp bands at 7.63 τ and 6.23 τ respectively, as expected (4).

Can. J. Chem. Downloaded from www.nrcresearchpress.com by 210.87.254.40 on 09/05/12
For personal use only.

Can. J. Chem. Downloaded from www.nrcresearchpress.com by 210.87.254.40 on 09/05/12
For personal use only.

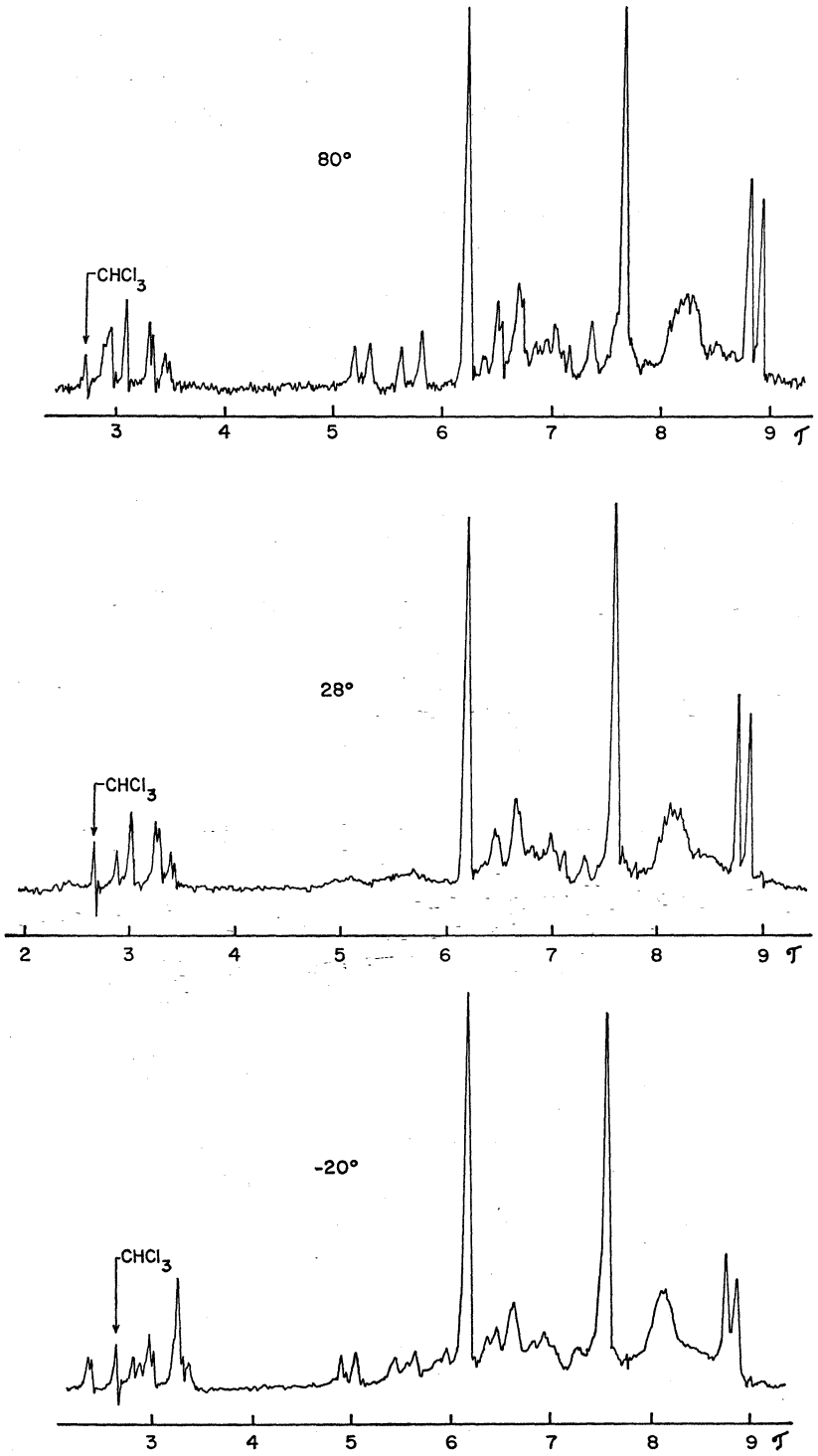

FIG. 1. Nuclear magnetic resonance spectra (60 Mc/sec) of strychnospermine in deuterated chloroform at various temperatures. The scale (3) is in tau units (p.p.m.). Tetramethylsilane was used as an internal standard. Spectra were measured on a high-resolution Varian spectrometer.

The aromatic region of the spectrum is, on the other hand, quite puzzling. Superficially, the bands around 3 τ have the appearance of two protons coupled together by about 8 c.p.s. with the upfield proton further coupled to a third proton by about 2 c.p.s. Unfortunately, there is no sign of bands for this third aromatic proton. To the extent that the spectrum can be interpreted, structure II is supported over structure III, but calculations of ABC spectra show that no theoretical spectra can be matched to the observed bands in the aromatic region.

One possibility is that the band of the third proton is so broad as not to be visible. This can be the case, for example, if the proton is coupled to the nitrogen atom of the dihydroindole ring. The broadening can then be due to quadrupole relaxation, provided this is of the correct magnitude, and that the coupling constant is sufficiently large. Although the α protons of pyridine have been found (5) to be very slightly broadened by such a mechanism, the coupling required in the present case seems to be unreasonably great. This possibility can in fact be eliminated since it is found that the spectrum is unchanged by double irradiation at the nitrogen resonance frequency.

Another reason for broadening can be the presence of the *N*-acetyl group. For example, in *N*,*N*-dimethylacetamide at room temperature, two different methyl signals are observed (6, 7) because of restricted, and hence slow, rotation about the N—CO bond. As the temperature is raised, the two bands become broad and finally coalesce. At still higher temperature, when the rate of rotation about the nitrogen–carbonyl bond has become sufficiently high, only a single, sharp band is observed. Such effects have not been observed in *N*-methylacetanilide (6), but it is not known whether the reason is that the barrier to rotation is too low or whether one conformation is so much more stable that practically none of the compound exists in the alternative conformation. A lower barrier than that in the aliphatic amides would be expected because the resonance interaction of the nitrogen lone pair of electrons with the benzene ring would decrease the amount of double-bond character in the N—CO bond.

Since the bands of the three methyl groups and two aromatic protons of strychnospermine were normal in appearance, it was at first considered that restricted rotation was unlikely as an explanation for the missing third aromatic proton. Nevertheless, measurements of the spectrum at various temperatures clearly reveal that restricted rotation is responsible for the anomalies previously mentioned in the room-temperature spectrum and confirm structure II for strychnospermine. Owing to a remarkable coincidence, the chemical shifts of the three methyl groups and of two aromatic protons change very little on going from one conformation of the *N*-acetyl group to the other. Thus (7) these bands are sharp at room temperature.

As the temperature is lowered, the n.m.r. spectrum of strychnospermine changes greatly. At about $-20°$, the spectrum (Figs. 1 and 2) is no longer changing, and at this temperature, therefore, the two conformations are 'frozen'. What is observed is now the superposition of two spectra, which can be interpreted, in part at least, when taken in conjunction with the high-temperature spectrum described below.

The doublet at 2.35 τ can be assigned to H-12 of conformation A; the low-field position is consistent with the strong magnetic anisotropy of the carbonyl group (3, 8). The band is a doublet ($J \sim 2.3$ c.p.s.) because of coupling with H-10. The band of the same proton in conformation B lies at about 3.25 τ but cannot be seen clearly because of overlap with H-10. H-9 has only slightly different chemical shifts in the two conformations and gives rise to the two overlapping, widely spaced doublets near 2.9 τ as a result of a coupling of ca. 8 c.p.s. to H-10 and practically zero coupling to H-12. The bands (Fig. 2) of H-10

Can. J. Chem. Downloaded from www.nrcresearchpress.com by 210.87.254.40 on 09/05/12
For personal use only.

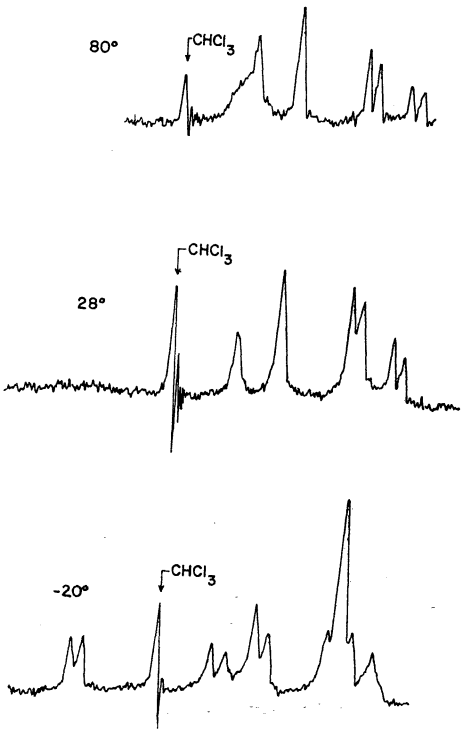

FIG. 2. Nuclear magnetic resonance spectra of the aromatic protons of strychnospermine in deuterated chloroform at various temperatures. The sweep rate is about the same for the three tracings.

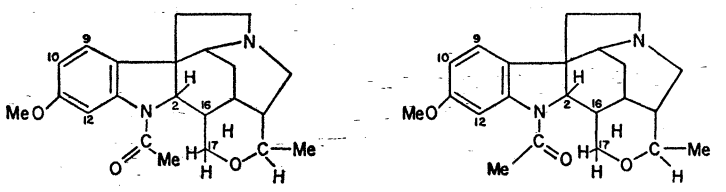

cannot be clearly analyzed because of overlap with part of H-12 and because the splitting pattern would in any case be expected to be complicated. In both conformations the chemical shift of H-10 is about 3.25 τ.

The bands of the methyl groups show practically no change with temperature. This is especially unexpected for the band of the acetyl group, in view of the large magnetic anisotropy of the benzene ring, which should cause a low-field shift of the methyl group in conformation B. The other *C*-methyl group does show slight broadening compared to the room-temperature band and this may be due to a small unresolved chemical shift in the two conformations.

As the temperature is raised from −20°, gradual changes take place, the first being a loss in the doublet character associated with the H-12 of conformation A and the chemical shift difference between H-9 in the two conformations. These changes take place at low temperatures because they involve averaging over only a few c.p.s. At room temperature

Can. J. Chem. Downloaded from www.nrcresearchpress.com by 210.87.254.40 on 09/05/12
For personal use only.

the band of H-12 is almost uniformly spread out over about 55 c.p.s., so that it is not surprising that it is almost completely obscured.

At 80°, the spectrum (Figs. 1 and 2) has become simpler, since rotation around the N—CO bond is now fast enough to cause almost complete averaging of all the protons of the two conformations. H-12 is now a single, rather broad band and at still higher temperatures it should become a sharp doublet (separation, ca. 2 c.p.s.), but measurements were not made above 80°. H-10 and H-11 give the expected bands, reminescent of those found at room temperature, but now of the correct intensities. These results are clearly consistent with structure II but not with III.

The bands at 4.8 to 6.0 τ also show interesting changes with temperature. The low-temperature spectrum is rather difficult to interpret because of superposition of bands. At room temperature all the bands in this region are extremely broad, but at 80° just two doublets of one proton each are left. The lower-field doublet (5.2 τ) (separation 8.7 c.p.s.) can be assigned to H-2, as this should be at quite low field. In *Aspidosperma* alkaloids (9), where H-2 is in a similar environment to the above, the chemical shift is about 5.5 τ. If the stereochemistry is similar to that of strychnine (10), this proton is axial and vicinal to another axial proton (H-16), in keeping with the large coupling constant found.

The other doublet at 5.71 τ (separation 11.3 c.p.s.) is assigned to one of the protons on C-17. Such a proton should show a large (geminal) coupling to the other proton on C-17 and might well show (3) a negligible coupling to H-16 provided that the dihedral angle between the CH bonds lies in the range 70–100°. Its rather low-field position is consistent with the attachment of an oxygen atom to C-17 and to the nearness in space of H-17 to the *N*-acetyl group. The skewness of the intensity of the band is also consistent with coupling to a proton on the same carbon atom and therefore not greatly chemically shifted.

A further confirmation of the position of the cyclic ether ring can be obtained from the *C*-methyl band. The two components of the doublet at 8.83 τ are nearly equal in intensity, suggesting that the proton to which the methyl group is coupled is well downfield, and thus that the methyl group is attached to a carbon atom bearing an electronegative substituent as well as a proton. Although the proton in question cannot be seen, its chemical shift can be determined precisely by double irradiation ("spin decoupling") (11). Thus the proton is found to be at 6.41 τ (145 c.p.s. from the methyl band) in agreement with II but not with a *C*-methyl group in the environment of partial structure IV.

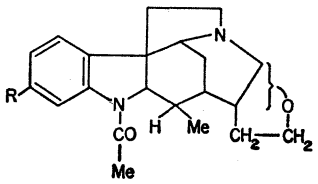

IV

The spectrum of spermostrychnine was studied only at room temperature. Apart from the aromatic region and the lack of a methoxyl band, it is identical with the spectrum of strychnospermine. The aromatic region consists of a single, not very sharp band, as expected.

Can. J. Chem. Downloaded from www.nrcresearchpress.com by 210.87.254.40 on 09/05/12
For personal use only.

The present results show that the n.m.r. spectra of natural products can yield valuable information if taken at different temperatures, and that techniques such as "spin decoupling" are useful.

REFERENCES

1. F. A. L. ANET and R. ROBINSON. J. Chem. Soc. 2253 (1955).
2. F. A. L. ANET, G. K. GUGHES, and E. RITCHIE. Australian J. Chem. **6**, 58 (1953).
3. L. M. JACKMAN. Applications of nuclear magnetic resonance spectroscopy in organic chemistry. Pergamon Press, New York. 1959.
4. N. S. BHACCA, L. F. JOHNSON, and J. N. SHOOLERY. NMR spectra catalog. Varian Associates, Palo Alto. 1962.
5. J. D. BALDESCHWIELER and E. W. RANDALL. Proc. Chem. Soc. 303 (1961).
6. H. S. GUTOWSKY and C. H. HOLM. J. Chem. Phys. **25**, 1228 (1956).
7. J. A. POPLE, W. G. SCHNEIDER, and H. J. BERNSTEIN. High-resolution nuclear magnetic resonance. McGraw-Hill Book Co. Inc., New York. 1959.
8. L. CROMBIE and J. W. LOWN. Proc. Chem. Soc. 299 (1961).
9. C. DJERASSI, H. W. BREWER, H. BUDZIKIEWICZ, O. O. ARAZI, and R. E. CORRAL. J. Am. Chem. Soc. **84**, 3480 (1962).
10. J. H. ROBERTSON and C. A. BEEVERS. Acta Cryst. **4**, 270 (1951).
11. S. L. MANATT and D. D. ELLEMAN. J. Am. Chem. Soc. **83**, 4095 (1961).

Can. J. Chem. Downloaded from www.nrcresearchpress.com by 210.87.254.40 on 09/05/12
For personal use only.

THE β-D-CONFIGURATION OF THE RIBOSYL NICOTINAMIDE PORTION OF DIPHOSPHOPYRIDINE NUCLEOTIDE

R. U. LEMIEUX AND J. W. LOWN[1]
Department of Chemistry, University of Alberta, Edmonton, Alberta
Received October 9, 1962

ABSTRACT

The configurations of the anomeric *N*-(tetra-*O*-acetyl-D-glucopyranosyl)-3-carboxamidopyridium bromides were established by nuclear magnetic resonance (n.m.r.) spectroscopy. The β-D-anomer was found to undergo deacetylation without anomerization. This compound on oxidation with periodate has been shown (M. Viscontini and E. Hürzeler-Jucker. Helv. Chim. Acta, **39**, 1620 (1956)) to yield a different product than did a synthetic *N*-(D-ribofuranosyl)-3-carboxamidopyridinium chloride. Therefore, the anomeric configuration of the latter compound must be α-D. Since its anomer was used (N. A. Hughes, G. W. Kenner, and A. Todd. J. Chem. Soc. 3733 (1957)) to synthesize diphosphopyridine nucleotide (DPN), the configuration of the anomeric center in this portion of the coenzyme must be β-D. Optical rotatory dispersion curves are reported for DPN, its component nucleotides, and the above-mentioned D-glucosides.

Can. J. Chem. Downloaded from www.nrcresearchpress.com by 210.87.254.5 on 09/05/12
For personal use only.

Because of its great biological importance, considerable interest attaches to the structure and configuration of diphosphopyridine nucleotide. The gross structure is well known and has been confirmed by synthesis (1, 2). However, the anomeric configuration of the ribosyl nicotinamide portion has remained an open question. The currently held view that the configuration is β-D rests on the following work by Todd and his co-workers (2). The anomeric *N*-(D-ribofuranosyl)-3-carboxamidopyridinium salts were known, the α-anomer having a specific rotation (D-line of sodium) of +49° (3) and the β-form −28° (1). DPN was synthesized (2) from a mixture of the α- and β-anomers of *N*-(D-ribofuranosyl)-3-carboxamidopyridinium chloride assumed to be present in a 1:4 ratio from arguments based on optical rotation. Since purified synthetic DPN was obtained in about 20% yield and had an active coenzyme content of 90%, it could be concluded that it had formed from the levorotatory D-ribofuranoside which was assigned to the β-series of anomers on the basis of Hudson's rules of isorotation (4). It was tentatively assumed to possess the 1,2-*trans*-configuration by analogy to the structure – optical activity correlations now well established for *O*-glycofuranosides (5). However, it has been recently shown (6) that pyrimidine deoxyribofuranosides may have rotations opposite to those expected on the basis of these rules. It has also been observed[2] that the tri-*O*-acetyl-2-deoxy-2-iodo derivatives of the β-D-glucopyranosyl and α-D-mannopyranosyl pyridinium perchlorates have specific rotations of +157°, +298°, +604°, +1270°, and +1740° for the β-D-isomer and of −4°, −4°, −92°, −380°, and −650° for the α-D-compound at wavelengths of 590, 450, 350, 300, and 280 mμ, respectively. Although these compounds are not anomers, as was found for thymidine and its α-anomer (6), the optical rotatory dispersion trends are definitely opposite to those which would be expected on the basis of Hudson's rules of isorotation. Thus, it can be anticipated that the anomers for these pyranosides, which have an absorbing group attached directly to the anomeric center, may well provide further exceptions to Hudson's rules of isorotation. Clearly, therefore, care must be exercised in the application of these empirical rules for structure – optical activity correlations. As it was pointed out by Todd *et al.* (2), the conclusion,

[1]*University of Alberta Postdoctoral Fellow, 1961–1962.*
[2]*Unpublished results by R. U. Lemieux and A. R. Morgan.*

reached by Viscontini and Hürzeler-Jucker (3) to the effect that the D-ribofuranosyl nicotinamide with rotation +49° possesses the β-configuration, is defective in several respects and can be neglected. As will be seen below, the assignment of the α-configuration to a synthetic D-glucopyranosyl nicotinamide was erroneous and the convention proposed for the assignment of the α- and β-designations to *N*-glycosides which is based on the sign of rotation of the product of oxidation by periodate should be abandoned.

There exists no direct evidence for the assignment of configuration on the basis of optical rotation for *N*-glycosides wherein the nitrogen is quaternized. It is now well established (7, 8) that the n.m.r. signal for the anomeric hydrogen often can be used to unequivocally establish anomeric configurations, since the anomeric hydrogen is generally considerably shifted from the envelope of other C—H resonances and the spin–spin splitting can be related to dihedral bond angle by employing the Karplus relation (9). The purpose of this communication is to demonstrate such an application in the determination of the configurations of the anomeric D-glucopyranosyl derivatives of nicotinamide. Published information (2, 3) could then be used to correlate the configurations of these compounds to the natural D-ribofuranosyl nicotinamide.

The *N*-(tetra-*O*-acetyl-D-glucopyranosyl)-3-carboxamidopyridinium bromides were prepared as described by Haynes and Todd (10). The product (I) which formed in preponderance could be purified simply by recrystallization. The mother liquors provided a residue the n.m.r. spectrum of which required the material to be a roughly equimolar mixture of I and its anomeric form. Repeated partition chomatography and fractional crystallization provided a pure compound (II) with the n.m.r. spectrum expected for the anomer of I.

Compound I, $[\alpha]_D$ −20.5°, provided the n.m.r. spectrum in Fig. 1A. The doublet of intensity one at 6.46 p.p.m. has a spacing of 9 c.p.s. Since the anomeric proton forms part of a strongly coupled system of protons extending around the pyranose ring, one may legitimately question whether the observed spacing reflects the true coupling constant between the protons at the 1- and 2-positions. In fact, such a spacing is influenced by "second order" effects (11, 12) so that, for example, if the protons at the 1,2- and 3-positions form a strongly coupled set, the spacing of the proton is dependent upon the ratio of the chemical shift between the 2- and 3-protons and their coupling constant. The spacing will approximate the true coupling constant more closely the larger the ratio becomes. If this system is regarded as an AMX then the theory of the system (13) states that the separation of the centers of gravity of the two main groups of lines comprising the X branch corresponds to J_{AX}. Therefore, an estimate of the centers of gravity of the two branches of the doublet for the anomeric center may be safely regarded as a *minimum* value of $J_{1,2}$. This is an important consideration when doublet spacings are used to decide anomeric configuration.

In the case of compound I, it is clear that $J_{1,2}$ is approximately 9 c.p.s. Since the compound has a six-membered ring, this value requires the 1- and 2-hydrogens to define a dihedral angle of about 180° (9). Therefore, the compound possesses the β-D-configuration as shown in Fig. 1A. Compound II, $[\alpha]_D$ +22.1°, provided the n.m.r. spectrum shown in Fig. 1B. The doublet of intensity one at 7.06 p.p.m. can be assigned to the anomeric hydrogen. The spacing of 3 c.p.s. requires a dihedral angle of about 60° and the substance therefore possesses the α-D-*gluco*-configuration.

Compounds I and II were deacetylated to afford the β- and α-anomers (III and IV, respectively) for *N*-(D-glucopyranosyl)-3-carboxamidopyridinium bromide. The n.m.r. spectra for these compounds are in obvious agreement with the structures shown in Fig. 2.

Can. J. Chem. Downloaded from www.nrcresearchpress.com by 210.87.254.5 on 09/05/12
For personal use only.

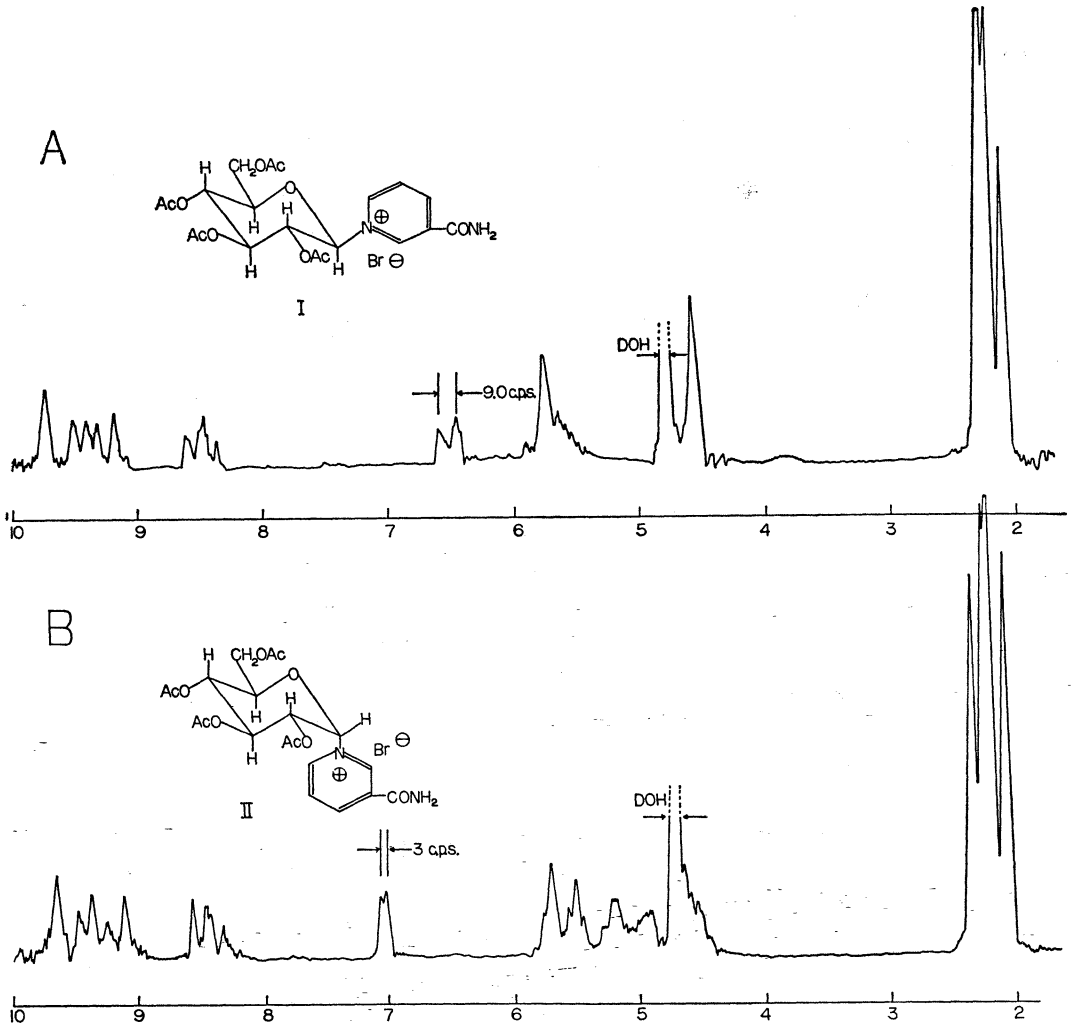

FIG. 1. Nuclear magnetic resonance spectra measured in deuterium oxide and the chemical shifts expressed in p.p.m. from the signal for tetramethylsilane as external reference. A. *N*-(Tetra-*O*-acetyl-β-D-glucopyranosyl)-3-carboxamidopyridinium bromide (I). B. *N*-(Tetra-*O*-acetyl-α-D-glucopyranosyl)-3-carboxamidopyridinium bromide (II).

Thus, the deacetylations proceeded without complication and the configuration of the products are those shown in Fig. 2. It is well established (7) that, for anomeric structures, barring the presence of unusually large screening effects, the axial anomeric proton resonates at higher field than does the equatorial proton. The greater shielding of the axial proton most likely arises from the diamagnetic anisotropy of C—C and C—O bonds in gauche relationship (7, 14). The above configurational assignments are consistent with this finding.

The n.m.r. spectra of DPN and DPNH are shown in Fig. 3. One of the doublets of intensity one at about 6 p.p.m. in the spectrum for DPN can be assigned to the anomeric proton of the ribose residue which is bonded to the pyridine base since one of these signals disappeared on reduction to DPNH. The anomeric configuration cannot be assigned directly from the observed spacing (4 or 5 c.p.s.) since coupling constants of this

Can. J. Chem. Downloaded from www.nrcresearchpress.com by 210.87.254.5 on 09/05/12
For personal use only.

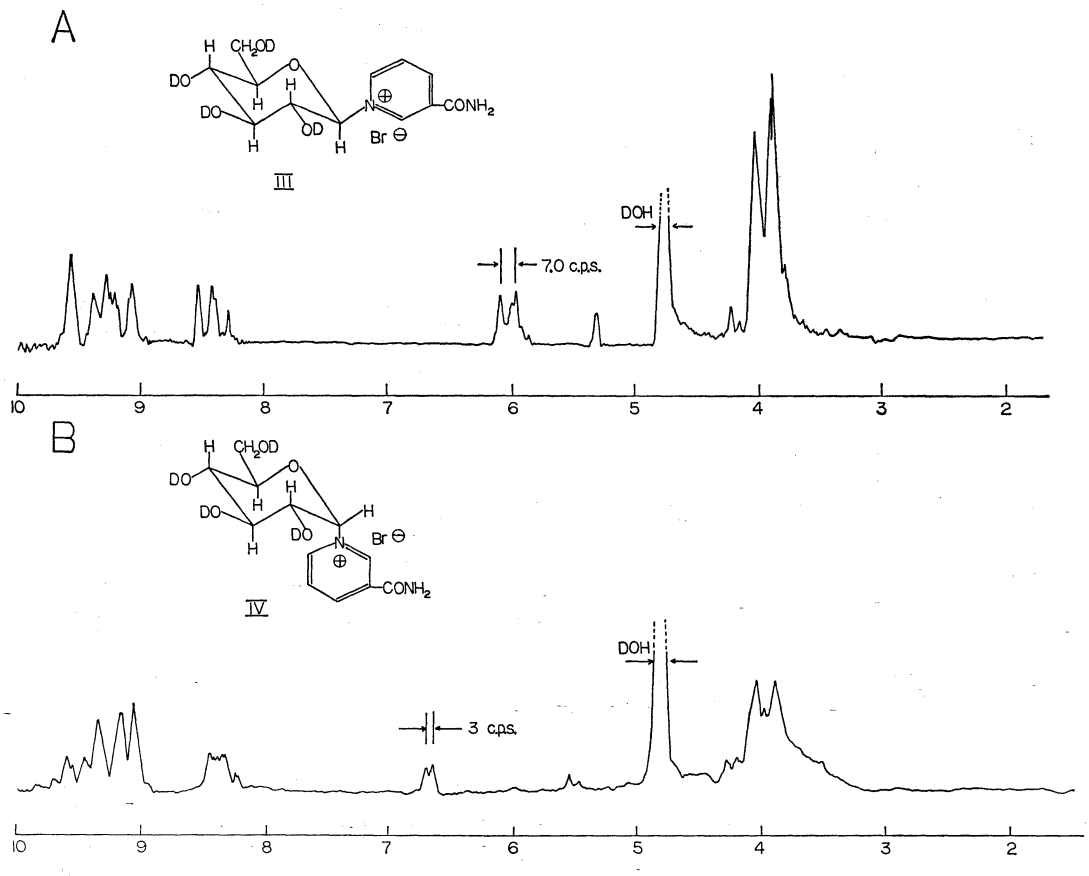

FIG. 2. Nuclear magnetic resonance spectra measured in deuterium oxide and the chemical shifts expressed in p.p.m. from the signal for tetramethylsilane as external reference. A. *N*-(β-D-Glucopyranosyl)-3-carboxamidopyridinium bromide (III). B. *N*-(α-D-Glucopyranosyl)-3-carboxamidopyridinium bromide (IV).

magnitude can arise from structures wherein the 1- and 2-hydrogens define dihedral angles of either about 40° or 140°. The 40° angle is readily possible for the hydrogens in either cis or trans relationships on a flexible five-membered ring (15). In fact, for cis-neighboring hydrogens, coupling constants in the range $J_{0°} \cong 8$ to $J_{46°} \cong 3$ c.p.s. can be reasonably expected. When the configurational relationship is trans, the coupling constants can fall in the range $J_{166°} \cong 9$ to $J_{74°} \cong 0.2$ c.p.s. Thus, a direct assignment of configuration can only be made when the coupling constant is very small (in view of the evidence (16) that the Karplus curve is subject to vertical displacements of at least 2 c.p.s., only values less than 1 c.p.s. should be taken as indicative of the trans configuration (17)). These considerations would of course not apply should it be possible to predict with reasonable certainty the conformations of anomeric furanosides.

Viscontini and Hürzeler-Jucker (3) oxidized the compound now known to be III with periodic acid to form a dialdehyde product with a specific rotation of +67°. We have confirmed this result. The periodic acid oxidation of a *N*-(D-ribofuranosyl)-3-carboxamidopyridinium chloride preparation with rotation of +49° provided (3) a dialdehyde with a specific rotation of −70°. Since both dialdehydes were derived from D-sugars, the diastereoisomeric compounds differ only in the configuration of the anomeric center. Since

Can. J. Chem. Downloaded from www.nrcresearchpress.com by 210.87.254.5 on 09/05/12
For personal use only.

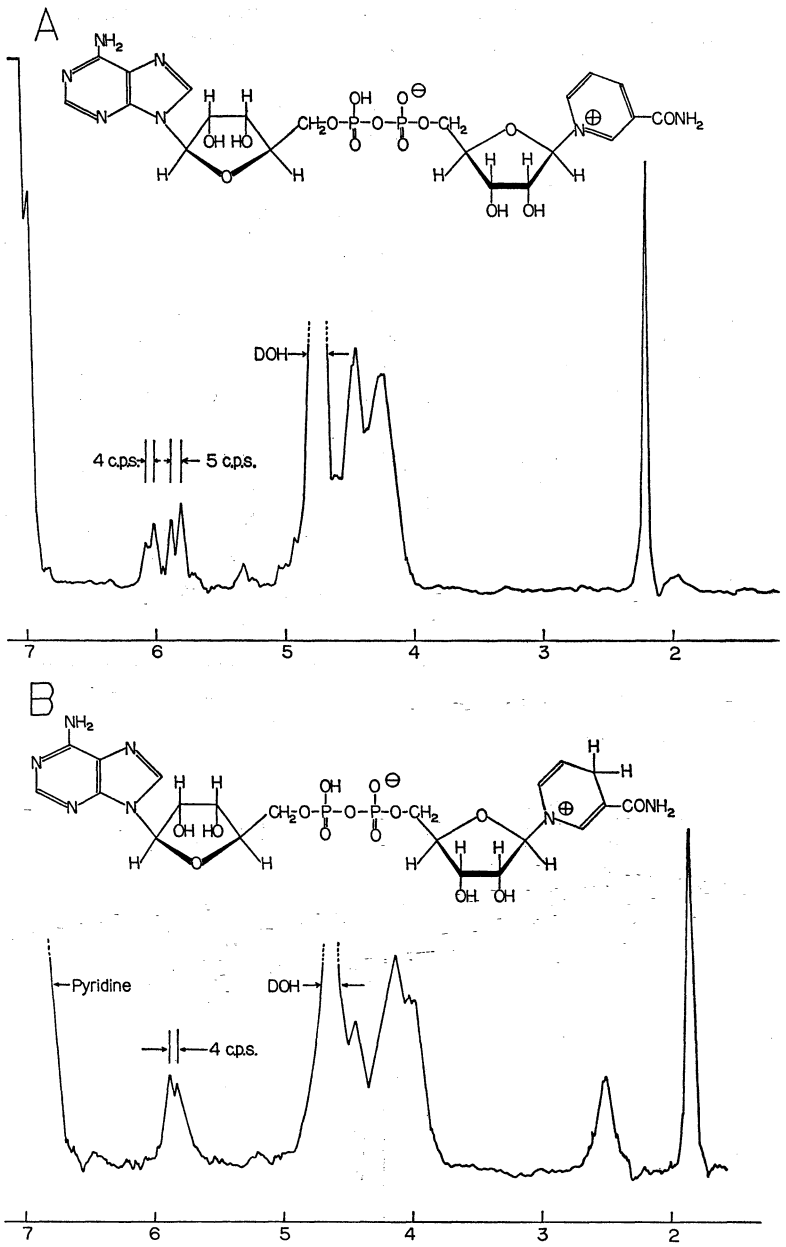

FIG. 3. Nuclear magnetic resonance spectra measured in 1:1 deuterium oxide – pyridine mixture and the chemical shifts expressed in p.p.m. from the signal for tetramethylsilane as external reference. A. Diphosphopyridine nucleotide (DPN). B. Reduced diphosphopyridine nucleotide (DPNH).

compound III is now known definitely to have the β-D-configuration, the dextrorotatory ribonucleoside which was oxidized must have had the α-D-configuration. Therefore, the levorotatory anomer used by Hughes, Kenner, and Todd (1) to synthesize DPN must have had the β-D-configuration and this must be the configuration of the anomeric center of the ribosyl nicotinamide portion of DPN.

Can. J. Chem. Downloaded from www.nrcresearchpress.com by 210.87.254.5 on 09/05/12
For personal use only.

The optical rotatory dispersion curves shown in Fig. 4 show that the rotations at all wavelengths for the β-D-glucopyranosides are less dextrorotatory than those for the

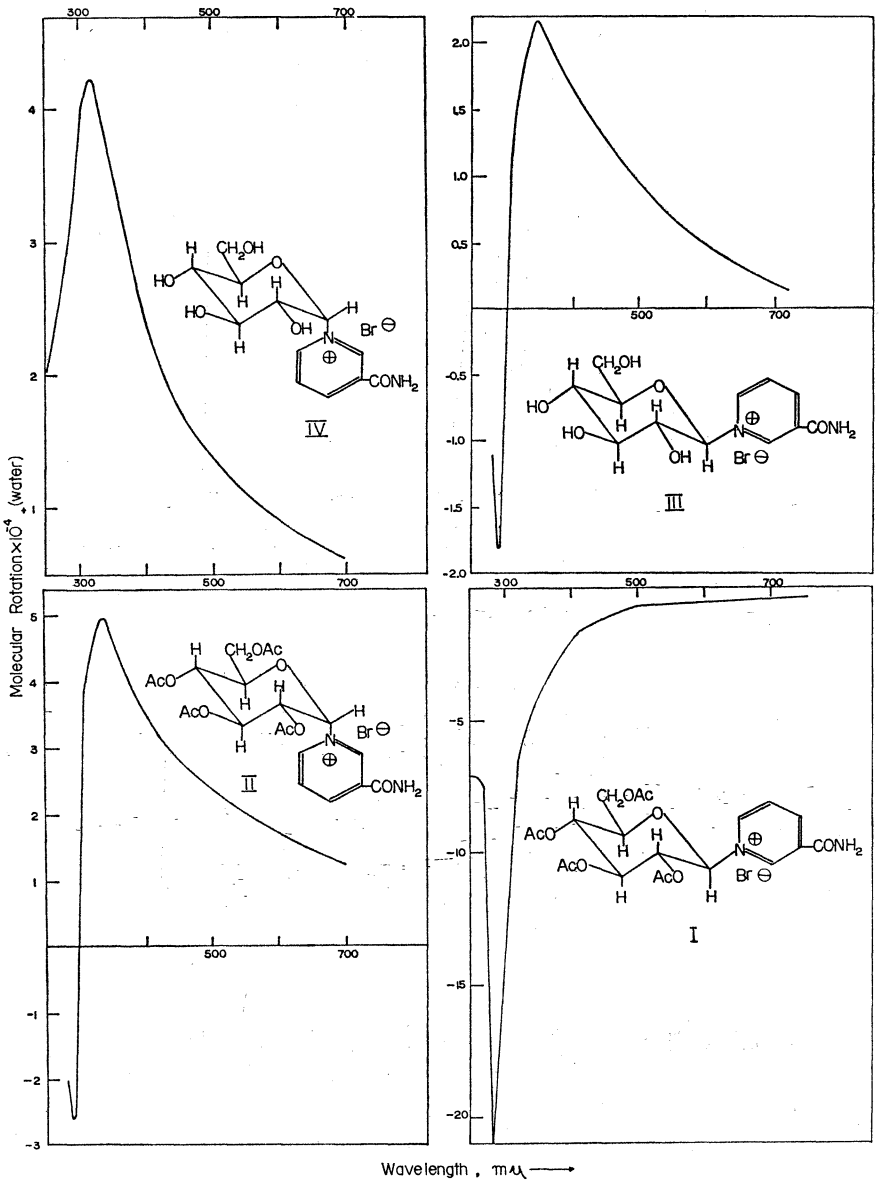

FIG. 4. Optical rotatory dispersion curves for the D-glucosyl nicotinamides I, II, III, and IV described in Figs. 1 and 2.

α-D-anomers. The marked effect of acetylation on the shape of the curve in the case of the β-anomers is noteworthy. Also, the resemblance of the curve for the unacetylated β-anomer to those for the α-anomers clearly demonstrates the hazard attending any attempt to establish the configuration of such a glycoside by optical rotation. The optical rotatory dispersion curves reproduced in Fig. 5 confirm the β-D-configuration for the ribosyl

Can. J. Chem. Downloaded from www.nrcresearchpress.com by 210.87.254.5 on 09/05/12
For personal use only.

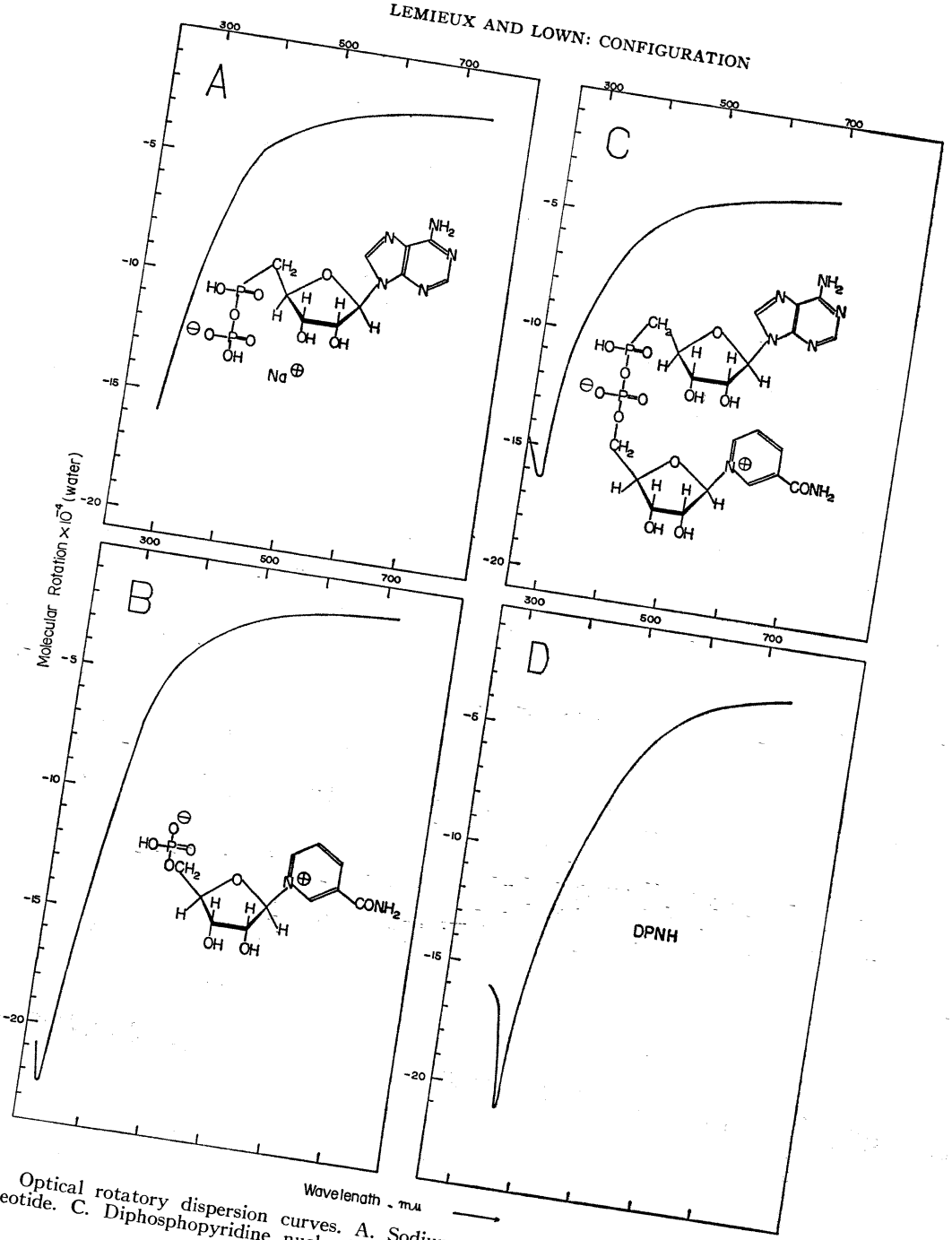

FIG. 5. Optical rotatory dispersion curves. A. Sodium adenosine-5′-diphosphate. B. Nicotinamide mononucleotide. C. Diphosphopyridine nucleotide (DPN). D. Reduced diphosphopyridine nucleotide (DPNH).

nicotinamide portion of DPN to the extent that the contribution to rotation by this portion of the molecule above 300 mμ is strongly levorotatory—the sign of rotation which would seem most likely in view of the rotational trends found for the compounds described in Fig. 4.

Can. J. Chem. Downloaded from www.nrcresearchpress.com by 210.87.254.5 on 09/05/12
For personal use only.

Can. J. Chem. Downloaded from www.nrcresearchpress.com by 210.87.254.5 on 09/05/12
For personal use only.

EXPERIMENTAL

All n.m.r. spectra were recorded on a Varian A-60 analytical spectrometer operating at a fixed radio frequency of 60 Mc/sec. The spectra were measured on approximately 20% (w/v) solutions in an appropriate solvent using tetramethylsilane as a standard.

The optical rotatory dispersion curves were measured on a Rudolph automatic recording spectropolarimeter, Model 260/655/850–614, using about 10^{-3} *M* aqueous solutions at room temperature. The nucleotides reported in Figs. 3 and 5 were purchased from Pabst Laboratories, Milwaukee, Wisconsin.

Tetra-O-acetyl-β-D-glucopyranosyl-3-carboxamidopyridinium Bromide (I) and its α-Anomer (II)

A solution of 15 g of freshly recrystallized tetra-*O*-acetyl-α-D-glucopyranosyl bromide and 5 g of nicotinamide in 70 ml of dry acetonitrile was heated on the steam bath for 4 hours under conditions similar to those employed by Haynes and Todd (10). The crystalline precipitate, 12 g (60% yield), was purified by recrystallization from methanol. The pure substance (I) melted with decomposition at 193–195° and possessed a $[\alpha]_D^{24} = -20.5°$ (*c*, 2.09 in water). The values reported (10) for these physical constants are m.p. 195–200° (decomp.) and $[\alpha]_D^{19} = -18.3°$. The n.m.r. spectrum is reported in Fig. 1A and the optical rotatory dispersion in Fig. 4.

The filtrate was evaporated to dryness under reduced pressure and the residual dark oil taken up in 30 ml of chloroform. After filtration, 150 ml of anhydrous ether was added. The resulting white precipitate was washed with ether and dried *in vacuo*. The n.m.r. spectrum showed two doublets, of approximately equal intensity, at 2.94 and 3.54 τ assignable to anomeric protons. The material was therefore subjected to partition chromatography (18) on Celite with *n*-butanol – diethyl ether (3:2) saturated with water as eluant. The fraction of the eluant which contained the α-nucleoside was identified by n.m.r. and was purified by several recrystallizations from a mixture of isopropanol and acetonitrile. The white crystalline powder (II), m.p. 185–190° and $[\alpha]_D^{24} = +22.1$ (*c*, 7 in water), possessed the n.m.r. spectrum reported in Fig. 1B, which showed it to be free of the β-anomer. The optical rotatory dispersion is shown in Fig. 4. Haynes and Todd (10) have reported an amorphous preparation of II with a specific rotation of +20.9° in water.

N-(β-D-Glucopyranosyl)-3-carboxamidopyridinium Bromide (III)

The acetylated glucoside (I), 2.03 g, was dissolved in 200 ml of a 3% solution of hydrobromic acid and the solution was kept at 45° for 20 hours. The solution was evaporated to dryness and the residual oil was treated with 1 ml each of isopropanol and acetonitrile and set aside at 0°. After 3 weeks, crystallization occurred and the solid was purified by recrystallization from a 1:1 mixture of isopropanol and ethanol. The yield was 0.624 g (39%) of material (III) with the physical constants, m.p. 151–152°, $[\alpha]_D^{27}$ +29.4 (*c*, 3.1 in water), in good agreement with the literature values (19). The n.m.r. spectrum is reported in Fig. 2A and the optical rotatory dispersion in Fig. 4.

A solution of 98.2 mg of the glucoside (III) in 5 ml of water was kept at 0° with 192 mg of sodium metaperiodate. After 4 hours, the rotation of the solution reached a steady value, $[\alpha]_D^{25} = +63.8°$ (*c*, 2.5 in water).

N-(α-D-Glucopyranosyl)-3-carboxamidopyridinium Bromide (IV)

The pure crystalline acetylated α-D-glucoside (II), 164 mg, was dissolved in 10 ml of a 3% solution of hydrobromic acid and kept at 45° for 24 hours. The solution was lyophilized to leave 100 mg of a dark gum which could not be induced to crystallize. The substance was dissolved in chloroform and reprecipitated as a yellow gum by the addition of anhydrous ether. The n.m.r. spectrum reproduced in Fig. 2B establishes beyond doubt the identity of the substance (IV) which gave the optical rotatory dispersion shown in Fig. 4.

ACKNOWLEDGMENTS

This research was supported in part by a National Research Council of Canada grant (T172) to R. U. L. The n.m.r. spectra and the optical rotatory dispersions were measured by R. N. Swindlehurst of this laboratory.

REFERENCES

1. N. A. HUGHES, G. W. KENNER, and A. R. TODD. J. Chem. Soc. 3733 (1957).
2. L. J. HAYNES, N. A. HUGHES, G. W. KENNER, and A. R. TODD. J. Chem. Soc. 3727 (1957).
3. M. VISCONTINI and E. HÜRZELER-JUCKER. Helv. Chim. Acta, **39**, 1620 (1956).
4. C. S. HUDSON. J. Am. Chem. Soc. **31**, 66 (1909).
5. O. KJØLBERG. Acta Chem. Scand. **14**, 1118 (1960). E. BERNER and O. KJØLBERG. Acta Chem. Scand. **14**, 909 (1960).
6. R. U. LEMIEUX and M. HOFFER. Can. J. Chem. **39**, 111 (1961).
7. R. U. LEMIEUX, R. K. KULLNIG, H. J. BERNSTEIN, and W. G. SCHNEIDER. J. Am. Chem. Soc. **80**, 6098 (1958).
8. R. U. LEMIEUX. Can. J. Chem. **39**, 116 (1961).

9. M. KARPLUS. J. Chem. Phys. **30**, 11 (1959).
10. L. J. HAYNES and A. R. TODD. J. Chem. Soc. 303 (1950).
11. F. A. L. ANET. Can. J. Chem. **39**, 2262 (1961).
12. J. I. MUSHER and E. J. COREY. Tetrahedron, **18**, 791 (1962).
13. J. D. ROBERTS. An introduction to spin-spin splitting in high resolution nuclear magnetic resonance spectra. W. A. Benjamin, Inc., New York. 1961.
14. L. M. JACKMAN. Applications of nuclear magnetic resonance spectroscopy in organic chemistry. Pergamon Press, New York. 1959.
15. K. S. PITZER and W. E. DONATH. J. Am. Chem. Soc. **81**, 3213 (1959).
16. R. U. LEMIEUX, J. D. STEVENS, and R. R. FRASER. Can. J. Chem. **40**, 1955 (1962).
17. K. L. RINEHART, JR., M. HICKENS, A. D. ARGOUDELIS, W. S. CHILTON, H. E. CARTER, M. P. GEORGIADIS, C. P. SCHAFFNER, and R. T. SCHILLINGS. J. Am. Chem. Soc. **84**, 3218 (1962).
18. R. U. LEMIEUX, C. T. BISHOP, and G. E. PELLETIER. Can. J. Chem. **34**, 1365 (1956).
19. M. VISCONTINI, R. HOCHREUTER, and P. KARRER. Helv. Chim. Acta, **36**, 1777 (1953).

Can. J. Chem. Downloaded from www.nrcresearchpress.com by 210.87.254.5 on 09/05/12
For personal use only.

HYDROLYTIC REACTIONS OF DISULPHUR MONOXIDE IN A HOMOGENEOUS MEDIUM

C. G. RAMACHANDRAN NAIR AND A. R. VASUDEVA MURTHY
Department of Inorganic and Physical Chemistry, Indian Institute of Science, Bangalore, India
Received September 27, 1962

ABSTRACT

The hydrolytic reactions of disulphur monoxide are studied in a homogeneous medium. Alkaline hydrolysis gives a mixture of sulphide, sulphite, and thiosulphate. Hydrolysis in the presence of sulphite in neutral medium gives equimolar amounts of trithionate and thiosulphate. These reactions are closely similar to the reactions of derivatives of thiosulphurous acid. The production of trithionate is explained on the basis of the formation of thiosulphurous acid as the primary product during hydrolysis and therefore it is suggested that disulphur monoxide is the true anhydride of this acid.

Can. J. Chem. Downloaded from www.nrcresearchpress.com by 210.87.254.105 on 09/05/12
For personal use only.

INTRODUCTION

It has recently been shown (1) that pure solutions of disulphur monoxide, S_2O, in carbon tetrachloride can be prepared by absorbing the products of combustion of sulphur in oxygen at 5 to 7 mm pressure, in the dry solvent kept cooled at $-16°$. Since the solubility of sulphur dioxide in carbon tetrachloride at this temperature is small, any dissolved sulphur dioxide could be conveniently pumped off. Somewhat more concentrated solutions could be prepared (2, 3) in toluene (at $-75°$) and anisole (at $-16°$), but these solutions were largely contaminated with sulphur dioxide, which could not be completely removed.

In view of the probable status of disulphur monoxide as the anhydride of the hypothetical thiosulphurous acid, $H_2S_2O_2$, an investigation of its hydrolytic reactions was undertaken in a homogeneous medium. It has been found advantageous to study the hydrolytic reactions in homogeneous media, since elemental sulphur and its compounds are more amenable to such studies (4, 5). Highly reactive species of sulphur compounds have been postulated as intermediate species during these reactions.

The hydrolytic reactions of disulphur monoxide in alkaline and sulphite solutions have been carried out. The products of reaction are sulphide, sulphite, and thiosulphate in alkaline hydrolysis and equimolar amounts of trithionate and thiosulphate in the reaction with sulphite.

EXPERIMENTAL

(a) Preparation of Disulphur Monoxide Solutions

The apparatus employed was essentially similar to that of Schenk (6) except that a quartz tube was used to burn sulphur (1). Sulphur was burnt in a stream of pure dry oxygen at a pressure of 5 to 7 mm and the products of combustion were absorbed in cooled organic solvents in suitable traps. The following organic solvents, kept cooled at the temperature noted against each, were used: toluene ($-75°$), anisole ($-25°$), carbon tetrachloride ($-16°$), and dioxane ($+20°$). All the solutions were clear yellow to orange-yellow in color.

(b) Analysis of the Disulphur Monoxide Solutions (1)

Aliquots of the disulphur monoxide solutions were shaken up with mercury in an all-glass assembly, when the disulphur monoxide decomposed, forming mercuric sulphide and sulphur dioxide in terms of the equation

$$2S_2O + 3Hg \rightarrow 3HgS + SO_2. \qquad [1]$$

The sulphur dioxide was swept off by a stream of pure dry nitrogen, absorbed in dilute alkali, and estimated iodometrically. The mercuric sulphide was estimated by the hydriodic acid method (7). It may be seen

from equation [1] that for a pure solution of disulphur monoxide, the ratio HgS/SO_2 should be 3. The results of the "mercury decomposition reaction" are presented in Table I.

TABLE I

Mercury decomposition of disulphur monoxide solutions*

(5-ml aliquots of S_2O solutions taken)

Expt. No.	Solvent	HgS formed	SO_2 formed	Total S	S_2O present (calc.)
1	Carbon tetrachloride	19.50	6.80	26.30	26.00
2	"	11.59	3.90	15.49	15.45
3	Toluene	31.40	329.10	360.50	41.87
4	"	31.60	413.50	445.10	42.13
5	Anisole	31.33	71.10	102.43	41.77
6	Dioxane	57.95	125.10	183.05	77.27

*Quantities of sulphur and sulphur compounds are all expressed in terms of g-atoms of $S \times 10^5$.

(c) Procedure for Hydrolytic Reactions

The hydrolytic reactions were carried out in a homogeneous medium as follows: Forty-five milliliters of an aqueous solution of carbonate-free sodium hydroxide (or sodium sulphite—for the sulphite reaction) was taken in a 500-ml stoppered conical flask, and 100 ml of aldehyde-free ethyl alcohol was added to it. To this solution was added 5 ml of the disulphur monoxide solution, and the mixture was shaken well, when a homogeneous solution was obtained. In the case of the dioxane solutions, addition of alcohol was not necessary for homogenization since dioxane is completely miscible with water. The yellow color of the disulphur monoxide solution disappeared quickly with the progress of the reaction.

The products of reaction were analyzed by the analytical procedures of Kurtenacker and co-workers (8) for a mixture of sulphide, sulphite, thiosulphate, and polythionates. Typical results of the alkaline hydrolysis and of the sulphite reaction are given in Tables II and III respectively.

TABLE II

Alkaline hydrolysis of disulphur monoxide solutions*

(Overall alkali strength 1.0 *N*; 5-ml aliquots of S_2O solutions taken)

Expt. No.	Solvent	S_2O content	Free SO_2 content	$S^=$ formed	$SO_3^=$ formed	$S_2O_3^=$ formed	Elemental S	Total S
1	Carbon tetrachloride	26.00	0.30	8.70	7.10	10.60	Nil	26.40
2	Toluene	41.87	318.60	6.30	307.60	52.10	"	366.00
3	"	42.13	403.00	11.60	396.80	40.40	"	448.80
4	Anisole	41.77	60.60	7.91	58.10	36.18	"	102.19
5	Dioxane	77.27	105.8	13.17	98.05	81.95	"	193.2
6†	Nil	—	—	37.4	1301.3	145.00	11.6	1495.3
7†	Nil	—	—	65.2	1150.0	151.8	22.0	1389.0

*Quantities of sulphur and sulphur compounds are all expressed in terms of g-atoms of sulphur $\times 10^5$.
†In these experiments the products of combustion were directly absorbed in 1 *N* NaOH (50% alcoholic solution). In expt. 7, a suspension of cadmium hydroxide was taken along with the sodium hydroxide solution.

It was of interest to study the reactions of disulphur monoxide with aqueous solutions of alkali and sulphite, without prior dissolution in organic solvents. The products of combustion were accordingly passed through aqueous alkali or sulphite solutions (containing alcohol to inhibit the oxidation of sulphite) at −5°. The results of these experiments are also included in Tables II and III.

All the hydrolytic reactions in homogeneous medium were carried out at the laboratory temperature (25±2°).

RESULTS

It may be seen from Table I that the HgS/SO_2 ratio is nearly 3 for solutions in carbon tetrachloride, indicating that these were fairly pure solutions of disulphur monoxide. The solutions in other solvents were largely contaminated with sulphur dioxide. The disulphur monoxide content of all the solutions could be computed in all cases from the mercury

Can. J. Chem. Downloaded from www.nrcresearchpress.com by 210.87.254.105 on 09/05/12
For personal use only.

TABLE III

Hydrolytic reaction of disulphur monoxide solutions with sulphite in homogeneous medium

(Amount of sulphite taken = 25 ml $M/4$ solution; 5-ml aliquots of S_2O solution taken)

Expt. No.	Solvent	S_2O content (moles$\times 10^5$)	Trithionate formed (moles$\times 10^5$)	Thiosulphate formed (moles$\times 10^5$)
1	Carbon tetrachloride	13.00	12.20	13.80
2	"	13.00	11.60	14.10
3	"	13.00	12.80	14.10
4	"	7.73	7.66	8.09
5	"	7.73	7.61	7.98
6	Toluene	20.94	11.77	29.80
7	"	20.94	12.07	29.70
8	"	20.94	12.13	29.80
9	"	21.07	12.77	30.85
10	Anisole	20.89	16.23	28.19
11	"	20.89	15.97	27.69
12	"	20.89	16.55	28.09
13	Dioxane	38.64	6.92	59.60
14*	Nil	—	98.70	109.10
15*	Nil	—	742.5	808.7

*In these experiments, the gaseous products of combustion were directly absorbed in sulphite solutions ($M/4$ and 1 M strengths for expts. 14 and 15 respectively).

decomposition reaction. It may be seen from equation [1] that, expressing quantities of sulphur compounds in terms of g-atoms of sulphur, $S_2O = 4/3\ HgS$.

Alkaline Hydrolysis

The products of alkaline hydrolysis of disulphur monoxide solutions in homogeneous medium were found to be sulphide, sulphite, and thiosulphate (Table II). For the carbon tetrachloride solutions, the percentage yields of sulphide, sulphite, and thiosulphate were about 32%, 28%, and 40% respectively. In the case of the other solutions, the sulphite yields were considerably higher, this being due to the free sulphur dioxide retained by these solvents.

Alkaline hydrolysis of disulphur monoxide solutions has been studied earlier employing a two-phase-reaction technique (1, 9). Solutions of disulphur monoxide in carbon tetrachloride were shaken with aqueous alkali containing some cadmium hydroxide suspension. The products obtained were sulphide (16%), sulphite (18%), thiosulphate (29%), and elemental sulphur (37%). No elemental sulphur is formed in the present homogeneous hydrolysis, because elemental sulphur is quantitatively hydrolyzed by alkali in homogeneous medium to a mixture of sulphide, thiosulphate, and a small quantity of sulphite (4).

When the products of combustion were directly absorbed in 1 N alkali containing 50% alcohol, colloidal white sulphur was rapidly formed. The other products were sulphide, thiosulphate, and sulphite (experiments 6 and 7 in Table II). The ratio of sulphide to thiosulphate was increased when a suspension of cadmium hydroxide was taken along with the sodium hydroxide solution, since the sulphide was now fixed as soon as it was formed (4).

Reaction with Sulphite

It may be seen from Table III that the products of reaction of disulphur monoxide with sulphite are trithionate and thiosulphate. Approximately equimolar amounts of trithionate and thiosulphate were obtained in the case of carbon tetrachloride solutions,

Can. J. Chem. Downloaded from www.nrcresearchpress.com by 210.87.254.105 on 09/05/12
For personal use only.

whereas considerably greater thiosulphate yields were obtained for the other solutions. It was interesting to find that the thiosulphate yield was only slightly higher than the trithionate yield when the products of combustion were directly absorbed in aqueous sulphite solution (experiments 14 and 15 in Table III). The solutions in this case were clear and colorless.

DISCUSSION

The results of the present investigation show that the hydrolytic reactions of disulphur monoxide are similar to those of disulphur dichloride (5), and of dialkyl thiosulphites and tetraalkyl dithiodiamines (10). All these compounds have been looked upon as derivatives of the hypothetical thiosulphurous acid, $H_2S_2O_2$; the common hydrolytic reactions may be considered as reactions of this acid, which is formed as primary product during the hydrolysis of these compounds:

$$S_2X_2 + 2H_2O \rightarrow H_2S_2O_2 + 2HX \qquad [2]$$

(where X = Cl, OR, or NR_2)

$$S_2O + H_2O \rightarrow H_2S_2O_2. \qquad [3]$$

Thiosulphurous acid has been known to give rise to sulphide, sulphite, and thiosulphate during the alkaline hydrolysis of its derivatives in a homogeneous medium (5, 10).

On the basis of the quantities of sulphide, sulphite, and thiosulphate produced during the hydrolytic reaction, it is possible to calculate the oxidation state of sulphur in disulphur monoxide and it is found to be +1.28. From the consideration of the structure of S_2O and also from the results of the oxidation studies of derivatives of S_2O such as the esters and amides of thiosulphurous acid, $S_2(OR)_2$, $S_2(NR_2)_2$, it has been shown that the average oxidation state of sulphur in S_2O is +1 (11). This average oxidation state of sulphur in S_2O also follows from the equation for complete oxidation:

$$S_2O + 5(O) \rightarrow 2SO_3,$$

where 10 equivalents of oxidant are required to bring both the sulphur atoms in S_2O to the sulphur trioxide stage. From this theoretical consideration also the oxidation state of sulphur in S_2O should be +1. However, the average oxidation state of sulphur obtained by hydrolytic reactions is slightly higher than the expected one. This discrepancy may perhaps be attributed to the complicated nature of the reaction involving hydrolysis, decomposition, and thionization of S_2O as well as the hydrolysis of elemental sulphur in homogeneous medium.

In addition to the above reactions, there is the possibility of polysulphide formation during the hydrolytic process. This has been observed in the hydrolytic reactions of the derivatives of thiosulphurous acid, of which disulphur monoxide is the anhydride. The formation of the polysulphide was indicated by a yellow color found at the initial stages which fades off gradually as thiosulphate forms. This particular step increases the positive oxidation state of the sulphur. However, it is difficult to evaluate this quantitatively.

The formation of equimolar amounts of trithionate and thiosulphate during the reaction with sulphite in a neutral medium is a characteristic reaction of thiosulphurous acid (12). The primary product would be tetrathionate, formed according to the equation

$$OH—S—S—OH + 2HSO_3^- \rightarrow {}^-O_3S—S—S—SO_3^- + 2H_2O. \qquad [4]$$

But tetrathionate is known to undergo quantitative degradation in a neutral or faintly

Can. J. Chem. Downloaded from www.nrcresearchpress.com by 210.87.254.105 on 09/05/12
For personal use only.

alkaline medium to give trithionate and thiosulphate, by the action of excess of sulphite:

$$S_4O_6^{=} + SO_3^{=} \rightarrow S_3O_6^{=} + S_2O_3^{=}. \quad [5]$$

It may be seen that disulphur monoxide answers this reaction almost quantitatively, as may be seen from the nearly equimolar amounts of trithionate and thiosulphate formed in the case of the carbon tetrachloride solutions as well as in the direct reaction of the gaseous product with sulphite solutions.

The considerably greater yields of thiosulphate and lower yields of trithionate in the experiments using solutions in toluene, anisole, and dioxane must be attributed to the complications arising from the large contamination of these solutions with sulphur dioxide. A direct thionization reaction,

$$2S_2O + 2SO_2 + 3H_2O \rightarrow 3H_2S_2O_3, \quad [6]$$

involving part of the disulphur monoxide, would perhaps explain this greater thiosulphate yield. It may be noted that significant amounts of trithionate are formed even in the case of these solutions.

The technique of homogeneous hydrolysis adopted in the present investigation enabled the reactions to be carried out fast, minimizing the chance for the decomposition of disulphur monoxide. The present studies seem to indicate that disulphur monoxide is the anhydride of the hypothetical thiosulphurous acid.

ACKNOWLEDGMENT

The authors wish to express their grateful thanks to Professor M. R. A. Rao for his kind interest in the work.

REFERENCES

1. A. R. Vasudeva Murthy. Proc. Indian Acad. Sci. Sect. A, **36**, 388, 425, 537 (1952).
2. P. W. Schenk, F. Thoma, and E. Bohm. Monatsh. Chem. **81**, 907 (1950).
3. K. Sharada and A. R. Vasudeva Murthy. J. Indian Inst. Sci. **44**, 49 (1962).
4. C. G. Ramachandran Nair and A. R. Vasudeva Murthy. Proc. Indian Acad. Sci. Sect. A, **55**, 168 (1962).
5. C. G. Ramachandran Nair and A. R. Vasudeva Murthy. Z. Anorg. Allgem. Chem. **318**, 155 (1962).
6. P. W. Schenk. Z. Anorg. Allgem. Chem. **220**, 268 (1934).
7. A. R. Vasudeva Murthy, V. A. Narayan, and M. R. A. Rao. Analyst, **81**, 373 (1956).
8. A. Kurtenacker. Analytische Chemie der Sauerstoffsäuren des Schwefels. Stuttgart 1938.
9. B. S. Rao. Proc. Indian Acad. Sci. **10**, 491 (1939).
10. C. G. Ramachandran Nair and A. R. Vasudeva Murthy. Proc. Indian Acad. Sci. Sect. A, **56**, 130 (1962).
11. C. G. Ramachandran Nair and A. R. Vasudeva Murthy. J. Sci. Ind. Res. (India), Sect. B, **21**, 146 (1962).
12. H. Stamm and M. Goehring. Z. Anorg. Allgem. Chem. **242**, 413 (1939).

Can. J. Chem. Downloaded from www.nrcresearchpress.com by 210.87.254.105 on 09/05/12
For personal use only.

THE STUDY OF VIBRATIONALLY EXCITED N_2 MOLECULES WITH THE AID OF AN ISOTHERMAL CALORIMETER[1]

J. E. MORGAN AND H. I. SCHIFF
Upper Atmosphere Chemistry Group, McGill University, Montreal, Que.

Received November 26, 1962

ABSTRACT

Vibrationally excited nitrogen molecules produced both by a microwave discharge in nitrogen and also by the reaction

$$N + NO \rightarrow N_2 + O + 75 \text{ kcal}$$

have been examined using an isothermal calorimetric probe.

In the first case the energy associated with an 'active' nitrogen stream, due to vibrationally excited N_2, was found to be 6.03 kcal mole^{-1} of total nitrogen. The subsequent relaxation of this species was found to occur almost entirely on the walls of the reaction vessel, with a collision efficiency of 4.5×10^{-4}. The addition of other gases greatly accelerated the homogeneous relaxation rate. Collisional efficiencies of N_2O, CO_2, and Ar were found to be 0.8×10^{-4}, 2.3×10^{-5}, and 1.0×10^{-6} respectively.

The vibrationally excited nitrogen produced by the N/NO reaction was found to possess 20 ± 4 kcal mole^{-1} of energy compared with the maximum of 75 kcal mole^{-1} allowed by the exothermicity of the reaction.

Can. J. Chem. Downloaded from www.nrcresearchpress.com by 210.87.254.6 on 09/05/12
For personal use only.

Calorimetric probes have been used extensively to measure atom concentrations. Such probes measure either the temperature rise (1) or the energy release (2, 3) resulting from atom recombination on a catalytic surface. They are, however, non-selective, and other energetic species, such as vibrationally and electronically excited molecules, can also be deactivated on these surfaces. While this places a serious restriction on the use of such probes for atom measurement, it affords a way of studying other excited species if the energy release due to atom recombination can be estimated independently.

The energy content of 'active' nitrogen, due to ground state (^4S) nitrogen atoms, can be calculated from their concentration determined by NO titration. This calculated energy content was compared in the present work with the energy content measured with an isothermal calorimetric probe. The discrepancy between these values clearly demonstrates the presence of energetic species other than ground state atoms in 'active' nitrogen. The presence of substantial quantities of vibrationally excited molecules in 'active' nitrogen has been inferred by Kaufman and Kelso (4) and observed spectroscopically by Dressler (5).

The nitrogen formed in the reaction

$$N + NO \rightarrow N_2 + O + 75 \text{ kcal} \qquad [1]$$

can also be expected to be vibrationally excited (6). Phillips and Schiff (7) have shown that the nitrogen produced in this reaction is capable of dissociating ozone, and must therefore be excited to at least the fourth vibrational level. This species was also investigated in the present study.

EXPERIMENTAL

Apparatus

The probe used in this study was of the 'isothermal' type described by Elias *et al.*(3). It consisted essentially of a filament through which an accurately measured electric current could be passed. In the absence of an

[1]*This work was supported in part by the U.S. Air Force Cambridge Research Laboratories and in part by the Defence Research Board of Canada.*

activated gas the power input to the probe has some arbitrary value P_0. When the gas is activated, the electrical power input is reduced to a value P_f sufficient to restore the resistance (and consequently the temperature) of the filament to its original value. The difference $P_0 - P_f$ can then be equated to the rate of energy release to the probe from the gas.

The essential features of the apparatus are shown in Fig. 1. The reaction vessel consisted of a 26 mm I.D.

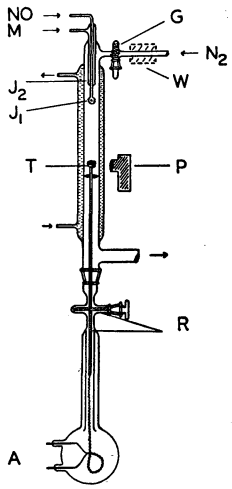

FIG. 1. Reaction vessel. W = microwave cavity; G = glass-wool plug; J_2 = inlet for M; J_1 = inlet for NO; P = photomultiplier; T = calorimetric probe; R = rack and pinion; A = leads from probe to resistance bridge.

pyrex tube surrounded by a water jacket. Nitrogen (Dinsmore Premium grade) was subjected to a 2450 Mc/s microwave discharge and was passed through the reaction tube at linear flow rates of 100–300 cm sec^{-1}. The relative N-atom concentration was determined as a function of the distance, d, along the reaction tube by measuring the afterglow intensity with a 1P21 photomultiplier. This detector was equipped with collimating slits and could be moved on rails parallel to the reaction tube. The absolute N-atom flow rate at J_1 ($t = 0$) was determined by NO titration.

The NO inlet jet, J_1, consisted of a spherical bulb containing 6 peripheral holes of 0.20 ± 0.01 mm diameter. The inlet J_2, concentric with J_1, was of similar construction. Close tolerances of the hole diameters were found to be essential for good mixing. The filament of the catalytic probe was made of approximately 100 cm of 28 B and S gauge platinum wire. Several catalytic surfaces were examined for use in the 'active' nitrogen system. Although freshly electroplated copper appeared to be very efficient in terminating the afterglow, volatile materials were found to be liberated during use, which contaminated the walls of the reaction tube. A cobalt surface electroplated from a dilute solution of ammoniacal cobalt sulphate was found to be equally efficient and free from this defect. It was therefore used throughout the work on the 'active' nitrogen system.

To examine the vibrationally excited nitrogen from the NO reaction (1), it was necessary to use a surface capable of recombining atomic oxygen. A silver peroxide coating formed by electroplating silver from a dilute solution of carefully purified $KAg(CN)_2$ followed by exposure to atomic oxygen was found to be very effective in this system.

'Active' Nitrogen System

A stream of partially dissociated nitrogen was first titrated with NO, which was added through inlet J_1. The end point of the titration is defined by the absence of either the blue NO emission obtained when N atoms are in excess, or the greenish NO_2 emission obtained when NO is in excess. After recording its value at the end point, the NO flow was discontinued. The relative nitrogen atom concentration along the reaction tube was then determined with the movable photomultiplier tube.

From these measurements the rate of energy release to the probe, arising from atom recombination, H_A, can be calculated from the relation

$$H_A = f_N(D/2) \text{ mcal sec}^{-1},$$

where f_N is the flow rate of atomic nitrogen in μmole sec^{-1} and D is the dissociation energy of N_2 in kcal $mole^{-1}$.

Can. J. Chem. Downloaded from www.nrcresearchpress.com by 210.87.254.6 on 09/05/12
For personal use only.

A typical plot of H_A against t is shown as curve A in Fig. 2. The rate of energy release actually measured by the probe, H_E, is shown as curve B. Curve C is a plot of ln ΔH, where $\Delta H = H_E - H_A$.

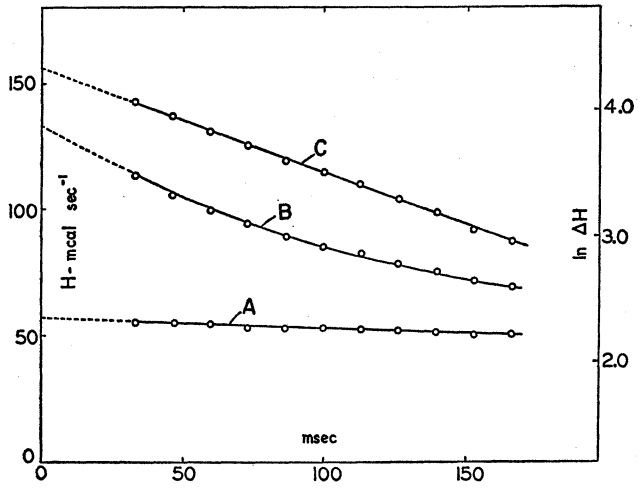

FIG. 2. Probe measurements on discharged nitrogen at $P_{N_2} = 1.65$ torr and $(P_N)_0 = 0.014$ torr. (A) H_A calculated from atom concentration at $t = 0$ and afterglow intensity; (B) H_E measured by cobalt-plated probe; (C) ln $(H_E - H_A)$.

The discrepancy between H_E and H_A indicates that some excited species, N_2^*, is being deactivated on the probe in addition to the recombination of atoms. The observed exponential decay of ΔH is consistent with a collisional deactivation mechanism such as

$$N_2^* + N_2 \rightarrow N_2 + N_2 \qquad [2]$$

$$N_2^* + \text{wall} \rightarrow N_2 + \text{wall} \qquad [3]$$

Such a mechanism would yield a pressure-dependent first-order rate constant given by

$$k_{obs} = k_2[N_2] + k_3$$

and a plot of k_{obs} against $[N_2]$ should permit evaluation of k_2 and k_3. Table I gives the results of four determinations of k_{obs} at different pressures. The independence of k_{obs} on $[N_2]$ suggests that $k_2 = 0$. The

TABLE I

Relaxation of N_2^* in the absence of added gas

P (torr)	$[N_2]\times10^7$ (moles cm^{-3})	$k_{obs} = \frac{1}{t}\ln\frac{[\Delta H]_0}{[\Delta H]_t}$ (sec^{-1})	$t_{\frac{1}{2}}$ (msec)
2.3	1.24	8.73	79.5
2.95	1.60	8.70	79.5
4.10	2.22	8.73	79.5
5.84	3.14	9.10	76.1
	Average	8.8±0.3	

homogeneous deactivation of N_2^* therefore appears to be extremely slow and virtually all the deactivation occurs on the walls. The average value of k_3 found in this way is 8.8±0.3 sec^{-1}. This can be expressed as a heterogeneous collisional deactivation coefficient, γ, by use of the familiar relation

$$\gamma = \frac{2k_3 r}{\bar{c}} = (4.5\pm0.2)\times10^{-4},$$

where r is the radius of the tube and $\bar{c}$ the average molecular velocity.

Can. J. Chem. Downloaded from www.nrcresearchpress.com by 210.87.254.6 on 09/05/12
For personal use only.

The magnitude of the energy $E_{N_2}^*$ associated with the excited molecules in the gas equals $\Delta H/f_{N_2}$, where f_{N_2} is the total molar flow rate of N_2. The value of $E_{N_2}^*$ just below the discharge should indicate the energy content of the excited molecules formed by the discharge. The varying geometry of the apparatus between the discharge and the reaction tube, as well as the ill-defined position of the discharge, make a direct extrapolation difficult. However, if the energy content of the gas stream leaving the discharge is independent of pressure, the value of $E_{N_2}^*$ at the *effective* discharge position can be obtained from the intersection of two or more plots of ln ΔH against d at different pressures. These plots will have different slopes due to the differences in time scales.

Figure 3 shows the data of four such experiments plotted in this way. The point of intersection corresponds to a value of $E_{N_2}^* = 6.03$ kcal mole^{-1}.

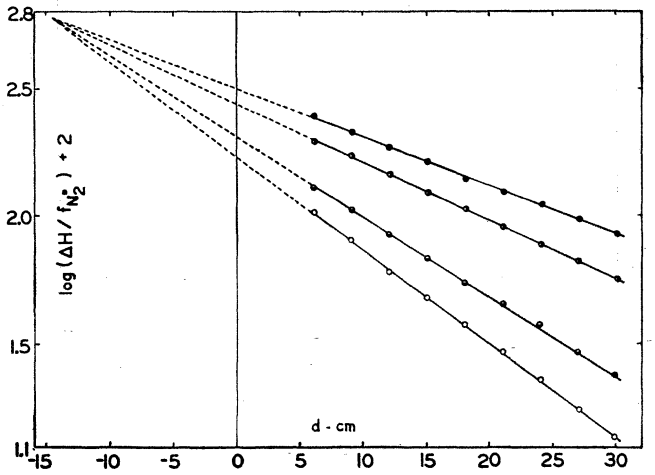

FIG. 3. Probe measurements of discharged nitrogen at four different linear flow rates f_{N_2}. ● $f_{N_2} = 200$ cm sec^{-1}, $P_{N_2} = 2.3$ torr, $(P_N)_0 = 0.0188$ torr; ◑ $f_{N_2} = 165$ cm sec^{-1}, $P_{N_2} = 2.95$ torr, $(P_N)_0 = 0.0229$ torr; ◒ $f_{N_2} = 126$ cm sec^{-1}, $P_{N_2} = 4.10$ torr, $(P_N)_0 = 0.0313$ torr; ○ $f_{N_2} = 110$ cm sec^{-1}, $P_{N_2} = 5.84$ torr, $(P_N)_0 = 0.0415$ torr.

Addition of N_2O through inlet J_2 was found to be an effective means of deactivating N_2^*, in agreement with the findings of Kaufman and Kelso (4). Figure 4 shows that the addition of N_2O at a rate approximately

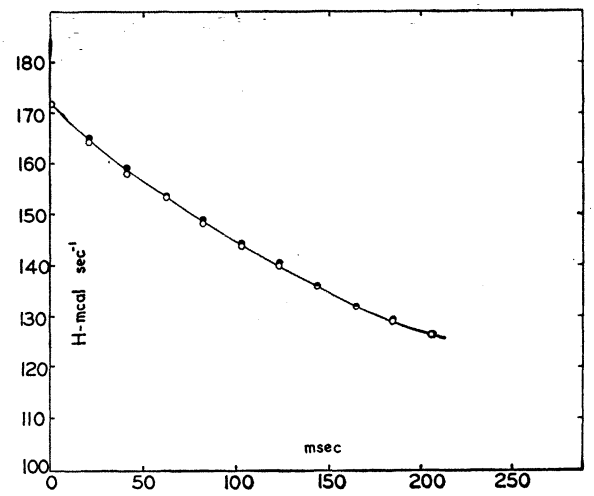

FIG. 4. Probe measurements of discharged nitrogen to which N_2O had been added. $P_{N_2} = 3.80$ torr; $P_{N_2O} = 0.37$ torr. ○ heat calculated from atom concentration at $t = 0$ and afterglow intensity; ● heat measured by probe.

Can. J. Chem. Downloaded from www.nrcresearchpress.com by 210.87.254.6 on 09/05/12
For personal use only.

0.1 that of the nitrogen flow rate resulted in the measured energy release to the probe being identical with that calculated for N atoms alone. These results also confirm the validity of the NO titration as a quantitative method for determining N-atom flow rates. In addition, it may be inferred that most of the N atoms are present in their ground state since the calculated energy release, H_A, was obtained using $D_{N_2} = 225$ kcal mole^{-1}.

To obtain a measure of the efficiency of N_2O, CO_2, and Ar in deactivating N_2* much lower flow rates of these gases were used. The observed relaxation rate constants were measured as a function of the concentration of added gas. The results, plotted in Fig. 5, suggest that deactivation occurs by reaction [3] and by

$$N_2^* + M \rightarrow N_2 + M. \qquad [4]$$

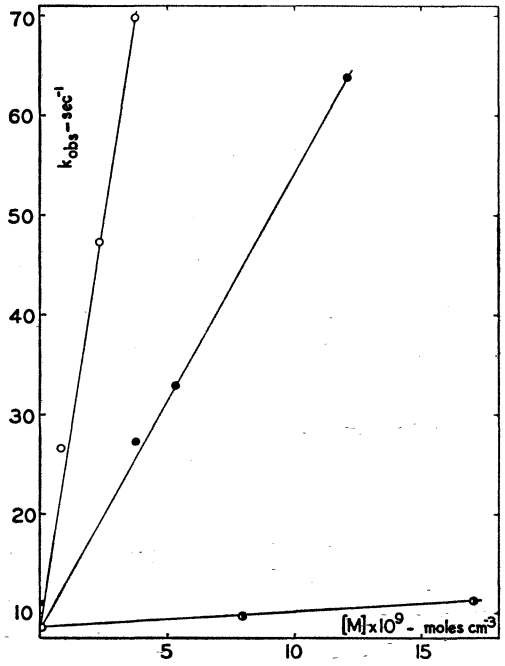

FIG. 5. Variation of deactivation rate of N_2* as a function of the concentration of added gas M. ○ N_2O; ● CO_2; ◑ Ar.

The overall rate constant will be given by

$$k_{obs} = k_4[M] + k_3.$$

Values of k_4 obtained from the slopes of these plots are given in Table II. The values of the homogeneous

TABLE II

Homogeneous deactivation of N_2* by inert gases

M	k_4 (cm^3 mole^{-1} sec^{-1})	σ^* (Å)	α_M
Ar	1.62×10^8	3.64	1.0×10^{-6}
CO_2	4.56×10^9	4.64	2.3×10^{-5}
N_2O	1.63×10^{10}	4.66	0.8×10^{-4}
N_2	$<3\times10^6$	3.74	$<2\times10^{-8}$

*From viscosity data given in S. W. Benson, Foundations of chemical kinetics, McGraw-Hill, 1960; and J. O. Hirschfelder, C. F. Curtiss, and R. B. Bird, Molecular theory of liquids and gases, Wiley and Sons, 1954.

Can. J. Chem. Downloaded from www.nrcresearchpress.com by 210.87.254.6 on 09/05/12
For personal use only.

collisional efficiencies, α_M, were calculated from the relation

$$\alpha_M = k_4/[1.142\times10^4(\sigma_{N_2}{}^*+\sigma_M)^2\left(\frac{M_{N_2}+M_M}{M_{N_2}\cdot M_M}\right)^{\frac{1}{2}}\cdot T^{\frac{1}{2}}],$$

where σ and M represent collision diameters and molecular weights respectively.[2] Although α_{N_2} was found to be zero in these experiments, an upper limit of 2×10^{-8} can be set from the magnitude of the experimental errors.

Vibrationally Excited $N_2{}^+$ Produced in the NO-titration Reaction

The titration of 'active' nitrogen with NO produces atomic oxygen and molecular nitrogen which may possess all or part of the exothermicity of the reaction. Such a system will, however, contain excited $N_2{}^*$ produced in the discharge as well as the excited $N_2{}^+$ produced by the reaction. The concentration of $N_2{}^+$ cannot be higher than that of atomic oxygen, i.e. about 1% of the total gas stream. Its contribution to the total energy content of the gas will therefore be smaller than that due to the $N_2{}^*$ from the discharge. It was, however, possible to remove the $N_2{}^*$ molecules from the gas stream before the titration.

In the previous section, it was shown that $N_2{}^*$ is deactivated by pyrex with an effective collision efficiency of 4.5×10^{-4}. Since the corresponding value for recombination of atomic nitrogen on pyrex is about 2×10^{-5} (8–10), it was possible to remove $N_2{}^*$ preferentially by insertion of a glass-wool plug between the discharge and the NO-inlet position. The effect of this plug is illustrated in Fig. 6, which shows that, according to

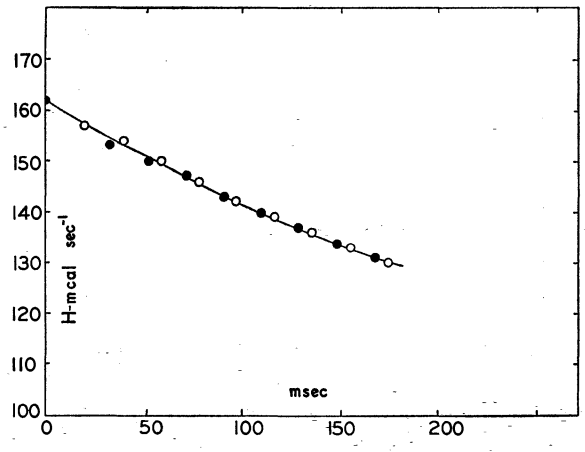

FIG. 6. Probe measurements of discharged nitrogen with pyrex-wool plug, located between discharge and reaction vessel. ○ heat measured by probe; ● heat calculated from atom concentration at $t = 0$ and afterglow intensity.

the calorimetric probe, all the $N_2{}^*$ has been removed without a drastic reduction of nitrogen atoms.

Titration of such a 'filtered' nitrogen atom stream should therefore produce oxygen atoms and excited nitrogen molecules in equimolar amounts. This system was examined with a silver-peroxide-coated probe. The results of a typical experiment are shown in Fig. 7. Curve A is a plot of H_A' calculated from the reaction

$$H_A' = f_O(D'/2),$$

where f_O is the flow rate of O atoms and D' is the dissociation energy of O_2. The value of f_O at $t = 0$ was obtained from the titration, and the variation of f_O with t was calculated from the O-atom recombination rate obtained previously for a similar system (11). The rate of O-atom recombination in this experiment is so small that no appreciable error will be introduced by neglecting the effect of any $O_2{}^*$ which might possibly be formed by the recombination.

The differences between the experimental points H_E', shown in curve B, and H_A' are small but significant. Curve C is a plot of ln $\Delta H'$ against t. Since $\Delta H'$ represents a small difference between relatively large quantities, the precision is not high. However, the slopes of a number of such plots gave a relaxation rate constant of 8.5 ± 0.3 sec^{-1}, which agrees quite well with the value found for the relaxation of $N_2{}^*$ produced in the discharge. This suggests that $N_2{}^*$ and $N_2{}^+$ are similar species.

The energy $E_{N_2}{}^+$ associated with $N_2{}^+$ equals $\Delta H'/f_O$ at $t = 0$. The results of a number of experiments are shown in Table III and yield an average value for $E_{N_2}{}^+$ of 20 ± 4 kcal mole^{-1}.

[2] $\sigma_{N_2}{}^*$ was assumed to be the same as σ_{N_2}.

Can. J. Chem. Downloaded from www.nrcresearchpress.com by 210.87.254.6 on 09/05/12
For personal use only.

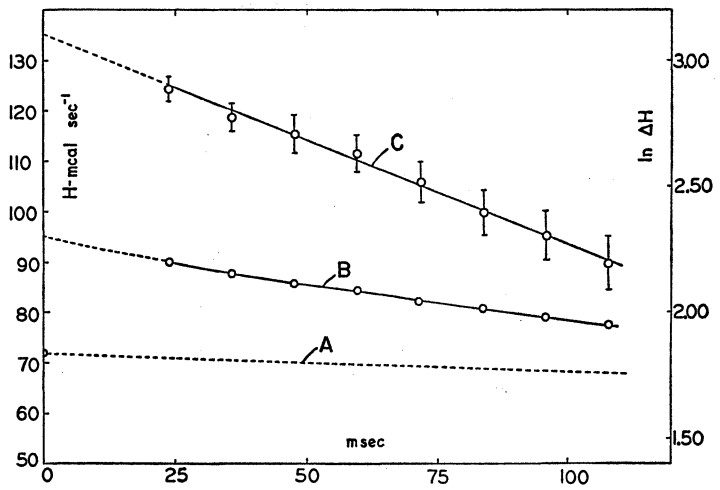

FIG. 7. Probe measurements of 'filtered' discharged nitrogen, titrated by NO. P_{N_2} = 1.3 torr; $(P_O)_0$ = 0.15 torr. (A) H_A' calculated from titration value of [O] and known decay rate of O atoms; (B) H_E' measured by silver-plated probe; (C) ln $(H_E'-H_A')$.

TABLE III

Relaxation of N_2^* formed from reaction [1]

P (torr)	$f_{N_2^*}$ (μmole sec^{-1})	$\Delta H_{(d=0)}$ (mcal sec^{-1})	$\Delta H_{(d=0)}/f_{N_2^*}$ (kcal mole^{-1})	k (sec^{-1})
1.3	1.223	22.2	18.2	8.20
2.1	0.970	17.9	18.5	8.77
2.60	0.985	23.0	23.4	8.06
3.35	1.02	21.8	21.4	9.10
			Average	8.5±0.3

DISCUSSION

The results can most readily be interpreted on the assumption that the N_2^* molecules formed by the discharge are vibrationally excited. The results of previous studies (12–16) on vibrational deactivation, summarized in Fig. 8, indicate that about 10^{10} collisions are necessary to effect homogeneous collisional deactivation of vibrationally excited N_2 at 300° K. This is consistent with the failure to observe any significant homogeneous deactivation of N_2^* in the present work.

The marked increase in relaxation rate upon addition of other gases also agrees with the vibrational relaxation measurements of Huber and Kantrowitz (14) and with the theoretical considerations of Schwartz *et al.* (15). The high deactivation efficiency of N_2O has been discussed recently by Callear (17). He considers the deactivation to be due to the energy exchange process

$$N_2^*(v = 1) + N_2O(v = 0) \rightarrow N_2(v = 0) + N_2O^*(v = 1).$$

Since N_2O has a fundamental vibrational frequency at 2223 cm^{-1}, which is only 129 cm^{-1} below that of N_2, he calculates that such an exchange should occur at every 10^3 collisions. The subsequent deactivation of N_2O is probably governed by its lowest vibrational frequency at 588 cm^{-1}, which Callear calculates should have a deactivation probability of about 10^{-4}. This probability should correspond to the rate of energy loss in the present study and is, in fact, in fair agreement with our observed efficiency of N_2O of 0.8×10^{-4}.

Can. J. Chem. Downloaded from www.nrcresearchpress.com by 210.87.254.6 on 09/05/12
For personal use only.

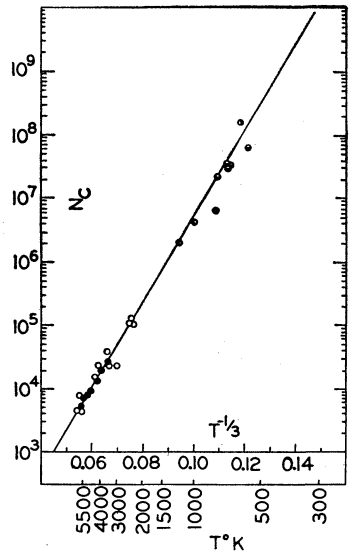

FIG. 8. Plot of number of collisions, N_c, required to deactivate vibrationally excited nitrogen as a function of temperature. ○ Strenlow and Cohen, ref. 16 (shock tube); ● Blackman, ref. 12 (shock tube); ◐ Lukasik and Young, ref. 13 (acoustical); ◒ Huber and Kantrowicz, ref. 14 as corrected in ref. 13 (impact tube); ◑ Schwartz, Slawsky, and Herzfeld, ref. 15 (calc.).

The same reasoning could probably also be applied to deactivation by CO_2. In this case the matching is almost perfect since CO_2 has a fundamental frequency of 2349 cm^{-1} compared with 2352 cm^{-1} for N_2. The subsequent energy loss from the CO_2* is probably also governed by its lowest vibrational frequency at 667 cm^{-1}, which might explain the lower deactivation efficiency of CO_2 relative to N_2O.

The collisional deactivation coefficient, γ, used above to characterize the heterogeneous deactivation of N_2*, does not necessarily represent the probability of complete deactivation of a molecule upon collision with the wall. This macroscopic collision efficiency will probably depend upon the energy distribution and cannot be directly related to the detailed, microscopic deactivation mechanism.

The experimental results simply show that the rate of loss of total energy can be represented as

$$-\frac{dE}{dt} = kE.$$

Now $E = \sum_i n_i\epsilon_i$, where ϵ_i is the energy and n_i is the concentration of molecules in the ith vibrational level. Thus

$$-\frac{d\sum_i n_i\epsilon_i}{dt} = k\sum_i n_i\epsilon_i.$$

There are two different ways in which a molecule can lose its energy:

(1) It may lose all its energy in one deactivating collision. This implies that the energy ϵ_i associated with each excited molecule remains constant so that the total energy loss is governed by the decrease in the number of excited molecules and its rate of decrease will be

$$-V\epsilon_i\frac{dn_i}{dt} = \frac{\gamma_i A n_i \epsilon_i \bar{c}}{4},$$

where V is the volume, A the surface area, and γ_i the efficiency for this process.

Can. J. Chem. Downloaded from www.nrcresearchpress.com by 210.87.254.6 on 09/05/12
For personal use only.

(2) It may lose only a fraction of its energy on each deactivating collision. In this case n_i will remain constant and the rate of energy loss will be equal to the rate of decrease of ϵ_i.

$$-Vn_i\frac{d\epsilon_i}{dt}=\frac{\gamma_i'An_i\epsilon_i\bar{c}}{4},$$

where γ_i' defines the efficiency for this kind of collision. If both processes occur simultaneously, the total rate of energy loss will be given by the sum over all i's:

$$-V\left(\sum_i \epsilon_i\frac{dn_i}{dt}+\sum_i n_i\frac{d\epsilon_i}{dt}\right)=\frac{A\bar{c}}{4}\sum_i(\gamma_i+\gamma_i')n_i\epsilon_i.$$

The bracketed term on the left-hand side is simply

$$\frac{d\sum_i n_i\epsilon_i}{dt}=k\sum_i n_i\epsilon_i.$$

The experimental results show, however, that k is a constant as $\sum_i n_i\epsilon_i$ changes. This implies that $(\gamma_i'+\gamma_i)$ must also be constant and the expression reduces to

$$k=\frac{A\bar{c}}{4V}(\gamma_i+\gamma_i').$$

For a cylindrical tube, therefore,

$$(\gamma_i+\gamma_i')\equiv\gamma=\frac{2kr}{\bar{c}}.$$

For a system in which there is simultaneous relaxation from different vibrational levels, γ_i and γ_i' would not be expected to be individually constant. The value of γ_i, the probability of complete deactivation on a single collision, should decrease with increasing vibrational quantum number, i. On the other hand the value of γ_i', the probability of the loss of a single vibrational quantum, should increase with increasing values of i because the vibrational levels get closer together. However, it is improbable that γ_i and γ_i' should vary in such a way as to retain $(\gamma_i+\gamma_i')$ constant for all values of i.

The constancy of γ observed in the present study is perhaps more readily understandable if the N_2* molecules were mainly in the first vibrational level. It is conceivable that the 'active' nitrogen may have been formed initially with considerable excitation of a relatively small fraction of the molecules. There might then be a rapid redistribution to a condition in which a large fraction of the molecules is present in the first vibrational level. The final relaxation of vibrational to kinetic energy ($v = 1$ to $v = 0$) would be relatively slow and be the one measured here. There may therefore be some significance to the observation that the measured energy content of N_2* corresponds to 6.03 kcal mole^{-1} of the total gas present, which is quite close to the first vibrational level of nitrogen (6.7 kcal mole^{-1}).

The extrapolation method used to determine the energy content of the N_2* does not preclude the presence of short-lived species which are deactivated before reaching the reaction vessel. In fact, Beale and Broida (18) have recently presented convincing evidence for the production of very energetic short-lived species by microwave discharge of nitrogen.

It is apparent that experiments of this type are incapable of providing detailed relaxation mechanisms unless independent information is available concerning the variation of the energy distribution with time.

The vibrationally excited N_2^+ formed in the titration reaction was found to possess an average energy of excitation of 20 ± 4 kcal mole^{-1}. The maximum energy available for

Can. J. Chem. Downloaded from www.nrcresearchpress.com by 210.87.254.6 on 09/05/12
For personal use only.

excitation is 75 kcal mole^{-1}. Again, the measurements made here cannot give detailed information regarding the distribution of energy.

Basco and Norrish (6) favor the hypothesis that molecules formed by reactions of this type possess, initially, all the exothermicity of the reaction, but their initial relaxation is so rapid that it is only possible to observe a distribution among lower levels. The present method measures the *total* energy of the $N_2^{\ddagger}$, which should not be altered by relaxation to different vibrational levels. This total energy will only be altered by vibrational–translational energy exchange, which was found to be relatively slow in this system. The value of 20 ± 4 kcal mole^{-1}, measured at the beginning of the reaction zone, can then be taken as evidence against an initial distribution in which all the molecules are formed with energy close to the exothermicity of the reaction.

REFERENCES

1. J. W. Linnett and D. G. H. Marsden. Proc. Roy. Soc. (London), Ser. A, **234**, 489 (1956).
2. J. R. Dingle and D. J. Le Roy. J. Chem. Phys. **18**, 1632 (1950).
3. L. Elias, E. A. Ogryzlo, and H. I. Schiff. Can. J. Chem. **37**, 1680 (1959).
4. F. Kaufman and J. R. Kelso. J. Chem. Phys. **28**, 510 (1958).
5. K. Dressler. J. Chem. Phys. **30**, 1621 (1959).
6. N. Basco and R. G. W. Norrish. Can. J. Chem. **38**, 1769 (1960).
7. L. F. Phillips and H. I. Schiff. J. Chem. Phys. **36**, 3282 (1962).
8. J. T. Herron, J. L. Franklin, P. Brandt, and J. H. Dibeler. J. Chem. Phys. **30**, 879 (1959).
9. T. Wentinck, Jr., J. O. Sullivan, and K. L. Wray. J. Chem. Phys. **29**, 231 (1958).
10. R. A. Young. J. Chem. Phys. **34**, 1292 (1961).
11. J. E. Morgan and H. I. Schiff. J. Chem. Phys. In press.
12. J. H. Blackman. J. Fluid. Mech. **1**, 61 (1956).
13. S. J. Lukasik and J. E. Young. J. Chem. Phys. **27**, 1149 (1957).
14. P. W. Huber and A. Kantrowitz. J. Chem. Phys. **15**, 275 (1947).
15. R. N. Schwartz, Z. I. Slawsky, and K. F. Herzfeld. J. Chem. Phys. **20**, 1591 (1952).
16. R. A. Strenlow and A. Cohen. J. Chem. Phys. **30**, 257 (1959).
17. A. B. Callear. Private communication.
18. A. E. Beale and H. P. Broida. J. Chem. Phys. **31**, 1030 (1959).

Can. J. Chem. Downloaded from www.nrcresearchpress.com by 210.87.254.6 on 09/05/12
For personal use only.

A STUDY OF THE VAPOR PHASE REACTION OF OZONE WITH OLEFINS IN THE PRESENCE AND ABSENCE OF MOLECULAR OXYGEN[1]

Y. K. WEI[2] AND R. J. CVETANOVIĆ
Division of Applied Chemistry, National Research Council of Canada, Ottawa, Canada
Received December 12, 1962

ABSTRACT

Relative rates of reaction of ozone with a number of olefins in the vapor phase have been determined at room temperature in the presence and absence of molecular oxygen. In the absence of oxygen the rates appear to follow more closely an electrophilic trend, although some of the deviations observed previously in the presence of oxygen still persist to some extent. The ratio of olefin to ozone consumed is unity in the absence of oxygen and varies from about 1.4 to 2 in its presence. In the presence of molecular oxygen, therefore, a secondary attack on the olefins takes place as well. The yields of products are similarly affected.

INTRODUCTION

Reactions of ozone with olefins in the vapor phase are of importance from the point of view of chemistry of air pollution and have been recently reviewed (1) in that connection. The reactions are complex and are not fully understood. Their study is subject to considerable experimental and analytical difficulties. As a result there are uncertainties in the literature regarding the reaction order, the ratio of olefin to ozone consumed, and the rate constants.

In a previous study carried out in this laboratory (2, 3) a certain amount of information was obtained on the type of products formed in the vapor phase reactions of ozonized oxygen with a number of olefins (2). At the same time a competitive technique was used to determine the relative rate constants (3). As anticipated, these showed a general electrophilic trend, but there were also strong deviations from it in the case of some olefins. Although feasible explanations for these deviations could be suggested, there were also large differences between some of the observed rates and the corresponding values in the literature, obtained by different techniques. The present work was undertaken primarily with the object of checking the rate constants determined previously and obtaining some information on the role of the presence of excess molecular oxygen. Reactions have been carried out in the presence and absence of molecular oxygen under conditions where no appreciable temperature increase in the reaction mixture was detectable in the course of the reaction. Relative rate constants, ratios of olefin to ozone consumption, and the yields of some of the reaction products have been determined and compared. Qualitative observations of the aerosol formation have also been made.

EXPERIMENTAL

The reaction apparatus was constructed of pyrex glass and was incorporated into a conventional high-vacuum line. It contained an ozone-generating and -purifying section with a storage bulb, a calibrated volume with a sulphuric acid manometer, a 500-ml ozone–nitrogen mixer, and two matched 100-ml spherical reaction vessels. The arrangement is shown schematically in Fig. 1.

The ozonized oxygen was produced in a standard Tower ozone apparatus. It was purified by passing the mixture through a liquid nitrogen trap and slowly pumping out the oxygen and subjecting the condensed ozone to repeated bulb-to-bulb distillation *in vacuo*. Precautions were taken to guard against possible explosions. The freezing trap was surrounded by a steel cylinder and use was made also of a heavy protective

[1]*Issued as N.R.C. No. 7239.*
[2]*National Research Council Postdoctoral Fellow 1960–1962.*

Can. J. Chem. Downloaded from www.nrcresearchpress.com by 210.87.254.5 on 09/05/12
For personal use only.

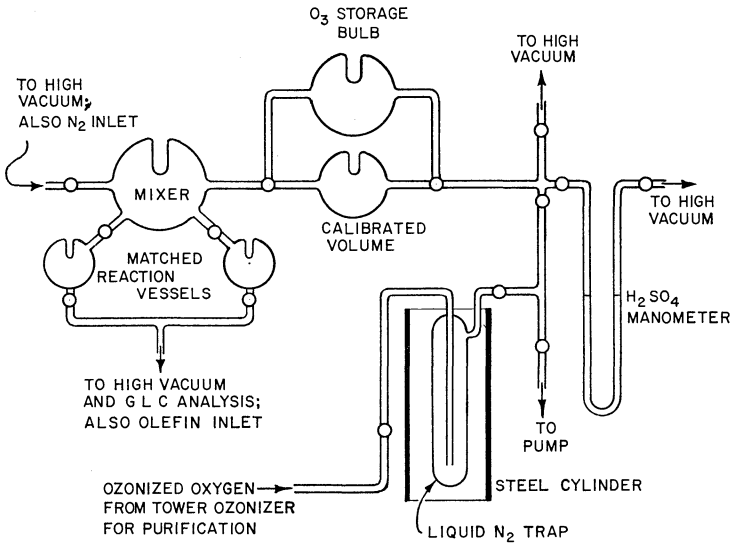

FIG. 1. Schematic diagram of a part of the reaction system.

safety glass shield. Only relatively quite small amounts of ozone (not greater than about 2 mmole) were handled at a time. Several small explosions occurred but the damage was slight and was limited mainly to the freezing trap.

The purity of the ozone was determined iodometrically and found to be 97±2 mole%. The calibrated volume provided with the sulphuric acid manometer was used to measure the required amount of ozone. This was then frozen into the mixer, where a known amount of nitrogen was admitted and allowed to mix with the ozone. The necessary amounts of the olefins were measured and transferred into the two reaction vessels. A known pressure of the diluent gas, nitrogen or oxygen, was then also introduced into the reaction vessels. After bringing up the mixtures of the gases to room temperature (25±2° C), the ozone–nitrogen mixture was expanded in turn into the two reaction vessels through the connecting capillaries. The amounts of ozone admitted into each of the two reaction vessels could be readily calculated and controlled by adjusting the pressures of the gases in the mixer and in the reaction vessels.

Batch procedure was employed. In most cases the same olefin, or mixture of a pair of olefins, was in both reaction vessels and different diluent gases (oxygen and nitrogen) were used so that the products and the relative rates could be compared. In some cases both vessels contained the same diluent gas but one contained a single olefin to monitor its products while the other contained the same olefin mixed with another olefin in order to determine their relative rate. In all cases the reactions in the two vessels were carried out under as similar conditions as possible.

The amounts of olefin and ozone used in the studies of the reaction products were 120±20 and 20±5 μmoles, respectively. Their initial concentrations in the diluent gases, before mixing for the reaction, were 2.0±0.2 mole% in the case of ozone, and 20±2 mole% in the case of the olefins. In the determinations of the relative rates, the total concentration of the two olefins was 30±5 mole% while the concentration of ozone remained unchanged. The total pressures of the gases in the mixer and in the reaction vessels were, respectively, 360±35 mm and 100±20 mm.

Care was taken to prevent the ozone from coming in contact with mercury or its vapors. Halofluorocarbon grease* was used for stopcocks exposed to gas mixtures containing ozone. With freshly greased stopcocks the ozone concentration calculated from the amounts of products formed was lower than the value calculated from the sharing ratios and the partial pressure of ozone in the mixer. However, the difference was not large and a good agreement was restored after two or three runs. The experimental arrangement used, with two matched reaction vessels operated under closely similar conditions, would compensate for any small consumption of ozone by the grease. Low ozone values were also observed when the sulphuric acid manometer was in use for a longer period of time, and it was then necessary to replace the acid.

The condensable reaction products were retained by pumping off the non-condensable gases slowly through a regulating stopcock, a capillary constriction, and three liquid nitrogen traps in series. The condensables were analyzed by gas–liquid chromatography (GLC) using a 12-ft, 1/4 in. I.D. copper column

**Kel–F 90 grease, obtained from the Chemical Division of Minnesota Mining and Manufacturing Company, St. Paul, Minn.*

Can. J. Chem. Downloaded from www.nrcresearchpress.com by 210.87.254.5 on 09/05/12
For personal use only.

packed with β,β'-thiodipropionitrile on firebrick and operated at 50±1° C. The reactant olefins were analyzed on the same column, although in a few cases their purity was checked on a 18-ft, 1/4 in. I.D. pyrex glass column packed with propylene carbonate on firebrick and operated at room temperature. Quantitative calibrations were made with standard samples. No attempt was made to analyze the non-condensable gases and only the main (non-hydrocarbon) products observed by GLC were followed quantitatively.

The olefins used were either Phillips research grade or American Petroleum Institute standard samples, with the exception of 4-methyl-2-pentene and 2-hexene, which were Phillips pure grade. The 2-hexene was a mixture of the cis and trans isomers with apparently less than about 10% of trans (as estimated roughly from the gas–liquid chromatogram).

The diluent gases used, oxygen and nitrogen, were passed through concentrated sulphuric acid, followed by a tube packed with potassium hydroxide and a tube packed with glass wool.

Thermocouples placed in wells in each of the two reaction vessels at a distance of about 2 cm from the orifice of the ozone inlet tube were used to determine any temperature change in the reacting gases taking place in the course of the reaction. No noticeable temperature increase was observed.

RESULTS

The major products of the vapor phase reaction of ozone with a number of olefins in the presence and absence of oxygen, as analyzed by GLC, are listed in Table I. The quantities are expressed as moles of products formed per mole of ozone originally employed. It should be pointed out that, as in the previous (2) work, the quantities reported are those observed *after* the passage of the condensables through the GLC column and may include any products of decomposition of the original compounds in the course of the analysis. In several experiments, in particular with 2,3-dimethyl-2-butene, the reaction mixture was left overnight in the reaction vessel (in the presence of oxygen) before removing the non-condensable gases and analyzing the condensables. In such cases there was a substantial increase in the yields of the main carbonyl products and a smaller increase in carbon dioxide.

For the olefins investigated the olefin consumption per mole of ozone was always close to unity when only nitrogen was used as the diluent. In the presence of oxygen, on the other hand, the ratios of olefin to ozone consumed were greater than unity and varied from 1.4 to 2.0 for different olefins. These values and the ratios of the main reaction products observed in the presence of oxygen (O_2) and its absence (N_2) are listed in Table II.

Formation of an aerosol in the course of the reaction was observed in many cases. It formed within a very short time after mixing the reactants, along the path of the inlet stream of ozone–nitrogen mixture, and diffused quickly throughout the reaction vessel. Only visual observations were made and crude estimates of its relative abundance for various olefins are given in the last column of Table II.

In some cases, mostly with olefins of more than four carbons, a non-volatile semi-transparent liquid deposited on the reaction vessel wall. It was of low volatility and could be pumped out only on heating (for example around 120° C). Inasmuch as this liquid was left in the reaction vessel, it appeared to affect the results of the subsequent run. In most cases a white film remained on the wall of the liquid nitrogen trap in which the products were condensed on pumping off the non-condensable gases. This deposit also was volatile when heated.

The competitive method described previously (3) was used to determine the relative rate constants. Two olefins (A_1, A_2) are made to compete for ozone in the reactions

$$A_1 + O_3 \rightarrow \alpha_1 P_1 + \text{other products} \quad [1]$$

$$A_2 + O_3 \rightarrow \alpha_2 P_2 + \text{other products.} \quad [2]$$

P_1 and P_2 are the main carbonyl products observed in the two reactions. The relative rate constants (k_1/k_2) were calculated by comparing the GLC peak heights (ΔP) of these

Can. J. Chem. Downloaded from www.nrcresearchpress.com by 210.87.254.5 on 09/05/12
For personal use only.

Can. J. Chem. Downloaded from www.nrcresearchpress.com by 210.87.254.5 on 09/05/12
For personal use only.

TABLE I

Yield of carbon dioxide, aldehydes, and ketones in the reactions of olefins with ozone in the presence and absence of oxygen
(Yields are expressed as number of moles formed per mole of ozone consumed; no analysis has been carried out for formaldehyde)

			Aldehydes*						Ketones†		
Olefin	Diluent	CO_2	A	P	B	*i*-B	V	*i*-V	Ac	ME	MP
Monoalkyl ethylenes											
Propylene	N_2	n.d.	0.27								
	O_2	n.d.	0.34								
1-Butene	N_2	0.15	0.10	0.26							
	O_2	0.25	0.11	0.38							
1-Pentene	N_2	0.16	0.053	0.053	0.24						
	O_2	0.24	0.019	0.087	0.32						
1-Hexene	N_2	0.14	0.035	0.015	0.035		0.25				
	O_2	0.20	0.010	0.015	0.055		0.30				
3-Methyl-1-butene	N_2	0.18	0.125			0.25			0.040		
	O_2	0.29	0.040			0.36			0.050		
3-Methyl-1-pentene	N_2	0.16	0.115	0.016				0.23‡	0.004	0.035	
	O_2	0.26	0.050	0.003				0.30‡	0.002	0.050	
4-Methyl-1-pentene	N_2	0.15	0.060			0.030		0.23§	0.020		
	O_2	0.24	0.010			0.080		0.30§	0.020		
1,1-Dialkyl ethylenes											
Isobutene	N_2	0.15	0.006						0.33		
	O_2	0.35	0.008						0.52		
2-Methyl-1-butene	N_2	0.14	0.105						0.070	0.26	
	O_2	0.30	0.205						0.050	0.44	
2-Methyl-1-pentene	N_2	0.14	0.035	0.075					0.035		0.22
	O_2	0.32	0.045	0.150					0.015		0.36

Can. J. Chem. Downloaded from www.nrcresearchpress.com by 210.87.254.5 on 09/05/12
For personal use only.

1,2-Dialkyl ethylenes									
cis-2-Butene	N_2	0.19	0.68						
	O_2	0.35	0.98						
trans-2-Butene	N_2	0.17	0.71						
	O_2	0.31	1.20						
cis-2-Pentene	N_2	0.20	0.32	0.30					
	O_2	0.36	0.52	0.45					
trans-2-Pentene	N_2	0.14	0.33	0.31					
	O_2	0.24	0.52	0.45					
2-Hexene (cis + trans)‖	N_2	0.18	0.32	0.040	0.25				
	O_2	0.32	0.46	0.052	0.34				
4-Methyl-2-pentene	N_2	0.18	0.30	0.010		0.33			
	O_2	0.30	0.40	0.002		0.48			
Trialkyl ethylenes									
2-Methyl-2-butene	N_2	0.15	0.40				0.33		
	O_2	0.41	0.76				0.56		
2-Methyl-2-pentene	N_2	0.13	0.036	0.36			0.26		
	O_2	0.40	0.076	0.63			0.48		
3-Methyl-2-pentene	N_2	0.11	0.39				0.001	0.30	
	O_2	0.32	0.73				0.005	0.50	
Tetraalkyl ethylenes									
2,3-Dimethyl-2-butene	N_2	0.11					0.65		
	O_2	0.42					1.45		

NOTE: n.d. = not determined.
*A = acetaldehyde, P = propionaldehyde, B = butyraldehyde, *i*-B = isobutyraldehyde, V = valeraldehyde, *i*-V = isovaleraldehyde.
†Ac = acetone, ME = methyl ethyl ketone, MP = methyl propyl ketone.
‡2-Methylbutanal.
§3-Methylbutanal.
‖Mixture of cis and trans (trans isomer estimated by GLC to be less than 10%).

Can. J. Chem. Downloaded from www.nrcresearchpress.com by 210.87.254.5 on 09/05/12
For personal use only.

TABLE II

Ratios of the yields of the major products and of the olefin consumption per mole of ozone in the presence of molecular oxygen (R_{O_2}) and its absence (R_{N_2}) and qualitative (visual) observations of aerosol formation (vsc = very slightly cloudy; sc = slightly cloudy; c = cloudy, vc = very cloudy)

	R_{O_2}/R_{N_2}				Aerosol formation	
Olefin	Olefin consumption	CO_2	Aldehydes*	Ketones*	O_2†	N_2‡
Monoalkyl ethylenes						
Propylene	1.4	n.d.	A 1.25		vsc	vsc
1-Butene	1.4	1.65	P 1.45		c	sc
1-Pentene	1.5	1.50	B 1.40		c	c
1-Hexene	1.5	1.45	V 1.20		vc	vc
3-Methyl-1-butene	1.5	1.60	*i*-B 1.42		c	sc
3-Methyl-1-pentene	1.5	1.60	*i*-V 1.45§		vc	c
4-Methyl-1-pentene	1.5	1.60	*i*-V 1.30‖		c	c
1,1-Dialkyl ethylenes						
Isobutene	1.5	2.30		Ac 1.55	vsc	vsc
2-Methyl-1-butene	1.6	2.15		ME 1.70	c	sc
2-Methyl-1-pentene	1.6	2.30		MP 1.62	vc	c
1,2-Dialkyl ethylenes						
cis-2-Butene	1.5	1.85	A 1.45		vsc	vsc
trans-2-Butene	1.5	1.85	A 1.70		vsc	vsc
cis-2-Pentene	1.5	1.80	A 1.60; P 1.50		sc	sc
trans-2-Pentene	1.5	1.60	A 1.60; P 1.50		sc	sc
2-Hexene (cis + trans)	1.5	1.75	A 1.50; B 1.35		vc	vc
4-Methyl-2-pentene	1.5	1.65	A 1.35; *i*-B 1.45		vc	vc
Trialkyl ethylenes						
2-Methyl-2-butene	1.7	2.70	A 1.90	Ac 1.70	sc	sc
2-Methyl-2-pentene	1.7	3.05	P 1.75	Ac 1.85	c	sc
3-Methyl-2-pentene	1.7	2.90	A 1.85	ME 1.65	c	sc
Tetraalkyl ethylenes						
2,3-Dimethyl-2-butene	2.0	3.80		Ac 2.20	c	sc

NOTE: n.d. = not determined.
*Same symbols as in footnotes * and † of Table I.
†Experiments in the presence of oxygen.
‡Experiments in the absence of oxygen.
§2-Methylbutanal.
‖3-Methylbutanal.

products at different ratios of the concentrations of the two olefins (A_1/A_2):

$$\frac{\Delta P_1}{\Delta P_2} = \frac{k_1}{k_2}\frac{\alpha_1}{\alpha_2}\frac{(A_1)}{(A_2)}. \qquad [a]$$

For the competitive reaction of isobutene and ethylene the following expression was used instead (P_1 = acetone):

$$\frac{\Delta P_1}{\Delta P_1{}^* - \Delta P_1} = \frac{k_1}{k_2}\frac{(A_1)}{(A_2)}. \qquad [b]$$

ΔP^* is the amount of product formed when one of the competing olefins is taken singly, and $\alpha = \Delta P^*/\Delta O_3$.

Experimental data gave in most cases fairly good linear plots, in agreement with these expressions, and from their slopes the mean values of the relative rate constants given in Table III were obtained. The major products used in these determinations are indicated in the table. For some internal olefins both major carbonyl compounds produced in the reaction could be conveniently measured. In such cases the relative rates of these olefins could be checked for consistency from two or more linear plots using different combinations of the major carbonyl compounds from the same set of experimental data. An example of such plots is given in Fig. 2.

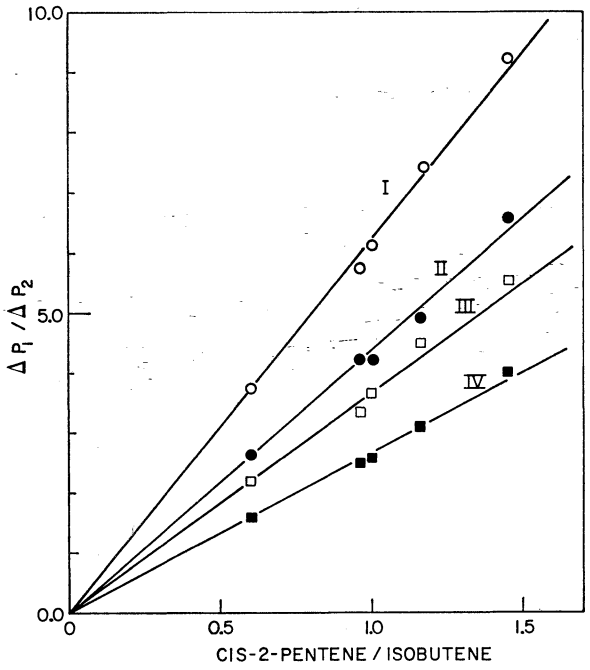

FIG. 2. Plots of equation [a] for *cis*-2-pentene and isobutene. The curves are: I and II for P_1 = acetaldehyde, P_2 = acetone, in the presence (I) and absence (II) of oxygen; III and IV for P_1 = propionaldehyde, P_2 = acetone, in the presence (III) and absence (IV) of oxygen.

A greater number of values of relative rate constants was obtained for 2,3-dimethyl-2-butene competing for ozone with a number of different olefins. The values obtained, expressed relative to isobutene as unity, are shown in Table IV and are discussed in the following section.

Can. J. Chem. Downloaded from www.nrcresearchpress.com by 210.87.254.5 on 09/05/12
For personal use only.

Can. J. Chem. Downloaded from www.nrcresearchpress.com by 210.87.254.5 on 09/05/12
For personal use only.

TABLE III

Relative rate constants determined in the presence of molecular oxygen (k_{O_2}) and its absence (k_{N_2}) (the values for isobutene are taken as unity)

Details of determinations					
		Products measured*		Rate constants	
Olefin (A_1)	Competing olefin (A_2)	P_1	P_2	k_{O_2}	k_{N_2}
Ethylene					
Ethylene	Isobutene	—	Ac	0.32	0.21
Monoalkyl ethylenes					
Propylene	Isobutene	A	Ac	1.30	0.95
1-Butene	Isobutene	P	Ac	1.10	0.85
1-Pentene	Isobutene	B	Ac	1.10	0.85
1-Hexene	Isobutene	V	Ac	1.25	1.05
3-Methyl-1-butene	Isobutene	*i*-B	Ac	0.95	0.75
3-Methyl-1-pentene	Isobutene	*i*-V†	Ac	0.90	0.75
4-Methyl-1-pentene	Isobutene	*i*-V‡	Ac	1.15	0.85
1,1-Dialkyl ethylenes					
Isobutene	Taken as standard for comparison			1.00	1.00
2-Methyl-1-butene	1-Butene	ME	P	1.30	1.25
2-Methyl-1-pentene	1-Pentene	MP	B	1.30	1.25
1,2-Dialkyl ethylenes					
cis-2-Butene	Isobutene	A	Ac	3.4	2.0
trans-2-Butene	Isobutene	A	Ac	4.3	2.2
cis-2-Pentene	Isobutene	A	Ac	3.4	2.4
		P	Ac	3.4	2.4
trans-2-Pentene	Isobutene	A	Ac	4.1	2.7
		P	Ac	4.3	2.8
2-Hexene (cis + trans)	Isobutene	A	Ac	3.6	2.7
		B	Ac	3.6	2.6
	2-Methyl-2-pentene	A	P	3.3	2.3
		B	Ac	3.4	2.7
4-Methyl-2-pentene	Isobutene	A	Ac	3.5	2.3
		i-B	Ac	3.5	2.4
Trialkyl ethylenes					
2-Methyl-2-butene	1-Butene	Ac	P	3.5	3.2
2-Methyl-2-pentene	3-Methyl-2-pentene	P	Ac	3.5	3.2
		A	Ac	3.3	3.2
3-Methyl-2-pentene	Isobutene	A	Ac	3.4	3.2
		ME	Ac	3.5	3.3
Tetraalkyl ethylenes					
2,3-Dimethyl-2-butene	Mean values, see Table IV for details			4.8	5.5

*Symbols as in footnotes * and † of Table I.
†2-Methylbutanal.
‡3-Methylbutanal.

TABLE IV

Relative rate of reaction of ozone with 2,3-dimethyl-2-butene (isobutene taken as unity) as determined competitively with different olefins (In all cases A_1 = 2,3-dimethyl-2-butene, P_1 = acetone)

Competing olefin (A_2)	Products from A_2 used in determinations (P_2)	Mean rate constants k_{O_2}*	Mean rate constants k_{N_2}†
A. Competition with monoalkyl ethylenes			
1-Butene	Propionaldehyde	4.0	5.4
1-Pentene	Butyraldehyde	4.2	5.5
1-Hexene	Valeraldehyde	4.6	6.6
3-Methyl-1-butene	Isobutyraldehyde	4.0	5.3
B. Competition with 1,1-dialkyl ethylenes			
2-Methyl-1-butene	Methyl ethyl ketone	3.0	4.5
C. Competition with 1,2-dialkyl ethylenes			
cis-2-Butene	Acetaldehyde	5.6	5.5
cis-2-Pentene	Acetaldehyde	5.5	5.9
	Propionaldehyde	5.6	5.8
2-Hexene (cis + trans)	Acetaldehyde	5.2	5.8
	Butyraldehyde	6.0	6.2
4-Methyl-2-pentene	Acetaldehyde	5.1	5.2
	Isobutyraldehyde	6.3	6.4
D. Competition with trialkyl ethylenes			
3-Methyl-2-pentene	Acetaldehyde	4.0	4.7
	Methyl ethyl ketone	4.0	4.7
	Mean values	4.8	5.5

*Determined in the presence of O_2.
†Determined in the absence of O_2.

DISCUSSION

Of primary interest for the present work have been the determinations of the relative rate constants and these will be discussed first.

Equations [*a*] and [*b*], used in the evaluation of the rate constants, are valid provided the ratios of the monitored products (P_1, P_2) formed per mole of ozone consumed are always proportional to the rates of the respective primary reactions [1] and [2] of ozone with the olefins, both when the olefins react singly and in pairs. This presupposes that no cross interaction of any kind occurs which would tend either to decrease or increase the yields of these products relative to each other when two olefins compete for ozone. Absence of such interactions has to be verified by cross checking the relative rate constants obtained with a number of different overlapping pairs of competing olefins. The results of a number of experiments of this kind are given in Table III and in particular in Table IV. If the attention is focussed for the moment on the relative values of rate constants obtained in the absence of molecular oxygen (k_{N_2}), there seems to be a fairly good overall consistency. Some scatter of the k_{N_2} values in Table IV is probably explainable by the cumulative experimental errors. At the same time some cross interaction cannot be ruled out, although it seems justifiable to assume that this cannot be large. In view of this the k_{N_2} values in Table III are believed to represent to a good approximation the relative second-order rate constants of the primary reactions of ozone with the olefins. A support for this view comes also from the simple stoichiometry observed in the absence of molecular oxygen.

The relative rate constants in the absence of molecular oxygen (k_{N_2}) are seen in Table III to be distinctly dependent on the number of alkyl groups attached to the two doubly bonded carbon atoms. They increase continuously with the number of substituents and

Can. J. Chem. Downloaded from www.nrcresearchpress.com by 210.87.254.5 on 09/05/12
For personal use only.

evidently follow an electrophilic trend, as anticipated. At the same time one anomaly is immediately evident: the rates of 1,1-dialkyl ethylenes are appreciably smaller than those of the 1,2-dialkyl derivatives, although they would be expected to be comparable in magnitude. This is perhaps brought out more clearly in the "free energy" plot against the corresponding rates of the oxygen atom reactions (k_O) in Fig. 3. The latter exhibit an

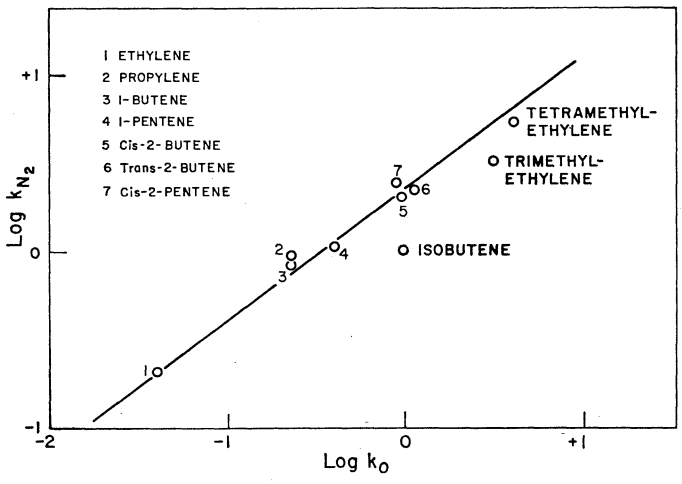

FIG. 3. Free energy plot for the reactions of olefins with ozone in the absence of molecular oxygen (k_{N_2}) and with the ground-state oxygen atoms (k_O).

electrophilic trend (4) and the plot shows therefore that there is also a general electrophilic trend in the k_{N_2} values. This trend is considerably better than that shown by k_{O_2} values obtained previously (3) or in the present work. At the same time, as observed earlier with the k_{O_2} values, the 1,1-dialkyl, trialkyl, and tetraalkyl ethylenes still show smaller rates than would be expected although the deviations are now smaller. As suggested previously, these deviations can be explained either by a large steric hindrance of two alkyl groups on the same carbon atom of the double bond or by their adverse inductive effect which slows down the nucleophilic ring closure in the formation of the "initial ozonides". This is discussed in greater detail in the earlier communication (3) and the same views appear to be still pertinent.

In the presence of molecular oxygen there is a departure from the simple stoichiometry and the ratios of olefin to ozone consumed are greater than unity. Evidently a secondary attack of some kind on the olefins takes place. If this secondary attack on the olefins were only due to a regeneration of ozone in some manner, i.e. involving chain reactions of very short chain length, the k_{O_2} and k_{N_2} values could be expected to be the same. Although the two are seen in Tables III and IV to be roughly similar, they are not the same and it appears therefore likely that in the presence of molecular oxygen active species other than ozone may be involved in the process as well. This in itself could be responsible for an effect on the relative rates determined by the present technique similar in its consequences to the cross interaction discussed above. The k_{O_2} values in Table IV are indeed appreciably less mutually consistent than the k_{N_2} values.

In the case of the 1,2-dialkyl ethylenes the k_{O_2} values are in particular much greater than the corresponding k_{N_2} values. Inasmuch as these differences may be still further accentuated under drastically different experimental conditions, an explanation could

Can. J. Chem. Downloaded from www.nrcresearchpress.com by 210.87.254.5 on 09/05/12
For personal use only.

perhaps be found for the discrepancies in some of the literature values of the rate constants mentioned in the Introduction, notably those of the 1,2-dialkyl ethylenes. However, definite conclusions would have to be based on systematic studies of the effect of such large variations of experimental conditions. At the moment, in comparing the rate data in the literature, invariably obtained in the presence of molecular oxygen, a potential importance of the particular conditions employed should be borne in mind.

The rate constants obtained in the presence of molecular oxygen (k_{O_2}) agree reasonably well with the previous determinations of Vrbaski and Cvetanović (3). In the earlier work some temperature increase probably did occur in the course of the reaction and it was feared that this might have affected the values of the rate constants. However, this effect could not have been large in view of the fair agreement of the rates with the present k_{O_2} values. In the present experiments, with increased amounts of diluent gases and still slower ozone introduction, no temperature increase was observed in the reaction vessels.

The yields of the products formed in the presence of molecular oxygen agree in general reasonably well with the values obtained previously (2). However, lower yields of carbon dioxide have been obtained in a number of cases. This may be due to the fact that, as pointed out, some temperature increase in the course of the reaction probably did occur in the earlier work. The yields of ketones agree well with the previous data, while those of aldehydes show some differences, perhaps in part due to different GLC column temperature used (50° in present work and 125° in the earlier work). However, such differences in the yields of the products as have been observed have evidently not resulted in large differences in the relative rate constants (k_{O_2}). This is no doubt due to the fact that in each study the experiments with single olefins and the competing olefin pairs have been done under mutually comparable conditions.

The trend in the rates of ozone–olefin reactions is very similar to that of the corresponding photochemical reactions of NO_2 with olefins in the presence of molecular oxygen. This is true both for the k_{N_2} and k_{O_2} values. A log k – log k plot of the k_{O_2} values obtained in the present work and the corresponding "maximum" rates determined by Schuck and Doyle (5, 1) for the latter reactions (k_{NO_2}) is shown in Fig. 4. The plot indicates a close similarity in the electronic and steric requirements of the electrophilic species responsible for olefin consumption in the two processes, although this does not mean that they are necessarily identical. It should be noted that isobutene deviates significantly from the linear plot and the slope is appreciably different from unity. (With the k_{N_2} values isobutene deviates much less, but the slope is again about the same and there is also a certain amount of scatter in the case of some olefins.) Considerable similarity between the two systems may be expected, since it is likely that in the photochemical reaction of NO_2 and olefins in air the reaction of the ozone generated in the process with the olefins is important (1, 6). The photochemical NO_2 reactions with olefins play a very important role in the formation of "photochemical smog" and have received considerable attention in recent years (1, 6–8). There can be little doubt that this process has much in common with the corresponding ozone reactions, although both processes are complex and their full understanding will require considerable further work.

The yields of the major products observed are invariably higher in the presence of molecular oxygen than in its absence, as is shown in Table II. It is also seen that in the presence of molecular oxygen olefin consumption is greater than stoichiometric. Under such conditions, a secondary attack on the olefins evidently takes place. The exact nature of these secondary processes and the significance of the apparently systematic trends with olefin structure shown in Table II would be difficult to ascertain on the basis of the

Can. J. Chem. Downloaded from www.nrcresearchpress.com by 210.87.254.5 on 09/05/12
For personal use only.

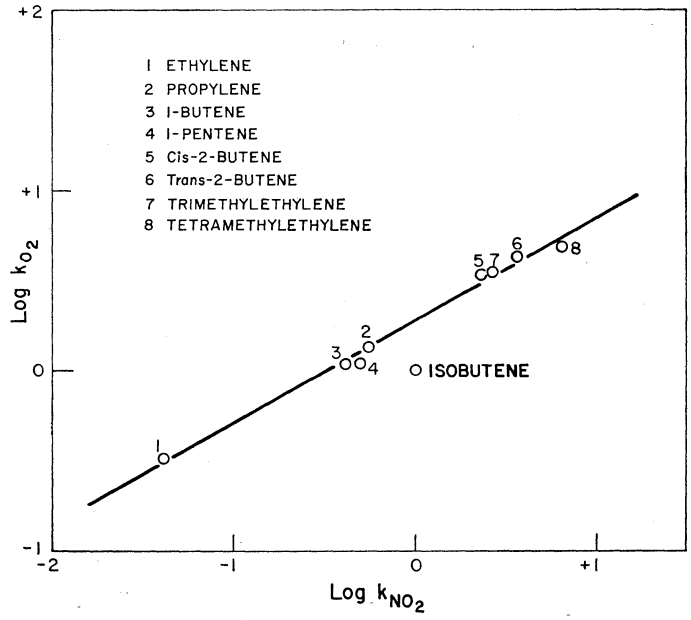

FIG. 4. Log k – log k plot for the reactions of ozone with olefins in the presence of molecular oxygen (k_{O_2}) and the photochemical reactions of NO_2 with olefins in air (k_{NO_2}). (The k_{O_2} values are those obtained in this work, the k_{NO_2} values have been taken from the data summarized in reference 1.)

experimental information available at present. In this connection the formation of the "abnormal" carbonyl products formed in these reactions is of interest.

It was shown in the earlier work (2) that in addition to the major carbonyl compounds, i.e. the expected "normal" products of ozonolysis, smaller amounts of carbonyl compounds containing fewer carbon atoms (one or more) were also produced. These degradations were visualized as perhaps being induced by "peroxide–formate" rearrangement, or other types of rearrangement of the initially formed zwitterions, followed by decomposition, or as being due to secondary oxidation. However, it is found now that these products are not restricted to the reactions in the presence of molecular oxygen but occur also in its absence, as shown in Table I. Furthermore these products seem to fall largely into two groups, those in which the yields are smaller and those in which they are larger when molecular oxygen is present, the latter more or less following the same trend as the "normal" carbonyl products.

A unique explanation of these observations cannot be given but it may be useful to consider some tentative possibilities, subject to modifications or rejection as more extensive experimental results become available. That these degradations do not occur only as a result of secondary attack by molecular oxygen is evident, and, at least in its absence, rearrangement of zwitterions is likely to play an important role. This, again, can occur in various ways, such as single and consecutive 1,2 carbon-to-carbon shifts of H and alkyl groups or via formation of intermediate cyclic complexes. For purposes of illustration, the following example of a possible course of rearrangement of this latter kind may be given:

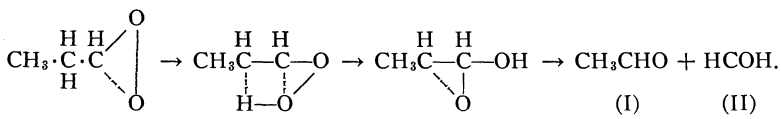

Can. J. Chem. Downloaded from www.nrcresearchpress.com by 210.87.254.5 on 09/05/12
For personal use only.

By allowing internal interactions of this kind with H-atoms and alkyl groups not only on β but also on γ (etc.) carbon atoms, and assuming that the fragments (II) are as a rule not stabilized to the corresponding carbonyl compounds except in some very simple cases, formation of the degradation carbonyl products in Table I can be qualitatively explained. It seems that in most cases the yields of the degradation products formed by interaction with the substituents on the γ carbon atom decrease in the presence of molecular oxygen, while those involving β-carbon interaction increase. This would suggest that there may be an attack by molecular oxygen on β-C—H bonds of the zwitterions in competition with internal rearrangement and that this may be responsible for the increase of the yields of the degradation products formed by β-carbon interaction and the decrease of the products formed by γ-carbon interaction. Interactions of this kind involving oxygen could conceivably be also responsible for the generation of active species which induce the secondary attack on the olefins in the presence of molecular oxygen. At the same time, it should be stressed that there are some exceptions (β product yields *decreasing* in the presence of molecular oxygen) which require further refinements of this simple picture. It is also possible that degradations may be occurring as a result of internal rearrangements of zwitterions followed by molecular detachment of olefins, as discussed briefly in the earlier work (2), with simultaneous formation of zwitterions containing fewer carbon atoms. Such a mechanism, however, is not likely to be able to explain all the "abnormal" carbonyl products.

The observed increased complexity of the reaction of ozone with olefins in the presence of molecular oxygen is in agreement with some earlier conclusions by other workers (1). Smith and Eastman (9) have recently studied the reaction of ozonized oxygen with 2,3-dimethyl-2-butene in the vapor phase and have observed a consumption of about two moles of olefin per mole of ozone, in close agreement with the present findings. They suggest that two reactions occur simultaneously, attack of ozone at the carbon–carbon double bond and attack of oxygen at the allylic position of the olefin. This is similar to the tentative possibilities discussed here. However, the details of such interactions, as already stressed, must remain uncertain at present.

REFERENCES

1. P. A. LEIGHTON. Photochemistry of air pollution. *In* Physical chemistry. A series of monographs. Vol. IX. Academic Press, New York. 1961.
2. T. VRBASKI and R. J. CVETANOVIĆ. Can. J. Chem. **38**, 1063 (1960).
3. T. VRBASKI and R. J. CVETANOVIĆ. Can. J. Chem. **38**, 1053 (1960).
4. R. J. CVETANOVIĆ. Can. J. Chem. **38**, 1678 (1960).
5. E. A. SCHUCK and G. J. DOYLE. Air Pollution Foundation Report 29, San Marino, California. 1959.
6. E. R. STEPHENS. Chemical reactions in the lower and upper atmosphere. Interscience, New York. 1961. p. 51.
7. C. S. TUESDAY. Chemical reactions in the lower and upper atmosphere. Interscience, New York. 1961. p. 15.
8. S. SATO and R. J. CVETANOVIĆ. Can. J. Chem. **36**, 279, 970, 1668 (1958); **37**, 953 (1959).
9. H. E. SMITH and R. H. EASTMAN. J. Am. Chem. Soc. **83**, 4274 (1961).

Can. J. Chem. Downloaded from www.nrcresearchpress.com by 210.87.254.5 on 09/05/12
For personal use only.

5-ARYL- AND 5-ALKYL-1,2,3,4-THIATRIAZOLES

SYNTHETIC, SPECTROSCOPIC, AND DEGRADATIVE STUDIES[1, 2]

EUGENE LIEBER[3] AND C. N. R. RAO[4]

Department of Chemistry, Roosevelt University, Chicago, Illinois, U.S.A.

AND

R. C. ORLOWSKI

Department of Chemistry, DePaul University, Chicago, Illinois, U.S.A.

Received November 8, 1962

ABSTRACT

A number of 5-(*p*-substituted)phenyl-1,2,3,4-thiatriazoles have been synthesized by the diazotization of *p*-substituted thiobenzhydrazides or by the reaction of sodium thiobenzoylthioglycollates with sodium azide. The thermal decomposition of these thiatriazoles yields nitriles, nitrogen, and sulphur. 5-Alkyl-1,2,3,4-thiatriazoles are very unstable and readily decompose to nitriles. Infrared and ultraviolet absorption spectra of 5-(*p*-substituted)phenyl-1,2,3,4-thiatriazoles have been studied. Infrared spectra of several thiohydrazides have also been studied and there appears to be no thiol–thione tautomerism in these derivatives. The thiatriazole ring is found to be electron withdrawing.

INTRODUCTION

The existence of the 1,2,3,4-thiatriazole system was firmly established by Lieber and co-workers (1–5). It has been shown that the diazotization of 4-substituted thiosemicarbazides, as well as the reaction of alkyl- and aryl-isothiocyanates with hydrazoic acid, leads to 5-(substituted)amino-1,2,3,4-thiatriazoles (1, 2). The reaction product of azide ion with carbon disulphide has been shown to possess the 1,2,3,4-thiatriazoline-5-thione structure and not the acyclic azidodithiocarbonic acid structure (4). The esters of the so-called azidodithiocarbonic acid have been found to be either 5-substituted mercapto-1,2,3,4-thiatriazoles or 4-substituted-1,2,3,4-thiatriazoline-5-thiones (5). In the present communication, we report the synthesis of 5-alkyl- and 5-(substituted)phenyl-1,2,3,4-thiatriazoles (I) by two independent methods.* We have also investigated the

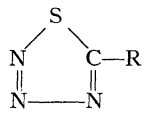

I

R = alkyl or *p*-substituted phenyl

thermal decomposition and infrared and near-ultraviolet absorption spectra of these thiatriazoles (I). In addition, we have studied the infrared spectra of 4-(substituted)-thiobenzhydrazides and aliphatic thiohydrazides.

[1]*This work was supported by Contract DA-44-009-ENG-4798, Basic Research Group, ERDL, Basic Research Group, Fort Belvoir, Virginia.*

[2]*Abstracted in part from the Master's thesis, DePaul University, of R. C. Orlowski, June 1960.*

[3]*To whom all the correspondence should be addressed, at the Department of Chemistry, Roosevelt University, Chicago 5, Illinois.*

[4]*Department of Physical Chemistry, Indian Institute of Science, Bangalore, India.*

**After the completion of these studies, it was noted that Kirmse (6) and Smith and Kenny (7) had synthesized some of the compounds of type I.*

Can. J. Chem. Downloaded from www.nrcresearchpress.com by 210.87.254.105 on 09/05/12
For personal use only.

Can. J. Chem. Downloaded from www.nrcresearchpress.com by 210.87.254.105 on 09/05/12
For personal use only.

EXPERIMENTAL*

Thiobenzoylthioglycolic Acid

To an ethanolic solution of potassium sulphide (equivalent of 1 mole), 97.8 g (0.5 mole) of phenyl chloroform was added slowly with stirring at about 50° C. The reaction mixture was stirred for another 15 minutes after the addition was complete (addition time 80 minutes) and was cooled to about 0° C. A solution of 62.4 g of chloroacetic acid and 38 g of sodium carbonate in 250 ml of water was then added and the temperature of the reaction mixture was maintained at about 5° C for 48 hours. The reaction mixture was then acidified with 95 ml of ice-cold aqueous sulphuric acid (50%). A dark red compound precipitated, which was washed with 200 ml of water, dried under vacuum, and recrystallized from 250 ml of benzene. The yield was 47.5 g (44.8%), m.p. 126–128° C, lit. m.p. 126.5–128° C (8, 9). Anal. Calc. for $C_9H_8O_2S_2$: S, 29.2. Found: S, 28.8.

p-Chlorothiobenzoylthioglycolic Acid

An orange crystalline solid, m.p. 118° C, was prepared starting from carbon disulphide and *p*-chlorophenylmagnesium bromide. The resulting product was treated with ice and to the aqueous layer a solution of chloroacetic acid and sodium carbonate was added. After standing for 48 hours at 5° C, the reaction mixture was acidified with ice-cold aqueous sulphuric acid. The resulting orange solid was crystallized from benzene, furnishing a yield of 24%, m.p. 117–118.5° C. Anal. Calc. for $C_9H_7O_2S_2Cl$: S, 25.9. Found: S, 25.8. This procedure is essentially the same as that of Smith and Kenny (7) but the yield in this investigation was considerably higher.

p-(N,N-Dimethylamino)thiobenzoylthioglycolic Acid

A yellowish brown solid, m.p. 168–172° C (decomp.), was prepared in 58% yield from *p*-bromo-N,N-dimethylaniline following the procedure described for the *p*-chloro analogue. Anal. Calc. for $C_{11}H_{13}O_2NS_2$: N, 5.48; S, 25.1. Found: N, 5.36; S, 24.8.

p-Methoxythiobenzoylthioglycolic Acid

To a solution of 68.1 g (0.5 mole) of *p*-anisaldehyde in 150 ml of 95% ethanol at 80° C, ammonium polysulphide solution was added dropwise with stirring. The reaction mixture was refluxed for 10 minutes and cooled to room temperature. The mother liquor was then decanted from the resinous precipitate. To the resinous precipitate in the flask was added a solution of 20 g of sodium hydroxide in 100 ml of 95% ethanol. The resulting solution was kept at 50° C for 16 hours with continuous stirring. The solution was then filtered and the precipitate washed with 50 ml of warm water. The filtrate, washings, and the mother liquor were taken in a 2-liter beaker and covered with 500 ml of ethyl ether. *p*-Methoxydithiobenzoic acid was then liberated by the slow, careful addition of 400 ml of ice-cold 6 *N* hydrochloric acid. The ether layer was extracted with 200-ml portions of 1.25 *N* potassium hydroxide. The basic extracts were treated with a solution of 62.4 g of chloroacetic acid and 38 g of sodium carbonate in 250 ml of water. This solution was kept at 5° C for 48 hours, after which the sodium salt precipitated. The solution and precipitate were acidified with 200 ml of 6 *N* hydrochloric acid. The product was crystallized from 95% ethanol to furnish 32.5 g (26.8%) of orange-yellow crystals, m.p. 125–127° C, lit. m.p. (7) 124–125° C. Anal. Calc. for $C_{10}H_{10}O_3S_2$: S, 26.5. Found: S, 26.1. Smith and Kenny (7) have prepared *p*-methoxythiobenzoylthioglycolic acid in 10% yield starting from *p*-bromoanisole and carbon disulphide.

p-Hydroxybenzoylthioglycolic Acid

A red solid, m.p. 196° C (decomp.), was prepared in 24% yield starting from *p*-hydroxybenzaldehyde, by a procedure similar to that described for the *p*-methoxy analogue. Anal. Calc. for $C_9H_8O_3S_2$: S, 28.1. Found: S, 28.2. A small amount of *p,p'*-dihydroxybenzyldisulphide was also isolated.

p-Methylthiobenzoylthioglycolic Acid

An orange-red solid, m.p. 121–122° C, was prepared in 20% yield starting from *p*-bromotoluene and carbon disulphide employing the procedure described for the *p*-chloro analogue. Anal. Calc. for $C_{10}H_{10}O_2S_2$: S, 28.3. Found: S, 28.6.

Phenylthioacetylthioglycolic Acid

A yellow solid, m.p. 77–79° C (10), was prepared in 28% yield starting from benzylmagnesium bromide and carbon disulphide by the procedure described for the *p*-chlorothiobenzoyl analogue. Anal. Calc. for $C_{10}H_{10}O_2S_2$: S, 28.3. Found: S, 28.0.

Sodium Cyclohexanethiocarbonylthioglycolate

A yellow solid, m.p. 230–245° C (decomp.), was prepared in 23% yield starting from cyclohexylmagnesium bromide. Anal. Calc. for $C_9H_{13}O_2S_2Na$: S, 26.7. Found: S, 26.4. The free acid was not prepared. Smith and Kenny (7) have obtained a 3% yield of the acid.

**All melting points are uncorrected and were determined on a Fisher–Johns apparatus. Microanalyses were by Dr. C. Weiler and Dr. F. B. Strauss, Oxford, England.*

p-Nitrobenzoylthioglycolic Acid

It was not possible to prepare this compound by any of the procedures described. Another possibility studied was the reaction of *p*-nitroethylthionbenzoate with hydrazine. However, it was found that the reaction of ethylthionbenzoate with 85% hydrazine in ethyl ether did not yield thiobenzhydrazide, as reported by Matusi (11). The only product isolated was a clear oil (b.p. 188–191° C) which contained nitrogen.

p-Substituted Thiobenzhydrazides and Aliphatic Thiohydrazides

A solution of hydrazine hydrate was added dropwise with stirring to an alkaline solution of the thioglycolic acid at 0° C. The solution was then acidified with glacial acetic acid and the product recrystallized from ethanol–water solvent. The data on all the hydrazides thus prepared are given in Table I. In the

TABLE I

p-Substituted thiobenzhydrazides and aliphatic thiohydrazides, $RC(S)NHNH_2$

R	% yield	M.p. (°C)	Cryst. form	Formula	% S Calc.	% S Found	% N Calc.	% N Found
C_6H_5*	60	70–71	White plates	$C_7H_8N_2S$	21.06	20.75	18.41	18.49
4-ClC_6H_4†	73	123–124.5	Yellow plates	$C_7H_7N_2SCl$	17.18	17.18	15.01	15.28
4-$CH_3OC_6H_4$‡	62	127	White plates	$C_8H_{10}ON_2S$	17.60	18.04	15.38	15.40
4-$CH_3C_6H_4$	65	138–139	Yellow plates	$C_8H_{10}N_2S$	19.29	19.40	16.68	16.38
4-OHC_6H_4	60	215	White needles	$C_7H_8ON_2S$	19.06	18.95	16.66	16.90
4-$N(CH_3)_2C_6H_4$	72	165–168	Orange powder	$C_9H_{13}N_3S$	16.42	16.80	21.52	21.90
$C_6H_5CH_2$§	50	67–68	Yellow plates	$C_8H_{10}N_2S$	—	—	—	—
Cyclo-C_6H_{11}	51	105–107	White plates	$C_7H_{14}N_2S$	20.26	20.60	17.71	17.90

*Reference 8, m.p. 71–72° C.
†Reference 7, m.p. 123–124° C.
‡Reference 7, m.p. 123.5–124° C.
§Decomposes on standing at room temperature.
‖Reference 7, m.p. 106–107° C.

case of the *p*-hydroxythiobenzhydrazide, acetic acid was added just to the point of neutralization since this compound does not precipitate from acidic solutions. In the preparation of thiobenzhydrazide, a small quantity of 2,5-diphenyl-1,3,4-thiadiazole, m.p. 141–142.5° C, lit. (8) m.p. 141–142° C, was isolated.

p-Nitrophenylhydrazone Derivatives

One gram of the hydrazide and 0.8 g of *p*-nitrobenzaldehyde were dissolved in 10 ml of 95% ethanol, and a drop of concentrated hydrochloric acid was added. The mixture was vigorously shaken and warmed in a hot-water bath for 10 minutes and then allowed to cool to room temperature. The *p*-nitrophenylhydrazones, 4-$NO_2C_6H_4NNHC(S)R$, thus prepared were: (1) R = $C_6H_5CH_2$, m.p. 174–176° C, red powder, 83% yield. Anal. Calc. for $C_{15}H_{13}O_2N_3S$: S, 10.2; N, 13.4. Found: S, 10.4; N, 13.6. (2) R = cyclo-C_6H_{11}, m.p. 124–126° C (lit. (7) m.p. 125–126° C), 87% yield. Anal. Calc. for $C_{14}H_{17}O_2N_3S$: S, 10.5; N, 13.8. Found: S, 10.4; N, 13.6. (3) R = 4-$(CH_3)_2NC_6H_4$, m.p. 174–176° C, red powder, 83% yield. Anal. Calc. for $C_{16}H_{16}O_2N_4S$: S, 9.4; N, 16.4. Found: S, 9.8; N, 16.4.

1-Naphthylhydrazone Derivatives

The derivatives, $C_{10}H_7CHNNHC(S)C_6H_4R$, were obtained as white felted needles from 1-naphthaldehyde using a procedure analogous to that described for the *p*-nitrophenylhydrazones: (1) R = H, m.p. 136.5–138° C, 86% yield. Anal. Calc. for $C_{18}H_{14}N_2S$: S, 11.0; N, 9.6. Found: S, 10.8; N, 9.7. (2) R = 4-Cl, m.p. 166.5–168° C, 90% yield. Anal. Calc. for $C_{18}H_{13}N_2SCl$: S, 9.9; N, 8.6. Found: S, 9.7; N, 8.5. (3) R = 4-CH_3, m.p. 142–143.5° C, 88% yield. Anal. Calc. for $C_{19}H_{16}N_2S$: S, 10.5; N, 9.2: Found: S, 10.3; N, 9.0. (4) R = 4-OH, m.p. 174–177° C, 85% yield. Anal. Calc. for $C_{18}H_{14}ON_2S$: S, 10.5; N, 9.2. Found: S, 10.6; N, 9.4. (5) R = 4-CH_3O, m.p. 122.5–124° C, 89% yield. Anal. Calc. for $C_{19}H_{16}ON_2S$: S, 10.0; N, 9.6. Found: S, 9.6; N, 8.5.

5-(p-Substituted)phenyl-1,2,3,4-thiatriazoles

Procedure A

The *p*-substituted thiobenzhydrazide (0.01 mole) was dissolved in 22 ml of 1 N hydrochloric acid. The solution was cooled in an ice–salt bath, and a solution of 0.8 g (0.01 mole) of sodium nitrite in 25 ml of water was added dropwise with stirring. The product which separated was immediately washed with water and recrystallized from ethanol–water mixture.

Procedure B

The *p*-substituted thiobenzoylthioglycolic acid (0.01 mole) was dissolved in 20 ml of 1 *N* sodium hydroxide, and a solution of 1.3 g (0.02 mole) of sodium azide in 15 ml of water was added. The reaction mixture was agitated at room temperature for 24 hours, the compound gradually precipitating. Both procedures A

Can. J. Chem. Downloaded from www.nrcresearchpress.com by 210.87.254.105 on 09/05/12
For personal use only.

and B were employed and the results are summarized in Table II. Similar procedures have also been employed by Kirmse (6) and Smith and Kenny (7).

TABLE II

5-(*p*-Substituted)phenyl-1,2,3,4-thiatriazoles

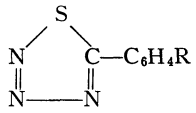

R	Procedure*	% yield	M.p. (°C)	Cryst. form	Formula	% S Calc.	% S Found	% N Calc.	% N Found
H†	B	72	95–96	White plates	$C_7H_5N_3S$	19.65	19.64	25.80	25.40
4-Cl‡	B	69	96–97	Tan plates	$C_7H_4N_3SCl$	16.22	16.00	21.27	21.30
4-OCH_3§	B	62	104–106	White needles	$C_8H_7ON_3S$	16.59	16.80	21.75	21.60
4-CH_3	B	71	93–95	White plates	$C_8H_7N_3S$	19.29	19.40	16.86	16.38
4-OH	A	70	151–153	White needles	$C_7H_5ON_3S$	17.89	18.20	23.45	23.70
4-$N(CH_3)_2$	A	70	168–171	Yellow plates	$C_9H_{10}N_4S$	15.83	15.48	27.19	27.30

*Where procedure B was used, procedure A may also be used, yields being generally 10% lower.
†Reference 6, m.p. 94–95° C.
‡Reference 7, m.p. 97–98° C.
§Reference 7, m.p. 103–104° C.

Attempted Synthesis of 5-Benzyl- and 5-Cyclohexyl-1,2,3,4-thiatriazoles

Diazotization of thiophenylacetylhydrazide and cylohexanethiocarbonylhydrazide yielded oils which showed nitrile absorption in the infrared spectra due to the decomposition of the thiatriazole. These results are similar to those of Kirmse (6) and Smith and Kenny (7). Kirmse (6), however, obtained the 5-benzyl derivative in crystalline form. While an attempt to distill the oily product was being made a mild explosion resulted, in the case of the 5-benzyl derivative.

Infrared Absorption Spectra

The infrared spectra of *p*-substituted thiobenzhydrazides, aliphatic thiohydrazides, and 5-(*p*-substituted)-phenyl-1,2,3,4-thiatriazoles were recorded on a Perkin–Elmer, Model 21-C spectrometer with rock salt optics. The samples were prepared as mulls in mineral oil.

Ultraviolet Absorption Spectra

The near-ultraviolet absorption spectra of 5-(*p*-substituted)phenyl-1,2,3,4-thiatriazoles were studied in 95% ethanol using Beckman DK-1 and DK-2 spectrometers.

Thermal Decomposition Studies

Thermal decompositions of some of the 5-(*p*-substituted)phenyl-1,2,3,4-thiatriazoles were studied as a function of time using a gas volumetric apparatus. The thiatriazole (0.0015 mole) was mixed with fine, dry sand and the flask containing the mixture was lowered into an oil bath maintained at 90° C, and the decompositions were studied up to 20% completion of decomposition. The *p*-substituents studied were Cl, H, and $N(CH_3)_2$. Total decompositions were studied for most of the thiatriazoles and the expected stoichiometric quantities of nitrogen were obtained in all the cases.

RESULTS AND DISCUSSION

Diazotization of *p*-substituted thiobenzhydrazides (II), as well as reaction of *p*-substituted thiobenzoylthioglycolic acids (III), with azide ion, produces 5-(*p*-substituted)-phenyl-1,2,3,4-thiatriazoles (IV). The infrared spectra of the products do not show the

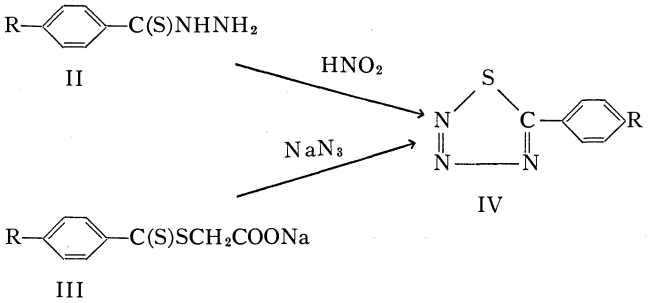

Can. J. Chem. Downloaded from www.nrcresearchpress.com by 210.87.254.105 on 09/05/12
For personal use only.

characteristic azide stretching frequencies (12), but exhibit the thiatriazole frequencies (3, 5) in the regions 1615–1515, 1300–1270, 1120–1100, and 1080–1030 cm^{-1}. Thus, the acyclic azide structure (V) for thioacyl azides, suggested by Oliveri-Mandala (13), must be eliminated from consideration.

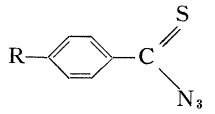

V

Phenyl-1,2,3,4-thiatriazole (IV, R = C_6H_5) does not dissolve in dilute mineral acids. It is also inert to concentrated hydrochloric and nitric acids, but decomposes in sulphuric acid at concentrations above 55%. The decomposition products are benzonitrile, nitrogen, and sulphur. A 2% solution of IV (R = C_6H_5) in reagent carbon tetrachloride showed signs of decomposition after standing for 5 days at room temperature. Precipitation of sulphur was observed and the solution exhibited the characteristic nitrile stretching frequency in the infrared.

The 5-(*p*-substituted)phenyl-1,2,3,4-thiatriazoles are relatively stable at room temperature but decompose rapidly when heated.* The products of thermal decomposition are a nitrile, sulphur, and nitrogen. Photodecomposition, however, gives rise to isothiocyanates and nitriles (6). Studies of the thermal decomposition of IV are in good agreement with the observations of Smith and Kenny (7). The mode of thermal decomposition may be represented by VI involving heterolytic bond breaking. The instability of 5-alkyl-1,2,3,4-thiatriazoles (IV, R = alkyl) may be due to the electron-donating nature

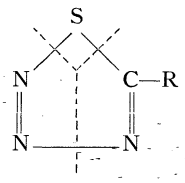

VI

of the alkyl groups, which would be expected to decrease the stability of the ring. The identification of nitriles in the attempted syntheses of IV (R = alkyl) derivatives and the occurrence of explosions during their preparation clearly indicate that these derivatives were formed, at least momentarily. The kinetics of the thermal decomposition of IV (R = *p*-substituted phenyl), studied by a volumetric gas apparatus, showed no dependence on the *p*-substituent.

The near-ultraviolet absorption spectra of IV (R = *p*-substituted phenyl) (Table III) show an interesting trend in the position of the absorption maximum with the *p*-substituent. There is progressive bathochromic shift with increase in the electron-donating ability of the *p*-substituent. This trend is similar to that found in 5-substituted phenylamino-1,2,3,4-thiatriazoles (14) and 1-substituted phenyl-5-amino-tetrazoles (15). On the basis of the correlations of ultraviolet absorption maxima of benzenoid derivatives with electrical effects of substituents (16), it may be concluded that the 1,2,3,4-thiatriazole ring is as electronegative as a tetrazole ring. Smith and Kenny (7) have also arrived at a similar conclusion.

**A sample of IV* (R = C_6H_5) *stored for 4 months at room temperature showed no nitrile absorption in the infrared.*

Can. J. Chem. Downloaded from www.nrcresearchpress.com by 210.87.254.105 on 09/05/12
For personal use only.

TABLE III

Near-ultraviolet absorption spectra of 5-(*p*-substituted)phenyl-1,2,3,4-thiatriazoles

p-Substituent	λ_{max} (mμ)	log ϵ_{max}	*p*-Substituent	λ_{max} (mμ)	log ϵ_{max}
H	237	3.41	OCH_3	260	3.52
Cl	246	3.69	OH	262.5	3.55
CH_3	248.5	3.61	$N(CH_3)_2$*	297	3.51

*Another peak at 223 mμ (log ϵ 3.94) and a shoulder at 324 mμ (log ϵ 3.64) were also observed.

Thiohydrazides show no SH stretching absorption in the infrared spectra, but exhibit the characteristic —N—C=S bands (17) in the regions 1545–1495, 1325–1300, and 1050–1010 cm^{-1}. Apparently there is no thione–thiol tautomerism in these derivatives in the solid state just as in the case of thiosemicarbazides (3). Thiohydrazides exhibit the characteristic frequencies due to the hydrazino group (3, 18, 19) in the regions 1600–1585, 1250–1190, 995–930, and 840–710 cm^{-1}.

REFERENCES

1. E. Lieber, C. N. Pillai, and R. D. Hites. Can. J. Chem. **35**, 832 (1957).
2. E. Lieber and J. Ramachandran. Can. J. Chem. **37**, 101 (1959).
3. E. Lieber, C. N. R. Rao, C. N. Pillai, J. Ramachandran, and R. D. Hites. Can. J. Chem. **36**, 801 (1958).
4. E. Lieber, C. N. Pillai, J. Ramachandran, and R. D. Hites. J. Org. Chem. **22**, 1750 (1957).
5. E. Lieber, E. Oftedahl, and C. N. R. Rao. J. Org. Chem. **28**, 000 (1963).
6. W. Kirmse. Chem. Ber. **93**, 2353 (1960).
7. P. A. S. Smith and D. H. Kenny. J. Org. Chem. **26**, 5221 (1961).
8. B. Holmberg. Arkiv. Kemi. Mineral. Geol. **A17**, No. 23 (1943).
9. A. Kjaer. Acta. Chem. Scand. **4**, 1347 (1950).
10. A. Kjaer. Acta Chem. Scand. **6**, 327 (1952).
11. M. Matusi. Mem. Coll. Sci. Eng. Kyoto Imp. Univ. **3**, 247 (1912); **10**, 79 (1926).
12. E. Lieber, C. N. R. Rao, T. S. Chao, and C. W. W. Hoffman. Anal. Chem. **29**, 916 (1957).
13. E. Oliveri-Mandala. Gazz. Chim. Ital. **44**, 670 (1914); **51**, 195 (1921); **52**, 98 (1922).
14. E. Lieber, J. Ramachandran, C. N. R. Rao, and C. N. Pillai. Can. J. Chem. **37**, 563 (1959).
15. E. Lieber, C. N. R. Rao, and C. N. Pillai. Current Sci. (India), **26**, 167 (1957).
16. C. N. R. Rao. Chem. Ind. (London), 666 (1956).
17. C. N. R. Rao and R. Venkataraghavan. Spectrochim. Acta, **18**, 541 (1962).
18. E. Lieber, D. R. Levering, and L. J. Patterson. Anal. Chem. **23**, 1594 (1951).
19. H. M. Randall, R. G. Fowler, N. Fuson, and J. R. Dangl. Infrared determination of organic structures. Van Nostrand Co., New York. 1949.

Can. J. Chem. Downloaded from www.nrcresearchpress.com by 210.87.254.105 on 09/05/12
For personal use only.

Can. J. Chem. Downloaded from www.nrcresearchpress.com by 210.87.254.40 on 09/05/12
For personal use only.

CO-CATALYSIS IN FRIEDEL–CRAFTS REACTIONS

VI. POLYMERIZATION OF 2-BUTENE BY BORON FLUORIDE – METHANOL[1, 2]

H. R. ALLCOCK[3] AND A. M. EASTHAM
Division of Applied Chemistry, National Research Council, Ottawa, Canada

Received November 26, 1962

ABSTRACT

2-Butene is polymerized by boron fluoride and methanol in ethylene dichloride solution at ordinary temperatures to give very low molecular weight polymers. The rate of polymerization shows exactly the same dependence on catalyst concentration as did the rate of isomerization of the *cis*- and *trans*-2-butenes, i.e. first order both in free boron fluoride and in the boron fluoride – methanol complex. The polymerization, however, shows a first-order dependence in olefin over a concentration range where the isomerization is, experimentally, virtually independent of the olefin concentration.

The polymerization of olefins by strong acids is generally considered to proceed by a mechanism of the type

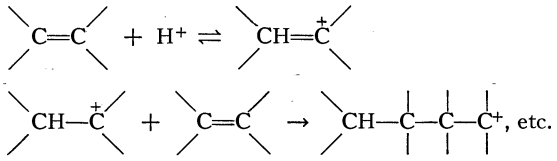

In previous work we have attempted to obtain information about the protonation step in this process by studying the acid-catalyzed equilibration of the three isomeric olefins *cis*-2-, and *trans*-2-, and 1-butene, on the assumption that the basic difference between this isomerization and a polymerization lies simply in the relative rates with which the initial carbonium ion undergoes either deprotonation or olefin addition. The *n*-butenes were chosen for this work because they do not polymerize easily and hence conditions can be found where the isomerization can be observed without serious interference from polymerization.

The results of our studies seem to show quite clearly that isomerization takes place according to the following reaction scheme (1), which is essentially a modification of the Polanyi–Evans mechanism for the polymerization of isobutene (2).

$$BF_3 + HX \rightleftharpoons HBF_3X \qquad [1]$$

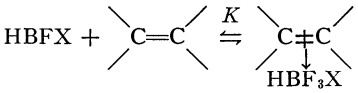

[2]

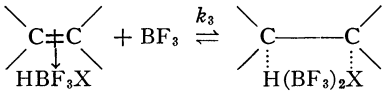

[3]

Here HX, the co-catalyst, is a proton-donating material such as water, methanol, or acetic acid which reacts with the catalyst, BF_3, to form the strong acid, HBF_3X. This acid reacts rapidly with the olefin (reaction [2]) to form a labile complex (π-complex?)

[1] *Issued as N.R.C. No. 7237.*
[2] *For Part V see ref. 1.*
[3] *N.R.C. Postdoctoral Fellow, 1958–1960.*

without disrupting the olefin double bond. Isomerization occurs when this complex reacts with a molecule of free boron fluoride but the kinetics do not show whether the rearrangement occurs during the addition of this second molecule of boron fluoride or in some subsequent process such as an ionization of the complex so formed.

The rate expression for the isomerization takes the form

$$\text{rate of isomerization} = \frac{k_3[BF_3][BF_3 \cdot HX][\text{butene}]}{K + [\text{butene}]},$$

where k_3 is the rate constant for the forward process in reaction [3] (the rate-controlling step) and K is the equilibrium constant for reaction [2]. However, since the values of k_3 and K differ for each isomer, the equation in this form applies only to the initial rate of isomerization of a pure isomer. For the present purpose it is sufficient to point out that the rate is directly dependent upon the concentrations of the free boron fluoride and of the boron fluoride – methanol complex but will depend on butene concentration in a manner determined by the value of K in the ratio [butene]/K+butene. With acetic acid as co-catalyst at 20° C, K has the values 0.1, 0.4, and 0.5 mole l^{-1} respectively for the isomers *cis*-2-, *trans*-2-, and 1-butene, so the experimental order in butene varies markedly over the usual concentration range. However, in addition to this kinetic effect of changes in butene concentration, there is a medium effect which operates in the opposite direction, and the net result of the two effects is to make the observed rate virtually independent of the butene concentration over the concentration range 0.2–2.0 mole l^{-1} with either methanol or acetic acid as co-catalyst.

With the mechanism for isomerization seemingly established, it seemed worthwhile to extend the measurements to the polymerization in order to test the assumption that polymerization and isomerization are related as described above. In doing so, we have made no attempt to determine the detailed polymerization kinetics but have confined ourselves to the measurement of initial rates of monomer disappearance in ethylene dichloride solution at 0° C, using methanol – boron fluoride as the catalyst system. In order to minimize interference from the somewhat more rapid isomerization reaction we have employed as monomer a mixture of *cis*- and *trans*-2-butene in approximately the ratio they are found in the equilibrium mixture (1:3), but 1-butene, which is also a component (3%) of the equilibrium mixture, was not added because preliminary experiments indicated that the small initial fluctuations in the concentration of this monomer should not cause significant errors in the measurements.

EXPERIMENTAL

(a) Materials

Ethylene dichloride, butenes, methanol, and boron fluoride were prepared and manipulated essentially as previously described (3, 4).

(b) Rate Measurements

The rates were followed by observing the decrease in vapor pressure of butene over the reaction mixture by means of a mercury manometer closely coupled to the reaction flask. The volume of the flask and manometer was about 75 ml. For each run the methanol was distilled into the flask and was followed by 20 ml of ethylene dichloride and then by the boron fluoride. At this point the mixture was brought to 0° C, thoroughly mixed by means of a magnetic stirrer, and its vapor pressure determined as a check on its composition. It was then frozen down to remove vapor from the manometer, the manometer isolated by means of a stopcock, and the mixture again brought to 0°. The butene was rapidly vaporized into the reaction system from a small bulb attached to the reaction flask, and a few minutes allowed for equilibration of the system. The stopcock to the manometer was opened and readings taken at intervals. The readings were plotted against time, the initial rate obtained from the slope of the smoothed curve, and the results converted to concentration by means of a calibration chart prepared for the system.

Can. J. Chem. Downloaded from www.nrcresearchpress.com by 210.87.254.40 on 09/05/12
For personal use only.

(c) Reaction Products

Reactions carried out with a low catalyst/monomer ratio stop short of completion because of catalyst consumption; the yield of polymer varies with the conditions but several hundred molecules of monomer are consumed per molecule of methanol. In order to obtain some information about catalyst destruction the vapor above the reaction mixture was circulated continuously through a gas cell in an Infracord infrared spectrophotometer and the strong boron fluoride band at 1500 cm^{-1} observed during the course of the polymerization. The gases were circulated rapidly through the system by means of a high-speed, magnetically driven platinum fan mounted on Teflon bearings within the system. The sodium chloride windows of the absorption cell were sealed with lead–mercury amalgam and the reference cell was filled with ethylene dichloride vapor at a pressure just sufficient to balance the absorption due to solvent vapor in the reaction cell.

In measuring the boron fluoride absorption it is necessary to make a small correction for a butene peak in the same region. Since butene disappears during the reaction the correction must be made continuously, so a manometer was introduced into the system and the pressure decrease observed. Correction was then made for butene absorption on the assumption that the pressure drop was due entirely to the decrease in butene, an assumption which may not be entirely justified but which is consistent with the change in butene absorption in other regions of the spectrum. The results thus obtained showed that the absorption due to boron fluoride remained substantially constant throughout the runs and we are satisfied that consumption of this reagent is small, perhaps well below 1% of its concentration, over the period of the rate measurements. This point is of considerable importance because the rates were followed by the fall in pressure in the system, and boron fluoride in some cases makes up a substantial part of that pressure.

Since the boron fluoride concentration seems to remain constant during the runs, we conclude that it is the co-catalyst, methanol, which is consumed, but we have been unable to devise a direct test of this point. We do know, however, that under certain rather restricted conditions, methanol can be added to butene to form the ether,

$$CH_3—CH=CH—CH_3 + CH_3OH \xrightarrow{BF_3} CH_3—CH_2—CHOCH_3—CH_3,$$

so it seems very likely that a reaction of this kind is a termination process in the polymerization (1).

No effort was made to examine the products of the rate runs but a few larger-scale runs were made for this purpose, typically as follows. Methanol (0.076 g), boron fluoride (0.22 g), and *trans*-2-butene (43 g) were added, on the vacuum line, to ethylene dichloride (700 ml) and allowed to stand 4 days at room temperature. Boron fluoride and most of the solvent was then distilled off to leave a residue of about 100 ml, which was fractionally distilled first at atmospheric and then under reduced pressure. The fractions were found, by gas chromatography, carbon and hydrogen analysis, and cryoscopy in cyclohexane, to be hydrocarbons having molecular weights below 350. Over half of the product was made up of a mixture of butene tetramers but the range included dimers to hexamers, and in all, nearly 20 different compounds. The large number of products presumably results from a mixture of 1- and 2-butene units in the polymers.

(d) Concentrations

Except in the case of boron fluoride, concentrations have been expressed in mole l^{-1} calculated from the amount of solvent and reactant measured into the reaction flask. However, since the boron fluoride has limited solubility, the concentration of this reagent in solution, $[BF_3]_{soln}$, has been used; in the present work at 0° C the dissolved boron fluoride is very close to one third of the total free boron fluoride present in the system. In calculating the concentrations it has been assumed, on the basis of earlier work (3), that methanol is always present as the 1:1 complex with boron fluoride.

RESULTS

The dependence of the rate of polymerization on the free boron fluoride concentration is shown in Fig. 1, where some typical results are plotted for a number of methanol concentrations. The dependence on methanol is obtained from the slopes of these lines and is shown in Fig. 2. There is a small and erratic "blank" in the absence of added methanol which may be due to adventitious moisture in the reagents or reaction system. It seems clear from the results that the polymerization depends on catalyst in exactly the same way as did the isomerization, i.e., directly on the concentrations of free boron fluoride and of boron fluoride – methanol complex.

The variation of rate with monomer concentration over the concentration range 0.2–1.0 mole l^{-1} is shown in Fig. 3 and is, experimentally, approximately of the first order. In the case of the isomerization reaction, under slightly different experimental conditions (1, 3), the order in butene approaches zero in this region so one is tempted to conclude

Can. J. Chem. Downloaded from www.nrcresearchpress.com by 210.87.254.40 on 09/05/12
For personal use only.

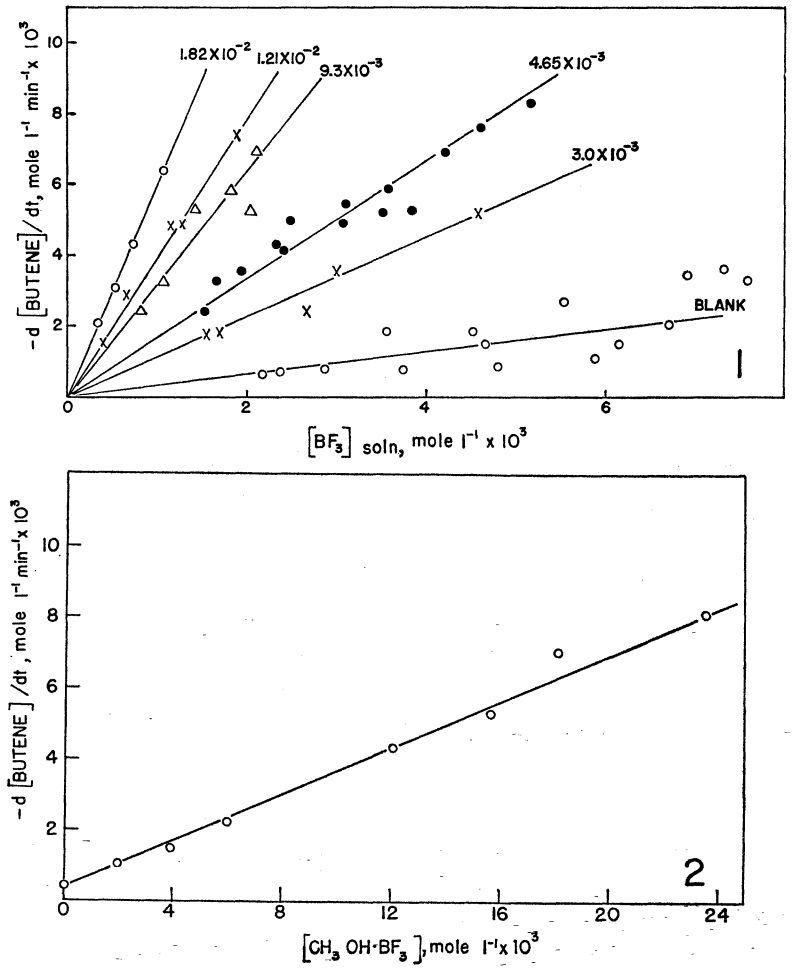

FIG. 1. Dependence of the rate of disappearance of butene on the concentration of free boron fluoride; [butene] 0.40 mole l^{-1}, [$CH_3OH \cdot BF_3$] as indicated on the curves.

FIG. 2. Dependence of the rate of polymerization on the concentration of methanol; [butene] 0.40 mole l^{-1}, $[BF_3]_{soln}$ 1.15×10^{-3} mole l^{-1}.

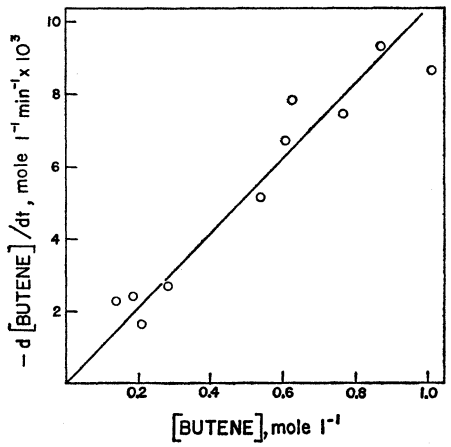

FIG. 3. Dependence of the rate of polymerization on butene concentration; [methanol] 4.65×10^{-3} mole l^{-1}, $[BF_3]_{soln}$ 4.2×10^{-3} mole l^{-1}.

Can. J. Chem. Downloaded from www.nrcresearchpress.com by 210.87.254.40 on 09/05/12
For personal use only.

that in the polymerization the overall rate of disappearance of monomer is about one order higher in monomer concentration than is the rate of initiation. While this conclusion seems reasonable and may in fact be true, it is a dangerous one because the dependence of the rate of initiation (isomerization) upon monomer concentration is complex (1) and any comparison of this kind, to be valid, should be made over a much wider concentration range than the present one. Unfortunately the range of the present method is restricted by the high rates at one end of the scale and the low vapor pressure of monomer at the other, but it seems rather doubtful that it is worth pursuing the subject further with this monomer because the complexity of the system is such that there is little hope for a solution to the polymerization equation. The chains are so short that each monomer unit will probably add at a different rate to the previous one, and furthermore the monomer itself is a mixture of three isomers each presumably with its own rate of addition. We therefore conclude only that the order in butene is somewhat higher for polymerization than for isomerization.

The rate expression governing these *experimental* results is thus

$$-d[\text{butene}]/dt = k[BF_3]_{soln}[BF_3 \cdot CH_3OH][\text{butene}]$$

and k has the value 6.5×10^2 l^2 mole^{-2} min^{-1} at 0° in ethylene dichloride solution.

REFERENCES

1. J. M. Clayton and A. M. Eastham. J. Chem. Soc. In press.
2. A. G. Evans and M. Polanyi. J. Chem. Soc. 242 (1947).
3. J. M. Clayton and A. M. Eastham. Can. J. Chem. **39**, 138 (1961).
4. A. M. Eastham. J. Am. Chem. Soc. **78**, 6040 (1956).

Can. J. Chem. Downloaded from www.nrcresearchpress.com by 210.87.254.40 on 09/05/12
For personal use only.

THE REACTION OF POLYISOPRENE WITH TITANIUM TETRACHLORIDE[1]

MORTON A. GOLUB AND JORGE HELLER
Stanford Research Institute, Menlo Park, California, U.S.A.
Received August 27, 1962

ABSTRACT

The reaction of titanium tetrachloride with hevea, balata, and synthetic *cis*-polyisoprene in benzene at 80° C has been studied. The most prominent change in the infrared spectra of these polymers is the nearly total disappearance of the 12 μ band after prolonged reaction with $TiCl_4$. The diminution of this band, associated with the loss of the original $-C(CH_3)=CH-$ units, whether cis or trans, followed pseudo-first-order kinetics, the rate varying with $[TiCl_4]^n$, where n is 1.0 in the case of the cis polymers and 1.5 in the case of the trans polymer. Contrary to previous reports, practically no cis–trans isomerization of polyisoprene occurs in the course of this reaction, the data being explained entirely by cyclization. With the help of *cis*-1,4 polymers of isoprene-3-*d* and 2-methyl-d_3-1,3-butadiene-1,1-d_2, it was concluded that cyclization, involving a $TiCl_4$-induced carbonium ion mechanism, leads to the formation of six-membered rings fused into predominantly bicyclic structures, connected by methylene groups and/or uncyclized monomer units. Each of the fused ring structures contains a single tetra-, tri-, or di-substituted double bond, the relative amounts of which are in the order tetra- > tri- > di-substituted.

INTRODUCTION

It is well known that natural rubber when treated at 60 to 80° C with strong acids such as H_2SO_4, or Lewis acids such as $SnCl_4$, BF_3, $TiCl_4$, $FeCl_3$, undergoes a progressive resinification with the formation of so-called cyclized rubber (1). Synthetic polyisoprenes also undergo cyclization quite readily (2), but polybutadienes require fairly drastic conditions (3). This reaction has been considered for some time to involve a carbonium ion mechanism, although there is a controversy as to whether the product consists of monocyclic (2, 4–8) or polycyclic (3, 9, 10) ring structures. Thus, Gordon (4–6), who studied the kinetics of cyclization of hevea latex, considered the reaction to involve the protonation of a double bond in *cis*-polyisoprene, followed by an attack of the resulting carbonium ion on an adjacent double bond, both occurring in the Markownikoff sense, to form a cyclic carbonium ion which then deprotonates to give structure I. Similar views were held by D'Ianni *et al.* (2) and various other workers. Flory (11) calculated that if monocyclic rings are formed a definite proportion (13.5%) of the isoprene units should end up as "widows", i.e., not cyclized by virtue of their neighbors having already reacted, so that the final unsaturation of the completely cyclized rubber should be about 57% of that of the original rubber instead of the 50% unsaturation indicated by structure I. This view accounted for the early unsaturation determinations on cyclized rubber by Fisher and McColm (12). On the other hand, van Veersen (9), who contends that unsaturation measurements on cyclized rubber involving iodine monochloride are not reliable because of complications due to substitution reactions, claims that cyclized rubber consists of fused cyclohexyl rings, such as II, connected by unreacted isoprene segments. Van Veersen's mechanism is similar to Gordon's except that the cyclic carbonium ion attacks still another, adjacent double bond to form a condensed ring structure, and this reaction proceeds until eventually it is terminated by a deprotonation process. According to this picture, totally cyclized rubber contains about 20 to 30% of the original unsaturation consisting of widowed double bonds as well as undetermined double bonds somewhere

[1]*Presented at the 11th Canadian High Polymer Forum, Windsor, Ontario, September 1962.*

Can. J. Chem. Downloaded from www.nrcresearchpress.com by 210.87.254.42 on 09/05/12
For personal use only.

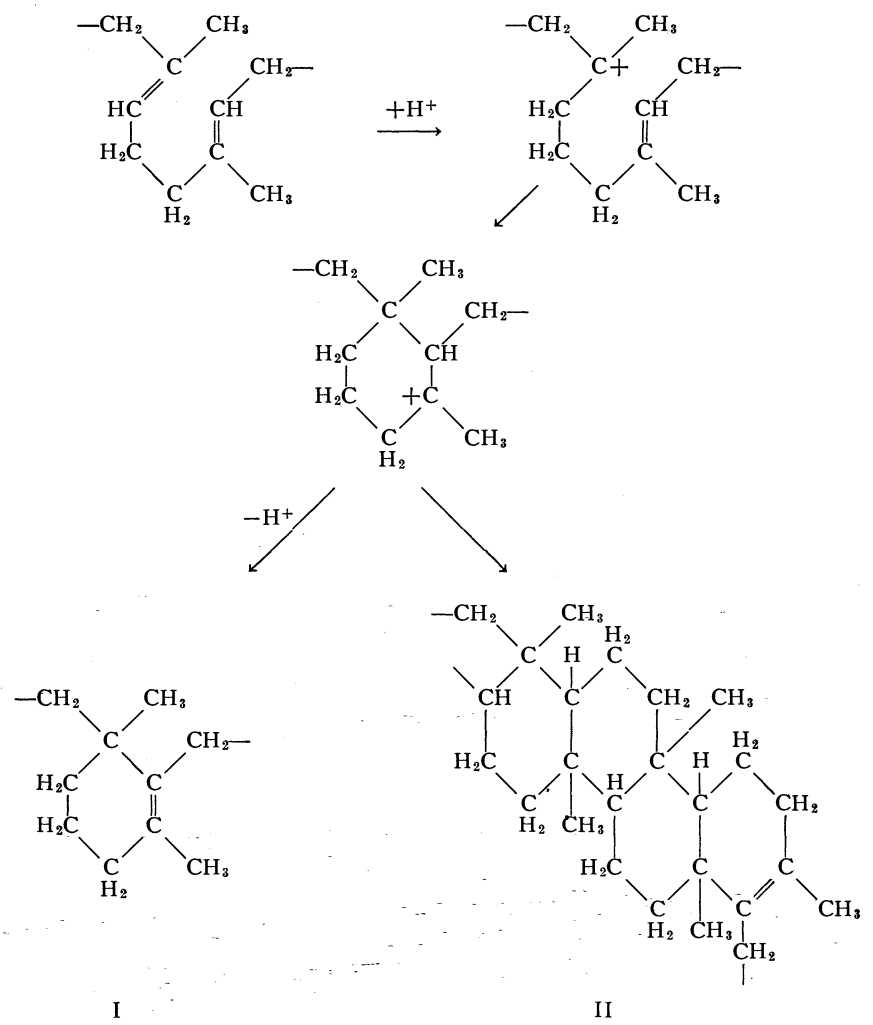

I II

in the fused rings. Clearly, there is a need for further work to try to settle the controversy regarding the structure of cyclized rubber.

If the protonation step is reversible (4), some cis–trans isomerization might occur during the cyclization reaction since release of the proton from its original point of attachment would re-establish the double bond. On thermodynamic grounds, the new double bond would be expected to be predominantly trans. This is in line with the observed cis–trans isomerization of polyisoprene under the influence of such agents as sulphur dioxide or thiol acids (13, 14) or selenium (15) which can reversibly add to or complex with carbon–carbon double bonds. The possibility of isomerization accompanying cyclization was apparently not considered by Gordon nor, with the possible exception of Ferri (16), by earlier workers who investigated the cyclization of polyisoprene. Ferri showed that treatment of both hevea and balata with chlorostannic acid or titanium tetrachloride led to closely similar products which he considered had structures intermediate between the two isomeric forms of naturally occurring polyisoprene. In view of our present knowledge about the cyclizing tendencies of the materials employed, Ferri's results can

Can. J. Chem. Downloaded from www.nrcresearchpress.com by 210.87.254.42 on 09/05/12
For personal use only.

probably best be explained in terms of the transformation of hevea and balata into essentially the same cyclized structure, rather than by cis–trans isomerization.

Recently, Dolgoplosk and co-workers (17–19) reported that natural rubber in benzene undergoes such an isomerization when treated at 80 to 90° C with titanium tetrachloride, anhydrous hydrogen chloride, or various organometallic compounds. Their results, however, are open to question on the following grounds. Firstly, they did not show the infrared spectra of the treated polymer samples over a reasonably wide range of wavelengths but confined their attention to the diminution of the 12 μ band (associated with the —$C(CH_3)$=CH— units, whether cis or trans). Although a decrease in this band could indicate cis–trans isomerization (the absorption coefficient of the trans —$C(CH_3)$=CH— unit is approximately 70% of that of the corresponding cis unit), it could also signify loss of the original double bonds through cyclization. Thus, in order to establish that cis → trans isomerization has taken place in natural rubber, it is necessary to adduce definite proof of the formation of new trans —$C(CH_3)$=CH— units. This might possibly be indicated, for example, by characteristic infrared absorption at around 7.5 μ and in the 8.5 to 10.0 μ region (13–15). Dolgoplosk and co-workers stated that they observed such characteristic absorption (18), but they neglected to present the appropriate spectra. As will be shown in this paper, the changes which do appear in these regions of the spectra of $TiCl_4$-treated polyisoprene are associated, not with the formation of trans —$C(CH_3)$=CH— units, but with the loss of unsaturation, and other structural modifications involved in cyclization. A second point of criticism is that these workers did not explain how they calculated the cis and trans content in their reacted polymers from data on the relative intensity of the 12 μ band and the residual unsaturation as determined chemically. Nor did they present such intensity data to enable the reader to see how those calculations were carried out. In fact, close examination of the data they did present (17, 18) indicates that these workers overlooked the important point that accompanying the disappearance of the original double bonds in cyclization new double bonds are formed, as in structure I or II. Thus, the relative intensity of the 12 μ band must be compared with the residual —$C(CH_3)$=CH— units, cis or trans, and not with the overall unsaturation; otherwise, one may be led into concluding that cis–trans isomerization has occurred even where it has not.

For the various reasons given above, it was considered worthwhile to reinvestigate the reaction of $TiCl_4$ with polyisoprene. Accordingly, this paper presents the results of an infrared, n.m.r., and kinetic study of the reaction of natural *cis*-, synthetic *cis*-, and natural *trans*-polyisoprenes with $TiCl_4$.

EXPERIMENTAL

Natural rubber (hevea) and balata were obtained through the courtesy of the B. F. Goodrich Company Research Center, Brecksville, Ohio; synthetic polyisoprene having a very high *cis*-1,4 structure as well as a relatively high 3,4 content was a gift of the Shell Chemical Company, Torrance, California. In addition, samples of *cis*-polyisoprene-3-*d* and *cis*-poly(2-methyl-d_3-1,3-butadiene-1,1-d_2), prepared by Dr. David Craig and Mr. Harold Tucker of the Goodrich Research Center, were kindly donated to us.

The *cis*-polyisoprenes were purified by precipitation from benzene solution using methanol as precipitant. The *trans*-polyisoprene was dissolved in refluxing hexane and allowed to crystallize out of solution at −20° C. Stock solutions were then prepared by dissolving the purified polymers in sodium-dried benzene to a polymer concentration of about 20 g/l., and stored under dry nitrogen.

Kinetic runs on the reaction of polyisoprene with $TiCl_4$ were carried out in 500-ml flasks equipped with a nitrogen inlet, stirrer, reflux condenser, and a self-sealing neoprene cap. All equipment was dried overnight in an oven at 140° C, assembled while hot, and allowed to cool under a stream of purified nitrogen. The reaction vessel was immersed in a constant-temperature bath maintained at 80±0.5° C, and 200 ml of stock solution was introduced by means of a volumetric pipette. After stirring the solution for 20 to 30 minutes

Can. J. Chem. Downloaded from www.nrcresearchpress.com by 210.87.254.42 on 09/05/12
For personal use only.

to reach the bath temperature, a measured volume of a 1 *M* solution of $TiCl_4$ in petroleum ether was injected by means of a hypodermic syringe through the neoprene cap. Aliquots were withdrawn from the reaction system at periodic intervals by means of a syringe, the reacted polymer samples precipitated with methanol, washed with additional alcohol, and dried in a vacuum oven at 60° C. The treated polymers were analyzed for chemical unsaturation by means of addition of iodine monochloride in acetic acid to the double bonds (20). Structural changes were analyzed by means of infrared absorption spectra of thin films cast from benzene solution onto rock salt plates, using a Beckman IR-4 spectrophotometer. In order to obtain spectra of the fully cyclized polymers free of benzene absorption bands, it was necessary to heat the films under vacuum for about 5 to 6 hours at 50° C. In addition, n.m.r. spectra of the cyclized perprotio and partially deuterated polyisoprenes were obtained at room temperature with a Varian HR-60 spectrometer on 5% polymer solutions in carbon tetrachloride containing 1% tetramethylsilane as an internal standard.

The reactions of the perprotio *cis* and *trans*-polyisoprenes with $TiCl_4$ were followed by measuring the decrease in the intensity of the 12 μ band relative to that of the 7.25 μ band (due to CH_3 groups) as an internal standard. The relative optical density of the 12 μ band, D, given by $O.D._{12\,\mu}/O.D._{7.25\,\mu}$, drops from about 0.79 in the case of natural rubber, 0.74 in synthetic *cis*-polyisoprene, and 0.49 in natural *trans*-polyisoprene (balata) to an ultimate D_∞ value of about 0.09 in the fully reacted *cis*- or *trans*-polyisoprene. Strictly speaking, the optical density measurements were made at 11.95 μ in the case of the cis polymers and at 11.85 μ in the case of the trans polymers. However, it has been convenient to refer to these bands in the text simply as the 12 μ band. The ratio of the extinction coefficients for the cis and trans absorption bands at 11.95 and 11.85 μ in hevea and balata, respectively, may therefore be taken to be equal to 0.79/0.49 or 1.61, which is in very good agreement with the corresponding value of 1.64 indicated by the work of Richardson and Sacher (21). Measurements were also made of the relative optical density of the 11.3 μ band, D', given by $O.D._{11.3\,\mu}/O.D._{7.25\,\mu}$, which provided a measure of the exomethylene units ($\rangle C{=}CH_2$) in the various polyisoprenes.

RESULTS AND DISCUSSION

Infrared Spectroscopy

Typical infrared spectra of the synthetic *cis*- and natural *trans*-polyisoprenes before and after reaction with $TiCl_4$ are presented in Figs. 1 and 2. The most pronounced change in the spectra of the fully reacted polymers is the nearly total disappearance of the 12 μ band. Accompanying this change in each case is a marked reduction in intensity and alteration of the shape of the various bands in the 7.5 to 10.0 μ region, bands which are characteristic of the isomeric forms of polyisoprene. At the same time, the absorption peak at 6.0 μ, corresponding to the C=C stretching vibration in an internal double bond, is greatly diminished. These facts all signify that the cis or trans $-C(CH_3){=}CH-$ units originally present in the two polymers disappear practically completely in the course of the polyisoprene–$TiCl_4$ reaction. The remaining absorption in the 7.5 to 10.0 μ region is too weak and indefinite to indicate whether the residual double bonds in either polymer comprise both cis and trans units, although under certain favorable conditions such an analysis is possible (13–15). The changes observed in the polyisoprene spectra can be accounted for entirely by cyclization without having to invoke any contribution from cis–trans isomerization, as will be confirmed later. For the present, it should be noted that the spectra of the final reaction products obtained from the two isomers of polyisoprene (Figs. 1C, 2C) are practically identical, indicating that essentially the same polymeric structures are produced. This result is in full accord with the experience of Ferri (16), who obtained very similar products on treating hevea and balata with $TiCl_4$. Moreover, the spectra in Figs. 1C and 2C are in qualitative agreement with the results of D'Ianni *et al.* (2) and others (22 and references cited therein) concerning the disappearance of the 12 μ band in polyisoprene on cyclization.

An additional feature of the spectra of the fully reacted perprotio polyisoprenes which should be mentioned is the band at 6.1 μ. This probably represents the C=C stretching vibration in an external double bond such as the exomethylene group for which direct evidence is provided by the band of medium intensity at 11.3 μ. As may be seen, the

Can. J. Chem. Downloaded from www.nrcresearchpress.com by 210.87.254.42 on 09/05/12
For personal use only.

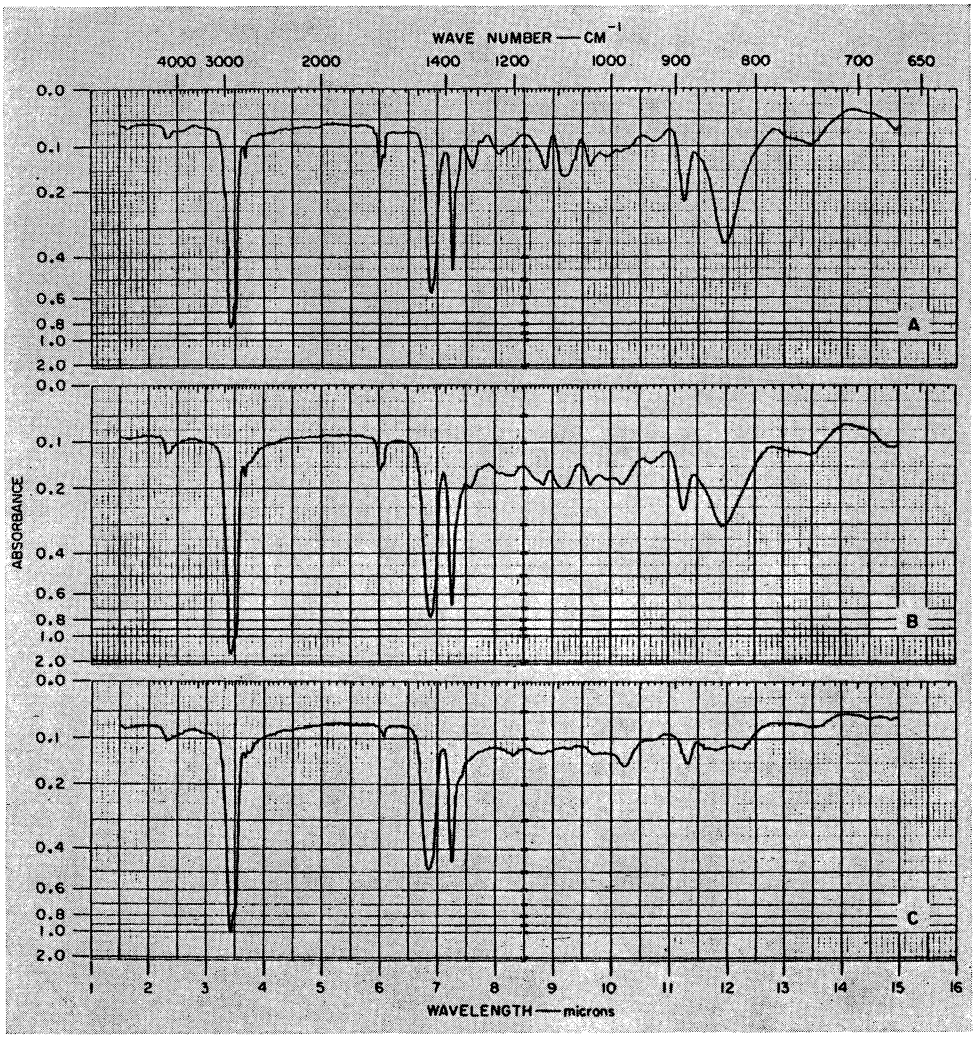

FIG. 1. Infrared spectra of synthetic *cis*-polyisoprene before and after reaction with $TiCl_4$ in benzene at 80° C. (A) Initial polymer; (B) partially cyclized polymer; (C) completely cyclized polymer.

latter band develops in the spectra of natural *trans*-polyisoprene and decreases somewhat in those of the synthetic cis polymer. Although not presented here, the spectrum of cyclized hevea was found to have an 11.3 μ band of intensity comparable to that obtained with cyclized balata. Examination of Fig. 3B reveals that this band also appears in the spectrum of cyclized *cis*-polyisoprene-3-*d* and is likewise attributed to the formation of $\diagdown C{=}CH_2$ units in this polymer.

Corresponding to the nearly complete disappearance of the 12 μ band in the perprotio polymers is the complete elimination of the 14.7 μ band in cyclized polyisoprene-3-*d* representing the loss of the original —$C(CH_3)$=CD— units in this polymer. Inspection of another infrared spectrum covering the wavelength range of 10 to 25 μ confirmed the disappearance of the 14.7 μ band in the deuterated polymer. Examination of Fig. 3B

Can. J. Chem. Downloaded from www.nrcresearchpress.com by 210.87.254.42 on 09/05/12
For personal use only.

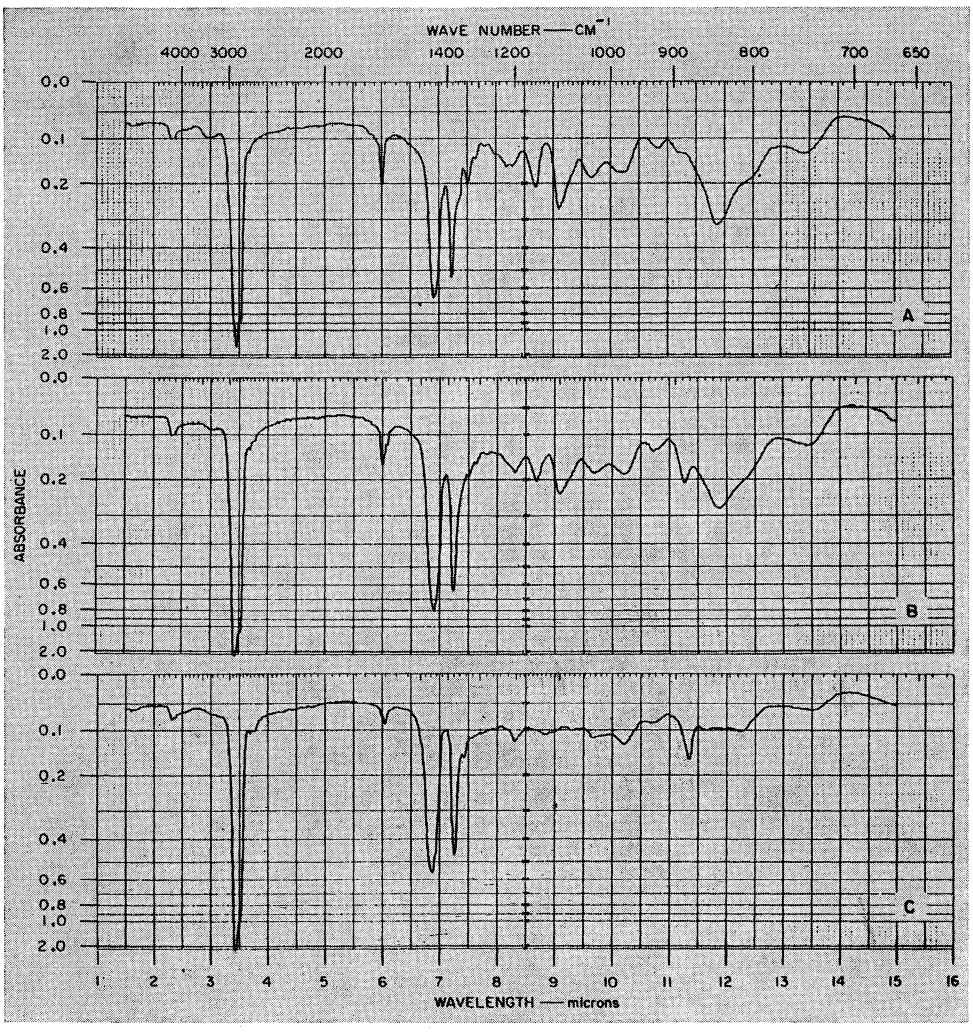

Fig. 2. Infrared spectra of natural *trans*-polyisoprene before and after reaction with $TiCl_4$ in benzene at 80° C. (A) Initial (amorphous) polymer; (B) partially cyclized polymer; (C) completely cyclized polymer.

shows also that the sharp band at 4.5 μ (C—D stretching vibration for an olefinic carbon atom) has been replaced by the broader band at 4.65 μ (C—D stretching vibration associated with a saturated carbon atom). This spectral change not only verifies the loss of the original —$C(CH_3)$=CD— units in monodeuterio polyisoprene through cyclization but it also indicates that these double bonds have become saturated to give $\rangle C(CH_3)$—CDH— and/or $\rangle C(CH_3)$—CD$\langle$ units.[2] On the basis of a monocyclic structure, these units could be found in structures III and IV. However, these structures involving tri- and di-substituted double bonds, respectively, cannot be important since there is very

[2]*Reference to examples of absorption at around 4.65 μ by* —CDH— *and tertiary* C—D *groups are given in reference 23 of this paper.*

Can. J. Chem. Downloaded from www.nrcresearchpress.com by 210.87.254.42 on 09/05/12
For personal use only.

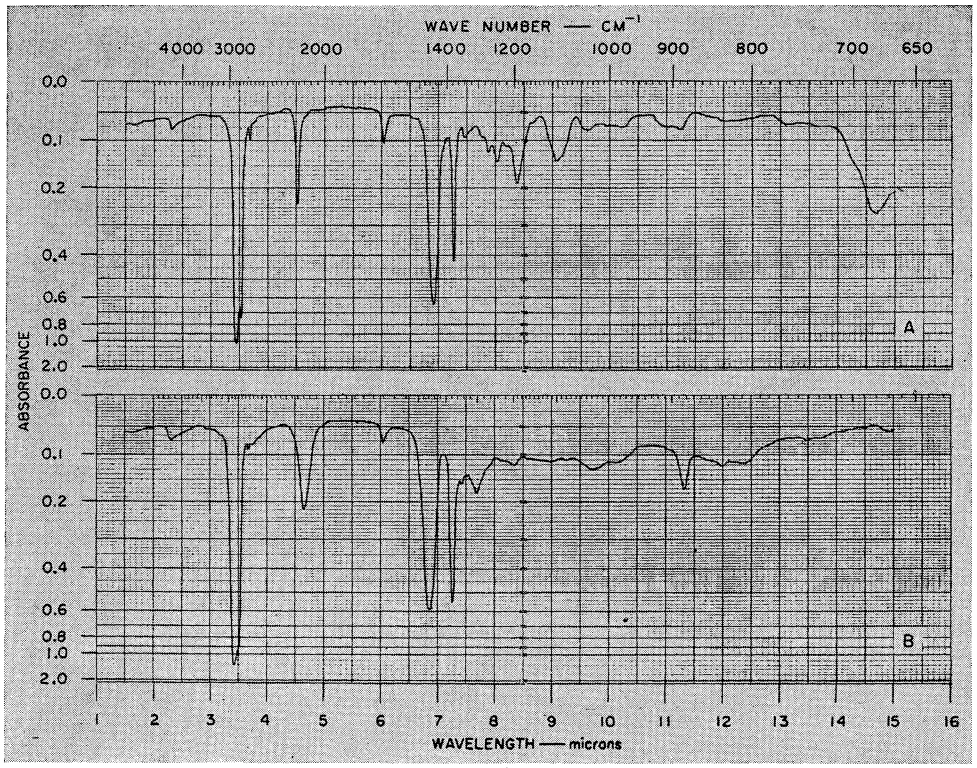

FIG. 3. Infrared spectra of *cis*-polyisoprene-3-*d*, $[-CH_2-C(CH_3)=CD-CH_2-]_n$, before and after reaction with $TiCl_4$ in benzene at 80° C. (A) Initial polymer and (B) completely cyclized polymer.

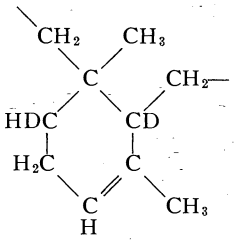

III

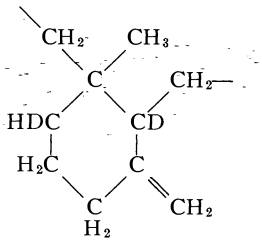

IV

little absorption at 12 μ and at 11.3 μ in the spectra of the cyclized polyisoprenes. Moreover, the deuterio analogue of the D'Ianni–Gordon structure I, viz., structure I*a*,

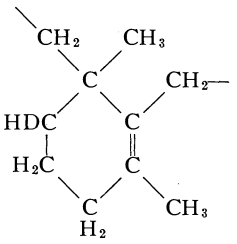

I*a*

containing a CDH group instead of a CD_2 group, and an essentially infrared-invisible

Can. J. Chem. Downloaded from www.nrcresearchpress.com by 210.87.254.42 on 09/05/12
For personal use only.

tetrasubstituted double bond, can be dismissed since it is incompatible with the nearly complete retention of deuterium in cyclized polyisoprene-3-*d*.[3] Furthermore, the alternative structure I*b*, which has the same D/H ratio as the starting polymer, would also

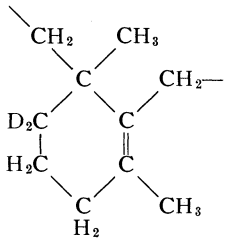

I*b*

be ruled out on the grounds that whereas CD_2 groups produce a pair of absorption bands at 4.5 and 4.75 μ (23, 24), we see only a fairly symmetrical singlet at 4.65 μ in Fig. 3B. In order to rationalize the infrared results, it is necessary to postulate that cyclized polyisoprene-3-*d* consists of fused rather than monocyclic rings. As we shall see shortly, the fused ring structure is supported by n.m.r. data which point to a predominantly bicyclic structure for cyclized rubber. Thus, cyclized polyisoprene-3-*d* may be depicted by the following structures, the relative importance of which is probably in the order

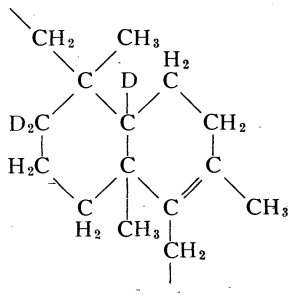

V

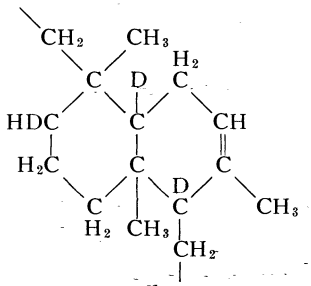

VI

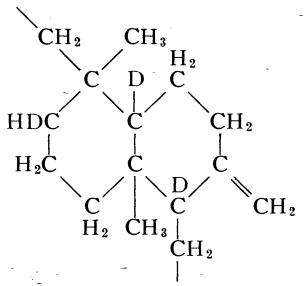

VII

V > VI > VII. The contribution of these structures, combined with that from some monocyclic rings and various other highly fused rings which perhaps also occur in cyclized rubber, gives rise to more —CDH— and tertiary C—D groups than CD_2 groups. This could account for the shape and relative intensity of the 4.65 μ band, which is probably the unresolved envelope of a weak doublet from CD_2 groups and a strong singlet from CDH and tertiary C—D groups.

The completeness with which the 14.7 μ band in Fig. 3B has disappeared compared to the incomplete removal of the 12 μ band in Figs. 1C and 2C deserves comment. In terms of a predominantly bicyclic structure for cyclized polyisoprene-3-*d*, we would expect to find some 10% of the original double bonds ending up as widows. The absence of the 14.7 μ absorption indicates that the widowed —$C(CH_3)$=CD— units have probably been replaced by —$C(CH_3)$=CH— units through a $TiCl_4$-induced double-bond shift. If this is so, there should be some residual absorption at around 12 μ instead of at 14.7 μ. Significantly, the 11.5 to 13 μ regions in the spectra of all three cyclized polyisoprenes presented in this paper are very similar in both overall shape and in relative intensity.

[3]*The deuterium content of the original polymer was 0.98 deuterium atom per isoprene unit and that of the cyclized polymer was 0.94 deuterium atom per isoprene unit, indicating only 4.3% deuterium–hydrogen exchange. The deuterium analysis was done by Mr. Joseph Nemeth, 303 Washington Ave., Urbana, Illinois.*

Can. J. Chem. Downloaded from www.nrcresearchpress.com by 210.87.254.42 on 09/05/12
For personal use only.

Can. J. Chem. Downloaded from www.nrcresearchpress.com by 210.87.254.42 on 09/05/12
For personal use only.

It may be noted that Figs. 1C and 2C, but not 3B, show a band at 10.25 μ. At first glance this band might be thought to represent the formation of some trans —CH=CH— units in ordinary polyisoprene on cyclization since such units are known to absorb at around 10.35 μ (24). However, this cannot be the case because then either the same kind of double bonds and/or the analogous —CD=CH— units would have to appear in cyclized polyisoprene-3-*d* and they do not. Thus, the absence of absorption at 10.25 to 10.35 μ in Fig. 3B rules out the former possibility while the absence of absorption at 11.2 μ (24) rules out the latter possibility. To be sure, there is a band at 11.3 μ in this figure but its shape and intensity, compared to those of the corresponding bands in Figs. 1C and 2C, clearly indicate the presence of $\diagdown\!\!\diagup C{=}CH_2$ groups. The most likely interpretation of the 10.25 μ band in cyclized polyisoprene-d_0 is that it is due to the CH_2 deformation vibrations associated with some ring structure. At the present time there is not much that can be said about such absorption other than to point out that if it involves a coordinated vibration of a number of adjacent methylene groups the absorption would be disturbed and its wavelength changed by the introduction of a CDH or CD_2 group into a sequence of CH_2 groups. This could explain why there is no 10.25 μ band in the spectrum of cyclized polyisoprene-3-*d*, the structure of which is considered to consist principally of the bicyclic rings V, VI, and VII.

To conclude the discussion of the spectrum in Fig. 3B, mention may be made of the 7.7 μ band, which is probably also related to the CDH groups (23).

Nuclear Magnetic Resonance Spectroscopy

A typical n.m.r. spectrum of the product obtained from the reaction of *cis*-polyisoprene with $TiCl_4$ is shown in Fig. 4 as the uppermost curve bounding the areas A, B, C, and D. The extensive overlapping of resonance peaks throughout the 7 to 10 τ region of this spectrum is due to the cyclic structure of the reaction product, which contains a variety

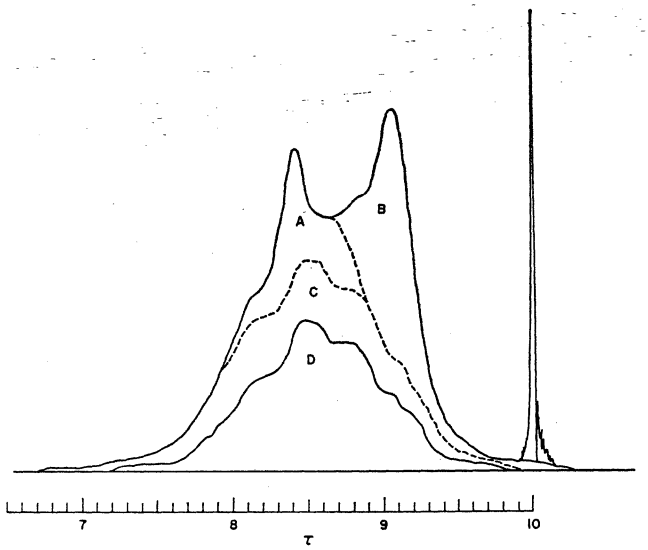

FIG. 4. Proton n.m.r. spectra of cyclized polyisoprenes at 60 Mc. The uppermost curve, comprising the envelope of the combined areas A, B, C, and D, corresponds to the cyclized perprotio polyisoprene. The curve which bounds area D corresponds to the cyclized poly(2-methyl-d_3-1,3-butadiene-1,1-d_2). For description of A, B, and C, see the text.

of non-equivalent methylene groups with different chemical shifts. Despite the obvious complexity of this spectrum, two prominent peaks stand out at around 8.4 and 9.1 τ, which correspond to protons on methyl groups attached to olefinic and saturated carbon atoms, respectively. Unfortunately, it is impossible to determine from this spectrum alone the relative amounts of the two types of methyl groups in cyclized rubber. Otherwise, we would be able to say at once that the latter material consists of mono-, bi-, tri-, or poly-cyclic rings according to whether the ratio of the methyl groups on saturated carbon atoms to the methyls on olefinic carbon atoms was one, two, three, or even higher. In an effort to resolve this question, the n.m.r. spectrum of cyclized poly(2-methyl-d_3-1,3-butadiene-1,1-d_2), viz., the curve bounding area D, was superimposed on that of the cyclized perprotio polymer. Due allowance was made for the fact that the pentadeuterio polymer has only 37.5% of the proton content of the perprotio polymer; hence, the area D was adjusted, by suitable control of the gain in the spectrometer, to 37.5% of the combined area A+B+C+D.

It is obvious from a comparison of the n.m.r. spectra of the two cyclized polymers shown in Fig. 4 that substitution of CH_3 by CD_3 resulted in the elimination of the two prominent methyl peaks. Moreover, there was a more pronounced loss in nuclear resonance in the "saturated" methyl region than in the "unsaturated" methyl region. This suggested that in the n.m.r. spectrum of cyclized perprotio polyisoprene the $CH_3-\overset{|}{\underset{|}{C}}-$peak is at least about twice as intense as the $CH_3-\underset{|}{C}=$peak. In fact, careful examination of the *differential* n.m.r. spectrum represented by the areas A, B, and C show that the most probable structure for cyclized rubber is the one consisting predominantly of bicyclic rings. Thus, if structures VIII and VIII*a* represent the cyclized perprotio and pentadeuterio polyisoprenes, respectively, it is clear that area A+B+C must represent the protons of the following groups in VIII: the three methylenes shown in bold print and also the three methyls. If we now make the reasonable assumption that these six methylene protons have essentially the same chemical shifts as the other eight methylene protons, with the one tertiary proton lying somewhere in between, we can regard C, which is drawn with the same contour as D and with an area of 6/9 or 2/3 of that of D, as representing the former six methylene protons. The methyl groups would then fall into the remaining area, A+B, which has been divided into two parts in accordance with what is known of the chemical shifts of the two types of methyl protons involved. As a result the area corresponding to the methyls on saturated carbon atoms, viz., B, is found to be about twice the area corresponding to the methyls on olefinic carbon atoms, or A. Although this

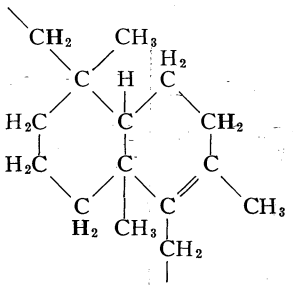

VIII

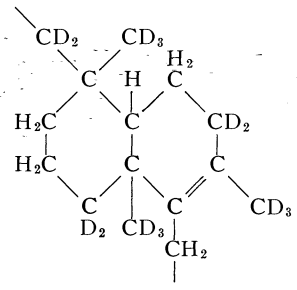

VIII*a*

Can. J. Chem. Downloaded from www.nrcresearchpress.com by 210.87.254.42 on 09/05/12
For personal use only.

analysis of the differential n.m.r. spectrum is not rigorous, it is nevertheless reliable enough to indicate that we are dealing with a predominantly bicyclic structure rather than with a predominantly monocyclic or other polycyclic structure.

Preliminary examination of the n.m.r. spectrum of cyclized polyisoprene in the 4.5 to 5.5 τ region indicated the presence of 3.4% olefinic protons distributed as follows: 1.4% in —C(CH_3)=C*H*— units, as in IX (4.7 τ); 1.2% in uncyclized —C(CH_3)=C*H*— units (4.9 τ); and 0.8% in $\diagdown$C=CH_2 groups (5.4 τ), as in X. On the basis of an exclusively bicyclic structure, we can calculate that structures IX and X would comprise 33 and 9%,

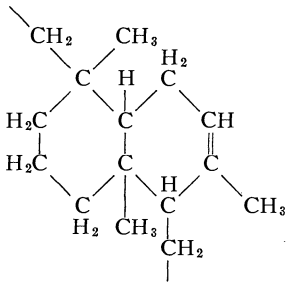

IX

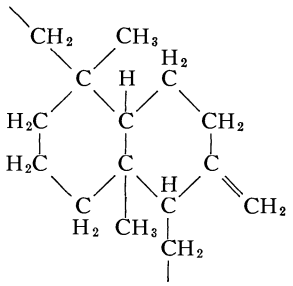

X

respectively, of the isoprene units, with 10% in the form of widows, and the remaining 48% of the isoprene units contained in structure VIII. However, it may be presumed that cyclized rubber contains, in addition to a very large concentration of bicyclic rings, some monocyclic rings and some tri-, tetra-, and other poly-cyclic rings, so that the above calculations for the relative amounts of structures VIII, IX, and X can only be regarded as approximations.

In order to arrive at a fully definitive structure for cyclized rubber, the cyclization of another partially deuterated polyisoprene, —CD_2—C(CH_3)=CH—CD_2—, will be investigated. It is expected that this polymer on cyclization will yield an n.m.r. spectrum in which the two characteristic methyl peaks will be clearly resolved, thus enabling their relative areas to be determined accurately and hence also the average number of fused rings per polycyclic group.

Kinetics and Mechanism

Results of typical kinetic runs for the reaction of synthetic *cis*- and natural *trans*-polyisoprenes with $TiCl_4$ are given in Table I. The values of the optical density, D, at infinite reaction time are only approximations since the residual absorption at around 12 μ is very broad and non-specific (Figs. 1C, 2C). Thus, no particular significance can be attached to the value of 0.090 for D_∞. It was, therefore, more reasonable to calculate the percentage of residual —C(CH_3)=CH— units as $100(D-D_\infty)/(D_0-D_\infty)$ rather than as $100D/D_0$. However, for such calculations, it was not practical to follow the reactions to completion.

Attention is called to the similarity of the unsaturation values, determined both spectroscopically and chemically, for samples of *cis*- and *trans*-polyisoprenes after different periods of reaction with $TiCl_4$. The spectroscopic unsaturation values were calculated on the assumption that the disappearance of the 12 μ band is due entirely to cyclization of the polymers to bicyclic ring structures. Consider, for example, the 60-minute run for the cis polymer in which there are assumed to be 74.5% residual —C(CH_3)=CH— units.

Can. J. Chem. Downloaded from www.nrcresearchpress.com by 210.87.254.42 on 09/05/12
For personal use only.

TABLE I

Kinetics of disappearance of the 12 μ band in polyisoprenes

Time, min	D	$(D-D_\infty)$	$1+\log(D-D_\infty)$*	% residual† —C(CH$_3$)=CH— units	Unsaturation	
					Spectroscopic	Chemical‡
		Synthetic *cis*-polyisoprene ([TiCl$_4$] = 0.99×10^{-2} M)				
0	0.740	0.650	0.813	100.0	100.0	100.0
60	0.574	0.484	0.685	74.5	83.0	85.7
120	0.446	0.356	0.551	54.8	69.9	76.9
180	0.386	0.296	0.471	45.5	63.7	70.0
240	0.319	0.229	0.360	35.2	56.8	66.7
∞	0.090	—	—	—	—	46.5§
		Natural *trans*-polyisoprene ([TiCl$_4$] = 0.50×10^{-2} M)				
0	0.492	0.402	0.604	100.0	100.0	100.0
60	0.379	0.289	0.461	71.9	81.3	85.2
120	0.337	0.247	0.393	61.4	74.3	77.5
180	0.312	0.222	0.346	55.2	70.1	75.4
240	0.291	0.201	0.303	50.0	66.7	72.6
∞	0.090	—	—	—	—	43.8§

*The plots of log $(D-D_\infty)$ vs. time were linear, giving pseudo-first-order rate constants $k' = 4.02$ and 1.83×10^{-3} min^{-1} for the *cis*- and *trans*-polyisoprenes, respectively.
†Calculated as $100(D-D_\infty)/(D_0-D_\infty)$.
‡Based on ICl titrations. For convenience in the calculations, the double bonds in the starting polymers were arbitrarily taken to be 100% —C(CH$_3$)=CH— units. The small contribution of the exomethylene units in the various polymer samples was neglected in these calculations.
§Corresponding unsaturation, based on n.m.r. results, is estimated as about 40%.

This corresponds to the loss of 25.5% of the original double bonds. On the basis of cyclization, whether to ring structure VIII, IX, or X, one-third of the 25.5% unsaturation lost, or 8.5%, would reappear as new double bonds. The resulting total unsaturation (spectroscopic), 83.0%, is only slightly less than the chemical unsaturation value of 85.7% determined by iodine monochloride titration of the polymer double bonds. The agreement between the two sets of unsaturation values is, however, somewhat poorer at the higher degrees of cyclization. This disparity is considered to arise from an inherent difficulty with the spectroscopic estimate inasmuch as there is a broadening of the 12 μ band with disappearance of the original unsaturation. This makes the value of D somewhat less than it otherwise would be. Significantly, the calculated unsaturation values were less than the corresponding chemical values by approximately the same amounts for both *cis*- and *trans*-polyisoprenes. Nevertheless, the spectroscopic and chemical unsaturation values are in close enough agreement to show that isomerization cannot be an important part of the overall reaction of polyisoprene with $TiCl_4$ as claimed by Dolgoplosk and co-workers (17–19). Accordingly, we are justified in disregarding changes in D due to possible isomerization when calculating the residual —C(CH$_3$)=CH— units in the manner shown in Table I. Finally, it should be pointed out that the chemical unsaturation of the completely cyclized *cis*- and *trans*-polyisoprenes (43 to 46%) are in good agreement with the unsaturation value indicated by n.m.r. data for a bicyclic structure for cyclized rubber, *viz.*, 40%.[4] The latter values obviously differ from the values of 56 to 58% reported by previous workers (5, 7, 12) for monocyclic structures.

Representative kinetic plots for the disappearance of the 12 μ band in the spectra of *cis*- and *trans*-polyisoprenes are shown in Figs. 5 and 6. The essential first-order character of the reaction indicates that the rate is given by a kinetic expression of the form

$$[1] \qquad -dU/dt = kUT^n = k'U,$$

[4]*Assuming 10% widowed double bonds, the consumption of 90% of the original double bonds in cyclization results in the formation of 30% new double bonds for a total unsaturation of about 40%.*

Can. J. Chem. Downloaded from www.nrcresearchpress.com by 210.87.254.42 on 09/05/12
For personal use only.

where U denotes the concentration of cyclizable isoprene segments, as measured by the relative intensity of the 12 μ absorption band, T is the concentration of the effective catalyst for the reaction, and k' is the pseudo-first-order rate constant which depends on the catalyst concentration. The linearity of the semilogarithmic plots throughout the course of the reaction shows that the effective catalyst, whether the original $TiCl_4$ molecules and/or the proton by-products, maintains a steady-state concentration in the system. In analogy to the carbonium ion mechanism proposed for the acid-catalyzed cyclization to hevea latex (4, 5), but involving the formation of bicyclic rings, the overall reaction of polyisoprene with $TiCl_4$ may be written as

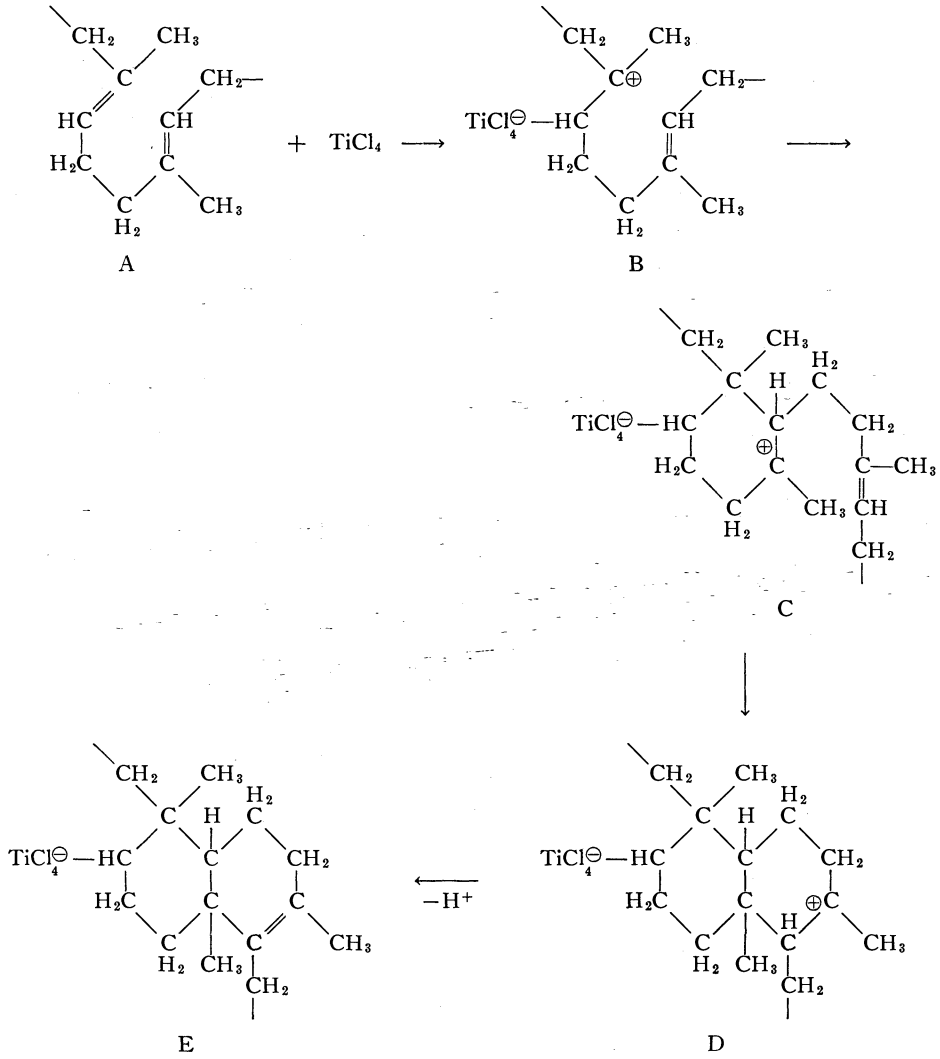

In this sequence of steps, for every $TiCl_4$ molecule attached to the isoprene double bond a proton is released which can either initiate further cyclization or exchange with the attached $TiCl_4$ as in E to give, finally, structure VIII and a regenerated Lewis acid catalyst. Thus, the combined concentration of free $TiCl_4$ molecules and available protons

Can. J. Chem. Downloaded from www.nrcresearchpress.com by 210.87.254.42 on 09/05/12
For personal use only.

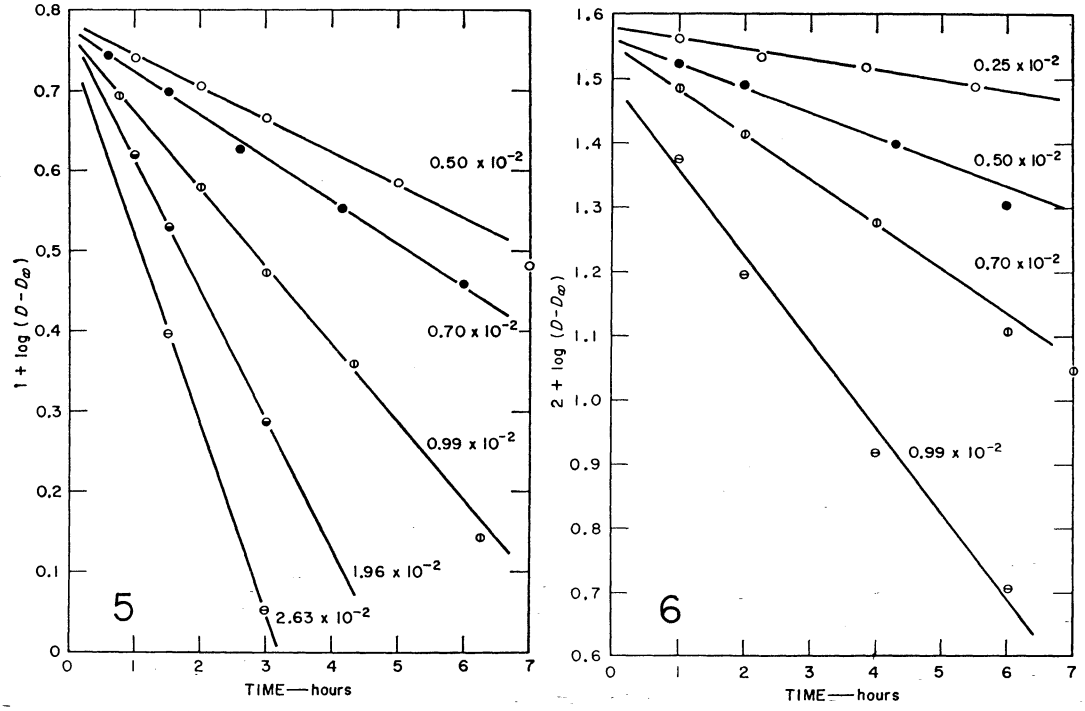

FIG. 5. Kinetic plots for the disappearance of the 12 μ band in synthetic *cis*-polyisoprene on reaction with $TiCl_4$. Concentrations of $TiCl_4$ are given in mole/l.

FIG. 6. Kinetic plots for the disappearance of the 12 μ band in natural *trans*-polyisoprene on reaction with $TiCl_4$. Concentrations of $TiCl_4$ are given in mole/l.

must remain essentially constant, and this is consistent with the first-order character of the kinetic plots. Furthermore, the proton and the $TiCl_4$ molecule must attack the isoprene double bond with comparable ease to form the carbonium ion, which is rapidly followed by cyclization of two adjacent isoprene units.

In addition to the one shown above, there are two other routes for the deprotonation of D involving hydrogens on carbon atoms adjacent to the carbonium ion site. These yield structures IX and X. Since the relative stabilities of the different possible double bonds are probably in the order tetra- > tri- > di-substituted, it is not surprising that VIII is the predominant cyclic structure, followed by IX, with only a small amount of exomethylene units, as in X, formed in the course of the cyclization reaction.

Since there is no a priori reason for the cyclization to stop after only three monomer units have been involved in forming bicyclic structures VIII to X, it is quite possible that some more highly fused rings are also formed in the polyisoprene–$TiCl_4$ reaction. However, the experimental data presented here show that for some unknown reason, probably steric in origin, most of the cyclization ceases at the bicyclic stage.

Although considerable effort was made to exclude moisture in this work, it is entirely possible that traces of water were present in the reaction system which could serve as a co-catalyst in the $TiCl_4$-induced cyclization of polyisoprene.

It should be pointed out that any reversibility to the attachment of $TiCl_4$ onto the isoprenic double bond cannot be significant since it would lead to cis–trans isomerization.

Can. J. Chem. Downloaded from www.nrcresearchpress.com by 210.87.254.42 on 09/05/12
For personal use only.

Presumably, the carbonium ion XI, as soon as it is formed, undergoes ring closure with

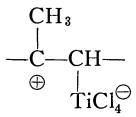

XI

an adjacent isoprenic double bond, if available for cyclization, before detachment of $TiCl_4$ can take place. However, in the case of a widowed double bond, where the opportunity for cyclization to monocyclic rings no longer exists, such a detachment with consequent isomerization may take place. On the other hand, it is possible for double-bond shift in a widowed segment to occur according to the process

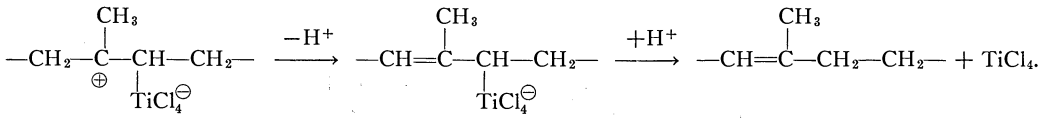

Obviously, in the cyclization of the monodeuterio polyisoprene to form structure V, deuterons released in the "deprotonation" step proceed to initiate further cyclization, while the protons released in the formation of structures VI and VII likewise go on to induce cyclization. Since practically all the released deuterons and protons are consumed in what is essentially a "closed" chain reaction system, it would be expected that the resulting cyclized polyisoprene-3-*d* should show little or no isotope exchange. The fact that the latter polymer actually has a slightly lower deuterium content than the starting polymer may be explained by assuming that some $TiCl_4$ which is complexed to the cyclized polymer is replaced by protons from methanol in the course of precipitating the polymer from solution at the end of the cyclization reaction.

The slopes of the plots of Figs. 5 and 6, as well as those of the corresponding plots for natural *cis*-polyisoprene, multiplied by 2.3, give the pseudo-first-order constants k', which are plotted against the $TiCl_4$ concentrations in Fig. 7. The data for both synthetic and natural *cis*-polyisoprenes fall on a common line the slope of which has the value of 1.08, which determines the exponent n in equation [1]. The cyclization reaction, in addition to being first order in isoprene double bonds, is thus also first order in $TiCl_4$. On the other hand, the kinetic data for the natural *trans*-polyisoprenes fall on a different line having a slope of 1.51. We have no explanation for the apparent 1.5-order in $TiCl_4$ in the cyclization of balata.

Figure 8 shows the growth of the 11.3 μ band due to exomethylene structure in the naturally occurring *cis*- and *trans*-polyisoprenes in the course of the reaction with $TiCl_4$. There has been some controversy as to whether these polyisoprenes actually contain $\diagdown C{=}CH_2$ units. Thus, Binder and Ransaw (25) hold that 2.2% of the double bonds in hevea and 1.3% in balata are of the isopropenyl $CH_2{=}C(CH_3)-$ type, whereas Fraga (26) contends that such units are absent in these polymers, which he assumes to have an essentially 100% *cis*- or *trans*-1,4 structure. The latter point of view has been supported recently by high-resolution n.m.r. studies (27). Nevertheless, there is a band at 11.2 μ in the spectra of the naturally occurring polyisoprenes which, with the development of the 11.3 μ absorption, merges into the broad band centered at the latter wavelength.

Can. J. Chem. Downloaded from www.nrcresearchpress.com by 210.87.254.42 on 09/05/12
For personal use only.

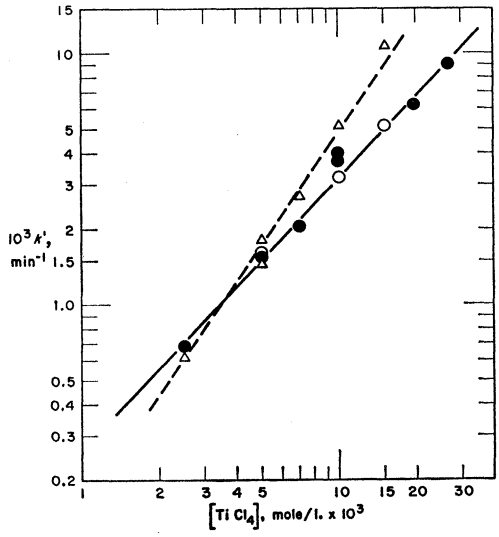

FIG. 7. Dependence of the pseudo-first-order rate constant for the disappearance of the 12 μ band in polyisoprene on the concentration of $TiCl_4$. Synthetic *cis*- (●), natural *cis*- (○), and natural *trans*- (△) polyisoprenes.

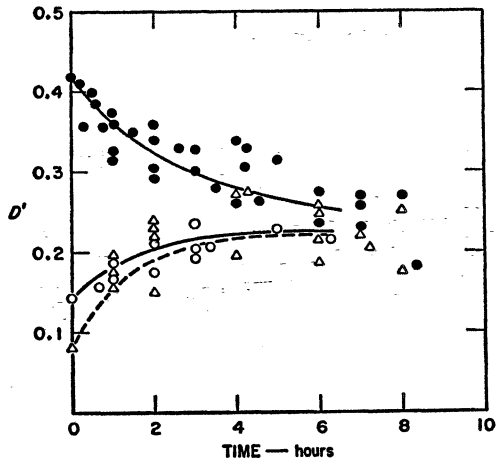

FIG. 8. Growth or decay of the 11.3 μ band in various polyisoprenes. Synthetic *cis*- (●), natural *cis*- (○), and natural *trans*- (△) polyisoprenes.

Since it is difficult to determine the relative amounts of the 11.2 and 11.3 μ components in this band, especially in the early stages of the reaction, the initial absorption intensities at 11.2 μ are treated, for convenience, just as though they were at 11.3 μ, and this is reflected in the particular values for hevea and balata indicated in Fig. 8. However, these initial values are not considered to have any special significance here. Figure 8 also shows the decay of the 11.3 μ band in a synthetic *cis*-polyisoprene containing a relatively high concentration (4.4%) of isopropenyl groups initially. As can be seen, the exomethylene content in all three polymers tends to reach a more or less equilibrium value (about 2.5%

Can. J. Chem. Downloaded from www.nrcresearchpress.com by 210.87.254.42 on 09/05/12
For personal use only.

of the *original* double bonds). It is not known whether this results from an isomerization of the type

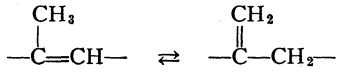

or whether, as seems more likely, the processes for the formation and decay of the exomethylene units are independent. Thus, it is easy to imagine that some of the initially present $\diagdown C{=}CH_2$ units in the synthetic *cis*-polyisoprene are consumed in cyclization much like the ordinary isoprenic double bonds, while other exomethylene units are formed as a result of the cyclization.

ACKNOWLEDGMENTS

The authors wish to record their appreciation to Mrs. Harriett H. Johnson, who performed the unsaturation measurements on the various polymers, and to William R. Anderson, Jr., for providing n.m.r. data on the cyclized polyisoprenes.

REFERENCES

1. N. Grassie. Chemistry of high polymer degradation processes. Butterworth Scientific Publications, London, 1956. pp. 315–319.
2. J. D. D'Ianni, F. J. Naples, J. W. Marsh, and J. L. Zarney. Ind. Eng. Chem. **38**, 1171 (1946).
3. J. R. Shelton and Lieng-Huan Lee. Rubber Chem. Technol. **31**, 415 (1958).
4. M. Gordon. Ind. Eng. Chem. **43**, 386 (1951); Rubber Chem. Technol. **24**, 940 (1951).
5. M. Gordon. Proc. Roy. Soc. (London), Ser. A, **204**, 569 (1951); Rubber Chem. Technol. **24**, 924 (1951).
6. M. Gordon and J. S. Taylor. J. Appl. Chem. **3**, 537 (1953); Rubber Chem. Technol. **28**, 297 (1955).
7. N. V. C. Rao. Makromol. Chem. **16**, 198 (1955).
8. C. S. Ramakrishnan, S. Dasgupta, and N. V. C. Rao. Makromol. Chem. **20**, 46 (1956).
9. G. J. Van Veersen. Rec. Trav. Chim. **69**, 1365 (1950); Rubber Chem. Technol. **24**, 957 (1951).
10. F. T. Wallenberger. Monatsh. **93**, 74 (1962).
11. P. J. Flory. J. Am. Chem. Soc. **61**, 1518 (1939).
12. H. L. Fisher and E. M. McColm. Ind. Eng. Chem. **19**, 1325, 1328 (1927).
13. J. I. Cunneen, G. M. C. Higgins, and W. F. Watson. J. Polymer Sci. **40**, 1 (1959).
14. J. I. Cunneen. Rubber Chem. Technol. **33**, 445 (1960).
15. M. A. Golub. J. Polymer Sci. **36**, 523 (1959).
16. C. Ferri. Helv. Chim. Acta, **20**, 1393 (1937); Rubber Chem. Technol. **11**, 350 (1938).
17. B. A. Dolgoplosk, E. N. Kropacheva, and K. V. Nelson. Dokl. Akad. Nauk SSSR, **123**, 685 (1958); Rubber Chem. Technol. **32**, 1036 (1959).
18. I. I. Boldyreva, B. A. Dolgoplosk, E. N. Kropacheva, and K. V. Nelson. Dokl. Akad. Nauk SSSR, **131**, 830 (1960); Rubber Chem. Technol. **33**, 985 (1960).
19. B. A. Dolgoplosk, G. P. Belonovskaja, I. I. Boldyreva, E. N. Kropacheva, K. V. Nelson, JA. M. Rosinoer, and J. D. Chernova. J. Polymer Sci. **53**, 209 (1961).
20. A. R. Kemp and G. S. Mueller. Ind. Eng. Chem., Anal. Ed. **6**, 52 (1934).
21. W. S. Richardson and A. Sacher. J. Polymer Sci. **10**, 353 (1953).
22. M. B. Evans, G. M. C. Higgins, D. F. Lee, and W. F. Watson. J. Appl. Polymer Sci. **4**, 367 (1960).
23. J. J. Shipman and M. A. Golub. J. Polymer Sci. **58**, 1063 (1962).
24. M. A. Golub and J. J. Shipman. Spectrochim. Acta, **16**, 1165 (1960).
25. J. L. Binder and H. C. Ransaw. Anal. Chem. **29**, 503 (1957).
26. D. W. Fraga. J. Polymer Sci. **41**, 522 (1959).
27. M. A. Golub, S. A. Fuqua, and N. S. Bhacca. J. Am. Chem. Soc. **84**, 4981 (1962).

Can. J. Chem. Downloaded from www.nrcresearchpress.com by 210.87.254.42 on 09/05/12
For personal use only.

THE APPARENT IONIZATION CONSTANTS OF SOME ORGANOSILYLMETHYLBENZOIC ACIDS

H. R. ALLCOCK[1]
Chemistry Department, University of Leicester, Leicester, England
Received November 27, 1962

ABSTRACT

The apparent ionization constants of several organosilylmethylbenzoic acids of formula p-$R_3SiCH_2C_6H_4CO_2H$ were measured in 39 wt% aqueous methanol using a spectrophotometric method. p-$(CH_3)_3SiCH_2C_6H_4CO_2H$ was found to be a slightly stronger acid than p-$(C_2H_5)_3SiCH_2C_6H_4CO_2H$ and p-$(n$-$C_3H_7)_3SiCH_2C_6H_4CO_2H$, but replacement of $(CH_3)_3Si$ in p-$(CH_3)_3SiCH_2C_6H_4CO_2H$ by $(C_6H_5)(CH_3)_2Si$—, $(p$-$CH_3C_6H_4)(CH_3)_2Si$—, and $(C_6H_5)_3Si$— brought about no significant change in acid strength. All the organosilylmethlybenzoic acids studied were weaker acids than p-toluic acid.

INTRODUCTION

Several investigators have attempted to correlate the dissociation constants of organosilylcarboxylic acids with the inductive and mesomeric properties of the R_3Si group (where R is alkyl or aryl). For example, Sommer *et al.* (1) reported that the dissociation constant of the acid $(CH_3)_3SiCH_2CO_2H$ was less than that of acetic acid, and Eaborn and Parker (2) found that the compounds o-, m-, and p-$(CH_3)_3SiCH_2C_6H_4CO_2H$ were weaker acids than the corresponding toluic acids. These effects were ascribed to a strong inductive electron supply by the $(CH_3)_3Si$ group.

In compounds where silicon is bonded to an aromatic ring, a mesomeric effect is also possible due to $d\pi$–$p\pi$ bonding between silicon and the phenyl group (3). Thus, Chatt and Williams (4) found that the acid p-$(CH_3)_3SiC_6H_4CO_2H$ was very slightly stronger than benzoic acid. In this compound the mesomeric electron withdrawal by the $(CH_3)_3Si$ group is presumably of greater influence than the inductive electron supply of the same group. However, successive replacement of methyl groups in this compound by phenyl groups resulted in a progressive increase in acid strength (5), which indicated that the inductive electron withdrawal by the phenyl groups in this position slightly outweighed the mesomeric electron supply to silicon.

It was of interest, therefore, to examine the dissociation constants of acids of type p-$R_3SiCH_2C_6H_4CO_2H$, in which R is methyl, ethyl, n-propyl, or aryl, since such variations would affect only the electron supply to silicon. The transmission of this effect to the carboxyl group would not be complicated by mesomeric or steric factors, and the influence of the group R should be more readily discernible.

RESULTS AND DISCUSSION

Dissociation constants of the organosilylmethylbenzoic acids and p-toluic acid were measured in 39 wt% aqueous methanol using an ultraviolet spectrophotometric method. The insolubility of the acids in water necessitated the use of an aqueous methanolic medium and, since no correction is applied for the solvent, the values obtained are considered as apparent dissociation constants. The results are shown in Table I.

The acid strength of p-$(CH_3)_3SiCH_2C_6H_4CO_2H$ is slightly lower than that of p-toluic acid. This result is in agreement with the data of other authors (2, 6), and reflects the

[1]*Present address: American Cyanamid Company, Stamford, Connecticut.*

Can. J. Chem. Downloaded from www.nrcresearchpress.com by 210.87.254.6 on 09/05/12
For personal use only.

TABLE I

Dissociation constants for p-$XCH_2C_6H_4CO_2H$ at 25° C

X	λ (mμ)	$\frac{D_{alk}-D_{buf}}{D_{buf}-D_{acid}}$*	pK_a	10^6K_a
H	240–258	2.90	5.75	1.78†
$(CH_3)_3Si$	256–272	3.65	5.85	1.41‡
$(C_2H_5)_3Si$	254–270	4.65	5.96	1.01
$(n\text{-}C_3H_7)_3Si$	258–274	4.66	5.96	1.01
$(C_6H_5)(CH_3)_2Si$	256–274	3.71	5.85	1.41
$(p\text{-}CH_3C_6H_4)(CH_3)_2Si$	256–272	3.62	5.85	1.41
$(C_6H_5)_3Si$	256–270	3.83	5.87	1.35

*D_{alk}, D_{buf}, and D_{acid} refer to optical densities in alkaline, buffered, and acidic media respectively.
†Compare with value of 1.74 reported by Bott, Eaborn, Pande, and Swaddle (6) in 39 wt% methanol–water at 25° C.
‡Compare with value of 1.35 obtained by the same authors.

strong inductive electron supply by the $(CH_3)_3Si$ group when separated from the benzoic acid system by a methylene group. Replacement of the $(CH_3)_3Si$ group in this compound by $(C_2H_5)_3Si$ or $(n\text{-}C_3H_7)_3Si$ brings about a further lowering of the acid strength, and this effect is consistent with the increased inductive electron supply to silicon from the ethyl and propyl groups (7). The lowering of the dissociation constants for the ethyl and propyl compounds is of particular significance in view of the separation of these groups from the carboxyl group, and provides a measure of the sensitivity of the method. The result is also of interest in view of the data of Chatt and Williams (4), who found that the acid strengths of the compounds p-$(CH_3)_3SiC_6H_4CO_2H$ and p-$(C_2H_5)_3SiC_6H_4CO_2H$ were almost equal. In these compounds, the inductive effects of the alkyl groups are probably masked by mesomeric influences resulting from the direct silicon–phenyl bonding.

Replacement of the $(CH_3)_3Si$ group in p-$(CH_3)_3SiCH_2C_6H_4CO_2H$ by $(C_6H_5)(CH_3)_2Si$, $(p\text{-}CH_3C_6H_4)(CH_3)_2Si$, or $(C_6H_5)_3Si$ brought about no significant change in the dissociation constant. Thus, the inductive electron withdrawal by phenyl groups attached to silicon (5) is not apparent in these compounds. The results suggest that, for phenyl groups in R_3Si, a mesomeric electron supply from phenyl to silicon counteracts the inductive electron withdrawal from silicon, and the overall effect approximates to that of a methyl group attached to silicon. A phenyl group attached to silicon is, therefore, weakly electron supplying. The report by Sommer *et al.* (1) that the compound $(C_6H_5)(CH_3)_2SiCH_2CO_2H$ is a weaker acid than $(CH_3)_3SiCH_2CO_2H$ can thus be attributed to the effects of electron supply to silicon by the phenyl group.

Eaborn and Parker (2) reported a bathochromic shift of the main peak in ultraviolet spectra of p-$(CH_3)_3SiCH_2C_6H_4CO_2H$ compared with p-toluic acid. This effect was attributed to an electron supply from the trimethylsilyl group by a delocalization effect. Table II lists the positions of the absorption maxima for the acids, anions, and buffered mixtures studied in the present series. Replacement of methyl groups in $(CH_3)_3Si$ by phenyl groups brought about no significant shift in the position of the absorption peak, indicating that there is little interaction between phenyl groups and other groups attached to silicon.

EXPERIMENTAL

p-(Trimethylsilylmethyl)benzoic Acid

This acid, m.p. 197° C, was prepared in 50% yield by the method described by Eaborn and Parker (8).

p-(Triethylsilylmethyl)benzoic Acid

The Grignard reagent was prepared from p-chlorobenzyl chloride (80 g) and magnesium turnings (12.5 g) in dry ether (300 ml), and was added slowly to a stirred, cooled solution of tetrachlorosilane (85 g) in ether

Can. J. Chem. Downloaded from www.nrcresearchpress.com by 210.87.254.6 on 09/05/12
For personal use only.

TABLE II

Absorption maxima and log ϵ* values for acids of type p-$XCH_2C_6H_4CO_2H$ in 39 wt% aqueous methanol

X	λ_{max}† (mμ)		
	0.1 *N* NaOH	Buffer, pH 5.29	0.1 *N* H_2SO_4
H	233 (4.0)	238 (4.07)	239.5 (4.11)
$(CH_3)_3Si$	245 (4.21)	253.5 (4.23)	254.5 (4.26)
$(C_2H_5)_3Si$	246 (4.23)	253.5 (4.24)	254 (4.26)
$(n\text{-}C_3H_7)_3Si$	246 (4.17)	253 (4.17)	253.5 (4.20)
$(C_6H_5)(CH_3)_2Si$	247 (4.26)	252 (4.27)	254.5 (4.28)
$(p\text{-}CH_3C_6H_4)(CH_3)_2Si$	246 (4.27)	253.5 (4.26)	255 (4.29)
$(C_6H_5)_3Si$	247 (4.31)	253 (4.33)	255 (4.29)

*Log ϵ values are in parentheses.
†Ill-defined inflections were also observed in spectra of the anions in the 272–280 mμ region.

(222 ml). The mixture was refluxed for 3 hours and was then treated with the Grignard reagent prepared from ethyl bromide (164 g) and magnesium turnings (36 g) in ether (400 ml). This mixture was refluxed for 26 hours, and was then treated with aqueous 10% sulphuric acid. The ethereal layer was separated, washed with water, and dried (Na_2SO_4). Removal of the ether and fractionation gave an impure sample of *p-chlorobenzyltriethylsilane* (20 g, 17%), b.p. 141–143° C at 10 mm, $n_D^{20°}$ 1.5146. (Found: C, 62.3; H, 8.62%. $C_{13}H_{21}SiCl$ requires: C, 65.0; H, 8.8%.) The lithium reagent was prepared from this compound (20 g) and lithium (1.5 g) in ether (100 ml), with high-speed stirring and gentle heating during the reaction. The mixture was then poured onto a slurry of dry ice and ether, excess lithium was removed by filtration through glass wool, and the filtrate was treated with aqueous 10% sulphuric acid. The ethereal layer was separated and washed with 0.2 *N* aqueous sodium hydroxide solution, and the extracts were added immediately to aqueous hydrochloric acid (1 *N*). The precipitated solid was extracted with ether and was recrystallized from aqueous acetone and from an acetone – petroleum ether mixture to give *p-(triethylsilylmethyl)benzoic acid* (0.5 g), m.p. 235° C. (Found: C, 66.7; H, 8.82%. $C_{14}H_{22}O_2Si$ requires: C, 67.0; H, 8.85%.)

p-(Tri-n-propylsilylmethyl)benzoic Acid

This compound was prepared by essentially the same method as described for the previous acid. Tetrachlorosilane was treated with *p*-chlorobenzylmagnesium chloride and with *n*-propylmagnesium bromide to yield an impure form of *p-chlorobenzyltri-n-propylsilane*, b.p. 176–180° C at 10 mm, $n_D^{20°}$ 1.5191. (Found: C, 63.9; H, 8.61%. $C_{16}H_{27}SiCl$ requires: C, 67.8; H, 9.63%.) This compound (16 g) was converted to the lithium derivative and was carbonated to give *p-(tri-n-propylsilylmethyl)benzoic acid* (0.5 g), m.p. 197° C.

p-(Phenyldimethylsilylmethyl)benzoic Acid

A solution of phenylmagnesium bromide, prepared from bromobenzene (78.5 g) and magnesium turnings (12.5 g) in ether (300 ml), was added slowly to dimethyldichlorosilane (70 g) in dry ether (100 ml). The mixture was refluxed for 2 hours and was treated with the Grignard reagent prepared from *p*-chlorobenzyl chloride (80.5 g) and magnesium turnings (12.5 g) in ether (400 ml). The mixture was refluxed for 20 hours, hydrolyzed with aqueous 10% sulphuric acid, and the ethereal layer was washed and dried ($NaSO_4$). Distillation yielded a colorless oil, b.p. 190–200° C at 29 mm, which solidified when cooled. This material was recrystallized from petroleum ether to give *p-chlorobenzylphenyldimethylsilane* (25 g, 19%), m.p. 55° C. (Found: C, 69.1; H, 6.58%. $C_{15}H_{17}SiCl$ requires: C, 69.1; H, 6.57%.) The lithium reagent was prepared from this compound (8 g) and lithium (1 g) in ether (50 ml), and the mixture was carbonated and separated as described previously. Recrystallization from aqueous ethanol and from aqueous acetone yielded *p-(phenyldimethylsilylmethyl)benzoic acid* (2 g, 22%), m.p. 165° C. (Found: C, 71.1; H, 6.86%. $C_{16}H_{18}SiO_2$ requires: C, 71.0; H, 6.72%.)

p-(p-Tolyldimethylsilylmethyl)benzoic Acid

The Grignard reagent, prepared from *p*-chlorobenzyl chloride (40 g) and magnesium turnings (7 g) in ether (200 ml), was added slowly to a cooled, stirred solution of dimethyldichlorosilane (42 g) in ether (50 ml). The mixture was refluxed for 10 hours and was then treated with a solution of *p*-methylphenylmagnesium bromide, prepared from *p*-bromotoluene (42 g) and magnesium turnings (7 g) in ether (150 ml). After the mixture was refluxed for 50 hours it was hydrolyzed, washed, dried, and distilled to give a colorless liquid, b.p. 240° C at 10 mm, which, when fractionated, yielded *p-chlorobenzyl-p-tolyldimethylsilane* (10 g, 14%), b.p. 185° C at 6 mm, 150° C at 3 mm, $n_D^{20°}$ 1.5581. (Found: C, 72.2; H, 7.51%. $C_{16}H_{19}SiCl$ requires: C, 70.0; H, 6.96%.) This compound (8 g) was converted to the lithium derivative, was carbonated with dry ice, and the acid was isolated as described previously. Recrystallizations from aqueous ethanol and from aqueous acetone yielded *p-(p-tolyldimethylsilylmethyl)benzoic acid* (2.5 g, 27%), m.p. 174° C. (Found: C, 71.8; H, 7.01%. $C_{17}H_{20}SiO_2$ requires: C, 71.9; H, 7.10%.)

Can. J. Chem. Downloaded from www.nrcresearchpress.com by 210.87.254.6 on 09/05/12
For personal use only.

p-(Triphenylsilylmethyl)benzoic Acid

Triphenylchlorosilane (75 g) in ether (100 ml) was added slowly to the Grignard reagent prepared from *p*-chlorobenzyl chloride (40 g) and magnesium turnings (6 g) in ether (200 ml). The mixture was refluxed for 24 hours, hydrolyzed, washed, and dried. Removal of the ether yielded a mixture of *p*-chlorobenzyltriphenylsilane and triphenylsilanol. The former was extracted from the latter with petroleum ether (b.p. 40–60° C), and was recrystallized from aqueous ethanol to give *p-chlorobenzyltriphenylsilane* (5 g, 5%), m.p. 111° C. (Found: C, 78.4; H, 5.39%. $C_{25}H_{21}SiCl$ requires: C, 78.0; H, 5.50%.) This compound (2.25 g) was converted to the carboxylic acid through formation of the lithium reagent and carbonation. After isolation of the product as described previously, and recrystallization from aqueous ethanol and from an ether – petroleum ether mixture, there was obtained *p-triphenylsilylmethyl)benzoic acid* (1 g, 44%), m.p. 233° C. (Found: C, 78.8; H, 5.77%. $C_{26}H_{22}SiO_2$ requires: C, 79.2; H, 5.62%.)

Dissociation Constants

Dissociation constants were measured using an ultraviolet spectrophotometric method. The method depends on the difference in ultraviolet absorption spectra of the anion and the undissociated form of the acid, and requires that absorption measurements be taken in alkaline and acidic media, and in a buffer solution of known pH. pK_a values were calculated using the equation

$$pK_a = pH + \log_{10}[(D_{alk} - D_{buf})/(D_{buf} - D_{acid})],$$

where D_{alk}, D_{buf}, and D_{acid} are optical densities in the appropriate media. pK_a values were converted to K_a values using the equation $pK_a = -\log_{10} K_a$.

Solvent

The acids p-$R_3SiCH_2C_6H_4CO_2H$ are not sufficiently soluble in water to allow acid strength measurements to be obtained in that medium. Dissociation constants were, therefore, measured in 39 wt% water in methanol. The methanol was redistilled "Analar" grade material, diluted with carbon-dioxide-free distilled water and checked to a specific gravity of 0.896 at 15° C.

Stock Solutions

Stock solutions of the carboxylic acids were made to a concentration of 1×10^{-4} *M* in 39 wt% aqueous methanol. A 0.195 *N* sodium hydroxide stock solution was prepared by dissolving "Analar" grade sodium hydroxide pellets in 39 wt% aqueous methanol followed by standardization against potassium hydrogen phthalate solution. A 0.212 *N* sulphuric acid stock solution was prepared using the same solvent, and was standardized against standard sodium hydroxide solution. The acetate buffer stock solution was prepared from "Analar" grade sodium acetate (6.8044 g) and glacial acetic acid (10.4091 g) in 39 wt% aqueous methanol (250 ml). The pH of this solution was 5.15, and when diluted with an equal volume of 39 wt% aqueous methanol the pH was 5.29.

Experimental Procedure

Equal volumes (10 ml) of carboxylic acid stock solution and reagent stock solution were measured by pipette into a clean, dry mixing bottle and the solutions were thoroughly mixed by shaking. A portion of the mixed solution was then transferred by dropper to a 10-mm stoppered silica cell, which was placed in a thermoblock, thermostatically controlled at 25° C in the cell compartment of a Unicam S.P.500 spectrophotometer. The blank solution for the optical density measurements was prepared by mixing equal volumes (10 ml) of reagent stock solution and solvent. The cells were allowed to remain in the thermoblock for 15 minutes for temperature equilibration before the first readings were taken. In order to obtain maximum accuracy and to determine the most favorable region for spectral measurements, complete absorption spectra were plotted for acidic, alkaline, and buffered solutions from 224 mμ to 290 mμ, and a series of at least eight accurate optical density measurements was taken at different wavelengths in the most favorable region.

ACKNOWLEDGMENTS

The author wishes to thank Professor C. Eaborn for suggesting the topic and for his helpful advice and interest. A Research Scholarship from the University of Leicester is gratefully acknowledged.

REFERENCES

1. L. H. Sommer, J. R. Gold, G. M. Goldberg, and N. S. Marans. J. Am. Chem. Soc. **71**, 1509 (1949).
2. C. Eaborn and S. H. Parker. J. Chem. Soc. 939 (1954).
3. C. Eaborn. Organosilicon compounds. Butterworths Scientific Publications, London. 1960. p. 91.
4. J. Chatt and A. A. Williams. J. Chem. Soc. 4403 (1954).
5. J. Chatt and A. A. Williams. J. Chem. Soc. 688 (1956).
6. R. W. Bott, C. Eaborn, K. C. Pande, and T. W. Swaddle. J. Chem. Soc. 1217 (1962).
7. C. K. Ingold. Structure and mechanism in organic chemistry. G. Bell and Sons Ltd., London. 1953. pp. 60–66.
8. C. Eaborn and S. H. Parker. J. Chem. Soc. 126 (1955).

Can. J. Chem. Downloaded from www.nrcresearchpress.com by 210.87.254.6 on 09/05/12
For personal use only.

AZA STEROIDS

III. SYNTHESIS OF 11-AZA STEROIDS—A NOVEL CLASS OF STEROIDAL SAPOGENIN ANALOGUES

JAMES P. KUTNEY, I. VLATTAS, AND GANTI VENKAT RAO[1]
Department of Chemistry, University of British Columbia, Vancouver, British Columbia
Received December 3, 1962

ABSTRACT

The cyclization of a 9,12-seco-11-nor keto acid in the hecogenin series in the presence of benzylamine and anhydrous ammonia is described. The benzylamine reaction follows an unusual course whereas the ammonia reaction proceeds normally to provide an enol lactam. The sequence represents the first synthesis of an 11-aza derivative in the steroidal sapogenin series.

In previous papers of this series (1, 2) we reported on the introduction of a nitrogen function into ring B of the steroid skeleton, and this work provided some 6-aza steroidal analogues. In extending these studies, we considered the synthesis of ring C aza steroids since these steroidal derivatives with an unexpanded C-ring system were not known (3 and references cited therein pertaining to 12*a*-aza-C-homo steroids). However, a very recent article by Engel and Rakhit (4) on the first synthesis of 11-aza steroids possessing the normal skeleton prompts us to report some of our results in this area.

In considering a synthetic sequence, it was obvious that an extension of our work in ring B should provide an entry into this series. It was therefore necessary to prepare the appropriate 9,12-seco steroidal intermediates which, in turn, could be cyclized in the presence of an amine to provide the 11-aza steroid. The most direct approach to the desired 9,12-seco steroids involved ozonolysis of a 9,11-unsaturated 12-keto steroid since this type of reaction had been successfully employed by the present authors (1, 2) and by Jacobs and Brownfield (5) in the synthesis of ring B seco derivatives and by Engel and co-workers (4, 6, 13) in the synthesis of some 9,12-seco steroids. An attractive starting material for the ring-opening reaction was 9,11-dehydrohecogenin acetate, which was readily available from hecogenin acetate (7). When we subjected this substance to ozonolysis we obtained in low yield, from the acidic fraction of the reaction product, a crystalline, high-melting compound which exhibited the expected properties of the desired 9,12-seco keto acid (I). The infrared spectrum indicated two bands in the carbonyl region (5.80 μ, 5.93 μ) and still retained the characteristic spiroketal bands (8, 9), indicating that the spiroketal side chain remained unaffected under these conditions. In spite of numerous experiments, we were not able to improve the yield in this reaction and we turned to consider another approach to this problem. An attractive alternative was the use of the Lemieux reagent (10, 11) since, just at this time, Edward (12) published his work which indicated that this reagent was superior to ozone in the instance of cholest-4-en-3-one. Consequently, 9,11-dehydrohecogenin acetate was treated with this reagent and a crystalline acidic product was obtained from this reaction. This substance was shown to be identical with the ozonolysis product (I). In addition, another crystalline compound was obtained from the acidic fraction of the reaction product which on the basis of its infrared spectrum (5.68 μ) is tentatively assigned an enol lactone structure

[1]*National Institutes of Health Postdoctoral Fellow, 1960–1961.*

(IX). Our present evidence does not fully establish this structure and further investigation will be necessary. The overall yield of the desired keto acid (I) was substantially higher in the Lemieux reaction particularly since a large proportion of the neutral fraction in this reaction was unreacted starting material. In addition to the improved yield, it was also more convenient to utilize this reagent in large-scale preparations of I and we have used this procedure in all our subsequent preparations. After this phase of the work was completed, a detailed study of the ozonolysis of $\Delta^{9,11}$-12-keto steroids was reported by Engel (4, 13).

Because of our success with benzylamine in our previous work on ring B aza steroids, we decided to study the cyclization of the keto acid (I) with this amine. When the keto acid was treated with refluxing benzylamine and the reaction mixture extracted with ether, there were obtained from the neutral portion of the reaction product two crystalline compounds. The minor component was a high-melting substance which exhibited strong absorption at 6.01 μ and 6.06 μ in the infrared spectrum and also possessed an absorption maximum at 255 mμ in the ultraviolet spectrum. This spectral data led us to believe that the desired enol lactam (X) had been obtained but the subsequent analytical data was not in agreement with this structure. The structure of this product will be discussed in a later portion of this paper. The major product of the benzylamine reaction was a lower-melting crystalline compound which possessed strong carbonyl absorption in the infrared at 5.88 μ and 6.15 μ. The substance did not possess any absorption in the ultraviolet and the nuclear magnetic resonance (n.m.r.) spectrum of this material showed an intense signal in the aromatic proton region (2.75 τ). It was therefore clear that this substance did not represent a cyclic enol lactam structure but was most probably the keto amide (III). The analytical data supported this structure for the substance. In view of the apparent difference in reaction of the keto acid (I) when compared to the corresponding keto acid in the ring B series (1, 2), it was necessary to establish fully the assigned structure (III) for this keto amide. The following results provide conclusive proof of structure III.

The presence of the hydroxyl group at C_3 was readily demonstrated by the formation of a monoacetate (IV) which now showed, apart from the ketone and amide absorption, a new band at 5.80 μ in its infrared spectrum. In addition, the n.m.r. spectrum indicated a new signal for the acetate methyl group (8.0 τ). Reduction of the keto amide with sodium borohydride or with lithium aluminum hydride under mild conditions provided a dihydroxy amide (V) in good yield. Chromatographic purification of this reduction product indicated a predominance of only one isomer. The infrared spectrum of this compound indicated a disappearance of the acetate and ketone absorption but still indicated the amide band at 6.15 μ. Similarly, a disappearance of the acetate methyl signal was likewise noted in the n.m.r. spectrum for this substance. A similar reduction of the acetate, IV, with sodium borohydride provided the hydroxy acetate, VI, which in turn, was also obtained from a mild acetylation of the dihydroxy amide, V. This last reaction demonstrated that it was possible to obtain preferential acetylation at C_3 without affecting the hydroxyl function at C_9. This series of reactions served to demonstrate the functionality present in the major reaction product from the benzylamine reaction and allowed us to assign structure III to this substance.

It was now clear that the cyclization of 9,12-seco keto acids of the type indicated above could not be accomplished under the influence of refluxing benzylamine to provide N-benzyl 11-aza steroid analogues. We felt that the steric influence of the angular methyl group at C_{10} was probably the reason why the cyclization with the relatively large

N-benzyl function had failed. In order to obtain more information about the cyclization reaction we subjected the keto acid, I, to a reduction with sodium borohydride in the hope that the resulting hydroxy acid could be cyclized to provide a δ-lactone structure (VII). Indeed when we completed this reduction we obtained, as one of the reaction products, a crystalline substance which showed only one carbonyl absorption in the infrared spectrum (5.81 μ). The n.m.r. spectrum of this material showed the absence of a carboxylic proton and the analytical data was in good agreement with a lactone structure. Consequently, we tentatively assign the lactone structure VII to this reduction product, although it will be necessary to carry out a more careful study of this reaction at a later date. It is to be noted that Atwater, in his paper on oxasteroids (14), has reported a complex mixture of lactones and lactols in his work on ring B seco steroids and it would be of some interest to see whether similar results are also obtained in ring C. However, as far as the present phase of the investigation was concerned, it was merely necessary to realize that the cyclization of 9,12-seco steroids could indeed be successfully accomplished.

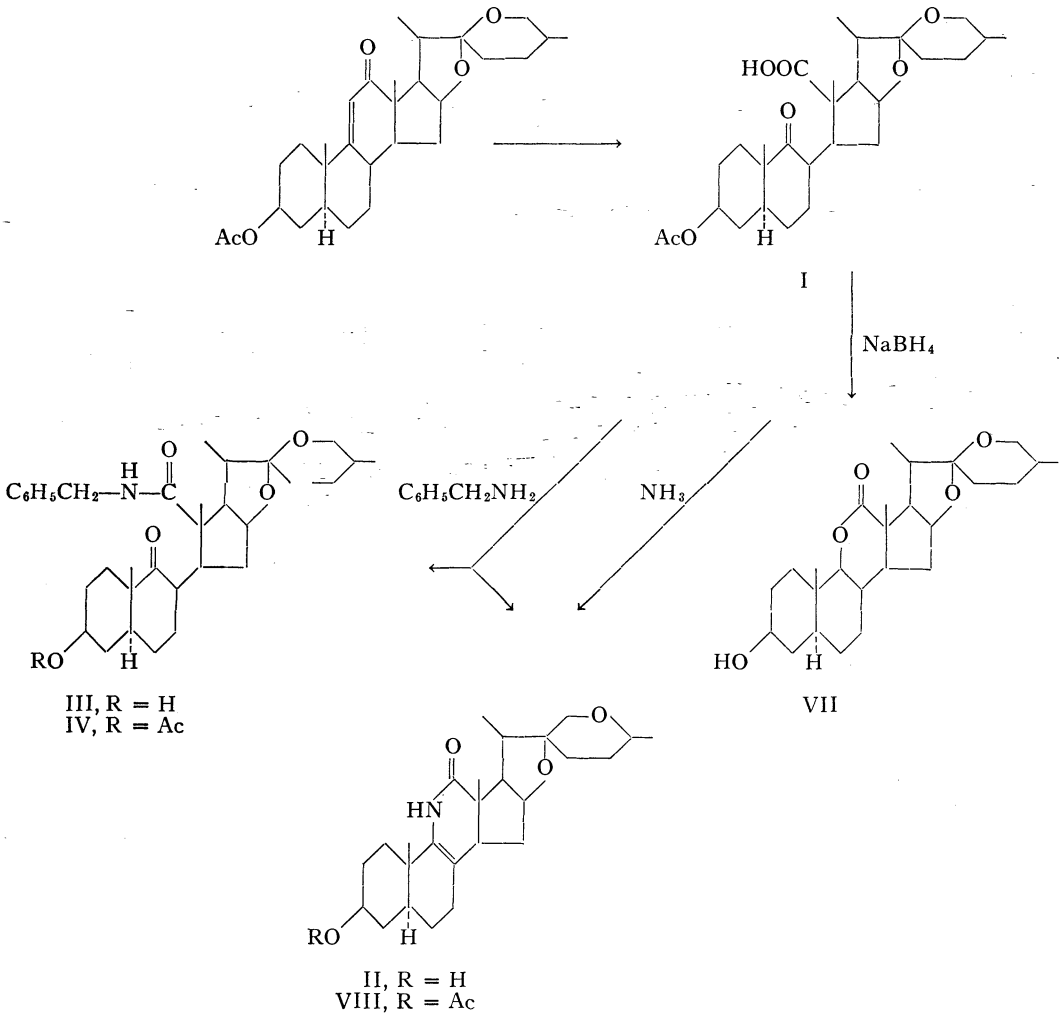

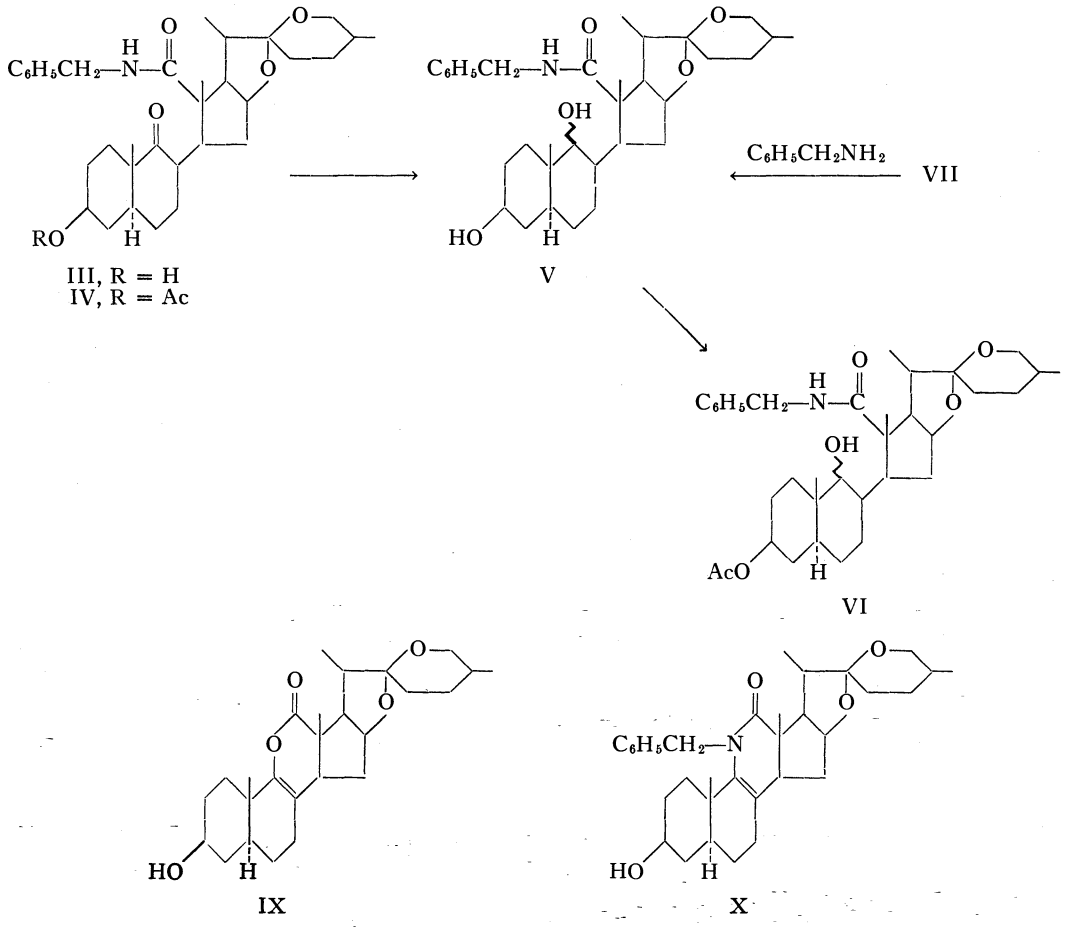

With the above information at hand, we treated an alcoholic solution of the keto acid, I, with anhydrous ammonia in a sealed tube at 150° C for 15 hours (5) and obtained an excellent yield of the expected enol lactam (II). This compound possessed an absorption at 255 mμ in its ultraviolet spectrum as expected for this type of chromophore (1, 2, 4, 5) and its high melting point was immediately reminiscent of the minor product which we had previously isolated in the reaction of benzylamine with I. Indeed, infrared, n.m.r., and mixed melting point comparison established beyond any doubt that the two products were *identical*. This very interesting result revealed several important aspects of the cyclization reaction. Firstly, the cyclization of 9,12-seco keto acids can be accomplished very successfully with ammonia and, most probably, with relatively small amines to generate 11-aza steroid derivatives. As already mentioned above, Engel has recently reported this reaction in another series of compounds (4), and our results amplify the generality of this type of reaction. Secondly, if a sterically larger amine such as benzylamine is employed, the reaction path takes an unusual course wherein an unexpected cyclic product is obtained. It is not known at this time whether the mechanism of the benzylamine reaction involves debenzylation at some stage or whether perhaps ammonia possibly formed by prolonged heating of the benzylamine is the actual reactant. We hope to present more evidence about this reaction in the future.

Further investigations with some of the above compounds will be the subject of future publications.

EXPERIMENTAL

All melting points were determined on a Fischer–Johns apparatus and are uncorrected. The ultraviolet spectra were recorded in 95% ethyl alcohol on a Cary 14 recording spectrophotometer and the rotations were taken in 1% chloroform solutions except where stated otherwise. The infrared spectra were determined on a Perkin–Elmer Model 21 spectrophotometer. The n.m.r. spectra were taken at 60 Mc on a Varian A60 instrument. The values are given in the Tiers τ scale with the signal of tetramethylsilane, which was used as the internal standard, set at 10.0 τ units. Analyses were performed by Mrs. Aldridge, University of British Columbia, and by A. Bernhardt and his associates, Mulheim (Ruhr) Germany.

Ozonolysis of 9,11-Dehydrohecogenin Acetate

A solution of 9,11-dehydrohecogenin acetate (2.7 g, prepared according to the procedure of Bowers *et al.* (7)) in methylene chloride (100 ml) was ozonized at −78° C over a period of 1 hour with an ozone stream producing 0.1 mole ozone per hour. The reaction mixture was then brought to room temperature, and water (5 ml) and 30% hydrogen peroxide (5 ml) were added. The reaction mixture was stirred for 4 hours at room temperature and then the organic layer was separated. The aqueous layer was extracted with several small portions of methylene chloride and the combined organic extracts were evaporated to dryness. The residue was taken up in ether (250 ml) and washed with a saturated solution of sodium bicarbonate (100 ml) to remove acidic components. The sodium bicarbonate layer was then made acidic with dilute hydrochloric acid and extracted with ether. The ether extract was dried over anhydrous magnesium sulphate and the solvent removed to yield an insignificant amount (0.15 g) of a solid, acidic material.

The original ether extract, which had been washed with the sodium bicarbonate solution, was now washed with cold aqueous 7% sodium hydroxide to remove any remaining acidic products. The alkaline layer was then acidified with hydrochloric acid and this mixture now extracted exhaustively with ether. The ether extract was dried over anhydrous magnesium sulphate and the solvent removed to yield 0.73 g (total, 0.88 g) of crystalline, acidic product with a melting point of 262–264°. Several recrystallizations from methanol provided a pure sample (0.7 g) of 3β-acetoxy-9-oxo-9,12-seco-11-nor-25-iso-5α,22β-spirostan-12-oic acid (I), m.p. 264–265; $[\alpha]_D$ −87°; infrared (KBr): 5.80 μ, 5.93 μ. Found: C, 68.94; H, 8.89; O, 22.53. Calc. for $C_{28}H_{42}O_7$: C, 68.54; H, 8.63; O, 22.83.

Lemieux Oxidation of 9,11-Dehydrohecogenin Acetate

A solution of 9,11-dehydrohecogenin acetate (3.0 g) in a *t*-butanol – water mixture (220.6 ml, prepared from 200 ml *t*-butanol and 20.6 ml water) was treated with an aqueous solution of potassium carbonate (1.375 g) in water (39 ml). The stirred mixture was then treated with an aliquot (25 ml) of a stock solution of sodium metaperiodate (prepared from sodium metaperiodate (9.81 g) in water (123 ml)) and 0.8% aqueous potassium permanganate (2.5 ml) and the stirring was continued. The remainder of the periodate solution was added slowly to the reaction mixture over a period of 10 minutes, and after this time, another portion (2.5 ml) of 0.8% aqueous permanganate was added. The whole mixture was stirred at room temperature for another 30 minutes, a third portion (3.75 ml) of permanganate was added, and the mixture stirred at room temperature for 4 hours. The excess permanganate was destroyed by the addition of sodium bisulphite and the resultant brownish reaction mixture was concentrated on a steam cone *in vacuo* to about one-half the original volume (until most of the volatile materials had been removed). The reaction mixture was cooled in ice, acidified with ice-cold 50% aqueous sulphuric acid, and extracted with ether. The ether extract was then washed several times with cold, dilute aqueous sodium hydroxide and finally with water. The alkaline and water washings were combined and treated with concentrated hydrochloric acid until the solution was acidic and then extracted with ether. The ether extract was dried over anhydrous magnesium sulphate and the solvent was removed to provide a crystalline, acidic product (1.1 g). Several recrystallizations from methanol–chloroform (1:1) provided the pure product (0.75 g). Infrared and mixed melting point comparison established that this product was identical with the ozonolysis product (I). The mother liquors from the above crystallizations were concentrated and another crop (300 mg) of crystals was collected, m.p. 230–240°. Repeated recrystallization of this material from aqueous methanol provided a crystalline substance (200 mg) which exhibited a somewhat improved melting point (235–238°) but it was clear that this sample was not analytically pure. The infrared spectrum of this substance with only *one* strong carbonyl absorption at 5.68 μ suggests an enol lactone structure IX but further work will be necessary before any definite conclusions can be made.

The original ether extract, which had been washed with sodium hydroxide and water, was dried over anhydrous magnesium sulphate. The solvent was removed to yield 1.3 g of a crystalline, neutral product which proved to be unreacted starting material.

This procedure has been utilized in all subsequent preparations of I.

Benzylamine Reaction on Keto Acid

The keto acid (I, 2.57 g) was dissolved in benzylamine (10 ml) and refluxed for 26 hours under a nitrogen

atmosphere. The cooled reaction mixture was then taken up in ether (200 ml) and the ethereal mixture was washed several times with 5% aqueous hydrochloric acid solution, water, and finally with 5% aqueous potassium carbonate. The ether extract was dried over anhydrous magnesium sulphate and the solvent removed to provide a semisolid neutral substance (1.9 g). This material was taken up in a small amount of ether and the small quantity of white solid which remained undissolved was removed by filtration. On allowing the ether solution to stand at room temperature for 1 hour, a second crop of the white solid precipitated. Both crops of the solid were combined and weighed (0.7 g). This substance was recrystallized from benzene to provide pure, white needles (0.55 g) melting at 274–276° (with some decomposition). This compound was subsequently shown to be *identical* with the lactam, II, by means of infrared, ultraviolet, nuclear magnetic resonance, and mixed melting point comparison. The preparation and complete characterization of II is given in a later portion of this experimental part.

The ether solutions remaining after the removal of the keto amide, II, was diluted with petroleum ether and after standing overnight deposited another crop of crystals. Several more crops of crystals were obtained upon concentration of this solution and a total of 1.0 g of this compound melting at 172–174° was obtained. Two further recrystallizations from ether – petroleum ether provided an analytical sample (0.85 g) of 3β-hydroxy-9-oxo-9,12-seco-11-nor-25-iso-5α,22β-spirostan-12-N-benzylcarboxamide (III), m.p. 174–175°; $[\alpha]_D$ −143°; infrared (KBr): 5.88 μ, 6.15 μ; infrared ($CHCl_3$): 5.90 μ, 6.08 μ, and spiroketal bands at 10.19 μ, 10.85 μ, 11.11 μ, 11.50 μ (8, 9); n.m.r. ($CDCl_3$): 2.75 τ (aromatic H). Found: C, 73.32; H, 8.83; O, 15.48; N, 2.70. Calc. for $C_{33}H_{47}O_5N$: C, 73.70; H, 8.81; O, 14.88; N, 2.61.

3β-Acetoxy-9-oxo-9,12-seco-11-nor-25-iso-5α,22β-spirostan-12-N-benzylcarboxamide (IV)

The keto amide (III, 300 mg) was treated with pyridine (8 ml) and acetic anhydride (5 ml) and the reaction mixture was allowed to stand at room temperature for 24 hours. The excess anhydride was destroyed by the cautious addition of water and the reaction mixture was extracted with ether. The ether extract was first washed with 5% aqueous hydrochloric acid and then with ice-cold 5% aqueous sodium carbonate and finally dried over anhydrous magnesium sulphate. The solvent was removed and the crystalline solid (310 mg) was recrystallized from ether – petroleum ether to provide the analytical sample of the acetate (IV, 300 mg), m.p. 168–170°; $[\alpha]_D$ −132°; infrared (KBr): 5.80 μ, 6.15 μ; n.m.r. ($CDCl_3$): 2.74 τ (aromatic H), 8.0 τ ($-\overset{\overset{O}{\|}}{C}-CH_3$). Found: C, 72.09; H, 8.42; N, 2.67. Calc. for $C_{35}H_{49}O_6N$: C, 72.51; H, 8.52; N, 2.92.

3β,9ξ-Dihydroxy-9,12-seco-11-nor-25-iso-5α,22β-spirostan-12-N-benzylcarboxamide (V)

(a) By Lithium Aluminum Reduction of Keto Amide (III)

The keto amide (III, 140 mg) was dissolved in anhydrous tetrahydrofuran and refluxed for 6 hours with lithium aluminum hydride (400 mg) which was initially placed in a Soxhlet extractor and gradually brought into the vessel by the refluxing solvent. The excess hydride was destroyed by careful addition of water and the ether layer was separated. After drying the ether extract over anhydrous magnesium sulphate, the solvent was removed to yield a white solid (150 mg). This solid was recrystallized several times from ether to provide an analytical sample of dihydroxy amide, V (120 mg), m.p. 223–224°; $[\alpha]_D$ −108°; infrared (KBr): 2.86 μ, 2.91 μ, 3.01 μ, 6.15 μ; n.m.r. ($CDCl_3$): 2.75 τ (aromatic H), complete disappearance of signal at 8.0 τ present in the spectrum of IV. Found: C, 73.37; H, 9.32; N, 2.78. Calc. for $C_{33}H_{49}O_5N$: C, 73.43; H, 9.15; N, 2.66.

(b) By Sodium Borohydride Reduction of Acetoxy Keto Amide (IV)

A solution of the acetoxy keto amide (IV, 110 mg) in methanol (8 ml) was treated with a solution of sodium borohydride (65 mg) in methanol (6 ml), and the mixture was stirred at room temperature for 1 hour. After this time, more sodium borohydride (75 mg) was added to the reaction mixture and the stirring was continued at room temperature for a further 3 hours. The mixture was concentrated *in vacuo*, water was added, and the whole mixture was acidified by the addition of 10% aqueous acetic acid. The organic product was extracted from the reaction mixture with ether and the ether extract was then washed with ice-cold 5% potassium carbonate solution and finally with water. The ether layer was dried over anhydrous magnesium sulphate and the solvent removed to yield an oily product (110 mg) which did not crystallize too well. This product was taken up in benzene and chromatographed on silica gel (50 g). Elution with benzene–chloroform (1:1) provided 35 mg of the 3-acetoxy-9-hydroxy amide, VI, which is characterized below. Elution with chloroform–benzene (9:1) yielded 65 mg of another solid which was shown to be identical with the lithium aluminum hydride reduction product, V, by infrared and mixed melting point comparison.

3β-Acetoxy-9ξ-hydroxy-9,12-seco-11-nor-25-iso-5α,22β-spirostan-12-N-benzylcarboxamide (VI)

The dihydroxy amide (V, 100 mg) was dissolved in pyridine (5 ml) and treated with acetic anhydride (3 ml), and the reaction mixture was left to stand at room temperature for 24 hours. The excess anhydride was destroyed by the addition of water and the resulting reaction mixture was extracted with ether. The ether extract was washed with 5% aqueous hydrochloric acid, then with 5% aqueous sodium carbonate, and finally dried over anhydrous magnesium sulphate. Evaporation of the solvent yielded a white solid (100 mg) which on recrystallization from ether – petroleum ether provided an analytical sample of the acetate, VI

(90 mg), as white needles, m.p. 166–167°; $[\alpha]_D$ −59°; infrared (KBr): 5.80 μ, 6.17 μ; n.m.r. ($CDCl_3$): 2.78 τ (aromatic H), 8.0 τ (—C(=O)—CH_3). Found: C, 72.50; H, 8.75; N, 2.70. Calc. for $C_{35}H_{51}O_6N$: C, 72.25; H, 8.84; N, 2.41.

3β-Hydroxy-11-aza-5α,22β-spirost-8(9)-ene-12-one (II)

The keto acid (I, 500 mg) was taken up in 95% ethyl alcohol (50 ml) and anhydrous ammonia was bubbled through the solution for 1 hour at 0° C. The mixture was then heated in an autoclave kept at 150° C for 15 hours. At the end of this heating period, the mixture was allowed to come to room temperature and a small amount (50 mg) of a yellowish solid which had precipitated was removed by filtration. The filtrate was concentrated on a steam bath *in vacuo* to yield a yellowish solid (460 mg). Both crops of the solid material were combined and recrystallized from benzene to provide the enol lactam, II, as yellowish needles. Further recrystallization from benzene, after treatment with Norite, provided the pure enol lactam as white needles (450 mg), m.p. 274–276° (with some decomposition); $[\alpha]_D$ +163° (due to solubility difficulties, this rotation was taken on 1% tetrahydrofuran solution); ultraviolet: λ_{max} 255 mμ (log ϵ 3.68); infrared (KBr): 6.01 μ, 6.06 μ; Found: C, 73.11; H, 9.10; N, 3.45. Calc. for $C_{26}H_{39}O_4N$: C, 72.69; H, 9.15; N, 3.26.

3β-Acetoxy-11-aza-5α,22β-spirost-8(9)-ene-12-one (VIII)

The enol lactam (II, 100 mg) was acetylated in exactly the manner described in the preparation of VI. The white solid product (105 mg) was recrystallized from methyl alcohol to provide the pure acetate, VIII, as white needles (95 mg), m.p. 283–285° (decomp.); $[\alpha]_D$ +132° (due to solubility difficulties this rotation was taken on a 1% solution of the substance in a 1:1 mixture of methyl alcohol–chloroform); ultraviolet: λ_{max} 255 mμ (log ϵ 3.69); infrared ($CHCl_3$): 5.81 μ, 6.0 μ, and spiroketal bands at 10.18 μ, 10.85 μ, 11.11 μ, and 11.53 μ. Found: C, 71.05; H, 8.60; N, 2.85. Calc. for $C_{28}H_{41}O_5N$: C, 71.30; H, 8.76; N, 2.97.

3β-Hydroxy-11-oxa-5α,22β-spirostan-12-one (VII)

The keto acid (I, 230 mg) was dissolved in a mixture of wet methyl alcohol (18 ml) and chloroform (10 ml) and treated with a solution of sodium borohydride (150 mg) in methyl alcohol (10 ml). The reaction mixture was stirred at room temperature for 1 hour and then more sodium borohydride (300 mg) was added and stirring continued for a further 2.5 hours. After this time the solvent was removed *in vacuo* and the residue treated with a small amount of water and then acidified by the addition of 10% aqueous acetic acid. The reaction mixture was extracted with ether and the ether extract dried over anhydrous magnesium sulphate. Evaporation of the solvent left a white solid which was recrystallized from aqueous methanol to provide a first crop (150 mg) of the lactone, VII. Concentration of the mother liquors provided an additional crop (20 mg) of the same material but subsequent concentrations of the mother liquors provided small crops (total 50 mg) of solid materials which were obviously mixtures and still remain to be characterized.

The first two crops (170 mg) were combined and recrystallized from aqueous methanol to yield the pure lactone, II (140 mg), m.p. 274–276°; $[\alpha]_D$ −22°; infrared (KBr): 5.81 μ; infrared ($CHCl_3$): 5.78 μ and spiroketal bands at 10.18 μ, 10.83 μ, 11.11 μ, and 11.53 μ; n.m.r. ($CDCl_3$): complete absence of any signals for acetate methyl group and carboxylic proton. Found: C, 72.46; H, 9.20; O, 18.27. Calc. for $C_{26}H_{40}O_5$: C, 72.19; H, 9.32; O, 18.49.

Benzylamine Reaction on Lactone (VII)

The lactone (VII, 115 mg) was dissolved in benzylamine (2 ml) and refluxed for 22 hours under a nitrogen atmosphere. The cooled reaction mixture was taken up in ether and the ethereal mixture was washed with 5% aqueous hydrochloric acid and then with 5% aqueous sodium carbonate solution. After drying of the ether extract over anhydrous magnesium sulphate, the solvent was removed to yield a white solid (130 mg). Crystallization of this substance from ether yielded a pure sample (105 mg), m.p. 222–224°. Subsequent comparison of the infrared spectrum of this product with the spectrum of the dihydroxy amide, V, indicated that the two substances were identical. This identity was further confirmed by a mixed melting point determination and comparison of the nuclear magnetic resonance spectra.

ACKNOWLEDGMENTS

Financial aid from the National Research Council of Canada and from the National Cancer Institute of the National Institutes of Health, U.S. Public Health Service, grant No. CY-5037, is very gratefully acknowledged. We would also like to thank Syntex S.A., Mexico City, for generous gifts of hecogenin acetate.

REFERENCES

1. J. P. KUTNEY and R. A. JOHNSON. Chem. Ind. (London), 1713 (1961).
2. J. P. KUTNEY, R. A. JOHNSON, and I. VLATTAS. Can. J. Chem. **41**, 613 (1963).
3. R. H. MAZUR. J. Am. Chem. Soc. **81**, 1454 (1959).

4. CH. R. ENGEL and S. RAKHIT. Can. J. Chem. **40**, 2153 (1962).
5. T. L. JACOBS and R. B. BROWNFIELD. J. Am. Chem. Soc. **82**, 4033 (1960).
6. CH. R. ENGEL and W. W. HUCULAK. Can. J. Chem. **37**, 2031 (1959).
7. A. BOWERS, E. DENOT, M. B. SANCHEZ, F. NEUMANN ,and C. DJERASSI. J. Chem. Soc. 1859 (1961)
8. C. R. EDDY, M. E. WALL, and M. K. SCOTT. Anal. Chem. **25**, 266 (1953).
9. R. N. JONES, E. KATZENELLENBOGEN, and K. DOBRINER. J. Am. Chem. Soc. **75**, 158 (1953).
10. R. U. LEMIEUX and E. VON RUDLOFF. Can. J. Chem. **33**, 1701, 1710 (1955).
11. E. VON RUDLOFF. Can. J. Chem. **33**, 1714 (1955); **34**, 1413 (1956).
12. J. T. EDWARD, D. HOLDER, W. H. LUNN, and I. PUSKAS. Can. J. Chem. **39**, 599 (1961).
13. CH. R. ENGEL, S. RAKHIT, and W. W. HUCULAK. Can. J. Chem. **40**, 921 (1962).
14. N. W. ATWATER. J. Am. Chem. Soc. **83**, 3071 (1961).

PROTON MAGNETIC RESONANCE SHIFTS AND THE ELECTRON DENSITY DISTRIBUTION IN AROMATIC SYSTEMS[1]

T. SCHAEFER[2] AND W. G. SCHNEIDER
Division of Pure Chemistry, National Research Council, Ottawa, Canada

Received October 22, 1962

ABSTRACT

The quantitative nature of the empirical linear correlation between the proton resonance shifts in aromatic molecules and the local electron density on the carbon atom to which the proton is bonded has been investigated. The application of this relationship to the determination of the electron density distribution of a variety of aromatic molecules, as well as the main limitations inherent in this application, are discussed. Electron density distributions have been derived for aniline, anisole, azulene, acepleiadylene, pyridine, pyridinium ion, and for the aromatic ions pentalenyl, indenyl, fluorenyl, triphenylmethyl cation, and azulene dianion, and are compared with those calculated by molecular orbital methods. In general there is a fairly good correspondence between the experimental and calculated density values, although for the aromatic ions the excess charge tends to be somewhat more uniformly distributed over the molecule than would be indicated by simple MO calculations.

I. THE CORRELATION BETWEEN π-ELECTRON DENSITY AND THE PROTON RESONANCE SHIFT

It has been recognized for some time that the proton resonance shift in aromatic molecules tends to reflect the π-electron density on the carbon atom to which the proton is bonded. For example in substituted benzenes, a strong electron-withdrawing substituent decreases the shielding of ring protons, whereas electron-releasing substituents cause increased shielding (1, 2, 3). The non-alternant hydrocarbon azulene provides another example; it is not possible to account for the observed proton resonance spectrum unless one invokes a contribution due to the unequal electron density at different carbon atoms (4). It is therefore of some interest to examine the possible quantitative aspects of such correlations and to what extent proton resonance shifts can provide useful information about the electron density distribution in aromatic systems.

Previous work (5, 6, 7) has provided evidence for a simple linear correlation between the proton chemical shift, δ, and the local "excess" charge, $\Delta\rho$ (located on the carbon atom), in aromatic systems; thus,

$$\delta = k\Delta\rho, \qquad [1]$$

where the constant k was found empirically to have a value near 10 p.p.m./electron. In the present work attempts have been made to examine more carefully the experimental basis of this relationship, as well as its application to a wide variety of aromatic systems. The main limitations and sources of error in evaluating π-electron densities in individual cases have also been considered.

For convenience benzene has been chosen as the reference base, both for the proton chemical shifts, δ, and for the excess charge densities, $\Delta\rho$. Thus since the π-electron density on the carbon atoms in benzene is unity, $\Delta\rho = 0$. We adopt the further convention that δ is positive for proton resonances appearing to higher field of the benzene resonance, and

[1]*Issued as N.R.C. No. 7258.*
[2]*Research Associate, National Research Council, Summer, 1962. Permanent address: Chemistry Department, University of Manitoba, Winnipeg, Manitoba.*

Can. J. Chem. Downloaded from www.nrcresearchpress.com by 210.87.254.42 on 09/05/12
For personal use only.

negative for resonances at lower field. On this basis k is found experimentally to be a positive constant. Accordingly a negative δ, associated with decreased proton screening, corresponds to a negative $\Delta\rho$ on the carbon atom, that is, an electron deficiency relative to the carbon atoms in benzene.

The constant k can be evaluated empirically in either of two ways:

(i) by measuring δ for systems in which $\Delta\rho$ is known, and

(ii) by forming positive or negative aromatic ions

$$\mathrm{Ar} \pm \mathrm{e} = [\mathrm{Ar}]^{\pm}.$$

The total π-electron density has now been altered by exactly one unit charge. If the shifts of all protons are measured relative to benzene, the sum of these shifts must correspond to $\Delta\rho = 1$, whence $\sum\delta_1 = k$. This is essentially a normalization condition, which can also be adapted to neutral molecules.*

In applying eq. [1] to the valuation of local π-electron densities several perturbing effects are frequently encountered. These arise from contributions to the measured proton resonance shifts in addition to those caused by the altered electron density. These additional contributions are due to:

(*a*) the magnetic anisotropy of substituents or of hetero atoms in the aromatic ring,

(*b*) ring current effects of neighbor rings in polycyclic aromatic compounds,

(*c*) ion association effects of aromatic ions, and

(*d*) solvent effects.

Large contributions arising from any one of these effects seriously limit the reliability with which the electron density can be evaluated. Frequently, however, adequate corrections can be made to the measured chemical shifts, or the perturbing effect can be avoided by an appropriate choice of the experimental conditions.

The magnitude of the proton resonance shift arising from the magnetic anisotropy of substituent groups in individual molecules cannot be estimated with sufficient accuracy at present to permit a satisfactory correction to the measured shifts. Since this contribution has a $1/R^3$ dependence, it will affect primarily those protons in the molecule close to the anisotropic center. For example, in nitrobenzene there is a substantial contribution to the chemical shift of the ortho protons arising from the magnetic anisotropy of the nitro group (3). At the meta and para positions the contribution is greatly attenuated and, for the present purpose, it can be neglected. Other substituents, such as —HCO, —CH_3CO, —COCl, —SO_3, —Cl, —Br, and —I, also give rise to magnetic anisotropy effects. Hetero atoms in aromatic rings may give rise to similar effects. For example the magnetic anisotropy of the N atom in pyridine gives rise to a slight unshielding contribution to the resonance shift of the α-protons (8). An empirical evaluation of this contribution, which is undoubtedly possible, would permit extension of the present methods to a considerable number of heterocyclic aromatic molecules.

The ring current effects (9) can be dealt with more readily. Since benzene has been chosen as the basic reference, no correction is required for monocyclic (benzenoid) systems. The corrections required for 5- or 7-membered rings are small and introduce little error. For a polycyclic ring system the resonance shift of a particular ring proton must be corrected for the ring current of neighbor rings to bring the shift in line with the benzene reference. For this purpose the dipole model due to Pople (10) has been employed.

**The additivity of chemical shifts and electron charges implied here depends on the validity of eq. [1].*

Can. J. Chem. Downloaded from www.nrcresearchpress.com by 210.87.254.42 on 09/05/12
For personal use only.

For benzene itself this gives a contribution to the proton shift of magnitude

$$-\frac{e^2}{2mc^2}\frac{a^2}{R^3} \approx -1.75 \text{ p.p.m.}$$

Here a is the radius of the benzene ring and R the distance of the proton from the center of the ring. The simple dipole model evidently slightly overestimates the ring current contribution in benzene (11). An improved value of 1.5 p.p.m., used for the present work, was obtained by measuring the difference between the resonance shift of benzene and the shift of the olefinic protons in 1,3-cyclohexadiene.* With this adjustment the correction for a particular proton due to the ring current in a neighbor ring, designated δ^1, becomes

$$[2] \qquad \delta^1 = 12.0\left(\frac{a^2}{R^3}\right).$$

Here δ^1 is expressed in p.p.m.; a and R (expressed in Å units) are respectively the radius of the *neighbor* ring, and the distance of the proton being considered from the center of the neighbor ring. For bicyclic systems this correction is fairly reliable and the uncertainty is probably no greater than about 0.1 p.p.m. For larger molecules containing several fused ring systems the corrections, and hence also the errors, begin to mount. For such molecules a greater portion of the electron current circulates around the periphery of the molecule and the ring current within any one ring may differ somewhat from that of benzene.

With aromatic positive or negative ions an association with counterions in solution may be anticipated. Considered as a perturbing electric field, the counterion will cause a shift of the proton resonance of the aromatic ion being measured (12, 13, 14). With small aromatic ions, and more particularly in ions where the charge is largely concentrated at one atom in the molecule, as for example in the anilinium ion, association with the counterion occurs selectively at this point and involves a close approach, on the average, to the highly charged atom. The result is a non-averaged contribution to the resonance shifts of the ring protons, which differs in magnitude at each non-equivalent proton. In the case of anilinium ion, it has been observed (15) that these contributions to the proton resonance shift are reduced by the substitution of bulky alkyl groups on the nitrogen atom. By this means the close approach of the counterion is prevented, thus reducing the strength of the perturbing ionic field. In larger aromatic ions, and particularly those in which the excess charge is well distributed over the molecule, the effects of counterion association may be expected to be averaged out and to be much smaller in magnitude. In general such effects may be expected to be further minimized by a high degree of dilution of the ionic species with a solvent of high dielectric constant.

Closely related is the problem of residual solvent effects, which may also give rise to small contributions to the proton shifts (16). With neutral aromatic molecules this can usually be avoided by an appropriate choice of solvent, and by using a dilute solution together with a suitable internal reference. These conditions must necessarily be somewhat compromised for aromatic ions which require polar solvents. If the charge distribution in the ion is highly asymmetric, the resulting "reaction field" in the solvent may contribute to the proton shift. It is difficult to estimate the magnitude of this effect in individual cases, although when it is non-negligible it can certainly be detected and investigated by direct experimentation.

Returning now to the question of the quantitative basis for eq. [1], probably the most direct evaluation of the proportionality constant k is based on the proton resonance

Both compounds were measured as a 3 mole% solution in cyclohexane.

Can. J. Chem. Downloaded from www.nrcresearchpress.com by 210.87.254.42 on 09/05/12
For personal use only.

shifts of the symmetrical species $C_5H_5^-$, C_6H_6, $C_7H_7^+$, and $C_8H_8^=$. Although the measurements were originally made by Leto, Cotton, and Waugh (17), the most extensive ones of the first three members of the series have been carried out by Fraenkel, Carter, McLachlan, and Richards (5). The proton resonance of cyclooctatetraene dianion has been measured previously by Katz (18) and by Fritz and Keller (19) and the C^{13} resonance by Spiesecke and Schneider (7). Because of the importance of the quantitative evaluation of the constant k it was considered desirable to confirm these measurements and, in particular, to investigate the possible effects of solvent and ion association. Table I shows

TABLE I

Proton resonance shifts of monocyclic aromatic ions

	Solvent	Concentration (mole%)	δ[a] (c/s at 60 Mc/s)
$(C_5H_5)^-Na^+$	THF[b]	8	102.4±0.5
		4	100.3±0.3
		2	97.9±0.2
		1	96.1±0.3
		0.5	95.4±0.1
		0 (extrapolated)	94.5
$(C_5H_5)^-Li^+$	CH_3CN	4	109.6±0.4
		2	109.7±0.5
		1	109.5±0.2
$(C_7H_7)^+Br^-$	CH_3CN	0.2	−114.8±0.2
$(C_8H_8)^=2Na^+$	CH_3CN	3	95.9±0.2
	THF	3	95.4±0.1

[a]Relative to an internal benzene reference.
[b]Tetrahydrofuran.

the measured proton shifts of $(C_5H_5)^-Na^+$ as a function of concentration in tetrahydrofuran and of $(C_5H_5)^-Li^+$ in acetonitrile. The results for a 0.2 mole% solution of tropylium bromide in CH_3CN and of $(C_8H_8)^=2Na^+$ in tetrahydrofuran and acetonitrile are also shown.

It is apparent from the results of Table I that there is a measurable solvent dilution shift for $(C_5H_5)^-Na^+$ in tetrahydrofuran. It will be noted that the direction of this dilution shift is toward lower applied (magnetic) field, contrary to that expected for decreasing ion association with dilution. No explanation can be offered for this behavior. However, one suggestion worth considering is the possibility of complex formation of the sodium cyclopentadienide with tetrahydrofuran. A specific etherate complex, $K_2C_8H_8.THF$, has been reported (19). On the other hand $(C_5H_5)^-Li^+$ in CH_3CN shows a negligible dilution shift and, moreover, the proton shift itself is larger (relative to benzene) than that of $(C_5H_5)^-Na^+$ in tetrahydrofuran. Table II shows a comparison of some of the present measurements with the corresponding results reported by Fraenkel, Carter, McLachlan,

TABLE II

	Solvent	Concentration (mole%)	δ (p.p.m. relative to benzene) Ref. 5	Present results
$(C_5H_5)^-Na^+$	THF	2	1.72	1.63
$(C_5H_5)^-Na^+$	CH_3CN	2	1.78_5	
$(C_5H_5)^-Li^+$	CH_3CN	2		1.83

Can. J. Chem. Downloaded from www.nrcresearchpress.com by 210.87.254.42 on 09/05/12
For personal use only.

and Richards (5), who quote a measurement error in δ of ± 0.004 p.p.m. On this basis the discrepancy in the two sets of measurements for $(C_5H_5)^-Na^+$ in THF is unacceptably large. The difference between the measurements in CH_3CN is about 0.04 p.p.m., which is probably within a more realistic margin of error.

On the basis of the solvent dilution measurements shown in Table I, the results for $(C_5H_5)^-Li^+$ in CH_3CN are considered the more reliable. These have been combined with the $(C_7H_7)^+Br^-$ measurement (also shown in Table I) for the purpose of evaluating the constant k. Since the ions $C_5H_5^-$ and $C_7H_7^+$ also have six π-electrons, the aromatic ring current is taken to be the same as in benzene, and corrections, amounting to -0.10 and $+0.07$ p.p.m., respectively, were applied to allow for the effect of different ring size on the proton chemical shift. The final shifts are -1.98, 0, and $+1.73$ p.p.m. respectively for $C_7H_7^+$, C_6H_6, and $C_5H_5^-$, to be compared with differences in π-electron densities, $\Delta\rho$, of -0.143, 0, and $+0.20$. The best straight line through these points (with equal residuals) results in a value of $k = 10.7 \pm 0.2$ p.p.m./electron. Here ± 0.2 p.p.m. refers to the actual deviation of the individual points and accordingly a more realistic "error" may be in the neighborhood of ± 1.0 p.p.m.

It is difficult to give a reliable assessment of the actual precision of the above determination. In the first place the validity of eq. [1] has been assumed, which neglects possible contributions of higher-order terms. Inclusion of a square term has been suggested by Musher (20), but lacking further confirmation the use of the simple first-order term is to be preferred for the present. Moreover the application of this expression to a variety of aromatic systems, as shown in the results following, leads to a fairly satisfactory internal consistency. It should be pointed out that the measurements for $(C_8H_8)^{=}2Na^+$ were not included in the above evaluation of k. The much larger ring size and four additional π-electrons as compared to benzene would involve additional uncertainties with respect to the actual contribution of the ring current effect to the proton shift. (The measured shift relative to benzene, as shown in Table I, is actually less than that of $C_5H_5^-$ in CH_3CN.) Finally there is the question of small differences in the degree of hybridization of the carbon orbitals in the 5-, 6-, 7-, and 8-membered aromatic rings. This will undoubtedly make some contribution to the measured proton shifts, but the magnitude of this contribution cannot be reliably estimated. In any event, relative to benzene, it may be expected to be largest for the C_8H_8 dianion.

Method (ii) for the evaluation of k, mentioned earlier, involves the measurement of the proton shifts of aromatic positive or negative ions relative to those of the corresponding neutral molecule. Unfortunately there are not many compounds suitable for this purpose, but the method does provide a useful "self-consistency" check of the value of k determined by the methods already described. In their study of benzene carbonium ions MacLean and Mackor (6) derived an independent value of k equal to 13.5 p.p.m./electron. This was based on the assumption that the contribution of the "ring current" effect to the proton shift in benzene is 1.88 p.p.m. With the value 1.5 p.p.m. for this contribution used here, which we regard as a more appropriate value, the value of k based on the benzene carbonium ion shifts reported by the above authors becomes 11.8 p.p.m./electron. While this value is somewhat higher than that derived above, it nevertheless represents a satisfactory confirmation by an independent method which involves only six-membered aromatic rings. A further "self-consistency" check based on aromatic ions can be illustrated with reference to the indenyl ion as an example. (See Table III below.) This involves two aromatic rings with seven protons. The two carbon atoms joining the two rings do not contain a bonded proton, and hence their π-electron charge cannot be determined by the

Can. J. Chem. Downloaded from www.nrcresearchpress.com by 210.87.254.42 on 09/05/12
For personal use only.

present methods. However, since the ion contains unit excess charge, an approximate value for the density at the 8,9-carbon atoms can be derived by application of the normalization condition mentioned earlier. Thus we have

$$\Delta\rho_{8,9} = \frac{1}{2}\left(1 - \sum \frac{\delta_1}{k}\right) = 0.17,$$

where δ_1 represents the shifts of individual protons bonded to the other carbon atoms, and k = 10.7 p.p.m./electron. If the indenyl negative ion had a uniform charge distribution, the π-electron density on each carbon atom would be 1.11. The value at the 8,9-positions would not be expected to differ from this by an "unreasonable" amount. The actual value, 1.17, determined in the above manner is necessarily approximate since it contains the accumulated errors of all δ_1, but the result nevertheless provides a further internal self-consistency test to the value of k.

One rather important point, however, which emerges from the experimental data presented in the next section, is that in all cases the measured proton shifts, when used in eq. [1], give the correct sign of the excess charge, $\Delta\rho$. This has also been noted in connection with measurements of benzene carbonium ions (6) and indicates that higher-order terms (which have been neglected in eq. [1]) can make but a relatively minor contribution.

The complete expression for the change in the proton screening due to a perturbing field E (here regarded as arising from the excess charge concentrated on the carbon atom) may be written (12, 14)

$$\Delta\sigma = aE + bE^2 + \ldots . \qquad [3]$$

The inclusion of the square term on the right-hand side to represent the proton shift measurements of $C_5H_5^-$ and $C_7H_7^+$ has been suggested (20) and its magnitude has been estimated.

In this connection it is of some interest to compare the proton shifts of H_3O^+ and OH^- relative to H_2O. In *both* these ions, though oppositely charged, the protons are *less* screened relative to H_2O by 10–11 p.p.m. (21, 22). To account for this it has been proposed (23) that only the square term in eq. [3] is involved. In contrast, as already mentioned, in the aromatic carbonium ions and carbanions the linear term is definitely dominant. This rather curious difference remains to be intrepreted, although the comparison may not be wholly justified. For example, the ions H_3O^+ and OH^-, when measured in aqueous solution, form hydrogen bonds and are known to undergo very rapid proton exchange. Accordingly the direct application of equation [3] to their "proton averaged" species in solution may not be appropriate.

II. APPLICATION TO ELECTRON DENSITY DETERMINATION IN AROMATIC SYSTEMS

In order to investigate further the quantitative nature of the correlation of proton resonance shifts and π-electron densities, the electron densities have been evaluated on the basis of the methods described in the preceding section, for a variety of aromatic systems. These include both neutral molecules and positive or negative aromatic ions. The value of k (cf eq. [1]) employed throughout is 10.7 p.p.m./electron. The results are summarized in Table III, where the notation

$$\delta_{corr} = \delta + \delta'$$

has been employed, δ' being given by eq. [2], and ρ ($=1+\Delta\rho$) represents the derived

Can. J. Chem. Downloaded from www.nrcresearchpress.com by 210.87.254.42 on 09/05/12
For personal use only.

total π-electron density. The experimental conditions employed for the proton resonance shift measurements are outlined below.

There is, unfortunately, at present no wholly reliable information on charge densities for comparison with the present derived values. The only recourse is to the various molecular orbital calculations. Depending on the type of approximation employed these often differ considerably in the individual electron density values. However, the general trend of the electron density distribution and the alternation of the densities within the molecule is broadly similar in the various approximations. (A comparison of the electron

TABLE III

Proton chemical shifts, derived electron densities, and calculated electron densities of aromatic systems

	Position	δ (p.p.m.)[a]	δ' (p.p.m.)[b]	δ_{corr} (p.p.m.)	ρ_{exp}		ρ_{calc}		
Aniline							HMO (M)[c]	HMO (M)[d]	HMO[i]
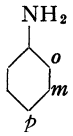	*o*	$+0.75_5$			1.071		1.081	1.043	1.034
	m	$+0.20_3$			1.019		0.997	0.998	0.999
	p	$+0.62_5$			1.059		1.064	1.037	1.027
Anisole									
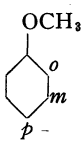	*o*	+0.42			1.039				
	m	+0.04			1.004				
	p	+0.37			1.035				
Azulene							HMO, CI[e]	SCF[f]	VESCF[g]
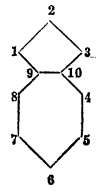	2	-0.58_3	+0.29	−0.29	0.97	1.047	0.979	0.997	0.988
	1,3	-0.06_7	+0.55	+0.49	1.05	1.173	1.096	1.049	1.059
	4,8	-0.94_5	+0.52	−0.43	0.96	0.855	0.879	0.908	0.954
	5,7	+0.28	+0.17	+0.45	1.04	0.986	1.049	1.034	1.011
	6	−0.17	+0.12	−0.05	0.99	0.870	0.948	0.938	0.969
	9,10				(0.97)	1.027	1.013	1.042	0.998
Acepleiadylene							HMO[h]		
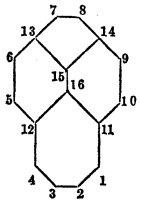	7,8	−0.50	+0.74	+0.24	1.02		1.095		
	6,9	−0.96	+0.94	−0.02	1.00		0.943		
	5,10	−0.58	+1.05	+0.63	1.06		1.055		
	1,4	−0.42	+0.96	+0.54	1.05		0.934		
	2,3	+0.48	+0.43	+0.91	1.09		0.938		
	11 → 16 (Av.)				(0.93)		(1.010)		
Pyridine							SCF, CI[i]	VESCF[i]	
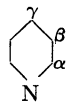	α	−1.31			—		0.951	0.952	
	β	$+0.15_5$			1.014		1.010	1.004	
	γ	−0.26			0.976		0.979	0.981	

Can. J. Chem. Downloaded from www.nrcresearchpress.com by 210.87.254.42 on 09/05/12
For personal use only.

TABLE III (*Continued*)

	Position	δ (p.p.m.)[a]	δ' (p.p.m.)[b]	δ_{corr} (p.p.m.)	ρ_{exp}	ρ_{calc}
Pyridinium ion						VESCF[i]
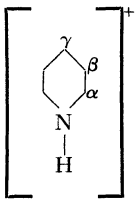	N	−6.11			(1.60)	1.520
	α	−1.56			0.854	0.899
	β	−0.91			0.915	0.927
	γ	−1.48			0.862	0.829
Pentalenyl dianion						HMO
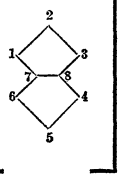	1,3,4,6	+2.29	+0.55	+2.84	1.27	1.314
	2,5	+1.54	+0.29	+1.83	1.17	1.173
	7,8				(1.29)	1.198
Indenyl ion						HMO
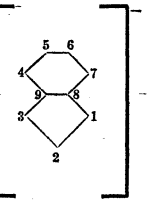	5,6	+0.78	+0.18	+0.96	1.09	1.06
	4,7	−0.12	+0.46	+0.33	1.03	1.04
	1,3	+1.31	+0.48	+1.80	1.17	1.25
	2	+0.64	+0.27	+0.91	1.09	1.11
	8,9				(1.16_5)	1.10
Fluorenyl ion						HMO
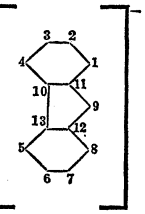	1,8	−0.09	+0.60	+0.51	1.05	1.029
	2,7	+0.42	+0.26	+0.68	1.06	1.058
	3,6	+0.80	+0.28	+1.08	1.10	1.077
	4,5	−0.68	+0.82	+0.14	1.01	1.009
	9	+1.31	+0.97	+2.28	1.21	1.322
	10,13				(1.09)	1.110
	11,12				(1.09)	1.056
Triphenyl methyl cation						HMO[k] SCF[k]
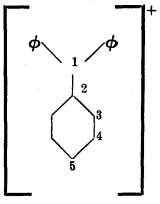	1				$(0.95)_{av}$	0.69 0.75
	2					1.00 1.15
	3	−0.35			0.97	0.92 0.95
	4	−0.60			0.94	1.00 0.94
	5	−1.0			0.91	0.92 0.81

Can. J. Chem. Downloaded from www.nrcresearchpress.com by 210.87.254.42 on 09/05/12
For personal use only.

TABLE III (*Concluded*)

Position	δ (p.p.m.)[a]	δ' (p.p.m.)[b]	δ_{corr} (p.p.m.)	ρ_{exp}	ρ_{calc} HMO
Azulene dianion					
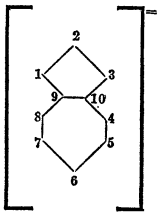					
2	+1.48	+0.29	+1.77	1.17	1.24
1,3	+1.48	+0.55	+2.03	1.19	1.18
4,8	+0.71	+0.52	+1.23	1.11	1.30
5,7	+2.22	+0.17	+2.39	1.22	1.01
6	+1.74	+0.12	+1.86	1.18	1.39
9,10				(1.29)	1.20

NOTE: Abbreviations: HMO, Hückel molecular orbitals; (M), modified; CI, configurational interaction included; SCF, self consistent field molecular orbitals; VESCF, variable electronegativity self-consistent field molecular orbitals.
[a]Proton resonance shifts in p.p.m. from benzene.
[b]Correction due to induced currents in neighbor rings.
[c]H. Baba and S. Suzuki. J. Chem. Phys. **32**, 1706 (1960).
[d]C. Sandorfy. Bull. Soc. Chim. France, **16**, 615 (1949).
[e]R. Pariser. J. Chem. Phys. **25**, 1112 (1956).
[f]A. Julg. J. Chim. Phys. **52**, 377 (1955).
[g]R. D. Brown and M. L. Heffernan. Australian J. Chem. **13**, 38 (1960).
[h]B. Pullman, A. Pullman, G. Berthier, and J. Pontes. J. Chim. Phys. **49**, 20 (1952).
[i]R. McWeeny and T. E. Peacock. Proc. Phys. Soc. (London), Sect. A, **70**, 41 (1957).
[j]R. D. Brown and M. L. Heffernan. Australian J. Chem. **12**, 554 (1959).
[k]J. A. Pople. J. Phys. Chem. **61**, 6 (1957).
[l]Reference 24, p. 353.

density values calculated by various approximations for azulene, for example, is given by Streitwieser (24, p. 456).) The calculated densities included in Table III for comparison with the densities derived from n.m.r. data were either taken from the literature or else were calculated for the present purpose using simple Hückel MO methods.

(1) Aniline, Anisole

As mentioned above the main difficulty in the employment of proton resonance shifts to evaluate the electron density in substituted aromatics arises from the magnetic anisotropy of substituent groups. With substituents such as CH_3, NH_2, OH, and OCH_3, such effects are relatively small. Table III shows the π-electron densities for aniline and anisole derived from the proton resonance shifts previously reported (3). The results exhibit the anticipated excess density at the ortho and para positions and an almost negligible contribution at the meta positions.* The MO calculations for substituted benzenes are difficult, and the results depend largely on the assumptions made to take account of the electronic effects of the substituent. Three such calculations are shown for aniline. While a quantitative comparison with the n.m.r. data may not be too meaningful, the general trend of the density distributions is very similar.

(2) Non-alternant Hydrocarbons Azulene, Acepleiadylene

The electron density distribution of azulene derived from proton resonance shifts has been reported previously (25). A re-evalution of the densities of azulene is included in Table III, employing the present revised values for k and for the aromatic ring current. The proton resonance shifts employed were measured for a 3 mole% solution of azulene in cyclohexane. Accordingly solvent effects are not in question, and the main source of error in evaluating the electron densities arises from the corrections to the proton shifts, δ', due to current circulations in the "other" ring. These corrections, evaluated by eq. [2],

**The density values previously reported in ref. 5 for aniline differ significantly at the para position. This is doubtless due to a different value of the proton resonance shift employed.*

Can. J. Chem. Downloaded from www.nrcresearchpress.com by 210.87.254.42 on 09/05/12
For personal use only.

are shown in the fourth column in the table. It was assumed that the currents in the 5- and 7-membered rings are equal to those in benzene, an assumption which derives some justification from a theoretical calculation due to Pople (26). The corrections are largest for the 1,3-positions and the 4,8-positions. A rather liberal estimate of the possible error in the electron density due to uncertainties in the "other" ring corrections might be ± 0.02 for the 1,3- and 4,8-positions, and probably less than ± 0.01 at the other positions. The value given in parenthesis in the table for the 9,10-positions was obtained by difference, using the normalization condition referred to earlier. Since this value is subject to cumulative errors, it will be somewhat less reliable than the other density values. It does, however, provide a useful internal self-consistency check. Of the various MO calculations for azulene included in Table III for comparison, those of Brown and Heffernan (27) (VESCF) have been adjusted to give the best agreement with the measured dipole moment of azulene. In general, the electron densities derived from n.m.r. data show a somewhat smaller variation than those evaluated by MO methods, but the density alternations around the two rings are well reproduced.

The non-alternant hydrocarbon acepleiadylene, which contains four aromatic rings in a pyrene-type structure, is less satisfactory for the present purposes than azulene. Each proton resonance shift must be corrected for current circulation in three other rings. These corrections become rather large, and no doubt also involve proportionately greater errors. The *average* density evaluated for carbons 11, 12, 13, 14, 15, and 16 was found to be 0.93. This was again obtained by taking the difference of the sum of the densities derived for all the other carbon atoms which have a bonded proton, and the total number of π-electrons (16). The low value of 0.93 for the inner carbon atoms might be interpreted to mean that the excess charge tends to be concentrated mainly on the outer perimeter of the molecule. However, in view of the possibility of accumulated errors in the "other ring" corrections this cannot be substantiated on the basis of the present results. Comparison of the charge densities derived for the remaining carbon atoms indicates a preference for the excess charge to reside in the 7-membered ring, rather than in the 5-membered ring at the opposite end of the molecule as indicated by simple Hückel MO calculations (28). This discrepancy appears to be real and outside the probable limits of the experimental uncertainties. It would also imply a direction of the molecular dipole moment opposite to that indicated by the MO calculations. The actual direction of the molecular dipole moment is not known.

(3) Pyridine, Pyridinium Ion

Pyridine and the pyridinium ion illustrate some features common to many heterocyclic aromatic systems. As already mentioned, the N atom in pyridine gives rise to a magnetic anisotropy. The presence of this anisotropy, which has been demonstrated by the nitrogen resonance measurements of Baldeschwieler and Randall (8), gives a non-negligible contribution to the screening of the α-protons in pyridine. In order to evaluate the electron density at the α-position this contribution must be subtracted out. At present a quantitative estimate of such contributions is lacking. They are very much attenuated at the β- and α-positions, and accordingly the electron densities at these positions, derived from the measured proton shifts, should be fairly reliable. They are listed in Table III together with two sets of calculated densities, with which they show a rather good correspondence.

In the pyridinium ion the magnetic anisotropy of the N atom, which now contains a bonded proton, is greatly reduced. The proton resonance shifts of the pyridinium ion have

Can. J. Chem. Downloaded from www.nrcresearchpress.com by 210.87.254.42 on 09/05/12
For personal use only.

been reported previously (29). The derived electron densities are listed in Table III. The density shown for the N atom is again obtained by difference. If the shift of the N—H proton is employed in conjunction with that in pyrrole as a reference state, and with the same value of k as employed here for aromatic C—H bonds, the value of the density on the N atom is found to be 1.57. However, this latter procedure is very rough. The calculated results of Brown and Heffernan (30) for the pyridinium ion (Table III) show a fair correspondence with the present results.

The proton resonance measurements for pyridine were carried out in a dilute solution of cyclohexane, and solvent effects may be assumed to be absent. The pyridinium ion shifts were measured in a dilute solution (~5 mole%) in trifluoroacetic acid. Accordingly the measured proton shifts may be affected somewhat by solvent interaction and ion association.

(4) The Carbanions Pentalenyl, Indenyl, and Fluorenyl

The pentalenyl dianion has been prepared by Katz and Rosenberger (31). The proton resonance shifts (measured in a dilute solution of tetrahydrofuran) reported by these authors have been employed to evaluate the π-electron densities. These are shown in Table III together with the density values calculated by simple Hückel MO methods. There is a fairly good correspondence between the two sets of results. The experimental value in parenthesis shown for the 7,8-positions was obtained by difference and may be somewhat less reliable.

The indenyl and fluorenyl ions were prepared by reacting dilute solutions (2–5 mole%) of the parent hydrocarbons, indene and fluorene, in tetrahydrofuran with sodium. Figure 1

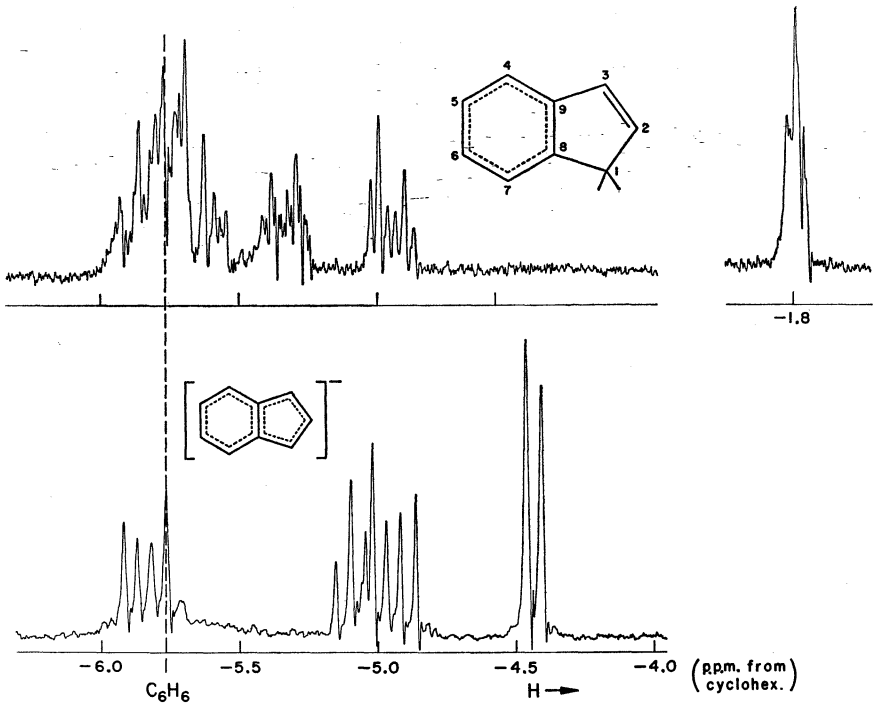

FIG. 1. Proton resonance spectrum at 60 Mc/s for indene and indenyl ion. The reference scale is in p.p.m. relative to internal cyclohexane.

Can. J. Chem. Downloaded from www.nrcresearchpress.com by 210.87.254.42 on 09/05/12
For personal use only.

shows the proton resonance spectra (at 60 Mc/s) of both indene and the indenyl ion, on a common scale. The proton resonance of benzene on this scale is indicated by the broken line. The proton resonance spectrum of indene has been previously assigned and analyzed by Elleman and Manatt (32). Starting from the right, the signals at −1.8 p.p.m. (from cyclohexane) arise from the methylene protons at the 1-position; those centered near −4.9 from proton 2, and those centered near −5.3 from proton 3. The latter signals show additional splitting due to long-range spin-coupling with proton 4. Finally the complex pattern of signals centered near −5.7 is due to the four protons in the 6-membered ring. The assignment of the proton spectrum of the more symmetrical indenyl ion is straightforward. The three protons in the 5-membered ring give rise to an AB_2 system; the doublet at −4.4 p.p.m. is accordingly assigned to the 1,3-protons, and the triplet centered near −5.1 to the 2-proton. The four protons in the 6-membered ring form an A_2B_2 system; the lower-field half of the spectrum, centered near −5.8, has broader lines than the higher-field half centered near −4.9 p.p.m. Assuming that the broader lines are due to long-range spin-coupling with the 1,3-protons, they are accordingly assigned to the 4,7-protons. Thus, in the ion the 5,6-proton signals are shifted up field to a greater extent by the excess charge. The signals of protons 1, 2, and 3 also show a large up-field shift, but this is partly compensated by the appearance of a ring current in the 5-membered ring.

The density distribution evaluated from the proton resonance shifts (Table III) shows the largest density at the 1,3-positions and the smallest at the 4,7-positions. In this respect there is a parallel with the density distribution in azulene. The density at the 8,9-position was obtained by difference as explained above, and is accordingly subject to greater error. The densities calculated by HMO methods show a remarkably good correspondence with the n.m.r. values, and the density alternation around the rings is identical.

The proton resonance shifts in the fluorenyl ion were generally larger than those in the indenyl ion and a first-order analysis of the spectrum was adequate for the present purpose. The proton assignment was made on the basis of the spin-coupling patterns, but there remains an ambiguity, as between protons 2,7 and 3,6 and between protons 1,8 and 4,6. Of the various possible combinations of assignments, only that shown in Table III gives a reasonable pattern for the density distribution and compares favorably with that calculated by HMO. As in a number of other examples, the spread between maximum and minimum density is smaller than that in the calculated density distribution. This difference is particularly apparent at the 9-position.

(5) The Triphenyl Methyl Cation

As an example of a carbonium ion, the triphenylmethyl cation has been investigated. The proton resonance spectrum of the ion has been reported previously (33), and was repeated for the present study under conditions of higher resolution. The main problem encountered in evaluating the electron density is the assessment of the contribution to the proton shifts due to neighboring ring currents. The most reasonable assumption to make is that the molecular framework is essentially planar (i.e. carbon 1 trigonally hybridized) but with the phenyl groups tending to be tilted out of the plane like the blades of an air fan. A completely planar structure would appear to be ruled out because of strong repulsions between protons in ortho positions. If in addition the phenyl rings are assumed to librate or rotate, the contribution of the ring current to the proton shifts of a neighboring phenyl group will be largely averaged out. In any event the effect at the meta and para protons will be negligibly small, although some average residual

Can. J. Chem. Downloaded from www.nrcresearchpress.com by 210.87.254.42 on 09/05/12
For personal use only.

contribution could be present at the ortho protons. Accordingly in evaluating the electron densities shown in Table III no corrections for neighbor ring effects were made. Comparison with the theoretically calculated values shown indicates a much closer correspondence with the SCFMO results than with those from simple Hückel molecular orbitals. The value 0.95 shown in parenthesis may be regarded as a rough indication of the average density of the 1- and 2-positions. It represents one third of the total electron density at positions 1, 2, 2′, and 2″, obtained by subtracting the sum of the density at all other positions from 18, the total number of π-electrons.

(6) The Azulene Dianion

Aromatic negative ions of a large number of compounds are readily formed by treating a dilute solution of the parent aromatic hydrocarbon in a suitable solvent with alkali metals. With most hydrocarbons the formation of a paramagnetic mononegative ion, which has the added electron in the lowest antibonding molecular orbital, is favored. Azulene on the other hand readily forms the dinegative ion on treatment with excess lithium.* Since the two electrons are paired in the same orbital the ion is diamagnetic. Its proton resonance spectrum bears a close resemblance to that of azulene itself, except that the whole spectrum is considerably displaced toward higher applied field and the signals of the 1-, 2-, and 3-protons are coalesced to a single line. This assignment of the ion was confirmed by measuring 1,3-dideuteroazulene. As an additional confirmatory check, deuterated dimethoxyethane was used as solvent. This was desirable because the spectrum of the ion, occurring at higher field, was partially overlain by the C^{13} satellite resonance peaks of the protons in the undeuterated solvent.

In evaluating the electron density distribution the assumption was made that the ring current induced by the magnetic field in the dinegative ion is similar in magnitude to that in azulene itself. Addition of two electrons to the first antibonding orbital will not increase the aromatic ring current; in fact the ring current is probably somewhat decreased (26). Certainly if all five antibonding orbitals were completely filled the induced ring current would be reduced to zero. Since the magnitude of the reduction in the ring current for the dinegative ion is not readily estimated, the above assumption is probably the best one can make under the circumstances. That this assumption cannot be far wrong is borne out by the density values derived on this basis (Table III); the value 1.29 obtained for the 9,10-positions by difference, in the usual way, is not unreasonable in the context of the overall charge distribution, particularly in view of the fact that this value will involve some accumulation of errors. Had the ring current in the dianion been very substantially reduced relative to that in azulene, the resulting value at the 9,10-positions may have been expected to deviate rather widely.

Comparison of the experimentally derived charge distribution for the dianion with that calculated from simple Hückel orbitals shows the excess charge to be more uniformly distributed, i.e. more delocalized, than would be anticipated from the calculated results. This point is perhaps more clearly demonstrated by comparing the density distribution of the dianion with auzlene itself. Table IV shows the density increments at each position for the process [azulene] $\rightarrow$ [azulene]$^{=}$. In other words, these are the density increments at each position resulting from the addition of two electrons to the lowest antibonding orbital in azulene. Discounting those at the 9,10-positions (which contain the compounded errors of both density distributions), the increments derived experimentally are moderately uniform at each position. On the other hand the calculated increments are large at the

We are indebted to Professor J. Hoijtink for pointing this out to us.

Can. J. Chem. Downloaded from www.nrcresearchpress.com by 210.87.254.42 on 09/05/12
For personal use only.

TABLE IV

Charge density increments for [azulene] → [azulene]⁼

Position	Δρ	
	Experimental	Calc. (HMO)
2	0.20	0.20
1,3	0.14	0.01
9,10	(0.32)	0.17
4,8	0.15	0.44
5,7	0.18	0.02
6	0.19	0.52

2-, 4-, and 6-positions and negligible at the 3- and 5-positions. These results, based on HMO calculations, represent, of course, a highly idealized system. In any real system it may be anticipated that an excess charge of 0.5 electron placed on any one carbon atom, as at the 6-position, would cause the molecular system to relax and part of this charge would be distributed over the neighboring carbon atoms, the 5- and 7-positions.

The greater degree of charge delocalization indicated in the charge distributions derived from n.m.r. data as compared to the MO results appears to be common also to the other aromatic ions investigated (Table III). A similar observation has also been made previously in relation to the benzene carbonium ion (6). Colpa, MacLean, and Mackor (34) have given an interpretation of this behavior in terms of π–σ interaction. As discussed above, the proton resonance responds to an altered π-electron density on a carbon atom due to an essentially electrostatic polarization of the C—H sigma bond. It is thus to be anticipated that the sigma bonds to neighboring carbon atoms will be similarly polarized, resulting in some contribution to the resonance shift of their bonded protons. Consequently the densities derived from proton resonance shifts give a measure of the combined local density alteration in both the π- and σ-electron systems. In contrast the densities calculated by simple MO theory yield an "idealized" local density for the π-electron system only. In neutral molecules, where the π-electron densities differ but slightly from unity this basic difference in the results of the two methods is not very pronounced. However, in the aromatic ions, and particularly double-charged ions, where the excess charges are greater, the disparity in the resulting density distributions is increased.

III. CONCLUSIONS

The present investigations provide strong support for a simple empirical correlation between the proton resonance shift and the local electron density on the bonded carbon atom in aromatic systems. When this relationship is applied to a variety of suitable aromatic systems a satisfactory reproduction of the electron density distribution, as indicated by chemical and theoretical methods, is obtained. The assumption that the proton screening depends linearly (to a good approximation) on the excess electron density of the bonded carbon atom appears to be well borne out. In all cases this gives the correct sign of the proton shifts, and accordingly, if square terms or higher-order interactions are involved, they must be relatively small. In favorable cases, therefore, the charge densities determined from proton shifts can be expected to be quite reliable; they are probably more accurate than those calculated by simple MO methods and compare favorably with those obtained by more refined calculations.

Can. J. Chem. Downloaded from www.nrcresearchpress.com by 210.87.254.42 on 09/05/12
For personal use only.

On the other hand many aromatic systems represent "unfavorable" cases and the determination of the electron density distribution by the present methods has serious limitations. Among these are molecules with magnetically anisotropic substituents, heterocyclic molecules, and large polycyclic molecules, for which the effects due to induced ring currents are proportionately large. The extent to which useful information on charge densities can be derived in these cases will ultimately depend on the extent to which the perturbing effects can be treated, either theoretically or empirically, in a more quantitative manner. In some cases solvent effects could give rise to additional uncertainties although these are usually less serious.

For aromatic positive or negative ions, which involve much larger excess charges than neutral molecules, the charge density distributions derived from n.m.r. data generally indicate a somewhat more uniform distribution of the excess charge than those calculated by MO methods. This may be indicative of π–σ interaction, the proton screening being thus altered by the polarized σ-orbitals as well as by the excess charge in the π-orbitals.

EXPERIMENTAL

General

The carbanions whose cations were sodium were prepared by shaking with sodium in a solvent vapor atmosphere. They were transferred to sample cells through a sintered-glass filter. The apparatus was self-contained so that contact was never made with air or water. Tetrahydrofuran (THF) had been purified by vacuum distillation after shaking with sodium and anthracene. Acetonitrile was dried over P_2O_5 and was vacuum distilled.

The carbanions whose cations were lithium were prepared from a solution of *n*-butyl lithium in hexane. After precipitation of the salt the hexane was removed by vacuum distillation and the appropriate solvent was added. Again no contact with air or water was allowed, all transfers of solvent being done on a vacuum line.

The proton resonance measurements were made at 60 Mc/s. Internal references were either benzene or cyclohexane, present in the purified solvent at a concentration between 0.5 and 1 mole%. The internal shift between benzene and cyclohexane was 351.4 c/s in THF. The same shift was found in a THF solution which had been shaken with sodium for 1 day, demonstrating the reliability of the reference positions.

Cyclopentadienyl Sodium

Separate solutions (series I) of varying concentrations were prepared from measured amounts of reactants and solvent as described above. Dicyclopentadiene was freshly distilled. A second series of dilution studies was made on an 8 mole% solution by the addition of known volumes of solvent to the initial solution in a self-contained apparatus. This arrangement precluded spinning the sample but as a check the 8 mole% solution, retrieved by vacuum removal of the correct amount of solvent, was spun, and the measurement was found to agree exactly with the original one. Table I gives the results. In the higher concentration regions (6–10 mole%) the difference in shifts between the two types of measurement differ by as much as 1.0 c/s. This is probably due to the difficulty of getting accurate concentrations with such small amounts of material (the solutions in the first series of dilution experiments were made from 1 cc of solvent). However, plots of the two series of points extrapolate to the same point at zero concentration. The shifts for the 10 mole% and 6 mole% solutions (series I) gave virtually the same peak intensities and shifts, so that a limited solubility in THF is indicated.

Cyclopentadienyl Lithium

Dilution studies were carried out from 4 mole% down to 1 mole% in acetonitrile. The dilution shift was zero to within experimental error and the shift relative to benzene was 1.83 p.p.m.

Tropylium Bromide

A 0.2 mole% solution in CH_3CN had a strong peak at -1.91 p.p.m. relative to benzene. The salt was insufficiently soluble in THF to give a resonance.

$C_8H_8{=}2Na^+$

Solutions, 3 mole%, of this compound were prepared from freshly distilled cyclooctatetraene in both THF and CH_3CN, as described above. The THF solution threw down a dark brown precipitate which partially redissolved to give a greenish-yellow solution. The CH_3CN solution was brown. The shifts were 1.60 and 1.59 p.p.m. relative to C_6H_6, respectively. A previous measurement of this ion, reported by Fritz and Keller (19), differs excessively. Our values agree with those of Katz (18).

Can. J. Chem. Downloaded from www.nrcresearchpress.com by 210.87.254.42 on 09/05/12
For personal use only.

Triphenylcarbonium Ions

Both the chloride and the carbinol of triphenylmethane dissolved to form 5 mole% orange solutions in trifluoroacetic acid. The ring proton spectra, of the A_2B_2C type, were virtually identical for the two solutions. They were analyzed to give approximate shifts (Table III). The spectra were very similar to those of Connor *et al.* for the carbinol at 40 Mc/s, allowing for the difference in spectrometer frequencies.

Crystal violet, the chloride of the symmetrically trisubstituted *p*-N,N-dimethyltriphenylmethane, gave a single broad line for the ring protons in CF_3COOH, about -0.3 p.p.m. from internal C_6H_6. Since at least partial protonation of the $N(CH_3)_2$ groups occurs, no conclusions can be drawn. Solutions in various solvents of dielectric constants as high as 65 all gave nearly the same A_2B_2 spectra for the ring protons, all a few tenths of a p.p.m. to high field of internal benzene. It was concluded that ionization was not occurring.

Experiments with $AlCl_3$ and the chloride as well as crystal violet, in an attempt to get the carbonium ion, were unsuccessful.

Triphenylmethyl sodium in THF gave a broad line at about 0.2 p.p.m. to high field of internal benzene, indicating no appreciable ionization and possibly some radical species present.

Indenyl Sodium

Freshly distilled indene gave a light orange or yellowish 5 mole% solution in THF after shaking for about a day. The spectrum of the molecule and the ion are shown in Fig. 1. The experiment was repeated at a lower concentration (~3 mole%). The shifts obtained agreed to within 0.04 p.p.m.

Fluorenyl Sodium

Solutions, 5 mole% and 3 mole%, in THF gave orange solutions after shaking with sodium for a few days. The 5 mole% solution was not completely converted to the ion but conversion was very nearly complete in the 3 mole% solution. The shifts relative to benzene in the two solutions agreed to within 0.05 p.p.m. at worst and to within 0.01 p.p.m. at one position.

Azulene Dianion

Solutions, 4 mole%, were prepared by shaking with lithium in dimethoxyethane and in deuterated dimethoxyethane, both solvents having been purified with sodium and anthracene. The solution was deep purple in color.

ACKNOWLEDGMENTS

We gratefully acknowledge our indebtedness to Mr. Y. Lupien for the preparation of samples, to Mr. J. Nicholson for technical assistance, and also to Dr. E. Mackor for providing us with his results prior to publication and to Dr. J. Martin for informative discussions.

REFERENCES

1. P. L. Corio and B. P. Dailey. J. Am. Chem. Soc. **78**, 3043 (1956).
2. A. A. Bothner-By and R. E. Glick. J. Chem. Phys. **26**, 1651 (1957).
3. H. Spiesecke and W. G. Schneider. J. Chem. Phys. **35**, 731 (1961).
4. W. G. Schneider, H. J. Bernstein, and J. A. Pople. J. Am. Chem. Soc. **80**, 3497 (1958).
5. G. Fraenkel, R. E. Carter, A. McLachlan, and J. H. Richards. J. Am. Chem. Soc. **82**, 5846 (1960).
6. C. MacLean and E. L. Mackor. Mol. Phys. **4**, 241 (1961).
7. H. Spiesecke and W. G. Schneider. Tetrahedron Letters, No. 14, 468 (1961).
8. J. D. Baldeschwieler and E. W. Randall. Proc. Chem. Soc. 303 (1961).
9. J. A. Pople, W. G. Schneider, and H. J. Bernstein. High resolution nuclear magnetic resonance. McGraw Hill Book Co., Inc., New York. 1959. p. 180.
10. J. A. Pople. J. Chem. Phys. **24**, 1111 (1956).
11. N. Jonathan, S. Gordon, and B. P. Dailey. J. Chem. Phys. **36**, 2443 (1962).
12. T. W. Marshall and J. A. Pople. Mol. Phys. **1**, 199 (1958).
13. M. J. Stephen. Mol. Phys. **1**, 223 (1958).
14. A. D. Buckingham. Can. J. Chem. **38**, 300 (1960).
15. G. Fraenkel. Private communication.
16. A. D. Buckingham, T. Schaefer, and W. G. Schneider. J. Chem. Phys. **32**, 1227 (1960).
17. J. R. Leto, F. A. Cotton, and J. S. Waugh. Nature, **180**, 978 (1957).
18. T. J. Katz. J. Am. Chem. Soc. **82**, 3784 (1960).
19. H. P. Fritz and H. Keller. Z. Naturforsch. **16b**, 231 (1961).
20. J. I. Musher. J. Chem. Phys. **37**, 34 (1962).
21. H. S. Gutowsky and A. Saika. J. Chem. Phys. **21**, 1688 (1953).
22. G. C. Hood, O. Redlich, and C. A. Reilly. J. Chem. Phys. **22**, 2067 (1954).
23. J. I. Musher. J. Chem. Phys. **35**, 1989 (1961).
24. A. Streitwieser. Molecular orbital theory for organic chemists. John Wiley and Sons, New York. 1961.
25. S. S. Danyluk and W. G. Schneider. Can. J. Chem. **40**, 1777 (1962).

Can. J. Chem. Downloaded from www.nrcresearchpress.com by 210.87.254.42 on 09/05/12
For personal use only.

26. J. A. POPLE. Mol. Phys. **1**, 175 (1958).
27. R. D. BROWN and M. L. HEFFERNAN. Australian J. Chem. **13**, 38 (1960).
28. B. PULLMAN, A. PULLMAN, G. BERTHIER, and J. PONTIS. J. Chim. Phys. **49**, 20 (1952).
29. I. C. SMITH and W. G. SCHNEIDER. Can. J. Chem. **39**, 1158 (1961).
30. R. D. BROWN and M. L. HEFFERNAN. Australian J. Chem. **12**, 554 (1959).
31. T. J. KATZ and M. ROSENBERGER. J. Am. Chem. Soc. **84**, 865 (1962).
32. D. D. ELLEMAN and S. L. MANATT. J. Chem. Phys. **36**, 2346 (1962).
33. R. B. MOODIE, T. M. CONNOR, and R. STEWART. Can. J. Chem. **37**, 1402 (1959).
34. J. P. COLPA, C. MACLEAN, and E. L. MACKOR. Private communication.

Can. J. Chem. Downloaded from www.nrcresearchpress.com by 210.87.254.42 on 09/05/12
For personal use only.

DIFFUSION WITH MIGRATION IN THE DIFFUSE DOUBLE LAYER

S. K. RANGARAJAN
Central Electrochemical Research Institute, Karaikudi, India
Received June 12, 1962

ABSTRACT

The polarization characteristics of the concentration of the reactive species are discussed when the effects of migration in the diffuse layer are accounted for. A limiting case ($\xi_0 \rightarrow \infty$) and some particular cases ($|Z_i/Z| = 0, 1, 2, 3, 4$) are derived both for attraction and repulsion in the double layer. Linear approximations (and conditions sufficient to validate these) are presented. Some general results which relate the functional forms of the transforms of the interfacial concentrations for the cases of attraction and repulsion are also pointed out.

Can. J. Chem. Downloaded from www.nrcresearchpress.com by 210.87.254.40 on 09/05/12
For personal use only.

The effect of the diffuse double layer is usually neglected in the quantitative formulations of the problems in electrode kinetics. It is the object of the present paper to examine the polarization characteristics* of the concentrations of the reactive species when the effect of migration in the diffuse double layer is taken into account. As has been pointed out (1) the effect of the diffuse layer is mainly twofold, viz., the manner in which it affects the effective concentrations of the reactants in the plane of closest approach and the potentials for the forward and the backward reactions. Detailed investigations on the corrections that must be applied necessarily to account for the effects of the diffuse double layer have been made by various authors,† and in particular the derivations of Matsuda and Delahay (2) will be examined with reference to the expressions obtained in this paper.

1. The Formulation of the Problem and its Solution

The changes in the concentrations of the reactive species C_i(i = O, oxidant; R, reductant) in the plane of closest approach is given by the solution of the diffusion equation

$$\frac{\partial C_i}{\partial t} = D_i\left[\frac{\partial}{\partial x}\left(\frac{\partial C_i}{\partial x} + \frac{Z_iF}{RT}\frac{d\phi}{dx}C_i\right)\right] \qquad [1]$$

where the second term in the R.H.S. accounts for the "flux due to the migration effects in the diffuse double layer".

The initial condition is

$$C_i(t = 0) = C_i^{\,0}\exp\left(\frac{-Z_iF\phi}{RT}\right) \qquad [2]$$

(Z_i: valency of the species i *with sign*)

The boundary conditions are given as

$$D_i\left(\frac{\partial C_i}{\partial x} + \frac{Z_iF}{RT}\frac{d\phi}{dx}C_i\right) = \pm\frac{I}{nF} \qquad (\text{at } x = 0) \qquad [3]$$

(positive sign for i = O and negative for i = R,
if the net cathodic current is taken as positive)

**By 'polarization characteristics' of the concentrations, we mean the deviation of the final state, the concentration distribution which exists at the moment due to the application of an electric field vis-a-vis the initial state (viz. the equilibrium state).*

†For a comprehensive bibliography, see reference 1.

where n is the number of electrons transferred in the rate-determining step

$$O^{z_O} + ne \rightleftharpoons R^{z_R}$$

$$Z_O = Z_R + n$$

and

[4] $$C_i(x \to \infty) \to C_i^0.$$

It is assumed that:

(a) the diffuse double layer structure is determined entirely by a Z–Z supporting electrolyte;

(b) the potential distribution $\phi(x)$ in the layer obeys Gouy–Chapman theory, i.e.,

[5] $$\frac{d\phi}{dx} = -\left(\frac{2RT}{|Z|F}\right)\kappa \sinh\left(\frac{|Z|F\phi}{2RT}\right)$$

and

[5′] $$1/\kappa = (RT\epsilon/8\pi Z^2F^2C_t)^{1/2};$$

(c) convection is negligible; and

(d) the mobility is given by

$$\mu = \frac{Z_iD_iN}{RT}.$$

Defining the Laplace's transformation* of $f(t)$ as

$$\bar{f}(p) = p\int_0^\infty e^{-pt}f(t)dt$$

equation [1] can be transformed into an ordinary differential equation, viz.,

[6] $$D_i\frac{d}{dx}\left(\frac{d\bar{C}_i}{dx} + \frac{Z_iF}{RT}\frac{d\phi}{dx}\bar{C}_i\right) - p\left[\bar{C}_i - C_i^0\exp\left(\frac{-Z_iF\phi}{RT}\right)\right] = 0.$$

Following Matsuda and Delahay, we write

[7] $$\bar{C}_i(p) = \exp\left(\frac{-Z_iF\phi}{RT}\right)\cdot[C_i^0 - v_i(p)]$$

and

[7′] $$\xi = \exp\frac{|Z|\,F\,|\phi|}{2\,R\,T}$$

so that

[8] $$v_i \to 0 \text{ as } x \to \infty \text{ (since } \phi \to 0 \text{ as } x \to \infty).$$

By using equation [7], equation [6] can be transformed into

$$D_i\exp\left(\frac{Z_iF\phi}{RT}\right)\frac{d}{dx}\left[\exp\left(\frac{-Z_iF\phi}{RT}\right)\frac{dv_i}{dx}\right] - pv_i = 0.$$

It can be shown by using equations [5] and [7′] that

$$d\xi = -\frac{\kappa}{2}(\xi^2 - 1)dx$$

The transform variable 'p' here is not to be confused with the parameter $p = \pm|Z_i/Z| - 1$ introduced in reference 2. p of reference 2 $= (l - \frac{1}{2})$ of this paper.

Can. J. Chem. Downloaded from www.nrcresearchpress.com by 210.87.254.40 on 09/05/12
For personal use only.

and

$$[9] \qquad \xi^{(2l+1)}(\xi^2-1)\frac{d}{d\xi}\left[\xi^{-(2l+1)}(\xi^2-1)\frac{dv_i}{d\xi}\right]-\left(\frac{2}{\kappa}\right)^2 pv_i = 0$$

where $(2l+1)$ is written for $\pm|Z_i/Z|$ (the positive sign is to be taken in the case of repulsion ($Z_i\phi > 0$) and negative for attraction ($Z_i\phi < 0$). The corresponding boundary conditions are, now:

$$[10] \qquad v_i \to 0 \text{ as } \xi \to 1$$

and

$$[11] \qquad \left(\frac{dv_i}{d\xi}\right)_{\xi=\xi_0} = \mp 2\frac{\overline{I(p)}}{nFD_i\kappa}\cdot\frac{\xi_0^{(2l+1)}}{\xi_0^2-1}$$

where $\xi_0 = \exp(\{|Z|\,F\,|\phi_0|\}/2RT)$ (ϕ_0 being the potential drop across the entire diffuse double layer, i.e., $\phi(x \to 0)-\phi(x \to \infty)$).

It can be easily seen that any approximation used must be compatible with the boundary conditions; for example, it needs justification to rewrite (ξ^2-1) as ξ^2 *in the differential equation itself* (assuming $\xi^2 \gg 1$) and also use the resulting solution (which is valid only for $\xi^2 \gg 1$) to fit in with the boundary conditions at $\xi = 1$ (cf. Matsuda and Delahay (2)). Moreover, the first-order differential equation [5] is uniquely solved once the boundary condition $\phi = \phi_0$ at $x = 0$ is assumed. Actually, the solution can be written in the form

$$[5''] \qquad \frac{\xi-1}{\xi+1} = \frac{\xi_0-1}{\xi_0+1}e^{-\kappa x}$$

where κ is the *parameter* defined by equation [5']. It can easily be verified that $\xi \neq 1$ when $x = 1/\kappa$, though, of course, $1/\kappa$ gives a measure of how steep the fall is, at sufficient distances away from the electrode. (For example, at $x = 1/\kappa$, $\xi_{1/\kappa} = [\xi_0(e+1)+(e-1)]/[\xi_0(e-1)+(e+1)]$; for $\phi_0 \simeq 50$ mv and $Z = 2$, $\xi_0 = e^2$ and $\xi_{1/\kappa} \simeq 1.8$.) Also, the independent variable ξ is *not* independent of x and hence any chosen value of x leaves no choice for ξ. At the best, it can be approximated. Hence, yet another but less serious inconsistency exists while stating that $\xi = 1$ when $x = \delta$ (cf. Matsuda and Delahay). An attempt is made here to solve the equation [1] without fitting in the solutions obtained in the two different regions (viz. $0 < x \leqslant \delta_k$ and $x \geqslant \delta_k$ (cf. Matsuda and Delahay).

A fundamental method of solving this* will be to express the solution as a power series in ξ. As we are interested in the domain $1 \leqslant \xi \leqslant \xi_0$ it is but natural to express the solution of [9] as a power series in $(1 - 1/\xi^2)$. Writing $\zeta = 1 - 1/\xi^2$, the equation is transformed into

$$[12] \qquad (1-\zeta)\zeta^2 v''+\zeta[(1-\zeta)-(l+1)\zeta]v'-k^2v = 0$$

where

$$k = \frac{1}{\kappa}\sqrt{\left(\frac{p}{D_i}\right)}; \qquad [0 \leqslant \zeta \leqslant (1 - 1/\xi_0^2)].$$

The solution of this, which satisfies the boundary condition [10]; can easily be seen to be (refer to Appendix I),

$$[13] \qquad v = a_0\zeta^k F(k, k+l+1; 2k+1; \zeta)$$

**The solution of the equation [9] can be expressed in terms of hypergeometric functions by proper transformation of the variables and identifying the resulting differential equation with the Riemann P equation.*

Can. J. Chem. Downloaded from www.nrcresearchpress.com by 210.87.254.40 on 09/05/12
For personal use only.

where F is the Gaussian hypergeometric function, and a_0 is an arbitrary constant. Rewriting the boundary condition at $\xi = \xi_0$, [11], as

$$[14] \qquad \left(\frac{dv_i}{d\zeta}\right)_{\zeta=\zeta_0} = \pm\frac{\overline{I(p)}}{nF\sqrt{(D_i p)}}\left(\frac{1}{\kappa}\sqrt{\left(\frac{p}{D_i}\right)}\right)\frac{\xi_0^{(2l+4)}}{\xi_0^2-1},$$

it is shown in Appendix I that

$$[15] \qquad a_0 = \pm\frac{\overline{I(p)}}{nF\sqrt{(D_i p)}}\,\frac{\xi_0^{(2l+1)}(1-1/\xi_0^2)^{-k}}{F(k+1,\, k+l+1;\, 2k+1;\, \zeta_0)};$$

$$[16] \qquad (v_i)_{\xi=\xi_0} = \pm\frac{\overline{I(p)}}{nF\sqrt{(D_i p)}}\,\xi_0^{(2l+1)}\frac{F(k,\, k+l+1;\, 2k+1;\, \zeta_0)}{F(k+1,\, k+l+1;\, 2k+1;\, \zeta_0)}$$

and the distribution of the concentration with x is given as

$$[17] \qquad (v_i)_\xi = \pm\frac{\overline{I(p)}}{nF\sqrt{(D_i p)}}\,\xi_0^{(2l+1)}\left(\frac{1-1/\xi^2}{1-1/\xi_0^2}\right)^k\frac{F(k,\, k+l+1;\, 2k+1;\, 1-1/\xi^2)}{F(k+1,\, k+l+1;\, 2k+1;\, 1-1/\xi_0^2)}.$$

(The variable x is not explicitly present here but one can easily note that ξ is a function of x; refer to equation [5″].)

2. A Particular Case

At this stage, it may be interesting to observe how one obtains the concentration distribution for linear diffusion (with the effects due to diffuse double layer assumed negligible), as a limiting case of the equation [17].

The differential equation [1] and the condition [3] can be reduced to

$$[18] \qquad D_i\frac{\partial^2 C_i}{\partial x^2} = \frac{\partial C_i}{\partial t} \qquad \text{with} \qquad D_i\left(\frac{\partial C_i}{\partial x}\right)_{x=0} = \pm\frac{I}{nF}$$

by allowing Z_i to become zero, the other parameters, Z, ϕ_0, $1/\kappa$, etc. remaining unaltered. Hence, writing $(l+1) = \pm|z_i/z|+\frac{1}{2} = \frac{1}{2}$ in equation [17], we get

$$[19] \qquad (v_i)_\xi = \pm\frac{\overline{I(p)}}{nF\sqrt{(D_i p)}}\,\xi_0^{(2l+1)}\left(\frac{1-1/\xi^2}{1-1/\xi_0^2}\right)^k\frac{F(k,\, k+1/2;\, 2k+1;\, 1-1/\xi^2)}{F(k+1,\, k+1/2;\, 2k+1;\, 1-1/\xi_0^2)},$$

which is shown to reduce identically to the well-known (3) expression

$$[20] \qquad C_i^0 - \bar{C}_i = (v_i)_\xi = \pm\frac{\overline{I(p)}}{nF\sqrt{(D_i p)}}\,e^{-\sqrt{(p/D_i)}x} \qquad \text{(Appendix II).}$$

Though the transform of the concentrations are obtained exactly, the process of inverse transformation is not so simple in general. Approximations may have to be made or particular cases alone chosen.

3. A Limiting Case: $\xi_0^2 \gg 1$

Interesting results are obtained when the assumption $\xi_0^2 \gg 1$ (or $1-1/\xi_0^2 \cong 1$) (*irrespective of the magnitude of other parameters like k and l*) is made. The limiting cases ($\xi_0 \to \infty$) markedly depend upon the signs of (l) and ($l+1$). The results are tabulated below (Table I) (refer to Appendix III).

But, the above limiting results are not of much significance since the condition $\xi_0^2 \gg 1$ absolutely is not of practical importance—its magnitude in relation to other parameters (particularly k) alone is of interest to us. As a matter of fact, k can be taken to be so small in many cases that any condition for an approximation made must be specified in relation to k. It will be shown later that the necessary conditions for the validity of

Can. J. Chem. Downloaded from www.nrcresearchpress.com by 210.87.254.40 on 09/05/12
For personal use only.

TABLE I

$\lvert Z_i/Z\rvert$	$< \frac{1}{2}$	$= \frac{1}{2}$	$> \frac{1}{2}$
	Attraction		
l	< 0	< 0	< 0
$(l+1)$	> 0	$= 0$	< 0
$\frac{(v_i)}{\pm\overline{I(p)}/nF\sqrt{(D_i p)}}$	$\frac{\Gamma(-l).\Gamma(k+l+1)}{\Gamma(l+1).\Gamma(k-l)}$	$\frac{1}{k \ln \xi_0^2}$	$\xi_0^{-2\lvert l+1\rvert}\frac{\lvert l+1\rvert}{k}$
	Repulsion		
l	< 0	$= 0$	> 0
$(l+1)$	> 0	> 0	> 0
$\frac{(v_i)}{\pm\overline{I(p)}/nF\sqrt{(D_i p)}}$	$\frac{\Gamma(-l).\Gamma(k+l+1)}{\Gamma(l+1).\Gamma(k-l)}$	$k \ln \xi_0^2$	$\xi_0^{2l}\frac{k}{l}$

the first approximation, viz., expanding $(v_i)_0$ in the form $(a+bk)$ depends whether there is attraction or repulsion of the species in the diffuse layer.

Before examining the coefficient of k in the expansion of $(v_i)_0$ in its general form, some particular cases where exact expressions for $(v_i)_0$ can be obtained are also presented.

4. Particular Cases

(a) Attraction: $|Z_i| = |Z|$; $(l+1) = \pm|Z_i/Z| + 1/2 = -1/2$

$$[21] \qquad (v_i)_0 = \pm\frac{\overline{I(p)}}{nF\sqrt{(D_i p)}}\,\xi_0^{-1}\frac{F(k, k-1/2; 2k+1; 1-1/\xi_0^2)}{F(k+1, k-1/2; 2k+1; 1-1/\xi_0^2)}$$

It is shown in Appendix IV that

$$[22] \qquad F(k, k-1/2; 2k+1; 1-1/\xi_0^2) = \left(\frac{2\xi_0}{\xi_0+1}\right)^{2k}\frac{2k+\xi_0}{\xi_0(2k+1)}$$

and

$$[23] \qquad F(k+1, k-1/2; 2k+1; 1-1/\xi_0^2) = \left(\frac{2\xi_0}{\xi_0+1}\right)^{2k}\frac{1+2k\xi_0}{\xi_0(2k+1)}$$

so that

$$[24] \qquad (v_i)_0 = \pm\frac{\overline{I(p)}}{nF\sqrt{(D_i p)}}\left(\frac{1+2k/\xi_0}{1+2k\xi_0}\right) = \pm\frac{\overline{I(p)}}{nF\sqrt{(D_i p)}}\left[1-(\xi_0-1/\xi_0)\frac{2k}{1+2k\xi_0}\right],$$

which $\rightarrow (\overline{I(p)})/(nF\sqrt{(D_i p)})$ as $|k| \rightarrow 0$ or as $\xi_0 \rightarrow 1$.

The first term represents what one would have derived had there been no perturbation due to the diffuse layer. The variation of the perturbation in the interfacial concentration with time is as that of the inverse transform of

$$\mp\frac{I(p)}{nF\sqrt{(D_i)}}\,(1-1/\xi_0^2)/(\alpha+\sqrt{(p)})$$

where $\alpha = [\kappa\sqrt{(D_i)}]/[2\xi_0]$. The inverse transform of $(v_i)_0$ is

$$[25] \qquad \frac{1}{nF\sqrt{(D_i)}}\int_0^t \frac{I(t-u)}{\sqrt{(\pi u)}}\,du - \frac{(1-1/\xi_0^2)}{nF\sqrt{D_i}}\left[\int_0^t \frac{I(t-u)}{\sqrt{(\pi u)}}\,du - \alpha\int_0^t I(t-u)e^{\alpha^2 u}\,\mathrm{Erfc}\,(\alpha u^{\frac{1}{2}})du\right].$$

Can. J. Chem. Downloaded from www.nrcresearchpress.com by 210.87.254.40 on 09/05/12
For personal use only.

The first term in the right hand side of equation [25] alone will be present if the effects due to the migration in diffuse layer are assumed negligible.

If $k = (1/\kappa)\sqrt{(p/D_i)}$ is so small that $(k\xi_0)^2 \ll 1$, $(v_i)_0$ can be written as

$$[26] \qquad \pm\frac{\overline{I(p)}}{nF\sqrt{(D_i p)}}[1-2k(\xi_0 - 1/\xi_0)].$$

If $2k\xi_0 \gg 1$,

$$[27] \qquad (v_i)_0 \rightarrow \pm\frac{\overline{I(p)}}{nF\sqrt{(D_i p)}}\xi_0^{-1}\frac{1}{2k} \qquad \text{(refer to Table I).}$$

(b) Attraction: $|Z_i| = 2|Z|$; $(l+1) = -3/2$

It follows from Appendix V that

$$[28] \qquad (v_i)_0 = \pm\frac{\overline{I(p)}}{nF\sqrt{(D_i p)}}\xi_0^{-3}\frac{F(k, k-3/2; 2k+1; 1-1/\xi_0^2)}{F(k+1, k-3/2; 2k+1; 1-1/\xi_0^2)}$$

$$= \pm\frac{\overline{I(p)}}{nF\sqrt{(D_i p)}}\frac{(3+6k/\xi_0+4k^2/\xi_0^2+2k/\xi_0^3)}{(3+6k\xi_0+4k^2\xi_0^2+2k\xi_0^3)},$$

which $\rightarrow \pm[\overline{I(p)}]/[nF\sqrt{(D_i p)}]$ as $|k| \rightarrow 0$ or as $\xi_0 \rightarrow 1$. But, if $k\xi_0^3 \gg 1$ (such that the other terms in the denominator can be neglected in comparison with $k\xi_0^3$),

$$[29] \qquad (v_i)_0 \cong \pm\frac{\overline{I(p)}}{nF\sqrt{(D_i p)}}\xi_0^{-3}\frac{3}{2k} \qquad \text{(refer to Table I).}$$

Expanding $(v_i)_0$ as a power series in k and neglecting coefficients of k^2 and higher powers,

$$[30] \qquad (v_i)_0 = \pm\frac{\overline{I(p)}}{nF\sqrt{(D_i p)}}\{1-2k[(\xi_0-1/\xi_0)+\tfrac{1}{3}(\xi_0^3-1/\xi_0^3)]\}.$$

It can be noted that (i) the coefficient of $2k$ is negative and (ii) the necessary and sufficient condition for such an expansion is $(k\xi_0^3)^2 \ll 1$ (so that it follows that k^2, $(k^2\xi_0^2)^2$, etc. are also negligible as compared with 1).

The inverse transform of $(v_i)_0$ can be expressed in integral form by making use of the convolution theorem.

(c) Attraction: $|Z_i| = 3|Z|$; $(l+1) = -5/2$

Referring to Appendix V, it can be seen that

$$[31] \qquad (v_i)_0 = \pm\frac{\overline{I(p)}}{nF\sqrt{(D_i p)}}\frac{F(k, k-5/2; 2k+1; 1-1/\xi_0^2)}{F(k+1, k-5/2; 2k+1; 1-1/\xi_0^2)}$$

$$= \pm\frac{\overline{I(p)}}{nF\sqrt{(D_i p)}}\frac{f_3(k, 1/\xi_0)}{f_3(k, \xi_0)}$$

where

$$f_3(k, \xi_0) = \frac{15+30k\xi_0+24k^2\xi_0^2+(10k+8k^3)\xi_0^3+12k^2\xi_0^4+6k\xi_0^5}{(2k+1)(2k+3)(2k+5)}$$

$$\rightarrow \pm\frac{\overline{I(p)}}{nF\sqrt{(D_i p)}} \text{ as } k \rightarrow 0 \text{ or as } \xi_0 \rightarrow 1;$$

and

$$[32] \qquad \rightarrow \pm\frac{\overline{I(p)}}{nF\sqrt{(D_i p)}}\xi_0^{-5}\frac{5}{2k} \qquad \text{(cf. Table I)}$$

Can. J. Chem. Downloaded from www.nrcresearchpress.com by 210.87.254.40 on 09/05/12
For personal use only.

Can. J. Chem. Downloaded from www.nrcresearchpress.com by 210.87.254.40 on 09/05/12
For personal use only.

if $k\xi_0^5 \gg 1$ such that other terms in the denominator can be neglected. For small k, $(v_i)_0$ can be expanded as

$$[33] \qquad \pm\frac{\overline{I(p)}}{nF\sqrt{(D_i p)}}\{1-2k[(\xi_0 - 1/\xi_0)+\tfrac{1}{3}(\xi_0^3 - 1/\xi_0^3)+\tfrac{1}{5}(\xi_0^5 - 1/\xi_0^5)]\},$$

other powers in k being neglected—the condition for this being $(k\xi_0^5)^2 \ll 1$.

(d) Attraction: $|Z_i| = 4|Z|$; $(l+1) = -7/2$

In this case,

$$[34] \qquad (v_i)_0 = \pm\frac{\overline{I(p)}}{nF\sqrt{(D_i p)}}\,\xi_0^{-7}\,\frac{F(k, k-7/2; 2k+1; 1-1/\xi_0^2)}{F(k+1, k-7/2; 2k+1; 1-1/\xi_0^2)}$$

$$= \pm\frac{\overline{I(p)}}{nF\sqrt{(D_i p)}}\,\frac{f_4(k, 1/\xi_0)}{f_4(k, \xi_0)}$$

where

$$f_4(k, \xi_0) = [105+210k\xi_0+180k^2\xi_0^2+(70k+80k^3)\xi_0^3+(104k^2+16k^4)\xi_0^4$$
$$+(42k+48k^3)\xi_0^5+60k^2\xi_0^6+30k\xi_0^7]/[(2k+1)(2k+3)(2k+5)(2k+7)]$$

$$\to \pm\frac{\overline{I(p)}}{nF\sqrt{(D_i p)}} \text{ as } k \to 0 \text{ or as } \xi_0 \to 1 \qquad \text{(refer to Appendix V)}$$

and

$$[35] \qquad \to \pm\frac{\overline{I(p)}}{nF\sqrt{(D_i p)}}\,\xi_0^{-7}\,\frac{7}{2k} \text{ for } k\xi_0^7 \gg 1.$$

For small k, an approximate expression for $(v_i)_0$, linear in k, will be

$$[36] \qquad \pm\frac{\overline{I(p)}}{nF\sqrt{(D_i p)}}\{1-2k[(\xi_0 - 1/\xi_0)+\tfrac{1}{3}(\xi_0^3 - 1/\xi_0^3)+\tfrac{1}{5}(\xi_0^5 - 1/\xi_0^5)+\tfrac{1}{7}(\xi_0^7 - 1/\xi_0^7)]\}$$

$$((k\xi_0^7)^2 \ll 1)$$

(e) Repulsion: $|Z_i| = |Z|$; $(l+1) = 3/2$

It can be proved in this case (Appendix IV) that

$$[37] \qquad (v_i)_0 = \pm\frac{\overline{I(p)}}{nF\sqrt{(D_i p)}}\,\xi_0^3\,\frac{F(k, k+3/2; 2k+1; 1-1/\xi_0^2)}{F(k+1, k+5/2; 2k+1; 1-1/\xi_0^2)}$$

$$= \pm\frac{\overline{I(p)}}{nF\sqrt{(D_i p)}}\left(\frac{1+2k\xi_0}{1+2k/\xi_0}\right),$$

which

$$[38] \qquad \to \pm\frac{\overline{I(p)}}{nF\sqrt{(D_i p)}} \text{ as } k \to 0 \text{ or as } \xi_0 \to 1.$$

Note that if one writes

$$(v_i)_0^{\text{rep}} = \pm\frac{\overline{I(p)}}{nF\sqrt{(D_i p)}}\,w_{\text{rep}}(\xi_0),$$

and similarly define $w_{\text{attr}}(\xi_0)$,

$$w_{\text{rep}}(\xi_0)\,.\,w_{\text{attr}}(\xi_0) = 1;$$

also, refer to Section 7.

If k is small enough to satisfy the inequality $k^2 \ll 1$, $(v_i)_0$ can be expanded as

$$[39] \qquad (v_i)_0 = \pm\frac{\overline{I(p)}}{nF\sqrt{(D_i p)}}\{1+2k(\xi_0 - 1/\xi_0)+\text{terms in } k^2, k^3, \ldots\}.$$

For $k\xi_0 \gg 1$,

$$[40] \qquad (v_i)_0 \rightarrow \pm\frac{\overline{I(p)}}{nF\sqrt{(D_i p)}}\,2k\xi_0 \qquad \text{(refer to Table I).}$$

The condition for neglecting terms in second and higher powers of k in $(v_i)_0$ is less strict in the case of repulsion. The inverse transform for $(v_i)_0$ can, of course, be expressed in this case too—as was done previously for the case of attraction.

(f) Repulsion: $|Z_i| = 2|Z|$; $(l+1) = 5/2$

$(v_i)_0$ can be written as

$$[41] \qquad (v_i)_0 = \pm\frac{\overline{I(p)}}{nF\sqrt{(D_i p)}}\,\xi_0^{\,5}\,\frac{F(k, k+5/2; 2k+1; 1-1/\xi_0^{\,2})}{F(k+1, k+3/2; 2k+1; 1-1/\xi_0^{\,2})}$$

$$= \pm\frac{\overline{I(p)}}{nF\sqrt{(D_i p)}}\,\frac{(3+6k\xi_0+4k^2\xi_0^{\,2}+2k\xi_0^{\,3})}{(3+6k/\xi_0+4k^2/\xi_0^{\,2}+2k/\xi_0^{\,3})} \qquad \text{(Appendix V).}$$

If $k^2\xi_0^{\,2} \ll 1$ such that terms in k^2 and higher powers can be neglected,

$$[42] \qquad (v_i)_0 \cong \pm\frac{\overline{I(p)}}{nF\sqrt{(D_i p)}}\{1+2k[(\xi_0 - 1/\xi_0)+\tfrac{1}{3}(\xi_0^{\,3} - 1/\xi_0^{\,3})]\}.$$

For $k\xi_0^{\,3} \gg 1$, it is possible to express $(v_i)_0$ as

$$[43] \qquad \pm\frac{\overline{I(p)}}{nF\sqrt{(D_i p)}}\,\xi_0^{\,3}\,\frac{2k}{3} \qquad \text{(cf. Table I).}$$

(g) Repulsion: $|Z_i| = 3|Z|$; $(l+1) = 7/2$

It can easily be proved, as in the other cases, that

$$[44] \qquad (v_i)_0 = \pm\frac{\overline{I(p)}}{nF\sqrt{(D_i p)}}\,\xi_0^{\,7}\,\frac{F(k, k+7/2; 2k+1; 1-1/\xi_0^{\,2})}{F(k+1, k+7/2; 2k+1; 1-1/\xi_0^{\,2})}$$

$$= \pm\frac{\overline{I(p)}}{nF\sqrt{(D_i p)}}\,\frac{f_3(k, \xi_0)}{f_3(k, 1/\xi_0)}$$

where

$$f_3(k, \xi_0) = \frac{15+30k\xi_0+24k^2\xi_0^{\,2}+(10k+8k^3)\xi_0^{\,3}+12k^2\xi_0^{\,4}+6k\xi_0^{\,5}}{(2k+1)(2k+3)(2k+5)},$$

which

$$\rightarrow \pm\frac{\overline{I(p)}}{nF\sqrt{(D_i p)}} \quad \text{as } k \rightarrow 0 \text{ or as } \xi_0 \rightarrow 1.$$

For large ξ_0 such that $k^2\xi_0^{\,4}$ can be neglected in comparison with 1, $(v_i)_0$ can be expressed by

$$[45] \qquad (v_i)_0 \cong \{1+2k[(\xi_0 - 1/\xi_0)+\tfrac{1}{3}(\xi_0^{\,3} - 1/\xi_0^{\,3})+\tfrac{1}{5}(\xi_0^{\,5} - 1/\xi_0^{\,5})]\}.$$

If $k^2\xi_0^{\,4} = 0(1)$, the expansion must include terms in k^2 also. For $k\xi_0^{\,5} \gg 1$, such that other terms in the numerator can be neglected,

$$[46] \qquad (v_i)_0 = \pm\frac{\overline{I(p)}}{nF\sqrt{(D_i p)}}\,\xi_0^{\,5}\,\frac{2k}{5} \qquad \text{(cf. Table I).}$$

Can. J. Chem. Downloaded from www.nrcresearchpress.com by 210.87.254.40 on 09/05/12
For personal use only.

(h) Repulsion: $|Z_i| = 4|Z|$; $(l+1) = 9/2$

$(v_i)_0$ can be written as

[47] $$(v_i)_0 = \pm\frac{\overline{I(p)}}{nF\sqrt{(D_i p)}}\,\xi_0^{9}\,\frac{F(k, k+9/2; 2k+1; 1-1/\xi_0^{2})}{F(k+1, k+9/2; 2k+1; 1-1/\xi_0^{2})}$$

$$= \pm\frac{\overline{I(p)}}{nF\sqrt{(D_i p)}}\,\frac{f_4(k, \xi_0)}{f_4(k, 1/\xi_0)} \qquad \text{(Appendix V)}$$

where

$$f_4(k, \xi_0) = [105+210k\xi_0+180k^2\xi_0^2+(70k+80k^3)\xi_0^3+(104k^2+16k^4)\xi_0^4 + (42k+48k^3)\xi_0^5+60k^2\xi_0^6+30k\xi_0^7]/[(2k+1)(2k+3)(2k+5)(2k+7)]$$

which

$$\to \pm\frac{\overline{I(p)}}{nF\sqrt{(D_i p)}} \text{ as } k \to 0 \text{ or as } \xi_0 \to 1$$

and

[48] $$\to \pm\frac{\overline{I(p)}}{nF\sqrt{(D_i p)}}\,\xi_0^{7}\,\frac{2k}{7} \quad (\text{as } \xi_0 \to \infty).$$

A linear approximation in k for $(v_i)_0$ will yield

[49] $$(v_i)_0 = \pm\frac{\overline{I(p)}}{nF\sqrt{(D_i p)}}\{1+2k[(\xi_0 - 1/\xi_0)+\tfrac{1}{3}(\xi_0^3 - 1/\xi_0^3)+\tfrac{1}{5}(\xi_0^5 - 1/\xi_0^5) + \tfrac{1}{7}(\xi_0^7 - 1/\xi_0^7)]\}.$$

5. A Linear Expression in k for $(v_i)_0$

In general, the exact functional expressions of $(v_i)_0$ will not be simple rational functions of k. It is of interest to expand $(v_i)_0$ as a power series in k and to obtain the coefficient of k, whatever be the value of the parameter l. This coefficient alone will serve the purpose satisfactorily, as k can be assumed to be very small. It has been shown in Appendix VI that $(v_i)_0$ can be written as

[50] $$(v_i)_0 = \pm\frac{\overline{I(p)}}{nF\sqrt{(D_i p)}}\,(1+a_i k)$$

(positive sign for the oxidant and negative for the reductant, assuming net cathodic current to be positive)

neglecting higher powers of k, where

[51] $$a_i = \int_0^{1-1/\xi_0^2} \frac{(1-z)^{-(l+1)} - (1-z)^{l}}{z}\,dz$$

$$= 2\int_1^{\xi_0} \frac{\xi^{2(l+1)} - \xi^{-2l}}{\xi(\xi^2-1)}\,d\xi$$

$$= k\int_0^{\infty}\left[\exp\left(\pm\frac{|Z_i|\,F\,|\phi|}{RT}\right) - \exp\left(\mp\frac{|Z_i|\,F\,|\phi|}{RT}\right)\right]dx$$

$$= \pm 2k\int_0^{\infty} \sinh\frac{|Z_i\phi|F}{RT}\,dx;$$

Can. J. Chem. Downloaded from www.nrcresearchpress.com by 210.87.254.40 on 09/05/12
For personal use only.

positive sign for repulsion ($Z_i\phi > 0$) and negative for attraction ($Z_i\phi < 0$) (whereas the integral

$$\int_0^\infty \exp\left[\pm(Z_iF\phi)/(RT)\right]dx$$

is divergent, a_i, as given above, can easily be proved to be convergent).

This differs from the expressions for a_i derived by Matsuda and Delahay (2). It will be shown later that the results may vary appreciably in some instances, while the order of the values as regards ξ_0 will be very much the same for $\xi_0 \to \infty$. Also $(a_i)_{rep} > 0$.

[52] $$(a_i)_{attr} < 0 \text{ and } (a_i)_{rep} = -(a_i)_{attr}$$

As illustrations, we can consider the following cases.

(i) $|Z_i| = |Z|$

[53]
$$\begin{aligned} a_i &= \pm 2\kappa \int_0^\infty \sinh\left(\frac{|Z\phi|F}{RT}\right)dx \\ &= \pm 4\kappa \int_0^\infty \cosh\frac{|Z\phi|F}{RT}\left(-\frac{|Z|F}{2RT}\frac{1}{\kappa}\frac{d\phi}{dx}\right)dx \\ &= \mp 4\int_{x=0}^{x=\infty} \cosh y\, dy \text{ where } y = \frac{|Z\phi|F}{2RT} \\ &= \pm 4 \sinh\frac{|Z|\ F\ |\phi_0|}{2RT} \text{ (since } \phi = \phi_0 \text{ at } x = 0 \text{ and } \to 0 \text{ as } x \to \infty) \\ &= \pm 2(\xi_0 - 1/\xi_0), \end{aligned}$$

as has already been proved. (The positive sign to be taken when there is repulsion and the negative when there is attraction.)

(ii) $|Z_i| = |Z|/2$; $l+1 = 1$ for repulsion and $l+1 = 0$ for attraction

[54]
$$\begin{aligned} a_i &= \pm 2\kappa \int_0^\infty \sinh\frac{|Z_i\phi|F}{2RT}dx \\ &= \mp\frac{|Z|F}{RT}\int_0^\infty \frac{d\phi}{dx}dx = \mp\frac{|Z|F}{RT}[\phi_\infty - \phi_0] \\ &= \pm\frac{|Z|F}{RT}\phi_0 \text{ or } \pm\ln \xi_0^2. \end{aligned}$$

It can be shown that the term $k(|Z|F/RT)\phi_0$ (or $k \ln \xi_0^2$) is the dominant term as regards the order of ξ_0 in the expansion of $F(k, k+1; 2k+1; 1 - 1/\xi_0^2)$ and hence in the case of repulsion ($l+1 = 1$),

$$(v_i)_0^{rep} \cong \frac{\overline{I(p)}}{nF\sqrt{(D_ip)}}\, k \ln \xi_0^2 \qquad (\text{since } k \ln \xi_0^2 \gg 1).$$

In the case of attraction, $(l+1) = 0$, and

[55] $$(v_i)_0^{attr} \cong \frac{\overline{I(p)}}{nF\sqrt{(D_ip)}}\frac{1}{k \ln \xi_0^2} \qquad \text{(cf. Table I).}$$

Can. J. Chem. Downloaded from www.nrcresearchpress.com by 210.87.254.40 on 09/05/12
For personal use only.

(iii) $|Z_i| = 3|Z|/2$

[56] $$a_i = \pm 2\kappa \int_0^\infty \sinh \frac{3|Z|\,F\,|\phi|}{2RT}\,dx$$

$$= \mp \int_{x=0}^{x=\infty} (2\cosh y + 1)dy \text{ where } y = \frac{|Z|\,F\,|\phi|}{RT},$$

since $\sinh 3Z = \sinh Z\,(2\cosh 2Z - 1)$

[57] $$a_i = \pm 2\left[\sinh \frac{|Z|\,F\,|\phi|}{RT} + \frac{|Z|\,F\,|\phi|}{2RT}\right]$$

$$= \pm[\xi_0^2 - 1/\xi_0^2 + \ln \xi_0^2].$$

(iv) $|Z_i| = |Z|/3$; $(l+1) = 5/6$ for repulsion and $= 1/6$ for attraction

[58] $$a_i = \pm 2 \int_1^{\xi_0} \frac{\xi^{2(l+1)} - \xi^{-2l}}{\xi(\xi^2-1)}\,d\xi$$

$$= \pm 6 \int_{1/\xi_0^{1/3}}^1 \frac{1-z^4}{1-z^6}\,dz \qquad \text{(by substituting } z^{-3} = \xi,\ d\xi = -3z^{-4}dz)$$

[59] $$= \pm\sqrt{3}\left[\pi - 2\tan^{-1}\frac{\sqrt{3}\,\xi_0^{1/3}}{\xi_0^{2/3}-1}\right]$$

$$\to \pm\sqrt{3}\,\pi \qquad \text{as } \xi_0 \to \infty.$$

Thus we see that a_i can be evaluated exactly for almost all the values (relevant to our problem) of the parameter l.

6. Validity of the Approximations

It will be of use to us to find out the range of approximation, i.e. the inequalities that the parameters are to satisfy to validate the linear approximation for $(v_i)_0$.

It is proposed to find the conditions to be satisfied in order that $(v_i)_0$ may be expressed as $(a+bk)$, (a, b, independent of k). It is proved in Appendix VI that the coefficients of k^2 in the expansion of $F(k, k+l+1; 2k+1; \zeta_0)$ and $F(k+1, k+l+1; 2k+1; \zeta_0)$ are

[60] $$S_2 = \int_0^{\zeta_0} \frac{(1-\zeta)^l S_1 - \phi_1}{\zeta}\,d\zeta \qquad \text{and}$$

$$\phi_2 = \int_0^{\zeta_0} \frac{(1-\zeta)^{-(l+1)}\phi_1 - S_1}{\zeta}\,d\zeta$$

respectively.

Table I can help us in obtaining some information about the dominant terms (i.e. for large ξ_0) in the expression for $(v_i)_0$ (the order of k being assumed to be independent of ξ_0). One can easily conclude from this and the functional forms of S_2 and ϕ_2 that the second and higher powers of k can be *confidently* neglected in the expansion of $(v_i)_0$ provided

$$\left(\frac{1}{\kappa}\sqrt{\left(\frac{p}{D_i}\right)}\right)^2 \xi_0^{2l} \ll 1 \qquad \text{(repulsion)}$$

and

$$\left[\frac{1}{\kappa}\sqrt{\left(\frac{p}{D_i}\right)}\,\xi_0^{2|l+1|}\right]^2 \ll 1 \qquad \text{(attraction)}.$$

Can. J. Chem. Downloaded from www.nrcresearchpress.com by 210.87.254.40 on 09/05/12
For personal use only.

Note that these are *confident* inequalities since a less strict condition may suffice in some cases. For example,

$$\text{for } |Z_i| = |Z| \text{ (repulsion)}$$
$$(l+1) = +3/2$$

and the condition as stated above reads

$$\left(\frac{1}{\kappa}\sqrt{\left(\frac{p}{D_i}\right)}\right)^2 \xi_0 \ll 1.$$

But, the *exact* expression for $(v_i)_0$ in this case is

$$\pm\frac{\overline{I(p)}}{nF\sqrt{(D_i p)}}\frac{1+2k\xi_0}{1+2k/\xi_0},$$

which can be expanded as

$$\pm\frac{\overline{I(p)}}{nF\sqrt{(D_i p)}}(1+2k\xi_0)\left(1-\frac{2k}{\xi_0}+\frac{4k^2}{\xi_0^2}-\ldots\right), \text{ provided } (2k/\xi_0) < 1;$$

and wherein the terms in k^2 and higher powers can be neglected if

$$k^2 = \left(\frac{1}{\kappa}\sqrt{\left(\frac{p}{D_i}\right)}\right)^2 \ll 1.$$

7. Two Theorems

Some results concerning the functional forms of $(v_i)_0$ in the case of attraction and repulsion are given in the two theorems presented below.

Theorem No. 1

For a *given* Z_i, if $(v_i)_0^{\mathrm{A}}$ represents the expression of $(v_i)_0$ at the electrode surface *if there is attraction in the diffuse layer* and $(v_i)_0^{\mathrm{R}}$ the expression for $(v_i)_0$ for repulsion,

$$\frac{(v_i)_0^{\mathrm{A}}}{\pm\overline{I(p)}/nF\sqrt{(D_i p)}} \times \frac{(v_i)_0^{\mathrm{R}}}{\pm\overline{I(p)}/nF\sqrt{(D_i p)}} = 1.$$

Theorem No. 2

If $F(k, k+|Z_i/Z|+1/2; 2k+1; 1-1/\xi_0^2) = g(k, \xi_0)$, then

$$(v_i)_0^{\mathrm{A}} = \pm\frac{\overline{I(p)}}{nF\sqrt{(D_i p)}}\xi_0^{2k}\frac{g(k, 1/\xi_0)}{g(k, \xi_0)}$$

and

$$(v_i)_0^{\mathrm{R}} = \pm\frac{\overline{I(p)}}{nF\sqrt{(D_i p)}}\xi_0^{-2k}\frac{g(k, \xi_0)}{g(k, 1/\xi_0)}$$

(For proofs and discussion refer to Appendix VII.)

CONCLUSIONS

The diffusion equations for the concentration of the reactive species are solved, taking into account the migration in the diffuse double layer (Section 1).

The expression for the known solution of the diffusion equation where the effect of double layer is neglected is derived as a limiting case (Section 2).

Can. J. Chem. Downloaded from www.nrcresearchpress.com by 210.87.254.40 on 09/05/12
For personal use only.

The asymptotic forms ($\xi_0 \to \infty$) of the interfacial concentrations are obtained (Section 3).

Exact functional expressions for the transforms of the interfacial concentrations in the form of rational fractions in k are given for the particular cases $|Z_i| = |Z|$, $2|Z|$, $3|Z|$, and $4|Z|$, for the cases of both attraction and repulsion (Section 4).

Under certain conditions, $(v_i)_0$ can be related linearly to k, and such a linear expansion is given, for all the values of $|Z_i/Z|$. As illustration, the double layer corrections for the cases $|Z_i| = |Z|$, $|Z|/2$, $3|Z|/2$, and $|Z|/3$ are deduced from the formulae (Section 5).

The conditions which must hold to validate such a linear expansion are discussed (Section 6).

Lastly, some results which relate the functional forms of $(v_i)_0$ for the cases of attraction and repulsion are derived (Section 7).

APPENDIX I

With the substitution $\zeta = 1 - 1/\xi^2$, equation [9] of the text, viz.,

$$\xi^{(2l+1)}(\xi^2-1)\frac{d}{d\xi}\left[\xi^{-(2l+1)}(\xi^2-1)\frac{dv_i}{d\xi}\right] - \left(\frac{2}{\kappa}\right)^2 \frac{pv_i}{D_i} = 0, \tag{A.1}$$

can be transformed into

$$(1-\zeta)^{-l}\zeta[(1-\zeta)^{l+1}\zeta v_i']' - k^2 v_i = 0; \tag{A.2}$$

(a prime indicating the differential with respect to ζ and $k = (1/\kappa)\sqrt{(p/D_i)}$).

Rewriting (A.2) as

$$(1-\zeta)\zeta^2 v'' + [(1-\zeta) - (l+1)\zeta]\zeta v' - k^2 v = 0 \tag{A.3}$$

we seek a solution which will converge at $\zeta = 0$, i.e., at $\xi = 1$ (this is equivalent to the statement: $v_i \to 0$ as $x \to \infty$). Assuming the solution to be of the form

$$\zeta^s \sum_{r=0}^{\infty} a_r \zeta^r$$

and substituting this series solution in (A.3), we obtain the indicial equation for s as

$$s^2 - k^2 = 0. \tag{A.4}$$

Hence that solution which converges at $x \to \infty$ will have $s = +k$; also

$$\sum_{r=0}^{\infty} a_r\{[(s+r)^2 - k^2] - x[(s+r)^2 + (s+r)(l+1)]\}x^{s+r} = 0, \tag{A.5}$$

which leads to the equations

$$a_r[(s+r)^2 - k^2] - a_{r-1}(s+r-1)(s+r+l) = 0; \; r = 1, 2, 3, \ldots \tag{A.6}$$

For $s = k$, (A.6) gives

$$a_r = \frac{(k+r-1)(k+r+l)}{r(2k+r)} a_{r-1}, \tag{A.7}$$

so that

$$a_1 = a_0 \frac{k(k+l+1)}{2k+1}; \qquad a_2 = a_0 \frac{k(k+l+1)(k+1)(k+l+2)}{(2k+1)(2k+2)\cdot 1\cdot 2}; \text{ etc.}$$

Can. J. Chem. Downloaded from www.nrcresearchpress.com by 210.87.254.40 on 09/05/12
For personal use only.

It is thus seen that the required solution is

$$v_i = a_0\zeta^k\left\{1 + \frac{k(k+l+1)}{2k+1}\zeta + \frac{k(k+l+1)(k+1)(k+l+2)}{(2k+1)(2k+2)}\frac{\zeta^2}{2!} + \frac{k(k+1)(k+2)(k+l+1)(k+l+2)(k+l+3)}{(2k+1)(2k+2)(2k+3)}\frac{\zeta^3}{3!} + \ldots\right\},$$

where $\zeta = 1 - 1/\xi^2 < 1$;
In terms of hypergeometric functions, this solution is

$$v_i = a_0\zeta^k F(k, k+l+1; 2k+1; 1 - 1/\xi^2). \tag{A.8}$$

The arbitrary constant a_0 is to be found by making use of the boundary condition [11], which can be rewritten as

$$\left(\frac{dv_i}{d\zeta}\right)_{\zeta=\zeta_0} = \pm\frac{\overline{I(p)}}{nF\sqrt{(D_i p)}}\left(\frac{1}{\kappa}\sqrt{\left(\frac{p}{D_i}\right)}\right)\cdot\frac{\xi_0^{2l+4}}{\xi_0^2-1}; \tag{A.9}$$

since it is known that

$$\frac{d}{dz}[z^a F(a, b; c; z)] = az^{a-1}F(a+1, b; c; z),$$

$$\frac{dv_i}{d\zeta} = a_0 k\zeta^{k-1}F(k+1, k+l+1, 2k+1; \zeta); \tag{A.10}$$

and hence, with the help of (A.9), we conclude that

$$a_0 = \pm[\overline{I(p)}\xi_0^{(2l+2)}/nF\sqrt{(D_i p)}](1 - 1/\xi_0^2)^k F(k+1, k+l+1; 2k+1; \zeta_0) \tag{A.11}$$

where

$$\zeta_0 = 1 - 1/\xi_0^2 \quad \text{and} \quad \xi_0 = \exp(|Z|\, F\, |\phi_0|/2RT);$$

consequently,

$$(v_i)_{\xi=\xi_0} = a_0\zeta_0^k F(k, k+l+1; 2k+1; \zeta_0) \tag{A.12}$$

$$= \pm\frac{\overline{I(p)}}{nF\sqrt{(D_i p)}}\xi_0^{2(l+1)}\frac{F(k, k+l+1; 2k+1; \zeta_0)}{F(k+1, k+l+1; 2k+1; \zeta_0)}$$

(positive sign for the oxidant, negative for the reductant; cathodic current being taken as positive).

APPENDIX II

The equation

$$D_i\frac{\partial}{\partial x}\left(\frac{\partial C_i}{\partial x} + \frac{Z_i F}{RT}C_i\frac{d\phi}{dx}\right) = \frac{\partial C_i}{\partial t} \tag{A.13}$$

and the boundary condition

$$D_i\frac{\partial}{\partial x}\left(\frac{\partial C_i}{\partial x} + \frac{Z_i F}{RT}C_i\frac{d\phi}{dx}\right) = \pm\frac{I(t)}{nF} \qquad (\text{at } x = 0) \tag{A.14}$$

reduce to

$$D_i\frac{\partial^2 C_i}{\partial x^2} = \frac{\partial C_i}{\partial t} \quad \text{and} \quad D_i\frac{\partial C_i}{\partial x} = \pm\frac{I(t)}{nF} \tag{A.15}$$

respectively, by allowing Z_i to become zero.

Can. J. Chem. Downloaded from www.nrcresearchpress.com by 210.87.254.40 on 09/05/12
For personal use only.

The solution of equation (A.13) must, therefore, tend to that of (A.15), which is well known (3), viz.,

$$\bar{C}_i(x = 0) = C_i^0 \mp \frac{\overline{I(p)}}{nF\sqrt{(D_i p)}} e^{-\sqrt{(p/D_i)}x}. \tag{A.16}$$

(Note: only the Laplace transform of C (with respect to t) is given instead of the original. That there is no loss of generality is ensured by the uniqueness property of a function and its Laplace transform.)

It has been proved that

$$v_i = \pm\frac{\overline{I(p)}}{nF\sqrt{(D_i p)}} \xi_0^{2(l+1)} \left(\frac{1 - 1/\xi^2}{1 - 1/\xi_0^2}\right)^k \frac{F(k, k+l+1; 2k+1; \zeta)}{F(k+1, k+l+1; 2k+1; \zeta_0)} \tag{A.17}$$

and

$$(l+1) = \pm\left|\frac{Z_i}{Z}\right| + \frac{1}{2};$$

and hence $(l+1)$ becomes $= 1/2$. It is known that

$$F(k, k + 1/2; 2k+1; \zeta) = \left(1/2 + \frac{\sqrt{(1-\zeta)}}{2}\right)^{-2k} \tag{A.18}$$

and

$$F(k+1, k + 1/2; 2k+1; \zeta_0) = \left(1/2 + \frac{\sqrt{(1-\zeta_0)}}{2}\right)^{-2k} \Big/ \sqrt{(1-\zeta_0)}. \tag{A.19}$$

Substituting $\zeta = 1 - 1/\xi^2$,

$$\begin{aligned}(v_i) &= \pm\frac{\overline{I(p)}}{nF\sqrt{(D_i p)}} \xi_0 \left(\frac{1 - 1/\xi^2}{1 - 1/\xi_0^2}\right)^k \left(\frac{\xi}{\xi+1}\right)^{2k} \left(\frac{\xi_0+1}{\xi_0}\right)^{2k} \frac{1}{\xi_0} \\ &= \pm\frac{\overline{I(p)}}{nF\sqrt{(D_i p)}} \left(\frac{\xi-1}{\xi+1}\right)^k \left(\frac{\xi_0+1}{\xi_0-1}\right)^k; \end{aligned} \tag{A.20}$$

$$\xi = \exp\frac{|Z|\,F\,|\phi|}{2RT};$$

but

$$\frac{\xi-1}{\xi+1} = \frac{\xi_0-1}{\xi_0+1} e^{-\kappa x}$$

and hence,

$$(v_i) = \pm\frac{\overline{I(p)}}{nF\sqrt{(D_i p)}} (e^{-\kappa x})^k = \pm\frac{\overline{I(p)}}{nF\sqrt{(D_i p)}} e^{-\sqrt{(p/D_i)}x}. \tag{A.21}$$

Also

$$v_i = C_i^0 - \bar{C}_i \exp(Z_0 F\phi/RT),$$

and since $Z_0 = 0$,

$$v_i = C_i^0 - \bar{C}_i$$

or

$$\bar{C}_i = C_i^0 \mp \frac{\overline{I(p)}}{nF\sqrt{(D_i p)}} e^{-\sqrt{(p/D_i)}x},$$

which is (A.16).

Can. J. Chem. Downloaded from www.nrcresearchpress.com by 210.87.254.40 on 09/05/12
For personal use only.

It may be mentioned, in passing, that the same limit can be attained through the path $1/\kappa \rightarrow 0$ (which also implies $\phi \rightarrow 0$ and $\xi \rightarrow 1$). By observing that

$$\xi, \xi_0 \rightarrow 1$$

but

$$\left[\left(\frac{\xi-1}{\xi+1}\right)\left(\frac{\xi_0+1}{\xi_0-1}\right)\right]^k \rightarrow e^{-\sqrt{(p/D_i)}x},$$

it can be proved that (A.16) can be regained in this case too.

APPENDIX III

To obtain the asymptotic behavior $\xi \rightarrow \infty$ (or equivalently $\zeta_0 \rightarrow 1$) of the solution, we must distinguish between the cases of attraction and repulsion and also the signs of the parameters (l) and ($l+1$).

We assume here the following limiting behavior of hypergeometric functions (4):

(a) If $(\nu-\alpha-\beta) < 0$,

$$\text{(A.22)} \qquad \underset{x\rightarrow 1-0}{\text{Limit}}\, F(\alpha, \beta; \nu; x) \div \left\{\frac{\Gamma(\nu)\cdot\Gamma(\alpha+\beta-\nu)}{\Gamma(\alpha)\cdot\Gamma(\beta)}\,(1-x)^{\nu-\alpha-\beta}\right\} \rightarrow 1.$$

(b) If $(\nu-\alpha-\beta) = 0$,

$$\text{(A.23)} \qquad \underset{x\rightarrow 1-0}{\text{Limit}}\, F(\alpha, \beta; \nu; x) \div \left\{\frac{\Gamma(\alpha+\beta)}{\Gamma(\alpha)\Gamma(\beta)}\,\log\frac{1}{1-x}\right\} \rightarrow 1.$$

(c) If $(\nu-\alpha-\beta) > 0$,

$$\text{(A.24)} \qquad \underset{x\rightarrow 1-0}{\text{Limit}}\, F(\alpha, \beta; \nu; x) = F(\alpha, \beta; \nu; 1) = \frac{\Gamma(\nu)\cdot\Gamma(\nu-\alpha-\beta)}{\Gamma(\nu-\alpha)\cdot\Gamma(\nu-\beta)}.$$

Also,

$$\text{(A.25)} \qquad l = \pm\left|\frac{Z_i}{Z}\right| - 1/2 \qquad l+1 = \pm\left|\frac{Z_i}{Z}\right| + 1/2$$

(positive sign to be taken in the case of repulsion and negative for attraction in the diffuse layer)

The asymptotic behavior of the hypergeometric functions $F(k, k+l+1; 2k+1; \zeta_0)$ and $F(k+1, k+l+1; 2k+1; \zeta_0)$ depends essentially on the signs of l and $(l+1)$ respectively.

It can be easily seen that $l < 0$ for attraction and $(l+1) > 0$ for repulsion, whatever be Z_i. Hence, we obtain the following:

(*a*) For attraction, in view of (A.24),

$$\text{(A.26)} \qquad F(k, k+l+1; 2k+1; \zeta_0) \cong \frac{\Gamma(-l)\cdot\Gamma(2k+1)}{\Gamma(k+1)\cdot\Gamma(k-l)} \qquad \text{(for large } \xi_0\text{)}.$$

The behavior of the denominator, namely, $F(k+1, k+l+1; 2k+1; \zeta_0)$, varies depending on whether $(l+1) > 0$, $= 0$, or < 0 (i.e. depending on whether $|Z_i/Z| < 1/2$, $= 1/2$, or $> 1/2$):

Can. J. Chem. Downloaded from www.nrcresearchpress.com by 210.87.254.40 on 09/05/12
For personal use only.

(i) $|Z_i/Z| < 1/2$; $(l+1) > 0$.
Using (A.22), one obtains,

$$\Gamma(k+1, k+l+1; 2k+1; \zeta_0) \cong \frac{\Gamma(2k+1)\cdot\Gamma(l+1)}{\Gamma(k+1)\cdot\Gamma(k+l+1)} (1-\zeta)^{-(l+1)}; \tag{A.27}$$

also by (A.12), it is seen that

$$(v_i)_{\xi=\xi_0} \cong \pm\frac{\overline{I(p)}}{nF\sqrt{(D_i p)}} \frac{\Gamma(-l)\cdot\Gamma(k+l+1)}{\Gamma(l+1)\cdot\Gamma(k-l)}. \tag{A.28}$$

(ii) $|Z_i/Z| = 1/2$; $(l+1) = 0$.
By making use of (A.23) and (A.12), it can be proved that

$$F(k+1, k+l+1; 2k+1; \zeta_0) = \frac{\Gamma(2k+1)}{\Gamma(k)\Gamma(k+1)} \ln \xi_0^2$$

and

$$(v_i)_{\xi=\xi_0} \cong \pm\frac{\overline{I(p)}}{nF\sqrt{(D_i p)}} \frac{1}{k \ln \xi_0^2}.$$

(iii) $|Z_i/Z| > 1/2$; $(l+1) < 0$
As in the above cases, the asymptotic form of v_i will be

$$\cong \pm\frac{\overline{I(p)}}{nF\sqrt{(D_i p)}} \xi_0^{-2|l+1|} \frac{|l+1|}{k}, \tag{A.29}$$

where $|l+1|$ denotes the numerical value of $(l+1)$.
(*b*) For repulsion, in view of (A.22),

$$F(k+1, k+l+1; 2k+1; \zeta_0) \cong \frac{\Gamma(2k+1)\cdot\Gamma(l+1)}{\Gamma(k+1)\cdot\Gamma(k+l+1)} \xi_0^{2(l+1)}. \tag{A.30}$$

The behavior of the numerator varies depending on whether ($l < 0$, $= 0$, or > 0 (i.e., $|Z_i/Z| < 1/2$, $= 1/2$, or $> 1/2$):

$$F(k, k+l+1; 2k+1; 1 - 1/\xi_0^2) \cong \begin{cases} \dfrac{\Gamma(-l)\cdot\Gamma(2k+1)}{\Gamma(k+1)\cdot\Gamma(k-l)}; & l < 0 \\ \dfrac{\Gamma(2k+1)}{\Gamma(k)\cdot\Gamma(k+1)} \ln \xi_0^2; & l = 0 \\ \dfrac{\Gamma(2k+1)\cdot\Gamma(l)}{\Gamma(k)\cdot\Gamma(k+l+1)} \xi_0^{2l}; & l > 0 \end{cases} \tag{A.31}$$

Hence, the behavior of $(v_i)_{\xi=\xi_0}$, in the case of repulsion, for large ξ_0 will be as

$$\frac{(v_i)_{\xi=\xi_0}}{(\pm\overline{I(p)}/nF\sqrt{(D_i p)})} \cong \begin{cases} \dfrac{\Gamma(-l)\cdot\Gamma(k+l+1)}{\Gamma(l+1)\cdot\Gamma(k-l)}; & l < 0 \\ k \ln \xi_0^2; & l = 0 \\ \xi_0^{2l} \dfrac{k}{l}; & l > 0 \end{cases} \tag{A.32}$$

The above results are tabulated in Table I.

Can. J. Chem. Downloaded from www.nrcresearchpress.com by 210.87.254.40 on 09/05/12
For personal use only.

APPENDIX IV

$|Z_i| = |Z|$; for attraction,

$$l+1 = -\left|\frac{Z_i}{Z}\right| + 1/2 = -1/2$$

$$(v_i)_{\xi=\xi_0} = \pm\frac{\overline{I(p)}}{nF\sqrt{(D_i p)}}\,\xi_0^{-1}\,\frac{F(k, k-1/2; 2k+1; 1-1/\xi_0^2)}{F(k+1, k-1/2; 2k+1; 1-1/\xi_0^2)}.$$

Assuming the relationship

$$F(k, k+1/2; 2k+1; \zeta_0) = \left(\frac{1}{2}+\frac{\sqrt{(1-\zeta_0)}}{2}\right)^{-2k}, \tag{A.33}$$

and the identity

$$\frac{d}{d\zeta}\left[\zeta^{c-a}(1-\zeta)^{a+b-c}F(a, b; c; \zeta)\right] = (c-a)\zeta^{c-a-1}(1-\zeta)^{a+b-c-1}F(a-1, b; c; \zeta), \tag{A.34}$$

we find that

$$F(k, k+1/2; 2k+1; 1-1/\xi_0^2) = \left(\frac{2\xi_0}{\xi_0+1}\right)^{2k} \tag{A.35}$$

and

$$\frac{d}{d\zeta}\left[(\xi^2-1)^{k+1/2}\xi^{-2k-1}\xi\left(\frac{2\xi}{\xi+1}\right)^{2k}\right] = \frac{\xi^3}{2}\frac{d}{d\xi}\left[2^{2k}\sqrt{(\xi^2-1)}\left(\frac{\xi-1}{\xi+1}\right)^{k}\right], \tag{A.36}$$

from which we obtain that

$$F(k, k-1/2; 2k+1; 1-1/\xi_0^2) = \frac{1}{\xi_0}\left\{\frac{(2k+\xi_0)}{(2k+1)}\right\}\left(\frac{2\xi_0}{\xi_0+1}\right)^{2k}. \tag{A.37}$$

Also

$$F(k+1, k+1/2; 2k+1; \zeta) = \left(\frac{1}{2}+\frac{\sqrt{(1-\zeta)}}{2}\right)^{-2k} \Big/ \sqrt{(1-\zeta)}\,; \tag{A.38}$$

and hence, by (A.36),

$$\frac{d}{d\zeta}\left[\zeta^{k+1/2}(1-\zeta)^{1/2}\frac{(1/2+\sqrt{(1-\zeta)}/2)^{-2k}}{\sqrt{(1-\zeta)}}\right] = \tfrac{1}{2}\zeta^{k-1/2}(1-\zeta)^{-1/2}\left(\frac{1}{2}+\frac{\sqrt{(1-\zeta)}}{2}\right)^{-2k-1}\left(1+\sqrt{(1-\zeta)}\left(k+\frac{\sqrt{(1-\zeta)}}{2}\right)\right),$$

which can be rewritten as

$$(k+1/2)\zeta^{k-1/2}(1-\zeta)^{-1/2}F(k+1, k-1/2; 2k+1; \zeta). \tag{A.39}$$

Therefore,

$$F(k+1, k-1/2; 2k+1; \zeta) = \frac{(1/2+\sqrt{(1-\zeta)}/2)^{-2k}(k+\sqrt{(1-\zeta)}/2)}{(k+1/2)},$$

Can. J. Chem. Downloaded from www.nrcresearchpress.com by 210.87.254.40 on 09/05/12
For personal use only.

i.e.,

$$F(k+1, k-1/2; 2k+1; 1-1/\xi_0^2) = \left(\frac{2\xi_0}{\xi_0+1}\right)^{2k} \frac{1+2k\xi_0}{(1+2k)\xi_0}. \tag{A.40}$$

The resulting expression for $(v_i)_{\xi=\xi_0}$ is

$$(v_i)_0 = \pm\frac{\overline{I(p)}}{nF\sqrt{(D_i p)}}\,\xi_0^{-1}\left\{\frac{(1/\xi_0)\{(2k+\xi_0)/(2k+1)\}(2\xi_0/\xi_0+1)^{2k}}{(1/\xi_0)\{(1+2k\xi_0)/(2k+1)\}(2\xi_0/\xi_0+1)^{2k}}\right\} \tag{A.41}$$

$$= \pm\frac{\overline{I(p)}}{nF\sqrt{(D_i p)}}\left(\frac{1+2k/\xi_0}{1+2k\xi_0}\right).$$

An alternate method for deriving the above expression for $F(k+1, k-1/2; 2k+1; \zeta)$ by making use of the known results for $F(k, k+1/2; 2k+1; \zeta)$ and $F(k, k-1/2; 2k+1; \zeta)$ will be to make use of the Gaussian relation among contiguous functions:

$$F(a,b;c;\zeta)+aF(a+1,b;c;\zeta)-bF(a,b+1;c;\zeta) = 0 \tag{A.42}$$

and identifying a, b, and c with k, $k-1/2$, and $2k+1$ respectively.

$$kF(k+1, k-1/2; 2k+1; \zeta) = (k-1/2)F(k, k+1/2; 2k+1; \zeta) + \tfrac{1}{2}F(k, k-1/2; 2k+1; \zeta), \tag{A.43}$$

i.e.,

$$F(k+1, k-1/2; 2k+1; 1-1/\xi_0^2) \tag{A.44}$$

$$= \frac{1}{k}\left\{(k-1/2)\left(\frac{2\xi_0}{\xi_0+1}\right)^{2k} + \frac{1}{2\xi_0}\left(\frac{2k+\xi_0}{2k+1}\right)\left(\frac{2\xi_0}{\xi_0+1}\right)^{2k}\right\}$$

$$= \left(\frac{2\xi_0}{\xi_0+1}\right)^{2k}\cdot\frac{1}{2k}\left[(2k-1) + \frac{2k+\xi_0}{(2k+1)\xi_0}\right]$$

$$= \left(\frac{2\xi_0}{\xi_0+1}\right)^{2k}\cdot\left\{\frac{2k\xi_0+1}{(2k+1)\xi_0}\right\}.$$

APPENDIX V

We define the functions $U(k, \xi)$ and $f_n(k, \xi)$ $(n = 1, 2, 3, 4)$ as follows:

$$U(k, \xi) = \left(\frac{2\xi}{\xi+1}\right)^{2k};$$

$$f_1(k, \xi) = (1+2k\xi)/(2k+1);$$

$$f_2(k, \xi) = \frac{3+6k\xi+4k^2\xi^2+2k\xi^3}{(2k+1)(2k+3)};$$

$$f_3(k, \xi) = \frac{15+30k\xi+24k^2\xi^2+(10k+8k^3)\xi^3+12k^2\xi^4+6k\xi^5}{(2k+1)(2k+3)(2k+5)};$$

$$f_4(k, \xi) = \frac{105+210k\xi+180k^2\xi^2+(70k+80k^3)\xi^3+(104k^2+16k^4)\xi^4 + (42k+48k^3)\xi^5+60k^2\xi^6+30k\xi^7}{(2k+1)(2k+3)(2k+5)(2k+7)}.$$

Can. J. Chem. Downloaded from www.nrcresearchpress.com by 210.87.254.40 on 09/05/12
For personal use only.

Then

$$F(k, k - 1/2; 2k+1; 1 - 1/\xi^2) = U(k, \xi) \cdot f_1(k, 1/\xi)$$

and

$$F(k+1, k - 1/2; 2k+1; 1 - 1/\xi^2) = U(k, \xi) \cdot f_1(k, \xi)/\xi.$$

By repeated application of the identity

$$\frac{d}{d\zeta}[\zeta^{c-a}(1-\zeta)^{a+b-c}F(a, b; c; \zeta)] = (c-a)\zeta^{c-a-1}(1-\zeta)^{a+b-c-1}F(a-1, b; c; \zeta),$$

or by using the contiguous relationship, we can prove the following:

(A.45) $F(k, k - 3/2; 2k+1; 1 - 1/\xi_0^2) = U(k, \xi_0) \cdot f_2(k, 1/\xi_0);$

(A.46) $F(k+1, k - 3/2; 2k+1; 1 - 1/\xi_0^2) = U(k, \xi_0) \cdot f_2(k, \xi_0)/\xi_0^3;$

(A.47) $F(k, k - 5/2; 2k+1; 1 - 1/\xi_0^2) = U(k, \xi_0) \cdot f_3(k, 1/\xi_0);$

(A.48) $F(k+1, k - 5/2; 2k+1; 1 - 1/\xi_0^2) = U(k, \xi_0) \cdot f_3(k, \xi_0)/\xi^5;$

(A.49) $F(k, k - 7/2; 2k+1; 1 - 1/\xi_0^2) = U(k, \xi_0) \cdot f_4(k, 1/\xi_0);$

(A.50) $F(k+1, k - 7/2; 2k+1; 1 - 1/\xi_0^2) = U(k, \xi_0) \cdot f_4(k, \xi_0)/\xi_0^7;$

(A.51) $F(k, k + 3/2; 2k+1; 1 - 1/\xi_0^2) = U(k, \xi_0) \cdot f_1(k, \xi_0);$

(A.52) $F(k+1, k + 3/2; 2k+1; 1 - 1/\xi_0^2) = U(k,\xi_0) \cdot f_1(k, 1/\xi_0)\xi_0^3;$

(A.53) $F(k, k + 5/2; 2k+1; 1 - 1/\xi_0^2) = U(k, \xi_0) \cdot f_2(k, \xi_0);$

(A.54) $F(k+1, k + 5/2; 2k+1; 1 - 1/\xi_0^2) = U(k, \xi_0) \cdot f_2(k, 1/\xi_0) \cdot \xi_0^5;$

(A.55) $F(k, k + 7/2; 2k+1; 1 - 1/\xi_0^2) = U(k, \xi_0) \cdot f_3(k, \xi_0);$

(A.56) $F(k+1, k + 7/2; 2k+1; 1 - 1/\xi_0^2) = U(k, \xi_0) \cdot f_3(k, 1/\xi_0) \cdot \xi_0^7;$

(A.57) $F(k, k + 9/2; 2k+1; 1 - 1/\xi_0^2) = U(k, \xi_0) \cdot f_4(k, \xi_0);$

(A.58) $F(k+1, k + 9/2; 2k+1; 1 - 1/\xi_0^2) = U(k, \xi_0) \cdot f_4(k, 1/\xi_0) \cdot \xi_0^9.$

It may be of interest to mention here that the sequence of polynomials $f_r(k, \xi)$ satisfies the identity

$$(2k+2r+1)\, f_{r+1}(k, \xi) = (2r+1)f_r(k, \xi)+2k\xi^{2r+1}f_r(k,1/\xi).$$

APPENDIX VI

If $F(k, k+l+1; 2k+1; 1 - 1/\xi_0^2)$ can be expanded in the form $S_0+S_1k+S_2k^2+ \ldots$ the coefficients S_0, S_1, S_2, etc., can be found as follows.

It can be noted that $S_0 = 1$ by studying the behavior at $k = 0$ on both sides.

Expressing

(A.59) $$F(k, k+l+1; 2k+1; \zeta_0) = S_0+S_1k+S_2k^2+ \ldots$$

$$= 1 + \frac{k(k+l+1)}{2k+1}\zeta_0 + \frac{k(k+1)(k+l+1)(k+l+2)}{(2k+1)(2k+2)}\frac{\zeta_0^2}{2!} + \ldots$$

Can. J. Chem. Downloaded from www.nrcresearchpress.com by 210.87.254.40 on 09/05/12
For personal use only.

one can collect the coefficients of k in the various terms and write S_1 as

$$(l+1)\zeta_0 + \frac{(l+1)(l+2)}{2!}\frac{\zeta_0^2}{2} + \frac{(l+1)(l+2)(l+3)}{3!}\cdot\frac{\zeta_0^3}{3} + \ldots$$

so that

$$\frac{dS_1}{d\zeta_0} = (l+1) + \frac{(l+1)(l+2)}{2!}\zeta_0 + \frac{(l+1)(l+2)(l+3)}{3!}\zeta_0^2 + \ldots$$

or

$$\zeta_0\frac{dS_1}{d\zeta_0} = (l+1)\zeta_0 + \frac{(l+1)(l+2)}{2!}\zeta_0^2 + \ldots = (1-\zeta_0)^{-(l+1)} - 1,$$

which gives

$$S_1 = \int_0^{\zeta_0}\frac{(1-\zeta_0)^{-(l+1)}-1}{\zeta_0}\,d\zeta_0, \tag{A.60}$$

making use of the fact that $S_1 = 0$ for $\zeta_0 = 0$; or

$$S_1 = 2\int_1^{\xi_0}\frac{\xi^{2(l+1)}-1}{\xi(\xi^2-1)}\,d\xi. \tag{A.61}$$

Similarly expressing $F(k+1,\ k+l+1;\ 2k+1;\ \zeta_0)$ as

$$(1-\zeta_0)^{-(l+1)}\{1+\phi_1 k+\phi_2 k^2+\ldots\} \tag{A.62}$$

one can apply the identity

$$\frac{d}{dz}[z^{c-a}(1-z)^{a+b-c}F(a, b; c; z)] = (c-a)z^{c-a-1}(1-z)^{a+b-c-1}F(a-1, b; c; z),$$

which gives

$$\frac{d}{d\zeta}[\zeta^k(1-\zeta)^{l+1}(1-\zeta)^{-(l+1)}(1+\phi_1 k+\phi_2 k^2+\ldots)] = k\zeta^{k-1}(1-\zeta)^l(1+kS_1+k^2S_2+\ldots),$$

i.e.,

$$\zeta^k k\frac{d\phi}{d\zeta} + (1+k\phi_1)\frac{k}{\zeta}\zeta^k + \zeta^k k^2\frac{d\phi_2}{d\zeta} + \ldots = k\frac{\zeta^k}{\zeta}(1-\zeta)^l(1+kS_1+k^2S_2+\ldots).$$

Equating the coefficients of k, we get

$$\frac{d\phi_1}{d\zeta} + \frac{1}{\zeta} = \frac{(1-\zeta)^l}{\zeta} \quad \text{or} \quad \phi_1 = \int_0^{\zeta}\frac{(1-\zeta)^l-1}{\zeta}\,d\zeta. \tag{A.63}$$

(Note: ϕ_0 is taken as equal to 1 in the above equation, since $F(k+1,\ k+l+1;\ 2k+1;\ \zeta) \to (1-\zeta)^{-(l+1)}$ as $k \to 0$, so that comparing the terms independent of k, ϕ_0 can be identified with 1.)

It can be shown by equating the coefficients of k^2,

$$\frac{d\phi_2}{d\zeta} + \frac{\phi_1}{\zeta} = \frac{(1-\zeta)^l}{\zeta}S_1$$

so that

$$\phi_2 = \int_0^{\zeta}\frac{(1-\zeta)^l S_1 - \phi_1}{\zeta}\,d\zeta, \tag{A.64}$$

Can. J. Chem. Downloaded from www.nrcresearchpress.com by 210.87.254.40 on 09/05/12
For personal use only.

where the expressions for ϕ_1 are given in (A.60) and (A.63). Substituting in the identity

$$\frac{d}{dz}[z^a F(a, b; c; z)] = az^{a-1}F(a+1, b; c; z),$$

k, $k+l+1$, $2k+1$, and ζ for a, b, c, and z respectively, it is seen that

$$k\zeta^{k-1}F(k+1, k+l+1; 2k+1; \zeta) = \frac{d}{d\zeta}[\zeta^k F(k, k+l+1; 2k+1; \zeta)].$$

With the help of (A.59) and (A.62), it can be seen that

$$\frac{k}{\zeta}(1-\zeta)^{-(l+1)}(1+k\phi_1+k^2\phi_2+\ldots) = \frac{k}{\zeta}(1+S_1k+S_2k^2+\ldots) + k\frac{dS_1}{d\zeta} + k^2\frac{dS_2}{d\zeta} + \ldots$$

Comparing the coefficients of k and k^2 we obtain

$$\frac{(1-\zeta)^{-(l+1)}}{\zeta} = \frac{1}{\zeta} + \frac{dS_1}{d\zeta} \quad \text{or} \quad S_1 = \int_0^\zeta \frac{(1-\zeta)^{-(l+1)}-1}{\zeta}\,d\zeta$$

(a result that has been derived already by a different method) and

$$\frac{\phi_1(1-\zeta)^{-(l+1)}}{\zeta} = \frac{S_1}{\zeta} + \frac{dS_2}{d\zeta}.$$

Integrating one can obtain S_2 as

$$\int_0^\zeta \frac{(1-\zeta)^{-(l+1)}\phi_1 - S_1}{\zeta}\,d\zeta. \tag{A.65}$$

APPENDIX VII

For *attraction* in the diffuse layer,

$$(v_i)_0 = \pm\frac{\overline{I(p)}}{nF\sqrt{(D_ip)}}\,\xi_0^{(-2|z_i/z|+1)}\,\frac{F(k, k+1/2-|Z_i/Z|; 2k+1; \zeta_0)}{F(k+1, k+1/2-|Z_i/Z|; 2k+1; \zeta_0)}. \tag{A.66}$$

Since

$$F(a, b; c; z) = (1-z)^{c-a-b}F(c-a, c-b; c; z), \tag{A.67}$$

$$(v_i)_0 = \pm\frac{\overline{I(p)}}{nF\sqrt{(D_ip)}}\,\xi_0^{(-2|z_i/z|+1)}\,\frac{1}{\xi_0^2}\,\frac{F(k+1, k+1/2+|Z_i/Z|; 2k+1; \zeta_0)}{F(k, k+1/2+|Z_i/Z|; 2k+1; \zeta_0)}; \tag{A.68}$$

$$= \pm\frac{\overline{I(p)}}{nF\sqrt{(D_ip)}}\,\xi_0^{-(2|z_i/z|+1)}\,\frac{F(k+1, k+1/2+|Z_i/Z|; 2k+1; \zeta_0)}{F(k, k+1/2+|Z_i/Z|; 2k+1; \zeta_0)}.$$

For *repulsion* ($l+1 = |Z_i/Z| + 1/2$)

$$(v_i)_0 = \pm\frac{\overline{I(p)}}{nF\sqrt{(D_ip)}}\,\xi_0^{(2|z_i/z|+1)}\,\frac{F(k, k+1/2+|Z_i/Z|; 2k+1; 1-1/\xi_0^2)}{F(k+1, k+1/2+|Z_i/Z|; 2k+1; 1-1/\xi_0^2)}. \tag{A.69}$$

For a *given* Z_i, if $(v_i)_0^{\mathrm{A}}$ represents the expressions of v_i at the electrode surface *if there is attraction* in the diffuse layer, and $(v_i)_0^{\mathrm{R}}$ the expression of v_1 for repulsion

$$\left\{\frac{(v_i)_0^{\mathrm{A}}}{\pm\overline{I(p)}/nF\sqrt{(D_ip)}}\right\}\left\{\frac{(v_i)_0^{\mathrm{R}}}{\pm\overline{I(p)}/nF\sqrt{(D_ip)}}\right\} = 1. \tag{A.70}$$

This helps one in calculating the functional form of $(v_i)_0$ for the case of attraction, given the form for the case of repulsion and vice versa.

Can. J. Chem. Downloaded from www.nrcresearchpress.com by 210.87.254.40 on 09/05/12
For personal use only.

To illustrate, let us investigate the case when $|Z_i| = |Z|$; if there is attraction,

$$\frac{(v_i)_0}{(\pm\overline{I(p)}/nF\sqrt{(D_ip)})} = \frac{1+2k/\xi_0}{1+2k\xi_0}.$$

Had there been repulsion, for $|Z_i| = |Z|$, one would therefore, have obtained

$$\frac{(v_i)_0}{(\pm\overline{I(p)}/nF\sqrt{(D_ip)})} = \frac{1+2k\xi_0}{1+2k/\xi_0},$$

a result that has been proved already. (Refer to equation [37] of the text.)

The above relationship between $(v_i)_0^{A}$ and $(v_i)_0^{R}$ is not so obvious, (nor can it be at once understood explicitly) since

$$(v_i)_0 = \pm\frac{\overline{I(p)}}{nF\sqrt{(D_ip)}}\frac{F(k, k+l+1; 2k+1; 1-1/\xi_0^2)}{F(k+1, k+l+1; 2k+1; 1-1/\xi_0^2)}$$

and l assumes *different* values for the *same* $|Z_i/Z|$ depending on whether there is attraction or repulsion and could be seen only through the identity (A.67) relating the hypergeometric functions with different parameters.

Also, by making use of the functional relationship

$$F(a, b; c; z) = (1-z)^{-a}F(a, c-b; c; z/z-1) \tag{A.71}$$

it is seen that if

$$F(k, k+l+1; 2k+1; 1-1/\xi^2) = g(k, l, \xi), \tag{A.72}$$

$$F(k+1, k+l+1; 2k+1; 1-1/\xi^2) = \xi^{2(k+l+1)}g(k, l, 1/\xi). \tag{A.73}$$

Abbreviating, for convenience, the function $g(k, l, \xi)$ as $g(\xi)$, $(v_i)_0$ can be written in the form

$$(v_i)_0 = \pm\frac{\overline{I(p)}}{nF\sqrt{(D_ip)}}\cdot\xi_0^{-2k}\cdot\frac{g(\xi_0)}{g(1/\xi_0)}, \tag{A.74}$$

which shows that it is enough if the hypergeometric function in the numerator (or denominator) is evaluated to obtain the function $(v_i)_0$.

Also, if

$$F(k, k+|Z_i/Z|+1/2; 2k+1; 1-1/\xi^2) = g(\xi),$$

then

$$(v_i)_0 = \pm\frac{\overline{I(p)}}{nF\sqrt{(D_ip)}}\xi_0^{-2k}\frac{g(\xi_0)}{g(1/\xi_0)} \qquad \text{(for repulsion)} \tag{A.75}$$

and

$$(v_i)_0 = \pm\frac{\overline{I(p)}}{nF\sqrt{(D_ip)}}\xi_0^{2k}\frac{g(1/\xi_0)}{g(\xi_0)} \qquad \text{(for attraction)}. \tag{A.76}$$

To illustrate, let us take the particular case when $|Z_i| = |Z|$:

$$F(k, k+3/2; 2k+1; 1-1/\xi_0^2) = \left(\frac{2\xi_0}{\xi_0+1}\right)^{2k}\left(\frac{1+2k\xi_0}{1+2k}\right)$$

$$= g(\xi_0)$$

$$g(1/\xi_0) = \left(\frac{2}{1+\xi_0}\right)^{2k}\left(\frac{1+2k/\xi_0}{1+2k}\right),$$

Can. J. Chem. Downloaded from www.nrcresearchpress.com by 210.87.254.40 on 09/05/12
For personal use only.

so that *for repulsion*, using (A.75), we can write,

$$(v_i)_0 = \frac{\overline{I(p)}}{nF\sqrt{(D_i p)}} \frac{g(\xi_0)}{g(1/\xi_0)}$$

$$= \pm\frac{\overline{I(p)}}{nF\sqrt{(D_i p)}} \left(\frac{1 + 2k\xi_0}{1 + 2k/\xi_0}\right)$$

as has been shown already (equation [37] of the text). Similarly, *for attraction*, using (A.76),

$$(v_i)_0 = \pm\frac{\overline{I(p)}}{nF\sqrt{(D_i p)}} \xi_0^{2k} \cdot \frac{g(1/\xi_0)}{g(\xi_0)}$$

$$= \pm\frac{\overline{I(p)}}{nF\sqrt{(D_i p)}} \left(\frac{1 + 2k/\xi_0}{1 + 2k\xi_0}\right)$$

as has been shown (equation [24] of the text).

NOTATIONS

$C_i(x,t)$	instantaneous concentration of the species i, (O for oxidant; R for reductant) at a distance x from the electrode surface
$C_i(O,t)$	instantaneous interfacial concentration of the species i
C_i^0	bulk concentration of the species i
D_i	diffusion coefficient of the species i
Z_O	valency (with sign) of the oxidant
Z_R	valency (with sign) of the reductant
Z	valency of the supporting electrolyte.
$\phi(x)$	potential distribution in the diffuse (Gouy) layer, viz., $\phi(0) - \phi(\infty)$
$I(t)$	Faradaic current
κ	Debye parameter for the reciprocal thickness of the double layer
p	transform variable (Laplace)
$\overline{C_i}(x,p)$	Laplace transform of $C_i(x,t)$
$\overline{I(p)}$	Laplace transform of $I(t)$
$F(a,b,c;Z)$	Gaussian hypergeometric function of argument Z
$\Gamma(x)$	gamma function of x
l	$\pm\lvert Z_i/Z\rvert - 1/2$ (positive sign for repulsion; negative for attraction)
$(v_i)_0 = [v_i(p)]_0$	$= C_i^0 - \overline{C_i}(0,p) \exp(Z_i F\phi/RT)$
$(v_i)_\xi = [v_i(p)]_\xi$	$= C_i^0 - \overline{C_i}(x,p) \exp(Z_i F\phi/RT)$
ξ	$\exp \lvert Z\rvert F \lvert\phi\rvert/2RT$
ξ_0	$\exp \lvert Z\rvert F \lvert\phi_0\rvert/2RT$
ζ	$1 - 1/\xi^2$
ζ_0	$1 - 1/\xi_0^2$
k	$\frac{1}{\kappa}\sqrt{(p/D_i)}$
$\cong$	asymptotically equal to

ACKNOWLEDGMENT

The author wishes to thank Professor K. S. G. Doss, Director, Central Electrochemical Research Institute, Karaikudi, for his keen interest and valuable discussions.

REFERENCES

1. A. N. Frumkin. Z. Elektrochem. **59**, 807 (1955). M. Breiter, M. Kleinerman, and P. Delahay. J. Am. Chem. Soc. **80**, 511 (1958).
2. H. Matsuda and P. Delahay. J. Phys. Chem. **64**, 332 (1960).
3. S. K. Rangarajan. J. Electroanal. Chem. **1**, 396 (1960).
4. E. T. Whittaker and C. N. Watson. A course of modern analysis. Cambridge at the University Press. 1958. p. 299.

Can. J. Chem. Downloaded from www.nrcresearchpress.com by 210.87.254.40 on 09/05/12
For personal use only.

FARADAIC IMPEDANCE: EFFECT OF MIGRATION IN THE DIFFUSE DOUBLE LAYER

S. K. RANGARAJAN
Central Electrochemical Research Institute, Karaikudi, India

Received June 12, 1962

ABSTRACT

The expressions for the elements of the equivalent circuit are derived by making use of the modified solutions for the diffusion equation (with migration in the diffuse layer) obtained earlier. The impedance (faradaic) characteristics are discussed. Also, the results are compared with those of Matsuda and Delahay.

Can. J. Chem. Downloaded from www.nrcresearchpress.com by 210.87.254.42 on 09/05/12
For personal use only.

1. *The Steady-State Concentrations*

The study of the a-c. impedance of an electrode serves as a powerful tool in measuring the kinetic parameters of rapid electrode reactions. The conditions existing at the electrode–solution interface can be represented by an equivalent circuit whose elements R_r and C_r are given through the expressions (1)

[1] $$R_r = \frac{RT}{nF}\left\{\frac{1}{I_0} + \frac{1}{nF\sqrt{(2\omega)}}\left(\frac{1}{C_O^0\sqrt{(D_{O2})}} + \frac{1}{C_R^0\sqrt{(D_{R2})}}\right)\right\}$$

and

[2] $$\frac{1}{\omega C_r} = \frac{RT}{n^2F^2}\left\{\frac{1}{\sqrt{(2\omega)}}\left(\frac{1}{C_O^0\sqrt{(D_{O2})}} + \frac{1}{C_R^0\sqrt{(D_{R2})}}\right)\right\}$$

(R_r and C_r refer to the faradaic process only).

In obtaining these, it has been assumed that only small departures from equilibrium are of interest and diffusion is the sole mode of mass transfer.

In the above formulation, the effects due to migration in the double layer were assumed absent. It will be of importance to examine how the elements of the equivalent circuit are modified if the structure of the diffuse layer is taken into account.

Detailed investigations on this aspect have been made by Matsuda (2), based on the expressions for the interfacial concentrations obtained earlier by Matsuda and Delahay (3). It has been shown by the author (4) that the solutions derived by Matsuda and Delahay (and consequently the results of Matsuda) are to be modified. It is the object of the present paper to examine these modifications in the expressions for the elements of the equivalent circuit.

Denoting the interfacial concentration of the species i (i = O, oxidant; R, reductant) by $C_i(0,t)$ and its Laplace transform as $\bar{C}_i(0,p)$, it has been shown that

[3] $$\bar{C}_i(0, p) = \exp\left(\frac{-Z_0F\phi}{RT}\right)[C_i^0 - v_i(p)],$$

where

[4] $$v_i(p) = \pm\frac{\overline{I(p)}}{nF\sqrt{(D_ip)}}\,\xi_0^{2(l+1)}\,\frac{F(k, k+l+1; 2k+1; 1 - 1/\xi_0^2)}{F(k+1, k+l+1; 2k+1; 1 - 1/\xi_0^2)}$$

(for details, see reference 4),

$$(l+1) = \pm\left|\frac{Z_i}{Z}\right| + 1/2$$

(positive sign for the case of repulsion ($Z_i\phi > 0$) and negative sign for attraction ($Z_i\phi < 0$)), p is the transform variable, and

$$\xi_0 = \exp \frac{|Z|\ F\ |\phi_0|}{2RT}.$$

Assuming the sinusoidal component of the faradaic current as $I \cos \omega t$, it can be rigorously proved that the *steady-state* components of the concentration will assume the form

$$C_i^0 \mp \Delta C_i \cos\ (\omega t - \theta_i).$$

Hence, confining our interest only to the alternating components of the concentration, at the interface, it may be noted that

$$[5] \qquad C_i(0, t) = \exp\left(\frac{-Z_0 F\phi}{RT}\right)\left[C_i^{\,0} \mp \text{Real Part of } \frac{Ie^{j\omega t}}{nF\sqrt{(D_i\omega)}} j^{-1/2} G_i\right]$$

where $j = \sqrt{(-1)}$ and G_i stands for

$$[6] \qquad \xi_0^{\,2(l+1)} \frac{F(k_\omega, k_\omega+l+1; 2k_\omega+1; 1 - 1/\xi_0^{\,2})}{F(k_\omega+1, k_\omega+l+1; 2k_\omega+1; 1 - 1/\xi_0^{\,2})}$$

where

$$k_\omega = \frac{1}{\kappa}\sqrt{\left(\frac{j\omega}{D_i}\right)}.$$

For particular values of the parameter l, G_i takes the functional form of

$$P(k_\omega)/Q(k_\omega),$$

where $P(Z)$ and $Q(Z)$ are polynominals in Z of the same degree.

In general,

$$\frac{F(k_\omega, k_\omega+l+1; 2k_\omega+1; 1 - 1/\xi_0^{\,2})}{\Gamma(2k_\omega+1)}$$

and

$$\frac{F(k_\omega+1, k_\omega+l+1; 2k_\omega+1; 1 - 1/\xi_0^{\,2})}{\Gamma(2k_\omega+1)},$$

where

$$k_\omega = \frac{1}{\kappa}\sqrt{\left(\frac{j\omega}{D_i}\right)},$$

are entire analytic functions in k_ω, so that the only infinities of G_i are the poles, which, incidentally, are the zeros of $F(k_\omega+1, k_\omega+l+1; 2k_\omega+1; 1 - 1/\xi_0^2)$. Also observing that *no real positive* ω exists which will satisfy the equation $F(k_\omega+1, k_\omega+l+1; 2k_\omega+1; 1 - 1/\xi_0^2) = 0$, we may expand the numerator and the denominator of the function G_i in the form

$$[7] \qquad G_i = \frac{1 + k_\omega S_1(\xi_0) + (k_\omega)^2 S_2(\xi_0) + \ldots}{1 + k_\omega \phi_1(\xi_0) + (k_\omega)^2 \phi_2(\xi_0) + \ldots},$$

Can. J. Chem. Downloaded from www.nrcresearchpress.com by 210.87.254.42 on 09/05/12
For personal use only.

where

$$S_1(\xi_0) = 2\int_1^{\xi_0} \frac{\xi^{2(l+1)}-1}{\xi(\xi^2-1)}\,d\xi,$$

$$\phi_1(\xi_0) = 2\int_1^{\xi_0} \frac{\xi^{-2l}-1}{\xi(\xi^2-1)}\,d\xi,$$

[8]

$$S_2(\xi_0) = \int_0^{1-1/\xi_0^2} \frac{(1-\zeta)^{-(l+1)}\phi_1 - S_1}{\zeta}\,d\zeta, \quad \text{and}$$

$$\phi_2(\xi_0) = \int_0^{1-1/\xi_0^2} \frac{(1-\zeta)^{l} S_1 - \phi_1}{\zeta}\,d\zeta$$

(cf. reference 4, Appendix VI).

Conforming to the notation used by Matsuda (2), one can write

$$(-j)^{1/2}G_i = (h_i)_{\text{re}} - j(h_i)_{\text{im}},$$

where

[9]

$$(h_i)_{\text{re}} = \frac{1 + \frac{1}{\kappa}\sqrt{\left(\frac{2\omega}{D_i}\right)}S_1(\xi_0) + \left(\frac{1}{\kappa}\sqrt{\left(\frac{\omega}{D_i}\right)}\right)^2 S_1(\xi_0)\phi_1(\xi_0)}{H_i(\omega)},$$

[10]

$$(h_i)_{\text{im}} = \frac{1 + \frac{1}{\kappa}\sqrt{\left(\frac{2\omega}{D_i}\right)}\phi_1(\xi_0) + \left(\frac{1}{\kappa}\sqrt{\left(\frac{\omega}{D_i}\right)}\right)^2 S_1(\xi_0)\phi_1(\xi_0)}{H_i(\omega)},$$

and

$$H_i(\omega) = 1 + \frac{1}{\kappa}\sqrt{\left(\frac{2\omega}{D_i}\right)}\phi_1(\xi_0) + \left(\frac{1}{\kappa}\sqrt{\left(\frac{\omega}{D_i}\right)}\right)^2 \phi_1^2(\xi_0).$$

Note that $S_1(\xi_0)$ and $\phi_1(\xi_0)$ are functions of the parameter $l = \pm|Z_i/Z| - 1/2$ (positive sign for the case of repulsion ($Z_i\phi > 0$) and negative for the case of attraction ($Z_i\phi < 0$)).

Thus, the steady-state interfacial concentrations are

[11]

$$C_i(0, t) = \exp\left(\frac{-Z_0F\phi}{RT}\right)[C_i^{\,0} \mp \Delta C_i \cos(\omega t - \theta_i)],$$

where

$$\Delta C_i = \left(\frac{I}{nF}\right)(2\omega D_i)^{-1/2}[(h_i)_{\text{re}}^{\,2} + (h_i)_{\text{im}}^{\,2}]^{1/2}$$

and

$$\cot\theta_i = (h_i)_{\text{re}}/(h_i)_{\text{im}}$$

(the sign accompanying ΔC_i in the above equation is to be taken positive for the oxidant and negative for the reductant. Note that (i) the functions $(h_i)_{\text{re}}$ and $(h_i)_{\text{im}}$ defined above are only approximate, since terms in $[(1/\kappa)\sqrt{(\omega/D_i)}]^2$ and higher powers are neglected, and (ii) the functions $(h_i)_{\text{re}}$ and $(h_i)_{\text{im}}$ defined above are *different* from those given by Matsuda (2).

Can. J. Chem. Downloaded from www.nrcresearchpress.com by 210.87.254.42 on 09/05/12
For personal use only.

Can. J. Chem. Downloaded from www.nrcresearchpress.com by 210.87.254.42 on 09/05/12
For personal use only.

An interesting particular case arises for $|Z_i| = |Z|$. Under this condition, the solution of the diffusion equation shows (4) that

$$G_i = \frac{1 + 2k_\omega\xi_0}{1 + 2k_\omega/\xi_0} \quad (|Z_i| = |Z|;\ \text{repulsion},\ Z_i\phi > 0) \tag{12}$$

and

$$G_i = \frac{1 + 2k_\omega/\xi_0}{1 + 2k_\omega\xi_0} \quad (|Z_i| = |Z|;\ \text{attraction},\ Z_i\phi < 0). \tag{13}$$

These are *exact* expressions for G_i and, hence,

$$(h_i)_{re} = \frac{1 + \frac{1}{\kappa}\sqrt{\left(\frac{2\omega}{D_i}\right)}2\xi_0 + 4\left(\frac{1}{\kappa}\sqrt{\left(\frac{\omega}{D_i}\right)}\right)^2}{1 + \frac{2}{\kappa}\sqrt{\left(\frac{2\omega}{D_i}\right)}\frac{1}{\xi_0} + 4\left(\frac{1}{\kappa}\sqrt{\left(\frac{\omega}{D_i}\right)}\frac{1}{\xi_0}\right)^2} \tag{14}$$

and $(h_i)_{im}$ can be similarly expressed.

2. The Impedance Characteristics

The faradaic current $I(t)$ is related to the potential as

$$I(t) = (I_0)_{app}\left\{\frac{C_O(0,t)}{C_O^0}\exp(Z_O F\phi_0/RT)[\exp(-\alpha nF/RT)v] - \frac{C_R(0,t)}{C_R^0}\exp(Z_R F\phi_0/RT)\exp[((1-\alpha)nF/RT)v]\right\}. \tag{15}$$

Here, $(I_0)_{app}$ stands for the apparent exchange current density (Frumkin correction) and is related to $I_0 = nF\,\kappa_s C_O^{0(1-\alpha)} C_R^{0\,\alpha}$ by

$$(I_0)_{app} = I_0 \exp[(\alpha n - Z_0)F\phi_0/RT]. \tag{16}$$

Considering the a-c. impedance measurements for small deviations from the equilibrium conditions (i.e. as a relaxation method), we may linearize the exponentials in the rate equation [15] and write

$$I = (I_0)_{app}\left\{\frac{C_O(0,t)}{C_O^0}\exp\left(\frac{Z_O F\phi_0}{RT}\right) - \frac{C_R(0,t)}{C_R^0}\exp\left(\frac{Z_R F\phi_0}{RT}\right) - \frac{nFv}{RT}\right\}. \tag{17}$$

Substituting for $C_i(0,t)$ from equation [11] in [17] and identifying with

$$-v = iR_s + \frac{\int idt}{C_s} \tag{17a}$$

(the negative sign in the left hand side of [17*a*] is necessary so as to conform to the convention chosen: electrode solution potential positive and net cathodic current positive), the elements of the equivalent circuit can be derived to be

$$R_s = \frac{RT}{nF}\left\{\frac{1}{(I_0)_{app}} + \frac{1}{nF\sqrt{(2\omega)}}\left[\frac{(h_0)_{re}}{C_O^0 D_O^{1/2}} + \frac{(h_R)_{re}}{C_R^0 D_R^{1/2}}\right]\right\}, \tag{18}$$

$$\frac{1}{\omega C_s} = \frac{RT}{nF}\left\{\frac{1}{nF\sqrt{(2\omega)}}\left[\frac{(h_0)_{im}}{C_O^0 D_O^{1/2}} + \frac{(h_R)_{im}}{C_R^0 D_R^{1/2}}\right]\right\}, \tag{19}$$

where $(h_i)_{re}$ and $(h_i)_{im}$ are defined through the equations [9] and [10].

It can also be seen that

$$[20]\quad R_s - \frac{1}{\omega C_s} = \frac{RT}{nF}\left\{\frac{1}{(I_0)_{app}} + \frac{1}{nF\sqrt{(2\omega)}}\left[\left(\frac{(h_0)_{re}-(h_0)_{im}}{C_O^0 D_O^{1/2}}\right) + \left(\frac{(h_R)_{re}-(h_R)_{im}}{C_R^0 D_R^{1/2}}\right)\right]\right\}$$

$$= \frac{RT}{nF}\left\{\frac{1}{(I_0)_{app}} + \frac{S_1(\xi_0)-\phi_1(\xi_0)}{nFC_O^0 \kappa D_O H_O(\omega)} + \text{a similar term for the reductant}\right\}.$$

If the denominator of the equations [9] and [10] can be approximated as 1,

$$[21]\quad \left(R_s - \frac{1}{\omega C_s}\right) = \frac{RT}{nF}\left\{\frac{1}{(I_0)_{app}} + \frac{1}{nF}\left(\frac{a_O}{\kappa C_O^0 D_O} + \frac{a_R}{\kappa C_R^0 D_R}\right)\right\},$$

where the non-dimensional parameter a_i is given by

$$[22]\quad a_i = S_1(\xi_0) - \phi_1(\xi_0)$$

$$= \pm 2\kappa \int_0^\infty \sinh\left(\frac{Z_i F \phi}{RT}\right) dx$$

(positive sign to be taken for the case of repulsion and negative for the attraction). Recalling the classical method of measuring the exchange current density by a-c. impedance measurements, one writes

$$[23]\quad R_s - \frac{1}{\omega C_s} = \frac{RT}{nF(I_0)_{ms}},$$

where the measured exchange current density is related to $(I_0)_{app}$, and consequently to I_0, by the relationship

$$[24]\quad \frac{1}{(I_0)_{ms}} = \frac{1}{(I_0)_{app}} + \frac{1}{nF}\left(\frac{a_O}{\kappa C_O^0 D_O} + \frac{a_R}{\kappa C_R^0 D_R}\right).$$

The form of this result is identical with that derived by Matsuda, though a_O and a_R, as given here, are different from those derived therein (2, 3).

Theoretical curves $(I_0)_{ms}$ vs. ϕ_0 are drawn in Figs. 1 and 2 for some particular cases, which are compared with those of Matsuda and Delahay (3).

Under the conditions assumed in deriving equation [21], it may be seen that

$$[25]\quad R_s = R_r + \frac{RT}{n^2F^2}\left(\frac{a_O}{\kappa C_O^0 D_O} + \frac{a_R}{\kappa C_R^0 D_R}\right)$$

$$[26]\quad \frac{1}{\omega C_s} = \frac{1}{\omega C_r},$$

where R_r and C_r are the expressions obtained for the *classical case* (1).

Even if the migration in the diffuse double layer is taken into account, a linear relationship between R_s (or $1/\omega C_s$) and $1/\sqrt{(\omega)}$ is obtained. While the slopes are preserved, the intercept of the R_s vs. $1/\sqrt{(\omega)}$ plot is changed. This intercept is denoted by $RT/nF(I_0)_{ms}$ and is expressed through equation [24].

3. The Equivalent Circuits

To obtain the equivalent circuit for the case when $v_i(p)$ is written as*

$$[27]\quad \frac{\overline{I(p)}}{nF\sqrt{(D_i p)}}\left(\frac{1 + 1/\kappa\sqrt{(p/D_i)}S_1}{1 + 1/\kappa\sqrt{(p/D_i)}\phi_1}\right),$$

**Though, for simplicity, no subscript (i) is added to S_1 and ϕ_1, it must be remembered that S_1 and ϕ_1 depend on the species and are* different *for the oxidant and the reductant.*

Can. J. Chem. Downloaded from www.nrcresearchpress.com by 210.87.254.42 on 09/05/12
For personal use only.

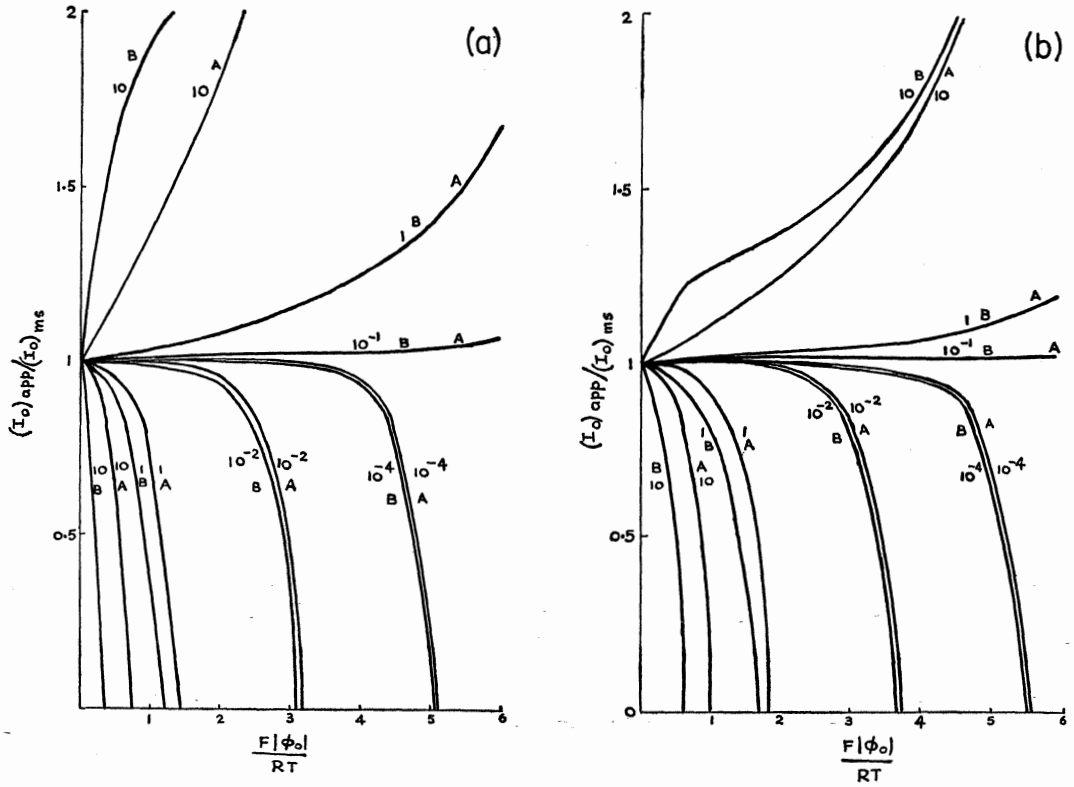

FIG. 1. Theoretical curves for the variation of $(I_0)_{app}/(I_0)_{ms}$ with the diffuse layer potential ϕ_0 (see equation [24] of the text). The numbers noted along the curves denote the values assumed for the exchange current densities. Data used: $\alpha = 0.5$; $Z_O = n = 2$; $Z_R = 0$; $C_O = 10^{-6}$ mole cm^{-3}; $D_O = 10^{-5}$ cm^2 sec^{-1}. A represents the curve obtained by calculating $(I_0)_{app}/(I_0)_{ms}$ from the equation of Matsuda and Delahay (3); B is drawn from the modified formulae derived by the author (4).
(*a*): $1/\kappa = 10^{-7}$ cm; (*b*): $1/\kappa = 3\times10^{-8}$ cm.
It may be noted that $(I_0)_{app}/(I_0)_{ms} > 1$ for the case of repulsion and <1 for the case of attraction.

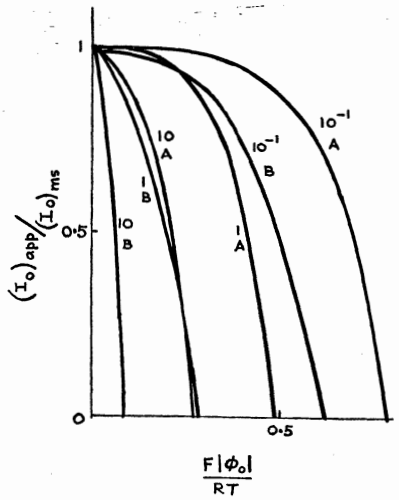

FIG. 2. Theoretical plot of $(I_0)_{app}/(I_0)_{ms}$ vs. $|\phi_0|$ (assuming *attraction* in the diffuse layer) for the case $Z_O = -3$; $Z_R = -4$; $n = 1$; $Z = 1$; $C_O = C_R = 10^{-5}$; $D_O = D_R = 10^{-6}$; $I_0 = 10$, 1, and 10^{-1} (noted along the curves); $1/\kappa = 10^{-7}$ cm. A and B calculated using the equations derived by Matsuda and Delahay (3) and the author (4), respectively.

Can. J. Chem. Downloaded from www.nrcresearchpress.com by 210.87.254.42 on 09/05/12
For personal use only.

we substitute for $v_i(p)$ in the linearized rate equation [17] to obtain

$$\left\{\frac{\overline{I(p)}}{(I_0)_{app}} + \frac{\bar{I}}{nF\sqrt{(D_i p)}C_i^0}\left(\frac{1+1/\kappa\sqrt{(p/D_i)}S_1}{1+1/\kappa\sqrt{(p/D_i)}\phi_1}\right) + \left\{\begin{array}{c}\text{(a similar expression corresponding}\\ \text{to the reductant)}\end{array}\right\}\right\}$$

$$\equiv -\frac{nF}{RT}v.$$

Expressing

$$\frac{RT}{n^2F^2\sqrt{(D_i p)}C_i^0}\left\{\frac{1+1/\kappa\sqrt{(p/D_i)}S_1}{1+1/\kappa\sqrt{(p/D_i)}\phi_1}\right\} \text{ as } Z_i^{d}(p)$$

we may write

[28] $$\frac{1}{Z_i^{d}} = n^2F^2C_i^0\frac{\sqrt{(D_i p)}}{RT}\left\{\frac{1+1/\kappa\sqrt{(p/D_i)}\phi_1}{1+1/\kappa\sqrt{(p/D_i)}S_1}\right\}$$

$$= \frac{n^2F^2}{RT}C_i^0\sqrt{(D_i p)} + \frac{1}{\kappa}\frac{(\phi_1 - S_1)n^2F^2C_i^0 p}{RT(1+1/\kappa\sqrt{(p/D_i)}S_1)}$$

[29] $$= \frac{1}{Z_1} + \frac{1}{Z_{2a}},$$

where

[30] $$Z_1 = \frac{RT}{n^2F^2C_i^0\sqrt{(D_i p)}} = W_i^{d}$$

and

[31] $$Z_{2a} = \frac{\kappa RT}{(-a_i)n^2F^2C_i^0}\frac{1}{p} + \frac{1}{\sqrt{(pD_i)}}\frac{RTS_1}{n^2F^2C_i^0(-a_i)}.$$

When the faradaic current is of the form $I\cos(\omega t)$, Z_1 stands for the Warburg impedance (1) and

[32] $$Z_{2a} = \frac{1}{j\omega C_i^{1}} + [W_i^{a1}]$$

with

[33] $$C_i^{1} = (-a_i)\frac{n^2F^2C_i^0}{RT\kappa}$$

and

$$W_i^{a1} = R_i^{a1} - \frac{j}{\omega C_i^{a1}}$$

$$= \frac{RTS_1}{n^2F^2C_i^0\sqrt{(2\omega D_i)}(-a_i)} - \frac{jRTS_1}{n^2F^2C_i^0\sqrt{(2\omega D_i)}(-a_i)}$$

so that

[34] $$R_i^{a1} = \frac{RTS_1}{n^2F^2C_i^0\sqrt{(2\omega D_i)}(-a_i)}$$

and

[35] $$C_i^{a1} = \frac{n^2F^2C_i^0(-a_i)}{RTS_1}\sqrt{\left(\frac{2D_i}{\omega}\right)}.$$

Can. J. Chem. Downloaded from www.nrcresearchpress.com by 210.87.254.42 on 09/05/12
For personal use only.

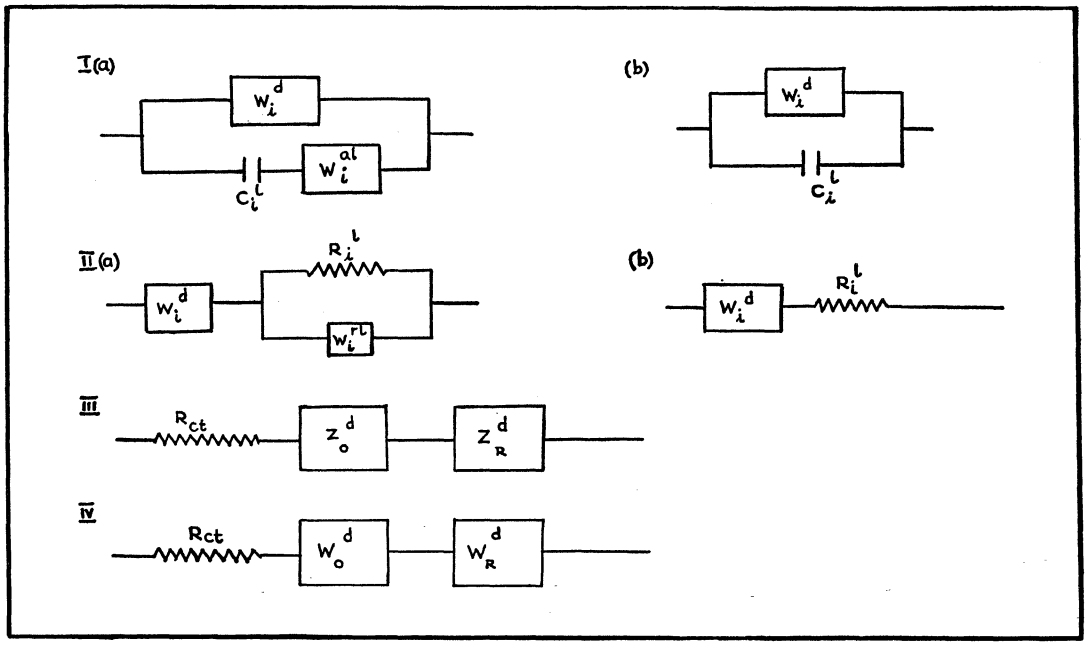

FIG. 3. Impedance characteristics—effect of migration in the diffuse layer.

Equivalent circuits for the reaction $O + ne \rightleftharpoons R$. Z_i^d: the contribution of the species i (= O, R) to the overall impedance Z (= $R_{ct}+Z_O^d+Z_R^d$); W_i^d: Warburg impedance; W_i^{al}: $[S_1/(-a_i)]W_i^d$ ($a_i < 0$); W_i^{rl}: $[a_i/\phi_1]W_i^d$ ($a_i > 0$); R_{ct}: charge transfer resistance.

I(a): formal schematic representation for Z_i^d; I(b): Z_i^d, as given by Senda and Delahay (5), for the particular condition $|(1/\kappa)\sqrt{(\omega/D_i)}S_1| \ll 1$; II($a$): Z_i^d, for the case of repulsion; II(b): Z_i^d, when $|(1/\kappa)\cdot\sqrt{(\omega/D_i)}\phi_1| \ll 1$ (see ref. 5); III: equivalent circuit for the faradaic impedance with (Z_O^d) and (Z_R^d) to be substituted from I or II depending on whether there is attraction or repulsion in the double layer; IV: the classical representation of Z (i.e. for the particular case $\phi_0 = 0$).

Hence, for the *case of attraction* (i.e. when $a_i < 0$), the impedance due to the polarization characteristics of the *species i* consists of the classical Warburg impedance in *parallel* with the impedance

$$Z_{2a} = \frac{1}{j\omega C_i^{\,l}} + R_i^{\,al} + \frac{1}{j\omega C_i^{\,al}}.$$

(Note that when the effects due to diffuse double layer are negligible, $\xi_0 \rightarrow 1$ and $a_i \rightarrow 0$ so that $R_i^{al} \rightarrow \infty$ and $C_i^{al} \rightarrow 0$.) For the case of repulsion, Z_i^d may be written as

[36] $$Z_i^{\,d} = \frac{RT}{n^2F^2\sqrt{(D_ip)}C_i^{\,0}} + \frac{a_iRT}{\kappa D_i(1 + 1/\kappa\sqrt{(p/D_i)}\phi_1)n^2F^2C_i^{\,0}}$$

$$= Z_1+Z_{2r}$$

with

[37] $$\frac{1}{Z_{2r}} = \frac{\kappa D_in^2F^2C_i^{\,0}}{RTa_i} + \frac{\sqrt{(pD_i)}\phi_1n^2F^2C_i^{\,0}}{RTa_i}$$

$$= \frac{1}{R_i^{\,l}} + \frac{1}{W_i^{\,rl}},$$

Can. J. Chem. Downloaded from www.nrcresearchpress.com by 210.87.254.42 on 09/05/12
For personal use only.

where

[38] $$W_i^{r1}(p) = \frac{RTa_i}{\phi_1\sqrt{(pD_i)}.n^2F^2C_i^0}$$

and

[39] $$R_i^1 = \frac{a_iRT}{\kappa D_i n^2F^2C_i^0}.$$

Thus, in the *case of repulsion* ($a_i > 0$) the impedance due to the polarization characteristics of the species i consists of the classical Warburg impedance *in series* with the impedance Z_{2r}. (Refer to Fig. 3.)

CONCLUSIONS

By making use of the modified expressions obtained recently for the interfacial concentrations $C_i(0,t)$ when the effect of the migration in the diffuse layer is taken into account, the alternating components of $C_i(0,t)$ are derived (Section 1).

With the help of the rate equation, the impedance characteristics are discussed. A comparison is made with those obtained by Matsuda (Section 2).

Equivalent circuits are derived for the cases of attraction (and repulsion) for the species i (Section 3).

ACKNOWLEDGMENT

The author wishes to thank Professor K. S. G. Doss, Director, Central Electrochemical Research Institute, Karaikudi, for his keen interest and valuable discussions.

REFERENCES

1. J. E. B. Randles. Discussions Faraday Soc. **1**, 11 (1947). B. V. Ershler. Discussions Faraday Soc. **1**, 269 (1947).
2. H. Matsuda. J. Phys. Chem. **64**, 339 (1960).
3. H. Matsuda and P. Delahay. J. Phys. Chem. **64**, 332 (1960).
4. S. K. Rangarajan. Can. J. Chem. This issue.
5. M. Senda and P. Delahay. J. Phys. Chem. **65**, 1580 (1961).

Can. J. Chem. Downloaded from www.nrcresearchpress.com by 210.87.254.42 on 09/05/12
For personal use only.

Can. J. Chem. Downloaded from www.nrcresearchpress.com by 210.87.254.5 on 09/05/12
For personal use only.

NOTES

THE NUCLEAR MAGNETIC RESONANCE SPECTRUM OF SULPHUR TETRAFLUORIDE

J. Bacon, R. J. Gillespie, and J. W. Quail

The F^{19} n.m.r. spectrum of SF_4 has previously been described by Cotton, George, and Waugh (1) and also by Muetterties and Phillips (2). Both of these groups found the F^{19} n.m.r. spectrum to consist of one very broad line at room temperature due to rapid exchange. Upon cooling the sample, these workers observed that this line broadened further and then split into two peaks. At $-100°$ C each of these peaks was further resolved into a triplet. This spectrum is entirely compatible with the known structure of the SF_4 molecule (3).

The symmetry of the SF_4 molecule is C_{2v}. The four fluorine atoms occupy four of the corners of a trigonal bipyramid around the sulphur, the fifth position being occupied by a lone pair of electrons. All of the F—S bonds are distorted away from the lone pair by lone pair – bond pair repulsions (4).

The resolution of the SF_4 spectrum into two triplets was observed at $-60°$, a higher temperature than that previously reported. At $-90°$ C all the peaks of both triplets were observed to split into doublets. The two halves of the spectrum are symmetrical about the center, and the low-field half of the spectrum is reproduced in Fig. 1. A complete

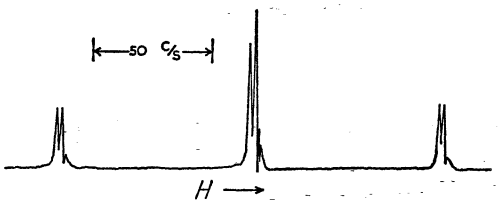

Fig. 1. Low-field half of fluorine resonance of SF_4 at $-101°$ C.

assignment of the spectrum can be achieved by treating SF_4 as an A_2B_2 system in which the two coupling constants between non-equivalent nuclei are equal.

The general theory of A_2B_2 spectra has been previously treated by Pople, Schneider, and Bernstein (5, 6). There are 24 possible transitions, of which 12 are A lines and 12 are B lines. The set of A lines is a mirror image of the set of B lines with respect to the central position, $1/2(\nu_A+\nu_B)$. Since the ratio $J/\nu_0\delta$ for SF_4 is very small, transitions giving rise to combination lines have extremely low probability and need not be considered. Because the two coupling constants between non-equivalent nuclei are equal, the spectrum is independent of the coupling constants between equivalent nuclei and depends only on the ratio $J/\nu_0\delta$. The frequency separation between transitions 1 and 3 of the n.m.r. spectrum is $2J$ and the separation between the 10,11 transition of the A spectrum and the corresponding transition of the B spectrum is $\nu_0\delta$. The values found for J and $\nu_0\delta$ at $-101°$ C are:

$$J = 76.3\pm0.3 \text{ c.p.s.}$$
$$\nu_0\delta \text{ (56.4 Mc)} = 2935\pm10 \text{ c.p.s.} = 52.1 \text{ p.p.m.}$$
$$J/\nu_0\delta = 0.0260$$

The expected spectrum of SF_4 was calculated using these values. The energies of the s_0 states have usually been obtained by perturbation methods. We obtained an explicit expression for the stationary-state energies of the s_0 levels by solving the appropriate secular determinant. It may be seen in Table I that there is good agreement between the observed and calculated spectra.

TABLE I

	Observed		Calculated	
Transition	Line position (c.p.s.)	Second-order splitting (c.p.s.)	Line position (c.p.s.)	Second-order splitting (c.p.s.)
1	−78.7±0.6	2.0±0.1	−78.3	1.9
2	−76.7±0.6		−76.4	
7	−2.0±0.1		−2.0	
6			−1.9	
10,11	0	2.0±0.1	0	1.9–2.0
3	74.2±0.6	1.9±0.1	74.3	1.9
4	76.1±0.6		76.2	

The F^{19} n.m.r. spectrum of SF_4 is an example of second-order splitting for an extremely small value of $J/\nu_0\delta$. The reason that a second-order effect is observed in this case is that the absolute values of both J and $\nu_0\delta$ are very large. The only other reported A_2B_2 spectra for which it is certain that the coupling constants between non-equivalent nuclei are equal due to the symmetry of the molecule are the SF_4 portion of the spectrum of $SF_4(SO_3F)_2$ (7) and the C^{13} satellite spectrum of allene (8). It has been suggested (9) that other n.m.r. spectra which have previously been explained as A_2B_2 with equal coupling constants between non-equivalent nuclei (β-propiolactone (10), ethyl monothiocarbonate (11), *trans*-dibromocyclopropane (12), and 2,3-dihydrofuran (12)) probably do not, in fact, have exactly equal coupling constants.

EXPERIMENTAL

The sulphur tetrafluoride used in this study was obtained from a commercial source and was contaminated with SOF_2, SCl_2, and CH_3CN. The latter two of these impurities and some of the SOF_2 were removed by fractional distillation in a vacuum line. Due to the similarity of the boiling points of SF_4 and SOF_2 it was not possible to obtain samples of SF_4 which were completely free from SOF_2. The oxyfluoride was usually present in a concentration of about 5%. Samples of SF_4 were distilled into 5 mm O.D. silica tubes, which were sealed under vacuum.

The fluorine n.m.r. spectra were obtained using a Varian high-resolution n.m.r. spectrometer and electromagnet at a frequency of 56.4 Mc and a field of 14,000 gauss. The spectra were calibrated using audio side bands generated with a D-890-A Muirhead Wigan Decade Oscillator. Peaks being measured were "bracketed" with modulation side bands from a reference peak (13). The chemical shift was measured by overlapping of the appropriate audio side bands from the A and B halves of the spectrum and recording the overlap pattern. Since the splitting between the multiplet peaks was known, $\nu_0\delta$ could be calculated.

ACKNOWLEDGMENTS

We are grateful to the Directorate of Chemical Sciences, United States Air Force Office of Scientific Research, and to the National Research Council for financial support. One of us (J. W. Q.) thanks the National Research Council for the award of a studentship.

Can. J. Chem. Downloaded from www.nrcresearchpress.com by 210.87.254.5 on 09/05/12
For personal use only.

1. F. A. COTTON, J. W. GEORGE, and J. S. WAUGH. J. Chem. Phys. **28**, 944 (1958).
2. E. L. MUETTERTIES and W. D. PHILLIPS. J. Am. Chem. Soc. **81**, 1084 (1959).
3. W. M. TOLLES and W. D. GWINN. J. Chem. Phys. **36**, 1119 (1962).
4. R. J. GILLESPIE. Can. J. Chem. **39**, 318 (1961); J. Chem. Phys. **37**, 2498 (1962).
5. J. A. POPLE, W. G. SCHNEIDER, and H. J. BERNSTEIN. Can. J. Chem. **35**, 1060 (1957).
6. J. A. POPLE, W. G. SCHNEIDER, and H. J. BERNSTEIN. High resolution nuclear magnetic resonance. McGraw-Hill. 1959.
7. J. M. SHREEVE and G. H. CADY. J. Am. Chem. Soc. **83**, 4521 (1961).
8. E. B. WHIPPLE, J. H. GOLDSTEIN, and W. E. STEWART. J. Am. Chem. Soc. **81**, 4761 (1959).
9. D. M. GRANT and H. S. GUTOWSKY. J. Chem. Phys. **34**, 699 (1961).
10. W. A. ANDERSON. Phys. Rev. **102**, 151 (1956).
11. P. L. CORIO. Chem. Rev. **60**, 396 (1960).
12. L. M. JACKMAN. Applications of nuclear magnetic resonance spectroscopy in organic chemistry. Pergamon Press. 1959. p. 84.
13. G. TIERS. J. Phys. Chem. **62**, 1151 (1958).

RECEIVED OCTOBER 23, 1962.
DEPARTMENT OF CHEMISTRY,
MCMASTER UNIVERSITY,
HAMILTON, ONTARIO.

Can. J. Chem. Downloaded from www.nrcresearchpress.com by 210.87.254.5 on 09/05/12
For personal use only.

AZOESTER–ANTHRACENE REACTIONS

C. W. HUFFMAN[1]

The known biological activity of various carbamates led us to prepare several hydrazo compounds which are a type of dicarbamate. However, none of the compounds recorded in this article were active as herbicides. An improvement in the preparation of stable ethyl azodicarboxylate and of varied labile azoester–anthracene adducts was achieved.

A recent review (1) of Diels–Alder syntheses states that the expected labile diene adduct from anthracene and ethyl azodicarboxylate cannot be isolated. This is incorrect. The labile isomer can be obtained and purified, if pure azoesters are used. The first report (2) on this reaction disclosed the preparation of labile compounds from anthracene and ethyl or methyl azodicarboxylate. These preparations have been confirmed and extended. A similar labile compound (I) was made from 2-chloroanthracene and ethyl azodicarboxylate. These labile compounds are converted to stable isomers (II) by acids. Others (3) had not been able to repeat the preparation of the labile compounds. Very likely, the azoester must be free of acid-forming by-products, to permit isolation of the labile adduct (I).

The ethyl azodicarboxylate, prepared as described, gave good yields of the labile adduct with anthracene after 21 months storage in a freezer. In his standard preparation of ethyl azodicarboxylate, Rabjohn (4) comments that chlorination by-products are formed if the reaction mixture containing ethyl hydrazodicarboxylate absorbs more than the theoretical amount of chlorine, thereby lowering the yields. His ethyl azoester yields were 81–83%. During this work it was found that appreciable quantities of unreacted ethyl hydrazodicarboxylate remained under Rabjohn's conditions. Consequently, an excess of chlorine was employed to obtain an improved azoester yield of 92%.

Alder and his co-workers (5) showed that the stable isomer from anthracene had a hydrazine structure. This means that monosubstituted anthracenes and azoesters should yield one labile ester (I), and could give two isomeric stable esters. It was surprising to find that 2-chloroanthracene gave a 74% yield of one sharply melting stable isomer (II*a* or II*b*), without prior purification of the labile ester (I). A chlorine substituent

[1]*Present address: International Minerals and Chemical Corporation, Skokie, Illinois, U.S.A.*

1. F. A. COTTON, J. W. GEORGE, and J. S. WAUGH. J. Chem. Phys. **28**, 944 (1958).
2. E. L. MUETTERTIES and W. D. PHILLIPS. J. Am. Chem. Soc. **81**, 1084 (1959).
3. W. M. TOLLES and W. D. GWINN. J. Chem. Phys. **36**, 1119 (1962).
4. R. J. GILLESPIE. Can. J. Chem. **39**, 318 (1961); J. Chem. Phys. **37**, 2498 (1962).
5. J. A. POPLE, W. G. SCHNEIDER, and H. J. BERNSTEIN. Can. J. Chem. **35**, 1060 (1957).
6. J. A. POPLE, W. G. SCHNEIDER, and H. J. BERNSTEIN. High resolution nuclear magnetic resonance. McGraw-Hill. 1959.
7. J. M. SHREEVE and G. H. CADY. J. Am. Chem. Soc. **83**, 4521 (1961).
8. E. B. WHIPPLE, J. H. GOLDSTEIN, and W. E. STEWART. J. Am. Chem. Soc. **81**, 4761 (1959).
9. D. M. GRANT and H. S. GUTOWSKY. J. Chem. Phys. **34**, 699 (1961).
10. W. A. ANDERSON. Phys. Rev. **102**, 151 (1956).
11. P. L. CORIO. Chem. Rev. **60**, 396 (1960).
12. L. M. JACKMAN. Applications of nuclear magnetic resonance spectroscopy in organic chemistry. Pergamon Press. 1959. p. 84.
13. G. TIERS. J. Phys. Chem. **62**, 1151 (1958).

RECEIVED OCTOBER 23, 1962.
DEPARTMENT OF CHEMISTRY,
MCMASTER UNIVERSITY,
HAMILTON, ONTARIO.

Can. J. Chem. Downloaded from www.nrcresearchpress.com by 210.87.254.5 on 09/05/12
For personal use only.

AZOESTER–ANTHRACENE REACTIONS

C. W. HUFFMAN[1]

The known biological activity of various carbamates led us to prepare several hydrazo compounds which are a type of dicarbamate. However, none of the compounds recorded in this article were active as herbicides. An improvement in the preparation of stable ethyl azodicarboxylate and of varied labile azoester–anthracene adducts was achieved.

A recent review (1) of Diels–Alder syntheses states that the expected labile diene adduct from anthracene and ethyl azodicarboxylate cannot be isolated. This is incorrect. The labile isomer can be obtained and purified, if pure azoesters are used. The first report (2) on this reaction disclosed the preparation of labile compounds from anthracene and ethyl or methyl azodicarboxylate. These preparations have been confirmed and extended. A similar labile compound (I) was made from 2-chloroanthracene and ethyl azodicarboxylate. These labile compounds are converted to stable isomers (II) by acids. Others (3) had not been able to repeat the preparation of the labile compounds. Very likely, the azoester must be free of acid-forming by-products, to permit isolation of the labile adduct (I).

The ethyl azodicarboxylate, prepared as described, gave good yields of the labile adduct with anthracene after 21 months storage in a freezer. In his standard preparation of ethyl azodicarboxylate, Rabjohn (4) comments that chlorination by-products are formed if the reaction mixture containing ethyl hydrazodicarboxylate absorbs more than the theoretical amount of chlorine, thereby lowering the yields. His ethyl azoester yields were 81–83%. During this work it was found that appreciable quantities of unreacted ethyl hydrazodicarboxylate remained under Rabjohn's conditions. Consequently, an excess of chlorine was employed to obtain an improved azoester yield of 92%.

Alder and his co-workers (5) showed that the stable isomer from anthracene had a hydrazine structure. This means that monosubstituted anthracenes and azoesters should yield one labile ester (I), and could give two isomeric stable esters. It was surprising to find that 2-chloroanthracene gave a 74% yield of one sharply melting stable isomer (II*a* or II*b*), without prior purification of the labile ester (I). A chlorine substituent

[1]*Present address: International Minerals and Chemical Corporation, Skokie, Illinois, U.S.A.*

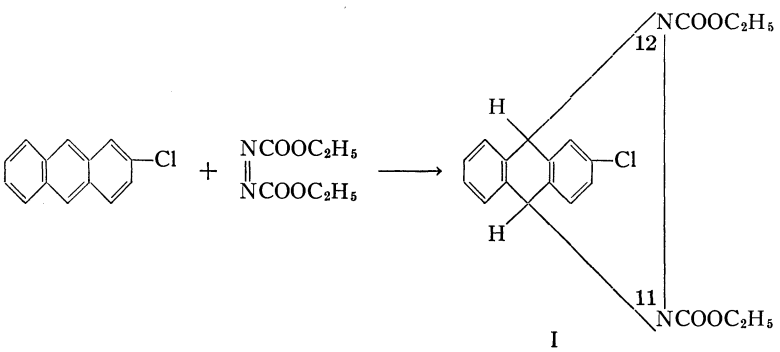

I
(labile)

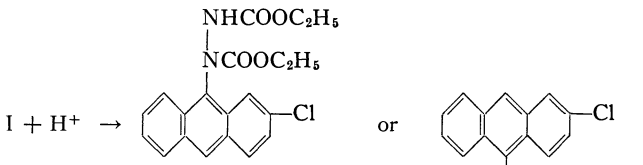

IIa
(stable)

IIb
(stable)

should stabilize intermediates which are formally related to parachlorophenyl compounds rather than the metachloro type. Furthermore, electron withdrawal by the chlorine should result in a slight increase in electrophilic attack by a proton on N-11 to give II*a* as the preferred isomer. Some II*b* should form too. Therefore, the effect of anthracene substituents (1, 2, or 9) on this ring-opening reaction warrants further study.

EXPERIMENTAL

Melting points were taken in a Hershberg-type apparatus. Initial determinations were made with ordinary 360° thermometers and the final uncorrected melting points with Anschutz thermometers.

Ethyl Azodicarboxylate

Slight modifications of the *Organic Syntheses* procedure of Rabjohn (4) gave a higher yield of stable product. Therefore, a detailed procedure is given. Ethyl hydrazodicarboxylate (4) (293 g), benzene (1470 ml), and water (1470 ml) were stirred in a 5-liter flask which was immersed in an ice bath (hood). Chlorine (cylinder on scale) was bubbled into the mixture through a plain glass tube,[2] when the reaction mixture temperature had reached 11°. A temperature of 6–7° was held constant while a total of 195 g of chlorine was added during a 1.5-hour period. The red-orange benzene layer was separated from the water layer. This water layer was extracted with 150 ml of benzene. The combined benzene solution was washed 10 times with 350-ml portions of 3% sodium carbonate before the water layer became alkaline (no doubt some of the preliminary washes could be combined). A final wash with 350 ml of 3% sodium carbonate was made, followed by two water washes with 350-ml portions of water. The final water wash was neutral. Sodium sulphate (200 g) was added to the benzene solution. The following day the sodium sulphate was removed by filtration and the benzene distilled from the solution under water-pump vacuum on the steam bath. The residue, in a 500-ml flask, was connected to a $1\frac{1}{4}\times 15$-in. column, packed half full with glass helices and wrapped with asbestos tape. An oil pump was used to maintain a pressure of 5 mm during a rapid distillation (shield). A small (4.5 g) forerun of orange-red oil was discarded. The main fraction of ethyl azodicarboxylate was orange-red, b.p. 110° at 5.0 mm, and weighed 266 g (92% yield). Most of the undistilled residue (25 g) crystallized.

[2]*Possibly an efficient gas dispersion tube would decrease the chlorine requirement. However, chlorine should be added until all the solid ethyl hydrazodicarboxylate dissolves, or the reaction mixture should be stirred until the solid dissolves (this did not take place in other experiments when the theoretical amount of chlorine was absorbed by the reaction mixture as determined by an increase in the weight of the reaction mixture).*

Can. J. Chem. Downloaded from www.nrcresearchpress.com by 210.87.254.5 on 09/05/12
For personal use only.

Redistillation of one sample of ethyl azodicarboxylate from a 200-ml flask heated by a Glascol mantle proceeded satisfactorily at 122° (24 mm pressure) until about 2 ml remained in the distillation flask. At this point, the residue in the flask *exploded violently*. Consequently, the distillation flask must not be overheated. If azoesters are to be redistilled, a small amount of a high-boiling stable solvent should be added to the distillation flask, prior to the distillation.

2-Chloro-9,10-endo-(N,N'-ethylhydrazocarboxylate)-9,10-dihydroanthracene (I)

Ethyl azodicarboxylate (32.2 g, 0.183 mole, a 14% excess), toluene (110 ml), and 2-chloroanthracene (6) (34.2 g, 0.161 mole, m.p. 223°) were refluxed overnight. The clear solution was treated with Nuchar C (1.5 g) and concentrated under vacuum on the steam bath to a dark red oil. Four precipitations of this material from isopropanol solutions, by water, gave 57.8 g (93%) of dried 2-chloro-9,10-*endo*-(N,N'-ethylhydrazodicarboxylate)-9,10-dihydroanthracene, which sintered at 84° and had m.p. 100–104°. An earlier preparation, using a 10% excess of ethyl azodicarboxylate, and a 7-hour reflux period, gave a 14% recovery of unreacted 2-chloroanthracene. This run was processed to give a 64% yield of product, m.p. 99–100°. Two recrystallizations from isopropanol–water gave light yellow crystals, which sintered at 75°, and had m.p. 99–102°. Anal. Calc. for $C_{20}H_{19}ClN_2O_4$: C, 62.1; H, 4.95; Cl, 9.17; N, 7.25. Found: C, 62.3; H, 5.03; Cl, 9.27; N, 7.17.

2-Chloro-9(or 10)-(N,N'-dicarboethoxy)hydrazinoanthracene (II)

Ethyl azodicarboxylate (10.44 g, 0.06 mole), toluene (50 ml), and 2-chloroanthracene (10.6 g, 0.05 mole) were refluxed 8 hours. The clear solution was placed in a freezer overnight. A filtration gave 0.4 g (4%) of yellow flakes of recovered 2-chloroanthracene, m.p. 213–221° with sintering at 135°. The filtrate was concentrated under vacuum to an orange-red oil (21.1 g), which was dissolved in warm acetic acid (65 ml). Concentrated hydrochloric acid (6 ml) was added to the yellow filtrate. In 15 minutes a solid mass had formed. The following day, the solid was removed by filtration and slurried with acetic acid to remove the yellow color. It was dried under vacuum at 88° to give 14.3 g (74%) of cream-colored 2-chloro-9(or 10)-(N,N'-dicarbethoxy)hydrazinoanthracene, m.p. 213–214.5°, with sintering at 208°. A small sample from an earlier preparation was recrystallized several times from benzene to give white crystals which sintered at 211°, and had m.p. 213–214°. Anal. Calc. for $C_{20}H_{19}ClN_2O_4$: C, 62.1; H, 4.95; Cl, 9.17; N, 7.25. Found: C, 62.2; H, 5.06; Cl, 9.21; N, 7.33.

Water (150 ml) was added to the acetic acid filtrate above to yield 1.5 g (7.7%) of a solid which sintered at 160° and had m.p. 180–186°. This solid may contain an isomer of the stable ester which melted at 214°.

ACKNOWLEDGMENTS

The author wishes to express his appreciation to Dr. R. C. Tallman for helpful suggestions and to Dr. S. E. Allen (Tennessee Valley Authorities Research Center, Muscle Shoals, Alabama) for conducting the herbicide tests. Analyses were performed by the Clark Microanalytical Laboratory of Urbana, Illinois.

1. S. B. Needleman and M. C. Chang Kuo. Chem. Rev. **62**, 413 (1962).
2. O. Diels, S. Schmidt, and W. Witte. Ber. **71**, 1187 (1938).
3. J. C. J. MacKenzie, A. Rodgman, and G. T. Wright. J. Org. Chem. **17**, 1666 (1952).
4. N. Rabjohn. Org. Syn. **28**, 59 (1948); also in Coll. Vol. III, 376 (1955).
5. K. Alder, H. Niklas, R. Aumüller, and B. Olsen. Ann. **585**, 81 (1954).
6. C. Liebermann and M. Beudet. Ber, **47**, 1011 (1914).

Received November 26, 1962.
Research Division,
Lion Oil Company, a Division of
Monsanto Chemical Company,
Creve Coeur, Missouri.

INFLUENCE OF A PULSED ELECTRIC FIELD ON LUMINESCENCE IN THE RARE GASES EXCITED BY IONIZING RADIATION

Aleksander Szymanski* and Jan A. Herman

Although luminescence in gases excited by ionizing radiation has been known for a long time (1), no satisfactory interpretation of this phenomenon has yet been found. One of the points of dispute has been the relative contribution of radiative ion–electron

**Present address: Department of Chemistry, Polytechnical Institute of Lodz, Lodz, Poland.*

Can. J. Chem. Downloaded from www.nrcresearchpress.com by 210.87.254.5 on 09/05/12
For personal use only.

Redistillation of one sample of ethyl azodicarboxylate from a 200-ml flask heated by a Glascol mantle proceeded satisfactorily at 122° (24 mm pressure) until about 2 ml remained in the distillation flask. At this point, the residue in the flask *exploded violently*. Consequently, the distillation flask must not be overheated. If azoesters are to be redistilled, a small amount of a high-boiling stable solvent should be added to the distillation flask, prior to the distillation.

2-Chloro-9,10-endo-(N,N'-ethylhydrazocarboxylate)-9,10-dihydroanthracene (I)

Ethyl azodicarboxylate (32.2 g, 0.183 mole, a 14% excess), toluene (110 ml), and 2-chloroanthracene (6) (34.2 g, 0.161 mole, m.p. 223°) were refluxed overnight. The clear solution was treated with Nuchar C (1.5 g) and concentrated under vacuum on the steam bath to a dark red oil. Four precipitations of this material from isopropanol solutions, by water, gave 57.8 g (93%) of dried 2-chloro-9,10-*endo*-(N,N'-ethylhydrazodicarboxylate)-9,10-dihydroanthracene, which sintered at 84° and had m.p. 100–104°. An earlier preparation, using a 10% excess of ethyl azodicarboxylate, and a 7-hour reflux period, gave a 14% recovery of unreacted 2-chloroanthracene. This run was processed to give a 64% yield of product, m.p. 99–100°. Two recrystallizations from isopropanol–water gave light yellow crystals, which sintered at 75°, and had m.p. 99–102°. Anal. Calc. for $C_{20}H_{19}ClN_2O_4$: C, 62.1; H, 4.95; Cl, 9.17; N, 7.25. Found: C, 62.3; H, 5.03; Cl, 9.27; N, 7.17.

2-Chloro-9(or 10)-(N,N'-dicarboethoxy)hydrazinoanthracene (II)

Ethyl azodicarboxylate (10.44 g, 0.06 mole), toluene (50 ml), and 2-chloroanthracene (10.6 g, 0.05 mole) were refluxed 8 hours. The clear solution was placed in a freezer overnight. A filtration gave 0.4 g (4%) of yellow flakes of recovered 2-chloroanthracene, m.p. 213–221° with sintering at 135°. The filtrate was concentrated under vacuum to an orange-red oil (21.1 g), which was dissolved in warm acetic acid (65 ml). Concentrated hydrochloric acid (6 ml) was added to the yellow filtrate. In 15 minutes a solid mass had formed. The following day, the solid was removed by filtration and slurried with acetic acid to remove the yellow color. It was dried under vacuum at 88° to give 14.3 g (74%) of cream-colored 2-chloro-9(or 10)-(N,N'-dicarbethoxy)hydrazinoanthracene, m.p. 213–214.5°, with sintering at 208°. A small sample from an earlier preparation was recrystallized several times from benzene to give white crystals which sintered at 211°, and had m.p. 213–214°. Anal. Calc. for $C_{20}H_{19}ClN_2O_4$: C, 62.1; H, 4.95; Cl, 9.17; N, 7.25. Found: C, 62.2; H, 5.06; Cl, 9.21; N, 7.33.

Water (150 ml) was added to the acetic acid filtrate above to yield 1.5 g (7.7%) of a solid which sintered at 160° and had m.p. 180–186°. This solid may contain an isomer of the stable ester which melted at 214°.

ACKNOWLEDGMENTS

The author wishes to express his appreciation to Dr. R. C. Tallman for helpful suggestions and to Dr. S. E. Allen (Tennessee Valley Authorities Research Center, Muscle Shoals, Alabama) for conducting the herbicide tests. Analyses were performed by the Clark Microanalytical Laboratory of Urbana, Illinois.

1. S. B. Needleman and M. C. Chang Kuo. Chem. Rev. **62**, 413 (1962).
2. O. Diels, S. Schmidt, and W. Witte. Ber. **71**, 1187 (1938).
3. J. C. J. MacKenzie, A. Rodgman, and G. T. Wright. J. Org. Chem. **17**, 1666 (1952).
4. N. Rabjohn. Org. Syn. **28**, 59 (1948); also in Coll. Vol. III, 376 (1955).
5. K. Alder, H. Niklas, R. Aumüller, and B. Olsen. Ann. **585**, 81 (1954).
6. C. Liebermann and M. Beudet. Ber, **47**, 1011 (1914).

Received November 26, 1962.
Research Division,
Lion Oil Company, a Division of
Monsanto Chemical Company,
Creve Coeur, Missouri.

INFLUENCE OF A PULSED ELECTRIC FIELD ON LUMINESCENCE IN THE RARE GASES EXCITED BY IONIZING RADIATION

Aleksander Szymanski* and Jan A. Herman

Although luminescence in gases excited by ionizing radiation has been known for a long time (1), no satisfactory interpretation of this phenomenon has yet been found. One of the points of dispute has been the relative contribution of radiative ion–electron

*Present address: Department of Chemistry, Polytechnical Institute of Lodz, Lodz, Poland.

Can. J. Chem. Downloaded from www.nrcresearchpress.com by 210.87.254.40 on 09/05/12
For personal use only.

recombination to the luminescence. Contrary to what was formerly believed (2), recent work (3) indicates that such recombination does play a role in the luminescence. In this note we present some preliminary results bearing on this point.

In contrast to previous work we have measured the variation in intensity of light emission at the beginning and end of a pulsed electric field. Since the luminescence intensity in general is proportional to the number of individual processes occurring in each of the possible radiative deactivation processes undergone by atoms, molecules, or ions, it will be also proportional in the special case of dissociative recombination. To calculate this recombination as a function of time, one must know the concentration of ions and electrons at the moment of application and removal of the electric field. The following reasoning applies only to an atomic gas which does not undergo electron attachment.

The kinetic equations (neglecting diffusion) are as follows:

$$\begin{aligned} dN/dt &= q-\alpha_1 n_1 N-\alpha_2 n_2 N+\mu^- NE \\ dn_1/dt &= q-\alpha_1 n_1 N-\beta n_1-\mu_1{}^+ n_1 E \\ dn_2/dt &= \beta n_1-\alpha_2 n_2 N-\mu_2{}^+ n_2 E, \end{aligned} \qquad [1]$$

where q is the number of ions formed per cc per sec, N is the electron concentration per cc, n_1 the concentration of atomic ions, n_2 the concentration of molecular ions, α_1 the coefficient for atomic ion–electron recombination, α_2 the coefficient for dissociative recombination, μ^- the electron mobility, $\mu_1{}^+$ the atomic ion mobility, $\mu_2{}^+$ molecular ion mobility, β the rate of conversion of atomic ions into molecular ions, and E the electric field intensity in v/cm.

Adopting the following assumptions: (*a*) that E is sufficiently weak to neglect the terms $\mu^- NE$, $\mu_1{}^+ n_1 E$, and $\mu_2{}^+ n_2 E$ and (*b*) that the atomic ion–electron recombination can be neglected, α_1 being very small (4) (i.e. $\alpha_1 n_1 N \ll \alpha_2 n_2 N$, also $\alpha_1 n_1 < \beta$), then the solution of the equations [1] reduces to:

$$n_1 = q/\beta, \qquad [2]$$

$$n_2 = n_{2\,\mathrm{st}} \frac{c\sqrt{\Delta_{\mathrm{st}}}\exp(\alpha_{\mathrm{st}} t\sqrt{\Delta_{\mathrm{st}}})}{1-c\exp(\alpha_{\mathrm{st}}\sqrt{\Delta_{\mathrm{st}}})} \qquad [3]$$

$$N = n_2+q/\beta, \qquad [4]$$

where $n_{2\,\mathrm{st}}$, c ($c = (n_{2\,\mathrm{in}}-n_{2\,\mathrm{st}})/(n_{2\,\mathrm{in}}-n_{2\,\mathrm{st}}+\sqrt{\Delta_{\mathrm{st}}})$), and Δ_{st}, ($\Delta_{\mathrm{st}} = (q^2/\beta^2)-(4q/\alpha_{2\,\mathrm{st}})$) are constants and $n_{2\,\mathrm{in}}$ and $n_{2\,\mathrm{st}}$ are respectively the initial and stationary concentrations of molecular ions. Equation [3] applies both for the beginning and the end of the pulse, as it describes the transition between two states of equilibrium; these states are associated with field off and field on.

By definition the number of recombinations, $I(t)$, is given by $I(t) = \alpha n(t)N(t)$. The coefficient of dissociative recombination in general decreases with increasing electron energy (5); it will therefore decrease under an applied electric field. On the other hand, independent of this effect, the number of dissociative recombinations of molecular ions, $I(t) = \alpha_2 n_2(t)N(t)$, in a weak field may be shown to be the same as that in zero field, from which: $I_o = \alpha_{2p} n_{2p} N_p = \alpha_{2o} n_{2o} N_o$, the subscripts "o" and "p" indicating respectively values in the absence and presence of a field. Since $\alpha_{2o} > \alpha_{2p}$, then $N_o < N_p$ and $n_{2o} < n_{2p}$; in other words, there is an interdependence between a change in the recombination coefficient and a change in ion and electron density. As a result the number

Can. J. Chem. Downloaded from www.nrcresearchpress.com by 210.87.254.40 on 09/05/12
For personal use only.

of dissociative recombinations at the beginning of the field pulse will be given by: $I(t_1) = \alpha_{2p} n_{2o} N_o < I_o$, and at the end of the field pulse by: $I(t_2) = \alpha_{2o} n_{2p} N_p > I_o$. The change in recombination at the start of the field pulse is therefore:

$$\Delta I_s = I(t_1) - I_o = (\alpha_{2p} - \alpha_{2o}) n_{2o} N_o \quad [5]$$

and at the end of the field pulse:

$$\Delta I_e = I(t_2) - I_o = (\alpha_{2o} - \alpha_{2p}) n_{2p} N_p. \quad [6]$$

Since $n_{2p} N_p > n_{2o} N_o$, then $\Delta I_e > \Delta I_s$. The change in light emission will be proportional to ΔI_s and ΔI_e at the beginning and the end of the field pulse respectively. Figure 1 expresses graphically the results given by equations [5] and [6].

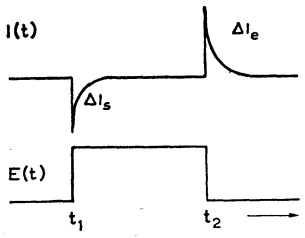

FIG. 1. Theoretical light pulse emission I, at the beginning and the end of an applied field pulse $E(t)$.

The abrupt increase or decrease in recombination rate at the beginning and end of the field pulse will be followed by a return to equilibrium rate with a decay constant given by equation [3]; however, it should be noted that the exponential in this equation is $\alpha_p qt(1+4\beta^2/q\alpha_p)^{1/2}$ at the start of the field pulse and $\alpha_o qt(1+4\beta^2/q\alpha_o)^{1/2}$ at the end of the field pulse. In addition ΔI_e depends on N_p and n_{2p}; therefore, it should diminish as the amplitude of field pulse increases.

The rare gases helium, neon, argon, krypton, xenon, and also nitrogen were studied. All, with the exception of helium and nitrogen, were spectroscopically pure. They were excited by a beam of X rays produced by a tube operated at 45 kv. The intensity was variable. The electric field was produced by a square wave generator with a rise and fall time of 8 μsec and 0.4 μsec respectively, an amplitude from 100 to 750 v/cm, pulse length of 50–500 μsec, and repetition rate of 250 to 1500 per sec. The light emitted was measured by a photomultiplier (E.M.I., type 9526-B). The output was observed on a Tetronix 545-A oscilloscope. The cell (6) contained aluminum electrodes and had a quartz window transparent to 2000 Å. Gas pressures used were from 70 to 300 mm.

In the case of helium, neon, and argon, no variation in light intensity characteristic of recombination was observed, other than that already described in the literature (2, 3, 6), and due to increased excitation by electrons accelerated by the pulsed field. Figure 2(*a*) shows the light pulse in argon; similar curves result in helium and neon. In nitrogen there is no change in luminescence that is in any way extraordinary.

However, the heavy rare gases behave differently, at the beginning of the field pulse a very weak decrease in luminescence occurs, which is almost completely masked by the increase produced by the increased excitation caused by accelerated electrons. On the other hand, at the end of the field pulse there is a large increase in luminescence (Fig. 2 (*b* and *c*)). These light pulses (peaks) can be identified without doubt with the impulses ΔI_s and ΔI_e described above. Another argument in favor of this theory is that

Can. J. Chem. Downloaded from www.nrcresearchpress.com by 210.87.254.40 on 09/05/12
For personal use only.

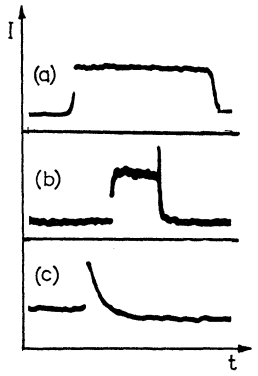

FIG. 2. (*a*) Light emission in argon; P = 224 mm Hg, E = 500 v/cm, field pulse time 0.6 msec. (*b*) Light emission in xenon: P = 664 mm Hg, E = 500 v/cm, field pulse time 0.4 msec. (*c*) Expanded trace showing peak at end of light pulse in xenon; P = 317 mm Hg, E = 400 v/cm, sweep time 20 μsec/cm.

the light pulse occurring at the end of the field pulse increases with increasing X-ray intensity, and decreases with increase in amplitude of the field pulse. Anderson (7) has observed a similar effect in the afterglow from microwave discharges in gases and assigned it to the same cause.

Similar experiments have been made using Po^{210} α-particles as the ionizing radiation; however, the large background of emission produced by ionizing radiation made it impossible to observe any changes.

The experiments described above show that in the case of krypton and xenon dissociative recombination plays an active role in the mechanism of luminescence. In the case of lighter gases either this process is less probable, or the light emitted is in a spectral region in which the photomultiplier is insensitive. In argon also, the expected phenomena were not observed, perhaps again because of experimental limitations.

The observed phenomena should permit: (*a*) measurement of recombination coefficients from the decay in the light pulse after the end of the field pulse, (*b*) relative measurements of molecular ion concentration at high pressures.

The authors would like to thank J. W. McGowan and D. G. H. Marsden for their interest in this work; and also Professor L. Kerwin, Head of the Physics Department, for the loan of equipment used in this work.

1. M. CURIE. Radioactivité. Paris. 1935.
2. J. STARK. Z. Physik, **7**, 892 (1906). H. GREINACHER. Z. Physik, **47**, 344 (1928). K. MICHAILOV'A. Sitz. Akad. Wiss. Wien, **143**, IIa (1934). A. WARD. Proc. Phys. Soc. (London), Sect. A, **67**, 841 (1954). L. KOCH. Thèse, Paris. 1959.
3. A. TAVENDALE. Proc. Phys. Soc. (London), **79**, 652 (1961).
4. H. MASSEY and E. BURHOP. Electronic and ionic impact phenomena. Oxford. 1952.
5. D. R. BATES. Phys. Rev. **78**, 492 (1950). C. CHEN, C. LEIBY, and L. GOLDSTEIN. Phys. Rev. **121**, 1391 (1961).
6. A. SZYMANSKI and J. A. HERMAN. J. Chim. Phys. In press.
7. L. GOLDSTEIN, J. N. ANDERSON, and C. L. CLARK. Phys. Rev. **90**, 486 (1953). J. N. ANDERSON. Phys. Rev. **108**, 898 (1957); Proceedings of the Fifth Conference on Ionizing Phenomena in Gases, Munich. 1961.

RECEIVED DECEMBER 3, 1962.
DEPARTMENT OF CHEMISTRY,
LAVAL UNIVERSITY,
QUEBEC, QUE.

Can. J. Chem. Downloaded from www.nrcresearchpress.com by 210.87.254.40 on 09/05/12
For personal use only.

THE HYDRATES OF FLUORAL[1]

D. E. McGreer, R. Stewart, and M. M. Mocek

Fluoral has been prepared by a number of procedures (1–5) and in each report some mention is given to the formation of a hydrate from the reaction of fluoral with water. The hydrate is reported to be a solid which sublimes at 50° (1) and has a melting point of 68–70° (3, 5) but it has never been fully characterized. Fluoral hydrate is also sold commercially (Columbia Organic Chemicals Co.) as a liquid.

In connection with our studies on the permanganate oxidation of fluoral hydrate (6) we have now characterized this compound more fully and find that its analysis and physical properties more closely fit those of a hemihydrate.

Reduction of trifluoroacetic acid by the procedure of Braid, Iserson, and Lawlor (5) gave the gas fluoral, which when reacted with less than the stoichiometric amount of water yielded a white moist solid hydrate (I). This solid gave non-reproducible melting points; however, when it was dried over phosphorus pentoxide a constant melting point of 93–94° (sealed tube) was obtained. Samples could be solidified and remelted with no change in the melting point.

The elemental analysis of I (C, 22.51; H, 1.92) does not fit well for fluoral hydrate II (C, 20.68; H, 2.59) but fits better for the hemihydrate III (C, 22.40; H, 1.88). Molecular

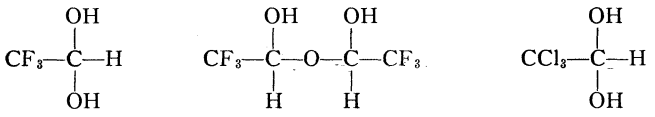

weight determinations (m.p. depression of camphor) gave a value of 223, which also favored structure III (mol. wt. 214) over structure II (mol. wt. 116).

The proton n.m.r. spectrum of I in acetone (Fig. 1A) shows two signals, at 3.44 τ

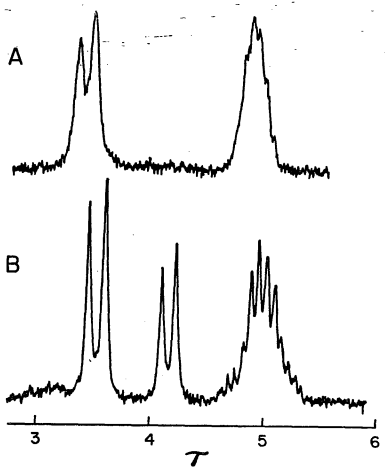

FIG. 1. A, I in acetone; B, I in acetone after standing several days in an open tube.

[1]*Taken from the thesis of M. M. Mocek submitted to the Graduate School of the University of British Columbia in partial fulfillment of the requirements for the degree of Doctor of Philosophy.*

Can. J. Chem. Downloaded from www.nrcresearchpress.com by 210.87.254.42 on 09/05/12
For personal use only.

and 4.90 τ, with relative areas of 1:1.07. The lower-field peak, which is a doublet, J = 8.5 c.p.s., is clearly due to an OH as it is markedly shifted to higher field on the addition of water. Both structures II and III would predict a doublet for the OH but III predicts an area ratio of 1:1 whereas II predicts an area ratio of 2:1 for OH and CH. The CH peak is a complex multiplet due to coupling of the CH with the OH (J = 8.5 c.p.s.) and with the CF (J = 4.3 c.p.s.).

The proton n.m.r. spectrum of chloral hydrate (IV) (Fig. 2) in acetone, on the other hand, is quite as expected for the monohydrate. There are two peaks at 3.98 τ and

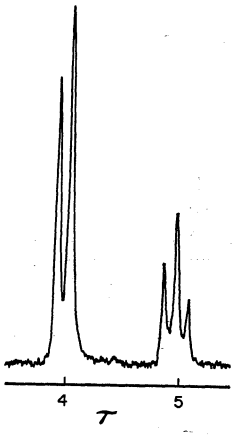

FIG. 2. Chloral hydrate in acetone.

4.96 τ with relative areas of 1.9:1. The low-field peak, which is a doublet (J = 6.7 c.p.s.) and is broadened and moves to higher field on the addition of water, is assigned to the OH. The high-field peak, which is a triplet (J = 6.6 c.p.s.), is assigned to the CH.

The fluorine n.m.r. spectrum for each of the possible structures for I would be expected to be a doublet. It is interesting therefore that the fluorine spectrum in acetone shows a number of doublets (Fig. 3). This would indicate that an acetone solution may in fact contain a number of species. This is also indicated by the fact that an acetone solution of I (Fig. 1B) which had been standing for a number of days was found to have a new but smaller doublet in the proton spectrum at 4.17 τ attributable to the OH of a second species. The development of this peak over a period of time may be due to the fact that the new species is formed slowly in the solution due to absorption of water or that on standing a reduction in the rate of exchange of the OH hydrogens (7) permits measurement of more than one species.

Addition of water in small amounts to an acetone solution of I (Fig. 3) changes the fluorine spectrum by reducing the relative area of the low-field signals with respect to the high-field signal until with excess water (mole ratio of water to I = 10:1) (Fig. 3D) the high-field peak becomes the major peak.

It is apparent from the n.m.r. evidence that in acetone there is present an equilibrium between the various hydrated fluorals. Whether this equilibrium is present in the solid I has not been determined. The major species in acetone would appear to be the hemihydrate III since the proton ratio is 1:1 and the major fluorine doublet is the second doublet from the high-field end. The high-field doublet is undoubtedly due to the hydrate II since it becomes the sole species on dilution with water. Shifts in the n.m.r. due to

Can. J. Chem. Downloaded from www.nrcresearchpress.com by 210.87.254.42 on 09/05/12
For personal use only.

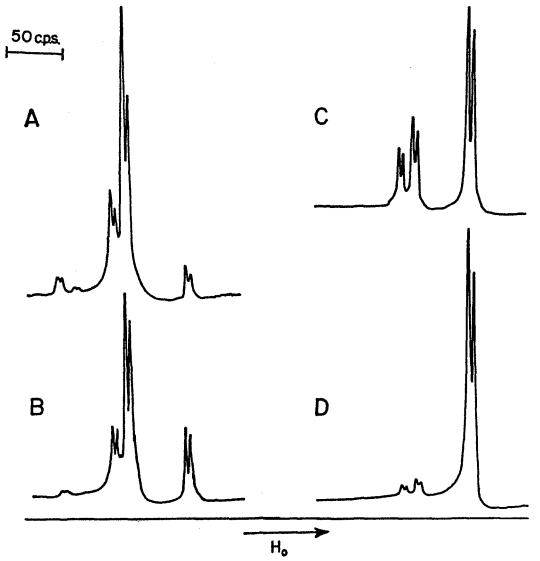

FIG. 3. A, fluorine resonance of I in acetone; addition of water gives mole ratio of water to I for B = 2:1, C = 3:1, and D = 10:1.

structural changes from condensation would be expected to be progressive; thus the first condensation product, III, would be expected to be the species leading to the second doublet. Other species which might exist in solution are the lower hydrates like V and the trioxane structure VI.

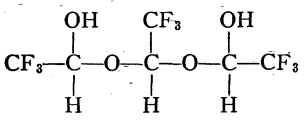

V

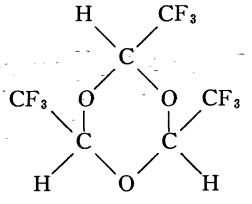

VI

EXPERIMENTAL

The proton n.m.r. spectra were obtained at 60 Mc on a Varian Associates A-60 instrument. The fluorine n.m.r. spectra were obtained at 40 Mc on a Varian Associates V4300 instrument. Reagent acetone dried over anhydrous magnesium sulphate was used as the n.m.r. solvent. The microanalyses were determined by A. Bernhardt, Mulheim, West Germany.

Fluoral Hemihydrate

Trifluoroacetic acid was reduced with the stoichiometric amount of lithium aluminum hydride by the procedure of Braid, Iserson, and Lawlor (5). The crude aldehydrol was dehydrated in a mixture of concentrated sulphuric acid and phosphorus pentoxide (5), and the fluoral which distilled was condensed at −78°. To this condensate at −78° was added less than the stoichiometric amount of water. The resulting white solid was dried over phosphorus pentoxide and gave in 43% yield a product, I, with a melting point of 93–94° (sealed tube). Calc. for $C_4H_4O_3F_6$ (III): C, 22.40; H, 1.88; mol. wt., 214 and for $C_2H_3O_2F_3$ (II): C, 20.68; H. 2.59; mol. wt., 116. Found: C, 22.51; H, 1.92; mol. wt., 223. On standing in a desiccator over phosphorus pentoxide a sample of I loses weight presumably due to slow dissociation to water and fluoral.

Can. J. Chem. Downloaded from www.nrcresearchpress.com by 210.87.254.42 on 09/05/12
For personal use only.

ACKNOWLEDGMENTS

This work has been generously supported by the National Research Council of Canada, to whom we are indeed grateful. Thanks are extended to Mrs. E. G. Brion for determining many of the n.m.r. spectra and to Mrs. A. Aldridge for determining the molecular weight.

1. A. L. HENNE, R. L. PELLEY, and R. M. ALM. J. Am. Chem. Soc. **72**, 3370 (1950).
2. H. SCHECTER and F. CONRAD. J. Am. Chem. Soc. **72**, 3371 (1950).
3. D. R. HUSTED and A. H. ALBRECHT. J. Am. Chem. Soc. **74**, 5422 (1952).
4. O. R. PIERCE and T. J. KANE. J. Am. Chem. Soc. **76**, 300 (1954).
5. M. BRAID, H. ISERSON, and F. E. LAWLOR. J. Am. Chem. Soc. **76**, 4027 (1954).
6. R. STEWART and M. M. MOCEK. To be published.
7. J. A. POPLE, W. G. SCHNIEDER, and H. J. BERNSTEIN. High-resolution nuclear magnetic resonance. McGraw-Hill Book Co., Inc., New York. 1959. p. 417.

RECEIVED NOVEMBER 26, 1962.
DEPARTMENT OF CHEMISTRY,
UNIVERSITY OF BRITISH COLUMBIA,
VANCOUVER, BRITISH COLUMBIA.

Can. J. Chem. Downloaded from www.nrcresearchpress.com by 210.87.254.42 on 09/05/12
For personal use only.

ORGANIC PEROXIDES
VI. REACTION OF PHENOLS AND SECONDARY AROMATIC AMINES WITH *p*-NITROBENZOYL AND *p,p'*-DINITROBENZOYL PEROXIDES

J. T. EDWARD AND S. A. SAMAD[1]

Benzoyl peroxide (I; Ar = Ph) reacts with secondary aromatic amines (II) to give substituted *o*-benzamidophenols (III; Ar = Ph) (1, 2), and with phenols (IV) to give *o*-benzoyloxyphenols (V or VI; Ar = Ph) (3). Yields in these reactions are at best only fair, and the availability of *p,p'*-dinitrobenzoyl peroxide (I; Ar = $C_6H_4 \cdot NO_2$-*p*), prepared

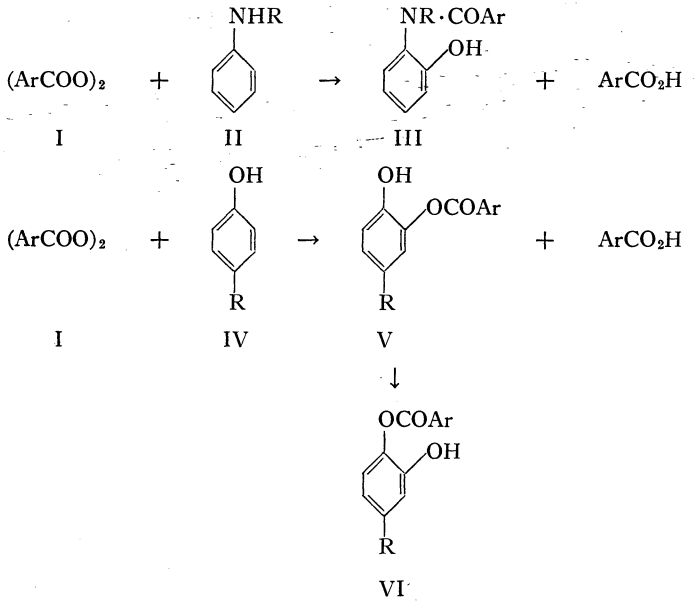

[1]*Holder of Colombo Plan Fellowship, 1957–1960.*

ACKNOWLEDGMENTS

This work has been generously supported by the National Research Council of Canada, to whom we are indeed grateful. Thanks are extended to Mrs. E. G. Brion for determining many of the n.m.r. spectra and to Mrs. A. Aldridge for determining the molecular weight.

1. A. L. HENNE, R. L. PELLEY, and R. M. ALM. J. Am. Chem. Soc. **72**, 3370 (1950).
2. H. SCHECTER and F. CONRAD. J. Am. Chem. Soc. **72**, 3371 (1950).
3. D. R. HUSTED and A. H. ALBRECHT. J. Am. Chem. Soc. **74**, 5422 (1952).
4. O. R. PIERCE and T. J. KANE. J. Am. Chem. Soc. **76**, 300 (1954).
5. M. BRAID, H. ISERSON, and F. E. LAWLOR. J. Am. Chem. Soc. **76**, 4027 (1954).
6. R. STEWART and M. M. MOCEK. To be published.
7. J. A. POPLE, W. G. SCHNIEDER, and H. J. BERNSTEIN. High-resolution nuclear magnetic resonance. McGraw-Hill Book Co., Inc., New York. 1959. p. 417.

RECEIVED NOVEMBER 26, 1962.
DEPARTMENT OF CHEMISTRY,
UNIVERSITY OF BRITISH COLUMBIA,
VANCOUVER, BRITISH COLUMBIA.

Can. J. Chem. Downloaded from www.nrcresearchpress.com by 210.87.254.40 on 09/05/12
For personal use only.

ORGANIC PEROXIDES
VI. REACTION OF PHENOLS AND SECONDARY AROMATIC AMINES WITH *p*-NITROBENZOYL AND *p,p'*-DINITROBENZOYL PEROXIDES

J. T. EDWARD AND S. A. SAMAD[1]

Benzoyl peroxide (I; Ar = Ph) reacts with secondary aromatic amines (II) to give substituted *o*-benzamidophenols (III; Ar = Ph) (1, 2), and with phenols (IV) to give *o*-benzoyloxyphenols (V or VI; Ar = Ph) (3). Yields in these reactions are at best only fair, and the availability of *p,p'*-dinitrobenzoyl peroxide (I; Ar = $C_6H_4 \cdot NO_2$-*p*), prepared

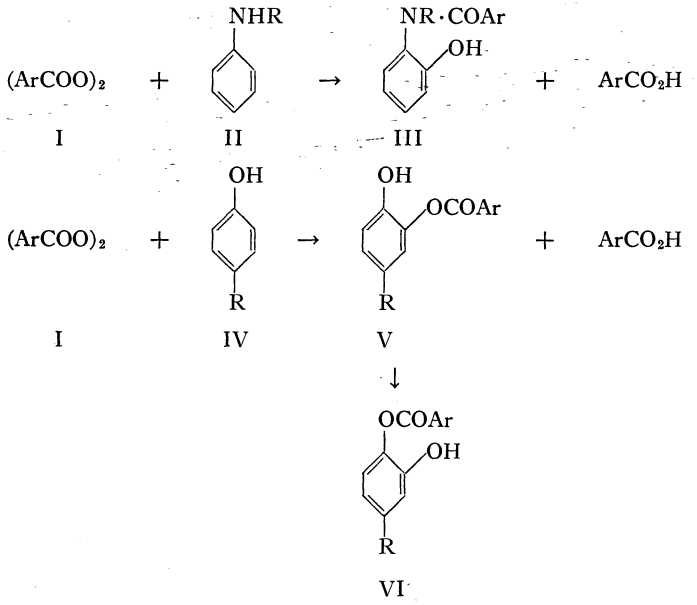

[1]*Holder of Colombo Plan Fellowship, 1957–1960.*

for another investigation (4), prompted us to study its reactions with a few amines and phenols. These are listed in Table I, in which are also shown the yields of phenolic products. These yields are about the same as those obtained earlier with benzoyl peroxide,

TABLE I

Yields from reactions of amines or phenols with *p,p'*-dinitrobenzoyl peroxide

	Phenolic product		*p*-Nitrobenzoic acid
Amine or phenol	Formula*	Yield (%)	Yield (%)
N-Methylaniline	III; R = Me	38	55
N-Ethylaniline	III; R = Et	45	59
N-Butylaniline	III; R = Bu	42	65
Diphenylamine	III; R = Ph	52	55
Phenol	—	—	90
p-Methoxyphenol	—	—	91
p-Cresol	VI; R = Me	44	61
p-Bromophenol	V; R = Br	16	80
α-Naphthol	VIII	40	62
β-Naphthol	VIII	80	59

*In all cases Ar = $C_6H_4 \cdot NO_2$-*p*.

but with *α*- and *β*-naphthol crystalline phenolic products could be obtained by oxidation with *p,p'*-dinitrobenzoyl peroxide but not with benzoyl peroxide.

The structures of the phenols obtained from the substituted anilines are without doubt represented by III (Ar = $C_6H_4 \cdot NO_2$-*p*), since they show no basic properties. The oxidation product of *p*-cresol (IV; R = Me) slowly gave a green color on treatment with *p*-aminodimethylaniline and sodium hypochlorite. This color reaction is considered diagnostic of a free para position in a phenol (3), so that the oxidation product probably has the structure VI (R = Me, Ar = $C_6H_4 \cdot NO_2$-*p*), similar to that found for the product from *p*-cresol and benzoyl peroxide (3); in each case the compound V (R = Me, Ar = Ph or $C_6H_4 \cdot NO_2$-*p*) is probably formed first, but rearranges by acyl migration. On the other hand, the phenol from the reaction of *p*-bromophenol (IV; R = Br) appears from the color reaction to have no free para position, and so is probably represented by V (R = Br; Ar = $C_6H_4 \cdot NO_2$-*p*). Both *α*- and *β*-naphthol reacted with *p,p'*-dinitrobenzoyl peroxide to give the same product, which accordingly must be VII or VIII. The latter was shown

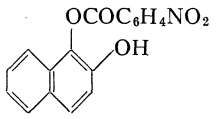

VII

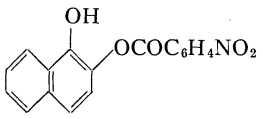

VIII

to be correct, since methylation of the product with diazomethane followed by alkaline hydrolysis gave 1-methoxy-2-naphthol. Evidently the compound (VII) first formed by reaction of *β*-naphthol rearranges to VIII.

The mechanisms of the reactions of benzoyl peroxide with amines (5) and phenols (6) have been investigated recently and shown to involve nucleophilic attack of the amino or hydroxyl group on a peroxide oxygen with displacement of a benzoate ion. With the unsymmetrical peroxide, *p*-nitrobenzoyl peroxide (X), this attack may take place on the oxygen (*α*) adjacent to the benzoyl group, with expulsion of a *p*-nitrobenzoate ion (route *a*) or on the oxygen (*β*) adjacent to the *p*-nitrobenzoyl group, with expulsion of a benzoate ion (route *b*). Dibenzylamine (IX; R = CH_2Ph) attacks by route *a* in boiling

Can. J. Chem. Downloaded from www.nrcresearchpress.com by 210.87.254.40 on 09/05/12
For personal use only.

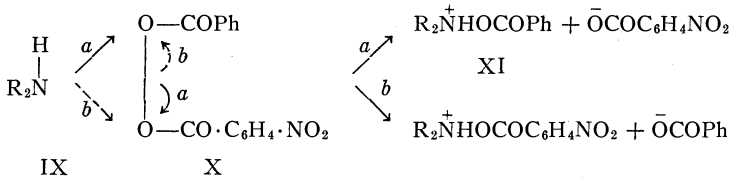

chloroform (7). Diphenylamine (IX; R = Ph) might accordingly be expected to react by this route to give *o*-(*N*-phenylbenzamido)phenol (III; R = Ar = Ph) (via the intermediate XI (R = Ph) (5)) and *p*-nitrobenzoic acid. In fact, evidence could be obtained only for its reaction by route *b*. A mixture of phenolic products was obtained, from which only the nitro derivative (III; R = Ph, Ar = $C_5H_4 \cdot NO_2$-*p*) could be obtained crystalline (17% yield). Infrared and combustion analysis indicated that the uncrystallizable phenolic fraction remaining was *not* a simple mixture of the two phenols (III; R = Ph; Ar = Ph and $C_6H_4 \cdot NO_2$-*p*).

The reaction of phenols with the unsymmetrical peroxide (X) also follows a complex course. *p*-Cresol gave a mixture of benzoic and *p*-nitrobenzoic acids, and a gummy phenolic fraction from which the *p*-nitrobenzoyloxy derivative (VI; R = Me, Ar = $C_6H_4 \cdot NO_2$-*p*) could be crystallized in 13% yield, but from which the benzoyloxy derivative (VI; R = Me, Ar = Ph) was absent, since nothing could be distilled from the phenolic fraction at temperatures up to 270° at 0.1 mm pressure (cf. ref. 3). β-Naphthol also gave a complex phenolic mixture, from which only the *p*-nitrobenzoyloxy derivative (VIII) could be obtained crystalline.

It is evident that, like tributylphosphine (8) and unlike dibenzylamine (7), phenols and secondary aromatic amines attack the β oxygen of *p*-nitrobenzoyl peroxide (X), although yields are low because of competing reactions giving complex phenolic products.

EXPERIMENTAL

Reactions of Secondary Aromatic Amines with p,p'-Dinitrobenzoyl Peroxide

The peroxide (0.01 mole) was added gradually to a stirred solution of the amine (0.01 mole) in benzene (50 ml) at 20–25°. After standing overnight, the solution was worked up in the usual way (2) for acid and phenol fractions (cf. Table I). *N*-Methylaniline gave *o*-(*N*-methyl-*p'*-nitrobenzamido)phenol (III; R = Me, Ar = $C_6H_4 \cdot NO_2$-*p*), colorless needles from ethanol, m.p. 197–198°. Calc. for $C_{14}H_{12}O_4N_2$: C, 61.76; H, 4.41; N, 10.29%. Found: C, 61.92; H, 4.26; N, 10.14%. *N*-Butylaniline gave *o*-(*N*-butyl-*p'*-nitrobenzamido)-phenol (III; R = Bu, Ar = $C_6H_4 \cdot NO_2$-*p*), colorless plates from benzene, m.p. 167°. Calc. for $C_{17}H_{18}O_4N_2$: C, 64.97; H, 5.73; N, 8.91%. Found: C, 64.86; H, 5.55; N, 8.69%. Diphenylamine gave *o*-(*N*-phenyl-*p'*-nitrobenzamido)phenol (III; R = Ph, Ar = $C_6H_4 \cdot NO_2$-*p*), yellow plates from ethanol, m.p. 240°. Calc. for $C_{19}H_{14}O_4N_2$: C, 68.26; H, 4.19; N, 8.38%. Found: C, 68.08; H, 4.16; N, 8.56%.

N-Ethylaniline gave *o*-(*N*-ethyl-*p'*-nitrobenzamido)phenol (III; R = Et, Ar = $C_6H_4 \cdot NO_2$-*p*), colorless plates from 50% aqueous ethanol, m.p. 152°. Calc. for $C_{15}H_{14}O_4N_2$: C, 62.93; H, 4.89; N, 9.78%. Found: C, 62.83; H, 4.93; N, 9.63%. This phenol crystallized from other solvents with a certain amount of firmly held solvent, probably entrapped by clathrate formation, which is known to be particularly easy for phenolic compounds (9). Thus it crystallized from benzene in plates which, after being dried at 80° at 3 mm for 24 hours, melted at 90–92°, solidified, and remelted at 118°. Calc. for $C_{15}H_{14}O_4N_2 + 1/6\ C_6H_6$: C, 64.21; H, 5.01%. Found: C, 63.82; H, 4.97%. The phenol crystallized from toluene in prisms, m.p. 120°. Calc. for $C_{15}H_{14}O_4N_2 + 1/12\ C_7H_8$: C, 63.68; H, 4.99; N, 9.53%. Found: C, 63.26; H, 5.18; N, 9.60%. It crystallized from bromobenzene in prisms, m.p. 130°. Calc. for $C_{15}H_{14}O_4N_2 + 1/3\ C_6H_5Br$: C, 60.29; H, 4.63; N, 8.28%. Found: C, 60.18; H, 4.93; N, 8.18%.

Reaction of Diphenylamine with p-Nitrobenzoyl Peroxide

Diphenylamine (3.32 g) in benzene (70 ml) was treated as above with *p*-nitrobenzoyl peroxide (5.74 g). The acid fraction (3.1 g) was composed of benzoic and *p*-nitrobenzoic acids, as shown by its melting point of 193–200°. It was dissolved in alkali, filtered, and reprecipitated with mineral acid. The dried precipitate was analyzed for nitrogen, and contained 5.31%, corresponding to 37% benzoic + 63% *p*-nitrobenzoic acid.

Removal of the acid fraction from the benzene solution left a precipitate of phenolic material (0.75 g), m.p. 206–208° (decomp.). Found: C, 65.72; H, 4.41; N, 6.80%. A further 0.8 g, m.p. 202–206° (decomp.),

Can. J. Chem. Downloaded from www.nrcresearchpress.com by 210.87.254.40 on 09/05/12
For personal use only.

was removed from the benzene solution from aqueous alkali. Crystallization from acetic acid yielded *o*-(*N*-phenyl-*p*′-nitrobenzamido)phenol (III; R = Ph, Ar = $C_6H_4 \cdot NO_2$-*p*) (1.05 g, 17%), m.p. and mixed m.p. 239°. No other pure compound could be obtained from the phenolic fraction.

Reaction with Phenols with p,p′-Dinitrobenzoyl Peroxide

Solutions of the phenol (0.01 mole) and peroxide (0.01 mole) in chloroform (50 ml) were refluxed for 4–6 hours. Carboxylic acids were removed by extraction with aqueous sodium bicarbonate, and the chloroform solution dried over sodium sulphate and evaporated. The residue was dissolved in the minimum quantity of hot benzene. The solution on cooling deposited crystals of phenolic compound. In this way, *p*-cresol gave pale yellow plates of 4-*p*-nitrobenzoyloxy-*m*-cresol (VI; R = Me, Ar = $C_6H_4 \cdot NO_2$-*p*), m.p. 164°. Calc. for $C_{14}H_{11}O_5N$: C, 61.54; H, 4.03; N, 5.13%. Found: C, 61.73; H, 4.12; N, 5.20%. *p*-Bromophenol gave colorless needles of 2-*p*-nitrobenzoyloxy-4-bromophenol (V; R = Br, Ar = $C_6H_4 \cdot NO_2$-*p*), m.p. 187–188°. Calc. for $C_{13}H_8O_5NBr$: C, 46.15; H, 2.36; N, 4.14%. Found: C, 46.19; H, 2.30; N, 4.15%. α-Naphthol and β-naphthol gave yellow needles of 2-*p*-nitrobenzoyloxy-1-naphthol (VIII), m.p. 182°. Calc. for $C_{17}H_{11}O_5N$: C, 66.02; H, 3.56; N, 4.53%. Found: C, 66.14; H, 3.57; N, 4.59%.

1-Methoxy-2-p-nitrobenzoyloxynaphthalene

A solution of diazomethane in dry ether was added to a solution of 2-*p*-nitrobenzoyloxy-1-naphthol (3.11 g) in ether until a yellow color persisted. After 20 minures, excess diazomethane was destroyed with dilute hydrochloric acid. The ether solution was washed with dilute aqueous potassium hydroxide and then water, dried, and concentrated. The residue crystallized from ethanol in yellow needles, m.p. 140°, of 1-methoxy-2-*p*-nitrobenzoyloxynaphthalene (1.65 g; 51%). Calc. for $C_{18}H_{12}O_5N$: OMe, 9.59%. Found: OMe, 9.49%.

1-Methoxy-2-naphthol

A solution of 1-methoxy-2-*p*-nitrobenzoyloxynaphthalene (1 g) and potassium hydroxide (5 g) in methanol–water (9:1 v/v; 100 ml) was refluxed for 3 hours. After removal of most of the methanol by distillation, the solution was acidified. The precipitate was removed by filtration and washed with aqueous sodium bicarbonate. The residue (0.32 g) crystallized from ligroin as colorless plates of 1-methoxy-2-naphthol, m.p. 90° (reported m.p. 90.5° (10); 2-methoxy-1-naphthol has been prepared recently, and has m.p. 53.5–54.5 (11)). Calc. for $C_{11}H_{10}O_2$: C, 75.86; H, 5.75%. Found: C, 75.51; H, 5.52%. The benzoate, prepared in the usual way with benzoyl chloride in pyridine, crystallized from methanol as colorless rods, m.p. 107°. Calc. for $C_{18}H_{14}O_3$: C, 77.40; H, 5.04%. Found: C, 77.59; H, 5.17%.

Reaction of p-Cresol with p-Nitrobenzoyl Peroxide

The reaction of the peroxide (2.87 g) with *p*-cresol (1.08 g) in chloroform (50 ml) gave a mixture of benzoic and *p*-nitrobenzoic acids (1.72 g), m.p. 198–210°. This melting point corresponds to that of a mixture of 75% of *p*-nitrobenzoic acid and 25% benzoic acid. The phenolic fraction afforded 4-*p*-nitrobenzoyloxy-*m*-cresol (0.35 g; 13%), m.p. and mixed m.p. 164°, and an uncrystallizable gum (1.63 g). This was separated by chromatography on alumina into several fractions showing strong infrared bands at 3350 cm^{-1} (bonded OH) and 1745 cm^{-1} (ester CO), but none of these could be induced to crystallize.

Reaction of β-Naphthol with p-Nitrobenzoyl Peroxide

Reaction of the peroxide (5.74 g) with β-naphthol (2.88 g) in chloroform (90 ml) gave an acidic mixture (2.78 g) indicated by its melting point (188–199°) to be made up of about 65% of *p*-nitrobenzoic and 35% of benzoic acid. The phenolic fraction gave 2-*p*-nitrobenzoyloxy-1-naphthol (0.678; 11%), m.p. and mixed m.p. 182°, and a gum (3.95 g) which by chromatography on alumina gave several gummy fractions.

ACKNOWLEDGMENT

Grateful acknowledgment is made to the National Research Council for financial support.

1. S. GAMBARJAN. Ber. **42**, 4003 (1909).
2. J. T. EDWARD. J. Chem. Soc. 1464 (1954).
3. S. L. COSGROVE and W. A. WATERS. J. Chem. Soc. 3189 (1949).
4. J. T. EDWARD, H. S. CHANG, and S. A. SAMAD. Can. J. Chem. **40**, 804 (1962).
5. D. B. DENNEY and D. Z. DENNEY. J. Am. Chem. Soc. **82**, 1389 (1960).
6. C. WALLING and R. B. HOGDON. J. Am. Chem. Soc. **80**, 228 (1958).
7. L. HORNER and W. KIRMSE. Ann. **597**, 66 (1955).
8. D. B. DENNEY and M. A. GREENBAUM. J. Am. Chem. Soc. **79**, 979 (1957).
9. H. M. POWELL. J. Chem. Soc. 61 (1948).
10. F. BEDZIK. Monatsh. **30**, 271 (1909).
11. J. T. EDWARD and H. S. CHANG. To be published.

RECEIVED DECEMBER 5, 1962.
DEPARTMENT OF CHEMISTRY,
MCGILL UNIVERSITY,
MONTREAL, QUE.

Can. J. Chem. Downloaded from www.nrcresearchpress.com by 210.87.254.40 on 09/05/12
For personal use only.

ALUMINUM ALKOXIDE INDUCED REARRANGEMENT DURING THE OPPENAUER OXIDATION OF CYCLOPROPYLCARBINOL

C. C. Lee and I. S. Bhardwaj*

In connection with a study in this laboratory on the radiolysis of aqueous solutions of cyclopropylcarbinol, it was necessary to synthesize cyclopropanecarboxaldehyde. This was accomplished by the lithium aluminum hydride reduction of cyclopropyl cyanide as described by Smith and Rogier (1). A possible alternative method is the Oppenauer oxidation of cyclopropylcarbinol. Smith and Rogier (1) reported that application of this oxidation, with benzil as hydrogen acceptor, failed to yield any aldehyde. However, a further investigation of the Oppenauer oxidation was undertaken as we were informed by Dr. R. H. Mazur (2) that among the unpublished results in his studies on small-ring compounds (3, 4) is the preparation of cyclopropanecarboxaldehyde from oxidation of cyclopropylcarbinol in the presence of cinnamaldehyde and a catalytic amount of aluminum isopropoxide.

About equimolar quantities of cyclopropylcarbinol and cinnamaldehyde and a catalytic amount of aluminum isopropoxide or aluminum *t*-butoxide were heated under reflux for 2 or 24 hours. The resulting mixture was distilled and the distillate analyzed by vapor phase chromatography. The results, as summarized in Table I, show the presence of some cyclopropanecarboxaldehyde as well as the formation of the rearranged alcohol, cyclobutanol. The yield of aldehyde was of the order of 20% regardless of whether the reaction mixture was refluxed for 2 or 24 hours. This is not surprising since the Oppenauer oxidation is reversible (5, 6) and no attempt was made to force the equilibrium in the forward direction by continual product removal during the reaction.

It has been well established that carbonium-ion-type reactions with cyclopropylcarbinyl derivatives will lead to mixtures of cyclopropylcarbinyl, cyclobutyl, and allylcarbinyl products (3, 7, 8). The cyclobutanol observed in the product of the Oppenauer oxidation of cyclopropylcarbinol very likely also resulted from some reaction involving intermediate carbonium ions. The metallic part of the aluminum alkoxide catalyst may act as a Lewis acid, cause formation of electron-deficient centers, and induce rearrangements typical of carbonium ions. To test this possibility, cyclopropylcarbinol was refluxed for 24 hours with either aluminum isopropoxide or aluminum *t*-butoxide under the same conditions as were used in the Oppenauer oxidation, but without any cinnamaldehyde. Vapor phase chromatographic analyses of the distillates obtained in these trials indeed showed the formation of cyclobutanol, and in amounts sufficient to account for all the cyclobutanol observed in the products of the Oppenauer oxidation (Table I). Thus, during the Oppenauer oxidation of cyclopropylcarbinol to cyclopropanecarboxaldehyde, an aluminum alkoxide induced rearrangement to cyclobutanol occurs as a side reaction. This rearrangement may be depicted by equation [1]. The intermediate cation or ion pair may be more complex in nature and probably may be better represented

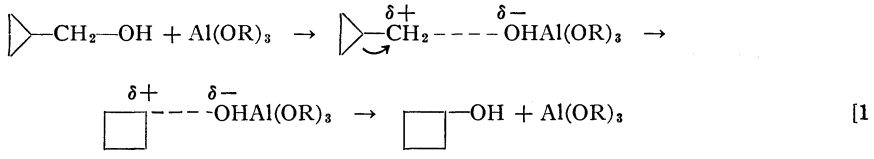

[1

Holder of a National Research Council of Canada Studentship, 1962–1963.

Can. J. Chem. Downloaded from www.nrcresearchpress.com by 210.87.254.105 on 09/05/12
For personal use only.

Can. J. Chem. Downloaded from www.nrcresearchpress.com by 210.87.254.105 on 09/05/12
For personal use only.

TABLE I

Analyses of distillates from Oppenauer oxidation and from aluminum alkoxide treatment

Reactions	Catalyst	Reaction time (hr)	Percentage composition					
			Cyclopropylcarbinol		Cyclobutanol		Cyclopropanecarboxaldehyde	
			Run 1	Run 2	Run 1	Run 2	Run 1	Run 2
Oxidation	$(i\text{-PrO})_3Al$	2	71.3		8.4		20.3	
		24	65.1	69.0	9.8	10.2	25.1	20.8
Oxidation	$(t\text{-BuO})_3Al$	2	69.0	74.0	5.0	5.5	26.0	17.5
		24	67.9	71.0	11.7	9.0	20.4	20.0
Treatment with catalyst	$(i\text{-PrO})_3Al$	24	87.7	84.5	12.3	15.5		
Treatment with catalyst	$(t\text{-BuO})_3Al$	24	83.8	83.7	16.2	16.3		

by nonclassical structures (7, 8). However, in the absence of further data, such as isotope position rearrangements as reported by Roberts and co-workers (7, 8), a simple 1,2-shift as shown in equation [1] is adequate to account for the formation of cyclobutanol.

EXPERIMENTAL

Standard Compounds for V.P.C. Calibration

Cyclopropylcarbinol was prepared by the lithium aluminum hydride reduction of cyclopropanecarboxylic acid (1, 7). Cyclobutanol was obtained from the treatment of an aqueous solution of cyclopropylcarbinol with concentrated hydrochloric acid (8). The product obtained consisted of about 93% cyclobutanol and 7% cyclopropylcarbinol. Cyclopropanecarboxaldehyde was prepared by the lithium aluminum hydride reduction of cyclopropyl cyanide (1). The product, boiling at 97–101° C as described by Smith and Rogier (1), consisted of about 90% aldehyde and 10% unreacted cyclopropyl cyanide according to v.p.c. analysis.

Oppenauer Oxidation

A mixture of 2.0 g (0.028 mole) of cyclopropylcarbinol, 3.5 g (0.027 mole) of cinnamaldehyde, and 0.2 g of aluminum isopropoxide or aluminum *t*-butoxide was refluxed for 2 or 24 hours and then distilled through a helix-packed column. The fraction collected boiled between 90–122° C. The recoveries were of the order of 1.2 g. These distillates were analyzed with a Beckman GC-2A gas chromograph using a column filled with type A packing (diisodecyl phthalate on Chromosorb) supplied by the Perkin–Elmer Corp.

Treatment of Cyclopropylcarbinol with Aluminum Alkoxide

A mixture of 2.0 g of cyclopropylcarbinol and 0.2 g of aluminum isopropoxide or aluminum *t*-butoxide was refluxed for 24 hours and then distilled through a helix-packed column. The materials distilling below 122° C were collected and analyzed by v.p.c. as described above.

ACKNOWLEDGMENT

The financial aid given by the National Research Council of Canada is gratefully acknowledged.

1. L. I. Smith and E. R. Rogier. J. Am. Chem. Soc. **73**, 4047 (1951).
2. R. H. Mazur. Private communications.
3. J. D. Roberts and R. H. Mazur. J. Am. Chem. Soc. **73**, 2509 (1951).
4. E. Renk, P. R. Shafer, W. H. Graham, R. H. Mazur, and J. D. Roberts. J. Am. Chem. Soc. **83**, 1987 (1961).
5. C. Djerassi. Organic reactions. R. Adams (*Editor-in-chief*). Vol. VI. John Wiley and Sons Inc., New York. 1951. pp. 207–272.
6. W. A. Waters. Organic chemistry. H. Gilman (*Editor-in-chief*). Vol. IV. John Wiley and Sons, Inc., New York. 1953. pp. 1238–1245.
7. R. H. Mazur, W. N. White, D. A. Semenow, C. C. Lee, M. S. Silver, and J. D. Roberts. J. Am. Chem. Soc. **81**, 4390 (1959).
8. M. C. Caserio, W. H. Graham, and J. D. Roberts. Tetrahedron, **11**, 171 (1960).

Received December 10, 1962.
Department of Chemistry,
University of Saskatchewan,
Saskatoon, Saskatchewan.

Can. J. Chem. Downloaded from www.nrcresearchpress.com by 210.87.254.105 on 09/05/12
For personal use only.

SOME 4-OXYGENATED CYCLOHEPTANONES

Peter Yates[1] and Charles D. Anderson[2]

Recent interest (1, 2) in the preparation and properties of certain 4-hydroxycycloheptanones and the corresponding cyclohexanones prompts us to record the results (3) of a related study carried out in connection with another investigation (4).

[1]*Present address: Department of Chemistry, University of Toronto, Toronto, Ontario.*
[2]*N.S.F. Fellow, 1952–1953; present address: Pacific Lutheran University, Tacoma, Washington.*

by nonclassical structures (7, 8). However, in the absence of further data, such as isotope position rearrangements as reported by Roberts and co-workers (7, 8), a simple 1,2-shift as shown in equation [1] is adequate to account for the formation of cyclobutanol.

EXPERIMENTAL

Standard Compounds for V.P.C. Calibration

Cyclopropylcarbinol was prepared by the lithium aluminum hydride reduction of cyclopropanecarboxylic acid (1, 7). Cyclobutanol was obtained from the treatment of an aqueous solution of cyclopropylcarbinol with concentrated hydrochloric acid (8). The product obtained consisted of about 93% cyclobutanol and 7% cyclopropylcarbinol. Cyclopropanecarboxaldehyde was prepared by the lithium aluminum hydride reduction of cyclopropyl cyanide (1). The product, boiling at 97–101° C as described by Smith and Rogier (1), consisted of about 90% aldehyde and 10% unreacted cyclopropyl cyanide according to v.p.c. analysis.

Oppenauer Oxidation

A mixture of 2.0 g (0.028 mole) of cyclopropylcarbinol, 3.5 g (0.027 mole) of cinnamaldehyde, and 0.2 g of aluminum isopropoxide or aluminum *t*-butoxide was refluxed for 2 or 24 hours and then distilled through a helix-packed column. The fraction collected boiled between 90–122° C. The recoveries were of the order of 1.2 g. These distillates were analyzed with a Beckman GC-2A gas chromograph using a column filled with type A packing (diisodecyl phthalate on Chromosorb) supplied by the Perkin–Elmer Corp.

Treatment of Cyclopropylcarbinol with Aluminum Alkoxide

A mixture of 2.0 g of cyclopropylcarbinol and 0.2 g of aluminum isopropoxide or aluminum *t*-butoxide was refluxed for 24 hours and then distilled through a helix-packed column. The materials distilling below 122° C were collected and analyzed by v.p.c. as described above.

ACKNOWLEDGMENT

The financial aid given by the National Research Council of Canada is gratefully acknowledged.

1. L. I. Smith and E. R. Rogier. J. Am. Chem. Soc. **73**, 4047 (1951).
2. R. H. Mazur. Private communications.
3. J. D. Roberts and R. H. Mazur. J. Am. Chem. Soc. **73**, 2509 (1951).
4. E. Renk, P. R. Shafer, W. H. Graham, R. H. Mazur, and J. D. Roberts. J. Am. Chem. Soc. **83**, 1987 (1961).
5. C. Djerassi. Organic reactions. R. Adams (*Editor-in-chief*). Vol. VI. John Wiley and Sons Inc., New York. 1951. pp. 207–272.
6. W. A. Waters. Organic chemistry. H. Gilman (*Editor-in-chief*). Vol. IV. John Wiley and Sons, Inc., New York. 1953. pp. 1238–1245.
7. R. H. Mazur, W. N. White, D. A. Semenow, C. C. Lee, M. S. Silver, and J. D. Roberts. J. Am. Chem. Soc. **81**, 4390 (1959).
8. M. C. Caserio, W. H. Graham, and J. D. Roberts. Tetrahedron, **11**, 171 (1960).

Received December 10, 1962.
Department of Chemistry,
University of Saskatchewan,
Saskatoon, Saskatchewan.

Can. J. Chem. Downloaded from www.nrcresearchpress.com by 210.87.254.6 on 09/05/12
For personal use only.

SOME 4-OXYGENATED CYCLOHEPTANONES

Peter Yates[1] and Charles D. Anderson[2]

Recent interest (1, 2) in the preparation and properties of certain 4-hydroxycycloheptanones and the corresponding cyclohexanones prompts us to record the results (3) of a related study carried out in connection with another investigation (4).

[1]*Present address: Department of Chemistry, University of Toronto, Toronto, Ontario.*
[2]*N.S.F. Fellow, 1952–1953; present address: Pacific Lutheran University, Tacoma, Washington.*

Can. J. Chem. Downloaded from www.nrcresearchpress.com by 210.87.254.6 on 09/05/12
For personal use only.

4-Benzoyloxycyclohexanone (I) (5, 6) was converted to 4-benzoyloxycycloheptanone (II) by treatment with diazomethane, generated *in situ* by addition of *N*-nitrosomethylurethane to a solution of I in methanol or ethanol containing a catalytic amount of potassium carbonate (7). The ketone II was isolated as its semicarbazone. Best results (49% yield of purified semicarbazone) were obtained when absolute ethanol was the solvent and the molar ratio of *N*-nitrosomethylurethane to I was 1.17. The substitution of methanol for ethanol resulted in a similar yield of crude product of reduced purity. Use of an increased proportion of the urethane (1.50 mole/mole of I) reduced the yield of II appreciably. The reaction proceeded at a considerably slower rate in ethanol than in methanol; a similar observation has been made by Gutsche and Peter (8) in the case of the reaction of *trans*-1-decalone with diazomethane. Purification of the semicarbazone by recrystallization was found to be greatly facilitated by prior continuous extraction with petroleum ether, which removed adhering oily by-products. The ketone II was regenerated from its semicarbazone either by treatment of the latter with sodium nitrite in acetic acid (9) or by continuous ether extraction of a solution of the semicarbazone in 8 *N* hydrochloric acid. The second process led to the better yield of II: 81% from the purified semicarbazone, i.e. 40% based on I. The genesis, infrared spectrum (*vide infra*), and reactions of this product secure the assigned structure. 4-Methoxycycloheptanone (IV) was similarly prepared from 4-methoxycyclohexanone (III) in 25% overall yield; this cycloheptanone has previously been prepared in impure form by Adamson and Kenner (10).

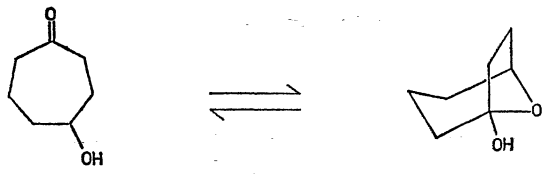

Va Vb

Hydrolysis of 4-benzoyloxycycloheptanone (II) with aqueous base gave 4-hydroxycycloheptanone (V). Doering and Sayigh (1) prepared this compound in high yield by the ring expansion of 4-hydroxycyclohexanone[3] and concluded on the basis of its infrared spectrum that it exists mainly as the bicyclic tautomer V*b*. We have reached the same conclusion in regard to solutions of V in carbon disulphide, since their infrared spectra show strikingly low-intensity carbonyl absorption (5.88 μ, apparent extinction coefficient less than that of the C—H stretching band). In chloroform solution, however, the carbonyl stretching band (5.90 μ) is very much more intense and it is considered that in this, more polar, solvent the hydroxy ketone tautomer V*a* is predominant. The spectra of V in either solvent possess a band at 9.82–9.83 μ, absent in the spectrum of II; the location of this band is very close to that of the C—O stretching band[4] of cycloheptanol (9.75 μ, liquid film) (12). The corresponding bands in the spectra of other saturated alicyclic secondary alcohols having three- to eight-membered rings are reported to occur at lower wavelengths (8.3–9.63 μ, liquid films) (12).

[3]*The fact that this compound gives a considerably better yield of ring-expanded product than do I and III under similar conditions lends support to the suggestion (1) that intramolecular catalysis by the hydroxyl group is involved in the former reaction.*

[4]*The vibrational assignment for this band is controversial (cf. ref. 11).*

The ethylene ketal of II, 4-ethylenedioxycycloheptyl benzoate (VI), was prepared in the usual manner (13) and was converted without purification to 4-ethylenedioxycycloheptanol (VII) by hydrolysis in aqueous methanolic base. The infrared spectrum of this compound has, in addition to O—H stretching bands at 2.82 and 2.93 μ, a band at 9.85 μ, presumably analogous to that discussed above in the case of the spectrum of V. Oxidation of VII with chromium trioxide – pyridine gave 4-ethylenedioxycycloheptanone (VIII).[5] This was characterized by conversion to the bis-2,4-dinitrophenylhydrazone of 1,4-cycloheptanedione (15). The infrared spectrum of VIII is noteworthy for the presence of bands at 2.94 and 9.87 μ, which resemble bands in the spectrum of VII associated with the presence of the hydroxyl group in that compound. The band at 2.94 μ, however, is not accompanied by a non-associated O—H stretching band at lower wavelength as is the case in the spectra of most alcohols and, in particular, of VII. Further, passage of a benzene solution of VIII over a column of activated alumina failed to change its infrared spectrum, demonstrating the absence of any hydroxylic component. It must be concluded that the band at 2.94 μ is an overtone of the carbonyl-stretching band at 5.88 μ; Stolow (2) has recently shown that bands at 2.92 μ in the spectra of 4-hydroxycyclohexanone and 4-hydroxy-4-phenylcyclohexanone have a similar origin.

Studies of the effect of ring size on the location of the carbonyl-stretching bands of cycloalkanones have indicated that these bands are shifted to slightly longer wavelengths when the ring size is increased from six to seven (16). The spectra of the four cycloheptanones prepared here (see Table I) are in accord with this conclusion.

TABLE I

Carbonyl-stretching bands of cycloheptanones and corresponding cyclohexanones

	Medium	Carbonyl band (μ)
Cycloheptanone	CCl_4	5.88*
Cyclohexanone	Liquid film	5.87†
	Liquid film	5.83†
4-Benzoyloxycycloheptanone (II)	CCl_4	5.84‡
4-Benzoyloxycyclohexanone (I)	CCl_4	5.80§
4-Methoxycycloheptanone (IV)	CCl_4	5.86
4-Methoxycyclohexanone (III)	CCl_4	5.82
4-Hydroxycycloheptanone (V*a*)	$CHCl_3$	5.90
	CS_2	5.88
4-Hydroxycyclohexanone	C_2Cl_4	5.80‖
	Unspecified	5.85¶
4-Ethylenedioxycycloheptanone (VIII)	$CHCl_3$	5.88
4-Ethylenedioxycyclohexanone	Unspecified	5.84**

*E. J. Corey. J. Am. Chem. Soc. **75**, 2301 (1953).
†Reference 16(*a*).
‡Shoulder on benzoate carbonyl band.
§Superimposed on benzoate carbonyl band.
‖Reference 2.
¶Reference 1.
**Reference 14.

EXPERIMENTAL[6]

Mixed cis- and trans-1,4-Cyclohexanediol Monobenzoate

The method used was that of Owen and Robins (5) as modified by Jones and Sondheimer (6). With commercial reagent chloroform as diluent instead of the specified ethanol-free chloroform a 49% yield (based on the diol) of mixed *cis*- and *trans*-1,4-cyclohexanediol monobenzoate, b.p. 162.5–166.5° at 3 mm,

[5]*Compound VIII has been prepared by an alternative route (14).*

[6]*The melting and boiling points are uncorrected. Pressure values <0.1 mm are nominal. The drying agent was magnesium sulphate, unless otherwise stated. The infrared spectra were calibrated against atmospheric water vapor or polystyrene.*

Can. J. Chem. Downloaded from www.nrcresearchpress.com by 210.87.254.6 on 09/05/12
For personal use only.

was obtained (reported yield 59%, b.p. 175–178° at 0.2 mm (6)). When 40% ethanol-free chloroform in dichloromethane was substituted for ethanol-free chloroform as the diluent for the pyridine and dichloromethane for ethanol-free chloroform as the diluent for the benzoyl chloride a 57% yield of distilled *cis*- and *trans*-monobenzoate was obtained.

The above procedures gave a 25–30% crude yield of the by-products, *cis*- and *trans*-1,4-cyclohexanediol dibenzoate. These remained as a distillation residue and were partially saponified to yield more monobenzoate mixture. Dibenzoate mixture (60.5 g, 0.187 mole; once recrystallized from ethanol) was dissolved in 350 ml of 95% ethanol and 50 ml of water. To this mixture at reflux was added dropwise a solution of 7.5 g (0.19 mole) of sodium hydroxide in 50 ml of water. Fifteen hours after the beginning of the sodium hydroxide addition, most of the alcohol was distilled from the refluxing mixture. Extraction of the residual liquid with chloroform afforded 19.3 g (47%) of additional *cis*- and *trans*-monobenzoate, b.p. 173–175° at 4–5 mm.

4-Benzoyloxycyclohexanone (I)

The mixture of *cis*- and *trans*-1,4-cyclohexanediol monobenzoate was oxidized with chromium trioxide in aqueous acetic acid (6) to give 73–80% of recrystallized I, m.p. 63–64.5° (lit. (17) m.p. 63–64°); infrared bands (CCl_4): 5.80, 7.89, and 9.01 μ; *semicarbazone*: white leaflets, m.p. 190–191° (lit. (5) m.p. 195–196°).

4-Benzoyloxycycloheptanone Semicarbazone

A suspension of anhydrous potassium carbonate (1.20 g, 0.0088 mole) in a solution of 4-benzoyloxycyclohexanone (I) (40.0 g, 0.184 mole) in 700 ml of absolute ethanol was cooled in an ice–salt bath. A solution of *N*-nitrosomethylurethane (18) (28.6 g, 0.216 mole) in 660 ml of absolute ethanol was added with mechanical stirring at such a rate that the temperature of the reaction mixture was maintained at −9 to −3°. The addition required 11 hours. After warming slowly to room temperature over an additional 17.5 hours, the mixture (still containing enough free diazomethane to be slightly yellow) was filtered and glacial acetic acid (1.0 ml) was added to the filtrate. The volume of the colorless solution was reduced to about 60 ml by distilling the ethanol at 60 mm, and the concentrate was added to a filtered solution of semicarbazide hydrochloride (20.5 g, 0.184 mole) and anhydrous sodium acetate (31 g) in 205 ml of water, with the use of 55–60 ml of 95% ethanol to complete the transfer. The resulting mixture was stoppered, heated in a 75° water bath for 0.5 hour, and then left in the bath to cool slowly. After about 15 hours, the mixture was cooled to 0° to give the crystalline semicarbazone (47.4 g), m.p. 143–163°. This crude product was extracted with petroleum ether (30–60°) in a Soxhlet apparatus for 2 hours. The dried, extracted 4-benzoyloxycycloheptanone semicarbazone weighed 33.5 g (63%), m.p. 158–167°. Recrystallization from 60% ethanol gave two crops: (*a*) 22.3 g, m.p. 167–170°, and (*b*) 3.69 g, m.p. 164–168°. These were pure enough for preparative purposes and represented a 49% yield. An analytical sample, m.p. 169–170°, was prepared by three recrystallizations of the product of an earlier run. Anal. Calc. for $C_{15}H_{19}N_3O_3$: C, 62.27; H, 6.62; N, 14.52. Found: C, 62.43; H, 6.74; N, 14.28.

Similar experiments carried out using absolute methanol as the solvent during the ring expansion gave a 44–47% yield of once-recrystallized product in four to six crops, the later ones having melting points down to 160–165°.

4-Benzoyloxycycloheptanone (II)

4-Benzoyloxycycloheptanone semicarbazone (21.1 g, 0.073 mole) was placed in a continuous liquid–liquid extractor and dissolved in 135 ml of 10.5 *N* hydrochloric acid by swirling at room temperature. The resulting yellowish solution was diluted with 35 ml of water and continuously extracted with ether for 30 hours. After the first 6 hours, the original ether was replaced with a fresh portion. Both portions (each of about 200-ml volume) were washed once with 40 ml of water, once with 30 ml of 1 *N* aqueous potassium carbonate, and twice with saturated aqueous sodium chloride. When dried, filtered, and stripped of ether, the first portion yielded 17.6 g and the second 3.8 g of nearly colorless liquid residue. These residues were combined and distilled from a modified Claisen flask, yielding 13.64 g (81%) of II, as a colorless oil, b.p. 145–149° at 10^{-3} mm, n_D^{20} 1.5371; infrared bands (CCl_4): 5.80, 5.84 (shoulder), 7.89, 9.01 μ (a strong band at 10.94 μ in the spectrum of I is absent in the spectrum of this product).

Liberation of the ketone with nitrous acid (9) gave a 62% yield of identical product.

Anal. Calc. for $C_{14}H_{16}O_3$: C, 72.39; H, 6.94. Found: C, 72.12; H, 7.06.

4-Methoxycyclohexanone (III)

The sample of 4-methoxycyclohexanone (III) used had b.p. 107–108.5° at 50 mm and n_D^{20} 1.4553 (lit. (19) b.p. 84–85° at 11 mm, n_D^{24} 1.4550); infrared bands (CCl_4): 5.82, 9.11, and these medium-intensity bands absent from the spectrum of 4-methoxycycloheptanone (see below): 7.68, 8.76, 9.27, and 11.05 μ. This afforded a *semicarbazone*, m.p. 179.5–181°, constant on repeated recrystallization from methanol (lit. m.p. 178° (20), 183–185° (10)); infrared bands ($CHCl_3$): 2.83, 2.94, 5.91, 6.39, and the following distinct bands not found in the spectrum of 4-methoxycycloheptanone semicarbazone: 8.66, 8.77, and 10.86 μ.

4-Methoxycycloheptanone Semicarbazone

A solution of 4-methoxycyclohexanone (III) (25.6 g, 0.200 mole) in 760 ml of absolute ethanol was cooled to −5° in an ice–salt bath. Anhydrous potassium carbonate (1.30 g, 0.0094 mole) was suspended in it, and a

Can. J. Chem. Downloaded from www.nrcresearchpress.com by 210.87.254.6 on 09/05/12
For personal use only.

solution of *N*-nitrosomethylurethane (27.9 g, 0.212 mole) in 720 ml of absolute ethanol was added with mechanical stirring at such a rate that the temperature of the reaction mixture did not exceed −1°. On completion of the addition, which required 11 hours, stirring was discontinued, and the mixture was allowed to come slowly to room temperature. Thirty-eight hours after completion of the addition, the mixture (still yellow) was filtered. Most of the ethanol was distilled *in vacuo* and the yellowish residue was dissolved in 200 ml of ether and washed with three 50-ml portions of water and two of saturated aqueous sodium chloride. The ethereal phase was dried and concentrated by distillation of the solvent. This afforded 21.0 g of yellow residual liquid. The major portion (20.8 g) was dissolved in 10 ml of 95% ethanol and mixed with a solution of semicarbazide hydrochloride (16.4 g, 0.147 mole) and anhydrous sodium acetate (24.6 g) in 155 ml of water. The mixture was heated at 75–80° for 1 hour, cooled, and scratched, when the semicarbazone began to crystallize. After standing overnight at room temperature, the mixture was cooled at 0° to give 13.3 g (33%) of 4-methoxycycloheptanone semicarbazone, m.p. 171–173° (lit. (10) m.p. 175.5°), unchanged by two recrystallizations from 60% ethanol (mixture m.p. with the semicarbazone of III 164–170.5°); infrared bands ($CHCl_3$): 2.85, 2.96, 5.91, 6.40, and a band at 11.32 μ absent from the spectrum of the lower homologue. Anal. Calc. for $C_9H_{17}N_3O_2$: C, 54.25; H, 8.60. Found: C, 54.61; H, 8.78.

4-Methoxycycloheptanone (IV)

4-Methoxycycloheptanone semicarbazone (9.34 g, 0.0469 mole) was placed in a liquid–liquid continuous extractor and dissolved in 90 ml of 8 *N* hydrochloric acid. As water (20–30 ml) was added with cooling, a colorless oil appeared on the surface of the solution. This mixture was continuously extracted with three successive 100-ml portions of ether for these respective periods: (*a*) 7 hours, (*b*) 11.5 hours, and (*c*) 11 hours. Each ethereal extract was washed with one 20-ml portion each of water, aqueous 5% sodium bicarbonate, and saturated aqueous sodium chloride and dried. The total crude product (5.65 g) obtained on distillation of the ether was evaporatively distilled at 5 mm and 45° (bath temperature), affording 5.07 g (76%, 25% overall from III) of colorless 4-methoxycycloheptanone (IV), n_D^{22} 1.4632; infrared bands (CCl_4): 5.86, 9.11, and the following weak- to medium-intensity bands absent from the spectrum of 4-methoxycyclohexanone (III): 7.95, 10.30, 11.40, and 11.74 μ. Anal. Calc. for $C_8H_{14}O_2$: C, 67.57; H, 9.92. Found: C, 67.52; H, 9.81.

4-Hydroxycycloheptanone (V)

Crude 4-benzoyloxycycloheptanone, prepared by treatment of the semicarbazone (1.78 g, 0.0062 mole) with nitrous acid (9), was suspended in 5.0 ml of 1.8 *N* aqueous sodium hydroxide, and the mixture was heated on a steam bath for 50 minutes, and finally refluxed for 25 minutes. The mixture was neutralized with concentrated hydrochloric acid and evaporated to dryness *in vacuo*. The residue was refluxed with chloroform (40 ml) for 3 hours, and the solution was decanted. This extract afforded crude V as a brown liquid. Evaporative distillation at 60–63° (bath temperature) and 1 mm yielded 0.29 g (37% overall) of partially crystalline V, n_D^{20} 1.4903 (liquid phase); infrared bands (CS_2): 2.82, 3.00, 3.43, 5.88 μ (about same intensity as 3.00 μ band, weaker than 3.43 μ band); ($CHCl_3$): 2.80, 2.97, 3.43, 5.90 μ (strongest band in spectrum). A portion of the liquid phase was used for analysis. Anal. Calc. for $C_7H_{12}O_2$: C, 65.60; H, 9.44. Found: C, 65.68; H, 9.42.

4-Ethylenedioxycycloheptanol (VII)

4-Benzoyloxycycloheptanone (II) (4.20 g, 0.0181 mole) and *p*-toluenesulphonic acid monohydrate (18 mg) were dissolved in 50 ml of benzene. Ethylene glycol (1.20 ml, 0.022 mole) was added, and the mixture was refluxed under a water separator for 3.2 hours. The cooled mixture was washed with three 10-ml portions of aqueous 5% sodium bicarbonate and two of water. After being dried over anhydrous potassium carbonate, the solution was decolorized by passing it over 1.0 g of Merck alumina; the alumina was washed with 35 ml of benzene. The combined eluates afforded 5.98 g of crude 4-ethylenedioxycycloheptyl benzoate (VI); infrared bands (CCl_4): 5.80, 7.88, 9.04 with shoulder at 9.12 μ; there was no hydroxyl absorption in the vicinity of 3 μ, and the ketone carbonyl shoulder which appears on the benzoate carbonyl band of II was absent.

The crude VI was hydrolyzed by refluxing with a solution of potassium hydroxide (1.50 g) in 50 ml of aqueous methanol (2:3 v/v) under nitrogen for 2.5 hours. Evaporative distillation of the product at 60–70° (bath temperature) and 1 mm afforded 4-ethylenedioxycycloheptanol (VII) (2.35 g, 76% overall from II) as a colorless, somewhat viscous liquid, n_D^{20} 1.4890; infrared bands ($CHCl_3$): 2.82, 2.93, 8.78, 8.89, 9.18, 9.85 μ (a weak band at 5.91 μ could indicate the presence of a trace of ketonic contaminant). Anal. Calc. for $C_9H_{16}O_3$: C, 62.76; H, 9.36. Found: C, 62.77; H, 9.11.

4-Ethylenedioxycycloheptanone (VIII)

Reagent grade pyridine (44 ml) was placed in the 250-ml extraction chamber of a continuous liquid–liquid extractor and cooled in tap water while chromium trioxide (4.4 g) was added in small portions with swirling (21). To the resulting suspension of chromium trioxide – pyridine complex was added 4-ethylenedioxycycloheptanol (VII) (2.31 g, 0.0134 mole) in pyridine (20 ml) with vigorous swirling, and the mixture was allowed to stand at room temperature for 18 hours. Saturated aqueous sodium sulphate (100 ml) was added, and the mixture was extracted continuously with ether for 24.5 hours. The extract was dried, filtered, and concentrated *in vacuo*. The residue was evaporatively distilled at 55–60° (bath temperature) and 1 mm, yielding VIII as a colorless liquid (1.52 g, 67%), n_D^{20} 1.4852 (lit. (14) b.p. 102° at 1.5 mm; n_D^{20} 1.4828);

Can. J. Chem. Downloaded from www.nrcresearchpress.com by 210.87.254.6 on 09/05/12
For personal use only.

infrared bands ($CHCl_3$): 2.94, 5.88, 8.79, 8.90, 9.10, 9.87 μ; no change in the relative intensities of the bands at 2.94, 5.88, and 9.87 μ was observed after passing 15–20 mg of this product in 5–6 ml of benzene over 200 mg of Merck alumina. Anal. Calc. for $C_9H_{14}O_3$: C, 63.51; H, 8.29. Found: C, 63.58; H, 8.34.

1,4-Cycloheptanedione Bis-2,4-dinitrophenylhydrazone

1,4-Cycloheptanedione bis-2,4-dinitrophenylhydrazone was prepared from VIII by the method of Shriner and Fuson (22). Two recrystallizations from pyridine afforded a yellow-orange hemisolvated product, m.p. 242–244° (lit. (15) m.p. 242.4–242.8° decomp. (unsolvated)). Anal. Calc. for $(C_{19}H_{18}N_8O_8)_2.C_5H_5N$: C, 49.10; H, 3.93; N, 22.64. Found: C, 48.85, 49.10; H, 3.75, 3.96; N, 22.49, 22.35.

1. W. von E. Doering and A. A.-R. Sayigh. J. Org. Chem. **26**, 1365 (1961).
2. R. D. Stolow. J. Am. Chem. Soc. **84**, 686 (1962).
3. C. D. Anderson. Ph.D. Thesis, Harvard University, Cambridge, Mass. 1958.
4. P. Yates and C. D. Anderson. J. Am. Chem. Soc. **80**, 1264 (1958).
5. L. N. Owen and P. A. Robins. J. Chem. Soc. 320 (1949).
6. E. R. H. Jones and F. Sondheimer. J. Chem. Soc. 615 (1949).
7. B. Eistert. *In* Newer methods of preparative organic chemistry. *Trans. and rev. by* F. W. Spangler. Interscience Publishers, Inc., New York. 1948. p. 513. C. D. Gutsche. Org. Reactions, **VIII**, 364 (1954).
8. C. D. Gutsche and H. H. Peter. J. Am. Chem. Soc. **77**, 5971 (1955).
9. St. Goldschmidt and W. L. C. Veer. Rec. Trav. Chim. **65**, 796 (1946); **66**, 238 (1947).
10. D. W. Adamson and J. Kenner. J. Chem. Soc. 181 (1939).
11. L. J. Bellamy. The infra-red spectra of complex molecules. 2nd ed. Methuen and Co. Ltd., London. 1958. p. 108.
12. H. H. Zeiss and M. Tsutsui. J. Am. Chem. Soc. **75**, 897 (1953).
13. E. J. Salmi. Ber. **71**, 1803 (1938).
14. N. J. Leonard, L. A. Miller, and J. W. Berry. J. Am. Chem. Soc. **79**, 1482 (1957).
15. A. C. Cope, T. A. Liss, and G. W. Wood. J. Am. Chem. Soc. **79**, 6287 (1957).
16. (*a*) W. M. Schubert and W. A. Sweeney. J. Am. Chem. Soc. **77**, 4172 (1955).
(*b*) E. D. Bergmann and S. Pinchas. J. Chem. Phys. **49**, 537 (1952).
17. K. Dimroth, E. Schmeil, and W. Daake. Ber. **75B**, 317 (1942).
18. W. W. Hartman and R. Phillips. *In* Organic syntheses. Coll. Vol. II. *Edited by* A. H. Blatt. John Wiley and Sons, Inc., New York. 1943. p. 464.
19. D. Papa, F. J. Villani, and H. F. Ginsberg. J. Am. Chem. Soc. **76**, 4446 (1954).
20. L. Helfer. Helv. Chim. Acta, **7**, 950 (1924).
21. G. I. Poos, G. E. Arth, R. E. Beyler, and L. H. Sarett. J. Am. Chem. Soc. **75**, 422 (1953).
22. R. L. Shriner and R. C. Fuson. The systematic identification of organic compounds. 3rd ed. John Wiley and Sons, Inc., New York. 1948. p. 171.

Received August 20, 1962.
Department of Chemistry,
Harvard University,
Cambridge, Mass., U.S.A.

Can. J. Chem. Downloaded from www.nrcresearchpress.com by 210.87.254.6 on 09/05/12
For personal use only.

THE NUCLEAR MAGNETIC RESONANCE SPECTRA OF SOME 2-METHYL-Δ^2-OXAZOLINES AND 2-METHYL-Δ^2-THIAZOLINES*

M. A. Weinberger and R. Greenhalgh

In connection with hydrolysis studies of 2-methyl-Δ^2-oxazoline (I) we have determined its n.m.r. spectrum and those of related compounds. An interesting feature of the spectrum of I (Fig. 1) is the coupling of the 2-methyl protons with one set of the ring methylenes.

The methylene proton spectrum was analyzable as an A_2B_2 system with equal J_{AB}'s, the upper-field half being further split by the coupling with the methyl group. Since the methyl spectrum is a triplet the two methylene protons must couple equally with the methyl protons, indicating that, unless this equality is accidental, the molecule is very likely planar. The spectrum of the 2-methyl group in 2,5,5-trimethyl-Δ^2-oxazoline (II) also shows a triplet but in the case of 2,4,4-trimethyl-Δ^2-oxazoline (III) only a single

Issued as D.R.C.L. Report No. 385.

infrared bands ($CHCl_3$): 2.94, 5.88, 8.79, 8.90, 9.10, 9.87 μ; no change in the relative intensities of the bands at 2.94, 5.88, and 9.87 μ was observed after passing 15–20 mg of this product in 5–6 ml of benzene over 200 mg of Merck alumina. Anal. Calc. for $C_9H_{14}O_3$: C, 63.51; H, 8.29. Found: C, 63.58; H, 8.34.

1,4-Cycloheptanedione Bis-2,4-dinitrophenylhydrazone

1,4-Cycloheptanedione bis-2,4-dinitrophenylhydrazone was prepared from VIII by the method of Shriner and Fuson (22). Two recrystallizations from pyridine afforded a yellow-orange hemisolvated product, m.p. 242–244° (lit. (15) m.p. 242.4–242.8° decomp. (unsolvated)). Anal. Calc. for $(C_{19}H_{18}N_8O_8)_2.C_5H_5N$: C, 49.10; H, 3.93; N, 22.64. Found: C, 48.85, 49.10; H, 3.75, 3.96; N, 22.49, 22.35.

1. W. von E. Doering and A. A.-R. Sayigh. J. Org. Chem. **26**, 1365 (1961).
2. R. D. Stolow. J. Am. Chem. Soc. **84**, 686 (1962).
3. C. D. Anderson. Ph.D. Thesis, Harvard University, Cambridge, Mass. 1958.
4. P. Yates and C. D. Anderson. J. Am. Chem. Soc. **80**, 1264 (1958).
5. L. N. Owen and P. A. Robins. J. Chem. Soc. 320 (1949).
6. E. R. H. Jones and F. Sondheimer. J. Chem. Soc. 615 (1949).
7. B. Eistert. *In* Newer methods of preparative organic chemistry. *Trans. and rev. by* F. W. Spangler. Interscience Publishers, Inc., New York. 1948. p. 513. C. D. Gutsche. Org. Reactions, **VIII**, 364 (1954).
8. C. D. Gutsche and H. H. Peter. J. Am. Chem. Soc. **77**, 5971 (1955).
9. St. Goldschmidt and W. L. C. Veer. Rec. Trav. Chim. **65**, 796 (1946); **66**, 238 (1947).
10. D. W. Adamson and J. Kenner. J. Chem. Soc. 181 (1939).
11. L. J. Bellamy. The infra-red spectra of complex molecules. 2nd ed. Methuen and Co. Ltd., London. 1958. p. 108.
12. H. H. Zeiss and M. Tsutsui. J. Am. Chem. Soc. **75**, 897 (1953).
13. E. J. Salmi. Ber. **71**, 1803 (1938).
14. N. J. Leonard, L. A. Miller, and J. W. Berry. J. Am. Chem. Soc. **79**, 1482 (1957).
15. A. C. Cope, T. A. Liss, and G. W. Wood. J. Am. Chem. Soc. **79**, 6287 (1957).
16. (*a*) W. M. Schubert and W. A. Sweeney. J. Am. Chem. Soc. **77**, 4172 (1955).
(*b*) E. D. Bergmann and S. Pinchas. J. Chem. Phys. **49**, 537 (1952).
17. K. Dimroth, E. Schmeil, and W. Daake. Ber. **75B**, 317 (1942).
18. W. W. Hartman and R. Phillips. *In* Organic syntheses. Coll. Vol. II. *Edited by* A. H. Blatt. John Wiley and Sons, Inc., New York. 1943. p. 464.
19. D. Papa, F. J. Villani, and H. F. Ginsberg. J. Am. Chem. Soc. **76**, 4446 (1954).
20. L. Helfer. Helv. Chim. Acta, **7**, 950 (1924).
21. G. I. Poos, G. E. Arth, R. E. Beyler, and L. H. Sarett. J. Am. Chem. Soc. **75**, 422 (1953).
22. R. L. Shriner and R. C. Fuson. The systematic identification of organic compounds. 3rd ed. John Wiley and Sons, Inc., New York. 1948. p. 171.

Received August 20, 1962.
Department of Chemistry,
Harvard University,
Cambridge, Mass., U.S.A.

Can. J. Chem. Downloaded from www.nrcresearchpress.com by 210.87.254.5 on 09/05/12
For personal use only.

THE NUCLEAR MAGNETIC RESONANCE SPECTRA OF SOME 2-METHYL-Δ^2-OXAZOLINES AND 2-METHYL-Δ^2-THIAZOLINES*

M. A. Weinberger and R. Greenhalgh

In connection with hydrolysis studies of 2-methyl-Δ^2-oxazoline (I) we have determined its n.m.r. spectrum and those of related compounds. An interesting feature of the spectrum of I (Fig. 1) is the coupling of the 2-methyl protons with one set of the ring methylenes.

The methylene proton spectrum was analyzable as an A_2B_2 system with equal J_{AB}'s, the upper-field half being further split by the coupling with the methyl group. Since the methyl spectrum is a triplet the two methylene protons must couple equally with the methyl protons, indicating that, unless this equality is accidental, the molecule is very likely planar. The spectrum of the 2-methyl group in 2,5,5-trimethyl-Δ^2-oxazoline (II) also shows a triplet but in the case of 2,4,4-trimethyl-Δ^2-oxazoline (III) only a single

Issued as D.R.C.L. Report No. 385.

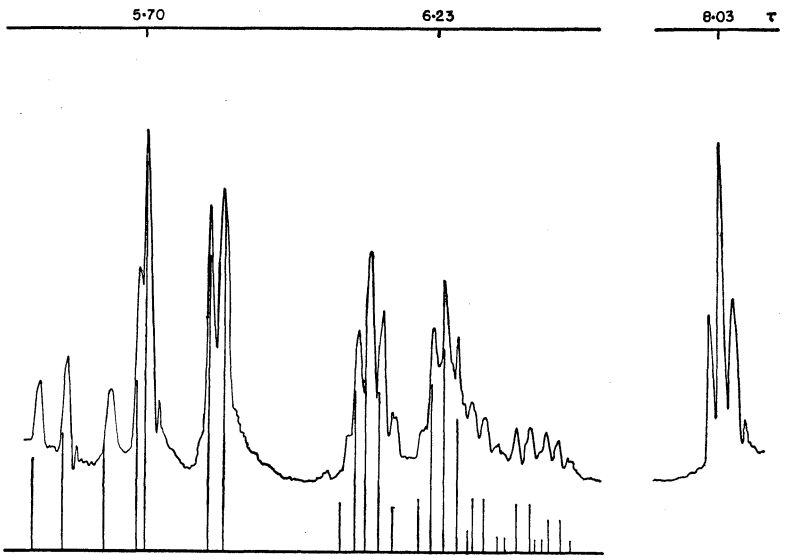

FIG. 1. The 60 Mc/s spectrum of 2-methyl-Δ^2-oxazoline in water. The theoretical spectrum for the CH_2—CH_2 portion was calculated as an A_2B_2 system with the parameters in Table I, and modified by the methyl group coupling.

peak is obtained. Thus it is the 4-position methylene protons which couple with the 2-methyl hydrogens.

The remainder of the spectrum of II consists of a low-field quartet for the methylene protons in the 4-position and a single peak for the *gem*-dimethyl protons. As expected, III only showed single peaks.

The corresponding thiazoline compounds were also investigated with similar results. 2-Methyl-Δ^2-thiazoline (IV) and 2,5,5-trimethyl-Δ^2-thiazoline (V) again show a triplet for the 2-methyl protons whilst a single peak is obtained for this set in 2,4,4-trimethyl-Δ^2-thiazoline (VI). The A_2B_2 system of IV was analyzable with $J_{AB} = J'_{AB}$, but here the half further split by the methyl protons occurs at lower field.

Long-range coupling between protons separated by five bonds has been observed previously, mainly in more highly conjugated systems (1(*a*), 2, 3). The coupling constants in our examples (1.38–1.65 c.p.s.) are comparable to that between the methyl protons of angelic acid (4), in which the trans type relationship of the groups and the degree of unsaturation are similar. In the latter cases, coupling is believed to involve hyperconjugation (1(*b*)).

Summarized in Table I are the spectral parameters together with the pK_a values for the various compounds.

The parallelism between pK_a and τ value of the N—CH_2 protons indicates that the factors which govern the electron density of the nitrogen atom similarly affect that of the hydrogen atoms. The τ values of the X—CH_2 protons depend on the electron-withdrawing character of X and are much lower for the oxazolines than for the thiazolines. In all cases substitution by *gem*-dimethyl groups increases the τ value of the unsubstituted CH_2 protons, as expected.

The τ values of the 2-methyl protons are mainly governed by X and are higher in the oxazoline series. It is believed that because of the mesomerism in oxazolines

Can. J. Chem. Downloaded from www.nrcresearchpress.com by 210.87.254.5 on 09/05/12
For personal use only.

Can. J. Chem. Downloaded from www.nrcresearchpress.com by 210.87.254.5 on 09/05/12
For personal use only.

TABLE I

N.M.R. parameters and pK_a values for alkyl-substituted 2-methyl-Δ^2-oxazolines and thiazolines

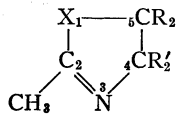

Compound	X	R	R′	pK_a	τ (p.p.m.) (4) H_2	(5) H_2	(4) Me_2	(5) Me_2	(2) Me	J (c.p.s.) $J_{CH_2—CH_2}$	$J_{CH_3—CH_2}$
I(A)	O	H	H	5.52*	6.225	5.695	—	—	8.029	9.57	1.38
(B)	O	H	H		6.329	5.886	—	—	8.150	9.56	1.38
IV	S	H	H	5.21†	5.883	6.768	—	—	7.857	8.22	1.61
III	O	H	Me	5.59	—	6.232	8.825	—	8.162	—	—
VI	S	H	Me	5.39	—	6.979	8.718	—	7.914	—	—
II	O	Me	H	6.12	6.613	—	—	8.685	8.174	—	1.45
V	S	Me	H	5.67	6.241	—	—	8.537	7.887	—	1.65

*Reference 5 quotes 5.51 ±0.05.
†Reference 6.

(—O—C(CH_3)=N— ↔ —$\dot{O}$=C(CH_3)—$\bar{N}$—) there is less demand on the 2-methyl to supply electrons to the ring than in thiazolines.

In aqueous solutions of I the field positions of the 2-methyl protons are very dependent on pH, as shown in Fig. 2. This sigmoid curve, which presumably depicts the number-

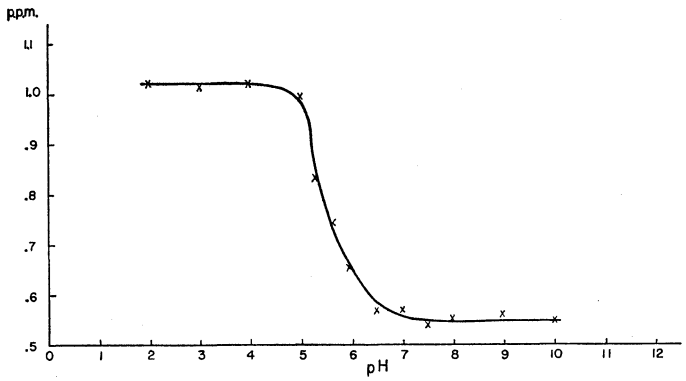

FIG. 2. Variation of chemical shift of methyl protons of 2-methyl-Δ^2-oxazoline with pH. Chemical shifts are referred to external cyclohexane.

average chemical shift of the protonated and unprotonated forms, is equivalent to a titration curve and the pK_a value deduced from it (5.5±0.1) agrees very closely with that shown in Table I. Similar chemical shift – pH curves have been reported for methyl groups attached directly to the nitrogen (7), but here the methyl protons are one atom further removed. The coupling constant $J_{CH_3-CH_2}$ also varies in an analogous manner from about 1.0 to 1.3 c.p.s. as the pH is increased.

EXPERIMENTAL

The n.m.r. spectra were determined on a Varian 4300*c* spectrometer at 60 Mc/s in CCl_4 solution (10% w/v). I was done in both H_2O (I(A), 40% w/v) and CCl_4 (I(B), 50% w/v). τ and J have standard deviations of 0.001–0.005 p.p.m. and 0.02–0.10 c.p.s. respectively.

All the compounds in Table I were prepared by the methods described by Wenker (8) and have physical properties in accord with those reported elsewhere (9, 10, 11). The pK_a values were determined in 0.1 *M* NaCl solution by titration of 2 m*M* base at 25°.

ACKNOWLEDGMENTS

The assistance of J. R. Blanchfield, B. Larose, and K. Oikawa is gratefully acknowledged.

1. (*a*) S. GRONOWITZ and R. A. HOFFMAN. Acta Chem. Scand. **13**, 1687 (1959).
   (*b*) R. A. HOFFMAN and S. GRONOWITZ. Arkiv Kemi, **16**, 471 (1960).
2. F. A. L. ANET. J. Chem. Phys. **32**, 1274 (1960).
3. T. SCHAEFER. J. Chem. Phys. **36**, 2235 (1962).
4. R. R. FRASER. Can. J. Chem. **38**, 549 (1960).
5. G. R. PORTER, H. N. RYDON, and J. A. SCHOFIELD. J. Chem. Soc. 2686 (1960).
6. R. B. MARTIN, S. LOWEY, E. L. ELSON, and J. T. EDSALL. J. Am. Chem. Soc. **81**, 5089 (1959).
7. E. GRUNWALD, A. LOEWENSTEIN, and S. MEIBOOM. J. Chem. Phys. **27**, 641 (1957).
8. H. WENKER. J. Am. Chem. Soc. **57**, 1079 (1935).
9. P. F. TRYON. U.S. Patent No. 2,372,409 (1945).
10. A. T. MEYERS and J. J. RITTER. J. Org. Chem. **23**, 1918 (1958).
11. P. E. FANTA and A. S. DEUSCH. J. Org. Chem. **23**, 72 (1958).

RECEIVED NOVEMBER 29, 1962.
DEFENCE RESEARCH CHEMICAL LABORATORIES,
OTTAWA, CANADA.

Can. J. Chem. Downloaded from www.nrcresearchpress.com by 210.87.254.5 on 09/05/12
For personal use only.

PYRIDINES FROM BASE TREATMENT OF BENZALMALONONITRILE

M. R. S. Weir, K. E. Helmer, and J. B. Hyne

Can. J. Chem. Downloaded from www.nrcresearchpress.com by 210.87.254.40 on 09/05/12
For personal use only.

In connection with a study of the reaction of benzalmalononitrile with basic reagents we have investigated its reaction with potassium hydroxide in methanol and ethanol.

Infrared spectral analysis of the product mixture from reaction of benzalmalononitrile with molar potassium hydroxide in ethanol at room temperature gave clear indication of the presence of benzaldehyde. Isolation of the 2,4-dinitrophenylhydrazone of benzaldehyde from the reaction mixture verified that a reverse aldol condensation was taking place in the reaction. No evidence of the formation of malononitrile was found, however, and in particular the characteristic CH_2 scissoring mode absorption was absent in the infrared. The other product isolated from the product mixture was a high-melting crystalline solid obtained in 15–20% yield. The infrared spectrum of this product (Fig. 1*a*) has several striking features: a very strong absorption at 4.4 μ indicative of conjugated CN; a strong absorption in the region 2.8–3.0 μ suggesting the presence of an OH or NH_2 group; and a complex absorption pattern between 12.5 and 14.5 μ suggesting skeletal vibration modes of a ring structure other than those of the phenyl group. Addition of malononitrile to the reaction mixture resulted in a doubling of the yield of the high-melting crystalline solid.

The absence of malononitrile in the product mixture coupled with the observed increase in yield on addition of malononitrile suggested that the malononitrile entity produced in the reverse aldol reaction was undergoing further reaction with unchanged benzalmalononitrile to yield a cyclic pyridine structure.

The formation of pyridines from 1,1,3,3-tetracyanopropenes by refluxing with concentrated sulphuric acid in alcohol solution has been previously reported (1). Urushibara (2) has also reported that ethoxymethylene malononitrile yields pyridines on refluxing with the sodium salt of malononitrile in alcohol. Comparison of the infrared spectrum of the high-melting crystalline product obtained from KOH treatment of benzalmalononitrile in methanol with that of an authentic sample of 2-amino-6-methoxy-3,5-dicyano-4-phenylpyridine (1) obtained by independent synthesis* showed that the two samples were identical. The n.m.r. spectra of the products from both ethanolic and methanolic KOH treatment (Figs. 1*c*, 1*d*) are in keeping with the fully substituted pyridine structures.

The experimental evidence noted above is in accord with the following proposed mechanism.

$$C_6H_5{-}CH{=}C(CN)_2 + KOH \rightarrow C_6H_5CHO + K^+CH(CN)_2^-$$

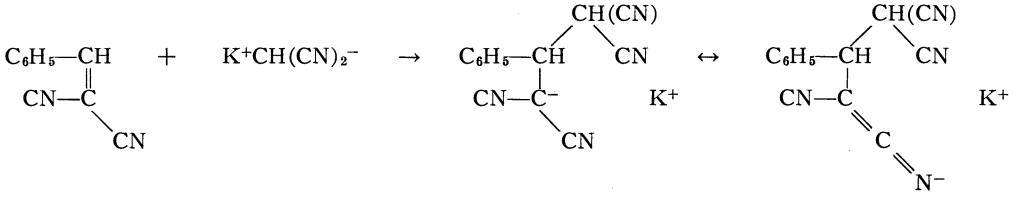

The authors are indebted to Dr. W. J. Middleton, Central Research Department, E. I. duPont de Nemours and Co., Wilmington, Delaware, for providing a sample of the fully substituted pyridine.

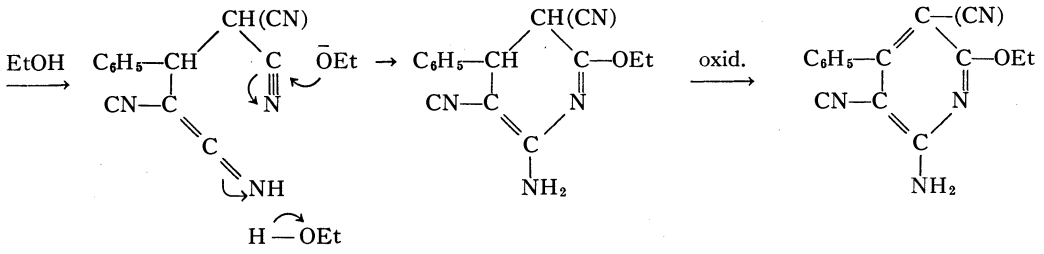

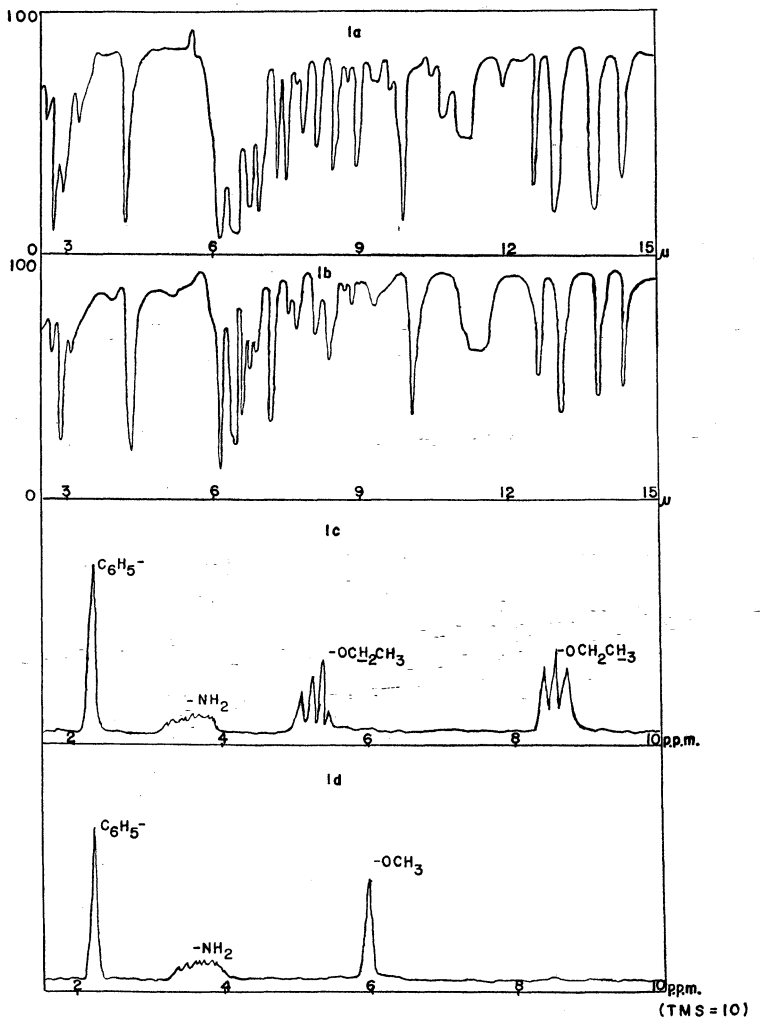

FIG. 1(*a*) The infrared spectrum of 2-amino-6-ethoxy-3,5-dicyano-4-phenylpyridine (KBr pellet).
(*b*) The infrared spectrum of 2-amino-6-methoxy-3,5-dicyano-4-phenylpyridine (KBr pellet).
(*c*) The n.m.r. spectrum of 2-amino-6-ethoxy-3,5-dicyano-4-phenylpyridine, 3–5% solution in CD_3CN. (CH_3—CN in CD_3—CN peak not shown.)
(*d*) The n.m.r. spectrum of 2-amino-6-methoxy-3,5-dicyano-4-phenylpyridine, 3–5% solution in CD_3CN. (CH_3—CN in CD_3—CN peak not shown.)

The low-field position and broadening of the NH_2 peak is due to hydrogen bonding with the CD_3—CN solvent.

Can. J. Chem. Downloaded from www.nrcresearchpress.com by 210.87.254.40 on 09/05/12
For personal use only.

The final oxidation step will obviously proceed very readily in view of the driving force to attain full aromatization of the ring. The oxidizing agent must be either aerobic oxygen or benzalmalononitrile. The latter possibility seems to be the more likely in view of the production of considerable quantities of tarry residue in the reaction probably resulting from the polymerization of the diene as it performs its role as an oxidizing agent.

It is clear from the above mechanism that variation of the solvent from methanol to ethanol will simply change the 6-alkoxy group. Both the methoxy and ethoxy pyridines were prepared and isolated, although characterization by identifying the product infrared spectrum with an authentic sample was carried out only in the methoxy case.

EXPERIMENTAL

Materials

Benzalmalononitrile was prepared by the method of Corson and Stoughton (3) by condensation of benzaldehyde with redistilled malononitrile in ethanol in the presence of catalytic amounts of piperidine. Recrystallization from ethanol gave benzalmalononitrile in 90% yield, m.p. 84.5–85° C (lit. 83.5–84° C). Reagent grade potassium hydroxide and commercial absolute ethanol and methanol were used without further purification.

Isolation of Benzaldehyde

Benzalmalononitrile (1 g, 0.0064 *M*) was stirred at room temperature for 6–8 hours in 50 ml of a molar solution of potassium hydroxide in ethanol. An aliquot of the resulting yellow solution was removed and treated with excess 2,4-dinitrophenylhydrazine reagent. This gave a solid derivative, m.p. 236–237 °C (lit. value for derivative of benzaldehyde 237° C). Mixed m.p. 236–237° C.

Isolation of Substituted Pyridine from Ethanol Solution

The remainder of the yellow product mixture solution noted above was poured into a large excess of water and the resulting precipitate filtered and recrystallized twice from 95% ethanol. The recovered pale yellow crystals were of 2-amino-6-ethoxy-3,5-dicyano-4-phenylpyridine, m.p. 235–236° C uncorr. (lit. 238–239° C). Analysis for $C_{15}H_{12}N_4O$: Calc.: C, 68.16; H, 4.58; N, 21.20. Found: C, 68.06; H, 4.50; N, 21.16. Infrared spectrum Fig. I*a*, n.m.r. spectrum Fig. I*c*.

Isolation of Substituted Pyridine from Methanol Solution

The procedure was the same as that used in the case of ethanol above but with absolute methanol as solvent. The recrystallized product had m.p. 259–260° C. Lit. value for m.p. of 2-amino-6-methoxy-3,5-dicyano-4-phenylpyridine 259–261° C. Mixed m.p. with authentic sample 260–261° C. Infrared spectrum Fig. 1*b*, n.m.r. spectrum Fig. 1*d*.

ACKNOWLEDGMENTS

The research for this paper was supported in part by the Defence Research Board of Canada, Grant No. 2001–01. The authors also wish to acknowledge the helpful discussions throughout the course of this work with Dr. H. L. Holmes, Suffield Experimental Station, Defence Research Board.

1. E. L. Little, W. J. Middleton, D. D. Coffman, V. A. Englehardt, and G. N. Sausen. J. Am. Chem. Soc. **80**, 2832 (1958).
2. Y. Urushibara. Bull. Chem. Soc. Japan, **2**, 278 (1927).
3. B. B. Corson and R. W. Stoughton. J. Am. Chem. Soc. **50**, 2825 (1928).

Received November 21, 1962.
Department of Chemistry,
University of Alberta, Calgary,
Calgary, Alberta.

Can. J. Chem. Downloaded from www.nrcresearchpress.com by 210.87.254.40 on 09/05/12
For personal use only.

THE DECOMPOSITION OF HYDRAZINE VAPOR IN ELECTRICAL DISCHARGES[1, 2]

R. A. JONES AND S. S. BARTON

A review of work done on the vapor phase decomposition of hydrazine has been given by Audrieth and Ogg (1), who represent the stoichiometry of the decomposition reaction by the general equation

$$3N_2H_4 = 4(1-x)NH_3 + (1+2x)N_2 + 6xH_2. \quad [1]$$

Values of x range from 0.06 for thermal decomposition to 0.96 for photochemical reaction. Intermediate products have been reported by Rice and Scherber (2), who, using a high-speed flow system, at liquid nitrogen temperature, trapped ammonia and a yellow labile substance from thermally decomposed hydrazine vapor (stoichiometry of the overall reaction giving $x = 0.1$) and by Foner and Hudson (3), who detected several higher hydronitrogens as well as ammonia by mass spectrographic analysis of hydrazine vapor decomposed in an electrodeless microwave discharge.

In the investigation described in this note hydrazine vapor was decomposed by passage through an electrodeless discharge. The stoichiometry of the reaction is given by $x = 0.5$ in equation [1]. Under certain conditions small amounts of a labile yellow substance were observed.

EXPERIMENTAL

The discharge tube terminated in a cold finger trap and was pumped by a high-speed mercury diffusion pump. After leaving the discharge zone, the decomposed vapor was allowed to traverse a predetermined volume (traversed volume) before reaching the trap. The traversed volume was changed by moving the discharge zone along the tube.

A Tesla coil connected to a narrow copper band clamped around the discharge tube was used to drive the discharge. The predominant output frequency of the coil was determined by a high-speed oscilloscope to be about 0.2 Mc. By adjustment of the spark gap and input voltage, the coil could be set to give a reproducible reading on a vacuum tube voltmeter.

Hydrazine was prepared in the vacuum system by the thermal decomposition of hydrazinium phthalyl hydrazide (4), thoroughly outgassed and stored as a solid at 0°. Hydrazine flow rate into the discharge tube was fixed by a capillary tube flow control. The linear flow rate in the discharge tube was about 10 cm sec^{-1}, much smaller than that used by Rice and Scherber (2) (2900 cm sec^{-1}). Pressures were measured with a Consolidated Electrodynamics micromanometer.

At the end of the discharge period, the system was evacuated and isolated from the pumps. Then the liquid air was removed from the trap, whereupon the condensed product vaporized completely. The trap was then refilled with liquid air to recondense the vapors; at this stage there was always a residual pressure which was noted. The non-condensable gas ("evolved gas") thus measured is considered to be a measure of the amount of labile compound in the original condensed product. (Any occluded hydrogen or nitrogen will also be included in this determination.) Finally the recondensed product was distilled into a titration vessel containing an aliquot of standard hydrochloric acid. Excess acid was titrated with sodium hydroxide to give the total ammonia and hydrazine content. The titrated solution was then rapidly acidified and titrated again with standard potassium iodate for hydrazine (5).

RESULTS AND DISCUSSION

Figure 1 shows the variation with voltage of hydrazine loss and of ammonia yield at constant traversed volume for 30-minute experiments. These yields are plotted as a

[1]*Paper presented at the 44th Annual Conference, Chemical Institute of Canada, Montreal, Quebec, August 3–5, 1961.*

[2]*This work was supported by D.R.B. Grant 9530–14.*

Can. J. Chem. Downloaded from www.nrcresearchpress.com by 210.87.254.5 on 09/05/12
For personal use only.

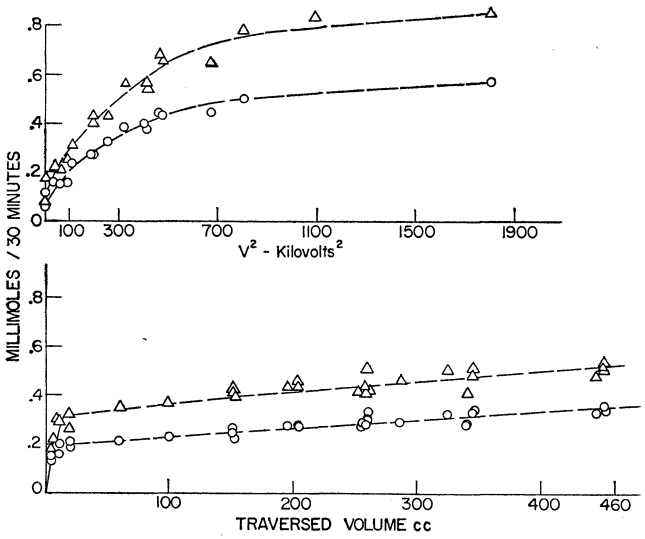

FIG. 1. Hydrazine loss and ammonia yield. Flow rate: 0.87 millimole/0.5 hr; pressure: 240±10 μ; upper figure: traversed volume = 196 cc; lower figure: voltage = 13.9 kv.

function of V^2 because Gill and Townsend found in a theoretical analysis of electrodeless discharges at electrical frequencies comparable to the molecular collision frequency of the gas (6) that the rate at which energy is transferred from the field to the gas by means of electron–molecule collisions is proportional to the square of the field strength. The apparent extent of decomposition of hydrazine for the overall reaction is about 21% for the lowest voltage to nearly 100% for the highest voltage used. The value of the ratio, millimoles ammonia produced to millimoles hydrazine lost, appears to be constant and independent of voltage over this range of percentage decomposition and is 0.69±0.03. This constant ratio is close to the value 0.67 demanded by

$$3N_2H_4 = 2NH_3 + 2N_2 + 3H_2 \text{ (i.e. } x = 0.5 \text{ in equation [1])}. \qquad [2]$$

Figure 1 also shows the variation of hydrazine loss and of ammonia yield at constant voltage with increasing traversed volume. The decomposition appears to proceed downstream away from the discharge zone in the same manner as in the discharge itself. Hydrazine is destroyed and ammonia formed in a constant ratio 0.65±0.04 independent of traversed volume up to the largest traversed volume allowed by the apparatus.

Figure 2 shows the influence of voltage and traversed volume on the production of evolved gas from the warmed product. The percentage yield of evolved gas (based on hydrazine loss) ranged from about 20% at low traversed volumes and low voltages to about 5% for the experiments done at higher traversed volumes and 13.9 kv. In the experiments done at very high voltages and 196-ml traversed volume the percentage yield approached zero. Possibly a certain amount of this evolved gas can be attributed to the presence of occluded or adsorbed nitrogen and hydrogen (7). However, this effect appears not to be significant, since the amount of gas drops to smaller values for larger apparent extent of hydrazine decomposition when the concentrations of nitrogen and hydrogen in the vapor impinging on the cold finger have higher values.

With increasing traversed volume, the amount of evolved gas suffers a rapid initial decrease followed by a much slower decrease as the traversed volume increases. The

Can. J. Chem. Downloaded from www.nrcresearchpress.com by 210.87.254.5 on 09/05/12
For personal use only.

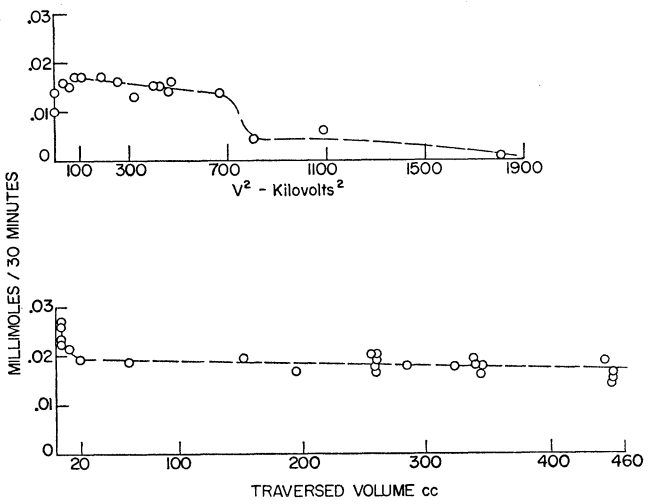

FIG. 2. Evolved gas. Flow rate: 0.87 millimole/0.5 hr; pressure: 240±10 μ; upper figure: traversed volume = 196 cc; lower figure: voltage = 13.9 kv.

condensed product was snow white in color except when formed from traversed volumes less than 10 cc, when it became straw-yellow.

The composition of the evolved gas was not systematically investigated during this work. However, one sample from an experiment done at 5.3-cc traversed volume (straw-yellow deposit) was analyzed by mass spectrometry and found to contain 16% H_2 and 84% N_2 by volume.[3]

Since the reaction in the traversed volume continues for an appreciable length of time after the gas has left the discharge, it is necessary to postulate the existence of some long-lived carriers of energy. These carriers could be activated hydrazine molecules formed by neutralization of hydrazine ions formed in the discharge, activated hydrazine molecules formed by electron collision in the discharge, or NH_2 radicals formed by the decomposition of such activated molecules. Both activated hydrazine molecules and NH_2 radicals are considered to re-form hydrazine on the cold finger. A mechanism for the reaction can be written as

$$N_2H_4^* \rightarrow 2NH_2 \qquad [3]$$

$$NH_2 + N_2H_4 \rightarrow NH_3 + N_2H_3 \qquad [4]$$

$$N_2H_3 \rightarrow N_2 + 3/2H_2. \qquad [5]$$

Reactions [3], [4], and [5] add up to give the overall stoichiometry which was observed (i.e. equation [2]). The immediate fate of the N_2H_3 radical is not clear. The vapor phase decomposition to hydrogen and nitrogen probably proceeds via the formation of other radicals and labile hydronitrogens. Rice and Scherber (2), using a high-speed flow system, regarded N_2H_3 as condensing to form their "tetrazane" (a yellow labile substance) at liquid nitrogen temperature in the thermal decomposition of hydrazine vapor:

$$2N_2H_3 \rightarrow N_4H_6. \qquad [6]$$

Tetrazane was then considered to decompose on warming according to

$$N_4H_6 \rightarrow 2NH_3 + N_2. \qquad [7]$$

[3]*Courtesy of Dr. A. W. Tickner, National Research Council, Ottawa, Ont.*

Can. J. Chem. Downloaded from www.nrcresearchpress.com by 210.87.254.5 on 09/05/12
For personal use only.

With the mechanism postulated here this reaction cannot be taking place to any appreciable extent since the stoichiometric yield of ammonia has already been accounted for by reaction [4]. Foner and Hudson (3) have observed a similar yellow deposit from a microwave discharge in hydrazine vapor which vaporized to give diimide (N_2H_2) and ammonia but no nitrogen and thus was not Rice and Scherber's tetrazane.

It is possible in our case that the straw-yellow color of the deposits which yield larger amounts of evolved gas is that of N_4H_6 formed from N_2H_3 radicals on the cold wall. The disappearance of the yellow color, together with the decrease in evolved gas yield as traversed volume is increased, suggests that this radical is not present in large concentrations at higher traversed volumes.

The mechanism given above, which partially describes the observed reaction, is similar to that of Rice and Scherber's thermal decomposition mechanism except that the production of ammonia via the N_2H_3 radical is not considered to be significant. When a low flow rate is used, almost all the N_2H_3 radicals will decompose by an alternate route in the vapor phase to yield nitrogen and hydrogen. Only at very low traversed volumes do small amounts of N_2H_3 survive to reach the cold surface, where it forms tetrazane, which gives the deposit a straw-yellow color and increases the yield of evolved gas.

1. L. F. Audrieth and B. A. Ogg. The chemistry of hydrazine. John Wiley and Sons, Inc., New York. 1951.
2. F. O. Rice and F. Scherber. J. Am. Chem. Soc. **77**, 291 (1955).
3. S. N. Foner and R. L. Hudson. J. Chem. Phys. **29**, 442 (1958).
4. H. J. Barber and W. R. Wragg. J. Chem. Soc. 1458 (1948).
5. R. A. Penneman and L. F. Audrieth. Anal. Chem. **20**, 1058 (1948).
6. E. W. B. Gill and J. S. Townsend. Phil. Mag. **26**, 290 (1938).
7. R. T. Brackman and L. F. Wade. J. Chem. Phys. **34**, 1572 (1961).

Received November 1, 1962.
Department of Chemistry,
Royal Military College of Canada,
Kingston, Ontario.

AN EXPLOSION WITH METHYL AZIDE[1]

C. L. Currie[2] and B. deB. Darwent

A violent explosion which occurred during the course of an investigation of the vapor-phase photolysis of methyl azide led us to investigate the cause of the phenomenon and especially the influence of impurities.

Approximately 1 liter of methyl azide gas at N.T.P., mixed with a smaller quantity of propane, had been condensed in a trap which was separated from the rest of the vacuum system by a mercury cutoff. The mixture had been warmed, until the vapor pressure was approximately 20 mm Hg, when the level of the mercury cutoff was lowered. The explosion occurred as soon as the mercury started to drop rapidly in the cutoff.

Attempts to reproduce the explosion, on a smaller scale, by causing mercury to move rapidly in a closed-arm manometer were unsuccessful whether the azide was pure or mixed with propane, stored in the dark, or exposed to the laboratory illumination. However, the explosion could be induced by the discharge of a Tesla coil. In those experiments

[1]*This work was supported by the United States Army Engineer Research and Development Laboratories, Fort Belvoir, Va., under Contract Numbers DA-44-009-ENG-4139 and DA-44-009-ENG-3574.*
[2]*Present address: Woodstock College, Woodstock, Maryland.*

Can. J. Chem. Downloaded from www.nrcresearchpress.com by 210.87.254.5 on 09/05/12
For personal use only.

With the mechanism postulated here this reaction cannot be taking place to any appreciable extent since the stoichiometric yield of ammonia has already been accounted for by reaction [4]. Foner and Hudson (3) have observed a similar yellow deposit from a microwave discharge in hydrazine vapor which vaporized to give diimide (N_2H_2) and ammonia but no nitrogen and thus was not Rice and Scherber's tetrazane.

It is possible in our case that the straw-yellow color of the deposits which yield larger amounts of evolved gas is that of N_4H_6 formed from N_2H_3 radicals on the cold wall. The disappearance of the yellow color, together with the decrease in evolved gas yield as traversed volume is increased, suggests that this radical is not present in large concentrations at higher traversed volumes.

The mechanism given above, which partially describes the observed reaction, is similar to that of Rice and Scherber's thermal decomposition mechanism except that the production of ammonia via the N_2H_3 radical is not considered to be significant. When a low flow rate is used, almost all the N_2H_3 radicals will decompose by an alternate route in the vapor phase to yield nitrogen and hydrogen. Only at very low traversed volumes do small amounts of N_2H_3 survive to reach the cold surface, where it forms tetrazane, which gives the deposit a straw-yellow color and increases the yield of evolved gas.

1. L. F. Audrieth and B. A. Ogg. The chemistry of hydrazine. John Wiley and Sons, Inc., New York. 1951.
2. F. O. Rice and F. Scherber. J. Am. Chem. Soc. **77**, 291 (1955).
3. S. N. Foner and R. L. Hudson. J. Chem. Phys. **29**, 442 (1958).
4. H. J. Barber and W. R. Wragg. J. Chem. Soc. 1458 (1948).
5. R. A. Penneman and L. F. Audrieth. Anal. Chem. **20**, 1058 (1948).
6. E. W. B. Gill and J. S. Townsend. Phil. Mag. **26**, 290 (1938).
7. R. T. Brackman and L. F. Wade. J. Chem. Phys. **34**, 1572 (1961).

Received November 1, 1962.
Department of Chemistry,
Royal Military College of Canada,
Kingston, Ontario.

AN EXPLOSION WITH METHYL AZIDE[1]

C. L. Currie[2] and B. deB. Darwent

A violent explosion which occurred during the course of an investigation of the vapor-phase photolysis of methyl azide led us to investigate the cause of the phenomenon and especially the influence of impurities.

Approximately 1 liter of methyl azide gas at N.T.P., mixed with a smaller quantity of propane, had been condensed in a trap which was separated from the rest of the vacuum system by a mercury cutoff. The mixture had been warmed, until the vapor pressure was approximately 20 mm Hg, when the level of the mercury cutoff was lowered. The explosion occurred as soon as the mercury started to drop rapidly in the cutoff.

Attempts to reproduce the explosion, on a smaller scale, by causing mercury to move rapidly in a closed-arm manometer were unsuccessful whether the azide was pure or mixed with propane, stored in the dark, or exposed to the laboratory illumination. However, the explosion could be induced by the discharge of a Tesla coil. In those experiments

[1]*This work was supported by the United States Army Engineer Research and Development Laboratories, Fort Belvoir, Va., under Contract Numbers DA-44-009-ENG-4139 and DA-44-009-ENG-3574.*
[2]*Present address: Woodstock College, Woodstock, Maryland.*

Can. J. Chem. Downloaded from www.nrcresearchpress.com by 210.87.254.5 on 09/05/12
For personal use only.

we found the presence of a small amount of mercury to be essential to the explosion. In a large number of experiments in which mercury was carefully excluded no explosion occurred when either pure azide or azide–propane mixtures were subjected to the Tesla discharge. Explosions always occurred when mercury was added to the system and the discharge applied.

These experiments show that methyl azide, if pure, is a relatively safe substance but that a trace of mercury makes the mixture extremely treacherous. This suggests that the explosion was initiated by a shock wave set up by the detonation of minute crystals of mercury azide. The detonation of the mercury azide was possibly caused by the friction of mercury on glass.

Received December 14, 1962.
The Maloney Chemistry Laboratory,
The Catholic University of America,
Washington 17, D.C.

Can. J. Chem. Downloaded from www.nrcresearchpress.com by 210.87.254.5 on 09/05/12
For personal use only.

Canadian Journal of Chemistry

Issued by THE NATIONAL RESEARCH COUNCIL OF CANADA

VOLUME 41 MAY 1963 NUMBER 5

Can. J. Chem. Downloaded from www.nrcresearchpress.com by 210.87.254.40 on 09/05/12
For personal use only.

ALKYLALUMINUM HYDRIDE TRIMETHYLAMINE COMPLEXES

F. M. PETERS, B. BARTOCHA,[1] AND A. J. BILBO

U.S. Naval Ordnance Laboratory, Corona, California, U.S.A.

Received November 19, 1962

ABSTRACT

Alkylaluminum hydride trimethylamine complexes have been obtained by several different methods: (*a*) reduction of an alkylaluminum halide trimethylamine complex with lithium hydride, (*b*) alkylation of aluminum hydride trimethylamine with dialkylmercury, (*c*) reaction of trialkylaluminum trimethylamine and aluminum hydride trimethylamine, and (*d*) reaction of dialkylaluminum chloride with lithium aluminum hydride and trimethylamine. Some physical properties of the compounds are reported, including the infrared and proton magnetic resonance spectra. Cryoscopic molecular weight determinations indicate that the compounds are associated in cyclohexane. Their possible structures are discussed.

INTRODUCTION

Trimethyldialuminum trihydride, $(Me_3Al_2H_3)_n$, and dimethylaluminum hydride, $(Me_2AlH)_n$, were originally prepared by subjecting a mixture of trimethylaluminum and hydrogen to an electric discharge (1). The latter compound was subsequently obtained from the reaction of trimethylaluminum and lithium aluminum hydride (2). Higher alkyl monohydrides have since been prepared (3, 4), but no uncomplexed dihydrides have been characterized. Since trivalent aluminum has empty $3p$ and $3d$ orbitals in addition to the three sp^2 hybrid bonding orbitals, it can further hybridize to make one or two additional orbitals available for coordination with electron donor groups. There are many examples of coordination compounds of this type, among them $AlH_3 \cdot NMe_3$, $AlH_3 \cdot 2NMe_3$, and $Et_3Al \cdot OEt_2$.

The coordinating power of aluminum suggested the possibility of stabilizing the alkylaluminum dihydrides by complex formation with a Lewis base. This was shown to be the case with the isolation of the stable trimethylamine complexes $EtAlH_2 \cdot NMe_3$ and $MeAlH_2 \cdot NMe_3$. The methylaluminum and ethylaluminum monohydride trimethylamine complexes were also prepared (5). In the following equations, which summarize the methods of synthesis, R = CH_3— and C_2H_5—. The reaction between ethylaluminum dichloride trimethylamine and lithium hydride did not yield a product free of chlorine.

$$\begin{aligned} Et_2AlCl \cdot NMe_3 + LiH &\longrightarrow Et_2AlH \cdot NMe_3 + LiCl \\ EtAlCl_2 \cdot NMe_3 + 2LiH &\longrightarrow EtAlH_2 \cdot NMe_3 + 2LiCl \end{aligned} \qquad [A]$$

$$\begin{aligned} R_2Hg + AlH_3 \cdot NMe_3 &\longrightarrow R_2AlH \cdot NMe_3 + H_2 + Hg \\ \tfrac{1}{2}R_2Hg + AlH_3 \cdot NMe_3 &\longrightarrow RAlH_2 \cdot NMe_3 + \tfrac{1}{2}H_2 + \tfrac{1}{2}Hg \end{aligned} \qquad [B]$$

[1]*Present address: Naval Propellant Plant, Indian Head, Maryland.*

$$AlH_3 \cdot NMe_3 + 2R_3Al \cdot NMe_3 \longrightarrow 3R_2AlH \cdot NMe_3$$
$$2AlH_3 \cdot NMe_3 + R_3Al \cdot NMe_3 \longrightarrow 3RAlH_2 \cdot NMe_3 \qquad [C]$$

$$R_2AlCl + LiAlH_4 \xrightarrow{NMe_3} 2RAlH_2 \cdot NMe_3 + LiCl \qquad [D]$$

EXPERIMENTAL

Apparatus

Because the alkylaluminum compounds are sensitive to air and moisture, all synthetic work was carried out either in a high-vacuum system or in a nitrogen atmosphere. Transfers were conducted in an inert atmosphere chamber.[2] For the vapor tension measurements of the triethylaluminum complex, a tensimeter was used (6).

Preparation of Starting Materials

Commercially available lithium hydride (75% pure, based on hydrogen evolution) and lithium aluminum hydride (95% pure) were obtained from Metal Hydrides, Inc. Lecture bottles of the organoaluminum starting materials were supplied by the Ethyl Corporation and Texas Alkyls, Inc. Anhydrous aluminum trichloride was obtained from Matheson Company, Inc. All other starting materials were prepared in this laboratory.

A method based on the procedure of Wiberg, Graf, and Usón (7) was used to prepare aluminum hydride trimethylamine. Lithium aluminum hydride, 32 g (0.8 mole), was refluxed in 500 ml of diethyl ether for 4 hours. After the insoluble material had settled to the bottom of the flask, the supernatant liquid was filtered into a 1-liter flask. An ether solution of 25 g (0.2 mole) of aluminum trichloride was added to the $LiAlH_4$ solution with continuous stirring. After 20 minutes, 50 ml (0.6 mole) of trimethylamine, dissolved in cold ether, was added to the reaction mixture. The product was collected by filtering the supernatant liquid of the reaction mixture, removing the ether under vacuum, and subliming the residue at 60° C (1 mm Hg). The pure $AlH_3 \cdot NMe_3$ melted at 76° C and was free of chlorine. The yield was 65% based on $AlCl_3$. Anal. Calc. for $C_3H_{12}NAl$: C, 40.44; H, 13.57; N, 15.72; Al, 30.28. Found: C, 40.42; H, 13.94; N, 15.49; Al, 30.53.

Triethylaluminum trimethylamine was made on the vacuum line, by the reaction of a hexane solution of Et_3Al and gaseous trimethylamine. The product, after purification by vacuum distillation, boiled at 38–39° C (10^{-3} mm Hg). Anal. Calc. for $C_9H_{24}NAl$: C, 62.38; H, 13.96; N, 8.09; Al, 15.57. Found: C, 62.68; H, 14.25; N, 8.30; Al, 16.03. Vapor pressure data and additional physical properties of triethylaluminum trimethylamine are shown in Tables I and II.

TABLE I

Vapor tensions of liquid triethylaluminum trimethylamine

t (°C)	69.8	101.7	109.8	124.9	138.1
P_{obs} (mm Hg)	1.21	6.8	10.2	20.2	35.2
P_{calc} (mm Hg)	1.22	6.8	10.0	20.1	35.2

TABLE II

Physical properties of triethylaluminum trimethylamine

M.p. (°C)	−41.0
B.p. (°C)*	229.5
A†	−3017.0
B†	8.882
H_{vap} (kcal mole^{-1})	13.801
Trouton const. (cal deg^{-1} mole^{-1})	27.4
Mol. wt.‡	180.0
Mol. wt. (calc.)	173.3

*By extrapolation of vapor pressure equation.
†$\text{Log}_{10} P$ (mm Hg) = $A/T + B$.
‡In cyclohexane.

Trimethylaluminum trimethylamine (8) was prepared in a manner analogous to that of the triethyl compound.

[2]*Model HE-43/HE-73, D. L. Herring Co., Inc., Sherman Oaks, California.*

406704

Can. J. Chem. Downloaded from www.nrcresearchpress.com by 210.87.254.40 on 09/05/12
For personal use only.

Ethylaluminum dichloride (9) was prepared by refluxing a mixture of aluminum trichloride (8.7 g, 0.065 mole) and Et_2AlCl (7.8 g, 0.065 mole). The purified material boiled at 54–55° C (1 mm Hg) and melted at 32° C.

Dimethylmercury and diethylmercury were prepared by reaction of an excess of alkylmagnesium bromide with mercuric chloride in ethyl ether (10).

Preparation of Reaction Intermediates

In order to understand the nature of the intermediates in the reactions of lithium hydride and alkylaluminum chlorides, the trimethylamine adducts of the alkylaluminum chlorides were prepared. Two methods led to the same products: (*a*) direct union of the reactants, and (*b*) their reaction in ethyl ether. In the presence of excess trimethylamine only the monoamine adducts were formed. The diethyl compound melted at −33 to −32° C. Anal. Calc. for $C_7H_{19}ClNAl$: Cl, 19.74; Al, 15.02. Found: Cl, 20.23; Al, 15.52. Ethylaluminum dichloride trimethylamine melted at 50–52° C. Anal. Calc. for $C_5H_{14}Cl_2NAl$: C, 32.27; H, 7.58; Cl, 38.11; N, 7.53; Al, 14.50. Found: C, 31.76; H, 7.74; Cl, 38.02; N, 7.58; Al, 14.04.

Preparation of Diethylaluminum Hydride Trimethylamine

Method A

Diethylaluminum chloride, 19.0 g (0.16 mole), was placed in 250 ml of diethyl ether in a three-necked, 500-ml flask equipped with reflux condenser and drying tube, N_2 gas inlet, and NMe_3 gas inlet. Excess trimethylamine was bubbled into the solution, which was kept at −20° C for 1 hour. After the ether solution of $Et_2AlCl \cdot NMe_3$ had reached room temperature, 1.7 g of powdered 75% LiH (0.16 mole pure LiH) was added. The reaction mixture was then maintained at reflux temperature for 9 hours. The solids were allowed to settle overnight. The clear supernatant liquid was filtered into a distilling flask, and the ether was removed in vacuum. During the slow, high-vacuum distillation that followed, the distillation flask was kept at 40° and the receiving trap at −196° C. A sample of the distillate redistilled at 63–65° C (1 mm Hg). The melting point was −28° C. Methanolysis of a 0.2643 g sample gave the following results: calc. for H_2: 40.8 ml at S.T.P., found: 39.6 ml; calc. for Al: 18.58%, found: 18.86%. The analytical data are summarized in Table III.

TABLE III

The ethylaluminum and methylaluminum hydride trimethylamine complexes

Compound	M.p. (°C)	B.p. (°C) (1 mm Hg)	Anal. calc.	Anal. found A	B	C	D
$Et_2AlH \cdot NMe_3$	−28	63–65	C, 57.89	57.92	57.66	56.98	
			H, 13.88	13.70	13.84	13.52	
			N, 9.65	9.62	10.03	8.84	
			Al, 18.58	18.34	18.39	18.03	
$EtAlH_2 \cdot NMe_3$		39–40	C, 51.25		51.29	51.18	50.97
			H, 13.76		13.93	14.06	13.64
			N, 11.96		11.95	11.94	12.13
			Al, 23.03		22.72	22.73	22.77
$Me_2AlH \cdot NMe_3$	33–35	42–43	C, 51.25		51.43	51.50	
			H, 13.76		13.60	12.97	
			N, 11.96		11.83	12.10	
			Al, 23.03		22.77	23.20	
$MeAlH_2 \cdot NMe_3$	−35	25–26	C, 46.58		46.26	47.04	46.71
			H, 13.68		13.67	12.88	13.61
			N, 13.58		13.30	13.77	13.59
			Al, 26.16		25.83	26.66	26.03

Method B

Aluminum hydride trimethylamine, 4.0 g (0.045 mole), was placed in a three-necked, 500-ml flask, and 250 ml of hexane was added. A hexane solution of diethylmercury, 11.6 g (0.045 mole), was added dropwise to the $AlH_3 \cdot NMe_3$ with stirring and heating. A grey precipitate of mercury was visible after 10 minutes of reaction. The system was kept at 60° C for 4 hours and then permitted to stand for 5 days at room temperature. The supernatant liquid was filtered into a distilling flask, and the solvent was removed in vacuum. Purification of the residue by high-vacuum distillation produced a liquid that boiled at 63–65° C (1 mm Hg). Methanolysis of a 0.4363-g sample gave the following results: calc. for H_2: 67.2 ml at S.T.P., found: 61.2 ml; calc. for Al: 18.58%, found: 19.19%.

Can. J. Chem. Downloaded from www.nrcresearchpress.com by 210.87.254.40 on 09/05/12
For personal use only.

Method C

Triethylaluminum trimethylamine, 4.0 g (0.023 mole), and 1.0 g (0.011 mole) of $AlH_3 \cdot NMe_3$ were placed in a flask and heated with stirring for 30 minutes at 40°. Stirring was continued for 2 hours at room temperature. Distillation yielded a compound boiling at 63–64° C (1 mm Hg).

Preparation of Ethylaluminum Dihydride Trimethylamine

Method A

Several attempts to synthesize the ethylaluminum dihydride amine complex by using lithium hydride in ethyl ether were only partially successful. Although reduction took place, as indicated by the presence of an Al—H band in the infrared spectrum of the reaction mixture, no compound free of chlorine could be obtained.

Method B

The compound was prepared by Method B and gave the following hydrolytic results for a 0.4828-g sample: calc. for H_2: 184.7 ml at S.T.P., found: 181.0 ml; calc. for Al: 23.03%, found: 22.93%.

Method C

The compound was also prepared by Method C given above.

Method D

A solution of 5.9 g (0.155 mole) $LiAlH_4$ in 300 ml of ether was prepared. To this was added dropwise 18.6 g (0.155 mole) of Et_2AlCl in ether. White solids began to precipitate immediately. After the mixture had been refluxed for 20 minutes the solids were allowed to settle, the liquid was filtered into a flask, and the ether was removed in vacuum. A gelatinous material remained. A portion of the gelatinous residue was allowed to react with gaseous trimethylamine. The mixture became quite warm and liquefied while ether and some hydrogen were evolved. A grey solid, presumably metallic aluminum, also formed. When the reaction mixture was subjected to vacuum in a sublimation apparatus, a small amount of white solid collected on the cold finger. According to the melting point (88–92° C) it was $AlH_3 \cdot 2NMe_3$ (7). Fractionation under vacuum of the liquid residue yielded $EtAlH_2 \cdot NMe_3$ as well as some $Et_2AlH \cdot NMe_3$ (the latter was identified by its infrared spectrum and boiling point).

Preparation of Dimethylaluminum Hydride Trimethylamine

Dimethylaluminum hydride trimethylamine was prepared according to Methods B and C. It is interesting that dimethylaluminum chloride, following treatment with trimethylamine in ether solution, was found unreactive toward lithium hydride at 36° C.

Preparation of Methylaluminum Dihydride Trimethylamine

Successful preparation was effected by Methods B, C, and D. A variation of Method D, where the hydride was not isolated from solution prior to addition of trimethylamine, yielded only $MeAlH_2 \cdot NMe_3$. This behavior is in contrast to the corresponding ethyl reaction, where both the monohydride and dihydride were found among the reaction products.

Analytical Results

The alkylaluminum hydride trimethylamine complexes were purified by vacuum distillation and were analyzed for the elements. The analytical results,[3] melting points,[4] and boiling points of the compounds are shown in Table III. The capital-letter designations under the column heading "Anal. found" refer to the methods of synthesis used.

Molecular Weights

Molecular weights were determined cryoscopically in an airtight glass apparatus fitted with a magnetically driven stirrer.[5] The alkylaluminum hydride trimethylamine solutions in cyclohexane were prepared in the dry box. Outside the dry box the charged airtight glass vessel was placed in the ice-cooled glass jacket of the cryoscopic molecular weight apparatus and the electromagnet that drives the stirrer was attached. The freezing point of pure solvent was determined immediately prior to each solution determination. The apparent molecular weights of the alkylaluminum hydride trimethylamine complexes are given in Table IV.

Spectral Data

A model IR-5 Beckman double-beam infrared spectrophotometer with sodium chloride optics was used to record spectra. A NaCl cell with a 0.001-in. lead spacer was used for the samples. The major absorptions in the infrared of the new alkylaluminum complexes are summarized in Table V.

Proton magnetic resonance spectra of the alkylaluminum hydride trimethylamine complexes in cyclohexane solution, tabulated in Table VI, were obtained at 60 Mc, using a Varian model V-4302 nuclear magnetic resonance spectrometer.

[3]*Elemental analyses were conducted by the Schwarzkopf Microanalytical Laboratory, Woodside, New York.*

[4]*Melting points are uncorrected and were determined by the capillary method or the Stock magnetic plunger technique, depending upon the physical state of the material at room temperature.*

[5]*Bender and Hobein, G.m.b.H., Munich, Germany.*

Can. J. Chem. Downloaded from www.nrcresearchpress.com by 210.87.254.40 on 09/05/12
For personal use only.

TABLE IV

Molecular weights of ethylaluminum and methylaluminum hydride trimethylamine complexes*

Compound	Form. wt.	Molal concn.	Mol. wt.	Av. deg. of assoc.
$Et_2AlH \cdot NMe_3$	145.2	0.053	169	1.18
		0.063	172	
		0.072	173	
$EtAlH_2 \cdot NMe_3$	117.2	0.080	187	1.60
		0.082	189	
		0.083	186	
$Me_2AlH \cdot NMe_3$	117.2	0.071	157	1.34
		0.074	157	
		0.076	157	
		0.078	159	
$MeAlH_2 \cdot NMe_3$	103.1	0.091	204	1.95
		0.105	198	
		0.110	199	
		0.118	203	

*Molecular weight measurements were taken cryoscopically in cyclohexane.

TABLE V

Major absorptions in the infrared spectra of the ethylaluminum and methylaluminum hydride trimethylamine complexes

Compound	Absorption (cm^{-1})*†
$Et_2AlH \cdot NMe_3$	2980 (sh, m); 2960 (sh, s); 2880 (vs); 2760 (m); 2700 (w); 1730 (vs); 1480, 1465 (d, vs); 1410 (m); 1370 (w); 1245, 1233 (d, m); 1190 (m); 1103 (m); 997 (vs, b, u); 950 (m); 918 (m); 897 (m); 818 (s); 770 (vs, b)
$EtAlH_2 \cdot NMe_3$	2970 (s); 2900 (vs); 2880 (m); 2710 (w); 1750 (vs, b); 1487, 1470 (d, vs); 1410 (s); 1370 (w); 1250 (s); 1190 (m); 1107 (s); 1000 (vs, b); 952 (s); 920 (s); 898 (s, b); 822 (vs)
$Me_2AlH \cdot NMe_3$	3000 (sh, s); 2970 (s); 2900 (vs); 2800 (sh, s); 1750 (vs); 1480, 1470 (d, vs); 1410 (m); 1250 (s); 1190 (vs); 1108 (s); 1002 (vs); 823 (s)
$MeAlH_2 \cdot NMe_3$	2970 (ms); 2900 (s); 1750 (vs); 1480, 1470 (d, vs); 1410 (m); 1250 (ms); 1192 (ms); 1108 (m); 1002 (vs); 823 (m)

*Spectra were calibrated against the standard spectrum of polystyrene.
†w = weak, m = medium, s = strong, v = very, sh = shoulder, d = doublet, b = broad, u = unsymmetrical.

TABLE VI

Nuclear magnetic resonance spectra of the ethylaluminum and methylaluminum hydride trimethylamine complexes*

	δ†			
Compound	H	N—CH_3	CH_3	CH_2
$Et_2AlH \cdot NMe_3$	‡	−0.94	0.35	1.59‖
$EtAlH_2 \cdot NMe_3$	−2.10	−1.04	0.47	1.64‖
$Me_2AlH \cdot NMe_3$	‡	−0.95	2.27, 2.32§	
$MeAlH_2 \cdot NMe_3$	−2.10	−1.02	2.24, 2.34§	

*Cyclohexane, as the standard, is arbitrarily given the value of $\delta = 0$. Solutions are approximately 10% by weight.
†δ (the chemical shift) $= [(Hr - H)/Hr] \times 10^6$.
‡Not observed.
§Doublet.
‖Some splitting observed.

Can. J. Chem. Downloaded from www.nrcresearchpress.com by 210.87.254.40 on 09/05/12
For personal use only.

DISCUSSION

Synthetic Methods

The reduction of $Et_2AlCl \cdot NMe_3$ to $Et_2AlH \cdot NMe_3$ with lithium hydride was found to be more sluggish than the corresponding reaction using Et_2AlCl-etherate (3). Approximately half the calculated amount of hydride was collected after 9 hours of refluxing of the reactants in ether solution. Times up to 24 hours were used to attempt the lithium hydride conversion of $EtAlCl_2 \cdot NMe_3$ to $EtAlH_2 \cdot NMe_3$. Partial conversion was attained in numerous instances; a strong Al—H absorption repeatedly appeared in the infrared spectra of the ether-soluble fractions of the reaction mixtures. The pure dihydride, free of chlorine, was never obtained, however. In contrast to the diethyl compound, dimethylaluminum chloride trimethylamine did not react with lithium hydride in refluxing ether. Consequently, reduction of methylaluminum dichloride trimethylamine was not attempted.

Replacement of the hydrogen atoms in $AlH_3 \cdot NMe_3$ and $LiAlH_4$ by alkylmercury and arylmercury compounds has been shown to be a general reaction. A mechanism for the reaction has been proposed (11,12). Divinylmercury (13) and bisperfluorovinylmercury (14) react analogously with aluminum hydride trimethylamine, the latter reaction being violent at room temperature in ethyl ether. The partial substitution of alkyl groups for hydrogen on $AlH_3 \cdot NMe_3$ was accomplished by carefully controlling the stoichiometry of the reactants. Diethylmercury was found slightly more reactive towards $AlH_3 \cdot NMe_3$ than dimethylmercury. Hexane was found to be a better reaction medium than ether, even though the $AlH_3 \cdot NMe_3$ is insoluble in hexane, because a higher reaction temperature could be employed. A temperature of 60° C for several hours was usually required to complete the reaction. The yields of products were high since the evolution of hydrogen and the precipitation of mercury cause the equilibrium to shift continually to the right.

The mixing of stoichiometric quantities of $R_3Al \cdot NMe_3$ and $AlH_3 \cdot NMe_3$ has led to nearly quantitative yields of the alkylaluminum hydride compounds. Nuclear magnetic resonance spectra, boiling points, and cryoscopic molecular weight determinations have indicated that single compounds are formed in each case and not equilibrium mixtures containing the reactants.

Whereas reaction of Groups I and II metal alkyls with lithium aluminum hydride leads to the formation of the corresponding metal hydrides (15), the trialkyls of boron, aluminum, and gallium react according to the equation (2)

$$LiAlH_4 + R_3M \rightarrow R_2AlH + LiMRH_3.$$

It must be pointed out, however, that the reactions of Groups I and II metal alkyls with lithium aluminum hydride were carried out in diethyl ether whereas those of Group III were accomplished in the absence of solvent. To check the possibility of further exchange in the reaction of trialkylaluminum and lithium aluminum hydride, the reaction was conducted in diethyl ether using a 3:1 molar ratio of $LiAlH_4$ to Me_3Al. The product was first isolated as the etherate, and was subsequently treated with trimethylamine for easy identification. Only the monohydride was found, indicating that R_2AlH is the reaction product in the absence of or in the presence of diethyl ether. Thus, the formation of the alkylaluminum dihydride trimethylamine complexes by reaction of lithium aluminum hydride and dialkylaluminum halide with subsequent addition of trimethylamine may proceed by the following route:

Can. J. Chem. Downloaded from www.nrcresearchpress.com by 210.87.254.40 on 09/05/12
For personal use only.

$$LiAlH_4 + R_2AlX \xrightarrow{Et_2O} R_2AlH + [LiAlH_3X] \downarrow LiX + AlH_3$$

$$AlH_3 + R_2AlH \rightarrow 2RAlH_2 \xrightarrow{NMe_3} 2RAlH_2 \cdot NMe_3.$$

In the case of R = methyl, the reaction product is all $MeAlH_2 \cdot NMe_3$. The corresponding reaction where R = ethyl yields a mixture of $EtAlH_2 \cdot NMe_3$, $Et_2AlH \cdot NMe_3$, and $AlH_3 \cdot 2NMe_3$, possibly indicating that the combination of AlH_3 and Et_2AlH did not proceed to completion before trimethylamine was introduced into the system. Since excess trimethylamine was used, the very stable $AlH_3 \cdot 2NMe_3$ was formed. This compound does not appear to react with either $R_3Al \cdot NMe_3$ or $R_2AlH \cdot NMe_3$.

Physical Properties

At room temperature the ethylaluminum and the monomethylaluminum hydride trimethylamine complexes are mobile liquids that can be distilled without disproportionation or dissociation under high vacuum. The dimethylaluminum complex is a low-melting solid which sublimes readily under vacuum at room temperature without change. However, the evolution of trimethylamine from each of the complexes was observed during the attempt to obtain their mass spectra at a pressure of 10^{-7} mm Hg. The complexes appear to be unstable at temperatures above 80° C.

The molecular weight determinations show that the methylaluminum and ethylaluminum hydride trimethylamine complexes are associated in cyclohexane. The degree of association appears to be a function of the number and the size of the alkyl groups attached to aluminum (Table IV). Thus, steric hindrance seems to offset the tendency for aluminum to increase its coordination number to 5 by using 3*d* orbitals in its hybridization. If the association is occurring by way of hydrogen bridges, then the hybridization of pentacoordinated aluminum must be considered. If two symmetrical bipyramids are joined on an edge by two hydrogen atoms, each aluminum atom will exhibit the sp^3d state. However, according to the estimate of the Al—H bridge distance in the aluminum hydride trimethylamine dimer by Ruff and Hawthorne (16), the Al—Al bond distance will be less than twice the normal covalent radius of aluminum in the sp^3d structure. Gillespie (17) has proposed an sp^3spd hybridization for the carbon atom which utilizes three normal sp^3 orbitals and two equivalent *spd* orbitals which are formed from the remaining sp^3 orbital and a 3*d* orbital. Ruff and Hawthorne find that a reasonable Al—Al bond distance can be calculated from the sp^3spd interpretation of the aluminum atom and their estimated Al—H bridge distance. A similar interpretation appears reasonable in the case of the analogous alkyl dimers. If the double hydrogen bridge is considered to be rigid, several isomers of each compound in the dimeric state are expected. The resulting nonequivalent alkyl groups may contribute to the methyl and methylene splitting observed in the nuclear magnetic resonance spectra of the alkylaluminum hydride amines (Table VI).[6] It must be pointed out, however, that a number of species may be present in a solution of each of the compounds in cyclohexane, since cryoscopy gives only an average molecular weight value of the species under consideration. Hence, the existence of the dimer is only postulated. The phenomenon of association may even be the result

[6]*A referee has suggested that the splitting observed may be explained in terms of an alternate structure for the dimer which involves bridging methyl or ethyl groups. Low-temperature n.m.r. studies will be required to determine the cause of the splitting.*

Can. J. Chem. Downloaded from www.nrcresearchpress.com by 210.87.254.40 on 09/05/12
For personal use only.

of dipole–dipole interactions rather than hydrogen bridging. Further studies are required to elucidate the structures and the modes of association in these electron-deficient aluminum compounds.

ACKNOWLEDGMENTS

The authors wish to thank D. W. Moore of the U.S. Naval Ordnance Test Station, China Lake, California, for the n.m.r. spectra. We desire to express our appreciation also for the continued interest of Drs. Charles P. Haber and Peter J. Slota of the Naval Ordnance Laboratory, Corona. The financial support by the Advanced Research Projects Agency through the Navy Department, Bureau of Naval Weapons, is also gratefully acknowledged.

REFERENCES

1. O. Stecker and E. Wiberg. Chem. Ber. **75**, 2003 (1942).
2. T. Wartik and H. I. Schlesinger. J. Am. Chem. Soc. **75**, 835 (1953).
3. K. Ziegler, H. Gellert, H. Martin, K. Nagel, and T. Schneider. Ann. Chem. **589**, 91 (1954).
4. K. Ziegler, K. Schneider, and J. Schneider. Ann. Chem. **623**, 9 (1959).
5. F. M. Peters and B. Bartocha. Chem. Ind. (London), 1271 (1961).
6. A. B. Burg and H. I. Schlesinger. J. Am. Chem. Soc. **59**, 780 (1937).
7. E. Wiberg, H. Graf, and R. Usón. Z. Anorg. Allgem. Chem. **272**, 221 (1953).
8. N. Davidson and H. C. Brown. J. Am. Chem. Soc. **64**, 316 (1942).
9. A. von Grosse and J. M. Mavity. J. Org. Chem. **5**, 106 (1940).
10. H. Gilman and R. E. Brown. J. Am. Chem. Soc. **52**, 3314 (1930).
11. T. G. Traylor. Chem. Ind. (London), 1223 (1959).
12. J. K. Ruff. J. Am. Chem. Soc. **83**, 1798 (1961).
13. B. Bartocha, A. J. Bilbo, and M. Y. Gray. Angew. Chem. **72**, 36 (1960).
14. B. Bartocha and A. J. Bilbo. J. Am. Chem. Soc. **83**, 2202 (1961).
15. G. D. Barbaras, C. Dillard, A. E. Finholt, T. Wartik, K. E. Wilzbach, and H. I. Schlesinger. J. Am. Chem. Soc. **73**, 4585 (1951).
16. J. K. Ruff and M. F. Hawthorne. J. Am. Chem. Soc. **82**, 2141 (1960).
17. R. J. Gillespie. J. Chem. Soc. 1002 (1952).

Can. J. Chem. Downloaded from www.nrcresearchpress.com by 210.87.254.40 on 09/05/12
For personal use only.

REACTION OF CHROMYL CHLORIDE WITH SOME OLEFINS

PART I. THE PRODUCTS FROM CYCLOHEXENE, CYCLOPENTENE, 1-HEXENE, AND 2-METHYL-1-PENTENE

R. A. STAIRS
Department of Chemistry, Queen's University, Kingston, Ontario

AND

D. G. M. DIAPER AND A. L. GATZKE
Department of Chemistry, Royal Military College of Canada, Kingston, Ontario

Received November 30, 1962

ABSTRACT

Chromyl chloride in carbon tetrachloride solution reacts in the cold with cyclohexene, cyclopentene, and 1-hexene to give the various isomeric chlorohydrins as the major products. The major product from 2-methyl-1-pentene was 2-methylpentanal. Significant amounts of α-chloro carbonyl compounds and some α,β-unsaturated carbonyl compounds were also produced. The significance of these results is discussed.

INTRODUCTION

The reaction of chromyl chloride with olefins has received little attention in contrast to the better known Étard reaction, involving the oxidation of an alkyl side chain of an aromatic hydrocarbon. Étard (1), and later Henderson and others (see references quoted in ref. 2), oxidized olefinic terpenes to obtain brown complexes containing about two atoms of chromium per molecule of olefin. On hydrolysis these complexes yield aldehydes, ketones, and chlorinated compounds that were for the most part unidentified. The first significant study of the chromyl chloride – olefin reaction was made by Cristol and Eilar (3). They reported that oxidation of cyclohexene gave *trans*-2-chlorocyclohexanol, and a series of terminal olefins yielded the chlorohydrins corresponding to anti-Markownikoff addition of hypochlorous acid. It was postulated that only 1 mole of chromyl chloride took part in the main reaction. This was later verified by Stairs (4).

From these results it was concluded that the reaction involves electrophilic attack on the double bond by an oxygen of chromyl chloride. A cyclic oxonium ion intermediate would then account for the observed positional isomerism and stereoisomerism.

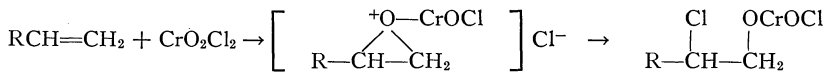

More recently Sulima and Gragerov (5) have shown by use of O^{18} tracers that in the case of cyclohexene all the oxygen in the 2-chlorocyclohexanol comes from the chromyl chloride. This suggests that the most probable structure of the complex is A (or as is highly likely, a polymer of A containing cyclohexane and chlorochromate residues, possibly linked through oxygen–chromium bridges) and that hydrolysis involves the O—Cr bond of the chlorochromate IV ester.

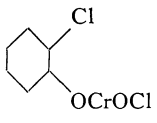

A

Can. J. Chem. Downloaded from www.nrcresearchpress.com by 210.87.254.5 on 09/05/12
For personal use only.

Reinvestigation of the chromyl chloride – olefin reaction, using gas chromatography to separate the products, has revealed a number that were previously unreported. The nature of these products permit certain speculations regarding the mechanism of the reaction.

RESULTS AND DISCUSSION

Reaction of chromyl chloride with cyclohexene in carbon tetrachloride solution gave a nearly quantitative yield of a brown precipitate assumed to be $C_6H_{10} \cdot CrO_2Cl_2$. Hydrolysis with aqueous sodium bisulphite followed by distillation gave as the major fraction what was believed to be *trans*-2-chlorocyclohexanol. However, infrared spectral comparison of this product with authentic samples of *cis*- and *trans*-2-chlorocyclohexanol indicated that the product of the oxidation was a mixture of both isomers. This was confirmed by the preparation of both α-naphthylurethan derivatives, and by quantitative analysis with alkali (6). Treatment of the product mixture with α-naphthylisocyanate afforded the derivative of the trans chlorohydrin in a fairly pure state. To obtain the derivative of the cis chlorohydrin, the trans isomer was converted to cyclohexene oxide by treatment with aqueous alkali and removed from the mixture by distillation. Since this treatment was essential, the failure of Cristol and Eilar to detect the cis isomer is easily understood.

The more volatile fractions of the distillate showed infrared absorptions at 1710 and 1680 cm^{-1} which were attributed to a non-conjugated and an α,β-unsaturated ketone. Chromatography on a Bentonite–Celite column of the 2,4-dinitrophenylhydrazone obtained from this fraction resulted in separation of the 2,4-dinitrophenylhydrazones of cyclohexanone and Δ^2-cyclohexenone (7). Quantitative estimation was made of the reaction of 0.167 mole of cyclohexene with 0.160 mole of chromyl chloride. The yields (in parentheses) of the products formed were: *trans*-2-chlorocyclohexanol (21%), *cis*-2-chlorocyclohexanol (14%), cyclohexanone (5.5%), Δ^2-cyclohexenone (17%). In addition 21% of unreacted cyclohexene was recovered, and 21.5% was unidentified high-boiling material. A similar oxidation of cyclopentene yielded *trans*-2-chlorocyclopentanol (6%), *cis*-2-chlorocyclopentanol (18%), and a small amount of 2-chlorocyclopentanone.

The reaction of 1-hexene with an equimolar amount of chromyl chloride gave a liquid which was separated by preparative gas chromatography into five chromatographically pure products. These were found to be 2-chloro-1-hexanol (32.6%), 1-chloro-2-hexanol (9.3%), 2-chlorohexanal (1.7%), 1-chloro-2-hexanone (4.6%), and a 1.8% yield of a substance having an ultraviolet absorption maximum at 217 mμ in ethanol, which could be either 2-hexenal or 1-hexene-3-one. Oxidation of 2-methyl-1-pentene gave mainly 2-methylpentanal. The chlorohydrins, if they were formed at all, represented less than 10% of the major product.

The formation of cis as well as trans chlorohydrins from both cyclohexene and cyclopentene indicates that a cyclic oxonium ion intermediate, B, cannot represent the only reaction route. On the other hand, an intermediate such as C would be expected to yield entirely cis chlorohydrin. Finally, an intermediate such as D would lead to both

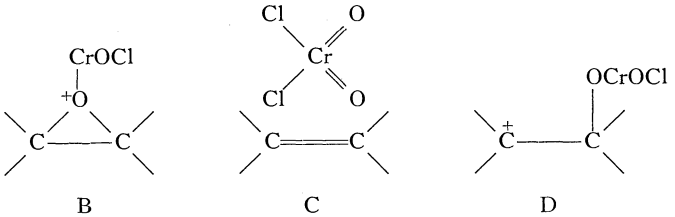

B C D

Can. J. Chem. Downloaded from www.nrcresearchpress.com by 210.87.254.5 on 09/05/12
For personal use only.

cis and trans chlorohydrins with proportions of the isomers thermodynamically controlled. Unfortunately, the thermodynamic information is not available. The situation is complicated by the possibility of selective overoxidation of one of the isomeric chlorohydrins, either during the first step as the chlorochromate IV ester or during the hydrolysis. This is probably the origin of the α-chloro carbonyl compounds.

A further source of complication lies in the possible elimination of hydrogen chloride from both the α-chloro carbonyl compounds and from the chlorohydrins. The conjugated unsaturated compounds found among the products from cyclohexene and 1-hexene may arise in this way, and not, as we first supposed, by an Étard reaction on the allylic carbon of the olefin. That this elimination does not appear to happen with 2-chlorocyclopentanone may be due to steric difficulty in the flat cyclopentane ring. The configuration of 2-chlorocyclohexanone, on the other hand, with an axial chlorine atom (8) is very favorable for trans elimination. Elimination of hydrogen chloride from 2-methyl-2-chloropropanol has been shown to occur readily (9). If it is assumed that 2-methylpentanal, the main product from 2-methyl-1-pentene, arose in this manner, the ratio of 2-chloro-1-ol to 1-chloro-2-ol is 10:1 or greater for the 2,2-dialkylethylene, as compared to about 3:1 for the monoalkyl, i.e. 1-hexene. This is reasonable for a weak Markownikoff effect, with chlorine acting as the negative, and CrO_2Cl as the positive, part of the addend. Depending on whether the ratio is kinetically or thermodynamically controlled, this corresponds to a $\Delta(\Delta G^*)$ or $\Delta(\Delta G)$ of about 0.7 kcal/mole for 1-hexene and >1.5 kcal/mole for 2 methyl-1-pentene. This is compatible with any of the intermediates B, C, or D, though the small size of the effect favors C.

It is clearly not possible to favor any single route or particular combination of routes for the reaction on the basis of the products reported here. A kinetic study would be simpler if there were fewer products and higher yields, but it is clearly needed before the mechanism can be further discussed. Such a study is now in progress.

EXPERIMENTAL

Melting points were determined by the capillary tube method and are uncorrected. Gas chromatograms were obtained using a Burrell Model K-3 for qualitative work and a Burrell Model K-2 for preparative separations and analysis. Nuclear magnetic resonance spectra were obtained on the Varian A60 spectrometer with tetramethylsilane as external standard, this being set at 10.0 τ on the Tiers scale.

Reagents

Chromyl chloride (Allied Chemical) was purified by bubbling dry nitrogen through the liquid to remove traces of hydrogen chloride and was then distilled through a 30-cm Vigreaux column. The fraction boiling at 114–115° was retained. The reagent was protected from light during the distillation and storage and was repurified when any turbidity was noticeable. The olefins were dried and distilled before use and the purity was shown to be greater than 99% by gas chromatography using a silver nitrate – ethylene glycol column. This column efficiently separated a mixture of 1-hexene and 2-hexene prepared by the dehydration of 2-hexanol.

Reaction of Chromyl Chloride with Cyclohexene

A solution of 20.09 g (0.24 mole) of cyclohexene in carbon tetrachloride (500 ml) was treated with 38 g (0.24 mole) chromyl chloride in carbon tetrachloride (200 ml) during a 1-hour period. The temperature was maintained at 0–5°. Precipitation of the brown complex began on the addition of the first few drops of the chromyl chloride solution. The complex was hydrolyzed *in situ* by the addition of a mixture of water (200 ml), ice (100 g), and sodium metabisulphite (15 g). The mixture was stirred for 15 minutes and the organic layer was then separated, washed with saturated sodium chloride solution, dried over sodium sulphate, and the solvent removed. A gas chromatogram (115°, Apiezon T on Embacel, H_2, 55 ml/min) of crude product showed peaks with retention times of 40 seconds (solvent), 125 seconds (small), 145 seconds (medium), and 290 seconds (large). Distillation under reduced pressure through a 15-cm Vigreaux column gave the following fractions: (1) 0.30 g, b.p. 36° at 150 mm; (2) 0.66 g, b.p. 68–84° at 90 mm; (3) 1.18 g, b.p. 84–85° at 80 mm; (4) 2.26 g, b.p. 104–109° at 60 mm; (5) 2.18 g, b.p. 96–98° at 40 mm; (6) 3.15 g, b.p. 98–100° at

Can. J. Chem. Downloaded from www.nrcresearchpress.com by 210.87.254.5 on 09/05/12
For personal use only.

36 mm; (7) 2.24 g, b.p. 92–97° at 20 mm; (8) 1.69 g, b.p. 90–92° at 20 mm; (9) 0.70 g, b.p. 92–97° at 20 mm. The following compounds were identified in the distillate.

(*a*) *Cyclohexanone and* Δ^2*-Cyclohexenone*

Gas chromatography of fraction 3 from the distillation showed two major peaks (125 and 145 seconds). The infrared spectrum of this fraction in carbon tetrachloride had absorption maxima attributed to the carbonyl absorption frequencies at 1710 and 1680 cm^{-1}. Treatment of fraction 3 with 2,4-dinitrophenylhydrazine gave a precipitate from which cyclohexanone-2,4-dinitrophenylhydrazone and Δ^2-cyclohexenone 2,4-dinitrophenylhydrazone were obtained after chromatography on a Bentonite–Celite column (7). The first eluted, a yellow band, when crystallized from ethanol, had m.p. 160–161°. The mixed melting point and infrared spectrum were identical with those of cyclohexanone 2,4-dinitrophenylhydrazone as was the retention time on gas chromatography of the original ketone. The second band on elution chromatography was a deep red-orange which when crystallized from ethanol had m.p. 162–163°. Lit. m.p. 163° (10). The infrared spectrum and mixed melting point were identical with those of an authentic sample of Δ^2-cyclohexenone 2,4-dinitrophenylhydrazone (11). Anal. Calc. for $C_{12}H_{12}N_4O_4$: C, 52.19; H, 4.38; N, 20.27. Found: C, 51.91; H, 4.25; N, 20.27.

(*b*) *cis and trans-2-Chlorocyclohexanols*

Fractions 5 to 9 showed strong infrared absorption at 3600 cm^{-1} assigned to the hydroxyl group. The spectra differed from that of authentic *trans*-2-chlorocyclohexanol prepared by the addition of hypochlorous acid to cyclohexene (12), and that of *cis*-2-chlorocyclohexanol prepared by the aluminum isopropoxide reduction of 2-chlorocyclohexanone (13), and appeared to be a composite of these. Known mixtures of these isomers were not resolved by gas chromatography under the conditions used. Treatment of the oxidation product mixture with α-naphthylisocyanate on the steam bath for 30 minutes gave *trans*-2-chlorocyclohexanol α-naphthylurethan which when recrystallized twice from hexane had m.p. and mixed m.p. 164–165°. Lit. m.p. 164° (6). Anal. Calc. for $C_{17}H_{18}NO_2Cl$: C, 67.19; H, 6.32; Cl, 11.68. Found: C, 66.70; H, 5.92; Cl, 11.40. Separation of the cis isomer from the mixture by the method of Bartlett (6) followed by treatment with α-naphthylisocyanate on the steam bath for 2 hours afforded *cis*-2-chlorocyclohexanol α-naphthylurethan, m.p. and mixed m.p. 93–94°. Lit. 93° (6). Calc. for $C_{17}H_{18}NO_2Cl$: C, 67.19; H, 6.32; Cl, 11.68. Found: C, 66.92; H, 6.34; Cl, 11.46.

Quantitative Analysis of the Cyclohexene – Chromyl Chloride Reaction

(*a*) *Unreacted Cyclohexene*

The reaction was carried out as previously outlined and the brown complex was then collected by filtration, washed with carbon tetrachloride, and dried under vacuum. Escaping vapor from both the filter flask and the vacuum desiccator were trapped in a dry ice–acetone trap and returned to the main filtrate. This filtrate was then diluted to 1000 ml with carbon tetrachloride and aliquots were titrated for cyclohexene with a standard solution of bromine according to the method of Siggia (14). The analysis was found to be accurate to within 2% when samples of known concentration were titrated.

(*b*) *cis and trans-2-Chlorocyclohexanols*

The reaction was carried out as previously described. The organic layer was extracted several times with saturated sodium chloride solution to remove any hydrochloric acid formed during the hydrolysis. The carbon tetrachloride was distilled off and the residue made up to volume with ethanol. Suitable aliquots were titrated with standard sodium hydroxide by Bartlett's method (6) for both chlorohydrins.

(*c*) Δ^2*-Cyclohexenone and Cyclohexanone*

These products were determined from their retention volumes on gas chromatography after calibration with known volumes of the pure liquids.

Reaction of Chromyl Chloride and 1-Hexene

1-Hexene (20 g, 0.24 mole) and chromyl chloride (20 ml, 0.24 mole) were reacted as described for cyclohexene. A gas chromatogram of the crude product, after removal of the solvent (125°, neopentylglycol sebacate on Embacel, He, 40 ml/min), showed five major peaks with retention times 420 seconds (small), 595 seconds (small), 730 seconds (medium), 1030 seconds (medium), 1235 seconds (large). These components were gas chromatographically separated and the various fractions condensed and collected. About 20 injections of 100 μl each were required to obtain a workable sample for the identification of the components.

(*a*) *2-Chlorohexanal*

The infrared spectrum showed absorption maxima at 1730 and 2720 cm^{-1} assigned to carbonyl and aldehyde carbon–hydrogen absorption frequencies respectively. This fraction gave positive Schiff's and Fehling's tests, and contained chlorine (Beilstein's test). Treatment with 2,4-dinitrophenylhydrazine gave yellow needles, m.p. 106–107°. An authentic sample of 2-chlorohexanal prepared by the α-chlorination of hexanal with sulphuryl chloride (15) was identical with the chromyl chloride oxidation product in every way (retention time on gas chromatography, infrared spectrum, m.p. and mixed m.p. of the 2,4-dinitrophenylhydrazone).

(*b*) *Unsaturated Carbonyl Compound*

The component with retention time 595 seconds could not be obtained in sufficient quantity for complete

Can. J. Chem. Downloaded from www.nrcresearchpress.com by 210.87.254.5 on 09/05/12
For personal use only.

characterization because of failure to condense in the fraction collector. However, sufficient sample was obtained for an ultraviolet spectrum, which showed a single maximum at λ_{max} 217 mμ. A value for the extinction coefficient was not obtained.

(*c*) *1-Chloro-2-hexanone*

The infrared spectrum of this oxidation product showed a carbonyl absorption at 1720 cm^{-1}. This compound failed to react with 2,4-dinitrophenylhydrazine. Analysis of the liquid for chlorine by the Schoeniger combustion method gave: Cl, 25.2. Calc. for $C_6H_{11}OCl$, 26.4. The n.m.r. signals were as follows: distorted triplet centered at 8.62 τ (terminal methyl, area = 3 H), large number of lines centered at 8.11 τ (β- and γ-methylenes area = 4 H), triplet centered at 6.08 τ (α-methylene, area = 2 H), and singlet at 5.64 τ (α-chloromethyl, area = 2 H).

(*d*) *1-Chloro-2-hexanol*

This component showed strong hydroxyl absorption in the infrared and gave a positive Beilstein's test for chlorine. Upon admixture of this product with an authentic sample prepared by the hypochlorous acid addition to 1-hexene, and gas chromatography of the mixture, a single peak was obtained. Treatment with an equivalent of α-naphthylisocyanate for 3 hours at 100° C gave the α-naphthylurethan, m.p. and mixed m.p. 86–87°. (The authentic 1-chloro-2-hexanol had to be gas chromatographically purified to remove about 10% 2-chloro-1-hexanol before a good α-naphthylurethan could be obtained.) Anal. Calc for $C_{17}H_{20}NO_2Cl$: C, 66.80; H, 6.58; Cl, 11.60. Found: C, 66.85; H, 6.65; Cl, 11.33.

(*e*) *2-Chloro-1-hexanol*

This component showed strong hydroxyl absorption in the infrared and contained chlorine. The α-naphthylurethan had m.p. 93–94°. Anal. Calc for $C_{17}H_{20}NO_2Cl$: C, 66.8; H, 6.80; Cl, 11.60. Found: C, 66.21; H, 6.90; Cl, 11.21.

(*f*) *Yields*

1-Hexene (5.0 g, 0.0591 mole) and chromyl chloride (4.8 ml, 0.059 mole) were reacted in the usual way. The carbon tetrachloride was distilled off until a volume of 30 ml was obtained as a residue. This residue was then transferred to a 50-ml volumetric flask and made up to volume with the rinse from the distilling flask. The yields of the various components were determined from the retention volumes on gas chromatography. The instrument was calibrated by obtaining retention volume versus volume injected for each of the gas chromatographically pure components.

Reaction of Chromyl Chloride with Cyclopentene

Cyclopentene (8.0 g, 0.12 mole) was oxidized with chromyl chloride (9.0 ml, 0.11 mole) in the previously described manner. A gas chromatogram (125°, neopentylglycol sebacate on Embacel, He, 40 ml/min) of the crude product showed three major peaks and one minor peak with retention times 310 seconds (small), 700 seconds (large), 950 seconds (medium), 1170 seconds (medium). These products were separated in pure fractions by the same method as applied with 1-hexene and then identified.

(*a*) *trans-2-Chlorocyclopentanol*

This fraction showed a strong infrared absorption at 3470 cm^{-1} (pure liquid) assigned to the hydroxyl group, and gave a positive Beilstein's test for chlorine. The α-naphthylurethan had m.p. 106–107°. Lit. m.p. 105° (16). Anal. Calc for $C_{16}H_{16}NO_2Cl$: C, 66.40; H, 5.57; Cl, 12.24. Found: C, 66.22; H, 5.72; Cl, 11.79. The oxidation product was found to be identical in every way (retention time on gas chromatography, infrared spectrum, m.p. and mixed m.p. of the α-naphthylurethan) with an authentic sample of *trans*-2-chlorocyclohexanol prepared by the addition of hypochlorous acid to cyclopentene.

(*b*) *cis-2-Chlorocyclopentanol*

The infrared spectrum of this component showed a strong absorption attributed to the hydroxyl group. The α-naphthylurethan had m.p. 100–101°. Anal. Calc for $C_{16}H_{16}NO_2Cl$: C, 66.40; H, 5.57; Cl, 12.24. Found: C, 66.56; H, 5.77; Cl, 11.96. This compound was identical in the infrared spectrum, in retention time on gas chromatography, and in m.p. and mixed m.p. of the α-naphthylurethan derivative with authentic *cis*-2-chlorocyclopentanol, prepared by the aluminum isopropoxide reduction of 2-chlorocyclopentanone and purification through gas chromatography.

(*c*) *2-Chlorocyclopentanone*

This product showed an infrared absorption at 1750 cm^{-1} assigned to carbonyl stretching, and it was found to contain chlorine. Authentic 2-chlorocyclopentanone, prepared by the chlorination of cyclopentanone (17), had an infrared spectrum and retention time on gas chromatography identical with those of this product.

(*d*) *Yields*

The products of the reaction of chromyl chloride with cyclopentene were determined quantitatively by the same method used for 1-hexene.

Reaction of Chromyl Chloride and 2-Methyl-1-pentene

2-Methyl-1-pentene (10 g, 0.12 mole) and chromyl chloride (9.7 ml, 0.12 mole) were reacted in the usual fashion. A gas chromatogram of the crude product showed one major product along with four very minor

Can. J. Chem. Downloaded from www.nrcresearchpress.com by 210.87.254.5 on 09/05/12
For personal use only.

products. The infrared spectrum of the crude product showed absorption maxima at 2720 and 1720 cm^{-1} attributed to aldehyde carbon–hydrogen and carbonyl absorption respectively. Distillation of the product gave a fraction weighing 3 g, b.p. 55° at 22–26 cm, and leaving a large pot residue. The fraction distilled was identified as consisting mainly of 2-methylpentanal by a positive Fehling's test, and a 2,4-dinitrophenylhydrazone melting point of 104–105°. Lit. m.p. 102–104° (18). Anal. Calc. for $C_{12}H_{16}N_4O_4$: N, 20.0. Found: 19.8. The distilled fraction on gas chromatography had the same retention time as that of the major peak of the crude product.

ACKNOWLEDGMENTS

The financial support of the National Research Council and the Defence Research Board is gratefully acknowledged. We thank Dr. J. F. Hanlan of the Du Pont Research Centre, Kingston, Ontario, for the determination of the n.m.r. spectra, and Dr. S. Wolfe for many helpful discussions.

REFERENCES

1. A. Étard. Ann. Chim. Phys. **22**, 218 (1881).
2. W. H. Hartford and M. Darrin. Chem. Rev. **58**, 40 (1958).
3. S. J. Cristol and K. R. Eilar. J. Am. Chem. Soc. **72**, 4353 (1950).
4. R. A. Stairs. Can. J. Chem. **38**, 2028 (1960).
5. L. V. Sulima and I. P. Gragerov. J. Gen. Chem. USSR (Eng. Transl.), 3787 (1959).
6. P. D. Bartlett. J. Am. Chem. Soc. **57**, 224 (1935).
7. R. P. Linstead, J. A. Elvidge, and M. Whalley. A course in modern techniques of organic chemistry. Butterworths Scientific Publications, London. 1955. p. 5.
8. E. J. Corey. J. Am. Chem. Soc. **75**, 2301 (1953).
9. A. A. Petrov. J. Gen. Chem. USSR, **15**, 690 (1945).
10. P. D. Bartlett and G. F. Woods. J. Am. Chem. Soc. **62**, 2933 (1940).
11. F. C. Whitmore and G. W. Pedlow, Jr. J. Am. Chem. Soc. **65**, 758 (1943).
12. G. H. Coleman and H. F. Johnstone. *In* Organic syntheses. Coll. Vol. I. 2nd ed. John Wiley and Sons, New York. 1948. p. 158.
13. H. C. Stevens and O. Crummitt. J. Am. Chem. Soc. **74**, 4876 (1952).
14. S. Siggia. Quantitative organic analysis via functional groups. John Wiley and Sons, New York. 1949. p. 33.
15. L. Herzfeld, B. Prijs, and H. Erlenmeyer. Helv. Chim. Acta, **36**, 1842 (1953).
16. L. H. Owen and P. N. Smith. J. Chem. Soc. 4026 (1952).
17. A. Kotz, K. Blendermann, E. Karpati, and R. Rosenbusch. Ann. **400**, 50 (1913).
18. K. C. Brannock and J. R. Lappin. J. Am. Chem. Soc. **77**, 6052 (1955).

Can. J. Chem. Downloaded from www.nrcresearchpress.com by 210.87.254.5 on 09/05/12
For personal use only.

THE PROTONATION OF THE CARBONYL GROUP

III. DIARYL KETONES

ROSS STEWART, M. R. GRANGER, R. B. MOODIE, AND L. J. MUENSTER
Department of Chemistry, University of British Columbia, Vancouver, British Columbia

Received December 26, 1962

ABSTRACT

The basicities of 14 diaryl ketones have been determined. Except for 4,4′-bis(dimethylamino)benzophenone, which protonates on nitrogen, the pK_{BH^+} values range from −4.19 for 4,4′-dihydroxybenzophenone to −10.12 for 4,4′-dinitrobenzophenone. The basicities are not correlated well by either σ or σ^+ substituent constants and it is believed that this is due either to a variation in the degree of rotation (and hence conjugation) of the two aryl rings or to a departure of carbonyl basicities from the conventional acidity scale based on ammonia bases. The effect on the basicity of joining the ortho positions by bridges of various sizes has also been determined and the results are discussed in terms of steric and electronic effects.

Can. J. Chem. Downloaded from www.nrcresearchpress.com by 210.87.254.6 on 09/05/12
For personal use only.

Previous work in this laboratory has been concerned with the protonation of very weakly basic groups such as carbonyl (1), carboxyl (2, 3), and carboxamido (4, 5). We now wish to report the basicities of two series of diaryl ketones. In one series the para or

$$Ar_2C{=}O + H^+ \rightleftharpoons Ar_2C{=}\overset{+}{O}H$$

meta substituents in benzophenone are varied and in the other the angle of the aryl rings with the carbonyl group is varied by means of ortho–ortho bridges.

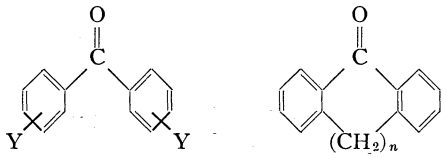

The basicities of benzophenone and anthrone have been previously measured by Handa and Koboyashi (6) and those of benzophenone and some of its alkyl derivatives by Fischer, Grigor, Packer, and Vaughan (7).

RESULTS AND DISCUSSION

The basicities and the ultraviolet spectral data for the diaryl ketones are given in Table I. Unlike the series of monoaryl ketones and aldehydes (1) whose basicities correlate quite well with the modified Hammett substituent constants, σ^+ (8), the present series (compounds I to VIII) does not give a very satisfactory fit with any of the parameters commonly used in linear free energy correlations. This may be due to the presence of two potentially conjugating rings each of which can rotate and whose actual degrees of conjugation may vary considerably with the identity of the para substituents. Another possibility to be considered is that carbonyl compounds are not following the conventional Hammett acidity function, H_0, which is based on protonation of amine bases (9, 10). The satisfactory correlations with σ^+ previously observed for benzaldehydes and acetophenones do not cover nearly the range of acidities spanned by the benzophenones. Recent work suggests that the anomalous ionization curves often obtained with carbonyl bases are due less to solvent effects on spectra than to the compounds' ionization not following the function H_0 (9). It should be pointed out in this connection that most of the

TABLE I

pK_{BH^+} and ultraviolet spectral data for diaryl ketones

Compound		Basicity		Neutral compound*		Conjugate acid†		
		pK_{BH^+}	% H_2SO_4 at half ionization	λ_{max} (mμ)	$10^{-4}\epsilon_{max}$	λ_{max} (mμ)	$10^{-4}\epsilon_{max}$	Δλ (mμ)
$(C_6H_5)_2C{=}O$	(I)	−6.16‡	73.8	258	1.70	344 292	2.44 1.36	86
$(p\text{-}CH_3C_6H_4)_2C{=}O$	(II)	−5.67	70.0	273	1.96	375 302	3.90 1.27	102
$(p\text{-}CH_3OC_6H_4)_2C{=}O$	(III)	−4.39	59.5	299 225	2.20 1.28	404 319 246	4.30 1.06 0.67	105
$(p\text{-}HOC_6H_4)_2C{=}O$	(IV)	−4.19	57.6	300 230	2.10 1.30	390 305 240	3.74 0.97 0.67	90
$(p\text{-}ClC_6H_4)(C_6H_5)C{=}O$	(V)	−6.64	77.6	267	2.05	363 299	3.30 1.20	96
$(p\text{-}ClC_6H_5)_2C{=}O$	(VI)	−6.96	80.0	264§	2.60	377 311	4.24 1.50	(113)
$(m\text{-}NO_2C_6H_4)_2C{=}O$	(VII)	−9.85‖	99.3	258¶	2.81	322**	2.05	64
$(p\text{-}NO_2C_6H_4)_2C{=}O$	(VIII)	−10.12‖	99.6	280¶	2.70	324**	1.74	44
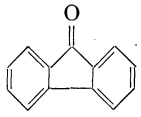	(IX)	−6.65	77.6	257	8.3	266	5.3	9
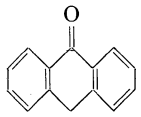	(X)	−5.02	64.7	275	1.5	351	2.4	76
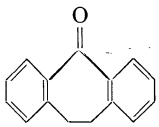	(XI)	−5.69	70.2	276	1.3	358	2.3	82
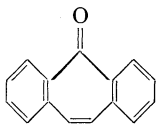	(XII)	−5.25	66.6	262	4.0	293	9.1	31
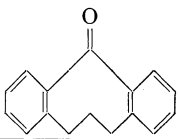	(XIII)	−5.80	71.1	277	1.3	353	2.5	76

*Solvent is EtOH–H_2O (1:10).
†Solvent is 95% H_2SO_4.
‡Literature values, −5.5 (6) and −6.18 (7).
§The low solubility of this compound required the use of 95% EtOH.
‖The pK_{BH^+} of nitrobenzene is −11.26 (J. C. D. Brand, J. Chem. Soc., 997, (1950)); the nitro groups in the ketones will be less basic than this and so carbonyl, not nitro, protonation must be occurring here.
¶Solvent is 80% H_2SO_4.
**Solvent is 30% fuming H_2SO_4, nitro protonation has probably occurred here.

compounds studied in the present work gave excellent ionization curves with slopes very near unity for the logarithmic plots (Figs. 1 and 2). Following the suggestions of Professors N. C. Deno and E. M. Arnett (personal communications) we have also listed in

Can. J. Chem. Downloaded from www.nrcresearchpress.com by 210.87.254.6 on 09/05/12
For personal use only.

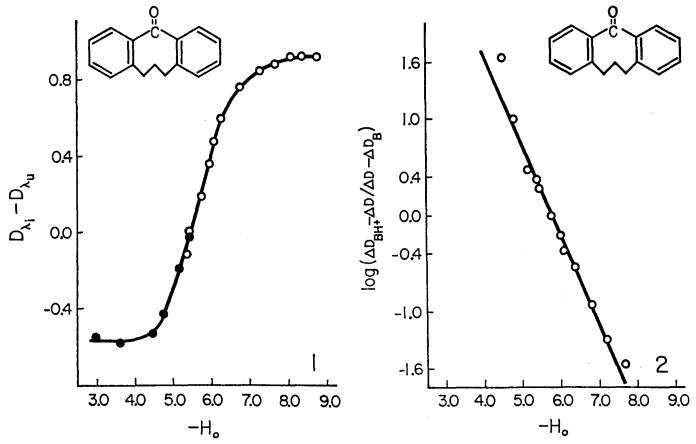

FIG. 1. The function $D\lambda_i - D\lambda_u$ plotted against $-H_0$ for 2,3;7,8-dibenzcyclooctadienone (XIII). $\lambda_i = 353$ mμ, $\lambda_u = 277$ mμ. ○, 3.93×10^{-5} *M*; ●, 4.68×10^{-6} *M*.

FIG. 2. The function log $(\Delta D_{BH^+} - \Delta D/\Delta D - \Delta D_B)$ plotted against $-H_0$ for 2,3;7,8-dibenzcyclooctadienone (XIII). ΔD, ΔD_{BH^+}, and ΔD_B are equal to $D_{353} - D_{277}$ in acid solutions in which XIII is partly ionized, completely ionized, and completely unionized, respectively.

Table I the basicities in terms of % H_2SO_4 in which the compounds are half ionized. Should it be found, in fact, that different scales are required for amine bases, carbonyl bases, etc., such an indication of a compound's basicity will still be meaningful.

Infrared Spectra of the Ketones

We have previously observed very good correlations between the basicities of substituted acetophenones and their carbonyl stretching frequencies (1). This is because the carbonyl stretching frequency and the basicity constant both tend to follow σ^+. However, when values for $\nu_{C=O}$ for diaryl ketones are plotted against both σ and σ^+ a roughly linear relation is obtained in each case. In fact, the correlation coefficients for the two lines are identical (0.978).* This probably reflects a somewhat diminished resonance effect between the carbonyl group and the para substituents in the benzophenones compared to both the acetophenone and the benzaldehyde conjugate acids, in agreement with the p*K* results.

Ultraviolet Spectra of the Cations

A red shift ($\Delta\lambda$, Table I) of roughly 100 mμ in the ultraviolet maxima results from protonation of the carbonyl group, in most cases. This is about twice as large as the shift in the case of acetophenones and benzaldehydes (1). The effect of substituents on the absorption maximum of benzophenone conjugate acid is the same as on that of the diphenylmethyl cation, $(C_5H_6)_2CH^+$ (11). The derivatives of the latter carbonium ion each absorb at about 100 mμ longer wavelength than do the corresponding protonated benzophenone ions reported herein. However, there is a marked resemblance in the shape of the spectra of the isoelectronic ions $Ar_2\overset{+}{C}OH$ and $Ar_2\overset{+}{C}CH_3$ (12).

**When a parameter gives plots with the same degree of linearity (same correlation coefficient) with both σ and σ^+ this is usually reflected in a low value of the correlation coefficient. This is not always the case, however. A plot of σ against σ^+ for the following 14 groups, p-NMe_2, p-NH_2, p-OH, p-OMe, p-C_6H_5, p-F, p-Cl, p-Br, m-F, m-I, m-Cl, m-CO_2Et, m-Br, m-CF_3, using the data of Brown and Okamoto (8), gives an excellent linear relation (correlation coefficient, 0.998). It is obvious that no decision whatever could be reached about whether σ or σ^+ was being followed if one chose only substituents in this list.*

Can. J. Chem. Downloaded from www.nrcresearchpress.com by 210.87.254.6 on 09/05/12
For personal use only.

4,4′-Bis(dimethylamino)benzophenone

This compound protonates on nitrogen and the expected blue shift accompanies the formation of the doubly charged cation (348 to 251 mμ). The first and second protonation steps occur at approximately pH 3.0 and 1.2, respectively. We were interested in seeing if the presence of the resonance-stabilized cation XV, which should be in equilibrium with the ammonium monocation XIV, could be detected. By analogy with the behavior

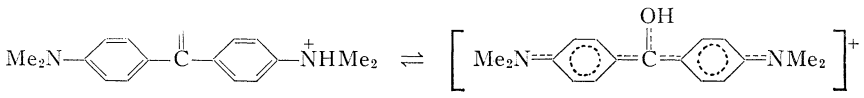

XIV XV

of the other benzophenones we would expect the carbonyl-protonated ion, XV, to absorb at about 500 mμ with an extinction coefficient in the range $3–5\times10^4$. The monocation produced in aqueous solution has no peak in the visible and, in fact, absorbs at about 380 mμ with an extinction coefficient somewhat smaller than that of the neutral compound. This is clearly the ammonium ion, XIV. Interestingly enough, in solvents such as acidified methanol and ethanol a small peak appears at 500 mμ and this is probably due to the ion XV. As the solution is made more acidic the intensity of this peak rises and then falls again as the ammonium dication is formed. Even in these solvents, however, only a small proportion, possibly 1%, of the monocation is in the form XV. Pfeiffer *et al.* (13) prepared the crystalline mono- and di-perchlorates of 4,4′-bis(dimethylamino)benzophenone; the diperchlorate is colorless but the monoperchlorate has a yellow cast and dissolves in ethanol and acetone to give a brown-red solution. The latter color is presumably due to the presence of the ion XV in the system.

Bridged Diaryl Ketones

The basicities of these compounds are listed in Table I. There are two effects, electronic and steric, which are clearly operative in this series. Fluorenone (IX) and dibenztropone (XII) each possess special electronic features which set them apart from the other ketones. Fluorenone is a derivative of cyclopentadienone and the well-known reluctance of that ring system to donate charge is reflected in fluorenone's low basicity; this, despite the increased conjugation of the aryl rings with the protonated carbonyl group which results from the rigid planar geometry of the molecule.

Dibenztropone (XII), on the other hand, possesses the highly basic tropone unit. The pK_{BH^+} value of -5.25 shows that this compound is more basic than its saturated analogue (XI), as expected, but it is clearly many powers of 10 weaker than tropone itself. This is in agreement with its known physical and chemical properties. Unlike tropone (14) it has a normal dipole moment, its carbonyl stretching frequency (1660 cm^{-1}) (15) is similar to that of benzophenone, and it forms a 2,4-dinitrophenylhydrazone. From this evidence it has been concluded that the molecule is folded (16).

Anthrone (X) is considerably more basic than benzophenone and this must be due chiefly to the increased conjugation between the protonated carbonyl group and the two rings. Although anthrone is not actually planar it is closer to this condition than is benzophenone (17, 18).

Increasing the number of carbons in the bridge forces the aromatic rings out of the plane of the carbonyl group and this causes the decrease in basicity observed in going from X to XI to XIII. The decrease due to steric factors would probably be greater than this were it not partly compensated by the increasing inductive effect of the alkyl substituents.

Can. J. Chem. Downloaded from www.nrcresearchpress.com by 210.87.254.6 on 09/05/12
For personal use only.

That is, the ortho substituent in the case of anthrone (X) is really a benzyl group containing a carbonyl substituent. In the case of dibenzcyclooctadienone (XIII) the ortho substituent is essentially alkyl in character.

It is worth noting that the effect of two ortho methyl groups in reducing the basicity of benzophenone by lowering the planarity of the system is considerably greater than the effect of a trimethylene bridge. Thus the pK_{BH^+} value of 2,6-dimethylbenzophenone is −6.6 (7) compared to −6.2 for benzophenone and −5.8 for 2,3;7,8-dibenzcyclooctadienone (XIII).

EXPERIMENTAL

Reagents

The benzophenones which were commerically available reagents were crystallized several times to constant melting point as follows: benzophenone, 48–49°; 4-chlorobenzophenone, 75.5–76.5°; 4,4′-dimethylbenzophenone, 94–95°; 4,4′-dichlorobenzophenone, 148–149°; 4,4′-dimethoxybenzophenone, 144–145°; 4,4′-dihydroxybenzophenone, 210–212°; 4,4′-bis(dimethylamino)benzophenone, 174.5–175.5°; anthrone, 153–156°; fluorenone, 80–80.5°. 3,3′-Dininitrobenzophenone was prepared by the method of Barnett and Mathews (19). Nitration of diphenylmethane gave 4,4′-dinitrodiphenylmethane, which was oxidized with chromium trioxide to 4,4′-dinitrobenzophenone, m.p. 156–158°. 2,3;6,7-Dibenzsuberone was prepared from benzalphthalide (20) by the method of Cope and Fenton (21), b.p. 149–151° (0.3 mm). 2,3;6,7-Dibenztropone was prepared from the suberone by bromination with N-bromosuccinimide and subsequently dehydrobrominated with triethylamine (21), m.p. 88–89°. (All melting points are uncorrected.)

2,3;7,8-Dibenzcyclooctadienone

This compound was prepared from 2-(γ-phenylpropyl)benzoyl chloride (colorless oil, b.p. 153° at 0.65 mm, n_D^{20} 1.5812) by cyclization using the extreme dilution technique of Hedden and Brown (22). This procedure appears to be more successful than that used by Gutsche and co-workers (23).

To 7.5 g of aluminum chloride in 160 ml carbon disulphide was added, over a period of 10 hours, 6 g of 2-(γ-phenylpropyl)benzoyl chloride dissolved in 70 ml of carbon disulphide. The brown complex thus formed was decomposed on 200 g of crushed ice and became a cream-colored solid. The carbon disulphide was removed and the solid collected and dried in an Abderhalden pistol at 60°. The crude product was purified by sublimation (0.03 mm, 110°) followed by recrystallization from a 1:6 acetone – ethyl alcohol mixture. The colorless needles had m.p. 148–149°. Calc. for $C_{16}H_{14}O$: C, 86.46; H, 6.35. Found: C, 86.72; H, 6.65. (Thanks are due to Mr. D. Dolman for preliminary work on this preparation.)

2,4-Dinitrophenylhydrazone

The cyclooctadienone was kept for 3 weeks at 60° in a solution of 2,4-dinitrophenylhydrazine in diethyleneglycol containing a few drops of concentrated hydrochloric acid. The reaction mixture was then left for several weeks at room temperature. The crude product was recrystallized from glacial acetic acid. The obtained orange platelets turned yellow on grinding and had m.p. 195–196°. Calc. for $C_{22}H_{18}N_4O_4$: C, 65.66; H, 4.51; N, 13.92. Found: C, 65.42; H, 4.50; N, 13.67.

Oxime

White needles, m.p. 146–148°. Calc. for $C_{16}H_{15}NO$: C, 80.98; H, 6.37; N, 5.90. Found: C, 81.12; H, 6.37; N, 5.68.

Basicity Measurements

The pK measurements were made as previously described (1–4). In addition, since the absorption maxima of the neutral compounds and their conjugate acids were very far apart in most cases, a check was made by using absorption data at a single wavelength. Excellent agreement was obtained.

The ionization curve for 2,3;7,8-dibenzcyclooctadienone (XIII) using measurements at two different wavelengths is shown in Fig. 1. Low solubility of the neutral molecule required the use of two different substrate concentrations for the measurements. The logarithmic plot (3) should give a straight line of unit slope if the ionization behavior is normal. The slope of the line in Fig. 2 is close to unity, 0.94, with a correlation coefficient of 0.99.

The well-behaved character of both ionization plots in Figs. 1 and 2 may result from the fact that the absorption maxima of the neutral molecule and the cation are well separated. Tailing of the plots of $D_{\lambda i} - D_{\lambda u}$ against H_0 was not observed and it was not necessary to choose for $D_{\lambda u}$ and $D_{\lambda i}$ values which were 1.5 H_0 units away from the pK, as was done in a previous case (3).

In the case of the dinitro compounds the H_0 values of the solutions used were determined by indicator measurements. This is essential if one works with solutions whose H_0 value changes rapidly with concentration, since titration with base cannot hope to give sufficiently precise values of the acidity function.

Can. J. Chem. Downloaded from www.nrcresearchpress.com by 210.87.254.6 on 09/05/12
For personal use only.

ACKNOWLEDGMENT

The financial support of the National Research Council is gratefully acknowledged.

REFERENCES

1. R. STEWART and K. YATES. J. Am. Chem. Soc. **80**, 6355 (1958); Can. J. Chem. **37**, 664 (1959).
2. R. STEWART and K. YATES. J. Am. Chem. Soc. **82**, 4059 (1960).
3. R. STEWART and M. R. GRANGER. Can. J. Chem. **39**, 2508 (1961).
4. J. T. EDWARD, H. S. CHANG, K. YATES, and R. STEWART. Can. J. Chem. **38**, 1518 (1960).
5. R. STEWART and L. J. MUENSTER. Chem. Ind. (London), 1906 (1961).
6. T. HANDA and M. KOBAYASHI. Yoki Gosei Kagaka Kyoksai Shi, **13**, 580 (1955); Chem. Abstr. **51**, 8439 (1957).
7. A. FISCHER, B. A. GRIGOR, J. PACKER, and J. VAUGHAN. J. Am. Chem. Soc. **83**, 4208 (1961). D. S. NOYCE and M. J. JORGENSON. J. Am. Chem. Soc. **84**, 4312 (1962).
8. H. C. BROWN and Y. OKAMOTO. J. Am. Chem. Soc. **79**, 1913 (1957).
9. J. T. EDWARD and I. C. WANG. Can. J. Chem. **40**, 966 (1962). A. J. KRESGE, G. W. BARRY, K. R. CHARLES, and Y. CHIANG. J. Am. Chem. Soc. **84**, 4343 (1962), and references therein.
10. R. W. TAFT. J. Am. Chem. Soc. **82**, 2965 (1960). R. W. TAFT and P. L. LEVINS. Anal. Chem. **34**, 436 (1962).
11. N. C. DENO, J. J. JARUZELSKI, and A. SCHRIESHEIM. J. Am. Chem. Soc. **77**, 3044 (1955).
12. V. GOLD and F. L. TYE. J. Chem. Soc. 2172 (1952).
13. P. PFEIFFER, K. SCHWENZER, and K. KUMETAT. J. Prakt. Chem. **143**, 143 (1935).
14. H. J. DAUBEN, JR. and H. J. RINGOLD. J. Am. Chem. Soc. **73**, 876 (1951). W. VON E. DOERING and F. L. DETERT. J. Am. Chem. Soc. **73**, 877 (1951).
15. E. D. BERGMANN and D. GINSBURG. Bull. Res. Council Israel, **1**, No. 3, 120 (1951).
16. A. J. BIRCH. Ann. Repts., Chem. Soc. (London), **48**, 188 (1951).
17. R. N. JONES. J. Am. Chem. Soc. **67**, 2127 (1945).
18. R. BRAMLEY and R. J. W. LEFEVRE. J. Chem. Soc. 56 (1962).
19. E. DE B. BARNETT and M. A. MATHEWS. J. Chem. Soc. **125**, 767 (1924).
20. R. WEISS. Organic syntheses. Coll. Vol. II. John Wiley and Sons Inc., New York. 1943. p. 61.
21. A. C. COPE and S. W. FENTON. J. Am. Chem. Soc. **73**, 1673 (1951).
22. G. D. HEDDEN and W. G. BROWN. J. Am. Chem. Soc. **75**, 3744 (1953).
23. C. D. GUTSCHE, E. F. JASON, R. S. COFFEY, and H. E. JOHNSON. J. Am. Chem. Soc. **80**, 5766 (1958).

Can. J. Chem. Downloaded from www.nrcresearchpress.com by 210.87.254.6 on 09/05/12
For personal use only.

PHTHALIDE FORMATION

IV. CONDENSATIONS WITH 5-METHOXY-3-METHYLBENZOIC ACID[1]

E. H. Charlesworth and Leon Levene
Department of Chemistry, University of Manitoba, Winnipeg, Manitoba

Received December 14, 1962

ABSTRACT

The products of the condensation of 5-methoxy-3-methylbenzoic acid with aqueous formaldehyde and hydrochloric acid in the presence of glacial acetic acid are dependent on the length of the heating period. A very short period of heating (2 minutes) yields 6-methoxy-4-methylphthalide and the two chloromethylphthalides of m.p. 135° and 154° C, related to the unisolated 4-methoxy-6-methylphthalide. If the period of heating is 20 minutes or longer, the above chloromethylphthalide melting at 135° is formed and in addition some of the 6-methoxy-4-methylphthalide is chloromethylated to 6-methoxy-7-chloromethyl-4-methylphthalide, melting at 179°. The orientation of all three chloromethylphthalides has been established.

Can. J. Chem. Downloaded from www.nrcresearchpress.com by 210.87.254.6 on 09/05/12
For personal use only.

INTRODUCTION

In 1945, Charlesworth *et al.* (1) reported the isolation of two products from the condensation of 5-methoxy-3-methylbenzoic acid (I) with formaldehyde and concentrated hydrochloric and acetic acids. Of these, the compound which melted at 176–178° C was established as a chloromethylphthalide, but its orientation was not proved. The present paper establishes the orientation of this and other products isolated in this reaction.

The phthalide ring may form in two ways to produce the simple phthalides II and III. On further reaction a chloromethyl group may enter positions 5 or 7 in II or 5 or 7 in III. Thus, four chloromethylphthalides (IV–VII) are theoretically possible. All condensations were carried out using the Edwards, Perkin, and Stoyle (2) method as modified by Rây and Robinson (3) by the addition of glacial acetic acid to the formaldehyde – hydrochloric acid mixture. The length of the heating period determined the number and nature of the products isolated.

When the mixture was heated for 2 minutes or less, that is, just for the length of time to put everything into solution, only the simple phthalide II and the chloromethylphthalides VI and VII were formed. The chloromethylphthalide IV, m.p. 178–179° C, of the earlier paper was not formed under these conditions. It was formed along with II and VI if the condensation time was extended to 20 minutes or more. It (IV) can also be formed alone from phthalide II in continued condensation of 20 minutes or more. Phthalide III was not isolated from any of the condensations and apparently is chloromethylated as fast as produced.

The orientation of phthalide II was established by mixed melting point and infrared spectra comparison with this phthalide produced by the Fritsch reaction. Meldrum (4) synthesized and established the orientation of both the simple phthalides by this method. When phthalide III formed by the Meldrum method was subjected to further chloromethylation VI and VII are produced, but not IV. Thus, chloromethylphthalides VI and VII have been proved to be related to phthalide III, and IV, as previously, to phthalide II. In establishing the orientation of the three isolated chloromethylphthalides it was thus necessary to determine the orientation of IV (or V) as derived from the simple phthalide II and one of the two chloromethylphthalides VI or VII as formed from simple phthalide III. Once a definite orientation could be affixed to either VI or VII the other was also known.

[1]*For Part III of this series, see Can. J. Chem.*, **32**, *941 (1954).*

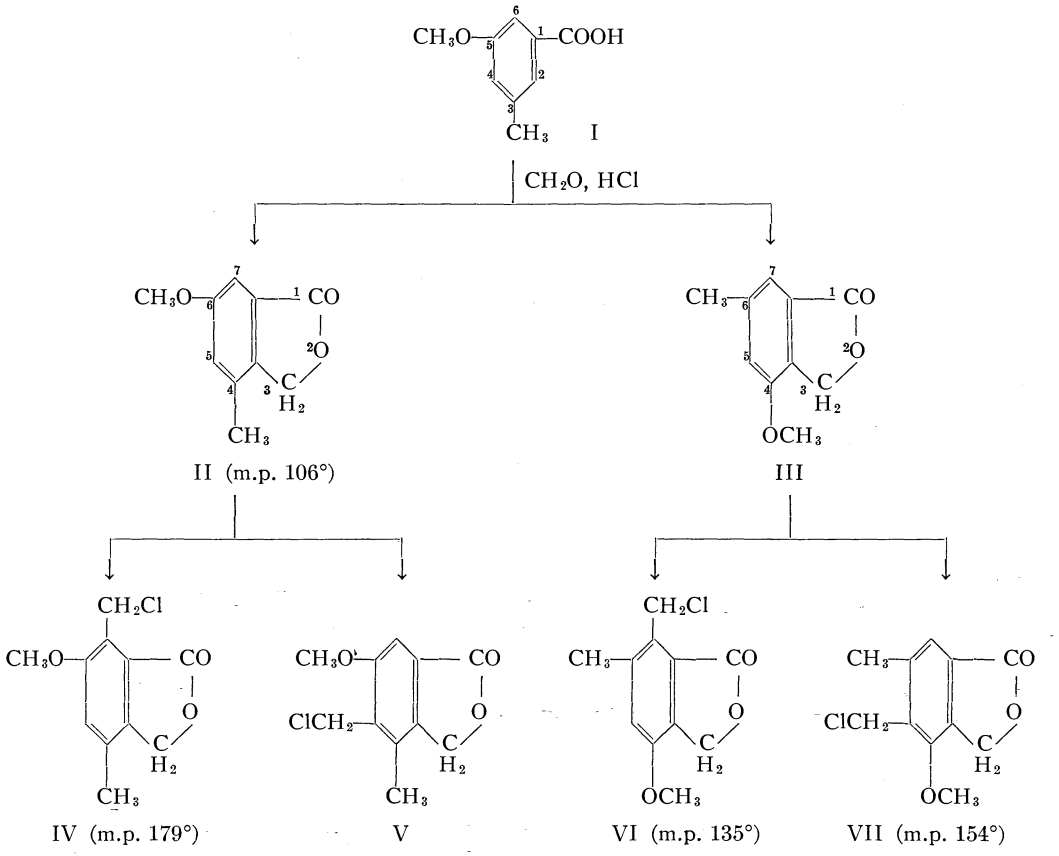

A successful attack on this problem involved a synthesis of the two substituted aromatic acids VIII and X. Once these acids were available they were subjected to the normal condensation reaction to produce the corresponding phthalides IX and XI.

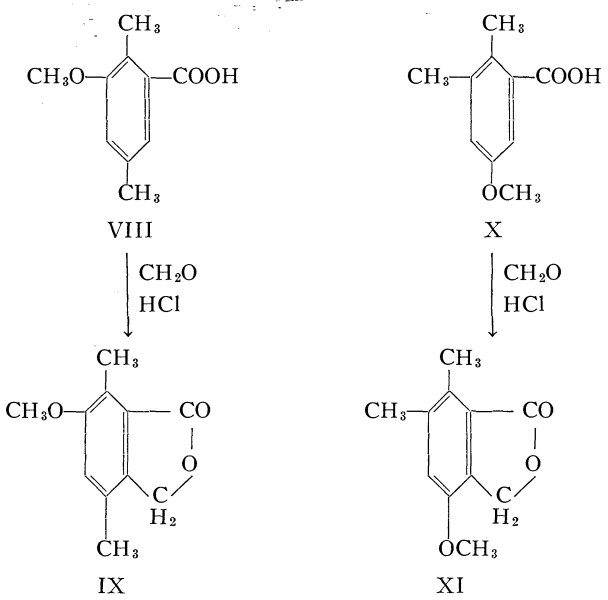

Can. J. Chem. Downloaded from www.nrcresearchpress.com by 210.87.254.6 on 09/05/12
For personal use only.

Reduction of the four theoretically possible chloromethylphthalides, IV, V, VI, and VII, derived from 5-methoxy-3-methylbenzoic acid with zinc and hydrochloric acid would yield the corresponding chlorine-free phthalides A, B, C, and D.

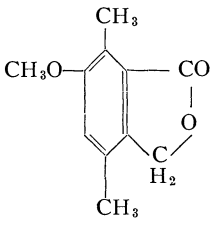

A

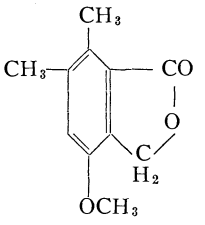

C

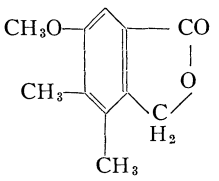

B

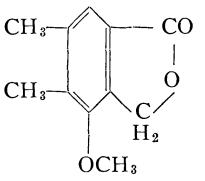

D

The phthalide IX prepared synthetically from 2,5-dimethyl-3-methoxybenzoic acid (VIII), whose orientation is proved below, was found to be identical with phthalide A, in turn derived from the chloromethylphthalide IV of melting point 178–179° C. In this way the orientation of IV was definitely established. Similarly, phthalide XI formed from 2,3-dimethyl-5-methoxybenzoic acid (X) was shown to be identical with phthalide C, thus definitely establishing the orientation of chloromethylphthalide (VI) of melting point 134–135° C. The remaining chloromethylphthalide melting at 152.5–154° C must by elimination have the structure VII.

The synthesis of 2,5-dimethyl-3-methoxybenzoic acid (VIII) was carried out as follows:

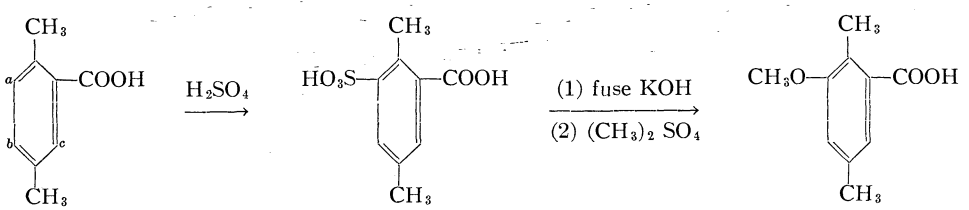

XII VIII

There are three possible positions of sulphonation in the starting molecule of 2,5-dimethylbenzoic acid (XII). If the sulphonic acid group had entered position *c* it would yield, after alkali fusion and methylation, the acid of structure XIII. It would be impossible for this acid to form a phthalide because there is no position ortho to the carboxyl group

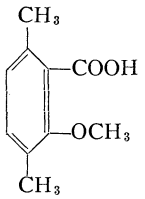

XIII

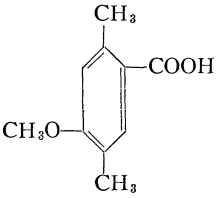

XIV

Can. J. Chem. Downloaded from www.nrcresearchpress.com by 210.87.254.6 on 09/05/12
For personal use only.

unsubstituted. The phenol corresponding to XIII would be expected to yield a color with ferric chloride solution. The actual acid obtained did not give a ferric chloride reaction, but does form a phthalide. Thus structure XIII can be ruled out.

If the sulphonic acid group had entered position *b* the final methyl ether would be identical with 4-methoxy-2,5-dimethylbenzoic acid (XIV), first produced by Gattermann (5) from 2,5-dimethylphenol by a Gattermann reaction, followed by methylation of the phenolic aldehyde and oxidation of the aldehyde to the corresponding acid. We have synthesized this acid by a modification of the original procedure and it is not identical with our acid (VIII), which thus must have the structure indicated.

The synthesis of 5-methoxy-2,3-dimethylbenzoic acid (X) was carried out in a similar manner from hemimellitene (XV). This was oxidized by dilute nitric acid to the acid XVI

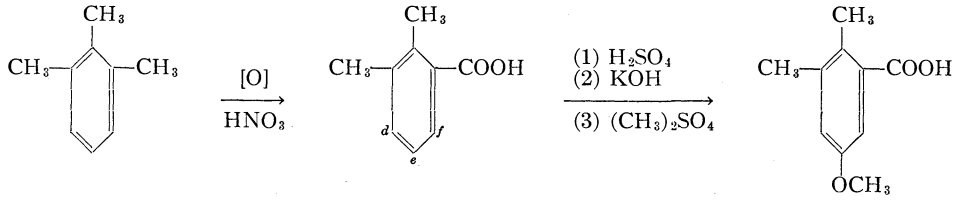

XV XVI X

first reported by Jacobsen (6), which was then sulphonated and subjected to alkali fusion and methylation. As in the previous case, the sulphonic acid substituent can enter three possible positions. Our phenol did not give a ferric chloride reaction, but its methyl ether did form a phthalide. Position *f* is thus ruled out on both counts. It was now a relatively simple matter to establish whether carbon *d* or *e* was sulphonated. 3,4-Dimethylphenol and 2,3-dimethylphenol are solids and commercially available. Decarboxylation of our phenol formed a product identical with 3,4-dimethylphenol. Thus position *e* has been established for the sulphonation of acid XVI.

An earlier plan of attack to establish the orientation of the three isolated chloromethylphthalides (IV, VI, and VII) was oxidative attack on the reduced phthalides A, C, and D to obtain the corresponding dicarboxylic acids. These were then to have been decarboxylated and the resulting methyl ethers demethylated and compared with the commercially available solid phenols. Two of these dicarboxylic acids were isolated in the form of their anhydrides, but attempts at decarboxylation were unsuccessful.

EXPERIMENTAL

Condensation of 5-Methoxy-3-methylbenzoic Acid

The general method followed was that of Edwards, Perkin, and Stoyle (2) as modified by Rây and Robinson (3). This procedure was employed in all condensations carried out, with modifications in the period of heating, the proportion of formaldehyde, and the method of isolation of the resultants. The 5-methoxy-3-methylbenzoic acid was made from *m*-toluic acid as described in the first paper of this series (1).

Condensation Time Two Minutes or Less

5-Methoxy-3-methylbenzoic acid (4.0 g), concentrated hydrochloric acid (25.0 ml), aqueous formaldehyde (10 ml, 37%), and glacial acetic acid (25 ml) were mixed in a small flask fitted with a reflux condenser and heated on a steam bath just long enough to permit the 5-methoxy-3-methylbenzoic acid to dissolve. This usually took about 2 minutes. The flask was then cooled in ice to prevent further reaction. On standing overnight in the refrigerator a yellowish precipitate formed, which was filtered off and washed.

Isolation of 6-Methoxy-4-methylphthalide (II)

Cold water was added to the filtrate obtained above, when a white precipitate settled out. After standing the solution overnight in the cold this precipitate was filtered off and washed with water. Repeated crystallization from ethyl alcohol (95%) gave the 6-methoxy-4-methylphthalide (0.7–0.9 g), which melted at 105–106° C. Found: C, 66.9; H, 5.64%. Calc. for $C_{10}H_{10}O_3$: C, 67.4; H, 5.62%.

Can. J. Chem. Downloaded from www.nrcresearchpress.com by 210.87.254.6 on 09/05/12
For personal use only.

A small amount of material insoluble in ethyl alcohol and with a melting point above 275° C was found. It was considered to be a diphenylmethane type of material and was not examined further.

Isolation of the Two Chloromethylphthalides VI and VII

The yellowish precipitate, mentioned above, obtained directly from the reaction mixture, was crystallized from alcohol (charcoal). The dry colorless crystals were washed on the filter funnel with four or five portions (5.0 ml) of boiling alcohol. This treatment dissolved the more soluble chloromethylphthalide and left the less soluble on the funnel. The latter was recrystallized from glacial acetic acid and finally from alcohol. This chloromethylphthalide, VII (0.6 g), melted at 153–154° C. Found: C, 58.2; H, 5.06; Cl, 15.4%. Calc. for $C_{11}H_{11}O_3Cl$: C, 58.3; H, 4.86; Cl, 15.7%.

The more soluble chloromethylphthalide, VI (1.0 g), was also purified by recrystallization from acetic acid and from alcohol. It melted at 134–135° C. Found: C, 58.3; H, 5.21; Cl, 15.4%. Calc. for $C_{11}H_{11}O_3Cl$: C, 58.3; H, 4.86; Cl, 15.7%.

Condensation Time Twenty Minutes or Longer

The Chloromethylphthalide IV

The procedure was as above except that the time of heating was increased to 20 minutes. The 6-methoxy-4-methylphthalide (II) was isolated as before. Two chloromethylphthalides were separated by portions of hot alcohol, the more soluble being the previously mentioned VI of melting point 134–135° C and the less soluble, IV (2.1 g) of melting point 178–179° C. Found: C, 58.4; H, 5.07; Cl, 15.6%. Calc. for $C_{11}H_{11}O_3Cl$: C, 58.3; H, 4.86; Cl 15.7%. The infrared spectrum of IV differs from that of VI and VII by not possessing characteristic peaks at 6.91 and 8.90 μ.

6-Methoxy-4-methylphthalide (II) and 4-Methoxy-6-methylphthalide (III)

These two simple phthalides were produced by the Fritsch method as reported by Meldrum (4), who also established their orientation. Mixed melting point determination and infrared spectra comparison of the simple phthalide obtained from the condensation above proved its identity with 6-methoxy-4-methylphthalide (II), m.p. 104–105° C, produced by Meldrum's directions.

Condensation of the Meldrum Phthalides II and III with Formaldehyde and Hydrochloric Acid

When 6-methoxy-4-methylphthalide II (0.85 g) was condensed with formaldehyde solution, hydrochloric acid, and glacial acetic acid for 1½ hours in the standard manner, a chloromethylphthalide (0.6 g) which melted at 178–179° C was isolated. This proved identical with the product of the same melting point isolated from the main reaction. None of the other chloromethylphthalides were found in the reaction mixture. Thus chloromethylphthalide IV must be related to simple phthalide II. If the condensation time was only 2 minutes the chloromethylphthalide was not formed, but the unchanged simple phthalide (II) could be recovered.

When the simple Meldrum phthalide III (2.0 g) was subjected to further chloromethylation for 2 minutes, a solid separated on cooling, which on crystallization from alcohol in the manner previously described gave a product (0.4 g) which melted at 153–154° C. Dilution of the reaction mixture with water and repeated crystallization of the separated product from alcohol gave the second chloromethylpthalide (0.32 g), which melted at 133–134°. These two substances were identical with the products VII and VI of the same melting points isolated from the main condensation. Thus VI and VII must be related to the simple phthalide III.

Formation of the Three Chlorine-free Phthalides (A, C, and D)

6-Methoxy-4-methyl-7-chloromethylphthalide (3.5 g) of melting point 178–179° C, zinc dust (3.7 g), concentrated hydrochloric acid (10 ml), and ethyl alcohol (75 ml, 95%) were refluxed for 15 hours. Excess hydrochloric acid was added until the zinc had completely dissolved. The solution was cooled and cold water (75 ml) added, when a thick white paste was formed. The solid was collected, washed well with water, and dried. Crystallization from ethyl alcohol produced colorless crystals (3.2 g) of 6-methoxy-4,7-dimethylphthalide (A) which melted at 169–170° C. Found: C, 68.3; H, 6.15%. Calc. for $C_{11}H_{12}O_3$: C, 68.8; H, 6.26%.

Reduction of 4-methoxy-6-methyl-7-chloromethylphthalide (VI) of melting point 134–135° C by the same method gave 4-methoxy-6,7-dimethylphthalide (C) which melted at 179–180° C. Found: C, 68.5; H, 6.29%. Calc. for $C_{11}H_{12}O_3$: C, 68.8; H, 6.26%.

Reduction of 4-methoxy-6-methyl-5-chloromethylphthalide (VII) of melting point 153–154° C gave 4-methoxy-5,6-dimethylphthalide (D) which melted at 174–175° C. Found: C, 68.5; H, 6.19%. Calc. for $C_{11}H_{12}O_3$: C, 68.8; H, 6.26%.

Formation of the Three Phthalic Acids (Anhydrides) from the Phthalides A, C, and D

6-Methoxy-4,7-dimethylphthalide (3.0 g) was dissolved in warm potassium hydroxide solution (100 ml, 6 *N*). After cooling, finely powdered potassium permanganate (3.8 g) was added slowly over a 10-minute period. The dark solution was allowed to stand at room temperature for 36 hours. The brown manganese dioxide was filtered off, leaving a green filtrate. On acidification with dilute sulphuric acid a white precipitate of 4-methoxy-3,6-dimethylphthalic acid was formed. This relatively pure product (2.1 g) was collected, washed with water, and allowed to dry. It melted at 181–182° C and effervesced vigorously with sodium

Can. J. Chem. Downloaded from www.nrcresearchpress.com by 210.87.254.6 on 09/05/12
For personal use only.

bicarbonate solution. Found: C, 58.4; H, 5.41%. Calc. for $C_{11}H_{12}O_5$: C, 58.9; H, 5.36%. Crystallization from either ethyl alcohol or glacial acetic acid converted the acid into the corresponding anhydride, which melted at 185–186° C and no longer effervesced with bicarbonate solution. Found: C, 63.9; H, 5.10%. Calc. for the anhydride $C_{11}H_{10}O_4$: C, 64.1; H, 4.85%.

6-Methoxy-3,4-dimethylphthalic anhydride (1.2 g) was prepared in a similar manner from phthalide C (3.0 g). On crystallization from acetic acid it melted at 230–231° C. Found: C, 63.8; H, 4.98%. Calc. for $C_{11}H_{10}O_4$: C, 64.1; H, 4.85%.

3-Methoxy-4,5-dimethylphthalic anhydride was prepared from 4-methoxy-5,6-dimethylphthalide (D) as in the two previous cases. It melted at 174–175° C. Found: C, 63.8; H, 4.75%. Calc. for $C_{11}H_{10}O_4$: C, 64.1; H, 4.85%.

Attempts to decarboxylate the 4-methoxy-3,6-dimethylphthalic acid with copper chromite and quinoline were unsuccessful. Solid material recovered from this attempt proved to be the corresponding 4-methoxy-3,6-dimethylphthalic anhydride.

Preparation of 3-Methoxy-2,5-dimethylbenzoic Acid (VIII)

(a) Sulphonation of 2,5-Dimethylbenzoic Acid

2,5-Dimethylbenzoic acid (11.0 g, Eastman No. 7270) was heated at 110° with stirring for 2 hours with a mixture of concentrated sulphuric acid (15 ml) and fuming sulphuric acid (35 ml, 20% SO_3). After cooling, the solution was poured cautiously into ice-cold water (200 ml). After further cooling the acid was partially neutralized by the slow, careful addition of sodium bicarbonate (10 g). Sodium chloride (25 g) was added and the mixture warmed until solution was complete. The clear liquid was cooled in an ice bath, when a brown solid began to separate. This sodium salt of 2,5-dimethyl-3-sulphobenzoic acid (15 g) was collected on a sintered-glass funnel, washed well with a small quantity of saturated sodium chloride solution, and dried in an oven.

(b) 3-Hydroxy-2,5-dimethylbenzoic Acid

The above sodium salt (14 g) was fused with potassium hydroxide (80 g) in the conventional manner. The melt was dissolved in water (300 ml) and neutralized with dilute sulphuric acid. The solution was made slightly alkaline, cooled, and the precipitated potassium sulphate removed. The mother liquor was concentrated (charcoal) to about one third the original volume, filtered, cooled, and a second crop of potassium sulphate removed. On acidification with concentrated hydrochloric acid the required 3-hydroxy-2,5-dimethylbenzoic acid (5.8 g) separated. It was recrystallized from water and melted at 163–165° C. It did not give a color with ferric chloride solution. Found: C, 65.0; H, 5.99%; neut. equiv., 163. Calc. for $C_9H_{10}O_3$: C, 65.1; H, 6.03%; neut. equiv., 166.

(c) 3-Methoxy-2,5-dimethylbenzoic Acid (VIII)

3-Hydroxy-2,5-dimethylbenzoic acid (5.2 g) was methylated in the conventional manner with sodium hydroxide solution and dimethyl sulphate (10 g). The 3-methoxy-2,5-dimethylbenzoic acid (2.3 g) was crystallized from aqueous alcohol, and melted at 143–144° C. Found: C, 67.0; H, 6.74%. Calc. for $C_{10}H_{12}O_3$: C, 66.8; H, 6.68%.

6-Methoxy-4,7-dimethylphthalide (IX)

3-Methoxy-2,5-dimethylbenzoic acid (1.5 g), concentrated hydrochloric acid (11.0 ml), glacial acetic acid (11 ml), and formaldehyde solution (9 ml, 35%) were heated on a steam cone for 45 minutes. Complete solution did not take place. The flask was then cooled and the solid collected and washed with water. On crystallization from alcohol, the 6-methoxy-4,7-dimethylphthalide (1.3 g) was obtained, and melted at 169–170° C. Found: C, 68.4; H, 6.24%. Calc. for $C_{11}H_{12}O_3$: C, 68.8; H, 6.25%.

A mixed melting point of this material and the chlorine-free phthalide A of the same melting point formed by the reduction of the chloromethylphthalide IV of m.p. 179° C showed no depression. Thus the orientation of chloromethylphthalide IV has been established.

Preparation of 5-Methoxy-2,3-dimethylbenzoic Acid (X)

(a) Oxidation of 1,2,3-Trimethylbenzene

The oxidation of 1,2,3-trimethylbenzene (hemimellitene) (XV) with dilute nitric acid was first reported by Jacobsen (6). His experimental details are scanty, but the following procedure was satisfactory. It appeared impossible, however, to stop at the required monocarboxylic stage without the production of some dicarboxylic acid.

1,2,3-Trimethylbenzene (60 ml, Aldrich Chemical Co.) was refluxed with a mixture of nitric acid (50 ml, 70%) and water (140 ml) for about 20 hours, a magnetic stirrer operating throughout the heating period. The mixture was poured into cold water (400 ml). On standing in the refrigerator, the crude acid, which separated as an oil, solidified. It was separated and dissolved in sodium hydroxide solution (200 ml, 10%). The cold dark red alkaline solution was extracted with ether to remove unoxidized hemimellitene, warmed with decolorizing carbon, and filtered. The warm filtrate was acidified with dilute hydrochloric acid, when the acid separates as a brown solid. On recrystallization from ethyl alcohol (charcoal) the required 2,3-dimethylbenzoic acid (8.0 g) was obtained. It melted at 139–141° C. Jacobsen gives a value of 144° C for the melting point, but it was considered sufficiently pure for sulphonation purposes.

Can. J. Chem. Downloaded from www.nrcresearchpress.com by 210.87.254.6 on 09/05/12
For personal use only.

(b) 5-Hydroxy-2,3-dimethylbenzoic Acid

The sulphonation of 2,3-dimethylbenzoic acid (12 g) was carried out exactly as described above for 2,5-dimethylbenzoic acid, and the sodium salt of the required 1,2-dimethyl-5-sulphobenzoic acid was isolated. This salt was fused with alkali as described above and the 5-hydroxy-2,3-dimethylbenzoic acid obtained. It was crystallized from water and melted at 179.0–179.5° C. Found: C, 64.6; H, 6.04%; neut. equiv., 161. Calc. for $C_9H_{10}O_3$: C, 65.1; H, 6.03%; neut. equiv., 166. This phenolic acid did not yield a color with ferric chloride solution.

(c) Decarboxylation of 5-Hydroxy-2,3-dimethylbenzoic Acid

Attempts to decarboxylate this acid by refluxing with quinoline and copper chromite were unsuccessful. However, when the acid was heated with soda lime a product was obtained which melted at 62–63° C. This did not effervesce with sodium bicarbonate solution nor give a color with ferric chloride solution. A mixed melting point with commercial 3,4-dimethylphenol gave no depression.

(d) 5-Methoxy-2,3-dimethylbenzoic Acid (X)

Methylation of 5-hydroxy-2,3-dimethylbenzoic acid (0.6 g) in the conventional manner gave 5-methoxy-2,3-dimethylbenzoic acid (0.47 g). On crystallization from aqueous ethyl alcohol it melted at 102–103° C. Found: C, 66.7; H, 6.68%. Calc. for $C_{10}H_{12}O_3$: C, 66.8; H, 6.68%.

4-Methoxy-6,7-dimethylphthalide (XI)

The above 5-methoxy-2,3-dimethylbenzoic acid, X (0.4 g), was condensed as described above for the preparation of 6-methoxy-4,7-dimethylphthalide. After crystallization from ethyl alcohol the 4-methoxy-6,7-dimethylphthalide (0.3 g) melted at 179–180° C. Found: C, 68.5; H, 6.38%. Calc. for $C_{11}H_{12}O_3$: C, 68.8; H, 6.25%. A mixed melting point of this material and the chlorine-free phthalide C, formed by the reduction of the chloromethylphthalide VI of m.p. 135° C, showed no depression. Thus the orientation of the chloromethylphthalide VI has been established.

Synthesis of 4-Methoxy-2,5-Dimethylbenzoic Acid

(a) 4-Hydroxy-2,5-dimethylbenzaldehyde

This aldehyde, m.p. 130–132° C, was synthesized from 2,5-dimethylphenol by a Gattermann reaction as modified by Adams and Montgomery (7) employing zinc cyanide and anhydrous aluminum chloride as the condensing agent.

(b) 4-Methoxy-2,5-dimethylbenzaldehyde

The aldehyde of the previous paragraph was methylated as described by Clemo *et al.* (8). It boiled at 147–179° at 12 mm and melted at 32–33° C.

(c) 4-Methoxy-2,5-dimethylbenzoic Acid

The methoxyaldehyde (23.5 g) of the previous paragraph was oxidized by boiling for 40 minutes with acetone (300 ml) containing finely powdered potassium permanganate (35 g). The hot solution was filtered and the dark solid suspended in water and treated with sulphur dioxide gas to dissolve the manganese dioxide, leaving a thick white precipitate of the 4-methoxy-2,5-dimethylbenzoic acid. A further quantity of the acid could be obtained by concentration of the acetone filtrate and dilution with water. On crystallization from aqueous acetic acid the purified acid (14.6 g) melted at 164–165° C, in agreement with the figure reported by Clemo (8). This acid is not identical with the acid VIII described above.

ACKNOWLEDGMENT

The authors are grateful to the National Research Council of Canada for grants which have aided this research.

REFERENCES

1. E. H. Charlesworth, R. P. Rennie, J. E. Sinder, and M. M. Yan. Can. J. Res. Sect. B, **23**, 17 (1945).
2. G. A. Edwards, W. H. Perkin, and F. W. Stoyle. J. Chem. Soc. **127**, 195 (1925).
3. J. N. Rây and R. Robinson. J. Chem. Soc. **127**, 1618 (1925).
4. A. N. Meldrum. J. Chem. Soc. **99**, 1712 (1911).
5. L. Gattermann. Ann. **357**, 313 (1907).
6. O. Jacobsen. Ber. **19**, 2517 (1886).
7. R. Adams and E. Montgomery. J. Am. Chem. Soc. **46**, 1518 (1924).
8. G. R. Clemo, R. D. Haworth, and E. Walton. J. Chem. Soc. 2368 (1929).

Can. J. Chem. Downloaded from www.nrcresearchpress.com by 210.87.254.6 on 09/05/12
For personal use only.

THE BAKER–NATHAN EFFECT OBSERVED IN THE RELATIVE RATES OF REDUCTION OF SEVERAL PARA-ALKYLATED NITROBENZENES BY SODIUM HYDROSULPHIDE[1]

O. J. Cope and R. K. Brown
Department of Chemistry, University of Alberta, Edmonton, Alberta
Received September 27, 1962

Can. J. Chem. Downloaded from www.nrcresearchpress.com by 210.87.254.40 on 09/05/12
For personal use only.

ABSTRACT

By measuring the initial rates of production of hydrodisulphide during reductions by sodium hydrosulphide in aqueous ethanol, it has been shown that the relative rates of reduction of a number of para-alkylated nitrobenzenes are in the order *p*-H- > *p*-*t*-butyl- > *p*-isopropyl- = *p*-cyclohexyl- > *p*-ethyl- > *p*-methyl-nitrobenzene. This is in accord with the "hyperconjugative" order of electron release by these alkyl groups.

INTRODUCTION

It has been shown that the reduction of nitrobenzene by aqueous sodium hydrosulphide (at pH ~ 9–10) first produces phenylhydroxylamine, which in turn is reduced by the hydrosulphide much more slowly than is the original nitrobenzene (1). Hydrosulphide reduction of nitrobenzene, but apparently not of phenylhydroxylamine, is accompanied by the accumulation of hydro*di*sulphide ion, which, as well as reducing nitrobenzene more quickly than does hydrosulphide ion, is capable of reducing phenylhydroxylamine 2 to 3 times more rapidly than it does the nitrobenzene. Hydro*di*sulphide reduction of nitrobenzene is accompanied by an increase in hydro*di*sulphide ion whereas in contrast the hydroxylamine apparently only *consumes* hydrodisulphide ion. In all of these reactions thiosulphate ion is produced.

Goldschmidt and Larsen (2) have found that at a pH of 8, the reduction of nitrobenzene by sodium hydrosulphide quantitatively precipitates sulphur according to the following equation:

$$C_6H_5NO_2 + 2NaSH + H_2O \rightarrow C_6H_5NHOH + 2S^0\downarrow + 2NaOH. \qquad (a)$$

At higher pH, however, the sulphur is not precipitated. For example, in the reduction by sodium sulphide (pH ~ 12.5) (3, 4), where due to hydrolysis a considerable concentration of both sulphide and hydrosulphide ion exists, the elemental sulphur produced during reaction appears as the disulphide ($S_2^=$, HS_2^-) and as $S_2O_3^=$. Nitrobenzene becomes aniline with no evidence of phenylhydroxylamine appearing during the course of the reaction. The following reactions were presented to account for this observation:

$$C_6H_5NO_2 + 3S^= + 4H_2O \rightarrow C_6H_5NH_2 + 3S^0 + 6OH^- \qquad (b)$$

$$S^0 + S^= \rightarrow S_2^= \qquad (c)$$

$$4S^0 + 6OH^- \rightarrow S_2O_3^= + 2S^= + 3H_2O. \qquad (d)$$

At pH 9–10 reduction of nitrobenzene by hydrosulphide ion produces sulphur, which also appears as hydrodisulphide and thiosulphate ions (1).

Since hydrodisulphide ion concentration increases with time during the reduction of

[1]*Taken from the thesis of O. J. Cope submitted to the Faculty of Graduate Studies of the University of Alberta in partial fulfillment of the requirements for the degree of Doctor of Philosophy.*

nitrobenzene (1) it was thought that the measurement of the rate of increase of hydrodisulphide ion, by periodically estimating its absorption at 450 mμ, might be a suitable method for determining the relative rates of reduction of a series of alkylated nitrobenzenes. The growth in concentration of hydroxyl ion, a product of the reaction (cf. equations (*a*) and (*b*)), is known to increase the rate of reduction by sodium sulphide (4) and no doubt would have the same effect in the hydrosulphide reduction presently considered. As well, change in the hydroxyl ion concentration might well increase the colorless product $S_2O_3^=$ at the expense of the HS_2^- (cf. equations (*c*) and (*d*)). In the present work, this complication was minimized by employing hydrosulphide ion in large excess and consequently for the first few minutes of the reaction at least, the hydroxyl ion concentration should remain constant due to the buffering effect of the ammonium chloride used to obtain the sodium hydrosulphide solution.

Furthermore, in the first 10 to 15 minutes of the reaction, the amounts of phenylhydroxylamine and of hydrodisulphide ion produced are both quite small relative to the concentration of nitrobenzene and hydrosulphide ion. The rate of reaction of hydrodisulphide ion with the hydroxylamine is only 2 to 3 times greater than that of hydrodisulphide with nitrobenzene, while the reaction of hydrodisulphide ion with nitrobenzene is approximately 7 times that of the hydrosulphide ion with nitrobenzene (1). Hence loss of hydrodisulphide ion by reaction with the hydroxylamine, or change of hydrodisulphide ion concentration by reaction with nitrobenzene would be negligible in this short space of time. Thus the expression $d[HS_2^-]/dt = k[HS^-][RNO_2]$ can be employed, with $k[HS^-]$ being practically constant.

Accordingly, if a series of runs are made under these conditions and as well the initial concentrations of RNO_2 are identical, then $d(HS_2^-)/dt$ will vary according to the nature of R. Thus, at least in the initial stages, $d(HS_2^-)/dt$ will provide a measure of the relative rates of reduction of various nitro compounds.

The present paper describes the application of this technique to the study of the relative rates of reduction of nitrobenzene and some of its para alkyl homologues. The particular compounds examined in addition to nitrobenzene itself were *p*-methyl-, *p*-ethyl-, *p*-isopropyl-, *p*-*t*-butyl-, and *p*-cyclohexyl-nitrobenzene.

The reduction of a nitro group is believed to occur by an attack of the negatively charged reducing species on the electron-deficient nitrogen atom of the nitro group (5) and is thus favored by electron recession from the nitrogen atom. Accordingly, it is expected and actually has been found that electron-withdrawing substituents in the position para to the nitro group in the benzene ring accelerate, while electron-donating substituents retard, the reduction processes (3, 5, 7). Since the alkyl groups cited above are electron donors, it should be possible to examine their relative electron-donating capabilities by a study of the reduction rates of the *p*-alkylnitrobenzenes, and thus gain more information concerning the controversial question of electron donation via the hyperconjugative mechanism (8–12 and references therein).

It was not possible to carry out the comparative study using sodium sulphide as the reducing agent because under the highly alkaline conditions thus involved, polysulphide oxidation of the methyl group of nitrotoluene (13, 14) interferes significantly in the normal reduction and yields products whose absorption also interferes in the spectrophotometric determination of the polysulphide. Under the buffered conditions (and consequently lower pH) prevailing during hydrosulphide reductions, a similar loss of nitrotoluene, and interference of the product in the 450 mμ region, was not detected.

Can. J. Chem. Downloaded from www.nrcresearchpress.com by 210.87.254.40 on 09/05/12
For personal use only.

Can. J. Chem. Downloaded from www.nrcresearchpress.com by 210.87.254.40 on 09/05/12
For personal use only.

EXPERIMENTAL

Reagents

Nitrobenzene.—Fisher certified reagent was purified by distillation under vacuum. The material boiling at 85–86° at 10 mm was retained.

p-Nitrotoluene.—Fisher reagent material was crystallized from ethanol and melted sharply at 51.5°. Lit. m.p., 51.8–52.0° (10).

p-Ethylnitrobenzene, p-isopropylnitrobenzene, and p-t-butylnitrobenzene.—These reagents were all prepared by nitration of the corresponding alkylbenzenes (10 and references therein). The mixtures of isomers were separated by fractional distillation until a constant refractive index was obtained. The *p-t*-butylnitrobenzene was purified further by two successive crystallizations from methanol. M.p., 28°.

p-Cyclohexylnitrobenzene.—This reagent, prepared according to published procedures (15), was crystallized twice from ethanol. M.p., 58°, lit., 58.5°.

Sodium hydrosulphide solution.—A stock solutions of 0.900 *M* sodium sulphide containing sufficient ammonium chloride to form the sodium hydrosulphide was prepared as previously described (1).

95% Ethanol.—Commercial 95% ethanol was deaerated by heating the alcohol to its boiling point and then cooling it under nitrogen.

Experimental Procedure for the Kinetic Runs

The apparatus and general method described in the previous publication (1) were used in the present work with the following minor modification. Fifty milliliters of a 0.150 *M* stock solution of nitrobenzene in 95% ethanol was added to the reaction flask containing 200 ml of the deaerated 95% ethanol. Volume measurements were made at 25°. When this solution had reached 50°, a 50-ml quantity of the sodium sulphide – ammonium chloride solution (measured at 25° then brought to 50°) was added from an automatic pipette under nitrogen pressure. An aliquot of this final solution was used to fill the absorption cell and measurements were made of hydrodisulphide concentration in terms of absorbance.

RESULTS

By conducting all of the reductions under identical conditions, and employing the same initial concentrations of reactants, it was considered a reasonable assumption that any difference in the rate of intensification of the yellow color due to hydrodisulphide formation could be ascribed to the electron-releasing ability of the para substituent. The greater reducing power of hydrodisulphide (1), frequently present as a trace impurity in hydrosulphide solutions, made it imperative that the initial concentrations of the contaminating hydrodisulphide in the various solutions of sodium hydrosulphide be identical in all determinations. This required each reduction to be carried out at least twice, and in some cases three or four times in order to obtain a comparable series. The effect of a small change in initial concentration of hydrodisulphide is demonstrated in Fig. 1 for the reduction of *p*-nitrotoluene (0.0250 *M*) by 0.150 *M* hydrosulphide. Plot I, Fig. 1, is

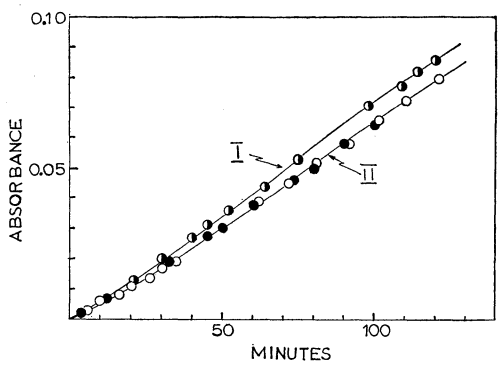

FIG. 1. The effect of initial small amounts of contaminating HS_2^- on the relative rate of reduction of 0.0250 *M* *p*-nitrotoluene with 0.150 *M* HS^- in aqueous media. Plot I—for 0.150 *M* HS^- containing HS_2^-, whose concentration is expressed by an absorbance of 0.023 (◑) at 450 mμ. Plot II—two separate reductions, with initial absorbances at 450 mμ of contaminating HS_2^-, 0.008 (○) and 0.006 (●).

that for the reduction in a solution with initial absorbance of hydrodisulphide at 450 mμ of 0.023, whereas plot II, Fig. 1, is a composite of two such reductions having initial absorbances of their solutions at 450 mμ of 0.006 and 0.008. The latter plot also demonstrates the degree of reproducibility of the measurements when all initial concentrations are practically the same.

A comparable series, obtained in the manner described above, is shown in Fig. 2. Solutions for all five runs had an initial absorbance at 450 mμ, due to contaminating

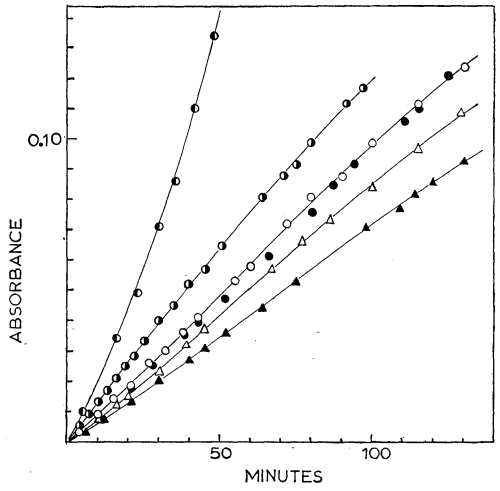

FIG. 2. The change in absorbance at 450 mμ during the reduction of the *p*-alkylnitrobenzenes (0.0250 *M*) by 0.150 *M* hydrosulphide ion in aqueous ethanol (76.5% by weight ethanol) at 50.0° C. The para substituents are H, ◐; CH_3, ▲; C_2H_5, △; *i*-C_3H_7, ○; cyclohexyl, ●; and *t*-C_4H_9, ◑.

disulphide, of 0.025±0.002. The results of the reductions of the *p*-alkylnitrobenzene, shown in Fig. 2, certainly indicate a qualitative order of electron release in the sequences methyl > ethyl > isopropyl ≈ cyclohexyl > *t*-butyl. Quantitatively, the initial slopes in each case gave a measure of the relative reduction rates of the compounds. These relative rates are shown in Table I.

TABLE I

Relative initial rates of reduction by sodium hydrosulphide of para-substituted nitrobenzenes

R in *p*-R—$C_6H_4NO_2$	H	CH_3	C_2H_5	*i*-C_3H_7	Cyclohexyl	*t*-C_4H_9
Relative rate	1.0	0.33	0.39	0.46	0.46	0.65

NOTE: Concentration of hydrosulphide, 0.150 *M*; of nitro compound, 0.0250 *M*. Solvent, 76.5% by weight ethanol in water. Temperature, 50°.

Previous work (3, 4) has shown that in the reduction of nitrobenzene by sodium sulphide an induction period exists wherein reduction of nitrobenzene by sulphide ion occurred very slowly with simultaneous production of disulphide ion. The much greater reducing ability of the disulphide species, compared with that of the monosulphide ion, caused a sharp acceleration of rate. This increase of rate was found to be due only to the disulphide ion produced in the reaction. Reduction of nitrobenzene by hydrosulphide ion also shows a similar but much less pronounced "induction" period because the rate of reduction of nitrobenzene by hydrodisulphide ion is only about 7 times that for hydrosulphide ion

Can. J. Chem. Downloaded from www.nrcresearchpress.com by 210.87.254.40 on 09/05/12
For personal use only.

(1). In a reaction well protected from air oxidation, the appearance of disulphide or hydrodisulphide ion occurs *only when reduction of the nitro group is taking place* (1, 3, 4). Hence any increase in hydrodisulphide concentration is a measure of the reduction occurring, at least in the initial stages of the reaction, when loss of hydrodisulphide ion by reaction with the intermediate hydroxylamine is unimportant. Thus, measurement of the production of hydrodisulphide ion at periodic intervals should give a comparison of the relative rates of reduction of the nitro group in these substituted nitrobenzenes.

The plots in Fig. 2 show the acceleration of rate of reduction as hydrodisulphide ion accumulates. The change from increasing to decreasing slope occurs as loss of this hydrodisulphide by reaction with the hydroxylamine becomes more important. The plot of unsubstituted nitrobenzene (◐) does not exhibit the decreasing slope, due to the limited size of the figure, but previous work has shown that when the reaction is continued for 50 minutes or more a similar decrease in slope does occur (1).

The composition of the solvent used was 76.5% by weight of ethanol in water. Schubert *et al.* (10), by examination of the principal band in the ultraviolet absorption spectra of *p*-alkylnitrobenzenes in various solvents as well as in the gas phase, showed that the excitation energies of these alkylnitrobenzenes in the *gas* phase and in *hydrocarbon* solvents are in the inductive order, while in other solvents (alcohols, water, amine, ethers, acids) there is a tendency towards the hyperconjugative order of electron release by alkyl groups. It was hoped in a like manner that observations could be made on the effect of change of solvent on the relative rates of reduction of the alkylnitrobenzenes. The compatibility and solubilities of both the nitro compounds and the inorganic reagents required for reduction greatly limited the choice of solvents. Hence we were confined to the use of aqueous alcoholic solutions containing not more than 51% nor less than 23% of water. Accordingly, only the two extremes of alcohol–water mixtures, compatible with the solutes, were used to show the effect of change in solvent composition on the rate of reduction. It was found that the ratio of 1.9 of the initial reduction rates of *p*-nitrotoluene and *p*-*t*-butylnitrobenzene in a solution 50.5% by weight of ethanol in water was practically identical with that found for the reductions in the solvent containing 76.5% ethanol in water.

The original concept of hyperconjugation involved a second means of electron release, in addition to the normal inductive mechanism, which was operative when the alkyl groups were subjected to a high electron demand occurring in the transition state. The phenomenon was thus considered to be electromeric (16). However, Baker, Nathan, and Shoppee (17) illustrated also the mesomeric nature of electron release in demonstrating the retardation of the sodium-ethoxide-catalyzed prototropy of benzylidene-*p*-alkylbenzylamines, a reaction facilitated by electron recession from the reaction site.

The work described in the present paper is another example of a reaction whose rate is increased by electron recession from the reaction center and again demonstrates the mesomeric character of the hyperconjugative electron release of alkyl groups in *p*-alkylnitrobenzenes. The results obtained do not assist in clarifying the *origin* of the Baker–Nathan effect—a problem which has been the subject of considerable investigation (8–12, 16–19).

ACKNOWLEDGMENTS

The authors gratefully acknowledge the generous financial assistance given by the National Research Council of Canada in support of this work.

Can. J. Chem. Downloaded from www.nrcresearchpress.com by 210.87.254.40 on 09/05/12
For personal use only.

REFERENCES

1. O. J. Cope and R. K. Brown. Can. J. Chem. **40,** 2317 (1962).
2. H. Goldschmidt and H. Larsen. Z. Physik. Chem. **71,** 437 (1910).
3. J. L. Bullock and G. S. Forbes. J. Am. Chem. Soc. **55,** 232 (1933).
4. O. J. Cope and R. K. Brown. Can. J. Chem. **39,** 1695 (1961).
5. M. Hojo, Y. Takagi, and Y. Ogata. J. Am. Chem. Soc. **82,** 2459 (1960).
6. Y. Ogata and I. Sugiyama. Science (Tokyo), **19,** 232 (1949); Chem. Abstr. **45,** 5116 (1951).
7. J. R. Sampey. J. Am. Chem. Soc. **52,** 88 (1930).
8. J. W. Baker. Hyperconjugation. Oxford University Press, London. 1953.
9. Conference on Hyperconjugation. Tetrahedron, **5,** 105 (1959).
10. W. M. Schubert, J. Robins, and J. L. Haun. J. Am. Chem. Soc. **79,** 910 (1957).
11. F. A. Matsen, W. W. Robertson, and R. L. Chuoke. Chem. Rev. **41,** 273 (1947).
12. L. M. Stock and A. Himoe. J. Am. Chem. Soc. **83,** 4605 (1961).
13. H. G. Beard and H. H. Hodgson. J. Chem. Soc. 4 (1944).
14. R. Schroter. Methoden der organischen chemie. Georg Thieme Verlag, Vol. XI. Stuttgart. 1954.
15. H. A. Mayes and E. E. Turner. J. Chem. Soc. 500 (1929).
16. J. W. Baker and W. S. Nathan. J. Chem. Soc. 1844 (1935).
17. J. W. Baker, W. S. Nathan, and C. W. Shoppee. J. Chem. Soc. 1847 (1935).
18. C. Earborn and R. Taylor. J. Chem. Soc. 247 (1961).
19. W. M. Schubert and R. G. Minton. J. Am. Chem. Soc. **82,** 6188 (1960).

Can. J. Chem. Downloaded from www.nrcresearchpress.com by 210.87.254.40 on 09/05/12
For personal use only.

SUBSTITUTED PHENYLACETYLENES. INFRARED SPECTRA

A. D. ALLEN AND C. D. COOK[1]
Department of Chemistry, University of Toronto, Toronto, Ontario
Received December 4, 1962

ABSTRACT

A series of substituted phenylacetylenes has been prepared and their infrared spectra recorded. The C≡C and ≡C—H stretching frequencies are only slightly affected by substituents in the phenyl ring. Substituents in the 4-position cause a splitting of the ≡C—H band into two clearly resolved bands of similar intensity, about 10 cm^{-1} apart.

As part of an investigation into the formation of complexes between unsaturated organic molecules and transition metals, a series of substituted phenylacetylenes has been prepared and their infrared spectra recorded. Nuclear magnetic resonance spectra of these compounds have already been reported (1). In this paper we give the principal features of the infrared spectra of these compounds and the methods used for their preparation.

EXPERIMENTAL

A wide variety of substituted phenylacetylenes may be prepared by one of two general methods: (*a*) from the substituted acetophenone by chlorination followed by dehydrochlorination with alkali (2), and (*b*) from the substituted cinnamic acid by bromination followed by dehydrobromination with base.

Method (*a*) was used for the following compounds, the first four of which have not been reported previously, although Dessy (3) has described mercury acetylides derived from two of them (4-fluoro- and 3-methyl-phenylacetylene).

2-Methylphenylacetylene.—A mixture of 9.5 g phosphorus pentachloride and 5.5 g 2-methylacetophenone was maintained at 70–80° for 30 minutes. The resulting dark orange solution was distilled and the fraction boiling between 80–95° at 15 mm was collected (4.4 g). This fraction was refluxed overnight with 5 g potassium hydroxide in 15 ml absolute ethanol. After adding 150 ml iced water the solution was extracted with ether, and the extract was washed with iced water and dried over sodium sulphate. Distillation at reduced pressure gave the crude product, which was stored over potassium hydroxide pellets overnight at room temperature and then distilled from fresh pellets of potassium hydroxide. The product (1.8 g, 38%) was a colorless oil, b.p. 49–50° at 13 mm. Calc. for C_9H_8: C, 93.1; H, 6.9. Found: C, 93.0; H, 6.5.

2-Fluorophenylacetylene.—Prepared from 2-fluoroacetophenone (Pierce Chemical Co.) by the procedure used for 2-methylphenylacetylene. The product (5.8 g, 42%) was an oil, b.p. 31–32° at 10 mm. Calc. for C_8H_5F: C, 80.0; H, 4.2. Found: C, 80.0; H, 4.7.

4-Fluorophenylacetylene.—Prepared from 4-fluoroacetophenone (Pierce Chemical Co.) by the procedure used for 2-methylphenylacetylene. The product (7.5 g, 61%) was a solid, m.p. 25°, b.p. 34–35° at 10 mm, 140° at 758 mm. Calc. for C_8H_5F: C, 80.0, H, 4.2. Found: C, 80.1; H, 4.3.

3-*Methylphenylacetylene.*—Phosphorus pentachloride (83.5 g) was added to 50 g 3-methylacetophenone in 100 ml dry benzene. The mixture was cooled in ice during the initial vigorous reaction and then stirred overnight at room temperature, protected from moisture. The resulting solution was distilled at reduced pressure and the fraction boiling at 105–110° at 16 mm was collected (62 g). This fraction was refluxed for 5 hours with 75 g potassium hydroxide in 150 ml 95% ethanol. Dilution with 250 ml water, extraction with ether, drying and distillation of the ether extract gave the crude product, b.p. 75–80° at 23 mm, which was stored over potassium hydroxide pellets overnight. Distillation from fresh potassium hydroxide gave the product (16 g, 37%) as a colorless oil, b.p. 58–59° at 14 mm. Calc. for C_9H_8: C, 93.1; H, 6.9. Found: C, 92.1; H, 7.1.

4-Methylphenylacetylene.—Prepared from 4-methylacetophenone by the procedure used for 2-methylphenylacetylene. The product was an oil, b.p. 59–60° at 16 mm (lit. (2) b.p. 65–67° at 18 mm).

3-Methoxyphenylacetylene.—Prepared from 3-methoxyacetophenone by the method of Johnson *et al.* (4), b.p. 80° at 12 mm (lit. (4) b.p. 85° at 13 mm).

4-Bromophenylacetylene.—Prepared from 4-bromoacetophenone as described by Jacobs (5), m.p. 63° (lit. (2) m.p. 63.5°).

[1]*Present address: Department of Chemistry, University College, London, England.*

Can. J. Chem. Downloaded from www.nrcresearchpress.com by 210.87.254.105 on 09/05/12
For personal use only.

4-Chlorophenylacetylene.—Prepared from 4-chloroacetophenone as described by Jacobs (5), b.p. 62–63° at 13 mm, m.p. 43° (lit. (2) m.p. 43.5–44°). This compound is best purified by sublimation.

2-Chlorophenylacetylene.—Prepared from 2-chloroacetophenone by the same method as was used for 2-methylphenylacetylene, b.p. 44–45° at 11 mm (lit. (2) b.p. 71° at 18 mm).

Method (*b*) was used for the following compounds.

2-Methoxyphenylacetylene.—The following procedure is a modification of those described by Manchot (6) and Smissman (7). A solution of 48 g bromine in 200 ml dry chloroform was added during 2 hours to 50 g 2-methoxycinnamic acid in 250 ml dry chloroform. During the addition the mixture was stirred vigorously and kept between 0° and 5°. After the addition the solution was stirred for a further 30 minutes and then cyclohexene was added to remove excess bromine. The solvent was removed in a stream of dry air and the resulting crystalline mass was washed with cold carbon tetrachloride. The yield of 2-methoxy-α,β-dibromocinnamic acid was quantitative. This product was heated on a steam bath for 2 hours with 600 ml 10% sodium carbonate solution. The cooled solution was extracted with ether, and the ether extract was washed, dried, and evaporated. The residue was refluxed for 4-hours with 400 ml tertiary butanol in which 8 g potassium metal had been dissolved. Most of the solvent was then removed by distillation at reduced pressure and the residue treated with 500 ml water. Ether extraction, followed by washing, drying, and distillation of the extract, gave the crude product, b.p. 88–92° at 8 mm. This was stored overnight over pellets of potassium hydroxide and then distilled from fresh potassium hydroxide, giving a colorless liquid (12 g, 33%), b.p. 89–90° at 8 mm (lit. (8) b.p. 93° at 10 mm).

4-Methoxyphenylacetylene.—Prepared from 4-methoxycinnamic acid by the procedure used for 2-methoxyphenylacetylene, b.p. 86° at 9 mm, m.p. 29° (lit. (7) b.p. 90–95° at 10 mm).

2-Nitrophenylacetylene.—2-Nitrocinnamic acid was converted into *cis*-2-nitro-β-bromostyrene by the method of Dann *et al.* (9). The product (11.5 g) was stirred for 30 minutes at room temperature with 20 g sodium hydroxide in 250 ml 95% ethanol. The resulting solution was neutralized with glacial acetic acid, and 200 ml solvent was removed by distillation at reduced pressure. The crude product was precipitated by adding 500 ml iced water. Recrystallization from aqueous ethanol gave the pure product (3.4 g, 45%) as colorless needles, m.p. 81° (lit. (10) m.p. 81–82°).

3-Nitrophenylacetylene.—Prepared from 3-nitrocinnamic acid by the procedure used for 2-nitrophenylacetylene, b.p. 118–120 at 20 mm, m.p. 27° (lit. (11) m.p. 27°).

4-Nitrophenylacetylene.—Prepared by the method of Cristol *et al.* (12), m.p. 149–150° (lit. (12) m.p. 148–149°).

Other methods were used for the following compounds.

2-Hydroxyphenylacetylene.—Coumarilic acid (benzofuran-2-carboxylic acid) was prepared from coumarin by the method of Fuson *et al.* (13). An intimate mixture of 20 g coumarilic acid, 20 g powdered calcium oxide, and 1 g copper bronze powder was heated in a small distilling flask with a free flame until distillation stopped. The crude benzofuran (14 g) was washed with 10% sodium hydroxide solution, dried over sodium sulphate, and distilled, b.p. 170°.* A mixture of 11.8 g benzofuran, 6.9 g sodium, and 94 g pyridine (freshly distilled from potassium hydroxide) was heated in an oil bath at 190° for 4 hours. The cooled mixture was treated with pyridine and water and then acidified (to congo red) with dilute hydrochloric acid. Extraction with ether, followed by drying and distillation of the ether extract, gave the crude product, which was then dissolved in 10% aqueous potassium hydroxide. The resulting solution was extracted with ether to remove any unreacted benzofuran, and the acetylene was regenerated by the addition of dilute hydrochloric acid to the alkaline solution. The resulting acidic solution was extracted with ether, and the ether extract was washed, dried, and distilled at reduced pressure to give the pure product (3.8 g, 32%), b.p. 63° at 7 mm (lit. (8) b.p. 73–74° at 11 mm).

2-Aminophenylacetylene.—Prepared by the reduction of 2-nitrophenylacetylene as described by Schofield and Swain (10). The product was purified by precipitating the amine hydrochloride from benzene solution, and recovering the free amine by treating the precipitate with aqueous alkali. Extraction with ether, followed by washing, drying, and distillation of the ether extract, gave the product as a yellowish oil, b.p. 99–101° at 13 mm (lit. (10) b.p. 98–100° at 12 mm).

4-Aminophenylacetylene.—Prepared by reduction of 4-nitrophenylacetylene, as described by Burawoy and Critchley (14), m.p. 99–100° (lit. (14) m.p. 100°).

Phenylacetylene.—The commercial material was distilled from pellets of potassium hydroxide and the fraction boiling between 140–144° was collected and stored over potassium hydroxide. Fractional distillation gave the pure material, b.p. 44° at 23 mm (lit. (15) b.p. 140°).

Infrared Spectra

The infrared spectra of dilute solutions (ca. 5%) of the compounds in carbon tetrachloride (Fisher 'Spectranalysed') were obtained using a Perkin–Elmer 221G prism-grating spectrometer. The instrument was calibrated against indene and routinely checked against polystyrene film. The spectra were recorded at 30±1°, at a scanning speed of approximately 1 cm^{-1}/sec, in the regions of interest. Standard 221G

**Details of this method for the decarboxylation of coumarilic acid, developed by H. Gilman, were kindly provided by Professor A. G. Brook.*

Can. J. Chem. Downloaded from www.nrcresearchpress.com by 210.87.254.105 on 09/05/12
For personal use only.

settings used were: slit schedule 927, attenuator speed 11.00, amplifier gain 4.5, and scan suppression at 4–5. A 0.1-mm sodium chloride fixed cell was used and the position of the weak band at 2100 cm^{-1} was checked if necessary by using scale expansion or a 0.5-mm cell. Reproducibility was ± 1 cm^{-1}, and the precision of the band maxima is estimated to be ± 2 cm^{-1}.

DISCUSSION

Table I shows details of the C≡C and ≡C—H stretching frequencies observed for these compounds.

TABLE I

Stretching frequencies ν for compounds X—$C_6H_4C_2H$

X	ν (cm^{-1}) ≡C—H	ν (cm^{-1}) C≡C	X	ν (cm^{-1}) ≡C—H	ν (cm^{-1}) C≡C
4-Amino	3328, 3313	2114	Hydrogen	3319, 3308 (sh)	2119
2-Amino	3316	2103	4-Fluoro	3319, 3305	2119 (w)
4-Methoxy	3324, 3310	2116	2-Fluoro	3320	2125, 2113 (sh)
3-Methoxy	3322	2118	4-Chloro	3317, 3310	2119 (w)
2-Methoxy	3320	2116	2-Chloro	3308	2112 (w)
2-Hydroxy	3310	2109	4-Bromo	3318, 3307	2119 (w)
4-Methyl	3323, 3307	2115	4-Nitro	3322, 3308	2122 (w)
3-Methyl	3313	2112	3-Nitro	3314	2126 (w)
2-Methyl	3312	2111	2-Nitro	3314	2119 (w)

The carbon–hydrogen stretching mode gives a strong absorption in all cases. The carbon–carbon stretching mode gives a much weaker absorption, the maximum observed for the series being about 10% of the ≡C—H absorption. Those compounds in which the C≡C absorption is markedly less than 10% of that of ≡C—H are shown as weak (w) in the table. It may be significant that such compounds all contain electron-withdrawing substituents.

It will be seen that there is little correlation between the electron-withdrawing or -donating ability of the ring substituent and the frequency of either stretching vibration. If the variations observed do indicate significant trends then these are that electron-withdrawing substituents tend to decrease the ≡C—H and increase the C≡C stretching frequencies.

A weak band showing up as a shoulder on the low-frequency side of the ≡C—H absorption has been reported for a variety of acetylenes by Brand *et al.* (16). They found this band to be most intense in the spectra of the aryl acetylenes studied and suggest that this absorption results from a combination tone intensified by Fermi resonance. Nyquist and Potts (17), in a more detailed examination of phenylacetylene, arrived at the same conclusion and propose that the absorption results from the summation of the first overtone of the ≡C—H bending mode (at about 1220–1250 cm^{-1}) and the C≡C stretching fundamental, the intensity being increased by Fermi resonance with the ≡C—H stretching fundamental. However recent work by West and Kraihanzel (15), which included a study of the spectrum of deuterophenylacetylene ($C_6H_5C_2D$), may invalidate the earlier proposals since these authors report that side bands also accompany the C—D stretching absorption at 2595 cm^{-1}.

We find that compounds with substituents in the 2- and 3-positions give a single, sharp band at about 3315 cm^{-1}, with perhaps a very weak unresolved shoulder, but that when the substituent is in the 4-position this band is split into two bands about 10 cm^{-1} apart. The lower-frequency band of this pair is usually of slightly lower intensity than the other,

Can. J. Chem. Downloaded from www.nrcresearchpress.com by 210.87.254.105 on 09/05/12
For personal use only.

but only in the unsubstituted phenylacetylene is it sufficiently poorly resolved to be described as a shoulder. These spectra are complex in the 1000–1500 cm^{-1} region and in many cases it is difficult to assign a band to the first overtone of the ≡C—H bending mode, but the suggestion of Nyquist and Potts is supported by the fact that the 4-substituted compounds usually have a strong band between 1220–1230 cm^{-1}, which may be attributed to this overtone, whereas the 2- and 3-substituted compounds usually do not.

Grateful acknowledgment is made to the National Research Council of Canada for financial support and to the Shell Oil Company of Canada Limited for a fellowship (to C. D. C.).

REFERENCES

1. C. D. Cook and S. S. Danyluk. Tetrahedron. In press.
2. M. M. Otto. J. Am. Chem. Soc. **56**, 1393 (1934).
3. R. E. Dessy and J. Y. Kim. J. Am. Chem. Soc. **83**, 1167 (1961).
4. W. S. Johnson, D. K. Banerjee, W. P. Schneider, C. D. Gutsche, W. E. Shelberg, and L. J. Chinn. J. Am. Chem. Soc. **74**, 2832 (1952).
5. T. L. Jacobs. Organic reactions. Vol. 5. John Wiley, New York. 1949.
6. W. Manchot. Ann. **387**, 283 (1912).
7. E. E. Smissman, R. H. Jonsen, A. W. Carlson, and B. F. Aycock. J. Am. Chem. Soc. **78**, 3395 (1956).
8. V. Prey and H. Berbalk. Monatsh. **82**, 990 (1951).
9. A. T. Dann, A. Howard, and W. Davies. J. Chem. Soc. 605 (1928).
10. K. Schofield and T. Swain. J. Chem. Soc. 2398 (1949).
11. F. Willring. Ber. **47**, 108 (1914).
12. S. J. Cristol, A. Begoon, W. P. Norris, and R. S. Ramey. J. Am. Chem. Soc. **76**, 4558 (1954).
13. R. C. Fuson, J. W. Kueisley, and E. W. Keises. Organic syntheses. Coll. Vol. 3, John Wiley, New York. 1955. p. 209.
14. A. Burawoy and J. P. Critchley. Tetrahedron, **5**, 340 (1959).
15. R. West and C. S. Kraihanzel. J. Am. Chem. Soc. **83**, 765 (1961).
16. J. C. D. Brand, E. Eglinton, and J. F. Morman. J. Chem. Soc. 2526 (1960).
17. R. A. Nyquist and W. J. Potts. Spectrochim. Acta, **16**, 419 (1960).

Can. J. Chem. Downloaded from www.nrcresearchpress.com by 210.87.254.105 on 09/05/12
For personal use only.

CRITICAL PHENOMENA IN THE SYSTEM ACETIC ACID – CHLOROFORM – WATER

A. N. CAMPBELL AND E. M. KARTZMARK
Department of Chemistry, University of Manitoba, Winnipeg, Manitoba
Received November 30, 1962

ABSTRACT

This paper is an experimental study of (*a*) the solid–liquid equilibria at low temperatures; (*b*) equilibrium compositions at temperatures other than 25° C; (*c*) the critical phenomena, L_1–L_2, L_1–V, and L_2–V, in the acetic acid – chloroform – water system. No previous study has been made of critical phenomena in a system exhibiting partial liquid miscibility.

Can. J. Chem. Downloaded from www.nrcresearchpress.com by 210.87.254.6 on 09/05/12
For personal use only.

The system acetic acid – chloroform – water is one of the classical examples of partial miscibility in a ternary system, first studied by Wright, Thompson, and Leon in 1891 (1). Thanks to the subsequent workers Brancker, Hunter, and Nash (2), the equilibrium relations at 25° are very well known, as far as the compositions of equilibrium liquid layers are concerned. Nothing, however, is known about:

(*a*) the solid–liquid equilibria at low temperatures;
(*b*) equilibrium liquid compositions at temperatures other than 25°;
(*c*) the critical phenomena, L_1–V (L_1 = chloroform layer) and L_2–V (L_2 = aqueous layer).

So far no study has been made of critical phenomena in any system exhibiting partial miscibility in the liquid state and the results arrived at in this paper have general applicability to all systems of this kind.

A previous paper (3) has dealt with the thermodynamics of this system, as exemplified by the vapor pressures and densities. Further work is proceeding on the isobaric boiling points, dielectric constants, and heats of mixing.

RESULTS AND DISCUSSION

Because of the chemical natures of the substances named in the title, formation of compounds or of solid solutions is inherently improbable and therefore the study of the freezing point curves was expected to yield little of interest. The study was, however, carried out for the binary systems chloroform – acetic acid and chloroform – water, and for the ternary system, using a double-junction copper–constantan thermocouple, a Brown Elektronik recorder, and liquid nitrogen as a coolant. The system acetic acid – water was previously studied by various workers (4) and the eutectic found to lie at 58.1% acetic acid and −28.5 to −27.0°. The eutectic of the chloroform – acetic acid system was found to lie at 91.8% $CHCl_3$ by weight, and −67.5° (Fig. 1). In the system chloroform–water, the eutectic lies at 0.1% H_2O and −64.0°. The ternary eutectic was found to lie at −70° and 90.7% chloroform, 8.3% acetic acid, and 1.0% water. The eutectic trough leading from the acetic acid – water eutectic to the acetic acid – chloroform eutectic was determined experimentally. The results are given in Fig. 2, on which has been superimposed the partial miscibility gap for 0°.

Two types of temperatures of homogeneity are to be distinguished in this work, namely, the temperature at which two partially miscible liquids become completely miscible ($L_1 + L_2 \rightarrow L$) and the true critical temperatures ($L_1 + V \rightarrow V$ and/or $L_2 + V \rightarrow V$);

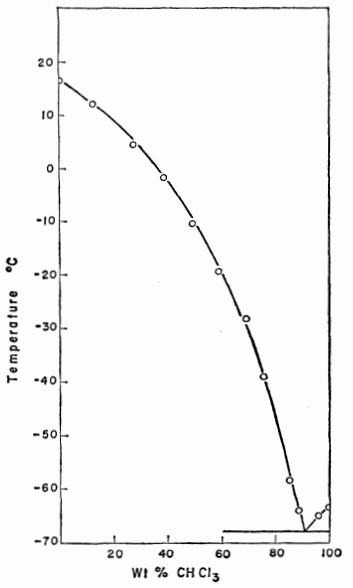

FIG. 1. Freezing point diagram of system chloroform – acetic acid. Eutectic: −67.5° C, 91.8% $CHCl_3$.

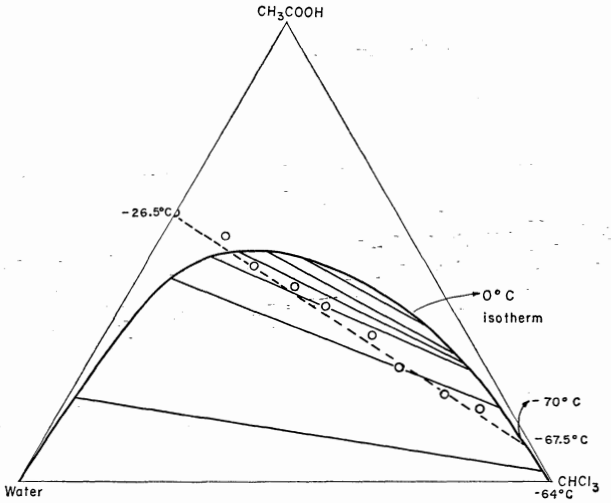

FIG. 2. 0° isotherm superimposed on a projection of the ternary freezing point diagram.

certain of the mixtures, though not all, will exhibit all three temperatures. For the determination of all three types of temperatures, the simple apparatus shown in the photograph (Fig. 3) worked very well. It consists essentially of a cylindrical block of copper, weighing about 75 lb and having a radial boring of 1-cm diameter. Slots parallel to the boring permit light to pass through. A sealed capillary tube placed in the central boring can be viewed in a telescope at a safe distance. Two heating circuits in parallel, wound around the copper cylinder, make it possible to raise the temperature to 350° in about 3 hours. An ordinary mercury-in-glass thermometer placed in a separate boring of the copper block gives the temperature. The temperature was corrected for exposed stem but with

Can. J. Chem. Downloaded from www.nrcresearchpress.com by 210.87.254.6 on 09/05/12
For personal use only.

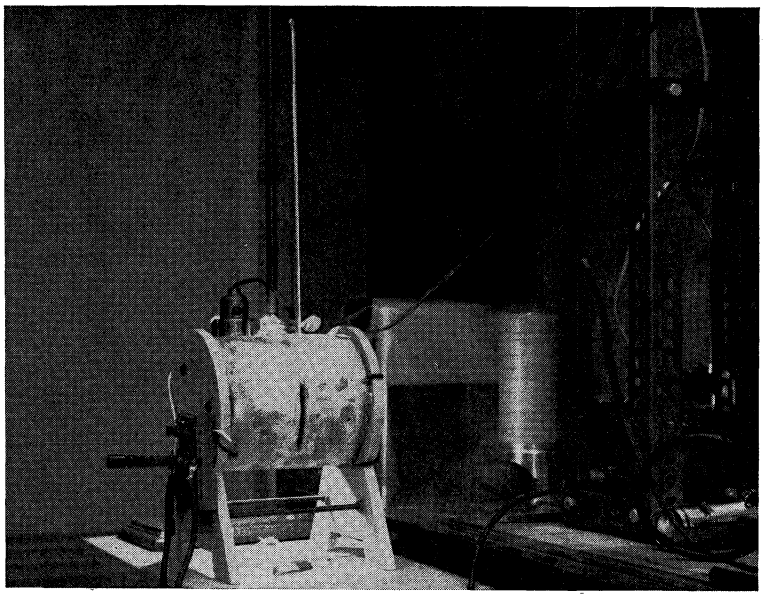

FIG. 3. Apparatus.

this relatively crude arrangement we do not believe the results to be more accurate than ±1°. We saw no reason to refine the temperature measurement, although it would have been easy to do so. Temperature was easily controlled and occasional explosions constituted no hazard to the operators.

A possible criticism of this method, as applied to L–V critical temperatures, is that, unless the amount of the mixture and the volume of the container are such as to represent the critical density, the temperature of disappearance of the meniscus is not the true critical temperature. Nevertheless, the phenomena as observed usually presented the fluctuating striae said to be characteristic of critical phenomena. It is true that the temperature of reappearance of the meniscus was frequently 5–10° lower than that of disappearance but this may be a characteristic of mixtures as distinct from pure liquids: we reproduce only the temperature of disappearance. The results were also reproducible in different experiments and the curve of critical temperature vs. composition was smooth. The explanation is, no doubt, that in the four-dimensional representation of pressure, volume, temperature, and concentration, all curves are very flat in the neighborhood of the critical point, or, in plain words, the critical temperature is not very sensitive to small changes in volume of the system. At all events, we repeat that in all cases the disappearance of the meniscus appeared to be a critical phenomenon: cases where the meniscus disappeared by exhaustion of the one or other phase were always discarded. If our figures are not true critical temperatures they are sufficiently close for the present purpose. We note that the critical temperatures of the pure liquids as determined by us are in good agreement with accepted literature values.

The critical temperatures of the homogeneous binary systems acetic acid – water and acetic acid – chloroform are reproduced graphically in Figs. 4 and 5. The critical temperatures of homogeneous ternary mixtures are given in Table I, since they cannot be expressed graphically on a plane diagram to any purpose.

Can. J. Chem. Downloaded from www.nrcresearchpress.com by 210.87.254.6 on 09/05/12
For personal use only.

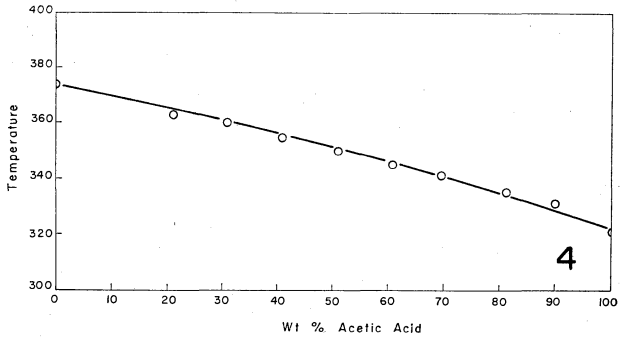

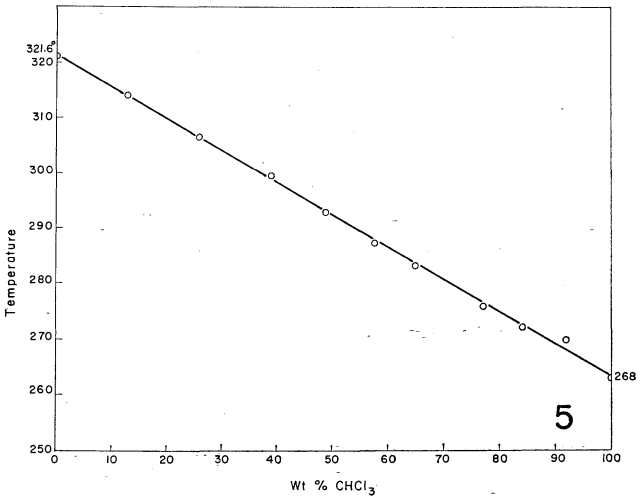

FIG. 4. Acetic acid – water critical temperatures.
FIG. 5. Chloroform – acetic acid critical temperatures.

TABLE I

Composition of mixture in wt%			Critical temperature in °C
Acetic acid	Water	Chloroform	
88.7	5.7	5.7	317.5
76.6	9.3	14.1	327.0
69.7	17.3	13.0	326.0
66.7	8.2	25.1	318.0
60.1	27.1	12.8	330.0
55.2	18.0	21.8	323.0
54.2	9.3	36.5	317.5
50.2	36.0	13.9	342.0
47.9	25.8	26.4	342.0
49.4	15.3	35.2	315.5
52.0	8.2	39.7	307.5
42.0	52.4	5.6	355.0
41.7	9.2	49.2	306.5
42.5	13.4	44.0	309.5
35.9	58.8	5.2	358.5
31.6	9.4	59.0	284.5

Can. J. Chem. Downloaded from www.nrcresearchpress.com by 210.87.254.6 on 09/05/12
For personal use only.

Within the region of heterogeneity, as mentioned in the introduction, two, and sometimes three, temperatures of homogeneity (2 phase) have to be determined. The $L_1 - L_2 \rightarrow L$ temperature was easily determined in the apparatus described as the temperature at which one or the other liquid layer vanished by exhaustion (method of Alexejew). In order to do this accurately, it is necessary to heat very slowly in the neighborhood of the temperature of homogeneity, to remove the tube and shake vigorously to produce a fine suspension, and then to determine if the suspension persists at the temperature of the furnace.

As a preliminary to the above work, however, the isothermal area of heterogeneity was determined at such temperatures as were readily accessible, viz. 0°, 48.5°, and 91.5°. Such quantities of the three components as would give approximately equal volumes of the two layers were stirred in thermostat for 24 hours and then each layer sampled for analysis. The method of analysis was that of determining acetic acid by titration. A weighed amount of acetic acid was then added to a separate sample and the density determined. A previous calibration had been made, at 25°, of the densities of mixtures lying without the area of heterogeneity (3). These data yielded a complete analysis. We have subsequently found that the determination of refractive index gives a more sensitive determination. The results are represented graphically in Figs. 6, 7, and 8. The plait point compositions are given in Table II.

TABLE II

	Composition in wt%		
Temperature in °C	Chloroform	Water	Acetic acid
0	45.0	14.0	41.0
25.0 (Brancker, Hunter and Nash (2))	41.5	16.1	42.4
48.5	44.0	17.0	39.0
91.5	45.0	19.0	36.0

The results of the Alexejew method for the heterogeneous region are represented graphically in Figs. 9, 10, 11, 12, and 13, each of which represents a pseudobinary section of the solid model having a fixed amount of acetic acid. Some comment is necessary. In systems containing less than 20% acetic acid, the surface of heterogeneity (L_1–L_2) intersects the critical surface L_1–V, where L_1 represents the chloroform layer. This means that the chloroform layer has a constant composition when passing through the critical change L_1–V, and this change therefore takes place at a constant temperature, independent of the total composition, so long as the composition lies within the miscibility gap at the temperature of the L_1–V transition. The L_1–V transition exhibits experimentally all the characteristics of a true critical point, except that a (separate) liquid layer, the aqueous layer, remains behind and this in turn goes through the L_2–V critical transition at, however, a much higher temperature. Since, however, there is only one liquid, its composition varies with the total composition of the mixture and therefore the second critical temperature (L_2–V) is not constant but is a function of total composition.

As the concentration of acetic acid in the pseudobinary mixtures is increased, the L_1–L_2 surface separates from the L–V surface and the temperatures of L–V transition now also become a function of total composition. This is clearly shown in the pseudobinary sections Figs. 9, 10, 11, 12, and 13.

Can. J. Chem. Downloaded from www.nrcresearchpress.com by 210.87.254.6 on 09/05/12
For personal use only.

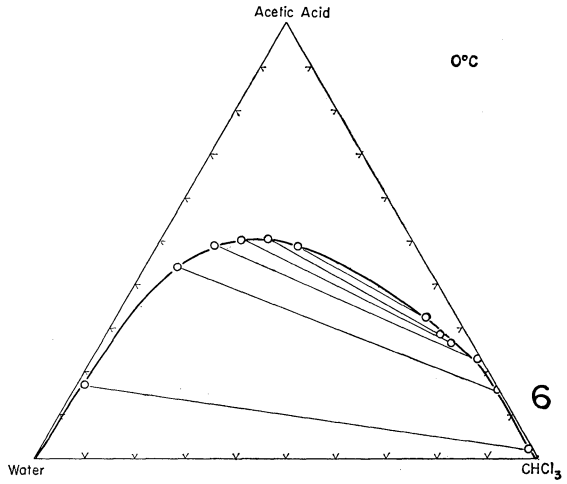

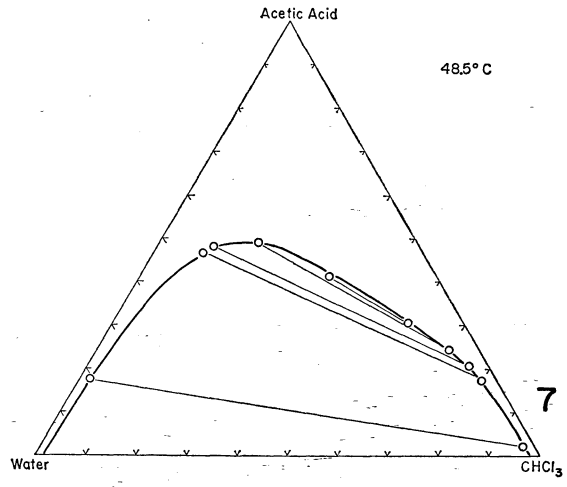

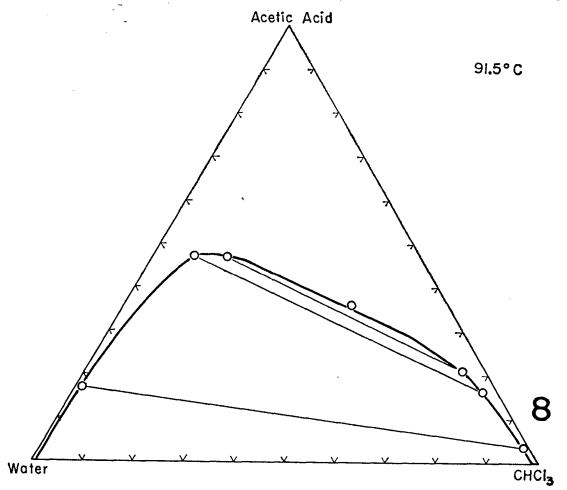

FIG. 6. 0° C isotherm.
FIG. 7. 48.5° C isotherm.
FIG. 8. 91.5° C isotherm.

Can. J. Chem. Downloaded from www.nrcresearchpress.com by 210.87.254.6 on 09/05/12
For personal use only.

Can. J. Chem. Downloaded from www.nrcresearchpress.com by 210.87.254.6 on 09/05/12
For personal use only.

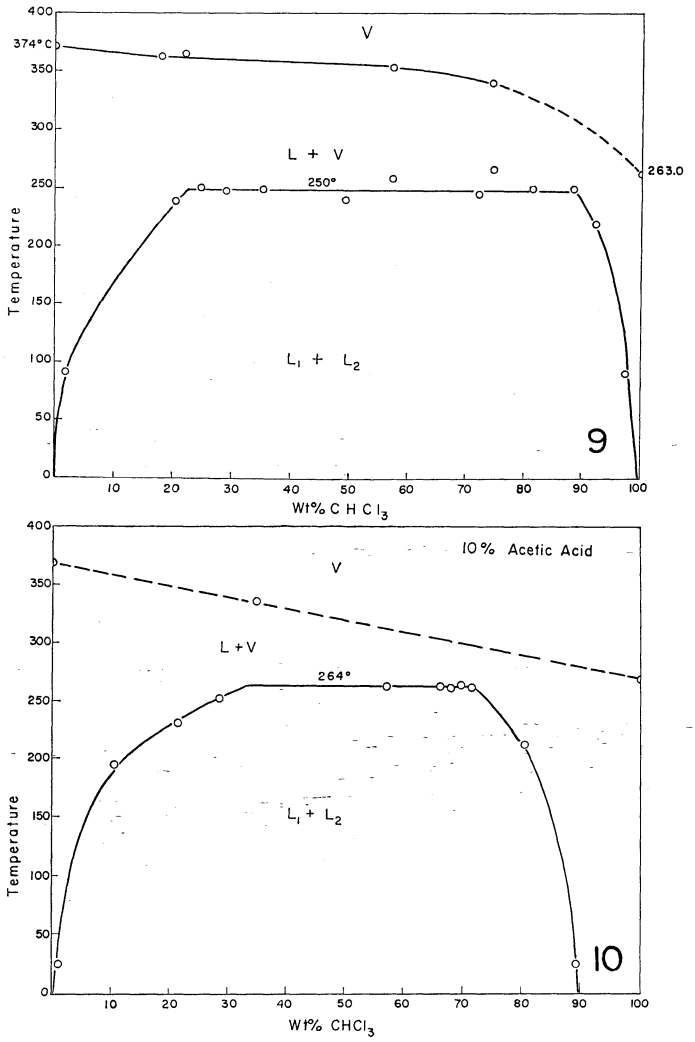

FIG. 9. Critical data in system chloroform–water.
FIG. 10. Critical data in pseudobinary system containing 10% acetic acid.

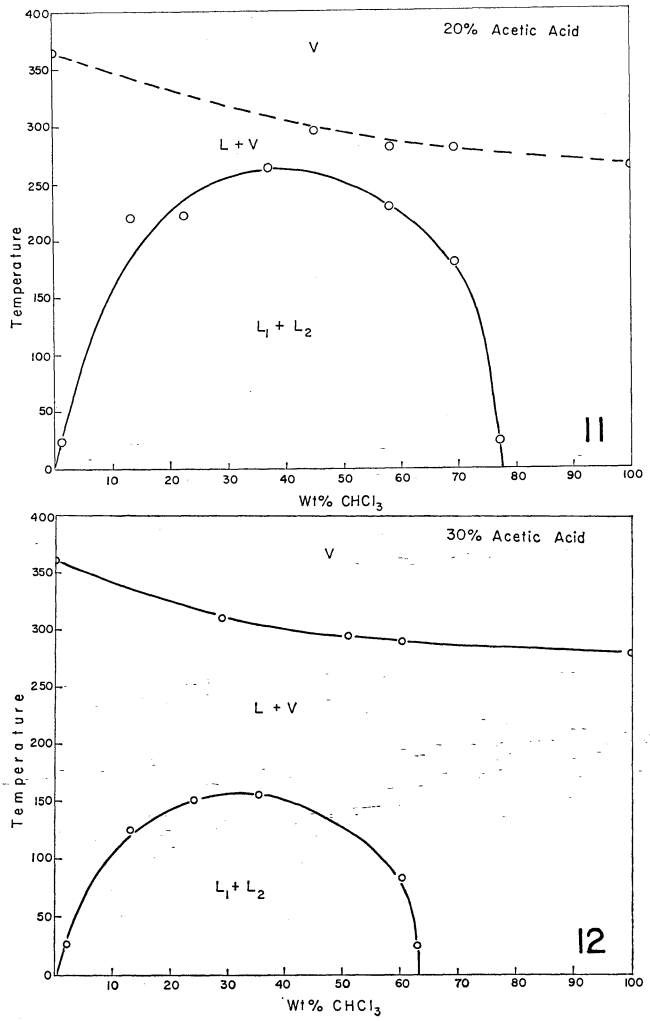

Fig. 11. Critical data in pseudobinary system containing 20% acetic acid.
FIG. 12. Critical data in pseudobinary system containing 30% acetic acid.

Can. J. Chem. Downloaded from www.nrcresearchpress.com by 210.87.254.6 on 09/05/12
For personal use only.

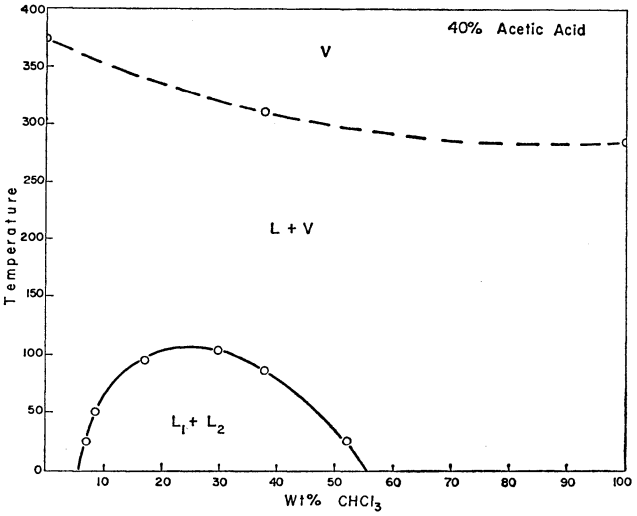

FIG. 13. Critical data in pseudobinary system containing 40% acetic acid.

From the data given it is readily possible to construct the solid (composition–temperature) model, on an equilateral triangular base, and we have done this as an aid to the teaching of advanced phase rule. The experimental data of this paper are available on application.

REFERENCES

1. C. R. A. WRIGHT, C. THOMPSON, and J. T. LEON. Proc. Roy. Soc. (London), **49**, 174 (1891).
2. A. V. BRANCKER, T. G. HUNTER, and A. W. NASH. J. Phys. Chem. **44**, 683 (1940).
3. A. N. CAMPBELL, E. KARTZMARK, and J. M. T. M. GIESKES. Can. J. Chem. **41**, 407 (1963).
4. A. FAUCON. Ann. Chim. Phys. **19**, 70 (1910). M. HIRATA, Y. HIROSE, and K. KOBAYASHI. Kagaku Kagaku, **23**, 403 (1959).

Can. J. Chem. Downloaded from www.nrcresearchpress.com by 210.87.254.6 on 09/05/12
For personal use only.

THE REACTION OF ACTIVE NITROGEN WITH METHANOL[1]

M. J. Sole and P. A. Gartaganis[2]
Chemistry Department, Ontario Research Foundation, Toronto, Ontario
Received April 30, 1962

ABSTRACT

The reaction of active nitrogen with methanol has been investigated at several temperatures in the range 30 to 480° C using a fast-flow system. The only condensable products found in appreciable amounts were water and hydrogen cyanide. The overall activation energy is 3.0 and 3.2 kcal/mole and the steric factors 1.3×10^{-3} and 2.1×10^{-3} for streamline and turbulent flow respectively.

It is postulated that the mechanism consists of the initial formation of a collision complex, $[NCH_3OH]$, which breaks down to two fragments, NCH_3 and OH, from which the two condensable products are formed,

$$N + CH_3OH \rightarrow [NCH_3OH] \rightarrow NCH_3 + OH$$

$$NCH_3 \rightarrow HCN + 2H \text{ or } H_2$$

$$OH + H \rightarrow H_2O.$$

Attack of the methanol molecules by hydrogen atoms resulting from the main reaction occurs to a lesser extent and is responsible for the production of small quantities of methane, carbon monoxide, and additional water.

INTRODUCTION

Studies of the reactions of active nitrogen, produced by electrical discharge in a low-pressure nitrogen stream, with organic compounds have been in progress for many years and have received particular attention recently through the discovery that these species exist in the upper atmosphere (1). Except for two preliminary studies on the reactions of active nitrogen with methanol, acetone, and dimethyl ether (2) and with several aromatic and aliphatic oxygenated compounds (3) and a recent study on the reactions with liquid siloxane heptamer (4), no other work has been reported on the kinetics of active nitrogen with simple oxygen-containing organic compounds. The present investigation was undertaken with a view to studying the reaction of active nitrogen with methanol.

It is now established that the major chemically active species present in active nitrogen is nitrogen atom in the ^4S ground state; recent investigations (5–7) have shown that the second active species is the $A^3\Sigma_u^+$ state of N_2.

EXPERIMENTAL

The apparatus used was similar to that described in detail by Gartaganis and Winkler (8). It consisted essentially of a condensed discharge Wood–Bonhoeffer fast-flow system with additional features for the measurement of reactants and analysis of products. The spherical reaction vessel was replaced in the present study by a 100-cm reaction tube of a 16-mm i.d. which contained thermocouple wells at regular intervals.

The duration of an experiment varied from 200 to 1600 seconds. The products were collected in traps surrounded with liquid air and were distilled at the end of each run into an absorber containing 1 *N* KOH or methanol. Hydrogen cyanide was measured by titration with 0.100 *N* $AgNO_3$ solution. Water was determined with Karl–Fischer reagent by means of a specially constructed apparatus for the direct transference of the products to the analytical system. Mass spectrometric analyses supplied information on the purity of the reagents and the nature of the non-condensable products. The ratio of water to hydrogen cyanide was established by determining their concentrations in aliquot parts withdrawn from the absorber. The

[1]*Presented at the 45th Annual Conference of the Chemical Institute of Canada, Edmonton, May, 1962.*
[2]*Present address: Dominion Tar and Chemical Company Ltd. Central Research Laboratories, Cornwall, Ontario.*

Can. J. Chem. Downloaded from www.nrcresearchpress.com by 210.87.254.6 on 09/05/12
For personal use only.

results obtained with the above techniques were verified by means of gas phase chromatography (Vapor Fractometer, Model 154, Perkin Elmer Corp.). A column comprising polyethylene glycol on teflon powder separated, in a satisfactory way, unreacted methanol, hydrogen cyanide, and water in that order.

RESULTS

The reaction of active nitrogen with methanol was accompanied by a peach-violet colored flame, similar to those observed in reactions with hydrocarbons. There was a gradual change in the flame characteristics as the flow rate of methanol and/or the temperature were increased. The atomic and the total nitrogen flow rates were 1.55 and 23.2 μmoles/sec respectively.

Hydrogen cyanide and water in approximately equal amounts were the only condensable products found regardless of methanol flow rate or temperature. Mass spectrometric analysis of non-condensable products revealed the presence of a substantial amount of hydrogen and small quantities of carbon monoxide and methane. No ammonia was detected.

The amount of hydrogen cyanide, the only nitrogen-containing product, recovered in different experiments at various flow rates and at different temperatures in the range 30 to 480° C is shown in Fig. 1.

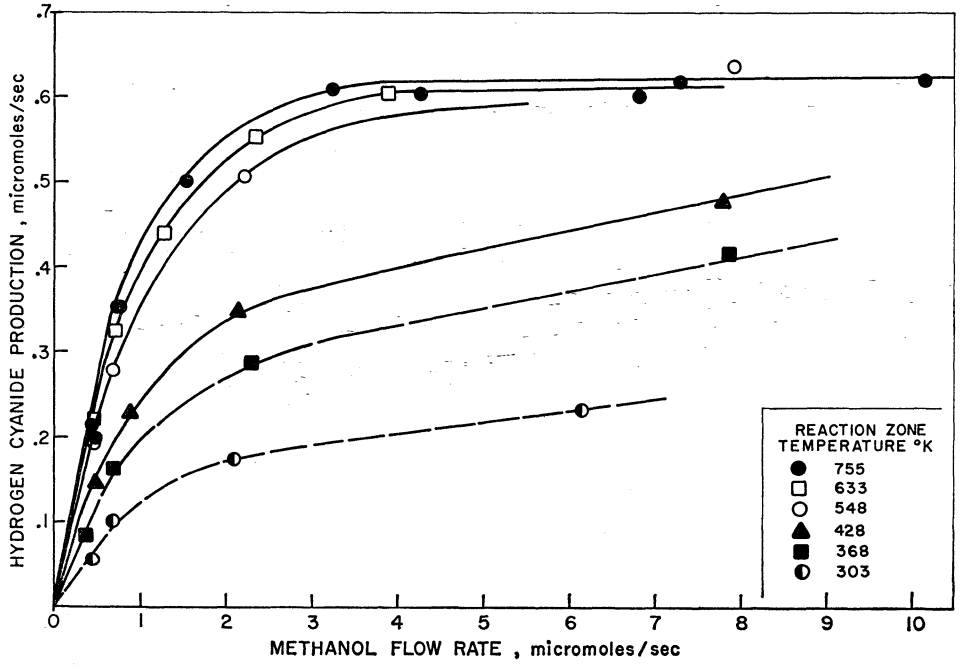

FIG. 1. Hydrogen cyanide production as a function of methanol flow rate at different temperatures in the reaction of atomic nitrogen with methanol.

It is reasonable to assume that the initial attack of the nitrogen atom on the methanol molecule is the rate-determining step of the overall reaction. If it is further assumed that pressure gradients in the reaction vessel are small and that changes in the total gas flow rate due to reaction may be neglected, second-order rate constants may be calculated from the rate of formation of hydrogen cyanide for streamline and turbulent flow (9).

Can. J. Chem. Downloaded from www.nrcresearchpress.com by 210.87.254.6 on 09/05/12
For personal use only.

$$\text{Streamline flow: } k_1 = \frac{(b+c)^2R^2T^2}{(a-b)VP^2}\ln\frac{b(a-x)}{a(b-x)} \quad [1]$$

$$\text{Turbulent flow: } k_2 = \frac{x(b+c)^2R^2T^2}{(a-x)(b-x)VP^2}, \quad [2]$$

where a, b, x = flow rates of atomic nitrogen, methanol, and hydrogen cyanide respectively, moles/sec;
c = total nitrogen flow rate (molecular and atomic), moles/sec;
V = volume of reaction zone, liters;
P = pressure in reaction tube, atm.

The initial slopes of the hydrogen cyanide curves, Fig. 1, are an approximate measure of the overall reaction rates. Values of k_1 and k_2 calculated from equations [1] and [2] are shown in Table I.

TABLE I

Calculation of second-order rate constants for the reaction of methanol with atomic nitrogen (pressure 1.06×10^{-3} atm)

Methanol flow rate, μmoles/sec	Hydrogen cyanide production, μmoles/sec	k_1, liters/mole-sec $\times10^7$	k_2, liters/mole-sec $\times10^7$
	Reaction zone temperature 755° K		
0.423	0.216	23.3	35.4
0.490	0.197	17.3	23.9
0.738	0.352	23.4	36.7
0.812	0.350	22.5	30.9
	Reaction zone temperature 633° K		
0.460	0.440	11.0	16.5
0.709	0.220	15.2	23.0
1.300	0.324	15.3	23.2
	Reaction zone temperature 548° K		
0.458	0.191	9.35	13.2
0.688	0.279	9.56	13.7
	Reaction zone temperature 428° K		
0.471	0.147	3.88	4.85
0.870	0.227	3.28	4.22
	Reaction zone temperature 368° K		
0.372	0.085	1.83	2.27
0.690	0.162	2.04	2.62
	Reaction zone temperature 303° K		
0.444	0.056	0.59	0.74
0.671	0.120	0.84	0.97

According to the collision theory (10)

$$k = PZ\exp(-E/RT). \quad [3]$$

P is the steric factor and Z is the collision number, which is equal to

$$10^{-3}\sigma_{AB}^2N[8\pi RT(M_A+M_B)/M_AM_B]^{\frac{1}{2}}, \quad [4]$$

where $R = 8.3144\times10^7$ ergs/deg-mole;
M_A, M_B = molecular weights of methanol and atomic nitrogen respectively.

Can. J. Chem. Downloaded from www.nrcresearchpress.com by 210.87.254.6 on 09/05/12
For personal use only.

The mean collision diameter, σ_{AB}, was calculated using values of 2.85 and 2.98 Å (11) for the collision diameters of methanol and atomic nitrogen respectively. Equation [3] can be written in terms of its temperature-independent part Z' and $T^{\frac{1}{2}}$, so that,

$$k = PZ'T^{\frac{1}{2}} \exp(-E/RT). \qquad [5]$$

According to equations [3] and [5] the energy of activation can be calculated from the slope of a plot of log k against $1/T$ and log $(k/T^{\frac{1}{2}})$ against $1/T$ respectively.

The calculated values and corresponding Arrhenius plots are shown in Tables II and III and Fig. 2.

TABLE II

Average values from the data in Table I

Temp., °K	$\frac{10^3}{T_{°K}}$	k_1 average, liters/mole-sec	k_2 average, liters/mole-sec	log k_1	log k_2	log $(k_1/T^{\frac{1}{2}})$	log $(k_2/T^{\frac{1}{2}})$
303	3.30	7.15×10^6	8.50×10^6	6.854	6.929	5.614	5.688
368	2.72	1.93×10^7	2.45×10^7	7.286	7.389	6.002	6.106
428	2.34	3.58×10^7	4.53×10^7	7.554	7.656	6.238	6.339
548	1.83	9.46×10^7	1.34×10^8	7.975	8.127	6.607	6.758
633	1.58	1.38×10^8	2.09×10^8	8.140	8.320	6.739	6.919
755	1.33	2.16×10^8	3.17×10^8	8.335	8.501	6.895	7.061

TABLE III

Kinetic constants for the reaction of atomic nitrogen with methanol

Flow condition assumed	Temp., °K	A	Z	P	E, kcal/mole
		By equation $k = PZ \exp(-E/RT)$			
Streamline	500	3.4×10^8	1.68×10^{11}	2.0×10^{-3}	3.4
Turbulent	500	6.2×10^8		3.7×10^{-3}	3.7
		By equation $k = PZ'T^{\frac{1}{2}} \exp(-E/RT)$			
Streamline	500	9.8×10^{6}*	7.53×10^9†	1.3×10^{-3}	3.0
Turbulent	500	15.8×10^{6}*		2.1×10^{-3}	3.2

*Value for A'.
†Value for Z'.

DISCUSSION

Whereas the identity of the two major chemically reactive species in active nitrogen, i.e. atoms in the ^4S and molecules in the $A^3\Sigma_u^+$ state, has been firmly established, their relative concentration and its variation with experimental conditions is still under investigation (5–7). The nitric oxide "titration" in conjunction with the determination of the extent of hydrogen cyanide production from ethylene provides a measure of the concentrations of these two species. The experimental conditions adopted in this study—particularly the considerable decay time from the discharge tube to the methanol inlet—ensured the almost exclusive presence of nitrogen atoms in the active nitrogen stream. The N atom concentration was measured from the reaction with ethylene at 385° C.

The reaction of nitrogen atoms with methanol may be represented by the following mechanism:

$$CH_3OH + N \rightarrow [NCH_3OH] \rightarrow NCH_3 + OH. \qquad [6]$$

Can. J. Chem. Downloaded from www.nrcresearchpress.com by 210.87.254.6 on 09/05/12
For personal use only.

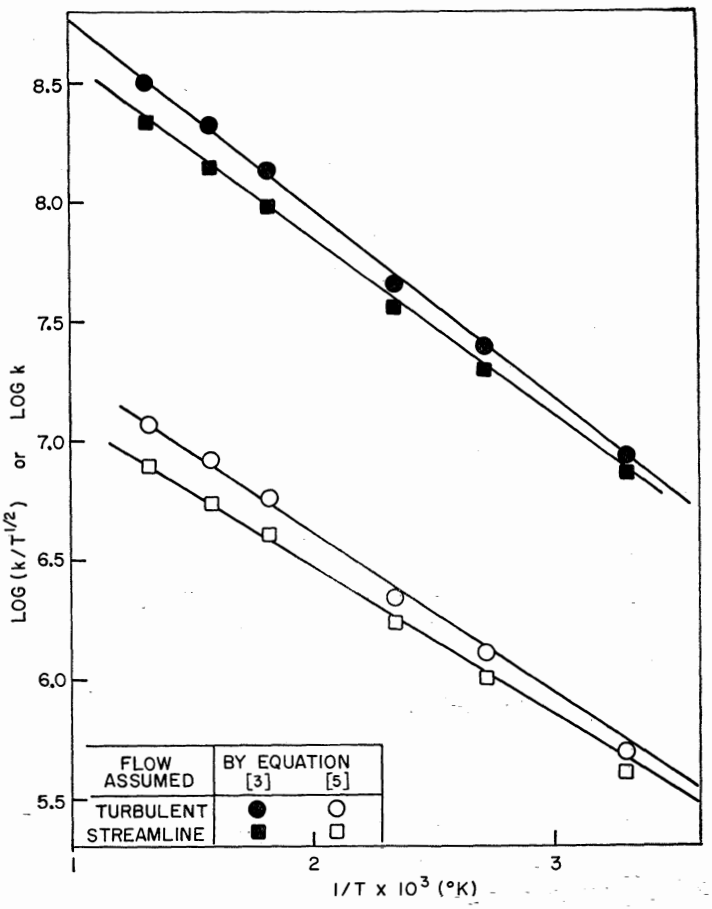

FIG. 2. Arrhenius plot of log k vs. $1/T$ and log $(k/T^{\frac{1}{2}})$ vs. $1/T$ for the reaction of atomic nitrogen with methanol.

The two fragments react further to produce hydrogen cyanide and water, which were the only two condensable products found in appreciable quantities:

$$NCH_3 \rightarrow HCN + 2H \quad [7]$$

or

$$NCH_3 \rightarrow HCN + H_2 \quad [8]$$

and

$$OH + H \rightarrow H_2O \quad [9]$$

$$OH + H_2 \rightarrow H_2O + H. \quad [10]$$

Reaction [8] is much more favorable energetically than reaction [7]; however, the latter may conserve spin while the former does not. Spin considerations are important as well as the energy relations. Reaction [9] probably requires a third body, and water production from equation [10] probably depends on prior recombination of hydrogen atoms.

Small amounts of methane and carbon monoxide were found among the products besides the three main ones, i.e. hydrogen cyanide, water, and hydrogen. In addition, a slight excess of water over hydrogen cyanide was consistently produced. Both these observations can best be explained by the direct attack on methanol by hydrogen atoms.

Can. J. Chem. Downloaded from www.nrcresearchpress.com by 210.87.254.6 on 09/05/12
For personal use only.

Indeed, Geib (12) investigated the reaction of hydrogen atoms with methanol by the discharge tube method and reported water, carbon monoxide, and methane as the main products. The small yield of CH_4 and CO can be attributed to the relatively small concentration of hydrogen atoms, which are produced according to equation [7]. Loss of hydrogen atoms results also from: (*a*) recombination of hydrogen atoms by three-body collisions with methanol molecules (13) and with nitrogen (14):

$$H + H + N_2 \rightarrow H_2 + N_2; \qquad [11]$$

(*b*) consumption of hydrogen atoms by other concomitant reactions, for instance reaction [9]. No significant amount of oxygen was found among the products, which is in accordance with the observations of Oldenberg and Rieke (15) that hydroxyl radicals react more readily with hydrogen than with themselves. Similarly, Rodebush *et al.* (16) indicated that the reaction

$$OH + OH \rightarrow H_2O + O \qquad [12]$$

does not occur.

It is noteworthy that no detectable quantities of ammonia or hydrazine were formed. Of the electronegative atomic reactants that have been studied, nitrogen atom appears to be the only one for which the direct attack is favored over hydrogen abstraction (17).

The products of the reaction of active nitrogen with methanol do not react further with the former to any significant extent. It has been established that simple hydrides, H_2, CH_4 (18), NH_3 (19) are relatively inert to atomic nitrogen; therefore, it would not be an unreasonable assumption to extend these observations to the reaction of the water molecules with active nitrogen.

The maximum yield of hydrogen cyanide (ca. 0.63 μmole/sec) does not correspond to the maximum nitrogen atom concentration indicated from the ethylene reaction (ca. 1.55 μmoles/sec). It would seem, therefore, that the consumption of nitrogen atoms does not proceed exclusively according to equation [6]. Reactions leading to nitrogen atom "wastage" must also be considered. The simplest explanation for the consumption of more than half the atomic nitrogen with no product formation in the presence of methyl alcohol is the reaction

$$N + N + CH_3OH \rightarrow N_2 + CH_3OH, \qquad [13]$$

where the alcohol is an efficient third body. According to Geib (12) there is evidence of catalytic recombination of hydrogen atoms in the presence of methyl alcohol. Alternatively the "wastage" could result from intermediate formation of NO or NOH. On the basis of the available data it is rather difficult to decide which approach to a mechanism of nitrogen atom wastage would be the best. It is hoped that pertinent information from the reactions of active nitrogen with other simple alcohols will elucidate this interesting phenomenon.

CONCLUSION

On the basis of the available evidence the mechanism of the reaction of active nitrogen with methanol appears to consists of an initial formation of a collision complex, $[NCH_3OH]$, which breaks down to two fragments, NCH_3 and OH, according to reaction [6]. These two fragments produce directly by reactions [7], [8] and [9], [10] the only two condensable products present in appreciable amounts, i.e. hydrogen cyanide and water, in a 1:1 ratio. Concomitant attack of the methanol molecule by hydrogen atoms is responsible for the production of small amounts of carbon monoxide, methane, and additional water.

Can. J. Chem. Downloaded from www.nrcresearchpress.com by 210.87.254.6 on 09/05/12
For personal use only.

ACKNOWLEDGMENTS

Acknowledgments are gratefully made to Drs. C. A. Winkler and A. N. Wright for valuable discussions. The authors are also indebted to Dr. A. G. Harrison for mass spectrometric analyses. Thanks are due to U. DeBoni for assistance in the experimental work.

REFERENCES

1. J. A. RATCLIFFE. Physics of the upper atmosphere. Academic Press, Inc., New York. 1960.
2. R. H. C. VERSCHINGEL. Ph.D. Thesis, McGill University, Montreal, Que. 1955.
3. P. M. ARONOVICH and B. M. MIKHAILOV. Bull. Acad. Sci. USSR, Div. Chem. Sci. 541 (1956).
4. J. L. WEININGER. J. Am. Chem. Soc. **83,** 3388 (1961).
5. K. D. BAYES. Can. J. Chem. **39,** 1074 (1961).
6. H. B. DUNFORD. 141st Annual American Chemical Society Meeting, Washington, D.C. March 21–24, 1962.
7. A. N. WRIGHT, R. L. NELSON, and C. A. WINKLER. Can. J. Chem. **40,** 1082 (1962).
8. P. A. GARTAGANIS, and C. A. WINKLER. Can. J. Chem. **34,** 1457 (1956).
9. R. A. BACK. Ph.D. Thesis, McGill University, Montreal, Que. 1953.
10. K. J. LAIDLER. Chemical kinetics. McGraw-Hill Inc., New York. 1950.
11. G. J. VERBEKE, and C. A. WINKLER. J. Phys. Chem. **64,** 319 (1960).
12. K. H. GEIB. Ergeb. Exakt. Naturw. **15,** 44 (1936).
13. E. W. R. STEACIE. Atomic and free radical reactions. Reinhold, New York. 1954.
14. H. GESSER, C. LUNER, and C. A. WINKLER. Can. J. Chem. **31,** 346 (1953).
15. O. OLDENBERG and F. F. RIEKE. J. Phys. Chem. **7,** 435 (1939).
16. W. H. RODEBUSH, C. W. J. WENDE, and R. W. CAMPBELL. J. Am. Chem. Soc. **59,** 1924 (1937).
17. H. G. V. EVANS, G. R. FREEMAN, and C. A. WINKLER. Can. J. Chem. **34,** 1271 (1956).
18. H. BLADES and C. A. WINKLER. Can. J. Chem. **29,** 1022 (1951).
19. G. R. FREEMAN and C. A. WINKLER. J. Phys. Chem. **59,** 371 (1955).

Can. J. Chem. Downloaded from www.nrcresearchpress.com by 210.87.254.6 on 09/05/12
For personal use only.

THE RADIOLYSIS OF HCl–HBr MIXTURES

R. C. Rumfeldt and D. A. Armstrong
Department of Chemistry, University of Alberta, Calgary, Alberta
Received August 7, 1962

ABSTRACT

Bromine was the only halogen formed in irradiated mixtures of HCl and HBr. A study of its effect on the hydrogen yield from HCl showed that it reacted with the first hydrogen-forming species (or its precursor), and indicated the same yield for this species as did the earlier experiments with chlorine. The results were consistent with thermal hydrogen atoms, formed in the reaction

$$e + H—Cl \cdots H—Cl \rightarrow H + Cl—H \cdots Cl^-,$$

as the first hydrogen-forming species, and hot hydrogen atoms, resulting from the dissociation of excited HCl molecules, as the second species.

The hydrogen yield from liquid HBr at −79° C was a factor of two larger than that from liquid HCl at the same temperature, and in mixtures of the two the hydrogen yield increased gradually from a value characteristic of pure HCl ($G_{H_2} = 6.5$) to one characteristic of pure HBr ($G_{H_2} = 12.4$). The smaller yield from HCl cannot be explained by radical combinations:

$$H + Cl + M \rightarrow HCl + M$$

$$H + H + M \rightarrow H_2 + M$$

in the radiation tracks and must be attributed either to differences in the ion-combination reactions in the two liquids or to a genuinely greater yield of ions and/or dissociative excited molecules in HBr. The hydrogen yield from solid HBr at −196° C was $G_{H_2} = 10.5$.

INTRODUCTION

A recent publication (1) from this laboratory described a study of the radiolysis of liquid and solid hydrogen chloride. This paper reports the results of a similar study of the radiolysis of hydrogen bromide, and also presents further evidence for the existence of two hydrogen-forming species in irradiated hydrogen chloride. Because the decomposition yield of hydrogen bromide was found to be twice that of hydrogen chloride, hydrogen and halogen yields in mixtures of the two were also studied in the hope that a reason for the difference in radiation sensitivity of the two compounds would become apparent.

EXPERIMENTAL

Materials

Hydrogen chloride and hydrogen bromide were obtained from the Matheson Co. and purified by the preirradiation procedure already described. Reagent grade bromine was thoroughly dried by treatment with $CaCl_2$ and subjected to several bulb-to-bulb distillations. It was stored over P_2O_5 at −80° C.

Apparatus

The apparatus and technique used for the preparation of samples and measurement of hydrogen yields were essentially as previously described. In this study a spectroscopic technique was also employed to observe the halogen production in the irradiated mixtures. Optical cells, which were shielded from the direct Co^{60} beam during irradiations, were attached to the pyrex irradiation cells. On completion of an irradiation the hydrogen halide – halogen solution was transferred to the optical cell, where its spectrum over the range 3000–5000 Å was taken with a Beckman D.U. spectrometer fitted with a cell compartment for use at −80° C. This consisted of an aluminum block machined to receive the optical cell and to permit passage of the light beam. The block was insulated with styrofoam on all sides and attached to two plates, which were bolted to the monochromator and photocell of the D.U. spectrometer. Quartz plates isolated the cell compartment from the D.U. spectrometer and it was purged by streams of dry nitrogen. The temperature of the compartment was maintained within a few degrees of −80° C by means of a liquid nitrogen cooling bath. Optical densities were measured relative to air as blank. The optical density of the cell over the wavelength range used with liquid HCl or HBr in it at −80° C was the same, within experimental error, as that

of the cell with water at room temperature. This is in accord with expectation, as HCl and HBr do not absorb appreciably above 2500 Å (2). For the pure hydrogen halides changes in optical density on irradiation may be associated with the halogen generated by the radiolysis.

Dosimetry

Dose rates were calculated in units of ev per gram per minute from measurements of ferrous–ferric conversion in the Fricke dosimetry solution. Corrections for differences in the number of electrons per gram in liquid HCl, liquid HBr, and the dosimetry solution were made on the basis of the Compton scattering process alone. The scattering cross sections per electron were assumed to be identical in all three liquids. In mixtures of HCl and HBr the total dose was taken as the sum of the individual doses calculated separately.

RESULTS

The hydrogen yields from pure liquid and solid HBr have been presented in Table I. Within experimental error they were independent of dose over the range used. Hydrogen

TABLE I

Hydrogen yields from γ-irradiated HBr–HCl mixtures

Composition, mole%		Molecules H_2/g HX $\times 10^{-17}$	Dose $\times 10^{-18}$, ev/g HX	Temp.,* °C	G_{H_2}
HCl	HBr				
0	100	0.785	0.639	−79	12.3
0	100	2.287	1.841	−79	12.4
0	100	4.986	4.057	−79	12.3
0	100	6.106	4.902	−79	12.4
0	100	7.096	5.729	−79	12.4
0	100	1.235	1.194	−196	10.4
0	100	1.867	1.777	−196	10.5
0	100	3.413	3.239	−196	10.5
97.4	2.6	0.753	1.050	−79	7.17
97.4	2.6	3.599	5.014	−79	7.18
95.0	5.0	2.136	2.898	−79	7.37
95.0	5.0	3.462	4.661	−79	7.43
92.4	7.6	3.137	3.965	−79	7.91
92.4	7.6	4.464	5.615	−79	7.95

*Experiments at −79° C refer to liquid samples; experiments at −196° C refer to solid samples.

yields from liquid mixtures of HCl and HBr have also been given in Table I and have been plotted in Fig. 1 as a function of the "electron fraction" of HBr. The effect of bromine on hydrogen yields from HCl is shown in Table II.

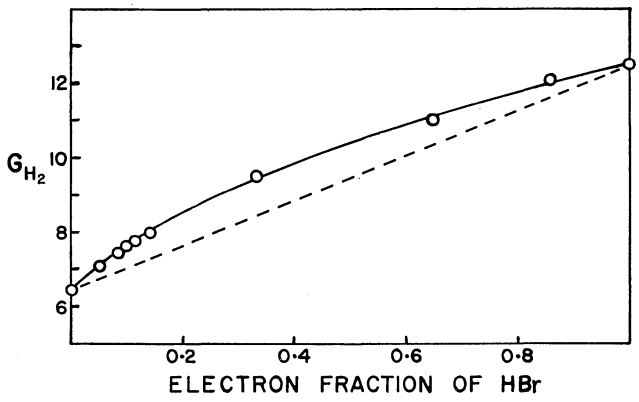

FIG. 1. Hydrogen yields from irradiated liquid mixtures of HCl and HBr at −79° C plotted as a function of the electron fraction of HBr.

TABLE II

Hydrogen yields from γ-irradiated solutions of Br_2 in HCl at $-79°$ C

$[Br_2]\times10^4$, mole/g	G_{H_2}	ΔG_{H_2}	$[Br_2]\times10^4$, mole/g	G_{H_2}	ΔG_{H_2}
0.00	6.53	0.00	0.620	4.72	1.81
0.118	5.67	0.86	0.635	4.75	1.78
0.167	5.50	1.03	1.143	4.56	1.97
0.246	5.15	1.38	2.056	4.14	2.39
0.345	5.03	1.50			

Measurement of the halogen yields by the spectroscopic technique described served as a check on the purity of the hydrogen halides. It was in fact the use of this technique which led to the development of the preirradiation procedure, and irradiated samples of either hydrogen halide exhibited absorption bands other than those of the corresponding halogen unless this procedure was employed. The absorption spectra of Br_2 and Cl_2 generated by irradiation in the liquid hydrogen halides (see Fig. 2) were very similar to their spectra

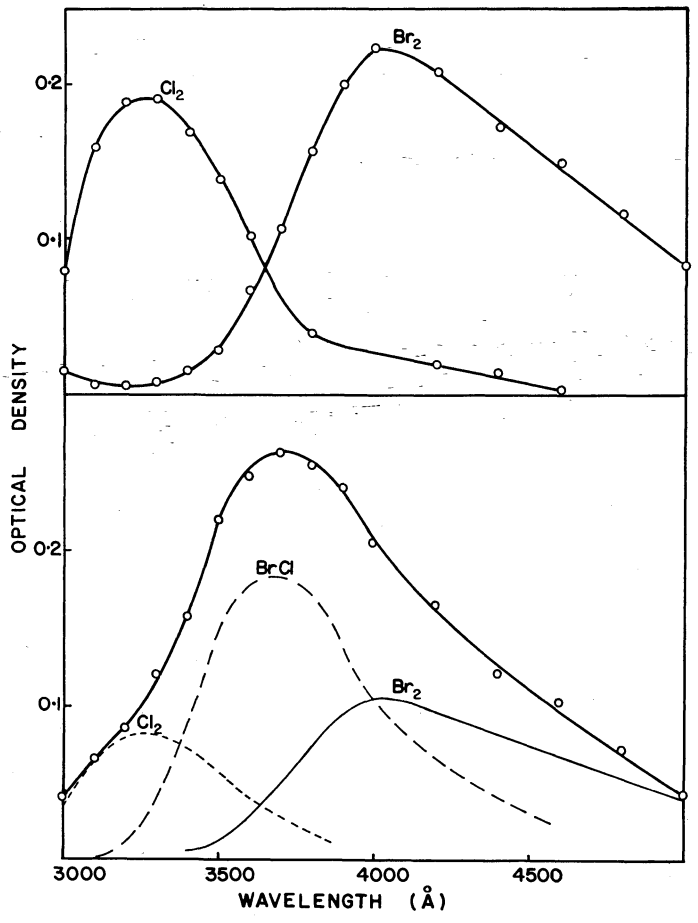

FIG. 2. Top: typical spectra of Cl_2 and Br_2 in the liquid hydrogen halides at $-79°$ C; bottom: spectrum of an irradiated 0.004 M solution of HBr in liquid HCl at $-79°$ C after complete oxidation of the HBr.

obtained under more normal conditions (3, 4). The optical densities at 3300 Å taken after successive irradiations of a sample of HCl, which had been purified by preirradiation, have been plotted as a function of dose in Fig. 3, line A. After this data had been obtained

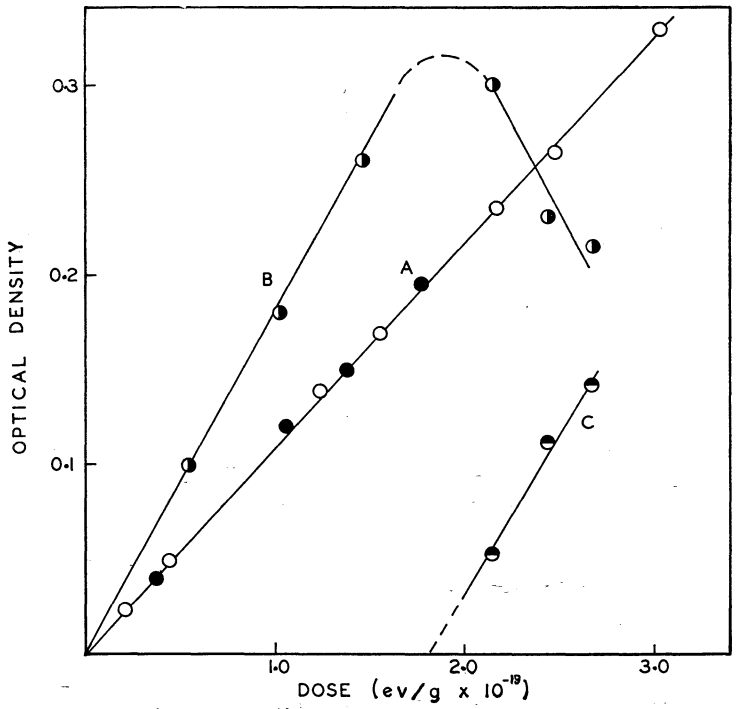

FIG. 3. Optical density – dose plots for irradiated HCl solutions. These plots illustrate: A: ● optical density at 3300 Å of Cl_2 produced in an irradiated sample of pure HCl, ○ same experiment repeated; B: ◑ optical density at 4000 Å of Br_2 produced in the irradiation of a 0.004 *M* solution of HBr in HCl; C: ◓ optical density at 3700 Å of BrCl produced in the irradiation of a 0.004 *M* solution of HBr in HCl.

the sample was distilled into the vacuum line, purified from chlorine, replaced in the irradiation cell, and then subjected to a second set of irradiations. After each of these the optical density at 3300 Å was again taken. The optical densities for both sets of irradiations have been included in Fig. 3, line A. Bromine yields from preirradiated HBr were similarly linear with dose. Extinction coefficients for solutions of the halogens in their respective hydrides were calculated from the slopes of the optical density – dose plots on the assumption that the hydrogen and halogen yields were identical. The values obtained at the absorption maxima (viz. ϵ_{Br_2} at 4000 Å = 198 in HBr; ϵ_{Cl_2} at 3300 Å = 88 in HCl) were slightly lower than those observed in carbon tetrachloride (viz. ϵ_{Br_2} at 4110 Å = 206; ϵ_{Cl_2} at 3300 Å = 97) (3, 4), but such a trend is in accordance with the behavior of these molecules in polar acidic solvents (4). From these figures and the observed linearity of the optical density – dose plots it may be concluded that the preirradiation procedure was effective in removing the impurities which interfered with halogen formation in the hydrogen halide samples not subjected to this procedure.

In mixtures of the hydrogen halides containing more than 1 mole% HBr bromine was the only halogen detected after irradiation. In dilute solutions of HBr in HCl, however, bromine was produced until all of the HBr had been oxidized, and then on further irradiation the absorption maximum of the solution began to shift toward shorter wavelengths,

indicating the formation of bromine monochloride and chlorine. The spectra of these solutions can be resolved as is the one in Fig. 2 (bottom). A plot of the contribution of bromine to the total optical density at 4000 Å of an irradiated 0.004 *M* HBr solution in HCl is shown in Fig. 3, curve B. The optical density rose until the HBr had been consumed, and thereafter decreased. Production of BrCl (see C in Fig. 3) commenced at the point where the bromine concentration passed through a maximum. From the spectrum taken after the final irradiation (see Fig. 2, bottom) it would appear that Cl_2, Br_2, and BrCl exist in equilibrium, as they do at room temperature. In support of this it was found that the value of the equilibrium constant for the reaction

$$Cl_2 + Br_2 \rightleftharpoons 2ClBr \qquad [1]$$

calculated from the present data agreed with the work of Buckles and Mills (4).

As nothing is known about the rates of the reactions which may occur between the halogens and HBr under these conditions, viz:

$$BrCl + HBr \rightarrow HCl + Br_2 \qquad [2]$$

$$Cl_2 + HBr \rightarrow HCl + BrCl, \qquad [3]$$

a solution of bromine monochloride (in equilibrium with smaller amounts of chlorine and bromine) in liquid HCl was prepared and frozen at liquid nitrogen temperature in an optical cell. A slight excess of HBr was then frozen on the surface of this. Spectroscopic examination carried out immediately after melting of this mixture showed that the bromine monochloride and chlorine oxidized the HBr to bromine, the above reactions being complete in a few minutes. Since these spontaneous reactions would have occurred prior to spectroscopic examination of the irradiated samples, the failure to observe Cl_2 and BrCl in the dilute solutions of HBr in HCl does not mean that all of the chlorine atoms escaped from the radiation tracks to undergo the reaction

$$Cl + HBr \rightarrow HCl + Br. \qquad [4]$$

There should in fact be a "molecular yield" of chlorine similar to the "molecular yield" of H_2O_2 observed in irradiated water.

DISCUSSION

The earlier paper from this laboratory showed that two hydrogen-forming species, which were scavenged with different efficiencies by chlorine, were present in irradiated HCl. The results with bromine confirm the presence of two species, and a plot of $1/\Delta G_{H_2}$ versus $1/[Br_2]$ has been presented in Fig. 4 in accordance with equation (i) of reference 1. The *G* value for the formation of the first hydrogen-forming species and the ratio of its rate constants for reaction with bromine and HCl as deduced from this plot have been presented in Table III together with the corresponding data obtained from the work

TABLE III

	Cl_2		Br_2	
	G	k_{HCl}/k_{Cl_2}	*G*	k_{HCl}/k_{Br_2}
First species	2.3	1.7×10^{-3}	2.4	7.9×10^{-4}
Second species	4.2	0.10	4.1	—

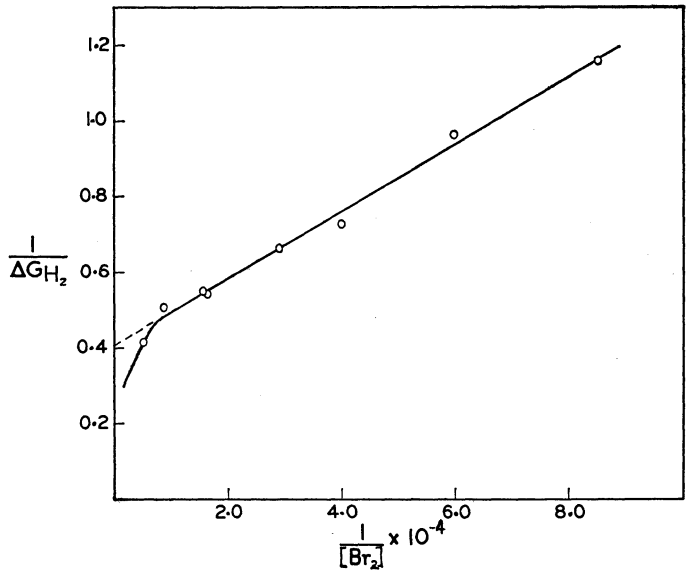

FIG. 4. The reciprocal of the reduction in the hydrogen yield ($1/\Delta G_{H_2}$) plotted against the reciprocal of the bromine concentration ($1/[Br_2]$) measured in moles/g.

with chlorine. Unfortunately the low solubility of bromine in liquid HCl at −80° C (approximately 3×10^{-4} mole/g) precluded experiments at higher concentrations, where the scavenging of the second species should have occurred. The ratio of its rate constants for reaction with bromine and HCl could not therefore be evaluated.

In view of the fact that added bromine reduced the hydrogen yields from HCl, one might suggest that its accumulation in the irradiated mixtures could have reduced the decomposition yield as the irradiations proceeded. However, since the concentration of bromine generated in the mixtures of HBr and HCl (and also in pure HBr) was always at least an order of magnitude less than the lowest concentration of bromine listed in Table II, and since HBr reacts more rapidly both with hydrogen atoms and electrons than does HCl (see below), it may be concluded that scavenging of the first hydrogen-forming species would have been unimportant at the doses used in the present work. The dose independence of the hydrogen yields in Table I leads to the same conclusion and we may assume that they are true initial yields. Similar considerations do not apply to an earlier study (5) of the radiolysis of liquid HBr, in which much larger doses were given and much lower yields obtained. In view of this and the more extensive study reported here, we feel that the present results are more trustworthy.

Although in the initial study it was not clear whether chlorine was scavenging electrons or hydrogen atoms, it seemed probable that the first (or more readily scavenged species) was the thermal hydrogen atom and the second species the "hot" hydrogen atom. Recent mass spectrometric investigations (6, 7) have shown that the energy thresholds of the electron capture reactions

$$e + Cl_2 \rightarrow Cl + Cl^- \quad [5]$$

$$e + HCl \rightarrow H + Cl^- \quad [6]$$

$$e + Br_2 \rightarrow Br + Br^- \quad [7]$$

are respectively 1.6_0, 0.6_5, and 0.0_0 ev. Since electrons are thermalized very rapidly in liquid media (8), reaction [5] could not have competed with reaction [6] unless chlorine molecules were present in such high concentrations (ca. 10 mole%) that a significant number of electrons would have collided with them prior to falling below the threshold energy. Identification of the first species as the thermal hydrogen atom is thus supported. Further, bromine, as well as reacting with these hydrogen atoms, would have been an efficient scavenger for electrons at or just above the thermal energy range, and at the concentrations used (0.1 to 1 mole%, see reference 9) reaction [7] should have competed with reactions [8*a*] and [8*b*]:

$$e + H_2Cl^+ \rightarrow H^* + HCl \qquad [8a]$$

$$e + H_2Cl^+ \rightarrow H_2 + Cl \qquad [8b]$$

for electrons which were not captured in reaction [6]. Thus the fact that it indicated the same yields of the two hydrogen-forming species as did chlorine is an indication that reactions [8*a*] and [8*b*] are not the major source of the second (or less readily scavenged) component of the hydrogen yield. In fact for reasons already stated (1) it is highly likely that the threshold energy for electron capture in liquid HCl is much lower than that in the gas phase, and that all electrons are captured* in a process which is best represented by the equation

$$e + H—Cl\cdots H—Cl \rightleftharpoons H + Cl—H\cdots Cl^-. \qquad [6a]$$

Highly energetic electrons undergoing this reaction could conceivably produce a number of hot hydrogen atoms. However, the rapid rate of energy loss for electrons and the fact that the capture process is restricted to a fairly narrow energy range (see ref. 7) would operate against this. Reaction [9]:

$$HCl \text{—}\!\!\sim\!\!\rightarrow HCl^* \rightarrow H^* + Cl, \qquad [9]$$

is therefore postulated as the major source of hot hydrogen atoms in this system.

Since the energy threshold for capture of electrons by HBr molecules is lower than that for HCl molecules (0.22 ev and 0.65 ev for HBr and HCl respectively (7)) and the capture cross section higher (10), we conclude, as did Eyring, Hirschfelder and Taylor (11), that the analogous reaction will also be the predominate fate of electrons in irradiated HBr. Because of hydrogen bonding effects, the liquid capture reaction should be written:

$$e + H—Br\cdots H—Br \rightarrow H + Br—H\cdots Br^-. \qquad [10]$$

Although positive fragment ions (Br^+ and Br^{++}) are more frequent in the mass spectrum of HBr than of HCl (12), they are not likely to be formed in great abundance in the liquid phase, where the excited molecule–ions from which they arise should be rapidly stabilized. The parent ions, HBr^+ and HCl^+, should therefore be the predominate ionic species resulting from ionization in both compounds:

$$HCl \text{—}\!\!\sim\!\!\rightarrow HCl^+ + e \qquad [11]$$

$$HBr \text{—}\!\!\sim\!\!\rightarrow HBr^+ + e. \qquad [12]$$

The analogous ion–molecule reactions:

$$HCl^+ + HCl \rightarrow H_2Cl^+ + Cl \qquad [13]$$

and

$$HBr^+ + HBr \rightarrow H_2Br^+ + Br \qquad [14]$$

*NOTE ADDED IN PROOF: *This argument has been substantiated by more recent experiments and for reasons which will be presented elsewhere we do not believe that an alternative non-dissociative electron capture by the halogen molecules to form the negative molecule–ions* Cl_2^- *and* Br_2^- *recently discussed in some detail by Person (J. Chem. Phys.* **38**, *109 (1963)) competes with reaction [6] in liquid* HCl.

occur with roughly equal rate constants (13), and in the liquid phase should be complete within about 10^{-13} seconds of formation of the parent ions. Because conventional electrochemical studies (14) have shown that pure liquid HCl undergoes autoprotolysis, it has been inferred (1) that neutralization of the H_2Cl^+ and Cl—H - - Cl^- ions formed in it by radiation will proceed via the reverse of the autoprotolysis reaction:

$$H_2Cl^+ + Cl—H - - Cl^- \rightleftharpoons 3HCl, \quad [15]$$

and that this will be a relatively slow process. Though the electrochemistry of HBr has not been studied as extensively, the similar dielectric constants (D.C. of HCl = 10; D.C. of HBr = 7 at −80° C (15)) and generally analogous electrochemical properties (16) of the two liquids suggest that the corresponding process:

$$H_2Br^+ + Br—H - - Br^- \rightleftharpoons 3HBr, \quad [16]$$

should occur in HBr. On this basis one hydrogen atom, resulting from the electron capture processes [6*a*] and [10], would be formed per ionization in both HCl and HBr, and the difference in hydrogen yield could not be attributed to differences in ionic reactions. However, the possibility of alternative neutralization reactions in HBr, such as reaction [17]:

$$H_2Br^+ + Br—H - - Br^- \rightarrow H + Br + 2HBr, \quad [17]$$

cannot be overlooked. Since this would produce a second hydrogen atom per ionization, we offer it as a possible explanation for the higher hydrogen yield from HBr.

The free-radical reactions which H and Br atoms are likely to undergo in irradiated HBr are analogous to those already discussed for the corresponding atoms in HCl. In both liquids hot atoms should react rapidly with hydrogen halide molecules. On the basis of existing kinetic knowledge from conventional gas phase studies the ratio of the rate constants for the thermal hydrogen atom reactions

$$H + HCl \rightarrow H_2 + Cl \quad [18]$$

$$H + HBr \rightarrow H_2 + Br \quad [19]$$

$$H + H + M \rightarrow H_2 + M \quad [20]$$

$$H + Cl + M \rightarrow HCl + M \quad [21]$$

$$H + Br + M \rightarrow HBr + M \quad [22]$$

at −80° C can be estimated to be about 10^{-4}: 10^{-1}: 1: 1: 1 respectively (17). Thus in pure HCl the probability of reactions [20] and [21] competing with reaction [18] would be somewhat greater than that of the corresponding competition in liquid HBr. However, since the *G* value for thermal hydrogen atoms determined from the chlorine experiments was only 2.4, it is very unlikely that more than half of this number undergo combination in the tracks. In fact, since they probably are produced in reaction [6*a*], they would be formed at some distance from the track centers and the possibility of reactions [20] and [21] occurring would be even less. Analogy with water, which should have a similar ion density and for which Dyne and Kennedy (18), Kupperman (19), and others have computed estimates of the track combination reactions at different scavenger concentrations, supports these conclusions. Furthermore a much steeper initial slope would have been observed at the lower HBr concentrations in Fig. 1 had reactions [20] and [21] been very important in pure HCl. Hydrogen atom combination in the HCl tracks could at the most, therefore, account for only one *G* unit of the rather large difference in the hydrogen yields from HCl and HBr. The only explanation for this difference, other than the one offered above, would be that the primary yield of ions and/or dissociating

excited molecules is much larger in HBr than in HCl. Since the ionization potentials of the two molecules are similar (I_{HCl} = 12.8 ev, I_{HBr} = 12.0$_4$ ev (20)) large differences in the ion yields are not to be expected, and it may well be that fast electron excitation produces a greater number of dissociative excited molecules in HBr than in HCl.

ACKNOWLEDGMENT

We wish to acknowledge the financial assistance of the National Research Council of Canada.

REFERENCES

1. D. A. Armstrong. Can. J. Chem. **40**, 1385 (1962).
2. J. Romand. Ann. Phys. **4** (12), 527 (1948).
3. A. I. Popov and J. J. Mannion. J. Am. Chem. Soc. **74**, 222 (1952).
4. R. E. Buckles and J. F. Mills. J. Am. Chem. Soc. **75**, 552 (1953).
5. S. C. Lind. Le Radium, **8**, 289 (1911).
6. D. C. Frost and C. A. McDowell. Can. J. Chem. **38**, 407 (1960).
7. D. C. Frost and C. A. McDowell. J. Chem. Phys. **29**, 503 (1958).
8. A. H. Samuel and J. L. Magee. J. Chem. Phys. **21**, 1080 (1952).
9. J. R. Nash and W. H. Hamill. J. Phys. Chem. **66**, 1097 (1962). L. J. Forrestal and W. H. Hamill. J. Am. Chem. Soc. **83**, 1535 (1961).
10. N. S. Buckelnikova. Soviet Phys.-Tech. Phys. **35**, 783 (1959).
11. H. Eyring, J. O. Hirschfelder, and H. S. Taylor. J. Chem. Phys. **4**, 570 (1936).
12. W. H. Johnston and J. R. Arnold. J. Chem. Phys. **21**, 1499 (1953).
13. D. O. Schissler and D. P. Stevenson. J. Chem. Phys. **24**, 926 (1956).
14. G. Glockner and R. E. Peck. J. Chem. Phys. **4**, 658 (1936). M. E. Peach and T. C. Waddington. J. Chem. Soc. 2329 (1960); 1238 (1961).
15. C. P. Smyth and C. S. Hitchcock. J. Am. Chem. Soc. **55**, 1830 (1933).
16. S. S. Danyluk and G. Janz. Chem. Rev. **62**, 209 (1960).
17. S. W. Benson. The Foundations of chemical kinetics. McGraw-Hill Book Co., Toronto. 1960.
18. P. J. Dyne and J. M. Kennedy. Can. J. Chem. **36**, 1518 (1958).
19. A. Kupperman. The chemical and biological action of radiations. Academic Press, London. 1961.
20. W. C. Price. Proc. Roy. Soc. London, Sect. A, **167**, 216 (1938).

Can. J. Chem. Downloaded from www.nrcresearchpress.com by 210.87.254.5 on 09/05/12
For personal use only.

THE STEREOCHEMISTRY OF MALEOPIMARIC ACID AND THE LONG RANGE SHIELDING EFFECT OF THE OLEFINIC BOND[1]

W. A. AYER AND C. E. MCDONALD
Department of Chemistry, University of Alberta, Edmonton, Alberta

AND

J. B. STOTHERS
Department of Chemistry, University of Western Ontario, London, Ontario

Received October 9, 1962

ABSTRACT

Nuclear magnetic resonance studies of methyl maleopimarate and closely related derivatives clearly establish the stereochemistry of methyl maleopimarate and, consequently, levopimaric acid. An extension of this study to other related compounds, 22 in all, provides evidence, on the basis of an intercomparison of the chemical shifts for the angular methyl protons, to support the original suggestion by Jackman (Applications of NMR in organic chemistry. Pergamon, New York. 1959. Chap. 7) that the long range shielding effect of the olefinic linkage is analogous to that of the carbonyl double bond. Coupling constants and chemical shifts for some of the protons of the bicyclo[2.2.2]octene system present in these compounds are also discussed.

INTRODUCTION

Levopimaric acid (I) reacts quantitatively with maleic anhydride in benzene at room temperature (1) to yield an adduct, maleopimaric acid, which has recently been assigned the stereochemistry shown in II (R = H) (2). This assignment was based mainly on

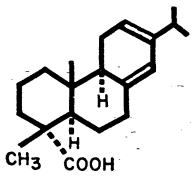

I

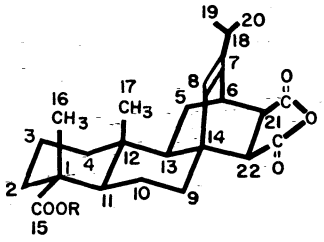

II

studies of molecular models coupled with the observation that a single isomer is formed in the reaction (2). At that time the configuration at C-13 in levopimaric acid had not been definitely established and, in fact, Klyne (3), using the method of molecular rotation differences, had assigned the β-configuration. Recent chemical (4) and rotatory dispersion (5) evidence has supported the α-orientation at C-13. We wish to report some proton magnetic resonance studies on methyl maleopimarate (II, R = CH_3) and related compounds which confirm structure II, and hence the α-orientation at C-13 in levopimaric acid. We have examined the N.M.R. spectra of a series of 22 compounds derived from II, and an intercomparison of *all* of these data leads to the conclusion that these compounds have the α-orientation at C-13. The compounds examined, prepared in connection with

[1]*This paper represents Part III in the series Nuclear Magnetic Resonance Studies from one of our laboratories (J. B. S.).*

another investigation, are of three types: A (II–XIII, XXI, and XXII), those with an endocyclic double bond at the 7,8-position; B (XIV–XVI), those with an exocyclic

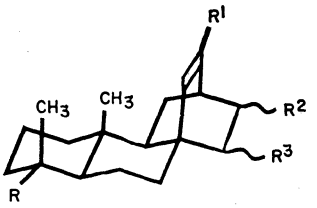

A

III R = $COOCH_3$; R^1 = $CH(CH_3)_2$; $R^2 = R^3$ = endo - $COOCH_3$

IV R = $COOCH_3$; R^1 = $CH(CH_3)_2$; R^2 = exo - $COOCH_3$; R^3 = endo - $COOCH_3$

V R = CH_2OH; R^1 = $CH(CH_3)_2$; R^2, R^3 = endo - anhydride

VI R = CH_2OH; R^1 = $CH(CH_3)_2$; $R^2 = R^3$ = endo - $COOCH_3$

VII R = CH_2OH; R^1 = $CH(CH_3)_2$; R^2 = exo - $COOCH_3$; R^3 = endo - $COOCH_3$

VIII R = CH_3; R^1 = $CH(CH_3)_2$; R^2, R^3 = endo - anhydride

IX R = CH_3; R^1 = $CH(CH_3)_2$; $R^2 = R^3$ = endo - $COOCH_3$

X R = $COOCH_3$; R^1 = $CH(CH_3)_2$; $R^2 = R^3$ = H

XI R = $COOCH_3$; R^1 = $COCH_3$; $R^2 = R^3$ = endo - $COOCH_3$

XII R = $COOCH_3$; R^1 = $COCH_3$; R^2 = exo - $COOCH_3$; R^3 = endo - $COOCH_3$

XIII R = CH_3; R^1 = $COCH_3$; $R^2 = R^3$ = endo - $COOCH_3$

XXII R = $OCOCH_3$; R^1 = $CH(CH_3)_2$; R^2, R^3 = endo - anhydride

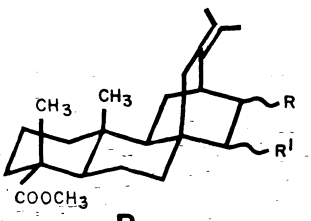

B

XIV R = exo - $COOCH_3$; R^1 = endo - $COOCH_3$

XV R = endo - $COOCH_3$; R^1 = -CO-O-(C_8)

XVI R = exo - $COOCH_3$; R^1 = -CO-O-(C_8)

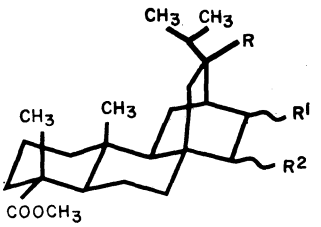

C

XVII R, R^1 = (C_7)-O-CO-(C_{21}); R^2 = endo - $COOCH_3$

XVIII R, R^1 = (C_7)-O-CO-(C_{21}); R^2 = endo - COOH

XIX R = OH; R^1 = exo - $COOCH_3$; R^2 = endo - $COOCH_3$

XX R = -O-(C_{18}); R^1 = endo - $COOCH_3$; R^2 = -CO-O-(C_8)

Can. J. Chem. Downloaded from www.nrcresearchpress.com by 210.87.254.5 on 09/05/12
For personal use only.

double bond at the 7,18-position; and C (XVII–XX), those with no carbon–carbon double bond. These results provide evidence that an olefinic linkage exhibits a long range shielding effect similar to that of the carbonyl grouping (6, 7), and therefore, tends to shield nuclei above or below the plane of the trigonal carbons and to deshield nuclei in or close to this plane. This interpretation of the long range effect of the olefinic group was suggested some time ago (8), but little evidence bearing on this point was available. More recently an alternative model which predicts that the region of maximum shielding will be on the transverse axis *in the plane* of the double bond has also been discussed (9). The conclusion that the former model is the more appropriate for the interpretation of the long range effect of the double bond (i.e. that it is analogous to that of the carbonyl group) has been reached by other workers from studies of other cyclic systems (10, 11) since this study was initiated.

EXPERIMENTAL

N.M.R. Spectra

All spectra were determined at 60 Mc/s using either a Varian DP-60 or an A-60 spectrometer. With the former instrument, the peak positions were measured by the usual audio side-band method. The chemical shift data are given in p.p.m. relative to an internal tetramethylsilane (TMS) signal, and the precision is estimated to be within ±0.01 p.p.m. for the chemical shifts and ±0.2 c/s for the coupling constants. For most cases, the solute concentrations were approximately 10% (w/v) in either carbon tetrachloride or deuterochloroform. To check for differences between these two solvents, 10 of the examples were examined in both.

Materials[2]

Methyl maleopimarate (II, R = CH_3) was prepared by esterification of commercial (Distillation Products Industries) maleopimaric acid. The triester III was prepared as previously described (12) or more conveniently by treatment of a methanolic solution of maleopimaric acid with ethereal diazomethane. Compound IV was obtained by refluxing maleopimaric acid with methanolic potassium hydroxide followed by esterification (CH_2N_2) of the tricarboxylic acid thus obtained, or by the addition of fumaric acid to abietic acid (13) followed by esterification. The assignment of the C-21 exo, C-22 endo configuration rests mainly on the observation that the oxidation of the C-15 monoester corresponding to IV (prepared by the addition of fumaric acid to methyl abietate) with lead tetracetate in pyridine yields the γ-lactone XVI. A second product of this oxidation was the $\Delta^{21,22}$ compound corresponding to X, which on hydrogenation over platinum yielded X. The alcohol V was prepared by sodium borohydride reduction of the acid chloride of maleopimaric acid. Dissolution of V in methanolic diazomethane yielded the diester VI. Reduction of the C-15 monoester corresponding to IV with lithium–ammonia–alcohol followed by esterification gave the diester VII, which was also obtained by equilibration (methanolic KOH) of VI. The ketone XI was prepared by ozonolysis of III as previously described (14). Treatment of XI with methanolic KOH followed by esterification of the resulting acid gave XII. The anhydride VIII was prepared by addition of maleic anhydride to abieta-7,14(9)-diene. Methanolic diazomethane transformed VIII to IX and ozonolysis of IX gave the ketone XIII.

The lactone XVII was prepared by the method of Brus and co-workers (15). The acid XVIII was prepared by partial saponification of XVII, and the hydroxy compound XIX was obtained by treatment of XVII with hot 1 *N* sodium hydroxide for 96 hours followed by esterification. The tricarboxylic acid corresponding to XIX failed to lactonize or readily form an anhydride. Dehydration of XIX with phosphorus oxychloride – pyridine yielded the isopropylidine compound XIV, contaminated with a small amount (less than 10% by N.M.R. analysis) of the endo isomer IV. Compound XV was obtained by alkaline permanganate oxidation of maleopimaric acid (16). The structure of this oxidation product has recently been established independently by Zalkow, Ford, and Kutney (17). The oxide XX was prepared by ozonization of XV.

Compounds XXI and XXII resulted from the lead tetraacetate – pyridine oxidation of maleopimaric acid, followed by (in the case of XXI) methanolysis and esterification with diazomethane. The configuration at C-1 in XXII rests on the observation that the C-17 protons are not shifted relative to methyl maleopimarate (II, R = CH_3). If the acetoxyl group were β, a downfield shift of the C-17 protons would be expected (18).

The ketone XXIII was kindly provided by Professor L. H. Zalkow, Oklahoma State University.

[2]*Complete details of the preparation of all new compounds and of the structural assignments will be presented in a separate communication. All new compounds reported gave satisfactory analytical results.*

Can. J. Chem. Downloaded from www.nrcresearchpress.com by 210.87.254.5 on 09/05/12
For personal use only.

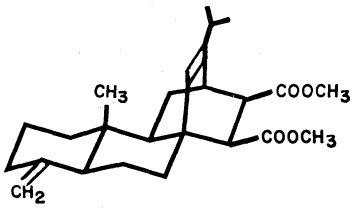

XXI

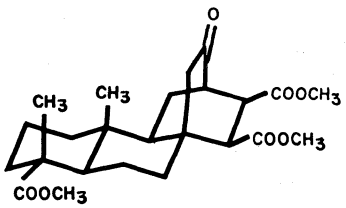

XXIII

RESULTS

In the N.M.R. spectra of this series of compounds, there are two principal types of information provided. First, there are the chemical shift data for the various kinds of methyl protons and these are collected in Table I. Secondly, in a number of cases a critical examination of the region from 110 to 200 c/s from TMS allows a determination of the chemical shifts and coupling constants for the protons at C-6, C-21, and C-22, and thus provides evidence for the relative configuration of substituents on C-21 and C-22. The data for these protons are given in Table II.

DISCUSSION

General Features

To illustrate the gross features of the N.M.R. spectra for the three basic formulations, A, B, and C, some typical curves are reproduced in Figs. 1(*a*) and (*b*), and 2(*a*) and (*b*). In these figures, two examples of type A (II, R = CH_3 and III), and one example of each of B (XIV) and C (XIX) are included, and the line positions are given in c/s from TMS. It can be seen that marked differences occur in the C-methyl region (<100 c/s) as the double bond is changed in position or is removed. The number of separately resolved peaks in the carbomethoxyl region (~220 c/s) appears to depend on the double bond position as well as on the relative configuration of these groups. A third general feature to be noted is the variation in the appearance of the spectral pattern in the region 100–200 c/s for these structural modifications.

Stereochemistry of Maleopimaric Acid, II

If one examines the spectrum of the parent compound, methyl maleopimarate (II, R = CH_3), Fig. 1(*a*), in more detail, a number of the signals can be assigned directly. The single olefinic proton must give rise to the slightly broadened peak at 332 c/s (5.53 δ), while the carbomethoxyl protons absorb as a singlet at 220 c/s (3.67 δ) and the C-methyl groups appear as four equally intense peaks near 36, 56, 63, and 70 c/s. The highest-field peak can be assigned to the angular methyl group, C-17, (0.59 δ), on the basis of a published survey of the N.M.R. spectra of some resin acids (19) and from the results discussed below. Since the separations between the three remaining signals are approximately equal and since one would expect the isopropyl methyl protons to appear as a doublet with a coupling constant of ca. 7 c/s (19), two assignments are possible. The C-16 protons absorb at either 56 or 70 c/s. The more reasonable choice is that the lower-field peak arises from these protons (1.16 δ). Thus, the C-19 and C-20 protons, which are equivalent, absorb at 1.00 δ with J = 6.9 c/s. Support for this assignment is provided by the spectrum of III, Fig. 1(*b*), in which the relative intensities of the C-methyl peaks clearly show the C-16 protons to be at 68.8 c/s (1.14 δ), overlapping one band of an isopropyl methyl doublet (the isopropyl methyls are clearly non-equivalent in this case). Again, the angular methyl protons appear at highest field, 0.62 δ.

Can. J. Chem. Downloaded from www.nrcresearchpress.com by 210.87.254.5 on 09/05/12
For personal use only.

Can. J. Chem. Downloaded from www.nrcresearchpress.com by 210.87.254.5 on 09/05/12
For personal use only.

TABLE I

Chemical shifts* of methyl protons

Type	Cpd.	Position of methyl protons					
A		C-16	C-17	R	R¹†	R², R³	
	II	1.16	0.59	3.67	1.00 [6.9]	—	—
	III	1.15 (1.10)	0.62 (0.60)	3.67 (3.63)	1.05, 1.09 [7.1] (1.03 ,1.07)	3.53 (3.47)	3.53 (3.47)
	IV	1.11	0.58	3.69	1.07 [6.0]	3.64	3.59
	V	0.76	0.61	—	1.01 [7.2]	—	—
	VI	0.76 (0.73)	0.65 (0.63)	—	1.06, 1.10 [6.8] (1.05, 108)	3.57 (3.48)	
	VII	0.75 (0.70)	0.61 (0.58)	—	1.09 [7.0] (1.08)	3.72 (3.67)	3.63 (3.56)
	VII*a*‡	0.81 (0.81)	0.61 (0.60)	—	1.08 [6.8] (1.08)	3.73 (3.66)	3.63 (3.57)
	VIII	0.82 (0.82)	0.58 (0.57)	0.91 (0.90)	1.01 [6.9] (1.01)	—	—
	IX	0.81 (0.80)	0.59 (0.59)	0.87 (0.87)	1.05, 1.09 [7.0] (1.03, 1.07)	3.53 (3.49)	3.53 (3.46)
	X	(1.10)	(0.58)	(3.63)	[7.0] (1.00)	—	—
	XI	1.14 (1.11)	0.51 (0.52)	3.66 (3.64)	2.36 (2.26)	3.49 (3.47)	3.55 (3.50)
	XII	1.14 (1.10)	0.48 (0.51)	3.69 (3.64)	2.33 (2.28)	3.60 (3.58)	3.73 (3.72)
	XIII	0.80 (0.80)	0.49 (0.50)	0.89 (0.89)	2.37 (2.26)	3.52 (3.48)	3.58 (3.52)
	XXII	1.41	0.57	1.97	0.98 [6.3]	—	—
	XXI	—	0.49	4.48 4.85 (=CH_2)	1.05, 1.09 [6.6]	3.55	3.55

B		C-16	C-17	C-15 (COOMe)	C-18, C-19 isopropylidene	R	R¹
	XIV	1.14 (1.10)	0.81 (0.80)	3.68 (3.65)	1.55 (1.55)	3.73 (3.60)	3.70 (3.60)
	XV	1.16	0.74	3.65	1.80	3.65	—
	XVI	1.16	0.70 (0.70)	3.67	1.79	3.76 (3.72)	—
	XXIII	1.14	0.84	3.66	—	3.60	3.62

C		C-16	C-17	C-15 (COOMe)	$(CH_3)_2$-C(18)	R¹	R²
	XVII	1.15	0.95	3.65	0.97 [6.5]	—	3.65
	XVIII	1.15	0.95	3.67	0.95, 1.06 [6.5]	—	—
	XIX	1.17	0.95	3.67	1.06	3.73	3.73
	XX	1.19	0.94	3.66	1.39, 1.43	3.66	—

*In p.p.m. from TMS; ca. 10% solution in $CDCl_3$, shifts in parentheses are for CCl_4 solution.
†Values in square brackets indicate coupling constant, CH_3—CH, in c/s.
‡Acetyl derivative of VII.

TABLE II

Chemical shifts* of methine protons
(ca. 10% solution in $CDCl_3$)

Cpd.	Substituent C-7	C-21	C-22	δ C_{21}-H A	δ C_{22}-H B	Rel. confign. of A, B	J_{AB}, c/s	J_{AX}, c/s	δ C_6-H
XI	$\Delta^{7(8)}$-7-Ac	COOMe	COOMe	3.05	2.88	Cis	11.1	1.7	3.5
XIII	$\Delta^{7(8)}$-7-Ac	COOMe	COOMe	3.05	2.83	Cis	11.0	1.7	3.6
XV	7-$(CH_3)_2C=$	$COOC_8$	COOMe	2.42	2.89	Cis	10.1	1	3.1
XX	7-$(Me)_2C$— O	$COOC_8$	COOMe	2.55	3.13	Cis	10.0	1	2.2
XII	$\Delta^{7(8)}$-7-Ac	COOMe	COOMe	2.5	3.0	Trans	6.0	3	3.6
XIX	7-*i*-Pr, 7-OH	COOMe	COOMe	3.3	2.9	Trans	4.0	4	2.4

*In p.p.m. from TMS.

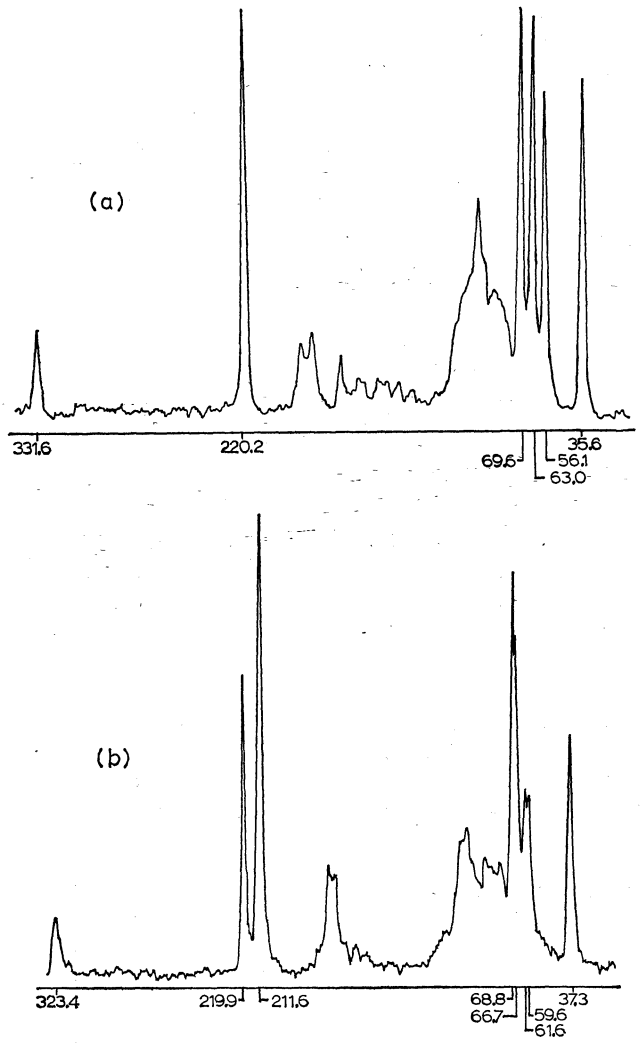

FIG. 1. Typical spectra (in $CDCl_3$) of compounds having the A type skeleton: (*a*) methyl maleopimarate, II, and (*b*) compound III. Line positions are indicated in c/s from TMS at 60 Mc/s.

Can. J. Chem. Downloaded from www.nrcresearchpress.com by 210.87.254.5 on 09/05/12
For personal use only.

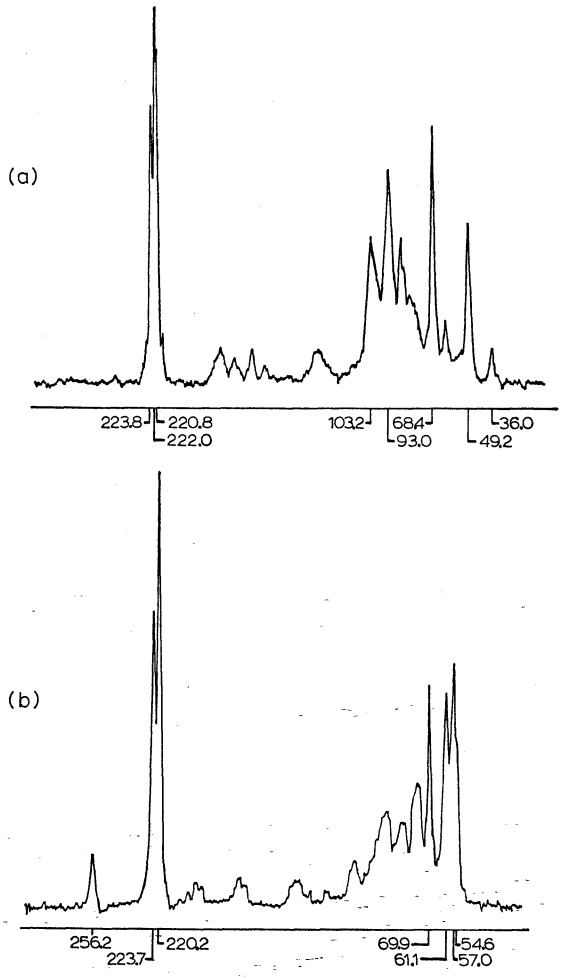

FIG. 2. Spectra at 60 Mc/s (in $CDCl_3$) of compounds (*a*) XIV and (*b*) XIX, having the B and C type skeletons, respectively. Line positions are given in c/s from TMS. (In (*a*), a small amount of IV is also present, as shown by the peak at 36 c/s.)

The virtually constant position of the angular methyl group at $0.60\pm0.03\ \delta$ for the closely related compounds II–X (see Table I) clearly indicates that the C-17 protons are strongly shielded by some similar means. Although four possible isomeric structures may be envisaged for the parent compound, maleopimaric acid, only two of these possibilities, II and its exo isomer, provide a common mechanism which could explain the similar shifts of the angular methyl protons for all the compounds II–X. It is apparent from the data in Table I that the carbonyl functions on C-21 and C-22 do not contribute to this shift, since not only is the shift independent of the change anhydride to diester but it is unchanged even when the carbonyl groups are replaced by hydrogen as in X. Proof that the C-15 substituent is without effect on the angular methyl shift is provided by the data for the same series, in which the C-15 grouping is changed from $—COOCH_3$ (II–IV, X) to $—CH_2OH$ (V–VII), to $—CH_3$ (VIII, IX), or to $—OCOCH_3$ (XXII). The only common feature potentially capable of producing the observed high-field shift is the C-7, C-8 double bond in compounds II–X and XXII. It follows, therefore, that this

Can. J. Chem. Downloaded from www.nrcresearchpress.com by 210.87.254.5 on 09/05/12
For personal use only.

bond must be responsible for the observed effect and, furthermore, it must be relatively close to C-17. These facts require the α-configuration at C-13 in maleopimaric acid and, since the reaction conditions for its formation (in benzene at room temperature (1)) would not be expected to epimerize levopimaric acid (I) at C-13, the recent assignment of the 13α-H configuration in I (4, 5) is confirmed.[3]

The remaining uncertainty concerns only the configuration of the anhydride group in II. This problem, however, has been answered by the observation (17, 20) that a number of lactones may be prepared from II, for example, XV, XVII, XVIII, and XX. The formation of these derivatives requires an interaction of the anhydride grouping and the double bond, and only in the endo isomer, II, are these groups suitable oriented. Further support for this assignment from the N.M.R. spectrum is presented in a later section of this paper. It should be noted that the stereochemistry as now established is exactly that which would be predicted on the basis of mechanistic arguments and molecular models.

Long Range Shielding Effect of the Olefinic Bond

A definitive, qualitative evaluation of the long range effect of a carbon–carbon double bond due to its diamagnetic anisotropy should be possible from the results of this study because of two important factors. (*a*) All of the methyl protons in the compounds of the entire series give rise to sharply defined signals which can be assigned unequivocally. (*b*) The orientation of each of these methyl groups relative to the double bond position can also be assigned, in the majority of the cases, with certainty. A critical examination of the trends exhibited by the chemical shifts of these protons in similar positions should, therefore, provide evidence as to the spatial characteristics of the shielding effect of the olefinic bond. To this end, the observed shifts for each of the various types of methyl groups are discussed in the following.

(a) C-17 Angular Methyl Protons

As already mentioned, the chemical shift of the angular methyl protons is found to be virtually independent of the functional groups on C-21 and C-22 and at C-15 as shown by the data for compounds II–X and XXII (Table I). A small increase in the shielding of ca. 0.1 p.p.m., however, is observed when the isopropyl grouping is replaced by a methyl ketone function (on C-7). The data for three examples, XI–XIII, are included in Table I. Again, no significant effect is noted for a change either at C-15 from —$COOCH_3$ to —CH_3 or for configurational differences of the carbomethoxyl groups on C-21 and C-22 (XV and XVI). The origin of this enhanced shielding in the methyl ketones, however, is obscure.

An examination of molecular models (Dreiding) indicates that the expected effect of the carbonyl group would tend to deshield the C-17 protons slightly, assuming either an S-cis or S-trans conformation for the α,β-unsaturated carbonyl system; but this effect should be small, since the average distance between these protons and the carbonyl bond is large (ca. 4 Å). The effect of the isopropyl grouping cannot be estimated reliably, since the long range shielding effects of carbon–carbon single bonds are not clearly established. Although some successful semiquantitative evaluations of the shielding effects of carbon–carbon single bonds have appeared using the point-dipole approximation (21, 22, 23, 24) in each case, rather limited systems were examined. A recent systematic

[3]*After the completion of this manuscript, a preliminary communication (W. L. Meyer and R. W. Hoffman. Tetrahedron Letters, No. 16, 691 (1962)) appeared in which conclusions similar to ours were reached, but on the basis of less extensive evidence.*

Can. J. Chem. Downloaded from www.nrcresearchpress.com by 210.87.254.5 on 09/05/12
For personal use only.

study of the shielding effects of the methyl group in an extensive series of closely related compounds, 36 methylated cyclohexanols, has shown the weakness of this approach for single bonds (25). At any rate, the present results indicate that the isopropyl group may be *deshielding* the angular methyl protons, since the angular methyl shift is up-field when the isopropyl group is replaced by an acetyl group which has a carbonyl bond at C-18. An additional complexity is that the effect of changing the polarization of the C-7, C-8 double bond cannot be predicted with any degree of certainty. The fact remains that the C-17 protons absorb at relatively high field in all compounds having the C-7, C-8 double bond as a common feature.

One other example, having the basic skeleton A, requires comment. Compound XXI differs from the others in that C-15 and C-16 are replaced by an exo methylene group. The N.M.R. spectrum of XXI clearly shows these protons at 4.48 and 4.85 δ as well as the C-8 proton at 5.46 δ. The positions of the carbomethoxyl and isopropyl methyl signals are virtually unchanged from those in III, as expected. The angular methyl peak, however, appears at 0.49 δ, showing an increased shielding of 0.13 p.p.m. relative to III. Part of this change, if not all, may be attributed to the loss of the C-16 methyl group, since it has been shown in the steroid series (26) that the C-19 protons are deshielded by 0.05–0.10 p.p.m. by a 6β-methyl, a 1,3-diaxial arrangement comparable to the C-16, C-17 positions in the present series. Since the observed shift is slightly larger, we have an indication that the exocyclic double bond at C-1 may exert a small shielding effect on the C-17 protons.

Turning now to the compounds having the B skeleton, with an exocyclic double bond at C-7, C-18 (XIV–XVI), it can be seen that the angular methyl group appears at lower field than in the A series, namely, 0.70–0.81 δ (Table I). The spectrum of a typical example, XIV, is shown in Fig. 2(*a*). It is reasonable to assume that the effect of the C-15 and C-21 carbomethoxyls and the C-16 methyl group is the same as above, II–IV and X–XII, and, hence, the downfield shift relative to these must be attributed to the change in position of the double bond to C-7, C-18. Apparently, an additional effect enters into two of these cases, XV and XVI, in which C-8 bears an oxygen of a lactonic link to C-22. It is not surprising that such an effect is observed since an oxygen atom will be closer to the C-17 protons than in any of the previous examples. A closely related compound, XXIII, shows the angular methyl group at 0.84 δ, in good agreement with the position of this peak for XIV. The key feature in each of these cases is the common location of a double bond at C-7, C-18, and it appears that the effect of the carbonyl bond in XXIII is qualitatively similar to that of the carbon–carbon double bond in XIV–XVI.

For the third group, the members of which have the basic skeleton C, with no double bond, XVII–XX, it can be seen from Table I that the angular methyl protons absorb at the lowest field of any so far discussed. The general appearance of the spectra of these compounds is illustrated in Fig. 2(*b*) (compound XIX). The virtually constant position of the C-17 signals at 0.95 ± 0.01 δ clearly shows that these compounds lack some shielding factor present in the others (i.e., the double bond). As before the shift of the angular methyl group is independent of the nature of the functional groups at C-21 and C-22. There is a possibility that an oxygen atom on C-7 or C-8 influences this shift in some manner, but all that can be concluded from the present results is that this effect is similar for both positions since each of the examples has this feature.

It can also be noted that the angular methyl protons for all examples absorb at a similar field (within 0.02 p.p.m.) in either solvent.

Can. J. Chem. Downloaded from www.nrcresearchpress.com by 210.87.254.5 on 09/05/12
For personal use only.

(b) C-16 Methyl Protons

The chemical shift of the C-16 protons throughout this series is found to depend only on the nature of the C-15 group. In those cases in which there is a carbomethoxyl group at C-15, the C-16 protons appear near 1.14 δ in chloroform and 1.10 δ in carbon tetrachloride solution. This small difference is probably due to an association of chloroform with the carbonyl group of the substituent. An indication that this is indeed the case is given by the fact that the shift of the C-16 protons is *not* solvent dependent when C-15 is a methyl (VIII, IX, and XIII) or a hydroxymethyl group (V–VII). In all cases the shifts are unexceptional.

As mentioned before, the relative configuration at C-1 in XXII was assigned from the N.M.R. spectrum, since the alternative configuration of the acetoxyl group would tend to deshield the angular methyl protons by ca. 0.1 p.p.m. and this is not observed.

(c) Carbomethoxyl Protons

The protons of the various carbomethoxyl groups present in this series of compounds give rise to signals in the range 3.52–3.76 δ, and an examination of these data reveals some consistent trends for the shifts of these groups in the different environments. From the positions of these protons in II, X, and XVIII, in which the assignment is straightforward, together with the previous observation that the C-16 protons are unaffected by structural changes at C-21 and C-22, it is possible to assign the appropriate peak for the C-15 carbomethoxyl groups in the rest of the series. The data in the last two columns of Table I indicate certain chemical shift changes with structure for these groups at C-21 and C-22. For compounds III, VI, IX, and XXI, having a C-7, C-8 double bond and the cis $COOCH_3$ groups in the endo configuration, the methoxyl protons are equivalent and appear at relatively high field, but when one $COOCH_3$ group is exo (IV and VII) these groups are non-equivalent and absorb at lower field. In XI and XIII, the two carbomethoxyl groups, although cis and endo, are no longer equivalent but these peaks are also at relatively high field. Furthermore, in a saturated example, XIX, the trans C-21 and C-22 carbomethoxyl protons are equivalent and appear at lower field than the examples above. One can conclude, therefore, that the protons of an endo carbomethoxyl group at C-21 and C-22 tend to absorb at slightly higher field than those of an exo carbomethoxyl because of the shielding effect of the endocyclic double bond.

(d) Other Methyl Groups

The chemical shifts of the other various types of methyl protons encountered in this series of compounds are listed in Table I. All of the data are unexceptional. A downfield shift of the methyl protons is observed in chloroform relative to carbon tetrachloride solution when a carbonyl grouping is adjacent. Presumably this is a result of an association of chloroform with the carbonyl grouping.

The Diamagnetic Anisotropy of the Carbon–Carbon Double Bond

On the basis of the chemical shift results for the methyl groups in these compounds, it is apparent that the olefinic bond exerts an appreciable effect on those protons which lie close to it (<3 Å). The effect is most striking for the angular methyl protons (on C-17) particularly in the A series with the C-7, C-8 double bond, and it is definitely a shielding contribution. A smaller shielding effect is observed for the angular methyl protons in those compounds having the exocyclic double bond (C-7, C-18, series B), and in fact, the shift of these protons in XXIII (7-keto) was found to be comparable. These observations clearly support the original suggestion by Jackman (8) that the anisotropy

Can. J. Chem. Downloaded from www.nrcresearchpress.com by 210.87.254.5 on 09/05/12
For personal use only.

of the carbon–carbon double bond is analogous to that of the carbonyl double bond. In terms of the McConnell point-dipole approximation (27) for the carbonyl group, the anisotropic effect can be considered to produce a 'shielding cone' whose axis is centered on the C=O bond (or, at the electrical center of gravity) and is orthogonal to the trigonal plane and whose apical angle is approximately 70°. The shielding effect at a given nucleus near the carbonyl bond depends on the distance, R, between that nucleus and the center of the bond and the angle, θ, described by R and the bond axis. This model predicts a maximum shielding for $\theta = 90°$ and a zero effect at $\theta = 54°44'$; while a minimum shielding (i.e., maximum deshielding) would be expected at $\theta = 0°$. Although this is an idealized model, the limitations of which have been discussed in detail (8), it is qualitatively valid and a number of examples of its use in stereochemical studies have appeared (8, 28, 29, 30). By analogy, therefore, protons lying above the trigonal plane of an olefinic bond will experience a shielding effect and those in this plane will be deshielded. Although the shielding is appreciable in the present system one would expect a still larger effect for a suitably located proton if that proton were fixed. Presumably, the shifts are reduced for the angular methyl protons as a result of free rotation of the methyl group.

On the basis of the point-dipole approximation (27), the contribution of the anisotropic double bond to the total shielding of a given proton, $\Delta\sigma$, may be related in terms of R and θ by the expression $\Delta\sigma = (1/R^3)(1 - 3\cos^2\theta)\Delta\chi$, where $\Delta\chi$ is the difference between the longitudinal and transverse magnetic susceptibilities which defines the diamagnetic anisotropy of a group of electrons. Although, in principle, three susceptibilities are required to express the anisotropy of the double bond, two will suffice if one is significantly larger than the others. From models with an assumed staggered conformation for the angular methyl group it is possible to evaluate the terms for R and θ in this expression for these protons in the A and B type skeletons and so calculate the ratio $\Delta\sigma_A/\Delta\sigma_B$ for the two structures. This calculation yields the value 2.9. An experimental determination of this ratio from the observed shifts for compounds IV, XIV, and XIX, using the expression $\Delta\sigma_A/\Delta\sigma_B = (\delta_{XIX}-\delta_{IV})/(\delta_{XIX}-\delta_{XIV})$, leads to the value 2.8, which is in good agreement with the theoretical, and thereby provides further support for our conclusion regarding the diamagnetic anisotropy of the double bond.

Stereochemistry at C-21 and C-22

In all of the spectra of these compounds, II–XXIII, patterns of varying complexity are observed in the region 130–200 c/s and while some of the spectra defy analysis in this region, others are much simpler and can be analyzed in detail. As an example of the latter, the 140–200 c/s region of the spectrum of XI is reproduced in Fig. 3(*a*). The integral curve showed that these peaks are due to two protons and the absorption pattern appears to be of the AB type, one half of which is further split by coupling with another nucleus with spacings of 11.0 and 1.7 c/s. In XI, only those protons at C-6, C-21, and C-22 would be expected to absorb in this region and the observed pattern eliminates the C-6 proton as a possibility. Since the integral curve clearly shows 10 protons in the carbomethoxyl region, the bridgehead proton probably absorbs near 210 c/s. The AB pattern, therefore, arises from the C-21 and C-22 hydrogens, with the former showing additional coupling with the bridgehead proton. Since Anet (31) has shown that 1,3-coupling involving a bridgehead proton is not observed in the bicyclo[2.2.1]heptane system, it is reasonable to assume that this is also the case in the present bicyclo[2.2.2]-octene system. It follows that the vicinal coupling of the cis-oriented protons gives the larger splitting, of 11 c/s, a value which is considerably larger than that predicted by

Can. J. Chem. Downloaded from www.nrcresearchpress.com by 210.87.254.5 on 09/05/12
For personal use only.

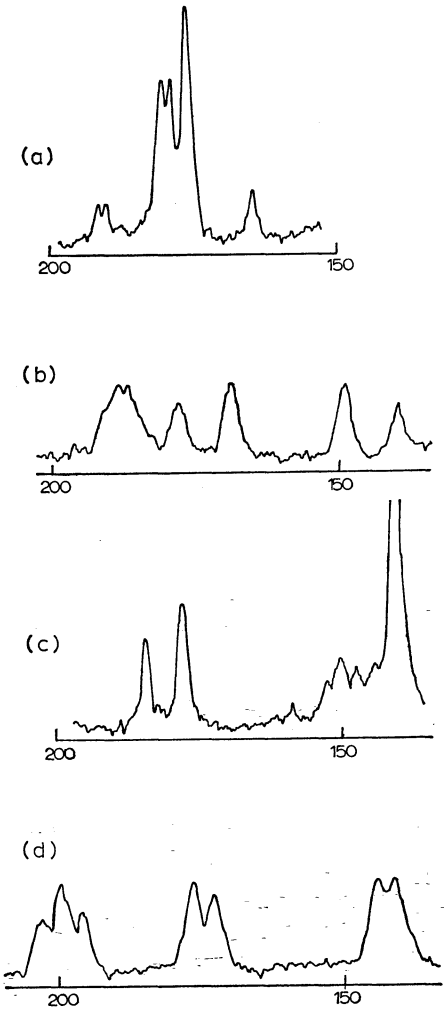

FIG. 3. Intermediate-field region (130–210 c/s from TMS) for the following compounds: (*a*) XI, (*b*) XV, (*c*) XII, and (*d*) XIX.

Karplus (32). It can be noted that recent reports of coupling constants of comparable magnitude have appeared for other fused ring systems (12, 14, 33, 34) having protons in a similar orientation and also for vicinal cases in which there are small dihedral angles of ca. 20° (35, 36).

To illustrate some of the variations in these patterns, portions of the spectra for XV, XII, and XIX are shown in Figs. 3(*b*), (*c*), and (*d*), respectively. Since a few of the observed patterns can be analyzed as the AB portions of ABX systems, it is possible to determine the chemical shifts and coupling constants for the C-21 and C-22 protons in a number of the examples. In all cases, the bridgehead proton gives a broad, unresolved multiplet, the center of which has been taken as the approximate chemical shift. These data are collected in Table II.

It is clear that a large coupling is observed for those cases in which the protons on C-21 and C-22 are in a cis and exo orientation. The nature of the ring system requires that the dihedral angle for these vicinal protons must be close to 0°. Small variations

Can. J. Chem. Downloaded from www.nrcresearchpress.com by 210.87.254.5 on 09/05/12
For personal use only.

in this coupling are observed for structural changes which would be expected to alter the dihedral angle. For example, the coupling constant is 11.0 c/s for the diesters, XI and XIII, and decreases to 10.0 c/s in the lactone esters, XV and XX. It is reasonable that the formation of the lactone would alter the C-21, C-22 dihedral angle and, since a maximum coupling is expected for 0° (32), an increase in the dihedral angle would tend to decrease the coupling, as is observed. The concomitant change in the coupling of the bridgehead and C-21 protons is a further indication that the skeletal geometry is indeed different from that of the diesters and that the dihedral angle between the bridgehead and C-21 protons increases upon formation of the lactone relative to the diesters. Qualitatively, the general behavior of these coupling constants is that predicted by Karplus (32) but the magnitude of the constants for very small dihedral angles is significantly larger than the calculated values.

An indication of the magnitude of the trans vicinal coupling between the C-21 and C-22 protons is given by the spectra of XII and XIX (Figs. 3(*c*) and (*d*)). In each of these cases, a well-defined doublet appears near 175 c/s which can be assigned to the C-22 proton from the results in the cis examples discussed above. The spacing of these doublets, 6 and 4 c/s, respectively, will be approximately equal to the trans vicinal coupling constant and these values are of the order expected for dihedral angles near 120° (32). Since the coupling constant is much more sensitive to changes in the dihedral angles of this magnitude, the observed difference is not unexpected because of the marked difference in flexibility, between the bicyclo[2.2.2]octene ring system and its saturated analogue. The coupling between the bridgehead and the C-21 protons is also changed from the cis cases and appears to be approximately 3–4 c/s. Again, the agreement with theoretical predictions is reasonable.

For the examples discussed above, there are some interesting changes in the chemical shifts of the C-21, C-22, and bridgehead (C-6) protons. In the doubly unsaturated compounds, XI–XIII, the bridgehead proton absorbs at the lowest field of the three, ca. 3.5 δ. Presumably this shift is a result of the combined effects of the two neighboring double bonds since, in the most favorable conformation, the C-6 proton is in the plane of both (i.e., the region of maximum deshielding). This proton is shifted up-field in XV, in which only one double bond is adjacent, and a further shift to higher field is observed upon removal of the double bond as in XIX and XX. A part of the high-field shift observed for the bridgehead proton in XX may arise from a shielding contribution by the neighboring epoxide ring. Since it has been shown recently (37) that this grouping tends to deshield nuclei near the plane of the three-membered ring, it follows that a shielding effect may be operative in the region above this plane. In general, however, the changes in shift for the C-21 and C-22 protons are in agreement with those expected on the basis of the anisotropic nature of the double bond as discussed earlier. A marked shielding effect is observed for the change from the exo to the endo configuration in compounds with the endocyclic double bond (cf. XI and XII). This change can be attributed to the anisotropic olefinic grouping since, in the endo orientation, the C-21 proton would be in the shielding region of the C-7, C-8 bond.

These assignments are based on the observed splittings and on the intensities (i.e., the skewed nature of the bands), and, although not unequivocally, clearly indicate that there is a marked dependence of the shift on the orientation of the protons in the vicinity of anisotropic groups. Further work is planned, using simpler model compounds, to test these assignments and to study the coupling constants in this bicyclic system in more detail.

Can. J. Chem. Downloaded from www.nrcresearchpress.com by 210.87.254.5 on 09/05/12
For personal use only.

C-8 Protons

In the series of compounds containing the endocyclic double bond at C-7, C-8, the proton on C-8 appears in the characteristic olefinic region and exhibits minor variations in chemical shift with structural changes. In the C-21, C-22 diesters this band appears at $5.40\pm0.03\ \delta$ ($CDCl_3$) and $5.34\pm0.02\ \delta$ (CCl_4). This peak is shifted to lower field in the anhydrides and is found at $5.57\pm0.03\ \delta$ ($CDCl_3$). As is usual, an additional deshielding is experienced by this proton when it is beta to a carbonyl group (e.g., XI–XIII) and the peak appears at $6.90\pm0.03\ \delta$ ($CDCl_3$) and $6.81\pm0.03\ \delta$ (CCl_4). Finally, for compounds XV and XVI, in which C-8 is part of a lactone ring to C-22, the C-8 proton appears at $5.00\ \delta$ ($CDCl_3$).

ACKNOWLEDGMENTS

The authors wish to express their thanks to Dr. L. H. Zalkow, Oklahoma State University, for the sample of compound XXIII, and to the National Research Council of Canada for financial assistance.

REFERENCES

1. R. G. R. Bacon and L. Ruzicka. Chem. Ind. (London), 546 (1936). H. Wienhaus and W. Sandermann. Ber. **69**, 2202 (1936).
2. W. D. Lloyd and G. W. Hedrick. J. Org. Chem. **26**, 2029 (1961).
3. W. Klyne. J. Chem. Soc. 3074 (1953).
4. W. H. Schuller and R. V. Lawrence. J. Am. Chem. Soc. **83**, 2563 (1961).
5. A. W. Burgstahler, H. Ziffer, and U. Weiss. J. Am. Chem. Soc. **83**, 4660 (1961).
6. J. A. Pople. Proc. Roy. Soc. (London), Ser. A, **239**, 550 (1957).
7. P. T. Narasimhan and M. T. Rogers. J. Phys. Chem. **63**, 1388 (1959).
8. L. M. Jackman. Applications of NMR in organic chemistry. Pergamon, New York. 1959. Chap. 7.
9. H. Conroy. Advances in organic chemistry. Vol. 2. Interscience, New York. 1960. pp. 285–286.
10. G. Slomp, F. A. MacKellar, and L. A. Paquette. J. Am. Chem. Soc. **83**, 4472 (1961).
11. R. R. Fraser. Can. J. Chem. **40**, 78 (1962).
12. L. Ruzicka, P. J. Ankersmit, and B. Frank. Helv. Chim. Acta, **15**, 1289 (1932).
13. N. J. Halbrook and R. V. Lawrence. J. Am. Chem. Soc. **80**, 368 (1958).
14. L. Ruzicka and St. Kaufman. Helv. Chim. Acta, **23**, 1346 (1940). 28, 865 (1952)
15. S. Brus, Le-van-thoi, H. Francois, and C. Fines. Peintures, Pigments, Vernis, ~~29, 36 (1953)~~.
16. L. Ruzicka and W. A. Lalande, jr. Helv. Chim. Acta, **23**, 1357 (1940).
17. L. H. Zalkow, R. A. Ford, and J. P. Kutney. J. Org. Chem. In press.
18. Y. Kawazoe, Y. Sato, M. Natsume, H. Hasegawa, T. Okamoto, and K. Tsuda. Chem. Pharm. Bull. (Tokyo), **10**, 338 (1962).
19. J. C. W. Chien. J. Am. Chem. Soc. **82**, 4762 (1960).
20. W. A. Ayer and C. E. McDonald. Unpublished observations.
21. A. A. Bothner-By and C. Naar-Colin. Ann. N.Y. Acad. Sci. **70**, 833 (1958).
22. J. I. Musher. J. Chem. Phys. **35**, 1159 (1961); **37**, 192 (1962).
23. R. F. Zurcher. Helv. Chim. Acta, **44**, 1380 (1961).
24. P. T. Narasimhan and M. T. Rogers. J. Chem. Phys. **31**, 1302 (1959).
25. E. L. Eliel, M. H. Gianni, Th. H. Williams, and J. B. Stothers. Tetrahedron Letters, No. 17, 741 (1962).
26. G. Slomp and B. R. McGarvey. J. Am. Chem. Soc. **81**, 2200 (1959).
27. H. M. McConnell. J. Chem. Phys. **27**, 226 (1957).
28. L. M. Jackman and R. H. Wiley. J. Chem. Soc. 2881, 2886 (1960).
29. L. Crombie and J. W. Lown. Proc. Chem. Soc. 299 (1961).
30. W. A. Ayer, R. Hayatsu, P. de Mayo, S. T. Reid, and J. B. Stothers. Tetrahedron Letters, No. 18, 648 (1961).
31. F. A. L. Anet. Can. J. Chem. **39**, 789 (1961).
32. M. Karplus. J. Chem. Phys. **30**, 11 (1959).
33. G. Albergs-Schönberg and H. Schmid. Helv. Chim. Acta, **44**, 1447 (1961).
34. J. S. Webb, R. W. Broschard, D. B. Cosulich, J. H. Mowat, and J. E. Lancaster. J. Am. Chem. Soc. **84**, 3183 (1962).
35. K. L. Williamson and W. S. Johnson. J. Am. Chem. Soc. **83**, 4623 (1961).
36. W. A. Ayer and D. A. Law. Can. J. Chem. **40**, 2088 (1962).
37. A. D. Cross. J. Am. Chem. Soc. **84**, 3206 (1962).

Can. J. Chem. Downloaded from www.nrcresearchpress.com by 210.87.254.5 on 09/05/12
For personal use only.

THE INFRARED SPECTRA OF TRIMETHYLAMINE OXIDE SALTS[1]

DENYS COOK
Exploratory Research Laboratory, Dow Chemical of Canada, Limited, Sarnia, Ontario
Received January 2, 1963

ABSTRACT

Several salts of trimethylamine oxide have been prepared. A species common to all these salts, the $(CH_3)_3NOH^+$ ion, has been inferred from the infrared spectra of the solids, but with varying degrees of interaction in the hydrogen bond O—H · · · X, depending on the anion. These variations have been investigated in detail, and with the help of deuterium replacement, confident assignments for the OH stretching, bending, and torsional modes have been made. A splitting of about 80 cm^{-1} in the bending mode has been noted, and has been ascribed to correlation field coupling. With one exception, the assignments are in good agreement with those previously determined by Giguère and Chin.

INTRODUCTION

An analysis of the vibrational spectrum of trimethylamine oxide, its dihydrate, and its hydrochloride has recently been published by Giguère and Chin (1). The earlier work was summarized by them. The structure of the hydrochloride has also been determined by Rérat using the techniques of X-ray diffraction (2).

The present work complements the existing data, for while the general assignments were satisfactory, the definition of the OH group modes needed further elaboration. This has been achieved by the study of several hydrohalides and also more complex salts of trimethylamine oxide, using deuterium substitution to aid identification of bands due to the hydroxyl hydrogen atom.

This work forms part of an attempt to determine donor characteristics of functional groups for both Lewis acids and protonating acids. The interaction of donors with the latter category yields salts whose XH stretching modes are of little diagnostic use but whose bending modes show promise of becoming useful group frequencies.

RESULTS

The spectrum of the HBr salt is shown in Fig. 1. Bands from all the spectra are listed in Table I and those bands arising from vibrations of the OH group are summarized in Table II.

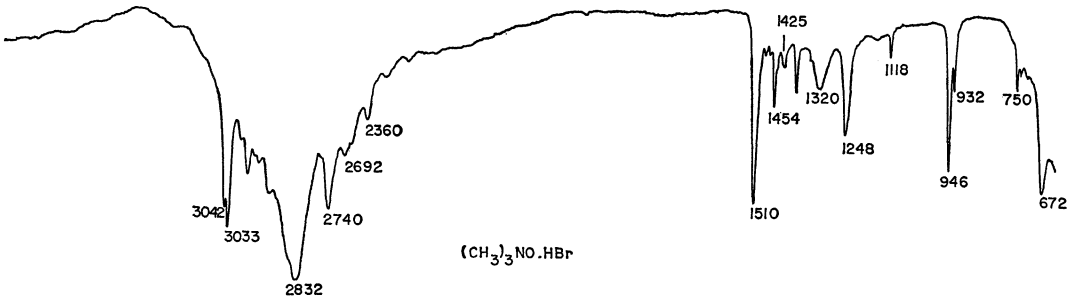

FIG. 1. Infrared spectrum of trimethylamine oxide.HBr.

[1]*Contribution No. 92.*

Can. J. Chem. Downloaded from www.nrcresearchpress.com by 210.87.254.5 on 09/05/12
For personal use only.

Can. J. Chem. Downloaded from www.nrcresearchpress.com by 210.87.254.5 on 09/05/12
For personal use only.

TABLE I

Bands in spectra of $(CH_3)_3NO$ salts

	Cl^-		Br^-		I^-		ClO_4^-		BF_4^-		BPh_4^-		PF_6^-	
	H	D	H	D	H	D	H	D	H	D	H	D	H	D
νCH	3049 s	3048 m, sh	3042 s	3042 m	3027 s	3030 m	3062 m		3070 m	3071 m			3068 m	3068 m
νCH	3040 s	3039 m	3033 s	3033 s	3017 s	3020 m	3052 m, sh		3060 m, sh	3060 m, sh				
	3030 m, sh	3031 m, sh		3028 m, sh										
			2998 w											
		2260 w	2975 m											
	2790 m	2210 w	2942 w	2340 w		2398 w								
	2710 s	2130 s	2910 m	2230 s		2323 w								
	2668 s	2105 m, sh	2856 s, sh	2212 s	3184 w	2291 m		2450 m, sh						
νOH	2628 vs	2048 s, b	2832 s, b	2170 s	3042 vs, b	2260 s	3225 s, b	2412 s, b	3332 vs, b	2480 s, b	3338 m, b	2482 s	3450 s, b	2552 s
	2590 s, sh	1984 s	2740 s	2090 s, sh	2974 s, sh	2220 m, sh	3012 w	2340 m, sh		2450 m, sh				
	2456 m		2692 m, sh	2078 s	2964 s	2178 m	2936 w	2195 vw						
	2028 w		2630 m	1975 m	2900 s	2067 m	2047 vw	1735 vw						
			2580 w		2870 s	1960 w								
			2005 vw		2861 s									
					2833 s, sh									
					2768 s, sh									
					2722 m									
					2670 m									
					2604 w									
					2499 w									
	1550 w, sh													
	1532 s, sh													

δ_{OH}	1525 vs	1148 m	1510 s	1144 m	1495 s	1139 m	1505 m		1507 s	1145 vs?	1490 m, sh	1150 m	1496 s, sh	1140 m
	1512 m, sh												1510 m, sh	1510 m, sh
	1490 w	1487 m	1480 w	1485 m	1474 m	1468 m	1488 s	1488 s	1490 s	1492 s	1479 s	1474 vs	1486 s	1489 s
δ_{CH}	1474 m	1470 s	1468 w	1466 m	1457 m	1460 m	1469 s	1469 s	1470 s	1470 s			1465 s	1465 s
		1460 w	1454 m	1460 m, sh	1448 m	1446 m	1455 m		1453 m	1458 m, sh			1456 s, sh	1458 s, sh
$2\gamma_{OH}$	1458 m	1070 m	1320 m	962 w	1155 m	840 m								
			1445 w	1450 w	1443 m, sh									1445 s, sh
		1424 w		1440 w	1432 m	1435 w								
δ_{OH}	1435 m	1055 m	1425 m	1050 m	1421 m	1035 s	1440 m	1060 s	1443 m	1040 s	1400 w	1019 m	1414 s	1028 m
δ_{CH}	1398 m	1396 m	1390 m	1392 m	1390 m	1392 m	1402 m	1402 m	1404 m	1404 m			1395 s	1397 s
				1388 w	1386 m, sh	1387 m								
	1340 w	1340 w		1340 w	1340 w	1338 w	1340 w	1340 w	1345 w		1340 w		1342 w	1340 w
		1298 w		1295 w		1291 m	1302 vw	1298 vw	1292 m	1290 w	1295 w	1300 w	1282 m	1288 w
δ_{CH_3}	1258 s	1258 m	1248 s	1252 m	1251 m	1256 m, sh	1255 m, sh	1256 m	1260 m	1258 w	1255 m	1258 m	1246 m	1250 m
	1251 s, sh		1240 m, sh		1234 m	1248 s	1240 s	1240 w	1242 m		1228 m		1229 m	1230 m
	1123 m		1118 m		1114 m				1122?				1111 m	
		1055 m, sh												
		1020 w												
	953 s		948 m, sh	942 m	941 s, sh									
ν_{CN}	950 s	948 s	946 s		937 s	933 s	948 vs	944 s	948 s	942 s	943 m	940 w	948 s	949 s
ν_{NO}	940 m	940 s	932 m, sh	930 m	923 m	923 m	931 vs	932 s	932 vs	930 s	924 m	920 m	929 s	931 s
γ_{OH}	752 s		672 s		585 m		622 s							
ν_{CN}		750 w	750 m	745 w	740 w	745 m	743 m	741 w	743 w	740 w				
			736 vw		733 m	730 m								
	510 w		504 w											
δ_{OCN}	492 m		488 m											
δ_{OCN}	458 m		457 m											

Can. J. Chem. Downloaded from www.nrcresearchpress.com by 210.87.254.5 on 09/05/12
For personal use only.

TABLE II

OH and OD stretching and deformation vibrations

	Cl^-	Br^-	I^-	ClO_4^-	BF_4^-	BPh_4^-	PF_6^-
ν_{OH}	2628	2832	3042	3225	3332	3338	3450
$\Delta\nu_{\frac{1}{2}}$	130	125		250	145	80	115
ν_{OD}	2048	2170	2260	2412	2480	2482	2552
$\Delta\nu_{\frac{1}{2}}$	75	80	65	90	55	50	80
Ratio	1.28	1.31	1.36	1.34	1.34	1.34	1.35
δ_{OH}	1525	1510	1495	1505	1507	1490	1496
δ_{OD}	1148	1144	1139		1145?	1150	1140
Ratio	1.33	1.32	1.31		1.32	1.30	1.31
δ_{OH}	1435	1425	1421	1440	1443	1400	1414
δ_{OD}	1055	1050	1035	1060	1040	1019	1028
Ratio	1.36	1.36	1.37	1.36	1.39	1.37	1.38
$2\gamma_{OH}$	1458	1320	1156				
$2\gamma_{OD}$	1070	962	840				
Ratio	1.36	1.37	1.38				
γ_{OH}	752	672	585	622			

DISCUSSION

Hydrogen Stretching Modes

The strong band designated ν_{OH} in the tables has been assigned to the OH stretching vibration. This varies from a strong, broad band with much structure centered at 2628 cm^{-1}, for the HCl salt, to a slightly narrower band in the HPF_6 salt at about 3450 cm^{-1}. In the analogous deuterated salt the vibration is found at a lower frequency which bears a ratio to the hydrogen stretching frequency varying from about 1.28 in the HCl salt to about 1.35 in the HPF_6 salt. The half-widths in the deuterated salts are also smaller.

This behavior is characteristic of protonated species and has been observed for the salts of pyridine (3), γ-pyrones (4), γ-pyridones (5), etc. It has been suggested that the structure in many XH stretching vibrations is due to a combination of a fundamental (or possibly two, if splitting occurs) with a low-lying lattice mode and its overtones, i.e. $\nu_{XH} \pm n\nu_L$, where ν_L is a lattice mode. Raman shifts due to some of these lattice modes in crystalline acids have been measured recently by Gross (6) near 200 cm^{-1}. These lattice modes also showed some fine structure, a series of small peaks with a separation increasing from 10 to 20 cm^{-1} being observed.

Similar behavior has been noted in the OH stretching band in the HPF_6 salt of trimethylamine oxide. This salt has one strong, broad absorption band at 3450 cm^{-1} ($\Delta\nu_{1/2} \sim 115$ cm^{-1}) in the H salt and at 2552 cm^{-1} ($\Delta\nu_{1/2} \sim 80$ cm^{-1}) in the D salt. The contours of the band suggest a series of shoulders which are spaced approximately 10 cm^{-1} apart on both sides of the main peak. Inspection of one of the salts with low ν_{OH}, for example, the HCl salt, shows the displacements of the satellites from the main peak to be larger, of the order of 35 to 40 cm^{-1}. Consequently the resolution of these bands in the spectra of such compounds is greater. On deuteration the usual shift to lower frequency occurs. The structure in the salts with low ν_{OD}, for example, the DCl salt, is better resolved than in the H salt, but in the DPF_6 salt the shoulders are still not resolved.

Hydrogen Bending Modes

The in-plane hydrogen-bending mode, δ_{OH}, is, by contrast, a relatively sharp band ($\Delta\nu_{1/2} \sim 20$ cm^{-1}). It occurs near 1500 cm^{-1} (see Table II) and is always split with another

Can. J. Chem. Downloaded from www.nrcresearchpress.com by 210.87.254.5 on 09/05/12
For personal use only.

component near 1430 cm^{-1}. This second component is generally somewhat weaker than the other. The deuteration shifts are normal, giving ratios of about 1.33 and 1.37 for each component respectively. The splitting of this mode recalls a similar splitting in salts of γ-pyrones (4) and γ-pyridones (5), where the values were $\sim$1300 and 1210 cm^{-1}, and $\sim$1300 and 1230 cm^{-1} respectively. Some light can be thrown on the origin of the splitting in the present case as the structure of trimethylamine oxide hydrochloride is known (2).

The crystals belong to the space group *Pnam*, have orthorhombic symmetry, and contain four molecules per unit cell. The structure is made up of layers consisting of alternating rows, each molecule in each row being related to the other by an S_2 symmetry operation. The layer above is similarly constituted except that the O—H . . . Cl bonds point in the reverse direction. Cohesive forces between layers are due to coulombic interaction between Cl^- and N^+. Two site symmetries are involved; some molecules are related by a center of symmetry and have site group C_i (two molecules from different layers) while others (in the same layer) have C_s site symmetries (7). There can be no site group splitting, therefore, since the ion symmetry is C_s (the H, O, N, and one C atom are in the same plane). The space group, however, D_{2h}^{16} being isomorphous with the irreducible representation D_{2h}, will permit some splitting, the number of components being determined by the species of the site group involved. For the C_s site group the A' modes of the ion would be split with two components, while the A'' modes would show no splitting in the infrared spectrum. For the C_i site group, however, both A' and A'' modes should be split in the Raman and infrared spectra into three components (see Table III).

TABLE III

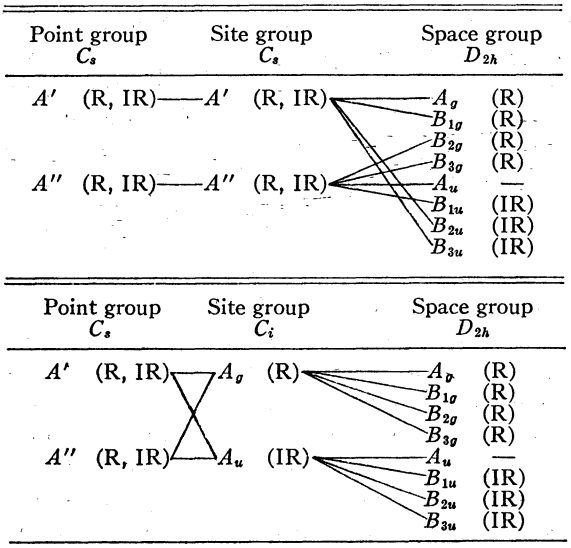

The actual behavior in the infrared spectrum seems to be more in keeping with splitting due to the C_s site symmetry. Two components have been observed in the OH in-plane bending mode (A') for all the compounds studied, the magnitude of the splitting decreasing somewhat as the hydrogen bond gets weaker in the salts with larger anions (see Table II). The detailed structure of the OH stretching band in some of the salts with low ν_{OH} may be due to splitting from such coupling. Although this structure disappears in the

Can. J. Chem. Downloaded from www.nrcresearchpress.com by 210.87.254.5 on 09/05/12
For personal use only.

salts with more complex anions, the band is still broad enough to accommodate two components. A larger splitting would be expected in the hydrohalides which have stronger hydrogen bonds and would be more strongly coupled. The out-of-plane hydrogen deformation does not seem to be split. Although the low-frequency region is somewhat inaccessible, only one band has been observed between 450 and 750 cm^{-1} in the HCl salt, and probably in the HBr salt, that shifts on deuteration. It seems unlikely that splitting of this mode could be as much as 300 cm^{-1}.

The presence of these bands in the infrared spectrum seems to show that the site group symmetry responsible for the splitting is C_s, and the coupling is between molecules lying on zigzag chains running in the direction of the *c* axis, or in almost linear chains making an angle of about 45° with the *c* axis. In terms of intermolecular contacts the OH groups of molecules on these chains are probably close enough to permit this coupling (the oxygen atoms are 4.4 Å apart; compare 5.4 Å between those in the same plane, and 7 Å for those related by the center of symmetry).

Dilute isotopic solid solutions have been used previously to distinguish between static field and correlation field effects (8, 9). The vibration of the bond containing the dilute isotope is then uncoupled from those of its neighbors, and its frequency should then be the average of all correlation field components. This type of behavior has been confirmed for dilute solutions of $(CH_3)_3NO.HX$ in $(CH_3)_3NO.DX$. The two coupled components near 1500 and 1420 cm^{-1} practically disappear, leaving two small shoulders, and a band at about 1465 cm^{-1} that is not present in the HX salt appears strongly. Occasionally this band can only be observed as an enhancement of a band already present. The frequency of the uncoupled vibration is sufficiently close to the mean value of the two components to make it reasonably certain that these are the only infrared-active components. Dilute solutions of the D salt in the H salt have not given unambiguous results, since the presence of the 1123 cm^{-1} band in the H salt, close to the mean of the two bending components ($1/2(1148+1055) = 1102$ cm^{-1}), has interfered with the observation of weak new bands. A small shoulder, however, at 1112 cm^{-1}, has been observed in such solid solutions. This is further support for the view that the site group symmetry responsible for the splitting is C_s. Without the Raman shifts, though, this cannot be proved.

Torsional Modes

The symmetric CN stretching vibration was assigned by Giguère and Chin (1) to the strong band at 752 cm^{-1} in the hydrochloride. This band, however, disappears in the deuterated salt (a very small component at 745 cm^{-1} remains, see below), and is probably due to the out-of-plane (or torsional) mode. A similar band, which also disappears on deuteration, is at 672 cm^{-1} in the HBr salt, at 585 cm^{-1} in the HI salt, and at 622 cm^{-1} in the $HClO_4$ salt. These bands do not appear to be split, in accordance with the selection rules for the solid. The trend in these frequencies to lower values with weaker hydrogen bonds duplicates that for the in-plane hydrogen-bending mode, though in this case, too, the relationship between ν_{OH} and γ_{OH} is far from precise. Wavelength limitations prevented observation of γ_{OD} so no value of the ratio γ_{OH}/γ_{OD} can be determined. However, it must be greater than $752/550 = 1.37$ since 550 cm^{-1} is the low-frequency cutoff of the spectrometer used.

Several other bands which shift on deuteration are seen at 1458, 1320, and 1155 cm^{-1} in the HCl, HBr, and HI salts respectively; the deuterated materials have bands at 1070, 962, and 840 cm^{-1}. They are weak bands and are plausibly assigned to the overtone of the out-of-plane hydrogen deformation. The isotopic ratios are 1.36, 1.37, and 1.38 respec-

Can. J. Chem. Downloaded from www.nrcresearchpress.com by 210.87.254.5 on 09/05/12
For personal use only.

tively for these three salts. No band in the appropriate region has been found for the other salts.

In all the salts there is a weak band at about 1120 cm^{-1} which disappears on deuteration. It seems unlikely that this can be a fundamental, partly on account of its intensity, partly since all the OH fundamentals have been assigned. Neither is it likely to be another component of the in-plane hydrogen-bending mode. It can be accounted for by a combination tone of the NO stretching mode (or the CN asymmetric stretching mode), and a low-lying lattice mode, thus 950+170 = 1120. If on deuteration the lattice mode is displaced by a factor 1.37 to lower frequency then the combination tone should be seen at 950+(170/1.37) = 950+124 = 1054. Since δ_{OD}, the low-frequency component of the bending mode, absorbs near 1050 cm^{-1}, one would have to assume that the combination tone is obscured by δ_{OD}, an unsatisfactory assumption, but with little plausible alternative.

Other Vibrational Modes

Although the strong band at 752 cm^{-1} in the HCl salt is not due to the symmetric CN stretching vibration as suggested by Giguère and Chin (1), there is in the DCl salt, and in all the other salts, a weak band at about 745 cm^{-1} which is probably due to this vibration. Its weakness is a little surprising but becomes more reasonable when it is appreciated that the greater part of the dipolar structure resides in the NO bond.

The doublet near 950 cm^{-1} has been assigned to the NO stretching mode and the CN asymmetric stretching mode. In many of the salts studied further structure in this doublet was observed as a high-frequency shoulder. This is probably the splitting of ν_{CN}, which is doubly degenerate in $(CH_3)_3NO$. This should be apparent too for the OCN bending mode, previously (1) assigned to the 472 cm^{-1} band. Wavelength limitations do not permit observation below the 460 cm^{-1} band, presumably the high-frequency component of the doublet.

EXPERIMENTAL

Materials

Trimethylamine oxide dihydrate and hydrochloride were obtained from the K and K Laboratories. Other salts were made by adding the requisite amount of aqueous acid to the dihydrate and allowing the salt to crystallize. The following exceptions were made. The HBr salt was prepared by passing HBr gas through a solution of the dihydrate in a little methanol with excess ether. The solid so formed was recrystallized from methanol. The tetraphenylboron compound was precipitated when aqueous solutions of the hydrochloride and sodium tetraphenylboron were mixed. Deuterium exchange of the labile proton was achieved by dissolving the salt in excess D_2O and removing the latter by evacuation, except that the insoluble tetraphenylboron salt was made from D_2O solutions in the manner described.

Spectra

The spectra were those of emulsions of the finely ground solid in nujol and fluorolube. They were recorded on a Perkin–Elmer 221 prism-grating spectrometer with NaCl optics over the range 4000 to 650 cm^{-1}, and from 650 to 550 cm^{-1} on a Perkin–Elmer 421 double-grating spectrometer. A KBr prism-grating spectrometer (10) was used to record the spectra of two of the salts down to 450 cm^{-1}.

ACKNOWLEDGMENTS

The assistance of Miss C. D. Anderson in preparing some of the salts and recording their spectra is gratefully acknowledged. The facilities of the Perkin–Elmer 421 spectrometer and the KBr prism-grating spectrometer were kindly made available by Mr. D. G. Barnes and Dr. W. J. Potts, Jr. (The Dow Chemical Company, Midland, Michigan, U.S.A.) respectively.

REFERENCES

1. P. A. Giguère and D. Chin. Can. J. Chem. **39**, 1214 (1961).
2. C. Rérat. Acta Cryst. **13**, 63 (1960).
3. D. Cook. Can. J. Chem. **39**, 2009 (1960).

Can. J. Chem. Downloaded from www.nrcresearchpress.com by 210.87.254.5 on 09/05/12
For personal use only.

4. D. Cook. Can. J. Chem. **41**, 505 (1963).
5. D. Cook. Unpublished results.
6. E. F. Gross. *In* Hydrogen bonding. *Edited by* D. Hadži. Pergamon Press, New York. 1959. p. 203.
7. R. S. Halford. J. Chem. Phys. **14**, 8 (1946).
8. W. Vedder and D. F. Hornig. *In* Advances in spectroscopy. Vol. II. *Edited by* H. W. Thompson. Interscience, New York. 1961. p. 189.
9. D. F. Hornig and G. L. Hiebert. J. Chem. Phys. **27**, 752 (1957).
10. L. W. Herscher. Spectrochim. Acta, **15**, 91 (1959).

Can. J. Chem. Downloaded from www.nrcresearchpress.com by 210.87.254.5 on 09/05/12
For personal use only.

THE STABILITY OF METALLIC COMPLEXES OF TWO DIMETHYLPHENANTHROLINES

D. A. BRISBIN[1] AND W. A. E. MCBRYDE[1]
Department of Chemistry, University of Waterloo, Waterloo, Ontario
Received November 26, 1962

ABSTRACT

The stepwise formation constants for the complexes formed by 5,6-dimethyl- and 4,7-dimethyl-1,10-phenanthroline with bivalent iron, cobalt, nickel, copper, and zinc were determined by a partition method. The measurements were made at 25° C and in aqueous solutions having an ionic strength maintained at 0.1. The enhanced basicity of the ligands compared to the parent phenanthroline is paralleled by increased stability of the metallic complexes. The abnormally high formation constants of the cobalt complexes suggest oxidation to cobalt (III).

Can. J. Chem. Downloaded from www.nrcresearchpress.com by 210.87.254.6 on 09/05/12
For personal use only.

A number of studies to determine the stability of metal complexes of the phenanthrolines have been published (1–8), among the most complete of which are those of Irving and co-workers (2, 4). In an extension of these studies the present investigation has sought formation curves, and hence formation constants, for the complexes formed by 5,6- and 4,7-dimethyl-1,10-phenanthroline with a selected group of ions of the first transition series.

The inductive effect of substituent methyl groups in increasing the basic strength of phenanthroline is apparent from the data of the following table:

Compound	pK_a	Investigators	Compound	pK_a	Investigators
1,10-Phenanthroline	4.96	Ref. 6	2,9-Dimethylphenanthroline	5.85	Ref. 2
	4.93	This work		5.79	This work
	5.0	Ref. 2			
2-Methylphenanthroline	5.42	Ref. 2	5,6-Dimethylphenanthroline	5.60	This work
5-Methylphenanthroline	5.28	Ref. 3	4,7-Dimethylphenanthroline	5.95	This work
	5.23	Ref. 7			
	5.26	Ref. 8			

From these data it is seen that the basic strength of these compounds is enhanced by the presence of each methyl group in the conjugated ring system, and that the extent of this enhancement is related to the propinquity of the methyl groups to the nitrogen atoms. In agreement with expectations, the increased basicity of the compounds investigated is paralleled by an increase in stability of the complexes investigated except, as noted elsewhere, when steric hindrance to coordination about the metal atom occurs (5).

METHOD

The experimental method used was based on partition of the ligand between an aqueous solution and a solvent immiscible with water. The principle of the method is old, but its extension to the study of formation of complexes involving stepwise equilibria was first suggested by Kolthoff *et al.* (9), and subsequently extended and refined by Irving and co-workers (2). A measured volume of a solution of the ligand of known concentration in a selected solvent was shaken with a measured volume of aqueous solution containing

[1]*Formerly of the Department of Chemistry, University of Toronto, where most of the experimental work was done.*

the metal (and also buffer and indifferent electrolyte sufficient to maintain constant ionic strength) until a steady state was reached. The initial and final optical densities of the solution of free ligand were measured, and, as necessary, the pH of the aqueous solution. The distribution of unbound ligand was assumed to follow the distribution law, and after allowance had been made for any protonated ligand that might have formed, the amount bound to metal was found by difference. This quantity, divided by the number of moles of metal taken, yields the degree of complex formation, $\bar{n}$, while the concentration of ligand in the aqueous phase furnishes a corresponding value of pL. Thus, for equal volumes of the two liquid phases,

$$[1] \qquad \bar{n} = \frac{C_L - C_L' - C_L'(1 + H/K_a)q^{-1}}{C_M}$$

$$[2] \qquad pL = \log q - \log C_L',$$

in which C_L = initial concentration of ligand in solvent,
C_L' = final concentration of ligand in solvent,
C_M = total concentration of metal in aqueous phase,
q = partition coefficient for free ligand,
H = antilog (−pH),
K_a = dissociation constant for protonated ligand.

Each distribution experiment thus yields a point on the formation curve ($\bar{n}$ vs. pL).

An assumption implicit in the use of this method for studying complex formation is that no species other than free ligand occurs in the solvent phase throughout the distribution experiment. A ready check on this can be made by examining the absorption spectrum of the solvent phase after shaking with an aqueous solution containing metal; in the case of iron (II) the intense color of the metallic complexes would readily disclose the presence of any metal in the organic solvent. Except for the cases noted below, no evidence was found for the presence of any species other than ligand in the organic solvent.

The range of pL that could be encompassed by a single solvent was limited by practical upper and lower limits in C_L'. The lower limit in this case was set by the smallest optical density that could be measured with precision, the upper limit by the necessity to define accurately the difference $C_L - C_L'$. The upper limit in C_L was fixed in some solvents by the solubility of the ligand; in another (chloroform) by the number of dilutions required to produce a solution whose optical density could be measured in a 1-cm cell. For the investigation of all ranges of pL appropriate to the formation curves of the complexes examined chloroform and carbon tetrachloride were selected as solvents, but some experiments were performed with a mixed solvent consisting of these two substances mixed in such proportions as to give a convenient value of q between those of the single solvents.

EXPERIMENTAL

The two dimethylphenanthrolines were purchased from the G. F. Smith Chemical Co. and purified before use. Some of the material was recrystallized from warm benzene, and some by dissolving in dilute hydrochloric acid and reprecipitating by the addition of dilute aqueous sodium hydroxide. The latter method produced a whiter crystalline product than the former, although both melted sharply. The melting points and analyses showed that whereas the 4,7-dimethyl derivative crystallized from aqueous solution as the monohydrate, the 5,6-dimethyl analogue was obtained as the anhydrous compound.

The solutions of the metallic ions were made up from reagent-grade salts; and in any instance where the composition of the salt was in doubt, for instance as a result of deliquescence, the solutions were standardized by familiar gravimetric methods. Chloroform and carbon tetrachloride, of U.S.P. grade, were distilled in all-glass apparatus before use as solvents for the ligands.

Can. J. Chem. Downloaded from www.nrcresearchpress.com by 210.87.254.6 on 09/05/12
For personal use only.

Measurements of ultraviolet absorption were made in 1-cm covered silica cells with a Beckman Model DU spectrophotometer. The cell compartment was flanked by thermospacers through which water, maintained thermostatically at 25° C, was circulated. When spectra over a wide range of wavelengths were desired these were measured by a Beckman Model DK-1 spectrophotometer. The pH of aqueous solutions was measured by a Beckman Model G meter fitted with the manufacturer's small electrodes. The circuit was calibrated with freshly prepared buffer solutions as follows: 0.05 *M* potassium hydrogen phthalate (pH 4.00); 0.01 *M* potassium tetroxalate (pH 2.15); a suitable dilution of Radiometer concentrated buffer (pH 6.50). All distribution experiments were carried out in 40-ml glass-stoppered tubes; these were shaken in a water bath maintained at 25° for a minimum of 20 hours.

Acidity Constants of Ligands

The pK_a values for the protonated forms of the ligands were obtained absorptiometrically. Solutions of a suitable concentration of ligand containing buffer and indifferent electrolyte to give ionic strength of 0.1 were prepared to have pH values ranging from 2 to 12. The optical densities of these at various selected wavelengths were plotted against pH, and at the points of inflection on the resulting skew-shaped curves the pH was noted and identified with pK_a. The values found in this way are listed above.

Partition Coefficients

Measured volumes of a solution of ligand in non-aqueous solvent and of an aqueous solution containing various amounts of hydrochloric acid and potassium chloride sufficient to yield an ionic strength of 0.1 were shaken together in a thermostat, and analysis of the ligand solution carried out as described above in connection with measurement of $\bar{n}$. The partition coefficient was given by the equation

$$q = \frac{D_2V_2}{(D_1-D_2)V_1}(1 + H/K_a), \qquad [3]$$

in which D_1 = optical density of ligand solution before shaking,
D_2 = optical density of ligand solution after shaking,
V_1 = volume of the organic solvent solution,
V_2 = volume of the aqueous solution,
and the remaining terms apply as above.

FORMATION CONSTANTS

Formation curves depicting the relationship between $\bar{n}$ and pL were drawn from the experimental results. Except as noted below for cobalt and iron (II), the formation constants were obtained from these by a system of approximations suggested by Bjerrum (10).

This procedure did not work for the iron (II) or the cobalt data. The curves were peculiarly steep, as the iron (II) curve also is with orthophenanthroline. In the latter case the steepness is due to the value of K_3 being appreciably larger than those for K_1 and K_2. To a first approximation the iron (II) curves can be represented by the equation

$$\bar{n} = \frac{3\beta_3[L]^3}{1+\beta_3[L]^3}, \qquad [4]$$

in which

$$\beta_3 = K_1K_2K_3.$$

The formation curve can, therefore, give little information about the constants K_1 and K_2. This is illustrated in Table I, in which values of $\bar{n}$ calculated by the above equation are compared with values from the experimental formation curves for these two ligands reacting with iron (II). The values of β_3 for the calculations were those found to give the best fit to the experimental curves.

For establishing values of K_1 recourse was made to the procedure of Kolthoff *et al.* (11). In this, solutions containing a molar excess of iron (II) over reagent ($\bar{n}$ = 0.1 to 0.3) and

Can. J. Chem. Downloaded from www.nrcresearchpress.com by 210.87.254.6 on 09/05/12
For personal use only.

TABLE I
Curve fitting for iron (II) complexes

	Iron (II)-5,6-dimethylphenanthroline			Iron (II)-4,7-dimethylphenanthroline	
pL	β function 1	β function 2	$\bar{n}$ observed	β function 1	$\bar{n}$ observed
7.20	2.88	2.87	2.92	2.90	—
7.30	2.78	2.76	2.80	2.80	—
7.40	2.59	2.57	2.62	2.64	2.67
7.50	2.28	2.26	2.32	2.34	2.40
7.60	1.83	1.82	1.82	1.92	1.84
7.70	1.33	1.32	1.18	1.41	1.23
7.80	0.85	0.85	0.69	0.93	0.78
7.90	0.50	0.51	0.44	0.55	0.59
8.00	0.27	0.29	0.28	0.30	0.29
8.10	0.14	0.16	0.16	0.16	0.16
8.20	—	—	—	0.08	0.09

NOTE: β function 1 = $(3\beta_3[L]^3)/(1+\beta_3[L]^3)$, β function 2 = $(K_1[L]+3\beta_3[L]^3)/(1+K_1[L]+\beta_3[L]^3)$; the values of K_1 and β_3 used are those shown in Table III.

adjusted to pH $\sim$ 5 were prepared, and their optical densities measured at the wavelength of maximum absorption by the tris-complex. The following relationships apply:

$$K_1 = \frac{[FeL]}{[Fe][L]} \quad [5]$$

$$\beta_3 = \frac{[FeL_3]}{[Fe][L]^3} \quad [6]$$

$$[L]_T = 3[FeL_3]+[FeL]+[L](1 + H/K_a) \quad [7]$$

$$[Fe]_T = [FeL_3]+[FeL]+[Fe]. \quad [8]$$

We have assumed, as did Kolthoff, that no significant concentration of FeL_2 is present in these solutions and that the final term in equation [7] is negligible compared with the first two. The second assumption can subsequently be verified when values of [L] have been obtained. From the measured optical density and $[L]_T$ we obtain [Fe] by equation [8], and thence [L] with equation [6]. For each solution prepared this way, $\bar{n}$ and pL are known, and a value of K_1 may be calculated. Such measurements provide additional points at the lower end of the formation curves for the iron (II) complexes. Concerning K_2 no more can be said than that its value cannot lie above 10^7; values much greater than this would produce a detectable difference in the middle and lower parts of the formation curves from the values obtained by equation [4].

RESULTS AND DISCUSSION

The characteristic absorption of the ligands in the three solvents used, and the partition coefficients for the ligands between these solvents and dilute aqueous solutions are given in Table II.

The formation curves are shown in Figs. 1 and 2. The circles show the experimental points; the solid lines are calculated from the formation constants derived as explained in the previous section. These formation constants are given in Table III.

Certain anomalies, not encountered in similar studies with the simpler phenanthrolines, came to light in this work. For instance, in the partition experiments with iron (II) or nickel and 4,7-dimethylphenanthroline, where chloroform was the solvent, evidence was

Can. J. Chem. Downloaded from www.nrcresearchpress.com by 210.87.254.6 on 09/05/12
For personal use only.

TABLE II
Characteristics of ligands

Ligand	Property	Chloroform	0.3 $CHCl_3$, 0.7 CCl_4	Carbon tetrachloride
5,6-Dimethylphenanthroline	λ_{max} (mμ)	273	273	273
	ϵ_{max}	33,000	32,800	32,800
	q	12,350	1,050	11.3
4,7-Dimethylphenanthroline	λ_{max} (mμ)	266	266	266
	ϵ_{max}	36,000	36,000	36,500
	q	6,500	530	13.5

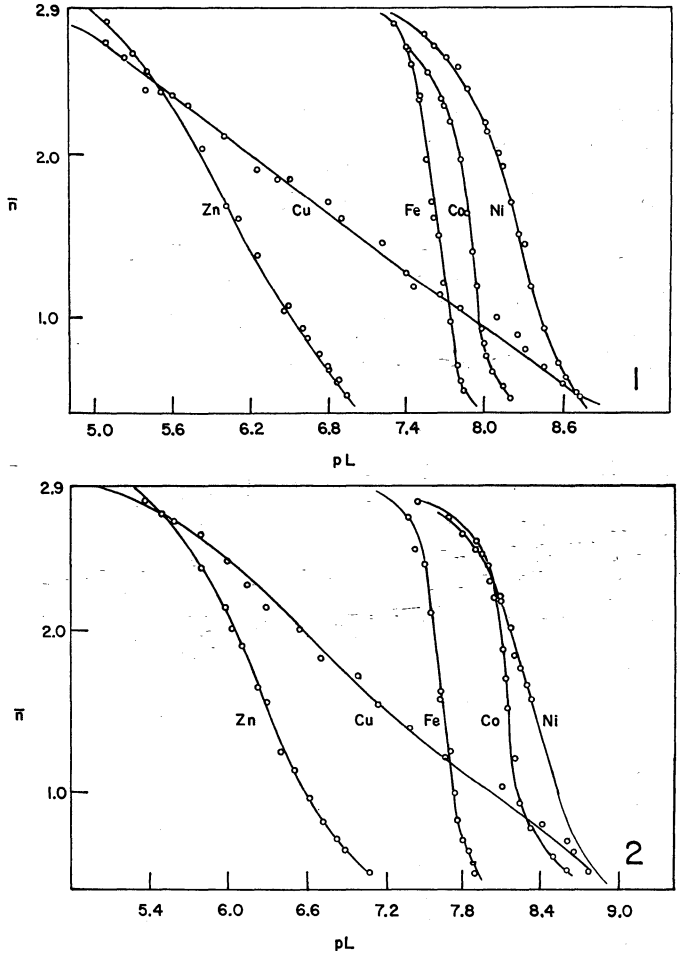

FIG. 1. Formation curves for 5,6-dimethylphenanthroline and the indicated metals. Not shown are four points at the lower end of the iron (II) curve determined by a spectrophotometric method.
FIG. 2. Formation curves for 4,7-dimethylphenanthroline and the indicated metals. Not shown are four points at the lower end of the iron (II) curve determined by a spectrophotometric method.

observed that some of the metallic complex had entered the solvent phase. This was plainly visible in the case of the colored iron complex, and in both cases was detected by a marked shift of the points for the experimental formation curve along the pL axis. Fortunately

Can. J. Chem. Downloaded from www.nrcresearchpress.com by 210.87.254.6 on 09/05/12
For personal use only.

TABLE III
Formation constants

Ligand	Metal	log K_1	log K_2	log K_3	log β_3
5,6-Dimethylphenanthroline	Nickel	8.25	8.30	8.21	24.76
	Cobalt	7.47	8.00	8.14	23.62
	Zinc	6.87	6.02	5.71	18.60
	Iron (II)	6.37*			23.00
	Copper	8.71	6.99	5.41	21.11
4,7-Dimethylphenanthroline	Nickel	8.44	8.20	8.40	25.04
	Cobalt	8.08	8.00	8.43	24.51
	Zinc	6.90	6.18	6.04	19.12
	Iron (II)	5.60*			23.05
	Copper	8.76	7.26	5.97	21.99

*Average of four determinations made spectrophotometrically.

this effect was not observed in distributions with the 3:7 mixed solvent, and most of the formation curves could be obtained with this solvent. The formation curve for nickel with this ligand is incomplete, and the value of K_1 given in Table III has been estimated on the assumption that the formation curve would continue parallel to that of the 5,6-dimethyl analogue.

A second difference is shown by cobalt; here oxidation has undoubtedly occurred with formation of a more stable cobalt (III) complex. This oxidation had been noted previously with the simpler phenanthrolines, but could be prevented by the addition of hydroxylamine (2). The steeper cobalt formation curves and the large values for β_3 in these cases suggest that very stable complexes with large values of K_3 have been formed in a manner similar to the iron (II) complexes with which they are isoelectronic. However, the results must be interpreted with some care in this case, since no proof of the reversibility of the reactions by which these postulated cobalt (III) complexes were formed can be given; it might be better to regard the values of β_3 etc. derived from these curves as "apparent" formation constants.

The results reported here, taken with those for 1,10-phenanthroline and its 5-methyl derivative, provide a good example of the correlation between the stability of metallic complexes and the proton affinity of the ligands. This is portrayed in Fig. 3 in which

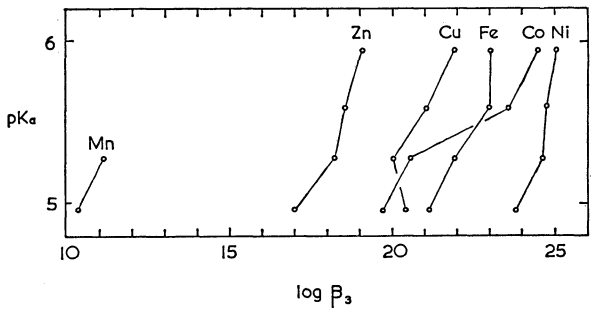

FIG. 3. Correlation between log β_3 of metallic complexes and pK_a of phenanthrolines. Data for orthophenanthroline from reference 2, for 5-methylphenanthroline from reference 3, for the dimethylphenanthrolines from this paper.

log β_3 for the indicated metallic complexes is compared with pK_a of the ligand. The exceptional behavior of the cobalt complexes noted in the previous paragraph is also

Can. J. Chem. Downloaded from www.nrcresearchpress.com by 210.87.254.6 on 09/05/12
For personal use only.

evident. A similar representation of log K_1 plotted against pK_a shows the same trend except that the relative positions of iron (II) and copper are different. As has been noted elsewhere (1, 12) the large β_3 of the iron (II) complexes resides mainly in the abnormally large K_3. Copper (II), on the other hand, shows a large K_1 (see the Irving–Williams order of stability) but this is not carried over into the β_3 owing to the reluctance on the part of copper to accept ligands beyond a coordination number of four.

ACKNOWLEDGMENTS

This investigation was supported by grants from the National Research Council of Canada, for which the authors record their appreciation. We also wish to thank Professor H. M. Irving of the University of Leeds for helpful discussions.

REFERENCES

1. C. V. BANKS and R. I. BYSTROFF. J. Am. Chem. Soc. **81**, 6153 (1959).
2. H. M. IRVING and D. H. MELLOR. J. Chem. Soc. 5222, 5237 (1962).
3. W. A. E. McBRYDE, D. A. BRISBIN, and H. M. IRVING. J. Chem. Soc. 5245 (1962).
4. H. M. IRVING and D. H. MELLOR. J. Chem. Soc. 3457 (1955).
5. H. M. IRVING, M. J. CABELL, and D. H. MELLOR. J. Chem. Soc. 3417 (1953).
6. T. S. LEE, I. M. KOLTHOFF, and D. L. LEUSSING. J. Am. Chem. Soc. **70**, 2348 (1948).
7. W. W. BRANDT and D. K. GULLSTROM. J. Am. Chem. Soc. **74**, 3532 (1952).
8. M. YASUDA, K. SONE, and K. YAMASAKI. J. Phys. Chem. **60**, 1667 (1956).
9. I. M. KOLTHOFF, D. L. LEUSSING, and T. S. LEE. J. Am. Chem. Soc. **73**, 390 (1951).
10. J. BJERRUM. Metal ammine formation in aqueous solution. P. Haase and Son, Copenhagen. 1941.
11. I. M. KOLTHOFF, D. L. LEUSSING, and T. S. LEE. J. Am. Chem. Soc. **72**, 2173 (1950).
12. H. M. IRVING and R. J. P. WILLIAMS. J. Chem. Soc. 3192 (1953).

Can. J. Chem. Downloaded from www.nrcresearchpress.com by 210.87.254.6 on 09/05/12
For personal use only.

Can. J. Chem. Downloaded from www.nrcresearchpress.com by 210.87.254.6 on 09/05/12
For personal use only.

THE ORIGIN OF CARBON ATOMS 4, 5, AND 6 OF RICININE[1]

J. M. Essery,[2] P. F. Juby,[2] Léo Marion, and E. Trumbull[3]
Division of Pure Chemistry, National Research Council, Ottawa, Canada

Received January 4, 1963

ABSTRACT

Degradations to isolate the carbon atoms at positions 4, 5, and 6 of the alkaloid ricinine from *Ricinus communis* L. are described. Tracer experiments with glycerol-1-^{14}C and glycerol-2-^{14}C suggest that glycerol or a closely related metabolic compound is a biosynthetic precursor of these carbon atoms.

Previous studies (1, 2) on the biosynthesis of ricinine (I) from *Ricinus communis* L. implicated succinic acid or a closely related four-carbon dicarboxylic acid found in the Krebs tricarboxylic acid cycle as the source of the carbon atoms at positions 2, 3, and 7. Also, the distribution of radioactivity in ricinine from feeding experiments with sodium acetate-1-^{14}C and sodium acetate-2-^{14}C was consistent with the initial formation of appropriately labelled succinic acid via the Krebs cycle.

The fact that carbon atoms 4, 5, and 6 were not significantly labelled by either acetate-^{14}C or succinic acid-^{14}C indicated that these three carbon atoms arose from a precursor or precursors not contained in the Krebs cycle and not derived under the experimental conditions used from the Krebs cycle. Consequently glycerol-1-^{14}C and glycerol-2-^{14}C were fed in separate experiments (1) to young *Ricinus* plants. Both precursors were incorporated into ricinine to almost the same extent as the acetate and succinic acid, but an appreciable proportion of the activity was concentrated on the carbon atoms of the methyl groups and nitrile group. Some of the glycerol may have been converted to acetate through glycolysis. Significant incorporation of activity into ricinine from labelled glycerol-^{14}C feeding experiments has been reported by other workers (3) but the location of the activity within the α-pyridone ring was not determined. Further progress was hampered by the lack of suitable degradative procedures for isolating the carbon atoms under study.

It is the object of this present paper to describe the individual isolations of carbon atoms 4, 5, and 6 of the ricinine molecule and to report and discuss the results obtained from the labelled acetate, succinic acid, and glycerol feeding experiments. A brief account of this work has already been reported (4).

Carbon 4 of ricinine (I) was isolated as the carbon of the carboxyl group of benzoic acid by the scheme outlined in Fig. 1. Ricinine was converted by hydrolysis followed by

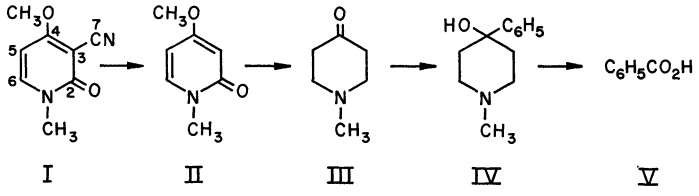

FIG. 1. Isolation of C-4 of ricinine.

[1]*Issued as N.R.C. No. 7269.*
[2]*National Research Council Postdoctoral Fellow.*
[3]*American Chemical Society Petroleum Research Fellow. Present address: Colgate University, Hamilton, N.Y.*

decarboxylation (5) to 4-methoxy-1-methyl-2-pyridone (II), which on treatment with lithium aluminum hydride followed by an acid work-up gave 1-methyl-4-piperidone (III). Reaction of this ketone with phenyllithium provided the known 4-hydroxy-1-methyl-4-phenylpiperidine (IV), which on oxidation with potassium permanganate gave benzoic acid (V), the carboxyl carbon of which originated at C-4 of ricinine.

Use was made again of the 'bromopicrin split' (2, 6) for the isolation of carbon 5 of ricinine. Electrophilic substitution of the nucleus of N-methyl-2-pyridones occurs in the 3- and 5-positions (7, 8). A methoxyl group at position 4 will activate position 3 for electrophilic substitution. A nitrile group at position 3 will deactivate position 6 for electrophilic substitution. Ricinine (I) readily underwent nitration to a mononitro derivative with the orientation of the incoming group being, necessarily, to the 5-position (Fig. 2). Treatment of the 5-nitroricinine (VI) with calcium hypobromite liberated carbon 5

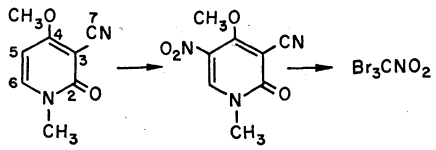

I VI VII

FIG. 2. Isolation of C-5 of ricinine

of ricinine as the carbon atom of tribromonitromethane (bromopicrin) (VII). The liquid bromopicrin was purified by gas–liquid chromatography.

A degradative procedure for the isolation of carbon atom 6 of ricinine has already been described by Tamir and Ginsburg (9). These authors claimed that ozonolysis of 4-methoxy-1-methyl-2-pyridone (II), followed by an oxidative decomposition of the resulting ozonides, gave methyl hydrogen oxalate, N-methyloxamic acid, and one equivalent of carbon dioxide. The carbon dioxide was assumed to have arisen from carbon 6 of ricinine. In our hands application of this degradative procedure gave initially between two and four equivalents of carbon dioxide. Part of the carbon dioxide obtained was shown to have arisen from attack of ozone upon the solvent used in the reaction. By employing techniques designed to eliminate this source of error, approximately one equivalent of carbon dioxide was eventually obtained from the pyridone. However, the activity at carbon 6 of ricinine from the succinic acid-2,3-^{14}C feeding experiment (1, 2) by this method was found to be 31% of the total activity of the ricinine, when 95.7% of the activity had already been accounted for (2) on carbons 2, 3, 7 and the methyl carbons.

In order to check the usefulness of this ozonolysis procedure for carbon 6, a sample of ricinine-6,7-^{14}C (VIII), equally labelled on each of the two carbon atoms, was synthesized by the route outlined in Fig. 3. The scheme is based on a synthesis of ricinine first described by Schroeter, Seidler, Sulzbacher, and Kanitz (10).

Removal of the nitrile group from this synthetic ricinine (VIII) gave 4-methoxyl-1-methyl-2-pyridone (II) specifically labelled at position 6. Ozonolysis of this pyridone with oxidative cleavage of the resulting ozonides gave approximately one equivalent of carbon dioxide, which was isolated as barium carbonate. Instead of the expected activity of 50% of the total activity of the parent ricinine, carbon 6 was experimentally found to account for only 1.8%. Clearly most of the carbon dioxide from this degradation comes from some source other than carbon 6, probably from carbon 2 or 3 if the result obtained

Can. J. Chem. Downloaded from www.nrcresearchpress.com by 210.87.254.6 on 09/05/12
For personal use only.

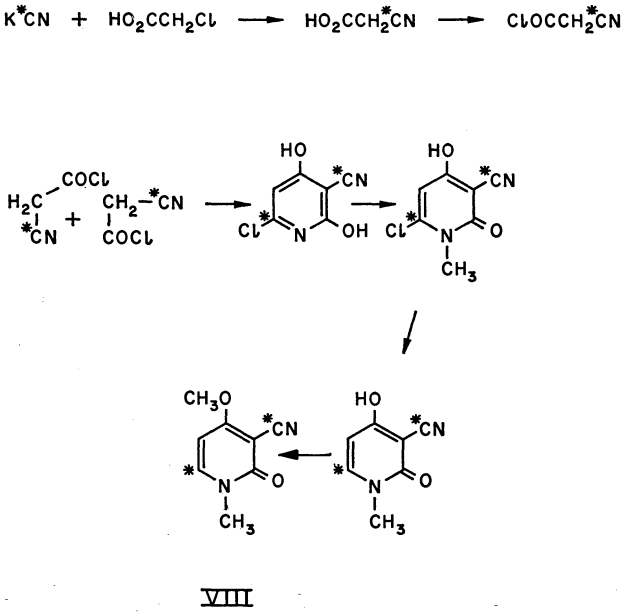

FIG. 3. Synthesis of ricinine-6,7-^{14}C. *C signifies ^{14}C.

from the ozonolysis degradation of ricinine from succinic acid-2,3-^{14}C is taken into account. More important, the degradative procedure must be rejected as a method of isolating carbon 6 of ricinine.

Carbon 6 was eventually isolated by the procedure outlined in Fig. 4 as formaldehyde

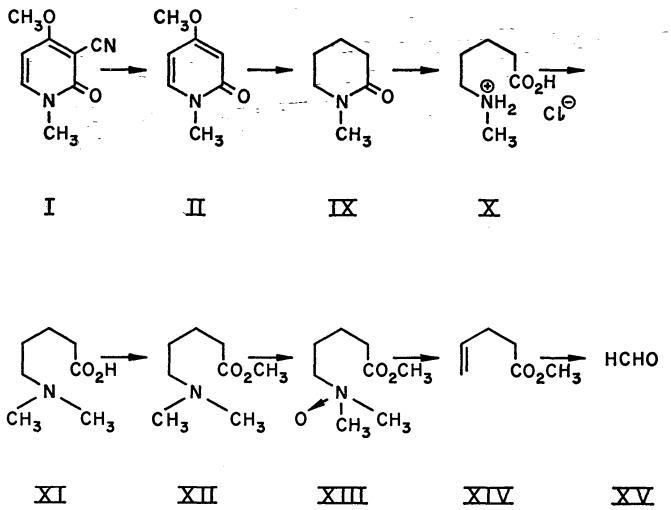

FIG. 4. Isolation of C-6 of ricinine.

characterized as its dimedone derivative. Conversion of ricinine (I) to 4-methoxy-1-methyl-2-pyridone (II) has been described above. In a previous paper (2) it was reported that the only product obtained from treatment of the pyridone (II) with hydrogen and

Can. J. Chem. Downloaded from www.nrcresearchpress.com by 210.87.254.6 on 09/05/12
For personal use only.

Adams' catalyst in methanol was 4-methoxy-1-methyl-2-piperidone. Subsequently it has been found impossible to repeat this result under the conditions stated. The main product now obtained, under similar conditions but using a fresh batch of catalyst, is 1-methyl-2-piperidone (IX) with only ca. 10% of the 4-methoxy-1-methyl-2-piperidone. By addition of a trace of hydrochloric acid to the reaction mixture, it is possible to obtain almost complete hydrogenolysis. The 1-methyl-2-piperidone was hydrolyzed with concentrated hydrochloric acid to the corresponding amino acid (X), which was readily converted to the dimethylamino derivative (XI) on treatment with formaldehyde, formic acid, and sodium formate. The order of addition of the N-methylation reagents to the free amino acid (X) was found to be important if rapid recyclization was not to occur. Esterification of XI with diazomethane gave methyl dimethylaminovalerate (XII). The amine (XII) was converted to its N-oxide (XIII) with 98% hydrogen peroxide. Pyrolysis of the N-oxide yielded the methyl ester of allylacetic acid (XIV), the identity of which was confirmed by comparison with a sample prepared by esterification of allylacetic acid (11) with diazomethane. The olefin was cleaved by the action of sodium periodate in the presence of a catalytic amount of osmium tetroxide, and the liberated formaldehyde (XV), containing carbon 6 of ricinine, was isolated as the dimedone derivative (12).

The degradative procedures described above were applied to samples of ricinine obtained from the acetate-2-^{14}C, succinic acid-2,3-^{14}C, glycerol-1-^{14}C, and glycerol-2-^{14}C feeding experiments (1). Samples of ricinine, benzoic acid, bromopicrin, and the dimedone derivative of formaldehyde were separately converted by combustion to carbon dioxide, which was collected in barium hydroxide solutions as barium carbonate. All radioactivity measurements were made on barium carbonate samples. The percentages of the incorporated activity located at carbon atoms 4, 5, and 6 for the various samples are recorded in Table I.

TABLE I

Location of radioactivity in ricinine

Precursor	Percentage of activity of ricinine		
	C-4	C-5	C-6
Acetate-2-^{14}C	0.0	0.3	*
Succinic acid-2,3-^{14}C	0.0	0.0	*
Glycerol-1-^{14}C	25.8	2.2	19.7
Glycerol-2-^{14}C	2.2	38.8	0.0

*Activity not determined.

As was to be expected, carbon atoms 4 and 5 from ricinine obtained from the acetate-2-^{14}C and succinic acid-2,3-^{14}C feeding experiments showed little or no activity, since in both cases nearly 100% of the total incorporated activity already had been accounted for (2). The activities at carbon 6 in these two samples were not determined due to insufficient material.

From the results reported previously for glycerol-1-^{14}C and glycerol-2-^{14}C (1) it was apparent that there was considerable breakdown of the glycerol molecule to simpler units prior to incorporation, since the nitrile, N-methyl, and O-methyl carbon atoms of both samples of ricinine were all significantly labelled. However, the fact that carbon 5 of ricinine from the glycerol-2-^{14}C feeding experiment holds an appreciable percentage of the total activity of the ricinine molecule, whilst very little activity is located at carbons 4 and 6, suggests that some of the glycerol was incorporated intact into the ricinine

Can. J. Chem. Downloaded from www.nrcresearchpress.com by 210.87.254.6 on 09/05/12
For personal use only.

molecule. The high activity at both carbons 4 and 6 and the low activity at carbon 5 after the feeding of glycerol-1-^{14}C lend support to this suggestion.

It is now proposed that carbon atoms 4, 5, and 6 of ricinine are derived from a three-carbon unit such as glycerol or a closely related metabolic compound. The slight inequality of activity at carbons 4 and 6 from the glycerol-1-^{14}C experiment points to the possibility that the actual precursor, unlike glycerol, is chemically non-symmetrical. If glycerol itself were the only source of this non-symmetrical intermediate, then the latter should be labelled equally at the terminal carbon atoms. However, with the rather long time lapse (3 days) between the feeding of the labelled glycerol and the harvesting of the plants, some of the actual non-symmetrical precursor could have been synthesized from the previously mentioned breakdown products of glycerol, with unequal labelling of the terminal carbons. In this connection further tracer experiments with labelled glycerol with a much shorter time interval between feeding and harvesting the plants are being carried out.

It has already been suggested (2) that carbon atoms 2 and 3 of the pyridine nucleus of nicotine are derived from the same source as carbon atoms 2 and 3 of the α-pyridone nucleus of ricinine. Recently Byerrum and his co-workers (13, 14) have reported the incorporation of activity derived from labelled glycerol into the pyridine ring of nicotine. Although only a small fraction of the activity (8%) was located at C-3 it could well be that at least part of the glycerol was incorporated intact into positions 4, 5, and 6 of the pyridine ring of the nicotine molecule. Hence it is possible that the carbon atoms of the α-pyridone ring of ricinine and the pyridine ring of nicotine are derived from the same basic units. This is not so surprising if it is remembered that nicotinic acid occupies an important position towards the end of the biosynthetic pathways of both molecules.

It should be noted that Ortega and Brown have proposed (15), although with little experimental proof, that resting cells of *Eschericia coli* synthesize nicotinic acid by an initial reaction between a three-carbon compound (either glycerol or a compound closely related to glycerol) and a four-carbon dicarboxylic acid.

Further studies are now required to determine more precisely the precursors of the carbon atoms of ricinine, and to determine the route by which the ring nitrogen atom (16) enters the molecule.

EXPERIMENTAL

Melting points were determined on a Kofler block and corrected. Radioactive samples were counted as thin layers on aluminum planchets in either a Radiation Counter Laboratories internal sample proportional counter or a Baird-Atomic end window proportional counter, as indicated in the text. Appropriate corrections were made for background count and sample self-absorption. Glycerol-1-^{14}C and glycerol-2-^{14}C were supplied by the California Corporation for Biochemical Research. Potassium cyanide-^{14}C was supplied by Merck, Sharp and Dohme of Canada Ltd.

Growth of Ricinus Plants and Administration of the Tracers

Plants of *R. communis* L. were grown and the tracers fed as described previously (1, 2). The glycerol-1-^{14}C (1.53 mg) in water (0.5 ml) was fed to 42 plants, and had a total activity of 2.22×10^8 d.p.m. The glycerol-2-^{14}C (2.13 mg) in water (0.8 ml) was fed to 50 plants, and had a total activity of 2.22×10^8 d.p.m.

Isolation of Ricinine

The ricinine was isolated and purified as described previously (1, 2).

Ricinine (418 mg), m.p. 202° (17), with radioactivity of 20,500 d.p.m./mg (Radiation Counter Laboratories instrument, previously reported (1) in c.p.m./mg) was obtained from the plants fed glycerol-1-^{14}C, which represents an incorporation of 3.9%.

Ricinine (470 mg), m.p. 202°, with radioactivity of 12,900 d.p.m./mg (Radiation Counter Laboratories instrument, previously reported (1) in c.p.m./mg) was obtained from the plants fed glycerol-2-^{14}C, which represents an incorporation of 2.7%.

Can. J. Chem. Downloaded from www.nrcresearchpress.com by 210.87.254.6 on 09/05/12
For personal use only.

Ricinine from Succinic Acid-2,3-^{14}C and Acetate-2-^{14}C Feeding Experiments

The same two samples of active ricinine which were used in the isolations of carbon atoms 2, 3, 7 and the N-methyl and O-methyl carbons (2) were also used in the isolations of the carbon atoms at positions 4 and 5, as described below.

Successful Degradation Procedures for Carbon Atoms 4, 5, and 6

The degradation of the ricinine from the glycerol-2-^{14}C feeding experiment will be taken as typical. The Baird-Atomic Counter was used in all the following experiments.

Carbon 4

The radioactive ricinine (I) (40 mg) was diluted with pure, inactive ricinine by a factor of approximately 30. The active ricinine was cocrystallized with the inactive sample. A small sample of the diluted ricinine was sublimed and then converted by combustion to carbon dioxide, which was collected in a barium hydroxide solution as barium carbonate. The barium carbonate had an activity of 36.5 d.p.m./mg.

4-Methoxy-1-methyl-2-pyridone (II)

The diluted ricinine (1.25 g) was hydrolyzed and decarboxylated (5) with 57% sulphuric acid solution to 4-methoxy-1-methyl-2-pyridone (820 mg). The product was purified by sublimation at 80° at 5×10^{-4} mm and had m.p. 114–116°.

1-Methyl-4-piperidone (III)

A solution of the pyridone (II) (820 mg) in hot, dry tetrahydrofuran (8 ml) was added, with stirring, to an excess of lithium aluminum hydride in dry ether (30 ml) and the mixture heated under reflux for 5½ hours. The excess lithium aluminum hydride was destroyed with water, and the complex decomposed with 10% hydrochloric acid. The mixture was shaken well and the aqueous layer separated, made alkaline, and extracted with chloroform. The solvent was removed from the extract, and 1-methyl-4-piperidone (116 mg) was distilled from the residue as a colorless oil, air-bath temperature 55–60° at 12 mm (18). An inactive sample of the piperidone (III), prepared from inactive ricinine as above, formed a hydrochloride derivative (18), m.p. 164–166°, and was identified with an authentic sample of 1-methyl-4-piperidone by comparison of infrared and n.m.r. spectra.

4-Hydroxy-1-methyl-4-phenylpiperidine (IV)

A solution of the ketone (III) (116 mg) in dry ether (10 ml) was added, with cooling and shaking, to a suspension of an excess of phenyllithium in ether (15 ml). The reaction mixture was stirred at room temperature for 2 hours, then poured onto ice and 10% hydrochloric acid. After shaking well, the aqueous layer was separated, made alkaline with sodium hydroxide, and extracted with ether. Evaporation of the dried extracts left an oily solid which was purified by sublimation at 80–85° at 5×10^{-4} mm to afford 4-hydroxy-1-methyl-4-phenylpiperidine (71 mg) as colorless prisms, m.p. 115–116° (19) undepressed on admixture with an authentic synthetic sample.

Benzoic Acid (V)

A solution of the carbinol (IV) (71 mg) in water (25 ml) was heated under reflux with an excess of potassium permanganate (0.5 g) for 2½ hours. The excess permanganate was destroyed by the addition of ethanol and the precipitated manganese dioxide removed by filtration. The filtrate was acidified and extracted with ether. Evaporation of the dried ether extracts left a residue which was purified by repeated sublimation at 100–105° at 12 mm to yield benzoic acid (10 mg), m.p. 121–122° with no depression on admixture with a pure authentic sample. The benzoic acid was converted to carbon dioxide by combustion, and the carbon dioxide collected in a barium hydroxide solution as barium carbonate which had a specific activity of 0.9 d.p.m./mg.

Similar Degradations

The activity at carbon 4 of ricinine from the glycerol-1-^{14}C, succinic acid-2,3-^{14}C, and acetate-2-^{14}C feeding experiments was determined likewise. The results are recorded in Table II.

TABLE II

Precursor	Activity of $BaCO_3$ from diluted ricinine, d.p.m./mg	Activity of $BaCO_3$ from benzoic acid, d.p.m./mg
Glycerol-1-^{14}C	77.3	10.2*
Succinic acid-2,3-^{14}C	24.0	0.0
Acetate-2-^{14}C	142.0	0.0

*In the degradation involving the glycerol-1-^{14}C experiment, it was necessary to dilute the intermediate, radioactive 4-hydroxy-1-methyl-4-phenylpiperidine with a pure synthetic and inactive sample, by a factor of 31.3/14.0. This factor has to be taken into account in calculating the percentage of activity (25.8, Table I) at C-4 in the ricinine derived from glycerol-1-^{14}C.

Can. J. Chem. Downloaded from www.nrcresearchpress.com by 210.87.254.6 on 09/05/12
For personal use only.

Carbon 5

The radioactive ricinine (20 mg) from the glycerol-2-^{14}C feeding experiment was diluted with inactive ricinine by a factor of approximately 18, as described for carbon 4. The barium carbonate obtained by combustion of the diluted ricinine had an activity of 62.5 d.p.m./mg.

5-Nitroricinine (VI)

The diluted ricinine (300 mg) was dissolved in a solution of concentrated sulphuric acid (5 ml) and 90% nitric acid (1.0 ml) and the solution allowed to stand at room temperature for 2 hours. The solution was poured onto ice, and sodium hydroxide added until the solution was just acid. Chloroform extraction of the aqueous solution yielded 5-nitroricinine (275 mg), which was recrystallized from methanol as pale yellow needles, m.p. 163–164°. Found: C, 45.94; H, 3.39; N, 20.19. Calc. for $C_8H_7O_4N_3$: C, 45.94; H, 3.37; N, 20.09%.

Tribromonitromethane (Bromopicrin) (VII)

The bromopicrin was produced from the 5-nitroricinine (275 mg) by treatment with calcium hydroxide and bromine as described for the preparation of bromopicrin from 4-methoxy-1-methyl-3-nitro-2-pyridone (2). The purified bromopicrin was identified by comparison of its infrared spectrum with that of an authentic sample prepared from picric acid (20). Gas–liquid chromatography (2) of a small sample of the purified material showed only one component with a retention time almost identical with that obtained for authentic bromopicrin. The pure bromopicrin was converted by combustion to carbon dioxide, which was collected in a barium hydroxide solution as barium carbonate. The barium carbonate had an activity of 194.0 d.p.m./mg.

Similar Degradations

The activity at carbon 5 of ricinine from the glycerol-1-^{14}C, succinic acid-2,3-^{14}C, and acetate-2-^{14}C feeding experiments was determined likewise. The results are recorded in Table III.

TABLE III

Precursor	Activity of $BaCO_3$ from diluted ricinine, d.p.m./mg	Activity of $BaCO_3$ from bromopicrin, d.p.m./mg
Glycerol-1-^{14}C	84.0	15.0
Succinic acid-2,3-^{14}C	29.5	0.5
Acetate-2-^{14}C	229.0	4.65

Carbon 6

The radioactive ricinine (60 mg) from the glycerol-2-^{14}C feeding experiment was diluted with inactive ricinine by a factor of approximately 13, as described for carbon 4. The barium carbonate from the diluted ricinine had an activity of 84.0 d.p.m./mg.

4-Methoxy-1-methyl-2-pyridone (II)

The diluted ricinine (750 mg) was hydrolyzed and decarboxylated (5) with 57% sulphuric acid solution to 4-methoxy-1-methyl-2-pyridone (536 mg). The product was purified by sublimation at 80° at 5×10^{-4} mm and had m.p. 114–116.°

1-Methyl-2-piperidone (IX)

A solution of the pyridone (II) (536 mg) in methanol containing drops of concentrated hydrochloric acid was shaken in an atmosphere of hydrogen with Adams' catalyst at room temperature and under pressure of a small head of mercury, until no further uptake of hydrogen was observed. The catalyst and methanol were removed and the residue dissolved in water which was made basic with sodium hydroxide. Chloroform extracts of the aqueous solution yielded an oil which was distilled over a short path at 12 mm. 1-Methyl-2-piperidone (IX) (360 mg) distilled at an air-bath temperature of 100–105° (21). An inactive sample prepared from inactive ricinine as above formed a mercuric chloride derivative, m.p. 117–120° (21), and was identified with an authentic sample by comparison of their infrared spectra.

5-Methylaminovaleric Acid Hydrochloride (X)

A solution of 1-methyl-2-piperidone (IX) (360 mg) in concentrated hydrochloric acid (6 ml) was heated under reflux for 55 hours. The solvent was removed by heating on a steam bath at 25 mm. A small quantity of methanol was added to the residue and removed in the same way. The residue was heated with a lamp while under vacuum on the steam bath, and 5-methylaminovaleric acid hydrochloride (515 mg) crystallized on cooling as clusters of needles (21). The salt is hygroscopic.

Methyl 5-Dimethylaminovalerate (XII)

The 5-methylaminovaleric acid hydrochloride was dissolved in 98% formic acid (1.2 ml) and 37% formaldehyde (0.5 ml). Sodium formate (197 mg) was added and the mixture heated on the steam bath for 3 hours. Very little undissolved material remained at this point. The solvents were removed by distillation at 25 mm on the steam bath and a solution of hydrogen chloride in anhydrous methanol added to the residue.

Can. J. Chem. Downloaded from www.nrcresearchpress.com by 210.87.254.6 on 09/05/12
For personal use only.

A white crystalline precipitate formed. The methanol and excess acid were removed by heating at 25 mm and were flushed out by adding fresh methanol to the residue and distilling again. The residue was treated successively with three portions of methanol (5 ml). Each portion was decanted from an insoluble white salt. The combined methanolic extracts were treated with a solution of diazomethane in ether, when an additional quantity of the white solid precipitated. Excess diazomethane was destroyed with acetic acid, the solution was decanted from the solid, and the solvents removed at atmospheric pressure on the steam bath. The residue was distilled at 25 mm, air-bath temperature 90–130°, and was identified as methyl 5-dimethylaminovalerate (247 mg) by comparison of its infrared spectrum with that of an authentic sample prepared by the methods described above from inactive synthetic 1-methyl-2-pyridine. The authentic methyl 5-dimethylaminovalerate had b.p. 90° at 20 mm (22) and formed a methiodide, m.p. 140–141°. Found for the methiodide: C, 35.89; H, 6.81; N, 4.77; I, 42.02. Calc. for $C_9H_{20}O_2NI$: C, 35.88; H, 6.69; N, 4.65; I, 42.13%. In several preparations, the yield of the ester was 50–55%.

Methyl Allylacetate (XIV)

The methyl 5-dimethylaminovalerate (XII) (247 mg) was dissolved in anhydrous methanol (1.0 ml), cooled in water at 23°, and treated with 98% hydrogen peroxide (ca. 150 mg). The reaction mixture was kept at 22–24° until a negative test with phenolphthalein was obtained (5 hours). The excess peroxide was destroyed by the addition of a small quantity of platinum black. The initial reaction was violent and the solution was cooled in water at 18–20°. The solution was allowed to stand overnight at room temperature, when a negative test with moistened lead sulphide paper showed no peroxide. The solution was filtered to remove platinum and the methanol removed at 45° at 25 mm. The residue was extracted with chloroform (2 ml). The chloroform was removed at 25 mm whilst the heating bath temperature was gradually raised to 50°. The temperature was gradually raised again until a product distilled at 130–155°. The product, which was collected in a receiver cooled in a dry ice – butyl cellosolve bath, was treated with carbon disulphide (0.5 ml) and water (1.0 ml). The carbon disulphide was removed and the aqueous layer re-extracted four times with fresh solvent. The combined carbon disulphide extracts were dried (sodium sulphate). An infrared spectrum of this solution (3.0 ml) showed the presence of methyl allylacetate (ca. 48 mg) by comparison with an infrared spectrum of authentic inactive methyl allylacetate. The latter, b.p. 127–128° at 760 mm, was synthesized by alkylating malonic ester with allyl bromide, hydrolysis, decarboxylation of the product to allylacetic acid (11), and treatment of the allylacetic acid with diazomethane. Found: C, 63.3; H, 8.86. Calc. for $C_6H_{10}O_2$: C, 63.13; H, 8.83%. Methyl iodide (0.2 ml) was added to the solution of methyl allylacetate from the degradation of the ricinine, and the mixture allowed to stand at 5° for 30 minutes. The small amount of methyl 5-dimethylaminovalerate methiodide which precipitated was removed by filtration of the mixture through a short column of anhydrous magnesium sulphate. The carbon disulphide was removed from the filtrate by distillation. The residue was treated with dry pentane, and the solution decanted from a small amount of solid residue. Removal of the pentane left a liquid residue (59 mg) consisting mainly of methyl allylacetate. It was identified with the synthetic sample by comparison of their infrared absorption spectra.

Formaldehyde (XV)

The sample of methyl allylacetate prepared above was dissolved in dioxane (2 ml) containing osmium tetroxide (11 mg). Water (3.0 ml) was added and the solution stirred at 27° for several minutes. Sodium metaperiodate (189 mg) was added in one portion, and the slurry stirred for 90 minutes. To this slurry was added water (10 ml) and concentrated sulphuric acid (3 ml). The mixture was heated at 30° at 30 mm, when an orange-yellow distillate was obtained and discarded. The mixture was then heated with continual stirring to 60° at 30 mm until approximately 10 ml of distillate had been collected. This distillate was brought to pH 4.5 with sodium acetate and acetic acid, then warmed on a steam bath and treated with 5,5-dimethyl-1,3-cyclohexandione (dimedone reagent). After 5 minutes the mixture was cooled in ice and the solid collected, washed well with water, and dried briefly at 105°. The grey material (50 mg) was purified by sublimation at 130–135° at 0.01 mm to give a colorless cubic crystalline product, m.p. 191–192° undepressed on admixture with a dimedone derivative prepared from authentic formaldehyde (12). The formaldehyde dimedone derivative was converted by combustion to carbon dioxide, which was collected in barium hydroxide solution as barium carbonate. The barium carbonate was inactive.

Carbon 6 from Glycerol-1-^{14}C

The radioactive ricinine from the glycerol-1-^{14}C feeding experiment was diluted with inactive ricinine by a factor of approximately 20, as described for carbon 4. The barium carbonate from the diluted ricinine had an activity of 75.6 d.p.m./mg. The degradation of the diluted ricinine was carried out as described above. The barium carbonate from the dimedone derivative of formaldehyde had an activity of 7.0 d.p.m./mg.

Synthesis of Ricinine-6,7-^{14}C

Cyanoacetyl Chloride-^{14}CN

Potassium cyanide-^{14}C (3.2 mg of total activity 5.9×10^8 d.p.m.) was diluted with inactive potassium cyanide (20 g). The diluted $K^{14}CN$ was allowed to react (23) with chloracetic acid to give cyanoacetic acid-^{14}CN. Treatment of the cyanoacetic acid with phosphorus pentachloride (23) gave cyanoacetyl chloride-^{14}CN.

Can. J. Chem. Downloaded from www.nrcresearchpress.com by 210.87.254.6 on 09/05/12
For personal use only.

Ricinine-6,7-^{14}C (VIII)

The labelled ricinine (3 g) was prepared from the dimerization of the cyanoacetyl chloride-^{14}CN by a method similar to that described for a synthesis of inactive ricinine from inactive cyanoacetyl chloride by Schroeter *et al.* (10). The ricinine-6,7-^{14}C was purified by alternate crystallization from methanol and by sublimation at 180° at 5×10^{-4} mm.

Ozonolysis Degradative Procedure for Carbon 6

Active ricinine from the succinic acid-2,3-^{14}C feeding experiment (1, 2) and the synthetic ricinine-6,7-^{14}C were separately degraded by a method similar to that described by Tamir and Ginsburg (9).

Ricinine from Succinic Acid-2,3-^{14}C

The active ricinine was diluted with inactive ricinine by a factor of approximately 20 as described previously. A sample of barium carbonate from the diluted ricinine had an activity of 29.5 d.p.m./mg.

4-Methoxy-1-methyl-2-pyridone (II)

The diluted ricinine from above was converted to 4-methoxy-1-methyl-2-pyridone as described previously.

Ozonolysis of 4-Methoxy-1-methyl-2-pyridone

Ozonized oxygen was passed through a solution of the pyridone (II) (110 mg) in methylene chloride (7 ml), cooled by a solid carbon dioxide – acetone bath, until the solution turned blue. Pure oxygen was passed through until the solution was colorless. The solution, in an atmosphere of oxygen, was allowed to warm to room temperature, and oxygen bubbled through the solution for a further 20 minutes. Hydrogen peroxide (30%, 3 ml) was added to the tube containing the reaction solution, and the tube connected to a trap containing a barium hydroxide solution. Pure oxygen was passed through the system until no further precipitate was obtained in the trap (3–4 hours). The precipitated barium carbonate (ca. 90% of one equivalent based on the pyridone) had an activity of 73.0 d.p.m./mg.

A blank experiment, run as above but without the pyridone, gave a negligible precipitate. A precipitate was continuously formed when a blank experiment was run with the barium hydroxide trap connected to the reaction vessel while the ozonized oxygen was being passed through the reaction vessel. Experiments with inactive pyridone gave between two and four equivalents of barium carbonate after 3–4 hours when the barium hydroxide trap was connected during the passage of the ozonized oxygen.

Ricinine-6,7-^{14}C (VIII)

A small sample of the synthetic ricinine was converted by combustion to carbon dioxide, which was collected in a barium hydroxide solution as barium carbonate. The barium carbonate had an activity of 2670 d.p.m./mg. The synthetic ricinine was treated as described above for ricinine from the succinic acid-2,3-^{14}C experiments. The barium carbonate isolated from the ozonolysis reaction had an activity of 384.0 d.p.m./mg.

ACKNOWLEDGMENTS

The authors are indebted to Dr. L. C. Leitch and Mr. N. Kraut for the synthesis of ricinine-6,7-^{14}C. Thanks are also due to Mr. H. Seguin for the microanalysis and sample combustions.

REFERENCES

1. P. F. Juby and L. Marion. Biochem. Biophys. Res. Commun. **5**, 461 (1961).
2. P. F. Juby and L. Marion. Can. J. Chem. **41**, 117 (1963).
3. G. R. Waller and L. M. Henderson. Biochem. Biophys. Res. Commun. **5**, 5 (1961).
4. J. Essery, P. F. Juby, L. Marion, and E. Trumbull. J. Am. Chem. Soc. **84**, 4597 (1962).
5. E. Winterstein, J. Keller, and A. B. Weinhagen. Arch. Pharm. **255**, 513 (1917).
6. A. J. Birch, C. J. Moye, R. W. Rickards, and Z. Vanek. J. Chem. Soc. 3586 (1962).
7. H. Decker and A. Kaufmann. J. Prakt. Chem. **84**, 425 (1911).
8. O. Fischer and M. Chur. J. Prakt. Chem. **93**, 363 (1916).
9. H. Tamir and D. Ginsburg. J. Chem. Soc. 2921 (1959).
10. G. Schroeter, C. Seidler, M. Sulzbacher, and R. Kanitz. Ber. **65**, 432 (1932).
11. R. P. Linstead and H. N. Rydon. J. Chem. Soc. 580 (1933).
12. R. E. Reeves. J. Am. Chem. Soc. **63**, 1476 (1941).
13. T. Griffith, K. P. Hellman, and R. U. Byerrum. Biochemistry, **1**, 336 (1962).
14. T. Griffith and R. U. Byerrum. Federation Proc. **21**, 398 (1962).
15. M. J. Ortega and G. M. Brown. J. Biol. Chem. **235**, 2939 (1960).
16. G. R. Waller and L. M. Henderson. Abstracts of Papers, American Chemical Society Meeting. Sept. 1961. p. 30Q.
17. E. C. Taylor and A. J. Crovetti. J. Am. Chem. Soc. **78**, 214 (1956).
18. R. E. Lyle, R. E. Adel, and G. G. Lyle. J. Org. Chem. **24**, 342 (1959).
19. Aktieselskabet 'Ferrosan.' Dan. 60,592 (1943); Chem. Abstr. **40**, 4086^5 (1946).
20. J. Baddiley, G. Ehrensvärd, E. Klein, L. Reio, and E. Saluste. J. Biol. Chem. **183**, 777 (1950).
21. C. Räth. Ann. **489**, 107 (1931).
22. R. Willstatter and W. Kahn. Ber. **37**, 1853 (1904).
23. G. Schroeter and C. Seidler. J. Prakt. Chem. **105**, 165 (1922).

Can. J. Chem. Downloaded from www.nrcresearchpress.com by 210.87.254.6 on 09/05/12
For personal use only.

THE REACTION OF CHLOROSULPHATE ESTERS OF SUGARS WITH PYRIDINE

H. J. Jennings and J. K. N. Jones
Department of Chemistry, Queen's University, Kingston, Ontario
Received November 26, 1962

ABSTRACT

Hexoside and hexitol derivatives with vicinal chlorosulphate ester groups in different configurations were treated with pyridine. The corresponding cyclic sulphate esters were produced except in the case of the diaxial configuration, which gave an anyhdro derivative. The axial–equatorial configuration gave in addition a keto-deoxy compound. The structures of the cyclic sulphate esters and of other reaction products are proposed and their mode of formation is discussed.

Can. J. Chem. Downloaded from www.nrcresearchpress.com by 210.87.254.42 on 09/05/12
For personal use only.

INTRODUCTION

Sulphuryl chloride is the only reagent which has been reported to yield cyclic sulphate ester derivatives of carbohydrates (1–5) and although other methods of forming diol cyclic sulphates are known they do not seem to be applicable in this field (6). Helferich and co-workers first isolated cyclic sulphate derivatives of methyl α- and methyl β-D-glucopyranoside, of mannitol, and of trehalose (1–3) and this work has been extended more recently (4, 5). The cyclic sulphate ester groups were shown to bridge adjacent hydroxyl groups on C_2 and C_3 of the glycopyranosides and possibly across C_3 and C_4 of the D-mannitol derivative (4, 5). Comparison of the reaction conditions which yielded the cyclic sulphate esters (1, 4) with more recent work which described the preparation of 2,3-dichlorosulphate ester derivatives of reducing sugars (7) showed that the ratio of pyridine to sulphuryl chloride had been approximately halved in the latter series of reactions. Therefore the effect of excess pyridine on the chlorosulphate esters of model compounds of different configurations was investigated, with particular emphasis on the 2,3-dichlorosulphate esters. This led to a new synthesis of cyclic sulphate esters in sterically favorable cases.

DISCUSSION

The reactions of pyridine on the 2,3-dichlorosulphate esters in the equatorial–equatorial configuration were carried out using derivatives of methyl α-D-glucopyranoside. Methyl α-D-glucopyranoside when treated with sulphuryl chloride gave a syrupy product which was dechlorosulphated (sodium iodide) to yield crystalline methyl 4,6-dichloro-4,6-dideoxy-α-D-galactopyranoside (4). This evidence indicated that the initial reaction product was methyl 4,6-dichloro-4,6-dideoxy-α-D-galactopyranoside 2,3-dichlorosulphate. The syrupy dichlorosulphate ester when reacted with pyridine gave methyl 4,6-dichloro-4,6-dideoxy-α-D-galactopyranoside 2,3-cyclic sulphate (4). Methyl 4,6-*O*-benzylidene-α-D-glucopyranoside when similarly treated gave a crystalline compound which was identified as the 2,3-dichlorosulphate ester (I) by isolation of the initial reactant after dechlorosulphation with sodium iodide. Treatment of the dichlorosulphate ester with pyridine in the cold yielded crystalline methyl 4,6-*O*-benzylidene-α-D-glucopyranoside 2,3-cyclic sulphate (4). When this reaction was carried out at 60° no cyclic sulphate derivative was formed and methyl α-D-glucopyranoside and its 4,6-*O*-benzylidene derivative were isolated.

The reaction of methanolic sodium methoxide on the 2,3-dichlorosulphate ester produced no cyclic sulphate ester and a poor yield of methyl 4,6-*O*-benzylidene-2,3-anhydro-α-D-alloside (9) was isolated. This evidence indicates that the basicity of the reagent is an important factor in the formation of the cyclic sulphate ester. The reactions probably proceed by the basic hydrolysis of the chlorosulphate ester on C_2 of I as in the case of the formation of the 2,3-anhydro derivatives from the ditosylate esters (9, 11), and the mechanism can be represented by the partial formulae (I, I*a*, and I*b*) (cf. ref. 10).

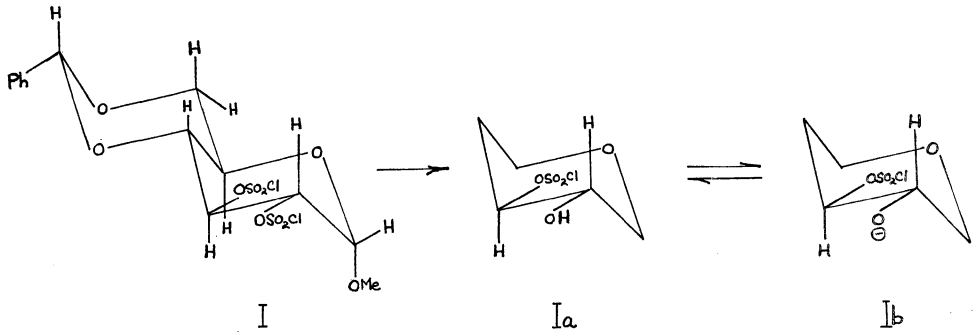

I Ia Ib

Sodium methoxide produced the 2,3-anhydro derivative due to the large concentration of oxide ion (I*b*), whereas in the less basic reagent (pyridine) the concentration of I*b* would be much smaller, enabling the formation of the cyclic sulphate from I*a* to take place.

The reaction of pyridine on the 2,3-dichlorosulphate ester in the axial–equatorial configuration was carried out using the 2,3-dichlorosulphate derivative of methyl 4,6-*O*-ethylidene-α-D-mannopyranoside (II), the structure of which was proved by the isolation and identification of the following reaction products. The dichlorosulphate ester was treated with pyridine to give two crystalline products identified as methyl 4,6-*O*-ethylidene-α-D-mannopyranoside 2,3-cyclic sulphate, and methyl 4,6-*O*-ethylidene-2-deoxy-3-keto-α-D-*erythro*-hexoside. The structure of the cyclic sulphate derivative was indicated by its analysis and desulphation followed by hydrolysis (4) to give syrupy D-mannose (identified as the crystalline phenylhydrazone).

The structure of the 2-deoxy-3-keto compound was confirmed by sodium borohydride reduction of the 3-keto group and hydrolysis of the reduced product to give 2-deoxy-D-*ribo*-hexose (13). This reduction appears to be stereospecific in absolute ethanol and practically so in ethanol–water (1:1). Although 2-deoxy-D-glucose was detected when ethanol–water (1:1) was used it seems that solvent effects of the type reported by Eliel (14) are insignificant and that the main factor is steric hindrance of the reducing species. Models of the 2-deoxy-3-keto compound (II*d*) indicate possible interaction between the axial glycosidic group on C_1 of the molecule and the axial approach of the borohydride complex (14) needed for reduction of the keto group on C_3 to form an equatorial hydroxyl group. The bulky group would therefore be expected to approach from the less hindered equatorial side of the molecule, producing a hydroxyl group in the axial configuration (15).

The reaction of the axial–equatorial vicinal chlorosulphate ester groups with pyridine to give the cyclic sulphate and 2-deoxy-3-keto derivatives can be explained by the same mechanism as proposed previously and is represented by the partial formulae II, II*a*, and

Can. J. Chem. Downloaded from www.nrcresearchpress.com by 210.87.254.42 on 09/05/12
For personal use only.

II*b*. The formation of the 2-deoxy-3-keto compound using pyridine indicates that hydrolysis of the chlorosulphate ester group on C_2 of II must take place slowly for diaxial

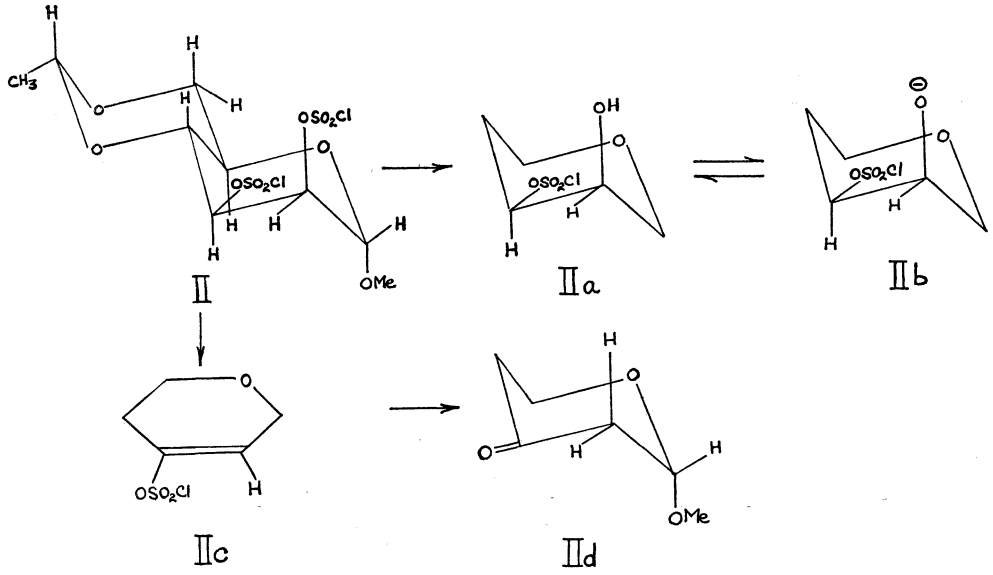

elimination (16), with the subsequent formation of the transient compound (II*c*). This compound (II*c*) in the basic medium would be rapidly converted to the 2-deoxy-3-keto compound (II*d*) via an intermediate enolate. Sodium methoxide produced no keto-deoxy compound because the hydrolysis of II to II*a* was rapid. The formation of the cyclic sulphate derivative probably takes place via II*a* using pyridine and II*b* using sodium methoxide, as the formation of a 2,3-anhydro compound from II*b* is sterically unfavorable.

The reaction of pyridine on the 2,3-dichlorosulphate esters in the axial–axial configuration was carried out using the 4,6-*O*-benzylidene derivative of methyl α-D-altroside. Methyl 4,6-*O*-benzylidene-α-D-altropyranoside was treated with sulphuryl chloride to give a crystalline dichlorosulphate ester derivative (III), which decomposed rapidly and could not be analyzed. When a chloroform solution of the compound was allowed to evaporate to dryness another crystalline derivative was obtained which had lost the benzylidene group and which was indicated by analysis to be methyl α-D-altropyranoside 2,3-dichlorosulphate. The removal of the benzylidene group was probably facilitated by the presence of traces of acid caused by the partial decomposition of the chlorosulphate ester groups. The 4,6-*O*-benzylidene dichlorosulphate ester was treated immediately with pyridine to give crystalline methyl 4,6-*O*-benzylidene 2,3-anhydro-α-D-mannopyranoside (11).

The formation of the 2,3-anhydro derivative from III using pyridine indicates that the small concentration of III*b* is in a sterically more favorable position to react than III*a*. Models show that the distance between the groups on C_2 and C_3 of III*a* is much greater than for the equatorial–equatorial and axial–equatorial configurations, which gave cyclic sulphate derivatives with ease. Also the trans–axial configuration of III*b* is the most preferred configuration for nucleophilic attack of the oxide ion on C_3 to give the 2,3-anhydro derivative.

The reactions of pyridine on vicinal dichlorosulphate esters in the open chain form were carried out on derivatives of D-mannitol. D-Mannitol when treated with sulphuryl

Can. J. Chem. Downloaded from www.nrcresearchpress.com by 210.87.254.42 on 09/05/12
For personal use only.

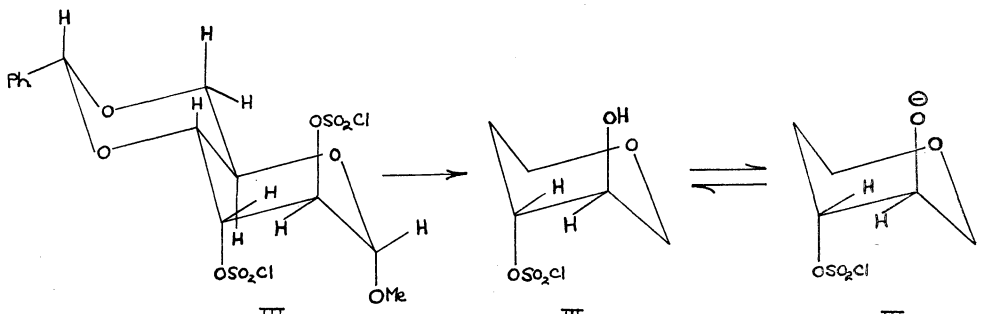

III IIIa IIIb

chloride gave a crystalline tetrachlorotetradeoxy dichlorosulphate ester (IV). The ester (IV) when treated with pyridine gave a crystalline derivative which was shown by analysis to be a tetrachlorotetradeoxy cyclic sulphate ester (2, 4). This evidence indicates that the chlorosulphate groups in the original compound (IV) must have been vicinal. There is also some evidence that they are situated on C_3 and on C_4, as 1,2:5,6-di-*O*-isopropylidene mannitol gave an unstable dichlorosulphate ester which with pyridine yielded a crystalline cyclic sulphate derivative.

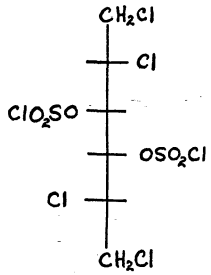

IV

Because of the free rotation of the bond between C_3 and C_4 of IV it is possible for the two chlorosulphate groups to approach each other closer than is possible for structures I, II, and III. It might therefore be expected that the reaction of pyridine on the vicinal dichlorosulphate ester would form the cyclic sulphate derivative with ease. The fact that sodium iodide also produced the cyclic sulphate derivative is unusual as the same treatment of the 2,3-dichlorosulphate esters in the equatorial–equatorial configuration (7) has so far resulted in dechlorosulphation to give the 2,3-dihydroxy compound. A possible explanation for this could be that the proximity of the two groups is favorable for cyclic sulphate formation in this case.

1,2:5,6-Di-*O*-isopropylidene-D-glucose when treated with sulphuryl chloride gave a crystalline monochlorosulphate ester as shown by analysis and dechlorosulphation (sodium iodide) to form the starting product. The monochlorosulphate ester when treated with pyridine also gave 1,2:5,6-di-*O*-isopropylidene-D-glucose, which indicates that pyridine can hydrolyze the chlorosulphate ester.

EXPERIMENTAL

Optical rotations were measured at 21±3°. Melting points were determined on a Kofler hot stage and were uncorrected. All solutions were concentrated under reduced pressure below 50°. Paper chromatography

Can. J. Chem. Downloaded from www.nrcresearchpress.com by 210.87.254.42 on 09/05/12
For personal use only.

was carried out by the descending method on Whatman No. 1 filter paper using the following solvent systems (v/v): (*a*) butan-1-ol, ethanol, water (3:1:1), (*b*) ethyl acetate, acetic acid, formic acid, water (18:3:1:4), and (*c*) 2-butanone, acetic acid, saturated aqueous boric acid (9:1:1). Reducing sugars were located on chromatograms by *p*-anisidine hydrochloride (17) or alkaline silver nitrate (18) spray reagents and keto-sugars by orcinol – trichloracetic acid spray reagent (19); the rates of movement are quoted relative to that of D-xylose (R_x). Paper electrophoresis was performed using Whatman 3MM filter paper impregnated with 0.05 *M* borate buffer and the sugars were detected on the electrophoretograms by *p*-anisidine hydrochloride spray reagent (17). The rates of movement of compounds on paper electrophoretograms are given relative to that of D-glucose (M_g). Infrared spectra were measured in chloroform solution (unless otherwise stated) using a Perkin–Elmer Model 21 spectrophotometer.

The reactions with sulphuryl chloride and the isolation of the chlorosulphate esters were carried out by the method described in a previous communication ("general method") (7), except that in most cases the reaction mixture was homogeneous.

Methyl 4,6-Dichloro-4,6-dideoxy-α-D-galactopyranoside 2,3-Dichlorosulphate

Methyl-α-D-glucoside (10 g) was treated with sulphuryl chloride (26 ml) and pyridine (40 ml) in chloroform solution (7). Concentration of the chloroform extracts gave a yellow syrup (12 g, 55%) which had $[\alpha]_D$ +115° (*c*, 1.2 in chloroform) and gave a positive test with aniline–pyridine (7). The syrup showed strong absorption frequencies in the infrared spectrum at 1427 cm^{-1} and 1195 cm^{-1}.

Dechlorosulphation of Methyl 4,6-Dichloro-4,6-dideoxy-α-D-galactopyranoside 2,3-Dichlorosulphate

The above syrup (10 g) was dissolved in methanol (150 ml), and a solution of sodium iodide (8 g dissolved in 20 ml of methanol–water (1:1)) was added, producing an immediate formation of iodine and the evolution of sulphur dioxide. The solution was neutralized with barium carbonate, filtered, and concentrated to a semicrystalline mass, which was dissolved in water. Following the addition of a few crystals of sodium thiosulphate to remove traces of iodine, the aqueous solution was continuously extracted with chloroform. Concentration of the chloroform solution gave a crystalline mass which was recrystallized from chloroform – light petroleum (b.p. 40–60°) to give colorless needle-shaped crystals (4.5 g, 82%) of $[\alpha]_D$ +179° (*c*, 2.0 in water) and m.p. 158°, undepressed on admixture with authentic methyl 4,6-dichloro-4,6-dideoxy-α-D-galactopyranoside (4).

Methyl 4,6-Dichloro-4,6-dideoxy-α-D-galactopyranoside 2,3-Cyclic Sulphate

The syrupy 2,3-dichlorosulphate (9.7 g) was dissolved in redistilled pyridine (40 ml) and the solution was kept at 60° for 8 hours. The resultant dark brown solution, which still gave a positive test with aniline–pyridine (7), was poured into water and extracted (×2) with chloroform. The chloroform solution was washed with dilute sulphuric acid (5%), saturated sodium bicarbonate solution, and distilled water before being dried over anhydrous sodium sulphate. The chloroform solution was treated with charcoal, filtered, and concentrated to a pale yellow syrup (5 g, 76%). The syrup crystallized on standing, and the crude crystals gave a negative test with aniline–pyridine (7) and showed absorption frequency in the infrared spectrum at 1412 cm^{-1}. No strong absorption was detected in the 1200 cm^{-1} region as with the chlorosulphate esters (7). Recrystallization from ether – light petroleum (b.p. 40–60°) gave large needles (3 g, 46%) of $[\alpha]_D$ +139° (*c*, 1.75 in methanol) and m.p. 103–104°, undepressed on admixture with authentic methyl 4,6-dichloro-4,6-dideoxy-α-D-galactopyranoside 2,3-sulphate (4).

Methyl 4,6-O-Benzylidene-α-D-glucopyranoside 2,3-Dichlorosulphate

Methyl 4,6-*O*-benzylidene-α-D-glucoside (8) (5 g) was treated with sulphuryl chloride (13 ml) and pyridine (20 ml) in chloroform solution (7). Concentration of the chloroform extracts gave a syrup (8 g, 94%) which crystallized immediately. Recrystallization from chloroform – light petroleum (b.p. 60–80°) gave large colorless crystals of m.p. 133–136° (decomp.) and $[\alpha]_D$ +41.5° (*c*, 1.5 in chloroform). The crystals gave a positive test with aniline–pyridine (7) and showed strong absorption frequencies in the infrared spectrum at 1415 cm^{-1} and 1190 cm^{-1}. Analysis: Calc. for $C_{14}H_{16}O_{10}Cl_2S_2$: C, 35.1; H, 3.3; Cl, 14.8; S, 13.4. Found: C, 35.0; H, 3.3; Cl, 14.5; S, 13.2.

Dechlorosulphation of Methyl 4,6-O-Benzylidene-α-D-glucopyranoside 2,3-Dichlorosulphate

The crystals (3 g) were dechlorosulphated by the method described previously in the dechlorosulphation of methyl 4,6-dichloro-4,6-dideoxy-α-D-galactoside 2,3-dichlorosulphate except that barium carbonate (8 g) was stirred into the methanol solution before the addition of the sodium iodide (3 g). This kept the solution neutral and prevented the removal of the benzylidene group. The solution was filtered, concentrated to small volume, and, on the addition of water, the reaction product was precipitated. The precipitate was filtered from the solution and recrystallized from acetone–water to give crystals of m.p. 165°, undepressed on admixture with authentic methyl 4,6-*O*-benzylidene-α-D-glucopyranoside (8).

Methyl 4,6-O-Benzylidene-α-D-glucopyranoside 2,3-Cyclic Sulphate

The crystals of the dichlorosulphate ester above (5 g) were dissolved in pyridine and kept at 0° for 8 hours, after which time the solution still gave a positive test with aniline–pyridine (7). The product was isolated as described previously for the 4,6-dichlorodideoxy cyclic sulphate derivative to yield a syrup which

Can. J. Chem. Downloaded from www.nrcresearchpress.com by 210.87.254.42 on 09/05/12
For personal use only.

crystallized on standing and gave a negative test with aniline–pyridine (7). Recrystallization from chloroform – *n*-hexane gave needles (2 g, 72%) which had m.p. 103–106° (decomp.) and $[\alpha]_D$ +69° (*c*, 2.28 in chloroform). The crystals showed a strong absorption frequency in the infrared spectrum at 1405 cm^{-1} and a weak absorption frequency at 1203 cm^{-1}. Analysis: Calc. for $C_{14}H_{16}O_8S$: C, 48.8; H, 4.7; S, 9.3. Found: C, 48.8; H, 4.7; S, 9.4. This compound was isolated previously by Bragg *et al.* (4).

When the above reaction was carried out at 60° as with the 4,6-dichlorodideoxy derivative, methyl 4,6-*O*-benzylidene-α-D-glucopyranoside and methyl α-D-glucoside were isolated and characterized as the only products.

Methyl 4,6-O-Benzylidene-2,3-anhydro-α-D-alloside

Methyl 4,6-*O*-benzylidene-α-D-glucoside 2,3-dichlorosulphate (0.25 g) was treated with 4.8 moles of sodium methoxide (1 ml of 2.5 *N* solution in methanol) by the method of Richtmyer and Hudson (20). It was observed that the chloroform solution gave a negative test with aniline–pyridine (7) immediately after the addition of the sodium methoxide. Therefore the chloroform solution was washed with distilled water, dried (anhydrous $NaSO_4$), and concentrated to a crystalline solid (0.032 g, 23.2%). Recrystallization from methanol gave needles of m.p. 200–201°, undepressed on admixture with authentic methyl 4,6-*O*-benzylidene-2,3-anhydro-α-D-alloside (9).

Methyl 4,6-O-Ethylidene-α-D-mannopyranoside 2,3-Dichlorosulphate

Methyl 4,6-*O*-ethylidene-α-D-mannoside (12) (4.2 g) was treated with sulphuryl chloride (10 ml) and redistilled pyridine (16 ml) in chloroform solution (7). Concentration of the chloroform extracts gave a brown syrup which was redissolved in chloroform and treated with charcoal. Filtration and concentration of the solution gave a yellow syrup which slowly crystallized (7.2 g, 90%). Recrystallization from light petroleum (b.p. 60–80°) gave colorless crystals (5 g, 63%) of m.p. 94–96° and $[\alpha]_D$ −10° (*c*, 1.8 in chloroform). The crystals gave a positive test with aniline–pyridine (7) and showed strong absorption frequencies in the infrared spectrum at 1417 cm^{-1} and 1200 cm^{-1}. Analysis: Calc. $C_9H_{14}O_{10}Cl_2S_2$: C, 25.9; H, 3.4; Cl, 17.0; S, 15.4. Found: C, 25.7; H, 3.3; Cl, 17.0; S, 15.2.

Methyl 4,6-O-Ethylidene-α-D-mannopyranoside 2,3-Cyclic Sulphate

The crystals above (4 g) were treated with redistilled pyridine (40 ml) by the same method as used previously with methyl 4,6-dichloro-4,6-dideoxy-α-D-galactopyranoside 2,3-dichlorosulphate. After treatment with charcoal the chloroform solution was filtered and concentrated to a light yellow syrup (1.5 g) which partially crystallized and gave a negative test with aniline–pyridine (7). The strong absorption frequencies shown by the product in the infrared spectrum at 1740 cm^{-1} and 1405 cm^{-1} indicated that it was a mixture containing a keto compound and a cyclic sulphate derivative. The presence of the keto compound was further substantiated by chromatographic analysis of the mixture in solvents (*a*) and (*b*), which showed the presence of one component at R_x 4.0 with *p*-anisidine hydrochloride (brown) and orcinol – trichloracetic acid (green) sprays. The cyclic sulphate ester was obtained by repeated crystallizations from methanol as colorless plates (0.35 g, 12%) of m.p. 163–164° (slow decomp.) and $[\alpha]_D$ −23° (*c*, 1.2 in chloroform). Analysis: Calc. for $C_9H_{14}O_8S$: C, 38.3; H, 5.0; S, 11.4. Found: C, 38.4; H, 5.5; S, 11.3.

Methyl 4,6-O-Ethylidene-2-deoxy-3-keto-α-D-erythro-hexoside

The mother liquors from the reaction above were concentrated to a syrup and dissolved in a small quantity of ether from which solution crystallization occurred. The crystals were recrystallized from ether – *n*-hexane, giving colorless needles (0.25 g, 14.5%) of m.p. 103–104° and $[\alpha]_D$ +155° (*c*, 1.23 in methanol). Analysis: Calc. for $C_9H_{14}O_5$: C, 53.4; H, 6.9. Found: C, 53.0; H, 6.6.

Reaction of Methyl 4,6-O-Ethylidene-α-D-mannopyranoside 2,3-Dichlorosulphate with Sodium Methoxide

The crystals of the 2,3-dichlorosulphate ester (2 g) were dissolved in methanol (25 ml) and treated with 3.8 moles of sodium methoxide (64 ml of 0.2 *N* solution in methanol). Both the solutions were previously cooled in an ice bath before mixing and the reaction mixture was kept at 0° for 16 hours. Excess sodium methoxide was decomposed by the addition of solid carbon dioxide and the methanol solution was concentrated to a syrup, which was dissolved in chloroform. The chloroform solution was washed with dilute sulphuric acid (10%) in order to disperse a gel formation and then with saturated sodium bicarbonate solution and distilled water. The chloroform solution was dried (anhydrous Na_2SO_4) and concentrated to a syrup (0.9 g) which gave a negative test with orcinol – trichloracetic acid (19) and showed the absence of carbonyl absorption in the infrared spectrum. Crystallization of the syrup occurred from ether – light petroleum (b.p. 40–60°) and two recrystallizations from methanol gave colorless plates (0.05 g) of m.p. 162–163° (decomp.) and $[\alpha]_D$ −26.5° (*c*, 1.25 in chloroform). Mixed melting point with the cyclic sulphate derivative obtained previously by the reaction of pyridine on the dichlorosulphate ester of methyl 4,6-*O*-ethylidene-α-D-mannoside was 159–164° (decomp.). The two cyclic sulphate esters also gave identical infrared spectrums (0.8% in potassium bromide).

Desulphation of Methyl 4,6-O-Ethylidene-α-D-mannopyranoside 2,3-Cyclic Sulphate

The crystals of the cyclic sulphate ester (0.35 g) were desulphated by the method of Bragg *et al.* (4) using methanolic ammonia and sulphuric acid to yield a syrup (0.15 g). Chromatographic examination of the

Can. J. Chem. Downloaded from www.nrcresearchpress.com by 210.87.254.42 on 09/05/12
For personal use only.

Can. J. Chem. Downloaded from www.nrcresearchpress.com by 210.87.254.42 on 09/05/12
For personal use only.

syrup in solvents (*a*) and (*b*) indicated that it was a reducing sugar which co-chromatographed with D-mannose. The phenylhydrazone derivative of the syrup had m.p. 186–187° (decomp.), undepressed on admixture with authentic D-mannose phenylhydrazone.

*Reduction of Methyl 4,6-O-Ethylidene-2-deoxy-3-keto-α-*D-erythro-*hexoside with Sodium Borohydride*

The crystals of the 2-deoxy-3-keto compound (0.35 g) were dissolved in ice-cold absolute ethanol (20 ml). Sodium borohydride (0.35 g) was added at 0° and the solution was stirred continuously until it gave a negative test with orcinol – trichloracetic acid (19) (40 hours). Acetone was then added to the solution to destroy the excess sodium borohydride. The solution was deionized (Amberlite IR.120 (H form) ion exchange resin) and the eluate was concentrated to a syrup, which was co-distilled with methanol to constant weight in order to remove boric acid. The resultant pale yellow syrup (0.33 g), which could not be obtained crystalline, was dissolved in 0.2 *N* sulphuric acid and the solution was heated at 60° for 14 hours. The solution was neutralized with barium carbonate, filtered, and passed through Amberlite IR.120 (H form) and Duolite A.4 (OH form) ion exchange resins and concentrated to a syrup (0.27 g, 88%) which crystallized on standing. Chromatographic analysis of the crystals in solvent (*c*) indicated one component at R_x 1.7 which chromatographed with 2-deoxy-D-allose (2-deoxy-D-*ribo*-hexose). Electrophoresis showed one component at M_g 0.64 which ran at the same speed as 2-deoxy-D-allose and a faint unidentified spot at M_g 0.77. Recrystallization from ethanol–ether gave colorless needles of $[\alpha]_D$ +57° (*c*, 0.76 in water) and m.p. 138°, undepressed on admixture with authentic 2-deoxy-D-allose (13).

The reduction was repeated using ethanol–water (1:1) as the solvent and crystalline 2-deoxy-D-allose was again isolated as the main product. In this case chromatographic analysis in solvent (*c*) did indicate a faint spot at R_x 1.5 which was found to chromatograph with authentic 2-deoxy-D-glucose, and this was confirmed by electrophoresis as it showed a trace of material at M_g 0.33 which ran at the same speed as 2-deoxy-D-glucose. However, 2-deoxy-D-glucose was not present in sufficient quantities to allow its isolation.

*Reaction of Methyl 4,6-O-Ethylidene-α-*D-*mannopyranoside 2,3-Cyclic Sulphate with Pyridine*

The crystals of the cyclic sulphate were treated with redistilled pyridine at 60° by the same method previously used with the dichlorosulphate ester of methyl 4,6-*O*-ethylidene-α-D-mannopyranoside (12). The pyridine solution gave a negative test with orcinol – trichloracetic acid spray (19) and the chloroform-soluble crystalline product was recrystallized from methanol and gave colorless plates of m.p. 163°, undepressed on admixture with the starting material.

*Methyl 4,6-O-Benzylidene-α-*D-*altropyranoside 2,3-Dichlorosulphate*

Methyl 4,6-*O*-benzylidene-α-D-altroside (20) (1.2 g) was treated with sulphuryl chloride (3.2 ml) and redistilled pyridine (5 ml) in chloroform solution (7). Concentration of the chloroform gave a syrup which rapidly crystallized. Recrystallization from chloroform – light petroleum (b.p. 30–60°) gave colorless needles (1.65 g, 82%) of m.p. 105–108° (slow decomp.) and $[\alpha]_D$ +25.5° (*c*, 1.2 in chloroform). The crystals gave a positive test with aniline–pyridine (7) and showed strong absorption frequencies in the infrared spectrum at 1410 cm^{-1}, 1192 cm^{-1} (chlorosulphate ester), 3010 cm^{-1}, and 1605 cm^{-1} (aromatic) and no hydroxyl absorption. The substance began to decompose rapidly and it was therefore quickly dissolved in chloroform. A fraction (A) of the chloroform solution was kept and the remainder was concentrated to a crystalline solid (B) and was treated with pyridine.

*Methyl α-*D-*Altroside 2,3-Dichlorosulphate*

The chloroform was allowed to evaporate slowly from fraction A, leaving a comparatively stable crystalline compound. Recrystallization from chloroform–ether gave colorless needles of the 2,3-dichlorosulphate of m.p. 120–122° (decomp.) and $[\alpha]_D$ +44° (*c*, 1.09 in dioxane). The crystals showed strong absorption frequencies at 3550 cm^{-1}, 3315 cm^{-1} (hydroxyl), 1410 cm^{-1}, and 1192 cm^{-1} (chlorosulphate ester) and no aromatic absorption in the infrared spectrum. Analysis: Calc. for $C_7H_{12}O_{10}Cl_2S_2$: C, 21.5; H, 3.0; Cl, 18.2; S, 16.4. Found: C, 21.3; H. 3.0; Cl, 18.5; S, 16.2.

*Reaction of Methyl 4,6-O-Benzylidene-α-*D-*altropyranoside 2,3-Dichlorosulphate with Pyridine*

The crystalline mass (B) from above (1 g) was dissolved in pyridine and left at 0° for 16 hours. The chloroform-soluble component was isolated as described in previous reactions with pyridine, and gave a negative test with aniline–pyridine (7). The solution was concentrated to a crystalline mass which was recrystallized from methanol–water to give needles (0.33 g, 60%) of m.p. 146° and $[\alpha]_D$ 107° (*c*, 0.98 in chloroform). Analysis: Calc. for $C_{14}H_{16}O_5$: C, 63.6; H, 6.1. Found: C, 63.5; H, 5.9. The physical constants and the analysis are consistent with those of methyl 4,6-*O*-benzylidene-2,3-anhydro-α-D-mannopyranoside (11). Chromatographic analysis of the methanol–water mother liquors in solvents (*a*) and (*b*) showed the presence of a component R_x 3.7 which gave a faint green color with orcinol – trichloracetic acid (19). The infrared spectrum of the residue from the mother liquors also showed a weak absorption frequency at 1700 cm^{-1} indicating the presence of a ketonic compound. However, it was not present in sufficient quantities for isolation.

Tetrachlorotetradeoxyhexitol Dichlorosulphate

D-Mannitol (10 g) was treated with sulphuryl chloride (26 ml) and pyridine (40 ml) in chloroform solution

(7). The chloroform extract was treated with charcoal, filtered, and concentrated to a yellow syrup, which slowly crystallized (16.7 g, 67%). Recrystallization from chloroform – light petroleum (b.p. 40–60°) gave colorless crystals of the dichlorosulphate derivative of m.p. 134° and $[\alpha]_D$ +41° (*c*, 1.07 in chloroform). Analysis: Calc. for $C_6H_8O_6Cl_6S_2$: C, 15.9; H, 1.8; Cl, 47.0; S, 14.1. Found: C, 15.9; H, 1.8; Cl, 47.8; S, 14.2.

Tetrachlorotetradeoxyhexitol Cyclic Sulphate

The crystalline hexitol derivative (3 g) was dissolved in pyridine (26 ml) and allowed to stand at ambient temperature for 24 hours. The chloroform-soluble product was isolated from the reaction mixture as described in previous reactions with pyridine. The chloroform extract was concentrated to a syrup (1.7 g, 80%) which crystallized on standing. Two recrystallizations from chloroform – light petroleum (b.p. 40–60°) gave yellow plates (0.5 g, 23%) of the cyclic sulphate derivative of m.p. 105° and $[\alpha]_D$ +104° (*c*, 1.0 in methanol). Analysis: Calc. for $C_6H_8O_4Cl_4S$: C, 22.6; H, 2.5; Cl, 44.7. Found: C, 22.6; H, 2.4; Cl, 44.8. The infrared spectrum of the compound showed a strong absorption frequency at 1410 cm^{-1} and a weak one at 1197 cm^{-1} (cyclic sulphate ester), and the physical constants and analysis indicate that it is identical with the compound isolated by Helferich *et al.* (2).

An attempt was made to dechlorosulphate the tetrachlorotetradeoxyhexitol dichlorosulphate (12 g) with sodium iodide (5 g) by the method used previously in the dechlorosulphation of methyl 4,6-*O*-benzylidene-α-D-glucopyranoside 2,3-dichlorosulphate. The resultant chloroform solution was treated with charcoal, filtered, and concentrated to a syrup (4.2 g, 50%) which crystallized on standing. Recrystallization from ether – light petroleum (b.p. 40–60°) gave pale yellow plates of $[\alpha]_D$ +103° (*c*, 1.06 in methanol) and m.p. 105°, undepressed on admixture with the tetrachloro cyclic sulphate ester derivative obtained above.

1,2:5,6-Di-O-isopropylidene-D-mannitol 3,4-Cyclic Sulphate

1,2:5,6-Di-*O*-isopropylidene-D-mannitol (21) (6.5 g) was treated with sulphuryl chloride (13 ml) and pyridine (26 ml) in chloroform solution (7). The chloroform extract was concentrated to a syrup (10 g, 82%) which gave a positive test with aniline–pyridine (7) and which began to decompose rapidly. The syrup was dissolved in pyridine (40 ml) and left at ambient temperature for 8 hours and the chloroform-soluble product was isolated as described in previous reactions with pyridine. The resultant chloroform solution was concentrated to a syrup (3.5 g, 48%) which crystallized on standing. Successive recrystallizations from ether, methanol, and light petroleum (b.p. 30–60°) gave long colorless needles of m.p. 114–118° and $[\alpha]_D$ +41° (*c*, 0.6 in chloroform). Analysis: Calc. for $C_{12}H_{20}O_8S$: C, 44.4; H, 6.2; S, 9.9. Found: C, 44.6; H, 6.1; S, 9.8.

1,2:5,6 Di-O-isopropylidene-D-glucose 3-Chlorosulphate

Diacetone glucose (10 g) (22) was treated with sulphuryl chloride (26 ml) and pyridine (40 ml) in chloroform solution (7). Concentration of the chloroform extract gave a syrup which crystallized immediately and recrystallization from light petroleum (b.p. 60–80°) gave colorless needles (10 g, 72%) which had m.p. 92° and $[\alpha]_D$ −40° (*c*, 1.36 in chloroform). Analysis: Calc. for $C_{12}H_{29}O_8ClS$: C, 40.2; H, 5.3; Cl, 9.9; S, 8.9. Found: C, 40.2; H, 5.7; Cl, 9.9; S, 8.9. It was found to decompose rapidly in the atmosphere but could be kept for a longer period of time under vacuum over phosphoric oxide.

Dechlorosulphation of 1,2:5,6-Di-O-isopropylidene-D-glucose 3-Chlorosulphate

The crystals above (2 g) were dechlorosulphated using sodium iodide (2 g) as described previously for the dechlorosulphation of methyl 4,6-*O*-benzylidene-α-D-glucopyranoside 2,3-dichlorosulphate. The barium carbonate was filtered from the methanol solution and the filtrate was concentrated to a syrup, which was dissolved in water and extracted with ether. Concentration of the ethereal extract gave a crystalline mass, which was recrystallized from light petroleum (b.p. 40–60°) to give needles (0.6 g, 41%) of m.p. 107–108°, undepressed on admixture with authentic 1,2:5,6 di-*O*-isopropylidene-D-glucose (22).

When the monochlorosulphate ester of di-*O*-isopropylidene-D-glucose was dissolved in pyridine and the solution was kept at 0° for 8 hours, di-*O*-isopropylidene-D-glucose was isolated in good yield (melting point undepressed on admixture with an authentic sample).

ACKNOWLEDGMENTS

The authors wish to thank the National Research Council (N.R.C. T-19) and the Ontario Research Foundation for grants which made this work possible. They also thank Dr. T. Reichstein for a gift of 2-deoxy-D-*ribo*-hexose (2-deoxy-D-allose) and Dr. E. Buncel for helpful discussion on the reaction mechanisms.

REFERENCES

1. B. Helferich. Ber. **54,** 1082 (1921).
2. B. Helferich, A. Lowa, W. Nippe, and H. Riedel. Ber. **56,** 1083 (1923).
3. B. Helferich, G. Sproek, and E. Besler. Ber. **58,** 886 (1925).
4. P. D. Bragg, J. K. N. Jones, and J. C. Turner. Can. J. Chem. **37,** 1412 (1959).
5. J. K. N. Jones, M. B. Perry, and J. C. Turner. Can. J. Chem. **38,** 1122 (1960).

Can. J. Chem. Downloaded from www.nrcresearchpress.com by 210.87.254.42 on 09/05/12
For personal use only.

6. J. S. BRIMACOMBE, A. B. FOSTER, E. B. HANCOCK, W. G. OVEREND, and M. STACEY. J. Chem. Soc. 201 (1960).
7. H. J. JENNINGS and J. K. N. JONES. Can. J. Chem. **40,** 1408 (1962).
8. K. FREUDENBERG, H. TOEPFFER, and C. ANDERSON. Ber. **61,** 1758 (1928).
9. G. J. ROBERTSON and C. F. GRIFFITH. J. Chem. Soc. 1193 (1935).
10. S. PEAT. Advan. Carbohydrate Chem. **2,** 37 (1946).
11. G. J. ROBERTSON and W. WHITEHEAD. J. Chem. Soc. 319 (1940).
12. G. O. ASPINALL and G. ZWEIFEL. J. Chem. Soc. 2271 (1957).
13. R. JEANLOZ, D. A. PRINS, and T. REICHSTEIN. Experimenta, **1,** 336 (1945).
14. H. HAUBENSTOCK and E. L. ELIEL. J. Am. Chem. Soc. **84,** 2368 (1962).
15. O. THEANDER. Acta Chem. Scand. **12,** 1883 (1958).
16. D. H. R. BARTON and W. J. ROSENFELDER. J. Chem. Soc. 1048 (1951) and previous papers.
17. L. HOUGH, J. K. N. JONES, and W. H. WADMAN. J. Chem. Soc. 1702 (1950).
18. W. E. TREVELYAN, D. P. PROCTOR, and J. S. HARRISON. Nature, **166,** 444 (1950).
19. R. KLEVSTRAND and A. NORDAL. Acta Chem. Scand. **4,** 1320 (1950).
20. N. K. RICHTMYER and C. S. HUDSON. J. Am. Chem. Soc. **63,** 1727 (1941).
21. E. BAER. J. Am. Chem. Soc. **67,** 338 (1945).
22. H. VAN GRUNENBERG, C. BREDT, and W. FREUDENBERG. J. Am. Chem. Soc. **60,** 1507 (1938).

Can. J. Chem. Downloaded from www.nrcresearchpress.com by 210.87.254.42 on 09/05/12
For personal use only.

THE MECHANISMS OF PERMANGANATE OXIDATION

VII. THE OXIDATION OF FLUORAL HYDRATE[1, 2]

ROSS STEWART AND MICHAEL M. MOCEK[3]
Department of Chemistry, University of British Columbia, Vancouver, British Columbia
Received December 26, 1962

ABSTRACT

The kinetics of the permanganate oxidation of fluoral hydrate have been examined over a very wide range of acidities. In the region between pH 2 and pH 8 the reaction is extremely slow but as the basicity is increased the reaction rate rises and can be correlated with the increasing concentration of the anions $CF_3—\underset{|}{\overset{O^-}{C}}HOH$ and $CF_3CHO_2^-$. The latter is oxidized extremely rapidly. The mechanism is discussed in terms of hydride ion or hydrogen atom transfer from the anions to permanganate. Large isotope effects are observed in the oxidation of $CF_3CD(OH)_2$.

In strong acid the oxidation rate rises again and this is interpreted in terms of a reaction between neutral fluoral hydrate and neutral permanganic acid. The acidity constant for the latter has been determined.

Previous work on the mechanism of the permanganate oxidation of alcohols gave strong indication that the reactive species were the alkoxide ions and that the rate-controlling step was a hydride transfer from alkoxide ion to permanganate ion (1, 2). In order to investigate this type of reaction more closely we have examined the permanganate oxidation of fluoral hydrate to trifluoroacetic acid:

$$CF_3CH(OH)_2 \xrightarrow{Mn^{VII}} CF_3CO_2H.$$

This is a useful model system since the first ionization occurs in only mildly basic solution and the effect on the reaction rate of the substrate's charge can be conveniently determined.

EXPERIMENTAL

Materials

Fluoral hydrate and its deuterio derivative were prepared by the reduction of trifluoroacetic acid by lithium aluminum hydride and deuteride essentially by the procedure of Braid, Iserson, and Lawlor (3). The white solid materials which were obtained were found to be not monomeric and the details of the structure proof of these compounds are presented elsewhere (4, 5). In aqueous solution it is clear that fluoral hydrate exists as the monomer, however.

Kinetic Methods

Both titration and spectrophotometric methods were used and these have been previously described (1, 6). The molar ratio of permanganate to reductant used was 2:1 above pH 12 and 2:3 below pH 11 because of the different stoichiometries. Typical rate plots are shown in Fig. 1.

In the experiments in sulphuric acid solution complications arose because of the decomposition of the permanganate and because of the heat of mixing of the reacting solutions. Blank experiments helped correct for the first problem and the following procedure for the second. The acid solution was momentarily cooled in ice and the aqueous permanganate solution was added. The substrate was then added and the volume of the solution adjusted quickly to the mark with sulphuric acid of the appropriate concentration. Since the substrate did not mix immediately with the remainder of the solution the reaction could be conveniently started by agitating the mixture. Since the temperature of the reaction mixture was slightly below the temperature of the run the heat of mixing could be used to bring the temperature close to the desired value.

[1]*From part of the thesis presented by M. M. M. in partial fulfillment of the requirements for the Ph.D. degree, 1962.*
[2]*For the previous paper in the series see R. Stewart and R. Van der Linden, Can. J. Chem.,* ***38****, 2237 (1960).*
[3]*Present address: Cyanamid of Canada Ltd., Niagara Falls, Ontario.*

Can. J. Chem. Downloaded from www.nrcresearchpress.com by 210.87.254.40 on 09/05/12
For personal use only.

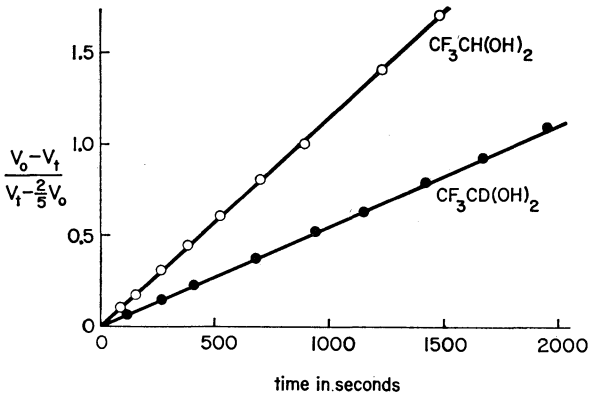

FIG. 1. Rate plots for the permanganate oxidation of fluoral hydrate and fluoral-1-*d* hydrate at pH 10.20. (Multiply units on ordinate by 2 and on abscissa by 5 for the latter.) $T = 25°$.

The solution was then thermostated. With practice it was found that the initial temperature could be brought to within a degree of the desired reaction temperature.

Acidity Constant of Fluoral Hydrate

The method which was employed makes use of the glass electrode and was similar to that previously described (7). The results of pK_a measurements at different ionic strengths are shown in Table I. The

TABLE I

Acidity constants of fluoral hydrate and fluoral-1-*d* hydrate in water at 25°

	$CF_3CH(OH)_2$		$CF_3CD(OH)_2$	
Ionic strength	$K\times10^{11}$	pK	$K\times10^{11}$	pK
0.01	6.17	10.21	6.03	10.22
0.05	6.46	10.19		
1.00	9.78	10.01	9.33	10.03

difference in the acidity of the protio and deuterio compounds is within experimental error (±0.02 pK units) but suggests that the deuterio acid may be slightly weaker than the protio acid. This would be in the same direction as that found by Halevi for carboxylic acids (8).

The enthalpy of ionization for the protio compound was measured by the same means and found to be approximately 6.2 kcal mole^{-1}. This is somewhat higher than the value for aliphatic acids (9, 10) but is in accord with the findings of other investigators (11, 12, 13).

Acidity Constant for Permanganic Acid

This was determined spectrophotometrically in sulphuric acid essentially as previously described (14) except that the substrate was added as the salt ($KMnO_4$) in aqueous solution. The absorption measurements for permanganate ion were made at 525 mμ and for permanganic acid at 458 mμ, near the absorption maxima. Symons has previously determined the pK_a to be −2.25 in aqueous perchloric acid (15).

The plot of optical densities (at 458 and 525 mμ) versus the H_- function showed, except for one point, the behavior of typical ionization curves (Fig. 2). The pK_a was calculated from the data at 525 and 458 mμ and then by modified Davis-Geissman method (14), using optical data at both wavelengths (Fig. 3). Since the plot of log $\{(\epsilon_{B^-}-\epsilon_{\lambda 525})/(\epsilon_{\lambda 525}-\epsilon_{BH})\}$ versus H_- did not show a slope of unity, the logarithms of the extinction coefficients were also plotted against the H_0 and H_R (J_0) functions in order to determine whether the dependence on the H_- function is real. It was found that the slope was essentially the same when H_0 or H_- function was used. This is not surprising, since both functions are almost parallel in the region studied. The slope, using H_R function was, however, much less than unity. The optical data used in the calculations are shown in Table II and the pK_a's summarized in Table III. The pK_a calculated with the aid of the H_R function was rejected on the basis of the small slope. The pK_a calculated with the H_- function appears to be the most satisfactory. The low slope (using data at 525 mμ) is perhaps due to interference of the ionization (16),

$$HMnO_4 + H^+ \rightleftharpoons MnO_3^+ + H_2O.$$

Can. J. Chem. Downloaded from www.nrcresearchpress.com by 210.87.254.40 on 09/05/12
For personal use only.

TABLE II

Spectroscopic data for ionization of permanganic acid

% H_2SO_4	Optical density at 525 mμ	Extinction coefficient at 525 mμ	Optical density at 458 mμ	Extinction coefficient at 458 mμ
Neutral solution	0.761	2370	0.099	308
41.5	0.740	2310	0.102	310
52.2	0.630	1965	0.107	331
57.6	0.515	1603	0.123	383
62.9	0.362	1178	0.160	499
67.5	0.212	660	0.186	579
72.3	0.142	443	0.199	620
82.2	0.060	187	0.199	620
97.0	0.041	128	0.158	493

NOTE: $[MnO_4^-] = 0.000321\ M$ (in water). Values obtained in 97.0% H_2SO_4 were not used in calculation of the pK_a. Measurements made in 1-cm cells. Spectrum of MnO_4^- remains unchanged from aqueous solutions up to 30% H_2SO_4.

TABLE III

Summary of pK_a's of permanganic acid evaluated with aid of H_0, H_-, and H_R (J_0) functions*

Wavelength (mμ)	$-pK_a$	Slope	Acidity function used in evaluation of pK_a
525	5.10	0.68	H_-
458	5.11	1.06	H_-
525	4.57	0.65	H_0
458	4.61	1.09	H_0
525	9.15	0.3	H_R
458	9.26	0.5	H_R
Evaluation of pK_a using modified Davis-Geissman method			
	5.10	0.71	H_-
	4.57	0.71	H_0
	9.17	0.32	H_R

*See R. H. Boyd, J. Am. Chem. Soc., **83**, 4288 (1961), and N. C. Deno, H. E. Berkheimer, W. L. Evans, and H. J. Peterson, J. Am. Chem. Soc., **81**, 2344 (1959).

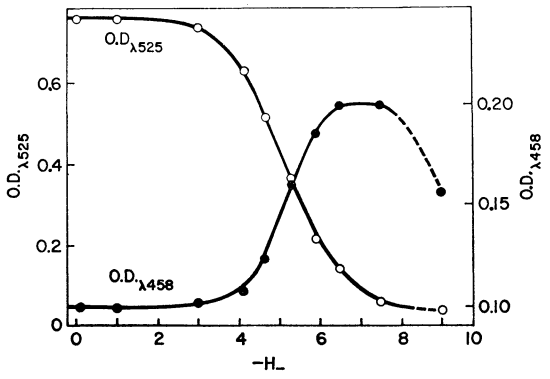

FIG. 2. Spectral changes for permanganate in aqueous sulphuric acid as a function of the acidity of the medium.

Can. J. Chem. Downloaded from www.nrcresearchpress.com by 210.87.254.40 on 09/05/12
For personal use only.

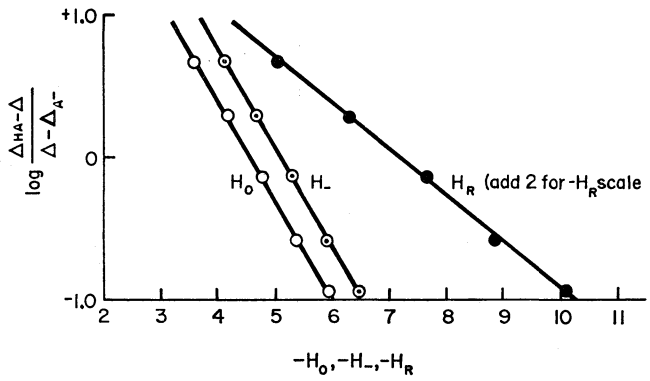

FIG. 3. Logarithm of the fraction of permanganic acid ionized plotted against different acidity functions.

RESULTS

Stoichiometry and Kinetics

Since fluoral hydrate is subject to hydrolytic cleavage in basic solution it was important to show that the oxidation reaction being followed was not that of the hydrolysis product, formic acid. The rate of the latter's reaction over the entire pH range is known and it was easy to show that the fluoral hydrolysis is much slower than its oxidation. This was done by allowing fluoral hydrate to stand in 0.15 *M* sodium hydroxide for 30 minutes (about 34 half-lives for the oxidation at this basicity), then quenching the hydrolysis by adding acid and buffering the solution to pH 6.5 and titrating the amount of formic acid formed with permanganate. At this pH the oxidation of formic acid is fast and of fluoral hydrate very slow. At most, 2% of the fluoral hydrate had been hydrolyzed during the period.

Similar experiments with chloral hydrate showed that the hydrolysis seriously interfered with the oxidation reaction even though chloral hydrate appears to be oxidized somewhat faster than fluoral hydrate (4).

In the alkaline solution the stoichiometry of the reaction is given by the equation

$$2MnO_4^- + CF_3CH(OH)_2 + 3OH^- \rightarrow 2MnO_4^= + CF_3CO_2^- + 3H_2O.$$

The manganate which accumulates in the reaction mixture oxidizes fluoral hydrate only about 1/64th as fast as permanganate in 0.1 *M* sodium hydroxide and hence it would not interfere with the kinetics until a very late stage of the oxidation.

Below approximately pH 12 the manganate disproportionates to permanganate and manganese dioxide and the stoichiometry becomes

$$2MnO_4^- + 3CF_3CH(OH)_2 + OH^- \rightarrow 2MnO_2 + 3CF_3CO_2^- + 5H_2O.$$

Figure 2 shows the results for two typical kinetic runs, one of which is taken to about 75% completion. Excellent fits with second-order kinetics were obtained except in the region pH 11 to 12.5 where the manganate disproportionation rate becomes comparable to the oxidation rate. Neither a 2:1 nor a 2:3 ratio of reactants is satisfactory in this region.

Variation of Oxidation Rate with Acidity

Figures 4 and 5 show the effect of changing acidity on the oxidation rate of fluoral hydrate. The paucity of points near pH 11 in Fig. 5 is caused by the difficulties with manganese (VI) disproportionation referred to earlier.

Can. J. Chem. Downloaded from www.nrcresearchpress.com by 210.87.254.40 on 09/05/12
For personal use only.

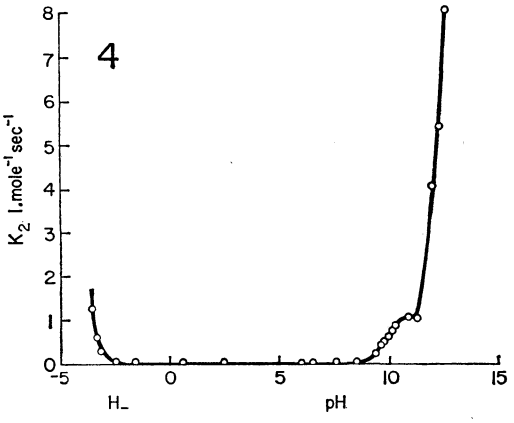

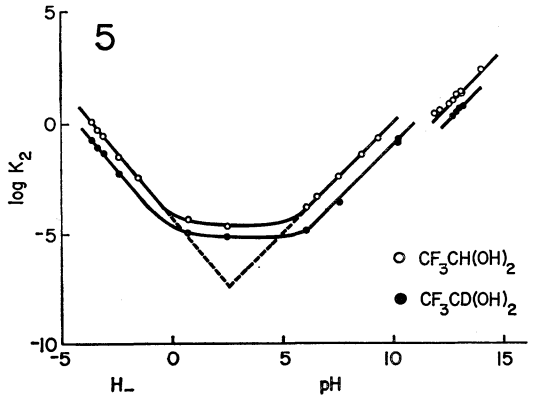

FIG. 4. Rate of the permanganate oxidation of fluoral hydrate as a function of the acidity of the medium.
FIG. 5. The logarithm of the rate of the permanganate oxidation of fluoral hydrate as a function of the acidity of the medium.

Between pH 6 and pH 11 the oxidation rate of fluoral hydrate rises by a factor of about 10^4. Using the pK_a of 10.01 determined for fluoral hydrate one can show that the reaction rate in this region is linearly dependent on the concentration of the monoanion,

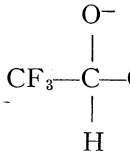

$CF_3CH(O^-)OH$, (Fig. 6). As the concentration of monoanion nears its maximum the rate

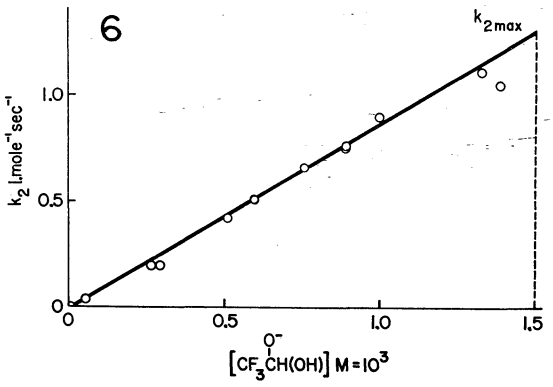

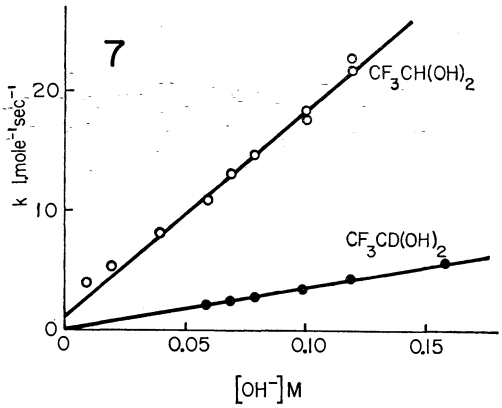

FIG. 6. The permanganate oxidation rate as a function of the fluoral hydrate monoanion concentration.
FIG. 7. Rate dependence on hydroxyl ion concentration.

levels off but soon rises again much more sharply as the much more reactive dianion begins to form. The first-order dependence of the rate on the hydroxyl ion concentration above pH 12 (Figs. 7 and 5) shows that the rate in this region becomes directly proportional to the concentration of the dianion, $CF_3CHO_2^=$. The reaction rate in 0.1 *N* NaOH is increased by a factor of more than three when the ionic strength is raised from 0.1 to 1.0. This is outside the region where the Debye–Hückel treatment can be applied but it is clearly in accord with the reactants possessing like charges.

Can. J. Chem. Downloaded from www.nrcresearchpress.com by 210.87.254.40 on 09/05/12
For personal use only.

In the weakly acidic region, pH 2 to 3, the oxidation of fluoral hydrate is extremely slow but one can detect a reaction which is some 100 times faster than that due to the minute amount of anion present at these acidities. This is presumably the oxidation of the neutral fluoral hydrate molecule by permanganate ion.

As the acidity is increased the rate of oxidation rises once more and becomes dependent on the acidity function again (Fig. 5). In this region, up to 46% sulphuric acid, the H_- function is used to denote the latter quantity. The oxidation in this region is believed due to the reaction of the neutral fluoral hydrate molecule with permanganic acid, $HMnO_4$. The latter is a strong acid which is about half dissociated in 60% sulphuric acid. The determination of the pK_a of this acid is described in the Experimental section.

Activation Parameters

The effect of the reactants' charge on the activation parameters of the oxidation is shown in Table IV. Figure 8 shows the effect of changing temperature on the oxidation rate

TABLE IV
Activation parameters

Oxidant	Substrate	Acidity	$\Delta H^{\ddagger}$ (kcal mole^{-1})	$\Delta S^{\ddagger}$ (e.u.)
MnO_4^-	$CF_3-C(O^-)(O_-)-H$	$[OH^-] = 0.07\ M$	6.6	−31.4
MnO_4^-	$CF_3-C(O^-)(O_-)-D$	$[OH^-] = 0.07\ M$	7.5	−31.8
MnO_4^-	$CF_3-C(O^-)(OH)-H$	pH = 10.20	12.4	−18.4
MnO_4^-	$CF_3-C(O^-)(OH)-D$	pH = 10.20	14.3	−16.7
$HMnO_4$	$CF_3-C(OH)(OH)-H$	41.8% H_2SO_4	12.9	−17.8

of the monoanion. The rate constants used to calculate the activation parameters for the monoanion oxidation are true bimolecular rate constants corrected for incomplete ionization but in the case of the dianion oxidation and in the case of the permanganic acid oxidation they necessarily include the pre-equilibrium step. The true enthaplies of activation for the rate-controlling step may be either somewhat larger or somewhat smaller than those listed; the entropies of activation are certainly more negative for these two reactions.

The effect of the reactants' charge type is entirely reasonable. The greatly increased rate of oxidation of the dianion results from a greatly lowered activation enthalpy, which more than overcomes the unfavorable entropy term. The latter results from the repulsion between the anionic oxidant and the dianionic reductant.

Can. J. Chem. Downloaded from www.nrcresearchpress.com by 210.87.254.40 on 09/05/12
For personal use only.

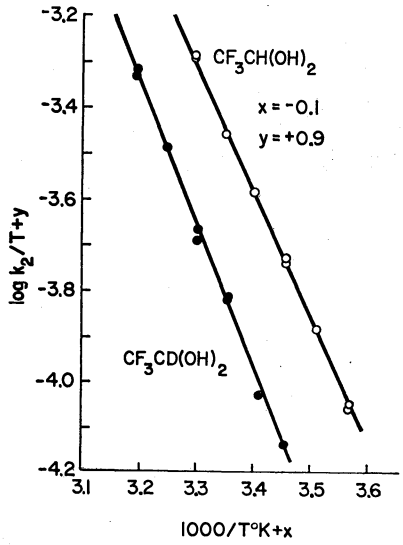

FIG. 8. Effect of changing temperature on the rate of the permanganate oxidation of the fluoral hydrate monoanion.

Isotope Effects

The carbon–hydrogen bond is clearly cleaved in the rate-controlling step in all of the reaction paths detected in the present study (Table V). Values are not listed in Table V for the very slow reaction which occurs in the weakly acidic region because of the difficulty

TABLE V

Isotope effects in the permanganate – fluoral hydrate reaction, 25°

Conditions	Principal reactants	k_H (l. mole^{-1}sec^{-1})	k_D (l. mole^{-1}sec^{-1})	k_H/k_D
[OH$^-$] = 0.12 *M*	MnO_4^-, $CF_3C(O^-)(O_-)H$	22.5	4.4	5.1
[OH$^-$] = 0.10 *M*	MnO_4^-, $CF_3C(O^-)(O_-)H$	0.29	0.060	4.8
pH = 10.2	MnO_4^-, $CF_3C(O^-)(OH)H$	0.75	0.074	10.1
pH = 7.6	MnO_4^-, $CF_3C(O^-)(OH)H$	3.4×10^{-3}	2.5×10^{-4}	13.6
44.1% H_2SO_4	$HMnO_4$, $CF_3CH(OH)_2$	0.27	0.043	6.3

Can. J. Chem. Downloaded from www.nrcresearchpress.com by 210.87.254.40 on 09/05/12
For personal use only.

of making accurate measurements for these very slow reactions. However, an isotope effect clearly exists for this reaction also, which we presume is that between permanganate ion and neutral fluoral or its hydrate.

The discrepancy in the isotope effect of 10.1 and 13.6 observed at pH's 10.2 and 7.6 is not easily accounted for since they are both presumed to refer to the reaction between permanganate ion and fluoral hydrate monoanion. The fact that they are larger than the "normal" value of 7, which corresponds to complete loss of the C—H stretching mode in the transition state at 25°, occasions no surprise since large isotope effects had been previously observed for the permanganate oxidation of fluoroalcohols (2). (An isotope effect of close to 20 has been observed in the permanganate oxidation of $(CF_3)_2CDOH$ (17).) Experiments were conducted at a much higher temperature in order to throw some light on the possibilities of proton tunnelling as a cause of the high isotope effects at room temperature. A non-classical penetration of the reaction barrier should also result in a curved Arrhenius plot and this has been observed by Hullett in at least one case (18). The present work showed no deviation from linearity in the Arrhenius plots but as a check a rate experiment was conducted at 78°. We found an isotope effect of 6.3 at this temperature. This is the exact value calculable from the activation parameters of the protio and deuterio compounds obtained at the lower temperatures. It appears as if proton tunnelling is not the cause of the large isotope effect. Changes in the bending modes in the transition state could account for the present results and this may be associated with the fact that the reactants bear a similar charge and, as a consequence of this repulsion, will tend to be further apart in the transition state. The reaction between the dianion and permanganate, which should exhibit this effect more strongly, actually has a smaller isotope effect. The activation enthalpy for this reaction is very small, however, and the transition state must resemble the reactants rather closely, suggesting that the C—H bond is only slightly stretched in the transition state of the dianion–permanganate reaction. We have observed in other work that the isotope effect in the oxidation of structurally related compounds tends to decrease as the reaction rate increases (19). It should be pointed out that the C—H and C—D stretching vibrations in fluoral hydrate are unexceptional (2980 cm^{-1} and 2220 cm^{-1}).

DISCUSSION

Except for one feature of the reaction the present results can be explained quite satisfactorily in terms of a hydride transfer from the reductant to the oxidant. On this basis

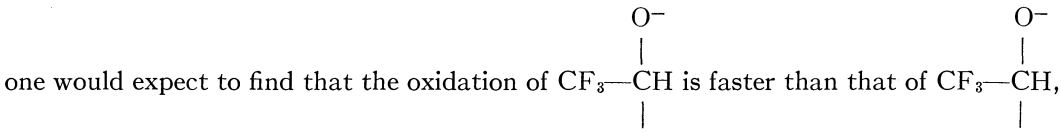

one would expect to find that the oxidation of $CF_3—CH(O^-)—O^-$ is faster than that of $CF_3—CH(OH)—O^-$, which is faster than that of $CF_3—C(OH)_2—H$, and that oxidation by $HMnO_4$ is faster than that by MnO_4^-. This is indeed what is observed.

The profound effect of charge on the oxidizability of the substrate is shown in Table VI. The surprising aspect of these results is the relatively small effect of group polarities on the reaction rate. That is, such groups as $—CF_3$ and —H, with vastly different inductive

Can. J. Chem. Downloaded from www.nrcresearchpress.com by 210.87.254.40 on 09/05/12
For personal use only.

TABLE VI

Effect of substituents on the rate* of permanganate oxidation of $CF_3—\underset{\displaystyle Y}{\overset{\displaystyle Z}{\overset{|}{\underset{|}{C}}}}—H$

Y	Z	Relative rate	Reference
OH	OH	0.0001	Present work
C_6H_5	OH	0.001	2
CF_3	O^-	0.2	
OH	O^-	0.6	Present work
H	O^-	1	
m-BrC_6H_4	O^-	3	
C_6H_5	O^-	3	
p-$CH_3C_6H_4$	O^-	4	2
m-$NO_2C_6H_4$	O^-	4	
p-$CH_3OC_6H_4$	O^-	4	
O^-	O^-	1000	Present work

*Ionic strength not constant, rate values rounded off.

effects, produce only a fivefold rate difference when directly attached to the reacting C—H group. (The very low rho value in the permanganate oxidation of $Ar—\underset{|}{\overset{O^-}{\overset{|}{C}}}HCF_3$ is similar and has been commented on before (2).) If a hydride ion is expelled from $Z—\underset{|}{\overset{O^-}{\overset{|}{C}}}HCF_3$ a drastic change in rate would be expected when the electronic properties of the substituent Z are varied. It is true that when Z is the strongly electron-donating group $—O^-$ the rate soars but this again seems to indicate the importance of negative charge on the reductant. The increased charge results in a greater electrostatic repulsion between the reactants and this shows up in the less favorable activation entropy for the fluoral hydrate dianion – permanganate reaction but this is much more than compensated for by the lowered activation enthalpy.

In view of the above discussion it is worth examining a hydrogen atom abstraction mechanism. There appears little doubt that the rate-controlling step is between the alkoxide and permanganate ions and the following step can be considered.

$$CF_3—\underset{|}{\overset{O^-}{\overset{|}{C}}}—H + MnO_4^- \rightarrow CF_3—\underset{|}{\overset{O^-}{\overset{|}{C}}}\cdot + HMnO_4^-$$

$$\underset{|}{\overset{O^-}{\overset{|}{C}}}\cdot \xrightarrow[\text{fast}]{Mn^{VI} \text{ or } Mn^{VII}} CF_3CO_2H$$

The driving force for such a reaction would be the greater stability of Mn(VI) (compared to Mn(V) formed by hydride transfer) and the fair stability of the ketyl type radical–anion, $CF_3\underset{|}{\overset{O^-}{\overset{|}{C}}}\cdot$. Moreover, recent work by Halpern and Candlin (20) on the permanganate

Can. J. Chem. Downloaded from www.nrcresearchpress.com by 210.87.254.40 on 09/05/12
For personal use only.

oxidation of the formate – Co(III) complex can only be interpreted in terms of a hydrogen atom abstraction by permanganate.

Further work is required to determine whether hydride ion or hydrogen atom abstraction from the fluoral hydrate anion is occurring. The reaction in strong acids, on the other hand, appears to be between neutral fluoral or its hydrate and permanganic acid.

ACKNOWLEDGMENT

The financial support of the National Research Council is gratefully acknowledged.

REFERENCES

1. R. STEWART. J. Am. Chem. Soc. **79**, 3057 (1957).
2. R. STEWART and R. VAN DER LINDEN. Discussions Faraday Soc. **29**, 211 (1960).
3. M. BRAID, H. ISERSON, and F. E. LAWLOR. J. Am. Chem. Soc. **76**, 4027 (1954).
4. M. M. MOCEK. Ph.D. Thesis, University of British Columbia, Vancouver, B.C. October, 1962.
5. D. E. MCGREER, R. STEWART, and M. M. MOCEK. Can. J. Chem. **41**, 1024 (1963).
6. K. B. WIBERG and R. STEWART. J. Am. Chem. Soc. **77**, 1786 (1955).
7. R. STEWART and L. G. WALKER. Can. J. Chem. **35**, 1561 (1957).
8. N. A. HALEVI and N. NUSSIM. Bull. Res. Council Israel, **4**, 263 (1956).
9. H. S. HARNED and R. W. EHLERS. J. Am. Chem. Soc. **55**, 652 (1933); **55**, 2379 (1933).
10. H. S. HARNED and N. D. EMBREE. J. Am. Chem. Soc. **56**, 1042 (1934).
11. H. M. PAPEE, W. J. CANADY, T. W. ZAWIDSKI, and K. J. LAIDLER. Trans. Faraday Soc. **55**, 1743 (1959).
12. K. D. LOUISE. Trans. Faraday Soc. **56**, 1633 (1960).
13. G. F. ALLEN, R. A. ROBINSON, and V. E. BOWER. J. Phys. Chem. **66**, 171 (1962).
14. R. STEWART and K. YATES. J. Am. Chem. Soc. **82**, 4059 (1960).
15. N. BAILEY, A. CARRINGTON, K. A. K. LETT, and M. C. R. SYMONS. J. Chem. Soc. 290 (1960).
16. D. J. ROYER. J. Inorg. Nucl. Chem. **17**, 159 (1961).
17. M. M. MOCEK and R. STEWART. To be published.
18. J. R. HULLETT. Proc. Roy. Soc. (London), Ser. A, **251**, 274 (1959).
19. R. STEWART and D. G. LEE. To be published.
20. J. HALPERN and J. CANDLIN. Personal communication.

Can. J. Chem. Downloaded from www.nrcresearchpress.com by 210.87.254.40 on 09/05/12
For personal use only.

FLUORIDE COMPLEXES OF GERMANIUM (IV) IN AQUEOUS SOLUTION[1]

R. L. BENOIT AND J. PLACE
Department of Chemistry, University of Montreal, Montreal, Que.
Received December 21, 1962

ABSTRACT

The germanium (IV) – fluoride species in various acid media have been investigated by solvent extraction, solubility, and potentiometric methods. The results are interpreted in terms of a series of mononuclear fluorohydroxygermanium (IV) species in which the number of fluorides bound per germanium tends to a maximum value of 5. The formation curve in 0.50 *M* perchloric acid is explained in terms of stability constants of species $GeF_4(OH)_i^{i-}$ and $GeF_5(OH)_i^{(i+1)-}$.

INTRODUCTION

The chlorogermanium (IV) species in acid media have recently been investigated (1, 2), and this work is now extended to the fluorogermanium (IV) species.

$H_2(GeOF_4).2H_2O$ and $H_2(GeF_6).2H_2O$ have been shown to exist as solid phases in the system GeO_2–HF–H_2O (3) at high HF concentrations, but information on the nature and stability of the species in solution is meagre. An approximate method for comparing the stabilities of various fluoride complexes (4) indicated that the germanium complexes were very weak, and conductance data relating to GeF_6^{2-} have been interpreted in terms of partial hydrolysis (5). Adsorption of Ge(IV) from mixed HF–HCl solutions on an anionic resin revealed the presence of negatively charged fluorogermanic species (6).

In this work three methods have been employed to investigate the equilibria involving fluorogermanium (IV) species, each method being useful at certain levels of acidity. The solvent extraction method (1) has been first used to study the distribution of Ge (IV) between CCl_4 and HCl (8–11 molal) as a function of added hydrofluoric acid. In the second place, the solubilities of GeO_2 in HF (0–1 *M*), and, as functions of HF added, in $HClO_4$ (5.7 and 7.0 molal) and HCl (4.5 molal) were measured. The solubility data were supported by measurements of pH and fluoride concentrations. Finally, a potentiometric method, the so-called "ferri" method (7), was used to investigate the fluorogermanium (IV) species in 0.50 *M* perchloric acid.

EXPERIMENTAL

Reagents

Chemicals used were of reagent grade. Germanium dioxide, of 99.9% purity, was used to make up stock solutions. Potassium fluorogermanate was prepared according to the procedure of Müller (8) and was recrystallized from hot water in polythene vessels. The preparation of stock solutions for the "ferri" method has been described by Hepler *et al.* (9).

Apparatus coming into contact with hydrofluoric acid was either made of polythene or protected by paraffin wax. Volumetric apparatus, of glass or polythene, was calibrated before use.

Procedure

Solvent Extraction

The procedure followed was similar to that for the experiments on the chlorogermanium (IV) system (1). The phases were shaken in a tightly sealed polythene bottle at 23±1° C and separated by decantation. The aqueous phase was also analyzed for germanium when the distribution ratio D was high ($\log D \geqslant +0.5$), and when the total germanium added was small because traces of germanium were found to be adsorbed by the polythene. Analysis for germanium was by the phenylfluorone method (10); a Beckman DU spectrophotometer was used.

[1]*Part of this work was carried out at the Department of Chemistry, Laval University, Quebec, Que.*

Can. J. Chem. Downloaded from www.nrcresearchpress.com by 210.87.254.6 on 09/05/12
For personal use only.

Solubility Experiments

The aqueous and solid phases were shaken together in polythene bottles for 4 days at room temperature, 25±1° C. The solid phase was then allowed to settle (several hours) and aliquots of the clear liquid were removed by pipette. After dilution of the sample, analysis for germanium was made by the phenylfluorone method (10); the data of the solvent extraction experiments were used to ensure that sufficient HCl was added to give adequate separation in the presence of fluoride.

Hydrogen ion concentrations were determined by means of the quinhydrone electrode, and fluoride by the "ferri" method.

Potentiometric Measurements

A Radiometer pH meter 4c was used, and potentials were read to ±0.1 mv. Electrodes were of bright platinum wire or foil; a calomel–saturated KCl electrode served as the reference electrode.

The setup for the "ferri" method was based on that described by Hepler *et al.* (9), the chief difference being that the potential of the Fe^{2+}/Fe^{3+} system was measured against a calomel reference electrode. An atmosphere of nitrogen was maintained over the solution, and stirring was by means of a stream of nitrogen. The salt bridge for the experiments at ionic strength 0.5 was of 0.5 *M* $NaClO_4$ in 3% agar-agar; one end of the bridge and the reference electrode dipped into saturated NaCl. The temperature of the reaction vessel was maintained at 25.0±0.1° C in a water bath. The salt bridges for the experiments in 5.70 and 7.00 molal $HClO_4$ media were of perchloric acid of the same concentrations, connection to the reaction vessel being made by narrow, flexible polythene tubing with a platinum wire clip and to the reference electrode by a solution of saturated NaCl.

EXPERIMENTAL RESULTS

Solvent Extraction

Preliminary experiments showed that the amounts of hydrofluoric acid extracted from concentrated hydrochloric acid by carbon tetrachloride were negligible at the concentrations involved: at 10.2 molal HCl, the HF distribution coefficient $(HF)_{CCl_4}/(HF)_{aq}$ is about 2×10^{-4}.

Irvine *et al.* (11) have reported small changes in relative volumes on equilibrating equal volumes of concentrated HCl solutions and CCl_4; however, under the present conditions the volumes of the two phases were found to be unchanged within 0.5% provided that clean separations were ensured.

It has been shown that germanium is extracted by CCl_4 from germanium solutions in concentrated HCl media and that addition of HF lowers the germanium distribution ratio (2). The variation of the distribution ratio with the HF concentration can be interpreted in terms of solution equilibria involving fluorogermanium species if mixed fluoro–chloro species $GeF_i(OH)_jCl_m$ are unimportant.

Assuming first that hydrated $GeF_i(OH)_j$ is the only fluorogermanium (IV) species present in a given concentration interval, calling K_{ij} the mass action constant for the equilibrium, and ignoring the charge of the fluorogermanium (IV) species,

$$GeCl_4 + i\,HF + j\,H_2O \rightleftarrows GeF_i(OH)_j + 4Cl^- + (i+j)H^+,$$

the following expression is found:

$$D_{ij} = \frac{P}{K_{ij}} \times \frac{|Cl^-|^4 |H^+|^{i+j}}{|HF|^i \, |H_2O|^j} \times f_{ij}, \qquad [1]$$

where

$$D_{ij} = \frac{(GeCl_4)_{CCl_4}}{(GeF_i(OH)_j)}, \qquad P = \frac{(GeCl_4)_{CCl_4}}{|GeCl_4|_{aqueous}},$$

vertical rules designate activity, parentheses concentration, and f_{ij} is the activity coefficient of $GeF_i(OH)_j$.

Can. J. Chem. Downloaded from www.nrcresearchpress.com by 210.87.254.6 on 09/05/12
For personal use only.

If activity coefficients and water activity are kept constant equation [1] gives:

$$\left[\frac{d \log D_{ij}}{d \log (HF)}\right]_{(H^+),(Cl^-)} = -i. \qquad [2]$$

Assuming now that various mononuclear $GeF_i(OH)_j$ and $GeCl_m(OH)_n$ species are present simultaneously, the distribution ratio becomes

$$\frac{1}{D} = \sum \frac{1}{D_{ij}} + \sum \frac{1}{D_{mn}}.$$

Taking the derivatives with respect to log (HF),

$$\frac{d \log D}{d \log (HF)} = D \sum \frac{1}{D_{ij}} \times \frac{d \log D_{ij}}{d \log (HF)}. \qquad [3]$$

Combining equations [2] and [3],

$$\left[\frac{d \log D}{d \log (HF)}\right]_{(H^+),(Cl^-)} = \sum \frac{-iD}{D_{ij}}.$$

For the fluorogermanium species the average number of F bound per Ge atom is:

$$\bar{i} = \frac{\sum i(GeF_i(OH)_j)}{\sum (GeF_i(OH)_j)} = \frac{C_{Ge}}{\sum (GeF_i(OH)_j)} \sum \frac{iD}{D_{ij}},$$

where C_{Ge} is the total germanium concentration in the aqueous phase. Finally

$$\left[\frac{d \log D}{d \log (HF)}\right]_{(H^+),(Cl^-)} = -\bar{i} \frac{\sum (GeF_i(OH)_j)}{C_{Ge}}.$$

In other words, the plot of log D against log (HF) at constant (H^+) and (Cl^-) gives $\bar{i}$, the average number of fluoride bound per germanium, when the chloride species are in negligible concentration, i.e. $\sum (GeF_i)(OH)_j)/C_{Ge} \simeq 1$. When chloride species are also present, $\bar{i}$ is obtained by multiplying the slope by $C_{Ge}/\sum (GeF_i(OH)_j)$; this correction factor is taken as being equal to $D_0/(D_0-D)$, where D_0 is the distribution ratio for (HF) $=0$.

At the levels of acidity involved, 8–11 molal HCl, HF is practically undissociated and the concentration of the species F^- and HF_2^- is negligible (12). The values of the equilibrium concentration (HF) were calculated from the added concentration C_{HF} by subtracting a correction term for fluoride bound to germanium, $\bar{i} \sum (GeF_i(OH)_j)$. $\sum (GeF_i(OH)_j)$ was calculated from the values of C_{Ge} and D_0, and $\bar{i}$ was obtained, by using successive approximations, from the corrected value of the slope of log D against log (HF). Germanium distribution and $\bar{i}$ are plotted as functions of (HF) in Figs. 1 and 2 respectively.

The Potentiometric Method

In the so-called "ferri method" the redox potential of the ferric–ferrous system is used to indicate the equilibrium HF concentration present in an acid solution (9).

A run was first made with ferrous and ferric ions and the potential measured with a platinum electrode was plotted on a graph as a function of added HF. Then a run was made under identical conditions but with germanium added and the potentials read off as a measure of free HF; a correction for the fluoride bound to Fe^{3+}, $\sum x(FeF_x)$, was calculated from the equilibrium constants for the ferric fluoride system (9). The concentration of fluoride bound to germanium was obtained as $C_F - [(HF) + \sum x(FeF_x)]$, where C_F is the total concentration of HF added.

Can. J. Chem. Downloaded from www.nrcresearchpress.com by 210.87.254.6 on 09/05/12
For personal use only.

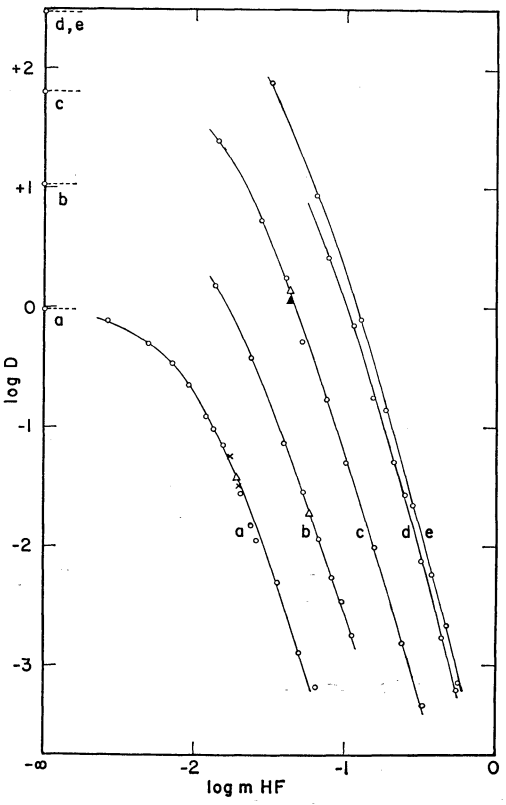

FIG. 1. Germanium distribution as a function of HF concentration at various levels of molality.
The molalities and the initial Ge concentrations in the aqueous phases are: (*a*) 8.12 molal HCl, (Ge) added = 1.76×10^{-3} molal;(*b*) 9.07 molal HCl, (Ge) added = 1.74×10^{-3} molal; (*c*) 10.13 molal HCl, (Ge) added = 3.84×10^{-3} molal; (*d*) 9.07 molal HCl+2.06 molal LiCl, (Ge) added = 5.61×10^{-3} molal; (*e*) 11.12 molal HCl, (Ge) added = 1.70×10^{-3} molal.
▲, (Ge) added reduced by a factor of 10; △, (Ge) added reduced by a factor of 100; ×, germanium added as K_2GeF_6.

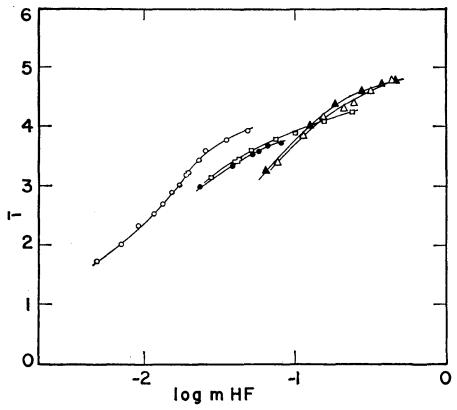

FIG. 2. Complexity of the germanium (IV) – fluoride system in media of high acidity: ○ 8.12 molal HCl; ● 9.07 molal HCl; □ 10.13 molal HCl; △ 9.07 molal HCl+2.06 molal LiCl; ▲ 11.12 molal HCl.

Can. J. Chem. Downloaded from www.nrcresearchpress.com by 210.87.254.6 on 09/05/12
For personal use only.

Experiments were carried out in a perchlorate medium with $(H^+) = 0.497\ M$ and the ionic strength was made up to 0.500 with $LiClO_4$. The temperature of the thermostat was 25.0±0.1° C. The initial volume for each run was 25.17 ml, the initial concentrations of ferrous and ferric ion were $4.91\times10^{-4}\ M$ and $2.82\times10^{-4}\ M$ respectively, and runs were made at initial germanium concentrations of $1.00\times10^{-2}\ M$ and $2.16\times10^{-3}\ M$. The results of several runs are consolidated in Table I. In calculating the ionic strength of the solutions, the contributions of GeO_2 and HF were neglected although the formation of ionic germanium species will have some effect as more HF is added. At this level of acidity the predominant hydrofluoric species is HF since $(F^-)/(HF) = 2.5\times10^{-4}$ (13).

TABLE I

Complexing of germanium (IV) by fluoride at $(H^+) = 0.50\ M$

Run	Fluoride complexed to Ge (IV), mmoles/l.	C_{Ge}, mmoles/l.	(HF), mmoles/l.	$\bar{\imath}$
III	0.23	10.01	3.67	0.023
V	0.07	2.01	3.83	0.035
III	1.58	9.35	5.84	0.169
IV	2.34	10.01	6.41	0.234
III	3.19	8.78	7.33	0.363
VI	0.95	2.01	7.78	0.472
III	4.78	8.27	8.48	0.578
IV	7.25	9.35	9.27	0.775
III	6.42	7.82	9.30	0.821
IV	12.2	8.78	11.17	1.39
III	10.41	7.41	11.12	1.40
VI	3.68	1.88	12.8	1.96
IV	16.5	8.27	12.9	2.00
III	14.2	7.05	12.6	2.01
III	17.4	6.72	14.2	2.58
IV	20.2	7.82	14.6	2.58
III	19.9	6.42	15.9	3.10
IV	23.1	7.41	16.5	3.11
VI	5.87	1.77	17.5	3.33
III	21.7	6.14	18.1	3.53
IV	25.2	7.05	18.8	3.58
III	22.7	5.89	20.7	3.86
IV	26.8	6.72	21.1	3.99
VI	6.81	1.66	22.6	4.10
III	23.5	5.66	23.2	4.16
IV	27.2	6.42	24.3	4.24
VI	6.92	1.57	27.8	4.40
III	24.0	5.44	25.8	4.42
III	24.5	5.24	32.9	4.68
III	23.4	5.06	41.0	4.63

The formation curve is plotted in Fig. 3 in the form of $\bar{\imath}$ against log (HF), where

$$\bar{\imath} = \frac{C_F - [(HF) + \sum x(FeF_x)]}{C_{Ge}}.$$

The values of $\bar{\imath}$ tend to a maximum of 5. Further information on the nature and stability of the species formed can be obtained by finding the minimum number of parameters necessary to fit the formation curve satisfactorily. As GeO_2, probably hydrated, is present in non-complexing acid media (14), addition of HF to the Ge (IV) solution leads to equilibria such as

$$GeO_2 + i\,HF + (j-2)H_2O \rightleftarrows GeF_i(OH)_j + (i+j-4)H^+ \qquad [4]$$

ignoring the charges of the fluorogermanium (IV) species.

Can. J. Chem. Downloaded from www.nrcresearchpress.com by 210.87.254.6 on 09/05/12
For personal use only.

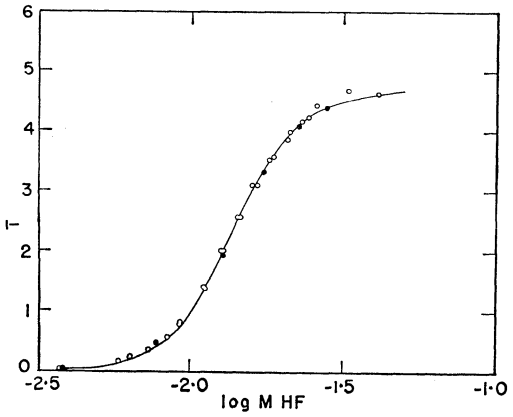

FIG. 3. Complexity of the germanium (IV) – fluoride system at $(H^+) = 0.50$ M: ○ (Ge) initial = 1.076×10^{-2} M; ● (Ge) initial = 2.16×10^{-3} M. The curve is calculated from $\beta_4' = 2.0\times10^7$, $\beta_5' = 8.8\times10^8$.

The overall stoichiometric stability constant, β_{ij}, for this equilibrium is

$$\beta_{ij} = \frac{(GeF_i(OH)_j)(H^+)^{(i+j-4)}}{(GeO_2)(HF)^i}.$$

When (H^+) is held constant at a particular level, a constant β_{ij}' may be defined such that

$$\beta_{ij}' = \frac{(GeF_i(OH)_j)}{(GeO_2)(HF)^i}. \qquad [5]$$

If N is the maximum coordination number of Ge (IV), constants β_i' may be determined under the particular conditions of ionic strength and acidity, where

$$\beta_i' = \sum_{j=0}^{j=N-i} \beta_{ij}' = \frac{\sum_{j=0}^{j=N-i} (GeF_i(OH)_j)}{(GeO_2)(HF)^i}. \qquad [6]$$

A graphical extrapolation method of Rossotti and Rossotti (15, p. 110) using the function

$$\frac{\bar{i}(HF)^{-5}}{5-\bar{i}} = \beta_5' + \beta_4' \frac{4-\bar{i}}{5-\bar{i}}(HF)^{-1} + \sum_{i=1}^{i=3} \frac{i-\bar{i}}{5-\bar{i}} \beta_i'(HF)^{i-5}$$

gave the following values:

$$\beta_5' = 8.8(\pm0.2)\times10^8,\ \beta_4' = 2.0(\pm0.3)\times10^7,\ \beta_3' \leqslant 10^4.$$

The approximate limits of error quoted were estimated from the graphs used to evaluate the constants. Satisfactory agreement between the experimental and calculated formation curves was obtained by using β_5' and β_4' only, as can be seen in Fig. 3.

To check whether the maximum value of i is in fact 5, a plot was made of $[\beta_4' + \beta_5'(HF)]$ against (HF); this gave a linear relation over the explored range of (HF), implying that complexes in which $i > 5$ are not present in appreciable concentration under these conditions (15, p. 116).

Solubility Measurements

Solubility of GeO_2 in HF at Constant Levels of Acidity and Molality

Stability constants are easily obtained from solubility measurements when added and

Can. J. Chem. Downloaded from www.nrcresearchpress.com by 210.87.254.6 on 09/05/12
For personal use only.

free ligand can to a first approximation be regarded as equal (16), i.e. when the solubility remains low.

Determinations of GeO_2 solubility were carried out for solutions containing increasing HF concentrations at 4.50 molal HCl, 5.70 molal $HClO_4$, and 7.00 molal $HClO_4$. By working at constant and high acidity one of the variables of the system is eliminated with the further advantage that the GeO_2 solubility is appreciably depressed by a salting-out effect (14). Results are given in Table II and the values of C_{Ge} are plotted against C_F in Fig. 4.

TABLE II

Effect of HF on the solubility of GeO_2 in various acid media (concentrations expressed in molalities)

	C_F	C_{Ge}	(HF)	$\bar{\imath}$	$\frac{C_F-(HF)}{C_{Ge}-S_0}$
HCl = 4.50 molal					
	0	0.0120			
	0.0306	0.0206			
	0.0571	0.0289			
	0.117	0.0463			
	0.168	0.0618			
	0.247	0.0838			
	0.365	0.116			
	0.474	0.146			
	0.606	0.178			
$HClO_4$ = 5.70 molal					
	0	0.00426	—	—	—
	0.0525	0.0179	0.0087	2.44	3.20
	0.105	0.0337	0.0098	2.84	3.25
	0.163	0.0510	0.0106	2.98	3.25
	0.284	0.0866	0.0133	3.13	3.29
$HClO_4$ = 7.00 molal					
	0	0.00153	—	—	—
	0.0483	0.0163	0.0106	2.31	2.55
	0.0966	0.0304	0.0128	2.76	2.90
	0.150	0.0471	0.0160	2.84	2.94
	0.261	0.0800	0.0182	3.04	3.10

The equation

$$(C_{Ge}-S_0)\mathbf{a} = C_F, \qquad [7]$$

where $\mathbf{a} = 3.3\pm0.1$ and S_0 is the solubility when $C_F = 0$, accounts for the results at all three levels of acidity over the range $C_F = 0$ to $C_F = 0.3$ molal. With $\bar{\imath}' = [C_F-(HF)]/[C_{Ge}-S_0]$, the results set an upper limit of $\mathbf{a} = 3.3$ for $\bar{\imath}'$ which is the average number of fluoride bound per germanium for species other than GeO_2. A further interpretation of these data, according to the method described in reference 16, is not feasible and as the rise in solubility in relation to C_F is considerable another approach must be found.

Solid GeO_2 is in equilibrium with dissolved GeO_2, so, with (GeO_2) and (H^+) constant, from [6],

$$\sum (GeF_i(OH)_j) = \sum \beta_i' S_0 (HF)^i.$$

Thus, taking into account the experimental relation [7],

$$\mathbf{a} \sum \beta_i' S_0 (HF)^i = (HF) + \sum i\beta_i' S_0 (HF)^i. \qquad [8]$$

Can. J. Chem. Downloaded from www.nrcresearchpress.com by 210.87.254.6 on 09/05/12
For personal use only.

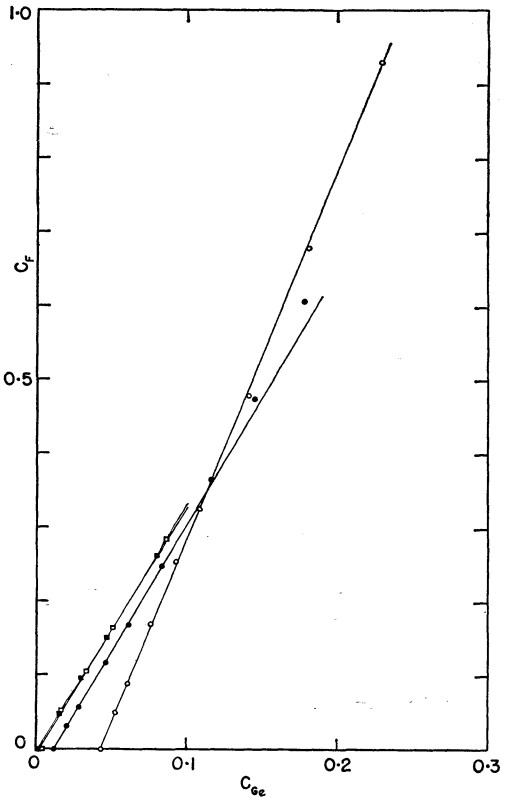

FIG. 4. The solubility of GeO_2 in HF in various media: C_{Ge} as a function of C_F. ○ in HF (in molarities); ● in 4.50 molal HCl (in molalities); □ in 5.70 molal $HClO_4$ (in molalities); ■ in 7.00 molal $HClO_4$ (in molalities).

A set of solutions to this equation is obtained if (HF) is negligible, i.e. (HF) $\ll C_F$, and all the values of β_i' except one are nil: e.g. with $\beta_i' = \beta_2' = \beta_4' \ldots = 0$ and $\beta_3' \neq 0$,

$$\mathbf{a}_3 = \frac{3\beta_3' S_0(\mathrm{HF})^3}{\beta_3' S_0(\mathrm{HF})^3} = 3.$$

Thus by assuming the presence of only $GeF_3(OH)_j$ species in addition to GeO_2 and a small free ligand concentration, it is possible to account for the experimental relation [7]. However, approximate solutions can also be found for equation [8]: a nearly linear relation with $\mathbf{a} = 3.3$ is obtained by choosing two arbitrary constants β_3' and β_4' such that the ratio $\beta_3'/\beta_4' = 50$ and varying (HF) but little around 10^{-2} molal. Therefore in order to obtain less ambiguous information on the nature of the fluorogermanium (IV) species in these solutions, some measurements of (HF) were made by the "ferri" method, allowing the direct calculation of $\bar{\imath}$. These data are given in Table II.

The interpretation given by Kleiner for the rise of solubilities of stannic (17) and antimonous (18) oxides in fluoride solutions involved an expression of the type log $(M(OH)_{N-i}F_i) = i$ log (HF) + constant, neglecting or correcting for S_0. On this basis the data of Table II would have been interpreted in terms of the formation of species where $i = 1$. Consequently this simplified treatment of such solubility data would seem to be misleading.

Can. J. Chem. Downloaded from www.nrcresearchpress.com by 210.87.254.6 on 09/05/12
For personal use only.

Solubility of GeO_2 in HF (0–1 M)

The measurements of the solubility of GeO_2 in HF up to 1 M are listed in Table III, expressed in molarities. C_{Ge} as a function of C_F is plotted in Fig. 4. Near 1 M HF the solubility values agree with the results of Tananaev and Avduevskaya (3), which start at $C_F = 1$ M. The solubility is represented up to $C_F = 1$ M by the relation [7], $(C_{Ge} - S_0)\mathbf{a} = C_F$, with $\mathbf{a} = 5.0$.

TABLE III

Solubility of GeO_2 in HF (concentrations expressed in molarities)

C_F	C_{Ge}	$C_{Ge}-S_0$	(H^+)
0	0.0433*	—	—
0.0488	0.0527	0.0094	0.0110
0.0883	0.0607	0.0174	0.0195
0.107	0.0645†	0.0212	0.0216
0.169	0.0762	0.0329	0.0340
0.253	0.0930	0.0497	—
0.322	0.109	0.066	—
0.478	0.142	0.099	0.096
0.679	0.181	0.136	0.131
0.929	0.229	0.186	0.163

*Reference 19.
†By interpolation.

Some supporting measurements of (H^+) were made by comparing the quinhydrone electrode potentials given by the germanium (IV) – HF solutions and a series of standard hydrochloric acid solutions. This implied that equimolar germanium and HCl solutions would be of comparable ionic strength. The results are given in Table III. (H^+) can be related to the solubility increase $C_{Ge}-S_0$ as

$$(H^+) = (F^-)+(HF_2^-)+\bar{n}(C_{Ge}-S_0),$$

where $\bar{n}$ is the average negative charge of the $GeF_i(OH)_j$ species other than GeO_2. As (F^-) and (HF_2^-) are low, $\bar{n} \simeq (H^+)/[C_{Ge}-S_0]$, and this ratio is seen to be near 1.

DISCUSSION

In the solvent extraction experiments the concentration of Ge was varied by factors of 10 and 100 without significant deviation from the distribution ratio (Fig. 1), and in the potentiometric investigations a fivefold variation in Ge concentration had no effect on the formation curve (Fig. 3), so polynuclear germanium species are unimportant in the range of variables studied, as implicitly assumed above.

The formation curve in 0.50 M perchloric acid was satisfactorily interpreted by using only the overall stability constants β_4' and β_5', corresponding to species $GeF_4(OH)_j^{j-}$ and $GeF_5(OH)_j^{(j+1)-}$. The relative abundances of the fluorogermanium (IV) species over the range of (HF) studied are illustrated in Fig. 5. This formation curve was the only one to cover a satisfactory range of $\bar{\imath}$ and (HF) values with sufficient accuracy to warrant the determination of stability constants.

In the experiments concerning the solubility of GeO_2 in HF at constant acidity, the (HF) values as measured by the "ferri" method varied over only a small range, as did the values of $\bar{\imath}$. As indicated in Table II the average number of F bound per Ge for species other than GeO_2, $\bar{\imath}' = [C_F-(HF)]/[C_{Ge}-S_0]$, is in the region 2.5–3.3. It is also apparent that the range of C_F studied corresponds to a limited range of (HF). Under these circumstances the value of **a** obtained from the linear variation of the solubility with added

Can. J. Chem. Downloaded from www.nrcresearchpress.com by 210.87.254.6 on 09/05/12
For personal use only.

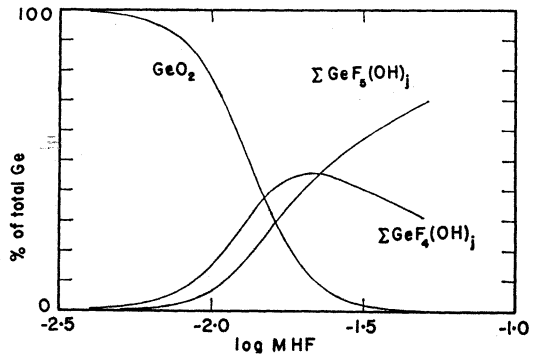

FIG. 5. The percentages of species in the germanium (IV) – fluoride system at $(H^+) = 0.50\ M$.

HF can give no more than a maximum value for $\bar{\imath}'$. The solubility method as used here was of little value as such since the free ligand concentration had to be measured to resolve ambiguity in the interpretation.

Considering the solubility of GeO_2 in HF alone, it is interesting that the solubility still varies linearly with added HF even though (H^+) and the ionic strength vary. The value of **a** again gives a maximum for $\bar{\imath}'$, since some free HF is present and "S_0" may decrease somewhat with increasing ionic strength. This ratio remains close to 5, not only in the range studied here but up to 3 molal added HF (3), subsequently decreasing to 4.2 when the added HF is about 30 molal with respect to the added H_2O and when the solid phase is still GeO_2. The value of **a** suggests that $GeF_4(OH)_j$ and $GeF_5(OH)_j$ species play a prominent part at these low acid levels, as they do when $(H^+) = 0.5\ M$. In this connection it was calculated that, using the values of β_4' and β_5' obtained for the medium 0.50 M $HClO_4$, the solubility of GeO_2 would also vary nearly linearly with added HF according to relation [7] with **a** = 4.6 up to at least 0.3 M added HF, provided that the very considerable effect of the germanium (IV) – fluoride species on the ionic strength was ignored. The average charge $(\bar{\imath}+\bar{\jmath}-4)$ of the $GeF_i(OH)_j$ species other than GeO_2, deduced from a comparison of the solubility increase and (H^+), is approximately -1; this would lead to species of the nature $GeF_4(OH)^-$ and GeF_5^-.

The formation curves obtained at the highest levels of molality and acidity by the distribution method (Fig. 2) show qualitatively that $\bar{\imath}$ again tends towards a maximum value of 5. The more flattened nature of these curves compared with the curve obtained in 0.5 M perchloric acid suggests greater participiation of complexes with $i < 4$ at higher levels of acidity, and a similar effect was observed in the solubility experiments. The replacement of about 18% of the H^+ of the medium by Li^+ at the highest level of molality (11.12 molal) had little effect on either the measured distribution (Fig. 1) or formation (Fig. 2) curves. Investigation of the number of bound hydroxy groups would have required a much wider variation in (H^+), to which the methods used did not lend themselves.

Equilibrium in the system at 8.12 molal HCl was achieved rapidly whether the germanium was added as GeO_2 or as K_2GeF_6; in other words there is no very slow step in the equilibria and GeF_6^{2-} is much more labile than, for example, AsF_6^- (20) or BF_4^- (21). This is confirmed by the fact that K_2GeF_6 and similar salts of GeF_6^{2-} are readily recrystallized from their aqueous solutions whose acidity (pH $\simeq$ 3) indicates hydrolysis. Thus the trend to decreasing lability in the isoelectronic series $AlF_6^{3-} > SiF_6^{2-} > PF_6^- > SF_6$ (22) is followed to the extent that $GeF_6^{2-} \gg AsF_6^-$.

Can. J. Chem. Downloaded from www.nrcresearchpress.com by 210.87.254.6 on 09/05/12
For personal use only.

In conclusion, the fluorogermanium (IV) species in acid media are much more stable than the chlorogermanium (IV) species, which are only formed at high HCl concentrations (1), although quantitative comparisons cannot be made. It has not been possible to demonstrate conclusively the presence of fluorogermanium (IV) species with $i > 5$ in aqueous solution, just as complete formation of $GeCl_6^{2-}$ in acid media was not obtained (1). Comparisons with other metal–fluoride systems (23) are difficult owing to the hydrolyzed nature of the complexed and uncomplexed metal species and to the unknown stability of the first Ge–F complex.

ACKNOWLEDGMENTS

The authors wish to thank the National Research Council of Canada for a grant and the American Metal Climax Corporation for a gift of germanium dioxide. One of the authors (J. P.) gratefully acknowledges a bursary from Canadian Industries Limited.

REFERENCES

1. R. L. Benoit and P. Clerc. J. Phys. Chem. **65**, 676 (1961).
2. P. Clerc. M.Sc. Thesis, Université Laval, Québec, Qué. 1960.
3. I. V. Tananaev and K. A. Avduevskaya. Zh. Neorgan. Khim. **3**, 2165 (1958).
4. A. K. Babko and L. G. Shimadina. Zh. Neorgan. Khim. **4**, 1060 (1959).
5. R. H. Schmitt, E. L. Grove, and R. D. Brown. J. Am. Chem. Soc. **82**, 5292 (1960).
6. F. Nelson, R. M. Rush, and K. A. Kraus. J. Am. Chem. Soc. **82**, 339 (1960).
7. C. Brosset and J. Orring. Svensk Kem. Tidskr. **55**, 101 (1943).
8. J. H. Müller. J. Am. Chem. Soc. **43**, 1087 (1921).
9. L. G. Hepler, J. W. Kury, and Z. Z. Hugus, Jr. J. Phys. Chem. **58**, 26 (1954).
10. E. B. Sandell. Colorimetric determination of traces of metals. Interscience Publ., New York, N.Y. 1959. p. 482.
11. G. O. Brink, P. Kafalas, R. A. Sharp, E. L. Weiss, and J. W. Irvine, Jr. J. Am. Chem. Soc. **79**, 1303 (1957).
12. H. H. Broene and T. DeVries. J. Am. Chem. Soc. **69**, 1644 (1947).
13. R. E. Connick *et al.* J. Am. Chem. Soc. **78**, 1827 (1956).
14. G. Brauer and H. Müller. Z. Anorg. Allgem. Chem. **287**, 71 (1956).
15. F. J. C. Rossotti and H. Rossotti. The determination of stability constants. McGraw-Hill Book Co., New York. 1961.
16. K. B. Yatsimirskii and V. P. Vasil'ev. Instability constants of complex compounds. Pergamon Press Inc., New York. 1960. p. 16.
17. K. E. Kleiner and V. T. Vasilenko. Zh. Neorgan. Khim. **5**, 112 (1960).
18. K. E. Kleiner and G. I. Gridchina. Zh. Neorgan. Khim. **4**, 2020 (1959).
19. A. W. Laubengayer and D. S. Morton. J. Am. Chem. Soc. **54**, 2317 (1932).
20. H. M. Dess and R. W. Parry. J. Am. Chem. Soc. **79**, 1589 (1957).
21. C. A. Wamser. J. Am. Chem. Soc. **70**, 1209 (1948).
22. H. Taube. Chem. Rev. **50**, 69 (1952).
23. R. E. Connick. J. Am. Chem. Soc. **76**, 5313 (1954).

Can. J. Chem. Downloaded from www.nrcresearchpress.com by 210.87.254.6 on 09/05/12
For personal use only.

THE INFRARED ABSORPTION OF SOME CRYSTALLINE INORGANIC FORMATES

K. B. HARVEY, B. A. MORROW,[1] AND H. F. SHURVELL
Department of Chemistry, University of British Columbia, Vancouver, British Columbia

Received January 2, 1963

ABSTRACT

The infrared absorption of some polycrystalline alkali metal and alkaline earth formates has been measured in the region of 500 cm^{-1} to 3000 cm^{-1}. The observed crystal splitting of the formate fundamentals is discussed in terms of a vibrational analysis under the factor group.

INTRODUCTION

Apart from some Raman studies of aqueous solutions (1, 2, 3) little has been reported concerning the vibrational spectrum of the formate ion. We have therefore undertaken the investigation of the infrared absorption spectra of a number of crystalline inorganic formates. The present report concerns a preliminary survey of the infrared absorption of polycrystalline samples.

EXPERIMENTAL

Those formates not directly obtainable were prepared from formic acid and the corresponding carbonate. All materials used were reagent grade and the salts were further purified by recrystallization from aqueous solution. The lithium and potassium salts are quite hygroscopic and a certain amount of care was necessary in their manipulation.

The spectra were obtained on a Perkin–Elmer, Model 421, double-beam grating spectrometer. All of the samples were polycrystalline and were suspended, in the usual manner, in KBr pellets. Under the scanning conditions employed the accuracy would be of the order of ± 2 cm^{-1} and the resolution 2 cm^{-1} or better.

RESULTS AND DISCUSSION

Assignments

The frequencies of the observed absorption peaks are summarized completely in Tables I and II and representative spectra are shown in Figs. 1 and 2. The vibrational

TABLE I

Infrared absorption of alkali metal formates (frequencies in cm^{-1})

	$Li(HCO_2)$ I.R., cryst.	$Na(HCO_2)$ I.R., cryst.	$K(HCO_2)$ I.R., cryst.	$Na(DCO_2)$ I.R., cryst.	$Na(HCO_2)$ R., H_2O (Fonteyne)	$Na(DCO_2)$ R., H_2O (Fonteyne)
ν_T	622					
ν_T	658					
		755 ?				
$\nu_3(a_1)$	789	769	755	762	773	757
$\nu_6(b_2)$	1060 ?	1062	1060 ?	912	1069	918
$\nu_1(a_1)$	1367.5	1355	1345	1327	1352	1329
	1372.5					
$\nu_5(b_1)$	1380					
	1385 ?	1385 ?	1382	1010	1386	1028
$\nu_4(b_1)$	1560 ?	1590	1580	1580	1584	1580
	1588	1630 ?				
$2\nu_6$					2126	1831
$2\nu_5$	2748	2715	2705	2017	2732	2032
$\nu_1+\nu_3$				2080		
$\nu_2(a_1)$	2856	2828	2790	2130	2825	2122
$2\nu_4$	3120	2950	2950			

[1]*Present address: Department of Organic Chemistry, University of Cambridge, Cambridge, England.*

Can. J. Chem. Downloaded from www.nrcresearchpress.com by 210.87.254.105 on 09/05/12
For personal use only.

TABLE II

Infrared absorption of some formates of divalent cations (frequencies in cm^{-1})

	$Ca(HCO_2)_2$ I.R., cryst.	$Sr(HCO_2)_2$ I.R., cryst.	$Ba(HCO_2)_2$ I.R., cryst.	$Ba(HCO_2)_2$ I.R., H_2O	$Ba(DCO_2)_2$ I.R., cryst.	$Pb(HCO_2)_2$ I.R., cryst.
	778	763	756		745	763
$\nu_3(a_1)$		780			755	768.5
	796	784	765			778
$\nu_6(b_2)$	1060	1070	1060		905	1060 ?
	1072	1082	1069		912	
	1349	1350	1345	1345	1320	1326
$\nu_1(a_1)$	1359	1360	1355		1330	1348
		1369				
	1386	1381	1385	1380	1028	1360
$\nu_5(b_1)$	1397	1387.5	1398			1372
	1582	1580	1570		1545	1563
$\nu_4(b_1)$	1618		1600		1580	1575
	1650					1623
$2\nu_1$	2694	2720	2700		2645	
	2745		2745	2730	2043	
$2\nu_5$	2775	2775	2765			
	2868		2822	2820	2112	2800
$\nu_2(a_1)$	2890	2872	2865		2160	
			2912		2881	2905
$\nu_1+\nu_4$	2942	2925	2920		2900	
$2\nu_4$	3000	2980	2975		2950	

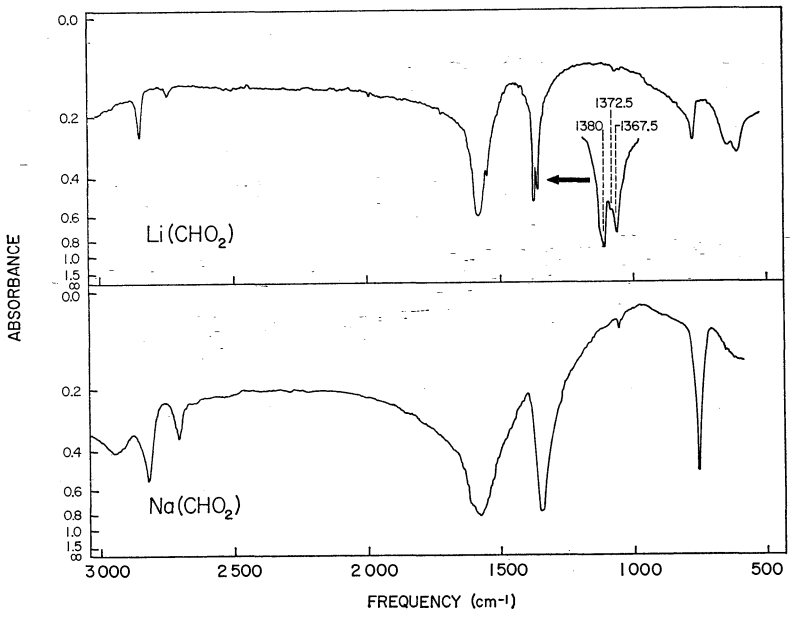

FIG. 1. Infrared absorption spectra of lithium and sodium formates.

analysis of Fonteyne (3), employing a Urey–Bradley potential function, was used as a basis for the assignments. For the most part, the assignments are straightforward but some ambiguities exist, especially in the assignment of the overtones and combinations. Thus, two fundamentals, ν_1 and ν_5, fall in the region 1340 cm^{-1} to 1400 cm^{-1}. In the spectra of the formates of divalent cations, the assignment of these two fundamentals would appear to be straightforward, with two strong, easily resolved absorption bands

Can. J. Chem. Downloaded from www.nrcresearchpress.com by 210.87.254.105 on 09/05/12
For personal use only.

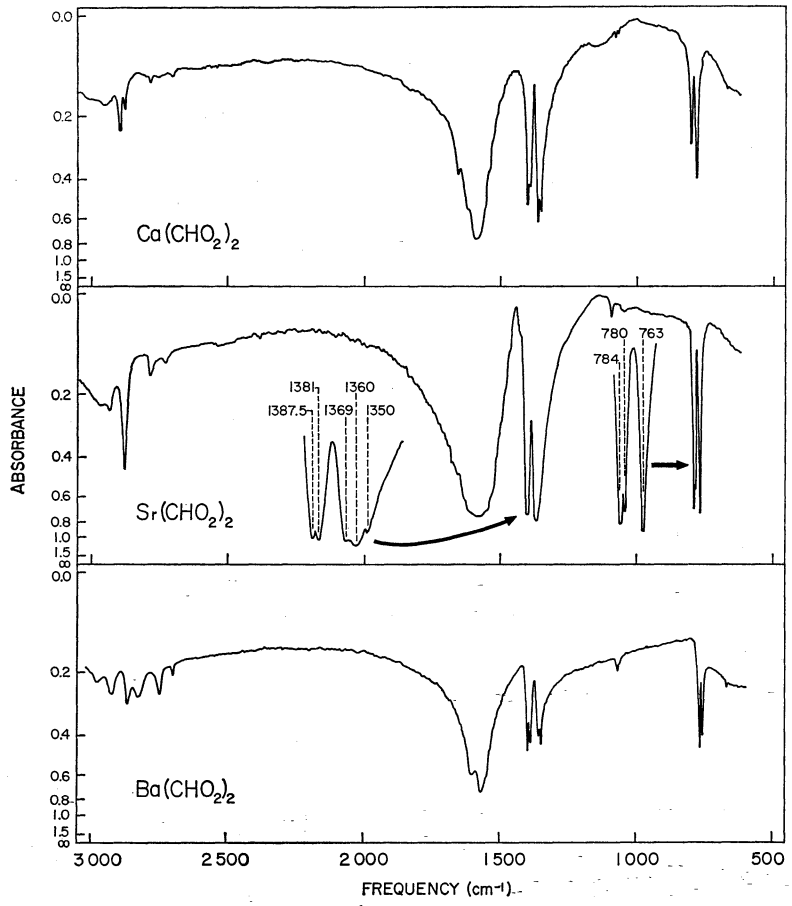

FIG. 2. Infrared absorption spectra of some alkaline earth formates.

being observed in each case. The spectrum of lithium formate also exhibits this feature but those of the sodium and potassium salts differ rather markedly in this region. Presumably this results from the different crystal structure of the formates of potassium and sodium (Table III). Similar ambiguities exist in the assignment of $2\nu_5$. On a frequency basis this would appear to be the only plausible assignment, especially for the 2017 cm^{-1} peak of the $Na(DCO_2)$ spectrum, but in view of the weak fundamental it is surprising that the overtone is observed. That it is seen in every case must be the result of Fermi resonance with the fundamental ν_2. Such an explanation also provides a means for rationalizing the variations in the difference between the observed and calculated values for the frequency of $2\nu_5$.

Fine Structure of the Absorption Bands

Since the C_{2v} symmetry of the free formate ion precludes any degeneracy, the fine structure of the absorption due to the formate, internal vibrations may be ascribed to crystal-field splitting. That such fine structure is to be expected can be seen from the factor group analyses summarized in Tables IV, V, and VI. These tables and the correlation table (Table VII) were prepared by the well-known procedure described by

Can. J. Chem. Downloaded from www.nrcresearchpress.com by 210.87.254.105 on 09/05/12
For personal use only.

TABLE III

Crystal structures of formates studied

	System	Space group	Z	Lattice constants	Comments
$Li(HCO_2)$	Orthorhombic	$V_h^{16}(Pnma)$ or $C_{2v}^9(Pna2_1)$	4	$a = 6.49, b = 10.01, c = 4.85$	
$Na(HCO_2)$	Monoclinic	$C_{2h}^6(C2/c)$	4	$a = 6.19, b = 6.72, c = 6.49, \beta = 121°42'$	Formate and sodium ions on 2-fold axes
$K(HCO_2)$	(Not known, presumable similar to structure of sodium formate)				
$Ca(HCO_2)_2$	Orthorhombic	$D_{2h}^{15}(Pcab)$	8	$a = 10.16, b = 13.38, c = 6.27$	All atoms on general positions
$Sr(HCO_2)_2$	Orthorhombic	$D_2^4(P2_12_12_1)$	4	$a = 6.87, b = 8.75, c = 7.27$	Formate ions on two sets of 4-fold general positions
$Ba(HCO_2)_2$	Orthorhombic	$D_2^4(P2_12_12_1)$	4	$a = 6.81, b = 8.91, c = 7.67$	Formate ions on two sets of 4-fold general positions
$Pb(HCO_2)_2$	Orthorhombic	$D_2^4(P2_12_12_1)$	4	$a = 6.52, b = 8.75, c = 7.74$	Formate ion on two sets of 4-fold general positions

TABLE IV

Factor group vibrational analysis of crystalline $Na(HCO_2)$

C_{2h}	E	C_2	i	σ_h	n_i	n_i (T)	n_i (T′)	n_i (R′)	n_i'
a_g	1	1	1	1	6	0	2	1	3
b_g	1	−1	1	−1	9	0	4	2	3
a_u	1	1	−1	−1	6	1	1	1	3
b_u	1	−1	−1	1	9	2	2	2	3

Bhagavantum (4) and Halford (5). In addition to the character table, giving the symmetry of the vibrations, the tables list the following:

n_i, the total number of optically active vibrations of the symmetry species i under the factor group analysis;

n_i (T), the number of purely translational modes of symmetry species i;

n_i (T′), the number of lattice modes of translational origin of symmetry species i;

n_i (R′), the number of lattice modes of rotational origin of symmetry species i;

n_i', the number of internal formate vibrations of symmetry species i.

The crystal structures on which these analyses are based have been summarized in Table III. It should be noted that while the number of molecules (Z) in the conventional unit cell of sodium formate is four, the primitive cell will contain only two molecules.

In the case of the formates of divalent cations the factor group analysis is almost trivial because, in each case, the atoms all lie on general positions. The unit cell of $Ca(HCO_2)_2$, for example, contains 16 formate ions composed of two sets of 8 crystallographically equivalent units. A set of eight formate ions, each member of which is executing the same normal vibration, gives rise to eight different combinations with the ions vibrating in phase or 180° out of phase relative to one of their number arbitrarily chosen; each combination corresponds to one of the irreducible representations. The other set of ions will exhibit eight identical combinations but, since the two sets are not related by symmetry, in-phase or out-of-phase combinations of the two sets are of the same symmetry species. Thus a single internal formate vibration has 16 components in the spectrum of the crystal. Only vibrations of three symmetry species are active, however, so that, if completely resolved, the infrared spectrum should reveal each internal vibration to be

Can. J. Chem. Downloaded from www.nrcresearchpress.com by 210.87.254.105 on 09/05/12
For personal use only.

Can. J. Chem. Downloaded from www.nrcresearchpress.com by 210.87.254.105 on 09/05/12
For personal use only.

TABLE V

Factor group vibrational analysis of crystalline $Ca(HCO_2)_2$

$V_h \equiv D_{2h}$	E	$C_2(z)$	$C_2(y)$	$C_2(x)$	i	$\sigma(xy)$	$\sigma(zx)$	$\sigma(yz)$	n_i	n_i (T)	n_i (T′)	n_i (R′)	n_i'
a_g	1	1	1	1	1	1	1	1	27	0	9	6	12
b_{1g}	1	1	−1	−1	1	1	−1	−1	27	0	9	6	12
b_{2g}	1	−1	1	−1	1	−1	1	−1	27	0	9	6	12
b_{3g}	1	−1	−1	1	1	−1	−1	1	27	0	9	6	12
a_u	1	1	1	1	−1	−1	−1	−1	27	0	9	6	12
b_{1u}	1	1	−1	−1	−1	−1	1	1	27	1	8	6	12
b_{2u}	1	−1	1	−1	−1	1	−1	1	27	1	8	6	12
b_{3u}	1	−1	−1	1	−1	1	1	−1	27	1	8	6	12

TABLE VI

Factor group vibrational analyses of crystalline $Ba(HCO_2)_2$, $Sr(HCO_2)_2$, and $Pb(HCO_2)_2$

D_2	E	$C_2(z)$	$C_2(y)$	$C_2(x)$	n_i	n_i (T)	n_i (T′)	n_i (R′)	n_i'
a	1	1	1	1	27	0	9	6	12
b_1	1	1	−1	−1	27	1	8	6	12
b_2	1	−1	1	−1	27	1	8	6	12
b_3	1	−1	−1	1	27	1	8	6	12

TABLE VII

Correlation table for $Na(HCO_2)$

Molecular group	Site group	Factor group
C_{2v}	C_2	C_{2h}
a_1	a	a_g
a_2		b_g
b_1	b	a_u
b_2		b_u

split into six components, two each of species b_{1u}, b_{2u}, and b_{3u}. Examination of Table II shows that in most cases only a doublet is observed, so that one might tentatively assume that each component of the doublet is composed of three unresolved absorption peaks corresponding to vibrations of symmetry b_{1u}, b_{2u}, and b_{3u}.

Similar considerations apply in the case of the formates which have the space group $D_2^4(P2_12_12_1)$. Each formate internal vibration will have eight components in the crystal spectrum but only six of these are infrared active, two each of species b_1, b_2, and b_3. Again, most of the internal vibrations are split into doublets, so that one is tempted to propose that each component of the doublet is composed of three unresolved absorption peaks corresponding to vibrations of symmetry b_1, b_2 and b_3.

In the case of sodium formate each internal formate vibration should give rise to two components, one of which is infrared active. In addition, because the twofold axes of the ions are coincident with those of the crystal, there is a correspondence between the a_1 modes of the free ion and the a_u modes of the crystal, and the b_1 and b_2 modes of the free ion and the b_u modes of the crystal (Table VII). These conclusions would appear to be in agreement with the observed spectrum.

It will be apparent from the above discussion that a study of single crystals of these materials using polarized radiation would be of considerable assistance in deciding the origin of the observed fine structure. Such an investigation of barium formate is nearly completed and will be reported upon shortly. In the case of lithium formate, a single crystal study would likely permit specific characterization of the space group and reveal whether or not the formate ions lie on special positions. In addition, because of the light cation, it is probable that many of the lattice modes will be in regions which are experimentally accessible.

ACKNOWLEDGMENTS

The authors are indebted to Mr. Rudolf Muelchen for his very capable assistance in the construction and maintenance of the apparatus. We wish also to gratefully acknowledge the financial assistance of the National Research Council of Canada.

Can. J. Chem. Downloaded from www.nrcresearchpress.com by 210.87.254.105 on 09/05/12
For personal use only.

RESUMÉ

On a mesuré l'absorption infrarouge de quelques formiates inorganiques dans l'état polycristallin. La multiplicité des bands d'absorption fondamentales de l'ion formiate est discuté en function de l'analyse vibrationale du groupe facteur.

REFERENCES

1. J. LECOMTE. Compt. Rend. **208**, 1401 (1939).
2. J. LECOMTE. Cahiers Phys. **17**, 1 (1943).
3. R. FONTEYNE. Natuurw. Tijdschr. (Ghent), **25**, 173 (1943).
4. S. BHAGAVANTAM and T. VENKATARAYUDU. Theory of groups and its application to physical problems. Andhra University, Waltair. 1951.
5. R. S. HALFORD. J. Chem. Phys. **14**, 8 (1946).

Can. J. Chem. Downloaded from www.nrcresearchpress.com by 210.87.254.105 on 09/05/12
For personal use only.

PREMELTING PHENOMENA IN LONG-CHAIN FATTY ACIDS

M. R. BARR, B. A. DUNELL, AND R. F. GRANT[1]
Chemistry Department, University of British Columbia, Vancouver, British Columbia
Received October 25, 1962

ABSTRACT

Nuclear magnetic resonance spectra and the infrared absorption between 700 and 750 cm^{-1} have been observed at temperatures near the melting points of the even-numbered fatty acids from C_{18} to C_{10}. The results are interpreted as indicating breakdown of crystalline character and onset of liquid-like motion at scattered points in the solid structure several degrees below the melting point, and increasing in extent as the melting point is approached.

Can. J. Chem. Downloaded from www.nrcresearchpress.com by 210.87.254.105 on 09/05/12
For personal use only.

A proton magnetic resonance study of anhydrous stearic acid (1) gave some quantitative indication of liquid-like molecular motion occurring in part of an otherwise rigid lattice at temperatures several degrees below the melting point. It seemed appropriate to look for this behavior, which was considered to be a premelting phenomenon (2), in other fatty acids and by other methods. Acids with an even number of carbon atoms from palmitic (C_{16}) to capric (C_{10}) have been examined by nuclear magnetic resonance, and the change with temperature of the shape of the infrared absorption band at about 720 cm^{-1} has been studied for the even-numbered acids from stearic (C_{18}) to lauric (C_{12}). This infrared band, which is characteristic of hydrocarbon chains $(CH_2)_n$ with $n \geqslant 4$, is frequently a doublet below the melting points of the compounds showing it, and a singlet above the melting point or for the compound in solution. It has been assigned to the CH_2 rocking mode (3, 4). A series of higher normal modes of CH_2 rocking has been identified in the spectra of *n*-paraffins in the range 720–1050 cm^{-1} (4). These bands are of much lower intensity than the first mode at 720 cm^{-1}, and their number depends on the length of the methylene chain. Stein has used the strong absorption of the first mode in an investigation of the crystallinity of polyethylene (5), attributing the component of the doublet at 720 cm^{-1} equally to crystalline and amorphous parts of the polymer and the component at 730 cm^{-1} exclusively to crystalline parts. The splitting of the band was explained by the perturbation of the CH_2 rocking vibration by the interaction of nearest-neighbor methylene chains in the crystalline array. It was shown (6) that the crystal field shifted the frequency of the out-of-phase rocking mode only slightly to higher energy and that the frequency of the in-phase mode was moved much further to higher energy. In an amorphous substance (solid, liquid, or solution) the unperturbed band occurs at essentially the same frequency as the out-of-phase mode in the crystalline substance. Changes with temperature in the intensity of this band have also been used to study phase transitions in waxes (7). In the work reported here, the variation with temperature of the integrated intensity of the components of the doublet has been examined as a possible indication of loss of crystalline character in fatty acids below the melting point.

EXPERIMENTAL

The acids used in this investigation were all Eastman Kodak white label grade that were further purified by repeated recrystallizations from acetone following the method of Brown and Kolb (8). Melting points were run on a hot stage microscope using a heating rate of about 0.2° C/min, and freezing points were obtained from the plateau of a time–temperature cooling curve. Values obtained are compared in Table I with those quoted by Markley (9).

[1]*Present address: Canadian Services College, Royal Roads, Victoria, B.C.*

TABLE I
Melting and freezing points of fatty acids used

	N.M.R. sample	I.R. sample		Literature (9)	
Acid	F.p.	F.p.	M.p.	F.p.	M.p.
Stearic (C_{18})	69.3	69.4	69.5–69.8	69.3	69.6
Palmitic (C_{16})	62.7	62.7	63.0	62.8	63.1
Myristic (C_{14})	54.1	54.1	54.3–54.5	54.1	53.9*
Lauric (C_{12})	43.9	43.7	44.0–44.3	43.9	44.2
Capric (C_{10})	31.2			31.2	31.6

*54.4 quoted by Francis and Piper, J. Am. Chem. Soc., **61**, 577 (1939).

Broad line n.m.r. spectra were obtained with a marginal oscillator spectrometer operating at 28 Mc/sec and a 6-in. Varian electromagnet. This spectrometer and the arrangements for temperature control have been described previously (1).

Infrared spectra were run on a Perkin–Elmer 21B double-beam spectrometer. Samples were prepared as solid films from a melt between sodium chloride plates and as pellets pressed with potassium bromide. Compensation was provided in the reference beam with a double-thickness sodium chloride plate or a pure potassium bromide pellet. The sample was heated with a standard Perkin–Elmer heating unit or cooled with vapor from liquid nitrogen flowing over the face of the NaCl plates, the sample and beam path being enclosed in a box. Temperature was measured with a copper–constantan thermocouple mounted in a small notch between the NaCl plates, and extending into the beam, or soldered into a well set into the KBr pellet holder. Temperature gradients around the KBr pellet were such that the thermocouple temperature in that case was probably good only to within 3°. For the samples between NaCl plates, temperatures are probably reliable to within 0.5°. Preliminary studies of the full spectrum of stearic acid from 4000 to 600 cm^{-1} were made at several temperatures from 30° C to 20° above the melting point. Expanded spectra (50 cm per 100 cm^{-1}) were then run in the range 750 to 700 cm^{-1}. Expanded runs for each acid were commenced at about 30°, made at successive temperatures down to about 60° below the melting point, then at increasing temperatures to some 20° above melting and back to 30° C.

RESULTS

The n.m.r. spectra of these acids are all comparable to those of stearic acid as their melting points are approached. A narrow line, whose width is determined on the broad line spectrometer by the depth of modulation at any temperature, can be resolved from the broad line. As the melting point of an acid is approached the intensity of the narrow component increases relative to the intensity of the rest of the line. The qualitative nature of this behavior has been shown in Fig. 1 of reference 1 for stearic acid. The derivative curves for n.m.r. absorption can be resolved very readily, and the relative integrated areas under the component absorption curves determined. The fraction, area under narrow component/area under both components, equals the fraction of protons involved in very rapid and extensive motion, corresponding to a liquid-like condition. This fraction is plotted in Fig. 1 as a function of $T_M - T$ for the acids studied, where T_M is the melting point of the acid, and T the temperature at which the spectrum was taken.

The infrared spectra of the acids all showed two peaks of the CH_2 rocking mode very clearly resolved at temperatures sufficiently below the melting points. This is illustrated by the four spectra of Fig. 2, all taken near 0° C and between 750 and 700 cm^{-1}. In addition, a third peak at frequency higher than the other two is very distinctly resolved in palmitic acid; it sometimes appears as a resolved peak and sometimes as a shoulder in lauric acid, and is seen as a shoulder in stearic acid, the more clearly the higher the temperature to within a couple of degrees of the melting point. There is some indication that myristic acid behaves like stearic but its shoulder at higher frequency is not as distinct, and no attempt was made to resolve it. These low- to medium-intensity

Can. J. Chem. Downloaded from www.nrcresearchpress.com by 210.87.254.105 on 09/05/12
For personal use only.

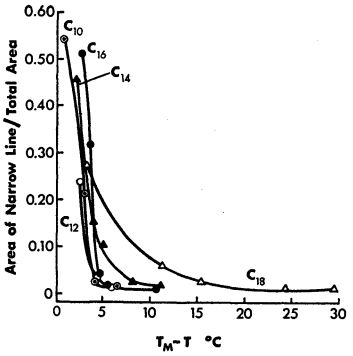

FIG. 1. Fraction of protons in rapid motion as obtained from n.m.r. study.

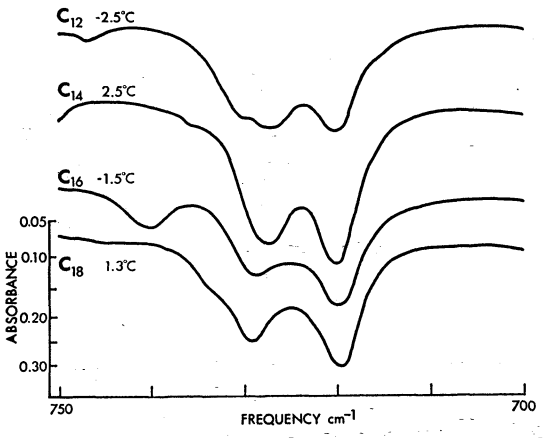

FIG. 2. Spectra of lauric, myristic, palmitic, and stearic acids near 0° C in the range 700–750 cm^{-1}. For each spectrum the absorbance at 750 cm^{-1} is 0.07. For convenience the ordinate has been displaced for each spectrum.

absorptions at about 735 cm^{-1} must arise from higher normal modes of the CH_2 rocking motion (4).

Graphical resolution of the whole band from 745 to 700 cm^{-1} was attempted in order to obtain the integrated intensity for each of the two principal peaks. Maximum transmission for the whole of the range 4000 to 600 cm^{-1} occurs near 750 cm^{-1} for these acids, and it was assumed that absorbance was zero at 750 cm^{-1} or at the point of maximum transmission close to 750 cm^{-1} for myristic and lauric acids. Absorbance was plotted on a linear scale against frequency (cm^{-1}) and it was assumed, for the purpose of resolving the bands, that absorbances were additive, that each peak was symmetrical about its maximum, and that no appreciable portion of a band was included in a long tail (4). Table II shows the frequencies of the peaks that were thus resolved for the solid acids.

Since the observed absorbances were all less than 0.35 (for 100% transmission at approximately 750 cm^{-1}), the difference between observed and true absorbance attributable to non-uniformity of sample thickness in those samples prepared from a melt cooled between sodium chloride plates was minimal and can probably be ignored without significant error (10).

Can. J. Chem. Downloaded from www.nrcresearchpress.com by 210.87.254.105 on 09/05/12
For personal use only.

TABLE II

Frequencies of resolved peaks in the infrared band for the CH_2 rocking mode in solid fatty acids

Acid	Frequencies (cm^{-1})		
Stearic (C_{18})	719.5	726–729*	733.5–736
Palmitic (C_{16})	720	726–728.5*	740.5
Myristic (C_{14})	720	726.5–728*	
Lauric (C_{12})	720	724–727*	731

*The frequency of the middle peak decreased as the melting point was approached.

The change in the appearance of the two lower-frequency peaks of the observed band with change in temperature is similar for all four acids studied, and is shown for stearic acid in Fig. 3. The behavior with changing temperature of the shoulder or peak at about

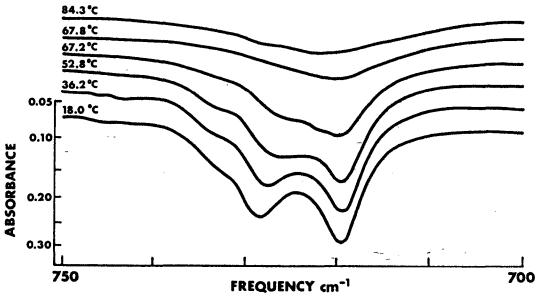

FIG. 3. Spectrum of stearic acid in the range 700–750 cm^{-1} at various temperatures. For each spectrum the absorbance at 750 cm^{-1} is 0.07. For convenience the ordinate has been displaced for each spectrum.

735 cm^{-1} varies considerably from one acid to another. At and above the melting point of each acid, resolution could only be made on the basis of asymmetry of the total band about its maximum, which now appears at approximately 720.5 cm^{-1}. The significance of such resolution as might be made is very questionable. One sample of myristic acid behaved irregularly by showing two just distinguishable peaks even at temperatures above the melting point. Determination of the integrated intensity above the melting point is also of doubtful significance because the peak is broadened to such an extent that it is very difficult to determine the shape of the wings, which apparently extend beyond 700 and 750 cm^{-1}, overlapping with other bands. A general increase in absorbance in the wings of the curve, both with film samples between NaCl plates and with samples pressed in KBr disks, may be in part due to change in scattering by the sample when the melting point is passed.

The spectra obtained from samples pressed in KBr pellets were qualitatively the same as those obtained from films of the acids. Three peaks could be resolved for each of the acids except myristic, which again showed a small, not easily resolvable shoulder near 735 cm^{-1}. The ratio of integrated areas under each peak did not agree with those obtained from film samples, although the progressive decrease in sharpness of resolution of the 727 cm^{-1} peak could be followed clearly as the melting point was approached. Lack of quantitative agreement between the two forms of sample might correspond with the observation of Kirkland that the absorptivity of bands associated with crystalline character is affected by particle size in the KBr pellet technique of sampling (11). More

Can. J. Chem. Downloaded from www.nrcresearchpress.com by 210.87.254.105 on 09/05/12
For personal use only.

probably, however, the effect is the result of preferential orientation in the sample film between the NaCl plates.

The variation in the integrated intensity under each of the 720 and 727 cm^{-1} peaks is shown as a function of temperature for four of the acids in Figs. 4 to 7. The intensities

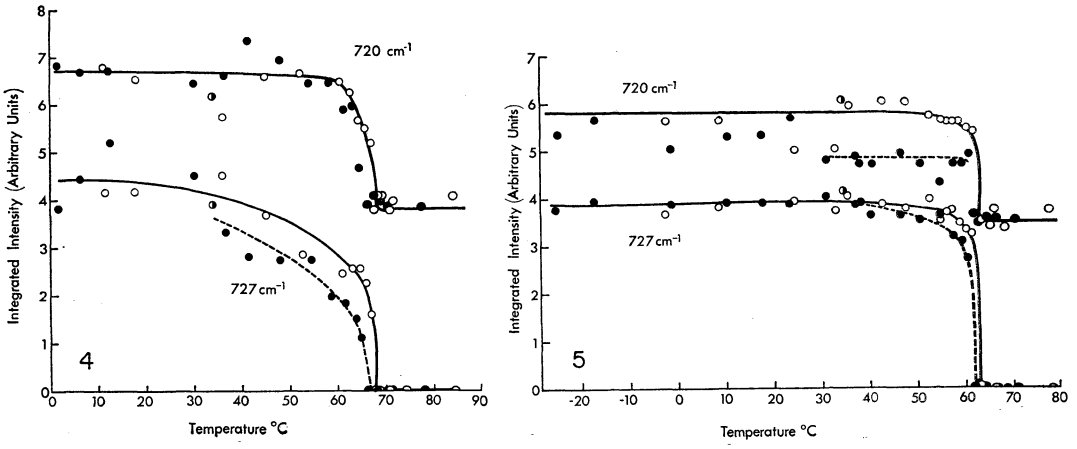

FIG. 4. Integrated intensities of the 720 and 727 cm^{-1} bands of stearic acid. Half-filled circles, starting temperature; open circles, increasing temperature; filled circles, decreasing temperature.

FIG. 5. Integrated intensities of the 720 and 727 cm^{-1} bands of palmitic acid. Half-filled circles, starting temperature; open circles, increasing temperature; filled circles, decreasing temperature.

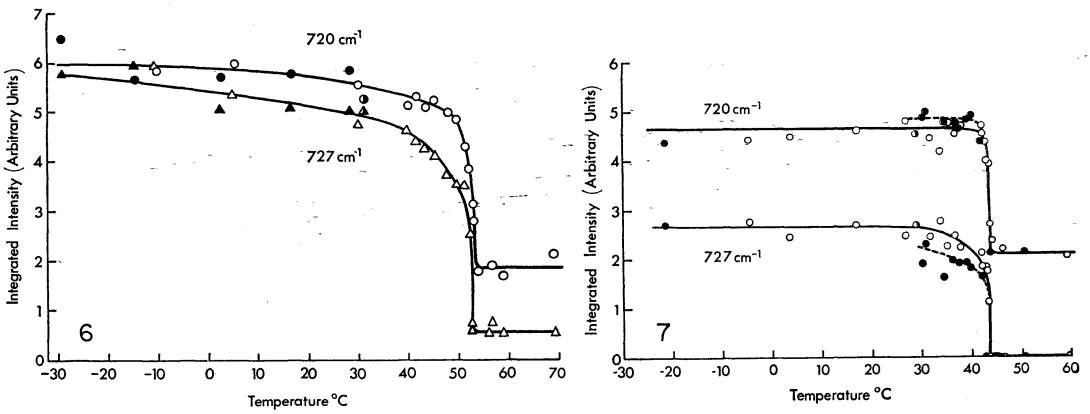

FIG. 6. Integrated intensities of 720 and 727 cm^{-1} bands of myristic acid. Half-filled points, starting temperature; open points, increasing temperature; filled points, decreasing temperature.

FIG. 7. Integrated intensities of 720 and 727 cm^{-1} bands of lauric acid. Half-filled circles, starting temperature; open circles, increasing temperature; filled circles, decreasing temperature.

are in arbitrary units, unrelated from one acid to another, and are taken from spectra obtained from film samples between NaCl plates. A hysteresis loop is found for each acid because of differences in behavior as the temperature is raised twoard the melting point or lowered from it. Using the notation of Stein and Sutherland from their work on the crystallinity of polyethylene (5), one can say that if x is the fraction of the sample which

Can. J. Chem. Downloaded from www.nrcresearchpress.com by 210.87.254.105 on 09/05/12
For personal use only.

is crystalline, or well ordered, and I_{720} and I_{727} are the integrated intensities in the 720 and 727 cm^{-1} bands,

$$\frac{I_{727}}{I_{720}} = \frac{xB_c}{xA_c+(1-x)A_a},$$

where A_a is the integrated intensity of the 720 cm^{-1} band for a completely amorphous sample, A_c is the same for a completely crystalline sample, and B_c is the integrated intensity of the 727 cm^{-1} band for a completely crystalline sample. Snyder (4) has indicated that the integrated intensities of the two bands need not be the same in a crystalline substance, and if we assume that the fatty acids are approaching a completely crystalline condition at low temperature, we can consider that B_c/A_c equals the low-temperature limiting value of the ratio of integrated intensities of 727 and 720 cm^{-1} bands, $(I_{727}/I_{720})_0$. If the ratio A_a/A_c is represented by ρ,

$$x = \frac{(I_{727}/I_{720})\rho}{(I_{727}/I_{720})_0+(I_{727}/I_{720})(\rho-1)}.$$

It is difficult to arrive at a value for the parameter ρ. Even if A_a is taken as the integrated absorption of the 720 cm^{-1} band above the melting point and A_c the corresponding quantity at lowest temperature, there is still difficulty in determining A_a. Resolution of the absorption curve above and just below the melting point is difficult, but one can construct a symmetrical band about 720 cm^{-1}. The remainder of the liquid phase absorption is a fairly symmetrical peak centered at about 735 cm^{-1}, corresponding, presumably, to a higher normal mode of the CH_2 rocking motion (4). Small variation in the optical density at the edges of the CH_2 rocking absorption (at 750 cm^{-1} and 700 cm^{-1}) as one passes through the melting point may be due to changes in scattering of radiation with the change of phase. Such changes in optical density which move the whole band make a significant increment in the integrated intensity. In spite of these uncertainties, and failing a better method of determining ρ, we have estimated ρ by taking the ratio of the integrated intensity of a resolved 720 cm^{-1} peak above the melting point to that of the 720 cm^{-1} peak at the lowest temperatures. Values of ρ of 0.57, 0.60, 0.42, and 0.46 have been obtained from the curves of Figs. 4 to 7 for stearic, palmitic, myristic, and lauric acids, respectively. Stein and Sutherland (5) estimate ρ to be in the range 1.4 to 2 for long-chain hydrocarbons. Such a large value of ρ appears, however, to be inconsistent with the observed decrease of the integrated intensity of the 720 cm^{-1} band with increasing temperature in fatty acids. From the relation

$$I_{720} = A_a+x(A_c-A_a)$$

it is seen that if x decreases with increasing temperature and I_{720} is to decrease with increasing temperature, $A_c > A_a$, which requires that $\rho < 1$. The quantity $1-x$, measuring the extent of disorder in the alignment of the CH_2 chains, is plotted using the appropriate value of ρ for each of the acids as a function of temperature difference from the melting point, T_M-T, in Fig. 8.

DISCUSSION

It is not considered that the fraction, $1-x$, of disordered material as obtained from the infrared study should be directly comparable to the fraction of protons in rapid, liquid-like motion as measured by the area of the narrow n.m.r. absorption peak divided

Can. J. Chem. Downloaded from www.nrcresearchpress.com by 210.87.254.105 on 09/05/12
For personal use only.

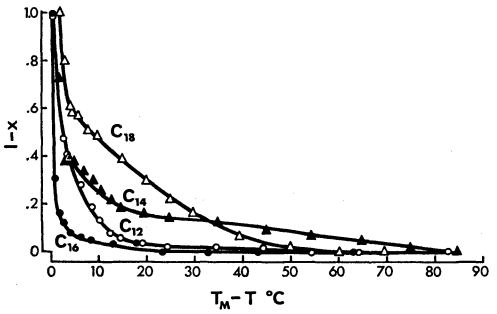

FIG. 8. Fraction of the lattice which is disordered, $1-x$, as a function of the temperature interval from the melting point, $T_M - T$, for stearic, palmitic, myristic, and lauric acids.

by the total area under the n.m.r. absorption curve. Apart from the uncertainties inherent in the calculation of x, the two quantities may not agree because it is quite possible that disordered chains may be rigid as far as n.m.r. observations are concerned (reorientations less frequent than approx. $\gamma\Delta H = 4(10^5)$ cycles/sec), and consequently contribute to decreasing x, but not to the area of the narrow n.m.r. signal. The n.m.r. results show that in all the fatty acids studied a significant fraction of the protons are in liquid-like motion at least 4° C below the melting point of the acid, and the fraction increases as the melting point is approached. Since 1% of palmitic acid impurity in stearic acid has been found to lower the freezing point of stearic acid by 0.24° C (12), it is probable that none of the acids contains more than 1% impurity, and most samples much less. Thus one can in no case attribute the narrow line of the n.m.r. spectrum solely to motion of impurities, although the impurities may serve as centers at which disordering of the main lattice may occur below its melting point. It is presumed (1) that liquid-like regions appear at defect or impurity centers in the crystal and spread from there as the melting point is closely approached. A study of the effect on this phenomenon of introducing known amounts of impurity is indicated, and preliminary results point to the existence of a larger amount of liquid-like motion at lower temperatures when the sample is more impure. Variation from acid to acid of the percentage of protons in liquid-like motion as a function of temperature interval to the melting point may be dependent only on the purity of the samples, except in the case of stearic acid, for which the purity is considered to be very high. If this is correct, the unusually large amounts of liquid-like motion in stearic acid must be dependent on the crystal structure of stearic acid rather than on a high impurity content.

The infrared results suggest that lack of crystalline order appears well below the melting points of the fatty acids and as the melting point is approached increases rather more rapidly in extent than does the liquid-like motion evidenced by the n.m.r. behavior. It is possible that disordering of the crystal lattice around imperfection sites, without significantly rapid chain motion accompanying the disorder, precedes the appearance of the liquid-like regions. The infrared studies of Davison and Corish on polyesters (13) and dicarboxylic acids (14) indicate, contrary to the review by Bellamy (3), that the 720 cm^{-1} peak in the compounds they studied is virtually eliminated upon melting and they conclude that the extended trans configuration of the methylene chain is virtually absent from the molten state of these substances. Bradbury, Elliott, and Fraser (15) find that the 720 cm^{-1} band is greatly reduced in intensity with increasing temperature in polyethylene and polyethylene suberate, but that it does not disappear. From this and other

Can. J. Chem. Downloaded from www.nrcresearchpress.com by 210.87.254.105 on 09/05/12
For personal use only.

evidence they conclude that there are many configurations of the hydrocarbon chain which, in amorphous material, do not contribute to the 720 cm^{-1} CH_2 rocking band. If it is supposed that the fraction of the CH_2 groups which is in disordered configurations which do not contribute to the 720 cm^{-1} peak remains effectively constant within the temperature range involved in this study, then the factor ρ includes the necessary compensation for the failure of certain conformations to contribute to the observed band. The measure $1-x$ of the extent of disordering of hydrocarbon chains should be, then, reliable to within the extent to which ρ is correctly evaluated, and to which the fraction of non-contributing disordered conformations is independent of temperature.

An alternative approach (16) also assumes that the sample is 100% crystalline (or of ordered configuration) at low temperature and that the distribution of chain conformations in the liquid just above the melting point is the same as the distribution in the regions of disorder below the melting point. Then if C is integrated intensity of the whole doublet at low temperature ($C = A_c+B_c$), and A is the integrated intensity of the 720 cm^{-1} band just above the melting point (where the 727 cm^{-1} band has disappeared; $A = A_a$), and I_T is the integrated intensity of the doublet at intermediate temperature T ($I_T = I_{720}+I_{727}$), the fraction of chains undergoing melting is

$$f = \frac{C-I_T}{C-A}.$$

The fraction f is plotted in Fig. 9 as a function of T_M-T, having been calculated from the results shown in Figs. 4–7 as

$$f = \frac{(I_{720}+I_{727})_0-(I_{720}+I_{727})_T}{(I_{720}+I_{727})_0-A_a}.$$

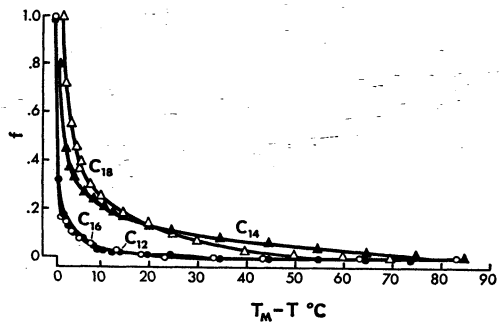

FIG. 9. The fraction f of chains which are disordered as calculated from total integrated intensity of both components of the doublet is plotted as a function of temperature interval from the melting point for stearic, palmitic, myristic, and lauric acids.

In terms of the previous assumptions, namely, $I_{720} = xA_c+(1-x)A_a$, and $I_{727} = xB_c$, the right-hand side of this expression reduces to $1-x$. The curves of Figs. 8 and 9 for $1-x$ and f, respectively, as functions of T_M-T are not identical, but are very close to one another for palmitic and myristic acids and are sufficiently alike for stearic and lauric acids that they lead to the same qualitative picture of the premelting behavior in these acids. Such discrepancy as exists may be due to failure of the assumption that the distribution of conformations in the disordered portions is independent of temperature or to difficulties associated with preferential orientation in the film samples between NaCl

Can. J. Chem. Downloaded from www.nrcresearchpress.com by 210.87.254.105 on 09/05/12
For personal use only.

plates. The infrared results do, however, support the n.m.r. evidence for the existence of premelting behavior well below the accepted melting points of these fatty acids.

ACKNOWLEDGMENTS

The authors wish to thank the National Research Council of Canada for financial assistance by the award of a grant-in-aid for research and of a studentship to R. F. G.

REFERENCES

1. R. F. GRANT and B. A. DUNELL. Can. J. Chem. **38**, 359 (1960).
2. A. R. UBBELOHDE. Trans. Faraday Soc. **34**, 282 (1938).
3. L. J. BELLAMY. The infra-red spectra of complex molecules. Methuen and Co., Ltd., London. 1958. p. 27.
4. R. G. SNYDER. J. Mol. Spectry. **4**, 411 (1960); **7**, 116 (1961).
5. R. S. STEIN and G. B. B. M. SUTHERLAND. J. Chem. Phys. **22**, 1993 (1954).
6. R. S. STEIN. J. Chem. Phys. **23**, 734 (1955).
7. J. M. MARTIN, JR., R. W. B. JOHNSTON, H. J. CANNON, and M. J. O'NEAL. Anal. Chem. **30**, 1005 (1958).
8. J. R. BROWN and D. K. KOLB. Progress in the chemistry of fats and other lipids. Vol. 3. Pergamon Press, Ltd., London. 1955. p. 58.
9. K. S. MARKLEY. Fatty acids. Interscience Publishers, Inc., New York. 1947. p. 114.
10. R. N. JONES and C. SANDORFY. *In* Chemical applications of spectroscopy. *Edited by* W. West. Interscience Publishers, New York. 1956. p. 268.
11. J. J. KIRKLAND. Anal. Chem. **27**, 1537 (1955).
12. F. FRANCIS, F. J. E. COLLINS, and S. H. PIPER. Proc. Roy. Soc. (London), Ser. A, **158**, 691 (1937).
13. W. H. T. DAVISON and P. J. CORISH. J. Chem. Soc. 2428 (1955).
14. P. J. CORISH and W. H. T. DAVISON. J. Chem. Soc. 2431 (1955).
15. E. M. BRADBURY, A. ELLIOTT, and R. D. B. FRASER. Trans. Faraday Soc. **56**, 1117 (1960).
16. E. M. BRADBURY. Private communication.

Can. J. Chem. Downloaded from www.nrcresearchpress.com by 210.87.254.105 on 09/05/12
For personal use only.

THE PHOTOLYSIS OF TRIFLUOROACETIC ACID VAPOR[1]

A. M. MEARNS[2] AND R. A. BACK
Division of Pure Chemistry, National Research Council of Canada, Ottawa, Canada

Received December 22, 1962

ABSTRACT

The photolysis of CF_3COOH vapor has been studied at temperatures between about 90 and 190° C, using light of wavelengths between 2000 and 2200 Å. The major products were CO_2 and C_2F_6, with smaller amounts of CO, H_2, and CF_3H. A marked reduction in the yields of CO_2, CO, and H_2 with increasing pressure of added isobutane or 1-butene has been interpreted to imply the presence of free COOH radicals in the system, which is supported by the tentative identification of formic and oxalic acids as products of the photolysis. It is thought that the reaction

$$CF_3COOH + h\nu \rightarrow CF_3 + COOH$$

represents the main primary photolytic process, with the minor processes

$$CF_3COOH + h\nu \rightarrow CF_3 + CO_2 + H$$

and

$$CF_3COOH + h\nu \rightarrow CF_3 + CO + OH$$

accounting for no more than 27 and 7% respectively of the total at 165° C.

Some tentative conclusions have been drawn about the reactions of COOH radicals. In the present system, the disproportionation reaction,

$$2COOH \rightarrow CO_2 + HCOOH,$$

appears to predominate, with the decomposition reaction,

$$COOH \rightarrow CO_2 + H,$$

apparently of minor importance at 165° C.

INTRODUCTION

Previous studies of the vapor-phase photolysis of acetic acid have indicated a mechanism, partly intramolecular and partly free radical, which was complicated by secondary reactions of radicals with the parent compound (1, 2, 3). It was thought that the photolysis of trifluoroacetic acid should be very much simpler, by analogy with the perfluoroketones, and might yield some useful information about the primary photolysis process in carboxylic acids, and about the stability and reactions of the COOH radical.

EXPERIMENTAL

The photolysis vessel was a quartz cylinder, 10 cm long and 5 cm in diameter, with plane windows at both ends, whose temperature was controlled to ±0.5° C with an air thermostat. The light source was a medium-pressure Hanovia S-500 mercury arc, used without a filter, and collimated to give approximately uniform illumination throughout the vessel. The absorption spectrum of the acid vapor showed a strong, apparently continuous absorption beginning at about 2200 Å, so that the light effective in the photolysis was of wavelength between 2200 and 2000 Å. In a few experiments in which it was desired to selectively photolyze perfluoroacetone in mixtures with CF_3COOH, Corning filter 9700 was used to eliminate light with wavelengths below 2600 Å. In almost all the experiments, the time of irradiation was about 200 minutes.

In the first series of experiments, the reaction vessel was attached through a metal diaphragm valve (Hoke 413) to conventional high-vacuum preparation and analytical lines. When it became evident that non-volatile products were accumulating in the reaction vessel, and were decomposing to yield CO and CO_2, a different technique was adopted. Before each experiment, the photolysis vessel was fitted with a break-seal and attached to the preparation line through a constricted Pyrex lead, and was baked overnight at 350° C under vacuum. The reagent vapors were then metered out and condensed in the vessel at −196° C, and after evacuation to a pressure of 10^{-5} mm, the vessel was sealed at the constriction, removed from the preparation

[1]*Issued as N.R.C. No. 7287.*

[2]*National Research Council of Canada Postdoctoral Fellow, 1959–1961. Present address: Constantine College of Technology, Middlesbrough, Yorkshire, England.*

Can. J. Chem. Downloaded from www.nrcresearchpress.com by 210.87.254.42 on 09/05/12
For personal use only.

line, and mounted in a reproducible position in the air thermostat. After irradiation, the vessel was removed again, and attached through the break-seal to the analytical line. This technique was found to give consistent and reproducible results, and was used in all but the first few preliminary experiments.

The products of the reaction were condensed at −196° C, and CO and H_2 were removed through a trap at −210° C, measured in a gas burette, and analyzed by combustion on copper oxide. Mass-spectrometric analysis showed that H_2 and CO were the only gases non-condensable at −210° C. The remaining products were transferred to two low-temperature stills in series, and C_2F_6, CF_3H, and CO_2 were removed at −145° C and measured in a gas burette. This fraction was then analyzed by gas chromatography, using a 2-m column of silica gel at 76° C. In some experiments, an analysis was made for higher-boiling products. Isobutane, when present, was removed at −125° C, and the remaining material analyzed by gas chromatography, using a column with 20% glyceryl monooleate on firebrick.

Trifluoroacetic acid was obtained from three different sources. The acid itself was purchased from both the Minnesota Mining and Manufacturing Co., and the Columbia Chemical Co. The acid was then distilled at atmospheric pressure, a middle fraction being collected, which was treated with anhydrous sodium sulphate, and distilled again on a Vigreaux-type column. The vapor was dried again over sodium sulphate in the vacuum line, was degassed thoroughly by the usual methods, and stored at −80° C. The third source of acid was its preparation by the addition of water to an excess of the acid anhydride, which was obtained from Matheson, Coleman and Bell, the excess anhydride being distilled off. Acid from all three sources gave identical results, and no impurities were detectable by gas chromatography.

Hexafluoroacetone was obtained from Merck and purified by methods described elsewhere (4). Perfluorobutane was obtained from Minnesota Mining and Manufacturing Company, while isobutane and 1-butene were Phillips' research-grade, all used without further purification.

RESULTS

Preliminary experiments in the fixed reaction vessel at 150° C showed that CO_2, C_2F_6, and CO were the main products of the photolysis, with much smaller amounts of CF_3H and H_2. In a series of experiments, a single sample of acid was irradiated three times, volatile products being removed after each irradiation, and it was observed that the yields of CO_2 and CO increased progressively by about 30% between the first and the third experiments, while the C_2F_6 yield remained almost constant. Subsequently it was found that irradiating the "empty" reaction vessel, or heating it to 200° C, caused the evolution of appreciable quantities of CO and CO_2, and it was concluded that a very slightly volatile material, possibly oxalic acid, or perhaps some higher product of the photolysis, was condensed on the walls of the vessel, and decomposed either thermally or by photolysis to give CO and CO_2 in approximately equal quantities. It proved very difficult to eliminate these effects in the fixed reaction vessel, so that finally a detachable vessel, which could be thoroughly baked out between experiments, as previously described, was adopted, and used in all subsequent experiments.

In Table I are shown the gaseous products of the photolysis at 165° C, at several pressures of CF_3COOH, and in Fig. 1, values of $CO + CO_2$ and of $CF_3H + 2C_2F_6$ are

TABLE I

Products of the photolysis of CF_3COOH at 165° C

CF_3COOH pressure (mm)	Rates of product formation (μmoles/min×100)				
	C_2F_6	CF_3H	CO_2	CO	H_2
10.5	0.219	0.047	0.666	0.133	0.021
28.0	0.610	0.071	1.645	0.252	0.044
50.7	1.025	0.110	2.570	0.420	0.063
98.0	1.520	0.150	3.500	0.463	0.162

plotted against the pressure of acid. Several features are evident from these data. The yield of C_2F_6 was much greater than that of CF_3H, indicating that abstraction of hydrogen from the acid by CF_3 radicals was very inefficient, and also that the intramolecular

Can. J. Chem. Downloaded from www.nrcresearchpress.com by 210.87.254.42 on 09/05/12
For personal use only.

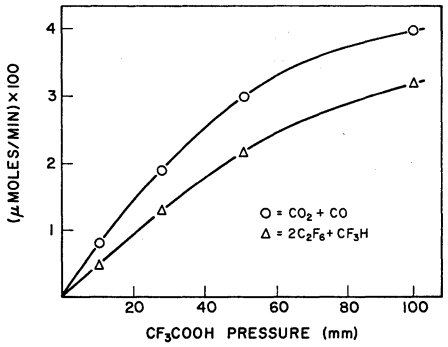

FIG. 1. Products of the photolysis vs. pressure of CF_3COOH vapor, showing the deficit of CF_3-containing products.

formation of CF_3H and CO_2 was not an important primary process. The yield of CO_2 was much greater than that of CO, and the ratio CO_2/CO increased from 5.0 to 7.6 with increasing pressure of acid. The material balance evident in Fig. 1 indicates an apparent loss of CF_3 radicals which varied from about 40% to 20% with increasing pressure of acid. There was also a marked shortage of hydrogen in the gaseous products, with the H_2 and CF_3H accounting for only about 9 to 13% of the yield of CO_2. The general pressure dependence of the yields of gaseous products (Fig. 1) appears to parallel approximately the absorption of light in the system, although because the light was not monochromatic, no precise measurement of the absorption was possible.

A series of experiments was made at 165° C with a constant pressure of CF_3COOH and varying amounts of isobutane added to see whether the yield of CF_3-containing products might be improved by providing a substrate for the abstraction of hydrogen. The results are shown in Figs. 2 and 3. As expected, the yield of C_2F_6 fell rapidly to zero

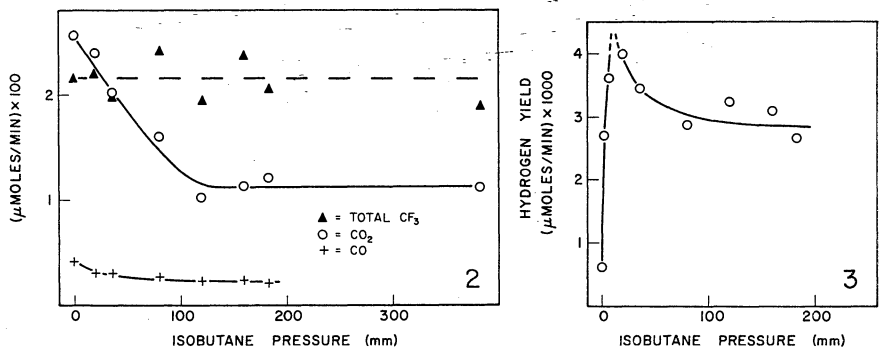

FIG. 2. The effect of added isobutane on the products of the photolysis at 165° C, with an acid pressure of 50.7 mm.

Fig. 3. The effect of added isobutane on the hydrogen yield from the photolysis at 165° C, with an acid pressure of 50.7 mm.

with increasing isobutane pressure, while the yield of CF_3H rose accordingly. However, the final rate of production of CF_3H at high isobutane pressure was, within a rather large experimental scatter, just equal to twice that of C_2F_6 in the pure acid, so that the total yield of CF_3-containing products was unchanged. The isobutane, however, had a

Can. J. Chem. Downloaded from www.nrcresearchpress.com by 210.87.254.42 on 09/05/12
For personal use only.

marked effect on all the other products. The yield of H_2 rose sharply, passed through a maximum of about 20 mm pressure of isobutane, and decreased again at higher pressures of isobutane. The yields of CO_2 and CO were both reduced to about one-half their original values by the addition of isobutane.

In order to determine whether the effect of isobutane might be due simply to collisional deactivation, some experiments were made with added C_4F_{10}, both with and without isobutane present (Table II). Like isobutane, the C_4F_{10} appeared to have little effect on

TABLE II

Effect of C_4F_{10} on the photolysis products
(T = 165° C, CF_3COOH = 50.7 mm)

C_4H_{10} pressure (mm)	C_4F_{10} pressure (mm)	Rates of product formation (μmoles/min$\times$100)				
		C_2F_6	CF_3H	CO_2	CO	H_2
—	—	1.03	0.11	2.57	0.42	0.06
35.5	—	—	2.00	2.02	0.31	0.34
37.5	78.5	—	2.01	1.77	Not	measured
38.0	174.0	—	2.09	1.68	Not	measured
—	122.0	0.90	0.15	2.42	0.39	0.09

the yield of CF_3-containing products. There was a slight decrease in the yield of CO_2, both with and without isobutane also present, but C_4F_{10} was about 10 times less effective than isobutane in reducing the yield.

In Fig. 4 is shown the effect of temperature on the products of the photolysis, with 50

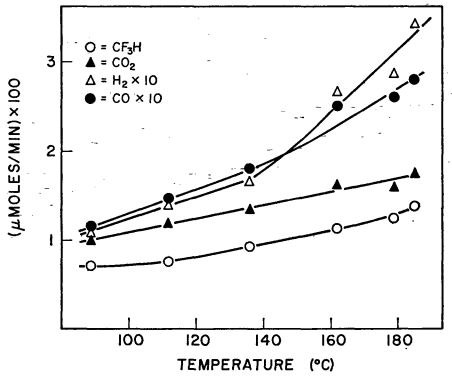

FIG. 4. The effect of temperature on the photolysis of CF_3COOH, at a constant pressure of 50.7 mm of acid and 80 mm of isobutane.

mm pressure of CF_3COOH and 80 mm of isobutane. All the products increased with increasing temperature, H_2 the most markedly and CF_3H the least. The light intensity was somewhat less than for the experiments in Figs. 1 and 2, so that the data are not exactly comparable.

In Table III is shown the effect of 1-butene on the photolysis of CF_3COOH. The only products observed in the presence of the olefin were CO_2 and CO, and these were reduced to about one-third and one-half respectively of their original yields.

Can. J. Chem. Downloaded from www.nrcresearchpress.com by 210.87.254.42 on 09/05/12
For personal use only.

TABLE III

The effect of butene-1 on the photolysis of CF_3COOH (T = 165° C, CF_3COOH pressure = 50.7 mm)

Butene-1 pressure (mm)	Rates of product formation (μmoles/min $\times$ 100)	
	CO_2	CO
—	2.57	0.42
19	0.79	0.21
71	0.73	0.20
168	0.83	0.19

DISCUSSION

Molecular Association in CF_3COOH Vapor

Trifluoroacetic acid, like other carboxylic acids, is known to be partially associated into hydrogen-bonded dimer molecules in the vapor phase (5), and the effect of such association on the photolysis must be considered. The degree of association depends upon both temperature and pressure. Most of the present results were obtained at 165° C and a pressure of 50.7 mm, and from the data of Taylor and Templeman (5), one may calculate a monomer/dimer ratio of 144. It seems unlikely that acid dimers present in such low concentration played any important role in the photolysis mechanism. At 90° C, the lowest temperature used, with a pressure of 50.7 mm, the monomer/dimer ratio was about 6. The lack of any profound changes in the products of the photolysis with changing pressure and temperature suggests that the presence of dimer molecules had little effect in the present experiments.

Primary Processes

The experimental evidence suggests that the main primary process in the photolysis was

$$CF_3COOH + h\nu \rightarrow CF_3 + COOH. \qquad [1]$$

While this reaction presumably proceeded through some excited state of CF_3COOH, the almost negligible effect of C_4F_{10}, the relatively small effect of temperature, and the nature of the dependence of the product yields on the pressures of acid, isobutane, and 1-butene all indicate that any such excited intermediate was too short lived under the experimental conditions to suffer appreciable deactivation before decomposing. This is not surprising in view of the energy of 130 to 140 kcal/einstein of the absorbed light.

The formation of free CF_3 radicals in the photolysis seems beyond doubt. The production of C_2F_6 in the pure acid, its replacement by CF_3H in the presence of isobutane, and the complete suppression of both products by 1-butene can only be explained by reactions of free CF_3 radicals, and it appears that the intramolecular production of CF_3-containing products, in particular the formation of CF_3H and CO_2, played no part in the photolysis. This is in contrast to the photolysis of CH_3COOD, in which intramolecular formation of CH_3D and CO_2 was thought to be a minor ($\sim$10%) primary process (1).

The evidence for the presence of free COOH radicals in the system is less certain, but still fairly convincing. The ability of isobutane to reduce by about one-half the yields of CO_2 and CO, without seriously affecting the production of CF_3-containing products, strongly suggests the removal, by reaction, of some precursor of CO_2 and CO. This view is confirmed by the effect of 1-butene on the yields of CO_2 and CO. The effect of isobutane on the yield of H_2 suggests that hydrogen atoms were formed in the photolysis, which,

Can. J. Chem. Downloaded from www.nrcresearchpress.com by 210.87.254.42 on 09/05/12
For personal use only.

in the pure acid, disappeared, probably by reaction with the acid, without forming H_2. These hydrogen atoms reacted efficiently with added isobutane, and the H_2 production rose sharply (Fig. 3). The subsequent decrease in hydrogen production as more isobutane was added approximately parallelled the decreases in CO_2 and CO, and suggests that a common precursor of CO_2, CO, and H was being removed by reaction with isobutane. The carboxyl radical is the most probable such precursor. The suppression by 1-butene of the CO_2 and CO yields to approximately the same extent as caused by isobutane indicates that the precursor can also disappear by reaction with 1-butene, while the complete suppression of hydrogen production suggests that all the hydrogen was formed by reactions of hydrogen atoms or carboxyl radicals.

There is some additional supporting evidence for the presence of free carboxyl radicals. In two experiments at 117° C with 50.7 mm of acid and 88 mm of isobutane, appreciable amounts of formic acid were detected in the products by gas chromatography. In three similar experiments at 166° C, and in one other experiment at 117° C, however, formic acid was not found. This rather capricious behavior was probably due to the difficulties in detecting micromolar amounts of formic acid in a large excess of CF_3COOH, which tended to flood the chromatographic column, so that formic acid appeared as a small peak superimposed on a large "tail". In the experiments at 117° C, the reaction vessel was also fitted with a second break-seal, so that after removal of all the volatile products in the usual way, the vessel was sealed again and baked overnight at 300° C. Several micromoles of gas were produced which was found to consist of CO and CO_2 in almost equal amounts, of water vapor, and of traces of H_2 and C_8-hydrocarbon, perhaps a dimer of butyl radicals. The formation of CO, CO_2, and water in the observed proportions suggests that oxalic acid may have been the involatile compound which was deposited on the walls of the vessel, and which decomposed thermally. Similar deposition of a compound which yielded CO and CO_2 on heating or on photolysis had also been observed in the fixed reaction vessel used in preliminary experiments. The formation of formic and oxalic acids in the system is most simply explained as resulting from abstraction and dimerization reactions of free carboxyl radicals.

The continued production of some CO and CO_2 in the presence of 1-butene suggests the occurrence of two other primary processes,

$$CF_3COOH + h\nu \rightarrow CF_3 + CO_2 + H \quad [2]$$

and

$$CF_3COOH + h\nu \rightarrow CF_3 + CO + OH, \quad [3]$$

which from the data in Table III may be estimated to represent 27 and 7% respectively of the primary photolysis process, with reaction [1] accounting for the remainder.

In this estimate, no account was taken of carboxyl radicals which reacted to form products other than CO and CO_2. It is also possible that some of the CO_2, and perhaps the CO, formed in the presence of 1-butene came from disproportionation reactions of COOH with hydrocarbon radicals. For these reasons, the values of 27 and 7% for reactions [2] and [3] should be regarded as upper limits.

Reactions of CF_3 Radicals

In the pure acid, from 90 to 95% of the CF_3 radicals found in the products were accounted for by C_2F_6, which was almost certainly formed by simple dimerization. The remainder was CF_3H, and this apparently did not arise by abstraction of hydrogen from CF_3COOH. This was shown by several experiments in which CF_3 radicals were generated by the selective photolysis of perfluoroacetone in the presence of CF_3COOH, and no CF_3H

Can. J. Chem. Downloaded from www.nrcresearchpress.com by 210.87.254.42 on 09/05/12
For personal use only.

was observed. The most probable source of CF_3H in the photolysis of the acid is the disproportionation reaction

$$CF_3 + COOH \rightarrow CF_3H + CO_2. \quad [4]$$

The material balance of the volatile products, shown in Fig. 1, indicated a considerable loss of CF_3 radicals in the photolysis of the pure acid. This loss was most likely due to an addition reaction,

$$CF_3 + CF_3COOH \rightarrow (CF_3)_2\dot{C}—OH, \quad [5]$$

followed by further reactions of the resulting radical to form higher-weight products. Such addition of perfluoro radicals to carbonyl double bonds has been observed previously (6, 7).

When the experiments with added isobutane were done, it was thought that the reaction

$$CF_3 + C_4H_{10} \rightarrow CF_3H + C_4H_9 \quad [6]$$

would effectively scavenge all the CF_3 radicals, so that the limiting rate of production of CF_3H at high isobutane pressure would be a measure of the CF_3 radicals initially formed. It has since become evident that this simple condition cannot in practice be attained with isobutane (8). At a very early stage in the reaction, isobutene, formed by disproportionation of butyl radicals, begins to compete effectively with isobutane for CF_3 radicals,

$$CF_3 + C_4H_8 \rightarrow CF_3C_4H_8—. \quad [7]$$

Olefin is used up in the process, and rapidly reaches a very low steady-state concentration, which because of the relatively high value of the ratio k_7/k_6 is achieved after less than 0.1% reaction. The $CF_3C_4H_8$ radicals probably undergo further reactions, resulting in CF_3-containing compounds with 5 to 10 carbon atoms. Under certain conditions, reaction of CF_3 radicals with C_4H_9 or other radicals may also compete with reaction [6]. The net result of these complications is that, for example, in the photolysis of hexafluoroacetone in the presence of isobutane at 120° C, a limiting rate of production of CF_3H at high isobutane pressure corresponded to only about 70% of the CF_3 radicals formed (8). It appears almost certain that in the photolysis of CF_3COOH there was a similar loss of CF_3 radicals in the presence of isobutane, the exact extent depending on a number of parameters of the system. Thus in the pure acid, CF_3 radicals were probably lost by addition to the carbonyl double bond, while with isobutane added, they disappeared chiefly by addition to the isobutene which was present in a low steady-state concentration. The loss by these two mechanisms appears to have been fortuitously about the same, within the rather large experimental scatter.

Reactions of COOH Radicals

There is some uncertainty about the thermochemistry of the carboxyl radical. Most previous workers have assumed that the reaction

$$COOH \rightarrow CO_2 + H \quad [8]$$

was endothermic by only a few kilocalories, and that the carboxyl radical decomposed rapidly in this way even at room temperature. However, there are at present two sets of conflicting data. Gorden and Ausloos (9) have estimated reaction [8] to be almost thermoneutral; this estimate was based on Glockler's values for the dissociation energies of the

Can. J. Chem. Downloaded from www.nrcresearchpress.com by 210.87.254.42 on 09/05/12
For personal use only.

C—C bond in acetic acid (93 kcal) and the C—H bond in formic acid (99.9 kcal), which were calculated from a correlation of bond length with bond energy (10), and which lead to $\Delta H_f(\text{COOH}) = -43$ kcal. On the other hand, Back and Sehon have estimated, from a toluene-carrier measurement of the bond-dissociation energy of phenylacetic acid (11), that $\Delta H_f(\text{COOH}) = -62$ kcal/mole, which would make reaction [8] about 20 kcal endothermic, and which would lead to dissociation energies of about 85 and 78 kcal for the C—H and C—C bonds in formic acid and acetic acid respectively. These latter bond energies seem slightly low, and those estimated by Glockler rather high, by comparison with similar C—C and C—H bonds, and an intermediate value for $\Delta H_f(\text{COOH})$ is perhaps most probable, as there are considerable uncertainties in both estimates. Thus an endothermicity of 10 ± 10 kcal may be assigned to reaction [8], which, combined with a probable activation energy for the reverse reaction of at least 10 kcal, suggests that carboxyl radicals may well be stable enough to undergo a variety of reactions in the present system. The alternative decomposition,

$$\text{COOH} \rightarrow \text{CO} + \text{OH}, \qquad [9]$$

is well established to be 25 kcal more endothermic than reaction [8], and should certainly be unimportant by comparison at the temperatures of the present study.

In the photolysis of the pure acid, several combination and disproportionation reactions are possible:

$$2\text{COOH} \rightarrow (\text{COOH})_2 \qquad [10]$$
$$\rightarrow \text{CO}_2 + \text{HCOOH} \qquad [11]$$
$$\rightarrow 2\text{CO}_2 + \text{H}_2 \qquad [12]$$
$$\rightarrow \text{CO}_2 + \text{CO} + \text{H}_2\text{O}. \qquad [13]$$

In the presence of isobutane, the situation is somewhat complex. The simplest way to account for the reduced yields of CO_2, CO, and H_2 is by the reaction

$$\text{COOH} + \text{C}_4\text{H}_{10} \rightarrow \text{HCOOH} + \text{C}_4\text{H}_9. \qquad [14]$$

The thermochemistry of this reaction is in some doubt due to the uncertainty in the C—H bond in formic acid, and it may or may not be exothermic. It also seems probable, as discussed earlier, that in the trifluoroacetic acid – isobutane system there was a low steady-state concentration of olefin formed by disproportionation of isobutyl radicals, and reaction with this olefin may account for a considerable part of the loss of COOH radicals. The effect of 1-butene on the photolysis shows that olefins can remove carboxyl radicals very efficiently, probably by an addition reaction followed by further reactions of the resulting radicals, leading eventually to higher carboxylic acids.

From the products of the photolysis, and assuming a mechanism involving reactions [1] to [14], some simple stoichiometric estimates may be made of the relative importance of the several possible reactions of carboxyl radicals. The rates of product formation were all measured at a temperature of 165° C and 50.7 mm pressure of acid, and are expressed in units of μmoles/min$\times$100.

$R_2 = H_2$ production at high isobutane pressure = 0.30

$R_3 =$ CO production at high pressure of isobutane or butene = 0.20

$R_4 = CF_3H$ production in pure acid = 0.11

R_8+R_{12} = reduction in H_2 yield (from a rather arbitrary maximum value of 0.46 estimated from Fig. 3) caused by removal of COOH at high pressures of isobutane = 0.16

$R_{12} = H_2$ production from pure acid = 0.06

R_{13} = reduction in CO production at high pressures of isobutane or butene = 0.22

Can. J. Chem. Downloaded from www.nrcresearchpress.com by 210.87.254.42 on 09/05/12
For personal use only.

The rate of reaction [2] estimated above is too low, perhaps by about a factor of 2, because of loss of hydrogen atoms by addition to the olefin generated in the system, as discussed earlier, and 0.60 is probably a better estimate for R_2. This may be compared with the yield of CO_2 of 0.80 in the presence of 1-butene, which should also be a measure of reaction [2]. The excess CO_2, and the much larger excess at high isobutane pressure ($R_{CO_2} = 1.10$) could be due to disproportionation reactions between COOH and hydrocarbon radicals,

$$COOH + R \rightarrow CO_2 + RH, \qquad [15]$$

which may be very favorable because of the relatively weak COO—H bond.

The decrease in CO_2 production on the addition of 1-butene should have equalled the sum $R_4+R_8+2R_{12}+R_{13}+R_{11}$. The first four terms, from the estimates above, can account for a total of 0.55, leaving a yield of 1.25 to be formed by reaction [11] to make up the observed total decrease of 1.80. Thus reaction [11] apparently represented the predominant fate of carboxyl radicals in the photolysis of the pure acid, with the reactions of carboxyl in order of importance being 11 (1.25), 13 (0.22), 4 (0.11), 8 (0.10), and 12 (0.06). The extent of occurrence of reaction [10] is difficult to estimate. The simple decomposition of carboxyl (reaction [4]) appears to be relatively unimportant under the present experimental conditions, which would tend to support the higher value for the COO—H bond strength. This behavior is in contrast to that in the photolysis of formic acid (9), in which the carboxyl radical apparently decomposed rapidly, so that added olefin had almost no effect on the yields of CO and CO_2. Excess energy from the primary photolytic process may account for this difference in behavior, as the carboxyl radical would undoubtedly carry away more of the excess energy from formic acid than from the larger CF_3COOH molecule with its additional degrees of freedom.

The suggested mechanism appears to account fairly well for the observed results, but in the absence of more complete product analysis it must be regarded as tentative. All the calculations above apply to the photolysis of the acid at 165° C and 50.7 mm pressure. The temperature dependence of the products (Fig. 4), from the photolysis in the presence of isobutane, requires some comment. The increasing yields of CO_2, CO, and H_2 suggest that primary processes [2] and [3] are favored by the higher temperatures. The increase in CF_3H, and part of the sharp increase in H_2, may reflect a more efficient scavenging of CF_3 and H by isobutane.

In summary, the photolysis of CF_3COOH appears to proceed by three concurrent primary processes, the most important being the simple decomposition into CF_3 and COOH. The carboxyl radicals so formed were apparently stable enough to undergo a variety of reactions before decomposing, and some tentative conclusions about these reactions have been drawn. The main fate of COOH in the photolysis of the pure acid appears to have been a mutual disproportionation reaction yielding CO_2 and formic acid. A more detailed product analysis, particularly of heavier products, would be required for a full understanding of the photolysis mechanism.

The authors wish to thank Dr. K. O. Kutschke for his interest and useful suggestions throughout the course of this work.

REFERENCES

1. P. Ausloos and E. W. R. Steacie. Can. J. Chem. **33**, 1530 (1955).
2. M. Burton. J. Am. Chem. Soc. **58**, 692, 1645 (1936).
3. L. Farkas and O. H. Wansborough-Jones. Z. Physik. Chem. Sect. B, **18**, 124 (1932).
4. J. L. Holmes and K. O. Kutschke. Trans. Faraday Soc. **58**, 333 (1962).

Can. J. Chem. Downloaded from www.nrcresearchpress.com by 210.87.254.42 on 09/05/12
For personal use only.

5. M. D. TAYLOR and M. B. TEMPLEMAN. J. Am. Chem. Soc. **78**, 2950 (1956).
6. A. S. GORDON. J. Chem. Phys. **36**, 1330 (1962).
7. A. STRACHAN and K. O. KUTSCHKE. Private communication.
8. S. A. MCINTOSH and K. O. KUTSCHKE. Private communication.
9. R. GORDEN, JR. and P. AUSLOOS. J. Phys. Chem. **65**, 1033 (1961).
10. G. GLOCKLER. J. Phys. Chem. **62**, 1049 (1958).
11. M. H. BACK and A. H. SEHON. Can. J. Chem. **38**, 1261 (1960).

Can. J. Chem. Downloaded from www.nrcresearchpress.com by 210.87.254.42 on 09/05/12
For personal use only.

THE REACTIONS OF ELECTRONICALLY EXCITED NITRIC OXIDE MOLECULES WITH HYDROCARBONS[1]

O. P. STRAUSZ AND H. E. GUNNING
Department of Chemistry, University of Alberta, Edmonton, Alberta

Received November 9, 1962

ABSTRACT

The reactions of $NO(^4\Pi)$ molecules, generated by Hg $6(^3P_1)$ photosensitization, with methane, ethane, propane, neopentane, and benzene have been studied at room temperature in a circulatory system. In the case of ethane the following reaction products were identified: N_2, N_2O, H_2O, NO_2, CO, CO_2, C_2H_4, acetaldehyde, nitroethane, ethyl nitrite, ethyl nitrate, nitroethylene, nitromethane, methyl nitrite, methyl nitrate, formaldehyde. For hydrocarbon consumption, under comparable conditions, the following quantum yield values were established: $\Phi_{-(C_6H_6)} < 0.04$, $\Phi_{-(CH_4)} > 0.045$, $\Phi_{-(C_2H_6)} > 0.063$, $\Phi_{-(\text{neopentane})} \simeq 0.1$ mole/einstein. The most probable primary process may be represented by the sequence

$$Hg^* + NO \rightarrow Hg + NO(^4\Pi)$$
$$NO(^4\Pi) + RH \rightarrow NO + R + H.$$

Alkyl free radicals catalyze the chain disproportionation of nitric oxide at room temperature according to the stoichiometric equation

$$4NO\ (+ R) \rightarrow N_2 + 2NO_2\ (+ R).$$

A minimal value of 12 was established for the average chain length.

INTRODUCTION

It was shown in a previous paper (1) that the Hg $6(^3P_1)$-photosensitized decomposition of nitric oxide proceeds via the formation of an electronically excited species, very likely in the $(^4\Pi)$ state (2) and its subsequent reactions with ground-state molecules. On this basis it appeared instructive to obtain additional information concerning the reactivity of $NO(^4\Pi)$ molecules with other species, since this type of reaction would involve both atomic and molecular photosensitization and as such is of special interest in itself. In addition, nitric oxide has been used extensively as a free-radical trap in reaction kinetics, and recently the possibility of an attack of nitric oxide on substrate molecules has been considered (3). In the present study, the reactions of $NO(^4\Pi)$ molecules with methane, ethane, propane, neopentane, and benzene are reported.

EXPERIMENTAL

The static reaction system used will be described in another publication (4). The circulatory reaction system consisted of a rotary pump of commercial design (Precision Glass), a differential manometer, a U-trap, a Pirani gauge, and a cylindrical reaction cell made of optical quartz, 50 mm in diameter and 40 mm in length. The cell was attached to the system by standard tapers. The entire system was equipped with mercury float valves. The reaction cell was positioned in a water thermostat in such a fashion that its plane windows were opposite ports of Vycor 7910 glass in the sides of the thermostat. Radiation at 2537 Å was taken from a Hanovia SC-2537 mercury resonance source.

The methane, ethane, propane, neopentane (all Phillips Research Grade), nitric oxide (Matheson), trideuteroethane (Merck), and benzene (Fisher, Reagent Grade) were purified by standard low-temperature distillation techniques. Their purity was checked by gas–liquid partition chromatography (G.L.P.C.). The reaction products were fractionated by low-temperature distillation and the various fractions analyzed by G.L.P.C. The following columns were used: 6 ft of Burrell, 13X molecular sieves; 6 ft of Burrell, medium activity silica gel; 10 ft of Carbowax 600–6% by weight on "Celite".

The product identifications were performed by mass spectrometry and confirmed against predetermined retention time values in the G.L.P.C. analysis.

[1]*Part of this work was presented at the 44th National Meeting of the Chemical Institute of Canada, Montreal, August 2–5, 1961.*

Can. J. Chem. Downloaded from www.nrcresearchpress.com by 210.87.254.6 on 09/05/12
For personal use only.

Can. J. Chem. Downloaded from www.nrcresearchpress.com by 210.87.254.6 on 09/05/12
For personal use only.

RESULTS

Preliminary experiments had shown that the addition of a small amount of a hydrogen-containing compound to pure nitric oxide which was undergoing mercury photosensitization resulted in a marked increase in the nitrogen and nitrous oxide yields. The results of some experiments, carried out under static conditions, are tabulated in Table I. A more

TABLE I

The effect of various addends on the rates of N_2 and N_2O formation in the reaction of NO with Hg $6(^3P_1)$ atoms

Addend	$P_{(Ad)}$, mm	$P_{(NO)}$	N_2	N_2O	CO	Cond. at −160°
			μmoles			
—	—	22.3	3.53	0.41	—	—
CH_4	3.0	22.5	17.4	—	4.2	10.7
C_2H_6	1.7	35.0	19.8	2–3	3.9	—
$(Me)_4C$	8.2	24.4	81.2	8.0	12.3	—
CF_3H	4.68	26.8	3.86	—	—	—
H_2O	1.5	27.5	6.15	1.12	—	—

NOTE: I_a = 33.4 μeinstein/min; exposure time = 60 minutes.

detailed analysis of the ethane – nitric oxide system revealed the following reaction products: N_2, N_2O, NO_2, CO, CO_2, H_2O, C_2H_4, acetaldehyde, ethyl nitrite, ethyl nitrate, nitroethane, nitromethane, methyl nitrate, nitroethylene, and traces of formaldehyde and methyl nitrite. The yields of some of these products as a function of exposure time are shown graphically in Fig. 1. It can be seen that with exposure times not exceeding 5

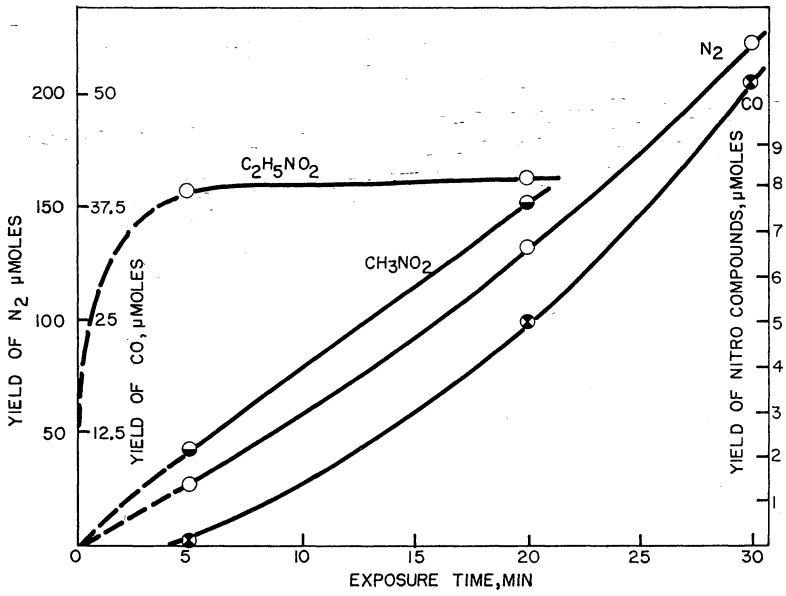

FIG. 1. Yield of products formation as a function of exposure time.

minutes, the secondary reactions are comparatively minor. The analysis of two runs, each 5 minutes in duration, are given in Table II. After these preliminary experiments

TABLE II

The products of the reaction of NO($^4\Pi$) molecules with ethane*

Product	μmoles	Product	μmoles
N_2	21.4; 25.1	C_2H_4	1.5
N_2O	12.1; 8.6	C_2H_5ONO	1.5
CO	0.6; 0.6	CH_3CHO	3.9
H_2O	14.7	CH_3NO_2	0.9
$-\Delta C_2H_6$	27.7	$C_2H_5NO_2$	6.4

NOTE: I_a = 120 μeinstein/min; exposure time = 5 minutes; temperature = 28°.
*$P_{(NO)}$ = 50.0 mm; $P_{(C_2H_6)}$ = 10.0 mm.

the reactions were further investigated in the circulatory apparatus to avoid depletion of mercury vapor in the cell through reaction with NO_2.

The quantum yield of N_2 formation ($\Phi_{(N_2)}$) as a function of the total pressure, with $P_{(C_2H_6)}/P_{(NO)} = 1.11$, is shown in Fig. 2. This curve, after an initial steep rise, seems to

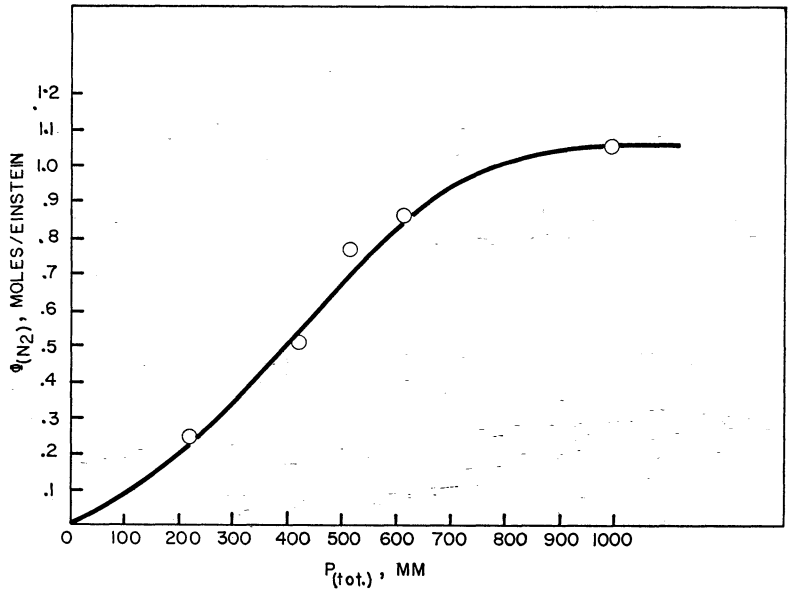

FIG. 2. The quantum yield of nitrogen formation as a function of total pressure, for $P_{(C_2H_6)}/P_{(NO)} = 1.11$.

level off at a pressure of ca. 1000 mm. The highest measured value of $\Phi_{(N_2)}$ at 30° was 1.06 moles/einstein at a total pressure of 995 mm.

It was also found that nitrogen formation continued in the reaction mixture even after termination of the photochemical reaction. The apparent $\Phi_{(N_2)}$ values, as a function of the dark reaction time following 12-minute exposures, are given in Fig. 3. At a total pressure of 430 mm and a $[C_2H_6]/[NO]$ ratio of 1.10, $\Phi_{(N_2)}$ increased from 0.51 mole/einstein, when the analysis was started immediately after the lamp was shut off, to a value of 1.27 moles/einstein, when the analysis was delayed 6 hours. This dark reaction was found to be much less pronounced at longer exposures as shown by the data of Table III. The decrease of $\Phi_{(N_2)}$ at longer exposures is not due to a mercury depletion in the system, since the quantum yield of the condensable products increased rather than decreased with longer exposure periods. It will be shown later that a more plausible explanation of this effect

Can. J. Chem. Downloaded from www.nrcresearchpress.com by 210.87.254.6 on 09/05/12
For personal use only.

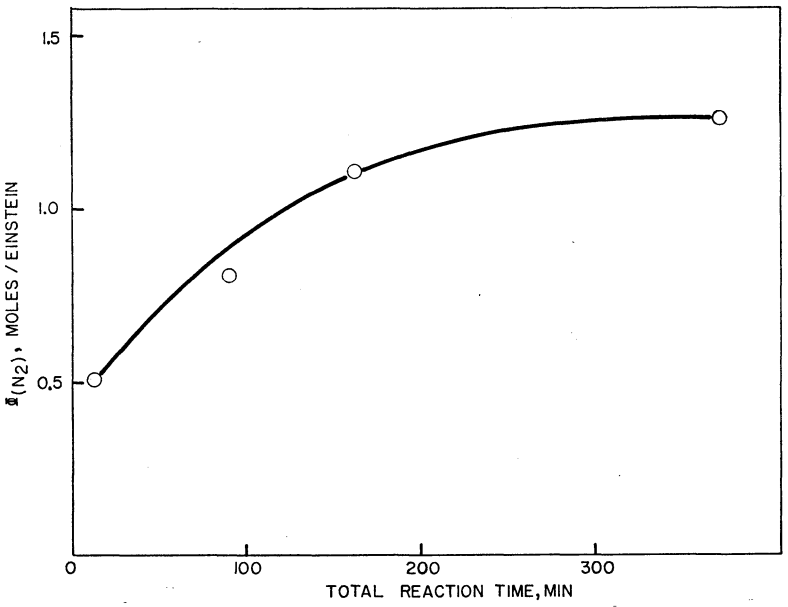

FIG. 3. The apparent quantum yield of nitrogen formation as a function of total dark reaction time, following 12-minute exposures at $P_{(C_2H_6)}/P_{(NO)} = 1.10$, and a total pressure of 430 mm.

TABLE III

The effect of exposure duration, and post-irradiation dark period on the apparent quantum yield of nitrogen in the reaction of NO($^4\Pi$) molecules with ethane

$P_{(tot)}$		Exposure duration	Dark Period	$\Phi_{(N_2)}$
mm	$[C_2H_6]/[NO]$	min		moles/einstein
430	1.11	12	360	1.27
438	1.12	33	680	0.73
466	1.10	50	180	0.50
430	1.14	12	150	1.12

is that the nitrogen-producing reaction between alkyl free radicals and nitric oxide is a chain reaction in which the most likely chain-terminating step is the combination reaction of an alkyl radical with NO_2 or NO_3. Since the concentration of NO_2 increases progressively with increasing exposure time, the relative rate of chain propagation to chain termination will progressively decrease. Since nitrogen is a chain product, the apparent $\Phi_{(N_2)}$ will have lower values with longer exposure periods.

In connection with the quantum yield measurements for C_2H_6 consumption, the experimental difficulties encountered should be briefly mentioned. First of all, one of the major reaction products was NO_2, and this product reacted rapidly with mercury to form $HgNO_2$. The amount of NO_2 formed was in almost all cases several times that of the C_2H_6 consumed; that is, the corrosion of the mercury surface and the depletion of mercury vapor was disproportionately faster than the reaction under study. This necessitated the use of a comparatively large reaction volume. Furthermore, it was necessary to confine the study to high nitric oxide concentrations at high total pressure, in order to

Can. J. Chem. Downloaded from www.nrcresearchpress.com by 210.87.254.6 on 09/05/12
For personal use only.

ensure that the ethane decomposition resulted from NO($^4\Pi$) photosensitization. Thus there was always a large excess of the reactants present in the reaction mixtures, which prevented the quantitative determination of some of the products.

To illustrate the procedure for the estimation of $\Phi_{-(C_2H_6)}$ a representative run will be considered, for which the quantum yield data are listed in Table IV. The total condensables at −130° C amounted to 35.92 μmoles, excluding the higher nitrogen oxides which

TABLE IV

Quantum yield data for a representative run in the reaction of NO^4(II) molecules with ethane

Product formed	μmoles	Φ moles/einstein
N_2	136.8	0.50
Condensable	35.92	0.133
CH_3CHO	6.16	2.27×10^{-2}
$C_2H_5ONO_2$	2.27	0.84×10^{-2}
C_2H_5ONO	2.32	0.86×10^{-2}
$C_2H_5NO_2$	1.18	0.44×10^{-2}
CH_3NO_2	0.18	0.07×10^{-2}
$CH_2{=}CHNO_2$	~0.1	
CH_2O }	<0.6	
CH_3ONO }		

NOTE: I_a = 5.42 μeinstein/min; exposure time = 50 minutes; temperature = 30° C; $P_{(C_2H_6)}$ = 244 mm; $P_{(NO)}$ = 222 mm; dark period following exposure = 180 minutes.

were previously absorbed by mercury. The total yields of C_1 and C_2 compounds were 0.29 and 11.93 μmoles respectively, and in this oxidation of ethane, 9.53 μmoles of water must have formed. The sum of the condensables is therefore 21.75 μmoles, leaving 35.92 − 21.75 or 14.17 μmoles of condensables unaccounted for. Now each mole of unrecovered product, condensable at −130°, could represent, at the most, 1 mole of ethane consumed where the oxidation yields ethylene and water, and in the least, one-third of a mole of ethane consumed where all of the hydrogen in the ethane is converted to water. Therefore the minimum and maximum values for $\Phi_{-(C_2H_6)}$ will be $(12.22 + 14.17/3)/(5.42\times50) = 0.063$, and $(12.22+14.17)/(5.42\times50) = 0.098$ mole/einstein respectively. Since both CO_2 and C_2H_4 were detected in the products the true quantum yield value should be about 0.08–0.09 mole/einstein. In either case the actual value is considerably higher than the quantum yield for the reaction between C_2H_6 and Hg $6(^3P_1)$ atoms, corrected for quenching by NO, for which an effective value of <0.005 mole/einstein is obtained.

The analytical data for a number of runs performed under various conditions are given in Table V. It is apparent from the table that the total C_2 yield found was in each case only a fraction of the condensable products and well below the stoichiometric ratio. This ratio was considerably higher at longer exposure times.

The effect of temperature was studied in the short range, 30–77° C. The data obtained seem to suggest a small positive activation energy for the reaction forming condensable products, and a small negative activation energy for the N_2-producing reaction. A plot of $\ln \Phi_{(cond.)}$ against $1/T$ gave a satisfactory straight line, as can be seen from Fig. 4, and from the slope a value of 2.0 kcal/mole was obtained for ΔE_a. A similar plot for $\Phi_{(N_2)}$ showed a strong curvature, thus indicating some complexity in the reaction mechanism.[2]

[2]*Only a part of the reaction system was temperature regulated, therefore the* $\Phi(N_2)$ *values at elevated temperature have only qualitative significance.*

Can. J. Chem. Downloaded from www.nrcresearchpress.com by 210.87.254.6 on 09/05/12
For personal use only.

Can. J. Chem. Downloaded from www.nrcresearchpress.com by 210.87.254.6 on 09/05/12
For personal use only.

TABLE V

Quantum yield data and chain length values for the reaction of NO($^4\Pi$) molecules with ethane

$P_{(C_2H_6)}$	$P_{(NO)}$	Temp.	Exposure duration	Dark period	$\Phi_{(N_2)}$	Φ(cond.)†	C_2+H_2O fraction of condensables	Min. chain length	Max. chain length
mm		°C	min		moles/einstein		mole%		
228	214	30	33	180	0.76	0.13	69	11.3	17.4
231	207	30	33	680	0.73	—	—	—	—
412	205	30	41.5	0	0.60	0.12	60	9.5	6.1
236*	211	30	61	0	0.58	0.17	49	4.3	7.5
217	200	30	12	720	—	0.11	—	12.5	30.7
229	201	30	12	150	1.12	0.11	21	10.5	25.3
325	291	30	18	0	0.87	0.13	—	—	—
226	206	50	12	304	1.21	0.13	30	10.4	22.7
230	221	77	12	292	0.82	0.17	—	6.0	13.5

NOTE: I_a = 5.75 μeinstein/min.
*CH_3CD_3.
†Condensables at −130° C.

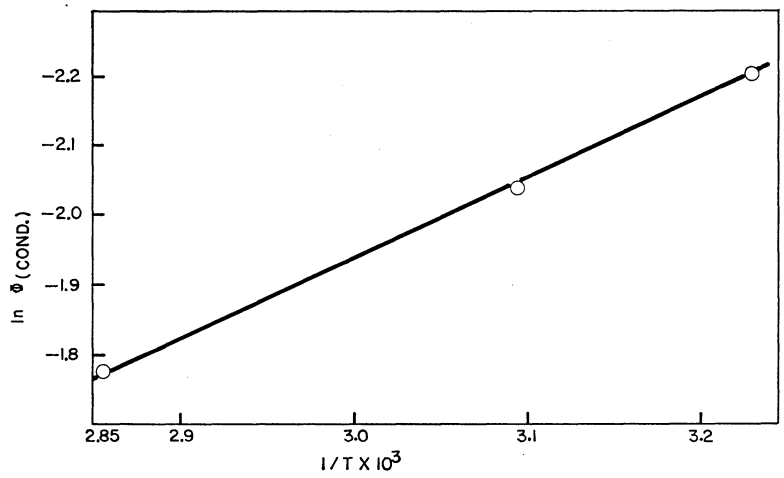

FIG. 4. Plot of ln $\Phi_{(cond.)}$ versus $1/T$.

To study the isotope effect on the reaction, one run was performed with 1,1,1-trideuterioethane. The quantum yield data for this run are given in Table VI, together with

TABLE VI

Quantum yield data for the CH_3CD_3 + NO($^4\Pi$) reaction

Product	Φ mole/einstein	Product	Quantity μmoles
N_2	0.58	Nitroethane	~1.4
Condensables	0.17	Nitromethane	~0.4
Acetaldehyde	0.021	Methyl nitrate	
$CH_3CD_2ONO_2$	0.007	H_2O	Very large
$CD_3CH_2ONO_2$	0.005		
CH_3CD_2ONO	0.006		
CD_3CH_2ONO	0.004		

NOTE: $\Phi_{(min.)}$ for ethane disappearance = 0.077 mole/einstein; $\Phi_{-(CH_3CD_3)}$ calculated on a competitive quenching basis was <0.005 mole/einstein; CH_3CD_2/CD_3CH_2 = 1.4 as determined from the ethyl nitrate, ethyl nitrite, and nitroethane products by mass spectrometric analysis; I_a = 5.42 μeinstein/min; exposure time = 61 minutes; temperature = 30°; $P_{(CH_3CD_3)}$ = 236 mm; $P_{(NO)}$ = 211 mm; dark period = 0.

the isotopic composition of the products as obtained from mass spectrometric analysis. It is interesting to note the increase in the quantum yield for CH_3CD_3 consumption compared to that for C_2H_6. The corresponding minimum values are $\Phi_{-(C_2H_6)} = 0.063$ and $\Phi_{-(C_2H_3D_3)} = 0.077$, which represent approximately a 22% increase in reactivity for the deuterated compound. The isotopic analysis data suggested that the reactivity of CD_3 with respect to NO($^4\Pi$) molecules is about 40% higher than that of the CH_3 in CH_3CD_3. Combining this result with the quantum yield values, it follows that the reactivity of CH_3 in C_2H_6 and CH_3CD_3 is about the same.

One more qualitative run, carried out under static conditions, should be mentioned. In this run (27 mm C_2H_6 and 39 mm NO), after completion of the exposure, 172 mm NO was added to the reaction mixture. Within a few minutes a deep brown color developed in the cell. No color formation could be observed in similar experiments omitting the addition of a further amount of nitric oxide. This experiment suggests the presence of

Can. J. Chem. Downloaded from www.nrcresearchpress.com by 210.87.254.6 on 09/05/12
For personal use only.

some reactive species in the reaction mixture capable of combining with NO if the concentration of the latter is sufficiently high. At this point it appeared to be instructive to examine the reaction of some other hydrocarbon with NO($^4\Pi$) molecules.

The quantum yield data for three runs performed with methane are given in Table VII. The non-condensable fraction, in addition to N_2 and unreacted CH_4 and NO, contained a small amount of H_2. The middle fraction was composed of N_2O and CO_2 and the condensable fraction contained water, formaldehyde, methyl nitrite, methyl nitrate, nitromethane, and some other unidentified compounds. For the disappearance of CH_4 a minimum quantum yield value of 0.045 mole/einstein was obtained, while the one calculated on a competitive quenching basis is negligibly small.

TABLE VII

Quantum yield data for the $CH_4 + NO(^4\Pi)$ reaction

$P_{(CH_4)}$	$P_{(NO)}$	Exposure time	Dark period	$\Phi_{(N_2)}$	$\Phi_{(cond.)}$	$\Phi_{(N_2O)}$	$\Phi_{(CO_2)}$
mm		min		mole/einstein			
237	207	14.7	60	0.44	0.09	~0.07	—
292	263	30.0	0	—	0.06	0.05	0.005
109.5	103.5	30.0	820	—	0.07	0.05	0.02

NOTE: $\Phi_{(min.)}$ for CH_4 disappearance = 0.045 mole/einstein; I_a = 5.42 μeinstein/min; temperature = 30°.

One qualitative run was also done using nitrosomethane dimer and nitric oxide. No reaction was observed at room temperature in several hours. It was concluded that the nitrosomethane dimer is much less reactive than the monomer (5, 6).

The products identified in the reaction of propane with NO($^4\Pi$) molecules along with the corresponding quantum yield data are listed in Table VIII. The ratio of *n*-propyl/*i*-propyl in the products was 0.86.

TABLE VIII

Quantum yield data for the $C_3H_8 + NO(^4\Pi)$ reaction

Product formed	μmoles	Φ mole/einstein
N_2	175.6	0.42
Condensables	16.32	3.91×10^{-2}
$CH_3CH(ONO)CH_3$	0.86	0.21×10^{-2}
CH_3COCH_3	0.97	0.23×10^{-2}
$CH_3CH(ONO_2)CH_3$	1.40	0.34×10^{-2}
$CH_3CH(NO_2)CH_3$	0.68	0.16×10^{-2}
$CH_3CH_2CH_2ONO$	0.62	0.15×10^{-2}
CH_3CH_2CHO	0.78	0.19×10^{-2}
$CH_3CH_2CH_2ONO_2$	1.43	0.34×10^{-2}
$CH_3CH_2CH_2NO_2$	0.42	0.10×10^{-2}
$CH_3CH_2CH_2OH$	0.13	0.03×10^{-2}

NOTE: Total propyl = 7.3 μmoles; *n*-propyl/*i*-propyl = 0.86; I_a = 5.42 μeinstein/min; exposure time = 77 minutes; temperature = 30°; $P_{(C_3H_8)}$ = 26.58 mm; $P_{(NO)}$ = 233 mm.

The data from one run performed with benzene are given in Table IX. The low quantum yields of N_2 and N_2O indicate that this reaction is very slow.

The results of five runs with neopentane are shown in Table X. The highest measured quantum yield for N_2 production was 1.75 moles/einstein. The quantum yield of the

Can. J. Chem. Downloaded from www.nrcresearchpress.com by 210.87.254.6 on 09/05/12
For personal use only.

TABLE IX

Quantum yield data for the C_6H_6 + NO($^4\Pi$) reaction

$P_{(C_6H_6)}$	$P_{(NO)}$	Temp.	Exp. time	$\Phi_{(N_2)}$	$\Phi_{(N_2O)}$
mm		°C	min	mole/einstein	
100	130	30	12	0.01	0.015

NOTE: I_a = 5.42 μeinstein/min.

TABLE X

Quantum yield data for the neopentane + NO($^4\Pi$) reaction

$P_{(NP)}$	$P_{(NO)}$	Reaction time	Dark period	$\Phi_{(N_2)}$	$\Phi_{(cond.)}$*	$\Phi_{(N_2O)}$
mm		min		mole/einstein		
223	205	12	Nil	0.79	0.21	0.14
226	202	10	600	1.47	0.17	0.09
332	301	10	600	1.75	0.20	0.13
113.5	103.5	10	600	1.19	0.20	0.12
415	207	10	Nil	0.70	0.17	0.11

NOTE: I_a = 5.42 μeinstein/min; temperature = 30°.
*Condensable at −98°.

condensable products was also high and varied between 0.17 and 0.21 mole/einstein. The quantum yield data for N_2O in the table are high since they include the CO_2 which was formed in the reaction, the amount of which varied between 10 and 20 mole%.

In common with the ethane and methane systems, a dark reaction was also observed in this system, as is evident from the data in Table X. The condensables contained at least 18 compounds, among them trimethylacetaldehyde and water.

DISCUSSION

The hydrocarbon molecules selected for this study are characterized by their low reactivity with respect to Hg $6(^3P_1)$ atoms, due either to their low quenching or low quantum efficiencies, or both. The corresponding σ_Q^2 and Φ values are listed in Table XI.

TABLE XI

Quenching cross section and quantum yield values for Hg $6(^3P_1)$-photosensitized reactions

Substrate	σ_Q^2 Å^2	Φ mole/einstein	References
CH_4	0.059	0.008 (98°)	7, 8
C_2H_6	0.11; 0.10	1.0	9, 10, 11
$(Me)_4C$	1.5	0.004	9, 12
C_6H_6	41.9	0.00	7, 13
NO	24.7	0.002	7, 1

In the case of two substrate molecules, the fraction of each that quenches the sensitizer atoms is determined by the formula $F_A = 1/[1+(Z_BP_B)/(Z_AP_A)]$, where Z_A and Z_B are the collision numbers and P_A and P_B are the pressures of components A and B respectively. Possessing the values of the quenching cross sections and quantum yields, one can

Can. J. Chem. Downloaded from www.nrcresearchpress.com by 210.87.254.6 on 09/05/12
For personal use only.

calculate, using the above formula, the amount of each substrate disappearing in the reaction. The computed values are as follows: $\Phi_{(CH_4)} < 0.001$, $\Phi_{(C_2H_6)} < 0.005$, $\Phi_{(neopentane)} < 0.001$, which can be compared to the measured values of 0.045, 0.063, and 0.1 mole/einstein respectively for the minimum Φ value obtained in this study. The case of neopentane is of special interest. For the Hg $6(^3P_1)$-photosensitized decomposition of this molecule, under conditions similar to those prevailing in this study, a quantum yield value of 0.004 mole/einstein has been reported (12). When, however, an approximately equal amount of NO is added, the quantum yield increases about 25-fold, even though the amount of energy transferred directly from the Hg $6(^3P_1)$ atoms to neopentane has decreased by ca. 25-fold. This fact, taken in conjunction with the quantum yield data for the NO–CH_4 and NO–C_2H_6 systems, can best be explained by the formation and subsequent reactions of NO($^4\Pi$) molecules in these systems according to the following sequence:

$$Hg + h\nu_{(2537)} \rightarrow Hg^* \quad [1]$$

$$Hg^* + NO \rightarrow NO(^4\Pi) + Hg \quad [2]$$

$$NO(^4\Pi) + RH \rightarrow NO + R + H. \quad [3]$$

The role of NO as a photosensitizer is evident from this mechanism.

The results obtained from the CH_3CD_3 study are also in agreement with and lend further support to the proposed mechanism. Recent investigations of the Hg $6(^3P_1)$-photosensitized reactions of partially and fully deuterated saturated hydrocarbon molecules (14–18) have concordantly shown that replacement of H-atoms in the molecule by D-atoms led to a more or less marked decrease in the reactivity of the molecule with respect to Hg $6(^3P_1)$ atoms. In the present instance, however, a marked increase appeared in the minimum quantum yield from 0.063 to 0.077. Furthermore, in the Hg $6(^3P_1)$ reaction, the C—H bond rupture in all cases predominates over C—D bond scission, contrary to the inverted isotope effect of 1.4 favoring C—D rupture found here. It should also be noted that the reactivity of hydrocarbons with respect to Hg $6(^3P_1)$ atoms follows the order $CH_4 < (Me)_4C < C_2H_6$, while for NO($^4\Pi$)-photosensitization the reactivity sequence is $CH_4 < C_2H_6 < (Me)_4C$.

The measured quantum yield values are of the order of one tenth. Naturally, unit efficiency cannot be expected, owing to the activation energy required (2.0 kcal for the C_2H_6 + NO system) and because of the deactivating effect of the nitric oxide on the NO($^4\Pi$) species (1), which is likely very efficient.

The ratio of primary to secondary C—H bond cleavage in the reaction of NO($^4\Pi$) molecules with propane is 0.86 (Table VIII), nearly identical with the value obtained in the Hg $6(^3P_1)$-photosensitized reaction (14, 15).

The alkyl free radicals produced in reaction [3] react with nitric oxide to form the corresponding nitroso compounds (19–25):

$$R + NO \rightarrow RNO. \quad [4]$$

This reaction is likely to be second order for ethyl and the higher alkyl radicals (the corresponding reaction with O_2 is second order (26)). The reaction of H-atoms with NO will be discussed in another publication (4). The subsequent reactions of the alkyl nitroso monomers are complex and not fully understood. Generally, there are three possible ways for their disappearance: (1) dimerization leading to the formation of the stable, solid

Can. J. Chem. Downloaded from www.nrcresearchpress.com by 210.87.254.6 on 09/05/12
For personal use only.

alkyl nitroso dimers as shown in step [5]; (2) isomerization to the corresponding oxime (reaction [6]); (3) further reaction with nitric oxide (reaction [7]):

$$2RNO \rightarrow (RNO)_2 \quad [5]$$

$$RNO \rightarrow R{=}NOH \quad [6]$$

$$RNO + 2NO \rightarrow RNO\cdot(NO)_2. \quad [7]$$

Reaction [5] is slow (5, 6, 27) and the dimer formed is not capable of further reactions (5, 6). The isomerization reaction, [6], has an activation energy of 39 kcal in the case of nitrosomethane (6) but it may proceed rapidly in ultraviolet light or in the presence of an active surface (6, 28). Reaction [7], under the conditions of this study (high pressure of nitric oxide, room temperature), must be considerably faster than [5] and [6], since neither oxime nor nitroso dimer was found in the products. That nitroso monomers react with NO was first shown by Bamberger (29), who obtained phenyldiazonium nitrate from nitrosobenzene and NO in the liquid phase. More recently Burkhard *et al.* (30) have reported on the reaction of hydrocarbons with nitric oxide. Brown (31, 32) studied a number of reactions involving various hydrocarbons and nitric oxide. With isobutylene, 45 liquid and solid organic fractions were isolated from the crude product. This author has proposed that the reaction occurs via a diazo nitrate, the formation of which can be visualized as

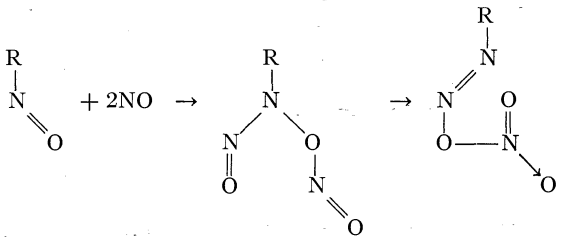

[8]

It was further proposed that this intermediate diazo nitrate can decompose by either homolytic or heterolytic bond rupture. The homolytic process regenerates the original radical and hence accomplishes a simple disproportionation of the NO into N_2 and NO_2, which is a thermodynamically feasible reaction ($\Delta F = -59.6$ kcal):

$$R\cdot + 3NO \rightarrow RN_2ONO_2 \quad [9]$$

$$RN_2ONO_2 \rightarrow R\cdot + N_2 + NO_3\cdot \quad [10]$$

$$NO_3\cdot + NO \rightarrow 2NO_2 \quad [11]$$

$$4NO \rightarrow N_2 + 2NO_2 \quad [12]$$

The heterolytic route yields sequentially diazonium nitrate, carbonium nitrate, nitroolefin, and nitric acid. A conversion of NO to NO_2 is also achieved but less efficiently than by the homolytic route:

$$NO_2 + \text{olefin} \rightarrow R'\cdot \quad [13]$$

$$R'\cdot + 3NO \rightarrow R'N_2ONO_2 \quad [9a]$$

$$R'N_2ONO_2 \rightarrow [R'N_2^+\cdot NO_3^-] \rightarrow [R'^+\cdot NO_3^-] + N_2 \quad [14]$$

$$[R'^+\cdot NO_3^-] \rightarrow \text{nitroolefin} + HNO_3 \quad [15]$$

$$HNO_3 + 0.5NO \rightarrow 0.5H_2O + 1.5NO_2 \quad [16]$$

$$\text{olefin} + 3.5NO \rightarrow \text{nitroolefin} + 0.5H_2O + 0.5NO_2 + N_2, \quad [17]$$

Can. J. Chem. Downloaded from www.nrcresearchpress.com by 210.87.254.6 on 09/05/12
For personal use only.

where R′· is a nitroalkyl free radical. Donaruma and Carmody (33) have studied the reaction of nitric oxide with bisnitrosocyclohexane. They obtained cyclohexyl nitrate, nitrocyclohexane, and cyclohexyl nitrite as the major reaction products. Their kinetic findings—a rate equation zero order in NO pressure, a high activation energy coupled with a high positive entropy of activation, along with the spectroscopic and thermochemical evidence for the association complex formation—were interpreted in terms of Brown's (31, 32) mechanism. In order to account for the final reaction products the following reactions between R and NO_2, formed in reactions [10] and [11], were suggested:

$$R + NO_2 \rightarrow RNO_2^* + RONO^* \quad [18]$$

$$RNO_2^* + M \rightarrow RNO_2 + M \quad [19]$$

$$RONO^* \rightarrow RO + NO \quad [20]$$

$$RONO^* + M \rightarrow RONO \quad [21]$$

$$RO + NO_2 \rightarrow RONO_2. \quad [22]$$

Burrell (5) has also measured the specific rate constant for the reaction of nitric oxide with nitrosocyclohexane monomer. The results and their interpretation are in line with those of Donaruma and Carmody (33).

There is also evidence in the literature from gas phase kinetic studies which gives support to the above mechanism. Levy (34) found that in the thermal decomposition of *t*-butyl nitrite the HCN product is replaced by nitromethane when the reaction is carried out in the presence of NO. The explanation advanced was that the HCN originated from the thermal decomposition of nitrosomethane by the equation

$$CH_3NO \rightarrow CH_2{=}NOH \rightarrow HCN + H_2O \quad [23]$$

while CH_3NO_2 originated from the reaction of CH_3NO with NO. Indeed, separate experiments showed that the reaction of nitrosomethane with nitric oxide produced nitromethane (35). Christie (27) found that CH_3NO reacts with nitric oxide in the ratio of 1:2 to give a product which is stable in the gas phase at room temperature, but decomposes on freezing and rewarming. Batt and Gowenlock (6) have also reported that nitrosomethane monomer in the gas phase reacts with NO. The reaction product could be condensed at liquid air temperatures but decomposed on standing to give a mixture of gases about one-half of which was condensable in liquid air. They suggested the mechanism

$$CH_3{-}\underset{\underset{N{=}O}{|}}{N}{-}O{-}N{=}O \rightarrow CH_3N_2^+ \cdot NO_3^- \rightarrow CH_3ONO_2 + N_2, \quad [24]$$

which is essentially identical with the heterolytic route [14] proposed by Brown (32). Finally, McMillan (36) reported very recently that when diisopropyl peroxide is decomposed in the presence of nitric oxide, at room temperature, the products include methyl nitrate and nitrogen among others. The formation of these products was explained on the basis of Batt and Gowenlock (6) and Christie's (27) experimental observations of the reaction between methyl free radicals and nitric oxide.

In conclusion it may be stated that all the publications which have appeared in the literature in connection with the reactions between alkyl and aryl nitroso compounds and nitric oxide appear to be in favor of the mechanism first proposed by Brown (31, 32). The results of the present work may also be conveniently explained in terms of this mechanism and, as such, lend additional support to its validity.

It is likely that in the gaseous phase the homolytic process predominates over the

Can. J. Chem. Downloaded from www.nrcresearchpress.com by 210.87.254.6 on 09/05/12
For personal use only.

heterolytic route. The proposed mechanism to account for the products found in this work is as follows:

$$RNO + 2NO \rightleftarrows R{-}N(O{-}N{=}O)(N{=}O) \quad [25]$$

$$R{-}N(O{-}N{=}O)(N{=}O) \rightarrow R{-}N{=}NONO_2 \quad [26]$$

$$R{-}N{=}NONO_2 \rightarrow R + N_2 + NO_3 \quad [10]$$

$$R{-}N{=}NONO_2 \rightarrow [RN_2^+ \cdot NO_3^-] \quad [27]$$

$$[RN_2^+ \cdot NO_3^-] \rightarrow [R^+ \cdot NO_3^-] + N_2 \quad [28]$$

$$[R^+ \cdot NO_3^-] \rightarrow \text{olefin} + HNO_3 \quad [29]$$

$$NO_3 + NO \rightarrow 2NO_2 \quad [11]$$

$$HNO_3 + 0.5NO \rightarrow 1.5NO_2 + 0.5H_2O \quad [16]$$

$$R + NO_2 \rightarrow RNO_2^* \quad [18a]$$

$$\rightarrow RONO^* \quad [18b]$$

$$RNO_2^* + M \rightarrow RNO_2 + M \quad [19]$$

$$RONO^* \rightarrow RO^* + NO \text{ or } R'CHO + HNO \quad [30]$$

$$RONO^* + M \rightarrow RONO + M \quad [21]$$

$$RO^* + NO \rightarrow R'CHO + HNO \quad [31]$$

$$RO^* + M \rightarrow RO + M \quad [32]$$

$$RO + NO_2 \rightarrow RONO_2 \quad [22]$$

$$R'CHO + h\nu \text{ (or Hg* or NO}(^4\Pi)) \rightarrow R' + CHO \quad [33]$$

$$CHO + NO \rightarrow CO + HNO \quad [34]$$

$$R' + NO + M \rightarrow R'NO + M. \quad [35]$$

The N-nitroso-N-alkyl-hydroxylamine nitrite intermediate formed in reaction [25] appears to be in equilibrium with the nitrosoalkyl monomer, in agreement with Burrell's (5) but contrary to Donaruma and Carmody's (33) proposal. This view is supported by our observation that the reaction mixture, after the excess NO was distilled off at −183° C, releases nitric oxide on standing at room temperature. The rate-determining step is the isomerization of this intermediate to the corresponding diazonium nitrate, [26], the latter then rapidly decomposes, mainly homolytically, [10], to regenerate the alkyl radical, and simultaneously a small fraction cleaves heterolytically, [29], to yield olefin. Donaruma and Carmody (33) obtained a value of 47,700 cal/mole for $\Delta H^{\ddagger}$ and 77.9 e.u. for $\Delta S^{\ddagger}$ in the reaction of bisnitrosocyclohexane with nitric oxide in cyclohexane solution. This value for $\Delta H^{\ddagger}$ may be compared to the small negative activation energy found for the nitrogen-producing reaction in this work and also to the results of Batt and Gowenlock (6), for the gas-phase reaction of nitrosomethane monomer with nitric oxide, which indicate that there is little effect of temperature upon the reaction rate. The following reason can be advanced to explain this discrepancy, which far exceeds the experimental error. Donamura and Carmody (33) measured the rate of dimer disappearance by determination of its absorption band at 8.28 μ. Now it is apparent from Burrell's (6) work that

Can. J. Chem. Downloaded from www.nrcresearchpress.com by 210.87.254.6 on 09/05/12
For personal use only.

the rate of dissociation for the dimer is about two orders of magnitude slower than the rate of the monomer reaction with nitric oxide at the nitric oxide pressures encountered in their experiments. The half-period of reaction at 25° was found to be 0.23 sec for the nitric oxide and 13.5 sec at 51° for the dissociation reactions. The rate-controlling step is obviously the dissociation of the dimer, which reaction has a high activation energy. Donaruma and Carmody incorrectly assigned this activation energy and the related entropy of activation to the subsequent reactions with nitric oxide. The view that the activation energy is due to the dissociation process is further substantiated by Burrell's (6) qualitative observation that chloronitrosocyclohexane in cyclopentane solution reacts rapidly at −80° with nitric oxide, indicating a low activation energy process leading to the formation of nitrate. Chloronitrosocyclohexane is known to be monomeric in solution. It may be mentioned here that for an association reaction leading to equilibrium, a low activation energy would be expected also on theoretical grounds. If, however, the activation energy is very low, the entropy of activation, in contrast to Donaruma and Carmody's value, ca. 80 e.u., should rather have a negative value, since the reaction rate is comparatively slow. A negative value for the entropy of activation may be expected if the molecule in the activated state contains more bonds than the original molecule (37), or, in other words, if the isomerization of N-nitroso-N-alkyl-hydroxylamine nitrite intermediate to the alkyl diazonium nitrate occurs via a cyclic activated complex as was originally proposed by Brown (32). It also follows from this line of reasoning that the rate-determining step is this isomerization reaction, the slowness of which is related to the low probability of formation of the activated complex.

Reaction [18*a*] illustrates the autoinhibited character of the reaction. Under favorable conditions, when the NO to NO_2 ratio is kept sufficiently high, long chains could probably build up. Some calculated values of the average chain lengths, from the ethane – nitric oxide system, are given in the last column of Table V. The minimum and maximum values were obtained by dividing the nitrogen quantum yields by the maximum and minimum values respectively of the estimated quantum yield of ethane consumption. As can be seen from the table, an increase in NO pressure or dark reaction time causes an increase in the average chain length.

The significant difference between gas and liquid phase reactions as far as the final product distribution is concerned lies in the fact that in the latter case only nitration occurs whereas in the former case, both nitration and oxidation products are formed (32), with oxidation assuming major importance. This deviation may be explained in terms of the cage effect, which favors nitrate formation, and the more efficient collisional deactivation of excited species in the liquid phase.

The aldehyde is formed from the decomposition of RONO (38), either through excited alkoxy radicals, in reactions [30] and [31], or directly from RONO* [30]. Some alkoxy radicals have to be present in the gas phase system since the formation of the nitrate product directly from R and NO_3 is very unlikely. If RONO* dissociates, the excess energy of about 20 kcal/mole likely remains in the newly formed C—O bond.

The nitroethylene, which was tentatively identified by a peak at mass 73 in the mass spectrum of the condensable products, may arise from the secondary reactions of C_2H_4 by the heterolytic process, as suggested by Brown (32).

The discussion of such secondary reactions as the photolytic and oxidative decomposition of the primary products leading to CO and CO_2 formation will be omitted here.

Finally, as will be shown in another publication (4), both the nature of the products and the kinetics of the reaction of hydrogen atoms with nitric oxide molecules seem to

Can. J. Chem. Downloaded from www.nrcresearchpress.com by 210.87.254.6 on 09/05/12
For personal use only.

be in favor of a reaction between nitroxyl molecule and nitric oxide in close analogy with alkyl and aryl nitroso compounds and nitric oxide. This reaction, however, according to the quantum yield data is not a chain process. Therefore it is assumed that during the isomerization of the nitrosohydroxylamine nitrite intermediate to diazonium nitrate a proton shift from the nitrogen to the oxygen occurs and the reaction yields directly N_2 and HNO_3 without going through the diazonium nitrate state. Alternately hydrogen diazonium nitrate may be formed, and decompose via the heterolytic route [29].

CONCLUSIONS

Electronically excited nitric oxide molecules, most likely in the ($^4\Pi$) state, produced in Hg $6(^3P_1)$ photosensitization, react with hydrocarbons. The primary step is a carbon–hydrogen split. The rate of reaction follows the order benzene < methane < ethane < neopentane. In the case of the CH_3CD_3 molecule an inverted isotope effect appears. Propane yields normal and isopropyl radicals in nearly equal quantities.

Monomeric alkyl nitroso compounds in the gas phase react with nitric oxide. These reactions lead to an alkyl-radical-catalyzed chain disproportionation of nitric oxide into nitrogen and nitrogen dioxide at room temperature. Nitrogen dioxide inhibits the chain propagation.

ACKNOWLEDGMENTS

The authors wish to express their deep appreciation to Mr. Gene Fried for his assistance in some of the experimental work and to Mr. R. K. Taylor for the mass spectrometric analysis.

This study was partially supported by the National Research Council of Canada under N.R.C. Grant No. T–162. This assistance is gratefully acknowledged.

REFERENCES

1. O. P. Strausz and H. E. Gunning. Can. J. Chem. **39**, 2549 (1961).
2. R. J. Fallon, J. T. Vanderslice, and E. A. Mason. J. Phys. Chem. **63**, 2082 (1959).
3. B. W. Wojciechowski and K. J. Laidler. Can. J. Chem. **38**, 1027 (1960). B. W. Wojciechowski and K. J. Laidler. Proc. Roy. Soc. (London), Ser. A, **260**, 103 (1961). N. H. Sagert, B. W. Wojciechowski, and K. J. Laidler. 45th Canadian Chemical Conference and Exhibition. Edmonton. May 28–30, 1962. D. R. Blackmore and Sir C. Hinshelwood. Proc. Roy. Soc. (London), Ser. A, **268**, 21 (1962).
4. O. P. Strausz and H. E. Gunning. To be published.
5. E. J. Burrell. J. Phys. Chem. **66**, 401 (1962).
6. L. Batt and B. G. Gowenlock. Trans. Faraday Soc. **56**, 682 (1960).
7. J. R. Bates. J. Am. Chem. Soc. **52**, 3825 (1930); **54**, 569 (1932).
8. K. Morikawa, W. S. Benedict, and H. S. Taylor. J. Chem. Phys. **5**, 212 (1937).
9. B. deB. Darwent. J. Chem. Phys. **18**, 1532 (1950).
10. R. J. Cvetanovic. J. Chem. Phys. **23**, 1208 (1955).
11. R. A. Back. Can. J. Chem. **37**, 1834 (1959).
12. B. deB. Darwent and E. W. R. Steacie. Can. J. Res. Sect. B, **27**, 181 (1949).
13. E. J. Y. Scott and E. W. R. Steacie. Can. J. Chem. **29**, 233 (1951).
14. G. N. C. Woodall and H. E. Gunning. Paper presented at the Sixth Informal Photochemistry Conference, Brussels. June 18–22, 1962; Bull. Soc. Chim. Belges, **71**, 725 (1962).
15. Y. Rousseau and H. E. Gunning. Can. J. Chem. **41**, 465 (1963).
16. M. Avrahami and P. Kebarle. Can. J. Chem. **41**, 335, 347 (1963).
17. J. P. Chesick. J. Am. Chem. Soc. **84**, 2448 (1962).
18. C. S. Coe and T. F. Doumani. J. Am. Chem. Soc. **70**, 1516 (1948).
19. E. W. R. Steacie. Atomic and free radical reactions. Reinhold, N.Y. 1954.
20. J. Jach, F. J. Stubbs, and C. Hinshelwood. Proc. Roy. Soc. (London), Ser. A, **224**, 283 (1954).
21. W. A. Bryce and K. U. Ingold. J. Chem. Phys. **23**, 1968 (1955).
22. K. Yang. J. Phys. Chem. **65**, 42 (1961).
23. D. E. Hoare. Can. J. Chem. **40**, 2012 (1962).
24. J. G. Calvert, S. Sandra, and P. L. Hanst. J. Am. Chem. Soc. **82**, 1 (1960).
25. B. G. Gowenlock and W. Luttke. Quart. Rev. (London), **12**, 321 (1958).
26. J. G. Calvert. Private communications.
27. M. I. Christie. Proc. Roy. Soc. (London), Ser. A, **249**, 248, 258 (1958).

Can. J. Chem. Downloaded from www.nrcresearchpress.com by 210.87.254.6 on 09/05/12
For personal use only.

28. B. G. GOWENLOCK, J. TROTMAN, and L. BATT. Chem. Soc. Spec. Publ. **10**, 75 (1957).
29. E. BAMBERGER. Ber. **51**, 634 (1918).
30. C. A. BURKHARD, J. F. BROWN, C. S. HERRICK, R. L. MYERS, and D. T. HURD. Abstract of Papers, 126th Meeting of American Chemical Society. 1954.
31. J. F. BROWN. Abstracts of Papers, 126th Meeting of American Chemical Society. 1954.
32. J. F. BROWN. J. Am. Chem. Soc. **79**, 2480 (1957).
33. L. G. DONARUMA and D. J. CARMODY. J. Org. Chem. **22**, 635 (1957).
34. J. B. LEVY. Ind. Eng. Chem. **48**, 762 (1956).
35. S. W. BENSON. The foundations of chemical kinetics. McGraw-Hill, N.Y. 1960.
36. G. R. MCMILLAN. J. Am. Chem. Soc. **83**, 3018 (1961).
37. S. GLASSTONE, K. F. LAIDLER, and H. EYRING. The theory of rate processes. McGraw-Hill, N.Y. 1941.
38. H. W. BROWN and G. C. PIMENTEL. J. Chem. Phys. **29**, 883 (1958).

Can. J. Chem. Downloaded from www.nrcresearchpress.com by 210.87.254.6 on 09/05/12
For personal use only.

THE METHYL 2-O-(BENZYLTHIO)CARBONYL DERIVATIVE AS A PRECURSOR TO PARTIAL ESTERS OF METHYL α-D-GLUCOPYRANOSIDE

J. J. WILLARD,[1] JOANNE SADOWSKI,[2] AND WILLIAM VITALE[2]
Cellulose Research Institute, State University of New York College of Forestry, Syracuse, N.Y., U.S.A.

Received December 26, 1962

ABSTRACT

The utility of the thiocarbonyl group for blocking the C_2 hydroxyl in methyl glucosides has been demonstrated. Methyl 2-*O*-(benzylthio)carbonyl-α-D-glucopyranoside has been synthesized in good yield and its structure proved. Use of this 2-*O*-thiocarbonyl derivative in conjunction with acid-labile blocking groups has permitted the first syntheses of the following esters of methyl α-D-glucopyranoside: 3-*O*-benzoyl-, 3,4-di-*O*-benzoyl-, and 3,4,6-tri-*O*-benzoyl-, and the crystalline 2-*O*-(*p*-toluene)sulphonate derivative of each.

INTRODUCTION

In a previous communication (1) the synthesis of methyl 2,3-di-*O*-(benzylthio)-carbonyl-α- and -β-D-glucopyranosides and the use of these compounds for the synthesis of methyl 4,6-di-*O*-benzoyl-α- and -β-D-glucopyranosides were described. Thiocarbonate derivatives of carbohydrates are conveniently prepared, are stable to mild aqueous acid conditions, but are readily decomposed by oxidation with hydrogen peroxide in glacial acetic acid or by reduction with Raney nickel, conditions which do not generally disturb other ester groups. Thus, a (benzylthio)carbonyl derivative can be used in conjunction with acid-sensitive blocking groups to furnish several classes of partial ester derivatives of the methyl glucosides.

It has been found that crystalline methyl 4,6-*O*-benzylidene-2-*O*-(benzylthio)carbonyl-α-D-glucopyranoside (III), as seen in Fig. 1, can be isolated in 58% yield after treating

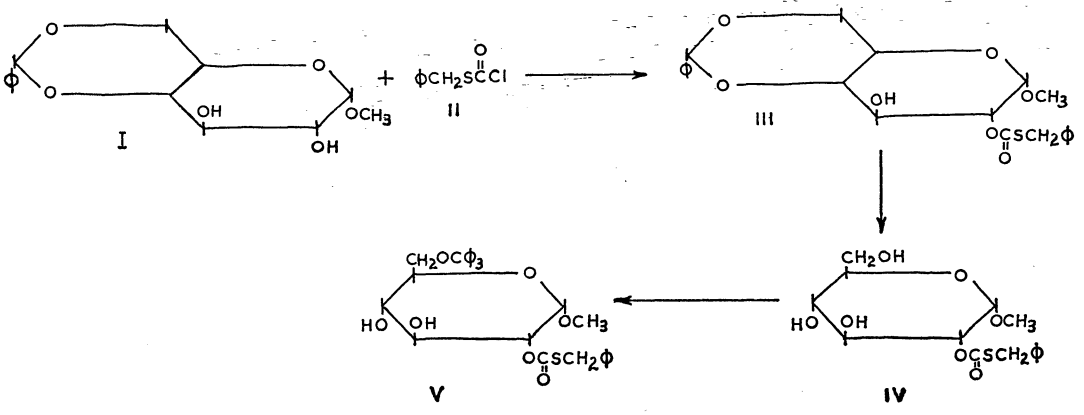

FIG. 1.

methyl 4,6-*O*-benzylidene-α-D-glucopyranoside (I) with 1 mole of (benzylthio)carbonyl chloride (II) in pyridine solution. Removal of the benzylidene group by mild acid

[1]*Present address: Chemistry Department, The University, Edgbaston, Birmingham 15, England.*
[2]*Supported by the National Science Foundation Undergraduate Summer Program at the College of Forestry, Summer, 1961.*

Can. J. Chem. Downloaded from www.nrcresearchpress.com by 210.87.254.105 on 09/05/12
For personal use only.

hydrolysis gave, in 98% yield, a crystalline product which was shown to be methyl 2-*O*-(benzylthio)carbonyl-α-D-glucopyranoside (IV). These compounds serve as useful intermediates in the synthesis of 3-, 3,4-di-, and 3,4,6-tri-*O*-substituted derivatives of methyl α-D-glucopyranoside in the following ways: (i) esterification of III followed by removal of the benzylidene and (benzylthio)carbonyl groups provides 3-*O*-substituted methyl glucosides, (ii) esterification of IV and subsequent removal of the (benzylthio)-carbonyl group gives 3,4,6-tri-*O*-substituted derivatives, and (iii) formation of the triphenylmethyl (trityl) ether of IV provides a compound (V) which is suitable for the formation of 3,4-di-*O*-substituted methyl glucosides. This is the first general synthetic route to each of these three classes of partial ester derivatives of methyl α-D-glucopyranoside.

This article describes the proof of structure of methyl 4,6-*O*-benzylidene-2-*O*-(benzylthio)carbonyl-α-D-glucopyranoside (III) and the syntheses of each of the above classes of partial esters as benzoates of methyl α-D-glucopyranoside; crystalline 2-*O*-(*p*-toluene)-sulphonates of each partially benzoated derivative were prepared.

DISCUSSION

Problems encountered in the use of previously reported blocking groups for the synthesis of partial esters of carbohydrates (namely the trifluoroacetate (2), the dichloroacetate (3), and the tosylate groups (4)) are largely overcome by making use of the thiocarbonate radical. The latter is stable under a wide range of conditions but is readily decomposed, when desired, by oxidative or reductive cleavage. It is now possible to synthesize a large number of previously inaccessible partial ester derivatives of the sugars.

There is ample evidence that the hydroxyl groups at C_2 and C_6 in methyl α-D-glucopyranoside are more reactive than those at C_3 and C_4 (5–7). Similarly, in methyl 4,6-*O*-benzylidene-α-D-glucopyranoside (I) the hydroxyl at C_2 is more reactive in substitution reactions than that at C_3 (8–11). When I was treated with 1 mole of (benzylthio)-carbonyl chloride in pyridine solution, the 2-thiocarbonate derivative was isolated in 58% yield together with 10% of the disubstituted product, methyl 4,6-*O*-benzylidene-2,3-di-*O*-(benzylthio)carbonyl-α-D-glycopyranoside. These two products are readily separated by fractional crystallization from ethanol. Attempts to isolate another product from the mother liquors which might be the 3-thiocarbonate derivative were not successful. The 2-thiocarbonate gave a crystalline acetate, phenylcarbamate, and benzoate derivative.

In order to establish the position of substitution of the thiocarbonate group in III, use was made of its benzoate derivative, VI, Fig. 2, since removal of the thiocarbonate group would furnish one of the isomeric monobenzoate derivatives of I, both being well characterized (2). Attempts to remove the thiocarbonate group from VI by oxidation with hydrogen peroxide in glacial acetic acid resulted in loss of the benzylidene group. It was found, however, that the thiocarbonate radical is decomposed by treatment with Raney nickel in boiling ethanol. In order to accomplish this desulphurization, it was discovered that it is essential to shake the ethanol solution of VI with Raney nickel at room temperature for at least 24 hours prior to refluxing for 3 hours. Omission of this step resulted in the recovery of mostly starting material, in low yield, together with small amounts of other products which were difficult to separate from VI. Under the above conditions, a mixture of the isomeric monobenzoates was obtained containing 24% of the C_2 benzoate (VII) and 56% of the C_3 benzoate (VIII); in another experiment the yield of VIII was 71%. Both monobenzoates were characterized as their tosylates, IX and X. Replacement of the (benzylthio)carbonyl group in VIII yielded a product indistinguishable from that (VI)

Can. J. Chem. Downloaded from www.nrcresearchpress.com by 210.87.254.105 on 09/05/12
For personal use only.

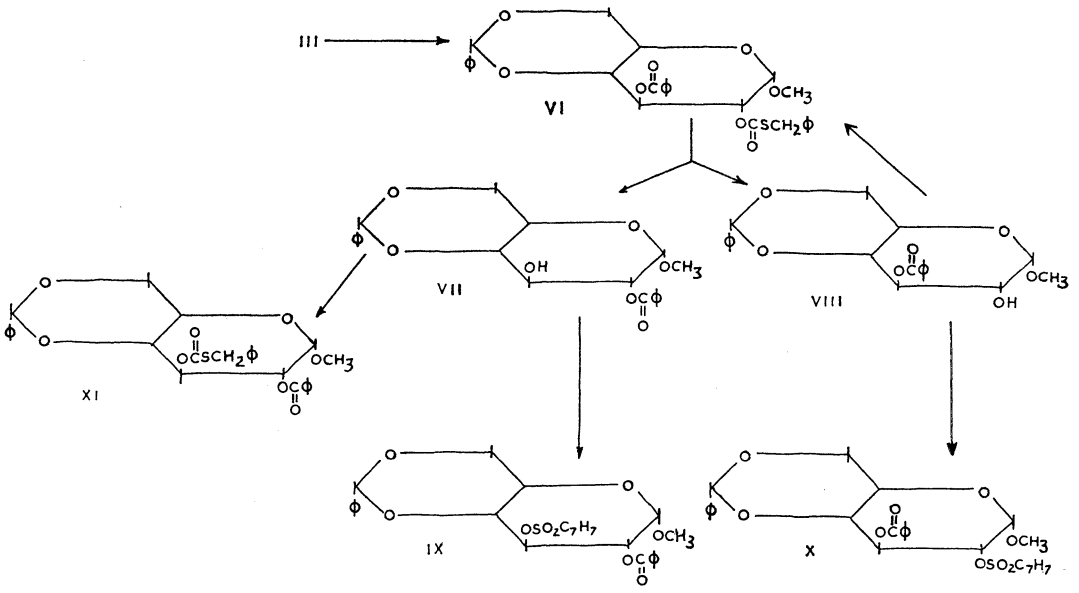

FIG. 2.

obtained by benzoylation of III. Since VIII and its tosylate (X) are well characterized as having the benzoyl group on C_3, the structure of VI must be as shown. Resubstitution of the (benzylthio)carbonyl group in VII yielded a product (XI) quite different from VI in melting point and specific rotation. The occurrence of VII as a product of Raney nickel desulphurization of VI must therefore have resulted from migration of the benzoyl group from the C_3 to the C_2 hydroxyl, possibly catalyzed by traces of alkali still present in the Raney nickel.

The migrations of ester groups in sugar derivatives are assumed to occur through orthoester intermediates (12) but factors which influence the direction of migration are not clearly understood. In derivatives of I there are reports of both C_3 to C_2 (2) and C_2 to C_3 (2, 13) migrations of ester groups; the present work provides another example of a C_3 to C_2 migration in these derivatives.

Benzoylation of IV gave a sirupy product XII, Fig. 3, which on treatment with hydro-

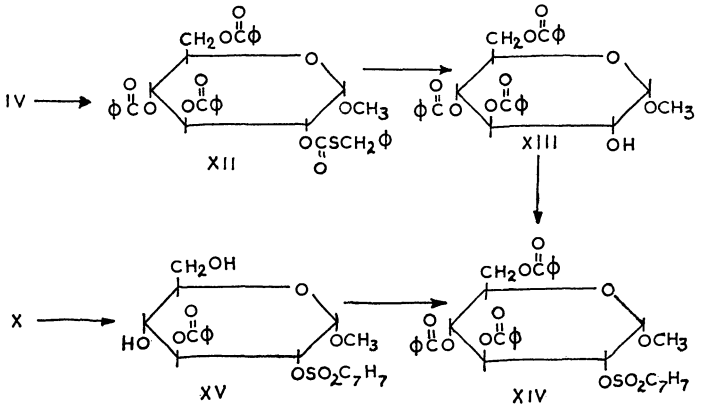

FIG. 3.

Can. J. Chem. Downloaded from www.nrcresearchpress.com by 210.87.254.105 on 09/05/12
For personal use only.

gen peroxide in glacial acetic acid gave 72% of the new crystalline tribenzoate of methyl α-D-glucopyranoside (XIII); this compound yielded a crystalline tosylate (XIV). The same tosylate was obtained from the known compound X by removal of the benzylidene group to give XV and benzoylation to yield methyl 3,4,6-tri-*O*-benzoyl-2-*O*-(*p*-toluene)-sulphonyl-α-D-glucopyranoside (XIV). Compound XIII was therefore proved to be methyl 3,4,6-tri-*O*-benzoyl-α-D-glucopyranoside.

The trityl derivative V of IV gave on benzoylation, XVI, Fig. 4. Detritylation to XVII followed by oxidative removal of the thiocarbonate group gave an amorphous solid,

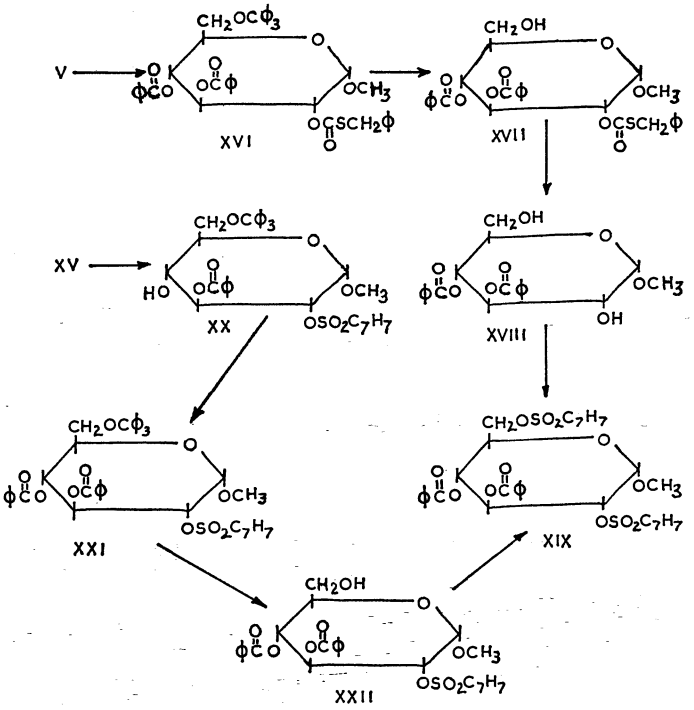

FIG. 4.

XVIII, which, however, gave a crystalline ditosylate derivative, XIX. To prove the structure of this compound, the known compound X was converted through three new crystalline products to an identical ditosylate dibenzoate derivative of methyl α-D-glucopyranoside. Contrary to the usual experience found in this laboratory with sugars having a free primary hydroxyl group, XV did not react with trityl chloride (1 mole) during 2 days at room temperature in pyridine solution. However, when the reaction mixture was warmed on the steam bath for 2 hours, a 93% yield of the crystalline trityl derivative XX was obtained. Benzoylation of the C_4 hydroxyl gave XXI, which was detritylated to give the crystalline 2-tosylate derivative of methyl 3,4-di-*O*-benzoyl-α-D-glucopyranoside. Tosylation of XXII gave a product indistinguishable from XIX obtained from XVIII. Thus, the structure of XVIII was also established.

Removal of the benzylidene group from the known 3-*O*-benzoyl derivative VIII furnished, in 70% yield, an hydroscopic amorphous solid, methyl 3-*O*-benzoyl-α-D-glucopyranoside. Its purity was established when the resynthesis of the benzylidene derivative, VIII, was accomplished in 93% yield.

Can. J. Chem. Downloaded from www.nrcresearchpress.com by 210.87.254.105 on 09/05/12
For personal use only.

These reactions confirm the assignment of structure to the monothiocarbonate derivative III as methyl 4,6-*O*-benzylidene-2-*O*-(benzylthio)carbonyl-α-D-glucopyranoside and to the compound IV, methyl 2-*O*-(benzylthio)carbonyl-α-D-glucopyranoside. Furthermore, the synthesis of the three new partial benzoate derivatives in good yield further demonstrates the use of the thiocarbonate group as a valuable blocking group for carbohydrate reactions.

EXPERIMENTAL[3]

Methyl 4,6-O-Benzylidene-2-O-(benzylthio)carbonyl-α-D-glucopyranoside (III)

Methyl 4,6-*O*-benzylidene-α-D-glucopyranoside (I) was prepared by a standard method (14), as was (benzylthio)carbonyl chloride (15). To 15.0 g of I in 30 ml of anhydrous pyridine was added dropwise 9.0 ml of II during ½ hour, the solution being cooled with an ice bath. The mixture was kept an additional half hour at room temperature and was then poured into 300 ml of ice water. The sirupy product was extracted into 100 ml of chloroform, and the latter solution was extracted successively with 100 ml of *N* hydrochloric acid, *N* sodium hydroxide, and water. The chloroform layer was dried over magnesium sulphate. The sirup obtained by evaporation of the chloroform was dissolved in 150 ml of hot ethanol. When cooled to room temperature, this solution gave after 3 hours 3.1 g (10%) of methyl 4,6-*O*-benzylidene-2,3-di-*O*-(benzylthio)carbonyl-α-D-glucopyranoside (1), which was recrystallized from ethanol; there was thus obtained 2.7 g of product with m.p. 133–134°. The original ethanol solution was cooled overnight at −5° and furnished 14.4 g of product having m.p. 118–121°. After recrystallization from 1 liter of ligroin there was obtained 13.3 g (58%) of fine needles, m.p. 121–122°. The melting point was not changed after recrystallization from ethanol, and this product showed $[\alpha]_D^{22}$ +80.60° (*c* 2, $CHCl_3$). Anal. Calc. for $C_{22}H_{24}O_7S$: C, 61.06; H, 5.77; S, 7.37. Found: C, 61.21; H, 5.41; S, 7.45.

In some instances, a third product, m.p. 42.5–44° and optically inactive, was obtained, which cocrystallized with III from ethanol. It was isolated by recrystallization of the mixture from ligroin, coming down last from that solvent. Its infrared spectrum and elemental analysis indicated that this compound was di(benzylthio)carbonyl, $(C_6H_5CH_2S)_2CO$, reported (16) previously as an oil. This same compound was sometimes encountered in low yield during the preparation of II from phosgene and benzylmercaptan, and can be distilled under high vacuum. Its formation during the synthesis of III can be attributed to a reaction of II with water, followed by loss of carbon dioxide to give benzylmercaptan, which reacts in turn with another mole of II. The use of strictly anhydrous pyridine was found to be essential for high yields of III. Anal. for di(benzylthio)carbonyl: Calc. for $C_{15}H_{14}OS_2$: C, 65.69; H, 5.12; S, 23.38. Found: C, 65.33; H, 5.23; S, 23.29.

Derivatives of III

The following derivatives of III were synthesized by standard procedures in pyridine solutions.

Methyl 3-O-Acetyl-4,6-O-benzylidene-2-O-(benzylthio)carbonyl-α-D-glucopyranoside

Yield: 59%; m.p. 135–136°; $[\alpha]_D^{22}$ +74.30° (*c* 2, $CHCl_3$). Anal. Calc. for $C_{24}H_{26}O_8S$: C, 60.75; H, 5.48; S, 6.74. Found: C, 59.61; H, 5.62; S, 6.99.

Methyl 4,6-O-Benzylidene-2-O-(benzylthio)carbonyl-3-O-phenylcarbamoyl-α-D-glucopyranoside

Yield: 84%; m.p. 120–121°; $[\alpha]_D^{22}$ +99.15° (*c* 2, $CHCl_3$). Anal. Calc. for $C_{29}H_{29}O_8NS$: C, 63.16; H, 5.26; S, 5.78; N, 2.54. Found: C, 63.68; H, 5.36; S, 5.78; N, 2.59.

Methyl 3-O-Benzoyl-4,6-O-benzylidene-2-O-(benzylthio)carbonyl-α-D-glucopyranoside (VI)

Yield: 87%; m.p. 138–139°; $[\alpha]_D^{25}$ +44.5° (*c* 2, $CHCl_3$). Anal. Calc. for $C_{29}H_{28}O_8S$: C, 64.92; H, 5.23; S, 5.97. Found: C, 64.87; H, 5.21; S, 6.08.

Methyl 2-O-(Benzylthio)carbonyl-α-D-glucopyranoside (IV)

To 1.0 g of III dissolved in 40 ml of acetone was added 12 ml of 0.2 *N* hydrochloric acid, and the solution was refluxed for 2 hours. After neutralization with excess barium carbonate and filtration, the solution was evaporated to dryness and the residue was extracted with several portions of warm ether, the insoluble barium chloride being removed by filtration. On cooling, the ether solution gave 0.78 g (98%) of product as large needles, m.p. 135–137°. After recrystallization from acetone – petroleum ether the product had m.p. 136–137° and $[\alpha]_D^{22}$ +112.2° (*c* 2, $CHCl_3$). Anal. Calc. for $C_{15}H_{20}O_7S$: S, 9.30. Found: S, 9.18.

Methyl 2-O-(Benzylthio)carbonyl-3,4,6-tri-O-phenylcarbamoyl-α-D-glucopyranoside

Compound IV was treated with phenyl isocyanate in pyridine solution by the usual procedure. The product had m.p. 192.5–193° and $[\alpha]_D^{22}$ +107.6° (*c* 2, $CHCl_3$). Anal. Calc. for $C_{36}H_{35}O_{10}N_3S$: C, 61.62; H, 4.99; N, 5.99; S, 4.57. Found: C, 60.95; H, 5.08; N, 6.01; S, 4.64.

Methyl 2-O-(Benzylthio)carbonyl-6-O-triphenylmethyl-α-D-glucopyranoside (V)

To 1.0 g of IV in 5 ml of anhydrous pyridine was added 0.81 g of triphenylmethyl chloride. The solution

[3]*Melting points are uncorrected. Solvents were removed in vacuo at 50°.*

Can. J. Chem. Downloaded from www.nrcresearchpress.com by 210.87.254.105 on 09/05/12
For personal use only.

stood for 2 days at room temperature, with protection from moisture, and was then poured into ice water. The product was extracted into chloroform and isolated in the usual way. The sirup obtained on evaporation of the chloroform turned to a glass on standing over phosphorus pentoxide, but failed to crystallize. It had $[\alpha]_D^{22}$ +46.7° (*c* 1, $CHCl_3$).

Reaction of Methyl 3-O-Benzoyl-4,6-O-benzylidene-2-O-(benzylthio)carbonyl-α-D-glucopyranoside with Raney Nickel

A solution of 5.4 g of VI in 500 ml of ethanol was treated with 8 g of Raney nickel (suspension in ethanol). The mixture was shaken for 24 hours at room temperature and then was refluxed for 3 hours. After filtering the hot solution, 100 ml of water was added. After concentrating this solution to 250 ml and cooling it at −25° for 3 hours, 2.2 g (56%) of product, m.p. 210–212°, was obtained. After recrystallization from acetone – petroleum ether the product had m.p. 216–217° and $[\alpha]_D^{25}$ +34.0° (*c* 1, $CHCl_3$). Reported for VIII: m.p. 217–218° and $[\alpha]_D^{19}$ +33.5° (*c* 2.6, $CHCl_3$).

Further concentration of the original solution gave two additional crops totaling 0.94 g, m.p. 160–163°. After recrystallization from acetone – petroleum ether this product had m.p. 166–168° and $[\alpha]_D^{25}$ +106° (*c* 2, $CHCl_3$). Reported (2) for VII, m.p. 165–166° and $[\alpha]_D^{15}$ +109.5° (*c* 2.1, $CHCl_3$). A mixed melting point with I (m.p. 163–164°) was depressed to 133–150°.

In a separate experiment, 50 mg of VI was shaken for 3 days at room temperature with 200 mg of Raney nickel prior to refluxing for 3 hours. Isolation as above gave, on cooling the ethanol solution, 26 mg (71%) of VIII, m.p. 217–218°.

Methyl 3-O-Benzoyl-4,6-O-benzylidene-2-O-(p-toluene)sulphonyl-α-D-glucopyranoside (X)

To 100 mg of VIII in 2 ml of anhydrous pyridine was added 58 mg of (*p*-toluene)sulphonyl chloride. After being left to stand overnight, the solution was poured into 50 ml of ice water. A solid product was obtained which was recovered by filtration and washed with water. It crystallized from ethanol, giving 125 mg (91%), m.p. 213–214° and $[\alpha]_D^{25}$ +52.4° (*c* 0.8, $CHCl_3$). Reported for X: m.p. 212–213°, $[\alpha]_D^{15}$ +51.6° (*c* 2.9, $CHCl_3$).

Methyl 2-O-Benzoyl-4,6-O-benzylidene-3-O-(p-toluene)sulphonyl-α-D-glucopyranoside (IX)

Compound VII (200 mg) was tosylated as described above except that 4 days' reaction time was required. The yield of IX was then 50%; the product, crystallized from ethanol, had m.p. 185–186° and $[\alpha]_D^{25}$ +78.9° (*c* 2.8, $CHCl_3$). Reported (2): m.p. 184–186° and $[\alpha]_D^{15}$ +83.8° (*c* 4.2, $CHCl_3$).

Resynthesis of VI from VIII

To 240 mg of VIII dissolved in 1 ml of anhydrous pyridine was added 140 mg of II. After 10 hours at room temperature, the product was isolated by the usual procedure. Evaporation of the chloroform gave a sirup which crystallized from ethanol, giving 220 mg (73%) after recrystallization from that solvent. This product had m.p. 138–139° and $[\alpha]_D^{25}$ +45.0° (*c* 2, $CHCl_3$). Found before: the same m.p. and $[\alpha]_D^{25}$ +44.5°. The melting point was not depressed after admixture with VI obtained by benzoylation of III.

Methyl 2-O-Benzoyl-4,6-O-benzylidene-3-O-(benzylthio)carbonyl-α-D-glucopyranoside (XI)

To 196 mg of VII in 1 ml of anhydrous pyridine was added 186 mg of II. The solution stood for 3 hours at room temperature (drying tube), and was then poured into 50 ml of ice water, giving a solid which was recovered by filtration. Two crystallizations from ethanol gave 130 mg (48%) of product as needles having m.p. 133–135° and $[\alpha]_D^{25}$ +107° (*c* 2, $CHCl_3$). Anal. Calc. for $C_{29}H_{28}O_8S$: C, 64.93; H, 5.23; S, 5.97. Found: C, 65.37; H, 5.43; S, 5.73.

Methyl 3,4,6-Tri-O-benzoyl-2-O-(benzylthio)carbonyl-α-D-glucopyranoside (XII)

To 0.5 g of IV in 5 ml anhydrous pyridine was added 1 ml of benzoyl chloride. Isolation in the usual way gave a sirup with $[\alpha]_D^{25}$ +28.0° (*c* 2, $CHCl_3$) which failed to crystallize.

Methyl 3,4,6-Tri-O-benzoyl-α-D-glucopyranoside (XIII)

The product XII from above was dissolved in 10 ml of glacial acetic acid containing 1 ml of chloroform. Sodium acetate (150 mg) and 2 ml of 30% hydrogen peroxide were added and the solution was kept for 5 days at room temperature. The solution was then poured into 200 ml of ice water containing sufficient sodium bicarbonate to neutralize the acetic acid. The product was extracted into chloroform, and the latter was dried and evaporated, leaving a sirupy product which crystallized from ligroin. After recrystallization from ligroin there was obtained 391 mg (72%) of product as needles having m.p. 103–105° and $[\alpha]_D^{25}$ +75.5° (*c* 2, $CHCl_3$). Anal. Calc. for $C_{28}H_{26}O_9$: C, 66.40; H, 5.14. Found: C, 66.52; H, 5.09.

Methyl 3,4,6-Tri-O-benzoyl-2-O-(p-toluene)sulphonyl-α-D-glucopyranoside (XIV)

To 100 mg of XIII in 1 ml of pyridine was added 100 mg of (*p*-toluene)sulphonyl chloride. After being left to stand overnight, the solution was poured into 50 ml of ice water; a solid product was obtained which crystallized from ligroin. There was obtained after recrystallization from that solvent 103 mg (79%) of product having m.p. 158–159° and $[\alpha]_D^{25}$ +67.2° (*c* 2, $CHCl_3$). Anal. Calc. for $C_{35}H_{32}O_{11}S$: C, 63.64; H, 4.85; S, 4.85. Found: C, 63.50; H, 5.35; S, 4.91.

Can. J. Chem. Downloaded from www.nrcresearchpress.com by 210.87.254.105 on 09/05/12
For personal use only.

Methyl 3-O-Benzoyl-2-O-(p-toluene)sulphonyl-α-D-glucopyranoside (XV)

Compound X (125 mg) was treated as described before for the synthesis of IV. After two crystallizations from acetone – petroleum ether, the product (82 mg, 80%) was obtained as large needles having m.p. 192–193° and $[\alpha]_D^{25}$ +114° (*c* 2, acetone). Anal. Calc. for $C_{21}H_{24}O_9S$: C, 55.77; H, 5.32; S, 7.08. Found: C, 55.40; H, 5.66; S, 6.78.

Benzoylation of 15 mg of XV by the usual procedure gave 11 mg of product having $[\alpha]_D^{25}$ +66.5° (*c* 0.2, $CHCl_3$) and m.p. 157–158°. Admixture of this product with XIV synthesized from XIII did not depress the melting point.

Methyl 3,4-Di-O-benzoyl-2-O-(benzylthio)carbonyl-α-D-glucopyranoside (XVII)

One gram of IV was tritylated as described before and 1.2 ml of benzoyl chloride was added to the pyridine solution after 2 days. After a third day, the product was isolated by the usual procedure and was obtained as a glass having $[\alpha]_D^{25}$ +19° (*c* 2, $CHCl_3$). This product was dissolved in 6 ml of glacial acetic acid, and 1 ml of acetic acid saturated with hydrogen bromide was added, the solution being kept cool with an ice bath. The triphenylmethyl bromide (0.75 g) was recovered by filtration, and the solution was poured into 100 ml of ice water containing 1 g of sodium bicarbonate. The water was decanted from the sirup, and the latter was then dissolved in chloroform. After washing, drying, and evaporating the chloroform, there was obtained a sirup with $[\alpha]_D^{25}$ +13° (*c* 2, $CHCl_3$).

Methyl 3,4-Di-O-benzoyl-α-D-glucopyranoside (XVIII)

The product from the above reaction was dissolved in 10 ml of glacial acetic acid containing 3 ml of chloroform. Sodium acetate (275 mg) and 3 ml of hydrogen peroxide were added and the solution was kept for 4 days at room temperature. It was then poured into 200 ml of ice water containing sufficient sodium bicarbonate to neutralize the acetic acid. Evaporation of the chloroform left the product as a solid suspended in the water. This product was recovered by filtration and washed thoroughly with water. It could not be induced to crystallize. The yield was 0.69 g (59% based on IV) and the amorphous product had $[\alpha]_D^{25}$ +32° (*c* 0.5, acetone). Anal. Calc. for $C_{21}H_{22}O_8$: C, 62.68; H, 5.48. Found: C, 61.83; H, 5.61.

Methyl 3,4-Di-O-benzoyl-2,6-di-O-(p-toluene)sulphonyl-α-D-glucopyranoside (XIX)

To 60 mg of XVIII in 1 ml of anhydrous pyridine was added 200 mg of (*p*-toluene)sulphonyl chloride. After 3 days the solution was poured into 50 ml of ice water; a solid product was obtained, which was recovered by filtration. After two crystallizations from ligroin, there was obtained 51 mg of product (48%) as needles which had m.p. 189–190° and $[\alpha]_D^{25}$ +25.9° (*c* 1, $CHCl_3$). Anal. Calc. for $C_{35}H_{34}O_{12}S_2$: C, 59.16; H, 4.78; S, 9.02. Found: C, 60.29; H, 5.06; S, 9.41.

Methyl 3-O-Benzoyl-2-O-(p-toluene)sulphonyl-6-O-trityl-α-D-glucopyranoside (XX)

To 300 mg of XV in 5 ml anhydrous pyridine was added 240 mg of triphenylmethyl chloride. While being protected with a drying tube, the solution was warmed on the steam bath for 2 hours, after which it was poured into ice water. The solid product thus obtained was recovered by filtration and crystallized from ethanol, giving 429 mg (93%), m.p. 174–176°. Recrystallization from ligroin did not change the melting point of the product, which had $[\alpha]_D^{25}$ +90.0° (*c* 2, $CHCl_3$). Anal. Calc. for $C_{40}H_{38}O_9S$: C, 69.16; H, 5.48; S, 4.61. Found: C, 69.39; H, 5.37; S, 4.64.

Methyl 3,4-Di-O-benzoyl-2-O-(p-toluene)sulphonyl-6-O-trityl-α-D-glucopyranoside (XXI)

To 330 mg of XX in 3 ml of anhydrous pyridine was added 120 mg of benzoyl chloride and this solution was heated for 1 hour on the steam bath (drying tube). The addition of ice water (50 ml) gave a solid product, which was crystallized from ethanol and then ligroin; there was thus obtained 210 mg (61%) of product in a low-melting crystalline form (m.p. 89–91°). Recrystallization from ligroin gave large needles, m.p. 179–181° and $[\alpha]_D^{25}$ +38.0° (*c* 1, $CHCl_3$). Anal. Calc. for $C_{47}H_{42}O_{10}S$: C, 70.67; H, 5.27; S, 4.01. Found: C, 70.56; H, 5.25; S, 4.30.

Methyl 3,4-Di-O-benzoyl-2-O-(p-toluene)sulphonyl-α-D-glucopyranoside (XXII)

Compound XXI (140 mg) was detritylated as previously described; there was obtained 50 mg (52%) of product which was crystallized twice as fine needles from ligroin. The product had m.p. 70–72° and $[\alpha]_D^{25}$ +18.0° (*c* 0.5, $CHCl_3$). Anal. Calc. for $C_{28}H_{28}O_{10}S$: C, 60.43; H, 5.04; S, 5.76. Found: C, 60.80; H, 5.07. For an unexplained reason, sulphur analyses were high, 6.7 and 7.1

This product (24 mg) was tosylated as previously described, giving 16 mg of product, which after two crystallizations from ligroin had m.p. 190–192°. The m.p. was not depressed after admixture with XIX obtained from tosylation of XVIII.

Methyl 3-O-Benzoyl-α-D-glucopyranoside

This compound was synthesized from 0.5 g of VIII by a method previously described. The product was obtained as an amorphous solid having $[\alpha]_D^{25}$ +169° (*c* 2, $CHCl_3$). Anal. Calc. for $C_{14}H_{18}O_7$: C, 56.37; H, 6.04. Found: C, 55.71; H, 6.34.

To 100 mg of this product dissolved in 1 ml of benzaldehyde was added 100 mg of anhydrous zinc chloride. After the mixture was shaken for 3 hours, it was treated with ice water and petroleum ether; the product

Can. J. Chem. Downloaded from www.nrcresearchpress.com by 210.87.254.105 on 09/05/12
For personal use only.

was thus obtained as a solid, which was recovered by filtration and crystallized twice from ethanol. There was obtained 120 mg (93%) of product having m.p. 216–217° and $[\alpha]_D^{25}$ +34.0° (*c* 1, $CHCl_3$). The melting point was not depressed after admixture with VIII.

ACKNOWLEDGMENT

This investigation was carried out during the tenure of a Postdoctoral Fellowship supported by the National Science Foundation.

REFERENCES

1. J. J. WILLARD. Can. J. Chem. **40**, 2035 (1962).
2. E. J. BOURNE, A. J. HUGGARD, and J. C. TATLOW. J. Chem. Soc. 735 (1953).
3. D. J. BELL. J. Chem. Soc. 1180 (1935).
4. G. W. KENNER and M. A. MURRAY. J. Chem. Soc. 5178 (1949).
5. TH. LIESER and R. SCHWEIZER. Ann. **519**, 217 (1935).
6. M. L. WOLFROM and M. A. EL-TARABOULSI. J. Am. Chem. Soc. **75**, 5350 (1953).
7. R. W. LENZ. J. Am. Chem. Soc. **82**, 182 (1960).
8. G. J. ROBERTSON and C. F. GRIFFITH. J. Chem. Soc. 1193 (1935).
9. H. R. BOLLIGER and D. A. PRINS. Helv. Chim. Acta, **28**, 465 (1945).
10. B. R. BAKER, K. HEWSON, L. GOODMAN, and A. BENITEZ. J. Am. Chem. Soc. **80**, 6577 (1958).
11. J. SUGIHARA. Advan. Carbohydrate Chem. **8**, 1 (1953).
12. E. PACSU. Advan. Carbohydrate Chem. **1**, 77 (1945).
13. J. HONEYMAN and J. W. W. MORGAN. J. Chem. Soc. 3660 (1955).
14. K. FREUDENBERG, H. TOEPFFER, and C. ANDERSON. Ber. **61**, 1750 (1928).
15. H. TILLES. J. Am. Chem. Soc. **81**, 714 (1959).
16. G. BULMER and F. G. MANN. J. Chem. Soc. 666 (1945).

Can. J. Chem. Downloaded from www.nrcresearchpress.com by 210.87.254.105 on 09/05/12
For personal use only.

Can. J. Chem. Downloaded from www.nrcresearchpress.com by 210.87.254.6 on 09/05/12
For personal use only.

NOTES

THE NUCLEAR MAGNETIC RESONANCE SPECTRUM OF SODIUM METHYLCYCLOPENTADIENIDE

STEWART MCLEAN AND PETER HAYNES

The nuclear magnetic resonance spectrum of sodium cyclopentadienide in several solvents has already been described (1). Our results, obtained with a *colorless* 4 mole% solution of sodium cyclopentadienide in tetrahydrofuran, confirm the previous report that the proton spectrum consists of a single line (at 4.38 τ in our system) and that addition of free cyclopentadiene to the solution produces a spectrum that is a simple superimposition of those of the two components, showing that proton exchange between cyclopentadiene and cyclopentadienide anion is a relatively slow process.

The distillate obtained on thermal cracking of methylcyclopentadiene dimer consists principally of a mixture of 1- and 2-methylcyclopentadienes in the ratio of 1:1.2 (2, 3). The mixture can be converted to a single sodium methylcyclopentadienide by several methods, including treatment with sodium sand in a suitable medium.

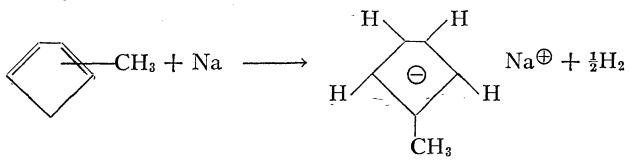

The n.m.r. spectrum of a colorless 4 mole% solution of sodium methylcyclopentadienide in tetrahydrofuran consisted of only two peaks other than those from the solvent: one at 4.58 τ (relative area 4) due to the ring protons, and the other at 7.87 τ (relative area 3) due to the methyl protons. The peaks, which had widths at half height of 1.0 and 1.3 c.p.s. respectively, showed no resolvable fine structure. Two pairs of non-equivalent protons are present on the ring and it must be presumed that the negative charge on the ring produces a "levelling" effect on their environment. The spectrum was relatively insensitive to changes of concentration in the range 4 to 15 mole% sodium methylcyclopentadienide, the shift to higher field at the higher concentration being 5.4 c.p.s. for the ring protons and 3.9 c.p.s. for the methyl protons.

Although it is obvious that throughout the study of these systems a thorough analysis cannot ignore completely the influence of the cation associated with the ring system, it is interesting to note that the introduction of a methyl substituent on the cyclopentadienide anion shifts each of the ring protons 12 c.p.s. to higher field, giving a total effect of +48 c.p.s. for the four protons; this is almost exactly the value obtained by Reddy and Goldstein (4) for the effect of a methyl substituent on the ring proton chemical shifts in a number of uncharged aromatic systems.

The spectrum of the mixture of methylcyclopentadienes is, needless to say, very complex; we merely note at this stage that a solution of our material in tetrahydrofuran gave rise to characteristic spectral patterns at 3.6 to 4.2 τ (vinyl protons), 7.02 to 7.25 τ (methylene protons), and 7.97 to 8.07 τ (methyl protons). Addition of this mixture of isomers to a solution of sodium methylcyclopentadienide produced a spectrum that was

a simple superimposition of the spectra of the components. Once again proton exchange must be a slow process on the scale of nuclear relaxation times.

The addition of methylcyclopentadiene to sodium cyclopentadienide or of cyclopentadiene to sodium methylcyclopentadienide allows proton exchange to be examined on a considerably expanded time scale since products and reactants are no longer indistinguishable. When fractions of an equivalent of cyclopentadiene were added stepwise to a solution of sodium methylcyclopentadienide in tetrahydrofuran, it was possible to observe the growth of the peak attributed to the cyclopentadienide anion at the expense of the methylcyclopentadienide peaks, and it was convenient to use the areas of the peaks associated with ring protons to calculate the relative concentrations of the two anions.* When a full equivalent of cyclopentadiene had been added, the spectrum of the solution did not change appreciably on longer standing. From a comparison of the peak areas associated with the anionic species it is possible to deduce that the equilibrium

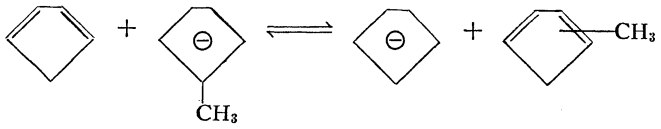

lies to the right and that the methylcyclopentadienide ion is an appreciably stronger base than the cyclopentadienide anion. We are as yet unable to express this quantitatively, and a refinement of technique will be necessary before we can do so. The spectrum obtained on addition of methylcyclopentadiene to sodium cyclopentadienide confirmed that the equilibrium could be approached from either direction.

We were interested to observe that the spectrum of the mixture of methylcyclopentadienes produced from sodium methylcyclopentadienide and cyclopentadiene was identical with that of the material obtained by cracking the dimer. Thermal cracking of the dimer must, therefore, lead to the equilibrium mixture of methylcyclopentadienes, as we had suspected from other evidence.

EXPERIMENTAL

Cyclopentadiene and *methylcyclopentadiene* were prepared by thermally cracking the appropriate dimer (at 170° and 200° respectively).

Sodium cyclopentadienide and *sodium methylcyclopentadienide* solutions of the required concentration were prepared by adding a calculated amount of the corresponding diene to a stirred suspension of sodium sand in dry tetrahydrofuran (distilled from $LiAlH_4$ and stored over sodium wire) under an atmosphere of dry, oxygen-free nitrogen. When the reaction was complete, the colorless solution was transferred via a side arm incorporating a sintered-glass filter into the n.m.r. sample tube, which was then sealed. A stream of nitrogen was used to drive the solution through the side arm and the whole apparatus was blanketed with another stream of nitrogen. The concentration of the filtered solution was determined by adding an aliquot to an excess of standard HCl solution and back-titrating (pH meter) with standard NaOH solution.

Nuclear magnetic resonance spectra were obtained at 22° using a Varian DP 60 high-resolution spectrometer operating at 60 Mc/sec and equipped with a field stabilizer. A precision bore (5 mm) spinning tube with a gas-tight ground-glass stopper was used. Operations requiring the addition of a further component to the solution in the tube were carried out under nitrogen. Chemical shifts (τ values (5)) were determined using tetramethylsilane (1–2%) as an internal reference and utilizing the audio side-band technique; a preliminary check showed that the addition of tetramethylsilane did not change the character of the spectrum.

**It is of interest that when the two peaks were of equal height, the width at half height of the methylcyclopentadienide peak was 1.8 c.p.s. while that of the cyclopentadienide peak was 0.9 c.p.s., indicative of unresolved coupling in the former case.*

Can. J. Chem. Downloaded from www.nrcresearchpress.com by 210.87.254.6 on 09/05/12
For personal use only.

ACKNOWLEDGMENTS

Nuclear magnetic resonance spectra were measured by Mr. S. Cawley through the courtesy of Dr. S. S. Danyluk. Methylcyclopentadiene dimer was a gift from Enjay Chemical Company, Elizabeth, N.J. This research was supported by a grant from the National Research Council.

1. G. Fraenkel, R. E. Carter, A. McLachlan, and J. H. Richards. J. Am. Chem. Soc. **82,** 5846 (1960). J. R. Leto, F. A. Cotton, and J. S. Waugh. Nature, **180,** 978 (1957).
2. S. M. Csicsery. J. Org. Chem. **25,** 518 (1960).
3. S. McLean and P. Haynes. Unpublished observations.
4. G. S. Reddy and J. H. Goldstein. J. Am. Chem. Soc. **83,** 5020 (1962).
5. G. V. D. Tiers. J. Phys. Chem. **62,** 1151 (1958).

Received November 26, 1962.
Department of Chemistry,
University of Toronto,
Toronto 5, Ontario.

Can. J. Chem. Downloaded from www.nrcresearchpress.com by 210.87.254.6 on 09/05/12
For personal use only.

ORGANIC PEROXIDES
V. OXIDATION OF ARYLLITHIUM COMPOUNDS TO PHENOLS

H. S. Chang and J. T. Edward

Low yields of phenols are obtained by the oxidation of arylmagnesium halides with molecular oxygen, but they may be improved by carrying out the oxidation in the presence of an aliphatic Grignard reagent (1). The reasons for this improvement have been discussed by Walling and Buckler (2). Aryllithium compounds are also oxidized to phenols by molecular oxygen in low yields (3, 4), and we have carried out the oxidation in the presence of butyllithium in the hope of improving the yield. This hope proved illusory, as shown by the results in Table I. Better yields were obtained when oxidation was effected by *t*-butyl hydroperoxide (cf. ref. 4), but were still sometimes low. The oxidations of the α-furyllithium compounds were suggested by the successful oxidation of α-thienyllithium (5), and expected to yield the unsaturated lactones tautomeric with the α-furanols (6); in the event, only intractable, high-boiling tars were obtained.

TABLE I

Yields (%) of phenols from the oxidation of aryllithium compounds with different oxidizing agents

	Oxidizing agent		
Compound	O_2*	O_2 + BuLi*	Bu^{t}OOH†
Phenyllithium	30‡	30	93§
p-Biphenylyllithium	18‖	19	—
2-Methoxy-1-naphthyllithium	7	—	23
α-Furyllithium	0	—	0
5-Methyl-2-furyllithium	0	—	0

*Yield based on aryllithium compound.
†Yield based on peroxide.
‡Gilman and Pacevitz (3) reported 22–25% yield.
§Müller and Töpel (4), using α-tetralyl hydroperoxide, reported 96% yield.
‖Müller and Töpel (4) reported 3% yield.

ACKNOWLEDGMENTS

Nuclear magnetic resonance spectra were measured by Mr. S. Cawley through the courtesy of Dr. S. S. Danyluk. Methylcyclopentadiene dimer was a gift from Enjay Chemical Company, Elizabeth, N.J. This research was supported by a grant from the National Research Council.

1. G. Fraenkel, R. E. Carter, A. McLachlan, and J. H. Richards. J. Am. Chem. Soc. **82,** 5846 (1960). J. R. Leto, F. A. Cotton, and J. S. Waugh. Nature, **180,** 978 (1957).
2. S. M. Csicsery. J. Org. Chem. **25,** 518 (1960).
3. S. McLean and P. Haynes. Unpublished observations.
4. G. S. Reddy and J. H. Goldstein. J. Am. Chem. Soc. **83,** 5020 (1962).
5. G. V. D. Tiers. J. Phys. Chem. **62,** 1151 (1958).

Received November 26, 1962.
Department of Chemistry,
University of Toronto,
Toronto 5, Ontario.

Can. J. Chem. Downloaded from www.nrcresearchpress.com by 210.87.254.42 on 09/05/12
For personal use only.

ORGANIC PEROXIDES
V. OXIDATION OF ARYLLITHIUM COMPOUNDS TO PHENOLS

H. S. Chang and J. T. Edward

Low yields of phenols are obtained by the oxidation of arylmagnesium halides with molecular oxygen, but they may be improved by carrying out the oxidation in the presence of an aliphatic Grignard reagent (1). The reasons for this improvement have been discussed by Walling and Buckler (2). Aryllithium compounds are also oxidized to phenols by molecular oxygen in low yields (3, 4), and we have carried out the oxidation in the presence of butyllithium in the hope of improving the yield. This hope proved illusory, as shown by the results in Table I. Better yields were obtained when oxidation was effected by *t*-butyl hydroperoxide (cf. ref. 4), but were still sometimes low. The oxidations of the α-furyllithium compounds were suggested by the successful oxidation of α-thienyllithium (5), and expected to yield the unsaturated lactones tautomeric with the α-furanols (6); in the event, only intractable, high-boiling tars were obtained.

TABLE I

Yields (%) of phenols from the oxidation of aryllithium compounds with different oxidizing agents

Compound	Oxidizing agent		
	O_2*	O_2 + BuLi*	Bu^{t}OOH†
Phenyllithium	30‡	30	93§
p-Biphenylyllithium	18‖	19	—
2-Methoxy-1-naphthyllithium	7	—	23
α-Furyllithium	0	—	0
5-Methyl-2-furyllithium	0	—	0

*Yield based on aryllithium compound.
†Yield based on peroxide.
‡Gilman and Pacevitz (3) reported 22–25% yield.
§Müller and Töpel (4), using α-tetralyl hydroperoxide, reported 96% yield.
‖Müller and Töpel (4) reported 3% yield.

EXPERIMENTAL

Oxidation with Molecular Oxygen

The preparations of phenyllithium (7), *p*-biphenylyllithium (7), α-furyllithium (8), and 5-methyl-2-furyllithium (8) were carried out according to the literature; 2-methoxy-1-naphthyllithium was prepared in 80% yield (estimated by titration) from 1-bromo-2-methoxy naphthalene by the conventional procedure (7). Dry oxygen was bubbled through the ether solutions of the organolithium compounds for several hours. This represents a large excess of oxygen over that stoichiometrically required; in separate experiments it was shown that use of the stoichiometric quantity offered no advantage. The ether solutions were then worked up in the usual way.

Phenol, extracted from the ether solution with aqueous sodium hydroxide, was estimated in the extract by titration (9); this accounts for yields slightly higher than those reported (3, 4), which were based on the isolation of the product. *p*-Hydroxybiphenyl was isolated as a crystalline solid, m.p.161°, identified by mixed m.p. The phenolic fraction from the oxidation of 2-methoxy-1-naphthyllithium (0.014 mole) was obtained as a brown gum (0.58 g), which was chromatographed on Woelm alumina (activity II–III) in hexane solution. Elution with hexane–benzene 4:1 (v/v) gave 2-methoxy-1-naphthol as a gummy solid, crystallizing from hexane as colorless needles (0.17 g; 7%), m.p. 53.5–54.5°. Calc. for $C_{11}H_{10}O_2$: C, 75.86; H, 5.75%. Found: C, 75.70; H, 5.78%. Infrared spectrum: $\nu_{max}^{CCl_4}$ in cm^{-1}: 3530 (m), 3040 (m), 2940 (m), 2820 (m), 1650 (m), 1600 (m), 1490 (s), 1410 (m), 1380 (m), 1360 (s), 1280 (s), 1200 (m), 1180 (w), 1100 (s), 1060 (s), 905 (s). Treatment of this compound with benzoyl chloride in pyridine gave an oily product. The oil in benzene solution was washed with aqueous alkali, dried over magnesium sulphate, and recovered by evaporation. It was then taken up in hexane and chromatographed on Woelm alumina (activity II–III). Elution with hexane–benzene 4:1 (v/v) gave 2-methoxy-1-naphthyl benzoate, crystallizing from hexane in colorless rods, m.p. 104–105°. Calc. for $C_{18}H_{14}O_3$: C, 77.69; H, 5.03%. Found: C, 77.48; H, 4.93%. Infrared spectrum: $\nu_{max}^{CCl_4}$ in cm^{-1}: 3050 (w), 3020 (w), 2985 (w), 2860 (w), 1750 (s), 1645 (m), 1609 (m), 1515 (w), 1485 (w), 1459 (m), 1385 (m), 1353 (w), 1318 (w), 1280 (s), 1247 (s), 1190 (m), 1175 (s), 1155 (m), 1150 (m), 1100 (s), 1080 (s), 1067 (s), 1023 (s), 923 (w), 695 (m). Chakravarti and Pasupati (10), who oxidized 2-methoxy-1-naphthylmagnesium bromide with molecular oxygen, did not isolate the napthol, but converted it to 2-methoxy-1-naphthyl benzoate, m.p. 110°, in low, unspecified overall yield.

Oxidation with t-Butyl Hydroperoxide

Commercial hydroperoxide (84% by titration; 1 mole) in anhydrous ether was added slowly to a stirred ether solution of the aryllithium compound (2.2 moles). Stirring was continued for 2–3 hours, and the mixture then poured into ice water and worked up in the usual fashion. Crystallization from hexane of the gummy phenolic fraction obtained from 2-methoxy-1-naphthyllithium gave white crystals (7% yield) decomposing above 288°, presumably of *4,4′-dihydroxy-3,3′-dimethoxy*-1,1′-*binaphthyl* (cf. ref. 11), although a satisfactory analysis could not be obtained for the compound. Calc. for $C_{22}H_{18}O_4$: C, 76.30; H, 5.20%. Found: C, 75.39; H, 5.02%. (Chakravarti and Pasupati (10) reported obtaining in unspecified yield from the oxidation of 2-methoxy-1-naphthylmagnesium bromide with molecular oxygen a solid melting above 300°, which they did not analyze.) However, the *dibenzoate*, obtained by treatment of the binaphthol with benzoyl chloride in pyridine, crystallized from benzene in colorless rods, m.p. 346–348°, of satisfactory purity. Calc. for $C_{36}H_{25}O_6$: C, 77.97; H, 4.67%. Found: C, 77.98; H, 4.88%. The mother liquors from 4,4′-dihydroxy-3,3′dimethoxy-1,1′-binaphthyl were chromatographed as before to yield 2-methoxy-1-naphthol (Table I).

ACKNOWLEDGMENTS

We are grateful to Harchem Limited for a gift of *t*-butyl hydroperoxide and to the National Research Council for financial support.

1. M. S. Kharasch and W. B. Reynolds. J. Am. Chem. Soc. **65**, 501 (1943).
2. C. Walling and S. A. Buckler. J. Am. Chem. Soc. **77**, 6032 (1955).
3. H. A. Pacewitz and H. Gilman. J. Am. Chem. Soc. **61**, 1603 (1939).
4. E. Müller and T. Töpel. Ber. **72**, 273 (1939).
5. C. D. Hurd and H. J. Anderson. J. Am. Chem. Soc. **75**, 5124 (1953).
6. R. H. Thompson. Quart. Rev. (London), **10**, 27 (1956).
7. H. Gilman, E. A. Zoellner, and W. M. Selby. J. Am. Chem. Soc. **55**, 1252 (1933).
8. W. E. Truce and E. Wellisch. J. Am. Chem. Soc. **74**, 5177 (1952).
9. N. H. Furman. Scott's standard methods of chemical analysis. Vol. II. D. van Nostrand Co. Inc., New York. 1947. p. 2253.
10. S. N. Chakravarti and V. Pasupati. J. Chem. Soc. 1859 (1937).
11. F. Straus, O. Bernoully, and P. Mautner. Ann. **444**, 165 (1925).

Received October 23, 1962.
Department of Chemistry,
McGill University,
Montreal, Que.

Can. J. Chem. Downloaded from www.nrcresearchpress.com by 210.87.254.42 on 09/05/12
For personal use only.

Can. J. Chem. Downloaded from www.nrcresearchpress.com by 210.87.254.105 on 09/05/12
For personal use only.

Symposium on Organometallic Compounds

The papers that follow were presented at a symposium held at the University of British Columbia, Vancouver, British Columbia, on September 4, 5, and 6, 1962, under the joint auspices of the Inorganic Chemistry Division of the Chemical Institute of Canada, and the Department of Chemistry of the University of British Columbia.

THE EFFECT OF SUBSTITUENTS ON THE STABILITIES OF COMPLEXES OF PLATINUM WITH ARYL ACETYLENES AND PHOSPHINES[1]

A. D. Allen and C. D. Cook
Department of Chemistry, University of Toronto, Toronto, Ontario

Received October 29, 1962

ABSTRACT

Compounds of platinum (0) with aryl phosphines are stabilized by electron-withdrawing substituents. A maximum coordination number of three is observed in such cases, suggesting that platinum tetracarbonyl cannot be prepared. Compounds in which one phosphine is replaced by an aryl acetylene are also stabilized by electron withdrawal by the acetylene and quantitative data are given on the relative stabilities of these compounds. These data indicate that a two-coordinated diphosphine platinum (0) compound might be stable if an appropriate substituted phosphine is used. The effect of substituents on the stabilities of these compounds is discussed.

Ligands which stabilize zero oxidation states of the transition metals are generally those which are capable of donating electrons to and accepting electrons from the metal atom. The clearest example of this is carbon monoxide in the metal carbonyls. It follows that the ability of the metal atom to accept and donate electrons is an important factor in the formation of such compounds. The stabilities, occurrence, and absence of carbonyls of the various transition metals have been the subject of much speculation (1), and in particular the absence of carbonyls of palladium and platinum, in contrast to the ready formation of nickel carbonyl, has been related to the higher ionization potential of the d^{10} spin-paired state of these two elements (1). Although no tetracarbonyls of palladium or platinum have been prepared, mixed derivatives containing carbon monoxide and ligands such as phosphines (2), amines, and halogens (3) exist, presumably because these other ligands are stronger electron donors and weaker electron acceptors than carbon monoxide and thus do not compete so strongly for the metal *d* electrons. No compound with more than two molecules of carbon monoxide attached to platinum has been prepared. Even for nickel carbonyl there is evidence (4) that loss of one carbon monoxide occurs readily, leaving a relatively stable tricarbonyl intermediate.

It appears that the requirement for ligands which are most likely to stabilize the zero oxidation state of platinum is that they should be slightly better electron donors and weaker electron acceptors than carbon monoxide. Phosphines, arsines, sulphides, and unsaturated hydrocarbons are obvious possibilities, and various compounds containing these ligands have been prepared (5). These ligands form an ideal system for study, since their donor and acceptor properties can be modified by introducing suitable substituents, particularly if an aromatic nucleus is attached to the bonding atoms.

[1]*Presented at the Symposium on Organometallic Compounds, Vancouver, British Columbia, September 4–6, 1962, sponsored by the Inorganic Chemistry Division, Chemical Institute of Canada, and the Department of Chemistry, University of British Columbia, with the support of the National Research Council, Ottawa, in cooperation with the University Extension Department.*

Can. J. Chem. Downloaded from www.nrcresearchpress.com by 210.87.254.105 on 09/05/12
For personal use only.

Malatesta and Cariello (5) observed that triphenylphosphine forms compounds with platinum (0) containing three and four phosphines. Recently Chopoorian, Lewis, and Nyholm (6) have reported that these compounds should be regarded as hydrides of bivalent platinum. We have found (7) that the triphenylphosphine–platinum system is complicated and that both hydrides and non-hydrides are formed under different conditions, but that the products are difficult to characterize adequately, the composition changing during purification procedures. Malatesta and Cariello also found that not more than three tri-*p*-chlorophenylphosphine ligands could be attached to platinum (0). We find the same behavior with tri-*p*-fluorophenylphosphine and have demonstrated (8) that the very stable three-coordinated compound formed is not a hydride. These results indicate that triphenylphosphine is just too weak an electron acceptor to give very stable platinum (0) compounds, but that when electron-withdrawing groups are introduced the substituted phosphine strongly stabilizes the three-coordinated compound. Since there is no steric change on going from triphenylphosphine to the substituted compound, failure to obtain the four-coordinating compound must be attributed to the nature of the bonding involved. Monodentate ligands which can accept electrons sufficiently strongly apparently do stabilize the zero oxidation state of platinum, but only three such ligands can then be attached. Thus it is extremely unlikely that platinum tetracarbonyl could form, and it seems that carbon monoxide depends too strongly on electron acceptance even to form a stable tricarbonyl. A platinum dicarbonyl might be kinetically unstable, but there is some evidence from our work with acetylenic complexes that a relatively stable reaction intermediate is formed with only two triphenylphosphines attached to platinum. The possibility of increasing the stability of the two-coordinated compound by using bulky substituents on the phosphines is currently being investigated.

Towards platinum (0), aryl acetylenes behave in a manner very similar to that of the aryl phosphines. Compounds of the general formula $(Ph_3P)_2Pt\cdot ac$, where ac is a substituted acetylene, were first reported by Chatt, Rowe, and Williams (9) in 1957. These may be regarded as tricoordinated compounds in which the triple bond of the acetylene occupies one position. The most stable compound reported was that of di-*p*-nitrophenylacetylene, showing that electron withdrawal by aryl groups attached to the triple bond stabilizes the compound. We have now made a detailed study of the effect of substituents on the stabilities of these compounds (10). The ligand exchange reaction: $(Ar_3P)_2Pt\cdot ac + ac' \rightleftarrows (Ar_3P)_2Pt\cdot ac' + ac$, proceeds smoothly at room temperature in an inert solvent such as cyclohexane, and we have been able to determine spectrophotometrically both the equilibrium position and the kinetic form of the reaction for a wide range of substituted aryl acetylenes and diaryl acetylenes. As an example of the effects observed the results obtained with a series of para-substituted phenyl acetylenes are given in Table I.

The equilibrium constants show clearly that electron-withdrawing substituents stabilize these complexes relative to phenylacetylene. Confirmation of this is given by the kinetic measurements. The initial rates of both the forward and backward reactions are independent of the nature and concentration of the reagent, and are first order with respect to the complex. The rate-determining step thus appears to be the breaking of the metal–acetylene bond, and the rate of the reaction provides a measure of the relative strength of this bond. The complex with the slowest rate of reaction is that of *p*-nitrophenylacetylene and so we may conclude that the bond is strengthened by the strongly electron-withdrawing nitro group.

TABLE I

First-order rate coefficients (k_1) and equilibrium constants (K) for the reactions, in cyclohexane at 28°,

$$(Ph_3P)_2Pt\text{-}p\text{-}X\text{-}C_6H_4CCH + PhCCH \underset{k_1}{\overset{K}{\rightleftharpoons}} (Ph_3P)_2PtPhCCH + p\text{-}X\text{-}C_6H_4CCH$$

p-X-	10^4k_1 (sec^{-1})	$1/K$
p-Nitro-	1.5	105
p-Bromo-	5	10
p-Chloro-	7	10
p-H-	15	1
p-Methoxy-	19	~1

A more detailed examination of the kinetics of these, and other related reactions, particularly when more than one acetylene is present in the reaction mixture, indicates that the intermediate formed in the rate-determining step, $(Ar_3P)_2Pt$, has a significant stability, there being a small activation energy for its reaction with the available acetylenes which varies with the nature of the acetylene, e.g. is less for p-nitrophenylacetylene than for phenylacetylene.

The reaction steps may be written:

$$(Ph_3P)_2Pt\cdot ac \underset{k_{-1}}{\overset{k_1}{\rightleftharpoons}} (Ph_3P)_2Pt + ac$$

$$(Ph_3P)_2Pt + ac' \xrightarrow{k_2} (Ph_3P)_2Pt\cdot ac'.$$

If we assume a steady state for the intermediate $(Ph_3P)_2Pt$, the rate expression for the initial forward reaction is:

$$v = k_1[(Ph_3P)_2Pt\cdot ac]/\left(\frac{k_{-1}}{k_2}\frac{[ac]}{[ac']}\right)+1.$$

In the absence of added acetylene ac, the initial concentration [ac] is zero and a simple first-order expression is obtained, $v = k_1[(Ph_3P)_2Pt\cdot ac]$. If ac is added at a concentration equal to ac′, the denominator becomes $(k_{-1}/k_2)+1$. The effect on the rate of reaction of addition of ac thus depends on the relative magnitudes of k_{-1} and k_2. If both are very large, as would be the case with a very reactive intermediate, k_{-1}/k_2 would approach unity and the denominator would approach a value of 2. Thus for a reactive intermediate we would expect the rate to be approximately halved when [ac] = [ac′]. If k_{-1} is much greater than k_2 a strong retardation of rate will be observed, but if k_2 is much greater than k_{-1} there will be little, if any, inhibition. We find that the rate of the reaction of the phenylacetylene complex with p-nitrophenylacetylene is virtually unaffected by added phenylacetylene, but that the reverse reaction is strongly inhibited by small amounts of added p-nitrophenylacetylene. Thus the intermediate reacts at different rates with different acetylenes, showing that the process involves some activation energy.

The limited availability of the metal d electrons and the competition for them that exists between the various ligands is illustrated by a comparison between complexes of substituted phenyl phosphines. Under the same conditions the phenylacetylene complex with tri-p-fluorophenylphosphine reacts about twice as rapidly, and that with tri-p-tolylphosphine about twice as slowly as the triphenylphosphine complex. Electron

Can. J. Chem. Downloaded from www.nrcresearchpress.com by 210.87.254.105 on 09/05/12
For personal use only.

donation by the methyl groups in tri-*p*-tolylphosphine will reduce the acceptor properties of the phosphorus and hence allow the acetylene to increase the degree of double bonding between it and the metal. This strengthens the metal–acetylene bond and reduces the rate of reaction. The opposite occurs with tri-*p*-fluorophenylphosphine.

The rather delicate balance between the ability of these ligands to stabilize the zero oxidation state of platinum is illustrated by their methods of preparation. Treatment of a suspension of *cis*-dichlorobis(triarylphosphine)platinum (II) in alcohol with hydrazine gives a clear solution which reacts further in a way which depends on the substituent in the aryl phosphine, as shown below:

Substituent in phosphine	Clear solution at room temp. gives	Heating to 70° for 5 minutes gives
p-Methoxy	No product	No product
p-Methyl	No product	No product
p-H	No product	$(Ph_3P)_nPtH_m$?
p-Fluoro	$((p\text{-F—Ph})_3P)_3Pt$ rapidly	—
p-Chloro	$((p\text{-Cl—Ph})_3P)_3Pt$ rapidly	—

Thus electron-donating groups inhibit the formation of the phosphine complexes, and electron-withdrawing groups facilitate their formation. When the clear solution resulting from the reduction of the dichloro complex with hydrazine is treated with excess phenylacetylene, the tri-*p*-methoxy-, tri-*p*-totyl-, and triphenyl-phosphine compounds give the acetylene complexes, the ease and rapidity of formation increasing in the above sequence. With the tri-*p*-fluoro- and tri-*p*-chloro-phenylphosphine compounds the trisphosphine is formed too rapidly to permit the preparation of the acetylene complex in this way. If, however, an excess of the acetylene is added before reduction with hydrazine, the *p*-fluorophenylphosphine compound gives the acetylene complex, but the *p*-chlorophenylphosphine compound still gives only the trisphosphine of platinum (0). We have been unable to prepare an acetylene complex from the *p*-chlorophenylphosphine compound.

These reactions show that by the use of suitable substituents the tendency of this type of ligand to stabilize platinum (0) compounds can be significantly modified. Preliminary results with substituted aryl sulphides indicate that these ligands behave in a similar manner.

ACKNOWLEDGMENTS

We are indebted to the National Research Council for financial support, to the Shell Oil Company of Canada Limited for a Fellowship (to C. D. C.), and to Dr. J. Chatt for his interest and helpful advice.

REFERENCES

1. R. S. Nyholm. Proc. Chem. Soc. 273 (1961).
2. L. Malatesta and C. Cariello. J. Inorg. Nucl. Chem. **8**, 561 (1958).
3. R. J. Irving and E. A. Magnusson. J. Chem. Soc. 1860 (1956); 2018 (1957).
4. F. Basolo and R. G. Pearson. Advances in inorganic chemistry and radiochemistry. Vol. 3. Academic Press, New York. 1961. p. 72.
5. L. Malatesta and C. Cariello. J. Chem. Soc. 2323 (1958). J. Chatt and G. A. Rowe. Nature, **191**, 1191 (1961).
6. J. A. Chopoorian, J. Lewis, and R. S. Nyholm. Nature, **190**, 528 (1961).
7. A. D. Allen, R. Asselestine, and C. D. Cook. Unpublished results.
8. A. D. Allen and C. D. Cook. Proc. Chem. Soc. 218 (1962).
9. J. Chatt, G. A. Rowe, and A. A. Williams. Proc. Chem. Soc. 208 (1957).
10. A. D. Allen and C. D. Cook. Proc. 7th I.C.C.C., Stockholm. June, 1962. p. 299.

Can. J. Chem. Downloaded from www.nrcresearchpress.com by 210.87.254.105 on 09/05/12
For personal use only.

ORGANOTIN CHEMISTRY

II. THE REACTION OF DIORGANOTIN OXIDES WITH PHENOLS[1, 2]

WM. J. CONSIDINE, J. J. VENTURA, A. J. GIBBONS, JR., AND A. ROSS
Research Laboratory, Metal and Thermit Corp., Rahway, New Jersey, U.S.A.

Received October 29, 1962

ABSTRACT

The reaction of diorganotin oxides with many compounds containing active hydrogen proceeds to the formation of di-derivatives. With phenols the reaction stops at the distannoxane stage. The synthesis and characterization of several 1,3-diphenoxydistannoxanes is described. On the basis of molecular weights and other evidence, a structure is proposed for these compounds.

Can. J. Chem. Downloaded from www.nrcresearchpress.com by 210.87.254.105 on 09/05/12
For personal use only.

The literature (1) reports the reaction of diorganotin oxides with acids, phenols, alcohols, and mercaptans. In the case of phenols the expected product, the diorganotin diphenoxide, would be formed according to reaction [1]. Compounds of structure I have

$$R_2SnO + 2ArOH \rightarrow R_2Sn(OAr)_2 + H_2O \qquad [1]$$

I

been reported in the literature (1 and references cited therein, 2) but without any description of their synthesis or analytical, or other, data to support the claims.

We reacted dibutyltin oxide with 4-methoxyphenol and 4-*tert*-butylphenol. Toluene was used as solvent and the water of reaction was removed by azeotropic distillation and collected in a Dean–Stark trap. The final, constant amount of water isolated never equalled that predicted by [1] and the product which crystallized from the reaction mixture was the starting phenol.

These results caused us to reconsider the applicability of [1] to the reaction of diorganotin oxides and phenols. The insufficiency of water produced and the recovery of starting phenol both suggested that reaction [2] might be an accurate description of the reaction. Compounds of structure II have been disclosed in the patent literature (3) but have never been described in any detail.

$$2R_2SnO + 2ArOH \rightarrow (R_2SnOAr)_2O + H_2O \qquad [2]$$

II

In order to decide between [1] and [2] as the course of the reaction, we reacted a variety of diorganotin oxides and phenols according to the stoichiometries of [1] and [2]. For example, when 2 moles of phenol itself was reacted in toluene with 1 mole of dibutyltin oxide, only 56% of the amount of water required by [1] could be isolated. When equimolar quantities of the two were reacted, the amount of water predicted by [2] was isolated and the compound tetrabutyl-1,2-diphenoxydistannoxane (II, R = *n*-C_4H_9; Ar = C_6H_5) was isolated in a 95% yield.

To give more examples, dimethyl- and diphenyl-tin oxide were reacted with phenol, and dibutyltin oxide was reacted with 4-methoxyphenol, 4-*tert*-butylphenol, 4-nitrophenol,

[1]*Presented at the Symposium on Organometallic Compounds, Vancouver, British Columbia, September 4–6, 1962, sponsored by the Inorganic Chemistry Division, Chemical Institute of Canada, and the Department of Chemistry, University of British Columbia, with the support of the National Research Council, Ottawa, in cooperation with the University Extension Department.*

[2]*Part I: Wm. J. Considine and J. J. Ventura. Chem. Ind. In press.*

β-naphthol, hydroquinone, and 2,2-bis(4-hydroxyphenyl)propane (bisphenol A). In every case, when 2 moles of the phenol was reacted with 1 mole of the oxide, only about 50% of the water required by [1] was isolated. When equimolar amounts of reactants were used, high yields of water, according to [2], and the corresponding distannoxanes were isolated. The distannoxanes from hydroquinone and bisphenol A were apparently polymeric in nature. No reaction was observed between dibutyltin oxide and 2,6-di-*tert*-butyl-4-methylphenol due to the steric hinderance of the bulky *tert*-butyl groups.

Tetrabutyl-1,3-diphenoxydistannoxane was isolated as white prisms; m.p. 137–139.5°. The molecular weights, by the Rast procedure, both in camphor and cyclopentadecanone, gave values corresponding to a monomer. When the molecular weight was determined in benzene or carbon tetrachloride solutions at 37.5° in a thermistor osmometer, the results clearly showed a dimer to be present. These observations require a structure which is a dimer, but which allows for an easy thermal dedimerization at the higher temperatures of the Rast determination.

Okawara (4), on the basis of X-ray analysis, has determined the structure of tetramethyl-1,3-bis(trimethylsiloxy)distannoxane as III. Alleston, Davies, and Figgis (5) were unable to choose between IV and V, as structures for tetrabutyl-1,3-dichlorodistannoxane

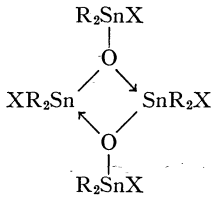

III, R = CH_3, X = $(CH_3)SiO$ V, R = *n*-C_4H_9, X = Br
IV, R = *n*-C_4H_9, X = Cl VI, R = *n*-C_4H_9, X = OC_6H_5

and tetrabutyl-1,3-dibromostannoxane, and related structures in which the halogens were only on the exocyclic tin atoms. Their conclusions were based on dimeric molecular weights and the occurrence of two overlapping peaks of approximate area, and with chemical shifts close to those of the corresponding dibutyl dihalides, in the ^{119}Sn magnetic resonance spectra of IV and V.

We propose VI as the structure of tetrabutyl-1,3-diphenoxydistannoxane. The molecular weight data is accommodated by the unique four-membered ring. It would be reasonable to expect that the strength of the coordinate bond could be offset by thermal energy and the dimer would revert to the monomers. This dimeric structure also is supported by the melting point behavior of the diphenoxydistannoxanes. Most of the members of this class have a constant, but broad, melting point due to the fact that the phase change observed is not a simple melting point, but rather a dedimerization. The same melting behavior is shown by the nitroso compounds, which are also dimers.

We have not considered any alternates to VI in which the exocyclic tins each bear two phenoxy groups. Dibutyltin diphenoxide (6) is extremely sensitive to hydrolysis, whereas the distannoxane is quite indifferent to water. For this reason it does not seem reasonable to advance a structure which has two phenoxy groups on the same tin.

VI was independently synthesized by reaction [3].

$$[([n\text{-}C_4H_9]_2ClSn)_2O]_2 + 4C_6H_5OH + 4(CH_3CH_2)_3N \rightarrow [([n\text{-}C_4H_9]_2C_6H_5OSn)_2O]_2 + 4(CH_3CH_2)_3N.HCl \quad [3]$$

Mention was made of the extreme sensitivity of the diphenoxide to hydrolysis. It is our view that this fact explains the failure of the diphenoxydistannoxanes to react further

Can. J. Chem. Downloaded from www.nrcresearchpress.com by 210.87.254.105 on 09/05/12
For personal use only.

with phenols. The further reaction of phenol, to form dibutyltin diphenoxide, would produce water. This water then would hydrolyze the product back to the distannoxane. Dibutyltin oxide does react with, for example, 4-*tert*-butylthiophenol to form dibutyltin di-4-*tert*-butylthiophenoxide in toluene. However, the Sn—S bond is much more resistant to hydrolysis (7) than is the Sn—O bond so the water of reaction does not destroy the product in this case.

EXPERIMENTAL

All melting points are uncorrected.

In the reactions of diorganotin oxides with various phenols described below, the reactions were run under two conditions. In condition A the ratio of moles diorganotin oxide to *equivalents* of the phenol was 1:2. In condition B this ratio was 1:1.

Reactions of Bu_2SnO with Phenol

A (1:2). Phenol (47.1 g, 0.5 mole) was added to a stirred suspension of dibutyltin oxide (67.2 g, 0.25 mole) in 500 ml of anhydrous toluene contained in a 1-liter three-necked flask equipped with a Dean–Stark apparatus, a mechanical stirrer, a reflux condenser, and a drying tube. After 3 hours' refluxing, a constant volume of only 2.5 ml water (0.14 mole, 56%) collected in the trap.

Tetrabutyl-1,3-diphenoxydistannoxane

B (1:1). Phenol (47.1 g, 0.5 mole) was reacted as in A, above, with dibutyltin oxide (124.5 g, 0.5 mole). After 2 hours' reflux a constant volume of 4.5 ml water (0.25 mole, 100%) had been collected. The hazy solution was filtered and the toluene removed by vacuum distillation to give 159.0 g (0.12 mole; 95%) of a yellow oil which set to a light tan solid. Repeated recrystallizations from hexane gave white prisms; m.p., 137–139.5° constant. Anal. Calc. for $C_{56}H_{62}O_6Sn_4$: C, 50.34; H, 6.94; Sn, 35.54; M.W., 1336.10. Found: C, 50.36; H, 6.96; Sn, 35.48; M.W., 661, 682 (Rast, cyclopentadecanone); 675, 692 (Rast, camphor); 1291, 1374 (thermistor osmometer, carbon tetrachloride); 961, 982, 985 (thermistor osmometer, benzene).

Reactions of Bu_2SnO with p-Methoxyphenol

A (1:2). In this example, 78% of the theoretical amount of water could be isolated. The crude reaction product was dissolved in benzene. Upon the addition of pentane, *p*-methoxyphenol was obtained in a recovery of 29%. Its identity was established by a mixed melting point determination, after recrystallization from hexane.

Tetrabutyl-1,3-bis(4-methoxyphenoxy)distannoxane

B (1:1). Water was isolated in the theoretical amount. Removal of the solvent gave the crude product as a solid in 101% yield. Three recrystallizations from pentane gave crystalline material with a constant melting point of 86–89°. Anal. Calc. for $C_{60}H_{100}O_{10}Sn_4$: Sn, 32.61; C, 49.48; H, 6.92. Found: Sn, 32.57, 32.61; C, 49.82, 49.68; H, 6.97; 6.91.

Reactions of Bu_2SnO with p-tert-Butylphenol

A (1:2). Water was isolated in 59% of theory. Recrystallization of the crude product gave *p-tert*-butylphenol as shown by a mixed melting point determination.

Tetrabutyl-1,3-bis(4-tert-butylphenoxy)distannoxane

B (1:1). Water was isolated in the theoretical amount and removal of the solvent gave the product in a yield of 97%. Three recrystallizations from pentane gave white crystals with a constant melting point of 139–142°. Anal. Calc. for $C_{72}H_{122}O_6Sn_4$: Sn, 30.43; C, 55.41; H, 8.01. Found: Sn, 30.15; C, 55.20, 55.19; H, 8.02, 8.11.

Reactions of Bu_2SnO with p-Nitrophenol

A (1:2). Only 53% of the calculated amount of water was obtained.

Tetrabutyl-1,3-bis(4-nitrophenoxy)distannoxane

B (1:1). Water was isolated in 100% yield and the product was obtained directly as a yellow powder by filtration of the reaction mixture, in which it was insoluble. The yield was 99%. The melting point of the crude product, 247–248°, was unchanged when a small portion was recrystallized from toluene. The crude product was dried at 100° and a pressure of 1 mm Hg for 6 hours before analysis. Anal. Calc. for $C_{56}H_{88}N_4O_{14}Sn_4$: C, 44.08; H, 5.61; N, 3.72; Sn, 31.32. Found: C, 43.92; H, 5.71; N, 3.80; Sn, 31.55.

Reactions of Bu_2SnO with β-Naphthol

A (1:2). Only 49% of the theoretical amount of water was isolated.

Can. J. Chem. Downloaded from www.nrcresearchpress.com by 210.87.254.105 on 09/05/12
For personal use only.

Tetrabutyl-1,3-bis(β-naphthoxy)distannoxane

B (1:1). Water was obtained in 100% yield. Removal of the toluene by vacuum distillation gave the product as a brown oil which solidified to a brown solid upon cooling. The yield of the crude product was 104%. Repeated recrystallizations from pentane, including charcoal clarification, gave the product as light tan crystals with a constant melting point of 94–100°. Anal. Calc. for $C_{12}H_{100}O_6Sn_4$: C, 56.29; H, 6.56; Sn, 30.91. Found: C, 56.39, 56.11; H, 6.61, 6.65; Sn, 30.68.

Reactions of Bu_2SnO with Hydroquinone

A (1:1). Only 58% of the calculated amount of water was obtained.

B (1:0.5). Water was obtained in 100% of calculated yield. The reaction mixture was a thick slurry of a white solid which was separated from the toluene by filtration. The product, when dry, was a brown, friable powder, insoluble in toluene, ether, or methanol, which decomposed, without melting, at 310°. It was obtained in 100.5% yield. Anal. Calc. for $(C_{22}H_{40}O_3Sn_2)_x$: Sn, 40.24. Found: Sn, 40.68.

Reactions of Bu_2SnO with 2,2-Bis(p-hydroxyphenyl)propane

Dibutyltin oxide (248.8 g, 0.1 mole) and 2,2-bis(*p*-hydroxyphenyl)propane were added to 200 ml of benzene contained in a three-necked flask equipped with a mechanical stirrer, a Dean–Stark apparatus, and a reflux condenser with a drying tube. During stirring, the reaction mixture was heated to, and held at, the reflux temperature for 3 hours. Two milliliters of water (0.08 mole; 80%) was collected in the trap. The reaction mixture was filtered, while hot, and allowed to cool.

Overnight, white solids formed, which were isolated by filtration and air-dried; yield 20 g (66%). Washing of the crude product with cold methanol caused a weight loss of 1 g and gave material with m.p. 268–274°. Recrystallization from toluene raised the melting point to 302–305° (decomp.). Anal. Calc. for $(C_{31}H_{50}O_3Sn_2)_x$: Sn, 33.53; C, 52.57; H, 7.12. Found: Sn, 32.87; C, 52.59; H, 7.18.

Reactions of Diphenyltin Oxide with Phenol

A (1:2). Only 50% of the theoretical amount of water was obtained.

Tetraphenyl-1,3-diphenoxydistannoxane

B (1:1). The reaction mixture was a very thick, pasty, white mass, and an additional 250 ml of anhydrous toluene had to be added to get efficient stirring. The water isolated amounted to 83% of the theoretical amount. The crude reaction product was insoluble in toluene and it was isolated by filtration in a yield, when dry, of 89%. The melting point of the crude material was broad and centered around 250°. Attempts to recrystallize the material were unsuccessful due to its extreme insolubility in all of the solvents tried. It was analyzed without further purification. Anal. Calc. for $C_{72}H_{60}O_6Sn_4$: Sn, 31.74. Found: Sn, 33.12.

Reactions of Dimethyltin Oxide with Phenol

A (1:2). Under these conditions only 53% of the theoretical amount of water could be isolated.

Tetramethyl-1,3-diphenoxydistannoxane

B (1:1). Water was isolated in the theoretical yield. Removal of the solvent gave a 94% yield of the product as a white solid. Recrystallizations from both hexane and cyclohexane gave a crystalline product with a constant, but broad, melting range of 190–197° C. Anal. Calc. for $C_{32}H_{22}O_6Sn_2$: Sn, 47.51. Found: Sn, 48.24, 48.28, 48.21.

Reactions of Bu_2SnO with 2,6-Di-tert-butyl-p-methylphenol

A (1:2). This reaction was not run under condition A.

B (1:1). After 12 hours' reflux the water isolated was only a constant 2.5% of the theoretical.

Synthesis of Tetrabutyl-1,3-diphenoxydistannoxane from Tetrabutyl-1,3-dichlorodistannoxane

Phenol (0.1 g; 107 mmoles) and tetrabutyl-1,3-dichlorodistannoxane (28.3 g, 27 mmoles) were dissolved in 100 ml of anhydrous benzene. During stirring, triethylamine (10.8 g, 107 mmoles) was added over a period of 5 minutes. The temperature rose from ambient to 42° and a white precipitate formed. Stirring was continued for 2 hours.

The reaction mixture was washed with a 100-ml and a 50-ml portion of water to remove triethylamine hydrochloride. The organic layer dried over anhydrous magnesium sulphate and was freed of benzene to give 33.0 g (24 mmoles, 89%) of off-white crystals with a melting point of 137.5–139°, undepressed when admixed with the material prepared as above. The infrared spectra of the materials prepared by both methods were congruent.

After recrystallization from hexane, the X-ray powder pattern of the product was identical with that of the material prepared as above.

Treatment of Tetrabutyl-1,3-diphenoxydistannoxane

Tetrabutyl-1,3-diphenoxydistannoxane (33.4 g, 25 mmoles) and phenol (9.4 g, 100 mmoles) were dissolved in 50 ml of anhydrous toluene and the solution was heated to reflux in a flask fitted with a Dean–Stark apparatus, a reflux condenser, and a drying tube. After 48 hours' reflux, 0.2 ml of water (11 mmoles, 22%) had collected in the trap. After an additional 48 hours of reflux no more water had collected.

Can. J. Chem. Downloaded from www.nrcresearchpress.com by 210.87.254.105 on 09/05/12
For personal use only.

The toluene was removed by distillation, at atmospheric pressure, to a pot temperature of 160°. The stripped residue was subjected to vacuum distillation and 2.9 g (31 mmoles, 31%) passed over at 63° at 5 mm. These white needles were identified as phenol by their melting point of 37–41°, undepressed when admixed with authentic material.

The distillation residue, a brownish crystalline solid, weighed 38.3 g. Recrystallization from hexane raised the melting point considerably but pure tetrabutyl-1,3-diphenoxydistannoxane could not be recovered. The infrared spectra showed the presence of an —OH band which points to phenol as the difficultly removable contaminant.

Synthesis of Dibutyltin Di-p-tert-butylthiophenol

Dibutyltin oxide (106.2 g, 427 mmoles) and *p-tert*-butylthiophenol (142.0 g, 854 mmoles) were added to 500 ml of anhydrous benzene contained in a 1-liter three-necked flask fitted with a mechanical stirrer, a Dean–Stark apparatus, a reflux condenser, and a drying tube. During stirring the mixture was heated to ithe reflux and held there for 3½ hours, during which period 7.7 ml of water (427 mmoles, 101%) was collected n the trap. Removal of benzene left 229 g (406 mmoles, 95%) of a hazy yellow liquid. Fractionation gave material boiling at 191–200° at 0.1 mm Hg, N_D^{29} 1.5744. Anal. Calc. for $C_{28}H_{44}S_2Sn$: Sn, 21.07; S, 11.40. Found: Sn, 20.72, 20.66, 20.83; S, 11.61.

ACKNOWLEDGMENTS

The analyses were performed by Mr. H. Corbin and his associates with the exception of C, H determinations, which were done by Spang Microanalytical Laboratory, Ann Arbor, Michigan. The molecular weights and spectra were determined by Mr. I. Simmons and his associates.

REFERENCES

1. R. K. INGHAM, S. D. ROSENBERG, and H. GILMAN. Chem. Rev. **60**, 459 (1960).
2. T. HARADA. Sci. Papers Inst. Phys. Chem. Res. (Tokyo), **35**, 304 (1939).
3. U. S. Patent No. 2,789,105.
4. R. OKAWARA. Proc. Chem. Soc. 383 (1961) and private communication quoted in D. L. Alleston, A. G. Davies, and B. N. Figgis. Proc. Chem. Soc. 457 (1961).
5. D. L. ALLESTON, A. G. DAVIES, and B. N. FIGGIS. Proc. Chem. Soc. 457 (1961).
6. Unpublished work.
7. W. T. REICHLE. J. Org. Chem. **26**, 4634 (1961).

Can. J. Chem. Downloaded from www.nrcresearchpress.com by 210.87.254.105 on 09/05/12
For personal use only.

ORGANOGERMANIUM COMPOUNDS

PART II. INFRARED SPECTRA OF SOME ACETOXYGERMANES AND THE RELATIVE INDUCTIVE EFFECTS OF TRIMETHYLSILYL AND TRIMETHYLGERMYL GROUPS[1, 2, 3]

T. N. SRIVASTAVA[4] AND M. ONYSZCHUK

Inorganic Chemistry Laboratory, McGill University, Montreal, Que.

Received October 29, 1962

ABSTRACT

The infrared spectra of GeH_3OCOCH_3 and $(CH_3)_3GeOCOCH_3$ have been measured in the gas phase over the range 650–3800 cm^{-1}. Assignments for the principal bands have been made and their values compared with those of analogous alkyl, methylsilyl, methyltin, and methyllead acetates. Carbonyl absorption bands shift to lower frequencies and carbon–oxygen (skeletal) absorptions to higher frequencies as M changes from C to Si to Ge in the series of acetates represented by $(CH_3)_3MOCOCH_3$. These results suggest that the Ge—O bond is more polar than the Si—O bond and that the order of electron release in acetate derivatives is $(CH_3)_3Ge > (CH_3)_3Si > (CH_3)_3C$, which is consistent with the electronegativity order: C > Si > Ge.

INTRODUCTION

The infrared spectra of all but the germanium compound in the series of acetates with general formula $(CH_3)_3MOCOCH_3$, where M is a Group IV*b* element, have now been reported. Okawara, Webster, and Rochow (1) examined the infrared spectra of several methylsilicon and methyltin acetates, and they concluded, on the basis of the positions of the carbonyl stretching bands, that the Si—O bonds in the former are covalent while the Sn—O bonds in the latter are ionic. Later, Okawara and Sato (2) interpreted the infrared spectrum of trimethyllead acetate as the superimposition of absorptions due to the acetate anion and the trimethyllead cation.

We have examined the infrared spectra of acetoxygermane, GeH_3OCOCH_3, and trimethylacetoxygermane, $(CH_3)_3GeOCOCH_3$, with the object of determining the nature of the Ge—O bond. These new compounds have been prepared recently in this laboratory in connection with our interests in the preparation and properties of germyl (3) and trimethylgermyl (4, 5) compounds.

EXPERIMENTAL

The interaction of silver acetate with monobromogermane and trimethylbromogermane in a vacuum was used for the preparation of acetoxygermane (3) and trimethylacetoxygermane (5), respectively. Both compounds were purified by fractional distillation in a vacuum and tensimetrically pure samples were used for infrared spectral measurements (vapor pressures were 9.7 mm at 0° for GeH_3OCOCH_3 and 7.1 mm at 15° for $(CH_3)_3GeOCOCH_3$). The spectrum of *tert*-butyl acetate (Eastman Kodak, redistilled) was also recorded because we were unable to find its spectrum in the chemical literature.

Spectra were recorded on a Perkin–Elmer, Model 21, double-beam spectrometer equipped with a NaCl prism and calibrated with CO_2 and H_2O. In the range 650 to 2000 cm^{-1} wave numbers are accurate to ± 3 cm^{-1}, and to ± 10 cm^{-1} above 2000 cm^{-1}. Samples were examined as liquids in capillary film or in carbon tetrachloride solution, and/or as gases contained at measured pressures in glass cells of 10-cm length and 5-cm diameter fitted with 5 mm thick NaCl end plates.

[1]*Presented at the Symposium on Organometallic Compounds, Vancouver, British Columbia, September 4–6, 1962, sponsored by the Inorganic Chemistry Division, Chemical Institute of Canada, and the Department of Chemistry, University of British Columbia, with the support of the National Research Council, Ottawa, in cooperation with the University Extension Department.*

[2]*Financial assistance for this work was received from the National Research Council.*

[3]*Part I: J. E. Griffiths and M. Onyszchuk. Can. J. Chem.* ***39****, 339 (1961).*

[4]*Holder of an N.R.C. Postdoctoral Research Fellowship at McGill University; on leave from the Department of Chemistry, University of Lucknow, Lucknow, India.*

RESULTS AND DISCUSSION

The spectra of acetoxy- and trimethylacetoxy-germane are shown in Fig. 1, and the frequency assignments are summarized in Table I; these assignments are discussed separately as follows.

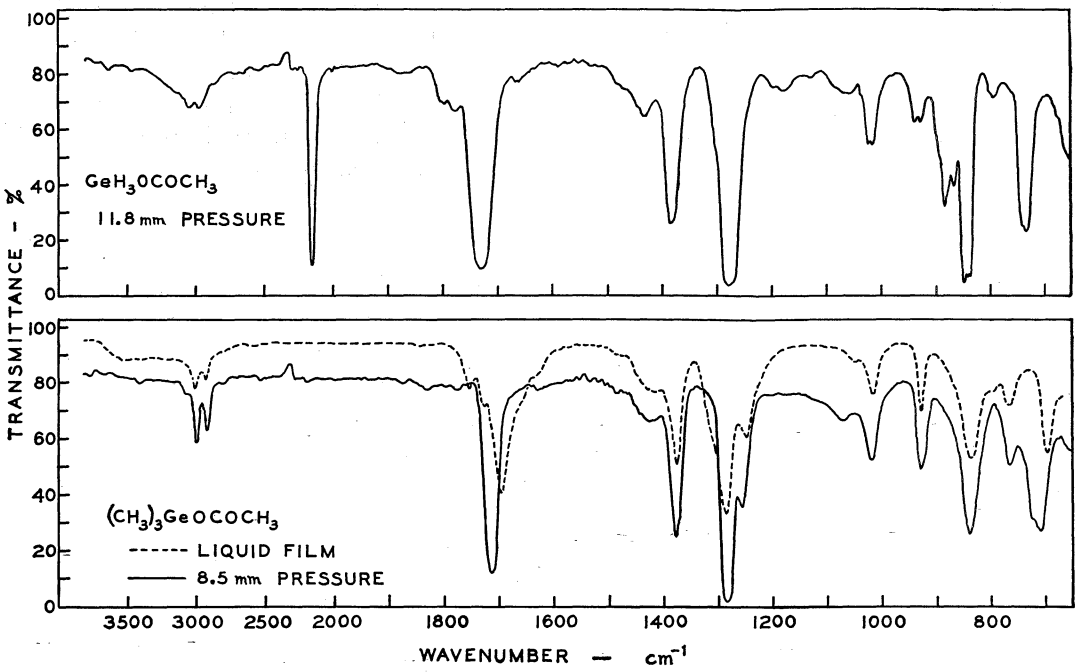

FIG. 1. Infrared spectra of GeH_3OCOCH_3 and $(CH_3)_3GeOCOCH_3$.

TABLE I

Vibrational assignments for gaseous GeH_3OCOCH_3 and $(CH_3)_3GeOCOCH_3$

GeH_3OCOCH_3 bands (cm^{-1})	$(CH_3)_3GeOCOCH_3$ bands (cm^{-1})	Assignment
3045 w	2995 w	C—H asym. stretching (CH_3—C)
2970 w	2920 w	C—H sym. stretching (CH_3—C)
2150 vs	—	Ge—H asym. and sym. stretching (GeH_3—)
1727 vs	1715 vs	C=O stretching
1432 w	1426 w	C—H asym. deformation (CH_3—C & CH_3(—Ge))
1383 s	1376 s	C—H sym. deformation (CH_3—C)
1275 vs	1285 vs	Skeletal (C—CO—O—)
—	1257 s	C—H sym. deformation (CH_3(—Ge))
1065 w	1072 w	Combination or CH_3 rocking (CH_3—C)
1017 m	1018 m	Skeletal (C—CO—O—) coupled with CH_3 rocking
932 w	927 m	Skeletal (C—CO—O—) coupled with CH_3 rocking
880 m 862 m 842 s		Ge—O stretching, skeletal (C—CO—O—) coupled, and GeH_3 deformation
	837 s	Ge—O stretching, skeletal (C—CO—O—) coupled, and CH_3(—Ge) rocking
790 w		Combination
730 s	707 s	Skeletal (C—CO—O—) coupled with Ge—O stretching

NOTE: w = weak; m = medium; s = strong; v = very.

C—H Stretching Vibrations

The two distinct weak bands which occur at 3045 and 2970 cm^{-1} in the spectrum of acetoxygermane are attributed to the asymmetrical and symmetrical C—H stretching vibrations of the methyl carboxyl group (CH_3—C), respectively. In methyl acetate (6) the same vibrations are about 10 times weaker than those of the ester methoxy group (—OCH_3). Two weak bands appear at 2995 and 2920 cm^{-1} in the spectrum of trimethylacetoxygermane; they are probably also due to C—H stretching modes of the methyl carboxyl group. However, these bands are remarkably similar in position, shape, and relative intensity to those exhibited by trimethylgermyl halides and pseudohalides (5), in which they are entirely due to C—H stretching vibrations of methyl groups bonded to germanium (CH_3(—Ge)). This strongly suggests that these vibrations also contribute appreciably to the absorptions at 2995 and 2920 cm^{-1} in trimethylacetoxygermane.

Ge—H Stretching Vibrations

In germyl halides (7) and pseudohalides (8) the Ge—H stretching vibrations of the GeH_3 group produce strong and sharp bands in the range 2110–2140 cm^{-1}. The strong and sharp band at 2150 cm^{-1} in acetoxygermane is definitely due to this vibration, but the symmetrical and asymmetrical modes were not resolved by the NaCl prism.

C=O Stretching Vibrations

In acetoxygermane the C=O stretching absorption band is very strong and appears at 1727 cm^{-1}, which is 44 cm^{-1} lower than the corresponding band in gaseous methyl acetate (9). In trimethylacetoxygermane this vibration occurs at 1715 cm^{-1} in the gaseous phase, at 1696 cm^{-1} in the liquid phase, and at 1695 cm^{-1} in carbon tetrachloride solution. These values are significantly lower than those observed for *tert*-butyl acetate and trimethylacetoxysilane as evident from the comparisons made in Table II. The significance of these differences is discussed in a separate section.

TABLE II

Comparison of some vibrational frequencies of Group IV*b* acetates

R (in $ROCOCH_3$)	C=O stretching (cm^{-1})	C—CO—O— skeletal (cm^{-1})	CO—O asymmetric stretching (cm^{-1})	CO—O symmetric stretching (cm^{-1})	Ref.
CH_3	$1771_{(g)}$	$1248_{(g)}$	—	—	9
SiH_3*	—	—	—	—	—
GeH_3	$1727_{(g)}$	$1275_{(g)}$	—	—	This work
$(CH_3)_3C$	$1750_{(g)}$, $1738_{(l)}$, $1738_{(s)}$	$1265_{(s)}$	—	—	This work
$(CH_3)_3Si$	— — $1725_{(s)}$	$1267_{(s)}$	—	—	1
$(CH_3)_3Ge$	$1715_{(g)}$, $1696_{(l)}$, $1695_{(s)}$	$1280_{(s)}$	—	—	This work
$(CH_3)_3Sn^+$	—	—	1576	1428	1
$(CH_3)_3Pb^+$	—	—	1560	1408	2
Na^+	—	—	1582	1425	16

NOTE: g = gas phase; l = pure liquid; s = solution in CCl_4 (1%).
*This compound has not yet been prepared.

C—H Deformation Vibrations

The weak band at 1432 cm^{-1} and the stronger one at 1383 cm^{-1} in acetoxygermane are due respectively to asymmetrical and symmetrical deformation vibrations of the methyl carboxyl group. Bands of similar shape and relative intensity occur at 1426 and 1376 cm^{-1} in trimethylacetoxygermane, which contains two types of methyl groups, CH_3—C and

CH_3(—Ge), the C—H deformation vibrations of which undoubtedly overlap. In methyl acetate, absorptions near 1430 and 1370 cm^{-1} have been assigned to CH_3—C asymmetrical and symmetrical C—H deformation vibrations, respectively (6, 9). The corresponding C—H deformation modes of CH_3(—Ge) methyl groups in trimethylgermyl halides and pseudohalides (5) appear near 1415 and 1250 cm^{-1}, respectively. These comparisons lead us to suggest that in trimethylacetoxygermane: (i) the 1426 cm^{-1} band results from superimposition of asymmetrical C—H deformation vibrations of CH_3—C and CH_3(—Ge) methyl groups, (ii) the 1376 cm^{-1} band is due only to symmetrical C—H deformation mode of the CH_3—C methyl group, and (iii) the 1257 cm^{-1} band arises from symmetrical deformation vibrations of CH_3(—Ge) methyl groups.

"C—O Stretching Vibrations"

The intense band between 1280 and 1150 cm^{-1} in alkyl carboxylic esters was first assigned to a stretching vibration of the C—O bond adjacent to the carbonyl bond, but it was later shown to involve coupled vibrations of C—C and C—O bonds and is better described as a skeletal stretching vibration of the acetoxy group (C—CO—O—) (10). The strong bands at 1275 and 1285 cm^{-1} in acetoxy- and trimethylacetoxy-germane, respectively, are attributed to this skeletal vibration. These bands are at significantly higher frequencies than the corresponding ones in analogous methyl, *tert*-butyl, and trimethylsilyl acetates (Table II).

Absorption Bands in the Range 1100–650 cm^{-1}

There is much confusion in the literature about assignments of absorption bands below 1100 cm^{-1} in spectra of alkyl acetates. Methyl rocking, C—C stretching, C—O stretching, and acetoxy skeletal vibrations are expected in this region and considerable overlapping and coupling of vibrations is possible. This region is further complicated in acetoxy- and trimethylacetoxy-germane by the presence of Ge—O stretching, GeH_3 deformation, and CH_3(—Ge) rocking vibrations.

The weak bands at 1065 and 1072 cm^{-1} in acetoxy- and trimethylacetoxy-germane, respectively, may be due to combination tones or to CH_3—C methyl rocking vibrations. Stronger bands are observed at 1017 and 1018 cm^{-1} in acetoxy- and trimethylacetoxy-germane, respectively. Similar bands have been reported at 1060 cm^{-1} in methyl acetate (9), at 1046 cm^{-1} in ethyl acetate (11), at 1016 cm^{-1} in methyl laurate (12), and in the range 1020–995 cm^{-1} in a variety of saturated methyl esters (13). Wilmshurst (9) assigned the 1060 cm^{-1} band in methyl acetate to the C—O stretching of the methoxy group, but this has been questioned by Katritzky *et al.* (13) and by Jones (12). Jones suggests that it is more reasonable to regard this band, like the one between 1280 and 1150 cm^{-1}, as a skeletal stretching vibration of the C—CO—O— linkage system. On this basis we assign the bands at 1017 and 1018 cm^{-1} in acetoxy- and trimethylacetoxy-germane, respectively, to C—CO—O— skeletal stretching modes.

Acetoxy- and trimethylacetoxy-germane also exhibit similar bands at 932 and 927 cm^{-1}, respectively. The corresponding band in methyl acetate occurs at 980 cm^{-1} and Wilmshurst (9) has assigned it to a CH_3—C methyl rocking vibration, while Katritzky *et al.* (13) regard it as due to coupling of methyl rocking and C—CO—O— skeletal modes. The latter assignment appears to be more realistic and is proposed for the 932 and 927 cm^{-1} bands in the two acetoxygermanes.

The strongest band in the 800–900 cm^{-1} region of acetoxygermane occurs at 842 cm^{-1} and is undoubtedly due to deformation vibrations of the GeH_3 group, since these occur between 830 and 875 cm^{-1} in germyl halides (7). Two other weaker bands at 880 and 835

cm^{-1} are more difficult to assign. The band at 880 cm^{-1} is attributed to the Ge—O stretching vibration, which occurs near 880 cm^{-1} in alkylgermanium oxides (14). The band at 862 cm^{-1} probably corresponds to a band at 846 cm^{-1} in methyl acetate (13) which, like the band at 980 cm^{-1}, has been assigned to a coupling of methyl rocking and C—CO—O— skeletal vibrations.

The absorption band at 837 cm^{-1} in trimethylacetoxygermane probably results from overlap of the Ge—O stretching vibration, the coupling of methyl rocking with C—CO—O— skeletal vibrations, and rocking vibrations of methyl groups bonded to germanium, all of which are known to occur near 850 cm^{-1}. Since CH_3(—Ge) methyl rocking vibrations also give a band near 750 cm^{-1} in trimethylgermyl halides and pseudohalides (5), it is likely that the band at 767 cm^{-1} in trimethylacetoxygermane is associated with this vibration. The weak band at 790 cm^{-1} in acetoxygermane is probably a combination band. The strong bands at 730 and 707 cm^{-1} in acetoxy- and trimethylacetoxygermane, respectively, are probably due to C—CO—O— skeletal vibrations coupled with the polar Ge—O bond.

Polarity and Relative Inductive Effects

The positions of the carbonyl and carbon–oxygen (skeletal) stretching vibrations are of particular interest because, as Okawara *et al.* (1) have pointed out, they reflect the type of bonding between the acetate group and the group attached to it. Carbonyl stretching vibrations near 1750 cm^{-1} are indicative of covalent bonding, while values near 1570 and 1425 cm^{-1} are characteristic of ionic bonding. This differentiation has been questioned recently by Beattie and Gilson (15),* who examined the effect of acetate bridging on the infrared spectra of some metal acetates. They concluded that there is "no simple way of distinguishing between a discrete acetate ion and a bridging acetate group". If this is true, the positions of carbonyl stretching vibrations cannot be used to distinguish between covalent and ionic bonding in acetates in their solid phase.

The comparisons made in Table II reveal that acetoxy- and trimethylacetoxy-germane resemble alkyl and methylsilyl acetates more than they do sodium, trimethyltin, and trimethyllead acetates. Therefore, it seems reasonable to conclude that the Ge—O bond in acetoxygermanes, like the C—O and Si—O bonds in alkyl and methylsilyl acetates, respectively, is predominantly covalent. The carbonyl stretching frequency is 44 cm^{-1} lower in acetoxygermane than in methyl acetate; there is also a significant decrease from top to bottom in the series of methyl-substituted acetates (Table II). The shift to lower frequencies is probably associated with increasing polarity of the metal–oxygen bond; thus the Ge—O bond is more polar than the Si—O and C—O bonds in acetate derivatives.

Hartwell *et al.* (17) concluded, after a thorough examination of the infrared spectra of a variety of alkyl acetates and related compounds, that variations in carbonyl stretching frequencies are not due to mass effects but mainly to electronic effects induced by attached groups. In support of this Freeman (18) has shown that electronegative groups attached to the α-oxygen atom of carboxylic acid derivatives raise the carbonyl stretching frequency by 15–70 cm^{-1}. This he attributes to inductive effects, although these cannot be differentiated from direct field effects. We found that substitution of a *tert*-butyl group for the methyl group in methyl acetate lowers the carbonyl stretching frequency by 21 cm^{-1} (Table II). This is probably due mainly to the greater positive inductive effect (+I) of

**We are grateful to Dr. R. J. O'Brien of The University of British Columbia for drawing our attention to this paper.*

the *tert*-butyl group, which decreases the electron density at the carbonyl bond thereby decreasing its vibrational frequency. Similarly, the lowering of carbonyl stretching frequencies in methyl-substituted acetates (Table II) is attributed to decreasing electron release in the order $(CH_3)_3Ge > (CH_3)_3Si > (CH_3)_3C$. The positive inductive effect of the first two groups in this series is opposed by a negative inductive effect (−I) resulting from electron release from oxygen to silicon or germanium through supplementary d_π–p_π bonding. If the latter effect were predominant, carbonyl stretching frequencies of trimethylsilyl and trimethylgermyl acetates would be higher than that of *tert*-butyl acetate, contrary to the observed trend.

The order of electron release suggested by our results differs from the following order established by nuclear magnetic measurements on tetramethyl Group IV*b* compounds (19, 20): $(CH_3)_3Si \approx (CH_3)_3Sn > (CH_3)_3Ge \gg (CH_3)_3Pb > (CH_3)_3C$. The interpretation of these measurements has been disputed (21). Our order supports the results described recently by Bott *et al.* (22). They concluded from the rates of some cleavage reactions that towards a methylene group the trimethylgermyl group is slightly more electron releasing than the trimethylsilyl group, which implies that silicon is slightly more electronegative than germanium, contrary to the new electronegativity scale proposed by Allred and Rochow (19). Seyferth and Kahlen (23) suggested that the shift to lower frequencies of N=C stretching vibrations in $RN{=}C{-}Fe(CO)_4$ compounds might be due to decreasing electron release in the series $R = (CH_3)_3Sn \approx (CH_3)_3Ge \approx (CH_3)_3Si > (CH_3)_3C > CH_3$. Apparently the N=C stretching vibrations in these compounds are not sufficiently sensitive to the small differences which undoubtedly exist in the inductive effects of the trimethyl-substituted groups. More work is obviously necessary to clarify the relative inductive effects of these groups.

ACKNOWLEDGMENTS

We thank the National Research Council for a Postdoctoral Fellowship (to T. N. S.) and for an Annual Grant (to M. O.). We are grateful to Mr. J. P. Guertin and Mr. J. M. Miller for technical assistance, and to Dr. R. N. Jones for helpful discussions.

REFERENCES

1. R. Okawara, D. E. Webster, and E. G. Rochow. J. Am. Chem. Soc. **82**, 3287 (1960).
2. R. Okawara and H. Sato. J. Inorg. Nucl. Chem. **16**, 204 (1961).
3. T. N. Srivastava, J. E. Griffiths, and M. Onyszchuk. Can. J. Chem. **40**, 739 (1962).
4. J. E. Griffiths and M. Onyszchuk. Can. J. Chem. **39**, 339 (1961).
5. T. N. Srivastava and M. Onyszchuk. Unpublished work.
6. B. Nolin and R. N. Jones. Can. J. Chem. **34**, 1382 (1956).
7. J. E. Griffiths, T. N. Srivastava, and M. Onyszchuk. Can. J. Chem. **40**, 579 (1962).
8. T. N. Srivastava and M. Onyszchuk. Unpublished work.
9. J. K. Wilmshurst. J. Mol. Spectry. **1**, 201 (1957).
10. R. N. Jones and C. Sandorfy. *In* Technique of organic chemistry. Vol. IX. *Edited by* A. Weissberger. Interscience Publishers, Inc., New York. 1956. p. 502.
11. B. Nolin and R. N. Jones. Can. J. Chem. **34**, 1392 (1956).
12. R. N. Jones. Can. J. Chem. **40**, 301 (1962).
13. A. R. Katritzky, J. M. Lagowski, and J. A. T. Beard. Spectrochim. Acta, **16**, 964 (1960).
14. M. P. Brown, R. Okawara, and E. G. Rochow. Spectrochim. Acta, **16**, 591 (1960).
15. I. R. Beattie and T. Gilson. J. Chem. Soc. 2585 (1961).
16. K. Ito and H. J. Bernstein. Can. J. Chem. **34**, 170 (1956).
17. E. J. Hartwell, R. E. Richards, and H. W. Thompson. J. Chem. Soc. 1436 (1948).
18. J. P. Freeman. J. Am. Chem. Soc. **80**, 5954 (1958).
19. A. L. Allred and E. G. Rochow. J. Inorg. Nucl. Chem. **5**, 269 (1958).
20. A. L. Allred. J. Inorg. Nucl. Chem. **17**, 215 (1961).
21. R. S. Drago. J. Inorg. Nucl. Chem. **15**, 237 (1960).
22. R. W. Bott, C. Eaborn, K. C. Pande, and T. W. Swaddle. J. Chem. Soc. 1217 (1962).
23. D. Seyferth and N. Kahlen. J. Am. Chem. Soc. **82**, 1080 (1960).

RECENT DEVELOPMENTS IN THE ORGANOMETALLIC CHEMISTRY OF TECHNETIUM. PREPARATION AND PROPERTIES OF A POLYNUCLEAR TETRACARBONYL[1,2,3]

H. D. KAESZ AND D. K. HUGGINS
Department of Chemistry, University of California, Los Angeles, California, U.S.A.
Received October 29, 1962

ABSTRACT

A polynuclear tetracarbonyl of technetium, constituting a novel class of carbonyls for the manganese subgroup metals, is formed during the treatment of the pentacarbonyl, $Tc_2(CO)_{10}$, with sodium amalgam and subsequent acidification. The new derivative is characterized, and its possible structure is discussed.

INTRODUCTION

In a recent synthesis of the pentacarbonyl hydride of technetium (1) the less volatile residues were observed to contain infrared absorption bands due both to technetium pentacarbonyl, $Tc_2(CO)_{10}$, as well as some additional product(s) not then identified. It is significant that in the preparation of the intermediate, $Na^+Tc(CO)_5^-$, from the treatment of the carbonyl with sodium amalgam, appreciable evolution of carbon monoxide and a reddish coloration of the solution had occurred in competition with the normal cleavage of the metal–metal bond in $Tc_2(CO)_{10}$ (2). We now wish to report a new carbonyl of technetium, $[Tc(CO)_4]_n$, which we have isolated from the above-mentioned reaction mixture, which is not observed in similar treatment of the pentacarbonyls of manganese or rhenium.

EXPERIMENTAL

The following procedures were carried out in an atmosphere and with materials rigorously freed of oxygen.

In a typical experiment, $Tc_2(CO)_{10}$ (2) (0.500 g, 1.05 mmole) in 15 ml of tetrahydrofuran (THF) was treated with 100 g of 0.5% sodium amalgam (containing 22 mg-atom of Na). The mixture was agitated at room temperature for 15 hours, resulting in a dark red coloration of the THF solution, and evolution of 6.9 cc at S.T.P. (0.31 mmole) of CO gas. The THF solution was separated from the excess amalgam by decantation and washing, under inert atmosphere. The solvent was stripped off under vacuum, and 30 ml of cyclohexane was distilled onto the remaining red solids, which were insoluble in that medium. Infrared spectrophotometric examination of the cyclohexane at this point revealed no absorptions in the carbonyl stretching region, indicating that no unreacted $Tc_2(CO)_{10}$ had remained.

The contents of the flask were gradually treated with a solution of 5 ml of H_3PO_4 in 20 ml of H_2O at 0° C. The flask was warmed to room temperature, and the immiscible solid and liquids were agitated over a 24-hour period, with provision for release of the H_2 gas which was formed (1). An aliquot of cyclohexane was withdrawn at this point, and dried over $CaSO_4$. This displayed a multitude of bands in the carbonyl stretching region of the infrared, given in the center spectrum, Fig. 1. The maxima were measured[4] at the following positions (cm^{-1}): $2093._3$ (m), $2064._3$ (m), 2052 (m), $2036._5$ (s), $2020._8$ (s), $2016._8$ (s), $2014._4$ (s), $1989._6$ (m), and $1984._2$ (m). By contrast, the cyclohexane solution resulting from a completely analogous treatment of the carbonyls of manganese and rhenium displayed only the absorptions of the respective pentacarbonyl hydrides (1), as shown on the upper and lower traces in Fig. 1.

[1]*Presented at the Symposium on Organometallic compounds, Vancouver, British Columbia, September 4–6, 1962, sponsored by the Inorganic Chemistry Division, Chemical Institute of Canada, and the Department of Chemistry, University of British Columbia, with the support of the National Research Council, Ottawa, in cooperation with the University Extension Department.*

[2]*This work received financial assistance from the National Science Foundation (U.S.A.) under Grant No. G16819.*

[3]*Contribution No. 1470.*

[4]*Each spectrum was calibrated against the 1988.5 cm^{-1} band in the v_2 fundamental of water vapor; cf. band No. 50, Table 5, ref. 3.*

Can. J. Chem. Downloaded from www.nrcresearchpress.com by 210.87.254.5 on 09/05/12
For personal use only.

Can. J. Chem. Downloaded from www.nrcresearchpress.com by 210.87.254.5 on 09/05/12
For personal use only.

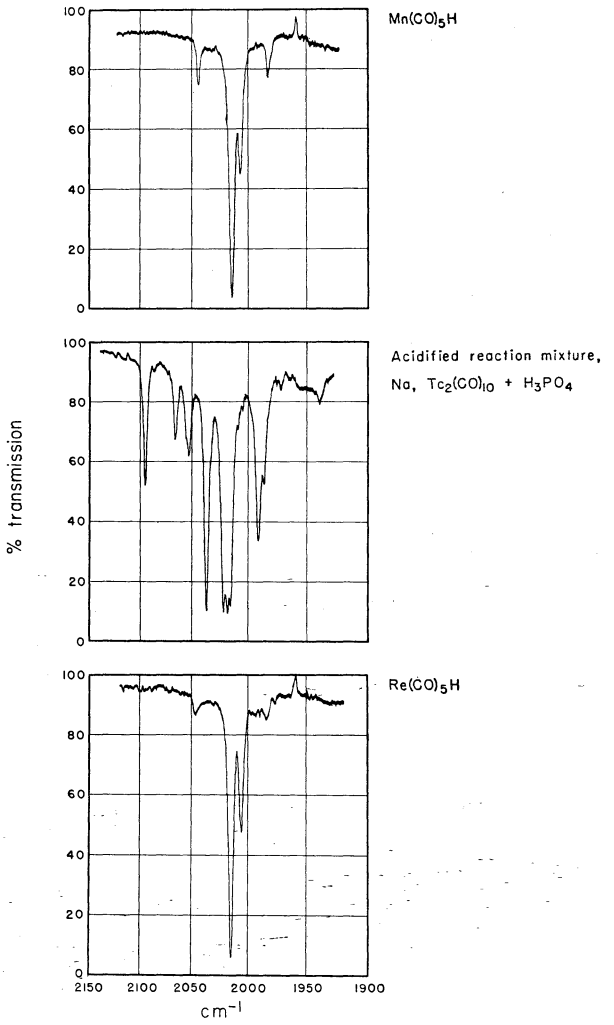

FIG. 1. Comparison of the high-resolution infrared absorption spectra in the carbonyl stretching region after acidification of the reaction mixtures resulting from the treatment of Group VII*b* metal carbonyls with sodium amalgam. LiF prism, cyclohexane solutions.

The small amount of $Tc(CO)_5H$ present in the reaction mixture of the compounds of technetium may be identified by the presence of the band at $2020._8$ cm^{-1} (1), and is removed by stripping off a quantity of cyclohexane at reduced pressure (15–20 mm Hg). When diethyl ether is used in place of cyclohexane during the acidification step, the solids are dissolved and the yield of $Tc(CO)_5H$ is much higher and, also, almost none of the new derivative reported here could be observed.

The less volatile residues were extracted with 10 portions of 8 ml each of cyclohexane, and the combined solutions evaporated to dryness in a stream of nitrogen at room temperature. The extracted solids were subjected to sublimation at 50° C and 0.05 mm Hg, with the probe cooled to 0° C. After 6 hours, $Tc_2(CO)_{10}$, which was present in the gross reaction product, was removed and identified by the bands at $2064._3$ (m), $2016._8$ (s), and $1984._2$ (m) cm^{-1} (also present in the pattern shown in Fig. 1). A cyclohexane extract of the residue displayed four prominent absorptions, at $2093._3$ (m), $2036._5$ (s), $2014._4$ (s), and $1989._6$ (s) cm^{-1}, as shown in Fig. 2. The four bands, taken together with those for $Tc(CO)_5H$ and $Tc_2(CO)_{10}$, account for all but one of the bands observed in the gross reaction mixture above (Fig. 1), that of medium intensity at 2052 cm^{-1}. This band was observed to decrease slowly in relative intensity and to finally disappear, over a period of 3 or 4 hours, from the solution stored in the infrared cell. It is due to some less robust species which we have as yet not identified.

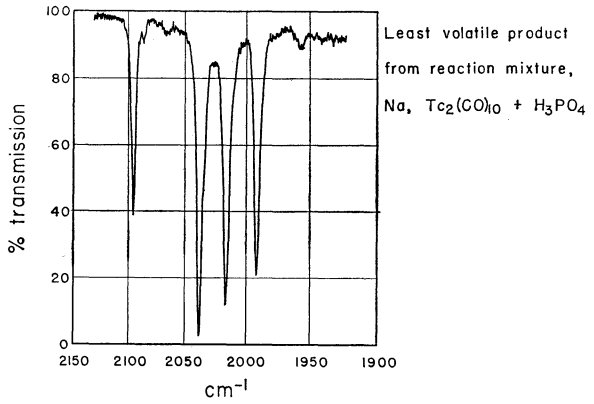

FIG. 2. High-resolution infrared absorption spectrum in the carbonyl stretching region of the least volatile product isolated from the acidified reaction mixture resulting from the treatment of technetium carbonyl with sodium amalgam. LiF prism, cyclohexane solvent.

The sublimation residue was extracted with five portions of 5 ml each of cyclohexane, which were combined and concentrated to a volume of 1 ml in a stream of nitrogen, in a 12-ml centrifuge tube. Solids, consisting mostly of the product giving rise to the four absorptions shown in Fig. 2, crystallized from solution. Precipitation was brought to a maximum by cooling the tube to 0° C, and then allowing it to warm up just enough to melt the cyclohexane. The tube was quickly centrifuged, and the reddish filtrate discarded. The solids in the centrifuge tube were washed with two succeeding 1-ml portions of cyclohexane, and finally recrystallized from 5 ml of solvent by essentially the same cooling and centrifugation procedure mentioned above. A light tan, flocculent product (I) consisting of small platelets was obtained, weighing approximately 25 mg. Analysis[5] yielded 47.0% Tc, 23.35% C, and 0.0% H; required, for $[Tc(CO)_4]_n$, 46.9% Tc, 22.8% C.

The product (I) appeared to be quite stable in air as the solid. Its solutions in cyclohexane (giving the infrared absorptions shown in Fig. 2) appeared to decompose only slowly in contact with the atmosphere. Treatment of the product (I) with dilute solution of Br_2 in cyclohexane resulted in a solution in which only the bands of $[Tc(CO)_4Br]_2$ could be observed, namely, 2117 (m), 2046 (s), 2013 (s), and 1975 (s), which compared exactly with those of an authentic sample in this solvent (a previous report lists the bands observed in CCl_4 (1), in which the maxima were only slightly shifted from these results). By comparison, bromination under identical conditions of $Tc_2(CO)_{10}$ yields $Tc(CO)_5Br$, initially (1), which slowly loses CO over *several days'* standing in solution at room temperature to give mixtures also containing $[Tc(CO)_4Br]_2$. It is reasonable to assume then that bromination of I indicates the presence of $Tc(CO)_4$ and absence of $Tc(CO)_5$ groups in that compound.

The product (I) could be converted to $Tc_2(CO)_{10}$ by carbonylation in an autoclave, in which the products were handled in a Von Grosse tube, as already described (1). The carbonylation occurred at 220° C, for 17 hours, initial pressure of 3100 p.s.i. CO at room temperature, which rose to 5300 p.s.i. at the reaction temperature. Conversion to $Tc_2(CO)_{10}$ was complete; the infrared spectrum showed no evidence for any other compound.

A molecular weight of the product was determined with a Mechrolab Vapor Pressure Osmometer[6] (Mechrolab Inc., Mountain View, Calif.), using cyclohexane as a solvent and $Re_2(CO)_{10}$ as standard. Because of relative low solubility of (I), the concentration of the standard and unknown solutions were of the order of 0.0016 *M*. The average of eight determinations of the molecular weight was 625, with a standard deviation of 37.

DISCUSSION

Analytical data and the results of bromination indicate that I is a tetracarbonyl of technetium. This is further supported by the fact that I is produced only under conditions where cleavage of a carbonyl group from the pentacarbonyl has occurred. The four infrared absorptions of I are extremely similar to the tetracarbonyl halide dimers of technetium (4) in which each Tc atom is octahedrally surrounded by four CO groups, and

[5]*Schwartzkopf Microanalytical Laboratory, Woodside 77, New York; cf. ref. 1.*

[6]*This instrument was kindly made available to us by Dr. Charles Haber of the Naval Research Laboratories, Corona, California.*

Can. J. Chem. Downloaded from www.nrcresearchpress.com by 210.87.254.5 on 09/05/12
For personal use only.

two (cis) bridging halogen atoms (C_{2v} local symmetry). When the absorptions of I are compared to those of the tetracarbonyl halides, Fig. 3, it is seen that a uniform progression in the positions of the bands are observed. Those of $[Tc(CO)_4Cl]_2$ are the most

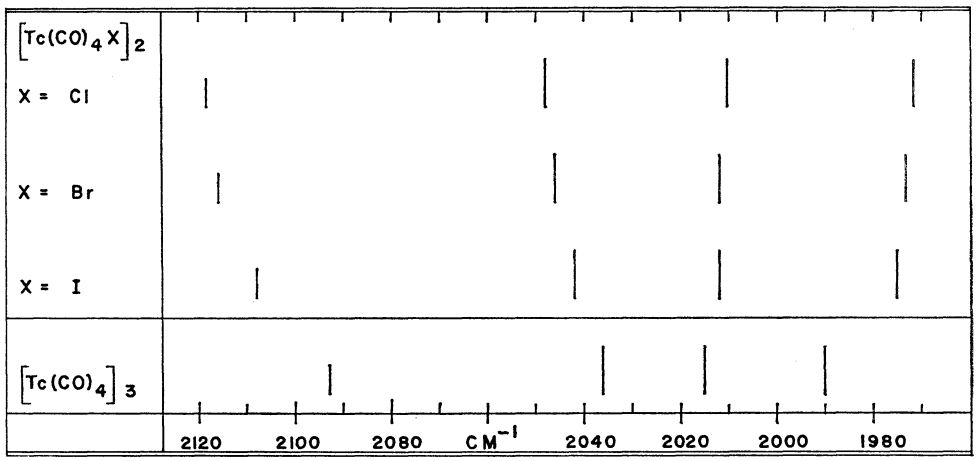

FIG. 3. Comparison of the infrared absorption spectra in the carbonyl stretching region of the series of derivatives $[Tc(CO)_4X]_2$ and $[Tc(CO)_4]_3$.

widely spaced, with a minimum reached in the bands of I. This is in keeping with a similar local symmetry for each Tc atom in this series of compounds, where in I metal–metal bonds have replaced the bridging halogen atoms in the tetracarbonyl halides. The molecular weight indicates that we have isolated a trimer: found 625 (see above); required for $[Tc(CO)_4]_3$, 633, and in that case would possess the structure shown in I*a*. This structure would then be extremely similar to that recently determined for $[Os(CO)_4]_3$ (5).

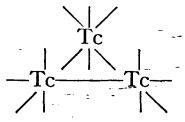

I*a*

Both of these possess C_{2v} local symmetry for each metal, and overall symmetry of D_{3h}, for which four infrared-active carbonyl stretching modes would be expected.[7]

A reliable determination of the magnetic susceptibility of the product has been hindered by the low solubility of the compound in suitable solvents and, also, by the lack of sufficient sample, so far. A preliminary attempt to determine the magnetic properties of I was carried out, using the n.m.r. method of Evans, adapted to coaxial sample tubes as previously described (2). Measurement of the proton resonance of solvent of a saturated solution of I in cyclohexane (0.0093 molal) in the inner tube gave a separation of 19.5 c.p.s. (at 60 Mc) from the resonance of the methyl protons of toluene in the annular space. Neat cyclohexane yields essentially the same separation under these conditions. We assume this to indicate diamagnetism for I. This conclusion must be held as only tentative at this time since the observed value is not sufficiently separated from that which might be expected from a paramagnetic complex. A trimer containing one unpaired electron,

[7]*Six, rather than four, prominent carbonyl stretching absorptions have been reported (6) for* $Os_3(CO)_{12}$. *We have redetermined the spectrum of a sample of that compound purified by elution chromatography, and observed only four prominent bands, as expected: 2068 (s), 2034.5 (s), 2014 (m), and 2002 (m)* cm^{-1}, *in cyclohexane.*

Can. J. Chem. Downloaded from www.nrcresearchpress.com by 210.87.254.5 on 09/05/12
For personal use only.

for instance, would be expected to yield a separation of approximately 18 c.p.s. under these conditions, assuming no factors restricting paramagnetism are in operation. We are therefore presently engaged in obtaining more definitive magnetic data.

If the trimer is diamagnetic, however, as appears most likely at this time, some moiety such as an H atom or CH or OH group would be required in the complex in addition to the odd number of $Tc(CO)_4$ units. Any one of the three above-mentioned additional groups, if present, would not markedly affect the analytical results, and furthermore, if placed symmetrically in the center of the trimeric structure drawn above (I*a*), would not greatly perturb the local symmetry of the $Tc(CO)_4$ units. No evidence is yet available about whether such an additional group does exist, and the search for this would be predicated on more reliable magnetic measurements. It is of course possible to account for a diamagnetic species of polymers containing only $Tc(CO)_4$ units, but then in an even total number. Such might also have been synthesized in the above-mentioned reaction sequence. Further work is in progress to answer these and other questions about the new derivative of technetium. It is also our intent to ascertain whether similar species of manganese and rhenium[8] may be obtained, though requiring perhaps, different preparative routes.

REFERENCES

1. J. C. Hileman, D. K. Huggins, and H. D. Kaesz. Inorg. Chem. **1**, 933 (1962).
2. J. C. Hileman, D. K. Huggins, and H. D. Kaesz. J. Am. Chem. Soc. **83**, 2953 (1961).
3. E. K. Plyler, A. Danti, L. R. Blaine, and E. D. Tidwell. J. Res. Natl. Bur. Stand., A, **64**, 1 (1960).
4. M. A. El-Sayed and H. D. Kaesz. Inorg. Chem. **2**, 158 (1963).
5. E. R. Corey and L. F. Dahl. Inorg. Chem. **1**, 521 (1962).
6. W. Beck and K. Lottes. Chem. Ber. **94**, 2578 (1961).
7. W. A. G. Graham and A. R. Gatti. Proceedings of the Conference on the Ultra-purification of Semiconductor Materials. M. S. Brooks and J. K. Kennedy (*Editors*). The Macmillan Co., New York. 1962. p. 136.

[8]*During the discussion following the presentation of this paper, it was pointed out by Dr. W. A. G. Graham (present address: Department of Chemistry, University of Alberta, Edmonton) that, in some recent work with A. R. Gatti, a brown solid of empirical formula* $ReC_{3.87}O_{3.96}H_{1.85}$, *perhaps* $[Re(CO)_4H_2]_n$ ($n = 20$), *had been obtained from the photolysis of rhenium pentacarbonyl in a hydrocarbon solvent (7).*

Can. J. Chem. Downloaded from www.nrcresearchpress.com by 210.87.254.5 on 09/05/12
For personal use only.

ELEMENTAL ORGANIC COMPOUNDS

VI. SIGNIFICANCE OF π-RADICAL HYBRIDIZATION: NEW SYNTHETIC METHOD FOR BIS-ARENE π-COMPLEXES[1,2]

MINORU TSUTSUI AND GEORGE CHANG
New York University, Departments of Chemical Engineering and Chemistry, New York, N.Y., U.S.A.

Received October 29, 1962

ABSTRACT

The hypothesis of the existence of π-radical hybridization in aryl (M. Tsutsui. Ann. N.Y. Acad. Sci. **93**, 133 (1961)) and vinyl (M. Tsutsui. Abstracts of Papers, 141st Meeting of the American Chemical Society, Washington, D.C. March, 1962. p. 3-O) coupling reactions has led us to a further investigation of the reactivity of highly active transition metal atoms in the so-called "radical state". As a result, a new synthetic method for bis-benzene-type π-complexes of transition metals has been discovered.

The following methods (1) for the preparation of bis-arene π-complexes have been reported previously.

(1) Grignard Method (2)

The reaction of an aryl Grignard solution and a transition metal halide in ether or tetrahydrofuran yields arene π-complexes. This method, at present, is limited to the preparation of chromium π-complexes.

$$RMgX + MCl_n \rightarrow \text{bis-arene } \pi\text{-complexes}$$

(R is limited to a phenyl or tolyl group; M = transition metal; n = 2 or 3)

(2) Reductive Friedel–Crafts Method (3)

Heating of a mixture of a transition metal halide, arene, aluminum metal powder, and aluminum chloride under atmospheric pressure or increased pressure affords arene π-complexes. This method seems to be widely applicable. It has, however, been shown to be non-usable for certain elements and arenes.

$$3MCl_3 + 2Al + AlCl_3 + 6C_6H_6 \rightarrow 3M(C_6H_6)_2^+ \cdot (AlCl_4)^-$$

(3) Cyclic Polymerization of Disubstituted Acetylenes by Organotransition Metals (4)

The reaction of an organotransition metal and disubstituted acetylene yields an aromatic hydrocarbon, a trimer of the acetylene, and a bis-arene π-complex. This method has afforded manganese and cobalt π-complexes which could not be prepared via the reductive Friedel–Crafts method.

(4) Cyclic Polymerization of Disubstituted Acetylenes with a Transition Metal Halide and Trialkylaluminum (5)

Except for the reductive Friedel–Crafts method, all the methods involve the reduction of either di- or tri-valent chromium to the zerovalent state. In the case of the reductive Friedel–Crafts method, chromium seems to be reduced from trivalent to monovalent. The question whether chromium is reduced from trivalent to monovalent or from trivalent

[1]*Presented at the Symposium on Organometallic Compounds, Vancouver, British Columbia, September 4–6, 1962, sponsored by the Inorganic Chemistry Division, Chemical Institute of Canada, and the Department of Chemistry, University of British Columbia, with the support of the National Research Council, Ottawa, in cooperation with the University Extension Department.*

[2]*Paper V: M. Tsutsui. Z. Chem. In press.*

Can. J. Chem. Downloaded from www.nrcresearchpress.com by 210.87.254.40 on 09/05/12
For personal use only.

to zerovalent has arisen from the observation that bis-benzene-chromium (0) forms a brownish addition complex with aluminum trichloride in benzene (6). Upon hydrolysis of the brownish complex with oxygen-free water or oxygen-free alkaline water solution, bis-benzene-chromium(0) was obtained accompanied by bis-benzene-chromium cation. The formation of bis-benzene-chromium cation is explained with difficulty by a mechanism involving simple hydrolysis of such a complex under an inert gas atmosphere. Fischer and Fritz (7) have formulated the complex as $3Cr^{+1}(C_6H_6)_2[AlCl_4]\cdot 4AlCl_3$. The addition reaction of bis-benzene-chromium and aluminum trichloride in benzene was thus expressed as follows:

$$3Cr^0(C_6H_6)_2 + 8AlCl_3 + 6C_6H_6 \rightarrow 3Cr^{+1}(C_6H_6)_2[AlCl_4]\cdot 4AlCl_3.$$

The mechanism of the hydrolysis of the addition complex was also described by an electron disproportionation shown as follows:

$$2Cr(C_6H_6)_2^+ \rightarrow Cr(C_6H_6)_2 + Cr^{+2} + 2C_6H_6$$
$$Cr^{+2} \rightarrow Cr^{+3} + e^-$$

Hein and Kartte (8) have provided strong evidence that the addition reaction of bis-arene-chromium and aluminum trichloride may cause an electron transfer. A complex, $[(C_6H_5C_6H_5)_2Cr]_3Al_4Cl_{12}$, was obtained from the addition reaction of bis-diphenyl-chromium(0) and aluminum trichloride in benzene. The empirical formula of the complex is $[(C_6H_5C_6H_5)_2Cr][AlCl_4]$. The following similar type complexes have been obtained from the reaction of bis-arene-chromium(0) and aluminum halide in various solvents: $[(C_6H_5C_6H_5)_2Cr]_3Al_4Br_{12}$; $[(C_6H_5C_6H_5)_2Cr][AlBr_4]\cdot\frac{1}{4}C_6H_4$; $(C_6H_5C_6H_5)_2CrAlI_4$; $(C_6H_5C_6H_5)_2CrAlCl_4\cdot\frac{1}{4}C_6H_6\cdot\frac{1}{4}CH_2Cl_2$; $(C_6H_6)(C_6H_5C_6H_5)CrAlCl_4\cdot\frac{1}{2}C_6H_6$.

Although the formulations of the addition products by the two groups of investigators are not exactly the same, it seems to be conclusively established that oxidation, an electron transfer, occurs during an addition reaction of a bis-arene-chromium compound and aluminum halide. These results, however, have not yet provided conclusive elucidation of the mechanism of the formation of bis-arene π-complex by the reductive Friedel–Crafts reaction. Even in this reaction, it is not unreasonable to assume that a highly active metal is produced in the course of π-complex formation. Immediately after the formation of bis-arene-chromium(0) through the transition stage of π-radical hybridization of arene and "radical metal", the π-complex may be oxidized with aluminum trichloride, forming a new addition complex.

Based upon the hypothesis of the existence of a so-called "radical metal" during the course of the formation of π-complex by most of the reported preparative methods, other new synthetic methods for π-complex may be found by devising ways of producing such a "radical metal" in the presence of arene. If a suitable reducing agent for transition metal halide in an arene environment were found, a new synthetic method for bis-arene π-complexes, more pertinent and more broadly applicable than the known methods, might result. For this purpose, triethylaluminum was chosen as the reducing agent.

A mixture of triethylaluminum, a transition metal halide, and an arene in a normal hydrocarbon solution (e.g. *n*-heptane) was heated at 130–140° (bath temperature) for 10 to 30 minutes. The reaction mixture was digested with a small amount of methanol below 0°. The slurry was hydrolyzed with water under an atmosphere of air. In most cases, the filtrate contained a π-complex ion (hydroxide) which could be isolated as the iodide, tetraphenylboron salt, or other salt forms. If π-complex ion is sparingly soluble in water, it should be extractable with methanol or acetone from a precipitate. By this method, a

Can. J. Chem. Downloaded from www.nrcresearchpress.com by 210.87.254.40 on 09/05/12
For personal use only.

number of known chromium π-complexes with arenes, e.g. toluene, xylene, mesitylene, diphenyl, and fluorene, have been prepared.

A bis-mesityl-iron π-complex and several other new arene π-complexes, e.g. a bridged bis-benzene-chromium-1,1′(β,γ-diphenyltetramethylene)-bis-benzene-chromium iodide, have been prepared. These new π-complexes will be described in detail after completion of the characterization of their structure and properties. This new method has proved to be extraordinarily successful and widely applicable. This method, at least, has one advantage: no rearrangement or fission of an alkyl group in the arene molecule occurs during the reaction, while aluminum chloride, in the reductive Friedel–Crafts reaction, may cause such undesirable reactions.

EXPERIMENTAL

Bis-mesitylene-chromium Salt

To a mixture of 2.4 g (0.02 mole) of mesitylene, 1.58 g (0.01 mole) of chromic trichloride anhydride, and 10 ml of *n*-heptane in a Schlenk tube, 0.01–0.03 mole of triethylaluminum was added at room temperature. The mixture was stirred and was heated by an oil bath in which the temperature was gradually raised to 140°. After the mixture was heated at 140° for about 15–30 minutes, the temperature was gradually dropped to room temperature during a period of 1 hour. The reaction mixture was cooled by a dry ice – acetone mixture or ice water and was decomposed under a nitrogen gas stream with methanol, which was carefully added dropwise. The decomposed mixture was finally hydrolyzed with water. An additional 100 ml of water was added to the hydrolyzed solution and the solution was filtered. To the filtrate, a solution of sodium tetraphenylboron salt in water was added until no further precipitation was observed. A golden yellow bis-mesitylene-chromium π-complex salt was isolated by filtration. A π-complex iodide salt can be obtained by the addition of a potassium iodide solution in water instead of an aqueous sodium tetraphenylboron salt solution.

These π-complexes thus obtained were shown to be identical, by infrared spectroscopy, with known authentic samples prepared by the reductive Friedel–Crafts method. Other known complexes, and the new bis-arene π-complexes previously mentioned, were prepared in a similar fashion.

Hydrolysis of Reaction Mixture

During another preparation of bis-mesitylene-chromium π-complex as described above, the reaction mixture was hydrolyzed with oxygen-free water at 0 to ~5° C. A total of 100 ml of water was added. After hydrolysis, some oxygen-free benzene was added to the mixture followed by vigorous shaking. The hydrocarbon layer was crystal clear and did not contain any π-complex in the zerovalent state. The yellowish filtrate from the water layer gave bis-mesitylene-chromium tetraphenylboron salt by the addition of an aqueous solution of sodium tetraphenylboron.

DISCUSSION

There have been several methods described for producing a highly active transition metal in the radical state:

(*a*) a homolytic cleavage of the metal–carbon bond of an organotransition metal (9);

(*b*) reduction of a transition metal halide with aluminum metal (3);[3]

(*c*) treatment of iron metal with diluted acid followed by washing with water, alcohol, and ether (10).

π-Complexes have been produced from methods (*a*) and (*b*). Method (*a*) is a clear case of producing a so-called "radical metal". The course of the mechanism of the aryl coupling reaction based on the new hypothesis of the existence of π-radical hybridization is shown in Fig. 1.

In II, Fig. 1, dotted loops indicate the sp^2 orbitals on the benzene rings and 3*d* orbitals of the metal, when the covalent bond between the metal and carbon atoms cleaves homolytically. Electrons in the center shell of the metal and the π-system P_z electrons of the carbon atoms are stimulated to an excited state. An antibonding π–π^* system on the

[3]*As previously described, it is not clear whether the transition metal halide is reduced to the cation or the zerovalent state.*

Can. J. Chem. Downloaded from www.nrcresearchpress.com by 210.87.254.40 on 09/05/12
For personal use only.

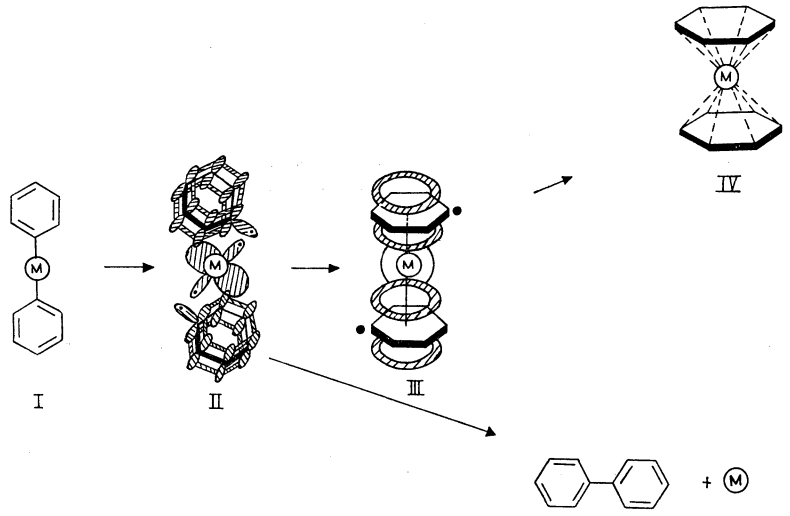

FIG. 1.

benzene rings hybridizes with the very close excited electron orbital of the metal atom. Formation of a hypothetical diradical π-complex III or a coupling reaction of the excited phenyl rings to form biphenyl with the elimination of the metal atom may then follow. It has been assumed with supporting evidence (9) that a π-complex forms through π-radical hybridization in the Grignard method.

The explanation of the course of the mechanism of π-complex formation by applying the simple molecular orbital picture described above well visualizes the role of the "radical transition metal atom". As previously mentioned, trivalent chromium might also be reduced to an active chromium state, possibly to a "radical metal atom" state, during the course of the reaction in the reductive Friedel–Crafts method. In this case, chromium (III) is reduced in an arene environment to an active chromium atom which hybridizes with π-systems on the arene to form a π-complex (0) which might then be oxidized to a cation with aluminum chloride. The sequence of π-radical hybridization occurring in the two methods, the decomposition of aryl transition metal and the reductive Friedel–Crafts reaction, is quite different. Arene π-ligands in the latter case are not attached to the metal atom before the occurrence of "π-radical hybridization", while the arene π-ligand in the former case is attached with a σ-covalent bond and thus it never leaves the metal atom from the beginning to the end of π-complex formation.

In the new method reported here, the situation between the metal atom and arene is quite similar to that of the reductive Friedel–Crafts method. No experimental evidence has been provided as to whether the π-radical metal atom forms π-bonding with the arene after formation of the radical metal, or at precisely the time when it forms by the reduction of metal halide with the reducing agent.

The following experiment has revealed that bis-arene π-complex cation is the sole product of the reaction by the new method. When the reaction mixture was hydrolyzed with oxygen-free water, only bis-arene-chromium cation was produced as π-complex. Since the formation of aluminum chloride is expected from the reaction of chromic chloride and triethyl aluminum, bis-arene-chromium(0) should be oxidized with aluminum trichloride as seen in the reductive Friedel–Crafts reaction.

Can. J. Chem. Downloaded from www.nrcresearchpress.com by 210.87.254.40 on 09/05/12
For personal use only.

Considering the results of the formation of 1,1′-(β,γ-diphenyltetramethylene)-bis-benzene-chromium iodide from the reaction of chromic chloride, triethylaluminum, and *trans*-stilbene by the new method, a reductive coupling reaction of *trans*-stilbene evidently occurred and thus chromic hydride might be formed as an intermediate in the formation of "radical metal atom". The details of the formation and properties of new bridged bis-benzene-chromium will be reported elsewhere.

We gratefully acknowledge financial support from the Petroleum Research Fund, administered by the American Chemical Society, the Arakawa Rinsan Kagaku Company, Osaka, Japan, and the Division of Medicinal Chemistry, United States Public Health Service, Grant (RG-8921).

REFERENCES

1. L. PAUSON. Quart. Rev. (London), **9**, 391 (1955). F. A. COTTON and G. WILKINSON. Progress in inorganic chemistry. Vol. 1. *Edited by* F. A. Cotton. Interscience Publishers, New York. 1959. p. 1. E. O. FISCHER and H. P. FRITZ. Advances in inorganic and radiochemistry. Vol. 1. Academic Press, New York. 1959. p. 55. M. TSUTSUI. Chem. Ind. Japan, No. 4 (1961). H. ZEISS. Organometallic chemistry. American Chemical Society monograph No. 147, Reinhold. 1960. G. E. COATES. Organometallic compounds. John Wiley & Sons, Inc., New York. 1961.
2. F. HEIN. Ber. **52**, 195 (1919). H. ZEISS and M. TSUTSUI. J. Am. Chem. Soc. **79**, 3062 (1957).
3. E. O. FISCHER and W. Z. HAFNER. Z. Anorg. Allgem. Chem. **286**, 146 (1956).
4. H. ZEISS and W. HERWIG. J. Am. Chem. Soc. **80**, 2913 (1958). M. TSUTSUI and H. ZEISS. J. Am. Chem. Soc. **83**, 825 (1961).
5. G. W. WILKE and M. KRONER. Angew. Chem. **18**, 574 (1959).
6. M. TSUTSUI and H. ZEISS. Abstracts of Papers, 133rd Meeting, American Chemical Society, San Francisco, Calif. April 14, 1958. p. 3*N*.
7. E. O. FISCHER and H. P. FRITZ. Angew. Chem. **73**, 353 (1961).
8. F. HEIN and K. KARTTE. Z. Anorg. Allgem. Chem. **307**, 52 (1960).
9. M. TSUTSUI. Ann. N.Y. Acad. Sci. **93**, 133 (1961).
10. G. M. AFANASYEN and P. A. TSYGANOREA. Zhur. Obshch. Khim. **21**, 285 (1951). M. TSUTSUI. Abstracts, 138th American Chemical Society Meeting at St. Louis, Mo. March, 1961. p. 28-O.

Can. J. Chem. Downloaded from www.nrcresearchpress.com by 210.87.254.40 on 09/05/12
For personal use only.

ELECTRONIC EFFECTS IN ORGANOMAGNESIUM REACTIONS[1,2]

JOEL D. CITRON[3] AND ERNEST I. BECKER[4]
Chemical Laboratories, Polytechnic Institute of Brooklyn, Brooklyn, N.Y., U.S.A.

Received October 29, 1962

ABSTRACT

The kinetics of the first part of the reaction between para-substituted benzonitriles and diethylmagnesium have been studied. The rarely isolated intermediate products, the ketimines, have been isolated and identified. The kinetic constants fit a Hammett plot, with rho equal to +1.57.

Can. J. Chem. Downloaded from www.nrcresearchpress.com by 210.87.254.40 on 09/05/12
For personal use only.

Recently, a precise, convenient procedure was reported for following kinetics of the Grignard reaction (1). The purpose of this investigation was to use this method in evaluating the electronic effect of *p*-substituents in the reactions between the substituted benzonitriles and diethylmagnesium.

EXPERIMENTAL

Reagents

The magnesium used has been previously described (1). All other reagents for kinetics, with the exceptions noted below, were purified in the usual manner. Diethylmagnesium in tetrahydrofuran was prepared by the method of Storfer and Becker (1). The solutions were colorless and were standarized by the method of Gilman *et al.* (2). No precipitate was observed when test portions of the diethylmagnesium solutions (approximately 0.5 to 1 ml) were hydrolyzed in acidified silver nitrate solution. All work with organomagnesium compounds was carried out in an atmosphere of either nitrogen or argon.

α,α,α-Trifluoro-p-tolunitrile

A solution of α,α,α-trifluoro-*p*-tolylmagnesium bromide was prepared in the usual manner from 40 g (0.18 mole) of α,α,α-trifluoro-*p*-bromotoluene in 175 ml anhydrous ether. The Grignard solution was then filtered through a glass-wool plug into an addition funnel.

In a 500-ml flask equipped with stirrer, gas inlet tube, and condenser was placed 125 ml of anhydrous ether. Twelve grams (0.20 mole) of cyanogen chloride (3) were distilled into the flask. The cyanogen chloride solution was cooled in an ice bath and the Grignard solution added over a period of 2.5 hours. After standing overnight, the mixture, which had separated into two layers, was hydrolyzed with cracked ice and then dilute sulphuric acid. The ether layer was dried with anhydrous sodium sulphate, distilled on a steam bath, and the residue was then vacuum distilled, yielding two fractions: the first, 10.1 g, boiling from 35 to 58° at 6 mm; the second, 6.1 g, boiling from 58 to 62° at 5.5–6.0 mm (total 16.2 g, 0.094 mole, 52.5%). The higher-boiling fraction was then purified for analysis by three-stage fractional freezing and one crystallization from pentane, m.p. 36.4–37.4° (reported (4) 36–37°). The total yield of purified nitrile was 5.9 g (0.035 mole, 19.1%). Anal. Calc. for $C_8H_4F_3N$: C, 56.15; H, 2.36; N, 8.19. Found: C, 56.07; H, 2.60; N, 8.10.

4′-(Trifluoromethyl)-propiophenone

The title compound was made via bis(α,α,α-trifluoro-*p*-tolyl)cadmium by the method of Gilman and Nelson (5). The organocadmium was prepared through the corresponding Grignard reagent using 10 g (0.044 mole) α,α,α-trifluoro-*p*-bromotoluene and 4.5 g (0.025 mole) cadmium chloride. The mixture was then treated with 3.8 ml (0.044 mole) propionyl chloride. After hydrolysis, the organic layer was concentrated on a steam bath and the residue extracted with Girards "T" reagent. After hydrolyzing the Girard derivative with hydrochloric acid, and extracting the ketone with ether, 1.25 g (0.0057 mole, 12.9%) of a solid, m.p. 35.6–36.8°, was obtained. The ketone was crystallized twice from pentane and once from ethanol–water, m.p. 35.6–37.0°. Anal. Calc. for $C_{10}H_9F_3O$: C, 59.41; H, 4.49. Found: C, 59.45; H, 4.58.

[1]*Presented at the Symposium on Organometallic Compounds, Vancouver, British Columbia, September 4–6, 1962, sponsored by the Inorganic Chemistry Division, Chemical Institute of Canada, and the Department of Chemistry, University of British Columbia, with the support of The National Research Council, Ottawa, in cooperation with the University Extension Department.*

[2]*Taken in part from the thesis submitted by J. D. Citron to the Faculty of the Polytechnic Institute of Brooklyn in partial fulfillment of the requirements for the degree of Bachelor of Science in Chemistry, June 1962.*

[3]*National Science Foundation Undergraduate Research Participant, Summer 1961 (NSF-G-15814); Research Assistant, Summer 1962 (NSF-G-14558).*

[4]*To whom inquiries should be directed.*

Method of Analysis

This method is based upon that described in reference 1. An aliquot of the solution under study was hydrolyzed in a known excess of sulphuric acid (10.00 ml of 0.06–0.10 *N*) containing ethanol (about 10 ml) to dissolve the organic materials present. The solution was heated to just below the boiling point for 15 minutes to dissolve the magnesium compounds present, and was then back-titrated while hot with sodium hydroxide solution (0.04–0.06 *N*) to the methyl red end point.

Blanks were run to determine whether the organic species present affected the results. Approximately 0.1–0.2 g each of nitrile and substituted propiophenone were added to a mixture of 5 ml sulphuric acid and 5 ml ethanol. After heating to just below the boiling point for 15 minutes, the solutions were back-titrated while hot using methyl red indicator. The results were the same within experimental error as a blank using only sulphuric acid.

Kinetics

The apparatus and reaction conditions have been previously described (1). Before starting a run, a measured volume of a standardized solution of diethylmagnesium in tetrahydrofuran was introduced into the reaction vessel. At time zero, a thermostatted standard solution of the nitrile in tetrahydrofuran was introduced into the diethylmagnesium solution. At appropriate intervals, samples were withdrawn by syringe for analysis. All solutions remained homogeneous during and after the kinetic runs. The ratios of nitrile to diethylmagnesium ranged from 1:1 to 2.5:1, and the concentration of diethylmagnesium ranged from 0.10 to 0.22 *M*.

Reaction Products

(1) 2,4,6-Tris-(*p*-chlorophenyl)-*s*-triazine was isolated in preliminary runs with *p*-chlorobenzonitrile when the nitrile:Et_2Mg ratio exceeded 2:1. At 30° in tetrahydrofuran, with a 3:1 ratio, a precipitate, the triazine, appeared after 24 hours, m.p. 332.0–332.9°. It was identified by elemental analysis, mixed melting point, 332.3–333.2°, with an authentic sample, m.p. 332.6–333.6° (reported (6) 335°), and identity of their infrared spectra. The triazine was very insoluble in tetrahydrofuran at 30°.

An attempt was made to increase the yield of triazine. Twenty-five milliliters of a 0.5 *M* Et_2Mg (0.0125 mole) solution in tetrahydrofuran and 5.0 g (0.0445 mole) *p*-chlorobenzonitrile were refluxed for 3 days. A precipitate appeared after the first 24 hours. A mixture of 20 ml of water and 5 ml of concentrated hydrochloric acid was added, filtration affording 1.49 g (45.6% theoretical, after subtracting the amount of nitrile consumed in ketimine formation) of crude triazine.

(2) 2,4-Dinitrophenylhydrazone derivatives of *p*-substituted propiophenones were prepared by adding the ketone to an excess of a stock solution (1) of 2,4-dinitrophenylhydrazine and recrystallizing the precipitates. The data are summarized in Table I.

TABLE I

2,4-Dinitrophenylhydrazones of *p*-substituted propiophenones

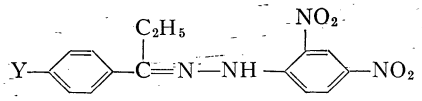

Y	Yield, %*	Melting point, °C	Empirical formula	Analyses, % C Calc.	C Found	H Calc.	H Found	N Calc.	N Found
CF_3	44, orange	188.9–190.3†	$C_{16}H_{13}F_3N_4O_4$	50.27	50.32	3.43	3.72	14.66	14.65
Cl	95, orange	219.6–220.5‡	$C_{15}H_{13}ClN_4O_4$§	51.65	51.68	3.76	3.64	16.07	16.12
C_6H_5	97, orange-red	216.5–218.5‖ (decomp.)	$C_{21}H_{18}N_4O_4$	64.61	64.90 64.85	4.65	4.94 4.78	14.35	14.54 14.32
CH_3	44, red	200.0–205.5¶							
OCH_3	64, deep red	194.0–197.2**							

*Starting with 120 mg of ketone in each case. Yields are after one recrystallization; melting points are uncorrected.
†Recrystallized from ethanol, chloroform–methanol, and ethanol – ethyl acetate.
‡Recrystallized twice from ethanol – ethyl acetate and twice from ethanol.
§Calc.: Cl, 10.17. Found: Cl, 9.99.
‖Recrystallized twice from ethanol – ethyl acetate and twice from chloroform–methanol.
¶Reported m.p. 200–202° (L. M. Long and H. R. Henze. J. Am. Chem. Soc. **63**, 1939 (1941)).
**Reported m.p. 195° (N. M. Cullinane, S. J. Chard, and D. M. Leyshon. J. Chem. Soc. 376 (1952)).

Ketimines

The method used was that of Pickard and Tolbert (7). Ethylmagnesium bromide was employed with the nitrile in ether. The imines were handled under anhydrous conditions at all times, as they appeared to be very sensitive to hydrolysis. The physical constants will be found in Table II.

Can. J. Chem. Downloaded from www.nrcresearchpress.com by 210.87.254.40 on 09/05/12
For personal use only.

TABLE II

p-Substituted phenyl ethyl ketimines

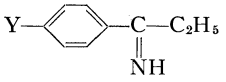

Y	Color	Boiling point, °C (mm of Hg)*	Empirical formula	Analyses, % C Calc.	C Found	H Calc.	H Found	N Calc.	N Found
Cl	Yellow liquid	115 (4.4)	$C_9H_{10}ClN$†	64.48	64.60	6.01	5.81	8.36	8.58
C_6H_5	White solid	84.0–87.0‡	$C_{15}H_{15}N$	86.08	86.08	7.22	7.40	6.69	6.95
CH_3	Yellow liquid	101–105 (4.5)	$C_{10}H_{13}N$	81.58	81.72	8.90	9.15	9.52	9.40
OCH_3	White solid	128 (4.7)§	$C_{10}H_{13}NO$	73.59	73.58	8.03	7.99	8.58	8.78

*Block temperature of a molecular still.
†Calc.: Cl, 21.15. Found: Cl, 21.19.
‡Melting point.
§M.p. 46.7–48.6°. Reported m.p. 38–40° (P. L. Couturier. Ann. Chim. **10**, 559 (1938)).

RESULTS

The initial concentration of nitrile was calculated from the number of moles added and the initial volume of the reaction mixture. The initial concentration of diethylmagnesium was obtained by the above method, or by extrapolating the early points (less than 10% reaction) back to zero time; the agreement between the two methods was an internal check on the technique for each run (see reference 1).

A second-order rate equation, first order in diethylmagnesium and first order in nitrile, gave consistent values for the rate constant (eq. [1]). The rates thus obtained are shown

$$\text{rate} = k[Et_2Mg][\text{nitrile}] \quad [1]$$

in Table III, together with the appropriate data for the Hammett plot. The Hammett

TABLE III

Kinetic data

Y	k*	Number of runs	log k/k_0	sigma†
CF_3	23.8 ±0.0	2	0.848	0.550
Cl	7.47±0.10	2	0.344	0.227
C_6H_5	3.65±0.22	5	0.033	0.009
H	3.38‡		0.000	0.000
CH_3	1.60±0.10	5	−0.325	−0.170
OCH_3	1.30±0.00	2	−0.415	−0.268

*In liter/mole-sec×10^4; ± values are average deviations from the mean.
†See ref. 8.
‡Rate constant from ref. 1.

plot is given in Fig. 1, and the ρ is +1.57. The Hammett plot and all kinetic curves were fitted by the method of least squares.

DISCUSSION

The precision of the analytical procedure made possible the study of the initial rates of the reaction. This point is significant, since it was shown earlier (1) that only half of the available ethyl groups react, and that for this half two reaction rates are observed. It is within the time for reaction of this first quarter of the available ethyl groups that the data were obtained in the present work.

Can. J. Chem. Downloaded from www.nrcresearchpress.com by 210.87.254.40 on 09/05/12
For personal use only.

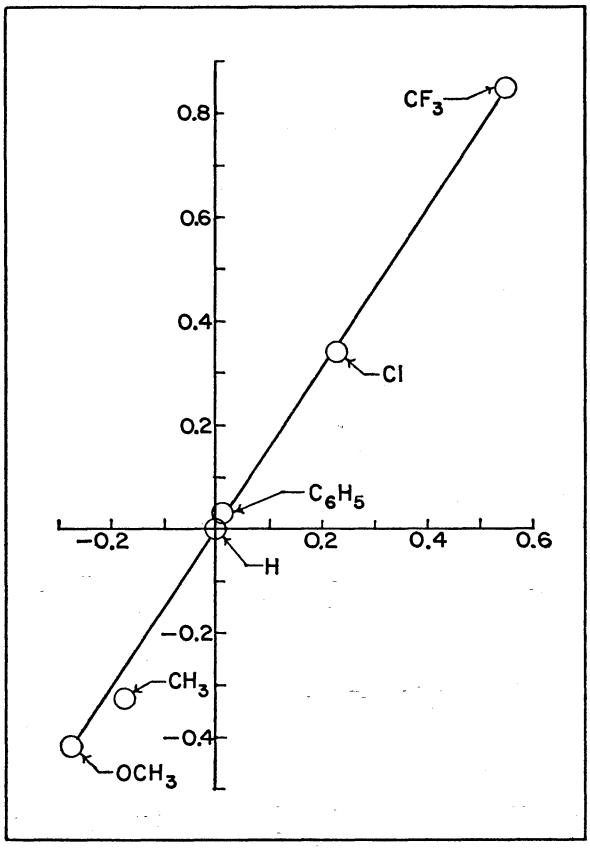

FIG. 1. Hammett plot of reaction rate constants. Slope (ρ) = +1.57. Ordinate: log (k/k_0); abscissa: σ.

The linearity of the Hammett plot affirms that the nitriles taken here react by the same mechanism. The value of ρ, +1.57, indicates that the rate-determining step involves a dipolar, but probably not ionic, species as befits a solvent of low dielectric constant such as tetrahydrofuran.

The mechanism previously proposed (1) for the first part of the reaction can be used to explain the electronic effects of the substituents. The role of the solvent is not considered in this mechanism. The increased rate with the electron-attracting chlorine atom in the

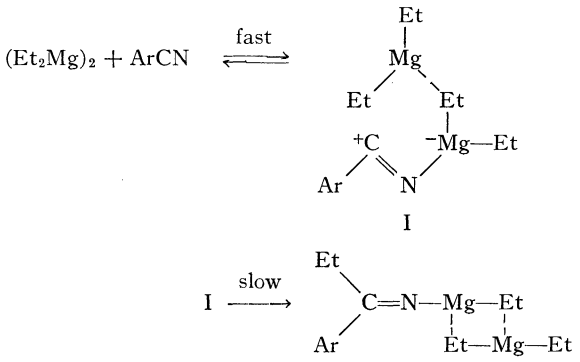

Can. J. Chem. Downloaded from www.nrcresearchpress.com by 210.87.254.40 on 09/05/12
For personal use only.

para position is consistent with the rearrangement of the complex as the slow step, since that step requires the transfer of a negative ethyl group to an electron-deficient center—the nitrile carbon atom. Conversely, electron-releasing groups, such as CH_3 and OCH_3, should decrease the rate by increasing the electron density at the nitrile carbon atom, making the transfer of a negative ethyl group there more difficult, which is the case.

Prior workers in this area of research have employed competition experiments and found the effect of substituents to be in qualitative agreement with the results obtained here. Thus, Gilman and Lichtenwalter (9) found the order of reactivities to be $Cl > H > CH_3 > OCH_3 > N(CH_3)_2$ for the reaction between phenylmagnesium bromide and the *p*-substituted benzonitriles in ethyl ether. In a study of the competitive reaction between *p*-substituted benzophenones and 1-naphthol against methylmagnesium iodide in phenetole, Lewis and Wright (10) obtained a ρ of $+0.362$.

The appreciable changes in the rate with changes in substituent obtained in the reactions with benzonitriles appear to be significantly different from those reported by Dessy and Salinger (11) for the reaction of *p*-substituted benzalanilines with ethylmagnesium bromide in ethyl ether. In that study the authors claim that essentially no change in rate is observed with the methoxy or chloro groups.

REFERENCES

1. S. J. Storfer and E. I. Becker. J. Org. Chem. **27**, 1868 (1962).
2. H. Gilman, P. D. Wilkinson, W. P. Fishel, and C. H. Meyers. J. Am. Chem. Soc. **45**, 150 (1923).
3. G. H. Coleman, R. W. Leeper, and C. C. Schulze. Inorganic syntheses. Vol. II. McGraw-Hill Book Co., Inc. New York. 1946.
4. J. Bernstein, H. L. Yale, K. Losee, M. Hölsing, J. Martins, and W. A. Lott. J. Am. Chem. Soc. **73**, 906 (1951).
5. H. Gilman and J. F. Nelson. Rec. Trav. Chim. **55**, 518 (1936).
6. A. H. Cook and D. G. Jones. J. Chem. Soc. 278 (1941).
7. P. L. Pickard and T. L. Tolbert. J. Org. Chem. **26**, 4886 (1961).
8. H. H. Jaffe. Chem. Rev. **53**, 191 (1953).
9. H. Gilman and M. Lichtenwalter. Rec. Trav. Chim. **55**, 588 (1936).
10. R. N. Lewis and J. R. Wright. J. Am. Chem. Soc. **74**, 1257 (1952).
11. R. E. Dessy and R. M. Salinger. J. Am. Chem. Soc. **83**, 3530 (1961).

Can. J. Chem. Downloaded from www.nrcresearchpress.com by 210.87.254.40 on 09/05/12
For personal use only.

THE VAPOR PHASE POLYMERIZATION OF ETHYLENE ON AN ORGANOTITANIUM CATALYTIC SURFACE[1]

F. H. C. EDGECOMBE
Du Pont of Canada Limited, Research Division, Kingston, Ontario
Received October 29, 1962

ABSTRACT

The polymerization of ethylene has been studied in the gas phase on a solid catalyst formed by the reaction of an organotitanium vapor with a solid crystalline titanium compound deposited on the walls of a reaction vessel.

The rate of polymerization of ethylene was found to be, initially, of first order but as the reaction proceeded departure from the first-order case was observed.

Experiments conducted under the condition of constant pressure as well as the usual constant-volume state enabled us, with the aid of an analogue computer, to devise a mathematical model which explained the experimental results in an unique fashion.

A measure of the rate constant for catalyst decay was also obtained as well as the activation energy for the overall propagation step in the polymerization of ethylene.

Can. J. Chem. Downloaded from www.nrcresearchpress.com by 210.87.254.42 on 09/05/12
For personal use only.

The discovery of stereospecific polymerization processes capable of leading, by poly-addition of olefinic units, to high yields of sterically regulated polymers has created a tremendous surge of interest in polymer chemistry.

In spite of all the effort which numerous investigators have expended upon the study of coordination catalysis no adequate description of the mechanism of action of the catalyst nor complete kinetic analysis of the polymerization process has been formulated to date.

The catalyst systems themselves are many and varied. The majority of catalysts do involve a complex of a transition metal and a metal organic compound. Nonetheless even the most cursory survey of what is now an immense patent literature concerning these systems will indicate the diversity of materials capable of the polymerization of alpha olefins. There are very few of the elements in the periodic table which cannot be found playing some role in some system of what is now rather loosely termed coordination catalysis.

The work which we are about to describe deals with the study of one of the more common types of catalyst, the system of transition metal and metal organic compound previously mentioned, but differs from the majority of such systems in that the active species contains but one metal element. The choice of a single-metal system was made in order to simplify so far as possible the mechanism of the catalytic function.

All the polymerizations studied have been carried out by the reaction of a gaseous monomer at a solid catalytic surface under conditions of constant temperature and either constant volume or constant pressure.

EXPERIMENTAL

Apparatus

The apparatus, illustrated in Fig. 1, was in essence a simple two-manifold high-vacuum system provided with a high-capacity two-stage rotary vacuum pump; liquid nitrogen cooled traps; a reaction vessel, to be described later, immersed in a water bath the temperature of which was controlled within ±0.1° C; glass

[1]*Presented at the Symposium on Organometallic Compounds, Vancouver, British Columbia, September 4–6, 1962, sponsored by the Inorganic Chemistry Division, Chemical Institute of Canada, and the Department of Chemistry, University of British Columbia, with the support of the National Research Council, Ottawa, in cooperation with the University Extension Department.*

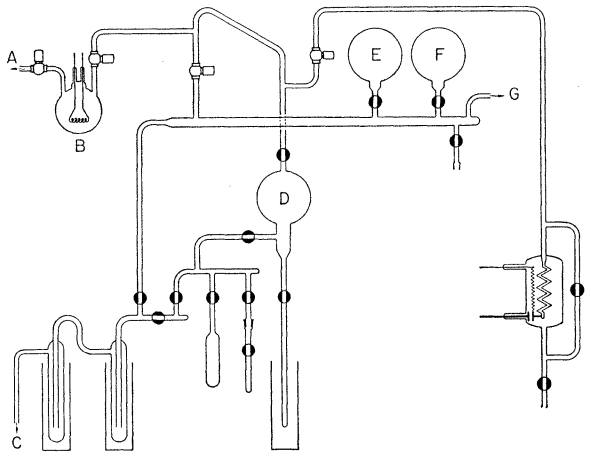

FIG. 1. Apparatus. A, to gas chromatograph; B, reaction vessel; C, to pump; D, mixing bulb; E, hydrogen; F, ethylene; G, to mercury manometer.

bulbs for the storage of monomer and other gaseous reactants; storage facilities for catalyst components; an all-glass pressure-measuring device; mercury manometer and automatic apparatus which could be used to maintain the pressure of the system constant.

The reaction vessel was a pyrex glass bulb into which was sealed, through uranium glass, a tungsten electrode of the sort found in fluorescent light fixtures. Entrance into the reaction vessel from the vacuum manifold was through a Springham greaseless stopcock fitted with a Viton A diaphragm and O ring. Exit from the vessel into an automatic gas chromatograph was made by means of a Hoke A431 all-metal bellows valve attached by a kovar glass to metal seal. Similar Hoke valves were used in those places where catalyst contact with greased stopcocks was deemed to be undesirable.

Since the catalyst has been found to be photochemically unstable to room lighting all transparent parts of the reaction line with which catalyst came in contact were externally blackened with a dispersion of colloidal graphite.

Pressures were automatically recorded to a precision of ± 0.05 cm of Hg by means of a small glass spiral used in a differential fashion and accurately calibrated against a mercury manometer. This pressure-measuring device, previously described by Edgecombe and Jardine (1), was constructed in such a way that pressure changes within the system varied the capacitance of a simple plate condensor. These capacitance variations were in turn fed to a capacitance transducer which transposed them into a voltage, a form suitable for amplification and strip chart recording.

The course of the polymerization could also be followed by gas chromatography. An automatic gas chromatograph was devised (2) which could remove at regular intervals very small samples of gaseous monomer from the system and record their concentration.

When it was necessary to carry out the polymerization under conditions of constant pressure two procedures were used. In the first instance the pressure of monomer in the reaction vessel was manually returned to the initial pressure after a short period of polymerization and this process repeated so that the record of pressure change with time as recorded on the strip chart recorder gave a sawtooth pattern. At a later stage of our investigation a more refined method was used to maintain a constant pressure. This device took the form of an automatic gas burette and is described elsewhere (3). It consisted essentially of a servo actuated screw raising the level of a container of mercury which was connected to a calibrated gas burette. Control was obtained by using the pressure-measuring device described previously and the pressure of the system could be maintained constant to within less than 0.01 cm of the initial pressure of 10 cm of Hg. The device was also capable of providing a continuous record of the time rate of volume change within the system.

Preparation of Materials

Ethylene

The ethylene used was a chemically pure grade supplied by Matheson Inc. and was taken directly from its cylinder by a suitable feed system and stored in a large bulb on the vacuum line. Although high-sensitivity gas chromatography could detect no impurity in the stored material several experiments were carried out in which the ethylene to be used was first passed through a purification train consisting of a 10-ft column of silica gel, a 2-ft column of ascarite, two washings with triisobutyl aluminum, and a 2-ft column of alumina. Ethylene thus treated reacted in no way different from that taken directly from the cylinder.

Can. J. Chem. Downloaded from www.nrcresearchpress.com by 210.87.254.42 on 09/05/12
For personal use only.

Hydrogen and Helium

The hydrogen used in the reaction for the formation of titanium trichloride was of chemically pure grade and was not subjected to further purification.

The helium used as a carrier gas in the gas chromatographic system was of very high purity and was not treated in any way before use.

Titanium Tetrachloride

Fisher certified reagent grade titanium tetrachloride was used in the catalyst formation. It was distilled from a trap on the vacuum line immediately before use.

Titanium Trichloride

The titanium trichloride used in the catalyst preparation was formed within the reaction vessel by the action of $TiCl_4$ vapor and hydrogen at a tungsten filament heated to bright red. The reaction may be represented as

$$2TiCl_4 + H_2 \xrightarrow{\text{heat}} 2TiCl_3 + 2HCl.$$

The HCl vapor was immediately pumped off. The $TiCl_3$ formed was the alpha variety, i.e. purple $TiCl_3$. Experiments have shown that the $TiCl_3$ is laid down each time on the walls of the reaction vessel in a consistent pattern and if similar voltages are applied to the filament for identical periods of time reproducible quantities of $TiCl_3$ are produced.

A study was carried out in which the $TiCl_3$ deposit was carefully washed out of the reaction vessel with dilute nitric acid and a Volhard analysis performed to determine the chloride content. The amount of $TiCl_3$ deposited for a 35-minute reaction period with a voltage of 22 v a-c. applied to the filament from 1 cm pressure of $TiCl_4$ in a volume of 400 ml was determined to be 7.95×10^{-5} mole (average of 17 experiments).

Dimethyl Zinc

Dimethyl zinc was used in the formation of the catalyst precursor CH_3TiCl_3. It was prepared in the following manner. Anhydrous zinc chloride was melted in a glass container and then cooled in an atmosphere of dry nitrogen. The fused zinc chloride was powdered in a mortar and transferred in the nitrogen atmosphere to a three-neck round-bottom flask purged with nitrogen. One neck of the flask was closed off. A condenser was fitted into one of the remaining necks and a dropping funnel containing trimethyl aluminum adapted to the third neck.

The entire system was purged with nitrogen. A stream of nitrogen was directed over any openings to the atmosphere in the system. Trimethyl aluminum was slowly added to the zinc chloride and the mixture heated to 50° C until it was evident that a reaction had commenced. The heat was removed and the reaction

$$(CH_3)_3Al + ZnCl_2 \rightarrow (CH_3)_2Zn + CH_3AlCl_2$$

continued, the material refluxing under its own heat of reaction. When all signs of reaction had disappeared the vessel was cooled in a dry ice – acetone mixture and transferred to a spinning band column through which the $(CH_3)_2Zn$ was distilled into a cooled glass container and finally redistilled into a storage trap on the vacuum line.

Formation of Catalyst

Five millimeters of Hg pressure of dimethyl zinc contained in a 4-liter mixing bulb was condensed and isolated in a cold finger surrounded by liquid nitrogen. The bulb was next pumped out and 10 mm of Hg pressure of titanium tetrachloride vapor distilled into it. The $(CH_3)_2Zn$ in the cold finger was quickly warmed to slightly above room temperature and was expanded into the bulb, where it mixed and reacted with the $TiCl_4$. The reaction represented by the following equation takes place:

$$Zn(CH_3)_2 + 2TiCl_4 \rightarrow 2CH_3TiCl_3 + ZnCl_2.$$

CH_3TiCl_3 is a vapor and $ZnCl_2$ a solid. The $ZnCl_2$ settles out leaving CH_3TiCl_3, which has been shown by infrared spectroscopy to be free of zinc compounds and unreacted $TiCl_4$.

CH_3TiCl_3 was then expanded into the evacuated reaction vessel upon which a layer of $TiCl_3$ had been deposited. The reaction between CH_3TiCl_3 and $TiCl_3$ was allowed to proceed for a fixed time after which the residual CH_3TiCl_3 and the $TiCl_4$ produced by the reaction was pumped out.

$$CH_3TiCl_3 + TiCl_3 \rightarrow TiCl_4 + CH_3TiCl_2$$

CH_3TiCl_2 is the active catalyst and is thought of as an alkylated $TiCl_3$ surface.

Infrared Instrumentation

In the discussion reference will be made to several infrared analyses. A Perkin–Elmer Model 221 double-beam spectrophotometer fitted with sodium chloride optics was used to record the infrared spectra from 4000 to 650 cm^{-1}. A Perkin–Elmer single-beam, double-pass Model 112 spectrophotometer with cesium bromide optics was used for the region 650 to 290 cm^{-1}.

Can. J. Chem. Downloaded from www.nrcresearchpress.com by 210.87.254.42 on 09/05/12
For personal use only.

The infrared gas cells used in this work were of pyrex, 10 cm in length and fitted with a vacuum stopcock. CsBr windows were sealed on with glyptal in such a manner that the cells were vacuum tight.

THE CATALYTIC SYSTEM

Before presentation of the kinetic data, a few comments on the catalytic system which we have used are in order.

The existence of methyl titanium trichloride has been known for some time. During the years 1955 and 1956 this laboratory carried out a rather exhaustive study of its physical and catalytic properties. It was found that CH_3TiCl_3 vapor alone was extremely stable in the dark at room temperature, Fig. 2, and that in the pure form either in

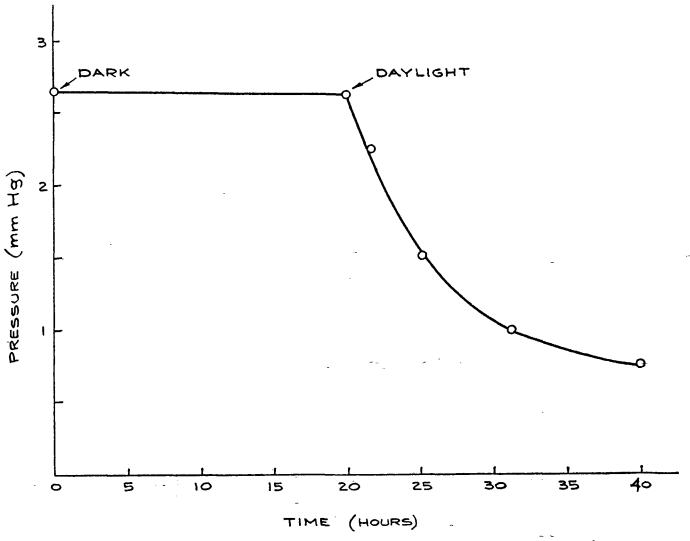

FIG. 2. Stability of gaseous $TiCl_3CH_3$.

hydrocarbon solution or the vapor state possessed little or no catalytic activity. If, on the other hand, one partially decomposed CH_3TiCl_3 by photochemical or thermal means, a catalyst, active for the polymerization of ethylene, was formed. It was also found, by an infrared technique, that during the decomposition of CH_3TiCl_3 in cyclohexane solution $TiCl_4$ was formed, Fig. 3.

Van Heerden (4), discussing a paper by Natta, drew attention to a Hoechst patent (5) which mentioned that $TiCl_3$ forms an active system for polymerization when reacted with tetravalent alkyl titanium halides. Dr. Van Heerden further reported that in his own laboratory the combination of CH_3TiCl_3 and brown $TiCl_3$ formed by the thermal decomposition of CH_3TiCl_3 was an extremely active system. His explanation of the experimental results is applicable to the system which we are describing and consequently warrants repetition.

The Ti—C bond in the tetravalent titanium alkyl halide seems too stable to give a rapid "aufbau" reaction under the mild conditions of low-pressure ethylene polymerization. The unique character of the Ti—C bond has become apparent in an infrared analysis (6) of CH_3TiCl_3 carried out in this laboratory and to be published shortly. It has become evident that the CH_3 group present in CH_3TiCl_3 does not possess the infrared character of the normal metal organic methyl group and therefore the Ti—C bond is

Can. J. Chem. Downloaded from www.nrcresearchpress.com by 210.87.254.42 on 09/05/12
For personal use only.

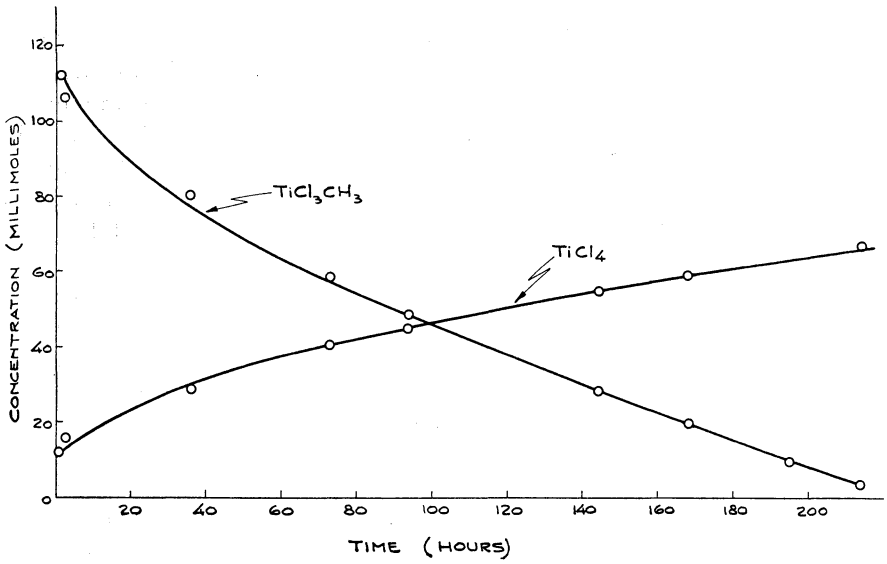

FIG. 3. Decomposition of $TiCl_3CH_3$ in cyclohexane in the dark at 25° C.

not a normal metal carbon bond. (Rodriguez's (7) work using D_2O to hydrolyze methyl titanium trichloride also emphasizes this last fact since he found all of the mixed CDH groups present in his products.) Van Heerden's studies also show that a solution of CH_3TiCl_3 in the absence of $TiCl_3$ does not give the aufbau reaction or at least the rate of such a reaction is very small in comparison with the polymerization rate in coordination catalyst systems. De Vries' (8) work in the same laboratory as Van Heerden found that only those alkyl titanium chlorides are unstable which can decompose in a bimolecular reaction by the disproportionation of two alkyl groups to an olefin and an alkane, i.e. those compounds having an H atom on a β-C atom in the alkyl group. CH_3TiCl_3 lacking H atoms on β carbon atoms is consequently stable.

Arlman and De Jong (9) discussed the work of Beerman and Bestian (10) regarding the decomposition of CH_3TiCl_3. The decomposition appeared autocatalytic and the addition of extra $TiCl_3$ increased the rate of decomposition. It was suggested that the reaction takes place predominantly at the surface of $TiCl_3$ crystals.

The preparation of the catalyst system used in our study is described in detail in the section of this paper dealing with experimental methods. The CH_3TiCl_3 vapor is reacted with a deposit of purple $TiCl_3$, i.e. the alpha form prepared in a pure state. An infrared examination of the formation of this catalyst has shown that $TiCl_4$ is formed during the reaction of the vapor and the solid. If the surface is pumped for an hour or more to remove any remaining $TiCl_4$ and then a small quantity of moist helium is brought into contact with it, methane is formed and has been detected by gas chromatography. No ethane has been found in the system.

From the foregoing discussion we postulate the following reaction to explain the formation of a catalyst active for ethylene polymerization:

$$TiCl_3 + CH_3TiCl_3 \rightarrow CH_3TiCl_2 + TiCl_4,$$

CH_3TiCl_2 being the active species. The active site might well be a chlorine vacancy in the crystal lattice, a mechanism well described by Cossee (11).

Can. J. Chem. Downloaded from www.nrcresearchpress.com by 210.87.254.42 on 09/05/12
For personal use only.

Can. J. Chem. Downloaded from www.nrcresearchpress.com by 210.87.254.42 on 09/05/12
For personal use only.

KINETICS

The literature which has been built up since the advent of the polymerization of olefines by coordination catalysts contains many discussions of the kinetics of ethylene polymerization. A large variety of catalytic systems has been studied and numerous postulations made as to the factors controlling the rate of reaction. The majority of such investigations have dealt with polymerization in hydrocarbon solution and have involved catalysts generally formed *in situ*. Relatively few investigations have been carried out in the absence of solvent and the investigation of Eden and Feilchenfeld (12) represents one of these. It should be mentioned that we do not consider the fixed bed catalysts such as the chromium oxide system of Phillips Petroleum and the nickel, cobalt, and molybdenum oxide systems of Standard Oil as belonging to the class of coordination catalysts which we are considering.

Most investigations dealing primarily with catalysts formed by the reaction of aluminum alkyls and titanium or vanadium halides have shown that the rate curves for ethylene polymerization are complex. Ludlum, Anderson, and Ashby (13) divide their observed rate curve into three regions. Fukui (14) and his co-workers, using a somewhat different system than Ludlum, have delineated four regions in their overall rate curve. Badin (15) and Chien (16) have two regions and Gilchrist (17) by virtue of the time period of his observations finds but one. Most authors do, however, in spite of their divisions of the rate curve, observe a region in which the rate of polymerization of ethylene is first order in ethylene. Several people, among them Fukui (14) and Gilchrist (17), have found second-order dependence but often it is possible to postulate ethylene being a necessary substituent in the catalyst-forming step of their reaction scheme. It is commonly observed that the rate eventually departs from first order, and several explanations to be discussed later have been postulated to explain this fact.

Figure 4 represents the change in ethylene concentration with time for a constant-volume system in which gaseous ethylene is polymerized on the alkylated $TiCl_3$ surface previously described. Figure 5 is the same experiment plotted as a first-order reaction. It is evident that the rate of reaction obeys the first-order rate law during the first 50 minutes but then departs from that law and must be expressed in some different form.

Figure 6 shows the polymerization of ethylene under a condition approximating constant pressure; this condition was obtained in the manner previously described, i.e. returning the pressure to the initial value at frequent, regularly spaced intervals. It is obvious from this figure that the initial rate is changing. Figure 7 shows the polymerization of an alpha olefin under conditions of constant pressure using the automatic gas burette to control the pressure. The curve represents the volume change as a function of time. If one considers the general equation for a first-order process,

$$dn/dt = -k_1C,$$

where $n \equiv$ number of moles and $C \equiv$ number of moles/liter $= n/V$, assuming perfect gas $n = PV/RT$, $C = P/RT$ it is easily shown that

$$dV/dt = -k_1,$$

i.e. for a first-order process the rate of change of volume should be constant.

Since the result of the constant-pressure experiment is not a straight line it is evident

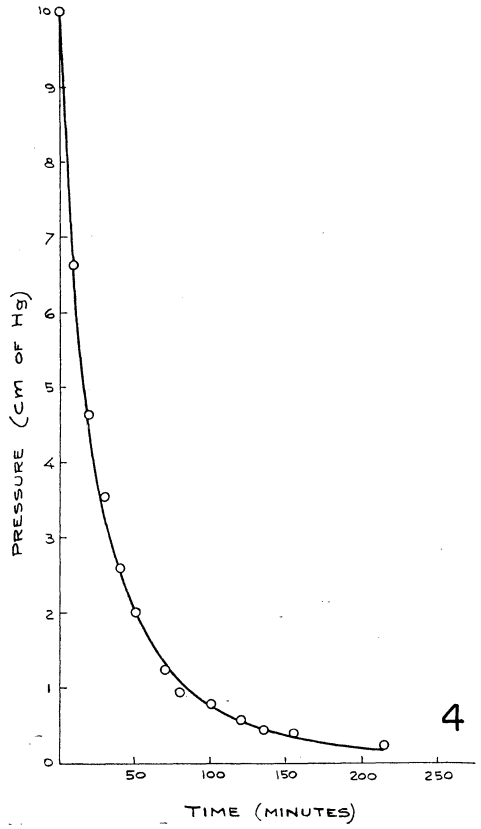

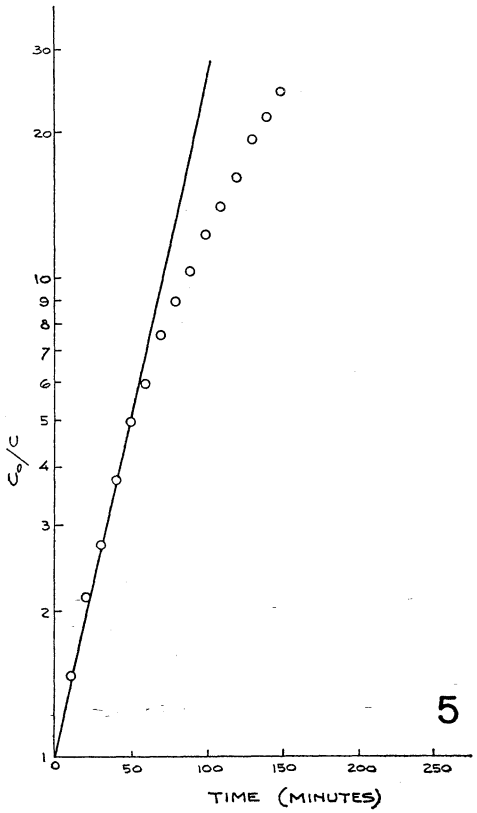

FIG. 4. The polymerization of ethylene. Ethylene concentration as a function of time.
FIG. 5. The polymerization of ethylene. First-order plot.

that the reaction is not entirely first order. A consideration of a second-order process at constant pressure would give

$$dV/dt = -k_2P,$$

which would also be a straight line under the conditions of reaction.

The amount of curvature evident in the time rate of change of volume of Fig. 7 is a measure of the departure from either first or second order. From the constant-volume experiments it is evident that the rate deviates from the first-order case.

The initial attempt to explain our kinetic data was based on the following mathematical analysis. In the first approximation the following differential equations were said to govern the progress of the polymerization step. It is to be borne in mind that the catalyst is preformed and active. No initiation reaction is necessary.

[1] $$-dE/dt = k_1E$$

[2] $$-dC/dt = k_2(E_0-E)C$$

[3] $$k_1 = k_3C$$

$E \equiv$ concentration of ethylene at time t, $E_0 \equiv$ initial concentration of ethylene, $C \equiv$ concentration of catalyst at time t, $C_0 \equiv$ initial concentration of catalyst.

Can. J. Chem. Downloaded from www.nrcresearchpress.com by 210.87.254.42 on 09/05/12
For personal use only.

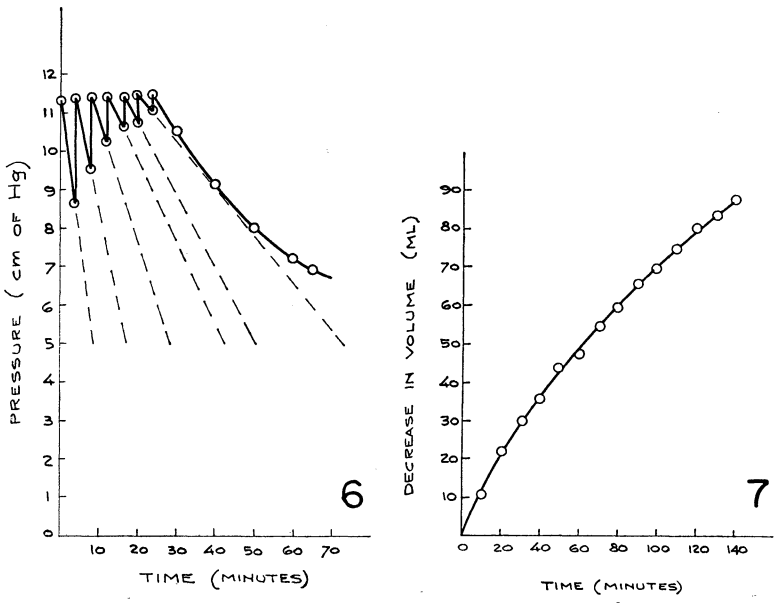

FIG. 6. The polymerization of ethylene at constant pressure.
FIG. 7. The polymerization of an α olefin at constant pressure (automatic gas burette).

Equation [1] represents the first-order polymerization mechanism.

Equation [2] was derived in an intuitive fashion and represents the decrease in effective catalyst concentration (i.e. number of active sites) brought about by buildup of polymer around the site. This explanation for the decrease in polymerization rate has been suggested by Feilchenfeld and Jeselson (18) and also by Ludlum and his co-workers (13).

Equation [3] links the rate of polymerization with the concentration of catalyst.

Rewriting [1]

$$dE/dt = -k_3CE.$$

For ease in manipulation we shall make concentration and time terms dimensionless. Dividing by E_0 and letting E/E_0 be represented by Y

$$dY/dt = -k_3CY.$$

Dividing by C_0 and letting C/C_0 be represented by X

[4] $$dY/dt = -k_3C_0XY.$$

Transposing [2]

[5] $$dX/dt = -k_2E_0(1-Y)X.$$

At $t = 0$, $k_3C_0 = k_{1_0}$ (the initial rate constant) and $X = Y = 1$. Let $k_3C_0 \equiv \lambda$ and $\lambda t \equiv \tau$, and normalizing time, [4] becomes

[6] $$dY/d\tau = -XY$$

and [5] becomes

[7] $$dX/d\tau = -\alpha(1-Y)X,$$

where $\alpha = k_2E_0/k_3C_0$.

Can. J. Chem. Downloaded from www.nrcresearchpress.com by 210.87.254.42 on 09/05/12
For personal use only.

Equations [6] and [7] were then set up on an analogue computer and a family of solutions developed for various values of α. The solutions thus generated were then compared with the experimental curve and it was found that the solution obtained for an α value of 0.32 closely fitted the experimental results.

The experimental results just applied to the theoretical equations have been obtained from measurements made in a constant-volume system. If the theory is to be correct it should also apply to measurements made under constant pressure. The analogue computer was wired so as to perform a hypothetical constant-pressure experiment using the theoretical equations outlined previously. The results of this experiment showed that the theoretical equations were not adequate to describe the changing initial rate data found experimentally.

A new system of equations was then set up. The rate of catalyst decay was said to be proportional to the *rate* of ethylene polymerization. In this particular case equation [6] does not change but equation [7] becomes

$$dX/d\tau = -\alpha(X\,Y)X. \qquad [8]$$

It was found that the solutions generated using equations [6] and [8] fitted the constant-pressure experiments, but failed to satisfy the constant-volume data.

The third case considered was that in which the catalyst decayed in a purely exponential fashion. In this instance equation [7] takes the form

$$dX/d\tau = -kX. \qquad [9]$$

Once again, it was found that the solutions of the differential equations did not fit all of the experimental situations.

The mathematical expressions were again studied and it was found that if both constant-pressure and constant-volume conditions were to be met, another term would have to be introduced into equation [7]. The expressions

$$dY/d\tau = -X\,Y$$

and

$$dX/d\tau = -\{\alpha(1-Y)X + \beta X\}, \qquad [10]$$

where βX represents exponential catalyst decay, gave a solution which satisfied all conditions. β is a constant equal to K/k_3C_0 in the normalized expressions given above, K being the decay rate constant.

The specific solution fitting the experimental measurements has a value of $\alpha = 0.38$ and a value of $\beta = 0.10$. It is evident from the expressions given above that in the initial stages of reaction the falloff in rate is due solely to catalyst decay, which has been shown to be slow from a study of experiments in which the catalyst was aged previous to the introduction of ethylene. As polymer builds up around the active site less monomer is able to reach it and the rate begins to drop.

The diffusion processes which have some influence on the chemical process are at present under study.

Estimation of the Rate Constant for Catalyst Decay

If we consider the initial stages of the polymerization and also assume that the only catalyst decay process of importance during that particular stage is normal exponential decay the constant-pressure experiments may be used to estimate the rate constant

Can. J. Chem. Downloaded from www.nrcresearchpress.com by 210.87.254.42 on 09/05/12
For personal use only.

of this decay process. It is recognized that the above approximation is rather great but nonetheless the calculation is included since the method might find application to other processes.

Consider the curvature of the time rate of change of volume depicted in Fig. 7. Under conditions of constant pressure

$$dV/dt = -k_E n_{cat}, \tag{11}$$

where $V \equiv$ volume, $t \equiv$ time, $k_E \equiv$ a rate constant for volume change, $n_{cat} \equiv$ number of moles of catalyst or number of active sites.

Making use of our aforementioned assumption involving first-order catalyst decay

$$dn_{cat}/dt = -k_{cat} n_{cat}. \tag{12}$$

Integrate [12] and apply the condition that $n_{cat} = n_0$ at $t = 0$

$$n_{cat} = n_0 \epsilon^{-k_{cat} t}. \tag{13}$$

Put [13] into [11]

$$dV/dt = -k_E n_0 \epsilon^{-k_{cat} t}.$$

At $t = 0$

$$dV/dt = -k_E n_0.$$

Let $\phi = (k_E/k_{cat})n_0$, then at $t = 0$,

$$dV/dt = -k_{cat}\phi.$$

Also it may be shown that

$$\begin{aligned} \Delta V &= (k_E/k_{cat})n_0[\epsilon^{-k_{cat} t} - 1] \\ &= \phi[\epsilon^{-k_{cat} t} - 1]. \end{aligned}$$

Select any pair of values of ΔV and t. Find, by trial and error, various values of ϕ and k_{cat} which fit. Plot ϕ as a function of k_{cat}. Repeat for other values of ΔV and t which are widely separated.

The intersection of the family of curves, Fig. 8, denotes unique values of k_{cat} and ϕ.

A value of $k_{cat} = 1.6 \times 10^{-2}$ min^{-1} has been determined from a number of experiments.

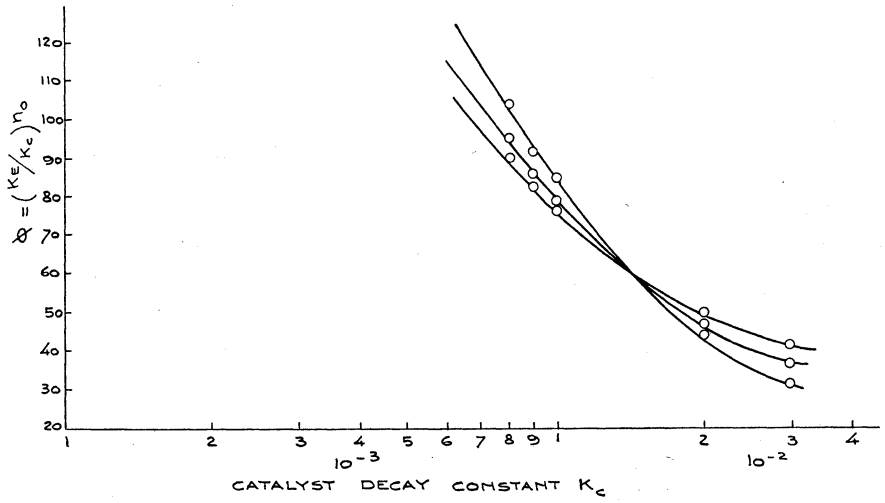

FIG. 8. Estimation of rate constant for catalyst decay.

Can. J. Chem. Downloaded from www.nrcresearchpress.com by 210.87.254.42 on 09/05/12
For personal use only.

Activation Energy for the Polymerization of Ethylene

The initial rate constant of polymerization of ethylene was measured at temperatures of 30° C and 40° C as well as 21° C. (The catalyst in all cases was formed at 21° C.) A plot of the log of the rate constant as a function of reciprocal absolute temperature was drawn. A straight line resulted and the activation energy for the overall polymerization reaction was calculated from the slope. This was found to be approximately 10 kcal/mole in agreement with Badin's (15) value of 10 kcal/mole for the polymerization of ethylene in the catalyst system $TiCl_4$ + $(isobutyl)_3Al$ and Natta's (19) value of 11.7 kcal/mole for a cyclopentadienyl catalyst system.

REFERENCES

1. F. H. C. Edgecombe and D. A. Jardine. Can. J. Chem. **39**, 1728 (1961).
2. K. Casey, F. H. C. Edgecombe, and D. A. Jardine. Analyst, **87**, 835 (1962).
3. F. H. C. Edgecombe and D. A. Jardine. Rev. Sci. Inst. **33**, 240 (1962).
4. C. Van Heerden. J. Polymer Sci. **34**, 21 (1959).
5. A. G. Farbwerke Hoechst. Ger. Patent No. 1,023,766 (1958).
6. A. P. Gray, F. H. C. Edgecombe, and A. B. Callear. Can. J. Chem. In press. 1963.
7. L. Rodriguez, J. Gabant, and B. Hargitay. Tetradedron Letters, **17**, 7 (1959).
8. H. de Vries. Rec. Trav. Chim. **80**, 866 (1961).
9. E. J. Arlmann and J. R. De Jong. Rec. Trav. Chim. **79**, 1319 (1960).
10. C. Beerman and H. Bestian. Angew. Chem. **71**, 618 (1959).
11. P. Cossee. Tetrahedron Letters, **17**, 12 (1960).
12. C. Eden and H. Feilchenfeld. J. Phys. Chem. **64**, 935 (1960).
13. D. B. Ludlum, A. W. Anderson, and C. E. Ashby. J. Am. Chem. Soc. **80**, 1380 (1958).
14. K. Fukui, T. Shimidau, T. Yagi, S. Fukumoto, T. Kagiya, and S. Yuasa. J. Polymer Sci. **55**, 321 (1961).
15. E. J. Badin. J. Am. Chem. Soc. **80**, 6545 (1958).
16. J. C. W. Chien. J. Am. Chem. Soc. **81**, 86 (1959).
17. A. Gilchrist. J. Polymer Sci. **34**, 49 (1959).
18. H. Feilchenfeld and M. Jeselson. J. Phys. Chem. **63**, 720 (1959).
19. G. Natta, I. Pasquen, and E. Grachetti. Makromol. Chem. **24**, 258 (1957).

Can. J. Chem. Downloaded from www.nrcresearchpress.com by 210.87.254.42 on 09/05/12
For personal use only.

NEW CONSIDERATIONS IN ORGANOGERMANIUM-SULPHUR CHEMISTRY[1]

MALCOLM C. HENRY AND WENZEL E. DAVIDSON[2]
Organic Chemistry Laboratory, Pioneering Research Division, U.S. Army Laboratories, Natick, Mass., U.S.A.
Received October 29, 1962

ABSTRACT

The successful synthesis of sodium triphenylgermanethiol (1), $(C_6H_5)_3GeSNa$, and disodium diphenylgermanedithiol, $(C_6H_5)_2Ge(SNa)_2$, have made it possible to carry out reactions with RX type compounds yielding a variety of organogermanium-sulphur compounds. In addition, triphenylgermanethiol, $(C_6H_5)_3GeSH$, has been synthesized for the first time. Reactions of these compounds are related to analogous group IV element compounds. Physical and chemical properties of these new compounds are also discussed.

Although many organogermanium compounds have been prepared within the last 20 years, only relatively few papers (17 out of about 400) have dealt with thiogermanium compounds. Basically two methods are available for synthesizing tetraalkyl- and tetraaryl-thiogermanes (2–6):

$$GeCl_4 + 4NaSR \rightarrow Ge(SR)_4 + 4NaCl$$

$$GeCl_4 \cdot 2C_5H_5N + 4RSH \rightarrow Ge(SR)_4 + 2C_5H_5N \cdot HCl$$

Bis-trialkyl(aryl) sulphides, $R_3GeSGeR_3$, have been prepared by Burschkies (7) by the reaction of substituted monobromogermanes with sodium sulphide. Anderson (8, 9) has synthesized a group of triethylgermanethiol derivatives as follows:

$$Et_3GeOAc + ArSH \rightleftharpoons Et_3GeSAr + HOAc.$$

It should be noted that this method is limited to those cases where the product acid is the most volatile compound of the reaction mixture.

Finally, a few compounds of the types R_2GeS (10–15), $R_2Ge(SCN)_2$ (16), and $(R_2GeS)_2S$ (17), where R is usually an alkyl substituent, have also been reported.

The sparsity of information about this general area of organogermanium chemistry and more specifically about the chemistry of di- and tri-phenylgermanethiol derivatives prompted us to investigate possible methods for preparing these general types of compounds.

RESULTS AND DISCUSSION

Generally considered, organogermanium and organosilicon compounds exhibit rather similar properties. Considerable difference exists, however, between the hydrolytic stability of germanium–sulphur and silicon–sulphur bonds.

Due to the stability of the recently described sodium triphenylgermanethiol, $(C_6H_5)_3GeSNa$ (1), attempts were made to prepare the analogous compounds of the other group IV elements. Sodium triphenylsilanethiol, $(C_6H_5)_3SiSNa$, could not be formed under the preparative conditions used (hydrated sodium sulphide) probably due to

[1]*Presented at the Symposium on Organometallic Compounds, Vancouver, British Columbia, September 4–6, 1962, sponsored by the Inorganic Chemistry Division, Chemical Institute of Canada, and the Department of Chemistry, University of British Columbia, with the support of the National Research Council, Ottawa, in cooperation with the University Extension Department.*

[2]*Research Fellow sponsored by the Germanium Research Committee, New York City.*

Can. J. Chem. Downloaded from www.nrcresearchpress.com by 210.87.254.6 on 09/05/12
For personal use only.

hydrolysis of the initially formed product. Sodium triphenyltinthiol, $(C_6H_5)_3SnSNa$, was prepared and one derivative, $[(C_6H_5)_3SnSGe(C_6H_5)_3]$, prepared from the salt. The initial sodium salt for the case of the tin compound could not be recrystallized and the crude powder was used directly for the subsequent reaction with the RX compound, in this case triphenylbromogermane. Other work in our laboratories (18) has shown that sodium triphenylleadthiol, $(C_6H_5)_3PbSNa$, existed in solution only and was not stable enough to be isolated. Reactions with RX type compounds were carried out in solution, however, and derivatives were prepared to establish the existence of the unstable salt.

Attempts to prepare bis-triphenylgermanium disulphide by halogenation of sodium triphenylgermanethiol failed. Instead a cleavage of the germanium–sulphur bond was observed. Reaction of the sodium salt with sulphonyl chlorides or hydrogen peroxide yielded the bis-triphenylgermanium disulphide, a bright yellow compound melting at 171° C. The reaction is as follows:

$$Ph_3GeSNa + RSO_2Cl \rightarrow [Ph_3GeSSO_2R + NaCl]$$

$$2Ph_3GeSNa + RSO_2Cl \rightarrow Ph_3GeSSGePh_3 + RSO_2Na + NaCl$$

$$(C_6H_5)_3GeSNa \xrightarrow{H_2O_2} (C_6H_5)_3GeSSGe(C_6H_5)_3,$$

where R = $-CH_3$, $-C_6H_4CH_3$-*p*. It is interesting to note that the analogous carbon compound, bis-triphenylmethyl disulphide, $(C_6H_5)_3CSSC(C_6H_5)_3$, is colored only in solution. Analogous silicon, tin, and lead compounds are unknown. The bis-triphenylgermanium trisulphide (obtained by the reaction of sodium triphenylgermanethiol with sulphur chloride, SCl_2 (1)) is slightly yellow.

Etienne's method (19) for the synthesis of triphenylsilanethiol was successfully used for the preparation of the analogous triphenyl germanethiol, $(C_6H_5)_3GeSH$, as follows:

$$(C_6H_5)_3GeBr + H_2S + C_5H_5N \rightarrow (C_6H_5)_3GeSH + C_5H_5N \cdot HBr.$$

This white, crystalline compound is stable in dry air; however, in the presence of moist air a slight hydrogen sulphide odor developed. It is known that triphenylmethylthiol easily splits off hydrogen sulphide in the presence of moisture in contrast to the more stable aliphatic thiols (20).

Oxidation of triphenylgermanethiol with iodine produced bis-triphenylgermanium disulphide as follows:

$$2(C_6H_5)_3GeSH + I_2 \rightarrow (C_6H_5)_3GeSSGe(C_6H_5)_3 + 2HI.$$

Reaction with acrylonitrile under a variety of conditions gave no addition to the carbon–carbon double bond. Instead, bis-triphenylgermanium sulphide was produced along with the evolution of hydrogen sulphide. Similar results were obtained when the thiol was reacted with benzoyl chloride or other halides in the presence of equivalent amounts of pyridine. If pyridine was used as solvent, reactions between the thiol and RX compounds could be carried out without difficulty and the expected products, $(C_6H_5)_3GeSR$, isolated in good yield as follows:

$$(C_6H_5)_3GeSH + RX \xrightarrow{C_5H_5N} (C_6H_5)_3GeSR + HX.$$

Reaction of triphenylgermanethiol with dithiocyanogen, $(SCN)_2$, did not yield the expected sulphur-thiocyanogen compound but rather the simpler germanium-thiocyanogen compound and elemental sulphur. This reaction will be further studied since

Can. J. Chem. Downloaded from www.nrcresearchpress.com by 210.87.254.6 on 09/05/12
For personal use only.

the formation of elemental sulphur indicates that the thiocyanate derivative of triphenylgermanethiol at least existed as an intermediate as follows:

$$(C_6H_5)_3GeSH + (SCN)_2 \rightarrow [(C_6H_5)_3GeSSCN] + HSCN$$
$$\downarrow \text{ decomp.}$$
$$(C_6H_5)_3GeSCN + S^0.$$

Since the syntheses of sodium triphenylgermanethiol and triphenylgermanethiol were reasonably facile and useful for synthesizing a variety of organogermanium derivatives, it was of interest to prepare the corresponding disubstituted compounds, which should lead to interesting polymer-forming materials. The same method used in the synthesis of the monosodium salt was applied with success to diphenyldibromogermane as follows:

$$(C_6H_5)_2GeBr_2 + 2Na_2S \rightarrow (C_6H_5)_2Ge(SNa)_2 + 2NaBr.$$

A white crystalline material was isolated in good yield which, upon examination, turned out to be the trihydrate of disodium diphenylgermanedithiol. This compound is not soluble in benzene but soluble in alcohol, acetone, tetrahydrofuran, and dimethylformamide. The dehydrated product is not as stable as the hydrate and seems to decompose.

Thus far, only a few reactions have been performed with this compound. It reacts with triphenylbromogermane forming the expected, known bis-triphenylgermylthio diphenylgermane, $(C_6H_5)_2Ge[(SGe(C_6H_5)_3]_2$ (1). Reaction of the trihydrate with methyl iodide produced a liquid which according to its infrared spectrum is probably diphenyldimethylthiogermane. Elemental analyses and molecular weight determinations indicate that the compound was not analytically pure.

Benzoyl chloride (and *p*-nitrobenzoyl chloride) react with the trihydrate to form diphenylgermanium sulphide and benzoic acid (*p*-nitrobenzoic acid). It is probable that the halide reacted first with the water of the hydrate to form hydrochloric acid, which then interacted with the sodium salt to form diphenylgermanium sulphide, $[(C_6H_5)_2GeS]_n$. This sulphide exists, as shown by melting points and molecular weight determinations, in both dimeric and trimeric forms:

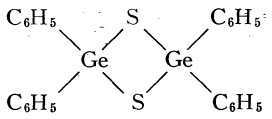

m.p. 203° C

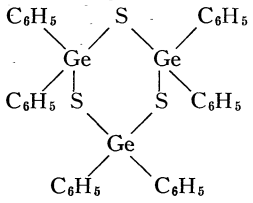

m.p. 170° C

Similar dimers and trimers are known in the case of dialkylsilicon sulphides (21). Diphenylsilicon sulphide is reported to exist only in the dimeric form (22) while analogous organotin and -lead sulphides apparently form only trimers (14). Thus far, there is no evidence for the existence of an open-chain structure of the type

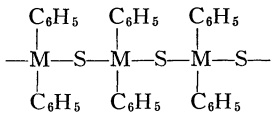

where M = Si, Ge, Sn, or Pb.

Successful attempts to synthesize diphenylgermanedithiol have not been realized. There is some evidence that it may exist in solution; however, it is analogous to carbon-*gem*-thiols and not expected to exhibit a high degree of stability.

Can. J. Chem. Downloaded from www.nrcresearchpress.com by 210.87.254.6 on 09/05/12
For personal use only.

Can. J. Chem. Downloaded from www.nrcresearchpress.com by 210.87.254.6 on 09/05/12
For personal use only.

EXPERIMENTAL

Melting points were carried out on a Kofler hot stage or a Thomas-Hoover melting point apparatus and are uncorrected. Molecular weight determinations were carried out using a Mechrolab vapor pressure osmometer, Model 301A.

Synthesis of Triphenylgermanethiol

Triphenylbromogermane, 10 g, was dissolved together with 2.1 g pyridine in 150 ml benzene in a round-bottom flask. The clear solution was stirred (magnetic stirrer) at room temperature while hydrogen sulphide gas was bubbled through for a period of 90 minutes. A white precipitate (4.1 g) of pyridine hydrobromide formed during the reaction period and was subsequently filtered. The filtrate was evaporated in vacuum at 25–30° C to dryness. A white crystalline substance (8.65 g; 97% yield), m.p. 110–114, remained in the flask. After recrystallization from benzene, there was obtained 7.6 g of white prisms with a yield of 86% pure triphenylgermanethiol. The molecular weight found was 336 (in benzene); calculated 336.88. The infrared spectrum showed the characteristic SH absorption, at 2450 cm^{-1}. Found: Ge, 21.57; S, 9.49; C, 64.08; H, 4.83. Calc. for $C_{18}H_{16}GeS$: Ge, 21.55; S, 9.52; C, 64.10; H, 4.79.

Oxidation of Triphenylgermanethiol with Iodine

A solution of 0.5 g of triphenylgermanethiol dissolved in 25 ml benzene was added to 25 ml distilled water in a separatory funnel. Iodine, 0.19 g, dissolved in 25 ml benzene was added in four parts to the mixture, which was thoroughly agitated after each addition in order to remove the hydrogen iodide as it is formed. The iodine color disappeared after 2 minutes. After separation of the aqueous phase, the benzene solution was washed with 20 ml of 1% sodium hydroxide, 20 ml water, then dried with anhydrous sodium sulphate, filtered, and evaporated in vacuum. A yellow crystalline substance, 0.45 g, with m.p. 160–170° C, was isolated. Recrystallization from toluene yielded 0.25 g yellow, bis-triphenylgermanium disulphide, m.p. 171–172. A mixed melting point with an authentic sample gave no depression.

Reaction of Triphenylgermanethiol with Benzoyl Chloride in Pyridine

Benzoyl chloride, 1.67 g (11.9 mmoles), was added to a stirred solution of triphenylgermanethiol, 4 g (11.9 mmoles), during the course of a few minutes. Heat was evolved and the solution turned slightly yellow. It was stirred 30 minutes and then evaporated in vacuum. The residue was dissolved in 20 ml benzene and transferred into a separatory funnel. To remove the last traces of pyridine, the benzene solution was extracted twice with dilute sulphuric acid (1–2%), then washed twice with water. After the benzene phase had been dried with anhydrous sodium sulphate, it was filtered and again evaporated in vacuum. Yield: 4.7 g of crude benzoylthiophenylgermane (90%). It was recrystallized from petroleum ether (60–110°) and yielded 3.7 g of the pure compound (70%), m.p. 145.5° C.

Reaction of Triphenylgermanethiol with Thiocyanogen

*(1) Preparation of $(SCN)_2$ (Lit.: H. Lecher and K. Simon. Ber. **54**, 632 (1921))*

One milliliter bromine was dissolved in 150 ml of ice-cold ether (anhydrous), and 7.5 g lead thiocyanate was added immediately. The mixture was stirred until the bromine color disappeared (about 30 minutes), the solution filtered into a round-bottom flask, and the filtrate washed with 20 ml ether.

(2) Reaction of Triphenylgermanethiol with the $(SCN)_2$ Solution

A solution of 6.2 g triphenylgermanethiol in 30 ml ether was added rapidly to the stirred $(SCN)_2$ solution. After 15 minutes, the clear solution was evaporated in vacuum at normal temperature and the slightly yellow residue (m.p. 100–105°) was recrystallized from petroleum ether 60–110°. Yield: 3.8 g white crystals, m.p. 105°. From the filtrate an additional 0.8 g was isolated and about 150 mg of bright yellow crystals which were identified as elemental sulphur. Yield: 68% for $(C_6H_5)_3GeSCN$. Analysis: Calc. for $(C_6H_5)_3GeSCN$: Ge, 20.00; S, 8.85; C, 63.10; H, 4.18. Found: S, 9.04; C, 62.90; H, 4.20. Mol. wt.: Calc.: 362. Found: 352.

A heated aqueous suspension of the compound with ferric ion gave the characteristic red color of ferric thiocyanate.

Preparation of the Thiocyanate from the Reaction of Triphenylgermaniumbromide with Leadthiocyanate

One gram $(C_6H_5)_3GeBr$ was stirred with a suspension of 2 g lead thiocyanate in benzene (20 ml) for 1 hour. It was filtered, the filtrate evaporated, and the residue recrystallized from petroleum ether 60–110°. Yield: 0.4 g (42%) white crystals, m.p. 105°. Mixed m.p. 105° (with $(C_6H_5)_3GeSCN$). (The filtrate was discarded.)

Synthesis of Disodium Diphenylgermanedithiol, $(C_6H_5)_2Ge(SNa)_2 \cdot 3H_2O$

Diphenyldibromogermane, 5 g (16 mmoles), dissolved in 25 ml of benzene, was added dropwise over a 30-minute period into a round-bottom flask (cooled in an ice bath) containing an alcoholic suspension of sodium sulphide pentahydrate, 10 g (60 mmoles). The solution was stirred for 1 hour and filtered. The filtrate was evaporated to dryness, leaving a slightly yellow residue (12.5 g), which was extracted with 40 ml benzene at room temperature for 30 minutes. After filtration and a final washing of the insoluble residue with an

additional 15 ml of benzene, the combined filtrates were evaporated to about a 20-ml volume. Shiny crystalline plates formed upon standing. Filtration of the crystals and washing with small amounts of benzene resulted in more crystals being formed in the filtrate. In this manner, a second and third crop of crystals could be collected. (Yield based on total three fractions, 4 g (79%). Final evaporation of the filtrate yielded a yellow "oil like" residue. These fractions are all transparent crystalline plates soluble in alcohol and water with a strong alkaline reaction, insoluble in benzene, hexane, heptane, carbon tetrachloride, and petroleum ether. In addition, there was no melting point up to 330° C. Attempts at recrystallization by dissolution in alcohol and addition of benzene or petroleum ether were not successful.

Analytical Results and Conclusions

Elemental analyses of the disodium diphenylgermanedithiol were as follows: Calc. for $(C_6H_5)_2Ge(SNa)_2$: C, 42.80; S, 19.02; H, 2.99. Found: C, 36.60; S, 16.12; H, 4.25.

As a result of the above analyses and because the S:C ratio in the analyzed product is 1:6 in agreement with the proposed disodium diphenylgermanedithiol, we suspected that the compound contained water of hydration. Therefore, 0.4549 g of the compound was stored for 2 days in a vacuum desiccator over phosphorus pentoxide. During this period the crystals lost 0.0608 g of weight, an amount equal to a 13.4% weight loss. Further standing produced no additional weight loss. The theoretical amount of water in disodium diphenylgermanedithiol trihydrate is 13.5%.

Thus, upon re-examination of the analytical data, based upon a trihydrate, it appeared that this compound was the stable organogermanium trihydrate. Calc. for $(C_6H_5)_2Ge(SNa)_2 \cdot 3H_2O$: C, 36.90; S, 16.35; H, 4.10.

Reaction with Diphenyldibromogermane

One gram of the trihydrate was dissolved in 20 ml ethanol, and 0.99 g diphenyldibromogermane dissolved in 20 ml benzene was added. The mixture was stirred for 1 hour. A white crystalline precipitate appeared and H_2S was developed. The mixture was evaporated in vacuum, the residue extracted with benzene, filtered, and again evaporated to yield 1.44 g of product with m.p. 165–197° C. After two recrystallizations from benzene, two fractions were isolated.

Fraction 1.—0.3 g fine needles, m.p. 198.5–200.5°. Mol. wt. found: 516 (benzene); 531 (chloroform). Theoretical molecular weight based on dimer: 517.7.

Fraction 2.—0.3 g small plates with m.p. 170–173°. Mol. wt. found: 754 (benzene); 774 (chloroform). Theoretical mol. wt. calculated for trimer: 776.

Reaction with Triphenylbromogermane

A solution of 229.5 mg of triphenylbromogermane was added to a solution of 100 mg of disodium diphenylgermanedithiol trihydrate dissolved in 20 ml of absolute alcohol. The mixture was stirred for 90 minutes and then evaporated to dryness. The residue was extracted with boiling benzene and cooled. The crystals which separated were identified as bis-triphenylgermylthio diphenylgermane by melting point and mixed melting point with an authentic sample, 162° C.

ACKNOWLEDGMENT

The authors are grateful to C. DiPietro of these laboratories for the microanalyses.

REFERENCES

1. M. C. Henry and W. E. Davidson. J. Org. Chem. **27**, 2252 (1962).
2. E. W. Abel. J. Chem. Soc. 3746 (1958).
3. H. J. Backer and F. Stienstra. Rec. Trav. Chim. **52**, 1033 (1933); **54**, 607 (1935).
4. E. Krause and G. Renwanz. Ber. **65**, 777 (1932).
5. R. Schwarz and W. Reinhardt. Ber. **65**, 1743 (1932).
6. G. K. Teal. Thesis, Brown University, Providence, R.I. May, 1931.
7. K. Burschkies. Ber. **69**, 1143 (1936).
8. H. H. Anderson. J. Am. Chem. Soc. **72**, 2089 (1950).
9. H. H. Anderson. J. Org. Chem. **21**, 869 (1956).
10. H. H. Anderson. J. Am. Chem. Soc. **78**, 1692 (1956).
11. Brit. Thomson-Houston Co. Ltd. Brit. Patent No. 654,571; Chem. Abstr. **46**, 45616 (1952).
12. E. G. Rochow. U.S. Patent No. 2,506,386 (May 2, 1950).
13. E. G. Rochow. J. Am. Chem. Soc. **72**, 198 (1950).
14. W. T. Reichle. J. Org. Chem. **26**, 4634 (1961).
15. R. West. J. Am. Chem. Soc. **75**, 6080 (1953).
16. E. G. Rochow and J. Allred. J. Am. Chem. Soc. **77**, 4489 (1955).
17. M. Rothermundt and K. Burschkies. Z. Immunitätsforsch. **87**, 445 (1932).
18. M. C. Henry and A. W. Krebs. J. Org. Chem. **28**, 225 (1963).
19. Y. Etienne. Bull. Soc. Chim. France, 791 (1953).
20. D. Vorländer and E. Mittag. Ber. **46**, 3450 (1913); **52**, 412 (1919).
21. Gmelins Handbuch der anorganischen Chemie, Band Si (C). 8th ed. 1958. p. 305.
22. L. S. Moody. General Electric Co., U.S. Patent No. 2,567,724 (1951); Chem. Abstr. **145**, 7534 (1953).

Can. J. Chem. Downloaded from www.nrcresearchpress.com by 210.87.254.6 on 09/05/12
For personal use only.

THE ELECTRONIC STRUCTURES AND REACTIVITIES OF $Mn(CO)_5X$ COMPLEXES[1, 2]

HARRY B. GRAY AND ERNST BILLIG
Department of Chemistry, Columbia University, New York, N. Y., U.S.A.
AND
ANDREW WOJCICKI AND M. FARONA
Department of Chemistry, Ohio State University, Columbus, Ohio, U.S.A.

Received November 15, 1962

ABSTRACT

The bonding in $Mn(CO)_5X$ complexes is described in terms of molecular orbitals. The axial CO group is assumed to be bonded much more strongly to Mn than the other four CO groups. The molecular orbital energy level scheme thus derived successfully accounts for the principal features of the electronic spectra of $Mn(CO)_5X$ complexes in different solvents. The first charge transfer band is assigned as an $n(Mn) \rightarrow \pi^*(CO)$ type transition. This $n \rightarrow \pi^*$ assignment is supported by the fact that the maximum of the band for $Mn(CO)_5Br$ is shifted to higher energies on increasing the polarity of the solvents employed.

Kinetic studies of $Mn(CO)_5X$–^{14}CO exchange reveal that the axial CO is more inert than the other four CO groups; also, the rates of ^{14}CO exchange of the four equivalent CO groups in $Mn(CO)_5X$ complexes depend strikingly on the nature of the X^- ligand. A consistent interpretation of the above results and the observed kinetics of some typical substitution reactions of $Mn(CO)_5X$ complexes is presented in terms of the derived electronic structural description.

Carbon monoxide, cyanide ion, and nitric oxide form the simplest transition metal complexes in which π-bonding involving empty π-antibonding ligand molecular orbitals is an important part of the overall electronic structural description. The $Mn(CO)_5X$ complexes (X = Cl, Br, I, NO_3, CH_3, etc.) are of particular interest since they are representative of the important class of metal carbonyls and nitrosyls which have a distorted octahedral structure with one particularly strong metal–ligand bond (1).

This paper presents a molecular orbital description of the electronic structures of the $Mn(CO)_5X$ complexes. The spectral properties and chemical reactivities of the complexes are discussed in terms of the derived molecular orbital energy level scheme.

MOLECULAR ORBITALS FOR $Mn(CO)_5X$ COMPLEXES

The $Mn(CO)_5X$ complexes have a distorted octahedral structure (C_{4v}), as shown in Fig. 1. Both infrared (2) and kinetic studies (3, 4, 5) (*vide infra*) indicate that the axial CO is bound considerably more tightly to Mn than the four CO's in the *xy* plane. This implies that there is more [Mn—C]O π-bonding for the axial CO, with the result that the Mn—C(5) distance is shorter than Mn—C(1–4), and the C—O(5) distance is longer than C—O(1–4).

The orbital transformation scheme for the C_{4v} symmetry is summarized in Table I. The general bonding scheme is rather complicated, since all metal and ligand orbitals of the same symmetry may interact. However, it is useful to describe the principal features of the electronic structure.

There is a strong σ-bond between the Mn and CO(5), involving mainly the $(3d_{z^2}+4s)$ metal orbital combination and the carbon $2s$ and $2p_z$ orbitals. The π-bonding between Mn

[1] *Presented at the Symposium on Organometallic Compounds, Vancouver, British Columbia, September 4–6, 1962, sponsored by the Inorganic Chemistry Division, Chemical Institute of Canada, and the Department of Chemistry, University of British Columbia, with the support of the National Research Council, Ottawa, in cooperation with the University Extension Department.*

[2] *Acknowledgment is made to the donors of the Petroleum Research Fund, administered by the American Chemical Society, for partial support of this research.*

Can. J. Chem. Downloaded from www.nrcresearchpress.com by 210.87.254.40 on 09/05/12
For personal use only.

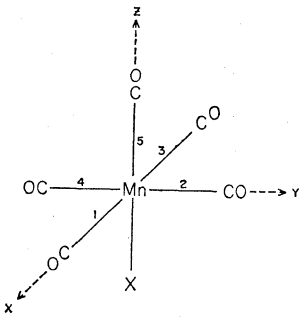

FIG. 1. Structure of $Mn(CO)_5X$.

TABLE I

Orbital transformation scheme for $Mn(CO)_5X$ complexes with C_{4v} symmetry

		Ligand orbital totals	
Representation	Mn orbitals	σ	π
a_1	$3d_{z^2}$, $4s$, $4p$	3	1
a_2	—	—	1
b_1	$3d_{x^2-y^2}$	1	1
b_2	$3d_{xy}$	—	1
e	($3d_{xz}$, $3d_{yz}$) ($4p_x$, $4p_y$)	1	4

and CO(5) involves mainly the metal $3d_{xz}$, $3d_{yz}$, and the CO(5) π-bonding (π^b) and π-antibonding (π^*) molecular orbitals. The $4p_x$, $4p_y$ metal orbitals may also interact in this π-molecular orbital system to some extent, although they participate mainly in σ-bonding. This Mn—CO(5) π-interaction yields one strongly bonding, one virtually nonbonding, and two antibonding molecular orbitals.

The four σ-bonds between Mn and the four CO's in the xy plane are formed using the $(4s-3d_{z^2})$, $3d_{x^2-y^2}$, $4p_x$, and $4p_y$ metal orbitals and the $(2s+2p_z)$ carbon orbitals. The metal $4p_z$ orbital may be used to σ-bond with the σ-orbital of the axial X^- ligand.

For π-bonding purposes the four CO's in the xy plane have exclusive claim only to the $3d_{xy}$ metal orbital. The other metal orbitals of the right symmetry for π-bonding with the planar CO's ($4p_x$, $4p_y$, $4p_z$, $3d_{xy}$, $3d_{yz}$) all are involved either in σ-bonding ($4p_x$, $4p_y$, $4p_z$) or stronger π-bonding ($3d_{xy}$, $3d_{yz}$). The p_x, p_y π-orbitals of the X^- ligand may interact with the $3d_{xz}$, $3d_{yz}$ metal orbitals. As a result, the nonbonding π-molecular orbital (mostly composed of the Mn $3d_{xz}$, $3d_{yz}$) from the Mn—CO(5) π-system is made more unstable, while the π-molecular orbital mostly localized on the X^- ligand is made slightly bonding.

The single electron molecular orbital energy level scheme for the bonding situation described above is shown in Fig. 2. Coulomb energies are taken in the order

$$\sigma(CO,X) < \pi^b(CO) < \pi(X) < 3d < 4s < \pi^*[CO(5)] < \pi^*[CO(1\text{–}4)] < 4p.$$

The π^*[CO(5)], π^*[CO(1–4)] energy order is taken consistent with the infrared (2) and kinetic evidence (3, 4, 5) (*vide infra*). To simplify the diagram (Fig. 2), all the single electron π^b and π^* molecular orbitals mostly localized on the planar CO's are grouped together in a box and are indicated as [π^b, CO(1–4)] and [π^*, CO(1–4)], respectively.

Can. J. Chem. Downloaded from www.nrcresearchpress.com by 210.87.254.40 on 09/05/12
For personal use only.

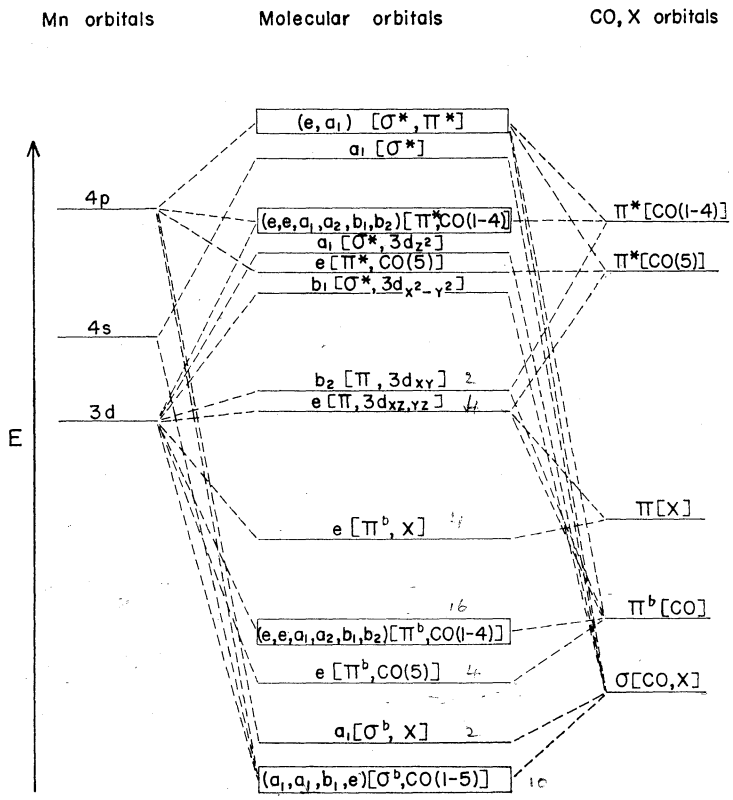

FIG. 2. Single electron molecular energy level scheme for $Mn(CO)_5X$.

ELECTRONIC SPECTRA OF $Mn(CO)_5X$ COMPLEXES

A $Mn(CO)_5X$ complex contains Mn^+ ($3d^6$), five CO's (10 σ, 20 π^b electrons), and one X^- (2 σ, 4 π electrons). Thus a total of 42 electrons are assigned to the single electron molecular orbital level scheme. The ground state is $[\sigma^b, CO(1\text{–}5)]^{10}[\sigma^b, X]^2[\pi^b, CO(5)]^4$-$[\pi^b, CO(1\text{–}4)]^{16}[\pi^b, X]^4[\pi, 3d_{xz,yz}]^4[\pi^*, 3d_{xy}]^2 = {}^1A_1$. The electronic transitions of lowest energy fall into five categories and will be considered separately. In order to estimate the energy range of each type of transition it is necessary to have values for some of the coulomb energies. These values (with references) are given in Table II.

A. Transitions Mostly Localized on the Central Mn, or the d–d transitions

These are the transitions

$$b_2[\pi^*, 3d_{xy}] \rightarrow b_1[\sigma^*, 3d_{x^2-y^2}] \ ({}^1A_1 \rightarrow {}^1A_2),$$
$$b_2[\pi^*, 3d_{xy}] \rightarrow a_1[\sigma^*, 3d_{z^2}] \ ({}^1A_1 \rightarrow {}^1B_2),$$
$$e[\pi, 3d_{xz,yz}] \rightarrow b_1[\sigma^*, 3d_{x^2-y^2}] \ ({}^1A_1 \rightarrow {}^1E),$$
$$e[\pi, 3d_{xz,yz}] \rightarrow a_1[\sigma^*, 3d_{z^2}] \ ({}^1A_1 \rightarrow {}^1E).$$

Since the value (6) of the d–d splitting parameter Δ for $Cr(CO)_6$ is considerably greater than 30,000 cm^{-1}, 30,000 cm^{-1} will be taken as a lower limit for Δ in the $Mn(CO)_5X$ complexes. Therefore the d–d bands for $Mn(CO)_5X$ complexes may reasonably be expected to appear at such high energies that they will be masked by charge transfer bands.

Can. J. Chem. Downloaded from www.nrcresearchpress.com by 210.87.254.40 on 09/05/12
For personal use only.

TABLE II
Estimated orbital energies for $Mn(CO)_5X$ complexes

Orbital	Energy (cm^{-1})
$3d$(Mn)	− 70,000[a]
	− 85,000 (I)[b]
π(X)	− 90,000 (Br)[b]
	− 95,000(Cl)[b]
π^b[CO(1–4)]	−110,000[c]
π^*[CO(5)]	− 40,000[d]
π^*[CO(1–4)]	− 30,000[d]

[a]Data for Mn(I) from Moore (C. E. Moore. Atomic energy levels. U.S. Natl. Bur. Std. Circ. 467. 1949 and 1952).
[b]Ionization potentials corrected for the estimated residual negative charges, −0.25 (Cl), −0.20 (Br), and −0.15 (I).
[c]Ionization potential of CO from Field and Franklin (F. H. Field and J. L. Franklin. Electron impact phenomena. Academic Press, New York. 1957. p. 280), which gives an upper limit for the orbital energy.
[d]From spectroscopic data, see G. Herzberg, Spectra of diatomic molecules, Van Nostrand, New York, 1950, p. 452; π^* level for CO(5) is estimated to be 10,000 cm^{-1} more stable than π^* for CO(1–4), in agreement with kinetic and infrared evidence.

B. Charge Transfer from X to Mn

The first such transition would be $e[\pi^b, X] \rightarrow b_1[\sigma^*, 3d_{x^2-y^2}]$ ($^1A_1 \rightarrow {}^1E$). The energy of this transition is expected to fall in the range 50,000–60,000 cm^{-1}, considering that the $e[\pi^b, X]$ is more stable than −85,000 cm^{-1}. The next transition is $e[\pi^b, X] \rightarrow a_1[\sigma^*, 3d_z]$ ($^1A_1 \rightarrow {}^1E$), of even higher energy.

C. Charge Transfer from π^b Molecular Orbitals Mostly Localized on the CO's to Mn

The lowest-energy transitions of this type would be $(e,e,a_1,a_2,b_1,b_2)[\pi^b, CO(1–4)] \rightarrow b_1[\sigma^*, 3d_{x^2-y^2}]$ ($^1A_1 \rightarrow {}^1E$, ^1E, $^1B_1$, $^1B_2$, $^1A_1$, $^1A_2$), calculated to appear in the range 70,000–80,000 cm^{-1}.

D. Charge Transfer from Mn to π^* Molecular Orbitals Mostly Localized on the CO's

The lowest-energy transition is $b_2[\pi^*, 3d_{xy}] \rightarrow e[\pi^*, CO(5)]$ ($^1A_1 \rightarrow {}^1E$), estimated at about 30,000 cm^{-1}. There are a number of excited states at slightly higher energies, due to the transitions $e[\pi, 3d_{xz,yz}] \rightarrow e[\pi^*, CO(5)]$ ($^1A_1 \rightarrow {}^1A_1$, $^1A_2$, $^1B_1$, $^1B_2$) and $b_2[\pi^*, 3d_{xy}] \rightarrow (e,e,a_1,a_2,b_1,b_2)[\pi^*, CO(1–4)]$ ($^1A_1 \rightarrow {}^1E$, ^1E, $^1B_1$, $^1B_2$, $^1A_1$, $^1A_2$). The highest-energy excited states of the $Mn \rightarrow CO(\pi^*)$ type are due to the transition $e[\pi, 3d_{xz,yz}] \rightarrow (e,e,a_1, a_2,b_1,b_2)[\pi^*, CO(1–4)]$ ($^1A_1 \rightarrow {}^1A_1$, $^1A_2$, $^1B_1$, $^1B_2$, $^1A_1$, $^1A_2$, $^1B_1$, $^1B_2$, ^1E, ^1E, ^1E, ^1E) and are expected to appear around 45,000 cm^{-1}.

E. Charge Transfer from X to π^* Molecular Orbitals Mostly Localized on the CO's

The first transition of this type is $e[\pi^b, X] \rightarrow e[\pi^*, CO(5)]$ ($^1A_1 \rightarrow {}^1A_1$, $^1A_2$, $^1B_1$, $^1B_2$), expected to appear at about 50,000 cm^{-1}.

A summary of these transitions and their expected energies is given in Table III.

The electronic spectra of $Mn(CO)_5X$ complexes (X = Cl, Br, I) show two bands below 50,000 cm^{-1}, one in the 43,000–50,000 cm^{-1} and one in the 25,000 cm^{-1} region. These spectra are given in Table IV. It is clear from the discussion above that $Mn[3d(\pi^*)] \rightarrow CO(\pi^*)$ charge transfer will appear at lowest energy, and thus the two bands are assigned as follows: 25,000 cm^{-1} band: $b_2[\pi^*, 3d_{xy}] \rightarrow e[\pi^*, CO(5)]$ ($^1A_1 \rightarrow {}^1E$); 43,000–50,000 cm^{-1} band: $e[\pi, 3d_{xz,yz}] \rightarrow (e,e,a_1,a_2,b_1,b_2)[\pi^*, CO(1–4)]$ ($^1A_1 \rightarrow {}^1A_1$, $^1A_2$, $^1B_1$, $^1B_2$, $^1A_1$, $^1A_2$, $^1B_1$, $^1B_2$, ^1E, ^1E, ^1E, ^1E). The 25,000 cm^{-1} band in $Mn(CO)_5X$ complexes may be considered as being related to the 35,780 cm^{-1} band ($^1A_{1g} \rightarrow {}^1T_{1u}{}^{(1)}$) in $Cr(CO)_6$,

Can. J. Chem. Downloaded from www.nrcresearchpress.com by 210.87.254.40 on 09/05/12
For personal use only.

TABLE III

Electronic transitions for $Mn(CO)_5X$ complexes

	Transition type	Energy expected (cm^{-1})
A.	$Mn[3d(\pi^*)] \rightarrow Mn[3d(\sigma^*)]$	30,000–40,000
B.	$X[\pi^b] \rightarrow Mn[3d(\sigma^*)]$ charge transfer	50,000–60,000
C.	$CO[\pi^b] \rightarrow Mn[3d(\sigma^*)]$ charge transfer	70,000–80,000
D.	$Mn[3d(\pi^*)] \rightarrow CO[\pi^*]$ charge transfer	30,000–45,000
E.	$X[\pi^b] \rightarrow CO[\pi^*]$ charge transfer	50,000–60,000

TABLE IV

Electronic Spectra of $Mn(CO)_5X$ Complexes

	Band assignments—maxima reported in cm^{-1}		
Complex	$[\pi^*, 3d_{xy}] \rightarrow [\pi^*, CO(5)]$	$[\pi, 3d_{xy,yz}] \rightarrow [\pi^*, CO(1-4)]$	$[\pi^b, X] \rightarrow [\sigma^*, 3d_{x^2-y^2}], [\pi^*, CO(5)]$
$Mn(CO)_5Cl$	26,520 (ϵ = 620)[a]	49,600 (ϵ = 25,000)[b]	> 52,500[b]
$Mn(CO)_5Br$	25,870 (ϵ = 420)[a]	44,200 (ϵ = 15,000)[b]	> 52,500[b]
$Mn(CO)_5I$	24,750 (ϵ = 390)[a]	43,480 (ϵ = 19,800)[b]	48,830 (ϵ = 44,600)[b]
$Mn(CO)_5ONO_2$	26,670 (ϵ = 1200)[a]	[c]	[c]

[a]In chloroform solution. Values agree with those of Addison *et al.* (C. C. Addison, M. Kilner, and A. Wojcicki. J. Chem. Soc. 4839 (1961)).
[b]In cyclohexane solution. Spectra taken with a Cary 14 spectrophotometer.
[c]Not measured above 30,000 cm^{-1}.

just as the 43,000–50,000 cm^{-1} $Mn(CO)_5X$ band may be related to the 44,480 cm^{-1} band ($^1A_{1g} \rightarrow {}^1T_{1u}{}^{(2)}$) in $Cr(CO)_6$ (6).

The assignment of the 25,000 cm^{-1} band as due to a charge transfer transition is supported by the sensitivity of the band maxima to solvent changes (1). No appreciable solvent shift would be expected for a *d–d* transition. The large intensity of the 43,000–50,000 cm^{-1} band is consistent with a charge transfer process.

The bands due to the transitions $b_2[\pi^*, 3d_{xy}] \rightarrow (e,e,a_1,a_2,b_1,b_2)[\pi^*, CO(1-4)]$ and $e[\pi, 3d_{xz,yz}] \rightarrow e[\pi^*, CO(5)]$ probably do not differ appreciably in energy from the observed high- and low-energy bands and consequently are not resolved, or, more likely, are simply buried under the intense 43,000–50,000 cm^{-1} band.

A third band, at 48,830 cm^{-1}, is observed for the $Mn(CO)_5I$ complex. This band is assigned as a combination of $I[\pi^b] \rightarrow Mn[3d(\sigma^*)]$ and $I[\pi^b] \rightarrow CO(5)[\pi^*]$ charge transfer. Of the complexes investigated, the $Mn(CO)_5I$ complex would be expected to show this type of charge transfer at the lowest energy (ca. 50,000 cm^{-1} estimated—see Table III). The fact that this band obviously lies at considerably higher energies in $Mn(CO)_5Cl$ and $Mn(CO)_5Br$ strongly supports the assignment.

INFRARED SPECTRA OF $Mn(CO)_5X$ COMPLEXES

The $Mn(CO)_5X$ complexes show three bands in the 2000 cm^{-1} infrared region. The vibrations in $Mn(CO)_5X$ expected to appear with some intensity in the 2000 cm^{-1} region are

$$Mn\text{—}\overleftarrow{C}\text{—}\overrightarrow{O}(5)\ A_1{}^{(1)}$$

$$Mn\text{—}\overleftarrow{C}\text{—}\overrightarrow{O}(1\text{–}4)\ A_1{}^{(2)}$$

$$(1)\overrightarrow{O}\text{—}\overleftarrow{C}\text{—}Mn\text{—}\overleftarrow{C}\text{—}\overrightarrow{O}(3)\ E$$

$$(2)\overrightarrow{O}\text{—}\overleftarrow{C}\text{—}Mn\text{—}\overleftarrow{C}\text{—}\overrightarrow{O}(4)$$

Can. J. Chem. Downloaded from www.nrcresearchpress.com by 210.87.254.40 on 09/05/12
For personal use only.

The expected intensities are $E > A_1^{(1)} \gg A_1^{(2)}$; this feature is discussed by Orgel (2).

The infrared spectra and assignments for the $Mn(CO)_5X$ complexes are given in Table V. In all cases, the $A_1^{(1)}$ vibration occurs at the lowest energy, indicating that

TABLE V

Infrared spectra of $Mn(CO)_5X$ complexes[a]

Complex	Vibration[b]		
	$A_1^{(1)}$	$A_1^{(2)}$	E
$Mn(CO)_5Cl$	2005	2145	2055
$Mn(CO)_5Br$	2010	2140	2050
$Mn(CO)_5I$[c]	2017	2136	2056

[a]Similar spectra have been obtained in cyclohexane and carbon tetrachloride solutions. See ref. 7.
[b]In chloroform solutions. Intensities are in the order $E > A_1^{(1)} \gg A_1^{(2)}$. All spectra taken using a Perkin–Elmer Model 421 spectrophotometer.
[c]From Abel *et al.* (E. W. Abel, M. H. Bennett, and G. Wilkinson. Chem. Ind. (London), 441 (1960)).

CO(5) has lower bond order than CO(1–4). In terms of the molecular orbital bonding scheme, this means that the π^*[CO(5)] orbitals participate more than the π^*[CO(1–4)] orbitals in the π-molecular orbitals mostly localized on Mn. This is, of course, just the result that was used as a guide earlier.

REACTIONS OF $Mn(CO)_5X$ COMPLEXES

The discussion of reactions of $Mn(CO)_5X$ complexes will be divided into two parts: carbon monoxide exchange reactions and substitution reactions involving displacement of CO.

A. Carbon Monoxide Exchange Reactions

The kinetics and mechanism of carbon monoxide exchange with $Mn(CO)_5X$ (X = Cl, Br, and I) were reported earlier (3); the kinetic data are summarized in Table VI. Three

TABLE VI

Rates of equatorial CO exchange in $Mn(CO)_5X$ in toluene at 31.8° C[a]

Complex	$k \times 10^4$ (sec^{-1})
$Mn(CO)_5Cl$	30
$Mn(CO)_5Br$	1.2
$Mn(CO)_5I$	0.15

[a]From ref. 3.

definite conclusions can be drawn: (1) at 31.8° C and in toluene, one carbon monoxide exchanges more slowly than do the other four, (2) the rate of exchange of the four CO's does not depend on the concentration of carbon monoxide, and (3) the rate of CO exchange depends on X, with $Mn(CO)_5Cl > Mn(CO)_5Br > Mn(CO)_5I$.

That four CO's exchange faster than the fifth is consistent with the molecular orbital bonding scheme for $Mn(CO)_5X$. There is more [Mn—C]O π-bonding for the axial CO, and since exchange proceeds by dissociation, the nonequivalence with respect to exchange of the five carbon monoxides is to be expected. Furthermore, the results indicate that the

Can. J. Chem. Downloaded from www.nrcresearchpress.com by 210.87.254.40 on 09/05/12
For personal use only.

active intermediate with reduced coordination number must contain nonequivalent carbonyls in order to account for the experimental observations.

The relative rates of exchange of the four equatorial CO's at 31.8° C are in the order 200:8:1 for $Mn(CO)_5Cl$, $Mn(CO)_5Br$, and $Mn(CO)_5I$, respectively. This order is consistent with the ultraviolet and infrared spectra. The transition $e[\pi, 3d_{xz,yz}] \rightarrow (e,e,a_1,a_2, b_1,b_2)[\pi^*, CO(1\text{–}4)]$ occurs at 49,600 cm^{-1} for $Mn(CO)_5Cl$, 44,200 cm^{-1} for $Mn(CO)_5Br$, and 43,480 cm^{-1} for $Mn(CO)_5I$. The energies of these electronic transitions indicate that the $e[\pi, 3d_{xz,yz}] \rightarrow (e,e,a_1,a_2,b_1,b_2)[\pi^*, CO(1\text{–}4)]$ separation is greatest for the chloride and smallest for the iodide. This is to be expected since highest π-polarizability of the iodide ion raises the energy of its $e[\pi, 3d_{xz,yz}]$ orbitals with respect to those of the bromide and chloride complexes. Thus, $\pi^*[CO(1\text{–}4)]$ participation is greatest with the iodide and least with the chloride, which effectively means strongest equatorial Mn—CO bonds for $Mn(CO)_5I$.

The infrared spectra of $Mn(CO)_5X$ complexes show that the frequency of the $A_1^{(2)}$ carbon–oxygen vibrational mode decreases from the chloride to the iodide (see Table V). This is consistent with stronger Mn—C equatorial bonds in the carbonyl iodide.

Recently, Hieber and Wollmann (4) showed that if the CO exchange is carried out at higher temperatures (40° C, benzene solvent) somewhat different results are obtained. With the chloride and bromide, all five CO's exchange, four faster than the fifth, as evidenced by a nonlinear semilogarithmic plot of the data. However, with the iodide, all five CO's seem to exchange at about the same rate. Approximate relative rates of exchange of the four equatorial CO's are 110:9:1 for the chloride, bromide, and iodide, respectively.

These results can be explained on the basis of the infrared spectra and values of activation energy for dissociation of equatorial carbonyls in these compounds, obtained by Angelici and Basolo (5). These values are 27.4, 29.8, and 32.2 kcal, for the chloride, bromide, and iodide, respectively, consistent with the order of reactivity of these complexes. The infrared spectra indicate that all axial CO's are bound more tightly than the equatorial CO's and that the axial Mn—C bond is strongest in $Mn(CO)_5Cl$ and weakest in $Mn(CO)_5I$. Thus activation energies for dissociation of the fifth CO are higher than those for the planar carbonyls and probably follow the reverse trend, that is, the chloride would have the highest activation energy. Therefore, it is possible that at a higher temperature the rates of exchange of two different kinds of CO's in the iodide become comparable, whereas in the chloride and bromide, nonequivalence is still observed.

B. Substitution Reactions

That the axial CO's are bonded more strongly than the four equatorial CO's is further supported by recent kinetic studies of Angelici and Basolo (5). The results are summarized in Table VII.

Many tertiary phosphines, arsines, and stibines, as well as phosphites and pyridine react with $Mn(CO)_5X$ according to the equation

$$Mn(CO)_5X + L \rightarrow Mn(CO)_4LX + CO,$$

where L is one of the above neutral ligands. With some ligands L the reaction proceeds further to yield disubstituted products, $Mn(CO)_3L_2X$.

Kinetic studies of the former reaction show that the formation of monosubstituted products is independent of the nature and concentration of the entering ligand, but depends on the first power of the $Mn(CO)_5X$ concentration. Thus, a dissociative (S_N1) mechanism has been proposed.

Can. J. Chem. Downloaded from www.nrcresearchpress.com by 210.87.254.40 on 09/05/12
For personal use only.

TABLE VII

Rates of reaction of $Mn(CO)_5X$ with various ligands in chloroform[a]

$$Mn(CO)_5X + L \rightarrow Mn(CO)_4LX + CO$$

Complex	Concentration (mole/liter) $Mn(CO)_5X$	Concentration (mole/liter) L	Ligand L	Temp. (°C)	$k \times 10^{-5}$ (sec^{-1})
$Mn(CO)_5Cl$	0.0199	0.224	$As(C_6H_5)_3$	30.2	59.2
	0.0218	0.243	$P(OC_4H_9)_3$	30.2	65.0
	0.0190	0.232	C_5H_5N	30.2	61.6
$Mn(CO)_5Br$	0.0301	0.133	$P(C_6H_5)_3$	30.1	6.67
	0.0301	0.387	$As(C_6H_5)_3$	30.1	6.59
	0.0297	0.135	$Sb(C_6H_5)_3$	30.1	6.59
			$P(C_6H_5)_3$	31.8	13[b]
			C_5H_5N	31.8	13[b]
$Mn(CO)_5I$	0.0171	0.208	$As(C_6H_5)_3$	35.1	0.824
	0.0175	0.203	$P(C_6H_5)_3$	35.1	0.844

[a]From ref. 5.
[b]In toluene; concentrations of $Mn(CO)_5Br$ and L were not specified. See ref. 5.

Since the rate of replacement of CO by L is the same as the rate of exchange of the four equatorial carbon monoxides, it follows that L enters an equatorial position. Thus, the structure of monosubstituted products must be

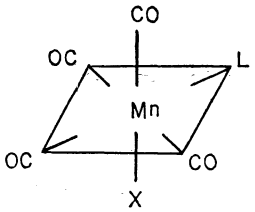

As before, the rate of replacement of CO is affected by the nature of X, with $Mn(CO)_5Cl > Mn(CO)_5Br > Mn(CO)_5I$. Such an order is to be expected since the reactions proceed by dissociation of an equatorial CO. Thus, the combined substitution and exchange kinetic results strongly support the bonding scheme presented earlier.

It would be of interest to compare reactivities of the manganese group pentacarbonyl halides. On the basis of infrared spectra of these compounds (7), one might predict that with all three metals—manganese, technetium, and rhenium—one carbon monoxide will be more inert than the other four. Also, for exchange or substitution of the equatorial CO's, the chloride complexes will react more readily than the bromide complexes, and the bromide complexes still faster than the iodide complexes. Thus all of these compounds would fit the molecular orbital bonding description presented above. Furthermore, the infrared spectra indicate that the equatorial carbonyls should be most labile with rhenium and least so with manganese, and the metal–carbon bond strength of the axial CO's should follow the reverse order, that of manganese being the strongest. Experimental results on the technetium and rhenium compounds are still lacking.

REFERENCES

1. H. B. Gray, I. Bernal, and E. Billig. J. Am. Chem. Soc. **84**, 3404 (1962).
2. L. E. Orgel. Inorg. Chem. **1**, 25 (1962).
3. A. Wojcicki and F. Basolo. J. Am. Chem. Soc. **83**, 525 (1961).
4. W. Hieber and K. Wollmann. Ber. **95**, 1552 (1962).
5. R. J. Angelici and F. Basolo. J. Am. Chem. Soc. **84**, 2495 (1962).
6. H. B. Gray. To be published.
7. M. A. El-Sayed and H. D. Kaesz. Private communication.

Can. J. Chem. Downloaded from www.nrcresearchpress.com by 210.87.254.40 on 09/05/12
For personal use only.

METALLOCENE CHEMISTRY—A DECADE OF PROGRESS[1]

M. D. RAUSCH

Research and Engineering Division, Monsanto Chemical Company, Saint Louis, Mo., U.S.A. and Department of Chemistry, University of Kansas, Lawrence, Kan., U.S.A.

Received October 29, 1962

ABSTRACT

One of the most significant new frontiers in chemistry during the past decade has been the stabilization and study of π-organic derivatives of the transition metals. Over 60 elements are now known to form one or more cyclopentadienyl compounds. The aromatic-type reactions displayed by ferrocene and related complexes have also been extensively investigated. Ferrocene will undergo alkylation, acylation, sulphonation, metalation, arylation, formylation, aminomethylation, and other reactions characteristic of a highly reactive aromatic system. π-Cyclopentadienyl derivatives of vanadium, chromium, manganese, ruthenium, and osmium as well as certain π-arene complexes of chromium exhibit ring substitution reactions in varying degrees. Other metallocenes undergo ring addition reactions.

The orientation effects of substituents on reactions of substituted ferrocenes have been studied. A variety of unique oxidation, reduction, dehydration, and rearrangement reactions are known in metallocene chemistry. Haloferrocenes and mercuriferrocenes are readily converted to biferrocenyl. Recent rate investigations have established that carbonium ions adjacent to metallocene nuclei possess unusual stabilization as a result of direct metal participation.

Can. J. Chem. Downloaded from www.nrcresearchpress.com by 210.87.254.40 on 09/05/12
For personal use only.

The chemistry of organometallic compounds has always intrigued chemists since the very beginning of this field over a century ago. Through the intervening years many outstanding discoveries have been made, and these discoveries have had a profound effect on the science of chemistry and chemical technology. In spite of extensive research in organometallic chemistry during the period from about 1830 to 1950, the preparation and study of organic derivatives of transition metals remained largely an enigma. The early work along these lines is well summarized in a recent review by Cotton (1).

The accidental discovery of ferrocene in 1951 was a major event in organometallic chemistry. The isolation of this unique organo-iron compound has provided a tremendous stimulus for research leading to many other types of novel organo-transition metal derivatives. Detailed studies on these derivatives in turn have contributed greatly to a better understanding of carbon – transition metal bonding.

Certainly the most extensively investigated organo-transition metal complexes during the period from 1951 to the present have been those in which the cyclopentadienyl group is present. Over 60 of the chemical elements have now been shown to form cyclopentadienyl derivatives. No doubt the ability of this group to form organometallic and organometalloidal compounds with so many elements results from the variety of ways it can enter into bonding. In a very broad sense cyclopentadienyl compounds of metals and metalloids can be classified according to whether the ring-metal bonding is principally ionic, principally covalent, or principally π-type. It must be emphasized that these distinctions are not mutually exclusive, and that a given metal-cyclopentadienyl may possess bonding characteristics of several of these types. The chemistry of cyclopentadienyl compounds of metals and metalloids has recently been summarized by the present author (2).

[1]*Presented at the Symposium on Organometallic Compounds, Vancouver, British Columbia, September 4–6, 1962, sponsored by the Inorganic Chemistry Division, Chemical Institute of Canada, and the Department of Chemistry, University of British Columbia, with the support of the National Research Council, Ottawa, in cooperation with the University Extension Department.*

Can. J. Chem. Downloaded from www.nrcresearchpress.com by 210.87.254.40 on 09/05/12
For personal use only.

During the past 10 years many other organic groups containing π-electron systems have been shown to form π-metallo derivatives. Groups of this sort include ethylene, the allyl group, various cyclobutadienes, arenes, the cycloheptatrienyl group, cyclooctatetraene, and many others. When one considers the large number of potential π-ligands and the fact that nearly all the transition metals have now been found to form organometallic π-complexes, it is no wonder that this area has been such a fertile new frontier in chemistry!

Ferrocene itself has been shown to possess a pentagonal antiprismatic structure in the crystal state (I) (3). The compound is diamagnetic and has a dipole moment of zero. The high symmetry of ferrocene results in a strikingly simple infrared spectrum (4). The nuclear magnetic resonance spectrum shows only one type of hydrogen resonance at about 4 p.p.m. downfield from tetramethylsilane.

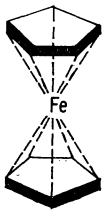

I

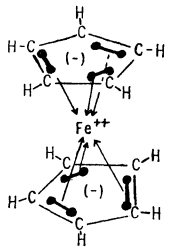

II

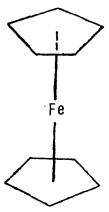

III

While the "sandwich" structure of ferrocene is well established, the precise nature of the ring-metal bond is still in dispute (5). Two hypotheses can be briefly mentioned. Fischer and co-workers (6) regard ferrocene and related compounds as penetration complexes in which two negatively charged rings, each containing three pairs of π-electrons, are coordinated in an approximately octahedral arrangement around a positively charged metal atom. In ferrocene the metal is Fe^{II}, and the complete filling of hybrid d^2sp^3 metal orbitals results in an inert gas configuration (II).

Moffitt (7) and others regard the ring-metal bonding in ferrocene to result largely from a delocalized covalent bond between the metal atom and two cyclopentadienyl radicals. A two-electron bond of this sort results from overlap of a π-orbital of suitable symmetry in each ring with the $3d_{xz}$ and $3d_{yz}$ orbitals of iron. Four π-electrons thus remain in each ring and are not involved in the principal bonding, while filled $3d$ orbitals of the metal lie in the xy-plane between the two cyclopentadienyl rings (III).

A variety of chemical and physical properties of ferrocene and related substances can be advantageously explained using either concept of bonding. The essential difference between these hypotheses appears to be in the *degree* in which π-electrons participate in bonding with metal orbitals.

Shortly after the isolation of ferrocene, a subsequent important discovery was made by Woodward, Rosenblum, and Whiting (8). These investigators noted the failure of ferrocene to undergo Diels–Alder type reactions and its resistance to catalytic hydrogention. They reasoned that because of its remarkable stability, ferrocene might behave like an aromatic substance. These suppositions proved to be correct as ferrocene was readily acylated under Friedel–Crafts conditions to form acyl derivatives. Indeed, the name *ferrocene* was given to biscyclopentadienyliron because of its chemical similarity to benzene.

Can. J. Chem. Downloaded from www.nrcresearchpress.com by 210.87.254.40 on 09/05/12
For personal use only.

The successful acylation of ferrocene set off a vigorous research effort that has resulted in the establishment of a new field of chemistry, metallocene chemistry. In recent years, a variety of π-cyclopentadienyl derivatives of ruthenium, osmium, manganese, vanadium, and chromium have been shown to exhibit certain aromatic-type reactions in varying degrees. Metallocenes can thus be broadly classified as ferrocene-type compounds which exhibit aromatic substitution reactions. In addition, the name *metallocene* has been applied to many other metal-cyclopentadienyl compounds which might be expected to possess aromatic character but which fail to survive the reaction conditions required for aromatic substitution. It should be noted, however, that certain compounds in this category do exhibit various addition reactions. Metallocenes represent a new class of heterocyclic compounds in which a transition metal, in a manner similar to nitrogen, oxygen, and sulphur in classical heterocycles, not only is an integral part of the structure but actually participates in many reactions.

Although metallocene chemistry is only 10 years old, the literature is already profuse. In this view, a brief outline of the many aromatic-type substitution reactions of metallocenes will first be presented. Emphasis will be given to specific substituent and metal effects, and to the synthetic utility of each type of ring-substitution reaction. Finally, a number of important recent topics in metallocene chemistry will be discussed. These will include the formation of biferrocenyl and polyferrocenylenes, interannular resonance effects, α-carbonium ion stabilization, rearrangements, and ring-addition reactions.

Acylation

The acylation of metallocenes has been investigated more extensively than any other substitution reaction. The Friedel–Crafts reaction between ferrocene and acetyl chloride in the presence of aluminum chloride serves as a good example. When equimolar amounts of these reactants are employed, monoacetylferrocene is formed almost exclusively (9, 10). When an excess of acetyl chloride and aluminum chloride is employed, a mixture of two isomeric diacetylferrocenes is produced, and the products can be separated by careful chromatography on activated alumina (9). It should be noted that nearly all metallocenes are highly colored and can be advantageously separated by column chromatography.

The major product is the heteroannular disubstituted derivative, 1,1′-diacetylferrocene (IV), while a very small amount of a homoannular isomer, 1,2-diacetylferrocene (V), is also obtained. The first acetyl group appears to deactivate the substituted ring toward further electrophilic substitution, and the second acetyl group preferentially enters the opposite ring.

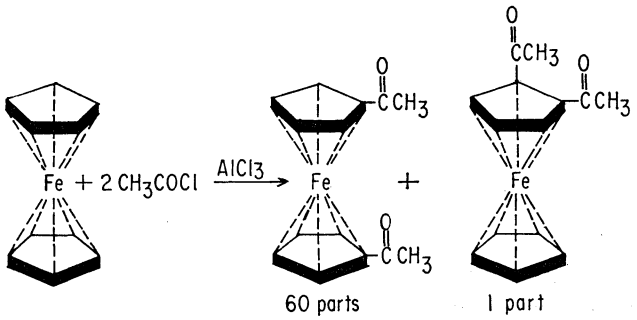

IV V

The structure of isomer IV was confirmed by degradative evidence. Under conditions of high temperature and pressure, this product was catalytically hydrogenated to ethylcyclopentane to the exclusion of cyclopentane and diethylcyclopentane (11). The structure of isomer V was shown by haloform oxidation to the diacid followed by facile anhydride formation (12).

The exceedingly high reactivity of ferrocene in Friedel–Crafts acylations is exemplified by the fact that mild catalysts such as stannic chloride (13), boron trifluoride (14), zinc chloride (15), and phosphoric acid (16) can be used with considerable success. When ferrocene and anisole were allowed to compete for a limited amount of acetyl chloride and aluminum chloride, acetylferrocene was the sole product isolated (10).

The remarkable reactivity of ferrocene in acylation reactions is reminiscent of the marked reactivity of thiophene in classical heterocyclic chemistry. A novel means of comparing the reactivities of these two aromatic systems has recently been reported by Schlögl and Pelousek (17). 2-Thenylferrocene (ferrocenyl-2-thienylmethane) was prepared by acylation of ferrocene with thenoyl chloride and subsequent reduction. Acetylation of 2-thenylferrocene produces a variety of acetylated derivatives. From the products obtained, it appears that ring substitution occurs in the following decreasing order: thiophene (5-position); ferrocene (heteroannular ring); ferrocene (homoannular ring, 3-position).

The acylation of other substituted ferrocenes has also received increasing attention in recent years. The nature of the substituent markedly affects the location of the entering acetyl group. Acetylation of monoethylferrocene, for example, produces three isomeric acetylethylferrocenes: the 1,2-isomer (VI, R = C_2H_5), the 1,3-isomer (VII, R = C_2H_5), and the 1,1′-isomer (VIII, R = C_2H_5) (9). The isolation of three positional isomers of

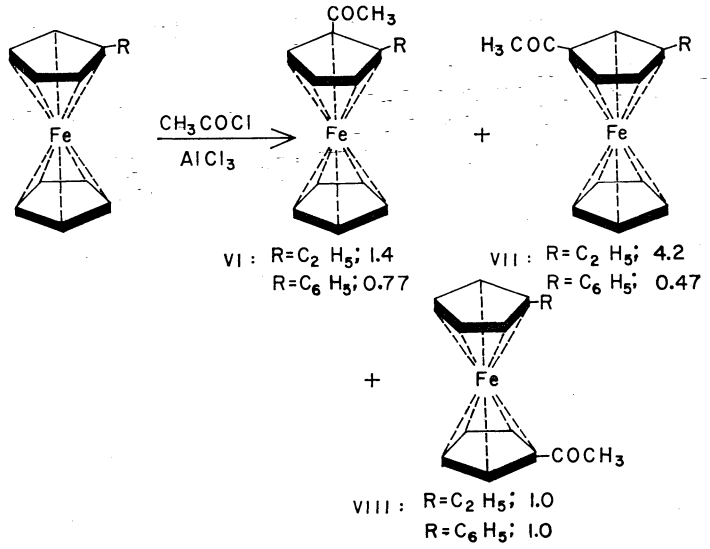

this type is completely consistent with the concept that the two cyclopentadienyl rings in ferrocene are rotating in all but the crystalline state. From the amounts of each isomer formed and the number of non-equivalent ring positions, site reactivities can be calculated, the 1′-position being arbitrarily assigned a value of unity.

Can. J. Chem. Downloaded from www.nrcresearchpress.com by 210.87.254.40 on 09/05/12
For personal use only.

From the site reactivities given under each isomer, it can readily be seen that acylation is enhanced in the substituted ring compared to the unsubstituted ring, as might be expected by the presence of an electron-releasing alkyl group. Further, substitution at the 3-position is favored over the 2-position. This result is corroborated by similar studies involving the acetylation of 1,1′-dimethylferrocene, in which it was found that the 3-position was also favored (18). Acylation at the 3-position was even more pronounced in the case of 1,1′-diisopropylferrocene, suggesting that steric factors play an important role in determining the mechanism of homoannular acylation of alkylferrocenes.

While acetylation of phenylferrocene also produces three similar acetylphenylferrocenes (VI, VII, VIII; R = C_6H_5) (as well as a very small amount of an isomer in which the phenyl group is acetylated), the site reactivities are quite different (19, 20). It can be seen that the ring bearing the phenyl substituent is deactivated compared to the unsubstituted ring. In contrast to alkylferrocenes, the 2-position is favored over the 3-position. It has been postulated that this is the result of enhanced resonance stabilization of the transition state in substitution involving electrophilic attack at the 2-position.

Preliminary studies involving the acetylation of aralkylferrocenes such as benzylferrocene indicate substitution occurs in the unsubstituted ring (17). Detailed site reactivity studies have not yet been reported.

Another interesting series of reactions involving acylation concerns bridging or cyclization of ω-ferrocenylcarboxylic acids. β-Ferrocenylpropionic acid (IX, n = 2), when

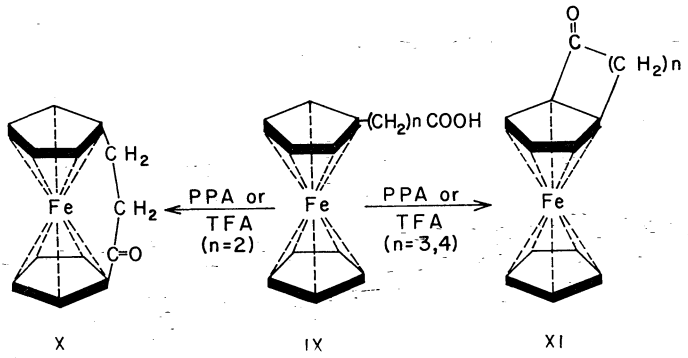

X IX XI

treated with either polyphosphoric acid or trifluoroacetic anhydride, yields the bridged ketone 1,1′-α-ketotrimethyleneferrocene (X) (21). Ferrocenylbutyric or valeric acids (IX, n = 3, 4) produce homoannular cyclized products (XI, n = 3, 4). By means of related sequences of reactions, ferrocenes containing two (22), three (23), and four (24) trimethylene bridges have now been prepared. Indeed, it appears that the interesting situation may soon arise in which the centrosymmetric iron atom is completely enclosed in an "alkylene cage"!

While acylations of metallocenes are usually carried out with acid halides, acid anhydrides, or carboxylic acids, a number of other acylating agents have been reported. The reaction of ferrocene with various isocyanates and aluminum chloride leads to N-substituted ferrocenecarboxamides (XII) (25). Use of ruthenocene in place of ferrocene leads to analogous results (26). The preparation of N-phenylferrocenecarboxamide from phenyl isocyanate in this manner has been used as a proof of structure for the product obtained from the Beckmann rearrangement of benzoylferrocene oxime (27).

Can. J. Chem. Downloaded from www.nrcresearchpress.com by 210.87.254.40 on 09/05/12
For personal use only.

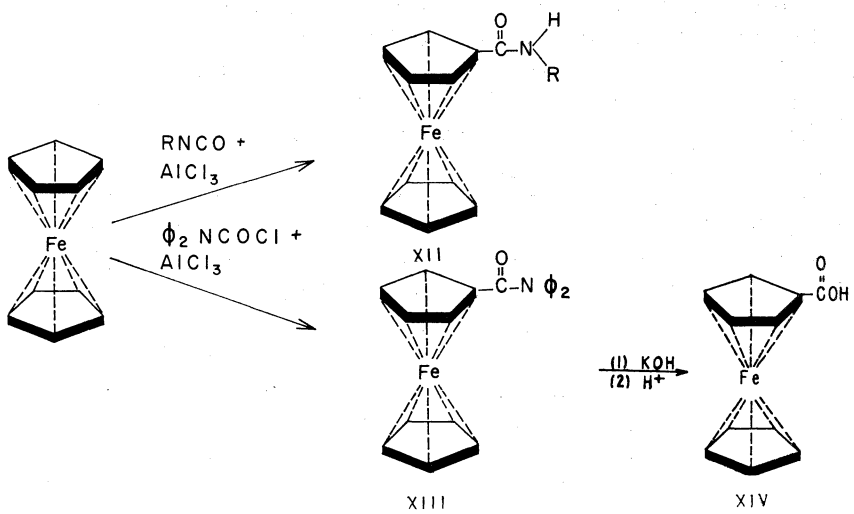

A useful synthetic technique involves the acylation of ferrocene with diphenylcarbamyl chloride (28). The product, diphenylcarbamylferrocene (XIII), is readily hydrolyzed to ferrocenecarboxylic acid (XIV). Acylation of diphenylcarbamylferrocene followed by hydrolysis produces good yields of 1′-acylferrocenecarboxylic acids.

Several years ago Rausch, Fischer, and Grubert found that the ruthenium and osmium analogues of ferrocene, viz., ruthenocene and osmocene, likewise undergo acylation in varying degrees (26, 29). Under identical conditions in which the acylation of ferrocene leads solely to 1,1′-diacylferrocenes, mixtures of mono- and di-acylruthenocenes were obtained from ruthenocene acylations, and osmocene yielded only monoacylation products. These studies as well as competition experiments indicate that the electrophilic reactivity of Group VIII metallocenes markedly decreases proceeding from ferrocene to osmocene.

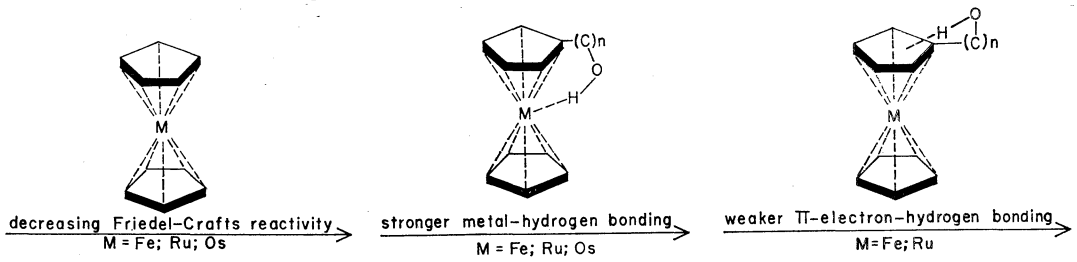

The precise reason for this marked gradation in electrophilic reactivity is not yet clear. It has been tentatively suggested that the availability of bonding π-electrons in each cyclopentadienyl ring decreases in the order ferrocene > ruthenocene > osmocene as a result of stronger ring-metal bonding in the case of the heavier metal complexes (26). Such a trend in metal–ligand bond strength is known to occur in metal–olefin complexes, and might result from enhanced back-donation from filled metal orbitals to ring antibonding π-orbitals. Enhanced d_π–p_π bonding of this sort would tend to strengthen the metal–ligand bond as a whole. It should be mentioned that infrared (4, 26), thermochemical (30), and

Can. J. Chem. Downloaded from www.nrcresearchpress.com by 210.87.254.40 on 09/05/12
For personal use only.

mass spectra studies (31) are in accord with the concept of stronger ring-metal bonding in ruthenocene and osmocene compared to ferrocene.

Other investigators have recently defined several types of hydrogen bonding in metallocenyl alcohols (32, 33). They have shown that hydrogen bonding between the hydroxyl hydrogen and the central metal atom becomes stronger proceeding from the ferrocenyl to the osmocenyl alcohol. Conversely, hydrogen bonding to the π-electron density of the cyclopentadienyl ring appears weaker in ruthenocenyl alcohols compared to ferrocenyl alcohols. It has also been shown that ruthenocenecarboxylic acid is nearly twice as acidic as its iron analogue, XIV (26).

Another topic that is closely related to these results concerns the protonation of metallocenes. A number of metallocenyl hydrides of rhenium, molybdenum, and tungsten have been shown to behave as bases and are soluble in dilute aqueous acids (34). The remarkable basicities of these compounds have been ascribed to the presence of filled metal orbitals that are not involved in primary ring-metal bonding, and to a possible angular configuration of the rings. Although much less basic, Group VIII metallocenes can be protonated in boron trifluoride hydrate (35). High-resolution nuclear magnetic resonance studies on these protonated metallocenes show the presence of a proton resonance at very high fields relative to tetramethylsilane, and indicate the presence of a highly shielded proton that is bonded directly to the metal atom.

The nuclear magnetic resonance data further indicate that the apparent ease of protonation of Group VIII metallocenes decreases from ferrocene to osmocene. It is striking that this gradation in reactivity parallels the trends observed in acylation studies. Hydrogen atoms of ferrocene are known to be readily substituted by deuterium when ferrocene is dissolved in anhydrous deuterosulphuric acid (36). Protonation can thus be considered as a simple form of electrophilic substitution. It is possible that the transition state for other electrophilic substitution reactions involves initial interaction of the electrophile with a filled metal orbital, followed by rearrangement to an endocyclic σ-complex (37).

Metallocenes may therefore undergo electrophilic substitution by a mechanism fundamentally more complex than that which pertains to substitution in benzenoid systems. Clearly, more studies are needed along these lines in order to define specific metal effects on the properties and reactions of these remarkable compounds.

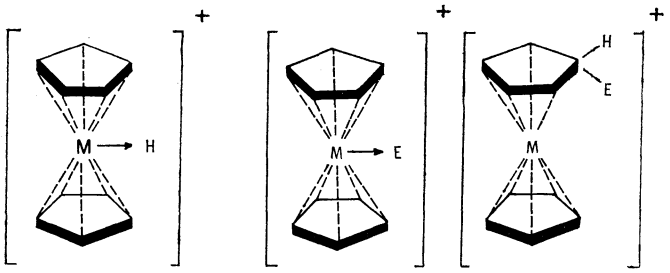

decreasing ease of protonation: M = Fe, Ru, Os

E = Electrophile

Acylmetallocenes undergo many reactions shown by acylbenzenes, and a detailed discussion will not be presented here (38). Reductions with either lithium aluminum hydride or sodium borohydride give the corresponding carbinols, while Clemmensen

Can. J. Chem. Downloaded from www.nrcresearchpress.com by 210.87.254.40 on 09/05/12
For personal use only.

reduction, reduction with lithium aluminum hydride plus aluminum chloride, catalytic hydrogenation, etc., yield corresponding alkyl derivatives. Acetylferrocenes undergo a variety of base condensation reactions and can be oxidized to ferrocenecarboxylic acids without apparent oxidation of the iron atom.

Still other π-cyclopentadienyl-metal compounds have been shown to undergo acylation. The successful acylation of cyclopentadienylmanganese tricarbonyl has opened up yet another interesting aromatic-type system for exploration (39–43). An example of this type concerns the benzoylation of methylcyclopentadienylmanganese tricarbonyl (XV) (40). Both 1-methyl-2-benzoylcyclopentadienylmanganese tricarbonyl (XVI) and the corresponding 1,3-isomer (XVII) are readily obtained. Cyclopentadienylvanadium tetracarbonyl (44, 45) and cyclopentadienylchromium dicarbonyl nitrosyl (46) can also be acylated under Friedel–Crafts conditions.

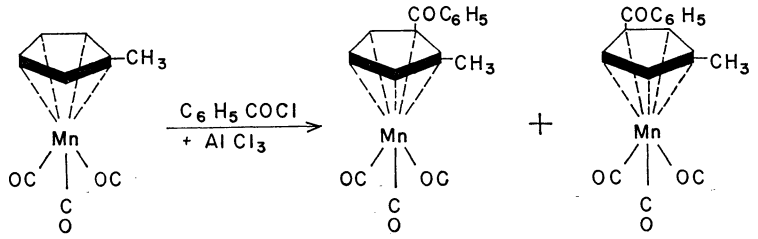

XV XVI XVII

Attempts to bring about acylation reactions of bisbenzenechromium and bistoluenechromium have thus far failed, the ring-metal bond being readily cleaved under the reaction conditions involved (47). On the other hand, benzenechromium tricarbonyl (XVIII) has recently been acylated to produce acetophenonechromium tricarbonyl (XIX), the ring-metal bond in this case remaining intact (48, 49).

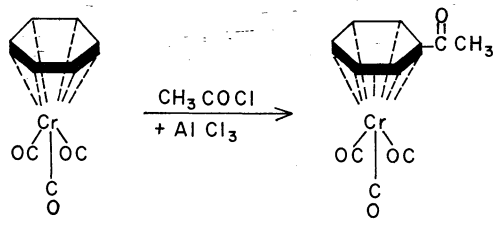

XVIII XIX

Formylation

Ferrocene is similar to other highly reactive aromatic systems in that it is readily formylated by N-methylformanilide in the presence of phosphorus oxychloride (16, 50–53). Only the monosubstituted product, ferrocenecarboxyaldehyde (XX), is produced even when a large excess of formylating agent is used. Ferrocenecarboxaldehyde, like benzaldehyde, is readily reduced to the corresponding carbinol and undergoes the Cannizzaro reaction with alcoholic potassium hydroxide solution. While ferrocenecarboxaldehyde apparently does not undergo a self-benzoin condensation it will condense with benzaldehyde to form a mixed benzoin. The low carbonyl stretching frequency

Can. J. Chem. Downloaded from www.nrcresearchpress.com by 210.87.254.40 on 09/05/12
For personal use only.

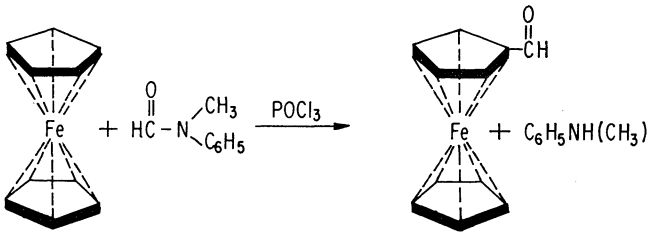

XX

(1670 cm^{-1}) compared to the value for benzaldehyde (1704 cm^{-1}) indicates strong polarization of the carbonyl group. This point is also reflected in the remarkable basicity of ferrocenecarboxaldehyde, since it forms a solid hydrochloride from ether solution and hydrogen chloride (52).

It is timely at this point to mention some recent studies of Arnett and Bushick (54). These investigators have determined the pK_A values for the conjugate acids of ferrocenyl ketones in aqueous sulphuric acid. They have found, for example, that acetylferrocene is over 2000 times more basic than is acetophenone and 85 times more basic than is *p*-hydroxyacetophenone. These data support the concept (*vide infra*) that metallocenyl groups are strongly electron releasing compared to the phenyl group and that they possess extraordinary ability to delocalize adjacent positive charges.

Alkylation

Ferrocene is readily alkylated by alkyl halides, alcohols, or olefins to produce alkylated derivatives (55, 56). The exceedingly great reactivity of ferrocene under these conditions results in the formation of mixtures of mono-, di-, tri-, and poly-alkylated products, and the yield of any one alkylation product is usually low. As in benzenoid chemistry, the

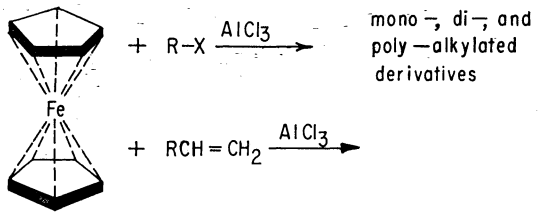

introduction of an alkyl group into the ferrocene nucleus facilitates subsequent alkylation in the same ring. Aralkylferrocenes can be conveniently prepared by reaction of ferrocene with substituted carbinols such as triphenylcarbinol in the presence of a Lewis acid, the reactions being carried out in the melt phase (57).

Alkylferrocenes can serve as useful synthetic intermediates, since it has recently been shown that they are conveniently oxidized by activated manganese dioxide to carbonyl compounds (58). Methylferrocene, for example, can be converted to ferrocenecarboxaldehyde without apparently oxidizing the iron atom. Another interesting oxidation involves conversion of the 1,1′-dimethylcobalticinium cation to the corresponding dicarboxylic acid cation by means of alkaline potassium permanganate solution (59).

The Friedel–Crafts alkylation of ferrocene with ethylene chloride has been the subject of considerable investigation. It was initially reported by Nesmeyanov and co-workers

Can. J. Chem. Downloaded from www.nrcresearchpress.com by 210.87.254.40 on 09/05/12
For personal use only.

that the reaction produced "diferrocenylethane" and appreciable amounts of polymeric material (60). Rinehart and co-workers later proved that the low molecular weight product was 1,1-diferrocenylethane (XXI) instead of the expected 1,2-isomer (61). The anomalous

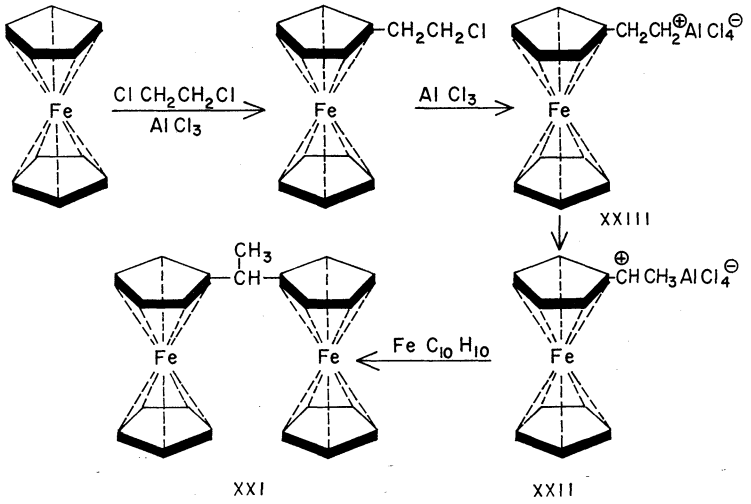

product is postulated to result from a hydride ion rearrangement in the transition state, the driving force resulting from the enhanced stability of the α-ferrocenylcarbonium ion XXII compared to the primary carbonium ion XXIII formed initially.

Nesmeyanov and co-workers have also recently reported that this reaction produces yet another alkylated product, pentaethylenediferrocene, in which two ferrocene units are purported to be connected by five ethylene bridges (62).

Aldehyde Condensation

The reaction of ferrocene and formaldehyde in either concentrated sulphuric acid or liquid hydrogen fluoride, followed by reduction, produces a compound containing two ferrocenyl and two methylene groups (63–65). After several incorrect assignments had

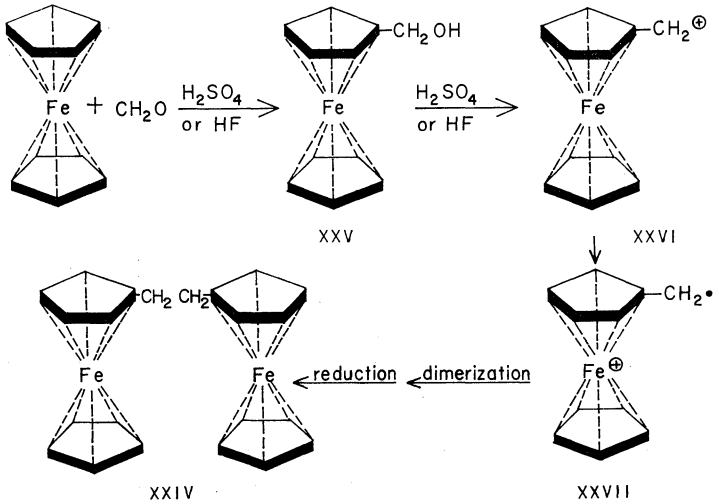

Can. J. Chem. Downloaded from www.nrcresearchpress.com by 210.87.254.40 on 09/05/12
For personal use only.

been proposed for the structure of this condensation product, Rinehart and co-workers showed by an unequivocal synthesis that the product was 1,2-diferrocenylethane (XXIV) (66). The mechanism of this reaction presumably involves the initial formation of ferrocenylcarbinol (XXV), followed by ionization in the strongly acidic media to the ferrocenylmethylcarbonium ion (XXVI). Conversion to radical ion XXVII followed by dimerization and subsequent reduction produces the product. This mechanism is supported by the fact that ferrocenylcarbinol under the same acidic conditions also yields 1,2-diferrocenylethane. Further, the intermediate dicationic dimerization product has been isolated as a dipicrate.

Ferrocenecarboxaldehyde and ferrocene condense to form a deep blue diferrocenylmethine cation. The cation can be isolated in crystalline form as a perchlorate (67).

Arylation

The great reactivity of ferrocene toward electrophilic reagents prompted an early examination of its behavior with aryldiazonium salts. Azoferrocenes were expected to be formed by analogy to the reactions of phenol and related reactive aromatic compounds. The reactions instead were found to proceed with elimination of nitrogen and the products were arylferrocenes (XXVIII). Conversions of this sort now constitute the most convenient means of preparing these substances, an alternative method being direct synthesis from arylcyclopentadienes and iron chlorides (68).

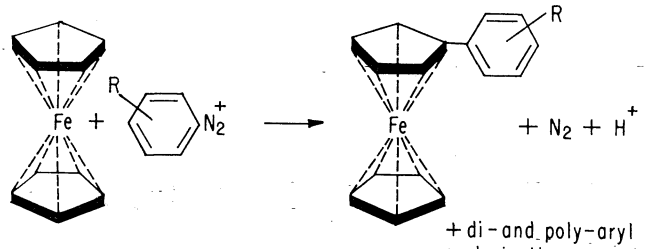

XXVIII

Various investigators have studied this reaction using aqueous acetic acid (19, 69) or water–ether mixtures (13, 70) as the reaction medium. Weinmayr has reported the successful arylation of ferricenium salts in aqueous sulphuric acid (71). The products of the arylation reactions are mono-, di-, and poly-arylferrocenes. While earlier studies indicated that the diaryl products had a 1,1′-configuration, Rosenblum and co-workers have recently found that all possible structurally isomeric diarylferrocenes (1,1′; 1,2; 1,3) are produced in this manner (72). Ferrocene can also be phenylated in cyclohexane solution in the presence of N-nitrosoacetanilide (69) although the free-radical mechanisms originally proposed for this reaction and the diazonium arylation are questionable (72).

Monosubstituted alkyl-, acyl- and aryl-ferrocenes undergo arylation to form primarily heteroannular disubstituted ferrocenes (69, 73). Attempts to arylate 1,1′-diacylferrocenes, however, result in rupture of the ring-metal bond. Bozak and Rinehart have recently presented spectral evidence that the iron-free product resulting from the reaction of 1,1′-diacetylferrocene and benzenediazonium chloride is 6-methyl-6-hydroxy-2-phenylazofulvene (74), rather than a 1,2,3-oxadiazine structure originally proposed (73, 75, 76).

Aminomethylation

Hauser and Lindsay first showed that ferrocene undergoes a Mannich-type reaction with formaldehyde and dimethylamine to form dimethylaminomethylferrocene (XXIX)

Can. J. Chem. Downloaded from www.nrcresearchpress.com by 210.87.254.40 on 09/05/12
For personal use only.

(77). This amine is readily converted to a methiodide, and the latter quaternary salt has proved to be an important synthetic intermediate in ferrocene chemistry. Reduction of the methiodide of XXIX with sodium amalgam, for example, produces methylferrocene

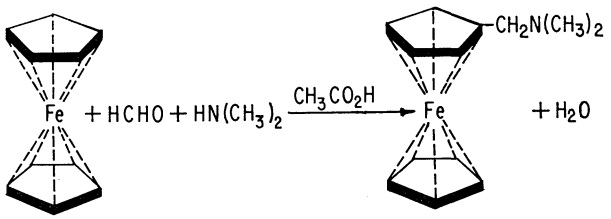

XXIX

in high yield (78). Treatment with solutions of potassium cyanide or potassium hydroxide yields ferrocenylacetonitrile and ferrocenylcarbinol, respectively (77, 79, 80). Reaction with potassium amide in liquid ammonia results in a Stevens rearrangement to give β-dimethylaminoethylferrocene (81, 82).

Aminomethylation of methylferrocene results in substitution apparently at the 3-position, while phenylferrocene reacts in a similar manner to produce primarily the heteroannular aminomethylated product (83, 84). Pauson and co-workers have reported that aminomethylation of 1,1′-dithiomethylferrocene results in introduction of the dimethylaminomethyl group at both the 2- and 3-positions, the ratio being 1.9:1 (85).

Sulphonation

Ferrocene can readily be sulphonated by either sulphuric acid or chlorosulphonic acid in acetic anhydride (64, 86). The products, ferrocenesulphonic acid (XXX) and ferrocene-1,1′-disulphonic acid (XXXI) are obtained together with products resulting from

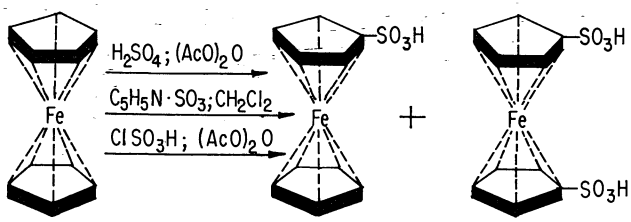

XXX XXXI

oxidation. A second synthetic technique has employed either pyridine or dioxane adducts of sulphur trioxide as sulphonating agents. Ferrocene, phenylferrocene, and ferrocene-carboxylic acid have been sulphonated in this manner (84, 87, 88). These substituents deactivate the substituted ring, and the products are the heteroannular sulphonic acids. Sulphonation of cyclopentadienylmanganese tricarbonyl is also readily accomplished (89).

The sulphonic acids of these metallocenes can be converted to sulphonyl chlorides, sulphonamides, etc., by appropriate reagents. Reduction of ferrocenesulphonyl chloride by lithium aluminum hydride produces the rapidly oxidized ferrocenethiol in quantitative yield (86). Both the sulphonic acid of cyclopentadienylmanganese tricarbonyl as well

Can. J. Chem. Downloaded from www.nrcresearchpress.com by 210.87.254.40 on 09/05/12
For personal use only.

as the corresponding sulphinic acid (obtained by sodium sulphite reduction of the sulphonic acid) have been converted to sulphones (89).

Mercuration

Ferrocene, like thiophene, furan, and other so-called "superaromatic" systems, reacts readily with mercuric acetate to form mercurated derivatives. Nesmeyanov and co-workers first reported that ferrocene could be mercurated under relatively mild conditions in either ethyl ether – alcohol or benzene–alcohol solution (13). The acetoxymercuri-ferrocenes formed in this manner are usually treated with an alcoholic solution of an alkali metal halide. The resulting products, chloromercuriferrocene (XXXII) and 1,1′-di(chloromercuri)ferrocene (XXXIII), can be conveniently separated by extraction with *n*-butyl alcohol.

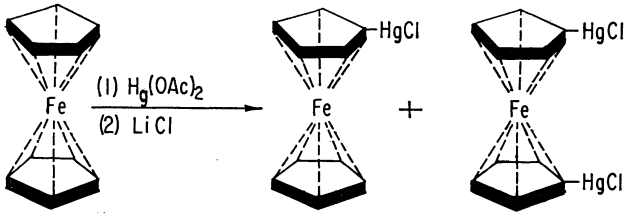

XXXII XXXIII

In a more detailed study of this reaction, Rausch, Vogel, and Rosenberg determined optimum conditions for the synthesis of either mercurated ferrocene (90). Ruthenocene has also been mercurated using glacial acetic acid as the solvent, but pure products could not be separated (26).

Mercurated ferrocenes have proved to be useful intermediates in the synthesis of various halogenated ferrocenes. Iodoferrocene, for example, is readily formed by treatment of chloromercuriferrocene with iodine, followed by decomposition of the resulting iodine complex with aqueous sodium thiosulphate (91). Dihaloferrocenes can be prepared in low yield starting with 1,1′-di(chloromercuri)ferrocene and either iodine or bromine. This indirect route to haloferrocenes, as well as the method involving cupric halide cleavage of ferrocenylboronic acids (*vide infra*), has been of much value in ferrocene chemistry. Attempts to bring about halogenation directly lead either to halogen-containing complexes or oxidative rupture of the ring-metal bond with formation of pentahalocyclopentanes (11, 65, 91).

A well-known reaction in organomercury chemistry consists of the conversion of arylmercuric chlorides to diarylmercury compounds by means of solutions of sodium iodide or sodium thiosulphate. Treatment of chloromercuriferrocene readily produces diferrocenylmercury (XXXIV) under these conditions (13, 90).

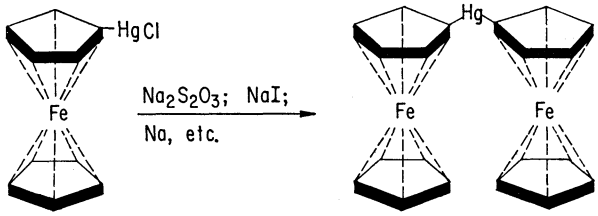

XXXIV

Can. J. Chem. Downloaded from www.nrcresearchpress.com by 210.87.254.40 on 09/05/12
For personal use only.

Both chloromercuriferrocene and diferrocenylmercury undergo metal interchange reactions with organolithium reagents to form ferrocenyllithium (92–94). Ferrocenyl Grignard reagents can also be prepared by the reaction of haloferrocenes and magnesium under controlled conditions (95).

Reaction of 1,1′-di(chloromercuri)ferrocene with sodium iodide or sodium thiosulphate solutions might be expected to lead to higher homologues of diferrocenylmercury in which ferrocene units are bridged by atoms of mercury. Reactions of this type have produced apparently polymeric products whose spectra and composition are consistent with structures such as XXXV, although the very limited solubility of the products has thus far precluded reliable molecular weight measurements (96).

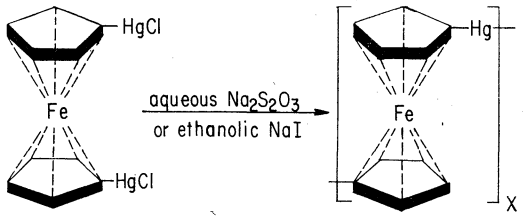

XXXV

Metalation

Another very important substitution reaction of ferrocene is its ability to undergo metalation with organolithium and organosodium compounds. Metalation with *n*-butyllithium in ethyl ether, first reported by Nesmeyanov and co-workers (13) and independently by Benkeser, Goggin, and Schroll (97), leads to rather low yields of ferrocenyllithium (XXXVI, M = Li) and 1,1′-ferrocenylenedilithium (XXXVII, M = Li).

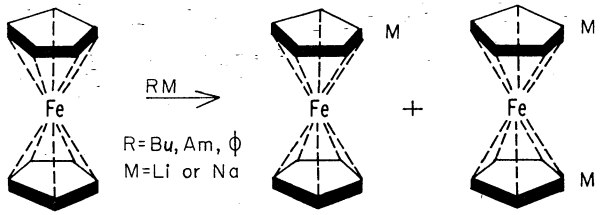

XXXVI XXXVII

It was subsequently shown that the use of the mixed solvent ethyl ether – tetrahydrofuran 1:1 leads to greatly improved yields of lithioferrocenes, and this procedure has been extensively used in further synthetic applications (98).

Similar reactions of ferrocene with phenylsodium or *n*-amylsodium lead to the corresponding sodiated products (XXXVI, XXXVII, M = Na) (99, 100). The steric course of both metalation reactions has been studied, and it has been proved that dimetalation occurs in opposite cyclopentadienyl rings (101).

Several investigations have been directed at the metalation of substituted ferrocenes (100, 102). Rinehart and co-workers have recently found that 1,1′-dimethylferrocene is metalated in the ring and not at the methyl group, in contrast to the metalation of toluene.

Can. J. Chem. Downloaded from www.nrcresearchpress.com by 210.87.254.40 on 09/05/12
For personal use only.

Both ruthenocene and osmocene have been metalated with *n*-butyllithium (26). It has been shown that under comparable conditions ruthenocene is metalated to a greater extent than is ferrocene.

Carbonation and subsequent hydrolysis of either lithiated or sodiated metallocenes lead to the corresponding carboxylic acids. Ferrocenecarboxylic acid and ferrocene-1,1′-dicarboxylic acid are readily produced in this manner and can be conveniently separated by extraction of the former with ethyl ether or benzene. The reaction of metalated ferrocenes with various chlorosilanes has led to a variety of trialkylsilylferrocenes (90, 97, 101).

Metalated ferrocenes have served as very valuable intermediates for the synthesis of a number of other derivatives. Treatment of lithiated ferrocenes with tributyl borate followed by hydrolysis leads to ferroceneboronic acid (XXXVIII) as well as the diboronic acid (103). Ferroceneboronic acid, like benzeneboronic acid, is readily cleaved by cupric bromide or cupric chloride to form the corresponding halo derivatives (XXXIX). Ferrocene-1,1′-diboronic acid reacts in the same manner, and either one or two carbon–boron bonds can be cleaved. Further reactions of this type have led to a variety of mixed dihaloferrocenes (103, 104).

Another important reaction of ferroceneboronic acid and haloferrocenes consists of their facile conversion to ferrocenyl acetate on treatment with cupric acetate. Ferrocenyl acetate in turn has been hydrolyzed to hydroxyferrocene, the ferrocene analogue of phenol (105).

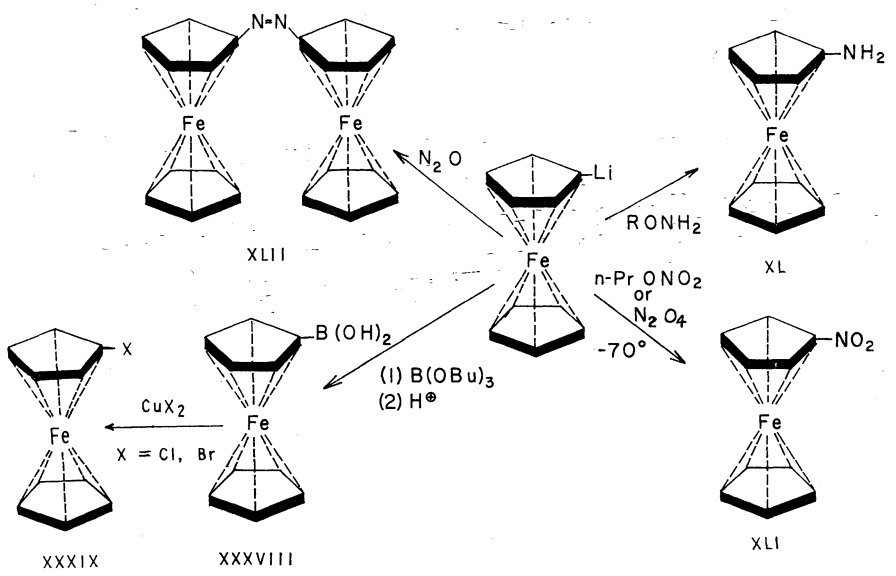

Aminoferrocene (XL) can be prepared in low yield by treatment of O-methylhydroxylamine or O-benzylhydroxylamine with ferrocenyllithium (106, 107). Nitroferrocene (XLI), unattainable by direct nitration of ferrocene, can be isolated from the reaction of ferrocenyllithium and either *n*-propyl nitrate or dinitrogen tetraoxide at −70° (108, 109). A similar reaction between ferrocenyllithium and nitrous oxide leads to azoferrocene (XLII) (110).

Although attempts to acylate bisbenzenechromium under Friedel–Crafts conditions have thus far resulted in cleavage of the ring-metal bond, the successful metalation of

Can. J. Chem. Downloaded from www.nrcresearchpress.com by 210.87.254.40 on 09/05/12
For personal use only.

this π-arene complex using amylsodium has been recently reported (111). The resulting metalated products can be carbonated and esterified to yield a mixture of mono-, di-, and poly-substituted carbmethoxy derivatives of bisbenzenechromium. Gas chromatographic analysis of the dicarbmethoxy portion indicates that the meta isomer is the main component (112). Homoannular dimetalation of bisbenzenechromium is therefore in contrast to heteroannular dimetalation of Group VIII metallocenes.

Oxidation and Reduction

Various oxidation and reduction reactions of substituted metallocenes have already been discussed. It should be mentioned in addition that a large number of substituted metallocenes have been oxidized chronopotentiometrically at a platinum foil in acetonitrile solution (113, 114). Electron-withdrawing substituents decrease the ease of oxidation, while electron-donating substituents increase the ease of oxidation, with respect to the parent metallocenes. A plot of chronopotentiometric quarter-wave potentials, $E_{1/4}$, versus Hammett para sigma constants shows a definite linear relationship. The $E_{1/4}$ values for ruthenocene and osmocene indicate that these metallocenes are more difficultly oxidized than ferrocene, in agreement with earlier qualitative observations (30).

Ferrocene can also be oxidized to the ferricenium cation, $(FeC_{10}H_{10})^+$, by polarographic oxidation, by chemical oxidizing agents such as ferric chloride or ceric sulphate, or simply by passing air through a suspension of it in concentrated acid (115). The deep blue, dichroic cation can readily be reduced to ferrocene by means of reducing agents such as stannous chloride or ascorbic acid (71, 115).

Stronger conditions of oxidation lead to complete rupture of the cyclopentadienyl–iron bond. Attempts to nitrate ferrocene using ethyl nitrate in the presence of sodium alkoxides led to considerable amounts of nitrocyclopentadienylsodium and iron oxides (53). It is interesting to note, however, that a similar reaction of phenylferrocene and ethyl nitrate leads to low yields of *p*-nitrophenylferrocene, the cyclopentadienyl ring remaining attached to the iron in this case (84). Earlier studies have shown that the introduction of a phenyl substituent into ferrocene results in a marked decrease in the oxidation potential (116). Treatment of ferrocene with bromine or chlorine is also reported to result in destruction of the ferrocene nucleus, the products including pentahalocyclopentanes (11).

While initial attempts to hydrogenate ferrocene under relatively mild conditions were not successful, extensive treatment with hydrogen in the presence of a nickel catalyst at 300–350° and under 280 atm absolute pressure results in the formation of cyclopentane (11). Although ferrocene is extremely resistant to catalytic hydrogenation, it can be readily reduced by lithium, in ethylamine the products being metallic iron and cyclopentadiene (117).

Interannular Electronic Effects

We have seen how a substituent on one cyclopentadienyl ring in ferrocene markedly affects subsequent ring substitution reactions. While certain transformations of this type are at least partially determined by steric factors, it seems certain that resonance and inductive interactions also play a very important role in determining orientation. A detailed knowledge of electronic transmissions both within and across the cyclopentadienyl rings is as yet not fully understood, since the precise nature of the bonding in ferrocene is still uncertain.

Several additional studies have confirmed interannular electronic interactions in ferrocene. Early investigations by Nesmeyanov and co-workers and by others demonstrated the electron donor properties of the ferrocenyl group (118). Aminoferrocene, for

Can. J. Chem. Downloaded from www.nrcresearchpress.com by 210.87.254.40 on 09/05/12
For personal use only.

example, is approximately 20 times stronger a base than is aniline, while benzoic acid is several times more acidic than is ferrocenecarboxylic acid. Moreover, acidities and basicities of this sort are markedly affected by substituents on the opposite cyclopentadienyl ring.

A portion of this data is summarized in Table I, in which the acidities of a number of heteroannular ferrocenecarboxylic acids are compared. It can readily be seen that introduction of an electron-releasing alkyl group into the unsubstituted ring lowers the acidity of the corresponding acid, while the introduction of an electron-withdrawing group increases the acid strength.

TABLE I

Interannular electronic effects in ferrocene

	R	pK_A	(68% CH_3OH, 20°)
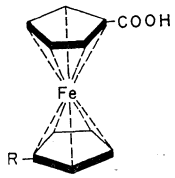	H	6.29	(ϕ-COOH, 5.93)
	C_2H_5	6.43	
	C_4H_9	6.50	
	$COOCH_3$	6.08	
	$COCH_3$	5.91	
	CN	5.82	
	SO_2NH_2	5.56	

In related studies, Little and Eisenthal have found that a plot of similarly obtained pK_A values for substituted forrrocenecarboxylic acids versus Hammett para sigma constants yields a satisfactory straight line (119). These investigators have also recently measured the second-order rate constants for the esterification of a series of heteroannular substituted ferrocenecarboxylic acids with diphenyldiazomethane (120). Logarithms of the rate constants correlated well with the corresponding acid constants and with Hammett para sigma constants. These results quantitatively relate interannular electronic effects in ferrocene and suggest that resonance interactions across the cyclopentadienyl rings parallel the effects between substituents in para-substituted benzoic acids.

The carbonyl stretching frequencies of a number of heteroannular ferrocenecarboxylic acids have been measured (121). The spectral shifts vary in the direction expected from the electronic effects of the substituent groups, and parallel the effects of these substituents on the acid constants. Little and Clark have also demonstrated resonance interaction of the ferrocenyl group in ferrocenylazobenzenes by measuring shifts in the absorption maxima in the visible and ultraviolet spectra (122).

Biferrocenyl and Polyferrocenylenes

During the course of studies relating to the synthesis of certain trialkylsilylferrocenes from lithiated ferrocenes and trialkylchlorosilanes, Rausch and co-workers detected minute amounts of a dark orange crystalline substance which was subsequently shown to be biferrocenyl on the basis of analytical evidence (123, 124). In order to provide an unequivocal synthesis and a more satisfactory route to this compound, several alternative routes were investigated.

It was reasoned that if ferrocene behaved as an aromatic system, then haloferrocenes should undergo the Ullmann coupling reaction. Biferrocenyl (XLIII) was obtained from this reaction and was shown to be identical in every respect with the anomalous material isolated previously (125, 126). Surprisingly, it was found that the reaction of iodoferrocene

Can. J. Chem. Downloaded from www.nrcresearchpress.com by 210.87.254.40 on 09/05/12
For personal use only.

and copper produces biferrocenyl in practically quantitative yield, even at temperatures as low as 60°.

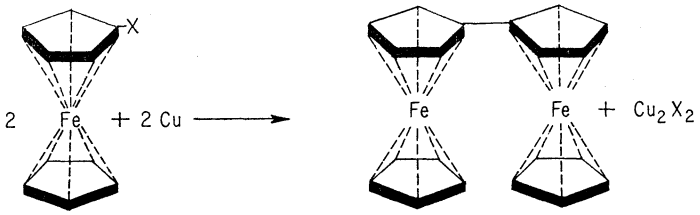

XLIII

Additional studies showed that iodoferrocene was approximately as reactive as 1-iodo-2-nitrobenzene under Ullmann conditions. A mixed Ullmann reaction involving these two reactive aryl halides produced 2-nitrophenylferrocene. Ullmann condensations of iodoferrocene with various sodium phenoxides and sodium arenethiolates likewise lead to ferrocenyl aryl ethers and sulphides, respectively (126, 127).

Another approach to the synthesis of biferrocenyl was suggested by the work of Wittig and Herwig (128). These investigators found that *o*-biphenylenemercury (XLIV; actually this compound has been shown to be a cyclic tetramer) and silver when heated at 300° resulted in the elimination of mercury and the formation of biphenylene (XLV). Rausch showed that a similar reaction involving diferrocenylmercury and silver at elevated temperatures produced biferrocenyl in yields of 30–61%, depending on the conditions

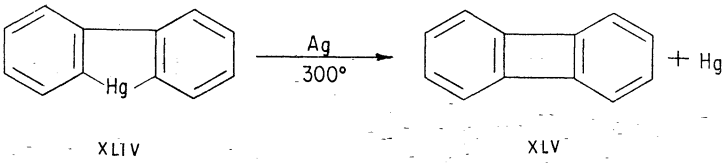

XLIV XLV

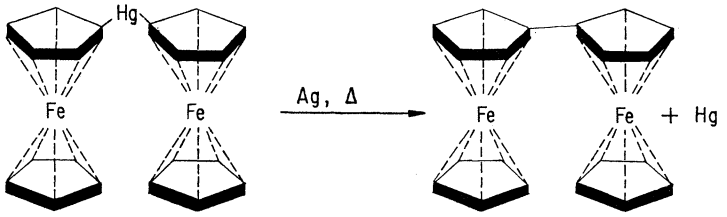

XLIII

(92, 96). The other products from the reaction included mercury, ferrocene, and quite probably polyferrocenylenes.

Nesmeyanova and Perevalova in some related studies involving diferrocenylmercury and palladium black obtained similar results (129). Their yields of biferrocenyl amounted to only 1–6%, however. It is postulated that the reactions proceed via homolytic scission of the carbon–mercury bond with the formation of ferrocenyl radicals.

Can. J. Chem. Downloaded from www.nrcresearchpress.com by 210.87.254.40 on 09/05/12
For personal use only.

Biferrocenyl has also been obtained from the interaction of ferroceneboronic acid with ammoniacal silver oxide solution (103). Ferrocenyl Grignard reagents decompose at elevated temperatures to give ferrocene and biferrocenyl (95). Treatment of ferrocenylmagnesium bromide with cobaltous chloride likewise gives biferrocenyl in high yield (95).

Korshak and co-workers have reported that the reaction of ferrocene and butyl peroxide produces polyferrocenylenes. The benzene-soluble portion of this polymer is reported to melt over 300° and to have a molecular weight between 2500 and 7000 (130). Polyferrocenylenes prepared in this manner have been shown to be paramagnetic compared to diamagnetic ferrocene (131).

α-Metallocenyl Carbonium Ions

A number of observations have been made which qualitatively suggest that carbonium ions adjacent to metallocene systems possess unusual stability. Ferrocenecarboxaldehyde, for example, is soluble in dilute hydrochloric acid (15), ferrocenyl carbinols such as ferrocenylphenylcarbinol form ethers with great ease (27), and ferrocenylmethylcarbinol can be dehydrated to vinylferrocene under exceedingly mild conditions (132). The concept of stabilizations of this type has also been used to explain certain anomalous ring substitution reactions as explained in the preceding sections.

Richards and Hill have recently obtained quantitative evidence for the stabilization of α-metallocenyl carbonium ions (133, 134). They have shown that solvolyses of methylmetallocenylcarbinyl acetates proceed via a carbonium ion mechanism, and that these acetates solvolyze with rates greater than even that of triphenylmethyl (trityl) acetate. Further, the relative rates of solvolysis and thus the order of carbonium ion stabilities increase proceeding from the iron to the osmium acetate. A portion of this data is summarized in Table II.

TABLE II

Relative rates of solvolysis of methylmetallocenylcarbinyl acetates

Acetate	Relative rate (80% acetone, 30°)
Trityl	0.15
Methylferrocenylcarbinyl	1.00
Methylruthenocenylcarbinyl	1.36
Methylosmocenylcarbinyl	5.37

Buell, McEwen, and Kleinberg have observed that weak acids such as hydrogen azide and acetic acid add readily across the double bond of vinylferrocene (XLVI, M = Fe) (135). They have postulated that the mechanism of addition proceeds via intermediate formation of the α-ferrocenylcarbonium ion (XLVII, M = Fe), followed by conversion to the acetate (XLVIII, M = Fe). Stabilization of carbonium ions of this type can result from overlap of filled metal orbitals with the vacant *p*-orbital of the carbonium ion.

The extraordinary reactivity of vinylferrocene under these conditions prompted a study of the rates of addition of absolute acetic acid to vinylmetallocenes (XLVI, M = Fe, Ru, Os). The relative rates are given in Table III.

It is interesting to note that the relative rate data closely parallel the results obtained in the solvolysis studies. Such a result might be expected from reactions proceeding through similar transition states. The observed order of relative rates may result from better overlap as the size of the central metal atom and the polarizability of its electron

Can. J. Chem. Downloaded from www.nrcresearchpress.com by 210.87.254.40 on 09/05/12
For personal use only.

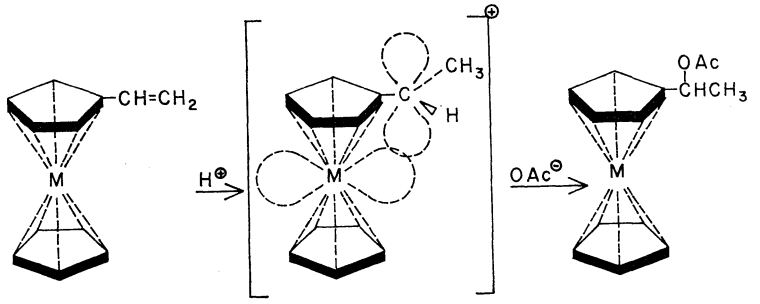

XLVI XLVII XLVIII

TABLE III

Relative rates of addition of acetic acid to vinylmetallocenes

Metallocene	Relative rate (100% HOAc, 40°)
Vinylferrocene	1.00
Vinylruthenocene	1.19
Vinylosmocene	4.62

shell increase. This would result in increased stabilization and therefore ease of formation of the carbonium ions proceeding from lighter to heavier metal complexes.

Trifan and Bacskai as well as Hill and Richards have reported the preparation and solvolysis of exo acetate XLIX and endo acetate L (134, 136). It was shown that the

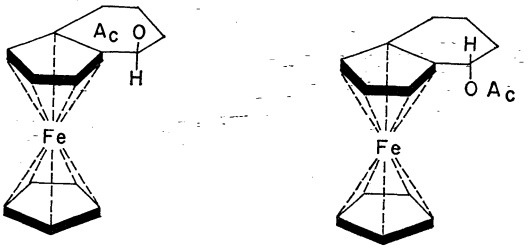

XLIX L

relative rate of solvolysis for the exo acetate was several thousand times greater than for the endo isomer, indicating it is much more favorable for the acetate group to leave in a position trans to the metal rather than cis. Metal electrons must therefore be directly participating in backside displacement of the acetate anion in the rate-determining ionization process. The fact that the exo alcohol is the *sole* alcohol formed from either solvolysis reaction is further evidence for backside metal participation in the transition state.

Rearrangements

The remarkable aromatic reactivity of metallocenes has prompted a number of investigations in which substituted metallocenes have been subjected to conditions which promote molecular rearrangements in benzenoid chemistry.

Can. J. Chem. Downloaded from www.nrcresearchpress.com by 210.87.254.40 on 09/05/12
For personal use only.

Weliky and Gould obtained the pinacol of benzoylferrocene by bimolecular reduction of this ketone using methylmagnesium bromide and cobaltous chloride (27). The pinacol rearranged with remarkable ease in the presence of hydrogen chloride to the pinacolone, phenylbenzoyldiferrocenylmethane, indicating that the ferrocenyl group had migrated.

These investigators also found that benzoylferrocene oxime rearranges under alkaline conditions via its *p*-benzenesulphonate ester to give N-phenylferrocenecarboxamide. This result indicates that the phenyl group is anti to the hydroxyl group in the oxime. Attempts to rearrange the oxime under the usual acidic Beckmann conditions were not successful.

A number of investigators have observed the ease with which ferrocenoyl azide undergoes Curtius rearrangement to ferrocenyl isocyanate (107, 137–139). This rearrangement has been useful for the synthesis of a variety of ferrocenylamines and urethanes.

The rearrangements described above involve migration of a ferrocenyl group, together with its pair of bonding electrons, to an electron-deficient terminus. In 1,2-shifts of this type, rearrangement occurs on a side chain to which the migrating groups are attached.

Attempts to bring about rearrangements which are known to proceed via cyclic transition states have thus far been unsuccessful in metallocene chemistry. Attempts to effect Claisen rearrangement of ferrocenyl allyl ether have led to hydroxyferrocene instead of the expected rearrangement product (140). The mechanism of the Claisen rearrangement is believed to involve a cyclic transition state in which a dienone intermediate is formed. Cyclic intermediates of this sort are apparently not favored in ferrocene chemistry, due to the complex electronic interactions of the ring π-electrons with the iron atom.

Azoferrocene has been subjected to the benzidine rearrangement under conditions which readily promote the rearrangement of azobenzene (141). Again the rearrangement fails, the products instead being aminoferrocene and iron oxide. While the mechanism of the benzidine rearrangement is still in doubt, it also probably involves a cyclic transition state.

Treatment of the methiodide of N,N-dimethylaminomethylferrocene with potassium amide in liquid ammonia results in a Stevens-type rearrangement to produce N,N-dimethylaminoethylferrocene (82). The corresponding benzene analogue behaves quite differently, the product being derived from an ortho substitution rearrangement. Such a rearrangement in the ferrocene series would involve a transition state consisting of two fused five-membered rings (142).

The most thoroughly studied rearrangement to date in metallocene chemistry has concerned the acid-catalyzed decomposition of metallocenylphenylcarbinyl azides. Reaction of the ferrocenyl azide (LI, M = Fe) with concentrated sulphuric acid in chloroform solution afforded nitrogen and a complex mixture of products, including ferrocenecarboxaldehyde, aniline, the diasterioisomeric dications of 1,2-diferrocenyl-1,2-diphenylethane (LII), and these diasterioisomers in their neutral state (143). The isolation

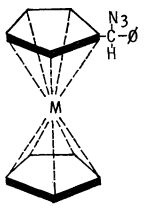

LI

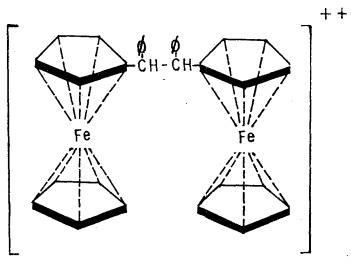

LII

Can. J. Chem. Downloaded from www.nrcresearchpress.com by 210.87.254.40 on 09/05/12
For personal use only.

of ferrocenecarboxaldehyde and aniline to the exclusion of benzaldehyde and aminoferrocene clearly indicates preferential migration of the phenyl group in this reaction. It is postulated that the reaction mechanism involves protonation of both the azido group and the iron atom. In the rearrangement step the phenyl group would be better able to migrate to the electron-deficient nitrogen than the protonated ferrocenyl group. The formation of the dications LII can be explained by partial formation of the ferrocenylphenylcarbonium ion, followed by intramolecular oxidation–reduction to a radical–ion and subsequent coupling of the latter. The dications are in part reduced to the neutral diasterioisomers by oxidation–reduction reactions with other ferrocene derivatives present in the reaction system.

In related studies involving ruthenocenylphenylcarbinyl azide (LI, M = Ru) preferential phenyl migration was again found to occur, and the reaction products included ruthenocenecarboxaldehyde and aniline (144). The corresponding osmium azide (LI, M = Os) behaved quite differently than the iron and ruthenium analogues in that no products of rearrangement could be detected.

Ring Addition Reactions

Attempts to promote ring substitution reactions on the biscyclopentadienyls of nickel (nickelocene) and cobalt (cobaltocene) have not yet been successful. On the other hand, these metallocenes do exhibit certain remarkable ring addition reactions, and it is appropriate to consider such reactions at this point.

Cobaltocene (LIII) contains one unpaired electron and is readily oxidized to the cobalticinium ion (LIV). This cation is remarkably stable, since it is isoelectronic with

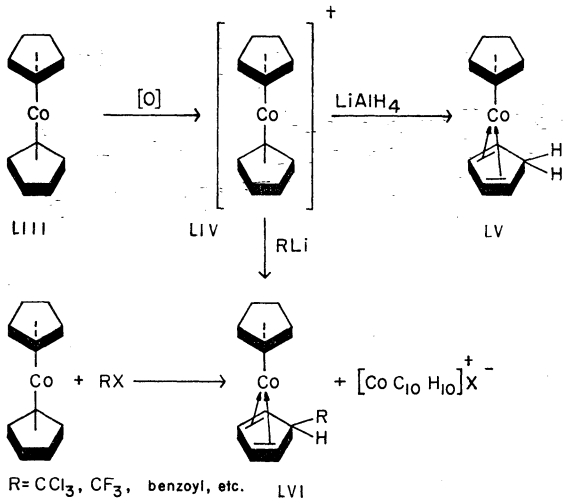

ferrocene, and is not attacked by oxidizing agents such as ozone or boiling aqua regia. Attempts to reduce cation LIV by means of lithium aluminum hydride or sodium borohydride lead to partial hydrogenation of one of the cyclopentadienyl rings, the product being cyclopentadienylcobalt-cyclopentadiene (LV) (145).

Cobaltocene reacts directly with a variety of organic halides to produce equimolar amounts of cobalticinium halides and 1-endo-substituted compounds (LVI) (59, 145–148). Cobalticinium ion readily undergoes nucleophilic addition with various organolithium

Can. J. Chem. Downloaded from www.nrcresearchpress.com by 210.87.254.40 on 09/05/12
For personal use only.

reagents to produce 1-endo-substituted compounds of the same type. Attempts to transform the latter into asymmetric substituted cobalticinium ions have not been successful (59).

Treatment of nickelocene (LVII) with sodium amalgam in ethanol results in partial reduction of one of the cyclopentadienyl rings, thus enabling nickel to attain an inert gas electronic configuration (149). The structure of the product, cyclopentenyl-cyclopentadienylnickel (LVIII) has been confirmed by nuclear magnetic resonance studies

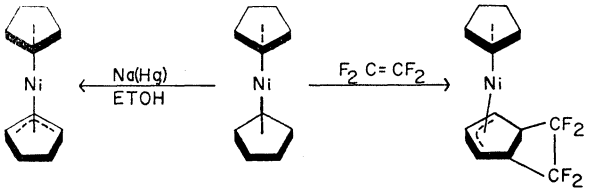

LVIII LVII LIX

as well as by an independent synthesis. Nickelocene undergoes facile addition of dimethyl acetylenedicarboxylate to give an adduct possessing a norbornadienyl group (150). Tetrafluoroethylene likewise adds to one of the cyclopentadienyl rings of nickelocene (151). On the basis of proton and F^{19} nuclear magnetic resonance studies, the product is believed to have a structure such as LIX.

Cobaltocene also undergoes addition of tetrafluoroethylene to yield the unusual binuclear bridged compound LX (152).

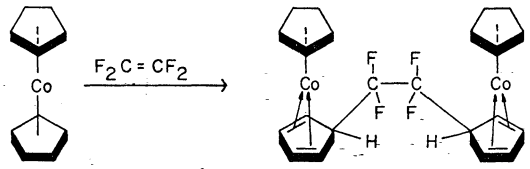

LX

REFERENCES

1. F. A. Cotton. Chem. Rev. **55**, 551 (1955).
2. M. D. Rausch. J. Chem. Educ. **37**, 568 (1960).
3. J. D. Dunitz, L. E. Orgel, and A. Rich. Acta Cryst. **9**, 373 (1956).
4. E. R. Lippincott and R. D. Nelson. J. Chem. Phys. **21**, 1307 (1953); J. Am. Chem. Soc. **77**, 4990 (1955); Spectrochim. Acta, **10**, 307 (1958).
5. G. Wilkinson and F. A. Cotton. Progr. Inorg. Chem. **1**, 1 (1959).
6. E. O. Fischer and H. P. Fritz. Advan. Inorg. Chem. Radiochem. **1**, 55 (1959).
7. W. Moffitt. J. Am. Chem. Soc. **76**, 3386 (1954).
8. R. B. Woodward, M. Rosenblum, and M. C. Whiting. J. Am. Chem. Soc. **74**, 3458 (1952).
9. M. Rosenblum and R. B. Woodward. J. Am. Chem. Soc. **80**, 5443 (1958).
10. G. D. Broadhead, J. M. Osgerby, and P. L. Pauson. J. Chem. Soc. 650 (1958).
11. A. N. Nesmeyanov, E. G. Perevalova, R. V. Golovnya, T. V. Nikitina, and N. A. Simukova. Izv. Akad. Nauk SSSR, Otd. Khim. Nauk, 739 (1956).
12. J. H. Richards and T. J. Curphey. Chem. Ind. (London), 1456 (1956).
13. A. N. Nesmeyanov, E. G. Perevalova, R. V. Golovnya, and O. A. Nesmeyanova. Dokl. Akad. Nauk SSSR, **97**, 459 (1954).
14. C. R. Hauser and J. K. Lindsay. J. Org. Chem. **22**, 482 (1957).
15. M. D. Rausch. Unpublished studies.
16. P. J. Graham, R. V. Lindsey, G. W. Parshall, M. L. Peterson, and G. M. Whitman. J. Am. Chem. Soc. **79**, 3416 (1957).
17. K. Schlögl and H. Pelousek. Ann. **651**, 1 (1962).
18. K. L. Rinehart, Jr., K. L. Motz, and S. Moon. J. Am. Chem. Soc. **79**, 2749 (1957).
19. M. Rosenblum. J. Am. Chem. Soc. **81**, 4530 (1959).

Can. J. Chem. Downloaded from www.nrcresearchpress.com by 210.87.254.40 on 09/05/12
For personal use only.

20. M. ROSENBLUM and W. G. HOWELLS. J. Am. Chem. Soc. **84**, 1167 (1962).
21. K. L. RINEHART, JR. and R. J. KIRBY. J. Am. Chem. Soc. **79**, 3290 (1957).
22. K. SCHLÖGL and H. SEILER. Tetrahedron Letters, No. 7, 4 (1960).
23. K. L. RINEHART, JR., D. E. BUBLITZ, and D. H. GUSTAFSON. Abstracts of Papers, 141st National Meeting, American Chemical Society, Washington, D.C. March 21–29, 1962. p. 19–O.
24. K. SCHLÖGL. Personal communication.
25. M. D. RAUSCH, P. SHAW, D. MAYO, and A. M. LOVELACE. J. Org. Chem. **23**, 505 (1958).
26. M. D. RAUSCH, E. O. FISCHER, and H. GRUBERT. J. Am. Chem. Soc. **82**, 76 (1960).
27. N. WELIKY and E. S. GOULD. J. Am. Chem. Soc. **79**, 2742 (1957).
28. W. F. LITTLE and R. EISENTHAL. J. Am. Chem. Soc. **82**, 1577 (1960).
29. M. D. RAUSCH, E. O. FISCHER, and H. GRUBERT. Chem. Ind. (London), 756 (1958).
30. E. O. FISCHER and H. GRUBERT. Chem. Ber. **92**, 2302 (1959).
31. L. FRIEDMAN, A. P. IRSA, and G. WILKINSON. J Am. Chem. Soc. **77**, 3689 (1955).
32. D. S. TRIFAN and R. BACSKAI. J. Am. Chem. Soc. **82**, 5010 (1960).
33. E. A. HILL and J. H. RICHARDS. J. Am. Chem. Soc. **83**, 3840 (1961).
34. M. L. H. GREEN, J. A. MCCLEVERTY, L. PRATT, and G. WILKINSON. J. Chem. Soc. 4854 (1961), and references cited therein.
35. T. J. CURPHEY, J. O. SANTER, M. ROSENBLUM, and J. H. RICHARDS. J. Am. Chem. Soc. **82**, 5249 (1960).
36. A. N. NESMEYANOV, D. N. KURSANOV, V. N. SETKINA, N. V. KISLYAKOVA, and N. S. KOCHETKOVA. Tetrahedron Letters, No. 2, 41 (1961).
37. J. H. RICHARDS. Abstracts of Papers, 135th National Meeting, American Chemical Society, Boston, Mass. April 5–10, 1959. p. 86-O.
38. M. D. RAUSCH, M. VOGEL, and H. ROSENBERG. J. Org. Chem. **22**, 903, 1016 (1957). M. D. RAUSCH and L. E. COLEMAN. J. Org. Chem. **23**, 107 (1958). K. SCHLÖGL *et al.* Monatsh. **88**, 601 (1957); **92**, 219, 533 (1961). N. WELIKY and E. S. GOULD. J. Am. Chem. Soc. **79**, 2742 (1957). C. R. HAUSER *et al.* J. Org. Chem. **22**, 482 (1957); **23**, 1142 (1958); **25**, 1982 (1960); **26**, 1030, 1795, 1800 (1961).
39. E. O. FISCHER and K. PLESSKE. Chem. Ber. **91**, 2719 (1958); **92**, 2841 (1959).
40. J. KOZIKOWSKI, R. E. MAGINN, and M. S. KLOVE. J. Am. Chem. Soc. **81**, 2995 (1959). M. CAIS and J. KOZIKOWSKI. J. Am. Chem. Soc. **82**, 5667 (1960).
41. F. A. COTTON and J. R. LETO. Chem. Ind. (London), 1592 (1958).
42. R. RIEMSCHNEIDER and H. G. KASSAHN. Z. Naturforsch. **14b**, 348 (1959); Chem, Ber. **92**, 3208 (1959).
43. M. CAIS and A. MODIANO. Chem. Ind. (London), 202 (1960); Tetrahedron Letters, No. 18, 31 (1960). M. CAIS and M. FELDKIMEL. Tetrahedron Letters, No. 13, 440 (1961).
44. E. O. FISCHER and K. PLESSKE. Chem. Ber. **93**, 1006 (1960).
45. R. RIEMSCHNEIDER, O. GOEHRING, and M. KRÜGER. Monatsh. **91**, 305 (1960).
46. E. O. FISCHER and K. PLESSKE. Chem. Ber. **94**, 93 (1961).
47. H. P. FRITZ and E. O. FISCHER. Z. Naturforsch. **12b**, 65 (1957).
48. R. ERCOLI, F. CALDERAZZO, and E. MANTICA. Chim. Ind. (Milan), **41**, 404 (1959).
49. R. RIEMSCHNEIDER, O. BECKER, and K. FRANZ. Monatsh. **90**, 571 (1959).
50. M. ROSENBLUM. Chem. Ind. (London), 72 (1957).
51. K. SCHLÖGL. Monatsh. **88**, 601 (1957).
52. G. D. BROADHEAD, J. M. OSGERBY, and P. L. PAUSON. Chem. Ind. (London), 209 (1957); J. Chem. Soc. 650 (1958).
53. A. I. TITOV, E. S. LISITSYNA, and M. R. SHEMTOVA. Dokl. Akad. Nauk SSSR. **130**, 341 (1960).
54. E. M. ARNETT and R. D. BUSHICK. J. Org. Chem. **27**, 111 (1962).
55. A. N. NESMEYANOV and N. S. KOCHETKOVA. Dokl. Akad. Nauk SSSR, **109**, 543 (1956); **114**, 800 (1957); **117**, 92 (1957); Izv. Akad. Nauk SSSR, Otd. Khim. Nauk, 242 (1958).
56. M. VOGEL, M. D. RAUSCH, and H. ROSENBERG. J. Org. Chem. **22**, 1016 (1957).
57. E. W. NEUSE and D. S. TRIFAN. J. Am. Chem. Soc. **84**, 1850 (1962).
58. K. L. RINEHART, JR., A. F. ELLIS, C. J. MICHEJDA, and P. A. KITTLE. J. Am. Chem. Soc. **82**, 4112 (1960).
59. E. O. FISCHER and G. E. HERBERICH. Chem. Ber. **94**, 1517 (1961).
60. A. N. NESMEYANOV and N. S. KOTCHETKOVA. Dokl. Akad. Nauk SSSR, **109**, 543 (1956).
61. K. L. RINEHART, JR., P. A. KITTLE, and A. F. ELLIS. J. Am. Chem. Soc. **82**, 2082 (1960).
62. A. N. NESMEYANOV and N. S. KOCHETKOVA. Dokl. Akad. Nauk SSSR, **126**, 307 (1959); **136**, 1096 (1961).
63. A. N. NESMEYANOV and I. I. KRITSKAYA. Izv. Akad. Nauk SSSR, Otd. Khim. Nauk, 253 (1956).
64. V. WEINMAYR. J. Am. Chem. Soc. **77**, 3009 (1955).
65. R. RIEMSCHNEIDER and D. HELM. Chem. Ber. **89**, 155 (1956).
66. K. L. RINEHART, JR., C. J. MICHEJDA, and P. A. KITTLE. J. Am. Chem. Soc. **81**, 3162 (1959).
67. C. JUTZ. Tetrahedron Letters, No. 21, 1 (1959).
68. P. L. PAUSON. J. Am. Chem. Soc. **76**, 2187 (1954).
69. G. D. BROADHEAD and P. L. PAUSON. J. Chem. Soc. 367 (1955).
70. A. N. NESMEYANOV, E. G. PEREVALOVA, and R. V. GOLOVNYA. Dokl. Akad. Nauk SSSR, **99**, 539 (1954).
71. V. WEINMAYR. J. Am. Chem. Soc. **77**, 3012 (1955).
72. M. ROSENBLUM, W. G. HOWELLS, A. K. BANNERJEE, and C. BENNETT. J. Am. Chem. Soc. **84**, 2726 (1962).

Can. J. Chem. Downloaded from www.nrcresearchpress.com by 210.87.254.40 on 09/05/12
For personal use only.

73. E. G. PEREVALOVA, N. A. SIMUKOVA, T. V. NIKITINA, P. D. RESHETOV, and A. N. NESMEYANOV. Izv. Akad. Nauk SSSR, Otd. Khim. Nauk, 77 (1956).
74. R. E. BOZAK and K. L. RINEHART, JR. J. Am. Chem. Soc. **84**, 1589 (1962).
75. A. N. NESMEYANOV, E. G. PEREVALOVA, R. V. GOLOVNYA, N. A. SIMUKOVA, and O. V. STAROVSKY. Izv. Akad. Nauk SSSR, Otd. Khim. Nauk, 638 (1957).
76. A. N. NESMEYANOV, E. G. PEREVALOVA, N. A. SIMUKOVA, Y. N. SHEINKER, and M. D. RESHETOVA. Dokl. Akad. Nauk SSSR, **133**, 851 (1960).
77. C. R. HAUSER and J. K. LINDSAY. J. Org. Chem. **21**, 382 (1956); **22**, 355 (1957).
78. A. N. NESMEYANOV, E. G. PEREVALOVA, L. S. SHILOVTSEVA, and Z. A. BEINORAVICHUTE. Dokl. Akad. Nauk SSSR, **121**, 117 (1958).
79. D. LEDNICER, K. J. LINDSAY, and C. R. HAUSER. J. Org. Chem. **23**, 653 (1958).
80. J. M. OSGERBY and P. L. PAUSON. J. Chem. Soc. 656 (1958).
81. C. R. HAUSER, J. K. LINDSAY, D. LEDNICER, and C. E. CAIN. J. Org. Chem. **22**, 717 (1957).
82. C. R. HAUSER, J. K. LINDSAY, and D. LEDNICER. J. Org. Chem. **23**, 358 (1958).
83. A. N. NESMEYANOV, E. G. PEREVALOVA, L. S. SHILOVTSEVA, and Y. A. USTYNYUK. Dokl. Akad. Nauk SSSR, **124**, 331 (1959).
84. A. N. NESMEYANOV, E. G. PEREVALOVA, S. P. GUBIN, T. V. NIKITINA, A. A. PONOMERENKO, and L. S. SHILOVTSEVA. Dokl. Akad. Nauk SSSR, **139**, 888 (1961).
85. G. R. KNOX, P. L. PAUSON, and G. V. D. TIERS. Chem. Ind. (London), 1046 (1959).
86. G. R. KNOX and P. L. PAUSON. J. Chem. Soc. 692 (1958).
87. A. N. NESMEYANOV, E. G. PEREVALOVA, and S. S. CHURANOV. Dokl. Akad. Nauk SSSR, **114**, 335 (1957).
88. A. N. NESMEYANOV and O. A. REUTOV. Izv. Akad. Nauk SSSR, Otd. Khim. Nauk, 926 (1959).
89. M. CAIS and J. KOZIKOWSKI. J. Am. Chem. Soc. **82**, 5667 (1960).
90. M. D. RAUSCH, M. VOGEL, and H. ROSENBERG. J. Org. Chem. **22**, 900 (1957).
91. A. N. NESMEYANOV, E. G. PEREVALOVA, and O. A. NESMEYANOVA. Dokl. Akad. Nauk SSSR, **100**, 1099 (1955).
92. M. D. RAUSCH. Inorg. Chem. **1**, 414 (1962).
93. D. SEYFERTH and J. F. HELLING. Chem. Ind. (London), 1568 (1961).
94. D. SEYFERTH, H. P. HOFMANN, R. BURTON, and J. F. HELLING. Inorg. Chem. **1**, 227 (1962).
95. H. SHECHTER and J. F. HELLING. J. Org. Chem. **26**, 1034 (1961).
96. M. D. RAUSCH. Abstracts of Papers, 140th National Meeting, American Chemical Society, Chicago, Ill. Sept. 3–8, 1961. p. 34-Q.
97. R. A. BENKESER, D. GOGGIN, and G. SCHROLL. J. Am. Chem. Soc. **76**, 4025 (1954).
98. D. W. MAYO, P. D. SHAW, and M. D. RAUSCH. Chem. Ind. (London), 1388 (1957).
99. A. N. NESMEYANOV, E. G. PEREVALOVA, and Z. A. BEINORAVICHUTE. Dokl. Akad. Nauk SSSR, **112**, 439 (1957).
100. A. N. NESMEYANOV, E. G. PEREVALOVA, Z. A. BEINORAVICHUTE, and I. L. MALYGINA. Dokl. Akad. Nauk SSSR, **120**, 1263 (1958).
101. S. L. GOLDBERG, D. W. MAYO, M. VOGEL, H. ROSENBERG, and M. D. RAUSCH. J. Org. Chem. **24**, 824 (1959).
102. K. L. RINEHART, JR., L. WESTMAN, H. GRUBERT, D. H. GUSTAFSON, J. T. MARVEL, and T. L. SHEDROFF. Abstracts of Papers, 17th International Congress of Pure and Applied Chemistry, Munich, Germany. Aug. 30–Sept. 6, 1959. p. 28.
103. A. N. NESMEYANOV, V. A. SAZONOVA, and V. N. DROZD. Dokl. Akad. Nauk SSSR, **126**, 1004 (1959).
104. A. N. NESMEYANOV, V. A. SAZONOVA, V. N. DROZD, and L. A. NIKONOVA. Dokl. Akad. Nauk SSSR, **131**, 1088 (1960).
105. A. N. NESMEYANOV, V. A. SAZONOVA, and V. N. DROZD. Dokl. Akad. Nauk SSSR, **129**, 1060 (1960); Tetrahedron Letters, No. 17, 13 (1959); Dokl. Akad. Nauk SSSR, **130**. 1030 (1960).
106. A. N. NESMEYANOV, E. G. PEREVALOVA, R. V. GOLOVNYA, and L. S. SHILOVTSEVA. Dokl. Akad. Nauk SSSR, **102**, 535 (1955).
107. E. M. ACTON and R. M. SILVERSTEIN. J. Org. Chem. **24**, 1487 (1959).
108. H. GRUBERT and K. L. RINEHART, JR. Tetrahedron Letters, No. 12, 16 (1959).
109. J. F. HELLING and H. SHECHTER. Chem. Ind. (London), 1157 (1959).
110. A. N. NESMEYANOV, E. G. PEREVALOVA, and T. V. NIKITINA. Tetrahedron Letters, No. 1, 1 (1960); Dokl. Akad. Nauk SSSR, **138**, 1118 (1961).
111. E. O. FISCHER and H. BRUNNER. Z. Naturforsh. **16b**, 406 (1961).
112. E. O. FISCHER and H. BRUNNER (as quoted by K. Plesske). Angew. Chem. **74**, 309 (1962).
113. T. KUWANA, D. E. BUBLITZ, and G. HOH. J. Am. Chem. Soc. **82**, 5811 (1960).
114. G. L. HOH, W. E. MCEWEN, and J. KLEINBERG. J. Am. Chem. Soc. **83**, 3949 (1961).
115. G. WILKINSON, M. ROSEMBLUM, M. C. WHITING, and R. B. WOODWARD. J. Am. Chem. Soc. **74**, 2125 (1952).
116. J. G. MASON and M. ROSENBLUM. J. Am. Chem. Soc. **82**, 4206 (1960).
117. D. S. TRIFAN and L. NICHOLAS. J. Am. Chem. Soc. **79**, 2746 (1957).
118. A. N. NESMEYANOV and O. A. REUTOV. Dokl. Akad. Nauk SSSR, **115**, 518 (1958); Izv. Akad. Nauk SSSR, Otd. Khim. Nauk, 926 (1959).
119. W. F. LITTLE and R. EISENTHAL. J. Org. Chem. **26**, 3609 (1961).
120. W. F. LITTLE and R. EISENTHAL. J. Am. Chem. Soc. **83**, 4936 (1961).
121. L. A. KAZITSYNA, B. V. LOKSHIN, and N. A. NESMEYANOV. Dokl. Akad. Nauk SSSR, **127**, 333 (1959).
122. W. F. LITTLE and A. K. CLARK. J. Org. Chem. **25**, 1979 (1960).

Can. J. Chem. Downloaded from www.nrcresearchpress.com by 210.87.254.40 on 09/05/12
For personal use only.

123. M. D. RAUSCH, M. VOGEL, H. ROSENBERG, D. MAYO, and P. SHAW. Wright Air Development Center Tech. Rept. 57–62, Part II. February, 1958; ASTIA Document No. 150979. (This report has been released to the Office of Technical Services, U.S. Department of Commerce, Washington 25, D.C., for sale to the general public.)
124. S. I. GOLDBERG and D. W. MAYO. Chem. Ind. (London), 671 (1959).
125. M. D. RAUSCH. J. Am. Chem. Soc. **82**, 2080 (1960).
126. M. D. RAUSCH. J. Org. Chem. **26**, 1802 (1961).
127. M. D. RAUSCH. J. Org. Chem. **26**, 3579 (1961).
128. G. WITTIG and W. HERWIG. Chem. Ber. **87**, 1511 (1954).
129. O. A. NESMEYANOVA and E. G. PEREVALOVA. Dokl. Akad. Nauk SSSR, **126**, 1007 (1959).
130. V. V. KORSHAK, S. L. SOSIN, and V. P. ALEXSEEVA. Dokl. Akad. Nauk SSSR, **132**, 360 (1960); J. Poly. Sci. **52**, 213 (1961).
131. A. N. NESMEYANOV, A. M. RUBINSHTEIN, G. L. SLONIMSKII, A. A. SLINKIN, N. S. KOCHETKOVA, and R. B. MATERIKOVA. Dokl. Akad. Nauk SSSR, **138**, 125 (1961).
132. K. SCHLÖGL and H. SEILER. Naturwiss. **48**, 376 (1961).
133. J. H. RICHARDS and E. A. HILL. J. Am. Chem. Soc. **81**, 3484 (1959); **83**, 3840 (1961).
134. E. A. HILL and J. H. RICHARDS. J. Am. Chem. Soc. **83**, 4216 (1961).
135. G. R. BUELL, W. E. MCEWEN, and J. KLEINBERG. Tetrahedron Letters, No. 5, 16 (1959); J. Am. Chem. Soc. **84**, 40 (1962).
136. D. S. TRIFAN and R. BACSKAI. Tetrahedron Letters, No. 13, 1 (1960).
137. F. S. ARIMOTO and A. C. HAVEN, JR. J. Am. Chem. Soc. **77**, 6295 (1955).
138. K. SCHLÖGL and H. SEILER. Naturwiss. **45**, 337 (1958).
139. M. ROSENBLUM. Ph.D. Thesis, Harvard University, Cambridge, Mass. 1953.
140. A. N. NESMEYANOV, V. A. SAZONOVA, V. N. DROZD, and L. A. NIKONOVA. Dokl. Akad. Nauk SSSR, **133**, 126 (1960).
141. E. G. PEREVALOVA, A. N. NESMEYANOV, and T. V. NIKITINA. Dokl. Akad. Nauk SSSR, **138**, 1118 (1961).
142. J. M. OSGERBY and P. L. PAUSON. Chem. Ind. (London), 196 (1958).
143. A. BERGER, W. E. MCEWEN, and J. KLEINBERG. Chem. Ind. (London), 204 (1960); J. Am. Chem. Soc. **83**, 2274 (1961).
144. D. E. BUBLITZ, W. E. MCEWEN, and J. KLEINBERG. Chem. Ind. (London), 936 (1960); J. Am. Chem. Soc. **84**, 1845 (1962).
145. M. L. H. GREEN, L. PRATT, and G. WILKINSON. J. Chem. Soc. 3753 (1960).
146. H. H. HOEHN, L. PRATT, K. F. WATTERSON, and G. WILKINSON. J. Chem. Soc. 2738 (1961).
147. S. KATZ, J. F. WEIHER, and A. F. VOIGT. J. Am. Chem. Soc. **80**, 6459 (1958).
148. G. WILKINSON, F. A. COTTON, and J. BIRMINGHAM. J. Inorg. Nucl. Chem. **2**, 95 (1956).
149. M. DUBECK and A. H. FILBEY. J. Am. Chem. Soc. **83**, 1257 (1961).
150. M. DUBECK. J. Am. Chem. Soc. **82**, 6193 (1960).
151. D. W. MCBRIDE, R. L. PRUETT, E. PITCHER, and F. G. A. STONE. J. Am. Chem. Soc. **84**, 497 (1962).
152. K. F. WATTERSON and G. WILKINSON. Chem. Ind. (London), 1358 (1960).

Can. J. Chem. Downloaded from www.nrcresearchpress.com by 210.87.254.40 on 09/05/12
For personal use only.

ELECTRONEGATIVITY

III. ORBITAL ELECTRONEGATIVITIES AND ELECTRON AFFINITIES OF TRANSITION METALS[1, 2]

JÜRGEN HINZE[3] AND H. H. JAFFÉ
Department of Chemistry, University of Cincinnati, Cincinnati, Ohio, U.S.A.
Received October 29, 1962

ABSTRACT

The orbital electronegativities of the neutral transition metals of the first transition series have been calculated by the Mulliken formula for a wide variety of hybrid states. The electron affinities needed in the process have been calculated by isoelectronic and isoconfigurational extrapolation.

Can. J. Chem. Downloaded from www.nrcresearchpress.com by 210.87.254.40 on 09/05/12
For personal use only.

ORBITAL ELECTRONEGATIVITIES

In the first article (1) of this series electronegativities have been evaluated and reported for a variety of valence states of the neutral elements of rows one and two of the periodic system. Mulliken's definition (3) of electronegativity, given as

$$\chi = \frac{I+E}{2}, \qquad [1]$$

has been used for the evaluation since this definition has the best theoretical foundation (4, 5) and can account sensitively for any valence state variations, provided the appropriate valence state ionization potentials and valence state electron affinities are used. In the second article (2) of this series the entire much-confused concept of electronegativity has been reinvestigated, and the following conclusions have been reached:

(*a*) Electronegativity is the property, not of an atom, but of an orbital of an atom in its valence state.

(*b*) The values of such orbital electronegativities depend strongly on the valence state considered, and, in the case of hybrids between *s* and *p* electrons, increase linearly with increasing *s* character of the hybrid orbital considered.

(*c*) Orbital electronegativity has meaning only for an orbital before it has formed a bond. For the analogous but distinctly different property of an orbital after bond formation and charge exchange the term *bond* electronegativity is suggested.

(*d*) Mulliken's definition does not yield orbital electronegativities of vacant (virtual) orbitals or doubly occupied orbitals. However, a new definition was arrived at which includes Mulliken's definition as a special case for singly occupied orbitals.

This definition was given as

$$\chi_j = \partial E(n_j)/\partial n_j \qquad [2]$$

[1]*Presented at the Symposium on Organometallic Compounds, Vancouver, British Columbia, September 4–6, 1962, sponsored by the Inorganic Chemistry Division, Chemical Institute of Canada, and the Department of Chemistry, University of British Columbia, with the support of the National Research Council, Ottawa, in cooperation with the University Extension Department.*
[2]*For Part II see reference 2.*
[3]*Present address: Department of Chemistry, Rice University, Houston 1, Texas.*

where n_j is the occupation of the orbital considered, j, and E is the energy of the atom as a function of this occupation. The energy relation postulated for this function is

$$E = a+bn_j+cn_j^2, \qquad [3]$$

in which the constants a, b, and c can be determined from the known valence state ionization potentials and electron affinities. With this definition it is possible to evaluate orbital electronegativities for vacant and doubly occupied orbitals, and for partially charged atoms and groups. Combination of [2] and [3] gives eq. [1] for singly occupied orbitals, i.e., $n = 1$.

It is the purpose of this work to examine the dependence of the orbital electronegativity in the transition series on the *valence* state, not *oxidation* state. Here the picture is considerably complicated by the much larger variety of possible hybrids due to the availability of d orbitals. Computations of orbital electronegativities for a few hybrids of the transition elements have already been done (6), but the need for a more extensive investigation becomes apparent if it is realized that a priori quantum mechanical computations do not readily yield answers for molecules containing transition elements, since such systems are too complex. It is possible, however, to obtain valuable information in such complex systems by different semiempirical methods, such as ligand field theory (7), Mulliken's "Magic Formula" (8), or various forms of molecular orbital theory. Such semiempirical methods can make good use of electronegativities as well as valence state ionization potentials, electron affinities, and promotion energies, all of which are obtained and reported in this work.

The essential part of the evaluation of orbital electronegativities, following eq. [1], is the determination of the valence state ionization potentials, I_v, and valence state electron affinities, E_v. The valence state ionization potentials are obtained by subtracting and adding to the ground state ionization potential the corresponding promotion energies of the atom, P^0, and of the positive ion, P^+, respectively. Analogously the valence state electron affinities are obtained by adding and subtracting to the ground state electron affinities the promotion energies of the atom, P^0, and negative ion, P^-, respectively. Methods for the computation of promotion energies of atoms and positive ions are known (1), and ground state ionization potentials obtainable from spectroscopy are tabulated (9), hence the evaluation of valence state ionization potentials is straightforward. However, difficulties arise in the evaluation of valence state electron affinities. The promotion energy of negative ions, although not directly obtainable, can be extrapolated, as generally done, from isoelectronic sequences (1). However, no ground state electron affinities of the transition elements are available, consequently such values had to be determined in this work, as described in Part I (1).

Procedure

The computations of the promotion energies and hence the valence state ionization potentials and electronegativities are in general the same as described in detail in the first paper of this series (1).

(1) The hybrids listed in Table I, to which the computations are confined, are constructed using group theory and the procedure outlined by Kimball (10).

(2) The valence state promotion energies for these hybrids are evaluated using the method of Mulliken (3) and Van Vleck (11), i.e., the valence state energies are expressed as linear combinations of Slater parameters, the valence state equations.[4]

[4]*The coefficients of the valence state equations are evaluated using an IBM 650 electronic computer and a program written and described by Zung (12).*

Can. J. Chem. Downloaded from www.nrcresearchpress.com by 210.87.254.40 on 09/05/12
For personal use only.

TABLE I

The hybrids considered

Point group	Configuration	Orbitals	Geometry
Two-orbital hybrids			
$D_{\infty h}$	(sp)	$\frac{1}{\sqrt{2}}s \pm \frac{1}{\sqrt{2}}z$	Linear
$D_{\infty h}$	(dp)	$\frac{1}{\sqrt{2}}\sigma \pm \frac{1}{\sqrt{2}}z$	Linear
C_{2v}	(p^2)	x, y	Rectangular
C_{2v}	(ds)	$\frac{1}{\sqrt{2}}s \pm \frac{1}{\sqrt{2}}\delta$	Rectangular
C_{2v}	(d^2)	$-\frac{1}{\sqrt{2}}\sigma \pm \frac{1}{\sqrt{2}}\delta$	Rectangular
Three-orbital hybrids			
D_{3h}	(sp^2)	$\frac{1}{\sqrt{3}}s + \frac{\sqrt{2}}{\sqrt{3}}x$ $\frac{1}{\sqrt{3}}s - \frac{1}{\sqrt{6}}x \pm \frac{1}{\sqrt{2}}y$	Trigonal planar
D_{3h}	(dp^2)	$-\frac{1}{\sqrt{3}}\sigma + \frac{\sqrt{2}}{\sqrt{3}}x$ $-\frac{1}{\sqrt{3}}\sigma - \frac{1}{\sqrt{6}}x \pm \frac{1}{\sqrt{2}}y$	Trigonal planar
D_{3h}	(d^2s)	$\frac{1}{\sqrt{3}}s + \frac{\sqrt{2}}{\sqrt{3}}\delta$ $\frac{1}{\sqrt{3}}s - \frac{1}{\sqrt{6}}\delta \pm \frac{1}{\sqrt{2}}\delta'$	Trigonal planar
D_{3h}	(d^3)	$-\frac{1}{\sqrt{3}}\sigma + \frac{\sqrt{2}}{\sqrt{3}}\delta$ $-\frac{1}{\sqrt{3}}\sigma - \frac{1}{\sqrt{6}}\delta \pm \frac{1}{\sqrt{2}}\delta'$	Trigonal planar
C_{3v}	(d^2p)*	$\frac{1}{\sqrt{3}}z + \frac{\sqrt{2}}{\sqrt{3}}\delta$ $\frac{1}{\sqrt{3}}z - \frac{1}{\sqrt{6}}\delta \pm \frac{1}{\sqrt{2}}\delta'$	Trigonal pyramid
Four-orbital hybrids			
T_d	(sp^3)	$\frac{1}{2}(s+x+y+z)$‡	Tetrahedral
T_d	(d^3s)	$\frac{1}{2}(s+\pi+\pi'+\delta)$‡	Tetrahedral
D_{4h}	(dsp^2)	$\frac{1}{2}(s+x+y+\delta)$‡	Square planar
D_{4h}	(d^2p^2)	$\frac{1}{2}(\sigma+x+y+\delta)$‡	Square planar
C_{3v}	(d^2sp)	$\frac{1}{2}(s+z+\delta+\delta')$‡	Trigonal pyramid
C_{3v}	(dp^3)	$\frac{1}{2}(\sigma+x+y+z)$‡	Trigonal pyramid
C_{3v}	(d^3p)	$\frac{1}{2}(\sigma+\pi+\pi'+z)$‡	Trigonal pyramid
C_{4v}	(d^4)	$\frac{1}{2}(\sigma+\delta+\pi+\pi')$‡	Tetragonal pyramid

Can. J. Chem. Downloaded from www.nrcresearchpress.com by 210.87.254.40 on 09/05/12
For personal use only.

TABLE I (*Concluded*)

Point group	Configuration	Orbitals	Geometry
Five-orbital hybrids			
D_{3h}	(dsp^3)†	$0.314s-0.485\sigma+\frac{\sqrt{2}}{\sqrt{3}}x$	
		$0.314s-0.485\sigma-\frac{1}{\sqrt{6}}x\pm\frac{1}{\sqrt{2}}y$	Trigonal bipyramid
		$0.594s+0.384\sigma\pm\frac{1}{\sqrt{2}}z$	
D_{3h}	(d^3sp)*	$\frac{1}{\sqrt{3}}s+\frac{\sqrt{2}}{\sqrt{3}}\delta$	
		$\frac{1}{\sqrt{3}}s-\frac{1}{\sqrt{6}}\delta\pm\frac{1}{\sqrt{2}}\delta'$	Trigonal bipyramid
		$-\frac{1}{\sqrt{2}}\sigma\pm\frac{1}{\sqrt{2}}z$	
C_{4v}	(d^2sp^2)†	$0.059s-0.496\sigma\pm\frac{1}{\sqrt{2}}x+\frac{1}{2}\delta$	
		$0.059s-0.496\sigma\pm\frac{1}{\sqrt{2}}y-\frac{1}{2}\delta$	Tetragonal pyramid
		$0.993s+0.117\sigma$	
C_{4v}	(d^4s)	$\frac{1}{\sqrt{5}}s-\frac{1}{\sqrt{20}}\sigma\pm\frac{1}{\sqrt{2}}\pi+\frac{1}{2}\delta$	
		$\frac{1}{\sqrt{5}}s-\frac{1}{\sqrt{20}}\sigma\pm\frac{1}{\sqrt{2}}\pi'-\frac{1}{2}\delta$	Tetragonal pyramid
		$\frac{1}{\sqrt{5}}s+\frac{2}{\sqrt{5}}\sigma$	
C_{4v}	(d^4p)	$\frac{1}{\sqrt{5}}z-\frac{1}{\sqrt{20}}\sigma\pm\frac{1}{\sqrt{2}}\pi+\frac{1}{2}\delta$	
		$\frac{1}{\sqrt{5}}z-\frac{1}{\sqrt{20}}\sigma\pm\frac{1}{\sqrt{2}}\pi'-\frac{1}{2}\delta$	Tetragonal pyramid
		$\frac{1}{\sqrt{5}}z+\frac{2}{\sqrt{5}}\sigma$	
Six-orbital hybrids			
O_h	(d^2sp^3)	$\frac{1}{\sqrt{6}}s\pm\frac{1}{\sqrt{2}}z+\frac{1}{\sqrt{3}}\sigma$	
		$\frac{1}{\sqrt{6}}s\pm\frac{1}{\sqrt{2}}x-\frac{1}{\sqrt{12}}\sigma+\frac{1}{2}\delta$	Octahedral
		$\frac{1}{\sqrt{6}}s\pm\frac{1}{\sqrt{2}}y-\frac{1}{\sqrt{12}}\sigma-\frac{1}{2}\delta$	

*No choice of coefficients yields equivalent orbitals; thus, standard coefficients are chosen.
†The coefficients are chosen so that all orbitals are equivalent, i.e., yield the same overlap integral in an iron (ψ) – carbon (sp^3) bond.
‡The other three hybrids are given by the same combinations, but with signs: $++--$, $+-+-$, and $+--+$.

(3) Substitution of the Slater parameters, Table II, into the valence state equations derived gives the promotion energies required of atoms, positive ions, and negative ions, P^0, P^+, and P^-, respectively.

(4) The valence state ionization potentials and electron affinities are obtained from the corresponding ground state potentials, Table III, as

$$I_v = I_g + P^+ - P^0$$

and

$$E_v = E_g + P^0 - P^-.$$

Can. J. Chem. Downloaded from www.nrcresearchpress.com by 210.87.254.40 on 09/05/12
For personal use only.

Can. J. Chem. Downloaded from www.nrcresearchpress.com by 210.87.254.40 on 09/05/12
For personal use only.

TABLE II

Slater–Condon parameter used

	(d^n)	$(d^{n-1}s)$	$(d^{n-1}p)$	$(d^{n-2}s^2)$	$(d^{n-2}sp)$	$(d^{n-2}p^2)$	$F_2(pp)$	$F_2(pd)$	$F_2(dd)$	$F_4(dd)$	$G_1(pd)$	$G_3(pd)$	$G_1(sp)$	$G_2(sd)$
Ca	46,662	21,103	37,840	0	19,458	40,097	93	108	(400)	(10)	364	8	4,195	746
Sc	41,958	18,588	38,349	101	21,821	(47,811)	(200)	68	580	22	182	32	2,744	1,095
Ti	51,825	25,988	46,945	7,689	32,161	(60,386)	(220)	229	770	47	326	26	2,092	1,534
V	59,273	35,556	69,532	18,052	58,439	(97,125)	(240)	786	747	51	1,169	114	3,618	1,813
Cr	70,925	64,771	84,588	46,520	80,396	(114,300)	(260)	35	953	82	3	14	10,320	1,462
Mn	67,566	64,119	104,024	71,228	105,667	(144,437)	(280)	217	1,141	97	914	−14	2,841	1,192
Fe	43,472	34,343	65,528	44,665	88,375	(132,000)	(300)	211	1,190	76	24	36	4,078	1,285
Co	27,886	18,226	47,518	31,157	(68,610)	(106,000)	(320)	201	1,408	119	159	0	(2,500)	1,143
Ni	14,729	2,071	32,071	14,763	(58,653)	(102,000)	(340)	130	1,629	121	200	16	(3,000)	1,339
Cu	—	0	30,701	12,020	(66,683)	(121,000)	(360)	315	—	—	391	35	(6,200)	(1,600)
Sc^+	11,282	1,323	28,966	11,736	47,473	(77,574)	(300)	242	737	51	380	3	8,243	1,218
Ti^+	16,059	10,904	41,374	25,100	64,399	(104,000)	(350)	434	797	32	450	32	7,275	1,182
V^+	32,569	29,801	61,053	(35,000)	75,088	(115,000)	(370)	382	961	70	310	36	5,690	1,942
Cr^+	61,815	58,593	95,001	69,088	(110,000)	(151,000)	(390)	459	1,051	81	483	58	(7,000)	1,747
Mn^+	52,752	71,029	111,343	90,809	(134,000)	(180,000)	(410)	(350)	480	134	1,660	12	(13,000)	1,302
Fe^+	29,330	56,713	104,727	108,061	(155,000)	(210,000)	(430)	319	1,346	113	261	30	(4,000)	1,591
Co^+	(13,354)	(46,767)	(88,585)	(95,556)	(140,000)	(186,000)	(450)	353	(1,500)	(120)	(250)	(30)	(4,000)	(1,237)
Ni^+	603	26,584	75,184	(90,000)	(145,000)	(200,000)	(470)	342	1,637	122	238	32	(4,000)	1,541
Cu^+	0	24,457	72,907	86,979	139,358	(193,000)	(490)	159	1,720	132	266	21	7	2,894
Ca^-	67,857	26,272	35,324	−24,898	−20,757	−8,378	50	−298	363	12	−86	32	−1,787	378
Sc^-	71,081	22,175	32,837	−19,622	−10,766	5,772	70	76	579	24	342	16	−1,506	1,126
Ti^-	56,731	12,519	44,063	−32,984	6,878	43,250	90	1,113	443	21	1,855	170	236	1,879
V^-	89,098	58,513	57,833	2,231	26,792	48,600	110	−280	1,426	30	−1,654	16	7,640	1,622
Cr^-	105,802	71,525	103,321	34,395	56,334	78,874	130	115	936	81	1,567	−289	1,682	793
Mn^-	73,590	21,919	42,471	−6,226	36,750	78,000	150	69	880	32	−202	12	4,156	1,333
Fe^-	55,169	9,868	19,852	−27,686	−7,780	12,000	170	60	1,179	116	80	−32	1,000	745
Co^-	29,458	−20,315	−8,765	−57,453	−22,052	11,000	190	101	1,538	110	134	11	5,993	−216

TABLE III
Ground state electron affinities and ionization potentials

Element	E_g (ev)	I_g (ev)
Ca	0.11	6.11
Sc	0.46	6.56
Ti	1.25	6.83
V	1.19	6.74
Cr	3.54	6.76
Mn	1.17	7.34
Fe	3.13	7.90
Co	3.29	7.86

Finally, the orbital electronegativities are given in Mulliken's scale as

$$\chi_M = \frac{I_v + E_v}{2},$$

which are converted to Pauling units by (1):

[4] $$\chi_P = 0.336(\chi_M - 0.615).$$

The Slater Parameters

The Slater parameters used for the evaluation of the valence state promotion energies of atoms and positive ions are those obtained previously (13) by an extensive fitting of Slater equations to the corresponding observed atomic energy levels (9). For the evaluation of promotion energies more Slater parameters are needed than can be obtained from one configuration alone. Consequently it is necessary to use those Slater parameters which are obtained when several configurations are fitted simultaneously. This implies that equivalent parameters have the same value in different configurations. That this is not true is known. However, it has been shown (13) that the uncertainties inherent in Slater's treatment of the many-electron atom are not increased significantly by assuming that the Slater parameters are equal for different configurations. In fact, the representation of spectroscopic data by Slater's equations is often better if different configurations are considered simultaneously rather than any one configuration individually. Thus, in the level of the approximations necessary to use empirical Slater parameters, it is valid to use values obtained from fitting several configurations simultaneously. The values used are listed in Table II, where the values in parentheses, not obtainable directly, had to be estimated as follows.

The values of $G_1(sp)$ of Co, Ni, and Cr^+ through Ni^+ are estimated so that they follow the same general trend indicated by the parameters determined. The parameters $G_1(sp)$ and $G_2(sd)$ of Cu cannot be evaluated independently from the atomic energy levels observed; however, the parameter $G_1(sp)+G_2(sd)$ is obtained, which gives the value of $G_1(sp)$ after $G_2(sd)$ has been estimated. The values of $W(d^{n-2}sp)$ of Co, Ni, and Fe^+ are obtained by adding to the corresponding apparent $W(d^{n-2}sp)$'s determined, which include some $G_1(sp)$, the values of $G_1(sp)$ estimated. Similarly the value of $W(d^{n-2}sp)$ of Mn^+ is obtained by adding to the value determined the values of $G_1(sp)$ and $F_2(pd)$ estimated. The $W(d^{n-2}sp)$'s of Cr^+, Co^+, and Ni^+ as well as the $W(d^{n-2}s^2)$'s of V^+ and Ni^+ are determined so that they follow the trend indicated by the other parameters. Only the value of $F_2(pp)$'s must be assumed freely. Fortunately the $F_2(pp)$'s are known to be small and of

Can. J. Chem. Downloaded from www.nrcresearchpress.com by 210.87.254.40 on 09/05/12
For personal use only.

no great importance here, since they will influence only the energies of valence states with several p electrons, and such states are rather high in energy anyway. With the $F_2(pp)$ assumed, it is possible to calculate the values of $W(d^{n-2}p^2)$ of the elements Sc, Ti, V, Mn, and Sc^+ from the apparent values computed which contain $-5F_2(pp)$. All other $W(d^{n-2}p^2)$ which had to be extrapolated are obtained from the relation

$$W(d^{n-2}p^2) \approx 2W(d^{n-2}sp) - W(d^{n-2}s^2), \quad [5]$$

which implies that the promotion of two s electrons to p electrons requires twice as much energy as the promotion of one. Here the change of the electronic interaction of the different configurations is neglected. This is not too serious, since the d electron configuration is kept constant and the other changes, involving only one electron pair, are small.

The values of $F_2(dd)$ and $F_4(dd)$ of Ca cannot be obtained separately, thus they had to be assumed inside the range of the values determined. The same is true for Co^+, where the parameter obtained is $F_2(dd)-5F_4(dd)$. Here $F_2(dd)$ is calculated after $F_4(dd)$ has been assumed. The assumed $F_4(dd)$ of Co^+ permits also the evaluation of $G_2(sd)$ from the parameter $G_2(sd)+21F_4(dd)$ computed. With the values of $G_1(pd)$ and $G_3(pd)$ which have been estimated for Co^+ it is finally possible to calculate the values of $W(d^n)$, $W(d^{n-1}s)$, $W(d^{n-1}p)$, and $W(d^{n-2}s^2)$ from the parameters obtained from spectral data, $W(d^n)-49F_4(dd)$, $W(d^{n-1}s)-147F_4(dd)$, $W(d^{n-1}p)-18G_1(pd)-189G_3(pd)-147F_4(dd)$, and $W(d^{n-2}s^2)-294F_4(dd)$, respectively.

The Slater parameters for negative ions cannot be determined from spectral data, since no spectra of negative ions are observed. Their magnitude is extrapolated linearly from the corresponding parameters of atom and positive ion in an isoelectronic sequence. Such a linear relation has been shown for lighter elements by Rohrlich (14) and is here assumed to hold also for the transition series, since there is no other method on hand to estimate the parameters or valence state promotion energies of negative ions. However, it must be pointed out that the Slater parameters of negative ions reported in Table II are relatively uncertain, since only two known numbers in an isoelectronic sequence could be used for the extrapolation. Furthermore, it should be noted that the W's given for negative ions have no *absolute* significance, since they are not based on the ground state of the negative ions; the same is true for the valence state promotion energies reported for negative ions.

Results

The present paper considers only the elements Ca through Cu, and the ions Sc^+ through Cu^+. This restriction is necessary because of the limitations of experimental information on spectroscopic states involving incompletely filled d shells; for other elements of the third period the evaluation of the Slater–Condon parameters needed is not possible. Consequently, P^- values, and hence electronegativities of d-hybrid orbitals are obtainable only for the elements Sc to Co.

In Table IV the resulting orbital electronegativities of these elements are given in Pauling's units together with the corresponding promotion energies P^0, P^+, and P^- and the valence state ionization potentials and electron affinities, I_v and E_v, respectively.

There are numerous possible ways of distributing the non-valence electrons of the valence shell. Only distributions of maximum multiplicity have been considered, in keeping with Hund's rule, except where the s orbital is not included in the hybrid; s^2 configurations were also considered. In no case was occupation of hybrid orbitals by valence electrons considered.

Can. J. Chem. Downloaded from www.nrcresearchpress.com by 210.87.254.40 on 09/05/12
For personal use only.

TABLE IV

Electronegativities of transition metals

Element	Hybrid	Configuration*	P^0	P^+	P^-	I_v	E_v	χ
Sc	sp^2	000000	3.58	6.70	−6.35	9.68	7.36	2.66
	dp^2	000000	5.31	5.96	−1.29	7.21	4.03	1.68
	d^2s	000000	2.41	0.68	1.43	4.82	−1.60	0.33
	d^3	000000	4.48	1.04	7.98	3.12	−6.08	−0.69
	d^2p	000000	5.01	3.09	3.28	4.64	−0.85	0.43
Ti	sp	100010	2.68	2.20	−3.86	6.36	2.70	1.32
	dp	001010	4.55	2.53	1.89	4.81	−1.19	0.40
	p^2	100010	6.11	4.08	−2.21	4.80	4.48	1.35
	ds	011000	1.63	0.57	−2.36	5.77	0.15	0.79
	d^2	001010	4.23	1.00	5.59	3.59	−5.21	−0.47
	sp^2	000010	6.22	8.85	−3.76	9.46	6.14	2.41
	dp^2	000010	6.74	7.42	−1.65	7.51	4.55	1.82
	d^2s	100000	2.05	0.81	−1.18	5.59	−0.62	0.63
	d^3	001000	4.43	1.12	5.73	3.52	−5.15	−0.47
	dsp	100000	3.17	3.55	−2.59	7.21	1.91	1.33
	d^2p	100000	4.93	3.53	1.67	5.43	−0.59	0.61
	sp^3	000000	11.21	19.77	−3.68	15.39	11.04	4.23
	d^3s	000000	1.91	0.95	−1.00	5.88	−0.93	0.62
	dsp^2	000000	6.64	11.63	−3.21	11.82	6.00	2.79
	d^2p^2	000000	6.88	9.06	−1.51	9.01	4.55	2.07
	d^2sp	000000	3.96	5.52	−2.69	8.39	2.81	1.67
	dp^3	000000	10.87	16.22	−3.40	12.19	10.43	3.59
	d^3p	000000	5.49	4.52	3.02	5.86	−1.38	0.55
	d^4	000000	4.43	1.09	5.75	3.48	−5.17	−0.48
V	sp	100110	3.67	3.07	−1.41	6.13	2.18	1.19
	dp	001110	4.47	3.03	2.87	5.30	−1.32	0.46
	p^2	101010	7.34	5.06	4.39	4.46	0.04	0.55
	ds	011010	1.47	0.74	−0.19	6.02	−1.25	0.59
	d^2	011010	3.36	0.57	7.39	3.95	−6.95	−0.70
	sp^2	100010	8.15	9.12	2.78	7.71	2.46	1.50
	dp^2	001010	7.73	8.21	4.77	7.22	0.04	1.01
	d^2s	011000	1.92	1.41	1.52	6.23	−2.52	0.41
	d^3	011000	3.77	1.10	8.00	4.07	−7.15	−0.71
	d^2p	011000	5.33	4.22	4.56	5.63	−2.15	0.38
	sp^3	100000	14.14	18.29	10.99	10.89	0.23	1.66
	d^3s	000010	2.15	2.03	1.79	6.63	−2.56	0.48
	dsp^2	100000	8.26	11.42	3.11	9.89	2.24	1.83
	d^2p^2	001000	7.74	9.99	5.15	8.99	−0.33	1.25
	d^2sp	100000	4.76	6.10	0.79	8.08	1.05	1.33
	dp^3	000010	11.96	15.90	9.63	10.68	−0.59	1.49
	d^3p	000010	5.26	5.02	5.11	6.49	−2.77	0.42
	d^4	000010	3.97	1.37	8.30	4.14	−7.24	−0.72
	dsp^3	000000	14.20	20.34	11.05	12.88	0.23	1.99
	d^3sp	000000	4.37	7.53	1.44	9.91	0.01	1.46
	d^2sp^2	000000	8.46	12.75	4.14	11.02	1.40	1.88
	d^4s	000000	2.16	2.09	2.13	6.66	−2.89	0.43
	d^2p^3	000000	11.89	16.55	9.81	11.41	−0.84	1.57
	d^4p	000000	5.43	5.60	5.00	6.91	−2.48	0.54
Cr	sp	011110	3.84	4.32	−5.72	7.24	10.19	2.72
	dp	011110	4.72	3.74	4.19	5.79	1.15	0.96
	p^2	111010	8.58	6.48	−0.69	4.66	9.90	2.24
	ds	111010	1.59	1.61	1.23	6.78	0.98	1.10
	d^2	011020	5.69	3.68	11.52	4.74	−5.21	−0.27
	sp^2	011010	10.78	11.40	−9.84	7.38	21.25	4.60
	dp_2	011010	10.11	10.02	1.64	6.67	9.10	2.44
	d^2s	111000	2.55	2.86	3.13	7.07	.04	0.99
	d^3	012000	5.97	4.04	11.74	4.83	−5.15	−0.25
	d^2p	111000	5.81	5.99	5.96	6.94	0.47	1.04
	sp^3	100010	21.30	21.13	−13.98	6.59	35.91	6.93
	d^3s	100010	2.98	3.44	4.04	7.22	−0.44	0.93
	dsp^2	011000	12.29	14.16	−7.77	8.63	20.69	4.72
	d^2p^2	000002	10.61	13.16	5.76	9.31	5.47	2.28

Can. J. Chem. Downloaded from www.nrcresearchpress.com by 210.87.254.40 on 09/05/12
For personal use only.

TABLE IV (*Continued*)

Element	Hybrid	Configuration*	P^0	P^+	P^-	I_v	E_v	χ
	d^2sp	011000	6.35	8.34	−0.92	8.75	7.90	2.59
	dp^3	000002	16.51	18.79	0.98	9.04	16.16	4.03
	d^3p	000110	6.41	6.81	6.39	7.16	0.64	1.10
	d^4	000020	5.97	4.07	11.71	4.86	−5.12	−0.24
	dsp^3	000010	22.71	23.68	−11.72	7.74	35.06	6.98
	d^3sp	001000	7.03	10.38	−0.54	10.10	8.21	2.87
	d^2sp^2	001000	13.81	16.04	−5.01	8.99	19.44	4.57
	d^4s	000010	3.33	3.90	4.67	7.33	−0.72	0.90
	d^4p	000010	6.65	7.42	6.85	7.53	0.42	1.13
	d^2sp^3	000000	23.32	25.63	−11.58	9.08	35.53	7.29
Mn	sp	111110	3.44	3.22	−10.67	7.22	10.41	2.75
	dp	011120	6.96	5.57	−1.44	6.04	4.70	1.60
	p^2	111110	8.01	5.36	−20.89	4.78	25.20	4.83
	ds	211010	3.56	3.51	−1.67	7.38	1.52	1.29
	d^2	012002	4.86	7.20	17.30	9.77	−16.15	−1.27
	sp^2	110110	10.80	11.90	−18.61	8.53	25.71	5.55
	dp^2	011110	9.86	9.87	−15.32	7.44	21.48	4.65
	d^2s	211000	4.31	4.45	0.10	7.57	0.50	1.15
	d^3	022000	6.58	5.00	8.91	5.85	−6.04	−0.23
	d^2p	211000	8.06	7.52	0.65	6.89	3.71	1.57
	sp^3	011010	19.85	24.55	−32.08	12.12	48.23	9.93
	d^3s	100020	4.68	5.05	1.37	7.80	−0.40	1.04
	dsp^2	011010	12.07	15.54	−15.35	10.91	23.72	5.61
	d^2p^2	011010	10.88	12.40	−12.30	8.95	19.48	4.57
	d^2sp	111000	6.47	8.52	−5.29	9.48	8.06	2.74
	dp^3	011010	18.00	20.45	−29.89	9.89	44.18	8.88
	d^3p	000120	8.13	7.91	1.73	7.20	2.69	1.45
	d^4	000012	3.21	8.43	−2.83	12.66	2.34	2.31
	dsp^3	001010	21.29	28.02	−29.51	14.17	47.09	10.09
	d^3sp	011000	6.71	10.75	−3.09	11.46	6.10	2.74
	d^2sp^2	001010	13.00	18.13	−14.07	12.56	23.37	5.83
	d^4s	000020	4.71	5.21	1.74	7.93	−0.74	1.00
	d^2p^2	001010	18.78	21.72	−28.48	10.37	43.56	8.85
	d^4p	000020	8.26	8.41	2.31	7.57	2.25	1.44
	d^2sp^3	000010	21.80	30.71	−26.71	16.34	44.81	10.06
	d^4sp	100000	7.40	10.56	−3.21	10.59	6.91	2.73
	d^5p	000001	7.09	10.94	−3.12	11.29	6.51	2.78
	d^3p^3	001000	19.55	25.10	−24.90	12.98	40.75	8.82
Fe	sp	111120	1.57	2.87	−9.21	9.20	7.25	2.56
	dp	012120	5.59	4.94	−1.30	7.24	3.36	1.57
	p^2	211110	4.17	5.28	−13.55	9.02	14.18	3.69
	ds	211020	2.19	2.21	−2.85	7.92	1.50	1.38
	d^2	022020	4.56	2.76	6.84	6.10	−5.82	−0.15
	sp^2	111110	0.94	10.60	−16.05	17.56	13.46	5.00
	dp^2	011120	5.63	11.29	−10.07	13.55	12.17	4.11
	d^2s	122000	2.97	3.82	−1.44	8.75	0.87	1.41
	d^3	012002	2.31	8.59	−5.26	14.18	4.04	2.85
	d^2p	122000	6.23	7.43	0.01	9.10	2.68	1.77
	sp^3	011110	4.37	28.28	−20.45	31.82	21.29	8.71
	d^3s	200020	2.79	3.62	−0.81	8.73	0.07	1.27
	dsp^2	111010	2.80	16.09	−13.31	21.19	12.58	5.47
	d^2p^2	012010	6.39	14.29	−7.96	15.80	10.82	4.27
	d^2sp	211000	4.19	10.19	−5.29	13.90	5.96	3.13
	dp^3	011110	4.41	21.43	−20.46	24.92	21.34	7.57
	d^3p	000220	6.69	8.72	0.89	9.94	2.26	1.84
	d^4	000022	2.31	8.63	−5.29	14.22	4.07	2.86
	dsp^3	011010	5.79	33.70	−18.40	35.81	20.66	9.28
	d^3sp	012000	4.64	13.06	−3.94	16.32	5.05	3.38
	d^2sp^2	011010	3.84	19.99	−11.25	24.04	11.56	5.77
	d^4s	000000	3.91	7.63	−2.81	11.61	3.19	2.28
	d^4p	000012	4.23	19.50	−7.60	23.17	8.30	5.08
	d^2sp^3	001010	6.83	38.01	−16.48	39.08	19.78	9.68
	d^4sp	200000	4.77	12.62	−4.11	15.75	5.35	3.34
	d^5p	000002	4.25	20.19	−7.50	23.84	8.22	5.18
	d^3p^3	011000	6.49	28.73	−16.38	30.14	19.35	8.11

Can. J. Chem. Downloaded from www.nrcresearchpress.com by 210.87.254.40 on 09/05/12
For personal use only.

TABLE IV (*Concluded*)

Element	Hybrid	Configuration*	P^0	P^+	P^-	I_v	E_v	χ
Co	sp	211120	3.42	3.73	−6.73	8.18	4.73	1.96
	dp	022120	5.11	4.61	−2.41	7.36	2.10	1.38
	p^2	211120	7.11	6.02	−4.36	6.77	6.05	1.95
	ds	122020	1.56	2.34	−5.39	8.64	1.53	1.50
	d^2	012022	1.66	8.98	−7.66	15.18	3.90	3.00
	sp^2	111120	8.43	9.88	−3.42	9.31	6.42	2.43
	dp^2	012120	8.95	11.40	−3.17	10.31	6.70	2.65
	d^2s	222000	2.71	4.90	−3.86	10.04	1.15	1.67
	d^3	022002	1.66	9.17	−7.87	15.37	4.11	3.07
	dsp	211020	4.95	5.73	−4.82	8.64	4.35	1.97
	sp^3	111110	14.86	17.99	1.33	10.99	8.10	3.00
	dsp^2	211010	10.23	13.41	−2.79	11.05	7.60	2.92
	d^2p^2	022010	9.55	13.77	−2.44	12.08	6.57	2.92
	d^2sp	122000	6.04	9.06	−4.59	10.88	5.21	2.49
	dp^3	011120	14.13	20.47	−1.23	14.20	9.94	3.85
	dsp^3	011110	17.25	21.54	2.23	12.14	9.59	3.44
	d^3sp	022000	6.16	10.94	−4.77	12.64	5.51	2.84
	d^2sp^2	012010	11.56	14.99	−1.47	11.30	7.61	2.97
	d^2p^3	011020	15.19	21.98	−0.05	14.65	9.82	3.90
	d^4p	000022	8.26	13.91	−5.31	13.52	8.15	3.43
	d^2sp^3	011010	18.83	25.15	3.04	14.18	10.36	3.92
	d^3p^3	012000	16.14	26.03	0.03	17.75	10.69	4.57

*The six numbers of this column refer, in order, to the number of electrons occupying the $d_{z^2} = \sigma$, $d_{xz} = \pi$, $d_{yz} = \pi'$, $d_{x^2-y^2} = \delta$, $d_{xy} = \delta'$, and s orbitals.

Computations have been made for all possible arrangements of the non-bonding electrons in the available orbitals. Reported, however, are only those arrangements of the non-valence electrons which give rise to the lowest promotion energy of the atom.[5] These distributions of the electrons in the orbitals not involved in hybridization are given in column 3 of Table IV.

GROUND STATE ELECTRON AFFINITIES

The extensive efforts made to evaluate or determine electron affinities have been carefully reviewed by Pritchard (16), but in spite of all attempts no electron affinities of transition elements have been reported so far. Experimental and extrapolation methods seem to fail; the previous, as well as the more recently derived, extrapolation methods (17, 18) are reported to hold only for the first two rows of the periodic system. The method of Ginsberg and Miller (19), which they claim will hold for heavier elements as well, cannot be applied in the transition series.

Most of the extrapolations of electron affinities described are based on a relation between the ionization potentials of atoms in successive states of ionization in an isoelectronic sequence. Such methods must fail when the ground states in the isoelectronic sequence considered are not identical, which is the case in the transition series. Generally such extrapolation formulas will require the use of equivalent ionizations in an isoelectronic sequence. This may be illustrated on the sequence of ionizations required to extrapolate the electron affinity of scandium. The corresponding ground state ionizations are:

$$\begin{array}{llll} Sc^- & d^2s^2\ (^3F_2) \rightarrow Sc & ds^2\ (^2D_{1\frac{1}{2}}) & = E_g \\ Ti & d^2s^2\ (^3F_2) \rightarrow Ti^+ & d^2s\ (^4F_{1\frac{1}{2}}) & = I_1 \\ V^+ & d^4\ (^5D_0) \rightarrow V^{++} & d^3\ (^4F_{1\frac{1}{2}}) & = I_2 \\ Cr^{++} & d^4\ (^5D_0) \rightarrow Cr^{+++} & d^3\ (^4F_{1\frac{1}{2}}) & = I_3 \end{array}$$

[5]*A complete listing of the results for all distributions of non-valence electrons is given by Hinze (15).*

Can. J. Chem. Downloaded from www.nrcresearchpress.com by 210.87.254.40 on 09/05/12
For personal use only.

A sequence of equivalent transitions, which could be used for the extrapolation is:

Sc^-	$d^3s\ (^5F_1) \rightarrow Sc$	$d^3\ (^4F_{1\frac{1}{2}}) = T_0$
Ti	$d^3s\ (^5F_1) \rightarrow Ti^+$	$d^3\ (^4F_{1\frac{1}{2}}) = T_1$
V^+	$d^3s\ (^5F_1) \rightarrow V^{++}$	$d^3\ (^4F_{1\frac{1}{2}}) = T_2$
Cr^{++}	$d^3s\ (^5F_1) \rightarrow Cr^{+++}$	$d^3\ (^4F_{1\frac{1}{2}}) = T_3$

Generally, ionizations of type $d^ns \rightarrow d^n$ have been chosen here for the equivalent transitions, since only in such cases are sufficient spectral data available.

Extrapolation Procedure

Edlén's extrapolation method (18) was chosen here since it appears to give the best representation with a minimum of initial information. The method suggested by Johnson and Rohrlich (17), apparently equally reliable, requires higher and more ionization potentials for the extrapolation, which is a decided disadvantage, especially in the transition series, where higher ionization potentials are quite uncertain. Edlén obtains the electron affinity T_0 from the successive *equivalent* ionizations T_1, T_2, and T_3 respectively by the following expression,

$$[6] \qquad T_0 = 3T_1-3T_2+T_3+\frac{3\left(T_1-2T_2+T_3-\frac{2R}{n^2}\right)\left(-T_1+2T_2-T_3+\frac{6R}{n^2}\right)}{T_1-4T_2+3T_3-\frac{12R}{n^2}},$$

where R is the Rydberg constant and n the principal quantum number.

Since equivalent ionization processes of an isoelectronic sequence should be used in this expression, it is necessary to reduce the ground state ionizations to such values. This is done by adding and subtracting the appropriate term values, W, to the ground state potentials.

In the above example we obtain,

$$\begin{array}{lllll} \text{Ti} & d^2s^2\ (^3F_2) & \xrightarrow{I_1} & \text{Ti}^+ & d^2s\ (^4F_{1\frac{1}{2}}) \\ & \Big\downarrow W \quad 0.81\text{ ev} & & & \Big\downarrow W^+ \quad 0.11\text{ ev} \\ \text{Ti} & d^3s\ (^5F_1) & \xrightarrow[6.12\text{ ev}]{T_1 = I_1-W+W^+} & \text{Ti}^+ & d^3\ (^4F_{1\frac{1}{2}}) \end{array}$$

$$I_1 = 6.82\text{ ev}$$

The required ground state ionization potentials and term values are obtained from Moore's tables (9). The T values generally calculated for the transition $d^ns \rightarrow d^n$ are listed in Table V together with the T_0 values obtained by extrapolation.

TABLE V

Isoelectronic electron affinities and ionization potentials

		T_1 (ev)	T_2 (ev)	T_3 (ev)	T_0 (ev)	
$d^2s\ (^4F_1)$	$d^2\ (^3F_2)$	5.71	13.57	23.86	0.74	Ca^-
$d^3s\ (^5F_1)$	$d^3\ (^4F_1)$	6.12	14.33	24.82	0.56	Sc^-
$d^4s\ (^6D_1)$	$d^4\ (^5D_0)$	6.48	15.01	25.94	0.75	Ti^-
$d^5s\ (^7S_3)$	$d^5\ (^6S_2)$	6.76	15.64	26.91	0.65	V^-
$d^6s\ (^6D_4)$	$d^6\ (^5D_4)$	7.09	16.18	27.73	0.85	Cr^-
$d^7s\ (^5F_5)$	$d^7\ (^4F_4)$	7.24	16.63	28.50	0.71	Mn^-
$d^8s\ (^4F_4)$	$d^8\ (^3F_4)$	7.43	17.11	29.29	0.62	Fe^-
$d^9s\ (^3D_3)$	$d^9\ (^2D_2)$	7.60	17.57	30.02	0.47	Co^-
$d^{10}s\ (^2S)$	$d^{10}\ (^1S_0)$	7.72	17.96	30.70	0.33	Ni^-

Can. J. Chem. Downloaded from www.nrcresearchpress.com by 210.87.254.40 on 09/05/12
For personal use only.

A major difficulty is the determination of the ground state electron affinities from the calculated T_0 values. For this it is necessary to know the energy difference between the state considered of configuration $d^n s$ and the ground state of the negative ion. These values must be calculated since no spectra of negative ions are observed. These energy differences have been evaluated by setting up the Slater equations of the required states and using the Slater–Condon parameters for the corresponding negative ions, Table II. The extrapolation of these parameters needed has been described above. In Table III the ground state electron affinities obtained are listed, together with the ground state ionization potentials of the same atoms.

Discussion

There are two major sources of error in the method described, and the electron affinities obtained cannot be expected to be highly accurate. One uncertainty is introduced by the use of Edlén's extrapolation and the possible inaccuracy of the ionization potentials used. This uncertainty is believed to be small, an opinion supported by the small variation of the T_0 values extrapolated.

The second source of error is considerably more serious, as the method of obtaining the term values, W^-, for negative ions is much more doubtful. The linear extrapolation of Slater–Condon parameters from the corresponding isoelectronic sequence is quite questionable, especially since in many cases only two members of such a sequence are known. Unfortunately there exists no better simple method to obtain the values required.

In spite of such uncertainties inherent in the procedure, the values obtained are not only of the right order of magnitude, but they reflect also the changes and trends expected on chemical grounds. It is expected and observed that the values increase in going from Ca to V; the value calculated for Ti seems somewhat too large. The sudden rise observed for the electron affinity of Cr must be anticipated, since here the transition $d^5s^2 \rightarrow d^5s$ gives rise to the ground state electron affinity, i.e., removal of an s electron, while in all other cases the transition is $d^n s^2 \rightarrow d^{n-1}s^2$, removal of a d electron. The low value obtained for Mn appears reasonable because of the special stability of the half-filled shell. The removal of the extra d electron beyond the half-filled shell will not require much energy on account of the missing additional exchange energy of state d^6s^2 with respect to d^5s^2.

The sudden rise to the values of Fe and Co seems to be too drastic and values about 1 ev lower would be anticipated in the light of the Ca $\rightarrow$ V rise. This inconsistency is undoubtedly due to an overestimation of the term splitting of the negative ion. Unfortunately there is no method known at the moment by which more reliable values for the electron affinities of the transition metals can be obtained. But these roughly estimated values obtained here give at least a lead about magnitude and order, and are sufficient for the use in electronegativity calculations, for which purpose they have been determined. This is especially true here since the electronegativity computations are made especially to investigate the valence state dependence of the orbital electronegativities, and the differences between the electronegativities for different valence states of the same atom are not affected by the ground state electron affinities used. On the other hand, an uncertainty in the ground state electron affinity of 1 ev results only in an error of 0.16 Pauling electronegativity units in the electronegativities computed. This weakens the comment frequently made about Mulliken's definition of electronegativity, saying, although Mulliken's definition is best justified and should give the most reliable values, it cannot be used since the electron affinities are not available. However, it will always be possible to estimate the electron affinities with an uncertainty limit of less than 1 ev.

Can. J. Chem. Downloaded from www.nrcresearchpress.com by 210.87.254.40 on 09/05/12
For personal use only.

It is remarkable to what degree the orbital electronegativities obtained depend on the hybrids considered. Unfortunately, due to the complexity of the hybrids, it is rather difficult to obtain a general and simple relation about the value of the orbital electronegativity as a function of s, p, or d character of the hybrids involved. Universally the electronegativities increase slightly with increasing s character of the orbitals and steeply with increasing p character. Similarly, the orbital electronegativity is generally higher for higher bonding valence states than for lower bonding ones. These increases, especially the steep increase with increasing p character, lead to some electronegativity values which are astonishingly high. Such are, for example, the values for the octahedral valence state d^2sp^3 of Cr, Mn, Fe, and Co. The explanation of such high values for just this valence state with an extremely high promotion energy cannot be given immediately. The meaning of these high values however will be investigated. Readily explainable are the unfamiliar high electronegativity values of other hybrids with high p character, and consequently high promotion energy. All these unstable hybrids can be substituted either completely or to any intermediate amount by other linear combinations of atomic orbitals, giving rise to more stable hybrids with the same geometry but electronegativities more in the familiar range. In this sense it is possible to substitute the unstable trigonal hybrids sp^2 and dp^2 by the hybrids d^2s or d^3. The tetrahedral hybrid sp^3 can be substituted by the more stable d^3s; actually any intermediate substitution of the three p orbitals by the corresponding d orbitals will lead to a tetrahedral hybrid. The low-energy hybrids d^3p and d^2sp can substitute for the unstable dp^3. By substituting the s orbital by the d_{z^2} orbital, the high-energy dsp^2 hybrid can be reduced to the more stable d^2p^2 hybrid with the same symmetry; similarly the unstable dsp^3 hybrid is transformed into the low-energy d^3sp hybrid by substituting d for p orbitals.

A relation between the s, p, and d character of the hybrid orbitals and the electronegativity seems desirable. From the orbital electronegativity data given, the relation

$$\chi_h = a\chi_s + b\chi_p + c\chi_d \qquad [7]$$

is suggested. Here χ_h, χ_s, χ_p, and χ_d are the orbital electronegativities of the hybrid, the s, the p, and the d orbitals respectively, and a, b, and c give the amount of s, p, and d character respectively of the hybrid considered. From the data reported for different hybrids, the electronegativities of pure s, p, and d orbitals are easily evaluated using eq. [7], which in turn, with these electronegativities of the pure orbitals, can be used to evaluate the electronegativity of any intermediate and second-order hybrids. However, eq. [7] holds only if similar hybrids are considered, that means hybrids which will form the same number of bonds, and if the distribution of the non-valence electrons is equal.

ACKNOWLEDGMENTS

This work was performed under contract with Wright Air Development Division, United States Air Force. The authors would like to acknowledge many helpful discussions with Dr. M. A. Whitehead, preliminary work by Dr. I. Goldfarb, and J. T. Zung, and technical assistance by Mr. C. Schare and Mr. B. Free. The Computing Center of the University of Cincinnati made considerable machine time available, thanks to a NSF Grant G19281.

REFERENCES

1. J. Hinze and H. H. Jaffé. J. Am. Chem. Soc. **84**, 540 (1962).
2. J. Hinze, M. A. Whitehead, and H. H. Jaffé. J. Am. Chem. Soc. **85**, 184 (1963).
3. R. S. Mulliken. J. Chem. Phys. **2**, 782 (1934).

Can. J. Chem. Downloaded from www.nrcresearchpress.com by 210.87.254.40 on 09/05/12
For personal use only.

4. R. S. MULLIKEN. J. Chem. Phys. **46**, 497 (1949).
5. W. MOFFITT. Proc. Roy. Soc. (London), Ser. A., **202**, 534 (1950).
6. H. A. SKINNER and F. H. SUMNER. J. Inorg. Nucl. Chem. **4**, 245 (1955).
7. L. E. ORGEL and J. S. GRIFFITH. Quart. Rev. (London), **11**, 381 (1957).
8. R. S. MULLIKEN. J. Phys. Chem. **56**, 295 (1952).
9. C. E. MOORE. Atomic energy levels. Natl. Bur. Std. (U.S.), Circ. No. 467. Vol. I–III, and private communication.
10. G. E. KIMBALL. J. Chem. Phys. **8**, 188 (1940).
11. J. H. VAN VLECK. J. Chem. Phys. **2**, 20 (1934).
12. J. ZUNG. Ph.D. Dissertation, University of Cincinnati, Cincinnati, Ohio. 1960.
13. J. HINZE and H. H. JAFFÉ. J. Chem. Phys. In press.
14. F. ROHRLICH. Phys. Rev. **101**, 69 (1956).
15. J. HINZE. Ph.D. Dissertation, University of Cincinnati, Cincinnati, Ohio. 1962.
16. H. O. PRITCHARD. Chem. Rev. **52**, 529 (1953).
17. H. R. JOHNSON and F. ROHRLICH. J. Chem. Phys. **30**, 1608 (1959).
18. B. EDLÉN. J. Chem. Phys. **33**, 98 (1960).
19. A. P. GINSBERG and J. M. MILLER. J. Inorg. Nucl. Chem. **7**, 351 (1958).

Can. J. Chem. Downloaded from www.nrcresearchpress.com by 210.87.254.40 on 09/05/12
For personal use only.

Can. J. Chem. Downloaded from www.nrcresearchpress.com by 210.87.254.5 on 09/05/12
For personal use only.

A KINETIC INVESTIGATION OF THE REACTION OF METHYLMAGNESIUM BROMIDE WITH BENZOPHENONE[1, 2, 3, 4]

NORBERT M. BIKALES[5] AND ERNEST I. BECKER[6]
Chemical Laboratories, Polytechnic Institute of Brooklyn, Brooklyn, N.Y., U.S.A.

Received October 29, 1962

ABSTRACT

The reaction of methylmagnesium bromide with benzophenone in tetrahydrofuran was found to be homogeneous and essentially quantitative. The rates of this reaction were measured by following the decrease in absorbance of benzophenone in the ultraviolet as a function of time. Variables examined were concentrations of reactants, magnesium bromide, and temperature. Values were derived for the rate constants, and the energy and entropy of activation. The reaction was found to be initially first order in each reactant, but the rate decreased faster with time than would be predicted from the simple second-order rate equation. The implications of these findings are discussed.

In the present investigation, the second (1) in a series concerned with the study of Grignard kinetics, an analytical procedure was developed which made it possible to study the kinetics of the reaction between benzophenone and methylmagnesium bromide or dimethylmagnesium. It is the purpose of this paper to report the results and to discuss their significance to the mechanism of the Grignard reaction.

EXPERIMENTAL[7]

Apparatus

Instrumentation

A Cary Model 14 recording spectrophotometer was used for recording the ultraviolet spectra. This instrument was equipped with a jacketed cell compartment permitting temperature control and a gas inlet allowing the compartment to be flushed with nitrogen. Vapor phase chromatographs were obtained on a Perkin–Elmer Fractometer, Model 154.

Glassware

Kinetic runs were carried out in stoppered, calibrated, matched quartz cells (American Instrument Co.) of either 1-, 10-, or 20-mm lengths. A 20-mm cell was especially constructed with a jacket to permit circulation of coolant.

Calibrated syringes equipped with stainless steel needles were used for transfer and measurement of reagents. Deliveries could be reproduced with an average of 2 parts per thousand.

All glassware was dried in an oven at 130° and stored in an atmosphere of dry nitrogen until use.

Temperature Control

Water from a constant temperature bath (±0.02°) was pumped through the jacket of the Cary cell compartment as well as through the jacket of the cell itself (in the case of the 20-mm cell). Temperature readings were made in the bath and inside the compartment using calibrated thermometers reading to 0.1° and 0.2°, respectively (estimates possible to 0.02° and 0.04°). Heat exchange from the compartment walls to the cell was greatly facilitated by a rapid flow of nitrogen (ca. 20 liters min^{-1}), which also provided an inert atmosphere.

Timer

An electric stopwatch ("Time-It") allowing readings to 0.01 minute was used.

[1]*Presented at the Symposium on Organometallic Compounds, Vancouver, British Columbia, September 4–6, 1962, sponsored by the Inorganic Chemistry Division, Chemical Institute of Canada, and the Department of Chemistry, University of British Columbia, with the support of the National Research Council, Ottawa, in cooperation with the University Extension Department.*

[2]*From the dissertation submitted by N. M. B. to the Faculty of the Polytechnic Institute of Brooklyn in partial fulfillment of the requirements for the degree of Doctor of Philosophy (Chemistry), June 1961.*

[3]*Supported in part by the National Science Foundation NSFG-14558.*

[4]*A preliminary communication of these results has appeared in Chem. Ind. (London), 1831 (1961).*

[5]*Present address: Gaylord Associates, 20 Mt. Pleasant Avenue, Newark, N.J.*

[6]*To whom inquiries should be directed.*

[7]*Additional details, including kinetic data for all runs, may be found in the reference cited in footnote 2.*

Preparation of Reagents

Reagents were prepared, stored, and transferred in an atmosphere of dry nitrogen. In order to avoid the possible introduction of moisture through repeated sampling, fresh reagents were prepared at frequent intervals. Thus, a total of four preparations of methylmagnesium bromide and seven preparations of benzophenone were carried out for the kinetic runs.

Magnesium

Ingots of sublimed magnesium (Dow) were milled into turnings using a Carballoy cutting tool, with special care being taken to prevent contamination. The turnings were washed with ether, dried *in vacuo* and stored in an atmosphere of dry nitrogen. Methyl bromide (Matheson) was purified by passage successively through concentrated sulphuric acid and phosphorus pentoxide (2, p. 213). Vapor phase chromatographic analysis indicated the presence of a possible maximum of 0.018% of impurities. Tetrahydrofuran (DuPont) was stored over lithium aluminum hydride and fractionally distilled under nitrogen as required. Vapor phase chromatographic analysis showed that impurities amounted to a maximum of 0.007%. 1,2-Dibromoethane (Eastman) was fractionally frozen twice and then distilled from phosphorus pentoxide; b.p. 130.5°; $n_D^{26.5}$ 1.5350, (lit. (2, p. 239) b.p. 131.6°; n_D^{15} 1.5416, dn/dt −0.00058). Dioxane was purified by the method of Fieser (3) and stored over sodium in the dark in an atmosphere of nitrogen. Ethyl ether anhydrous (Mallinkrodt) was distilled from lithium aluminum hydride immediately prior to use. Nitrogen prepurified (Air Reduction) was passed through a 20-cm drying tower containing Ascarite and Drierite.

Methylmagnesium bromide was prepared under nitrogen from magnesium and methyl bromide in the conventional fashion. At the completion of the reaction, the mixture was forced through a fritted-glass filter directly into the storage vessel with nitrogen pressure. The filtrate was clear and virtually colorless. The solution was analyzed for base content by the Gilman method (4) and for halogen content by a Mohr titration (5). A typical analysis of a Grignard solution gave a base content of 0.936 *N* and a halogen concentration of 0.980 *N*, corresponding to a Br/CH_3 ratio of 1.047.[8]

Care was necessary to avoid the presence of residual methyl bromide at the end of the reaction. In several cases, where large excesses of methyl bromide were allowed to remain in solution, the Grignard reagent was completely consumed in a coupling reaction:

$$(CH_3)_2Mg \cdot MgBr_2 + 2CH_3Br \rightarrow 2MgBr_2 + 2C_2H_6.$$

This reaction produced in about a day a saturated solution of magnesium bromide giving a negative Gilman test (14). The precipitated magnesium bromide was a white, crystalline solid, solvated by 3 moles of tetrahydrofuran, as indicated by Mohr titration. Anal. Calc. for $3C_4H_8O \cdot MgBr_2$: Br, 39.9%. Found: Br, 38.2%. The infrared spectrum showed a bathochromic shift of the strong tetrahydrofuran bands from 1075 to 1040 cm^{-1} and from 920 to 885 cm^{-1}.

Dimethylmagnesium in tetrahydrofuran was prepared by the procedure which Storfer and Becker (1) had used in preparing diethylmagnesium.

Magnesium bromide was prepared from 1,2-dibromoethane and magnesium directly in tetrahydrofuran. The solution was clear and only faintly yellow, unlike the product from magnesium and bromine which was invariably dark.

Benzophenone

Benzophenone (Eastman) was washed successively with dilute alkali, dilute acid, and then recrystallized successively from chloroform, petroleum ether (three times), and ethanol to a melting point of 47.9–48.0°. Solutions were handled only in subdued light. The product was stored under dry nitrogen in the dark.

Standard solutions were prepared by distilling tetrahydrofuran directly into the storage vessel containing the ketone. Analyses were carried out by ultraviolet spectroscopy.

Ultraviolet Spectra

All spectra were measured in freshly distilled tetrahydrofuran.

Benzophenone

There were two major peaks in the ultraviolet spectrum: a strong peak at 251 mμ, ϵ 1.82×10^4, and a much weaker maximum at 343.5 mμ, ϵ 128±1. There was also a trough at 308 mμ.

The peak at 343.5 mμ followed Beer's law over the range of concentrations from 6.47×10^{-4} *M* to 1.09×10^{-1} *M*. Little or no photolysis was observed when a 5.5×10^{-3} *M* solution was irradiated in the spectrophotometer with monochromatic light (343.5 mμ) for 12 hours.

1,1-Diphenylethanol

1,1-Diphenylethanol absorbed at the following peaks: 253 mμ, ϵ 380; 258 mμ, ϵ 453; 264 mμ, ϵ 356. A less distinct maximum was present at 268 mμ, ϵ 247, and a shoulder at 248 mμ. There was no absorption in the 300–400 mμ range.

Methylmagnesium Bromide and Magnesium Bromide

A 0.086 *M* solution of methylmagnesium bromide had only a slight absorption in the 340–400 mμ range

[8]*Wotiz et al. (6–12) have used a* Br/Mg *ratio in describing their Grignard reagents. Thus a reagent consisting of* $R_2Mg + \frac{1}{2}MgBr_2 = 0.66$. *We prefer to express this information by a* Br/R *ratio (= 0.50 in this case) from which the molar ratio is more easily derived (1, 13).*

Can. J. Chem. Downloaded from www.nrcresearchpress.com by 210.87.254.5 on 09/05/12
For personal use only.

($A \leqslant 0.02$; 20-mm cell). The absorbance increased with decreasing wavelength, reaching 0.85 at 300 mμ. Solutions of magnesium bromide did not absorb in the 300–400 mμ range.

Mixtures of Benzophenone and Magnesium Bromide

A yellow color formed upon mixing benzophenone with methylmagnesium bromide; simultaneously, the absorbance increased in the 300–400 mμ range. The formation of a yellow color and the spectral changes were noted even when the molar ratio of magnesium bromide to benzophenone was as low as 0.018.

While the yellow color was invariably present, it was observed, however, that the spectral changes were not reproducible because of a faint haziness present even at the 0.018 *M* ratio cited above.

The color was found to vanish immediately upon the addition of even small amounts of methylmagnesium bromide, with regeneration of the benzophenone spectrum.

To 0.50 ml of 0.100 *M* (0.050 mmole) of benzophenone in a 1-mm cell, there was added 0.70 ml of 0.224 *M* (0.16 mmole) magnesium bromide. The solution immediately turned yellow and the absorbance exceeded the limit of the instrument (2.0) at 344 mμ. A few minutes after the addition of the bromide, 0.050 ml of 0.52 *M* (0.026 mmole) methylmagnesium bromide was added with shaking. The color vanished instantly. The benzophenone spectrum reappeared with an absorbance of 0.52 at the 344 mμ maximum, which was exactly the value calculated taking into account the dilution of the original benzophenone solution (little reaction had yet taken place).

The Reaction of Methylmagnesium Bromide with Benzophenone

Product Analysis

To 1.82 g (0.0100 mole) of benzophenone in 10 ml of tetrahydrofuran, there was added 10.5 ml of 0.520 *M* (0.0109 equiv) methylmagnesium bromide. A moderate exotherm was noted. The solution was diluted to 25.00 ml and allowed to stand in a dry box protected from light for 5 days. The solution was clear throughout this time. Three 1.00-ml aliquots were then withdrawn, diluted to 100 ml each with tetrahydrofuran containing 0.10 ml of 6 *M* HCl, and examined in the ultraviolet. The spectrum matched that of pure 1,1-diphenylethanol. The remainder of the reaction mixture was treated with 20 ml of saturated ammonium chloride solution in water and extracted three times with a total of 100 ml of ether. After having been dried with Drierite, the ether solution was evaporated, yielding 1.70 g (97.7%) of a white solid, m.p. 79.5–80.5° (lit. (15) m.p. 81°). Recrystallization successively from ethanol, petroleum ether, and ethanol gave a product, m.p. 80.0–80.4°. The infrared spectrum of the crude material likewise matched that of the recrystallized material, with the possible exception of a trace (<2%) of residual ketone. Fractional crystallization (petroleum ether – methanol) failed to reveal any other impurities.

Analytical Procedure

The benzophenone peak at 343.5 mμ was found to lie in a region where neither the product nor the Grignard reagent had any significant absorption. A direct measure of concentration could therefore be obtained from the absorbance at that wavelength, either after quenching or more simply during reaction itself. The validity of this method was confirmed in experiments wherein methylmagnesium bromide was added to benzophenone solutions containing a reagent capable of destroying the Grignard reagent. Thus, when 0.0236 g (1.30×10^{-4} mole) of benzophenone was dissolved in 49.00 ml of tetrahydrofuran containing 0.20 ml (5.0×10^{-3} mole) of methanol, and 1.00 ml of 0.873 *M* (8.73×10^{-4} mole) methylmagnesium bromide was added slowly with good agitation, the absorbance found (20-mm cell) was 0.667 vs. 0.666 calculated from the absorptivity of pure benzophenone. Similar experiments gave absorbance readings of 0.828 and 0.414 vs. the calculated values of 0.820 and 0.410, respectively. Methanol, in the amounts used, had no effect on the absorptivity of benzophenone itself. Quenching of partially reacted mixtures likewise gave good agreement of observed absorbance values with those calculated based on benzophenone content.

An additional check on the accuracy of the method consisted in the extrapolation of the experimental curve of absorbance vs. time obtained in kinetic runs from the first measured point (ca. 10 seconds after mixing of reagents) to time zero. Invariably, the extrapolated curve was smooth and corresponded at time zero with the calculated absorbance.

Kinetics

(a) Exploratory runs.—A number of experiments were made in order to obtain an estimate of the rate to be expected in the kinetic runs. In a typical case, the initial concentrations were $[BP]_0 = 0.140$ *M* and $[MMB]_0 = 0.195$ *M*. Samples (1 ml) were withdrawn from the reaction mixture, quenched with tetrahydrofuran containing some methanol, diluted to 25 ml, and analyzed spectroscopically. After 11 minutes of reaction at 30.0°, the benzophenone had been completely consumed (no absorbance at 343.5 mμ) and the normal spectrum of 1,1-diphenylethanol had appeared with an absorbance at 258 mμ, agreeing with the expected value. For the 5.00-mm cell: calc.: *A*, 1.27; found: *A*, 1.30.

(b) General procedure.—To the well-dried cell there was added a measured amount of standard benzophenone solution and, if needed, tetrahydrofuran. The cell was then placed into the compartment of the Cary spectrophotometer and sufficient time was allowed for temperature equilibrium to be reached. The benzophenone spectrum was measured in the 300–400 mμ range, after which the wavelength setting of the instrument was fixed at 343.5 mμ. A measured amount of standard Grignard reagent was added, a timer was started, and the recording of absorbance was begun. Inasmuch as the chart was driven by a synchronous

Can. J. Chem. Downloaded from www.nrcresearchpress.com by 210.87.254.5 on 09/05/12
For personal use only.

motor, a direct plot of absorbance at the peak vs. time was obtained. The time elapsed between the addition of the Grignard reagent and the beginning of the recording of absorbance was about 10 to 15 seconds. When the initial, fast reaction had subsided, complete spectra in the 300–400 mμ range were obtained periodically. The cell was kept tightly stoppered throughout the reaction. For the lower concentrations of benzophenone (ca. 5×10^{-3} M), the jacketed 20-mm cell was used. Higher concentrations required either a 10-mm or a 1-mm cell. When the reaction was allowed to proceed for long periods (for example for 5 hours, or overnight), the spectrum of benzophenone was occasionally observed to change in appearance; a decrease in the depth of the trough at 308 mμ and the appearance of a new maximum at 333 mμ were noted. Absorbance readings when this occurred were rejected in the calculations. Reaction mixtures were completely homogeneous and colorless, except as noted before; only reactions in which homogeneity was observed throughout were used in the kinetic study.

Calculations

Benzophenone concentrations were obtained from an equation derived from Beer's law:

$$[\mathrm{BP}] = \frac{A}{\epsilon \times l} = \frac{A}{128 \times l}\ , \qquad [1]$$

where A was the absorbance, [BP] was in moles/liter, and l, the length of the cell, was in cm. Volumes of reaction mixtures were calculated from the volumes of methylmagnesium bromide and benzophenone solutions added.

Concentrations of methylmagnesium bromide at time t were obtained from

$$[\mathrm{MMB}]_t = [\mathrm{MMB}]_0 - x = [\mathrm{MMB}]_0 - [\mathrm{BP}]_0 + [\mathrm{BP}]_t \qquad [2]$$

on the assumption that the stoichiometry of the reaction involves 1 mole of each species (eq. [3]):

$$\mathrm{C_6H_5{-}\underset{\underset{\mathrm{O}}{\|}}{C}{-}C_6H_5} + (\mathrm{CH_3})_2\mathrm{Mg\cdot MgBr_2} \rightarrow \mathrm{CH_3{-}\overset{\overset{\mathrm{C_6H_5}}{|}}{\underset{\underset{\mathrm{C_6H_5}}{|}}{C}}{-}O{-}Mg_2(CH_3)Br_2.} \qquad [3]$$

Since the spectrophotometer gave a continuous record of absorbance vs. time, i.e., an infinite number of points, sufficient values of absorbance (corrected, if necessary, for absorbance of the blank) were converted to concentrations to obtain an adequate representation of the reaction. Thus, in the early, rapid part of the reactions, 5- or 10-second intervals were chosen. Later, concentrations were calculated only for every 20 or 30 seconds. Toward the end of the reaction, absorbance values were taken at intervals of several minutes. Data thus obtained for [BP] and [MMB] at various times of reaction were plotted using log {[BP]/[MMB]} or log {[MMB]/[BP]} as the ordinate and time as the abscissa to test agreement with the second-order equation (16):

$$kt = \frac{2.303}{(a-b)} \log \frac{b(a-x)}{a(b-x)}\ .$$

Inasmuch as the data thus plotted did not lie on a single straight line in any of the experiments, a line was fitted in each run for the early part of the reaction only (as in Fig. 1). This line was drawn visually (16) so as to accommodate as many points as possible, including the point at time zero, without exceeding the estimated precision of the measurements. From the slope of this line there was obtained a rate constant for the early part of the reaction, k(initial):

$$k(\mathrm{initial}) = \frac{2.303\left(\log \frac{[\mathrm{BP}]_2}{[\mathrm{MMB}]_2} - \log \frac{[\mathrm{BP}]_1}{[\mathrm{MMB}]_1}\right)}{(t_2-t_1)([\mathrm{BP}]_0-[\mathrm{MMB}]_0)}\ .$$

Data for the early parts of all runs, including those illustrated in Figs. 3 and 4, were plotted on a scale similar to that shown on Fig. 1.

The initial rate, $-d[\mathrm{BP}]/dt$, was derived from the change in absorbance during the first 5 seconds actually recorded (not extrapolated) in a run by inserting the data into the unintegrated rate equation and fitting the results using a computer.

RESULTS

Order of the Reaction

Benzophenone and methylmagnesium bromide have been reported to react without the side reactions of enolization and reduction (18, 21); the high yield of 96% of addition product was verified in these experiments.

Can. J. Chem. Downloaded from www.nrcresearchpress.com by 210.87.254.5 on 09/05/12
For personal use only.

The speed of the reaction in tetrahydrofuran precluded a sampling technique for following the reaction. However, the rate could be measured spectrophotometrically by observing continuously the decrease in absorbance of the 343.5 mμ peak of benzophenone. The absorbance followed Beer's law over a 170-fold range of concentrations.

Twelve runs were made to test the reproducibility of the reaction rate constant. That the reaction was initially second order was determined from the slopes of the straight lines afforded by the second-order plots for the first phase of the reaction (Fig. 1). Second-order plots made for approximately the first 60 seconds gave k(initial) = 0.192±0.013 liter mole^{-1} sec^{-1} at 25.0° (Table I). Furthermore, mathematical analysis of the data

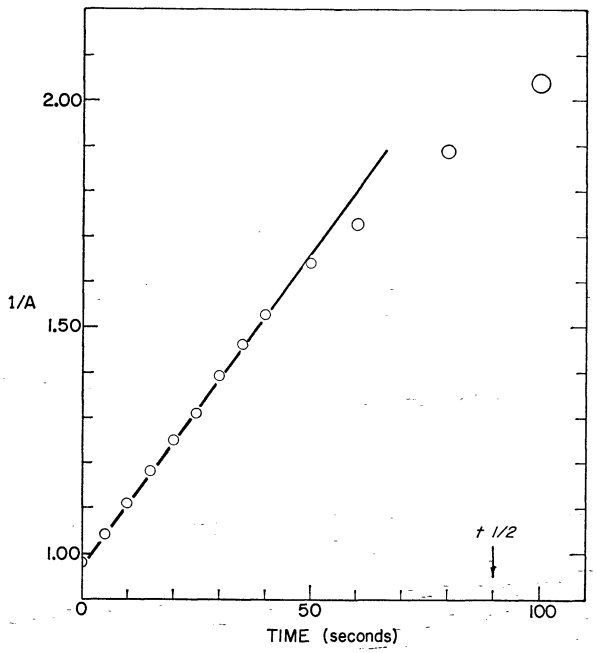

FIG. 1. Second-order plot for the first half-life of run 4 ([MMB]$_0$/[BP]$_0$ = 1.01). Plot of the reciprocal of the absorbance at 343.5 mμ vs. time. Data for the early parts of all runs were plotted on a larger scale so as to permit a more accurate determination of k(initial).

TABLE I

Rate constants derived from initial rates (25.0°)

Run	[BP]$_0$ ×10^2, M	[MMB]$_0$ ×10^2, M	[MMB]$_0$/[BP]$_0$	k(initial), liter mole^{-1} sec^{-1}
1	8.70	5.12	0.589	0.196
2	8.42	6.15	0.730	0.198
3	9.36	2.83	0.302	0.19
4	7.96	8.07	1.01	0.175
5	7.03	10.9	1.55	0.214
6	0.941	2.08	2.21	0.182
7	13.0	4.89	0.376	0.214
8	0.552	1.77	3.21	0.186
9	0.541	1.75	3.24	0.176
15	10.3	5.25	0.507	0.181
17	7.55	2.60	0.344	0.19
23	5.55	5.15	0.928	0.199
			Average	0.192±0.013

Can. J. Chem. Downloaded from www.nrcresearchpress.com by 210.87.254.5 on 09/05/12
For personal use only.

showed that the following equation described the initial rate:

$$-\frac{d[\mathrm{BP}]}{dt} = 0.18[\mathrm{BP}]^{0.89}[\mathrm{MMB}]^{1.1},$$

where 0.18 is in liter mole^{-1} sec^{-1}. These results establish the first-order dependence in each component.

However, graphical analysis also showed that the simple second-order dependence was not followed throughout the reaction. After about 30–40% conversion, the data deviated increasingly from a straight line. Correlations for 0, 0.5, 1, 1.5, 2, and 3 orders likewise failed to give a straight line over the whole range of the data.

A further characteristic of the kinetics was that after half of the methyl groups in the solution was consumed, the rate of further consumption of methyl groups decreased to, at most, 1/85th of that of the first half of the total methyl groups. For kinetic analysis of the initial phase of the reaction, one half of the methyl groups could therefore be regarded as inactive. Thus, the term "half-life" refers to the consumption of one-half of the kinetically significant methyl groups, or to one-quarter of the total methyl groups present in solution at the beginning of reaction.[9] The spectrophotometric method of measurement was not sufficiently accurate in the later stages of reaction to permit an evaluation of the order throughout since measurements of the rate were much less precise.

Similarly to the findings at 25°, a straight line of log {[MMB]/[BP]} vs. t could be fitted to the data only for the early part of the reaction in runs made at other temperatures. The initial-rate constants calculated from the slopes were found to be 0.0312 liter mole^{-1} sec^{-1} at 1.0°, 0.119 at 15.0°, 0.181 at 25.0°, and 0.248 at 35.0° (Table II).

TABLE II
Effect of temperature on the rate

Run	Temperature, °C	$[BP]_0$ $\times 10^3$, M	$[MMB]_0$ $\times 10^2$, M	k(initial), liter mole^{-1} sec^{-1}
11	1.0	5.57	1.81	0.0320
20	1.0	5.07	2.00	0.0303
16	15.0	5.18	1.78	0.119
8	25.0	5.52	1.77	0.186
9	25.0	5.41	1.75	0.176
10	35.0	5.29	1.71	0.251
19	35.0	5.50	1.74	0.244

The logarithms of the rate constants obtained at the various temperatures were plotted as a function of the reciprocal of absolute temperature (Fig. 2), as required by the Arrhenius equation (16). Since the data deviated somewhat from linearity, the slope was calculated by the method of least squares. The energy of activation derived from this calculation was E_a = 11 kcal/mole. Lines were also drawn with a minimum and maximum slope for the data. They indicated that E_a fell in the range of 10–13 kcal/mole. The entropy of activation $\Delta S^{\ddagger}$ corresponding to these extremes was −28 and −18 e.u., while E_a = 11 kcal/mole gave a value for the entropy of activation of −25 e.u. at 25°.

Effect of Magnesium Bromide

The effect of magnesium bromide on the rate was investigated at 25° in three ways:

(*a*) magnesium bromide was premixed with methylmagnesium bromide and the mixture was added to benzophenone (runs 13 and 14);

[9] *A similar assumption was made by Storfer and Becker in the case of the kinetics of addition to nitriles (1).*

Can. J. Chem. Downloaded from www.nrcresearchpress.com by 210.87.254.5 on 09/05/12
For personal use only.

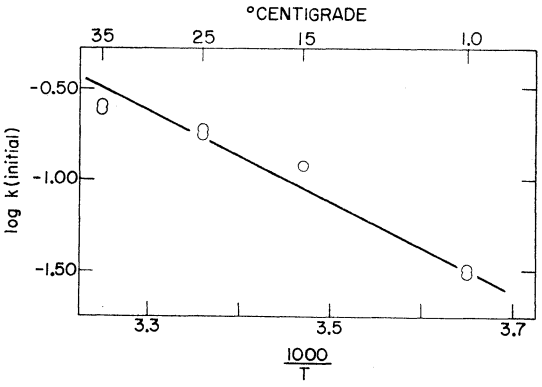

FIG. 2. Effect of temperature on rate.

(*b*) methyl Grignard reagent free of magnesium bromide (i.e., dimethylmagnesium) was allowed to react with benzophenone (runs 21, 22, 24, and 25);

(*c*) magnesium bromide was added to dimethylmagnesium, and the mixture was allowed to react with benzophenone (run 23).

In method (*a*), when sufficient magnesium bromide was added to the Grignard reagent to give a $[MgBr_2]/[BP]_0$ ratio of about 1 in the reaction mixture, the rate decreased as compared to a similar run with no added magnesium bromide. Thus, under comparable conditions, except for the presence of added magnesium bromide, the rate constant fell to 0.045 liter mole^{-1} sec^{-1} from an average of 0.192 for the ordinary Grignard reagent. The time for which the MMB–$MgBr_2$ mixture was allowed to stand did not seem to affect the results; in run 13, the mixture was allowed to stand for 40 minutes before use, while in run 14 it was used immediately (see Table III and Fig. 3). Yet, the rate constants

TABLE III

Effect of magnesium bromide on rate (25.0°)

		Methylmagnesium compound		
Run	$[BP]_0$ $\times 10^2$, *M*	Concn. at t_0 $\times 10^2$, *M*	Br/CH_3	*k*(initial), liter mole^{-1} sec^{-1}
21	0.482	1.66	0.00	0.407
22	7.08	7.32	0.00	0.403
24	7.08	7.32	0.00	0.403
25	7.73	4.04	0.00	0.40
Average of 12 runs			0.99–1.05	0.192±0.013
23	5.55	5.15	1.00	0.199
13	0.537	1.70	1.29	0.044
14	0.530	1.67	1.29	0.045

were virtually identical. The spectrum of benzophenone had a normal appearance in these experiments.

The experiments with dimethylmagnesium [DMM], $(CH_3)_2Mg$, method (*b*), showed that this reagent was slightly more reactive than the ordinary Grignard reagent, the initial rate giving a constant of 0.40 liter mole^{-1} sec^{-1}, as compared to an average of 0.192 for $(CH_3)_2Mg \cdot MgBr_2$ (Fig. 4). The concentrations investigated covered about the

Can. J. Chem. Downloaded from www.nrcresearchpress.com by 210.87.254.5 on 09/05/12
For personal use only.

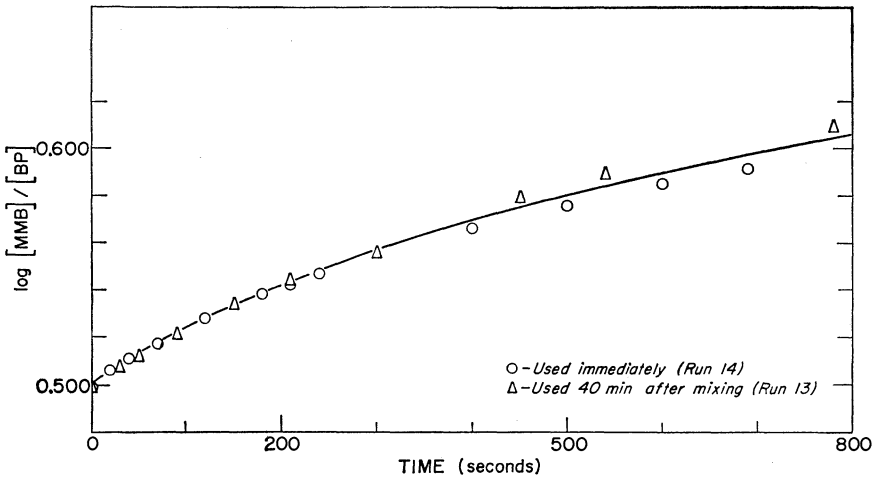

FIG. 3. Runs with added magnesium bromide ($Br/CH_3 = 1.29$).

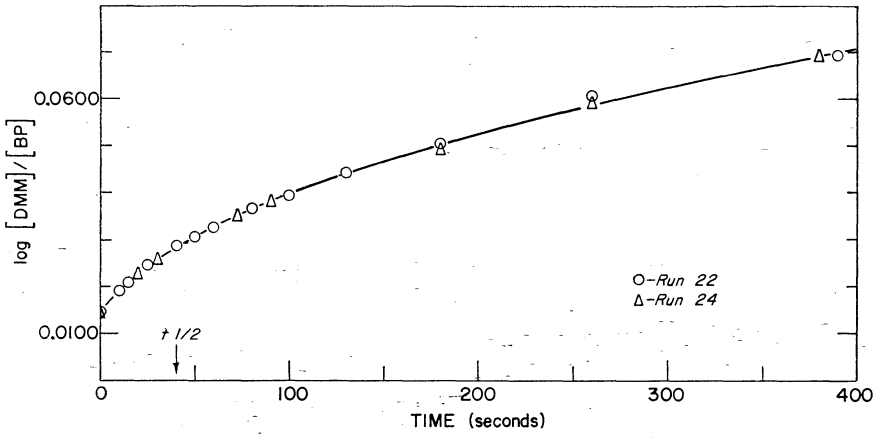

FIG. 4. Runs with dimethylmagnesium.

same range as that studied for methylmagnesium bromide. As with methylmagnesium bromide, the initial stages of the reaction followed second-order kinetics (Table III). On the other hand, no agreement in rate constants was found when the data were tested for adherence to third-order kinetics: runs 21, 22, 24, and 25 gave values of 26, 7.1, 7.1, and 13 liter^2 mole^{-2} sec^{-1}, respectively, for the third-order initial-rate constants.

The equivalency of an equimolar mixture of dimethylmagnesium and magnesium bromide to that of methylmagnesium bromide (1) (method (*c*)) was tested in run 23. The specific rate constant found was 0.199 liter mole^{-1} sec^{-1} in good agreement with that observed with the Grignard reagent made from methyl bromide and magnesium (Table II).

When magnesium bromide was mixed with benzophenone, a deep yellow color appeared with concurrent increase in absorbance in the 300–400 mμ range. These effects were noted even at a molar ratio of 0.018 of magnesium bromide to ketone and could be ascribed at least in part to gradual precipitation of what probably was a complex. The color

Can. J. Chem. Downloaded from www.nrcresearchpress.com by 210.87.254.5 on 09/05/12
For personal use only.

disappeared instantly with regeneration of the benzophenone spectrum when either methylmagnesium bromide or dimethylmagnesium was added to the mixture.[10]

Effect of Products on Rate

An experiment was carried out to determine the influence of products of the reaction upon a subsequent run. A kinetic run was first made under normal conditions, $[BP]_0 = 0.0871\ M$, $[MMB]_0 = 0.0696\ M$, at a temperature of 37.0°. The rate of disappearance of benzophenone was measured, and reaction was allowed to go to completion, based on a 1:1 stoichiometry (equation [3]). The value of k(initial) was 0.299 liter mole^{-1} sec^{-1}. More benzophenone was then added followed by a second quantity of methylmagnesium bromide, giving $[BP] = 0.0909\ M$ and $[MMB] = 0.0638\ M$. The rate was then measured again and found to be only 0.189 liter mole^{-1} sec^{-1}. Thus the rate was slower by 37% in the presence of products of the reaction.

DISCUSSION

The study reported here represents one of the first successful kinetic investigations of the reaction of a Grignard reagent with a ketone.[11] In view of past failures, our success may be attributed to the choice of the methylmagnesium bromide – benzophenone system offering a minimum of problems with side reactions, to the availability of a recording instrument permitting a continuous measurement of a property proportional to concentration, to careful handling of reagents, and to the use of a solvent wherein the reaction mixture is homogeneous.

The observations made in the past that reactions of Grignard reagents with carbonyl compounds were rapid have been confirmed in the present experiments. The rates observed readily serve to explain previous failures to obtain kinetic data. A rough approximation of the relative reactivity of benzophenone as compared to benzonitrile may be derived from our results and those of Storfer and Becker (1). Both sets of experiments were conducted in tetrahydrofuran, but in the previous investigation ethylmagnesium bromide was used while our runs were made with methylmagnesium bromide. At 30°, Storfer and Becker found an initial rate constant of 6.4×10^{-4} liter mole^{-1} sec^{-1}. Interpolation of our data (Fig. 2) gave a value of 2.4×10^{-1} for k(initial) at that temperature. The rate with benzophenone was therefore 370 times as fast as that with benzonitrile. The difference in reactivity between benzophenone and benzonitrile may actually be even larger since Wotiz *et al.* (6) have found that ethylmagnesium bromide reacted 17 times as fast as methylmagnesium bromide. Assuming the same ratio of reactivities is applicable here, then benzophenone is 6300 times as reactive as benzonitrile toward the same Grignard reagent.

Since the Grignard reagent is now believed to have the $R_2Mg\cdot MgX_2$ structure (40), the question as to whether both alkyl groups have the same reactivity has recently received some attention. Thus, Wotiz (6–12) assumed that such differences existed and assigned rate constants of 1.3×10^{-2} and 2.5×10^{-3} liter mole^{-1} sec^{-1} for reaction of the first and second ethyl groups, respectively, toward 1-hexyne. It has previously been demonstrated that in some cases reaction of the second 50% of the alkyl groups could

[10]*The benzophenone spectrum was normal in appearance when the organomagnesium reagent was added within a few minutes after mixing of the magnesium bromide with benzophenone. When the complex was allowed to stand for about 15 minutes or longer, coagulation had proceeded to such an extent that quantitative regeneration was more difficult because of heterogeneity of the mixture. These difficulties have thus far prevented a comparison of rates of method (a) with an alternative where magnesium bromide is premixed with benzophenone followed by addition of methylmagnesium bromide.*

[11]*Apparently, Anteunis' work (27) was carried out simultaneously and independently.*

Can. J. Chem. Downloaded from www.nrcresearchpress.com by 210.87.254.5 on 09/05/12
For personal use only.

actually be so slow as to be negligible (1). Thus, alkylmagnesium reagents gave only 50% conversions based on ethyl when benzonitrile was the substrate, but higher conversions could be obtained with benzaldehyde. Dessy and Salinger (17) likewise found only 50% conversion of ethyl groups in the reaction with Schiff bases.

In our own case the reaction of methylmagnesium bromide and dimethyl magnesium with benzophenone eventually resulted in consumption of all the methyl groups. Lewis and Wright (18) likewise had obtained yields of about 86% when the reaction was allowed to proceed in ether for 5 hours at reflux. The intermediate I must therefore have been capable of further reaction, and the overall process can then be represented as:

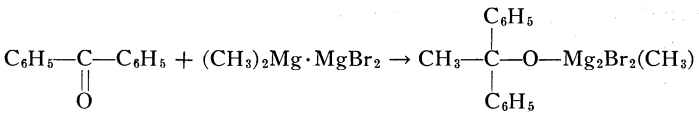

[4]

I

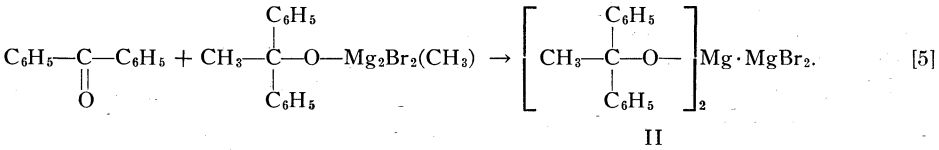

[5]

II

However, here too the reactivity of the intermediate I was probably much lower than that of methylmagnesium bromide since the specific rate had fallen by a factor of at least 85 when 50% conversion based on the total original methyl content was exceeded. This significant decrease in rate permitted us to neglect reaction [5] for kinetic purposes, although the reaction was shown to take place and should be taken into account for synthetic purposes.

From these considerations it appears that there are differences in reactivity between Grignard reagents and intermediates of the type I which still contain alkyl groups attached to magnesium, and that the reactivity of the latter can vary depending on the nature of the substrate. The lesser reactivity of alkyl groups in compounds such as I can be rationalized on the ground that they are attached to magnesium atoms with lower electron densities than in the Grignard reagent. Stated another way, the greater electronegativity of oxygen and of nitrogen than of carbon causes the O—Mg and the N—Mg bonds to be more ionic than the C—Mg bond in the Grignard reagent. Since reaction of these compounds with substrates such as nitriles or ketones probably involves transfer of the alkyl group with its pair of electrons, such a reaction would be hindered.

Mechanism of the Reaction

The mechanism most frequently cited for the addition of a Grignard reagent to a ketone is that proposed by Swain. According to Swain, a complex of ketone and Grignard reagent is first formed which can be converted to the product only by the intervention of a second mole of Grignard reagent:

$$G + K \underset{k_2}{\overset{k_1}{\rightleftharpoons}} C \qquad [6]$$

$$C + G \xrightarrow{k_3} P + G, \qquad [7]$$

Can. J. Chem. Downloaded from www.nrcresearchpress.com by 210.87.254.5 on 09/05/12
For personal use only.

where G is the Grignard reagent, K is the ketone, C is the complex, P is the product, and III is the transition state in the step *b* represented by equation [7].

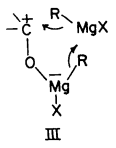

III

No product was stated to form with equimolar or less than equimolar amounts of Grignard reagent (19) because of stability of the complex toward internal reaction. A necessary implication of this hypothesis is that the equilibrium must be far toward the complex and that it must be reached very rapidly in relation to reaction [7]. Otherwise, the uncomplexed Grignard reagent could play the role of the second mole of G, and reaction [7] would take place. A further result is that kinetically the reaction is of third order, first order in ketone and second order in Grignard reagent. The validity of this mechanism may be questioned for the following reasons:

(1) Our kinetic measurements indicate that the reaction is initially first order in benzophenone and first order in methylmagnesium bromide.[12] This finding is in harmony with the results recently published by Miller, Gregoriou, and Mosher (20), who determined from the relative amounts of addition versus reduction in a hindered ketone that the reaction proceeds by consecutive, *second-order* kinetics.

(2) We have found the reaction of methylmagnesium bromide with benzophenone to take place in tetrahydrofuran at ratios of $[MMB]_0/[BP]_0$ as low as 0.302. Even on the basis of the RMgX formulation for the Grignard reagent, this would correspond to a ratio of $[CH_3MgBr]_0/[BP]_0$ of only 0.604, or less than 1. Furthermore, at equimolar concentrations based on the RMgX formulation, product analyses showed essentially quantitative yields of 1,1-diphenylethanol, thus substantiating the belief that the disappearance of benzophenone observed spectroscopically led to product, and not solely to a complex of starting materials.

(3) It has been reported (18) that the reaction in ether of equivalent amounts of methylmagnesium bromide and benzophenone gave yields of about 86% of product regardless of whether the ketone was added slowly to the Grignard reagent, or whether inverse addition was used. No product other than complex should have been formed by the inverse addition technique, if Swain's mechanism held.

(4) The evidence on which the existence of a stable complex has been based is in our view by no means conclusive. In the frequently cited (1, 21–25) paper by Pfeiffer and Blank (26), the contents of which were incorrectly credited by Swain (19) to Gilman and Jones (24), the following experiment is reported: "We examined the behavior of benzophenone toward ethylmagnesium bromide. Experiment I. Both components were reacted in a molar ratio of 1:1 in ethereal solution while cooling with ice. A dirty, white precipitate formed which rapidly changed to an oily mass and hence could not be filtered or analyzed. The ethereal solution as well as the precipitate was heated for 5 hrs. at reflux on a water bath. After cooling, the reaction mixture was treated with water and aqueous ammonia until the odor of ammonia was detected. After having been shaken well, the ethereal solution was separated, washed with water, dried with sodium sulfate,

[12]*It is worth noting that from a kinetic point of view, the order in Grignard reagent does not depend on the fact that it is* $R_2Mg \cdot MgX_2$ *rather than* RMgX.

Can. J. Chem. Downloaded from www.nrcresearchpress.com by 210.87.254.5 on 09/05/12
For personal use only.

and concentrated on the water bath. The residue was at first oily, but most of it solidified after having been seeded with a few crystals of benzophenone. After having been pressed dry on a porous plate, the crystals melted at 49–51°. A mixed m.p. with benzophenone gave no depression. The greater part of the benzophenone was therefore recovered unchanged."[13]

It is to be noted that the authors hydrolyzed *the entire reaction mixture together*. Thus, the recovery of some benzophenone could be ascribed simply to incomplete reaction (possibly because of lesser reactivity of an intermediate similar to I). No quantities, yields, analyses, or isolation were reported to justify in any way the conclusion that the precipitate was a complex of starting materials. It is because of these serious defects that it is felt that the experiment does not merit the importance that has been attached to it. This has already been pointed out by Nesmeyanov and Sazanova (28), who repeated Pfeiffer and Blank's work, but isolated the precipitate immediately. They found that the latter gave, upon hydrolysis, the desired carbinol in 79% yield.[14]

(5) Swain's experiments with added magnesium bromide (30), which he considered to support his mechanism, may be open to different interpretations. McBee, Pierce, and Meyer (31) found no detectable amounts of complexing between magnesium bromide and fluorinated carbonyl compounds. Yet the presence of magnesium bromide in ethylmagnesium iodide favored the addition reaction at the expense of reduction. This is the same effect which Swain had ascribed to prior complexing of the carbonyl compound with magnesium bromide. The authors (31) also found that addition was favored in the absence of magnesium bromide when pyridine was used as solvent and believed that changes in polarity of the medium may be the important factor.[15]

Cram (32) has pointed out that the added magnesium bromide may have shifted the Schlenk equilibrium (equation [8]) (21) toward RMgX and that the results may be rationalized if it is assumed that R_2Mg is a better reducing agent than RMgX. In the light of Dessy's work on the constitution of the Grignard reagent, this is tantamount to stating that R_2Mg is a better reducing agent than $R_2Mg \cdot MgX_2$.

$$R_2Mg + MgX_2 \rightleftharpoons 2RMgX \qquad [8]$$

In our own work, spectral evidence has been presented that magnesium bromide was *not* complexed with benzophenone in the presence of methylmagnesium bromide. It

[13]*A complete translation of Pfeiffer and Blank's main experiment is given here, because language difficulties may have hindered its full understanding by some of the authors who have referred to it. Kharasch and Reinmuth, for example, erroneously believed that the oil was separated before hydrolysis (21, p. 141). Anteunis (27) similarly stated that the complex was "isolated".*

[14]*The work of Meisenheimer (29) has also been cited (21, 24, 26) in support of a complex. A precipitate obtained in the reaction of benzaldehyde with ethylmagnesium bromide was filtered and found to release some ethane upon hydrolysis. This fact was considered by Meisenheimer to be strong evidence for the presence of benzaldehyde complexed with Grignard reagent in the precipitate.*

Based on the RMgX *structure then in use, such a conclusion was reasonable. On the other hand, in view of Dessy's recent work on the structure of ethylmagnesium bromide (40) and the growing evidence for lesser reactivity of the second half of the alkyl groups, one may assume that the ethane could have originated from the product (IV) as well as from a possible complex (V).*

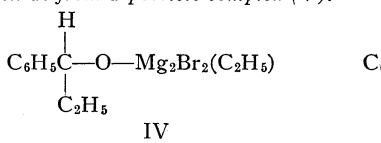

IV

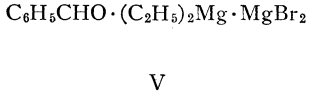

V

[15]*It is worth noting that in Swain's experiment the reaction mixture was heterogeneous since concentrated solutions of magnesium bromide form two phases in ether. Furthermore, no experiments were reported wherein 1 mole of Grignard reagent was actually replaced by a mole of magnesium bromide—the Grignard reagent was present in both experiments in a 2:1 ratio to the ketone, based on the* RMgX *formulation.*

Can. J. Chem. Downloaded from www.nrcresearchpress.com by 210.87.254.5 on 09/05/12
For personal use only.

may instead have been complexed with the Grignard reagent,[16] in analogy to the proposals of Doering and Noller (33) and of Stewart and Ubbelohde (34). Attention has been called to such a possibility by Meyer (25), by Smith (35), and by Hamelin (36).

(6) The recently published investigation by Anteunis (27, 37) which purports to support the Swain mechanism appears to us to suffer from two major defects. The data published do *not* support the conclusion that the reaction is of third order, and the reaction was carried out in an ether–benzene solvent system wherein the reaction is *heterogeneous*. The concentrations were varied only over a less than a fourfold range, yet the third-order rate "constants" varied from 0.165 to 0.425 liter^2 mole^{-2} sec^{-1}. Furthermore, the calculated rate constants at equal Grignard concentrations were significantly different depending on whether the rate was measured in the beginning or toward the middle of the reaction; thus, k_3 when measured in a run starting at 0.159 M of Grignard reagent was 0.36 liter^2 mole^{-2} sec^{-1}, but k_3 was only 0.158 when a reaction beginning at 0.350 M had decreased to 0.157 M. These inconsistencies are not compatible with third-order kinetics. For the reaction of benzophenone with dimethylmagnesium, Anteunis (37) reports for only one concentration and one temperature. A calculation for second-order k from his data at $-15.2°$ gives 0.316 liter mole^{-1} sec^{-1} to be compared with 0.0312 liter mole^{-1} sec^{-1} obtained here at 1.0°. The difference in rate is probably due to the different solvent systems employed, Anteunis using ether–benzene, which would be much less coordinated to magnesium.

It may be concluded, therefore, that the concept of the Grignard reaction with a ketone proceeding via a *stable* complex of the type described by Swain is not supported by the published evidence nor by the results of the present investigation.

While we feel that the Swain and Pfeiffer–Blank mechanism is ruled out, the results of the present investigation do not permit us to draw any firm conclusions as to a possible substitute. The kinetics were found to be complex and additional work is required, especially to establish the reasons for the decrease in rate with time and with added magnesium bromide.

It is noteworthy that similar deviations from simple second-order kinetics have been observed in the past in the case of reaction with alkynes (6–12) and with benzonitrile (1). In both cases, competitive, consecutive second-order reactions were assumed to account for the deviation. In the latter case, it was further believed that the Grignard reagent was composed of various species with different reactivities. Both of these assumptions appear to be reasonable and a detailed analysis of the mechanism may have to await a better understanding of the constitution of Grignard reagents.

From the information presently available, the following mechanism is tentatively proposed:

$$G + K \underset{k_{-1}}{\overset{k_1}{\rightleftharpoons}} C_1 \overset{k_2}{\rightarrow} I \qquad [9]$$

$$I + K \underset{k_{-3}}{\overset{k_3}{\rightleftharpoons}} C_2 \overset{k_4}{\rightarrow} II, \qquad [10]$$

where the rate-determining steps are k_2 and k_4 and the equilibrium is far toward the

[16] *If complexing of magnesium bromide with Grignard reagent did take place, its rate must have been rapid since the spectrum of benzophenone was regenerated immediately upon addition of methylmagnesium bromide to a mixture of magnesium bromide and benzophenone. Also, there was no difference in rates between run 14, where a mixture of magnesium bromide with methylmagnesium bromide was used immediately, and run 13, where the mixture was allowed to stand for 40 minutes before reaction with benzophenone.*

Can. J. Chem. Downloaded from www.nrcresearchpress.com by 210.87.254.5 on 09/05/12
For personal use only.

reactants. The transition states for the rate-determining steps may then be visualized as VI and VII wherein use is made of Dessy's structure of the Grignard reagent:[17]

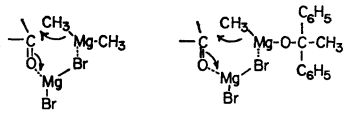

VI VII

This mechanism is in accord with our finding of second-order kinetics for the early part of the reaction, and with Mosher's conclusion (20) that addition and reduction proceed by the same kinetic order. Since reduction is believed to proceed by way of a six-membered cyclic transition state, it is reasonable to assume that addition would also. This is further supported by analogy with the Meerwein–Ponndorf–Verley reduction, which is believed to have a similar transition state. A recent investigation has shown that the energy and entropy of activation for the reaction of benzophenone with aluminum isopropoxide are 14 kcal/mole and −31 e.u., respectively (39). The similarity with our results of 11 kcal/mole and −25 e.u. is striking. For pinacolone – methylmagnesium bromide in ether, Anteunis found E_a 14.5±0.6 kcal/mole.

Finally, some comments may be made as to the structure of the Grignard reagent. We have provided additional confirmation that equimolar mixtures of dimethylmagnesium and magnesium bromide are equivalent to the Grignard reagent. The fact that even small amounts of magnesium bromide drastically altered the ultraviolet spectrum of benzophenone but that nevertheless the spectrum was normal in the presence of methylmagnesium bromide permits the conclusions that less than 1.8%, if any, free magnesium bromide is present in this Grignard reagent and that dimethylmagnesium may complex with more than 1 mole of magnesium bromide (33, 34, 36).

ACKNOWLEDGMENTS

The authors wish to thank the American Cyanamid Company, in whose laboratories these experiments were carried out. They are indebted to N. B. Colthup for the infrared measurements and to A. Schneider for the calculations of initial rates using a digital computer.

REFERENCES

1. S. J. Storfer and E. I. Becker. J. Org. Chem. **27**, 1868 (1962). S. J. Storfer. Doctoral Dissertation, Polytechnic Institute of Brooklyn, Brooklyn, N.Y. June, 1960.
2. J. Timmermans. Physico-chemical constants of pure organic compounds. Elsevier, New York. 1950.
3. L. F. Fieser. Experiments in organic chemistry. Heath, New York. 1941. p. 368.
4. H. Gilman, E. A. Zoellner, and J. B. Dickey. J. Am. Chem. Soc. **51**, 1576 (1929).
5. W. Rieman, J. D. Neuss, and B. Naiman. Quantitative analysis. McGraw-Hill Book Co., New York. 1942. p. 65.

[17] *Mosher et al. (20) and Hamelin (36) have independently arrived at the same conclusion. By analogy, reduction and enolization may be visualized as proceeding via VIII and IX respectively, where the carbonyl group is coordinated to the magnesium atom bearing the* alkyl *groups. The proposal for transition state VIII is in agreement with Mosher's finding (38) that* R_2Mg *and the Grignard reagent behave alike in asymmetric reduction and by studies with molecular models which confirm that* steric *hindrance with alkyl groups bulkier than methyl would favor coordination as in VIII.*

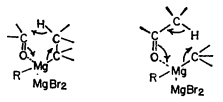

VIII IX

Can. J. Chem. Downloaded from www.nrcresearchpress.com by 210.87.254.5 on 09/05/12
For personal use only.

6. J. H. WOTIZ, C. A. HOLLINGSWORTH, and R. E. DESSY. J. Am. Chem. Soc. **77**, 103 (1955).
7. R. E. DESSY, C. A. HOLLINGSWORTH, and J. H. WOTIZ. J. Am. Chem. Soc. **77**, 4410 (1955).
8. J. H. WOTIZ, C. A. HOLLINGSWORTH, and R. E. DESSY. J. Org. Chem. **20**, 1545 (1955).
9. J. H. WOTIZ, C. A. HOLLINGWSORTH, and R. E. DESSY. J. Am. Chem. Soc. **78**, 1221 (1956).
10. R. E. DESSY, J. H. WOTIZ, and C. A. HOLLINGSWORTH. J. Am. Chem. Soc. **79**, 358 (1957).
11. J. H. WOTIZ, C. A. HOLLINGSWORTH, R. E. DESSY, and L. C. LIN. J. Org. Chem. **23**, 228 (1958).
12. J. H. WOTIZ, C. A. HOLLINGSWORTH, and A. W. SIMON. J. Org. Chem. **24**, 1202 (1959).
13. R. HAMELIN and S. GOYPIRON. Compt. Rend. **246**, 2382 (1958).
14. H. GILMAN and F. SCHULZE. J. Am. Chem. Soc. **47**, 2002 (1925).
15. H. MASSON. Compt. Rend. **135**, 533 (1902).
16. A. A. FROST and R. G. PEARSON. Kinetics and mechanism. John Wiley & Sons, Inc., New York. 1953. pp. 8–99.
17. R. E. DESSY and R. M. SALINGER. J. Am. Chem. Soc. **83**, 3530 (1961).
18. R. N. LEWIS and J. R. WRIGHT. J. Am. Chem. Soc. **74**, 1253 (1952).
19. C. G. SWAIN. J. Am. Chem. Soc. **69**, 2306 (1947).
20. J. A. MILLER, G. GREGORIOU, and H. S. MOSHER. J. Am. Chem. Soc. **83**, 3966 (1961). D. O. COWAN and H. S. MOSHER. J. Org. Chem. **27**, 1 (1962).
21. M. S. KHARASCH and O. REINMUTH. Grignard reactions of nonmetallic substances. Prentice-Hall, New York. 1954.
22. F. DRAHOWZAL and H. KÖNIG. Monatsh. Chem. **85**, 654 (1954).
23. R. N. LEWIS and J. R. WRIGHT. J. Am. Chem. Soc. **74**, 1257 (1952).
24. H. GILMAN and R. G. JONES. J. Am. Chem. Soc. **62**, 1243 (1940).
25. D. D. MEYER. Doctoral Dissertation, Purdue University, Lafayette, Ind. 1954.
26. P. PFEIFFER and H. BLANK. J. Prakt. Chem. **153**, 242 (1939).
27. M. ANTEUNIS. J. Org. Chem. **26**, 4214 (1961).
28. A. N. NESMEYANOV and V. A. SAZANOVA. Bull. Acad. Sci. URSS Classe Sci. Chim. 499 (1941); Chem. Abstr. **37**, 2723 (1943).
29. J. MEISENHEIMER. Ann. **446**, 76 (1926).
30. C. G. SWAIN and H. B. BOYLES. J. Am. Chem. Soc. **73**, 870 (1951).
31. E. T. MCBEE, O. R. PIERCE, and D. D. MEYER. J. Am. Chem. Soc. **77**, 83 (1955).
32. D. J. CRAM, A. ELHAFEZ, and H. L. NYQUIST. J. Am. Chem. Soc. **76**, 22 (1954).
33. W. VON E. DOERING and C. R. NOLLER. J. Am. Chem. Soc. **61**, 3436 (1939).
34. R. STEWART and A. R. UBBELOHDE. J. Chem. Soc. 2649 (1949).
35. G. B. SMITH. Doctoral Dissertation, University of Pittsburgh, Pittsburgh, Penn. 1959.
36. A. KIRRMANN and R. HAMELIN. Compt. Rend. **251**, 2990 (1960). R. HAMELIN. Bull. Soc. Chim. France, 692, 915 (1961).
37. M. ANTEUNIS. J. Org. Chem. **27**, 596 (1962).
38. H. S. MOSHER and P. K. LOEFFLER. J. Am. Chem. Soc. **78**, 4959 (1956).
39. W. N. MOULTON, R. E. VAN ATTA, and R. R. RUCH. J. Org. Chem. **26**, 290 (1961).
40. R. E. DESSY, G. S. HANDLER, J. H. WOTIZ, and C. A. HOLLINGSWORTH. J. Am. Chem. Soc. **79** 3476 (1957). R. E. DESSY and G. S. HANDLER. J. Am. Chem. Soc. **80**, 5824 (1958).

Can. J. Chem. Downloaded from www.nrcresearchpress.com by 210.87.254.5 on 09/05/12
For personal use only.

OBSERVATIONS ON ALKYLBORANES[1, 2, 3]

C. A. LUTZ AND D. M. RITTER
Department of Chemistry, University of Washington, Seattle, Wash., U.S.A.

Received October 29, 1962

ABSTRACT

Some synthesis and exchange reactions of diborane and its alkyl derivatives and of the higher boron hydrides were reviewed as background for new work.

In pursuit of an idea prompted by knowledge of the deuterium and B^{10} exchanges found for the reactive and unstable higher boron hydrides B_4H_{10} and B_5H_{11}, mono- and di-methyldihydropentaborane and methyltetraborane have been prepared by direct reaction between the parent higher hydrides and 1,2-dimethyldiborane or monomethyldiborane. The identity and the reactions of each product have been delineated by gas chromatographic separation, gas density, and mass, infrared, and n.m.r. spectrometry. The H^1 n.m.r. spectrum of dihydropentaborane has been reinterpreted and used to decide that monomethyldihydropentaborane is probably a B_{III} derivative which displays stereoisomerism.

To confine the topic within proportions suitable for a symposium this paper concerns mostly alkylation reactions in which carbon atoms are transferred from sites in one boron compound to sites in another, thus excluding almost completely the extensive material on hydroboration.

As a preliminary, consider some facts about the boron hydrides. They occur in two types, the open pyramidal and the closed pyramidal structures, with the commonest members, diborane, tetraborane-10, pentaborane-11, as examples of the first class and pentaborane-9 and decaborane-14 of the second. The former are the labile, reactive hydrides, the latter the ones of lesser reactivity. Exchange and interconversion reactions show the labile hydrides to maintain effective steady-state concentrations of reactive fragments;[4] the more stable ones do not (1, 2).

Diborane is convertible to the other hydrides by pyrolysis (3) and by interactions such as that with tetraborane (4):

$$B_4H_{10} + B_2H_6 \rightleftharpoons B_5H_{11} + H_2.$$

Three boron and deuterium exchanges exemplify models for alkylation reactions: (*a*) self-exchange of diborane, (*b*) diborane exchange with pentaborane-9, and (*c*) diborane exchange with pentaborane-11. The first is 3/2 order involving successively dissociation of diborane and a borane–diborane displacement reaction with $E^{\ddagger} = 22$ kcal. Deuterium exchanges three times faster than boron. Similarly, the second is 1/2 order in diborane (dissociation) and first order with respect to pentaborane-9, but without boron exchange, $E^{\ddagger} = 27$ kcal. Since the third, pentaborane-11 – diborane exchange, is 1/2 order with respect to the higher hydride and first order in diborane the dissociation is that of pentaborane-11 and the displacement is borane–diborane. With these varying patterns

[1] *Presented at the Symposium on Organometallic Compounds, Vancouver, British Columbia, September 4–6, 1962, sponsored by the Inorganic Chemistry Division, Chemical Institute of Canada, and the Department of Chemistry, University of British Columbia, with the support of the National Research Council, Ottawa, in cooperation with the University Extension Department.*

[2] *Portions of the work discussed here were financed by the U.S. Air Force, Air Research and Development Command, Washington 25, D.C., through contracts AF 18(600)-1541 and AF 49(638)-937. Reproduction in whole or in part for any purpose of the United States Government is permitted.*

[3] *The work on the methyl higher boranes was largely performed by Dr. Lutz during his tenure as a National Science Foundation Cooperative Fellow academic years 1959–1961.*

[4] *Diborane dissociates into two BH_3 fragments with a bridge-bond dissociation energy estimated at 28.5±2.0 kcal (2), and methylation lowers this about 0.5–1.0 kcal per methyl group (14).*

Can. J. Chem. Downloaded from www.nrcresearchpress.com by 210.87.254.6 on 09/05/12
For personal use only.

available there remains now to observe to what degree the alkylation reactions coincide in type with the isotopic exchanges and the hydride interconversion reactions.

In the case earliest examined, methyl–hydrogen exchange gave all the possible methyl derivatives in the reactions begun by treating diborane with trimethylborane (5, 6). From organo group transfer the results so far include also higher *n*-alkyl diboranes (7), phenyl derivatives (8), carborocyclic diboranes (9), and B-methylborazoles (10). Qualitatively the lower alkyl diboranes disproportionate at comparable rates without regard for what group is the substituent, but in mono-*n*-butyldiborane some degree of kinetic stability appears (11). The cause may resemble the entropy-determined stability of the carborocyclic derivatives (9), and also govern the relative stability of the 1,2-disubstituted diboranes (6, 12). The kinetic stabilities of the methyldiboranes are in the order 1,2-di $\gg$ 1,1-di > tri > mono > tetra. From curiosity an investigation was begun a few years ago concerning this ordering, and the nature of the reactions of formation and disproportionation. This has developed into a general inquiry into kinetics and equilibria in the alkylation of the boranes with some results summarized in the next paragraphs.

The reaction between diborane and trimethylborane appears first order in each reactant. Since one of these is itself a borane, through analogy with the boron and deuterium exchange reactions it seemed logical to search for borane–borane reactions, together with displacements, as the means of methyl group transfer. An early interpretation of the results seemed consistent with this conclusion (13), but subsequent determination of an activation energy of ~11 kcal (14) was inconsistent with any scheme for which the activation energy would need to have a value at least half the bridge-bond dissociation energy for diborane as one of several components. Presently the data can be best interpreted as denoting two consecutive second-order reactions at temperatures 0–35° C:

$$\tfrac{3}{2}B_2H_6 + BMe_3 \xrightarrow{k_1} 1,1\text{-}B_2H_4Me_2 + B_2H_5Me$$

$$B_2H_5Me + BMe_3 + \tfrac{1}{2}B_2H_6 \xrightarrow{k_2} 2\ 1,1\text{-}B_2H_4Me_2.$$

Viewed as reactions with B_3 transition states these can be seen to be analogous with the borane displacement step in the diborane self-exchange, and in the B_5H_{11} exchange sequence.

The monomethyldiborane dismutation, quite unlike the easily predicted course of dissociation and reassembly, appears to proceed through a second-order process. In pyrex glass reactors induction periods and several-fold variations in the velocity constants suggest a heterogeneous reaction, but no pronounced influence is exerted upon the rate by tenfold increase in surface–volume ratio. The reaction proceeds to an equilibrium:

$$2MeB_2H_5 \rightleftharpoons B_2H_6 + (BH_2Me)_2,$$

which has been completely defined at ordinary temperatures[5] (11, 14).

Reaction of trimethylborane with pentaborane-9 at temperatures up to 135° C gives no methylation (15), though at 235° C methyldiboranes with hydrogen give methylated derivatives of pentaborane-9 (16) in a reaction probably so drastic as to defy logical analysis. Alkyl pentaborane-9 and alkyldecaborane derivatives have been synthesized by methods not involving other alkylboron compounds as reagents (17, 18, 19). Since the less stable hydrides, tetraborane, B_4H_{10}, and dihydropentaborane or pentaborane-11, B_5H_{11}, could scarcely be alkylated by such drastic means, though dimethylenetetraborane is made in the hot–cold reactor (20), reactions analogous to the synthesis reaction for

[5]*In the range 273.2° K to 309.7° K, through equilibrium constants described by the equation* $\ln(K \pm 5 \times 10^{-4}) = -1.5971 - (281.46/T)$. *(*$\Delta H$ *= 559 cal/mole,* F_{298}^0 *= 1505 cal/mole, and* $\Delta S^\circ = -3.17$ *e.u.)*

Can. J. Chem. Downloaded from www.nrcresearchpress.com by 210.87.254.6 on 09/05/12
For personal use only.

B_5H_{11} and to the isotope exchange processes for B_5H_{11} and B_4H_{10} were adopted, using in each case momomethyldiborane or 1,2-dimethyldiborane as the reactants, instead of diborane, as described in the equations

$$B_4H_{10} + \tfrac{1}{2}(BH_2Me)_2 \rightleftharpoons B_5H_{10}Me + H_2$$
$$B_5H_{11} + B_2H_5Me \rightleftharpoons B_5H_{10}Me + B_2H_6$$
$$B_4H_{10} + B_2H_5Me \rightleftharpoons B_4H_9Me + B_2H_6.$$

The results obtained illustrate that these alkylation reactions, like those of the diboranes, proceed in conformance with the analogies suggested by the exchange processes.

EXPERIMENTAL

The vacuum line operations used were those developed by Stock (21) and by Schlesinger and his co-workers, and described by Sanderson (22). Separation of products was accomplished by gas chromatography in almost all cases. The design, construction, and operation of the type of chromatograph employed has been described previously (23). The purity of samples used for physical measurements was monitored by gas chromatography before and after each measurement. In no case did the impurities exceed 0.5%.

Molecular Weights

Molecular weights were determined in duplicate by the gas density method. Care was taken to minimize contact with stopcock grease.

Infrared Spectra

Infrared spectra were obtained with a Perkin–Elmer Model 21 spectrometer using both sodium chloride and calcium fluoride optics and cells of either 5 or 10 cm length constructed with minimum cell volume. Atmospheric absorption peaks were used for calibration and reported values are accurate within ~5 cm^{-1}.

Nuclear Magnetic Resonance Spectra

A Varian (Model 4311) high-resolution nuclear magnetic resonance spectrometer operating at 60 Mc was used. The substances B_5H_{11} and $B_5H_{10}Me$ were used neat without an internal reference. All sample tubes were prepared in vacuum and stored in liquid nitrogen to prevent decomposition. The scales of the spectra were established in all instances by the standard side-band technique.

Analysis of the H^1 spectrum of B_5H_{11}, needed as a reference for characterizing $B_5H_{10}Me$, was begun by recognizing that peaks 1, 2, 10 (Fig. 1(*b*)) with an area ratio 1.95:4.05:1.00 represent respectively the lowest-field members of two quartets, *a* and *b*, and the highest-field member of a third, *c*. These quartets were

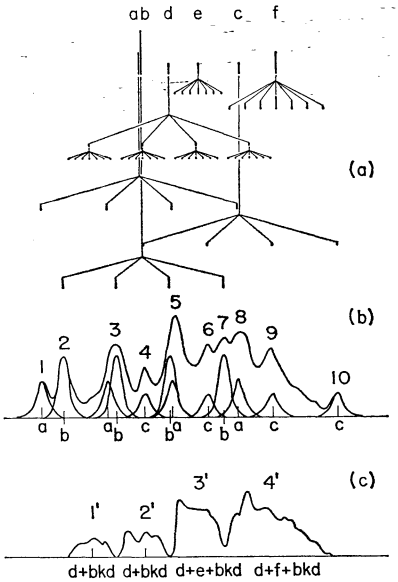

FIG. 1. H^1 n.m.r. spectrum of B_5H_{11} (field increasing to right): (*a*) diagrammatic display of resonances; (*b*) experimental trace with components *a*, *b*, *c*; (*c*) difference trace containing *d*, *e*, *f*, and background (*bkd*).

Can. J. Chem. Downloaded from www.nrcresearchpress.com by 210.87.254.6 on 09/05/12
For personal use only.

subtracted from the total band envelope to give the difference trace shown in Fig. 1(*c*). This was recognized as the sum of a quartet, each member broadened by splitting into unresolved septets, *d*, and two unresolved septets, *e* and *f*. Resonances *d* overlap *e* and *f*.

The presence of B^{10} nucleii makes these comparisons somewhat less correct than desirable but not fatally so.[6] The intensities of the B^{11}-split resonances are reduced slightly, and there appear as background unresolvable resonances of B^{10} origin, for which correction can be made in the following way. The whole original band envelope had an area 22.47 cm²; the difference trace was 14.99 cm² comprising 1′, 2′, 3′, 4′ of area 1.18, 1.93, 4.38, and 7.50 cm², respectively. Peak 10, taken as unity, had an area 0.60 cm², and from this and the areas of 1′, 2′ backgrounds of 0.58 cm² and 1.33 cm², respectively, were calculated for those peaks. For 3′ the background was taken equal to that of 2′, 1.33 cm², and the sum of backgrounds for 1′ and 2′ was assumed as background for 4′. Then from 3′ and 4′ each 0.60 cm² was subtracted for the *d* component. The remainders were, for 3′ 2.45 cm^{-2} and for 4′ 5.09 cm² in the ratio approximately 1:2, representing respectively four units and eight units of intensity.

Mass Spectra

All mass spectra were obtained with a Consolidated Model 20–103 mass spectrometer using a rhenium filament. The fractionation effect at varying pressures was often used to detect impurities. Ionizing voltages of 70 v and 8–14 v were used.

The isotopic ratio $B^{11}/B^{10} = 4.00$ was used, as is customary (25), to reduce the polyisotopic abundances to the monoisotopic values, and for the methyl derivatives a C^{13} content of 1.108% was assumed.

Gas–Liquid Chromatographic Properties

To separate compounds with a wide range of retention times as quickly as possible a variety of flow rates and columns was used. The flow rates of helium carrier gas were in the range of 1–70 ml/min. The columns had "Standard White Oil #9" as the stationary phase supported on Johns-Mansville firebrick (crushed and sieved to 32–65 Taylor mesh) in a weight ratio of 0.38:1. After removal of the solvent for the white oil the column packing was dried *in vacuo* for at least 24 hours. Diborane was passed through the column a number of times before use. Column lengths varied from 25–95 cm and internal diameters from 0.4 to 1.0 cm.

The relative retention times of all relevant compounds are found in Table I.

TABLE I

Gas chromatographic properties—relative retention times

Compound	Relative retention time	Compound	Relative retention time
B_2H_6	3.2	B_4H_9Me	97
B_2H_5Me	7.3	B_5H_9	100
BMe_3	11.1	B_5H_{11}	148
1,1-$B_2H_4Me_2$	16.5	B_5H_8Me	278
1,2-$B_2H_4Me_2$	21.3	$B_5H_{10}Me$	410
B_4H_{10}	29.5	B_6H_{10}	477
$B_2H_3Me_3$	53.2	$B_5H_9Me_2$	847

Preparations and Reactions

Tetraborane and dihydropentaborane were prepared from diborane by the "hot–cold" tube reactor method (26). The crude products were purified by repeated passes through the gas chromatograph with appropriate cuts, until the products were chromatographically pure.

All the methyldiboranes except 1,2-dimethyldiborane were obtained by fractionating the desired compound from a large storage bulb containing diborane, boron trimethyl, and mixed methyldiboranes. Final purification was accomplished by repeated passes through the gas chromatograph. Dimethyldiborane was prepared by allowing monomethyldiborane to disproportionate to diborane and 1,2-dimethyldiborane at room temperature followed by gas chromatographic separation.

Methyldihydropentaboranes were prepared by use of monomethyl- and dimethyl-diboranes in (*a*) reaction with tetraborane or (*b*) exchange with dihydropentaborane.

(*a*) Tetraborane (0.2 mmole) and a methyldiborane mixture (mostly dimethyldiboranes) (0.2 mmole) were heated at ~1 atm pressure and 100° C for 15 minutes. Diborane was removed by passing the mixture through a U-tube cooled to −145°, and the remaining components were separated by gas chromatography. The components were methyldiboranes, tetraborane, pentaborane, dihydropentaborane, identified

[6] *From the isotope distribution for the pyramidal* B_5 *system, previously calculated for* B_4H_9 *(24), the attenuations and the* B^{10}*-derived intensities can be calculated for the various resonances. The fractional attenuations and the overall (unsplit) relative* B^{10} *resonance intensities are, for "a" and "b" 0.099, for "c" and "d" 0.161, for "e" 0.179, and for "f" 0.128.*

Can. J. Chem. Downloaded from www.nrcresearchpress.com by 210.87.254.6 on 09/05/12
For personal use only.

by their infrared spectra (27, 28); 2-methylpentaborane, identified by its infrared spectrum, 0° vapor pressure, and mass spectrum (16); and the two new substances methyl- and dimethyl-dihydropentaborane. The yield of all methylpentaboranes combined was less than 5%, and solid hydrides formed extensively.

(*b*) Dihydropentaborane (0.2 mmole) and a mixture of mono- and di-methyldiboranes (0.2 mmole) were held at 35° for 15 minutes. Diborane was removed by passing the mixture through a U-tube cooled to −145°, and the reaction was continued at 35° for another 15-minute period. Gas chromatography served to separate the residual starting materials, diborane, pentaborane-9, and the new substance methyldihydropentaborane, the latter two in yields of 7% and 64%, respectively, based upon the original dihydropentaborane. A trace of dimethyldihydropentaborane was always formed, and from larger-scale preparative experiments it was accumulated until sufficient material was obtained for characterization. $B_5H_{10}CH_3$ v.p. 0° C 21.0 mm; mol. wt.: found 79.2, 80.0; calc. 79.2.

Methyltetraborane was prepared from tetraborane (5.0 mmoles) and a mixture of monomethyldiborane and dimethyldiboranes (15.0 mmoles) contained in a 500-ml bulb, allowed to stand at room temperature for 2 days, and then heated to 45° C with a water bath for 4 hours. The reaction mixture was fractionated through a U-tube cooled to −90° C and the portion retained by the bath was passed through the gas chromatograph. Because the g.l.c. relative retention times of methyltetraborane and pentaborane differ only as 97 and 100, respectively, repeated passage through the chromatographic column was necessary, with sample partition practiced at each step, until a single peak for a substance of constant properties was attained. Approximately 0.4 mmole of B_4H_9Me was obtained. Molecular weight: found 66.8, 68.0; calculated 67.4. The compound was also characterized by infrared and mass spectra shown in Tables XII, and IX, and X respectively.

Methyldihydropentaborane decomposition was observed in two experiments.

(*a*) A sample of the purified substance was left standing for 30 minutes at room temperature. The gas chromatograph trace of the material then showed $B_5H_{10}Me$ 83.8%, B_5H_{11} 10.1%, $B_5H_9Me_2$ 6.1%. The inequality of the latter two amounts can be explained by further disproportionation to give $B_5H_8Me_3$ with a too long retention time for observation.

(*b*) After 15 minutes of heating at 90° a sample of $B_5H_{10}Me$ contained 70% starting material, 7.2% B_5H_{11}, ~1% B_5H_8Me, a trace of B_5H_9, and 7.6% diborane and methyldiboranes. The material balance was 85.8%; the unaccounted for balance was presumably converted to solid hydrides and possibly to $B_5H_9Me_2$.

Reactions of methyldihydropentaborane were observed with (*a*) diborane and with (*b*) diethyl ether (29).

(*a*) Methyldihydropentaborane (0.3 mmole) and diborane (3.0 mmole) were mixed for 30 minutes at room temperature. The products, separated by gas chromatography and identified by infrared spectra, contained methyldiboranes, a trace of pentaborane, dihydropentaborane (72% conversion), some starting material, with a material balance of 96%.

(*b*) Methyldihydropentaborane (0.5 mmole) was condensed with a slight excess of diethyl ether. The tube was held at −78° C for 5 minutes and at 0° C for 10 minutes. The products, separated by gas chromatography and identified by their infrared spectra, were pentaborane, dihydropentaborane, starting material. Only a very small sample of material with a long retention time was obtained, heavily contaminated with dimethyldihydropentaborane. A polyisotopic mass spectrum of the sample is shown in Table II.

TABLE II

Polyisotopic mass spectrum of the fraction of longest retention time from the $B_5H_{10}Me$–Et_2O reaction*

m/e	Intensity	*m/e*	Intensity	*m/e*	Intensity
60	67.13	72	55.23	83	36.26
61	85.74	73	63.13	84	46.67
62	100.00	74	62.56	85	52.82
63	70.92	75	51.28	86	50.92
64	63.59	76	57.85	87	39.33
65	12.78	77	43.59	88	44.77
66	19.82	78	39.48	89	42.56
67	28.20	79	16.48	90	36.92
68	41.59	80	15.54	91	16.49
69	45.38	81	17.22	92	8.35
70	39.33	82	23.58	93	0.56
71	48.72				

*Ionizing voltage 14 v.

RESULTS AND DISCUSSION

Identification and characterization of the compounds $B_5H_{10}Me$, $B_5H_9Me_2$, B_4H_9Me rest upon data collected by mass, n.m.r., and infrared spectroscopy, necessitating that

Can. J. Chem. Downloaded from www.nrcresearchpress.com by 210.87.254.6 on 09/05/12
For personal use only.

results for the parent substances be examined for comparison. The older data were obtained on samples, purified by fractional condensation, which inescapably contained impurities now removable by gas chromatography.

Polyisotopic mass spectra of B_5H_{11} are found in Table III. The parent group and the

TABLE III

Polyisotopic mass spectra of B_5H_{11}

	Intensity			Intensity	
m/e	70 v	11 v	*m/e*	70 v	11 v
10	7.16		45	31.12	0.63
11	30.60		46	46.46	2.90
12	15.11		47	67.28	7.94
13	32.13		48	51.16	12.17
14	1.22	1.24	49	26.16	
			50	16.42	
20	0.08		51	4.40	
21	0.42		52	4.29	
22	2.36	0.50	53	7.84	
23	7.20	3.44	54	19.14	
24	13.17	7.42	55	27.24	0.20
25	9.96	7.37	56	29.85	0.97
26	15.49	20.64	57	35.45	3.71
27	20.52	24.37	58	33.58	12.11
28	8.61		59	82.84	31.13
29	1.86		60	100.00	62.95
30	1.42		61	98.13	100.00
31	0.64		62	91.25	98.82
32	2.05		63	29.85	50.30
33	4.74		64	21.64	38.50
34	11.94	0.21	65	0.86	0.59
35	21.27	1.12	66		0.20
36	25.75	6.37			
37	25.93	21.56	Doubly charged ions		
38	25.49	28.68			
39	4.48	1.66	$23\frac{1}{2}$	0.01	
40	2.50		$27\frac{1}{2}$	Trace	
41	5.11		$28\frac{1}{2}$	0.03	
42	2.35		$29\frac{1}{2}$	0.02	
43	2.72		$30\frac{1}{2}$	Trace	
44	17.57				

subgroups, readily distinguished in the B_5H_{11} spectrum at 11 v, are a small parent peak $(B_5H_{11})^+$ at *m/e* 66, and subgroups at *m/e* 52, *m/e* 39, *m/e* 27, and *m/e* 14 composed of ions of the type $(B_4H_8)^+$, $(B_3H_6)^+$, $(B_2H_5)^+$, and $(BH_3)^+$ respectively. A partial monoisotopic mass spectrum for B_5H_{11} is shown in Table IV. The previously noted tendency of boron hydrides to lose hydrogen atoms in pairs (29) is also observed in the monoisotopic B_5H_{11} spectrum and in that for the $(B_4H_8)^+$ subgroup.

Polyisotopic mass spectra of $B_5H_{10}Me$ at ionizing voltages of 70 and 12 v are found in Table V. A parent peak at *m/e* 80 is observed in neither spectrum. Although the spectrum at 70 v is essentially continuous from *m/e* 21 to 79, making it difficult to identify the subgroups, certain similarities between this spectrum and the spectrum of B_5H_{11} can be seen. The peak with highest intensity in both the B_5H_{11} and $B_5H_{10}Me$ spectrum occurs at six mass units below the parent peak at *m/e* 60 in the B_5H_{11} spectrum and at *m/e* 74 in the $B_5H_{10}Me$ spectrum. Doubly charged ions are observed at *m/e* $34\frac{1}{2}$, *m/e* $35\frac{1}{2}$, and *m/e* $36\frac{1}{2}$, which correspond, considering the methyl group in $B_5H_{10}Me$, to the ions observed in the B_5H_{11} spectrum in the range *m/e* $27\frac{1}{2}$–$30\frac{1}{2}$.

Can. J. Chem. Downloaded from www.nrcresearchpress.com by 210.87.254.6 on 09/05/12
For personal use only.

TABLE IV

Partial monoisotopic mass spectrum of B_5H_{11}*

Ion species	Intensity	Ion species	Intensity	Ion species	Intensity
BH_3^+	1.50	$B_4H_2^+$	0.18	$B_5H_2^+$	0.29
		$B_4H_3^+$	0.25	$B_5H_3^+$	0.87
B_2H^+	0.41	$B_4H_4^+$	9.26	$B_5H_4^+$	0.83
$B_2H_2^+$	8.35	$B_4H_5^+$	0.83	$B_5H_5^+$	20.21
$B_2H_3^+$	2.23	$B_4H_6^+$	17.48	$B_5H_6^+$	1.53
$B_2H_4^+$	11.53	$B_4H_7^+$	0.37	$B_5H_7^+$	100.00
$B_2H_5^+$	33.35	$B_4H_8^+$	7.56	$B_5H_8^+$	3.64
				$B_5H_9^+$	51.94
$B_3H_2^+$	0.03			$B_5H_{10}^+$	0.47
$B_3H_3^+$	0.99			$B_5H_{11}^+$	0.27
$B_3H_4^+$	0.87				
$B_3H_5^+$	37.64				
$B_3H_6^+$	2.27				

*Ionizing voltage 11 v.

TABLE V

Polyisotopic mass spectra of $B_5H_{10}Me$

	Intensity			Intensity			Intensity	
m/e	70 v	12 v	*m/e*	70 v	12 v	*m/e*	70 v	12 v
14	1.46	3.53	38	23.78	6.67	59	54.10	7.48
15	3.80	1.24	39	12.75	17.77	60	50.34	17.58
16	0.48	1.04	40	13.95	31.30	61	63.69	34.64
			41	24.18		62	70.04	46.52
21	0.32		42	1.90		63	36.45	46.64
22	1.49		43	5.83		64	27.94	46.02
23	1.19	2.43	44	4.58		65	7.85	9.51
24	9.69	5.39	45	21.46		66	12.54	8.25
25	10.75	6.63	46	49.90	2.84	67	19.49	
26	25.68	22.91	47	73.20	12.21	68	24.77	
27	49.82	35.49	48	74.44	24.52	69	25.76	1.41
28	3.51	2.01	49	60.56	43.72	70	31.74	4.87
29	0.75		50	50.34	54.17	71	48.36	11.13
30	0.12		51	26.44	39.18	72	66.19	22.39
31	0.32		52	26.44	44.59	73	84.30	43.35
32	1.61		53	4.98	1.04	74	100.00	72.76
33	4.40		54	10.82		75	88.35	100.00
34	13.08	0.93	55	20.10		76	79.67	95.46
35	25.56	5.12	56	29.36		77	28.54	39.12
36	38.45	13.37	57	39.63	0.83	78	17.12	28.59
37	48.36	19.59	58	46.18	2.76	79	0.59	0.87

In the polyisotopic spectrum of $B_5H_{10}Me$ at 12 v the subgroups are clearly visible and can be compared with the subgroups observed in the B_5H_{11} spectrum at low ionizing voltage. The first subgroup below the parent group in the $B_5H_{10}Me$ spectrum, beginning at *m/e* 66, is composed of ions of the type $(B_4H_7Me)^+$. This corresponds to the $(B_4H_8)^+$ subgroup from the B_5H_{11} molecule. Another subgroup may be hidden under the $(B_4H_7Me)^+$ subgroup, namely the $(B_5H_{10})^+$ group, which would appear at *m/e* 65 as a result of the loss of the methyl group from the $B_5H_{10}Me$ molecule. The subgroup beginning at *m/e* 53 probably is composed of ions of the type $(B_3H_5Me)^+$, and corresponds to the $(B_3H_6)^+$ subgroup which begins at *m/e* 39 in the B_5H_{11} spectrum. Another subgroup, resulting from the loss of a BH_2Me group from the $B_5H_{10}Me$ molecule, is probably hidden beneath the $(B_3H_5Me)^+$ subgroup. The subgroup beginning at *m/e* 41 is most likely composed of ions of the type $(B_2H_4Me)^+$ and $(B_3H_6)^+$, while the subgroup beginning at *m/e* 28 contains

Can. J. Chem. Downloaded from www.nrcresearchpress.com by 210.87.254.6 on 09/05/12
For personal use only.

ions of the type $(BH_3Me)^+$ and $(B_2H_5)^+$. The purity of the sample and the correctness of the molecular formula for $B_5H_{10}Me$ were confirmed by the monoisotopic spectrum calculated for the parent peak as shown in Table VI. The qualitative agreement between

TABLE VI

Polyisotopic mass spectra of $B_5H_9Me_2$

	Intensity				Intensity		
m/e	14 v	11 v	9 v	*m/e*	14 v	11 v	9 v
27	60.39	59.74		61	46.01	26.32	
28	2.65	2.35		62	60.62	40.07	32.95
29	1.13			63	50.39	43.70	72.87
30	0.10			64	46.64	44.73	81.12
31	1.63			65	12.46	13.13	39.28
32	0.52			66	11.91	13.18	44.99
33	0.22			67	0.81	0.74	
34	1.15	0.49		68	1.10	0.20	
35	4.08	2.03		69	3.03	0.55	
36	11.28	5.49		70	6.46	1.58	
37	17.87	10.76		71	12.59	3.50	
38	16.33	13.75		72	19.16	6.83	2.53
39	10.20	8.77		73	27.48	12.36	6.34
40	32.99	33.82		74	35.43	18.22	24.71
41	100.00	100.00		75	36.24	22.94	46.89
42	2.60	2.10		76	39.63	26.51	83.02
43	2.50	0.69		77	25.72	21.41	91.25
44	1.00	0.30		78	21.57	18.60	69.46
45	3.35	0.90		79	4.08	5.05	28.90
46	2.78	3.65		80	3.45	3.97	29.78
47	21.32	10.38		81	0.79	0.64	
48	33.02	17.46		82	1.69	0.94	
49	33.88	21.22		83	3.49	2.14	
50	38.84	30.38		84	5.63	4.13	
51	36.56	35.87		85	8.66	6.89	
52	39.57	42.61		86	11.27	9.35	2.53
53	3.92	3.84		87	13.94	12.46	6.34
54	1.47	1.88		88	19.19	19.09	20.91
55	2.28	2.58		89	24.44	25.12	37.16
56	1.38	0.52		90	23.23	24.82	100.00
57	4.10	1.07		91	12.51	12.27	98.60
58	7.24	2.03		92	8.92	8.31	27.88
59	17.32	5.48		93	0.45	0.31	1.90
60	27.30	12.48					

the monoisotopic spectra of $B_5H_{10}Me$ and B_5H_{11} is excellent. The alternation of intensities observed in the monoisotopic spectrum of B_5H_{11} and other boron hydrides is also observed in the $B_5H_{10}Me$ spectrum. The three most intense ions in the parent group of $B_5H_{10}Me$, in order of decreasing intensity, are $(B_5H_6Me)^+$, $(B_5H_8Me)^+$, and $(B_5H_4Me)^+$, while in the parent group of B_5H_{11} the three most intense ions are $(B_5H_7)^+$, $(B_5H_9)^+$, and $(B_5H_5)^+$, in the same order.

Polyisotopic mass spectra of $B_5H_9Me_2$ are found in Table VI. Considerably more cracking to fragments of low mass occurs in the $B_5H_9Me_2$ spectra than in the spectra of B_5H_{11} or $B_5H_{10}Me$. At an ionizing voltage of 9 v the parent group and the subgroup can be clearly distinguished. The subgroup beginning at *m/e* 80 contains ions of the type $(B_4H_6Me_2)^+$ and is analogous to the subgroups containing ions of the type $(B_4H_8)^+$ and $(B_4H_7Me)^+$ in the spectra of B_5H_{11} and $B_5H_{10}Me$, all the result of BH_3 loss. It is likely that a subgroup resulting from the loss of a methyl group from the molecule underlies the $(B_4H_6Me_2)^+$ subgroup. The subgroup beginning at *m/e* 66 probably is the result of

Can. J. Chem. Downloaded from www.nrcresearchpress.com by 210.87.254.6 on 09/05/12
For personal use only.

the loss of a BH_2Me group from the molecule, leaving a subgroup composed of ions of the type $(B_4H_7Me)^+$.

A partial monoisotopic mass spectrum of $B_5H_9Me_2$ is found in Table VII. The parent group is very similar to those of B_5H_{11} and $B_5H_{10}Me$. The loss of hydrogen atoms in

TABLE VII

Partial monoisotopic mass spectra of $B_5H_{10}Me$ and $B_5H_9Me_2$

$B_5H_{10}Me$*		$B_5H_9Me_2$†	
Ion species	Intensity	Ion species	Intensity
$B_5H_9CH_3^+$	0.82	$B_5H_8C_2H_6^+$	1.01
$B_5H_8CH_3^+$	37.68	$B_5H_7C_2H_6^+$	46.22
$B_5H_7CH_3^+$	4.87	$B_5H_6C_2H_6^+$	10.66
$B_5H_6CH_3^+$	100.00	$B_5H_5C_2H_6^+$	100.00
$B_5H_5CH_3^+$	2.59	$B_5H_4C_2H_6^+$	5.74
$B_5H_4CH_3^+$	32.13	$B_5H_3C_2H_6^+$	38.54
$B_5H_3CH_3^+$	1.91	$B_5H_2C_2H_6^+$	4.42
$B_5H_2CH_3^+$	5.91	$B_5H_1C_2H_6^+$	21.58
$B_5H_1CH_3^+$	1.63	$B_5C_2H_6^+$	4.06
$B_5H_0CH_3^+$	0.02	$B_5C_2H_5^+$	3.97
		$B_5C_2H_4^+$	1.48

*Ionizing voltage 12 v.
†Ionizing voltage 11 v.

pairs is again observed. The ion $(B_5H_5Me_2)^+$, the most intense in the parent group, is analogous to the ions $(B_5H_6Me)^+$ and $(B_5H_7)^+$, which are the most intense ions in the parent groups of the monoisotopic $B_5H_{10}Me$ and B_5H_{11} spectra.

The mass spectrum of a sample of $B_5H_9Me_2$ which had been allowed to stand at room temperature for a few minutes contains a group of ions in the range *m/e* 96–107, which is very likely the parent group of the compound $B_5H_8Me_3$. This indicates that $B_5H_9Me_2$ probably undergoes a disproportionation reaction to form $B_5H_{10}Me$ and $B_5H_8Me_3$ similar to the disproportionation of $B_5H_{10}Me$.

Polyisotopic mass spectra of B_4H_{10} and B_4H_9Me are found in Tables VIII and IX. No parent peaks are found in either the B_4H_{10} or B_4H_9Me spectra. At 70 v the highest masses for B_4H_{10} and B_4H_9Me occur at *m/e* 52 and *m/e* 66 respectively, in each case two mass units below the parent peak. Highest intensities occur at *m/e* 49 and *m/e* 63 respectively, in each case five mass units below the parent peaks. Doubly charged ions are observed at *m/e* $22\frac{1}{2}$, *m/e* $23\frac{1}{2}$, and *m/e* $24\frac{1}{2}$ in the B_4H_{10} spectrum and at *m/e* $28\frac{1}{2}$, *m/e* $29\frac{1}{2}$, and *m/e* $30\frac{1}{2}$ in the B_4H_9Me spectrum. Both these series of doubly charged ions have masses 9, 7, and 5 mass units less than their respective parent peaks. Doubly charged ions probably occur at the even masses in these regions of the spectra but are masked by more intense singly charged ions.

At 11 v highest intensities occur at *m/e* 50 and *m/e* 64 for B_4H_{10} and B_4H_9Me respectively. Since the subgroups and the parent group do not overlap in the B_4H_9Me spectrum at 11 v it is possible to identify some of the subgroups. The subgroup which begins at *m/e* 53 is most likely composed of $(B_4H_9)^+$, $(B_4H_8)^+$, . . . ions. The subgroup beginning at *m/e* 41 could be composed of ions of the type $(B_3H_8)^+$ or of ions of the type $(B_2H_4Me)^+$.

Partial monoisotopic mass spectra of B_4H_{10} and B_4H_9Me at 11 v are found in Table X. In the calculation for B_4H_9Me the assumption which led to minimum residues was that the subgroups at *m/e* 45–53 and *m/e* 34–41 were composed solely of ions of the type $(B_4H_9)^+$ and $(B_2H_4Me)^+$.

The interpretation of the H^1 n.m.r. spectra of B_5H_{11} and $B_5H_{10}Me$ rests upon the structure determination for the parent substance (30, 31). Owing to the presence of B_5H_9

Can. J. Chem. Downloaded from www.nrcresearchpress.com by 210.87.254.6 on 09/05/12
For personal use only.

TABLE VIII
Polyisotopic mass spectra of B_4H_{10}

	Intensity			Intensity	
m/e	70 v	11 v	*m/e*	70 v	11 v
10	6.02		41	0.44	
11	24.42	0.13	42	2.44	
12	10.41	0.39	43	3.08	
13	20.45	1.15	44	20.38	0.14
14	0.38	0.19	45	31.51	1.19
15	0.26		46	50.70	6.63
			47	73.66	21.27
20	0.07		48	92.85	50.49
21	0.48		49	100.00	94.88
22	1.87		50	97.85	100.00
23	4.56	0.13	51	17.56	17.73
24	7.39	0.32	52	6.53	12.80
25	4.87	1.18	53	0.37	0.32
26	3.78	3.89			
27	4.53	4.40			
28	1.18				
31	0.39				
32	2.53				
33	7.41				
34	17.38	0.26			
35	28.01	0.52			
36	26.15	2.91			
37	25.86	9.65	Doubly charged ions		
38	24.70	12.41	$22\frac{1}{2}$	0.13	
39	2.91	0.52	$23\frac{1}{2}$	0.39	
40	0.11		$24\frac{1}{2}$	0.04	

TABLE IX
Polyisotopic mass spectra of B_4H_9Me

	Intensity			Intensity	
m/e	70 v	11 v	*m/e*	70 v	11 v
14	1.59	0.64	45	15.04	0.16
15	4.43	0.50	46	28.39	1.09
16	0.43	0.65	47	43.32	3.80
			48	48.36	9.84
20	0.04		49	54.83	22.13
21	0.38		50	57.28	32.84
22	1.59		51	40.93	28.69
23	3.82	0.49	52	29.83	24.43
24	8.47	1.03	53	5.81	4.43
25	10.47	2.02	54	2.38	
26	25.48	7.36	55	6.90	
27	46.25	22.38	56	14.74	
28	1.93	1.18	57	20.76	0.42
29	0.11		58	21.37	1.61
30	0.09		59	26.25	4.75
31	0.10		60	32.22	13.79
32	1.79		61	59.07	33.88
33	5.13		62	90.45	63.77
34	15.29	0.63	63	100.00	97.81
35	30.00	2.78	64	97.61	100.00
36	42.96	6.83	65	13.13	12.84
37	53.69	14.10	66	4.40	7.60
38	27.68	19.85	67	0.41	0.26
39	12.14	6.45			
40	6.98	8.20			
41	4.67	4.67	Doubly charged ions		
42	0.96		$28\frac{1}{2}$	0.02	
43	3.04		$29\frac{1}{2}$	0.10	
44	7.52		$30\frac{1}{2}$	0.02	

Can. J. Chem. Downloaded from www.nrcresearchpress.com by 210.87.254.6 on 09/05/12
For personal use only.

TABLE X

Partial monoisotopic mass spectra of B_4H_{10} and B_4H_9Me*

B_4H_9Me		B_4H_9Me		B_4H_9Me		B_4H_{10}	
Ion species	Intensity	Ion species	Intensity	Ion species	Intensity	Ion species	Intensity
$B_4H_8CH_3^+$	0.19	$B_4H_9^+$	4.77	$B_2H_4CH_3^+$	4.96	$B_4H_9^+$	0.40
$B_4H_7CH_3^+$	7.92	$B_4H_8^+$	21.56	$B_2H_3CH_3^+$	6.33	$B_4H_8^+$	13.79
$B_4H_6CH_3^+$	4.79	$B_4H_7^+$	7.60	$B_2H_2CH_3^+$	3.30	$B_4H_7^+$	5.71
$B_4H_5CH_3^+$	100.00	$B_4H_6^+$	19.44	$B_2H_1CH_3^+$	19.31	$B_4H_6^+$	100.00
$B_4H_4CH_3^+$	3.57	$B_4H_5^+$	0.24	$B_2CH_3^+$	5.45	$B_4H_5^+$	2.18
$B_4H_3CH_3^+$	27.31	$B_4H_4^+$	2.59	$B_2CH_2^+$	3.42	$B_4H_4^+$	15.87
$B_4H_2CH_3^+$	1.51	$B_4H_3^+$	0.18	$B_2CH_1^+$	0.85	$B_4H_3^+$	0.80
$B_4H_1CH_3^+$	2.23					$B_4H_2^+$	0.20
$B_4H_0CH_3^+$	0.69						

*Ionizing voltage 11 v.

impurity, almost impossible to remove completely by fractional condensation but easily eliminated by gas chromatography, the earlier normal spectra (32, 33) can scarcely have been interpreted satisfactorily, although multiplet structure collapse by "spin saturation" did resolve four types of H^1 in the proper ratio of 6 as B—H, 3 as B—H—B, and 1 as unique apical B—H (32).

The most recent H^1 n.m.r. spectrum for highly purified B_5H_{11}, shown in Fig. 1, was dissected as described in the experimental part. The observed peaks, 1 through 10, have been assigned as: quartet *a* to the two H^1 linked to the two back-based B_{II} atoms; quartet *b* to the four H^1 linked to the two forward-based B_{III} atoms; quartet *c* to the single H^1 linked to the apical B_I atom and projected upward from the pyramid. From the difference trace there have been assigned to account for intensity groups, 1′ through 4′: the quartet *d* arising from the unique H^1, bonded to the apical B_I atom at a distance 1.09 ± 0.19 Å (30); additionally each member of the quartet appears broadened through splitting into an unresolved septet owing to the bridge-bonding of this H^1 to the two B_{III} atoms at distances 1.77 ± 0.19 Å (30); the unresolved septet *e* from the back bridge-bond B_{II}—H—B_{II} atoms and the unresolved septet *f* from the two side bridge-bonds B_{II}—H—B_{III}. The assigned areas are in the proper ratio *a*:*b*:*c*:*d*:*e*:*f* as 2:4:1:1:1:2, and the locations of the band centers without exception are consistent with the excess charge densities calculated for the B_5H_{11} framework (34), as (B_I) $-0.14e$, (B_{II}) $+0.08e$, and (B_{III}) $-0.01e$. The *J* values calculated from the spectrum are, in c.p.s.: *a*, $B_{II}H$, 152; *b*, $B_{III}H$, 123; *c*, B_IH, 148; *d*, B_IH (unique), ~124; *e*, $B_{II}HB_{II}$, ≈18; *f*, $B_{II}HB_{III}$, ≈33; unique $B_{III}HB_{III}$, ≈15.

The H^1 n.m.r. spectrum of methyldihydropentaborane is shown in Fig. 2, where it is compared with the H^1 spectrum for B_5H_{11}. The low-field resonances belonging to quartets *a* and *b* are the ones detectably influenced by the methylation. The separation of peaks 1 and 2 has been obliterated; peak 1 has been diminished slightly; peaks 2, 3, 5, 8 have been diminished to a greater extent, and a tendency toward fusion can be noted between peaks 8 and 9. The largest contribution to peaks 2, 3, 5 is from resonances *b*, assigned to protons on B_{III} atoms. It is proposed that one of these, a frontal pyramid-base boron atom, is the site of the methyl group.

Resonances from the methyl group protons arise prominently in the spectrum, as a pair, probably owing to stereoisomerism which can be deduced by examining the *a* and *c* resonances. An apical location is excluded by the unaltered intensity of peak 10, a *c* quartet member. While the *a* intensity, peak 1, is slightly diminished this has another

Can. J. Chem. Downloaded from www.nrcresearchpress.com by 210.87.254.6 on 09/05/12
For personal use only.

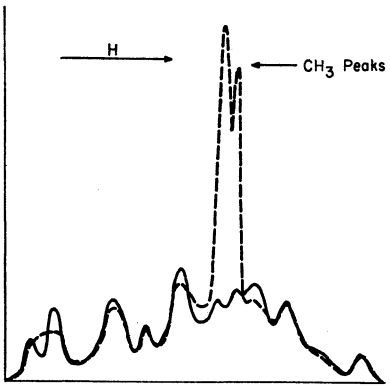

FIG. 2. H^1 n.m.r. spectrum of $B_5H_{10}Me$.

interpretation than assignment of B_{II} boron atoms as sites of isomeric methyl groups. Instead this must be considered together with the intensity increment between peaks 1, 2 and 8, 9. Suppose the degeneracy of the resonances from the B_{II}-linked protons were removed so each had a slightly different chemical shift. There then would be two resonances a and a'. Such alteration could occur through inductive (+I) feeding of electron density into the polyhedron from the methyl group, whereby one site of lowest excess charge, B_{II}, would experience an increase in charge density, disymmetrically, owing to the disymmetric location of the methyl group. Thus would one resonance be shifted slightly to higher field. It is to be concluded therefore that the methyl group is located on a B_{III} atom, that the isomerism is geometric, and that an inductive effect has possibly been observed in a delocalized polyhedral system.

The infrared spectra of the B_5 molecules are shown in Fig. 3, Table XI, and of the B_4

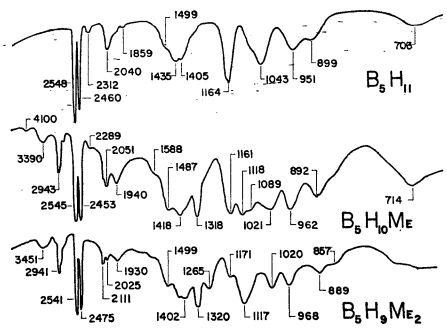

FIG. 3. Infrared spectra of B_5H_{11} and its methyl derivatives.

molecules in Fig. 4, Table XII.[7] The assignments are tentative ones, made by analogy and without detailed consideration of the molecular dynamics. To a degree B_5H_9 can be considered a model for B_5H_{11}. The symmetry of the latter is lower, and there are additional structural features: BH_2, three distinct BHB bridge types, one possibly unsymmetrical, and an open edge on the pyramid. Regardless of these departures, the assignments were made consistent with those for B_5H_9 (24), with reference to data on the non-pyramidal

[7]*Though similar results on the parent molecules have been published previously (28), never have they been tabulated in detail from measurements on highly purified samples. They are therefore included for comparison.*

Can. J. Chem. Downloaded from www.nrcresearchpress.com by 210.87.254.6 on 09/05/12
For personal use only.

Can. J. Chem. Downloaded from www.nrcresearchpress.com by 210.87.254.6 on 09/05/12
For personal use only.

TABLE XI

Infrared spectra of dihydropentaborane and its methyl derivatives

B_5H_{11}			$B_5H_{10}Me$			$B_5H_9Me_2$		
ν (cm^{-1})	Intensity	Assignment	ν (cm^{-1})	Intensity	Assignment	ν (cm^{-1})	Intensity	Assignment
			4100	v w				
			3390	w		3451	w	
			2943	m	CH str asym.	2941	m	CH str asym.
			2820	v w	CH str sym.	2815	w sh	CH str sym.
2548	s	BH_2 asym. str	2545	s	BH_2 asym. str	2541	s	BH_2 asym. str
2460	s	BH_2 sym. str	2453	s	BH_2	2475	s	BH_2 sym. str
		BH			BH			BH
2312	v w	BH′	2289	w	BH′			
2040	m	BH′	2100	m sh	BH′	2111	m	BH′
			2051	m	BH′	2025	m	BH′
1940	w sh	BH′	1940	m	BH′	1930	m	BH′
1859	v w	BH′						
			(1588)	m sh	BH	(1625)	m sh	BH
1499	m sh	BH bend	1487	s	BH	1499	s	BH
1435	m	BH bend	1418	s	BH	1420	s	BH
					$B—CH_3$ def asym.			$B—CH_3$ def asym.
1405	m	BH bend				1402	s	BH′
			1318	s	CH_3 def	1320	s	CH_3 def sym.
			(1275)	m sh	CH_2 wag, twist	1265	s	CH_2 wag, twist
1164	s	BH_2 sci BH bend	1161	s	BH_2 sci BH bend	1171	m	BH_2 sci BH bend
			1118	s	CH_3 rock	1117	s	CH_3 rock
			1089	s sh	BH in plane			
1043	m	BH in plane bend	1021	s	BCH_3 str	1020	m	BCH_3 str
951	m	BH_2 wag	962	s	BH_2 wag BCH_3 rock	968	m	BH_2 wag BCH_3 rock
899	m sh	BH apical	892	m	BH apical	889	m	BH apical
			859	m sh		857	m sh	
703	w b	B—B frame work	714	m b	B—B frame work	?		B—B frame work

NOTE: s = strong; m = medium; w = weak; sh = shoulder; str = stretch; def = deformation; v = very; H′ = bridge hydrogen.

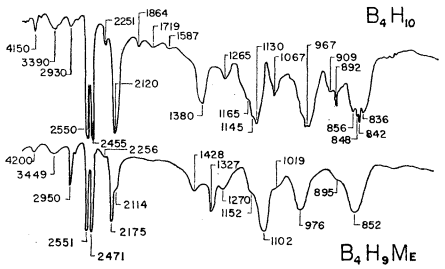

FIG. 4. Infrared spectra of B_4H_{10} and its methyl derivative.

TABLE XII

Infrared spectrum of tetraborane and methyltetraborane

B_4H_{10}			B_4H_9Me		
$\nu(cm^{-1})$	Intensity	Assignment	$\nu(cm^{-1})$	Intensity	Assignment
4150	w		4200	w	
3390	w		3449	w	
2930	w				
			2950	m	CH str asym.
2800	w		2834	w	
2550	s	BH_2 asym. str	2551	s	BH_2 asym. str
2455	s	BH_2 sym. str	2471	s	BH_2 sym. str
		BH single			BH single
2251	w	BH′	2256	v w	
2120	s	BH′	2175	s	BH′
			2114	m sh	BH′
1864	w	BH′			
1719	w	BH′			
1587	w	BH′			
			1428	m	B—CH_3 def asym.
1380	m	BH′	1327	m	BH′
1265	m	BH′	1270	m	BH′
1165	m sh	BH_2 sci	1152	m	BH_2 sci
1145	s sh	BH_2 sci			
1130	s	BH	1102	s	BH
1067	m	BH	1062	m b	BH
967	s	BH_2 wag	990	s	BH_2 wag
909	m	BH asym.			
892	m	BH sym.	895	m b	
856	m	BH_2′B str	852	m	BH_2′B str
848	m	BH_2′B str			
842	m	BH_2′B str			
836	m	BH_2′B str			
780	v w b	B—B	780	v w b	B—B

NOTE: The code is the same as in Table XI.

methyldiboranes (27) for the other structural features. In general the spectra of the two methyl derivatives of B_5H_{11} are simply the sum of the B_5H_{11} features, sometimes displaced about 10–20 wave numbers, and the methyl group frequencies scarcely altered from those in the methyldiboranes (27).

In B_4H_{10} the most prominent structural feature is the dual pair of bridges holding the molecule together. If a charge density relation for B_{II} and B_{III} atoms in tetraborane is assumed similar to that in dihydropentaborane, the bridge vibrations should give such changes in dipole moment as to make the bridge frequencies a prominent feature in the B_4H_{10} spectrum. So it is found that the band at 2120 cm^{-1}, assignable as a bridge stretching

Can. J. Chem. Downloaded from www.nrcresearchpress.com by 210.87.254.6 on 09/05/12
For personal use only.

frequency, is more intense than the similar band in any other boron hydride, excepting tetramethyldiborane.

The shape of the 2120 band in B_4H_{10} is altered in the methyl derivative. The original band intensity is lowered and a new component almost as intense appears 60 cm^{-1} higher. This would seem to arise from the introduction of disymmetry and to the introduction of an increased reduced mass at the outer end of the bridge system. A similar alteration occurs in the dimethylene tetraborane spectrum, where the shift is to 2150 cm^{-1}, and the intensity loss by the original band is much greater (20). In general the alteration of 5–50 cm^{-1} in B_4H_{10} frequencies upon methylation is somewhat greater than that found for B_5H_{11}.

The methyl-derived frequencies clearly discernable in the B_4H_9Me spectrum are the CH stretch and the B—CH_3 deformation at 2950 and 1428 cm^{-1}, respectively. Others in the 900–1100 cm^{-1} domain are so nearly coincident with bands of B—H origin as not to be separately assignable.

One interesting result of methylation is the obliteration of resolution for the bands between 836 and 856 cm^{-1}. This region is much too low for observation of methyl-derived frequencies, and tentatively the assignment has been made to BH_2B stretching modes. These could be increased in number by methylation of the B_{III} boron atom.

REFERENCES

1. W. S. Koski. Advan. Chem. Ser. No. 32, 78 (1961).
2. S. H. Bauer. J. Am. Chem. Soc. **78**, 5775 (1956).
3. J. K. Bragg, L. V. McCarty, and F. J. Norton. J. Am. Chem. Soc. **73**, 2134 (1951). R. P. Clark and R. N. Pease. J. Am. Chem. Soc. **73**, 2132 (1951).
4. H. I. Schlesinger and A. B. Burg. J. Am. Chem. Soc. **55**, 4009 (1933).
5. H. I. Schlesinger and A. O. Walker. J. Am. Chem. Soc. **57**, 621 (1935).
6. H. I. Schlesinger, N. W. Flodin, and A. B. Burg. J. Am. Chem. Soc. **61**, 1078 (1939).
7. H. I. Schlesinger, L. Horvitz, and A. B. Burg. J. Am. Chem. Soc. **60**, 2297 (1938).
8. E. Wiberg, J. E. F. Evans, and H. Nöth. Z. Naturforsch. **13b**, 263 (1958).
9. R. Koster. Angew. Chem. **72**, 626 (1960).
10. H. I. Schlesinger, D. M. Ritter, and A. B. Burg. J. Am. Chem. Soc. **60**, 2297 (1938).
11. D. M. Ritter. Unpublished results.
12. I. J. Solomon, M. J. Klein, and K. Hattori. J. Am. Chem. Soc. **80**, 4520 (1958).
13. L. Van Alten, G. R. Seely, J. P. Oliver, and D. M. Ritter. Advan. Chem. Ser. No. 32, 107 (1961).
14. J. P. Oliver. Ph.D. Thesis, University of Washington, Seattle, Wash. 1959.
15. H. I. Schlesinger. Private communication.
16. L. Lamneck and S. Kaye. Natl. Advisory Committee for Aeronautics. Research Memorandum E58 E12, Sept. 1958.
17. J. Gallagher and B. Siegel. J. Am. Chem. Soc. **81**, 504 (1959).
18. B. Figgis and R. L. Williams. Spectrochim. Acta. **15**, 331 (1959).
19. N. J. Blay, J. Williams, and R. L. Williams. J. Chem. Soc. 424 (1960).
20. B. C. Harrison, I. J. Solomon, R. P. Hites, and M. J. Klein. J. Inorg. Nucl. Chem. **14**, 195 (1960).
21. A. Stock. Hydrides of boron and silicon. Cornell University Press, Ithaca, N.Y. 1933.
22. R. T. Sanderson. Vacuum manipulation of volatile compounds. John Wiley and Sons, New York. 1948.
23. G. R. Seely, J. P. Oliver, and D. M. Ritter. Anal. Chem. **31**, 1993 (1959).
24. H. J. Hrostowski and G. C. Pimentel. J. Am. Chem. Soc. **76**, 998 (1954).
25. I. Shapiro, C. O. Wilson, J. F. Ditter, and W. J. Lehmann. Advan. Chem. Ser. No. 32, 127 (1961).
26. M. J. Klein, B. C. Harrison, and I. J. Solomon. J. Am. Chem. Soc. **82**, 4149 (1958).
27. W. J. Lehmann and I. Shapiro. Spectrochim. Acta, **17**, 396 (1961).
28. L. V. McCarty, G. C. Smith, and R. S. McDonald. Anal. Chem. **26**, 1027 (1954).
29. M. W. Forsyth, W. V. Hough, M. D. Ford, G. T. Hefferan, and L. J. Edwards. Abstracts of Papers, Division of Inorganic Chemistry, 135th Meeting, American Chemical Society. April, 1959. p. 40M.
30. L. Lavine and W. N. Lipscomb. J. Chem. Phys. **22**, 614 (1956).
31. E. B. Moore, Jr., R. E. Dickerson, and W. N. Lipscomb. J. Chem. Phys. **27**, 209 (1957).
32. R. Schaeffer, J. N. Schoolery, and R. Jones. J. Am. Chem. Soc. **79**, 4606 (1957).
33. R. E. Williams, S. G. Gibbins, and I. Shapiro. J. Chem. Phys. **30**, 320 (1959).
34. W. N. Lipscomb. J. Chem. Phys. **25**, 38 (1956).

Can. J. Chem. Downloaded from www.nrcresearchpress.com by 210.87.254.6 on 09/05/12
For personal use only.

Can. J. Chem. Downloaded from www.nrcresearchpress.com by 210.87.254.40 on 09/05/12
For personal use only.

SOME REACTIONS OF ORGANOALUMINUM COMPOUNDS WITH NITROGEN-CONTAINING BASES[1]

NEIL R. FETTER, BODO BARTOCHA,[2] FREDERICK E. BRINCKMAN, JR.,[2] AND DONALD W. MOORE[3]

Chemistry Division, U.S. Naval Ordnance Laboratory, Corona, Calif., U.S.A.

Received October 29, 1962

ABSTRACT

The reactions of Me_3Al with Me_2NNMe_2 and $Me_2NCH_2NMe_2$ have yielded complexes whose n.m.r. spectra suggest cyclic structures. They have the formulas $Me_3Al{:}Me_2NNMe_2$ and $Me_3Al{:}Me_2NCH_2NMe_2$ respectively. Me_3Al reacts with $Me_2NCH_2CH_2NMe_2$ to form a complex with a linear structure and the formula $Me_3Al{:}Me_2NCH_2CH_2NMe_2{:}AlMe_3$.

The reactions of $H_3Al{:}NMe_3$ with several methyl hydrazines have yielded the following compounds: $[-Al(HNNHMe)NHNMe-]_n$, $[-HAlNNMe_2-]_n$, $H_2Al-NHNEt_2$, $[(-HAlNNEt_2-){:}NMe_3]_n$, and $H_2Al-NMe_2$. No reaction occurred between $H_3Al\cdot(Et_2O)_n$ and tetramethylhydrazine and the reaction of 3 moles of H_2NNMe_2 with 1 mole of $H_3Al{:}NMe_3$ yielded a compound for which no structural formula could be assigned, but which had emperical formula $C_4H_{15}N_5Al$.

INTRODUCTION

Our recently reported (1) studies of the reactions of aluminum trialkyls and their trimethylamine complexes with methyl hydrazines have led to a number of new compounds which are formed by two general reactions established by Brown and Davidson (2) and Wiberg and May (3):

$$R_3Al + R_2NNR_2 \rightarrow R_3Al{:}R_2NNR_2 \quad [1]$$

$$R_3Al + HRNNR_2 \rightarrow R_2Al-NRNR_2 + RH. \quad [2]$$

Also recently reported (4, 5) was a study of the reactions of tetramethyltetrazene with Me_3Al, $Me_3Al{:}NMe_3$, and $H_3Al{:}NMe_3$. This work may also be summarized by two general reactions:

$$R_3Al + Me_2NN{=}NNMe_2 \rightarrow R_3Al{:}Me_2NN{=}NNMe_2 \quad [3]$$

$$2R_3Al \text{ (or } 2R_3Al{:}NMe_3) + Me_2NN{=}NNMe_2 \rightarrow 2R_2Al-NMe_2 + N_2 + RH + (NMe_3) + C_hH_{2h}N_2\cdot \quad [4]$$

An n.m.r. investigation of the trimethylaluminum–tetramethyltetrazene adduct (reaction [3]) indicated that it had a symmetric structure and that upon pyrolysis, not only were $Me_2Al-NMe_2$ and nitrogen obtained, but also a red polymer, tetramethyltetrazene, and small amounts of methyl azide and methane. From these data, the following structural formula was proposed:

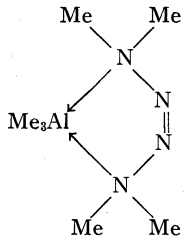

[1]*Presented at the Symposium on Organometallic Compounds, Vancouver, British Columbia, September 4–6, 1962, sponsored by the Inorganic Chemistry Division, Chemical Institute of Canada, and the Department of Chemistry, University of British Columbia, with the support of the National Research Council, Ottawa, in cooperation with the University Extension Department.*

[2]*U.S. Naval Propellant Plant, Indian Head, Maryland.*

[3]*U.S. Naval Ordnance Test Station, China Lake, California.*

The purpose of this paper is to report a study of the reactions of aluminum hydride trimethylamine with alkyl hydrazines and to report the results of structural studies of compounds formed from the reactions of Me_3Al and $M_3Al{:}NMe_3$ with tetramethylhydrazine, N,N,N′,N′-tetramethylmethylenediamine, and N,N,N′,N′-tetramethylethylenediamine.

The reactions of methyl hydrazines with aluminum hydride produce compounds which are more difficult to characterize than the corresponding compounds obtained from the Me_3Al and $Me_3Al{:}NMe_3$ reactions. Most of the products had low vapor pressures and were not distillable or sublimable and the reactions generally did not follow the scheme set forth in reactions [1] and [2]. In a few cases the products were shock sensitive and exploded when handled.

The reactions of Me_3Al and $H_3Al{:}NMe_3$ with difunctional tertiary amines have yielded complexes whose n.m.r. spectra suggest pentacoordinated aluminum involved in four- and five-membered ring systems (see the above structural formula for $Me_3Al{:}Me_2NN{=}NNMe_2$).

EXPERIMENTAL

Apparatus and Reagents

The apparatus and procedures employed have been described previously (1, 4). The amines and hydrazines were distilled from CaH_2 before use and the hydrocarbon solvents, which were reagent grade, were used without treatment. The trimethylaluminum was vacuum distilled at 25° C before use and the $Me_3Al{:}NMe_3$ and $H_3Al{:}NMe_3$ were vacuum sublimed before use. The elemental analyses were performed by the Schwarzkopf Microanalytical Laboratory, Woodside, New York.

The n.m.r. spectra were obtained with a Varian Associates Model V-4302 spectrometer at 60 Mc. Liquid samples, containing approximately 5% benzene, were sealed under vacuum in 5-mm pyrex tubes. The solid samples were dissolved in benzene to approximately 15% by weight and then sealed in the tubes. All spectra were taken at 30° C.

Reaction of Aluminum Hydride Trimethylamine with Hydrazine and Methylhydrazine

The reaction of $H_3Al{:}NMe_3$ with hydrazine in *n*-octane produced a white solid which detonated when handled after the solvent had been removed. This extreme shock sensitivity made characterization difficult; however, a hydrolysis with methanol yielded no active hydrogen and an aluminum assay gave the value 35.0%. The infrared spectrum also showed no Al—H band at 5.5 μ, but an NH band at 3.1 μ and an NH_2 band at 6.3 μ. These data suggest the reaction

$$n\mathrm{H_3Al{:}NMe_3} + 2n\mathrm{H_2NNH_2} \rightarrow \left[\begin{array}{c} \text{NHNH}_2 \\ | \\ \text{—Al—NHNH—} \end{array}\right]_n + 3n\mathrm{H_2} + n\mathrm{NMe_3}.$$

The calculated percentage aluminum is 32.6% for the product of the above equation.

The reaction of $H_3Al{:}NMe_3$ with methylhydrazine resulted in a product which was not as shock sensitive as the hydrazine product and hence a somewhat better characterization was possible. With methylhydrazine being used as the reaction medium, 8.57 g of H_2NNHMe was vacuum transferred onto 0.206 g (2.32 mmole) of $H_3Al{:}NMe_3$ at −196° C. After the reaction mixture had warmed to room temperature, 143.6 ml (6.42 mmole) of hydrogen and 52.2 ml (2.24 mmole) of trimethylamine were evolved. The powdery white solid which remained after the excess methylhydrazine was removed gave an elemental analysis which is in fair agreement with the formula $C_2H_9N_4Al$: Anal. Calc.: C, 20.69; H, 7.81; N, 48.26; Al, 23.24. Found: C, 18.39; H, 7.81; N, 52.80; Al, 23.56.

Hydrolysis of the product yielded no active hydrogen and the infrared spectrum showed no Al—H band at 5.6 μ, but did show an NH band at 3.15 μ. These data suggest the following reaction:

$$n\mathrm{H_3Al{:}NMe_3} + 2n\mathrm{H_2NHNMe} \rightarrow \left[\begin{array}{c} \text{NHNHMe} \\ | \\ \text{—Al—NHNMe—} \end{array}\right]_n + 3n\mathrm{H_2} + n\mathrm{NMe_3}.$$

The reaction may also be conducted in hydrocarbon solvent.

Reaction of Aluminum Hydride Trimethylamine with 1,1-Dimethylhydrazine and 1,1-Diethylhydrazine

The reactions of $H_3Al{:}NMe_3$ with H_2NNMe_2 and H_2NNEt_2 appear, on the basis of analytical data, to produce different compounds of unusual structure.

Can. J. Chem. Downloaded from www.nrcresearchpress.com by 210.87.254.40 on 09/05/12
For personal use only.

With 1,1-dimethylhydrazine being used as the reaction medium, 20 g of H_2NNMe_2 was vacuum transferred to a vessel containing 0.461 g (5.18 mmole) of $H_3Al{:}NMe_3$ at −196° C. After the resulting mixture was warmed to room temperature and left to stand overnight, a crop of clear crystals deposited on the walls of the reaction flask and 296 ml (12.7 mmole) of hydrogen was evolved. The crystalline product (m.p. 193–194° C) could not be vacuum sublimed (0.05 mm at 70° C), but an elemental analysis gave values which are in good agreement with the formula $C_4H_{15}N_5Al$: Anal. Calc.: C, 29.99; H, 9.44; N, 43.73; Al, 16.84. Found: C, 30.16; H, 9.43; N, 43.80; Al, 16.84.

The infrared spectrum of the product showed no Al—H band at 5.5 μ and no NH_2 band at 6.3 μ, but did have a band at 3.05 μ for N—H. As expected, hydrolysis with methanol showed no active hydrogen. The same product may be obtained by reacting 3 moles of H_2NNMe_2 per mole of $H_3Al{:}NMe_3$ in heptane.

In another experiment, a starting ratio of 2 moles of H_2NNMe_2 per mole of $H_3Al{:}NMe_3$ was used in a reaction carried out in pentane. A white, powdery solid was obtained which showed no melting or apparent decomposition up to 250° C, and elemental analysis gave results which agree with the formula $C_2H_7N_2Al$: Anal. Calc.: C, 27.91; H, 8.19; N, 32.55; Al, 31.34. Found: C, 27.01; H, 8.69; N, 31.90; Al, 31.17. The infrared spectrum of the product showed a strong Al—H band at 5.6 μ, but no band for either NH at 3.0 μ or NH_2 at 6.3 μ. The structures of these two materials will be discussed later.

The reaction of $H_3Al{:}NMe_3$ with H_2NNEt_2 gave a white non-volatile solid when the starting ratio of reagents was 1:1 and a non-volatile, viscous liquid when the starting ratio of reagents was 2 moles of H_2NNEt_2 per mole of $H_3Al{:}NMe_3$. In a typical reaction using a 2:1 ratio of reagents, 0.688 g (7.72 mmole) of $H_3Al{:}NMe_3$ in 25 ml of *n*-heptane was combined with 1.27 g (16.3 mmole) of H_2NNEt_2 at −196° C. After the mixture had warmed to room temperature and was allowed to stand overnight, the solvent was removed and the product analyzed. The analysis gave values which agree with the formula $C_7H_{20}N_3Al$: Anal. Calc.: C, 48.53; H, 11.64; N, 24.25; Al, 15.57. Found: C, 48.41; H, 11.04; N, 24.60; Al, 16.00. Also, 360 ml (16.1 mmoles) of hydrogen and 53.5 ml (2.38 mmole) of trimethylamine were evolved. Hydrolysis of 0.1780 g (1.03 mmole) of the product with methanol gave 13.3 ml (0.594 mmole) of hydrogen. The infrared spectrum had a strong Al—H band at 5.55 μ and a weak N—H band at 3.1 μ.

From these data, the reaction appears to be:

$$n\mathrm{H_3Al{:}NMe_3} + n\mathrm{H_2NNEt_2} \longrightarrow \left[\begin{array}{c} \mathrm{H} \\ \mathrm{-Al-N-} \\ \cdots \quad \diagdown \\ \mathrm{NMe_3\ NEt_2} \end{array}\right]_n + 2n\mathrm{H_2}.$$

In a reaction where the starting ratio was 1:1, 0.936 g (12.0 mmole) of H_2NNEt_2 was vacuum transferred to a 50-ml vessel containing 0.919 g (10.3 mmole) of $H_3Al{:}NMe_3$ and 20 ml of *n*-heptane at −196° C. The mixture was allowed to warm to room temperature and to stand overnight. By the end of this period most of the solids had dissolved and 314 ml (14.0 mmole) of hydrogen had evolved. An attempt was made to separate the trimethylamine from the heptane, but only 81.8 ml (3.65 mmole) of pure material could be recovered. Elemental analysis of the crude product gave results which agreed with the formula H_2Al—$NHNEt_2$: Anal. Calc.: C, 41.36; H, 11.28; N, 24.13; Al, 23.23. Found: C, 42.06; H, 10.72; N, 24.06; Al, 23.56.

Hydrolysis of 0.231 g (1.97 mmole) of crude product with methanol gave 52.5 ml (2.34 mmole) of hydrogen and pyrolysis of 0.330 g (2.81 mmole) at 100° C for 6 hours (gas evolution ceased) yielded 66.0 ml (2.95 mmole) of hydrogen. From these data the reaction appears to be:

$$\mathrm{H_3Al{:}NMe_3} + \mathrm{H_2NNEt_2} \rightarrow \mathrm{H_2Al{-}NHNEt_2} + \mathrm{H_2} + \mathrm{NMe_3}.$$

Reaction of Aluminum Hydride Trimethylamine with Trimethylhydrazine

In absence of solvent, 1.58 g (12.3 mmole) of $HNMeNMe_2$ was transferred to 1.80 g (20.2 mmole) of $H_3Al{:}NMe_3$ at −196° C. After the mixture had warmed to room temperature (30 minutes), 234 ml (10.5 mmole) of hydrogen and 132 ml (5.90 mmole) of trimethylamine were evolved. The crude product was then pumped to remove any traces of $HNMeNMe_2$. A white crystalline solid (m.p. 93–95° C) remained which, when analyzed, proved to be H_2Al—NMe_2: Anal. Calc.: C, 32.87; H, 11.03; N, 19.17; Al, 36.92. Found: C, 32.72; H, 10.82; N, 19.70; Al, 36.55. A quantitative yield of H_2Al—NMe_2 was obtained.

Reaction of Aluminum Hydride Etherate with Tetramethylhydrazine

From 1.50 g of $LiAlH_4$ and 1.00 g of $AlCl_3$ an etherate solution of $AlH_3 \cdot n\mathrm{Et_2O}$ was prepared. After the LiCl had been removed by filtration, 20 ml of Et_2O containing 1.00 g of Me_2NNMe_2 was added to the $AlH_3 \cdot n\mathrm{Et_2O}$. The mixture was refluxed for an hour and then the ether and any excess Me_2NNMe_2 were removed under vacuum. A powdery white solid remained which could not be sublimed at 55° C under 0.05 mm vacuum. An infrared spectrum of the solid showed only the very broad band of polymeric aluminum hydride at 5.5 μ. Treatment of a portion of the solid with a large excess of trimethylamine gave a quantitative yield of $H_3Al(NMe_3)_2$. From these data it was concluded that no reaction had occurred.

The reaction was repeated with $H_3Al{:}NMe_3$, but the starting materials were recovered unreacted.

Reaction of Trimethylaluminum with N,N,N′,N′-Tetramethylethylenediamine

Into 5.55 g (75.7 mmole) of Me_3Al at −196° C was distilled 9.12 g (78.6 mmole) of $Me_2N(CH_2)_2NMe_2$ and 20 ml of *n*-heptane. The mixture was allowed to warm to room temperature and to stand for 2 hours.

Can. J. Chem. Downloaded from www.nrcresearchpress.com by 210.87.254.40 on 09/05/12
For personal use only.

The solvent and any unreacted starting materials were removed by vacuum transfer, leaving a white crystalline mass in the reaction vessel. Also obtained from the reaction was 81.0 ml (3.61 mmole) of methane.

The crude product was vacuum sublimed at 75° C and a 76 mole% yield of white crystals (m.p. 136–137.5 (decomp.)) was obtained. Elemental analysis gave results which agreed with the formula $Me_2N(CH_2)_2$-$NMe_2(Me_3Al)_2$: Anal. Calc.: C, 55.35; H, 13.16; N, 10.76; Al, 20.72. Found: C, 54.92; H, 13.07; N, 10.92; Al, 19.61.

Hydrolysis of 0.268 g (1.03 mmole) of sublimed material with methanol yielded 139 ml (6.23 mmole) of methane. These data indicate that the reaction

$$Me_3Al + Me_2N(CH_2)_2NMe_2 \rightarrow \begin{matrix} Me_3Al & & AlMe_3 \\ \cdot\cdot & & \cdot\cdot \\ Me_2N(CH_2)_2NMe_2 \end{matrix}$$

had occurred.

This complex has been found to react almost quantitatively with trimethylamine. Treatment of 0.630 g (2.62 mmole) of $(Me_3Al)_2$:$Me_2N(CH_2)_2NMe_2$ with 7.37 mmole of NMe_3 gave 0.660 g (5.03 mmole) of Me_3Al:NMe_3 (composition confirmed by elemental analysis).

Reaction of Trimethylaluminum with N,N,N′,N′-Tetramethylmethylenediamine

Under vacuum, 3.23 g (31.7 mmole) of $Me_2NCH_2NMe_2$ was transferred to a 50-ml reaction vessel containing 2.26 g (30.0 mmole) of Me_3Al and 20 ml of *n*-heptane at −196° C. The mixture was allowed to warm to room temperature and stand for an hour. The heptane and any excess amine were removed by vacuum transfer. The remaining white solid was vacuum sublimed at room temperature onto a −78° C cold finger. The sublimate (m.p. 33–35° C) was obtained in approximately 80 mole% yield.

Elemental analysis of the sublimate gave values which agree with the formula Me_3Al:$Me_2NCH_2NMe_2$: Anal. Calc.: C, 55.10; H, 13.24; N, 16.07; Al, 15.47. Found: C, 55.24; H, 13.55; N, 15.84; Al, 15.73. Hydrolysis of 0.364 g (2.46 mmole) of sublimate with methanol gave 146 ml (6.51 mmole) of methane. These data indicate that a 1:1 adduct is formed.

Reaction of Aluminum Hydride Trimethylamine with N,N,N′,N′-Tetramethylmethylenediamine

In the absence of solvent, 1.64 g (16.1 mmole) of $Me_2NCH_2NMe_2$ was vacuum transferred to a 50-ml vessel containing 1.34 g (15.0 mmole) of H_3Al:NMe_3 at −196° C. The mixture was allowed to warm to room temperature and stand for 2 hours. During this period the H_3Al:NMe_3 dissolved in the amine. The solution was then vacuum sublimed at room temperature onto a −78° C cold finger. The sublimate melted at room temperature (25–26° C) and elemental analysis gave results which agree with the formula H_3Al:Me_2NCH_2 NMe_2. Anal. Calc.: C, 45.42; H, 12.97; N, 21.20; Al, 20.41. Found: C, 45.21; H, 12.97; N, 21.00; Al, 20.22.

Hydrolysis of 0.167 g (1.26 mmole) of the sublimate with methanol gave 156 ml (3.74 mmole) of hydrogen. These data indicate the formation of a 1:1 complex by the reaction

$$H_3Al{:}NMe_3 + Me_2NCH_2NMe_2 \rightarrow H_3Al{:}Me_2NCH_2NMe_2 + NMe_3.$$

The yield of sublimate was approximately 60 mole% of initial H_3Al:NMe_3.

DISCUSSION

Reaction of Aluminum Hydride Trimethylamine with Hydrazines

From the experimental data presented above, a few preliminary observations may be made about these reactions. In contrast to the reactions of aluminum alkyls with hydrazines (equations [1] and [2]), aluminum hydride does not appear to follow any systematic reaction scheme. The products vary depending upon the starting ratios of reagents and the solvents employed. Also, in almost all reactions, the products could not be purified, because of their insolubilities and low vapor pressures. It appears that most materials obtained were polymeric, having no sharp melting points or crystalline character.

An illustration of the problems encountered is the variety of results obtained from the reactions of aluminum hydride trimethylamine with 1,1-dimethylhydrazine and 1,1-diethylhydrazine. In the case of 1,1-dimethylhydrazine one reaction was carried out with the hydrazine acting as solvent and heat sink. A sharp-melting crystalline solid was obtained which several elemental analyses indicated has the emperical formula $C_4H_{15}N_5Al$. The structure of this compound is difficult to determine, because the Al/N ratio is odd and Al/C ratio is even. If it had formed via reaction [1] or [2] the Al/N ratio would be even, i.e., 1:2, 1:4, etc., or if trimethylamine were still adducted to the molecule, the Al/C ratio would be odd. The structure which fits all the data available is:

Can. J. Chem. Downloaded from www.nrcresearchpress.com by 210.87.254.40 on 09/05/12
For personal use only.

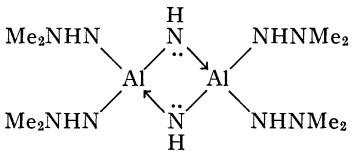

or:

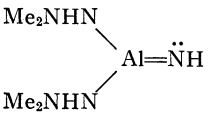

In the other example cited above when the starting ratio of H_2NNMe_2 to $H_3Al{:}NMe_3$ was 2:1 and the reaction was run in pentane, a material with the formula $C_2H_7N_2Al$ was obtained. The best formula for the analytical and infrared data is the previously unreported polymer

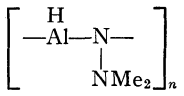

This structure is unusual because both hydrogen atoms have been removed from the hydrazine nitrogen atom.

However, 1,1-diethylhydrazine also appears to react with $H_3Al{:}NMe_3$ in a similar manner when the starting ratio of the hydrazine to $H_3Al{:}NMe_3$ is 2:1. In this case a trimethylamine molecule still appears to be associated with the aluminum atom; hence, the structure may be

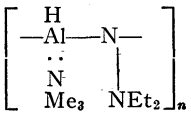

If the starting ratio of reagents is changed to 1:1, a reaction which follows equation [2] occurs and the compound $H_2Al{-}NHNEt_2$ is produced. It is one of the few examples of the behavior observed in the corresponding trimethylaluminum – alkyl hydrazine reactions.

The reaction of aluminum hydride trimethylamine with trimethylhydrazine did not produce the expected $H_2Al{-}NMeNMe_2$, but instead gave a quantitative yield of $H_2Al{-}NMe_2$. This result creates a problem of accounting for the hydrazine residues. So far we have been able to detect only trimethylamine in the condensables, but it would appear that another material, perhaps methylamine or dimethylamine, is present.

Our final surprise in this series of reactions was the fact that freshly prepared aluminum hydride etherate would not react with tetramethylhydrazine yet would react with trimethylamine to form aluminum hydride bis-trimethylamine. As a first approximation, it was assumed that trimethylamine and tetramethylhydrazine were compounds of equal basicity, but it appears that trimethylamine is basic enough to break up the aluminum hydride polymer and aluminum–ether bonds while tetramethylhydrazine is not.

Trimethylaluminum Difunctional Amine Complexes

Our recent finding (5) that trimethylaluminum forms a symmetric complex with tetramethyltetrazene and the recent report by Bains and Bradley (6) of the preparation of $(i\text{-PrO})_3Al{:}H_2NNH_2$ have led us to examine the reactions of trimethylaluminum with

Can. J. Chem. Downloaded from www.nrcresearchpress.com by 210.87.254.40 on 09/05/12
For personal use only.

tetramethylhydrazine, N,N,N′,N′-tetramethylmethylenediamine, and N,N,N′,N′-tetramethylethylenediamine. We have proposed the structure shown in the Introduction for the tetrazene complex and Bains and Bradley (6) have suggested the chelate

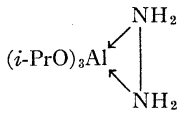

as one of two possibilities for the structure of the tris-isopropoxy-aluminum – hydrazine complex.

Trimethylaluminum forms a 1:1 complex with tetramethylhydrazine and two cryoscopic molecular weight determinations on 0.086 and 0.083 molal solutions showed the complex to be monomeric in cyclohexane. The n.m.r. spectrum of a 15% solution in benzene (Fig. 1) shows only one peak for both Al-methyl protons and N-methyl protons. This

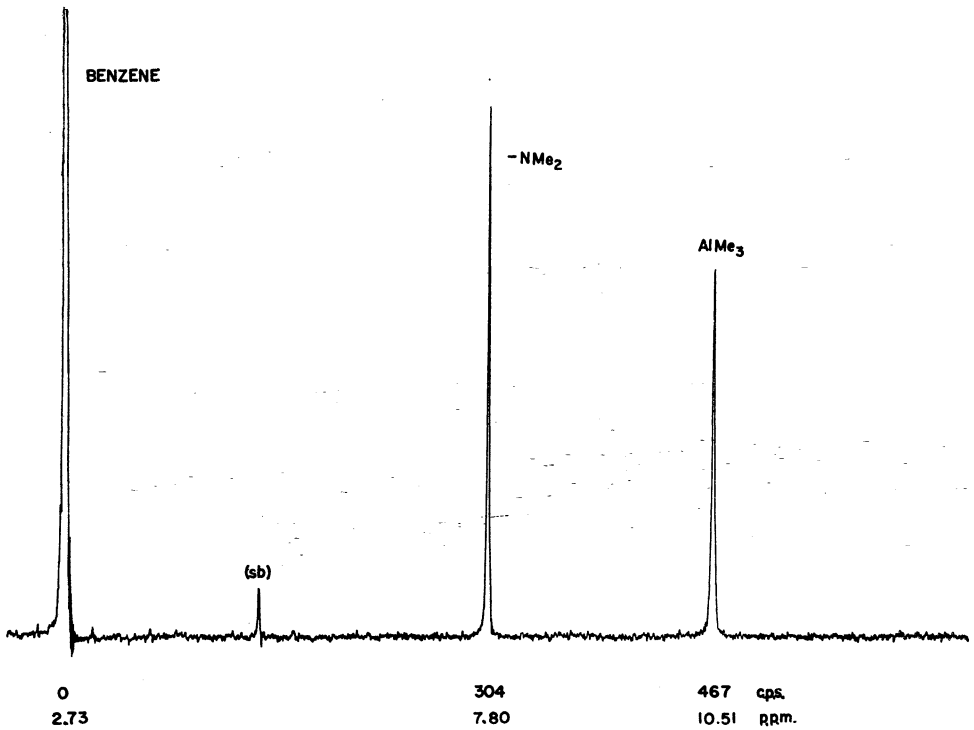

FIG. 1. The n.m.r. spectrum of $Me_3Al:Me_2NNMe_2$ (m.p. 66.0° C), at 60 Mc, of a 15 wt% solution in benzene.

information leads us to the chelate structure proposed earlier by Fetter and Bartocha (1) for this type of complex, namely,

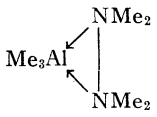

The 1:1 complex formed in the reaction of trimethylaluminum with N,N,N′,N′-tetramethylmethylenediamine appears to be slightly associated in benzene, for two freezing

Can. J. Chem. Downloaded from www.nrcresearchpress.com by 210.87.254.40 on 09/05/12
For personal use only.

point depression molecular weight measurements of 0.048 molal and 0.051 molal solutions gave the values 246 and 232 respectively (calc. for monomer: 174). The n.m.r. spectrum of a 15% solution in benzene (Fig. 2) shows one peak each for Al-methyl proton, N-methyl

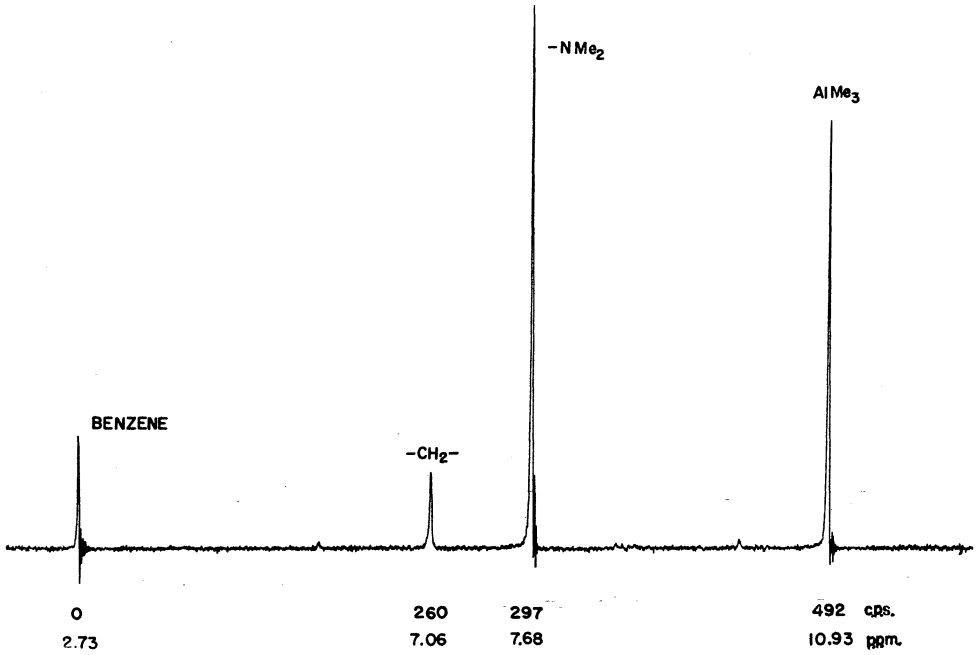

FIG. 2. The n.m.r. spectrum of $Me_3Al{:}Me_2NCH_2NMe_2$ (m.p. 35° C), at 60 Mc, of a 15 wt% solution in benzene.

protons, and methylene protons. This result also suggests a chelated complex with the structure

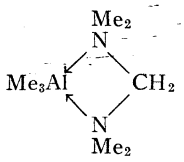

Aluminum hydride trimethylamine also appears to form a complex of similar structure as a result of reaction with N,N,N′,N′-tetramethylmethylenediamine. This complex also appears to be associated in benzene, for two measurements on 0.125 molal and 0.107 molal solutions gave the values 167 and 164 respectively (calc. for monomer: 132). The n.m.r. spectrum (Fig. 3) shows a single peak only for N-methyl protons. The methylene protons appear to be split and the Al-protons were not detectable at the concentration of complex used in the sample. Although the n.m.r. spectrum is not as clear as in the trimethylaluminum case, the structure

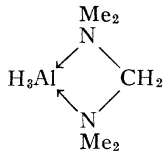

appears to fit the available data best.

Can. J. Chem. Downloaded from www.nrcresearchpress.com by 210.87.254.40 on 09/05/12
For personal use only.

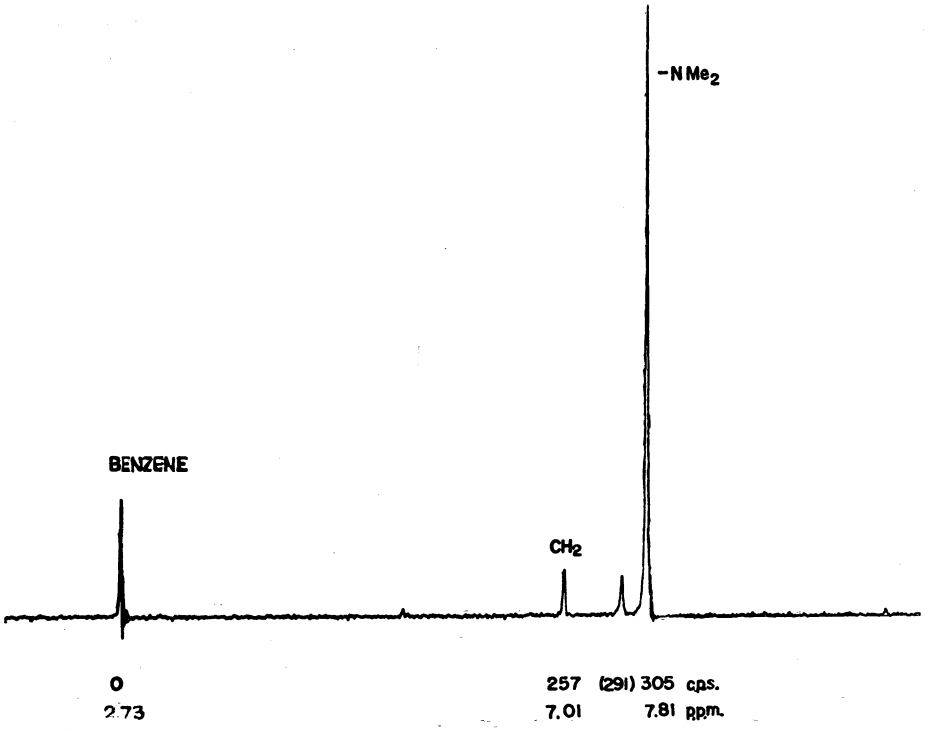

FIG. 3. The n.m.r. spectrum of $H_3Al{:}Me_2NCH_2NMe_2$ (m.p. 25° C), at 60 Mc, of a 15 wt% solution in benzene.

When another methylene group is present in the difunctional tertiary amine, as in the case of N,N,N′,N′-tetramethylethylenediamine, the nature of the bonding to trimethylaluminum changes considerably. Instead of obtaining the anticipated five-membered chelate ring

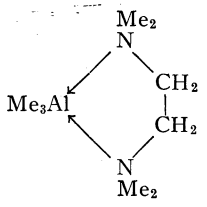

obtained by Davidson and Wartik (7) for the corresponding aluminum hydride complex, a trimethylaluminum molecule bonds to each of the —NMe_2 groups. Cryoscopic molecular weights also indicate that this complex is associated. Two determinations with 0.069 and 0.084 molal solutions gave the values 359 and 342 respectively (calc. for monomer: 260).

It is tempting from the data presented to make the generalization that any difunctional tertiary amine will form a bis-adduct with trimethylaluminum if there are two or more intervening carbon atoms, and that with one or no carbon atoms intervening, a chelate complex will form. Other reactions with model amines are planned to determine the validity of this hypothesis.

The status of aluminum hydride complexes appears to be somewhat different. The work of Wartik and Davidson (7) and the work presented here suggest that cyclic complexes

Can. J. Chem. Downloaded from www.nrcresearchpress.com by 210.87.254.40 on 09/05/12
For personal use only.

are formed with difunctional tertiary amines with up to at least two intervening methylene groups.

Some of the structures proposed above involve pentacoordinate aluminum. As the ligand chemistry of aluminum becomes more extensive the appearance of what seems to be a rather stable pentacoordinate condition appears more frequently. Ruff and Hawthorne (8) first proposed the pentacoordinate state for dimeric aluminum hydride trimethylamine and recently Ruff (9) has reported the compound $HAl(NMe_2)_2 \cdot 2BH_2NMe_2$ for which he proposed (among others) the structure

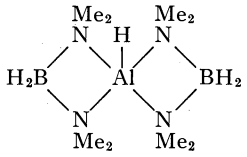

Aluminum hydride bis-trimethylamine, which is thermally more stable than the monocomplex, also requires a pentavalent aluminum. The data available so far, however, do not provide conclusive evidence in most cases and the final proof may be obtained from single crystal X-ray studies.

A word of caution should be made concerning molecular weight data. In most cases the compounds appear to be associated in freezing benzene, but it would require a more thorough study of concentration effects and perhaps vapor phase determinations to get a clearer understanding of association of monomeric species. Also, low-temperature n.m.r. studies of some of the above complexes are being studied to determine whether association occurs.

ACKNOWLEDGMENTS

The authors wish to acknowledge the assistance given by Dr. Peter J. Slota and Dr. Charles P. Haber of the U.S. Naval Ordnance Laboratory, Corona, California.

The work was supported by funds from the Advanced Research Projects Agency and the U.S. Navy Department, Bureau of Naval Weapons.

REFERENCES

1. N. R. FETTER and B. BARTOCHA. Can. J. Chem. **39**, 2001 (1961).
2. H. C. BROWN and B. DAVIDSON. J. Am. Chem. Soc. **64**, 316 (1942).
3. E. WIBERG and A. MAY. Z. Naturforsch. **10b**, 232 (1955).
4. N. R. FETTER and B. BARTOCHA. Can. J. Chem. **40**, 342 (1962).
5. N. R. FETTER, F. E. BRINCKMAN, JR., and D. W. MOORE. Can. J. Chem. **40**, 2184 (1962).
6. M. S. BAINS and D. C. BRADLEY. Can. J. Chem. **40**, 1351 (1962).
7. J. M. DAVIDSON and T. WARTIK. J. Am. Chem. Soc. **82**, 5506 (1960).
8. J. K. RUFF and M. F. HAWTHORNE. J. Am. Chem. Soc. **82**, 2141 (1960).
9. J. K. RUFF. Inorg. Chem. **1**, 613 (1962).

Can. J. Chem. Downloaded from www.nrcresearchpress.com by 210.87.254.40 on 09/05/12
For personal use only.

MECHANISMS OF THE REACTIONS OF DIETHYLZINC WITH ISOPROPANOL AND WATER[1]

R. J. HEROLD, S. L. AGGARWAL, AND V. NEFF
Central Research Laboratories, The General Tire & Rubber Company, Akron, Ohio, U.S.A.
Received November 22, 1962

ABSTRACT

Reactions of diethylzinc with isopropanol and water were studied by means of infrared absorption and gas evolution. The former method was found to be more reliable. Ethylzinc isopropoxide, formed from diethylzinc and isopropanol, was shown to be stable in the presence of excess isopropanol. The reaction of diethylzinc with water was found to proceed in a two-step manner, the product of the first being ethylzinc hydroxide. The decomposition of ethylzinc hydroxide was found to be first order with respect to itself and independent of diethylzinc.

INTRODUCTION

The reaction of zinc alkyls with compounds containing active hydrogens has been used in the past for qualitative and quantitative estimation of active hydrogen concentrations (1, 2). Generally, such procedures have been carried out with an excess of metal alkyl and little attention has been paid to the zinc-containing reaction products. Haurowitz noted that in many cases reaction of zinc alkyls with organic compounds containing active hydrogens is not complete. Specifically in the case of benzyl alcohol only 60% of the expected ethane is evolved. Tolkatschev (3) and Menard and Aston (4) found, however, that both ethyl groups can be removed from diethyl zinc with methanol and acetoxime respectively.

Current interest in the reaction products of zinc alkyls with water and with alcohols is derived from their use as catalysts. Furukawa *et al.* (5, 6, 7) and Stewart (8) have shown the usefulness of such reaction products for the polymerization of epoxides and of aldehydes. Furukawa concluded that the reaction product of diethylzinc with water results from the initial formation of ethylzinc hydroxide followed by reaction of this intermediate with diethyl zinc. Although quite plausible, his suggestion is not supported by proof of the existence of the intermediate, nor by kinetic data to show the bimolecular nature of its reaction with diethylzinc.

In the studies reported herein, we have: (1) shown that ethylzinc isopropoxide formed from diethylzinc and isopropanol is stable in the presence of excess isopropanol in heptane solution; (2) shown that ethylzinc hydroxide is formed as an intermediate in the reaction of diethylzinc and water in ether solution; and (3) worked out the kinetics of the disappearance of ethylzinc hydroxide in the presence of various concentrations of diethylzinc in dimethoxyethane (glyme) solution. Two methods were used to study this latter reaction, namely, measurements of (1) the change in infrared absorption intensity at 2.9 μ (hydroxyl) and (2) ethane gas evolution as a function of time. However, these two methods give rate curves which are quite different. Since a lag in the evolution of ethane appeared to be the reason for this discrepancy, the kinetic analysis was based on the infrared results. The initial portions of the gas evolution rate curves were nevertheless useful in obtaining an indication of the activation energy of the process.

[1]*Presented at the Symposium on Organometallic Compounds, Vancouver, British Columbia, September 4–6, 1962, sponsored by the Inorganic Chemistry Division, Chemical Institute of Canada, and the Department of Chemistry, University of British Columbia, with the support of the National Research Council, Ottawa, in cooperation with the University Extension Department.*

Can. J. Chem. Downloaded from www.nrcresearchpress.com by 210.87.254.42 on 09/05/12
For personal use only.

Can. J. Chem. Downloaded from www.nrcresearchpress.com by 210.87.254.42 on 09/05/12
For personal use only.

EXPERIMENTAL

Reactions of Diethylzinc with Isopropanol

These reactions were carried out in heptane solution under nitrogen by adding the alcohol slowly to stirred solutions of diethylzinc. Gas was evolved and slightly hazy solutions were formed which cleared slowly, giving very small amounts of precipitate. The solid may have been the reaction product of traces of water in the isopropanol with the diethylzinc. Evaporation of the clear liquid yielded a white solid which was unstable in air. Infrared absorption measurements were used to determine the nature and extent of the reaction.

Reactions of Diethylzinc with Isomeric Butanols

The reactions of diethylzinc with normal, secondary, and tertiary butanols were studied in 1,2-dimethoxyethane (glyme) solution. The reactions were carried out at 0° and the extents of reaction measured by means of both gas evolution and infrared absorption. Clear solutions were obtained up to ratios of 2 to 1 of normal and secondary butanols to diethylzinc. Cloudy solutions and copious precipitates resulted from the 1:1 reaction product of diethylzinc with tertiary butanol. Cloudy solutions also resulted upon the addition of solutions of each of the alcohols to solutions of ethylzinc hydroxide.

Reactions of Diethylzinc with Water

These reactions were carried out in 12-oz beverage bottles sealed with perforated crown caps backed with butyl rubber which allowed additions, gas evolution, and sampling through the use of syringes and stainless steel hypodermic needles. Early experiments were started with a nitrogen atmosphere but later it was realized that the data were more reliable when all of the solutions were saturated with ethane. Such a solution of water in glyme was added to a solution of diethylzinc in glyme at 0° C. The addition was made along the side of the bottle with vigorous agitation by means of a magnetic stirring bar. The addition was made with the aid of a mechanically driven syringe since the times of addition of the water solution sometimes required as long as 40 minutes in order to minimize temperature rise. The syringe used in the transfer was cooled with dry ice to avoid degassing. Clear colorless solutions resulted from this technique. The gas liberated by the reaction was allowed to evolve as formed through a wet test meter filled with water saturated with ethane. After the addition was completed a sample was usually removed for infrared measurement and the beverage bottle was removed from the ice bath and placed in a constant-temperature bath for the gas evolution measurement.

Table I summarizes the conditions and results of the kinetic experiments. Most of the experiments were done at the same initial diethylzinc concentration (column 1). However, since part of this was reacted

TABLE I

Representative kinetic experiments

Et_2Zn initial (moles/l.)	H_2O added (moles/mole Et_2Zn)	Concn. at start of kinetic measurements (moles/l.)		C_2H_6 evolved (moles/mole H_2O)	
		EtZnOH	Et_2Zn	First step	Second step
0.87	0.31	0.27	0.60	1.02	0.86
0.87	0.62	0.53	0.34	1.00	0.87
1.25	0.61	0.76	0.49	1.01	0.95
0.87	0.92	0.80	0.07	1.00	0.65
0.87	0.97	0.84	0.03	1.00	0.90

away by water at various mole ratios (column 2), it was the excess diethylzinc concentrations (column 4) and the initial ethylzinc hydroxide concentrations (column 3) which were of interest kinetically. As shown in column 5 the ethane evolved during the first step was very nearly 1 mole per mole of water except at very low water ratios. This may have been associated with inherent measurement errors which were larger in proportion to the amounts measured in these experiments. The amounts of gas liberated in the second step were always less than, but usually close to, 1 mole per mole of water.

The infrared measurements were made at room temperature (30° C), but most of the gas evolution measurements were made at 15° C because the decomposition was sufficiently rapid and exothermic at 30° C that the temperature rose significantly in the beverage bottles. No such temperature rise is expected to have occurred in the infrared cell due to the large surface-to-volume ratio.

The infrared samples were pressured into cells closed at each end with stopcocks. Pressure helped minimize bubbling in the cells. It was found that cells smaller than 0.10 mm were often unsatisfactory in that the bubbles were sometimes trapped in the center areas of such cells and thus vitiated the results.

The rates measured in the infrared experiments cannot be taken as absolute measurements since the temperature was not measured or controlled beyond being in a thermostated room. It is supposed that a

slight temperature adjustment occurred during the first 2 to 4 minutes of each experiment, after which time a steady state was reached and maintained.

Two methods of following the decrease of hydroxyl absorption were used. The first is illustrated in Fig. 1. The spectrometer was set to repeat the 2.5 to 3.5 μ region once each 100 seconds. The depth of the peak

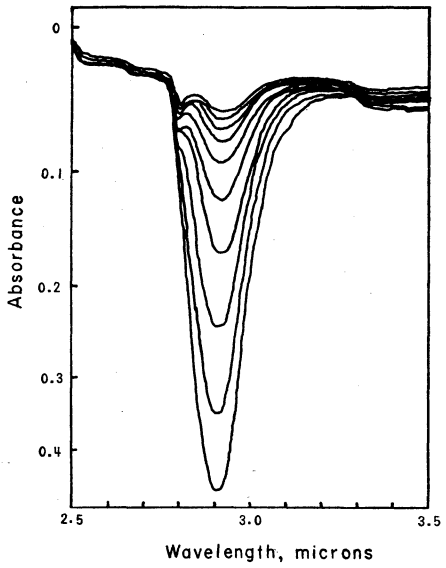

FIG. 1. Disappearance of EtZnOH at 30° C (100-second time intervals).

(log I/I_0) from the background estimated for each experiment was taken as a measure of relative concentration. The other method consisted of running the spectrometer at a fixed wavelength (2.91 μ) and making a mark at intervals of from 20 to 60 seconds.

RESULTS AND DISCUSSION

Reactions of Diethylzinc and Alcohols

Figure 2 shows the significant portions of the infrared spectra of ~5% solutions of isopropanol in heptane, and the 1:1 reaction product of isopropanol and diethylzinc in heptane. Cells of the same thickness were used (0.047 mm). The absorbances and assignments of the important bands in these spectra are given in Table II. The marked increase in the intensities of these absorption bands in the spectrum of the 1:1 reaction product

TABLE II

Absorbances and assignments of isopropanol and ethylzinc isopropoxide absorption bands

Wavelength (μ)	Assignment	Absorbance*		Vibrational mode
		Isopropanol	Ethylzinc isopropoxide	
2.93–2.95	ν(O—H)	0.351	0.0	Hydrogen-bonded stretching
8.63–8.64	δ(H—C)	0.223	0.223	Deformation of H on secondary C
8.85–8.83	ν(C—O), ν(C—C)	0.285	0.565	Coupled skeletal
9.05–8.95	ν(C—O), ν(C—C)	0.049	1.67	Coupled skeletal
10.50–10.53	$\gamma(CH_3)$, ν(C—O), ν(C—C)	0.669	2.23	Coupled methyl and skeletal
12.22–12.15	$\gamma(CH_3)$	0.231	0.859	Rocking

*Absorbance of ~5% solution in heptane in 0.047-mm cell.

Can. J. Chem. Downloaded from www.nrcresearchpress.com by 210.87.254.42 on 09/05/12
For personal use only.

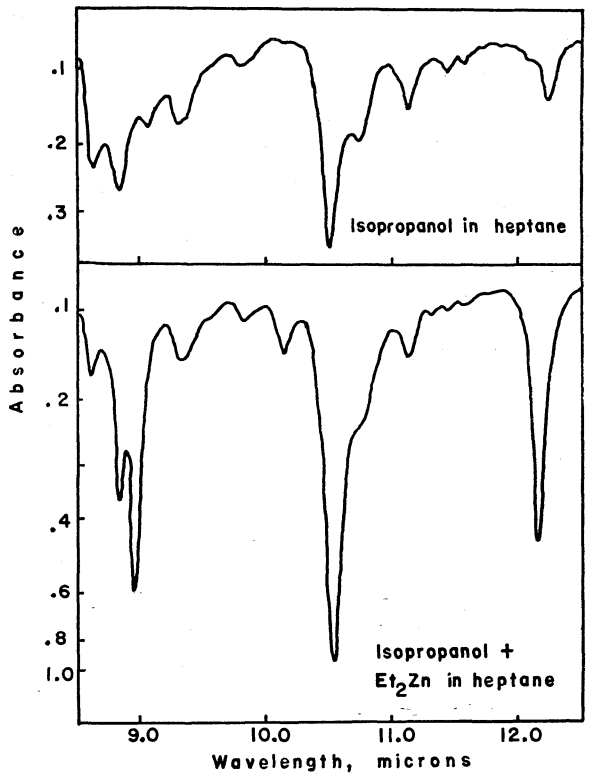

FIG. 2. Infrared spectra of isopropanol and of Et_2Zn–isopropanol reaction products in heptane.

over that of isopropanol may be attributed to the formation of a more heteropolar carbon–oxygen band in the zinc alkoxide.

In Table III are given absorbances at 2.95 μ (hydroxyl) and at 8.96 μ and 12.15 μ (isopropoxyl) for solutions of diethylzinc and isopropanol at various mole ratios of the

TABLE III

Absorbances of diethylzinc–isopropanol reaction products

Isopropanol to diethylzinc (mole ratio)	Absorbances		
	2.95 μ	8.96 μ	12.15 μ
0.674	0	1.04	0.662
0.956	0	1.66	1.051
1.91	0.621	1.68	0.993
2.87	1.23	1.63	0.981

reactants. These solutions were prepared by adding the required amounts of isopropanol to solutions containing about 0.42 mole of diethylzinc per liter of heptane. As shown, the intensities of the bands at 8.96 μ and 12.15 μ do not increase for mole ratios of isopropanol to diethylzinc greater than 1:1, suggesting that the reaction proceeds according to the equation

$$(C_2H_5)_2Zn + i\text{-}C_3H_7OH \rightarrow C_2H_5ZnOC_3H_7 + C_2H_6. \quad [1]$$

Can. J. Chem. Downloaded from www.nrcresearchpress.com by 210.87.254.42 on 09/05/12
For personal use only.

At the mole ratio of 0.674:1 isopropanol to diethylzinc the decrease in intensities of the alkoxyl bands is approximately that expected from the reaction as shown above. Further, no hydroxyl absorption occurs in the 0.674:1 and 0.956:1 mole ratio experiments, whereas hydroxyl absorption does occur for mole ratios greater than 1:1. The intensities of the hydroxyl band for the 1.91:1 and 2.87:1 mole ratio experiments are, within experimental error, equal to that expected on the above 1:1 reaction between isopropanol and diethylzinc. Furthermore the absorption band at 10.1 μ assigned to the ethyl group attached to zinc is present in all of the spectra, even at mole ratios of 2.87:1.

These results show that the alcoholysis of diethylzinc does indeed proceed according to reaction [1] above, and unexpectedly, the second ethyl group bonded to zinc is not replaced in the presence of an excess of the alcohol. No satisfactory explanation for the stability of the second ethyl group has yet been deduced. Three possible explanations have occurred to us as follows: (1) that electronic changes are induced by the zinc–oxygen bond to strengthen the zinc–carbon bond; (2) that a stable complex is formed between one or more alcohol molecules and an ethylzinc isopropoxide molecule; and (3) that diethylzinc, which has been shown (9) to exist as an ion pair, ($ZnEt^+Et^-$), reacts toward active hydrogen containing compounds in a two-step manner, the first, much more rapid step involving the ethyl anion.

The reactions of diethylzinc with normal, secondary, and tertiary butanols were studied in the hope of developing a method for the determination of excess diethylzinc in the presence of compounds containing ethyl–zinc–oxygen structures. This would have been useful in the kinetic studies reported later in this paper. They were carried out in 1,2-dimethoxyethane (glyme) in order to make them applicable in that system. However, reactions of these alcohols in glyme solution did not stop at a ratio of 1 to 1. Both gas evolution and infrared absorption indicated partial reaction of a second mole of each of the alcohols. Here again, however, there remained considerable unreacted alcohol in the presence of zinc–ethyl bonds. The difference between these results and the prior results with isopropanol is supposed to be due to the effects of the solvents used. Heptane would of course tend to suppress ion separation and promote hydrogen bonding as compared to an ether as solvent.

Nature of the Reaction of Diethylzinc with Water

Initial attempts to determine the nature of the diethylzinc reaction products by infrared absorption indicated the absence of hydroxyl groups. These experiments were done after indeterminate periods of aging. Gas evolution data, however, strongly suggested that hydroxyl groups should have been present, since at low temperatures only 1 mole of gas per mole of water appeared to be evolved. More careful analysis of the gas evolution showed, moreover, that following the initial rapid evolution of 1 mole of gas per mole of water slow evolution continued, finally amounting to very nearly another mole of gas. This prompted us to observe the infrared spectra of the solution immediately after the water addition was completed. Figure 3 shows a portion of the spectrum of such a sample with a strong hydroxyl absorption at 2.90 μ. It should be noted that there is no companion band at 6.12 μ as would have been expected if the hydroxyl band was due to residual water. Rerunning the spectra after aging the solution overnight or for short periods in the infrared cell reduced or completely eliminated this absorption. Measurements of the hydroxyl band at various concentrations of water and diethylzinc have shown it to vary in the manner expected for the formation of ethylzinc hydroxide by reaction [2].

$$(C_2H_5)_2Zn + H_2O \rightarrow C_2H_5ZnOH + C_2H_6 \qquad [2]$$

Can. J. Chem. Downloaded from www.nrcresearchpress.com by 210.87.254.42 on 09/05/12
For personal use only.

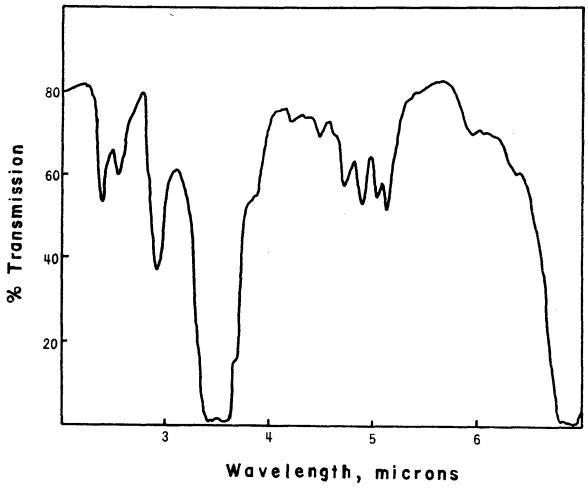

FIG. 3. Infrared spectrum of Et_2Zn–H_2O reaction product in glyme immediately after addition of H_2O.

So far the properties of ethylzinc hydroxide have only been observed in solution. The molar absorptivity of its hydroxyl absorption is 97 ± 9 (liters/mole cm). As shown later, it has half-life periods in the range of 6 minutes at 30° C, 35 minutes at 15° C, and 220 minutes at 0° C. From these data it may be inferred to be a "stable" compound at -60° C and below. This was confirmed at -78° C, at which temperature there was no change in its infrared spectra over a 4-day period.

No such intermediate was isolated from the reaction of triethylaluminum with water at 0° C. Also, when triethylaluminum is added to a solution of ethylzinc hydroxide at 0° C, practically instantaneous evolution of the theoretical amount of ethane (based on the active hydrogen concentration) occurs. It is inherent in the data presented in the following that diethyl zinc reacts very slowly, if at all, with ethylzinc hydroxide. This appears to be in contradiction to the reactivity of zinc and aluminum alkyls toward active hydrogens as reported by Nelson (10).

KINETICS OF THE DISAPPEARANCE OF ETHYLZINC HYDROXIDE

Infrared Studies

Figure 4 shows representative data from early infrared measurements of the disappearance of ethylzinc hydroxide plotted as concentration of hydroxyl versus time. The general shape of the curves is exponential. However, it will be noted that there are short initial periods of linear or actually increasing slope in some of the plots. Figure 5 shows the first-order plots of these same data and another run at a ratio of [EtZnOH] to [Et_2Zn] equal to 0.17. It is of interest to notice that the reactions follow first-order kinetics during an appreciable extent of the reaction in all of these cases. First-order kinetics did not fit the reaction scheme suggested by Furukawa for the reaction of this intermediate, namely,

$$C_2H_5ZnOH + (C_2H_5)_2Zn \rightarrow C_2H_5ZnOZnC_2H_5 + C_2H_6 \quad [3]$$

$$2C_2H_5ZnOH \rightarrow C_2H_5ZnOZnOH + C_2H_6. \quad [4]$$

The other salient fact from the early data is that the rates are not affected to an appreciable extent by the concentration of excess diethylzinc. This may be seen by

Can. J. Chem. Downloaded from www.nrcresearchpress.com by 210.87.254.42 on 09/05/12
For personal use only.

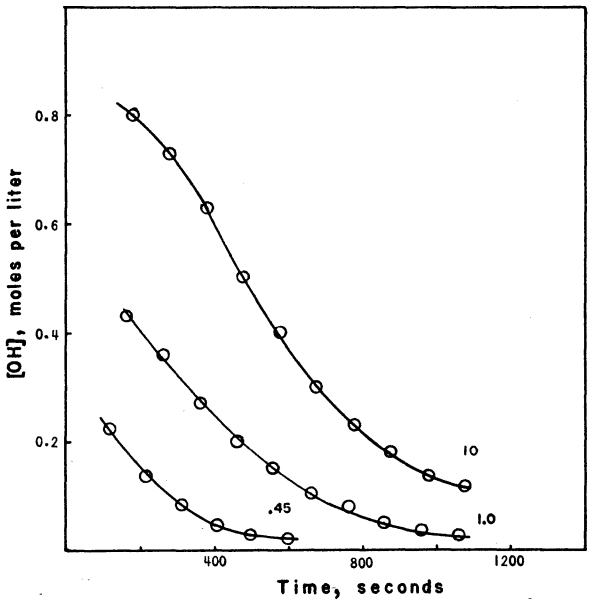

FIG. 4. Disappearance of EtZnOH as measured by infrared at 30° C for different (EtZnOH)/(Et_2Zn) ratios.

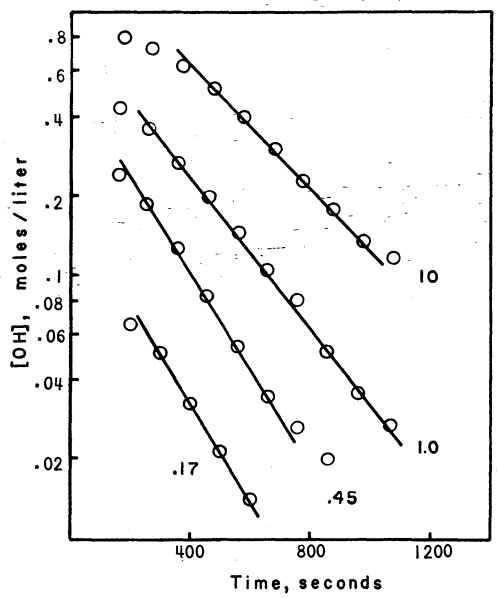

FIG. 5. Disappearance of EtZnOH as measured by infrared at 30° C for different (EtZnOH)/(Et_2Zn) ratios.

comparing the rate constants for runs made with ratios of initial concentrations of ethylzinc hydroxide to diethylzinc of 0.18 and 11.5. The rate constants were 4.2×10^{-3} and 2.8×10^{-3} sec^{-1} respectively.

With these facts in mind more accurate experiments were carried out at the extremes

Can. J. Chem. Downloaded from www.nrcresearchpress.com by 210.87.254.42 on 09/05/12
For personal use only.

of concentrations of these reactants, i.e. at ratios of ethylzinc hydroxide to diethylzinc of 0.05 and 32 as well as at equal concentrations. By means of the rate equation:

$$-\frac{d[\mathrm{OH}]}{dt} = k[\mathrm{C_2H_5ZnOH}]^n[(\mathrm{C_2H_5})_2\mathrm{Zn}]^m, \qquad [5]$$

separation of the possibility of pseudo orders from real reaction orders was made. The overall orders of these reactions were calculated by the fractional life period method (11). These were found to be 0.80, 0.83, and 0.83 for the experiments at ratios of [EtZnOH] to $[(Et)_2Zn]$ of 0.05, 1.0, and 32 respectively. The latter value was for the part of the curve following the initial slow portion. Including this portion would have resulted in a lower value.

Thus, at the low ratio of [EtZnOH] to $[Et_2Zn]$, where $[\mathrm{EtZnOH}] \ll [\mathrm{Et_2Zn}]$

$$-\frac{d[\mathrm{OH}]}{dt} = k'[\mathrm{C_2H_5ZnOH}]^n,$$

where $k' = k'[(\mathrm{C_2H_5})_2\mathrm{Zn}]^m$; therefore $n = 0.80$. At equal concentrations of these species, i.e. where $[\mathrm{EtZnOH}] = [(Et)_2Zn]$,

$$-\frac{d[\mathrm{OH}]}{dt} = k[\mathrm{C_2H_5ZnOH}]^{m+n}.$$

Since $m+n = 0.83$, and $n = 0.80$, the value of $m \cong 0$. This result agrees with the prior one that diethylzinc concentration is not a part of the rate expression for this reaction. The low order of reaction in the case of the experiment in which the ratio of [EtZnOH] to $[Et_2Zn]$ was high, i.e. where $[\mathrm{EtZnOH}] \gg [(Et)_2Zn]$, shows that the disappearance of hydroxyl cannot be accounted for by a bimolecular reaction of ethylzinc hydroxide with itself as in equation [4].

The deviations from first-order behavior at the beginning of the reaction suggested that the mechanism might involve a reaction in which the concentration of an intermediate built up until a steady state was reached. One such mechanism involves the assumption that ethylzinc hydroxide exists in this system as a dimer. The known tendency of zinc to coordinate with oxygen atoms suggested this to be a reasonable possibility. Decomposition of this dimer may be considered to take place in the following set of first-order series reactions:

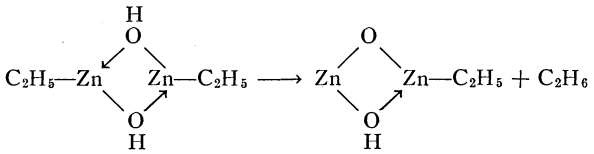

[6]

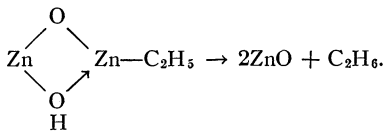

[7]

The fact that zinc oxide is one of the products could account for the apparent colloidal nature of the system as judged from Tyndall scattering of light. Excess diethylzinc perhaps stabilizes the zinc oxide particles in ether solution.

As will be shown in the following detailed analysis of this pair of first-order series reactions the mechanism accounts very well for the decomposition kinetics at and below a 1.2 ratio of [EtZnOH] to $[Et_2Zn]$. However, it does not account for the initial slow

Can. J. Chem. Downloaded from www.nrcresearchpress.com by 210.87.254.42 on 09/05/12
For personal use only.

phase of the reaction at high ratios of these reactants. In order to account for this it seems necessary to suggest that the reaction is autocatalytic at high ratios of [EtZnOH]. On the other hand excess diethylzinc may act as a catalyst at low ratios of these reactants.

Detailed analyses of first-order series reactions similar to those in [6] and [7] have been made by Esson (13) and French (14). Applying a similar analysis to reactions [6] and [7], we obtained a theoretical rate expression as follows:

$$A \xrightarrow{k_1} B + D$$

$$B \xrightarrow{k_2} C + D$$

where A = $[C_2H_5ZnOH]_2$; B = $[C_2H_5ZnOZnOH]$; C = 2ZnO; D = C_2H_6.
Setting

$$\alpha = \frac{[A]}{[A]_0} \quad \text{and} \quad \beta = \frac{[B]}{[A]_0}$$

and defining

$$\tau = k_1 t \quad \text{and} \quad \kappa = \frac{k_2}{k_1}$$

the following differential equations express the above reactions:

$$\frac{d\alpha}{d\tau} = -\alpha \qquad [8]$$

$$\frac{d\beta}{d\tau} = \alpha - \kappa\beta. \qquad [9]$$

Substituting the solution of equation [8], $\alpha = e^{-\tau}$, into equation [9] gives:

$$\frac{d\beta}{d\tau} + \kappa\beta = e^{-\tau}. \qquad [10]$$

The solution of differential equation [10] is:

$$\beta = \frac{1}{\kappa - 1}[e^{-\tau} - e^{-\kappa\tau}].$$

We know that [OH] = 2[A]+[B]. By letting ϵ = [OH]/$[OH]_0$, where $[OH]_0 = 2[A]_0$, we obtain

$$\epsilon = \frac{[A]}{[A]_0} + \frac{[B]}{2[A]_0}$$

or

$$\epsilon = \alpha + \frac{\beta}{2}$$

or

$$\epsilon = e^{-\tau} + \frac{1}{2(\kappa - 1)}[e^{-\kappa} - e^{-\kappa\tau}].$$

A family of plots of ϵ versus log τ were obtained for different values of κ between 100 and 0.02. The experimental plots of ϵ versus log t were matched to one of the family, thus determining κ, by shifting horizontally along the log t axis. From the amount of shift along log t with respect to log τ, values of k_1 were determined. The data for [EtZnOH] to [Et_2Zn] ratios of 1.2 and below fit quite well for $\kappa = 2$. The fit of the theoretical and experimental data are shown for [EtZnOH]/[Et_2Zn] ratios of 0.05, 1.0 and 32 in Fig. 6.

Can. J. Chem. Downloaded from www.nrcresearchpress.com by 210.87.254.42 on 09/05/12
For personal use only.

As noted previously the absolute values of the rate constants are not significant probably because of temperature variation.

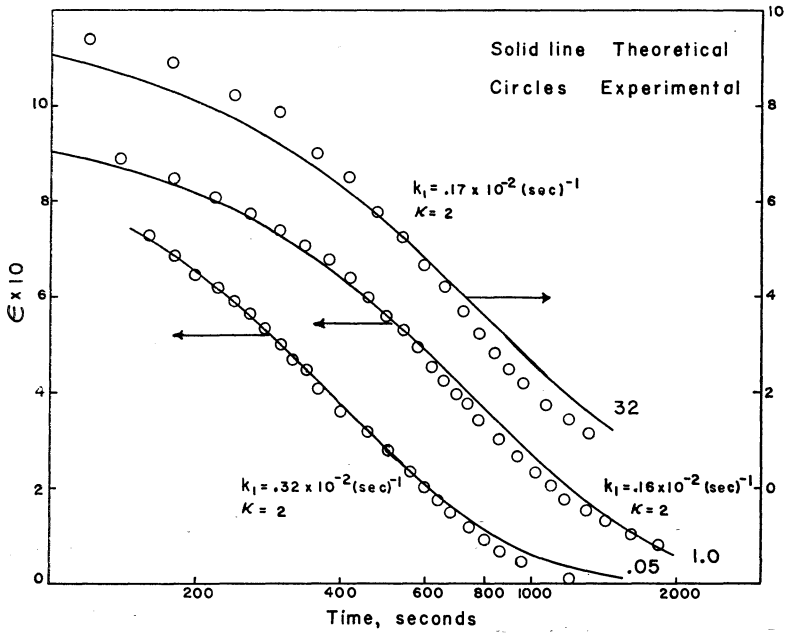

FIG. 6. Fit of experimental data and theoretical expression for various (EtZnOH)/(Et_2Zn) ratios.

An alternate suggestion is that ethylzinc hydroxide coordinates with diethylzinc as well as with itself. The decomposition of this "mixed dimer", i.e.

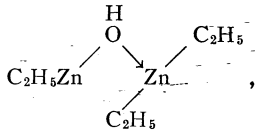

would be expected to be first order with respect to ethylzinc hydroxide. At low [EtZnOH] to [Et_2Zn] ratios, where this form would be favored, the initial deviation from first-order behavior could be ascribed to temperature equilibration. On the other hand at high [EtZnOH] to [Et_2Zn] ratios, where the ethylzinc hydroxide dimer would be favored, the very much larger deviation could be considered as characteristic of this chemical species and need not be considered as anomalous behavior. The similarity of the stabilized first-order rates at high and low ratios of [EtZnOH] to [Et_2Zn] would be taken as coincidentally similar behavior of the two dimeric species. The similar kinetic behavior between experiments at [EtZnOH] to [Et_2Zn] ratios of 0.05 and 1.0 suggests that formation of the "mixed dimer" may be favored over the ethylzinc hydroxide dimer. In the ethylzinc hydroxide dimer case the colloid which is believed to be formed during these reactions would be zinc oxide. For the case involving a complex of ethylzinc hydroxide and diethylzinc it would be necessary to suppose a colloid formed of the molecule EtZnOZnEt.

Gas Evolution Studies

Figure 7 shows representative first-order plots of the gas evolution data. These plots also show slight to considerable deviation from first-order behavior at the start, just as

Can. J. Chem. Downloaded from www.nrcresearchpress.com by 210.87.254.42 on 09/05/12
For personal use only.

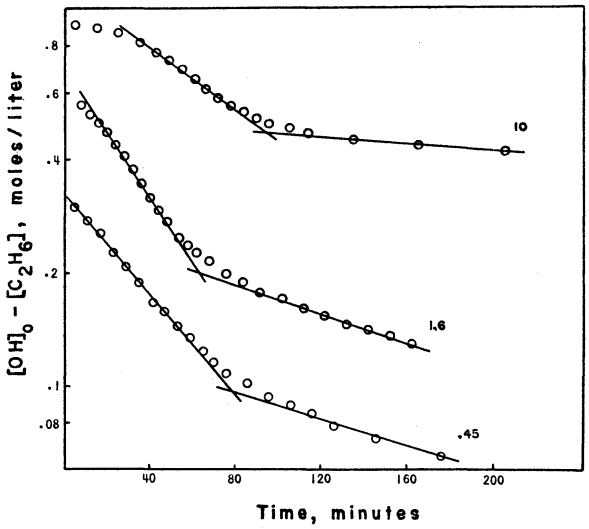

FIG. 7. Apparent disappearance of EtZnOH as measured by ethane evolution at 15° C.

was noted in the plots of data from infrared measurements. However, the plots degenerate from first-order behavior between 40 and 70% reaction (compared to over 90% in most of the experiments measured by infrared). There follow in some cases what appear to be another first-order region.

The discrepancy between the two methods is brought into focus by examination of Figure 8, which shows the results of an experiment in which both the gas evolution and hydroxyl absorption decrease were measured on the same solution at 15° C. It shows that not only does the gas evolution first-order plot deviate at a smaller extent of reaction but that the apparent rate is appreciably slower than that indicated by infrared absorption. In the absence of a clear-cut indication of the reason for this discrepancy the writers

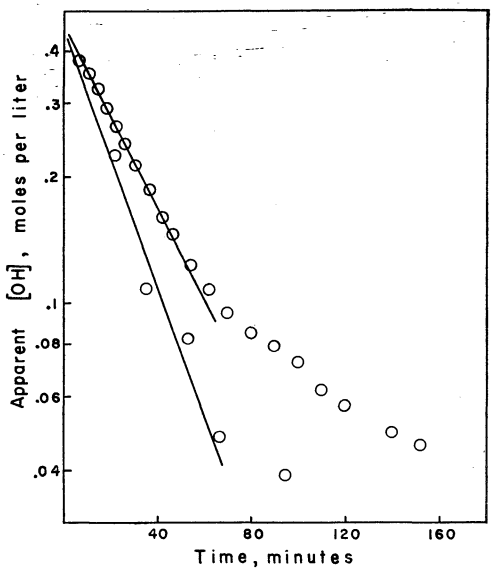

FIG. 8. Decomposition of EtZnOH at 15° C.

Can. J. Chem. Downloaded from www.nrcresearchpress.com by 210.87.254.42 on 09/05/12
For personal use only.

have intuitively supposed that the infrared method was less open to systemic error than was the gas evolution method. The volume of ethane equivalent to the maximum discrepancy between the two methods in the above experiment is in the range of one third of its solubility. Such a solubility variation might be expected in a developing colloidal dispersion. That such a colloidal phase was present was suggested (1) by light scattering measurements and (2) by the yellow color of the solutions combined with their lack of distinct ultraviolet absorption bands. The yellow color always developed during the evolution of the second mole of ethane per mole of water originally added. Saegusa and co-workers (12) found that the "soluble" portion of the reaction product of diethylzinc and water prepared in hexane was of colloidal nature in benzene.

Among alternate ideas to explain this discrepancy the following were considered: (1) This discrepancy was caused by the difference in surfaces of the reaction vessels used, i.e. the glass of the beverage bottles and the sodium chloride of the infrared cells. To check this a gas evolution experiment was carried out with dried powdered salt in a beverage bottle. The evolution of gas was somewhat faster in this experiment. However, the apparent hydroxyl decrease slowed down drastically as in the other experiments in the range of 50% disappearance. (2) It was possible that the infrared measured only half of the reaction, i.e. that the absorption occurring at 2.9 μ was specific for ethylzinc hydroxide, and that other products also containing hydroxyl groups, such as EtZnOZnOH, absorbed elsewhere or much less strongly. The weak absorption at 2.8 μ as shown in Fig. 1 is within the hydroxyl range. It decreases with time at a somewhat slower rate than does the strong absorption at 2.9 μ. If this were the correct interpretation an explanation of the large difference in extinction coefficient between these two absorptions would be required. However, the data shown in Fig. 7 do not rule out this alternative.

The following similarities between the infrared absorption decrease and gas evolution data appear to make conclusions on the basis of the latter data reasonable: (1) The first-order rates were affected very little by excess diethylzinc concentration. (2) Experiments at high ratios of [EtZnOH] to [Et_2Zn] showed slow initial rates. Accordingly, the first-order rates from gas evolution measurements were used to estimate the overall activation energy of the process. The rather low order of reliability of the 30° C experiment may be appreciated by examination of its first-order plot (Fig. 9). The initial slow portion was

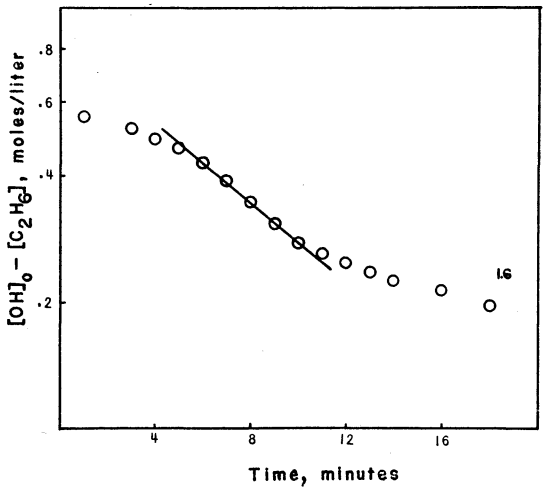

FIG. 9. Apparent disappearance of EtZnOH as measured by ethane evolution at 30° C.

Can. J. Chem. Downloaded from www.nrcresearchpress.com by 210.87.254.42 on 09/05/12
For personal use only.

due to temperature equilibration from 0° to 30°, which took up an appreciable part of the reaction time. However, use of this rate along with first-order rates at 15° and 0° gave the Arrhenius plot as shown in Fig. 10. The activation energy on this basis was 19 kcal/mole.

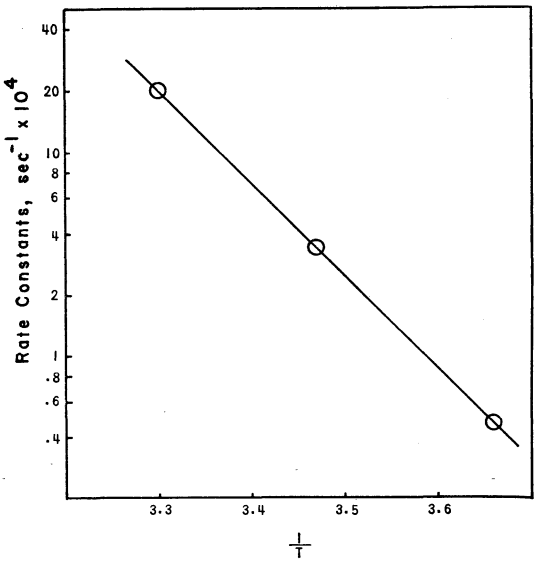

FIG. 10. Temperature dependence of rates of decomposition of EtZnOH.

The overall conclusion from these experiments appears to be that the second ethyl group of diethylzinc is less liable to reaction than the first. This conclusion may be necessarily limited to reactions involving active hydrogens and to cases in which the first carbon zinc bond is transformed into an oxygen–zinc bond.

ACKNOWLEDGMENTS

The writers wish to acknowledge the encouragement and helpful suggestions of Dr. E. E. Gruber, Dr. R. A. Briggs, and Dr. R. Livigni of the General Tire Laboratories, as well as of Dr. J. P. Fugassi of Carngeie Institute of Technology and Dr. C. C. Price of the University of Pennsylvania. Our thanks also to Dr. W. O. Phillips for help in programming the computer, to Mr. P. Suman for the infrared measurements, and to Mr. J. L. Cowell for experimental assistance.

REFERENCES

1. L. FRIEDMAN and A. P. IRSA. Anal. Chem. **24**, 876 (1952).
2. F. HAUROWITZ. Mikrochemie, **7**, 88 (1929).
3. S. TOLKATSCHEV. Chem. Zentr. **II**, 1200 (1901).
4. D. F. MENARD and J. G. ASTON. J. Am. Chem. Soc. **56**, 1601 (1934).
5. J. FURUKAWA, T. SAEGUSA, and T. TSURUTA. Makromol. Chem. **32**, 90 (1959).
6. J. FURUKAWA, T. SAEGUSA, T. TSURUTA, and G. KAKOGAWA. J. Poly. Sci. **35**, 541 (1959).
7. J. FURUKAWA, T. SAEGUSA, T. TSURUTA, and G. KAKOGAWA. Makromol. Chem. **36**, 25 (1960).
8. D. G. STEWART, D. WADDAN, and E. BORROWS. (Shell Dev. Co.) U.S. Patent No. 2,870,100 (1959).
9. W. V. EVANS and R. PEARSON. J. Am. Chem. Soc. **64**, 2865 (1942).
10. J. F. NELSON. Iowa State Coll. J. Sci. **12**, 145 (1937).
11. A. A. FROST and R. G. PEARSON. Kinetics and mechanism. Wiley. p. 43.
12. T. SAEGUSA. Private communication.
13. W. ESSON. Phil. Trans. Roy. Soc. London, **156**, 220 (1866).
14. D. FRENCH. J. Am. Chem. Soc. **72**, 4806 (1950); *also* A. A. FROST and R. G. PEARSON. Kinetics and mechanism. Wiley. p. 169.

Can. J. Chem. Downloaded from www.nrcresearchpress.com by 210.87.254.42 on 09/05/12
For personal use only.

Canadian Journal of Chemistry

Issued by THE NATIONAL RESEARCH COUNCIL OF CANADA

VOLUME 41 JUNE 1963 NUMBER 6

CHARACTERIZATION OF THREE HEMICELLULOSES FROM THE WOOD OF AMABILIS FIR (ABIES AMABILIS)

E. C. A. SCHWARZ[1] AND T. E. TIMELL[2]

Department of Chemistry, McGill University, and the Pulp and Paper Research Institute of Canada, Montreal, Que.

Received January 9, 1963

ABSTRACT

An arabino-4-*O*-methylglucuronoxylan (10:14:76), a water-soluble galactoglucomannan (1:1:3), and an alkali-soluble galactoglucomannan (0.1:1:3) have been isolated in yields of 7, 4, and 8% from the wood of amabilis fir (*Abies amabilis*). The structure of the polysaccharides was established by methylation and periodate oxidation techniques. The xylan ($\bar{P}_n$ 106) contained side chains of (1 → 2)-linked 4-*O*-methyl-α-D-glucuronic acid and (1 → 3)-linked α-L-arabinofuranose residues, both attached directly to a linear framework of (1 → 4)-linked β-D-xylose residues. The galactoglucomannans ($\bar{P}_n$ 76 and 95) contained (1 → 6)-linked α-D-galactopyranosyl residues attached directly to a backbone of (1 → 4)-linked β-D-mannose and β-D-glucose residues. Partial hydrolysis of the two hexosans yielded 10 and 13 oligosaccharides, respectively, containing (1 → 4)-β-D-mannose, (1 → 4)-β-D-glucose, and (1 → 6)-α-D-galactopyranose residues. The molecular rotations of a series of mannooligosaccharides corresponded to a value of −54° for the specific rotation of an infinitely long mannan. It is concluded that the main hemicelluloses in amabilis fir wood are the same as those occurring in the wood of gymnosperms from other genera. The same three hemicelluloses are also present in the bark of this species.

Among the gymnosperms, members of the genera *Ginkgo*, *Larix*, *Picea*, *Pinus*, *Thuja*, and *Tsuga* have been extensively studied with regard to their main hemicellulose constituents (1). No member of the genus *Abies*, however, has so far been similarly investigated although many fir species are both widespread and valuable. The present investigation is concerned with the isolation and constitution of the three principal hemicelluloses in the wood of amabilis fir (*Abies amabilis*) (Douglas) Forbes). The polysaccharides occurring in the bark of this tree have previously been examined in detail (2, 3).

RESULTS AND DISCUSSION

When amabilis fir wood was partially hydrolyzed, the acid portion of the hydrolyzate consisted of galacturonic acid, 4-*O*-methylglucuronic acid, a galacturonosyl rhamnose, probably admixed with a galacturonosyl glucose, and a 4-*O*-methylglucuronosyl xylose. The first aldobiouronic acid has previously been isolated from pine wood (4, 5). The third was fully identified as 2-*O*-(4-*O*-methyl-α-D-glucosyluronic acid)-D-xylopyranose. It probably originated from the xylan portion of the wood.

For isolation of the hemicelluloses, the wood was partially delignified with chlorous acid and the holocellulose was extracted with aqueous potassium hydroxide, giving two polysaccharides, which were separated by repeated treatment with barium hydroxide.

[1]*Present address: E. I. du Pont de Nemours and Company, Kinston, N.C.*
[2]*Present address: Department of Forest Chemistry, State University College of Forestry, Syracuse, N.Y.*

Can. J. Chem. Downloaded from www.nrcresearchpress.com by 210.87.254.5 on 09/05/12
For personal use only.

Can. J. Chem. Downloaded from www.nrcresearchpress.com by 210.87.254.5 on 09/05/12
For personal use only.

TABLE I

General characteristics of three hemicelluloses

Polysaccharide	Percentage of wood	$[\alpha]_D$, deg	Solvent	$\bar{P}_n$	Constituent sugar residues						Periodate consumed per repeating unit	
					Gal	Glu	Man	Ara	Xyl	Uron. acid	Calc.	Found
Arabino-4-*O*-methyl-glucuronoxylan	7.0	−40	Water	106				10	76	14	86	81
Galactoglucomannan A	4.1	−8	Water	76	1	1	3				6.0	6.0
Galactoglucomannan B	8.1	−38	Alkali	95	0.1	1	3				4.2	4.3

The soluble portion was an arabino-4-*O*-methylglucuronoxylan, while the barium hydroxide complex gave a water-soluble galactoglucomannan. Extraction of the residual holocellulose with aqueous sodium hydroxide – borate yielded an alkali-soluble galactoglucomannan. Yields, sugar composition, and other characteristics of the hemicelluloses are presented in Table I.

The wood contained approximately 25% hemicelluloses. The combined yield of pure polysaccharides was 19.2%, corresponding to a recovery of 77%. The relative sugar compositions and specific rotations were typical of each of the three polysaccharides. Number-average degrees of polymerization ($\bar{P}_n$) were determined by osmometry with organo-soluble derivatives. The value for the xylan was similar to those reported for other softwood xylans (1). The water-soluble galactoglucomannan (A) had a lower molecular weight than the alkali-soluble type. All three hemicelluloses had probably been degraded by the action of the chlorous acid used for delignification.

The xylan was methylated, giving a fully substituted derivative with 95 xylose residues per average molecule. The partly methylated sugars obtained on hydrolysis were separated on columns of exchange resin and charcoal–Celite, resulting in the six compounds in Table II. These results, in conjunction with the nature of the 4-*O*-methylglucuronosyl

TABLE II

Sugars obtained on hydrolysis of the methylated arabino-4-*O*-methylglucuronoxylan

Component	Moles	Component	Moles
2-*O*-Methyl-D-xylose	10	2,3,4-Tri-*O*-methyl-D-xylose	1
3-*O*-Methyl-D-xylose	3	2,3,5-Tri-*O*-methyl-L-arabinose	10
2,3-Di-*O*-methyl-D-xylose	48	2-*O*-(2,3,4-tri-*O*-methyl-α-D-glucuronic acid)-3-*O*-methyl-D-xylopyranose	14

xylose, show that the hemicellulose consisted of at least 100 (1 → 4)-linked β-D-xylopyranose residues, every fifth of which carried a (1 → 2)-linked 4-*O*-methyl-α-D-glucuronic acid residue directly linked to the xylan backbone. The arabinofuranose residues, one per eight xylose, all occurred as non-reducing end groups, linked (probably directly) to position 3 of the xylose residues. In analogy with other softwood xylans (6), the arabinose was probably present in the α-L-configuration. The polysaccharide contained only 1.2 non-reducing xylose end groups per average molecule, virtually equivalent to a linear structure.

The two galactoglucomannans were methylated to completion and hydrolyzed. The mixtures of partly methylated hexoses were resolved on charcoal–Celite, giving the compounds presented in Table III. Polysaccharide A evidently consisted of a backbone

TABLE III

Sugars obtained on hydrolysis of methylated galactoglucomannans A and B

Component	Moles		Component	Moles	
	A	B		A	B
2,3,Di-*O*-methyl-D-mannose	5.7	0.2	2,3,6-Tri-*O*-methyl-D-glucose	5.3	12.5
3,6-Di-*O*-methyl-D-mannose	0.6	Nil	2,3,4,6-Tetra-*O*-methyl-D-galactose	5.5	1.3
2,3-Di-*O*-methyl-D-glucose	1.1	1.5	2,3,4,6-Tetra-*O*-methyl-D-mannose	1.0	1.0
2,3,6-Tri-*O*-methyl-D-mannose	15.6	33.1	2,3,4,6-Tetra-*O*-methyl-D-glucose	Trace	Trace

of (1 → 4)-β-linked mannose and glucose residues, three of which formed non-reducing end groups, suggesting the presence of two branch points per average macromolecule. All

Can. J. Chem. Downloaded from www.nrcresearchpress.com by 210.87.254.5 on 09/05/12
For personal use only.

Can. J. Chem. Downloaded from www.nrcresearchpress.com by 210.87.254.5 on 09/05/12
For personal use only.

TABLE IV

Oligosaccharides obtained on partial hydrolysis of galactoglucomannans A and B

Oligosaccharide*	Galactoglucomannan A				Galactoglucomannan B			
	Yield, mg	D.P.	M.p., °C	$[\alpha]_D$, deg†	Yield, mg	D.P.	M.p., °C	$[\alpha]_D$, deg†
M → M	310		212–213	−8.3	240		209–210	−8.0
M → G	30			+14	14			+29
M → M → M	240		166–168	−24	126		167–168	−25
G → G	22		231–233	+35	18		220–221‡	+34
Gal → M → M → M					35	3.7		−7
M → M → M → M	94	3.7		−30	40			−29
G → M	185		137–138	+7	90			+10
M → M → M → M → M	40	5.1		−35				
Gal → M → M → M → M					28	4.7		−11
G → M → M	87			−9	42			−9
M → M → M → M → M → M	78	5.8		−39				
M → M → M → M → G	48	5.0		−23				
M → M → G → M	50			−17				
M → G → M	65	2.8		+5.5				
G → G → M	62			+9	30			+9

*M →, β-D-mannosyl-(1 → 4)-; G →, β-D-glucosyl-(1 → 4)-; Gal →, α-D-galactopyranosyl-(1 → 6)-.
†In water.
‡Octaacetate derivative.

galactose residues were present as non-reducing end groups. Most likely, they occurred as α-D-galactopyranose residues, linked directly to the hexosan framework by (1 → 6)-glycosidic bonds. Although it contained 10 times less galactose residues, the structure of galactoglucomannan B was evidently the same.

Additional structural evidence was obtained by an examination of the 23 oligosaccharides formed on partial hydrolysis of the two hemicelluloses. The results are summarized in Table IV. The two galactose-containing oligosaccharides on partial hydrolysis gave 6-*O*-α-D-galactopyranosyl-D-mannose, thus showing the mode of attachment of the galactose residues. All other oligosaccharides contained only (1 → 4)-β-links. Methyl β-D-mannopyranoside is hydrolyzed by acids 3.0 times faster than the corresponding glucoside (7) while mannobiose is hydrolyzed 2.5 times more rapidly than cellobiose (8). As pointed out by Lindberg (9), a trisaccharide of the type G → G → M would therefore be present in noticeable amounts during the earlier stages of a partial hydrolysis in spite of the 1:3 ratio between the randomly distributed glucose and mannose residues. It is interesting to note that for polysaccharide B approximately equal quantities were found of compounds G → G → M and M → G → M. The amount of the former was in both cases much larger than that of cellobiose, as can be expected from statistical considerations (9). Many of the oligosaccharides obtained here have previously been isolated from similar galactoglucomannans (10, 11). With the exception of the mannotetraose, however, none of the tetra-, penta- or hexa-saccharides have so far been reported.

If molecular rotations and degrees of polymerizations of the five mannooligosaccharides are plotted according to Freudenberg (12), a straight line can be drawn, extrapolation of which gives a specific rotation of −54° for an infinitely long polysaccharide composed exclusively of (1 → 4)-linked β-D-mannose residues. Assuming a degree of polymerization of 15 for mannan A from vegetable ivory (13), its calculated specific rotation in water or aqueous alkali (6) should be −48°. Experimental values reported are −46° and −48° (14, 15), a good agreement in spite of the probable presence of some α-(1 → 4)- and perhaps also (1 → 6)-linkages in ivory nut mannan A.

When the three polysaccharides were oxidized with periodate, the results presented in Table I were obtained. The calculated and found values agreed quite well, thus confirming the other structural evidence.

The combined evidence shows that the three main hemicelluloses in the wood of amabilis fir, and probably in all other species of the genus *Abies*, are a water-soluble arabino-4-*O*-methylglucuronoxylan, a water-soluble galactoglucomannan, and an alkali-soluble galactoglucomannan with only a few galactose residues. One or both of the hexosans might be partly acetylated in the native state (16). The relative amount, molecular weight, and detailed structure of the polysaccharides are the same as has been previously found for corresponding hemicelluloses from the wood of other gymnosperms. The latter thus appear to be very uniform with respect to the nature of their major polysaccharides, the larches forming a notable exception. It is interesting to note that the same also applies to the nature of their lignin, which is of the coniferyl type except in trees from a few genera (17). All three polysaccharides studied here have previously (2, 3) been isolated from the bark of the same tree.

EXPERIMENTAL

Specific rotations were measured at equilibrium at 25° and referred to 589 mμ. Melting points are corrected. Demethylations were carried out with boron trichloride (18). Degrees of polymerization of polysaccharides (19) and oligosaccharides (20, 21) were determined as described elsewhere. Evaporations were carried out *in vacuo* at 50°.

Can. J. Chem. Downloaded from www.nrcresearchpress.com by 210.87.254.5 on 09/05/12
For personal use only.

Paper Chromatography

Solvents used for separating the sugars were ethyl acetate – acetic acid – water (A) (9:2:2) and (B) (18:7:8), (C) *n*-butanol–pyridine–water (10:3:3), (D) ethyl acetate – pyridine – water (8:2:1), and (E) butanone–water–ammonia (90:8:2). Whatman No. 1 and 3MM filter papers were used for the first four solvents. For solvent E a 3MM paper provided with a wick of No. 50 paper was used. Paper electrophoresis was carried out with No. 3MM paper and 0.05 *M* borate at 750 v for 5 hours. *o*-Aminodiphenyl was used as spray reagent and for quantitative sugar analysis (22).

Wood

Standard methods of analysis (23) indicated that the wood meal (40–60 mesh, extractive free) contained 44% cellulose, 29.2% lignin, 6.3% pentosans, 2.6% uronic anhydride, 1.4% acetyl, and 0.2% ash.

Partial Hydrolysis of Wood

Wood meal (200 g) was hydrolyzed with sulphuric acid in the usual way. After neutralization (barium hydroxide), filtration through Celite, treatment with Amberlite IR-120 (acid form) exchange resin, filtration, and concentration, acidic sugars were adsorbed on a column of Dowex 1-X4 (acetate form) exchange resin and subsequently removed by elution with aqueous acetic acid. The mixture of sugar acids (5.0 g) was resolved into four fractions on a column of Darco G-60 charcoal–Celite by gradient elution with 2 to 40% aqueous ethanol. The first two acids corresponded in rate of movement on the paper chromatogram (solvent A) to galacturonic acid (0.93 g) and 4-*O*-methylglucuronic acid (0.41 g). The fourth fraction (0.045 g) on hydrolysis gave rise to galacturonic acid, rhamnose, and a trace of glucose.

The third fraction consisted of an aldobiouronic acid which gave xylose and 4-*O*-methylglucuronic acid on hydrolysis and had $[\alpha]_D$ +86° (*c*, 1.0 in water). Anal. Calc. for $C_{12}H_{20}O_{11}$: OCH_3, 9.1%. Found: OCH_3, 9.2%. The derived methyl ester methyl glycoside of the trataacetate derivative (24) had m.p. and mixed m.p. 202° and $[\alpha]_D$ +101° (*c*, 0.5 in chloroform). The infrared spectra of the two compounds were identical with those of authentic samples.

Isolation of Hemicelluloses

Chlorite holocelluloses were prepared in two experiments from wood (2×1200 g) by the method of Wise, Murphy, and D'Addieco (25). Yields: 73.1 and 76.0%. Holocellulose(700 g) was exhaustively extracted with 24% (w/w) aqueous potassium hydroxide to give a mixture of polysaccharides (106 g, 11.1% of wood). Addition of barium hydroxide to an alkaline solution of the mixture gave a precipitate, which was recovered. This process was repeated twice. The final solution yielded an arabino-4-*O*-methylglucuronoxylan (67 g, 7.0%) which contained arabinose, uronic acid, and xylose (solvents A and D) in a ratio of 10:14:76 and had $[\alpha]_D$ −40° (*c*, 1.5 in water). Anal. OCH_3, 3.05%; uronic anhydride, 15.0%. The first two barium hydroxide precipitates were combined, and the polysaccharides were recovered and dissolved in alkali for a second precipitation with barium hydroxide. After a third similar precipitation the product (galactoglucomannan A) contained only traces of arabinose and xylose and had a ratio of galactose:glucose:mannose of 2:120:59. Yield: 39 g, 4.1% of wood, $[\alpha]_D$ −8° (*c*, 3.0 in water).

The residual holocellulose was extracted with 17% aqueous sodium hydroxide containing 4% boric acid to yield a polysaccharide (77 g, 8.1% of wood) which contained galactose, glucose, and mannose residues in a ratio of 0.1:1:3 and had $[\alpha]_D$ −38° (*c*, 2.4 in 10% sodium hydroxide).

Xylan

On oxidation with 0.05 *M* sodium metaperiodate the xylan consumed 81 moles of oxidant per 76 anhydroxylose units. The number-average molecular weight of the fully acetylated xylan (osmometry) was 31,000, corresponding to 106 xylose residues in the backbone of the average macromolecule.

Methylation of the Xylan

Xylan (13.5 g) was methylated four times with dimethyl sulphate and alkali to give a partly methylated product (11.5 g), which was further methylated by the procedure of Kuhn and co-workers (26) .The fully methylated product (8.5 g) showed a negligible band in the hydroxyl region of the infrared spectrum and had $[\alpha]_D$ −42° (*c*, 2.0 in chloroform). Anal. Calc. for a fully methylated and esterified xylan: OCH_3, 39.6%. Found: OCH_3, 39.5%. The molecular weight of the methylated xylan (osmometry) was 21,400, corresponding to 95 xylose residues in the xylan framework.

The methylated xylan (4.1 g) was subjected to methanolysis and acidic and neutral glycosides were separated with anion exchange resin, giving 1.0 and 2.9 g of material, respectively. The acid glycoside was a partly methylated aldobiouronic acid whose methyl ester was reduced with lithium aluminum hydride to give methyl 2-*O*-(2,3,4-tri-*O*-methyl-α-D-glucosyl)-3-*O*-methyl-β-D-xylopyranoside, m.p. and mixed m.p. 164–165°, $[\alpha]_D$ +84° (*c*, 1.5 in water). Its infrared spectrum was identical with that of an authentic specimen. Anal. Calc. for $C_{16}H_{30}O_{10}$: OCH_3, 40.6%. Found: OCH_3, 40.4%. The neutral fraction was hydrolyzed and the sugars were separated by gradient elution with aqueous ethanol from charcoal–Celite. The five compounds obtained are given in Table II.

Identification of Methylated Sugars

Preliminary examination of all sugars was carried out by paper chromatography (solvent E) and by paper electrophoresis, using authentic specimens as comparison.

Can. J. Chem. Downloaded from www.nrcresearchpress.com by 210.87.254.5 on 09/05/12
For personal use only.

*2-O-Methyl-*D*-xylose.*—The crystalline sugar had m.p. and mixed m.p. 133–134° and $[\alpha]_D$ +35.5° (*c*, 1.5 in water). Anal. Calc. for $C_6H_{12}O_5$: OCH_3, 18.9%. Found: OCH_3, 18.4%.

*3-O-Methyl-*D*-xylose.*—The sirupy compound had $[\alpha]_D$ +17° (*c*, 1.8 in water). The aniline derivative had m.p. and mixed m.p. 136–137°. Anal. Calc. for $C_6H_{12}O_5$: OCH_3, 18.9%. Found: OCH_3, 18.7%.

*2,3-Di-O-methyl-*D*-xylose.*—The sirup, $[\alpha]_D$ +21.5° (*c*, 1.5 in water), was crystallized from ethyl acetate, m.p. 92°. The aniline derivative had m.p. 130° and $[\alpha]_D$ +194° (*c*, 1.3 in ethyl acetate). Anal. Calc. for $C_7H_{14}O_5$: OCH_3, 34.8%. Found: OCH_3, 34.6%.

*2,3,4-Tri-O-methyl-*D*-xylose.*—This compound, which could not be induced to crystallize, had $[\alpha]_D$ +19.8° (*c*, 2.5 in ethanol). Demethylation gave only xylose. Anal. Calc. for $C_8H_{16}O_5$: OCH_3, 48.4%. Found: OCH_3, 47.6%.

*2,3,5-Tri-O-methyl-*L*-arabinose.*—Demethylation of this sirupy compound gave only arabinose. The 2,3,5-tri-*O*-methyl-L-arabonamide had m.p. 130–132° and $[\alpha]_D$ +17.5° (*c*, 1.0 in water).

Galactoglucomannan A

Periodate oxidation of the polysaccharide gave a consumption of oxidant of 1.20 mole per anhydrohexose residue. The molecular weight of the nitrated polysaccharide (osmometry) was 27,000, corresponding to 76 glucose and mannose residues per average molecule.

Methylation of Galactoglucomannan A

The polysaccharide was methylated successively in the usual way by the Haworth, Kuhn, and Purdie methods to give a product (4.3 g) which exhibited no hydroxyl absorption in the infrared and had $[\alpha]_D$ −7° (*c*, 2.0 in chloroform). Anal. Calc. for a fully methylated hexosan: OCH_3, 45.6%. Found: OCH_3, 45.0%. The molecular weight was 21,400, corresponding to a $\bar{P}_n$ of 84. The product was subjected to methanolysis and hydrolysis and the methylated sugars were separated by gradient elution with aqueous ethanol on charcoal–Celite. Six fractions were obtained, giving the sugars listed in Table III.

Identification of Methylated Sugars

*2,3- and 3,6-Di-O-methyl-*D*-mannose.*—The first fraction was a mixture of these two sugars in an approximate ratio of 10:1, as indicated by paper electrophoresis, using authentic compounds as comparison. Demethylation gave only mannose.

*2,3-Di-O-methyl-*D*-glucose.*—This sugar had $[\alpha]_D$ +45° (*c*, 1.0 in water) and gave only glucose on demethylation. It was chromatographically and electrophoretically identical with an authentic sample.

*2,3,6-Tri-O-methyl-*D*-mannose.*—This sirupy compound had $[\alpha]_D$ −12.2° (*c*, 3.0 in water). The 1,4-di-*p*-nitrobenzoate had m.p. and mixed m.p. 188–189° and $[\alpha]_D$ +33° (*c*, 1.0 in chloroform). The aniline derivative had m.p. and mixed m.p. 125–127° and $[\alpha]_D$ −152° (*c*, 1.0 in methanol).

*2,3,6-Tri-O-methyl-*D*-glucose.*—The crystalline compound had m.p. and mixed m.p. 120–121° and $[\alpha]_D$ +70.5° (*c*, 1.0 in water). The 1,4-di-*p*-nitrobenzoate derivative had m.p. and mixed m.p. 189–190° and $[\alpha]_D$ −33.5° (*c*, 1.0 in chloroform).

*2,3,4,6-Tetra-O-methyl-*D*-galactose.*—The sirupy compound had $[\alpha]_D$ +109° (*c*, 1.0 in water) and gave galactose on demethylation. The aniline derivative had m.p. and mixed m.p. 192–193°.

*2,3,4,6-Tetra-O-methyl-*D*-mannose.*—This fraction on demethylation gave mannose and a trace of glucose and had $[\alpha]_D$ +5.5° (*c*, 4.0 in water).

Partial Hydrolysis of Galactoglucomannan A

The polysaccharide (10 g) was partially hydrolyzed at 98° with 45% aqueous formic acid (200 ml) for 3.5 hours. Chromatographic examination (solvents A, B, and C) indicated the presence of approximately 50% monosaccharides, 30% lower (D.P. 2–6) oligosaccharides and 20% higher oligomers. The mixture (8 g) was resolved on a charcoal–Celite column with 2–35% aqueous ethanol after removal of monosaccharides with water. Many of the oligosaccharides obtained (D.P. 3–6) were further purified by preparative paper chromatography (solvents B and C). The sugars are presented in Table IV in the approximate order in which they were eluted from the column. The 10 oligosaccharides were characterized, whenever possible, through their melting point and specific rotation. Total hydrolysis before and after reduction with sodium borohydride established the component sugars and the nature of the reducing end group. Partial hydrolysis, with or without prior reduction, and characterization by paper chromatography of the oligosaccharides formed yielded information concerning the sequence of the constituent sugar residues. Whenever possible, the degree of polymerization was also determined. The procedures are described in detail only for the two galactose-containing compounds.

*O-α-*D*-Galactopyranosyl-(1 → 6)-O-β-*D*-mannopyranosyl-(1 → 4)-O-β-*D*-mannosyl-(1 → 4)-*D*-mannose.*—This compound had $[\alpha]_D$ −7° (*c*, 3.5 in water) and on complete hydrolysis gave mannose and galactose in a ratio of 3:1. The degree of polymerization was 3.7. Partial hydrolysis yielded 6-*O*-α-D-galactopyranosyl-D-mannose, and (1 → 4)-β-linked mannobiose and mannotriose, all three chromatographically identical with authentic specimens. Complete hydrolysis of the reduced oligosaccharide gave mannose and galactose in a ratio of 2:1.

*O-α-*D*-Galactopyranosyl-(1 → 4)-O-β-*D*-mannopyranosyl-(1 → 4)-O-β-*D*-mannosyl-(1 → 4)-O-β-*D*-mannosyl-(1 → 4)-*D*-mannose.*—This compound had $[\alpha]_D$ −11° (*c*, 2.0 in water) and on total hydrolysis yielded mannose and galactose in a ratio of 4:1. The degree of polymerization was 4.7. Partial hydrolysis gave 6-*O*-α-D-galactopyranosyl-D-mannose, mannobiose, mannotriose, and mannotetraose.

Can. J. Chem. Downloaded from www.nrcresearchpress.com by 210.87.254.5 on 09/05/12
For personal use only.

Galactoglucomannan B

This polysaccharide on oxidation with sodium metaperiodate consumed 1.05 mole of oxidant per anhydrohexose unit. The nitrate derivative had a molecular weight of 27,000, corresponding to 95 glucose and mannose residues per average molecule.

Methylation of Galactoglucomannan B

The polysaccharide (18 g) was methylated in succession by the methods of Haworth, Kuhn, and Purdie to give a material (8.5 g) with $[\alpha]_D$ −23° (*c*, 2.0 in chloroform) and a methoxyl content of 45.1%. Its infrared diagram contained no hydroxyl band. After methanolysis and hydrolysis, the mixture of methylated sugars was resolved by charcoal chromatography into six main fractions.

Identification of Methylated Sugars

*2,3-Di-O-methyl-*D*-glucose and -mannose.*—These sugars had rates of movement on the paper chromatogram and electrophoretogram identical with those of authentic compounds. Demethylation gave glucose and mannose, respectively.

*2,3,6-Tri-O-methyl-*D*-mannose.*—This sirup had $[\alpha]_D$ −11.8° (*c*, 3.5 in water). The 1,4-di-*p*-nitrobenzoate had m.p. and mixed m.p. 188–189° and $[\alpha]_D$ +33° (*c*, 0.6 in chloroform). The aniline derivative had m.p. and mixed m.p. 125–126° and $[\alpha]_D$ −149° (*c*, 0.9 in methanol).

*2,3,6-Tri-O-methyl-*D*-glucose.*—This compound had m.p. and mixed m.p. 120–121° and $[\alpha]_D$ +69° (*c*, 3.1 in water).

*2,3,4,6-Tetra-O-methyl-*D*-galactose.*—Demethylation of this fraction, which had $[\alpha]_D$ +101° (*c*, 1.0 in water), gave galactose with traces of glucose and mannose.

*2,3,4,6-Tetra-O-methyl-*D*-mannose.*—This fraction gave mannose on demethylation and had $[\alpha]_D$ +5.3° (*c*, 3.3 in water).

Partial Hydrolysis of Galactoglucomannan B

Partial hydrolysis was carried out as described for galactoglucomannan A. The sugar mixture was resolved by a combination of charcoal and paper chromatography to give 13 oligosaccharides, given in Table IV in the approximate order in which they were eluted from the charcoal column. The oligomers were characterized as described above.

ACKNOWLEDGMENTS

The authors are thankful to Dr. R. L. Whistler, Purdue University, for a generous gift of 6-*O*-α-D-galactopyranosyl-D-mannose. Financial support from the National Research Council of Canada is also acknowledged. E. C. A. Schwarz wishes to express his gratitude to the American Viscose Corporation and the National Research Council of Canada for financial assistance.

REFERENCES

1. G. O. Aspinall. Advan. Carbohydrate Chem. **14**, 429 (1959).
2. T. E. Timell. Svensk Papperstid. **64**, 651, 685, 744, 748 (1961); **65**, 843 (1962).
3. S. S. Bhattacharjee and T. E. Timell. Unpublished results.
4. A. J. Roudier and L. Eberhard. Bull. Soc. Chim. France, 2074 (1960); 976 (1961).
5. S. K. Banerjee and T. E. Timell. Tappi, **43**, 849 (1960).
6. R. H. Marchessault and T. E. Timell. To be published.
7. C. N. Riiber and N. A. Sörensen. Kgl. Norske Videnskab. Selskabs, Skrifter, No. 1 (1938).
8. T. E. Timell. Unpublished results.
9. B. G. Lindberg. Personal communication (August 1960).
10. O. Perila and C. T. Bishop. Can. J. Chem. **39**, 815 (1961).
11. H. Meier. Acta Chem. Scand. **14**, 749 (1960).
12. K. Freudenberg. Tannin, Cellulose und Lignin. Julius Springer Verlag, Berlin. 1933. pp. 90, 104.
13. H. Meier. Biochim. Biophys. Acta, **28**, 229 (1958).
14. G. O. Aspinall, E. L. Hirst, E. G. V. Percival, and I. R. Williamson. J. Chem. Soc. 3184 (1953).
15. G. O. Aspinall, R. B. Rashbrook, and G. Kessler. J. Chem. Soc. 215 (1958).
16. H. Meier. Acta Chem. Scand. **15**, 1381 (1961).
17. R. D. Gibbs. *In* The physiology of forest trees. *Edited by* K. V. Thimann. 269 (1958).
18. T. G. Bonner, E. J. Bourne, and S. McNally. J. Chem. Soc. 2929 (1960).
19. C. P. J. Glaudemans and T. E. Timell. Svensk Papperstid. **61**, 1 (1958).
20. S. Peat, W. J. Whelan, and J. G. Roberts. J. Chem. Soc. 2258 (1956).
21. T. E. Timell. Svensk Papperstid. **63**, 668 (1960).
22. T. E. Timell, C. P. J. Glaudemans, and A. L. Currie. Anal. Chem. **28**, 1916 (1956).
23. T. E. Timell. Tappi, **40**, 568 (1957).
24. T. E. Timell. Can. J. Chem. **37**, 827 (1959).
25. L. E. Wise, M. Murphy, and A. A. D'Addieco. Paper Trade J. **122**, No. 2, 35 (1946).
26. R. Kuhn, H. Trischmann, and I. Löw. Angew. Chem. **67**, 32 (1955).

Can. J. Chem. Downloaded from www.nrcresearchpress.com by 210.87.254.5 on 09/05/12
For personal use only.

CONSTITUTION OF THREE HEMICELLULOSES FROM THE WOOD OF ENGELMANN SPRUCE (PICEA ENGELMANNI)

A. R. MILLS[1] AND T. E. TIMELL[2]

Department of Chemistry, McGill University, and the Pulp and Paper Research Institute of Canada, Montreal, Que.

Received January 14, 1963

ABSTRACT

An arabino-4-*O*-methylglucuronoxylan (10:70:12), a water-soluble galactoglucomannan (1:1:3), and an alkali-soluble galactoglucomannan (0.2:1:3) have been isolated in yields of 8.0, 1.0, and 8.1% from the wood of Engelmann spruce (*Picea engelmanni*). The xylan consisted of a linear framework of (1 → 4)-linked β-D-xylose residues to which were directly attached single side chains of (1 → 2)-linked 4-*O*-methyl-α-D-glucuronic acid and (1 → 3)-linked α-L-arabinofuranose residues. The galactoglucomannans were both composed of a backbone of (1 → 4)-linked β-D-mannose and β-D-glucose residues, some of which carried directly attached side chains of (1 → 6)-linked α-D-galactopyranose residues. Partial hydrolysis of the water-soluble galactoglucomannan yielded, among other oligosaccharides, a trisaccharide composed of galactose, glucose, and mannose residues. It is concluded that the main polysaccharides in the wood of Engelmann spruce are the same as those in most other gymnosperms. In the bark of this tree, the water-soluble galactoglucomannan is replaced by one or several polysaccharides of an entirely different composition.

Can. J. Chem. Downloaded from www.nrcresearchpress.com by 210.87.254.40 on 09/05/12
For personal use only.

In connection with a study of the polysaccharides occurring in the bark of Engelmann spruce (*Picea engelmanni* Parry), it became of interest to establish the nature of the hemicelluloses present in the wood of the same species, thus making possible a comparison. The present paper is concerned with the isolation and constitution of the three main hemicelluloses in Engelmann spruce wood.

RESULTS AND DISCUSSION

Partial acid hydrolysis of the wood gave three sugar acids, namely galacturonic acid, 4-*O*-methylglucuronic acid, and 2-*O*-(4-*O*-methyl-α-D-glucosyluronic acid)-D-xylopyranose, the last two probably originating from an acidic xylan.

Extraction of chlorite holocellulose with alkali and application of the barium hydroxide method as described earlier (1) gave an arabino-4-*O*-methylglucuronoxylan and two galactoglucomannans, the properties of which are summarized in Table I. Since the wood contained approximately 24% hemicelluloses, the total recovery was 75%. Losses occurred in the isolation of galactoglucomannan A, but it is nevertheless probable that the present wood contained less of this hemicellulose than did other softwoods (2). The degree of polymerization of the same polysaccharide was higher than that of other galacotglucomannans of this type (2). This might have been the result of a preferential loss of low molecular weight material during the isolation. In other respects, the three hemicelluloses appeared to be typical of those generally occurring in the wood of gymnosperms.

After complete methylation, the xylan contained 88 xylose residues per average molecule and on methanolysis and hydrolysis gave the six compounds given in Table II. The results show that the xylan consisted of at least 90 (1 → 4)-linked β-D-xylose residues, forming a framework to which were directly attached (1 → 3)-linked L-arabinofuranose and (1 → 2)-linked 4-*O*-methyl-α-D-glucuronic acid residues. Evidence presented elsewhere (3) indicates that the former groups were probably present in the α-L-configuration. Partial

[1]*Present address: Shell Development Company, Emeryville 8, Calif.*
[2]*Present address: Department of Forest Chemistry, State University College of Forestry, Syracuse, N.Y.*

Can. J. Chem. Downloaded from www.nrcresearchpress.com by 210.87.254.40 on 09/05/12
For personal use only.

TABLE I
General characteristics of hemicelluloses

Polysaccharide	Percentage of wood	$[\alpha]_D$, deg	Solvent	$\bar{P}_n$	Constituent sugar residues						Branch points per average molecule	Periodate consumed per repeating unit	
					Gal	Glu	Man	Ara	Xyl	Uron. acid		Calc.	Found
Arabino-4-*O*-methyl-glucuronoxylan	8.0	−35	Water	92				10	70	12	None	80	80
Galactoglucomannan A	1.8	−7	Water	100	1	1	3				One	6.0	5.9
Galactoglucomannan B	8.1	−40	Alkali	107	0.2	1	3				None	4.4	4.2

TABLE II

Sugars obtained on hydrolysis of original (A) and partially hydrolyzed (B) *O*-methylxylans

Component	Moles A	Moles B	Component	Moles A	Moles B
2-*O*-Methyl-D-xylose	8	2	2,3,4-Tri-*O*-methyl-D-xylose	1	1
3-*O*-Methyl-D-xylose	2	4	2,3,5-Tri-*O*-methyl-L-arabinose	9	0.1
2,3-Di-*O*-methyl-D-xylose	49	55	2-*O*-(2,3,4-Tri-*O*-methyl-α-D-glucuronic acid)-3-*O*-methyl-D-xylopyranose	10	12

hydrolysis of the arabino-4-*O*-methylglucuronoxylan gave a 4-*O*-methylglucuronoxylan almost devoid of arabinose but with nearly the same degree of polymerization (82). The relative amounts and the nature of the sugars obtained on hydrolysis of this polysaccharide (Table II) show that removal of the arabinose groups produced no additional non-reducing xylose end groups in the macromolecule. *All* arabinose residues were accordingly attached directly to the xylan backbone. In addition, it is also clear that the original polysaccharide was linear.

The two galactoglucomannans, after complete methylation, contained 93 and 103 glucose and mannose residues per average molecule. The sugars obtained on hydrolysis are presented in Table III. Both polysaccharides evidently consisted of a backbone of

TABLE III

Sugars obtained on hydrolysis of methylated galactoglucomannans A and B

Component	Moles A	Moles B	Component	Moles A	Moles B
2,3-Di-*O*-methyl-D-mannose	4	1.2	2,3,6-Tri-*O*-methyl-D-glucose	8	18
2,3-Di-*O*-methyl-D-glucose	4	0.7	2,3,4,6-Tetra-*O*-methyl-D-galactose	8	2
2,3,6-Tri-*O*-methyl-D-mannose	25	56	2,3,4,6-Tetra-*O*-methyl-D-mannose	1	1

approximately 100 (1 → 4)-linked β-D-mannose and β-D-glucose residues to which were attached various amounts of (1 → 6)-linked α-D-galactopyranose end groups. Galactoglucomannan A contained on the average 1.2 and compound B 0.3 branch points per molecule.

These conclusions were corroborated by the nature of the oligosaccharides obtained on partial hydrolysis of the two polysaccharides, given in Table IV. The occurrence of a galactopyranosyl-(1 → 6)-mannosyl-(1 → 4)-mannose suggests that the galactose residues were attached directly to the glucomannan framework in galactoglucomannan A. The isolation of a trisaccharide consisting of galactose, glucose, and mannose residues is noteworthy. This compound, albeit not fully characterized, was chromatographically homogeneous in several solvent systems. Its composition offers the first proof of a chemical linkage between galactose, glucose, and mannose residues in this type of wood. It also constitutes strong evidence for the triheteropolymer nature of the water-soluble galactoglucomannans occurring in the wood of all gymnosperms so far investigated (2, 4). That the latter should consist of a mixture of a galactomannan and a glucomannan, as has been suggested (5), now appears highly unlikely.

Results obtained on oxidation of the three polysaccharides with periodate are given in Table I. The data agree well with the other structural evidence.

Can. J. Chem. Downloaded from www.nrcresearchpress.com by 210.87.254.40 on 09/05/12
For personal use only.

Can. J. Chem. Downloaded from www.nrcresearchpress.com by 210.87.254.40 on 09/05/12
For personal use only.

TABLE IV

Oligosaccharides obtained on hydrolysis of galactoglucomannans A and B

		Galactoglucomannan A			Galactoglucomannan B		
Oligosaccharide*	R_C†	Weight, %	M.p., °C	$[\alpha]_D$, deg‡	Weight, %	M.p., °C	$[\alpha]_D$, deg
Mannobiose	1.15	6.4	200–202	−9	3.8	210–211	−9
Cellobiose	1.00	0.2	219–220§	+32	0.2	231–232	+34
Mannosyl glucose	0.71	1.3	197–198	+24	0.6	168–170	+22
Glucosyl mannose	1.65	1.3	180–182	+12	1.3	180–182	+8
Mannotriose	0.33	2.8			3.0	170–171	−21
Mannotetraose	0.16				0.3	230–232	−30
Mannosyl glucosyl mannose	0.46				1.0		−15
Glucosyl mannosyl mannose	0.23	0.8					
Galactosyl mannosyl mannose	0.45	0.5					
A triose (galactose, glucose, mannose)	0.63	0.2					

*β-D-Mannosyl-(1 → 4)-, β-D-glucosyl-(1 → 4)-, α-D-galactopyranosyl-(1 → 6)-.
†Rate of movement on the paper chromatogram relative to cellobiose in *n*-butanol–pyridine–water (10:3:3).
‡In water.
§Octaacetate derivative.

The principal hemicelluloses in Engelmann spruce wood are the same as those found in the wood of other gymnosperms, such as Norway spruce (6–10), Sitka spruce (11, 12), and white spruce (13, 14). In amabilis fir, the same three hemicelluloses occur both in the wood and the bark of the tree (1). Interestingly enough, this is not the case with Engelmann spruce. The bark of this tree contains an alkali-soluble galactoglucomannan and probably also an acidic arabinoxylan. The water-soluble galactoglucomannan, however, is entirely missing, its place being taken by one or several polysaccharides of an entirely different composition (15). The nature of these hemicelluloses will form the subject of a later communication.

EXPERIMENTAL

General experimental conditions and methods of paper chromatography were the same as those used in an earlier paper (1).

Wood

Standard analytical methods showed that the wood (40–60 mesh, extractive free) contained 43% cellulose, 28.0% lignin, 9.2% pentosans, 3.3% uronic anhydride, 1.3% acetyl, and 0.3% ash.

Acidic Sugars

Wood meal (100 g) was hydrolyzed with sulphuric acid, acidic sugars in the hydrolyzate were separated from neutral sugars, and the mixture of uronic acids was finally resolved by charcoal chromatography as described earlier (1). Three fractions were obtained. The first (0.50 g) consisted of galacturonic acid. The second was an *O*-methylated hexuronic acid (1.20 g) with $[\alpha]_D$ +50° (*c*, 1.7 in water). Anal. Calc. for $C_7H_{12}O_7$: OCH_3, 15.0%; equiv. wt., 208. Found: OCH_3, 15.0%; equiv. wt., 203. Reduction of the methyl ester methyl glycoside with lithium aluminum hydride gave a compound chromatographically identical with 4-*O*-methyl-D-glucose, $[\alpha]_D$ +47° (*c*, 2.0 in water). Anal. Calc. for $C_7H_{14}O_6$: OCH_3, 16.0%. Found: OCH_3, 16.1%. The third fraction (2.5 g) was an aldobiouronic acid with $[\alpha]_D$ +84° (*c*, 1.8 in water), giving 4-*O*-methylglucuronic acid and xylose in hydrolysis. The tetraacetate derivative of its methyl ester methyl glycoside had m.p. and mixed m.p. 201–202° and $[\alpha]_D$ +98° (*c*, 1.0 in chloroform). Anal. Calc. for $C_{22}H_{32}O_{15}$: OCH_3, 17.3%. Found: OCH_3, 17.3%. Its infrared diagram was identical with that of an authentic sample.

Isolation of Hemicelluloses

Chlorite holocellulose (890 g, 72% of wood) was extracted with aqueous potassium hydroxide and the mixture of polysaccharides (180 g, 14.5% of the wood) was resolved by the barium hydroxide method into an arabino-4-*O*-methylglucuronoxylan (98 g, 8.0%) and galactoglucomannan A (22 g, 1.8%) as described previously (1). The residual holocellulose was extracted with aqueous sodium hydroxide – borate to give galactoglucomannan B (100 g, 8.1%).

Xylan

When oxidized with 0.05 *M* sodium metaperiodate, the xylan consumed 80 moles of oxidant per repeating unit. The number-average molecular weight of the acetate derivative, as determined by osmometry, was 26,200, corresponding to a degree of polymerization of 92.

Methylation of the Xylan

The xylan (20 g) was methylated by the procedures of Haworth and Kuhn to give a fully methylated derivative with $[\alpha]_D$ −56° (*c*, 1.0 in chloroform) and no hydroxyl band in its infrared spectrum. Anal. Calc. for the fully methylated and esterified xylan: OCH_3, 39.6%. Found: OCH_3, 39.2%. The molecular weight (osmometry) was 20,600 ($\bar{P}_n$ = 88).

After methanolysis, the acid (1.71 g) and the neutral (5.60 g) glycosides were separated with exchange resin. The methyl ester of the acid fraction was reduced with lithium aluminum hydride, giving methyl 2-*O*-(2,3,4-tri-*O*-methyl-α-D-glucosyl)-3-*O*-methyl-α,β-D-xylopyranoside, m.p. and mixed m.p. 167–168° and $[\alpha]_D$ +84° (*c*, 1.0 in water). Hydrolysis gave 3-*O*-methylxylose and 2,3,4-tri-*O*-methylglucose. Anal. Calc. for $C_{16}H_{30}O_{10}$: OCH_3, 40.6%. Found: OCH_3, 40.7%. The infrared spectrum of the compound was the same as that of an authentic sample.

The mixture of neutral glycosides was hydrolyzed and resolved on charcoal–Celite by gradient elution with aqueous ethanol, giving six partly methylated compounds (Table II).

*2-O-Methyl-*D*-xylose.*—This compound (315 mg) had m.p. and mixed m.p. 134–135° and $[\alpha]_D$ +30° (*c*, 1.2 in methanol). Anal. Calc. for $C_6H_{12}O_5$: OCH_3, 18.9%. Found: OCH_3, 18.5%.

*3-O-Methyl-*D*-xylose.*—This sirup (66 mg) had $[\alpha]_D$ +18° (*c*, 1.2 in water) and gave an aniline derivative with m.p. and mixed m.p. 134–135°. Anal. Found: OCH_3, 18.6%.

*2,3-Di-O-methyl-*D*-xylose.*—This fraction (2.15 g) contained no 3,4-di-*O*-methylxylose as indicated by paper electrophoresis. Crystallization from ethanol gave a product with m.p. 98–100° and $[\alpha]_D$ +24° (*c*, 1.7 in water). Anal. Calc. for $C_7H_{14}O_5$: OCH_3, 34.8%. Found: OCH_3, 34.7%. The aniline derivative, when

Can. J. Chem. Downloaded from www.nrcresearchpress.com by 210.87.254.40 on 09/05/12
For personal use only.

crystallized from ethyl acetate, had m.p. 140–142° and $[\alpha]_D$ +197° (*c*, 2.3 in ethyl acetate). Anal. Calc. for $C_{13}H_{19}O_4N$: OCH_3, 24.5%. Found: OCH_3, 23.5%.

*2,3,4-Tri-O-methyl-*D*-xylose.*—This compound (47 mg), when crystallized from benzene, had m.p. and mixed m.p. 90–91° and $[\alpha]_D$ +17° (*c*, 0.9 in ethanol). Anal. Calc. for $C_8H_{16}O_5$: OCH_3, 48.4%. Found: OCH_3, 48.2%.

*2,3,5-Tri-O-methyl-*L*-arabinose.*—This sirup had $[\alpha]_D$ −27° (*c*, 0.7 in water) and gave only arabinose on demethylation with boron trichloride. Anal. Found: OCH_3, 48.0%. The 2,3,5-tri-*O*-methyl-L-arabonamide had m.p. 129–130°.

Methylation of the Partially Hydrolyzed Xylan

Arabino-4-*O*-methylglucuronoxylan (20 g) was dissolved in aqueous hydrochloric acid (350 ml) and the pH adjusted to 2.3. After being kept at 90° for 4 hours, the solution was poured into ethanol (4 liters) and the precipitate (14.2 g) was collected. Chromatographic analysis indicated only traces of arabinose residues. The partly hydrolyzed xylan (14 g) was methylated in the usual way to give a product (8 g) which contained no hydroxyl groups and had a methoxyl content of 39.8%. The partially methylated sugars obtained on hydrolysis (3.5 g) were resolved by charcoal chromatography to give four compounds and a trace of tri-*O*-methylarabinose. 2-*O*-Methylxylose (95 mg) and 3-*O*-methylxylose (192 mg) were only characterized chromatographically.

*2,3-Di-O-methyl-*D*-xylose.*—This compound (2.79 g) had m.p. and mixed m.p. 98–100° and $[\alpha]_D$ +25° (*c*, 1.6 in water). Anal. Found: OCH_3, 34.4%. The aniline derivative had m.p. and mixed m.p. 140–142°.

*2,3,4-Tri-O-methyl-*D*-xylose.*—This sugar (55 mg) had m.p. and mixed m.p. 91–92° and $[\alpha]_D$ +17° (*c*, 1.2 in ethanol). Anal. Found: OCH_3, 48.3%.

Galactoglucomannan A

The galactoglucomannan, after three precipitations with barium hydroxide, contained residues of galactose, glucose, and mannose in a ratio of 1:1:3. This ratio remained unchanged after one additional precipitation with Fehling's solution. The polysaccharide consumed 1.18 mole of periodate per anhydrohexose residue. The molecular weight of the nitrate derivative was 35,000 ($\bar{P}_n$ = 100).

Methylation of Galactoglucomannan A

Galactoglucomannan A (15 g) was methylated successively by the procedures of Haworth, Kuhn, and Purdie to give an almost fully substituted product (5 g). Anal. Calc. for a fully methylated hexosan: OCH_3, 45.6%. Found: OCH_3, 45.0%. The molecular weight was 23,800 ($\bar{P}_n$ = 93). Methylated sugars obtained on hydrolysis (0.5 g) were separated by preparative paper chromatography (solvent E) to give six fractions.

*2,3-Di-O-methyl-*D*-mannose.*—This fraction (30 mg) on demethylation gave mannose and a small amount of glucose. Paper electrophoresis indicated the presence of the 2,3-derivative.

*2,3-Di-O-methyl-*D*-glucose.*—Demethylation of this fraction (29 mg) gave only glucose. The sugar was chromatographically and electrophoretically identical with an authentic specimen.

*2,3,6-Tri-O-methyl-*D*-mannose.*—This sirupy sugar (206 mg) had $[\alpha]_D$ −7° (*c*, 1.1 in water). The di-*p*-nitrobenzoate derivative had m.p. and mixed m.p. 187–188°.

*2,3,6-Tri-O-methyl-*D*-glucose.*—The crystalline sugar (64 mg) had m.p. and mixed m.p. 118–119° and $[\alpha]_D$ +72° (*c*, 1.0 in water).

*2,3,4,6-Tetra-O-methyl-*D*-galactose.*—The sirup (67 mg) had $[\alpha]_D$ +109° (*c*, 2.3 in water). The aniline derivative had m.p. and mixed m.p. 190–191° and $[\alpha]_D$ −135° (*c*, 0.3 in pyridine).

*2,3,4,6-Tetra-O-methyl-*D*-mannose.*—This fraction (9 mg) had $[\alpha]_D$ +17° (*c*, 0.9 in chloroform) and on demethylation gave mannose only.

Partial Hydrolysis of Galactoglucomannan A

The hemicellulose (10 g) was treated with 45% aqueous formic acid (400 ml) at 100° for 2 hours. Yield: 9.4 g. Oligosaccharides were separated by gradient elution with aqueous ethanol from a charcoal–Celite column and further purified by preparative paper chromatography. The eight oligosaccharides obtained are given in Table IV.

Galactosyl mannosyl mannose.—This sugar contained galactose and mannose in a ratio of 1:2. Partial hydrolysis gave mannobiose and a compound chromatographically identical with 6-*O*-α-D-galactopyranosyl-D-mannose.

Glucosyl mannosyl mannose.—This trisaccharide gave glucose and mannose in a ratio of 1:2 on complete hydrolysis while partial hydrolysis gave glucosyl mannose and mannobiose.

A triose (galactosyl glucosyl mannose).—This trisaccharide was chromatographically homogeneous in several solvent systems. Complete hydrolysis gave galactose, glucose, and mannose in equimolar portions while partial hydrolysis gave glucosyl mannose. After reduction with sodium borohydride, only galactose and glucose were observed.

Galactoglucomannan B

After two precipitations with barium hydroxide, galactoglucomannan B contained residues of galactose, glucose, and mannose in a ratio of 0.2:1:3. Fehling's solution was less suited for removal of residual xylan. The hemicellulose consumed 1.02 mole of periodate per anhydrohexose unit. The nitrate derivative had a molecular weight of 37,500 ($\bar{P}_n$ = 107).

Can. J. Chem. Downloaded from www.nrcresearchpress.com by 210.87.254.40 on 09/05/12
For personal use only.

Methylation of Galactoglucomannan B

The polysaccharide (15 g) was methylated successively by the methods of Haworth, Kuhn, and Purdie to give a product (7 g) with a methoxyl content of 44.8% and a molecular weight of 22,700 ($\bar{P}_n$ = 103). The mixture of partly methylated sugars obtained on hydrolysis (1.5 g) was resolved by preparative paper chromatography (solvent E) to give six fractions.

*2,3-Di-O-methyl-*D*-mannose and -glucose.*—These two compounds (18 and 11 mg) on demethylation gave mannose and glucose, respectively. They were tentatively characterized from their behavior on paper chromatography and electrophoresis.

*2,3,6-Tri-O-methyl-*D*-mannose.*—This sirupy compound (859 mg), $[\alpha]_D$ −10° (*c*, 2.3 in water), gave a di-*p*-nitrobenzoate derivative with m.p. and mixed m.p. 188–189° and $[\alpha]_D$ +33° (*c*, 1.0 in chloroform).

*2,3,6-Tri-O-methyl-*D*-glucose.*—This sugar (282 mg) had m.p. and mixed m.p. 117–118° and $[\alpha]_D$ +70° (*c*, 1.7 in water).

*2,3,4,6-Tetra-O-methyl-*D*-galactose.*—The sirup (30 mg), $[\alpha]_D$ +95° (*c*, 0.7 in water), gave only galactose on demethylation. The aniline derivative had m.p. and mixed m.p. 192–193° and $[\alpha]_D$ −135° (*c*, 0.7 in pyridine).

*2,3,4,6-Tetra-O-methyl-*D*-mannose.*—This fraction had $[\alpha]_D$ +25° (*c*, 0.5 in chloroform) and gave mannose on demethylation.

Partial Hydrolysis of Galactoglucomannan B

Galactoglucomannan B (20 g) was treated with 45% aqueous formic acid (400 ml) at 100° for 3 hours to give a mixture of glycoses (14 g). The oligosaccharides were separated in the usual way to give the compounds presented in Table IV.

Mannosyl glucosyl mannose.—Complete hydrolysis of this compound gave mannose and glucose in a ratio of 2:1. Partial hydrolysis yielded mannosyl glucose and glucosyl mannose.

ACKNOWLEDGMENT

The authors wish to express their gratitude to the National Research Council of Canada for financial assistance.

REFERENCES

1. E. C. A. Schwarz and T. E. Timell. Can. J. Chem. This issue.
2. T. E. Timell. Tappi, **44**, 88 (1961); **45**, 734, 799 (1962).
3. R. H. Marchessault and T. E. Timell. To be published.
4. J. K. Hamilton, E. V. Partlow, and N. S. Thompson. J. Am. Chem. Soc. **82**, 451 (1960).
5. H. Meier. Acta Chem. Scand. **14**, 749 (1960).
6. J. Saarnio. Suomen Kemistilehti, B, **29**, 35 (1956).
7. G. O. Aspinall and M. O. Carter. J. Chem. Soc. 3744 (1956).
8. B. Lindberg and H. Meier. Svensk Papperstid. **60**, 785 (1957).
9. I. Croon and B. Lindberg. Acta Chem. Scand. **12**, 453 (1958).
10. A. J. Morak and K. Ward, Jr. Tappi, **44**, 12 (1961).
11. G. O. Aspinall, R. A. Laidlaw, and R. B. Rashbrook. J. Chem. Soc. 4444 (1957).
12. G. G. S. Dutton and K. Hunt. J. Am. Chem. Soc. **80**, 4420, 5697 (1958); **82**, 1682 (1960).
13. G. A. Adams. Can. J. Chem. **37**, 29 (1959).
14. A. Tyminski and T. E. Timell. J. Am. Chem. Soc. **82**, 2823 (1960).
15. K. V. Ramalingam and T. E. Timell. Unpublished results.

Can. J. Chem. Downloaded from www.nrcresearchpress.com by 210.87.254.40 on 09/05/12
For personal use only.

REACTIONS OF IODINE ATOMS WITH *n*-BUTENES

I. CIS–TRANS ISOMERIZATION OF BUTENE-2[1]

MARGARET H. BACK[2] AND R. J. CVETANOVIĆ
Division of Applied Chemistry, National Research Council, Ottawa, Canada

Received January 28, 1963

ABSTRACT

In the interaction of iodine atoms with butene-2 at 65° C no addition products are observed although cis–trans isomerization of the butene occurs readily. Iodine atoms have been generated by photolyzing iodine in three spectral regions. The limiting quantum yield of the isomerization reaction is about 0.1 at 4358 Å. The low quantum yield shows that chain reactions, similar to those observed in olefin photochlorinations and photobrominations, do not take place. A mechanism involving initial formation of π-complexes between iodine atoms and butene-2 is tentatively considered.

Can. J. Chem. Downloaded from www.nrcresearchpress.com by 210.87.254.6 on 09/05/12
For personal use only.

INTRODUCTION

A study of the relative rates of addition of various reagents to olefins in the gas phase has been in progress for the past several years (1). Such studies provide information on the nature of the process of addition to double bonds and whether in this process the attacking species behaves as an electrophilic, nucleophilic, or radical reagent. The variation of the rate constants for addition with structure of the olefins has shown that in their reactions with olefins, oxygen atoms (2) and ozone (3) behave as electrophilic reagents, while hydrogen atoms (4) have the character of radical (electroneutral) reagents. As an extension of this series a study of the addition of iodine atoms to olefins was begun and this paper reports the first results.

The photoiodination of the butenes, propylene, and ethylene in chloroform solution was studied by Forbes and Nelson (5) and quantum yields for disappearance of iodine were found to be of the order of 1. The addition product of iodine atoms with the butenes, diiodobutane, was found to be unstable at room temperature and the reaction was done at −70° C. Since the diiodobutane was not stable at temperatures required for the gas phase study (6), butene-2 was chosen for the reference olefin in the present work in the hope that the cis–trans isomerization would provide a measure of the rate of reaction of iodine atoms with the double bond.

EXPERIMENTAL

Materials

Reagent grade iodine was sublimed once and sealed off in a reservoir. Phillips Research Grade butene was used after two bulb-to-bulb distillations. *cis*-Butene was found to contain less than 0.1% *trans*-butene. Oxygen was prepared by heating potassium permanganate, and Red-band grade of nitrogen was obtained from Linde Air Company.

Apparatus

The experiments were done in a cylindrical Pyrex cell 10 cm long and 5 cm in diameter. A high-pressure mercury arc lamp, Mazda type ME/D, was used and a roughly parallel beam was obtained using a 250-cc flask as a spherical lens. A 935 phototube and microammeter, placed beyond the reaction vessel, were used to measure relative light intensities. The lamp, flask, reaction cell, and phototube were mounted on an optical bench and the reaction cell was enclosed in a thermostatted oven.

For experiments with light of wavelength greater than 5000 Å, Corning filter 3-69 was used and the

[1]*Issued as N.R.C. No. 7294.*

[2]*National Research Council Postdoctoral Fellow 1959–1961. Present address: Chemistry Department, University of Ottawa, Ottawa, Canada.*

flask was filled with a dilute solution of copper sulphate. For some experiments a solution of $NdCl_3$ (7) was used to isolate the mercury line 5461 Å. For light of wavelength less than 5000 Å, a filter solution was made of 6.2 g of copper sulphate and 75 cc of concentrated ammonium hydroxide diluted to 1 liter (8). The flask provided a path length of about 8 cm for absorption. To isolate the mercury line 4358 Å, Corning filter 3-74 was used with this solution.

A few experiments were done using a low-pressure mercury resonance lamp and Corning filter 7-54. In this case a quartz reaction vessel of similar dimensions replaced the Pyrex cell and the flask was not used.

Iodine was admitted to the reaction vessel at its equilibrium vapor pressure from a constant-temperature reservoir through a heated stopcock. The pressure was calculated from the expression (9)

$$\log_{10} p_{\text{atm}} = -\frac{3512.8}{T} - 2.013 \log_{10} T + 13.3740.$$

The reaction vessel and iodine reservoir were separated from the main manifold by a large trap filled with glass beads and maintained at −78° C. This provided an effective means of keeping iodine from the main manifold and mercury from the reaction vessel.

Procedure

It was found necessary, in order to eliminate heterogeneous reaction, to avoid condensation of butene and iodine together. After allowing the iodine pressure to equilibrate for 10 minutes the reservoir was closed and butene admitted by momentarily connecting the reaction vessel to a bulb containing the appropriate quantity of gaseous butene. The pressure of butene always exceeded that of iodine so that no iodine escaped the cell. Nitrogen and oxygen were admitted in a similar manner from a much larger reservoir and in this case the pressure of nitrogen or oxygen was much greater than the combined pressures of iodine and butene.

Pressures of iodine ranged from 0.5 mm to 5 mm and of butene from 1 to 25 cm. Highest pressure of nitrogen used was 46 cm and of oxygen 20 cm. Most of the experiments were done at 65° C and at conversions of about 2%, where a back reaction could be neglected. Fine copper or nickel screens were used to reduce the incident light intensity.

Analysis

The hydrocarbon products were analyzed on a 50-ft gas chromatographic column of dimethylsulpholane on firebrick at 25° C.

Measurement of Light Intensity

Potassium ferrioxalate was used as an external actinometer (10) with light of wavelengths 4358 Å and 2537 Å. A cylindrical cell about 1 cm thick and of the same diameter as the reaction cell was placed first in front of and then behind the reaction vessel, and measurements were taken with and without iodine in the vessel.

RESULTS

The reaction of iodine atoms with *cis*-butene-2 caused isomerization to *trans*-butene-2 and at conversions of less than 3% no other products were observed. Experiments with long times of irradiation showed that the final ratio of *trans*-butene/*cis*-butene approached the equilibrium value at 65° C, 0.726 (11). Even at these high conversions there was no evidence for the formation of heavier products and it may be assumed that the diiodobutane was not an important product.

Several series of experiments were done with constant iodine pressure and variable butene pressure, utilizing light from three spectral regions for production of iodine atoms: region (*a*) $\lambda > 5000$ Å; region (*b*) $\lambda < 5000$ Å; region (*c*) $\lambda = 2537$ Å. Only wavelengths transmitted by Pyrex were included in region (*b*). The two regions (*a*) and (*b*) correspond to the banded region and the continuum, respectively, of the iodine spectrum. In the banded region predissociation occurs, yielding two ground state atoms (12), while in the continuum direct dissociation gives one ground state, $^2P_{3/2}$, and one excited state, $^2P_{1/2}$, atom (13).

In regions (*a*) and (*b*) the initial rapid increase in the rate as the butene pressure was increased was followed by a much slower increase at higher butene pressures. Typical series of results are shown in Fig. 1(*a*, *b*, and *c*). A few series of experiments were done with constant butene pressure and variable iodine pressure, with incident light of wave-

Can. J. Chem. Downloaded from www.nrcresearchpress.com by 210.87.254.6 on 09/05/12
For personal use only.

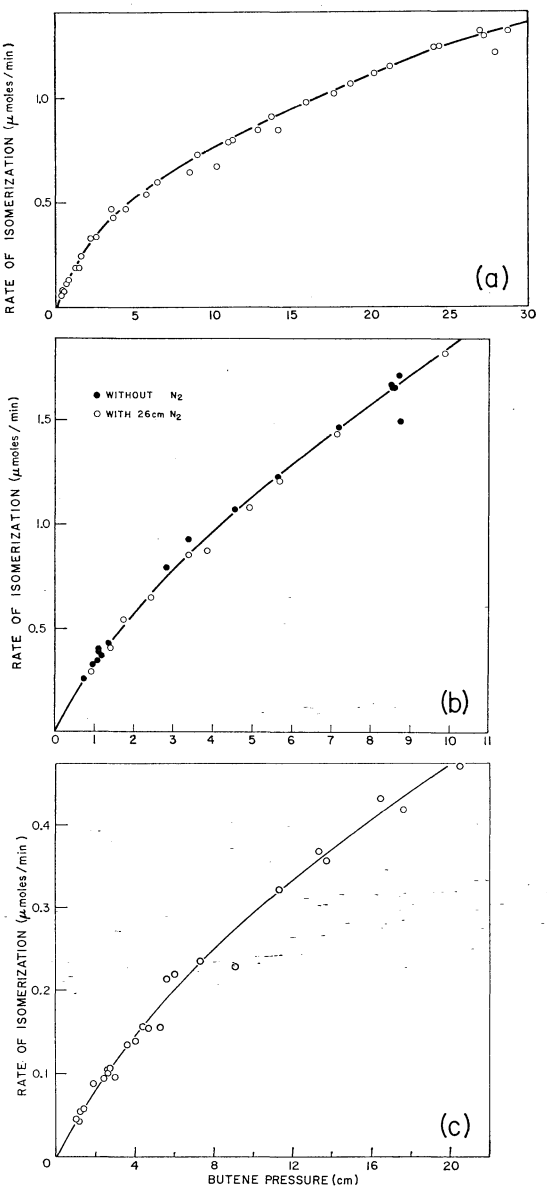

FIG. 1(*a*). Dependence of rate of isomerization on butene pressure at wavelengths > 5000 Å (temp. 54° C, iodine pressure 2 mm).

(*b*). Effect of nitrogen additions on the rate of isomerization at wavelengths > 5000 Å (temp. 65° C, iodine pressure 4 mm).

(*c*). Dependence of rate of isomerization on butene pressure at 4358 Å (temp. 65° C, iodine pressure 4 mm).

length greater than 5000 Å, one of which is shown in Fig. 2. In this case a limiting rate was reached at about 4 mm of iodine.

The dependence of the rate on the absorbed light intensity at various pressures of iodine and of butene is shown in Fig. 3(*a–f*). At high light intensities the rate was a linear function of the intensity, but in each case extrapolated to a small positive intercept.

Can. J. Chem. Downloaded from www.nrcresearchpress.com by 210.87.254.6 on 09/05/12
For personal use only.

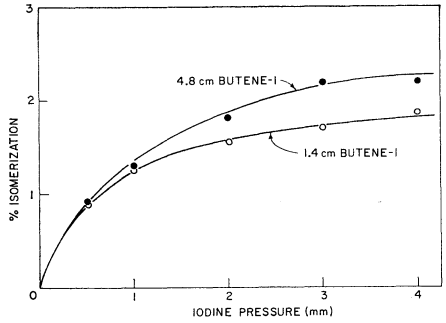

FIG. 2. Dependence of rate of isomerization on iodine pressure (temp. 65° C, wavelength > 5000 Å).

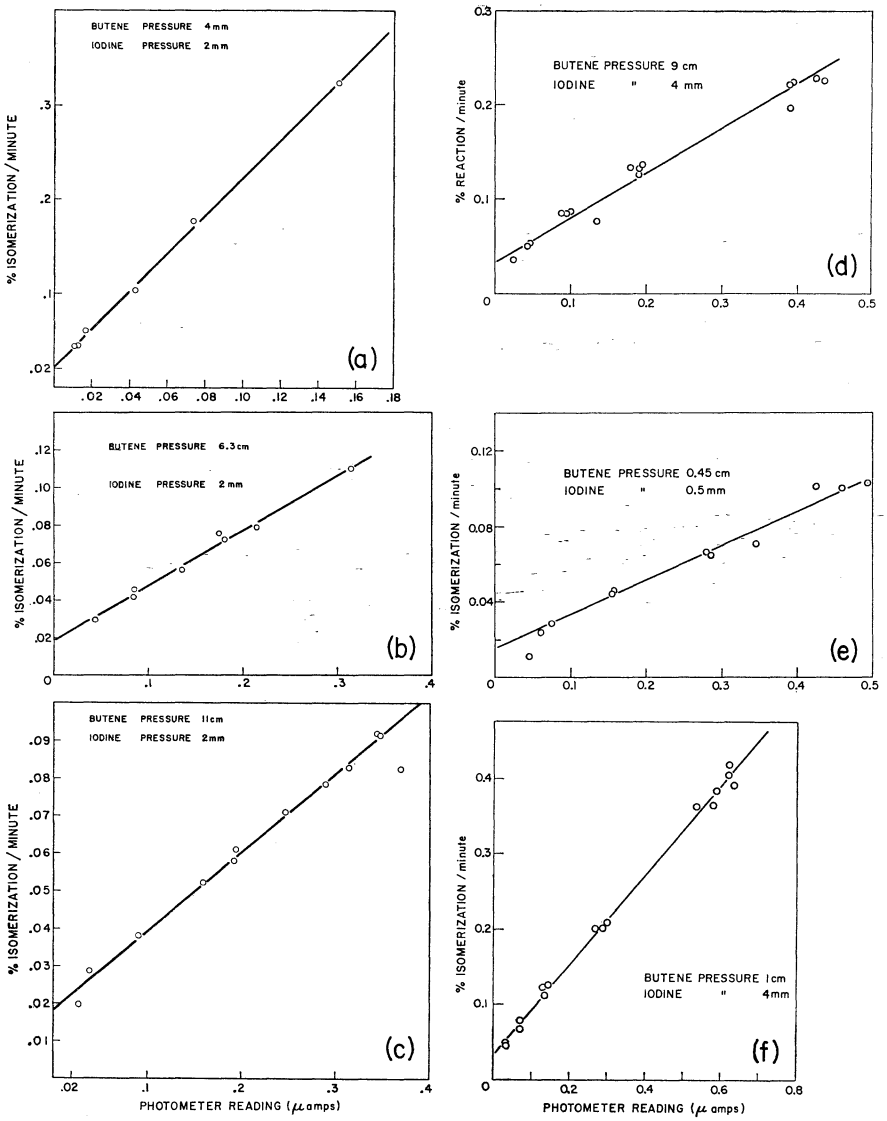

FIG. 3(*a–f*). Dependence of rate of isomerization on light intensity.

Can. J. Chem. Downloaded from www.nrcresearchpress.com by 210.87.254.6 on 09/05/12
For personal use only.

In the banded region, using the mercury green line, 5461 Å, addition of butene or nitrogen to iodine caused an increase in the light absorbed by the iodine, as measured by the phototube. A maximum increase of about 28% was observed. The ratio of the absorption with added gas to the absorption with iodine alone as a function of added gas is shown in Fig. 4. This increased absorption is most probably the effect of pressure on

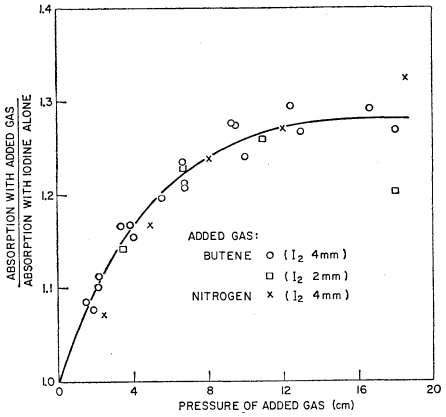

FIG. 4. Effect of additions of butene and nitrogen on light absorption by iodine in the banded region.

the width of the absorption band of the iodine molecule. Obviously such an effect would not occur in a region of continuous absorption and indeed was not observed with light of wavelength less than 5000 Å.

Addition of nitrogen, on the other hand, did not appear to increase the concentration of iodine atoms in the banded region by increased predissociation of the iodine molecule (Fig. 1(*b*)). Pressures of up to 45 cm of nitrogen were added to 4 cm of butene and 2 mm of iodine, under which conditions the indirect effect of the nitrogen on the rate as a result of the increased light absorption by the iodine was almost within the experimental error in rate measurements. The rate of isomerization itself was not increased and in fact gradually decreased slightly, probably due to the effect of nitrogen as a third body in removing iodine atoms.

Oxygen caused a more pronounced drop in the rate of isomerization, but still a large excess (about 10 times that of butene) was required to decrease the rate by 25%. It seems likely that this decrease was again the result of removal of iodine atoms by recombination on oxygen, which might be much more efficient than recombination on nitrogen. With still greater pressures of oxygen, reactions with butene took place, but this aspect was not pursued further.

A series of experiments was done at a temperature of 98° C with 4 mm of iodine using light in the banded region. The rate of isomerization was increased by about a factor of three and approached a limiting rate higher than that at 65° C.

The Quantum Yield

Region (b)

The quantum yield measurements were made with light of wavelength 4358 Å since the potassium ferrioxalate solution absorbs too weakly at wavelengths greater than 5000 Å to permit a reliable measurement of the light intensity in that region. The average incident intensity at 4358 Å was 4×10^{19} quanta/min. Absorption by iodine at 4 mm was

Can. J. Chem. Downloaded from www.nrcresearchpress.com by 210.87.254.6 on 09/05/12
For personal use only.

16% or 6.6×10^{18} quanta/min. Using the values for the rate of isomerization shown in Fig. 1(*c*) a plot of $1/\phi$ against $1/p$ is shown in Fig. 5. From the intercept the upper limit

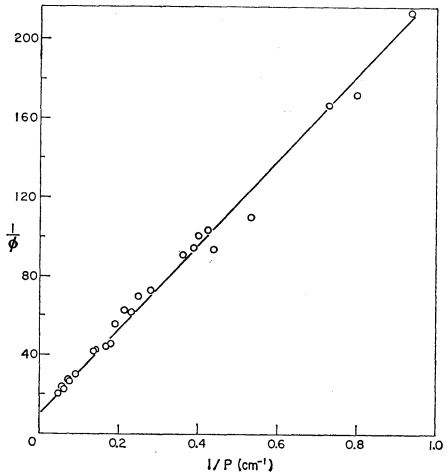

FIG. 5. Plot of the reciprocal quantum yield against reciprocal pressure at 4358 Å. (The data are from Fig. 1(*c*).)

of ϕ is seen to be approximately 0.1. The assumption is made, of course, that the primary quantum yield for production of iodine atoms is 2, but there seems little doubt of this for wavelengths less than 5000 Å. This very low value makes it at once apparent that the reaction is not a chain process with iodine atoms as the chain carriers, such as is observed in the similar reactions of bromine and chlorine atoms.

Region (c)

The few experiments done with the low-pressure mercury resonance lamp, region (*c*), are shown in Fig. 6. At 2537 Å the average total incident intensity was 3×10^{17} quanta/

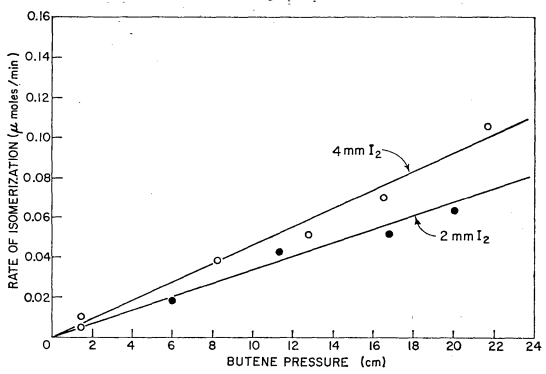

FIG. 6. Dependence of rate of isomerization on butene pressure at 2537 Å (temp. 65° C).

min, with about 2×10^{16} quanta/min absorbed by 4 mm of iodine. Under these conditions of low light intensity absorbed the rate was a linear function of the butene pressure over the range of pressures studied.

Can. J. Chem. Downloaded from www.nrcresearchpress.com by 210.87.254.6 on 09/05/12
For personal use only.

DISCUSSION

Of the two possible species which may cause isomerization, an iodine atom or an excited iodine molecule, the former appears the more probable in the present system. Only light of wavelength greater than 5000 Å would form an excited iodine molecule with sufficient lifetime to undergo energy transfer. However, the similarity of the kinetics of isomerization with incident light of wavelength both above and below 5000 Å suggests that the same species is operative in both cases. Furthermore, addition of nitrogen, and oxygen, especially, would be expected to quench excited molecules more efficiently than is indicated by the results.

Mechanism of Isomerization

Regions (a) and (b)

In discussing the mechanism of isomerization of *cis*-butene by iodine atoms the following observations must be considered:

(*a*) The rate of isomerization was not first order with respect to butene.

(*b*) The rate was linearly dependent on the light intensity for high light intensities, extrapolating to a small positive intercept.

(*c*) The limiting quantum yield for isomerization was about 0.1.

The first result indicates that isomerization does not occur entirely by the simple addition of an iodine atom to *cis*-butene followed by dissociation of the radicals so formed to give a certain fraction, α, of *trans*-butene:

$$C + I \rightarrow R \qquad [1]$$

$$R \rightarrow \alpha T + (1-\alpha)C + I, \qquad [2]$$

where C and T refer to *cis*- and *trans*-butene respectively. In this case the rate of isomerization would be a linear function of the butene pressure. However, if butene is also an efficient third body for recombination of iodine atoms, then an increase in butene pressure would have the effect of reducing the iodine atom concentration. If the rate of recombination is appreciable compared to the rate of isomerization, then the rate of isomerization will not increase linearly with butene pressure but will approach a limiting value.

$$R + I \rightarrow \alpha T + (1-\alpha)C + I_2 \qquad [2a]$$

The fact that the quantum yield approached a limiting value much less than 1 may be interpreted to mean that butene acts as a third body for the recombination of iodine atoms without necessarily undergoing isomerization. In other words the reaction of an iodine atom with butene does not always form a radical in which rotation about the C—C bond may occur. The interaction complex then must preserve the rigidity of the double bond and be sufficiently stable to allow recombination of iodine atoms by further reaction of the complex with another iodine atom. Such a structure may be a π-complex of an iodine atom with the double bond. These have been postulated (14) to occur in the recombination of iodine atoms with various third bodies and in the reaction of oxygen atoms and ozone with olefins (13).

$$C + I \rightarrow C{:}I \qquad [3]$$

$$C{:}I \rightarrow C + I \qquad [4]$$

$$C{:}I + I \rightarrow C + I_2 \qquad [5]$$

The linear dependence of the rate of isomerization on the absorbed light intensity raises the problem of the order of the recombination reaction of iodine atoms in the present

Can. J. Chem. Downloaded from www.nrcresearchpress.com by 210.87.254.6 on 09/05/12
For personal use only.

system. In the flash photolysis experiments (14, 15) the rate of recombination of iodine atoms is second order in iodine atoms. In the present system the concentration of iodine atoms is less than that under the conditions of flash photolysis. Hence in this case, also, recombination will be second order in iodine atoms and the concentration of iodine atoms will depend on the square root of the absorbed light intensity. In order for the rate to appear linear with respect to light intensity under these conditions the rate of isomerization must also be second order in iodine atom concentration. Reactions [2] and [2*a*] will not give this dependence.

This situation will occur if isomerization proceeds not only by reactions [1] and [2] but by a certain fraction of the encounters represented by reaction [5]. If this reaction takes place by the simple abstraction of the iodine atom from the π-complex formed in [3] then isomerization would not be expected to occur. However, if 2,3-diiodobutane is formed as an intermediate, rotation about the C—C bond becomes possible and in the subsequent decomposition to butene and iodine isomerization may occur.

$$\mathrm{C{:}I} + \mathrm{I} \rightarrow \mathrm{CI_2} \qquad [6]$$

$$\mathrm{CI_2} \rightarrow \alpha\mathrm{T} + (1-\alpha)\mathrm{C} + \mathrm{I_2} \qquad [7]$$

The linear dependence of the rate on the absorbed light intensity rules out the occurrence of isomerization by reaction [2*a*], which would lead to a dependence on the square root of intensity. Thus recombination of iodine atoms on butene appears to occur entirely by reactions [3], [4], [5], and [6]. This would suggest that the complex formed in [3] has a longer life than the radical formed in [1]. The heat of formation of the C_4H_8I radical may be very roughly estimated to be 25 kcal/mole.* With this value the radical is unstable toward the formation of butene-1 by 7 kcal/mole and slightly more for butene-2. On the other hand Christie *et al.* (15) have found values of a few kcal/mole for the heats of formation of several complexes formed by interaction of an iodine atom and a hydrocarbon molecule. Rand and Strong (16) also found a complex formation between iodine atoms and benzene when iodine was flash photolyzed in benzene solution. They found that the complex disappeared by a second-order mechanism and might be more stable than the complex formed between iodine molecules and benzene. By analogy, the complex formed in [3] might well be more stable than the radical and have a lower energy barrier for formation.

If the mechanism of isomerization may be described by the following reactions,

$$h\nu + \mathrm{I_2} \rightarrow 2\mathrm{I} \qquad [1a]$$

$$\mathrm{I} + \mathrm{C} \rightarrow \mathrm{R} \qquad [1]$$

$$\mathrm{R} \rightarrow \alpha\mathrm{T} + (1-\alpha)\mathrm{C} + \mathrm{I} \qquad [2]$$

$$\mathrm{I} + \mathrm{C} \rightarrow \mathrm{C{:}I} \qquad [3]$$

$$\mathrm{C{:}I} \rightarrow \mathrm{C} + \mathrm{I} \qquad [4]$$

$$\mathrm{C{:}I} \rightarrow \mathrm{R} \qquad [1a]$$

$$\mathrm{C{:}I} + \mathrm{I} \rightarrow \mathrm{C} + \mathrm{I_2} \qquad [5]$$

$$\mathrm{C{:}I} + \mathrm{I} \rightarrow \mathrm{CI_2} \qquad [6]$$

$$\mathrm{CI_2} \rightarrow \alpha\mathrm{T} + (1-\alpha)\mathrm{C} + \mathrm{I_2} \qquad [7]$$

$$\mathrm{I} + \mathrm{I_2} \rightarrow \mathrm{I_3} \qquad [8]$$

$$\mathrm{I_3} \rightarrow \mathrm{I} + \mathrm{I_2} \qquad [9]$$

$$\mathrm{I_3} + \mathrm{I} \rightarrow 2\mathrm{I_2}, \qquad [10]$$

**Values used in this estimation (17): $H_{f25}(C_4H_{10}) = -29.8$; $D(sec\text{-}C_4H_9\text{—}H) = D(sec\text{-}C_3H_7\text{—}H) = 94$; $D(H_2) = 103.2$; $D(I_2) = 35.35$; $D(sec\text{-}C_4H_9\text{—}I) = 48$; $D(sec\text{-}C_4H_8I\text{—}H) = D(sec\text{-}C_4H_9\text{—}H)$.*

Can. J. Chem. Downloaded from www.nrcresearchpress.com by 210.87.254.6 on 09/05/12
For personal use only.

the rate of isomerization (r_i) equals $\alpha[k_2(R)+k_7(CI_2)]$. Therefore, for second-order atomic recombination (i.e. $k_9 \gg k_{10}(I)$ and $k_4 \gg (k_5+k_6)(I)$),

$$r_i = \frac{\alpha\left(k_1+k_{1a}\frac{k_3}{k_4}\right)(C)\sqrt{I_a}}{\sqrt{\left(k_6\frac{k_3}{k_4}(C)\right)}\sqrt{\left(\frac{k_5+k_6}{k_6}+\frac{k_{10}k_8k_4(I_2)}{k_6k_9k_3(C)}\right)}} + \frac{\alpha I_a}{\frac{k_5+k_6}{k_6}+\frac{k_{10}k_8k_4(I_2)}{k_6k_9k_3(C)}}$$

and

$$r_i\,(\%) = \frac{100\alpha\left(k_1+k_{1a}\frac{k_3}{k_4}\right)\sqrt{I_a}}{\sqrt{\left(k_6\frac{k_3}{k_4}(C)\right)}\sqrt{\left(\frac{k_5+k_6}{k_6}+\frac{k_{10}k_8k_4(I_2)}{k_6k_9k_3(C)}\right)}} + \frac{100\alpha}{(C)}\times\frac{I_a}{\frac{k_5+k_6}{k_6}+\frac{k_{10}k_8k_4(I_2)}{k_6k_9k_3(C)}}.$$

At constant pressures of C and I_2

$$r_i = K_1\sqrt{I_a} + K_2I_a.$$

The intensity dependence plots (Fig. 3(*a–f*)) extrapolated to a small intercept and it may be seen that such behavior is consistent with this mechanism. Plots of $r_i/I_a^{\frac{1}{2}}$ against $I_a^{\frac{1}{2}}$ for each series of intensity dependence curves gave straight lines from which values for K_1 and K_2 were obtained. The ratio $(k_1k_4+k_{1a}k_3)^2/k_3k_4k_6$ was equal to the (intercept)^2/slope. Table I shows this ratio as well as values for K_1, K_2, $K_1I_a^{\frac{1}{2}}$, and K_2I_a for each series

TABLE I

Determination of the constants in the rate equation

I_2 (mm)	Butene (mm)	$\frac{I_2}{\text{Butene}}$	K_1	K_2	$K_1\sqrt{I_a}$	K_2I_a	$\frac{r_1+r_{1a}^*}{r}$ (%)	$\frac{r_6^*}{r}$ (%)	$\frac{(\text{intercept})^2}{\text{slope}}$, $\frac{(k_1k_4+k_{1a}k_3)^2}{k_3k_4k_6}$
2	4	0.50	0.24	1.50	0.0936	0.228	29.1	70.9	0.0384
2	60	0.033	0.10	0.235	0.0561	0.074	43.0	57.0	0.0429
2	110	0.0182	0.081	0.125	0.0478	0.0435	52.4	47.6	0.0525
4	10	0.40	0.155	0.460	0.122	0.285	30.0	70.0	0.052
4	90	0.0445	0.195	0.246	0.127	0.105	55.0	45.0	0.154
0.5	4.5	0.111	0.068	0.110	0.0477	0.0542	46.8	53.3	0.0416

*r_1, r_{1a}, r_6, and r are, respectively, rates of reactions [1], [1*a*], [6], and the total isomerization.

of experiments covering a wide range of iodine and butene concentrations. The proportion of the isomerization which occurs by reactions [6] and [7] is greatest when the I_2/butene ratio is largest. Absolute values for the ratio $k_{10}k_8k_4/k_6k_9k_3$ may not be obtained from these plots since only relative values for I_a were measured.

The observed dependence of the isomerization rate on the concentration of the reactants is qualitatively in agreement with the considered mechanism. A detailed quantitative treatment is precluded by the appreciable experimental scatter and by the complexity of the rate expressions. The proposed reaction mechanism is therefore of a tentative character. Both reactions [1] and [1*a*] have been included into the mechanism to show that the kinetic expressions are independent of whether the iodobutyl radicals (R) are assumed to be formed by direct addition of iodine atoms or by rearrangement of π-complexes (C:I).

Region (c)

Reactions [5] and [6] would be expected to be less efficient at low light intensities and

Can. J. Chem. Downloaded from www.nrcresearchpress.com by 210.87.254.6 on 09/05/12
For personal use only.

this is shown by the experiments using the mercury resonance line 2537 Å (Fig. 6). The light absorbed in this region was about 300 times less than that at 4358 Å. Although the points are scattered there appeared to be no curvature in the plot of rate against butene pressure. The quantum yield divided by the equilibrium trans/cis value reached unity at about 7 cm of butene and continued to increase as the butene pressure was increased. The rate of reaction [6] thus appears to be considerably reduced at these light intensities. At the same time, the more highly energetic iodine atom formed in this region may make reaction [1] much faster relative to [3].

REFERENCES

1. R. J. Cvetanović. Can. J. Chem. **38**, 1678 (1960).
2. R. J. Cvetanović. J. Chem. Phys. **30**, 19 (1959).
3. T. Vrbaski and R. J. Cvetanović. Can. J. Chem. **38**, 1053 (1960).
4. K. R. Jennings and R. J. Cvetanović. J. Chem. Phys. **35**, 1233 (1961).
5. G. S. Forbes and A. F. Nelson. J. Am. Chem. Soc. **59**, 693 (1937).
6. G. B. Kistiakowsky and J. E. Cline. J. Chem. Phys. **5**, 990 (1937).
7. C. Arnot and C. A. McDowell. Can. J. Chem. **36**, 114 (1958).
8. E. J. Bowen. Chemical aspects of light. 2nd ed. Oxford. 1946.
9. L. J. Gillespie and L. H. D. Fraser. J. Am. Chem. Soc. **58**, 2260 (1936).
10. C. G. Hatchard and C. A. Parker. Proc. Roy. Soc. (London), Ser. A, **235**, 518 (1956).
11. Selected Values of Properties of Hydrocarbons. Natl. Bur. Standards Circ. 461. 1947.
12. E. Rabinovitch and W. C. Wood. Trans. Faraday Soc. **31**, 689 (1935).
13. R. Mulliken. Phys. Rev. **36**, 1440 (1930).
14. G. Porter and J. A. Smith. Proc. Roy. Soc. (London), Ser. A, **261**, 28 (1961).
15. M. I. Christie, R. G. W. Norrish, and G. Porter. Proc. Roy. Soc. (London), Ser. A, **216**, 152 (1953).
16. S. J. Rand and R. L. Strong. J. Am. Chem. Soc. **82**, 5 (1960).
17. T. L. Cottrell. The strengths of chemical bonds. Butterworths, London. 1958.

Can. J. Chem. Downloaded from www.nrcresearchpress.com by 210.87.254.6 on 09/05/12
For personal use only.

REACTIONS OF IODINE ATOMS WITH *n*-BUTENES

II. INTERCONVERSION OF BUTENE-1 AND BUTENE-2[1]

MARGARET H. BACK[2] AND R. J. CVETANOVIĆ
Division of Applied Chemistry, National Research Council, Ottawa, Canada

Received January 28, 1963

ABSTRACT

In the vapor phase reaction of iodine atoms with *n*-butenes at 65° C appreciable double-bond migration takes place in addition to the readily occurring geometrical isomerization. No detectable quantities of iodine-containing hydrocarbons are observed. In contrast to this, appreciable amounts of 1,3-butadiene and the corresponding amounts of hydrogen iodide are formed although direct abstraction of a hydrogen atom from butene by an iodine atom is unlikely in view of the endothermicity of this reaction. Formation of 1,3-butadiene is counterbalanced by its hydrogenation back to the original butene and its isomers and a steady state concentration is reached in the course of the reaction. As a consequence of this balancing of dehydrogenation and hydrogenation steps there is an induction period in the formation of butene-2 in the reaction of iodine atoms with butene-1 and a large part of butene-2 is found to be derived from the butadiene initially produced. To explain the occurrence of the endothermic steps, it is assumed that the initial iodine atom – butene adduct (iodobutyl radical or π-complex) interacts with a second iodine atom. Reaction mechanism is tentatively discussed.

Can. J. Chem. Downloaded from www.nrcresearchpress.com by 210.87.254.5 on 09/05/12
For personal use only.

INTRODUCTION

In the study of the interaction of iodine atoms with *cis*-butene-2 (1) (Part I) it was found at large conversions, used in order to determine the final equilibrium ratio of *trans*-butene/*cis*-butene, that small amounts of butene-1 and butadiene were formed as well. The following results report the investigation of this additional reaction of iodine atoms with *n*-butenes.

EXPERIMENTAL

The apparatus and methods were the same as those used in Part I. Butadiene was Phillips Research Grade and was analyzed by gas chromatography with the column described in Part I. Fully deuterated butadiene was obtained from Merck, Sharpe and Dohme, Montreal, and was shown by mass spectrometric analysis to consist of 66.7% C_4D_6 and 33.3% C_4D_5H. Hydrogen iodide was analyzed by titration with silver nitrate using eosin as indicator and also with sodium hydroxide using phenolphthalein as indicator. Small amounts of oxygen were added by first mixing with a large amount of nitrogen.

RESULTS

The reaction of iodine atoms with butene-1 produced butadiene and *cis*- and *trans*-butene-2 and the reaction with *cis*-butene-2 produced *trans*-butene-2, butadiene, and butene-1. Hydrogen iodide was analyzed from 11 experiments and found to be approximately twice the molar quantity of butadiene formed. The results are given in Table I. The variation in the yield of products with time of reaction is shown in Figs. 1 and 2. The formation of butadiene from *cis*-butene was about 15 times slower than the rate of cis–trans isomerization. The rate of production of butadiene was roughly about one and a half times as fast from butene-1 as from butene-2 (Fig. 3), while the overall conversion of butene-1 to butene-2 was about seven to eight times faster than the reverse reaction (Fig. 4).

[1]*Issued as N.R.C. No. 7295.*
[2]*National Research Council Postdoctoral Fellow 1959–1961. Present address: Chemistry Department, University of Ottawa, Ottawa, Canada.*

TABLE I

Comparison of yields of HI and butadiene in the reaction of iodine atoms with butene-1

Expt. No.	2×butadiene (μmoles)	HI (μmoles)	Method of titration
381	10.8	12–13	$AgNO_3$
382	10.0	12.5	$AgNO_3$
383	6.4	8.0	$AgNO_3$
386	5.22	7.3	Acid–base
388	10.8	7.7	$AgNO_3$
389	9.68	11.8	Acid–base
392	7.82	8.2	$AgNO_3$
393	7.66	6.7	Acid–base
394	10.1	8.9	$AgNO_3$
395	9.52	8.3	$AgNO_3$
396	7.86	7.7	Acid–base
		7.5	$AgNO_3$

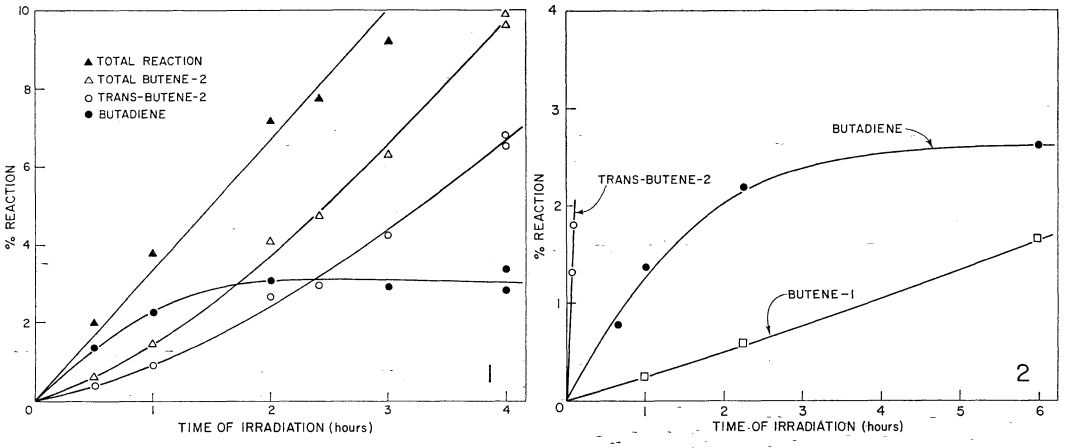

FIG. 1. Time dependence of the yields of products of the reaction of butene-1 with iodine atoms (temp. 65° C, wavelength > 5000 Å, pressure of butene-1 1.7 cm, pressure of I_2 4 mm).

FIG. 2. Time dependence of the yields of products of the reaction of *cis*-butene-2 with iodine atoms (temp. 65° C, wavelength > 5000 Å, pressure of *cis*-butene-2 1.4 cm, pressure of I_2 4 mm).

The recovery of C_4 hydrocarbons, or compounds volatile at −78° C, was never less than 98% and the loss was not related to the extent of reaction. The same loss occurred in blank experiments with no irradiation in which no products were formed and was probably due to some absorption of butene in stopcock grease. It was therefore concluded that non-volatile products were not formed in the reaction to a significant extent.

Addition of butadiene to butene-1 in approximately 1:1 ratio increased the production of butene-2 by almost a factor of two. Results of experiments with added butadiene-d_6 are shown in Table II. Only about half of the product butene-2 was formed from the deuterated butadiene, although the deuterated butadiene was greatly in excess over that formed in the reaction.

The composition of the butene-2 fraction from the reaction with butene-1 is shown as a function of reaction time in Fig. 5. Although the extrapolation is not precise it seems likely that *cis*- and *trans*-butene-2 are formed initially in approximately equal amounts, but by subsequent reaction with iodine atoms, gradually approach their equilibrium proportions.

Can. J. Chem. Downloaded from www.nrcresearchpress.com by 210.87.254.5 on 09/05/12
For personal use only.

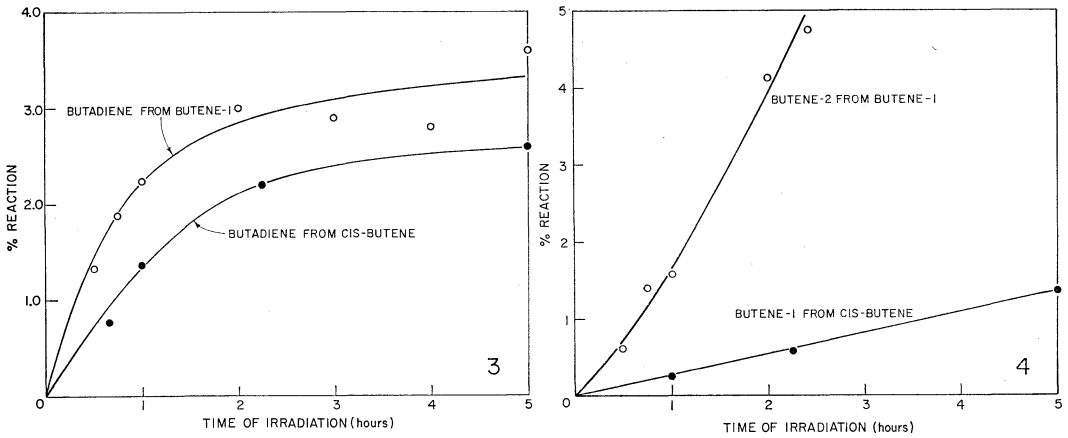

FIG. 3. Comparison of butadiene yields in the reactions of iodine atoms with *cis*-butene-2 and butene-1 (temp. 65° C, wavelength > 5000 Å; in both reactions iodine pressure 4 mm, olefin pressure 1.7 cm).

FIG. 4. Comparison of the rates of double-bond isomerization in the reactions of iodine atoms with *cis*-butene-2 and butene-1 (temp. 65° C, wavelength > 5000 Å; in both reactions iodine pressure 4 mm, olefin pressure 1.7 cm).

TABLE II

Isotopic composition of the product butene-2 formed in the reaction of iodine atoms with a 1:1 mixture of C_4H_8-1 and 1,3-C_4D_6

	Isotopic composition at various times of irradiation (%)					
Product	1 hr		2 hr		3 hr	
C_4H_8	47		42		30	
C_4H_7D	7	54	7	49	15	45
$C_4H_6D_2$						
$C_4D_4H_4$	0.9				2	
$C_4D_5H_3$	10		11		12	
$C_4D_6H_2$	17	43	26	51	17	55
C_4D_7H	11		11		19	
C_4D_8	4.2		3		5	

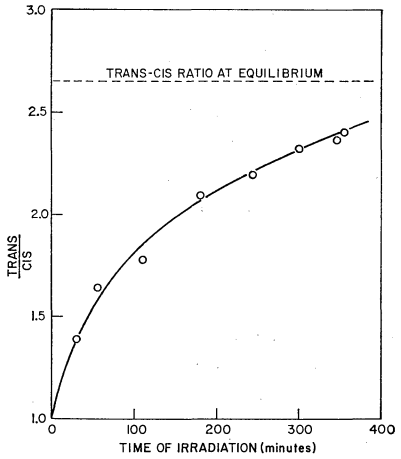

FIG. 5. Time dependence of the isomeric composition of butene-2 formed in the reaction of iodine atoms with butene-1 (temp. 65° C, wavelength > 5000 Å, pressure of butene-1 1.7 cm, pressure of iodine 4 mm).

Can. J. Chem. Downloaded from www.nrcresearchpress.com by 210.87.254.5 on 09/05/12
For personal use only.

The effect of pressure of butene-1 on the rate of reaction (Fig. 6) was similar to that observed for the isomerization of butene-2, and, as in the latter reaction, the effect of

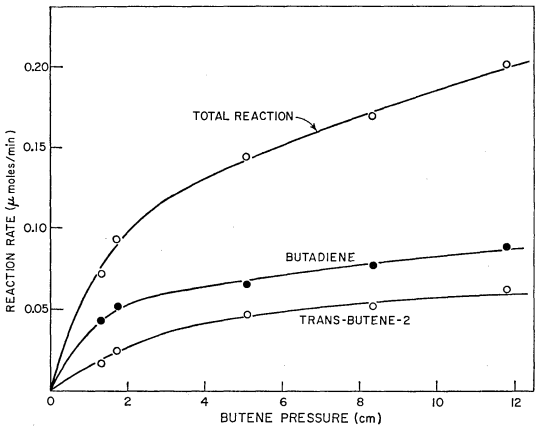

FIG. 6. Dependence of the rates of product formation on pressure of butene-1 in the reaction of iodine atoms with butene-1 (temp. 65° C, wavelength > 5000 Å, pressure of iodine 4 mm, irradiation time 1 hour).

the butene as a third body for the recombination of iodine atoms presumably resulted in the tendency for the levelling off of the rate at high butene pressures.

The rate of production of butadiene from butene-1 was a linear function of the light intensity over the range studied (Fig. 7). Since the rate of recombination of iodine atoms

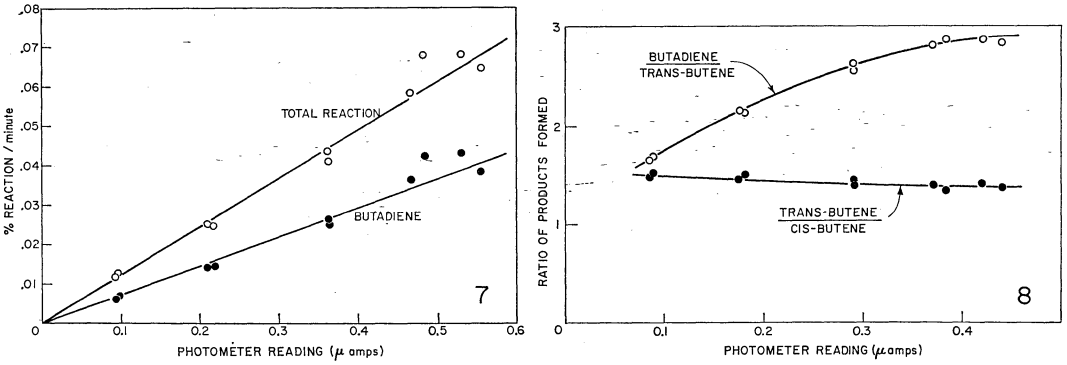

FIG. 7. Dependence of the reaction rates on light intensity in the reaction of iodine atoms with butene-1 (temp. 65° C, wavelength > 5000 Å, pressure of butene-1 ca. 14 mm, pressure of iodine 4 mm, % reaction ca. 2.5).

FIG. 8. Light intensity dependence of the ratios of the products formed in the reaction of iodine atoms with butene-1 (temp. 65° C, wavelength > 5000 Å, pressure of butene-1 1.4 cm, pressure of iodine 4 mm).

in the present system was proportional to $(I)^2$, this suggests that the rate of formation of butadiene was also dependent on the square of the iodine atom concentration and was probably a type of reaction similar to that suggested in Part I for iodine atom induced cis–trans isomerization of butene-2. The ratio of *trans*-butene-2/*cis*-butene-2 formed was practically independent of the light intensity for constant percentage conversion. The ratio of butadiene to *trans*-butene-2, however, increased with increasing light intensity. These ratios are shown in Fig. 8.

Addition of nitrogen had no effect on the rate of reaction of butene-1, except for a

Can. J. Chem. Downloaded from www.nrcresearchpress.com by 210.87.254.5 on 09/05/12
For personal use only.

slight decrease due to the competition of the nitrogen as third body for removal of iodine atoms. The ratios of the products, butadiene and *cis*- and *trans*-butene-2, remained the same. The effect of oxygen on the products at constant pressures of butene, iodine, and nitrogen and constant reaction time is shown in Fig. 9. The yield of butadiene was

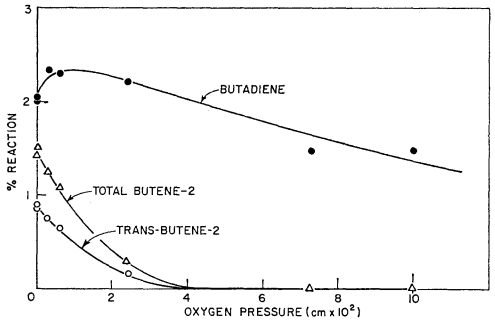

FIG. 9. Effect of additions of oxygen on the products formed in the reaction of iodine atoms with butene-1 (temp. 65° C, wavelength > 5000 Å, pressure of butene-1 1.4 cm, pressure of iodine 4 mm; HI was not determined).

increased somewhat with very small amounts of oxygen and then gradually decreased in a manner similar to the decrease in the rate of isomerization of butene-2 on addition of oxygen. The effect of oxygen on the production of butene-2 was more drastic. A ratio of oxygen/butene-1 of about 0.03 was sufficient to reduce the percentage formation of butene-2 from 1.5 to less than 0.04. The effect of oxygen on the yield of butadiene as a function of time is shown in Fig. 10. A fixed quantity of air was added in each experiment

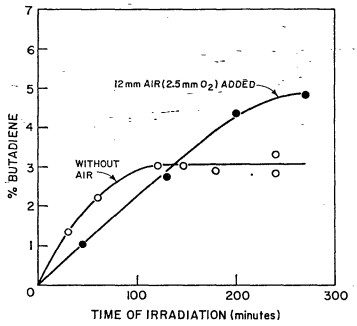

FIG. 10. Effect of oxygen additions on the yields of butadiene at various irradiation times in the reaction of iodine atoms with butene-1 (temp. 65° C, wavelength > 5000 Å, pressure of butene-1 1.4 cm, pressure of iodine 4 mm).

and the pressure of oxygen was sufficient to suppress completely the production of butene-2. The yield of butadiene was first below that found without oxygen, as was expected from Fig. 9. However, the final steady state yield of butadiene was about 50% greater than that observed with no added oxygen. In these experiments an estimate of the oxygen consumed was made by gas chromatographic analysis of the oxygen/nitrogen ratio before and after the irradiation. In each case the oxygen consumed was roughly equivalent to the yield of butene-2 in the absence of oxygen.

Can. J. Chem. Downloaded from www.nrcresearchpress.com by 210.87.254.5 on 09/05/12
For personal use only.

DISCUSSION

Butadiene was an unexpected product of the reaction of iodine atoms with butene-1 and butene-2 because hydrocarbons have not generally been found to lose hydrogen atoms by reaction with iodine atoms (2, 3). Excited molecules of iodine activated by 1849 Å light (4) were found to attack C—H bonds in methane and ethane, but the energy content of such molecules was so large that the reaction was not endothermic. Recently (5), both *n*-propyl iodide and isopropyl iodide and hydrogen iodide have been found as products of the reaction of iodine atoms with propane at 49° C, although the quantum yield was low, about 2×10^{-4}. The reaction was thought to occur by the formation of a collision complex RHI with subsequent attack by another iodine atom. A similar type of mechanism is indicated by the present results and with olefins the second iodine atom reacts faster than with paraffins.

The time dependence of the reaction products both from butene-1 and butene-2 and the production of deuterated butene-2 when deuterated butadiene was added to butene-1 are strong indications that butadiene was an intermediate product in the interconversion of butene-1 and butene-2 by reaction with iodine atoms. The butadiene was accompanied by hydrogen iodide and as this accumulated in the system a back reaction occurred to regenerate, finally, butene. In other words, the product butene was a secondary product and not formed by direct isomerization, through the formation of a short-lived C_4H_8I radical, for example. The rate of formation of butadiene and hydrogen iodide from butene-1 and butene-2 was roughly similar, but the rate of formation of butene-2 from butadiene was much faster than that of butene-1, as might be expected from the greater thermal stability of butene-2.

Butadiene Formation

It is rather unlikely that the initial step in the formation of butadiene is the abstraction of a hydrogen atom from butene by an iodine atom. This process is at least 10 kcal/mole endothermic and would be very slow at 65° C. Nevertheless the formation of butadiene from butene requires the removal of two hydrogen atoms by two iodine atoms to form two molecules of hydrogen iodide. This may occur by two slightly different mechanisms.

(*a*) An iodine atom may abstract a hydrogen atom from the radical or the π-complex formed by addition of an iodine atom to butene (C_4H_8I):

$$I + C_4H_8 \rightarrow (C_4H_8I) \quad [1]$$

$$I + (C_4H_8I) \rightarrow C_4H_7I + HI. \quad [2]$$

In either case the process would be exothermic and the product would be a molecule of iodobutene. Since the recovery of butene (as butene or butadiene) was virtually complete even at very long periods of irradiation the yield of this product could have been only very small so that fast subsequent reactions, keeping its steady state concentration low, would have to be assumed. A repetition of this sequence would yield butadiene:

$$C_4H_7I + I \rightarrow C_4H_7I_2 \quad [3]$$

$$C_4H_7I_2 + I \rightarrow C_4H_6I_2 + HI \quad [4]$$

$$C_4H_6I_2 \rightarrow C_4H_6 + I_2. \quad [5]$$

The formation of butadiene would thus occur in two steps, the molecule C_4H_7I being the intermediate.

(*b*) The cis–trans isomerization of butene-2 was postulated in Part I to occur through the intermediate formation of 2,3-diiodobutane. The subsequent dissociation of this

Can. J. Chem. Downloaded from www.nrcresearchpress.com by 210.87.254.5 on 09/05/12
For personal use only.

unstable compound, usually to give butene and iodine, could be assumed to give, a small fraction of the time, butadiene and two molecules of hydrogen iodide in one step:

$$C_4H_8I_2 \rightarrow C_4H_6 + 2HI. \quad [6]$$

An analogous process is direct formation of 2HI and butadiene in reaction [2]. The probability of each of these mechanisms will be considered later.

Butene Formation

A detailed mechanism of the reverse formation of butene from butadiene would be difficult to propose at present. Several broadly similar alternatives are possible. The process probably begins by addition of an iodine atom to form a C_4H_6I radical (or a π-complex) followed by reaction with hydrogen iodide. This could give one of the iodobutene isomers and a further similar series of steps could then yield $C_4H_8I_2$. Since significant amounts of non-volatile products were not formed it may be concluded that the diiodobutane molecule, $C_4H_8I_2$, dissociates rapidly to butene and iodine and the 1,4-diiodobutane (a stable compound) is not formed. This would require that the initial addition of iodine atoms occurs at one of the two internal carbon atoms and, furthermore, that the addition and abstraction occur in such a way that both butene-1 and butene-2 may be formed. The following reaction scheme, for example, would meet these requirements:

$$C_4H_6 + I \rightarrow H_2C{=}CH{-}\overset{H}{\underset{\cdot}{C}}I{-}CH_2 \quad [7]$$

$$C_4H_6I + HI \rightarrow H_2C{=}CH{-}CHI{-}CH_3 + I \quad [8]$$

$$C_4H_7I + I \rightarrow H_2\dot{C}{-}CHI{-}CHI{-}CH_3 \quad [9]$$

$$H_2C{-}CHI{-}CHI{-}CH_3 \rightarrow H_2\dot{C}{-}CH{=}CH{-}CH_3 + I_2 \quad [10]$$

$$\rightarrow H_2C{=}CH{-}\dot{C}H{-}CH_3 + I_2 \quad [11]$$

$$C_4H_7 + HI \rightarrow C_4H_8 + I. \quad [12]$$

If the radical formed in [9] is stable and reacts with hydrogen iodide before decomposing the result would be the formation of 2,3-diodobutane, which would then decompose to give butene-2 and iodine. However, the formation of butene-1 could not occur without hydrogen-atom migration. Intermediate formation of resonance-stabilized methallyl radicals, as in reactions [10] and [11], would be more likely to produce butene-1 and butene-2 in ratios consistent with their thermal stability by abstracting hydrogen from HI (reaction [12]). Inasmuch as methallyl radicals are indeed formed as intermediates, it is not necessary to postulate the unlikely non-terminal addition of iodine atoms in reaction [7].

The probability of mechanism (*a*) and (*b*) may now be discussed in more detail. The fact that the production of butadiene is not, or is very slightly, inhibited by oxygen may be adequately explained by mechanism (*b*) whereby butadiene is formed without the intermediate formation of a radical. However, the probability of simultaneous formation of two molecules of HI in reaction [6] may be quite low. Mechanism (*a*) accounts more easily for the results of the experiments with added butadiene-d_6 which showed that about half the product butene was not formed from butadiene. If the molecule C_4H_7I appears in both the breakdown to butadiene and the buildup to butene it follows that the C_4H_7I molecule may be converted back to C_4H_8 without necessarily going all the way to C_4H_6. This would still allow an induction period for the formation of the product butene-2 since the reaction [12] depends on a sufficient concentration of hydrogen iodide in the system. Thus the product butene may not all be formed by the buildup from butadiene.

Can. J. Chem. Downloaded from www.nrcresearchpress.com by 210.87.254.5 on 09/05/12
For personal use only.

The effect of oxygen on the series of reactions [1] to [5] is difficult to predict. The production of butadiene may not be inhibited if oxygen reacts with the C_4H_8I radical in the same way as the iodine atom reacts, to abstract a hydrogen atom. This may even increase the production of butadiene and in fact a small increase was observed. This effect is shown both in Fig. 8 and Fig. 9, where the increase occurs at a different percentage reaction for different amounts of added oxygen. With larger amounts of oxygen the additional effect of an efficient third body for recombination of iodine atoms may lower the overall rate of reaction as discussed in Part I.

The abstraction of hydrogen by oxygen may also inhibit the re-formation of butene-1 and butene-2 since the hydrogen atom thus abstracted would very likely be made unavailable for the reactions involving conversion of butadiene to butene. Inhibition by oxygen in this sequence could, however, also occur after reaction [11].

The linear dependence of the rate of production of butadiene on light intensity is the result of either mechanism (*a*) or (*b*). In each case the rate of butadiene formation is proportional to $(I)^2$ and since $(I)^2$ is proportional to I_a, the rate of formation of butadiene is thus proportional to I_a. It should be noted that in contrast to the cis–trans isomerization of butene-2 no evidence for an additional rate proportional to the first power of the iodine atom concentration was observed.

ACKNOWLEDGMENTS

The authors are grateful to the Analytical Section of this division for hydrogen iodide determinations by NaOH titration and to Dr. A. W. Tickner for mass spectrometric analyses.

REFERENCES

1. M. H. Back and R. J. Cvetanović. Can. J. Chem. This issue.
2. J. F. Hornig, G. Levy, and J. E. Willard. J. Chem. Phys. **20**, 1556 (1952).
3. J. Zimmerman and R. M. Noyes. J. Chem. Phys. **18**, 658 (1958).
4. T. A. Gover and J. E. Willard. J. Am. Chem. Soc. **82**, 3816 (1960).
5. S. V. Filseth and J. E. Willard. J. Am. Chem. Soc. **84**, 3806 (1962).

Can. J. Chem. Downloaded from www.nrcresearchpress.com by 210.87.254.5 on 09/05/12
For personal use only.

THE X-RAY DIFFRACTION PATTERNS OF ALUMINUM CARBIDE Al_4C_3 AND ALUMINUM OXYCARBIDE Al_4O_4C

J. H. Cox and L. M. Pidgeon
Department of Metallurgical Engineering, University of Toronto, Toronto, Ontario
Received December 20, 1962

ABSTRACT

An X-ray investigation of the compounds aluminum carbide, Al_4C_3, and aluminum oxycarbide Al_4O_4C yielded data which differed from that in the A.S.T.M. files. The aluminum carbide pattern was similar in many ways to that calculated by Stackelberg and Schnorrenberg (Z. Physik. Chem., Sect. B, **27**, 37 (1934). Minor differences occurred in the Al_4O_4C pattern.

INTRODUCTION

During an investigation of the aluminum–oxygen–carbon system (2), an X-ray powder analysis of the high-temperature reaction products indicated that either there were unknown compounds present in the system or there was some error existing in the standard X-ray files. Since a differential thermal analysis indicated that there were no reactions occurring to produce any unknown compounds, it was thought that errors in the patterns for the compounds in this range (the oxycarbide, Al_4O_4C, and the carbide, Al_4C_3) were responsible. Therefore, samples of Al_4O_4C and Al_4C_3 were prepared and analyzed.

EXPERIMENTAL

Apparatus

The samples were prepared in a graphite crucible in the high-temperature, resistance-heated, vacuum furnace described elsewhere (2). Subsequently, they were removed from the furnace and examined with a high-angle diffractometer using a copper target and nickel filter. The X-ray samples were prepared according to the recommendations of Klug and Alexander (3) and were scanned at speeds ranging from 1° per min to 1/8° per minute.

Method

Aluminum carbide was prepared by reacting the stoichiometric proportions of aluminum and graphite at 1250° C, and subsequently holding the product at 1500° C for 12 hours under an atmosphere of argon. A second method of production consisted of reacting alumina and graphite for 6 hours at 1900° C under argon.

The oxycarbide was prepared by holding for 24 hours a stoichiometric mixture of alumina and carbon just above the equilibrium temperature (determined elsewhere (2)) of 1695° C under a pressure of 90 mm Hg.

The Al_4C_3 prepared by the reaction of metal and graphite possessed the characteristic yellow color associated with the compound and tended to give an X-ray pattern in which the peaks were somewhat wider than those of the carbide obtained by the reaction of alumina and carbon. The latter form was composed of very hard purplish black crystals. The oxycarbide Al_4O_4C was found as a mauve powder.

RESULTS AND DISCUSSION

Table I is a comparison of the *d* values and relative intensities produced from samples of the carbide obtained by reacting alumina and carbon (type A) and aluminum and carbon (type B). It can be seen that type A (obtained from the alumina–carbon reaction) produced a pattern which showed several high-angle values which were not present in type B. These values were of low intensity and it was probable that in the more "amorphous" type B carbide they were indistinguishable from the background in the diffractograms.

According to Stackelberg and Schnorrenberg (1), the aluminum carbide lattice is rhombohedral with $a = 8.53$ Å, $\alpha = 22°28'$. For presentation purposes, the X-ray patterns have been converted to a hexagonal basis. Table II compares the hexagonal indices for

Can. J. Chem. Downloaded from www.nrcresearchpress.com by 210.87.254.40 on 09/05/12
For personal use only.

TABLE I

Experimental values for Al_4C_3 prepared by different methods

Type A d (Å)	Type A I/I_o	Type B d (Å)	Type B I/I_o	Type A d (Å)	Type A I/I_o	Type B d (Å)	Type B I/I_o
4.14	30	4.14	16	1.194	8	1.195	11
2.86	40	2.86	45	1.121	8	1.121	9
2.81	70	2.81	100	1.087	5	1.087	8
2.77	35	2.77	20	1.066	5	1.066	10
2.49	35	2.50	55	1.043	7	1.043	20
2.24	70	2.24	100	1.039	9		
2.12	8	2.11	8	1.029	5	1.029	7
2.08	100	2.08	55	1.014	7	1.015	6
1.887	20	1.888	25	0.9990	3	0.999	4
1.781	14	1.783	18	0.9830	3	0.983	4
1.665	65	1.671	95	0.9715	3	0.9718	6
1.516	25	1.517	35	0.9618	7	0.9620	18
1.441	3	1.440	7	0.9302	7	0.9310	11
1.434	7	1.433	8	0.9102	5		
1.429	4			0.8819	11	0.8822	17
1.386	8	1.385	9	0.8754	3	0.8761	6
1.337	13	1.337	16	0.8732	14	0.8738	20
1.306	14	1.308	11	0.8114	1		
1.299	35	1.300	50	0.8361	3	0.8392	5
1.248	3	1.248	6	0.8334	10	0.8334	13
1.216	2	1.217	4				

TABLE II

Comparison of patterns for Al_4C_3

hkl hex.	Calc. d (Å)	Schnorrenberg d (Å)	A.S.T.M. d (Å)	I/I_o	Expt. d (Å)	I/I_o	Expt. d (Å)	I/I_o
003	8.4						1.299	35
006	4.16				4.14	30	1.248	3
101	2.86		2.87	100	2.86	40	1.216	2
		2.83						
102	2.81		2.80	100	2.81	70	1.194	8
009	2.77				2.77	35	1.121	8
104	2.62						1.087	5
105	2.50	2.50	2.49	60	2.49	35	1.066	5
107	2.24	2.24	2.24	80	2.24	70	1.043	7
108	2.12	2.12	2.12	4	2.12	8	1.039	9
0012	2.08	2.08	2.08	32	2.08	100	1.029	5
1010	1.888	1.89	1.88	20	1.887	20	1.014	7
1011	1.784	1.79	1.78	16	1.781	14	0.9990	3
0015	1.664						0.9830	3
		1.66	1.66	100	1.665	65		
110	1.665						0.9715	3
113	1.634						0.9618	7
1013	1.599	1.60					0.9302	7
116	1.546						0.9102	5
1014	1.517	1.52	1.52	20	1.516	25	0.8819	11
201	1.440		1.440	12	1.441	3	0.8754	3
202	1.433				1.434	7	0.8732	14
119	1.428				1.429	4	0.8664	1
			1.388	4	1.386	8	0.8361	3
			1.340	12	1.337	13	0.8334	10
			1.302	40	1.306	14		

some low-angle planes and their corresponding d spacings calculated from the work of Schnorrenberg *et al.* (1, 4) with the experimental values presented by Stackelberg and Schnorrenberg (1), the A.S.T.M. files, and the type A carbide of the present work. It can

Can. J. Chem. Downloaded from www.nrcresearchpress.com by 210.87.254.40 on 09/05/12
For personal use only.

be seen that the experimental pattern is much closer to that calculated than either the standard files or Schnorrenberg's own work.

The standard pattern for the Al_4O_4C was from the work of Foster *et al.* (5), who have also commented upon the appearance of unknown planes during the X-ray analysis of some Al–O–C melts. Their findings are listed in Table III and are compared with the experimental pattern obtained in the present work.

TABLE III

Comparison of patterns for Al_4O_4C

Expt.		A.S.T.M.		Expt.		A.S.T.M.		Expt.		A.S.T.M.	
d (Å)	I/I_o	*d* (Å)	I/I_o	*d* (Å)	I/I_o	*d* (Å)	I/I_o	*d* (Å)	I/I_o	*d* (Å)	I/I_o
4.23	100	4.22	100	1.730	4	1.73	10	1.274	4	1.28	20
3.86	84	3.87	90	1.699	2			1.262	6	1.26	20
3.29	46	3.30	70	1.682	9	1.68	30	1.242	7	1.24	40
3.11	67	3.11	80	1.644	6	1.65	20	1.226	2		
2.55	7	2.57	30	1.636	2			1.214	1		
		1.31	40			1.61	30				
2.47	22			1.603	7			1.177	2	1.18	10
		2.48	50								
2.46	21			1.564	5			1.111	5	1.11	20
						1.56	20				
2.43	34	2.43	50	1.555	3			1.066	3		
2.31	55	2.32	70	1.499	8			1.055	2		
						1.49	60				
2.28	8			1.490	32			1.035	2		
2.22	5	2.23	20	1.446	38	1.45	70	1.006	3		
2.14	4			1.436	16			0.9960	4		
2.11	4			1.407	8	1.41	30	0.9875	4		
2.05	3			1.384	4	1.39	20	0.9643	1		
2.01	9	2.02	30	1.356	8	1.36	30	0.9490	2		
1.952	26	1.96	50	1.346	1			0.9389	5		
1.873	3	1.88	20	1.341	6	1.34	30	0.9134	1		
1.848	3	1.84	20	1.328	1			0.8390	2		
						1.31	40				
1.785	6	1.78	10	1.303	7			0.8344	2		
								0.8328	3		

It is suggested that difference between the two patterns was due to the small size of the samples used by Foster *et al.* (5) and to the non-equilibrium manner in which they were formed. Their samples were small crystals which had condensed onto the cold portions of their reaction assembly under extreme conditions while the samples used in the present work were obtained under equilibrium conditions.

CONCLUSIONS

An expanded X-ray diffraction pattern for aluminum carbide, Al_4C_3, was obtained which was more similar to that obtained by Stackelberg and Schnorrenberg (1) than to the A.S.T.M. standard pattern. The pattern also possessed many high-angle peaks not listed by either Schnorrenberg or the A.S.T.M. files.

A pattern for the aluminum oxycarbide Al_4O_4C was found which differed in detail from that of Foster *et al.* (5). The difference was thought to be due to non-equilibrium conditions of formation in the earlier work.

REFERENCES

1. M. V. Stackelberg and E. Schnorrenberg. Z. Physik. Chem. Sect. B, **27**, 37 (1934).
2. J. H. Cox and L. M. Pidgeon. To be published.
3. H. P. Klug and L. E. Alexander. X-ray diffraction procedures. John Wiley and Sons Inc., New York. 1954. pp. 290–305.
4. M. V. Stackelberg, E. Schnorrenberg, R. Paulus, and K. F. Spiess. Z. Physik. Chem. Sect. A, **175**, 127 (1935).
5. L. M. Foster, G. Long, and M. S. Hunter. J. Am. Ceram. Soc. **39**, 1 (1956).

Can. J. Chem. Downloaded from www.nrcresearchpress.com by 210.87.254.40 on 09/05/12
For personal use only.

PERIODATE OXIDATION OF MESQUITE GUM[1]

G. G. S. DUTTON AND A. M. UNRAU[2]
Department of Chemistry, University of British Columbia, Vancouver, British Columbia
Received January 14, 1963

ABSTRACT

Mesquite gum was subjected to the Smith procedure involving periodate oxidation, reduction, and mild hydrolysis. The main D-galactose chain was fragmented to a greater extent than expected. The quantity of glycerol formed indicated the presence of a considerable number of $1 \rightarrow 6$ linkages while the formation of threitol showed the presence of $1 \rightarrow 4$ linkages. Several small oligosaccharides terminated by a glycerol residue were isolated together with an oligosaccharide of D.P. 30. Further periodate oxidation of the latter gave a product with D.P. 24 which was in turn oxidized to a compound consisting largely of D-galactose and glycerol. Reduction of the acidic fraction gave mainly 2-*O*-methyl-D-erythritol.

Can. J. Chem. Downloaded from www.nrcresearchpress.com by 210.87.254.40 on 09/05/12
For personal use only.

Mesquite gum contains L-arabinose, D-galactose, and 4-*O*-methyl-D-glucuronic acid. The results of methylation studies and graded hydrolysis on the gum have been reviewed (1) and a generalized structure for the polysaccharide has been proposed. The methylation data do not permit the deduction of a unique structure but it is clear that the gum is highly branched and the isolation of relatively large amounts of 2,4-di-*O*-methyl-D-galactose suggests that the main chain is composed of galactose units linked $1 \rightarrow 6$ and/or $1 \rightarrow 3$. The main chain is known to be substituted by arabinofuranose units and by uronic acid units. If the majority of the D-galactopyranose units are substituted at C_3, either by linkage to another unit of the main chain or by a side chain, then the main structure should undergo little degradation on oxidation with periodate. The terminal uronic acid and arabinofuranose units should, however, be readily removed by periodate oxidation followed by reduction ($NaBH_4$) and mild acid hydrolysis (2). This technique has been successfully applied to oat glucan (2), brome grass hemicellulose (3), oat hull hemicellulose (4), laminarin (5), apple and cherry wood hemicelluloses (6). When mesquite gum was oxidized with periodate, reduced, and hydrolyzed in this manner considerably more degradation occurred than was expected.

The gum (8 g) was dissolved in water and oxidized in the dark with periodic acid for 96 hours. Periodate and iodate ions were removed by the addition of barium carbonate and the polyaldehyde was reduced with sodium borohydride. Excess hydride was destroyed and the solution was evaporated to dryness and the residue treated several times with methanol to remove borate.

A sample of the polyalcohol was completely hydrolyzed and gave threitol, glycerol, arabinose, and galactose in an approximate molar ratio of 1:10:30:10. The 1:4 glycerol: sugar ratio suggested that some glycerol probably arose from $1 \rightarrow 6$-linked galactopyranose units in the main chain in addition to that from arabinofuranose and galactopyranose end-units. The presence of threitol confirmed the existence in the polymer of $1 \rightarrow 4$ galactopyranose residues (1). The major part of the polyalcohol was hydrolyzed with 0.2 *N* hydrochloric acid for 10 hours at room temperature and the acid neutralized with lead carbonate. The filtered solution was passed through cation and anion exchange resins and the neutral eluate was evaporated to small volume. The acidic materials on the anion resin were subsequently eluted and examined (0.91 g). The neutral eluate was concentrated to a small volume and poured into an acetone–alcohol mixture, yielding a

[1]*Presented at the 142nd American Chemical Society Meeting, Atlantic City, New Jersey, September, 1962.*
[2]*Present address: Department of Plant Science, University of Manitoba, Winnipeg, Manitoba.*

precipitate, oligosaccharide A (2.60 g), which was subsequently further degraded to oligosaccharide B. The supernatant from this precipitation contained compounds of low molecular weight (2.71 g). The balance from the 8 g of gum presumably consisted of volatile two-carbon fragments such as glycollic aldehyde.

The present paper is concerned with the nature of the neutral, low molecular weight components; oligosaccharides A and B; and the acidic material. The degradation is shown schematically in Fig. 1. The results presented here show that the Smith degradation is a powerful method for the investigation of the fine structure of polysaccharide gums.

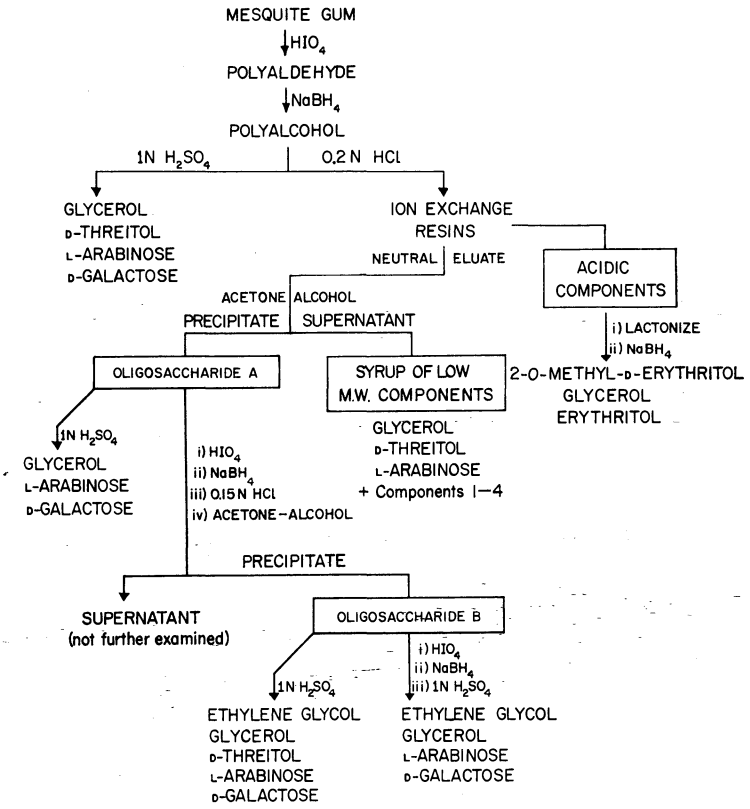

FIG. 1. The periodate degradation of mesquite gum.

The Low Molecular Weight Material

Chromatographic examination of the neutral sirup showed it to contain three non-reducing compounds with R_f values less than glucose (components 2, 3, and 4), presumably substituted arabinose and/or galactose units, and other components which corresponded in R_f values to threitol, glycerol, and arabinose. A non-reducing compound (component 1) with a greater mobility than threitol was also present; however, no ethylene glycol was detected. D-Threitol and glycerol were identified as their *p*-nitrobenzoates, L-arabinose as the crystalline sugar, and the other components as follows.

Component 1, $[\alpha]_D$ 5° in water, had an R_g of 2.31 in ethyl acetate – acetic acid – water (8:2:2) (solvent A), 2.22 in ethyl acetate – pyridine – water (9:2:2) (solvent B), and upon hydrolysis with mineral acid gave arabinose and glycerol in a molar ratio of 1:1. Periodate

Can. J. Chem. Downloaded from www.nrcresearchpress.com by 210.87.254.40 on 09/05/12
For personal use only.

Can. J. Chem. Downloaded from www.nrcresearchpress.com by 210.87.254.40 on 09/05/12
For personal use only.

oxidation, reduction ($NaBH_4$), and hydrolysis gave glycerol and ethylene glycol in a 1:1 molar ratio. In the periodate degradation of this component, formaldehyde was formed, and assuming that one arabinofuranose unit was linked to the primary hydroxyl of glycerol, the calculated degree of polymerization (D.P.) was found to be 2. Component 1 is therefore 1-*O*-L-arabinofuranosyl glycerol.

Component 2, $[\alpha]_D$ 39° in water, had an R_g of 0.90 in solvent A, 0.98 in solvent B, and upon hydrolysis gave glycerol and arabinose in an approximate molar ratio of 1:3. Periodate degradation gave formaldehyde corresponding to a D.P. of 3 to 4 and hydrolysis of the derived polyalcohol gave ethylene glycol, glycerol, and arabinose in an approximate molar ratio of 1:3:1. As in the periodate degradation of component 1, ethylene glycol arose from glycerol glycosidically bonded through C_1. Glycerol arose from arabinofuranose end-units and internal units presumably linked through C_5. The majority of molecules apparently also contained one arabinofuranose unit linked through C_2 or C_3, presumably C_2 from the methylation data (1).

Component 3, $[\alpha]_D$ 87° in water, had an R_g of 0.59 in solvent A, 0.46 in solvent B, and upon hydrolysis gave glycerol and arabinose in a molar ratio of about 1:4. Periodate oxidation gave formaldehyde corresponding to an approximate D.P. of 5 and hydrolysis of the derived polyalcohol gave ethylene glycol, glycerol, and arabinose in a molar ratio of approximately 1:4:1. Here again, it is believed that ethylene glycol arose from a glycerol unit glycosidically bonded at C_1 whereas arabinofuranose end-residues and internal arabinofuranose units linked through C_5 would furnish glycerol. Apparently almost all of the molecules contained one arabinofuranose unit linked through C_2.

Component 4, $[\alpha]_D$ 64° in water, had an R_g of 0.21 in solvent A and 0.22 in solvent B. Hydrolysis gave glycerol, arabinose, and galactose in an approximate molar ratio of 1:5:1. A trace of threitol appeared to be present. Oxidation with periodate resulted in the formation of formaldehyde the quantity of which corresponded to a D.P. of about 7. Hydrolysis of the polyalcohol gave ethylene glycol, glycerol, and arabinose in a ratio of approximately 1:4:3. Each molecule apparently contained one galactose unit and since no appreciable threitol was formed upon periodate degradation, the hexose residue must have been linked through C_6. Consequently, this hexose moiety was thus most likely linked through C_6 and C_3 in the original polymer. About 60% of the molecules apparently contained an arabinofuranose unit linked through C_2 while the other pentose units were apparently linked through C_5 in order to furnish glycerol in the periodate oxidation. Ethylene glycol would again have arisen from a glycerol residue linked through C_1.

The similarity in the structure of components 1–4 indicates that the arabinose side chains are of unequal length and the composition of component 4 suggests that the maximum number of arabinose units which may be joined together is six. There is, however, no evidence at present to show that all the arabinose units are linked to each other and the possibility of having two arabinose chains joined to galactopyranose at C_6 and C_3 etc. cannot be discounted. It would appear that the shorter arabinose chains are joined $1 \rightarrow 6$ to galactopyranose units rather than $1 \rightarrow 3$ and that these galactopyranose units are oxidized by periodate.

Examination of Oligosaccharides A and B

Acid hydrolysis of the non-reducing oligosaccharide A gave galactose, arabinose, and glycerol in an approximate molar ratio of 12:18:1. By analogy with components 1–4 it was assumed that each molecule was terminated by a glycerol residue linked through C_1. On this basis the amount of formaldehyde liberated on periodate oxidation of oligo-

saccharide A corresponded to a D.P. of 28. Reduction of the polyaldehyde and repetition of the mild acid hydrolysis gave a product (oligosaccharide B) which was precipitable in a 3:1 acetone–alcohol mixture. The supernatant contained only glycerol and a small amount of polymeric material, indicating that oligosaccharide A was not greatly degraded by periodate oxidation. Complete hydrolysis of oligosaccharide B gave ethylene glycol (from glycerol residues linked through C_1), glycerol (from terminal, non-reducing arabinofuranose and 1 → 6-linked galactopyranose units), D-threitol (from 1 → 4-linked galactopyranose units), L-arabinose, and D-galactose in an approximate ratio of 1:6:1.5:13:11. The nearly 1:1 ratio of galactose:arabinose indicated that each galactose unit was still substituted by an arabinofuranose unit at C_3 with a few hexose units still carrying two pentose residues. The presence of some threitol suggested that some galactose residues were linked by 1 → 4 bonds. The amount of ethylene glycol found by the periodate – chromotropic acid analysis (7) and by weight corresponded to an approximate D.P. of 30, hence in close agreement with that obtained by formaldehyde analysis of the periodate oxidation mixture. The alcohols were converted to the corresponding *p*-nitrobenzoates and the sugars were obtained crystalline.

A small quantity of twice-degraded mesquite gum, i.e. oligosaccharide B, was oxidized with periodate as described above. A small quantity of formaldehyde was released, presumably from some glycosidically bound threitol end-residues. Reduction ($NaBH_4$) and complete acid hydrolysis gave ethylene glycol, glycerol, arabinose, and galactose in an approximate molar ratio of 1:9:2:10. The amount of ethylene glycol found suggested a D.P. of about 22. Assuming that the small quantity of formaldehyde formed in the periodate oxidation came from threitol end-groups and adding this to the molar proportion of ethylene glycol, the estimated D.P. would then be about 24. This value indicated that about six or seven arabinose units were removed from each oligosaccharde molecule in the third periodate degradation. The rather large proportion of glycerol can be explained, as indicated above, as arising from arabinofuranose units and from a few threitol end-residues.

The Acidic Components

The acidic material obtained from the initial mild acid hydrolysis was eluted from the anion exchange resin with alkali and deionized. The residue obtained on evaporation was heated under vacuum to effect lactonization and the product dissolved in aqueous methanol to which sodium borohydride was added. The reduction proceeded overnight when the solution was evaporated to dryness and treated with methanolic hydrogen chloride to remove borate. Deionization finally yielded a sirup which was shown to contain 2-*O*-methyl-D-erythritol as the major component together with smaller amounts of glycerol and erythritol. The molar ratio was 19.4:1.6:1.

The 2-*O*-methyl-D-erythritol was obtained as expected from terminal units of 4-*O*-methyl-D-glucuronic acid. Glycerol would arise from terminal glucuronic acid units and erythritol from a glucuronic acid substituted at C_4 by a group other than methoxyl, e.g. arabinofuranose. About 1 in 20 of the acid groups occurred in this latter manner while 2 in 20 appeared to be unsubstituted glucuronic acid. It seemed unlikely that the glycerol and erythritol were artifacts arising from an incomplete separation of the acidic and neutral components since erythritol was not detected in the latter. Similar results have been obtained in the investigation of the acidic constituents of applewood and cherrywood xylans (6).

This periodate study on mesquite gum confirms the complexity and highly branched

Can. J. Chem. Downloaded from www.nrcresearchpress.com by 210.87.254.40 on 09/05/12
For personal use only.

nature of the polysaccharide. The isolation and characterization of D-threitol provide definite evidence for 1 → 4-substituted galactopyranose units and examination of the acidic fraction indicates the probable occurrence of acids other than 4-*O*-methyl-D-glucuronic acid in the gum.

EXPERIMENTAL

Chromatographic separations were carried out on Whatman No. 1 and No. 3MM papers for analytical and preparative purposes respectively using the descending technique and the following solvents: A, ethyl acetate – acetic acid – water, 8:2:2; B, ethyl acetate – pyridine – water, 9:2:2; C, butanone–water azeotrope.

Reducing compounds were detected with *p*-anisidine trichloroacetate and non-reducing compounds with ammoniacal silver nitrate. R_g values refer to D-glucose = 1.00.

Reducing sugars were determined by the phenol – sulphuric acid method (8) and polyols by periodate oxidation to formaldehyde, which was determined with chromotropic acid (7).

Evaporations were carried out under reduced pressure with a bath temperature of 40° C. Melting points are uncorrected. Specific rotations are equilibrium values determined at 22±2° C in water unless otherwise stated.

1. Periodate Degradation

Mesquite gum (8.0 g) was dissolved in water (200 ml), the solution was cooled (5° C), and periodic acid (40 mmoles dissolved in 50 ml water) added. The oxidation proceeded at 5° C and in the dark. After 96 hours, 0.46 mole of periodate per sugar unit had been consumed and no change was observed in the periodate uptake thereafter. The periodate and iodate ions were removed by precipitation with barium carbonate and the polyaldehyde was reduced with sodium borohydride (250 mg per gram of original gum). After 34 hours, the solution was neutralized and evaporated to dryness. The residue was treated several times with methanolic hydrogen chloride to remove borate.

2. Complete Acid Hydrolysis of Polyalcohol

A small portion (about 40 mg) of the residue was boiled with mineral acid (1 *N* H_2SO_4, 15 ml) for 8 hours, after which the solution was neutralized ($BaCO_3$), deionized, and evaporated. The residue was chromatographed in solvents A, B, and C, and glycerol, threitol, arabinose, and galactose were found to be present. The ratio of the components was determined chromatographically and a typical analysis gave 1.3, 13.2, 40.1, and 12.9 μmoles of threitol, glycerol, arabinose, and galactose, respectively, or a molar ratio of approximately 1:10:30:10.

3. Mild Acid Hydrolysis of Polyalcohol

The bulk of the residue was dissolved in 0.2 *N* hydrochloric acid (50 ml) and left at room temperature for 10 hours, when the acid was neutralized with lead carbonate. The filtered solution was passed through cation and anion exchange resin columns in that order and the neutral effluent evaporated to a small volume (25 ml). Addition of this solution with vigorous stirring to a 1:1 acetone–alcohol mixture gave an amorphous, white precipitate which was collected by centrifugation and dried by solvent exchange to yield 2.6 g (oligosaccharide A). The acidic material was later eluted from the anion exchange resin, see Section 6. The experiments on oligosaccharide A are reported in Section 5 and the nature of the non-precipitable components in the mother liquor is described in Section 4.

4. Characterization of Low Molecular Weight Components

The supernatant from the precipitation of oligosaccharide A and the combined washings were evaporated to a thick sirup (2.71 g). Chromatographic examination revealed the presence of glycerol, threitol, and arabinose and four other non-reducing components (components 1 to 4), one with an R_f greater than arabinose, the other three with R_g values less than 1.0. The sirupy mixture was resolved on sheets of Whatman 3 MM paper using solvent A. Where necessary, components were rechromatographed to attain maximum homogeneity. *Glycerol*, 280 mg, treated with *p*-nitrobenzoyl chloride and pyridine in the usual manner, gave the corresponding tri-*p*-nitrobenzoate, m.p. and mixed m.p. 189–191° C (9). D-*Threitol*, 185 mg, was converted to the tetra-*p*-nitrobenzoate, m.p. and mixed m.p. 222–224° (5). L-*Arabinose*, 415 mg, crystallized spontaneously, m.p. and mixed m.p. 158–159°, $[\alpha]_D$ 103° (*c*, 0.3).

Component 1

Component 1, 135 mg, $[\alpha]_D$ 5° (*c*, 1.4), R_g 2.31 in solvent A, 2.22 in B, gave upon hydrolysis (1 *N* H_2SO_4, 8 hours) arabinose and glycerol. Typical paper chromatographic analysis of the hydrolyzate gave 5.0 μmoles arabinose and 4.85 μmoles glycerol, hence a molar ratio of arabinose:glycerol of 1:1. A portion (65 mg) of component 1 was oxidized with periodate (25 ml 0.5 *M* periodic acid) at 5° C. Formaldehyde was determined after 48 hours (constant) and amounted to 8.1 mg, which corresponded to a D.P. of 2. Periodate and iodate were precipitated ($BaCO_3$) and sodium borohydride (30 mg) was added to the solution, which was left for 24 hours at room temperature. The solution was evaporated, treated with several volumes (15 ml) of methanolic hydrogen chloride (2%) to remove borate, and the residue was boiled with acid (1 *N* H_2SO_4,

Can. J. Chem. Downloaded from www.nrcresearchpress.com by 210.87.254.40 on 09/05/12
For personal use only.

15 ml) for 8 hours. After neutralization ($BaCO_3$), deionization of the filtrate, and evaporation, chromatographic examination of the residue showed the presence of glycerol and ethylene glycol. A typical chromatographic assay gave glycerol, 2.40 μmoles, and ethylene glycol, 2.55 μmoles. The approximate molar ratio of glycerol:ethylene glycol is therefore 1:1. Hence component 1 is 1-*O*-L-arabinofuranosyl glycerol.

Component 2

Component 2, 164 mg, $[\alpha]_D$ 39° (*c*, 1.6), R_g 0.90 in solvent A, 0.98 in B, gave upon hydrolysis glycerol and arabinose in a molar ratio of approximately 1:3. Treatment of a portion (82 mg) with periodate, as described for component 1, released 6.05 mg formaldehyde, corresponding to a D.P. of 4. Hydrolysis of the polyalcohol gave ethylene glycol and glycerol in an approximate molar ratio of 1:3.

Component 3

Component 3, 139 mg, $[\alpha]_D$ 87° (*c*, 1.4), R_g 0.59 in solvent A, 0.46 in B, was analyzed as described for component 1. Acid hydrolysis of a portion gave glycerol and arabinose in a 1:4 molar ratio. Traces of threitol and galactose also appeared to be present. Periodate oxidation of a portion (69 mg) released 3.70 mg formaldehyde, corresponding to an approximate D.P. of 5. Hydrolysis of the polyalcohol gave ethylene glycol and glycerol in molar ratio of approximately 1:4.

Component 4

Component 4, 76 mg, $[\alpha]_D$ 64° (*c*, 0.8), R_g 0.21 in solvent A, 0.22 in B, gave upon acid hydrolysis glycerol, arabinose, and galactose in a molar ratio of 1:5:1. A trace of threitol was also noted. Periodate oxidation of a portion (37 mg) released 1.13 mg formaldehyde, which corresponded to an approximate D.P. of 8. Hydrolysis of the polyalcohol gave ethylene glycol, glycerol, and arabinose in a ratio of about 1:4:3.

The hydrolyzates of components 4, 5, 6, and 7 were combined and the mixture resolved using Whatman 3MM paper and solvent A. *Glycerol*, treated with *p*-nitrobenzoyl chloride in the usual manner, gave the tri-*p*-nitrobenzoate, m.p. and mixed m.p. 189–191° C. L-*Arabinose* crystallized spontaneously, m.p. and mixed m.p. 157–159° C, $[\alpha]_D$ 102° (*c*, 0.4). D-*Galactose* sirup crystallized on nucleation, m.p. and mixed m.p. 164–165°, $[\alpha]_D$ 78° (*c*, 0.5). *Threitol* was present in very small quantity and identified only by paper chromatography.

The hydrolyzates of the polyalcohols of components 4, 5, 6, and 7 were also combined and the mixture resolved as described above. *Ethylene glycol* was converted to the corresponding di-*p*-nitrobenzoate, m.p. and mixed m.p. 138–141° C (10). *Glycerol* likewise was converted to the tri-*p*-nitrobenzoate, m.p. and mixed m.p. 188–191° C. L-*Arabinose* sirup crystallized on nucleation, m.p. and mixed m.p. 156–158° C, $[\alpha]_D$ 100° (*c*, 0.35). *Galactose* was present in small quantity and identified by paper chromatography.

5. Characterization of Oligosaccharide A

(a) Acid Hydrolysis

A portion (0.80 g) of the oligosaccharide, $[\alpha]_D$ 14° (*c*, 0.8), was boiled with 1 *N* sulphuric acid (25 ml) for about 10 hours. The solution was neutralized ($BaCO_3$), deionized, and evaporated to a sirup. Chromatographic examination revealed the presence of glycerol (minor quantity), arabinose, and galactose in a molar ratio of about 1:18:12. The apparent D.P. of the non-reducing oligosaccharide was thus about 31. The sirup was resolved using Whatman 3 MM paper and solvent A. L-*Arabinose*, 375 mg, crystallized spontaneously, m.p. and mixed m.p. 157–159° C, $[\alpha]_D$ 102° (*c*, 0.8). D-*Galactose*, 302 mg, also crystallized spontaneously, m.p. and mixed m.p. 165–166° C, $[\alpha]_D$ 79° (*c*, 0.5). *Glycerol*, 13 mg, was transformed to the tri-*p*-nitrobenzoate in the usual manner, m.p. and mixed m.p. 187–190° C.

(b) Periodate Oxidation

A quantity of the oligosaccharide, 1.0 g, was suspended in 0.1 *M* periodic acid solution (60 ml) and kept at 5° C. After 48 hours, 2.99 mmoles of periodate was consumed and 3.01 mmoles after 72 hours with no change thereafter. Formaldehyde was determined and the 7.16 mg found corresponded to an approximate D.P. of 28. Periodate and iodate were removed ($BaCO_3$) and the polyaldehyde was reduced ($NaBH_4$, 350 mg). After 24 hours, the solution was evaporated, borate was removed, and the solution acidified with hydrochloric acid (to 0.15 *N*). When the solution had stood at room temperature for 2 hours, the acid was neutralized and the filtered solution was passed through anion and cation exchange resin columns and the effluent evaporated to a small volume. The product was precipitable in a 1:3 alcohol–acetone mixture to give a white amorphous material (oligosaccharide B). Part (150 mg) of this solid was saved for further periodate oxidation (see (*c*) below) and the remainder (about 250 mg) was boiled with mineral acid (1 *N* H_2SO_4, 20 ml) for 8 hours. After neutralization and evaporation of the solution, chromatographic examination of the residue revealed the presence of galactose, arabinose, glycerol, ethylene glycol, and threitol. The molar ratio was 11:13:6:1:1.5 respectively. The mixture was resolved by paper chromatography. *Ethylene glycol*, 11 mg, was converted to the di-*p*-nitrobenzoate, m.p. and mixed m.p. 138–141° C (9). *Glycerol*, 55 mg, gave the tri-*p*-nitrobenzoate, m.p. and mixed m.p. 189–191° C. *Threitol*, 15 mg, was converted to the tetra-*p*-nitrobenzoate, m.p. and mixed m.p. 221–223° C. L-*Arabinose*, 120 mg, crystallized spontaneously, m.p. and mixed m.p. 157–158° C, $[\alpha]_D$ 101.5° (*c*, 0.45). D-*Galactose*, 100 mg, crystallized upon nucleation, m.p. and mixed m.p. 165–166°, $[\alpha]_D$ 78.5° (*c*, 0.85).

(c) Periodate Oxidation of Twice-Degraded Gum (Oligosaccharide B)

A small quantity (53 mg) of oligosaccharide B obtained in the previous experiment (Section 5(*b*)) was

Can. J. Chem. Downloaded from www.nrcresearchpress.com by 210.87.254.40 on 09/05/12
For personal use only.

dissolved in 0.1 *M* periodic acid solution (25 ml) and left at 5° C for 96 hours. A small quantity (about 2.0 μmoles) of formaldehyde was released. The periodate and iodate were removed ($BaCO_3$) and to the solution was added sodium borohydride (20 mg). After 24 hours at room temperature, the solution was evaporated, borate was removed, and the residue boiled with mineral acid (1 *N* H_2SO_4, 20 ml) for 8 hours. After neutralization ($BaCO_3$), deionization, and evaporation of the solution, paper chromatographic examination of the sirup revealed the presence of ethylene glycol, glycerol, arabinose, and galactose in an approximate molar ratio of 1:9:2:10. The formaldehyde:ethylene glycol:glycerol:arabinose:galactose ratio was approximately 2:1:9:2:10.

6. Isolation and Characterization of Acidic Residues

The anion exchange resin was eluted with alkali and the sodium ions subsequently adsorbed on a cation exchange resin. The acidic solution was evaporated and traces of hydrochloric acid were removed by repeated evaporation of 20-ml volumes of methanol. The residue was finally transferred to a tube fitted with a cold finger kept packed with solid carbon dioxide and the contents heated, under vacuum, for 2 hours at 80–90° C. The residue was dissolved in aqueous methanol, sodium borohydride was added (1.35 g), and the solution was left overnight. Evaporation of the solution to dryness followed by treatment with methanolic hydrogen chloride to remove borate and deionization gave a neutral sirup (0.905 g). Chromatographic analysis of the sirup revealed the presence of 2-*O*-methyl-D-erythritol in major amount and minor quantities of glycerol and erythritol. A portion of the sirup was resolved using Whatman 3 MM paper and solvent C. *Glycerol*, 7.8 mg, was converted to the corresponding tri-*p*-nitrobenzoate, m.p. and mixed m.p. 187–189° C. *Erythritol*, 6.5 mg, gave the tetra-*p*-nitrobenzoate, m.p. and mixed m.p. 248–250° C (10). *2-O-Methyl-D-erythritol*, 140 mg, $[\alpha]_D$ 30° (*c*, 2.8 in methanol), was converted to the corresponding tri-*p*-nitrobenzoate (6), m.p. and mixed m.p. 218–220° C, $[\alpha]_D$ −18° (*c*, 0.9 in pyridine). The molar ratio of erythritol:glycerol:2-*O*-methyl-D-erythritol was 1:1.6:19.4. The ratio of uronic acid to other sugar units estimated from the above results is approximately 1:7.

ACKNOWLEDGMENTS

The technical assistance of Miss Judith Hunter is gratefully acknowledged and we are indebted to the National Research Council of Canada for continued financial support.

REFERENCES

1. F. SMITH and R. MONTGOMERY. *In* Chemistry of plant gums and mucilages. Reinhold Publ. Corp., New York. 1959.
2. I. J. GOLDSTEIN, G. W. HAY, B. A. LEWIS, and F. SMITH. Abstracts, 135th American Chemical Society Meeting, Boston. April, 1959. p. 3D.
3. D. V. MYHRE and F. SMITH. Abstracts, 139th American Chemical Society Meeting, St. Louis. March, 1961. p. 6D.
4. G. W. HAY and F. SMITH. Abstracts, 139th American Chemical Society Meeting, St. Louis. March, 1961. p. 6D.
5. A. M. UNRAU. Ph.D. Thesis, University of Minnesota, St. Paul, Minn. 1960.
6. G. G. S. DUTTON and A. M. UNRAU. Can. J. Chem. **40**, 348 (1962).
7. A. M. UNRAU and F. SMITH. Chem. Ind. (London), 330 (1957).
8. M. DUBOIS, J. K. HAMILTON, K. A. GILLES, P. A. REBERS, and F. SMITH. Anal. Chem. **28**, 350 (1956).
9. F. WILD. *In* Characterization of organic compounds. C.U.P., London. 1958. p. 82.
10. G. G. S. DUTTON and A. M. UNRAU. Can. J. Chem. **40**, 1196 (1962).

Can. J. Chem. Downloaded from www.nrcresearchpress.com by 210.87.254.40 on 09/05/12
For personal use only.

THE LOW-FREQUENCY DIELECTRIC PROPERTIES OF ETHYLENE OXIDE AND ETHYLENE OXIDE HYDRATE[1]

D. W. DAVIDSON AND G. J. WILSON[2]
Division of Applied Chemistry, National Research Council, Ottawa, Canada
Received October 3, 1962

ABSTRACT

The static dielectric constant of liquid ethylene oxide has been measured between 158 and 286° K. The hydrate of ethylene oxide exhibits a dispersion–absorption region characterized by static dielectric constants about one-third as large as those of ice and by relatively large "high-frequency" dielectric constants ($\epsilon_1 = 7.5$ at 0° C). This region may be approximately described as a circular arc locus, but may be represented somewhat better by a superposition of two (or three) semicircular dispersions. In either case, the activation energy for the relaxation of water molecules, to which this region is ascribed, is ca. 6.7 kcal/mole, except at low temperatures, where it becomes smaller. Experimental values of ϵ_1 agree roughly with those calculated for comparatively rapid orientation of ethylene oxide molecules in the cavities of the hydrate. Such orientation may account for absorption maxima observed at 11 Mc/sec and above 100 Mc/sec at 90° K.

Can. J. Chem. Downloaded from www.nrcresearchpress.com by 210.87.254.40 on 09/05/12
For personal use only.

Within the past 12 years the crystal structures of the so-called "gas hydrates" have been determined. The gas molecules occupy cavities in a solid framework which consists of hydrogen-bonded water molecules. The arrangement of the oxygen atoms in the simplest class of gas hydrate, as outlined by Claussen (1), Pauling and Marsh (2), and von Stackelberg and Müller (3), corresponds to the cubic space group O_h^3—$Pm3n$, with a_0 equal to about 12 Å, and 46 molecules in the unit cell. Each unit cell of this structure contains 6 large cavities enclosed by 2 parallel hexagons and 12 pentagons of hydrogen-bonded water molecules, and 2 small cavities enclosed by 12 penatgons. The diameters of the cavities are, respectively, 5.9 and 5.2 Å (3).

The dielectric properties of these hydrates should be capable of providing information about two important aspects of their behavior: (*a*) the nature of the relaxation of the water molecules, which form a solid structure somewhat looser than that in ice, and (*b*) the nature of the barriers which oppose reorientation or rotation of the gas molecules occluded in the cavities.

This report presents results of a dielectric study of the hydrate of ethylene oxide whose structure conforms (4) to von Stackelberg's structure I as outlined above. Observations have been made of a relatively low-frequency dispersion–absorption region attributed to the relaxation of water molecules in this hydrate, and some study has been made of a second absorption region at relatively high frequencies and low temperatures which is possibly related to the rotation of the ethylene oxide molecules in the cavities. To ensure that these absorption effects cannot be ascribed to the presence of ethylene oxide as a separate phase, the dielectric properties of liquid and solid ethylene oxide were also examined.

EXPERIMENTAL METHODS

Ethylene Oxide

Samples of ethylene oxide (Matheson, 99.7% minimum purity) for measurements on the liquid were crudely fractionated at reduced pressure, followed by direct distillation of the middle fraction into the dielectric cell. The vapor pressure of one sample before the cell was filled was 49.6 cm at 0° (vs. 49.51 cm from the equation of Giauque and Gordon (5)). Ethylene oxide directly from the cylinder was used in the

[1]*Issued as N.R.C. No. 7306.*
[2]*N.R.C. Postdoctoral Fellow, 1961–1962.*

preparation of the hydrate. Gas chromatographic analysis with a hydrogen-flame detector showed negligible content of combustible impurities.

Preparation of the Hydrate

A number of attempts to prepare hydrates of various gases by bubbling the gas through liquid water near 0° in cells of different design did not provide satisfactory samples for electrical measurements, mainly because of incomplete filling of the interelectrode region. Because of its high boiling point (11°) and miscibility with water, ethylene oxide readily formed a hydrate *in situ*. Aqueous solutions in the cell were slowly frozen from below. Usually the ethylene oxide concentration was initially slightly in excess of the composition $C_2H_4O \cdot 5.75H_2O$ corresponding to all the cavities filled. The growth of a crack-free layer of uniform thickness could be followed initially by observation through the Lucite windows of the cell used for the bridge measurements. Later stages of freezing could not readily be followed because of the limited transparency of the samples. Subsequent cooling to dry ice temperature caused cracking ("starring") in the vicinity of the windows.

Electrical Measurements

Measurements were made in the frequency range between 0.040 and 500 kc/sec with a General Radio Model 716 Capacitance Bridge and Guard Circuit and conventional oscillators and tuneable detectors. The cell used in conjunction with the bridge was similar to the one of Auty and Cole (6). The guarded electrode (diameter 1 in.) and guard ring (outer diameter 2 in.), separated by a 0.010-in. gap, were mounted on a Teflon plate attached to a shaft extending through the top of the cell, by which the distance between the upper electrode assembly and the parallel lower electrode (diameter 2 in.) could be adjusted. Electrode separations were in the range 0.6 to 1.0 cm. In the initial measurements bare brass electrodes were used; later the electrodes were gold-plated. Gold-plating appeared not to affect appreciably the experimental properties, even at low frequencies. Temperature control and measurement were essentially as previously described (7).

Some measurements were also made with a Boonton RX Meter at temperatures between +5° and −40° and also near the boiling point of liquid nitrogen. The cell, for these high-frequency measurements, consists of two cylindrical coaxial electrodes of stainless steel, of which the outer (inside diameter 1/2 in.) is screwed into a brass tube so as to bear against a Teflon disk which forms the bottom of the cell. The tube in turn is threaded to fit the coaxial adapter of the RX Meter. The inner electrode (3/8 in. long, 1/16-in. diameter) penetrates the Teflon disk and ends in a pin which fits the central socket of the adapter. For the measurements near liquid nitrogen temperature, a center electrode of 1/4-in. diameter was used. The required temperature was achieved by circulation of cold liquid through a brass jacket. Since the metal connections between the bottom of the cell and the Meter cabinet were only 2.5 in. long (to minimize inductance effects) there was considerable heat conduction to the sample. This did not appear to affect appreciably the sample temperature for fast circulation rates at −40°, but was serious when liquid nitrogen was passed through the jacket. In the latter case the sample temperature was some 10° to 20° above liquid nitrogen temperature and a temperature gradient of several degrees occurred across the sample; there was also a cooling effect on the zero balance controls of the Meter which served to increase the uncertainties of the measurements.

A number of transient measurements were also made at temperatures below −130° with photographic and pen-recorder techniques. These results are not reported in detail because of lack of reproducibility and comparably large experimental uncertainties, which made their analysis ambiguous (see below).

Samples of ethylene oxide itself were studied in a three-electrode cell of the Gross–Taylor type (8), enclosed in a copper can provided with fittings which permitted the sample to be distilled into the cell. Measurements were made at at least two frequencies, including 100 and 200 kc/sec.

The conductivity of liquid ethylene oxide at relatively high temperatures was sufficiently great that it was thought possible that the value of the static dielectric constants calculated from the bridge data might be affected. Application of a d-c. "deionizing field" of 1000 volts/cm considerably reduced the conductivity. After 15 minutes, the conductivity of a sample at −25° was reduced from 5×10^{-7} to 4×10^{-8} $ohm^{-1}cm^{-1}$. Some hours were required at −25° for the conductivity to return to half its original value, the rate of increase increasing with temperature. Values of the dielectric constant measured at 100 kc/sec were insignificantly affected by change in conductivity. After one sample had been subjected to the field for several hours at 0° and the sample distilled off, the cell constant was found to have increased by 0.3% and the cathode to be coated with a thin layer of gelatinous material not readily soluble in benzene or water. Similar observations, following pre-electrolysis of nitrobenzene, were reported by Parry (9). It is possible that some polymerization of ethylene oxide took place at the cathode.

A d-c. forefield was also applied to a sample of ethylene oxide hydrate, as discussed below.

RESULTS AND DISCUSSION

Ethylene Oxide

The static dielectric constants of liquid ethylene oxide, measured for three samples at 41 temperatures between 158 and 286° K, may be expressed by $\epsilon_0 = -6.89 + 5842/T$

Can. J. Chem. Downloaded from www.nrcresearchpress.com by 210.87.254.40 on 09/05/12
For personal use only.

with an average deviation of ±0.4%. Consistent differences between the measured dielectric constants and those given by the above expression were noted only at temperatures near 160° K, where the experimental values were greater by about 0.2. The experimental values are plotted vs. temperature in Fig. 1.

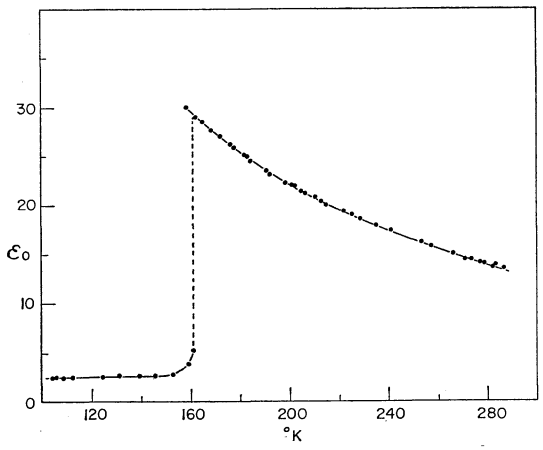

FIG. 1. Static dielectric constants of ethylene oxide.

The values of ϵ_0 previously reported (10) at temperatures to −30° are lower than our values by some 6%.

Studies of gaseous ethylene oxide have given dipole moments in the range 1.88 to 1.91 D (11, 12). The dipole moment μ_0 calculated from the liquid data (ϵ_0 = 14.50, d = 0.8917 g/cm³ at 0° C (13)) by use of the Onsager equation is greatly dependent upon the value taken for n_∞^2, as derived from A, the intercept of the molar polarization vs. $1/T$ curve of the gas. For A = 11.4 cm³/mole (11), μ_0 = 1.97 D, and for A = 12.9 cm³/mole (12), μ_0 = 1.88 D, both at 0° C. Values of μ_0 calculated from the density data of Maass and Bloomer (14) show little dependence on temperature to −50°.

The small dielectric constant of solid ethylene oxide (ca. 2.7, see Fig. 1) shows no contribution from dipolar orientation.

ETHYLENE OXIDE HYDRATE

(a) Relaxation Attributable to Water Molecules

Nature of the Relaxation Behavior

Several complex plane loci, all for the same sample, are illustrated in Fig. 2. The locus of Fig. 2 (*e*) resembles the Cole–Cole circular arc (15), modified by an additional (and variable) polarization effect at lower frequencies. Even at frequencies high enough that the latter effect may be assumed to have a negligible influence on the shape of the locus, however, the circular arc does not accurately describe the experimental behavior, as is shown by the tendency for ϵ'' to approach the real axis at right angles at high frequencies and by the departure from linearity of the log v/u vs. log f plot (15) of Fig. 3, where $v^2 = (\epsilon_0-\epsilon')^2+(\epsilon'')^2$ and $u^2 = (\epsilon'-\epsilon_1)^2+(\epsilon'')^2$.

A somewhat more satisfactory representation (illustrated in Fig. 4) is by a superposition of two semicircular dispersion regions whose relaxation times differ by a factor of about 3 and whose relative amplitudes are in a ratio of about 2:1, the greater contribution

Can. J. Chem. Downloaded from www.nrcresearchpress.com by 210.87.254.40 on 09/05/12
For personal use only.

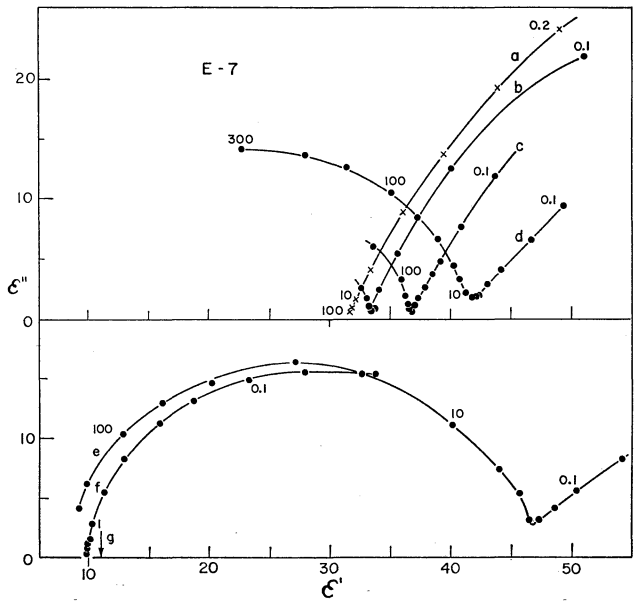

FIG. 2. Cole–Cole plots for ethylene oxide hydrate at: *a* 2.2°, *b* −16.8°, *c* −35.5°, *d* −52.0°, *e* −77.2°, *f* −130.0°, *g* −162.5°. Numbers are frequencies in kc/sec.

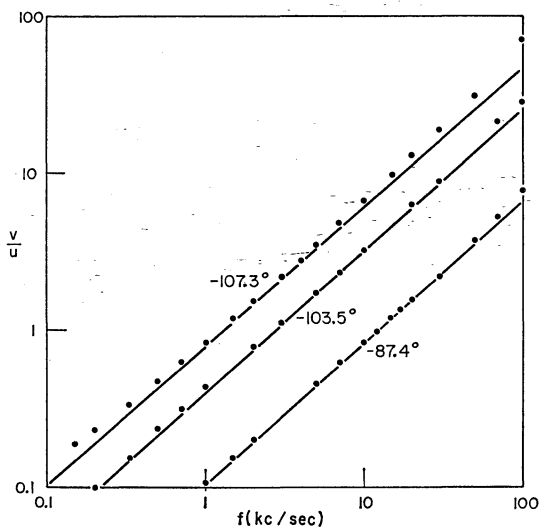

FIG. 3. Plots of log (v/u) vs. log (frequency) for three different samples. v and u are the lengths of lines between points in the complex plane and ϵ_0 and ϵ_1 respectively.

being made by the region with the larger relaxation times. Because of overlap at low frequencies with the additional polarization effect, it is difficult to assess the adequacy of this representation in the low-frequency range. Most samples, like that of Fig. 4, showed some indication of the presence of a small, third dispersion region, although some did not.

In view of the degree of arbitrariness connected with resolution of the observed loci

Can. J. Chem. Downloaded from www.nrcresearchpress.com by 210.87.254.40 on 09/05/12
For personal use only.

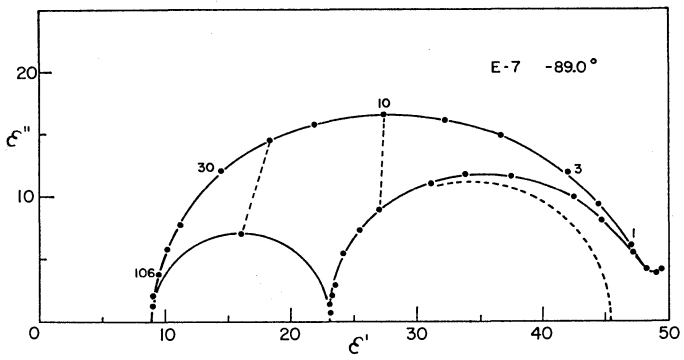

FIG. 4. Plot illustrating approximate resolution into two semicircles.

into two or three semicircles, we have preferred to represent the experimental behavior approximately in terms of the Cole–Cole α function, particularly for evaluation of relaxation times. As in the similar case of acetone hydrate (16) we attribute this dispersion–absorption region to relaxation of the water molecules of the hydrate structure and refer to the corresponding limiting value of ϵ' at low frequencies as the "static dielectric constant" ϵ_0.

Before discussing this dispersion region further, we shall briefly consider the effects of air gaps, of possible contamination of the sample with ice or liquid phase, and of the low-frequency polarization.

Effect of Air Gaps

In spite of attempts to allow the upper electrode assembly to follow the contraction of the samples with decrease of temperature, they invariably appeared to crack at low temperatures. Below about −70° the measured static dielectric constants of the best samples tended to decrease, or to remain almost unchanged, as the temperature fell.

An air gap of uniform thickness a fraction δ of the total interelectrode distance results in an apparent complex dielectric constant $\epsilon^*_{(app)}$, for the sample, which is related to the true complex dielectric constant ϵ^* of the hydrate by the series condenser formula

$$\frac{1}{\epsilon^*_{(app)}} = \delta + \frac{1-\delta}{\epsilon^*}$$

or

$$\epsilon^*_{(app)} = \frac{\epsilon^*}{1+\delta(\epsilon^*-1)}.$$

This results in lower apparent values of the limiting low- and high-frequency dielectric constants

$$\epsilon_{0\,(app)} = \frac{\epsilon_0}{1+\delta(\epsilon_0-1)}$$

$$\epsilon_{1\,(app)} = \frac{\epsilon_1}{1+\delta(\epsilon_1-1)}.$$

Since ϵ_0 is more than four times as large as ϵ_1, a finite δ has a more pronounced effect on the apparent value of the static dielectric constant than on the limiting high-frequency value. In fact (cf. Fig. 7, below) the experimental values of ϵ_1 always increased with decreasing temperature. In general our results are consistent with the presence of δ's less than 0.01 at temperatures above −150°.

Can. J. Chem. Downloaded from www.nrcresearchpress.com by 210.87.254.40 on 09/05/12
For personal use only.

For a single relaxation process, the relaxation time in the presence of an air gap becomes

$$\tau_{(app)} = \frac{1+\delta(\epsilon_1-1)}{1+\delta(\epsilon_0-1)}\tau_0,$$

and for less simple relaxation processes the effect is qualitatively the same: a shift of the dispersion regions toward higher frequencies. It is apparent that an air gap in series with parallel linearly independent relaxing units will reduce the separation in frequency of the resulting dispersion regions by shifting the low-frequency region more. At the same time the linear independence is removed. For the small δ's associated with temperatures at which dispersion occurred at bridge frequencies some small reduction in the slope of $d(\ln \tau_0)/d(1/T)$ with decreasing temperature is to be expected, but no qualitative change in the shape of the dispersion.

Effects of Ice and Excess Ethylene Oxide

One sample, after a series of runs, exhibited deep channels extending downward from the upper electrodes which may have been escape routes for ethylene oxide. Some ethylene oxide may also have been lost during the freezing process. Since the relaxation rate of hexagonal ice is some 1000 times slower than that of the water in the hydrate at 0° and this ratio increases with decreasing temperature, one should expect small quantities of ice merely to result in somewhat lower values of the complex dielectric constant. However, analysis shows that a thin layer of ice, in series with the hydrate sample, gives rise to a secondary absorption region at lower frequencies than that of the hydrate, but at considerably higher frequencies than that characteristic of ice itself. Thus a layer of ice of thickness a fraction 0.02 of the sample thickness would show, in addition to the relatively unchanged absorption of the hydrate, a second absorption maximum at a frequency some 35 times as great as a sample of ice alone. It is possible that the presence of ice may contribute to the polarization observed on the low-frequency side of the hydrate dispersion curve, but it cannot account for its principal characteristics.

From the broad, flat top of the liquidus curve of the ethylene oxide – water system (14), we infer that ethylene oxide present in excess will appear as a small quantity of almost water-free liquid. The measurements on liquid ethylene oxide showed no dispersion in the frequency range of that shown by the hydrate. There were no breaks in the ϵ_1 vs. $1/T$ curves (Fig. 7, below) to suggest the abrupt formation of an appreciable quantity of liquid above a eutectic temperature.

Low-frequency Polarization

The rise in ϵ'' and ϵ' observed in all samples at low frequencies is approximately proportional to $\omega^{-1/2}$. This dependence on frequency is considerably less than that which would follow from the charging and discharging of an air-sample interface for a sample displaying a finite air gap and a finite d-c. conductance. At frequencies sufficiently low that there are no contributions from the dispersion region defined by ϵ_0 and ϵ_1 the apparent dielectric constant, given above, reduces to

$$\epsilon^*_{(app)} = \frac{\epsilon_0 - i\epsilon''}{1+\delta(\epsilon_0-1)-i\delta\epsilon''},$$

where ϵ'' is related to k, the conductivity in ohm^{-1}cm^{-1}, and ω, the frequency in radians sec^{-1}, by

$$\epsilon'' = \frac{1.13\times10^{13}k}{\omega}.$$

Can. J. Chem. Downloaded from www.nrcresearchpress.com by 210.87.254.40 on 09/05/12
For personal use only.

Separating the real and imaginary parts of $\epsilon^*_{(app)}$ gives, for small values of δ,

$$\epsilon''_{(app)} = \frac{1.13\times10^{13}k(1-\delta)}{\omega[1+\delta(\epsilon_0-1)]^2}$$

$$\epsilon'_{(app)} = \frac{\epsilon_0}{1+\delta(\epsilon_0-1)} + \frac{\delta}{\omega^2}\frac{(1.13\times10^{13}k)^2}{[1+\delta(\epsilon_0-1)]^2}.$$

As with similar effects in ice (17) and acetone hydrate (16), application of a d-c. field results in a considerable reduction of the low-frequency polarization (Fig. 5). This suggests

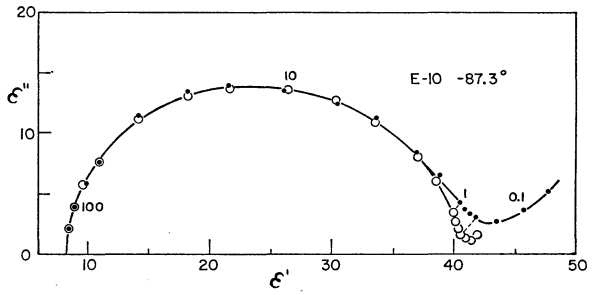

FIG. 5. Effect of application of a d-c. voltage of 1000 v/cm for 17 hours.

that the origin lies in a relatively slow buildup of space charge arising from the presence of ions in the sample. It can be shown that contributions to the complex dielectric constant which are proportional to $\omega^{1/2}$ on the high-frequency side of a polarization region are equivalent to a charging current which is proportional, for short times after application of a ramp voltage, to $(\text{time})^{1/2}$, as found for acetone hydrate (16).

Relaxation Times

Relaxation times, expressed in terms of the τ_0 of the circular arc representation, are shown in Fig. 6. The straight line drawn corresponds to an activation energy for orientation of the water molecules in ethylene oxide hydrate of 6.7 kcal/mole.

Analysis of a number of dispersion curves in terms of the two semicircles mentioned above yields two sets of relaxation times, each of which shows very nearly the same temperature dependence as τ_0.

The experimental relaxation times of Fig. 6 show a trend toward a smaller dependence on $1/T$ with decreasing temperature, which is the direction to be expected from the presence of an increasing air gap. However, this trend is already apparent at comparatively high temperatures where appreciable air gaps are not to be expected. Moreover, the transient measurements at much lower temperatures show the trend to become much more pronounced. An instance of this is given by the data of Table I, which refers to the transient current (expressed in units of capacitance equal to the cell constant) following application of ramp voltage pulse. The experimental data may be represented, about equally well, by

(I) $$\epsilon(t) = \epsilon_1+(\epsilon_0-\epsilon_1)\sum_{n=1}^{\infty}\frac{(-1)^{n-1}x^{n(1-\alpha)}}{\Gamma[1+n(1-\alpha)]},$$

with $\epsilon_1 = 11.57$, $\epsilon_0 = 50.74$, $\alpha = 0.313$, $x = 1/46.25$, and by

(II) $$\epsilon(t) = 11.57+14.66(1-e^{-t/9.5})+24.51(1-e^{-t/109}).$$

Can. J. Chem. Downloaded from www.nrcresearchpress.com by 210.87.254.40 on 09/05/12
For personal use only.

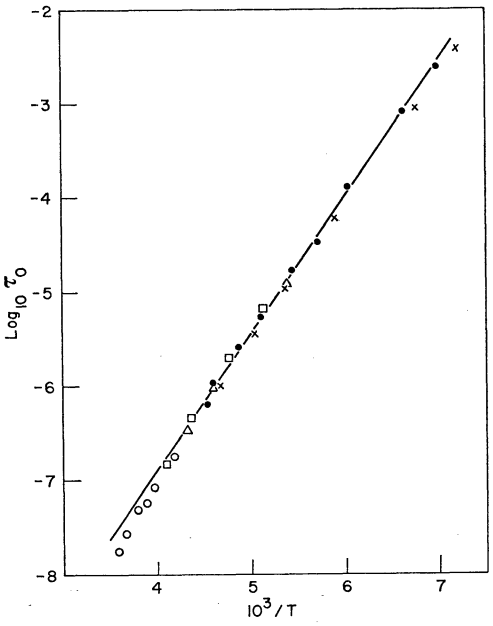

FIG. 6. Dependence of relaxation times on temperature: O, RX Meter results; other points, bridge measurements on various samples.

TABLE I

Comparison of experimental transient data at −182.7° with calculated values

Time (sec)	Experimental $\epsilon(t)$	Calculated $\epsilon(t)$	
		I	II
0	11.57 (bridge data)	(11.57)	(11.57)
4.75	18.6	19.3	18.4
9.5	22.9	23.1	22.9
19	28.0	27.8	28.2
38	33.2	33.4	33.2
76	38.8	38.8	38.6
95	40.5	40.4	40.6
124	42.4	42.0	42.9

Equation (I) results from integration of the current response function (for systems showing the circular arc behavior) for a step voltage pulse (18).[3] Equation (II) is equivalent to the previously mentioned resolution of the complex $\epsilon(i\omega)$ locus into two semicircles. On either basis, the relaxation times at this temperature are of the order of 100 times smaller than those given by linear extrapolation in $1/T$ of relaxation times given by analysis of the bridge data at higher temperatures. We are unable to offer an explanation of this fall in apparent activation energy at low temperatures, which is supported by other transient results.

Static Dielectric Constants

These values for ethylene oxide hydrate are only about one-third as great as the static

[3]*We are indebted to Mrs. M. Helfenstein and Dr. S. D. Baxter of the N.R.C. Computation Centre for evaluation of the sums of (I) for various values of* α.

Can. J. Chem. Downloaded from www.nrcresearchpress.com by 210.87.254.40 on 09/05/12
For personal use only.

dielectric constants of ice at comparable temperatures. This result points to an almost complete lack of correlation between the direction of the dipole moment of a water molecule and the average resultant dipole moment of surrounding molecules, that is, to a Kirkwood correlation parameter g of the order of unity. The explanation may lie in the mirror symmetric arrangement of the six water molecules around any pair in the hydrate structure, in contrast to the predominantly centrosymmetric arrangement in hexagonal ice (19). This is accompanied by the presence of pentagonal rings whose resultant moments tend to be small (16).

High-frequency Dielectric Constants

The experimental values of ϵ_1 are shown in Fig. 7. These tended to increase with

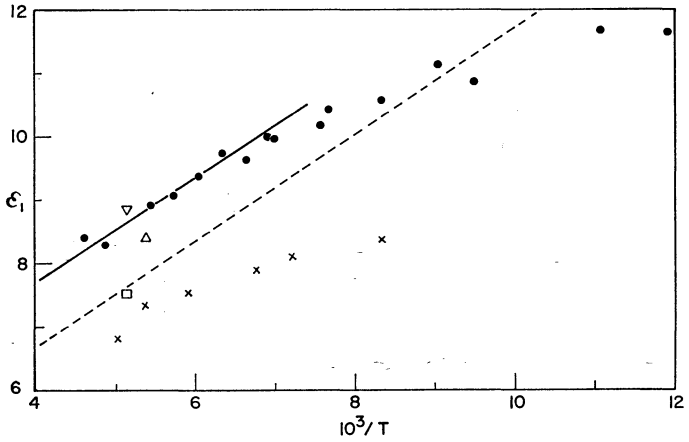

FIG. 7. "High-frequency" dielectric constants (various samples).

decreasing temperature, although less so at low temperatures than would be expected if no cracks were present in the samples. Some variation in ϵ_1 may also be associated with different degrees of cavity occupation.

The high value of ϵ_1 may be ascribed to a considerable freedom of orientation of ethylene oxide molecules in the cavities. The previous treatment (16), based on the presence of acetone molecules in the larger cavities of von Stackelberg's structure II, must be modified for ethylene oxide to take into account the presence of molecules in the small as well as the large cavities of structure I. In the terminology of reference 16, the radii of the large and small cavities of structure I are $a_L = 2.95$ Å, $a_S = 2.6$ Å. For ethylene oxide $\mu_0 = 1.90\times10^{-18}$ e.s.u. and $\alpha = 4.5\times10^{-24}$ cm^3/molecule, which, together with $T = 273°$ and $\epsilon_\infty = 3$, leads to a contribution to the Maxwell polarization from the orientation of the occluded molecules of $P_2 = (5.7\times10^{-23}y_L\nu_L+6.3\times10^{-23}y_S\nu_S)E$. For values of the cavity concentrations ν_L and ν_S obtained from the unit cell dimensions and for all cavities filled ($y_L = y_S = 1$), one finds $\epsilon_1 = 6.4$; for only the large cavities filled ($y_L = 1$, $y_S = 0$), $\epsilon_1 = 5.5$. The experimental value of ϵ_1 for the "best" samples is about 7.5 at 0° C.

The broken line in Fig. 7 represents the variation of the computed value of ϵ_1 with temperature, with all the cavities assumed filled and variations in the cavity concentrations neglected. The highest experimental values are about one unit higher than, and tend to run parallel to, the computed line, down to temperatures of about −120°. At lower temperatures cracks in the samples apparently cause the experimental values to fall below the calculated ones.

Can. J. Chem. Downloaded from www.nrcresearchpress.com by 210.87.254.40 on 09/05/12
For personal use only.

(b) Relaxation Probably Attributable to Ethylene Oxide Molecules

RX Meter measurements on two of three samples cooled to about 90° K showed absorption and dispersion behavior as illustrated in Fig. 8. The third showed a rise in

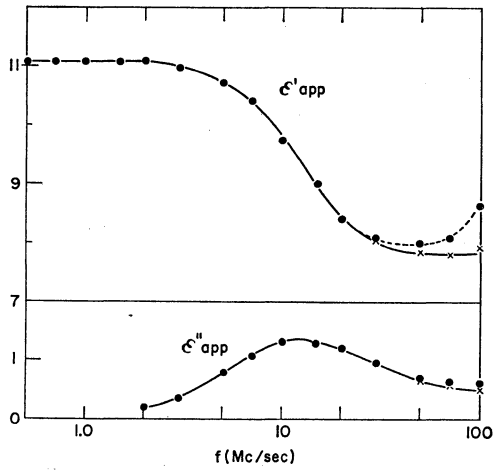

FIG. 8. Dependence of apparent dielectric constants and loss on frequency near 90° K. Points × have been corrected for inductance.

ϵ'' at high frequencies, but not the maximum near 11 Mc/sec. The considerable uncertainties of measurements at this temperature (see *Electrical Measurements*, above), especially in the absolute values of ϵ' and ϵ'', should be emphasized. One may speculate that the absorption peak at 11 Mc/sec arises from the restricted rotation of ethylene oxide molecules in the smaller cavities, the one at some frequency above 100 Mc/sec from rotation in the larger cavities, and the absence of the first peak in one sample from a low ethylene oxide content. Unfortunately the difficulties of proper temperature control at low temperatures have so far prevented an estimate of the activation energy involved.

CONCLUSIONS

The general relaxation behavior of the water molecules in ethylene oxide hydrate is consistent with the crystal structure. In particular, an activation energy for orientation of water molecules no more than one-half as great as that in ice may be related to the presence of O—O—O angles which may be as small as 103.8° and as large as 125.2° (based on the water coordinates of Pauling and Marsh (2)) and to O—O distances which are apparently some 0.05 Å longer than those in ice (3). This looser hydrogen-bonded structure should lead both to a greater concentration of Bjerrum defects (19) and to their greater mobility, provided the latter involves a classical diffusion process.

Within the space group O_h^3—$Pm3n$ the water molecules occur at three different site types (*k*, *i*, *c*), around which the positions of neighboring water molecules differ. There are four types of hydrogen bond (*k*–*k*, *k*–*i*, *k*–*c*, *i*–*i*), of which some may be "weaker" than others. For example, at the *k* sites within the hexagonal rings the angles between the *k*–*k* and *k*–*c* bonds (125.2°) show the greatest departure from the tetrahedral value and these bonds may be somewhat weaker than those of the *k*–*i* or *i*–*i* type. Such a non-equivalence of molecules and bonds is consistent with a broader absorption than that found in ice, particularly if the absorption is due to the relaxation of individual molecules

Can. J. Chem. Downloaded from www.nrcresearchpress.com by 210.87.254.40 on 09/05/12
For personal use only.

by the migration of orientational defects rather than by some cooperative process involving a great many molecules, as appears to occur in liquids exhibiting strong intermolecular hydrogen bonding.

The general similarity between the low-frequency dielectric properties of the hydrates of ethylene oxide and acetone (16) may be significant, in view of their different structures. Ethylene oxide forms a "gas hydrate" (von Stackelberg's structure I) (4), whereas acetone forms a "liquid hydrate" (structure II) (20). The question of the generality of this kind of behavior within the group of clathrate hydrates awaits study of other hydrates. As is apparent from the foregoing, certain experimental difficulties stand in the way of accurate low-frequency measurements on these systems. Preliminary study of other structure I hydrates suggests that the general dielectric characteristics are similar to those of ethylene oxide hydrate, but that the precise relaxation rates of the water molecules vary with the nature of the occluded molecules.

REFERENCES

1. W. F. CLAUSSEN. J. Chem. Phys. **19**, 1425 (1951).
2. L. PAULING and R. E. MARSH. Proc. Natl. Acad. Sci. **38**, 112 (1952).
3. M. VON STACKELBERG and H. R. MÜLLER. Z. Elektrochem. **58**, 25 (1954).
4. M. VON STACKELBERG and B. MEUTHEN. Z. Elektrochem. **62**, 130 (1958).
5. W. F. GIAUQUE and J. GORDON. J. Am. Chem. Soc. **71**, 2176 (1949).
6. R. P. AUTY and R. H. COLE. J. Chem. Phys. **20**, 1309 (1952).
7. D. W. DAVIDSON. Can. J. Chem. **35**, 458 (1957).
8. P. M. GROSS, JR. and R. C. TAYLOR. J. Am. Chem. Soc. **72**, 2075 (1950).
9. J. V. L. PARRY. Proc. Phys. Soc. (London), **68**, 431 (1955).
10. J. D. NICKERSON and R. MCINTOSH. Can. J. Chem. **35**, 1325 (1957).
11. A. A. MARYOTT and F. BUCKLEY. Tables of dielectric constants and electric dipole moments of substances in the gaseous state. Natl. Bur. St. Circ. No. 537. 1953.
12. W. L. G. GENT. J. Chem. Soc. 58 (1957).
13. J. TIMMERMANS. Physico-chemical constants of pure organic compounds. Elsevier Publishing Co., New York. 1950.
14. O. MAASS and E. H. BLOOMER. J. Am. Chem. Soc. **44**, 1709 (1922).
15. K. S. COLE and R. H. COLE. J. Chem. Phys. **9**, 341 (1941).
16. G. J. WILSON and D. W. DAVIDSON. Can. J. Chem. **41**, 264 (1963).
17. H. GRANICHER, O. JACCARD, P. SCHERRER, and A. STEINEMANN. Helv. Phys. Acta, **28**, 300 (1955).
18. K. S. COLE and R. H. COLE. J. Chem. Phys. **10**, 98 (1942).
19. N. BJERRUM. Kgl. Danske Videnskab. Selskab, Mat. Fys. Medd. **27**, 31 (1951).
20. A. S. QUIST and H. S. FRANK. J. Phys. Chem. **65**, 560 (1961).

Can. J. Chem. Downloaded from www.nrcresearchpress.com by 210.87.254.40 on 09/05/12
For personal use only.

THE PREPARATION, PROPERTIES, AND STRUCTURE OF 2,6-BIS-(ALKYLAMINO)-2,5-HEPTADIEN-4-ONES[1]

DENYS COOK
Exploratory Research Laboratory, Dow Chemical of Canada, Limited, Sarnia, Ontario
Received January 21, 1963

ABSTRACT

2,6-Bis-(alkylamino)-2,5-heptadien-4-ones have been prepared by the action of aqueous amines on (1) 3-acetyl-4-hydroxy-6-methyl-2-pyrone (dehydroacetic acid), (2) 3-(1-alkyliminoethyl)-4-hydroxy-6-methyl-2-pyrone, (3) 3-carboxy-2,6-dimethyl-4-pyrone, (4) 2,6-dimethyl-4-pyrone, (5) 2,6-dihydroxy-2,5-heptadien-4-one. The reactions are facile and proceed smoothly at temperatures near, or slightly above, room temperature. In (1) the first products are 3-(1-alkyliminoethyl)-4-hydroxy-6-methyl-2-pyrones, followed by the 2,6-bis-(alkylamino)-2,5-heptadien-4-one. The other reactions yield only the latter product, but in all cases it decomposes to the 4-pyridone at higher temperature, or on prolonged reaction or by the action of acid.

The 2,6-bis-(alkylamino)-2,5-heptadien-4-ones are pale yellow compounds with a slight violet fluorescence. Infrared, n.m.r., and ultraviolet spectra are consistent with an open-chain, internally hydrogen-bonded structure.

INTRODUCTION

The reaction of dehydroacetic acid (I) (3-acetyl-4-hydroxy-6-methyl-2-pyrone) with amines to give 4-pyridones (IV) has been known for a very long time (1). It has now been found that precursers to the pyridones are open-chain compounds 2,6-bis-(alkylamino)-2,5-heptadien-4-ones (III), which are isolable, stable compounds. The preparation of these compounds from 4-pyrones has been noted by Spooner (2), whose work has been confirmed.

Several other methods of preparation of the 2,6-bis-(alkylamino)-2,5-heptadien-4-ones from substituted 2- and 4-pyrones have been discovered, and will be described, together with some comments on the reaction paths.

EXPERIMENTAL

2,6-Bis-(alkylamino)-2,5-heptadien-4-ones (III)

These were prepared by the following methods.

1A. Reaction of 3-Acetyl-4-hydroxy-6-methyl-2-pyrone (Dehydroacetic Acid) (I) with Aqueous (~25% w/v) CH_3NH_2

The quantities in Table I were warmed on a steam bath (~50°) for 0.5 hour (i, 24 hours; ii, 16 hours) then allowed to cool.

TABLE I

	DHA (I)		aq. CH_3NH_2			H_2O		Yield
	g	mole	ml	mole	Ratio	g	Product	g
i	16.8	0.1	12.5	0.1	1	27	IIa	20.9
							(IIa + IVa)	4.1
ii	16.8	0.1	25.5	0.2	2	20	IIa + IVa	20.0
iii	16.8	0.1	50.0	0.4	4	0	IIIa	12.6
							(IVa)	9.1
iv	16.8	0.1	75.0	0.6	6	0	IVa	23.3
v	16.8	0.1	100.0	0.8	8	0	IVa	20.5

[1]*Contribution No. 93.*

Can. J. Chem. Downloaded from www.nrcresearchpress.com by 210.87.254.42 on 09/05/12
For personal use only.

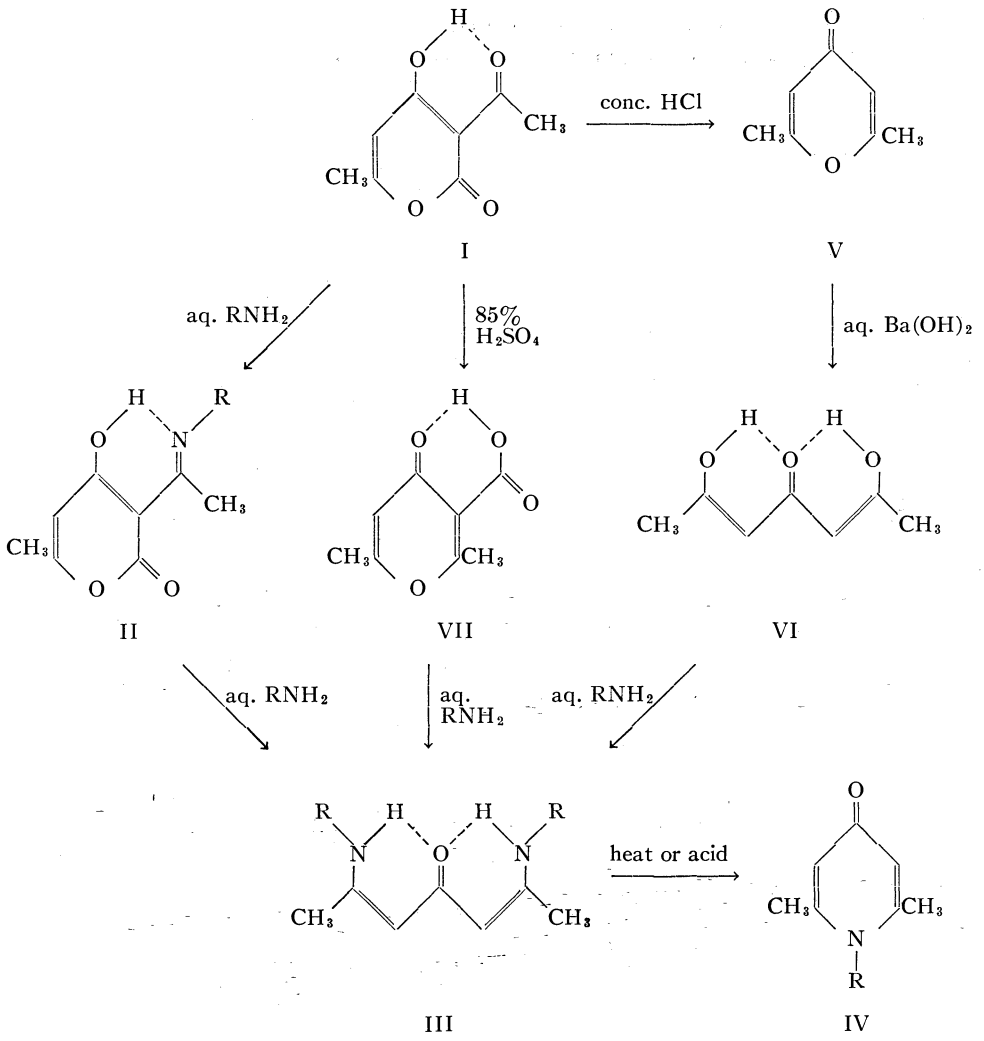

a, R = CH_3
b, R = C_2H_5

In iii, after about 0.2 hour, pale yellow crystals with a slight violet fluorescence appeared (III*a*). The products in parentheses crystallized from the filtrate.

II*a*, 3-(1-methyliminoethyl)-4-hydroxy-6-methyl-2-pyrone, m.p. 127–128° (anhydrous—by efflorescence of hydrate, by gentle heating *in vacuo*).

III*a*, 2,6-bis-(methylamino)-2,5-heptadien-4-one, m.p. 164.5–165.5° (from ligroin, b.p. 35–60°). Found: C, 64.40%; H, 9.69%; N, 16.60%. Calc. for $C_9H_{16}N_2O$: C, 64.25%; H, 9.59%; N, 16.65%. Infrared (CCl_4, CS_2): 1571 vs, 1436 m, 1413 m, 1312 m, 1283 s, 1168 w, 1068 m, 1029 w, 812 w, 796 m, 786 w, sh, 704 w cm^{-1}. Nuclear magnetic resonance (CCl_4): CH_3, 110; CH_3(N), doublet at 174 (J = 6); CH, 280; NH, ~600, very broad. All values in c.p.s. downfield from tetramethysilane as internal reference. Integrated intensities in the ratio 6, 6, 2, ~2, respectively.

IV*a*, 1,2,6-trimethyl-4-pyridone.$3H_2O$, m.p. 110–111° (hydrate from water). Found: C, 50.39%; H, 8.61%; N, 7.31%. Calc. for $C_8H_{11}NO.3H_2O$: C, 50.31%; H, 8.97%; N, 7.33%. M.p. 244–246° (anhydrous—by gentle heating *in vacuo*) (3).

1B. Reaction of Dehydroacetic Acid (I) with Aqueous $C_2H_5NH_2$

The quantities in Table II were warmed on a steam bath (~50°) for 1 hour (ii, 2 hours, vi, vii, 0.5 hour) then allowed to cool.

Can. J. Chem. Downloaded from www.nrcresearchpress.com by 210.87.254.42 on 09/05/12
For personal use only.

TABLE II

	DHA (I)		$C_2H_5NH_2$			H_2O		Yield
	g	mole	g	mole	Ratio	g	Product	g
i	16.8	0.1	4.5	0.1	1	36	II*b*	14.0
ii	16.8	0.1	9.0	0.2	2	36	II*b*	18.1
iii	16.8	0.1	13.5	0.3	3	36	II*b*	16.3
iv	16.8	0.1	18.0	0.4	4	36	III*b*	15.0
							(II*b*)	3.0
							(IV*b*)	Trace
v	16.8	0.1	22.5	0.5	5	36	III*b*	18.9
							(II*b*)	3.0
							(IV*b*)	1.0
vi	10.0	0.06	15.0	0.33	5.5	35	III*b*	
vii	50.0	0.30	75.0	1.65	5.5	175	III*b*	33.7
							(IV*b*)	24.0
viii	16.8	0.1	36.0	0.8	8	36	III*b*	20.6
							(IV*b*)	1.0

In experiments iv to viii, after about 0.5 hour, pale yellow crystals with a slight violet fluorescence appeared (III*b*). The products in parentheses crystallized from the filtrate.

II*b*, 3-(1-ethyliminoethyl)-4-hydroxy-6-methyl-2-pyrone, m.p. 68–69° (hydrate from 50% v/v aq. acetone), m.p. 85–86° (anhydrous — by efflorescence of hydrate, or by gentle heating *in vacuo*). Found: C, 61.60%; H, 6.35%; N, 7.33%. Calc. for $C_6H_{13}NO_3$: C, 61.52%; H, 6.71%; N, 7.18%.

III*b*, 2,6-bis-(ethylamino)-2,5-heptadien-4-one, m.p. 91–92° (from ligroin, b.p. 35–60°). Found: C, 67.53%; H, 9.45%; N, 14.04%. Calc. for $C_{11}H_{20}N_2O$: C, 67.30%; H, 10.27%; N, 14.27%. Infrared (CCl_4, CS_2): 1571 vs, 1436 m, 1369 w, 1300 m, 1260 m, 1133 m, 1090 m, 1060 w, 1030 w, 1000 w, 791 m cm^{-1}. Ultraviolet (methylcyclohexane): 370, 360, 285 sh, 232 mμ. Nuclear magnetic resonance (CCl_4): $CH_3(CH_2)$, triplet at 75 (J = 7); CH_3, 109; CH_2, quintet at 194 (J = 6.5); CH, 265; NH, ~600, very broad. All values in c.p.s. downfield from tetramethylsilane as internal reference. Integrated intensities in the ratio 6, 6, 4, 2, ~2, respectively.

IV*b*, 1-ethyl-2,6-dimethyl-4-pyridone.$3H_2O$, m.p. 72–74° (hydrate from water). Found: N, 6.94%. Calc. for $C_8H_{11}NO.3H_2O$: N, 6.83%. M.p. 158–161° (anhydrous—by gentle heating *in vacuo*) (3).

2. Reaction of 3-(1-Methyliminoethyl)-4-hydroxy-6-methyl-2-pyrone (IIa) with Aqueous Amine

3-(1-Methyliminoethyl)-4-hydroxy-6-methyl-2-pyrone (II*a*) (4.5 g) was warmed on the steam bath (~50°) for 0.2 hour with 12.5 ml 25% aqueous CH_3NH_2 (0.1 mole), when the typical pale yellow, violet fluorescing solid precipitated. After the mixture was cooled and filtered, 2.28 g 2,6-bis-(methylamino)-2,5-heptadien-4-one (III*a*) was obtained, identical in all respects with that prepared previously; 1.03 g 1,2,6-trimethyl-4-pyridone.$3H_2O$ (IV*a*) crystallized from the filtrate.

3. Reaction of 3-Carboxy-2,6-dimethyl-4-pyrone (VII) with Aqueous Ethylamine

3-Carboxy-2,6-dimethyl-4-pyrone was prepared from dehydroacetic acid by the action of 85% H_2SO_4 as described by Collie and Hilditch (4). 3-Carboxy-2,6-dimethyl-4-pyrone (8.4 g, 0.05 mole) was slurried with 18 g H_2O, then 18 g $C_2H_5NH_2$ was added. The solid went into solution as an exothermal reaction took place, followed very quickly by precipitation of a light yellow solid with typical pale violet fluorescence. This product (19.5 g) was the 2,6-bis-(ethylamino)-2,5-heptadien-4-one, identical in all respects with that previously prepared.

4. Reaction of 2,6-Dimethyl-4-pyrone (V) (DMP) with Aqueous Ethylamine

The quantities in Table III were warmed on a steam bath (~50°) for 1 hour (iii, 0.7 hour) then allowed to cool.

In all these experiments after ~0.5 hour light yellow crystals with typical pale violet fluorescence (III*b*) appeared in solution. The products in parentheses crystallized from the filtrate.

5. Reaction of 2,6-Dihydroxy-2,5-heptadien-4-one (VI) (Diacetylacetone) with Aqueous Ethylamine

2,6-Dihydroxy-2,5-heptadien-4-one was prepared from 2,6-dimethyl-4-pyrone (V) (12.4 g, 0.1 mole) in 40 ml H_2O to which was added 17.1 g $Ba(OH)_2$ (0.1 mole) in 500 ml hot water, precipitating the barium salt of VI, 22.9 g. This was dissolved in 100 ml 3 *N* HCl and extracted with $CHCl_3$ (2×100 ml), which on evaporation gave VI, 7.27 g, 52%, m.p. 58–59°. Found: C, 59.10%; H, 6.90%. Calc. for $C_7H_{10}O_3$: C, 59.14%; H, 7.08%. Infrared (CCl_4/CS_2): 1590 vs, 1482 s, 1471 m, 1460 m, 1228 s, 1183 m, 1139 s, 1030 m, 1005 w, 950 w, 898 s, 818 s, 782 w, 745 m cm^{-1}. Ultraviolet (methylcyclohexane): 328 sh, 322, 316 mμ. Nuclear magnetic resonance (CCl_4): CH_3, 118; CH, 304; OH, 842. All values in c.p.s. downfield from tetramethylsilane as internal reference. Some weak resonances at slightly lower field are indicative of a small amount of the keto form. They are being investigated further and will be reported in due course.

Can. J. Chem. Downloaded from www.nrcresearchpress.com by 210.87.254.42 on 09/05/12
For personal use only.

TABLE III

	DMP (V)		$C_2H_5NH_2$			H_2O		Yield
	g	mole	g	mole	Ratio	g	Product	g
i	12.4	0.1	4.5	0.1	1	36	III*b*	1.4
							(V)	6.0
ii	12.4	0.1	9.0	0.2	2	36	III*b*	9.6
							(V)	5.2
iii	12.4	0.1	18.0	0.4	4	36	III*b*	17.2
							(IV*b*)	3.0
iv	12.4	0.1	27.0	0.6	6	36	III*b*	15.4
							(IV*b*)	4.0

2,6-Dihydroxy-2,5-heptadien-4-one, (6.6 g, 0.047 mole), 18 g ethylamine (0.40 mole), and 18 g H_2O were heated on a steam bath. After 1 minute all the solid was in solution, but after 3 minutes a pale yellow solid with typical pale violet fluorescence developed, and the reaction was apparently complete in 8 minutes. This solid, 9.46 g, 81%, was the 2,6-bis-(ethylamino)-2,5-heptadien-4-one, identical in all respects with that prepared previously. The filtrate yielded 0.75 g 1-ethyl-2,6-dimethyl-4-pyridone.$3H_2O$ (IV*b*).

Reaction of 2,6-Dimethyl-4-pyrone with Anhydrous Amine

2,6-Dimethyl-4-pyrone (12.4 g, 0.01 mole) was treated with 9.0 g anhydrous ethylamine (0.2 mole). No reaction was observed, and after evaporation of the ethylamine the pyrone was recovered completely, and had the same infrared spectrum as the starting material.

Reaction of Dehydroacetic Acid with Anhydrous Amine

Dehydroacetic acid (I) (16.8 g, 0.1 mole) was treated with 9.0 g anhydrous ethylamine (0.2 mole). An exothermal reaction took place accompanied by partial solution of the acid in the amine. After evaporation of the excess amine the remaining solid was recrystallized from absolute ethanol, giving 15.9 g, 82%, anhydrous 3-(1-ethyliminoethyl)-4-hydroxy-6-methyl-2-pyrone (II*b*).

Dehydroacetic acid (I) (3.36 g, 0.02 mole) was dissolved in a small amount of $CHCl_3$ and excess ether. About 1.8 g anhydrous ethylamine (0.04 mole) was added, giving a white precipitate, ethylammonium dehydroacetate (X), m.p. 71–73°. Found: C, 56.40%; H, 7.41%; N, 6.19%. Calc. for $C_{10}H_{15}NO_4$: C, 56.32%; H, 7.09%; N, 6.57%. When dry ethylammonium dehydroacetate was heated overnight on a steam bath (~50°) the resulting product was 3-(1-ethyliminoethyl)-4-hydroxy-6-methyl-2-pyrone (II*b*), identical with previous preparations.

Reaction of 2,6-Bis-(ethylamino)-2,5-heptadien-4-one with H_2O

2,6-Bis-(ethylamino)-2,5-heptadien-4-one (III*b*) (1.33 g) and 20 g H_2O were boiled together for 0.5 hour. On cooling the solution and evaporation of excess water a white solid, recrystallized from water as long needles, 0.72 g, 52%, proved, from its infrared spectrum, to be identical with 1-ethyl-2,6-dimethyl-4-pyridone.$3H_2O$ prepared previously.

Reaction of 2,6-Bis-(ethylamino)-2,5-heptadien-4-one with HCl

2,6-Bis-(ethylamino)-2,5-heptadien-4-one (III*b*) (2.12 g) was dissolved in $CHCl_3$, and dry HCl gas was passed into the solution. A white solid precipitated immediately. This gave an infrared spectrum containing a superposition of the bands due to 1-ethyl-2,6-dimethyl-4-pyridone.HCl and $C_2H_5NH_2$.HCl.

The infrared spectra were recorded on a Perkin–Elmer 221 prism-grating spectrometer. A Varian A–60 spectrometer was used to record the n.m.r. spectra, and the ultraviolet spectra were determined on a Beckman DK–2 spectrophotometer. Melting points were determined in sealed capillary tubes and are uncorrected. Microanalyses were done in the Analytical Laboratory, Dow Chemical of Canada, Limited.

DISCUSSION

The experimental results have shown that 2,6-bis-(alkylamino)-2,5-heptadien-4-ones can be made, under the appropriate conditions, from 2,6-dihydroxy-2,5-heptadien-4-one (VI), 3-carboxy-2,6-dimethyl-4-pyrone (VII), and 3-(1-alkyliminoethyl)-4-hydroxy-6-methyl-2-pyrone (II). All these reactions proceed smoothly and quickly and can be considered in turn.

The clue to the structure of the 2,6-bis-(alkylamino)-2,5-heptadien-4-ones came from the reaction of 2,6-dihydroxy-2,5-heptadien-4-one (VI) with RNH_2. The infrared spectra of these compounds (see Experimental and Figs. 1 and 2) have many similarities, both showing

Can. J. Chem. Downloaded from www.nrcresearchpress.com by 210.87.254.42 on 09/05/12
For personal use only.

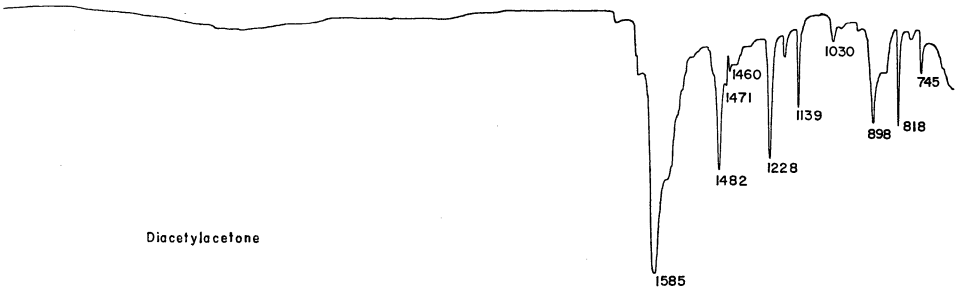

FIG. 1. Infrared spectrum of 2,6-dihydroxy-2,5-heptadien-4-one.

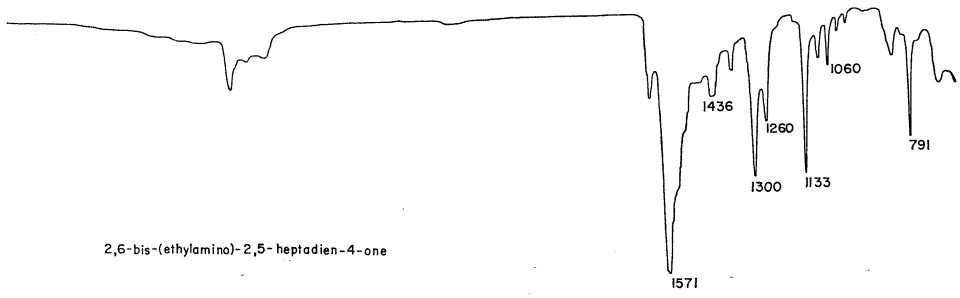

FIG. 2. Infrared spectrum of 2,6-bis-(ethylamino)-2,5-heptadien-4-one.

an intense carbonyl band at ~1571 cm^{-1} for the amino compound (III), and at about ~1590 cm^{-1} for the hydroxy compound (VI). These values are in keeping with our knowledge of carbonyl frequencies, as the following rough calculation shows: 1715 (aliphatic carbonyl) − 2×35 (conjugation) − 2×32 (internal hydrogen bond) = 1581 cm^{-1}. This is also confirmatory evidence that the compounds, as solids and in CCl_4/CS_2 solution, are in the dienol and diamino form. A heptane-2,4,6-trione should have a carbonyl absorption near 1715 cm^{-1}. VI is a white solid (λ_{max} = 316 mμ) whereas compounds III are pale yellow (λ_{max} = 370 mμ) with pale violet fluorescence. These facts tend to confirm that the oxygen atom in the OH group in VI participates in the conjugation in the system to a smaller extent than the nitrogen atom in the RNH group in III (3). The latter shifts the absorption into the visible region, and alters other excited molecular levels to permit fluorescence.

The reaction between 3-carboxy-2,6-dimethyl-4-pyrone and aqueous amines to give III involves opening the 4-pyrone ring. This probably occurs by nucleophilic attack on the carbon atom in the 2- or 6-position by OH^- or amine. The resulting compound, VIII, is seriously hindered and while rotation about the 3,4- and 4,5-bonds relieves some of this strain (IX) the carboxyl group is still hindered. Facile decarboxylation is therefore permitted to give III either directly or from the diketo form of IX.

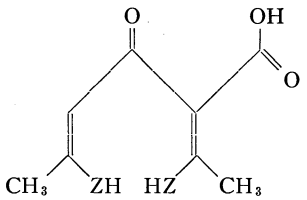

VIII

Z = O or NR

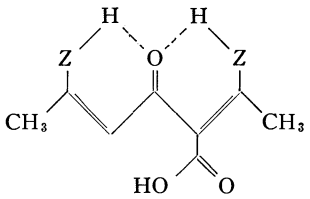

IX

Z = O or NR

Can. J. Chem. Downloaded from www.nrcresearchpress.com by 210.87.254.42 on 09/05/12
For personal use only.

3-(1-Alkyliminoethyl)-4-hydroxy-6-methyl-2-pyrone already contains (in the keto-amine form) a replica of half of the 2,6-bis-(alkylamino)-2,5-heptadien-4-one structure. Opening of the 2-pyrone ring by nucleophilic attack of hydroxyl ion or amine at position 6, followed by rotation about the 4,5-bond, would produce a structure analogous to IX. The subsequent reaction would be exactly as for the 3-carboxy-2,6-dimethyl-4-pyrone just described.

It remains to consider the reactions of dehydroacetic acid and 2,6-dimethyl-4-pyrone with aqueous amines. In the case of dehydroacetic acid the reaction with low molecular ratios of amine produces only the 3-(1-alkyliminoethyl)-4-hydroxy-6-methyl-2-pyrone, suggesting that the condensation proceeds more easily than the ring opening. A concomitant effect may be an insufficiently basic medium to effect ring opening. The solubility of the compounds, too, plays an undetermined part in the reactions. When the anhydrous amine is used in the reaction the only compound resulting is the 3-(1-alkyliminoethyl)-4-hydroxy-6-methyl-2-pyrone, and the reaction is very fast. When the two reactants are mixed in an inert medium, for example, by the action of anhydrous amine on a $CHCl_3$/ether solution of dehydroacetic acid, precipitation of the insoluble ethylammonium dehydroacetate (X) results. This is easily and irreversibly transformed, under mild

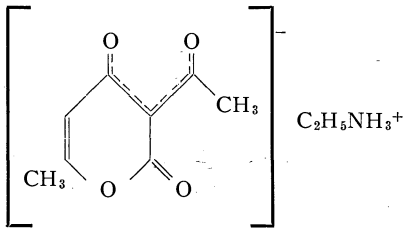

X

conditions, into 3-(1-alkyliminoethyl)-4-hydroxy-6-methyl-2-pyrone (II), by elimination of water. It seems likely, then, that the first reaction product of dehydroacetic acid with aqueous amines is the condensation product, subsequent reaction being as described above for 3-(1-alkyliminoethyl)-4-hydroxy-6-methyl-2-pyrone with aqueous amines.

Aqueous amines react quickly with 2,6-dimethyl-4-pyrone, opening the ring to form the open-chain compound with the OH groups replaced at some stage in the reaction by RNH groups. Again, nucleophilic attack by hydroxyl ion or amine at carbon atoms 2 or 6 seems to be responsible for ring opening.

The ease with which these reactions proceed suggests some of the possible facile mechanisms for synthesis of nitrogen heterocycles of biogenetic significance.

ACKNOWLEDGMENTS

The assistance of Miss C. D. Anderson in preparing some of the compounds and recording their spectra is gratefully acknowledged. The microanalyses were kindly performed by Mr. K. Sketris and Mr. G. A. Whitehouse, and the ultraviolet spectra were taken by Mr. W. T. Sanders. Dr. J. S. McIntyre is thanked for recording the n.m.r. spectra.

REFERENCES

1. L. Haitinger. Chem. Ber. **18**, 452 (1885).
2. A. B. Spooner. Ph.D. Thesis, University of Notre Dame, Notre Dame, Ind. 1950.
3. D. Cook. Can. J. Chem. **41**, 515 (1963).
4. J. N. Collie and T. P. Hilditch. J. Chem. Soc. **91**, 787 (1907).

Can. J. Chem. Downloaded from www.nrcresearchpress.com by 210.87.254.42 on 09/05/12
For personal use only.

THE NON-LINEARITY OF BIS-ARYLMERCURY COMPOUNDS

W. C. Horning, F. Lautenschlaeger, and G. F Wright
Department of Chemistry, University of Toronto, Toronto, Ontario
Received November 30, 1962

ABSTRACT

The measured distortion polarizations of a group of bis-arylmercury compounds show that they do not exhibit exalted atom polarizations. The apparent orientation polarization of each is appreciable. Two of them, which are substituted symmetrically with methoxyl or nitro, exhibit moments expected from the rotation which is generated in such substances. By comparison of bis-4-bromophenylmercury^{202} with the analogue containing the ordinary isotopic mixture of mercury the apparent moments are shown to be unrelated to nuclear asymmetry. The conclusion is unaltered that the apparent moments of bis-arylmercury compounds are due to effective non-linearity in the C—Hg—C bond.

Can. J. Chem. Downloaded from www.nrcresearchpress.com by 210.87.254.5 on 09/05/12
For personal use only.

In continuation of our search to explain the apparently anomalous electric moments of bis-arylmercury compounds (1) we have re-examined and extended the work of Hampson (2), who originally observed the anomalies. Essentially we have arrived at a conclusion which partakes of Hampson's original explanation as a "flexibility moment", which was later generally endorsed by Sidgwick (3) as not unexpected when mercury is involved.

Hampson's opinion that he had measured an orientation polarization of bis-phenylmercury and its symmetrical *p*-methyl, fluoro, chloro, and bromo analogues was not generally accepted. In particular there were some (4) who tried to attribute the anomaly to atom polarization, an argument which Coop and Sutton themselves questioned on the basis of the unrealistic force constant which would be required. Finally the question whether diphenylmercury exhibited an abnormally high atom polarization was for the first time put to the test of experiment (1, 5) and was answered in the negative.

Indeed the value obtained by direct measurement of distortion polarization (P_D, i.e. P_{E+A}) for diphenylmercury was found to be lower than that expected according to the commonly used methods of calculating molecular refraction (MR, i.e. P_E) by addition of the constituent atom refraction according to Eisenlohr (6) or of the bond refractions according to Vogel (7). Since the low distortion polarization implies a definite dipole moment which is unexpected among bis-mercurials it is necessary to decide why these distortion polarizations are low. Consequently the distortion polarizations of a series of bis-mercurials have been examined by the method of dielectric constant determination with compressed wafers of randomly oriented powders together with a number of other substances more or less related. The results are shown in Table I, where the differences between P_D and an average of MR_D by the methods of Eisenlohr and Vogel are shown in the last column.

The distortion polarization (P_D) of diphenylmercury has been redetermined with a result in good agreement with the 57.1 cc reported previously (1). The low value (negative difference) is reflected in comparable differences for the series of substituted diphenylmercurys, items 2–8 inclusive. On the other hand item 9, dimesitylmercury, shows a distortion polarization which is higher than the average of MR_D. But this exception at least conforms with the least of the negative differences among items 2–8 inclusive, namely di-*p*-tolylmercury. Evidently methyl groups exert a compensating effect.

It has been suggested earlier (8) that the negative discrepancy wherein the experimentally determined distortion polarization is lower than the summation value of atom (6) or bond (7) polarizabilities might be ascribed to "negative exaltation" due to substituent phenyl groups. This suggestion was based on the low molecular refractions found for substances in which resonance hydridization exists (9).

This hypothesis seems to be supported by the results of Table I. It may be seen (item 16) that a typical alkyl bis-mercurial does not have P_D lower than MR_D. Alternatively examination of items 12 and 14 as well as 17–34 shows that the presence of phenyl groups or of polynuclear aromatization leads to P_D values which are less than the MR_D calculation.

Of course, these negative values are abnormal in the sense that P_D ought always exceed MR_D since the latter is the measure of the electronic polarization P_E of which P_D is inclusive. In view of the many abnormalities we have encountered it is gratifying to find that a series of saturated alcohols and amines (items 32–37, item 50) seems to behave normally. However, esters, lactones, and lactams (items 40–42 incl.) show positive differences which probably indicate abnormally high atom polarization (P_A).

High atom polarizations have been found previously (10) for nitramines and this series has been extended with items 28–30 inclusive. It is of interest that the lowest of these values (benzylnitroguanidine) involves a substance containing a phenyl group. The high

TABLE I

Measured distortion polarization

Substance	ϵ	d_4^{20}	P_{E+A} exptl.	Electronic polarization: Eisenlohr	Vogel C_{ar}	Vogel C—C C=C	Diff.
1. Diphenylmercury	2.803	2.321	57.4	61.6	62.1	62.6	−4.7
2. Dibenzylmercury	2.852	2.262	64.6	70.9	71.4	71.9	−6.8
3. Di-*p*-tolymercury	3.062	2.228	70.0	70.9	71.4	71.9	−1.4
4. Di-*p*-bromophenylmercury	3.009	2.784	73.9	77.1	77.5	78.8	−3.6
5. Di-*p*-methoxyphenylmercury	2.521	1.964	71.1	74.1	74.9	75.5	−3.7
6. Di-*p*-xenylmercury	2.542	1.704	101.0	109.8	110.3	111.4	−9.5
7. Di-*m*-nitrophenylmercury	2.618	2.170	71.7	74.0	77.8	78.4	−5.0
8. Di-β-naphthylmercury	3.008	2.006	90.9	92.3	95.6	93.8	−3.0
9. Dimesitylmercury	2.945	1.825	94.6	89.3	90.0	90.5	+4.7
10. *p,p'*-Dinitrobibenzyl	2.769	1.371	73.7	73.1	72.5	73.0	+0.8
11. Di-*m*-Nitrophenylmethane	3.135	1.435	74.8	68.4	68.4	68.9	+6.3
12. *p,p'*-Difluorobiphenyl	2.599	1.379	48.0	49.8	49.8	50.4	−2.0
13. *m,m'*-Dinitrobiphenyl	3.213	1.480	70.3	63.8	64.3	63.7	+6.4
14. *p,p'*-Dibromobiphenyl	2.654	1.867	59.5	65.9	65.7	66.3	−6.4
15. *m,m'*-Dinitrobimesityl	2.942	1.205	106.4	91.5	91.6	92.3	+14.7
16. Dicyclohexylmercury*	2.428	1.819	65.2	64.4		65.5	+0.2
17. *cis*-Cinnamic acid	2.433	1.284	37.3	40.7		41.5	−3.8
18. α-Phenylcinnamic acid	2.312	1.137	60.0	65.3	65.3	65.9	−5.5
19. *p*-Phenylazobenzoic acid	2.373	1.214	58.5	62.2	62.5	63.0	−4.4
20. *meso*-Hydrobenzoin monomethyl ether	2.423	1.199	61.2	67.4	67.5	68.1	−6.4
21. *meso*-Hydrobenzoin dimethyl ether	2.275	1.202	65.1	72.2	72.5	73.0	−7.5
22. *dd,ll*-2,5-Dimethyl-3,4-diphenylhexane	2.395	1.036	81.6	89.4	87.4	87.5	−6.1
23. 2,5-Dichloro-*p*-xylene	2.529	1.390	42.5	45.3	45.1	45.4	−2.6
24. α,α'-Hexachloroxylene	2.649	1.743	63.7	64.8	64.5	64.8	−1.0
25. Naphthacene	4.430	1.850	65.8	72.3	68.5	71.9	−5.1
26. Triphenylene	2.757	1.275	66.1	72.3	72.4	73.2	−6.8
27. Acridine	2.293	1.101	49.0	54.6	54.6	55.2	−5.8
28. Carbazole	3.039	1.522	44.3	51.8	51.9	52.4	−7.7
29. 1,4-Dibromobenzene	2.860	2.279	39.6	41.8	41.6	41.9	−2.1
30. Pentabromobenzene	3.201	3.209	62.3	65.1	64.8	65.0	−2.6
31. 1,2,4,5-Tetrabromobenzene	2.873	3.032	49.9	57.4	57.0	57.3	−7.3

Can. J. Chem. Downloaded from www.nrcresearchpress.com by 210.87.254.5 on 09/05/12
For personal use only.

TABLE I (*Concluded*)

Substance	ϵ	d_4^{20}	P_{E+A} exptl.	Electronic polarization: Eisenlohr	Vogel C_{ar}	Vogel C—C C=C	Diff.
32. δ-Carboline	3.030	1.293	49.1	59.2	50.6		−1.8
33. 2,4,7-Trinitro-9-fluorenone	3.002	1.811	69.6	72.3	72.5	73.0	−3.3
34. 3,4-Dibenzoylfurazan-2-oxide	2.813	1.531	72.5		76.3	76.8	−4.0
35. Benzylnitroguanidine	2.855	1.357	54.7	50.3	52.3	52.5	+3.2
36. *sym*-Tetramethylnitroguanidine	3.261	1.129	50.0	43.4		43.3	+6.7
37. 3-Nitro-3-aza-[3,2,2]-bicyclononane	2.994	1.358	50.0	44.9		46.9	+4.1
38. 2,3-Dinitro-2,3-dimethylbutane	2.942	1.340	51.1	42.3		41.2	+9.4
39. Menthol	2.105	0.891	47.1	47.7		46.5	0
40. 2,5-Di-*tert*-butylhydroquinone	2.445	1.078	67.1	66.3	66.7	66.4	+0.7
41. *cis*-1,2,-Cyclohexanediol	2.375	1.150	31.7	30.8		30.9	+1.1
42. *cis*-2,2,4,4-Tetramethylcyclobutane-1,3-diol	2.345	1.094	40.8	40.0		40.2	+0.7
43. *trans*-2,2,4,4-Tetramethylcyclobutane-1,3-diol	2.157	1.023	39.2	40.0		40.2	−0.9
44. *trans*-1,4-Cyclohexanedimethanol	2.371	1.085	41.7	40.0		40.2	+1.6
45. Bicyclotriethylenediamine	2.278	0.907	36.9	33.4		33.4	+3.5
46. α-*sym*-Hexachlorocyclohexane	2.514	1.776	54.9	56.9		56.9	−2.0
47. β-*sym*-Hexachlorocyclohexane	2.458	1.774	53.6	56.9		56.9	−3.3
48. γ-*sym*-Hexachlorocyclohexane	2.443	1.777	53.2	56.9		56.9	−3.7
49. δ-*sym*-Hexachlorocyclohexane	2.425	1.775	52.8	56.9		56.9	−4.1
50. Di-*n*-butyl imidazole-4,5-dicarboxylate	2.572	1.229	70.8	67.1		67.7	+3.4
51. Cyclohexane-2,3-↓↓-dicarboxylic acid-dilactam	2.518	1.359	44.1	41.8		39.7	+3.4
52. 2,2-Dimethyl-3-isopropylidene-β-propiolactone	2.618	1.188	41.3	37.0		36.9	+4.3
53. *cis,cis-o*-Nitroacetophenone azine	3.067	1.344	99.0	84.8	86.2	86.7	+13.1
54. *trans,trans-o*-Nitroacetophenone azine	2.845	1.350	92.0	84.8	86.2	86.7	+6.1
55. Tetraphenylbutatriene†	2.823	1.191	113.1	115.7	115.7	116.8	−3.1
56. Tetraphenylallene†	2.595	1.137	105.3	111.6	111.6	112.6	−6.9
57. 2,2,5,5-Tetraphenyl-3-hexyne†	2.459	1.115	113.5	124.3	124.7	125.8	−13.7
58. Triethanolamine borate	3.020	1.601	39.4	39.2			+0.2

*Incorporated with 2% of 2,5-di-*tert*-butylhydroquinone.
†Polyethylene wax (2%) has been used to consolidate these wafers and correction has been made for contribution of this contaminant to the dielectric constant.

value for 2,3-dinitrohexane (item 38) is also of interest, indicating that it may be the nitro group in all of these compounds which is responsible for the high P_D. For example the nitro group seems to compensate for the lowering of P_{E+A} by phenyl in *p,p'*-dinitrobibenzyl (item 10).

An unexpected group of low P_D values has been found for four of the diastereomers of 1,2,3,4,5,6-hexachlorocyclohexane, especially unexpected since the effect of aliphatic halogen seems to compensate the aromatic effect in α,α'-hexachloroxylene. The group indicates that the distortion polarization effects are still not entirely explainable.

Discrepancy between experimentally determined P_D and the MR_D summations may arise from positive as well as negative exaltation. The high positive differences shown by the *o*-nitroacetophenone azines (items 53 and 54, kindly supplied by Fleming and Harley-Mason, Cambridge (11)) may reasonably be attributed to exaltation of P_E due to the conjugated system between the nitro groups. It is significant that the cis–cis isomer shows a much higher enhancement than the trans–trans.

Probably these distortion polarizations of the azines would be yet higher were it not for some negative effect of the phenyl groups. Such compensation seems to occur in the unsaturated aromatics of items 55–57 inclusive in Table I, which have been furnished to

Can. J. Chem. Downloaded from www.nrcresearchpress.com by 210.87.254.5 on 09/05/12
For personal use only.

us by Dr. Hoffman of American Cyanamide Company (12), to whom we are grateful. The effect of individual phenyl groups is exemplified by 2,2,5,5-tetraphenyl-3-hexyne, where the high negative exaltation is remindful of substances such as tetraphenylethylene and 1,2,3,4-tetraphenylbutadiene (1). By contrast the tetraphenylallene shows about half the negative exaltation of the alkyne, while the more cumulated butatriene shows less than half again. It is reasonable to assume that the negative effect of four phenyl groups is compensated by positive exaltation of the cumulated unsaturation.

It must be admitted that designation of exaltation in cumulenes is highly speculative, necessarily because no measurements of P_E have been made. The determination of refractive index in respect of the several axes of organic chemical crystals in general is difficult and unprecise. In conesquence few studies have been made. It is to be hoped that a novel method for determination of reactance of crystals at optical frequencies will be developed, and work is proceeding in this laboratory. Meanwhile positive abnormalities in distortion polarization must be assigned vaguely to either atom or electron exitation.

We choose to attribute the positive values of items 11, 13, and 15, Table I, to exaltation of P_E, if for no other reason than the ostensible difference between items 7 and 13 as well as items 7 and 9 and item 15, namely a mercury atom. This barrier should prevent exaltation arising from conjugation in biphenyl, although it must be noted that a large positive value is found for item 11 wherein a methylene group appears to interrupt conjugation. However, conjugative characteristics have been observed before among diphenylmethanes (13, 14). This small interposing atom will allow steric interaction between the phenyl groups which would be obliterated by a mercury atom.

To summarize the data of Table I it would appear that the experimental method for wafer dielectric constant gives usable values of distortion polarization. To be sure, there are anomalies, but the discrepancies between the P_D from the wafer method and P_E by summation of atom or bond refractions would seem to be due more to deficiencies in the summation method than to error in the experimental method with wafers. In the calculation of dipole moments we shall use distortion polarization values derived by both methods, but we rely principally on the experimental value.

In Table II we have recalculated the dipole moments reported by Hampson in terms of experimentally determined P_D. Besides diphenylmercury we have redetermined only one of Hampson's substances. An apparent moment lower than his is reported in Table III for bis-*p*-bromophenylmercury but our solvent and temperature are different and indeed we were not trying to check his result. Instead we wished to compare the substance made from mercury of symmetrical isotope 202 with that prepared from ordinary mercury which contains 16.9% of Hg^{199} and 13.2% of Hg^{201}, both of which nuclei are unsymmetrical. As may be seen from Table III the moment of the sample containing 97% of Hg^{202} is indistinguishable from that containing the ordinary isotopic mixture. The result (that dissymmetry of the nucleus, especially when it is heavy, will not affect valence stereochemistry) is not unexpected.

The apparent moment of bis-*p*-xenylmercury (Table III) is higher than that of diphenylmercury, roughly by the amount that conforms with calculation of the greater charge separation between para hydrogen and mercury in the xenyl versus the phenyl group when a C—Hg—C bond angle of about 140° is assumed. On the other hand the apparent moments of divinylmercury and bis-β-naphthylmercury are appreciably lower than has been observed for diphenylmercury, as would be expected in consideration of the lesser resultant charge separation, by contrast with the *p*-hydrogen of the phenyl group, in either the vinyl or β-naphthyl substituents.

Can. J. Chem. Downloaded from www.nrcresearchpress.com by 210.87.254.5 on 09/05/12
For personal use only.

Can. J. Chem. Downloaded from www.nrcresearchpress.com by 210.87.254.5 on 09/05/12
For personal use only.

TABLE II

Hampson's dipole moment studies with substituted diphenylmercury

R in $(RC_6H_4)_2Hg$	P_T (cc)	P_E (cc)	P_O (cc)	Solvent	Temp. (°C)	μ (D)	μ recalc. on P_{E+A}
H	68.8*	65.3	3.5	Benzene	25°	0.41	0.74
H	69.3	65.3	4.0	Decalin	25°	0.44	0.76
H	69.6	65.3	4.3	Decalin	142°	0.54	0.91
p-CH_3	83.2	75.1	8.1	Decalin	142°	0.74	0.90
p-F	76.5	65.3	11.2	Decalin	142°	0.87	
p-Cl	95.4	75.7	19.7	Decalin	142°	1.15	
p-Cl	93.2	75.7	17.5	Decalin	134°	1.08	
p-Br	93.6	80.9	12.7	Decalin	142°	0.92	1.15

*Similar values have subsequently been obtained by a number of workers. These values in absence of appreciable P_A would indicate a moment despite the absence of negative Kerr effect reported in J. Chem. Soc. 371 (1957).

TABLE III

Present dipole moment of R_2Hg and related compounds in benzene at 20°

Bisymmetric substance	$V_{solvent}$	$V_{extrap.}$	$\epsilon_{solvent}$	$\epsilon_{extrap.}$	P_T	α	β	MR_D	P_D	$\frac{\mu}{MR_D}$	$\frac{\mu}{P_D}$
Vinylmercury*	0.6270	0.6270	2.2463	2.2461	35.45	0.29	−0.256	31.44		0.44	
p-Bromophenylmercury[200.6]	1.13796	1.13798	2.2836	2.2838	88.22	0.30	−0.750	77.14	73.9	0.73	0.83
p-Bromophenylmercury[202]	1.13815	1.13817	2.2814	2.2812	88.51	0.32	−0.762	77.14	73.9	0.74	0.83
p-Methoxyphenylmercury	1.13817	1.13816	2.2826	2.2829	128.3	0.86	−0.640	74.1	71.1	1.60	1.65
p-Xenylmercury	1.13813	1.13818	2.2826	2.2829	121.6	0.52	−0.586	109.8	101.0	1.04	1.22
m-Nitrophenylmercury†	0.9812	0.9809	2.2477	2.2475	132.9	0.51	−0.436	76.7	71.7	5.52	5.61
β-Napthylmercury	1.13817	1.13812	2.2828	2.2832	92.5	0.212	−0.591	92.3	90.9	0.10	0.28
Ethanomercuribenzene	1.13810	1.13808	2.2852	2.2848	72.5	0.50	−0.660	47.2		1.10	
m,m'-Dinitrobiphenyl	1.13854	1.13857	2.2835	2.2835	416	7.95	−0.420	63.9	70.3	4.1	4.0
Dinitrobimesityl	1.13853	1.13846	2.2825	2.2829	514	7.02	−0.274	91.5	106.4	4.5	4.4
m,m'-Bis-nitrophenylmethane	1.13792	1.13787	2.2829	2.2796	613	11.63	−0.450	68.6	74.8	5.1	5.0

*Analyzed in carbon tetrachloride at 20° instead of benzene.
†Analyzed in dioxane at 40° instead of benzene at 20°.

Two of the entries of Table III are those of bis-mercurials in which the substituent constitutes a rotator of appreciable polarity. Therefore, a symmetrical bis-arylmercury of this kind will be comprised of either two or three rotators depending whether the C—Hg—C linkage is linear or angular. In fact the 3-rotator molecule ought to have a higher orientation polarization than the corresponding 2-rotator version according to the generalized equation (15), where ϕ is the C—Hg—C bond angle and θ is the moment angle of the other rotators:

$$\text{(I)} \qquad \mu_{obs}^2 = 2m_1^2+2m_2^2+2[-m_1^2\cos^2\theta\cos(180°-\phi)-2m_1m_2\cos\theta\cos(180°-\phi) +2m_1m_2\cos\theta - m_2^2\cos(180°-\phi)].$$

The first of these substances, bis-*p*-anisylmercury, has been chosen because the electric moment of 4,4′-dimethoxybiphenyl (the same constellation of atoms except for mercury) has been determined (16) with care, and has been found to correspond with that which would be expected if the phenyl groups were colinear and the methoxy groups were randomly rotating. This moment of di-*p*-anisyl is 1.52 D in benzene at 25°, i.e. only slightly lower than the apparent moment in benzene (1.60 or 1.65 D at 20° depending on choice of P_D) of bis-*p*-anisylmercury. This small difference does not imply near linearity of the C—Hg—C bond, but rather that the moment is not very sensitive to differences in bond angle at the central linkages. With this limitation a C—Hg—C bond angle may be calculated by use of reported bond moments.

The bond moment of the aromatic C—O—CH_3 bond has been specified (17) as $m_2 = 1.30$ D with a moment angle of 55°. A zero bond moment for C—Hg has been assigned (18, 19) for C—Hg—X (X = halogen), which is realistic in view of the extreme resistance of primary and secondary alkylmercuric halides toward acid fission (16). But it is not realistic for bis-mercurials, which split easily upon acid treatment. Consequently a bond moment for C—Hg in bis-mercurials was devised (20) from the polarizations of mercuracyclohexane and mercuracycloheptane after assuming a C—Hg—C bond angle of 140°. This bond moment, 1.3 D with mercury positive in respect of carbon, will be used in the current calculations as one limit, with zero C—Hg bond moment as the other.

Together with the observed moment of bis-*p*-anisylmercury (1.63 D) one may apply these bond moments to equation (I) to find that the C—Hg—C bond angle ϕ (Fig. 1) is

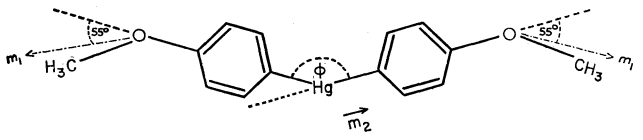

I

FIG. 1.

about 160° if the C—Hg bond is taken at 1.3 D or about 130° if it is taken at zero. Therefore, if the methoxyl groups in bis-*p*-anisylmercury and bis-*p*-anisyl are freely rotating the mercurial and the biphenyl cannot both be colinear.

Comparison between *m*,*m*′-dinitrobiphenyls and bis-*m*-nitrophenylmercury is not so direct because rotation does not seem to be free in the biphenyl. If free rotation existed in *m*,*m*′-dinitrobiphenyl the observed measurement ought to be 4.9 D according to the relationship (21)

$$\text{(II)} \qquad \mu_{res} = 2\mu_{C-NO_2}\sin\theta\cos\phi/2$$

Can. J. Chem. Downloaded from www.nrcresearchpress.com by 210.87.254.5 on 09/05/12
For personal use only.

for all possible values of ϕ, where $\theta = 60°$ and ϕ is the angle between the radial components of the C—NO_2 group moments, here assumed to be 4.0 D. It may be seen that this resultant moment for free rotation is the same as that for ϕ fixed at 90°.

According to Table III the observed moment of *m,m'*-dinitrobiphenyl is 4.0 D in benzene at 20°, indicating that the trans conformation is strongly favored; in terms of a fixed structure the angle ϕ is 130°. This value is 19° lower than that reported (22) from a consideration of Kerr constants but an azimuthal angle greater than 90° is indicated by either consideration.

According to the moments of nitrated biphenyls which have been determined here and elsewhere the circumstance of free rotation is unlikely. Indeed, the value nearest to the 4.9 D indicative of free rotation is 5.12–5.23 in benzene at 25° reported (22, 23, 24) for *o,o'*-dinitrobiphenyl, in which the ortho groups would certainly be obstructive. Alternatively one may calculate a fixed angle ϕ of 83° (92–93° according to ref. 22) by means of equation (II), presuming that this artificiality reflects the mean position of axial rotation in the molecule. On the same basis ϕ for 2,2',4,4'-tetranitrobiphenyl ($\mu_{obs} = 4.38$ D in benzene at 25°) (24) may be specified as 101° from the cis–cis coplanar conformation assuming that the para nitro groups are not involved (25).

Our values may be realistic in view of the observed moment (4.5 D., Table III) of dinitrobimesityl. Here fixation ought to be most closely approximated because of the methyl group obstruction, so the calculated angle ϕ, 99°, ought roughly to describe the actual condition of the molecule.

Obviously the methyl group obstruction in dinitrobimesityl prevents the trans as well as the cis conformation. According to the moment (4.0–4.1 D, Table III) observed for *m,m'*-dinitrobiphenyl there is a tendency in the meta isomer (in contrast to ortho) for transalignment of nitro groups since ϕ, 109° from cis coplanarity, is greater than the angle observed when methyl obstruction is present.

These results from the nitrated biphenyl series are of interest and deserve further study, which is at present being made here in respect of temperature. However, they contribute little for comparison with *m,m'*-diphenylmercury so the necessarily non-linear bis-*m*-nitrophenylmethane (26, 27) has also been examined. Assuming that the phenyl groups are freely rotating, that $\mu_{C-H} = 0.3$ with hydrogen positive, and that methylene valences are tetrahedral the resultant moment ought to be 5.5 D. Since the observed moment (Table III) is 5.1 D one might guess that the methylene group is not tetrahedral. Calculation of the C_6H_5—CH_2—C_6H_5 angle (which will be close to the bond angle) in terms of the observed moment gives an apparent value of 97°. Any deviation from the tetrahedral angle might be expected to be higher than 109° in view of the spectral evidence (13, 14) and of the 115° angle suggested for unsubstituted diphenylmethane (28). Moreover a diminution to 97° ought seriously to affect free rotation because of nitro group interaction. In consequence we are inclined toward the view that free rotation does not occur in bis-*m*-nitrophenylmethane, but as a consequence of resonance hybridization rather than obstruction.

These nitrophenyl models have been chosen for comparison with bis-*m*-nitrophenylmercury, for which the C—Hg—C bond angle is sought. If this bond were linear and the phenyl groups were freely rotating the moment ought to be that calculated under the same circumstances for *m,m'*-dinitrobiphenyl, namely 4.9 D if $\mu_{C-NO_2} = 4.0$. The observed moment is 5.61 D in dioxane at 40°. This moment would be obtained with linear C—Hg—C only if the nitro groups were in the cis quadrant, in terms of a fixed structure if they were radially inclined at 72°. But experience with the *m*-nitrobiphenyls shows that lack of free-

Can. J. Chem. Downloaded from www.nrcresearchpress.com by 210.87.254.5 on 09/05/12
For personal use only.

dom in rotation tends toward the trans conformation. The information about bis-*m*-nitrophenylmethane does not contradict the tendency. Therefore, no explanation for the high moment of bis-*m*-nitrophenylmercury is apparent except that of a non-linear C—Hg—C linkage (Fig. 2) especially since the chance of conjugative effects via the large

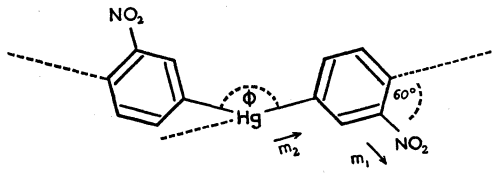

II

FIG. 2.

mercury atom is remote. In any case such conjugative effects would themselves tend to create non-linearity in C—Hg—C.

The calculation of the C—Hg—C angle according to equation (I) is of interest. Depending on choice of C—Hg bond moment from 0 to 1.3 D the resultant C—Hg—C angle will vary from 94° to 123°.

Of course the dioxane at 40°, which is required by solubility limitation, may be expected to enhance the moment by about 0.2 D (20) over that which would be observed in benzene, but a recalculation on the basis of a resultant moment of 5.4 D gives C—Hg—C angles of 110° for $\mu_{C-Hg} = 0$ and 133° for $\mu_{C-Hg} = 1.3$ D. Since there is no present evidence for postulation of a C—Hg bond moment greater than 1.3 D it would seem that the angle in bis-*m*-nitrophenylmercury is more acute than any yet encountered among bis-mercurials. This circumstance is not abnormal if the groups attached to a mercury atom are relatively free to assume positions directed by their own force fields with minimal influence of the large central atom.

EXPERIMENTAL

Bis-p-bromophenylmercury

(a) Using Ordinary Mercury

A solution of 4.95 g (0.248 mole) of *p*-bromophenylboronic acid, m.p. 286–290° C (29), in 110 ml of boiling 1% aqueous sodium hydroxide was filtered and then stirred just below the boiling point while a solution of 3.40 g (0.00992 mole) of mercuric nitrate in 50 ml of 0.4% nitric acid was added during 30 minutes. The resulting suspension was boiled for 15 minutes and then maintained below the boiling point for 2 hours until all traces of mercuric oxide had disappeared. The suspension was then suction-filtered and the cake was washed with 100 ml of distilled water, 5.25 g (103%, vacuum-dried at 50° C). This crude product was crystallized from 125 ml of 7:3 dioxane–water. The water-washed, vacuum-dried white needles melted at 246–251° C (4.25 g, 83%). A second crop (0.74 g, 15%) melted at 244–249° C.

The melting point range seems to be caused by polymorphism. The microcrystalline plates melt on the Koffler microstage at 224–230° C and transform to long prismatic needles. Transformation usually is not complete although conversion was complete in one instance, with remelting at 254.5–256° C. The mercurial is soluble in dioxane, benzene, dimethylformamide, and chloroform but only slightly soluble in other common solvents.

(b) Using Hg^{202}

To the solution of 1.558 g (0.00775 mole) of 4-bromophenylboronic acid in 100 ml of 10% aqueous sodium hydroxide at 80° C was added dropwise during 30 minutes a solution of 0.52 g of 97.66% mercuric^{202} nitrate in nitric acid estimated to be about 3 *N* (sample was used as received from Oak Ridge, Tennessee). Yellow

Can. J. Chem. Downloaded from www.nrcresearchpress.com by 210.87.254.5 on 09/05/12
For personal use only.

colloidal mercuric oxide began to form during the initial addition, but 10 minutes elapsed before the product began to appear. Finally 3 *N* nitric acid was added until the pH was 8–9, and the resulting orange-tinted suspension was boiled for 15 minutes and allowed to cool during 3 hours, after which the suspension was colorless although the aqueous phase was faintly greenish-yellow. The cold system was filtered, the product being washed with 150 ml of water in three portions. Thus, bis-mercurial, 1.373 g, was dissolved in hot 70:30 dioxane–water, leaving 0.0389 g of grey-green insoluble matter. The cooled solution yielded 1.1223 g, m.p. 245.5–250° C. Dilution of the filtrate to 1:9 dioxane–water ratio yielded 0.001 g, m.p. 244–247.5° C. Total yield is 96.4% of theoretical.

Recovery of isotopic mercury from residues or solutions was effected by evaporation to dryness, then solution of the residue in 5% oleum and concentrated nitric acid (2:1). The solution was diluted with water, evaporated almost to dryness, and the residue was dissolved in an amount of water such that the sulphuric acid concentration was about 50%.

4-Bromophenylmercuric Chloride

A solution of 0.190 g (0.00037 mole) of bis-4-bromophenylmercury in 20 ml of boiling acetone was treated during 10 minutes with a solution of 0.203 g (0.00075 mole) of mercuric chloride in 25 ml of acetone. The slightly milky suspension was treated with 20 ml of water, the mixture let stand overnight and filtered, 0.230 g, m.p. 256–259° C. Distillation of acetone and addition of water to the filtrate gave 0.035 g more, m.p. 256–260° C. The total yield was 91% of theoretical.

m,m'-Dinitrobiphenyl

To a dark brown solution of 27.4 g (0.1 mole) of *m,m'*-dinitrobenzidine (30), m.p. 265°, prepared by mortar grinding in 65 ml of concentrated sulphuric acid, was added dropwise into the mortar not more than 50 ml of water. The slurry was transferred to an Erlenmeyer flask by means of 10 ml of concentrated sulphuric acid. To this system at −15° was added ground potassium nitrate at such a rate as to maintain, with stirring, a temperature of −5°. To the completed reaction (test portion water soluble) was added 220 ml of absolute ethanol. The system was boiled until nitrogen evolution was complete, then diluted with 200 ml of water. The filtered precipitate was washed acid free by means of water, air dried 21 g (86%), m.p. 193–196° C. Crystallization twice from benzene, then from acetic acid, and finally repeatedly from absolute ethanol would not raise the melting point above 200° (31) but the yellow product was not highly crystalline. A benzene solution (1.55 g in 60 ml) was then chromatographed on an alumina (160–170 mesh, 180° for 8 days) column (I.D. 2 cm by 20 cm long) using benzene as developer. The colorless first eluates yielded dinitrobiphenyl, m.p. 201.5–203°, which may be obtained as long needles by crystallization from acetone. The substance was characterized by conversion to *m,m'*-diacetaminobiphenyl, m.p. 256–257.5° C (32).

Bis-m-nitrophenylmethane

The substance was prepared by the method of Schoepff (26) but his melting point as well as that of Thorpe and Wildman (27) was exceeded by successive crystallizations from benzene, acetic anhydride, and petroleum ether (b.p. 90–100°, 550 ml/g). The last melting point, 176–178.5°, was not increased by elution from alumina (180° activation) by means of chloroform.

Physical Measurements of Solid Substances

These measurements were identical with those described in previous papers (1) except that flotation densities are now more satisfactory since we have used hexafluorobenzene (d_4^{20}, 1.63) – hexane mixtures as flotation media. Most organic substances are insoluble in this system and less trouble is encountered in removal of bubbles by centrifugation.

The solid dielectric constant measurement of dicyclohexylmercury was complicated by the tendency of the sample (prepared by reduction of cyclohexylmercuric bromide by means of hydrazine hydrate in ether) to decompose to mercury, cyclohexane, and cyclohexene in air. It was found that the sample was stable in air at 25° for 60 hours if 2% of 2,5-di-*tert*-butylhydroquinone was intimately incorporated with it. The dielectric constant and density were measured for this mixture and then corrected for the corresponding constants of the antioxidant.

The extrapolation plots of wafer thickness versus apparent dielectric constant for *trans*-2,2,4,4-tetramethylcyclobutane-1,3-diol (A), dicyclohexylmercury (B), *m,m'*-dinitrobimesityl (C), dimesitylmercury (D), and *m,m'*-dinitrobiphenyl (E) have been selected as typical of the 58 entries of Table I, and are shown in Fig. 3.

Physical Measurements of Solutions

The total polarizations recorded in Table III were determined by methods outlined previously (1). Acceptance of a result was dependent on the correlation of $V_{solvent}$ and $\epsilon_{solvent}$ with extrapolated value of V and ϵ when apparent V and ϵ for the several concentrations fitted an extrapolatable straight line. Typical extrapolations of specific volume (V) and dielectric constant (ϵ) are shown for *m,m'*-dinitrobiphenyl (A) and dinitrobimesityl (B) in Fig. 4.

Can. J. Chem. Downloaded from www.nrcresearchpress.com by 210.87.254.5 on 09/05/12
For personal use only.

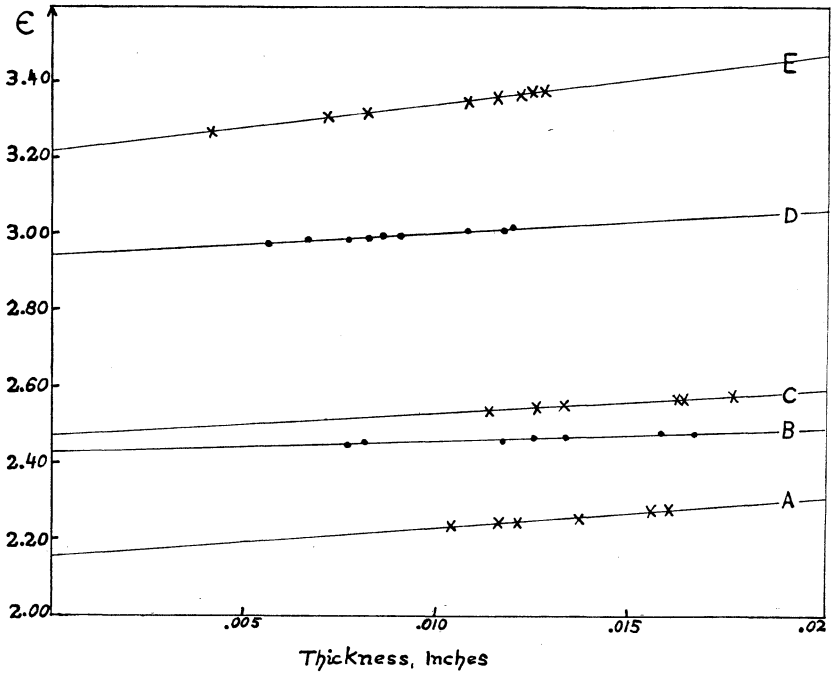

FIG. 3.

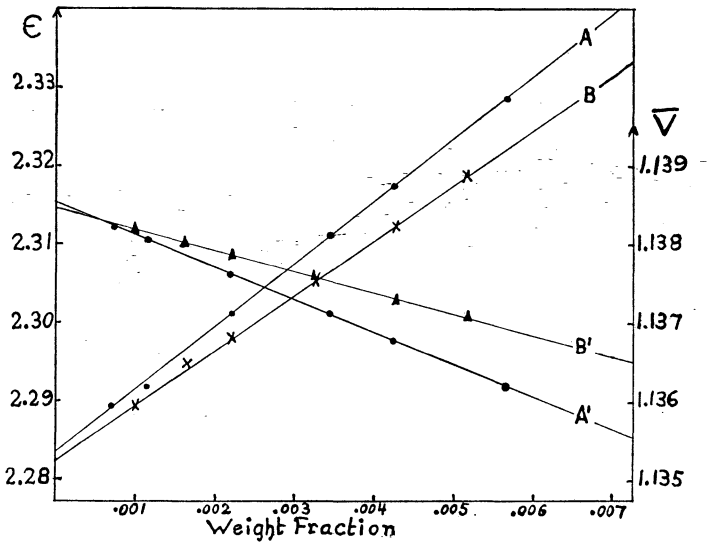

FIG. 4.

ACKNOWLEDGMENTS

The authors are indebted to Professor Raymond Dessy, University of Cincinatti, for samples of aromatic bis-mercurials, to Dr. Ronald Henry of N.O.T.S. for the divinylmercury, and to Professor Roger Adams for the dinitrobimesityl. The research has been supported generously by the National Research Council and the Defence Research Board of Canada.

Can. J. Chem. Downloaded from www.nrcresearchpress.com by 210.87.254.5 on 09/05/12
For personal use only.

REFERENCES

1. H. SAWATZKY and G. F WRIGHT. Can. J. Chem. **36**, 1555 (1958).
2. G. C. HAMPSON. Trans. Faraday Soc. **30**, 877 (1934).
3. N. V. SIDGWICK. The chemical elements and their compounds. Oxford, London. 1950. p. 309.
4. I. E. COOP and L. E. SUTTON. J. Chem. Soc. 1269 (1938).
5. J. SIPOS, H. SAWATZKY, and G. F WRIGHT. J. Am. Chem. Soc. **77**, 2759 (1955).
6. F. EISENLOHR. Z. Physik. Chem. **75**, 585 (1910); **79**, 129 (1912).
7. A. VOGEL, W. T. CRESWELL, G. H. JEFFREY, and J. LEICESTER. J. Chem. Soc. 514 (1952).
8. C. C. MEREDITH and G. F WRIGHT. Can. J. Chem. **38**, 1177 (1960).
9. A. WEISSBERGER. Techniques of organic chemistry. 1st ed. Interscience Publ., New York. 1945. p. 1676.
10. M. V. GEORGE and G. F WRIGHT. J. Am. Chem. Soc. **80**, 1200 (1958).
11. I. FLEMING and J. HARLEY-MASON. J. Chem. Soc. 5560 (1961).
12. HOFFMAN *et al.* J. Am. Chem. Soc. In press.
13. H. P. KOCH. J. Chem. Soc. 1123 (1948).
14. E. A. BRAUDE. J. Chem. Soc. 1902 (1949).
15. H. EYRING. Phys. Rev. **39**, 746 (1932).
16. E. BRETSCHER. Helv. Chim. Acta, **1**, 355 (1928).
17. C. P. SMYTH. Dielectric behaviour and structure. McGraw-Hill, New York. 1957.
18. C. P. SMYTH. J. Org. Chem. **6**, 421 (1941).
19. B. C. CURRAN. J. Am. Chem. Soc. **57**, 2162 (1935).
20. M. J. ABERCROMBIE, A. RODGMAN, K. R. BHARUCHA, and G. F WRIGHT. Can. J. Chem. **37**, 1328 (1959).
21. J. W. WILLIAMS. Z. Physik. Chem. **138**, 75 (1928).
22. J. Y. H. CHAU, C. G. LE FEVRE, and R. J. W. LE FEVRE. J. Chem. Soc. 2666 (1959).
23. E. BRETSCHER. Helv. Chim. Acta, **2**, 257 (1929).
24. R. J. W. LE FEVRE and H. VINE. J. Chem. Soc. 967 (1938).
25. P. PODLESCHKA, L. WESTLAND, and G. F. WRIGHT. Can. J. Chem. **36**, 574 (1958).
26. M. SCHOEPFF. Ber. **27**, 2321 (1894).
27. L. THORPE and E. A. WILDMAN. J. Am. Chem. Soc. **37**, 372 (1915).
28. G. C. HAMPSON, R. H. FARMER, and L. E. SUTTON. Proc. Roy. Soc. (London), Ser. A, **143**, 147 (1933).
29. F. R. BEAN and J. R. JOHNSON. J. Am. Chem. Soc. **54**, 4415 (1932).
30. O. L. BRADY and G. P. MCHUGH. J. Chem. Soc. **123**, 2051 (1923).
31. F. ULLMAN and L. FRENTZEL. Ber. **38**, 725 (1905).
32. F. ULLMAN and J. BIELECKI. Ber. **34**, 2177 (1901).

Can. J. Chem. Downloaded from www.nrcresearchpress.com by 210.87.254.5 on 09/05/12
For personal use only.

EFFETS STÉRÉOÉLECTRONIQUES DANS LA DÉSAMINATION NITREUSE DES *tert*-BUTYL-4 AMINOMÉTHYL-1 CYCLOHEXANOLS *cis* ET *trans*

H. FAVRE ET D. GRAVEL[1]
Département de Chimie, Université de Montréal, Montréal, Qué.
Reçu le 31 Août, 1962

RÉSUMÉ

La désamination nitreuse du *tert*-butyl-4 aminométhyl-1 cyclohexanol *cis* (groupe —CH_2NH_2 axial) conduit à la *tert*-butyl-4 cycloheptanone (89%), à l'époxyde *cis* du *tert*-butyl-4 méthylène-1 cyclohexane (6%) et à la *tert*-butyl-4 cyclohexanone (5%). L'isomère *trans* (groupe —CH_2NH_2 équatorial) donne la cétone agrandie (79%), l'époxyde correspondant (20%) et la *tert*-butyl-4 cyclohexanone (1%). L'aminométhyl-1 cyclohexanol se comporte comme l'isomère *trans*. Ces résultats indiquent que tout se passe comme si le cours de la réaction dépendait de la conformation de départ du groupe —NH_2, avec comme intermédiaire un ion diazonium ou un ion carbonium reflétant la conformation de l'ion diazonium.

Dans une note récente nous signalions la présence d'époxyde de *tert*-butyl-4 méthylène-1 cyclohexane *cis* (VIII) à côté de la *tert*-butyl-4 cycloheptanone (IX) dans les produits de la désamination nitreuse du *tert*-butyl-4 aminométhyl-1 cyclohexanol *cis* (II*b*) (1). Nous retrouvons dans cette réaction le comportement stéréospécifique de deux amino-alcools à géométrie bien définie: l'amino-2 cyclohexanol *trans*, diéquatorial (Fig. 1: A, D = CH_2; B, C = H; E = OH), qui par désamination engendre le formyl cyclopentane (2) par migration d'un groupe méthylène, et l'amino-2β 5α-cholestanol-3α *trans*, diaxial (Fig. 1: B, E = CH_2; A, C = H; D = OH), qui engendre l'époxyde correspondant -2α,3α (3). Tout se passe comme si l'amine de départ engendrait un ion diazonium qui réagira par migration ou réaction du groupe *trans-dans un plan*. D'autres exemples sont donnés d'orientation du cours de la réaction par l'ion diazonium dans la réaction d'extension de cycle de Tiffeneau (4, 5).

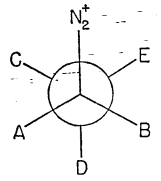

FIG. 1.

Il nous a paru intéressant de tenter de définir, pour la réaction de Tiffeneau, les facteurs stéréoélectroniques. Notre but était d'étudier principalement la formation des époxydes et de déterminer le rapport cétone agrandie-époxyde. Les *tert*-butyl-4 aminométhyl-1 cyclohexanols *cis* et *trans* (II*b*) et (II*a*) nous ont paru particulièrement appropriés à cette fin: la symétrie de ces molécules fait qu'il ne se formera qu'un époxyde dans chaque cas, et une seule et même cétone agrandie pour lesquels la chromatographie en phase gazeuse offre d'intéressantes possibilités de dosage. De plus, la présence stabilisatrice du groupe *tert*-butyle (6) assure la présence d'un groupe aminométhyle axial dans l'isomère *cis* et équatorial dans l'isomère *trans*,[2] ce qui nous semble couvrir les aspects conformationnels

[1]*Boursier du Conseil National de Recherches du Canada, 1958–1962.*
[2]*Nous avons adopté comme configurations cis et trans les relations spatiales entre les substituants carbonés.*

Can. J. Chem. Downloaded from www.nrcresearchpress.com by 210.87.254.105 on 09/05/12
For personal use only.

principaux de la réaction de Tiffeneau. Pour fins de comparaison, nous avons repris l'étude de la désamination nitreuse de l'aminométhyl-1 cyclohexanol (7), pour laquelle un mécanisme mettant en jeu un ion carbonium était avancé (8).

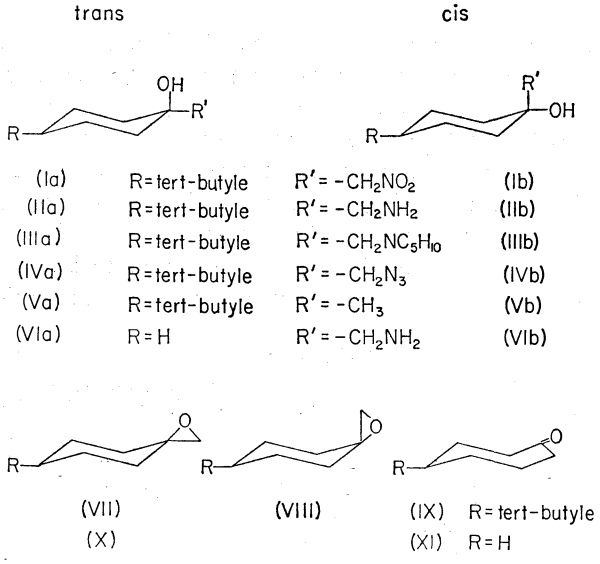

RÉSULTATS

Nous avons déjà montré (1) que l'action du nitrométhane sur la *tert*-butyl-4 cyclohexanone en présence d'éthylate de sodium conduisait aux deux nitro-alcools isomères I*a* et I*b*: l'isomère *cis* I*b*, p.f. 86–87°, constitue 95% environ du mélange et s'isole très facilement par cristallisation; sa réduction conduit à l'amino-alcool *cis* II*b*, caractérisé comme chlorhydrate, p.f. 235–236° (décomp.). Le nitro-alcool *trans* I*a*, p.f. 56–57°, fut isolé des nitro-alcools bruts après de nombreuses cristallisations.

Nous montrons dans ce mémoire que le nitro-alcool *trans* se réduit en amino-alcool de même configuration II*a*, dont le chlorhydrate fond à 254–255° (décomp.). Il est évident que le passage par le nitro-alcool I*a* ne convenait pas à la préparation de grandes quantités d'amino-alcool *trans*. Cross et Whitham (9) ayant fait une brève mention que le mélange des époxydes VII et VIII obtenu par l'action de l'acide perbenzoïque sur le *tert*-butyl-4 méthylène-1 cyclohexane était riche en époxyde *trans* VII, nous avons vu dans ce mélange un produit de départ convenable pour la synthèse de l'amino-alcool *trans* II*a*. En traitant en effet ce mélange d'époxydes par l'azoture de sodium, puis en réduisant sur platine le mélange des azido-alcools IV*a* et IV*b* nous avons obtenu un mélange des amino-alcools *cis* II*b* et *trans* II*a* duquel il est facile, par cristallisation, d'isoler le *tert*-butyl-4 aminométhyl-1 cyclohexanol *trans* (II*a*), dont le chlorhydrate fond à 254–255° (décomp.).

Le mélange des époxydes VII et VIII fut réduit par l'hydrure de lithium et d'aluminium en un mélange des méthyl-1 *tert*-butyl-4 cyclohexanols *cis* (V*b*) et *trans* (V*a*) connus (10, 1, 11, 12) contenant 70% d'isomère *trans* selon l'analyse par chromatographie en phase gazeuse. Cette technique montre que le mélange des époxydes VII et VIII est également de 30.4–69.6%, ce qui nous permet d'attribuer à ces composés les configurations *cis* et *trans*: c'est donc bien, comme le mentionnent Cross et Whitham (9), l'époxyde *trans* qui se forme en prépondérance.

Can. J. Chem. Downloaded from www.nrcresearchpress.com by 210.87.254.105 on 09/05/12
For personal use only.

Les désaminations nitreuses furent réalisées selon le procédé décrit par Tchoubar (7), soit l'action *in situ* d'acide nitreux sur l'amino-alcool en solution dans de l'acide acétique aqueux 25%. Deux méthodes analytiques ont été employées pour doser les époxydes: (*a*) chromatographie en phase gazeuse et (*b*) isolement des pipéridino-alcools issus des époxydes.

(*a*) Le mélange brut des composés neutres issus de la désamination nitreuse des amino-alcools II*a*, II*b* et VI*a* a été chromatographié en phase gazeuse: le chromatogramme montre bien séparés la cétone agrandie (soit IX, soit XI) et l'époxyde semicyclique (VII, VIII ou X). La présence d'un troisième composé est, de plus, décelée. Au départ des *tert*-butyl-4 aminométhyl-1 cyclohexanols *cis* et *trans* il s'agit de la *tert*-butyl-4 cyclohexanone, qui fut isolée et caractérisée par son point de fusion et son spectre infrarouge. La désamination nitreuse de l'aminométhyl-1 cyclohexanol engendre de la cyclohexanone, caractérisée par chromatographie en phase gazeuse par la technique du rehaussement des pics (13, p. 27). Les valeurs quantitatives sont rapportées au Tableau I.

TABLEAU I

Résultats qualitatifs et quantitatifs des désaminations nitreuses des *tert*-butyl-4 aminométhyl-1 cyclohexanols *cis* et *trans* et de l'aminométhyl-1 cyclohexanol

Produit de départ	Méthode*	Époxyde	Cétone agrandie	Cétone de rétrogradation
tert-Butyl-4 aminométhyl-1 cyclohexanol *cis*	Chim.	VIII 5.5%	—	—
	Chim.	VIII 6.1%	—	—
	Chim.	VIII 5.7%	—	—
	Chrom.§	VIII 6.1%	IX 89.2%	4.6%†
	Chrom.§	VIII 4.6%	IX 90.3%	5.1%†
tert-Butyl-4 aminométhyl-1 cyclohexanol *trans*	Chim.	VII 18.3%	—	—
	Chim.	VII 24.5%	—	—
	Chrom.§	VII 20.0%	IX 78.8%	1.2%†
Aminométhyl-1 cyclohexanol	Chrom.§	X 19.4%	XI 80.6%	<1%‡
	Chrom.§	X 20.0%	XI 80.0%	<1%‡

*Chim.: méthode chimique, par pesée des pipéridino-alcools issus des époxydes. Chrom.: par dosage par chromatographie en phase gazeuse.
†*tert*-Butyl-4 cyclohexanone.
‡Cyclohexanone.
§Les valeurs trouvées par chromatographie en phase gazeuse sont précises à ±1–2%.

(*b*) Les époxydes, dans la série *tert*-butylée, ont aussi été dosés gravimétriquement par la formation et l'isolement des pipéridino-alcools III*a* et III*b* (1). Les résultats sont très satisfaisants et concordent avec ceux obtenus par chromatographie en phase gazeuse, mais la méthode est extrêmement laborieuse.

Nous avons cherché à mettre en évidence le diol décrit par Tchoubar (7), mais sans succès. Nous sommes en mesure d'affirmer qu'il ne se forme pas comme produit primaire de la réaction. Nous avons par contre isolé, dans la désamination de l'amino-alcool II*b*, un composé azoté, p.f. 216–218°, dont la constitution n'a pas été élucidée; comme il ne se forme qu'en très petite quantité (2.6% environ) sa présence dans les produits de désamination n'altère pas la validité de nos dosages.

DISCUSSION

Il ressort clairement des résultats rapportés au Tableau I qu'il existe une différence appréciable dans les rapports cétone agrandie-époxyde entre les *tert*-butyl-4 aminométhyl-1 cyclohexanols *cis* et *trans*. Il apparait aussi que l'aminométhyl-1 cyclohexanol,

Can. J. Chem. Downloaded from www.nrcresearchpress.com by 210.87.254.105 on 09/05/12
For personal use only.

en donnant une proportion d'époxyde de 20%, réagit à la manière du *tert*-butyl-4 aminométhyl-1 cyclohexanol *trans*, donc avec le groupe aminométhyle en conformation équatoriale: on pouvait prévoir que l'aminométhyl-1 cyclohexanol allait exister plutôt sous la conformation VI*a* que VI*b*, le groupe $—CH_2NH_3^+$ axial amenant une plus grande énergie d'interactions non liées que le groupe —OH axial (valeurs A: —OH = 0.8 (6), $—CH_2CH_3$ = 1.86 (14) kcal/mole; le groupe $—CH_2NH_3^+$ est en effet l'isostère du groupe $—CH_2CH_3$).

Les différences entre les *tert*-butyl-4 aminométhyl-1 cyclohexanols *cis* et *trans* sont de deux ordres: l'isomère *trans* donne environ trois fois plus d'époxyde que l'isomère *cis*; l'isomère *cis* conduit à 5% de *tert*-butyl-4 cyclohexanone (cétone de rétrogradation formée par perte d'un atome de carbone), tandis que l'isomère *trans* en donne 1%.

Le schéma de la désamination nitreuse semble bien établi (15) jusqu'à l'ion diazonium:

$$R—NH_2 \rightarrow R—NHNO \rightarrow R—N{=}NOH \rightarrow R—N_2^+ \rightarrow R^+$$

$$\searrow \quad \swarrow$$

produits

Ensuite, pour la formation même des produits de réaction, certains travaux (4, 5, 16, 17) permettent d'avancer l'ion diazonium, certains travaux par contre justifient l'ion carbonium (18, 19, 20, 21) comme source première.

Nous retiendrons, au début de cette discussion, l'ion diazonium pour engendrer les produits de réaction et par le fait même la théorie des "4 centres *trans-dans un plan*". Nous sommes de plus enclins à suivre Streitwieser (17) dans ses conclusions, à savoir que la réaction est amorcée par le départ d'une molécule d'azote qui entraîne à sa suite le centre D (Fig. 1) qui migre, plutôt que par l'attaque, par le centre D, du carbone porteur de l'ion diazonium pour en libérer la molécule d'azote.

Donc, en accord avec le principe de la migration *trans-dans un plan*, XV et XVI (équiprobables) donneront la cétone agrandie par migration d'un lien $C—CH_2$ et XIV fournira l'époxyde par migration d'un doublet électronique du groupe OH et élimination d'un proton. Si les trois conformères XIV, XV et XVI étaient équiprobables, il y aurait formation de 66.6% de cétone agrandie et de 33.3% d'époxyde.[3] L'examen des formules XII et XIII, combiné à celui des formules XIV à XVI, nous montre que les trois rotamères XIV, XV et XVI ne peuvent être équiprobables. En effet si l'on admet que les groupes NH_3^+ occupent le même volume qu'un groupe méthyle, on trouve, d'après les travaux d'Allinger et Shih-En Hu (14) sur l'éthylcyclohexane, que dans l'isomère *trans* (XII) les conformations XV et XVI sont favorisées par rapport à XIV par une différence d'énergie de 0.9 kcal. Cette différence d'énergie entre 0° et 27° donne d'après la formule de distribution des populations ($-\Delta F = 2.3\ RT \log K$) de 19 à 22% pour XIV et de 78 à 81% pour XV et XVI prises ensemble. L'expérience (voir Tableau I) montre que la désamination nitreuse de l'amino-alcool *trans* II*a* conduit en fait à 20% d'époxyde VII. Par le même raisonnement, pour l'isomère *cis* II*b* la population XIV (équivalente à XIII; D = NH_3^+ ou N_2^+; E, F, = —H) est à toute fin pratique inexistante, parce que de très haute énergie comparée aux populations XV et XVI. L'époxyde VIII ne devrait pas se former dans ces conditions. Il s'en forme pourtant 6%.

Pour expliquer cette formation un remplacement de type frontal du groupe N_2^+ par le groupe —OH de la molécule à la manière de la molécule d'eau avancée par Mills dans le cas de la rétention de configuration lors de la désamination nitreuse de certaines amines

[3]*Ce raisonnement n'est valable qui si les populations relatives des rotamères ne varient pas lorsque l'ion ammonium (l'amine) est transformé en ion diazonium.*

Can. J. Chem. Downloaded from www.nrcresearchpress.com by 210.87.254.105 on 09/05/12
For personal use only.

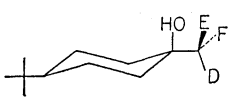

(XII)

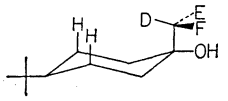

(XIII)

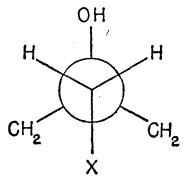

(XIV)

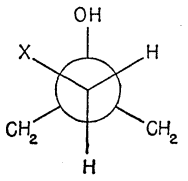

(XV)

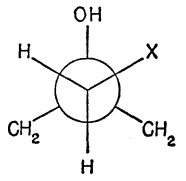

(XVI)

(X=NH_3^+, NH_2, N_2^+)

alicycliques (16, 22) a retenu notre attention. Le diagramme XVII illustre les conditions stéréoélectroniques du remplacement de type frontal que nous postulons dans le cas de l'amino-alcool *cis* XIII.

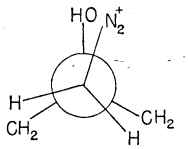

(XVII)

Ce remplacement frontal serait rendu possible par le fait que l'ion diazonium libère une molécule d'azote neutre et qu'il n'y a donc pas d'opposition de charges de même nature comme dans les déplacements S_N2 par exemple, où les espèces, celle qui se fixe et celle qui quitte le carbone, sont toutes deux négatives et demandent nécessairement une attaque "par l'arrière". De plus, le lien carbone–azote dans l'ion diazonium est long et faible, diminuant de ce fait l'encombrement stérique causé par le groupe diazonium lors d'une attaque sur le carbone. Et enfin le groupe —OH est à proximité immédiate de cet ion diazonium, au moment même de sa formation.

Il suffirait donc que l'ion diazonium subisse une rotation ou une oscillation de 60° environ pour passer des conformations XV et XVI à la conformation XVII. Il y aurait alors compétition entre la migration *trans-dans un plan* du groupe —CH_2— (XV et XVI) et la substitution frontale par l'un des doublets de l'oxygène du groupe —OH (XVII). La formation de 6% d'époxyde indique que seulement 6% des populations XV et XVI subiraient cette rotation.[4] Streitwieser et Coverdale (22) admettent que le mécanisme de déplacement frontal de Mills explique très bien les résultats obtenus dans la désamination de la cyclohexylamine (D)-2 *cis*.

Comme nous venons de le montrer la conformation de l'ion diazonium semble être responsable de l'orientation de la réaction vers l'extension de cycle ou la formation de

[4]*Il se pourrait que les populations XV et XVI, par des oscillations, conduisent naturellement à la formation d'époxyde; une partie des 20% d'époxyde trans pourrait ainsi être formée de cette manière. Il faudrait nécessairement admettre que la formation de l'époxyde serait plus lente que celle de la cétone agrandie.*

Can. J. Chem. Downloaded from www.nrcresearchpress.com by 210.87.254.105 on 09/05/12
For personal use only.

l'époxyde. De cette façon, les migrations seraient contrôlées par la conformation de moindre énergie de la molécule. Cependant, Collins et ses collaborateurs ont, dans la série des diaryl-propanolamines et diaryl-propylamines, proposé un ion carbonium classique comme intermédiaire donnant directement naissance aux produits de la réaction (18, 23, 24). Cette théorie, tout en écartant les possibilités d'avoir des ions carboniums pontés et de l'assistance de la part de groupes voisins dans l'étape intermédiaire de la réaction, ne réfute cependant pas l'idée de l'ion diazonium et du mécanisme *pull–push* de Streitwieser (17). En effet, Benjamin et Collins (18) mentionnent dans un article que leurs conclusions reposent sur la *supposition* que "l'attaque *topside* par un groupe phényle dans la proportion de 26.5% doit nécessiter une rupture complète du lien carbone–azote qui en retour implique qu'un ion carbonium classique doit être formé". Il est intéressant de noter que la théorie de l'ion carbonium de Benjamin, Collins et collaborateurs (18, 23, 24) et Felkin (19) peut aussi conduire à la même interprétation de nos résultats que la théorie de l'ion diazonium.

L'ion diazonium se décomposant en ion carbonium plat, les conformations XV et XVI deviennent alors XVIII et XIX, qui par rotation peuvent conduire à XX.

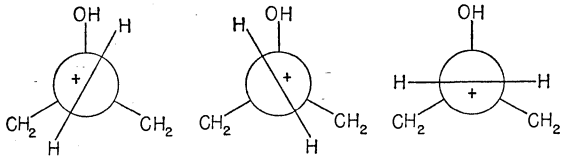

(XVIII) (XIX) (XX)

Dans le série *trans* les trois ions diazonium XIV (19–22%), XV (40%) et XVI (40%) engendreraient les ions carbonium XX, XVIII et XIX dans des rapports de 19–22, 40 et 40% qui réagiraient le premier pour donner l'époxyde, les deux autres pour donner l'agrandissement de cycle. Si le mécanisme en est un *topside* à la manière de Benjamin, Wilder et Collins (24) il n'y a strictement aucune différence entre le mécanisme par l'ion diazonium et ce mécanisme par ion carbonium. Dans la série *cis*, le rotamère XIV n'existant pas, il faudrait que 6% des rotamères XVIII et XIX tournent de 60° environ pour engendrer XX. Ce qui revient à dire que ce mécanisme de réaction est analogue à celui de Mills (16). Il est évident que les résultats obtenus dans ce travail ne permettent pas de trancher le noeud de l'épineuse question de savoir si l'intermédiaire véritable qui oriente et contrôle la réaction, est un ion diazonium ou un ion carbonium.

Il semble que tout se passe comme si l'ion diazonium agissait comme intermédiaire donnant directement naissance aux produits de réaction par un mécanisme de type concerté où la migration des groupes est contrôlée par les conformations de groupe ammonium (ou diazonium) dans la molécule. Ces conformations primaires peuvent être décelées par le truchement d'interactions non liées et peuvent servir à des fins de diagnostic et de prévision du cours que suivra la réaction.

Quant à la formation de cétone de rétrogradation, la divergence dans les pourcentages obtenus pour les isomères *cis* et *trans* (5% et 1%) nous paraît assez significative.

Elphimoff-Felkin et Gault (20) ont déjà observé la formation d'une quantité appréciable de cétone de rétrogradation (cyclohexanone) dans la désamination nitreuse de l'amino-alcool XXI. Ces auteurs expliquent ce résultat par un mécanisme faisant appel à un ion carbonium qui se réarrange, par analogie au cas de English et Bliss (25), qui ont observé des scissions dans les réactions de désamination nitreuse d'amino-alcools-1,3 aliphatiques.

Can. J. Chem. Downloaded from www.nrcresearchpress.com by 210.87.254.105 on 09/05/12
For personal use only.

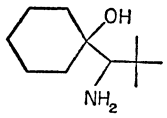

(XXI)

La formation de diazométhane (43%) a récemment été observée (26) dans la désamination nitreuse de l'aminométhyltriméthylsilane, dans lequel la liaison Si—CH_2NH_2 est faible; elle se brise lorsque l'amine est transformée en ion diazonium, probablement à cause du caractère fortement électrophile de celui-ci.

Ainsi un mécanisme selon lequel il y aurait formation de diazométhane nous paraît digne de mention, la différence dans la cétone de rétrogradation produite par chacum des amino-alcools *cis* II*b* et *trans* II*a* reflétant la décompression stérique plus grande dans le cas du groupe —CH_2—N_2^+ axial.

Remarque sur l'attribution des configurations cis–trans aux tert-butyl-4 aminométhyl-1 cyclohexanols IIb et IIa

La preuve de la configuration *cis* de l'amino-alcool II*b*, dont le chlorhydrate fond à 235–236° et que l'on prépare à partir du nitro-alcool I*b*, p.f. 86–87°, fut effectuée de la manière suivante (1). L'amino-alcool fut désaminé; le mélange de *tert*-butyl-4 cycloheptanone, de *tert*-butyl-4 cyclohexanone et d'époxyde fut réduit par l'hydrure de lithium et d'aluminium; le mélange des alcools secondaires et tertiaires résultant fut oxydé par l'acide chromique en un mélange d'alcool tertiaire et de cétones; par chromatographie sur alumine l'alcool tertiaire fut isolé et caractérisé comme *tert*-butyl-4 méthyl-1 cyclohexanol *cis*, par comparaison avec un échantillon authentique. Cette preuve de structure demande qu'il n'y ait aucun changement de configuration au cours des étapes: désamination, réduction et oxydation; c'est ce que nous avions admis (1).

Depuis la présentation de cette preuve nous avons repris l'étude de l'oxydation chromique des *tert*-butyl-4 méthyl-1 cyclohexanols *cis* et *trans* et nous avons constaté que, dans les conditions d'oxydation les deux alcools tertiaires subissent une certaine inversion de configuration: 29% d'inversion après 48 heures de contact et 37% après 72 heures pour l'isomère *cis*, 10% d'inversion après 72 heures pour l'isomère *trans*, tels que mis en évidence par chromatographie en phase gazeuse, sans compter la formation d'autres produits qui font présentement l'objet d'une étude particulière.

Devant ces résultats, qui auraient pu invalider la preuve de configuration présentée, nous avons repris la preuve en mettant en œuvre l'isomère *cis* et en omettant l'étape ambigüe qu'est l'oxydation, c'est-à-dire en analysant par chromatographie en phase gazeuse le mélange brut des alcools secondaires et tertiaires issu de la réduction: le chromatogramme montre l'absence totale d'alcool tertiaire *trans*, la présence de l'alcool tertiaire *cis* à côté des alcools secondaires. C'est donc bien le nitro-alcool de p.f. 86–87° et l'amino-alcool dont le chlorhydrate fond à 235–236° qui possèdent la configuration *cis*.

PARTIE EXPÉRIMENTALE

Les points de fusion ont été déterminés en tubes capillaires, avec un thermomètre étalonné avec des substances pures de point de fusion connu en provenance du Bureau des Standards de Washington. Les spectres infrarouges ont été déterminés au moyen d'un spectrophotomètre Perkin–Elmer, modèl 21, optique NaCl. Les chromatogrammes en phase gazeuse ont été obtenus au moyen d'un chromatographe Burrell, modèle K2, sauf indication contraire; les colonnes utilisées ont toujours un diamètre intérieur de 6 mm; les conditions variables (température, adsorbant, longueur de la colonne) sont indiquées pour chaque chromatogramme. Du point de vue qualitatif, les pics ont été repérés sur les chromatogrammes par la

Can. J. Chem. Downloaded from www.nrcresearchpress.com by 210.87.254.105 on 09/05/12
For personal use only.

méthode du rehaussement des pics avec des échantillons authentiques (13, p. 27). Du point de vue quantitatif, la méthode de triangulation fut mise en oeuvre (13, p. 33); nous avons vérifié par des mélanges appropriés que les surfaces mesurées correspondent bien aux pourcentages relatifs des composés analysés lorsque les fonctions étaient différentes, les conductivités thermiques pouvant être différentes. Les corrections qu'il faudrait apporter sont très petites: aussi ont-elles été négligées. Les résultats quantitatifs qui figurent dans ce travail en provenance de la méthode chromatographique en phase gazeuse sont donc les rapports des surfaces telles qu'elles apparaissent sur les chromatogrammes, sans corrections: les valeurs indiquées sont précises à ±1–2%. Les analyses centésimales sont de W. Manser, Ingénieur, Herrliberg, Suisse, et de C. Daesslé, Micro Analyses, Montréal.

(1) Chlorhydrate de tert-butyl-4 aminométhyl-1 cyclohexanol trans (IIa)

(1.1) Première méthode: par réduction du nitro-alcool trans Ia

En suivant fidèlement le mode opératoire décrit par Dauben *et al.* (27), on obtient à partir du nitro-alcool I*a*, p.f. 56–57° préparé selon la référence 1, 80 mg (78%) de chlorhydrate de *tert*-butyl-4 amino-éthyl-1 cyclohexanol (II*a*), paillettes incolores (méthanol–éther), p.f. 254–255° (décomp.). Calculé pour $C_{11}H_{24}ONCl$: C, 59.57; H, 10.91; N, 6.32%. Trouvé: C, 59.59; H, 10.99; N, 6.39%. Le point de fusion de ce chlorhydrate en mélange avec l'isomère *cis*, p.f. 235–236° (décomp.), décrit (1), est de 225–235°, avec décomposition partielle.

(1.2) Deuxième méthode: par réduction d'azido-alcools

(1.21) Époxydes cis et trans du tert-butyl-4 méthylène-1 cyclohexane (VIII et VII)

A 8.9 g de *tert*-butyl-4 méthylène-1 cyclohexane, préparé selon la référence 10, on ajoute d'un coup 157 ml d'une solution chloroformique d'acide perbenzoïque contenant 10.5 g de peracide. Le mélange s'échauffe et doit être refroidi sous le robinet. On ajoute un peu de sulfate de sodium anhydre et la fiole conique est déposée au réfrigérateur pendant 3 jours. La solution est filtrée et le filtrat lavé par une solution d'hydroxyde de sodium à 10%, une solution saturée de chlorure de sodium puis séché et évaporé. On obtient 9.5 g (96% brut) du mélange des époxydes *cis* et *trans* VIII et VII, p.é. 130° à 56 mm, n_D^{26} = 1.4590. Calculé pour $C_{11}H_{20}O$: C, 78.51; H, 11.98. Trouvé: C, 78.26; H, 11.61%.

L'analyse du produit brut par chromatographie en phase gazeuse, sur une colonne de 1 m contenant 15% de β,β′-oxydipropionitrile, adsorbé sur du Chromosorb-W, a donné à 136° deux pics. Le premier représente l'isomère *trans*, 69.6% du mélange, le deuxième l'isomère *cis*, 30.4%.

Les configurations *cis–trans* ont été établies par réduction du mélange des époxydes en méthyl-1 *tert*-butyl-4 cyclohexanols *cis* (V*b*) et *trans* (V*a*) connus (10, 1, 11, 12).

A une suspension agitée de 113 mg d'hydrure de lithium et d'aluminium dans 5 ml d'éther anhydre, on ajoute une solution de 500 mg du mélange des époxydes VII et VIII dans 10 ml d'éther. La solution est ajoutée goutte à goutte de façon à maintenir un léger reflux de l'éther. Le mélange est chauffé à reflux pendant 30 minutes, puis le complexe décomposé par addition à 0° de 1 ml d'eau, suivi de 5 ml d'une solution aqueuse d'acide sulfurique à 10%. Le mélange est extrait par de l'éther et la solution éthérée lavée par une solution de bicarbonate de sodium à 10%, de l'eau saturée de chlorure de sodium puis, séchée sur du sulfate de sodium anhydre et évaporée à travers une colonne de Widmer. On isole une huile incolore, 452 mg (90%), qui cristallise après quelques instants. L'analyse du produit brut par chromatographie en phase gazeuse, sur une colonne de 1 m contenant 13% de β,β′-oxydipropionitrile adsorbé sur Kromat F.B., a donné à 135° deux pics. Le premier correspond à 70% de méthyl-1 *tert*-butyl-4 cyclohexanol *trans* (V*a*), le deuxième correspond à 30% de l'isomère *cis* (V*b*). Nous en concluons que l'époxyde représentant 69.6% du mélange est l'isomère *trans* (VII) et que celui représentant 30.4% est l'isomère *cis* (VIII).

(1.22) tert-Butyl-4 azidométhyl-1 cyclohexanols cis (IVb) et trans (IVa)

Une solution de 2 g du mélange des époxydes VIII et VII préparé plus haut, dans 30 ml de méthanol, est chauffée à reflux. On y ajoute goutte à goutte 1.6 g d'azoture de sodium en solution dans 4 ml d'eau. La solution se colore en jaune dès le début de l'addition. Le mélange est agité et chauffé à reflux pendant 3 jours et 20 heures. Le méthanol est évaporé sous vide sur un bain d'eau à 40°. On isole un semi-solide blanc. Ce résidu est repris par de l'éther et la solution éthérée lavée par de l'eau distillée jusqu'à neutralité, séchée sur du sulfate de sodium anhydre et évaporée, à travers une colonne de Widmer.

On obtient 2.2 g d'une huile jaune dont la distillation fournit 2.07 g (83%) du mélange des *tert*-butyl-4 azidométhyl-1 cyclohexanols *cis* et *trans* (IV*b* et IV*a*), p.é. 138° à 13 mm, n_D^{21} = 1.4868. Spectre infrarouge (liquide pur): 3420 cm^{-1}; vibration O—H, lié; 2110 cm^{-1}: vibration —N═N═N (asymétrique); 1290 cm^{-1}; vibration —N═N═N (symétrique).

(1.23) tert-Butyl-4 aminométhyl-1 cyclohexanol trans (IIa)

Un gramme du mélange des azido-alcools IV*a* et IV*b* préparé plus haut, en solution dans 100 ml de méthanol, est hydrogéné en présence de 100 mg d'oxyde de platine sous une pression de 3.4 atm. Après 24 heures, le mélange est filtré et le filtrat acidifié par addition de 6 ml d'acide chlorhydrique concentré, puis évaporé sous vide sur un bain d'eau à 50°. On isole un solide blanc qui après lavage à l'éther pour enlever les neutres donne 710 mg (67.8%) du mélange des chlorhydrates des deux amino-alcools *cis* II*b* et *trans* II*a*. Après deux recristallisations dans un mélange méthanol–éther on isole 251 mg (23.9%) du chlorhydrate du

Can. J. Chem. Downloaded from www.nrcresearchpress.com by 210.87.254.105 on 09/05/12
For personal use only.

tert-butyl-4 aminométhyl-1 cyclohexanol trans (II*a*), p.f. 251–252° (décomp.), ne donnant pas de dépression de point de fusion en mélange avec l'échantillon préparé en (1.1).

(2) Désaminations nitreuses des amino-alcools IIa et IIb

(2.1) Dosage des époxydes par la méthode chimique

(2.11) Désamination du tert-butyl-4 aminométhyl-1 cyclohexanol trans (IIa)

A 940 mg du chlorhydrate de l'amino-alcool *trans* II*a*, en solution dans 20 ml d'eau, on ajoute 5.0 ml de soude 1.0 *N* pour libérer l'amine de son sel et 9.2 ml d'acide acétique glacial, ce qui donne une solution de l'amino-alcool dans l'acide acétique à 25%. La petite quantité de chlorure de sodium ne nuit pas à la réaction. Le mélange est refroidi à 0° et une solution de 0.88 g de nitrite de sodium dans 3.5 ml d'eau est ajoutée, goutte à goutte, en 45 minutes. Le mélange est ensuite agité à 0° pendant 2 heures, puis neutralisé par addition d'une solution d'hydroxyde de sodium à 20%, sans que la température ne s'élève au dessus de 0°. On cesse l'addition de la soude au moment où l'amino-alcool qui n'a pas réagi commence à se séparer sous forme de précipité blanc. On ajoute assez d'acide acétique glacial pour redissoudre le précipité puis 15 gouttes en excès. La solution légèrement acide est extraite par de l'éther. On obtient une solution aqueuse acide A et une solution éthérée B. La solution éthérée est lavée par une solution aqueuse de bicarbonate de sodium à 5%, par de l'eau saturée de chlorure de sodium puis séchée et évaporée à travers une colonne de Widmer. On obtient une huile jaune pesant 672 mg (94%), qui est reprise par 10 ml de méthanol et 1 ml de pipéridine puis chauffée à reflux pendant 2 heures. Le solvant est évaporé sous vide à 50° et le résidu repris par 100 ml d'éther anhydre. Cette solution éthérée est lavée par de l'eau jusqu'à neutralité, puis, extraite par trois portions de 10 ml d'acide chlorhydrique aqueux à 10%.

On examine séparément les solutions aqueuses acides (C) et la solution éthérée (D). Les solutions aqueuses acides (C) réunies sont évaporées sous vide (11 mm). On obtient 327 mg de chlorhydrate brut, qui par cristallisation dans un mélange méthanol–éther fournit le chlorhydrate de *tert*-butyl-4 pipéridinométhyl-1 cyclohexanol *trans*, p.f. 254–255° (décomp.). Calculé pour $C_{16}H_{32}ONCl$: C, 66.29; H, 11.13; N, 4.83%. Trouvé: C, 66.23; H, 11.22; N, 4.78%. Le spectre infrarouge du chlorhydrate brut montre une bande double à 1596 et 1620 cm^{-1}, correspondant à une fonction $—NH_3^+$ provenant du chlorhydrate de l'amino-alcool de départ II*a*; le mélange brut (327 mg) contient 75% et 25% des chlorhydrates de pipéridino-alcool III*a* et d'amino-alcool de départ II*a* respectivement. La solution éthérée (D) est lavée par une solution de bicarbonate de sodium (10%), par de l'eau saturée de chlorure de sodium, puis séchée et évaporée. On obtient ainsi 391 mg de *tert*-butyl-4 cycloheptanone brute (bande à 1705 dans le spectre infrarouge).

Les eaux-mères acides (A) obtenues plus haut sont rendues très alcalines par addition d'une solution d'hydroxyde de sodium à 20% et extraites par du chloroforme. L'extrait est lavé par de l'eau jusqu'à neutralité, puis l'amino-alcool II*a* en est extrait par trois lavages par de l'acide chlorhydrique aqueux à 10%. Les solutions d'acide chlorhydrique sont réunies et évaporées sous vide (11 mm), à 50°, pour abandonner 98 mg du chlorhydrate de l'amino-alcool II*a* qui n'a pas réagi, identifié par son spectre infrarouge.

Bilan de la réaction.—Des 940 mg de chlorhydrate de l'amino-alcool II*a* mis en réaction, 82 mg ont été récupérés en C et 98 en A. Les 760 mg d'amino-alcool II*a* qui ont effectivement réagi ont donné: 245 mg de pipéridino-alcool.HCl III*a* obtenus en C, soit 24.5% correspondant à autant d'époxyde *trans* VII, et 391 mg de *tert*-butyl-4 cycloheptanone isolée en D, soit 67.8%. Dans un deuxième dosage nous avons obtenu: 18.3% d'époxyde et 82% de *tert*-butyl-4 cycloheptanone.

(2.12) Désamination du tert-butyl-4 aminométhyl-1 cyclohexanol cis (IIb)

Par la méthode de dosage décrite en (2.11) nous avons obtenu à partir de 1.2 g du chlorhydrate de l'amino-alcool II*b*: 70.3 mg d'amino-alcool II*b* non entré en réaction, 82 mg (5.5%) du chlorhydrate du pipéridino-alcool III*b*, *cis*, correspondant à autant d'époxyde *cis* VIII, et 768 mg (89.3%) de cétone caractérisée comme *tert*-butyl-4 cycloheptanone dans un travail précédent (1); dans ce travail (1) nous avons également caractérisé le chlorhydrate du pipéridino-alcool III*b*. Nous montrons plus loin, à la section (2.21), que la *tert*-butyl-4 cycloheptanone décrite ici contient en fait de la *tert*-butyl-4 cyclohexanone, mais il n'est pas possible de la déceler par ce mode opératoire.

Deux autres essais ont donné 6.1 et 5.7% de chlorhydrate de pipéridino-alcool *cis* III*b*, correspondant à autant d'époxyde *cis* VIII.

(2.2) Dosage des époxydes par chromatographie en phase gazeuse

(2.21) Méthode expérimentale de la désamination nitreuse

La méthode de désamination dans ce cas-ci, est un peu différente de celle rapportée en (2.11). En effet, 1.5 g du chlorhydrate de l'amino-alcool, en solution dans 25 ml d'une solution aqueuse d'acide acétique à 25%, sont traités à 0° par un excès de nitrite de sodium (3 moles pour 1 mole d'amino-alcool) en solution à 25% dans l'eau.

Le mélange est agité à 0° pendant 2 heures, puis, neutralisé jusqu'à pH 10 par addition d'une solution de soude à 20%, sans que la température ne s'élève au dessus de 0°. Le mélange est extrait par de l'éther et la solution éthérée lavée par de l'eau saturée de chlorure de sodium, puis, séchée sur du sulfate de sodium anhydre et évaporée à travers une colonne de Widmer. On isole ainsi le produit brut de la réaction, en solution dans un peu d'éther. Les restes de l'éther ne sont pas évaporés sous vide afin de ne rien perdre des produits de la réaction.

Can. J. Chem. Downloaded from www.nrcresearchpress.com by 210.87.254.105 on 09/05/12
For personal use only.

(2.22) Dosage des époxydes

L'analyse du produit brut de la réaction est faite par chromatographie en phase gazeuse. Le produit brut des désaminations en solution dans un peu d'éther fut chromatographié sur une colonne de 2.5 m contenant du Kromat F.B. fixant 20% de Polyester de Craig (succinate); température: 210°; débit d'hélium: 40 ml/min.

Les résultats qualitatifs et quantitatifs des désaminations sont les suivants:

Désamination de l'amino-alcool cis IIb

1er essai: A = 6.1% d'époxyde *cis* VIII
B = 4.6% de *tert*-butyl-4 cyclohexanone
C = 89.2% de *tert*-butyl-4 cycloheptanone (IX)

2ième essai: A = 4.6% d'époxyde *cis* VIII
B = 5.1% de *tert*-butyl-4 cyclohexanone
C = 90.3% de *tert*-butyl-4 cycloheptanone (IX)

Désamination de l'amino-alcool trans IIa

A = 20.0% d'époxyde *trans* VII
B = 1.2% de *tert*-butyl-4 cyclohexanone
C = 78.8% de *tert*-butyl-4 cycloheptanone (IX)

Les pics correspondant aux époxydes *cis* VIII et *trans* VII ont été repérés en ajoutant le mélange des époxydes VIII et VII préparé plus haut en (1.21) au mélange de désamination. Il n'y a pas d'inconvénient à ajouter le mélange des époxydes *cis* et *trans*, car il est peu résolu sur la colonne utilisée. Les pics correspondant à la *tert*-butyl-4 cyclohexanone et à la *tert*-butyl-4 cycloheptanone ont été repérés sur le chromatogramme par la méthode du rehaussement des pics (13, p. 27), la *tert*-butyl-4 cyclohexanone pure, p.f. 50.5–52.5°, et la *tert*-butyl-4 cycloheptanone préparée en (2.11) servant d'échantillons authentiques.

Désamination de l'aminométhyl-1 cyclohexanol (VI)

1er essai: A = 19.4% d'époxyde X
B = trace (< 1%) de cyclohexanone
C = 80.6% de cycloheptanone (XI)

2ième essai: A = 20.0% d'époxyde X
B = trace (< 1%) de cyclohexanone
C = 80.0% de cycloheptanone (XI)

Par la méthode du rehaussement des pics (13, p. 27) nous avons repérés les composés A, B et C sur les chromatogrammes, l'époxyde étant préparé selon la méthode décrite en (1.21), la cycloheptanone et la cyclohexanone étant des échantillons commerciaux.

(2.23) Isolement de la tert-butyl-4 cyclohexanone des produits de la désamination nitreuse du tert-butyl-4 aminométhyl-1 cyclohexanol cis (IIb)

L'analyse par chromatographie en phase gazeuse, des produits de la désamination nitreuse de l'amino-alcool *cis* II*b*, montre qu'il y a environ 5% de *tert*-butyl-4 cyclohexanone de présent dans le mélange. L'analyse fut réalisée sur deux colonnes différentes: (*a*) 20% de Polyester de Craig (succinate) adsorbé sur du Kromat F.B.; longueur de la colonne: 2.5 m; température: 212°. (*b*) 30% d'huile de Silicone No. 550 adsorbée sur du Kromat F.B.; longueur de la colonne: 1 m; température: 195°.

Pour isoler la *tert*-butyl-4 cyclohexanone nous avons procédé de la manière suivante. Une désamination nitreuse fut réalisée sur 5.0 g du chlorhydrate de l'amino-alcool *cis* II*b*, à la façon décrite en (2.21). Le produit brut de la désamination est agité pendant la nuit avec 10 ml d'une solution aqueuse d'acide sulfurique à 1%, puis extrait par de l'éther. La couche éthérée est lavée par une solution de bicarbonate de sodium à 10%, par de l'eau saturée de chlorure de sodium puis séchée sur du sulfate de sodium anhydre et évaporée à travers une colonne de Widmer. On isole ainsi 3.6 g de mélange brut.

L'analyse par chromatographie en phase gazeuse montre deux pics, *tert*-butyl-4 cyclohexanone et *tert*-butyl-4 cycloheptanone, confirmés par la méthode du rehaussement des pics (13, p. 27).

Le produit brut (3.6 g), en solution dans 200 ml d'éther de pétrole (p.é. 30–40°), fut chromatographié sur 105 g d'alumine Fisher pour chromatographie. L'élution de la colonne donne: (*a*) par de l'éther de pétrole (p.é. 30–40°), 2.37 g d'une huile jaunâtre, constituée de 3.3% de *tert*-butyl-4 cyclohexanone et de 96.7% de cétone agrandie IX; (*b*) par un mélange éther de pétrole 90% – éther anhydre 10%, 0.46 g d'huile jaunâtre, constituée de 6.6% de *tert*-butyl-4 cyclohexanone et de 93.4% de cétone agrandie IX; (*c*) par un mélange éther de pétrole 50% – éther anhydre 50%, 0.06 g d'une huile avec un peu de solide; (*d*) par de l'éther anhydre, un mélange éther 95% – chloroforme 5% et un mélange éther 85% – chloroforme 15%, 0.15 g d'un solide blanc, p.f. 216–218°, après recristallisation dans du méthanol (fines aiguilles). La constitution de ce composé (trouvé: C, 68.25; H, 10.60; N, 9.47%) n'est pas connue.

Les fractions *a* et *b* sont réunies (2.83 g) et mises en solution dans 2 ml de méthanol. Le mélange est

Can. J. Chem. Downloaded from www.nrcresearchpress.com by 210.87.254.105 on 09/05/12
For personal use only.

ensuite injecté dans un appareil de chromatographie en phase gazeuse Fisher Prep/Partitioner, modèle 24, dans les conditions suivantes: une colonne (50×5 cm) suivie de trois colonnes (50×2.5 cm), chargées de Columpak sur lequel est adsorbé 20% de Dow-Corning Silicone Fluid No. 200. Températures: colonnes, 150°; "flash-evaporator", 270°; cellule, 200°. Eluant: azote, 1.6 atm.

On sépare aisément: premièrement le méthanol, qui ne fut pas isolé; deuxièmement la *tert*-butyl-4 cyclohexanone, isolée sous forme de solide blanc, p.f. 47–49°, caractérisée par point de fusion mixte et spectre infrarouge; troisièmement la *tert*-butyl-4 cycloheptanone (IX), isolée sous forme d'huile incolore.

(3) Oxydations chromiques

Une solution de 100 mg de l'alcool tertiaire (V*a* ou V*b*) dans 2.5 ml d'acide acétique glacial est agitée en présence de 100 mg d'anhydride chromique pulvérisé, à la température du laboratoire (25–26°).

Le mélange est étendu d'eau puis d'éther et l'acide acétique neutralisé par addition de bicarbonate de soude en poudre. Les solutions éthérées sont lavées par de l'eau saturée de chlorure de sodium, réunies, séchées et évaporées jusqu'à environ 2 ml.

L'analyse par chromatographie en phase gazeuse à 135° sur une colonne de 1 m contenant 13% β,β'-oxydipropionitrile adsorbé sur du Kromat F.B., montre les résultats suivants:

Alcool	Temps de contact	Alcool *cis* V*b*	Alcool *trans* V*a*
trans V*a*	70 heures	10%	90%
cis V*b*	70 heures	63%	37%
cis V*b*	47 heures	71%	29%

REMERCIEMENTS

Nous exprimons nos remerciements au Conseil National des Recherches du Canada, pour une bourse (D. G.) et un octroi de recherches (H. F.), ainsi qu'aux Etablissements Dow Chemical of Canada Limited, Montréal, pour la quantité généreuse de *tert*-butyl-4 cyclohexanone mise à notre disposition.

BIBLIOGRAPHIE

1. H. Favre et D. Gravel. Can. J. Chem. **39**, 1548 (1961).
2. G. E. McCasland. J. Am. Chem. Soc. **73**, 2293 (1951).
3. F. Winternitz et S. Ladabaum. Bull. Soc. Chim. France, 597 (1960).
4. P. A. S. Smith et D. R. Baer. Organic reactions. Vol. XI. John Wiley & Sons, Inc., New York. 1960. p. 157.
5. T. M. Jacob et S. Dev. J. Indian Chem. Soc. **38**, 674 (1961).
6. S. Winstein et N. J. Holness. J. Am. Chem. Soc. **77**, 5562 (1955).
7. B. Tchoubar. Bull. Soc. Chim. France, 164 (1949).
8. B. Tchoubar. Bull. Soc. Chim. France, 169 (1949).
9. B. Cross et G. H. Whitham. J. Chem. Soc. 3895 (1960).
10. B. Cross et G. H. Whitham. J. Chem. Soc. 3892 (1960).
11. C. H. DePuy et R. W. King. J. Am. Chem. Soc. **83**, 2743 (1961).
12. W. J. Houlihan. Abstracts, 140th American Chemical Society Meeting, Chicago. Sept. 1961. p. 18Q.
13. A. I. M. Keulemans. Gas chromatography. Reinhold Publishing Corporation, New York. 1959.
14. N. L. Allinger et Shih-En Hu. J. Am. Chem. Soc. **84**, 370 (1962).
15. J. H. Ridd. Quart Rev. (London), **15**, 418 (1961).
16. J. A. Mills. J. Chem. Soc. 260 (1953).
17. A. Streitwieser, Jr. J. Org. Chem. **22**, 861 (1957).
18. B. M. Benjamin et C. J. Collins. J. Am. Chem. Soc. **83**, 3662 (1961).
19. H. Felkin. Bull. Soc. Chim. France, 20 (1959).
20. I. Elphimoff-Felkin et Y. Gault. Compt. Rend. **246**, 1871 (1958).
21. D. J. Cram et J. E. McCarty. J. Am. Chem. Soc. **79**, 2866 (1957).
22. A. Streitwieser, Jr. et C. E. Coverdale. J. Am. Chem. Soc. **81**, 4275 (1959).
23. B. M. Benjamin, H. J. Schaeffer et C. J. Collins. J. Am. Chem. Soc. **79**, 6160 (1957).
24. B. M. Benjamin, P. Wilder, Jr. et C. J. Collins. J. Am. Chem. Soc. **83**, 3654 (1961).
25. J. English, Jr. et A. E. Bliss. J. Am. Chem. Soc. **78**, 4057 (1956).
26. R. Fessenden et F. J. Freenor. J. Org. Chem. **26**, 1681 (1961).
27. H. J. Dauben, Jr., H. J. Ringold, R. H. Wade et A. G. Anderson, Jr. J. Am. Chem. Soc. **73**, 2359 (1951).

Can. J. Chem. Downloaded from www.nrcresearchpress.com by 210.87.254.105 on 09/05/12
For personal use only.

THE EFFECT OF ELECTRIC FIELDS, AND A RELATED DEPENDENCE ON DOSE RATE, IN THE γ-RADIOLYSIS OF HYDROCARBON GASES[1]

T. W. WOODWARD[2] AND R. A. BACK
Division of Pure Chemistry, National Research Council of Canada, Ottawa, Canada
Received January 25, 1963

ABSTRACT

The effect of electric fields on the γ-radiolysis of ethane, propane, and the butanes has been investigated briefly at 800 mm pressure, with dose rates between 2×10^{10} and 400×10^{10} ev/cc sec. Yields of hydrogen were reduced when a saturation field was applied, except with ethane at low dose rate, where a slight increase in hydrogen yield was observed. With propane and *n*-butane, the yield of hydrogen in the presence of a saturation field was independent of dose rate, while with ethane, it decreased with decreasing dose rate. At the same time, a dose rate dependence was discovered in the simple radiolysis, in the absence of any field, of ethane, propane, and *n*-butane, a decrease in the yield of hydrogen at low dose rates being observed. An explanation of these observations is suggested in terms of a competition between neutralization of ions in the gas phase and diffusion of ions to the wall. High dose rates should favor the former process, and low dose rates the latter. At sufficiently high dose rates, all ions should be neutralized in the gas phase. At sufficiently low dose rates, all ions should diffuse to the wall before neutralization, and it is suggested that the radiolysis under these conditions should closely resemble that in the presence of a saturation field at higher dose rates.

The application of an electric field to a gas during irradiation offers a potential means of distinguishing between products arising from ions and those formed from neutral species. In practice, the interpretation of the results is very complex, and except for the work of Essex and his collaborators at Syracuse (1), mostly concerned with α-radiation, the method has not been widely used in radiation chemistry. The present work was undertaken to study the effects of electric fields on the γ-radiolysis of some simple hydrocarbon gases, using a saturation-current method (2) to measure absolute product yields. In the course of the work, a hitherto unsuspected dependence of hydrogen yield on dose rate was discovered, which appears to be closely related to the action of applied fields on the radiolysis.

EXPERIMENTAL

The preparation and purification of hydrocarbon samples for irradiation have been previously described (2, 3). Gases were irradiated in cylindrical vessels of 60-mm o.d. and about 500- to 600-cc volume. Two experiments with propane were done in a smaller vessel of the same design and length, but with about one-half the diameter and one-quarter the volume. The measurement of saturation ion current and of hydrogen yield has been described (2). Electric fields were always applied with the central electrode positive, so that the positive ions were drawn to the other electrode, the graphite-coated wall of the cylindrical vessel. Hydrogen was the only product measured, and the extent of decomposition was always small enough that "internal" scavenging was negligible, and the measured yields were very close to their true initial values (3). Ethylene scavenger was added in some experiments, in which case the hydrogen yield was extrapolated to zero scavenger concentration (3).

Two Co^{60} γ-ray sources were used, one of about 200 c,* the other a 1300-c A.E.C.L. "Gammacell". By a suitable choice of distance from the source, or appropriate shielding, dose rates varying from about 2×10^{10} to 300×10^{10} ev/cc sec were obtainable.

[1]*Issued as N.R.C. No. 7301.*
[2]*National Research Council of Canada postdoctoral fellow, 1960–1962. Present address: Department of Natural Philosophy, The University, Edinburgh, Scotland.*
**The authors are grateful to the Division of Applied Physics of these laboratories for the use of this γ-ray source.*

Can. J. Chem. Downloaded from www.nrcresearchpress.com by 210.87.254.5 on 09/05/12
For personal use only.

RESULTS AND DISCUSSION

Tables I to IV summarize the hydrogen yields from the radiolysis of ethane, propane, *n*-butane, and isobutane, measured under a variety of conditions of dose rate, electric field, and added scavenger. The dose rate in each case was calculated from the measured saturation current, combined with values of W of 24.9 for ethane, and 24.0 ev/ion pair for propane and the butanes (2). Values of M/N were obtained directly from the measure-

TABLE I

Radiolysis of ethane at 800 mm pressure

Expt. No.	Dose rate $\times 10^{-10}$ (ev/cc sec)	Applied field (kv)	Scavenger added (%)	Hydrogen yield M/N	Hydrogen yield G
1	6.2	0	0	1.74	7.00
2	61	0	0	2.02	8.10
3	216	0	0	2.15	8.60
4	216	0	0	2.10	8.40
5	6.0	1.5 (s)	0	1.78	7.15
6	218	1.4 (s)	0	1.95	7.84
7	6.3	0	2	0.65	2.61
8	6.4	0	4	0.69	2.77
9	6.3	1.0 (s)	2	0.68	2.73
10	6.3	2.0 (s)	2	0.79	3.18

NOTE: (s) indicates saturation field.

TABLE II

Radiolysis of propane at 800 mm pressure

Expt. No.	Dose rate $\times 10^{-10}$ (ev/cc sec)	Applied field (kv)	Hydrogen yield M/N	Hydrogen yield G
11	3.60	0	1.32	5.50
12*	9.90	0	1.50	6.25
13	85.0	0	1.79	7.45
14*	310	0	1.79	7.45
15†	315	0	1.79	7.45
16†	47.0	0	1.73	7.20
17	8.8	2.0 (s)	1.17	4.88
18	294	1.4 (s)	1.23	5.12
19	300	2.6 (s)	1.23	5.12

NOTE: (s) indicates saturation field.
*Average of several experiments.
†Experiments in small vessel.

TABLE III

Radiolysis of *n*-butane at 800 mm pressure

Expt. No.	Dose rate $\times 10^{-10}$ (ev/cc sec)	Applied field (kv)	Scavenger added (%)	Hydrogen yield M/N	Hydrogen yield G
20	2.25	0	0	1.18	4.92
21*	12.5	0	0	1.29	5.40
22*	394	0	0	1.30	5.41
23	390	2.5 (s)	0	0.98	4.08
24	11.4	0.8	0	1.12	4.67
25	10.8	2.2 (s)	0	0.98	4.08
26	11.8	4.0 (s)	0	0.96	4.00
27	11.4	2.0 (s)	6	0.34	1.42
28†	11.4	0	4	0.42	1.75

NOTE: (s) indicates saturation field.
*Average of several experiments.
†Taken from ref. 2.

Can. J. Chem. Downloaded from www.nrcresearchpress.com by 210.87.254.5 on 09/05/12
For personal use only.

TABLE IV
Radiolysis of isobutane at 800 mm pressure

Expt. No.	Dose rate $\times 10^{-10}$ (ev/cc sec)	Applied field (kv)	Hydrogen field	
			M/N	G
29*	11.5	0	1.20	5.00
30	12.1	0.7	1.05	4.37
31	11.2	2.2 (s)	0.80	3.33
32	11.6	4.0 (s)	0.80	3.33

NOTE: (s) indicates saturation field.
*Average of several experiments.

ments of saturation ion current and hydrogen production, while G-values were calculated from M/N via W. The experiment numbers in these tables are assigned arbitrarily, for reference purposes, and do not signify the order in which the experiments were done. In some instances, a single experiment number represents an average of several measurements.

Figure 1 shows the effect of an electric field on the yield of hydrogen from the radiolysis of n-butane at an approximately constant dose rate of about 11×10^{10} ev/cc sec. The

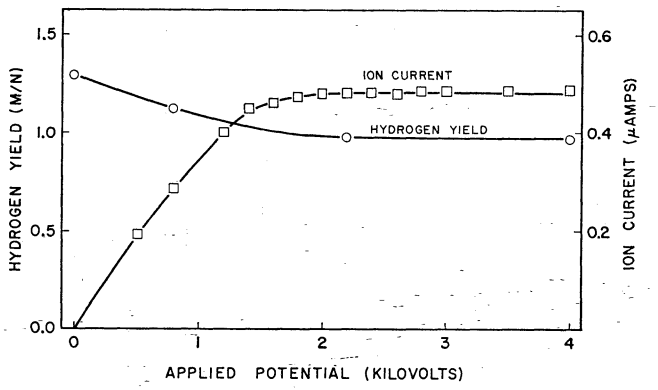

FIG. 1. The effect of electric fields on the yield of hydrogen from the γ-radiolysis of n-butane.

dependence of ion current on the applied voltage is also shown for comparison. It should be noted that in computing M/N for experiments at voltages below saturation, N was always the saturation value. The decrease in the hydrogen yield is seen to have parallelled the rise in the ion current, becoming constant in the saturation region. This behavior suggests that the effect of the field was simply associated with the removal of ions to the cathode, and became constant when this removal was complete. The lack of change in the saturation region shows that electron impact by electrons accelerated in the field was not contributing to the hydrogen production up to the highest voltages used. Similar data for isobutane may be seen in Table IV. Propane and ethane were studied only with saturation fields, somewhat above the minimum voltage required for saturation. This minimum voltage increased steadily in going from ethane to propane to butane, presumably due to differences in rates of diffusion of ions in the three gases. It also depended somewhat on the diameter of the central anode, which in several of the radiolysis vessels consisted of graphite-coated 5 mm o.d. Pyrex tubing instead of the 1.5-mm tungsten wire used in the original vessel (2). Slightly lower minimum voltages were required for saturation with the thicker central electrode, and the saturation current plateaus were perfectly

Can. J. Chem. Downloaded from www.nrcresearchpress.com by 210.87.254.5 on 09/05/12
For personal use only.

flat, eliminating the very slight increase in ion current evident in Fig. 1, which was presumably due to slight electron multiplication effects caused by the high local field strength immediately surrounding the tungsten wire.

In Fig. 2, the dependence of hydrogen yield on the $\log_{10}$ of the dose rate is shown for the radiolysis of ethane, propane, and *n*-butane, with no field applied. With propane and

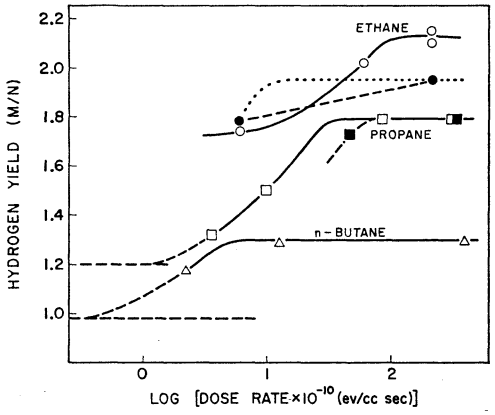

FIG. 2. The effect of dose rate on the yields of hydrogen from the γ-radiolysis of ethane, propane, and *n*-butane: ●, ethane with saturation field; ○, ethane with no field; □, propane with no field; ■, propane in small reaction vessel, with no field; △, *n*-butane with no field.

butane, the hydrogen yield was independent of dose rate at high dose rates, but showed a progressive decrease with decreasing dose rate at lower dose rates, with a maximum decrease of about 25% observed with propane at the lowest dose rate studied. Ethane showed a similar decrease, but a constant yield at high dose rate was not attained. The curves in Fig. 2 have been drawn, not as the simplest curves through the experimental points, but as will be seen shortly, to support a particular interpretation of the data.

With propane, *n*-butane, and isobutane, the application of a saturation field caused a marked reduction in the yield of hydrogen. With propane and *n*-butane, the values of these reduced yields of hydrogen were practically independent of dose rate (expts. 17–19, 23, 25–26), an observation which suggests a very simple explanation of the dose rate dependence in the absence of a field. With no applied field, neutralization may occur in the gas phase or at the surface of the vessel. Neutralization in the gas phase should be second order in ions, while diffusion to the wall is a first-order process, so that high dose rate, and consequent high ion concentration, should favor the former, and low dose rate the latter. In the one limit, at sufficiently high dose rate, gas phase neutralization should become fast enough that no ions reach the wall before being neutralized. In the other limit, at sufficiently low dose rate, all the ions should diffuse to the wall before appreciable neutralization can occur in the gas phase. If, as the effect of applied fields suggests, the hydrogen yield is lowered when ions are neutralized at the wall, then a sigmoid dependence of hydrogen yield on dose rate should be observed, with plateaus independent of dose rate at sufficiently high and low dose rates. Furthermore, if the effect of a saturation field is simply one of removing ions to the surface before neutralization, then the lower plateau should coincide with the dose-rate-independent hydrogen yield in the presence of a saturation field. The curves for propane and *n*-butane in Fig. 2 have been drawn in accordance with this hypothesis.

All the results obtained with propane and *n*-butane are, as far as they go, in agreement

Can. J. Chem. Downloaded from www.nrcresearchpress.com by 210.87.254.5 on 09/05/12
For personal use only.

with this simple explanation, although with neither gas was a lower plateau reached. The experiments with isobutane were done at constant dose rate, and so are no test of the theory. The results obtained with ethane are somewhat embarassing to the suggested explanation. The hydrogen yields from ethane measured in the absence of a field follow a sigmoid curve (Fig. 2), although neither an upper nor a lower plateau was reached. The hydrogen yield in the presence of a saturation field, however, was not independent of dose rate, and at the lowest dose rate, the application of a saturation field actually increased the hydrogen yield. This increase was barely within the accuracy of the measurements, but a similar increase was also found in the presence of scavenger (expts. 7–10), and it is interesting that Williams and Essex, using α-rays, found an increased yield of ethane decomposition when a field was applied (4).

Two explanations of the deviation of ethane from the simple theory seem possible. The first is that ethane is a special case, due to some peculiarity of the radiolysis mechanism, so that the hydrogen yield does not follow the simple behavior observed with propane and butane. The second explanation is that ethane is not a special case, but has merely been studied at dose rates low enough to show the fallacy of the simple theory, and that propane and butane would show similar deviations when studied at sufficiently low dose rates. Thus the hydrogen yield from ethane in the presence of a saturation field could follow the dotted curve in Fig. 2, and only the two experiments at the lowest dose rates would disagree with the simple theory.

In support of the suggested competition between gas phase neutralization and diffusion to the wall is the progressive shift of the sigmoid curves towards higher dose rate in going from butane to propane to ethane. Such a shift would be predicted by the dependence of the rate of diffusion on molecular weight of the medium, perhaps combined with larger cross sections for the neutralization of the larger ions; the same factors are reflected in the fact that a higher voltage was required for saturation in butane than in ethylene (2). Similar shifts of the sigmoid curves should also arise from a change in diameter of the radiolysis vessel, or from a change in pressure. Two experiments, 15 and 16, were done with propane in a smaller vessel, and the results are shown in Fig. 2 (filled squares). The vessel diameter was about one-half that of the regular vessels, so that the average distance of ions from the wall was roughly halved, and the rate of diffusion to the wall should have been approximately doubled. The results of these experiments are compatible with the expected shift towards higher dose rate, as the curves are drawn, but this is by no means conclusive.

Clearly, more data are required to determine the validity of the suggested explanation of the observed dependence on dose rate. The most obvious need is for further experiments at higher dose rates with ethane, and at lower dose rates for all three gases. Unfortunately, the lowest dose rates used are already becoming inconvenient: for example, at the lowest dose rate used with butane, 60 hours of irradiation yielded about 0.25 μmole of hydrogen. Keeping in mind that the scale in Fig. 2 is logarithmic, the extension of the present data much further towards lower dose rates begins to become impractical. A more hopeful approach would be to shift the sigmoid curves to higher, more convenient dose rates by working with lower pressures and smaller radiolysis vessels, which should favor diffusion to the walls.

Finally, if the suggested explanation of the present results proves correct, there are several interesting implications. The first of these is that in any study of the radiolysis of hydrocarbon gases, it is important to determine where the experiments lie on the dose rate dependence curve, keeping in mind that the sigmoid curve may be shifted by changes in molecular weight, pressure, and dimensions of the radiolysis vessel. There would seem

Can. J. Chem. Downloaded from www.nrcresearchpress.com by 210.87.254.5 on 09/05/12
For personal use only.

to be marked advantages, both practical and theoretical, in working at dose rates on the upper plateau, where neutralization occurs entirely in the gas phase. In this region, surface effects should be minimized, and the nature of the surface and the dimensions of the radiolysis vessel should have little influence on the measured yields. It might be noted that recent measurements of yields from the radiolysis of propane reported from this laboratory were made at dose rates well below the upper plateau (2).

A second implication is that the upper plateau of the dose rate dependence curve should also be the best region in which to study the effects of electric fields. The application of a saturation field should cause a change from neutralization entirely in the gas phase to neutralization entirely on the surface. Resultant changes in product yields should then be a maximum, and should permit the simplest possible interpretation in terms of a modification of the neutralization "cracking" reactions by their occurrence at a surface. In the present work, ethane, propane, *n*-butane, and isobutane showed, upon application of a saturation field in the high dose rate region, a loss of hydrogen of 0.18, 0.56, 0.33, and 0.40 molecule per ion pair. There is thus no obvious one-to-one correspondence between ions neutralized at the surface and loss of hydrogen. This may reflect an inefficiency in the quenching by the surface of the excited molecules formed by neutralization, or more probably means that not all ions yield hydrogen upon neutralization in the gas phase, with some undergoing dissociation of C—C bonds rather than splitting off H_2 or H. Loss of hydrogen atoms by reaction with the graphite electrode, following their formation by a neutralization reaction at the surface, is also a possibility. With *n*-butane, about 75% of the hydrogen lost when a saturation field was applied was "scavengeable" by ethylene, and presumably came from atomic hydrogen (expts. 21–23, 25, 26–28). The experiments with ethane in the presence of scavenger were not done in the upper plateau region of dose rate; the percentage change in hydrogen yield upon application of a saturation field was much the same as that found in experiments with pure ethane (Table I).

A further implication arises from a comparison of the rate of diffusion of ions to the wall, calculated from a simple random walk formula, with the rate of gas phase neutralization based on a recombination coefficient between 10^{-6} and 10^{-8} cc/sec (5). Despite the uncertainties of these calculations, it seems clear that the rate of diffusion of positive hydrocarbon ions to the wall is several orders of magnitude too slow to compete effectively with gas phase neutralization even at the lowest dose rates used in the present experiments. This implies that the diffusion of free electrons, which is many times faster than that of positive ions, must be the rate-controlling process in the competition (5, 6). Gas phase neutralization is prevented, of course, when the electrons reach the wall, even though the positive ions stay much longer in the gas phase. This conclusion is not unexpected, as it is known that saturated hydrocarbons do not readily form negative ions (7).

At the present time, there is almost nothing known about the modes of decomposition of the highly excited species that must be formed when a hydrocarbon ion is neutralized. Much more experimental work, using a variety of techniques, and with complete product analysis, will be required before much can be said about this very elusive phase of the radiolysis process.

REFERENCES

1. S. C. LIND. Radiation chemistry of gases. Reinhold, New York. 1961.
2. R. A. BACK, T. W. WOODWARD, and K. A. MCLAUCHLAN. Can. J. Chem. **40**, 1380 (1962).
3. R. A. BACK. J. Phys. Chem. **64**, 124 (1960).
4. N. T. WILLIAMS and H. ESSEX. J. Phys. Chem. **17**, 995 (1949).
5. A. VON ENGEL. Ionized gases. Oxford, London. 1955.
6. G. FRANCIS. Ionization phenomena in gases. Academic Press, New York. 1960. pp. 54–55.
7. C. E. MELTON and P. S. RUDOLPH. J. Chem. Phys. **31**, 1485 (1959).

Can. J. Chem. Downloaded from www.nrcresearchpress.com by 210.87.254.5 on 09/05/12
For personal use only.

ELECTRODE PROCESSES WITH A PRECEDING CHEMICAL REACTION: EFFECT OF THE DIFFUSE DOUBLE LAYER

S. K. RANGARAJAN
Central Electrochemical Research Institute, Karaikudi, India
Received December 10, 1962

ABSTRACT

The effect of migration in the diffuse double layer on the concentration field of the reactive species is analyzed assuming that the electrode reaction $O + ne \rightleftharpoons R$ is preceded by a chemical reaction $Y + \beta X \rightleftharpoons O$ ($Z_X = 0$). Comparison is made with the solutions derived already by Hurwitz and also by Matsuda for particular cases.

Can. J. Chem. Downloaded from www.nrcresearchpress.com by 210.87.254.42 on 09/05/12
For personal use only.

The influence of the migration in the diffuse double layer on the interfacial concentrations of the reactive species has been discussed in detail in a previous communication (1). Therein, it has been assumed that the reaction scheme is $O + ne \rightleftharpoons R$ with no preceding chemical reaction. (Specific adsorption will be assumed absent in the discussions.)

It is proposed to extend the treatment to a case where the electrode reaction is preceded by a chemical reaction $Y + \beta X \rightleftharpoons O$. Here, X is assumed to be a neutral substance so that $Z_Y = Z_O$. The steady-state solutions for this problem have been given by Hurwitz (2), and in the present paper we derive a modified expression for the same. The limiting behavior (viz. $\nu \gg 1$ or $\xi_0 \rightarrow \infty$) of the steady-state solutions do not differ appreciably. But otherwise, expressions obtained are different. In some cases at least, particularly for $|Z_i/Z| = m$, integer, the rigorous solutions assume relatively simpler forms.

Matsuda's solution (3) wherein the condition $Z_Y = Z_O$ has been relaxed at the expense of the inequality $K \ll 1$ has also been discussed. A general solution to the problem $Z_O \neq Z_R$ and K assuming any finite value is under investigation.

The reaction scheme is

[*a*] $$O^{z_O} + ne \rightleftharpoons R^{z_R}$$

[*b*] $$Y + \beta X \underset{k_b}{\overset{k_f}{\rightleftharpoons}} O^{z_O} \qquad (Z_X = 0).$$

The solution given below can as well be extended to the case $Y \rightleftharpoons O + \beta X$.

(i) Y and X are not reduced or oxidized; (ii) X is a neutral substance, so that $Z_Y = Z_O$; and (iii) a large excess of the species X as compared to O and Y is present, and consequently the concentration changes of X are negligible. Thus, the homogeneous chemical reaction [*b*] is *formally* monomolecular.

For such a case the concentration distribution is given by the system of equation [1] to [8]:

[1] $$\partial C_O/\partial t = -\partial Q_O/\partial x + k_f C_Y (C_X^0)^\beta - k_b C_O$$

[2] $$\partial C_Y/\partial t = -\partial Q_Y/\partial x - k_f C_Y (C_X^0)^\beta + k_b C_O$$

[3] $$(Q_O)_{x=0} = \pm I(t)/nF$$

[4] $$(Q_Y)_{x=0} = 0 \qquad \text{(cf. assumption (i))}$$

[5] $$[C_O(x,t)]_{x=\infty} = C_O^0$$

[6] $$[C_Y(x,t)]_{x=\infty} = C_Y^0$$

[7] $$C_O(x,0) = C_O^0 \exp(-Z_i F\phi/RT)$$

[8] $$C_Y(x,0) = C_Y^0 \exp(-Z_i F\phi/RT)$$

with

[9] $$Q_i = -D\{\partial C_i/\partial x + (Z_i F/RT)C_i(d\phi/dx)\} \qquad (i = O, Y).$$

In deriving the solution one must a priori know the dependence of ϕ on x. It is assumed in this paper that the diffuse double layer structure is determined entirely by a Z–Z supporting electrolyte and the potential distribution $\phi(x)$ in the layer obeys Gouy–Chapman theory, i.e.,

[10] $$d\phi/dx = -(2RT/|Z|F)\kappa \sinh(|Z|F\phi/2RT),$$

with

$$1/\kappa = (RT\epsilon/8\pi Z^2F^2C_i)^{\frac{1}{2}}.$$

Transforming the variables $C_O(x,t)$, $C_Y(x,t)$ into M and N, defined by

[11] $$M = C_Y(x,t)+C_O(x,t) \text{ and}$$

[12] $$N = [C_Y(x,t)-(1/K)C_O(x,t)] \exp(\mu t),$$

where

$$\mu = k_f(C_X^0)^\beta + k_b \text{ and } K = (k_f/k_b)(C_X^0)^\beta,$$

we rewrite the equations and the boundary conditions given by [1] to [8] as

[13] $$D\cdot\partial/\partial x[\partial M/\partial x + (Z_O F/RT)M(d\phi/dx)] = \partial M/\partial t$$

[14] $$D\cdot\partial/\partial x[\partial N/\partial x + (Z_O F/RT)N(d\phi/dx)] = \partial N/\partial t$$

[15] $$M_{t=0} = \exp(-Z_O F\phi_0/RT)(C_O^0+C_Y^0) = M^0 \exp(-Z_O F\phi_0/RT)$$

[16] $$M_{x=\infty} = (C_O^0+C_Y^0) = M^0$$

[17] $$N_{t=0} = 0$$

[18] $$N_{x=\infty} = 0$$

[19] $$D[\partial M/\partial x + (Z_O F/RT)M(d\phi/dx)] = \pm I(t)/nF$$

[20] $$D[\partial N/\partial x + (Z_O F/RT)N(d\phi/dx)] = \pm I(t)/nFK \exp(\mu t).$$

It may be noted that equations [13] and [14] are similar to those arising for the mass transfer of the species in the diffuse double layer that are directly discharged (without any chemical reaction preceding or following). Consequently, the solutions of these equations are similar to those given earlier (1). It can be proved that

[21] $$\bar{M}(0,p) = L[M(0,t)] = \exp(-Z_O F\phi_0/RT) \times\left[M^0 \mp \frac{I(p)}{nF\sqrt{(Dp)}}\,\xi_0^{2(l+1)}\,\frac{F(k, k+l+1; 2k+1; 1-1/\xi_0^2)}{F(k+1, k+l+1; 2k+1; 1-1/\xi_0^2)}\right]$$

and

Can. J. Chem. Downloaded from www.nrcresearchpress.com by 210.87.254.42 on 09/05/12
For personal use only.

[22] $$\bar{N}(0,p) = L[N(0,t)] = \exp(-Z_O F\phi_0/RT) \times\left[\pm\frac{L(I(t)\exp(\mu t))}{nF\sqrt{(Dp)}}\,\xi_0^{2(l+1)}\,\frac{F(k, k+l+1; 2k+1; 1-1/\xi_0^2)}{F(k+1, k+l+1; 2k+1; 1-1/\xi_0^2)}\right],$$

where

$$k = (1/\kappa)\sqrt{(p/D)}.$$

Hence

[23] $$L[N(0,t)\exp(-\mu t)] = (p/p+\mu)\bar{N}(p+\mu),$$

where $\bar{N}(o,p)$ is given by [22]. Also

[24] $$L[I(t)\exp(\mu t)] = \bar{I}(p-\mu)\cdot p/(p-\mu)$$

so that

$$\bar{N}(p+\mu) = \pm\exp\left(\frac{-Z_O F\phi_0}{RT}\right)\frac{\bar{I}(p)}{nF\sqrt{\{D(p+\mu)\}}}\,\xi_0^{2(l+1)} \times\frac{p+\mu}{p}\,\frac{F(\gamma, \gamma+l+1; 2\gamma+1; 1-1/\xi_0^2)}{F(\gamma+1, \gamma+l+1; 2\gamma+1; 1-1/\xi_0^2)},$$

where $\gamma = (1/\kappa)\sqrt{\{(p+\mu)/D\}}$. Equation [23] then gives

[25] $$L[N(0,t)\exp(-\mu t)] = L[C_Y^0(0,t) - (1/K)C_O(0,t)]$$
$$= \pm\exp\left(\frac{-Z_O F\phi_0}{RT}\right)\frac{I(p)}{nF\sqrt{\{(p+\mu)D\}}}\,\xi_0^{2(l+1)}\,\frac{F(\gamma, \gamma+l+1; 2\gamma+1; 1-1/\xi_0^2)}{F(\gamma+1, \gamma+l+1; 2\gamma+1; 1-1/\xi_0^2)}.$$

From [21] and [25] we may obtain the transforms of $C_O(0,t)$ and $C_Y(0,t)$ as

[26] $$\bar{C}_O(0,p) = K(\bar{M}-\bar{N})/(K+1)$$
$$= \frac{K}{K+1}\exp\left(\frac{-Z_O F\phi_0}{RT}\right)\left[M^0 \mp \frac{\bar{I}(p)}{nF\sqrt{(Dp)}}\,\xi_0^{2(l+1)} \times\frac{F(k, k+l+1; 2k+1; 1-1/\xi_0^2)}{F(k+1, k+l+1; 2k+1; 1-1/\xi_0^2)} \mp\frac{\bar{I}(p)}{nFK\sqrt{\{D(p+\mu)\}}}\,\xi_0^{2(l+1)}\,\frac{F(\gamma, \gamma+l+1; 2\gamma+1; 1-1/\xi_0^2)}{F(\gamma+1, \gamma+l+1; 2\gamma+1; 1-1/\xi_0^2)}\right]$$

and

[27] $$\bar{C}_Y(0,p) = (M+KN)/(K+1) = \exp(-Z_O F\phi_0/RT)/(K+1) \times\left[M^0 \mp\frac{\bar{I}(p)}{nF\sqrt{(Dp)}}\,\xi_0^{2(l+1)}\,\frac{F(k, k+l+1; 2k+1; 1-1/\xi_0^2)}{F(k+1, k+l+1; 2k+1; 1-1/\xi_0^2)} \pm\frac{\bar{I}(p)}{nF\sqrt{\{D(p+\mu)\}}}\,\xi_0^{2(l+1)}\,\frac{F(\gamma, \gamma+l+1; 2\gamma+1; 1-1/\xi_0^2)}{F(\gamma+1, \gamma+l+1; 2\gamma+1; 1-1/\xi_0^2)}\right].$$

Also from [12] and [25],

[28] $$\bar{C}_O(0,p) = K\{\bar{C}_Y(0,p) - L[N(0,t)\exp(-\mu t)]\}$$
$$= K\left\{\bar{C}_Y(0,p) \mp\frac{\bar{I}(p)\xi_0}{nFK\sqrt{\{D(p+\mu)\}}}\,\frac{F(\gamma, \gamma+l+1; 2\gamma+1; 1-1/\xi_0^2)}{F(\gamma+1, \gamma+l+1; 2\gamma+1; 1-1/\xi_0^2)}\right\}.$$

Can. J. Chem. Downloaded from www.nrcresearchpress.com by 210.87.254.42 on 09/05/12
For personal use only.

The relationship that one would obtain in the absence of chemical reaction can be deduced by allowing $K \rightarrow 0$ and $\mu \rightarrow 0$ so that $\gamma \rightarrow k$.

From [28] we obtain

$$\bar{C}_O(0,p) - K\bar{C}_Y(0,p) = \mp \frac{\bar{I}(p)\xi_0}{nF\sqrt{\{D(p+\mu)\}}} \frac{F(\gamma, \gamma+l+1; 2\gamma+1; 1-1/\xi_0^2)}{F(\gamma+1, \gamma+l+1; 2\gamma+1; 1-1/\xi_0^2)}.$$

Consequently, we observe that

$$[29] \qquad \lim_{t\rightarrow\infty} [C_O(0,t) - KC_Y(0,t)] = \mp [I(t)/nF\sqrt{(D\mu)}]\xi_0 U_l,$$

where

$$U_l = \frac{F(\nu, \nu+l+1; 2\nu+1; 1-1/\xi_0^2)}{F(\nu+1, \nu+l+1; 2\nu+1; 1-1/\xi_0^2)}$$

with

$$\nu = (1/\kappa)\sqrt{(\mu/D)}.$$

The corresponding result that one would obtain in the absence of double layer effects, viz., $\mp I(t)/nF\sqrt{(D\mu)}$, can be derived by allowing $\kappa \rightarrow \infty$ and $\xi_0 \rightarrow 1$.

For large values of t[1]

$$[30] \quad C_O(0,t) = \frac{K}{K+1}\left[M^* \mp \frac{I(t)}{nFD\kappa} a_i \mp \frac{I(t)}{nFK\sqrt{(D\mu)}} \xi_0^{2(l+1)} U_l\right] \exp(-Z_O F\phi_0/RT)$$

approximately, where M* is the value that would be obtained in the absence of chemical reaction and diffuse double layer, and

$$[31] \qquad C_Y(0,t) = (1/K+1)\left[M^* \pm \frac{I(t)a_i}{nFD\kappa} \pm \frac{I(t)\xi_0^{2(l+1)}U_l}{nF\sqrt{(D\mu)}}\right] \exp\left(\frac{-Z_O F\phi_0}{RT}\right).$$

Equation [29] can be rewritten as

$$[32] \qquad \lim_{t\rightarrow\infty} C_O(0,t) = \exp\left(\frac{-Z_O F\phi_0}{RT}\right) K\left\{C_Y^s \mp \frac{I(t)U_i\xi_0^{2(l+1)}}{nFK\sqrt{(D\mu)}}\right\},$$

$C_Y^s(0,t)$ being defined by

$$[33] \qquad C_Y(0,t) = C_Y^s(0,t) \exp(-Z_O F\phi_0/RT).$$

Equation [33] may be compared with that of Matsuda (equation 19 of reference 3) obtained under the assumption that

$$C_Y(0,t) = C_Y^s(0,t) \exp(-Z_O F\phi_0/RT) \qquad (x < \delta, \mu).$$

For the particular cases $|Z_O/Z| = n$ ($n = 1, 2, 3 \ldots$) the expressions take particularly simple forms. For such a case $\xi_0^{2(l+1)} U_l$ becomes

$$\frac{f_n^*(\nu, \xi_0)}{f_n^*(\nu, 1/\xi_0)} \quad \text{or} \quad \frac{f_n^*(\nu, 1/\xi_0)}{f_n^*(\nu, \xi_0)}$$

(refer to Appendix A).

[1]*Implicity assumed here is the inequality* $(1/\kappa\delta_i)\int_0 \exp(|Z_i| F|\phi|/RT)dx \ll 1$ *for the case of attraction, where* δ_i *is the thickness of the diffusion layer.*

Can. J. Chem. Downloaded from www.nrcresearchpress.com by 210.87.254.42 on 09/05/12
For personal use only.

Can. J. Chem. Downloaded from www.nrcresearchpress.com by 210.87.254.42 on 09/05/12
For personal use only.

DISCUSSION

Matsuda (3) and Hurwitz (2) have given the steady-state solutions for this problem assuming ξ_0 to be large. Whereas the former has limited his investigations to $K \ll 1$ (but making it more generalized by conceding $(Z_Y - Z_O)$ to be different from zero), the latter has solved it without restraining K. It is of interest to compare the steady-state solutions of these authors to that obtained here. A comparison of the functions $\xi_0 U_l$ of this paper, U_α of Hurwitz, and $\xi_0^{-(2p+1)} G_{II}$ of Matsuda (equation 20 of reference 3) will show that at least for integral values of $|Z_O/Z|$ the rigorous solution is simpler and more accurate. It may be proved that the functions $\xi_0 U_l$, U_α, and $\xi_0^{-(2p+1)} G_{II}$ given above become identical asymptotically (i.e. $\nu \to \infty$) (refer to Appendix B).

Hurwitz has discussed the possible dynamic ψ effects for this case. Though his treatment and the expressions for the interfacial concentrations are different from those given in this paper, it can be proved that no difference exists in the conclusions as regards these effects. It may be seen as follows:

[34] $$U_l = \frac{F(\nu, \nu+l+1; 2\nu+1; 1 - 1/\xi_0^2)}{F(\nu+1, \nu+l+1; 2\nu+1; 1 - 1/\xi_0^2)}$$
$$\to 1/\xi_0 \quad \text{for} \quad \nu \gg 1 \quad \text{and} \quad \nu/\xi_0 \gg 1$$
(refer to Appendix B).

Substituting this in equation [30] we show that

[35] $$C_O(0,t) \to \frac{K}{K+1}\left[M^* \mp \frac{I(t)a_i}{nFD\kappa} \mp \frac{I(t)}{nFK\sqrt{(D\mu)}}\xi_0^{(2l+1)}\right] \exp\left(\frac{-Z_O F\phi_0}{RT}\right).$$

Consequently for large ξ_0

[36] $$a_i \cong \xi_0^{2l}/l \quad \text{for} \quad |Z_i/Z| > \tfrac{1}{2} \quad \text{and}$$
$$\cong \ln \xi_0^2 \quad \text{for} \quad |Z_i/Z| = \tfrac{1}{2}.$$

Substituting [34] and [36] in the expression for $C_O(0,t)$ we get

$$C_O(0,t) = \frac{K}{K+1}\left\{M^* \mp \left(\frac{I(t)\xi_0^{(2l+1)}}{nFK\sqrt{(D\mu)}}\right)\left[1 + \frac{K}{l\kappa\xi_0}\sqrt{(\mu/D)}\right]\right\} \exp\left(\frac{-Z_O F\phi_0}{RT}\right)$$

for $|Z_i/Z| > \frac{1}{2}$. Hence if K is so small that $K\nu/\xi_0 \ll 1$ for $|Z_i/Z| > \frac{1}{2}$ and $K\nu \ln \xi_0^2/\xi_0 \ll 1$ for $|Z_i/Z| = \frac{1}{2}$, the limiting velocity V is approximately expressed by

[37] $$V \cong K\sqrt{(D\mu)} \exp(-Z_O F\phi_0/RT) = V_0 \exp(-Z_O F\phi_0/RT) \qquad \text{(static } \psi \text{ effect)}$$

where V_0 is the limiting kinetic rate in the absence of diffuse double layer effects. But, if K is such that $K\nu/\xi_0 \gg 1$ for $|Z_i/Z| > \frac{1}{2}$ and $(K\nu/\xi_0 \ln \xi_0^2 \gg 1$ for $|Z_i/Z| = \frac{1}{2}$, the limiting velocity V is no longer given by equation [37] and for this case

[38] $$V = D\kappa l \xi_0^{-2l} \quad \text{for} \quad |Zi/Z| > \tfrac{1}{2} \quad \text{and}$$
$$= D\kappa/\ln \xi_0^2 \quad \text{for} \quad |Z_i/Z| = \tfrac{1}{2} \qquad \text{(dynamic } \psi \text{ effect).}$$

Under the limiting conditions $\nu \gg 1$ and $\nu/\xi_0 \ll 1$,

$$U_l \to \nu/l\xi_0^2 \quad \text{for} \quad |Z_i/Z| > \tfrac{1}{2} \quad \text{and}$$
$$\to \nu \ln \xi_0^2 \quad \text{for} \quad |Z_i/Z| = \tfrac{1}{2} \qquad \text{(refer to Appendix B).}$$

Substituting in equation [35] we obtain

$$C_O(0,t) = \frac{K}{K+1}\left[M^* \mp \frac{I(t)\xi_0^{2l}}{nFD\kappa l}(1 + 1/K)\right]\exp\left(\frac{-Z_O F\phi_0}{RT}\right)$$

so that the limiting velocity for this case is given by

$$V = \frac{D\kappa l}{\xi_0^{2l}}(K/K+1) \quad \text{for } |Z_i/Z| > \tfrac{1}{2} \quad \text{and}$$

$$= \frac{D\kappa(K/K+1)}{\ln \xi_0^2} \quad \text{for } |Z_i/Z| = \tfrac{1}{2}.$$

It may be noted that the above limiting conditions are arrived at for all K.

The dynamic ψ effect can occur even when ν is small when $\xi_0 \gg 1$ as can be seen by making use of Table I.

TABLE I

Behavior of $U_l\xi_0^{2(l+1)}$ for large ξ_0

$\lvert Z_i/Z\rvert$	$< \frac{1}{2}$	$= \frac{1}{2}$	$> \frac{1}{2}$
	Attraction		
l	< 0	< 0	< 0
$l+1$	> 0	$= 0$	< 0
$U_l\xi_0^{2(l+1)}$	$\frac{\Gamma(-l)\cdot\Gamma(\nu+l+1)}{\Gamma(l+1)\cdot\Gamma(\nu-l)}$	$\frac{1}{\nu \ln \xi_0^2}$	$\xi_0^{-2\lvert l+1\rvert}\frac{\lvert l+1\rvert}{\nu}$
	Repulsion		
l	< 0	$= 0$	> 0
$l+1$	> 0	> 0	> 0
$U_l\xi_0^{2(l+1)}$	$\frac{\Gamma(-l)\cdot\Gamma(\nu+l+1)}{\Gamma(l+1)\cdot\Gamma(\nu-l)}$	$\nu \ln \xi_0^2$	$\xi_0^{2l}\frac{\nu}{l}$

To summarize, the solution of the diffusion equation for the concentration of the reactive species, accounting for the migration effects in the diffuse double layer, is given for the following reaction schematically represented as

$$Y + \beta X \rightleftharpoons O^{z_O} \text{ (or } Y \rightleftharpoons O^{z_O} + \beta X),\ Z_x = 0$$

$$O^{z_O} + ne \rightleftharpoons R^{z_R}.$$

The results obtained in this paper are compared with the steady-state solutions obtained by Hurwitz and Matsuda. It is also shown how their solutions converge to that of the rigorous solution under limiting conditions, (ν and $\xi_0 \to \infty$ so that ν/ξ_0 is finite).

The expressions for the limiting velocities (dynamic ψ effect) are found to be the same as those given by the treatment of Hurwitz.

ACKNOWLEDGMENT

The author is grateful to Professor K. S. G. Doss, Director, Central Electrochemical Research Institute, Karaikudi, for his kind encouragement and valuable discussions.

REFERENCES

1. S. K. Rangarajan. Can. J. Chem. **41**, 983 (1963).
2. L. Gierst and H. Hurwitz. Z. Elektrochem. **64**, 36 (1960). H. Hurwitz. Z. Elektrochem. **65**, 178 (1961).
3. H. Matsuda. J. Phys. Chem. **64**, 336 (1960).

Can. J. Chem. Downloaded from www.nrcresearchpress.com by 210.87.254.42 on 09/05/12
For personal use only.

APPENDIX A

The functions $f_n^*(k,\xi_0)$ are defined by

$$f_1^*(k,\xi_0) = 1+2k\xi_0;$$

$$f_2^*(k,\xi_0) = 3+6k\xi_0+4k^2\xi_0^2+2k\xi_0^3;$$

$$f_3^*(k,\xi_0) = 15+30k\xi_0+24k^2\xi_0^2+(10k+8k^3)\xi_0^3+12k^2\xi_0^4+6k\xi_0^5;$$

$$f_4^*(k,\xi_0) = 105+210k\xi_0+180k^2\xi_0^2+(70k+80k^3)\xi_0^3+(104k^2+16k^4)\xi_0^4 + (42k+48k^3)\xi_0^5+60k^2\xi_0^6+30k\xi_0^7.$$

An interesting property of the function $f_n^*(x,y)$ is the recurrence relation $f_{n+1}(x,y) = (2n+1)f_n+2xy^{2n+1}f_n(1/y)$.

APPENDIX B

By the analytic continuation of the hypergeometric functions

$$F(\nu,\nu+l+1;2\nu+1;1-1/\xi_0^2) = \frac{\Gamma(2\nu+1)\Gamma(-l)}{\Gamma(\nu+1)\Gamma(\nu-l)}F(\nu,\nu+l+1;l+1;1/\xi_0^2) + \frac{\Gamma(2\nu+1)\Gamma(-1)}{\Gamma(\nu)\Gamma(\nu+l+1)}\left(\frac{1}{\xi_0^2}\right)^{-l}F(\nu-l,\nu+l;1-l;1/\xi_0^2).$$

For large ν $(\to\infty)$ such that ν/ξ_0 is finite, we have

$$F(\nu,\nu+l+1;l+1;1/\xi_0^2) \to I_l(2\nu/\xi_0)\frac{\Gamma(l+1)}{(\nu/\xi_0)^l}$$

and

$$F(\nu-l,\nu+1;1-l;1/\xi_0^2) \to I_{-l}(2\nu/\xi_0)\frac{\Gamma(1-l)}{(\nu/\xi_0)^{-l}}.$$

Therefore

$$F(\nu,\nu+l+1;2\nu+1;1-1/\xi_0^2) \to I_l(2\nu/\xi_0) - \nu^{2l+1}\frac{\Gamma(\nu-l)}{\Gamma(\nu+l+1)}I_{-l}(2\nu/\xi_0)\frac{\Gamma(2\nu+1)l\Gamma(l)\Gamma(-l)}{\nu\Gamma(\nu)\cdot\Gamma(\nu-l)}\left(\frac{\xi_0}{\nu}\right)^l.$$

Since

$$\frac{\Gamma(Z+\alpha)}{\Gamma(Z+\beta)} \underset{(Z\to\infty)}{\simeq} Z^{\alpha-\beta},$$

$$\frac{\Gamma(\nu-l)}{\Gamma(\nu+l+1)}\nu^{2l+1} \to 1 \text{ as } \nu\to\infty,$$

and

$$Z\cdot\Gamma(Z)\cdot\Gamma(-Z) = -\pi \operatorname{cosec} \pi Z,$$

we have

$$F(\nu,\nu+1+l;2\nu+1;1-1/\xi_0^2) \to \frac{2\Gamma(2\nu+1)}{\nu\Gamma(\nu)\cdot\Gamma(\nu-l)}\left(\frac{\xi_0}{\nu}\right)^l K_l(2\nu/\xi_0),$$

Can. J. Chem. Downloaded from www.nrcresearchpress.com by 210.87.254.42 on 09/05/12
For personal use only.

where $K_r(x)$ is defined as equal to $(\pi/2)\{I_{-r}(x)-I_r(x)\}$ cosec $(\nu\pi)$ (appropriate *limit* is to be taken for integral r).

Similarly

$$F(\nu+1, \nu+l+1; 2\nu+1; 1-1/\xi_0^2) \rightarrow \frac{2\Gamma(2\nu+1)}{\Gamma(\nu)\cdot\Gamma(\nu-l)}\left(\frac{\xi_0}{\nu}\right)^{l+1} K_{1+l}(2\nu/\xi_0).$$

Hence

$$U_l = \frac{F(\nu, \nu+l+1; 2\nu+1; 1-1/\xi_0^2)}{F(\nu+1, \nu+l+1; 2\nu+1; 1-1/\xi_0^2)}$$

$$\rightarrow \frac{1}{\xi_0}\frac{K_l(2\nu/\xi_0)}{K_{l+1}(2\nu/\xi_0)} \text{ as } \nu \rightarrow \infty, \nu/\xi_0 \text{ being assumed finite.}$$

Assuming the well-known property of the Bessel functions

$$U_l \rightarrow 1/\xi_0 \quad \text{for} \quad \nu/\xi_0 \gg 1 \qquad \text{and}$$

$$U_l \rightarrow \nu/l\xi_0^2 \quad \text{for} \quad \nu/\xi_0 \ll 1.$$

NOTATIONS

$C_i(x,t)$	instantaneous concentration of i (= O or Y) at a distance x from the electrode surface.
C_X^0	bulk concentration of X
p	transform variable (Laplace)
$\bar{C}(x,p)$	Laplace transform of $C(x,t) = p\int_0^\infty C(x,t) \exp(-pt)dt = L(C(x,t))$
D	common diffusion coefficients of Z_Y and Z_O
M	$C_Y(x,t)+C_O(x,t)$
N	$[C_X(x,t)-(1/K)C_O(x,t)] \exp(\mu t)$
$\phi(x)$	potential distribution in the diffuse (Gouy) layer
ξ_0	$\exp(\lvert Z\rvert F\lvert\phi_0\rvert/2RT)$
κ	Debye parameter for the reciprocal thickness of the double layer
K	$(k_f/k_b)C_X^0$
k	$(1/\kappa)\sqrt{(p/D)}$
ν	$(1/\kappa)\sqrt{(\mu/D)}$
γ	$(1/\kappa)\sqrt{\{(p+\mu)/D\}}$
μ	$k_f(C_X^0)^\beta+k_b$
l	$\pm\lvert Z_i/Z\rvert-\frac{1}{2}$ (positive sign for repulsion and negative for attraction)
$I(t)$	Faradaic current
$F(a,b,c,z)$	Gaussian hypergeometric function of argument z
$\Gamma(x)$	gamma function of x
$I_l(Z)$, $K_l(Z)$	modified Bessel function of the first and second kind respectively
a_i	$\pm 2\kappa\int_0^\infty \sinh(\lvert Z_i\phi\rvert F/RT)dx$ (refer to ref. 1)

Can. J. Chem. Downloaded from www.nrcresearchpress.com by 210.87.254.42 on 09/05/12
For personal use only.

THE INTERACTION OF SILICON TETRAFLUORIDE WITH METHANOL

J. P. GUERTIN AND M. ONYSZCHUK
Inorganic Chemistry Laboratory, Department of Chemistry, McGill University, Montreal, Que.
Received January 7, 1963

ABSTRACT

Silicon tetrafluoride reacts with methanol in a 1:4 mole ratio, forming the complex $SiF_4.4CH_3OH$, which freezes to a glass at about −20° and is completely dissociated in the gaseous phase at 25°. Conductivity measurements show clearly that it is a very weak electrolyte in methanol solution. Its infrared spectrum does not contain an Si—O bond stretching absorption band. Proton magnetic resonance measurements provide strong evidence of hydrogen bonding between silicon tetrafluoride and methanol. These results indicate that the structure of the complex requires tetracovalent rather than hexacovalent silicon and strong hydrogen bonds between methanol and each of the four fluorine atoms.

Can. J. Chem. Downloaded from www.nrcresearchpress.com by 210.87.254.5 on 09/05/12
For personal use only.

INTRODUCTION

Many complexes of silicon tetrafluoride with nitrogen electron-pair donor molecules have been prepared and characterized (1–7); less is known about the interaction of silicon tetrafluoride with oxygen donors. Muetterties (6) has described $SiF_4.2(CH_3)_2SO$, $SiF_4.2(CH_3)_2NCHO$, and $SiF_4.xCH_3COCH_2COCH_3$; the last is a very weak complex of uncertain composition. Gierut *et al.* (8) reported briefly that silicon tetrafluoride reacts with alcohols in a 1:4 mole ratio, yielding unstable addition compounds $SiF_4.4ROH$, where R is CH_3, C_2H_5, iso-C_3H_7, and iso-C_5H_{11}; these results were confirmed by Topchiev and Bogomolova (9), who also suggested that the complex is ionic and contains hexacovalent silicon. However, Holzapfel *et al.* (10) reported that silicon tetrafluoride and methanol produce 1:6 and 1:8 complexes only. With the object of clarifying these conflicting results, we have investigated the interaction of silicon tetrafluoride with methanol using tensimetric titration, conductivity, infrared, and proton magnetic resonance methods. This research is part of a general investigation of the relative electron acceptor power of silicon and germanium tetrafluoride towards oxygen, sulphur, nitrogen, and phosphorus electron-pair donor molecules. This paper describes the peculiar nature of the silicon tetrafluoride – methanol system.

RESULTS AND DISCUSSION

Preparation of $SiF_4.4CH_3OH$

Silicon tetrafluoride (in excess) and methanol when slowly mixed together in a vacuum at 25° produced the 1:4 complex, $SiF_4.4CH_3OH$, a colorless liquid. It formed a glass at about −20° and was completely dissociated in the gaseous phase at 25°. The 1:4 combining ratio was not always reproducible and values in the range 1.00:3.75 to 1.00:4.20 were also obtained. Ratios lower than 1:4 are attributed to the formation of some dimethyl ether by the silicon tetrafluoride catalyzed dehydration of methanol (9); higher ratios are probably due to incomplete reaction of methanol with silicon tetrafluoride. The combining ratio was never 1:6 or 1:8, as claimed by Holzapfel *et al.* (10).

A tensimetric titration of silicon tetrafluoride with methanol (Fig. 1) confirmed the formation of only a 1:4 complex. After each successive addition of methanol to silicon tetrafluoride in this titration, the mixture was warmed to 25° and then cooled to −78°, at which temperature pressure measurements were made. As shown in Fig. 1 the pressure decreased linearly and approached zero after the mole ratio of methanol to silicon tetra-

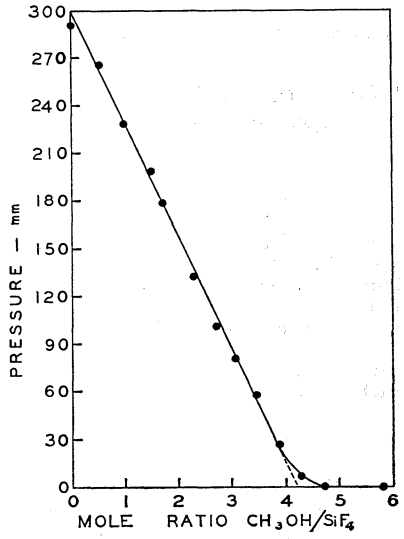

FIG. 1. Tensimetric titration of silicon tetrafluoride with methanol.

fluoride became greater than 4; extrapolation of the linear portion to zero pressure indicates a mole ratio of 4.2. In the reverse titration of methanol with silicon tetrafluoride (Fig. 2), the pressure remained zero until the mole ratio CH_3OH/SiF_4 decreased to 5, when

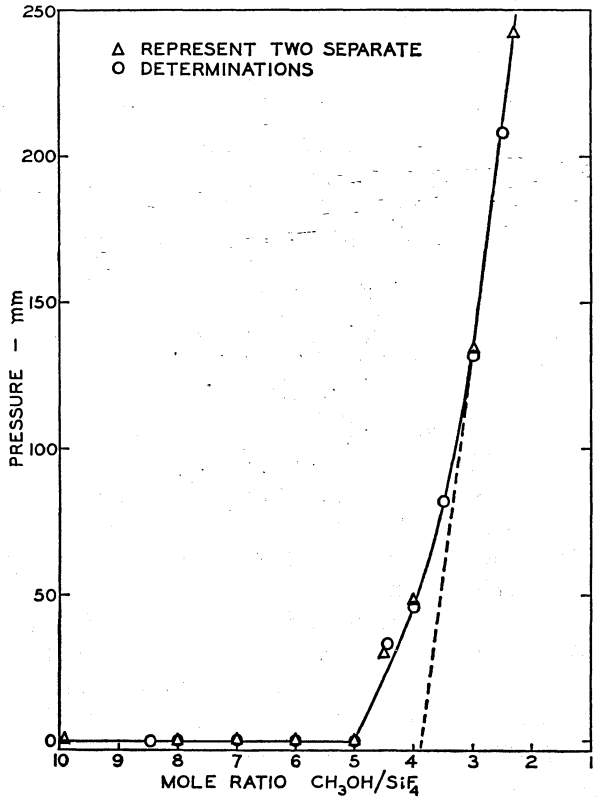

FIG. 2. Tensimetric titration of methanol with silicon tetrafluoride.

Can. J. Chem. Downloaded from www.nrcresearchpress.com by 210.87.254.5 on 09/05/12
For personal use only.

the pressure increased rapidly as the ratio decreased further; extrapolation of the linear part of this plot to zero pressure gives a mole ratio of 3.85, corresponding to the formation of the 1:4 complex, $SiF_4.4CH_3OH$. The two tensimetric titrations show conclusively that 1:6 and 1:8 complexes are not produced. Attempts were made to measure the dissociation pressure of $SiF_4.4CH_3OH$, but the values were not reproducible and therefore the heat of dissociation of the complex could not be obtained.

Conductivity of $SiF_4.4CH_3OH$

The conductivity of $SiF_4.4CH_3OH$ in methanol was measured to test the suggestion (9) that this complex has the ionic structure I, in which methoxy groups may be in

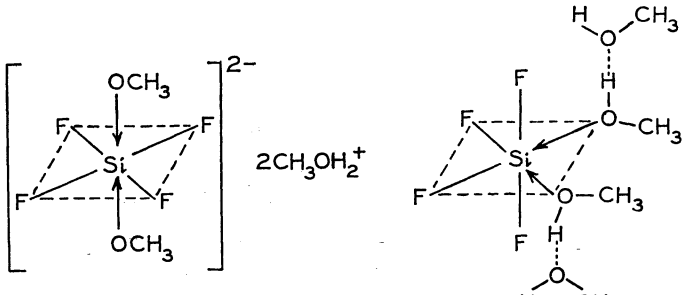

I II

either cis or trans arrangement. The conductivity measurements are given in Table I and plotted in Fig. 3, where they are compared with the molar conductances of acetic acid (11)

TABLE I

Conductivities of $SiF_4.4CH_3OH$ in methanol

$SiF_4.4CH_3OH$ concentration c, mole l^{-1}	Specific conductance k, mho cm^{-1}	Molar conductance μ, mho cm^2 $(g\text{-mole})^{-1}$ l^{-1}	$c^{1/2}$, $(\text{mole } l^{-1})^{1/2}$
3.75	3.0×10^{-3}	0.80	1.94
1.87	3.0×10^{-3}	1.60	1.37
0.47	1.0×10^{-3}	2.13	0.685
0.0094	4.0×10^{-4}	42.7	0.097
0.00090	1.2×10^{-4}	133	0.030
0.00019	4.7×10^{-5}	250	0.014
0*	5.0×10^{-6}	—	—

*Pure methanol (lit. (12)) value: 5×10^{-8} mho cm^{-1}.

and sodium chloride (12) in methanol. The results and comparisons reveal that $SiF_4.4CH_3OH$ is a very weak electrolyte in methanol; therefore, structure I or any other ionic structure is not valid. Using an empirical method recently described by Levitt (13), we estimated a molar conductance at infinite dilution of 830 mho cm^2 $(g\text{-mole})^{-1}$ l^{-1} for the complex, an equilibrium constant for dissociation of 2.76×10^{-5} mole l^{-1}, and a degree of dissociation of 4.8% for a solution of 0.01 mole l^{-1} concentration.

Infrared Spectrum of $SiF_4.4CH_3OH$

An alternative structure, II, involves octahedral bonding of silicon and hydrogen bonding between methanol and each of the coordinated methanol molecules. The infrared spectrum of such a species should contain an Si—O bond stretching absorption band;

Can. J. Chem. Downloaded from www.nrcresearchpress.com by 210.87.254.5 on 09/05/12
For personal use only.

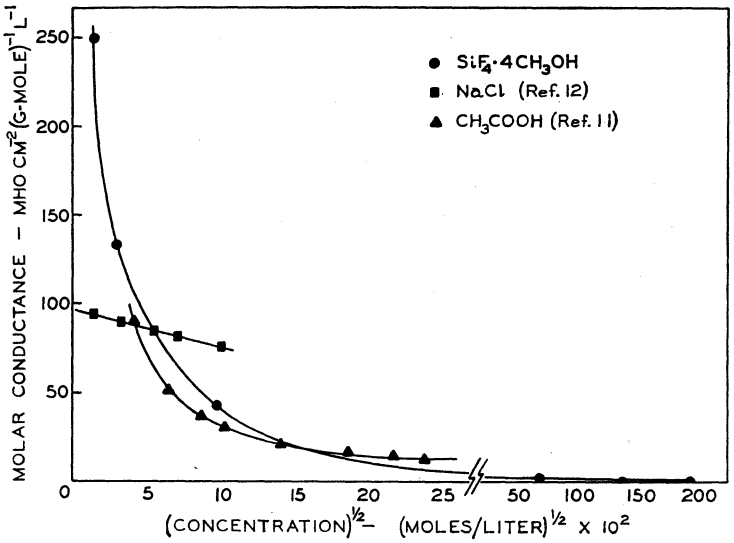

FIG. 3. Comparison of the molar conductances of $SiF_4.4CH_3OH$, NaCl, and CH_3COOH in methanol.

this is usually very strong and occurs at 1085–1105 cm^{-1} in methoxysilanes (14) and alkyldisiloxanes (15). Since the infrared spectra (Fig. 4) of liquid $SiF_4.4CH_3OH$ and its

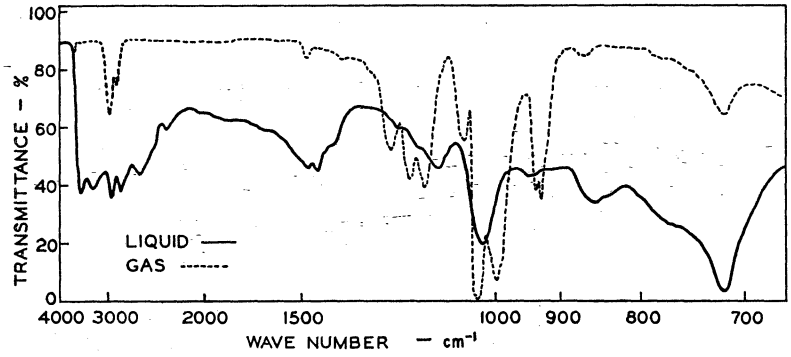

FIG. 4. Infrared spectrum of $SiF_4.4CH_3OH$ and its gaseous products.

gaseous products do not contain a strong band in this region, the complex is not octahedrally bonded and therefore structure II is not valid.

As shown in Table II, the infrared spectrum of the gaseous products of $SiF_4.4CH_3OH$ contains the bands characteristic of gaseous methanol and silicon tetrafluoride, together with bands of medium intensity at 1220, 1170, and 930 cm^{-1}. These bands are characteristic of dimethyl ether (16), which is formed in small amounts by dehydration of methanol with silicon tetrafluoride as catalyst. The fact that the 3680 cm^{-1} band, identified as the bond stretching vibration of the free O—H group, occurs in the same position as in gaseous methanol indicates that there was little or no hydrogen bonding between methanol and silicon tetrafluoride in the gaseous phase at 10 mm pressure. A further indication of the absence of "heavy" molecular species was the low molecular weight, 57.5, of the gaseous mixture.

Can. J. Chem. Downloaded from www.nrcresearchpress.com by 210.87.254.5 on 09/05/12
For personal use only.

TABLE II

Comparison and assignment of infrared absorption frequencies (cm^{-1})

$SiF_4.4CH_3OH$		CH_3OH		SiF_4	
Gas	Liquid	Gas	Liquid	Gas	Assignment
3680 w		3680 w			ν(O—H), free
	3300 s		3340 s		ν(O—H), H-bonded
2970 m	2950 s	2950 s	2950 s		ν(C—H), antisym.
2870 m	2830 s	2860 m	2840 m		ν(C—H), sym.
	2600 m		2500 w		Combination
	1450 m	1450 w	1460		$\delta(CH_3)$, antisym.
1220 m					Due to $(CH_3)_2O$
1170 m					impurity
1140 m	1110 m	1120 w	1120 m		$\delta(CH_3)$, sym.
1060 m				1070 w	SiF_4, combination band
1030 s	1025 s	1030 s	1030 s	1030 s	ν(Si—F) tetrahedral
1000 s					and ν(C—O)
930 m	950 vw				$(CH_3)_2O$ impurity
865 vw	855 w	860 w			Due to CH_3OH
		835 w			
782 w	762 w				Unidentified
718 w	720 s				ν(Si—F) octahedral for SiF_6^{2-}

NOTE: w = weak, m = medium, s = strong, v = very.

A comparison of the infrared absorption bands of liquid $SiF_4.4CH_3OH$ with those of liquid methanol and gaseous silicon tetrafluoride, also given in Table II, shows the following noteworthy features. (i) The band at 3300 cm^{-1} in methanol is shifted 40 cm^{-1} lower in $SiF_4.4CH_3OH$, indicating that there is stronger hydrogen bonding in the complex than in pure methanol. (ii) The strong and broad band at 1025 cm^{-1} in $SiF_4.4CH_3OH$ undoubtedly includes the C—O and Si—F bond stretching vibrations. (iii) The band at 720 cm^{-1} also occurs in the gaseous spectrum. This band appeared with almost the same intensity after the liquid sample was washed from the NaCl plates, and after the gaseous sample was removed from the NaCl gas cell. Moreover, the intensity of this band in the gas phase spectrum did not change when the sample pressure was doubled. These observations strongly suggest a surface effect involving the formation of a species which absorbs at 720 cm^{-1}. This species must be SiF_6^{2-} formed by the interaction of SiF_4 with the NaCl plates, as described recently by Heslop *et al.* (17).

Proton Magnetic Resonance Measurements

The indication by the infrared data that hydrogen bonding in liquid $SiF_4.4CH_3OH$ is greater than in pure methanol was investigated further by proton magnetic resonance measurements. Hydrogen bonding between methanol and the fluorine atoms of silicon tetrafluoride should change the electron density and the local magnetic polarizability of the electrons around the hydrogen atom of the OH group and, to a lesser extent, the hydrogen atoms of the CH_3 group of methanol. These effects were observed (Fig. 5) as large and small changes in the chemical shifts (τ) of the OH and CH_3 peaks, respectively. The effect of concentration of silicon tetrafluoride on these shifts was examined by measurements on silicon tetrafluoride – methanol solutions with mole ratios SiF_4/CH_3OH in the range 0 to 0.4. Solutions with ratios greater than 0.4 were not prepared because the

Can. J. Chem. Downloaded from www.nrcresearchpress.com by 210.87.254.5 on 09/05/12
For personal use only.

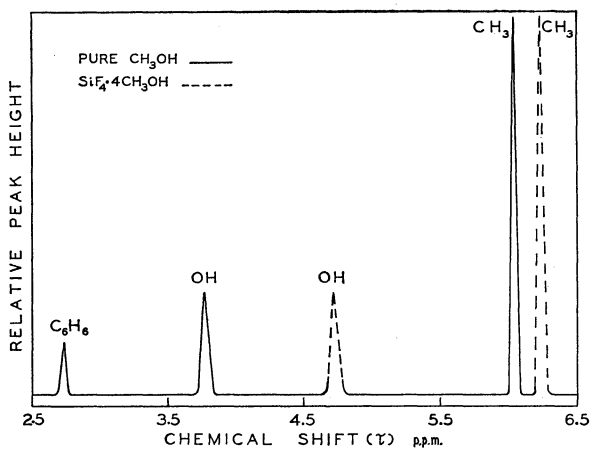

FIG. 5. Chemical shifts of pure methanol and methanol hydrogen bonded to silicon tetrafluoride.

sealed glass sample tubes might have exploded due to internal pressures in the tens of atmospheres.

The plot given in Fig. 6 shows that there is an initial linear and rapid decrease in

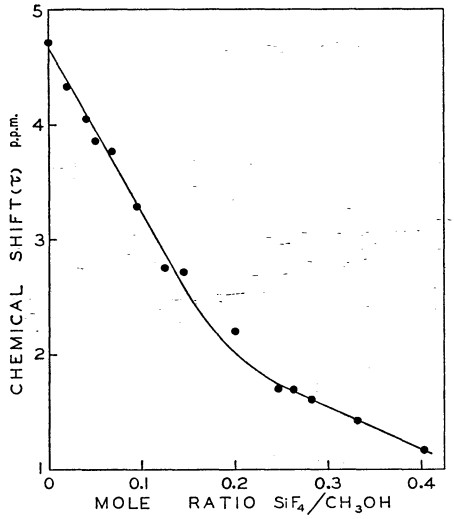

FIG. 6. Variation of the chemical shift of the OH peak with mole ratio of silicon tetrafluoride to methanol.

τ value of the OH peak as the amount of silicon tetrafluoride is increased. The slope of this line changes markedly near a mole ratio of 0.2 and finally becomes constant and smaller than initially. A comparison of the magnitude and direction (from high to low field) of the observed chemical shifts with those of the methanol – carbon tetrachloride and methanol–chloroform systems (18) reveals that (i) hydrogen bonding occurs to a greater extent between silicon tetrafluoride and methanol ($\Delta\tau \sim 3.5$ p.p.m.) than in methanol alone ($\Delta\tau \sim 3.0$ p.p.m.); (ii) successive addition of silicon tetrafluoride does not simply dilute the methanol; if it did, the chemical shift would be towards higher magnetic field strength.

Our interpretation of Fig. 6 is as follows. The chemical shift of the OH peak of pure

Can. J. Chem. Downloaded from www.nrcresearchpress.com by 210.87.254.5 on 09/05/12
For personal use only.

methanol (τ = 4.712 p.p.m.) decreases upon the successive addition of small amounts of silicon tetrafluoride because of the immediate formation of $SiF_4.4CH_3OH$ molecular species and rapid exchange between solvent methanol and methanol hydrogen bonded to silicon tetrafluoride. In order to observe the OH peaks of both types of methanol simultaneously the lifetime of each state must be longer than the reciprocal of the chemical shift (in cycles/sec) between the two states (19). Thus, the single OH peak observed at each mole ratio was an average value. These values decreased as the mole ratio SiF_4/CH_3OH increased, indicating that proportionately more methanol was hydrogen bonded to silicon tetrafluoride. When the ratio became 0.25 all of the methanol was used up in the formation of the $SiF_4.4CH_3OH$ complex. Further addition of silicon tetrafluoride produced secondary concentration effects which were directly proportional to the mole ratio SiF_4/CH_3OH.

The τ values of the CH_3 peak (Fig. 7) decreased gradually and finally levelled off as

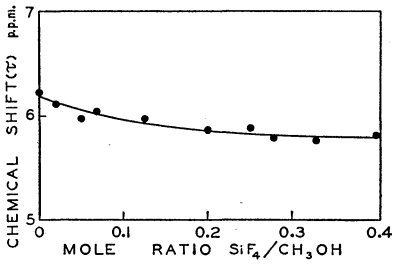

FIG. 7. Variation of the chemical shift of the CH_3 peak with the mole ratio of silicon tetrafluoride to methanol.

the concentration of silicon tetrafluoride increased. The decrease was not large because the protons of the CH_3 group were observing only secondary effects.

Structure of $SiF_4.4CH_3OH$

The experimental data reveals that the complex in the liquid or solid state (i) has the composition represented by $SiF_4.4CH_3OH$, (ii) is only very slightly dissociated into ions in methanol, (iii) does not contain Si—O bonds, (iv) contains strong hydrogen bonds. The most reasonable explanation of these data is that the complex is tetrahedral with strong hydrogen bonds between methanol and each of the four fluorine atoms (III).

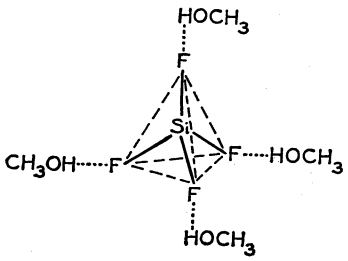

III

EXPERIMENTAL

Most of the materials used in this work were manipulated in a standard pyrex-glass high-vacuum system which had stopcocks and ground-glass joints lubricated with Kel-F grease. The purity of the volatile compounds was determined by measurements of their vapor pressures, molecular weights (M), and infrared spectra. Infrared spectra were recorded on a Perkin–Elmer Infracord double-beam spectrophotometer equipped with sodium chloride optics.

Can. J. Chem. Downloaded from www.nrcresearchpress.com by 210.87.254.5 on 09/05/12
For personal use only.

Anhydrous methanol was obtained by refluxing for a few hours 50 ml of the commercial grade material over about 1 g of freshly cleaned Mg turnings to which a few crystals of resublimed iodine had been added. The distillate boiling at 63–64° was collected and redistilled at −23° in the vacuum system. Commercial silicon tetrafluoride was purified by several low-temperature vacuum distillations.

Preparation of $SiF_4.4CH_3OH$

In a typical experiment SiF_4 (10.48 mmole) was combined in a vacuum with methanol (8.44 mmole), and the mixture was kept at 25° for 30 minutes and finally cooled slowly to −115°. Unreacted SiF_4 (8.32 mmole) was recovered by distillation first at −115° and then at −65°. Therefore, SiF_4 (2.16 mmole) had reacted with CH_3OH (8.44 mmole) in a mole ratio of 1:3.91, producing the complex $SiF_4.4CH_3OH$. Infrared and molecular weight measurements showed that the gas phase in equilibrium with the liquid at 25° consisted of SiF_4 and CH_3OH. (Found: M, 57.5. Calc. for CH_3OH: M, 32.1; for SiF_4: M, 104.1.)

Tensimetric Titrations

Preliminary experiments indicated that −78° was a suitable temperature at which to measure total pressures in the tensimetric titration of SiF_4 with CH_3OH. At this temperature the complex is not measurably dissociated and any excess SiF_4 (b.p. −94.8°) would be entirely in the gaseous phase. Measured amounts of methanol were added in successive small amounts (about 2 mmole at a time) to a fixed quantity of SiF_4 (5.43 mmole). After each addition the mixture was warmed to 25° for about 15 minutes before it was slowly cooled to −78°, at which temperature pressure measurements were made. A plot of total pressure against mole ratio of CH_3OH to SiF_4 is shown in Fig. 1. The reverse titration of CH_3OH by addition of SiF_4 gave the results shown in Fig. 2.

Conductivity of $SiF_4.4CH_3OH$

Conductivity measurements were made using a conductivity bridge (Industrial Instruments Model RC 16 B2) and a cell having a cell constant of 0.01. The instrument had a conductivity range of 4×10^{-9} to 5×10^{-2} mho cm^{-1}. Transfer of solutions and measurements were made in a nitrogen-filled dry box to avoid hydrolysis by atmospheric moisture. A sample with the highest concentration of $SiF_4.4CH_3OH$ (see Table I) was prepared in the vacuum system and then transferred to the conductivity cell in the dry box, and its conductivity was measured. Solutions of lower concentration were prepared by successive dilutions with methanol.

Proton Magnetic Resonance Measurements

Proton n.m.r. spectra were recorded on a high-resolution Varian spectrometer with a fixed frequency of 60 Mc. Pure benzene contained in a sealed capillary was used as the external standard (τ = 2.734 p.p.m.). It was placed in a pyrex glass tube, 17 cm long and 5 mm outside diameter, into which solutions of known mole ratio of SiF_4 to CH_3OH were condensed. The sample tube was sealed off in a vacuum at a constriction. The results are shown in Figs. 5, 6, and 7.

ACKNOWLEDGMENTS

We thank the National Research Council for financial assistance in the form of an annual grant (to M. O.). We are grateful to Dr. J. T. Edward for many helpful discussions and to Dr. A. Taurins and Dr. C. Stammer for the n.m.r. measurements.

REFERENCES

1. C. J. Wilkins and D. K. Grant. J. Chem. Soc. 927 (1953).
2. W. C. Schumb and P. S. Cook. J. Am. Chem. Soc. **75**, 5133 (1953).
3. T. S. Piper and E. G. Rochow. J. Am. Chem. Soc. **76**, 4318 (1954).
4. D. B. Miller and H. H. Sisler. J. Am. Chem. Soc. **77**, 4998 (1955).
5. J. E. Fergusson, D. K. Grant, R. H. Hickford, and C. J. Wilkins. J. Chem. Soc. 99 (1959).
6. E. L. Muetterties. J. Am. Chem. Soc. **82**, 1082 (1960).
7. V. Gutmann, P. Heilmayer, and K. Utvary. Monatsh. **93**, 322 (1961).
8. J. A. Gierut, F. J. Sowa, and J. A. Niewland. J. Am. Chem. Soc. **58**, 786 (1936).
9. A. V. Topchiev and N. F. Bogomolova. Dokl. Akad. Nauk SSSR, **88**, 487 (1953).
10. L. Holzapfel, E. Borchers, and H. Kettner. *In* Silicium Schwefel, Phosphate, Collog. Sek. Anorg. Chem. Intern. Union Reine u. Angew. Chem. Munster. 1954. p. 63.
11. T. Shedlovsky and R. L. Kay. J. Phys. Chem. **60**, 151 (1956).
12. J. P. Butler, H. I. Schiff, and A. R. Gordon. J. Chem. Phys. **19**, 752 (1951).
13. L. S. Levitt. Chem. Ind. (London), 1621 (1961).
14. B. Sternbach and A. G. MacDiarmid. J. Am. Chem. Soc. **81**, 5109 (1959).
15. E. A. V. Ebsworth, M. Onyszchuk, and N. Sheppard. J. Chem. Soc. 1453 (1958).
16. R. H. Pierson, A. N. Fletcher, and E. St. Clair Gantz. Anal. Chem. **28**, 1218 (1956).
17. W. R. Heslop, J. A. A. Ketelaar, and A. Buchler. Spectrochim. Acta, **16**, 513 (1960).
18. C. Reid and T. M. Connor. Nature, **180**, 1192 (1957).
19. W. G. Schneider. *In* Hydrogen bonding. *Edited by* D. Hadzi. Pergamon Press, London. 1959.

Can. J. Chem. Downloaded from www.nrcresearchpress.com by 210.87.254.5 on 09/05/12
For personal use only.

PSEUDACONITINE, AND THE STEREOCHEMICAL RELATIONSHIP OF THE HIGHLY OXYGENATED ACONITE ALKALOIDS[1]

Y. TSUDA[2] AND LÉO MARION
Division of Pure Chemistry, National Research Council, Ottawa, Canada
Received January 31, 1963

ABSTRACT

An alkaloid isolated from *Aconitum spicatum* Stapf has been found to be identical not only with the originally described pseudaconitine but also with 'α-pseudaconitine'. The product of the partial hydrolysis of the base, i.e., veratroylpseudaconine, is dextrorotatory, and not laevorotatory as recorded in the old literature. On heating, pseudaconitine undergoes pyrolysis, loses the elements of acetic acid, and gives rise to pyropseudaconitine. This substance, on treatment with lithium aluminum hydride, is converted to demethoxyisopyropseudaconine which is identical with the Wolff–Kishner reduction product of pyraconine. This correlation establishes that pseudaconitine and aconitine possess the same absolute configuration, which, in the light of previous knowledge, is extended also to indaconitine, delphinine, mesaconitine, and jesaconitine.

Can. J. Chem. Downloaded from www.nrcresearchpress.com by 210.87.254.105 on 09/05/12
For personal use only.

Pseudaconitine, $C_{36}H_{51}O_{12}N$, was first discovered by Wright and Luff (1) in 1878 and its properties were studied by Dunstan and Carr (2), who found that it was hydrolyzed by potassium hydroxide to acetic acid, veratric acid, and the base pseudaconine, $C_{25}H_{41}O_8N$, m.p. 93–94°, $[\alpha]_D$ +38.7° (H_2O). They also reported that mineral acids effected a partial hydrolysis only and gave rise to veratroylpseudaconine, m.p. 199°, $[\alpha]_D$ −38.18° (EtOH). Henry and Sharp (3, 4), who later investigated pseudaconitine further, did not prepare veratroylpseudaconine.

Much later, Marion and Edwards (5) isolated an alkaloid of the same empirical formula and physical properties as pseudaconitine which on hydrolysis gave acetic acid, veratric acid, and pseudaconine of the same formula, melting point, and optical rotation as reported by Dunstan and Carr (2). On partial hydrolysis, however, it gave dextrorotatory veratroylpseudaconine. Hence, the new base and its partial hydrolysis product were designated α-pseudaconitine and α-veratroylpseudaconine (5).

A. Identity of Pseudaconitine

From the roots of *Aconitum spicatum* Stapf,[3] an alkaloid has now been isolated, $C_{36}H_{51}O_{12}N$, which possesses the same physical properties as pseudaconitine. It forms a crystalline perchlorate, mono- and di-acetyl derivatives, and like pseudaconitine yields acetic acid, veratric acid, and pseudaconine, so that it contains two free hydroxyls and two ester groups. On the other hand, partial hydrolysis of the alkaloid gives dextrorotatory veratroylpseudaconine, m.p. 212–214°, $[\alpha]_D$ +38.5 (EtOH), +54.1 ($CHCl_3$), and indeed, the alkaloid is identical (by optical rotation, m.p., m.p. of the mixture, and infrared spectra comparison) with an authentic sample of the α-pseudaconitine of Marion and Edwards (5).

Because of the practically identical properties of the alkaloid from *A. spicatum* and its various derivatives (except the optical rotation of veratroylpseudaconine) with those of pseudaconitine and its corresponding derivatives, it was suspected that the two bases might be identical. It has been possible to obtain a sample of authentic pseudaconitine

[1]*Issued as N.R.C. No. 7299.*
[2]*National Research Council of Canada Postdoctoral Fellow.*
[3]*We wish to express our gratitude to S. B. Penick and Company, who kindly supplied the plant material.*

from the collection of the late Dr. T. A. Henry[4] and a comparison of it with our alkaloid (m.p. of the base and of the mixture, and infrared spectra) has shown the two to be identical. Hence, pseudaconitine is identical with α-pseudaconitine, and the latter designation should be deleted from the literature. Another conclusion is that the sign of the optical rotation of veratroylpseudaconine ($[\alpha]_D$ $-38°18'$, EtOH) recorded by Dunstan and Carr (2) is evidently in error, and the compound is dextrorotatory.

B. Correlation of Aconite Alkaloids

The absolute configuration of aconitine, $C_{34}H_{47}O_{11}N$ (I), has been established by the X-ray crystallographic analysis (6) of demethanolaconinone, II, and by conversion of the alkaloid into a series of lactones (7) of which III is typical. Delphinine, IV, $C_{33}H_{45}O_9N$, was correlated with aconitine by Wiesner *et al.* (8), who transformed both alkaloids into the common intermediate V. Whereas this correlation showed that aconitine and

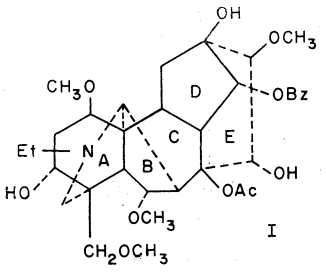

I

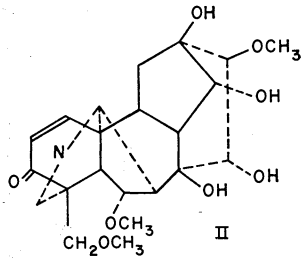

II

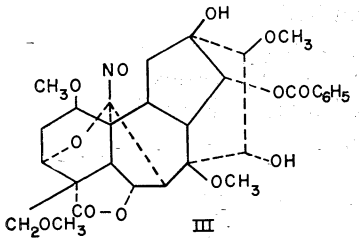

III

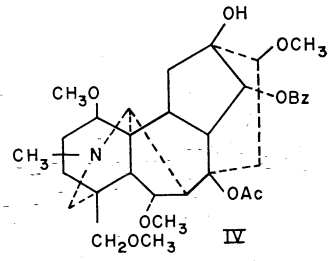

IV

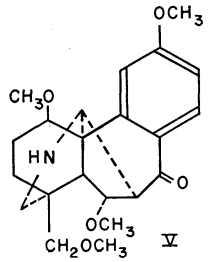

V

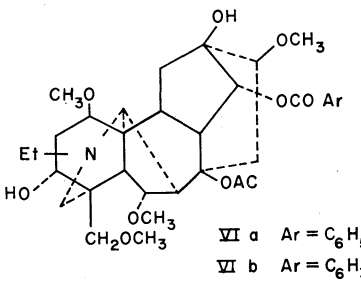

VI a Ar = C_6H_5
VI b Ar = $C_6H_3(OCH_3)_2$

delphinine possess the same stereochemistry in rings A, B, C, and the nitrogen ring, it did not establish the stereochemical relationships of the D/E ring systems, nor of the benzoyloxy groups in these alkaloids.

[4]*The sample of pseudaconitine was obtained through the kindness of Dr. H. T. Openshaw, The Wellcome Research Laboratories, to whom we express our thanks.*

Can. J. Chem. Downloaded from www.nrcresearchpress.com by 210.87.254.105 on 09/05/12
For personal use only.

Recently, the structure of indaconitine, $C_{34}H_{47}O_{10}N$ (VI*a*), an alkaloid hydrolyzable to acetic acid, benzoic acid, and pseudaconine, has been determined by conversion of the alkaloid into delphinine, IV (9). Since the reactions involved in this conversion do not disturb the asymmetric centers of the molecule except for the removal of the hydroxyl in ring A, the stereochemical arrangement present in delphinine is also present in indaconitine.

On the assumption that the ester groups in pseudaconitine and indaconitine are similarly located (for evidence of which see ref. 10), the correlation of the latter with delphinine also proves the structure of pseudaconitine (VI*b*), but it does not establish the position or the stereochemistry of the hydroxyl in ring A.

It has now been possible to correlate pseudaconitine with aconitine, and this not only establishes the stereochemistry of the hydroxyl of ring A in both indaconitine and pseudaconitine but also establishes that all the four alkaloids mentioned possess the same stereochemistry.

Pseudaconitine when heated *in vacuo* produced pyropseudaconitine, $C_{34}H_{47}O_{10}N$ (VII*a*), which could not be induced to crystallize. Sharp (4) described pyropseudaconitine as bundles of colorless stout needles, m.p. 132–135°, whereas Marion and Edwards (5) could not obtain the compound in a crystalline state. The n.m.r. spectrum of pyropseudaconitine contained a doublet (δ 5.57, J = 6 c/s) corresponding to one olefinic hydrogen. Further evidence of the olefinic character of the pyro compound was found in pyropseudaconine (VII*b*), its hydrolysis product, which had an infrared absorption spectrum containing a band at 1620 cm^{-1} and an n.m.r. spectrum showing a doublet (δ 5.55, J = 6 c/s), both of which indicated a double bond.

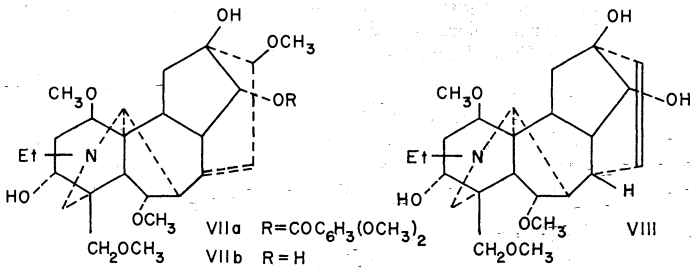

VII*a* R=$COC_6H_3(OCH_3)_2$
VII*b* R=H

VIII

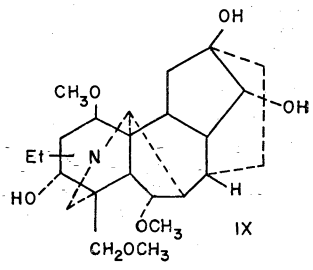

IX

The action of lithium aluminum hydride on VII*a* gave the solid but non-crystalline iso compound demethoxyisopyropseudaconine, $C_{24}H_{37}O_6N$ (VIII), which was well characterized as its crystalline perchlorate, m.p. 256–258° (decomp.). The n.m.r. spectrum of the free base confirmed the structure VIII in showing three methoxyl groups and two poorly resolved signals centered at δ 5.69, indicative of two olefinic protons. Reactions analogous to the bridgehead allylic rearrangement that results in the formation of VIII were reported in connection with neoline (11) and delphinine (12).

Catalytic hydrogenation of the isopyro compound (VIII) gave the saturated product $C_{24}H_{39}O_6N$ (IX), which formed a crystalline perchlorate, m.p. 230° (decomp.). This saturated product, which should have been identical with the Wolff–Kishner reduction product of pyraconitine (perchlorate, m.p. 258–259°, decomp.) described by McCaldin and Marion (13), was quite different. Re-examination of the latter substance revealed that it was not saturated as previously stated (13) but contained one double bond, and that it was identical (by melting point, that of the mixture, infrared and n.m.r. spectra comparison) with demethoxyisopyropseudaconine (VIII). Production of an unsaturated compound in the Wolff–Kishner reduction of an α-methoxyketone appears quite reasonable from a consideration of the reaction mechanism, and is not without precedent (14).

Can. J. Chem. Downloaded from www.nrcresearchpress.com by 210.87.254.105 on 09/05/12
For personal use only.

In the above series of transformations no inversions seem to be possible and, therefore, the conversion of both pseudaconitine and aconitine into a common intermediate supplies rigorous proof that the C-3 hydroxyl and the C-1 methoxyl of pseudaconitine have the same configuration respectively as in aconitine. It can also be concluded that aconitine, pseudaconitine, indaconitine, and delphinine all have the same absolute configuration with the possible but unlikely exception of the C-18 methoxyl group. This group is removed in the correlation of pseudaconitine with aconitine, but it is retained in the transformation of indaconitine into delphinine (9). Hence it has the identical configuration in delphinine, indaconitine, and pseudaconitine, and the configuration is most probably the same as that in aconitine. Concerning the aroyloxy group, its location at C-10 and its orientation are supported by n.m.r. evidence (10).

Mesaconitine, which is N-methyl-N-desethylaconitine (15, 16), and jesaconitine, a base hydrolyzable to acetic acid, *p*-anisic acid, and aconine (17), must also possess this same absolute configuration.

EXPERIMENTAL

The infrared spectra were measured on a Perkin–Elmer double-beam spectrophotometer Model 21B, and the n.m.r. spectra were obtained in $CDCl_3$ solution with tetramethylsilane as an internal reference on an A-60 instrument. The melting points were determined on a Kofler hot stage and were not corrected.

The ground root of *A. spicatum* Stapf was found to contain two major alkaloids, which were separated by chromatography on alumina.

Pseudaconitine

One of these alkaloids was crystallized from methanol, from which it separated as colorless prisms, m.p. 203–205°, $[\alpha]_D$ +24.0° (*c*, 2.5 in $CHCl_3$). Found: C, 62.63; H,7. 41; N, 2.31. Calc. for $C_{36}H_{51}O_{12}N$: C, 62.69; H, 7.45; N, 2.03%. The base agrees in its properties and empirical formula with those of pseudaconitine. It forms a perchlorate crystallizing from methanol–ether as colorless leaflets which on heating begin to sinter at 239° and decompose at 248°. Found: C, 54.49; H, 6.53. Calc. for $C_{36}H_{51}O_{12}N \cdot HClO_4$: C, 54.72; H, 6.58%.

Monoacetylpseudaconitine

Pseudaconitine (90 mg) in pyridine (2 ml) and acetic anhydride (2 ml) was kept overnight at room temperature. The mixture was poured into ice water, made basic with sodium carbonate, and extracted with methylene chloride. The extract was washed with water, dried over sodium carbonate, and evaporated to dryness. Monoacetylpseudaconitine (90 mg) was left as a residual gum which on trituration with *n*-hexane solidified, m.p. 143–147°. When recrystallized with cyclohexane it consisted of colorless needles, m.p. 135–140°. The product was solvated with cyclohexane as shown by the n.m.r. spectrum. It formed a perchlorate which crystallized from ethanol as colorless prisms, m.p. 247–248°, lit. (4) m.p. 225–228°. Found: C, 54.69; H, 6.44. Calc. for $C_{38}H_{53}O_{13}N \cdot HClO_4$: C, 54.84; H, 6.54%.

Diacetylpseudaconitine

Pseudaconitine (90 mg) in acetyl chloride (2 ml) was heated under reflux for 2 hours. The excess acetyl chloride was evaporated *in vacuo* and the residue dissolved in water. The solution was made basic, extracted with methylene chloride, and the extract evaporated to dryness. It left a residual semicrystalline mass, which was chromatographed in benzene solution over alumina (Grade IV, 5×70 mm column). The initial benzene eluate gave an amorphous fraction (18 mg). Further elution with benzene and benzene–chloroform gave pure diacetylpseudaconitine (45 mg). It crystallized from methanol as colorless elongated prisms, m.p. 227–229°, $[\alpha]_D$ +17° (*c*, 2.8 in $CHCl_3$) (lit. (4), m.p. 229°, $[\alpha]_D$ +24° in $CHCl_3$). Found: C, 62.73; H, 7.06. Calc. for $C_{40}H_{56}O_{14}N$: C, 62.09; H, 7.16%. The n.m.r. spectrum contains the signals for the protons of two acetate groups. Diacetylpseudaconitine was also obtained in better yield by acetylation with acetic anhydride and *p*-toluenesulphonic acid.

Pseudaconine

Pseudaconitine (90 mg) was hydrolyzed by heating with 3% methanolic potassium hydroxide (5 ml) for 1 hour on a steam bath. The reaction mixture when worked up in the usual way gave pseudaconine (acetone solvated, m.p. 87–88°, when crystallized from acetone; isopropanol solvated, m.p. 91–92°, when crystallized from that solvent) in excellent yield. Comparison with an authentic sample of pseudaconine (m.p. of the mixture and infrared spectra) confirmed the identity. Pseudaconine is also obtained in good yield by the action of lithium aluminum hydride on pseudaconitine. The isopropanol-solvated compound was used for the following determinations. $[\alpha]_D$ +49° (*c*, 1.9 in $CHCl_3$). Found: C, 62.19; H, 9.02. Calc. for $C_{25}H_{41}O_8N \cdot C_3H_8O$: C, 61.84; H, 9.08%.

Can. J. Chem. Downloaded from www.nrcresearchpress.com by 210.87.254.105 on 09/05/12
For personal use only.

Veratroylpseudaconine

A small quantity of pseudaconitine (100 mg) was dissolved in 0.1 *N* sulphuric acid (15 ml) and the solution heated in a sealed tube at 140° for 5 hours. The crude contents of the tube were made alkaline with 0.1 *N* potassium hydroxide and extracted with chloroform. The extract yielded 60 mg of basic material, which was chromatographed on alumina. The benzene–chloroform (2:3) eluate gave a colorless foam which was converted to a perchlorate, m.p. 228–230° after crystallization from ethanol. Found: C, 55.38; H, 7.00; OCH_3, 25.09. Calc. for $C_{34}H_{47}O_{10}N \cdot HClO_4$: C, 55.93; H, 6.63; 6 OCH_3, 25.51%. The base recovered from the salt crystallized from methanol–ether as colorless prisms, m.p. 212–214°; $[\alpha]_D$ +38.5° (*c*, 0.9 in EtOH), +54.1° (*c*, 1.5 in $CHCl_3$).

Pyropseudaconitine

Pseudaconitine (146 mg) was heated in a vacuum (5×10^{-2} mm) at 180° (air bath). An initial vigorous bubbling ceased after ca. 5 minutes. The product was dissolved in chloroform. The solution was washed with dilute sodium carbonate solution and with water, dried, and evaporated. It left a gum which was purified by chromatography on alumina (grade IV, 5×50 mm column). The benzene eluate gave crude pyropseudaconitine (20 mg) and the subsequent benzene–chloroform eluate gave pure (by thin layer chromatography) pyropseudaconitine (100 mg), which could not be induced to crystallize.

Demethoxyisopyropseudaconine

A mixture of pyropseudaconitine (490 mg) and an excess of lithium aluminum hydride in tetrahydrofuran (15 ml) was stirred overnight at room temperature. After the addition of a few drops of water, the reaction mixture was diluted with methylene chloride, filtered, and the solid washed thoroughly with methylene chloride. The combined filtrate and washings was evaporated on the steam bath under reduced pressure, and the residue extracted with 5% hydrochloric acid. The acid extract was washed with three portions of ether, made alkaline with sodium carbonate, and extracted with methylene chloride. This last extract, after drying and evaporation, left a gum which was chromatographed on alumina (grade IV, 5×70 mm column) and the column was eluted first with benzene, then with chloroform, and finally with chloroform containing 10% of methanol. The last two eluates gave pure demethoxyisopyropseudaconine (270 mg) as a colorless foam which could be distilled *in vacuo* (5×10^{-2} mm, air bath 190°). The solid distillate failed to crystallize but thin layer chromatography showed that it was homogeneous. $[\alpha]_D$ +53.5° (*c*, 0.75 in EtOH). It formed a perchlorate which crystallized from acetone–ether as colorless prisms, m.p. 256–258° (decomp.). $[\alpha]_D$ +21° (*c*, 0.85 in EtOH). Found: C, 53.59; H, 7.07. Calc. for $C_{24}H_{37}O_6N \cdot HClO_4$: C, 53.75; H, 7.14%. In admixture with the Wolff–Kishner reduction product of aconitine (13), the melting point was unchanged and the infrared absorption spectra of both compounds were superimposable.

Dihydrodemethoxyisopyropseudaconine

Demethoxyisopyropseudaconine (212 mg) in absolute ethanol (38 ml) was hydrogenated over Adams' catalyst (80 mg) for 15 hours at room temperature. The product, worked up as usual, consisted of a gum (197 mg), which was dissolved in ether, the solution filtered, and the filtrate evaporated to dryness. The residue in benzene solution was chromatographed over alumina (grade IV, 5×70 mm column). The column was eluted with benzene and with benzene containing 5% of chloroform. The second eluate gave a colorless gum (100 mg) which failed to crystallize but formed a perchlorate that crystallized from acetone–ether as colorless prisms, m.p. 229–231° (decomp.). $[\alpha]_D$ −24.8 (*c*, 1.45 in EtOH). Found: C, 53.08; H, 7.20. Calc. for $C_{24}H_{39}O_6N \cdot HClO_4$: C, 53.57; H, 7.49%. The n.m.r. spectrum did not contain any signal corresponding to olefinic protons.

REFERENCES

1. C. R. A. Wright and A. P. Luff. J. Chem. Soc. **33**, 151 (1878).
2. W. R. Dunstan and F. H. Carr. J. Chem. Soc. **71**, 350 (1897).
3. T. A. Henry and T. M. Sharp. J. Chem. Soc. 1105 (1928).
4. T. M. Sharp. J. Chem. Soc. 3094 (1928).
5. L. Marion and O. E. Edwards. J. Am. Chem. Soc. **68**, 2565 (1946).
6. M. Przybylska and L. Marion. Can. J. Chem. **37**, 1843 (1959).
7. F. W. Bachelor, R. F. C. Brown, and G. Büchi. Tetrahedron Letters, No. 10, 1 (1960).
8. K. Wiesner, D. L. Simmons, and L. R. Fowler. Tetrahedron Letters, No. 18, 1 (1959).
9. R. E. Gilman and L. Marion. Tetrahedron Letters, No. 20, 923 (1962).
10. Y. Tsuda and L. Marion. Can. J. Chem. This issue.
11. K. Wiesner, H. Brewer, D. L. Simmons, D. R. Babin, F. Bickelhaupt, J. Kallos, and T. Bogri. Tetrahedron Letters, No. 3, 17 (1960).
12. K. Wiesner, D. L. Simmons, and R. H. Wightman. Tetrahedron Letters, No. 15, 23 (1960).
13. D. J. McCaldin and L. Marion. Can. J. Chem. **37**, 1071 (1959).
14. E. W. Warnhoff and W. C. Wildman. Chem. Ind. (London), 1293 (1958).
15. W. A. Jacobs and D. W. Pelletier. Chem. Ind. (London), 591 (1960).
16. R. B. Turner, J. P. Jaschke, and M. S. Gibson. J. Am. Chem. Soc. **82**, 5182 (1960).
17. R. Majima and S. Morio. Ber. **57**, 1472 (1924).

Can. J. Chem. Downloaded from www.nrcresearchpress.com by 210.87.254.105 on 09/05/12
For personal use only.

THE SYNTHESIS OF D-*glycero*-D-*manno*-HEPTOSE

R. K. HULYALKAR, J. K. N. JONES, AND M. B. PERRY
Department of Organic Chemistry, Queen's University, Kingston, Ontario
Received December 15, 1962

ABSTRACT

The condensation of D-altrose with nitromethane in alkaline methanol gave the corresponding epimeric 1-deoxy-1-nitroheptitols from which 1-deoxy-1-nitro-D-*glycero*-D-*manno*-heptitol was obtained in 46% yield. The 1-deoxy-1-nitro-D-*glycero*-D-*manno*-heptitol was converted to D-*glycero*-D-*manno*-heptose in 61% yield.

DISCUSSION

D-*glycero*-D-*manno*-Heptose is a component of an extracellular polysaccharide synthesized by *Azotobacter indicum* (1, 2), whose mode of biosynthesis has been studied in this laboratory (3). In the course of these studies it became necessary to synthesize the heptose in order to devise a method for its stepwise degradation to determine the ^{14}C content at the individual carbon atoms in its chain, and to prepare D-*glycero*-D-*manno*-heptose-1-^{14}C.

D-*glycero*-D-*manno*-Heptose was first synthesised in 39% yield by the application of the Fisher cyanohydrin synthesis (4) to D-altrose. Sowden (5, 6) has shown that the sugar series may be ascended by reactions involving the condensation of nitromethane in alkaline media with the aldehyde function of a glycose to give a mixture of epimeric 1-deoxy-1-nitroglycitols which on treatment with acid (Nef reaction (7)) yield the corresponding glycoses. This procedure, which avoids the use of hydrogen cyanide and the reduction of aldonolactones to glycoses encountered in the use of the classical cyanohydrin method for the ascent of the sugar series (8), thus has several practical advantages.

In the present work it was found that D-altrose could be condensed with nitromethane in alkaline methanol solution to give the theoretical yield of the mixed crystalline salts of the epimeric 1-deoxy-1-nitroheptitols from which 1-deoxy-1-nitro-D-*glycero*-D-*manno*-heptitol was obtained crystalline in 46% overall yield. Treatment of the sodium salt of the 1-deoxy-1-nitro-D-*glycero*-D-*manno*-heptitol with 6 *N* sulphuric acid gave a product containing mainly D-*glycero*-D-*manno*-heptose which was contaminated with some unchanged starting material, D-altrose, and some D-*glycero*-D-*gluco*-heptose. Fractionation of this mixture by cellulose column chromatography (9) gave pure D-*glycero*-D-*manno*-heptose (60% yield), which remained a syrup. It is considered that the procedure offers a convenient route for the synthesis of D-*glycero*-D-*manno*-heptose-1-^{14}C using nitromethane-^{14}C.

Several derivatives of D-*glycero*-D-*manno*-heptose were prepared to investigate the possibility of using them for selective degradation studies directed to the determination of the distribution of ^{14}C in the heptose found in the extracellular polysaccharide produced by *Azotobacter indicum* grown in the presence of ^{14}C-labelled substrates. A degradation scheme for D-*glycero*-D-*manno*-heptose has been described in a recent paper (3).

Attempts to prepare D-mannose from the mixed anomeric methyl D-*glycero*-D-*manno*-heptopyranosides by selective scission of the exocyclic C_6–C_7 glycol system with periodate followed by reduction of the aldehyde group produced at C_6, in a way analogous to that used for the synthesis of D-gulose from D-*glycero*-D-*gulo*-heptose (10), gave a low yield

Can. J. Chem. Downloaded from www.nrcresearchpress.com by 210.87.254.5 on 09/05/12
For personal use only.

of D-mannose, which was isolated and characterized as its crystalline *p*-nitrophenylhydrazone (17% yield).

The D-*glycero*-D-*manno*-heptose gave a crystalline diethyldithioacetal derivative which on Raney nickel desulphurization gave 1-deoxy-D-*glycero*-D-*manno*-heptitol. The deoxyglycitol on periodate oxidation consumed the expected amount of periodate and liberated the theoretical amounts of formaldehyde and formic acid.

EXPERIMENTAL

Paper chromatography was carried out on Whatman No. 1 filter paper by the descending method (11) using the following solvent systems (v/v): (A) ethyl acetate – acetic acid – formic acid – water (18:3:1:4); (B) butan-1-ol – ethanol – water (3:1:1); (C) butan-1-ol – pyridine – water (10:3:3).

The sugars were located on the paper chromatograms using the *p*-anisidine hydrochloride spray reagent (12) and the alkaline silver nitrate spray reagent (13).

Condensation of D-*Altrose with Nitromethane*

To a stirred solution of D-altrose (30 g) (prepared by the method of Rosenfeld, Richtmyer, and Hudson (4)) in dry methanol (180 ml) and nitromethane (180 ml) was added a cold solution of sodium (6.3 g) in dry methanol (140 ml), and the reaction mixture was stirred for 7 hours at room temperature. The mixture was kept at −5° overnight and the precipitated sodium salts of the 1-deoxy-1-nitroheptitols (44 g) were collected by filtration, washed with cold methanol and ether, and then dried *in vacuo*.

The sodium salts of the 1-deoxy-1-nitroheptitols (44 g) were dissolved in water (300 ml), the solution was passed down a column of IR 120(H^+) ion-exchange resin to remove sodium ions, and the effluent was concentrated to a syrup. The syrup was dissolved in ethanol (60 ml) and was kept at 5° for 12 hours, when the resulting crystalline product (18.5 g) was collected by filtration, washed with ethanol, and then dried *in vacuo*; m.p. 105–108°.

Hydrolysis of a small portion of the product with sulphuric acid and paper chromatographic examination of the hydrolyzate indicated it to be mainly 1-deoxy-1-nitro-D-*glycero*-D-*manno*-heptitol contaminated with 1-deoxy-1-nitro-D-*glycero*-D-*gluco*-heptitol. A portion (1 g) of the product was recrystallized five times from methanol to give pure crystalline 1-deoxy-1-nitro-D-*glycero*-D-*manno*-heptitol (0.51 g), which had m.p. 109–110° and $[\alpha]_D^{20}$ −6.8° (*c*, 3.8, 75% ethanol). Anal. Calc. for $C_7H_{15}O_8N$: C, 34.85; H, 6.3; N, 5.8%. Found: C, 35.0; H, 6.8; N, 5.5%.

D-glycero-D-manno-*Heptose*

The crude 1-deoxy-1-nitro-D-*glycero*-D-*manno*-heptitol (9 g), dissolved in *N* sodium hydroxide solution (90 ml), was added dropwise with stirring to 6 *N* sulphuric acid (110 ml) cooled externally with ice. After 30 minutes the solution was diluted with water (200 ml) and was adjusted to pH 3 by the addition of saturated aqueous barium hydroxide solution, whereupon 12% aqueous barium acetate solution (100 ml) was added to complete the removal of sulphate ions. The precipitated barium sulphate was removed by filtration, the filtrate was passed down columns of IR 120(H^+) and Duolite A4 (OH^-) ion-exchange resins, and the deionized solution was concentrated to a syrup (7.7 g). Paper chromatographic examination of the syrup showed it to be composed of D-*glycero*-D-*manno*-heptose contaminated with small amounts of unreacted 1-deoxy-1-nitro-D-*glycero*-D-*manno*-heptitol, altrose, and D-*glycero*-D-*gluco*-heptose. The syrup (7 g) was fractionated chromatographically on a cellulose column (4.5×72 cm) using initially butan-1-ol three-quarters saturated with water as the mobile phase, which was changed to butan-1-ol one-half saturated with water after the D-altrose fraction had been eluted from the column. Using a flow rate of 16 ml of solvent per hour, the following fractions were collected in the order indicated: 1-deoxy-1-nitroheptitol (0.60 g, 8.6%); D-altrose (0.832 g, 12%); D-*glycero*-D-*manno*-heptose (4.23 g, 60.5%); mixed D-*glycero*-D-*manno*-heptose and D-*glycero*-D-*gluco* heptose (0.175 g, 2.5%); and D-*glycero*-D-*gluco*-heptose (1.05 g, 15%).

The D-*glycero*-D-*manno*-heptose, which had $[\alpha]_D^{25}$ +21° (equilib. value; *c*, 3.6 methanol), remained a syrup and on paper chromatography in solvent systems A, B, and C it was indistinguishable from an authentic sample; $R_{glucose}$ 0.90 in solvent A and 0.82 in solvent B.

D-glycero-D-manno-*Heptose p-Nitrophenylhydrazone*

The syrupy D-*glycero*-D-*manno*-heptose (0.2 g) in methanol (3 ml) was heated under reflux for 2 hours with *p*-nitrophenylhydrazine (0.2 g), and the mixture was concentrated and taken up in ethyl acetate (3 ml). On cooling, D-*glycero*-D-*manno*-heptose *p*-nitrophenylhydrazone (0.25 g, 63%), having m.p. 171–174°, was collected and after two recrystallizations from ethanol or aqueous acetone gave crystals (0.15 g) which had m.p. 176–177°. Anal. Calc. for $C_{13}H_{19}O_8N_3$: C, 45.2; H, 5.55; N, 12.2%. Found: C, 45.1; H, 5.7; N, 12.1%.

Hexa-O-acetyl-D-glycero-D-manno-*heptose*

D-*glycero*-D-*manno*-Heptose (1.9 g) was dissolved in acetic anhydride (30 ml) containing sulphuric acid (0.3 ml) and after 48 hours the mixture was poured onto ice; the acetate was extracted in the usual way to

Can. J. Chem. Downloaded from www.nrcresearchpress.com by 210.87.254.5 on 09/05/12
For personal use only.

give the derivative from methanol solution as crystals (2.5 g, 59%) having m.p. 135–136°. After two recrystallizations from chloroform – light petroleum (b.p. 40–60°) mixture the crystalline product (2.15 g) had m.p. 139–140° (lit. value m.p. 138–139° (4)) and $[\alpha]_D^{24}$ +65° (*c*, 2.25 chloroform).

D-glycero-D-manno-*Heptonic Acid*

A stirred solution of D-*glycero*-D-*manno*-heptose (0.5 g) in methanol (30 ml) containing iodine (1.4 g) was kept at 40° while 4% methanolic potassium hydroxide solution (25 ml) was added dropwise over 15 minutes. After cooling the mixture to 0° the precipitated potassium D-*glycero*-D-*manno*-heptonate (0.40 g) was collected, washed with methanol, and dried *in vacuo*. D-*glycero*-D-*manno*-Heptono-γ-lactone (0.2 g), prepared from the potassium salt, in water (2 ml), was heated with phenylhydrazine (0.2 ml) for 3 hours and on cooling of the mixture the phenylhydrazide derivative (0.15 g) was obtained. The D-*glycero*-D-*manno*-heptonic phenylhydrazide after two recrystallizations from methanol had m.p. 187–188° and $[\alpha]_D^{25}$ −6° (*c*, 3 water).

Methyl-D-glycero-D-manno-*Heptopyranosides*

D-*glycero*-D-*manno*-Heptose (0.75 g) was heated under reflux with 2% w/v methanolic hydrogen chloride solution (60 ml) for 48 hours. The isolated glycosides (0.75 g), $[\alpha]_D^{25}$ +47° (*c*, 1.7 methanol), failed to crystallize and paper chromatographic examination showed that no unchanged heptose was present.

One mole part of periodic acid (7.4 ml, 0.3 mole) was added slowly to a stirred solution of the methyl D-*glycero*-D-*manno*-heptosides (0.5 g) in water (10 ml) and after 5 hours the iodic acid was removed by passage of the solution through a column of Duolite A4 (OH^-) ion-exchange resin. The eluate was concentrated (ca. 10 ml) and sodium borohydride (0.5 g) was added. After 12 hours at 0°, IR 120 (H^+) resin was added and the solution was then concentrated to a syrup, from which the boric acid was removed by repeated distillation with methanol. The hydrolyzed (dil. H_2SO_4) product when examined by paper chromatography showed the presence of mannose, a trace of D-*glycero*-D-*manno*-heptose, and a non-reducing component tentatively identified as a pentitol. The concentrated hydrolyzate (0.29 g) in methanol (5 ml) was heated for 1 hour with *p*-nitrophenylhydrazine (0.3 g) to give crystalline D-mannose *p*-nitrophenylhydrazone (0.115 g, 17%) having m.p. and mixed m.p. 200–201°.

D-glycero-D-manno-*Heptose Diethyldithioacetal*

D-*glycero*-D-*manno*-Heptose (0.5 g) dissolved in ice-cold hydrochloric acid (0.6 ml) was shaken with ethanethiol (0.6 ml) at 0° for 30 minutes and then kept at −5° overnight. The resulting white crystals were collected and were combined with the crystals obtained on concentration of the neutralized ($PbCO_3$) reaction mixture. The product was recrystallized from ethanol to give D-*glycero*-D-*manno*-heptose diethyldithioacetal (0.48 g, 65%) which had m.p. 155–156° and $[\alpha]_D^{25}$ +29.6° (*c*, 2.1 water). Anal. Calc. for $C_{11}H_{24}O_6S_2$: C, 41.77; H, 7.65; S, 20.2%. Found: C, 41.73; H, 7.51; S, 20.6%.

1-Deoxy-D-glycero-D-manno-*heptitol*

D-*glycero*-D-*manno*-Heptose diethyldithioacetal (0.36 g) in aqueous methanol (10 ml) was desulphurized by refluxing the solution for 6 hours in the presence of Raney nickel (3 g). Concentration of the methanol solution gave 1-deoxy-D-*glycero*-D-*manno*-heptitol as a syrup (0.20 g) which had $[\alpha]_D^{25}$ 0° (*c*, 3.6 methanol).

The periodate oxidation of an aqueous solution of the 1-deoxy-D-*glycero*-D-*manno*-heptitol at room temperature was complete in 1 hour, giving the following final results: 5.10 mole periodate consumed, 3.90 mole formic acid, and 0.93 mole formaldehyde released per mole heptitol.

ACKNOWLEDGMENTS

The authors wish to thank the National Research Council for financial assistance and Queen's University for the award of a scholarship to one of us (R. K. H.). We wish to thank Dr. N. K. Richtmyer for a sample of hexa-*O*-acetyl-D-*glycero*-D-*manno*-heptose.

REFERENCES

1. C. M. Quinnell, S. G. Knight, and P. W. Wilson. Can. J. Microbiol. **3**, 277 (1957).
2. W. Sowa. Ph.D. Thesis, Queen's University, Kingston, Ontario. 1962.
3. J. K. N. Jones, M. B. Perry, and R. J. Stoodley. Can. J. Chem. **40**, 1798 (1962).
4. D. A. Rosenfeld, N. K. Richtmyer, and C. S. Hudson. J. Am. Chem. Soc. **73**, 4908 (1951).
5. J. C. Sowden. Advan. Carbohydrate Chem. **6**, 291 (1951).
6. J. C. Sowden and P. R. Strobach. J. Am. Chem. Soc. **82**, 954 (1960).
7. J. U. Nef. Ann. **280**, 263 (1894).
8. E. Fisher. Ber. **22**, 2204 (1889).
9. L. Hough, J. K. N. Jones, and W. H. Wadman. J. Chem. Soc. 2511 (1949).
10. N. J. Antia and M. B. Perry. Can. J. Chem. **38**, 1917 (1960).
11. S. M. Partridge. Biochem. J. **42**, 238 (1948).
12. L. Hough and J. K. N. Jones. J. Chem. Soc. 1702 (1950).
13. W. E. Trevelyan, D. D. Procter, and J. S. Harrison. Nature, **166**, 444 (1950).

Can. J. Chem. Downloaded from www.nrcresearchpress.com by 210.87.254.5 on 09/05/12
For personal use only.

THE OXYMERCURATION OF 1,4-↑↑-METHYLENE-Δ^5-CYCLOHEXENE-2-CARBOXYLIC ACIDS

M. MALAIYANDI AND GEORGE F WRIGHT
Department of Chemistry, University of Toronto, Toronto, Ontario
Received December 7, 1962

ABSTRACT

The oxymercuration of 1,4-↑↑-methylene-Δ^5-cyclohexene-2-↑-carboxylic acid yields two diastereomeric hydroxychloromercurials. Their configurations cannot be specified on the basis of information now available with certainty. The oxymercuration of 1,4-↑↑-methylene-Δ^5-cyclohexene-2-↓-carboxylic acid also yields two diastereomers, which are designated as 6-↓-hydroxy-5-↓-chloromercuri-1,4-↑↑-methylenecyclohexane-2-↓-carboxylic acid, γ-lactone and 6-↓-hydroxy-5-↑-chloromercuri-1,4-↑↑-methylenecyclohexane-2-↓-dicarboxylic acid, γ-lactone because the former is more easily deoxymercurated than the latter and because their dipole moments match relatively the corresponding moments of the analogous dicarboxylic acid γ-lactones, the configurations of which have been proved chemically. This is the first instance where two diastereomers of opposite configuration have been shown to be formed in an oxymercuration.

During a recent study of the oxymercuration of various substituted [2.2.1]-bicycloheptenes (1) an anomaly has become apparent. The [2.2.1]-bicycloheptenes behave differently from other cyclic alkenes because the oxymercuration is acid catalyzed and the oxymercurials have the ↑↓ (trans) configuration. The exception is the isolable oxymercurial III-C from 1,4-↑↑-methylene-Δ^5-cyclohexene-2,3-↓↓-dicarboxylic acid. The chemical behavior of III-C shows it to be 5-↓-hydroxy-6-↓-chloromercuri-1,4-↑↑-methylenecyclohexane-2,3-↓↓-dicarboxylic acid, γ-lactone. But if the reaction proceeds through an ionic intermediate, at least one other diastereomer (probably 5-↓-hydroxy-6-↑-chloromercuri-1,4-↑↑-methylenecyclohexane-2,3-↓↓-dicarboxylic acid, γ-lactone, IV-C, ought to be formed. However, this diastereomer, IV-C, has the same solubility characteristics as III-C. Its main chemical difference from III-C, a higher resistance toward deoxymercuration, would not be apparent if it were a contaminant of low concentration. Consequently its presence in small amount might be missed, especially if traces of other diastereomers were present.

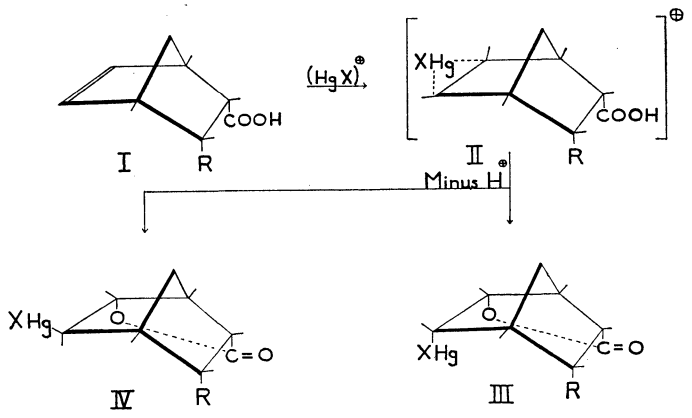

I TO IV (R=H)

I-C TO IV-C (R=COOH)

Can. J. Chem. Downloaded from www.nrcresearchpress.com by 210.87.254.6 on 09/05/12
For personal use only.

For this reason we decided to study the oxymercuration of a simpler substance, 1,4-↑↑-methylene-Δ^5-cyclohexane-2-↓-carboxylic acid, I. Since this acid is obtained from pentadiene and acrylic acid (2) in difficultly separable admixture with 1,4-↑↑-methylene-Δ^5-cylohexene-2-↑-carboxylic acid, IV, we have first effected a separation by an oxymercuration of the mixture. Fractional crystallization of the products of oxymercuration leads mainly to two oxymercurials which, when deoxymercurated by means of hydrochloric acid, regenerate I and IV separately. The ratio of 2-↓- to 2-↑-carboxylic acids in the mixture has been found by this method to be 12–13 to 1, thus more in agreement with the 9:1 ratio found by infrared analysis (3) than with the 77:23 ratio reported (4) by separation of I as its iodolactone.

We have treated 1,4-↑↑-methylene-Δ^5-cyclohexene-2-↓-carboxylic acid, I, in water with mercuric acetate, then with sodium chloride, and have obtained a crude 83% yield of mercurials m.p. 183–195°. When this mixture is fractionally crystallized the overall yield is found to be comprised of 77% of one mercurial and 3% of another, the remaining 3% being either more of the major product or else a yet unisolated isomer. We have assigned to the major product, III, the stereo-structure 6-↓-hydroxy-5-↓-chloromercuri-1,4-↑↑-methylenecyclohexane-2-↓-carboxylic acid, γ-lactone.

During the progress of the present investigation the oxymercuration of I was reported by Henbest and Nicholls (5), who assigned to their sole product (identical with our major product) the structure 6-↓-hydroxy-5-↑-chloromercuri-1,4-↑↑-methylenecyclohexane-2-↓-carboxylic acid, γ-lactone, IV, which we consider to be that of our minor product.

When our major product is treated in methanol with hydrazine a mixture is obtained consisting of 1,4-↑↑-methylenecyclohexane-2-↓-carboxylic acid and the mercurial which we specify as IV. Either of III or IV may be reduced by use of sodium borohydride (1, 5) to 6-↓-hydroxy-1,4-↑↑-methylenecyclohexane-2-↓-carboxylic acid, γ-lactone, V (6). The difference between the two mercurials must then rest entirely with the ↓↓ versus ↓↑ relationship of hydroxy and chloromercuri groups. Thus the expectation that acid-catalyzed oxymercuration ought to give more than one product has been realized.

On the basis of chemical reaction the assignment by Henbest and Nicholls is entirely arbitrary. These authors rely factually on the results of an X-ray diffraction study carried out earlier in our laboratory which has since been thought to be non-definitive (1). On the other hand our structure specifications are based on the observation that our minor product is more difficult to deoxymercurate than is our major product. Since the minor product also has a higher dipole moment than the major product we believe that our assignments (major product, III, and minor product, IV) are correct, because of these correlations with proven configurations among the mercurials from the 1,4-↑↑-methylene-Δ^5-cyclohexenedicarboxylic acids (7). Comparison in respect of dipole moment is shown in Table I. The dicarboxylic analogues are in each instance designated by the suffix "C".

The mechanism of oxymercuration for I is assumed to be the same as that for 1,4-↑↑-methylene-Δ^5-cyclohexene-2,3-↓↓-dicarboxylic acid, I-C (1). Although oxymercuration in [2,2,1]-bicycloheptenes is expected to proceed via a mercurinium-ion type of intermediate, II, and thus ought to lead chiefly to IV, the presence of the ↓-carboxylic group may be expected to alter this expectation by preference to an intramolecular addition which would proceed via the undissociated salt, VII. In the absence of external ion attack the major product would be III, similar to formation of III-C from I-C.

We were unable to oxymercurate 1,4-↑↑-methylene-Δ^5-cyclohexene-2-↑-carboxylic acid, VI, in purely aqueous medium because of product contamination with the mercuric salt of VI but we have successfully isolated two hydroxy-chloromercuri-1,4-↑↑-methylene-

Can. J. Chem. Downloaded from www.nrcresearchpress.com by 210.87.254.6 on 09/05/12
For personal use only.

TABLE I

Comparison of dipole moments of 1,4-↑↑-methylenecyclohexane (BCH) carboxylic acids and their hydroxychloromercuri derivatives in dioxane at 20°

Compound	μ (D)
BCH-2-↓-carboxylic acid	1.65
BCH-2,3-↓↓-dicarboxylic acid, I-C	2.78*
BCH-2-↑-carboxylic acid	1.61
BCH-2,3-↓↑-dicarboxylic acid, VI-C	2.49*
6-↓-Hydroxy BCH-2-↓-carboxylic acid, γ-lactone, V	4.70†
6-↓-Hydroxy BCH-2,3-↓↓-dicarboxylic acid, γ-lactone, V-C	4.85*
6-↓-Hydroxy-5-↓-chloromercuri BCH-2-↓-carboxylic acid, γ-lactone, III	3.39
6-↓-Hydroxy-5-↓-chloromercuri BCH-2,3-↓↓-dicarboxylic acid, γ-lactone, III-C	3.88*
6-↓-Hydroxy-5-↑-chloromercuri BCH-2-↓-carboxylic acid, γ-lactone, IV	6.99
6-↓-Hydroxy-5-↑-chloromercuri BCH-2,3-↓↓-dicarboxylic acid, γ-lactone, IV-C	7.18*
?-Hydroxy-?-chloromercuri-BCH-2-↑-carboxylic acid, IX	4.92
5-↑-Hydroxy-6-↓-chloromercuri BCH-2-↓-3-↑-dicarboxylic acid, C	4.75* ‡

*Moments reported in ref. 1.
†Checks value by Kwart and Kaplan (H. Kwart and L. Kaplan. J. Am. Chem. Soc. **76**, 4078 (1954)).
‡Compound XXIV, p. 1338, ref. 1.

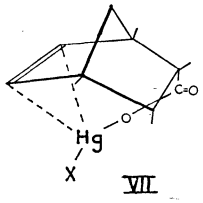

VII

cyclohexane-2-↑-carboxylic acids, VIII and IX, by inclusion of 2,5-dioxahexane into the reaction system. The ratio of high-melting (VIII) to low-melting diastereomer (IX) is 4:1. Unfortunately we have not found any chemical reaction by which we can specify either position or configuration for the added groups. The deoxymercuration of VIII is somewhat slower than that of IX. However, no definitive assignment of configuration can be made for them or for the 5-hydroxy-1,4-↑↑-methylenecyclohexane-2-↑-carboxylic acids obtained from them by reduction with sodium borohydride.

One may expect from consideration of the moments of the mercury-free mono- and di-carboxylic acids at the top of Table I that the values for the present pair of bicycloheptane-↓-monocarboxylic acid oxymercuration derivatives will be more meaningful than those obtained for the dicarboxylic acid derivatives (1). For the latter series, an artifically low C—COOH moment (1.2 D) had to be chosen, as would be expected because of mutual rotation interaction of the two carboxyl groups. By contrast, the moments of the bicycloheptanemonocarboxylic acids are approximate to those of many alkanecarboxylic acids, and they differ only by the contribution to polarity from the norbornane ring (1).

No such disparity is to be expected between 6-↓-hydroxy-1,4-↑↑-methylenecyclohexane-2-↓-carboxylic acid, γ-lactone and the analogue with a carboxyl group in the 3-position. Since the latter group is the only rotator, it is to be expected that 6-↓-hydroxy-1,4-↑↑-methylenecyclohexane-2,3-↓↓-dicarboxylic acid, γ-lactone would differ from its carboxylic-free analogue, V, only by the vectorial component due to this rotating carboxylic group. This expectation is confirmed in fact (Table I) by comparison of the moments of V and V-C.

Despite the small difference between μ for V-C and V it is to be expected that analysis of structure V should be less complicated than that of V-C.

Can. J. Chem. Downloaded from www.nrcresearchpress.com by 210.87.254.6 on 09/05/12
For personal use only.

This may be seen in the vector model:

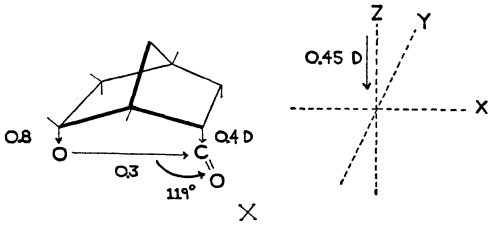

A slightly different set of bond moments and O—C=O bond angle than the one used for the comparable calculation of the 3-↓-carboxy analogue (1) has been assumed. When the O—C=O group moment resultant (2.54 D) is assumed to be directed 84° from the y-axis a close correlation with the observed value is obtained.

$$\mu_z = 0.4 \cos^2 18° + 0.8 \cos^2 18° + 2.54 \cos 30° + 0.45 = 3.735 \text{ D}$$
$$\mu_x = 0.4 \cos^2 18° - 0.8 \cos^2 18° + 2.54 \cos 119° = -0.88 \text{ D}$$
$$\mu_y = 0.8 \sin^2 18° - 0.4 \sin^2 18° + 2.54 \sin 84° = 2.64 \text{ D}$$
$$\mu_r^2 = \mu_z^2 + \mu_x^2 + \mu_y^2$$
$$\mu_r = 4.66 \text{ D} \qquad \text{found: } \mu = 4.70 \text{ D}$$

In order to calculate the moments of the two diastereomeric chloromercuri-1,4-↑↑-methylenecyclohexane-2-↓-carboxylic acid, γ-lactones III and IV one must add vectorially to the coordinate moments calculated above the Cl—Hg—C group, for which an angle of 96° is assumed in the present calculation. Then a Cl—Hg moment of 3.4 D is derived from the moment of *n*-propylmercuric chloride (3.70 D) by application of the 96° C—Hg—Cl angle and a C—Hg moment of 1.3 D (1).

The moment of 6-↓-hydroxy-5-↓-chloromercuri-1,4-↑↑-methylenecyclohexane-2-↓-carboxylic acid, γ lactone, III, has been calculated on the assumption that free rotation of the chloromercuri group is impossible, with this group diametrically opposed to the carbonyl group of the lactone. This assumption seems to be reasonable on the basis of the calculation for the carboxyl analogue of III with chloromercuri at the four quadrant positions (1).

$$\mu_z = 3.735 - 1.3 \cos 18° + 3.41 \cos 78°$$
$$\mu_x = -0.880 - 1.3 \cos 72° \cos 18° + 3.41 \cos 12° \cos 60°$$
$$\mu_y = 2.64 + 1.3 \cos^2 72° - 3.41 \cos 12° \cos 30°$$
$$\mu_r = 3.42 \text{ D} \qquad \text{found: } 3.39 \text{ D}$$

This calculation gives a moment value close to that actually determined in dioxane solution at 20°.

The test of the significance of this agreement between calculated and found values for III should be the application of the same parameters to the moment calculation of the diastereomer IV, although, in the absence of hindrance in this isomer, one should assume free rotation of the chloromercuri group. This rotation has been included by calculation of the two modes, 180° removed, of chloromercuri in the plane which includes the z-axis and the 2,5-positions of the norbornane skeleton.

Mode A:
$$\mu_z = 3.735 + 1.3 \cos 72° + 3.41 \cos 78°$$
$$\mu_x = -0.88 + 1.3 \cos^2 18° - 3.41 \cos 12° \sin 60°$$
$$\mu_y = 2.64 + 1.3 \cos 18° \cos 72° + 3.41 \cos 12° \cos 60°$$
$$\mu_r = 7.23 \text{ D}$$

Can. J. Chem. Downloaded from www.nrcresearchpress.com by 210.87.254.6 on 09/05/12
For personal use only.

Mode B: $\mu_z = 3.735 + 1.3 \cos 72° - 3.41 \cos 78°$
$\mu_x = -0.88 + 1.3 \cos^2 18° - 3.41 \cos 12° \cos 30°$
$\mu_y = 2.64 + 1.3 \cos 18° \cos 72° + 3.41 \sin 30° \cos 12°$
$\mu_r = 6.36$ D

The mean of these two resultant moments $[(52.2+40.5)/2]^{\frac{1}{2}}$ is 6.81 D, in reasonable agreement with the experimental value, 6.99 D. It may be noted that the discrepancy (0.18 D) is the same as was observed for the carboxy analogue of IV (1). This discrepancy may still be attributed to a slight obstruction to free rotation.

EXPERIMENTAL

Physical Constants

Dielectric constants of solids and solutions were determined as described previously (8). Melting points have been corrected against reliable standards (9). X-Ray diffraction patterns have been made with Cu K_α (Ni filtered) radiation and are expressed as relative intensities (I/I_1) for d spacings in Angstroms.

Separation of endo- and exo-1,4-Methylene-Δ⁵-cyclohexene-2-carboxylic Acids by Oxymercuration

A. Endo Acid

To a suspension of 28.0 g (0.2 mole) of the diastereomeric mixture of acids (2), m.p. −13° C, d_4^{25} 1.071, n_D^{20} 1.4850, in 500 ml of water was added 64.0 g (0.2 mole) of mercuric acetate. After 1 hour of stirring the system was treated with a slight excess of aqueous sodium chloride. The curdy precipitate, filtered, washed thrice with water, and dried, weighed 72 g (96%), m.p. 178–196° C. It was dissolved in a slight excess of cold 5% aqueous sodium hydroxide except for a small amount of yellow precipitate. After filtration the system was neutralized with 0.5 ml of 1% hydrochloric acid and then saturated with gaseous carbon dioxide. The precipitate, filtered, water-washed, and dried, melted at 195–200° C, 50 g. This precipitate was extracted with a mixture of dioxane and acetone (1:4) to leave 24 g, m.p. 217–219° C. Two crystallizations from the dioxane–acetone mixture left 22 g, m.p. 222–223° C.

This pure chloromercurial was deoxymercurated by warming for 3 minutes at 50° C a suspension of 23.9 g (0.064 mole) in 80 ml of methanol with 12.5 ml (0.13 mole) of conc. hydrochloric acid. The system, which was homogeneous within 15 minutes, was chilled after 1 hour and made alkaline (pH 8.3–10). The mercuric oxide was filtered off (13.6 g, 98.6%) and the filtrate was vacuum evaporated to remove the methanol. The aqueous residue was acidified to pH 3–4 and then was extracted with diethyl ether. Evaporation of the dried extract left 8 g of oil which, when crystallized at −30° C after solution in 30 ml petroleum ether (b.p. 40–60° C), gave 7.0 g (81%) of m.p. 41–42° C. Recrystallization from the same solvent raised this melting point to 44.3–45.0° C. The *p*-phenylphenacyl derivative melted at 134.9–135.4° C (9).

B. Exo Acid

The original liquor from which the oxymercurial m.p. 222–223° C was precipitated was combined with the crystallization liquors and was fractionally evaporated to yield crops of successively decreasing purity which still were mainly the oxymercurial m.p. 222–223° C. Final evaporation left 4.0 g, m.p. 160–178° C, which was crystallized from acetonitrile (10 ml/g) to give 3.0 g (6%) of mercurial m.p. 172–172.4° C.

Deoxymercuration of this mercurial by the procedure outlined above gave a 75% yield of impure 1,4-↑↑-methylene-Δ⁵-cyclohexene-2-↑-carboxylic acid m.p. 35–37° C. Crystallization from petroleum ether (b.p. 40–60° C) raised this melting point to 38–38.5° C. Although it gave the proper *p*-phenylphenacyl derivative (m.p. 131.5–132.2° C) (3) it was still impure. The separation of this exo acid from the diastereomeric mixture is much more satisfactorily accomplished via the iodolactone (4), especially if a mixture of diastereomers rich in exo acid is used. Actually such a mixture yielding 54% of 1,4-↑↑-methylene-Δ⁵-cyclohexene-2-↑-carboxylic acid b.p. 87–95° C (0.01–0.2 mm), m.p. 42–44° C was obtained by alkaline saponification of the 2-cyanonorbornene mixture prepared according to Bruson (10).

Hydroxymercuration of 1,4-↑↑-Methylene-Δ⁵-cyclohexene-2-↓-carboxylic Acid

To a stirred suspension of 9.0 g (0.067 mole) of the unsaturated endo acid in 100 ml of water was added 25.6 g (0.08 mole) of mercuric acetate in small amounts during 15 minutes. After 2 hours of subsequent stirring the system was treated with a slight excess of aqueous sodium chloride. The white precipitate was dissolved in a slight excess of 10% aqueous sodium hydroxide.

After filtration to remove mercuric oxide the system was neutralized by addition of two drops of 5% hydrochloric acid and by saturation with gaseous carbon dioxide. The precipitate was filtered off and washed successively with 5% aqueous acetic acid, water, acetone, and ether; dried weight 21 g (83%), m.p. 183–195° C.

This mixture was dissolved in 1500 ml of boiling dioxane. After filtration to remove 0.45 g of mercurous salt the solution was concentrated under reduced pressure in steps to yield crystal crops weighing 12.95 g,

Can. J. Chem. Downloaded from www.nrcresearchpress.com by 210.87.254.6 on 09/05/12
For personal use only.

m.p. 217–219° C. The final mother liquor (250 ml) was vacuum-evaporated to dryness. The residue (4.2 g, m.p. 167–180° C) was dissolved in 150 ml of hot methanol and this solution was concentrated to a volume of about 120 ml whereby 3.25 g more, m.p. 217–220° C, was obtained. The mother liquor was processed as described below.

The combined crops of crude 6-↓-hydroxy-5-↓-chloromercuri-1,4-↑↑-methylenecyclohexane-2-↓-carboxylic acid, γ-lactone, III, m.p. 217–220° C, 16.35 g (77%), were crystallized from 4:1 methanol–dioxane mixture (50 ml/g) to melt at 222–223° C. Anal. Calc. for $C_8H_9O_2HgCl$: C, 25.7; H, 2.41. Found: C, 25.9; H, 2.50.

The infrared spectrum (potassium chloride pellets at 20,000 p.s.i., 24° C) is expressed in wave numbers versus extinction as follows: (716) 6.80; (746) 6.85; (788) 6.94; (842) 7.88; (878) 4.85; (888) 7.71; (900) 8.86; (950) 12.7; (986) 23.9; (1010) 9.53; (1061) 7.88; (1100) 10.9; (1128) 6.75; (1146) 12.3; (1190) 22.6; (1242) 9.46; (1272) 9.60; (1304) 17.3; (1352) 15.0; (1450) 6.35; (1564) 3.79; (1768) 20.0; (1852) 3.65; (1930) 3.10; (1982) 2.95; (2580) 4.79; (2900) 8.42; (3010) 14.2.

The X-ray diffraction pattern was [10] 12.99, [8] 9.55, [7] 2.36, [6] 4.17, [5] 3.69, [4] 3.88, [3] 5.34, [2] 2.03, [1] 6.75.

The final mother liquor from which this crude chloromercurial was isolated yielded upon final vacuum evaporation 0.58 g, m.p. 184–186° C (3%). Crystallization from ethanol (80 ml/g) raised this melting point to 186.5–187° C. Anal. Calc. for $C_8H_9O_2HgCl$: C, 25.7; H, 2.41. Found: C, 25.8; H, 2.46. The X-ray diffraction pattern of this 6-↓-hydroxy-5-↑-chloromercuri-1,4-↑↑-methylenecyclohexane-2-↓-carboxylic acid, γ-lactone (IV) was [10] 9.06, [8] 3.14, [6] 4.88, [5] 2.84, [4] 4.50, [3] 5.26, [2] 4.58, [1] 2.36.

The infrared spectrum prepared and described as above is: (722) 31.4; (750) 13.8; (788) 10.6; (816) 7.96; (840) 14.8; (888) 25.0; (938) 13.9; (960) 13.2; (979) 56.7; (1010) 47.6; (1088) 45.2; (1138) 20.0; (1150) 14.7; (1192) 53.2; (1228) 11.2; (1248) 24.5; (1274) 15.9; (1300) 28.0; (1318) 25.5; (1344) 47.3; (1452) 14.1; (1470) 10.3; (1554) 7.52; (1758) 54.7; (2290) 16.5; (3020) 40.2.

This product, IV, also was formed when 7.4 g (0.02 mole) of III, m.p. 222–223° C, in 10 ml of methanol was stirred for 48 hours with 1.4 ml (0.022 mole) of hydrazine hydrate at 35–40° C. After removal of metallic mercury by filtration the system was vacuum-evaporated to leave a residue which was extracted with 100 ml of petroleum ether (b.p. 40–60° C). The extracted residue (vacuum-dried) was washed onto a filter with cold 5% hydrochloric acid, then redried and crystallized from 95% ethanol (10 ml/g) to yield 1.2 g (17%), m.p. 185–186° C. Recrystallization from ethanol (7 ml/g) raised this melting point to 186.5–187° C and a mixture melting point with that obtained by hydroxymercuration was not lowered.

The petroleum ether extract was vacuum-evaporated to leave a residue which was crystallized from acetonitrile (4 ml/g), m.p. 61–62° C, 1.8 g (64%) of crude 1,4-↑↑-methylenecyclohexane-2-↓-carboxylic acid. Two recrystallizations from acetonitrile raised the melting point to 64.5–65.3° C. A mixture melting point with an authentic sample (2) was not depressed.

1,4-↑↑-Methylene-Δ⁵-cyclohexene-2-↓-carboxylic Acid, I

A. By Deoxymercuration of III

To a suspension of 30.0 g (0.08 mole) of III, m.p. 222–223° C, in 150 ml of methanol was added 20 ml (0.208 mole) of 36% hydrochloric acid, and the system was warmed to 50° C for 5 minutes, then maintained without heating and with occasional stirring for 15 minutes. The homogeneous system was maintained for 1 hour longer, then was cooled in ice and made alkaline with a slight excess of 10% aqueous sodium hydroxide (pH 7.3–10). After filtration of mercuric oxide the solution was vacuum-evaporated until methanol was gone, then was acidified to pH 3 with hydrochloric acid and was extracted with diethyl ether. Evaporation of the dried extract left a residue (9.45 g, 85%) which when crystallized from petroleum ether (b.p. 40–60° C) melted at 44–45° C, not depressed by admixture with 1,4-↑↑-methylene-Δ⁵-cyclohexene-2-↓-carboxylic acid.

The deoxymercuration of III also may be effected completely in 5 minutes at 24° by treatment of 0.2 g of III with 0.5 ml of 36% hydrochloric acid. The same conversion to the endo unsaturated acid requires 15 minutes by use of 20.4% hydrochloric acid.

B. By Deoxymercuration of IV

When the methanolic deoxymercuration procedure described above was applied to IV a 3-hour reaction time was required to give an 80% yield of crude endo unsaturated acid, m.p. 36–38° C. Crystallization from petroleum ether (b.p. 40–60° C) raised this to 44.5–45.3° C whence a mixture melting point with pure 1,4-↑↑-methylene-Δ⁵-cyclohexene-2-↓-carboxylic acid proved the identity.

When 0.1 g of IV was treated with 0.25 ml of 36% hydrochloric acid for 5 minutes at 24° C, then diluted with 0.25 ml of water, the filterable portion, washed with water and then with diethyl ether, weighed 0.05 g and melted at 185–186° C. A mixture melting point with IV was not depressed. When the initial hydrochloric acid concentration was 20.4% only 15% of IV was deoxymercurated in 15 minutes.

C. By Deoxymercuration of III plus IV

To an intimate mixture of 0.2 g of III and 0.10 g of IV was added 0.5 ml of 36% hydrochloric acid. After 5 minutes at 24° C and then dilution with 0.5 ml of water the filtered solid phase was shown to be 0.045 g

Can. J. Chem. Downloaded from www.nrcresearchpress.com by 210.87.254.6 on 09/05/12
For personal use only.

(45%) of IV of high purity (m.p. 185–186° C). A mixture melting point was not lowered. When 20.4% hydrochloric acid was used the recovery of IV only was 90%, m.p. 184–185° C.

5-↓-Hydroxy-1,4-↑↑-methylenecyclohexane-2-↓-carboxylic Acid, γ-Lactone, V

A. From III

A clear solution of 7.4 g (0.02 mole) of 6-↓-hydroxy-5-↓-chloromercuri-1,4-↑↑-methylenecyclohexane-2-↓-carboxylic acid, γ-lactone, III, in 100 ml of 1% aqueous sodium hydroxide was cooled to −2° C and swirled while 2.6 g (0.022 mole) of sodium trimethoxyborohydride was added during 30 minutes. Then the black suspension was allowed to warm to 40° C and was filtered to remove 3.9 g (97%) of mercury.

The cold filtrate was carefully acidified with 5% aqueous sulphuric acid to pH 3 and then was extracted with diethyl ether. Evaporation of the dried extract left 2.15 g (76%), slightly sticky but melting at 146–149° C. After sublimation at 60–65° C at 0.7 mm and threefold crystallization from petroleum ether (b.p. 90–100° C) the melting point was raised to 155.5–156.5° C. A mixture melting point with an authentic specimen (6) was not lowered.

B. From IV

The identical procedure outlined above was applied to 6-↓-hydroxy-5-↑-chloromercuri-1,4-↑↑-methylenecyclohexane-2-↓-carboxylic acid, γ-lactone, IV, with identical result.

Hydroxymercuration of 1,4-↑↑-Methylene-Δ⁵-cyclohexene-2-↑-carboxylic Acid

To a stirred solution of 2.76 g (0.02 mole) of methylenecyclohexene-2-↑-carboxylic acid in 75 ml of 1:1 2,5-dioxahexane–water mixture at 65–70° C was added during 1 hour a solution of 6.4 g (0.02 mole) of mercuric acetate in 50 ml of 98:2 water – acetic acid. After 2 days of subsequent stirring the system was filtered to remove 0.2 g of grey solid and then was made alkaline to pH 10. More grey solid (50 mg) was filtered off and the filtrate, after 2.1 g of sodium chloride was dissolved in it, was acidified by addition of gaseous carbon dioxide. After filtration this solution at pH 5–6 was vacuum-evaporated. The residue was Soxhlet-extracted with absolute alcohol, leaving a solid residue, A, and an extract, B.

Hydroxy-chloromercuri-1,4-↑↑-methylenecyclohexane-2-↑-carboxylic Acid, VIII

The solid residue, A, was washed with 0.5% hydrochloric acid, then with water, and was filtered to remove 1.2 g (15%) of crude chloromercurial m.p. 199–206° C. Two crystallizations by solution in 25 ml of 1:4 dioxane–ethanol followed by dilution with 15 ml of commercial hexane raised this melting point to 216–217° C. The mother liquors were combined with extract A. The infrared spectrum (potassium chloride pellets at 20,000 p.s.i., 24° C) of the mercurial, VIII, is expressed as wave numbers versus extinction: (3144) 8.21; (2920) 6.26; (2584) 4.37; (1681) 14.6; (1441) 4.81; (1418) 5.60; (1361) 11.3; (1333) 8.46; (1297) 5.48; (1267) 4.81; (1247) 2.25; (1233) 3.99; (1209) 2.92; (1159) 0.84; (1126) 2.48; (1110) 1.00; (1055) 3.91; (1033) 4.99; (1020) 4.42; (1007) 7.17; (967) 2.74; (939) 0.56; (912) 2.58; (883) 2.74; (869) 2.58; (835) 1.92; (777) 2.07; (769) 2.58; (759) 3.81; (723) 4.37; (651) 3.27. Anal. Calc. for $C_8H_{11}O_3HgCl$: C, 24.6; H, 2.81. Found: C, 24.9; H, 3.09. The extrapolated dielectric constant of the pelleted solid (8, 11) (Fig. 1) was found to be 2.347 and its density by flotation was 2.004, so distortion polarization is 60.5 cc by contrast to 53.9 cc calculated additively from Eisenlohr values.

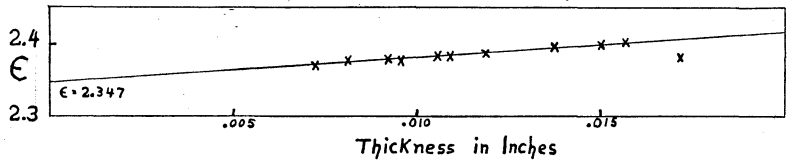

FIG. 1. Extrapolation of apparent ϵ to zero thickness, VIII.

Hydroxy-chloromercuri-1,4-↑↑-methylenecyclohexane-2-↑-carboxylic Acid, IX

The acid and water washings, together with the crystallization mother liquors obtained in the preceding experiment, were combined with extract A above and the whole was vacuum-evaporated to dryness. The residue was eluted with absolute ethanol. The vacuum-evaporated eluate was washed onto a filter with 25 ml of 0.5% hydrocholoric acid; 5 g (64%) of crude chloromercurial, m.p. 159–170° C, was obtained. After two crystallizations from acetonitrile (30 ml/g) the product melted at 171–172° C, identical, by mixture melting point, with that obtained during the original separation of norbornenecarboxylic acids. The infrared spectrum (pellets as described above) expressed as (cm^{-1}) is: (3236) 9.67; (2924) 5.42; (1695) 15.6; (1445) 0.77; (1443) 0.74; (1364) 3.94; (1324) 2.40; (1292) 3.35; (1250) 3.14; (1235) 5.29; (1178) 7.49; (1139) 9.05; (1065) 5.42; (1031) 2.33; (1013) 6.34; (1003) 6.34; (947) 1.74; (911) 3.07; (887) 1.79; (823) 2.07. Anal. Calc. for $C_8H_{11}O_3HgCl$: C, 24.6; H, 2.81. Found: C, 24.9; H, 3.20.

When the entire experiment was conducted without 2,5-dioxahexane for solubilization, the diastereomers

Can. J. Chem. Downloaded from www.nrcresearchpress.com by 210.87.254.6 on 09/05/12
For personal use only.

m.p. 216° C and 172° C were obtained in yields of 8 and 22% respectively; much exo acid was recovered unchanged.

Deoxymercuration Rates of VIII and IX

Into 5 ml of 20% hydrochloric acid at 25° was stirred 0.1 g of finely powdered chloromercurial IX, m.p. 171–172°. After 15 minutes the system was diluted with 10 ml of water and filtered to remove 0.008 g (8%) of the original mercurial. When these conditions were reproduced upon 0.1 g of VIII 52% was recovered unchanged.

When 0.1 g each of VIII and IX were stirred into 10 ml of 20% hydrochloric acid for 15 minutes and then diluted with 20 ml of water the recovered mercurial (0.048 g, 48%) melted at 212–215° and was shown by mixture melting point with an authentic specimen, m.p. 214–216°, to be chiefly VIII.

Reduction of VIII and IX with Sodium Borohydride

A solution of 3.4 g (8.7×10^{-3} mole) of either VIII or IX in 25 ml of 5% aqueous sodium hydroxide was chilled to −5°, and 0.38 g (0.01 mole) of sodium borohydride was added portionwise during 10 minutes. After 1 hour the cooling bath was removed and the system at room temperature was just acidified with 2 *N* hydrochloric acid. The metallic mercury (1.64 g, 94%) was filtered off. The filtrate was five times extracted, with a total of 75 ml of diethyl ether, and this extract, dried by use of sodium sulphate, was distilled under 0.3 mm.

The product from IX boiled at 157–160°, 0.45 g (30%), m.p. 105–110°. Crystallization from benzene raised this melting point to 114–115°. A Nujol mull of this product, X, showed strong hydroxyl absorption at 3430 cm^{-1} and carboxyl absorption at 1704 cm^{-1}. The hydroxyl absorption at 1010 cm^{-1} appeared as a doublet. Anal. Calc. for $C_8H_{12}O_3$: C, 61.5; H, 7.75. Found: C, 61.3; H, 7.59.

The product from VIII boiled at 146–152°, 0.36 g (22%). It melted at 131–135° after crystallization from 2 ml benzene. Recrystallization from the same solvent raised this melting point to 134–136°. The spectrum from this product, XI, resembled that of X except that only a single peak was found at 1008 cm^{-1}. Anal. Calc. for $C_8H_{12}O_3$: C, 61.5; H, 7.75. Found: C, 61.5; H, 7.52.

Electrical Polarization Studies

The high value of distortion polarization (P_D) found for VIII by extrapolation of the dielectric constants of various thicknesses of compressed wafers (11) (Fig. 1) indicates that the calculation of electronic polarization from summation of bond or group refractions may introduce a minor error in the results of Table I. These summations have been used in every instance except for IX, where P_D for VIII was subtracted from the total polarization to arrive at the orientation polarization from which the moment is calculated. The error is slight and it applies also to the determination of dielectric constants for the dicarboxylic acid series (1).

Two grades of dioxane were used for determination (11) of total solute polarizations. Dioxane of $\epsilon = 2.2183$ and $\bar{V} = 0.96803$ was used for the values shown in Fig. 2 and of $\epsilon = 2.2276$ with $\bar{V} = 0.96775$ for the values shown in Fig. 3. Both figures show extrapolations to zero concentration of ϵ and $\bar{V}$ for various strengths of solutions.

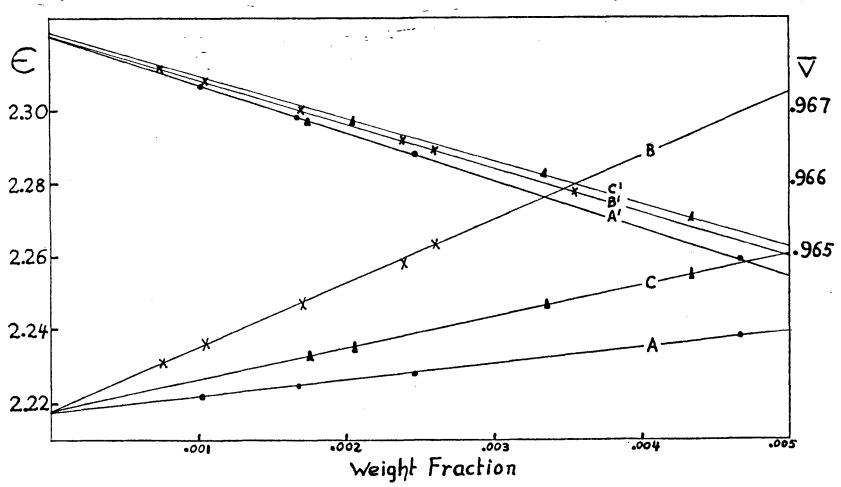

FIG. 2. Extrapolations of apparent ϵ and $\bar{V}$. A: 6-↓-Hydroxy-5-↓-chloromercuri-BCH-2-↓-carboxylic acid, γ-lactone, III; B: 6-↓-hydroxy-5-↑-chloromercuri-BCH-2-↓-carboxylic acid, γ-lactone, IV; C: ?-hydroxy-?-chloromercuri-BCH-2-↑-carboxylic acid, IX.

Can. J. Chem. Downloaded from www.nrcresearchpress.com by 210.87.254.6 on 09/05/12
For personal use only.

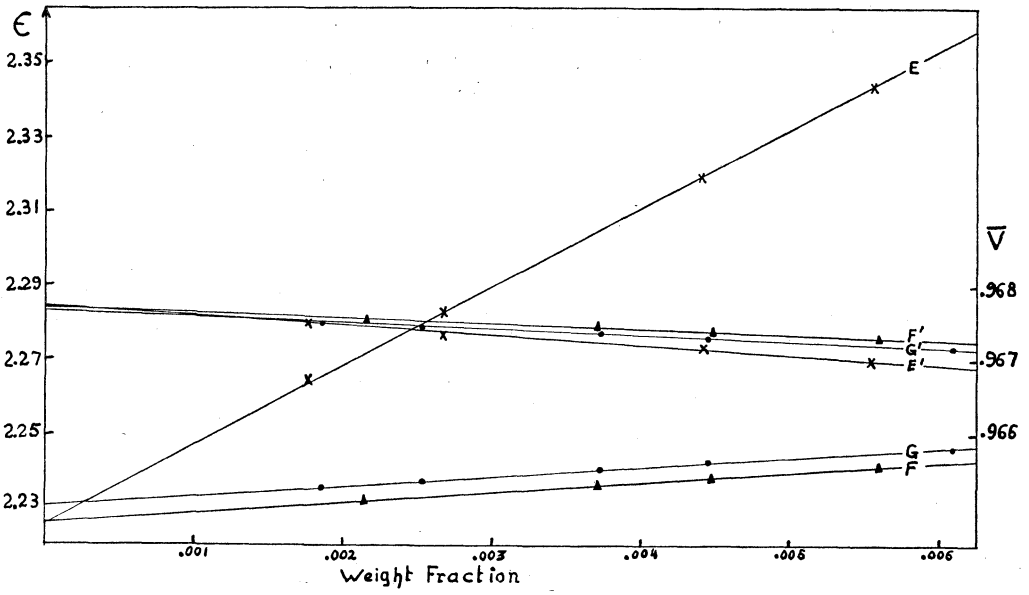

FIG. 3. Extrapolations of apparent ϵ and $\bar{V}$. E: 6-↓-Hydroxy-BCH-2-↓-carboxylic acid, γ-lactone, V; F: bicycloheptane-2-↓-carboxylic acid; G: bicycloheptane-2-↑-carboxylic acid.

REFERENCES

1. M. J. ABERCROMBIE, A. RODGMAN, K. R. BHARUCHA, and G. F WRIGHT. Can. J. Chem. **37**, 1328 (1959).
2. O. DIELS and K. ALDER. Ann. **460**, 117 (1928).
3. J. D. ROBERTS, E. R. TRUMBULL, JR., W. BENNETT, and R. ARMSTRONG. J. Am. Chem. Soc. **72**, 3116 (1950).
4. C. D. VER NOOY and C. S. RONDESTVEDT. J. Am. Chem. Soc. **77**, 3583 (1955).
5. H. B. HENBEST and B. NICHOLLS. J. Chem. Soc. 227 (1959).
6. K. ALDER, G. STEIN, E. ROLLAND, and G. SCHULZE. Ann. **514**, 211 (1934).
7. K. H. MCNEELY, A. RODGMAN, and G. F WRIGHT. J. Org. Chem. **20**, 714 (1955).
8. C. C. MEREDITH, L. WESTLAND, and G. F WRIGHT. J. Am. Chem. Soc. **79**, 2385 (1957).
9. G. F WRIGHT. Can. J. Technol. **34**, 89 (1956).
10. H. A. BRUSON. J. Am. Chem. Soc. **64**, 2457 (1942).
11. P. PODLESCHKA, L. WESTLAND, and G. F WRIGHT. Can. J. Chem. **36**, 574 (1958).

Can. J. Chem. Downloaded from www.nrcresearchpress.com by 210.87.254.6 on 09/05/12
For personal use only.

COORDINATION POLYMERIZATION OF OLEFINS

CATALYST STUDIES. PART I. THE INFRARED SPECTROSCOPIC INVESTIGATION OF THE SYSTEMS $(CH_3)_3Al$–$TiCl_4$ AND $(CH_3)_2Zn$–$TiCl_4$

A. P. GRAY,[1] A. B. CALLEAR,[2] AND F. H. C. EDGECOMBE
Du Pont of Canada Limited, Research Centre, Kingston, Ontario

Received August 14, 1962

ABSTRACT

An infrared spectroscopic investigation of the reaction between titanium tetrachloride and trimethyl aluminum in the vapor phase was carried out at six different reactant ratios. The study defined the course of the initial reactions; demonstrated the importance of equilibria among the products in this system as contrasted with dimethyl zinc – titanium tetrachloride; indicated the relative alkylating power of trimethyl, dimethylchloro, and methyldichloro aluminum toward titanium tetrachloride and methyl titanium trichloride; and supported the view that the active catalyst site in such systems is the titanium–carbon bond in reduced titanium alkyls. A new mode of decomposition of methyl titanium trichloride leading to active catalyst was found which can account for reported variable catalyst activities at Al/Ti ratios less than 1. Individual infrared spectra in the range 1500 to 300 cm^{-1} for trimethyl aluminum, dimethyl aluminum dichloride, methyl aluminum dichloride, methyl titanium trichloride, and dimethyl titanium dichloride as well as those of the initial reaction mixtures are presented.

INTRODUCTION

In spite of very widespread and intensive interest in olefin polymerization catalysts involving transition metal compounds with metal alkyls (coordination catalysts) (1–7), neither the reactions leading to the formation of active catalyst nor the nature of the catalyst species itself have been satisfactorily determined, and to a large extent remain matters for speculation. Aside from the work of Groenewege (8), who carried out an infrared study of the system dimethyl aluminum chloride plus titanium tetrachloride in heptane solution at two different reactant ratios, very little direct physical evidence pertaining to this problem has been published, no doubt because of the considerable experimental difficulties associated with such highly reactive systems. However, as will be demonstrated by the work to be reported, at least for the systems $(CH_3)_3Al + TiCl_4$ and $(CH_3)_2Zn + TiCl_4$, these difficulties may be largely overcome by working in the vapor phase. In this way, the initial and subsequent reactions between the catalyst components have been followed by infrared spectroscopy over essentially the whole range of practically significant reactant ratios.

As the compounds employed and produced in these investigations are in themselves of very great structural and spectroscopic interest, they are discussed at some length from this point of view in a paper which follows (9).

EXPERIMENTAL

Preparation of Materials

$TiCl_4$

The titanium tetrachloride was obtained from the Fisher Scientific Company. It was found to contain very small amounts of hydrogen chloride and phosgene, which were removed by pumping under vacuum. A final bulb-to-bulb fractionation *in vacuo*, the middle cut being retained, gave what appeared to be, on infrared analysis, a pure product.

$(CH_3)_6Al_2$

Trimethyl aluminum (a dimer at room temperature) was obtained from the Ethyl Corporation. This material was then distilled *in vacuo* and stored on the vacuum line.

[1]*Present address: Olin Mathieson Research Center, 275 Winchester Avenue, New Haven, Connecticut.*
[2]*Present address: Department of Physical Chemistry, University of Cambridge, Cambridge, England.*

Can. J. Chem. Downloaded from www.nrcresearchpress.com by 210.87.254.105 on 09/05/12
For personal use only.

$(CH_3)_2Zn$

It was found by C. T. Elston of this laboratory that the reaction between anhydrous zinc chloride and trimethyl aluminum produced $(CH_3)_2Zn$, which could be easily separated from the other products by efficient fractional distillation.

Trimethyl aluminum was added slowly from a dropping funnel to powdered anhydrous zinc chloride under nitrogen. The mixture was gently heated to about 50° C and allowed to reflux under its own heat of reaction. On completion of the reaction, dimethyl zinc was distilled from the mixture at 46° C, collected in a flask, cooled to 0° C, and finally redistilled onto the vacuum line, where it was stored. This method produced a very pure form of dimethyl zinc.

Infrared Instrumentation and Procedure

A Perkin–Elmer Model 21 double-beam spectrophotometer, fitted with sodium chloride optics, was used in this work to record the infrared spectra from 4000 to 650 cm^{-1}. A Perkin–Elmer single-beam, double-pass Model 112 spectrometer with caesium bromide optics was used for the region 650 to 290 cm^{-1}. The latter instrument was swept with dry nitrogen during the runs and was calibrated against reference lines of water vapor and methanol.

The infrared gas cells used were of Pyrex, 10 cm in length, and fitted with a vacuum stopcock and side arm. Kel-F grease was employed as a stopcock lubricant, and the CsBr windows were sealed on with glyptal in such a manner that the cells were vacuum-tight and had very little glyptal exposed to their interiors. After each run, the cell was taken apart, the windows repolished, and the cell body thoroughly cleaned and dried. The infrared solution work reported was carried out in a conventional sealed cell with CsBr windows and Teflon spacer.

The quantities of materials to be reacted were measured, using a sensitive spoon gauge. The infrared cell was connected to a high-vacuum system, pumped out, and then, to insure complete dryness and to render inert any potentially harmful materials used in the cell construction, was rinsed for 1 hour with a quantity of the metal alkyl vapor to be used. This vapor was then removed and the desired quantity of metal alkyl frozen out in the side arm of the cell. The required quantity of $TiCl_4$ was next measured and also frozen out in a different section of the side arm. The cell was isolated from the vacuum system and the side arm warmed quickly to allow the materials to react in the vapor phase.

RESULTS AND DISCUSSION

In order to facilitate the discussion, the individual spectra of the pure isolated components of the reaction mixtures will first be presented and briefly discussed to the extent necessary for consideration and understanding of the reaction mixtures. The spectra of the reaction mixtures at six different reactant ratios will next be interpreted. With the exception of carbon–hydrogen stretching vibrations, which occur essentially in the same range as that for hydrocarbons, no bands above 1500 cm^{-1} were observed in this study. Accordingly, the spectra presented cover the range from 1500 to 300 cm^{-1} only.

Individual Component Spectra

All major infrared absorption bands occurring in the spectra at the various ratios of titanium tetrachloride and trimethyl aluminum are found to be satisfactorily accounted for by absorption of the initial reactants, dimeric dimethyl aluminum chloride, dimeric methyl aluminum dichloride methyl titanium trichloride, and dimethyl titanium dichloride. This was established by infrared examination of the suspected compounds synthesized by totally independent means. The available data on the aluminum compounds were either incomplete or of doubtful quality at the time of this investigation, and the methyl titanium chlorides were unknown. Infrared investigations of trimethyl aluminum and the methyl aluminum chlorides in solution have since been reported by Groenewege (8) and more recently by Hoffmann (10), whose data, however, do not extend below 400 cm^{-1}. Spectra of methyl titanium trichloride have been reported by Groenewege (8) and by Karapinka, Smith, and Carrick (11). A more detailed comparison of the spectra will be made in the following paper (9), which deals with the purely spectroscopic aspects of the compounds involved in this research. It is sufficient to say at this point that, while some differences exist, most can be ascribed to frequency shifts and intensity changes between solution and vapor spectra.

Can. J. Chem. Downloaded from www.nrcresearchpress.com by 210.87.254.105 on 09/05/12
For personal use only.

$TiCl_4$

Figure 1 is the spectrum of titanium tetrachloride at a pressure of 10 mm Hg in the 10-cm cell. The observed bands are at 622, 522, and 500 cm^{-1}, in reasonable agreement with the published vapor spectrum (12).

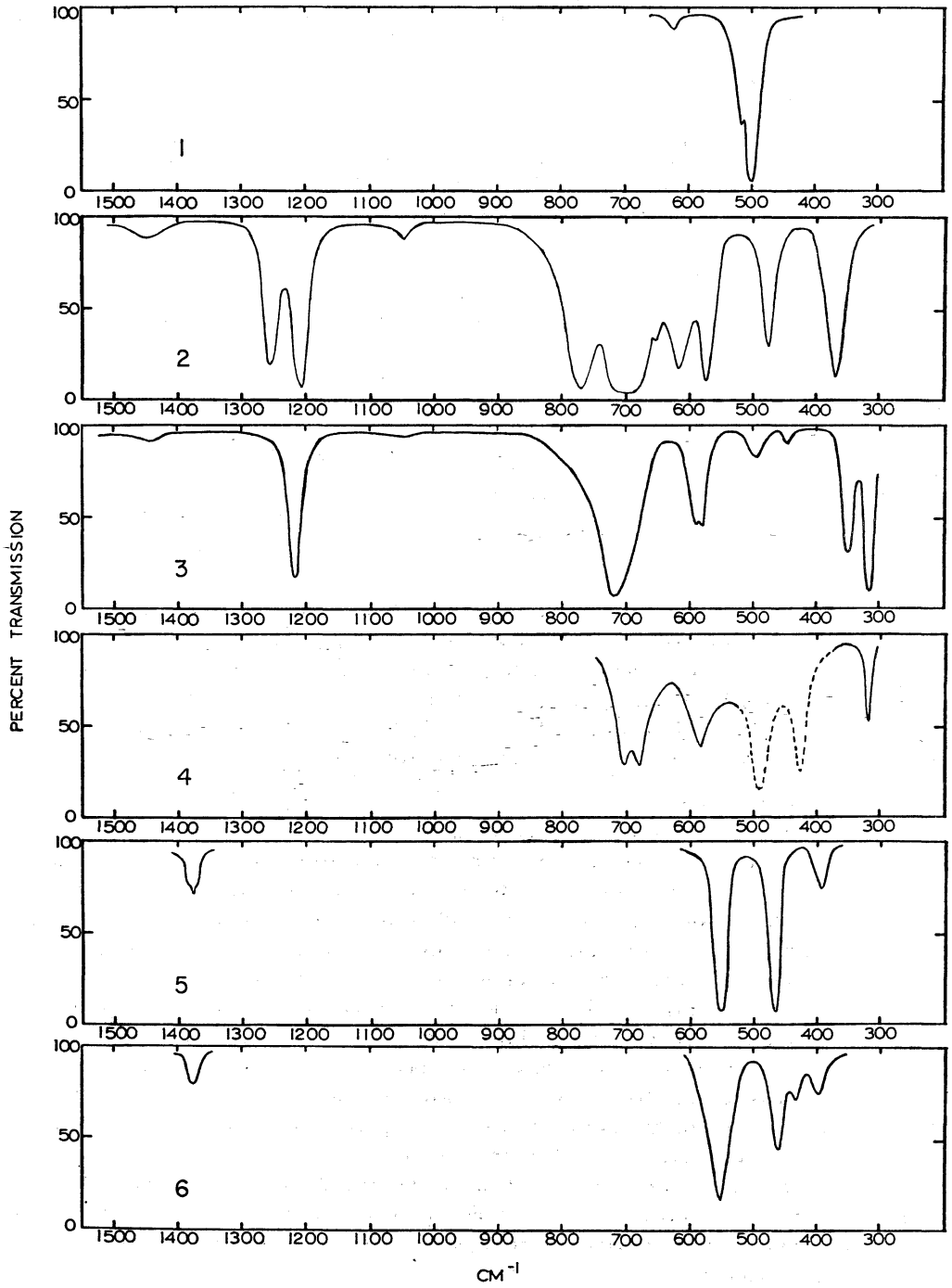

FIGS. 1–6. Individual component spectra.

Can. J. Chem. Downloaded from www.nrcresearchpress.com by 210.87.254.105 on 09/05/12
For personal use only.

$(CH_3)_6Al_2$

Figure 2 is the spectrum of dimeric trimethyl aluminum in the vapor. The absorption maxima occur at 1445, 1255, 1208, 1055, 772, 700, 652, 616, 572, 480, and 369 cm^{-1}.

$(CH_3)_4Al_2Cl_2$

Figure 3 is the spectrum of dimeric dimethyl aluminum chloride prepared by the reaction of hydrogen chloride with trimethyl aluminum in the vapor phase in the ratio of 2 moles of hydrogen chloride to 1 of dimer. The band positions are 1440, 1212, 1050, 720, 588, 581, 487, 440, 343, and 310 cm^{-1}.

$(CH_3)_2AlCl_4$

The caesium bromide spectrum of this compound obtained by reaction of hydrogen chloride and trimethyl aluminum in the appropriate ratio is shown in Fig. 4. Absorptions occur at 700, 675, 587, 483, 423, and 310 cm^{-1}. This spectrum is in excellent agreement with that of Groenewege with the exception of the 423 cm^{-1} band. There was initially some reason to believe that this absorption and the 483 cm^{-1} band, which are dashed in Fig. 4, were spurious. However, insofar as the practical application of these spectra to the identification of components in the reaction mixtures is concerned, the two absorptions at 700 and 675 cm^{-1} were taken to be characteristic of $(CH_3)_2Al_2Cl_4$, while the 720 and 343 cm^{-1} bands were similarly characteristic of the tetramethyldichloro dimer. The detailed consideration of these spectra presented in the following paper (9) substantiates these identifications and discusses the possible origin of the 423 cm^{-1} absorption. These matters, however, have no direct bearing on the results or conclusions of the reaction study.

CH_3TiCl_3

Figure 5 is the spectrum of this compound obtained in the vapor by reaction of dimethyl zinc with titanium tetrachloride in the mole ratio 1:2. In this case, the preparation was carried out on a vacuum line and the volatile product transferred to the cell entirely free from the completely nonvolatile zinc chloride. The bands occur at 1380, 550, 464, and 391 cm^{-1}, the 1380 cm^{-1} band having a barely discernible PQR structure. The pressure in the 10-cm cell was approximately 10 mm Hg, and no other absorptions were found under these conditions. The pure material in the vapor phase was completely stable when kept in the dark. However, exposure to room light did induce decomposition over a period of a day or two to produce a uniform brownish-yellow coating of titanium trichloride on the cell walls. Production of methane was also observed in the infrared cell as the decomposition proceeded. On freezing out, methyl titanium trichloride condenses to a yellow liquid which solidifies to a purple crystalline solid.

Methyl titanium trichloride was first observed by us in the reaction system $(CH_3)_3Al + TiCl_4$. The identity of the spectrum obtained from the independent preparation, using dimethyl zinc, conclusively demonstrated that it was not in any way complexed with aluminum compounds. Measurement of pressure changes during its preparation also showed the compound to be monomeric. All four bands observed decrease in proportion on decomposition, indicating that they are due to a single entity, and the infrared spectrum is entirely consistent with the proposed structure. The pure material when contacted with anhydrous aluminum chloride was shown by infrared to be converted to titanium tetrachloride. That the observed spectrum corresponds to a monomeric uncomplexed titanium compound of formula CH_3TiCl_3 is therefore beyond question.

$(CH_3)_2TiCl_2$

Figure 6 is the spectrum of this compound obtained by the mole-to-mole reaction of dimethyl zinc and titanium tetrachloride. The absorption bands are at 1380, 550, 462, 427, and 396 cm^{-1}. This material is unstable even in the dark and decomposes with a

Can. J. Chem. Downloaded from www.nrcresearchpress.com by 210.87.254.105 on 09/05/12
For personal use only.

"half-life" of about 2 hours under the conditions of the experiment. The pressure studies indicated that exposure to room light does not significantly increase the rate of decomposition.

Reaction Mixture Spectra

The reproducibility of the reactions carried out in the vapor phase by rapid volatilization of the separately condensed components was checked on many occasions and found to be very satisfactory. Wherever possible, the initial pressure of titanium tetrachloride was 9 mm Hg, and the dimeric trimethyl aluminum pressure was adjusted according to the ratio desired. The spectra shown represent the first scan of the reaction products immediately after mixing, and while some changes undoubtedly took place during the runs, it was established that the rate was such as to produce only minor variations in the relative intensities of the observed bands. The spectra were rescanned until no further changes took place. A single experiment frequently extended over several days. The reactant ratios will be expressed in terms of moles aluminum to moles titanium, and the aluminum compounds will be referred to in the discussion as monomers, their dimeric nature being understood. Moreover, the assignment to particular compounds of the various absorption bands found in the mixtures will not be discussed in detail, as they are obvious when reference is made to Figs. 1–6.

Figures 7 to 12 are the initial spectra at Al/Ti ratios of 1/3, 2/3, 1, 2, 8/3, and 4, respectively. At the equimolar reactant ratio, the initial reaction is simply

$$(CH_3)_3Al + TiCl_4 \rightarrow (CH_3)_2AlCl + CH_3TiCl_3. \quad [1]$$

At lower ratios, $(CH_3)_2AlCl$ also alkylates $TiCl_4$ to some degree, evidently achieving an equilibrium state, in agreement with Groenewege, according to the equation

$$(CH_3)_2AlCl + TiCl_4 \leftrightarrows CH_3AlCl_2 + CH_3TiCl_3. \quad [2]$$

At ratios >1, trimethyl aluminum further alkylates titanium tetrachloride to dimethyl titanium dichloride and apparently also when in sufficient excess to trimethyl titanium chloride, although this compound must have only a transient existence, since it is not observed directly. As excess trimethyl aluminum is present at the 4:1 ratio, complete alkylation is not achieved, at least under the conditions of these experiments. Thus,

$$2(CH_3)_3Al + TiCl_4 \rightarrow 2(CH_3)_2AlCl + (CH_3)_2TiCl_2 \quad [3]$$

$$3(CH_3)_3Al + TiCl_4 \rightarrow 3(CH_3)_2AlCl + (CH_3)_3TiCl \quad [4]$$

$$4(CH_3)_3Al + TiCl_4 \rightarrow 3(CH_3)_2AlCl + (CH_3)_3Al + (CH_3)_3TiCl. \quad [5]$$

At ratios of 1 and lower, the principal subsequent event was the photochemical decomposition of methyl titanium trichloride, which took place over periods of 50 to several hundred hours. This shifted the equilibrium of equation [2], causing dimethyl aluminum chloride and titanium tetrachloride to decrease in proportion. At the 1:3 ratio, all volatile products were eventually consumed, indicating an equilibrium according to the equation

$$CH_3AlCl_2 + TiCl_4 \rightleftarrows CH_3TiCl_3 + AlCl_3. \quad [6]$$

The equilibrium lies well to the left, as was independently shown by contacting pure CH_3TiCl_3 with anhydrous $AlCl_3$ to produce $TiCl_4$ almost quantitatively.

At the equimolar ratio, it was observed that, even in the dark, there was a very slow mutual disappearance of methyl titanium trichloride and dimethyl aluminum chloride. A product of this reaction was methyl aluminum dichloride, and the reaction must therefore have occurred according to the equation

$$(CH_3)_2AlCl + CH_3TiCl_3 \leftrightarrows (CH_3)_2TiCl_2 + CH_3AlCl_2. \quad [7]$$

Can. J. Chem. Downloaded from www.nrcresearchpress.com by 210.87.254.105 on 09/05/12
For personal use only.

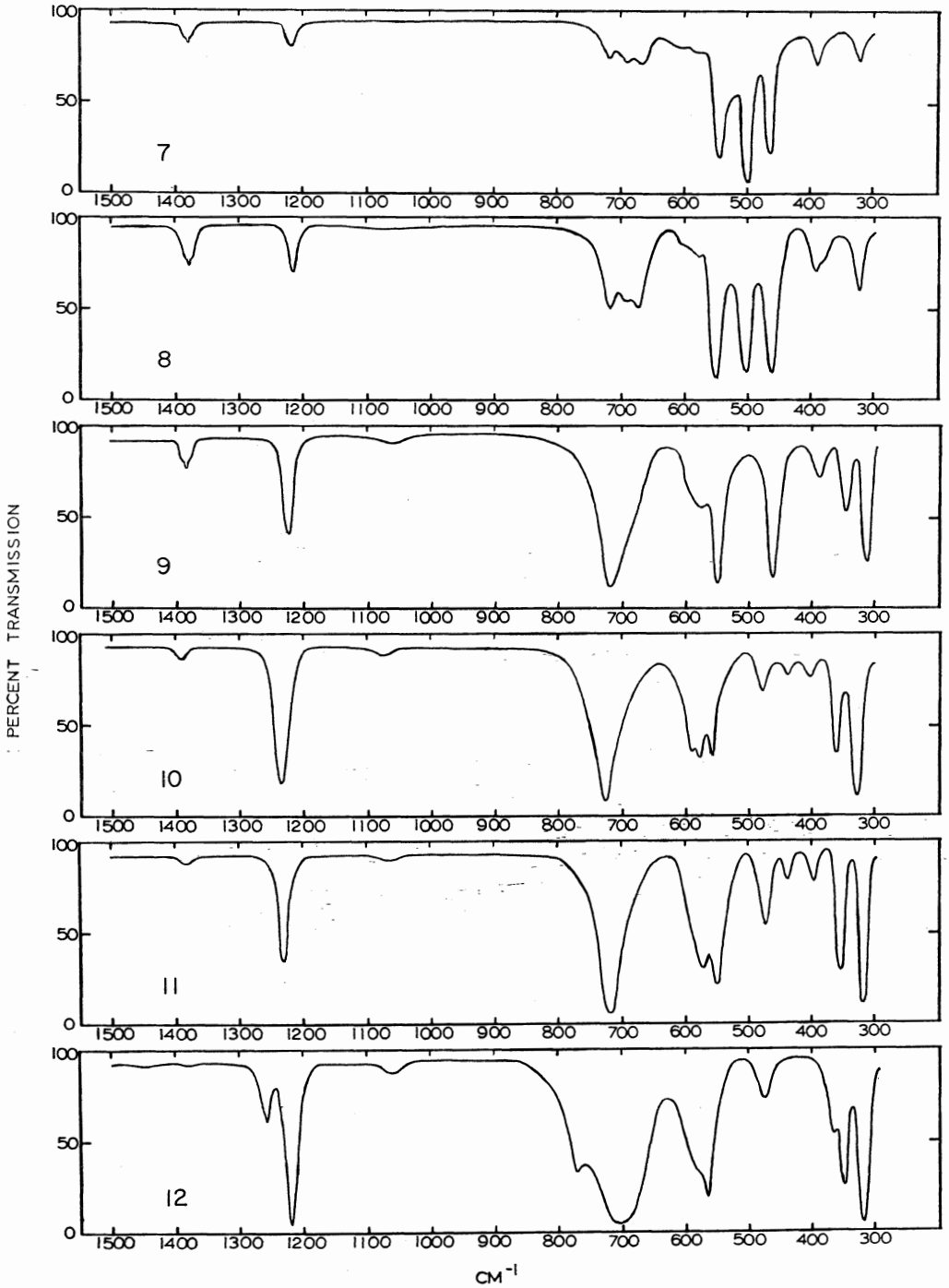

FIGS. 7–12. Reaction mixture spectra.

The equilibrium again lies far to the left, but is shifted by the decomposition of the thermally unstable dimethyl titanium dichloride.

Can. J. Chem. Downloaded from www.nrcresearchpress.com by 210.87.254.105 on 09/05/12
For personal use only.

At ratios >1, $(CH_3)_2TiCl_2$ decomposes thermally at essentially the same rate as when isolated from cocatalyst components.

That the nature of the catalyst-forming reactions found in the vapor phase is essentially the same in solution for the trimethyl aluminum – titanium tetrachloride system and, indeed, for longer-chain aluminum alkyls was demonstrated by subsequent unpublished work by C. T. Elston and, in some cases, by additional infrared data. For example, the transient existence of propyl titanium trichloride in hexane solution was shown by its synthesis from zinc dipropyl and titanium tetrachloride and the observation of absorption bands at 527, 483, and 386 cm^{-1}, which decreased together with time. An unexpected result of this same experiment was that titanium tetrachloride was found to increase as the titanium alkyl decomposed. This was the first time that this had been observed: it did not occur in the vapor phase decomposition studies and had not been noticed in our previous solution studies, where solid and supernatant phases were analyzed by usual methods. A subsequent careful infrared investigation of methyl titanium trichloride decomposition in cyclohexane, however, confirmed the generality of this phenomenon in solution. It was shown by quantitative calibration with known solutions of $TiCl_4$ that, upon completion of the reaction, one-half of the initial titanium content appeared as titanium tetrachloride. During the decomposition, which was followed over a period of 270 hours, the production of the tetrachloride was, moreover, directly correlated with the disappearance of the alkyl.

The usual thermal and photochemical mode of decomposition observed in our work and that of others results in the production of brown titanium trichloride and hydrocarbons:

$$CH_3TiCl_3 \rightarrow CH_3 + TiCl_3. \qquad [8]$$

The solid in this case is not an active catalyst. The production of titanium tetrachloride under the conditions of the infrared experiment is considered to have occurred via the disproportionation

$$2CH_3TiCl_3 \rightarrow (CH_3)_2TiCl_2 + TiCl_4. \qquad [9]$$
$$\downarrow$$
$$?$$

While other mechanisms are possible, this type of reaction is common in metal organic chemistry and offers a very satisfactory explanation of the infrared data. Since it has been demonstrated by ourselves and others that the decomposition of dimethyl titanium dichloride leads to an active catalyst, these observations at least partially account for those cases where activity has been observed at reactant ratios less than or equal to 1. At higher temperatures, the decomposition of methyl titanium trichloride is still more complex and is evidently autocatalytic, as shown by Beermann and Bestian (13).

CONCLUSIONS

The actual sequence of reactions occurring in the system appears to be the simplest imaginable and depends solely on the relative alkylating power of the various aluminum compounds and the stabilities of the titanium methyl products. The *absolute* reaction rates and stabilities for different aluminum alkyls and for different transition metal halides are quite variable, as shown, for example, by Beerman and Bestian (13). However, it seems probable that *relative* alkylating power and stabilities for the various components of other systems involving aluminum alkylating agents are the same as found for the trimethyl aluminum – titanium tetrachloride system.

The high efficiency of catalysts formed by the use of aluminum alkylating agents has

Can. J. Chem. Downloaded from www.nrcresearchpress.com by 210.87.254.105 on 09/05/12
For personal use only.

frequently been attributed to the formation of aluminum–titanium complexes which act as unusually active catalyst sites. This hypothesis may be necessary to account for the properties of certain stereospecific catalysts, but there seems to be no good reason to postulate complex formation in every case. Certainly there is no evidence for the formation of such complexes in this system. Independent gas phase kinetic studies carried out in this laboratory demonstrated that the catalytic activity of the decomposition products was only two or three times greater when decomposition occurred in the presence of "cocatalyst" components than when pure. If complex formation were necessary for catalytic activity, one would expect this difference to be several orders of magnitude. The particular efficacy of the aluminum alkylated catalysts could equally well be attributed to the more controlled and efficient production of active sites due to the gradation of alkylating power from the trialkyl to the dihaloalkyl. For example, the existence of slow acting, but effective, alkylating agents in equilibrium in the supernatant after initial catalyst formation may continuously generate active catalyst sites during the subsequent polymerization. This may be contrasted with the behavior of metal alkyls such as dimethyl zinc, where the second methyl group is effectively as powerful as the first in alkylating titanium tetrachloride. In this case, the initial reaction is rapid, complete, uncontrolled, and, one might expect, less efficient in producing the particular species which function as catalyst sites.

Although the decomposition products of the reactions were deposited in a uniform film over the cell body and windows, the thickness in the optical path was not sufficient for direct observation of the catalytically active species. The evolution of methane during the decomposition of the methyl titanium compounds was observed by infrared analysis, and methane, ethane, and ethylene were found and quantitatively determined by gas kinetic studies. Methyl groups, however, remain in the solid decomposition product at and above Al/Ti = 1. These observations, together with the fact that catalytic activity may be correlated with solid methyl content, strongly suggest that the modes of decomposition leading to catalytically active products are

$$(CH_3)_2TiCl_2 \rightarrow CH_3TiCl_2 + CH_3\cdot \quad [10]$$

$$(CH_3)_3TiCl \rightarrow CH_3TiCl + 2CH_3\cdot . \quad [11]$$

While these observations and conclusions are at variance with some suggested theories (14) concerning the catalytic activity of such systems, the available factual information from other sources can readily be interpreted in terms of the simple scheme that has been proposed.

In any event, it is apparent that the data considerably narrow the area of speculation permissible concerning the nature of the catalyst species. The body of evidence in our work suggests that the primary site of catalytic activity in this and analogous systems is the Ti—C bond. In view of the very large number of formulations which now appear to be effective in olefin polymerization and in the absence of sufficient detailed information regarding them, attempts to account for their activity in terms of any single hypothesis are premature. Nevertheless, it is clear that transition metal alkyl compounds must be accorded a more significant role in theories of catalyst activity than has sometimes been the case.

ACKNOWLEDGMENT

The authors wish to acknowledge the contribution of Mr. Heinz Demmler, who constructed the sensitive Pyrex spoon gauges essential to this investigation.

Can. J. Chem. Downloaded from www.nrcresearchpress.com by 210.87.254.105 on 09/05/12
For personal use only.

REFERENCES

1. E. J. BADIN. J. Phys. Chem. **63**, 1791 (1959).
2. R. HAVINGA and Y. Y. TAN. Rec. Trav. Chim. **79**, 56 (1960).
3. G. NATTA, P. PINO, G. MAZZANTI, and P. LONGI. Gazz. Chim. Ital. **87**, 553 (1957).
4. A. G. POZAMANTIV, A. A. KOROTKOV, and I. S. LISHANSKII. Vysokomolekul. Soedin. **1**, 1207 (1959).
5. A. SIMON, L. KOVACS, L. KOLLAR, and GY. DEZSENYI. Monatsh. Chem. **90**, 443 (1959).
6. R. VAN HELDEN, A. F. BICKEL, and E. C. KOOYMAN. Tetrahedron Letters, No. 12, 18 (1959).
7. K. ZIEGLER, H. MARTIN, and J. STEDEFEDER. Tetrahedron Letters, No. 20, 12 (1959).
8. M. P. GROENEWEGE. Z. Physik. Chem. (Frankfurt), **18**, 147 (1958).
9. A. P. GRAY. Can. J. Chem. This issue.
10. E. G. HOFFMANN. Z. Elektrochem. **64**, 616 (1960).
11. G. L. KARAPINKA, J. J. SMITH, and W. L. CARRICK. J. Polymer Sci. **50**, 143 (1961).
12. N. J. HAWKINS and D. R. CARPENTER. J. Phys. Chem. **23**, 1700 (1955).
13. C. BEERMANN and H. BESTIAN. Angew. Chem. **71**, 618 (1959).
14. H. UELZMANN. J. Polymer Sci. **32**, 457 (1958).

Can. J. Chem. Downloaded from www.nrcresearchpress.com by 210.87.254.105 on 09/05/12
For personal use only.

THE INFRARED SPECTRA OF TRIMETHYL ALUMINUM, DIMETHYL ALUMINUM CHLORIDE, METHYL ALUMINUM DICHLORIDE, METHYL TITANIUM TRICHLORIDE, DIMETHYL TITANIUM DICHLORIDE, AND SOME DEUTERIUM DERIVATIVES

A. P. GRAY[1]
Du Pont of Canada Limited, Research Centre, Kingston, Ontario
Received August 14, 1962

ABSTRACT

The vapor phase infrared spectra to 300 cm^{-1} are discussed and assignments made for the compounds $(CH_3)_6Al_2$, $(CD_3)_6Al_2$, $(CH_3)_4Al_2Cl_2$, $(CD_3)_4Al_2Cl_2$, $(CH_3)_2Al_2Cl_4$, CH_3TiCl_3, CD_3TiCl_3, and $(CH_3)_2TiCl_2$. The assignments differ significantly from those previously published, but are consistent throughout the series of aluminum compounds and with related spectra. The data are in agreement with a bridged structure for trimethyl aluminum of D_{2h} or C_{2h} symmetry and with a bridged structure of dimethyl aluminum chloride with chlorine bridging. The dimer $(CH_3)_2Al_2Cl_4$ is shown to exist in the trans configuration. Evidence is presented indicating that an impurity is commonly found in spectra of dimethyl aluminum chloride which is identified as the mixed dimer $(CH_3)_3Al_2Cl_3$, aluminum sesquichloride. A number of anomalies observed in the spectra of the methyl titanium compounds are pointed out and discussed.

INTRODUCTION

The compounds involved in the infrared spectroscopic study of the coordination catalyst system presented in the preceding paper (1) are in themselves of very considerable interest. Trimethyl aluminum is the simplest of a number of compounds known or suspected to be associated through bridge alkyl groups and has been the object of many investigational and theoretical studies. The halogen derivatives of trimethyl aluminum are similarly bridged dimers. Although there has been some controversy on the point (2–4), the bridging in these cases is through the halogen atoms. Alkyls of the transition elements are exceedingly rare and, in the case of titanium, only two which have reasonable stabilities have been isolated. The first was phenyltitanium triisopropylate, obtained by Herman and Nelson in 1952 (5), and the second, methyl titanium trichloride, was independently discovered a few years later by a number of workers concerned with coordination catalyst systems (1, 6). Dimethyl titanium dichloride is relatively unstable, but has a sufficient lifetime to allow infrared and possibly some other physical measurements to be made under the usual conditions.

In view of the unusual nature of these compounds, it is of interest to examine the spectra which have been briefly described in the preceding paper in considerably greater detail and to consider some others which are pertinent. It must be admitted, however, that the data to be discussed were for the most part incidental to the main object of the catalyst investigation and the experiments were not always as complete nor as well designed from the spectroscopic point of view as might be desired. Nevertheless, the information derived from the extension of the infrared data to 300 cm^{-1} and from the deuterium derivatives results in significant changes to previously made assignments which seem well founded. Since the spectra were in all cases those of the vapors at low pressure, relatively few fundamentals above 800 cm^{-1} were observed. The strong absorptions in the CsBr

[1]*Present address: Olin Mathieson Research Center, 275 Winchester Avenue, New Haven, Connecticut.*

Can. J. Chem. Downloaded from www.nrcresearchpress.com by 210.87.254.42 on 09/05/12
For personal use only.

region, however, are those most pertinent to structural considerations; and bands elsewhere are discussed only where relevant to the assignment of the skeletal modes.

EXPERIMENTAL

The preparation and origin of the compounds have been described (1). The fully deuterated trimethyl aluminum was obtained from Merck, Sharp and Dohme of Canada Limited, Research Chemicals Department, Montreal, Quebec. The infrared spectrum indicated that the material was of high isotopic purity. Fully deuterated dimethyl aluminum chloride was obtained as the only volatile product remaining 3 days after the reaction of deuterated trimethyl aluminum with titanium tetrachloride in the mole ratio Al/Ti = 1. The identity of this product was established by analogy with the product of the same reaction carried out several times using light trimethyl aluminum. This was identified as $(CH_3)_2AlCl$ by its independent preparation from $(CH_3)_3Al$ and HCl. A partial spectrum of deuterated methyl titanium trichloride was obtained during this same reaction shortly after mixing. The observed bands were associated with this compound on the basis of their correspondence with the rate of decomposition which had been found many times in the analogous undeuterated system.

The instrumentation and techniques employed have also been described (1). With the exception of the C—H stretching modes of trimethyl aluminum, which were measured with LiF in the Model 112, all other bands above 650 cm^{-1} were observed with NaCl optics in the Model 21. A minimum warm-up time of 4 hours was allowed prior to runs with CsBr. Calibrations in this region were derived from the lines of water vapor, carbon dioxide, and methanol recommended by Downie *et al.* (7).

RESULTS AND DISCUSSION

The observed absorption bands of the various compounds under consideration are summarized in Table I. The corresponding spectra are shown in Figs. 2 to 6 of the preceding paper and in three additional figures in this paper, Figs. 1–3. Reference to other spectra included among those of the preceding paper will sometimes be made.

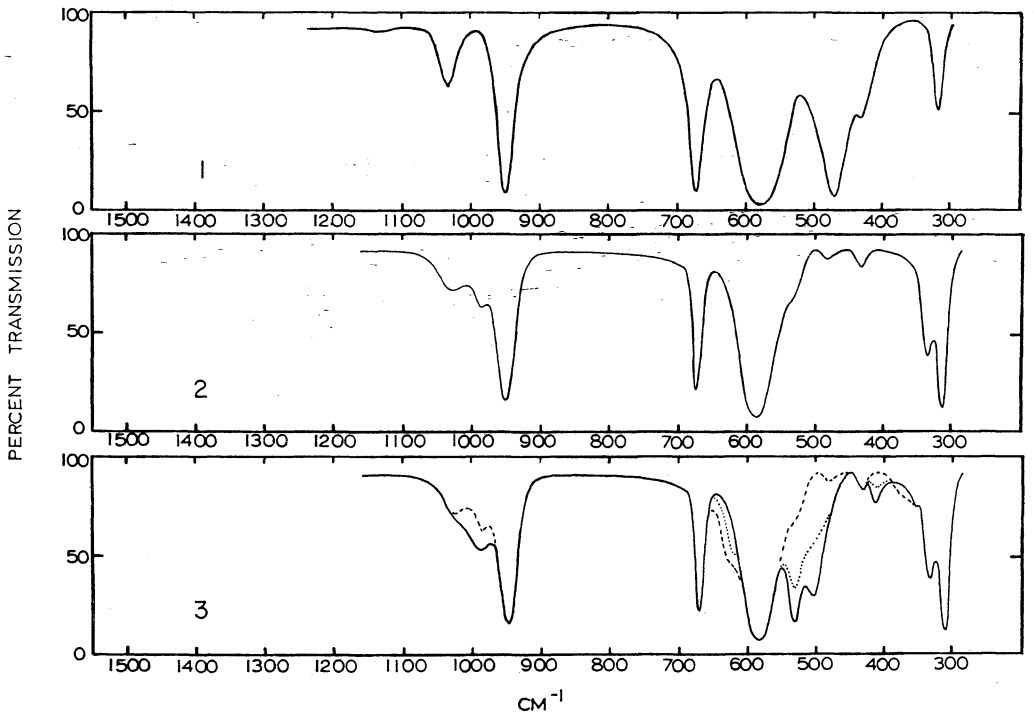

FIGS. 1–3. Deuterated compound spectra: 1, $(CD_3)_6Al_2$; 2, $(CD_3)_4Al_2Cl_2$; 3, $(CD_3)_6Al_2/TiCl_4$ = 1/2. — after mixing; .... 2 hours later; --- 3 days later.

Can. J. Chem. Downloaded from www.nrcresearchpress.com by 210.87.254.42 on 09/05/12
For personal use only.

Can. J. Chem. Downloaded from www.nrcresearchpress.com by 210.87.254.42 on 09/05/12
For personal use only.

TABLE I

Infrared Spectra

$Al_2(CH_3)_6$	$Al_2(CH_3)_4Cl_2$	$Al_2(CH_3)_2Cl_4$	$Al_2(CD_3)_6$	$Al_2(CD_3)_4Cl_2$	$TiCl_3CH_3$	$TiCl_2(CH_3)_2$	$TiCl_3CD_3$
2941 s			2200 m				
2899 m			2170 w				
2837 w			2110 w				
1445 vw	1440 vw		1140 vw		1380 Q w	1380 w	
1255 m			1036 m	1030 w			
1208 s	1212 s		955 s	957 s			
1055 vw	1050 vw						
772 s			677 s	664 s			
700 vs	720 vs	700 m	579 vs	583 vs	550 s	550 s	530 s
652 w							
616 m	588 R } m	675 m	472 vs	530 w	464 s	462 m	405 w
572 s	581 P }	587 m	435 m	483 ? w	391 w	427 w	
480 m	487 ? w	483 s	315 m	430 ? w		396 w	
369 s	440 ? w	423 ? m		331 m			
	343 m	310 m		307 s			
	310 s						

Trimethyl Aluminum

The generally accepted model of trimethyl aluminum dimer is that of Lewis and Rundle, who from X-ray data showed the skeletal symmetry of the molecule to be D_{2h}, the plane of the outer Al—C bonds being perpendicular to the plane of the bridge (8). The disposition of the methyl hydrogens of the bridge is not known, but if free-rotating, the effective overall symmetry of the molecule remains D_{2h}.

Infrared data on trimethyl aluminum have been reported by Pitzer and Gutowsky (9), Pitzer and Sheline (10), Schomburg (11), and more recently by Hoffmann (12). Previous work has been limited to the NaCl and KBr regions, and no deuterium analogues have been studied. The infrared data, together with the Raman results of Kohlrausch and Wagner (13) and of Hoffmann (12), are consistent with a dimeric formulation of symmetry D_{2h} or C_{2h} based on the number of observed fundamentals and the general absence of Raman–infrared coincidences.

The normal modes which are expected to give rise to infrared absorption or Raman scattering in the frequency range 800 to 300 cm^{-1} and their approximate descriptions are given in Table II, listed according to the symmetry species of the D_{2h} point group. Methyl deformations taking place perpendicular to the planes containing the carbon atoms are referred to as "wags", while those parallel to these planes are "rocks". The A_g and B_g species are Raman active, the B_u species are infrared active, and A_u is inactive in both infrared and Raman.

Previous authors have numbered the skeletal normal modes according to the scheme of Bell and Longuet-Higgins (16). To facilitate comparison, they are similarly numbered in Table II. Nonskeletal modes will be referred to by their approximate description and symmetry species. Where applicable, Table II also contains the frequency ratios of the corresponding modes in light and deuterated compounds.

The assignments given in Table II for the infrared-active species of trimethyl aluminum have been arrived at by application of the usual principles of vibrational analysis and by some arguments based on analogous systems. For example, since methyl rocking modes for dimethyl zinc and dimethyl mercury were found by Gutowsky at 707 and 787 cm^{-1}, respectively (15), it was considered unlikely that nonbridged methyl deformations would fall below 600 cm^{-1}. Bridge methyl deformations, on the other hand, where they occur in the same symmetry species as a skeletal bridge mode, might be expected to interact strongly and fall in frequency. The significance of shifts produced by deuterium substitution was determined by consideration of the deuterium displacements for the methyl deformation bands, 1440 to 1140 cm^{-1}, 1260 to 1036 cm^{-1}, and 1215 to 955 cm^{-1}, which are 1.26, 1.21, and 1.27, respectively. Modes exhibiting shifts in the range 1.2 to 1.3 were therefore considered to be primarily associated with methyl group vibrations, while a ν_H/ν_D ratio tending toward 1.09 was taken to indicate an approach to pure CH_3—Al stretching. Intermediate values are produced by a mixing of modes within the symmetry species. A useful criterion for the correctness of the assignment was the degree of consistency obtained by comparison with the closely related methyl aluminum halides and with the corresponding Raman spectra.

The correlation of the frequencies which has been chosen and indicated in Table II is considered to be the most satisfactory. However, it will be found to differ considerably from those previously proposed. Since the correct assignment of the band at 772 cm^{-1} in trimethyl aluminum is the key to the interpretation which is offered, it is considered in detail.

Comparing the spectrum of trimethyl aluminum (Fig. 2, preceding paper) with that of

Can. J. Chem. Downloaded from www.nrcresearchpress.com by 210.87.254.42 on 09/05/12
For personal use only.

Can. J. Chem. Downloaded from www.nrcresearchpress.com by 210.87.254.42 on 09/05/12
For personal use only.

TABLE II

Assignments

D_{2h} species	Approximate description	$Al_2(CH_3)_6$	ν_H/ν_D	$Al_2(CD_3)_6$	$Al_2Cl_2(CH_3)_4$	ν_H/ν_D	$Al_2Cl_2(CD_3)_4$	$Al_2Cl_4(CH_3)_2$	Al_2Cl_6
	Outer CH_3 rock								
A_g	Al—X stretch ν_1	592*			588*			582 492‡	506§
	Bridge stretch ν_2	453			330			342	340
	Al(X)(X) bend ν_3	313			282				217
A_u	Outer CH_3 wag								
	Outer CH_3 wag								
B_{1g}	Bridge CH_3 rock	632 ??†							
	Bridge stretch ν_6	495 ??							438
B_{2g}	Outer CH_3 rock	725			713			689	606
	Al—X stretch ν_{11}	683			620				
B_{3g}	Outer CH_3 wag								
	Bridge CH_3 wag								
	Al—X stretch ν_8	772	1.14	677	720	1.08	664		625
B_{1u}	Outer CH_3 rock	700	1.21	579	700	1.20	583		
	Bridge CH_3 wag	700	1.21	579					
	Outer CH_3 wag							675	
B_{2u}	Bridge stretch ν_{13}	652 ?						423 ?	420
	Outer CH_3 rock	700	1.21	579	700	1.20	583	700	
	Bridge CH_3 rock	572	1.21	472					
B_{3u}	Al—X stretch ν_{16}	616	1.08	570	585	1.10	530	587 483	484
	Bridge stretch ν_{17}	480	1.10	435	310	1.01	307	310	301
	Al(X)(X) bend ν_{18}	369	1.17	315	343	1.04	331		

*Raman data, ref. 12.
†For questionable assignments, see text.
‡Raman data, ref. 2.
§Infrared and Raman data, observed and calculated, ref. 14.

dimethyl aluminum chloride (Fig. 3, preceding paper), it is first observed that there is no band in the latter corresponding to the 772 cm^{-1} absorption, which suggests that it is in some way associated with the methyl bridges. Hoffmann, in fact, has assigned this band to the B_{3u} bridge methyl rock, additional evidence being cited based on mixed alkyl aluminum dimers with methyl bridging, which, at the time of this writing, has not been published. However, the corresponding band in the deuterium compound must be that found at 677 cm^{-1}, $\nu_H/\nu_D = 1.14$, which indicates that the band is more probably an Al—C stretch. This band is therefore taken to be ν_8. The deuterated spectrum of dimethyl aluminum chloride above 500 cm^{-1} (Fig. 2) is seen to be remarkably similar to that of deuterated trimethyl aluminum in contrast with those of the corresponding parent molecules (Figs. 2 and 3, preceding paper). This observation is critical, as it is especially difficult to rationalize this behavior on the basis of Hoffmann's assignment. The 664 cm^{-1} band in deuterated dimethyl aluminum chloride obviously corresponds to 677 cm^{-1} in deuterated trimethyl aluminum. It is of interest to apply the observed deuterium shift of the former band to the latter to arrive at a predicted position of ν_8 in trimethyl aluminum. The result, $1.08 \times 677 = 731$, is seen to be some 40 cm^{-1} lower than the observed value. This is, however, readily accounted for on the basis of a strong interaction with modes of the same species. The B_{1u} species for trimethyl aluminum contains three modes which reasonably may be expected to fall near 700 cm^{-1}: ν_8, an outer methyl rock, and a bridge methyl wag. Assuming accidental coincidence of two or all three of these at approximately 730 cm^{-1}, the displacement of ν_8 to 772 and of the other modes to approximately 700 cm^{-1} is readily understood. This hypothesis accounts for the observed features of the spectra; the interaction does not take place in dimethyl aluminum chloride due to the absence of the bridge methyl wag, and the similarity of the deuterated spectra of trimethyl aluminum and dimethyl aluminum chloride is due to the removal of the interaction on separating ν_8 from the methyl deformation modes.

The tentative assignment of the B_{2u} bridge mode, ν_{13}, to the relatively weak 652 band deserves some comment. Since ν_{13}, by analogy with Klemperer's assignment for aluminum chloride, is expected to be one of the higher bridge modes, it should be in the 600 cm^{-1} region. B_{2u} absorptions are, however, universally found to be weak in the series of compounds with which we are concerned and this mode may not be observed, particularly in this area of heavy overlapping in both light and heavy compounds. Its assignment to 652 cm^{-1} is, however, not unreasonable. While it could equally well be the B_{2u} outer methyl wag, a corresponding outer methyl wag is found at 675 cm^{-1} in methyl aluminum dichloride, and if anything, the trimethyl aluminum mode would be expected to be higher.

The Raman assignments of ν_1, ν_2, ν_3, and ν_{11} are in agreement with those of Hoffmann (12) and previous workers (3, 13). The depolarized 725 cm^{-1} band is taken to be the B_{2g} outer methyl rock solely on the grounds that the other Raman species seem to be weak, only two depolarized Raman lines being found above 300 cm^{-1}. Two other polarized lines are found, however: a weak 632 cm^{-1} shoulder and a quite strong line at 495 cm^{-1}. Hoffmann has assigned the latter to the A_g outer methyl rock. As previously discussed, this is considered to be too low for such a mode, and it would be preferable to consider it as an overtone enhanced by Fermi interaction with ν_2. However, it is interesting to note that the only significant consequence of the molecule's having a symmetry of C_{2h} rather than D_{2h}, but with the same principal axis of symmetry, is that the B_{1g} modes become totally symmetric. If this were the case, then the 632 and 495 cm^{-1} lines would be accounted for by the B_{1g} bridge methyl rock and the bridge stretch, ν_6. A Raman study of the deuterated

Can. J. Chem. Downloaded from www.nrcresearchpress.com by 210.87.254.42 on 09/05/12
For personal use only.

compound would be most helpful in settling this matter, but this information has not as yet been obtained.

Dimethyl Aluminum Chloride

The dimeric nature of this material has been established by Brockway and Davidson (17) by electron diffraction and by Davidson and Brown (18) by vapor pressure measurements. Infrared and Raman data have been reported by Groenewege (3) and by Hoffmann (12). Raman data on this compound, and on a variety of other halogen derivatives, were also reported by van der Kelen and Herman (2). It now seems well established that the bridging for this and analogous alkyl aluminum halides is through the halogen atoms.

Before proceeding with the new infrared data for this compound and its deuterium derivative, it is necessary to consider certain inconsistencies which appear in comparing both the present work and previously published spectra. The infrared spectrum of the vapor of dimethyl aluminum chloride (Fig. 3, preceding paper) shows two weak bands at 487 and 440 cm^{-1}. In solution, Hoffmann similarly finds two weak bands, one near 500 and the other at 443 cm^{-1}; the relative intensities are, however, reversed. Groenewege's solution spectra, on the other hand, only barely indicate absorption in this area, although a double-beam instrument was used and the intensity of the other bands indicates that it should be observed, if real. It is also noted that in Fig. 12, preceding paper, which is essentially a strong spectrum of dimethyl aluminum chloride containing some trimethyl aluminum, no 440 cm^{-1} band is found. Groenewege does not find the weak polarized lines at 480 and 410 cm^{-1} found by Hoffmann, although they are in agreement on other lines of comparable intensity. Groenewege has pointed out the discrepancies between his Raman work and that of van der Kelen and Herman, who found six additional lines at 94.5, 343, 480, 531, 685, and 727 cm^{-1}, all polarized. Groenewege considered the 480 and 531 lines as originating from 588 shifts of the *f* and *g* mercury lines, although Hoffmann finds the 480 line also.

All these observations are accounted for on the assumption that van der Kelen and Herman's material was quite heavily contaminated with aluminum sesquichloride, $(CH_3)_3Al_2Cl_3$, which evidently exists as a mixed dimer, and that the presently reported spectra, as well as Hoffmann's, are similarly but slightly impure. The sesquichloride is the initial product obtained in the usual preparation of dimethyl aluminum chloride from the reaction of methyl chloride and aluminum (19). The 487 cm^{-1} band in the infrared is probably an Al—Cl outer stretch and the 440 cm^{-1} band, a bridge mode of the sesquichloride corresponding to either ν_6 or ν_{13} in aluminum chloride, which occur at 438 and 420 cm^{-1}, respectively. Corresponding modes are found in the deuterated spectrum (Fig. 2) at 483 and 430 cm^{-1}. Note that the sesquichloride has no symmetry and all Raman lines are polarized, in agreement with those of the impurity.

Having disposed of these bands, the spectrum of dimethyl aluminum chloride dimer is seen to be quite simple, and the assignments follow from the discussion previously given for trimethyl aluminum. It is observed that the band centered at 585 cm^{-1} appears to be a doublet with maxima at 588 and 581 cm^{-1}, the lower frequency being somewhat stronger. However, a calculation of the expected band contour for a B_{3u} mode (20) predicts a separation of P and R branches of 6.8 cm^{-1}, in good agreement with that observed. Evidently, the Q branch is diffuse and shifted to lower frequency for this particular mode due to a difference in upper- and lower-state inertial moments and the population of many *K* levels (21). This behavior is common for heavy molecules.

Can. J. Chem. Downloaded from www.nrcresearchpress.com by 210.87.254.42 on 09/05/12
For personal use only.

The assignment of the Raman modes in this region is essentially the same as that of Groenewege (3).

Methyl Aluminum Dichloride

The infrared spectrum of this compound has been reported by Groenewege (3, 4) and the Raman by van der Kelen and Herman (2). A priori, there would seem to be little doubt, by analogy with its close relatives, that the molecule is dimeric and bridged through chlorine atoms, but one must consider three possible structures for the dimer, corresponding to those of dichloroethylene: the *trans*-1,2-dichloro (C_{2h}); *cis*-1,2-dichloro (C_{2v}); and 1,1-dichloro (C_{2v}) isomers.

The vapor phase spectrum of this compound is shown in Fig. 4, preceding paper. In order to obtain these bands with reasonable intensity, it was necessary to heat the gas cell to approximately 65° C. The spectrum was first scanned in the NaCl region with the Model 21 and was then transferred to the Model 112. No indication of any difficulty was noted until the cell was removed after the CsBr scan to be rerun on the 21. At this point, the contents became cloudy and a white crystalline material began to grow on the relatively cool cell windows. The subsequent NaCl spectrum indicated that the original compound had reacted, most probably because of a leak through the Kel-F stopcock grease, which has a high fluidity, even at these moderately elevated temperatures. Those bands in the CsBr spectrum which were not directly confirmed by observation in the reaction mixture spectra (Figs. 7 and 8, preceding paper) were considered questionable and are dashed in Fig. 4, preceding paper. Groenewege's spectrum is to be preferred.

A consideration of the selection rules for the various possible forms, utilizing the assignments which have been proposed for the compounds previously discussed, indicates that the observed spectra are those of the trans form. The cis isomer is predicted to have 13 infrared-active modes falling in the range 800 to 300 cm^{-1}, and the "symmetrical" isomer should have 11. Moreover, all of these should be Raman active. On the other hand, for the C_{2h} trans model one expects in the infrared, one methyl rock, one methyl wag, one Al—C stretch, one Al—Cl, stretch and two bridge modes. The observed bands fit this scheme extremely well, the corresponding modes being assigned to 700, 675, 587, 483, 402 (or 423), and 310 cm^{-1}, respectively. The Raman spectrum should show a similar distribution of lines, one methyl rock, one Al—C stretch, one Al—Cl stretch, and one bridge stretch (ν_2), all totally symmetric and therefore polarized. Depolarized lines should consist of one methyl wag and one bridge stretch (ν_6). Again, as seen in Table II, the Raman data of van der Kelen and Herman are in agreement with this scheme. The polarized methyl rock corresponding to that in A_g of the D_{2h} point group is not found, nor is the depolarized bridge stretch corresponding to ν_6. However, neither of these were found in any of the spectra of related molecules previously considered.

The assignments are collected in Table II, those associated with Cl modes and comparable to $AlCl_3$ to the right and those involving methyl modes and comparable to the methyl-containing compounds to the left of the column.

Methyl Titanium Trichloride

Infrared data on methyl titanium trichloride as a liquid have been reported by Karapinka, Smith, and Carrick (22) in the NaCl and KBr regions. They find a great many strong combination and overtone bands in addition to fundamentals at 1353, 530, and 460 cm^{-1}, which were also found by Groenewege (3) at 1366, 540, and 459 cm^{-1} in heptane solution. Groenewege attributed a band found by him at 498 cm^{-1} to an impurity, while

Can. J. Chem. Downloaded from www.nrcresearchpress.com by 210.87.254.42 on 09/05/12
For personal use only.

Karapinka *et al.* assigned a similar band at 490 cm^{-1} to the Ti—Cl unsymmetrical stretch. In both cases, this band is undoubtedly due to $TiCl_4$. No such absorption is found in the vapor phase spectrum of Fig, 5, preceding paper, where the fundamentals are located at 1380, 550, 464, and 391 cm^{-1}. Karapinka, Smith, and Carrick used the $TiCl_4$ combination band at 870 cm^{-1} as an indicator of $TiCl_4$ content, but since it is many times weaker than the 500 cm^{-1} fundamental, it is a relatively poor criterion of purity. Even if the sample of CH_3TiCl_3 were initially pure, $TiCl_4$ might well have been subsequently produced by the decomposition mechanism discussed in the preceding paper (1).

The simplest and most probable assumption to make as to the configuration of CH_3TiCl_3 is that, like $TiCl_4$, it is tetrahedral and therefore of C_{3v} symmetry. The skeletal stretching modes should consist of a degenerate —$TiCl_3$ stretch, a symmetrical —$TiCl_3$ stretch, and a symmetrical —Ti—CH_3 stretch. The symmetrical —$TiCl_3$ stretch is assigned to the 391 cm^{-1} band by analogy with the corresponding mode in $TiCl_4$, which is found at 386 cm^{-1} in the Raman effect. In the absence of any further information, one would have to agree with the reasoning of Groenewege in arriving at the assignment of the two remaining strong fundamentals in this region. Since, in all known comparable systems, the degenerate stretch is found at lower frequency than the corresponding mode in the T_d parent molecule, he has assigned his 459 cm^{-1} absorption to this vibration and consequently the 540 band to the Ti—C stretch.

Although the attempted preparation of CD_3TiCl_3 by reaction of $TiCl_4$ with $(CD_3)_3Al$ did not go as smoothly as might have been desired, two bands definitely attributable to this compound were identified at 530 and 405 cm^{-1} (Fig. 3). The band initially found in this spectrum at 500 cm^{-1} was definitely unreacted $TiCl_4$, which disappeared at a faster rate than the two other bands, which decreased in proportion. Additional evidence for the existence of CD_3TiCl_3 in this reaction mixture was the characteristic purple coloration of the condensate on freezing out with liquid nitrogen. The third fundamental was not located, although there was some evidence for a very weak band at 355 cm^{-1}. Previous experiments had shown that, as CH_3TiCl_3 decomposes, a broad band between 400 and 350 cm^{-1} grows in, which is due to the thin coating of $TiCl_3$ being deposited on the windows, so that the behavior of the indicated absorption at 355 cm^{-1} with time was difficult to determine.

In any event, since no band is found between 500 and 400 cm^{-1} other than that at 405 cm^{-1}, it must correspond to the 464 cm^{-1} in the light molecule. Otherwise, it would have to be assumed that the 464 absorption had so diminished in intensity on deuteration as not to be observed and that the 391 cm^{-1} band had shifted up to 405 cm^{-1}. Neither of these possibilities seems very likely. On the other hand, the deuterium shift 464 to 405 cm^{-1} ($\nu_H/\nu_D = 1.15$) seems quite large for a CH_3—Ti stretch, particularly since the product rule for the totally symmetric species would then limit the symmetrical methyl deformation to a shift of approximately 1.18, even if the symmetrical —$TiCl_3$ stretch did not shift at all. However, the small shift, 550 to 530 cm^{-1} ($\nu_H/\nu_D = 1.04$), is approximately that expected for the degenerate —$TiCl_3$ stretch, and everything considered, it seems necessary to reverse Groenewege's assignment and ascribe the 464 cm^{-1} band to the CH_3—Ti stretch. This departure from the usual behavior of non-transition-metal methyl-chloro compounds is but one example of several which are noted.

In particular, the unusually high value of what, at least initially, must be assumed to be the symmetrical methyl deformation at 1380 cm^{-1} has been discussed by Groenewege, who points out the very serious departure of this band from the electronegativity correlation of Sheppard (23) for previously studied methyl compounds. The observed PQR

Can. J. Chem. Downloaded from www.nrcresearchpress.com by 210.87.254.42 on 09/05/12
For personal use only.

structure and the magnitude of the PR splitting, however, tend to support the assignment to the symmetrical methyl deformation.

That CH_3TiCl_3 is monomeric and has the simplest formula indicated seems to have been well established (1, 5), and the tetrahedral conformation seems most reasonable, but the limited spectroscopic information obtained to date by no means proves this structure.

Dimethyl Titanium Dichloride

The infrared spectrum of $(CH_3)_2TiCl_2$ has not previously been reported. The vapor spectrum is shown in Fig. 6, preceding paper, the bands being found at 1380, 550, 462, 427, and 396 cm^{-1}. Again, the spectrum in the skeletal region is qualitatively what is expected for a tetrahedral compound of the given formula. By analogy with CH_3TiCl_3, the 550 absorption can be assigned to the unsymmetrical Ti—Cl stretch, the 396 band to the symmetrical Ti—Cl stretch, 462 to the unsymmetrical Ti—C stretch, and 427 to the symmetrical Ti—C stretch. Again, the essentially exact coincidence of the 550 and 462 cm^{-1} bands in this compound with those in CH_3TiCl_3 is unusual. The material is not detectably contaminated with CH_3TiCl_3, and its determined thermal stability is very much less than that of the monomethyl compound. In fact, on following the vapor phase decomposition of $(CH_3)_2TiCl_2$, the 462 cm^{-1} band was in the ratio of 1 to 2 with the 550 cm^{-1} band initially, but in the ratio of 1 to 4 towards the end of the decomposition. This behavior is opposite to that expected if the 462 band were due to CH_3TiCl_3, as this compound is the more stable, and one would anticipate that this ratio would approach 1:1 if it were a major contaminant. The change in relative intensities on dissociation does indicate, however, that two components of differing stabilities may be present. The 550 cm^{-1} band contour in the original spectra also indicates the presence of a fifth overlapping band on the high-frequency side. Trimethyl titanium chloride is not likely to be present, as it would be expected to have an extremely short lifetime, nor can any other volatile material be reasonably postulated, considering the method of preparation from $(CH_3)_2Zn$ and $TiCl_4$ in equimolar proportions.

A possible explanation of these observations is that $(CH_3)_2TiCl_2$ may have two isomeric configurations. A planar structure, although suggested with some reluctance, would more satisfactorily account for at least some of the anomalies.

The 1380 cm^{-1} band is again found, but with no resolvable structure. It is presumably a symmetrical methyl deformation.

In view of the spectroscopically unique behavior of the methyl titanium chlorides, a more thorough study than that presented is required in order to arrive at firm structural conclusions and band assignments. Since the deuterium analogues may be prepared readily and cleanly by reaction of $(CD_3)_2Zn$ with $TiCl_4$, data of higher quality may easily be obtained by extension of the preparative and spectroscopic techniques which have been described in this and the preceding paper.

Can. J. Chem. Downloaded from www.nrcresearchpress.com by 210.87.254.42 on 09/05/12
For personal use only.

REFERENCES

1. A. P. Gray, A. B. Callear, and F. H. C. Edgecombe. Can. J. Chem. This issue.
2. G. P. van der Kelen and M. A. Herman. Bull. Soc. Chim. Belges, **65**, 362 (1956).
3. M. P. Groenewege. Z. Physik. Chem. (Frankfurt), **18**, 147 (1958).
4. M. P. Groenewege. Rev. Universelle Mines, 9 Serie, **15**, 461 (1959).
5. D. F. Herman and W. K. Nelson. J. Am. Chem. Soc. **75**, 3877 (1953).
6. Farbwerke Hoechst. Belgian Patent No. 553,477 (1956).
7. A. R. Downie, M. C. Magoon, T. Purcell, and B. Crawford, Jr. J. Opt. Soc. Am. **43**, 942 (1953).
8. P. H. Lewis and R. E. Rundle. J. Chem. Phys. **21**, 986 (1953).
9. K. S. Pitzer and H. S. Gutowsky. J. Am. Chem. Soc. **68**, 2204 (1946).
10. K. S. Pitzer and R. K. Sheline. J. Chem. Phys. **16**, 552 (1948).
11. G. Schomburg. Dissertation, University of Aachen, Aachen. 1956.

12. E. G. HOFFMANN. Z. Elektrochem. **64**, 616 (1960).
13. K. W. F. KOHLRAUSCH and J. WAGNER. Z. Physik. Chem. Abt. B, **52**, 185 (1952).
14. W. KLEMPERER. J. Chem. Phys. **24**, 353 (1956).
15. H. S. GUTOWSKY. J. Chem. Phys. **17**, 128 (1949).
16. R. P. BELL and H. C. LONGUET-HIGGINS. Proc. Roy. Soc. (London), Ser. A, **183**, 357 (1945).
17. L. O. BROCKWAY and N. R. DAVIDSON. J. Am. Chem. Soc. **63**, 3287 (1941).
18. N. R. DAVIDSON and H. C. BROWN. J. Am. Chem. Soc. **64**, 316 (1942).
19. A. V. GROSSE and J. M. MAVITY. J. Org. Chem. **5**, 106 (1940).
20. R. M. BADGER and L. R. ZUMWALT. J. Chem. Phys. **6**, 711 (1938).
21. G. HERZBERG. Infrared and Raman spectra of polyatomic molecules. D. Van Nostrand Co., Inc., New York. p. 419.
22. G. L. KARAPINKA, J. J. SMITH, and W. L. CARRICK. J. Polymer Sci. **50**, 143 (1961).

Can. J. Chem. Downloaded from www.nrcresearchpress.com by 210.87.254.42 on 09/05/12
For personal use only.

OCCURRENCE OF D-GLUCURONIC ACID IN TAMARACK ARABINOGALACTAN[1]

B. URBAS,[2] C. T. BISHOP, AND G. A. ADAMS
Division of Applied Biology, National Research Council, Ottawa, Canada
Received February 13, 1963

ABSTRACT

The aldobiouronic acid 6-*O*-(β-D-glucopyranosyluronic acid)-D-galactose and D-glucuronic acid have been isolated from a hydrolyzate of an arabinogalactan from tamarack (*Larix laricina*). The identity of the aldobiouronic acid and the evidence for homogeneity of the polysaccharide showed that these acidic components are almost certainly constituents of the arabinogalactan.

Can. J. Chem. Downloaded from www.nrcresearchpress.com by 210.87.254.105 on 09/05/12
For personal use only.

During the past few years there have been numerous reports on the structural chemistry of water-soluble arabinogalactans from various coniferous woods. This topic has been included in recent reviews (1, 2) and it is clear that the major structural features of these polysaccharides are well established. However, as pointed out by Aspinall (1), several of these arabinogalactans contain small amounts (ca. 2%) of uronic acid. There has been no evidence to show whether these uronic acids are part of the arabinogalactan molecules or whether they occur in contaminating polysaccharides admixed with the arabinogalactans.

The present publication reports the isolation and identification of D-glucuronic acid and an aldobiouronic acid, 6-*O*-(β-D-glucopyranosyluronic acid)-D-galactose, from a hydrolyzate of an arabinogalactan from tamarack (*Larix laricina*). Evidence is presented to show that these acidic components almost certainly are constituents of the arabinogalactan.

The arabinogalactan was isolated from tamarack wood and gave no evidence of heterogeneity upon fractionation, free boundary electrophoresis, or ultracentrifugation (3). The main structural features of this polysaccharide were established by methylation studies (3) and by characterization of oligosaccharides produced by partial hydrolysis with acid (4). The results showed that the polysaccharide was a highly branched structure of 1 → 6- and 1 → 3-linked β-D-galactopyranose units to which L-arabinose units were attached, mainly in the form of the disaccharide unit 3-*O*-L-arabinopyranosyl-L-arabinofuranose.

Proof of the way in which the L-arabinose units are attached to the galactan portion of the molecule required isolation of an oligosaccharide which contained the arabinofuranosyl → galactose linkage. Two approaches to this problem were attempted: (*a*) enzymic hydrolysis and (*b*) Aspinall's application (5) of the Mehltretter (6) oxidation. No enzyme system could be found that would hydrolyze this polysaccharide to any significant extent and the oxidation was not successful. However, during the latter work the infrared spectrum of the arabinogalactan was recorded for comparison with the oxidized products. The unoxidized arabinogalactan showed a medium strength absorption band at 1625 cm^{-1} which was attributed to carboxyl groups. Chromatograms of a hydrolyzate of the arabinogalactan showed the presence of hexuronic acids; analysis (7) indicated 2–3% of uronic acid.

A large quantity of the arabinogalactan was hydrolyzed and the acidic components

[1]*Issued as N.R.C. No. 7326.*
[2]*National Research Council Postdoctoral Fellow, 1961–1963.*

were isolated by ion exchange resins. The mixture of acids was resolved by preparative paper chromatography to yield D-glucopyranuronic acid, and 6-*O*-(β-D-glucopyranosyluronic acid)-D-galactose. The first of these compounds was identified as crystalline D-glucofuranurono-(6 → 3)-lactone. The aldobiouronic acid yielded glucuronic acid and galactose on hydrolysis. On methylation the aldobiouronic acid gave a crystalline product having melting point and specific rotation in agreement with those reported for methyl 6-*O*-[methyl-(2,3,4,tri-*O*-methyl-β-D-glucosyl) uronate]-2,3,4-tri-*O*-methyl-β-D-galactoside (8, 9); the derived amide had a melting point in agreement with the reported value (9). As confirmatory evidence the fully methylated aldobiouronic acid was hydrolyzed to yield 2,3,4-tri-*O*-methyl-D-glucuronic acid and 2,3,4-tri-*O*-methyl-D-galactose, both characterized as crystalline derivatives.

It is extremely likely that these acidic components were part of the arabinogalactan, which should therefore be called an arabinogalactoglucuronoglycan. The polysaccharide was homogeneous upon fractionation, electrophoresis, and ultracentrifugation (3) and the known wood polysaccharides, if present as trace contaminants, could not give rise to 6-*O*-(β-D-glucopyranosyluronic acid)-D-galactose. The only uronic acid containing polysaccharides known to occur in woods are the glucurono- or arabino-4-*O*-methylglucuronoxylan and the pectic substances (1). In the former the glucuronic acid moiety is always joined to a D-xylose unit and the latter yields galacturonic rather than glucuronic acid on hydrolysis. Many plant gums which are exudates give rise to the same aldobiouronic acid as found in the present investigation (10). However, a gum could not have been a contaminant of the arabinogalactan which was extracted from wood from which the bark, and hence any exudates, had been removed.

Roudier and Eberhard (16) have isolated the same aldobiouronic acid from an acid hydrolyzate of maritime pine wood and reported that an arabinogalactoglucuronoglycan could be separated from the hot-water-soluble polysaccharides of that wood by fractionation. This was the first suggestion that this type of polysaccharide was present in wood. More recently Jones and Reid (17) have isolated an arabinogalactoglucuronoglycan from mountain larch. This polysaccharide contained 7.2% of uronic acid, yielded 6-*O*-(β-D-glucopyranosyluronic acid)-D-galactose on partial hydrolysis, and gave rise to 2,3,4-tri-*O*-methyl-D-glucuronic acid on methylation and hydrolysis. It is apparent that arabinogalactoglucuronoglycans may be of more widespread occurrence than has hitherto been indicated.

EXPERIMENTAL

Chromatograms were run by the descending method on Whatman No. 1 and No. 3 MM papers in the following solvent systems (v/v ratio): (A) ethyl acetate:water:acetic acid:formic acid, 18:4:3:1; (B) ethyl acetate:acetic acid:water, 3:1:3 (upper layer); (C) butanone saturated with water; (D) butanone:propan-1-ol:water, 5:3:2. Separated components were detected on the papers by the *p*-anisidine hydrochloride spray reagent (11). Solutions were evaporated under diminished pressure at 35° C or less, melting points are corrected, and all rotations are equilibrium values unless stated otherwise.

Polysaccharide

The isolation, fractionation, electrophoresis, and ultracentrifugation of the polysaccharide were described previously (3). The product showed $[\alpha]_D^{20}$ +12 (*c*, 4% in water); uronic acid, 2–3% (7); nitrogen, nil. The infrared spectrum in potassium bromide was recorded and showed the following absorption bands ((S)—strong, (M)—medium, (W)—weak) (frequencies in cm^{-1}); 3350 (S), 2890 (M), 1625 (M), 1375 (M), 1135 (S), 1050–1075 (S), 875 (W), 770 (W), 700 (W). Because the polysaccharide was devoid of nitrogen the absorption band at 1625 cm^{-1} could not represent amide groups from contaminating protein; this absorption was therefore attributed to uronic acid carboxyl groups.

Isolation of Uronic Acids

Heavily loaded chromatograms of a hydrolyzate of the polysaccharide (solvent A) showed the presence of glucofuranurono-3,6-lactone, glucuronic acid, and an aldobiouronic acid in addition to large amounts of

Can. J. Chem. Downloaded from www.nrcresearchpress.com by 210.87.254.105 on 09/05/12
For personal use only.

arabinose and galactose. The glucuronoarabinogalactan (65 g) was heated on a steam bath with *N* sulphuric acid (1300 ml) for 6 hours. The hydrolyzate was neutralized by barium carbonate, insoluble barium salts were removed by centrifugation, and the clear solution was passed through a column of Amberlite IR-120 ion exchange resin to remove soluble barium. Acidic components were then adsorbed on a column of Dowex 1-X4 (acetate form) which was washed with water until the neutral sugars had been removed (Molisch test). Uronic acids were eluted from the column with *N* formic acid; evaporation of the eluate yielded a mixture (0.5 g) of the acidic components, which was resolved by preparative paper chromatography (solvent A). Three compounds were recovered: D-glucofuranurono-3,6-lactone, D-glucuronic acid, and an aldobiouronic acid. The first two compounds were combined and crystallized from glacial acetic acid to yield D-glucofuranurono-3,6-lactone, m.p. 174–176° C unchanged on admixture with an authentic sample.

The aldobiouronic acid, which showed only one spot on chromatography in solvents A and B, was dissolved in water and neutralized by barium carbonate. The barium salt was precipitated from the aqueous solution by methanol as a white solid (0.28 g), $[\alpha]_D^{25}$ −5° (*c*, 2% in water). A sample (5 mg) of this product was heated with *N* sulphuric acid (1 ml) in a sealed tube at 100° C for 13 hours. Paper chromatography (solvent A) of the hydrolyzate showed the presence of glucuronic acid and galactose.

Methylation of Aldobiouronic Acid

The barium salt (0.28 g) was methylated twice by sodium hydroxide and dimethyl sulphate (12) and the product was recovered from the acidified solution by continuous extraction with chloroform for 3 days. The extract was dried (magnesium sulphate) and evaporated to yield a sirup (0.21 g) which was methylated twice by silver oxide and methyl iodide (13). The yellow, sirupy product (0.21 g) was distilled at 185–195° C (bath temperature) and 0.02 mm of mercury to yield the fully methylated aldobiouronic acid (0.15 g) having no hydroxyl absorption in the infrared. This product had $[\alpha]_D^{26}$ −32.3° (*c*, 1.3% in chloroform) and crystallized spontaneously after 1 week. Recrystallization from ether – light petroleum (b.p. 30–60° C) yielded methyl 6-*O*-[methyl-(2,3,4,tri-*O*-methyl-β-D-glucosyl) uronate]-2,3,4-tri-*O*-methyl-β-D-galactoside, m.p. 86–87° C; reported values for this compound are m.p. 94° C (8, 9), 86–87° C (14), $[\alpha]_D^{18}$ −35° (*c*, 1.2% in chloroform) (14).

In saturated methanolic ammonia the above compound yielded the derived amide, m.p. 194–195° C; N, 3.3%; calc. N, 3.09%; reported (9) m.p. 196° C.

Hydrolysis Products from Methylated Aldobiouronic Acid

The methylated aldobiouronic acid (0.14 g) was heated with *N* sulphuric acid (6 ml) at 95° C for 12 hours. The hydrolyzate was neutralized with barium carbonate and insoluble barium salts were removed by centrifugation and washed three times with water. The combined supernatant solutions were evaporated to dryness, yielding a yellow powder (0.11 g). This powder was extracted with dry ether and the extract was evaporated to give a sirup (0.05 g), $[\alpha]_D^{25}$ +64.6° (*c*, 3.08% in water), which had the same R_f value as 2,3,4-tri-*O*-methyl-D-galactose on paper chromatography in solvents C and D. The sirup was heated under reflux for 2 hours in a solution of absolute ethanol containing aniline (0.02 g). Ethanol was evaporated and the crystalline residue was recrystallized from ethyl acetate to yield *N*-phenyl-2,3,4-tri-*O*-methyl-D-galactosylamine (15), m.p. 164–165° C unchanged on admixture with an authentic sample, $[\alpha]_D^{25}$ +39° (*c*, 0.9% in methanol).

The ether-insoluble material was boiled under reflux for 7 hours with 3% methanolic hydrogen chloride (5 ml). The methanolyzate was neutralized with silver carbonate, filtered, and evaporated to a sirup. Extraction of this sirup with ether yielded methyl 2,3,4-tri-*O*-methyl-α-D-glucopyranosyluronic acid methyl ester, $[\alpha]_D^{22}$ +76° (*c*, 1.5% in water). This compound, in saturated methanolic ammonia, gave methyl 2,3,4-tri-*O*-methyl-α-D-glucopyranosyluronamide (15), m.p. 181–183° C, $[\alpha]_D^{22}$ +127° (*c*, 0.96% in water).

REFERENCES

1. G. O. Aspinall. Advan. Carbohydrate Chem. **14**, 429 (1959).
2. G. O. Aspinall. Ann. Rev. Biochem. **31**, 79 (1962).
3. G. A. Adams. Can. J. Chem. **38**, 280 (1960).
4. S. Haq and G. A. Adams. Can. J. Chem. **39**, 1563 (1961).
5. G. O. Aspinall and A. Nicolson. J. Chem. Soc. 2503 (1960).
6. C. L. Mehltretter. Advan. Carbohydrate Chem. **8**, 231 (1953).
7. R. M. McCready, H. A. Swenson, and W. D. MacLay. Ind. Eng. Chem., Anal. Ed. **18**, 290 (1946).
8. S. W. Challinor, W. N. Haworth, and E. L. Hirst. J. Chem. Soc. 258 (1931).
9. J. Jackson and F. Smith. J. Chem. Soc. 74 (1940).
10. F. Smith and R. Montgomery. The chemistry of plant gums and mucilages. Reinhold Publishing Corp., New York. 1959.
11. L. Hough, J. K. N. Jones, and W. H. Wadman. J. Chem. Soc. 1702 (1950).
12. W. N. Haworth. J. Chem. Soc. **107**, 8 (1915).
13. T. Purdie and J. C. Irvine. J. Chem. Soc. **83**, 1021 (1903).
14. A. J. Charlson, J. R. Nunn, and A. M. Stephen. J. Chem. Soc. 269 (1955).
15. F. Smith. J. Chem. Soc. 1724 (1939).
16. A. J. Roudier and L. Eberhard. Bull. Soc. Chim. France, 2074 (1960).
17. J. K. N. Jones and P. Reid. Abstracts, Fourth Cellulose Conference, Cellulose Research Institute, State University College of Forestry, Syracuse, New York. 1962.

Can. J. Chem. Downloaded from www.nrcresearchpress.com by 210.87.254.105 on 09/05/12
For personal use only.

THE ALKALINE CLEAVAGE OF *o*-NITROBENZYLTRIMETHYLSILANE SOLVENT EFFECTS IN THE DIOXANE–WATER SYSTEM

H. R. ALLCOCK[1]
Chemistry Department, University of Leicester, Leicester, England
Received January 16, 1963

ABSTRACT

The kinetics of alkaline cleavage of *o*-nitrobenzyltrimethylsilane were examined in aqueous dioxane media. At high water concentrations, increases in solvent polarity retard the cleavage, as required by a mechanism involving charge dispersion in the transition state. At high dioxane concentrations, solvent polarity increases are accompanied by increases in the rate of reaction, a result which may reflect association between the solvent components.

INTRODUCTION

Benzyl–silicon bonds are cleaved by alkali to yield toluene and silanol (1), and such reactions are known to be facilitated by electron-withdrawing substituents in the aromatic ring of the benzyl group (2). These reactions are believed to involve nucleophilic attack by hydroxide ion on silicon, either by a synchronous bimolecular (S_N2) process (i) or through the formation of a pentacovalent silicon intermediate (ii).

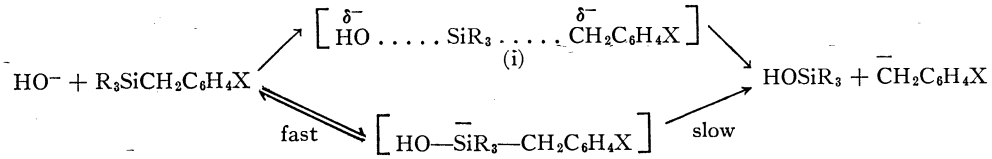

$$^{-}CH_2C_6H_4X + H_2O \longrightarrow CH_3C_6H_4X + OH^{-}$$

(where R is alkyl or aryl)

Eaborn and Parker (2) indicated that in both mechanisms the negative charge, formerly on the hydroxide ion, would become dispersed in the transition state, a fact which should render the reaction susceptible to solvent and salt effects. Since a charge delocalization would result in decreased solvation of the transition state, it can be predicted that an increase in the polarity of the solvent should bring about a small decrease in the rate of reaction (3). The same authors (2) found that the alkaline cleavage rates of several benzyltrimethylsilanes were faster in aqueous methanolic media which contained a higher proportion of water. However, they ascribed this result to the greater nucleophilicity of hydroxide ion than methoxide ion towards silicon, rather than to a solvent effect.

The present investigation was designed to study a solvent system which was free from complications of this type. The medium used was that of dioxane and water, and the silane chosen for this study was *o*-nitrobenzyltrimethylsilane. The rapid cleavage rate of this compound at very low alkali concentrations, coupled with the solubility in aqueous dioxane mixtures, made this silane particularly suitable for a study of solvent effects.

[1]*Present address: American Cyanamid Company, Stamford, Connecticut.*

Can. J. Chem. Downloaded from www.nrcresearchpress.com by 210.87.254.40 on 09/05/12
For personal use only.

EXPERIMENTAL

Materials

o-Nitrobenzyltrimethylsilane was prepared by the method described by Eaborn and Parker (2). The material used in this work was kindly provided by the same authors.

Distilled water was boiled for 30 minutes to expel dissolved carbon dioxide, and was then stored as described below.

Commercial dioxane (1 liter) was refluxed for 8 hours with *N* hydrochloric acid (1 liter) to hydrolyze ethylene acetal impurity. A steady stream of nitrogen was passed through the solution to remove volatile hydrolysis products. When cooled, the mixture was shaken with sodium hydroxide pellets to remove acid, water, and peroxides, and was allowed to stand overnight over the same reagent. The aqueous layer was separated from the dioxane, and the latter was refluxed for 3 days with finely divided sodium (20 g). The dioxane was then distilled in an all-glass apparatus designed to exclude moisture and, after rejection of the first 30 ml of distillate, the solvent was collected in a closed flask. The concentration of water in this solvent was determined by titration against Karl–Fischer reagent, and was found to be less than 0.5%.

Storage and Burette System

The cleavage of *o*-nitrobenzyltrimethylsilane required the use of very dilute alkali solutions and it was necessary, therefore, to store and measure solvents and reagent solutions in the absence of atmospheric carbon dioxide. The apparatus consisted of storage flasks connected to five microburettes, which were filled by suction, and which opened to the atmosphere through "carbazorb" carbon dioxide extractors and, where necessary, through phosphorus pentoxide drying tubes.

Stock Silane Solution

The silane stock solution was made up to a concentration of 7.5×10^{-4} *M* *o*-nitrobenzyltrimethylsilane in dry dioxane. The silane was weighed on a glass scoop and was washed rapidly with solvent into a graduated flask. The remainder of the solvent was then added after fitting the neck of the flask into a rubber stopper secured a short way up the nozzle of the dioxane-filled burette. The graduated flask was then connected by glass tubing to the microburette system. This procedure ensured that contamination by water vapor and carbon dioxide was reduced to a minimum.

Stock Alkali Solutions

The water-to-dioxane ratio was varied by mixing equal volumes of silane stock solution and diluted alkali solution, the latter being prepared in different mixtures of water and dioxane. A carbonate-free stock solution of 0.121 *N* sodium hydroxide in water was prepared and stored in a polyethylene bottle, which was connected by glass tubing to the appropriate burette. All subsequent alkali solutions were prepared from this stock, which was standardized from time to time against 0.1 *N* potassium hydrogen phthalate solution, using phenolphthalein as indicator. Kinetic measurements were made at three alkali concentrations, 9.65×10^{-3} *N*, 4.83×10^{-3} *N*, and 2.41×10^{-3} *N*, obtained by dilution of 4-ml, 2-ml, and 1-ml portions of the aqueous sodium hydroxide solution to 25 ml of the appropriate aqueous dioxane mixture in a closed flask. The diluted alkali solutions were then transferred by suction to the appropriate microburette. These solutions were prepared before each run and were used within 4 to 5 hours.

Method of Following Silane Cleavage

The disappearance of *o*-nitrobenzyltrimethylsilane was measured spectrophotometrically by the decrease in optical density at 330 mμ, using a Unicam S.P.500 spectrophotometer. The method utilized the difference in ultraviolet absorption spectra between the silane and its cleavage products, since the spectrum of *o*-nitrobenzyltrimethylsilane resembled that of *o*-nitrotoluene but was displaced towards the visible by about 7 mμ. Kinetic runs were carried out in stoppered silica cells contained in a thermoregulated brass block inside the cell compartment of the spectrophotometer. The electrically heated thermoblock contained vertical compartments for two 10-mm cells and apertures for the passage of light. Temperature regulation was by means of a Mullard temperature controller, type E.7594, connected to a thermistor at the base of the block. Temperature calibration was performed by immersing the bulb of a standardized thermometer into solvent contained in each cell, and cell temperatures were checked at regular intervals during the investigation. Temperature variations within the cells did not exceed ±0.02° C at 40° C.

Experimental Procedure

Silane stock solution (10 ml) was measured from the burette system into a 25-ml glass bottle. The bottle was protected from the atmosphere by a rubber stopper on the burette nozzle and by a carbon dioxide trap. By the same technique, diluted alkali in aqueous dioxane (10 ml) was added from the appropriate burette. The solutions were thoroughly mixed with a glass stopper in position. A portion of the mixture was then transferred rapidly by dropper to the prewarmed cell, and the cell stopper was placed in position. The momentary exposure to the atmosphere during filling of the cells appeared to have no effect on the reaction. The second cell was filled with a dioxane solvent blank.

Optical density readings were taken as soon as the solutions were in the cells, and the zero time reading

Can. J. Chem. Downloaded from www.nrcresearchpress.com by 210.87.254.40 on 09/05/12
For personal use only.

was obtained by extrapolation. The solutions reached the temperature of the thermoblock within 3 minutes of entering the cells at 40.15° C, and within 2 minutes at 30.23° C. This was demonstrated by the linearity of the kinetic plots after these times. Using this method, readings could be taken every 15 seconds and the kinetics of fast reactions could be followed accurately. Infinity values were obtained from optical density measurements at 10 times the half-life period. These readings were supplemented by values from portions of the reaction mixtures not used in the cell but placed in a closed reaction vessel in a thermostat bath for the required time. These values were also checked against synthetic end points prepared from solutions of *o*-nitrotoluene. All of the kinetic runs were performed in duplicate.

Calculation of Rate Constants

The rate constant k was calculated from the first-order equation of the form $k = [2.303/(t_2-t_1)] \log_{10} [(D_{t_1}-D_{t_\infty})/(D_{t_2}-D_{t_\infty})]$, where D_{t_1}, D_{t_2}, and D_{t_∞} are the optical densities at time t_1, t_2, and t_∞ respectively, determined at 330 mμ. The rate constants quoted are average values for duplicate runs. The first-order rate constants for a sample run are shown in Table I.

TABLE I

Variation of optical density and first-order rate constant during the alkaline cleavage of *o*-nitrobenzyltrimethylsilane ([NaOH], 4.83×10^{-3} N; temperature, 40.15° C; 26 vol% water in dioxane)

Time (min)	3	5	6	7	8	9	10	∞
10^3D (330 mμ)	636	577	552	529	510	492	474	318
10^3k (min^{-1})*	101	102	102	102	101	101	102	

*Graphical, $k = 1.02\times10^{-1}$ min^{-1}; duplicate run, $k = 1.00\times10^{-1}$ min^{-1}.

RESULTS AND DISCUSSION

Kinetic measurements were carried out in a series of water–dioxane mixtures containing from 8 to 75 vol% of water. The limitation of this system was that aqueous alkali solutions were immiscible with dioxane at high dioxane concentrations. This necessitated the use of low sodium hydroxide concentrations, in the range 2.42×10^{-3} N to 9.65×10^{-3} N, and required the use of special techniques to exclude carbon dioxide. Even so, the immiscibility of some solutions made it impossible to examine accurately the region below 16 vol% water at the highest alkali concentration. The results are shown in Table II.

TABLE II

Variation of first-order rate constants* with solvent, alkali concentration, and temperature

	30.23° C		40.15° C	
Vol% water in dioxane	[NaOH] 9.65×10^{-3} N	[NaOH] 4.83×10^{-3} N	[NaOH] 4.83×10^{-3} N	[NaOH] 2.41×10^{-3} N
8		157	312	
10		303	549	222
12		382	649	
16	1210	477	879	
26	1450	596	1010	
36	1490	594	1050	401
50	1260	479	838	
75	529	222	464	
	218†			

*Values quoted are 10^4k (min^{-1}).
†2 M $NaClO_4$ added.

The cleavage reactions were found to be first order in silane, reasonable constancy for the first-order rate constant k being obtained throughout a run. An exception to this behavior was provided by the reactions at the lowest water concentrations (8%), where first-order constants were maintained for the first 50% of the reaction only, a rapid falloff in rate being evident after that point. Evidence was obtained that this anomaly was due

Can. J. Chem. Downloaded from www.nrcresearchpress.com by 210.87.254.40 on 09/05/12
For personal use only.

to removal of alkali by a very slow reaction with residual traces of peroxide. This side reaction did not affect initial rates at low water concentrations and had no significant effect on reactions in media which contained more than 8% water. The rate changes which were observed in different water–dioxane mixtures can thus be attributed to solvent effects.

Cleavage rate measurements at different alkali concentrations demonstrated that the specific rate constant k_s (k/[NaOH]) invariably decreased on moving from a higher to a lower alkali concentration, even though the kinetic plots indicated that alkali was not consumed during the reaction. This may reflect a change in the order of reaction with respect to the alkali, a feature which contrasts with related kinetics in aqueous methanolic media (2).

The results in Table II show that the reaction rate was influenced by changes in the water-to-dioxane ratio of the solvent. As the water content of the medium was increased from 8 to 36 vol% the rate of cleavage increased to a maximum. The position of this rate maximum, between 26 and 36 vol% water, was not changed by the temperature variation or by the change in alkali concentration. As the water content of the solvent was increased above 36 vol%, a moderate decrease in the rate of reaction was evident.

For a reaction between an ion and a dipolar molecule, a plot of log k against the reciprocal of the dielectric constant of the medium should give a straight line of positive slope if the solvent effect is entirely dependent on changes in the solvent polarity (4, 5). The plot for this reaction is shown in Fig. 1. The curves show that, although the reaction may be

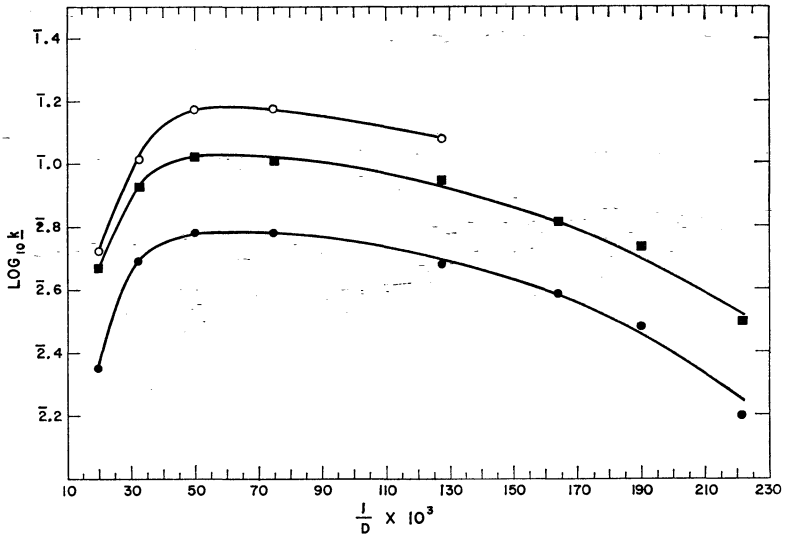

FIG. 1. Plot of the logarithm of rate constants versus the reciprocal of the dielectric constant of the water–dioxane solvent system. ○ [NaOH], 9.65×10^{-3} N; 30.23° C. ■ [NaOH], 4.83×10^{-3} N; 40.15° C. ● [NaOH], 4.83×10^{-3} N; 30.23° C.

dependent on the dielectric constant of the solvent at high water ratios in the manner predicted by theory, this interpretation is not valid in solvents containing less than 36 vol% water.

Rate constants were measured at 30.23° C and 40.15° C over a range of water concentrations from 8 to 75 vol% using 4.83×10^{-3} N sodium hydroxide. Activation energies and $\log_{10} A$ factors calculated from these values are listed in Table III. Changes in the rate

Can. J. Chem. Downloaded from www.nrcresearchpress.com by 210.87.254.40 on 09/05/12
For personal use only.

TABLE III

Activation energies and $\log_{10} A$ factors

Vol% water in dioxane	E (kcal/mole)	$\log_{10} A$
8	13.1	9.95
10	11.3	9.00
12	10.1	8.16
16	11.7*	9.41*
26	10.1	8.35
36	10.9	8.94
50	10.7	8.71
75	14.1	10.80

*The abnormal deviations for these values are probably due to experimental error.

of reaction are related to changes in both the activation energy and the frequency factor, since both E and $\log_{10} A$ reach a minimum in solvents which contain 12 to 26 vol% water. The absence of a simple linear relationship between E and $\log_{10} A$ over the whole range of solvent polarity changes suggests that water–dioxane mixtures which contain less than about 26 vol% of water have different solvation properties from those which contain a higher proportion of water (6).

The results of the present investigation demonstrate that, for solvent variations between 26 and 75 vol% water in dioxane, the reaction rate is decreased slightly by increases in the dielectric constant of the solvent, an effect which is consistent with the proposed reaction mechanism. The anomalous rate changes in the 8 to 26 vol% water region can be explained in terms of deviations from ideal solvation behavior. Deviations from ideal behavior in the water–dioxane system have been reported previously. The fluidity of water–dioxane mixtures reaches a minimum in the 40 to 50% water region (7, 8), and the density reaches a maximum at 32 wt% water (9). The kinetics of the exchange reaction and hydrolysis of *p*-nitrobenzyl bromide in water–dioxane mixtures show deviations from ideal behavior in media which contain less than 26 vol% of water (10). There is ample evidence that anomalous behavior of this type is due to hydrogen bonding between water and dioxane (11–14), which may reach a maximum in the 30 to 50% water region.

Hydrogen bonding within a solvent will seriously affect the nature of the solvation sheaths surrounding the reactants and the transition state, and will create local polarity effects in the vicinity of the reacting species which are not characteristic of the bulk solvent. It is possible that, as the dioxane concentration is increased beyond a limiting value, hydrogen bonding leads to the incorporation of dioxane molecules into the aqueous solvation sheaths of the polar species. At the highest dioxane concentrations it is likely that ionization of the alkali is retarded due to the absence of free water molecules.

ACKNOWLEDGMENTS

The author wishes to thank Professor C. Eaborn for suggesting the topic and for his helpful advice and interest. A Research Scholarship from the University of Leicester is gratefully acknowledged.

REFERENCES

1. C. Eaborn. Organosilicon compounds. Butterworths Scientific Publications Ltd., London. 1960. p. 143.
2. C. Eaborn and S. H. Parker. J. Chem. Soc. 126 (1955).
3. C. K. Ingold. Structure and mechanism in organic chemistry. G. Bell and Sons Ltd., London. 1953. pp. 345, 360.

Can. J. Chem. Downloaded from www.nrcresearchpress.com by 210.87.254.40 on 09/05/12
For personal use only.

4. K. J. LAIDLER. Chemical kinetics. McGraw-Hill, New York. 1950. Chap. 5.
5. K. J. LAIDLER and P. A. LANDSKROENER. Trans. Faraday Soc. **52**, 200 (1956).
6. J. E. LEFFLER. J. Org. Chem. **20**, 1209 (1955).
7. J. A. GEDDES. J. Am. Chem. Soc. **55**, 4832 (1933).
8. L. W. ÖHOLM. Finska Kemistsamfundets Medd. **48**, 19 (1938).
9. V. S. GRIFFITHS. J. Chem. Soc. 1326 (1952).
10. J. W. HACKETT and H. C. THOMAS. J. Am. Chem. Soc. **72**, 4962 (1950).
11. H. F. COOK. Trans. Faraday Soc. **47**, 751 (1951).
12. J. B. HASTED, G. H. HAGGIS, and P. HUTTON. Trans. Faraday Soc. **47**, 577 (1951).
13. J. DALY and C. G. SMITH. J. Chem. Soc. 2779 (1953).
14. R. L. STALLARD and E. S. AMIS. J. Am. Chem. Soc. **74**, 1981 (1952).

Can. J. Chem. Downloaded from www.nrcresearchpress.com by 210.87.254.40 on 09/05/12
For personal use only.

A NEW ASPIDOSPERMA ALKALOID: O-DEMETHYLASPIDOCARPINE[1]

C. FERRARI,[2] S. MCLEAN,[2] LÉO MARION, AND K. PALMER[2]
Division of Pure Chemistry, National Research Council, Ottawa, Canada
Received February 20, 1963

ABSTRACT

From the stem bark of *Aspidosperma album* four alkaloids have been isolated. Two of these (aspidoalbine and its N-acetyl-N-depropionyl homologue) have been reported recently and their structures established by Djerassi and his co-workers. The other two consist of aspidocarpine, and a new alkaloid, the structure of which has been determined. It is O-demethylaspidocarpine.

Can. J. Chem. Downloaded from www.nrcresearchpress.com by 210.87.254.105 on 09/05/12
For personal use only.

The alkaloids of the stem bark of *Aspidosperma album* (Vahl) R. Dent., collected in British Guiana,[3] have been under investigation in this laboratory for some time. A recent publication (1) reporting the structures of two alkaloids occurring in this plant prompts us to place on record some of our results.

Four bases have been isolated from the bark. Of these, alkaloids I and II are identical with aspidoalbine I*a* and its N-acetyl-N-depropionyl homologue I*b*, whose structures have

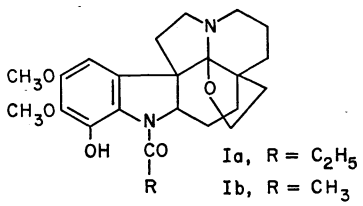

Ia, R = C_2H_5
Ib, R = CH_3

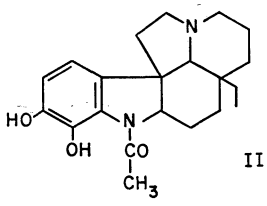

II

been determined by Djerassi[4] and his co-workers (1). Since they did not succeed in effecting a clean separation of these two bases and did not report the physical properties of the lower homologue, we now describe a method of separation and record the physical properties of both alkaloids (cf. Experimental). Thin layer chromatography tests showed that the method of separation was effective and produced both alkaloids in a chromatographically pure state.

Alkaloid I and its O-methyl derivative were compared directly with samples of aspidoalbine and O-methylaspidoalbine kindly supplied by Dr. C. Djerassi and found to be respectively identical. Alkaloid II analyzed correctly for N-depropionyl-N-acetylaspidoalbine. Both n.m.r. and infrared spectra indicated the presence of a hydrogen-bonded N-acetyl carbonyl. Alkaloid II gave rise to an O-methyl derivative which, although it had an infrared spectrum superimposable on that of N-depropionyl-N-acetyl-O-methylaspidoalbine, did not yield satisfactory analytical figures. The methyl derivative was hydrolyzed with hydrochloric acid and the product treated with propionic anhydride and pyridine. The purified product of the reaction showed no depression in melting point when mixed with O-methylaspidoalbine, and the two substances had the same optical rotation

[1]*Issued as N.R.C. No. 7320.*
[2]*National Research Council of Canada Postdoctoral Fellow.*
[3]*The plant material was obtained through the courtesy of Mr. R. Smeathers, Conservator of Forests, Kingston, Georgetown, British Guiana, whom we thank most cordially.*
[4]*We wish to thank Dr. C. Djerassi and Dr. B. Gilbert for their courtesy in giving us an advance copy of their manuscript.*

and superimposable infrared spectra. Hence alkaloid II is N-depropionyl-N-acetyl-aspidoalbine.

Alkaloid III appeared to be a new base not previously described while the fourth alkaloid proved to be identical in every respect with aspidocarpine (2). Alkaloid III was obtained from the ether eluate of a chromatogram of the crude alkaloids on a kieselguhr/phosphate buffer column. Its analytical figures corresponded to the empirical formula $C_{21}H_{28}O_3N_2$ (m.p. 156–158°). It was soluble in aqueous sodium hydroxide but not in sodium carbonate, and gave a violet coloration with a ferric chloride solution, so that at least one of its three oxygens must be present in a phenolic hydroxyl. It formed a monohydrochloride, m.p. 283°, and hence of the two nitrogens in the alkaloid one only appeared to be basic.

The n.m.r. spectrum of alkaloid III shows a striking resemblance to that of pyrifoline (3) and of aspidocarpine (2) except for the signals corresponding to the two methoxyl groups of the former and the one methoxyl of the latter, which are absent. The peak ($\delta = 11.0$) corresponding to the hydrogen-bonded hydroxyl in the n.m.r. spectrum of aspidocarpine (2) is also found in that of alkaloid III ($\delta = 11.3$). The ultraviolet spectrum (λ_{max} 227 mμ, log ϵ 4.25; 264 mμ, log ϵ 3.85) was similar to that of aspidocarpine (λ_{max} 228 mμ, log ϵ 4.42; 263.5 mμ, log ϵ 3.92). The infrared absorption spectrum contained bands indicative of hydroxyl groups and of an amide carbonyl. Since alkaloid III contained no methoxyl and its empirical formula contained CH_2 less than that of aspidocarpine it was thought probable in view of the foregoing spectral similarities that it could be O-demethylaspidocarpine. If alkaloid III be assumed to have the same skeleton as aspidocarpine, then a phenolic hydroxyl must be attached at C-17 because of its strongly hydrogen-bonded nature, evidenced in the infrared by the marked displacement to lower frequencies (1635 cm^{-1}) of the amide carbonyl absorption, and a characteristic signal in the n.m.r. spectrum.

The correctness of the assumption was confirmed by treatment of alkaloid III with dimethyl sulphate and sodium hydroxide. The reaction gave rise to a dimethyl derivative identical with O-methylaspidocarpine. Consequently, alkaloid III is O-demethylaspidocarpine and its structure is represented by formula II.

O-Demethylaspidocarpine provides a further example of a catechol type of alkaloid of which the first one reported in the aspidospermine series is spegazzinidine (5).

EXPERIMENTAL

All the n.m.r. spectra were taken with a Varian Associates A-60 instrument, and the infrared spectra with a Perkin–Elmer double-beam spectrophotometer Model 21B.

The ground stem bark was extracted first with petroleum ether and then with ethanol–ammonia (11 l. – 1 l.). A crystalline colorless material separated from the petroleum ether extract. It was heated with *n*-heptane to remove the accompanying fat. The insoluble crystalline basic substance was recrystallized from methanol, from which it separated as yellowish prisms. Several recrystallizations raised the melting point to 172–174°. A quantity of the same crystalline substance was also obtained from the basic ethanol extract. When the crude alkaloid of this extract was chromatographed in benzene solution on neutral alumina, the material was found in the first fractions of the eluate.

Aspidoalbine and N-Depropionyl-N-acetylaspidoalbine

The crystalline material was chromatographed on paper under the condition described by Taylor *et al.* (4) and found not to be homogeneous but to consist of two distinct components. This technique was modified to adapt it to the separation of relatively large amounts of material. Whatman No. 3 paper was used and the alkaloid mixture in chloroform was streaked along the base line. It was found convenient to use 240 mg of material for 130 cm of base line. When the chromatogram had developed and the paper had been allowed to hang overnight in air, thin vertical strips were cut from it at 15-cm intervals and sprayed with iodoplatinate reagent. This illustrated how the components had separated. The appropriate zones were cut out from the paper and each was thoroughly extracted with chloroform in a Soxhlet apparatus. Each extract

Can. J. Chem. Downloaded from www.nrcresearchpress.com by 210.87.254.105 on 09/05/12
For personal use only.

Can. J. Chem. Downloaded from www.nrcresearchpress.com by 210.87.254.105 on 09/05/12
For personal use only.

was evaporated to a volume of ca. 50 ml, was washed with 5% aqueous sodium carbonate and with water; it was dried over sodium sulphate and was evaporated to dryness. Each residue was dissolved in benzene, passed through a short column of alumina, and eluted with benzene; the products were crystallized from benzene–hexane and then from methanol. From 240-mg of mixture there was obtained 58 mg of alkaloid I (leading zone), colorless prisms, m.p. 174–177°, and 36 mg of alkaloid II (second zone), colorless prisms, m.p. 194–195°.

An easier but not complete separation of the two alkaloids can be achieved by chromatography of the mixture on low-activity (grade V) neutral alumina, and the use of *n*-hexane – chloroform as eluant. Under such conditions pure alkaloid I is first obtained, then a mixture of alkaloids I and II, and finally pure alkaloid II, but most of the mixture is separated into its components.

Alkaloid I, $[\alpha]_D^{25}$ +164° (*c*, 2.12 in chloroform). Found: C, 67.68; H, 7.71; N, 6.70; OCH_3, 14.68. Calc. for $C_{24}H_{32}O_5N_2$: C, 67.27; H, 7.53; N, 6.54; 2 OCH_3, 14.48%. A mixture of alkaloid I with a sample of aspidoalbine[5] (m.p. 168–173°) melted at 166–170°. On a silica gel chromatoplate with chloroform – *n*-hexane – diethylamine (10:20:3) as solvent, alkaloid I gave one spot while the sample of aspidoalbine gave two, one of which had the same mobility as the one spot of the former, and the other corresponded to alkaloid II.

On methylation with dimethyl sulphate and sodium hydroxide, alkaloid I gave rise to an O-methyl derivative, m.p. 128–131°, $[\alpha]_D^{25}$ +9.2° (*c*, 1.84 in methanol). Found: C, 68.17; H, 7.79; N, 6.30; OCH_3, 20.19. Calc. for $C_{25}H_{34}O_5N_2$: C, 67.85; H, 7.75; N, 6.33; 3 OCH_3, 21.04%. In admixture with a sample of O-methylaspidoalbine[5] (m.p. 120–123°), m.p. 120–132°. O-methyl alkaloid I gave one spot on a chromatoplate and the sample of O-methylaspidoalbine gave two, the major one of which corresponded in mobility with the one spot of the former.

Alkaloid II, m.p. 194–195°, had $[\alpha]_D$ +174° (*c*, 1.93 in chloroform). Found: C, 66.38; H, 7.29; N, 6.52; OCH_3, 15.06. Calc. for $C_{23}H_{30}O_5N_2$: C, 66.64; H, 7.30; N, 6.76; 2 OCH_3, 14.96%. λ_{max}^{EtOH} 227 mμ, log ε 4.43; 267 mμ, log ε 4.11. The only difference between the n.m.r. spectrum of alkaloid II and that of aspidoalbine is the replacement of the triplet at 1.26 δ (CH_3) and the quartet at 2.53 δ (CH_2) corresponding to the protons of the N-propionyl group of aspidoalbine by a peak at 2.36 δ corresponding to three protons (N-acetyl). The infrared absorption spectrum contains a band at 1625 cm^{-1} indicative of a hydrogen-bonded N-acetyl carbonyl. Alkaloid II therefore corresponds to the lower homologue of aspidoalbine.

Methylation of Alkaloid II

A quantity of alkaloid II was methylated with dimethyl sulphate and sodium hydroxide following the usual procedure. The product of reaction, after crystallization from aqueous methanol, was shown by thin layer chromatography not to be homogeneous. It was therefore chromatographed on a silica gel plate (20×20 cm), the main band (detected by spraying with water) scraped off and eluted with methanol–chloroform (1:1). The material recovered from the eluate was sublimed at 145° at 10^{-4} mm. Colorless needles were obtained, m.p. 169–173°, which after one more sublimation melted at 175–178.5°. This substance was found by thin layer chromatography to be homogeneous, and to have an infrared spectrum superimposable on that of N-depropionyl-N-acetyl-O-methylaspidoalbine.[5] The product, however, gave consistently low analytical figures. It was therefore hydrolyzed by boiling in 3 *N* hydrochloric acid under reflux for 2.5 hours. The solution was made alkaline and extracted with chloroform. The residue left after evaporation of the chloroform extract was heated on the steam bath for 2 hours with propionic anhydride and pyridine and the product of the reaction chromatographed on a silica gel plate (20×20 cm). The silica gel containing the main band was scraped off and extracted with methanol–chloroform. Evaporation of the extract left a residue which after sublimation consisted of colorless prisms, m.p. 134–137°, $[\alpha]_D$ +9.7° (*c*, 1.76 in MeOH). In admixture with O-methylaspidoalbine (m.p. 127–131°) it melted at 128–135°. Its infrared spectrum was superimposable on that of O-methylaspidoalbine.

Aspidocarpine and O-Demethylaspidocarpine

The alcoholic extract of the bark was fractionated on a 200 g/200 ml kieselguhr/phosphate buffer (pH 5.2) column, using first ether and then chloroform as eluting solvents. Only traces of base were left on the column, which was stripped with ammoniacal chloroform.

Evaporation *in vacuo* of the ether eluate at room temperature left a yellow resin, which was dissolved in boiling benzene and decolorized with charcoal. The filtered cooled solution, left to stand overnight, deposited long pale yellow needles, m.p. 139–140°. After two recrystallizations from benzene the substance consisted of colorless needles, m.p. 149–150°. Chromatography on Whatman No. 1 paper with butanol as solvent showed the substance to be a mixture of two components. Recrystallization from aqueous isopropanol effected a separation and gave pure alkaloid III as colorless plates. The basic mixture recovered from the ether eluate after separation of alkaloid III was chromatographed on grade V neutral alumina. *n*-Hexane – chloroform (4:1) removed first a portion of unidentified material and then the major component of the mixture which, after crystallization from methanol, consisted of colorless prisms, m.p. 166–168°, identical (by melting point of the mixture and infrared spectra) with an authentic sample of aspidocarpine. Further elution of the chromatogram with chloroform removed another portion of unidentified material, and finally with chloroform containing 5% of methanol gave another quantity of alkaloid III.

[5]*This sample was kindly sent to us by Dr. C. Djerassi, to whom we express our gratitude for his cooperation.*

Alkaloid III, m.p. 156–158°, was soluble in aqueous sodium hydroxide but not in sodium carbonate. It gave a violet coloration with ferric chloride solution. A sample of the base was dried at 100° *in vacuo* and used for analysis. Found: C, 70.7; H, 7.96; N, 7.90. Calc. for $C_{21}H_{28}O_3N_2$: C, 70.79; H, 7.86; N, 7.86%. No methoxyl group was present. $[\alpha]_D^{25}$ +125° (*c*, 0.95 in chloroform). The infrared spectrum contained bands at 3320, 2520, 1635 with a shoulder at 1615 and a band at 1584 cm^{-1}. (Aspidocarpine produced infrared bands at 1635 and 1586 cm^{-1}.)

The alkaloid formed a hydrochloride which separated from ethanol–ether as colorless needles containing solvent of crystallization, m.p. 283° (decomp.). On drying at 120° *in vacuo* the salt lost 11% of its weight. The dried sample was used for analysis. Found: C, 64.8; H, 7.48; N, 7.00; Cl, 9.37. Calc. for $C_{21}H_{28}O_3N_2.HCl$: C, 64.18; H, 7.18; N, 7.13; Cl, 9.02%.

Methylation of Alkaloid III

A small sample of alkaloid III was methylated under the usual conditions with dimethyl sulphate and sodium hydroxide. The product of the reaction was sublimed *in vacuo* to remove colored impurities and then chromatographed on silica gel plates with the use of chloroform – *n*-hexane – diethylamine (10:20:3) as solvent. The main band, detected by spraying with water, was scraped off and extracted with chloroform–methanol. The filtered solution was evaporated and the residue crystallized from aqueous methanol, from which it separated as colorless prisms, m.p. 146—150°, $[\alpha]_D^{25}$ −95.4° (*c*, 1.18 in chloroform). It was identical with O-methylaspidocarpine in optical rotation ($[\alpha]_D^{25}$ −94° in chloroform), in melting point and that of the mixture, in plate chromatographic mobility, and in infrared absorption spectra.

ACKNOWLEDGMENTS

We wish to express our thanks to Mr. A. Knoll for the extraction of the plant material, Mr. H. Séguin for the microanalyses, Mr. R. Lauzon for the infrared spectra, and Mr. M. Lesage for the n.m.r. spectra.

REFERENCES

1. C. Djerassi, L. D. Antonaccio, H. Budzikiewicz, J. M. Wilson, and B. Gilbert. Tetrahedron Letters, No. 22, 1001 (1962).
2. S. McLean, K. Palmer, and L. Marion. Can. J. Chem. **38**, 1547 (1960).
3. C. Djerassi, B. Gilbert, J. N. Shoolery, L. F. Johnson, and K. Biemann. Experientia, **17**, 162 (1961).
4. W. I. Taylor, N. Raab, H. Lehner, and J. Schmutz. Helv. Chim. Acta, **42**, 2750 (1959).
5. C. Djerassi, H. W. Brewer, H. Budzikiewicz, O. O. Orazi, and R. A. Corral. J. Am. Chem. Soc. **84**, 3480 (1962).

Can. J. Chem. Downloaded from www.nrcresearchpress.com by 210.87.254.105 on 09/05/12
For personal use only.

COUPLED GAS LIQUID – THIN LAYER CHROMATOGRAPHY

SIMULTANEOUS DETERMINATION OF PIPERITONE AND PIPERITONE OXIDE IN ESSENTIAL OILS

ISHWAR C. NIGAM,[1] M. SAHASRABUDHE, AND LEO LEVI
Food and Drug Directorate, Department of National Health and Welfare, Ottawa, Canada

Received November 7, 1962

ABSTRACT

Gas liquid and thin layer chromatography have been combined into a single microphysicochemical technique. The resolution of two terpenoids found in nature—piperitone and piperitone oxide—is described to illustrate the scope of the novel method of analysis. Occurrence of the epoxide in *Mentha arvensis* (Japanese mint), *Mentha piperita* (Mitcham peppermint), *Eucalyptus dives* Schauer, "Type" ("broad-leaved peppermint"), and *Eucalyptus numerosa* Maiden, var. "A" is reported for the first time. Its presence in these species should prove of biochemical as well as taxonomic interest.

Can. J. Chem. Downloaded from www.nrcresearchpress.com by 210.87.254.40 on 09/05/12
For personal use only.

Gas liquid partition and thin layer chromatography are extremely important techniques for the examination of complex natural and synthetic compositions. What were once considered tedious microchemical analyses have through their application become routine assays in research and industrial laboratories alike. Studies to combine both methods into a unified operation were begun in the authors' laboratory some time ago (1). A related investigation was published since by Casu and Cavalotti (2). It is the purpose of the present paper to record the experimental procedures we followed, to report some specific results, and to indicate future applications.

EXPERIMENTAL

Apparatus

Gas chromatograph.—Burrell Kromo-Tog K-2 equipped with thermal conductivity detector cell and separate heating baths for column and detector, respectively.

Column.—Glass tubing, 0.6-cm inside diameter, 215 cm long.

Packing.—Reoplex 400 (10 parts) deposited from ethanolic solution on 60- to 80-mesh, acid-washed Chromosorb W (90 parts). Length of packed column, 200 cm.

Carrier gas.—Helium, inlet pressure 1.1 atm; outlet pressure 1.0 atm.

Recorder.—0 to 1 mv full-scale deflection; 1 second.

Coupling device.—1 mm inside diameter platinum needle approximately 1 in. long, inserted into the exit of the chromatograph and bent slightly to deposit effluents directly on chromatoplates for concomitant TLC-analysis.

Thin layer chromatographic assembly.—According to Stahl; C. Desaga unit.

Materials

Essential oils.—Products from genera *Mentha* and *Eucalyptus*.

Essential oil constituents.—*l*-Piperitone obtained from a hybrid of *M. arvensis*. Experimental sample (1 g) purified by column chromatography over silica gel (25 g) using hexane–ether (10:1) as eluant; $\epsilon^{EtOH}_{max\ 318\ m\mu} = 50.4$; $\epsilon^{EtOH}_{max\ 234\ m\mu} = 13{,}950$. *l*-Piperitone oxide ex *M. sylvestris*: $\epsilon^{EtOH}_{max\ 296\ m\mu} = 48.6$.

Analytical Procedure

Samples ranging from 5 to 10 μl were injected from a Hamilton microliter syringe through silicone seals into the column, operated at 150±2° C. Helium served as carrier gas, its flow rate—measured by the soap bubble method at the exit—being maintained at 75±0.5 ml/min. A current of 200 ma was applied to the hot wire detector and the thermal conductivity cell operated at 200° C. Chart speed was 0.5 in./min.

Emerging fractions were spotted directly on chromatoplates coated with Silica Gel G (Merck) and activated by heating at 120° C for 24 hours prior to use. A 10:1 hexane – diethyl ether mixture was applied for development and a 5% solution of vanillin in concentrated sulphuric acid served as spray reagent.

[1]*National Research Council of Canada Postdoctoral Fellow, 1961–1962.*

Identification of Components and Quantitative Determinations

Hexane solutions containing known amounts of both ketones were prepared for use as reference standards and applied as controls for compound identification and the appraisal of product recovery by the combined technique.

RESULTS AND DISCUSSION

Detection of Ketones by Gas Liquid Partition and Thin Layer Chromatography

Figure 1 shows the gas chromatogram of a Japanese oil of mint (*M. arvensis*), an English

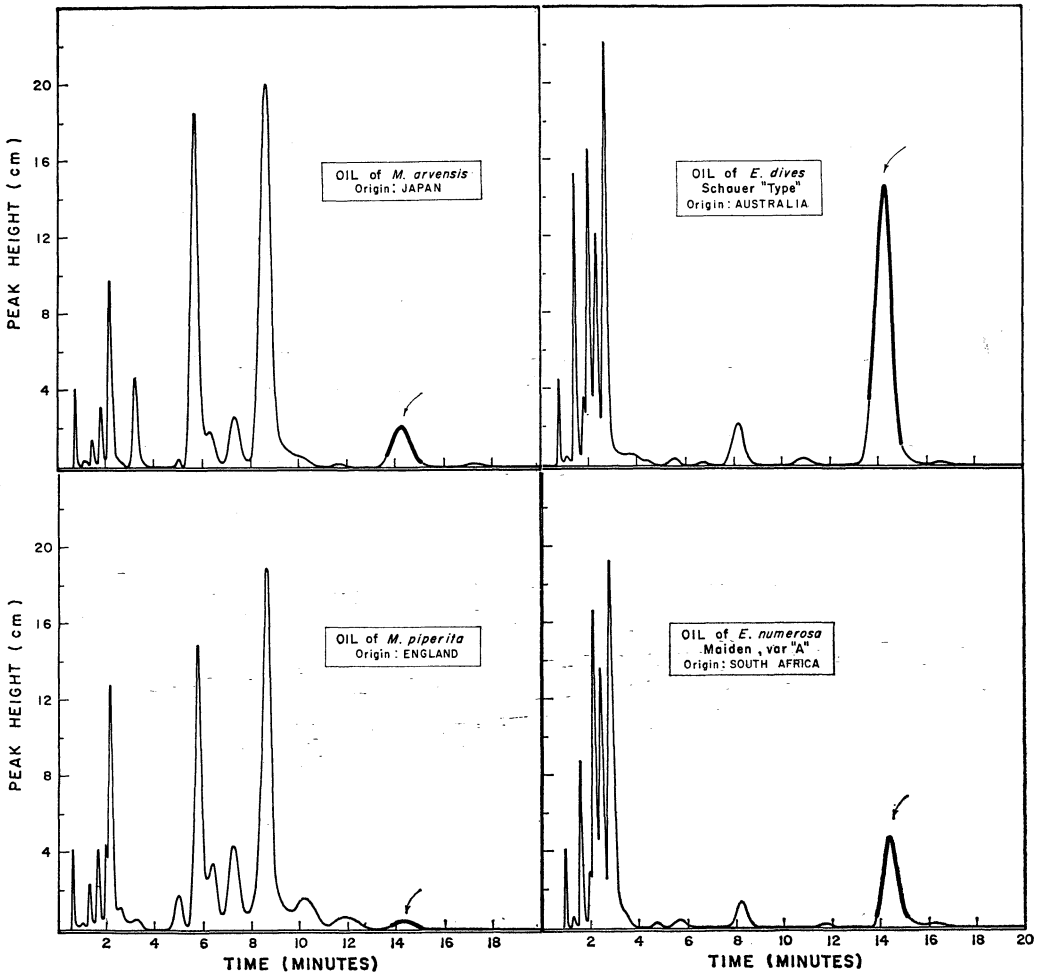

FIG. 1. Gas chromatograms of essential oils from genera *Mentha* and *Eucalyptus*. Analytical peaks reproduced in heavy lines.

oil of peppermint (*M. piperita*), an Australian oil of *E. dives* Schauer, "Type" ("broad-leaved peppermint"), and a South African oil of *E. numerosa* Maiden, var. "A". Analytical fractions examined in accordance with the technique described are reproduced in heavy lines.

Both piperitone and piperitone oxide were found to be present in each of the eluates—the epoxide appearing as a bright purple spot following treatment of the chromatoplate with a 5% solution of vanillin in sulphuric acid and turning dark violet on being heated

Can. J. Chem. Downloaded from www.nrcresearchpress.com by 210.87.254.40 on 09/05/12
For personal use only.

to 100° C for a period of 5 minutes. Sensitivity of spray reagent: 1 γ. Piperitone appeared as a light orange colored spot, becoming deep orange-brown on being heated to 100° C for a 5-minute interval. Sensitivity of spray reagent: 50 γ.

Infrared Examination of Gas Chromatographic Eluates

Characteristic bands permitting distinction of the two ketones are shown in Fig. 2,

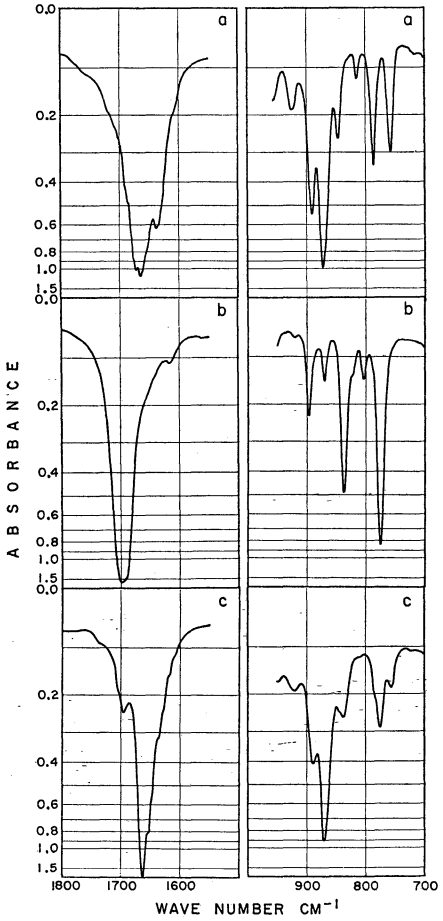

FIG. 2. Characteristic regions in infrared spectra of piperitone (*a*), piperitone oxide (*b*), and "piperitone" effluent from Japanese mint oil (*c*). Reference spectra measured in sealed sodium chloride cells of 0.025-mm path length (piperitone: 950–700 cm^{-1}) and 0.0155-mm path length (piperitone oxide). Carbonyl region of piperitone (1800–1550 cm^{-1}) charted as contact film. Spectrum of gas chromatographic effluent from essential oil obtained by direct deposition of analytical fraction on grooved salt plate (1) following 20-λ sample injection, with instrument (Perkin–Elmer Model 221 spectrophotometer) operated under 5-fold scale expansion.

along with the corresponding spectral features of the "piperitone" effluent from the Japanese mint oil.

Piperitone displays strong absorption at 1665 cm^{-1} (conjugated carbonyl) and exhibits sharp bands at 873, 785, and 760 cm^{-1}. Piperitone oxide shows an intense band at 1695 cm^{-1} (unconjugated carbonyl) and displays marked absorptions at 837 and 775 cm^{-1}.

These criteria of identity permitted detection of the epoxide in the analytical fraction

Can. J. Chem. Downloaded from www.nrcresearchpress.com by 210.87.254.40 on 09/05/12
For personal use only.

collected and examined as previously described (1), distinct bands being observed at 1695 and 775 cm^{-1}. Characteristic piperitone absorptions were found to occur at 1665 and 873 cm^{-1}, an inflection only being detected at 785 cm^{-1} because of marked absorbance by the epoxide at 775 cm^{-1}.

Similar infrared examination of the corresponding eluates from oil of *M. piperita*, *E. dives*, and *E. numerosa* failed to suggest the presence of any other but the major component, i.e., piperitone. Direct thin layer chromatography of the essential oils and their oxygenated fractions isolated via deterpenation over alumina yielded, likewise, negative results. Only coupled gas liquid – thin layer chromatography of the effluents established that both ketones occur in these oils along with still other components of identical or nearly identical retention times, as illustrated in Fig. 3 for Japanese mint oil.

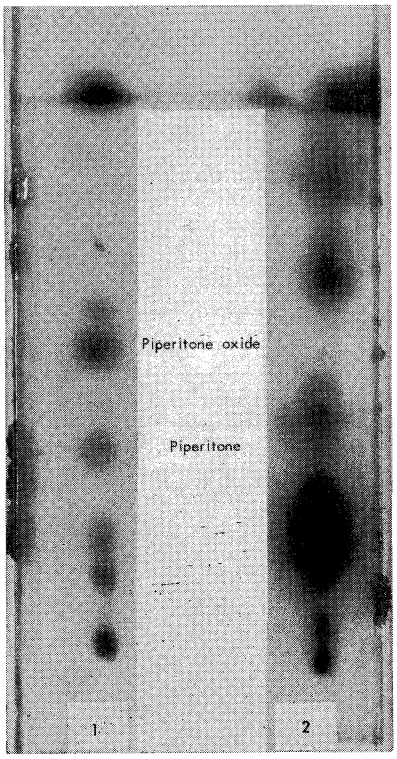

FIG. 3. CGT-chromatogram of "piperitone" effluent from Japanese mint oil (1), and TL-chromatogram of deterpenated sample (2).

Quantitative appraisal of the gas chromatogram recorded for the oil of *M. arvensis* indicated that the sample contained 7.1% of piperitone (3). Quantitative appraisal of the thin layer chromatogram obtained for the analytical peak revealed, however, admixture of the effluent with approximately 4% of piperitone oxide as a genuine constituent of the oil. Piperitone oxide content of whole oil $\sim 0.3\%$. Mere trace amounts of this ketone ($<0.1\%$) were detected in oils of peppermint and eucalyptus. Comparison of color intensities observed with those of comparable concentrations of binary mixtures of the ketones examined simultaneously revealed that product recoveries ranging from 90–95% were realized by the combined technique.

Smooth deposition of gas chromatographic eluates presented no difficulties. The tip of the needle was merely kept just barely touching the glass plate during collection. Surface

Can. J. Chem. Downloaded from www.nrcresearchpress.com by 210.87.254.40 on 09/05/12
For personal use only.

adsorption by the thin film of finely dispersed coating appears to insure efficient retention of the condensate. If, as in this study, isolated peaks only are being collected for analysis it is advisable to wipe the tip of the needle with a piece of soft tissue paper before deposition of the eluate in order to avoid contamination with material from preceding fractions, or to insert the needle into the apparatus just prior to emergence of the component or components to be examined.

Scope of Analytical Technique

Coupled gas liquid – thin layer chromatography has been applied successfully in our laboratory for the resolution of apparently symmetrical peaks observed in the gas chromatograms of many essential oils and their constituents and we are utilizing the technique routinely for the detection of trace components, the appraisal of sample authenticity, and quantitative determinations.

Because of its sensitivity the method allows for the investigation of oils from single leaf pairs of plants produced by controlled cultivation of pure species and thus eliminates the chance of extrapolation from results obtained with oils from mixed species or non-homozygous strains—a source of serious difficulty for the study of natural products and often justified doubts of the validity of biochemical deductions from physiochemical data (4). The value of the method to the plant breeder and taxonomist is thus obvious.

Since components resolved are characterized immediately by two specific criteria, namely retention time and R_f value, which constants are, in turn, codetermined by a number of closely related physiochemical parameters (5–8) their identities may often be staked and deduced directly from coupled gas liquid – thin layer chromatographic data. Permitting, furthermore, the exploration of all the variables of GLPC, e.g., column substrate, temperature, flow rate, as well as those of TLC, e.g., adsorbent, developer, spray reagent, and simultaneous performance of both analyses without interruption, the technique provides a simple, efficient method not only for the study of essential oils and their constituents but for the examination of complex natural and synthetic compositions generally on an ultramicro scale.

Because of the universal usefulness thus visualized for *C*oupled *G*as liquid – *T*hin layer *C*hromatography, we would like to suggest that it be designated the ***CGTC*** technique.

ACKNOWLEDGMENTS

The authors are indebted to Dr. F. J. Cramer, A. M. Todd Company, Kalamazoo, Mich., U.S.A., for courteously supplying samples of piperitone and piperitone oxide for this study. They also express their appreciation to Dr. Ernest Guenther, Fritzsche Brothers, Inc., New York, U.S.A., for a genuine sample of South African oil of *E. numerosa*, to Dr. Teikichi Hiraizumi, Takasago Perfumery Co., Ltd., Tokyo, Japan, for a representative specimen of oil of *M. arvensis*, and to Dr. F. R. Morrison, Museum of Applied Arts and Sciences, Sydney, Australia, for an authenticated sample of Australian oil of *E. dives*.

REFERENCES

1. I. C. NIGAM, M. SAHASRABUDHE, T. W. M. DAVIS, J. C. BARTLET, and L. LEVI. Perfumery Essent. Oil Record, **53**, 614 (1962).
2. B. CASU and L. CAVALLOTI. Anal. Chem. **34**, 1514 (1962).
3. D. M. SMITH and L. LEVI. J. Agr. Food Chem. **9**, 230 (1961).
4. H. REITSEMA. J. Am. Pharm. Assoc., Sci. Ed. **47**, 267 (1958).
5. D. M. SMITH, J. C. BARTLET, and L. LEVI. Anal. Chem. **32**, 568 (1960).
6. W. E. FALCONER and R. J. CVETANOVIĆ. Anal. Chem. **34**, 1064 (1962).
7. M. H. KLOUWEN and R. TER HEIDE. J. Chromatog. **7**, 297 (1962).
8. J. HERLING, J. SHABTAI, and E. GIL-AV. J. Chromatog. **8**, 349 (1962).

Can. J. Chem. Downloaded from www.nrcresearchpress.com by 210.87.254.40 on 09/05/12
For personal use only.

REACTIONS OF PHENYL-SUBSTITUTED HETEROCYCLIC COMPOUNDS

II. NITRATIONS AND BROMINATIONS OF 1-PHENYLPYRAZOLE DERIVATIVES[1]

MISBAHUL AIN KHAN[2]
Department of Chemistry, Memorial University of Newfoundland, St. John's, Newfoundland

AND

BRIAN M. LYNCH[3]
Departments of Chemistry, Memorial University of Newfoundland, St. John's, Newfoundland, and St. Francis Xavier University, Antigonish, Nova Scotia

AND

YUK-YUNG HUNG[4]
Department of Chemistry, St. Francis Xavier University, Antigonish, Nova Scotia

Received September 26, 1962

ABSTRACT

Nitrations of 1-phenylpyrazole (I), 1-*p*-biphenylylpyrazole (II), and 1,5-diphenylpyrazole by "acetyl nitrate" (nitric acid – acetic anhydride) occur selectively in the 4-position of the pyrazole ring, as do brominations of I and II in chloroform solution. These results are in agreement with R. D. Brown's calculations of localization energies for electrophilic substitution in pyrazole.

However, nitration of I by mixed acids at 12° yields 1-*p*-nitrophenylpyrazole, and bromination of I by bromine in concentrated sulphuric acid in the presence of silver sulphate yields 1-*p*-bromophenylpyrazole.

The variations in orientation of substitution can be rationalized if the reacting species of I in strongly acidic solvents is the conjugate acid, in which the pyrazole ring is deactivated by protonation.

INTRODUCTION

Electrophilic substitution in 1-phenylpyrazole (I) often leads to initial attack at the 4-position of the pyrazole ring (for example, bromination in inert solvents (1), Friedel–Crafts acylation (2, 3), chloromethylation (4), and mercuration (4)). However, nitration of 1-phenylpyrazole with mixed acids at 12° introduces the first nitro group into the para position of the phenyl ring, although further substitution occurs readily to yield 4-nitro-1-*p*-nitrophenylpyrazole (cf. Finar and Hurlock (5)).

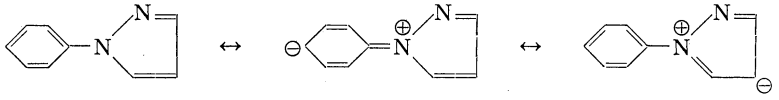

I Ia Ib

The present paper suggests a simple interpretation of this variation in orientation, and applies this interpretation in establishing conditions for selective 4-nitration of 1-*p*-biphenylylpyrazole (II) and 1,5-diphenylpyrazole (III), for the controlled dinitration of III, for the 4-bromination of II, and for the 1-*p*-bromination of I.

[1]*Financial assistance for this work was received from the National Research Council. Abstracted in part from a thesis presented by Misbahul Ain Khan in partial fulfillment of the requirements for the degree of Master of Science, Memorial University of Newfoundland.*

[2]*Graduate Research Assistant, 1961–1962. Present address: Florida State University, Tallahassee, Florida, U.S.A.*

[3]*Correspondence should be addressed to this author at the Department of Chemistry, St. Francis Xavier University, Antigonish, Nova Scotia.*

[4]*Graduate Research Assistant.*

Can. J. Chem. Downloaded from www.nrcresearchpress.com by 210.87.254.5 on 09/05/12
For personal use only.

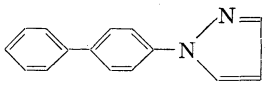

II

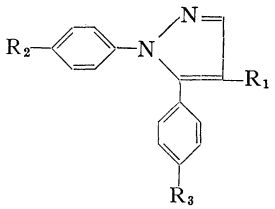

III: $R_1 = R_2 = R_3 = H$
V: $R_1 = NO_2$, $R_2 = R_3 = H$
VI: $R_2 = NO_2$, $R_1 = R_3 = H$
VII: $R_3 = NO_2$, $R_1 = R_2 = H$
VIII: $R_2 = R_3 = NO_2$, $R_1 = H$
IX: $R_1 = R_2 = NO_2$, $R_3 = H$

DISCUSSION

We suggest that the different orientation noted in the strongly acidic medium results from protonation of 1-phenylpyrazole to yield the conjugate acid (IV), in which the pyrazole ring would be deactivated towards attack by electrophils, while the +T effect of the 1-nitrogen atom would facilitate substitution at the para position of the phenyl group (cf. IV*a*). If this suggestion is correct, it should be possible to effect changes in the orientation of electrophilic substitution in 1-phenylpyrazole and its derivatives by varying the conditions of reaction so that either the neutral molecule or the conjugate acid is the reacting species.

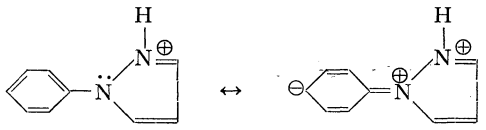

IV IV*a*

Examples

(a) Selective 4-Nitrations

Although no interpretation along the lines of the above suggestion has been offered previously, an instance of the predicted control of orientation exists in the literature, in that nitration of 1-phenylpyrazole by nitric acid in acetic anhydride at 0° is reported to give 4-nitro-1-phenylpyrazole (in unstated yield) (6). In confirmation (see Experimental) we find that fair yields of 4-nitro-1-phenylpyrazole are obtained. It seems almost certain that this reaction involves attack of protonated acetyl nitrate (the effective reagent in nitrations by nitric acid in acetic anhydride, cf. Bordwell and Garbisch (7)) on the neutral molecule of 1-phenylpyrazole, while Finar and Hurlock's nitration in mixed acids involves attack by nitronium ion on the conjugate acid (IV).

Since the normally favored position of attack by an electrophilic reagent on the neutral molecule of a 1-phenylpyrazole derivative is the 4-position of the pyrazole ring (cf. refs. 1–4), it would be predicted that nitrations of 1-*p*-biphenylylpyrazole and of 1,5-diphenylpyrazole by nitric acid in acetic anhydride would yield 4-substituted derivatives. The results from the nitrations of these compounds are consistent with this prediction, although the structures of the products were not proved absolutely. The structure assigned to the nitro-1-*p*-biphenylylpyrazole, m.p. 170° (i.e., 1-*p*-biphenylyl-4-nitropyrazole), is based on correlations with the infrared and ultraviolet absorption of nitrophenylpyrazoles and other substituted 1-phenylpyrazoles. The positions of the strong bands at the N—O stretching frequencies, in conjunction with others at ca. 690 and 760 cm^{-1}, as observed with compounds possessing monosubstituted phenyl groups (8), can be used to distinguish

Can. J. Chem. Downloaded from www.nrcresearchpress.com by 210.87.254.5 on 09/05/12
For personal use only.

between the various nitrophenylpyrazoles (see Table I): the similarities between the nitro-1-*p*-biphenylylpyrazole, m.p. 170°, and 4-nitro-1-phenylpyrazole indicate very strongly that the compound is 1-*p*-biphenylyl-4-nitropyrazole. Furthermore, we have noted (9) that a strong band in the region 925–960 cm^{-1} is associated with the C—H vibrations of the pyrazole carbons, and its position in substituted 1-phenylpyrazoles in diagnostic of substitution in the pyrazole ring: absorption in the range 925–942 cm^{-1} is noted for compounds without substituents in the pyrazole ring, while absorption in the range 950–960 cm^{-1} is observed with compounds carrying such substituents. This generalization is valid for approximately 50 substituted 1-phenylpyrazoles prepared in the course of the present series of papers. This band appears at 952 cm^{-1} in the infrared spectra of the nitro-1-*p*-biphenylpyrazole, m.p. 170°, thus providing further support for the assigned structure.

TABLE I

Infrared absorption bands of nitroarylpyrazoles

Compound	Infrared absorption regions (cm^{-1}) (all strong bands)		
	650–1000 (C—H deformation)	1300–1400 (ν_{N-O} sym.)	1500–1560 (ν_{N-O} asym.)
1-*o*-Nitrophenylpyrazole	750, 754, 760, 941	1371	1545
1-*m*-Nitrophenylpyrazole	738, 762, 940	1355	1535
1-*p*-Nitrophenylpyrazole	765, 852, 928	1341	1527
4-Bromo-1-*p*-nitrophenylpyrazole	750, 855, 960	1340	1527
1-(2,4-Dinitrophenyl)-pyrazole	740, 780, 832, 910, 940	1345 br	1530, 1545, 1555
4-Nitro-1-phenylpyrazole	690, 751, 770, 820, 950	1325	1545
Nitro-1-*p*-biphenylylpyrazole, m.p. 170°	692, 748, 765, 820, 952	1325	1541

Evidence from ultraviolet absorption is also consistent with the assigned structure: the ultraviolet absorption spectra of the various nitrophenylpyrazoles are characteristic, as 4-nitro-1-phenylpyrazole is the only isomer having two absorption maxima of approximately equal intensity above 220 mμ. The presumed 1-*p*-biphenylyl-4-nitropyrazole also exhibits two maxima, displaced bathochromically about 30 mμ, as would be expected from the presence of an extra *p*-phenyl substituent (compare 1-phenylpyrazole, λ_{max} 252 mμ, log ε 4.13, and 1-*p*-biphenylylpyrazole, λ_{max} 280 mμ, log ε 4.50). The absorption maxima are listed in Table II.

The nitro-1,5-diphenylpyrazole, m.p. 150°, obtained by nitration of 1,5-diphenylpyrazole in acetic anhydride, is almost certainly 1,5-diphenyl-4-nitropyrazole (V). The

TABLE II

Ultraviolet absorption spectra of nitro-1-arylpyrazoles

Compound	λ_{max} (mμ)	log ε
1-*o*-Nitrophenylpyrazole	238, 300	4.18, 3.27
1-*m*-Nitrophenylpyrazole	250	3.88
1-*p*-Nitrophenylpyrazole	318*	4.29
4-Bromo-1-*p*-nitrophenylpyrazole	315	4.21
4-Nitro-1-phenylpyrazole	228, 295	4.11, 4.07
Nitro-1-*p*-biphenylylpyrazole, m.p. 170°	265, 315	4.06, 4.08

*In chloroform solution.

Can. J. Chem. Downloaded from www.nrcresearchpress.com by 210.87.254.5 on 09/05/12
For personal use only.

only likely positions of attack are the 4-position of the pyrazole ring, or the para positions of either the 1- or 5-phenyl groups, and both 1-*p*-nitrophenyl-5-phenylpyrazole (VI), m.p. 117° (10), and 5-*p*-nitrophenyl-1-phenylpyrazole (VII), m.p. 93° (11), are known compounds.

(b) Nitrations in Mixed Acids

Under these conditions, we have assumed that the reacting species of substituted 1-phenylpyrazoles will be the appropriate conjugate acids. Attempted nitration of 1-*p*-biphenylylpyrazole, using the conditions employed for 1-phenylpyrazole (5), yielded mixtures from which no single substances were isolated. The infrared spectra of the mixtures showed broad, strong absorption in the 1350–1370 and 1530–1550 cm^{-1} regions, indicative of polysubstitution (compare the infrared absorption of 1-(2,4-dinitrophenyl)-pyrazole, Table I).

Nitration of 1,5-diphenylpyrazole was more successful: a dinitro-1,5-diphenylpyrazole, m.p. 185°, was obtained by reaction at 0°. This product is assigned tentatively as 1,5-di(*p*-nitrophenyl)pyrazole (VIII). In agreement with this assignment, nitration of 1-*p*-nitrophenyl-5-phenylpyrazole by mixed acids at 0° also yielded the dinitro-1,5-diphenylpyrazole, m.p. 185°, while similar nitration using nitric acid in acetic anhydride at 0° yielded a different dinitro-1,5-diphenylpyrazole, m.p. 147°, presumably 4-nitro-1-*p*-nitrophenyl-5-phenylpyrazole (IX).

(c) 4-Brominations

Balbiano (1) found that the initial product of bromination of 1-phenylpyrazole was 4-bromo-1-phenylpyrazole, while Brain and Finar (12) showed that further reaction took place readily to yield 4-bromo-1-*p*-bromophenylpyrazole. In the present work, in order to have authentic samples of these compounds for detailed comparison with 1-*p*-bromophenylpyrazole (cf. following section), we have repeated the preparations of these compounds using bromine in chloroform solution.

1-*p*-Biphenylylpyrazole underwent bromination in chloroform to yield 1-*p*-biphenylyl-4-bromopyrazole, m.p. 182°, whose structure was established by comparison with authentic samples prepared by two unambiguous routes. One used the sequence 4-bromo-1-phenylpyrazole → 4-bromo-1-*p*-nitrophenylpyrazole → 1-*p*-aminophenyl-4-bromopyrazole → 1-*p*-biphenylyl-4-bromopyrazole, and the other used the free-radical phenylation of 4-bromo-1-phenylpyrazole by benzoyl peroxide (cf. Lynch and Khan (13)). The presence of strong infrared absorption bands at 690 and 760 cm^{-1}, characteristic of a monosubstituted phenyl ring (cf. ref. 8), and at 952 cm^{-1}, assignable to a 1-phenylpyrazole carrying a pyrazole C-substituent (cf. ref. 9), provided additional evidence for the assigned structure of the bromination product of 1-*p*-biphenylylpyrazole.

(d) Selective 1-p-Bromination of 1-Phenylpyrazole

Derbyshire and Waters (14) have shown that solutions of bromine in concentrated sulphuric acid become extremely effective brominating agents on addition of silver sulphate; evidence summarized by Arotsky and Symons (15) indicates that $AgBr_2^+$, rather than protonated hypobromous acid or free bromine cations, is probably the effective electrophilic reagent in such solutions. Use of this Derbyshire–Waters reagent for the bromination of 1-phenylpyrazole gave good yields of 1-*p*-bromophenylpyrazole, m.p. 70°, identical (m.p., mixed m.p., superimposable ultraviolet and infrared spectra) with an authentic sample prepared by an unambiguous synthesis from *p*-bromophenylhydrazine and 1,1,3,3-tetramethoxypropane, and differing in melting point, ultraviolet and infrared absorption from other possible bromination products, i.e., 4-bromo-1-phenylpyrazole or 4-bromo-1-*p*-bromophenylpyrazole. Key differences in the infrared spectra of the three brominated

Can. J. Chem. Downloaded from www.nrcresearchpress.com by 210.87.254.5 on 09/05/12
For personal use only.

compounds include pyrazole C—H deformation bands at 952 and 955 cm^{-1} respectively for 4-bromo-1-phenylpyrazole and 4-bromo-1-*p*-bromophenylpyrazole, and at 935 cm^{-1} for authentic 1-*p*-bromophenylpyrazole and the bromo-1-phenylpyrazole, m.p. 70°, obtained using the Derbyshire–Waters reagent. The positions of these bands confirm that the bromo-1-phenylpyrazole, m.p. 70°, and, of course, authentic 1-*p*-bromophenylpyrazole, carry no C-substituents on the pyrazole ring (cf. ref. 9). Full details of the infrared spectra are given in the Experimental section.

Once again, the change in orientation noted in the sulphuric acid medium is readily interpreted in terms of protonation of 1-phenylpyrazole to the conjugate acid (IV), which undergoes bromination by $AgBr_2^+$ at the para position of the phenyl ring.

An Interpretation of 4-Substitution in the Neutral Molecule of 1-Phenylpyrazole: The Relevance of Localization Energies

Although initial 4-substitution is noted for many electrophilic substitutions in the neutral molecule of 1-phenylpyrazole (cf. above), no interpretation of this orientation has been offered previously. The preference for 4-substitution cannot result from inter-ring conjugation: although conjugative electron transfer by a +T mechanism is possible from the pyrazole ring to the para position of the phenyl ring (structure I*a*), charge transfer to the 4-position can involve only the heterocyclic ring (structure I*b*).

However, it is possible that differences in the electron densities at the 4-position and the para position account for the preferred 4-substitution. We explored this possibility by determining the pK_a values of isomeric acids having their functional groups at either the 4- or 1-*para*-substituted positions of 1-phenylpyrazole, since it is known that the electron density at a given position of a molecule influences the ionization constants of acids or bases whose functional groups are attached to that position (for a discussion of many instances of this influence, see Brown, McDaniel, and Hafliger (16)). The relevant pK_a values were: (*a*) in water at 25°: 4-amino-1-phenylpyrazole cation, 3.22±0.05; 1-*p*-aminophenylpyrazole cation, 3.42±0.20; anilinium ion, 4.58; (*b*) in 1:1 ethanol–water at 25°: 1-phenylpyrazole-4-carboxylic acid, 5.22±0.03; *p*-1-pyrazolylbenzoic acid, 5.32±0.03; benzoic acid, 5.67. Thus, in 1-phenylpyrazole, both the 4-position and the para position of the phenyl ring appear electron deficient with respect to a benzene position, and the results indicate that the electron density at the 4-position is slightly lower than that at the para position of the phenyl ring, since the 4-substituted acids are slightly stronger than the 1-*para*-substituted isomers. Consequently, we must discard the hypothesis that 4-substitution is a result of attack at the position of highest electron density; some other factor must control the orientation.

In this regard, Brown's molecular-orbital calculations for pyrazole (17) are of interest, since the localization energies for electrophilic substitution at various positions in pyrazole suggest that the 4-position is the most reactive; further, for reasonable choices of the relative electronegativity parameter h (defined by $h = (\alpha_N - \alpha_C)/\beta$, where α_N and α_C are the Coulomb integrals of nitrogen and carbon, and β is the standard resonance integral (approximately −20 kcal)), the localization energy for the 4-position in pyrazole is less than that for a benzene position. Typical values, in multiples of $-\beta$, are: benzene, 2.54; pyrazole, 2.10 ($h = 1/2$), 2.25 ($h = 1$). Accepting a current suggestion (18) that the bonds linking aromatic nuclei are essentially single, with minimal inter-ring conjugation, we propose that 1-phenylpyrazole should be regarded simply as a 1-substituted pyrazole with an inductively electron-attracting substituent, where the ease of localization of an electron pair at the 4-position approximates that for pyrazole; consequently, 4-substitution

Can. J. Chem. Downloaded from www.nrcresearchpress.com by 210.87.254.5 on 09/05/12
For personal use only.

is to be expected. Similarly, 1-*p*-biphenylylpyrazole is regarded as virtually independent biphenyl and pyrazole nuclei, and the ease of localization of an electron pair at the 4-position of the pyrazole ring is still product controlling (the localization energies for electrophilic substitution at the 2- or 4-positions of biphenyl (-2.38β and -2.44β respectively) are greater than that for the 4-position of pyrazole). For 1,5-diphenylpyrazole, where the three rings cannot be coplanar, we consider that the 5-phenyl group will have little effect on the localization energy, so 4-substitution is still favored.

Conclusions

Our assumption that the state of protonation of 1-phenylpyrazole derivatives controls the orientation of their electrophilic substitution reactions appears valid, as it satisfactorily predicts the results reported in this paper. It is realized, of course, that the attacking electrophilic reagents differ, in addition to the changes in the predominant substrate species. However, the products from the substitutions effected by both highly selective reagents (e.g., molecular bromine) and by the more reactive, less selective reagents (such as nitronium ion, or "positive bromine") are those of *selective* attack at a single position (*either* the 4- *or* the 1-*para*-position). This rules against any correlation between the nature of the attacking electrophilic reagent and the orientation of substitution, since such a correlation would be expected to reveal itself in a tendency of the more reactive reagents to attack both reactive positions (the 4- and the 1-*para*-position) to give mixtures of products. This is neither in agreement with our results, nor with the experience of previous workers.

EXPERIMENTAL

General

Analyses are by the Schwarzkopf Microanalytical Laboratory, Woodside, N.Y., U.S.A. Melting points were observed using a Fisher–Johns melting point apparatus, and are uncorrected. Infrared spectra were recorded using a Unicam SP 100 spectrophotometer equipped with a SP 130 grating accessory; samples were examined using the potassium chloride disk technique. Ultraviolet spectra refer to solutions in 95% ethanol, and were recorded using a Beckman DK-2A spectrophotometer. A Radiometer Model 4 pH meter was used for the potentiometric titrations.

Substituted 1-Phenylpyrazoles

The following compounds were prepared in excellent yields by the standard condensation of the appropriate substituted hydrazine with 1,1,3,3-tetramethoxypropane in ethanolic hydrochloric acid (cf. Jones (19) and Finar and Hurlock (5)): 1-phenylpyrazole, m.p. 11°, b.p. 246°, n_D^{25} 1.5957; 1-*o*-nitrophenylpyrazole, m.p. 89°; 1-*m*-nitrophenylpyrazole, m.p. 94–95°; 1-*p*-nitrophenylpyrazole, m.p. 170°; 1-(2,4-dinitrophenyl)-pyrazole, m.p. 107°; *p*-1-pyrazolylbenzoic acid, m.p. 268–270° (decomp.) (anal. calc. for $C_{10}H_8N_2O_2$: C, 63.82; H, 4.28%; found: C, 63.82; H, 4.47%); 1-*p*-bromophenylpyrazole, m.p. 70° (anal. calc. for $C_9H_7N_2Br$: C, 48.45; H, 3.16%; found: C, 48.70; H, 3.34%) (ultraviolet absorption: λ_{max} 262 mμ, log ϵ 4.29; infrared absorption: strong bands in the 650–1800 cm^{-1} region at 752, 810, 824, 935, 1050, 1075, 1125, 1205, 1340, 1398, 1495, 1525, and 1600 cm^{-1}); Brain and Finar (12) refer to 1-*p*-bromophenylpyrazole but quote no physical constants. 4-Nitro-1-phenylpyrazole, m.p. 127°, was prepared from sodium nitromalonaldehyde hydrate and phenylhydrazine (5, 6). 1-Phenylpyrazole-4-carboxylic acid, m.p. 220°, was prepared from 4-formyl-1-phenylpyrazole (20) by oxidation with alkaline potassium permanganate. 4-Amino-1-phenylpyrazole, m.p. 104°, and 1-*p*-aminophenylpyrazole, m.p. 45°, were obtained by reduction of the appropriate nitrophenylpyrazole with tin and hydrochloric acid. 1,5-Diphenylpyrazole, m.p. 55°, was prepared by condensation of hydroxymethyleneacetophenone and phenylhydrazine (21), and 1-*p*-nitrophenyl-5-phenylpyrazole, m.p. 117°, was prepared by a similar condensation using *p*-nitrophenylhydrazine (21).

1-p-Biphenylylpyrazole

This compound was obtained by condensation of *p*-hydrazinobiphenyl and 1,1,3,3-tetramethoxypropane, and also by the following route: 1-*p*-aminophenylpyrazole (10.7 g) was diazotized in 10 *N* hydrochloric acid at 0°, and the solution of the diazonium salt was stirred at 7° with benzene, after buffering to pH 5 with sodium acetate, and was allowed to reach room temperature. After 3 hours, evolution of nitrogen had ceased, and the benzene layer was separated and chromatographed on alumina. Evaporation of the eluate, followed by crystallization from ethanol, yielded 7.8 g (53%) of 1-*p*-biphenylylpyrazole, m.p. 126°. Anal. Calc. for $C_{15}H_{12}N_2$: C, 81.80; H, 5.50; N, 12.72%. Found: C, 82.00; H, 5.55; N, 13.00%.

Can. J. Chem. Downloaded from www.nrcresearchpress.com by 210.87.254.5 on 09/05/12
For personal use only.

Nitrations in Acetic Anhydride

(a) 1-Phenylpyrazole

A solution of nitric acid (*d* 1.52, 1.5 ml) in acetic anhydride (4 ml), prepared at 15–20°, was cooled to −5° and added to 1-phenylpyrazole (3 g) in acetic anhydride (6 ml) at −5° over 30 minutes. The reaction mixture was allowed to reach room temperature, and was poured onto ice. The precipitate was collected and crystallized from ethanol, yielding 4-nitro-1-phenylpyrazole, m.p. and mixed m.p. 125–127°, having ultraviolet and infrared absorption identical with authentic material. The yield of crystallized product was 2.1 g (53%). Reactions on a larger scale generally gave lower yields, although unreacted 1-phenylpyrazole was recovered.

(b) 1-p-Biphenylylpyrazole

Nitration of 1-*p*-biphenylylpyrazole (0.5 g) under the conditions of part (*a*) gave the presumed 1-*p*-biphenylyl-4-nitropyrazole (0.25 g, 42%), m.p. 170°, after crystallization from ethanol. Anal. Calc. for $C_{15}H_{11}N_3O_2$: C, 67.92; H, 4.18%. Found: C, 67.67; H, 4.41%. For ultraviolet and infrared absorption see tables.

(c) 1,5-Diphenylpyrazole

Nitration of 1,5-diphenylpyrazole (2 g) under the general conditions of part (*a*), except that the temperature of reaction was maintained at 0°, gave the presumed 1,5-diphenyl-4-nitropyrazole (ca. 1 g, 43%), m.p. 150°, after chromatography on alumina and crystallization from benzene. Anal. Found: C, 68.32; H, 4.04%.

(d) 1-p-Nitrophenyl-5-phenylpyrazole

Nitration of 1-*p*-nitrophenyl-5-phenylpyrazole (1 g) under the conditions of part (*c*) gave the presumed 4-nitro-1-*p*-nitrophenyl-5-phenylpyrazole (0.3 g, 26%), m.p. 147°, after chromatography on alumina and repeated recrystallization from ethanol. Anal. Calc. for $C_{15}H_{10}N_4O_4$: C, 58.06; H, 3.25%. Found: C, 57.71; H, 3.32%.

Nitrations in Mixed Acids

(a) 1-p-Biphenylylpyrazole

With mixed acids at 0°, using the conditions employed by Finar and Hurlock (5) for 1-phenylpyrazole, 1-*p*-biphenylylpyrazole yielded amorphous products, sparingly soluble in ethanol and in benzene, having infrared absorption indicative of polysubstitution (cf. Discussion), and giving bluish-violet colors on addition of aqueous sodium hydroxide to their solutions in acetone (Janovsky test, indicative of polynitro-substituted 1-phenylpyrazoles (cf. ref. 5)).

(b) 1,5-Diphenylpyrazole

1,5-Diphenylpyrazole (2 g) was dissolved in the minimum volume of sulphuric acid (*d* 1.84) and cooled to 0°. A mixture of nitric acid (*d* 1.42, 4 ml) and sulphuric acid (*d* 1.84, 5 ml) was added at 0°. The resultant mixture was maintained at 0° for 18 hours and then poured onto ice. The precipitate was collected and crystallized repeatedly from ethanol, yielding the presumed 1,5-di(*p*-nitrophenyl)pyrazole (1.5 g, 55%), m.p. 185°. Anal. Calc. for $C_{15}H_{10}N_4O_4$: N, 18.06%. Found: C, 58.57; H, 3.41; N, 17.94%.

(c) 1-p-Nitrophenyl-5-phenylpyrazole

Nitration of 1-*p*-nitrophenyl-5-phenylpyrazole (1 g) under the conditions of part (*b*), followed by chromatography on alumina and crystallization from ethanol, similarly yielded the presumed 1,5-di(*p*-nitrophenyl)-pyrazole (0.5 g, 44%), m.p. 185°, identical (mixed m.p.) with the product obtained in part (*b*).

Brominations in Chloroform Solution

(a) 1-Phenylpyrazole

Bromine (61 g) was added dropwise to 1-phenylpyrazole (50 g) in chloroform (1000 ml) at 0°. The resulting solution was shaken with an excess of sodium carbonate solution and dried over sodium carbonate. Removal of the solvent, followed by crystallization of the product from ethanol, gave 4-bromo-1-phenylpyrazole (50 g, 65%), m.p. 83° (lit. (12), 81.5–82.5°). Ultraviolet absorption: λ_{max} 263 mμ, log ϵ 4.24. Infrared absorption: strong bands in the 650–1800 cm^{-1} region at 690, 758, 845, 952, 1042, 1202, 1250, 1340, 1386, 1410, 1465, 1502, 1530, and 1600 cm^{-1}.

Further bromination, under conditions similar to the above, of either 4-bromo-1-phenylpyrazole or 1-*p*-bromophenylpyrazole yielded 4-bromo-1-*p*-bromophenylpyrazole, m.p. 81° (lit. (12), 84.5–85°) (mixed m.p. with 4-bromo-1-phenylpyrazole, ca. 72°). Ultraviolet absorption: λ_{max} 270 mμ, log ϵ 4.29. Infrared absorption: strong bands in the 650–1800 cm^{-1} region at 810, 825, 855, 955, 1080, 1340, 1385, 1400, 1500 cm^{-1}.

(b) 1-p-Biphenylylpyrazole

Bromination as for 1-phenylpyrazole, using 1-*p*-biphenylylpyrazole (10 g), yielded 1-*p*-biphenylyl-4-bromopyrazole (7.5 g, 55%), m.p. 182°, after crystallization from ethanol, identical in all respects with authentic samples as prepared below. Anal. Calc. for $C_{15}H_{11}BrN_2$: Br, 26.72%. Found: Br, 26.89%. Ultraviolet absorption: λ_{max} 284 mμ, log ϵ 4.42. Infrared absorption in the 650–1800 cm^{-1} region (cm^{-1}, intensity): 650 w, 690 s, 760 vs, 838 s, 952 vs, 1008 w, 1018 w, 1042 m, 1080 w, 1120 w, 1155 w, 1202 w, 1250 w, 1342 s, 1385 s, 1405 m, 1425 m, 1460 w, 1490 vs, 1535 s, 1610 m.

Can. J. Chem. Downloaded from www.nrcresearchpress.com by 210.87.254.5 on 09/05/12
For personal use only.

Syntheses of 1-p-Biphenylyl-4-bromopyrazole

(a) Via 4-Bromo-1-p-nitrophenylpyrazole

To 4-bromo-1-phenylpyrazole (10 g) in sulphuric acid (*d* 1.84, 20 ml) was added, at 0°, a mixture of nitric acid (*d* 1.42, 15 ml) and sulphuric acid (*d* 1.84, 20 ml). The reaction mixture was kept overnight at 0°, poured onto ice, and collected. After crystallization from ethanol, 4-bromo-1-*p*-nitrophenylpyrazole (4.8 g, 40%), m.p. 168° (lit. (22), 168–169°), was obtained. Anal. Calc. for $C_9H_6BrN_3O_2$: C, 40.31; H, 2.24; N, 15.69%. Found: C, 40.57; H, 2.33; N, 15.90%. For ultraviolet and infrared absorption, see tables.

The 4-bromo-1-*p*-nitrophenylpyrazole was reduced quantitatively to 1-*p*-aminophenyl-4-bromopyrazole, m.p. 83°, by tin and hydrochloric acid. The amine was diazotized and the diazo solution used to arylate benzene, employing the conditions noted above for the synthesis of 1-*p*-biphenylylpyrazole. Chromatography on alumina, followed by crystallization from ethanol, yielded 1-*p*-biphenylyl-4-bromopyrazole, m.p. 182°. Anal. Calc. for $C_{15}H_{11}BrN_2$: C, 60.22; H, 3.68%. Found: C, 60.03; H, 4.04; Br, 26.79%.

(b) By Free-radical Phenylation of 4-Bromo-1-phenylpyrazole

Benzoyl peroxide (10 g) was allowed to decompose in 4-bromo-1-phenylpyrazole at 90° for 66 hours. After removal of free benzoic acid (4.0 g) with sodium hydrogen carbonate solution, excess of substrate was removed by steam distillation followed by distillation under reduced pressure. The residue was chromatographed on alumina and crystallized repeatedly from ethanol, yielding 1-*p*-biphenylyl-4-bromopyrazole, m.p. 180°, having ultraviolet and infrared absorption identical with that of sample prepared as in part (*a*).

Derbyshire–Waters Bromination of 1-Phenylpyrazole

1-Phenylpyrazole (10.8 g) and bromine (5.2 ml) were dissolved in a mixture of sulphuric acid (*d* 1.84, 90 ml) and water (10 ml). Finely powdered silver sulphate (17 g) was added, and the mixture was shaken mechanically for 3 hours. Silver bromide was filtered off and the filtrate was poured onto ice. The precipitate was collected and extracted with boiling benzene. 1-*p*-Bromophenylpyrazole, m.p. 67–68°, crystallized on slow evaporation of the benzene. Crystallization from dilute methanol yielded 10.5 g (62%) of 1-*p*-bromophenylpyrazole, m.p. 70°, identical in all respects with an authentic sample (m.p., mixed m.p., superimposable ultraviolet and infrared spectra).

Ionization Constants

Ionization constants of the carboxylic acids were determined by potentiometric titration in 1:1 ethanol–water, and those of the conjugate acids of the aminophenylpyrazoles by differential ultraviolet spectrophotometry of the appropriate ionic species in buffers of varying pH.

ACKNOWLEDGMENTS

We thank the National Research Council for generous support through Operating and Equipment Grants, and Misses D. A. Chalker and J. Murphy, who provided skilled assistance with spectrophotometry.

REFERENCES

1. L. Balbiano. Gazz. Chim. Ital. **19**, 128 (1889).
2. A. Michaelis and C. A. Rojahn. Ber. **50**, 737 (1917).
3. C. A. Rojahn. Ber. **55**, 291 (1922).
4. I. L. Finar and K. E. Godfrey. J. Chem. Soc. 2293 (1954).
5. I. L. Finar and R. J. Hurlock. J. Chem. Soc. 3024 (1957).
6. D. DalMonte, A. Mangini, and R. Passerini. Gazz. Chim. Ital. **86**, 797 (1956).
7. F. G. Bordwell and E. W. Garbisch. J. Am. Chem. Soc. **82**, 3588 (1960).
8. L. J. Bellamy. The infrared spectra of complex molecules. Methuen, London. 1958. p. 77.
9. B. M. Lynch and M. A. Khan. To be published.
10. K. v. Auwers and H. Wunderling. Ber. Sect. B, **67**, 644 (1934).
11. S. Cusmando. Gazz. Chim. Ital. **70**, 227 (1940).
12. E. G. Brain and I. L. Finar. J. Chem. Soc. 2435 (1958).
13. B. M. Lynch and M. A. Khan. Can. J. Chem. In press.
14. D. H. Derbyshire and W. A. Waters. J. Chem. Soc. 573 (1950).
15. J. Arotsky and M. C. R. Symons. Quart. Rev. (London), **16**, 282 (1962).
16. H. C. Brown, D. H. McDaniel, and O. Hafliger. *In* Determination of organic structures by physical methods. *Edited by* E. A. Braude and F. C. Nachod. Academic Press, Inc., New York. 1955. p. 567.
17. R. D. Brown. Australian J. Chem. **8**, 100 (1955).
18. M. J. S. Dewar and H. N. Schmeising. Tetrahedron, **5**, 166 (1959).
19. R. G. Jones. J. Am. Chem. Soc. **71**, 3997 (1949).
20. I. L. Finar and G. H. Lord. J. Chem. Soc. 3314 (1957).
21. K. v. Auwers and H. Mauss. Ann. **452**, 182 (1927).
22. T. V. Protopopova, V. T. Kumko, and A. P. Skoldinov. Khim. Nauka i Prom. **4**, 803 (1959); Chem. Abstr. **54**, 11037 (1960).

Can. J. Chem. Downloaded from www.nrcresearchpress.com by 210.87.254.5 on 09/05/12
For personal use only.

THE SYNTHESIS AND PROPERTIES OF THE ANHYDROUS HEXACHLOROTITANATES OF RUBIDIUM AND CESIUM

R. L. LISTER AND S. N. FLENGAS
Department of Metallurgical Engineering, University of Toronto, Toronto, Ontario
Received February 1, 1963

ABSTRACT

The hexachlorotitanates of rubidium and cesium have been produced in a closed system, following the reaction

$$2MCl\ (s) + TiCl_4\ (g) = M_2TiCl_6\ (s),$$

where M is respectively Rb and Cs. With the titanium tetrachloride vapor at 1 atm, the optimum temperature for both reactions is 410±10° C.

INTRODUCTION

Because of their relatively high degree of thermal stability, the hexachlorotitanates of the alkali metals offer interesting possibilities as a source of titanium ions for the recovery of titanium metal by fused salt electrolysis.

The most recent methods for producing the hexachlorotitanates involve difficulties, either in producing the truly anhydrous salts or in yielding the stoichiometric compounds.

Thus, Ehrlich and Framm (1) prepared the compounds K_2TiCl_6, Rb_2TiCl_6, and Cs_2TiCl_6 by fractional crystallization at 0° C from an aqueous solution saturated with hydrogen chloride and containing titanium tetrachloride and the corresponding alkali metal chloride as solutes. Unsuccessful attempts were also made to produce the compounds directly in an autoclave by the reaction between titanium tetrachloride and the alkali chloride at 300° C (1).

Morozov and Toptygin (2) have produced the hexachlorotitanates by passing, over the corresponding alkali metal chloride at a specific temperature, chlorine gas saturated with titanium tetrachloride vapor. The method gave 100% yield for Cs_2TiCl_6 only, whereas the rubidium and potassium hexachlorotitanates were obtained mixed with unreacted alkali chlorides.

Pure potassium hexachlorotitanate (K_2TiCl_6) has been prepared in this laboratory by the direct reaction between titanium tetrachloride vapor and finely divided solid potassium chloride, in a closed system (3, 4).

In the present investigation, the method of preparation was further developed, and found to be applicable in the synthesis of the hexachlorotitanates of rubidium and cesium. The compounds obtained in this manner are anhydrous, and of stoichiometric composition.

EXPERIMENTAL

The titanium tetrachloride for use in the preparations was obtained by purification of the commercially pure material. This was achieved by refluxing in the presence of copper filing for about 2 hours and by fractional distillation in a dry atmosphere. The front and end tailings of the distillate were rejected, and the middle portion was stored in sealed containers.

The rubidium and cesium chlorides were of reagent grade and were further purified by sublimation at 800° C in a stream of anhydrous hydrogen chloride. The sublimate was finely ground inside a dry box, screened through a 325-mesh screen, and the −325 fraction was stored in a desiccator for future use.

Can. J. Chem. Downloaded from www.nrcresearchpress.com by 210.87.254.42 on 09/05/12
For personal use only.

The rubidium and cesium hexachlorotitanates were produced by the direct reaction, as indicated by the equation

$$2MCl\ (s) + TiCl_4\ (g) = M_2TiCl_6\ (s),$$

where M is respectively Rb and Cs.

Figure 1 shows the reaction apparatus, which was constructed from Pyrex glass.

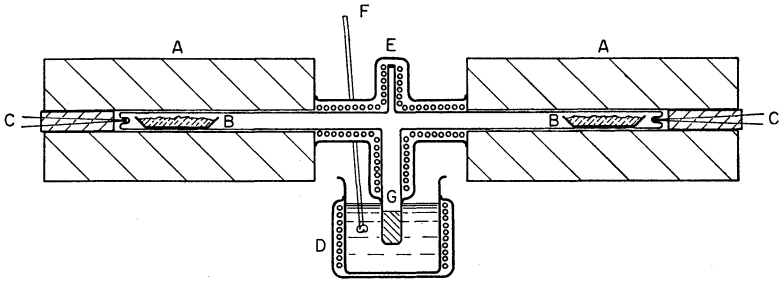

FIG. 1. Reaction apparatus. A = tube furnaces, B = pyrex boats containing the alkali metal chloride, C = temperature-measuring thermocouples, D = thermally regulated silicone oil bath, E = vacuum-sealed outlet, F = stirrer, G = titanium tetrachloride.

The titanium tetrachloride liquid was siphoned into the vertical arm of the reaction tube and frozen through the use of a dry ice – acetone mixture. Weighed amounts of the finely divided cesium and rubidium chlorides were transferred into the Pyrex boats using the dry box. The boats were then placed into the horizontal arms of the reaction tube and the ends were flame sealed. The entire apparatus was evacuated through a side arm tube at F, and sealed under vacuum. The two horizontal tubes containing the RbCl and CsCl respectively were then heated to about 410±10° C, while the titanium tetrachloride in the vertical tube was heated to 135±1° C by means of a temperature-controlled silicone bath oil. At this temperature, the pressure of titanium tetrachloride vapor in the system is slightly less than 1 atm.

After completion of the reaction, the reacted alkali chlorides in the horizontal tubes were cooled to about 150° C and held at this temperature, while the titanium tetrachloride in the reservoir was refrozen to condense the excess vapor still remaining in the reaction tube. The cell was then opened at E, and air was introduced through a calcium chloride drying tube. The products were removed by breaking the cell inside a dry box and were weighed to determine the composition of the reaction product. This determination was based on the weight of $TiCl_4$ reacted with the known amount of alkali metal chloride initially in the cell. The compound was then stored in a desiccator for further use.

Attempts to produce the corresponding compounds of Na_2TiCl_6 and Li_2TiCl_6 by this method were unsuccessful because of their instability.

RESULTS AND DISCUSSION

In all preparations, about 10 g of the −325 mesh alkali chloride was used, and the reaction time was 12 hours. It was found that the optimum reaction temperature was 410±10° C.

The composition of the reaction products from three typical runs is given in Table I.

TABLE I

	Rb_2TiCl_6 composition				Cs_2TiCl_6 composition			
	Weight (%)			Mole ratio of	Weight (%)			Mole ratio of
	Rb	Ti	Cl	$RbCl/TiCl_4$	Cs	Ti	Cl	$CsCl/TiCl_4$
Theoretical	39.60	11.10	49.30	2.00	50.49	9.10	40.41	2.00
Experimental	39.75	11.03	49.22	2.02	51.35	8.92	39.73	2.06
(3 runs)	39.72	11.05	49.23	2.01	50.84	9.09	40.07	2.01
	39.45	11.15	49.40	1.98	51.03	8.99	39.88	2.03

Can. J. Chem. Downloaded from www.nrcresearchpress.com by 210.87.254.42 on 09/05/12
For personal use only.

The slight excess of $TiCl_4$ found in some of the products represents adsorbed titanium tetrachloride that can be removed under vacuum.

Experiments done at 350° C and at 450° C yielded products of a lower titanium tetrachloride content. Granular alkali chloride reagent had also a similar inhibitive effect and the reaction with the coarse materials did not yield stoichiometric compounds. The microscopic investigation of such reacted particles indicated the existence of a surface layer of hexachlorotitanate and of an underlying core of unreacted alkali chloride. On the contrary, with the finely ground particles, the reactions proceeded to completion, as indicated by the results in Table I.

Although actual reaction rates were not investigated, it is reasonable to attribute the decreased yield at the higher temperatures to the sintering of the finely divided particles of the alkali chloride. Sintering was actually observed in all preparations done at 450° C, and the behavior of the sintered alkali chloride material should be compared with that of the granular particles mentioned above.

At temperatures below the optimum, sintering was not observed, but the rate of the reaction becomes too slow to complete the reaction within the time of observation. This is also in agreement with the results obtained by Ehrlich and Framm (1) during their autoclave experiments; at 300° C, the reacted titanium tetrachloride was always less than 1 mole%.

PROPERTIES OF THE HEXACHLOROTITANATES

At room temperature, rubidium hexachlorotitanate is light green, while the cesium hexachlorotitanate is yellow-green in color.

With respect to their stability in air, Cs_2TiCl_6 is the more stable, and its hydrolysis is very slow. On the other hand, Rb_2TiCl_6 and K_2TiCl_6 hydrolyze quite readily and should be handled in a dry atmosphere.

The approximate melting points of Rb_2TiCl_6 and Cs_2TiCl_6 were determined in sealed quartz tubes and found to be 686±5° C and 691±5° C respectively.

Diffractometer measurements were also taken on the various batches of the rubidium and cesium hexachlorotitanates. A copper target emitting a wavelength of $K\alpha$ radiation of 1.5418 Å was used with a nickel filter.

Engel (5) has shown that the rubidium and cesium hexachlorotitanates are cubic of the $Fm3m$ space group, and display the hexachloroplatinate crystal structure. Bland and Flengas (6) have shown that potassium hexachlorotitanate is also of this group.

The lattice parameter of the rubidium hexachlorotitanate was determined as 10.011± 0.005 Å, which agrees favorably with 9.9922 Å obtained by Engel (4). The calculated density of the rubidium hexachlorotitanate based on four formulae units per cell (3) is 2.85 g/cc, compared with 2.93 g/cc found by Engel. The experimental density found using reagent grade carbon tetrachloride in a standard density bottle was 2.92 g/cc. The cesium hexachlorotitanate exhibited a lattice parameter of 10.229±0.005 Å compared with 10.219 Å obtained by Engel. The calculated density for the cesium hexachlorotitanate is 3.28 g/cc compared with 3.29 g/cc calculated from the lattice parameter given by Engel. The experimental density was found to be 3.24 g/cc.

Relative peak intensities and the observed interplanar "d" spacings for Rb_2TiCl_6 and Cs_2TiCl_6 are given in Table II. The relative peak intensities and observed "d" spacings for K_2TiCl_6 as determined by Bland and Flengas (6) are also included.

Some of the physical properties of the hexachlorotitanates are summarized in Table III.

Can. J. Chem. Downloaded from www.nrcresearchpress.com by 210.87.254.42 on 09/05/12
For personal use only.

TABLE II

Plane	Rb_2TiCl_6 Observed "d" values	Rb_2TiCl_6 Relative intensity	Cs_2TiCl_6 Observed "d" values	Cs_2TiCl_6 Relative intensity	K_2TiCl_6* Observed "d" values	K_2TiCl_6* Relative intensity
111	5.8395	18	5.9060	45	5.575	23
200		10†	5.1157	45	4.840	8
220	3.5407	59	3.6187	80	3.382	8
310		13		10†	2.878	7
222	2.89020	100	2.9497	100	2.809	100
400	2.5039	82	2.5565	77	2.437	99
313		10†		29	2.214	2
420		10†	2.2893	38	2.149	4
422	2.0426	36	2.0872	38	1.985	8
511/333		10†	1.9689	29	1.880	16
440	1.7696	50	1.8085	26	1.728	79
531		20		33	1.653	12
422/600		10†		10†		2
620	1.5826	23		25	1.569	4
533		35		30		
622		26		29	1.475	49
444		28		30	1.412	19
551/711		20		20	1.371	8
640		10†		10†		
642						5

*The results for K_2TiCl_6 have been taken from Bland and Flengas (6), revised so that the 222 plane has a peak intensity equal to 100, allowing for a relative comparison between the three stable hexachlorotitanates.
†Represents values which have small peaks, the relative intensities of which could not be accurately measured.

TABLE III

Summary of properties

	K_2TiCl_6	Rb_2TiCl_6	Cs_2TiCl_6
Color at room temperature	Light yellow	Light green	Yellow-green
Crystal structure	Cubic (hexachloroplatinate)		
Lattice parameter (Å)	9.792	10.011	10.229
Space group	*Fm3m*	*Fm3m*	*Fm3m*
Density (g/cm³)			
Calculated	2.45	2.85	3.28
Experimental	2.40	2.92	3.24
Approximate melting point (°C)	695±5	686±5	691±5

ACKNOWLEDGMENTS

Acknowledgment is made to the National Research Council of Canada for a Fellowship to one of the authors (R. L. L.), and for its financial assistance in support of this work.

REFERENCES

1. P. VON EHRLICH and E. FRAMM. Z. Naturforsch. **9b**, 326 (1954).
2. I. S. MOROZOV and D. YA. TOPTYGIN. Russ. J. Inorg. Chem. **5**, 1, 42 (1960).
3. S. N. FLENGAS. Ann. N.Y. Acad. Sci. **79**, 11, 853 (1960).
4. S. N. FLENGAS and T. R. INGRAHAM. Can. J. Chem. **38**, 813 (1960).
5. G. ENGEL. Z. Krist. **90**, 341 (1935).
6. J. A. BLAND and S. N. FLENGAS. Can. J. Phys. **39**, 941 (1960).

Can. J. Chem. Downloaded from www.nrcresearchpress.com by 210.87.254.42 on 09/05/12
For personal use only.

Can. J. Chem. Downloaded from www.nrcresearchpress.com by 210.87.254.40 on 09/05/12
For personal use only.

THE PHOTOCHEMICAL DECOMPOSITION OF METHYL AZIDE[1]

C. L. CURRIE[2] AND B. deB. DARWENT
The Maloney Chemistry Laboratory, The Catholic University of America, Washington, D.C.

Received December 14, 1962

ABSTRACT

The photolysis of methyl azide has been investigated in the vapor phase at low conversions and over suitable ranges of pressure, temperature, intensity, and wavelength. Under all conditions the principal gaseous product was N_2 with small amounts of H_2 (5–11%), and traces of CH_4, C_2H_4, and C_2H_6. A condensate identified as $(CH_3N)_x$ was also found.

The quantum yield for the production of N_2 is approximately 2, independent of intensity (over a 45-fold range), temperature (17–100° C), and pressure (14–300 mm Hg). The quantum yield decreases slightly with increasing wavelength. Experiments with added CO_2, $CH_3N_2CH_3$, and C_2H_4 indicate the presence of a short chain carried mainly by the CH_3N radical. Excited species probably play some role in the reaction.

I. INTRODUCTION

The mechanism of the thermal decomposition of methyl azide, as proposed by Leermakers (1) and by Rice and Grelecki (2), appears to be rather complex and to involve more than one initial step. However, those experiments were carried to such high conversions that the initial reaction was obscured.

The photolysis of methyl azide has recently been investigated (3) in an inert matrix at low temperatures. Milligan (3) found bands in the infrared corresponding to methylenimine but not to the methylimino radical. He suggested that the methylimino radical isomerizes rapidly because of the excess energy from the photolysis:

$$CH_3N \rightarrow CH_2{=}NH.$$

The photolysis has now been investigated, in the gas phase, at small conversions, as functions of intensity, wavelength, pressure, and temperature. The effects of free radical scavengers and an inert gas have also been investigated.

II. EXPERIMENTAL

1. Materials

(a) Methyl azide.—Prepared by the methylation of sodium azide with methyl sulphate (4). The gaseous azide was dried with calcium chloride and condensed at −80° C. The condensate was distilled through a Vigreaux column and the fraction boiling at 20–21° C collected. That fraction was purified further by trap-to-trap distillation *in vacuo* at −80° C and the middle fraction retained.

(b) Azomethane.—Prepared by the oxidation of symmetrical dimethylhydrazine with cuprous chloride (5). The product was distilled and the middle fraction retained.

(c) Ethylene, carbon dioxide, and hydrogen sulphide.—Obtained commercially (Research Grade). Purified by trap-to-trap distillation *in vacuo* and stored in bulbs.

(d) Potassium ferrioxalate.—Prepared from reagent grade potassium oxalate and ferric chloride (6), with subsequent recrystallization.

2. Apparatus

The apparatus was a rather conventional all-glass high-vacuum system of the type used in gas kinetic studies. Mercury was rigorously excluded to avoid dangers of an explosion (7). A circulating pump, of the type designed by Watson (8), was included in the reaction system to ensure the proper mixing of the gases.

[1]*Presented in part at the meeting of the American Chemical Society, St. Louis, Missouri, March 1961. This is taken from the dissertation submitted by C. L. Currie to the Catholic University of America in partial fulfillment of the requirements for the degree of Doctor of Philosophy.*

This work was supported in part by the United States Army Engineer Research and Development Laboratories, Fort Belvoir, Va., under Contract Numbers DA-44-009-ENG-4139 and DA-44-009-ENG-3574.

[2]*Present address: Woodstock College, Woodstock, Maryland.*

The light source was a quartz-jacketed medium-pressure mercury arc. A grating monochromoter (Farrand Optical Co., Catalog No. 91087) was used in experiments where essentially monochromatic light was required.

3. Analysis

The products of the reaction were divided into three fractions: (*a*) uncondensable gases (N_2, H_2, CH_4), (*b*) C_2 fraction, and (*c*) heavy products.

The uncondensable gases were measured and analyzed by CuO oxidation and mass spectrometric methods.

The C_2 fraction was analyzed by GLPC using a silica gel column, which had been shown to separate ethane and ethylene.

The gaseous portion of the heavy products was also analyzed by GLPC with a column of silicone oil 203 (Dow Corning) on "Chromosorb W" (Fisher Scientific Co.) at room temperature. That column effected a satisfactory separation of HN_3, NH_3, HCN, $CH_3N_2CH_3$, CH_3N_3, and the trace impurities (H_2O, CH_3OCH_3, and CH_3Cl).

The higher-boiling products remained on the walls of the reaction cell and in the first trap, both of which were removable. The products were dissolved in water and analyzed. Hexamethylenetetramine (HMTA) was determined as formaldehyde, according to the spectrometric method of McFadyen (9), after hydrolysis with 2 *N* H_2SO_4. The first few experiments showed clearly that HMTA was equivalent to less than 10% of the N_2 formed and, in subsequent experiments, the solution of the heavy products was subjected to micro-Kjeldahl analysis[3] for total nitrogen.

4. Actinometry

The total incident intensity was measured by the use of potassium ferrioxalate as an actinometer (6, 10), the Fe^{++} produced was measured with a Beckman DU spcetrophotometer. The absorption coefficient of the azide was also measured with the spectrophotometer over the range of wavelengths used in this investigation. The quantum yield was measured at various wavelengths. using essentially monochromatic light from the monochrometer.

When using the full mercury arc, relative intensities were determined from the rate of formation of hydrogen in the photolysis of hydrogen sulphide (11). The intensity was altered by changing the diameter of a hole in a metal screen placed between the mercury arc and the collimating lens.

5. Effect of Added Gases

In these experiments CH_3N_3 was photolyzed alone, to very small conversion, and the rate of formation of N_2 measured. The second gas was then introduced to the residue and the photolysis repeated. The full mercury arc was used in all of these experiments.

III. RESULTS

1. Absorption Spectrum

The ultraviolet absorption of CH_3N_3 was found to exhibit maxima at 2880 Å and below 2400 Å. No structure was found in either band. The absorption obeyed Beer's law accurately between 14 and 300 mm Hg and between 2540 and 3130 Å.

2. Products

The gaseous products consisted predominantly of N_2. Other products were H_2 (6–11%); CH_4 (1%); C_2H_6 (1%). HCN was produced at approximately the same rate as H_2. This ratio of products persisted at all temperatures, pressures, intensities, and wavelengths used. Azomethane was not detected and so amounted to less than 5% of the N_2 formed. The rates of formation of the products were independent of time up to at least 2% conversion.

The heavy product contained small amounts of $(CH_2)_6N_4$ and much larger amounts of other N-containing compounds. The results of two analyses are given in Table I. It is evident that the number of atoms of N in the heavy product is very close to the number of moles of N_2 produced as a gas. This requires that the condensate have the empirical formula CH_3N for a satisfactory material balance. Hexamethylenetetramine accounted for only 3% of the total heavy products. Accordingly, the stoichiometry of the process is largely

$$x CH_3N_3 \rightarrow (CH_3N)_x + N_2,$$

[3]*We are indebted to Robert J. Koegel of the National Institutes of Health for those analyses.*

Can. J. Chem. Downloaded from www.nrcresearchpress.com by 210.87.254.40 on 09/05/12
For personal use only.

TABLE I

Nitrogen-containing products and material balance

		Products (moles×10⁶)		
			Condensate	
P (mm Hg)	Decomp. (%)	Gas N_2	$(CH_2)_6N_4$	Total N_2
97.5	5.2	5.06	0.16	2.68
101	4.7	4.70	0.15	2.42

and only a relatively small amount of the azide reacts by other paths leading to the minor amounts of H_2, CH_4, and $(CH_2)_6N_4$ found.

3. Quantum Yield

The effects of wavelength and pressure on the quantum yield of N_2 at 30° C are given in Table II. The conversion never exceeded 1% and was usually lower than 0.1%. ϕ_{N_2} is essentially independent of P and increases with decreasing λ from 1.7 in the region 2750–3130 Å to 2.3 at 2540 Å.

TABLE II

Quantum yields for N_2 production (reaction temp. = 30° C)

CH_3N_3 (mm Hg)	% absorp.	I_0 (einstein min^{-1} ×10⁹)	R_{N_2} (moles min^{-1} ×10⁹)	ϕ_{N_2}
2540 Å				
18	18.0	2.99	1.29	2.4
150	81.5	2.99	5.25	2.2
300	99.0	2.99	6.71	2.3
2652 Å				
150	91.0	2.42	4.16	1.9
300	99.0	2.42	5.34	2.2
2750 Å				
14	24.0	18.9	7.59	1.7
80	72.9	18.9	26.5	1.7
150	94.7	18.9	33.5	1.8
2925 Å				
14	26.4	6.50	2.41	1.4
80	82.2	6.50	8.82	1.7
150	96.2	6.50	10.2	1.6
300	99.3	6.50	11.4	1.8
3130 Å				
50	36.9	11.1	6.66	1.6
150	75.0	11.1	15.1	1.8
300	93.6	9.64	15.0	1.7

Consecutive determinations of the incident intensity with the actinometer did not vary by more than ±3%. The agreement with Beer's law was precise enough to suggest that the uncertainty in the measurement of the fraction of light absorbed in the spectrophotometer did not exceed ±1%. The only other factor in the calculation of the absorbed intensity was the path lengths in the spectrophotometer cell and in the reaction cell, 10.0 and 14 cm, respectively. The former was known accurately, but the latter was uncertain to ±1 cm because of the geometry of the cell. Thus the absolute values for the quantum

Can. J. Chem. Downloaded from www.nrcresearchpress.com by 210.87.254.40 on 09/05/12
For personal use only.

yields are probably accurate to ±10%. Accordingly, the dependence on wavelength is thought to be real, especially at the higher pressures, where the essentially complete absorption would minimize the uncertainties in the quantum yield determination.

The quantum yield for the production of nitrogen was also found to be independent of time within the percentage conversions studied (Fig. 1) and essentially independent of

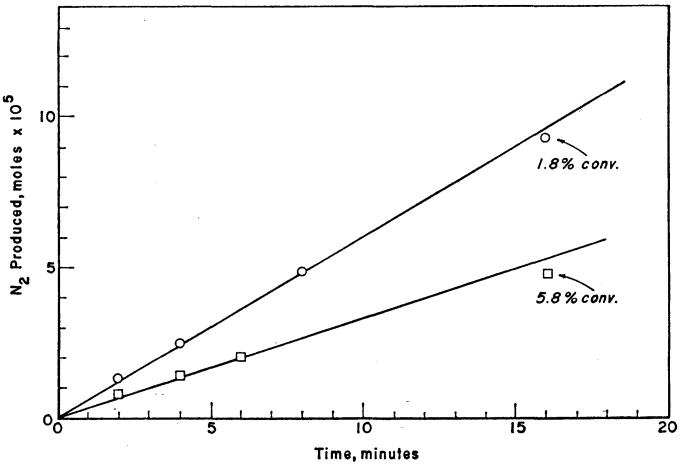

FIG. 1. Effect of time on the production of N_2 at room temperature. Pressure of azide: □ 15 mm Hg; ○ 100 mm Hg.

the intensity ($R_{N_2} \propto I_a^{0.9}$ rather than $I_a^{1.0}$) over a 45-fold variation in intensity and of temperature up to 100° C, the threshold of the thermal reaction.

4. Added Gases

The effect of free radical scavengers and inert gases on the rate of N_2 production was studied to determine the role of free radicals and excited species in the photolysis. The marked inhibition by both C_2H_4 and $CH_3N_2CH_3$, but much smaller inhibition by CO_2 is shown in Fig. 2. The addition of 10% of C_2H_4 reduced the rate of N_2 production by 35% (at 300 mm pressure) to 45% (at 15 mm pressure). The addition of 1% of $CH_3N_2CH_3$ gave the same inhibition as 10% C_2H_4, and as little as 0.03% of the former inhibited the rate of N_2 production by 10%. The inhibiting effect of CO_2 was very much smaller; even 120 times as much CO_2 did not reduce the rate by more than 20%.

5. Hydrogen

The ratio of H_2/N_2 was studied as a function of pressure, wavelength, percentage decomposition, and added gases in an attempt to elucidate the elementary reaction involved in its production. The data in Table III give the ratio as a function of pressure and wavelength. Since H_2 was measured as the difference between two relatively large numbers, the measurement is subject to an uncertainty of about 10%. With this qualification Table III shows that the H_2/N_2 ratio is independent of wavelength and intensity and that it decreases with increasing pressure. The rate of H_2 production was also found to be independent of percentage conversion and much less inhibited by C_2H_4 and $CH_3N_2H_3$ than the rate of N_2 production. The inhibition by CO_2 was about the same for H_2 as for N_2.

Can. J. Chem. Downloaded from www.nrcresearchpress.com by 210.87.254.40 on 09/05/12
For personal use only.

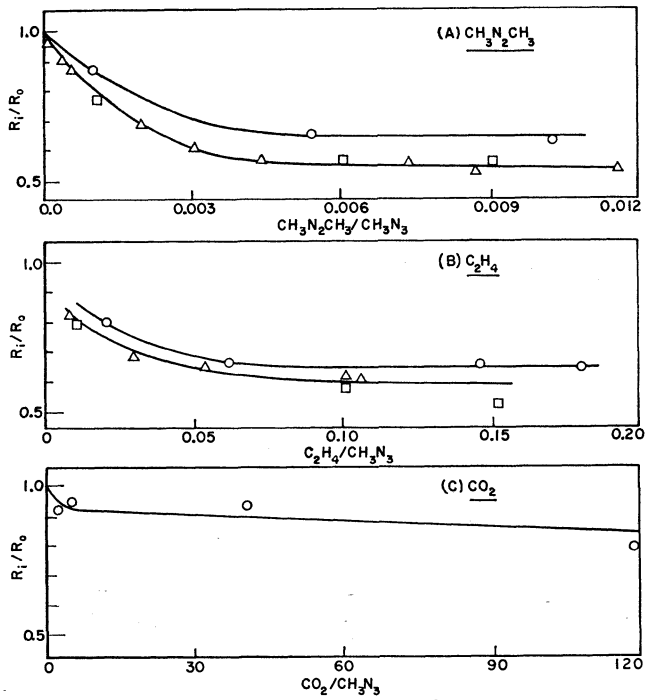

FIG. 2. Effect of free radical inhibitors (C_2H_4, $CH_3N_2CH_3$) and an inert gas (CO_2) on the rate of the reaction. R_i, rate of inhibited reaction; R_o, rate of uninhibited reaction. Pressure of azide: □ 15 mm Hg; △ 100 mm Hg; ○ 300 mm Hg.

TABLE III

Effect of pressure and wavelength on the ratio H_2/N_2

CH_3N_3 (mm Hg)	$(H_2/N_2)\times100$				
	Full arc	2540 Å	2650–2800 Å	2925 Å	3130 Å
5	10.6	—	—	—	—
15	9.0	10.4	8.4	10.4	—
50	7.3	—	—	—	7.2
50*	7.3	—	—	—	—
80	—	—	6.0	—	7.5
100	6.4	—	—	—	—
150	—	7.5	6.0	7.0	5.9
300	5.7	5.0	—	5.3	5.4

*Experiments with 45-fold decrease in intensity.

IV. DISCUSSION

1. *Primary Act*

The fact that N_2 is by far the most prevalent of the gaseous products suggests that the only important primary act is:

$$CH_3N_3 + h\nu \rightarrow CH_3N + N_2. \qquad [0]$$

The very small yields of CH_4, C_2H_4, C_2H_6, and HN_3 suggest that neither of the processes

$$CH_3N_3 + h\nu \nearrow CH_3 + N_3 \qquad [0']$$

$$\searrow CH_2 + HN_3 \qquad [0'']$$

Can. J. Chem. Downloaded from www.nrcresearchpress.com by 210.87.254.40 on 09/05/12
For personal use only.

is important. Evans *et al.* (12) have shown, on the basis of correlation rules and thermochemical data, that HN_3 should decompose into NH and N_2 rather than into H and N_3, and a similar argument should apply to CH_3H_3.

A previous investigation (1) of the thermal decomposition of CH_3N_3, which reported that C_2H_4 and HN_3 were important products, suggested that reaction [0″] accounted for 25% of the initial step. However, the conversions in that work were extensive, and sometimes complete. In the present investigation a few experiments, in which CH_3N_3 was decomposed thermally at 100° C, to very small conversions, showed that N_2 was the only important gaseous product. Accordingly, it is likely that the C_2H_4 and HN_3 arose from secondary processes and that reaction [0] is the only important initial step in the pyrolysis and in the photolysis.

The dependence of the quantum yield on wavelength suggests that either or both of the CH_3N and N_2 formed in reaction [0] is excited. Although no value for the $CH_3N—N_2$ bond dissociation energy is available, that of the $HN—N_2$ bond has been given as 33 ± 2 (3) and 37 (13) kcal mole^{-1}. Hence, the dissociation energy of the $CH_3N—N_2$ bond is probably not far from 40 kcal mole^{-1}. Since the energy of the incident radiation varied between 91 and 112 kcal mole^{-1}, the CH_3N and N_2 must have shared approximately 50 to 70 kcal mole^{-1} between them; the excess energy may be even greater.

2. Secondary Reactions

The fact that ϕ_{N_2} was always greater than unity in the uninhibited experiments and was decreased by very small concentrations of radical inhibitors suggests that the CH_3N radicals cause further decomposition of the azide, possibly by an insertion type of reaction:

$$CH_3N + CH_3N_3 \rightarrow (CH_3N)_2 + N_2, \qquad [1]$$

where the CH_3N may or may not be excited and the $(CH_3N)_2$ is probably azomethane.

The almost complete independence of ϕ_{N_2} on intensity requires the combination and disproportionation reactions

$$2CH_3N \rightarrow (CH_3N)_2 \qquad [a]$$

$$\rightarrow CH_3NH + CH_2N \qquad [b]$$

to be much less important than reaction [1], even at the lowest pressure of azide. The experiments with inhibitors show that the addition of very small amounts of azomethane drastically reduces the rate of formation of N_2. Accordingly, a reaction between CH_3N and azomethane, probably of the type

$$CH_3N + (CH_3N)_2 \rightarrow (CH_3N)_3, \qquad [2]$$

is considerably faster than reaction [1]. Actually, if azomethane is formed in reaction [1], the fact that no trace of it was detected in the products supports the suggestion that reaction [2] is very fast. The nature of the product of reaction [2] is quite unknown but it does correspond stoichiometrically with the analysis of the heavy products.

A mechanism based only on reactions [0], [1], and [2] gives

$$\phi_{N_2} = 1 + \frac{1}{1+\alpha}, \qquad [A]$$

where $\alpha = k_2(CH_3N_2CH_3)/k_1(CH_3N_3)$. Since the experiments have shown that ϕ_{N_2} is independent of time, it must be assumed that $CH_3N_2CH_3$ rapidly attains a steady state concentration, if it is formed at all. In that event $\alpha = 1$ and the maximum value of ϕ_{N_2}

Can. J. Chem. Downloaded from www.nrcresearchpress.com by 210.87.254.40 on 09/05/12
For personal use only.

would be 1.5. However, the quantum yield actually was within the range 1.7 to 2.3, for monochromatic light, and averaged 2.0 for the unfiltered light. The discrepancy between the calculated and observed values suggests that excited species (CH_3N^* and N_2^*) play some part in the reaction. Processes such as

$$CH_3N^* + CH_3N_3 \rightarrow 2CH_3N + N_2 \quad [3]$$

$$N_2^* + CH_3N_3 \rightarrow CH_3N + 2N_2 \quad [4]$$

would increase ϕ_{N_2} above 1.5. The increase in the quantum yield with decreasing wavelength supports the above suggestion. The experiments with CO_2 using unfiltered light show that ϕ_{N_2} may be reduced as much as 20% by an inert gas. If all the excited species were deactivated in those experiments, the resulting $\phi_{N_2} = 1.6$ agrees satisfactorily with that predicted by equation [A].

The results of the inhibition experiments (Fig. 2) show that the ratio R_1/R_0 is independent of the pressure of azide, as required by equation [A], between 15 and 100 mm. However, there is a decided effect of pressure between 100 and 300 mm; both ethylene and azomethane are less efficient inhibitors at 300 mm than at 100 mm. That effect is contrary to the requirements of equation [A]. The disagreement cannot be ascribed only to hot radical reactions; it does suggest that the reaction may be partly heterogeneous, but this is quite speculative.

Milligan (3) found no evidence for the presence of CH_3N when CH_3N_3 was photolyzed in an inert matrix at 4° K. He suggested that the isomerization:

$$CH_3N \rightarrow CH_2NH, \quad [5]$$

was very rapid. Although the CH_3N radicals may all react in the gas phase with CH_3N_3, in a matrix, in the absence of any other reactant, they may isomerize, as Milligan found.

3. H_2 Production

Since the H_2 formed is only 5–10% of N_2, its production has been neglected to a first approximation. However, the dependence of H_2 on various parameters does offer some information about the H_2 precursor, and thus is of some interest.

The independence of the rate of H_2 production on percentage of conversion indicates that H_2 is not produced from a stable product of the photolysis, e.g., from photolysis of the condensate. One possible reaction for its formation is:

$$CH_3N^* \rightarrow H_2 + HCN, \quad [7]$$

and actually HCN has been found to be produced at approximately the same rate as H_2. No closer correlation can be made between the two quantities since the amount of HCN represented the threshold of detection of the analysis.

The decrease of R_{H_2} with increasing pressure suggests that the H_2 originates from an excited species but the independence of wavelength argues against this, unless the energy of the precursor is approximately independent of wavelength. The pressure effect is probably due to competition between a first-order decomposition of the radical, reaction [7], and a second-order reaction involving the radical, reaction [1]. Another possible interpretation of the pressure effect is that the H_2 is formed by the radical decomposing on the wall and that fewer radicals reach the walls at the higher pressures.

REFERENCES

1. H. A. LEERMAKERS. J. Am. Chem. Soc. **55**, 3098 (1933).
2. F. O. RICE and C. J. GRELECKI. J. Phys. Chem. **61**, 830 (1957).
3. D. E. MILLIGAN. J. Chem. Phys. **35**, 1491 (1961).

Can. J. Chem. Downloaded from www.nrcresearchpress.com by 210.87.254.40 on 09/05/12
For personal use only.

4. O. DIMROTH and W. WISLICENUS. Ber. **38**, 1573 (1905).
5. F. P. JAHN. J. Am. Chem. Soc. **59**, 1761 (1937).
6. C. A. PARKER. Proc. Roy. Soc. (London), Ser. A, **220**, 104 (1953).
7. C. L. CURRIE and B. DEB. DARWENT. Can. J. Chem. **41**, 1048 (1963).
8. J. S. WATSON. Can. J. Tech. **34**, 373 (1956).
9. D. A. MCFADYEN. J. Biol. Chem. **158**, 107 (1945).
10. C. G. HATCHARD and C. A. PARKER. Proc. Roy. Soc. (London), Ser. A, **235**, 518 (1956).
11. B. DEB. DARWENT and R. ROBERTS. Proc. Roy. Soc. (London), Ser. A, **216**, 344 (1953).
12. B. L. EVANS, A. D. YOFFE, and P. GRAY. Chem. Rev. **59**, 515 (1959).
13. J. L. FRANKLIN, V. H. DIBELER, R. M. REESE, and M. KRAUSS. J. Am. Chem. Soc. **80**, 298 (1958).

Can. J. Chem. Downloaded from www.nrcresearchpress.com by 210.87.254.40 on 09/05/12
For personal use only.

THE PYROLYSIS OF TRIMETHYL GALLIUM

M. G. JACKO[1] AND S. J. W. PRICE
Department of Chemistry, Essex College, Assumption University of Windsor, Windsor, Ontario
Received October 31, 1962

ABSTRACT

The pyrolysis of trimethyl gallium has been studied in a toluene carrier flow system from 686° K to 983° K using total pressures from 6.1 mm to 31.1 mm. The progress of the reaction was followed by measuring the amount of methane, ethane, and ethylene formed. The rate constants decline rapidly if the toluene-to-alkyl ratio is decreased below 45. Part of this decrease has been shown to result from the loss of methyl radicals as ethylbenzene, propane, propylene, and xylenes. In an unseasoned vessel, the decomposition is markedly dependent on surface conditions. In the unpacked conditioned vessel, the reaction is 94% homogeneous in the first bond region and 97% homogeneous in the second bond region.

The decomposition occurs in two steps:

$$Ga(CH_3)_3 \rightarrow Ga(CH_3)_2 + CH_3 \quad [1]$$

$$Ga(CH_3)_2 \rightarrow Ga(CH_3) + CH_3. \quad [2]$$

The analysis of a black solid from the reaction zone is consistent with the formation of $(GaCH_3)_n$. Both rate constants depend on the total pressure in the system, the dependence of k_1 being very slight. A least-squares analysis of the experimental results gives:

$$\log_{10} k_1 (sec^{-1}) = 15.54 - (59{,}500/2.303RT)$$

$$\log_{10} k_2 (sec^{-1}) = 7.94 - (35{,}410/2.303RT).$$

INTRODUCTION

No previous kinetic studies of the thermal decomposition of trimethyl gallium have been reported. The heat of formation of trimethyl gallium has been obtained by the reaction of trimethyl gallium with iodine in benzene solution (1) and by the combustion of trimethyl gallium with oxygen (2). The mean gallium–carbon bond energies obtained from these studies are respectively 56.7±4 kcal/mole and 57.7±2 kcal/mole. In a recent review Long (3), using $D(CH_3—H) = 102.5$ kcal/mole, has recommended a value of 57.5 kcal/mole.

EXPERIMENTAL

Materials

(a) Trimethyl Gallium

Trimethyl gallium was prepared by refluxing pure gallium with dimethyl mercury in an atmosphere of dry nitrogen, using mercuric chloride as catalyst (4). The fraction boiling at 56° C (uncorrected) was degassed by bulb-to-bulb distillation and stored under vacuum at −190° C. Melting point and vapor pressure data were in agreement with literature values (2).

(b) Toluene

(i) Toluene was prepared by the diazotization of *o*-toluidine followed by deamination with sodium hypophosphite. The organic layer was dried over anhydrous calcium chloride and fractionally distilled. The fraction boiling 109–110° C (uncorrected) was dried by refluxing over sodium under vacuum and degassed by bulb-to-bulb distillation.

(ii) Toluene from sulphonic acid (Eastman Organic, X325) has been found to be as suitable as that described above. It was dried by refluxing over sodium under vacuum and then degassed by bulb-to-bulb distillation.

Apparatus and Procedure

The experiments were carried out in a typical toluene carrier flow system in which the reaction zone was 195 cc. In the runs with the vessel packed with quartz tubing, the surface area in the reaction zone was increased by a factor of 10 and its volume reduced to 145 cc. Pressures were measured using a mercury – dioctyl phthalate differential manometer designed to give a magnification of 10 to 1. The trimethyl gallium vapor was injected into the toluene stream through a capillary sealed to the barrel of a stopcock at the top

[1]*Recipient of a National Research Council of Canada Studentship.*

Can. J. Chem. Downloaded from www.nrcresearchpress.com by 210.87.254.5 on 09/05/12
For personal use only.

of the alkyl reservoir. The alkyl and toluene vessels were weighed at the end of each run to determine the amount of each used. In each experiment a pre-run of 4 to 6 minutes during which only toluene was passed was used to stabilize flow conditions. A similar post-run was used to remove all products from the reaction zone while conditions were still stabilized. In a few selected runs using the toluene from sulphonic acid, pre-runs were extended to 30 minutes. During the first 25 minutes the gaseous products were collected and measured. The rate constants obtained agreed with those obtained from the decomposition of toluene from *o*-toluidine (5). An acetone – dry ice trap removed toluene, ethylbenzene, dibenzyl, and similar products. The remaining products were transferred by a diffusion pump to a Le Roy still at −160° C to remove traces of toluene and hydrocarbons higher than C_2. The remaining H_2, CH_4, C_2H_6, and C_2H_4 were transferred past a non-return valve to a gas burette with the aid of a Toepler pump. After the gaseous mixture was measured, a sample was taken for chromatographic analysis.

The chromatographic analyses were carried out using a 2-m silica gel column at 40° C with a flow rate of approximately 20 cc/min. Internal standards were run with each set of analyses so that peak heights could be used. In a few selected runs, the contents of the acetone – dry ice trap were analyzed using a 2-m di-isodecyl phthalate on diatomaceous earth column at 130° C with a flow rate of 28.5 cc/min. This method is sensitive to better than 0.0002 part ethylbenzene or xylenes in toluene.

Analysis of a black solid recovered from the reaction zone was carried out by admitting concentrated hydrochloric acid (12 *N*) to an evacuated bulb containing a weighed sample. After 6 hours' digestion at 75° C, the bulb was cooled to −190° C. The non-condensable products were collected and measured and a sample taken for chromatographic analysis. The mixture in the flask was filtered through a weighed sintered-glass crucible to determine the weight of the insoluble materials. The remaining solution was then twice evaporated to near dryness and then analyzed for gallium by titration with 0.01 *M* potassium ferrocyanide using 3,3′-dimethylnaphthidine in the presence of a trace of ferricyanide as indicator (6).

RESULTS AND DISCUSSIONS

Selected experimental results are given in Tables I and II. Analysis of the data indicates that the thermal decomposition of trimethyl gallium does not occur by the simple release of three methyl radicals. It was found that even at 1075° K no more than two thirds of the theoretical quantity of methyl radicals could be accounted for. This is similar to the decomposition of trimethyl antimony (7) where the formation of $(SbCH_3)_n$ was indicated. To test for the possible formation of a similar gallium polymer, a black deposit scraped from the reaction zone was analyzed as previously described. The results of this analysis indicated: 80% gallium (I) oxide, 12% carbon, and 8% gallium methyl. The carbon is probably due to the decomposition of the carrier in the high-temperature runs. Since limited quantities of air were admitted to the reaction vessel between certain runs to test for surface effects, the Ga_2O could easily be formed from the reaction of O_2 with $(GaCH_3)_n$. Subsequently analyses were carried out on the contents of the acetone – dry ice trap and on the deposit in the furnace following each of a series of experiments. Under conditions such that less than one third of the theoretical yield of methyl radicals was observed, the gallium was found quantitatively in the acetone – dry ice trap. At temperatures above which two thirds decomposition occurred, the gallium was found quantitatively in the reaction vessel, as a thin, apparently non-metallic film. It therefore seems plausible that $GaCH_3$ does not decompose but deposits in the reaction vessel as $(GaCH_3)_n$.

The following mechanism is proposed:

$$Ga(CH_3)_3 \rightarrow Ga(CH_3)_2 + CH_3 \quad [1]$$

$$Ga(CH_3)_2 \rightarrow Ga(CH_3) + CH_3 \quad [2]$$

$$n(GaCH_3) \rightarrow (GaCH_3)_n \quad [3]$$

$$CH_3 + C_6H_5{-}CH_3 \rightarrow C_6H_5{-}CH_2 + CH_4 \quad [4]$$

$$2CH_3 \rightarrow C_2H_6 \quad [5]$$

$$2C_6H_5{-}CH_2 \rightarrow (C_6H_5{-}CH_2)_2. \quad [6]$$

The small amounts of ethylene formed were assumed to arise from the reactions

$$CH_3 + C_2H_6 \rightarrow C_2H_5 + CH_4 \quad [7]$$

$$C_2H_5 \rightarrow C_2H_4 + H. \quad [8]$$

Can. J. Chem. Downloaded from www.nrcresearchpress.com by 210.87.254.5 on 09/05/12
For personal use only.

Can. J. Chem. Downloaded from www.nrcresearchpress.com by 210.87.254.5 on 09/05/12
For personal use only.

TABLE IA

Temp. (°K)	Contact time (sec)	Total pressure (mm)	Length of run (min)		$GaMe_3$ (10^{-3}mole)	CH_4 (10^{-3}mole)	C_2H_6 (10^{-3}mole)	C_2H_4† (10^{-3}mole)	k_2 (sec^{-1})	$k_a/k_r^{1/2}$ ((cc/mole-sec)$^{1/2}$)
			Total	Alkyl						
983	1.103	13.0	50.0	40.0	0.765	1.205	0.0520	0.0160	1.258	1007
970	1.212	13.0	50.0	40.0	0.591	0.925	0.0222	0.0111	0.944	1066
961*	1.250	13.0	90.0	50.0	0.628	0.932	0.0244	0.0209	0.782	960
958	1.232	13.0	45.0	35.0	0.609	0.912	0.0267	0.0134	0.802	1020
936	1.300	13.0	45.0	35.0	0.852	1.070	0.0470	0.0160	0.399	942
934*	1.342	13.0	50.0	40.0	0.496	0.700	0.0161	0.0135	0.564	975
914	1.842	6.2	70.0	60.0	0.826	0.905	0.0662	0.0181	0.194	1142
914	1.462	9.2	60.0	50.0	0.930	1.032	0.0478	0.0179	0.198	1022
914	1.312	13.0	45.0	35.0	0.809	0.949	0.0860	0.0240	0.282	892
914	1.213	18.8	40.0	30.0	0.912	1.155	0.0417	0.0139	0.406	792
914	1.092	27.1	35.0	24.5	0.888	1.102	0.0224	0.0128	0.354	729
914	0.987	29.1	31.0	22.5	0.957	1.240	0.0335	0.0126	0.504	669
901*	1.369	13.0	63.0	50.0	0.669	0.838	0.0262	0.0210	0.365	800
894	1.342	13.0	40.0	30.0	0.913	1.088	0.0604	0.0158	0.195	890
869	1.355	13.0	38.0	30.0	1.042	1.008	0.0670	0.0194	0.105	750
868*	1.530	13.0	70.0	60.0	0.687	0.778	0.0312	0.0207	0.217	624
855*	1.400	13.0	60.0	50.0	0.661	0.677	0.0262	0.0131	0.110	670
848	1.390	13.0	33.0	25.0	1.130	1.040	0.0750	0.0240	0.0745	784
843	1.412	13.0	36.0	25.0	1.270	1.110	0.104	0.0250	0.0583	724
829*	1.474	13.0	50.0	40.0	0.476	0.443	0.0231	0.0154	0.0663	

*Packed vessel runs.
†Moles H_2 approximately equal to moles C_2H_4.

Can. J. Chem. Downloaded from www.nrcresearchpress.com by 210.87.254.5 on 09/05/12
For personal use only.

TABLE IB

Temp. (°K)	Contact time (sec)	Total pressure (mm)	Length of run (min)		$GaMe_3$ (10^{-3}mole)	CH_4 (10^{-3}mole)	C_2H_6 (10^{-3}mole)	C_2H_4† (10^{-3}mole)	k_1 (sec^{-1})	$k_a/k_r^{1/2}$ ((cc/mole-sec)$^{1/2}$)
			Total	Alkyl						
839	1.460	13.0	38.0	30.0	1.011	0.774	0.0497	0.0162	1.51	645
835	1.668	13.0	34.0	25.0	1.043	0.803	0.0490	0.0204	1.40	714
832	1.422	13.0	40.0	30.0	0.897	0.605	0.0343	0.0120	1.06	598
818	1.935	6.9	60.0	50.0	0.522	0.282	0.0150	0.0075	0.508	572
817	1.640	9.3	60.0	50.0	0.475	0.240	0.005	0.004	0.477	571
817	1.450	13.0	69.0	60.0	1.000	0.482	0.0156	0.0104	0.524	373
817	1.476	13.0	53.0	42.0	1.390	0.645	0.0136	0.0068	0.463	798
817	1.481	13.0	31.0	20.0	1.018	0.495	0.0209	0.0083	0.525	735
817	1.244	23.9	40.0	30.0	0.862	0.384	0.0086	0.0057	0.520	366
816*	1.535	13.0	50.0	40.0	0.620	0.430	0.0260	0.0130	1.170	468
816	1.165	31.1	38.0	25.0	0.556	0.280	0.0060	0.0040	0.660	280
811	1.150	30.8	50.0	40.0	0.973	0.338	0.007	0.004	0.400	291
809	1.197	27.7	37.0	27.0	0.791	0.255	0.004	0.003	0.350	298
813	1.510	13.0	38.0	30.0	0.984	0.345	0.0177	0.0020	0.329	553
810	1.568	13.0	40.0	30.0	1.280	0.624	0.032	0.016	0.525	588
805*	1.538	13.0	60.0	50.0	0.767	0.437	0.0270	0.0142	0.733	398
804	1.482	13.0	40.0	31.0	1.384	0.467	0.0208	0.0075	0.319	566
795*	1.588	13.0	50.0	40.0	0.626	0.210	0.0125	0.0069	0.319	314
794	1.490	13.0	40.0	30.0	1.245	0.230	0.0091	0.0030	0.154	426
776*	1.550	13.0	53.0	40.0	1.032	0.262	0.00505	0.00289	0.203	598
771	1.614	13.0	38.0	30.0	1.288	0.104	0.0026	0.0017	0.0570	313
765	1.565	13.0	38.0	30.0	1.210	0.0474	0.0009	0.0003	0.0275	308
758	1.640	13.0	54.0	45.0	1.95	0.0849	0.0020	0.0014	0.0287	231
757*	1.632	13.0	81.0	70.0	0.784	0.0885	0.00250	0.00220	0.0824	190
755	1.592	13.0	50.0	37.0	1.610	0.0416	0.0005	0.0003	0.0183	283
744	1.619	13.0	60.0	52.0	0.748	0.0796	0.00089	0.00067	0.0717	337
737	1.675	13.0	39.0	31.0	1.462	0.0410	0.0005	0.0003	0.0165	190
729*	1.842	13.0	125.0	115.0	1.405	0.0822	0.00052	0.00052	0.0337	282
686*	1.795	13.0	151.0	125.0	1.660	0.0648	0.00010	0.00000	0.0218	

*Packed vessel runs.
†Moles H_2 approximately equal to moles C_2H_4.

Can. J. Chem. Downloaded from www.nrcresearchpress.com by 210.87.254.5 on 09/05/12
For personal use only.

TABLE II

Temp. (°K)	Contact time (sec)	Total pressure (mm)	Length of run (min)		$GaMe_3$ (10^{-3}mole)	CH_4 (10^{-3}mole)	C_2H_6 (10^{-3}mole)	C_2H_4 (10^{-3}mole)	k_1 (sec^{-1})	toluene† / alkyl
			Total	Alkyl						
817	1.468	13.0	24.0	15.0	1.290	0.388	0.0181	0.0090	0.283	23.7
817	1.481	13.0	31.0	20.0	1.018	0.495	0.0209	0.0083	0.525	39.9
817	1.462	13.0	36.0	25.0	1.090	0.410	0.0209	0.0083	0.388	46.7
817	1.476	13.0	53.0	42.0	1.390	0.645	0.0136	0.0068	0.463	61.0
817	1.450	13.0	69.0	60.0	1.001	0.482	0.0156	0.0104	0.524	124.0
801*	2.05	13.0	30.0	18.0	2.02	0.494	0.711	0.0230	0.200	7.6
801*	1.536	13.0	25.0	15.0	0.969	0.0169	0.0119	0.0051	0.203	22.8
801*		13.0	← Packed vessel Arrhenius curve →						0.500	96.0

*Packed vessel runs.
†Molar ratio.

It was apparent from the analysis of the data that the second methyl radical was not released immediately after the first. The pattern of log $k_4/k_5^{1/2}$ shown in Fig. 1 indicates

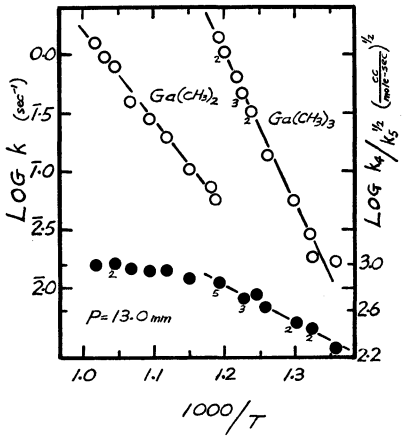

FIG. 1. Arrhenius plot for the pyrolysis of trimethyl and dimethyl gallium and the reaction of methyl radicals with toluene. ○ log k; ● log $k_4/k_5^{1/2}$. Subscripts denote the number of runs averaged to obtain the given points.

that the release of the first two methyl groups might be similar to the successive decomposition of dimethyl zinc, first to zinc methyl and only at much higher temperatures to zinc plus a methyl radical (8). The detailed calculations of k_1 and k_2 have therefore been carried out as for the decomposition of dimethyl zinc, assuming that below 820° K the decomposition of dimethyl gallium is not an important source of methyl radicals.

The mechanism further assumes that reaction [9] is unimportant. The following evidence

$$CH_3 + C_6H_5{-}CH_2 \rightarrow C_6H_5{-}CH_2CH_3 \qquad [9]$$

indicates the validity of this assumption under the experimental conditions used for most runs. First, values of k_1 obtained at 817° K and 13.0 mm pressure using toluene-to-alkyl ratios between 45 and 120 show little variation. Similarly values of k_2 at 916° K and 13.0 mm using toluene-to-alkyl ratios between 45 and 120 show little variation. Previous experiments and calculations (9) also indicate that under similar experimental conditions the loss of methyl radicals according to reaction [9] is negligible. However, as shown in Fig. 2, the value of log k_1 falls sharply when the toluene-to-alkyl ratio is decreased below 45. Values for k_2 are affected similarly. Additional gas chromatographic analyses have shown that the apparent falloff is due in part at least to the formation of propane, propylene, ethylbenzene, and xylenes. Analysis for butanes could not be made at present but these are probably also formed.

The Arrhenius plots shown in Fig. 1 were plotted using k_1's obtained using toluene-to-alkyl ratios of 45 to 120. The simple linear nature of these plots supports the method of calculation used. The curves may be represented by:

$$\log_{10} k_1 \text{ (sec}^{-1}) = 15.54 - (59{,}500/2.303RT)$$

$$\log_{10} k_2 \text{ (sec}^{-1}) = 7.94 - (35{,}410/2.303RT)$$

at 13.0 mm. No other plausible explanation of the results could be found.

The values of k_1 and k_2 were both extremely sensitive to the nature of the surface in the reaction zone. Admission of limited quantities of air to the conditioned vessel between

Can. J. Chem. Downloaded from www.nrcresearchpress.com by 210.87.254.5 on 09/05/12
For personal use only.

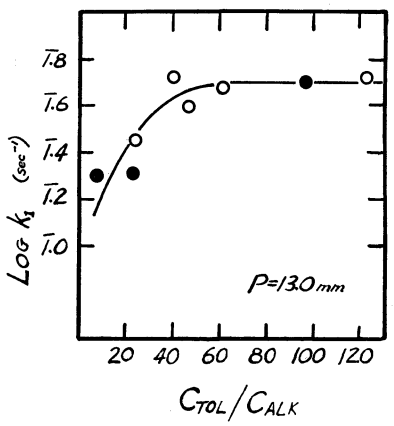

FIG. 2. Variation of k_1 with moles toluene to moles alkyl ratio using fixed toluene concentrations. ○ unpacked vessel at 817° K; ● packed vessel at 801° K.

runs resulted in approximately a 100% increase in k_1 and a 200% increase in k_2 even after pumping over a 48-hour period. Approximately three runs were required to bring values of k_1 and k_2 back to those normally observed in the conditioned vessels. Using a conditioned packed vessel with a surface-to-volume ratio 12 times that of the unpacked vessel gave values of k_1 2.0 times and values of k_2 1.4 times those observed in the unpacked conditioned vessel. It would therefore appear that in the conditioned unpacked vessel, both first and second bond ruptures are predominantly homogeneous processes with a 6% heterogeneous contribution in the first bond region and a 3% contribution in the second bond region.

Both k_1 and k_2 depend upon the total pressure in the system, although the dependence of k_1 is very slight (Fig. 3). The dependence of k_2 is similar to that observed for dimethyl

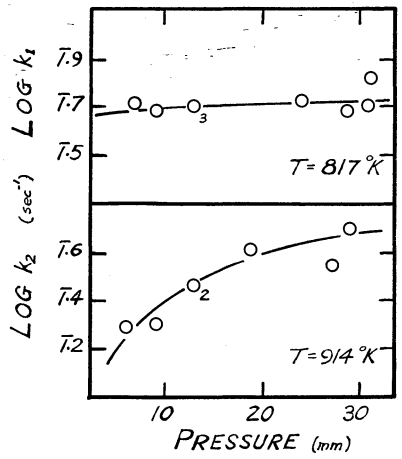

FIG. 3. Variation of k_1 and k_2 with pressure. Subscripts denote the number of runs averaged to obtain the given point.

mercury and dimethyl cadmium (9). Therefore, based solely on unimolecular pressure effects, the value of A_2 would be expected to be of the order 10^{11}–10^{13} sec^{-1}. However,

Can. J. Chem. Downloaded from www.nrcresearchpress.com by 210.87.254.5 on 09/05/12
For personal use only.

the observed A_2, 8.71×10^7, is much lower than expected. This is presumably due to a change in multiplicity from triplet to singlet state as the second methyl radical is released from trimethyl gallium.

The pressure dependence of log $k_4/k_5^{1/2}$ is shown in Fig. 4. The falloff with increasing

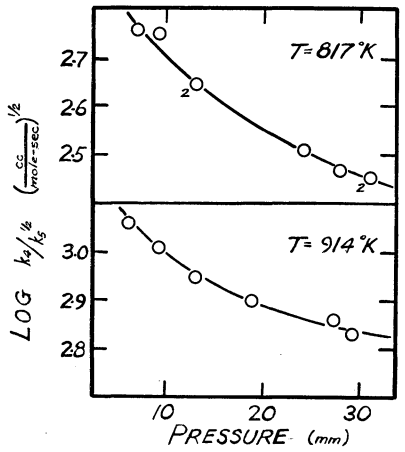

FIG. 4. Variation of $k_4/k_5^{1/2}$ with pressure at 817° K (first bond region) and 914° K (second bond region). Subscripts denote the number of runs averaged to obtain the given point.

pressure is similar to that previously observed (7, 8, 9) and may be attributed to the third-body reqirements of reaction [5].

The experimental evidence although complex would indicate that the activation energies may be approximately related to $D((CH_3)_2Ga—CH_3)$ and $D((CH_3)Ga—CH_3)$. Taking the total strength of the three gallium–carbon bonds equal to 172.4 kcal/mole (3) gives $D(Ga—CH_3)$ equal to 77.5 kcal/mole.

ACKNOWLEDGMENT

This work has been supported by a grant from the National Research Council of Canada.

REFERENCES

1. P. A. FOWELL and C. T. MORTIMER. J. Chem. Soc. 3734 (1958).
2. L. H. LONG and J. F. SACKMAN. Trans. Faraday Soc. **54**, 1797 (1958).
3. L. H. LONG. Pure Appl. Chem. **2**, 61 (1961).
4. G. E. COATES. J. Chem. Soc. 2003 (1951).
5. S. J. PRICE. Can. J. Chem. **40**, 1310 (1962).
6. R. BELCHER, A. T. NUTTEN, and W. I. STEPHAN. J. Chem. Soc. 2438 (1952).
7. S. J. W. PRICE and A. F. TROTMAN-DICKENSON. Trans. Faraday Soc. **54**, 1630 (1958).
8. S. J. W. PRICE and A. F. TROTMAN-DICKENSON. Trans. Faraday Soc. **53**, 1208 (1957).
9. S. J. W. PRICE and A. F. TROTMAN-DICKENSON. Trans. Faraday Soc. **53**, 937 (1957).

Can. J. Chem. Downloaded from www.nrcresearchpress.com by 210.87.254.5 on 09/05/12
For personal use only.

THE REACTION OF ATOMIC HYDROGEN WITH FORMAMIDE VAPOR

J. W. S. JAMIESON
Department of Chemistry, St. John's College, University of Manitoba, Winnipeg, Manitoba
Received June 29, 1962

ABSTRACT

Hydrogen cyanide was the main product of the reaction of hydrogen atoms with formamide vapor; its rate of production was fairly rapid and completely independent of reaction temperature over a wide range. If a hydrogen is abstracted from formamide it must be one of the hydrogens bonded to nitrogen. The results of this investigation suggest the possibility of another free radical chain mechanism, which does not involve hydrogen atoms, for the thermal decomposition of formamide vapor.

INTRODUCTION

When hydrogen atoms are abstracted from amines and similar compounds it is often difficult to determine whether the atom removed had been bonded to carbon or to nitrogen. Thermochemical calculations imply that C—H and N—H bonds have about equal strength.

The experimental evidence is conflicting. Steacie (1) noted that hydrogens attached to nitrogen are probably more labile since methyl radicals react four times more rapidly with ammonia than with methane. On the other hand, Spall and Steacie (2) found that methyl radicals reacted with CH_3COND_2 to give CH_4 predominately, rather than CH_3D.

In an investigation of the reaction of di-*t*-butyl peroxide with ethylenimine, Brinton and Volman (3) assumed that methyl radicals could abstract the imine hydrogen since the activation energy for the abstraction was much lower than the usual values for abstraction of a hydrogen atom from carbon. In 1956, hydrogen atoms were found to react with N-methylethylenimine much more slowly than with ethylenimine (4). Thus it seemed probable that the hydrogen bonded to nitrogen was abstracted from ethylenimine. This conclusion has been supported more recently by Brinton (5), who showed that the rate of hydrogen abstraction by methyl radicals from *t*-butylethylenimine was less than 10% of the rate of the analogous reaction from ethylenimine itself.

It was thought that more definite experimental indication of the site of hydrogen abstraction should be obtainable from a study of the reaction of atomic hydrogen with formamide vapor, particularly if hydrogen cyanide appeared as a major product, since the hydrogen atom of the HCN molecule would almost certainly be the hydrogen originally bonded to carbon in formamide.

EXPERIMENTAL

Materials

Hydrogen, supplied by the Linde Gases Division, Union Carbide Canada Limited, was dried by slow passage through a trap surrounded by liquid nitrogen.

Formamide, melting point 2–3° C, was purchased from Matheson, Coleman and Bell. Low-boiling impurities were removed by distillation.

Ethyl chloride, conforming to the British Pharmacopoeia, was obtained from Ingram and Bell Limited, and was further purified by bulb-to-bulb distillation under vacuum, the first and last fractions being discarded.

Ethylenimine, boiling point 55–56° C, was supplied by Brickman and Company, 546 Sebastopol St., Montreal 22, and was further purified by vacuum distillation.

Apparatus and Methods

The apparatus was a fast flow system of the conventional Wood–Bonhoeffer type. Dry hydrogen gas

Can. J. Chem. Downloaded from www.nrcresearchpress.com by 210.87.254.42 on 09/05/12
For personal use only.

flowed into both ends of the discharge tube, across the aluminum electrodes of which was a potential drop of about 1100 v a-c. at 300 ma, provided by two Hammond 717×60 transformers with the primaries in parallel and the secondaries in series. Disodium hydrogen phosphate was deposited on the walls of the discharge tube and the reaction vessel to retard the combination of hydrogen atoms.

The mixture of atomic and molecular hydrogen flowed down to the reaction vessel, into the center of which formamide vapor flowed. The rate of flow of formamide vapor was controlled by the temperature of the reservoir. Condensation of liquid formamide in the flow system was avoided by maintaining an increasing temperature gradient from the reservoir to the reaction vessel.

Condensable products of the reaction were trapped with liquid nitrogen below the reaction vessel. The products were then distilled into a removable trap for titration of the HCN formed, using the Liebig–Dénigès method (6) in which the solution was made ammoniacal and titrated with standard silver nitrate solution, potassium iodide being used as indicator. Alternatively, the products could be taken into a Le Roy still which was connected to a gas burette and to an apparatus for analysis by gas chromatography, in which a Beckman No. 17329 di-*n*-butyl maleate column was used with helium as carrier gas, a Gow-Mac thermal conductivity cell Model 9193, TE-II, and a Leeds and Northrup Speedomax Type G, Model "S", one second recorder.

RESULTS AND DISCUSSION

The reaction between formamide and hydrogen atoms was not visible but the extent of reaction could be measured by titration of hydrogen cyanide, which was found to be the main product. The results are shown in Fig. 1. The reaction was studied over a feasible

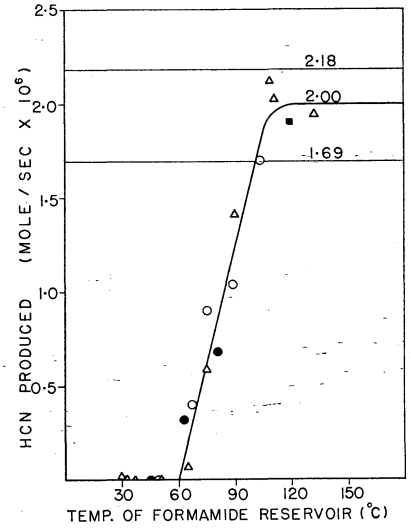

FIG. 1. Hydrogen cyanide produced in the reaction of atomic hydrogen with formamide vapor, over a feasible range of amide flow rates at 43° C (○), 95° C (●), and 195° C (△), and at a high flow rate and 275° C (■).

range of amide flow rates at 43°, 95°, and 195° C, with one experiment at a high flow rate and 275° C.

No reaction was detected until the amide had attained a vapor pressure about equal to the pressure in the reaction vessel, which was 1.10 mm, with the mixture of atomic and molecular hydrogen flowing. (The vapor pressure of formamide is about 0.6 mm at 60° C and 1 mm at 70.5° C.)

The actual flow rate of formamide was not measured but was estimated (7) using the formula of Knudsen for free molecular flow:

$$\text{flow rate} = \frac{4}{3}\sqrt{\left(\frac{2\pi RT}{M}\right)}\cdot\frac{r^3}{l}\cdot\frac{(p_1-p_2)}{RT}\ \text{moles/sec.}$$

Can. J. Chem. Downloaded from www.nrcresearchpress.com by 210.87.254.42 on 09/05/12
For personal use only.

At 110° C, where the vapor pressure of formamide is 12 mm, the calculated flow rate was about 3.9 μmoles/sec. Using Clausing's formula,

$$\text{flow rate} = \frac{20+8\left(\frac{l}{r}\right)}{20+19\left(\frac{l}{r}\right)+3\left(\frac{l}{r}\right)^2}\cdot r^2\sqrt{\left(\frac{\pi RT}{2M}\right)}\cdot\frac{(p_1-p_2)}{RT},$$

which is said to be accurate to within 1.5% for all values of tube length and radius, the calculated flow rate at the same temperature was 3.7 μmoles/sec.

There was no evidence of thermal decomposition of formamide to carbon monoxide and ammonia, which is said (8) to occur near the boiling point (210.5° C), and no production of HCN unless the hydrogen discharge was on. No condensable products other than HCN were detected by gas chromatography or the Le Roy still. (Ammonia should distill at −125° C and HCN at about −100° C.)

The production of hydrogen cyanide did not vary with the reaction vessel temperature over the entire range from 43° to 275° C. Either reactant was completely consumed in an excess of the other at all reaction temperatures. These observations suggest that the reaction is fairly rapid and may have a low activation energy.

At low formamide flow rates the production of HCN was limited only by the amount of formamide vapor available for reaction, while at high formamide flow rates the amount of HCN produced per second was constant and corresponded closely to the rate of flow of hydrogen atoms, which was 2.18 μmoles/sec when measured with ethyl chloride at 26° C and 1.69 μmoles/sec when measured with ethylenimine at 301° C. The data of Fig. 1 do not, however, establish unequivocally the existence of an HCN plateau despite the fact that the hydrogen atom flow rate was purposely kept low. Further experiments at higher formamide flow rates were not attempted due to the possibility of thermal decomposition of formamide in the reservoir at higher reservoir temperatures. It was decided instead to carry out another series of experiments in an unpoisoned reaction system at a still lower hydrogen atom flow rate, which was obtained by using a lower current (115 ma) in the discharge circuit. The results, given in Table I, definitely show the presence of a plateau in HCN production from hydrogen atom attack on formamide vapor.

TABLE I

Establishment of HCN plateau

Temperature of formamide reservoir (°C)	HCN produced (μmoles/sec)
63.5	0.040
87.5	0.21
107.0	0.40
131.0	0.46
157.0	0.46

NOTE: Reaction vessel temperature = 298±4° C.

The hydrogen atom flow rate, estimated from the ethyl chloride reaction in the same system at 300° C, is in agreement with the maximum HCN production from formamide.

Can. J. Chem. Downloaded from www.nrcresearchpress.com by 210.87.254.42 on 09/05/12
For personal use only.

Thus, if sufficient formamide is present, a molecule of HCN is produced for each hydrogen atom available for reaction.

The fairly fast primary reaction is probably

$$\begin{matrix} & O & H & & \\ & \| & | & & \\ H-C-N-H & + & H & \rightarrow & H-C\equiv N + H_2 + OH. \end{matrix} \quad [1]$$

The possibility that a hydrogen atom abstracts the hydrogen bonded to carbon seems to be eliminated by the fairly rapid appearance of HCN as the major product. Thus if abstraction occurs it must involve one of the hydrogens bonded to nitrogen. Since it is most improbable that a hydrogen atom would abstract the oxygen from formamide this is further evidence that N—H bonds are weaker and more reactive than C—H bonds, at least toward attack by hydrogen atoms.

It seems likely that reaction [1] occurs in two steps: hydrogen abstraction,

$$HCONH_2 + H \rightarrow HCONH + H_2, \quad [1a]$$

followed by rearrangement and decomposition of the radical,

$$HCONH \rightarrow HCN + OH. \quad [1b]$$

Since reaction [1*b*] is probably endothermic it appears to be necessary to postulate retention by the radical HCONH of the energy released in the first step. The only reasonable alternative would seem to be addition of a hydrogen atom to formamide, followed by molecular rearrangement and decomposition in one step according to reaction [1].

The presence of hydroxyl radicals in the system is inferred from the stoichiometry of reaction [1]. If these radicals had subsequently reacted with H-atoms to form water,

$$H + OH \rightarrow H_2O,$$

the HCN plateau would have been lower, but this reaction would require a third body and would likely be slow. Reaction of molecular hydrogen with OH,

$$H_2 + OH \rightarrow H_2O + H,$$

would have raised the HCN plateau. This reaction does not occur at ambient temperature (9) and is probably slow.

One might also expect hydroxyl radicals to be able to abstract hydrogens from formamide, especially at high formamide flow rates where all the available hydrogen atoms are consumed and formamide is present in excess. Occurrence of such a reaction would, however, almost certainly have raised the HCN plateau and would probably involve a chain reaction with reaction [1*b*] producing chain carriers. There is no evidence of attack on formamide by OH since the HCN plateau is at a flow rate equal to the hydrogen atom flow rate. Thus it appears that the reaction of OH with formamide is so slow that it does not occur.

The experiments reported here provide no indication of the fate of hydroxyl radicals in the present system, although it appears that they cannot undergo reactions such as

$$2OH \rightarrow H_2O + O,$$

since the oxygen atoms thus formed could then give subsequent reactions, such as

$$O + OH \rightarrow O_2 + H,$$

to destroy the simple 1:1 correspondence between available hydrogen atoms and HCN produced. Though there is a very remote possibility that the agreement between the H-atom flow rate and the HCN plateau is fortuitous, there is, however, absolutely no

Can. J. Chem. Downloaded from www.nrcresearchpress.com by 210.87.254.42 on 09/05/12
For personal use only.

evidence for the occurrence of any secondary reactions which consume or produce hydrogen atoms. Therefore it seems necessary to postulate the disappearance of hydroxyl radicals from the system by reactions such as

$$2OH \rightarrow H_2O_2 \qquad [2]$$

or

$$2OH \rightarrow H_2 + O_2 \qquad [3]$$

at the reaction vessel wall or in the cold trap, although neither oxygen nor peroxide was detected among the trapped products.

Discovery of the fairly rapid reaction of hydrogen atoms with formamide to yield HCN would seem to invalidate the mechanism proposed in 1955 by Luft (10) for the thermal decomposition of formamide. This reaction was studied by Berthelot and Gaudechon (8) and more recently by Schwab (11), who found that over 92% of the amide decomposed near its boiling point (170–200° C) to carbon monoxide and ammonia. The formation of HCN accounted for only 4 to 8% of the formamide decomposed.

Schwab calculated an experimental activation energy of 39.4 kcal/mole for the reaction

$$HCONH_2 \rightarrow CO + NH_3, \qquad [4]$$

which agreed reasonably well with a theoretical value of 35 kcal/mole obtained by means of Hirschfelder's rules (12).

Luft (10) thought it unlikely that the thermal decomposition took place by molecular rearrangement according to reaction [4] and postulated a chain mechanism with the primary step

$$HCONH_2 \rightarrow H + CONH_2 \qquad \Delta H \sim 85, \qquad E \sim 85 \qquad [5]$$

followed by several reactions of hydrogen atoms, such as

$$H + HCONH_2 \rightarrow HCO + NH_3 \qquad [6]$$

$$H + HCONH_2 \rightarrow H + CO + NH_3 \qquad [7]$$

$$H + CONH_2 \rightarrow CO + NH_3. \qquad [8]$$

It is, of course, not unlikely that reaction [5] or

$$HCONH_2 \rightarrow HCONH + H \qquad [9]$$

followed by reaction [1] would explain the small amount of HCN production, but there could hardly be extensive formation of hydrogen atoms in the thermal decomposition. Thus Luft's mechanism involving hydrogen atoms as chain carriers is quite unacceptable.

Now, at least, there are fewer possibilities for the correct mechanism of thermal decomposition. It is conceivable that a chain mechanism is still applicable and if so it appears that the major initiation step could only be

$$HCONH_2 \rightarrow HCO + NH_2. \qquad [10]$$

One is tempted, then, to suggest a new chain mechanism in which the NH_2 radicals abstract hydrogen from either formamide or HCO:

$$NH_2 + HCONH_2 \rightarrow NH_3 + CONH_2 \qquad [11]$$

$$NH_2 + HCO \rightarrow NH_3 + CO. \qquad [12]$$

Reaction [11] requires the drastic assumption that NH_2 radicals attack formamide at the formyl group despite the observation that hydrogen atoms abstract hydrogen from the amide group exclusively. The assumption does, however, seem inevitable if a free radical

Can. J. Chem. Downloaded from www.nrcresearchpress.com by 210.87.254.42 on 09/05/12
For personal use only.

chain mechanism, which cannot involve hydrogen atoms, is applicable. Spall and Steacie (2) found it necessary to postulate a reaction similar to reaction [11] to explain the formation of ammonia in the photolysis of acetamide.

The $CONH_2$ radicals formed in reaction [11] could decompose thermally according to the reaction

$$CONH_2 \rightarrow CO + NH_2 \qquad [13]$$

as in the photolysis of acetamide (2) with an activation energy of 29 kcal/mole and a frequency factor of 10^{13}. The chain could then be propagated by reactions [11] and [13] and could be terminated by reaction [12].

With the assumption that the radicals attain stationary state concentrations the overall rate of decomposition of formamide would be

$$-\frac{d(HCONH_2)}{dt} = k_{10}(HCONH_2)+k_{11}(NH_2)(HCONH_2)$$
$$= k_{10}(HCONH_2)+k_{11}\left(\frac{k_{10}}{k_{12}}\right)^{1/2}(HCONH_2)^{3/2}.$$

The experimental results (11) do not clearly establish the order of reaction as either first or second. Thus they might correspond to 3/2-order kinetics. The overall specific reaction rate for the chain mechanism now proposed is

$$k \sim k_{11}\left(\frac{k_{10}}{k_{12}}\right)^{1/2}$$

and

$$E_{\text{overall}} \sim E_{11} + \frac{E_{10}-E_{12}}{2}.$$

Heats of reaction may be calculated from known and estimated heats of formation and bond dissociation energies (2, 13, 14). Reaction [10] is about 89 kcal/mole endothermic. This should be approximately equal to the activation energy of reaction [10]. Reaction [11] would be about 24 kcal/mole exothermic, while reaction [12] would be about 78 kcal/mole exothermic.

If E_{11} and E_{12} are small, though not necessarily negligible, E_{overall} could very well have the magnitude to agree with Schwab's experimental data (11).

The proposed mechanism, then, could apply to the thermal decomposition of formamide vapor, although one might argue that the assumption of reaction [11] is too drastic to be acceptable and thus renders any chain mechanism untenable. Such a view would support Schwab's unimolecular decomposition of reaction [4]. It has, however, been pointed out (15) that some other mechanism, probably ionic, might be applicable to the thermal decomposition in the liquid state.

ACKNOWLEDGMENT

The author is grateful to the National Research Council for financial assistance.

REFERENCES

1. E. W. R. Steacie. Atomic and free radical reactions. American Chemical Society Monograph 125, Reinhold, New York. 1954.
2. B. C. Spall and E. W. R. Steacie. Proc. Roy. Soc. (London), Ser. A, **239**, 1 (1957).
3. R. K. Brinton and D. H. Volman. J. Chem. Phys. **20**, 25 (1952).
4. J. W. S. Jamieson and C. A. Winkler. J. Phys. Chem. **60**, 1542 (1956).

Can. J. Chem. Downloaded from www.nrcresearchpress.com by 210.87.254.42 on 09/05/12
For personal use only.

5. R. K. BRINTON. Can. J. Chem. **38**, 1339 (1960).
6. I. M. KOLTHOFF and E. B. SANDELL. Textbook of quantitative inorganic analysis. Macmillan, New York. 1948.
7. E. H. KENNARD. Kinetic theory of gases with an introduction to statistical mechanics. McGraw-Hill, New York. 1938.
8. D. BERTHELOT and H. GAUDECHON. Compt. Rend. **155**, 207 (1912).
9. J. S. BATZOLD, C. LUNER, and C. A. WINKLER. Can. J. Chem. **31**, 262 (1953).
10. N. W. LUFT. Monatsh. **86**, 671 (1955).
11. G-M. SCHWAB. Z. Anorg. Chem. **262**, 41 (1950).
12. J. HIRSCHFELDER. J. Chem. Phys. **9**, 645 (1941).
13. F. D. ROSSINI *et al.* Natl. Bur. Std. (U.S.), Circ. No. 500. 1952.
14. M. SZWARC. Chem. Rev. **47**, 75 (1950).
15. A. T. BLADES. Private communication.

Can. J. Chem. Downloaded from www.nrcresearchpress.com by 210.87.254.42 on 09/05/12
For personal use only.

A TISSUE-EQUIVALENT CHEMICAL DOSIMETER SENSITIVE TO 1 RAD[1]

W. A. Armstrong, R. A. Facey, D. W. Grant, and W. G. Humphreys
Defence Research Chemical Laboratories, Ottawa, Canada

Received January 29, 1963

ABSTRACT

The system 10^{-4} *M* terephthalic acid in 4×10^{-4} *M* NaOH is capable of measuring doses of ionizing radiation as low as 500 millirads. The concentration of hydroxyterephthalic acid, determined spectrophotofluorometrically, increases linearly with dose to at least 1000 rads and is independent of dose rate from 0.5 to 1000 rad/min. The energy dependence and stability of the system are also reported.

INTRODUCTION

The irradiation of an aqueous solution of an aromatic compound usually results in the hydroxylation of that compound and many hydroxy aromatics are highly fluorescent. The calcium benzoate dosimeter (1, 2), based on the fluorometric determination of the salicyclic acid formed on irradiation, was developed in this laboratory. Despite its limited usefulness below 30 rads this system exhibits many of the characteristics necessary for a good dosimeter. Consequently attempts were made to find a similar but more sensitive system. Aqueous terephthalic acid (TA) was chosen for investigation for a number of reasons. As its carboxyl groups are para to each other, there is only one isomer of hydroxyterephthalic acid (HTA) and no OH radicals are wasted in the formation of hydroxy acids that do not contribute to the fluorescence measured. In alkaline solution TA does not fluoresce nor does it interfere with the brilliant fluorescence of HTA. Preliminary results showed that the aqueous alkaline terephthalate system is five to six times as sensitive as the benzoate system and is capable of giving a measurable response on irradiation with 500 millirads.

EXPERIMENTAL

Water from a commercial still was redistilled from alkaline permanganate in an all Pyrex glass apparatus incorporating a splash column, and the distillate distilled once again from a similar apparatus. Reagent grade NaOH and Eastman "White Label" terephthalic acid (recrystallized three times from ethanol before being dried overnight at 55° C) were used to prepare the dosimeter solution. The hydroxyterephthalic acid was synthesized by the method of Kuhn (3, 4). Since a commercial sample of HTA was not available and very little information on its properties was found in the literature, the purity of this sample could not be determined accurately. The ultraviolet absorption spectrum of 10^{-4} *M* HTA in 4×10^{-4} *M* NaOH was measured at each major absorption band ($O.D._{246\,m\mu} = 1.099$ and $O.D._{312\,m\mu} = 0.400$). These values should be useful in comparing the relative purities of various samples of HTA. The results of an acid–base titration showed our sample to be 96.9% pure and the appropriate correction was applied to all data. Any unknown impurity in the HTA would change the numerical values of our data by a constant factor but would not change the characteristics of the dosimeter system.

Since widely scattered results have been obtained (5) when vessels cleaned in chromic acid were used for the measurement of very low doses, the Pyrex irradiation vessels were cleaned in an HNO_3–H_2SO_4 mixture (1:3) and washed many times with once-, twice-, and thrice-distilled water. Finally, steam from boiling thrice-distilled water was passed through them.

Samples of 5.0 ml were irradiated either with γ rays from 200 c of Co^{60} or with X rays from a 300 kvp Müller X-ray machine. Filtration of the X-ray beam was: (*a*) 0.9 g/cm² Cu and 0.13 g/cm² Al to give an effective energy of 105 kev when the machine was operated at 250 kvcp; and (*b*) 0.4 g/cm² Al to give an effective energy of 30 kev when the machine was operated at 100 kvcp. For the 50 kvcp X-ray experiments no filtration was used and the effective energy was estimated to be 12 kev (HVL 45.9 mg/cm³ Al).

When Co^{60} γ and 250 kvcp X rays were employed, the samples were irradiated in Pyrex tubes (i.d. 10 mm, o.d. 12 mm) clamped at right angles to the direction of the beam. In order to avoid filtering effects due to

[1]*Issued as D.R.C.L. Report No. 403.*

Can. J. Chem. Downloaded from www.nrcresearchpress.com by 210.87.254.105 on 09/05/12
For personal use only.

Pyrex, the 100 kvcp and 50 kvcp experiments were carried out by irradiating the samples from above in Pyrex petri dishes (i.d. 5 cm) covered with 1/2 thou Saran plastic sheet to prevent evaporation. These solutions were agitated gently during irradiation to insure homogeneous dose distribution. All dose rates were determined using the revised values for G(salicylic acid) of 0.66, 0.58, 0.52, and 0.46 for Co^{60} γ rays, 105 kev (effective), 30 kev (effective), and 12 kev (effective) X rays respectively (5).

It was confirmed by chromatographic analysis that HTA is the fluorescent compound produced on the irradiation of TA. An irradiated TA sample and a sample of standard HTA were spotted on paper and run with a chloroform:methanol:formic acid:water solvent (solvent system B) (6). After drying, an ultraviolet examination of the chromatogram showed the fluorescent compound in the irradiated sample to have run the same distance as the HTA.

The amount of HTA formed in an irradiated sample of 10^{-4} M TA in 4×10^{-4} M NaOH was determined by comparing its fluorescence intensity with that of a standard HTA solution 10^{-4} M in TA and 4×10^{-4} M in NaOH. The measurements were made with an Aminco-Bowman spectrophotofluorometer using an exciting wavelength of 310 mμ and recording the fluorescence emitted at 420 mμ. Over the range studied, the fluorescence intensity of HTA was found to increase linearly with concentration. The formula used in calculating the concentration of HTA in an irradiated sample is:

$$[\text{HTA}] = \frac{F-B}{F_S-B}\times S,$$

where F is the average of five readings of sample fluorescence, F_S is the average of five readings of standard fluorescence, B is the average of five readings of blank fluorescence, S is the concentration of HTA standard (kept to within a factor of two of the expected sample concentration for greater accuracy). Sample and standard were read alternately to minimize the effect of the fluctuations in the intensity of the xenon lamp light source. When standards less concentrated than 10^{-8} M HTA (equivalent to about 10 rads) were used, it was noticed that the fluorescence intensity increased with prolonged exposure to the ultraviolet light of the fluorometer. By comparing the exposed standard with a fresh one, this effect, presumably due to photochemical oxidation of TA, was corrected for when necessary.

RESULTS

As both TA and HTA are almost insoluble in neutral and acid solutions, the effect of changing pH on the dosimeter mechanism was not extensively investigated. However, the fluorescence characteristics of HTA were shown to be constant throughout the pH range 9 to 12.

The system investigated was 10^{-4} M TA in 4×10^{-4} M NaOH (pH = 10). The results listed in the tables below show the effects of such parameters as dose, dose rate, and radiation energy on G(HTA), the amount of HTA produced expressed in molecules per 100 ev. Each G value is reported as an arithmetic mean with its standard deviation.

The concentration of HTA increases linearly with dose from 1 to at least 1000 rads (Table I) and is independent of dose rate from 0.5 to 1000 rads/min (Table II). The energy dependence (Table II) is almost identical with that of the benzoate system (5). With respect to the value for Co^{60} γ rays, G(HTA) is 12.8% lower for 105 kev (effective) X rays, 24.5% lower for 30 kev (effective) X rays, and 33% lower for 12 kev (effective) X rays.

TABLE I

Linearity of [HTA] with Co^{60} γ dose

Dose rate (rads/min)	Dose (rads)	No. of samples	Average [HTA] (10^{-9} moles/l.)	G(HTA) (molecules/100 ev)
0.5	1.09	5	1.07	0.95±0.03
0.5	2.74	5	2.72	0.96±0.01
0.5	5.47	5	5.16	0.91±0.01
0.5	10.9	5	10.6	0.94±0.01
0.5	33.4	5	32.4	0.94±0.01
0.5	65.4	5	62.8	0.93±0.01
0.5	114.9	5	111.0	0.94±0.01
18.8	950.0	6	951.0	0.97±0.02

Can. J. Chem. Downloaded from www.nrcresearchpress.com by 210.87.254.105 on 09/05/12
For personal use only.

TABLE II

The effect of dose rate and radiation energy on G(HTA)

Effective energy (Mev)	Dose rate (rads/min)	Dose (rads)	No. of samples	G(HTA)
1.25	0.5	1–100	35	0.94±0.02
1.25	18.8	30.1	6	0.95±0.01
1.25	18.8	950	6	0.97±0.02
0.105	21	33.2	7	0.83±0.01
0.105	21	1050	14	0.81±0.02
0.030	21	30.5	7	0.73±0.03
0.030	21	1000	7	0.70±0.02
0.030	716	1430	5	0.69±0.01
0.012	21	147	19	0.63±0.03

The dosimeter solution is stable for at least a few weeks and exhibits no post-irradiation effect on standing overnight. However, HTA may be formed in small quantities by a photochemical reaction and solutions should be protected from light.

The precision of the dosimeter is about ±5% in the range 1 to 1000 rads. Below 1 rad the precision decreases greatly. This is due to the fact that the fluorescence of an unirradiated blank is equivalent to that produced by a 500-millirad dose. The error in measuring the difference in fluorescence between irradiated sample and unirradiated blank increases enormously when these fluorescences are comparable. This blank fluorescence is equivalent to that of 4×10^{-10} M HTA and is due partly to light scatter in the instrument and partly to trace impurities in the TA.

DISCUSSION

It is believed that the mechanism of the radiation-induced hydroxylation of terephthalic acid in aqueous solution is similar to that previously postulated for the hydroxylation of benzoic acid (7). Reaction with the OH radical is an important step in this process and as G(OH) decreases with decreasing energy G(HTA) will also decrease. Since no chain reaction is involved, no dose rate effect would be expected with the conditions used.

The outstanding characteristic of this system is its high sensitivity. That this sensitivity is due to the analytical technique rather than to high product yield is an important advantage since dosimeters that depend on high product yield for sensitivity are usually dose rate dependent. As this is an aqueous system and hence tissue equivalent, it is ideally suited for radiobiological work in the low dose range.

REFERENCES

1. W. A. Armstrong and D. W. Grant. Nature, **182**, 747 (1958).
2. W. A. Armstrong and D. W. Grant. Can. J. Chem. **38**, 845 (1960).
3. R. Kuhn, F. Zilliken, and H. Trischman. Hoppe-Seylers Z. Physiol. Chem. **286**, 264 (1951).
4. R. Kuhn, F. Zilliken, and H. Trischman. Chem. Ber. **83**, 304 (1950).
5. W. A. Armstrong, R. A. Facey, D. W. Grant, and W. G. Humphreys. Radiation Res. In press.
6. L. Reio. J. Chromatog. **1**, 338 (1958).
7. W. A. Armstrong, B. A. Black, and D. W. Grant. J. Phys. Chem. **64**, 1415 (1960).

Can. J. Chem. Downloaded from www.nrcresearchpress.com by 210.87.254.105 on 09/05/12
For personal use only.

POLYMÉRISATION PAR LES RAYONS-X DU CHLORURE DE VINYLE À L'ÉTAT DE VAPEUR

JAN A. HERMAN ET PIERRE M. HUPIN
Département de Chimie, Université Laval, Québec, Qué.
Reçu le 15 janvier 1963

ABSTRACT

The polymerization of vinyl chloride in the gas phase by X rays gives a solid polymer of 1140 average molecular weight. The G value of monomer disappearance varies from 100 to 400 and depends on pressure and temperature. From the measure of the rate of polymerization it was possible to deduce the activation energy of the chain propagation steps: 2.5 kcal/mole, and that of the hindered termination process: 7.4 kcal/mole. The negative temperature coefficient of the polymerization is explained by the importance of this hindered termination process.

INTRODUCTION

La polymérisation du chlorure de vinyle gazeux a été étudiée par Mund et ses collaborateurs (1–3) sous l'influence des particules α du radon. Les rendements ainsi obtenus en monomère consommé par 100 ev, $G(-C_2H_3Cl)$, varient entre 40 et 200 et dépendent des conditions expérimentales: dimensions du récipient, pression et température. Les résultats indiquent que, dans les conditions d'irradiation à l'aide des particules α, le polymère est produit par un mécanisme en chaîne, les chaînes cinétiques étant relativement courtes.

Récemment, Puig et Bretton (4) polymérisèrent le chlorure de vinyle à l'état de vapeur par les rayons γ. Dans leurs expériences, la pression varie de 0.5 à 2 atm et la température, entre 20 et 100° C. Les auteurs retrouvèrent sensiblement les mêmes phénomènes qu'avec l'irradiation par les particules α, mais, sous une pression de 1.5 atm et à température ambiante, le rendement $G(-C_2H_3Cl)$ était de l'ordre de 900, indiquant donc une longue chaîne cinétique.

Ces expériences de polymérisation par les particules α et les rayons γ ont le même défaut, les produits de polymérisation s'accumulant au fond du récipient sont soumis à une action constante du rayonnement ionisant, ce qui peut donner lieu à des phénomènes secondaires et compliquer la cinétique. D'autre part, dans les deux cas, la conversion en polymère fut poussée trop loin d'où une certaine difficulté à étudier le stade initial de la réaction de polymérisation.

Nous nous sommes proposés d'étudier la polymérisation par les rayons-X avec faible conversion en polymère de façon à examiner avec plus de détails la cinétique de la phase initiale de la réaction. L'emploi des rayons-X permet de diriger le faisceau rayonnant de telle sorte que le polymère, formé au cours de la réaction et qui se depose sur les parois inférieures du récipient, ne soit plus soumis à l'irradiation. En outre, un réglage facile de l'intensité des rayons-X donne plus de souplesse de manipulation que dans le cas d'irradiation par les particules α du radon ou les rayons γ de Co^{60}.

PARTIE EXPÉRIMENTALE

Le dispositif expérimental (Fig. 1) est essentiellement constitué d'une chambre d'irradiation, d'un manostat réuni à un enregistreur permettant du suivre la disparition du monomère et d'un système de prélèvement d'échantillons gazeux pour analyse.

Can. J. Chem. Downloaded from www.nrcresearchpress.com by 210.87.254.6 on 09/05/12
For personal use only.

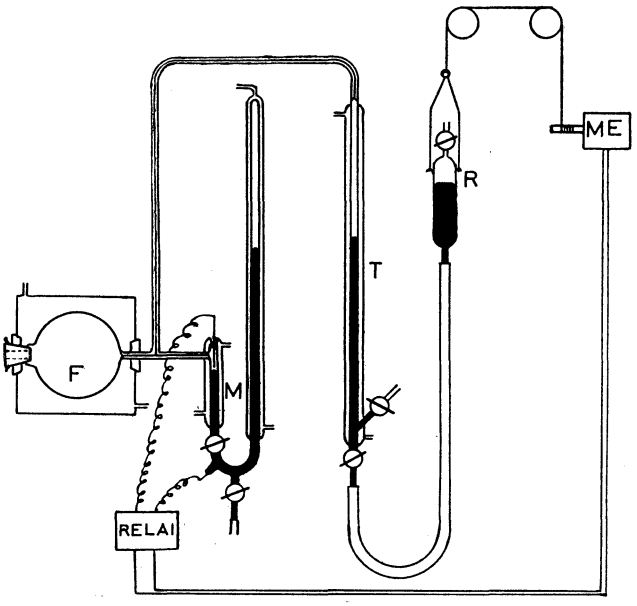

FIG. 1. Schéma de l'appareil de mesure.

La cellule d'irradiation (F) est un ballon sphérique de 500 ml muni d'un rôdage 40/50 où s'insère une pièce de laiton comprenant une fenêtre en aluminium de 0.06 mm d'épaisseur et 19 mm de diamètre. La position de la cellule d'irradiation est telle que les rayons-X la traversent horizontalement; un système de points de repère assure une position reproductible de la chambre de réaction par rapport à la source de rayonnement ionisant. Les rayons-X proviennent d'un tube "Machlett" OEG 60, fonctionnant à 45 kv.

Le manostat relié par un mine tube à la cellule d'irradiation est constitué d'un manomètre, M, porteur de commandes électriques pour le moteur, ME, qui soulève un réservoir de mercure, R, et dirige ainsi la montée du mercure dans le tube calibré, T, du manostat. Afin d'éviter l'influence des variations de la pression extérieure, on fait le vide au-dessus du mercure dans le réservoir R. La sensibilité du manostat dépend de la pression, pour des expériences faites à environ 400 mm Hg elle correspond à l'élévation de pression d'une variation de température de 0.01° C; ce qui exige une thermostatisation adéquate, ainsi l'ensemble manostat – cellule d'irradiation est-il maintenu à une température constante à 0.02° C près. Le moteur électrique, ME, est couplé à un potentiométre permettant l'enrégistrement de la variation de tension qui peut être convertie en volumes de déplacement du mercure dans le tube, T, du manostat.

Afin d'éviter le contact entre les gaz et le lubrifiant des robinets, on a remplacé ces derniers par des valves à mercure.

Le chlorure de vinyle, fourni par la "Matheson Company", est purifié par distillation de trappe à trappe, sous-vide, à la température de l'azote liquide. On a pris soin de n'admettre dans la cellule d'irradiation que la fraction médiane du distillat. L'analyse par chromatographie des gaz ne révèlait aucune impureté.

La dosimétrie du rayonnement ionisant est faite au moyen d'une mesure du courant d'ionisation dans l'argon pur, irradié dans les mêmes conditions que pour le monomère. A cet effet, nous nous sommes servis d'une cellule cylindrique de même diamètre, munie d'une fenêtre en aluminium de mêmes dimensions que pour la chambre de réaction. A l'intérieur de cette cellule, un système d'électrodes parallèles permet de mesurer le courant d'ionisation en fonction de la pression, de l'intensité des rayons-X et de la distance de la fenêtre où pénètre le rayonnement. La connaissance du spectre caractéristique du tube de rayons-X utilisé (5) ainsi que des coefficients d'atténuation atomique pour les rayons-X (6) permet de transposer les courants d'ionisation de l'argon en ceux du chlorure de vinyle.

RÉSULTATS EXPÉRIMENTAUX

Les expériences faites à pression constante portent sur l'influence de la pression, de la température et de l'intensité du rayonnement ionisant sur la vitesse de polymérisation. Au début de l'expérience, on constate quelquefois une période variable d'induction qui semble dépendre de la manière dont le contact électrique initial a été établi dans le manomètre. D'une manière générale, la courbe (Fig. 2) de disparition du monomère en

Can. J. Chem. Downloaded from www.nrcresearchpress.com by 210.87.254.6 on 09/05/12
For personal use only.

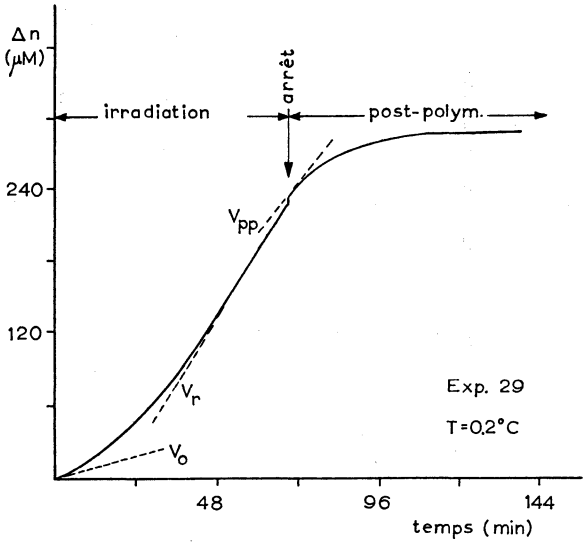

FIG. 2. Allure typique d'une courbe de disparition du monomère, Δn, dans le temps.

fonction du temps est caractérisée par une accélération plus ou moins marquée pouvant durer une vingtaine de minutes. La polymérisation prend ensuite une vitesse de régime, V_r, qui reste constante jusqu'au moins 5% de conversion. Habituellement, nous ne poussions pas cette conversion au-delà de 1%. En interrompant le rayonnement ionisant, une brusque chute de pression apparaît, qui est due au refroidissement interne du gaz. Ensuite, on assiste à une période de post-polymérisation qui débute avec une vitesse comparable à celle de régime et tombe exponentiellement à zéro après 40 minutes environ. La durée des expériences est de 150 minutes en moyenne.

Nous mentionnerons trois sortes de vitesse: V_0, vitesse initiale correspondant à la vitesse après la période d'induction; V_r, vitesse de régime correspondant à la pente stationnaire de disparition du monomère en fonction du temps, et V_{pp}, vitesse initiale de post-polymérisation. La vitesse initiale, V_0, est difficile à mesurer car elle dépend de la perfection de l'enregistrement; de même pour V_{pp}, qui étant partiellement masquée par la chute brusque de température, sa mesure est difficile.

La Fig. 3 illustre la variation des vitesses V_0 et V_r en fonction de la pression pour différentes températures à intensité constante des rayons-X. De façon générale, on constate qui si la vitesse initiale, V_0, augmente avec la température, la vitesse de régime, V_r, diminue, diminution qui a été signalée dans les travaux antérieurs sur la polymérisation du chlorure de vinyle par le rayonnement ionisant (1, 4). Le Tableau I donne les vitesses initiales de post-polymérisation, V_{pp}, en fonction de la pression et de la température.

TABLEAU I

Vitesses initiales de post-polymérisation

Exp. No.	P (cm Hg)	T (°C)	V_{pp} (μmoles/min)
2	73.4	25.2	1.11*
4	56.3	25.2	0.76*
5	40.9	25.2	0.39
29	52.6	0.2	1.65
31	58.7	16.5	1.34

*Moyenne de deux mesures.

Can. J. Chem. Downloaded from www.nrcresearchpress.com by 210.87.254.6 on 09/05/12
For personal use only.

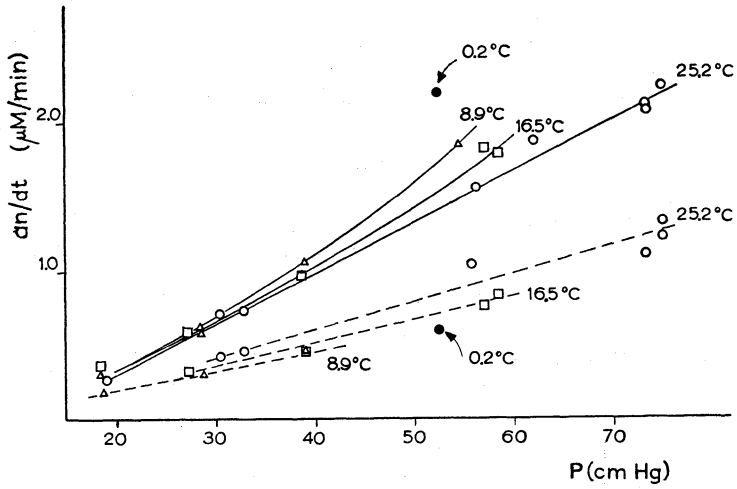

FIG. 3. Vitesse initiale, V_0 (trait pointillé), et vitesses de régime, V_r (trait plein), en fonction de la pression pour différentes températures.

La Fig. 4 montre la relation entre les logarithmes des vitesses et l'inverse de la température. Dans ce cas, les valeurs des ordonnées sont ramenées à une même densité, soit

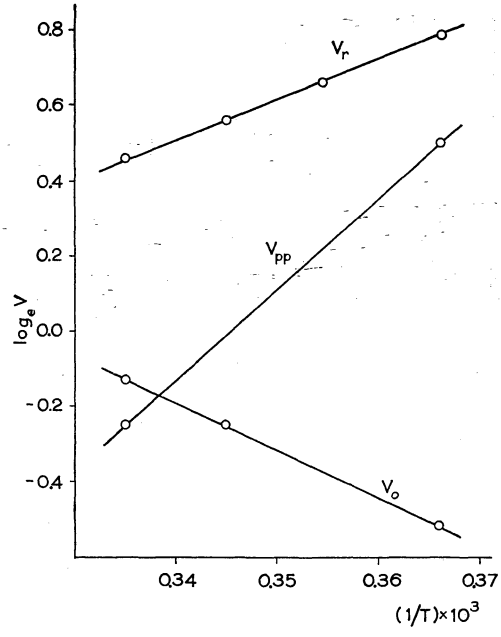

FIG. 4. Relation entre les logarithmes des vitesses et l'inverse de la température.

3.085×10^{-2} (25.2° C et 57 cm Hg). La vitesse de régime répond à une énergie d'activation de régime, E_a^r, négative dont la valeur, tirée de la pente de la Fig. 4, est de -2.1 kcal/mole. Puig et Bretton (4) trouvèrent, pour les rayons γ entre 20 et 100° C, une énergie d'activation de -5.8 kcal/mole pour une densité de 7×10^{-2} mole/litre; de même, Koisumi et ses

Can. J. Chem. Downloaded from www.nrcresearchpress.com by 210.87.254.6 on 09/05/12
For personal use only.

collaborateurs (7) trouvèrent aussi une énergie d'activation négative entre 10 et 95° C au cours d'une polymérisation du chlorure de vinyle photosensibilisée au mercure. La différence entre notre propre valeur et celle trouvée par Puig n'est qu'apparente, en effet, on constate que le coefficient de température négatif (Fig. 3) augmente avec la pression. D'après nos expériences il s'estompe à environ 30 cm Hg. L'énergie de la post-polymérisation, E_a^{pp}, correspondant à la vitesse initiale du post-effet, est également négative et a pour valeur -4.9 ± 1.0 kcal/mole.

Par contraste, l'énergie d'activation relative à la vitesse initiale, E_a^0, est positive et a pour valeur. 2.5 ± 1.0 kcal/mole; la marge d'erreur qui est importante provient des difficultés de mesures précises. En général, on constate que la polymérisation débute avec une vitesse d'environ 60% de celle de régime.

La Fig. 5 donne les relations, à pression et témperature constantes, entre les logarithmes des vitesses V_0 et V_r et le logarithme de l'intensité du rayonnement mesuré sous forme de

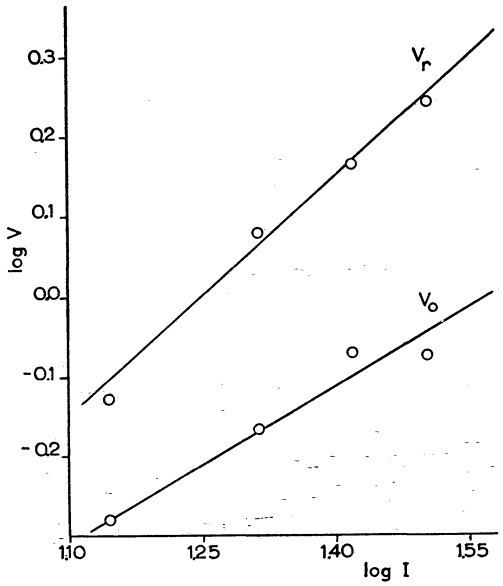

FIG. 5. Relation entre les vitesses initiale, V_0, et de régime, V_r, et l'intensité du rayonnement ionisant.

courant d'ionisation. On remarque de nouveau que l'influence du courant d'ionisation sur la vitesse de consommation du monomère n'est pas la même au départ et au cours du régime stationnaire de polymérisation. La valeur de la pente de la droite de la Fig. 5 est celle de l'exposant de l'intensité d'irradiation et est calculée par les moindres carrés. Au début de la polymérisation cet exposant est égal à 0.52 et devient 1.05 pour le régime stationnaire.

Le polymère apparaît comme un solide blanc qui se dépose au fond du récipient; aux pressions inférieures à 25 cm Hg, c'est un liquide brun, visqueux, qui semble avoir un très bas degré de polymérisation. Ces constations sont en accord avec celles déjà décrites (1) lors de l'irradiation par les rayons α. L'analyse chimique élémentaire du polymère solide (Tableau II) donne des valeurs correspondant assez bien aux valeurs théoriques.

En raison des faibles quantités de polymère recueillies, nous n'avons mesuré que le poids moléculaire global; cette mesure faite par cryoscopie dans le 1,2-dibromoéthane

Can. J. Chem. Downloaded from www.nrcresearchpress.com by 210.87.254.6 on 09/05/12
For personal use only.

TABLEAU II

Analyse chimique du polymère solide $(C_2H_3Cl)_n$

	%C	%H	%Cl
Trouvé	38.46	4.93	56.59
Théorique	38.43	4.84	56.73

suivant la méthode de Bianchi et Rossi (8) donne 1140, ce qui correspond à un degré de polymérisation moyen $\overline{DP} = 18.2$. Etant donné cette valeur relativement faible, il serait plus logique de parler de télomère.

L'analyse par chromatographie des gaz révèle de l'hydrogène, de l'acétylène, de l'éthylène et de l'acide chlorhydrique. Après une irradiation poussée jusqu'à 2% de conversion, on ne détecte pas de produits plus lourds en concentration supérieure ou égale à 10^{-3} mole/mole, c'est donc que même pas 5% du monomère converti ne se retrouve sous forme de dimère. Par ailleurs, le spectre de masse n'indique également aucune présence de fragment correspondant au dimère.

DISCUSSION

En se limitant au schéma simplifié de la cinétique de polymérisation, on peut représenter la vitesse de propagation, en supposant l'état stationnaire, par l'expression: $R_p = KR_i^x[M]^y$, où R_i est la vitesse d'amorçage, K une constante composée de vitesse, x et y des exposants affectés à la vitesse d'amorçage et à la concentration en monomère [M]. L'analyse de nos résultats donne les relations suivantes pour les vitesses initiales [1] et de régime [2] de la polymérisation:

[1] $$V_0 = K_1 I^{0.52} P^{1.10}$$

[2] $$V_r = K_2 I^{1.05} P^{1.02}.$$

Ces expressions sont équivalentes à celles de la vitesse cinétique de propagation, citée plus haut, puisque dans notre cas la concentration en monomère est représentée par la pression, P, le volume étant constant et la vitesse d'initiation est mesurée par le courant d'ionisation, I. En effet, si l'on considère que chaque paire d'ions conduit finalement à un nombre bien déterminé de radicaux capables d'amorcer des chaînes polymériques, on voit que le courant d'ionisation en est bien une mesure à une constante de proportionnalité près. L'expression [1] de la vitesse initiale correspond bien à une cinétique classique, homogène, la terminaison se faisant par destruction mutuelle des radicaux polymériques. Le fait que la cinétique de polymérisation se conforme initialement à l'expression classique de polymérisation radicalaire, homogène, semble être la meilleure preuve d'un mécanisme radicalaire dans le cas de polymérisation observé. Par contre, l'évolution ultérieure nous est donné par l'expression [2]; l'exposant supérieur à 0.5 dont le courant d'ionisation est affecté montre que la terminaison se fait par un mécanisme autre que la destruction mutuelle de chaînes radicalaires en croissance. Un tel exposant est normal lors de polymérisation en phases hétérogènes et en particulier dans les milieux précipitants; il a été observé à l'état liquide dans de nombreux cas, notamment pour le chlorure de vinyle polymérisé par les rayons γ (9) et par voie photochimique (10). Or, l'observation des phénomènes caractéristiques à la polymérisation à l'etat de vapeur montre bien qu'il s'agit d'une réaction comprenant tous les indices de polymérisation en milieu précipitant. Ce comportement de dépend pas de l'initiation radiochimique, puisqu'il existe des phénomènes identiques par initiation photochimique ou thermique (11–14), mais plutôt de la

Can. J. Chem. Downloaded from www.nrcresearchpress.com by 210.87.254.6 on 09/05/12
For personal use only.

nature du milieu, l'acrylonitrile polymérisé en masse en phase liquide ayant un exposant entre 0.7 et 0.8 pour la vitesse d'amorçage aussi bien avec les rayons γ (15, 18) qu'avec les initiateurs chimiques ou la lumière ultraviolette (16, 17). De plus, les systèmes hétérogènes montrent des accélérations initiales et des post-polymérisations semblables à celles de notre cas.

Que l'exposant de la vitesse d'amorçage dans l'expression cinétique [2] soit pratiquement égal à l'unité ne peut être interprété comme une terminaison linéaire des chaînes polymériques en croissance; il faut plutôt envisager une diminution de la vitesse de terminaison par occlusion des radicaux polymériques dans le polymère mort (16, 19).

L'image que nous nous faisons de la polymérisation est la suivante. Initialement les chaînes se terminent aisément, mais il y aurait déjà un important transfert de chaîne sur monomère s'effectuant de manière à garder la nouvelle chaîne en croissance liée physiquement au polymère mort. Il en résulterait un fort accroissement de volume des particules qui s'agglomèreraient par la suite en édifices colloidaux. On observe d'ailleurs un brouillard qui indique une grosseur des particules incompatible avec le degré de polymérisation. Nozaki (20) prévoyait, en considérant la stabilité des radicaux, que le transfert de chaîne est important dans la polymérisation du chlorure de vinyle, ce qui fut d'ailleurs vérifié expérimentalement (11, 21). Dans notre cas, le degré de polymérisation moyen, $\overline{DP}$ = 18.2, comparé à la longueur moyenne d'une chaîne cinétique (Tableau III), confirme ces considérations. Le fait que le transfert s'effectue tout en gardant la nouvelle chaîne en

TABLEAU III

Valeurs $G(-C_2H_3Cl)$ pour la polymérisation

Exp. No.	Pression (cm Hg)	Température (°C)	Courant d'ionisation (μa)	$G(-C_2H_3Cl)$, initial	$G(-C_2H_3Cl)$, de régime
7	74.8	25.2	32.9	252	425
8	55.8	25.2	31.2	207	310
9	32.8	25.2	25.9	110	178
10	18.9	25.2	21.6	—	76
31	58.7	16.5	31.8	163	354
32	58.1	16.5	26.3	200	348
33	57.6	16.5	20.6	208	360
34	57.0	16.5	14.0	258	324
56	57.2	17.1	31.6	146	361
24	54.7	8.85	31.5	—	368
29	52.6	0.2	31.5	118	437

croissance sur le polymère mort peut provoquer un emprisonnement du centre actif et une difficulté de croissance et de terminaison. Pourtant, l'occlusion du centre actif, même s'il ralentit la propagation, prolonge la vie moyenne de la chaîne cinétique et peut ainsi expliquer l'accélération initiale. Ces centres actifs emprisonnés sont aussi responsables de la post-polymérisation. Toutefois l'équilibre dynamique se maintient car il y a toujours autant de radicaux formés, autant de propagation avec terminaison "aisée" et autant de propagation avec terminaison "gênée", le polymère ayant une durée de vie propre. D'autre part, s'il y a transfert sur polymère, celui-ci sera constant si le nombre de particules de polymère mort en suspension est constant; or, ce dernier s'élimine spontanément puisque, par gravité, il tombe au fond du récipient.

Dans le cas de polymérisation radicalaire homogène, l'énergie d'activation positive est normale. On pourrait calculer l'énergie de propagation, E_p, à condition de connaître l'énergie de terminaison classique de destruction mutuelle de deux radicaux polymériques.

Can. J. Chem. Downloaded from www.nrcresearchpress.com by 210.87.254.6 on 09/05/12
For personal use only.

En général, on admet que la terminaison classique en phase gazeuse ne requiert pas d'énergie, on aurait donc pour E_p:

$$E_p = E_a^0 + \tfrac{1}{2}E_t' \sim 2.5 \text{ kcal},$$

et cette grandeur ne peut présenter qu'une valeur inférieure. Burnett (10) trouve pour la polymérisation du chlorure de vinyle en phase liquide une valeur de l'énergie de propagation de 3.7 kcal. Les valeurs sont donc du même ordre de grandeur. Les considérations cinétiques développées plus haut nous forcent toutefois à envisager la terminaison comme autre chose qu'un processus de recombinaison classique de radicaux sans énergie d'activation. En réalité, les terminaisons "gênées" pourraient nécessiter une énergie, E_t'', comparable ou même supérieure à E_p, si elles ont lieu entre radicaux emprisonnés dans un milieu plus ou moins rigide comme le polymère. Dans notre cas, cette énergie de terminaison aurait la valeur suivante:

$$E_t'' = E_p - E_a^{pp} = 2.5 - (-4.9) = 7.4 \text{ kcal}.$$

Dans ce calcul, nous utilisons l'énergie d'activation de post-polymérisation car elle seul correspond à la cinétique de la terminaison "génée" du polymère, toutes les terminaisons classiques de radicaux cessant immédiatement dès que la production de radicaux est arrêtée. Burnett trouve $E_t'' = 7.8$ kcal pour une terminaison qu'il qualifie de linéaire au cours d'une polymérisation hétérogène de C_2H_3Cl en phase liquide (10). La similitude entre cette valeur et la nôtre suggère que le mécanisme est de même nature dans les deux cas, ce qui est compréhensible puisque, suivant l'image que nous nous faisons, l'accessibilité du centre actif emprisonné dans le polymère solide détermine seule la terminaison. Une énergie de terminaison "gênée" plus élevée que l'énergie de propagation serait, par conséquent, à l'origine du coefficient de température négatif observé dans ce système.

L'énergie d'activation de régime, E_a^r, est la résultante de deux processus de terminaison, l'un classique, l'autre "gênée". Il est normal de penser que le processus classique soit d'autant plus important que la quantité de polymère en suspension et la masse moléculaire moyenne du polymère sont plus petits—ce qui aurait lieu à basse pression et/ou température élevée. Par contre, à pression élevée et/ou basse température, il y aurait une prépondérance du deuxième processus. Ceci doit se refléter dans les énergies d'activation de régime et, effectivement, le résultat de Puig et Bretton (4) confirme ce point de vue.

Nous donnons au Tableau III quelques valeurs $G(-C_2H_3Cl)$ de polymérisation sous différentes conditions expérimentales. Les valeurs G sont calculées à partir des rendements ioniques correspondants,* en admettant 25.5 ev pour la formation d'une paire d'ions dans le chlorure de vinyle, valeur proche de celle trouvée expérimentalement pour l'acétylène, l'éthylène et l'éthane (23). En tenant compte des nombreux facteurs, nous estimons l'exactitude de ces valeurs G à $\pm 10\%$.

La quantité $G(-C_2H_3Cl)$ représente, à un facteur de proportionnalité près, la longueur de la chaîne cinétique de polymérisation. Vue sous cet angle, elle permet de comparer les longueurs des chaînes dans diverses conditions.

Une première constatation se dégage de ces données: les valeurs G de la disparition du monomère sont comparables à celles trouvées aux mêmes conditions de pression et de température dans l'irradiation par les particules α (1–3).

Les expériences portant les numéros 31, 32, 33 et 34, faites à pression et température comparables mais à intensité d'irradiation variable, montrent que $G(-C_2H_3Cl)_{\text{régime}}$ ne change pratiquement pas, tandis que $G(-C_2H_3Cl)_{\text{initial}}$ diminue lorsque l'intensité

**Pour la définition et le calcul des rendements ioniques voir référence 22.*

Can. J. Chem. Downloaded from www.nrcresearchpress.com by 210.87.254.6 on 09/05/12
For personal use only.

d'irradiation augmente. L'explication en est aisée puisqu'au début la terminaison mutuelle des radicaux polymériques est d'autant plus favorisée que leur nombre est plus grand, c'est-à-dire lorsque l'intensité d'irradiation est plus forte. Il est donc naturel que pour une irradiation de faible intensité on trouve une chaîne cinétique moyenne plus longue. Par ailleurs, une fois que le polymère est apparu en suspension dans le gaz, la terminaison "gênée" détermine la longueur de la chaîne cinétique et elle ne devrait être que peu influencée par le rayonnement ionisant. Par contre, cette même terminaison "gênée" dépend de la pression (expériences 7, 8, 9 et 10) et de la température (expériences 8, 56, 24 et 29); en effet, à température constante, elle doit être d'autant plus facile que le télomère a un poids moléculaire plus faible, donc à basses pressions les chaînes cinétiques sont plus courtes. A pression constante, on doit trouver une terminaison "gênée" d'autant plus difficile que la température est plus basse puisque l'accessibilité du centre actif emprisonné dans le polymère, où la diffusion joue un rôle primordial, est le mécanisme déterminant. Les données expérimentales confirment ces deux aspects. Finalement, $G(-C_2H_3Cl)_{\text{initial}}$ augmente avec la température et la pression, le nombre de collisions donnant lieu à l'accroissement des chaînes étant d'autant plus grand que ces deux paramètres sont plus élevés.

La comparaison du poids moléculaire moyen et de la longueur des chaînes cinétiques, telle que représentée par les valeurs $G(-C_2H_3Cl)$, prouve qu'il y a un transfert important. Le nombre moyen de transfert serait estimable si l'on connaissait le nombre de radicaux formés par paire d'ions (ou par 100 ev) amorçant les chaînes polymériques. A partir des données obtenues il est impossible de déterminer cette grandeur, toutefois, une comparaison avec la valeur de $(k_p/k_t^{1/2}) = 0.05$, trouvée par Jones et Melville (24) lors de la photopolymérisation du chlorure de vinyle à l'état de vapeur, peut nous renseigner sur ce sujet. En exprimant les paramètres de l'équation [1] en unités adéquates: V_0 et I en mole litre^{-1} sec^{-1}, et P en mole litre^{-1}, on trouve pour l'expérience 32 une valeur du coefficient du rendement ionique radicalaire, k_1, de 0.5 ou $G_R = 1.8$. En général, on admet que chaque paire d'ions donne lieu à deux radicaux au moins (25), ce qui voudrait dire que dans notre cas il y aurait un radical susceptible d'amorcer une chaîne polymérique chaque fois que deux paires d'ions seraient formées. Cette valeur nous semble trop élevée, une valeur plus petite nous semblerait plus normale. La valeur de Jones et Melville est sujette à des réserves sérieuses puisqu'elle est calculée d'après l'hypothèse d'une cinétique de polymérisation homogène, ce qui, d'après la description des expériences, ne semble pas être le cas. Nous pouvons donc admettre que $G_R = 1.8$ représente, au plus, la limite supérieure.

Nous remercions le Conseil National des Recherches pour l'aide financière qui a permis de faire cette étude.

BIBLIOGRAPHIE

1. W. Mund, J. A. Herman et G. Verfaillie. Bull. Acad. Roy. Belges, **35**, 656 (1949).
2. W. Mund, J. A. Herman et P. Huyskens. Bull. Acad. Roy. Belges, **37**, 696 (1951).
3. W. Mund, M. van Meerssche et J. Momigny. Bull. Soc. Chim. Belges, 62, 109, 645 (1953).
4. J. R. Puig et R. H. Bretton. *Dans* Radiation chemistry of polymeric systems. *Cité par* A. Chapiro. Interscience. 1961.
5. R. C. Palmer. Thèse, Vanderbilt Univ. Nashville, Tenn. 1957.
6. G. W. Grodstein. Natl. Bur. Std. (U.S.), Circ. No. 583. 1957.
7. M. Koisumi, K. Nakatsuka, et. S. Kato. Bull. Chem. Soc. Japan, **27**, 185 (1954).
8. V. Bianchi et C. Rossi. Chim. Ind. (Milan), **41**, 875 (1959).
9. A. Chapiro. J. Chim. Phys. **53**, 512 (1956).
10. G. M. Burnett et W. W. Wright. Proc. Roy. Soc. (London), Ser. A, **221**, 28, 37, 41 (1954).
11. W. I. Bengough et R. G. W. Norrish. Proc. Roy. Soc. (London), Ser. A, **200**, 301 (1950).

Can. J. Chem. Downloaded from www.nrcresearchpress.com by 210.87.254.6 on 09/05/12
For personal use only.

12. E. J. ARLMAN et W. W. WAGNER. J. Polymer Sci. **9**, 583 (1952).
13. A. SCHINDLER et J. W. BREITENBACH. Ric. Sci., Suppl. 34 (1955).
14. F. DANUSSO et D. SIANESI. Chim. Ind. (Milan), **37**, 189, 278 (1955).
15. A. PREVOST-BERNAS et J. SEBBAN-DANON. J. Chim. Phys. **53**, 418 (1956).
16. C. H. BAMFORD et A. D. JEMKINS. Proc. Roy. Soc. (London), Ser. A, **216**, 515 (1953); Ser. A, **228**, 250 (1955).
17. W. H. THOMAS et J. J. PELLON. J. Polymer Sci. **13**, 329 (1954).
18. R. BENSASSON et A. PREVOST-BERNAS. J. Chim. Phys. **53**, 93 (1956).
19. R. BENSASSON et A. PREVOST-BERNAS. J. Polymer Sci. **30**, 163 (1958).
20. K. NOZAKI. Discussions Faraday Soc. **2**, 337 (1947).
21. D. J. MEAD et R. M. FUOSS. J. Am. Chem. Soc. **64**, 277 (1944).
22. S. C. LIND. Radiation chemistry of gases. American Chemical Society Monograph 151. 1961.
23. W. P. JESSE et J. SADAUSKIS. Phys. Rev. **109**, 2002 (1958).
24. T. T. JONES et H. W. MELVILLE. Proc. Roy. Soc. (London), Ser. A, **187**, 37 (1946).
25. L. REINISCH. J. Chim. Phys. **57**, 1064 (1960).

Can. J. Chem. Downloaded from www.nrcresearchpress.com by 210.87.254.6 on 09/05/12
For personal use only.

NICKEL–MAGNESIA CATALYST AS REVEALED BY ADSORPTION AND ELECTRON OPTICAL STUDIES

N. RAMASUBRAMANIAN[1] AND L. M. YEDDANAPALLI
Chemistry Department, Loyola College, Madras, India
Received February 4, 1963

ABSTRACT

A combined electron diffraction and hydrogen adsorption study on a nickel–magnesia catalyst with 36% nickel is reported. A comparison of the adsorption results with those on the previously reported 79% and 18% catalysts indicates the possibility of the unreduced nickel in the catalysts taking part in high-temperature fast adsorption. The electron optical studies show that there are structural changes taking place during the reduction treatment the catalyst undergoes. However, diffraction study *in situ* appears to be necessary to show, beyond doubt, the presence of reduced and unreduced nickel on the catalyst's surface.

Can. J. Chem. Downloaded from www.nrcresearchpress.com by 210.87.254.5 on 09/05/12
For personal use only.

Yamaguchi (1) has employed electron diffraction methods to study the behavior of combined catalysts and, using alternate wavelengths, reported three types. For chemisorption purposes the nature of the surface is of primary importance and an electron diffraction study, using the rather soft electrons, of a catalyst surface before and after the required hydrogen reduction treatment would provide additional information regarding the possible changes the catalyst may undergo during its preparation. In addition to the electron optical studies a study of the adsorption characteristics would enable one to examine the possible correlations existing between the structure and activity of the catalyst. Such a combined study on nickel–magnesia catalyst I is presented here. The adsorption results are compared with those reported earlier (2) on the two catalysts II and III.

EXPERIMENTAL

The method and materials have been fully described in references 2 and 3. It is sufficient to say here that the catalyst I was prepared by reducing the oxides, obtained by precipitation, using 400 ml 1 *N* sodium hydroxide, from the mixed nitrates solution (10 g nickel nitrate and 50 g magnesium nitrate in 300 ml water), at 475° C for 24 hours. The analysis gave a nickel content of 36.16% in the catalyst.

The electron diffraction photographs were taken using a camera length of 50 cm and an accelerating voltage of 50 kv. The specimens were mounted on carbon-coated copper grids for examination in the electron microscope.

RESULTS

The adsorption measurements on catalyst I were carried out in the temperature and pressure ranges 30 to 230° C and 8 to 60 cm Hg, respectively. The Elovich equation was used to analyze the data. The $q - \log t$ plots showed discontinuities and consisted of two linear portions. The initial portions of the room temperature plots were linearized using a t_0 chosen by the trial and error method (4).

Compared to 240° C obtained on catalyst II (2) the temperature at which $\alpha_1 = \alpha_2$ is found to be 90° C on catalyst I from the plots of the α values, at 55 cm Hg, of the two linear portions against temperature. The kinetic data obtained on the three catalysts I, II, and III at 55 cm Hg and 30 and 200° C are plotted in Fig. 1. The fast adsorption or the first-minute adsorption on catalyst I is about 1/10 of that on catalyst II at 30° whereas at 200° they are nearly equal to one another. On catalyst I the slow adsorption at both the

[1]*Present address: Division of Applied Chemistry, National Research Council, Ottawa, Canada.*

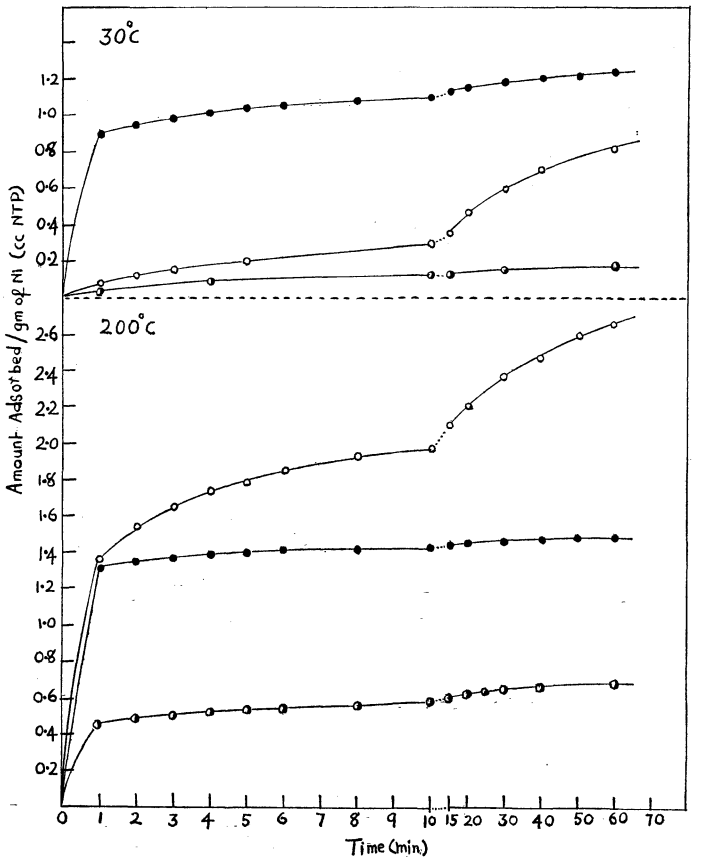

FIG. 1. Kinetics of hydrogen chemisorption on nickel–magnesia catalysts at 55 cm Hg: ○ catalyst I, ● catalyst II, and ◑ catalyst III.

temperatures is much higher than that on the other two catalysts. That there is a difference in activity between the catalysts I and II is also seen from the variation of the α values with pressure given in Table I. In contrast to catalyst II (2) the value of α_2 relative to

TABLE I

Hydrogen chemisorption on Ni–MgO catalyst I, 3.6 g, 36.16% Ni
Elovich parameters and initial pressure

30° C				207° C			
Run No.	Init. press. (cm Hg)	α_1	α_2	Run No.	Init. press. (cm Hg)	α_1	α_2
4	60.65	1.982	3.444	11	59.71	2.720	1.755
5	44.90	2.113	3.910	14	50.29	3.230	2.107
6	27.29	2.379	2.932	16	30.80	4.480	2.853
7	18.53	2.721	3.149	17	16.79	6.040	3.522
8	10.75	3.989	3.005	26	8.79	6.933	4.952
9	7.73	5.206	3.150	27	7.76	8.666	6.933

α_1 goes through a change at approximately 15 cm at the lower temperature of 30°. The α_2 at this temperature is almost independent of the initial pressure. These observations

Can. J. Chem. Downloaded from www.nrcresearchpress.com by 210.87.254.5 on 09/05/12
For personal use only.

show that both the temperature and pressure ranges of appearance of the kinetic stages are different on the two catalysts.

Considering the surface nickel available for chemisorption purposes it was pointed out that the poor hydrogen adsorptive capacity of catalyst III and the fast and the slow adsorptions on catalyst II could be explained on the basis of the presence of different amounts of pure or relatively pure, unreduced and unavailable nickel (2). On catalyst I there thus seems to be available a much higher percentage of unreduced nickel. The fast adsorption, which is much less at room temperature but which, with increasing temperature, becomes high and nearly equal to that on catalyst II, suggests, as discussed later, that unreduced nickel takes part in the fast adsorption also, at higher temperatures.

Generally, most of the catalysts undergo a reduction treatment in hydrogen before use. In the case of the supported metal catalysts, the metal oxide is reduced to the metal and the considerable volume change which results can be expected to have an effect on the structure, particularly of those prepared by the coprecipitation method. Therefore, it was thought that an electron diffraction study of the nickel oxide – magnesium oxide and the reduced oxides may provide some useful information. It is worth mentioning here that no solid solution series has been found between NiO and MgO (5). The electron diffraction patterns, in the case of catalyst I, of the oxides and the reduced oxides are given in Figs. 2(*a*), and 2(*b*) and 2(*c*), respectively, and in Table II the spacings and the

TABLE II

Comparison of the electron diffraction data obtained on Ni–MgO catalyst I with the literature values of NiO and MgO

Literature values*				Present study			
NiO		MgO		'*a*' mixed oxides		'*b*' reduced oxides	
d	I/I_o	*d*	I/I_o	*d*	I/I_o	*d*	I/I_o
2.410	91	2.431	10	2.420	15	2.414	57
2.088	100	2.106	100	2.115	100	2.088	100
1.476	57	1.489	52	1.493	50	1.481	62
1.206	13	1.216	12	1.226	15	1.207	16
0.958	7	0.966	2	0.965	14	0.937	23
0.934	21	0.942	17	0.858	11		
0.853	15	0.86	15				

*H. E. Swanson and E. Tatge. Natl. Bur. Std. Circ. No. 539. 1953.

relative intensities of the rings are compared with the literature values for nickel and magnesium oxides. There is a close correspondence between the spacings of nickel and magnesium oxides. The relative intensities of the rings, particularly of the first three, show that in the patterns 2(*a*) and 2(*b*) the major contributions come from magnesia and nickel oxide, respectively. In the pattern (2*b*) of the reduced oxides the strong rings of nickel are not distinctly visible; in the overexposed plate (2*c*) the indication of a faint ring at the spacing 1.75 (between the second and the third rings) becomes more clear. The electron micrographs of the oxides and the reduced oxides are shown in Fig. 3. The reduced oxides show a platelet-like structure, and more gaps than the oxides.

DISCUSSION

The fast and the slow adsorptions, the kinetic stages observed, and the variation of the slow rates of adsorption at the different temperature and pressure conditions studied on the three nickel–magnesia catalysts could be related to the availability of different

Can. J. Chem. Downloaded from www.nrcresearchpress.com by 210.87.254.5 on 09/05/12
For personal use only.

PLATE I

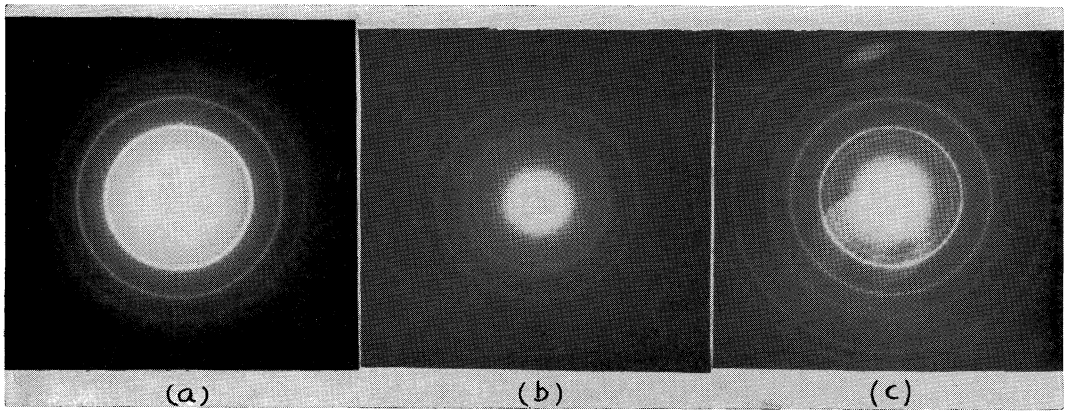

FIG. 2. Electron diffraction patterns, Ni–MgO catalyst I. (*a*) Mixed oxides; (*b*) reduced oxides; (*c*) reduced oxides, long exposure (1 minute) in the camera.

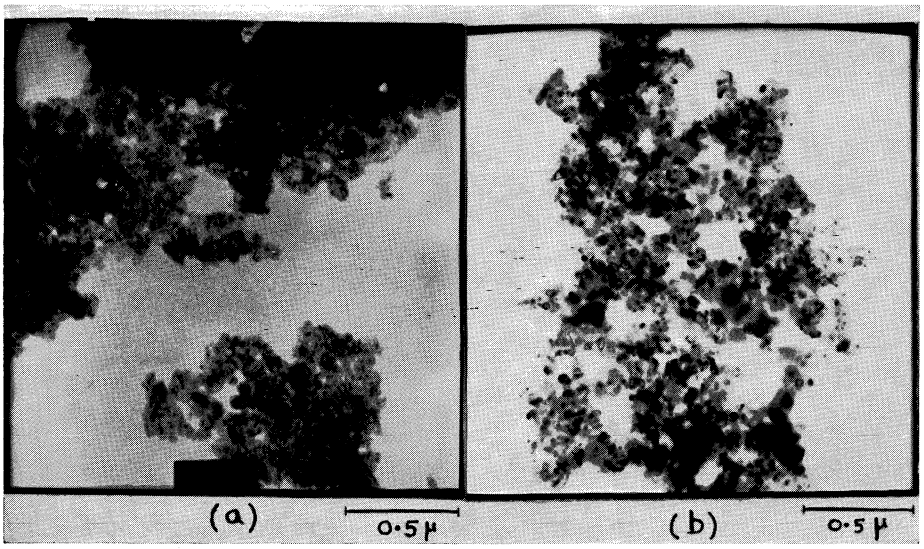

FIG. 3. Electron micrographs, Ni–MgO catalyst I, 40,000×. (*a*) Mixed oxides, (*b*) reduced oxides.

Can. J. Chem. Downloaded from www.nrcresearchpress.com by 210.87.254.5 on 09/05/12
For personal use only.

Can. J. Chem. Downloaded from www.nrcresearchpress.com by 210.87.254.5 on 09/05/12
For personal use only.

amounts of the three types of nickel on the surface. The higher nickel content catalyst II can thus be said to have a higher amount of pure or relatively pure nickel available as is evidenced by the high room-temperature fast adsorption and the low activated or slow adsorption. Moreover, the amount adsorbed compares favorably with that reported for unsupported nickel, prepared by the reduction of pure $Ni(OH)_2$ (6), indicating very little dispersion of nickel in this catalyst. The amount of unavailable nickel becoming high with increase in magnesia content explains the poor adsorptive capacity, and compared to catalyst I, the lower increase between the fast adsorption at 30° and at higher temperatures on catalyst III. The slow adsorption on catalyst I indicates a high percentage of unreduced nickel. This and the fact that compared to catalyst II there is observed a much larger increase between the fast adsorption at room temperature and that at the higher temperatures show that there is every possibility of the unreduced nickel becoming active for fast adsorption also, at the higher temperatures. The observation that in gas removal experiments the rapid desorption per unit pressure change is about eight times lower on catalyst I (3) even though the initial fast adsorption, from which this supposedly takes place, on the catalysts I and II is nearly the same confirms the idea of different types of sites being involved in the high-temperature fast adsorption on these two catalysts.

The electron beam used in the present study corresponds to the soft electrons in Yamaguchi's work (1) and therefore grazed the surface of the samples. The observation that in the reduced oxides' pattern the contribution from NiO is much greater than in the mixed oxides' shows that in the latter it is mainly magnesia that is on the surface, but after the reduction treatment much more nickel oxide becomes available on the surface. Considering the fact that during the reduction of the oxides there is an appreciable decrease in volume accompanying the conversion of NiO (4.1*a*) to Ni (3.5*a*) it is suggested that the mixed oxides is of the second type put forward by Yamaguchi (1) and that the volume decrease during reduction leads to the breakdown of the aggregates, exposing the nickel. It is seen from the width of the rings in the reduced oxides' pattern that the nickel particles are fine and the possibility of air oxidation of the reduced active nickel explains the absence of the distinct diffraction rings due to nickel. Therefore, it is hard to describe the state of nickel on the catalyst's surface, and carrying out the diffraction study of the reduction of the oxides *in situ* may prove beyond doubt the presence of both reduced and unreduced nickel on the surface. Nevertheless, the present study has shown that there are structural changes taking place during the reduction treatment. The effect of hydrogen reduction could also be seen from the micrographs of the oxides and the reduced oxides. The skeletal structure of the latter shows the effect of the decrease in volume during reduction.

REFERENCES

1. S. YAMAGUCHI. J. Chem. Phys. **27**, 1114 (1957).
2. N. RAMASUBRAMANIAN and L. M. YEDDANAPALLI. Can. J. Chem. **41**, 68 (1963).
3. N. RAMASUBRAMANIAN and L. M. YEDDANAPALLI. J. Phys. Chem. **66**, 1222 (1962).
4. M. J. D. LOW. Chem. Rev. **60**, 267 (1960).
5. C. PALACHE, H. BERMAN, and C. FRONDEL. Dana's system of mineralogy. Vol. I. John Wiley and Sons, New York. 1952. p. 498.
6. G. C. A. SCHUIT and N. H. DE BOER. Rec. Trav. Chim. **70**, 1067 (1951).

Can. J. Chem. Downloaded from www.nrcresearchpress.com by 210.87.254.5 on 09/05/12
For personal use only.

Can. J. Chem. Downloaded from www.nrcresearchpress.com by 210.87.254.5 on 09/05/12
For personal use only.

THE DEAMINATION OF ALICYCLIC α-AMINOKETONES[1,2]

O. E. EDWARDS AND M. LESAGE
Division of Pure Chemistry, National Research Council, Ottawa, Canada

Received February 8, 1963

ABSTRACT

The deamination of α-aminocyclohexanones has been shown to give cyclopentane carboxylic acids, bicyclo[3,1,0]hexane-2-ones, and 2-methyl-2-cyclopentene-1-ones. Deamination of 3-*endo*-aminocamphor gave cyclocamphanone, 6-isopropenyl-6-methyl-2-cyclohexen-1-one, and 6-(1′-hydroxy-1′-methylethyl)-6-methyl-2-cyclohexen-1-one.

The formation of bicyclo[3,1,0]hexane by deamination of cyclohexylamine is reported for the first time. The difference between the products from it and bornylamine and those from the corresponding α-aminoketones are rationalized on the basis of the amount of C—C participation in the corresponding carbonium ions.

The nature and fate of carbonium-ion-like intermediates in reactions are very much dependent on the way in which they are formed, on the solvent, and on the steric and electronic environment in which they are developed. The purpose of this study (1) was to examine the fate of carbonium ions located α to a ketone carbonyl. In order to ensure as pure carbonium ion states as possible we generated them by deamination of α-aminoketones.

Preparation of 2-aminocyclohexanone by stannous chloride reduction of 2-oximinocyclohexanone gave a 35% yield of 2-aminocyclohexanone hydrochloride (2). The 2-amino-6,6-dimethylcyclohexanone was prepared as its hydrochloride (I) by the illustrated sequence. The β-keto ester was obtained by the method of Linstead (3). In order to avoid

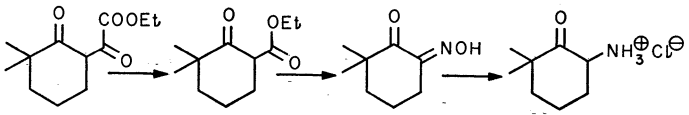

I

complicating the products unduly, the deaminations were carried out in water using acids whose anions had low nucleophilicity, i.e. sulphuric and perchloric acids, but without any attempt to remove the chloride ions from the original salt in the aminoketone cases.

The products from 2-aminocyclohexanone were separated into readily extractable neutral and acid fractions, and very water soluble material. The latter proved to be mainly adipic acid and 3-hydroxy-2-methylcyclopentanone.

The easily extracted acid (ca. 57%) yield had a strong unpleasant odor. It proved to be a mixture of a readily distillable acid (max. yield ca. 50%) and a non-volatile residue, which was not further studied. The volatile acid proved to be the expected cyclopentanecarboxylic acid, identified by comparison of its physical properties and those of its anilide and amide with authentic samples. This product had been observed earlier by Granger and Técher (4).[3] More recently Baumgarten and Anderson have reported the formation of this acid, and what are probably ϵ-hydroxycaproic and 5-hexenoic acids from 2-aminocyclohexanone (5). The readily extractable neutral products from the deamination of

[1]*Issued as N.R.C. No. 7346.*
[2]*Presented in part in the Merck lecture of the Chemical Institute of Canada, June 14, 1960. See Chem. Can.* ***13****, 40 (1961).*
[3]*We regret that we were unaware of their publication when our communications were submitted.*

2-aminocyclohexanone contained diazoketone as one component, as shown by the characteristic band at 2100 cm^{-1} in its infrared spectrum. The mixture was separated by vapor phase chromatography, which showed that at least eight components were present.[4] The two major components were isolated on a preparative scale, then used to make reference solutions. These were used to estimate absolute yields by comparison of areas under the v.p.c. curves.

The main component was formed in an average yield of 16%. It analyzed correctly for C_6H_8O, had λ_{max} 227 mμ (ε 11,200) and 305 mμ (ε 51), and ν_{max} 1705 and 1665 cm^{-1}. Its n.m.r. spectrum had peaks corresponding to an allylic methyl group (τ 8.3) and one vinyl hydrogen (τ 2.7). These correspond to a methylcyclopentenone, with 2-methyl- and 3-methyl-2-cyclopenten-1-ones being the most probable structures. Both were synthesized by known procedures, the 2-methyl isomer following Godchot (6) and the 3-methyl isomer following Robinson (7). The deamination product was identical in all respects with 2-methyl-2-cyclopenten-1-one (II).[5]

The second most abundant component (6.5–9% yield) again analyzed for C_6H_8O. It had strong end absorption in the ultraviolet and ν_{max} 1727 cm^{-1}. This, and the n.m.r. spectrum, which contained no vinyl hydrogen signal, seemed only consistent with the compound being bicyclo[3,1,0]hexan-2-one (III).[6] Comparison of the dinitrophenylhydrazone of the compound with a sample of the derivative of bicyclo[3,1,0] hexan-2-one kindly provided by Dr. N. A. Nelson (8) proved this to be correct.

The other components could not readily be obtained pure with the preparative columns at our disposal. However, the absence of absorption near 1675 cm^{-1} in the infrared spectrum of the neutral product indicated that not more than a trace of conjugated cyclohexenone was present.

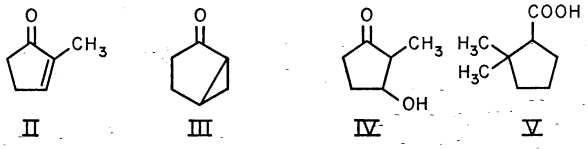

II III IV V

A product that we infer to be 3-hydroxy-2-methylcyclopentanone (IV) remained in the aqueous phase after the deamination and separation of the ether layer. When this aqueous solution was made weakly alkaline (pH 8–10) and stirred with ether, 2-methyl-2-cyclopenten-1-one was formed and accumulated in the ether layer. The yield of the hydroxyketone was 7–10%.

The deamination of 6,6-dimethyl-2-aminocyclohexanone (I) gave up to 35% weight yield of methylene-chloride-extractable acid, of which over half was readily distilled under 15 mm pressure. The distillate, which was mainly one component, was purified by further

[4]*In experiments with vapor phase chromatography of diazocamphor no peak was observed corresponding to the diazoketone or its thermal decomposition products. This behavior seems to be characteristic of compounds decomposing during passage through the column. Since no diazocyclohexanone passed unchanged through the v.p.c. columns, we conclude by analogy that none of the observed peaks were due to it or its thermal decomposition products. This conclusion was confirmed when the diazoketone in the total neutral products was destroyed by reaction with aqueous p-toluenesulphonic acid. Only minor changes in the quantity of the other products were observed, with no new product produced.*

[5]*The intensity of the ultraviolet maximum for 3-methyl-2-cyclopentenone cited by Robinson and co-workers is in error.*

[6]*With older instruments with more stray light, maxima in the vicinity of 210 mμ were observed with the bicyclic ketones obtained in this work. However, with a new Carey model 11 spectrophotometer these were absent. We hence consider it likely that all the maxima reported near 210 mμ for simple cyclopropyl ketones are spurious (see also ref. 9).*

Can. J. Chem. Downloaded from www.nrcresearchpress.com by 210.87.254.5 on 09/05/12
For personal use only.

distillation. The acid analyzed for $C_8H_{14}O_2$. The n.m.r. spectrum of its methyl ester had peaks corresponding to two C-methyl groups (τ 8.8 to 9.1), the O-methyl group (τ 6.4), six methylene hydrogens (τ 7.8 to 8.7), and a single deshielded hydrogen as an apparent doublet with a spacing of 8 c.p.s. centered at τ 7.6. These facts and the origin of the acid suffice to prove it to be 2,2-dimethylcyclopentanecarboxylic acid (V). Attempts to convert it to the known 2,2-dimethylcyclopentanone were abortive.

Attempts to prepare V from 2-chloro-6,6-dimethylcyclohexanone under the conditions of the Favorskii reaction[7] failed to give appreciable amounts of the acid. Similarly the action of silver nitrate in aqueous alcohol (11) on 2-bromo-6,6-dimethylcyclohexanone gave no detectable amount of V, although much water-soluble material was produced. It thus appears that the deamination may provide a useful alternative to the Favorskii reaction when one carbon α to the ketone carbonyl is quaternary.

The aqueous solution from the deamination after removal of the readily extractable neutral and acidic products was concentrated to small volume, made strongly acid, and continuously extracted with chloroform. The crystalline acid obtained was identified by analysis and melting point as 2,2-dimethyladipic acid. A sample of the aqueous solution immediately after the deamination failed to give any bisdinitrophenylhydrazone of 6,6-dimethyl-1,2-cyclohexanedione, hence any of the corresponding α-ketol which had been formed must have been completely oxidized to the adipic acid by nitrous acid.

The maximum weight yield of readily extractable neutral products obtained from 6,6-dimethyl-2-aminocyclohexanone was 78%. This was distilled under 15 mm pressure. A relatively non-volatile crystalline residue was obtained with empirical formula $C_{16}H_{24}N_2$. Its infrared spectrum had no carbonyl or isolated azomethine absorption, and its ultraviolet absorption (λ_{max} 289 mμ, ϵ 12,340) was consistent with it being the octahydrophenazine VI. Its n.m.r. spectrum indicated the absence of aromatic hydrogens, the presence of four identical methyl groups (τ 8.75), and two groups of methylene hydrogens centered around τ 7.17 (4 H) and τ 8.17 (8 H) in agreement with this assignment.[8] The volatile neutral products contained diazoketone (ν_{max} 2100 cm^{-1}) and at least nine other components as shown by gas chromatography. The two major ones were shown to be analogous to those from aminocyclohexanone, but in a reversed yield ratio.

The substance corresponding to the first major peak from the gas chromatogram analyzed for $C_8H_{12}O$ and had λ_{max} 228 mμ (ϵ 10,800) and 317 mμ (ϵ 60) and had ν_{max} 1710 cm^{-1}. Its n.m.r. spectrum was consistent with it being 2,5,5-trimethyl-2-cyclopenten-1-one (VII) (see the chemical shift assignments on the figure, given as τ value for deuterochloroform solutions). The other major component also gave correct analyses for $C_8H_{12}O$.

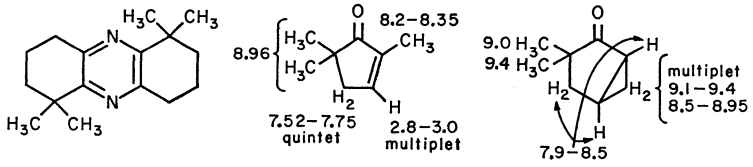

Its ultraviolet spectrum (intense end absorption, λ_{max} 284 mμ, ϵ 46) and its infrared spectrum (ν_{max} 1725 cm^{-1}) resembled those of bicyclo[3,1,0]hexanone. Its n.m.r. spectrum confirmed its identity as 3,3-dimethylbicyclo[3,1,0]hexan-2-one VIII (see assignments on

[7]*See reference 10 for leading references.*

[8]*Baumgarten and Bower (2) observed the formation of decahydrophenazine from 2-aminocyclohexanone. Presumably the nitrous acid dehydrogenated the decahydro derivative in our case.*

Can. J. Chem. Downloaded from www.nrcresearchpress.com by 210.87.254.5 on 09/05/12
For personal use only.

the figure). The ratio of the areas under the peaks from the gas chromatogram corresponding to the cyclopentenone and the bicyclic ketone were approximately 1:2. The minor components were not identified.

The bicyclic ketone gave no methylcyclopentanone when treated with dilute solutions of sodium hydroxide or perchloric acid in ethanol, hence it is very unlikely that VII was produced from VIII under the mild reaction conditions.

In order to provide the closest possible comparison of the above deaminations with that of a simple amine, we re-examined the deamination of cyclohexylamine. Under the same conditions as used for the aminocyclohexanone studies, the main product (ca. 80%) was cyclohexanol, as found by Hückel (12). Careful v.p.c. examination of the alcohol component failed to reveal the presence of any methylcyclopentanols or hydroxymethylcyclopentane. No cyclohexanone was present but a compound identified by its retention time on a v.p.c. column as cyclohexyl nitrite was formed in up to 14% yield. The hydrocarbon components gave a single peak using a polypropylene glycol column, but were resolved on a silver nitrate–glycol column into cyclohexene and bicyclo[3,1,0]hexane.[9] The yields of these averaged 4% and 2% respectively. No 1-methylcyclopentene was formed.

Finally, to extend our observations on the deamination of α-aminoketones we studied α-aminocamphor. Since the coupling of the 3-hydrogen (τ 5.5) with the bridgehead 4-hydrogen is 5 c.p.s. it appears that the amino group has the endo configuration[10] (13) shown in IX. Deamination of the aminoketone produced a small yield of crystalline acid. This appeared to be a mixture of isomers and was hence not further characterized. By analogy with the aminocyclohexanones this should have structure X.

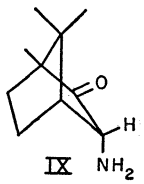

IX

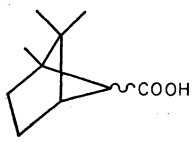

X

The neutral products contained around 18% of cyclocamphanone XI, identified by comparison with authentic material. Like the bicyclic ketones examined (III and VIII) this had no maximum near 210 mμ in its ultraviolet absorption spectrum.[6]

The major neutral product (62%) analyzed for $C_{10}H_{14}O$ and appeared to be a lightly substituted α,β-unsaturated ketone (λ_{max} 225 mμ (ϵ 13,940); ν_{max} 1680 cm^{-1}) containing a terminal methylene group (ν_{max} 898 cm^{-1}). Its n.m.r. spectrum showed the presence of one somewhat deshielded methyl group (singlet, τ 8.8), an allylic methyl group (singlet, τ 8.3), and the terminal methylene (τ 5.1 and 5.3, two hydrogens). The two vinyl hydrogens on the conjugated double bond appeared as a doublet centered at τ 4.1 (J = 10 c.p.s.) and a multiplet centered at τ 3.2. Reduction of the conjugated double bond with zinc and acetic acid gave a compound with ν_{max} 1710 and 898 cm^{-1}. Its n.m.r. spectrum showed little change except the loss of the signals at τ 4.1 and 3.2. Catalytic reduction of this product using palladium converted it to a dihydro compound, in whose infrared spectrum the 898 cm^{-1} band had disappeared. The signals at τ 5.1 and τ 5.3 were no longer present in its n.m.r. spectrum, and the low-field methyl of the parent compound now resonated at τ 9.1. Taking into account its origin, this evidence was only consistent with the deamination product being 6-isopropenyl-6-methyl-2-cyclohexene-1-one (XII). This

[9]*We are grateful to Dr. H. E. Simmons for a sample of pure bicyclo[3,1,0]hexane.*
[10]*We are grateful to Dr. F. A. L. Anet for suggesting this method of determining the configuration.*

Can. J. Chem. Downloaded from www.nrcresearchpress.com by 210.87.254.5 on 09/05/12
For personal use only.

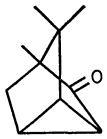
XI

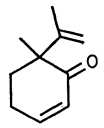
XII

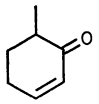
XIII

was proved correct by heating the compound in a 2:1 (v/v) mixture of 12 *N* sulphuric acid in methanol. A new α,β-unsaturated ketone was produced in good yield which analyzed for $C_7H_{10}O$. Its n.m.r. spectrum was in agreement with structure XIII and its 2,4-dinitrophenylhydrazone had the same melting point as that of 6-methyl-2-cyclohexen-1-one (14).

A third product of the deamination was at first missed because of its long retention time. It was observed, however, that if an ether solution of the neutral product was shaken with sodium carbonate solution, or if the mixture was chromatographed on neutral alumina, a new component appeared which was rapidly eluted from the v.p.c. column. This proved identical with XIII. Since XII is inert under these conditions, we conclude that the alkali or alumina was cleaving the alcohol XIV present in the products as shown:

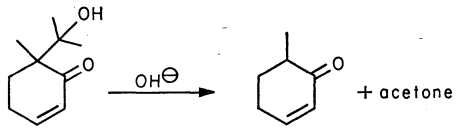

XIV

The yield of XIV was estimated to be around 4%. As far as we are aware XII and XIV represent a new type of fission product of the camphor skeleton.

When diazocamphor was treated with acid, the three products XI, XII, and XIII were produced. This confirms the conclusion of Applequist that protonation of diazoalkanes gives the corresponding alkyldiazonium ions (15).

DISCUSSION

The generation of a carbonium ion adjacent to a carbonyl is an energetically unfavorable process due to proximity of the positive charge to the positive end of the carbonyl dipole. This is well illustrated by the inertness of α-haloketones to S_N1 solvolysis (16). It is to be expected then that the developing positive charge in processes which would lead to such a carbonium ion would be delocalized if possible by participation of nearby carbon–carbon and carbon–hydrogen bonds. This expectation is borne out by the high yields of unusual products in the α-aminoketone deaminations.

That some α-ketol is produced in the aminocyclohexanone deaminations seems certain since the adipic acids must arise by oxidation of these by nitrous acid. The cyclopentanecarboxylic acids most likely arise by one of three mechanisms:

(*a*) Rearrangement synchronous with C—N bond rupture, giving the acylium ion:

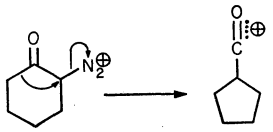

Can. J. Chem. Downloaded from www.nrcresearchpress.com by 210.87.254.5 on 09/05/12
For personal use only.

(*b*) Initial formation of a cyclopropanone as in the Favorskii reaction (8) followed by hydrolytic ring opening:

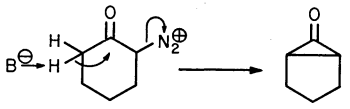

Since only very weak bases are present to accept the proton in the first stage, this would have the character of C—H bond participation in the dissociation.

(*c*) Hydration of the carbonyl followed by the concerted process shown:

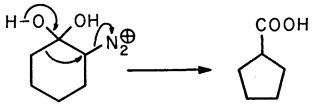

Since the dimethylcyclopentanecarboxylic acid was formed from 2-amino-6,6-dimethylcyclohexanone, for which mechanism (*b*) cannot operate, either (*a*) or (*c*) or both are valid mechanisms in this case.

Of the three mechanisms (*c*) seems to offer the path of least energy to the cyclopentanecarboxylic acids. The opposed dipoles in the amine salt and diazonium ion should favor hydration of the carbonyl (see for example chloral and mesoxalic acid). The diazonium ion could then dissociate, with participation of the 5,6 C—C bond aiding the electron release to the nitrogen. Since the *gem*-dimethyl group adjacent to the carbonyl would make the hydration less favorable on steric grounds, the lower yield of acid obtained in this case relative to aminocyclohexanone deamination can be accounted for.

The major neutral products from the aminocyclohexanones, the bicyclo[3,1,0]hexanones, methylcyclopentenones, and 3-hydroxy-2-methylcyclopentanones, are unusual, although other cases of cyclopropane ring formation in deaminations and deoxygenations in aliphatic compounds have recently been reported (17, 18, 19). The fact that cyclohexenones are absent, or are formed in very low yield, is striking. In addition the relatively low yield of products derived from the α-ketols is in marked contrast to the 94% yield of cyclohexanol and cyclohexyl nitrite from cyclohexylamine.

There appear to be only two simple routes, 1 or 2, to the methylcyclopentenones and 3-hydroxy-2-methylcyclopentanones:

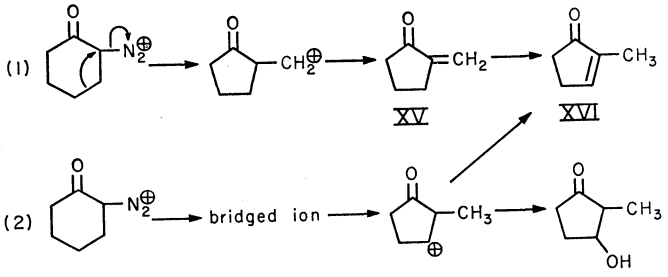

Route 1 is indirect and involves the high energy primary carbonium ion. In addition the rearrangement of XV go XVI would not be expected to take place under the reaction condition (short exposure to a weakly acid medium). We hence consider route 2 to be the most probable one. It has the added attraction of providing a direct path to the three major neutral products.

Can. J. Chem. Downloaded from www.nrcresearchpress.com by 210.87.254.5 on 09/05/12
For personal use only.

We suggest that the first ion produced is A, in which the positive charge is delocalized by participation of the 3,4 carbon–carbon bond. This is then converted by hydride migration to B, which collapses to the classical ion C, the immediate precursor of the methylcyclopentenone and 3-hydroxy-2-methylcyclopentanone. The hydride transfer in

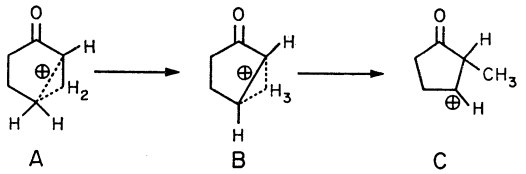

A B C

the transition of A to B could involve the protonated cyclopropane D or the hydrogen-bridged non-classical ion E. It seems likely that E is the intermediate ion since in dilute acid D would rapidly lose a proton to give the bicyclic ketone III.[11]

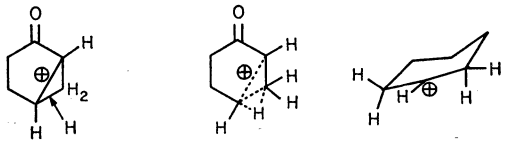

D E F

The bicyclohexanones could arise by proton expulsion from A, B, D, or E. An attractive possibility is that E can rearrange to D as well as to B, and that D in turn loses a proton to give the bicyclic ketones.

It now remains to reconcile the differences in product composition between the cyclohexylamine and aminocyclohexanone, and between the bornylamine and aminocamphor deaminations. We consider that these can be accounted for as follows:

The activation energy for the deamination of cyclohexylamine is so low that no assistance from external nucleophiles or neighboring C—C and C—H bonds is needed to aid the approach to the transition state.[12] The 'bare' carbonium ions that result react rapidly with nearby water molecules or nitrite ions.[13] The axial hydrogen on the α-carbon in the ideal planar state of the ion (F) is in a favorable stereo-electronic situation for elimination, and hence the few percent of cyclohexene formed probably arises from this state. The even smaller amount of bicyclo[3,1,0]hexane is presumably formed via a bridged-ion intermediate. No methylcyclopentene or 2-methylcyclopentanol could be detected among the products, which is consistent with the absence of well-developed C—C participation in the carbonium ion.

In contrast, the deamination of the α-aminocyclohexanones, for which we postulate a large amount of C—C participation, gave less than 25% of products derived from the simple carbonium ion. The major products, the bicyclic ketones and methylcyclopentenones, apparently arise from bridged ions as described above. No cyclohexenones could be detected, as expected if very little 'bare' carbonium ion was present in these cases.

[11]*There is good evidence (20, 21) that symmetrically protonated cyclopropanes (22) are not intermediates in methyl migration in carbonium ion rearrangements, but in our opinion unsymmetrical 'edge-protonated' cyclopropanes are not excluded from consideration by their work. However, we believe such intermediates would give rise in high yield to cyclopropane.*

[12]*This is in agreement with the views of Cram and McCarty (23) and Ridd (24).*

[13]*The retention of configuration in the cyclohexanol (25) could be the result of reaction with water before the ideal planar state of the ion is reached, or selective reaction with the water molecules which had solvated the diazonium ion, on the face of the carbon from which the nitrogen had departed.*

Can. J. Chem. Downloaded from www.nrcresearchpress.com by 210.87.254.5 on 09/05/12
For personal use only.

The deamination of 3-*endo*-aminocamphor gave as major products the monocyclic compounds XII and XIV (74%) and the tricyclic compound XI (18%). In contrast, the fairly comparable bornylamine (XVII) gave mainly camphene and camphene hydrate (XVIII) with 28% of α-terpeneol (XIX) (26). Isobornylamine (XX) gave over 90% camphene and camphene hydrate (27).

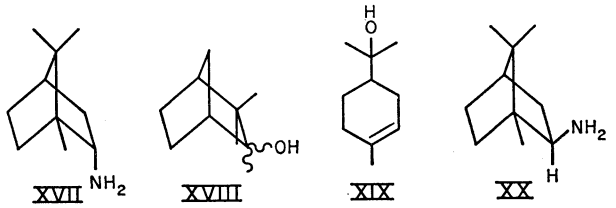

XVII XVIII XIX XX

As the positive charge develops on C-2 in the isobornylamine deamination it must be rapidly delocalized by formation of the bornonium ion G, which then gives nearly quantitatively camphene and camphene hydrate. Since in the deamination of bornylamine around 30% of the monocyclic α-terpineol was formed, we can thus conclude that at least this percentage of the molecules doesn't give rise to the ion G. The same conclusion follows from consideration of the fact that the participation of the 1,6 carbon–carbon bond would have to be subsequent to the departure of the nitrogen from the endo face of C-2. We hence suggest that in the bornylamine case an essentially bare carbonium ion is formed, which in part gives the bornonium ion and finally camphene and camphene hydrate, and in part captures the electron pair of the 1,7 carbon–carbon bond, giving the monocyclic terpineol.

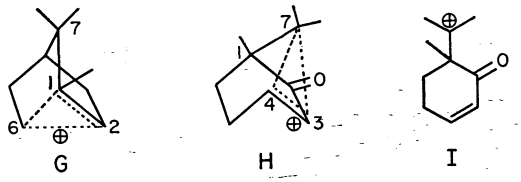

G H I

In the aminocamphor deamination no products with rearranged bicyclo[2,2,1]heptane skeleton were observed. We conclude that little bare carbonium ion was formed, consistent with the high activation energy which would be involved in juxtaposition of the two like charges. Instead the developing positive charge is delocalized by participation of the 4,7 carbon–carbon bond with formation of the rather high-energy bridged ion H. This collapses to the classical ion I in which good charge separation is achieved. I gives predominantly the diolefin XII but some of the tertiary alcohol is formed.

The cyclocamphanone formed from aminocamphor could arise from the bare carbonium ion or by conversion of H to the non-classical ion J followed by proton expulsion. The absence of tricyclic compound in the bornylamine case could be partly due to the lower

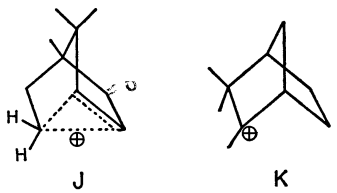

J K

Can. J. Chem. Downloaded from www.nrcresearchpress.com by 210.87.254.5 on 09/05/12
For personal use only.

energy of the tertiary carbonium ion K compared to the corresponding secondary carbonium ion from the aminocamphor. This would favor formation of the rearranged skeleton in the former and the tricyclene in the latter case.

It seems desirable to study the deamination of the at-present unknown 3-bornanamines in order to have more perfect comparison with the behavior of aminocamphor.

EXPERIMENTAL

Infrared spectra were taken on a Perkin–Elmer Model 21 spectrophotometer and ultraviolet spectra determined in 95% ethanol on a Cary Model 11 spectrophotometer. Vapor phase chromatography (v.p.c.) was carried out using a Perkin–Elmer Model 154C instrument with thermistor detector. The analytic columns used were 1 m and 2 m × 0.25 in. stainless steel columns with polypropylene glycol on diatomaceous earth packing (column R) and a 2 m×0.25 in. silver nitrate in diethylene glycol on diatomaceous earth packing (column H). The preparative chromatography was done with a 3 m×1 in. column with type R packing. Yields were estimated in the cyclohexylamine and 2-aminocyclohexanone cases by diluting the total neutral extract in ether to a known volume and comparison of the peak areas in the v.p.c. of an aliquot of this with those from ether solutions containing known concentrations of the corresponding substances. In the 2-amino-6,6-dimethylcyclohexanone and aminocamphor cases the yields were estimated roughly by assuming equivalent peak areas per gram for all the volatile products. The n.m.r. spectra were determined in deuterochloroform with tetramethylsilane as internal standard using a Varian A-60 spectrometer.

Deamination of Cyclohexylamine

A solution of 5 g of cyclohexylamine perchlorate and 5 g of sodium nitrite in 20 ml of water was prepared. Five milliliters of ether was added, then the mixture was cooled in ice. To this was added dropwise with stirring 15 ml of 0.1 *N* perchloric acid during 15 minutes. The escaping gas was bubbled through a trap containing cold ether.[14] The reaction mixture was left 10 minutes in the cold bath, then 5 minutes at room temperature. It was neutralized using sodium bicarbonate, then extracted thoroughly with ether. The liquid remaining after careful distillation of the ether was analyzed using vapor phase chromatography on a polypropylene glycol column (Perkin–Elmer R). The main products were cyclohexanol (~80%) and cyclohexyl nitrite (12–14%) with a smaller fraction rich in cyclohexene. Rechromatography of the cyclohexene fraction on Column H showed it to be a mixture of cyclohexene (3–5% yield) and bicyclo[3,1,0]hexane (~2% yield). The latter had retention time identical with that of an authentic specimen.[9]

2-AMINOCYCLOHEXANONE

2-Aminocyclohexanone Hydrochloride[15]

The method of Jaeger and van Dijk (28) was used to prepare 2-isonitrosocyclohexanone.

The isonitrosoketone (9.5 g) was slowly added with shaking to a solution of 40 g of stannous chloride in 50 ml of concentrated hydrochloric acid. Then 24 g of mossy tin was added and the reaction mixture heated on a steam bath for 15 minutes. The resulting solution was diluted with 1 l. of water, and the tin precipitated using hydrogen sulphide. After filtration the clear solution was reduced to dryness *in vacuo* at 40° in a rotating evaporator.

The residue was recrystallized from absolute ethanol, giving 3.85 g (35%) of hydrochloride, m.p. 150–155°. A further recrystallization from ethanol – ethyl acetate gave colorless needles, m.p. 154–155°. Found: C, 47.87; H, 8.15; N, 9.28. Calc. for $C_6H_{12}ClNO$: C, 48.15; H, 8.08; N, 9.36.

Deamination of 2-Aminocyclohexanone Hydrochloride

(*a*) 2-Aminocyclohexanone hydrochloride (800 mg) was dissolved in 3 ml of 0.05 *N* H_2SO_4. To this solution 1.7 g of sodium nitrite, dissolved in 2 ml of water, was added slowly with shaking. The reaction mixture was left at room temperature for ½ hour. It was then basified with sodium bicarbonate and extracted with methylene chloride. The methylene chloride solution was dried and the solvent distilled, giving 400 mg of neutral residue.

The aqueous solution was acidified with 6 *N* H_2SO_4 and extracted with methylene chloride. Then methylene chloride solution was dried over anhydrous sodium sulphate and distilled, leaving 280 mg of acidic material.

(*b*) 2-Aminocyclohexanone hydrochloride (500 mg) was dissolved in 1 ml of water and to this solution 0.5 g of sodium nitrite in 1 ml of water was added. The reaction mixture was cooled in ice water for 10 minutes. Then, with stirring, 1.5 ml of 0.1 *N* perchloric acid was added dropwise to steadily liberate nitrous acid (time 20 minutes). The reaction was left for 10 minutes more in the cold bath and at room temperature for 5 minutes.

An acid-neutral separation as in (*a*) gave 219 mg of acidic material and 88 mg of neutral.

[14]*The ether trap collected no significant amount of product.*

[15]*We thank Mr. Earl Brewer, who first prepared this compound.*

Can. J. Chem. Downloaded from www.nrcresearchpress.com by 210.87.254.5 on 09/05/12
For personal use only.

Many variations of these conditions were tried, including changing the nature of the acid and its concentration, and varying the temperature rate and order of addition. The conditions in (*b*) gave the highest yield of acid.

(*c*) 2-Aminocyclohexanone hydrochloride (200 mg) was dissolved in 2 ml of 0.2 *N* sulphuric acid and a solution of 0.5 g of sodium nitrite in 1 ml of water was added to it dropwise during 20 minutes. The reaction was then basified with sodium bicarbonate and a neutral acid separation was effected, giving 50 mg of neutral material and 48 mg of acid.

The Neutral Products

The bulk of the neutral product from deamination by method (*a*) was readily extractable into ether. An oil remained after careful distillation of the ether. This contained some 2-diazocyclohexanone, as indicated by the presence of a sharp band at 2100 cm^{-1} in the infrared spectrum of the residue. This absorption disappeared when the mixture was allowed to stand, or when an ether solution of the products was stirred in the presence of aqueous *p*-toluenesulphonic acid without significant change in the composition as indicated by v.p.c. The mixture was separated into two major and 5 minor components by a 2 m×1/4 in. column with R packing at 120° C and a flow rate of 120 cc/min. The minor components had retention times of 7, 13, 14, 15.5, and 22 minutes. The major components are described below.

The presence of another neutral component which remained in the aqueous layers was proved by treatment of the latter with sodium carbonate in the presence of ether. Vapor phase chromatography of the ether solution after concentration showed that 2-methyl-2-cyclopentene-1-one had been produced in 7 to 10% yield.

Bicyclo[3,1,0]hexane-2-one

Retention time 26.5 minutes, yield 6.5–9.2%. It had ν_{max} 1727 cm^{-1}; its ultraviolet spectra showed strong end absorption (ϵ, 1625 at 210 mμ) and λ_{max} 277 mμ (ϵ 370). Found: C, 75.42; H, 8.28. Calc. for C_6H_8O: C, 74.97; H, 8.39. It gave a 2,4-dinitrophenylhydrazone, m.p. 182–185°. This showed no mixed m.p. depression with an authentic sample (m.p. 175–183°) of the dinitrophenylhydrazone of bicyclo[3,1,0]hexane-2-one kindly provided by Dr. N. A. Nelson, and the X-ray powder patterns of the two were identical. The n.m.r. spectrum of the ketone had a series of signals between τ 8.7 and τ 9.2 with intensity equivalent to two protons.

2-Methyl-2-cyclopentene-1-one

Retention time 19.0 minutes. Yield 12.5–19.5%. It had $\nu_{max}^{CS_2}$ 1705 cm^{-1} (C=O), 1640 cm^{-1}, and 785 cm^{-1} (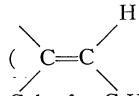); Its ultraviolet spectrum had λ_{max} 227 mμ (ϵ 11,220), 305 mμ (ϵ 51). Found: C, 74.80; H, 8.16. Calc. for C_6H_8O (96.12): C, 74.97; H, 8.39.

The n.m.r. spectrum of the ketone had a doublet (J = 1.5 c.p.s.) centered at τ 8.3 (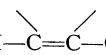), a series of signals from τ 7.8 to τ 7.3, and a multiplet centered at τ 2.7.

Cyclopentanecarboxylic Acid

The readily extractable acids from the deamination of 2-aminocyclohexanone were distilled over a short path at an air-bath temperature of 102° under 8 mm pressure. The clear colorless oil so obtained had a rancid odor. It had n_D^{18} 1.4540 (reported 1.4534) (29). Found: C, 62.64; H, 8.60. Calc. for $C_6H_{10}O_2$: C, 63.13; H, 8.83. The maximum yield obtained using the conditions in (*b*) was 50%.

Its amide was prepared via the acid chloride ($SOCl_2$). After recrystallization from aqueous methanol and sublimation at 70°, 1×10^{-3} mm, it melted at 178–179°. Found: C, 63.38; H, 9.96. Calc. for $C_6H_{11}ON$: C, 63.68; H, 9.80.

The anilide of the acid was prepared from the acid chloride. After sublimation at 90°, 5×10^{-4} mm, it melted at 164–165°. Found: C, 76.03; H, 7.85; N, 7.49. Calc. for $C_{12}H_{15}ON$: C, 76.15; H, 7.99; N, 7.40.

The above derivatives had the same melting point as the amide and anilide of cyclopentanecarboxylic acid prepared by hydrolysis of cyclopentyl cyanide, and showed no mixed melting point depression with the corresponding authentic derivative.

Adipic Acid

Extraction of the acidic aqueous solution in a continuous liquid–liquid extractor using chloroform gave a small quantity of adipic acid characterized by melting point and mixed melting point.

2-Amino-6,6-dimethylcyclohexanone

2,2-Dimethyl-6-ethoxycarboxylcyclohexanone

A mixture of di- and tri-methylcyclohexanones from alkylation of 2-methylcyclohexanone (30) was treated with ethyl oxalate in the presence of sodium ethoxide. Only the 2,2-dimethylcyclohexanone formed an oxalyl derivative (3). This was decarboxylated in the presence of crushed soft glass, the optimum temperature

Can. J. Chem. Downloaded from www.nrcresearchpress.com by 210.87.254.5 on 09/05/12
For personal use only.

being 170–180°. The resulting 2,2-dimethyl-6-ethoxycarbonylcyclohexanone was distilled: b.p. 125° C under 20 mm.

2,2-Dimethyl-6-isonitrosocyclohexanone

2,2-Dimethyl-6-ethoxycarbonylcyclohexanone (54 g) was stirred (vibro mixer) under nitrogen with a solution of 20 g of sodium hydroxide in 1 l. of H_2O until the solution clarified, i.e., the ester was completely in solution (3–5 hours).

The reaction mixture was cooled in ice and a solution of 17.5 g of sodium nitrite in 50 ml of water was added with stirring and sweeping with nitrogen. After 10 minutes, the solution was acidified with 3 *N* sulphuric acid and left for a further 15 minutes. The solution was then basified and extracted with ether to remove any unchanged ester. It was reacidified and extracted with ether. The ether extracts were dried over anhydrous sodium sulphate. On evaporation of the solvent, the isonitroso compound crystallized. Four crops of crystals totalling 26.7 g (63%) of the isonitroso compound were collected, melting from 110–114°. This was recrystallized from ether–pentane, giving 2,2-dimethyl-6-isonitrosocyclohexanone, m.p. 116–116.5°. Found: C, 62.10; H, 8.40; N, 9.21. Calc. for $C_8H_{13}O_2N$ (155.19): C, 61.91; H, 8.44; N, 9.03.

2-Amino-6,6-dimethylcyclohexanone Hydrochloride

2,2-Dimethyl-6-isonitrosocyclohexanone (3.24 g) was added slowly to a solution of 15 g of stannous chloride in 18 ml of concentrated hydrochloric acid. The mixture was then filtered and the filtrate evaporated to dryness under reduced pressure at 40° C. The residue was taken up in absolute ethanol, giving 2.26 g of crystals, m.p. 172–174° C. This was recrystallized from methanol – ethyl acetate to yield 2-amino-6,6-dimethylcyclohexanone hydrochloride, m.p. 181–182° C. Found: C, 53.47; H, 9.00; N, 7.92. Calc. for $C_8H_{16}ClNO$: C, 54.08; H, 9.07; N, 7.82. The carbon value was low because of traces of ammonium chloride that were difficult to remove.

Deamination of 2-Amino-6,6-dimethylcyclohexanone

(*a*) 2-Amino-6,6-dimethylcyclohexanone hydrochloride (500 mg) was dissolved in 2 ml of 0.05 *N* sulphuric acid and then a solution of 1 g of sodium nitrite in 1 ml of water was added (addition time 15 minutes). There was a vigorous evolution of gas and the reaction mixture became yellow. A layer of yellow oil separated from the solution.

The reaction mixture was basified with sodium bicarbonate and extracted with methylene chloride. The methylene chloride solution was dried over sodium sulphate and distilled, leaving a neutral residue of 230 mg. The aqueous solution was acidified with sulphuric acid and extracted with methylene chloride. The 114 mg of acid which was extracted contained some dimethyladipic acid and other high-boiling acids, so was purified by short-path distillation. The main fraction came over at 75°, 0.5 mm; yield around 60 mg.

(*b*) A solution of 500 mg of amine hydrochloride and 1 g of sodium nitrite in 3 ml of water was prepared. This was cooled to 0°, then 5 drops of 0.05 *N* perchloric acid added slowly with stirring. The mixture was left for 10 minutes in the ice bath, then 5 minutes in the air. A yellow oil separated during the reaction. The readily extractable product gave 273 mg of neutral material and 58 mg of acid.

(*c*) The amine hydrochloride (106 mg) was dissolved in 3 ml of 80% aqueous dioxane, and 1 ml of 5% acetic acid solution was added. This was cooled in an ice bath, then 250 mg of sodium nitrite added in small portions. After gas evolution ceased the reaction mixture was adjusted to pH 8 using sodium bicarbonate. Extraction with methylene chloride gave 30 mg of neutral product. The aqueous solution was then acidified and extracted with methylene chloride, giving 29 mg of acid. These conditions gave the highest yield of acid.

The neutral product from deaminations by method (*a*) was distilled over a short path at bath temperature up to 80° under 10 mm pressure. A residue remained which crystallized from acetone. The crystalline substance could also be obtained by solution of the total neutral product in acetone, from which solution it separated on standing. The more volatile neutral products were separated by vapor phase chromatography using a 2 m×0.25 in. column with R packing at 120° and a flow rate of 50 cc/min. The retention time will be cited in the description of the different compounds. Minor components with retention times of 12, 14, 21, 25, 38, and 42 minutes were not characterized.

sym-Octahydrophenazine VI

The crystalline solid after sublimation at 60°, 5×10^{-4} mm, melted at 125–126°. Its infrared spectrum had no OH, NH, or carbonyl stretching bands. It had λ_{max} 289(ϵ 12,340). Found: C, 78.61; H, 9.84; N, 11.57. Calc. for $C_{16}H_{24}NO$: C, 78.63; H, 9.90; N, 11.46.

2,5,5-Trimethyl-2-cyclopentene-1-one (VII)

Retention time 19 minutes. It had $\nu_{max}^{CS_2}$ 1710 cm^{-1} ($\diagdown$ C=O), 1355 and 1380 cm^{-1} (*gem*-dimethyl), 828 cm^{-1} (R_2C=CHR); λ_{max} 228 mμ (ϵ 10,840), 317 mμ (ϵ 60). The maximum yield was approx. 23%. Found: C, 76.90; H, 9.59. Calc. for $C_8H_{12}O$ (124.18): C, 77.37; H, 9.74.

3,3-Dimethylbicyclo[3,1,0]-2-hexanone (VIII)

Retention time 35 minutes. It had $\nu_{max}^{CS_2}$ 1725 cm^{-1} (C=O), 1355 and 1380 cm^{-1} (*gem*-dimethyl); λ_{max} 284 mμ (ϵ 46). The maximum yield was approx. 46%. Found: C, 77.26; H, 9.60. Calc. for $C_8H_{12}O$: C, 77.37;

Can. J. Chem. Downloaded from www.nrcresearchpress.com by 210.87.254.5 on 09/05/12
For personal use only.

H, 9.74. The compound in dilute ethanol solution of perchloric acid or sodium hydroxide did not give any α,β-unsaturated ketone after several hours at room temperature (followed by ultraviolet absorption).

2,2-Dimethylcyclopentanecarboxylic Acid

The acid fractions from the deamination of 2-amino-6,6-dimethylcyclohexanone were distilled over a short path. The bulk of the volatile acid distilled at a bath temperature of 75° under 0.5 mm pressure. It had $\nu_{max}^{CS_2}$ 1700 cm^{-1}. The maximum yield was 18%. Found: C, 67.34; H, 9.67. Calc. for $C_8H_{14}O_2$: C, 67.57; H, 9.93. The chloride of the acid was prepared by refluxing the acid for 0.5 hour with thionyl chloride This was converted to the *anilide.* After recrystallization from acetone–pentane and sublimation at 90°, 5×10^{-4} mm, this melted at 124.5–125.5°. Found: C, 77.49; H, 8.57; N, 6.44. Calc. for $C_{14}H_{19}NO$: C, 77.38; H, 8.81; N, 6.45.

The methyl ester of the acid, prepared using diazomethane, was distilled over a short path at 25° C under 0.5 mm pressure. It gave a single peak with retention time 30.5 minutes using a 2-m column with R packing at 120° C with flow rate 50 cc/min.

2,2-Dimethyladipic Acid

The acidic aqueous solution remaining after removal of the readily extractable neutral and acidic products from the deamination of 2-amino-6,6-dimethylcyclohexanone was concentrated under reduced pressure until salts began to crystallize. The mixture was extracted thoroughly with chloroform. The crystalline residue after evaporation of the chloroform melted at 88–89°. When recrystallized from chloroform–hexane it had m.p. 89–90° (lit. m.p. 89–90° (31)). Found: C, 54.98; H, 7.97. Calc. for $C_8H_{14}O_4$: C, 55.16; H, 8.10.

Favorskii and Cope Reactions

2-Chloro-6,6-dimethylcyclohexanone

The chlorination of 2,2-dimethylcyclohexanone was carried out under conditions described in Organic Syntheses (32). The product melted at 62–63° after recrystallization from ether followed by sublimation under 1×10^{-2} mm. It had $\nu_{max}^{CHCl_3}$ 1725 cm^{-1} and λ_{max} 287 mμ (ε 26). Found: C, 59.65; H, 8.09; Cl, 22.23. Calc. for $C_8H_{13}OCl$: C, 59.81; H, 8.15; Cl, 22.07.

Attempted Favorskii Reaction

(*a*) A solution of 2-chloro-6,6-dimethylcyclohexanone (300 mg) in 5 ml of 3% potassium hydroxide in 60% aqueous dioxane was heated on the steam bath for 1.5 hours then left at room temperature overnight. The bulk of the solvent was removed under reduced pressure, water added, and the neutral product (103 mg) extracted into methylene chloride. The aqueous layer was then acidified and extracted with the same solvent. No extractable acid was obtained.

(*b*) The chloroketone (250 mg) and 1.2 ml of 4% sodium ethoxide in ethanol were heated for 16 hours at 145°. After hydrolysis in aqueous alcohol 125 mg of neutral material but only a trace of readily extractable acid were obtained.

(*c*) To a solution of 284 mg of the chloroketone in 20 ml of ether was added 300 mg of dry powdered potassium hydroxide. The mixture was heated in the water bath for 2 hours. The readily extractable products were 172 mg of neutral material and 16 mg of acid. The latter had a different infrared spectrum from 2,2-dimethylcyclopentanecarboxylic acid.

2-Bromo-6,6-dimethylcyclohexanone

The bromoketone was formed rapidly when a solution of 1.05 molar equivalents of bromine in ethanol-free chloroform was added dropwise to 2,2-dimethylcyclohexanone in ethanol-free chloroform. After recrystallization from ether–pentane and sublimation at 40°, 1×10^{-3} mm, it melted at 57–58° and had $\nu_{max}^{CHCl_3}$ 1725 cm^{-1} and λ_{max} 292 mμ (ε 32). Found: C, 47.05; H, 6.26. Calc. for $C_8H_{13}OBr$: C, 46.84; H, 6.36.

Action of Silver Nitrate on 2-Bromo-6,6-dimethylcyclohexanone (11)

A very slow reaction took place when a solution of 215 mg of the bromoketone and 510 mg of silver nitrate in approx. 75% aqueous ethanol stood at room temperature. After 6 hours' refluxing, however, 176 mg of silver bromide (1 molar equivalent) had precipitated. The readily extractable products were 55 mg of neutral material and a trace of acid.

α-Aminocamphor

Deamination of α-Aminocamphor

α-Aminocamphor hydrochloride (33) (1.2 g) was dissolved in 8 ml of 0.2 *N* sulphuric acid. A solution of 2 g of sodium nitrite was added dropwise with stirring while the temperature was held at 25° C (addition time 20 minutes). The mixture was then left for 10 minutes, basified with sodium bicarbonate, and extracted with methylene chloride. The neutral products recovered from the methylene chloride were examined using v.p.c. (column R, 1 m, 120° C, flow rate 120 cc/min). Two components were readily eluted, with retention times of 14 and 20 minutes. Their peak areas were in the ratio 1:5 respectively. When a methylene chloride

Can. J. Chem. Downloaded from www.nrcresearchpress.com by 210.87.254.5 on 09/05/12
For personal use only.

solution of the neutral product was shaken with 5% sodium hydroxide solution and the contents of the organic phase re-examined a new component, with retention time 6 minutes under the above conditions, was observed. This component also appeared if the deamination mixture was adjusted to pH 9–10 after reaction, left for 0.5 hour, then extracted with methylene chloride.

Cyclocamphanone XI

Retention time, 14 minutes. It was identified by comparison of retention time and melting point with an authentic sample prepared according to Schiff (34) and Takeuchi (35).

Cyclocamphanone was unchanged after 1 hour in approx. 0.1 *N* sulphuric acid in 50% aqueous dioxane. A methylene chloride solution of the ketone was shaken for 10 minutes with 5% sodium hydroxide solution. No trace of other readily eluted compounds was detected by v.p.c. after this treatment. Hence, this ketone is not the source of other products under the conditions of deamination and subsequent work-up.

6-Isopropenyl-6-methyl-2-cyclohexene-1-one (XII)

Retention time 20 minutes. It was redistilled over a short path at 100°, 15 mm pressure, after recovery from the preparative v.p.c. column. It had λ_{max} 225 mμ (ε 8770) and 327 mμ (ε 57); $\nu_{max}^{CCl_4}$ 1680 cm^{-1} ($\diagdown$C=O), 1640 and 898 cm^{-1} ($\diagdown$C=CH$_2$). Found: C, 79.66; H, 9.32. Calc. for $C_{10}H_{14}O$: C, 79.95; H, 9.39.

6-Isopropenyl-6-methylcyclohexanone

6-Isopropenyl-6-methyl-2-cyclohexene-1-one (500 mg) was dissolved in glacial acetic acid. Zinc dust (ca. 0.5 g) was added, and the mixture stirred for 1 hour. It was then diluted with 10 ml of water, filtered, and the filtrate extracted with methylene chloride. The organic phase was washed with sodium bicarbonate solution, then with water. The product remaining in the methylene chloride was distilled over a short path at 100° under 15 mm pressure. It had $\nu_{max}^{CCl_4}$ 1710 cm^{-1} (C=O), 1640 and 895 cm^{-1}. Its n.m.r. spectrum contained a doublet centered at τ 5.2 (2 hydrogens, J = 10 c.p.s.). Found: C, 79.01; H, 10.46. Calc. for $C_{10}H_{16}O$: C, 78.98; H, 10.59.

6-Isopropyl-6-methylcyclohexanone

6-Isopropenyl-6-methylcyclohexanone in 95% ethanol over 30% Pd/C rapidly absorbed 1 mole of hydrogen. The product had $\nu_{max}^{CCl_4}$ 1705 cm^{-1}. Found: C, 77.92; H, 11.90. Calc. for $C_{10}H_{18}O$: C, 77.86; H, 11.76.

6-Methyl-2-cyclohexene-1-one

Retention time, 6 minutes. After collection from the preparative column it was distilled over a short path at 70° under 10 mm pressure. It had λ_{max} 225 mμ (ε 10,350), 317 mμ (ε 56); $\nu_{max}^{CCl_4}$ 1680 and 1620 cm^{-1}. Found: C, 76.58; H, 8.90. Calc. for $C_7H_{10}O$: C, 76.32; H, 9.15. It gave a dinitrophenylhydrazone, m.p. 161–162° (reported m.p. 162° (14)).

A solution of 6-isopropenyl-6-methyl-2-cyclohexene-1-one in a 2:1 mixture (v/v) of 12 *N* sulphuric acid and methanol was refluxed for 1 hour. The product had identical retention time on column R with the 6-methyl-2-cyclohexene-1-one from the deamination reaction.

Reactions of Diazocamphor

(*a*) Finely divided diazocamphor (34, 35) (50 mg) was suspended in 2 ml of 0.2 *N* sulphuric acid for a period of 1 hour. The mixture was basified with sodium carbonate and extracted with methylene chloride. The products were identified by v.p.c. using column R to be 6-isopropenyl-6-methyl-2-cyclohexene-1-one 6-methyl-2-cyclohexene-1-one, and cyclocamphanone.

(*b*) In order to simulate the deamination conditions, 50 mg of finely divided diazocamphor was suspended in 2 ml of 0.2 *N* sulphuric acid, and a solution of 0.5 g of sodium nitrite in 1 ml of water was added. The mixture was left at room temperature for 2 hours. It was then basified with sodium carbonate and extracted with methylene chloride. Vapor phase chromatography on column R showed the readily eluted products to be 6-isopropenyl-6-methyl-2-cyclohexene-1-one and cyclocamphanone.

ACKNOWLEDGMENTS

We are grateful to Dr. F. A. L. Anet for valuable discussions. We wish to thank Mr. H. Seguin for the analyses, Mr. R. Lauzon for the infrared spectra, and Mr. J. Nicholson for n.m.r. spectra.

REFERENCES

1. (*a*) O. E. Edwards and M. Lesage. J. Org. Chem. **24**, 2071 (1959).
   (*b*) O. E. Edwards and M. Lesage. Chem. Ind. (London), 1107 (1960).
2. H. E. Baumgarten and F. A. Bower. J. Am. Chem. Soc. **76**, 4561 (1954).
3. G. H. Elliot and R. P. Linstead. J. Chem. Soc. 776 (1938).

Can. J. Chem. Downloaded from www.nrcresearchpress.com by 210.87.254.5 on 09/05/12
For personal use only.

4. R. GRANGER and H. TÉCHER. Bull. Soc. Chim. France, 1317 (1958); Compt. Rend. **250**, 4378 (1960).
5. H. E. BAUMGARTEN and C. H. ANDERSON. J. Am. Chem. Soc. **83**, 399 (1961).
6. M. GODCHOT. Compt. Rend. **158**, 506 (1914).
7. R. M. ACHESON and R. ROBINSON. J. Chem. Soc. 1131 (1952).
8. N. A. NELSON and G. A. MORTIMER. J. Org. Chem. **22**, 1146 (1957).
9. V. GEORGIAN and N. KUNDU. Chem. Ind. (London), 1755 (1962).
10. R. B. LOFTFIELD. J. Am. Chem. Soc. **73**, 4707 (1951).
11. A. C. COPE and E. S. GRAHAM. J. Am. Chem. Soc. **73**, 4702 (1951).
12. W. HÜCKEL and R. KUPKA. Chem. Ber. **89**, 1694 (1956).
13. F. A. L. ANET. Can. J. Chem. **39**, 789 (1961).
14. G. STORK and W. N. WHITE. J. Am. Chem. Soc. **78**, 4604 (1956).
15. D. E. APPLEQUIST and D. E. MCGREER. J. Am. Chem. Soc. **82**, 1965 (1960).
16. R. L. SHRINER and R. C. FUSON. Identification of organic compounds. John Wiley and Sons, New York. 1940. p. 42.
17. M. S. SILVER. J. Am. Chem. Soc. **82**, 2971 (1960).
18. P. S. SKELL and I. STARER. J. Am. Chem. Soc. **82**, 2971 (1960).
19. W. G. DAUBEN and P. LANG. Tetrahedron Letters, No. 11, 453 (1962).
20. G. KARABATSOS and J. D. GRAHAM. J. Am. Chem. Soc. **82**, 5250 (1960).
21. P. S. SKELL, I. STARER, and A. P. KRAPCHO. J. Am. Chem. Soc. **82**, 5257 (1960).
22. J. D. ROBERTS, C. C. LEE, and W. H. SAUNDERS. J. Am. Chem. Soc. **76**, 4501 (1954).
23. D. J. CRAM and J. E. MCCARTY. J. Am. Chem. Soc. **79**, 2866 (1957).
24. J. H. RIDD. Quart. Rev. (London), **15**, 418 (1961).
25. A. STREITWEISER and C. E. COVERDALE. J. Am. Chem. Soc. **81**, 4275 (1959).
26. W. HÜCKEL and F. NERDEL. Ann. **528**, 57 (1937).
27. W. HÜCKEL and P. RIECKMAN. Ann. **625**, 1 (1959).
28. F. M. JAEGER and J. A. VAN DIJK. Proc. Acad. Sci. Amsterdam, **39**, 384 (1936).
29. N. ZELINSKY. Ber. **41**, 2627 (1908).
30. P. S. ADAMSON, A. M. MARLOW, and J. L. SIMONSEN. J. Chem. Soc. 774 (1938).
31. G. BLANC. Bull. Soc. Chim. **33** (3), 879 (1905).
32. Organic syntheses. Vol. XXV. John Wiley and Sons, Inc., New York. p. 22.
33. L. CLAISEN and O. MANASSE. Ann. **273**, 90 (1893).
34. R. SCHIFF. Ber. **14**, 1375 (1881).
35. K. TAKEUCHI. Inst. Phys. Chem. Res. (Japan) Sci. Papers, **23–24**, 288 (1934).

Can. J. Chem. Downloaded from www.nrcresearchpress.com by 210.87.254.5 on 09/05/12
For personal use only.

METHYL 3-NITRO- AND 3-AMINO-3-DEOXY-β-D-GALACTOPYRANOSIDE AND -MANNOPYRANOSIDE[1]

HANS HELMUT BAER AND FRANK KIENZLE
Department of Chemistry, University of Ottawa, Ottawa, Ontario
Received January 31, 1963

ABSTRACT

The steric course of the nitromethane cyclization of L′-methoxy-D-hydroxymethyldiglycolic aldehyde was investigated. Methyl 3-nitro-3-deoxy-β-D-galactopyranoside was shown to arise as a second major reaction product in addition to the previously isolated principal stereoisomer, the *gluco* derivative. The corresponding *manno* stereoisomer is formed to a smaller extent. The configurations of the new methyl nitrodeoxyglycosides were established by conversion into the corresponding amino derivatives and hydrolysis of these latter to the known 3-amino-3-deoxy-D-galactose and -D-mannose hydrochlorides. All the products were obtained in a crystalline state. The reaction lends itself to a facile preparation of the nitrogenous galactose derivatives.

Can. J. Chem. Downloaded from www.nrcresearchpress.com by 210.87.254.105 on 09/05/12
For personal use only.

In a previous paper (1) the cyclization with nitromethane of the dialdehyde L′-methoxy-D-hydroxymethyldiglycolic aldehyde (I), which is readily available by periodate oxidation of methyl β-D-hexopyranosides, was reported to furnish a crystalline methyl 3-nitro-3-deoxy-β-D-hexopyranoside in a yield of 40% or better. The product was subsequently (2) established to possess the *gluco* configuration (II). There was evidence that the condensation reaction proceeded to virtual completion although no studies were made concerning the stereoisomeric composition of more than one-half of the mixture of products that was obtained. In view of the results recently elaborated in the anomeric α-hexoside series (3) as well as in anhydro sugars (4, 5) a more thorough investigation of the nitromethane condensation of I appeared to be of interest.

When the cyclization of I had been carried out in methanol in the presence of sodium methoxide, and had been followed by deionization of the solution and collection of the crystallizing nitroglycoside (40% of II and small fractions of undetermined composition[2,3]), there remained in the mother liquor a material which, at the time, failed to crystallize. Hydrogenation of this amorphous residue produced a crystalline aminoglycoside that had not been characterized further.[2] We have now found that the compound so obtained was methyl 3-amino-3-deoxy-β-D-galactopyranoside (IV). It is obvious, therefore, that the parent nitro compound, methyl 3-nitro-3-deoxy-β-D-galactopyranoside (III), was one of the products formed in the nitromethane cyclization in methanolic medium.

In an attempt to improve the preparation of the *galacto* derivatives we investigated the possibility of epimerizing the sodium nitronate of the glucoside II. As was demonstrated recently (3), *aci*-nitroglycoside salts in aqueous solution undergo spontaneous epimerizations at carbon atoms adjacent to the nitro grouping. While the experiments pertaining to the behavior of the glucoside II in aqueous alkali have not yet been concluded, preliminary evidence indicates that II can in fact be converted partly into III in this way. We were thus prompted to transfer the mixture of *aci*-salts, produced in methanol, into an aqueous medium for a short time prior to deionization, or indeed to conduct the whole cyclization in water in the presence of one equivalent of sodium hydroxide. In either case

[1]*Part X in the series "Cyclizations of Dialdehydes with Nitromethane". For Parts IX and VIII see references 5 and 3, respectively.*
[2]*See p. 2869 of reference 1.*
[3]*These fractions have now been shown to contain some methyl 3-nitro-3-deoxy-β-D-mannopyranoside.*

the proportions of II and III appeared to be shifted in favor of the latter, for the yields of isolable II were decreased to 24–25%, and at the same time it became possible to isolate 34% of crystalline III. The results to be described were obtained from cyclization experiments carried out in aqueous solution.

When the mother liquor remaining after the collection of the crystalline nitroglucoside II was inspected by paper chromatography, a pattern of nitro compounds was observed consisting of two major spots (R_f 0.57 and R_f 0.68) and a number of faster-moving weak spots. Whereas a relatively strong spot (R_f 0.68) was due to residual II, an even stronger spot (R_f 0.57) represented two new nitroglycosides, III and VII, which were not separated on paper. Their isolation and configurational elucidation will be described here. The products migrating faster than II were present in small amounts only and have not been identified.[4]

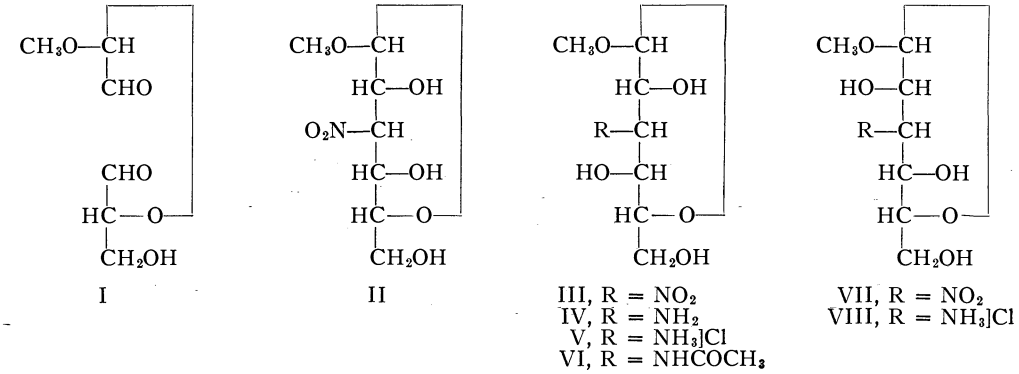

The three nitroglycosides II, III, and VII were separated by fractional crystallization. Methyl 3-nitro-3-deoxy-β-D-galactopyranoside (III) was obtained in 34% yield and hence represented a major reaction product. It melted at 131–132° and had a specific rotation of $[\alpha]_D$ +32.6°. Catalytic hydrogenation furnished the corresponding amine, methyl 3-amino-3-deoxy-β-D-galactopyranoside (IV), with m.p. 175–176° (decomp.) and $[\alpha]_D$ −3.7°. A crystalline hydrochloride (V) and an N-acetyl derivative (VI) of the amino compound were also prepared. The amine IV proved to be identical with the aminohexoside that had been obtained previously but had not been characterized.[2]

Preliminary assignment to IV of the *galacto* configuration was suggested by the proximity of its specific rotation to that of a nitrogen-free analogue, methyl β-D-galactopyranoside ($[\alpha]_D$ −0.4°). It is a well-known rule that substitution of an amino group for a hydroxyl in glycosides has little influence upon the rotation.[5] Final proof was established by acid hydrolysis of IV (or V), which readily furnished known (6) 3-amino-3-deoxy-α-D-galactose hydrochloride. The identification of this amino sugar hydrochloride was corroborated by N-acetylation to 3-acetamido-3-deoxy-β-D-galactose and direct comparison of the latter with an authentic sample (6, 3).

Methyl 3-nitro-3-deoxy-β-D-mannopyranoside (VII) was present in the reaction mixture to a smaller extent than either of the glycosides II or III. It was rather difficult to obtain in pure condition, as multiple recrystallizations, causing loss of product, were

[4]*At least three compounds appeared to be present in the R_f range of 0.77 to 0.90. Accurate values are not available since the products do not separate well. Despite its subordinate amount, part of this material is of peculiar interest as it possesses a distinct growth-inhibiting activity against Bacillus subtilis. This merits further investigation.*

[5]*For literature see reference 4.*

Can. J. Chem. Downloaded from www.nrcresearchpress.com by 210.87.254.105 on 09/05/12
For personal use only.

required. Eventually the pure compound was isolated in a yield of about 2%, although in the mixture it amounted to at least 13%. The higher figure was based on the isolation of the corresponding amine following hydrogenation. The nitromannoside VII melted at 136–138° and showed $[\alpha]_D$ −81.7°. Configurational assignment was accomplished by experiments similar to those just described for the galactoside III. Catalytic hydrogenation afforded an aminoglycoside that was crystallized as hydrochloride VIII (m.p. 230–231°, $[\alpha]_D$ −68.5°). It was noted that the molecular rotation of VIII (M_D −15,600) agreed well with that of the nitrogen-free analogue, methyl β-D-mannopyranoside (M_D −13,400). Acid hydrolysis of VIII produced known (7) 3-amino-3-deoxy-α-D-mannose hydrochloride, thus proving the configuration of the glycosides VIII and VII.

A comparison of the above results with those obtained earlier in the α-hexoside series leads to the following conclusion concerning the practical applicability of the nitromethane cyclization. The value of the method for the purpose of preparing nitrogenous hexose derivatives with *gluco*, *manno*, *galacto*, and *talo* configurations is complementary in the two anomeric series. In the α-series (3, 7), *manno* and *talo* derivatives are readily available by the method whereas *gluco* and *galacto* derivatives, although obtainable, are isolated only with some inconvenience. The β-series, on the other hand, lends itself to the facile preparation of *gluco* (1, 2) and, as was shown here, *galacto* derivatives.

EXPERIMENTAL

The melting points were determined in an aluminum block. The optical rotations were taken in 2-dm tubes and refer to solutions in carbon-dioxide-free water; *c*, approximately 1%. All evaporations were done *in vacuo* at 35–40° (bath temperature) unless otherwise indicated. Paper chromatography was performed by the descending technique on Whatman No. 1 paper. The nitro compounds were irrigated with 1-butanol – acetic acid – water (4:1:5, v/v, upper layer) and made visible by spraying with alkali (1 part *N* NaOH + 4 parts methanol + 5 parts butanol) and inspection under an ultraviolet lamp. The amino compounds were irrigated with pyridine – ethyl acetate – acetic acid – water (5:5:1:3, v/v, with pyridine – ethyl acetate – water, 11:40:6, v/v, in the bottom of the tank) and indicated with ninhydrin. R_{gm} = speed relative to glucosamine hydrochloride.

A. The Nitromethane Cyclization

(a) Condensation in Methanolic Solution Followed by Equilibration in Water

L′-Methoxy-D-hydroxymethyldiglycolic aldehyde (I) was prepared and condensed with nitromethane in the presence of sodium methoxide in methanolic solution as described previously (1). After the reaction period of 45 minutes, however, the solution was concentrated rapidly in an efficient evaporator at 20° (bath temperature) to the consistency of a thick sirup. The sirup was immediately dissolved in 10 parts of carbon-dioxide-free water and the solution was allowed to stand for 40 minutes at 23°. It was then cooled in ice water and deionized with Amberlite IR-120 (H^+). For deionization and subsequent crystallization and purification of the nitroglucoside II the earlier directions (1) were followed. There resulted a yield of 25% of purified II.

(b) Condensation in Aqueous Solution

A solution of dialdehyde I (0.08 mole, obtained from 15.52 g of methyl β-D-glucopyranoside) in 100 ml of water was carefully adjusted at 0° with sodium hydroxide to the point of a pink phenolphthalein coloration that persisted for at least 1 minute (3.6 ml of *N* NaOH was required). Upon addition of 4.44 ml of nitromethane (1 molar equiv.) another 80 ml of *N* NaOH was added over a period of 10 minutes at 0°. The solution was then brought to room temperature with running warm water and allowed to stand for 40 minutes. Thereupon the reaction mixture was deionized by being poured into an ice-cold aqueous suspension of 120 ml of Amberlite IR-120 (H^+); stirring was applied for 10 minutes. The solution was decanted from the resin, which was washed several times with water, and the combined liquid was passed over a column containing another 50 ml of fresh exchange resin. The column was finally rinsed with water. Evaporation of the effluent furnished a sirup which was dehydrated by two consecutive evaporations with ethanol and two with ethyl acetate. The partly crystalline residue was triturated with 30 ml of ethyl acetate and the crystals were collected after some standing in the refrigerator. The yield of crude nitroglucoside II was 4.3 g (24.1%).

(c) Methyl 3-Nitro-3-deoxy-β-D-galactopyranoside (III)

The mother liquor that remained after removal of the crystalline nitroglucoside II (cf. preceding Section (*b*)) was shown by paper chromatography to contain major components of R_f 0.57 and 0.68 as well as minor

Can. J. Chem. Downloaded from www.nrcresearchpress.com by 210.87.254.105 on 09/05/12
For personal use only.

components in the range of R_f 0.77–0.90. The mother liquor was concentrated to a sirup that was inoculated with crystalline nitrogalactoside III.[6] Copious crystallization occurred at 0° within a few hours. The material was triturated with a little ice-cold ethyl acetate and the solid matter isolated and washed with cold ethyl acetate. The yield was 5.6 g (31.6%) of crude III (R_f 0.57) containing some of the *gluco* isomer II (R_f 0.68). Another 400 mg of III which was even purer than the main crop was obtained from the mother liquor, but, curiously enough, only after the nitromannoside VII had been isolated (cf. Section (*d*)). Thus the total yield of III was 34%.

The product was recrystallized by dissolution in the minimum amount of hot acetone and addition of chloroform to incipient turbidity. When the solution was cooled fine thin needles of III separated quickly; $[\alpha]_D^{23}$ +27.8°. Accompanying traces of II were rather difficult to remove. A sample that had been recrystallized five times was at last chromatographically uniform and showed $[\alpha]_D^{23}$ +32.6°. The air-dried product evidently contained solvent of crystallization. It melted upon rapid heating at 87–90°, but upon very slow heating or after drying at 80° at 3 mm the melting point was 131–132°. Slight changes in the infrared spectrum (in nujol) occurred when the air-dried substance was dried at 80° *in vacuo* for several hours, and the same changes resulted when it was kept in the molten state at 95° for a few minutes. The high-melting product when triturated with acetone–chloroform gave again the original spectrum. Anal. Calc. for $C_7H_{13}NO_7$ (223.2): C, 37.67; H, 5.87; N, 6.28. Found: C, 37.02; H, 6.20; N, 6.10.

(d) Methyl 3-Nitro-3-deoxy-β-D-mannopyranoside (VII)

The ethyl acetate filtrate from the main crop of crystalline III contained, besides remnant II and III, the nitromannoside VII, which was isolated in two portions. The first portion (A) crystallized together with II upon concentration of the filtrate and addition of a little ether. The second portion (B) was obtained from the remaining mother liquor by column chromatography.

The crystalline fraction A, after being washed with ice-cold, ether-containing ethyl acetate, weighed 490 mg, melted at 161–164°, and was shown by paper chromatography to contain a considerable amount of II. The material was recrystallized thrice from acetone–chloroform and subsequently treated with a small amount of boiling ethyl acetate. There remained 45 mg of crystals that did not dissolve in the ester. By means of their melting point (201–202°) and infrared spectrum they were identified as nearly pure nitroglucoside II. The acetone–chloroform mother liquors of the successive recrystallizations and the ethyl acetate extract were combined and the solvents removed, leaving a crystalline residue. From this a further 140 mg of somewhat less pure II was separated by one more recrystallization followed by extraction. The combined mother liquor and extract of this second sequence gave upon evaporation a residue which was recrystallized once again from acetone–chloroform. Thus 95 mg of a product with m.p. 133–134° and $[\alpha]_D^{23}$ −66.7° was obtained. It was nitromannoside VII (R_f 0.59) which was still accompanied by a small amount of nitroglucoside II (R_f 0.68).

For the isolation of the second portion of VII (B) the mother liquor from which fraction A had been separated was first reduced to a smaller volume and placed in the refrigerator. In the course of a few days a crystalline deposit was formed (400 mg) which by melting point and infrared spectrum was shown to be additional nitrogalactoside III (cf. preceding Section (*c*)). The mother liquor therefrom was then chromatographed on a cellulose column (3.7 cm×58 cm), the aforementioned solvent system for nitroglycosides being used. Although no satisfactory separation of the remaining nitroglycosides could be so achieved, the process served to remove fast-moving yellow impurities and unidentified by-products. The effluent containing the nitroglycosides afforded a material from which 100 mg of a crystalline mixture of II and VII, and 390 mg (2%) of pure VII (m.p. 136–138°; $[\alpha]_D^{23}$ −81.3°), could be obtained by fractional crystallization with ethyl acetate – ether. Anal. Calc. for $C_7H_{13}NO_7$ (223.2): C, 37.67; H, 5.87; N, 6.28. Found: C, 37.93; H, 5.88; N, 6.27.

B. Amino Derivatives

For hydrogenation of the nitroglycosides, by the use of a platinum catalyst in the presence of one equivalent of dilute hydrochloric acid, the directions given earlier (1, 3) for similar experiments were followed. Chloride ion was removed from the hydrogenated solutions with Dowex-1 (OH^-), grade X2.

(a) Methyl 3-Amino-3-deoxy-β-D-galactopyranoside (IV)

Nitrogalactoside III (223 mg) was hydrogenated to give, after recrystallization from 95% ethanol, 105 mg (54.5%) of colorless needles of IV showing m.p. 173–174° decomp., $[\alpha]_D^{23}$ −3.7° and R_{gm} 1.38. The infrared spectrum, mixed melting point, and R_{gm} value established the identity of the product with the methyl aminodeoxyhexoside that had been obtained previously as a by-product but had not been characterized in detail.[2]

The analytical sample was recrystallized once more from moist ethanol and then showed m.p. 175–176° decomp.; the specific rotation remained unchanged. Anal. Calc. for $C_7H_{15}NO_5$ (193.2): C, 43.51; H, 7.83; N, 7.25; OCH_3, 16.06. Found: C, 43.39; H, 7.54; N, 7.25; OCH_3, 16.20.

For the preparation of IV on a larger scale we found it convenient to hydrogenate directly, i.e., without prior isolation of crystalline III, the total residue from the mother liquor as it was obtained in the nitromethane condensations following removal of the main portion of II (cf. Sections A(*a*) and/or A(*b*)). The

[6]*Seed crystals were first obtained when a similarly prepared sirup was left in a refrigerator for several days.*

Can. J. Chem. Downloaded from www.nrcresearchpress.com by 210.87.254.105 on 09/05/12
For personal use only.

overall yields of pure IV were about 21% (based on the original starting material, methyl β-D-glucopyranoside).

Hydrochloride (V).—Evaporation with dilute hydrochloric acid of a sample of IV, followed by trituration of the residue with methanol, furnished clusters of fine needles that were recrystallized from ethanol (95%) – ethyl acetate. It was the hydrochloride V; $[\alpha]_D^{23}$ −3.1°. It melted with decomposition at about 227° on rapid heating; slow heating resulted in gradual darkening without distinct melting.

(b) Methyl 3-Acetamido-3-deoxy-β-D-galactopyranoside (VI)

N-Acetylation of the free base IV (200 mg) as applied earlier to the *gluco* isomer (1, 2) yielded 174 mg (71.3%) of white needles of VI; m.p. 239°, $[\alpha]_D^{23}$ +52°. Anal. Calc. for $C_9H_{17}NO_6$ (235.2): C, 45.95; H, 7.29; N, 5.96. Found: C. 46.13; H, 7.10; N, 5.88.

Hydrolysis of a sample in 4 *N* hydrochloric acid for 3 hours at 100° gave 3-amino-3-deoxy-D-galactose hydrochloride as the only sugar detectable by paper chromatography.

(c) 3-Amino-3-deoxy-α-D-galactose Hydrochloride

Methyl aminodeoxygalactoside IV (160 mg) was hydrolyzed with 32 ml of 4 *N* HCl for 3 hours at 100°. The hydrolyzate was evaporated with addition of several successive portions of water and finally of toluene. The residue upon trituration with ethanol started to crystallize at once and was collected after standing for 2 hours at 0°. The yellowish-white product was recrystallized by dissolution in the minimum amount of water required and addition of excess ethanol. The yields found in several parallel runs were 80–85%. The colorless crystals were chromatographically uniform (R_{gm} 0.90). $[\alpha]_D^{23}$ +109° → +82.0° (final, after 2 hours); final values of samples from parallel runs, +82.1°, +82.7°. Reported values (6), $[\alpha]_D$ +115° → +89° (2 hours). We were unable to confirm the melting point quoted (6), but observed slow decomposition above 200°.

(d) 3-Acetamido-3-deoxy-β-D-galactose

The above hydrochloride (1.25 g) was N-acetylated according to a known procedure (8, 2). There was obtained 996 mg (78%) of an acetamido sugar melting at 162–164°. Repeated recrystallization from ethanol – ethyl acetate afforded a product of m.p. 173° and $[\alpha]_D^{23}$ +92.5° → +118.0° (final, 2.5 hours). Reported (6), m.p. 170–172° and $[\alpha]_D$ +99° → +119° (2.5 hours). Our product and an authentic sample of 3-acetamido-3-deoxy-β-D-galactose kindly supplied by Professor R. Kuhn, Heidelberg, gave identical infrared spectra and a mixed melting point of 171–173°.

(e) Methyl 3-Amino-3-deoxy-β-D-mannopyranoside Hydrochloride (VIII)

(*i*) A sample of 62 mg of nitromannoside VII (not quite pure; m.p. 133–134°) was hydrogenated and afforded, upon evaporation without prior removal of chloride ion, a partly crystalline material. This was recrystallized from ethanol – ethyl acetate to give 45 mg (67%) of oblong, rectangular prisms of VIII; m.p. 230–231° decomp., R_{gm} 1.27, $[\alpha]_D^{23}$ −68.5°.

(*ii*) A nitromethane condensation with 0.04 mole of dialdehyde I had been performed in aqueous solution and had furnished about 25% of crystalline nitroglucoside II. The mother liquor had then been hydrogenated, giving 20.5% of crystalline aminogalactoside as free base IV. (See Sections A(*b*) and B(*a*).) The filtrate therefrom was now evaporated and the residue taken up in water and acidified with 20 ml of *N* hydrochloric acid. Evaporation with several consecutive portions of water followed by ethanol gave a quickly crystallizing residue of amine hydrochlorides. The material was allowed to stand overnight under some ethanol at 0°. The crystals were collected, washed with cold ethanol, and dried. The product (1.184 g, 12.9%) was VIII and showed m.p. 228–229° decomp., and $[\alpha]_D^{23}$ −68.3° after one recrystallization from aqueous ethanol. It was chromatographically uniform (R_{gm} 1.24) and was identified by infrared spectroscopy with the preparation obtained under (*i*). Anal. Calc. for $C_7H_{16}O_5NCl$ (229.7): C, 36.61; H, 7.02; N, 6.10. Found: C, 36.04; H, 6.89; N, 6.39.

The mother liquor after the crystallization of VIII deposited, on standing and careful addition of a little ethyl acetate, a small amount of crystals (36 mg), also melting with decomposition at about 228°. They were, however, identified as aminogalactoside hydrochloride (V) from the results of rotation ($[\alpha]_D^{23}$ −3.15°) and chromatography (R_{gm} 1.39). This was confirmed by acid hydrolysis to yield crystalline 3-amino-3-deoxy-D-galactose, which was identified by its infrared spectrum and chromatogram.

(f) 3-Amino-3-deoxy-α-D-mannose Hydrochloride

A 30-mg sample of pure VIII was hydrolyzed with 6 ml of 4 *N* hydrochloric acid for 3 hours at 100°. The reducing amino sugar hydrocholoride was obtained in crystalline condition as in the previously described (7) hydrolysis of the anomeric glycoside, and was found identical with a specimen from that work by comparison of the infrared spectra, R_{gm} values (1.12), and mutarotation data. $[\alpha]_D^{23}$ +16.5° → +6.1° (2 hours, final).

ACKNOWLEDGMENTS

This work was made possible through generous support from the Ontario Research Foundation. Also, grants from the United States Public Health Service (Grant No.

Can. J. Chem. Downloaded from www.nrcresearchpress.com by 210.87.254.105 on 09/05/12
For personal use only.

E4697) and from the National Research Council of Canada were used in part and are gratefully acknowledged.

REFERENCES

1. H. H. BAER. Ber. **93**, 2865 (1960).
2. H. H. BAER. J. Am. Chem. Soc. **83**, 1882 (1961).
3. H. H. BAER. J. Am. Chem. Soc. **84**, 83 (1962).
4. A. C. RICHARDSON and H. O. L. FISCHER. J. Am. Chem. Soc. **83**, 1132 (1961).
5. H. H. BAER. J. Org. Chem. In press. 1963.
6. R. KUHN and G. BASCHANG. Ann. **636**, 164 (1960).
7. H. H. BAER and H. O. L. FISCHER. J. Am. Chem. Soc. **82**, 3712 (1960).
8. S. ROSEMAN and J. LUDOWIEG. J. Am. Chem. Soc. **76**, 301 (1954).

Can. J. Chem. Downloaded from www.nrcresearchpress.com by 210.87.254.105 on 09/05/12
For personal use only.

CORRELATION OF CHEMICAL COMPOSITION AND OPTICAL ROTATION OF NATIVE XYLANS

R. H. MARCHESSAULT, H. HOLAVA, AND T. E. TIMELL
State University College of Forestry at Syracuse University, Syracuse, N.Y., U.S.A.
Received February 11, 1963

ABSTRACT

The principle of optical superposition has been used to derive an equation relating the specific rotations of native xylans with their content of 4-O-methylglucuronic acid and/or arabinofuranose residues. The equation is in good agreement with literature data for the 4-O-methylglucuronoxylans and the arabinoxylans. Based on this correlation, an α-L-linkage is suggested for the arabinofuranose residues in various arabinose-containing xylans. Literature rotations for the 4-O-methylglucuronoarabinoxylans are consistently greater than values predicted by the equation. Finally, the rotatory dispersion behavior of acidic and neutral xylans is examined.

I. INTRODUCTION

There is good evidence (1) that the basic structure of many plant xylans and particularly those from wood consists either of a linear or moderately branched chain of β-D-xylopyranose residues, joined by (1 → 4)-glycosidic bonds. The configuration and position of branching, if such exists, has not been established. Wood xylans are known to be heavily substituted along the backbone by (1 → 2)-linked 4-O-methyl-α-D-glucuronic acid residues. Evidence so far accumulated indicates that these substituents occur randomly along the macromolecule. Thus, it has been possible to isolate xylan fractions even from the same plant with varying percentages of uronic acid (2, 3). Hydrolytic fragments averaging 30–60 xylose units completely free of uronic acid have also been isolated from xylans of relatively high acid content (4, 5). Finally, the X-ray diagrams of xylans with varying uronic acid content do not differ (6), whereas the opposite would be expected if the acid groups were regularly spaced.

The acidic softwood xylans also contain arabinofuranose residues. Such residues are especially abundant in the neutral arabinoxylans occurring in cereal gums (1). 4-O-Methylglucuronoxylans from hardwoods are esterified with O-acetyl groups in the xylan backbone (7, 8). Both these substituents can be removed by acidic and alkaline hydrolysis, respectively, in treatments which are very mild, and in the present study, therefore, will be assumed not to alter the remainder of the polymer chemically.

For the purposes of this study, plant xylans are divided into four categories: neutral xylans; acid xylans, i.e. those carrying the 4-O-methyl glucuronic acid side chains; arabinoxylans; and xylans containing both arabinose and acid moieties. The basic structure of the latter is illustrated in Fig. 1. It has been shown (9) that the neutral xylan has the

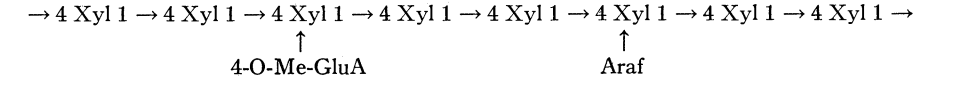

(Xyl = β-D-xylopyranose, 4-O-Me-GluA = 4-O-methyl-α-D-glucuronic acid, Araf = α-L-arabinofuranose)

FIG. 1. Schematic structure of an arabino-4-O-methylglucuronoxylan.

optical rotation which would be predicted on the basis of the rotation of the β-(1 → 4)-linked oligomers, viz. −102°. Acid xylans and arabinoxylans, however, have rotations

Can. J. Chem. Downloaded from www.nrcresearchpress.com by 210.87.254.42 on 09/05/12
For personal use only.

which differ widely from this value, ranging from −37° down to −108°. To some extent this variation is due to unavoidable contamination by other polysaccharides of significantly different structure and rotation. However, it seems reasonable to assume that most of this variation represents the contribution to the optical rotation by the appended acid and arabinose moieties. It should be possible, therefore, by application of the principle of optical superposition to predict the exact rotation of a xylan with any given composition of acid, arabinose, and xylose units, provided the respective linkages are the same in all polysaccharides of this class. It was the aim of this study to show that present data in the literature are generally in agreement with this hypothesis.

II. THEORETICAL

Let: n be the number of unsubstituted units in a linear xylan chain;
m be the molar rotation of an unsubstituted xylose unit in the chain;
u be the molar rotation of a 4-O-methyl-α-D-glucuronosyl xylose residue in the chain;
σ be the ratio of xylose to the above aldobiuronic acid residue;
ϕ be the molar rotation of a xylan chain with a ratio σ of xylose to aldobiuronic acid groups.

It will be assumed that the chains are long enough to ignore the special contribution of the two end groups, which are presumed to consist of xylose. Should they be acid groups, any special contribution due to their rotation because of this is probably negligible. Present data indicate that this assumption is entirely reasonable (9).

It follows from the principle of optical superposition that the molar rotation per xylose residue of a linear xylan chain with randomly occurring 4-O-methylglucuronic acid substituents is:

[1] $$\frac{\phi}{n\left(1+\frac{1}{\sigma}\right)} = \frac{m\cdot n + u\cdot n/\sigma}{n\left(1+\frac{1}{\sigma}\right)} = \frac{m+u/\sigma}{\left(1+\frac{1}{\sigma}\right)}.$$

Since

[2] $$[\alpha]_D = \frac{\phi}{n\left(1+\frac{1}{\sigma}\right)} \times \frac{1}{\left(132+\frac{190.35}{\sigma+1}\right)},$$

where the factor $[132 + 190.35/(\sigma+1)]$ is the average residue weight of each xylose unit in the polymer backbone with the 4-O-methylglucuronic acid averaged into each, it follows that:

[3] $$[\alpha]_D\left(132+\frac{190.35}{\sigma+1}\right)\left(1+\frac{1}{\sigma}\right) = m+\frac{u}{\sigma}.$$

A plot of the left-hand side of equation [3] for linear xylans of varying acid content should yield a straight line of intercept m and slope u.

The quantity m, available experimentally from the neutral xylan oligosaccharide series, is −13,500. The quantity u is not available at present since it could only be derived from the difference in molar rotations of xylobiose and the symmetrical 4-O-methyltetrauronic acid. It is expected, however, that u will be given to a sufficient approximation by the difference in molar rotation between the aldotetrauronic acid, derived from enzymatic hydrolysis of xylan (10(*a*)), and xylobiose; thus $u = +7900$.

Can. J. Chem. Downloaded from www.nrcresearchpress.com by 210.87.254.42 on 09/05/12
For personal use only.

Equation [3] is equally applicable to the arabinoxylans, in which case σ becomes the ratio of unsubstituted xylose to the arabinosyl xylose disaccharide and u is replaced by f, the molar rotation of the latter in the chain.

III. OBSERVED ROTATION AND STRUCTURE OF NATIVE XYLANS

The xylan samples used are listed in Table I together with references to the original literature describing their isolation and characteristics.

TABLE I

Optical rotation of neutral and acidic xylans as a function of acid content

Sample	$\sigma+1$	$[\alpha]_D^{20}$	ϕ/n	Ref.
Esparto	∞	−102*	−13,450	9
Milkweed	14	− 85.6	−13,280	10(*b*)
White birch	10	− 76.0	−12,855	11
Aspen	9	− 76.2	−13,000	12
White elm	7	− 66.7	−12,426	13

*Adjusted to value for infinite chain length.

The polysaccharides were dissolved in 10% aqueous sodium hydroxide by shaking the mixture overnight. Some turbidity often remained the following morning. It could be removed by centrifuging in a Servall centrifuge for 2 hours at 10,000 r.p.m. The loss in weight of the solution and change in rotation after centrifuging were shown to be negligible. Optical rotation measurements were made on a model 80 Rudolph polarimeter with photoelectric detection, which was kept in a controlled-temperature room at 19–20° C. Either a 2- or 1-dm tube was used depending on the clarity and/or concentration. Monochromatic radiation was provided by a sodium lamp.

The observed optical data are listed in Table I along with the values of ϕ/n which correspond to the left-hand side of equation [3]. Figure 2 is a plot of the data according

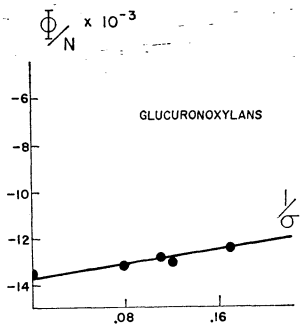

FIG. 2. The molar rotation per unsubstituted xylose residue versus the reciprocal ($1/\sigma$) of the xylose to aldobiouronic acid ratio for hardwood xylans.

to equation [3]. The line corresponds to a theoretical slope of +7900, which fits the data very well.

Similar data for arabinoxylans were compiled from the literature. These are summarized in Table II. Since some of these xylans are reportedly branched, application of equation [3] implies the tacit assumption that the configuration of the branchpoint is the same as that in the main chain and the molar rotation of the xylose at the branch is unaffected.

Can. J. Chem. Downloaded from www.nrcresearchpress.com by 210.87.254.42 on 09/05/12
For personal use only.

TABLE II

Optical rotation of arabinoxylans as a function of arabinose content

Sample	$\sigma+1$	$[\alpha]_D$	ϕ/n	Ref.
Corn cob	14.4	−103.0	−15,700	14
Wheat straw	12.0	−103.0	−14,800	14
Corn cob	9.0	− 87.0	−14,300	15
Barley husk	6.0	−102.0	−19,340	16
Rye flour	2.0	−107.0	−42,400	17
Barley flour	1.6	−104.0	−60,300	18
Wheat flour	1.5	−108.0	−71,400	19

The data in Table II cover an exceedingly broad range of σ values, e.g. when $\sigma = \infty$ there are no arabinose units while $\sigma = 0.5$ means more arabinoxylose than xylose units in the chain, yet all the data fall on a straight line. The slope of this line is −29,400, which should correspond to the molar rotation of an arabinosyl xylose residue in the chain. From the literature, the value for this disaccharide unit can be computed as the difference between the molar rotation of the symmetrical arabinosyl xylotriose and xylobiose:

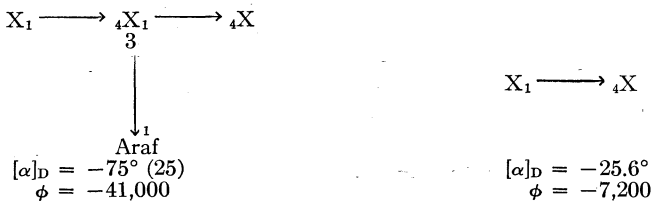

The calculated value of −33,800 is subject to the assumption that the same equilibrium mixture of anomers is present in solution for the two compounds. Thus, the calculated value and that derived from the plot in Fig. 3 are in reasonable agreement.

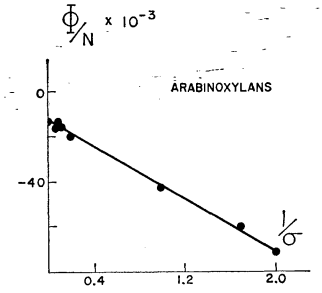

FIG. 3. The molar rotation per unsubstituted xylose unit versus the reciprocal of the xylose to arabinoxylose disaccharide ratio for arabinoxylans.

IV. DISCUSSION

The most important comment concerning the foregoing data, aside from the fact that they confirm the assumptions made in the derivation of equation [3], concerns the difference in sign of the slopes in Figs. 2 and 3. In both cases the slope represents the molar rotation of the disaccharide unit in the chain and since the α-D-configuration of the 4-O-methylglucuronosyl xylose is well established (29), the opposite sign strongly favors the assignment of an α-L-configuration for the arabinosyl xylose unit, which is known to contain an L-arabinofuranose sugar. Application of Hudson's rules to the molar rotation

Can. J. Chem. Downloaded from www.nrcresearchpress.com by 210.87.254.42 on 09/05/12
For personal use only.

for the arabinosyl xylose in the chain also favors the α-L-assignment. Finally, the same configuration was recently suggested by Perlin and co-workers (25) on the basis of enzyme studies.

The apparent value of −29,000 for the molar rotation of the arabinosyl xylose residue in the polymer chain corresponds to an average value of −14,500 for each sugar moiety. Since this is only slightly less than the value of −13,500 for each xylose unit, it is readily understood why arabinoxylans have specific rotations in the same range as the neutral esparto xylan, namely about −100°.

Many native xylans, such as those present in softwoods, contain both 4-O-methylglucuronic acid and arabinose side chains. By a derivation similar to that presented above, it is possible to show that for this class of polysaccharides the following relation holds:

$$[4] \qquad [\alpha]_D\left(132+\frac{190.35}{\sigma+1+\sigma/\mu}+\frac{132}{\mu+1+\mu/\sigma}\right)\left(1+\frac{1}{\sigma}+\frac{1}{\mu}\right)=m+\frac{u}{\sigma}+\frac{f}{\mu},$$

where μ is the ratio of xylose to arabinosyl xylose residues in the chain, f is the molar rotation of this disaccharide unit, and the other symbols are as before. Equation [4] reduces to equation [3] when $\mu = \infty$ (no arabinose side chains). Since σ and μ can be determined experimentally, it is again possible to compute $[\alpha]$ for a given xylan of this class. Table III shows some data taken from the literature for a number of such xylans along with the

TABLE III

Optical rotation of acidic arabinoxylans

Species	$\sigma+1$	$\mu+1$	$[\alpha]_D$ (obs.)	$[\alpha]_D$* (calc.)	Ref.
White pine	6.2	7.7	−65	−70	20
Ginkgo biloba	5.3	7.5	−35	−66	21
Norway spruce	5.4	5.0	−49	−70	22
Scots pine	4.8	6.1	−59	−64	23
Amabilis fir	5.4	8.3	−57	−65	24
Loblolly pine	6.0	∞	−20	−61	27
Cocksfoot grass	4.8	2.2	−67	−82	28

*Calculated from equation [4] with: $u = 7900$; $f = -29{,}400$; $m = -13{,}500$.

observed and calculated rotations. The lack of agreement between the experimental values and those derived from the equation is striking. Experimental values are consistently lower than those calculated. This suggests either that the assumed structure is actually not the one on hand or the samples are impure.

V. ROTATORY DISPERSION OF XYLANS

Rotatory dispersion measurements were made on several xylan samples used in this study. A model 80 Rudolph spectrapolarimeter was used over the 350 to 750 mμ wavelength range to record the optical rotation. The results were plotted according to the modified Drude equation:

$$\overline{[\alpha]}_\lambda\lambda^2 = k+\overline{[\alpha]}_\lambda\lambda_c^2$$

where k is the rotation constant and λ_c the dispersion constant. The latter was found to decrease slightly with increasing uronic acid content. The curves are shown in Fig. 4. The extrapolated value for λ_c for a neutral xylan is 207. A summary of the various rotation and dispersion constants for the neutral and acidic xylans is presented in Table IV.

Can. J. Chem. Downloaded from www.nrcresearchpress.com by 210.87.254.42 on 09/05/12
For personal use only.

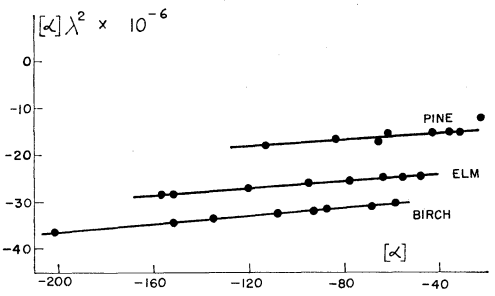

FIG. 4. Modified Drude plots for xylans with varying uronic acid content; solvent: 10% NaOH.

TABLE IV

Rotatory dispersion constants for neutral and acidic xylans

Sample	Xylose/uronic acid	$k \times 10^{-6}$	λ_c (mμ)	Solvent
White pine	5	−14.7	194	10% NaOH
White elm	7	−23.1	198	10% NaOH
White birch	10	−28.5	202	10% NaOH
Neutral xylan*	∞	—	207	10% NaOH
Xylohexaose	∞	−24.2	187	H_2O

*By extrapolation to zero acid content.

The distinct difference in λ_c for the neutral xylan and the oligosaccharide is reminiscent of the similar, albeit much greater, difference reported for an oligopeptide series (26). A decisive factor in the latter case is the hydrogen-bond-stabilized alpha-helix, which establishes a regular helical conformation in solution once the chain is composed of a minimum number of monomers. For polysaccharides in a good solvent, the situation is similar to that of a polypeptide in a non-helical solvent, where little or no change in λ_c would be expected. Nevertheless, the observed increase in the dispersion constant in going from the hexamer to the long chain is strongly suggestive of a conformational influence on the optical rotation even in a good solvent. This influence is most probably a simple energetic preference for a certain rotational isomer due to rotation around the bridge C_1—O—C_4 linkage. In this respect the influence of solvent is most probably important.

REFERENCES

1. G. O. ASPINALL. Advan. Carbohydrate Chem. **14**, 429 (1959).
2. C. P. J. GLAUDEMANS and T. E. TIMELL. Svensk Papperstid. **61**, 1 (1958).
3. I. CROON and B. F. ENSTROM. Tappi, **44**, 870 (1961).
4. C. T. BISHOP. Can. J. Chem. **31**, 793 (1953).
5. A. YUNDT. Tappi, **34**, 89 (1951).
6. R. H. MARCHESSAULT and T. E. TIMELL. J. Phys. Chem. **64**, 704 (1960).
7. H. O. BOUVENG, P. J. GAREGG, and B. LINDBERG. Acta Chem. Scand. **14**, 742 (1960).
8. T. E. TIMELL. J. Am. Chem. Soc. **82**, 5211 (1960).
9. R. H. MARCHESSAULT and T. E. TIMELL. J. Polymer. Sci. In press.
10. (*a*) T. E. TIMELL. Svensk Papperstid. **65**, 435 (1962); Can. J. Chem. **40**, 22 (1962).
(*b*) F. BARTH and T. E. TIMELL. J. Am. Chem. Soc. **80**, 6320 (1958).
11. C. P. J. GLAUDEMANS and T. E. TIMELL. J. Am. Chem. Soc. **80**, 941, 1207 (1958).
12. J. K. N. JONES, C. B. PURVES, and T. E. TIMELL. Can. J. Chem. **39**, 1059 (1961).
13. J. K. GILLHAM and T. E. TIMELL. Can. J. Chem. **36**, 1467 (1958).
14. R. MONTGOMERY and F. SMITH. J. Am. Chem. Soc. **76**, 5509 (1954).
15. R. L. WHISTLER and G. H. LAUTERBACH. J. Am. Chem. Soc. **80**, 1987 (1958).
16. G. O. ASPINALL and R. J. FERRIER. J. Chem. Soc. 4188 (1957).
17. G. O. ASPINALL and R. G. STURGEON. J. Chem. Soc. 4468 (1957).
18. G. O. ASPINALL and R. J. FERRIER. J. Chem. Soc. 638 (1958).
19. R. MONTGOMERY and F. SMITH. J. Am. Chem. Soc. **77**, 2834 (1955); **77**, 3325 (1955).
20. S. K. BANERJEE and T. E. TIMELL. Tappi, **43**, 849 (1960).

Can. J. Chem. Downloaded from www.nrcresearchpress.com by 210.87.254.42 on 09/05/12
For personal use only.

21. A. JABBAR and T. E. TIMELL. Svensk Papperstid. **64**, 21 (1960); **64**, 769 (1960).
22. J. SAARNIO. Suomen Kemistilehti, B, **29**, 35 (1956).
23. P. J. GAREGG and B. LINDBERG. Acta Chem. Scand. **14**, 871 (1960).
24. T. E. TIMELL. Svensk Papperstid. **64**, 748 (1961).
25. A. PERLIN. Private communication.
26. M. GOODMAN, E. E. SCHMITT, and D. YPHANTIS. J. Am. Chem. Soc. **82**, 3483 (1960).
27. J. K. N. JONES and T. J. PAINTER. J. Chem. Soc. 669 (1957); 573 (1959).
28. G. O. ASPINALL and I. M. CAIRNCROSS. J. Chem. Soc. 3877 (1960).
29. P. A. J. GORIN and A. S. PERLIN. Can. J. Chem. **36**, 999 (1958).

Can. J. Chem. Downloaded from www.nrcresearchpress.com by 210.87.254.42 on 09/05/12
For personal use only.

Can. J. Chem. Downloaded from www.nrcresearchpress.com by 210.87.254.40 on 09/05/12
For personal use only.

NOTES

THE INFLUENCE OF A VEHICLE-IMMISCIBLE, ADSORBABLE, THIRD COMPONENT ON THE FLOCCULATION OF LARGE-DIAMETER PARTICLES

J. J. Chessick, A. C. Zettlemoyer, and John B. Christian

INTRODUCTION

Flocculation processes of large-diameter (ca. 0.2 to 0.5 μ) solid particles as a function of the amount of vehicle-immiscible, adsorbable, third component present have rarely been studied. Definitive, mechanistic descriptions are lacking despite recent evidence that structural characteristics of such systems change with amount of flocculant present. Indeed, preliminary results indicate that flocculation processes of such polar solid particles in nonpolar organic vehicles with water as the flocculant should not be expected to conform to a general pattern.

Presentation of the brief results reported here was stimulated by a study of 14 m^2/g $BaSO_4$ – benzene – (flocculant) water systems reported by Smith and Puddington (1).

EXPERIMENTAL

In the prior work of Smith and Puddington (1) $BaSO_4$ evacuated at 200° and dry benzene were mixed asceptically before dispersion and before measurements of sedimentation volumes were made. Water was then introduced at definite and increasing concentrations, also prior to mixing and dispersion.

In the study reported here, a kaolin clay consisting of plate-like particles with an average size of ca. 0.3 μ and the dispersion medium decane were equilibrated at R.H.'s varying from 5.8 to 98% before mixing and dispersion. Dispersion was effected using a typical shaking apparatus for a period of 30 minutes; quantitative data are unavailable but there is little doubt that the systems were subjected to very small work levels. Systems consisting of solids dried over P_2O_5 at 100° and 200° before mixing with dried decane were also investigated. Other techniques used are described below. Sedimentation rates and final sediment volumes (heights) were determined.

RESULTS AND DISCUSSION

Final sedimentation heights for $BaSO_4$–benzene systens as a function of the amount of water associated with the solid, as determined by Smith and Puddington (1), are illustrated qualitatively in Fig. 1. These values were interpreted in terms of flocculation of $BaSO_4$ (the same number of dispersed particles per unit volume of benzene was apparently assumed) in benzene as a result of varying amounts of water adsorbed on the particle surfaces. The sedimentation height at zero water content reflected sedimentation of (little) flocculated, irregular particles (state A, Fig. 1). A voluminous, gel-like sediment (state B) due to rather small amounts of water at junction points between particles accounted for the maximum sediment volume. The formation of large, more sperical flocs at high water content was postulated (state C).

Sedimentation height and sedimentation rate data for the clay – decane – (flocculant) water systems are presented in Figs. 2 and 3, respectively. Final sedimentation heights represented by points I, II, and III of Fig. 2 are for suspensions containing solids dried over P_2O_5 at 100° or 200° before mixing and dispersion in dry decane. These heights decreased slightly with increasing severity of outgassing. Sedimentation rates for these dispersions were the second largest measured (curves D and E, Fig. 3). The combined results reveal that these low volumes resulted, not from minimal flocculation in water-free systems, but as a result of the increased resistance to dispersion of solid agglomerates.

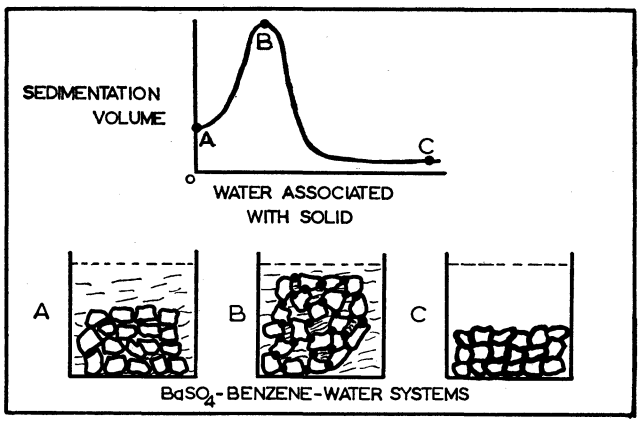

FIG. 1. Final sedimentation heights for $BaSO_4$–benzene suspensions as a function of water content (H. R. Smith and I. E. Puddington, Can. J. Chem., **38**, 1911 (1960); reproduction permission obtained).

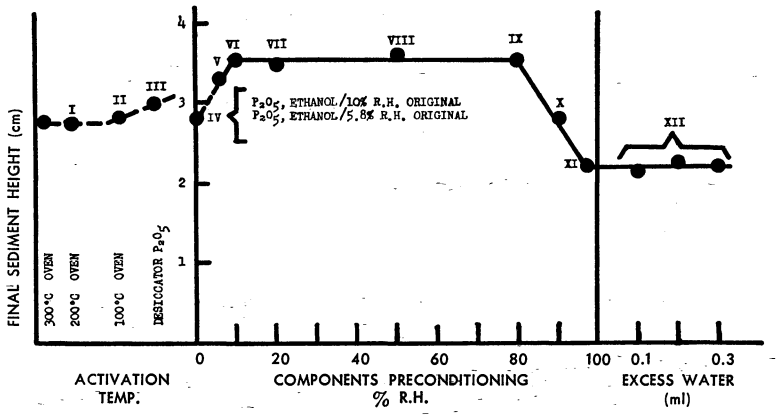

FIG. 2. Final sedimentation heights for kaolin–decane–water systems.

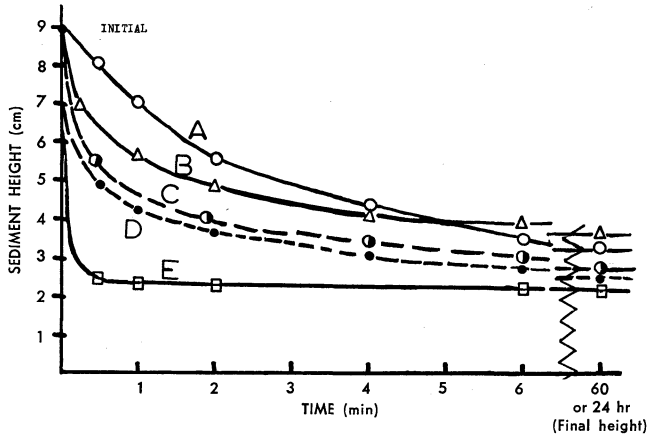

FIG. 3. Sedimentation rates for kaolin–decane–water system: ○ 10% R.H. (P_2O_5) or absolute alcohol); △ 10% R.H.; ◑ 90% R.H.; ● 100° C dried solid – dry decane; □ 0.1, 0.2 ml H_2O.

Can. J. Chem. Downloaded from www.nrcresearchpress.com by 210.87.254.40 on 09/05/12
For personal use only.

This strong agglomeration is due to capillary forces as water is removed progressively, at elevated temperatures, from interparticle pores between primary particles. The results of Smith and Puddington at zero and low water content for 200° activated $BaSO_4$ in benzene could be manifestations of this same phenomenon rather than the postulated (1) sedimentation of only moderately flocculated particles.

Systems made up of kaolin and decane equilibrated separately at 10, 20, 50, and 80% R.H. yielded essentially the same final sedimentation volumes and rates. Thus it is reasonable to conclude that similar initial states of dispersion were achieved. The conclusion that flocculation was due to and independent of the amount of water present in this R.H. range is therefore reasonable.

Equilibration of the components at 98% R.H. decreased the sedimentation volume to the lowest value observed; sedimentation of the 98% R.H. system was almost instantaneous (curve E, Fig. 3). The question arises as to whether excess water prevents dispersion. Upon dispersing 10, 20, 50, 90, or 98% systems and then injecting 0.1 and 0.2 ml H_2O, systems were produced having sedimentation heights all ca. 2.4 cm; this is equal to the value for the 98% R.H. equilibrated system. Adding excess water to these equilibrated systems prior to dispersion also produced a similar sedimentation volume.

Pretreatment of components at 5.8% R.H. led to a decreased sedimentation height relative to the maximum value. To eliminate the possibility of capillarity influences, 10% R.H. dispersed systems were injected with small amounts of P_2O_5 or absolute ethanol equivalent to that calculated amount of water originally present. The sedimentation height decreased to 2.8 cm (point IV, Fig. 2); the sedimentation rate (curve A, Fig. 3) was the *smallest* observed. These combined data support the contention that sedimentation occurred of particles which were less flocculated than in systems at higher water content.

The low sedimentation heights for temperature-evacuated samples (illustrated by points I, II, and III, Fig. 2) in the absence of rate data could have been ascribed to the sedimentation of small, sol-stabilized particles as suggested by Smith and Puddington (1).

Except for high temperature evacuated kaolin in dry decane systems the mechanisms of flocculation proposed by Smith and Puddington (1) can be used to explain the results of Figs. 1, 2, and 3. These are:

(1) The removal of interparticle water from pores between primary particles of an agglomerate by temperature evacuation decreases dispersability. Large irregular aggregates settle rapidly.

(2) Water removed in a manner that eliminates the influence of capillarity permits a sediment of irregular particles which are least flocculated by water. The lowest sedimentation rates are found in these systems.

(3) Water present in systems preconditioned at R.H.'s between 10 and 80% contains the same number of particles per unit volume after dispersion as in systems 2 and 4. Particles flocculate as a consequence of adsorbed water between particles; a more voluminous gel-like sediment results.

(4) At high water contents, more spherical flocs form, made up of a number of originally dispersed units, containing interparticle pore water; instantaneous sedimentation to the lowest volume is observed.

While the same mechanisms were proposed by Smith and Puddington (1), it is important to point out that their experimental findings possibly are not due alone to flocculation of solid particles in comparable initial states of dispersion, particularly at zero and low water contents.

Can. J. Chem. Downloaded from www.nrcresearchpress.com by 210.87.254.40 on 09/05/12
For personal use only.

Preliminary data obtained with another small-area oxide reveals the existence of significant differences in flocs formed at water levels different than reported here. A variety of systems need to be studied comprehensively. However, the data obtained in a similar manner for a chloride-process particle were in general agreement with the results of Smith and Puddington (1). Indeed, further investigations revealed that capillary forces due to water removal at 200° C from pores with $BaSO_4$ agglomerates were not important (2).

1. H. M. Smith and I. E. Puddington. Can. J. Chem. **38**, 1911 (1960).
2. I. E. Puddington. Private communication.

Received January 16, 1963.
Surface Chemistry Laboratory,
Lehigh University,
Bethlehem, Pennsylvania,
and
Aeronautical Systems Division,
Non-Metallic Materials Laboratory,
Wright-Patterson Air Force Base, Ohio.

Can. J. Chem. Downloaded from www.nrcresearchpress.com by 210.87.254.40 on 09/05/12
For personal use only.

THE ISOLATION OF 1,8-DIHYDROXY-3-METHYL-9-ANTHRONE FROM THE ROOT OF RUMEX CRISPUS LINN.

Ausat A. Khan

King *et al.* (1) have reported the isolation, from petroleum ether (60–80°), of an anthrone of the heartwood of *Ferrierea Spectabilis* (leguminose), which they named 1,8-dihydroxy-3-methyl-9-anthrone (I). Tsukida (2) has reported the presence of I in plants containing hydroxyanthraquinones and has found that the Japanese *Rumex* species (*Rumex Japonicus*) contains 'chrysophanic acid' (II), Emodin (III), I, and several other anthraquinones in minor quantities. In the present work it is found that the Argentine *Rumex Crispus* contains I as a major constituent and II and III as minor constituents.

I has been isolated in the present work in 0.3% yield from the finely divided roots of *Rumex Crispus* Linn., locally called 'lengua de vaca', as yellow needles, m.p. 206–208°. I was isolated by a convenient process of keeping the extract at 0° for 5 days to give a solid mass, which is deposited on the surface of the vessel. The solid mass was recrystallized from chloroform to give yellow needles of I. Removal of the solvent and fractional crystallization from benzene yielded chrysophanic acid, m.p. 194–196° (3), and Emodin, m.p. 254–256° (4). The total yield of II and III was 0.03% in this variety.

I gave an acetyl derivative, m.p. 234–236°, and with dimethyl sulphate yielded a methyl derivative, m.p. 140–142°.

EXPERIMENTAL

1. Extraction of I

Air-dried finely divided roots (1 kg) of *Rumex Crispus* Linn. (lengua de vaca) were extracted by being refluxed for 6 hours with 1.5 l. of petroleum ether (60–80°). Three more such extractions were carried out and the total extract was kept at 0° for 5 days whereby a solid mass (0.9 g) deposited. It was filtered and crystallized from chloroform as yellow needles, m.p. 206–208°.

The solvent was distilled under reduced pressure whereby a solid mass (0.3 g) separated which when

Preliminary data obtained with another small-area oxide reveals the existence of significant differences in flocs formed at water levels different than reported here. A variety of systems need to be studied comprehensively. However, the data obtained in a similar manner for a chloride-process particle were in general agreement with the results of Smith and Puddington (1). Indeed, further investigations revealed that capillary forces due to water removal at 200° C from pores with $BaSO_4$ agglomerates were not important (2).

1. H. M. Smith and I. E. Puddington. Can. J. Chem. **38**, 1911 (1960).
2. I. E. Puddington. Private communication.

Received January 16, 1963.
Surface Chemistry Laboratory,
Lehigh University,
Bethlehem, Pennsylvania,
and
Aeronautical Systems Division,
Non-Metallic Materials Laboratory,
Wright-Patterson Air Force Base, Ohio.

Can. J. Chem. Downloaded from www.nrcresearchpress.com by 210.87.254.42 on 09/05/12
For personal use only.

THE ISOLATION OF 1,8-DIHYDROXY-3-METHYL-9-ANTHRONE FROM THE ROOT OF RUMEX CRISPUS LINN.

Ausat A. Khan

King *et al.* (1) have reported the isolation, from petroleum ether (60–80°), of an anthrone of the heartwood of *Ferrierea Spectabilis* (leguminose), which they named 1,8-dihydroxy-3-methyl-9-anthrone (I). Tsukida (2) has reported the presence of I in plants containing hydroxyanthraquinones and has found that the Japanese *Rumex* species (*Rumex Japonicus*) contains 'chrysophanic acid' (II), Emodin (III), I, and several other anthraquinones in minor quantities. In the present work it is found that the Argentine *Rumex Crispus* contains I as a major constituent and II and III as minor constituents.

I has been isolated in the present work in 0.3% yield from the finely divided roots of *Rumex Crispus* Linn., locally called 'lengua de vaca', as yellow needles, m.p. 206–208°. I was isolated by a convenient process of keeping the extract at 0° for 5 days to give a solid mass, which is deposited on the surface of the vessel. The solid mass was recrystallized from chloroform to give yellow needles of I. Removal of the solvent and fractional crystallization from benzene yielded chrysophanic acid, m.p. 194–196° (3), and Emodin, m.p. 254–256° (4). The total yield of II and III was 0.03% in this variety.

I gave an acetyl derivative, m.p. 234–236°, and with dimethyl sulphate yielded a methyl derivative, m.p. 140–142°.

EXPERIMENTAL

1. Extraction of I

Air-dried finely divided roots (1 kg) of *Rumex Crispus* Linn. (lengua de vaca) were extracted by being refluxed for 6 hours with 1.5 l. of petroleum ether (60–80°). Three more such extractions were carried out and the total extract was kept at 0° for 5 days whereby a solid mass (0.9 g) deposited. It was filtered and crystallized from chloroform as yellow needles, m.p. 206–208°.

The solvent was distilled under reduced pressure whereby a solid mass (0.3 g) separated which when

crystallized from benzene yielded chrysophanic acid (II) as bright yellow needles, m.p. 196–198°, and Emodin (III) as bright orange needles, m.p. 254–256°.

Anal. Calc. for $C_{15}H_{12}O_3$ (I): C, 75.0; H, 5.0%. Found: C, 74.85; H, 4.91%. Anal. Calc. for $C_{15}H_{10}O_4$ (II): C, 70.86; H, 3.96%. Found: C, 70.51; H, 3.8%. Anal. Calc. for $C_{15}H_{10}O_5$ (III): C, 66.67; H, 3.73%. Found: C, 66.32; H, 3.9%.

2. Acetylation of I

A mixture of I (0.2 g), acetic anhydride (9 ml), and pyridine (1.5 ml) was refluxed for 2 hours. The reaction was then allowed to cool and poured onto crushed ice whereby a solid mass separated. It was filtered, washed well, and finally crystallized from aqueous alcohol to yield the acetyl derivatives as colorless needles, m.p. 234–236° (lit. m.p. 236–237°).

Anal. Calc. for $C_{21}H_{18}O_6$: C, 68.8; H, 4.95%. Found: C, 68.6; H, 4.7%.

3. Methylation of I

A mixture of 0.1 g of I, 0.5 ml of dimethyl sulphate in 200 ml of dry acetone, and 3 g of freshly ignited potassium carbonate was refluxed for 48 hours. At this stage a test sample did not give a color with ferric chloride.

The solution was filtered when cool; the residue obtained by removal of the solvent from the filtrate, when crystallized from dilute methanol, yielded colorless needles, m.p. 140–142° (lit. m.p. 142.5–143.5).

Anal. Calc. for $C_{17}H_{16}O_3$; C, 76.1; H, 6.0; 20 Me, 23.4%. Found: H, 6.3; 20 Me, 23.1%.

ACKNOWLEDGMENT

The author wishes to express his sincere thanks to Professor Anibal A. Sanguinetti, Director of the Institute of Chemical Sciences, for facilities and encouragement.

1. F. E. King, M. F. Grundon, and K. G. Niel. J. Chem. Soc. 4580 (1952).
2. K. Tsukida. J. Pharm. Soc. Japan, **74**, 294, 398, 401 (1954).
3. R. H. Thomson. Naturally occurring quinones. Academic Press, Inc., New York. 1957. p. 174.
4. E. H. Rodd. Chemistry of organic compounds. Vol. III B. Elsevier Publishing Co., Amsterdam. p. 1413.

Received November 13, 1962.
Departamento de Química Orgánica,
Instituto de Ciencias Químicas,
Universidad Nacional de Córdoba,
Cordoba, Argentina.

Can. J. Chem. Downloaded from www.nrcresearchpress.com by 210.87.254.42 on 09/05/12
For personal use only.

RELATIVE SIGNS OF PROTON COUPLING CONSTANTS IN 1-CHLORO-2,2-DIMETHYLCYCLOPROPANE

H. M. Hutton and T. Schaefer

Recent studies of the relative signs of spin–spin coupling constants have found that the geminal and vicinal coupling constants in substituted ethanes are opposite in sign (1), in disagreement with the theoretical calculations (2). It has now been established, following a suggestion by Karplus (3), that the one-bond C—H coupling has the same sign as the three-bond H—C—C—H vicinal coupling constants (4) and has the opposite sign to the two-bond H—C—H geminal coupling (5) in substituted ethanes. Since the directly bonded C—H coupling constants are almost certainly positive, one may conclude that J_{gem}^{H-H} is negative and J_{vic}^{H-H} is positive, which would in effect agree with the Dirac vector model (6).

To see whether these results hold true for substituted cyclopropanes, we have used Freeman's proton double-resonance technique (7) on 1-chloro-2,2-dimethylcyclopropane (8). The results of the ABX analysis for this cyclopropane in a 1:5 benzene solution are:

crystallized from benzene yielded chrysophanic acid (II) as bright yellow needles, m.p. 196–198°, and Emodin (III) as bright orange needles, m.p. 254–256°.

Anal. Calc. for $C_{15}H_{12}O_3$ (I): C, 75.0; H, 5.0%. Found: C, 74.85; H, 4.91%. Anal. Calc. for $C_{15}H_{10}O_4$ (II): C, 70.86; H, 3.96%. Found: C, 70.51; H, 3.8%. Anal. Calc. for $C_{15}H_{10}O_5$ (III): C, 66.67; H, 3.73%. Found: C, 66.32; H, 3.9%.

2. Acetylation of I

A mixture of I (0.2 g), acetic anhydride (9 ml), and pyridine (1.5 ml) was refluxed for 2 hours. The reaction was then allowed to cool and poured onto crushed ice whereby a solid mass separated. It was filtered, washed well, and finally crystallized from aqueous alcohol to yield the acetyl derivatives as colorless needles, m.p. 234–236° (lit. m.p. 236–237°).

Anal. Calc. for $C_{21}H_{18}O_6$: C, 68.8; H, 4.95%. Found: C, 68.6; H, 4.7%.

3. Methylation of I

A mixture of 0.1 g of I, 0.5 ml of dimethyl sulphate in 200 ml of dry acetone, and 3 g of freshly ignited potassium carbonate was refluxed for 48 hours. At this stage a test sample did not give a color with ferric chloride.

The solution was filtered when cool; the residue obtained by removal of the solvent from the filtrate, when crystallized from dilute methanol, yielded colorless needles, m.p. 140–142° (lit. m.p. 142.5–143.5).

Anal. Calc. for $C_{17}H_{16}O_3$; C, 76.1; H, 6.0; 20 Me, 23.4%. Found: H, 6.3; 20 Me, 23.1%.

ACKNOWLEDGMENT

The author wishes to express his sincere thanks to Professor Anibal A. Sanguinetti, Director of the Institute of Chemical Sciences, for facilities and encouragement.

1. F. E. King, M. F. Grundon, and K. G. Niel. J. Chem. Soc. 4580 (1952).
2. K. Tsukida. J. Pharm. Soc. Japan, **74**, 294, 398, 401 (1954).
3. R. H. Thomson. Naturally occurring quinones. Academic Press, Inc., New York. 1957. p. 174.
4. E. H. Rodd. Chemistry of organic compounds. Vol. III B. Elsevier Publishing Co., Amsterdam. p. 1413.

Received November 13, 1962.
Departamento de Química Orgánica,
Instituto de Ciencias Químicas,
Universidad Nacional de Córdoba,
Cordoba, Argentina.

Can. J. Chem. Downloaded from www.nrcresearchpress.com by 210.87.254.42 on 09/05/12
For personal use only.

RELATIVE SIGNS OF PROTON COUPLING CONSTANTS IN 1-CHLORO-2,2-DIMETHYLCYCLOPROPANE

H. M. Hutton and T. Schaefer

Recent studies of the relative signs of spin–spin coupling constants have found that the geminal and vicinal coupling constants in substituted ethanes are opposite in sign (1), in disagreement with the theoretical calculations (2). It has now been established, following a suggestion by Karplus (3), that the one-bond C—H coupling has the same sign as the three-bond H—C—C—H vicinal coupling constants (4) and has the opposite sign to the two-bond H—C—H geminal coupling (5) in substituted ethanes. Since the directly bonded C—H coupling constants are almost certainly positive, one may conclude that J_{gem}^{H-H} is negative and J_{vic}^{H-H} is positive, which would in effect agree with the Dirac vector model (6).

To see whether these results hold true for substituted cyclopropanes, we have used Freeman's proton double-resonance technique (7) on 1-chloro-2,2-dimethylcyclopropane (8). The results of the ABX analysis for this cyclopropane in a 1:5 benzene solution are:

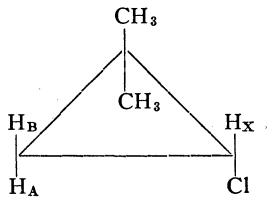

$|J_{AB}| = 5.98 \pm 0.17$ c.p.s.* $\quad \nu_B = 22.9$ c.p.s.†
$|J_{AX}| = 4.11 \pm 0.17$ c.p.s. $\quad \nu_A = 30.8$ c.p.s.
$|J_{BX}| = 7.39 \pm 0.17$ c.p.s. $\quad \nu_X = 156.3$ c.p.s.

To determine the relative signs by double irradiation (9), the transitions of this ABX system were labelled according to their origin as the ratio of the coupling constant to the chemical shift approaches zero, assuming $|J_{BX}| > |J_{AB}| > |J_{AX}|$. The decoupling frequencies were calculated for the two possibilities, namely, where the geminal and vicinal couplings have the same sign and the opposite sign. It was convenient to apply the high-amplitude radio-frequency field to the X transitions and observe the results in the AB spectrum. With the reverse procedure ambiguous results were obtained, probably due to the simultaneous disturbance of more than one pair of transitions. The results were as follows:

	Decoupling frequency (c.p.s.)			Decoupling frequency (c.p.s.)	
Signs of J_{AB} and J_{BX}	Calculated	Experimental	Signs of J_{AB} and J_{AX}	Calculated	Experimental
Same	124.5	118±1	Same	132.2	140±1
Opposite	116.5		Opposite	138.4	

The decoupling occurred gradually at the frequencies close to those listed for the case with opposite signs and then remained collapsed for a further increase of about 1 c.p.s. in the modulation frequency. The agreement between the calculated and observed decoupling frequencies is sufficiently good to show that the geminal coupling constant is opposite in sign to the vicinal couplings. In analogy to ethanes we conclude that in cyclopropanes the geminal coupling constant is negative and the vicinal coupling constants are positive. A similar conclusion is indicated by the direct analysis of the proton spectra of cyclopropanecarboxylic acid (10) and 2,2-diphenylcyclopropanecarboxylic acid (11) at low fields. Cyclopropane appears to differ from the substituted ethylene oxides, in which the geminal and vicinal coupling constants have the same sign.‡

ACKNOWLEDGMENTS

The authors wish to thank Dr. G. L. Closs, who generously donated the compound used in this experiment, and Mr. E. Erickson, who built the double-resonance apparatus for this work. We thank Dr. R. Freeman for advice on the construction of the apparatus. One of us (H. M. H.) thanks Canadian Industries Limited for Fellowship support.

This work was supported in part by the National Research Council of Canada and by the Research Corporation.

1. R. R. Fraser, R. V. Lemieux, and J. D. Stevens. J. Am. Chem. Soc. **83**, 3901 (1961). C. A. Reilly and J. D. Swalen. J. Chem. Phys. **35**, 1522 (1961). F. Kaplan and J. D. Roberts. J. Am.

**Root mean square deviation.*
†Chemical shift with respect to internal tetramethylsilane.
‡See Discussion, reference 4.

Can. J. Chem. Downloaded from www.nrcresearchpress.com by 210.87.254.42 on 09/05/12
For personal use only.

Chem. Soc. **83**, 4668 (1961). R. R. FRASER. Can. J. Chem. **40**, 1483 (1962). H. S. GUTOWSKY and C. JUAN. J. Chem. Phys. **37**, 120 (1962). K. A. MCLAUCHLAN and D. H. WHIFFEN. Proc. Chem. Soc. 144 (1962). H. FINEGOLD. Proc. Chem. Soc. 213 (1962).
2. M. KARPLUS. J. Chem. Phys. **30**, 11 (1959). H. S. GUTOWSKY, M. KARPLUS, and D. M. GRANT J. Chem. Phys. **30**, 1278 (1959).
3. M. KARPLUS. J. Am. Chem. Soc. **84**, 2458 (1962).
4. P. C. LAUTERBUR and R. J. KURLAND. J. Am. Chem. Soc. **84**, 3405 (1962).
5. F. A. L. ANET. J. Am. Chem. Soc. **84**, 3767 (1962).
6. H. M. MCCONNELL. J. Chem. Phys. **23**, 2454 (1955).
7. R. FREEMAN. Mol. Phys. **3**, 435 (1960).
8. G. L. CLOSS and L. E. CLOSS. J. Am. Chem. Soc. **82**, 5723 (1960).
9. J. P. MAHER and D. F. EVANS. Proc. Chem. Soc. 208 (1961). R. FREEMAN and D. H. WHIFFEN. Mol. Phys. **4**, 321 (1961). R. FREEMAN. Mol. Phys. **4**, 385 (1961). S. L. MANATT and D. D. ELLEMAN. J. Am. Chem. Soc. **84**, 1579 (1962).
10. K. WIBERG. Private communication.
11. J. I. MUSHER. Private communication.

RECEIVED FEBRUARY 4, 1963.
DEPARTMENT OF CHEMISTRY,
UNIVERSITY OF MANITOBA,
WINNIPEG, MANITOBA.

Can. J. Chem. Downloaded from www.nrcresearchpress.com by 210.87.254.42 on 09/05/12
For personal use only.

SOME NEW TRIARYLARSINES

W. R. CULLEN AND PAMELA E. YATES

During the course of a study of the electronic spectra of the arylarsines it became necessary to prepare some previously unknown triphenylarsines with substituents on the phenyl rings. The present communication describes the preparation of some compounds containing methoxy and trifluoromethyl groups.

The Wurtz-Fittig reaction was used by Michaelis and Weitz (1) to prepare tri(*p*-methoxyphenyl)arsine:

$$CH_3OC_6H_4Br + 6Na + AsCl_3 \rightarrow (CH_3OC_6H_4)_3As + 6NaCl.$$

We have now found that the *o*-methoxy and *m*-methoxy analogues can be prepared by the same method (Table I). However, when the Wutz-Fittig reaction was used to prepare trifluoromethyl-substituted phenylarsines no easily recognizable products were obtained. The successful synthesis of the compounds $(X—C_6H_4)_3As$ (X = *m*-CF_3 and *p*-CF_3) was achieved by reacting the Grignard reagent from the appropriate trifluoromethylphenyl bromide with arsenic trichloride (Table I). The product appeared to be contaminated in both these cases by partially substituted chloroarsines; however, these could be removed by distillation. The *m*-trifluoromethyl compound is most unusual in being a liquid at 20°.

The reaction of the Grignard reagent of *o*-trifluoromethylphenyl bromide with arsenic trichloride gave as a major product a compound which did not contain chlorine and which was shown, by analysis, to contain only two aryl groups for each arsenic atom. The infrared spectrum of the compound contained no —OH band and consequently the compound is best formulated as bis(*o*-trifluoromethylphenyl)arsine oxide (Table I). This suggests that the major product of the reaction was an incompletely substituted derivative of arsenic trichloride which was hydrolyzed to the oxide on working up the reaction mixture.

The authors wish to thank the National Research Council of Canada and the President's Research Fund of the University of British Columbia for financial support. Microanalyses were performed by Mrs. A. Aldridge in the Department of Chemistry, University of British Columbia.

Chem. Soc. **83**, 4668 (1961). R. R. FRASER. Can. J. Chem. **40**, 1483 (1962). H. S. GUTOWSKY and C. JUAN. J. Chem. Phys. **37**, 120 (1962). K. A. MCLAUCHLAN and D. H. WHIFFEN. Proc. Chem. Soc. 144 (1962). H. FINEGOLD. Proc. Chem. Soc. 213 (1962).
2. M. KARPLUS. J. Chem. Phys. **30**, 11 (1959). H. S. GUTOWSKY, M. KARPLUS, and D. M. GRANT J. Chem. Phys. **30**, 1278 (1959).
3. M. KARPLUS. J. Am. Chem. Soc. **84**, 2458 (1962).
4. P. C. LAUTERBUR and R. J. KURLAND. J. Am. Chem. Soc. **84**, 3405 (1962).
5. F. A. L. ANET. J. Am. Chem. Soc. **84**, 3767 (1962).
6. H. M. MCCONNELL. J. Chem. Phys. **23**, 2454 (1955).
7. R. FREEMAN. Mol. Phys. **3**, 435 (1960).
8. G. L. CLOSS and L. E. CLOSS. J. Am. Chem. Soc. **82**, 5723 (1960).
9. J. P. MAHER and D. F. EVANS. Proc. Chem. Soc. 208 (1961). R. FREEMAN and D. H. WHIFFEN. Mol. Phys. **4**, 321 (1961). R. FREEMAN. Mol. Phys. **4**, 385 (1961). S. L. MANATT and D. D. ELLEMAN. J. Am. Chem. Soc. **84**, 1579 (1962).
10. K. WIBERG. Private communication.
11. J. I. MUSHER. Private communication.

RECEIVED FEBRUARY 4, 1963.
DEPARTMENT OF CHEMISTRY,
UNIVERSITY OF MANITOBA,
WINNIPEG, MANITOBA.

Can. J. Chem. Downloaded from www.nrcresearchpress.com by 210.87.254.5 on 09/05/12
For personal use only.

SOME NEW TRIARYLARSINES

W. R. CULLEN AND PAMELA E. YATES

During the course of a study of the electronic spectra of the arylarsines it became necessary to prepare some previously unknown triphenylarsines with substituents on the phenyl rings. The present communication describes the preparation of some compounds containing methoxy and trifluoromethyl groups.

The Wurtz-Fittig reaction was used by Michaelis and Weitz (1) to prepare tri(*p*-methoxyphenyl)arsine:

$$CH_3OC_6H_4Br + 6Na + AsCl_3 \rightarrow (CH_3OC_6H_4)_3As + 6NaCl.$$

We have now found that the *o*-methoxy and *m*-methoxy analogues can be prepared by the same method (Table I). However, when the Wutz-Fittig reaction was used to prepare trifluoromethyl-substituted phenylarsines no easily recognizable products were obtained. The successful synthesis of the compounds $(X—C_6H_4)_3As$ (X = *m*-CF_3 and *p*-CF_3) was achieved by reacting the Grignard reagent from the appropriate trifluoromethylphenyl bromide with arsenic trichloride (Table I). The product appeared to be contaminated in both these cases by partially substituted chloroarsines; however, these could be removed by distillation. The *m*-trifluoromethyl compound is most unusual in being a liquid at 20°.

The reaction of the Grignard reagent of *o*-trifluoromethylphenyl bromide with arsenic trichloride gave as a major product a compound which did not contain chlorine and which was shown, by analysis, to contain only two aryl groups for each arsenic atom. The infrared spectrum of the compound contained no —OH band and consequently the compound is best formulated as bis(*o*-trifluoromethylphenyl)arsine oxide (Table I). This suggests that the major product of the reaction was an incompletely substituted derivative of arsenic trichloride which was hydrolyzed to the oxide on working up the reaction mixture.

The authors wish to thank the National Research Council of Canada and the President's Research Fund of the University of British Columbia for financial support. Microanalyses were performed by Mrs. A. Aldridge in the Department of Chemistry, University of British Columbia.

Can. J. Chem. Downloaded from www.nrcresearchpress.com by 210.87.254.5 on 09/05/12
For personal use only.

TABLE I

Reactant	Product‡	Yield (%)§	M.p. (°C)‖	B.p. (°C)	Analysis			
					Found		Calc.	
					C	H	C	H
o-$CH_3OC_6H_4Br$*	(*o*-$CH_3OC_6H_4)_3As$	9	200	—	63.5	5.34	63.6	5.31
m-$CH_3OC_6H_4Br$*	(*m*-$CH_3OC_6H_4)_3As$	11	108	—	63.9	5.43	63.6	5.31
p-$CF_3C_6H_4Br$†	(*p*-$CF_3C_6H_4)_3As$	10	90	156–160 (10^{-3} mm)	49.5	2.37	49.4	2.35
m-$CF_3C_6H_4Br$†	(*m*-$CF_3C_6H_4)_3As$	54	—	120–130 (10^{-3} mm) 202–204 (16 mm)	49.4	2.23	49.4	2.35
o-$CF_3C_6H_4Br$†	((*o*-$CF_3C_6H_4)_2As)_2O$	21	200	—**	45.7	2.10¶	45.1	2.14

*Wurtz-Fittig reaction using the procedure of Michaelis and Weitz (1): 50 g of the bromide were refluxed for 36 hours.

†Grignard reaction using the procedure of Challenger and Pritchard (2): 31 g of the bromide was used to make the Grignard reagent and after the arsenic trichloride had been added the mixture was refluxed for 8 hours.

‡All products are colorless.

§No attempt was made to obtain maximum yields. Solids were recrystallized from C_2H_5OH and C_6H_6.

‖Melting points are uncorrected.

¶Also found: Cl, 0.0; As, 20.6%. Calc.: Cl, 0.0; As, 20.1%.

**Working up the reaction mixture first gave an oil which distilled at 120° (10^{-3} mm). The solid oxide was obtained after recrystallization of this fraction from wet alcohol. Thus the oil was probably the compound $(CF_3C_6H_4)_2AsCl$.

1. A. MICHAELIS and L. WEITZ. Ber. **20**, 49 (1887).
2. F. CHALLENGER and F. PRITCHARD. J. Chem. Soc. 864 (1924).

RECEIVED JANUARY 24, 1963.
DEPARTMENT OF CHEMISTRY,
UNIVERSITY OF BRITISH COLUMBIA,
VANCOUVER, B.C.

Can. J. Chem. Downloaded from www.nrcresearchpress.com by 210.87.254.5 on 09/05/12
For personal use only.

STEROIDAL 3-CHLORO-3,5-DIENES

G. W. MOERSCH AND W. A. NEUKLIS

Some time ago, we found in studying the action of $POCl_3$ in dimethylformamide that this reagent converted steroidal Δ^4-3 ketones to 3-chloro-3,5-dienes, in which respect our experience resembled that since reported by Deghenghi and Gaudry (1).

Although previous work by Westphal *et al.* (2), Galinovsky *et al.* (3), Mamlok and Jacques (4), and Barber and Ehrenstein (5) as well as by Ruzicka and Fisher (6) and Kuwada and Miyasaki (7) had failed to indicate biological activity for other types of steroidal 3-chloro-3,5-dienes, we felt that the analogies might not be valid for 19-nor steroids nor in other assays such as myotrophic–androgenic ratio and in pituitary inhibition.

TABLE I

3-Chloro-3,5-dienes

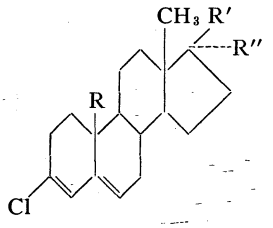

Number	R	R′	R″
I	CH_3	$OCCH_2CH_3$ (O)	H
II	H	$OCCH_3$ (O)	H
III	CH_3	OH	H (cf. ref. 3)
IV*	CH_3	$OCCH_3$ (O)	CH_3
V*	CH_3	CCH_3 (O)	H
VI	CH_3	CCH_3 (O)	OH
VII	CH_3	CCH_3 (O)	$OCCH_3$ (O)
VIII	CH_3	$OCCH_3$ (O)	C≡CH
IX	H	$OCCH_3$ (O)	C≡CH

*Our results for compounds IV and V were essentially the same as those reported by Deghenghi and Gaudry (1).

1. A. MICHAELIS and L. WEITZ. Ber. **20**, 49 (1887).
2. F. CHALLENGER and F. PRITCHARD. J. Chem. Soc. 864 (1924).

RECEIVED JANUARY 24, 1963.
DEPARTMENT OF CHEMISTRY,
UNIVERSITY OF BRITISH COLUMBIA,
VANCOUVER, B.C.

Can. J. Chem. Downloaded from www.nrcresearchpress.com by 210.87.254.40 on 09/05/12
For personal use only.

STEROIDAL 3-CHLORO-3,5-DIENES

G. W. MOERSCH AND W. A. NEUKLIS

Some time ago, we found in studying the action of $POCl_3$ in dimethylformamide that this reagent converted steroidal Δ^4-3 ketones to 3-chloro-3,5-dienes, in which respect our experience resembled that since reported by Deghenghi and Gaudry (1).

Although previous work by Westphal *et al.* (2), Galinovsky *et al.* (3), Mamlok and Jacques (4), and Barber and Ehrenstein (5) as well as by Ruzicka and Fisher (6) and Kuwada and Miyasaki (7) had failed to indicate biological activity for other types of steroidal 3-chloro-3,5-dienes, we felt that the analogies might not be valid for 19-nor steroids nor in other assays such as myotrophic–androgenic ratio and in pituitary inhibition.

TABLE I

3-Chloro-3,5-dienes

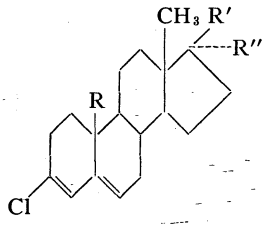

Number	R	R′	R″
I	CH_3	$OCCH_2CH_3$ (O)	H
II	H	$OCCH_3$ (O)	H
III	CH_3	OH	H (cf. ref. 3)
IV*	CH_3	$OCCH_3$ (O)	CH_3
V*	CH_3	CCH_3 (O)	H
VI	CH_3	CCH_3 (O)	OH
VII	CH_3	CCH_3 (O)	$OCCH_3$ (O)
VIII	CH_3	$OCCH_3$ (O)	C≡CH
IX	H	$OCCH_3$ (O)	C≡CH

*Our results for compounds IV and V were essentially the same as those reported by Deghenghi and Gaudry (1).

We found oxalyl chloride to be the most effective reagent, although PCl_5, $POCl_3$, and acetyl chloride could also be used. Hydroxyl groups were protected by acetylation and liberated by base hydrolysis.

The compounds prepared are given as the structures I–IX of Table I. Compounds IV and V were prepared with $POCl_3$ instead of oxalyl chloride. Our 3-chloro-3,5-dienes showed the characteristic ultraviolet absorption, in methanol, at 241–242 mμ with shoulders at 235 mμ and 250 mμ. The $\Delta^{3,5}$ band in infrared was at 1620 cm^{-1} in KBr.

Compounds II, III, and IV were active in a modification of the Hershberger androgenic–myotropic assay (8). We also noted improvement in the M/A ratio.

Compounds VI and IX showed activity in preventing litters in mice. Compounds VI and VII showed some progestational activity in the oral McPhail modification of the Clauberg assay (9). At 2.5-mg daily oral dose for 4 days, the uteri showed proliferation indices of 0.6 and 2.3 respectively.

EXPERIMENTAL[1]

3-Chloro-17β-propionoxyandrosta-3,5-diene (I)

A solution of 3.86 g of testosterone propionate in 40 ml of dimethylformamide (DMF) was added at room temperature with stirring to a reagent prepared by adding 1.1 ml $POCl_3$ to 6 ml DMF at <20° C. The reaction was warmed to 55–80° for 2.5 hours and the dark red reaction mixture cooled to room temperature and treated with 6 g of sodium acetate in 16 ml water, added dropwise with stirring. An orange precipitate formed which was partially dissolved on warming the mixture to 60–80° C for 30 minutes. The mixture was cooled in ice and filtered to collect the yellow product. The solid product was washed with water, dilute bicarbonate solution, and again with water before drying *in vacuo* at 50–60° to yield 3.5 g, m.p. 156–163° C.

Trituration with methanol removed most of the yellow color, leaving 2.27 g, m.p. 166–169°. Crystallization of 1 g from acetone–methanol gave 0.85 g of colorless needles, m.p. 170–172°; $[\alpha]_D^{23}$ −162° (0.53% in $CHCl_3$); λ_{max}^{MeOH} 242 mμ, log ε 4.36. Calc. for $C_{22}H_{31}O_2Cl$ (362.97): C, 71.87; H, 8.91; Cl, 10.15%. Found: C, 72.01; H, 8.74; Cl, 9.89%.

3-Chloro-17β-acetoxyestra-3,5-diene (II)

A solution of 1.0 g of 19-nortestosterone acetate in 25 ml of dry benzene was treated in the cold with 6 ml oxalyl chloride and let stand overnight at room temperature. The solution was then evaporated *in vacuo* at 40–55° C to give a mixture of amber solid and of gum. The product was warmed with dilute sodium bicarbonate solution and cooled in ice. A pale yellow solid was obtained, 0.98 g, m.p. 110–112° C. Two crystallizations from acetone–methanol gave 0.52 g of yellow plates, m.p. 118–120° C; $[\alpha]_D^{23}$ −192° (0.52% in $CHCl_3$); λ_{max}^{MeOH} 242 mμ, log ε 4.34. Calc. for $C_{20}H_{27}O_2Cl$ (334.87): C, 71.73; H, 8.12; Cl, 10.59%. Found: C, 71.65; H, 7.96; Cl, 10.57%.

3-Chloro-17β-hydroxyandrosta-3,5-diene (III)

A solution of 1.22 g of crude 3-chloro-17β-propionoxyandrosta-3,5-diene in 50 ml of 5% methanolic KOH was refluxed for 1 hour. The solution was filtered while hot and treated dropwise with 50 ml of water until a few crystals appeared. It was then cooled in ice and filtered to collect 0.86 g (81%), m.p. 145–147° C. Recrystallization from aqueous ethanol gave 0.53 g, m.p. 146–148° C in agreement with the melting point of 148° reported by Galinovsky *et al.* (3); $[\alpha]_D^{23}$ −150° (0.50% in $CHCl_3$); λ_{max}^{MeOH} 242, log ε 4.37. Calc. for $C_{19}H_{27}OCl$ (306.9): C, 74.35; H, 8.87; Cl, 11.55%. Found: C, 74.22; H, 9.07; Cl, 11.50%.

3-Chloro-17α-hydroxypregna-3,5-dien-20-one (VI)

This compound was prepared in the same manner as I. The yellow product, 1.8 g from 1.85 g of 17α-hydroxyprogesterone, was triturated with methanol (10 ml) and filtered to give 0.87 g, m.p. 190–193° C. Crystallization from methanol and acetone gave 0.54 g of tan crystals, m.p. 199–201° C; $[\alpha]_D^{23}$ −161° (0.50% in $CHCl_3$); λ_{max}^{MeOH} 241, log ε 4.37. Calc. for $C_{21}H_{29}O_2Cl$ (348.9): C, 72.29; H, 8.38; Cl, 10.16%. Found: C, 72.09; H, 8.56; Cl, 10.27%.

3-Chloro-17α-acetoxypregna-3,5-dien-20-one (VII)

Compound VI (2.65 g) in 165 ml of acetic acid was treated with 25 ml of acetic anhydride and 2.65 g of toluene sulphonic acid monohydrate and let stand at room temperature overnight. The reaction was then poured into 1 liter of ice water with shaking and the precipitated solid separated by filtration and washed with water and dilute sodium bicarbonate solution, 2.8 g, m.p. 155–160°. Two crystallizations from aqueous methanol gave 1.13 g of shiny white needles, m.p. 182–185°; $[\alpha]_D^{23}$ −127° (0.55% in $CHCl_3$); λ_{max}^{MeOH} 241, log ε 4.36. Calc. for $C_{23}H_{31}O_3Cl$ (390.9): C, 70.67; H, 7.99; Cl, 9.07%. Found: C, 70.45; H, 8.07; Cl, 9.08%.

[1]*Melting points were determined in capillary tubes and are uncorrected.*

Can. J. Chem. Downloaded from www.nrcresearchpress.com by 210.87.254.40 on 09/05/12
For personal use only.

Compound VII was less satisfactorily prepared by a procedure similar to that for compound I.

3-Chloro-17α-ethinyl-17β-acetoxyandrosta-3,5-diene (VIII)

Compound VIII was prepared from ethisterone acetate in similar reaction to that for compound I. The product was extracted with ether from the sodium acetate – water mixture diluted with 200 ml water. There was obtained 1.4 g from 2.0 g of ethisterone acetate. Crystallization of 0.9 g from heptane and acetone gave 0.19 g of pale yellow crystals, m.p. 181–184°; λ_{max}^{MeOH} 241, log ε 4.37; $[\alpha]_D^{23}$ −235° (0.9% in $CHCl_3$). Calc. for $C_{23}H_{29}O_2Cl$ (372.9): C, 74.08; H, 7.84; Cl, 9.51%. Found: C, 73.83; H, 7.79; Cl, 9.80%.

3-Chloro-17α-ethinyl-17β-acetoxyestra-3,5-diene (IX)

This compound was prepared in the manner of compound II. The product solidified on bicarbonate treatment to 2.02 g, m.p. 115–140° C. After two crystallizations from methanol, there was obtained 0.7 g, m.p. 138–140°; λ_{max}^{MeOH} 242, log ε 4.34. The analytical sample was obtained from aqueous acetone, m.p. 138–142° C; $[\alpha]_D^{23}$ −258° (0.58% in $CHCl_3$); λ_{max}^{MeOH} 242, log ε 4.34. Calc. for $C_{22}H_{27}O_2Cl$ (358.9): C, 73.62; H, 7.58; Cl, 9.88%. Found: C, 73.65; H, 7.59; Cl, 10.17%.

ACKNOWLEDGMENTS

We are indebted to Dr. M. R. Callatine, Dr. O. D. Bird, and Mr. R. Humphrey for the biological data; to Mr. C. E. Childs and staff for microanalytical data; and to Dr. J. M. Vandenbelt and staff for the physical measurements. We are grateful to Dr. L. M. Long for his support of this work.

1. R. Deghenghi and R. Gaudry. Can. J. Chem. **40**, 818 (1962).
2. U. Westphal, Y. L. Wang, and H. Hellmann. Ber. **72**, 1233 (1939).
3. F. Galinovsky, E. Kerschbaum, and H. Janisch. Monatsh. **84**, 193 (1953).
4. L. Mamlock and J. Jacques. Bull. Soc. Chim. France, 484 (1960).
5. G. W. Barber and M. Ehrenstein. Ann. **603**, 89 (1957).
6. L. Ruzicka and W. H. Fisher. Helv. Chim. Acta, **19**, 806 (1936).
7. S. Kuwada and M. Miyasaki. J. Pharm. Soc. Japan, **57**, 874 (1937).
8. D. A. McGinty and C. Djerassi. Ann. N.Y. Acad. Sci. **71**, 500 (1958).
9. M. K. McPhail. J. Physiol. (London), **83**, 145 (1934).

Received December 3, 1962.
Research Laboratories,
Parke, Davis and Company,
2800 Plymouth Road,
Ann Arbor, Michigan.

Can. J. Chem. Downloaded from www.nrcresearchpress.com by 210.87.254.40 on 09/05/12
For personal use only.

A PRELIMINARY STUDY OF SOME DITHIOSEMICARBAZONE–NICKEL(II) COMPLEXES[1]

B. A. Gingras, T. Suprunchuk, O. Bernardini,[2] and C. H. Bayley

We have reported earlier (1) that dithiosemicarbazones (ditscs) form solid 1:1 complexes with copper(II) in which the metal is coordinated tetrahedrally to two sulphur atoms and two nitrogen atoms. Monothiosemicarbazones, on the other hand, form 1:1 complexes with copper(I) whether Cu^+ (2) or Cu^{++} (3) salts are used, the metal in these being probably coordinated linearly in a polymeric structure (3). It has now been found that ditscs react with Ni^{++} salts in aqueous solution to form 1:1 complexes very likely similar in structure to the corresponding copper complexes described before (3).

Nickel complexes were readily obtained with benzil (R = R′ = C_6H_5), 2,3-heptanedione (R = Me; R′ = *n*-butyl), and 2,3-octanedione (R = Me; R = *n*-amyl) ditscs. Diacetyl (R = R′ = Me) and particularly glyoxal (R = R′ = H) ditscs gave complexes for which elementary analyses were variable and inconsistent at first with respect

[1]*Issued as N.R.C. No. 7302.*
[2]*N.R.C. Summer Student, 1962.*

Compound VII was less satisfactorily prepared by a procedure similar to that for compound I.

3-Chloro-17α-ethinyl-17β-acetoxyandrosta-3,5-diene (VIII)

Compound VIII was prepared from ethisterone acetate in similar reaction to that for compound I. The product was extracted with ether from the sodium acetate – water mixture diluted with 200 ml water. There was obtained 1.4 g from 2.0 g of ethisterone acetate. Crystallization of 0.9 g from heptane and acetone gave 0.19 g of pale yellow crystals, m.p. 181–184°; λ_{max}^{MeOH} 241, log ε 4.37; $[\alpha]_D^{23}$ −235° (0.9% in $CHCl_3$). Calc. for $C_{23}H_{29}O_2Cl$ (372.9): C, 74.08; H, 7.84; Cl, 9.51%. Found: C, 73.83; H, 7.79; Cl, 9.80%.

3-Chloro-17α-ethinyl-17β-acetoxyestra-3,5-diene (IX)

This compound was prepared in the manner of compound II. The product solidified on bicarbonate treatment to 2.02 g, m.p. 115–140° C. After two crystallizations from methanol, there was obtained 0.7 g, m.p. 138–140°; λ_{max}^{MeOH} 242, log ε 4.34. The analytical sample was obtained from aqueous acetone, m.p. 138–142° C; $[\alpha]_D^{23}$ −258° (0.58% in $CHCl_3$); λ_{max}^{MeOH} 242, log ε 4.34. Calc. for $C_{22}H_{27}O_2Cl$ (358.9): C, 73.62; H, 7.58; Cl, 9.88%. Found: C, 73.65; H, 7.59; Cl, 10.17%.

ACKNOWLEDGMENTS

We are indebted to Dr. M. R. Callatine, Dr. O. D. Bird, and Mr. R. Humphrey for the biological data; to Mr. C. E. Childs and staff for microanalytical data; and to Dr. J. M. Vandenbelt and staff for the physical measurements. We are grateful to Dr. L. M. Long for his support of this work.

1. R. Deghenghi and R. Gaudry. Can. J. Chem. **40**, 818 (1962).
2. U. Westphal, Y. L. Wang, and H. Hellmann. Ber. **72**, 1233 (1939).
3. F. Galinovsky, E. Kerschbaum, and H. Janisch. Monatsh. **84**, 193 (1953).
4. L. Mamlock and J. Jacques. Bull. Soc. Chim. France, 484 (1960).
5. G. W. Barber and M. Ehrenstein. Ann. **603**, 89 (1957).
6. L. Ruzicka and W. H. Fisher. Helv. Chim. Acta, **19**, 806 (1936).
7. S. Kuwada and M. Miyasaki. J. Pharm. Soc. Japan, **57**, 874 (1937).
8. D. A. McGinty and C. Djerassi. Ann. N.Y. Acad. Sci. **71**, 500 (1958).
9. M. K. McPhail. J. Physiol. (London), **83**, 145 (1934).

Received December 3, 1962.
Research Laboratories,
Parke, Davis and Company,
2800 Plymouth Road,
Ann Arbor, Michigan.

Can. J. Chem. Downloaded from www.nrcresearchpress.com by 210.87.254.40 on 09/05/12
For personal use only.

A PRELIMINARY STUDY OF SOME DITHIOSEMICARBAZONE–NICKEL(II) COMPLEXES[1]

B. A. Gingras, T. Suprunchuk, O. Bernardini,[2] and C. H. Bayley

We have reported earlier (1) that dithiosemicarbazones (ditscs) form solid 1:1 complexes with copper(II) in which the metal is coordinated tetrahedrally to two sulphur atoms and two nitrogen atoms. Monothiosemicarbazones, on the other hand, form 1:1 complexes with copper(I) whether Cu^+ (2) or Cu^{++} (3) salts are used, the metal in these being probably coordinated linearly in a polymeric structure (3). It has now been found that ditscs react with Ni^{++} salts in aqueous solution to form 1:1 complexes very likely similar in structure to the corresponding copper complexes described before (3).

Nickel complexes were readily obtained with benzil (R = R′ = C_6H_5), 2,3-heptanedione (R = Me; R′ = *n*-butyl), and 2,3-octanedione (R = Me; R = *n*-amyl) ditscs. Diacetyl (R = R′ = Me) and particularly glyoxal (R = R′ = H) ditscs gave complexes for which elementary analyses were variable and inconsistent at first with respect

[1]*Issued as N.R.C. No. 7302.*
[2]*N.R.C. Summer Student, 1962.*

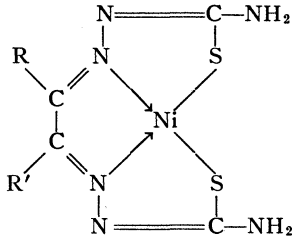

to the calculated values. In fact, it was believed in the early stages of this investigation that these two complexes contained a varying amount of oxygen, and it was only after repeated careful crystallizations that satisfactory analyses were obtained. It is now believed that the discrepancies in the analyses were due to varying amount of water of coordination in the complex, this water being retained fairly strongly.

It was found that glyoxal ditscs – Ni(II) did not lose water when heated for 3 days at 150° C, or in the drying pistol at 100° C, for the same period of time. An anhydrous glyxoal ditsc – Ni(II) complex for which elementary analyses were satisfactory was obtained only after several recrystallizations from dimethyl sulphoxide (DMSO). The complex dissolves fairly easily in warm DMSO but can only be recovered by addition of water or complete evaporation of the solvent. It is likely that DMSO adds on to the metal, which becomes hexacoordinated in an octahedral configuration (d^2sp^3). This adduct is not too stable as addition of a little water causes precipitation of the complex. When this process of solvation and precipitation is repeated three to four times, the elementary analyses for the resulting complex are satisfactory. It was observed that the addition of water must be carefully controlled since an excess of water favors the formation of the hydrated complex. It was found in two cases (glyoxal and diacetyl ditsc – Ni(II)) where the complexes had been prepared in the complete absence of water that after precipitation from DMSO with water, they contained a fair amount of water: e.g. glyoxal ditsc complex, about 14% and diacetyl ditsc, 8%.

Nickel(II) in a four-coordinated diamagnetic complex is usually square planar (dsp^2) but it is known that the configuration of many nickel(II) complexes changes with ease (4) when the complexes are dissolved in organic solvents. For instance, Willis and Mellor (5) found that a number of diamagnetic nickel(II) complexes react with two molecules of pyridine to form paramagnetic octahedral complexes. This was later confirmed by Basolo and Matoush (4), who were able to isolate some crystalline compounds of nickel(II) hexacoordinated complexes containing two molecules of pyridine. The change of configuration is reversible and the original complex is regenerated by removal of the solvent under vacuum or at elevated temperature.

DMSO is completely removed from the glyoxal complex by vacuum distillation. We have not been able as yet to separate and identify the addition compound formed with the solvent. Pyridine behaves in the same manner as DMSO but it was little used in this work as the various nickel complexes dissolved more readily in DMSO.

In the cases of the longer-chain ditscs (2,3-heptanedione, 2,3-octanedione, and benzil) it is possible that spatial arrangements do not allow further coordination of the metal with water, and good analyses were readily obtained. Identical compounds were obtained whether anhydrous or hydrated nickel salts were used.

Infrared spectra provide further evidence that coordinated water is responsible for the varying analytical results in the case of the nickel complex of glyoxal ditsc. The

Can. J. Chem. Downloaded from www.nrcresearchpress.com by 210.87.254.40 on 09/05/12
For personal use only.

spectra of five different samples of this complex, ranging from the anhydrous to the one containing 14% water, were found to be identical. It seems that the particularly broad N—H band of medium intensity in the region 3400–3500 cm^{-1} makes it impossible to detect the water absorption band.

Molecular weights of two ditsc–Ni(II) complexes were measured by the freezing point method in DMSO and the compounds were found to be monomers.* This is in agreement with the results reported by Bahr and Schleitzer (6) on some similar complexes.

EXPERIMENTAL

Ditscs were prepared as described previously (1). The nickel salts were "reagent grade" nickelous sulphate·$6H_2O$, nickelous chloride·$6H_2O$, and anhydrous nickelous sulphate. DMSO was purified by drying over CaO followed by distillation under reduced pressure in an atmosphere of nitrogen.

Glyoxal ditsc – Ni(II)

A solution of $NiSO_4 \cdot 6H_2O$ (2.62 g, 0.01 mole) in water (50 ml) was added dropwise to a boiling solution of glyoxal ditsc (2.04 g, 0.01 mole) in dimethylformamide (100 ml). Reflux was continued for 15 minutes as a dark blue precipitate was formed. After the mixture was cooled, the precipitate was collected by filtration, washed successively with hydrochloric acid (3%), water, dimethylformamide, alcohol, and acetone, and dried. Yield: 2.44 g, 90%; m.p. above 300° C. After repeated crystallizations from DMSO–water, the analysis was satisfactory. Calculated for $C_4H_6N_6S_2 \cdot Ni$: M.W. 260.7; C, 18.4; H, 2.3; N, 32.2; S, 24.3; Ni, 22.5%. Found: C, 19.3; H, 2.7; N, 31.8; S, 23.6; Ni, 21.5%. Several other samples of glyoxal ditsc – Ni(II) complex were prepared by this method or others using nickel chloride or anhydrous nickel sulphate but their analyses are not given since they were variable and showed indefinite amounts of oxygen. As mentioned earlier, however, their infrared spectra were identical.

Diacetyl ditsc – Ni(II)

This was prepared as above using diacetyl ditsc (2.32 g, 0.01 mole) in dimethylformamide (200 ml) and nickelous sulphate·$6H_2O$ (2.62 g, 0.01 mole) in water (50 ml). The precipitate was treated as described earlier and recrystallized from DMSO by careful addition of water. Yield: 2.25 g, 77%; m.p. above 300° C. Calculated for $C_6H_{10}N_6S_2 \cdot Ni$: C, 24.9; H, 3.5; N, 29.1; S, 22.2; Ni, 20.36%. Found: C, 25.2; H, 3.4; N, 29.2; S, 21; Ni, 20.3%.

Benzil ditsc – Ni(II)

The same method of preparation was used starting with benzil ditsc (2.56 g, 0.075 mole) in dimethylformamide (100 ml) and $NiSO_4 \cdot 6H_2O$ (2.62 g, 0.01 mole) in water (50 ml). The precipitate was collected, washed, and dried. After recrystallization from DMSO–water, it had m.p. 187–190° C; 2.2 g, 72%. Calculated for $C_{16}H_{14}N_6S_2 \cdot Ni$: C, 46.6; H, 3.4; N, 20.38; S, 15.5; Ni, 14.2%. Found: C, 46.5; H, 4.0; N, 20.1; S, 15.5; Ni, 13.9%.

This complex was also prepared by a different method using anhydrous nickel sulphate and carrying out the reaction in dimethylformamide alone. As the nickel salt was insoluble, the mixture was refluxed for 1 hour. After cooling of the mixture, and removal of some unreacted material, the solvent was distilled under vacuum. The resulting dark red residue was recrystallized from absolute alcohol; m.p. 190° C, 1.5 g, 50%. Found: C, 46.88; H, 3.26; N, 20.0; S, 14.7; Ni, 13.9%.

2,3-Heptanedione ditsc – Ni(II)

This was prepared by the usual method in dimethylformamide, and the resulting precipitate, after being washed, was recrystallized from absolute ethyl alcohol till constant melting point, 238° C, 1.7 g, 48%. Calculated for $C_9H_{16}N_6S_2 \cdot Ni$: C, 32.65; H, 4.84; N, 25.4; S, 19.35; Ni, 17.75%. Found: C, 32.42; H, 4.99; N, 24.65; S, 17.85; Ni, 17.75%.

2,3-Octanedione ditsc – Ni(II)

This was prepared in the same manner and the complex obtained, after the usual washing, was recrystallized from the DMSO–water mixture followed by two recrystallizations from absolute ethyl alcohol. It had m.p. 246° C, 1.2 g, 35%. Calculated for $C_{10}H_{18}N_6S_2 \cdot Ni$: C, 34.8; H, 5.2; N, 24.35; S, 18.55; Ni, 17.0%. Found: C, 34.3; H, 4.9; N, 24.1; S, 18.5; Ni, 17.1%.

1. B. A. GINGRAS, T. SUPRUNCHUK, and C. H. BAYLEY. Can. J. Chem. **40**, 1053 (1962).
2. B. A. GINGRAS, R. W. HORNAL, and C. H. BAYLEY. Can. J. Chem. **38**, 712 (1960).
3. B. A. GINGRAS, R. L. SOMORJAI, and C. H. BAYLEY. Can. J. Chem. **39**, 973 (1961).
4. F. BASOLO and W. R. MATOUSH. J. Am. Chem. Soc. **75**, 5663 (1953).

**Details of the method used for measuring molecular weights in* DMSO *will be given in a forthcoming publication.*

Can. J. Chem. Downloaded from www.nrcresearchpress.com by 210.87.254.40 on 09/05/12
For personal use only.

5. J. B. WILLIS and D. P. MELLOR. J. Am. Chem. Soc. **69**, 1237 (1947).
6. G. BAHR and E. SCHLEITZER. Z. Anorg. Allgem. Chem. **278**, 136 (1955).

RECEIVED DECEMBER 26, 1962.
DIVISION OF APPLIED CHEMISTRY,
NATIONAL RESEARCH COUNCIL,
OTTAWA, CANADA.

Can. J. Chem. Downloaded from www.nrcresearchpress.com by 210.87.254.40 on 09/05/12
For personal use only.

THE COORDINATION OF SEVEN ELECTRON PAIRS

DOYLE BRITTON

In a recent discussion of molecular shapes Gillespie (1)* pointed out that for two to nine electron pairs, coordinated at a fixed distance from a central nucleus with the geometry determined by repulsive forces between the electron pairs, only in the case of seven electron pairs did the geometry change when the assumed repulsive force law was changed. The three reasonable possibilities for seven coordination are shown in Fig. 1.

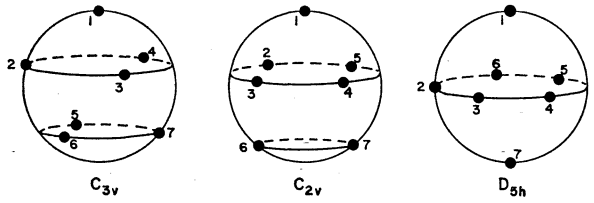

FIG. 1. Arrangements of seven particles on the surface of a sphere.

If the repulsive potential energy of the set of particles on the surface of the sphere is assumed to depend inversely upon the first power of the distance, which would be appropriate to ionic repulsion, the D_{5h} arrangement is found to be most stable. However, if the repulsive potential energy is assumed to depend inversely upon some large power of the distance, corresponding to Pauli forces, or in the limit, to a hard sphere model, the C_{3v} arrangement is found to be most stable. Gillespie suggested that the C_{2v} arrangement would also be stable for some intermediate inverse power dependence of the energy.

With a high-speed computer available to remove the tedium from the computations it seems of interest to check Gillespie's suggestion, and also to see how different in energy the various arrangements are.

For the C_{3v} arrangement there are two adjustable parameters: α = the north latitude of points 2, 3, 4, and β = the south latitude of points 5, 6, 7. For a sphere of radius = 1 the various interparticle distances are given by

$$r_{12}^2 = 2 - 2\sin\alpha$$
$$r_{15}^2 = 2 + 2\sin\beta$$
$$r_{23}^2 = 3\cos^2\alpha$$
$$r_{25}^2 = 2 - \cos\alpha\cos\beta + 2\sin\alpha\sin\beta$$
$$r_{27}^2 = 2 + 2\cos\alpha\cos\beta + 2\sin\alpha\sin\beta$$
$$r_{56}^2 = 3\cos^2\beta$$

and the repulsive energy is

$$E_{C_{3v}}(n) = \frac{3}{r_{12}^n} + \frac{3}{r_{15}^n} + \frac{3}{r_{23}^n} + \frac{6}{r_{25}^n} + \frac{3}{r_{27}^n} + \frac{3}{r_{56}^n}.$$

*This reference should be consulted for earlier literature references in this area.

5. J. B. WILLIS and D. P. MELLOR. J. Am. Chem. Soc. **69**, 1237 (1947).
6. G. BAHR and E. SCHLEITZER. Z. Anorg. Allgem. Chem. **278**, 136 (1955).

RECEIVED DECEMBER 26, 1962.
DIVISION OF APPLIED CHEMISTRY,
NATIONAL RESEARCH COUNCIL,
OTTAWA, CANADA.

THE COORDINATION OF SEVEN ELECTRON PAIRS

DOYLE BRITTON

In a recent discussion of molecular shapes Gillespie (1)* pointed out that for two to nine electron pairs, coordinated at a fixed distance from a central nucleus with the geometry determined by repulsive forces between the electron pairs, only in the case of seven electron pairs did the geometry change when the assumed repulsive force law was changed. The three reasonable possibilities for seven coordination are shown in Fig. 1.

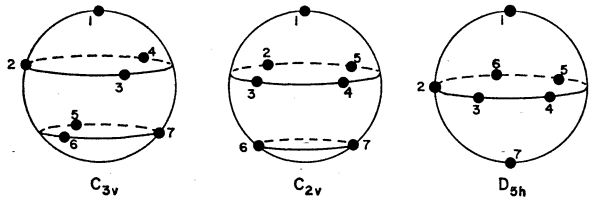

FIG. 1. Arrangements of seven particles on the surface of a sphere.

If the repulsive potential energy of the set of particles on the surface of the sphere is assumed to depend inversely upon the first power of the distance, which would be appropriate to ionic repulsion, the D_{5h} arrangement is found to be most stable. However, if the repulsive potential energy is assumed to depend inversely upon some large power of the distance, corresponding to Pauli forces, or in the limit, to a hard sphere model, the C_{3v} arrangement is found to be most stable. Gillespie suggested that the C_{2v} arrangement would also be stable for some intermediate inverse power dependence of the energy.

With a high-speed computer available to remove the tedium from the computations it seems of interest to check Gillespie's suggestion, and also to see how different in energy the various arrangements are.

For the C_{3v} arrangement there are two adjustable parameters: α = the north latitude of points 2, 3, 4, and β = the south latitude of points 5, 6, 7. For a sphere of radius = 1 the various interparticle distances are given by

$$r_{12}^2 = 2 - 2\sin\alpha$$
$$r_{15}^2 = 2 + 2\sin\beta$$
$$r_{23}^2 = 3\cos^2\alpha$$
$$r_{25}^2 = 2 - \cos\alpha\cos\beta + 2\sin\alpha\sin\beta$$
$$r_{27}^2 = 2 + 2\cos\alpha\cos\beta + 2\sin\alpha\sin\beta$$
$$r_{56}^2 = 3\cos^2\beta$$

and the repulsive energy is

$$E_{C_{3v}}(n) = \frac{3}{r_{12}^n} + \frac{3}{r_{15}^n} + \frac{3}{r_{23}^n} + \frac{6}{r_{25}^n} + \frac{3}{r_{27}^n} + \frac{3}{r_{56}^n}.$$

*This reference should be consulted for earlier literature references in this area.

Can. J. Chem. Downloaded from www.nrcresearchpress.com by 210.87.254.105 on 09/05/12
For personal use only.

For the C_{2v} arrangement there are three adjustable parameters: α = the north latitude of points 2, 3, 4, 5; β = the south latitude of points 6, 7; and γ = half the difference in longitude of points 2 and 3. For a sphere of radius = 1 the various interparticle distances are given by

$$\begin{aligned}
r_{12}^2 &= 2 - 2\sin\alpha \\
r_{16}^2 &= 2 + 2\sin\beta \\
r_{23}^2 &= 4\cos^2\alpha\sin^2\gamma \\
r_{24}^2 &= 4\cos^2\alpha \\
r_{25}^2 &= 4\cos^2\alpha\cos^2\gamma \\
r_{26}^2 &= 2 - 2\cos\alpha\cos\beta\cos\gamma + 2\sin\alpha\sin\beta \\
r_{27}^2 &= 2 + 2\cos\alpha\cos\beta\cos\gamma + 2\sin\alpha\sin\beta \\
r_{67}^2 &= 4\cos^2\beta
\end{aligned}$$

and the repulsive energy is

$$E_{C_{2v}}(n) = \frac{4}{r_{12}^n} + \frac{2}{r_{16}^n} + \frac{2}{r_{23}^n} + \frac{2}{r_{24}^n} + \frac{2}{r_{25}^n} + \frac{4}{r_{26}^n} + \frac{4}{r_{27}^n} + \frac{1}{r_{67}^n}.$$

For the D_{5h} arrangement there are no variable parameters, and for a sphere of radius = 1 the various interparticle distances are given by

$$\begin{aligned}
r_{12}^2 &= 2 \\
r_{17}^2 &= 4 \\
r_{23}^2 &= 4\sin^2(\pi/5) \\
r_{24}^2 &= 4\sin^2(2\pi/5)
\end{aligned}$$

and the repulsive energy is

$$E_{D_{5h}}(n) = \frac{10}{r_{12}^n} + \frac{1}{r_{17}^n} + \frac{5}{r_{23}^n} + \frac{5}{r_{24}^n}.$$

The first and simplest comparison to make is to assume that the particles are held at the distance appropriate to the hard sphere model. The results are given in Table I.

TABLE I

Relative repulsive energies at hard sphere distances

n	$\frac{E_{C_{3v}}}{E_{D_{5h}}}$	$\frac{E_{C_{2v}}}{E_{D_{5h}}}$	$\frac{E_{D_{5h}}}{E_{D_{5h}}}$	$E_{D_{5h}}$
0	1.0000	1.0000	1.0000	21.000
1	1.0039	1.0022	1.0000	14.453
2	1.0088	1.0051	1.0000	10.250
4	1.0166	1.0091	1.0000	5.5625
6	1.0130	1.0035	1.0000	3.2656
8	0.9908	0.9821	1.0000	2.0289
10	0.9489	0.9434	1.0000	1.3135
12	0.8907	0.8901	1.0000	0.87649
14	0.8218	0.8268	1.0000	0.59819
16	0.7476	0.7584	1.0000	0.41508
20	0.6007	0.6209	1.0000	0.20657
∞	0.0000	0.0000	1.0000	0.00000

NOTE: The boxes enclose the minimum values at each n.

Can. J. Chem. Downloaded from www.nrcresearchpress.com by 210.87.254.105 on 09/05/12
For personal use only.

Since only the relative values of the energy are of interest the actual values as a function of n are given only for D_{5h}, and the values relative to D_{5h} are given for the other geometries.

More realistic is a calculation of the energy where the distance are allowed to adjust to the minimum energy positions. These values were found by mapping the function in the neighborhood of the expected minimum position until the minimum position was found with the desired accuracy. The results are shown in Table II. As before, only the comparison with D_{5h} is given. The values for the positional parameters are also given.

It is apparent from the tables that Gillespie's suggestions are confirmed. First, the C_{2v} arrangement becomes most stable at intermediate values of n. For the hard sphere model this is for n from about 8 to 12; for the equilibrium model this is around $n = 4$. Second, and fairly striking, the energy differences among the forms are quite small fractions of the total energy, so that the actual arrangement will depend importantly upon factors other than the repulsive potential between the ligands.

TABLE II

Relative repulsive energies at equilibrium distances

n	$\frac{E_{C_{3v}}}{E_{D_{5h}}}$	sin α	sin β	$\frac{E_{C_{2v}}}{E_{D_{5h}}}$	sin α	sin β	sin γ	$\frac{E_{D_{5h}}}{E_{D_{5h}}}$
0	1.0000	—	—	1.0000	—	—	—	1.0000
1	1.0004	0.288	0.626	1.0003	0.159	0.811	0.755	1.0000
2	1.0010	0.284	0.630	1.0009	0.164	0.809	0.754	1.0000
3	1.0012	0.279	0.634	1.0009	0.169	0.807	0.753	1.0000
4	0.9999	0.274	0.639	0.9997	0.175	0.805	0.752	1.0000
6	0.9891	0.265	0.646	0.9893	0.184	0.802	0.752	1.0000
12	0.8602	0.246	0.661	0.8682	0.202	0.794	0.752	1.0000
20	0.5777	0.234	0.670	0.6018	0.210	0.790	0.755	1.0000
∞	0.0000	0.210	0.688	0.0000	0.219	0.781	0.768	1.0000

NOTE: The boxes enclose the minimum values at each n.

This work was supported in part by a grant from the National Science Foundation. The computations were done on the Control Data 1604 computer at the Numerical Analysis Center of the University of Minnesota.

1. R. J. GILLESPIE. Can. J. Chem. **38**, 818 (1960).

RECEIVED FEBRUARY 5, 1963.
DEPARTMENT OF CHEMISTRY,
UNIVERSITY OF MINNESOTA,
MINNEAPOLIS 14, MINNESOTA.

THE BENZOYLOXY GROUP OF ACONITINE*

Y. TSUDA† AND LÉO MARION

Although the structure of aconitine shown in the accompanying formula has been well established (1, 2), the position of the benzoyl ester group is perhaps less rigorously demonstrated than the rest of the structure.

*Issued as N.R.C. No. 7300.
†*National Research Council of Canada Postdoctoral Fellow.*

Can. J. Chem. Downloaded from www.nrcresearchpress.com by 210.87.254.105 on 09/05/12
For personal use only.

Since only the relative values of the energy are of interest the actual values as a function of n are given only for D_{5h}, and the values relative to D_{5h} are given for the other geometries.

More realistic is a calculation of the energy where the distance are allowed to adjust to the minimum energy positions. These values were found by mapping the function in the neighborhood of the expected minimum position until the minimum position was found with the desired accuracy. The results are shown in Table II. As before, only the comparison with D_{5h} is given. The values for the positional parameters are also given.

It is apparent from the tables that Gillespie's suggestions are confirmed. First, the C_{2v} arrangement becomes most stable at intermediate values of n. For the hard sphere model this is for n from about 8 to 12; for the equilibrium model this is around $n = 4$. Second, and fairly striking, the energy differences among the forms are quite small fractions of the total energy, so that the actual arrangement will depend importantly upon factors other than the repulsive potential between the ligands.

TABLE II

Relative repulsive energies at equilibrium distances

n	$\frac{E_{C_{3v}}}{E_{D_{5h}}}$	sin α	sin β	$\frac{E_{C_{2v}}}{E_{D_{5h}}}$	sin α	sin β	sin γ	$\frac{E_{D_{5h}}}{E_{D_{5h}}}$
0	1.0000	—	—	1.0000	—	—	—	1.0000
1	1.0004	0.288	0.626	1.0003	0.159	0.811	0.755	1.0000
2	1.0010	0.284	0.630	1.0009	0.164	0.809	0.754	1.0000
3	1.0012	0.279	0.634	1.0009	0.169	0.807	0.753	1.0000
4	0.9999	0.274	0.639	0.9997	0.175	0.805	0.752	1.0000
6	0.9891	0.265	0.646	0.9893	0.184	0.802	0.752	1.0000
12	0.8602	0.246	0.661	0.8682	0.202	0.794	0.752	1.0000
20	0.5777	0.234	0.670	0.6018	0.210	0.790	0.755	1.0000
∞	0.0000	0.210	0.688	0.0000	0.219	0.781	0.768	1.0000

NOTE: The boxes enclose the minimum values at each n.

This work was supported in part by a grant from the National Science Foundation. The computations were done on the Control Data 1604 computer at the Numerical Analysis Center of the University of Minnesota.

1. R. J. GILLESPIE. Can. J. Chem. **38**, 818 (1960).

RECEIVED FEBRUARY 5, 1963.
DEPARTMENT OF CHEMISTRY,
UNIVERSITY OF MINNESOTA,
MINNEAPOLIS 14, MINNESOTA.

THE BENZOYLOXY GROUP OF ACONITINE*

Y. TSUDA† AND LÉO MARION

Although the structure of aconitine shown in the accompanying formula has been well established (1, 2), the position of the benzoyl ester group is perhaps less rigorously demonstrated than the rest of the structure.

*Issued as N.R.C. No. 7300.
†National Research Council of Canada Postdoctoral Fellow.

Can. J. Chem. Downloaded from www.nrcresearchpress.com by 210.87.254.6 on 09/05/12
For personal use only.

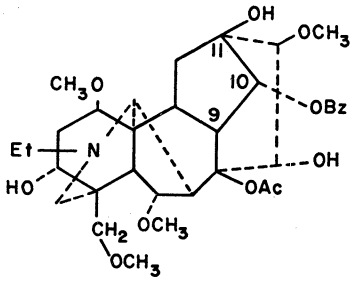

We wish to report n.m.r. evidence that favors the assignment of the benzoyloxy group at C-10 and its orientation (3).

All the alkaloids listed in Table I show in their n.m.r. spectra a doublet at $\delta \sim 4.9$, $J = 4.5$ c/s, corresponding to one proton. The doublet is at lowest field except for the

TABLE I

Nuclear magnetic resonance spectra*

	—OCOCH$_3$, δ	H —C—OCOAr, δ	J, c/s
Aconitine	1.39	4.89	4.5
Indaconitine	1.29	4.92	4.5
Pseudaconitine	1.33	4.87	4.5
Delphinine	1.28	4.92	4.5
Bikhaconitine†	1.30	4.87	4.5

*All spectra were taken in $CDCl_3$ solution, with tetramethylsilane as internal reference, on an A-60 instrument. Chemical shifts designated by $\delta = 10 - \tau$.
†The structure of bikhaconitine will be reported in a forthcoming publication.

aromatic protons. This signal must be attributable to a proton attached to a carbon carrying an ester group since it is no longer present in the spectra of the corresponding alkamines. Since the acetoxy group is known to be attached to a quaternary carbon next to a free secondary hydroxyl (4) the signal must be due to a proton attached to the same carbon as the aromatic ester group, and the splitting caused by a neighboring proton. This condition is fulfilled if the aromatic ester group is located at C-10 in which case there is a neighboring proton at C-9 and none at C-11, but would not hold were the aroyloxy group located at C-11, the only other possible position.

It is noteworthy that the magnitude of the coupling constant is in excellent agreement with the assigned configuration of the benzoate group. Dreiding models indicate an H—H dihedral angle of ca. 40° while the dihedral angle for the structure epimeric at C-10 is 80°. According to Karplus (5) $J_{40°}$ is ca. 4 c/s and $J_{80°}$ ca. 0 c/s.

The acetyl group protons in the spectra of the alkaloids listed show signals at unusually high field ($\delta \sim 1.3$). The shift is not due only to the tertiary nature of the acetyl group (cf. *tert*-butyl acetate, $\delta \sim 1.97$), nor is it due only to the ionic nature of the acetoxy group (cf. sodium acetate, $\delta \sim 1.80$).* The signal is shifted back to the usual position in tetraacetylpseudaconine and triacetylbikhaconine ($\delta \sim 1.96$).

The only plausible explanation of this marked shift is that the methyl protons in the acetoxy group come within the shielding range of the aromatic nucleus, and the strongly

**Measured in* D_2O *with tetramethylsilane as an external reference.*

Can. J. Chem. Downloaded from www.nrcresearchpress.com by 210.87.254.6 on 09/05/12
For personal use only.

anisotropic effect of the aromatic group causes large high-field shifts. This condition is satisfied when the aromatic ester group in the alkaloids is located at C-10, and possesses the configuration already assigned (6). In such an orientation the free rotation of the aromatic ester group is restricted. Since four of the alkaloids listed in the table have previously been correlated (6), it can be concluded that in these the position of the aromatic ester group and its orientation are the same.

1. M. PRZYBYLSKA and L. MARION. Can. J. Chem. **37**, 1843 (1959).
2. K. WIESNER, M. GÖTZ, D. L. SIMMONS, L. R. FOWLER, F. W. BACHELOR, R. F. C. BROWN, and G. BÜCHI. Tetrahedron Letters, No. 2, 15 (1959).
3. K. WIESNER, D. L. SIMMONS, and R. H. WIGHTMAN. Tetrahedron Letters, No. 15, 23 (1960).
4. D. J. MCCALDIN and L. MARION. Can. J. Chem. **37**, 1071 (1959).
5. M. KARPLUS. J. Chem. Phys. **30**, 11 (1959).
6. Y. TSUDA and L. MARION. Can. J. Chem. This issue.

RECEIVED JANUARY 31, 1963.
DIVISION OF PURE CHEMISTRY,
NATIONAL RESEARCH COUNCIL,
OTTAWA, CANADA.

Can. J. Chem. Downloaded from www.nrcresearchpress.com by 210.87.254.6 on 09/05/12
For personal use only.

POLAROGRAPHY OF 8-HYDROXYQUINALDINE

A. CORSINI AND R. P. GRAHAM

This note is concerned with the polarographic behavior of 8-hydroxyquinaldine (2-methyloxine), particularly in strongly basic solutions. The reduction process is shown to involve one electron and one hydrogen ion, the species undergoing reduction probably being the 2-methyloxine anion. The polarography of this reagent is favorable to its use for the indirect polarographic determination of metal ions.

EXPERIMENTAL

Apparatus

Polarographic measurements were made at 25.5±0.1° C using a pen-recording polarograph (Type 14/3, Tinsley Industrial Instruments, Ltd., London, England). Two capillaries were used; in 0.10 *M* potassium chloride on open circuit, their characteristics were: t = 7.67 sec and m = 0.956 mg/sec; t = 4.82 sec and m = 1.616 mg/sec. Under experimental conditions, at high negative potentials, t was reduced to 3–4 sec. A conventional H-type cell with a saturated calomel electrode was used for investigations of the polarographic behavior of 2-methyloxine.

Measurements of pH were made as described elsewhere (1).

Reagents

The 2-methyloxine and thorium nitrate were obtained as previously reported (1). All other chemicals were analyzed grade.

Polarography of 2-Methyloxine

Polarograms were recorded from aqueous solutions (pH 2.6–14.2) that were 7.0×10^{-4} *M* with respect to 2-methyloxine. Potassium hydrogen phthalate, potassium dihydrogen phosphate, boric acid, and disodium hydrogen phosphate (all examined polarographically for reducible impurities) were used to obtain pH values < 13; for values > 13, the 2-methyloxine was dissolved in 0.5–1.5 *M* sodium hydroxide.

In experiments having to do with the current as a function of the pressure of mercury in the capillary, h_e was varied from 20 to 65 cm.

Polarographic Determination of Thorium

The washed precipitate of the thorium 2-methyloxinate, $Th(C_{10}H_8ON)_4$, obtained as described elsewhere (1), was treated with hot 1.0 *M* sodium hydroxide, which metathesized it to hydrous thoria, freeing 2-methyloxine anion equivalent to the thorium. The solution of this passed through the filter, and was diluted to

anisotropic effect of the aromatic group causes large high-field shifts. This condition is satisfied when the aromatic ester group in the alkaloids is located at C-10, and possesses the configuration already assigned (6). In such an orientation the free rotation of the aromatic ester group is restricted. Since four of the alkaloids listed in the table have previously been correlated (6), it can be concluded that in these the position of the aromatic ester group and its orientation are the same.

1. M. PRZYBYLSKA and L. MARION. Can. J. Chem. **37**, 1843 (1959).
2. K. WIESNER, M. GÖTZ, D. L. SIMMONS, L. R. FOWLER, F. W. BACHELOR, R. F. C. BROWN, and G. BÜCHI. Tetrahedron Letters, No. 2, 15 (1959).
3. K. WIESNER, D. L. SIMMONS, and R. H. WIGHTMAN. Tetrahedron Letters, No. 15, 23 (1960).
4. D. J. MCCALDIN and L. MARION. Can. J. Chem. **37**, 1071 (1959).
5. M. KARPLUS. J. Chem. Phys. **30**, 11 (1959).
6. Y. TSUDA and L. MARION. Can. J. Chem. This issue.

RECEIVED JANUARY 31, 1963.
DIVISION OF PURE CHEMISTRY,
NATIONAL RESEARCH COUNCIL,
OTTAWA, CANADA.

Can. J. Chem. Downloaded from www.nrcresearchpress.com by 210.87.254.5 on 09/05/12
For personal use only.

POLAROGRAPHY OF 8-HYDROXYQUINALDINE

A. CORSINI AND R. P. GRAHAM

This note is concerned with the polarographic behavior of 8-hydroxyquinaldine (2-methyloxine), particularly in strongly basic solutions. The reduction process is shown to involve one electron and one hydrogen ion, the species undergoing reduction probably being the 2-methyloxine anion. The polarography of this reagent is favorable to its use for the indirect polarographic determination of metal ions.

EXPERIMENTAL

Apparatus

Polarographic measurements were made at 25.5±0.1° C using a pen-recording polarograph (Type 14/3, Tinsley Industrial Instruments, Ltd., London, England). Two capillaries were used; in 0.10 *M* potassium chloride on open circuit, their characteristics were: t = 7.67 sec and m = 0.956 mg/sec; t = 4.82 sec and m = 1.616 mg/sec. Under experimental conditions, at high negative potentials, t was reduced to 3–4 sec. A conventional H-type cell with a saturated calomel electrode was used for investigations of the polarographic behavior of 2-methyloxine.

Measurements of pH were made as described elsewhere (1).

Reagents

The 2-methyloxine and thorium nitrate were obtained as previously reported (1). All other chemicals were analyzed grade.

Polarography of 2-Methyloxine

Polarograms were recorded from aqueous solutions (pH 2.6–14.2) that were 7.0×10^{-4} *M* with respect to 2-methyloxine. Potassium hydrogen phthalate, potassium dihydrogen phosphate, boric acid, and disodium hydrogen phosphate (all examined polarographically for reducible impurities) were used to obtain pH values < 13; for values > 13, the 2-methyloxine was dissolved in 0.5–1.5 *M* sodium hydroxide.

In experiments having to do with the current as a function of the pressure of mercury in the capillary, h_e was varied from 20 to 65 cm.

Polarographic Determination of Thorium

The washed precipitate of the thorium 2-methyloxinate, $Th(C_{10}H_8ON)_4$, obtained as described elsewhere (1), was treated with hot 1.0 *M* sodium hydroxide, which metathesized it to hydrous thoria, freeing 2-methyloxine anion equivalent to the thorium. The solution of this passed through the filter, and was diluted to

volume with 1.0 M sodium hydroxide. The resultant solution (pH 14) was polarographed and, from the measured diffusion current and an appropriate calibration curve, the concentration of thorium in the original solution was assessed.

An excellent straight-line calibration curve was obtained for concentrations of thorium (in the original solution) over the 50-fold range from 6×10^{-5} to 3×10^{-3} M (corresponding to concentrations of 2-methyloxine, in the solution polarographed, of 1.2×10^{-4} to 6×10^{-3} M).

RESULTS AND DISCUSSION

We confirmed the observation (2) that the nature of the polarographic wave due to 2-methyloxine is markedly dependent on the pH of the solution, as indeed is so with oxine itself (3). At pH values below about 11, the shapes of the waves suggest complex reduction processes, all too common with heterocyclic nitrogen compounds (4).

Measurements of $i/h_e^{\frac{1}{2}}$ at six pH values in the range 7.6–14.2 were constant at each pH, indicating that the current is diffusion controlled throughout this range. The half-wave potential ($E_{\frac{1}{2}}$) becomes increasingly negative with increasing pH, indicating a reduction process involving hydrogen ions. The relationship between $E_{\frac{1}{2}}$ and pH is linear (at least over the pH range 11.2–14.2): $-E_{\frac{1}{2}} = 0.98+0.061$ pH. The slope of the line is in good agreement with that (0.059) for an electrode reaction involving hydrogen ions and electrons in equal numbers. (Other workers (2) have found 0.084 for the slope.) Plots of E_{de} vs. log $(i/(i_d-i))$ for five pH values in this range were linear, with slopes 0.055 ± 0.002, a value corresponding to that for a reversible electrode reaction involving one electron.

The one-electron, one-hydrogen-ion process in solutions of pH 11 and higher likely represents the reduction of the 2-methyloxine anion (2-methyloxine being substantially fully dissociated at pH $\geqslant$ 11) to a free radical such as:

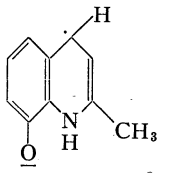

which undergoes dimerization or disproportionation. A reversible one-electron reaction, involving one hydrogen ion, to a free radical has been proposed (3) for the reduction of oxine at pH $\sim$ 10.

The diffusion coefficient of the 2-methyloxine anion, calculated from the Ilkovic equation using the diffusion currents at pH 11.2 and 12.6 ($\mu \simeq 0.2$–0.3), appropriately determined values of m and t, and taking $n = 1$, was $0.62\pm0.02\times10^{-5}$ cm²/sec. This may be compared with the value 0.80×10^{-5} cm²/sec, calculated (5) from equivalent conductance data, for the anion of quinaldinic acid at 25° C.

The waves obtained from solutions of pH < 11 are complex and resist analysis. Down to pH 7.6 at least, the current is diffusion controlled, and increases with decreasing pH. Some evidence was obtained that at pH 7.6 the reduction process involves two electrons: here, at the ionic strength of the solution, the reagent is largely (98.5%) in the form of undissociated 2-methyloxine (6), and the reduction may be that of the molecule to a dihydro derivative such as 1,4-dihydro-8-hydroxyquinaldine.

The form of the wave obtained from solutions of 2-methyloxine at pH 14 is excellent for analytical purposes, being similar to that of m-nitrobenzoic acid (7), which has been recommended for the indirect polarographic determination of thorium. The diffusion current of 2-methyloxine (or, rather, its anion) is directly proportional to the concentration of reagent, and is not significantly altered by changes in the concentration of

Can. J. Chem. Downloaded from www.nrcresearchpress.com by 210.87.254.5 on 09/05/12
For personal use only.

sodium hydroxide from 0.5 M to 1.5 M; these solutions are polarographically stable for at least 45 hours.

Suitable experiments proved that the decomposition of the thorium 2-methyloxinate with hot sodium hydroxide, and the separation of the organic anion from the hydrous thoria, are strictly quantitative. The precision of the polarographic method varies from $\pm 1\%$ (for a thorium concentration of 3×10^{-3} M) to $\pm 8\%$ (for a concentration of 6×10^{-5} M, or 14 p.p.m.).

This method is of course one for determining 2-methyloxine, and is therefore applicable to any metal ion that can be quantitatively precipitated by this reagent as a compound of reproducible stoichiometry. The method is particularly applicable to thorium, which does not lend itself to direct polarographic determination.

ACKNOWLEDGMENTS

This work was part of a project supported by the National Research Council of Canada and the International Nickel Company of Canada, Ltd. We also acknowledge the assistance of Mr. E. E. Wigg with some of the experimental work.

1. A. Corsini and R. P. Graham. Anal. Chim. Acta, **23**, 248 (1960).
2. Q. Fernando and J. P. Phillips. J. Am. Chem. Soc. **74**, 3103 (1952).
3. J. T. Stock. J. Chem. Soc. 586 (1949).
4. G. W. C. Milner. The principles and applications of polarography and other electroanalytical processes. Longmans, Green and Co., London. 1957. pp. 580–595.
5. J. T. Stock. J. Chem. Soc. 427 (1944).
6. R. Näsänen. Soumen Kemistilehti, B, **28**, 123 (1955).
7. R. P. Graham and G. B. Larrabee. Analyst, **82**, 415 (1957).

Received December 28, 1962.
Burke Chemical Laboratories,
McMaster University,
Hamilton, Ontario.

Can. J. Chem. Downloaded from www.nrcresearchpress.com by 210.87.254.5 on 09/05/12
For personal use only.

ORGANIC PEROXIDES
VII. OXIDATION OF PHENYLHYDRAZONES WITH BENZOYL PEROXIDE

J. T. Edward and S. A. Samad*

Benzoyl peroxide reacts with aromatic secondary amines to give *o*-benzamidophenols (1) and consequently was expected to react with benzophenone phenylhydrazone (I) to give the phenol VI.

However, the product of the reaction was not a phenol but a neutral yellow solid $C_{26}H_{20}N_2O_2$ having an absorption spectrum (λ_{max} 271 mμ, ϵ_{max} 8030; λ_{max} 400 mμ, ϵ_{max} 222, in ethanol: Fig. 1) characteristic of a phenylazo chromophore (2, 3). Recently Iffland and his colleagues have reported the preparation of phenylazodiphenylcarbinol benzoate (IV) from the reaction of benzophenone phenylhydrazone with lead tetrabenzoate (4), and comparison of a sample of this compound, kindly sent to us by Professor Iffland, with our own compound established their identity.† The mechanism (I → II → III → IV)

Holder of Colombo Plan fellowship, 1957–1960.

†Professor Iffland informs us that he also has established the identity of the products obtained from the reaction of benzophenone phenylhydrazone with lead tetrabenzoate and with benzoyl peroxide by a comparison of their infrared spectra, without isolating the product of the latter reaction.

sodium hydroxide from 0.5 M to 1.5 M; these solutions are polarographically stable for at least 45 hours.

Suitable experiments proved that the decomposition of the thorium 2-methyloxinate with hot sodium hydroxide, and the separation of the organic anion from the hydrous thoria, are strictly quantitative. The precision of the polarographic method varies from $\pm 1\%$ (for a thorium concentration of 3×10^{-3} M) to $\pm 8\%$ (for a concentration of 6×10^{-5} M, or 14 p.p.m.).

This method is of course one for determining 2-methyloxine, and is therefore applicable to any metal ion that can be quantitatively precipitated by this reagent as a compound of reproducible stoichiometry. The method is particularly applicable to thorium, which does not lend itself to direct polarographic determination.

ACKNOWLEDGMENTS

This work was part of a project supported by the National Research Council of Canada and the International Nickel Company of Canada, Ltd. We also acknowledge the assistance of Mr. E. E. Wigg with some of the experimental work.

1. A. Corsini and R. P. Graham. Anal. Chim. Acta, **23**, 248 (1960).
2. Q. Fernando and J. P. Phillips. J. Am. Chem. Soc. **74**, 3103 (1952).
3. J. T. Stock. J. Chem. Soc. 586 (1949).
4. G. W. C. Milner. The principles and applications of polarography and other electroanalytical processes. Longmans, Green and Co., London. 1957. pp. 580–595.
5. J. T. Stock. J. Chem. Soc. 427 (1944).
6. R. Näsänen. Soumen Kemistilehti, B, **28**, 123 (1955).
7. R. P. Graham and G. B. Larrabee. Analyst, **82**, 415 (1957).

Received December 28, 1962.
Burke Chemical Laboratories,
McMaster University,
Hamilton, Ontario.

Can. J. Chem. Downloaded from www.nrcresearchpress.com by 210.87.254.40 on 09/05/12
For personal use only.

ORGANIC PEROXIDES
VII. OXIDATION OF PHENYLHYDRAZONES WITH BENZOYL PEROXIDE

J. T. Edward and S. A. Samad*

Benzoyl peroxide reacts with aromatic secondary amines to give *o*-benzamidophenols (1) and consequently was expected to react with benzophenone phenylhydrazone (I) to give the phenol VI.

However, the product of the reaction was not a phenol but a neutral yellow solid $C_{26}H_{20}N_2O_2$ having an absorption spectrum (λ_{max} 271 mμ, ϵ_{max} 8030; λ_{max} 400 mμ, ϵ_{max} 222, in ethanol: Fig. 1) characteristic of a phenylazo chromophore (2, 3). Recently Iffland and his colleagues have reported the preparation of phenylazodiphenylcarbinol benzoate (IV) from the reaction of benzophenone phenylhydrazone with lead tetrabenzoate (4), and comparison of a sample of this compound, kindly sent to us by Professor Iffland, with our own compound established their identity.† The mechanism (I $\rightarrow$ II $\rightarrow$ III $\rightarrow$ IV)

Holder of Colombo Plan fellowship, 1957–1960.

†*Professor Iffland informs us that he also has established the identity of the products obtained from the reaction of benzophenone phenylhydrazone with lead tetrabenzoate and with benzoyl peroxide by a comparison of their infrared spectra, without isolating the product of the latter reaction.*

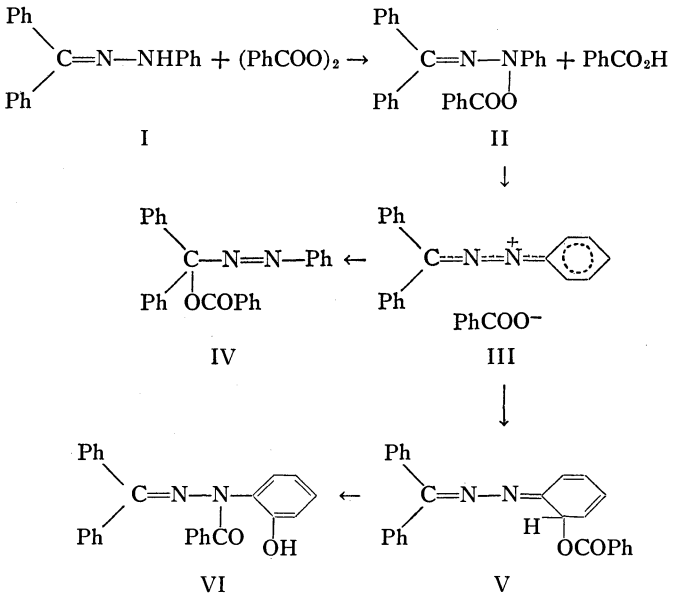

I II III IV V VI

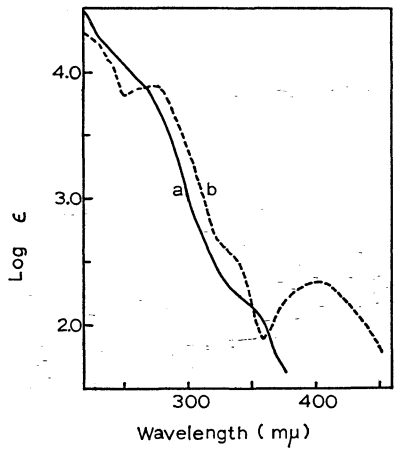

FIG. 1. Ultraviolet absorption of compounds produced by the reaction of benzoyl peroxide with (*a*) benzaldehyde phenylhydrazone, (*b*) benzophenone phenylhydrazone.

shown above seems likely from the studies of Denney and Denney (5) on the reaction of benzoyl peroxide with secondary amines. The reaction of the ion pair III to give the phenylazo benzoate (IV) rather than the phenol (VI) is probably a consequence of the higher activation energy which would be required in the step III → V leading to the phenol, since in this step a benzenoid is converted into a quinonoid compound.

The reaction of benzaldehyde phenylhydrazone (VII) with benzoyl peroxide gave a compound which was not phenolic and which lacked a phenylazo chromophore (Fig. 1). Its infrared spectrum showed peaks (at 3420 and 1670 cm^{-1}) indicative of an amide grouping (6), and it was identified as α,β-dibenzoylphenylhydrazine (XI) by comparison with an authentic sample prepared by benzoylation of phenylhydrazine hydrochloride in boiling benzene (7). It seems likely that initially the phenylazo compound (VIII) is

Can. J. Chem. Downloaded from www.nrcresearchpress.com by 210.87.254.40 on 09/05/12
For personal use only.

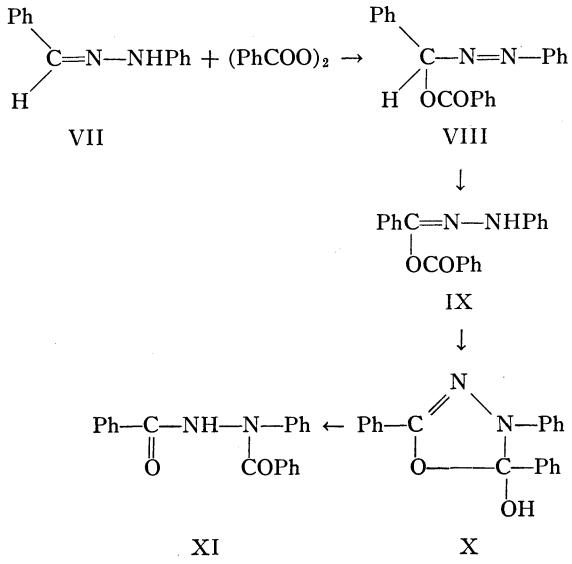

formed, but that in the presence of benzoic acid it rearranges as shown. Ample analogy is found in the literature for the tautomerization of the azo compound (VIII → IX) (3) and for the subsequent migration of the benzoyl group from oxygen to nitrogen via a cyclic intermediate (IX → X → XI) (8).

EXPERIMENTAL

Reaction of Benzoyl Peroxide with Benzaldehyde Phenylhydrazone

Benzoyl peroxide (12.3 g) was added to a solution of benzaldehyde phenylhydrazone (10 g) in benzene (125 ml), and the mixture was left at room temperature overnight. The benzene solution was then extracted with aqueous sodium bicarbonate to remove benzoic acid (6.3 g), washed with water, dried, and allowed to evaporate slowly. A crop of crystalline material (4.45 g; 27% yield) was obtained, and on complete evaporation, a tarry solid (8.5 g). The latter was chromatographed on alumina; elution with benzene–ether gave more crops of crystalline material (4.15 g; 25%). This material on recrystallization from ethanol was obtained as colorless needles, m.p. 181°, undepressed by admixture with authentic α,β-dibenzoylphenylhydrazine (reported m.p. 180° (7)), and having the same infrared spectrum: $\nu_{max}^{CHCl_3}$ 3420 m, 1672 s, 1600 m, 1585 m, 1470 m, 1420 m, 1345 s, 1306 m, 1078 w, 1075 w, 1027 w, 925 w, 732 w cm^{-1}.

Reaction of Benzoyl Peroxide with Benzophenone Phenylhydrazone

A mixture of benzophenone phenylhydrazone (6.0 g) and benzoyl peroxide (5.32 g) in benzene (50 ml) was stirred for 3 hours and then left overnight. After removal of benzoic acid (2.37 g), the benzene solution was washed with water, dried, and evaporated. The gummy residue crystallized from ethanol in yellow needles (5.43 g; 63%), m.p. 147°, raised to 149–152° (melting with gassing)* by recrystallization; this melting point was undepressed by admixture of the material with authentic phenylazodiphenylcarbinol benzoate (4). Calc. for $C_{26}H_{20}N_2O_2$: C, 79.59; H, 5.10; N, 7.14%. Found: C, 79.57; H, 5.15; N, 7.31%. Infrared spectrum: $\nu_{max}^{CCl_4}$ 3090 m, 1743 s, 1498 m, 1457 s, 1318 m, 1270 s, 1177 s, 1090 s, 1067 m, 914 w, 687 s.

The phenylazo benzoate (2.1 g), after hydrolysis with potassium hydroxide (5 g) in refluxing methanol–water (10:1 v/v; 165 ml) for 4 hours, gave benzophenone (isolated in 54% yield as its 2,4-dinitrophenylhydrazone, m.p. 236°) and benzoic acid (85% yield) (cf. ref. 4).

ACKNOWLEDGMENTS

We are grateful to Professor D. C. Iffland for a sample of phenylazodiphenylcarbinol benzoate and for helpful correspondence, and the National Research Council for financial support.

**Iffland and co-workers (4) report a melting point of 159–161°; however, later preparations showed a melting point of 150–152°, possibly because of polymorphism (D. C. Iffland. Private communication).*

Can. J. Chem. Downloaded from www.nrcresearchpress.com by 210.87.254.40 on 09/05/12
For personal use only.

1. S. GAMBARAJAN. Ber. **42**, 4003 (1909). J. T. EDWARD. J. Chem. Soc. 1464 (1954). L. HORNER and W. KIRMSE. Ann. **597**, 66 (1955).
2. W. HEROLD. Z. Physik. Chem. Sect. B, **18**, 277 (1932).
3. R. O'CONNOR. J. Org. Chem. **26**, 4375 (1961).
4. D. C. IFFLAND, L. SALISBURY, and W. R. SCHAFER. J. Am. Chem. Soc. **83**, 747 (1961).
5. D. B. DENNEY and D. Z. DENNEY. J. Am. Chem. Soc. **82**, 1389 (1960).
6. L. J. BELLAMY. The infrared spectra of complex molecules. John Wiley and Sons Inc., New York. 1958. p. 205.
7. H. FRANZEN. Ber. **42**, 2465 (1909).
8. W. BOTTCHER. Ber. **16**, 629 (1883). A. EINHORN and B. PFYL. Ann. 311, 34 (1900). K. AUWERS. Ann. **332**, 159 (1904). M. BERGMAN, R. ULPTS, and F. CAMACHO. Ber. **55**, 2796 (1922).

RECEIVED JANUARY 28, 1963.
DEPARTMENT OF CHEMISTRY,
MCGILL UNIVERSITY,
MONTREAL 2, QUE.

Can. J. Chem. Downloaded from www.nrcresearchpress.com by 210.87.254.40 on 09/05/12
For personal use only.

IONIZATION OF DEUTERATED ALCOHOLS IN ACID SOLUTION

MICHAEL M. MOCEK AND ROSS STEWART

We wish to report the effect of α-deuterium substitution on the ionization of 4,4′-disubstituted benzhydrols.*

$$Ar_2CHOH + H^+ \rightleftharpoons Ar_2CH^+ + H_2O \qquad K_H$$
$$Ar_2CDOH + H^+ \rightleftharpoons Ar_2CD^+ + H_2O \qquad K_D$$

The pK_{R^+} values for the alcohols are listed in Table I together with the stretching frequencies and the unobscured bending frequencies of the C—H and C—D bonds and the ultraviolet data for the cations. The sign of the isotope effects and their magnitude are

TABLE I

Ionization and spectral data for diarylmethyl cations at 25° in aqueous sulphuric acid

$(YC_6H_4)_2CZ^+$						
Y	Z	λ_{max} (mμ)	ϵ_{max}	$-pK_{R^+}$ (3)	K_H/K_D	Vibrational frequencies in corresponding carbinol (cm^{-1})
H	H	442		13.25	1.29	
H	D	442		13.36		2130, 998
Cl	H	483	110,000	13.97	1.35	1350
Cl	D	483	108,100	14.10		2140, 1000
CH_3	H	468	86,800	10.31	1.20	1357
CH_3	D	468	72,000	10.39		2150, 1002
CH_3O	H	504	116,200	5.85	1.18	1364
CH_3O	D	504	106,700	5.92		2138, 1004
C_2H_5O	H	505	127,000		1.17	
C_2H_5O	D	505				
$(CH_3)_2N$	H	605*	17,000*			(1400)
$(CH_3)_2N$	D	605*	14,500*			2120, 995
$(CH_3)_2N$	H	608†	156,500†		1.03†	
$(CH_3)_2N$	D	608†	156,500†			
NO_2‡	H	356	28,900	12.18§		

*5% acetone – 95% aqueous acetate buffer, carbonium ion formation incomplete.
†99% acetone – 1% aqueous sulphuric acid.

‡Protonates at nitro; structure of cation is $(HO_2\overset{+}{N}C_6H_4)_2CHOH$ (or possibly $(HO_2\overset{+}{N}C_6H_4)(O_2NC_6H_4)CHOH$).
§ $-pK_{BH^+}$.

**A preliminary account of part of this work appeared in a paper by Stewart et al. (1).*

1. S. GAMBARAJAN. Ber. **42**, 4003 (1909). J. T. EDWARD. J. Chem. Soc. 1464 (1954). L. HORNER and W. KIRMSE. Ann. **597**, 66 (1955).
2. W. HEROLD. Z. Physik. Chem. Sect. B, **18**, 277 (1932).
3. R. O'CONNOR. J. Org. Chem. **26**, 4375 (1961).
4. D. C. IFFLAND, L. SALISBURY, and W. R. SCHAFER. J. Am. Chem. Soc. **83**, 747 (1961).
5. D. B. DENNEY and D. Z. DENNEY. J. Am. Chem. Soc. **82**, 1389 (1960).
6. L. J. BELLAMY. The infrared spectra of complex molecules. John Wiley and Sons Inc., New York. 1958. p. 205.
7. H. FRANZEN. Ber. **42**, 2465 (1909).
8. W. BOTTCHER. Ber. **16**, 629 (1883). A. EINHORN and B. PFYL. Ann. 311, 34 (1900). K. AUWERS. Ann. **332**, 159 (1904). M. BERGMAN, R. ULPTS, and F. CAMACHO. Ber. **55**, 2796 (1922).

RECEIVED JANUARY 28, 1963.
DEPARTMENT OF CHEMISTRY,
MCGILL UNIVERSITY,
MONTREAL 2, QUE.

Can. J. Chem. Downloaded from www.nrcresearchpress.com by 210.87.254.5 on 09/05/12
For personal use only.

IONIZATION OF DEUTERATED ALCOHOLS IN ACID SOLUTION

MICHAEL M. MOCEK AND ROSS STEWART

We wish to report the effect of α-deuterium substitution on the ionization of 4,4′-disubstituted benzhydrols.*

$$Ar_2CHOH + H^+ \rightleftharpoons Ar_2CH^+ + H_2O \qquad K_H$$
$$Ar_2CDOH + H^+ \rightleftharpoons Ar_2CD^+ + H_2O \qquad K_D$$

The pK_{R^+} values for the alcohols are listed in Table I together with the stretching frequencies and the unobscured bending frequencies of the C—H and C—D bonds and the ultraviolet data for the cations. The sign of the isotope effects and their magnitude are

TABLE I

Ionization and spectral data for diarylmethyl cations at 25° in aqueous sulphuric acid

$(YC_6H_4)_2CZ^+$						Vibrational frequencies in corresponding carbinol (cm^{-1})
Y	Z	λ_{max} ($m\mu$)	ϵ_{max}	$-pK_{R^+}$ (3)	K_H/K_D	
H	H	442		13.25	1.29	
H	D	442		13.36		2130, 998
Cl	H	483	110,000	13.97	1.35	1350
Cl	D	483	108,100	14.10		2140, 1000
CH_3	H	468	86,800	10.31	1.20	1357
CH_3	D	468	72,000	10.39		2150, 1002
CH_3O	H	504	116,200	5.85	1.18	1364
CH_3O	D	504	106,700	5.92		2138, 1004
C_2H_5O	H	505	127,000		1.17	
C_2H_5O	D	505				
$(CH_3)_2N$	H	605*	17,000*			(1400)
$(CH_3)_2N$	D	605*	14,500*			2120, 995
$(CH_3)_2N$	H	608†	156,500†		1.03†	
$(CH_3)_2N$	D	608†	156,500†			
NO_2‡	H	356	28,900	12.18§		

*5% acetone – 95% aqueous acetate buffer, carbonium ion formation incomplete.
†99% acetone – 1% aqueous sulphuric acid.
‡Protonates at nitro; structure of cation is $(HO_2\overset{+}{N}C_6H_4)_2CHOH$ (or possibly $(HO_2\overset{+}{N}C_6H_4)(O_2NC_6H_4)CHOH$).
§ $-pK_{BH^+}$.

**A preliminary account of part of this work appeared in a paper by Stewart et al. (1).*

similar to that observed in the solvolysis of α-deuteroalkyl tosylates (2). In both cases the deuterated carbon undergoes a change from tetragonal towards trigonal hybridization as the reaction proceeds.

Electron-withdrawing groups in the aromatic rings appear to cause an increase in the size of the isotope effect. Unfortunately, nitro substituents which should reveal such an effect most clearly cause an unexpected change in the course of the reaction. They so depress the tendency of the alcohol group to ionize that the acid–base equilibrium which is actually set up is protonation of the nitro group itself. This is revealed by the changes which occur in the ultraviolet spectrum as the medium is made more acidic. Instead of a strong absorption band in the visible, which all diarylcarbonium ions exhibit (and which 4,4′,4″-tris(nitrophenyl)methylium ion exhibits (3)), the 4,4′-dinitrobenzhydrol cation is formed with a relatively small spectral change (λ_{max} = 289 mμ in 95% H_2SO_4 and 346 mμ in fuming 40% H_2SO_4) and is half formed in about 102.5% sulphuric acid. Nitrobenzene (λ_{max} = 286 mμ in 95% H_2SO_4) is half protonated in 100.1% sulphuric acid and the cation absorbs at about 350 mμ (4).

The isotope effect listed for Michler's Hydrol, 4,4′-bis(dimethylamino)benzhydrol, was obtained in acetone solution and it should be regarded as approximate only. The difficulty with this compound lies in its complex ionization pattern, in which nitrogen protonation competes with carbonium ion formation. In aqueous solution the maximum extinction coefficient obtained for the carbonium ion shows that the following equilibrium is well to the right:

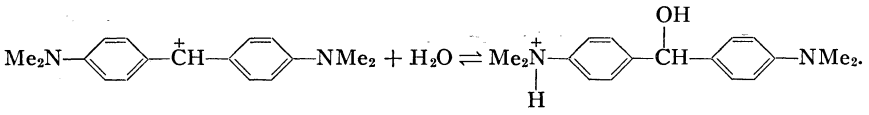

In acetone solution the equilibrium shifts toward the left as expected (5).

It is interesting that the only ring substituents which cause protonation of the benzhydrol at the substituent in preference to carbonium ion formation at the carbinol are nitro and dimethylamino, two groups which usually differ widely in behavior.

EXPERIMENTAL

Materials

The alcohols were prepared by reduction of the corresponding ketones with $LiAlH_4$ or $LiAlD_4$ essentially as previously described (6). The absence of the α-proton signal in the n.m.r. spectra of several of the alcohols was taken as indication of high isotopic purity.

pK_{R^+} Determination

The ionization constants of the alcohols were determined in sulphuric acid as before (7), the extinction coefficients at complete ionization being determined for both isotopic species. The fading of the carbonium ion color, which was slower for the deuterio ion in each case, required extrapolation to zero time in some cases when measurements near the pK were made.

Carbonium Salts

The perchlorate, fluoroborate, and hexachloroantimonate salts of several of the benzhydryl carbonium ions were prepared and their infrared spectra (mulls) examined. In all cases the intensities of the central C—H (or C—D) bands were too low to be detected. The hexachloroantimonate salt of benzhydrol can be conveniently prepared by simply mixing equivalent amounts of antimony pentachloride and benzhydryl chloride (each a 10% solution in carbon tetrachloride). The immediate yellow precipitate of the salt, $(C_6H_5)_2CH^+SbCl_6^-$, was stable for some time under carbon tetrachloride or even if kept "moist" with carbon tetrachloride. If the solid is "dried" completely, however, it begins almost at once to decompose to a brown tar.

Can. J. Chem. Downloaded from www.nrcresearchpress.com by 210.87.254.5 on 09/05/12
For personal use only.

1. R. STEWART, A. L. GATZKE, M. MOCEK, and K. YATES. Chem. Ind. (London), 331 (1959).
2. A. STREITWIESER, R. H. JAGOW, R. C. FAHEY, and S. SUZUKI. J. Am. Chem. Soc. **80**, 2326 (1958).
3. N. C. DENO, J. J. JARUZELSKI, and A. SCHRIESHEIM. J. Am. Chem. Soc. **77**, 3044 (1955).
4. J. C. D. BRAND. J. Chem. Soc. 997 (1950). J. C. D. BRAND, W. C. HORNING, and M. B. THORNLEY. J. Chem. Soc. 1374 (1952).
5. R. J. GOLDACRE and J. N. PHILLIPS. J. Chem. Soc. 1724 (1944). C. C. BARKER, G. HALLAS, and A. STAMP. J. Chem. Soc. 3790 (1960). S. F. MASON and R. GRINTER. *In* Steric effects in conjugated systems. *Edited by* G. W. Gray. Butterworths, Scientific Publications, London. 1958.
6. R. STEWART. J. Am. Chem. Soc. **79**, 3057 (1957).
7. R. STEWART and T. MATHEWS. Can. J. Chem. **38**, 602 (1960).

RECEIVED DECEMBER 26, 1962.
DEPARTMENT OF CHEMISTRY,
UNIVERSITY OF BRITISH COLUMBIA,
VANCOUVER 8, B.C.

Can. J. Chem. Downloaded from www.nrcresearchpress.com by 210.87.254.5 on 09/05/12
For personal use only.

5-(DISUBSTITUTED)AMINO-1,2,3,4-THIATRIAZOLES[1]

EUGENE LIEBER,[2] C. N. R. RAO,[3] C. B. LAWYER, AND J. P. TRIVEDI

Lieber and co-workers (1, 2) have synthesized 5-(monosubstituted)amino-1,2,3,4-thiatriazole derivatives (I) by the diazotization of 4-substituted thiosemicarbazides or by the addition of hydrazoic acid to organic isothiocyanates. The only 5-(disubstituted)amino derivative (III) that has been reported hitherto is that of the dimethyl derivative by Lieber *et al.*, synthesized by the diazotization of 4,4-dimethylthiosemicarbazide (1) and also by the reaction of dimethylamine with 5-chloro-1,2,3,4-thiatriazole (3). In this communication, we report the synthesis of 5-(disubstituted)amino-1,2,3,4-thiatriazoles (III) starting from N,N-disubstituted thiocarbamyl chlorides (II). Preliminary results on the relative thermal stabilities of some of these thiatriazole derivatives are also presented.

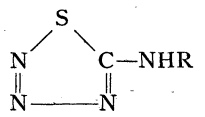

(I)

$R_1R_2NC(S)Cl$

(II)

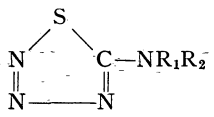

(III)

EXPERIMENTAL

N,N-Disubstituted Thiocarbamyl Chlorides (II)

In a three-necked flask equipped with a mechanical stirrer, a reflux condenser, and a dropping funnel were placed 0.2 mole of the secondary amine and 50 ml of anhydrous ether. The flask was immersed in an ice–salt–water bath. A solution of thiophosgene (0.1 mole) in 50 ml of anhydrous ether was slowly added from the dropping funnel, the reaction temperature being carefully kept below 5° C. The precipitation of amine hydrochloride was noticed immediately. Stirring was continued for about 45 minutes, at the end of which period the reaction mixture appeared oily. The precipitate of the amine hydrochloride formed in the flask was filtered off and the ethereal solution was concentrated. On cooling, pale yellow needles separated from the concentrate. Recrystallizations with chloroform and petroleum ether yielded colorless needles. Following this general procedure, the N,N-disubstituted thiocarbamyl chlorides (II) given in Table I were prepared.

[1]*This work was supported by Contract DA-44-009-ENG-4798, ERDL, Basic Research Group, Fort Belvoir, Virginia.*
[2]*To whom all the correspondence should be addressed, at the Department of Chemistry, Roosevelt University, Chicago 5, Illinois.*
[3]*Department of Physical Chemistry, Indian Institute of Science, Bangalore, India.*

1. R. STEWART, A. L. GATZKE, M. MOCEK, and K. YATES. Chem. Ind. (London), 331 (1959).
2. A. STREITWIESER, R. H. JAGOW, R. C. FAHEY, and S. SUZUKI. J. Am. Chem. Soc. **80**, 2326 (1958).
3. N. C. DENO, J. J. JARUZELSKI, and A. SCHRIESHEIM. J. Am. Chem. Soc. **77**, 3044 (1955).
4. J. C. D. BRAND. J. Chem. Soc. 997 (1950). J. C. D. BRAND, W. C. HORNING, and M. B. THORNLEY. J. Chem. Soc. 1374 (1952).
5. R. J. GOLDACRE and J. N. PHILLIPS. J. Chem. Soc. 1724 (1944). C. C. BARKER, G. HALLAS, and A. STAMP. J. Chem. Soc. 3790 (1960). S. F. MASON and R. GRINTER. *In* Steric effects in conjugated systems. *Edited by* G. W. Gray. Butterworths, Scientific Publications, London. 1958.
6. R. STEWART. J. Am. Chem. Soc. **79**, 3057 (1957).
7. R. STEWART and T. MATHEWS. Can. J. Chem. **38**, 602 (1960).

RECEIVED DECEMBER 26, 1962.
DEPARTMENT OF CHEMISTRY,
UNIVERSITY OF BRITISH COLUMBIA,
VANCOUVER 8, B.C.

Can. J. Chem. Downloaded from www.nrcresearchpress.com by 210.87.254.6 on 09/05/12
For personal use only.

5-(DISUBSTITUTED)AMINO-1,2,3,4-THIATRIAZOLES[1]

EUGENE LIEBER,[2] C. N. R. RAO,[3] C. B. LAWYER, AND J. P. TRIVEDI

Lieber and co-workers (1, 2) have synthesized 5-(monosubstituted)amino-1,2,3,4-thiatriazole derivatives (I) by the diazotization of 4-substituted thiosemicarbazides or by the addition of hydrazoic acid to organic isothiocyanates. The only 5-(disubstituted)amino derivative (III) that has been reported hitherto is that of the dimethyl derivative by Lieber *et al.*, synthesized by the diazotization of 4,4-dimethylthiosemicarbazide (1) and also by the reaction of dimethylamine with 5-chloro-1,2,3,4-thiatriazole (3). In this communication, we report the synthesis of 5-(disubstituted)amino-1,2,3,4-thiatriazoles (III) starting from N,N-disubstituted thiocarbamyl chlorides (II). Preliminary results on the relative thermal stabilities of some of these thiatriazole derivatives are also presented.

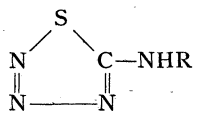

(I)

$R_1R_2NC(S)Cl$

(II)

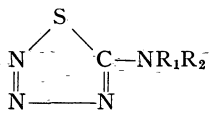

(III)

EXPERIMENTAL

N,N-Disubstituted Thiocarbamyl Chlorides (II)

In a three-necked flask equipped with a mechanical stirrer, a reflux condenser, and a dropping funnel were placed 0.2 mole of the secondary amine and 50 ml of anhydrous ether. The flask was immersed in an ice–salt–water bath. A solution of thiophosgene (0.1 mole) in 50 ml of anhydrous ether was slowly added from the dropping funnel, the reaction temperature being carefully kept below 5° C. The precipitation of amine hydrochloride was noticed immediately. Stirring was continued for about 45 minutes, at the end of which period the reaction mixture appeared oily. The precipitate of the amine hydrochloride formed in the flask was filtered off and the ethereal solution was concentrated. On cooling, pale yellow needles separated from the concentrate. Recrystallizations with chloroform and petroleum ether yielded colorless needles. Following this general procedure, the N,N-disubstituted thiocarbamyl chlorides (II) given in Table I were prepared.

[1]*This work was supported by Contract DA-44-009-ENG-4798, ERDL, Basic Research Group, Fort Belvoir, Virginia.*
[2]*To whom all the correspondence should be addressed, at the Department of Chemistry, Roosevelt University, Chicago 5, Illinois.*
[3]*Department of Physical Chemistry, Indian Institute of Science, Bangalore, India.*

TABLE I

R_1	R_2	% yield	M.p. (°C) Found	M.p. (°C) Lit.
CH_3	CH_3	43	41	41 (4)
C_2H_5	C_2H_5	58	45–46	46 (5)
CH_3	C_6H_5	38	34.5–35	35 (6)
C_2H_5	C_6H_5	60	56–57	57 (6)
$C_6H_5CH_2$	$C_6H_5CH_2$	50	49	49–50 (7)

5-(Disubstituted) amino-1,2,3,4-thiatriazoles (III)

A solution of 0.1 mole of sodium azide in 50 ml of water was placed in a three-necked flask fitted with a reflux condenser, a mechanical stirrer, and a dropping funnel. The flask was immersed in an ice–salt–water bath, and 0.05 mole of N,N-disubstituted thiocarbamyl chloride was added with stirring over a period of 30 minutes. The reaction mixture was kept for 12 to 24 hours at room temperature and was then extracted with ether. The ether layer was concentrated and the resulting solids were recrystallized from absolute ethanol. Following this procedure, the derivatives (III) given in Table II were prepared.

TABLE II

R_1	R_2	Yield	M.p. (°C)	% S Calc.	% S Found
CH_3	CH_3*	50	51	—	—
CH_3	C_6H_5†	45	56.5	16.60	16.30
C_2H_5	C_6H_5†	20	148.5–149	15.53	15.51
$C_6H_5CH_2$	$C_6H_5CH_2$†	50	89–90	11.30	11.40

*Lit. m.p. 49–51° C (1, 8).
†New compound.

Thermal Decomposition of 5-Substituted 1,2,3,4-Thiatriazoles

The thermal decompositions were studied by heating 0.0015 mole of thiatriazole admixed with sand at 90° C and measuring the nitrogen gas volumetrically at different intervals of time employing an apparatus similar to that described earlier (7, 9).

RESULTS AND DISCUSSION

A few 5-(disubstituted)amino-1,2,3,4-thiatriazoles (II) have been prepared by the reaction of N,N-disubstituted thiocarbamyl chlorides (III) with sodium azide.

Studies on the thermal decomposition of the 5-substituted 1,2,3,4-thiatriazoles have shown that the stability decreases in the order $N(CH_3)_2 > NH_2 > N(C_6H_5CH_2)_2 > C_6H_5NH > CH_3NH$.

1. E. Lieber, C. N. Pillai, and R. D. Hites. Can. J. Chem. **35**, 832 (1957).
2. E. Lieber and J. Ramachandran. Can. J. Chem. **37**, 101 (1959).
3. E. Lieber, C. B. Lawyer, and J. P. Trivedi. J. Org. Chem. **26**, 1644 (1961).
4. O. Billiter. Ber. **37**, 4319 (1904).
5. O. Billiter. Ber. **36**, 2274 (1903).
6. M. Mazzara. Gazz. Chim. Ital. **23**, 38 (1893).
7. R. C. Orlowski. M.S. Thesis, DePaul University, Chicago, Ill. 1960.
8. C. N. Pillai. M.S. Thesis, DePaul University, Chicago, Ill. 1958.
9. E. Lieber, C. N. R. Rao, and R. C. Orlowski. Can. J. Chem. **41**, 926 (1963).

Received February 8, 1963.
Departments of Chemistry,
Roosevelt University and DePaul University,
Chicago, Ill.

Can. J. Chem. Downloaded from www.nrcresearchpress.com by 210.87.254.6 on 09/05/12
For personal use only.

A SIMPLE METHOD FOR TRAPPING AND COLLECTING THE GASES NOT CONDENSABLE AT −196° IN A FAST-FLOWING, LOW-PRESSURE SYSTEM[1]

NICK DEMCHUK[2] AND H. GESSER

The separation and analysis of gases in a static system has been developed to the point of routine procedure (1). This includes gases not condensable in liquid nitrogen, such as N_2, CH_4, CO, O_2, and H_2 (2). Gas chromatography has now virtually eliminated such time consuming microanalysis. In a fast-flowing system under low pressures (about 1 mm of Hg) these gases, which are not condensable in liquid nitrogen, can be collected for analysis by sampling a small fraction of the flowing gas with a Toepler pump or a diffusion pump. This method was used by Jamieson and Winkler (3) for the mass spectrometric analysis of CH_4 and N_2 in a hydrogen flowing system. A novel method of collection was used by Versteeg (4), who collected the exhaust gases of the mechanical oil pump, and analysis for CH_4 and H_2 was possible in a nitrogen flowing system.

The use of silica gel as an adsorbing medium at low temperatures is well known but in a fast-flowing system the silica gel, when placed in appropriate traps, tends to restrict the flow of gas and alter the pressure in the reacting system (5). To overcome this difficulty, Steacie and Phillips (5) introduced a diffusion pump between the reaction system and the silica gel trap, which was followed by the mechanical oil pump. A similar system was used by Schiff and Steacie (6), but no quantitative data are given. We have successfully used a much simpler system without altering the characteristics of the flowing system by applying the silica gel to the inside walls of a trap which had previously been coated with a thin film of silicone grease. Such a surface can be removed from the system if the outside of the trap (containing the grease and the silica gel) is on a standard taper joint. Fast-flowing high-vacuum systems generally have two traps in series to insure complete collection of excess reactant and products. This second trap could conveniently serve to contain the silica gel.

The silica gel used (28/200 mesh) was obtained from Fisher Scientific. Dow Corning High Vacuum Silicone Grease was used to stick the gel to the glass trap, which was 15 cm long, with 30-mm O.D. The silica gel was degassed at 170° C prior to use in an experiment. The condensable gases were trapped in the first trap at −196° and the non-condensables were adsorbed in the silica gel trap maintained at −196°. After a reaction was completed, the non-condensable gases were removed from the silica gel at 170°, toeplered into a gas buret, measured, and analyzed.

The results of experiments to measure the trapping efficiency for CO, CH_4, and N_2 in a hydrogen flowing system at 1.05 mm pressure where the flow rate of hydrogen was 1530 μmoles/min are given in Table I.

The amount of gas put in was determined by PVT and time measurements and compared with the amount of gas recovered as measured in a gas buret.

Blank experiments with hydrogen alone showed that less than 1 μmole/min of gas, hydrogen, was trapped by the silica gel. From these results it seems reasonable that any two-component mixture of the above gases, or even the three-component mixture of

[1]*Grateful acknowledgment is made to the Petroleum Research Fund and the National Research Council of Canada for financial support.*

[2]*Holder of an Imperial Oil Graduate Research Fellowship.*

Can. J. Chem. Downloaded from www.nrcresearchpress.com by 210.87.254.42 on 09/05/12
For personal use only.

TABLE I

Trapping efficiency for CO, CH_4, and N_2, in a H_2 system

Time (min)	CO in (μmoles/min)	CO out (μmoles/min)	Time (min)	CH_4 in (μmoles/min)	CH_4 out (μmoles/min)	Time (min)	N_2 in (μmoles/min)	N_2 out (μmoles/min)
8.0	7.10	7.08	5.0	5.0	5.1	4.0	38.0	38.5
3.0	44.4	42.8	5.0	24.0	26.0	2.5	56.0	57.0
2.0	85.0	86.0	3.0	31.2	35.8	2.0	84.0	86.0
1.0	116	117	1.5	88.0	89.0	1.5	102	102
1.0	148	147	1.0	110	111	1.0	164	166
1.0	210	202	1.0	142	144	1.0	187	184
1.0	244	239	1.0	198	195	0.75	278	270
			0.75	248	239			

CH_4, CO, and N_2, could also be quantitatively trapped in the described manner. Actual experiments with a CO and CH_4 mixture showed from PVT measurements that the trapping is indeed quantitative but a mixing problem was encountered in the preparation of sample mixtures. As an example, a mixture having a prepared ratio for CO/CH_4 of 0.54 was trapped and collected completely but upon analysis by the standard combustion method in a CuO furnace at 210° C (7) it was shown to have the ratio of 0.51. The discrepancy was probably due to non-homogeneity of the original prepared mixture as well as to different rates of effusion of CH_4 and CO through the flowmeter constriction.

1. D. J. Le Roy. Can. J. Res. Sect. B, **29**, 492 (1950).
2. D. E. McElcheran, M. H. J. Wijnen, and E.W. R. Steacie. Can. J. Chem. **36**, 321 (1958).
3. J. W. S. Jamieson and C. A. Winkler. J. Phys. Chem. **60**, 1542 (1956).
4. J. Versteeg. Ph.D. Thesis, McGill University, Montreal, Que. 1952.
5. E. W. R. Steacie and N. W. F. Phillips. J. Chem. Phys. **4**, 461 (1934).
6. H. I. Schiff and E. W. R. Steacie. Can. J. Chem. **29**, 1 (1951).
7. H. Gesser and E. W. R. Steacie. Can. J. Chem. **34**, 113 (1956).

Received February 7, 1963.
Parker Chemical Laboratory,
University of Manitoba,
Winnipeg, Manitoba.

NOVEL SYNTHESIS OF 8-MERCAPTOQUINOLINE

H. S. Lee

8-Mercaptoquinoline, the sulphur analogue of 8-hydroxyquinoline, is a most interesting compound. Its dihydrate crystallizes as deep red needles, whereas its anhydrous form is a blue mobile liquid. It is easily oxidized when exposed to air, especially when dissolved in an alkaline solution. The presence of the sulphur atom in this compound might make it a good compound for spectral investigation of n–π^* electronic transition. Further, since its structure is very similar to that of 8-hydroxyquinoline, it may have wide use as an analytical reagent.

In 1908 Edinger (4) synthesized 8-mercaptoquinoline but relatively few investigators have studied the properties and possible uses of this substance. This paper reports a novel synthesis of 8-mercaptoquinoline, involving the reduction of quinoline-8-sulphonyl chloride directly to the corresponding mercaptan. The method has the advantage of requiring only

Can. J. Chem. Downloaded from www.nrcresearchpress.com by 210.87.254.42 on 09/05/12
For personal use only.

TABLE I

Trapping efficiency for CO, CH_4, and N_2, in a H_2 system

Time (min)	CO in (μmoles/min)	CO out (μmoles/min)	Time (min)	CH_4 in (μmoles/min)	CH_4 out (μmoles/min)	Time (min)	N_2 in (μmoles/min)	N_2 out (μmoles/min)
8.0	7.10	7.08	5.0	5.0	5.1	4.0	38.0	38.5
3.0	44.4	42.8	5.0	24.0	26.0	2.5	56.0	57.0
2.0	85.0	86.0	3.0	31.2	35.8	2.0	84.0	86.0
1.0	116	117	1.5	88.0	89.0	1.5	102	102
1.0	148	147	1.0	110	111	1.0	164	166
1.0	210	202	1.0	142	144	1.0	187	184
1.0	244	239	1.0	198	195	0.75	278	270
			0.75	248	239			

CH_4, CO, and N_2, could also be quantitatively trapped in the described manner. Actual experiments with a CO and CH_4 mixture showed from PVT measurements that the trapping is indeed quantitative but a mixing problem was encountered in the preparation of sample mixtures. As an example, a mixture having a prepared ratio for CO/CH_4 of 0.54 was trapped and collected completely but upon analysis by the standard combustion method in a CuO furnace at 210° C (7) it was shown to have the ratio of 0.51. The discrepancy was probably due to non-homogeneity of the original prepared mixture as well as to different rates of effusion of CH_4 and CO through the flowmeter constriction.

1. D. J. Le Roy. Can. J. Res. Sect. B, **29**, 492 (1950).
2. D. E. McElcheran, M. H. J. Wijnen, and E.W. R. Steacie. Can. J. Chem. **36**, 321 (1958).
3. J. W. S. Jamieson and C. A. Winkler. J. Phys. Chem. **60**, 1542 (1956).
4. J. Versteeg. Ph.D. Thesis, McGill University, Montreal, Que. 1952.
5. E. W. R. Steacie and N. W. F. Phillips. J. Chem. Phys. **4**, 461 (1934).
6. H. I. Schiff and E. W. R. Steacie. Can. J. Chem. **29**, 1 (1951).
7. H. Gesser and E. W. R. Steacie. Can. J. Chem. **34**, 113 (1956).

Received February 7, 1963.
Parker Chemical Laboratory,
University of Manitoba,
Winnipeg, Manitoba.

NOVEL SYNTHESIS OF 8-MERCAPTOQUINOLINE

H. S. Lee

8-Mercaptoquinoline, the sulphur analogue of 8-hydroxyquinoline, is a most interesting compound. Its dihydrate crystallizes as deep red needles, whereas its anhydrous form is a blue mobile liquid. It is easily oxidized when exposed to air, especially when dissolved in an alkaline solution. The presence of the sulphur atom in this compound might make it a good compound for spectral investigation of n–π^* electronic transition. Further, since its structure is very similar to that of 8-hydroxyquinoline, it may have wide use as an analytical reagent.

In 1908 Edinger (4) synthesized 8-mercaptoquinoline but relatively few investigators have studied the properties and possible uses of this substance. This paper reports a novel synthesis of 8-mercaptoquinoline, involving the reduction of quinoline-8-sulphonyl chloride directly to the corresponding mercaptan. The method has the advantage of requiring only

Can. J. Chem. Downloaded from www.nrcresearchpress.com by 210.87.254.6 on 09/05/12
For personal use only.

one step from the sulphonyl chloride to the final product instead of the several steps required by the old Edinger's method.

Best results were afforded when a 20% excess of lithium aluminum hydride was used. More or less hydride gave lower yields. The decomposition of the reduction complex and the excess lithium aluminum hydride with a calculated amount of water and 20% sodium hydroxide (2) (or 15% sodium hydroxide (5)) is not advised in the synthesis of 8-mercaptoquinoline, because it gives poor yields due to the formation of the corresponding sodium salt of the product. It is worth noting that no 8-mercaptoquinoline could be isolated by following the suggestion (1) to employ a 0.5 : 1 mole ratio for hydride to sulphonyl chloride.

EXPERIMENTAL

Quinoline-8-sulphonyl Chloride

A mixture of quinoline-8-sulphonic acid (20 g) and phosphorus pentachloride (25 g) was ground together for 5 minutes, and heated under reflux for 3 hours in an oil bath at 130° C. At the end of this period the contents of the flask became brown and almost all liquefied. After cooling, the crude product was poured onto crushed ice (180 g), neutralized with sodium bicarbonate, and extracted with ether. The ether extract was decolorized with charcoal (2 g) and filtered. After evaporation of the ether, the colorless crystalline sulphonyl chloride (21.1 g, 97%) was dried *in vacuo*. It melted at 118–122° (lit. 122° (4), 128.5–129° (3)).

8-Mercaptoquinoline

A solution of 0.55 g of lithium aluminum hydride in 250 ml of anhydrous ether was added, over a period of 1½ hours, to a solution of 1.83 g of quinoline-8-sulphonyl chloride and 600 ml of anhydrous ether in a 1-liter three-necked round-bottomed flask, fitted with a motor-driven stirrer and a condenser. Ice water was circulated through the condenser. The yellow intermediate was decomposed by the addition of 3 ml of water. Inorganic material was removed by filtration from the yellow ether solution. After the removal, by evaporation, of the solvent, some bluish red residue appeared. 8-Mercaptoquinoline dihydrate, shiny red needles (m.p. 58–59°; lit. 58–59° (4), 58.5° (6)), was obtained by dissolving the residue in dilute sodium hydroxide solution, and then neutralizing the mixture by adding dry ice. Anhydrous 8-mercaptoquinoline, a non-viscous blue liquid, was obtained by drying the red product in a nitrogen atmosphere over sodium hydroxide pellets. The yield was 0.78 g (61%).

ACKNOWLEDGMENT

The author wishes to thank his friends R. H. Ode, K. Lau, and J. L. Williams for reading this paper.

1. R. Adams *et al.* Organic reactions. Vol. VI. John Wiley & Sons. Inc., New York. 1951. p. 470.
2. L. H. Amundsen and L. S. Nelson. J. Am. Chem. Soc. **73**, 242 (1950).
3. G. M. Badger and R. G. Buttery. J. Chem. Soc. 3236 (1956).
4. A. Edinger. Ber. **41**, 937 (1908).
5. V. M. Micovie and M. L. Mihailovie. J. Org. Chem. **18**, 1190 (1953).
6. R. Ponci and F. Gialdi. Chem. Abstr. **49**, 11657b (1955).

Received February 14, 1963.
Department of Chemistry,
University of North Dakota,
Grand Forks, North Dakota.

STUDIES ON PIGMENTS OF PENICILLIUM FUNICULOSUM
I. PRODUCTION OF CHOLESTEROL[1]

Y. S. Chen[2] and R. H. Haskins

During investigations on pigments from an aberrant strain (PRL 1724) of *Penicillium funiculosum* Thom, the authors found that petroleum ether extracts of culture material

[1]*Issued as N.R.C. No. 7327.*
[2]*National Research Council of Canada Postdoctoral Fellow, 1960–1962. Present address: Department of Chemistry, University of Western Ontario, London, Ontario.*

Can. J. Chem. Downloaded from www.nrcresearchpress.com by 210.87.254.6 on 09/05/12
For personal use only.

one step from the sulphonyl chloride to the final product instead of the several steps required by the old Edinger's method.

Best results were afforded when a 20% excess of lithium aluminum hydride was used. More or less hydride gave lower yields. The decomposition of the reduction complex and the excess lithium aluminum hydride with a calculated amount of water and 20% sodium hydroxide (2) (or 15% sodium hydroxide (5)) is not advised in the synthesis of 8-mercaptoquinoline, because it gives poor yields due to the formation of the corresponding sodium salt of the product. It is worth noting that no 8-mercaptoquinoline could be isolated by following the suggestion (1) to employ a 0.5 : 1 mole ratio for hydride to sulphonyl chloride.

EXPERIMENTAL

Quinoline-8-sulphonyl Chloride

A mixture of quinoline-8-sulphonic acid (20 g) and phosphorus pentachloride (25 g) was ground together for 5 minutes, and heated under reflux for 3 hours in an oil bath at 130° C. At the end of this period the contents of the flask became brown and almost all liquefied. After cooling, the crude product was poured onto crushed ice (180 g), neutralized with sodium bicarbonate, and extracted with ether. The ether extract was decolorized with charcoal (2 g) and filtered. After evaporation of the ether, the colorless crystalline sulphonyl chloride (21.1 g, 97%) was dried *in vacuo*. It melted at 118–122° (lit. 122° (4), 128.5–129° (3)).

8-Mercaptoquinoline

A solution of 0.55 g of lithium aluminum hydride in 250 ml of anhydrous ether was added, over a period of 1½ hours, to a solution of 1.83 g of quinoline-8-sulphonyl chloride and 600 ml of anhydrous ether in a 1-liter three-necked round-bottomed flask, fitted with a motor-driven stirrer and a condenser. Ice water was circulated through the condenser. The yellow intermediate was decomposed by the addition of 3 ml of water. Inorganic material was removed by filtration from the yellow ether solution. After the removal, by evaporation, of the solvent, some bluish red residue appeared. 8-Mercaptoquinoline dihydrate, shiny red needles (m.p. 58–59°; lit. 58–59° (4), 58.5° (6)), was obtained by dissolving the residue in dilute sodium hydroxide solution, and then neutralizing the mixture by adding dry ice. Anhydrous 8-mercaptoquinoline, a non-viscous blue liquid, was obtained by drying the red product in a nitrogen atmosphere over sodium hydroxide pellets. The yield was 0.78 g (61%).

ACKNOWLEDGMENT

The author wishes to thank his friends R. H. Ode, K. Lau, and J. L. Williams for reading this paper.

1. R. Adams *et al.* Organic reactions. Vol. VI. John Wiley & Sons. Inc., New York. 1951. p. 470.
2. L. H. Amundsen and L. S. Nelson. J. Am. Chem. Soc. **73**, 242 (1950).
3. G. M. Badger and R. G. Buttery. J. Chem. Soc. 3236 (1956).
4. A. Edinger. Ber. **41**, 937 (1908).
5. V. M. Micovie and M. L. Mihailovie. J. Org. Chem. **18**, 1190 (1953).
6. R. Ponci and F. Gialdi. Chem. Abstr. **49**, 11657b (1955).

Received February 14, 1963.
Department of Chemistry,
University of North Dakota,
Grand Forks, North Dakota.

STUDIES ON PIGMENTS OF PENICILLIUM FUNICULOSUM
I. PRODUCTION OF CHOLESTEROL[1]

Y. S. Chen[2] and R. H. Haskins

During investigations on pigments from an aberrant strain (PRL 1724) of *Penicillium funiculosum* Thom, the authors found that petroleum ether extracts of culture material

[1]*Issued as N.R.C. No. 7327.*
[2]*National Research Council of Canada Postdoctoral Fellow, 1960–1962. Present address: Department of Chemistry, University of Western Ontario, London, Ontario.*

Can. J. Chem. Downloaded from www.nrcresearchpress.com by 210.87.254.42 on 09/05/12
For personal use only.

showed strong sterol color reactions. The material responsible for these reactions was isolated by column chromatography and was found to be a white crystalline substance (white plates from acetone), m.p. 148–149° C. This melting point was not depressed by admixture with cholesterol. The substance sublimed and was readily soluble in ether, acetone, chloroform, benzene, ethyl acetate, petroleum ether, and hot alcohol, and was slightly soluble in water and cold alcohol. It was optically active, $[\alpha]_D^{20}$ +39.8° (*c*, 2.123 in chloroform). Its color reactions in a series of seven tests were the same as those obtained with authentic cholesterol.

From the results of elementary analysis and of the osmometric method for molecular weight determination, it was confirmed that the molecular formula corresponded to $C_{27}H_{46}O$.

The substance gave a positive precipitation reaction with digitonin (8). The infrared spectrum in KBr and the ultraviolet spectrum (9) in ethanol were identical with those of cholesterol.

The substance formed the following derivatives: a monomethyl ether, $C_{28}H_{48}O$, m.p. 84° C, $[\alpha]_D^{20}$ −46.6° (*c*, 1.356 in chloroform); a monoacetate, $C_{29}H_{48}O_2$, m.p. 115° C, $[\alpha]_D^{20}$ −47.3° (*c*, 1.985 in chloroform); a benzoate, $C_{34}H_{50}O_2$, m.p. 146° and 180° C, $[\alpha]_D^{20}$ −13.9° (*c*, 1.562 in chloroform); a dibromide (8, 10, 11), $C_{27}H_{46}OBr_2$, m.p. 113° C, $[\alpha]_D^{20}$ −44.6° (*c*, 1.568 in chloroform).

All of the above properties of the substance and its derivatives are the same as those of cholesterol and its derivatives; therefore there seems to be no doubt that the substance is cholesterol.

There have been reports on the isolation of fungal sterols (12). The most abundant in microorganisms is ergosterol, with yields depending both on the species and on the conditions of cultivation (13). Among species of *Penicillium* (14) only traces of ergosterol could be found in mycelium grown in submerged culture, while the felts from surface cultures contained over 1% of the steroid. However, there has been no report on the isolation of cholesterol from fungal metabolic products. Indeed, among plants, only certain of the marine Rhodophyceae have been reported to produce this substance (15). It is very interesting, then, to find that *P. funiculosum* (PRL 1724) is capable of producing cholesterol.

EXPERIMENTAL

Organisms

Penicillium funiculosum Thom (PRL 1724) was used throughout this work. Its identity was confirmed by Miss Dorothy Fennel, who considered it to be an aberrant strain of *P. funiculosum*. Its culture and characteristics are being described elsewhere.

Cultural Methods for Sterol Production

The liquid medium used for shake-flask culture contained glucose 30 g, Difco Bacto-peptone 5 g, distilled water 1000 ml.

The medium was dispensed into 250-ml Erlenmeyer flasks in the amount of 25 ml per flask. The flasks containing the medium were plugged with cotton and autoclaved at 15 lb pressure for 15 minutes. Liquid cultures were grown for approximately 7 days at 24° C on a rotary shaker with a 1/2-in. radius of motion, operating at about 240 r.p.m.

Inoculum

Inoculum for shake-flask cultures was usually prepared from 7-day shake-flask cultures which had been originally inoculated with a suspension of a potato dextrose agar culture blended in distilled water.

Recovery of Sterol from Mycelium

When the wine-red pigmentation of the cultures visually appeared to have reached a maximum, the cultures were bulked and freeze-dried. The resulting solids were extracted with petroleum ether (b.p. 35–60° C) for 48 hours in Soxhlet apparatus. A pale yellow "oil" was recovered from the extract by removal of the petroleum ether by evaporation.

Can. J. Chem. Downloaded from www.nrcresearchpress.com by 210.87.254.42 on 09/05/12
For personal use only.

Column Chromatography

A slurry of aluminum oxide (30 g Brockman Grade 1) in benzene was used to prepare a column 15 cm long and 2.2 cm in diameter. The sample (1 g) of pale yellow "oil" was dissolved in a minimum amount of benzene and added to the column. The column was eluted, first with benzene and then with benzene – ethyl acetate (4:1). A white crystalline substance (24 mg) was left after evaporation of the solvent from the benzene – ethyl acetate eluates. This substance was recrystallized repeatedly from acetone to give white plates, m.p. 149° C, $[\alpha]_D^{20}$ +39.8 (*c*, 2.123 in chloroform). Found: C, 83.96; H, 12.01; OMe, 0. Calculated for $C_{27}H_{46}O$: C, 83.87; H, 11.99.

Characteristics of Crystalline Material

Solubility.—The substance sublimed and was readily soluble in ether, acetone, chloroform, benzene, ethyl acetate, petroleum ether, and hot alcohol and was slightly soluble in water and cold alcohol.

Molecular weight determination by osmometric method.—Found: 391, 385. Calculated for $C_{27}H_{46}O$: 386.44.

Precipitation reactions with digitonin (8).—One hundred milligrams of digitonin was dissolved in 10 ml of 90% alcohol. A small amount of the crystalline metabolic product was dissolved in alcohol and when added to digitonin alcoholic solution immediately gave a perceptible precipitate.

Color reactions.—The color reactions of the substance obtained from *P. funiculosum* and of authentic cholesterol were positive for the Liebermann (1), Liebermann–Burchard (2), Salkowski (3), Lifschütz (4), and Tshugajeff (5) reactions but negative for the Rosenheim (6) and Tortelli–Jaffe (7) reactions.

Derivatives

Monomethyl ether.—The substance (100 mg) was refluxed with dimethyl sulphate (2 ml) and 5% sodium hydroxide solution (15 ml) for 3 hours. The solution was cooled, neutralized, and extracted with ether. Purification by recrystallization from acetone gave white crystals (66 mg), m.p. 84° C, $[\alpha]_D^{20}$ −46.6° (*c*, 1.356 in chloroform). Found: C, 83.95; H, 12.1. Calculated for $C_{28}H_{48}O$: C, 83.93; H, 12.08.

Monoacetate.—The substance (200 mg) taken in freshly distilled acetic anhydride (5 ml) containing anhydrous sodium acetate (500 mg) was refluxed for 4 hours. The contents were poured onto broken ice, and white crystals separated. Purification by recrystallization from acetone gave white needles (142 mg), m.p. 115° C, $[\alpha]_D^{20}$ −47.3° (*c*, 1.985 in chloroform). Found: C, 81.28; H, 11.30. Calculated for $C_{29}H_{48}O_2$: C, 81.25; H, 11.29.

Benzoate.—The substance (100 mg) was dissolved in anhydrous pyridine (3 ml), and benzoyl chloride (500 mg) was added. The mixture was refluxed for 1 hour and poured onto broken ice. The precipitate was extracted with ether, washed with 5% sodium carbonate solution, and purified by recrystallization from 95% ethanol to give white prisms (52.5 mg), m.p. 146° C (the melting becomes clear at about 180° C), $[\alpha]_D^{20}$ −13.9° (*c*, 1.562 in chloroform). Found: C, 83.18; H, 10.3. Calculated for $C_{34}H_{50}O_2$: C, 83.21; H, 10.27.

Dibromide (8, 10, 11).—The substance (200 mg) in 5 ml of ether was gently warmed and 4 ml of a solution of bromine and sodium acetate in acetic acid added. The dibromide began to crystallize out in a few minutes. The crystalline paste was cooled in an ice bath and stirred with a rod for about 10 minutes to ensure complete crystallization. The crystals were collected on a small suction funnel and washed with an ice-cold ether – acetic acid (3:7) solution to remove the yellow mother liquor. The crystals were finally washed with a little methanol, and dried (111 mg), m.p. 113° C, $[\alpha]_D^{20}$ −44.6° (*c*, 1.568 in chloroform). Found: C, 59.42; H, 8.3; Br. 29.8. Calculated for $C_{27}H_{46}O_2Br_2$: C, 59.36; H, 8.40; Br, 29.28.

Each of these derivatives was prepared from authentic cholesterol with similar results.

ACKNOWLEDGMENTS

The authors wish to thank Mr. L. R. Nesbitt for the preparation of freeze-dried mycelium, Mr. W. C. Haid for the infrared spectra, Mr. M. Mazurek for the microanalyses and molecular weight determinations, and Miss Dorothy I. Fennel (Q. M. Research and Engineering Center, U.S. Army, Natick, Mass.) for her identification of the organism.

1. C. Liebermann. Ber. **18**, 1803 (1885).
2. H. Burchard. Chem. Ztbl. **I**, 25 (1890).
3. E. Salkowski. Z. Physiol. Chem. **57**, 521 (1908).
4. J. Lifschutz. Ber. **41**, 252 (1908).
5. L. Tschugajeff. Chem. Ztbl. **24**, 542 (1900).
6. O. Rosenheim. Biochem. J. **23**, 47 (1929).
7. M. Tortelli and E. Jaffe. Chem. Ztbl. **39**, 14 (1915).
8. A. Windaus. Ber. **39**, 518 (1906).
9. I. M. Heilbron, R. A. Morton, and W. A. Sexton. J. Chem. Soc. 47 (1928).
10. L. F. Fieser. J. Am. Chem. Soc. **75**, 5421 (1953).
11. E. Schwenk and N. T. Werthessen. Arch. Biochem. Biophys. **40**, 334 (1952).

Can. J. Chem. Downloaded from www.nrcresearchpress.com by 210.87.254.42 on 09/05/12
For personal use only.

12. M. W. MILLER. The Pfizer handbook of microbial metabolites. McGraw-Hill. 1961.
13. A. H. ROSE. Industrial microbiology. Butterworths, London. 1961 p. 270.
14. C. J. CAVALLITO. Science, **100**, 333 (1944).
15. K. TSUDA, S. AKAGI, and Y. KISHIDA. Science, **126**, 927 (1957).

RECEIVED FEBRUARY 1, 1963.
NATIONAL RESEARCH COUNCIL,
PRAIRIE REGIONAL LABORATORY,
SASKATOON, SASKATCHEWAN.

Can. J. Chem. Downloaded from www.nrcresearchpress.com by 210.87.254.42 on 09/05/12
For personal use only.

THIOHYDANTOINS
V. IONIZATION OF 2,4-DITHIOHYDANTOINS AS ACIDS

J. T. EDWARD AND O. J. CHIN

Thioamides are more acidic than amides (1) because the thiocarbonyl group is more polarized than the carbonyl group (2). Similarly, 2-thiohydantoin (I; R = H, X_1 = S, X_2 = O) (pK_a ~ 8.5 (3)) is more acidic than hydantoin (I; R = H, X_1 = X_2 = O) (pK_a 9.12 (4)), and so 2,4-dithiohydantoin (I; R = H, X_1 = X_2 = S) would be expected to be more acidic yet, with a pK_a of about 8. We have confirmed this expectation by determining the dissociation constant of the readily available 5,5-dimethyl-2,4-dithiohydantoin (I; R = Me, X_1 = X_2 = S); this should be only very slightly weaker as an acid than 2,4-dithiohydantoin (3).

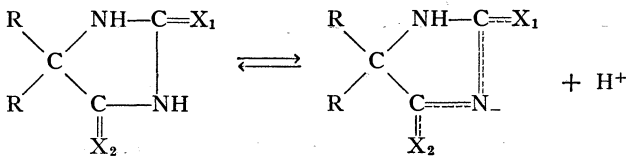

The absorption spectrum of 5,5-dimethyl-2,4-dithiohydantoin in weakly acidic aqueous solution shows a strong peak at 296 mμ (ϵ 27,600). A peak in this region has been found characteristic of 2,4-dithiohydantoins generally (5). In solutions more alkaline than pH 10 the peak has shifted to 318 mμ (Fig. 1A). In buffer solutions of pH between 5 and 10

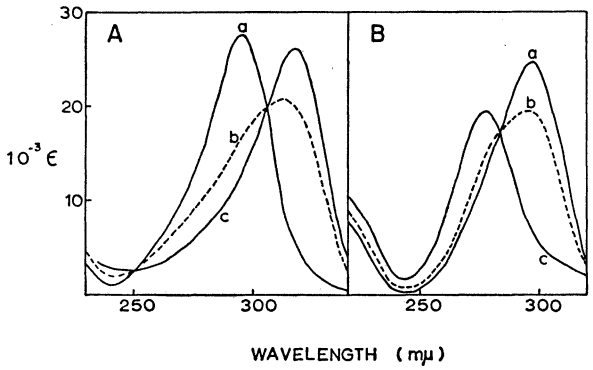

FIG. 1. Ultraviolet absorption of (A) 5,5-dimethyl-2,4-dithiohydantoin at pH (*a*) 2.05, (*b*) 8.00, (*c*) 10.00. (B) 3-methyl-5,5-pentamethylene-2,4-dithiohydantoin at pH (*a*) 6.5, (*b*) 9.71, and in (*c*) 0.1 *N* sodium hydroxide.

12. M. W. MILLER. The Pfizer handbook of microbial metabolites. McGraw-Hill. 1961.
13. A. H. ROSE. Industrial microbiology. Butterworths, London. 1961 p. 270.
14. C. J. CAVALLITO. Science, **100**, 333 (1944).
15. K. TSUDA, S. AKAGI, and Y. KISHIDA. Science, **126**, 927 (1957).

RECEIVED FEBRUARY 1, 1963.
NATIONAL RESEARCH COUNCIL,
PRAIRIE REGIONAL LABORATORY,
SASKATOON, SASKATCHEWAN.

Can. J. Chem. Downloaded from www.nrcresearchpress.com by 210.87.254.42 on 09/05/12
For personal use only.

THIOHYDANTOINS
V. IONIZATION OF 2,4-DITHIOHYDANTOINS AS ACIDS

J. T. EDWARD AND O. J. CHIN

Thioamides are more acidic than amides (1) because the thiocarbonyl group is more polarized than the carbonyl group (2). Similarly, 2-thiohydantoin (I; R = H, X_1 = S, X_2 = O) (pK_a ~ 8.5 (3)) is more acidic than hydantoin (I; R = H, X_1 = X_2 = O) (pK_a 9.12 (4)), and so 2,4-dithiohydantoin (I; R = H, X_1 = X_2 = S) would be expected to be more acidic yet, with a pK_a of about 8. We have confirmed this expectation by determining the dissociation constant of the readily available 5,5-dimethyl-2,4-dithiohydantoin (I; R = Me, X_1 = X_2 = S); this should be only very slightly weaker as an acid than 2,4-dithiohydantoin (3).

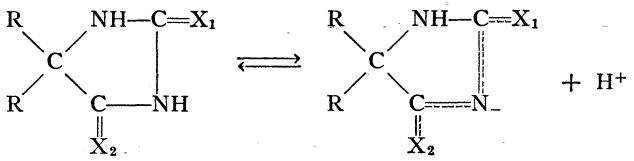

The absorption spectrum of 5,5-dimethyl-2,4-dithiohydantoin in weakly acidic aqueous solution shows a strong peak at 296 mμ (ϵ 27,600). A peak in this region has been found characteristic of 2,4-dithiohydantoins generally (5). In solutions more alkaline than pH 10 the peak has shifted to 318 mμ (Fig. 1A). In buffer solutions of pH between 5 and 10

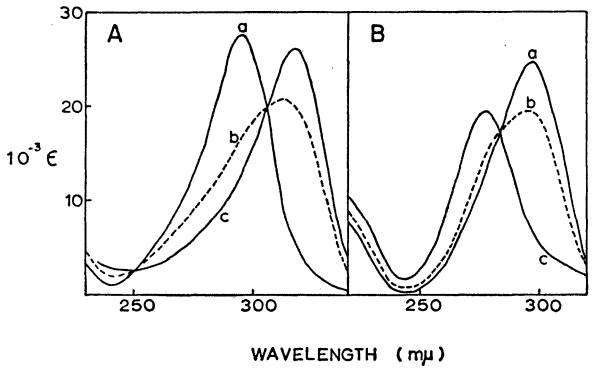

FIG. 1. Ultraviolet absorption of (A) 5,5-dimethyl-2,4-dithiohydantoin at pH (*a*) 2.05, (*b*) 8.00, (*c*) 10.00. (B) 3-methyl-5,5-pentamethylene-2,4-dithiohydantoin at pH (*a*) 6.5, (*b*) 9.71, and in (*c*) 0.1 *N* sodium hydroxide.

absorption curves intermediate in character are obtained, one of which is shown in Fig. 1A; all pass through an isobestic point at 306 mμ. Evidently ionization takes place in this pH range; from the change in absorption at 318 mμ a mixed dissociation constant pK_a^m (6) of 7.6±0.1* has been calculated by the usual methods (6). Taking account of the ionic strength of the buffer solutions, this indicates a thermodynamic pK_a of 7.7±0.1.

The relatively high acidity of 2,4-dithiohydantoins explains their solubility in aqueous sodium bicarbonate and acetate (7).

Ionization at $N_{(1)}$—H, in contrast to ionization at $N_{(3)}$—H, is accompanied by a shift in the main absorption peak to a shorter wavelength. This is shown in Fig. 1B for 3-methyl-5,5-pentamethylene-2,4-dithiohydantoin (III; $X_1 = X_2 = S$), which has an absorption

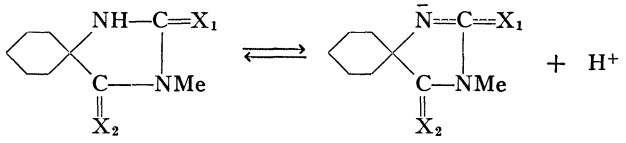

III IV

peak at 297 mμ (ε 24,800) in water at pH 6.5, and at 277.5 mμ (ε 19,300) in 0.1 *M* sodium hydroxide and more alkaline solutions. At pH values between 8 and 12 a family of curves passing through an isobestic point a 283 mμ is obtained. From the change in absorption at 260–310 mμ with pH, a pK_a^m of 10.05±0.03 and pK_a of 10.09±0.03 may be calculated. This compares with a pK_a^m of 11.23 for 3-methyl-5,5-pentamethylene-2-thiohydantoin (III; $X_1 = S$, $X_2 = O$) (4), illustrating again the acid-strengthening effect of replacing carbonyl by thiocarbonyl.

EXPERIMENTAL

3-Methyl-5,5-pentamethylene-2,4-dithiohydantoin was prepared according to Carrington and Waring (5), and 5,5-dimethyl-2,4-dithiohydantoin was obtained from Aldrich Chemical Co. Both compounds were crystallized to constant melting point. The spectrum of 5,5-dimethyl-2,4-dithiohydantoin was determined in buffer solutions of pH 2.05, 5.34, 7.00, 7.45, 7.60, 8.00, 8.22, 8.62, 9.04, 10.0, and 11.90, and ionic strength 0.06–0.14 *M* at 20–24°. The spectrum of 1-methyl-5,5-pentamethylene-2,4-dithiohydantoin was determined in buffer solutions of pH 6.5, 8.46, 9.20, 9.71, and 10.41; in sodium hydroxide of pH 11.87; and in 0.1 *M* and 1 *M* sodium hydroxide. The ionic strength of the latter buffer solutions was about 0.01 *M* and the temperature of the determinations 18–21°.

ACKNOWLEDGMENT

The financial assistance of the National Research Council is gratefully acknowledged.

1. J. T. Edward and H. Stollar. Can. J. Chem. **41**, 721 (1963).
2. C. M. Lee and W. D. Kumler. J. Org. Chem. **27**, 2052 (1962).
3. J. T. Edward and S. Nielsen. J. Chem. Soc. 5075 (1957).
4. L. W. Pickett and M. McLean. J. Am. Chem. Soc. **61**, 423 (1939).
5. H. C. Carrington and W. S. Waring. J. Chem. Soc. 554 (1950).
6. A. Albert and E. P. Serjeant. Ionization constants of acids and bases. Methuen, London. 1962. pp. 58, 69.
7. A. H. Cook, Sir I. Heilbron, and A. L. Levy. J. Chem. Soc. 201 (1948).

Received February 6, 1963.
Department of Chemistry,
McGill University,
Montreal 2, Que.

**The poor precision of this value probably came from using buffer solutions of too great ionic strength.*

Can. J. Chem. Downloaded from www.nrcresearchpress.com by 210.87.254.42 on 09/05/12
For personal use only.

SYNTHESIS OF DEUTERATED CHLOROSILANE AND BROMOSILANE[1]

R. D. VERMA AND L. C. LEITCH

Normal and deuterated chloro- and bromo-silanes were recently required to find out whether SiH_3 or SiD_3 radicals are formed by flash photolysis. Chloro- and bromo-silanes have always been prepared as reported by Stock and Somieski (1) from silane and hydrogen chloride or bromide in the presence of the corresponding aluminum halide. Trideuteriochlorosilane was similarly prepared from tetradeuteriosilane and deuterium chloride by Lord, Robinson, and Schumb (2). Peake (3) informed us in a private communication of the formation of bromosilane in small quantities when a slow current of anhydrous hydrogen bromide is bubbled into a solution of phenylsilane in diphenyl ether. Owing to the low yield of bromosilane obtained by us with this method and because a large amount of deuterium bromide would be required for the synthesis of the deuterated compound, the reaction was tried in a sealed tube with a slight excess of hydrogen or deuterium bromide. Bromo- and chloro-silanes were isolated in 70% yields without the liberation of hydrogen and the formation of di- and tri-halosilanes, unless the reaction time was prolonged from a few days to several months.

EXPERIMENTAL

Phenylsilane

Phenyltrichlorosilane was reduced with lithium aluminum hydride in ether as reported by Nebergall (4).

Bromosilane

Phenylsilane (10.0 g; 0.084 mole) and diphenyl ether (20 ml) were poured into a thick-walled glass tube of 250-ml capacity with a constriction to facilitate sealing later. The tube was attached to the vacuum line and evacuated. Hydrogen bromide (8.3 g; 3.0 ml at −78°; 0.12 mole) was distilled into the tube, which was cooled in liquid nitrogen. It was then carefully sealed at the constriction and transferred to a Dewar flask containing dry ice and acetone at −78°. The tube was allowed to warm up very slowly in the Dewar flask and kept for 1 day at room temperature. It was finally heated for a few hours at 50°. After the tube was cooled to −78° in dry ice and acetone, a nick was made just below the seal, and it was attached to the vacuum line with a piece of thick plastic tubing. The line was evacuated and the seal was broken off at the mark with a pair of pliers. The bromosilane was distilled into a trap and then fractionated from a Dewar at −78°. The yield of liquid with a vapor pressure of 10 mm at −78° was 4.5 ml (6.95 g) or 68.5%.

Chlorosilane

Hydrogen chloride (5.0 l.; 8.1 g; 0.12 mole) gave 4.5 ml (4.63 g) of chlorosilane from 10 g phenylsilane under the same conditions. Yield: 75.5%.

On one occasion the reactants were allowed to stand for 2 months at room temperature before the chlorosilane was isolated. In this instance there was considerable pressure in the tube when it was opened and dichloro- together with trichloro-silane was isolated. The identity of the dichlorosilane was established by vapor pressure measurements and also by the formation of SiHCl radical on flash photolysis of the compound.

Chloro- and Bromo-trideuteriosilane

These compounds were prepared by the same method from deuterium chloride and deuterium bromide and trideuteriophenylsilane. The yields were similar to those obtained with protiated reactants.

1. A. STOCK and C. SOMIESKI. Ber. **51**, 989 (1918); Ber. **52**, 695 (1919).
2. R. C. LORD, D. W. ROBINSON, and W. C. SCHUMB. J. Am. Chem. Soc. **78**, 1327 (1956).
3. J. S. PEAKE. Private communication.
4. W. H. NEBERGALL. J. Am. Chem. Soc. **72**, 4702 (1950).

RECEIVED FEBRUARY 6, 1963.
DIVISION OF PURE CHEMISTRY,
NATIONAL RESEARCH COUNCIL,
OTTAWA, CANADA.

[1]*Issued as N.R.C. No. 7335.*

Can. J. Chem. Downloaded from www.nrcresearchpress.com by 210.87.254.40 on 09/05/12
For personal use only.

Canadian Journal of Chemistry

Issued by THE NATIONAL RESEARCH COUNCIL OF CANADA

VOLUME 41 JULY 1963 NUMBER 7

THE SYNTHESIS AND SUBSTITUTION REACTIONS OF 3,5-DI-*tert*-BUTYLPHENOL[1]

JOHN W. ELDER[2] AND RAYMOND P. MARIELLA[3]

Department of Chemistry, Loyola University, Chicago, Ill., U.S.A.

Received March 4, 1963

ABSTRACT

3,5-Di-*tert*-butylphenol (I) was synthesized by two independent routes. It was possible to isolate a mononitro and a dinitro product. It was not possible to isolate a trinitrated product (3,5-di-*tert*-butylpicric acid). Bromination of I gave the dibrominated product, and chlorination of I gave a dichlorinated product and a tetrachloro product; the latter was shown to possess the dieneone structure.

Experience has shown that 3- and 3,5-alkyl-substituted phenols could be easily trinitrated to form substituted picric acids (1, 2). Even in the case of *m-tert*-butylphenol (3), where a steric problem might be present, the trinitration proceeded with the same ease as encountered by all the other *m*-alkylphenols previously investigated. In order to present an extreme case of steric crowding, it was decided to synthesize the previously unreported 3,5-di-*tert*-butylphenol (I) and to attempt its trinitration.

The phenol (I) was synthesized through two completely independent paths: one proceeding through 1-bromo-3,5-di-*tert*-butylbenzene, the other through the 3,5-di-*tert*-butylanilinium salt. The methods used in the two syntheses of I follow well-known procedures. These reactions and the substitution reactions carried out on the phenol are shown in Fig. 1.

There can be little doubt of the position of the substituents of 3,5-di-*tert*-butylphenol since the configuration of 3,5-di-*tert*-butyltoluene has been established by Wepster *et al.* (4).

Whether one starts with 3,5-di-*tert*-butyltoluene (IV) (5) or *sym*-tri-*tert*-butylbenzene (II) (6), the final phenol (I) is the same. However, the phenol (I) prepared through the bromo compound route requires less purification than the same phenol (I) obtained through the diazotization method.

The nitration of 3,5-di-*tert*-butylphenol met with considerable difficulties. Nitration by the usual method of adding nitric acid to a sulphuric acid solution of the phenol resulted in the separation of solid (chiefly the mononitro compound) almost as soon as the addition of nitric acid commenced. This could not be prevented even by very high dilutions of the phenol in sulphuric acid. Many variations of technique were attempted; the method of inverse addition given in the experimental part was the most successful, but the mononitro compound was still the major product. It was possible to isolate small quantities

[1]*Taken in part from the Ph.D. dissertation of J. W. Elder.*
[2]*Present address: Regis College, Willowdale, Ontario.*
[3]*To whom inquiries should be directed.*

Can. J. Chem. Downloaded from www.nrcresearchpress.com by 210.87.254.5 on 09/05/12
For personal use only.

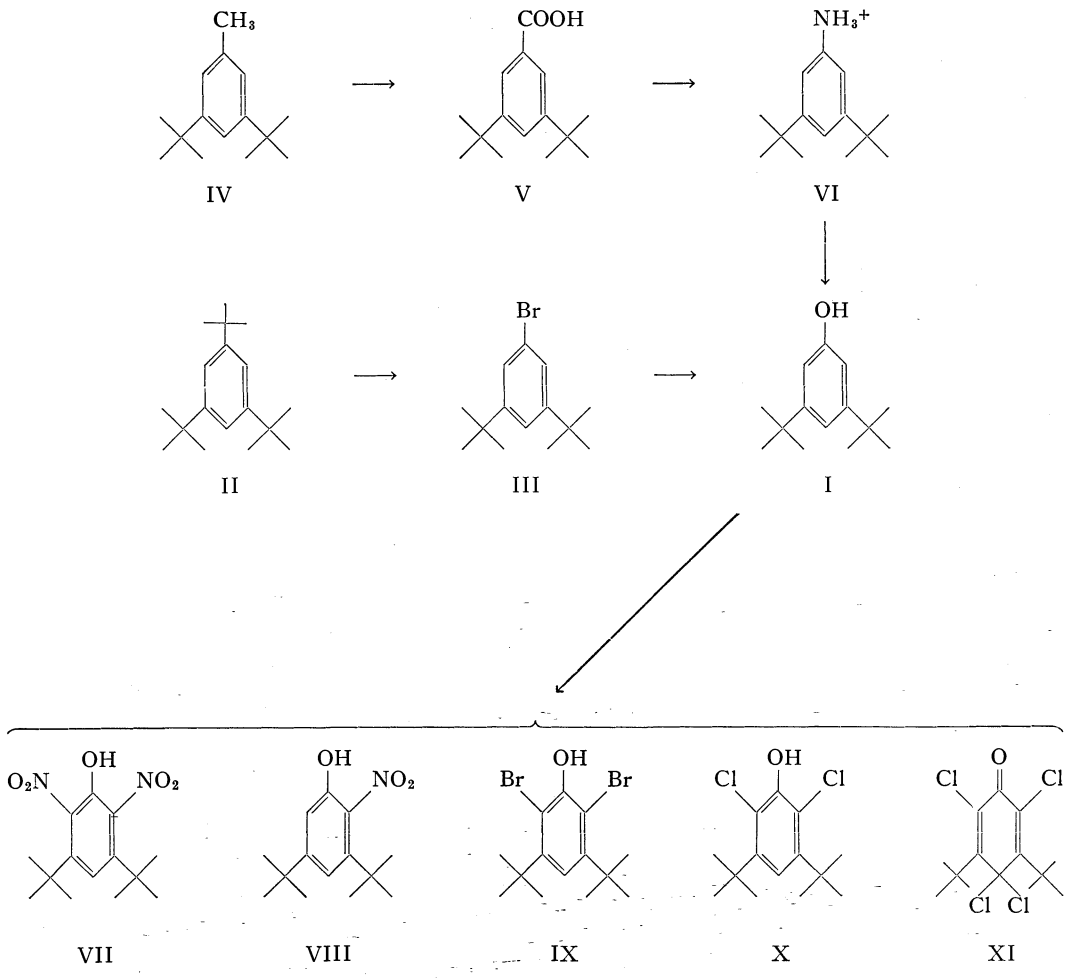

FIG. 1.

of the dinitrated product, but it was not possible to obtain any trinitrated product (3,5-di-*tert*-butylpicric acid).

Bromination of I led quite cleanly to the disubstituted compound, which can be presumed to be 2,6-dibromo-3,5-di-*tert*-butylphenol, since the para position is certainly highly hindered. The chlorination of I was not nearly as clean-cut as the bromination. There were two products formed: a dichloro compound (X) presumably the 2,6-isomer, and a tetrachloro compound (XI) which was analogous to a tetrachloro compound characterized by Zincke and Schaum (7).*

Denivelle and Fort (8) reported that 2,3,4,4,5,6-hexahalocyclohexadiene-2,5-one-1 compounds absorb at 250–280 mμ (in cyclohexane) and 2,2,3,4,5,6-hexahalocyclohexadiene-3,5-one-1 isomers absorb at 350–380 mμ; our compound (XI) had a maximum absorption at 255 mμ (isooctane), and a strong peak at 1685 cm^{-1}.

**By further chlorination of 2,4,6-trichlorophenol, they isolated 2,4,4,6-tetrachlorocyclohexadiene-2,5-one-1. We duplicated their work and found that the dieneone had a strong carbonyl absorption at 1675 cm^{-1}.*

Can. J. Chem. Downloaded from www.nrcresearchpress.com by 210.87.254.5 on 09/05/12
For personal use only.

EXPERIMENTAL

Melting points were taken on a Fisher–Johns melting point block and are corrected. Microanalyses were by Microtech Laboratories, Skokie, Illinois. Infrared spectra were determined with a Perkin–Elmer spectrophotometer, Model 21, and the ultraviolet spectra with a Beckman spectrophotometer, Model DU.

1-Bromo-3,5-di-tert-butylbenzene (III)

sym-Tri-*tert*-butylbenzene (II), prepared by the method of Barclay and Betts (9) or that of McCaulay, Lien, and Launer (6), was brominated by the method of Bartlett *et al.* (10) to give a 65% yield of 1-bromo-3,5-di-*tert*-butylbenzene, m.p. 62.5–65.0° C, reported (10) 63–64° C.

3,5-Di-tert-butylphenol (I) (Via the Bromo Route)

A suspension of 10 g (0.038 mole) 1-bromo-3,5-di-*tert*-butylbenzene (III), 1.5 g cupric oxide, and 0.5 g copper powder in 100 ml 10% sodium hydroxide solution was heated in an autoclave with stirring for 24 hours at 275° C. After the bomb had cooled, the contents were washed out with portions of ether and water. The solids were filtered off and the layers separated. The ether layer was extracted with methanolic KOH. The alkaline phase was added to the previous water layer and the methanol was distilled off. The remaining solution was acidified with sulphuric acid and the resultant solid collected. This was purified by vacuum sublimation, yielding 4.2 g (0.020 mole, 53%) 3,5-di-*tert*-butylphenol, m.p. 94–95° C. Anal. Calc. for $C_{14}H_{22}O$: C, 81.49; H, 10.75. Found: C, 81.43; H, 10.57.

The infrared spectrum (KBr disk) contained prominent bands at 3275, 1605, 1465, 1365, 1305, 1250, 955, 855, and 705 cm^{-1}.

Benzoate

The benzoate had m.p. 82.5–83.0° C. Anal. Calc. for $C_{21}H_{26}O_2$: C, 81.25; H, 8.44. Found: C, 81.44; H, 8.53.

1-Naphthylurethan

1-Naphthylurethan had m.p. 162.0–162.5° C. Anal. Calc. for $C_{25}H_{29}NO_2$: C, 79.97; H, 7.79. Found: C, 80.26; H, 7.97.

3,5-Di-tert-butylbenzoic acid (V)

This compound was prepared from 3,5-di-*tert*-butyltoluene (IV) following the method of Schlatter in a 64% conversion, m.p. 171–173° C, reported (5) 172.6–173.0° C.

3,5-Di-tert-butylanilinium sulphate (VI)

A mixture of 36 g (0.153 mole) 3,5-di-*tert*-butylbenzoic acid (V), 108 ml concentrated sulphuric acid, and 315 ml chloroform was stirred in a three-neck flask and heated to 45° C in an oil bath. In small portions, 10.8 g sodium azide was added over the course of 1 hour, and the mixture was stirred for another 4 hours. The mixture was cooled and the chloroform removed under reduced pressure. The residue was poured onto ice, the precipitated amine sulphate collected and recrystallized twice from ethanol, giving 40.0 g (0.071 mole, 93%) 3,5-di-*tert*-butylanilinium sulphate. The sulphate was used in the next step without conversion to the free amine.

3,5-Di-tert-butylphenol (I) (Via the Amine Route)

3,5-Di-*tert*-butylanilinium sulphate (VI) (39.4 g, 0.070 mole) was added to 1000 ml of 20% sulphuric acid solution. After addition of enough ice to bring the temperature to 0° C, 11.2 g, sodium nitrite in 60 ml water was added to the stirred solution over 10 minutes through a separatory funnel whose stem extended below the surface of the solution. The mixture was kept at 0° C for 1 hour with occasional stirring. The liquid was then decanted and added in portions to 300 ml of 20% sulphuric acid solution through which a current of steam was passing. After the liquid had been added, the solid was added in several portions, and the steam distillation continued until no more phenol came over in the distillate. The distillate was extracted with benzene, and the solvent removed by distillation. The remaining solid was purified by vacuum sublimation to give 23.4 g (0.113 mole, 80%) 3,5-di-*tert*-butylphenol, m.p. 93–95° C. This sample was shown to be identical with that obtained from 1-bromo-3,5-di-*tert*-butylbenzene by identical infrared spectra and undepressed mixed melting points.

Polynitration of 3,5-Di-tert-butylphenol

Red fuming nitric acid (75 ml) and 150 ml concentrated sulphuric acid were cooled to 10° C and rapidly agitated as 0.5 g (2.5 mmoles) 3,5-di-*tert*-butylphenol (I) dissolved in 50 ml concentrated sulphuric acid was added dropwise over a 20-minute period. After the addition was complete, the mixture was stirred at room temperature for 4 hours, and then poured on ice. The resulting solid was collected and recrystallized four times from 95% ethanol, giving a sample (0.2 g, 0.17 mmole, 28%) of 2,6-dinitro-3,5-di-*tert*-butylphenol (VII), m.p. 214–215° C (subl.). Anal. Calc. for $C_{14}H_{20}N_2O_5$: N, 9.46. Found: N, 9.00. The infrared spectrum shows a peak at 3450 cm^{-1} which is unchanged with dilution, indicating an intramolecular hydrogen-bonded phenol.

Can. J. Chem. Downloaded from www.nrcresearchpress.com by 210.87.254.5 on 09/05/12
For personal use only.

Mononitration of 3,5-Di-tert-butylphenol

3,5-Di-*tert*-butylphenol (I) (1.03 g, 5 mmoles) was dissolved in 100 ml of glacial acetic acid, and the mixture stirred at room temperature while a solution of 0.32 ml 70% nitric acid (5 mmoles) dissolved in 10 ml acetic acid was added over a 10-minute period. The reaction was stirred for another 15 minutes; then the reaction mixture was poured into water and partially neutralized by the addition of solid sodium bicarbonate. The solid was collected, washed with water, and recrystallized four times from pentane, giving 0.6 g (2.4 mmoles, 48%) 2-nitro-3,5-di-*tert*-butylphenol (VIII), m.p. 127.0–128.0° C. Anal Calc. for $C_{14}H_{21}NO_3$: N, 5.57. Found: N, 5.31. The infrared spectrum shows a peak at 3450 cm^{-1} which is unchanged with dilution, indicating an intramolecular hydrogen-bonded phenol.

Polybromination of 3,5-Di-tert-butylphenol

3,5-Di-*tert*-butylphenol (I) (1.03 g, 5 mmoles) was refluxed for 1 hour in 50 ml of acetic acid to which 3.2 g bromine had been added. Evaporation of the solvent and of the excess bromine gave a solid which was recrystallized three times from pentane to give colorless crystals (0.8 g, 2.2 mmoles, 44%) of 2,6-dibromo-3,5-di-*tert*-butylphenol (IX), m.p. 121.5–123.0° C. Anal Calc. for $C_{14}H_{20}Br_2O$: C, 46.17; H, 5.54. Found: C, 46.28; H, 5.72. The infrared spectrum shows a peak at 3430 cm^{-1} which is unchanged with dilution, indicating an intramolecular hydrogen-bonded phenol. A hydrolysis test (refluxing 5 minutes in 5% ethanolic potassium hydroxide, addition of silver nitrate solution) indicated that all halogen was attached to the aromatic ring.

Polychlorination of 3,5-Di-tert-butylphenol

3,5-Di-*tert*-butylphenol (I) (1.03 g, 5 mmoles) was dissolved in 100 ml carbon tetrachloride in a blackened flask. About 1 g of chlorine was bubbled through the mixture over a 10-minute period. The mixture was then refluxed for 30 minutes while chlorine addition was continued at the same rate. The mixture was then cooled, and excess chlorine and the solvent removed at reduced pressure. The residue was a semisolid. Repeated recrystallizations from pentane led to the isolation of two components. The first, a major constituent, was a colorless solid (X), which could not be completely purified (0.8 g, 2.9 mmoles, 58%), m.p. 88.0–89.5° C. Anal. Calc. for $C_{14}H_{20}Cl_2O$: C, 61.09; H, 7.33. Found: C, 60.20; H, 7.01. The infrared spectrum shows a peak at 3430 cm^{-1} which is unchanged with dilution, indicating an intramolecular hydrogen-bonded phenol. The spectrum also showed a small peak at 1685 cm^{-1} which indicates contamination by a small amount of the tetrachloro compound. The hydrolysis test as described above indicated that essentially all the halogen was attached to the aromatic ring.

The second product isolated, a lesser constituent, recovered after six recrystallizations from pentane, was in the form of long colorless needles (XI) (0.1 g, 0.29 mmole, 5.8%), m.p. 160.0–160.5° C. Anal. Calc. for $C_{14}H_{18}Cl_4O$: C, 48.86; H, 5.27. Found: C, 48.97; H, 5.29. The infrared spectrum of this compound shows a strong peak at 1685 cm^{-1} which corresponds to that of an α,β-unsaturated ketone (11). No hydroxyl peak is present in this spectrum.

The ultraviolet spectrum has a maximum at 255 mμ (isooctane), indicating a 2,5-cyclohexadieneone-1 structure (8).

The hydrolysis test, performed as above, indicated the presence of a large portion of alkyl type halide.

ACKNOWLEDGMENT

The authors wish to acknowledge their gratitude to Dr. M. J. Schlatter of California Research Corporation and Dr. A. McCaulay of American Oil Co. for generous gifts of 3,5-di-*tert*-butyltoluene.

REFERENCES

1. R. P. Mariella, M. J. Gruber, and John W. Elder. J. Org. Chem. **26**, 3217 (1961).
2. C. E. Moore and R. Peck. J. Org. Chem. **20**, 673 (1955).
3. C. E. Moore, M. M. Lally, R. L. Anderson, J. L. Brady, and J. J. McLafferty. Anal. Chim. Acta, **15**, 1 (1956).
4. J. Burger, W. Van Hartingsvedt, J. Van Keulen, P. E. Verkade, H. Visser, and B. M. Wepster. Rec. Trav. Chim. **75**, 1327 (1956).
5. M. J. Schlatter. U.S. Patent No. 2,634,114 (1953); Chem. Abstr. **48**, 7059 (1954).
6. D. A. McCauley, A. P. Lien, and P. J. Launer. J. Am. Chem. Soc. **76**, 2354 (1954).
7. T. Zincke and C. Schaum. Ber. **27**, 537 (1894).
8. L. Denivelle and R. Fort. Compt. Rend. **240**, 2423 (1955).
9. L. R. C. Barclay and E. E. Betts. Can. J. Chem. **33**, 672 (1955).
10. P. D. Bartlett, M. Roha, and R. M. Stiles. J. Am. Chem. Soc. **76**, 2349 (1954).
11. R. Mecke and K. Noack. Spectrochim. Acta, **12**, 391 (1958).

Can. J. Chem. Downloaded from www.nrcresearchpress.com by 210.87.254.5 on 09/05/12
For personal use only.

PALLADIUM COMPLEXES OF DI-2-THIENYLKETOXIME

WILLIAM J. HOLLAND AND LEO LEE
Department of Chemistry, Essex College, University of Windsor, Windsor, Ontario
Received October 3, 1962

ABSTRACT

The reaction between di-2-thienylketoxime and the palladium (II) ion has been studied. The compounds prepared were the complexes dichlorobis(di-2-thienylketoxime-N,N′)palladium (II), biaquobis(di-2-thienylketoxime-N,N′)palladium (II) half hydrate, and polymeric forms of the chelate bis(di-2-thienylketoxime)palladium (II).

INTRODUCTION

A recent investigation of complex formation between bivalent palladium and 2-thienyl-*trans*-aldoxime has illustrated the utility of a thiophene derivative as an analytical reagent (1). The purpose of the present work was to investigate complex formation between bivalent palladium and di-2-thienylketoxime.

A survey of the literature reveals a surprising lack of information regarding thiophene derivatives in complex formation with the transition metals. Although thenyltrifluoroacetone has been used for the separation of zirconium and hafnium (2) and the stability constants of metal complexes of 2-thiophenecarboxylic acid have been measured (3) no other thiophene derivatives seem to have been studied.

Oximes in general form stable complexes with metals, particularly with those of the transition triads of the Periodic Table, and are widely used for the detection and estimation of those metals. Examples are salicylaldoxime (4) and benzylmethylglyoxime (5).

EXPERIMENTAL

Di-2-thienylketoxime

A solution of 11.2 g of di-2-thienylketone (6), 11.2 g of hydroxylamine hydrochloride, and 44 g of potassium hydroxide in 500 ml of alcohol was refluxed for 2 hours. The reaction mixture was poured into 1000 ml of water and made acid to litmus by the addition of hydrochloric acid. The precipitate was filtered under suction and dissolved in alcohol. Water was added until the solution became turbid. On cooling, colorless needles separated which were filtered under suction and air-dried. There was obtained 10.3 g, 86% yield, of white needles, m.p. 134–136°. Anal. Calc. for $C_9H_7NOS_2$: C, 51.63; H, 3.37; N, 6.69. Found: C, 51.56; H, 3.46; N, 6.55.

Dichlorobis(di-2-thienylketoxime-N,N′)palladium (II)—Compound I

To a 400-ml beaker was added 1.0 g of di-2-thienylketoxime, 50 ml of alcohol, and 4.2 ml of concentrated hydrochloric acid. A solution of 0.40 g of anhydrous palladium (II) chloride in 5 ml of concentrated hydrochloric acid was prepared in a 100-ml beaker by warming on a hot plate. To the palladium (II) chloride solution was added 50 ml of water and the pH was adjusted to zero by dropwise addition of a concentrated potassium hydroxide solution. The palladium (II) chloride solution and 100 ml of 1 *N* hydrochloric acid were added with stirring to the oxime solution. After standing the solution for 1 hour the yellow precipitate was filtered under suction and air dried. There was obtained 1.30 g, 93% yield, of yellow crystals, m.p. 212–214° with decomp. Anal. Calc. for $PdC_{18}H_{14}Cl_2N_2O_2S_4$: Pd, 17.85; N, 4.70; Cl, 11.87. Found: Pd, 17.85; N, 4.58; Cl, 11.83.

On dissolving a few milligrams of I in 10 ml of alcohol and adding alcoholic silver nitrate, a clear solution was obtained which on standing for 3 hours became opalescent.

Regeneration of Di-2-thienylketoxime from I

To a 250-ml separatory funnel was added 0.3 g of I, 50 ml of acetone, 50 ml of chloroform, and 50 ml of concentrated hydrochloric acid. On shaking the mixture for 3 minutes, the solid went into solution and the chloroform layer became colored a pale yellow. The chloroform layer was withdrawn, washed first with a solution of 50 ml of acetone and 50 ml of concentrated hydrochloric acid, then four times with 50-ml portions of water, dried over anhydrous sodium sulphate, and filtered. On evaporation of the chloroform there was obtained a colorless, crystalline residue amounting to 0.22 g, 100% yield, m.p. 133–136°. A mixture melting

Can. J. Chem. Downloaded from www.nrcresearchpress.com by 210.87.254.105 on 09/05/12
For personal use only.

point determination with an authentic sample of di-2-thienylketoxime showed no depression; mixture m.p. 133–136°.

Biaquobis(di-2-thienylketoxime-N,N')palladium (II) Half Hydrate—Compound II

To a 250-ml separatory funnel was added 1.33 g of I, 50 ml of benzene, 50 ml of acetone, and 50 ml of water. The mixture was shaken for 10 minutes, at the end of which time all the solid had gone into solution to give a dark red-brown benzene layer. The benzene layer was washed with seventeen 50-ml portions of water and allowed to stand overnight. The yellow crystalline precipitate was filtered under suction and dried *in vacuo* over anhydrous calcium sulphate. The residue amounted to 0.80 g, 63% yield, m.p. 185–188° with decomp. Anal. Calc. for $PdC_{18}H_{14}N_2O_2S_4.2\frac{1}{2}\ H_2O$: Pd, 18.73; H_2O, 7.93. Found: Pd, 18.77; H_2O, 8.06.

The above procedure was repeated with 0.7221 g of I. The combined water washings were titrated with 0.102 *N* NaOH using phenolphthalein as indicator. Calc. for $PdC_{18}H_{14}Cl_2N_2O_2S_4$: HCl, 12.18. Found: HCl, 12.14.

Regeneration of Di-2-thienylketoxime from II

The procedure used for the regeneration of the ketoxime from I was followed with 0.15 g of II. There was obtained 0.11 g, 93% yield, of a crystalline residue, m.p. 133–136°. A mixture melting point determination with an authentic sample of di-2-thienylketoxime showed no depression; mixture m.p. 133–136°.

Bis(di-2-thienylketoxime)palladium (II) High Polymer—Compound III

On heating II at 120° for 3 hours, there was obtained a yellow-brown residue, m.p. 187–190° with decomp. Anal. Calc. for $PdC_{18}H_{12}N_2O_2S_4$: Pd, 20.35; N, 5.36. Found: Pd, 20.38; N, 5.46.

Ultraviolet absorption measurements in chloroform gave for III λ_{max} 288 mμ; $E^{1\%}_{1\ cm}$ 547.

On dissolving III in boiling benzene and allowing the solvent to evaporate at 50° a brown residue was obtained. This material in chloroform gave an ultraviolet absorption spectrum identical with that obtained with IV; λ_{max} 284 mμ; $E^{1\%}_{1\ cm}$ 507.

A cyroscopic molecular weight of III in nitrobenzene gave a value of 533. The calculated value for the monomer of IV is 523. Evaporation of the nitrobenzene on a steam bath under an air current gave a dark brown solid residue of IV.

A dipole moment measurement of III in carbon tetrachloride solution gave μ = 1.86 D.

Regeneration of Di-2-thienylketoxime from III

The procedure used for the regeneration of the ketoxime from I was followed with 0.15 g of III. There was obtained 0.12 g, 100% yield, of a crystalline residue, m.p. 133–136°. A mixture melting point determination with an authentic sample of di-2-thienylketoxime showed no depression; mixture m.p. 133–136°.

Bis(di-2-thienylketoxime)palladium (II) Low Polymer—Compound IV

To a 1-liter beaker was added 1.1 g of di-2-thienylketoxime, 5 ml of a saturated solution of potassium hydroxide, and 1500 ml of water. The pH of the solution was adjusted to 6.9 by the addition of hydrochloric acid. A solution of 0.4 g of palladium (II) chloride was prepared in 5 ml of concentrated hydrochloric acid with warming and diluted to 75 ml with water. The pH of the palladium (II) chloride solution was adjusted to 6.2 by the addition of potassium hydroxide solution and the solution diluted to 100 ml. To the boiling ketoxime solution was added alternately 2.0 ml of the palladium (II) chloride solution and 0.70 ml of 0.1024 *N* sodium hydroxide with vigorous stirring. When all the palladium (II) chloride had been added and a total of 35.0 ml of the sodium hydroxide solution, the reaction mixture was cooled to room temperature. The dark brown precipitate was filtered under suction and air dried. The dried residue was dissolved in benzene and filtered from a small amount of palladium (II) oxide. After evaporation of the benzene the residue was suspended in alcohol overnight to remove any unreacted ketoxime. The suspended chelate was filtered under suction and air dried. There was obtained 0.75 g of IV, m.p. 175–185° with decomp. Anal. Calc. for $PdC_{18}H_{12}N_2O_2S_4$: Pd, 20.35; N, 5.36. Found: Pd, 20.39; N, 5.44.

Ultraviolet absorption measurements of IV in chloroform gave λ_{max} 284 mμ; $E^{1\%}_{1\ cm}$ 509.

A dipole moment measurement of IV in carbon tetrachloride gave μ = 2.60 D.

A cyroscopic molecular weight determination of IV in nitrobenzene gave a value of 519. The calculated value for the monomer is 523. A similar determination in benzene gave a value of 1290. On standing, the cold benzene solution deposited yellow-brown crystals of III, m.p. 185–190° with decomp. The value 1290 corresponds to an average degree of polymerization of 2.5 for IV.

Regeneration of Di-2-thienylketoxime from IV

The procedure used for the regeneration of the ketoxime from I was followed with 0.15 g of IV. There was obtained 0.07 g, 60% yield, of a crystalline residue, m.p. 133–136°. A mixture melting point determination with an authentic sample of di-2-thienylketoxime showed no depression, mixture m.p. 133–136°.

DISCUSSION

In the present work di-2-thienylketoxime was found to form either a complex or a chelate with bivalent palladium, depending on the pH of the reaction medium. In 2 *N*

Can. J. Chem. Downloaded from www.nrcresearchpress.com by 210.87.254.105 on 09/05/12
For personal use only.

hydrochloric acid a small amount of the complex (I) formed and the major part of the reagent was recovered. In 1 *N* acid solution an almost quantitative yield of the complex (I) was obtained, while in neutral or slightly basic solution there was a good yield of the chelate (IV). In moderately acid solution in the pH range 1 to 6, mixtures of I and IV formed.

The complex (I) is a pale yellow crystalline solid insoluble in water and slightly soluble in benzene and chloroform, while the chelate (IV) is a dark brown solid insoluble in water and very soluble in benzene and chloroform, giving dark red-brown solutions.

When the complex (I) was treated with a mixture of benzene and water, hydrogen chloride was eliminated quantitatively as was shown by titration of the water layer with standard base. On standing, the benzene layer deposited a yellow crystalline solid which at 120° lost $2\frac{1}{2}$ moles of water to give a light brown solid (III) insoluble in water and slightly soluble in benzene and chloroform.

In alcoholic silver nitrate solution I gave no immediate precipitate, but on standing, the solution became turbid and silver chloride began to precipitate. This indicates that the chlorine atoms are bound covalently to the palladium. Analysis of I showed that two molecules of the ketoxime and two atoms of chlorine are associated with each palladium atom. Palladium therefore has a coordination number of four. This is to be expected since the existence of palladium (II) compounds with a coordination number greater than four has never been convincingly demonstrated (7). Although there is no experimental evidence to indicate whether coordination is with the nitrogen of the oxime group rather than with the sulphur of the thiophene ring, nevertheless the coordinating ability of the oxime group and the very strong donor properties of the oxime nitrogen are very well known (8). Further, one would expect the donor ability of the sulphur to be decreased because of resonance with the unsaturated ring.

Magnetic susceptibility measurements showed I and II to be diamagnetic. The complex (I) therefore is considered to be planar rather than tetrahedral. This is in accord with the fact that no tetrahedral structure for palladium (II) complexes has yet been identified positively, unless, of course, it is sterically impossible for the compound to assume a planar configuration. Also coordination theory predicts a planar configuration for ions such as bivalent palladium which have one *d*-orbital available for bond formation. In such a situation dsp^2 hybridization occurs and a square planar structure results.

The postulated hydrogen bonding for I eliminates the possibility of cis–trans isomerism. Such bonding would give rise to a more stable structure, since it has been long observed that an increase in the number of rings within a particular complex structure results in greater stability (9). Such a postulated bonding has precedent in the literature. For example, Brady and Meurs (10) proposed such bonding in their study of the nickel derivatives of biacetyl dioxime. That the complex (I) exists in the trans form is borne out by the facile elimination of hydrogen chloride. The ease of such elimination indicates that the hydrogen and chlorine atoms are adjacent to each other, whereas a cis configuration would place them on opposite sides of the molecule. Further molecular models reveal that a cis configuration would be more strained than a trans configuration. Infrared spectra of I indicate hydrogen bonding. Such spectra reveal no hydroxyl band present in the region 3400–3700 cm^{-1}, but do show a very broad band at 3100 cm^{-1}. Thus, the hydroxyl group band has been shifted considerably to a lower frequency. Such a shift is considered evidence for strong intramolecular bonding.

The structure shown for the hydrate (II) is based on the analysis and the course of the reaction used in its preparation. Thus, on shaking I in a mixture of benzene and water

Can. J. Chem. Downloaded from www.nrcresearchpress.com by 210.87.254.105 on 09/05/12
For personal use only.

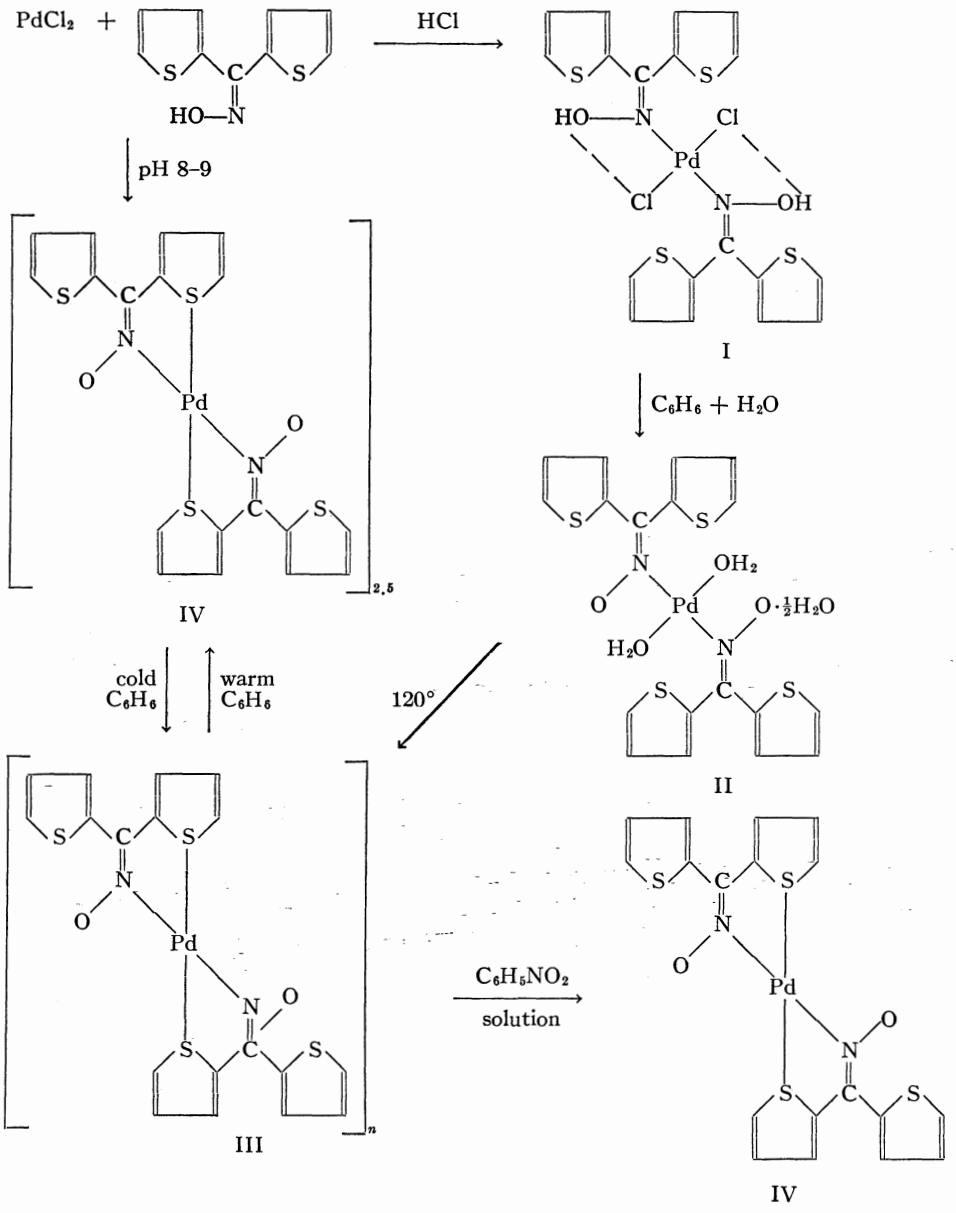

the benzene layer becomes colored a dark red-brown and hydrogen chloride is produced in the water layer. The color of the benzene layer indicates that a chelate has formed. On standing, the color disappears and a yellow crystalline precipitate forms. This is interpreted as being due to a displacement of the palladium–sulphur bond in the chelate with formation of a complex in which water molecules are coordinately bonded to palladium. Molecular models reveal that the two water molecules must be trans since a cis configuration would impart a large strain. The remaining one-half water molecule is considered to be involved in crystal formation.

Can. J. Chem. Downloaded from www.nrcresearchpress.com by 210.87.254.105 on 09/05/12
For personal use only.

The structure assigned to III is based on the analysis and on molecular weight determinations of III and IV. Thus IV in freezing benzene gave a molecular weight corresponding to that of a low polymer of IV, the average degree of polymerization being 2.5. On standing, the cold benzene solution deposited a yellow-brown solid with the same melting point as III. Thus IV is converted to III from cold benzene solution. This indicates that III is a polymer of IV. No direct molecular weight determination of III could be carried out in benzene owing to its insolubility in this solvent. On suspending III in boiling benzene and allowing the solvent to evaporate at 50° IV was obtained. Thus in hot benzene III is reconverted to IV. In freezing nitrobenzene III gave a molecular weight corresponding to that of a monomer of IV. On evaporation of the nitrobenzene a dark brown residue of IV was obtained. Substance III is thus converted to a low polymer of IV from warm nitrobenzene.

The analyses of III and IV showed these substances to be isomeric. That III and IV are not simply dimorphic is borne out by an examination of their ultraviolet absorption spectra in chloroform solution. Small, but definite, differences in their spectra were found.

The possibility of III and IV being cis–trans isomers was eliminated by dipole moment measurements in carbon tetrachloride solution. The moments of III and IV were 1.8 and 2.6 D respectively. If IV were a cis isomer the dipole moment would be expected to be much higher. Also a cis configuration for IV would mean that the two negatively charged oxygens of the nitrone groups would be adjacent to one another. It is highly unlikely that such a separation of like charges would take place since the resulting compound would be highly unstable.

The assignment of the chelate structure to IV is based on the analysis and on its solubility in benzene or chloroform to give highly colored solutions. Molecular weight determination in benzene indicates that IV is a low polymer of the structure shown. Similar determination in nitrobenzene reveals IV as the monomer in this solvent. That the structure contains two nitrone groups is inferred by reference to the studies made by Pfeiffer (11) on the nickel dimethylglyoxime chelate. In this case the author showed that a covalent linkage exists between nitrogen and the metal rather than between oxygen and the metal.

Finally, that the ketoxime reagent undergoes no change in structure is shown by the fact that it could be readily regenerated in high yield from each of I, II, III, and IV by treatment with strong hydrochloric acid solution.

ACKNOWLEDGMENT

This work has been supported by a grant from the National Research Council of Canada.

REFERENCES

1. S. G. Trandon and S. C. Bhattacharya. Anal. Chem. **32**, 194 (1960).
2. E. H. Huffman and L. J. Beaufait. J. Am. Chem. Soc. **71**, 3179 (1949).
3. P. O. Lumme. Suomen Kemistilehti, **33**, No. 2, 85 (1960).
4. E. Ephriam. Ber. **63**, 1930 (1928).
5. F. P. Dwyer and D. P. Mellor. J. Am. Chem. Soc. **57**, 605 (1935).
6. V. Thomas and V. Couderc. Bull. Soc. Chim. France, **23**, 288 (1918).
7. A. Martell and M. Calvin. Chemistry of the metal chelate compounds. Prentice-Hall Inc., New Jersey. 1959.
8. J. C. Bailar. Chemistry of the coordination compounds. Reinhold Publishing Corp., New York. 1956.
9. M. Calvin and R. H. Bailes. J. Am. Chem. Soc. **68**, 949 (1946).
10. G. L. Brady and M. M. Meurs. J. Chem. Soc. 1599 (1930).
11. P. Pfeiffer. Ber. **63**, 1811 (1930).

Can. J. Chem. Downloaded from www.nrcresearchpress.com by 210.87.254.105 on 09/05/12
For personal use only.

THE DECOMPOSITION OF 2-METHYL-Δ^2-OXAZOLINE IN AQUEOUS SOLUTION[1]

R. GREENHALGH, R. M. HEGGIE, AND M. A. WEINBERGER
Defence Research Chemical Laboratories, Ottawa, Canada

Received January 3, 1963

ABSTRACT

Nuclear magnetic resonance has been used to follow the decomposition of aqueous solutions of 2-methyl-Δ^2-oxazoline (0.29 *M*) at constant pH values in the range −1 to 14. The decomposition is first order with respect to total oxazoline at any specific pH, but deviates from the simple reaction of water with the protonated species above pH 5. At neutral pH values this is shown to be partially due to a second reaction involving 2-methyl-Δ^2-oxazoline and O-acetylethanolamine which yields N-2-acetoxyethyl N′-2-hydroxyethyl acetamidate. The decrease in rate constant at pH < 2 is accounted for by variation in the water concentration, which is related to the acidity function. A kinetic expression is derived for the decomposition over the whole pH range studied. The decomposition of the amidate is also discussed.

One of the more interesting properties of 2-methyl-Δ^2-oxazoline (I) is its decomposition in aqueous solution to give either O-acetylethanolamine (IV) or N-acetylethanolamine (III), both the rate of reaction and the product varying with pH. This decomposition has been examined kinetically in neutral and acid solutions by other workers (1, 2) and, except for pH < 2, the variation in the rate of decomposition was shown to be dependent on the concentration of the protonated species. Martin and Parcell suggested the following mechanism, which involves 2-hydroxy-2-methyloxazolidine (II) as a labile intermediate:

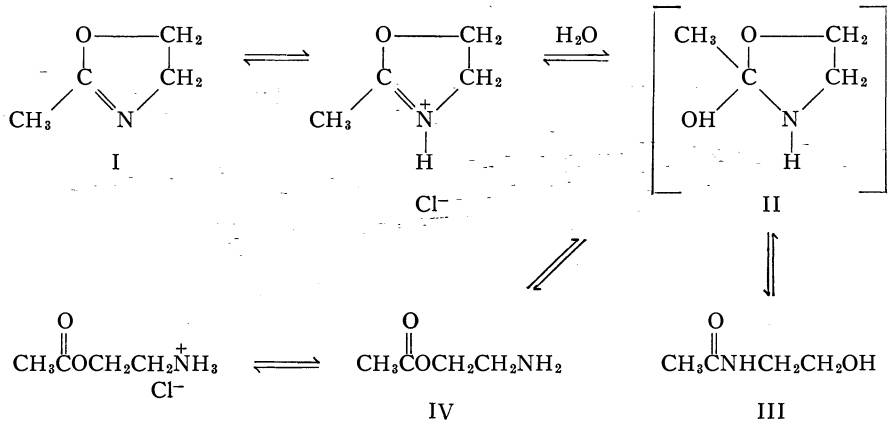

Earlier work in these laboratories (3) on the reaction of I in more concentrated solutions showed that this scheme did not account for the results at pH 7 and 8. Consequently, a study of the decomposition of I in aqueous solutions of pH −1 to 14 was undertaken.

Examination of the n.m.r. spectra of I and its known decomposition products, III and IV, in this pH range showed that they could be readily differentiated by the field position of the methyl protons. The minimum separation observed in these experiments was at pH 7 between I and III; however, since III is not a significant hydrolysis product of I at this pH, it did not produce any difficulties. At pH 7 the methyl triplet in I (4) is centered

[1]*Issued as D.R.C.L. Report No. 406.*

Can. J. Chem. Downloaded from www.nrcresearchpress.com by 210.87.254.6 on 09/05/12
For personal use only.

at 2.728 p.p.m. upfield from water, whilst III and IV give single methyl proton peaks at 2.709 and 2.571 p.p.m. respectively. Since n.m.r. can also be used under certain conditions to determine the relative amounts present (5), it appears to be a suitable method for following the decomposition of oxazoline.

Over the pH range studied, the decomposition of I at any specific pH was found to follow first-order kinetics. Typical first-order plots are shown in Fig. 1.

The pH dependence of the observed first-order rate constants (k_{obs}) is shown in Fig. 2.

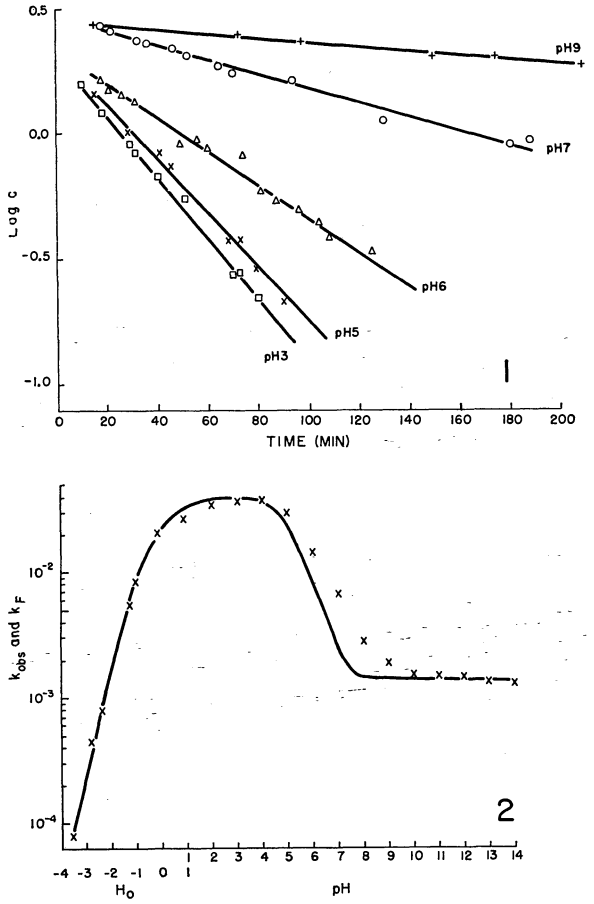

FIG. 1. Decomposition of I at 30° and constant pH. Concentration is expressed as the ratio of peak height of I to that of external standard.

FIG. 2. Variation with pH and H_0 of the observed first-order rate constant (points). The curve represents the values calculated from equation (F) with $k_1 = 4.58\times10^{-9}$ mole l^{-1} min^{-1}, $k_2 = 3.06\times10^{-2}$ min^{-1}, and $K_a = 3.16\times10^{-6}$ mole l^{-1}.

Examination of Fig. 2 reveals that the observed rate constants are virtually pH independent in alkaline solution. Therefore the decomposition of oxazoline above pH 10 is compatible with one or both of the following mechanisms, where B and BH^+ represent I and its protonated form:

$$BH^+ + OH^- \rightarrow \text{products}$$

$$B + H_2O \rightarrow \text{products.}$$

Can. J. Chem. Downloaded from www.nrcresearchpress.com by 210.87.254.6 on 09/05/12
For personal use only.

The former mechanism is preferred; however, our data do not allow us to differentiate between specific and general base catalysis. Both mechanisms lead to an expression for the first-order constant with respect to total oxazoline,

$$k_A = \frac{k_1}{K_a + [OH_3^+]}, \tag{A}$$

which is constant when $[OH_3^+] \ll K_a$, the ionization constant for the equilibrium $BH^+ \rightleftharpoons B + H^+$; k_1 is a composite constant, and k_A represents the theoretical approximation to k_{obs} given by equation (A). This nomenclature is used throughout to differentiate the theoretical first-order constants applicable to the various pH ranges.

In addition to the above mechanism the general shape of the k_{obs}/pH curve for the remaining pH region can, with some reservation at pH 6, 7, and 8, be accounted for by a mechanism proposed by Edward and Meacock (6(*a*), 6(*b*)) to explain the hydrolysis of benzamide and methyl benzimidate.

$$B + OH_3^+ \overset{1/K_1}{\rightleftharpoons} \overset{+}{B}H + H_2O \overset{K_2}{\rightleftharpoons} M^+ \overset{k}{\rightarrow} \text{products}$$

M^+ is the transition state for the hydrolysis, k a velocity constant, $1/K_1$ and K_2 are equilibrium constants. This mechanism leads to the expression

$$k_B = \frac{kK_2K_a}{K_1} \cdot \frac{[OH_3^+]}{K_a + h_0} \cdot \frac{f_B f_{OH_3^+}}{f_{M^+}}, \tag{B}$$

where h_0 is the non-logarithmic acidity function. The activity coefficient term is assumed not to vary and an overall constant (k_2) can therefore be defined:

$$k_2 = \frac{kK_2K_a}{K_1} \cdot \frac{f_B f_{OH_3^+}}{f_{M^+}}.$$

At any pH, then, the observed rate constant will be the sum of $k_A + k_B$. In the pH region around the pK_a, i.e. 5.5, this sum reduces to expression (C) since $h_0 \simeq [OH_3^+]$:

$$k_C = \frac{k_2[OH_3^+] + k_1}{K_a + [OH_3^+]}. \tag{C}$$

This describes the shape of the k_{obs}/pH curve in this region, apart from deviations which will be considered later.

For the range pH 2–4, since $K_a \ll h_0 = [OH_3^+]$ and the contribution from equation (A) is now negligible, equation (C) reduces to

$$k_D = k_2. \tag{D}$$

Finally, at high acid concentrations, where $h_0 \neq [OH_3^+]$, equation (B) becomes

$$k_E = k_2 \frac{[OH_3^+]}{h_0}. \tag{E}$$

The complete expression for the variation of the first-order constant with pH in the range -1 to 14 is therefore

$$k_F = \frac{k_2[OH_3^+] + k_1}{K_a + h_0}, \tag{F}$$

where $h_0 = [OH_3^+]$ at high pH's. The curve representing this expression is shown in Fig. 2 and, as can be seen, the observed rate constant at low pH is in good agreement with that

Can. J. Chem. Downloaded from www.nrcresearchpress.com by 210.87.254.6 on 09/05/12
For personal use only.

Can. J. Chem. Downloaded from www.nrcresearchpress.com by 210.87.254.6 on 09/05/12
For personal use only.

derived from equation (E). The decrease in k_{obs} is thus adequately described by the decrease in water concentration, which is proportional to $[OH_3^+]/h_0$. The treatment at high acid concentrations is equivalent to that of Bunnett (7(*c*)) for a base strong enough to be virtually completely protonated at the acid concentrations involved and with $\omega^* = 0$. The slope (ω^*) of the Bunnett plot (log k_{obs} − log [HCl] − H_0 vs. log a_{H_2O}) applicable in this case (7(*a*)) was found to be very close to zero. This implies that water is acting as a proton transfer agent in the rate-determining step (7(*b*)) and further that there is no change in hydration between the transition state and the reactants (7(*c*)). Martin and Parcell (2) have proposed an alternative expression which accounts for the falloff in k_{obs} with decrease in pH in terms of an equilibrium between BH^+ and 2-hydroxy-2-methyloxazolidine (II) which is reversed by high hydrogen ion concentration. This latter treatment has been applied to both I and 2-methyl-Δ^2-thiazoline, although very recently Martin has expressed some reservations about the applicability of his mechanism to the hydrolysis of I (8).

From Fig. 2 it is evident that agreement between the theoretical curve and the experimental points is poor in the range pH 5–9. This is due to a second reaction involving I that yields an amidate which at pH 7 is the primary product (9). This compound has been isolated, and spectral and analytical data showed it to be N-2-acetoxyethyl N′-2-hydroxyethyl acetamidate hydrochloride (V). The infrared spectrum showed peaks at 3325, 1060; 1660; 1740, and 1230 cm^{-1}, which were assigned to hydroxyl, imino, and ester groups. The presence of the hydroxyl group was confirmed by acetylation, which gave a crystalline derivative whose infrared spectrum showed an increase in intensity at 1740 cm^{-1} together with a new peak at 1245 cm^{-1}, whilst the peaks assigned to the hydroxyl group were missing. In order of appearance with increasing field, the n.m.r. spectrum of this acetyl derivative showed a triplet, a poorly resolved multiplet, and two single peaks at τ 7.544 and 7.917. The areas of the combined low-field multiplets and the single peaks were in the ratio 8.00:2.96:6.04, confirming that these peaks are due to the methylene protons, the methyl protons of the acetamidate group, and the methyl protons of the ester groups respectively. More recently the material and its acetyl derivative have been synthesized by the following scheme, thus confirming the structural assignment:

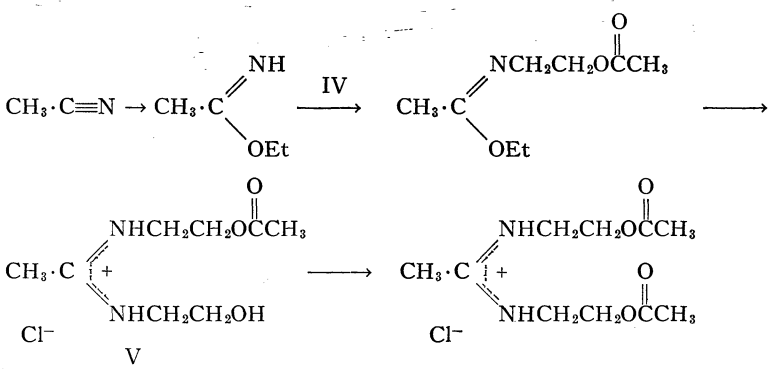

If we consider I as a cyclic imidate the formation of V is not unexpected since amidates are known to be formed from the reaction of imidates with primary or secondary amines (10). There are two possibilities for the amine component of this reaction, IV, and II, which has been postulated as an intermediate in the decomposition of I. To determine if IV was the reactant, the reaction of equimolar aqueous solutions of this amine and I was studied at pH 6, 7, and 8. At all three pH values the rates of both decomposition of I and appearance of V were greater when the amine was added. At pH 7, the disappearance of I could

be described by second-order kinetics (Fig. 3) with a rate constant of 2.8×10^{-1} l. mole^{-1} min^{-1}.

At pH 6 the first-order decomposition of I and at pH 8 the transformation of IV to III become significant competing reactions for the formation of V. The limitations of the method and the narrow pH range available for study make it impossible to determine the formation of V with sufficient accuracy for kinetic purposes.

Since V is formed by a second-order reaction it is surprising that the decomposition of I is apparently first order over the whole pH range studied. This can be explained at pH 6 and 8 by the fact that V is not the major reaction product. At pH 7, where V is the main product, the first-order treatment is still applicable since the concentration of IV rapidly reaches a low steady value. It is possible to calculate a value for the second-order rate constant (k_3) for amidate formation at this pH by use of equation (G), where k_C is the first-order rate constant derived from equation (C) and k_{obs} is the experimental value:

$$k_{obs} = k_C + k_3[IV]. \qquad (G)$$

The value of the second-order constant, 2.4×10^{-1} l. mole^{-1} min^{-1}, is found to be in good agreement with that obtained directly from the equimolar experiments at pH 7. All the above evidence supports the postulate that the amidate (IV) arises from the reaction of I with IV:

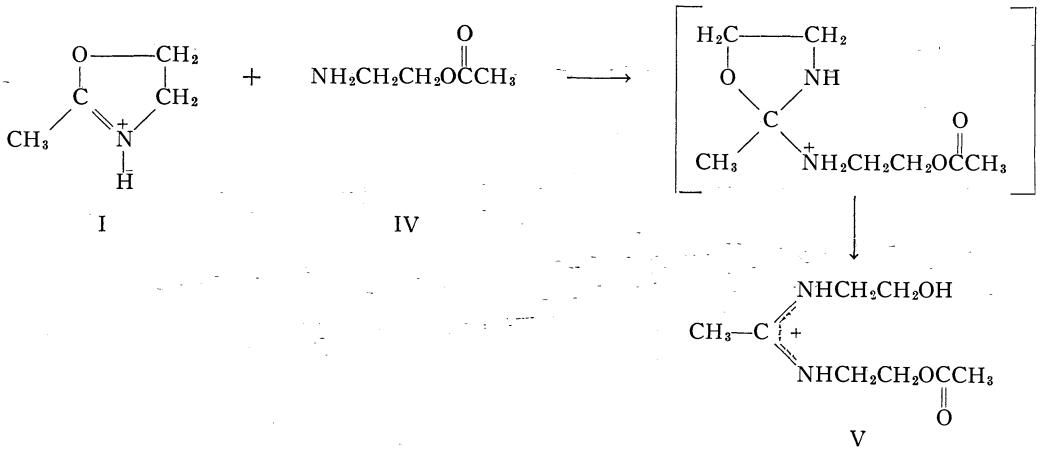

I IV V

Although I is stable in anhydrous methanol, if it is mixed with IV in this solvent it reacts to give V. When concentrations of reactants are used which are similar to those employed in the experiments in water, the reaction proceeds at about a quarter of the rate at pH 7. Since the absence of water would prevent the formation of II, it is felt that this evidence lends support to the mechanism derived from the kinetic data.

The properties of V were briefly examined, particularly its decomposition at various pH values. It was found to be stable at pH 4 and to decompose rapidly in alkaline solution. The formation of V and its subsequent decomposition at pH 7 are outlined in Fig. 4.

The persistence of IV long after I has disappeared indicates it to be a decomposition product of V, since it normally undergoes rapid transformation at this pH to III (see Table I). Thus at pH 7 the primary products of the decomposition of V are III and IV and a little acetate ion, with IV transforming to III as the ultimate product. At pH 10, however, the product ratio of III and acetate ion is reversed since acetate ion is now formed

Can. J. Chem. Downloaded from www.nrcresearchpress.com by 210.87.254.6 on 09/05/12
For personal use only.

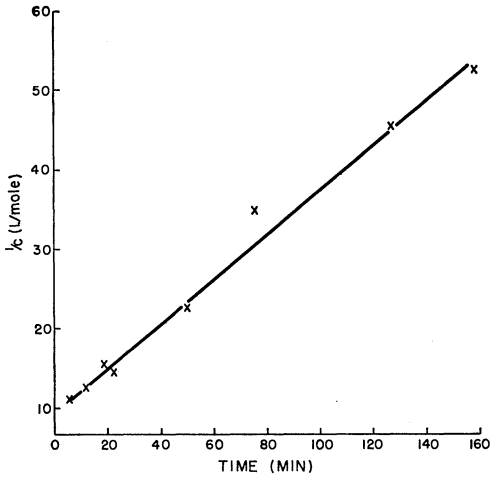

FIG. 3. The disappearance of I (0.14 *M*) at pH 7, 30°, in the presence of an equimolar amount of IV; $k_3 = 2.86 \times 10^{-1}$ l. mole^{-1} min^{-1}.

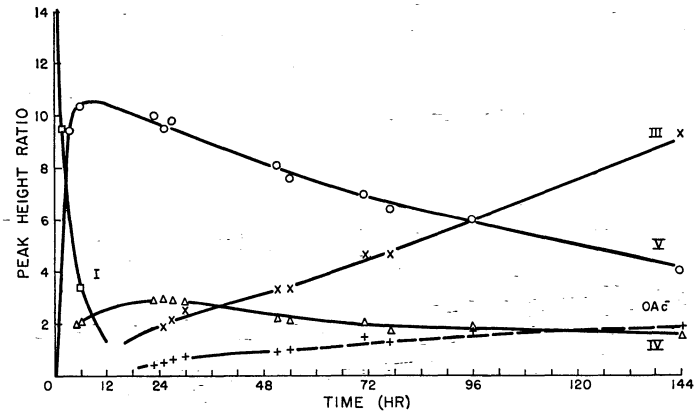

FIG. 4. The formation and decomposition of N-2-acetoxyethyl N′-2-hydroxyethyl acetamidate at pH 7 and 30°. Concentration is expressed as the peak height ratio of the particular methyl protons to the external standard. The conversion factor to moles/l. varies slightly between compounds.

very rapidly. By n.m.r. it is possible to show that the formation of the acetate ion is equivalent to the loss of the acetoxy group in V, and that the formation of III is equivalent to the loss of the methyl group of the amidate moiety. Thus two simultaneous reactions appear to be involved in the decomposition of V. Assuming that the k_{obs} for the decomposition of V is made up of the sum of the rate constants for these reactions, the ratio of these rate constants can be determined by product analysis. Comparison of the results at pH 7 and 10 indicates that the rate of formation of acetate ion increases by a factor of 10^3, whilst the rate for the reaction involving the amidate moiety increases at the most by a factor of 10. An intermediate, N,N′-bis-2-hydroxyethyl acetamidate, is postulated as being formed following cleavage of the acetoxy group. The two reactions are shown below, where with increasing pH the mechanism on the right-hand side predominates.

Reverting to the decomposition of I, it is found that the formation of V takes place only in the range pH 5 to 9, although V is found to be stable at pH values outside this range.

Can. J. Chem. Downloaded from www.nrcresearchpress.com by 210.87.254.6 on 09/05/12
For personal use only.

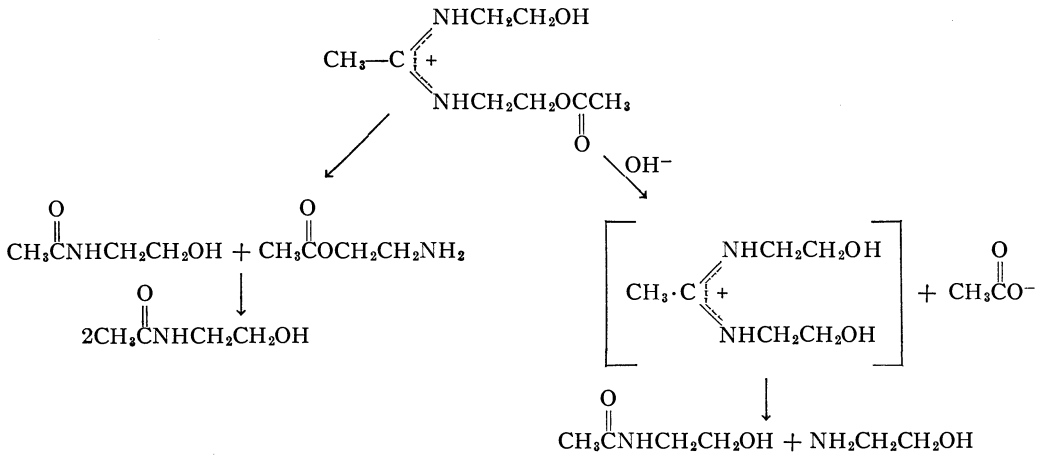

For pH < 5, this might be explained by the fact that both I and IV will be protonated, whereas amidate formation in general requires one or both reactants to be in the unprotonated form (10, 11). At pH 9 and above, any IV that is formed from I might be expected to transform preferentially into III. The fact that neither V nor its decomposition products were detected at pH 10 and above is in accord with this. The rates of transformation of IV to III are shown in Table I. As was noted above, when I and IV were mixed at pH 7

TABLE I

Rate constants for the transformation of O- to N-acetylethanolamine (30°)

pH	Rate constant, min^{-1}
6	1.2×10^{-3}
7	4.7×10^{-3}
8	3.8×10^{-2}
9	$>1.4\times10^{-1}$

III was not a significant early product. However, at pH 8 a substantial quantity of III was rapidly formed, apparently from isomerization of IV. This lends support to the above explanation.

In an attempt to determine the mode of ring opening of I, the n.m.r. spectra obtained during its decomposition were examined. The compounds of most interest in this respect are III and IV. Below pH 7, IV is found to the exclusion of III and above pH 9 the opposite is true; between these values signals due to both are observed. Two mechanisms have been postulated to explain these results. The first involves the decomposition of a transition complex of I and water to give IV, which at high pH is rapidly transformed to III. The second proposes hydration of the C=N bond to give II as a labile intermediate which yields III or IV depending on the pH. As no IV was detected above pH 8.5, and no signal was obtained in the experiments with I, I and IV, or IV which could be assigned to II, we are unable to differentiate between these two possibilities. The natural assumption that equation (A) also represents the direct formation of III was shown to be incorrect. At pH 7, equation (A) should account for approximately 40% of the decomposition of I, but as can be seen in Fig. 4, III is not present in significant amounts until after I has decomposed.

Can. J. Chem. Downloaded from www.nrcresearchpress.com by 210.87.254.6 on 09/05/12
For personal use only.

It has previously been suggested that 2-substituted Δ²-oxazolines behave like imidates in some of their reactions (3, 12). In the two reactions of I studied here, namely hydrolysis and amidate formation, the results are found to be in agreement with this hypothesis.

EXPERIMENTAL

Aqueous solutions of 2-methyl-Δ²-oxazoline (0.29 *M*) were held at 30° and maintained at the required pH by a Beckman automatic titrimeter. The n.m.r. spectra of aliquots were recorded at regular intervals using a Varian 4300C spectrometer at 60 Mc/s, with cyclohexane as an external reference. At least two spectra in the same sweep direction were recorded for each aliquot. The spectra were calibrated by the side-band technique using an electronic counter. Identification of peaks was checked by comparison of the field position of each compound separately at the appropriate pH and concentration. The reactions of O-acetylethanolamine hydrochloride (0.3 *M*) and O-acetylethanolamine hydrochloride (0.14 *M*) with 2-methyl-Δ²-oxazoline (0.14 *M*) were similarly studied.

For the sake of convenience, concentration was expressed as a ratio of the peak height of the methyl protons of the compound to that of the external standard. For O-acetylethanolamine, N-acetylethanolamine, and N-2-acetoxyethyl N′-2-hydroxyethyl acetamidate the peak height was used directly, whilst for 2-methyl-Δ²-oxazoline the height of the center peak of the triplet was doubled in order to determine the peak height ratio. The maximum deviation from linearity of the peak height to concentration relationship for 2-methyl-Δ²-oxazoline was found to be ±7% over the range 0.3 *M* to 0.03 *M*. It was necessary to reduce the peak height ratios of 2-methyl-Δ²-oxazoline by a factor of 0.71 to enable correlation with those obtained from O-acetylethanolamine.

Infrared spectra were recorded on a Perkin–Elmer 221 spectrophotometer. *2-Methyl-Δ²-oxazoline* was prepared by the method of Wenker (13), b.p. 109–111°. *O-Acetylethanolamine hydrochloride* was prepared from 2-methyl-Δ²-oxazoline by adjusting a 20% aqueous solution to pH 3 and allowing it to stand overnight at room temperature. The product was isolated after evaporation of the water under vacuum, and recrystallized from methanol/ether, m.p. 130–131° (lit. 128–130° (14)).

Isolation and Characterization of N-2-Hydroxyethyl N′-2-Acetoxyethyl Acetamidate Hydrochloride

A solution of oxazoline (1.25 g) in water (50 ml) which had been maintained at pH 7 and 30° overnight was taken to dryness under vacuum. The resulting oil (1.61 g) was chromatographed on Woelm acid alumina grade IV but was recovered unchanged on elution with 1:75 methanol:chloroform. Calc. for $C_8H_{17}O_3N_2Cl$: C, 42.81; H, 7.57; N, 12.50; Cl, 15.80%. Found: C, 41.06; H, 7.71; N, 11.26; Cl, 14.97%. Infrared (film): 3325 cm^{-1}, O—H; 3215 cm^{-1}, N—H; 3080 cm^{-1}, N—H; 1740 cm^{-1}, C=O (ester); 1660 cm^{-1}, C=N; 1230 cm^{-1}, C—OC (ester); 1060 cm^{-1} (sh), C—OH; 1050 cm^{-1}, C—C. The n.m.r. and infrared data are identical with those of the synthetic product, and with the analytical data support the assignment of the structure N-2-acetoxyethyl N′-2-hydroxyethyl acetamidate hydrochloride to this compound.

Some of the oil was warmed on a steam bath with acetic anhydride for 1/2 hour, and on evaporation a yellow oil resulted. Chromatography of this oil (600 mg) on Woelm acid alumina grade IV gave two fractions. The first fraction (79 mg) was eluted with chloroform and identified by its infrared spectrum and analysis as N,O-diacetylethanolamine. Elution with 1:75 methanol:chloroform gave a colorless oil (505 mg) which crystallized on standing. Recrystallization from acetone gave thick white needles, m.p. 106–108°. Calc. for $C_{10}H_{19}O_4N_2Cl$: C, 45.03; H, 7.13; N, 10.51; Cl, 13.30%. Mol. wt. 266. Found: C, 45.31; H, 7.21; N, 10.46; Cl, 13.01%. Mol. wt. 254 ($CHCl_3$), 145 (H_2O). Infrared (KBr): 3205 cm^{-1}, N—H; 3170 cm^{-1}, N—H; 3060 cm^{-1}; 3020 cm^{-1}; 1740 cm^{-1}, (C=O) ester; 1650 cm^{-1}, C=N; 1245 cm^{-1}, C—OC (ester); 1230 cm^{-1}, C—OC (ester); 1062 cm^{-1}, C—C. The relative intensities of the n.m.r. signal using a Varian electronic integrator were (CH_2), 8.00±0.12; (CH_3), 2.96±0.10; (CH_3, ester), 6.04±0.09. Comparison by mixed melting point and infrared spectrum indicated it to be identical with a synthetic sample of N,N′-bis-2-acetoxyethyl acetamidate hydrochloride.

Preparation of N-2-Acetoxyethyl Ethyl Acetimidate Hydrochloride

The procedure of Cornforth (15) was used; ethyl acetimidate hydrochloride (3 g) (16) was suspended in ether and stirred together with a solution of potassium carbonate (3.6 g) in water (10 ml). The ethereal solution containing the free base was decanted and to it O-acetylethanolamine hydrochloride (4.2 g) in water (10 ml) was added with cooling, and the mixture was stirred for 3/4 hour. The ether was again decanted, dried over sodium sulphate, and gave a yellow oil (1.53 g) on evaporation of the solvent. The oil was purified by distillation at 50° at 0.1 mm. Yield 25%. Calc. for $C_8H_{15}O_3N$: C, 55.5; H, 8.68; N, 8.09%. Found: C, 55.60; H, 8.80; N, 8.17%. Infrared (film): 1740 cm^{-1}, C=O (ester); 1628 cm^{-1}, C=N; 1465 cm^{-1}, C—CH_3; 1240 cm^{-1}, C—OC; 1048 cm^{-1}, C—C. pK_a (H_2O) 6.75.

Preparation of N-2-Acetoxyethyl N′-2-Hydroxyethyl Acetamidate Hydrochloride and its Acetyl Derivative

N-2-Acetoxyethyl ethyl acetimidate (1 g) was dissolved with cooling in anhydrous ether (10 ml) containing hydrogen chloride (208 mg). After the solvent was removed, the product was dissolved in absolute ethanol (10 ml), and ethanolamine (370 mg) in absolute ethanol (5 ml) was slowly added whilst the temperature

Can. J. Chem. Downloaded from www.nrcresearchpress.com by 210.87.254.6 on 09/05/12
For personal use only.

was maintained below 5°. The reaction mixture was stirred for 3 hours, after which the solvent was evaporated, leaving a yellow oil (940 mg). Although the oil was chromatographed on Woelm acid alumina grade IV its infrared spectrum remained unchanged, and the oil could not be induced to crystallize. Yield 72%. Calc. for $C_8H_{17}O_3N_2Cl$: C, 42.81; H, 7.57; N, 12.50; Cl, 15.80%. Found: C, 43.06; H, 7.71; N, 11.26; Cl, 15.4%. Ultraviolet: λ_{max} 207 mμ, ϵ 13,400 (0.3 mg/10 ml H_2O). pK_a 10.91 (H_2O).

The amidate hydrochloride (840 mg) was acetylated with acetic anhydride, giving a product (717 mg) which crystallized from acetone in the form of thick needles, m.p. 109–110°. Yield 71%. Calc. for $C_{10}H_{19}O_4N_2Cl$: C, 45.03; H, 7.13; N, 10.51; Cl, 13.30%. Found: C, 45.10; H, 7.39; N, 10.5; Cl, 13.00%. Ultraviolet: λ_{max} 207 mμ, ϵ 14,500 (0.28 mg/10 ml H_2O). pK_a 10.78 (H_2O). The spectral and analytical data are consistent with the structure of N,N′-bis-2-acetoxyethyl acetamidate hydrochloride.

ACKNOWLEDGMENTS

The authors would like to thank K. Oikawa for the n.m.r. spectra and J. Legari for technical assistance. Analytical determinations by J. Helie and infrared spectra by R. Gravelle are also gratefully acknowledged.

REFERENCES

1. G. R. Porter, H. N. Rydon, and J. A. Schofield. J. Chem. Soc. 2686 (1960).
2. R. B. Martin and A. Parcell. J. Am. Chem. Soc. **83**, 4835 (1961).
3. R. Greenhalgh. Can. J. Chem. **40**, 976 (1962).
4. M. A. Weinberger and R. Greenhalgh. Can. J. Chem. **41**, 1038 (1963).
5. R. B. Williams. Ann. N.Y. Acad. Sci. **70**, 890 (1958).
6. (*a*) J. T. Edward and S. C. R. Meacock. J. Chem. Soc. 2000 (1957).
   (*b*) J. T. Edward and S. C. R. Meacock. J. Chem. Soc. 2009 (1957).
7. (*a*) J. F. Bunnett. J. Am. Chem. Soc. **83**, 4956 (1961).
   (*b*) J. F. Bunnett. J. Am. Chem. Soc. **83**, 4968 (1961).
   (*c*) J. F. Bunnett. J. Am. Chem. Soc. **83**, 4973 (1961).
8. R. B. Martin. J. Am. Chem. Soc. **84**, 4130 (1962).
9. R. Greenhalgh. Nature, **196**, 267 (1962).
10. R. L. Shriner and F. W. Neumann. Chem. Rev. **35**, 351 (1944).
11. F. C. Cooper and M. W. Partridge. J. Chem. Soc. 5036 (1956).
12. A. A. Goldberg and W. Kelly. J. Chem. Soc. 1919 (1946).
13. H. Wenker. J. Am. Chem. Soc. **57**, 1079 (1935).
14. C. W. Crane and H. N. Rydon. J. Chem. Soc. 527 (1947).
15. J. W. Cornforth and R. H. Cornforth. J. Chem. Soc. 96 (1947).
16. S. M. McElvain and J. W. Nelson. J. Am. Chem. Soc. **64**, 1847 (1942).

Can. J. Chem. Downloaded from www.nrcresearchpress.com by 210.87.254.6 on 09/05/12
For personal use only.

THE USE OF ENZYMES IN STRUCTURAL STUDIES ON POLYSACCHARIDES

I. THE MODE OF ATTACK OF A β-D-(1 → 3)-GLUCANASE ON LAMINARIN[1]

T. E. NELSON, J. V. SCALETTI, F. SMITH, AND S. KIRKWOOD

Departments of Agricultural Biochemistry and Animal Husbandry, University of Minnesota, St. Paul, Minnesota, U.S.A.

Received October 19, 1962

ABSTRACT

A β-D-(1 → 3)-glucanase from the Basidiomycete sp. QM 806 of Reese and Mandels has been purified and shown to hydrolyze insoluble laminarin by removing glucose residues one at a time from the non-reducing end of the polysaccharide. The enzyme will also hydrolyze simple oligosaccharides and its mode of attack on these is similar to its action on laminarin. The products produced by the action of this preparation on laminarin are consistent with recent information on the structure of this polysaccharide.

Reese and Mandels (1), in a survey of the occurrence of β-D-(1 → 3)-glucanases in fungi, observed that an unidentified species of basidiomycete produced a very high level of β-D-(1 → 3)-glucanase activity when grown on a starch medium. The organism was designated Basidiomycete sp. QM 806. The criterion for activity was the extent of attack on the seaweed polysaccharide laminarin. The enzyme brought about the complete hydrolysis of laminarin, as judged by reducing value calculated as glucose. The hydrolysis products produced by the action of this enzyme were investigated (paper chromatography) and glucose was the only product observed. Reese and Mandels point out that this observation, coupled with the fact that the enzyme had a very slow rate of attack on a mixture of oligosaccharides produced from laminarin by the action of a glucanase from *Rhizopus arrhizus*, leads to the conclusion that the basidiomycete enzyme attacks laminarin in an exo or endwise splitting fashion.

Insoluble laminarin, a cold water insoluble polysaccharide from the brown algae *Laminaria cloustoni*, has been shown to contain mannitol (2) to which are attached chains composed of glucose residues. Furthermore, the glucose chains in laminarin are linked by both β-(1 → 6)and β-(1 → 3) bonds (3, 4). Recent investigations have shown that laminarin is heterogeneous and is composed of at least two components. One is a reducing substance, termed laminarose, which consists of glucose residues linked by both β-(1 → 6) and β-(1 → 3) bonds. The other component is a non-reducing substance, termed laminaritol, which appears to be two chains similar to laminarose, both terminating in the same mannitol residue (5). In view of these structural findings it is surprising that the basidiomycete enzyme produces only glucose from laminarin and one must assume that either the preparation is a mixture of enzymes or a single enzyme with a very low order of specificity. In either case the preparation should produce either mannitol or some fragment containing mannitol from that portion of the laminarin structure containing this substance.

In order to investigate these matters further, we have undertaken a study of the action pattern of a purified preparation of this enzyme with the view of using it in structural studies on laminarin and other polysaccharides of similar structure.

[1]*Paper No. 4964, Scientific Journal Series, Minnesota Agricultural Experiment Station. This work was supported by a grant from the National Institutes of Health.*

Can. J. Chem. Downloaded from www.nrcresearchpress.com by 210.87.254.40 on 09/05/12
For personal use only.

Action of the Purified Enzyme on Laminarin

The action of our purified preparation on laminarin[2] was investigated and compared with the results reported by Reese and Mandels. The enzyme was incubated with laminarin and the increase in reducing power with time followed by the Nelson–Somogyi method (6). Companion determinations of the glucose liberated were carried out by a procedure involving the use of glucose oxidase (7). The results of the experiment (Fig. 1)

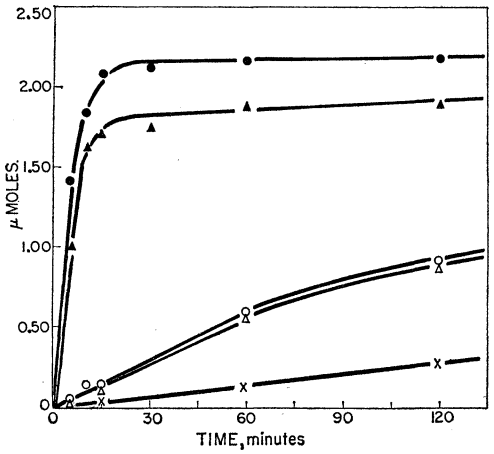

FIG. 1. Action of the enzyme at high concentration on laminarin, on periodate-oxidized and reduced laminarin. The concentration of enzyme used was fivefold that used in the laminarin experiment, the results of which are shown in Table I. The release of reducing power, as glucose and glyceritol, was negligible in the absence of enzyme. ● release of glucose equivalent from laminarin as determined by the Nelson–Somogyi procedure; ▲ release of glucose from laminarin as determined by glucose oxidase; ○ release of glucose equivalent from periodate-oxidized and reduced laminarin as determined by the Nelson–Somogyi procedure; △ release of glucose from periodate-oxidized and reduced laminarin as determined by glucose oxidase; × release of glyceritol from periodate-oxidized and reduced laminarin.

essentially confirm the observations of Reese and Mandels that the increase in reducing power upon enzymatic hydrolysis is due largely to the production of glucose. A further implication of these data is that contamination of this preparation with an endo-type glucanase must be small since the presence of such an enzyme would result in a large difference in the values obtained by the two methods. It should be pointed out also that the fact that the two determinations do not coincide indicates that the enzyme is producing significant amounts of reducing substances other than glucose. Such a result is to be expected on the basis of what is known of the structure of laminarin.

In order to make a more definite estimation of the extent of contamination by an endo-type enzyme, the preparation was incubated with purified undergraded samples of oat and barley gums at five times the enzyme level used in the laminarin experiment, the results of which are given in Table I. No increase in reducing capacity was observed (Table I). Since both oat and barley gums are known to contain both β-(1 → 3) and β-(1 → 4) linkages (8–11), the β-(1 → 3) linkages occurring both singly and together (12), it is reasonable to assume that an endo-type enzyme would attack these polysaccharides. In fact recent work by Parrish, Perlin, and Reese (13) has shown that the endo-glucanase from *R. arrhizus* does indeed produce extensive degradation of both of these polysaccharides. The conclusion may therefore be drawn that our preparation has little or no contamination with an endo-type enzyme. In addition, since cellulase has

[2]*The term "laminarin" is used throughout this paper to denote a preparation of L. cloustoni laminarin obtained from the Liverpool Borax Co., St. Paul's Square, Liverpool 3, England.*

Can. J. Chem. Downloaded from www.nrcresearchpress.com by 210.87.254.40 on 09/05/12
For personal use only.

TABLE I

Comparison of the rate of attack on laminarin with that on derivatives of laminarin and on oat and barley gum

Substrate	Enzyme units added	Increase in reducing capacity ΔOD_{660}/15 min
Laminarin	0.047	1.43
Periodate-oxidized and reduced laminarin	0.047	0.014
Periodate-oxidized, reduced, and mild acid hydrolyzed laminarin	0.047	1.07
Air-oxidized laminarin	0.047	1.03
Reduced laminarin	0.047	1.01
Oat poly-β-D-glucan	0.235	0.000
Barley poly-β-D-glucan	0.235	0.000

NOTE: All final substrate concentrations were at 0.05%. Determinations were made by adding to 0.50 ml substrate in 0.05 *M* acetate, pH 4.8, 0.50 ml enzyme solution in the same buffer and incubating for 15 minutes at 37°. The hydrolysis was stopped by the addition of 1.0 ml of Nelson–Somogyi alkaline copper reagent.

been shown to degrade oat and barley gums (13), it can be concluded that the cellulase contamination is negligible.

Action of the Enzyme on Chemically Modified Laminarins

In order to establish the mode of attack of the glucanase on laminarin, various derivatives of this polysaccharide were prepared in which the reducing and/or non-reducing ends had been altered. By comparing the rate of action of the enzyme on each of these with its rate of attack on unaltered laminarin, it has been possible to reach certain conclusions concerning its mode of attack.

Samples of laminarin in which the reducing end of the laminarose component had been altered were prepared by air oxidation in the presence of dilute alkali and by sodium borohydride reduction. The former procedure converts the reducing ends to acid residues, the latter procedure converts them to glucitol residues. In addition, a sample of laminarin that had been partially purified by dialysis and reprecipitation from water was oxidized with dilute sodium metaperiodate for several days in the dark at 4° and then reduced with sodium borohydride. This procedure alters both the reducing and non-reducing ends of laminarose (see Fig. 2) and laminaritol. The remaining 1 → 3-linked residues are, however, left intact (12, 14). A portion of this periodate-oxidized and reduced material was subjected to mild acid hydrolysis at room temperature. The hydrolysis regenerates the non-reducing ends by removing the altered residues and freeing the adjacent intact glucose moieties. It should be noted that this regenerated laminarin resembles the original material only at the non-reducing terminals, the other end of the molecule is probably terminated by an arabitol residue in the case of laminarose and a glyceritol residue in the case of laminaritol.

The action of the purified enzyme on these substrates is shown in Table I. An enzyme concentration was used such that the rate of attack on unaltered laminarin was at the maximum value that could be measured with any accuracy. This was done so that very low rates of attack on the modified substrates could be detected and compared with the rate on the unaltered material.

As can be seen in Table I, laminarin modified only at the reducing end of the molecule by air oxidation or sodium borohydride reduction is attacked at a rate only slightly less than that characteristic of untreated laminarin. Periodate-oxidized and reduced laminarin, in which both the reducing and non-reducing ends have been altered, is attacked at 1/100

Can. J. Chem. Downloaded from www.nrcresearchpress.com by 210.87.254.40 on 09/05/12
For personal use only.

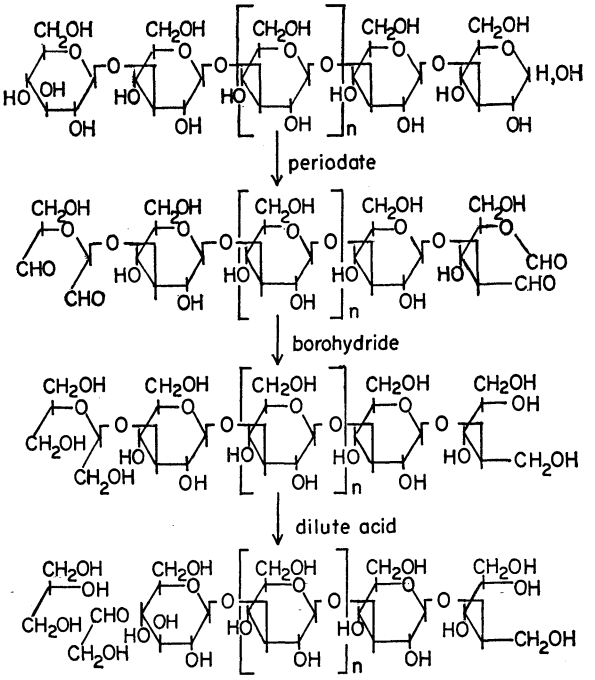

FIG. 2. Structural representation of periodate oxidation, reduction, and mild acid hydrolyses on the laminarose component of laminarin. The branching known to occur in this molecule is ignored for purposes of illustration. The ends of all branches will react in the same fashion as the non-reducing terminal illustrated in the drawing.

or less of this rate. The increase in reducing value was so low that it borders on experimental error. The rate of enzyme attack on the periodate-oxidized polysaccharide (tested prior to reduction) was also very low. However, in this case the high reducing value given by the substrate makes the rate of attack measurement much less accurate. Mild acid hydrolysis of the periodate-oxidized and reduced laminarin, which removes the blockage at the non-reducing end, resulted in a product that was almost as susceptible to enzymatic attack as the original laminarin. This is highly significant since it rules out the possibility that the failure of the enzyme to attack the periodate-oxidized and reduced molecule was due to a structural modification at a point other than the non-reducing terminal. Thus it can be stated conclusively that this glucanase preparation from Basidiomycete sp. QM 806 acts upon laminarin from the non-reducing end of the molecule, removing one residue at a time.

Modified laminarin is slowly degraded by the enzyme (Fig. 1). This may be attributed to a limited ability of the glucanase to attack the modified non-reducing end unit, to a slight endo-glucanase contamination, or to spontaneous hydrolysis of the non-reducing ends, allowing enzymatic attack on the exposed glucose residues. These possibilities can be differentiated readily by the fact that hydrolytic cleavage of the altered end unit liberates glyceritol, whereas this polyol would not be formed by attack along the interior of the chain. The data (Fig. 1) show a steady release of glyceritol as well as glucose, and since the modified polysaccharide does not decompose spontaneously at the pH of the enzymatic reaction, the glucanase preparation must have a limited ability to attack the altered non-reducing end unit.

Can. J. Chem. Downloaded from www.nrcresearchpress.com by 210.87.254.40 on 09/05/12
For personal use only.

Products of the Action of the Enzyme on Laminarin

Aliquots removed at various periods during the hydrolysis of laminarin by the glucanase were examined by paper chromatography. Glucose was the major observable product in all hydrolyses, and in those which were virtually complete it accounted for about 70% of the carbohydrate as measured by the phenol – sulphuric acid method (15). In addition, laminaribiose, gentiobiose, laminaritriose, and several higher oligosaccharides appeared. It was shown by elution of the material from the chromatogram, followed by acid hydrolysis and paper electrophoresis in borate, that at least two of the higher oligosaccharides contained mannitol. As the course of the hydrolysis proceeded, laminaritriose and most of the higher oligosaccharides gradually disappeared while gentiobiose remained constant and laminaribiose increased.

This pattern of the appearance and disappearance of products during the course of hydrolysis is consistent with recent work on the structure of laminarin (3, 16, 17, 18). The origin of the laminaribiose and laminaritriose is explicable on the basis that they result from the reducing ends of the laminarose component of laminarin. The enzyme apparently has the capacity to attack laminaritriose, since this substance gradually disappears, but it does not attack laminaribiose, which persists to the end of the hydrolysis. Gentiobiose (the β-(1 $\rightarrow$ 6)-linked disaccharide) arises from the 1 $\rightarrow$ 6 linkages that have been shown to occur in both laminarose and laminaritol. The enzyme is apparently incapable of hydrolyzing a 1 $\rightarrow$ 6 linkage but can bypass it, thus leaving gentiobiose from this structural feature. The mannitol-containing oligosaccharides result from the enzyme failing to totally hydrolyze the laminaritol chains. The action of the enzyme apparently ceases at some distance from the terminal mannitol unit.

Action of the Glucanase on Simple Oligosaccharides of Known Structure

The pattern of products produced by the action of the enzyme on laminarin suggests that it is incapable of attacking disaccharides but is capable of attacking a trisaccharide of the proper structure at a rate somewhat less than that characteristic of a longer-chain material. In order to confirm this, the action of the enzyme on laminaribiose, gentiobiose, and laminaritriose was investigated using the same conditions as those for laminarin (Table I). It was found that the two disaccharides were not attacked at all, while laminaritriose was acted on at about 1/10 the rate observed with laminarin. These results reinforce the conclusion that the glucanase attacks a β-(1 $\rightarrow$ 3)-linked chain of D-glucose residues from the non-reducing terminal and rapidly removes glucose residues one at a time, bypassing 1 $\rightarrow$ 6 linkages, until it approaches the reducing terminal. When the residue from the chain reaches the trisaccharide level, the action of the enzyme is slowed and then ceases after one more residue is removed. The final stages of this process are not established by the data since an attack on either glycoside bond in laminaritriose will yield the same products, namely glucose and laminaribiose. However, the accumulation of mannitol-containing oligosaccharides would indicate that the attack is stepwise, ceasing as the terminal is approached, even if the last residue is not glucose.

To establish the terminal process with more certainty, the action of the enzyme on laminaribiosyl-erythritol and laminaritriitol[3] was determined. If the attack is as predicted,

[3]*Common names have been used throughout to describe the oligosaccharides mentioned in this paper; their more formal designations are: laminaribiosyl-erythritol, O-β-D-glucopyranosyl-(1 → 3)-O-β-D-glucopyranosyl-(1 → 2)-D-erythritol; laminaritriitol, O-β-D-glucopyranosyl-(1 → 3)-O-β-D-glucopyranosyl-(1 → 3)-D-glucitol; laminaritriose, O-β-D-glucopyranosyl-(1 → 3)-O-β-D-glucopyranosyl-(1 → 3)-D-glucopyranose; laminaribiose, 3-O-β-D-glucopyranosyl-D-glucopyranose; gentiobiose, 6-O-β-D-glucopyranosyl-D-glucopyranose; laminaribiitol, 3-O-β-D-glucopyranosyl-D-glucitol; glucosyl-erythritol, 2-O-β-D-glucopyranosyl-D-erythritol.*

Can. J. Chem. Downloaded from www.nrcresearchpress.com by 210.87.254.40 on 09/05/12
For personal use only.

namely a single cleavage of the bond connecting the non-reducing terminal in the trisaccharide, then the former should give only glucose and glucosyl-erythritol, the latter only glucose and laminaribiitol. Both substrates were incubated with the enzyme and it was found, by paper chromatography and paper electrophoresis, that only the expected products were produced (Figs. 3 and 4). No erythritol or glucitol were produced even with very high concentrations of enzyme and long periods of incubation. These would be the products produced by any action of the enzyme on the "reducing" end of the chain.

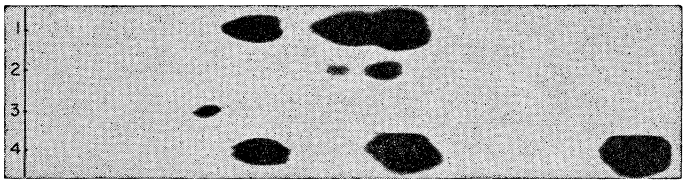

FIG. 3. Products of the action of the glucanase on laminaribiosyl-erythritol as shown by paper chromatography. All spots are named in order proceeding from the origin. Lane 1: laminaribiose, glucosyl-erythritol, and glucose standards; lane 2: the enzymatic hydrolyzate; lane 3: laminaribiosyl-erythritol standard; lane 4: laminaribiose, glucose, and erythritol standards. The enzyme concentration used in this experiment was 350-fold that used in the laminarin experiment reported in Table I, the substrate concentration was 0.2% and the incubation time 6 hours.

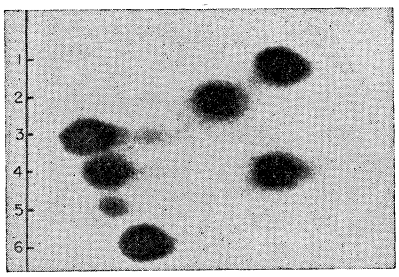

FIG. 4. Products of the action of the glucanase on laminaribiosyl-glucitol as shown by paper electrophoresis. All spots are named in order proceeding from the origin. Lane 1: glucose standard; lane 2: glucitol standard; lane 3: laminaritriitol standard; lane 4: enzymatic hydrolyzate; lane 5: laminaribiitol standard; lane 6: laminaribiose standard. The enzyme concentration used in this experiment was 350-fold that used in the laminarin experiment reported in Table I, the substrate concentration was 0.5% and the time of incubation was 18 hours.

EXPERIMENTAL

Preparation and Purification of the Enzyme

Basidiomycete sp. QM806 was grown on the 0.5% starch medium of Reese and Mandels (1). The crude culture filtrate was evaporated *in vacuo* at 37°, dialyzed, and then fractionated with ammonium sulphate. The ammonium sulphate precipitate was taken up in buffer, dialyzed, and refractionated on a diethylaminoethylcellulose column. The resulting preparation had a specific activity of 163 units per milligram of protein, which represents a 100-fold increase in specific activity over that of the crude culture filtrate. The full details of this and the further purification of this enzyme will be the subject of a separate publication.

Enzyme Assay and Unitage

To 0.5 ml of substrate solution (0.1% laminarin in 0.05 *M* acetate buffer, pH 4.8) was added 0.5 ml of an appropriate dilution of the enzyme preparation in the same acetate buffer. The mixture was incubated for 15 minutes at 37° and the reaction stopped by the addition of 1.0 ml of the alkaline copper reagent used in the Nelson–Somogyi reducing sugar estimation (6). The rate of reaction under these conditions is first order with respect to enzyme if the extent of hydrolysis does not proceed beyond 60%. One unit of enzyme is defined as that amount which will liberate 1 μmole of glucose equivalent per minute under the above conditions of incubation.

Other Incubation Procedures

Incubations carried out for purposes other than enzyme assay, such as investigation of the nature of products of hydrolysis etc., were done under the same general conditions as used for assay purposes. If the glucose

Can. J. Chem. Downloaded from www.nrcresearchpress.com by 210.87.254.40 on 09/05/12
For personal use only.

was to be estimated by the glucose oxidase procedure, the reaction was stopped by immersing the mixture in a boiling water bath for 5 minutes. In all cases where quantitative determinations were carried out, standards were included in the procedure and both reagent and substrate blanks used. In experiments involving the action of the enzyme on substrates other than laminarin, the latter was always run as a check on enzyme activity.

In the case of laminaribiosyl-erythritol and laminaritriitol, a micromethod of incubation was used. Ten microliters of buffered substrate and 5 μl of enzyme were incubated in a sealed capillary tube, heat-denatured in a boiling-water bath, and then spotted directly onto paper. This method permitted extreme economy in the use of valuable substrates.

Glyceritol Determination

The usual method (19, 20) was modified by carrying out the periodate oxidation in 0.05 *M* acetate buffer at pH 4.8 rather than in 1 *N* H_2SO_4. Under these conditions the altered non-reducing ends of the periodate-oxidized and reduced laminarin were not affected and only free glyceritol was determined. The excess periodate was destroyed by arsenious oxide. The glycerol values were corrected for the formaldehyde released by the action of periodate on the glycollic aldehyde produced during enzyme hydrolysis.

Paper Chromatography and Electrophoresis

All chromatography was done on Whatman No. 1 paper in the solvent system 1-propanol, ethyl acetate, water in the proportions 7:1:2 (21). The usual irrigation period was 36 hours. Paper electrophoresis was carried out with 0.1 *M* sodium borate in a potential gradient of 50 v/cm. The paper was dried and dipped through 10% HF in acetone to remove borate prior to developing the spots (22). The carbohydrate spots were developed by the Trevelyan modification of the Tollen's method (23).

Substrates

The "laminarin" used in these experiments was a preparation from *L. cloustoni* obtained from the Liverpool Borax Co., St. Paul's Square, Liverpool 3, England.

Air-oxidized laminarin.—Air-oxidized laminarin was obtained by passing a stream of air through a 0.5% solution of laminarin in 1.0% NaOH at reflux temperature. The reaction was discontinued when the reducing power of the solution had fallen to a negligible value. The solution was then neutralized with HCl, dialyzed in the cold against 0.05 *M*, pH 4.8 acetate buffer to remove salts, and used as the acetate buffer solution.

Reduced laminarin.—Reduced laminarin was prepared by reducing an aqueous solution of laminarin with excess sodium borohydride overnight at room temperature. The excess borohydride was destroyed by acidifying with acetic acid, the solution dialyzed in the cold against buffer as described above and used as the substrate solution. It should be noted that laminarin is partially dialyzable so that all dialyses were carried out in the cold, on a rocking dialyzer, for no more than 6 hours with two changes of dialyzing medium. All substrates that had been dialyzed were used on the basis of their total carbohydrate content as determined by the phenol – sulphuric acid method (15).

Periodate-oxidized and reduced laminarin.—Periodate-oxidized and reduced laminarin was prepared by Dr. B. Lewis of this laboratory and was dialyzed prior to use. The purified undegraded oat gum and the laminaribiosyl-erythritol used in this work were prepared by Dr. Lewis. The purified barley gum was prepared by Dr. G. Hay.

Laminaritriitol.—Laminaritriitol was prepared from chromatographically pure laminaritriose by sodium borohydride reduction. In this case the borate was removed by deionization with resin followed by evaporation to dryness several times in the presence of anhydrous methanol.

Laminaritriose, laminaribiose, and gentiobiose.—The first two substances were available in this laboratory, the last was obtained from the Pfanstiehl Co.

Other materials.—The glucose oxidase used was the "pure" grade supplied by Nutritional Biochemicals Corp. All glucose oxidase preparations that we have examined have been contaminated with a small amount of β-(1 → 3)-glucosidase activity. All determinations involving glucose oxidase reported in this paper were carried out with control procedures that eliminated this source of error. The peroxidase was a horseradish preparation from the Worthington Biochemical Corp.

ACKNOWLEDGMENTS

The authors would like to express their gratitude to Dr. B. Lewis and Dr. G. Hay of this laboratory for their generous gifts of substrates and to Dr. E. T. Reese of the Quartermaster Research Laboratories, Natick, Mass., for supplying us with the culture of Basidiomycete sp. QM 806.

REFERENCES

1. E. T. Reese and M. Mandels. Can. J. Microbiol. **5**, 173 (1959).
2. S. Peat, W. J. Whelan, and H. G. Lawley. Chem. Ind. (London), 35 (1955).
3. S. Peat, W. J. Whelan, and H. G. Lawley. J. Chem. Soc. 729 (1958).

Can. J. Chem. Downloaded from www.nrcresearchpress.com by 210.87.254.40 on 09/05/12
For personal use only.

4. A. BEATTIE, E. L. HIRST, and E. PERCIVAL. Biochem. J. **79**, 531 (1961).
5. I. J. GOLDSTEIN, F. SMITH, and A. M. UNRAU. Chem. Ind. (London), 124 (1959).
6. M. SOMOGYI. J. Biol. Chem. **195**, 19 (1952).
7. A. ST. G. HUGGETT and D. A. NIXON. Lancet, 368 (1957).
8. K. GILLES, W. O. S. MERIDITH, and F. SMITH. Cereal Chem. **29**, 314 (1952).
9. G. O. ASPINALL and R. G. J. TELFER. J. Chem. Soc. 3519 (1954).
10. R. A. AITKEN, B. P. EDDY, M. INGRAM, and C. WEURMAN. Biochem. J. **64**, 63 (1956).
11. S. PEAT, W. J. WHELAN, and J. G. ROBERTS. J. Chem. Soc. 3916 (1957).
12. I. J. GOLDSTEIN, G. W. HAY, B. A. LEWIS, and F. SMITH. American Chemical Society, 135th Meeting Abstracts, 3D. 1959.
13. F. W. PARRISH, A. S. PERLIN, and E. T. REESE. Can. J. Chem. **38**, 2094 (1960).
14. M. ABDEL-AKHER, J. K. HAMILTON, and F. SMITH. J. Am. Chem. Soc. **73**, 4691 (1951).
15. M. DUBOIS, K. A. GILLES, J. K. HAMILTON, P. A. REBERS, and F. SMITH. Anal. Chem. **28**, 350 (1956).
16. A. UNRAU and F. SMITH. Chem. Ind. (London), 330 (1957).
17. F. SMITH and A. M. UNRAU. Chem. Ind. (London), 636 (1959).
18. F. SMITH and A. M. UNRAU. Chem. Ind. (London), 881 (1959).
19. F. SMITH and R. MONTGOMERY. The chemistry of plant gums and mucilages. Reinhold, N.Y. 1959. pp. 215–216.
20. M. LAMBERT and A. C. NEISH. Can. J. Res. Sect. B, **28**, 83 (1950).
21. N. ALBON and D. GROS. Analyst, **77**, 410 (1952).
22. H. G. BRITTON. Biochem. J. **73**, 19p. (1959).
23. W. E. TREVELYAN, D. P. PROCTOR, and J. S. HARRISON. Nature, **166**, 444 (1950).

Can. J. Chem. Downloaded from www.nrcresearchpress.com by 210.87.254.40 on 09/05/12
For personal use only.

SULPHONIUM SALT SOLVOLYSIS

PART IV. SOLVENT EFFECTS

J. B. HYNE AND J. H. JENSEN
Department of Chemistry, University of Alberta, Calgary, Alberta
Received March 11, 1963

ABSTRACT

The variation of rate of solvolysis of dimethyl-*t*-butyl sulphonium iodide as a function of solvent composition is reported for various binary mixtures of water with ethanol, N,N-dimethylformamide, N-methylformamide, dioxane, and ethylene glycol. The inadequacy of solvent bulk dielectric constant as a correlating parameter is demonstrated and solvent *Y* and *Z* parameters are compared in this respect. The importance of the specific microscopic role of the solvent in the activation process is demonstrated and a possible important nucleophilic role for the amides suggested. Deviations in dioxane and ethylene glycol systems are discussed.

Can. J. Chem. Downloaded from www.nrcresearchpress.com by 210.87.254.6 on 09/05/12
For personal use only.

INTRODUCTION

The solvolysis of alkyl sulphonium salts has been repeatedly cited as a typical example of the class of reactions showing rate enhancement as dielectric constant of the solvolytic medium is reduced. This behavior follows from the fact that the mechanism commonly accepted for the solvolysis involves dispersal of the formal sulphonium ion charge in passing from the initial to the transition state of the rate-determing step (1 and references cited therein). In lower dielectric solvent media elimination becomes increasingly important, yielding olefins rather than the solvolysis product. The observation that the extent of elimination does not appear to be critically dependent on the nature of the leaving group (2) has been considered evidence in support of an E1 mechanism. Consequently, even in solvents where elimination is significant, the rate-determining step remains the same as in solvolysis, namely cleavage of the sulphonium salt to a neutral dialkyl sulphide leaving group and a carbonium ion entity.

Although the qualitative nature of the solvent dependence of sulphonium salt solvolysis rates is generally understood there has been little work done on the quantitative aspects of this problem. As part of our continuing study of the mechanism of sulphonium salt solvolysis (1, 3, 4) we report here the results of a study of the rates of solvolysis of dimethyl-*t*-butyl sulphonium iodide in a series of organic solvent mixtures with water. Among the organic solvents chosen was N-methylformamide, a liquid having a dielectric constant very much greater than water and one which would be expected to *reduce* the rate of solvolysis below that observed in water as the mole fraction in water mixtures is increased. The fact that no such result is observed, together with other conclusions that may be drawn from attempts to analyze the observed solvent effects quantitatively, lends further strong support to the growing volume of kinetic evidence which argues in favor of the critical role of specific solute–solvent interaction in kinetic processes and against the dominant role of bulk solvent medium effects.

EXPERIMENTAL

Reagents

N-Methylformamide was refluxed over calcium oxide and distilled, $n_{25}^{D} = 1.4303$, lit. $n_{25}^{D} = 1.4310$ (5), 1.4300 (6). N,N-Dimethylformamide was refluxed over calcium oxide and distilled, $n_{25}^{D} = 1.4285$, lit. $n_{25}^{D} = 1.4299$ (7). *p*-Dioxan, Matheson, Coleman and Bell spectroscopic grade, was used without further purification. Ethanol, reagent dry grade absolute, was used without further purification. Karl Fisher titration showed *less than* 0.14% water. Attempts to dry the ethanol further resulted in contamination as revealed

by its ultraviolet spectrum. Ethylene glycol, Fisher reagent grade, was used without further purification. Karl Fisher titration showed *less than* 0.2% water. The water used was doubly distilled, with conductance less than 1×10^{-7} mhos. Pyridine-1-oxide was purified by distillation. Fraction used: b.p. = 150–151° (15 mm), lit. b.p. = 146–147° (13 mm) (8). C^{14}-Dimethyl-*t*-butyl sulphonium iodide was prepared by the method of Hyne and Wolfgang (9), m.p. 159–160°.

Rate Determinations

Rate constants in all solvents except ethanol–water were determined by the radiochemical flow counting technique described previously (9). Rate constants in ethanol–water solvent mixtures were measured conductimetrically using an a-c. bridge at 1000 c.p.s. as described by Robertson (10).

Determination of Z′ Values

Solvent mixtures as recorded in Table II were prepared by weight from a stock solution to give final concentrations of pyridine-1-oxide of 5×10^{-5} *M*. The λ_{max} for each solvent in the ultraviolet was measured on a Beckman DK-1 recording ultraviolet spectrometer using 1-cm cells. At a chart scale of 5 mμ/inch λ_{max} values reproducible to ±0.2 mμ were obtained. *Z′* values were calculated from λ_{max} values using the Kosower equation (8).

RESULTS

The first-order rate constants for the solvolysis of dimethyl-*t*-butyl sulphonium iodide in a variety of organic solvent mixtures with water are recorded in Table I. The solvent mixtures were all chosen so as to maintain the bulk dielectric constant above 30. This restriction is necessary in view of the previously established onset of an alternative mechanism involving sulphonium salt ion pairs in media of dielectric constant less than 25 (3). The effect of onset of such a mechanism is illustrated in the dioxane–water solvent system where media of very low dielectric constant are possible. Below a dielectric constant value of 20 the rate increases rapidly due to the role played by the ion-pair mechanism.

Dielectric constant values in Table I were obtained from the literature as follows: ethanol–water (11); ethylene glycol – water (11); dioxane–water (12); N-methylformamide–water (5) and N,N-dimethylformamide–water (5). In the two latter cases interpolation was necessary to obtain the values required.

TABLE I

Rate of solvolysis of dimethyl-*t*-butyl sulphonium iodide in various organic solvent – water mixtures at 75.76° C

Mole fraction organic solvent	$k\times10^4$ (sec^{-1})*	*D*, 20° C†	*Z′*, 25° C‡	Mole fraction organic solvent	$k\times10^4$ (sec^{-1})*	*D*, 20° C†	*Z′*, 25° C‡
N-Methylformamide–water				Dioxane–water			
0.247	3.03(3)	130	109.9	0.060	2.35(4)	59.0	111.3
0.499	4.14(3)	163	108.0	0.151	2.28	38.0	110.1
0.800	6.63(3)	184	106.5	0.335	3.35(2)	17.5	108.4
0.936	7.98	188	105.9	0.658	7.82(2)	4.5	
				0.810	8.80	2.9	
N,N-Dimethylformamide–water				Ethanol–water			
0.131	3.03(3)	64.2	110.2	0.125	2.79(3)	65.0	111.9
0.300	4.06(2)	53.5	108.5	0.203	3.09(3)	57.0	110.9
0.500	6.75(3)	46.1	106.8	0.325	3.47(3)	47.8	110.2
0.598	7.15	44.5	106.0	0.411	3.78(3)	42.5	109.7
0.611	8.58	43.5	105.9	0.500	3.97(3)	38.3	109.3
Ethylene glycol – water				Pure water			
0.200	2.31(3)	66.1	111.6	0.000	2.50(3)	80.37	112.5
0.398	2.50(3)	56.4	110.7				
0.600	2.69(3)	48.4	110.1				

*Figures in parentheses indicate number of individual determinations. All rates ±1% uncertainty.
†Values of *D* for both amides interpolated from linear weight% vs. *D* plot.
‡Values interpolated from experimental data of Table II.

Can. J. Chem. Downloaded from www.nrcresearchpress.com by 210.87.254.6 on 09/05/12
For personal use only.

Z′ values shown in Table II for the various solvent mixtures used were obtained by the method of Kosower (8) as reported in the Experimental Section.

TABLE II

Z′ values for solvent mixtures with water at 25° C

Mole fraction organic solvent	*Z′*	Mole fraction organic solvent	*Z′*	Mole fraction organic solvent	*Z′*
N,N-Dimethylformamide		Ethanol		N-Methylformamide	
0.102	110.5	0.110	111.5	0.100	111.3
0.221	109.6	0.200	110.9	0.200	110.3
0.327	108.3	0.301	110.3	0.300	109.5
0.421	107.4	0.400	109.8	0.400	108.7
0.533	106.6	0.507	109.5	0.500	108.0
0.630	105.7	0.600	109.0	0.600	107.5
0.726	105.0	0.700	108.5	0.702	107.0
0.820	104.2			0.801	106.5
0.916	103.4			0.900	106.0
Dioxane		Ethylene glycol		Pure water	
0.096	110.8	0.100	112.2	0.000	112.4
0.200	109.6	0.200	111.6		
0.300	108.7	0.300	111.1		
0.400	108.0	0.400	110.7		
0.500	107.5	0.500	110.4		
		0.600	110.1		

Although neither the dielectric constant nor *Z′* values were determined at the same temperature as the rate measurements the temperature dependence of both of these solvent parameters is such that using values at the same temperature as the rate determinations would not significantly alter the form of the plots in either Fig. 1 or Fig. 2.

DISCUSSION

In the attempt to analyze the observed rate dependence on solvent composition in a quantitative manner three different parameters characteristic of the solvent medium were considered: the bulk dielectric constant; the polarity of the solvent as measured by the *Y* value of the Winstein, Grunwald, and Jones relationship; and the *Z′* parameter suggested by Kosower and obtainable from the ultraviolet spectral shift effect of the various solvents on a reference solute. These three approaches are considered separately.

Bulk Dielectric Constant

In the many previous attempts to correlate rate with solvent bulk dielectric constant a variety of terms involving *D* have been suggested. The simplest model based upon the assumption that the solvent is a structureless dielectric continuum leads to a linear relationship between log *k* and $1/D$ (13). While the application of this relationship to kinetic systems has met with some qualitative success quantitative agreement cannot be expected since there are no grounds for the assumption, inherent in the derivation, that the microscopic behavior of the dielectric in the vicinity of the reacting species will be related to the macroscopic bulk dielectric constant *D*. A similar criticism applies to the other common rate versus bulk dielectric constant relationships such as log *k* versus $(D-1)/(2D+1)$ derived for reactions between ions and polar molecules (14), and log *k* vs. *D*, proposed by Tommila and Hella (15). None of these relationships satisfactorily accounts for the rate variations with solvent shown in Table I. An adequate relationship

Can. J. Chem. Downloaded from www.nrcresearchpress.com by 210.87.254.6 on 09/05/12
For personal use only.

should produce a straight-line plot accommodating all of the rates irrespective of the molecular composition of the solvent. For illustrative purposes the simple log k versus D plot is shown in Fig. 1. Even the qualitative relationship, however, breaks down in the

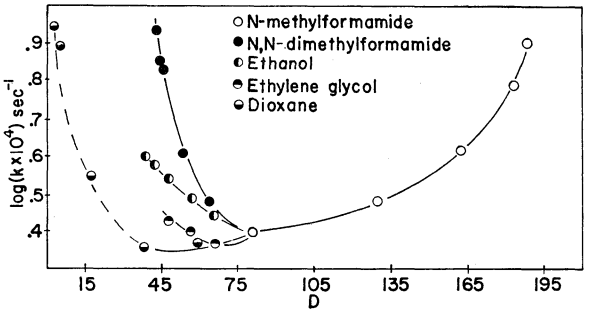

FIG. 1. Dependence of rate of solvolysis of dimethyl-*t*-butyl sulphonium iodide on the dielectric constant of various organic solvent – water mixtures.

case of N-methylformamide. As the bulk dielectric constant of the solvent medium increases with higher N-methylformamide mole fraction the qualitative prediction would be that the rate should decrease. Figure 1 clearly establishes the opposite behavior, leaving little doubt that the bulk dielectric constant of the solvent medium bears little if any relationship to the kinetic behavior of the sulphonium system. It is interesting to note that Ross and Labes (7) found a similar discrepancy in the bulk dielectric effect of N-methylpropionamide ($D^{30} = 164$) on the rate of solvolysis of *t*-butyl bromide. The rate of solvolysis in the propionamide is several powers of 10 *slower* than in water ($D^{30} = 80$) while the qualitative prediction would be the opposite.

Solvent Y Values

From the data in Table I for the rates of solvolysis of dimethyl-*t*-butyl sulphonium iodide in ethanol–water mixtures a value for the reactant constant $m = -0.062$ in the relationship $\log k/k_0 = mY$ (16) may be evaluated for the sulphonium salt using the known values of Y for ethanol–water mixtures (17). The negative sign of this m value compared with positive values close to unity for most alkyl halides is indicative of the charge dispersal character of the activation process in the sulphonium salt solvolysis compared with the charge creation character of the alkyl halide solvolysis. Using this m value, Y values for the N-methylformamide and N,N-dimethylformamide solvent mixtures may be calculated. The highest N-methylformamide composition used, 0.936 mole fraction, has a $Y = -4.7$ while 0.65 mole fraction N,N-dimethylformamide has a $Y = -5.2$. Ross and Labes (7) obtained a pure N,N-dimethylformamide value for various alkyl halide solvolyses which varied between -2.46 and -3.72. Our value for a much lower formamide concentration is considerably more negative. Ross and Labes did not use N-methylformamide as a solvent but their value for N-methylpropionamide, a similarly high dielectric solvent, was also variable between -2.60 and -3.14 depending on the alkyl halide used. It is clear, therefore, that the mY type relationship will not account for the solvent dependence of the rate of solvolysis of the sulphonium salts. The lack of agreement between Y values computed for the amide solvents using different reacting solutes and the high negative values obtained in the sulphonium case indicate that the solvent is playing a role other than one based solely on its polarity or solvating power. Solvents with large negative Y values in the Winstein, Grunwald, and Jones treatment are among

Can. J. Chem. Downloaded from www.nrcresearchpress.com by 210.87.254.6 on 09/05/12
For personal use only.

those to which Swain and co-workers attribute an important nucleophilic role in the four-parameter type relationship (18). As a typical example 97.5% acetic anhydride – 2.5% acetic acid mixtures have $Y = -3.29$ in the mY type relationship but the magnitude of the coefficient describing the nucleophilic role of this solvent in the Swain four-parameter equation is greater than the coefficient for the electrophilic role. Since the electrophilic role of the solvent in such solvolysis is largely a measure of the ability of the solvent to "solvate" the leaving group in the rate-determining step it is hardly surprising that this role is minimized in the sulphonium salt case where the leaving group (dialkyl sulphide) is neutral. Comparing the Y values obtained for the amides in this work with those obtained by Ross and Labes for alkyl halide solvolysis, it is seen that the larger negative values for the sulphonium cases reflect a proportionately larger nucleophilic role for the amides as a result of the reduced electrophilic role in a rate step involving a neutral leaving group. Although the nucleophilic role in the alkyl halide case is important the leaving halide anion has a greater solvation demand, which requires a significant electrophilic contribution from the solvent.

The apparently important nucleophilic role of the formamide solvents suggests that there may be a significant contribution in the rate-determining step for the solvolysis from covalent type bond formation leading to a quaternized ammonium intermediate. A similar solvent role was proposed by Ross and Labes. Subsequent decomposition of the

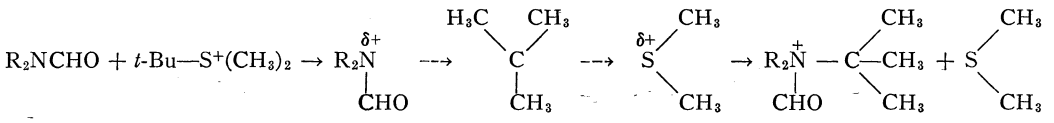

quaternary ammonium intermediate by either solvolysis or elimination would be rapid. It is interesting to note that this mechanism presumes transalkylation from sulphonium sulphur to nitrogen, a sulphonium salt role of considerable importance in biochemical transmethylations.

Correlation with Solvent Z′ Values

A test of the mY type relationship as applied to the solvent systems used in this work is limited to the comparison of Y values with those obtained for comparable amides by Ross and Labes since Y values are not available for the whole range of amide–water mixtures. Kosower has shown (8) that the energies associated with the charge-transfer band of pyridinium salts and related solutes in a wide variety of solvent mixtures (Z values) are linearly related to Y values where these parameters are available for comparison. The greater ease of measurement of the Z value, however, makes this solvent parameter a much more attractive one for use in rate–solvent correlation. Kosower has also illustrated (8) the quantitative correlation of rate variation with solvent using the Z parameter for several types of reaction. Z' values (using pyridine-1-oxide as solute) for all solvent systems used in this work were determined as described in the Experimental Section and are recorded in Table II.

In Fig. 2 the sulphonium salt solvolysis rate variation with solvent is correlated by using the Z' parameters for ethanol–water, N,N-dimethylformamide–water, and N-methylformamide–water mixtures. While there are deviations from both linearity and a single-curve representation, these deviations are minor compared with the inadequacy of the bulk dielectric constant type relationship illustrated in Fig. 1. In particular the kinetic role of the high dielectric constant N-methylformamide appears to be much more accurately described by the Z' value. The apparent success of the Z' value correlation

Can. J. Chem. Downloaded from www.nrcresearchpress.com by 210.87.254.6 on 09/05/12
For personal use only.

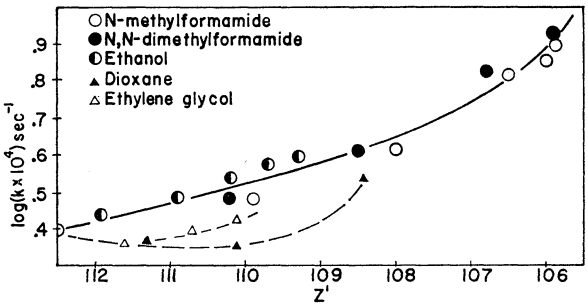

FIG. 2. Dependence of rate of solvolysis of dimethyl-*t*-butyl sulphonium iodide on Z' values.

is again a reflection of the importance of the microscopic solvent role in the activation process. The Z' value measures the specific effect of the solvent on a charge delocalization

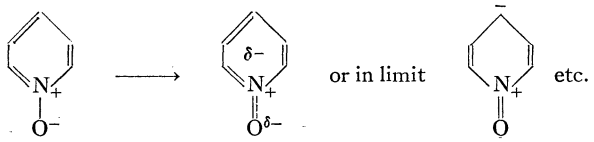

Charge transfer complex

process in passing from pyridine-1-oxide to the charge-transfer complex. This process has formal similarity to the activation process in the sulphonium salt solvolysis where a formal positive charge on sulphur is delocalized in the activation process.

Notwithstanding the apparent success of the Z' correlation in accounting for solvent effects in the ethanol and amide solvent mixtures it is clear from Fig. 2 that considerable deviations are still observed in the cases of ethylene glycol – water and dioxane–water solvent mixtures, especially in highly aqueous mixtures. While the specific role of solvent species in the activation process of the rate-determining step is still too imperfectly understood to warrant even a speculative interpretation of these observations it should be noted that in both these cases the non-aqueous component of the solvent mixture is a "bifunctional" molecule. Similar anomalies in the solvation behavior of dioxane have been noted previously (19) and solvent species of the general type X—CH_2—CH_2—Y, having the potential of existing in trans or gauche rotamer forms, have also been reported as exhibiting anomalous solvent behavior (20). The failure of the Z' correlation in these cases indicates that whatever the specific role of these "bifunctional" solvent molecules may be in the kinetic process it is not operative as a specific solvent effect in the charge-transfer process measured by Z'. Such anomalous observations, however, may be the key to the next stage in the refinement of the understanding of specific solute–solvent interactions.

ACKNOWLEDGMENTS

The authors acknowledge the experimental assistance of Mr. J. Gurst in the early stages of this work. A grant from the National Research Council of Canada was used in support of this work.

REFERENCES

1. J. B. HYNE. Can. J. Chem. **39**, 1207 (1961).
2. K. A. COOPER, E. D. HUGHES, C. K. INGOLD, and B. J. MACNULTY. J. Chem. Soc. 2038 (1948).

Can. J. Chem. Downloaded from www.nrcresearchpress.com by 210.87.254.6 on 09/05/12
For personal use only.

3. J. B. HYNE and J. W. ABRELL. Can. J. Chem. **39**, 1657 (1961).
4. J. B. HYNE and J. H. JENSEN. Can. J. Chem. **40**, 1394 (1962).
5. G. R. LEADER and J. F. GORMLEY. J. Am. Chem. Soc. **73**, 5731 (1951).
6. G. F. D'ALELIO and E. E. REID. J. Am. Chem. Soc. **59**, 109 (1937).
7. S. D. ROSS and M. M. LABES. J. Am. Chem. Soc. **79**, 4155 (1957).
8. E. M. KOSOWER. J. Am. Chem. Soc. **80**, 3253 (1958).
9. J. B. HYNE and R. WOLFGANG. J. Phys. Chem. **64**, 699 (1960).
10. R. E. ROBERTSON. Can. J. Chem. **33**, 1536 (1955).
11. G. AKERLOFF. J. Am. Chem. Soc. **54**, 4125 (1932).
12. G. AKERLOFF and O. SHORT. J. Am. Chem. Soc. **58**, 1241 (1936).
13. G. SCATCHARD. J. Chem. Phys. **7**, 657 (1939).
14. S. GLASSTONE, K. J. LAIDLER, and H. EYRING. The theory of rate processes. McGraw Hill, New York. 1941. p. 419.
15. E. TOMMILA and A. HELLA. Ann. Acad. Sci. Fennicae, Ser. A I, 153 (1954).
16. S. WINSTEIN, E. GRUNWALD, and H. W. JONES. J. Am. Chem. Soc. **73**, 2700 (1951).
17. A. FAINBERG and S. WINSTEIN. J. Am. Chem. Soc. **78**, 2770 (1956).
18. C. G. SWAIN, R. B. MOSELEY, and D. E. BROWN. J. Am. Chem. Soc. **77**, 3731 (1955).
19. J. B. HYNE. J. Am. Chem. Soc. **85**, 304 (1963).
20. Y. H. INAMI, H. K. BODENSEH, and J. B. RAMSEY. J. Am. Chem. Soc. **83**, 4745 (1961).

Can. J. Chem. Downloaded from www.nrcresearchpress.com by 210.87.254.6 on 09/05/12
For personal use only.

THE ANODIC OXIDATION OF AMMONIA AT PLATINUM BLACK ELECTRODES IN AQUEOUS KOH ELECTROLYTE

H. G. Oswin and M. Salomon[1]

Leesona Moos Laboratories, Lake Success, Long Island, N.Y., U.S.A.

Received February 19, 1963

ABSTRACT

Electrochemical kinetic studies are reported on the anodic oxidation of ammonia in aqueous potassium hydroxide solutions at platinum black electrodes. A kinetic scheme of consecutive reactions is proposed; Tafel slopes are deduced for various rate-determining mechanisms and compared with the experimental behavior. The reaction pathway is correlated with that involved in the analogous catalyzed ammonia vapor decomposition. The exchange currents obtained, compared with those for hydrogen oxidation, render the system unfavorable for fuel cell applications.

INTRODUCTION

Recently, ammonia has been considered as a possible fuel for use in fuel cell applications; it has the advantage of being a relatively cheap liquid fuel, and it appears to oxidize completely to nitrogen and water. It has, therefore, been considered a possible successor to hydrogen, but investigations that we have carried out with ammonia show that it is a far less reversible electrode than hydrogen over the temperature range 0° C to 200° C. Thus, although considerable current densities can be obtained from noble metal electrodes and ammonia, the polarization of these electrodes is excessively high and would preclude the use of ammonia where high thermal efficiency is required. It has been the object of this investigation to determine the rate-limiting steps in the overall mechanism of the anodic oxidation of ammonia which are responsible for the observed polarization levels.

A preliminary investigation of noble metal blacks indicated that platinum black appeared to be the most reversible of electrode systems and was chosen as the electrode for a detailed investigation of mechanisms. It was not possible to conduct these studies on a bright platinum surface because, under the experimental conditions, such surfaces exhibited very poor stability and reproducibility. This is considered to be a result of the low exchange current of the NH_3/Pt electrode relative to electrolyte impurity currents.

EXPERIMENTAL TECHNIQUE

The experimental cell used is shown in Fig. 1 and consists of four compartments. Compartments A and D contain the electrodes for pre-electrolysis, which was conducted for 24 hours at a current density of approximately 1 ma/cm^2. The study electrode and pre-electrolysis electrodes were prepared by electroplating platinum black onto platinum foil by the method described by Janz and Ives (1). High-purity nitrogen was bubbled through the pre-electrolysis compartments during the period of pre-electrolysis. The reference electrode was Hg/HgO/KOH. Electrolyte concentrations of 1, 5, and 10 molal KOH were prepared from analytical grade KOH and water triply distilled from alkaline permanganate solution.

The current–potential relationships were obtained by the galvanostatic method using a square-wave current generator. The potential transients were displayed on a Tektronix 545A oscilloscope and recorded photographically. The magnitude of the activation overpotential was measured at the point where $dV/dt = 0$.

The molal activity coefficients (2) for KOH solutions were used to calculate the reversible potential of the ammonia electrode. The activity of ammonia at 25° C was calculated from the experimental values of the solubility of ammonia in KOH and was estimated to be 0.0352. From the Nernst equation, E_0 was calculated to be −0.787 v versus the standard hydrogen electrode (S.H.E.). All potentials shown are referred to the standard hydrogen electrode (S.H.E.).

[1]*Present address: Department of Chemistry, University of Ottawa, Ottawa, Ont.*

Can. J. Chem. Downloaded from www.nrcresearchpress.com by 210.87.254.105 on 09/05/12
For personal use only.

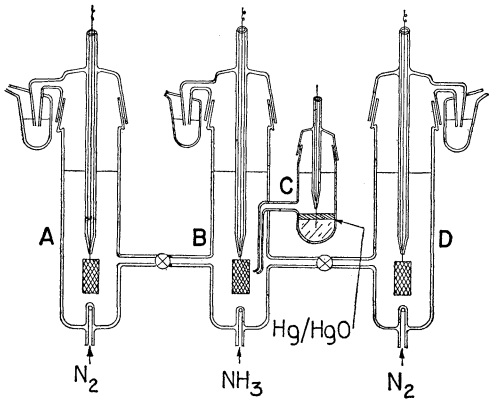

FIG. 1.

EXPERIMENTAL DATA

Experimental data are shown in Figs. 2–4. Table I lists the recorded open-circuit voltages (O.C.V.) and calculated exchange currents. The Tafel plots demonstrate two

TABLE I

Open-circuit voltages and exchange currents

Figure No.	Temperature (°C)	O.C.V. vs. S.H.E. (mv)	Current density, i_0 (amp/app. cm²)
1	27	−385	$\sim 10^{-8}$
2	32	−550	$\sim 10^{-8}$
3	70	−615	$\sim 10^{-8}$

distinct regions: a low-current linear region having a slope of (approximately) $2RT/3F$, and a high-current region where the slope approaches infinity. Visible gas evolution was observed in both regions, and the gas has been identified as pure nitrogen. The overall reaction appears to be

$$NH_3 + 3OH^- \rightarrow \tfrac{1}{2}N_2 + 3H_2O + 3e^- \qquad [A]$$

and the reaction appears to proceed with 100% coulombic efficiency. It might be noted that oxides of nitrogen would only be expected at potentials positive to S.H.E. All of the experiments reported herein were conducted in the potential region negative to S.H.E. It can be reasonably assumed, therefore, that over the whole current range observed, the currents correspond to the anodic oxidation of ammonia; also, the two different regions observed in the Tafel plots each have corresponding rate-limiting processes.

DISCUSSION OF RESULTS

An overall sequence of reactions must first be proposed. Considering the postulated mechanism of the vapor phase decomposition of ammonia to form nitrogen and hydrogen, it is presently believed that ammonia chemisorbs on the transition-metal surfaces, followed by dissociation to an amine radical which further dissociates to an imine radical (3–10). This can be represented by the following scheme, where (a) represents an adsorbed species.

Can. J. Chem. Downloaded from www.nrcresearchpress.com by 210.87.254.105 on 09/05/12
For personal use only.

Can. J. Chem. Downloaded from www.nrcresearchpress.com by 210.87.254.105 on 09/05/12
For personal use only.

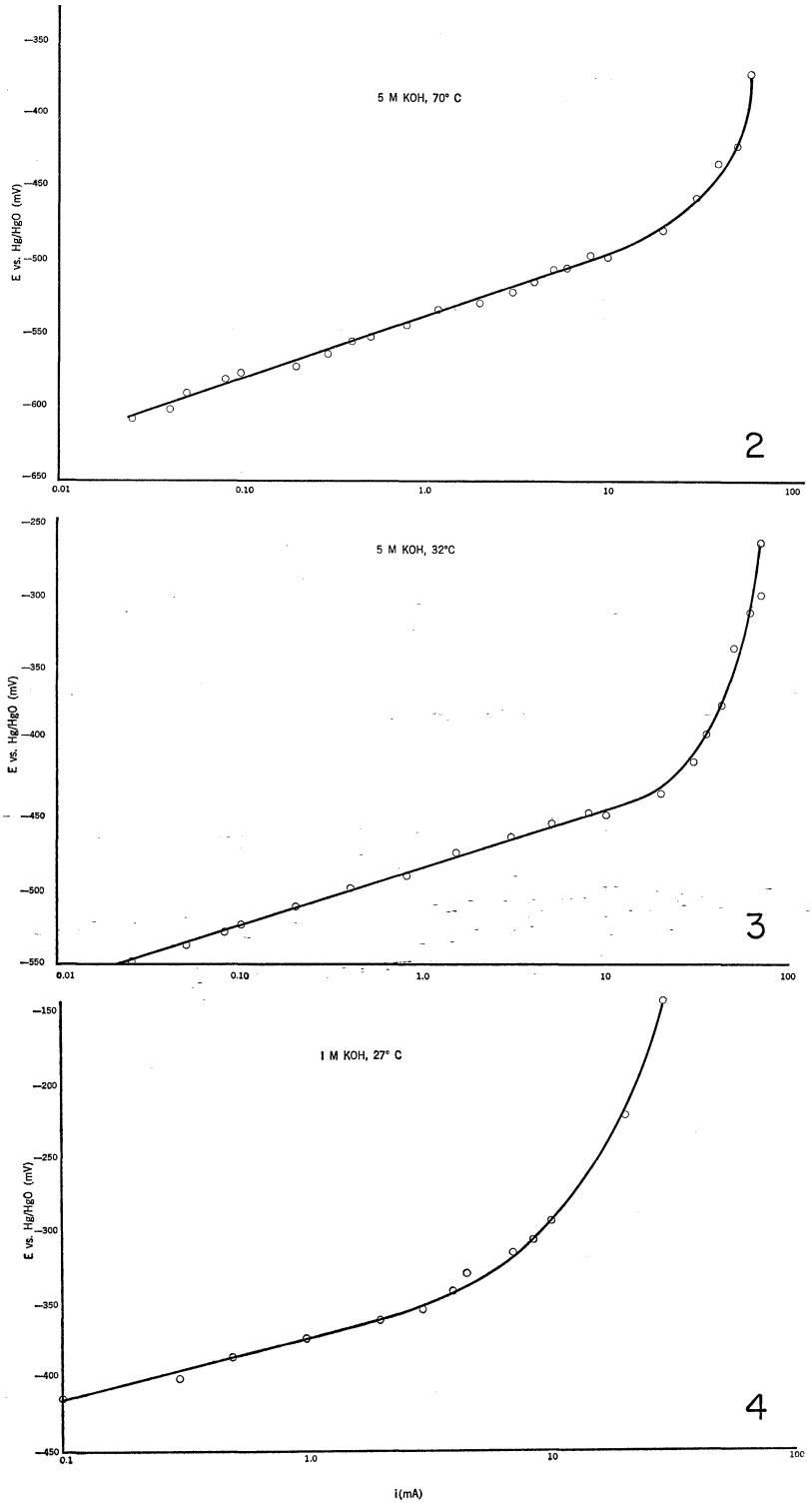

FIGS. 2–4.

$$NH_3 \rightarrow NH_2(a) + H(a) \quad [B]$$

$$NH_2(a) \rightarrow NH(a) + H(a) \quad [C]$$

$$NH(a) \rightarrow N(a) + H(a) \quad [D]$$

$$2H(a) \rightarrow H_2 \quad [E]$$

$$2N(a) \rightarrow N_2 \quad [F]$$

The overall gas phase equilibrium is

$$2NH_3 \rightleftharpoons 3H_2 + N_2.$$

Brunauer, Love, and Keenon (3) found that the energy of activation of adsorption increases linearly with coverage according to

$$\Delta E^{\ddagger} = \Delta E_0^{\ddagger} + r\theta, \quad [1]$$

where $\Delta E^{\ddagger}$ is the energy of activation at some finite coverage and $\Delta E_0^{\ddagger}$ is the energy of activation at zero coverage, r is a constant and has the dimensions of energy, and θ is the surface coverage. Similarly, for desorption, the energy of activation varies with coverage according to

$$\Delta E'^{\ddagger} = \Delta E_0'^{\ddagger} + r\theta.$$

From these experimental studies (3–5), it is concluded that reaction [F] (nitrogen recombination) is rate determining. Horiuti *et al.* (6–10) have proposed that the rate-determining step is one of the reactions [B], [C], or [D], although they favor reaction [D] (10). The conclusion that reaction [B], [C], or [D] is rate determining is based on the experimentally determined stoichiometric number of 2; that is, the number of times the rate-determining step has to occur for every complete reaction is two. The stoichiometric number is 2 for reactions [B], [C], and [D], 3 for reaction [E], and 1 for reaction [F]. These results for the vapor phase decomposition are important since we propose that two similar mechanisms occur during the anodic oxidation of ammonia in KOH solutions.

In strong acid electrolytes, the anodic oxidation of ammonia appears to be extremely slow. It is, therefore, proposed that the NH_3 molecule is the reacting species rather than the ammonium ion. It does not seem likely that the NH_4^+ ion can be chemisorbed without prior dissociation to NH_3 and H_3O^+, since the nitrogen does not have any electrons available to form a surface bond when in the NH_4^+ form. Therefore, we propose that the anodic oxidation of ammonia proceeds via the dissociation of an ammonia molecule in a manner similar to that believed to occur in the gas phase dissociation. Four sequential steps for the anodic oxidation of ammonia are proposed:

$$NH_3 + M + OH^- \rightarrow M{-}NH_2 + H_2O + e_m \quad [i]$$

$$M{-}NH_2 + OH^- \rightarrow M{=}NH + H_2O + e_m \quad [ii]$$

$$M{=}NH + OH^- \rightarrow M{=}N + H_2O + e_m \quad [iii]$$

$$M{\equiv}N + N{\equiv}M \rightarrow 2M + N_2. \quad [iv]$$

Three single electron-exchange steps are involved, followed by a non-electrochemical recombination of nitrogen atoms and the desorption of nitrogen molecules. The surface, therefore, would be covered with the chemisorbed species —NH_2, —NH, and —N. Since the potential region studied is greater than 200 mv positive to the reversible hydrogen potential in the electrolyte, it must be assumed that surface coverage of M—H species is very low and that θ_{MH} is negligible.

A comprehensive derivation of the kinetic parameters is treated for two cases. The first

Can. J. Chem. Downloaded from www.nrcresearchpress.com by 210.87.254.105 on 09/05/12
For personal use only.

case is where surface coverage is either low or high, i.e., $0.2 > \theta > 0.8$, which are the necessary conditions for applying the Langmuir isotherm. The second case is for intermediate coverages where the heat of chemisorption varies linearly as a function of θ and adsorption can be described by the Temkin isotherm (11).

Case I—Application of Langmuir Isotherm

When the initial stage [i] is the slow and rate-determining step, the rate of the reaction is given by the relation

$$V_1 = k_1 \cdot a_{NH_3} \cdot a_{OH^-}(1-\theta_t)e^{\beta VF/RT}, \qquad [2]$$

where k_1 is the electrochemical rate constant, β is the relative slope factor for the energy curves of the initial and final states at their point of intersection, θ_t is the total surface coverage, and all the other terms have their usual significance. Differentiation of eq. [2] yields a Tafel slope of $dV/d \ln i = RT/\beta F$ (noting that $i = zFV$). If $\beta = 0.5$, then the slope is 118 mv at 25° C.

When stage [ii] is rate determining, then [i] can be considered in quasi-equilibrium, and the reverse rate is

$$V_{-1} = k_{-1} \cdot a_{H_2O} \cdot \theta_{MNH_2} \cdot e^{-(1-\beta)VF/RT}. \qquad [3]$$

Since this step is regarded as being in equilibrium, the forward and reverse rates can be equated and the value of θ_{MNH_2} determined. Hence,

$$\theta_{MNH_2}/(1-\theta_t) = K_1 \cdot e^{VF/RT}, \qquad [3a]$$

where K_1 is the equilibrium constant. For low surface coverages

$$\theta_{MNH_2} = K_1 \cdot e^{VF/RT}. \qquad [4]$$

The velocity of the rate-determining mechanism is given by

$$V_2 = k_2 \cdot a_{OH^-} \cdot \theta_{MNH_2} \cdot e^{\beta VF/RT}. \qquad [5]$$

Substituting for θ_{MNH_2} from [4] and differentiating, we obtain

$$dV/d \ln i = 2RT/3F = 39 \text{ mv}. \qquad [6]$$

If step [iii] is rate determining, then [i] and [ii] can be considered to be in quasi-equilibrium. The reverse rate of step [ii] is

$$V_{-2} = k_{-2} \cdot a_{H_2O} \cdot \theta_{MNH} \cdot e^{-(1-\beta)VF/RT}. \qquad [7]$$

By equating eqs. [5] and [7]

$$\theta_{MNH} = K_2 \cdot \theta_{MNH_2} \cdot e^{VF/RT}.$$

Substituting for θ_{MNH_2} from eq. [4]

$$\theta_{MNH} = K_1 K_2 e^{2VF/RT} \qquad [8]$$

The velocity of step [iii] is

$$V_3 = k_3 \cdot a_{OH^-} \cdot \theta_{MNH} \cdot e^{\beta VF/RT}. \qquad [9]$$

Combining eqs. [8] and [9] and differentiating yields a Tafel slope of $2RT/5F$ or 24 mv. Similarly, where step [iv] is the rate-determining process

$$\theta_{MN} = K_1 K_2 K_3 e^{3VF/RT} \qquad [10]$$

Can. J. Chem. Downloaded from www.nrcresearchpress.com by 210.87.254.105 on 09/05/12
For personal use only.

and the rate is

$$V_4 = k_4 \cdot \theta_{MN}^2. \quad [11]$$

Equating [10] and [11]

$$V_4 = k_4[K_1K_2K_3]^2 \cdot e^{6VF/RT} \quad [12]$$

and differentiating, we obtain a Tafel slope of $RT/6F$ or 10 mv.

For the case of high coverages, i.e., as $\theta \rightarrow 1$, the coverage is no longer a function of potential. A Tafel slope of $RT/\beta F$ is predicted for all cases except the last, where the slope is infinite. Thus, when the nitrogen recombination stage is rate determining and surface coverage is high, a limiting-current condition is achieved (12).

It should be noted that application of Langmuir isotherm results in a decreasing Tafel slope when the assumed rate-determining step changes from the initial to the final step for the case of small surface coverages. It is quite possible, however, that intermediate surface coverages are involved and that the Langmuir isotherm is no longer applicable (see below).

Case II—Application of Temkin Isotherm

Recently, Thomas (13) has shown that linear Tafel lines can arise from the hydrogen evolution reaction in the region of intermediate coverage, i.e., $0.2 < \theta < 0.8$. Conway and Gileadi (14) have extended this treatment for a series of consecutive electrochemical reactions and have shown that the lowest Tafel slope obtainable for a terminal recombination step is $RT/2F$. This treatment for intermediate coverages is based upon the Temkin isotherm when there is a linear relation between heat of adsorption and coverage. This dependence can be represented by a form of eq. [1]. The exact form of eq. [1], which is applicable in the case of consecutive reactions, will depend upon the model used (14). The model which seems most probable is that of Boudart, which is based on the surface induction effect (15). This model is preferable to the one based on intrinsic heterogeneity of surface sites, since experimental investigations of the vapor phase decomposition of NH_3 on metals indicate that surface interactions not due to heterogeneity are involved (16, 17).

The r term in eq. [1] thus arises from dipole double-layer (surface potential) contributions from MNH_2, MNH, and MN. Hence, we can write equations analogous to [1] for the three species as

$$\begin{aligned}
\Delta H_A &= \Delta H_A^0 - r_A\theta_A - r_B\theta_B - r_C\theta_C \\
\Delta H_B &= \Delta H_B^0 - r_A\theta_A - r_B\theta_B - r_C\theta_C \\
\Delta H_C &= \Delta H_C^0 - r_A\theta_A - r_B\theta_B - r_C\theta_C,
\end{aligned}$$

where ΔH is the heat of adsorption. Replacing $r_A\theta_A + r_B\theta_B + r_C\theta_C$ by $f(\theta)$,

$$\begin{aligned}
\Delta H_A &= \Delta H_A^0 - f(\theta) \\
\Delta H_B &= \Delta H_B^0 - f(\theta) \\
\Delta H_C &= \Delta H_C^0 - f(\theta).
\end{aligned} \quad [13]$$

Since the heat of adsorption decreases linearly with the coverage, the free energy of activation is decreased by some fraction $1-\gamma$ of $f(\theta)$ (13, 14). The forward rate of step [i] can be written as

$$V_1 = k_1 \cdot a_{NH_3} \cdot a_{OH^-} \cdot (1-\theta_t) \cdot \exp\, -[\Delta G_{0_1}^{\ddagger} + \gamma f\theta - \beta VF]/RT. \quad [14]$$

Can. J. Chem. Downloaded from www.nrcresearchpress.com by 210.87.254.105 on 09/05/12
For personal use only.

Similarly, for the reverse reaction, the free energy of activation is increased by some fraction $1-\gamma$ of $f(\theta)$, and the reverse rate of step [i] is, therefore,

$$V_{-1} = k_{-1}\cdot\theta_{MNH_2}\cdot a_{H_2O}\cdot\exp\ -[\Delta G^{\ddagger}_{0_{-1}}-(1-\gamma)f\theta+(1-\beta)VF]/RT. \qquad [15]$$

If [i] is rate determining then θ_{MNH_2} is small and the simple discharge slope of $2RT/F$ can be derived. If [i] is fast (another step being slow), then it is assumed that [i] is in quasi-equilibrium. Equating [14] and [15]

$$f(\theta) = VF+K_1. \qquad [16]$$

Reactions [ii] and [iii] are radical–ion recombinations which involve charge transfer and production of a new surface species. Thus, the rate of [ii] is

$$V_2 = k_2\cdot\theta_{MNH_2}\cdot a_{OH^-}\cdot\exp\ -[\Delta G^{\ddagger}_{0_2}+\gamma f(\theta)-(1-\gamma)f(\theta)-\beta VF]/RT. \qquad [17]$$

Assuming that γ equals $1/2$

$$V_2 = K_2\cdot\theta_{MNH_2}\cdot a_{OH^-}\cdot\exp\ -[\Delta G^{\ddagger}_{0_2}-\beta VF]/RT. \qquad [17a]$$

For intermediate coverages, it follows that the pre-exponential terms in θ can be neglected compared to the exponential term in θ (13, 14). Using logs and differentiating [17*a*] yields a Tafel slope of $2RT/F$. Since mechanism [iii] is identical in form with mechanism [ii], it yields a Tafel slope of $2RT/F$.

The rate of terminal recombination step [iv] for non-activated chemisorption of nitrogen is

$$V_4 = k_4\cdot\theta^2_{MN}\cdot\exp\ -[\Delta G^{\ddagger}_{0_4}-2f(\theta)]/RT \qquad [18]$$

and for the activated adsorption of nitrogen is

$$V_4 = k_4\cdot\theta^2_{MN}\cdot\exp\ -[\Delta G^{\ddagger}_{0_4}-2\delta f(\theta)]/RT. \qquad [18a]$$

Here, δ is the symmetry factor of the energy barrier associated with activated chemisorption of nitrogen.

From equations [16] and [18] for non-activated adsorption

$$V_4 = k_4'\cdot\theta^2_{MN}\cdot\exp\ -[\Delta G^{\ddagger}_{0_4}-2VF]/RT. \qquad [19]$$

From eqs. [16] and [18*a*] and activated adsorption

$$V_4 = k_4'\cdot\theta^2_{MN}\cdot\exp\ -[\Delta G^{\ddagger}_{0_4}-2\delta VF]/RT. \qquad [20]$$

Therefore, the Tafel slopes corresponding to equations [19] and [20] are $RT/2F$ and $RT/2\delta F$, respectively.

Table II is a summary of the calculations performed and contains the derived Tafel slopes, assuming different rate-controlling mechanisms and either Langmuir or Temkin isotherms. In addition to the slopes for the Temkin isotherm (refer to Table II), other slopes can appear depending on the ratio of the coverages by intermediate species (14). Thus, if reaction [iii] is rate determining, both θ_{MNH_2} and θ_{MNH} can be significant depending upon the equilibrium constant for reaction [ii], i.e.,

$$\theta_{MNH}/\theta_{MNH_2} = K_2e^{VF/RT}. \qquad [21]$$

If step [iv] is rate determining, then there are three surface intermediates whose coverages are a function of the equilibrium constant for reaction [iii], i.e.,

$$\theta_{MN}/\theta_{MNH} = K_3e^{VF/RT} \qquad [22]$$

Can. J. Chem. Downloaded from www.nrcresearchpress.com by 210.87.254.105 on 09/05/12
For personal use only.

TABLE II
Tafel slopes

Mechanism	Langmuir case	Temkin case
(*a*) Calculated		
[i]	$2RT/F$	—
[ii]	$2RT/3F$	$2RT/F$
[iii]	$2RT/5F$	$2RT/F$
[iv]	RT/6F or ∞ ($\theta \rightarrow 1$)	RT/F (activated adsorption) or $RT/2F$ (non-activated)
(*b*) Observed		
	$2RT/3F$ $\rightarrow \infty$	Low-current region High-current region

and the equilibrium given above. Considering reaction [iii] to be rate determining and K_2 in eq. [21] $\ll 1$, then θ_{MNH} is small and exponentially dependent on potential. In addition, substitution for θ_{MNH} in the rate equation must be made. If the rate is

$$V_3 = k_3 \cdot a_{OH^-} \cdot \theta_{MNH} \cdot \exp -[\Delta G^{\ddagger}_{0_3} - \gamma f(\theta) + (1-\gamma) f(\theta) - \beta VF]/RT \qquad [23]$$

then substitution for θ_{MNH} yields

$$V_3 = k_3' \theta_{MNH_2} \cdot \exp VF/RT \cdot \exp \beta VF/RT. \qquad [24]$$

Since θ_{MNH_2} can be considered to be constant compared to the exponential term in θ, the Tafel slope is $2RT/3F$ or 39 mv.

Considering step [iv] to be rate determining and K_3 in eq. [22] $\ll 1$, then θ_{MN} is small and exponentially dependent upon potential. For activated nitrogen chemisorption,

$$V_4 = k_4'' \cdot \theta^2_{MNH} \cdot \exp 2VF/RT \cdot \exp 2\delta VF/RT \qquad [25]$$

is obtained from eqs. [20] and [22]. Assuming $\delta = 1/2$, the derived Tafel slope is $RT/3F$.

If both K_2 and K_3 are $\ll 1$, substitution must be made for θ^2_{MNH} in eq. [25]. The potential-dependent form for θ^2_{MNH} is obtained from eq. [21]. Substitution for θ^2_{MNH} yields

$$V_4 = K_4^* \cdot \theta^2_{MNH_2} \cdot \exp 4VF/RT \cdot \exp 2\delta VF/RT.$$

For $\delta = 1/2$

$$V_4 = k_4^* \cdot \theta^2_{MNH_2} \cdot \exp 5VF/RT \qquad [26]$$

and the Tafel slope is $RT/5F$.

Therefore, it is seen that a variety of slopes can be predicted which depend on equilibrium constants K_2 and K_3 in eqs. [21] and [22]. These constants are dependent on the relative bond strengths of the surface species involved. For example, K_2 will be closer to unity if the bond strength M=N > M—N. It is reasonable to assume that the bond strength will increase in the order M≡N > M=N > M—N. This is analogous to the case of carbon–nitrogen bonds (17). Therefore, slopes predicted by equations [21–26] can be rejected.

Comparison of Case I and II

The experimental values of $dV/d \ln i$ obtained from Figs. 2, 3, and 4 correspond to $2RT/3F$ in the low-current region and to infinity in the high-current region. Within the limitations and assumptions inherent in eqs. [2–26], it would seem that these experimental values can be interpreted in terms of the Langmuir isotherm. Thus, at low-current densities, the rate-controlling step would be the oxidation of the surface amine,

Can. J. Chem. Downloaded from www.nrcresearchpress.com by 210.87.254.105 on 09/05/12
For personal use only.

as shown in step [ii], while at high-current densities, the rate-determining process is nitrogen recombination and evolution (refer to step [iv]).

There appears to be some justification, therefore, for stating that there are similarities between the mechanisms of vapor phase decomposition and anodic oxidation of ammonia on a platinum electrode. However, there appears to be a significant difference between the two systems. In the anodic oxidation, the kinetic treatment using the Langmuir isotherm indicates both limiting low and high surface coverages. In the vapor phase decomposition, apparently the data can be explained on the basis of the Temkin isotherm, which requires that surface coverage be intermediate.

This difference might be expected in the case of the recombination step for the following reasons. During the vapor phase decomposition of ammonia, the overall nitrogen desorption rate would be influenced by surface coverage with chemisorbed hydrogen, which acts as a "poison" (3, 4). Thus, the rate of nitrogen recombination is reduced by the presence of chemisorbed hydrogen.

However, during the anodic oxidation of ammonia, the coverage with respect to chemisorbed hydrogen at potentials several hundred millivolts positive to the reversible hydrogen potential will be insignificant. This is clearly indicated from the approximate exchange current density values for the ammonia electrode, which are lower than that reported for hydrogen evolution (19) by a factor of about 10^5.

Therefore, it is suggested that in the anodic oxidation case no "poisoning" or blocking of surface sites by hydrogen ad-atoms occurs. In addition, nitrogen recombination can be rapid at low current densities. This is consistent with Horiuti *et al.* (6–10), except we conclude that step [ii] is rate determining at low-current densities; in the vapor phase, step [iii] is thought to be rate determining.

ACKNOWLEDGMENT

The authors would like to acknowledge the very helpful discussions with Professor B. E. Conway and Mr. E. Gileadi.

REFERENCES

1. G. J. Janz and D. J. G. Ives. Reference electrodes. Academic Press, New York. 1961.
2. G. C. Akerlof and P. Bender. J. Am. Chem. Soc. **70**, 2366 (1948).
3. S. Brunauer, K. S. Love, and R. G. Keenon. J. Am. Chem. Soc. **64**, 751 (1942).
4. K. S. Love and P. H. Emmett. J. Am. Chem. Soc. **63**, 3297 (1941).
5. M. Temkin and W. Pyzhev. Acta Phys. Chem. **17**, 327 (1940).
6. J. Horiuti and S. Enomoto. J. Res. Inst. Catalysis, Hokkaido Univ. **2**, 87 (1953).
7. J. Horiuti, S. Enomoto, and H. Kobayashi. J. Res. Inst. Catalysis, Hokkaido Univ. **3**, 185 (1955).
8. J. Horiuti and H. Kita. J. Res. Inst. Catalysis, Hokkaido Univ. **4**, 132 (1956).
9. J. Horiuti and I. Toyoshima. J. Res. Inst. Catalysis, Hokkaido Univ. **5**, 120 (1957).
10. J. Horiuti and I. Toyoshima. J. Res. Inst. Catalysis, Hokkaido Univ. **6**, 68 (1958).
11. M. Temkin. Zh. Fiz. Khim. **15**, 296 (1941).
12. A. Azzam and J. O'M. Bockris. Trans. Faraday Soc. **48**, 145 (1952).
13. J. G. N. Thomas. Trans. Faraday Soc. **57**, 1063 (1961).
14. B. E. Conway and E. Gileadi. Trans. Faraday Soc. **58**, 2493 (1962).
15. M. Boudart. J. Am. Chem. Soc. **72**, 3556 (1952).
16. K. J. Laidler and J. Weber. J. Chem. Phys. **19**, 1089 (1951).
17. J. H. deBoer. Electron emission and adsorption phenomena. Cambridge. 1935.
18. L. Pauling. Nature of the chemical bond. Cornell University Press. 1939.
19. J. O'M. Bockris. Modern aspects of electrochemistry. Butterworths, London. 1954. Chap. 4.

Can. J. Chem. Downloaded from www.nrcresearchpress.com by 210.87.254.105 on 09/05/12
For personal use only.

THE POLAROGRAPHY OF THE MAGNESIUM–ALIZARIN SYSTEM

D. G. Brewer[1] and John A. Page
Department of Chemistry, University of Toronto, Toronto, Ontario
Received March 13, 1963

ABSTRACT

The polarography of alizarin alone, and alizarin in the presence of magnesium, has been studied in an ammonia–ammonium chloride electrolyte. Alizarin was found to give a reduction wave with $E_{1/2} = -(0.14+0.059\ \text{pH})$ volts vs. S.C.E. and a polarographic diffusion coefficient D, equal to 1.20×10^{-6} cm^2 sec^{-1} over a range of pH from 7.4 to 10.0 in aqueous solution at 25° C. The slope of the wave corresponded to a two-electron reversible process. The addition of magnesium caused a decrease in the polarographic wave for alizarin, but the combining ratio of magnesium to alizarin was a function of pH, ranging from 1.02 at pH 9.0 to 1.28 at pH 10.1. The combining ratio greater than unity could be attributed to alizarin adsorbed on a 1:1 (MgAlz) precipitate. The removal of alizarin from the solution was not quantitative in the presence of excess magnesium, and there is evidence of the formation of soluble complex species. The reaction is potentially useful for the indirect polarographic determination of magnesium.

INTRODUCTION

The direct polarographic determination of magnesium has proved unsatisfactory, with hydrogen evolution accompanying the reduction of the magnesium at the dropping mercury electrode (1). In basic supporting electrolytes of tetraalkyl ammonium salts the polarographic wave for magnesium is irregular and abnormally large, with a half-wave potential of −2.2 volts vs. S.C.E. (2, 3, 4). However, magnesium has been determined polarographically utilizing a streaming mercury electrode in a tetramethyl ammonium chloride electrolyte of pH 5.4 to 6.8 (5).

A number of indirect polarographic procedures for magnesium have been reported in the literature. One method measures the amount of 8-hydroxyquinoline unused in the precipitation of magnesium (6), while a variation dissolves the magnesium precipitate in acid for a polarographic determination of the 8-hydroxyquinoline equivalent to the magnesium (7). Another indirect method involves the precipitation of the hexamine complex of either magnesium iodide or calcium–magnesium ferrocyanide (8). The precipitate is filtered, washed, dissolved in a potassium nitrate solution, and then the iodide is determined polarographically or the ferrocyanide is titrated amperometrically with a lead nitrate solution. Two methods employing ethylenediaminetetraacetic acid (EDTA) have also been reported. In one (9), magnesium is added to a buffered ammonia – ammonium chloride solution containing the zinc–EDTA complex. Zinc, equivalent to the magnesium, is liberated and determined polarographically. A second method (10) depends on the decrease in the anodic wave of EDTA caused by the presence of magnesium. All of these indirect methods are subject to numerous interferences.

A literature survey of reagents for the qualitative and quantitative determination of magnesium has revealed no reagent outstanding in specificity. However, the alizarin reagent family (Fig. 1(*a*)) is most prominent in magnesium spot tests and colorimetric procedures (11, 12, 13). Furman and Stone (14) have carried out a systematic polarographic study of these reagents in various aqueous buffer solutions containing 1% ethanol. In alkaline solutions they found that most of the alizarin reagents gave a single polarographic reduction wave with slopes close to that for a reversible two-electron process, indicating reduction to a hydroquinone form. However, some specific buffer effects were

[1]*Present address: Department of Chemistry, University of New Brunswick, Fredericton, New Brunswick.*

Can. J. Chem. Downloaded from www.nrcresearchpress.com by 210.87.254.6 on 09/05/12
For personal use only.

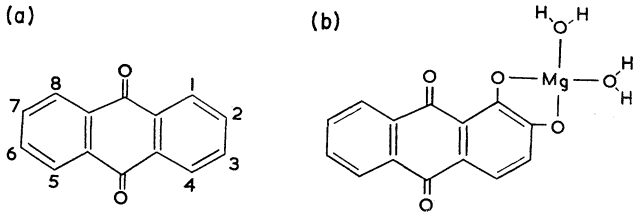

FIG. 1. (*a*) Hydroxyanthraquinone reagents: alizarin (1,2), quinizarin (1,4), anthrarufin (1,5), chrysazin (1,8), purpurin (1,2,4), anthrapurpurin (1,2,7), quinalizarin (1,2,5,8). (*b*) Structure of 1:1 magnesium–alizarin precipitate.

observed. In some cases, two polarographic waves, each with a one-electron slope, were obtained. This was taken as an indication of intermediate semiquinone formation. In the pH region of 4 to 8 a number of cases were found of single waves with slopes close to that for a one-electron process.

EXPERIMENTAL

Polarograms were recorded on a Leeds and Northrup Type E Electrochemograph with damping set at the No. 1 position. A conventional H-type cell with a saturated calomel reference electrode was used; the polarography was carried out at 25.0°. The dropping mercury electrode was used with a 50.0-cm head of mercury; the flow rate, m, was 1.178 mg sec^{-1}. Diffusion currents were measured at −1.00 volts vs. S.C.E. and corrected for residual current by graphical means; the drop time, t, was 5.25 sec at this potential in the supporting electrolyte. The capillary constant was equal to 3.11 $mg^{2/3}$ $sec^{-1/2}$.

Prepurified nitrogen (less than 20 p.p.m. nitrogen) was used to displace the oxygen from solutions for polarography. The pH measurements were made with a Beckman Model G meter employing external electrodes. The meter was standardized at 25.0° using Beckman 3501 pH 7.00 buffer. Most absorbance measurements were made on a Bausch and Lomb Spectronic 505 using matched quartz cells of 1-cm path length. One series of solutions (Table IV) was run on a Beckman DU spectrophotometer. Absorbances measured on both instruments differed appreciably, apparently due to a difference in the optical systems.

The alizarin used was supplied by the Fisher Scientific Company as a reagent grade material. It was recrystallized from carbon tetrachloride and dried at 110°. The purified reagent was confirmed by both infrared and n.m.r. spectra; it had a melting point of 280–283°. Standard stock solutions were prepared by dissolving known weights of the reagent in 25 ml of 0.1 M NaOH solution and then diluting to 500 ml with water. A number of preliminary experiments were carried out with a stock solution prepared by dissolving alizarin in 300 ml of ethanol and then diluting to 500 ml with stock NH_3–NH_4Cl buffer solution.

The stock NH_3–NH_4Cl buffer solution was prepared by dissolving 300 g of reagent NH_4Cl and 400 ml of concentrated aqueous NH_3 in water and diluting to 2000 ml. A 15-ml aliquot of this stock solution was used for each 100 ml of final solution, giving a system that was 0.45 M with respect to both NH_3 and NH_4Cl. Adjustment of the solution to the final pH was accomplished by addition of HCl or NH_3 before the final dilution. The standard magnesium solution was prepared by dissolving reagent grade MgO in a minimal amount of hydrochloric acid and then diluting. The solution was standardized by an EDTA titration employing Eriochrome Black T as indicator (15).

Determination of Alizarin

A method of analysis for alizarin in the presence of a large excess of magnesium or ammonium salts was developed. The procedure involves the dilution of an aqueous alizarin solution with concentrated H_2SO_4 to give a final solution 9 M in the acid. The final solution was yellow with an absorbance maximum at 428 mμ. A calibration curve prepared from weighed amounts of pure alizarin was found to obey Beer's law up to 5×10^{-5} M with a molar absorptivity, E, of 5.70×10^{-3} liter $mole^{-1}$ cm^{-1} at the absorbance maximum. Aliquots of the final buffered NH_3–NH_4Cl solutions containing known amounts of alizarin both alone and in the presence of large excess of magnesium gave results in agreement with the calibration curve.

Polarography of Alizarin

Alizarin was found to give a well-defined reduction wave with a regular diffusion current plateau in the buffer system. The stock solution of alizarin in NaOH was found to be stable for weeks, but the polarographic wave obtained from the buffered solutions deteriorated on several days' standing.

The diffusion current was found to be relatively independent of pH over the range from 8.8 to 10.8 with a mean diffusion coefficient of 4.13 μa $mmole^{-1}$ l^{-1} (Table I). Below pH 8, a buffered solution of alizarin containing 10% ethanol was found to give a precipitate with an accompanying decrease in the observed diffusion current (Fig. 2). The half-wave potential for the alizarin wave was found to shift with pH. Two

Can. J. Chem. Downloaded from www.nrcresearchpress.com by 210.87.254.6 on 09/05/12
For personal use only.

TABLE I

pH	Alizarin (mmolar) Taken	Found*	i_d (μa)	Wavelength of A_{max} (mμ)	A 525 mμ	550 mμ
Alizarin alone						
8.80	0.113	0.113	0.47	523	0.872	0.761
9.65	0.113	0.114	0.47	525	0.845	0.752
9.78	0.227	0.226	0.92	524	1.65	1.50
10.79	0.227	0.226	0.94	527	1.65	1.49
Alizarin in presence of 50-fold magnesium						
8.80	0.113	0.041_8	0.17	547	0.407	0.516
9.65	0.113	0.025_0	0.12	550	0.256	0.284
9.78	0.227	0.035_7	0.16	550	0.272	0.315
10.79	0.227	0.034_7	0.15	552	0.331	0.362

*Spectrophotometric determination in 9 M H_2SO_4 after filtration.

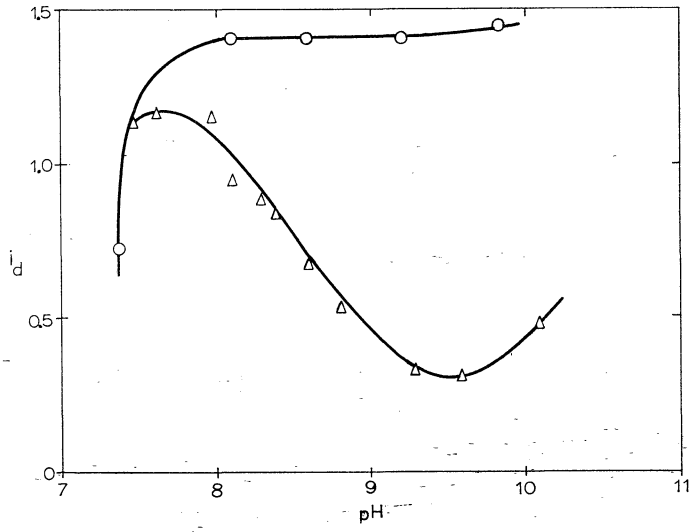

FIG. 2. pH dependence of diffusion current (μa). Upper line: 0.344 mmolar alizarin; lower line: 0.344 mmolar alizarin plus 0.500 mmolar Mg.

series of experiments using each of the stock solutions of alizarin in NaOH and ethanol gave similar shifts of -0.059 volts per pH unit but the presence of ethanol was found to shift the half-wave potentials to more negative values at a given measured pH (Fig. 3). Plots of log $(i/(i_d-i))$ vs. E_{dme} gave straight lines with slopes in close agreement with a 2 faraday per mole reduction (Table II). Thus the polarographic reduction presumably results in the formation of a hydroquinone species according to the equation

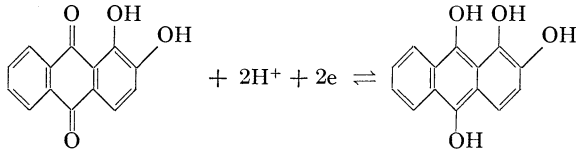

On the basis of the 2 faraday per mole reduction, a polarographic diffusion coefficient, D, equal to 1.20×10^{-6} cm^2 sec^{-1} can be calculated from the unmodified Ilkovic equation. Attempts to verify the 2 faraday per mole reduction by controlled potential coulometric reduction at a large isolated mercury cathode were not successful. Electrolysis in the buffered NH_3–NH_4Cl solution at -0.85 volts vs. S.C.E. was incomplete even after the passage of quantities of electricity several times larger than that predicted from the polarographic data.

Can. J. Chem. Downloaded from www.nrcresearchpress.com by 210.87.254.6 on 09/05/12
For personal use only.

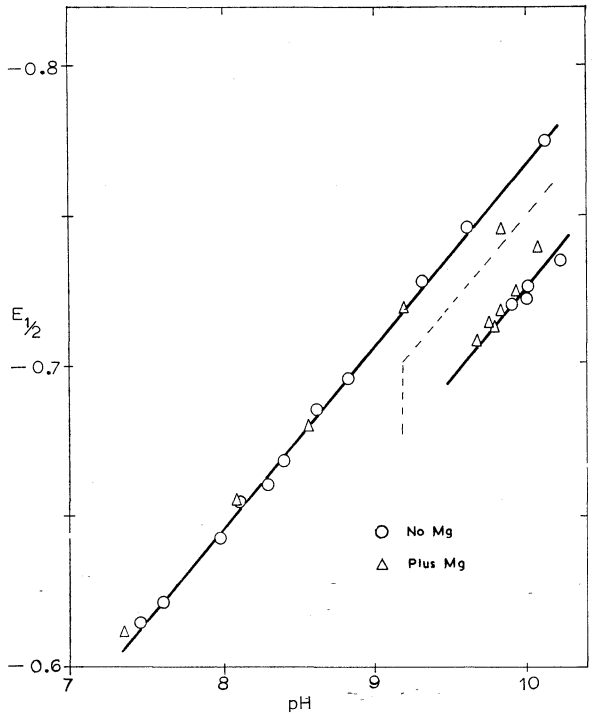

FIG. 3. pH dependence of half-wave potential (volts vs. S.C.E.). Upper line: 0.344 mmolar alizarin alone or with 0.499 mmolar Mg; lower line: 0.404 mmolar alizarin (ethanol) alone or with 0.232 mmolar Mg.

TABLE II

pH	Alizarin (mmolar)	Magnesium (mmolar)	i_d (μa)	n (faradays/mole)
9.50	1.087		4.49	2.02
9.53	0.944		3.90	1.76
9.67	1.124		4.64	1.82
9.81	1.316		5.43	1.87
10.10	0.908		3.75	2.09
9.43	0.768	0.231	2.63	1.95
9.51	1.236	0.231	3.95	2.18
9.54	0.931	0.231	2.90	1.94
9.61	0.936	0.231	2.96	1.80

Polarography of the Magnesium–Alizarin System

The effect of magnesium on the polarographic behavior of alizarin was studied by additions of magnesium to the buffered alizarin solutions before making up to final volume. Polarograms, taken at intervals, showed that approximately 3 hours at 25.0° were required to reach equilibrium (Fig. 4). A precipitate was observed to settle out of the solution over this period. The diffusion current at equilibrium in the presence of a fixed added amount of magnesium was found to be a function of pH (Fig. 2). The half-wave potential of the residual alizarin wave was not significantly shifted by added magnesium (Fig. 3), and plots of log $(i/(i_d-i))$ vs. E_{dme} again gave straight lines, in agreement with a 2 faraday per mole reduction (Table II).

The addition of a large excess of magnesium and subsequent filtration after equilibrium had been established left a residual polarographic wave with the same half-wave potential as free alizarin. The wavelength of maximum absorbance of the solution, however, was found to be shifted. The alizarin left in solution was determined spectrophotometrically in 9 M H_2SO_4 (Table I), and a mean polarographic diffusion coefficient of 4.50 μa mmole^{-1} l^{-1} was calculated.

The overall combining ratio of magnesium to alizarin was also determined. A series of solutions were prepared of fixed pH, fixed alizarin concentration, but varying concentrations of added magnesium. In each

Can. J. Chem. Downloaded from www.nrcresearchpress.com by 210.87.254.6 on 09/05/12
For personal use only.

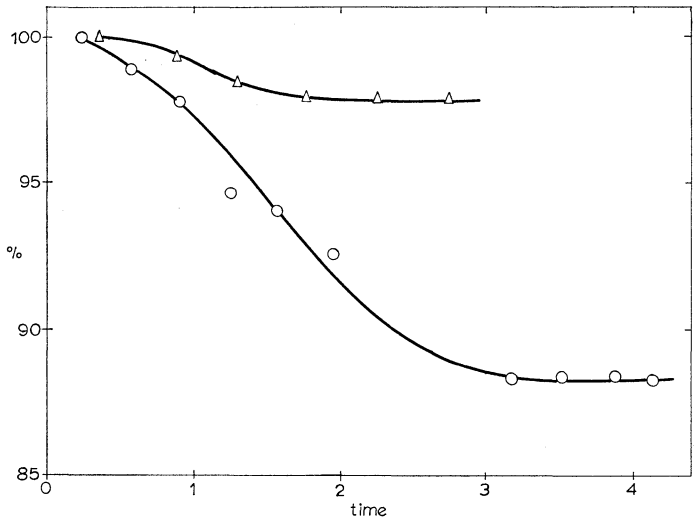

FIG. 4. Effect of standing at 25.0°. Diffusion current of alizarin (%) vs. time (hr). Upper line: 0.416 mmolar alizarin plus 0.231 mmolar Mg, pH 9.49; lower line: 1.002 mmolar alizarin plus 0.499 mmolar Mg, pH 9.71.

case investigated there was obtained an initial linear region in which the diffusion current decreased linearly with added magnesium, but also in each case the diffusion current approached zero only slowly on the addition of excess magnesium (Fig. 5). The initial linear region was extrapolated to zero diffusion current and the concentration of added magnesium corresponding to complete removal of the alizarin was determined. The overall combining ratio was found to be a function of pH (Table III), and the results have been confirmed by parallel absorbance measurements on each series of solutions (Table IV).

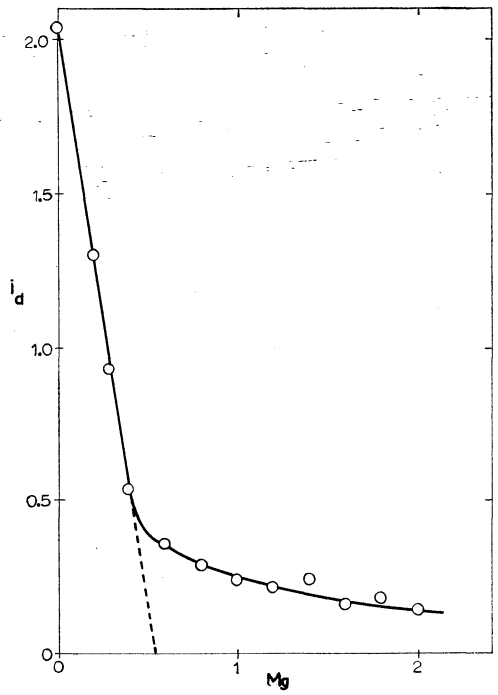

FIG. 5. Diffusion current (μa) vs. added Mg (mmolar); 0.539 mmolar alizarin, pH 9.15.

Can. J. Chem. Downloaded from www.nrcresearchpress.com by 210.87.254.6 on 09/05/12
For personal use only.

TABLE III

pH	Alizarin (mmolar)	Ratio alizarin/Mg	
		Polarographic	Spectrophotometric
9.00	0.678	1.02	
9.15	0.539	1.05	
10.11	0.748	1.26	
9.00	0.558	1.02	1.01
9.60	0.561	1.13	1.12
10.10	0.743	1.28	1.22

TABLE IV

Added Mg (mmolar)	i_d (μa)	A		Alizarin (mmolar)		K
		525 mμ	550 mμ	Free	Complexed	
0.557 mmolar alizarin, pH 9.00						
	2.30	4.24	3.73	0.558		
0.231	1.83	3.33	3.03	0.378	0.039	
0.462	0.86	1.51	1.37	0.170	0.019	
0.693	0.54	0.94	0.89	0.086	0.028	
0.924	0.48	0.85	0.80	0.079	0.024	0.036
1.38	0.35	0.64	0.62	0.053	0.024	0.025
1.85	0.31	0.52	0.52	0.036	0.024	0.021
2.31	0.23	0.48	0.48	0.030	0.025	0.021
0.561 mmolar alizarin, pH 9.60						
	2.32	4.14	3.72	0.561		
0.231	1.48	2.38	2.20	0.349	0.028	
0.462	0.53	0.89	0.85	0.091	0.023	
1.38	0.16	0.29	0.30	0.012	0.020	0.022
2.31	0.12	0.22	0.24	0.004	0.020	0.033
0.743 mmolar alizarin, pH 10.10*						
	3.07	4.47	3.89	0.743		
0.231	1.83	2.96	2.84	0.281	0.162	
0.348	1.23	1.98	1.90	0.186	9.109	
0.462	0.81	1.28	1.26	0.095	0.089	
0.693	0.77	0.99	1.06	0.006	0.121	
0.924	0.66	0.90	0.99		0.126	
1.15	0.65	0.82	0.92		0.124	
1.38	0.63	0.74	0.83		0.110	
1.62	0.62	0.69	0.77		0.109	
1.85	0.60	0.63	0.71		0.100	
2.08	0.64	0.64	0.72		0.102	

*Absorbances measured on Beckman DU spectrophotometer.

DISCUSSION

The acid dissociation constants for alizarin have been determined by Hüttig from solubility and absorption measurements (16). The values of K_1^H and K_2^H were found to be 6.61×10^{-9} and 1.07×10^{-12} at 18°. This would result in a distribution of the species H_2Alz, $HAlz^-$, and Alz^{2-} such that the predominant form over the range of pH studied would be $HAlz^-$.

Since the extrapolation of the linear region indicates a combining ratio near unity, the formula MgAlz may be assigned to the precipitate. A structure (Fig. 1(*b*)) can be postulated on the basis of a study of the reactions of other hydroxyanthraquinones. The reagents were relatively insoluble where there was the possibility of hydrogen bonding of all the hydroxyl groups to adjacent quinone oxygens; the solubility appeared to depend upon free hydroxyl groups. Of the reagents tested (Fig. 1(*a*)) only alizarin and quinalizarin precipitated with magnesium; the only reaction site consistent with insolubility

Can. J. Chem. Downloaded from www.nrcresearchpress.com by 210.87.254.6 on 09/05/12
For personal use only.

is across the 1- and 2-hydroxyl groups. Anthrapurpurin also provides this reaction site, but here the 7-hydroxyl group is available to give a soluble complex. Many other metals react with these anthraquinone reagents to form colored products. Some of these are the so-called "lakes" which are generally considered to be adsorbed dye on an insoluble hydroxide and are non-stoichiometric. However, some of the products are nearly stoichiometric and the two types may grade into each other. Sandell (13) has reviewed the chemistry of these anthraquinone products but could not establish if the bonding involved two adjacent hydroxyl groups or a quinone oxygen and its adjacent hydroxyl group.

In the present study, the combining ratio of alizarin to magnesium was close to that of a 1:1 precipitate at pH 9.00, but at a higher pH the ratio was significantly larger. These results could be explained by the formation of a mixed 1:1 and 1:2 magnesium–alizarin precipitate, the adsorption of alizarin on the 1:1 precipitate, or "lake" formation in which alizarin is adsorbed on a magnesium hydroxide precipitate in a ratio greater than 1:1. If the reaction between the alizarin and magnesium is quantitative, it would be expected that the measured diffusion current would decrease to zero in a linear fashion with added magnesium and this is not the case. The actual diffusion currents were found to approach zero slowly after an abrupt transition from the linear combining region. This behavior could not be explained on the basis of impurities in the alizarin reagent, for while the excess of magnesium did produce a spectral shift, the spectrum obtained on acidification of the solution to 9 M with H_2SO_4 was identical with that of pure alizarin.

Simple "lake" formation can also be rejected as an explanation of the behavior, for even in this case an excess of magnesium would cause the diffusion current to approach zero rapidly. Calculations based on the solubility product of $Mg(OH)_2$ (5.5×10^{-12} (17)) indicate the possibility of precipitation of the hydroxide, with the resultant buffering of the magnesium ion concentration at some maximum value. The concentration of unreacted alizarin and the diffusion current would then be expected to approach some limiting value with added magnesium, but the limiting value would increase with increasing pH; no such simple relationship was found.

The spectral shift obtained with a large excess of added magnesium may be taken as a positive indication of complex ion formation. If it is assumed that there is only one complex species in solution under these conditions, then the data of Table I can be used to calculate a mean extinction coefficient for the complex at the two wavelengths. The data of Table IV can then be resolved (18) in terms of the concentration of free and complexed alizarin using extinction coefficients for the free alizarin calculated from the absorption of the initial solution at each pH containing no added magnesium. The analysis shows significant concentrations of the complex species even at small additions of magnesium. The complex is evidently polarographically active with a half-wave potential close to that of free alizarin, and the complexation probably does not involve the quinone oxygens.

The formation of a 1:2 complex:

$$MgAlz + HAlz^- \rightleftharpoons MgAlz_2^{2-} + H^+,$$

is not in agreement with the experimental data, for the concentration of such a complex in equilibrium with the 1:1 precipitate would be a definite fraction of the free alizarin concentration at any pH. To fit the experimental results the complex must contain more magnesium than alizarin, e.g., 2:1:

$$MgAlz + Mg^{2+} \rightleftharpoons Mg_2Alz^{2+}.$$

The concentration of such a complex in equilibrium with the 1:1 precipitate would depend on the magnesium ion concentration in the solution; the concentrations calculated by

Can. J. Chem. Downloaded from www.nrcresearchpress.com by 210.87.254.6 on 09/05/12
For personal use only.

resolution of the spectra were found to decrease to a limiting value, indicating a maximum value of the free magnesium ion concentration.

If the primary reaction for the removal of alizarin from the solution is assumed to be the formation of a 1:1 precipitate:

$$Mg^{2+} + HAlz^{-} \rightleftharpoons MgAlz + H^{+},$$

then values of the equilibrium constant, K, can be calculated (Table IV). The concentration H^+ is known from the pH, and the concentration of $HAlz^-$ can then be calculated from the spectrally resolved free alizarin concentration and the known K^H values. The concentration of Mg^{2+} removed from the solution can be calculated if it is assumed that the combining ratio determined by extrapolation of the initial linear region holds over the whole range of added magnesium. The concentration of free Mg^{2+} can then be calculated if an allowance is made for the magnesium bound up in the known concentration of complexed alizarin (2 Mg:1 alizarin). The calculation is valid only in the intermediate range of added magnesium, for with small additions the free Mg^{2+} concentration is indeterminate, and with large additions the free alizarin concentration is indeterminate. A mean value of 2.6×10^{-2} mole^{-1} liter was obtained for the equilibrium constant.

It appears that the experimental data is not capable of further analysis as regards the nature of the reaction; none the less the initial linear decrease of diffusion current with added magnesium can be used as the basis of an indirect polarographic determination of magnesium (19).

ACKNOWLEDGMENTS

The authors are indebted to the National Research Council of Canada and the Advisory Committee of the University of Toronto for grants in aid of this research. One of us (D. G. B.) is further indebted to the National Research Council of Canada for aid in the form of a studentship. Thanks are also due to Miss H. Dolphin, University of New Brunswick, for n.m.r. spectra.

REFERENCES

1. J. Heyrovský and S. Berezicky. Collection Czech. Chem. Commun. **1**, 19 (1920).
2. G. Kimura. Collection Czech. Chem. Commun. **4**, 492 (1932).
3. O. H. Müller. Collection Czech. Chem. Commun. **7**, 321 (1935).
4. I. Zlotorvski and I. M. Kolthoff. J. Biol. Chem. **147**, 705 (1943).
5. K. Györobiró, L. Poós, and J. Proszt. Magy. Kém. Folyoirat, **61**, 102 (1956).
6. K. G. Stone and N. H. Furman. Ind. Eng. Chem., Anal. Ed. **16**, 596 (1944).
7. C. Carruthers. Ind. Eng. Chem., Anal. Ed. **15**, 412 (1943).
8. Z. Ferenczy, A. Almásy, and G. Szadelzky-Kardoss. Acta Chim. Acad. Sci. Hung. **9**, 179 (1956).
9. M. Ishibashi, J. Fujinaga, and J. Nagai. J. Chem. Soc. Japan, Pure Chem. Sec. **80**, 482 (1959).
10. D. Lydersen. Z. Anal. Chem. **139**, (1953).
11. Tables of Reagents for Inorganic Analysis. Edwards Brothers, Inc., Ann Arbor, Michigan. 1944.
12. F. Fiegl. Qualitative analysis by spot tests. 2nd English ed. Elsevier, Amsterdam. 1939. pp. 141–146.
13. E. B. Sandell. Colorimetric metal analysis. 3rd ed. Interscience Publishers Inc., New York. 1959.
14. N. H. Furman and K. G. Stone. J. Am. Chem. Soc. **70**, 3055 (1948).
15. H. H. Willard, N. H. Furman, and C. E. Bricker. Elements of quantitative analysis. 4th ed. D. Van Nostrand Co., New York. 1956. p. 136.
16. G. F. Hüttig. Z. Physik. Chem. (Leipzig), **87**, 129 (1914); **88**, 172 (1914).
17. W. D. Kline. J. Am. Chem. Soc. **51**, 2093 (1929).
18. L. Meites and H. C. Thomas. Advanced analytical chemistry. McGraw-Hill Book Co., Inc., New York. 1958. p. 281.
19. D. G. Brewer. Ph.D. Thesis, University of Toronto, Toronto, Ont. 1961.

Can. J. Chem. Downloaded from www.nrcresearchpress.com by 210.87.254.6 on 09/05/12
For personal use only.

STRESSES AND STRAINS IN ADSORBENT–ADSORBATE SYSTEMS

V. THERMODYNAMIC THEORY OF ADSORPTION-EXTENSION PHENOMENA[1]

E. A. FLOOD AND F. M. FARHAN[2]
Division of Pure Chemistry, National Research Council, Ottawa, Canada
Received February 25, 1963

ABSTRACT

The extensive thermodynamic variables of solids having large surface–volume ratios are usually not homogeneous functions of first degree in one another. In such systems mutual thermodynamic field potentials usually exist as between surface and interior regions. In general, mutual Helmholtz field potentials are not additive. When the lack of additivity of the Helmholtz potentials in adsorbate–adsorbent systems is independent of the quantity adsorbed, the changes in potentials of adsorbent and of adsorbate, due to adsorption, are additive and the equilibrium resembles the equilibrium of purely mechanical stresses. In such cases the adsorption potential is measured largely by the partial reversible relaxation of compressive and shear self-strain potentials of the solid adsorbent.

Can. J. Chem. Downloaded from www.nrcresearchpress.com by 210.87.254.105 on 09/05/12
For personal use only.

INTRODUCTION

Properties of porous materials such as their permeabilities, mechanical strengths, weather resistances, etc. are in many cases largely determined by their pore structures. Accordingly it is of considerable importance to obtain a description of these structures adequate to predict behaviors under various conditions.

In case of materials having considerable adsorptive capacities these pore structures are often very complex, very fine grained, and far from uniform. Such structures are usually not directly observable and we must resort to indirect measurements which yield various average quantities. Thus we must resort to describing these structures in terms of suitable distribution functions or in terms of a "statistical geometry".

With a view toward obtaining statistical descriptions of the structure of some activated carbons we have been studying their X-ray diffraction patterns, their permeabilities, densities, etc. We have been studying particularly the dimensional changes which these carbons undergo when subjected to mechanical stresses of various kinds, including such changes as accompany the immersion of the sample in fluids having various pressures. When the fluids are appreciably adsorbed the carbons usually expand as a result of the immersion, the phenomena being commonly referred to as adsorption-swelling or adsorption-extension.

Ideally, adsorption-extension measurements can provide a great deal of information concerning micropore structures that is difficult to obtain in almost any other way. The validity of this information depends, of course, on the validity of the theory assumed applicable to the adsorption-extension phenomena. Accordingly it is of considerable importance to obtain some notion of the validities of the various theories associated with this interesting phenomenon.

Adsorption-extension measurements have been carried out by a number of investigators using a variety of adsorbents and a variety of adsorbable gases and liquids. Notable

[1]*Issued as N.R.C. No. 7342.*
[2]*National Research Council of Canada Postdoctoral Fellow, 1961–1963 (on leave of absence from the University of Teheran, Iran).*

among these investigators are Bangham (1–3), McIntosh (4, 5), Yates (7, 8), Ambert (6), Dacey (9), Sereda (10, 11).*

In previous papers of this series (12–15) we have presented a theoretical description of adsorption extension based largely on the following assumptions:

Assumption A: The change in thermodynamic state of an adsorbent arising from physical adsorption is wholly equivalent to a change in its volumetric mean state of stress.

Assumption B: The thermodynamic conditions for equilibria of systems in hydrostatic states of stress and in scalar potential fields are adequate to describe physical adsorption equilibria.

Practically all of the existing theoretical equations describing adsorption-extension are based directly or indirectly on assumptions A and B. While a change in solid surface tension, if interpreted literally, is necessarily a change in volumetric mean state of stress, the converse statement does not hold.

While in many cases the theoretical equations based on A and B are in excellent agreement with experiment, the theory is difficult to reconcile with the "anomalous contractions" sometimes observed, i.e. with cases where adsorption leads initially to isotropic contractions instead of the predicted expansions.†

Assumption A is practically equivalent to describing the physical adsorption reaction as a purely mechanical interaction, i.e. as an interaction where forces associated with potential fields may be neglected in spite of the fact that it is just these forces which give rise to the whole adsorption phenomenon.

In what follows it is shown that assumption A is equivalent to assuming that the lack of additivity of the Helmholtz potentials of the adsorbent–adsorbate system is independent of the quantity adsorbed and that this will probably be the case when adsorption potentials are small compared with the lack of additivity of the Helmholtz potentials of the pure adsorbent, i.e. small compared with solid surface potentials.

It is also shown that the anomalous contractions cannot be strictly consistent with assumptions A and B but that if the thermodynamic conditions for equilibria include non-isotropic states of stress, thus modifying assumption B, contractions can be consistent with assumption A and are to be expected in some cases.

THERMODYNAMIC THEORY

Basic Postulates

In previous papers of this series it has been assumed that in cases of physical adsorption assemblies of volumes of adsorbate and of adsorbent can both exist separately in equilibrium with externally applied forces in states which are thermodynamically identical with their corresponding parts in the combined adsorbate–adsorbent systems; in these states the sums of the Gibbs potentials, Helmholtz potentials, volumes, etc. of the separate systems are assumed equal to the Gibbs potential, Helmholtz potential, volume, etc. of the combined system. Thus if v_a and v_c are the volumes of the adsorbate and adsorbent

**Maximum expansions of solid active adsorbents are of the order of 1 or 2% (i.e. $\delta V/V \simeq 0.015$), and are observed on immersion in liquids which "wet" the adsorbent and also on exposure to saturated vapors or to higher pressures of adsorbable gases. These expansions are more or less isotropic and show little specificity either with respect to the adsorbent or adsorbate and appear to be largely dependent on the net δG of the adsorption reaction. Expansions of this order are observed in H_2O, CCl_4, butane, alcohols, etc., also in some silicone oils, krypton, and methane at higher pressures, etc. The anomalous contractions seldom exceed 1/20 of the magnitude of maximum expansion.*

†They are normally observed only at low relative pressures and at coverages varying from small to large. They appear to be specific, depending both on the adsorbent and adsorbate. CCl_4 gives the largest contraction we have observed. Anomalous contractions are usually negligible in the case of the carbons having large micropores. Twisted rope-like adsorbents usually expand radially and contract axially—quite a different type of phenomena.

Can. J. Chem. Downloaded from www.nrcresearchpress.com by 210.87.254.105 on 09/05/12
For personal use only.

respectively and p_a, p_c the volumetric mean of the principal stresses of adsorbate and adsorbent respectively, and P is the hydrostatic pressure of the whole adsorbent–adsorbate system, then

$$[1] \qquad v_a p_a + v_c p_c = (v_a + v_c)P,$$

where $p_c = \sum \delta v_{ci}(p_{xi}+p_{yi}+p_{zi})/3v_c$ and $\sum \delta v_{ci} = v_c$; also p_{xi}, p_{yi}, p_{zi} are the principal stresses of the ith element of volume in the adsorbent; p_a is similarly defined.

Equation [1] will apply to any purely mechanical equilibrium where no "body forces" cross the surfaces over which p_a and p_c are summed.* Obviously the assumption that the two parts of the system can each exist separately in equilibrium with externally applied forces etc. applies literally to any purely mechanical interaction of two bodies. In the case of "physical" adsorption the assumption is that any mutual fields, stresses, etc. produce only such changes in the adsorbate and adsorbent as could be produced in bulk material by the application of suitable external forces, mechanical and other. While this would seem a more or less obvious definition of purely physical interaction, the assumption that in these states the potentials are additive imposes limits on the nature of the "externally applied forces". If these "forces" include forces associated with scalar field potentials (i.e. body forces, gravitational, electrostatic, van der Waals) as well as mechanical stresses, the potentials will not in general be additive unless the effect of the field on at least one of these two parts is thermodynamically equivalent to a change in state of stress only.

When we derive by "balancing mechanical forces" the relation $\Delta p = 2\gamma/r$ for the effect of surface tension on the pressure difference between the outside and inside of a spherical drop of water we assume that all "body forces" are contained within the thin spherical shell of the surface regions and that the Gibbs potentials, Helmholtz potentials, etc. of the spherical shell and the remaining spherical mass are additive. Theoretically, at least, both the water within the shell and the remainder can exist in equilibrium with externally applied stresses and suitable fields in states that are identical with those in the whole spherical mass and hence equation [1] is applicable. If, however, we consider a large self-gravitating spherical mass of water and suppose the sphere divided into two parts, which undoubtedly constitute a "physically" interacting system, body forces will pass the dividing surface and although each part separately can exist in equilibrium with externally applied forces and fields in states which are "identical" with those in the whole mass, the potentials will not be additive since the mutual field potential must be supplied by the external fields twice to the separate bodies and hence equation [1] will not hold.

Evidently assumption A and equation [1] are equivalent.

Hydrostatic States of Stress. Potentials Additive

In the first paper of this series the physical content of assumptions A and B was presented thermodynamically more or less as follows:

In order that the two separate bodies of adsorbate and adsorbent be reversibly convertible into the combined system, their natures and states remaining constant (i.e. the temperature, the pressures of the three systems, their positions in any fields, etc.) during the conversion, we must have

**The notions of stress, body force, etc. are quite sophisticated. In limiting cases the two types of force become indistinguishable. Some crude definitions are: Stress, force per unit area acting only on the surface of a volume. Principal stresses are normal stresses, i.e. p_x is the force per unit area normal to the plane yz, no shear stress being operative in the plane yz. Body force is the force per unit mass associated with a scalar potential field and may be thought of as operating at a point contained within a volume. Thus ideally we can change the shape of the surface, the volume contained by the surface, and the position of the "point" (within the surface or volume) on which the body forces operate—all independently.*

Can. J. Chem. Downloaded from www.nrcresearchpress.com by 210.87.254.105 on 09/05/12
For personal use only.

[2] $$G_a+G_c = G_{ac},$$

where G_a and G_c are respectively the Gibbs potentials of the separate assemblies of adsorbate and adsorbent; G_{ac} is the Gibbs potential of the combined systems.

In order that the systems to which G_a and G_c refer and the system to which G_{ac} refers remain reversibly interconvertible as any of the variables are changed, we must have

[3] $$dG_a+dG_c = dG_{ac}.$$

In the case of the gas remote from the surface forces, if the only changes are a change in hydrostatic pressure and the corresponding change in mass concerned (i.e. adsorbed), then

[4] $$dG_a = v_g\,dp_g+\mu_a dm_a = \frac{m_a}{\rho_g}\,dp_g+\mu_a dm_a.$$

If the combined system to which G_{ac} refers has the volume v and is immersed in the gas of pressure p_g, then

[5] $$dG_{ac} = v dp_g+\mu_a dm_a.$$

It is assumed that the solid and any reaction "products" are all contained within the volume v; i.e. they are insoluble in the gas. Hence we can write

[6] $$\delta G_c = \int_0^P v dp_g - \int_0^P \frac{m_a}{\rho_g}\,dp_g.$$

Equation [6] is applicable to any kind of reversible reaction between a gas and a solid (liquid) of zero vapor pressure, when the solid and all reaction products remain insoluble in the gas as the gas pressure changes from 0 to P.*

The volume v must include the volume of any residual pure solid as well as the volumes of any reaction products. While the volume of the solid component in its chemical compounds has no very definite meaning and cannot normally be treated as a thermodynamic entity, in the case of physical adsorption it is assumed that the volume of the pure solid remains distinct from that of the adsorbate so that the solid volume is a definite quantity, v_c. Thus v contains v_c and also the volume of all gas (adsorbate) under the influence of the surface field as well as any more or less arbitrary volume of normal gas. The total volume is thus the sum of v_c and v_a, where v_a must contain all of the gas under the influence of the field and also must contain the same mass of gas as the v_g of equation [4]. In the case of porous adsorbents it is convenient to take v as the total volume of the porous body; in this case v_a is the void volume.

Thus in the case of physical adsorption reactions we can write

[7] $$\delta G_c = \int_0^P (v_a+v_c)dp_g - \int_0^P \frac{m_a}{\rho_g}\,dp_g = \bar{v}_c \cdot P - \int_0^P \frac{v_a(\rho_a-\rho_g)}{\rho_g}\,dp_g,$$

An alternative expression for the δG_c accompanying the immersion of the solid in a large excess of gas at constant pressure and temperature is given by

$$G_a(p_g,m_a)+G_c(p_c = 0,\ m_c) = G_{ac}(p_g,m_a,m_c)+\delta G_c$$
$$\mu_a m_a+\mu_{c0}m_c = \mu_a m_a+\mu_c m_c+\delta G$$

since μ_a does not change.

$$\delta G = (\mu_{c0}-\mu_c)m_c = -\delta G_c.$$

If the rate of transfer of matter within the solid (i.e. its self-diffusion rate etc.) be negligible it is not necessary that μ_c be the same everywhere within the solid nor that $d\mu_c$ be the same everywhere. Thus δG_c is $(\bar{\mu}_c-\bar{\mu}_{c0})m_c$, where the bars represent the average quantities.

Can. J. Chem. Downloaded from www.nrcresearchpress.com by 210.87.254.105 on 09/05/12
For personal use only.

where $\bar{v}_c P$ is written for $\int_0^P v_c dp_g$* and ρ_a is the apparent mean density of the adsorbate. Evidently $v_a(\rho_a - \rho_g)$ is the mass adsorbed.

If assumptions A and B are valid,

$$[8] \qquad \delta G_c = \int_0^{p_c} v_c \cdot dp_c = \bar{v}_c \cdot \delta p_c$$

and equation [7] becomes

$$[9] \qquad \delta G_c = \bar{v}_c \cdot \delta p_c = \overline{v_a + v_c} \cdot P - \int_0^P \frac{m_a}{\rho_g} dp_g.$$

Since v_c and v_a are nearly constant we can obtain δp_c from experimental data, all the quantities on the right-hand side of equation [9] being measurable. In previous papers equation [9] was written in the form

$$[10] \qquad \delta p_c = \left[1 + \frac{v_a}{v_c}(1-\alpha)\right] P,$$

where $\int_0^P (\rho_a/\rho_g) dp_g = \alpha P$, defining α. If the solid is reasonably isotropic we can write

$$[11] \qquad \frac{\delta v_c}{v_c} = \frac{3\delta l}{l} = -A\delta p_c(1 - B\delta p_c),$$

where A is the compressibility and B measures the variation of the compressibility with compression. If δp_c were a uniform change in hydrostatic stress, $\delta v_c/v_c$ would be equal to $\delta v_a/v_a$ and hence to $\delta v/v$. Normally we cannot measure $\delta v_c/v_c$ directly but only $\delta v/v$.

In an assembly of solid spheres packed in some regular manner, if the spheres have markedly different radii, a uniform decrease in surface tension of the spheres would lead to different changes in their hydrostatic pressures. The resulting dilation of the whole assembly would be greater than the sum of the dilations of the solid spheres.

To provide for such geometric or "statistical" correlations we have written

$$[12] \qquad \frac{\delta v}{v} = -A\delta \bar{p}_c{}^L (1 - B\delta \bar{p}_c{}^L),$$

where

$$[13] \qquad \delta \bar{p}_c{}^L = \left[1 + f(p) \cdot K \cdot \frac{v_a}{v_c}(1-\alpha)\right] P,$$

where K is a characteristic constant for a particular solid structure and is a measure of the variation in cross-sectional area of representative solid filaments. Thus K measures what we have referred to as "persistence of configuration" in statistical geometric systems (13). Normally K will be greater than unity. The term $f(p)$ is a specific pressure-dependent factor measuring correlation of "surface potentials" and pore structure. The implication is that these terms are of the order of unity. As we shall see, if assumptions A and B are interpreted strictly, $f(p) \cdot K$ must be unity. Thus where $\delta v/v \neq \delta v_c/v_c$ shearing and similar stresses must be involved if assumption A is retained.

Turning our attention to the adsorbate and assuming with Polanyi that in the combined system the adsorbate behaves thermodynamically as a single substance in a scalar potential field and that only hydrostatic states of stress are involved, we can write

**In Lewis notation $\bar{X}$ represents a partial molar quantity. Throughout this paper $\bar{X}$ will represent a mean quantity.*

Can. J. Chem. Downloaded from www.nrcresearchpress.com by 210.87.254.105 on 09/05/12
For personal use only.

[14] $$\begin{aligned} dG_a &= v_g dp_g + \mu_a dm_a \\ &= \sum \delta v_{g\,i} dp_g + \mu_{a\,i} \sum dm_{a\,i} \\ &= \sum \delta v_{a\,i} dp_{a\,i} + \mu_{a\,i} \sum dm_{a\,i} \\ &= v_a dp_a + \mu_a dm_a, \end{aligned}$$

where $\sum \delta v_{a\,i} = v_a$ and $p_a = \sum \delta v_{a\,i} \cdot p_{a\,i}/v_a$, i.e. p_a is the volumetric mean hydrostatic pressure of the adsorbate. If p_a is not a uniform hydrostatic pressure equal to p_g it implies that scalar potential fields, say ϵ_i, exist between each element of volume of adsorbate, $\delta v_{a\,i}$, and the gas remote from the surface.

Assuming that dG_c is measured by its change in state of hydrostatic stress only we can write equation [3] in the form

[15] $$v_a dp_a + v_c dp_c = (v_a + v_c) dp_g,$$

where $v_a dp_a$ refers to assemblies of adsorbate volumes in the fields implied by equations [14], while $v_c dp_c$ refers to a separate adsorbent assembly, no field being explicitly involved. Thus the pure adsorbate is separated from the combined system, the pure adsorbent, and from the adsorbable gas by the field potentials implied by equations [14]. Evidently, equation [15] is implied by assumptions A and B.

Integrating equation [15] along a path where p_g increases from zero, i.e. along $0 \leqslant p_g \leqslant P$, gives

[16] $$\bar{v}_a \cdot p_a + \bar{v}_c \cdot p_c = \overline{v_a + v_c} \cdot P,$$

where $\bar{v}_a \cdot p_a$ is written for the integral $\int_0^{p_a} v_a \cdot dp_a$ etc.

It will be noted that equations [1], [15], and [16] cannot be mutually self-consistent when p_a or p_c differ from P unless $\delta v_c/v_c = \delta v/v$, $\bar{v}_c/v_c = \overline{v_a + v_c}/v_a + v_c$, etc., i.e. there can be no change in shape.

Thus in equation [13], $f(p) \cdot K$ must be unity and since δG_c is negative when adsorption occurs, $\delta v/v$ must be positive. Thus the "anomalous contractions" cannot be strictly consistent with assumptions A and B.

Non-isotropic States. Potentials Additive

The basic thermodynamic equation underlying equations [14] is

$$dE = TdS - pdv + fdx + \mu dm,$$

where f is the force function of a scalar potential field (i.e. a "body" force) and x is a suitable positional coordinate: the other symbols have their usual significance. If the system can increase in extent, i.e. grow in mass, volume, etc., its nature and state remaining constant, i.e. T, p, x, μ, then we can write for the corresponding increments

$$E = TS - pv + \mu m$$

and

$$G = E - TS + pv = \mu m.$$

Hence

$$dG = -SdT + vdp + fdx + \mu dm.$$

If shear stresses, polarization energies, etc. are included we must write the basic equation

[17] $$dE = TdS - pdv + \phi dq + fdx + \mu dm,$$

Can. J. Chem. Downloaded from www.nrcresearchpress.com by 210.87.254.105 on 09/05/12
For personal use only.

where ϕdq measures the work done on the system at constant S, v, x, and m; p is the effective mean principal stress. For reversible dilation $p = \frac{1}{3}(p_x+p_y+p_z)$.

In equation [17] only the independent variables, S, v and m, are "extensive" variables. Hence when the system grows reversibly (from a suitable source), its nature and state remaining constant (i.e. T, p, q, x, μ), the corresponding increment in the energy is $E = TS-pv+\mu m$ as before.* But for given values of p, μ will normally be greater when the principal stresses are not equal. Thus when non-isotropic forces are included we have

$$dG = -SdT+vdp+\phi dq+fdx+\mu dm. \qquad [18]$$

Applying this basic equation, equations [9], [15], [16] become respectively

$$\delta G_c = \bar{v}_c\cdot\delta p_c+\Phi_c = \overline{v_c+v_a}\cdot P - \int_0^P \frac{m_a}{\rho_g}\,dp_g \qquad [19]$$

$$v_a dp_a+\phi_a dq_a+v_c dp_c+\phi_c dq_c = (v_a+v_c)dp_g \qquad [20]$$

$$\bar{v}_a p_a+\Phi_a+\bar{v}_c p_c+\Phi_c = \overline{v_c+v_a}\cdot P, \qquad [21]$$

where $\Phi = \int_0^q \phi dq$ etc.

The potentials of the parts still being assumed additive, equation [1] holds, but now it is evident that in general $\delta v/v$ will not be equal to $\delta v_c/v_c$. Hence $f(p)K$ in equation [13] will differ from unity.

In an assembly of distinguishable volumes of matter, each of which is capable of having definable thermodynamic properties as in an assembly of solid granules, if the granules exert only mechanical forces upon one another, no body forces, no scalar potential fields being involved, the potentials are obviously additive. Hence the general thermodynamic equations for mechanical equilibrium can be written

$$\sum v_i p_i = vP \qquad [22]$$

and

$$\sum v_i dp_i + \sum \phi_i dq_i = vdp+\phi dq, \qquad [23]$$

where $\sum v_i = v$ and $p_i = \frac{1}{3}(p_{xi}+p_{yi}+p_{zi})$. Since $p_{xi}+p_{yi}+p_{zi}$ is invariant toward orthogonal transformation of coordinates, the directions of the principal stresses are largely immaterial in purely thermodynamic considerations. If the external pressure is a purely hydrostatic pressure the external work term ϕdq is zero, but this does not mean that $\sum \phi_i dq_i$ is necessarily zero by any means. Presumably $\phi_i dq_i$ will be expressible as a function of $(p_{xi}-p_{yi})^2$, $(p_{yi}-p_{zi})^2$, etc. as in elasticity theory. In any case these potentials, being scalar quantities, are independent of the choice of coordinating axes.

Evidently equations [22] and [23] are analogous to the equations of equilibrium for purely mechanical interaction,

$$\frac{\partial X_x}{\partial x}+\frac{\partial X_y}{\partial y}+\frac{\partial X_z}{\partial z} = 0, \qquad \frac{\partial Y_x}{\partial x}+\frac{\partial Y_y}{\partial y}+\frac{\partial Y_z}{\partial z} = 0, \text{ etc.}$$

When applicable to any reaction the equations virtually state that the "reaction potential" arises from a partial reversible relaxation of the mechanical self-strain potential of the solid. Since reversible compressive strain potentials can be very large, while reversible shear strain potentials are limited by shear strengths, large values of δG_c will be dominated

*The growth must take place in a definite manner in order that $\int_{v_0}^{v_0+\Delta v} pdv$ should have a definite value. When p_x, p_y, and p_z are not equal, Δv must be a pure dilation, i.e. $\Delta x/x = \Delta y/y = \Delta z/z$.

Can. J. Chem. Downloaded from www.nrcresearchpress.com by 210.87.254.105 on 09/05/12
For personal use only.

by $\bar{v}_c\delta p_c$ terms. Also, since most rigid solids have very limited compressibilities, $\bar{v}_c \approx v_c$, i.e. $\int_{p_{c0}}^{p_c} vdp = \bar{v}_c\delta p_c \approx v_c\delta p_c$, and we can write $\bar{v}_c = v_c + K_c\delta v_c$, $\bar{v}_a = v_a + K_a\delta v_a$, where K_c and K_a are of the order of $\pm\frac{1}{2}$. Hence equations [1] and [21] lead to

$$[24] \qquad K_a\frac{\delta v_a}{v_a} - K_c\frac{\delta v_c}{v_c} = \frac{\Phi_a + \Phi_c}{v_a(p_a - P)},$$

where $K_a\delta v_a/v_a$ and $K_c\delta v_c/v_c$ are small quantities. Hence if either ϕ_a or ϕ_c is comparable in magnitude with $v_a(p_a - P)$, ϕ_a and ϕ_c must be of comparable magnitudes but of opposite signs.

When the volume of the surface region is small compared with the solid volume, i.e. when the volume of solid and adsorbate under the influence of surface forces is small, equation [9] may be expressed in terms of the Gibbs adsorption equation if desired. Thus in the case of the spherical drop the change in Gibbs potential due to a change in surface tension is $\delta G = v\delta p = \frac{2}{3}\sigma d\gamma$, where σ is the surface area and γ the surface tension. The assumption that dimensional changes of an adsorbent are proportional to δG_c, the proportionality constant being directly related to the compressibility, is equivalent to assumption A whether we follow Bangham and measure δG_c via the change in "surface tension" and the Gibbs adsorption equation or by the more general equation [19]. The experimental evidence gives considerable support for assumption A. Thus in spite of the fact that the physical adsorption phenomenon is undoubtedly the result of mutual field potentials the systems appear to behave as mechanical systems, i.e., as systems in which the potentials of the adsorbent as a whole and that of the adsorbate as a whole are additive (equation [1] or [22]).

Referring again to the spherical drop of liquid of visible size, the volume of the surface region is so small compared to the whole that any changes in volume of the surface region are quite negligible and hence the change in volume of the drop as a whole due to changes in surface tension will be given by

$$\frac{\delta v}{v} = -A\delta p = -A\left(\frac{2\sigma}{3v}\right)\delta\gamma.$$

Thus lowering of the surface tension will cause an increase in volume of the whole drop. But since a reduction in tension is equivalent to an increase in pressure, other things being equal, the small surface volume should decrease when the surface tension is lowered. It must be emphasized that when adsorbents have "surface areas" of the order of $10^3\ m^2/g$ the volume of the surface region cannot be small compared to the whole solid volume. In this case a decrease in solid "surface tension", if construed at all literally, should lead to a net contraction. Further, in systems of such large surface areas the lack of additivity of potentials of the solid itself must be large and, paradoxically, one might conclude that there can be little or no correlation between dimensional changes and the corresponding changes in Gibbs potential. Evidently there is some special feature involved in physical adsorption reactions which must be brought out to resolve this apparent "paradox".

Any State of Stress. Potentials not Additive

Potentials which are inherent in the state of a body as distinct from any field potentials are commonly referred to as "intrinsic" potentials (16). Thus in an assembly of granules, the intrinsic potentials of the granules are necessarily additive, but if mutual field potentials exist these potentials are not strictly properties of any particular granule alone and are not normally additive. Thus if A_i is the Helmholtz potential of a granule and $A_i =$

Can. J. Chem. Downloaded from www.nrcresearchpress.com by 210.87.254.105 on 09/05/12
For personal use only.

$A_i^0 - \omega_i$, where ω_i is the Helmholtz potential of the field, then while $A^0 = \sum A_i^0$, A is not in general equal to $\sum A_i^0 - \sum \omega_i$ if the field potentials are "mutual" potentials.

While in any condensed system intermolecular "mutual potential fields" exist, usually these mutual "potential fields" only contribute to the "intrinsic" potentials and are thus not strictly thermodynamic field potentials. In the case of mobile fluids the time-average property of any small volume of the fluid (remote from surface regions) is the same as that of any other equal volume, while in the case of solids the "potentials" are periodic properties of position. In either case, if within any homogeneous phase a reasonably sized volume be interchanged with any other equal volume, temperature, pressure, etc., remaining constant during the interchange, no appreciable change in any thermodynamic property occurs. Thus in the case of solids for reasonably large volumes $\int_{x_0}^{x} \partial G/\partial x \cdot dx$ is virtually independent of the distance moved, any variation δG or δA with δx is negligible in comparison with G or A. For small volumes $\partial G/\partial x$ is a periodic function of x. In the case of mobile fluids remote from surface regions, $\partial G/\partial x = 0$. In such systems the thermodynamic properties are additive in the sense that no change in external systems accompanies the reversible combining of two identical systems. Thus it is possible for such systems to grow reversibly in "extent", i.e. in mass, volume, etc., from a suitable source, while the temperature, pressure, and thermodynamic potentials, etc., remain virtually constant during the process. Mathematically the extensive variables are homogeneous functions of first degree in one another (17, cf. also Butler's article in ref. 18).

Thus we can write

$$dG = \partial G/\partial m \cdot dm = \mu dm$$

and

$$G_i' = \partial G/\partial m \cdot m_i = \mu_i m_i$$

and

$$G = \sum G_i = \sum G_i' = \sum \mu_i m_i .$$

If $\sum G_i'$ refers to n separate identical bodies the combining of these separate bodies, the principal stresses, temperature, etc. remaining constant, involves no change in any thermodynamic property of any external body. If $\sum G_i'$ refers to n separate bodies which are different and have different principal stresses etc. and $\sum G_i$ refers to the n corresponding parts in the assembly, again no net change in any thermodynamic property of any external body accompanies the reversible combining of the separate parts. If, however, the parts exert forces upon one another and the separate bodies are placed in suitable fields so that $G_i' \equiv G_i$, then while $G = \sum \mu_i m_i = \sum G_i'$ work must be done during the combining of the separate systems, i.e. the process resembles a phase change or a reversible displacement in a field and $\sum G_i' \not\equiv G$.*

It is quite possible for a heterogeneous system, i.e., one of many phases, to grow in extent while T, p, μ_i, etc. remain constant. It is also possible for such a system to grow in extent in a field, say, along equipotential surfaces in the earth's field, while p (or rather $\bar{p}$ in this case), T, μ_i, etc. remain constant, and hence the potentials can be—and in fact on a laboratory scale they usually are—homogeneous functions of first degree in the mass or volume regardless of whether the systems are physically uniform and homogeneous or not. In such systems the potentials are additive in the sense that $\sum G_i' \equiv G$. However, if *mutual* potential fields exist between the parts of a system, then in general the potentials will not be additive and they will usually not be homogeneous functions of first degree in

*Not identical, $\not\equiv$.

Can. J. Chem. Downloaded from www.nrcresearchpress.com by 210.87.254.105 on 09/05/12
For personal use only.

the masses. While on a laboratory scale for n indentical parts, $\sum G_i' \equiv G$ to a high degree of accuracy, if the separate masses are too large or too numerous mutual gravitational potentials become large and $\sum G_i' \neq G$, $\sum A_i' \neq A$. Similarly when the volumes of the separate parts are too small or have too high a surface–volume ratio, again $\sum G_i' \neq G$, $\sum A_i' \neq A$. In both cases $\sum G_i' > G$ and the mutual potentials appear as "attractive" potentials.*

Active adsorbents have very high surface–volume ratios and hence are systems where large mutual surface potentials normally exist and where $\sum A_i' \neq A$. In addition these self-strained, highly porous bodies will not in general be in equilibrium everywhere with respect to "diffusive" interchange of material, i.e. the thermodynamic potential of the carbon will not be the same in regions relatively remote from one another (>20 atomic diameters when the transport is through the solid; > 2–3 atomic diameters if the transport involves evaporation and condensation, i.e. transport across a void space). However, in general these porous adsorbents will be in equilibrium with respect to mechanical and "body" forces and can undergo small elastic or reversible mechanical deformations. We cannot hope to describe in any detail the thermodynamics of such complex systems, but we can perhaps bring out the special "feature" by virtue of which these systems behave as mechanical systems in physical adsorption reactions.

As before we shall regard the solid body as made up of a number of granules. When no field potential exists, equations [22], [23] are applicable. When "intergranular" mutual field forces exist within the volume v, we can still write $G = A+pv$ as the Gibbs or displacement potential of the whole assembly, but in this case the Helmholtz potentials will not be additive. Thus $A = \sum A_i^0 - \sum\omega_i + \pi$, where π is the overlap potential, i.e. π measures the lack of additivity of the mutual Helmholtz field potentials ω_i. If each granule separately is in a field ω_i due to an external body, so that each granule is thermodynamically identical with the corresponding granule in the assembly, whose pressure is p_i and volume v_i, we can write for this system $\sum(A_i^0 - \omega_i + A_i^0 x) + \sum p_i v_i$, where $A_i^0 x$ is the intrinsic potential of an external body providing the field ω_i. We form the system $(\sum A_i^0 - \sum\omega_i + \pi + pv) + \sum A_i^0 x$, i.e. we form the assembly and the external bodies with their intrinsic potentials only. If this transformation can be carried out reversibly by a displacement or growth process where the pressures p_i and p remain constant, so that the net work done is $\sum p_i v_i - pv$ while the Helmholtz potentials of all the bodies concerned have increased by π, then $\sum p_i v_i - pv = \pi$. The relation between the various potentials, the stresses, etc. apart from any phase changes or chemical reaction, may be brought out perhaps more clearly by regarding each granule as a different substance or component. We assume that initially the system is a homogeneous function of first degree in the masses of its parts and write

$$dE = TdS - pdv + \phi dq + \sum \mu_i^0 dm_i,$$

where μ_i^0 is the intrinsic chemical or thermodynamic potential of each granule. We assume that the system is capable of growing reversibly from suitable sources of m_i, while T, p, q, the "composition", etc. remain constant. Accordingly we write as usual, $A+pv = \sum \mu_i^0 m_i = G$ where A, pv, etc. are the increments corresponding to the increments m_i, the ratios $m_i/\sum m_i$ remaining constant. However, if mutual attractive potentials develop

*This is the type of case referred to as "an apparent paradox" by Lewis and Randall (19). If by "molal free energy" we mean $\partial G/\partial m$, then when G is not a homogeneous function of first degree, $\partial G/\partial m$ is a function of m. Of course if $\partial G/\partial m$ refers not to all the variables other than m being held constant, but only to some of the m, the coefficient will be a function of the remaining variables. In the case discussed by Lewis and Randall, it would appear that $\partial A/\partial m$ was meant by "molal free energy".

Can. J. Chem. Downloaded from www.nrcresearchpress.com by 210.87.254.105 on 09/05/12
For personal use only.

during the growth we must write $G = A + pv = \sum \bar{\mu}_i m_i$, where in general $\bar{\mu}_i < \mu_i^0$, i.e., the system is not a homogeneous function of first degree in the masses. At this stage in the growth we assume that a small additional increment in the masses may occur without changing materially any of the various mutual fields, stresses, etc. that may have developed within the granular assembly, and we write for this small additional increment $\delta G = \delta A + p\delta v = \sum \bar{\mu}_i' dm_i$.

Focusing our attention on the individual granules during this increment we can write

$$[25] \quad dE = TdS - \sum p_i dv_i + \sum f_i \frac{\partial x_i}{\partial v_i} dv_i + \sum \phi_i dq_i + \sum f_i \frac{\partial x_i}{\partial q_i} dq_i + \sum \mu_i dm_i,$$

where $f_i \cdot dx_i/\partial v_i \cdot dv_i$, $f_i \cdot \partial x_i/\partial q_i \cdot dq_i$ are work terms against the mutual or internal field forces f_i.

Integrating over the increment $\sum \delta m_i$ with T, p_i, f_i, q_i and the "composition" constant,

$$dE = TdS - \sum p_i \delta v_i + \sum f_i \frac{\partial x_i}{\partial v_i} dv_i + \sum \bar{\mu}_i' dm_i,$$

and putting $d\pi = \sum f_i \cdot \partial x_i/\partial v_i \cdot dv_i$, we get

$$\delta G = \delta A + \sum p_i \delta v_i - \delta \pi = \delta A + p\delta v$$

and

$$\delta A = \sum (\delta A_i^0 - \delta \omega_i) + \delta \pi.$$

Evidently we can write

$$[26] \quad \sum p_i v_i - \pi = pv$$

and

$$[27] \quad dG = vdp + \phi dq = \sum v_i dp_i + \sum \phi_i dq_i + \sum \frac{\partial \pi}{\partial q_i} dq_i$$

as the thermodynamic equations describing the isothermal equilibrium between the mechanical and field forces within an assembly of solid particles and the stresses applied to the whole assembly.

Within the assembly the usual condition for equilibrium with respect to heat transfer will apply, i.e., the temperature must be uniform. If all of the "granules" are of the same kind of matter which may "interchange" by diffusive processes, independently of the other variables, the thermodynamic or chemical potentials must be the same everywhere. In the latter case $v_i dp_i + \phi_i dq_i + d\pi_i$ must be the same everywhere. If the granules are of the same kind of matter but diffusive interchange over appreciable distances is negligible, the system would be capable of elastic or reversible deformations where the μ_i and $d\mu_i$ of the parts were not the same everywhere.

Equations [26], [27] will apply to any system whose parts are capable of having individual thermodynamic properties, and we shall assume that we can apply these equations to solid adsorbents, when the elements of volume, v_i, are suitably chosen, i.e. we assume that such elements of volume exist. In these equations π is a measure of the lack of additivity of the potentials and is not the same in general as the "surface potential" although it can be a direct measure of it. When no mutual potentials exist anywhere π and any "surface potential" must both be zero.* For small elastic deformations of the

*While π is a function of the net internal Helmholtz field potential, π also depends on the distribution of these potentials and their influence on one another.

Can. J. Chem. Downloaded from www.nrcresearchpress.com by 210.87.254.105 on 09/05/12
For personal use only.

assembly the change in mutual field potentials would be small, so that if π were relatively large compared with $\sum p_i v_i$, $d\pi$ would be small compared with either $\sum v_i dp_i$ or $\sum \phi_i dq_i$ for relatively rigid and nearly incompressible systems.

Equations [26], [27] indicate that other things being equal the introduction of attractive mutual field potentials tends to increase the volumetric mean stresses and thus for the same external stresses these mutual potentials should lead to contractions. If no mutual field potentials exist within a solid and it is immersed in a liquid which is attracted toward the solid while the liquid pressure remote from solid is kept constant, then for the whole system after immersion

$$\sum p_i v_i - \pi = pv,$$

or distinguishing between the solid volume v_c and the volume of liquid v_a under the influence of the field,

$$p_c v_c + p_a v_a - \pi = P(v_a + v_c),$$

i.e. equation [1] will not hold.

If initially $\sum p_{ci0} v_{ci0} = p_{c0} v_{c0} \approx 0$, and after immersion $P(v_a + v_c) \approx 0$, the volumetric mean stress of the whole system must increase as a result of the immersion. If the equation of state of the liquid is not materially changed by the field, the density of the liquid must increase, while the density of solid may either increase or decrease depending on the shape of the dividing surface, the range and nature of the fields, etc. If a large fraction of the solid volume is directly under the influence of the field, the solid volume will almost certainly decrease. However, if the solid in its initial state has a large mutual attractive potential so that π is large,

$$\sum p_{ci0} v_{ci0} - \pi = p_{c0} v_{c0} \approx 0.$$

If these mutual potentials are largely confined to the surface regions, the outer surface being attracted toward the interior, then when immersed in a fluid which exerts attractive forces on these outer surface regions the interaction will reduce the potential gradients in the surface region and thus effectively reduce the mutual field forces within the solid. Thus we should have after immersion

$$\sum p_{ci}' v_{ci}' - \pi + \delta\pi_{ads}' = p_c' v_c' \quad [28]$$

while within the fluid we will now have potential gradients, and

$$\sum p_{ai} v_{ai} - \delta\pi_{ads}'' = p_a v_a. \quad [29]$$

Hence assuming $\delta\pi' = \delta\pi''$ we get

$$\sum p_{ci}' v_{ci}' - \pi + \sum p_{ai} v_{ai} = P(v_a + v_c) \quad [30]$$

and

$$\sum p_{ci}' v_{ci}' - \sum p_{ci0} v_{ci0} + \sum p_{ai} v_{ai} = P(v_a + v_c) - p_{c0} v_{c0}. \quad [31]$$

Thus the changes in volumetric mean states of stress are additive and the changes in Helmholtz potentials are additive. Thus in terms of the Helmholtz potentials we first suppose each element of volume of the solid and of the fluid placed in suitable fields of external bodies so that each element is identical with the corresponding element in the combined system, i.e., we have for the separate parts,

$$\sum A_{ci}^0 - \sum \omega_{ci} - \sum \omega_{cai} + \sum A_{cix}^0 + \sum A_{aj}^0 - \sum \omega_{acj} + \sum A_{ajx}^0, \quad [32]$$

Can. J. Chem. Downloaded from www.nrcresearchpress.com by 210.87.254.105 on 09/05/12
For personal use only.

which if removed from the external bodies to which A_{cix}, A_{ajx} refer, and combined, we get

[33] $$(\sum A_{ci}^0 - \sum \omega_{ci} + \pi - \delta\pi' + \sum A_{aj}^0 - \sum \omega_{acj}) + \sum A_{cix}^0 + \sum A_{ajx}^0.$$

The change in Helmholtz potential is $\delta A = \pi - \delta\pi' + \sum \omega_{cai}$ and when $\delta\pi' = \sum \omega_{cai}$, $\delta A = \pi$ and the additivity has not changed. If this can be carried out reversibly by a displacement process corresponding to

[34] $$\sum p_{ci}'v_{ci}' + \sum p_{aj}v_{aj} - P(v_a + v_c)$$

this work must be equal to π. Thus $\delta A_c + \delta A_a = \delta A_{ac}$ or

[35] $$A_c - A_{c0} + A_a = A_{ac} - A_{ac0} = A_{ac} - A_{c0}.$$

When adsorbent–adsorbate systems behave in this way they are special cases of systems where mutual field potentials exist but where the lack of additivity of the potentials π is independent of the quantity adsorbed. Accordingly the Gibbs potential changes which accompany the immersion of the adsorbent in an excess of fluid, whose pressure and temperature are kept constant, will be measured by the change in volumetric mean state of stress of the solid, i.e., assumption A will hold. In these cases,

[36] $$dG_c = \sum v_{ci}dp_{ci} + \sum \phi_{ci}dq_{ci} = v_c dp_c + \phi_c dq_c - d\pi = (v_a + v_c)dp_g - \frac{m_a}{\rho_g}dp_g$$

and

[37] $$\delta G_c = \bar{v}_c(\bar{p}_c - \bar{p}_{c0}) + \bar{\Phi}_c = \overline{v_a + v_c}\, p_g - \int_0^P \frac{m_a}{\rho_g}dp_g.$$

Note that while $\phi_c dq_c$ as applied to the outer surface of the solid volume is necessarily positive, $\sum \phi_{ci}dq_{ci}$ can be either positive or negative.

We would not expect the model systems and hence equations [36], [37] to be applicable if any solution or chemical reaction occurs, or if any material passes the dividing surface between solid and fluid or if for any reason the dividing surface largely ceases to exist.

When the model is applicable the additivity of the potentials should be independent of the quantity adsorbed when the adsorption potentials are much less than the initial solid surface potentials and when no adsorbent–adsorbate field forces of appreciable magnitude extend into the solid beyond the region where mutual solid potentials exist. When these conditions are met and adsorption potentials or energies are small compared with solid sublimation energies the equation of state of the solid should be substantially unchanged by the adsorption reaction, i.e. the compressibility should vary with compression very nearly as does the solid alone. Hence equation [13] should be reasonably valid and we should conclude that the "anomalous contractions" referred to above are mainly due to non-isotropic forces, i.e. to terms of the type $\sum \phi_{ci}dq_{ci}$. In the case of carbons of exceptionally high surface areas terms of the type $d\pi$ (i.e. variation in additivity or net internal field potential) might contribute to the anomalous contraction and would be very difficult to distinguish from $\sum \phi_{ci}dq_{ci}$ terms and other factors. However, if a given carbon physically adsorbs two different adsorbates with about equal δG_c values and the different adsorbate molecules are chemically similar and are of comparable sizes, but in one case the porous body expands more or less as predicted while in the other an "anomalous contraction" is observed, the implication is strong that the difference is due to terms of the type Φ_c and Φ_a, i.e. to rather highly specific "bridging" and similar mechanisms that might be associated with the mismatching field periodicities of the adsorbate and the

Can. J. Chem. Downloaded from www.nrcresearchpress.com by 210.87.254.105 on 09/05/12
For personal use only.

periodicities (20) of two or more adjacent surfaces with which it is in "contact" or with mechanisms associated with pore size and shape distributions and their compatibility with condensed adsorbate molecular configurations, etc. If for any reason the adsorbate tends to draw two adjacent surfaces together while tending to increase the area of the two surfaces, terms of the type Φ_c will be involved.

Gibbs Adsorption Equation

Finally a few remarks may be made concerning the Gibbs adsorption equation.

If we suppose a flat surface region capable of growth in extent in two dimensions only (i.e. constant thickness, h) and following Gibbs, we assume this region capable of thermodynamic properties and write

$$[38] \qquad dE = TdS - \bar{p}dv + \phi dq + \mu_1 dm_1 + \mu_2 dm_2,$$

where $\bar{p} = \frac{1}{2}(\bar{p}_x + \bar{p}_y)$, and $\bar{p}_x$, $\bar{p}_y$ are the principal surface or tangential stresses averaged over the thickness h, and $dv = hd\sigma$, where h is perpendicular to the interface (of area σ) and large enough to include all of the region under the influence of the surface fields, then this surface region can grow in area or extent while $\bar{p}$, T, q, μ_1 and μ_2 remain constant, i.e., although mutual potentials exist the potentials are homogeneous functions of first degree in the area, and masses. Hence, $G_s = \mu_1 m_1 + \mu_2 m_2$ or putting

$$\bar{\gamma} = -h\tfrac{1}{2}(\bar{p}_x + \bar{p}_y)$$

we get

$$[39] \qquad m_1 d\mu_1 + m_2 d\mu_2 = -\sigma d\gamma + \phi dq$$

and for μ_2 constant and $d\mu_1 = dp_g/\rho_g$, putting

$$m_1 = \sigma h(\rho_a - \rho_g) + \rho_g \sigma h = \sigma\Gamma + \rho_g \sigma h$$

we get the Gibbs equation in the form

$$[40] \qquad d\gamma - \phi_s dq = -\int_0^P \frac{\Gamma}{\rho_g} dp_g - h dp_g.$$

If we associate tangential surface tractions or surface tensions with such self-strained bodies as active carbons, it seems hardly possible that the principal surface tensions, i.e. the components of γ, can be equal everywhere. Thus it seems almost certain that terms of the type $\phi_s dq$ must be involved in adsorption reactions on the majority of solid surfaces.

The fact that in many cases dimensional changes can be correlated quite well ignoring terms of this type is probably due to the fact that strain potentials of the vdp type are generally much larger than those of the ϕdq type (cf. refs. 21–24).

REFERENCES

1. D. H. Bangham, N. Fakhoury, and A. F. Mohamed. Proc. Roy. Soc. (London), Ser. A, **138**, 162 (1932).
2. D. H. Bangham and R. I. Razouk. Trans. Faraday Soc. **33**, 1463 (1937).
3. D. H. Bangham. Proceedings of a conference on the ultrafine structure of coals and cokes. British Coal Utilization Research Association. 1944. pp. 18, 118.
4. E. W. Channen and R. L. McIntosh. Can. J. Chem. **33**, 172 (1955).
5. R. S. Haines and R. L. McIntosh. J. Chem. Phys. **15**, 28 (1947).
6. C. H. Amberg and R. L. McIntosh. Can. J. Chem. **30**, 1012 (1952).
7. D. J. C. Yates. Proc. Roy. Soc. (London), Ser. A, **224**, 526 (1954).
8. D. J. C. Yates. Advan. Catalysis, **12**, 265 (1960).
9. J. R. Dacey. Proceedings of Fourth Conference on Carbon. Pergamon Press, London and New York. 1960.

Can. J. Chem. Downloaded from www.nrcresearchpress.com by 210.87.254.105 on 09/05/12
For personal use only.

10. P. J. SEREDA and R. F. FELDMAN. J. Appl. Chem. To be published.
11. P. J. SEREDA and R. F. FELDMAN. J. Am. Ceram. Soc. To be published.
12. M. L. LAKHANPAL and E. A. FLOOD. Can. J. Chem. **35**, 887 (1957).
13. E. A. FLOOD. Proceedings of the Tenth Symposium of the Colston Research Society. Butterworth Scientific Publications, London. 1958. pp. 151–182.
14. E. A. FLOOD. Advan. Chem. Ser. **33**, 248 ff. (1961).
15. R. H. TOMLINSON and E. A. FLOOD. Can. J. Res. Sect. B, **26**, 38 (1948).
16. J. W. GIBBS. The collected works of J. Willard Gibbs. Vol. I. Yale University Press, New Haven, Conn. 1957. pp. 230, 234, etc.
17. L. E. COPELAND and T. F. YOUNG. Advan. Chem. Ser. **33**, 348 ff. (1961).
18. A COMMENTARY on the scientific writings of J. Willard Gibbs. Vol. I. Yale University Press, New Haven, Conn. 1936. pp. 71 ff.
19. G. N. LEWIS and M. RANDALL. Thermodynamics. McGraw-Hill Book Co., New York. 1961.
20. F. C. FRANK. Discussions Faraday Soc. **5**, 48 (1949).
21. F. O. KOENIG and R. C. SWAIN. J. Chem. Phys. **1**, 723 (1933).
22. E. A. GUGGENHEIM. Statistical thermodynamics. R. H. Fowler and E. A. Guggenheim (*Editors*). Cambridge University Press, London. 1949. pp. 422 ff.
23. F. P. BUFF. Advan. Chem. Ser. **33**, 340 ff. (1961).
24. J. J. BIKERMAN. Contributions to the thermodynamics of surfaces. Published by the author, Cambridge, Mass. 1961.

Can. J. Chem. Downloaded from www.nrcresearchpress.com by 210.87.254.105 on 09/05/12
For personal use only.

SYNTHESIS OF SOME PEPTIDES OF ε-N-ACETYL-L-LYSINE

LEO BENOITON
Department of Biochemistry, Faculty of Medicine, University of Ottawa, Ottawa, Ontario
Received February 8, 1963

ABSTRACT

ε-*N*-Acetyl-L-lysinamide, α-*N*-glycyl-ε-*N*-acetyl-L-lysine, ε-*N*-acetyl-L-lysylglycine, α-*N*-glycyl-ε-*N*-acetyl-L-lysylglycine, and ε-*N*-acetylglycyl-L-lysine have been synthesized for testing as substrates for the enzyme ε-lysine acylase.

Several years ago, the enzyme ε-lysine acylase was identified and partially purified from rat kidney (1). We have now purified ε-lysine acylase from a much more convenient source, hog kidney, and have tested its hydrolytic action on several derivatives of lysine including some peptides of ε-*N*-acetyl-L-lysine (2). This paper describes the synthesis of the peptides.

The compounds III, V, VII, and IX, and the synthetic routes employed, are illustrated in the accompanying scheme. In addition, the isomeric peptide ε-*N*-acetylglycyl-L-lysine was also prepared.

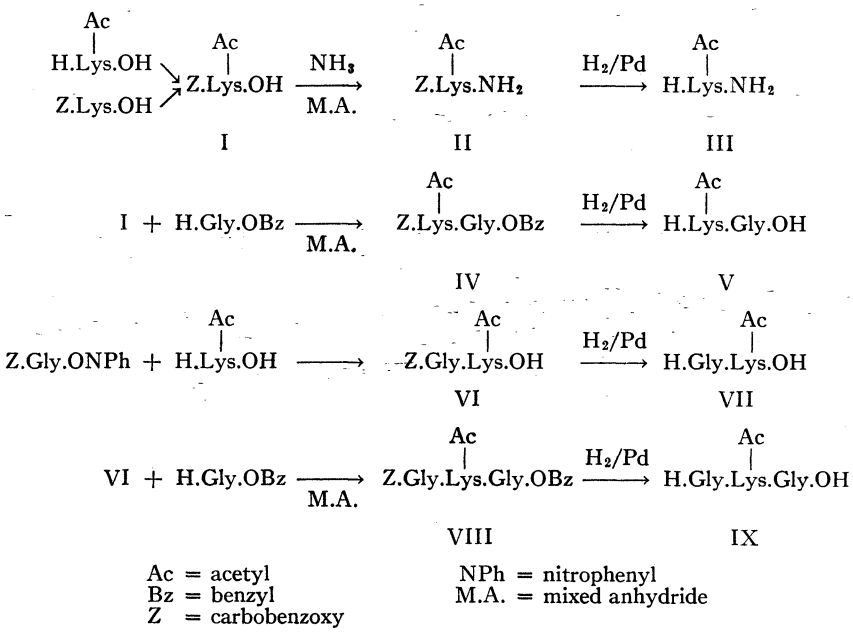

ε-*N*-Acetyl-L-lysine, prepared by acetylation of the copper salt of lysine (3), was carbobenzoxylated to the disubstituted derivative I, which was crystallized as the dicyclohexylammonium salt. I was also prepared by acetylation of α-*N*-carbobenzoxy-L-lysine, obtained through the ε-*N*-benzylidene derivative (4); however, our inability to obtain the reported yields for α-*N*-carbobenzoxy-L-lysine rendered this route less attractive. The mixed anhydride (5) of I, by treatment with anhydrous ammonia or glycine benzyl ester, gave the protected amide II and dipeptide IV respectively. Catalytic hydrogenolysis of these provided the ε-*N*-acetyl-L-lysine amide III and the ε-*N*-acetyl-L-lysine dipeptide

Can. J. Chem. Downloaded from www.nrcresearchpress.com by 210.87.254.105 on 09/05/12
For personal use only.

V. The isomeric glycyl dipeptide VII was made by hydrogenation of the protected intermediate VI, obtained in one step by the coupling of carbobenzoxyglycine *p*-nitrophenyl ester with ε-*N*-acetyl-L-lysine in hot acetic acid (6). The mixed anhydride (5) of VI plus glycine benzyl ester yielded the protected tripeptide VIII, which gave the free ε-*N*-acetyl tripeptide IX on hydrogenation. ε-*N*-Acetylglycyl-L-lysine was prepared directly by using a general procedure for the synthesis of ε-*N*-lysine peptides (7), namely, the coupling of the mixed anhydride of acetylglycine with the copper salt of lysine in aqueous solution.

Several of the optical rotations observed were extremely low, with one (for VII) actually being equal to zero. However, this was not due to racemization. If racemization had occurred, it would have been during the synthesis of VI by the nitrophenyl ester method. The optical purity of VI was established by measuring the optical rotation of a sample after hydrolysis in 5 *N* hydrochloric acid. The observed rotation was identical with that of a solution of lysine of corresponding concentration.

Enzymatic studies (2) have shown that the peptides are cleaved by ε-lysine acylase at rates of 85, 24, 109, and 70 for III, V, VII, and IX respectively, relative to a rate of 100 for ε-*N*-acetyl-L-lysine.

EXPERIMENTAL

General

Melting points were determined by the capillary method, using a thermometer calibrated against standard substances. Optical rotations were determined with a Rudolph Model 62 polarimeter using a 2-dm tube. Compounds were dried at 60° before analysis. Acetonitrile and chloroform were purified and distilled before use. The R_f values recorded are for the following solvents: R_f^B, *n*-butanol – acetic acid – water (4:1:5); R_f^F, *tert*-butanol – formic acid – water (70:15:15).

Starting Materials

ε-*N*-acetyl-L-lysine, $[\alpha]_D^{25}$ +22.7° (1, 5 *N* HCl), was prepared by acetylation of the copper salt of lysine with acetic anhydride (3) using two equivalents of lithium hydroxide as base (8). Yields of recrystallized, chromatographically pure material averaged 45%. Yields of 60%, obtained when using only one equivalent of base, have been reported (8). In our hands this procedure gave a product which was too highly contaminated with lysine to be purified by recrystallization. The original procedure (3) calls for two equivalents of base.

Carbobenzoxyglycine *p*-nitrophenyl ester (9) was prepared by the action of dicyclohexylcarbodiimide (10) on carbobenzoxyglycine (11) and *p*-nitrophenol in pyridine. After 12 hours, the mixture was filtered into ice water, and the precipitate which formed was washed by trituration with 1 *N* hydrochloric acid, water, and aq. sodium bicarbonate, and finally recrystallized from ethanol. Yield: 81%, m.p. 128°.

Glycine benzyl ester hydrochloride (12) was prepared from the corresponding *p*-toluenesulphonate (13) as described (14) except that the product was recrystallized from benzyl alcohol–ether. Yield: 80%.

Acetylglycine (15) was prepared by adding acetic anhydride to a hot solution of glycine in acetic acid.

α-N-Carbobenzoxy-ε-N-acetyl-L-lysine (Dicyclohexylammonium Salt (I))

(*a*) To a vigorously stirred cold solution of ε-*N*-acetyl-L-lysine (7.52 g; 0.04 mole) containing sodium bicarbonate (10 g) was added carbobenzoxy chloride (7 g) in four portions. After 3 hours, the solution was acidified (HCl) and extracted with ethyl acetate, the extract dried (Na_2SO_4) and evaporated to dryness. The residue was dissolved in ethyl acetate, and excess dicyclohexylamine was added. Crystals appeared immediately. After cooling, the product was filtered, recrystallized from acetonitrile, and washed with ether. Yield: 5.54 g (55%), m.p. 132–133°, $[\alpha]_D^{25}$ +8.6° (2, ethanol). Found: C, 66.7; H, 9.0; N, 8.3. $C_{28}H_{47}N_3O_5$ (503.7) requires: C, 66.8; H, 9.0; N, 8.3%.

(*b*) To a vigorously stirred solution of α-*N*-carbobenzoxy-L-lysine (4) (5.6 g; 0.02 mole) and sodium bicarbonate (3.78 g) in water (5°) was added, dropwise, acetic anhydride (2.3 g; 0.022 mole) during 30 minutes. Stirring was continued an additional hour at 25°, then the solution was acidified and the compound crystallized as described above. Yield: 5.54 g (55%), m.p. 132–133°.

α-N-Carbobenzoxy-ε-N-acetyl-L-lysinamide (II)

To I (3.02 g; 0.006 mole) suspended in chloroform was added 1 *N* sulphuric acid (6 ml). After shaking, the organic layer was taken and washed twice with water, dried overnight (Na_2SO_4), and concentrated down. The solution was cooled (0°), and triethylamine (0.83 ml; 0.006 mole) followed by ethyl chloroformate (0.54 ml; 0.006 mole) was added. After 30 minutes, anhydrous ammonia was bubbled through for 15 minutes,

Can. J. Chem. Downloaded from www.nrcresearchpress.com by 210.87.254.105 on 09/05/12
For personal use only.

the mixture being stirred by a magnetic stirrer. The mixture was kept an additional 15 minutes at 25°, then cooled and filtered. The product was washed with cold chloroform, and recrystallized from acetonitrile. Yield: 1.1 g (60%), m.p. 179°, $[\alpha]_D^{25}$ +3.4° (1, dimethylformamide). Found: C, 59.8; H, 7.1; N, 13.0. $C_{16}H_{23}N_3O_4$ (321.4) requires: C, 59.8; H, 7.2; N, 13.1%.

ε-N-Acetyl-L-lysinamide Hydrochloride (III)

A solution of II (0.96 g) in ethanol (25 ml) containing 1 *N* hydrochloric acid (3 ml) was hydrogenated over palladium black. The catalyst was filtered off, the solution evaporated to dryness, and the residue crystallized from ethanol containing a few drops of water. Ether was then added. Yield: 0.53 g (80%), m.p. 243°, $[\alpha]_D^{25}$ +17.9° (1, water), R_f^B 0.32, R_f^F 0.41. Found for a sample recrystallized from water–ethanol: C, 43.2; H, 8.1; N, 18.2. $C_8H_{18}ClN_3O_2$ (223.7) requires: C, 43.0; H, 8.1; N, 18.8%.

α-N-Carbobenzoxy-ε-N-acetyl-L-lysylglycine Benzyl Ester (IV)

The mixed anhydride of *α-N*-carbobenzoxy-*ε-N*-acetyl-L-lysine was prepared from I (4.02 g; 0.008 mole) as described for the synthesis of the amide (II). After 30 minutes, a cold chloroform solution of glycine benzyl ester hydrochloride (1.61 g; 0.008 mole) and triethylamine (1.11 ml; 0.008 mole) was added. The solution was kept at 0° for 1 hour, and at 25° overnight. The solution was then washed successively with 1 *N* hydrochloric acid, water, aq. sodium bicarbonate, and finally water, dried (Na_2SO_4), and evaporated to dryness. The residue, which solidified on trituration with ether, was collected and recrystallized from chloroform–ether. Yield: 2.85 g (80%), m.p. 113–114°. A sample recrystallized for analysis had m.p. 115–116°, $[\alpha]_D^{25}$ −6.3° (1, dimethylformamide). Found: C, 63.8; H, 6.8; N, 8.9. $C_{25}H_{31}N_3O_6$ (469.5) requires: C, 63.95; H, 6.65; N, 8.95%.

ε-N-Acetyl-L-lysylglycine (V)

A solution of IV (1.41 g) in ethanol (35 ml) containing water (5 ml) and acetic acid (2 ml) was hydrogenated over palladium black. After removal of the catalyst, the solution was evaporated down and the residue was crystallized from water–ethanol–ether. Yield: 0.59 g (80%). Recrystallization from water–ethanol gave 0.41 g (56%), m.p. 225–226°, $[\alpha]_D^{25}$ +74.3° (1, water), R_f^B 0.32, R_f^F 0.49. Found: C, 48.8; H, 8.0; N, 16.9. $C_{10}H_{19}N_3O_4$ (245.3) requires: C, 49.0; H, 7.8; N, 17.1%.

α-N-Carbobenzoxyglycyl-ε-N-acetyl-L-lysine (VI)

A mixture of *ε-N*-acetyl-L-lysine (3.76 g; 0.02 mole) and carbobenzoxyglycine *p*-nitrophenyl ester (7.2 g; 0.021 mole) in dry acetic acid was refluxed for 3 hours. The solvent was distilled off, and the residue was distributed between ethyl acetate and aq. sodium bicarbonate. The aqueous layer was acidified and extracted with ethyl acetate, the extract was dried (Na_2SO_4) and then evaporated to a white solid. The product was filtered with the aid of ether and recrystallized from acetonitrile. Yield: 4.4 g (58.7%), m.p. 126°, $[\alpha]_D^{25}$ −3.6° (1, dimethylformamide). Found: C, 56.9; H, 6.8; N, 11.2. $C_{18}H_{25}N_3O_6$ (379.4) requires: C, 57.0; H, 6.6; N, 11.1%. After hydrolysis of a sample (129.6 mg) in 5 ml of 5 N hydrochloric acid, α was +0.52° corresponding to $[\alpha]_D^{25}$ +26.0° when calculated for a lysine content of 49.9 mg. A solution of lysine had $[\alpha]_D^{25}$ +26.4° (1, 5 *N* HCl).

α-N-Glycyl-ε-N-acetyl-L-lysine (VII)

A solution of VI (1.54 g) in ethanol (50 ml) containing water (10 ml) and acetic acid (2 ml) was hydrogenated over palladium black. After removal of the catalyst by filtration, and solvent by evaporation, the residue was crystallized from water–ethanol. Yield: 0.7 g (72%), m.p. 220–221°, $[\alpha]_D^{25}$ 0 (water, or 5 *N* HCl), R_f^B 0.31, R_f^F 0.46. Found: C, 48.8; H, 7.9; N, 17.2. $C_{10}H_{19}N_3O_4$ (245.3) requires: C, 49.0; H, 7.8; N, 17.1%.

α-N-Carbobenzoxyglycyl-ε-N-acetyl-L-lysylglycine Benzyl Ester (VIII)

To VI (1.89 g; 0.005 mole) and triethylamine (0.70 ml; 0.005 mole) in dry chloroform at 0° was added ethyl chloroformate (0.45 ml; 0.005 mole). After 30 minutes, a cold chloroform solution of glycine benzyl ester hydrochloride (1.01 g; 0.005 mole) and triethylamine (0.70 ml; 0.005 mole) was added. After 1 hour at 0°, and 12 hours at 25°, the solution was successively washed with 1 *N* hydrochloric acid, water, aq. sodium bicarbonate, water, and then dried. The chloroform was evaporated off and the white residue was crystallized twice from acetonitrile. Yield: 1.2 g (46%), m.p. 170–171°, $[\alpha]_D^{25}$ −7.2° (1, dimethylformamide) Found: C, 61.4; H, 6.6; N, 10.7. $C_{27}H_{34}N_4O_7$ (526.6) requires: C, 61.6; H, 6.5; N, 10.6%.

α-N-Glycyl-ε-N-acetyl-L-lysylglycine (IX)

A solution of VIII (1.25 g) was hydrogenated as described for the preparation of VII. The product was crystallized twice from water–ethanol. Yield: 0.53 g (74%), m.p. 245–246°, $[\alpha]_D^{25}$ +1.5° (1, water), R_f^B 0.28, R_f^B 0.36. Found: C, 47.45; H, 7.4; N, 18.3. $C_{12}H_{22}N_4O_5$ (302.3) requires: C, 47.7; H, 7.3; N, 18.5%.

ε-N-Acetylglycyl-L-lysine

The mixed anhydride prepared from acetylglycine (1.17 g; 0.01 mole) in tetrahydrofuran was added quickly to a cold aqueous solution of the copper salt of lysine (1.83 g; 0.01 mole) containing 5 ml of 2 *N* lithium hydroxide. The mixture was kept cold and stirred for 2 hours. Next morning, the blue precipitate was collected, washed with water, then dissolved in hot water, and hydrogen sulphide was bubbled through

Can. J. Chem. Downloaded from www.nrcresearchpress.com by 210.87.254.105 on 09/05/12
For personal use only.

the solution. After subsequent charcoal treatment, the remaining solution was evaporated down and the residue crystallized twice from water–ethanol. Yield: 1.23 g (50%), m.p. 245–247°, $[\alpha]_D^{25}$ +17.1° (1, 5 *N* HCl), R_f^B 0.28, R_f^F 0.52. Found: C, 48.8; H, 7.9; N, 16.9. $C_{10}H_{19}N_3O_4$ (245.3) requires: C, 49.0; H, 7.8; N, 17.1%.

ACKNOWLEDGMENT

Financial support of this work by the Medical Research Council is gratefully acknowledged.

REFERENCES

1. W. K. Paik, L. Bloch-Frankenthal, S. M. Birnbaum, M. Winitz, and J. P. Greenstein. Arch. Biochem. Biophys. **69**, 56 (1957).
2. W. K. Paik and L. Benoiton. Can. J. Biochem. Physiol. **41**, 1643 (1963).
3. A. Neuberger and F. Sanger. Biochem. J. **37**, 515 (1943).
4. B. Bezas and L. Zervas. J. Am. Chem. Soc. **83**, 719 (1961).
5. R. A. Boissonas. Helv. Chim. Acta, **34**, 874 (1951). J. R. Vaughan and R. L. Osata. J. Am. Chem. Soc. **73**, 553 (1951).
6. F. Weygand and W. Steglich. Ber. **93**, 2983 (1960).
7. D. M. Theodoropoulus. J. Org. Chem. **23**, 140 (1958).
8. J. P. Greenstein and M. Winitz. Chemistry of the amino acids. Vol. 3. J. Wiley & Sons, Inc., New York, N.Y. 1961. p. 2117.
9. B. Iselin, W. Rittel, P. Sieber, and R. Schwyzer. Helv. Chim. Acta, **46**, 373 (1957).
10. M. Rothe and F. W. Kunitz. Ann. **609**, 88 (1957). D. F. Elliot and D. W. Russel. Biochem. J. **66**, 49-P (1957).
11. H. E. Carter, R. L. Frank, and H. W. Johnston. Org. Syn. **23**, 13 (1943).
12. C. R. Harrington and T. H. Mead. Biochem. J. **30**, 1598 (1936).
13. L. Zervas, M. Winitz, and J. P. Greenstein. J. Org. Chem. **22**, 1515 (1957).
14. P. Tailleur and L. Berlinguet. Can. J. Chem. **39**, 1309 (1961).
15. H. D. Dakin. J. Biol. Chem. **82**, 443 (1929).

Can. J. Chem. Downloaded from www.nrcresearchpress.com by 210.87.254.105 on 09/05/12
For personal use only.

QUELQUES METABOLITES POSSIBLES DE LA THALIDOMIDE[1]

MARCEL MÉNARD, LUCIEN ERICHOMOVITCH, MICHAEL LA BROOY
ET FRANCIS L. CHUBB
Frank W. Horner Limited, Montréal, Qué.

Reçu le 8 mars 1963

RÉSUMÉ

La synthèse de dérivés hydroxylés en positions 3 et 4 de 1′ α-phtalimidoglutarimide et de ses produits d'hydrolyse est décrite.

Can. J. Chem. Downloaded from www.nrcresearchpress.com by 210.87.254.5 on 09/05/12
For personal use only.

D'après les essais effectués dans nos laboratoires sur la thalidomide il semble que l'agent chimique responsable des malformations congénitales observées par Wiedemann (syndrome de Wiedemann) (1) ne soit pas la thalidomide elle-même, mais un produit de son métabolisme, vraisemblablement un dérivé hydroxylé dans les positions 3 ou 4 du groupe phtalyle. Williams et ses collaborateurs (2) pensent aussi que l'un des métabolites qu'ils ont isolés récemment est un dérivé hydroxylé en position 3. Dans le but d'obtenir des composés de référence connus pour l'identification et la détermination des activités biologiques de ces métabolites, la synthèse des hydroxy-3 et -4 phthalimidoglutarimides (hydroxy-3 et -4 thalidomides) et de leurs analogues à chaine ouverte, les hydroxy-3 et -4 phtalylglutamines fut entreprise et est décrite ici.

Les hydroxy-3 et -4 phtalylglutamines, V*a* et V*b*, s'obtiennent difficilement par réaction directe des anhydrides II*a* et II*b* avec la glutamine à cause de la facilité avec laquelle celle-ci se cyclise en acide pyrrolidone-2 carboxylique-4. Il s'est avéré profitable de protéger les fonctions hydroxylées des groupes phtalyles et de procéder par l'intermédiaire des anhydrides benzyloxyphtalimidoglutariques IV*c* et IV*d*. L'ouverture de ces anhydrides par l'ammoniac dans l'éthanol (3) donne les glutamines substituées V*c* et V*d* de préférence aux dérivés de l'isoglutamine; l'hydrazinolyse de V*c* et V*d*, par la phénylhydrazine suivant la méthode de Ujejski et Gaver (3), fournit uniquement la *dl*-glutamine. Les glutarimides VI*a* et VI*b* sont alors obtenues par cyclisation de V*c* et V*d* dans l'anhydride acétique et hydrogénolyse des groupes benzyles. L'hydroxy-4 phtalimidoglutarimide VI*a* peut aussi être preparée à partir de l'anhydride IV*a* et de l'urée mais il est préférable de passer par les intermédiaires III*c*, IV*c*, V*c* et VI*c*. Les produits obtenus sont optiquement inactifs.

Les essais biochimiques seront publiés bientôt.

PARTIE EXPÉRIMENTALE[2]

Acide benzyloxy-4 phtalique (Ic)

L'acide hydroxy-4 phtalique (4) (18.2 g, 0.1 mole) est dissous dans une solution de 17 g (0.3 mole) d'hydroxyde de potassium dans 46 ml d'eau; 13.9 g (0.11 mole) de chlorure de benzyle sont alors ajoutés en une fois et le mélange est vivement agité et reflué pendant 16 heures. Une solution de 8.5 g d'hydroxyde de potassium dans 46 ml d'eau est ajoutée et le tout chauffé à reflux jusqu'à l'obtention d'une solution limpide (3 heures). La solution est alors refroidie, lavée à l'éther et acidifiée au rouge congo par l'acide chlorhydrique concentré. Le précipité est filtré et recristallisé dans l'acide acétique pour donner 16 g (59%) du diacide fondant à 182–183°. Calculé pour $C_{15}H_{12}O_5$: C, 66.17; H, 4.44%. Trouvé: C, 66.11; H, 4.44%. Spectre

[1]α-*Phtalimidoglutarimide.*

[2]*Les points de fusion ont été déterminés en tubes capillaires et ne sont pas corrigés. Les spectres infrarouges ont été déterminés à l'aide d'un spectromètre Perkin–Elmer, modèle 237: des suspensions dans le nujol ont été employées là où le solvant n'est pas spécifié. Les spectres ultraviolets ont été déterminés au moyen d'un spectrophotomètre Beckman, modèle DK2. Les microanalyses sont du Dr. Claude Daesslé, 5757 Decelles, Montréal.*

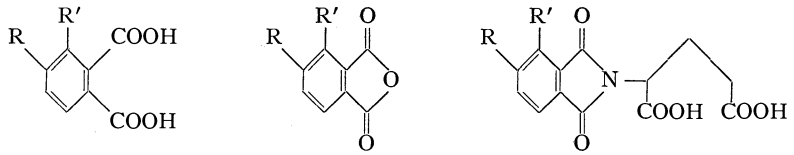

I II III

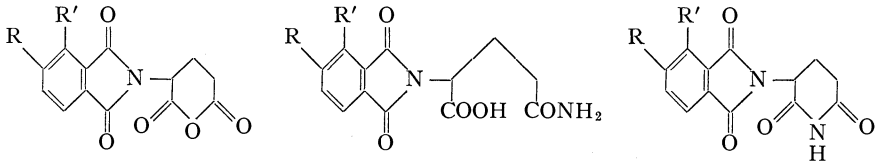

IV V VI

a: R = OH, R′ = H
b: R = H, R′ = OH
c: R = $OCH_2C_6H_5$, R′ = H
d: R = H, R′ = $OCH_2C_6H_5$
e: R = CH_3COO, R′ = H

infrarouge: —OH (acide), 3200 à 2100; =CO, 1675; aromatique, 1598 cm^{-1}. Spectre ultraviolet (CH_3OH): λ_{max} 252 mμ, log ϵ = 4.106.

Acide benzyloxy-3 phtalique (Id)

Préparé à partir de l'acide hydroxy-3 phtalique (5) suivant le procédé décrit plus haut. Rendement: 62%. P.f. 163–165° (eau). Calculé pour $C_{15}H_{12}O_5$: C, 66.17; H, 4.44%. Trouvé: C, 66.04; H, 4.33%. Spectre infrarouge: —OH (acide), 3400 à 2500; =CO, 1715 et 1665; aromatique, 1595 cm^{-1}. Spectre ultraviolet (CH_3OH): λ_{max} 293 mμ, log ϵ = 3.47.

Anhydride benzyloxy-4 phtalique (IIc)

Une mélange de 14 g (50 mmole) de I*c* et de 50 ml d'anhydride acétique est chauffé à reflux jusqu'à l'obtention d'une solution limpide (5–15 minutes). Celle-ci est évaporée sous vide au bain-marie et le résidu solide est recristallisé dans l'acétate d'éthyle – éther de pétrole pour donner 9 g (69%) de l'anhydride, p.f. 128–129°. Calculé pour $C_{15}H_{10}O_4$: C, 70.86; H, 3.96%. Trouvé: C, 70.81; H, 4.26%. Spectre infrarouge ($CHCl_3$): =CO, 1845 et 1775; aromatique, 1615 et 1600; —O— (éther), 1255 cm^{-1}. Spectre ultraviolet ($CHCl_3$): λ_{max} 311 et 277 mμ, log ϵ = 3.73 et 3.76.

Anhydride benzyloxy-3 phtalique (IId)

Preparé comme II*c*. Recristallisé dans le benzène – éther de pétrole après filtration d'une petite quantité de produit secondaire insoluble dans le benzène. P.f. 158–160°. Rendement: 75%. Calculé pour $C_{15}H_{10}O_4$: C, 70.86; H, 3.96%. Trouvé: C, 70.53; H, 3.72%. Spectre infrarouge: =CO, 1840 et 1770; aromatique, 1615 et 1595; —O— (éther), 1255 cm^{-1}. Spectre ultraviolet ($CHCl_3$): λ_{max} 331 mμ, log ϵ = 3.71.

Acide dl-(benzyloxy-4 phtalimido)-2 glutarique (IIIc)

On chauffe sous vide pendant une heure à 165–185° un mélange intime de II*c* (5 g, 19.7 mmole) et d'acide L-(+)-glutamique (3 g, 20.4 mmole). Après refroidissement, la masse vitreuse est triturée avec de l'eau et le solide ainsi obtenu est filtré et recristallisé dans l'acide acétique. Rendement: 5.5 g (73%). P.f. 235–240°. Calculé pour $C_{20}H_{17}O_7N$: C, 62.66; H, 4.47; N, 3.65%. Trouvé: C, 62.79; H, 4.36; N, 3.86%. Spectre infrarouge: —OH (acide), 3400 à 2200; =CO, 1770 et 1705; aromatique, 1610 et 1595; —O— (éther), 1250 cm^{-1}. Spectre ultraviolet (CH_3OH): λ_{max} 321 mμ, log ϵ = 3.35.

Acide dl-(hydroxy-4 phtalimido)-2 glutarique (IIIa)

(*a*) Un mélange d'anhydride hydroxy-4 phtalique (4) (12.5 g, 76 mmole) et d'acide L-(+)-glutamique (12.5 g, 85 mmole) dans 100 ml de pyridine est chauffé à reflux pendant 2 heures. L'excès d'acide glutamique est enlevé par filtration et la solution est évaporée sous vide au bain-marie. La trituration de l'huile résiduelle avec un excès d'acide chlorhydrique froid à 10% amène la formation d'un volumineux précipité blanc qui, après recristallisation dans l'eau, donne 14.3 g (64%) du diacide, p.f. 249–250°. Calculé pour $C_{13}H_{11}O_7N$: C, 53.24; H, 3.78; N, 4.78%. Trouvé: C, 53.33; H, 3.79; N, 4.87%. Spectre infrarouge: —OH, 3500 à 2300, sommet à 3285; =CO, 1775 et 1700; aromatique, 1615 et 1603; —O— (éther), 1255 cm^{-1}. Spectre ultraviolet (CH_3OH): λ_{max} 325 mμ, log ϵ = 3.16.

(*b*) III*c* (1 g) hydrogéné dans l'éthanol en présence de palladium à 10% sur charbon (0.5 g) donne 0.3 g (40%) de III*a*, p.f. 240–250°.

Can. J. Chem. Downloaded from www.nrcresearchpress.com by 210.87.254.5 on 09/05/12
For personal use only.

Anhydride dl-(acétyloxy-4 phtalimido)-2 glutarique (IVe)

Le produit brut, provenant de la réaction de 3 g d'acide L-(+)-glutamique avec 3 g de II*a* telle que décrite plus haut, est dissous dans un excès d'anhydride acétique sur le bain-marie. La solution est évaporée à sec sous vide et le résidu cristalisé par trituration avec de l'éther. P.f. 162–163° (acide acétique). Rendement: 2.6 g (50%). Calculé pour $C_{15}H_{11}O_7N$: C, 56.78; H, 3.50; N, 4.42%. Trouvé: C, 56.45; H, 3.64; N, 4.22%. Spectre infrarouge: =CO, 1815, 1760 et 1715; aromatique, 1610 cm^{-1}. Spectre ultraviolet (CH_3OH): λ_{max} 292 mμ, log ϵ = 3.19.

Anhydride dl-(benzyloxy-4 phtalimido)-2 glutarique (IVc)

IIIc (3.6 g) est chauffé à reflux avec un excès d'anhydride acétique (25 ml) jusqu'à dissolution complète (20 minutes). La solution est évaporée sous vide au bain-marie et le résidu est recristallisé dans l'acétate d'éthyle. Rendement: 2.7 g (80%). P.f. 164–165°. Calculé pour $C_{20}H_{15}O_6N$: C, 65.75; H, 4.14; N, 3.83%. Trouvé: C, 66.16; H, 4.18; N, 3.99%. Spectre infrarouge ($CHCl_3$): =CO, 1815, 1770 et 1715; aromatique, 1615 et 1603; —O— (éther), 1250 cm^{-1}. Spectre ultraviolet ($CHCl_3$): λ_{max} 325 mμ, log ϵ = 3.28.

Anhydride dl-(benzyloxy-3 phtalimido)-2 glutarique (IVd)

Obtenu en traitant le produit brut de la réaction de II*d* avec l'acide glutamique par l'anhydride acétique. Rendement: 80%. P.f. 194–197°. Calculé pour $C_{20}H_{15}O_6N$: C, 65.75; H, 4.14; N, 3.83%. Trouvé: C, 65.64; H, 3.85; N, 4.30%. Spectre infrarouge: =CO, 1815, 1770 et 1715; aromatique, 1615 cm^{-1}. Spectre ultraviolet ($CHCl_3$): λ_{max} 336 mμ, log ϵ = 3.93.

Benzyloxy-4 phtalyl glutamine (Vc)

A une solution refroidie d'ammoniac 1 *N* dans l'éthanol absolu (30 ml) on ajoute IV*c* (3 g) par portions successives. Après évaporation du solvant le résidu est émulsionné dans l'eau et acidié par l'acide chlorhydrique à 10% jusqu'au rouge congo. Les solvants sont décantés et la masse semi-solide est lavée à l'eau froide et recristallisée dans l'éthanol. Rendement: 2 g (47%). P.f. 165–168°. Calculé pour $C_{20}H_{18}O_6N_2$: C, 62.82; H, 4.74; N, 7.33%. Trouvé: C, 62.67; H, 4.54; N, 7.48%. Spectre infrarouge: —NH, —OH, 3500 à 2400, sommets à 3465 et 3320; =CO, 1775, 1700 et 1650; aromatique, 1610; —O— (éther), 1250 cm^{-1}. Spectre ultraviolet (CH_3OH): λ_{max} 322 mμ, log ϵ = 3.23.

L'hydrolyse de V*c* par la phénylhydrazine suivant la méthode décrite par Ujejski et Gaver (3) donne un produit identique (point de fusion mixte et spectres infrarouges) à la *dl*-glutamine preparée d'après ces auteurs.

Benzyloxy-3 phtalyl glutamine (Vd)

Preparé comme V*c*. Rendement: 72%. P.f. 196–197° (*n*-butanol). Calculé pour $C_{20}H_{18}O_6N_2$: C, 62.82; H, 4.74; N, 7.33%. Trouvé: C, 62.88; H, 4.92; N, 7.55%. Spectre infrarouge: —OH, —NH, 3500 à 2500, sommet à 3410; =CO, 1760, 1700 et 1640; —O— (éther), 1250 cm^{-1}. Spectre ultraviolet (CH_3OH): λ_{max} 332 mμ, log ϵ = 3.66.

Hydroxy-4 phtalyl glutamine (Va)

L'hydrogénolyse de V*c* (1 g) dans l'acide acétique (40 ml) en présence de palladium à 10% sur charbon (0.5 g) est complète en 30 minutes. Après filtration et évaporation du solvant le produit est obtenu sous forme solide par cristallisation dans l'eau. Rendement: 0.6 g (80%). P.f. 210–212°. Calculé pour $C_{13}H_{12}O_6N_2$: C, 53.42; H, 4.14; N, 9.59%. Trouvé: C, 53.14; H, 4.00; N, 9.66%. Spectre infrarouge: —OH, —NH, 3630 à 2300, sommets à 3600 et 3430; =CO, 1700 et 1650; aromatique, 1605 cm^{-1}. Spectre ultraviolet (CH_3OH): λ_{max} 326 mμ, log ϵ = 3.16.

Hydroxy-3 phtalyl glutamine (Vb)

Preparé comme V*a*. Rendement: 78%. P.f. 198–200° (eau). Calculé pour $C_{13}H_{12}O_6N_2$: C, 53.42; H, 4.14; N, 9.59%. Trouvé: C, 53.30; H, 4.30; N, 9.65%. Spectre infrarouge: —OH, —NH, 3500 à 2300, sommets à 3460 et 3350; =CO, 1735, 1695 et 1635; aromatique, 1610 et 1595 cm^{-1}. Spectre ultraviolet (CH_3OH): λ_{max} 335 mμ, log ϵ = 3.66.

α-(Benzyloxy-4 phtalimido)glutarimide (VIc)

V*c* (3 g) est chauffé au bain-marie pendant une heure avec un excès d'anhydride acétique (50 ml). Après évaporation du solvant le résidu est recristallisé dans le toluène. Rendement: 2.4 g (84%). P.f. 172–176°. Calculé pour $C_{20}H_{16}O_5N_2$: C, 65.93; H, 4.43; N, 7.69%. Trouvé: C, 65.93; H, 4.76; N, 7.64%. Spectre infrarouge: —NH, 3200 à 2550; =CO, 1765 et 1700; aromatique, 1605; —O— (éther), 1245 cm^{-1}. Spectre ultraviolet (CH_3OH): λ_{max} 321 mμ, log ϵ = 3.37.

α-(Benzyloxy-3 phtalimido)glutarimide (VId)

Preparé comme VI*c*. P.f. 230–234°. Calculé pour $C_{20}H_{16}O_5N_2$: C, 65.93; H, 4.43; N, 7.69. Trouvé: C, 66.07; H, 4.28; N, 8.06%. Spectre infrarouge: —NH, 3200; =CO, 1770 et 1705; aromatique, 1610 cm^{-1}. Spectre ultraviolet (CH_3OH): λ_{max} 335 mμ, log ϵ = 3.68.

α-(Hydroxy-4 phtalimido)glutarimide (VIa)

(*a*) Un mélange intime d'urée (0.5 g) et de IV*e* (1 g) est chauffé sous vide à 175–180° pendant 45 minutes.

Can. J. Chem. Downloaded from www.nrcresearchpress.com by 210.87.254.5 on 09/05/12
For personal use only.

Le produit de réaction est trituré avec de l'eau, filtré et recristallisé dans le DMF–eau. Rendement: 0.3 g (35%). P.f. 317–318°. Calculé pour $C_{13}H_{10}O_5N_2$: C, 56.93; H, 3.68; N, 10.22%. Trouvé: C, 57.20; H, 3.84; N, 10.08%. Spectre infrarouge: —OH, —NH, 3500 à 2550, sommet à 3250; =CO, 1770 et 1700; aromatique, 1605 cm^{-1}. Spectre ultraviolet (CH_3OH): λ_{max} 324 mμ, log ϵ = 3.31.

Dérivé acétylé: P.f. 217–220° (éthanol). Calculé pour $C_{15}H_{12}O_6N_2$: C, 56.96; H, 3.83; N, 8.86%. Trouvé: C, 56.71; H, 3.89; N, 8.96%.

(*b*) VI*a* est aussi obtenu par hydrogénolyse de VI*c* dans l'acide acétique en présence de palladium à 10% sur charbon. Rendement: 87%.

α-(Hydroxy-3 phtalimido)glutarimide (VIb)

Preparé par hydrogénolyse de VI*d* (58%). P.f. 273–275° (DMF–eau). Calculé pour $C_{13}H_{10}O_5N_2$: C, 56.93; H, 3.68; N, 10.22%. Trouvé: C, 56.89; H, 3.88; N, 10.24%. Spectre infrarouge: —OH, —NH, 3500 à 2550, sommet à 3275; =CO, 1770, 1750 et 1700; aromatique, 1610 cm^{-1}. Spectre ultraviolet (CH_3OH): λ_{max} 337 mμ, log ϵ = 3.60.

REMERCIEMENTS

Nous remercions le Dr. Willard J. Johnson qui a suggeré le project.

BIBLIOGRAPHIE

1. H. R. WIEDEMANN. Med. Wschr. **12**, 816 (1961); Med. Welt, **37**, 1863 (1961).
2. R. L. SMITH, R. A. D. WILLIAMS et R. T. WILLIAMS. Life sciences. No. 7. Pergamon Press Ltd., Great Britain. 1962. p. 333.
3. L. U. UJEJSKI et K. M. GAVER. U.S. Patent No. 2,951,090; Chem. Abstr. **55**, 4379 (1961).
4. W. H. BENTLEY et C. WEIZMANN. J. Chem. Soc. **91**, 98 (1896).
5. H. MÜHLEMANN. Pharm. Acta Helv. **23**, 257 (1948).

Can. J. Chem. Downloaded from www.nrcresearchpress.com by 210.87.254.5 on 09/05/12
For personal use only.

COLUMN AND GAS CHROMATOGRAPHIC ANALYSIS OF OIL OF WILD GINGER

IDENTIFICATION AND ESTIMATION OF SOME NEW CONSTITUENTS

ISHWAR C. NIGAM[1] AND LEO LEVI
Food and Drug Directorate, Department of National Health and Welfare, Ottawa, Canada

Received February 1, 1963

ABSTRACT

Oil of wild ginger was found to contain the following as yet unreported constituents: β-pinene, Δ^3-carene, β-caryophyllene, *ar*-curcumene, linalool, borneol, and α-terpineol. The presence of three ketones, one of them readily generated during gas chromatographic analysis from a non-ketonic sesquiterpenoid, was also demonstrated. Formation of a sesquiterpene alcohol as a compositional artefact of the oil occurred during column chromatography over alumina.

Oil of wild ginger, *Zingiber zerumbet* Smith, has been the subject of a number of chemical investigations (1–4). These established—though not unanimously—the presence of the following constituents: α-pinene, camphene, dipentene containing some limonene, α-humulene, humulene monoxide, humulene dioxide, cineole, camphor, zerumbone, and an unidentified alcohol. It is the purpose of this paper to describe the detection of hitherto unreported compounds in a genuine product. The oil from which the major portion of zerumbone had been removed by cooling to 5° C was fractionated by column chromatography and the various fractions were subjected to gas chromatographic analysis using Reoplex 400 and sucrose diacetate hexaisobutyrate (SAIB), respectively, as liquid phase. Constituents were identified by comparison of retention times on both columns as well as infrared characteristics with those of authenticated reference standards and determined by the sigma method developed in this laboratory (5, 6).

EXPERIMENTAL

I. Column Chromatography of Analytical Sample

The oil (1.433 g) was passed over alumina (Woelm Grade 1; 15 g) using as eluants petroleum ether (b.p. 40–60° C), benzene, and ether. Eight fractions were collected (see Table I) and, following removal of solvent in a rotating vacuum evaporator, examined by gas chromatography.

TABLE I

Column chromatography of oil of wild ginger

Fraction No.	Eluant	Volume of eluant (ml)	Weight of oil (%)
1	Pet. ether	10	48.1
2	Pet. ether	10	11.9
3	Pet. ether	20	3.2
4	Pet. ether	20	1.8
5	Benzene	25	11.8
6	Benzene	25	1.9
7	Ether	25	17.9
8	Methanol	25	0.7
		Recovery	97.3%

[1]*National Research Council of Canada Postdoctoral Fellow, 1962.*

Can. J. Chem. Downloaded from www.nrcresearchpress.com by 210.87.254.5 on 09/05/12
For personal use only.

II. Gas Chromatography of Essential Oil and Isolated Fractions

Apparatus and experimental procedures have been described (7, 8). Constituents were characterized by the serial dilution technique (9) and infrared examination of effluents collected following repeated sample injections and rechromatographed under optimal conditions of temperature and carrier gas flow rate (10). Rigorous comparison of retention times and infrared spectra with those of authentic specimens examined under the same experimental conditions was made for compound identification. Constituents detected for the first time are shown in the illustrations above the corresponding gas chromatographic peaks observed.

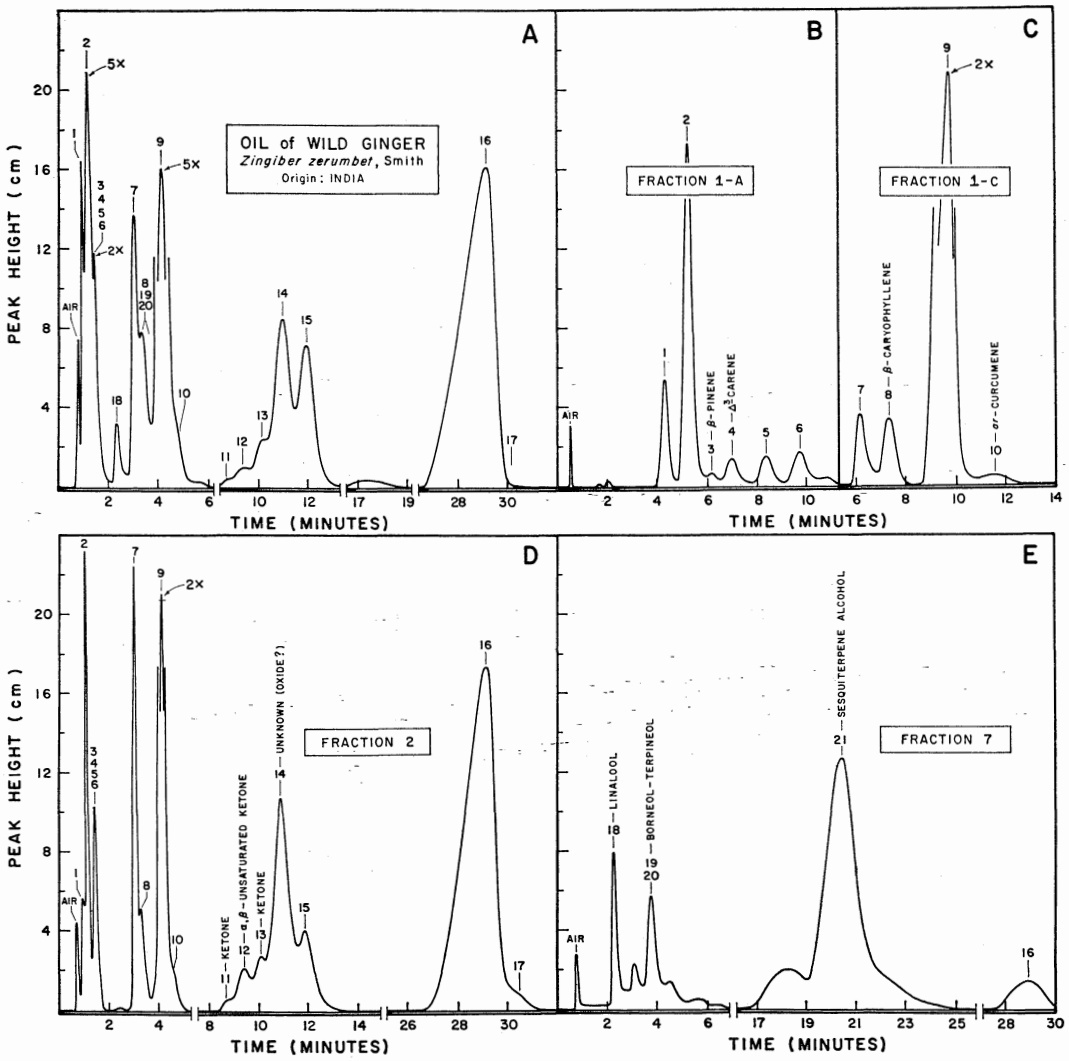

FIG. 1. Gas chromatographic examination of oil of wild ginger. Experimental conditions: A, D, E: column: Reoplex 400 (10%) on Chromosorb W (acid-washed); temp.: 200° C; helium: 25 ml/20 sec; sample vol.: 5 λ (A), 3 λ (D), 2 λ (E). B: column: SAIB (20%) on Chromosorb W (acid-washed); temp.: 130° C; helium: 25 ml/20 sec; sample vol.: 1 λ. C: column: Reoplex 400 (10%) on Chromosorb W (acid-washed); temp.: 170° C; helium: 25 ml/25 sec; sample vol.: 3 λ.

The chromatogram of the specimen prior to analytical treatment is reproduced in Fig. 1A. Monoterpenoids were not well resolved under the experimental conditions and in order to improve their separation from sesquiterpene compounds, fraction 1 was distilled at atmospheric pressure as illustrated in Table II.

Can. J. Chem. Downloaded from www.nrcresearchpress.com by 210.87.254.5 on 09/05/12
For personal use only.

TABLE II
Fractionation of petroleum ether eluate of oil of wild ginger

Fraction	Bath temp. (°C)	Weight of fraction (%)	Nature of isolate
1A	185–195	8.6	Monoterpenes
1B	195–210	12.8	Monoterpenes plus trace amounts of sesquiterpenes
1C	210–225	37.5	Sesquiterpenes plus trace amounts of monoterpenes
Residue		35.7	
		Recovery 94.6%	

RESULTS AND DISCUSSION

The following constituents were identified by means of the techniques described.

α-Pinene, β-Pinene, Δ³-Carene

These terpenes were readily detected in fraction 1A (see Fig. 1B) and trace amounts were found to be present in fraction 1B and 1C, respectively.

Camphor, β-Caryophyllene, ar-Curcumene

These compounds made up the major portion of fraction 1C (Fig. 1C). In addition to identification by infrared spectroscopy *ar*-curcumene was also characterized by its ultraviolet absorption (λ_{max}^{EtOH} 273, 267, 264, and 258 mμ).

Zerumbone, Humulene Monoxide

Both constituents were found to be present in fractions 2 and 3 (see Fig. 1D), with zerumbone occurring also in succeeding fractions.

Humulene Dioxide

Small amounts of this compound were detected in fraction 4.

Linalool, Borneol, α-Terpineol

These compounds were found to be present in fractions 7 and 8. Borneol and α-terpineol emerged together under the experimental conditions and were identified by comparison of the infrared spectrum of the effluent with that of a binary mixture of genuine reference specimens. Coupled gas liquid – thin layer chromatographic data served to confirm the identifications (11).

Unidentified Sesquiterpene Ketones

Infrared examination of carefully rechromatographed effluents of fraction 2 emerging within the 8- to 13-minute time interval (see Fig. 1D) indicated the presence of three ketones (peaks No. 11, 12, and 13), the latter of which displayed marked absorption at 1716 cm^{-1}; 1630 and 882 cm^{-1} (terminal methylene); and 802 cm^{-1} (trisubstituted double bond).

Treatment of fraction 2 with Girard-T reagent (12) followed by column chromatography of isolated carbonyls over alumina and gas chromatography through a Reoplex 400 column at 200° C led to recovery of the three ketones already detected but showed, moreover, that peak No. 12 was considerably enhanced. Comparable analyses of the ether eluate of the non-ketonic fraction revealed a closely related phenomenon—marked diminution of peak No. 14 accompanied by distinct enhancement of peak No. 12. Evidently, constituent No. 14 is an oxygenated, non-ketonic sesquiterpene—possibly an isomeric humulene oxide—rearranging partially to the carbonyl compound, constituent No. 12, during the course of the analysis. The infrared spectrum of the ketone, collected for

Can. J. Chem. Downloaded from www.nrcresearchpress.com by 210.87.254.5 on 09/05/12
For personal use only.

examination following column and gas chromatographic purification, displayed intense absorption at 1668 cm^{-1} and ultraviolet analysis demonstrated likewise the presence of α,β-unsaturation (maxima at 316 and 236 mμ, respectively).

Sesquiterpene Alcohol

Infrared examination of the main constituent occurring in fractions 7 and 8, peak No. 21, established that it was an alcohol. Yet the presence of this terpenoid was not detected in the original product. Correlation of these findings with the observation that the intensity of the humulene monoxide peak decreased following column chromatographic treatment of the essential oil (see Figs. 1A and 1D, respectively) suggested that significant amounts of the monoxide were apparently degraded and converted to the alcohol. Further experimental evidence for the observation was secured by chromatographing 20 mg of humulene monoxide over 1 g of grade 1 alumina (eluant diethyl ether). Infrared analysis of the isolate both prior to and following gas chromatographic examination proved that the major portion of material thus obtained was identical with the alcohol found as chief constituent of fraction 7 as well as fraction 8.

The findings illustrate that column chromatography of natural products may lead to the formation of artefacts and that the process of separation cannot always be considered entirely safe for the resolution of essential oils and the characterization of their constituents. Similar phenomena have also been observed in our laboratory during column chromatography of caryophyllene oxide. The nature of the alcohols thus produced will be described in a forthcoming publication.

Composition of Essential Oil

Quantitative results were obtained from the gas chromatographic data by determining peak areas in accordance with the sigma method previously reported (5, 6). The composition thus deduced for the essential oil is shown in Table III.

TABLE III

Composition of oil of wild ginger*

Peak No.	Constituents	Percent
1	α-Pinene	3.4
2	Camphene	21.9
3	β-Pinene	0.6
4	Δ^3-Carene	1.3
5	Limonene	1.5
6	Cineole	1.8
7	Camphor	4.2
8	β-Caryophyllene	1.6
9	α-Humulene	25.2
10	*ar*-Curcumene	0.8
11	Ketone	0.2
12	Ketone	0.6
13	Ketone	1.3
14	Unknown (oxide?)	5.4
15	Humulene monoxide	4.6
16	Zerumbone	21.2
17	Humulene dioxide	0.3
18	Linalool	0.9
19, 20	Borneol–α-terpineol	0.6
Unidentified	—	2.4

*Freed partially from zerumbone by storage at 5° C.

Can. J. Chem. Downloaded from www.nrcresearchpress.com by 210.87.254.5 on 09/05/12
For personal use only.

ACKNOWLEDGMENTS

The authors are indebted to Shri P. B. Kurup, Managing Director, Techno Chemical Industries, Ltd., Calicut, India, for kindly supplying an authentic sample of wild ginger oil and to Dr. S. C. Bhattacharyya, Assistant Director, National Chemical Laboratory, Poona, India, for courteously providing genuine specimens of humulene monoxide and dioxide for this study. They wish to thank also Mr. William Skakum of this laboratory for technical assistance rendered during the course of the investigation.

REFERENCES

1. V. K. Balakrishnan, R. K. Razdan, and S. C. Bhattacharyya. Perfumery Essent. Oil Record, **47**, 274 (1956).
2. S. K. Ramaswami and S. C. Bhattacharyya. Perfumery Essent. Oil Record, **51**, 65 (1960); Tetrahedron, **18**, 575 (1962).
3. S. Dev. Current Sci. (India), **20**, 296 (1951); Chem. Ind. (London), 1051 (1960); Tetrahedron, **8**, 171 (1960).
4. D. P. Parihar and S. Dutt. Indian Soap J. **16**, 123, 154 (1950).
5. J. C. Bartlet and D. M. Smith. Can. J. Chem. **38**, 2057 (1960).
6. D. M. Smith and L. Levi. J. Agr. Food Chem. **9**, 230 (1961).
7. I. C. Nigam and L. Levi. Can. J. Chem. **40**, 2083 (1962).
8. I. C. Nigam, W. Skakum, and L. Levi. Perfumery Essent. Oil Record, **54**, 25 (1963).
9. D. M. Smith, W. Skakum, and L. Levi. J. Agr. Food Chem. **11**, 268 (1963).
10. I. C. Nigam *et al.* Perfumery Essent. Oil Record, **53**, 614 (1962).
11. I. C. Nigam, M. Sahasrabudhe, and L. Levi. Can. J. Chem. **44**, 1535 (1963).
12. C. L. Teitelbaum. J. Org. Chem. **23**, 646 (1958).

Can. J. Chem. Downloaded from www.nrcresearchpress.com by 210.87.254.5 on 09/05/12
For personal use only.

REACTIONS WITH SUBSTITUTED XANTHENONES

V. MANNICH REACTION ON HYDROXY-9-XANTHENONES AND HYDROXY-10-THIAXANTHENONES

AHMED MUSTAFA, MAHMOUD M. SIDKY, AND FOUAD M. SOLIMAN

Chemistry Department, Faculty of Science, Cairo University, and the Laboratory of Synthetic Chemotherapy, National Research Centre, Cairo, Egypt

Received September 24, 1962

ABSTRACT

The application of the Mannich reaction to hydroxy-9-xanthenones and hydroxy-10-thiaxanthenones, which gives rise to the corresponding aminomethyl derivatives, is described. Experimental proof of the position taken by the aminomethyl group is given.

Can. J. Chem. Downloaded from www.nrcresearchpress.com by 210.87.254.5 on 09/05/12
For personal use only.

In continuation of our previous work (1), the behavior of hydroxy-9-xanthenones and hydroxy-10-thiaxanthenones towards the Mannich reaction has been investigated.[1]

Perusal of the literature reveals that hardly any work has been done on the application of the Mannich reaction to 9-xanthenone derivatives, though de Diesbach (2) has claimed the isolation of 2-trichloroacetylaminomethyl-9-xanthenone (IV*a*) via the action of N-hydroxymethyltrichloroacetamide on 9-xanthenone in the presence of concentrated sulphuric acid.

We have found that hydroxy-9-xanthenones as well as hydroxy-10-thiaxanthenones undergo the Mannich reaction. This seems to be of interest in view of the difference in behavior of the isomeric hydroxy-9-xanthenones. Thus, whereas 1-hydroxy-9-xanthenone (I*i*) shows reactions typical of phenols (3) by undergoing, for example, the Friedel–Crafts reaction and the Fries rearrangement (1, 4), 2-hydroxy-9-xanthenone (II*h*) fails to react with these reagents (5). 2-Hydroxy-10-thiaxanthenone (II*k*) was found in the present investigation to be similarly stable towards acetylation under the conditions of the Fries and Friedel–Crafts reactions.

The hydroxy-9-xanthenones (I*i*, I*j*, and II*h*) and hydroxy-10-thiaxanthenones (II*k* and III*d*) were allowed to undergo the Mannich reaction in the presence of formaldehyde. A number of secondary bases were used, namely, dimethyl-, diethyl-, and diethanolamine, piperidine, and morpholine.

When 1-hydroxy-9-xanthenone (I*i*) was allowed to condense with paraformaldehyde and a secondary base, in acetic acid, the corresponding aminomethyl derivative of I*i* was obtained in good yield. When ethanol and formaldehyde were used instead of acetic acid and paraformaldehyde, the yield of the respective Mannich bases was considerably reduced.

In I*i* substitution may occur in more than one way. In every case only one of the isomeric bases which can theoretically be formed was isolated. That substitution took place mainly at the ortho position finds confirmation from the following:

(*a*) Whenever an ortho position of a phenolic compound is free, monosubstitution via the Mannich reaction occurs preferentially at this position (6).

(*b*) The obtained Mannich bases reacted positively with 2,6-dichlorobenzoquinone chloroimide (Gibbs reagent). This shows that the position para to the hydroxyl group was unsubstituted (7).

[1]*The biological activity of these compounds is now under investigation.*

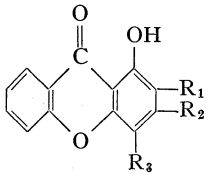

I

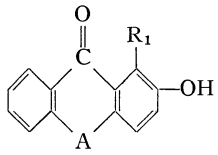

II

Ia, $R_1 = CH_2—N(CH_3)(CH_3)$, $R_2 = R_3 = H$

Ib, $R_1 = CH_2—N(C_2H_5)(C_2H_5)$, $R_2 = R_3 = H$

Ic, $R_1 = CH_2—N(CH_2CH_2OH)(CH_2CH_2OH)$, $R_2 = R_3 = H$

Id, $R_1 = CH_2—N(H)$, $R_2 = R_3 = H$

Ie, $R_1 = CH_2—N(H)O$, $R_2 = R_3 = H$

If, $R_1 = R_2 = H$, $R_3 = CH_2Cl$

Ig, $R_1 = R_2 = H$, $R_3 = CH_2—N(H)O$

Ih, $R_1 = CH_2—N(CH_3)(CH_3)$, $R_2 = CH_3$, $R_3 = H$

Ii, $R_1 = R_2 = R_3 = H$

Ij, $R_1 = R_2 = R_3 = H$

IIa, A = O, $R_1 = CH_2—N(CH_3)(CH_3)$

IIb, A = O, $R_1 = CH_2—N(C_2H_5)(C_2H_5)$

IIc, A = O, $R_1 = CH_2—N(CH_2CH_2OH)(CH_2CH_2OH)$

IId, A = O, $R_1 = CH_2—N(H)$

IIe, A = O, $R_1 = CH_2—N(H)O$

IIf, A = O, $R_1 = CH_2Cl$

IIg, A = O, $R_1 = CHO$

IIh, A = O, $R_1 = H$

IIi, A = S, $R_1 = CH_2—N(CH_3)(CH_3)$

IIj, A = S, $R_1 = CH_2—N(H)O$

IIk, A = S, $R_1 = H$

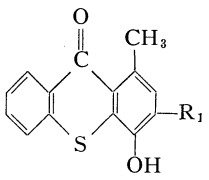

III

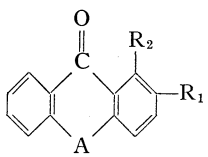

IV

Can. J. Chem. Downloaded from www.nrcresearchpress.com by 210.87.254.5 on 09/05/12
For personal use only.

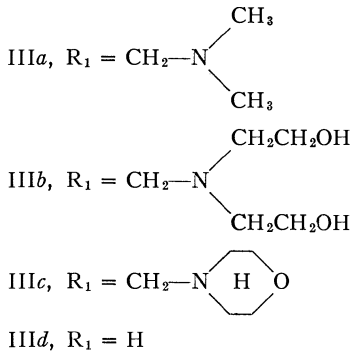

IIIa, $R_1 = CH_2—N(CH_3)_2$

IIIb, $R_1 = CH_2—N(CH_2CH_2OH)_2$

IIIc, $R_1 = CH_2—N(H)(O)$

IIId, $R_1 = H$

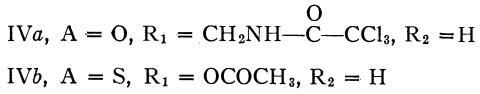

IVa, A = O, $R_1 = CH_2NH—C(=O)—CCl_3$, R_2 = H

IVb, A = S, $R_1 = OCOCH_3$, R_2 = H

(*c*) The phenolic bases did not respond to Millon's test (8), demonstrating that the ortho position to the hydroxyl group was substituted (9).

(*d*) Chloromethylation of I*i* yielded 4-chloromethyl-1-hydroxy-9-xanthenone, I*f*. The corresponding morpholino derivative I*g* was obtained by the action of morpholine on I*f*. The product (I*g*) reacted positively (9) with the Millon and negatively with the Gibbs reagent. It proved also to be different from that obtained by the action of morpholine and formaldehyde on I*i* (mixed m.p.).

(*e*) The behavior of I*i* towards the Mannich reaction finds analogy with its behavior towards the Friedel–Crafts reaction (1, 4) and the Claisen rearrangement (10).

We have also studied the behavior of 2-hydroxy-9-xanthenone, II*h*, and 2-hydroxy-10-thiaxanthenone, II*k*, towards the Mannich reaction.

The proposed structure for the Mannich base, e.g., II*a*, is based upon the fact that it could be converted into the corresponding 1-formyl-2-hydroxy-9-xanthenone, II*g*, by boiling with acetic acid in the presence of hexamine. The 1-aldehydo derivative II*g* was identical with that obtained from II*h* by the Duff reaction (11).

2-Hydroxy-9-xanthenone was chloromethylated to give 1-chloromethyl-2-hydroxy-9-xanthenone, II*f*. The position of the chloromethyl group was ascertained from the fact that upon treatment of II*f* with dimethylamine II*a* was obtained. The latter was identical with that obtained by the action of formaldehyde and dimethylamine on 2-hydroxy-9-xanthenone, II*h* (mixed m.p.), and was also converted to the known II*g*. Similarly, treatment of II*f* with morpholine gave the morpholinomethyl derivative II*e*.

By carrying out the Mannich reaction on 4-hydroxyl-1-methyl-10-thiaxanthenone, III*d*, the aminomethyl derivatives III*a*–III*c* were similarly obtained (cf. Table I).

With regard to the amine exchange reaction (12), the aminomethyl derivatives I*a*, II*a*, and II*i* behave in a manner similar to that of the phenolic Mannich bases (13). Thus, it was possible to substitute a secondary base such as morpholine for the dimethylamino group in each case.

EXPERIMENTAL

All melting points are uncorrected. The 1-hydroxy-9-xanthenone (14), 1-hydroxy-3-methyl-9-xanthenone (15), 2-hydroxy-9-xanthenone (11), 2-hydroxy-10-thiaxanthenone (16), and 4-hydroxyl-1-methy-10-thiaxanthenone (17) were prepared according to the published procedures.

Attempted Friedel–Crafts Acetylation

A mixture of 2-hydroxy-10-thiaxanthenone (2.2 g) and powdered anhydrous aluminum chloride (4.0 g) in nitrobenzene (20 ml) was treated under stirring with a solution of acetyl chloride (or acetic anhydride) (2.0 g) in nitrobenzene (5 ml). The reaction mixture was kept at room temperature for 5 days. After treatment with 2 N hydrochloric acid, followed by steam distillation to remove the nitrobenzene, only the starting material was obtained (mixed m.p.).

Can. J. Chem. Downloaded from www.nrcresearchpress.com by 210.87.254.5 on 09/05/12
For personal use only.

Can. J. Chem. Downloaded from www.nrcresearchpress.com by 210.87.254.5 on 09/05/12
For personal use only.

TABLE I

Aminomethyl derivatives of hydroxy-9-xanthenones and hydroxy-10-thiaxanthenones

Compound	Method of preparation	% yield*	Melting point (°C)		Formula	Molecular weight	Analysis†							
			Free bases	Hydrochloride salts			% C		% H		% N		% Cl	
							Calc.	Found	Calc.	Found	Calc.	Found	Calc.	Found
I*a*	A	60	—	223–225‡	$C_{16}H_{15}NO_3.HCl$	305.77	62.84	62.87	5.27	5.18	4.58	4.87	11.59	11.14
I*b*	A	75	—	191–192‡	$C_{18}H_{19}NO_3.HCl$	333.82	64.76	64.55	6.03	6.32	4.19	4.31	10.62	10.86
I*c*	B	40	—	201–203§	$C_{18}H_{19}NO_5.HCl$	365.82	—	—	—	—	3.82	3.87	—	—
I*d*	A	80	—	260–262‡	$C_{19}H_{19}NO_3.HCl$	345.83	65.98	65.87	5.82	5.95	4.05	4.45	10.25	10.61
I*e*	A	75	—	261–263‡	$C_{18}H_{17}NO_4.HCl$	347.81	62.15	62.04	5.21	5.48	4.03	4.44	10.19	10.35
I*h*	B	50	135§	—	$C_{17}H_{17}NO_3$	283.33	—	—	—	—	4.94	5.04	—	—
II*a*	B	30	120–122‖	—	$C_{16}H_{15}NO_3$	269.30	71.37	71.35	5.57	5.68	5.2	4.94	—	—
II*b*	B	50	—	202–204§	$C_{18}H_{19}NO_3.HCl$	333.82	64.76	64.42	6.03	6.21	4.19	4.24	10.62	10.53
II*c*	B	40	—	218–220§	$C_{18}H_{19}NO_5.HCl$	365.82	—	—	—	—	3.82	4.07	—	—
II*d*	B	40	131–132§	—	$C_{19}H_{19}NO_3$	309.36	73.9	73.62	6.15	5.78	4.53	4.37	—	—
II*e*	B	50	168–169§	—	$C_{18}H_{17}NO_4$	311.34	69.5	69.38	5.47	5.59	4.51	4.36	—	—
II*i*	B	20	102–104§	—	$C_{16}H_{15}NO_2S$	285.37	—	—	—	—	4.87	5.36	—	—
II*j*	B	15	168–170§	—	$C_{18}H_{17}NO_3S$	327.40	—	—	—	—	4.27	4.47	—	—
III*a*	B	40	120–121§	—	$C_{17}H_{17}NO_2S$	299.39	—	—	—	—	4.67	4.41	—	—
III*b*	B	50	—	182–184§	$C_{19}H_{20}NO_4S.HCl$	394.91	—	—	—	—	3.54	3.53	8.97	8.93
III*c*	B	45	145–146§	—	$C_{19}H_{19}NO_3S$	341.43	66.83	66.97	5.60	5.61	4.10	4.53	—	—

*Percentage yields based on free bases.
†Microanalyses carried out in the Microanalytical Laboratory of the National Research Centre, Dokki, Cairo, Egypt, U.A.R.
‡Crystallizing solvent was ethanol/ether.
§Ethanol was used as solvent for crystallization.
‖Crystallized from dilute ethanol.

Attempted Fries Rearrangement of 2-Acetoxy-10-thiaxanthenone

2-Acetoxy-10-thiaxanthenone (see below) (2.7 g) in nitrobenzene (25 ml) was treated with anhydrous aluminum chloride (3.5 g) and the mixture was left at room temperature for 4 days; only 2-hydroxy-10-thiaxanthenone was obtained almost in quantitative yield.

2-Acetoxy-10-thiaxanthenone, IV*b*, was obtained as colorless crystals by boiling II*k* in acetic anhydride – pyridine mixture for 2 hours. Crystallization from ethanol yielded IV*b*, m.p. 137–138°. Calc. for $C_{15}H_{10}O_3S$: C, 66.64; H, 3.72. Found: C, 66.43; H, 3.81.

Mannich Reaction on Hydroxy-9-xanthenones and Hydroxy-10-thiaxanthenones (General Procedure)

Method A

To a cooled suspension of the hydroxy-9-xanthenone (0.01 mole) in glacial acetic acid (30 ml) was added the secondary base (0.011 mole), followed by paraformaldehyde (0.011 mole). The reaction mixture was then heated under reflux for 4 hours and left overnight at room temperature. After the acetic acid was removed, in a vacuum, the residue was treated with dilute hydrochloric acid to dissolve the Mannich base formed. The reaction mixture was filtered and the cooled filtrate was made alkaline with ammonium hydroxide. The product was isolated either in the form of the solid free base or its hydrochloride (cf. Table I). The hydrochloride was formed by saturating the dry ethereal solution of the base with dry hydrogen chloride gas.

Method B

An aqueous solution of 40% formaldehyde (0.011 mole) was added dropwise to a mixture of the hydroxy-9-xanthenone (or hydroxy-10-thiaxanthenone) (0.01 mole) and the secondary amine (0.011 mole) in about 40 ml of ethanol. The temperature was kept below 10° and the solution was effectively stirred. The reaction mixture was then refluxed for 5 hours and left overnight at room temperature. After the volatile materials were removed, under reduced pressure, the residue was worked up as described in method A. Yields, physical data, and analytical data of the compounds are shown in Table I.

4-Chloromethyl-1-hydroxy-9-xanthenone

A mixture of 1-hydroxy-9-xanthenone (2.12 g), 20 ml of concentrated hydrochloric acid (sp. gr. 1.17), 1 ml of concentrated sulphuric acid (sp. gr. 1.84), and methylal (2.28 g) was stirred at 70° for 5 hours. During this time, dry hydrogen chloride gas was passed into the reaction mixture. After the mixture was cooled, the precipitate was collected, washed with cold water, and air-dried. Yield 2 g, m.p. 118–120°. Recrystallization from absolute ethanol gave an analytical sample, m.p. 120–122°. Anal. Calc. for $C_{14}H_{19}O_3Cl$: Cl, 13.6. Found: Cl, 13.4.

4-Morpholinomethyl-1-hydroxy-9-xanthenone

A mixture of 4-chloromethyl-1-hydroxy-9-xanthenone (2.5 g), morpholine (1 g), and dry benzene (50 ml) was refluxed for 5 hours. 4-Morpholinomethyl-1-hydroxy-9-xanthenone was isolated as its hydrochloride. Recrystallization from absolute ethanol gave the analytical sample, m.p. 258–260° (depressed when admixed with a sample of I*e*). Yield 70%. Anal. Calc. for $C_{18}H_{17}NO_4HCl$: N, 4.03. Found: N, 3.91.

1-Chloromethyl-2-hydroxy-9-xanthenone

This compound was obtained from II*h* using the above-described procedure for the preparation of 4-chloromethyl-1-hydroxy-9-xanthenone. An attempt to crystallize it resulted in its decomposition; the uncrystallized sample melts at 210–212°. It was directly converted into the corresponding aminomethyl compound II*a* (see below).

1-Dimethylaminomethyl-2-hydroxy-9-xanthenone

Dimethylamine gas was allowed to pass into a solution of 1-chloromethyl-2-hydroxy-9-xanthenone (2.5 g) in boiling benzene (70 ml) for 3 hours. After removal of the volatile materials under reduced pressure, the residue was treated with dilute hydrochloric acid to dissolve the aminomethyl compound formed. The reaction mixture was filtered and the cooled filtrate was made alkaline with ammonium hydroxide. The resulted solid was collected, washed with cold water, and crystallized from dilute ethanol to give II*a*, m.p. 120–122°. Admixture with a sample obtained by the Mannich reaction on II*h* as described above did not depress the melting point. Yield 55%.

Similarly the action of morpholine on 1-chloromethyl-2-hydroxy-9-xanthenone in boiling benzene gave II*e*. Recrystallization from ethanol gave the product melting at 168–169°. Its melting point was not depressed on admixture with a sample prepared from the reaction of 2-hydroxy-9-xanthenone with formaldehyde and morpholine in ethanol.

1-Formyl-2-hydroxy-9-xanthenone

A mixture of 1-dimethylaminomethyl-2-hydroxy-9-xanthenone (1 g), hexamine (1 g), and glacial acetic acid (20 ml) was refluxed for 1 hour. The reaction mixture was poured into dilute hydrochloric acid and left to stand overnight in the ice chest. The resulting yellow solid was collected, washed with water, dried, and crystallized from light petroleum (b.p. 100–120°) to give II*g*, m.p. 161–162°. Yield 45%. A mixed melting point with authentic 1-formyl-2-hydroxy-9-xanthenone (prepared by the Duff reaction) (11) was not depressed.

Can. J. Chem. Downloaded from www.nrcresearchpress.com by 210.87.254.5 on 09/05/12
For personal use only.

Amine Exchange Reaction of Hydroxyxanthenones Mannich Bases

A mixture of 2-dimethylaminomethyl-1-hydroxy-9-xanthenone (1.3 g) and morpholine (0.9 g) was heated in a nitrogen atmosphere at 130° for 2 hours. The oily product, thus obtained, was poured into cold water (10 ml) and then extracted with ether. The ethereal extract was washed with water and dried over anhydrous sodium sulphate. Saturation with dry hydrogen chloride gas gave the hydrochloride of I*e*. Admixture with a sample obtained by the Mannich reaction on I*i* using formaldehyde and morpholine in ethanol did not depress the melting point. Yield 60%.

Similarly, 1-morpholinomethyl-2-hydroxy-9-xanthenone, II*e*, and 1-morpholinomethyl-2-hydroxy-10-thiaxanthenone, II*j*, were obtained in 45% and 40% yield respectively.

ACKNOWLEDGMENTS

The authors are indebted to the National Research Centre for the award of a scholarship to one of us (F. M. S.).

REFERENCES

1. A. MUSTAFA and O. HISHMAT. J. Am. Chem. Soc. **79**, 2225 (1957).
2. H. DE DIESBACH. Helv. Chim. Acta, **23**, 1232 (1940).
3. R. C. ELDERFIELD. Heterocyclic compounds. Vol. II. John Wiley and Sons, Inc., New York. 1951. p. 439.
4. J. S. H. DAVIES, F. SCHEINMANN, and H. SUSCHITZKY. J. Chem. Soc. 2140 (1956).
5. F. LAMB and H. SUSCHITZKY. Tetrahedron, **5**, 1 (1959).
6. B. REICHERT. Die Mannich-Reaction. Springer-Verlag, Berlin-Göttingen-Heidelberg. 1959. p. 53.
7. F. E. KING, T. J. KING, and L. C. MANNING. J. Chem. Soc. 563 (1957).
8. F. FEIGEL. Spot tests in organic analysis. Elsevier Publishing Co. 1956. p. 183.
9. J. H. BURCKHALTER. J. Am. Chem. Soc. **72**, 5309 (1950).
10. F. SCHEINMANN and H. SUSCHITZKY. Tetrahedron, **7**, 31 (1959).
11. J. S. H. DAVIES, F. LAMB, and H. SUSCHITZKY. J. Chem. Soc. 1790 (1958).
12. H. R. SNYDER and J. H. BREWSTER. J. Am. Chem. Soc. **70**, 4230 (1948).
13. P. DA RE, L. VERLICCHI, and I. SETNIKAR. J. Org. Chem. **25**, 1097 (1960).
14. K. S. PANKAJAMANI and T. R. SESHADRI. J. Sci. Ind. Res. (India), **13B**, 396 (1954).
15. B. M. DESAI, P. R. DESAI, and R. D. DESAI. J. Indian Chem. Soc. **37**, 53 (1960).
16. H. CHRISTOPHER and S. SMILES. J. Chem. Soc. 2046 (1911).
17. R. N. SEN and S. C. SEN-GUPTA. J. Indian Chem. Soc. **6**, 267 (1929).

Can. J. Chem. Downloaded from www.nrcresearchpress.com by 210.87.254.5 on 09/05/12
For personal use only.

GAS–LIQUID CHROMATOGRAPHY OF TERPENES

PART VIII. THE VOLATILE OIL OF TANACETUM VULGARE L.[1, 2]

E. VON RUDLOFF

National Research Council of Canada, Prairie Regional Laboratory, Saskatoon, Saskatchewan

Received February 21, 1963

ABSTRACT

The chemical composition of the commercial oil of tansy and of that obtained from a local tansy species was determined by means of gas–liquid chromatography. Both oils contained *d*-isothujone as the major component (68.5%, 58%). The commercial oil contained fairly large amounts of *l*-camphor (13.9%), whereas that from local plants had only traces of camphor and 19.8% of *l*-thujone. The minor components isolated and identified in both oils were *l*-α-pinene, *l*-camphene, *d*-sabinene, *d*-limonene, 1:8-cineole, γ-terpinene, *p*-cymene, *d*-terpinen-4-ol, *l*-carvotanacetone, and *l*-borneol. Small amounts of α-thujene, β-pinene, α-terpinene, terpinolene, neoisothujyl and isothujyl alcohols, and dihydrocarvone were identified by retention characteristics only. Car-4-ene, isomeric alloocimenes, and carvomenthone may also be present. An unknown, crystalline monoterpene alcohol with a terminal methylene group was isolated in small amounts. A sesquiterpene (3.7%) was obtained from the oil of local plants.

Prefractionation of these oils by fractional distillation resulted in extensive isomerization of isothujone to *dl*-carvotanacetone. Such a rearrangement was not encountered during prefractionation by preparative gas–liquid chromatography.

An accurate qualitative and quantitative analysis of the volatile oil of the common tansy (*Tanacetum vulgare* L., fam. Compositae) was required for a biochemical study. Several early investigations have been reported (1), but no analysis with more modern techniques appears to have been published. Only two recent papers deal with this oil, Schenk and Heim (2) reporting that the highest oil content is found in the flowers shortly after opening (up to 1.42% of the dry weight of the plant) and Ionescu *et al.* (3) finding it to contain *d*-isothujone (60%, $[\alpha]_D$ +68.3°), a mixture of terpenes (10%), and a camphor (20%, n_D^{15} 1.4570, $[\alpha]_D$ +24°, oxime m.p. 141° C) which was not further characterized.

Semmler (4) was the first to recognize that the major constituent of the oil of tansy is thujone and Wallach (5) showed this to be dextrorotatory β-thujone (*d*-isothujone (6)). Persoz (7, cf. ref. 1) and Vohl (8, cf. ref. 1) found camphor which was later shown to be the rare *l*-form (9, cf. ref. 1). Small amounts of borneol appear to be present (9) and Bruylants (10) thought it likely that thujyl alcohol was a constituent of this oil. None of the terpene hydrocarbons have been isolated and identified.

In previous papers of this series (11, 12) the analysis of other thujone-containing oils by means of gas–liquid chromatography (GLC) has been reported. When this technique was applied to the analysis of the oil of tansy considerable difficulty was encountered in the complete separation and identification of the minor oxygenated monoterpenes. Since some of these components may have biochemical significance an attempt was made to improve the present technique, using temperature-programmed GLC, to a point where complete analysis may become possible. Two samples of the oil of tansy were investigated, one being of commercial origin, the other being obtained by steam distillation of local wild tansy plants.

EXPERIMENTAL

Isothermal GLC chromatograms were obtained as described previously (11–13). Temperature-programmed experiments were carried out with an Aerograph Autoprep model A-700 chromatograph (Wilkins

[1]*For Part VII, see Can. J. Chem.*, **41**, *1 (1963).*

[2]*Issued as N.R.C. No. 7354.*

Can. J. Chem. Downloaded from www.nrcresearchpress.com by 210.87.254.5 on 09/05/12
For personal use only.

Instrument and Research Inc., Walnut Creek, Calif., U.S.A.). This instrument is equipped with an automatic injector (0.03- to 2-ml capacity) and an automatic collector. Temperature programming was non-linear and the single-column technique was used. Fractions were automatically collected in 5-ml glass traps (ice-cooled) by a trip-switch which was actuated by the recording pen and which may be set for any particular peak height. Analytical runs were carried out on 4 mm I.D. (1/4 in. O.D.) coiled copper or stainless steel columns, and preparative runs on similar ones of 6-mm I.D. (3/8-in. O.D.).

Melting points were determined with a Leitz hot-stage microscope. Optical rotations were measured at 22–25° C in chloroform (1–5% solution) or, in case of the derived oximes and semicarbazones, in ethanol. The rotation of each oil sample was obtained with the undiluted material. Infrared spectra were recorded with a Perkin–Elmer model 21 double-beam spectrophotometer, liquid samples being mounted as films between sodium chloride plates and solid ones by the KBr-disk method.

Materials

The commercial oil (Fritzsche Bros. Inc., New York) had n_D^{24} 1.4590, $[\alpha]_D$ +39.7°. Steam distillation of the leaves and flowers of locally growing wild tansy plants (11.7 kg fresh weight), harvested near Saskatoon during September 1962, gave a light yellow oil (24.3 g) with n_D^{24} 1.4615, $[\alpha]_D$ +19.3°. Reference compounds were either commercial samples (purified by GLC where necessary) or those obtained from other plant sources (11–13). The four isomeric thujyl alcohols were prepared by reduction of *l*-thujone or *d*-isothujone with lithium aluminum hydride. Dihydrocarvone, carvotanacetone, and carvomenthone were obtained by reduction of *l*-carvone (14–17). A detailed description of these reductions and of the isolation of the individual products will be reported elsewhere.

The liquid phases used in the GLC columns were commercial products, except for adipate and azelate polyethylene glycol polyesters, which were kindly donated by Dr. B. M. Craig. The solid support was Chromosorb W (60–80 mesh) in the analytical columns, and Gas Chrom P (60–80 mesh) in most of the preparative columns. The ratio of liquid phase to solid support was 1 to 6, except in the 20-ft preparative polyethylene glycol column supplied with the Aerograph instrument (3/8 in. O.D. aluminum), which had 30% PEG 20 M on Chromosorb W.

Analytical Chromatograms

Aliquots (3 μl) of the two oils were analyzed on a 6-ft SE-30 column (at 65–180° C in 25 minutes in temperature-programmed runs; at 160° C in isothermal runs) to determine whether significant amounts of sesquiterpenes were present. In the commercial oil three peaks were recorded in trace amounts in the cedrene–cadinene range, but the oil from local plants had two minor and one fairly large component (approx. 4% of the oil) in this range. The latter was correlated with peak 26 of the PEG 20 M chromatogram (see Fig. 1(*b*)).

The oils were then systematically analyzed (isothermal runs) on all the analytical columns. The relative retention times (RRT) of monoterpene hydrocarbons (limonene = 1.00) on PEG 20 M (at 65° C; 64 ml helium/min); NGA polyester (18) (65° C; 160 ml); and ethylene glycol bis(propionitrile) (EGPN) (65° C;

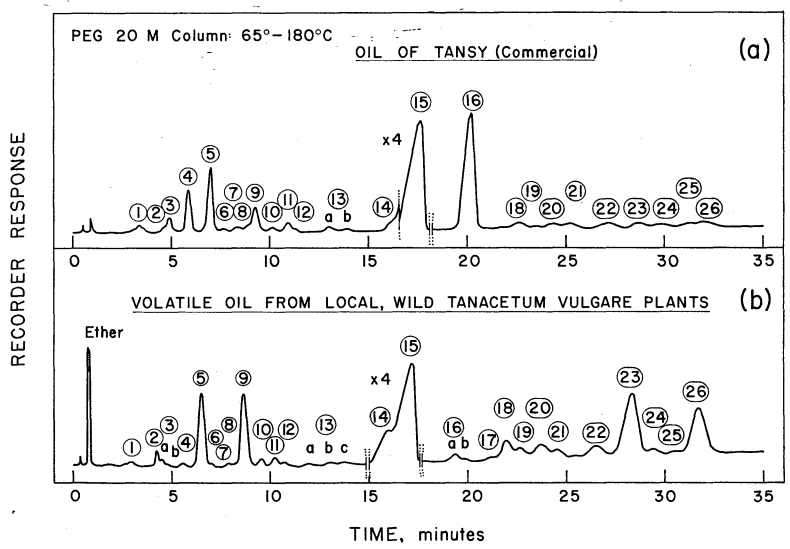

FIG. 1. Gas chromatograms of oil of tansy on a 6-ft polyethylene glycol column (temperature-programmed from 65° to 180° C). (*a*) Commercial oil; (*b*) oil from local tansy plants.

Can. J. Chem. Downloaded from www.nrcresearchpress.com by 210.87.254.5 on 09/05/12
For personal use only.

77 ml) and of the oxygenated monoterpenes (camphor = 1.00) on PEG 20 M (120° C; 92 ml); NGA (120° C; 109 ml); and QF-1 (19) (100° C; 115 ml) are shown in Table I. The relative retention times of *cis–trans*- and

TABLE I

Composition of the volatile oil of *Tanacetum vulgare* L.

Peak No.	Compound	Relative retention times*			Percent composition	
		A	B	C	I†	II‡
1	Unidentified	(3 unresolved peaks)			0.3	0.1
2	Unidentified	0.28	0.30	—	0.1	0.4
3*a*	*l*-α-Pinene	0.30	0.32	0.27	0.5	0.2
3*b*	(α-Thujene)	0.32	0.33	0.32	0.2	0.1
4	*l*-Camphene	0.42	0.41	0.45	2.3	0.2
5*a*	(β-Pinene)	0.59	0.57	0.54	Trace	Trace
5*b*	*d*-Sabinene	0.62	0.62	0.70	3.9	2.3
6	(? Car-4-ene)	0.71	0.76	—	Trace	0.1
7	(α-Terpinene)	0.94	0.90	0.98	0.2	0.1
8	*d*-Limonene	*1.00*	*1.00*	*1.00*	0.1	0.1
9	1:8-Cineole	1.07	1.15	1.68	1.5	2.3
10	γ-Terpinene	1.40	1.38	1.41	0.4	0.3
11	*p*-Cymene	1.63	1.38	2.38	0.6	0.4
12	(Terpinolene)	1.79	1.72	1.75	Trace	Trace
13	(? Alloocimene isomers)	(See experimental)			0.5	0.3
		D	E	F		
14	*l*-Thujone	0.61	0.70	0.68	1.0	19.4
15	*d*-Isothujone	0.67	0.75	0.70	68.5	58.0
16*a*	*l*-Camphor	*1.00*	*1.00*	*1.00*	13.9	0.8
16*b*	(? Carvomenthone)	1.15	1.33	1.06		0.2
17	Unidentified	1.30	—	—	Trace	Trace
18	*d*-Terpinen-4-ol	1.40	1.39	0.42	0.9	1.0
19	(Neoisothujyl alcohol)	1.68	1.34	0.34	0.2	0.7
	(Dihydrocarvone)	1.68	1.53	1.15		
20	(Isothujyl alcohol)	1.90	1.53	0.41	0.8	1.3
21	*l*-Carvotanacetone	2.06	2.00	1.24	0.5	0.7
22	*l*-Borneol	2.28	1.84	0.52	1.0	0.8
23	*l*-Carvone	2.66	2.32	1.53	0.8	5.8
24	Unidentified	2.98	—	—	0.5	0.5
25	(Crystalline alcohol and unidentified sesquiterpene)	3.30	2.46	0.68	0.5	0.3
26	Sesquiterpene	3.58	—	—	0.9	3.7

*Hydrocarbons (at 65° C; limonene = 1.00): A: polyethylene glycol 20 M column (PEG 20 M); B: neopentyl glycol adipate polyester column (NGA); C: ethylene glycol bis(propionitrile) (EGPN).
Oxygenated monoterpenes and sesquiterpenes (camphor = 1.00): D: PEG 20 M (at 120° C); E: NGA (at 120° C); F: QF-1 polymer column (at 100° C).
†Commercial oil.
‡Oil from local tansy plants.

trans–trans-alloocimene were RRT 4.14, 4.85 and 3.32, 3.90 on PEG 20 M and EGPN respectively. The data of known monoterpenes as determined on the other analytical columns have been reported previously (11, 12, 13, 20). When the retention times of a particular peak agreed with that of a known compound on every column, the peak was considered as tentatively identified.

Some higher-boiling trace components which were recorded in temperature-programmed runs (PEG 20 M and NGA, 65–180° C; see Fig. 1(*a* and *b*)) were absent on the charts from isothermal runs. Only after prefractionation were the concentrations of these trace components high enough to be clearly recorded by the latter technique. For this reason the quantitative composition was calculated (triangulation method) from the areas under the peaks as recorded in the temperature-programmed runs. The calculated data was reproducible within the errors of the method (11, 12, 13, 21) in repeat runs on the same, as well as on different columns. Use of internal standards (known amounts of *n*-decane, limonene, 1:8-cineole, camphor, 4-terpineol, carvone, and/or *n*-decanol added to a known weight of oil) showed that 98±2% of the oils could be accounted for, provided the trace components were included. Since isothujone (peak 15) was present in such large

Can. J. Chem. Downloaded from www.nrcresearchpress.com by 210.87.254.5 on 09/05/12
For personal use only.

amounts, it could not be recorded at the same attenuation as the other peaks when the aliquot of oil was large enough (5 to 10 μl) to permit recording of the trace components (see Fig. 1(*a* and *b*)). The use of a different attenuation and the skewing of the isothujone peak caused by the relatively large samples introduced fairly large errors (up to 5%) and it was found advantageous to calculate the quantitative data from runs with smaller aliquots (1–3 μl) and to add to this the respective amounts of trace components as recorded in runs with 5- to 10-μl samples.

Prefractionation

The commercial oil (100 ml) was fractionally distilled *in vacuo* (50 mm Hg) through a 1-mm×8-mm spinning band column (Podbielniak Inc., Chicago), using takeoff ratios from 1:60 to 1:100. Five fractions were collected and GLC analysis showed the following composition:

I (5 ml, b.p. 50–75° C) mainly monoterpene hydrocarbons;
II (10 ml, b.p. 75–100° C) hydrocarbons and isothujone;
III (55 ml, b.p. 100–108° C) mainly isothujone and some camphor;
IV (15 ml, b.p. 108–112° C) isothujone and midrange oxygenated monoterpenes;
V (10 ml, b.p. 112–120° C) mainly higher-boiling terpenes, including carvotanacetone and carvone, and sesquiterpenes.

The distillation residue showed extensive decomposition and polymerization and was not further investigated.

The oil from local plants was prefractionated in 0.2-ml aliquots on a 6-ft×3/8-in. SE-30 column at 90–180° C (in 15 minutes). Cuts similar to those obtained in the fractional distillation were collected, the collecting mechanism of the Autoprep being operated by hand. Recovery of the hydrocarbons varied between 40 and 80%, losses due to aerosol formation being highest for the minor constituents. No decomposition peaks were recorded on reinjection of each fraction on analytical columns. Overlaps of compounds between adjacent fractions were not as marked as in the distillation.

Hydrocarbons

Fractions I and II from distilled commercial oil were injected repeatedly (30- to 50-μl aliquots) onto a 6-ft×3/8-in. PEG 20 M column, which was temperature-programmed from 65° to 90° C during 12 minutes. The components which were isolated in sufficient amount and purity to permit recording of infrared spectra and physical data were identified by comparison with the corresponding data of authentic monoterpene hydrocarbons as: peak 3*a*, *l*-α-pinene (n_D^{24} 1.4606, $[\alpha]_D$ −21.6°) contaminated with a compound which had the same retention time as α-thujene (peak 3*b*, see Table I); peak 4, *l*-camphene (m.p. 30–42° C, $[\alpha]_D$ −111.1°); peak 5*b*, *d*-sabinene (n_D^{24} 1.4678, $[\alpha]_D$ +43.4°); peak 8, impure *d*-limonene (positive rotation); peak 9, 1:8-cineole (n_D^{23} 1.4584, $[\alpha]_D$ ±0); peak 10, γ-terpinene (n_D^{23} 1.4712, $[\alpha]_D$ ±0); peak 11, *p*-cymene (n_D^{24} 1.4800, $[\alpha]_D$ ±0). *p*-Cymene was further identified by its ultraviolet spectrum. The data of these components as isolated from fractions I and II of the oil from the local plants were in good agreement with those reported above.

Peaks 1 (mixture of at least 3 components) and 2 could not be identified, whereas peaks 3*b*, 5*a*, 6, and 7 were tentatively identified by relative retention times (cf. Table I). Peaks 13*a*, *b*, and *c* had retention times in the alloocimene range (see above) but none could be isolated pure as some decomposition was encountered.

Thujones

Fraction III from distilled commercial oil was fractionated on the same GLC column using a temperature range of 90–140° C. Essentially pure *d*-isothujone (peak 15) was obtained; n_D^{24} 1.4503, $[\alpha]_D$ +65.9° (*c*, 2.3, $CHCl_3$). The derived semicarbazone had m.p. 174–175° C, $[\alpha]_D$ +216.8° (*c*, 2.0, EtOH) after recrystallization from aqueous ethanol. Found: C, 63.38; H, 9.18; N, 20.22%. Calculated for $C_{11}H_{19}N_3O$: C, 63.12; H, 9.15; N, 20.08%.

Just ahead of the isothujone peak (peak 15), a shoulder (peak 14) was also recorded in preparative runs. This material was collected in small amounts. The infrared spectrum was similar to that of thujone and the optical rotation was negative; n_D^{24} 1.4500. GLC analysis showed contamination with about 10% isothujone.

In the oil from local plants peak 14 was a major constituent which was partially resolved from isothujone. By collecting the early portions of peak 14 and late ones of peak 15, both components were isolated fairly pure; n_D^{24} 1.4498 and 1.4501 and $[\alpha]_D$ −10° and +67° respectively. These data, as well as the infrared spectra, were in good agreement with those of *l*-thujone and *d*-isothujone respectively.

l-Camphor

Fraction III of the commercial oil also contained fairly large amounts of peak 16, which was isolated chromatographically pure in the above runs. The collected material had m.p. 150–170° C, $[\alpha]_D$ −39.8° (*c*, 2.2, $CHCl_3$). Further purification by recrystallization proved difficult and the material was converted to the oxime, m.p. 115.5–116.5° C, $[\alpha]_D$ +50.4° (*c*, 2.2, EtOH), after recrystallization from aqueous ethanol. Found: C, 72.08; H, 10.25; N, 8.57%. Calculated for $C_{10}H_{17}NO$: C, 71.81; H, 10.25; N, 8.38%.

In the oil from local plants peak 16 was only a trace component and analytical chromatograms showed an overlap with a second component (peak 16*b*). In the preparative runs these components were collected as one fraction. The infrared spectrum showed as characteristic absorption only a strong carbonyl band (1735–1715 cm^{-1}), indicating that both components are ketones.

Can. J. Chem. Downloaded from www.nrcresearchpress.com by 210.87.254.5 on 09/05/12
For personal use only.

Higher-Boiling Minor Components

The individual components from fraction IV could not be obtained pure by preparative GLC. All fractions collected, except peak 18, were subsequently shown to be mixtures of two or more components. Peak 18, as collected from the 6-ft×3/8-in. PEG column (120–190° C), had n_D^{24} 1.4754, $[\alpha]_D$ +17.0° (*c*, 1.3, $CHCl_3$) and its infrared spectrum was similar in all respects with that of terpinen-4-ol.

In analytical runs it was found that QF-1 polymer retained ketones and esters strongly with respect to alcohols and hydrocarbons (see Table I). A 6-ft×3/8-in. preparative column was made up and fraction IV was fractionated on a 0.03-g scale into alcohols and ketones. GLC analysis on the PEG 20 M column of the alcohol fractions showed the presence of six components with RRT 1.40, 1.68, 1.89, 2.28, 3.26, and 3.58 (peaks 18, 19, 20, 22, 25, and 26 respectively). Of these, peak 18 (RRT 1.40) was readily identified as *d*-terpinen-4-ol. Peaks 19 and 20 had RRT values corresponding with those of neoisothujyl and isothujyl alcohols respectively. However, neither component could be obtained pure in sufficient amount to confirm their identities. Peak 22 (RRT 2.28) was obtained crystalline (m.p. 120–180° C, $[\alpha]_D$ −23°) and its infrared spectrum agreed in all respects with that of borneol. α-Terpineol (RRT 2.24) could be a contaminant, but this was not confirmed by the infrared spectrum. Peak 25 (RRT 3.26) was also obtained crystalline (m.p. 45–60° C, $[\alpha]_D$ −43°). The infrared spectrum had strong bands at 3300, 2960–2860, 1655, 1465–1455, 1360, 1332, 1150, 1050, 975, and 882–877 cm^{-1} and well-defined weak bands at 3070, 850, and 765 cm^{-1}.

Of the ketonic components only carvotanacetone (peak 21, RRT 2.06) and carvone (peak 23, RRT 2.66) were positively identified (see below). A component of RRT 1.68, i.e. the same peak as 19, was isolated fairly pure and its infrared spectrum corresponded with that of dihydrocarvone. Because of paucity of material no crystalline derivative was obtained.

Carvotanacetone and Carvone

Fraction V of the commercial oil was composed of about 85% of peak 21 and smaller amounts of peaks 22, 23, 24, and 26. Peak 25 was not recorded and may have been lost in the distillation. Preparative GLC (using the QF-1 column first and then the PEG 20 M column) gave peak 21 practically pure; n_D^{24} 1.4808, $[\alpha]_D$ ±0. The infrared spectrum was similar to that of carvotanacetone. The oxime, m.p. 92.5–93.5° C, $[\alpha]_D$ +0.5°, after recrystallization from aqueous ethanol was obtained directly from fraction V. Found: C, 72.22; H, 10.32; N, 8.46%. Calculated for $C_{10}H_{17}NO$: C, 71.81; H, 10.25; N, 8.38%.

Peak 23 was isolated fairly pure in small amounts; n_D^{24} 1.4855, $[\alpha]_D$ −10.8°. The infrared spectrum was similar to that of *l*-carvone. During attempts to isolate peaks 24, 25, and 26 decomposition was encountered and these fractions from the commercial oil were not further investigated.

Peaks 21 and 23 were obtained fairly pure in small amounts from fraction IV of the oil from local plants. The infrared spectra agreed with those of carvotanacetone and carvone respectively and the optical rotations were negative (−45° and −11°).

Sesquiterpenes

In the oil from local plants peak 26 was recorded in fairly high amounts (about 3.7%). By using the SE-30 preparative column small amounts of this material were isolated fairly pure. The infrared spectrum resembled that of cadinene (strong infrared bands in the 2940–2860 cm^{-1} range, weak bands at 1645–1605 cm^{-1}, medium bands at 875 and 825 cm^{-1}), but the retention time on the PEG 20 M (41.5 min) and NGA column (71.0 min) at 120° C differed from that of cadinene (38.7 and 60.3 min respectively).

RESULTS AND DISCUSSION

Typical temperature-programmed chromatograms (as obtained on the PEG 20 M column) of the commercial oil of tansy and that obtained from local wild tansy plants are shown in Fig. 1(*a* and *b*). Nearly 30 different peaks were recorded and on comparison with chromatograms obtained in isothermal GLC runs the better detection of the higher-boiling minor components (peaks 18 to 26) in the temperature-programmed runs was evident. Therefore, it is likely that the values reported earlier for corresponding components in the volatile oils of the leaves of *Thuja occidentalis* L. (11), *Thuja plicata* D. Don (12), and black, white, and Colorado spruce (13) as determined by isothermal GLC require an upward correction. That the calculated values for oxygenated higher-boiling monoterpenes tended to be low in comparison with those of the lower-boiling hydrocarbons was already pointed out (20), but the error was thought to be mainly due to tailing. The use of internal standards in this study showed that 98±2% of the components of each oil were accounted for provided that all peaks were recorded at the same attenuation and trace components were included. The presence of a single component in excess of 50% caused inaccuracies in calculating quantitative data since fairly large aliquots (5–10 μl) of the oil had to be injected to record the trace components adequately. This

Can. J. Chem. Downloaded from www.nrcresearchpress.com by 210.87.254.5 on 09/05/12
For personal use only.

required a change of attenuation and resulted in considerable skewing of the large peaks (cf. Fig. 1). Both factors increased the error in quantitative calculations.

The preliminary runs on the SE-30 column showed that the commercial oil contained only traces of sesquiterpenes in the cedrene–cadinene range, and no oxygenated sesquiterpenes were recorded. The oil from the local plants, however, contained appreciable amounts of sesquiterpenes (peaks 24 to 26). Of these one (peak 26) was isolated fairly pure. The infrared spectrum showed it to be similar to cadinene but it was more strongly retained on GLC columns.

The average quantitative composition of the two oils as determined on a variety of columns in temperature-programmed runs is shown in Table I. All the major and several of the minor components were identified after isolation by preparative GLC. The results obtained confirm that *d*-isothujone (peak 15) is the major component in both oils. In the commercial oil the second largest component was *l*-camphor (peak 16), but this was only present in trace amounts in the oil from local tansy plants. Instead, *l*-thujone (peak 14) was a major constituent. The latter oil also contained fairly large amounts of *d*-sabinene (peak 5*b*), 1:8-cineole (peak 9), *l*-carvone (peak 23), and the unsaturated sesquiterpene (peak 26). In the commercial oil, the latter two components were only minor constituents and somewhat more *l*-α-pinene (peak 3*a*) and *l*-camphene (peak 4) were recorded. The presence of minor amounts of *l*-borneol (peak 21) was confirmed but no camphor having an oxime of m.p. 141° C, as reported by Ionescu *et al.* (3), was isolated. Of the other minor peaks *d*-limonene (peak 8), γ-terpinene (peak 10), *p*-cymene (peak 11), *d*-terpinen-4-ol (peak 18), and *l*-carvotanacetone (peak 21) were identified positively. Peaks 3*b*, 5*b*, 6, 7, 12, 19*a*, 19*b*, and 20 were identified tentatively by retention data (and to some extent by infrared spectra) as α-thujene, β-pinene, car-4-ene, α-terpinene, terpinolene, neoisothujyl alcohol, dihydrocarvone, and isothujyl alcohol respectively. Peaks 13*a* to *c* were recorded in the alloocimene range and the retention times of peaks 13*b* and *c* agreed fairly well with those of *trans–cis-* and *trans–trans*-alloocimene (see also ref. 22). By analogy, peak 13*a* could be *cis–cis*-alloocimene. Peak 25 appears to be a mixture of a sesquiterpene (trace amounts) and the unidentified crystalline alcohol of melting point 45–60° C, $[\alpha]_D$ −43°. The infrared spectrum of the latter indicated the presence of a terminal methylene group (sharp, medium strong bands at 1655 and 880 cm^{-1}). No reports of a crystalline monoterpene alcohol with such characteristics could be found in the literature.

Examination of the amount of carvotanacetone in the commercial oil as recorded by GLC and that present in fractions IV and V from the fractional distillation showed a considerable increase of this compound during distillation. Since the thujones have been isomerized to carvotanacetone at 280° C (23) it is likely that this rearrangement has occurred during distillation even though the pot temperature did not exceed 160° C. Disproportionation of carvone to carvacrol and more saturated ketones, including carvotanacetone (24, 25), may also have taken place. The fact that the compound isolated from the distilled fraction was optically inactive lends strong support that rearrangement from isothujone to carvotanacetone has occurred preferentially. When this compound was isolated by GLC from the oil of local plants a negative rotation was recorded. Also, when pure thujone, isothujone, and carvone were injected onto analytical GLC columns the relative amounts recorded were the same as those injected (within ±2%) and no sign of decomposition could be detected. Thus, the use of preparative GLC for the prefractionation of essential oils is to be preferred over fractional distillation. However, the poor recovery of some components (due to aerosol formation) is as yet a disadvantage.

Can. J. Chem. Downloaded from www.nrcresearchpress.com by 210.87.254.5 on 09/05/12
For personal use only.

Most of the oxygenated compounds found in the oil of tansy are substituted at C-2. This suggests a biogenetic relationship and it may be that a sequence in the formation of these compounds similar to the one described by Reitsema (26) for mint oils is operative. This aspect, as well as the effect of environmental changes on the composition of the oil, is being studied in this laboratory.

ACKNOWLEDGMENTS

The author wishes to thank Mr. M. Granat for technical assistance, Mr. M. Mazurek for the microanalyses, and Mr. W. C. Haid for recording the infrared spectra.

REFERENCES

1. E. GUENTHER. The essential oils. Vol. V. D. Van Nostrand Co., Inc., New York. 1952. p. 484.
2. G. SCHENK and W. H. HEIM. Pharmazie, **5**, 288 (1950); Chem. Abstr. **44**, 10266e (1950).
3. C. N. IONESCU, C. ANITESCU, W. LUNGU, and EL. STOICAN. Commun. Acad. Rep. Populare Romine, **8**, 279 (1958); Chem. Abstr. **54**, 14582*a* (1960).
4. F. W. SEMMLER. Ber. **25**, 3343 (1892).
5. O. WALLACH. Ann. **272**, 99 (1893).
6. A. G. SHORT and J. READ. J. Chem. Soc. 2016 (1938).
7. PERSOZ. Compt. Rend. **13**, 433 (1841).
8. VOHL. Arch. Pharm. **124**, 16 (1853).
9. BERICHTE SCHIMMEL & CO. October, 1895. p. 35.
10. G. BRUYLANTS. Ber. **11**, 449 (1878).
11. E. VON RUDLOFF. Can. J. Chem. **39**, 1200 (1961).
12. E. VON RUDLOFF. Phytochemistry, **1**, 195 (1962).
13. E. VON RUDLOFF. Tappi, **45**, 181 (1962).
14. O. WALLACH and H. SCHRADER. Ann. **279**, 377 (1894).
15. O. WALLACH. Ann. **381**, 64 (1911).
16. R. VAVON. Compt. Rend. **153**, 68 (1911).
17. J. READ and R. G. JOHNSTON. J. Chem. Soc. 226 (1934).
18. S. R. LIPSKY and R. A. LANDOWNE. Anal. Chem. **33**, 818 (1961).
19. W. J. A. VAN DEN HEUVEL, E. V. A. HAAHTI, and E. C. HORNING. J. Am. Chem. Soc. **83**, 1513 (1961).
20. E. VON RUDLOFF. Can. J. Chem. **39**, 1 (1961).
21. J. JANAK. J. Chromatog. **3**, 308 (1960).
22. M. H. KLOUWEN and R. TER HEIDE. J. Chromatog. **7**, 297 (1962).
23. F. W. SEMMLER. Ber. **27**, 895 (1894).
24. J. L. SIMONSEN. The terpenes. Vol. I. Cambridge University Press. 1947. p. 395.
25. R. P. LINSTEAD, K. O. A. MICHAELIS, and S. L. S. THOMAS. J. Chem. Soc. 1139 (1940).
26. R. H. REITSEMA. J. Am. Pharm. Assoc., Sci. Ed. **47**, 267 (1958).

Can. J. Chem. Downloaded from www.nrcresearchpress.com by 210.87.254.5 on 09/05/12
For personal use only.

THE INHIBITED AUTOXIDATION OF STYRENE

PART II. THE RELATIVE INHIBITING EFFICIENCIES OF META- AND PARA-SUBSTITUTED PHENOLS[1]

J. A. HOWARD[2] AND K. U. INGOLD
Division of Applied Chemistry, National Research Council, Ottawa, Canada

Received January 7, 1963

ABSTRACT

The relative rates of reaction of 11 meta- and para-substituted phenols with styrylperoxy radicals have been measured at 65° C and have been shown to give an excellent correlation with electrophilic substituent constants. The reaction is compared with a number of similar hydrogen abstraction reactions.

INTRODUCTION

In Part I of this series (1) it was shown by means of the deuterium isotope effect that the reaction of styrylperoxy radicals with 2,6-di-*tert*-butyl-4-methylphenol (BMP) involved a straightforward abstraction of the phenolic hydrogen by the radicals. That is,

$$RO_2\cdot + AH \rightarrow ROOH + A\cdot , \qquad [6]$$

where AH represents the phenol. In order to obtain further information about this reaction a number of meta- and para-substituted phenols have now been examined at 65° C in the same system, i.e., as inhibitors of the α,α'-azo-bis-isobutyronitrile (AIBN) initiated oxidation of styrene. The relative inhibiting efficiencies, i.e. the relative k_6 values, have been measured and have been found to give an excellent correlation with Brown's electrophilic substituent constants (σ^+ constants) (2). The implication of this correlation on the nature of the transition state of reaction [6] is discussed and the reaction is compared with a number of similar hydrogen abstraction reactions.

RESULTS

The experimental techniques and the kinetic treatment of the data have been described in Part I (1). In the present work, the inhibited rate was generally kept between 1% and 10% of the uninhibited rate in order to avoid the kinetic complexities associated with the self-termination reaction,

$$RO_2\cdot + RO_2\cdot \rightarrow \text{inactive products.} \qquad [5]$$

Under these conditions, theory predicts (1) that,

$$P = \rho - (2e-1)k_1[I_2] = \frac{ek_1k_3[RH][I_2]}{k_6[AH]},$$

where ρ is the measured inhibited rate, e is the efficiency of radical production by the initiator I_2, k_1 is its rate constant for decomposition, k_3 is the propagation rate constant, and RH represents the styrene. Although this equation fits the data for inhibition by BMP fairly well (1) it does not fit the data for any of the simple, unhindered phenols studied in the present work. Instead, the measured value of k_6 appears to decrease as the phenol concentration is increased. That is, although $P/[I_2]$ is independent of $[I_2]$ at constant [AH], when experiments are performed at constant $[I_2]$ then P[AH] increases as

[1]*Issued as N.R.C. No. 7348.*
[2]*N.R.C. Postdoctoral Fellow 1961–1963.*

Can. J. Chem. Downloaded from www.nrcresearchpress.com by 210.87.254.105 on 09/05/12
For personal use only.

[AH] is increased. A plot of P against $[I_2]/[AH]$ therefore shows a rather bad scatter of the experimental points since both $[I_2]$ and [AH] are generally varied from experiment to experiment. The points tend to be concave towards the $[I_2]/[AH]$ axis since $[I_2]/[AH]$ will, in part, be increased by decreasing [AH]. Over a limited range of conditions the rate law could appear to have the form $P \propto [I_2]/[AH]^{\frac{1}{2}}$ (or even $P \propto ([I_2]/[AH])^{\frac{1}{2}}$ if $[I_2]$ were not varied appreciably) but neither of these expressions fit the data over a large range in [AH].* It is therefore dangerous to attempt to draw conclusions as to the mechanism of the inhibition reaction on the basis of inadequate kinetic data involving only comparatively small changes in the concentrations of I_2 and AH.

Since reaction [5] is unimportant under the present experimental conditions the apparent decrease in k_6 as the inhibitor concentration is increased may be due either to intermolecular hydrogen bonding of the phenol (which would decrease the availability of free phenol for the inhibition reaction) or to chain transfer reactions of the type

$$XC_6H_4O\cdot + RH \longrightarrow XC_6H_4\dot{O}RH \qquad [9a]$$

or

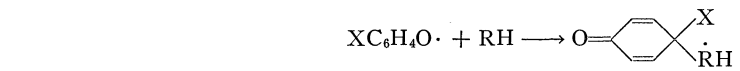

[9b]

or

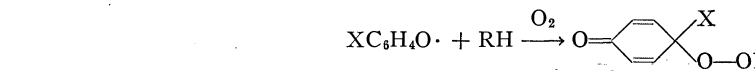

[9c]

That is, at high inhibitor concentrations these reactions will become of greater importance relative to the normal combination reaction

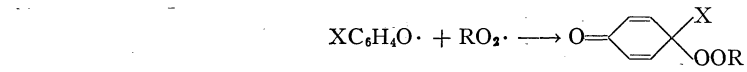

[7]

since, at constant $[I_2]$, the concentration of peroxy radicals will be decreased and the concentration of phenoxy radicals will be increased as [AH] increases. However, the destruction of phenol by direct oxidation or by reaction with an oxidation product is unlikely to account for this effect since the oxygen uptake curves would then show a fairly pronounced curvature whereas they are actually fairly good straight lines up to a phenol consumption of at least 20%. Whatever the causes of the apparent decrease in k_6 with increasing [AH] its true value can very easily be obtained from the measured values at different inhibitor concentrations by extrapolation to zero inhibitor concentration. A typical extrapolation is shown in Fig. 1, where the measured value of $1/k_6$ for phenol is plotted against the phenol concentration. Since a good straight line is obtained the limiting value of k_6 is found fairly accurately.† These k_6 values for a number of meta- and para-substituted phenols are given in Table I together with the slope of the line from which k_6 was obtained, i.e. slope $= [(1/k_6)_{[AH]} - (1/k_6)_{[AH]=0}]/[AH]$ in seconds. It can be seen that electron-releasing groups increase k_6 and decrease the slope. Rather high concentrations of 4-cyanophenol, the least active phenol studied, were required to reduce the rate to a reasonable fraction of its uninhibited value. For this reason, compounds such as 4-nitrophenol, which would be expected to be even less active, were not examined.

**It is interesting that similar equations are obtained under conditions where self-termination becomes of significant importance compared with reaction [6] (1).*

†k_6 values were calculated on the basis of the k_6 value obtained in Part I for BMP, *i.e. on the assumption $k_5 = 10^7$ liter/mole sec; then, for high concentrations of* BMP, *$k_6 = 7.95 \times 10^3$ liter/mole sec at 65°.*

Can. J. Chem. Downloaded from www.nrcresearchpress.com by 210.87.254.105 on 09/05/12
For personal use only.

TABLE I

k_6 for meta- and para-substituted phenols at 65° C based on k_6 (BMP) = 7.95×10^3 liter/mole sec

Substituent	σ^+	$k_6\times10^{-3}$ (liter/mole sec)	$\left(\frac{1}{k_6}\right)_{[AH]}-\left(\frac{1}{k_6}\right)_{[AH]=0}$ / [AH] (sec)
4-HO	−0.92	93.0	6.1×10^{-4}
4-CH_3O	−0.778	47.8	5.7×10^{-4}
4-CH_3	−0.311	9.17	1.3×10^{-3}
4-$C_2H_5(CH_3)_2C$	−0.250[a]	7.29	1.6×10^{-3}
4-$(CH_3)_3CCH_2(CH_3)_2C$	−0.248[a]	8.57	1.6×10^{-3}
3-CH_3	−0.066	3.07	2.9×10^{-3}
None	0.000	2.91	4.4×10^{-3}
3-CH_3O	0.047	2.57	7.4×10^{-3}
4-Cl	0.114	2.15	2.9×10^{-3}
3-Cl	0.399	0.56	4.9×10^{-2}
4-CN	0.659	0.29	4.3×10^{-1}

[a] σ^+constants estimated by the method outlined in reference 10 for E_s constants.

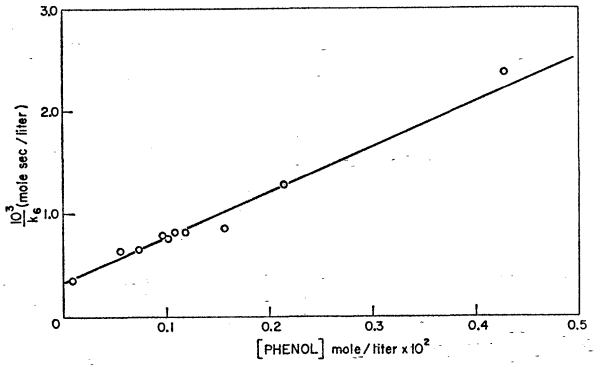

FIG. 1

The deuterium isotope effect on k_6 was examined for 4-*t*-amylphenol and phenol by the technique in which the phenol is maintained in its fully deuterated condition throughout the oxidation by the addition of heavy water (1). The results obtained with 4-*t*-amylphenol are rather more accurate than those obtained with phenol probably because of its lower solubility in water. For this phenol the limiting value of $(k_6)_D = 6.89\times10^2$ liter/mole sec, giving an isotope effect $(k_6)_H/(k_6)_D = 10.6$, in excellent agreement with the isotope effect found previously for BMP (1). Water has a negligible effect on $(k_6)_H$ and the slope for the light phenol; for the deuterated 4-*t*-amylphenol in the presence of D_2O the slope is 1.6×10^{-2} sec. In contrast, H_2O reduces the extrapolated value of k_6 for phenol to 2.1×10^3 liter/mole sec and reduces the slope to 3.2×10^{-3} sec. For deuterated phenol in the presence of D_2O the slope is 2.1×10^{-2} sec and $(k_6)_D = 1.4\times10^2$ liter/mole sec, giving an apparent isotope effect of 15. This rather large isotope effect may be due, in part, to experimental error arising from the high solubility of phenol in water.

An attempt to measure inhibitor stoichiometry (i.e. the number, n, of peroxy radicals destroyed by each inhibitor molecule) by the induction period method (1, 3) was frustrated by the discovery that n varied with inhibitor concentration. This is not too surprising since the apparent k_6 is a function of inhibitor concentration. However, it appears that a

Can. J. Chem. Downloaded from www.nrcresearchpress.com by 210.87.254.105 on 09/05/12
For personal use only.

second factor relating to the absolute magnitude of the true limiting k_6 may be even more important in determining apparent inhibitor stoichiometry. That is, the efficiency of radical production from AIBN, e, was found to be 0.74 at 65° with BMP as the inhibitor. As the concentration of BMP is decreased e at first stays constant but then also starts to decrease since self-termination by reaction [5] becomes important right from the start of the reaction. Therefore, to determine n for a less efficient inhibitor than BMP one must increase the concentration of this inhibitor to a point where reaction [5] is completely suppressed, i.e. to a point where the initial rate for a given AIBN concentration is at least as small as is found with the minimum concentration of BMP which gives a constant e. However, at 65° the uninhibited oxygen uptake curves are only linear for about 13,000 seconds owing to consumption of the AIBN. It is therefore impossible to suppress completely reaction [5] with a very weak inhibitor without adding so much that the inhibitor is not, itself, totally consumed before 13,000 seconds. For this reason measured values of n for inhibitors significantly weaker than BMP tend to be greater than the expected value of 2.0. This difficulty may well account for some of the non-integral stoichiometries greater than 2.0 reported by various authors (3, 4). It could probably be overcome by working at lower temperatures, where the half-life of the AIBN would be increased.

DISCUSSION

The limiting k_6 values given in Table I have, with the exception of hydroquinone, been plotted against the σ^+ substituent constants in Fig. 2. In the case of hydroquinone, k_6 has been halved to allow for the two hydroxyl groups. Both meta- and para-substituted phenols fall on a single line the equation for which is

$$\log_{10} k/k_0 = -0.010 - 1.49\sigma^+.$$

However, there seems to be some doubt as to the correct σ^+ constant for the 4-OH group (5). If the result for hydroquinone is excluded a rather better line of steeper slope is obtained which is given by

$$\log_{10} k/k_0 = 0.002 - 1.58_5\sigma^+.$$

Since σ^+ constants were mainly derived from the rates of hydrolysis of *tert*-cumyl chlorides (2) they give a measure of the effect of an aromatic nuclear substituent on the ease of formation of the transition state presumed to be involved in first-order solvolysis, i.e.,

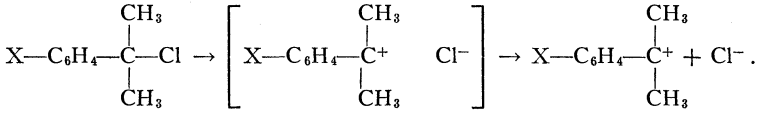

By analogy a similar transition state should be applicable to the reaction under study. That is, reaction [6] can be written

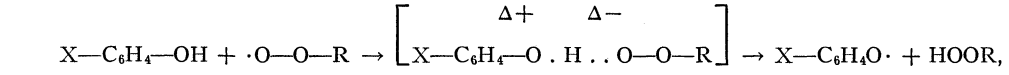

with the O—H bond becoming polarized to give at least a partial positive charge on the oxygen ($\Delta+$) and the electron being at least partially transferred to the attacking peroxy radical ($\Delta-$). However, in view of the very large deuterium isotope effect the rate-determining step cannot be an electron-transfer process, but it is not possible on the basis of kinetic evidence alone to decide whether electron transfer occurs prior to or during the

Can. J. Chem. Downloaded from www.nrcresearchpress.com by 210.87.254.105 on 09/05/12
For personal use only.

stretching of the O—H bond (6, 7). The excellent correlation by a single line of both meta- and para-substituted phenols, in particular 3-methyoxyphenol (8), indicates that there is no significant enhancement of resonance effects by meta substituents in this reaction (8).

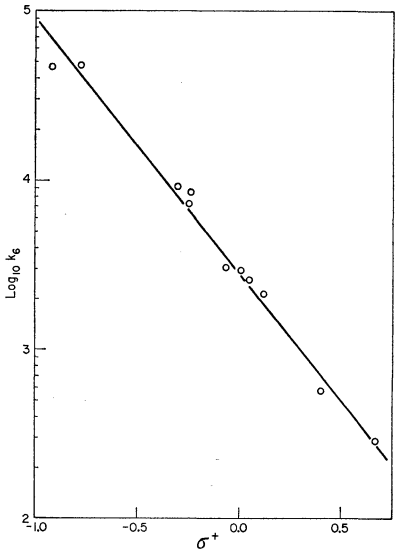

FIG. 2

The slopes of the lines from which limiting k_6 values are obtained very roughly obey the Hammett equation with $\rho \approx 2.2$ but with 3-chlorophenol showing a large positive deviation and 4-chlorophenol showing a large negative deviation (σ for 4-cyanophenol was taken as 1.00, and the other σ values were taken from McDaniel and Brown's compilation (9)). The positive sign of ρ is not unreasonable since the more acidic phenols may be expected to form stronger intermolecular hydrogen bonds. Alternatively, if the apparent decrease in k_6 with increasing inhibitor concentration is due chiefly to chain transfer it implies that the radical becomes more reactive the stronger the electron-withdrawing power of the substituents.

In some earlier work from this laboratory it was shown that the induction periods produced by 4-substituted-2,6-di-*tert*-butylphenols in a naphthenic hydrocarbon oil at 160° and at 140° C could be correlated extremely well by the Hammett σ constants and Taft steric substituent constants (E_s) of the group in the 4-position (10). The correlation with σ implies that under these conditions the transition state did not involve the formation of a phenoxy cation or partial phenoxy cation. It should, however, be added that owing to the apparent instability of 4-methoxy-2,6-di-*tert*-butylphenol at these reaction temperatures a highly polar transition state cannot be completely ruled out (11). Possible reasons for the differences in the two transition states are discussed below. The correlation with E_s, that is, the decreasing induction period associated with increasing size of the 4-alkyl substituents, was ascribed to a decrease in the rate of reaction [7] as the 4-position became sterically better protected. This effect appears to be of negligible importance in the present system probably both because of the smaller size of the peroxy radicals (i.e., they are secondary rather than tertiary as in the oil) and because of the unprotected nature of the ortho positions in these phenols.

Can. J. Chem. Downloaded from www.nrcresearchpress.com by 210.87.254.105 on 09/05/12
For personal use only.

The present data are compared in Table II with the available data for similar radical hydrogen abstraction reactions from compounds of the type XC_6H_4YH. This table includes the reactions, reaction temperatures, solvents, and the number of compounds used in the calculations. With the exception of reaction [2], compounds containing one or two ortho substituents have not been included in the determination of ρ. The original data have been recalculated in most cases* and the best correlation, i.e., that giving the smallest standard deviation (root mean square in $\log_{10}$ units), is given in heavy type. It can be seen that in aromatic solvents and in CCl_4 only reactions [7] and [14] are better represented by σ than by σ^+ and that for reactions [4] and [13] no distinction can properly be made.

There are several factors that might be expected to influence ρ, such as solvent (reactions [5] and [6]), temperature (reactions [10] and [11]), the nature of the attacking radical and the reactant, etc. Some of these effects are clearly brought out in this table but others still remain to be elucidated.

A change in ρ produced by a change in solvent might be due either to a change in the polarizability of the solvent or to a complexing of the radicals with the solvent, particularly if it is aromatic (27). It is difficult to evaluate the importance of the first factor from reactions [5] and [6] since benzene and CCl_4 have very similar polarizabilities. However, it would seem reasonable that an increase in the polarizability or dielectric constant of the solvent would tend to stabilize a charged transition state and thereby increase ρ, particularly for a reaction following σ^+ constants. Moreover, it is possible that a reaction following σ^+ constants in an aromatic system might follow σ constants in a less polarizable medium (cf. reactions [1] and [2] as a possible example of this phenomenon). If the radical complexes with the solvent one might expect a decreased sensitivity to polar effects, i.e., a decreased ρ, since polarization in the same direction will be involved in the complex as in the transition state. The overall reactivity of the radical will, of course, also be decreased by complexing. However, solvent effects must also depend on the nature of the attacking radical and reactant since, for reaction [12], ρ is the same in benzene as in CCl_4 even though chlorine atoms are known to complex with aromatic solvents (27). The possible importance of solvent effects suggests that ρ values obtained by competitive experiments in mixed reactants are less valuable than those obtained in a pure solvent since the polarizability of the medium will change as the reactants are changed.

The increase in ρ with decreasing temperature exemplified by reactions [10] and [11] appears to be a fairly general phenomena (28).

In addition to solvent effects, the magnitude of ρ for a given reactant may be expected to increase with increasing electron affinity of the attacking radical as originally proposed by van Helden and Kooyman (22). There is little or no evidence available at present to support this conclusion owing, in part, to the variety of solvents employed by different workers. However, it seems likely that this factor could become important in a series of reactions following σ^+ constants. Moreover, radicals with a very low electron affinity might follow σ rather than σ^+ constants. Reaction [7] may possibly be an example of this phenomenon. Similarly, the fact that reaction [15] definitely follows σ^+ constants whereas reactions [13] and [14] tend more to favor σ constants would also be in line with this suggestion.

For a given radical it seems probable that, in reaction series following σ^+ constants, ρ will increase with increasing polarizability of the YH bond, that is with increasing ease of formation of the $XC_6H_4Y^+H$ cation. Some evidence in favor of this is provided by a

**The difference in many of the ρ values listed in Table II and the values given in the original papers indicates that the method of least squares is "a custom more honour'd in the breach than the observance".*

Can. J. Chem. Downloaded from www.nrcresearchpress.com by 210.87.254.105 on 09/05/12
For personal use only.

Can. J. Chem. Downloaded from www.nrcresearchpress.com by 210.87.254.105 on 09/05/12
For personal use only.

TABLE II

Some typical hydrogen atom abstraction reactions

Reaction No.	Reaction	Solvent	No. of compounds used in calculations	σ		σ^+		Reference
				ρ	Std. deviation	ρ	Std. deviation	
1	$RO_2\cdot$ + phenols, 65°	Styrene	11[a]			**−1.49**	**0.024**	This work
			10[b]			**−1.58**$_5$	**0.016**	
2	$RO_2\cdot$ + 2,6-Bu_2^t phenols, 140°, 160°	Oil	7	**−1.01**[c]	**0.015**			10
3	$RO_2\cdot$ + phenols, 62.5°	Chlorobenzene		**−3.7**[d]				12
4	$RO_2\cdot$ + phenols, 44.4°	Methyl methacrylate	5	**−3.48**[e]	**0.114**	−2.28[e]	0.144	13
5	DPPH· + phenols, 30°	Benzene	13	−3.22	0.162	**−2.77**[f]	**0.090**	14
6	DPPH· + phenols, 20°	CCl_4	6	−6.4	0.301	**−4.54**	**0.064**	15
7	R· + thiophenols, 110°	Toluene	7	**−0.433**[g]	**0.008**	−0.287	0.025	16
8[h]	$RO_2\cdot$ + cumene, 60°	Chlorobenzene	6	−0.54	0.06	**−0.375**	**0.015**	17
9	$Cl_3C\cdot$ + toluene, 50°	Chlorobenzene	8			**−1.46**	**0.014**	19
10[i]	Br· + toluene, 80°	Benzene	6			**−1.39**	**0.03**	20
11	Br· + toluene, 19°	Benzene	4			**−1.78**	**0.06**	20
12[j]	Cl· + toluene, 40°	Benzene + CCl_4	8	−0.76	0.06	**−0.66**	**0.02**	17
13	$(CH_3)_3CO\cdot$ + toluene, 110°	γ-Picoline + reactant	4[k]	−0.741	0.037	**−0.646**	**0.030**	24
14	$(CH_3)_3CO\cdot$ + toluene, 40°	Reactants	5	**−0.821**	**0.008**	−0.695	0.015	25
15	$C_6H_5C(O)O\cdot$ + dibenzyl ether, 80–90°	Reactant	6	−0.957	0.047	**−0.647**	**0.016**	26

NOTE: The σ^+ constants have been taken from reference 2 and the σ constants from reference 9.

[a]With hydroquinone.

[b]Without hydroquinone.

[c]Of the 4-alkyl phenols, only 4-Me-2,6-Bu_2^t phenol was used in the calculations. 4-NO_2-2,6-Bu_2^t was not included and σ(4-CH_3O) was taken as −0.16 (10). ρ has been corrected for the observed 2/3 reaction order.

[d]The data are not in a form suitable to permit recalculation.

[e]Data not plotted by authors. Calculations based on 4-NO_2, 4-C_6H_5, 4-MeO, and 4-OH phenols and phenol. The reported efficiency for hydroquinone was not divided by 2.0.

[f]σ^+(4-CH_3CO) taken to equal σ(4-CH_3CO).

[g]σ(4-NO_2) taken as 1.00. 2,3-Benzo group not included in calculations.

[h]This data supersedes earlier data (18) for $RO_2\cdot$ + cumene, and $RO_2\cdot$ + toluene at 90° both in the reactants. The former gives σ correlation $\rho = -0.445 \pm 0.015$ and σ^+ correlation $\rho = -0.410 \pm 0.015$ and the latter gives a σ correlation $\rho = -0.756 \pm 0.035$ and $\sigma+$ correlation $\rho = -0.705 \pm 0.023$.

[i]This data supersedes the earlier work of Kooyman, van Helden, and Bickel (21) on Br· + toluene at 80° in CCl_4, and it is shown that virtually identical ρ values are obtained with Br_2, N-bromosuccinimide, N-bromotetrafluorosuccinimide, and N-bromotetramethylsuccinimide. van Helden and Kooyman's data give for Br_2 σ correlation $\rho = -1.33 \pm 0.062$, σ^+ correlation $\rho = -1.05 \pm 0.021$ and for N-bromosuccinimide σ correlation $\rho = -1.80 \pm 0.045$ and σ^+ correlation $\rho = -1.41 \pm 0.023$.

[j]This data supersedes the earlier work of van Helden and Kooyman (22) and Walling and Miller (23) on Cl· + toluene at 80° and 70°, in benzene and the reactants, respectively. The former workers' results give σ correlation $\rho = -1.32 \pm 0.043$, σ^+ correlation $\rho = -1.27 \pm 0.052$ and the latter workers' results give a σ correlation $\rho = -0.845 \pm 0.0196$ and a σ^+ correlation $\rho = -0.741 \pm 0.0203$.

[k]β-Picoline and γ-picoline were not included in the calculations. The value given for the 4-CH_3 group was not included either since it was derived from a comparison of cumene and *p*-cymene. In these two compounds the *tert*-hydrogen is abstracted and this hydrogen has a different local environment to that of a hydrogen atom in toluene (see text). The value given for the 4-CH_3 group is therefore not directly comparable with values given for the other substituted toluenes.

comparison of reaction [1] with reaction [8] since the OH bond is presumably more polarizable than the CH bond. Unfortunately the solvents are not identical but since they are both aromatic the comparison is probably justifiable.

The data given for $RO_2\cdot$ + toluene and $RO_2\cdot$ + cumene in footnote *h* to Table II suggests that there could be yet another factor influencing ρ since ρ is smaller for cumene than for toluene. This difference might be due to a smaller activation energy for hydrogen abstraction from cumene compared with toluene. However, it is also possible that this type of solvent effect arises from the local environment around the abstracted hydrogen. That is, in cumene the local environment will be more aliphatic in character than in toluene and will therefore be less polarizable and will presumably tend to give a smaller ρ. Some of our more recent work has shown that there is a similar decrease in ρ for reaction [1] when the phenols contain two ortho-alkyl groups. Such local environmental effects are known to be very important in determining the fundamental O—H stretching frequencies and intensities of sterically hindered phenols (29).

It is clear from the foregoing discussion that a great deal of further work on hydrogen abstraction reactions under carefully controlled conditions is required to elucidate the precise role of solvents in determining ρ. Further work is also needed to correlate ρ with radical electron affinities, with the ease of formation of the $XC_6H_4Y^+H$ cation, with the activation energies, and with the various steric and local environmental factors that may all play a part in the reaction mechanism and its transition state.

ACKNOWLEDGMENT

The authors wish to thank Dr. I. E. Puddington for his continuing interest and advice throughout the course of this work.

REFERENCES

1. J. A. Howard and K. U. Ingold. Can. J. Chem. **40**, 1851 (1962).
2. H. C. Brown and Y. Okamoto. J. Am. Chem. Soc. **80**, 4979 (1958).
3. C. E. Boozer, G. S. Hammond, C. E. Hamilton, and J. N. Sen. J. Am. Chem. Soc. **77**, 3233 (1955).
4. C. E. Boozer, G. S. Hammond, C. E. Hamilton, and C. Peterson. J. Am. Chem. Soc. **77**, 3380 (1955).
5. J. M. S. Tait, T. W. Shannon, and A. G. Harrison. J. Am. Chem. Soc. **84**, 4 (1962).
6. J. Kenner. Tetrahedron, **3**, 78 (1958); **8**, 350 (1960).
7. G. A. Russell. Tetrahedron, **5**, 101 (1959).
8. R. W. Taft, I. R. Fox, and I. C. Lewis. J. Am. Chem. Soc. **83**, 3349 (1961).
9. D. H. McDaniel and H. C. Brown. J. Org. Chem. **23**, 420 (1958).
10. K. U. Ingold. J. Phys. Chem. **64**, 1636 (1960).
11. K. U. Ingold. Chem. Rev. **61**, 563 (1961).
12. G. S. Hammond, C. E. Boozer, C. E. Hamilton, and J. N. Sen. J. Am. Chem. Soc. **77**, 3238 (1955).
13. R. G. Caldwell and J. I. Ihrig. J. Am. Chem. Soc. **84**, 2878 (1962).
14. J. S. Hogg, D. H. Lohmann, and K. E. Russell. Can. J. Chem. **39**, 1588 (1961).
15. J. C. McGowan, T. Powell, and R. Raw. J. Chem. Soc. 3103 (1959).
16. Y. Schaafsma, A. F. Bickel, and E. C. Kooyman. Rec. Trav. Chim. **76**, 180 (1957).
17. G. A. Russell and R. C. Williamson. Private communication.
18. G. A. Russell. J. Am. Chem. Soc. **78**, 1047 (1956).
19. E. S. Huyser. J. Am. Chem. Soc. **82**, 394 (1960).
20. R. E. Pearson and J. C. Martin. J. Am. Chem. Soc. **85**, 354 (1963).
21. E. C. Kooyman, R. van Helden, and A. F. Bickel. Koninkl. Ned. Akad. Wetenschap. Proc. Ser. B, **56**, 75 (1953).
22. R. van Helden and E. C. Kooyman. Rec. Trav. Chim. **73**, 269 (1954).
23. C. Walling and B. Miller. J. Am. Chem. Soc. **79**, 4181 (1957).
24. K. M. Johnston and G. H. Williams. J. Chem. Soc. 1446 (1960).
25. C. Walling and B. B. Jacknow. J. Am. Chem. Soc. **82**, 6113 (1960).
26. R. L. Huang, H. H. Lee, and S. H. Ong. J. Chem. Soc. 3336 (1962).
27. G. A. Russell. J. Am. Chem. Soc. **79**, 2977 (1957); **80**, 4987, 4997, 5002 (1958).
28. H. H. Jaffe. Chem. Rev. **53**, 191 (1953).
29. K. U. Ingold. Can. J. Chem. **40**, 111 (1962).

Can. J. Chem. Downloaded from www.nrcresearchpress.com by 210.87.254.105 on 09/05/12
For personal use only.

AROMATIC SUBSTITUTION

PART II. THE REACTION OF VARIOUS 3-SUBSTITUTED PYRIDINE DERIVATIVES AND OF QUINOLINE WITH PHENYLLITHIUM[1]

R. A. ABRAMOVITCH, K. S. AHMED, AND CHOO-SENG GIAM
Department of Chemistry, University of Saskatchewan, Saskatoon, Saskatchewan

Received March 7, 1963

ABSTRACT

Phenyllithium and pyridine-3-*N*,*N*-diethylsulphonamide gave the expected 2-phenyl derivative exclusively. Contrary to a previous report some 2,3-diphenylpyridine is formed with 3-phenylpyridine. No pyridyne intermediate seems to be formed in the reaction of phenyllithium with 3-bromopyridine. The reactions of phenyllithium with quinoline and with *N*-benzylpyridinium chloride have also been studied and are discussed.

In previous papers in this series (1, 2, 3) the reaction of phenyllithium with a number of 3-substituted pyridines was examined. With a 3-alkylpyridine (I) the main product was the 3-alkyl-2-phenylpyridine (II) when the alkyl group was methyl, ethyl, or isopropyl, but it was the 5-alkyl-2-phenylpyridine when the substituent was *t*-butyl. With nicotine (I; R = 2-*N*-methylpyrrolidyl) the isomer ratio was approximately 1:1. Two further examples were studied: R = NH_2 and R = OCH_3. In both cases the only isomer detected was the 2,3-disubstituted pyridine. It was suggested (2) that in these last two cases the exclusive substitution at the 2-position might be explained by assuming some coordination of the lithium atom with a pair of electrons on the 3-substituent such that the phenyl group would be suitably oriented for attack at the 2-position. No 4-phenylpyridine could be detected gas chromatographically in the reaction of phenyllithium with pyridine. A number of possible explanations were considered (3) to account for the observed orientation with 3-alkylpyridines.

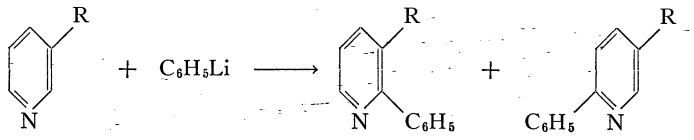

I II III

All the 3-substituents mentioned above are electron donating. The only reported example of such a reaction being carried out with a 3-substituted pyridine in which the 3-substituent may be considered to be electron attracting is that in which 3-phenylpyridine (I; R = C_6H_5) was the substrate used (4). In this case, and contrary to the expected electrical effect of a phenyl substituent group ($-I > +M$), it was reported that only 2,5-diphenylpyridine (III; R = C_6H_5) was isolated. It was postulated (1) that this might be attributed to steric inhibition of coplanarity in the transition state leading to the formation of the 2,3-isomer, whereas no such inhibition exists in the transition state for the 2,5-isomer. It seemed rather strange, though, that *no* 2,3-diphenylpyridine had been formed at all in this reaction. This has been reinvestigated. It was also important that the reaction of phenyllithium with 3-substituted pyridines in which the 3-substituent was electron attracting be studied: on the basis of simple electronic considerations (which fail to predict the correct behavior when R = CH_3, Et, or *i*-Pr (3)) it might be predicted that

[1]*Part I. Can. J. Chem.* **40**, *213 (1962).*

Can. J. Chem. Downloaded from www.nrcresearchpress.com by 210.87.254.6 on 09/05/12
For personal use only.

the 2,3-isomer should be formed predominantly in these cases. The choice of such a substituent was made difficult by the fact that most of the common electron-attracting groups (e.g. NO_2, CO_2R) themselves react with the organolithium reagent. It was decided to examine the reactions when R = SO_3CH_3 and Br, and also to try and determine whether coordination of the organolithium reagent at the pyridine nitrogen atom was important in determining the preferential orientation of the entering nucleophile, as had been suggested (5). The latter seemed unlikely since it has been reported that the reaction of benzylmagnesium chloride with 3,4-lutidine methiodide (where further coordination at nitrogen is not possible) gives the 1,2-dihydro-2-benzyl derivative (6). Other examples of such reactions are known (7). To this end it was decided to study the reaction of phenyllithium with *N*-benzylpyridinium chloride and with 3-methyl-*N*-benzylpyridinium chloride. Finally, it was suggested by Brown and Harcourt (8) that a "strong" nucleophilic reagent would attack the quinoline ring preferentially at $C_{(2)}$, whereas a "weak" one would attack it at the position of lowest nucleophilic atom localization energy, namely $C_{(4)}$. Phenyllithium is considered to be a strong nucleophile and it was, consequently, of interest to determine the orientation of the entering phenyl group with greater certainty than had been done before. Ziegler and Zeiser (9) carried out this reaction and obtained 2-phenylquinoline together with a small amount of a lower-melting compound which, they suggested but did not prove, was 4-phenylquinoline. Gilman and Gainer (10) repeated the reaction and obtained 2-phenylquinoline and 2,2-diphenyl-1,2-dihydroquinoline, but no 4-phenylquinoline. It was decided to re-examine this reaction and to attempt to detect by gas chromatographic analysis any 4-phenylquinoline formed.

Methyl 3-pyridinesulphonate (IV) could not be prepared by any of the standard reactions. Pyridine-3-sulphonic acid was recovered unchanged on treatment with diazomethane. When the acid chloride (V) was treated with methanolic sodium methoxide the betaine (VI) was obtained, identical with that prepared from potassium pyridine-3-sulphonate and methyl iodide in the presence of aqueous sodium hydroxide (11). It is conceivable that the required ester may have been formed in this reaction but that it underwent self-alkylation in the working-up process. Pyridine-3-*N*,*N*-diethylsulphonamide (VII) was used instead of the ester in the reaction with phenyllithium. When VII

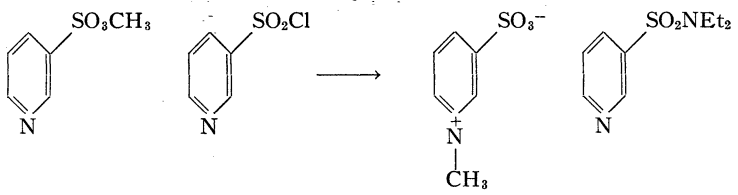

IV V VI VII

in excess was treated with phenyllithium and the product worked up by column chromatography only one product other than starting material was isolated, in low yield (20% based on phenyllithium). On the basis of its analysis and infrared spectrum (bands at 1578, 778, and 730 cm^{-1} (12, 13)) this is thought to be 2-phenylpyridine-3-*N*,*N*-diethylsulphonamide (II; R = SO_2NEt_2). No 2,5-isomer could be detected among the reaction products. The orientation observed is thus in accord with that expected on the basis of the electron-attracting character of the substituent.

The reaction of phenyllithium with 3-bromopyridine gave a mixture of neutral and basic products. Each of these fractions was analyzed by gas-phase chromatography. The neutral fraction was found to contain bromobenzene (43.4% of neutral components) together

Can. J. Chem. Downloaded from www.nrcresearchpress.com by 210.87.254.6 on 09/05/12
For personal use only.

with some biphenyl (some of which arises in the preparation of phenyllithium from bromobenzene) and an unknown product. No unreacted bromobenzene was present in the initial phenyllithium solution, however. The ether-soluble basic products were found to contain a small amount (1.8%) of 2-phenylpyridine together with a product which was different from 3-bromo-2-phenylpyridine (II; R = Br). A small amount of this substance was collected; its analysis was different from that expected for a bromophenylpyridine. Insufficient quantities were available to permit its structure to be investigated further at this time. Authentic 3-bromo-2-phenylpyridine could be prepared in low yield from 3-amino-2-phenylpyridine via the Sandmeyer reaction. A somewhat better yield (25.9%) was obtained by the use of Craig's perbromide hydrobromide method (14). Gilman and Spatz (15) similarly report (with L. Tolman) the isolation of 2-*p*-dimethylaminophenylquinoline from 3-bromoquinoline and *p*-dimethylaminophenyllithium. The reaction of 3-bromopyridine with butyllithium was shown (15) to give rise to a complex mixture of products. The 2-phenylpyridine and bromobenzene formed in the present reaction may arise as follows:

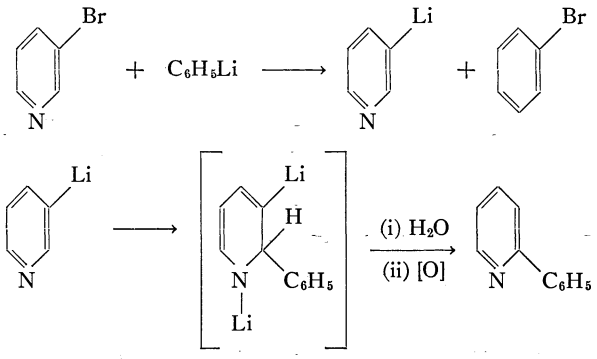

It is interesting to note that not only were no bromophenylpyridines isolated but neither was any 3- or 4-phenylpyridine detected gas chromatographically. This seems to rule out the formation of a 2- or 3-pyridyne intermediate in this case. In a recent report, Kauffmann and Boettcher (16) showed that the reaction of 3-chloro- or 3-bromo-pyridine with lithium piperidide and piperidine in ether involves the formation of a 3-pyridyne intermediate, with the resulting production of 3- (48%) and 4-piperidinopyridine (52%). Again, the formation of 4-phenacylpyridine and of 4-aminopyridine has been reported (17) in the reaction of 3-bromopyridine with sodioacetophenone and sodium in liquid ammonia, respectively, which has been postulated to take place by way of a pyridyne intermediate (VIII). Similarly, had a 2-pyridyne intermediate been formed one might have expected

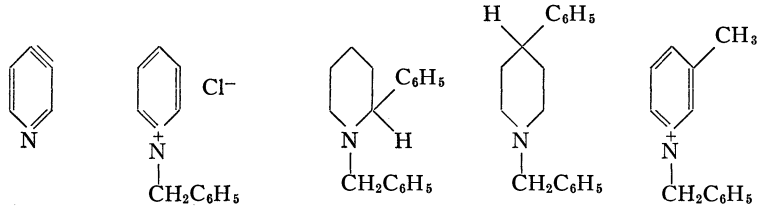

VIII IX X XI XII

some 3-phenylpyridine to be formed, particularly in view of the −I effect of the pyridine ring nitrogen atom (which would direct the entering nucelophile mainly to $C_{(3)}$ (see, for example, reference 18)).

The procedure reported (4) for the reaction of phenyllithium with 3-phenylpyridine

Can. J. Chem. Downloaded from www.nrcresearchpress.com by 210.87.254.6 on 09/05/12
For personal use only.

(I; R = C_6H_5) was modified somewhat in that a larger proportion of I (R = C_6H_5) compared with phenyllithium was used. Column chromatographic separation of the mixture of products formed confirmed that 2,5-diphenylpyridine (III; R = C_6H_5) was the main product formed (29% yield). A second product, m.p. 216–216.5° (5.7% yield), was also isolated which analyzed for a diphenylpyridine. That this was the expected 2,3-diphenylpyridine was established by a study of its n.m.r. spectrum in carbon disulphide solution. It exhibited a single proton doublet ($J_{\alpha\beta}$ 5 c.p.s.) centered at 534 c.p.s. (relative to tetramethylsilane as internal standard and using an oscillator frequency of 60 Mc/s) corresponding to H_α (1, 19), and another single proton doublet centered at 461 c.p.s. due to H_γ ($J_{\beta\gamma}$ 5 c.p.s.), which is only consistent with a 2,3-disubstituted pyridine derivative (the resolution was not high enough to separate the bands due to splitting between the α- and γ-protons). The n.m.r. spectrum of 2,5-diphenylpyridine was more complex because of the overlap of some of the phenyl proton peaks with the H_γ peak. The H_α proton peak consisted of a singlet at 530 c.p.s. whose intensity corresponded to that expected for one proton. A third fraction was isolated from the column chromatographic separation but this could neither be purified properly for analysis nor characterized at this time.

An ethereal suspension of *N*-benzylpyridinium chloride (IX) was treated with phenyllithium and the reaction products reduced catalytically (to change any dihydropyridines to the corresponding piperidine derivatives) and analyzed by gas chromatography. Most of the reaction products were high-boiling polymeric tars, which is not unexpected since the 1,2-dihydropyridine adduct is essentially a *cis*-butadiene system, which in this case, cannot aromatize under the conditions of the reaction and is formed in the presence of an efficient Zielger-type polymerization catalyst. The gas chromatogram consisted of four minor peaks followed by a fifth larger one. The latter was found to be due to *N*-benzyl-2-phenylpiperidine (X) (5.2% yield based on total reduction products). No peak corresponding to *N*-benzyl-4-phenylpiperidine (XI) or to either of the debenzylated products was detected. This is in contrast with the reaction of cyclopentadienyllithium with IX, which is reported to give the 4-substituted derivative (20) (it should be noted that in this case aromatization of the adduct to give the zwitterion is favored). When the phenyllithium reaction was carried out with *N*-benzyl-3-picolinium chloride (XII) only high-boiling tars were obtained. The preparation of authentic samples of *N*-benzyl-2- and -4-phenylpiperidine and of *N*-benzyl-3-methyl-2-phenylpiperidine is described in the Experimental section.

The reaction of phenyllithium with an excess of quinoline was examined next. Two products were detected by gas chromatography. The major product was, as expected, 2-phenylquinoline. The first, and very minor, peak corresponded to a compound whose retention time was different from that of authentic 4-phenylquinoline (21). A very small amount could be collected: its infrared spectrum and melting point (84–85° as compared with 61–62° for 4-phenylquinoline) were different from those of 4-phenylquinoline, whose presence was not detected among the reaction products. Similarly, no 2,2-diphenyl-1,2-dihydroquinoline appeared to be formed under these conditions. Unfortunately, insufficient quantities of the unknown component were obtained to permit any further structural work to be carried out. Though the possibility of an addition across the —C(H)=N— cannot be ruled out to explain the lack of formation of 4-phenylquinoline, with acridine, in which such an addition is not possible, phenyllithium gives 9,10-dihydro-9-phenylacridine readily (22).

EXPERIMENTAL

Melting points are uncorrected. Infrared spectra were measured on a Perkin–Elmer Model 21 spectrometer equipped with sodium chloride optics (only the main peaks are reported), and n.m.r. spectra on a Varian

Can. J. Chem. Downloaded from www.nrcresearchpress.com by 210.87.254.6 on 09/05/12
For personal use only.

A60 instrument, using carbon disulphide solutions of the compounds and tetramethylsilane as the internal standard. The oscillator frequency was 60 Mc/s.

Pyridine-3-*N,N*-diethylsulphonamide, m.p. 49–50°, was prepared according to the method of Zienty (23). 4-Phenylquinoline was prepared from β-chloropropiophenone as described by Kenner and Statham (21). 2-Phenylpyridine was prepared from pyridine and phenyllithium (24). 3-Phenylpyridine was obtained from the reaction of 3-pyridyllithium with cyclohexanone followed by dehydration and dehydrogenation (25). 2,2-Diphenyl-1,2-dihydroquinoline was prepared from 2-phenylquinoline and phenyllithium (10). 3-Amino-2-phenylpyridine was obtained by the reaction of phenyllithium on 3-aminopyridine (2). Treatment of dry pyridine with benzyl chloride gave *N*-benzylpyridinium chloride as a highly hygroscopic solid (26).

N-Methyl Betaine of Pyridine 3-Sulphonic Acid

(*a*) A solution of pyridine 3-sulphonyl chloride (4.54 g) in dry methanol (10.5 ml) containing sodium methoxide (from 0.60 g of sodium) was boiled under gentle reflux for 1 hour and then treated with water. The mixture was extracted repeatedly with ether, the ether layer washed with aqueous sodium bicarbonate and then with water, and the solvent evaporated to give the betaine as a pale yellow solid (0.6 g) which did not melt below 330° and was sparingly soluble in ether. (Calc. for $C_6H_7NO_3S$: C, 41.62; H, 4.08. Found: C, 41.79; H, 4.18.)

(*b*) Cf. Meyer (11). Potassium pyridine-3-sulphonate (0.8 g), 10% aqueous sodium hydroxide (1 ml), and methyl iodide (2 ml) were heated under reflux for 12 hours. The solution was evaporated to dryness and the residue recrystallized from hot water to give the betaine, m.p. > 330°, whose infrared spectrum was identical with that of the sample prepared above. Infrared spectrum (Nujol mull): 1646 (s), 1505 (s), 1235 (vs), 1215 (vs), 1135 (s), 1045 (vs), 1032 (vs), 820 (m), 720 (s), and 675 cm^{-1} (s).

Reaction of Phenyllithium with Pyridine-3-N,N-diethylsulphonamide

To a well-stirred solution of pyridine-3-*N,N*-diethylsulphonamide (18.2 g, 0.1 mole) in anhydrous ether (50 ml) and under nitrogen was added a solution of phenyllithium (0.05 mole, prepared from lithium and bromobenzene (3)) in dry ether (68 ml) at such a rate that the mixture boiled gently under reflux. At the end of the addition the ether was distilled off and simultaneously replaced with dry toluene. The solution was then boiled under reflux for 7.5 hours, cooled, treated with water, and extracted repeatedly with ether. The ether layer was extracted several times with hydrochloric acid, the acidic solution made strongly alkaline and extracted with several portions of ether. The dried (KOH) ether extract was evaporated and the residue chromatographed on a column of alumina (100 g). Elution with methanol (after preliminary elution with benzene and ether to remove unchanged VII) gave *2-phenylpyridine-3-N,N-diethylsulphonamide* as a waxy solid (2.8 g) which, after recrystallization from methanol, had m.p. 77–77.5°. (Calc. for $C_{15}H_{18}N_2O_2S$: C, 62.05; H, 6.25. Found: C, 62.12; H, 6.42.) Infrared spectrum (Nujol mull): 1578 (m), 1338 (s), 1155 (s), 778 (m), 730 (s), 700 (m), 690 (m), and 662 cm^{-1} (w).

3-Bromo-2-phenylpyridine

A solution of 3-amino-2-phenylpyridine (0.566 g) in 48% hydrobromic acid (2 ml) was cooled in an ice–salt mixture and bromine (0.8 ml) was added to it dropwise with stirring, when the solid orange perbromide separated. Sodium nitrite (1.0 g) in water (3 ml) was added with stirring at such a rate that the temperature remained at 0°. As the last of the sodium nitrite solution was added a vigorous evolution of gas occurred and the temperature rose to 10°. The reaction mixture was made strongly alkaline and steam-distilled, the distillate was extracted with ether, the ether extract dried (Na_2SO_4) and evaporated. The residue was distilled at 305–307° at 720 mm to give *3-bromo-2-phenylpyridine* (0.202 g) as a pale yellow liquid. (Calc. for $C_{11}H_8NBr$: C, 56.43; H, 3.44. Found: C, 56.74; H, 3.70.) Infrared spectrum (liquid film): 3030 (m), 1573 (s), 1432 (s), 1122 (s), 1088 (s), 1008 (s), 781 (s), 735 (s), and 682 cm^{-1} (s).

Reaction of Phenyllithium with 3-Bromopyridine

An ethereal solution of phenyllithium (28.5 ml, 0.0333 mole of phenyllithium, prepared from lithium and bromobenzene) was added dropwise under nitrogen to a stirred solution of 3-bromopyridine (15.8 g, 0.1 mole) in dry ether (100 ml). The mixture was stirred for another 2 hours, water was added followed by hydrochloric acid, the organic layer separated, and the aqueous layer extracted repeatedly with ether. The combined ether layers (A) containing the neutral products was concentrated and analyzed as described below. The acidic layer was basified with sodium hydroxide and extracted with ether. The ether extracts containing the basic material were evaporated, the residue distilled to remove unreacted 3-bromopyridine, and the residue (B) analyzed.

Fraction (A) was subjected to gas chromatography using a 3 ft×1/4 in. column packed with Apiezon N on Fluoropak (80–100 mesh) (1:10 by weight); the column temperature was 160° and the helium inlet pressure 30 p.s.i. Three peaks were observed, the first (retention time 1 min 20 sec) due to bromobenzene (43.4% of total neutral products), the second to biphenyl (retention time 12 min 40 sec), and the third to an unknown substance (retention time 29 min 20 sec).

Fraction (B) was subjected to gas chromatography on an 8 ft×1/4 in. column packed with ethylene glycol succinate on Chromosorb (1:10 by weight). The column temperature was 160° and helium inlet pressure 40 p.s.i. Two peaks were observed: the first (retention time 21 min 20 sec) was due to 2-phenylpyridine

Can. J. Chem. Downloaded from www.nrcresearchpress.com by 210.87.254.6 on 09/05/12
For personal use only.

(characterized by its retention time, infrared and ultraviolet spectra) (1.8% yield based on total amount of basic product); the second (retention time 44 min) was due to a compound of unknown structure. A small amount of the latter product was collected and analyzed: Found: C, 72.27; H, 5.94. Under these conditions the retention time of 3-bromo-2-phenylpyridine was 50 min. No 3- or 4-phenylpyridine could be detected.

Reaction of Phenyllithium with 3-Phenylpyridine

A solution of phenyllithium (0.0182 mole) in dry ether (47 ml) was added dropwise under nitrogen to a well-stirred solution of 3-phenylpyridine (3 g, 0.0193 mole) in ether (150 ml). The mixture was stirred for a further 24 hours and oxygen was then bubbled through the reaction mixture for 30 minutes. An excess of water was added and the mixture extracted exhaustively with ether. The dried (Na_2SO_4) ether extract was evaporated and the residue chromatographed on a column of alumina (110 g). Elution with light petroleum (b.p. 40–60°) – benzene mixture (4:1 v/v) gave 2,5-diphenylpyridine (0.947 g), m.p. 174–175° after recrystallization from alcohol. Wiley *et al.* (25) report m.p. 174–175° for this compound. Elution with light petroleum – benzene (1:1 v/v) gave unreacted 3-phenylpyridine (1.003 g). Elution with benzene – ether (4:1 v/v) brought down *2,3-diphenylpyridine* (0.169 g), which gave a bluish fluorescence in this solvent mixture. It was recrystallized from a benzene – light petroleum (b.p. 40–60°) mixture and had m.p. 216–216.5°. (Calc. for $C_{17}H_{13}N$: C, 88.28; H, 5.60. Found: C, 88.40; H, 5.61.) Infrared spectrum (KBr disk): 3060 (m), 1600 (m), 1538 (m), 1500 (m), 1457 (m), 1428 (m), 1121 (s), 903 (m), 800 (m), 767 (s), 748 (s), 698 (s), 678 cm^{-1} (m). Elution with ether and ethyl acetate gave a yellow powder (0.531 g), m.p. 112–113°, which could not be purified further. Infrared spectrum (KBr disk): 3090 (m), 1684 (s), 1610 (m), 1505 (s), 1465 (s), 758 (s), 698 cm^{-1} (s). The n.m.r. spectrum of this compound exhibited none of the peaks usually associated with pyridine ring protons.

2-Phenylpiperidine (27)

2-Phenylpyridine (1 g) in 1.1 *N* hydrochloric acid (6.6 ml) and 95% ethanol (50 ml) was reduced at atmospheric pressure in the presence of platinic oxide (50 mg). The catalyst was filtered off, the solvent evaporated, and the residue treated with dilute sodium hydroxide solution and extracted with ether. The dried (Na_2SO_4) ether extract was evaporated and the residue distilled to give 2-phenylpiperidine (0.855 g), b.p. 246–248° at 726 mm. Ushakov and Promyslov (27) give b.p. 255–256° at 766 mm for this compound.

4-Phenylpiperidine

This was prepared similarly by the reduction of 4-phenyl-1,2,3,4-tetrahydropyridine (28). The yield of product, b.p. 250–252° at 720 mm, was 74%. It had previously been prepared by the reduction of 4-phenylpyridine (29) and the reported boiling point was 255–257° at 727 mm.

N-Benzyl-2-phenylpiperidine

2-Phenylpiperidine (0.683 g) and benzyl chloride (0.53 g) were heated at 120–160° for 1/2 hour, the mixture was cooled, treated with dilute sodium hydroxide solution, and extracted with ether. The dried (Na_2SO_4) ether extract was evaporated, yielding *N-benzyl-2-phenylpiperidine* (0.728 g), which crystallized from ethanol and had m.p. 93–93.5°. (Calc. for $C_{18}H_{21}N$: C, 86.01; H, 8.42. Found: C, 86.00; H, 8.60.)

N-Benzyl-4-phenylpiperidine

Prepared in the same way as the 2-isomer it was obtained as a yellow oil, b.p. 149–150° at 0.4 mm. Boggiano, Petrov, Stephenson, and Wild (30), who prepared this compound by the reduction of *N*-benzyl-4-phenyl-4-propionoxypiperidine, report its b.p. as 151° at 0.4 mm.

Reaction of Phenyllithium with N-Benzylpyridinium Chloride

To a well-stirred suspension of *N*-benzylpyridinium chloride (15.87 g, 0.154 mole) in dry ether under nitrogen was added an ethereal solution of phenyllithium (0.077 mole) during 1/2 hour. The reaction mixture was stirred for 24 hours under nitrogen, treated with water, and extracted repeatedly with ether. The dried (Na_2SO_4) ether extract was evaporated to give a viscous dark red residue (11.82 g). A portion of this (1.18 g) was dissolved in a mixture of 95% ethanol (60 ml) and 1.1 *N* hydrochloric acid (4.8 ml) and hydrogenated at room temperature and pressure over platinic oxide. Uptake of hydrogen was very slow. The hydrogenated product was subject to gas chromatographic analysis on a 3 ft×1/4 in. Apiezon N on Fluoropak (80–100 mesh) (1:10 w/w) column operated at 220° and with a helium inlet pressure of 30 p.s.i. Five peaks were observed, the last one (retention time 15 min 15 sec) being due to *N*-benzyl-2-phenylpiperidine (5.2% yield based on reduced products) (retention time and infrared spectrum). The retention times and spectra of the compounds giving rise to the first four peaks were quite different from those of 2- and 4-phenylpiperidine and *N*-benzyl-4-phenylpiperidine. These substances were not investigated further.

3-Methyl-2-phenylpiperidine

This was prepared by catalytic reduction of 2-phenyl-3-picoline (1). The *product* (76.2% yield), b.p. 256–257° at 724 mm, was purified for analysis by gas chromatography using a 5 ft×1/4 in. 10% Apiezon N on Fluoropak column, followed by redistillation, but could not be obtained in an analytically pure state. (Calc. for $C_{12}H_{17}N$: C, 82.23; H, 9.78. Found: C, 80.55; H, 9.26.) Infrared spectrum (liquid film) 1497 (m), 1457 (s), 1383 (m), 1277 (m), 1130 (m), 1088 (m), 875 (m), 827 (s), 696 cm^{-1} (s).

Can. J. Chem. Downloaded from www.nrcresearchpress.com by 210.87.254.6 on 09/05/12
For personal use only.

N-Benzyl-3-methyl-2-phenylpiperidine

3-Methyl-2-phenylpiperidine (0.876 g; redistilled) and benzyl chloride at 120–160° for 1 hour gave, in a manner similar to that described for the unmethylated compound, *N-benzyl-3-methyl-2-phenylpiperidine* (0.8 g), b.p. 176–180° at 6 mm, m.p. 69–69.5° (after recrystallization from absolute alcohol). (Calc. for $C_{19}H_{23}N$: C, 85.92; H, 8.75. Found: C, 85.71; H, 8.92.) Infrared spectrum (KBr disk): 1610 (m), 1502 (s), 1462 (s), 1379 (m), 1272 (m), 1230 (m), 1142 (s), 738 (s), and 694 cm^{-1} (s).

Reaction of Phenyllithium with Quinoline

A solution of phenyllithium (0.024 mole) in dry ether (150 ml) was added dropwise under nitrogen to quinoline (9.29 g, 0.072 mole; purified via the zinc chloride complex) in dry ether (20 ml). When the addition was complete the ether was distilled off and simultaneously replaced by dry toluene (60 ml). The mixture was then boiled under reflux for 6 1/2 hours, the solution cooled and treated with water, and the toluene layer separated and extracted with hydrochloric acid. The acid layer was basified, extracted with ether, and the dried (NaOH) ether extract evaporated. The excess quinoline was distilled at 80° at 0.35 mm and the residue (1.434 g) analyzed by gas chromatography. A 3 ft × 1/4 in. 10% Apiezon N on Fluoropak column was used at a temperature of 220° and a helium inlet pressure of 45 p.s.i. Only two peaks, with retention times of 9.9 and 14.4 min, were observed. The latter (major peak) was due to 2-phenylquinoline (retention time and infrared spectrum). The first peak had a retention time and infrared spectrum different from that of 4-phenylquinoline. A small sample was collected and had m.p. 84–85°. Infrared spectrum (KBr disk): 1587 (s), 1494 (s), 1393 (s), 850 (m), 766 (s), and 698 cm^{-1} (s). This substance was not investigated further at this time.

ACKNOWLEDGMENTS

The authors are grateful to the National Research Council for financial support of this work and for the award of a studentship to C-S. G.

REFERENCES

1. R. A. Abramovitch, Giam Choo Seng, and A. D. Notation. Can. J. Chem. **38**, 761 (1960).
2. R. A. Abramovitch and A. D. Notation. Can. J. Chem. **38**, 1445 (1960).
3. R. A. Abramovitch and Choo-Seng Giam. Can. J. Chem. **40**, 213 (1962).
4. R. H. Wiley, C. H. Jarboe, P. X. Callahan, and J. T. Nielsen. J. Org. Chem. **23**, 780 (1958).
5. M. S. Howie. Ph.D. Thesis, Purdue University, Lafayette, Ind. 1960.
6. E. L. May and E. M. Fry. J. Org. Chem. **22**, 1366 (1957).
7. N. B. Eddy, J. G. Murphy, and E. L. May. J. Org. Chem. **22**, 1370 (1957). M. Freund and G. Bode. Ber. **42**, 1746 (1909).
8. R. D. Brown and R. D. Harcourt. J. Chem. Soc. 3451 (1959).
9. K. Ziegler and H. Zeiser. Ann. **485**, 174 (1931).
10. H. Gilman and G. C. Gainer. J. Am. Chem. Soc. **69**, 877 (1947).
11. H. Meyer. Monatsh. **24**, 195 (1903).
12. R. A. Abramovitch, Giam Choo Seng, and A. D. Notation. Can. J. Chem. **38**, 624 (1960).
13. H. E. Podall. Anal. Chem. **29**, 1423 (1957).
14. L. C. Craig. J. Am. Chem. Soc. **56**, 231 (1934).
15. H. Gilman and S. M. Spatz. J. Org. Chem. **16**, 1485 (1951).
16. T. Kauffmann and F. Boettcher. Chem. Ber. **95**, 1528 (1962).
17. R. Levine and W. W. Leake. Science, **121**, 780 (1955).
18. J. D. Roberts, D. A. Semenow, H. E. Simmons, Jr., and L. A. Carlsmith. J. Am. Chem. Soc. **78**, 601 (1956).
19. L. M. Jackman. Applications of nuclear magnetic resonance spectroscopy to organic chemistry. Pergamon Press, New York. 1959. p. 64.
20. D. N. Kursanov, N. K. Baranetskaya, and V. N. Setkina. Dokl. Akad. Nauk SSSR, **113**, 116 (1957). D. N. Kursanov and N. K. Baranetskaya. Bull. Acad. Sci. USSR, Div. Chem. Sci. **9**, 1586 (1961).
21. J. Kenner and F. S. Statham. J. Chem. Soc. **63**, 299 (1935).
22. E. Bergmann, O. Blum-Bergmann, and A. F. Von Christiani. Ann. **483**, 80 (1930).
23. M. F. Zienty. J. Am. Pharm. Assoc., Sci. Ed. **37**, 97 (1948).
24. J. C. W. Evans and C. F. H. Allen. Organic syntheses. Collective Vol. II. John Wiley & Sons. 1943. p. 517.
25. R. H. Wiley, P. X. Callahan, C. H. Jarboe, Jr., J. T. Nielsen, and B. J. Wakefield. J. Org. Chem. **25**, 366 (1960).
26. K. Tsuda, Y. Sato, and S. Saeki. Pharm. Bull. (Tokyo), **1**, 307 (1953); Chem. Abstr. **49**, 10946g (1955).
27. M. I. Ushakov and M. Sh. Promyslov. J. Gen. Chem. USSR, **17**, 1015 (1947); Chem. Abstr. **42**, 4584b (1948).
28. C. J. Schmidle and R. C. Mansfield. J. Am. Chem. Soc. **78**, 1702 (1956).
29. H. Adkins, L. F. Kuick, M. Farlow, and B. Wojcik. J. Am. Chem. Soc. **56**, 2427 (1934).
30. B. G. Boggiano, V. Petrow, O. Stephenson, and A. M. Wild. J. Chem. Soc. 1143 (1959).

Can. J. Chem. Downloaded from www.nrcresearchpress.com by 210.87.254.6 on 09/05/12
For personal use only.

ISOTOPE EFFECT STUDIES ON ELIMINATION REACTIONS

III. NITROGEN ISOTOPE EFFECTS IN THE E2 REACTION OF ETHYLTRIMETHYLAMMONIUM AND 2-PHENYLETHYLTRIMETHYLAMMONIUM IONS[1]

G. AYREY,[2] A. N. BOURNS, AND V. A. VYAS[3]

Department of Chemistry, Hamilton College, McMaster University, Hamilton, Ontario

Received February 14, 1963

ABSTRACT

Nitrogen isotope effects have been determined for the E2 reaction of two quaternary ammonium salts with ethoxide ion in ethanol. Ethyltrimethylammonium iodide gave k^{14}/k^{15} values of 1.017 at 60° and 1.015 at 95°, while 2-phenylethyltrimethylammonium bromide gave 1.012 at 40° and 1.009 at 60°. These results and the β-deuterium isotope effects reported by others have been interpreted in terms of the relative extent of C_α—N^+ and C_β—H bond weakening in the transition states of the two reactions.

Can. J. Chem. Downloaded from www.nrcresearchpress.com by 210.87.254.5 on 09/05/12
For personal use only.

INTRODUCTION

Although it was recognized by Ingold as early as 1927 (1) that bimolecular β-elimination reactions need not be fully synchronous processes, it has only been in recent years that the concept of a continuous spectrum of E2 reactions differing in the relative extent of C_α—X and C_β—H bond rupture in the transition state has been invoked to account for observed phenomena (2–13). The various factors, structural and environmental, which

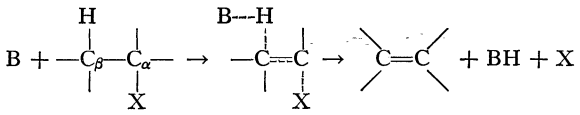

can be expected to influence the nature of the transition state have been discussed very recently by Bunnett (14), who, along with others (15, 16), has critically examined the limited number of tests now available for assessing the position of any particular elimination in the spectrum of E2 mechanisms.

Possibly the most definitive test is that based on the effect of isotopic mass of H and of X on reaction rate, i.e., the kinetic isotope effect. Although isotope effect theory has not been developed to the point that the magnitude of the isotope effect observed in an individual reaction can be used as any more than a semiquantitative measure of bond weakening in the transition state, a *comparison* of the isotope effects observed in a reaction series can allow certain conclusions to be drawn with respect to the influence of structural changes on the relative extent of bond rupture as one proceeds from reactant to reactant within the series. A complication arises, however, in the case of hydrogen isotope effects as a consequence of the fact that theory predicts (17, 18) a maximum effect when the proton is half transferred to the base at the transition state. If, then, for each of two related reactions, the proton is less than half transferred, that reaction showing the larger isotope effect will have the greater C_β—H bond weakening in the transition state. On the other hand, if the proton is more than half transferred at the transition state the relationship between the magnitude of the isotope effect and the extent of C_β—H bond rupture will be the reverse of this. Indeed, it is possible for two reactions to give rise to similar

[1]*Part II: G. Ayrey, E. Buncel, and A. N. Bourns. Proc. Chem. Soc. 458 (1961).*
[2]*Present address: Isotope Unit, Queen Elizabeth College, University of London, London, England.*
[3]*Present address: Rajkot, Bombay State, India.*

hydrogen isotope effects and yet differ markedly in the extent of C_β—H bond weakening at the transition state since this state for one reaction may be reached before the point of half transfer and for the other after half transfer. It is only when other considerations indicate that the transition states for both reactions find themselves on a particular side of the symmetrical situation that isotope effects give an indication of relative extents of C_β—H bond rupture. Alternatively, if it is known on the basis of other measurements, in particular, substituent effects on reaction rates, how C_β—H bond weakening at the transition state changes from reactant to reactant, then the direction of the variation in isotope effects will show the extent of proton transfer to base (14).

No such complication arises with respect to the isotope effect associated with the atom of the leaving group X which is attached to the α-carbon since this atom, unlike hydrogen, is not undergoing a three-center displacement. The magnitude of the isotope effect will therefore depend on the extent to which the composite force constant of the C—X bond is decreased in going from initial to the transition state (19). In other words, the X-isotope effect can be expected to increase regularly in a reaction series with the extent of bond weakening in the transition state. In spite of this straightforward relationship, few studies of X-isotope effects in elimination reactions have been reported. The reason for this is obvious. The effects are very small, amounting to never more than a few percent, and they require for their measurement very high precision mass spectrometry. When the necessary precision is achieved, however, the results can contribute in a significant way to our understanding of the nature of the transition state.

The first investigation of this kind was made by Saunders (20), who reported for the reaction of 2-phenylethyldimethylsulphonium ion with hydroxide ion in aqueous solution the extremely small sulphur isotope effect, k^{32}/k^{34}, of 1.0015, a value which may be compared to 1.018 in the S_N1 reaction of *t*-butyldimethylsulphonium ion. This result clearly indicates that the force constant of the C—S bond in the sulphonium salt elimination is essentially unchanged at the transition state and, together with the observed hydrogen isotope effect of 5.9 at 30° C (5) and a Hammett rho of +2.21 (21) for a series of phenyl-substituted sulphonium salts, it establishes that the transition state for the reaction possesses carbanionic character.

A similar study has been carried out in our laboratories on the $E_{CO}2$ elimination reaction of benzyl nitrate to benzaldehyde (15). The combination of a normal nitrogen isotope effect, k^{14}/k^{15}, of 1.020 and a hydrogen isotope effect of 5.0 at 60° indicates that both C_β—H and C_α—N bond rupture are well advanced at the transition state, although the large Hammett rho value of +3.4 (22) for the reaction shows that the former bond change is running ahead of the second.

We have now undertaken a study of the nitrogen isotope effect in the Hofmann elimination reaction of quaternary ammonium salts. This system has an advantage over the sulphonium salt studied by Saunders (20) since N^{14}:N^{15} isotope effects can be expected to be about twice as large as S^{32}:S^{34} effects (19) for the same extent of bond weakening at the transition state and can readily be measured with a precision of better than ±0.1%. The present paper reports the results obtained for the E2 reaction of ethyltrimethylammonium ion and 2-phenylethyltrimethylammonium ion with ethoxide ion in ethanol. The latter is the nitrogen analogue of the sulphonium salt studied by Saunders (20). Since the β-hydrogen isotope effects for the elimination reaction of both ammonium salts have already been reported (4, 5) the results of the present study make it possible to test the predictions of Bunnett (14) on the effect of a β-aryl group on the relative timing of the two bond changes.

Can. J. Chem. Downloaded from www.nrcresearchpress.com by 210.87.254.5 on 09/05/12
For personal use only.

EXPERIMENTAL

Materials

Ethyltrimethylammonium iodide.—The product formed by reaction at room temperature of equimolar quantities of trimethylamine and ethyl iodide in ethanol was repeatedly recrystallized from ethanol; m.p. 336° decomp.

2-Phenylethyltrimethylammonium bromide.—2-Phenylethyldimethylamine, prepared by the method of Icke *et al.* (23), was reacted with methyl bromide in benzene solution and the product was recrystallized several times from a methanol–water mixture; m.p. 251–252°.

Nitrogen Isotope Effect Measurements

The nitrogen isotope effects were obtained by comparing the nitrogen isotopic abundance in the trimethylamine formed in reactions carried to some small known extent of completion (7–20%) with the isotopic abundance in the starting compound. Isotopic analyses were performed mass spectrometrically on nitrogen gas samples prepared by oxidation of ammonia formed by Kjeldahl digestion of the quaternary salts and of the trimethylamine product. Compounds containing the natural abundance of the nitrogen isotopes were used throughout.

(a) Preparation of Nitrogen Samples from the Quaternary Ammonium Salts

Quaternary ammonium salt (ca. 0.2 mmole) was weighed into a 25-ml Kjeldahl flask, water (1.0 ml), 30% AnalaR hydrogen peroxide (0.5 ml), and sulphuric acid (0.5 ml) were added, and the mixture was boiled to expel the liberated iodine. After removal of most of the water by distillation, potassium sulphate (1.5 g), mercuric oxide (0.1 g), and sulphuric acid (2.5 ml) were added and the mixture digested in the usual way for 8 to 9 hours. Ammonia was liberated by addition of sodium hydroxide and distilled into excess standard sulphuric acid (average yield 97%).

The ammonium sulphate solution was concentrated to about 3 ml and then transferred to a high-vacuum system (Fig. 1) where, after thrice degassing in A, it was oxidized to nitrogen gas using degassed aqueous

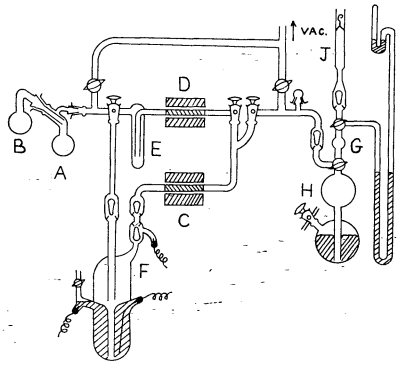

FIG. 1. Apparatus for preparation of nitrogen samples for mass spectrometric analysis.

sodium hypobromite (24, 25) transferred from B. The nitrogen was purified by repeated cycling by means of an automatic Urry Toepler pump (26), F, over copper (reduced oxide wire), C, and copper oxide wire, D, both at 750°, and through a trap, E, cooled in liquid nitrogen. After purification the gas was transferred to a standard volume, G, by means of the manual Toepler pump, H, where the yield (>95%) was determined. Finally, the nitrogen was pumped into the breakseal tube, J, which was then sealed. The need for such purification of nitrogen for precise mass spectrometry has been stressed by Hoering (27), and we can confirm that, in addition to the obvious interference by carbon monoxide at mass 28, the presence of oxygen has a deleterious effect upon the stability of the mass spectrometer.

(b) Partial Reactions and Preparation of Nitrogen Samples from Trimethylamine

Quaternary ammonium salt (ca. 2 mmole) was weighed into flask K (Fig. 2(*a*)) which was then restricted as shown. The required amount of alcoholic base (KOH in 95% ethanol or C_2H_5ONa in absolute ethanol) was added and the flask quickly attached to a vacuum manifold and cooled in liquid nitrogen. After triple degassing, the vessel was sealed and placed in a thermostatted bath for a predetermined time. The flask was then removed from the bath, cooled, opened, and the trimethylamine distilled into a liquid nitrogen cooled trap, L, (Fig. 2(*b*)) at below 0.1 mm pressure and 0° during 15–20 minutes. From time to time ethanol was added from the funnel, M, to avoid undue concentration of reactants. This distillation procedure was rigorously tested and it was shown that removal of trimethylamine was quantitative and no significant further reaction occurred during the time required. Trap L was then disconnected, stoppered at P, and the

Can. J. Chem. Downloaded from www.nrcresearchpress.com by 210.87.254.5 on 09/05/12
For personal use only.

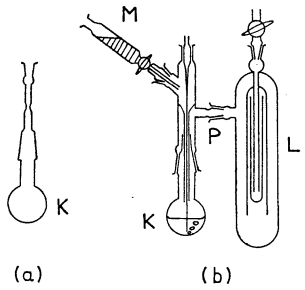

FIG. 2. (*a*) Apparatus for partial reactions.
(*b*) Apparatus for recovery of product.

trimethylamine and ethanol were distilled *in vacuo* into excess standard sulphuric acid, which was back titrated with standard alkali. The trimethylammonium sulphate solution was treated with sulphuric acid (1.0 ml), evaporated to a volume of about 1 ml, and transferred to a Kjeldahl flask for digestion. Nitrogen gas was prepared from the resulting ammonia by the method already described.

Mass Spectrometry and Evaluation of the Isotope Effect

The mass spectrometric analyses were carried out using a 90° sector-type instrument similar to one described by Wanless and Thode (28). It was capable of measuring *relative* isotopic abundance ratios, $N^{14}N^{14}/N^{14}N^{15}$, to ±0.02%. Twice the mass 28/29 ratio is equal to the N^{14}/N^{15} ratio in the compound degraded.

The kinetic isotope effect was calculated from the expression (29)

$$k^{14}/k^{15} = \frac{\ln (1-f)}{\ln (1-rf)},$$

where

$$r = \frac{(N^{14}/N^{15})_{\text{reactant}}}{(N^{14}/N^{15})_{\text{amine}}} = \frac{(N^{14}N^{14}/N^{14}N^{15})_{\text{reactant}}}{(N^{14}N^{14}/N^{14}N^{15})_{\text{amine}}}$$

and f is the fractional extent of reaction as determined by the trimethylamine yield.

RESULTS

The nitrogen kinetic isotope effect results for the Hofmann elimination reaction of 2-phenylethyltrimethylammonium ion and ethyltrimethylammonium ion are given in Table I. In the calculation of the individual k^{14}/k^{15} values, the $N^{14}N^{14}/N^{14}N^{15}$ ratios found for the nitrogen gas formed from a quaternary salt were averaged and the resulting value was combined in the above equation with the individual $N^{14}N^{14}/N^{14}N^{15}$ ratios for the nitrogen gas produced from the trimethylamine formed in each partial reaction of that salt. Although most partial reactions were carried out using as base sodium ethoxide in absolute ethanol, a few experiments were done using potassium hydroxide in 95% ethanol. A comparison of the results of experiments 14 and 15 with those of 16, 17, and 18 shows that, within the limits of measurement, the isotope effect is the same under the two reaction conditions. As a consequence no distinction is made between the two in the subsequent discussion.

DISCUSSION

Comparison of the E2 Reactions of 2-Phenylethyltrimethylammonium and 2-Phenylethyldimethylsulphonium Ions

In Table II are listed the nitrogen isotope effect found in the present study for the E2 reaction of 2-phenylethyltrimethylammonium ion in ethanol at 60° C, the sulphur isotope effect reported by Saunders (20) for reaction of the corresponding sulphonium ion in

Can. J. Chem. Downloaded from www.nrcresearchpress.com by 210.87.254.5 on 09/05/12
For personal use only.

TABLE I

N^{14}/N^{15} ratios and kinetic isotope effects in the E2 reaction of quaternary ammonium salts with sodium ethoxide in ethanol

Expt. No.	Reaction temp. (°C)	Extent of reaction (%)*	$N^{14}N^{14}/N^{14}N^{15}$ ratios†	k^{14}/k^{15}‡
		2-Phenylethyltrimethylammonium bromide		
1	—	S§	136.31	—
2	—	S	136.15	—
3	—	S	136.27	—
4	—	S	136.33	—
5	—	S	136.14	—
6	—	S	136.30	—
7	—	S	136.19	—
8	—	S	136.33	—
9	40	10.9	137.78	1.0119
10	40	11.4	137.66	1.0111
11	40	11.4	137.69	1.0113
12	40	12.4	137.89	1.0130
13	40	12.2	137.68	*1.0113*
				Mean 1.0117±0.0007
14	60.1	24.3	137.45	1.0099
15	60.1	19.1	137.42	1.0094
16‖	60.1	14.8	137.38	1.0088
17‖	60.1	11.3	137.48	1.0094
18‖	60.1	11.7	137.49	*1.0093*
				Mean 1.0094±0.0004
		Ethyltrimethylammonium iodide		
19	—	S	136.27	—
20	—	S	136.37	—
21	—	S	136.36	—
22	—	S	136.33	—
23	—	S	136.39	—
24	—	S	136.41	—
25‖	60.1	7.1	138.66	1.0173
26‖	60.1	15.3	138.55	1.0173
27‖	60.1	15.4	138.53	*1.0172*
				Mean 1.0173±0.0001
28	95	15.7	138.29	1.0156
29	95	10.0	138.35	1.0156
30	95	10.4	138.26	*1.0150*
				Mean 1.0154±0.0004

*Determined from the yield of trimethylamine.
†The ratios are relative to a standard nitrogen source whose $N^{14}N^{14}/N^{14}N^{15}$ ratio was arbitrarily chosen as 136.50.
‡The limits shown are standard deviations.
§S signifies Kjeldahl digestion on quaternary salt.
‖Reaction with potassium hydroxide in 95% (v/v) ethanol.

aqueous medium at the same temperature, the deuterium isotope effects for the two reactions, also previously reported by Saunders (5), and the Hammett rho values found in the reaction of a series of meta- and para-substituted 2-phenylethyltrimethylammonium and 2-phenylethyldimethylsulphonium salts (14, 21).

In contrast to the very low sulphur isotope effect found by Saunders (20) for the sulphonium salt, an effect of 0.9% is found for the reaction of the corresponding ammonium salt. This value is a little less than one-third the theoretical maximum effect of 3.2% calculated by the method of Bigeleisen and Wolfsberg (reference 19, equation II.30) using for the C—N^+ bond a value of 5.50×10^5 dynes cm^{-1} for the diagonal force constant (30) and 955 cm^{-1} for the stretching frequency (31). It is also only about one-half the isotope effect found in the E2 reaction of ethyltrimethylammonium ion (Table II). Nevertheless there is clearly a significant decrease in the composite force constant of the C—N^+ bond

Can. J. Chem. Downloaded from www.nrcresearchpress.com by 210.87.254.5 on 09/05/12
For personal use only.

TABLE II

Comparison of isotope effects found in the E2 reactions of ammonium and sulphonium salts

Substrate	$(k^L/k^H - 1)100$* at 60°	k^H/k^D	ρ
$PhCH_2CH_2\overset{\oplus}{N}(CH_3)_3$	0.94±0.04†	2.98‡	3.77§
$PhCH_2CH_2\overset{\oplus}{S}(CH_3)_2$	0.15±0.09‖	5.07¶ 5.93**	2.64†† 2.21‡‡
$CH_3CH_2\overset{\oplus}{N}(CH_3)_3$	1.73	3.90§§	—

*$k^L/k^H = k^{14}/k^{15}$ for the ammonium compound and k^{32}/k^{34} for the sulphonium compound.
†Present study. Ethoxide ion in ethanol.
‡Reference 5. Ethoxide in ethanol at 50° (estimated at 30°, 3.35).
§W. H. Saunders, Jr. and D. G. Bushman, reported in reference 14.
‖Reference 20. Hydroxide ion in water.
¶Reference 5. Ethoxide ion in ethanol at 30°.
**Reference 5. Hydroxide ion in water at 30°.
††Reference 21. Ethoxide ion in ethanol at 30°.
‡‡Reference 21. Hydroxide ion in water at 30°.
§§Reference 4. Basic ethylene glycol at 137°.

in passing from the initial to the transition state. Even after taking into account that, for the same percentage decrease in the C—X^+ force constant at the transition state, a sulphur isotope effect can be expected to be little more than half a nitrogen isotope effect, it is clear that C—N^+ bond rupture must be more fully advanced in the transition state of the 2-phenylethyltrimethylammonium ion reaction than is C—S^+ bond rupture for the corresponding sulphonium salt. This is so despite the fact that $-N^+(CH_3)_3$ is presumably the poorer leaving group (5, 14).

Interpretation of the relative magnitude of the deuterium isotope effects found in the reactions of the two salts requires a knowledge of the extent to which the proton is transferred from carbon to the oxygen base at the transition state. If for both salts it is more than half transferred, then that reaction in which C—H bond weakening is the greater will give the smaller deuterium isotope effect. If, on the other hand, the proton is less than half transferred the opposite will be the case. Light is shed on this matter by relating the observed isotope effects and the Hammett rho values found in the two reactions.

In a concerted process the negative charge released by the partial transfer of the hydrogen to the base at the transition state will reside in part on the β-carbon and its attached aryl group and in part on the leaving group X. A measure of the former is provided by the Hammett rho value for the reaction; the larger the rho the more charge is accommodated on the β-aryl group. A measure of the latter is provided by the magnitude of the isotope effect associated with X. Now it has already been shown from a comparison of nitrogen and sulphur isotope effects that C—N^+ bond weakening is more fully advanced in the transition state of the ammonium salt reaction than C—S^+ bond weakening for the sulphonium salt. Furthermore, the Hammett rho is considerably greater in the ammonium salt reaction (Table II). It therefore must be concluded that more electron charge is being accommodated *both* on the β-aryl group *and* on the leaving atom X in the reaction of the ammonium ion. This is only possible if there is more electron charge to be accommodated, that is, if C_β—H bond weakening is considerably more advanced in the transition state of the E2 reaction of the ammonium salt than in that of the sulphonium salt. Now reference to Table II reveals that the β-deterium isotope effect for the former reaction is considerably smaller than that for the latter and, furthermore, both effects are smaller than would be expected for a reaction in which the partial bonds of hydrogen to carbon and to oxygen are of equal strength at the transition state. Since,

Can. J. Chem. Downloaded from www.nrcresearchpress.com by 210.87.254.5 on 09/05/12
For personal use only.

then, it is the reaction with the greater C_β—H weakening which gives rise to the smaller isotope effect, it must be concluded that for the ammonium salt reaction, and very likely for the sulphonium salt reaction as well, the proton is more than half transferred to the base at the transition state. A similar conclusion has been reached by Bunnett (14) from a comparison of the deuterium isotope effects and Hammett rho values for the reaction of 2-phenylethyl tosylates, halides, and onium compounds. However, knowledge of the relative extent of C—X^+ weakening, which is provided in the present study from a comparison of the isotope effects associated with X, places this conclusion on a firmer basis.

It is somewhat surprising to find that both C_β—H and C_α—X bond rupture have made greater progress in the transition state for the 2-phenylethylammonium compound than for the corresponding sulphonium salt. More than one factor may be responsible for this. Firstly, the ammonium salt is less reactive, its free energy of activation being considerably greater than that of the sulphonium salt (32). One, therefore, might expect that the overall bond changes involved in the reaction might be more fully advanced in the transition state for the ammonium salt (33). Secondly, the nature of the medium may have an important influence on the extent to which bond rupture has progressed at the transition state. Saunders' (20) measurements on the sulphonium salt were carried out in aqueous solution while ethanol was the solvent in the present study on the ammonium salt reaction. It is possible that in this less polar medium the sulphonium salt reaction also might show a significant isotope effect with respect to the leaving group.

That the nature of the medium can influence to some degree the extent of bond weakening in the transition state is apparent from the deuterium isotope effect results obtained by Saunders (5) for the sulphonium salt (see Table II). In aqueous medium at 30°, k^H/k^D was found to have a value of 5.93. In ethanol the isotope effect was considerably lower, 5.07, which, since the proton is more than half transferred to base, means greater C_β—H bond weakening in the transition state for the reaction in the less polar solvent.

The foregoing explanation of the differences in the transition states for the two reactions is undoubtedly an oversimplification. Other factors, such as the ability of sulphur, but not of nitrogen, to use *d* orbitals in forming bonds with other atoms, may be more important than medium or transition state energy effects. Indeed, at this stage of our knowledge it is probably more fruitful to compare the isotope effects associated with reactants of the same reaction type than to attempt to account for the relative magnitude of the effects associated with two quite different leaving groups. A comparison of the former kind is to be found in E2 reaction of ethyltrimethylammonium and 2-phenylethyltrimethylammonium ions, which is discussed in the following section.

Comparison of the E2 Reactions of Ethyltrimethylammonium and 2-Phenylethyltrimethylammonium Ions

The relative magnitude of the isotope effects in the reaction of the two ammonium salts provides the first direct test for the hypothesis that, for reactants of the same type, any structural factor which facilitates the departure of one atom (H or X) will cause the bond to that atom to be weakened more and the bond to the other atom to be weakened less in the transition state than would be the case in the absence of this factor. A β-phenyl group, through its ability to conjugate with a developing carbanionic center on the β-carbon, can be expected to make proton transfer energetically easier. The pathway of lowest energy, therefore, should be that in which at the transition state C_β—H bond rupture has made greater progress and C_α—N^+ bond rupture less progress than in the case of the unsubstituted compound. The results given in Table II bear out this prediction.

Can. J. Chem. Downloaded from www.nrcresearchpress.com by 210.87.254.5 on 09/05/12
For personal use only.

The k^H/k^D ratio for 2-phenylethyltrimethylammonium ion is 3.0 at 50° C. For ethyltrimethylammonium ion the experimentally observed effect is 3.9 at 137°, which corresponds to an effect of between 5.5 and 6.5 at 50°. This value is twice the effect found for the phenyl-substituted compound and corresponds closely to the maximum expected for reaction in which the proton is half transferred to base at the transition state. It has been already shown (*vide supra*) that for the β-phenyl compound the proton is more than half transferred. The much smaller isotope effect observed for this compound must therefore mean a much greater C_β—H bond weakening at the transition state, which is in accordance with prediction.

The relative values of the nitrogen isotope effects for the two reactants bear out the prediction that the two bond changes are complementary; that is, the more C_β—H bond rupture the less C_α—N^+ bond rupture at the transition state. In contrast to an effect of 0.9% for the β-phenylethyl compound, the nitrogen isotope effect for the unsubstituted compound is 1.7%. This value is one of the highest nitrogen isotope effects observed in a rate process and is about one-half the maximum predicted from the Bigeleisen–Wolfsberg equation (*vide supra*).

It would appear then that the E2 reaction of ethyltrimethylammonium ion is a highly synchronous process with the two bond rupture processes having progressed to about the same extent at the transition state. The transition state for the reaction of the β-phenylethyl compound, on the other hand, has considerable carbanionic character.

The results of the present study demonstrate clearly how so-called heavy element isotope effects, when measured with sufficient precision, can be of great value in shedding light on the relative timing of concerted bond changes in elimination and related processes.

ACKNOWLEDGMENT

This work was supported by the National Research Council and one of us (G. A.) wishes to acknowledge financial assistance in the form of a N.R.C. Postdoctoral Fellowship.

REFERENCES

1. W. Hanhart and C. K. Ingold. J. Chem. Soc., 997 (1927).
2. D. J. Cram, F. D. Greene, and C. H. DePuy. J. Am. Chem. Soc. **78**, 790 (1956).
3. W. H. Saunders, Jr. and R. A. Williams. J. Am. Chem. Soc. **79**, 3712 (1957).
4. V. J. Shiner, Jr. and M. L. Smith. J. Am. Chem. Soc. **80**, 4095 (1958).
5. W. H. Saunders, Jr. and D. H. Edison. J. Am. Chem. Soc. **82**, 138 (1960).
6. C. H. DePuy and C. A. Bishop. J. Am. Chem. Soc. **82**, 2532, 2535 (1960).
7. S. J. Cristol and R. S. Bly, Jr. J. Am. Chem. Soc. **82**, 142 (1960).
8. E. D. Hughes and J. Wilby. J. Chem. Soc. 4094 (1960).
9. A. N. Bourns and E. Buncel. Ann. Rev. Phys. Chem. **12**, 1 (1961).
10. S. Ašperger, N. Ilakovac, and D. Pavlović. J. Am. Chem. Soc. **83**, 5032 (1961).
11. J. F. Bunnett, G. T. Davis, and H. Tanida. J. Am. Chem. Soc. **84**, 1606 (1962).
12. W. B. Smith and W. H. Watson, Jr. J. Am. Chem. Soc. **84**, 3174 (1962).
13. A. K. Colter and R. D. Johnson. J. Am. Chem. Soc. **84**, 3289 (1962).
14. J. F. Bunnett. Angew. Chem. Intern. Ed. **1**, 225 (1962).
15. E. Buncel and A. N. Bourns. Can. J. Chem. **38**, 2457 (1960).
16. C. K. Ingold. Proc. Chem. Soc. 265 (1962).
17. F. H. Westheimer. Chem. Rev. **61**, 265 (1961).
18. L. Melander. Isotope effects on reaction rates. Ronald Press, New York. 1960. p. 24.
19. J. Bigeleisen and M. Wolfsberg. Advan. Chem. Phys. **1**, 15 (1958).
20. W. H. Saunders, Jr. and S. Ašperger. J. Am. Chem. Soc. **79**, 1612 (1957).
21. W. H. Saunders, Jr., C. B. Gibbons, and R. A. Williams. J. Am. Chem. Soc. **80**, 4099 (1958).
22. J. W. Baker and T. G. Heggs. J. Chem. Soc. 616 (1955).
23. R. N. Icke, B. B. Wisegarver, and G. A. Alles. Org. Syn. **25**, 89 (1945).
24. H. C. Urey, J. R. Huffman, H. G. Thode, and M. Fox. J. Chem. Phys. **5**, 856 (1937).
25. D. Rittenberg. *In* Preparation and measurement of isotopic tracers. J. W. Edwards Co., Ann Arbor, Mich. 1946. p. 31.
26. G. Urry and W. H. Urry. Rev. Sci. Instr. **27**, 819 (1956).
27. T. Hoering. Science, **122**, 1233 (1955); Geochim. Cosmochim. Acta, **12**, 97 (1957).

Can. J. Chem. Downloaded from www.nrcresearchpress.com by 210.87.254.5 on 09/05/12
For personal use only.

28. R. K. WANLESS and H. G. THODE. J. Sci. Instr. **30**, 395 (1953).
29. W. H. STEVENS and R. W. ATTREE. Can. J. Res. Sect. B, **27**, 807 (1949).
30. R. K. SHELINE and K. S. PITZER. J. Chem. Phys. **18**, 595 (1950).
31. C. W. YOUNG, J. S. KOEHLER, and D. S. MCKINNEY. J. Am. Chem. Soc. **69**, 1410 (1947).
32. S. J. CRISTOL and F. R. STERMITZ. J. Am. Chem. Soc. **82**, 4692 (1960).
33. G. S. HAMMOND. J. Am. Chem. Soc. **77**, 334 (1955).

Can. J. Chem. Downloaded from www.nrcresearchpress.com by 210.87.254.5 on 09/05/12
For personal use only.

TWO-PHASE FLOW OF ADSORBED VAPORS

R. M. BARRER
Physical Chemistry Laboratories, Chemistry Department, Imperial College, London, England
Received March 8, 1963

ABSTRACT

Through a microporous medium, transport of a vapor may occur in an adsorbed film and in the gas phase. The formulation of this two-phase transport has been given in terms of forces and associated phenomenological coefficients, and the resultant expression for the total flux has then been related to the complex Darcy law and Fick law coefficients of flow and diffusion respectively. It is suggested how the various coefficients may be determined as functions of gas pressure or surface concentration of sorbate. The diffusive and hydrodynamic models of transport are considered as two limiting cases of the transport phenomenon, the former of increasing importance for decreasing sorption below monolayer coverage and the latter dominant above monolayer coverage. Steady state total concentration gradients are considered in presence and absence of blockage of gas phase flow by capillary condensate and multilayers, and when there is and is not interconversion between surface and gas phase fluxes along the direction of flow. Finally, the fluxes of each component in a two-phase two-component flow are derived. This problem is of major importance in the separation of mixtures by flow through microporous barriers.

Can. J. Chem. Downloaded from www.nrcresearchpress.com by 210.87.254.40 on 09/05/12
For personal use only.

1. INTRODUCTION

There are three ways in which one may attempt to formulate flow through a microporous medium, in which both surface and gas phase components of flux arise. These are, in terms of Fick's equation, Darcy's equation, and by means of irreversible thermodynamic procedures. The first two methods can be shown to be formally equivalent as will be seen from the following development of two-phase flow, although one emphasizes diffusion and the other hydrodynamic transport. The most fundamental procedure (see Section 4) seems to be that based on the thermodynamics of irreversible processes, which will be the method primarily developed here. It will then be the purpose of this paper to give some properties of the two-phase flow process and to indicate the conclusions which may be drawn from its measurement.

2. USEFUL THERMODYNAMIC PROPERTIES OF THE FLOWING COMPONENT

Consider the flow through unit cross section, in the x-direction. The flow occurs simultaneously in the adsorbed phase and the gaseous phase. In any plane $x = x$, normal to the direction of flow, it is assumed that the elements of each fluid are in thermodynamic equilibrium with each other, i.e.

$$\mu_s = \mu_g \quad [1]$$

$$d\mu_s = d\mu_g, \quad [2]$$

where μ_s and μ_g are the chemical potentials of the flowing component in the adsorbed film and the gaseous phase respectively. Also, for a single-component phase at constant temperature

$$d\mu_s = V_s dP_s \quad [3]$$

$$d\mu_g = V_g dP_g.$$

Equations [2] and [3] may be combined to give

[4] $$dP_s = \frac{V_g}{V_s} dP_g$$

and the total pressure drop between $x = 0$ and $x = l$ in the adsorbed film is then

[4a] $$\int dP_s = [P_s]_{x=0} - [P_s]_{x=l} = \Delta P_s = \int_{(P_g)_{x=l}}^{(P_g)_{x=0}} \frac{V_g}{V_s} dP_g.$$

If the concentration in the adsorbed film at $x = l$ (the outgoing face of the membrane) is very much smaller than at $x = 0$, we may write

$$\Delta P_s \sim [P_s]_{x=0} \sim \int_0^{(P_g)_{x=0}} \frac{V_g}{V_s} dP_g$$

and since $V_g \gg V_s$ it follows that $\Delta P_s \gg \Delta P_g$. Thus, the pressure drop in the adsorbed film, between $x = 0$ and $x = l$, is much larger than that in the gas phase, as noted for example by Flood (1).

3. FORMULATION OF FLOW

We now consider a porous medium with adsorbed and gaseous phases of sorbate, both phases diffusing (or flowing). Through any unit cross section normal to the direction of flow (the x-direction)

[5] $$J = J_s + J_g$$

where J_s is the flux of sorbed phase and J_g of gaseous phase.

Let ϵ and A denote pore volume and area per cm³ of porous medium. Let the degree of filling of pores with adsorbed phase be S at a given plane x, normal to the flow direction. Then the volume of adsorbed phase per unit volume of porous medium is $S\epsilon$, and the gaseous volume is $(1-S)\epsilon$. Unit cross section normal to x then contains an area equal to $S\epsilon$ of sorbed phase and $(1-S)\epsilon$ of gaseous phase. The total flux is then defined in terms of phenomenological coefficients λ_s and λ_g per unit cross-section of sorbed and gaseous phases respectively, and the total forces X_s and X_g acting respectively on sorbed and gaseous molecules through unit area of the sorbed phase and the gas phase:

[6] $$J = S\epsilon\lambda_s X_s + (1-S)\epsilon\lambda_g X_g$$

where the forces, X, are

[7] $$X_s = -\frac{C_s}{S\epsilon}\frac{d\mu_s}{dx}; \qquad X_g = -\frac{C_g}{(1-S)\epsilon}\frac{d\mu_g}{dx}.$$

C_s and C_g denote the total numbers of molecules per cm³ of porous medium on surface and in gas phase. If C_g' is the number of molecules per unit volume of gas phase, then

[8] $$(1-S)\epsilon C_g' = C_g$$
$$p_g = C_g' kT.$$

Then, using eq. [2]

[9] $$J = -\left[\lambda_s C_s \frac{d\mu_s}{dx} + \lambda_g C_g \frac{d\mu_g}{dx}\right]$$
$$= -[\lambda_s C_s + \lambda_g C_g]\frac{d\mu_g}{dx}.$$

Can. J. Chem. Downloaded from www.nrcresearchpress.com by 210.87.254.40 on 09/05/12
For personal use only.

Since

$$d\mu_g = RTd \ln C_g' = RTd \ln p_g$$

eq. [9] reduces, with the aid of eq. [8], to

$$[10] \qquad J = -\left[\lambda_s \frac{C_s}{C_g'} + (1-S)\epsilon\lambda_g\right] RT \frac{dC_g'}{dx}.$$

If, then, we define a diffusion coefficient, D, by Fick's law

$$[11] \qquad J = -D \frac{dC_g'}{dx}$$

we obtain

$$[12] \qquad D = \left[\lambda_s \frac{C_s}{C_g'} + (1-S)\epsilon\lambda_g\right] RT.$$

We may also use eq. [8] with eq. [10] to obtain Darcy's law:

$$[13] \qquad J = -\left[\lambda_s \frac{C_s}{C_g'} + (1-S)\epsilon\lambda_g\right] N_0 \frac{dp_g}{dx}$$

in which N_0 is Avogadro's number. The Darcy's law coefficient, K_D, defined by

$$[14] \qquad J = -K_D \frac{dp_g}{dx}$$

is then

$$[15] \qquad K_D = \left[\lambda_s \frac{C_s}{C_g'} + (1-S)\epsilon\lambda_g\right] N_0.$$

Darcy's and Fick's laws are thus seen to be equivalent.

4. PROPERTIES OF THE FLUX EQUATION

From eq. [13], by integration between $x = 0$ and $x = l$, we obtain

$$[16] \qquad Jl = \int_{p_1}^{p_0} \left[\lambda_s \frac{C_s}{C_g'} + (1-S)\epsilon\lambda_g\right] N_0 dp_g$$

so that

$$[17] \qquad l \frac{dJ}{d[p_g]_{x=0}} = \left[\lambda_s \frac{C_s}{C_g'} + (1-S)\epsilon\lambda_g\right]_{x=0} N_0 = [K_D]_{x=0}.$$

Similarly

$$[18] \qquad l \frac{dJ}{d[C_g']_{x=0}} = \left[\lambda_s \frac{C_s}{C_g'} + (1-S)\epsilon\lambda_g\right]_{x=0} RT = [D]_{x=0}.$$

Equations [17] and [18] give the differential concentration dependences of K_D or D for the medium at $x = 0$. The relation between $S\epsilon$ and C_s needs further consideration.

In the region of small sorption, before any multilayers or capillary condensate appear, perhaps up to sorptions approaching monolayer coverage, we will write for the effective sorption volume

$$[19] \qquad S\epsilon = Ad$$

Can. J. Chem. Downloaded from www.nrcresearchpress.com by 210.87.254.40 on 09/05/12
For personal use only.

where d is approximately the molecular diameter of the sorbate. Any molecule with its center within this distance from the surface is regarded as adsorbed. If its center is more than d from the surface the molecule is regarded as being in the gas phase. With this simplification, up to near the monolayer,

[20] $$\rho_s = \frac{C_s m}{S\epsilon} = \frac{C_s m}{Ad}$$

so that the film density ρ_s is proportional to C_s; m is the molecular weight of the sorbate.

After the monolayer region, $S\epsilon$ increases through the formation of multilayers and of capillary condensate, but the density will now be approximated as being close to that of the liquid sorbate:

[21] $$\rho_s \sim \rho_l.$$

In this event

[22] $$S\epsilon = \frac{C_s m}{\rho_l}$$

and so the degree of filling after monolayer coverage becomes proportional to C_s. This is the region in which a hydrodynamic mechanism of transport has largely replaced the diffusive, or random walk, mechanism appropriate for small values of C_s. The diffusive mechanism is dominant in the dilute Henry's law range of sorption. The two regions will in reality probably merge continuously into one another as in Fig. 1, curve iii. We will, however, assume that eq. [20] is valid up to the monolayer coverage, and eq. [22] thereafter (Fig. 1, curves i and ii).

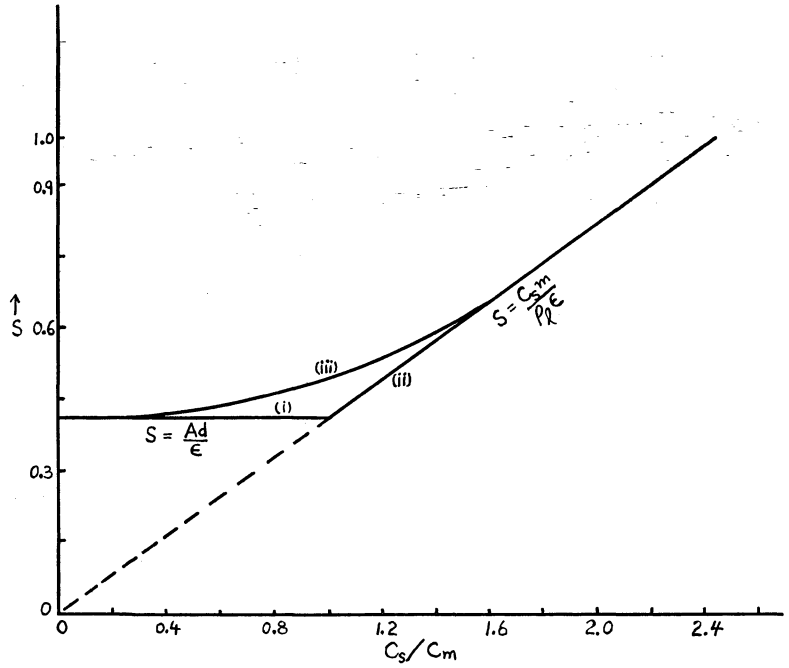

FIG. 1. The assumed variations of the fraction of saturation of the pore space below monolayer coverage (line (i)) and above monolayer coverage (line (ii)). Curve (iii) may represent behavior such as would be actually encountered.

Can. J. Chem. Downloaded from www.nrcresearchpress.com by 210.87.254.40 on 09/05/12
For personal use only.

In the region of applicability of eq. [20] $S\epsilon = Ad$ is a constant in eqs. [17] and [18]. When eq. [22] is valid, however, its substitution in eqs. [17] and [18] gives

$$[23] \qquad l\frac{dJ}{d[p_g]_{x=0}} = \left[\lambda_s \frac{C_s}{C_g'} + \left(\epsilon - \frac{C_s m}{\rho_l}\right)\lambda_g\right]_{x=0} N_0 = [K_D]_{x=0}$$

$$[24] \qquad l\frac{dJ}{d[C_g']_{x=0}} = \left[\lambda_s \frac{C_s}{C_g'} + \left(\epsilon - \frac{C_s m}{\rho_l}\right)\lambda_g\right]_{x=0} RT = [D]_{x=0}.$$

As the pore space fills, $(\epsilon - (C_s m)/\rho_l)$ approaches zero, and finally

$$[25] \qquad l\frac{dJ}{d[p_g]_{x=0}} \rightarrow \left[\frac{C_s}{C_g'}\lambda_s\right]_{x=0} N_0 = \left[\frac{S\epsilon\rho_l}{mC_g'}\lambda_s\right]_{x=0} N_0 = \left[K_D\right]_{x=0}.$$

This behavior further identifies the hydrodynamic term.

In their expression for transport Gilliland, Baddour, and Russell (2) followed Babbit (3) in that the driving force was regarded as the negative of the gradient of surface pressure rather than of chemical potential. In terms of adsorption thermodynamics (Hill (4); Everett (5))

$$[25a] \qquad d\mu_s = -S_s dT + V_s dp_g + A_s d\phi$$

so that in an isothermal system

$$[25b] \qquad \frac{d\mu_s}{dx} = V_s \frac{dp_g}{dx} + A_s \frac{d\phi}{dx}$$

where S_s, V_s, and A_s are the molar entropy, volume, and surface area of the adsorbate regarded as a single pure component phase. Flood (1) on the other hand considered the driving force to be proportional to $-dP_s/dx$ where the pressure, P_s, is defined by eq. [3]. However, in these expressions, V_s and A_s may be and usually are functions of p_g (or of amount sorbed). Moreover a limitation of these approaches is seen further when the temperature is not constant. The forces in the irreversible thermodynamic formulation are still clearly defined (De Groot (6)) as $-T\{d(\mu/T)/dx\}$ and $-(1/T)(dT/dx)$ in the flux equations such as

$$[25c] \qquad J_g = -\left\{\lambda_{11}{}^g C_g \cdot T\frac{d}{dx}(\mu_g/T) + \lambda_{12}{}^g C_g \frac{1}{T}\frac{dT}{dx}\right\}$$

where $\lambda_{12}{}^g$ is the cross-coefficient and $\lambda_{11}{}^g$ is the same as λ^g.

Blockage of the gas phase flux is also involved through the term $(\epsilon - C_s m/\rho)$. So long as there is any pore space unfilled there will be some vapor transport across it. This blockage will not in general be that measured by using an indicator gas non-sorbed and insoluble in the sorbate film, as was done by Ash, Barrer, and Pope (7), because towards such an indicator gas the pore system can become sealed by capillary condensate in bottle-necks while there still remains some pore volume unfilled by condensate. The present formulation is for the total flux in the gas phase (per cm² normal to the direction of flow) and for the reason given in the previous sentence is greater than that measured by the use of an indicator gas. The use either of a non-sorbed calibrating gas flowing through the sorbate-free medium (e.g. Barrer and Gabor (8)), or of the non-sorbed indicator gas (Ash, Barrer, and Pope (7)), leads to coefficients K_D and D for the combined or two-phase flow differently related to the terms of eqs. [12] or [15] (Barrer and Gabor (9)).

Can. J. Chem. Downloaded from www.nrcresearchpress.com by 210.87.254.40 on 09/05/12
For personal use only.

In the very dilute region of adsorption where Henry's law is valid, C_s/C_g' has its maximum value of $(Ak_s+S\epsilon)$, where k_s is the Henry's law constant. C_s denotes the total number of molecules in the adsorbed layer; this number exceeds that normally measured in a sorption experiment by $S\epsilon C_g'$. Accordingly $C_s/C_g' = AC_s'/C_g' + S\epsilon$ where C_s' is the measured surface excess in molecules per cm² of surface. In the Henry's law region, $k_s = C_s'/C_g'$. Above the monolayer coverage, from eq. [22],

$$[26] \qquad A\frac{C_s'}{C_g'}\frac{\rho_1}{(\rho_1-\rho_g)} = \frac{C_s}{C_g'}$$

where ρ_g is the density of the gas phase in equilibrium. In many cases $A(C_s'/C_g') \gg S\epsilon$ and the distinction between the surface excess per unit area and the *total* number of molecules in the sorbed phase per unit area is negligible. In microporous media of high area and low porosity one may find that $S\epsilon = Ad$ represents nearly all the pore space. This implies that there is little gas phase flow, and is a state which is approached by some active carbons well compacted into plugs and which is reached for the internal porosity of molecular sieve zeolites.

The rate of decline of $(\epsilon - C_s m/\rho_1)$ towards zero in eqs. [23] and [24], as p_g increases, is determined by the isotherm type in Brunauer's classification (Fig. 2). Equally interesting

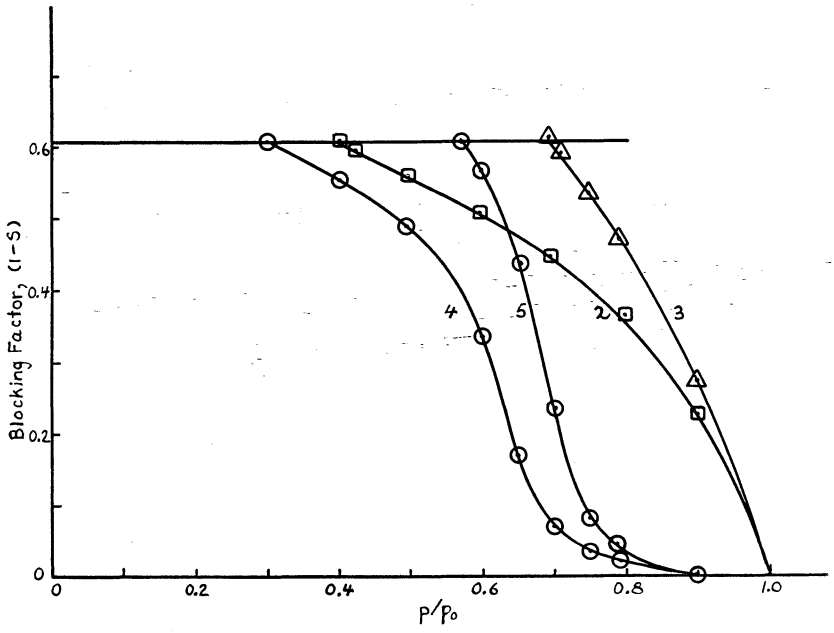

FIG. 2. The blockage factor $(\epsilon - C_s m/\rho_1)$ above monolayer coverage for isotherms of Types 2, 3, 4, and 5 in Brunauer's classification. Curves 2, 3, 4, and 5 correspond respectively to the isotherms 2, 3, 4, and 5 of Fig. 3. Monolayer coverage is taken as 78 cm³ at s.t.p. per cm³ of porous medium for isotherms 2 and 3 and as 70 cm³ at s.t.p. per cm³ for isotherms 4 and 5.

is the change in C_s/C_g' for various types of isotherm. This change is illustrated in Fig. 3. For Type I isotherms C_s/C_g' decreases continually, but for Type II isotherms this ratio may pass through a minimum, and for those of Type IV, may go through a minimum and

Can. J. Chem. Downloaded from www.nrcresearchpress.com by 210.87.254.40 on 09/05/12
For personal use only.

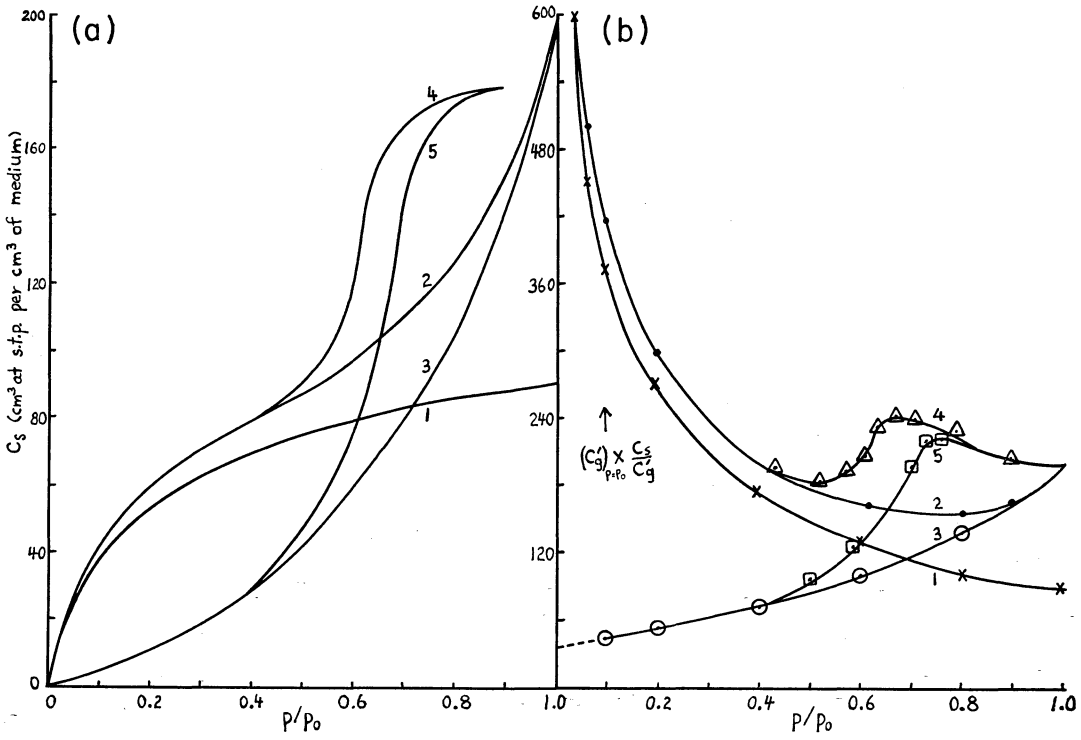

FIG. 3. (*a*) The isotherms of Types 1 to 5 in Brunauer's classification used to calculate the blockage factors of Fig. 2, and the ratios $(C_s/C_g')\times(C_g')_{p=p_0}$ in Fig. 3(*b*).
(*b*) The concentration dependence of the ratios $(C_s/C_g')\times(C_g')_{p=p_0}$ for the isotherms 1 to 5 in Fig. 3(*a*).

a maximum. In the case of Type III isotherms, C_s/C_g' increases continuously, and with those of Type V this quotient increases to a maximum and then decreases.

5. STEADY STATE DISTRIBUTION FOR DILUTE ADSORBED FILMS ($S\epsilon$ = CONSTANT)

For the purposes of Sections 5 and 6 it is convenient to transcribe the flux equations into the notation of Fick's law. Eq. [10] can be rewritten as

$$[27] \qquad J = -\left[\lambda_s RT \frac{d \ln C_g'}{d \ln C_s}\frac{dC_s}{dx} + (1-S)\epsilon RT\lambda_g \frac{dC_g'}{dx}\right]$$
$$= -\left[D_s \frac{dC_s}{dx} + (1-S)\epsilon D_g \frac{dC_g'}{dx}\right]$$

where the surface diffusion coefficient $D_s = \lambda_s RT(d \ln C_g'/d \ln C_s)$ and the gas phase diffusion coefficient $D_g = \lambda_g RT$. If there is no blockage and slip flow is occurring, $D_g = D_g^0(1+(D_p/D_g^0)C_g')$, where D_g^0 is the Knudsen flow diffusion coefficient and D_p is the coefficient appropriate for Poiseuille flow. Then

$$[28] \qquad Jx = -\int D_s dC_s - \int (1-S)\epsilon D_g dC_g' + B$$

where B is a constant. Also, we may set

$$[29] \qquad D_s = D_0(1+f(C_s))$$

Can. J. Chem. Downloaded from www.nrcresearchpress.com by 210.87.254.40 on 09/05/12
For personal use only.

so that provided we are in the dilute range of the adsorption (below monolayer coverage), in absence of blocking, and for slip-flow

$$[30] \qquad Jx = -\left\{D_0(C_s+F(C_s))+(1-S)\epsilon D_g^{\,0}\left(1+\frac{D_p}{2D_g^{\,0}}C_g'\right)C_g'\right\}+B$$

where $F(C_s) = \int f(C_s)dC_s$. When $x = l$, since C_s and C_g' are both very small at $x = l$, Henry's law should be valid, $f(C_s) \to 0$, and the Poiseuille term becomes negligible, giving

$$[31] \qquad Jl = -[D_0C_s+(1-S)\epsilon D_g^{\,0}C_g']_{x=l}+B.$$

When $x = 0$, $Jx = 0$ and so B is evaluated as

$$[32] \qquad B = \left[D_0(C_s+F(C_s))+(1-S)\epsilon D_g^{\,0}\left(1+\frac{D_p}{2D_g^{\,0}}C_g'\right)C_g'\right]_{x=0}.$$

Thus, finally,

$$[33] \qquad \frac{x}{l} = \left\{\left[D_0(C_s+F(C_s))+(1-S)\epsilon D_g^{\,0}\left(1+\frac{D_p}{2D_g^{\,0}}C_g'\right)C_g'\right]_{x=0} - \left[D_0(C_s+F(C_s))+(1-S)\epsilon D_g^{\,0}\left(1+\frac{D_p}{2D_g^{\,0}}C_g'\right)C_g'\right]_{x=x}\right\}$$
$$\div\left\{\left[D_0(C_s+F(C_s))+(1-S)\epsilon D_g^{\,0}\left(1+\frac{D_p}{2D_g^{\,0}}C_g'\right)C_g'\right]_{x=0} - [D_0C_s+(1-S)\epsilon D_g^{\,0}C_g']_{x=l}\right\}.$$

If, at $x = l$, C_s and C_g' are negligible compared with their values at $x = 0$, then eq. [33] reduces to

$$[34] \qquad 1-\frac{x}{l} = \frac{\left[D_0(C_s+F(C_s))+(1-S)\epsilon D_g^{\,0}\left(1+\frac{D_p}{2D_g^{\,0}}C_g'\right)C_g'\right]_{x=x}}{\left[D_0(C_s+F(C_s))+(1-S)\epsilon D_g^{\,0}\left(1+\frac{D_p}{2D_g^{\,0}}C_g'\right)C_g'\right]_{x=0}}.$$

6. RELATION BETWEEN THE STEADY STATE DISTRIBUTION FOR DILUTE FILMS, AND $D_s = D_0(1+f(C_s))$

If we differentiate eq. [34] with respect to x we obtain

$$[35] \qquad J = \frac{\left[D_0(C_s+F(C_s))+(1-S)\epsilon D_g^{\,0}\left(1+\frac{D_p}{2D_g^{\,0}}C_g'\right)C_g'\right]_{x=0}}{l}$$
$$= -\left[D_0(1+f(C_s))\frac{dC_s}{dC_g'}+(1-S)\epsilon D_g^{\,0}\left(1+\frac{D_p}{D_g^{\,0}}C_g'\right)\right]\frac{dC_g'}{dx}$$

while, at $x = l$, if Henry's law obtains, and molecular streaming is occurring in the gas phase,

$$[36] \qquad J = -\left\{\left[D_0(Ak_s+S\epsilon)+(1-S)\epsilon D_g^{\,0}\right]\frac{dC_g'}{dx}\right\}_{x=l}.$$

Two possibilities now arise:

(i) J_s and J_g are each constant between $0 < x < l$.
(ii) There is interconversion of fluxes J_s and J_g in this range.

Can. J. Chem. Downloaded from www.nrcresearchpress.com by 210.87.254.40 on 09/05/12
For personal use only.

When J_g is measured using a non-sorbed calibrating gas then condition (i) must necessarily be met, in an unblocked medium. This condition is also satisfied when J_g is measured using the calibrating gas as an indicator admixed with the sorbable gas, which partially blocks the medium. However, J_s (derived from J and J_g) is in both circumstances partly in the gas phase (Barrer and Gabor (9)) so that as noted previously D_s and D_g have here meanings different from those in eqs. [27] to [36].

If J_s and J_g are each constant over all x, we find

$$[37] \qquad \left(\frac{dC_g'}{dx}\right)_{x=l} \Big/ \left(\frac{dC_g'}{dx}\right)_{x=0} = \left(1 + \frac{D_p}{D_g^0} C_g'\right)_{x=0}$$

and by equating the terms for J_s in [35] and [36] we obtain (cf. Barrer (10))

$$[38] \qquad D_s = D_0(1+f(C_s))_{x=0} = D_0(Ak_s+S\epsilon)\left[\left(1 + \frac{D_p}{D_g^0} C_g'\right)\frac{dC_g'}{dC_s}\right]_{x=0}$$

$$= D_0(Ak_s+S\epsilon)\left[\left(1 + \frac{D_p}{D_g^0} C_g'\right)\frac{1}{A\dfrac{dC_s'}{dC_g'} + S\epsilon}\right]_{x=0}$$

where C_s' is the number of molecules adsorbed per cm^2 of surface. If there is only Knudsen flow in the gas phase then D_p in eq. [38] is zero.

When interconversion of fluxes occurs the theorem embodied in eq. [38] must be reformulated as follows. $(dC_g'/dx)_{x=l}$ can be evaluated from eq. [36], since J is known, and since D_g^0, D_0, and Ak_s can be evaluated from low-pressure flow and sorption data (Section 9). The ratio

$$[39] \qquad \left(\frac{dC_g'}{dx}\right)_{x=0} \Big/ \left(\frac{dC_g'}{dx}\right)_{x=l} = \phi = \frac{[D_0(Ak_s+S\epsilon)+(1-S)\epsilon D_g^0]_{x=l}}{\left[D_0(1+f(C_s))\dfrac{dC_s}{dC_g'} + (1-S)\epsilon D_g^0\left(1 + \dfrac{D_p}{D_g^0} C_g'\right)\right]_{x=0}}.$$

By rearrangement this equation gives

$$[40] \qquad \left\{D_0(1+f(C_s))\frac{dC_s}{dC_g'}\right\}_{x=0} = \left[\frac{D_0(Ak_s+S\epsilon)+(1-S)\epsilon D_g^0}{\phi}\right]_{x=l} - \left[(1-S)\epsilon D_g^0\left(1 + \frac{D_p}{D_g^0} C_g'\right)\right]_{x=0}.$$

7. STEADY STATE DISTRIBUTION WITH C_s ABOVE MONOLAYER VALUE AT $x = 0$

We may start with eq. [28], and proceed as previously, but recall that $S\epsilon$ is now proportional to C_s at $x = 0$ and also for other intermediate values of x. This leads to the steady state distribution

$$[41] \qquad \frac{x}{l} = \left\{\left[D_0(C_s+F(C_s))_{x=x} + \int_0^{(C_g')_{x=x}} (1-S)\epsilon D_g dC_g'\right] - \left[D_0(C_s+F(C_s))_{x=0} + \int_0^{(C_g')_{x=0}} (1-S)\epsilon D_g dC_g'\right]\right\} \div \left\{\left[D_0C_s+(1-S)\epsilon D_g^0 C_g'\right]_{x=l} - \left[D_0(C_s+F(C_s))_{x=0} + \int_0^{(C_g')_{x=0}} (1-S)\epsilon D_g dC_g'\right]\right\}$$

where, in the slip-flow region, $D_g = D_g^0(1+(D_p/D_g^0)C_g')$. Again, where C_s, C_g' are small

Can. J. Chem. Downloaded from www.nrcresearchpress.com by 210.87.254.40 on 09/05/12
For personal use only.

enough at $x = l$, the first term in the denominator is negligible compared with the second, and so

$$[42] \qquad 1 - \frac{x}{l} = \frac{D_0(C_s + r'(C_s))_{x=x} + \int_0^{(C_g')_{x=x}} (1-S)\epsilon D_g dC_g'}{D_0(C_s + F(C_s))_{x=0} + \int_0^{(C_g')_{x=0}} (1-S)\epsilon D_g dC_g'}.$$

Alternatively eq. [42] may be written

$$[43] \qquad \left(1 - \frac{x}{l}\right) = \frac{\int_0^{(C_g')_{x=x}} \left[\nu_0(1+f(C_s))\frac{dC_s}{dC_g'} + (1-S)\epsilon D_g{}^0\left(1 + \frac{D_p}{D_g{}^0} C_g'\right)\right] dC_g'}{\int_0^{(C_g')_{x=0}} \left[D_0(1+f(C_s))\frac{dC_s}{dC_g'} + (1-S)\epsilon D_g{}^0\left(1 + \frac{D_p}{D_g{}^0} C_g'\right)\right] dC_g'}.$$

Differentiating with respect to x gives

$$[44] \qquad J = \frac{1}{l}\int_0^{(C_g')_{x=0}} \left[D_0(1+f(C_s))\frac{dC_s}{dC_g'} + (1-S)\epsilon D_g{}^0\left(1 + \frac{D_p}{D_g{}^0} C_g'\right)\right] dC_g'$$

$$= -\left[D_0(1+f(C_s))\frac{dC_s}{dC_g'} + (1-S)\epsilon D_g{}^0\left(1 + \frac{D_p}{D_g{}^0} C_g'\right)\right]\frac{dC_g'}{dx}.$$

Also, at $x = l$, assuming Henry's law and Knudsen flow at this point, and that $f(C_s)$ here consequently tends to zero, one recovers eq. [36]:

$$[36] \qquad J = -\left[\{D_0(Ak_s + S\epsilon) + (1-S)\epsilon D_g{}^0\}\frac{dC_g'}{dx}\right]_{x=l}.$$

With $(dC_g'/dx)_{x=0}/(dC_g'/dx)_{x=l} = \phi$, as before, one obtains as the expression for the concentration dependence of D_s:

$$[45] \qquad \left[D_0(1+f(C_s))\frac{dC_s}{dC_g'}\right]_{x=0} = \frac{1}{\phi}[D_0(Ak_s + S\epsilon) + (1-S)\epsilon D_g{}^0]_{x=l}$$

$$-\left[\left(\epsilon - \frac{C_s m}{\rho_1}\right) D_g{}^0\left(1 + \frac{D_p}{D_g{}^0} C_g'\right)\right]_{x=0}.$$

8. FLUX INTERCONVERSION

It has been observed that, in a medium in which, according to helium flow measurements, only Knudsen flow was taking place in the gas phase, the permeability K for adsorbed vapors may increase with p_g (Ash, Barrer, and Logan (11)). The permeability K is defined as $K = Jl/[p_g]_{x=0}$ where J refers to unit cross section of the porous medium. On the basis of these experiments it was observed that

$$[46] \qquad \frac{Jl}{[p_g]_{x=0}} = K_0\{1 + \beta[p_g]_{x=0}\}$$

so that multiplying by p_g and differentiating with respect to p_g one has

$$[47] \qquad l\frac{dJ}{d[p_g]_{x=0}} = K_0\{1 + 2\beta[p_g]_{x=0}\}.$$

$l\{dJ/d[p_g]_{x=0}\}$ is, however, given by eq. [17], and combining this with eq. [13] leads to

Can. J. Chem. Downloaded from www.nrcresearchpress.com by 210.87.254.40 on 09/05/12
For personal use only.

$$[48] \qquad \left[\frac{dp_g}{dx}\right]_{x=0} = -\frac{J}{l}\frac{d[p_g]_{x=0}}{dJ} = -\frac{1}{l}\frac{d[p_g]_{x=0}}{d\ln J}$$

so that from a plot of p_g vs. $\ln J$ we can easily find $[dp_g/dx]_{x=0}$ as a function of $[p_g]_{x=0}$. Thus, in the systems considered,

$$[49] \qquad -\left[\frac{dp_g}{dx}\right]_{x=0} = \frac{[p_g]_{x=0}}{l}\left\{\frac{1+\beta[p_g]_{x=0}}{1+2\beta[p_g]_{x=0}}\right\}.$$

When surface flux is progressively transformed into gas phase flux as x increases we expect $-[dp_g/dx]_{x=0}$ to fall below and $-[dp_g/dx]_{x=l}$ to rise above the 'ideal' gradient $[p_g]_{x=0}/l$ for Knudsen flow. That is, in the absence of such interconversion, β should become zero, giving the 'ideal' gradient. The results expressed in eq. [49] therefore indicate interconversion of flows. Evidence obtained in these laboratories has shown flux interconversion for hydrocarbons in cracking catalyst plugs (Ash, Barrer, and Logan (11)) and for sulphur dioxide in carbon plugs (Ash, Barrer, and Pope (7)). There is no flux interconversion when Henry's law expresses the adsorption isotherm, nor in the region of still dilute adsorbed films outside the Henry's law range (Barrer and Strachan (12); Aylmore and Barrer (13), for various gases in carbon plugs).

9. ESTIMATION OF λ_s AND λ_g

The determination of λ_s and λ_g is not simple, because, as noted in Section 4, there are limitations in the use of helium as a non-sorbed calibrating gas to measure λ_g. In Section 8 it was also pointed out that according to our experiments $dJ/d[p_g]_{x=0}$ remains constant over a range of values of C_s appreciably outside the Henry's law range, and that then there is no interconversion of the fluxes J_s and J_g as x increases. In absence of flux interconversion and in the region of Knudsen flow in the gas phase, the relation of eq. [38] between D_s and isotherm curvature becomes

$$[38a] \qquad D_s = D_0(Ak_s+S\epsilon)\frac{dC_g'}{dC_s}.$$

The relation $D_s = \lambda_s RT(d\ln C_g'/d\ln C_s)$ can then be combined with eq. [38a] to give

$$[50] \qquad \lambda_s\frac{C_s}{C_g'} = \frac{D_0(Ak_s+S\epsilon)}{RT}$$

so that under these conditions the quotient $\lambda_s(C_s/C_g')$ is a constant. Accordingly in absence of flux interconversion each term in the relation

$$\frac{l}{N_0}\frac{dJ}{d[p_g]_{x=0}} = \left[\lambda_s\frac{C_s}{C_g'} + \lambda_g(1-S)\epsilon\right]_{x=0}$$

is separately constant. The intrinsic concentration dependence of λ_s is then that of the ratio C_g'/C_s, but the absolute value of λ_s (or of λ_g) cannot be obtained from the above argument. Two possible procedures are indicated below.

(a) λ_s in the Henry's Law Range

In this range the treatment of Barrer and Gabor (9) may lead to an estimate of λ_s. In their notation

$$[51] \qquad D_{ss}^* = \frac{D_{ss}}{(1-X)-X(J_s/J_g)_{\text{He method}}}$$

Can. J. Chem. Downloaded from www.nrcresearchpress.com by 210.87.254.40 on 09/05/12
For personal use only.

where $(J_s/J_g)_{\text{He method}}$ is the ratio of the surface flux to gas flux as found by the use of a non-sorbed indicator gas (Section 4) together with the flowing adsorbed gas (Ash, Pope, and Barrer (7)). X is the fraction of the plug length, or of the cross section A_c, along which or through which respectively the molecules comprising J_s are in the gas phase. Accordingly $(1-X)$ can be taken as a measure of the ratio J_s'/J_s where J_s' is now the flux which is only in the surface and J_s is the "surface" flux measured by means of the indicator gas and which is partly in the gas phase as noted above. D_{ss} is the steady state "surface" diffusion coefficient corresponding to J_s, and D_{ss}^* is this coefficient for an unbroken surface in which molecules comprising J_s are not involved in evaporative flights across cracks and blind pores. The physics of this situation has been described by Barrer and Gabor (9).

Different values of X are then tried in the eq. [51], and values of D_{ss}^* to correspond evaluated. For a given X, log D_{ss}^* is then plotted against $1/T$ to determine the Arrhenius energy of activation, E. The correct value of X is taken to be that for which $E/\Delta E$ lies between about 0.25 and 0.5. The ratio $E/\Delta E$ approaches the critical range of $E/\Delta E$ very sharply, i.e. over a narrow range of values of X, which is thus obtainable within a reasonable margin. Accordingly from $(1-X) = J_s'/J_s$ one may estimate J_s', and hence λ_s from

$$J_s' = \lambda_s \frac{C_s}{C_g'} N_0 \frac{[p_g]_{x=0}}{l} \qquad [52]$$

since $[p_g]_{x=l} \to 0$. The above expression is valid if unblocked Knudsen flow occurs in the gas phase.

(b) λ_g in the Absence of Flux Interconversion

If helium (or hydrogen) is used as a non-sorbed indicator gas along with the flowing adsorbed gas we may approximate to λ_g for not too large adsorptions. For the two gases we have, at any cross section

$$J_g = -\lambda_g(1-S)\epsilon RT\frac{dC_g'}{dx} = -D_g'\frac{dC_g'}{dx} \qquad [53]$$

$$J_g^{He} = -\lambda_g^{He}(1-S\theta)\epsilon RT\left(\frac{dC_g'}{dx}\right)^{He} = -(D_g^{He})'\left(\frac{dC_g'}{dx}\right)^{He}$$

where θ denotes the fraction of a monolayer covered by the adsorbed gas. The linear decrease in the product $\lambda_g^{He}(1-S\theta)$ corresponds quite well with the reduction in permeability of hydrogen as an indicator gas in admixture with SO_2 in carbon plugs (Ash, Barrer, and Pope (7)) in the pre-monolayer adsorption range. On the other hand the adsorption volume $S\epsilon = Ad$ is constant for the adsorbed gas in this range (eq. [19]). Then

$$\frac{D_g'}{(D_g^{He})'} = \frac{\lambda_g(1-S)}{\lambda_g^{He}(1-S\theta)}. \qquad [54]$$

As $\theta \to 0$

$$\frac{D_g'}{(D_g^{He})'} = \frac{\lambda_g(1-S)}{\lambda_g^{He}} = \sqrt{(M_{He}/M)}\cdot(1-S) \qquad [55]$$

and as $\theta \to 1$

$$\frac{D_g'}{(D_g^{He})'} = \frac{\lambda_g}{\lambda_g^{He}} \sim \sqrt{(M_{He}/M)}. \qquad [56]$$

This latter relation may serve to derive λ_g, but only provided that the pore geometry

Can. J. Chem. Downloaded from www.nrcresearchpress.com by 210.87.254.40 on 09/05/12
For personal use only.

plays the same role for the indicator gas at $\theta = 1$ as for the adsorbed gas. The relation as $\theta \rightarrow 0$ may be the more useful. Once λ_g is known, λ_s follows from the relation

$$\frac{l}{N_0}\frac{dJ}{d[p_g]_{x=0}} = \left(\lambda_s\frac{C_s}{C_g} + \lambda_g(1-S)\epsilon\right)_{x=0}.$$

10. TWO-PHASE FLOW OF TWO ADSORBED COMPONENTS IN A MIXTURE

This important problem relates directly to the separations possible for binary (or more complex) mixtures by flow through micropore systems. Such separations are attracting increasing attention, and can be remarkably effective (Kammermeyer and Wyrick (14); Ash, Barrer, and Pope (7)). Both components are present in each phase (vapor and adsorbed). The nomenclature is modified for convenience, 1 and 2 as subscripts denoting quantities related to species 1 and 2 respectively, while the superscripts s and g denote surface and gaseous phases. In the plane at x, normal to flow, equilibrium is assumed for distribution of the components between each phase:

$$[57] \qquad \begin{aligned} \mu_1^s &= \mu_1^g; & \mu_2^s &= \mu_2^g \\ d\mu_1^s &= d\mu_1^g & d\mu_2^s &= d\mu_2^g. \end{aligned}$$

In the steady state of flow

$$[58] \qquad \begin{aligned} J_1 &= J_1^s + J_1^g \\ J_2 &= J_2^s + J_2^g \end{aligned}$$

where J_1 and J_2 are independent of x. For these flows

$$[59] \qquad \begin{aligned} J_1^s &= S\epsilon(\lambda_{11}^s X_1^s + \lambda_{12}^s X_{21}^s) \\ J_2^s &= S\epsilon(\lambda_{22}^s X_2^s + \lambda_{12}^s X_{12}^s) \\ J_1^g &= (1-S)\epsilon(\lambda_{11}^g X_1^g + \lambda_{12}^g X_{21}^g) \\ J_2^g &= (1-S)\epsilon(\lambda_{22}^g X_2^g + \lambda_{12}^g X_{12}^g) \end{aligned}$$

where the X's denote forces and the λ's are the relevant phenomenological coefficients. The λ_{12} are the cross-coefficients, and in the formulation, although this is not essential, Onsager's reciprocal relations have been assumed. For the forces X we now have:

$$[60] \qquad \begin{aligned} X_1^s &= -\frac{C_1^s}{S\epsilon}\frac{d\mu_1^s}{dx}; & X_{21}^s &= -\frac{C_1^s}{S\epsilon}\frac{d\mu_2^s}{dx} \\ X_2^s &= -\frac{C_2^s}{S\epsilon}\frac{d\mu_2^s}{dx}; & X_{12}^s &= -\frac{C_2^s}{S\epsilon}\frac{d\mu_1^s}{dx} \\ X_1^g &= -\frac{C_1^g}{(1-S)\epsilon}\frac{d\mu_1^g}{dx}; & X_{21}^g &= -\frac{C_1^g}{(1-S)\epsilon}\frac{d\mu_2^g}{dx} \\ X_2^g &= -\frac{C_2^g}{(1-S)\epsilon}\frac{d\mu_2^g}{dx}; & X_{12}^g &= -\frac{C_2^g}{(1-S)\epsilon}\frac{d\mu_1^g}{dx}. \end{aligned}$$

Then, taking the flow of species 1 as an example

$$[61] \qquad J_1 = S\epsilon(\lambda_{11}^s X_1^s + \lambda_{12}^s X_{21}^s) + (1-S)\epsilon(\lambda_{11}^g X_1^g + \lambda_{12}^g X_{21}^g)$$

so that, substituting for the forces from eq. [60], utilizing eq. [57], and integrating from $x = 0$ to $x = l$, one obtains

$$[62] \qquad J_1 l = \int_{\mu_l^g}^{\mu_0^g} \left\{(\lambda_{11}^s C_1^s + \lambda_{11}^g C_1^g) + (\lambda_{12}^s C_1^s + \lambda_{12}^g C_1^g)\frac{\partial\mu_2^g/\partial x}{\partial\mu_1^g/\partial x}\right\} d\mu_1^g.$$

Can. J. Chem. Downloaded from www.nrcresearchpress.com by 210.87.254.40 on 09/05/12
For personal use only.

On differentiating with respect to μ_1^g, and recalling that $(1-S)\epsilon(C_1^g)' = C_1^g$ (where $(C_1^g)'$ denotes the number of molecules of species 1 per cm³ of gas phase), one finds from eq. [62] that

$$[63] \qquad \frac{l}{N_0}\frac{dJ_1}{d[p_1^g]_{x=0}} = \left\{\left(\lambda_{11}\frac{C_1^s}{(C_1^g)'} + (1-S)\epsilon\lambda_{11}^g\right) + \left(\lambda_{12}^s\frac{C_1^s}{(C_1^g)'} + (1-S)\epsilon\lambda_{12}^g\right)\frac{\partial\mu_2^g/\partial x}{\partial\mu_1^g/\partial x}\right\}_{x=0}.$$

In the region of pressures where Knudsen flow occurs in the gas phase, and when there is no interconversion of fluxes

$$-\frac{d(C_1^g)'}{dx} = \frac{(C_1^g)'_{x=0}}{l}; \qquad -\frac{d(C_2^g)'}{dx} = \frac{(C_2^g)'_{x=0}}{l}$$

and so $(\partial\mu_2^g/\partial x)/(\partial\mu_1^g/\partial x) = 1$. Then

$$[64] \qquad \frac{l}{N_0}\frac{dJ_1}{d[p_1^g]_{x=0}} = \left\{(\lambda_{11}^s+\lambda_{12}^s)\frac{C_1^s}{(C_1^g)'} + (1-S)\epsilon(\lambda_{11}^g+\lambda_{12}^g)\right\}_{x=0}.$$

Expressions similar to eqs. [63] and [64] may be written for $(l/N_0)(dJ_2/dp_2^g)_{x=0}$, and all these may be further simplified if in addition Henry's law is valid for each constituent. Moreover, since molecule–molecule collisions are negligible when Knudsen flow occurs, λ_{12}^g may vanish. Then

$$[65] \qquad \frac{l}{N_0}\frac{dJ_1}{d[p_1^g]_{x=0}} = \{(\lambda_{11}^s+\lambda_{12}^s)(Ak_s+S\epsilon)+(1-S)\epsilon\lambda_{11}^g\}_{x=0}.$$

I wish to acknowledge various helpful discussions with Dr. L. A. G. Sylmore, now of the University of Perth, W. Australia, and with Mr. R. Ash, of this department.

REFERENCES

1. E. A. Flood. Spec. Rept. 40, Highway Res. Board, Washington. p. 65.
2. E. R. Gilliland, R. F. Baddour, and J. L. Russell. J. Am. Inst. Chem. Engrs. **4**, 90 (1958).
3. J. D. Babbit. Can. J. Res. Sect. A, **28**, 449 (1950).
4. T. L. Hill. J. Chem. Phys. **18**, 246 (1950).
5. D. H. Everett. Trans. Faraday Soc. **46**, 453, 942, 957 (1950).
6. S. R. De Groot. Thermodynamics of irreversible processes. North Holland Publishing Co., Amsterdam. 1961. p. 98.
7. R. Ash, R. M. Barrer, and C. G. Pope. Proc. Roy. Soc. (London), Ser. A, **271**, 19 (1963).
8. R. M. Barrer and T. Gabor. Proc. Roy. Soc. (London), Ser. A, **251**, 353 (1959).
9. R. M. Barrer and T. Gabor. Proc. Roy. Soc. (London), Ser. A, **256**, 267 (1960).
10. R. M. Barrer. J. Appl. Phys., Suppl. No. 3, 49 (1954).
11. R. Ash, R. M. Barrer, and A. Logan. In preparation.
12. R. M. Barrer and E. E. Strachan. Proc. Roy. Soc. (London), Ser. A, **231**, 52 (1955).
13. L. A. G. Aylmore and R. M. Barrer. In preparation.
14. K. Kammermeyer and D. D. Wyrick. Ind. Eng. Chem. **50**, 1309 (1958).

Can. J. Chem. Downloaded from www.nrcresearchpress.com by 210.87.254.40 on 09/05/12
For personal use only.

INTERDIFFUSION IN THALLIUM AMALGAMS

W. T. FOLEY AND L. E. REID[1]
Department of Chemistry, St. Francis Xavier University, Antigonish, Nova Scotia
Received January 25, 1963

ABSTRACT

The interdiffusion coefficient of thallium in thallium amalgams was measured by the capillary reservoir technique. At 25° C the values of 10^5D in cm^2 sec^{-1} at 0.00365, 0.0536, 0.0895, 0.148, 0.188, 0.283, 0.323, and 0.404 mole fraction thallium were 1.08, 1.37, 1.50, 1.37, 1.14, 0.83, 0.95, and 1.11 respectively with standard deviations in 10^{-5}(cm^2 sec^{-1}) of 0.03, 0.06, 0.09, 0.10, 0.09, 0.08, 0.08, and 0.11 respectively. The minimum in the value of D at 0.288 mole fraction thallium shows that the compound Tl_2Hg_5 plays a significant role in the diffusion process. Values of $\partial \ln a/\partial \ln N$ for the thallium and for the compound were used to explain the dependence of D on the concentration.

This study of diffusion in thallium amalgams was undertaken because this unusual system is liquid at room temperature from 0 to 42 wt% thallium and because accurate thermodynamic data are available from the classic work of Richards and Daniels (1) on thallium amalgam concentration cells. For the concentration range 0.137–0.160 wt% thallium, von Wogau (2) reports that at 11.0–12.0° C the diffusion coefficient of thallium is 1.03×10^{-5} cm^2 sec^{-1}; and, for the concentration range 0.00216 to 0.00287 wt% thallium, Furnam and Cooper (3), from polarographic measurements at 25° C, found that the diffusion coefficient was 0.99×10^{-5} cm^2 sec^{-1}. Stromberg (4), from polarographic measurements on a 10^{-3} wt% amalgam, deduced a value of 1.60×10^{-5} cm^2 sec^{-1}.

The experimental method used was based on that employed by Anderson and Saddington (5) with the modification that a chemical rather than a radiochemical method of analysis was used. Fick's second law of diffusion for a one-dimensional system states that

$$\partial c/\partial t = D\cdot\partial^2 C/\partial x^2, \qquad [1]$$

where c is the concentration of the diffusing species, t is the time, and D is the diffusion coefficient with dimensions of area per unit of time. Consider a capillary of length l, with one end closed, having an initial concentration C_1 uniform throughout. Let the capillary be immersed in so large a volume of solution of composition C_∞ that at infinite time when diffusion is complete and the composition within the capillary and outside the capillary is the same the composition is still C_∞. The solution of equation [1] for time t under these circumstances is

$$\frac{C_{av}-C_\infty}{C_1-C_\infty} = \frac{8}{\pi^2}\sum_{n=0}^{n=\infty}\frac{1}{(2n+1)^2}\exp\left(\frac{2n+1}{2l}\right)^2\pi^2 Dt, \qquad [2]$$

where C_{av} is the average composition of the solution in the capillary at time t. The series on the right side of equation [2] is rapidly convergent.

In the derivation of equation [2] from equation [1] it was assumed that the diffusion coefficient is independent of the concentration. When the difference in concentrations of the two solutions is small, it may be assumed that the diffusion coefficient is constant. In this present work a chemical method of analysis was used to evaluate the terms on the left-hand side of equation [2] with the result that in both the numerator and the denomi-

[1]*Holder of National Research Council Bursary 1961–1962 and holder of National Research Council Studentship 1962–1963.*

Can. J. Chem. Downloaded from www.nrcresearchpress.com by 210.87.254.105 on 09/05/12
For personal use only.

nator there are small differences between large numbers. The success of the experiment depended upon having such a difference in concentration of the two solutions that the value for the left side of equation [2] would have accuracy, yet that the difference in concentration would not be so great as to render equation [2] inapplicable. The situation was not a happy one, but the results obtained for the concentration differences chosen are significant.

EXPERIMENTAL

The mercury used was purified by washing for long periods of time with dilute nitric acid while a stream of air was bubbled through it. After this treatment the metal was distilled. Thallium sulphate, which assayed 99.9%, was recrystallized once and the salt thus obtained was used to prepare the amalgams by electrolysis. The electrolyte was made 1 F with respect to sodium hydroxide and it contained hyrazine as an anodic depolarizaer. The metal was plated into the mercury at a controlled cathode potential of −0.53 v with respect to the standard hydrogen electrode. The normal reduction potential for lead in this electrolyte is −0.58 v so that there is no danger of lead being plated.

In a preliminary investigation of the diffusion coefficient, the more concentrated amalgam was placed in a 400-ml beaker and the amalgam was protected against corrosion by making it the cathode in an electrolysis cell. The electrolyte, which covered the amalgam to a depth of 1 inch, was 3% with respect to sodium sulphate and 1% with respect to hydrazine sulphate. A platinum anode, 2 cm^2 in area, dipped into the sulphate solution and the polarizing current of 5 ma was obtained by placing a 40,000-ohm resistor in series with the cell and a 200-v direct-current power supply. The diffusion cells, approximately 3 cm long and 1 mm in internal dimaeter, were made from pyrex capillary tubing of precision bore and the bottoms were made perfectly flat. A travelling microscope was used to measure the lengths of the capillaries. In an experiment, the beaker-reservoir was mounted on a stand in a constant-temperature bath regulated to 25±0.02° C. A capillary was filled with the less concentrated amalgam, and under a protecting atmosphere of carbon dioxide, this capillary was lowered into the reservoir until the top of the capillary was almost submerged into the amalgam. When it was felt that thermal equilibrium was reached, the capillary was lowered under the surface of the amalgam in the beaker and the time was noted. A stirrer, which rotated the capillary four times an hour in a circle with a radius of 1 inch, was attached to the capillary holder. An effort was made to have the average concentration of the amalgam in the capillary at the conclusion of a run about equal to the average of the initial concentration of the amalgam in the capillary and of the concentration of the amalgam in the reservoir; and, to that end, the diffusion was allowed to proceed for a period of from 20 to 60 hours. At the end of the run, the capillary was withdrawn, weighed, and its contents were removed with the aid of a centrifuge. The capillary was rinsed with dilute nitric acid which was then used to dissolve the amalgam. This solution was analyzed for thallium, and this result, along with a knowledge of the concentration of thallium in the two initial amalgams, the time t, and the capillary length l, was used in equation [2] to evaluate D.

The method used to analyze the amalgam was that described by Foley and Osyany (6), which method depends on the removal of mercury through the use of formic acid followed by the estimation of thallium by means of an iodate titration to an iodine monochloride end point. If the sample were micro or semi-micro, the thallium was estimated by coulometric titration with electrogenerated bromine in the manner described by Buck, Farrington, and Swift (7).

The procedure outlined above worked well only when mercury was used in the capillary. The apparatus shown in Fig. 1 was next adopted. In an experiment, vessel A was charged with the more dilute amalgam

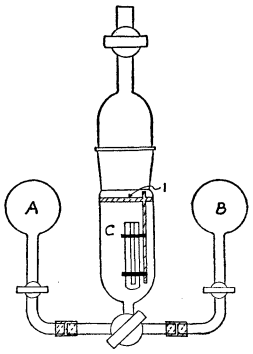

FIG. 1. Apparatus for diffusion measurements.

Can. J. Chem. Downloaded from www.nrcresearchpress.com by 210.87.254.105 on 09/05/12
For personal use only.

under vacuum, and vessel B was charged with the more concentrated amalgam. The reaction vessel C was evacuated and the more dilute amalgam was admitted into C until the solution covered the capillary supported by the holder I. The stopcock joining A and C was closed and purified nitrogen gas was admitted into chamber C until the pressure was 1 atm. The gas was now pumped off and the amalgam, except for that which was in the capillary, was restored to vessel A. The apparatus was now transferred to the constant-temperature bath; and, when it was felt that thermal equilibrium was established, the more concentrated amalgam was admitted to chamber C until the capillary was covered. The stopcock joining B and C was closed and purified nitrogen gas was admitted until the pressure was 1 atm. At the end of the run, the amalgam was restored to vessel B and the capillary was removed and treated as described above.

Even though the reaction vessel was firmly clamped to a sturdy stand while it was in the water bath, the surface of the amalgam was never quiescent. It is important that the amalgam just above the top of the capillary be always of the same concentration as that of the whole reservoir. Some users of the capillary-reservoir technique, for example, Burkell and Spinks (8), have assumed that stirring is unnecessary to maintain this boundary condition. To determine whether a stirrer should be added to the apparatus of Fig. 1, 10 runs were made with mercury in the capillary and with the same concentration of amalgam in the reservoir as was used in the open-beaker method. The average diffusion coefficient and the standard deviation of the diffusion coefficients obtained in the two cases were the same, and it was thus concluded that the boundary conditions were being met.

EXPERIMENTAL RESULTS

The experimental results are given in Table I and they are also displayed in Fig. 2 by the plot of the experimental diffusion coefficient against the mean mole fraction for the concentration interval used.

TABLE I

Interdiffusion of thallium at 25° C

Mole fraction thallium		$D \times 10^5$	Std. Deviation $\times 10^5$	Number
Capillary	Reservoir	(cm^2 sec^{-1})	(cm^2 sec^{-1})	of runs
0	0.00710	1.08	0.028	20
0.0462	0.0611	1.37	0.061	13
0.0797	0.0993	1.50	0.088	8
0.138	0.158	1.37	0.103	9
0.178	0.198	1.14	0.087	9
0.268	0.298	0.83	0.084	12
0.306	0.339	0.95	0.081	8
0.388	0.420	1.11	0.110	8

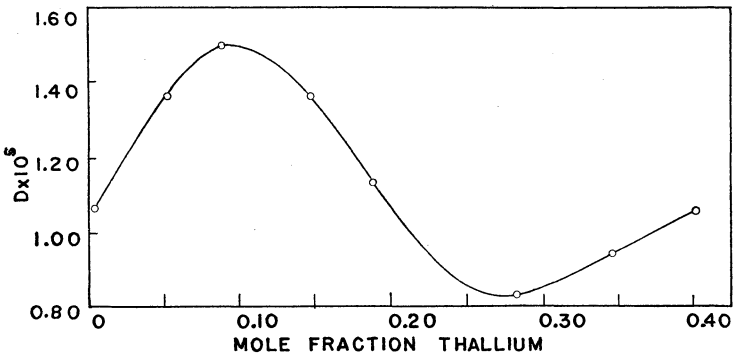

FIG. 2. Variation of D with concentration.

DISCUSSION

An understanding of the factors that determine the diffusion coefficient in a binary system would require a complete theory of the liquid state. With the information presently

Can. J. Chem. Downloaded from www.nrcresearchpress.com by 210.87.254.105 on 09/05/12
For personal use only.

available it is possible to give a qualitative explanation of the experimental results obtained in the thallium mercury system. Jost (9) gives equation [3] below to express the dependence of the rate of change of concentration with time of a diffusing species:

$$\frac{\partial c}{\partial t} = \frac{\partial}{\partial x}\left(\frac{cu}{N}\frac{\partial \mu}{\partial x}\right), \qquad [3]$$

where c = molar concentration, u = mobility of the diffusing particle per unit force, μ = chemical potential, and N = Avogadro's number. Introducing the activity a, we find

$$\frac{\partial c}{\partial t} = \frac{\partial}{\partial x}\left(D_0 \frac{\partial \ln a}{\partial \ln N_i}\frac{\partial c}{\partial x}\right), \qquad [4]$$

where $D_0 = ukT$ and $\partial \ln c = \partial \ln N_i$ and N_i is the mole fraction.

If we compare equations [1] and [4], we see that for non-ideal mixtures D should be replaced by

$$D = D_0 \frac{\partial \ln a}{\partial \ln N_i}.$$

The coefficient D_0, thus defined, is independent of deviations from ideal behavior, but it may still depend on concentration, since the mobility may depend on concentration.

The phase diagram for thallium and mercury (10) shows that at 28.95% thallium by weight there is a compound whose formula is Tl_2Hg_5. The electromotive force data of Richards and Daniels (1) were extrapolated to 14.9° C, the freezing point of the compound, and the activities of thallium and mercury were calculated from these extrapolated data for 14.9° C. The equilibrium constant for the chemical reaction leading to the formation of the compound is

$$K = (a_{Tl})^2 \times (a_{Hg})^5 / a_{Tl_2Hg_5}.$$

At 14.9° C and at 28.95% Tl the activity of the thallium is 1.92 and the activity of the mercury is 0.566. If we assume that at 14.9° C the activity of the compound is unity, the value of the equilibrium constant is about 0.2. At 25° C the activity of thallium in the amalgam increases very rapidly with increase of thallium content; but the activity of the mercury, on the other hand, more closely obeys the law of ideal solutions. This variation of activity with concentration may be accounted for by the fact that Tl_2Hg_5 removes from the solvent more mercury than thallium. The activity data at 325° C of Hildebrand and Eastman (11) show that the activity of thallium is so high in concentrated amalgams that one must conclude that the compound still exists in the liquid phase at this temperature. Hence, it is felt that the value of the equilibrium constant K will not change much when the temperature is raised from 14.9° C to 25° C and thus K is arbitrarily assigned a value of 0.2.

To account for the experimental curve of Fig. 2 values of $\partial \ln a/\partial \ln N$ were determined for thallium and for the compound Tl_2Hg_5. Richards and Daniels (1) obtained at 20° C and 30° C electromotive force data for concentration cells made up with a wide range of concentrations of thallium amalgams. These electromotive force data were interpolated to yield results valid for 25° C and the activities of mercury and thallium were calculated from these interpolated electromotive force data in the same manner as that described by Lewis and Randall (12). These activities are given in columns two and four of Table II. From a plot of log a_{Tl} against log N_{Tl} values of $\partial \ln a/\partial \ln N$ were obtained by measuring tangents to the curve. The results, shown in column three of Table II, reveal that $\partial \ln a/\partial \ln N$ increases very rapidly between mole fractions 0.005 and 0.10. This rise

Can. J. Chem. Downloaded from www.nrcresearchpress.com by 210.87.254.105 on 09/05/12
For personal use only.

TABLE II

Activities of Tl and Tl_2Hg_5 and values of $\partial \ln a/\partial \ln N$ at 25° C

N_1, mole fraction Tl	a_1, activity of thallium	$\frac{\partial \ln a_1}{\partial \ln N_1}$	a_2, activity of mercury	a_{12}, activity of compound	N_{12}, mole fraction Tl_2Hg_5	$\frac{\partial \ln a_{12}}{\partial \ln N_{12}}$
0.005	0.0052	1.06	0.994	1.32×10^{-4}	3.45×10^{-3}	2.60
0.010	0.012	1.10	0.988	6.78×10^{-4}	5.11×10^{-3}	2.60
0.020	0.026	1.21	0.979	3.03×10^{-3}	1.06×10^{-2}	2.50
0.040	0.092	1.41	0.967	3.39×10^{-2}	2.27×10^{-2}	2.40
0.050	0.100	1.50	0.945	3.77×10^{-2}	3.86×10^{-2}	2.35
0.080	0.190	1.65	0.895	1.03×10^{-1}	5.25×10^{-2}	2.25
0.10	0.240	1.70	0.852	1.27×10^{-1}	7.14×10^{-2}	2.00
0.15	0.570	1.85	0.770	5.60×10^{-1}	0.136	1.70
0.20	0.96	1.85	0.692	0.735	0.251	0.80
0.25	1.41	1.70	0.618	0.893	0.500	0.35
0.2875	1.76	1.70	0.572	0.948	1.00	0.00
0.35	2.42	1.65	0.493	0.839	0.590	−0.13
0.40	3.08	1.45	0.440	0.787	0.428	−0.62

accounts for the rapidly increasing values of D for the same concentration range because, as will be explained below, the rate of diffusion of the compound remains quite constant in this concentration interval.

To explain the minimum in the curve it was necessary to calculate the activity of the compound from the equilibrium constant and from the activities of mercury and thallium. These results are given in column five of Table II. In a manner similar to that described above values of $\partial \ln a/\partial \ln N$ were obtained for the compound and they are shown in column seven of Table II. The curve was parabolic so that $\partial \ln a/\partial \ln N$ falls to zero and then becomes negative. Between thallium mole fraction 0.08 and 0.2857 the tendency for the compound to diffuse falls steadily and the rate of diffusion of thallium atoms changes but little and this is reflected in the observed minimum in Fig. 2. For thallium mole fractions beyond 0.2857 the compound diffuses out of the capillary into the reservoir. The compound removes two and one-half times as much mercury as thallium so that the net result is an increase in the diffusion of thallium into the capillary. This is in contrast to the concentration range less than 0.2857 mole fraction because then the diffusion of the compound into the capillary increases the thallium content of the capillary.

Self-diffusion coefficients for thallium–mercury systems will be measured in this laboratory in the hope that further light will be shed on diffusion in these solutions.

ACKNOWLEDGMENT

Grateful acknowledgment is made by one of us, W. T. F., for a grant in aid of this research from the National Research Council of Canada.

REFERENCES

1. T. W. Richards and F. Daniels. J. Am. Chem. Soc. **41**, 1732 (1919).
2. M. von Wogau. Ann. Physik, **23**, 345 (1907).
3. N. H. Furman and W. C. Cooper. J. Am. Chem. Soc. **74**, 6183 (1952).
4. A. G. Stromberg. Dokl. Akad. Nauk SSSR, **85**, 831 (1952).
5. J. S. Anderson and K. Saddington. J. Chem. Soc. S381 (1949).
6. W. T. Foley and J. M. Osyany. Anal. Chem. **24**, 1195 (1952).
7. R. P. Buck, P. S. Farrington, and E. H. Swift. Anal. Chem. **24**, 1195 (1952).
8. J. E. Burkell and J. W. T. Spinks. Can. J. Chem. **30**, 311 (1952).
9. W. Jost. Diffusion. Revised ed. Academic Press, New York. 1960. p. 156.
10. R. N. Lyon (*Editor*). Liquid-metals handbook. 2nd ed. U.S. Gov. Printing Office, Washington. 1952. p. 93.
11. J. H. Hildebrand and E. D. Eastman. J. Am. Chem. Soc. **37**, 2452 (1915).
12. G. N. Lewis and M. Randall. J. Am. Chem. Soc. **43**, 233 (1921).

Can. J. Chem. Downloaded from www.nrcresearchpress.com by 210.87.254.105 on 09/05/12
For personal use only.

ON THE RELATIONSHIP BETWEEN INTERNAL PRESSURE AND ULTRASONIC VELOCITY[1,2]

S. C. SRIVASTAVA[3] AND N. BERKOWITZ
Coal Research Division, Research Council of Alberta, Edmonton, Alberta
Received December 26, 1962

ABSTRACT

Because of the relevance of internal pressure data to sonochemical kinetics, some interest attaches to expressions which permit evaluation of P_i from readily available or easily measured quantities. One such expression is developed in this paper. It relates P_i to the velocity u of ultrasonic waves transmitted through the liquid and takes the form $u\sqrt{D} = K'\sqrt{(R_m)}P_i$, where K' is a constant proportional to $\sqrt{(C_p/C_v)}\sqrt{(1/RT)}$, and D and R_m denote the density and molar refraction of the liquid.

The utility of this expression is tested against some 100 liquids (including a few binary liquid mixtures and aqueous electrolyte solutions), and it is shown that the equation offers an acceptable and quite general method for calculating P_i.

I. INTRODUCTION

Despite a considerable literature, details of sonochemical decomposition reactions remain generally uncertain and often controversial. In the case of *large* molecules (m.w. > ca. 5000) it is, however, at least possible to clearly discern the major variables that affect such reactions: as a rule, their rates depend upon the size of the reacting species, upon the frequency and intensity of the sound waves, and upon the intensity of cavitation in the liquid reaction medium. Decomposition or depolymerization in the absence of cavitation* is now conceded to be minimal (2).

No such view can be taken of sonochemical reactions involving *small* molecules, e.g. partial dehalogenation of $CHCl_3$, CCl_4, or KI. In most, if not in fact all, such instances, sound frequency and intensity are somewhat irrevelant (except insofar as they affect cavitation); and while cavitation is as necessary a prerequisite as in the case of large molecules, cavitation intensities per se, no matter how these might be defined, exert only an indirect control over reaction rates. For example, while *aqueous solutions* of $CHCl_3$ and CCl_4 will liberate Cl_2 at frequencies and intensities as low as 10 kc/s and 2 w/cm^2 and do so at increasing rates as the cavitation intensity is raised, *pure* $CHCl_3$ or CCl_4 will not measurably decompose even when they are made to cavitate with greater intensity than their solution counterparts (3). The same is qualitatively true of dichloro- and diiodo-methane, ethyl chloride, and dichloro- and dibromo-ethane (4), and of CS_2 which *inter alia* yields elemental sulphur (5).

In the light of these findings—which may, however, gain undue prominence from the fact that no serious study has yet been made of non-aqueous solutions—it is tempting to regard sonochemical decompositions of small molecules as in reality initiated and sustained by a peroxide mechanism which, as a first step, involves

$$H_2O \rightleftharpoons OH + H \qquad (a)$$

$$2OH \rightleftharpoons H_2O_2. \qquad (b)$$

[1]*Contribution No. 203 from the Research Council of Alberta, Edmonton.*
[2]*For a preliminary discussion of this topic, see ref. 1.*
[3]*RCA Postdoctoral Fellow, 1961–1963.*
**Cavitation can be virtually completely suppressed by thorough outgassing of the liquid reaction medium before exposure of the solution (or suspension) to the action of an ultrasonic field.*

Can. J. Chem. Downloaded from www.nrcresearchpress.com by 210.87.254.105 on 09/05/12
For personal use only.

(That some such conversion actually occurs when water is exposed to ultrasonic sound seems to be fairly conclusively established; cf. ref. 6.) But two pieces of evidence combine to make this a doubtful contention: (1) there is no indication of *oxidative* breakdown when aqueous suspensions or solutions of polymers are ultrasonically degraded, and (2) experiments in these laboratories indicate that aqueous solutions of, say, CCl_4 will decompose with liberation of Cl_2 at frequencies ($<$20 kc/s) at which water itself forms little H_2O_2.*

A better approach is therefore to suppose that sonochemical decomposition of small molecules will occur whenever the internal pressure (P_i) of the reaction medium exceeds some critical threshold value and to associate effective rate control with energy releases resulting from the collapse of cavitational 'holes'. (Since the internal pressure of water is 3–5 times greater than that of $CHCl_3$, CCl_4, etc., such a view would qualitatively account for the behavior of pure compounds vis-a-vis their aqueous solutions and, at the same time, assign an appropriate role to the cavitation intensity.)

In the prevailing absence of sufficient (and acceptable) sonochemical kinetic data, the mechanism here postulated must, of course, remain purely speculative. But it should be observed that it would, if valid, make P_i a uniquely important parameter in sonochemistry. In 'steady state' cavitation, i.e. when the number of developing 'holes' equals the number of collapsing 'holes', the cavitation intensity can be quite properly expressed in terms of the corresponding liquid volume increment Δv; and since the work entailed in forming the 'holes' may then be put as proportional to $P_i \Delta v$, where

$$P_i \simeq T(\partial P/\partial T)_v \simeq (\partial E/\partial v)_T,$$

it follows that the maximum energy released by 'hole' collapse (and therefore available for sonochemical reaction) should be proportional to $\int_0^{\Delta v} (\partial E/\partial v)_T dv$.

II. THE FUNCTION $u = f(P_i)$

With these considerations in mind, some interest attaches to expressions which permit evaluation of P_i from readily available or easily measured quantities. Such expressions are, of course, perfectly well known in principle. But since they entail the use of frequently unreliable (7) thermal expansion or compressibility coefficients or the direct measurement of $(\partial P/\partial T)_v$, the alternatives developed (and explored) in this paper may be thought to offer a worthwhile simplification.

It should perhaps also be noted here that while the derivation of the final form (equation (ix)) involves a number of approximations that do not enter into other expressions for P_i, the actual errors introduced by them do not exceed the errors normally incurred when estimating P_i by the various alternative methods. It is therefore possible to regard these approximations (and their more obvious shortcomings) with some equanimity.

A convenient starting point for deriving the desired relationship is afforded by Van der Waal's equation of state

$$(P + a/v^2)(v-b) = RT, \qquad \text{(i)}$$

which, when differentiated with respect to v at constant temperature and then multiplied by v, yields

$$-v(\partial P/\partial v)_T + 2a/v^2 = vRT/(v-b)^2 \qquad \text{(ii)}$$

**No hydrogen peroxide could, under these conditions, be detected by methods whose detection limits were of the order of 10^{-4} to 10^{-6} mole/100 cc. The primary reaction step must therefore be assumed to be $CCl_4 \rightarrow CCl_3 + Cl$, followed by $2Cl \rightarrow Cl_2$ and $2CCl_3 \rightarrow C_2Cl_6$. (A solid, white precipitate possibly corresponding to this latter compound has, in fact, been observed.)*

Can. J. Chem. Downloaded from www.nrcresearchpress.com by 210.87.254.105 on 09/05/12
For personal use only.

whence

$$-v(\partial P/\partial v)_T + 2a/v^2 = vRT/(v-b) - RTb/(v-b)^2 + RTb/(v-b)^2$$
$$= RT/(v-b) + (b/RT)[R^2T^2/(v-b)^2] \quad \text{(iii)}$$

or, after substitution of terms from (i),

$$-v(\partial P/\partial v)_T = P - a/v^2 + (b/RT)[P+(a/v^2)]^2. \quad \text{(iv)}$$

Replacing $-(1/v)(\partial v/\partial P)_T$ by the isothermal compressibility β_{iso}, and making use of the observation (8, 9, 10) that many liquids obey $a/v^2 = (\partial E/\partial v)_T \simeq P_i$, equation (iv) becomes

$$1/\beta_{iso} \simeq P - P_i + (b/RT)(P+P_i)^2 \quad \text{(v)}$$

or, since $P \ll P_i$,

$$1/\beta_{iso} \simeq (b/RT)P_i^2 - P_i. \quad \text{(vi)}$$

And since $(b/RT)P_i^2 \gg P_i$, $\beta_{iso}/\beta_{adia} = C_p/C_v$, and $1/\beta_{adia} = u^2D$, where β_{adia} and D denote the adiabatic compressibility and density of the liquid, and u the velocity of ultrasonic waves transmitted through it, (vi) may be written as

$$u^2D \simeq (C_p/C_v)(b/RT)P_i^2 \quad \text{(vii)}$$

which, after putting $b = 4M/D$, where M = molecular weight, becomes

$$uD \simeq K\sqrt{(M)}P_i, \quad \text{(viii)}$$

where $K = \sqrt{(C_p/Cv)}\sqrt{(4/RT)}$. Alternatively, remembering that

$$b = f\left(\frac{4}{3}\pi Nr^3\right),$$

where the bracketed term denotes the actual (as opposed to the apparent) molecular volume/mole, and that

$$\frac{n_\infty^2 - 1}{n_\infty^2 + 2}\frac{M}{D} = \frac{4}{3}\pi Nr^3$$

equation (viii) can be written in the form

$$u\sqrt{D} \simeq K'\sqrt{(R_m)}P_i, \quad \text{(ix)}$$

where $K' = \sqrt{(C_p/C_v)}\sqrt{(k_0/RT)}$ and R_m = molar refraction. k_0 (contained in K', is the proportionality constant connecting b with the RHS of the molar refraction equation.

While the Van der Waal's equation is an admittedly poor approximation for liquids—and here only preferred because of its simplicity—equations (viii) and (ix) turn out to be quite useful.

Table I offers a test of (viii) and (ix) by listing values of K and K' for several classes of compounds for which the necessary data (i.e. values of u, D, R_m, and P_i) were available in the literature. The bracketed numbers in column A indicate the number of compounds in each class, while columns B and C list the calculated (weighted arithmetic mean) values of K and K' and the maximum deviations from these. In general, equation (ix) leads to slightly narrower error limits than (viii) and appears therefore to be somewhat more useful. But the intraclass variation of *either* K *or* K' is sufficiently small to permit evaluation of P_i with no greater uncertainty than attaches to its determination by other means.

Can. J. Chem. Downloaded from www.nrcresearchpress.com by 210.87.254.105 on 09/05/12
For personal use only.

TABLE I

Class		K		K'	
1. Paraffins	(13)	3.64	$^{+0.24}_{-0.27}$	7.52	$^{+0.17}_{-0.07}$
2. Monoolefins	(8)	3.93	$^{+0.46}_{-0.39}$	7.52	$^{+0.25}_{-0.28}$
3. Aromatic hydrocarbons	(6)	4.00	$^{+0.37}_{-0.19}$	7.13	$^{+0.18}_{-0.17}$
4. Nitro compounds	(4)	3.67	$^{+0.17}_{-0.50}$	6.73	$^{+0.09}_{-0.08}$
5. Aliphatic chlorides	(8)	3.87	$^{+0.19}_{-0.10}$	7.55	$^{+0.31}_{-0.18}$
6. Aromatic chlorides	(8)	3.82	$^{+0.04}_{-0.10}$	6.89	$^{+0.26}_{-0.29}$
7. Aliphatic bromides	(8)	3.58	to 5.02	6.14	to 8.81
8. Aliphatic iodides	(4)	3.76	$^{+0.11}_{-0.07}$	6.88	$^{+0.06}_{-0.16}$
9. Esters	(10)	3.76	$^{+0.20}_{-0.16}$	7.21	$^{+0.68}_{-0.90}$
10. Alcohols (cf. note A)	(13)	3.29	$^{+0.72}_{-1.05}$	6.55	$^{+1.28}_{-1.59}$
11. Monocarboxylic acids (cf. note B)	(6)	3.58	$^{+0.86}_{-0.65}$	6.74	$^{+1.72}_{-0.78}$

NOTE A: If MeOH is omitted because of its abnormalities in other respects (7), K and K' become, respectively, 3.39 (+0.62, −0.55) and 6.89 (+0.96, −0.88), i.e. K' obeys the generalization $K' = 7 \pm 1$.
NOTE B: If C_{17} is omitted and consideration confined to C_3 to C_7, the values of K and K' become, respectively, 3.40 (+0.07, −0.47) and 6.40 (+0.35, −0.44).

On the other hand, both K and K' are distinctly structure dependent (cf. interclass variation of these constants); and in several instances, both constants show a systematic and more or less regular increase when proceeding from one member of a homologous series to the next. For example, for six straight-chain monocarboxylic acids, K' increased from 5.96 for C_3 to 6.75 for C_7 and 8.46 for C_{17}, i.e. $\Delta K'$ decreased progressively as the chain length increased. But among monoolefins, K' increased from 7.23 for C_7 (1-heptene) to 7.77 for C_{16} (1-hexadecene) at $\Delta K' = 0.05$ per incremental carbon atom; and for three *n*-alkyl bromides covering the range from C_2 to C_8, K' increased linearly at $\Delta K' = 0.07$ per incremental C atom. These observations, and the fact that the inclusion of several homologous series in any one class can, as in the case of aliphatic bromides, lead to fairly wide and occasionally seemingly erratic variations in K and K', suggest that both constants may be markedly affected by polarity, association, and (perhaps) molecular packing.

III. THE TEMPERATURE DEPENDENCE OF P_i

If equation (ix) is written in the form

$$u\sqrt{D} \simeq \sqrt{(C_p/C_v)}\sqrt{(k_0/R)}\sqrt{(1/T)}\sqrt{(R_m)}P_i$$

and C_p/C_v assumed to be effectively temperature independent over the range encompassed by liquidity, K' resolves itself into two terms of which one is temperature insensitive and the other equal to $\sqrt{(1/T)}$. By putting $K'' = \sqrt{(k/T)}$, where k is the temperature-insensitive component of K' (and therefore uniquely determined if K' is known at any one temperature), the variation of P_i with temperature can consequently be estimated by means of

$$u\sqrt{D} \simeq K''\sqrt{(R_m)}P_i, \qquad (x)$$

Can. J. Chem. Downloaded from www.nrcresearchpress.com by 210.87.254.105 on 09/05/12
For personal use only.

where u, D, and R_m are the ultrasonic velocity, liquid density, and molar refraction at the particular temperature T at which P_i is to be evaluated.

Table II shows some results calculated from published values of u by means of equation (x); the second and fifth columns list values of P_i and the third and sixth the corresponding values of $(\partial P/\partial T)_v$, i.e. P_i/T_{abs}. While their accuracy cannot be directly checked, Table III (taken from Hildebrand *et al.* (8)) suggests that they are unlikely to be much in error.

TABLE II

Toluene			*p*-Xylene		
Temperature, °C	P_i, atm	$(\partial P/\partial T)_v$	Temperature, °C	P_i, atm	$(\partial P/\partial T)_v$
3.0	3056	11.07	2.3	2448	8.89
10.0	3021	10.67	10.0	2428	8.57
20.0	3000	10.24	18.0	2408	8.27
31.8	2968	9.76			

TABLE III

Values of $(\partial P/\partial T)_v$—after Hildebrand *et al.* (8)

	$(\partial P/\partial T)_v$ at:		
	20° C	25° C	35° C
n-Heptane	8.66	8.41	7.93
Carbon tetrachloride	11.47	11.22	10.33
Benzene	12.58	12.23	11.49
Acetone	11.72	11.22	10.33

IV. LIQUID MIXTURES AND SOLUTIONS

For simple binary mixtures, equations (ix) assumes the form

$$u_{12}\sqrt{D_{12}} \simeq (K_1'x_1+K_2'x_2)\sqrt{(R_m)_{12}}(P_i)_{12}, \qquad \text{(xi)}$$

where x_1 and x_2 denote the mole fractions of the two components and the subscript '12' refers to the mixture.

A test of this expression is contained in Table IV, in which values of P_i (computed from published data and equation (xi)) and of $(\partial P/\partial T)_v$ (calculated via (x)) are compared with corresponding values given by Hildebrand *et al.* (8). The agreement appears to be aceptable.

TABLE IV

Mixture	Mole fraction	From equation (xi)		From Hildebrand (8)	
		P_i, atm	$(\partial P/\partial T)_v$	P_i, atm	$(\partial P/\partial T)_v$
C_6H_6 in CCl_4; 20° C	0	3087	10.53	3360	11.47
	50	3271	11.16	3572	12.19
	100	3410	11.64	3686	12.58
n-C_7H_{16} in CCl_4; 20° C	50	2783	9.49	2836	9.68
	100	2179	7.43	2573	8.66
C_6H_6 in *n*-C_7H_{16}; 20° C	50	2587	8.83	2889	9.86

For *dilute* solutions, $(K_1'x_1+K_2'x_2)$ becomes effectively equal to K_1', i.e. to the value of K' for the solvent, and equation (xi) then reduces to

$$u_{12}\sqrt{D_{12}} \simeq K'\sqrt{(R_m)_{12}}(P_i)_{12}$$

Can. J. Chem. Downloaded from www.nrcresearchpress.com by 210.87.254.105 on 09/05/12
For personal use only.

or

$$\simeq K'\sqrt{(R_m)_{12}}(P_i+\Delta P_i), \qquad \text{(xii)}$$

where P_i denotes the internal pressure of the solvent and $(P_i)_{12}$ that of the solution.

The major interest attaching to (xii) centers on the observation that for aqueous electrolyte solutions, ΔP_i turns out to be directly proportional to the osmotic pressure of the solution, and that π_{12} and the osmotic coefficient ϕ (the latter via (xiii)) can hence be estimated from a knowledge of u_{12}. Some examples of this proportionality between ΔP_i and π_{12} are shown in Figs. 1, 2, and 3. The values of π_{12} used in constructing these diagrams

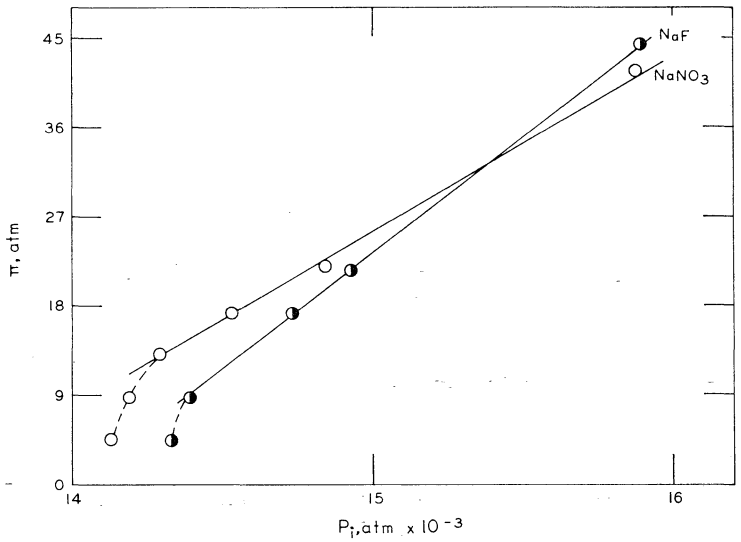

FIG. 1. Variation of osmotic pressure with internal pressure—aqueous solutions of NaF and $NaNO_3$.

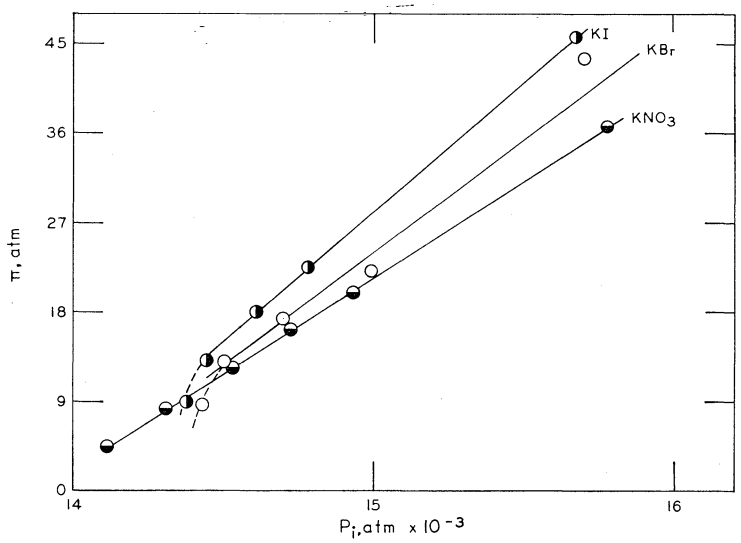

FIG. 2. Variation of osmotic pressure with internal pressure—aqueous solutions of KI, KBr, and KNO_3.

Can. J. Chem. Downloaded from www.nrcresearchpress.com by 210.87.254.105 on 09/05/12
For personal use only.

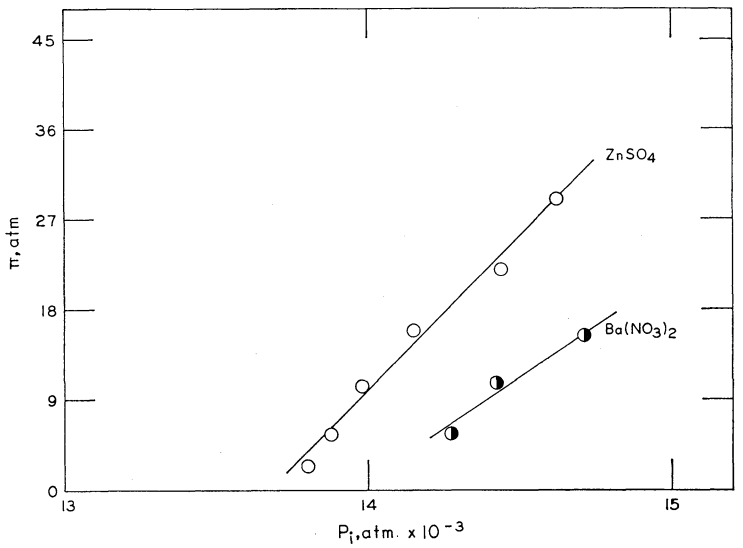

FIG. 3. Variation of osmotic pressure with internal pressure—aqueous solutions of $ZnSO_4$ and $Ba(NO_3)_2$.

were calculated from published values of ϕ by means of the usual relationship

$$\pi_{12} = \frac{RT\bar{n}mW_s}{V_s \cdot 1000}\,\phi, \qquad \text{(xiii)}$$

in which m is the molality of the solution, $\bar{n}$ the number of ions/molecule of electrolyte, and V_s and W_s the partial molal volume and molecular weight of the solvent.

Except at the very lowest concentrations, at which marked departures from linearity are observed in several instances, plots of P_i versus π_{12} are strictly linear with slopes of ca. 0.02 for NaF, 0.016 for $NaNO_3$, 0.02 for KNO_3, 0.025 for KI, 0.023 for KBr, 0.02 for $Ba(NO_3)_2$, and 0.03 for $ZnSO_4$.

REFERENCES

1. S. C. SRIVASTAVA. Indian J. Phys. **33**, 503 (1959).
2. A. WEISSLER. J. Appl. Phys. **21**, 171 (1950).
3. S. C. SRIVASTAVA. Nature, **182**, 47 (1958).
4. A. WEISSLER, H. W. COOPER, and S. SNYDER. J. Am. Chem. Soc. **72**, 1769 (1950). G. WAGNER. Mitt. Chem. Forschungs-Inst. Ind. Oesterr. **3**, 63 (1949). A. KLING and R. KLING. Compt. Rend. **223**, 1131 (1946).
5. S. C. SRIVASTAVA and N. BERKOWITZ. To be published.
6. R. O. PRUDHOME. Bull. Soc. Chim. Biol. **39**, 425 (1957). A. WEISSLER. J. Am. Chem. Soc. **81**, 1077 (1959).
7. J. H. HILDEBRAND and R. L. SCOTT. Solubility of non-electrolytes. Reinhold, New York. 1950. pp 96–97.
8. W. WESTWATER, H. W. FRANTZ, and J. H. HILDEBRAND. Phys. Rev. **31**, 135 (1928).
9. J. H. HILDEBRAND. Phys. Rev. **34**, 649, 984 (1929).
10. J. H. HILDEBRAND and J. M. CARTER. J. Am. Chem. Soc. **54**, 3592 (1932).

Can. J. Chem. Downloaded from www.nrcresearchpress.com by 210.87.254.105 on 09/05/12
For personal use only.

DEVIATIONS FROM THE "MIXTURE LAW" IN THE RADIOLYSIS OF HYDROCARBON MIXTURES

II. YIELDS OF LIQUID PRODUCTS IN MIXTURES OF CYCLOHEXANE AND CYCLOPENTANE[1]

P. J. DYNE AND J. DENHARTOG

Research Chemistry Branch, Atomic Energy of Canada Limited, Chalk River, Ontario

Received March 14, 1963

ABSTRACT

The radiolytic yields of olefins and dimers have been measured in mixtures of cyclohexane and cyclopentane. While the dimeric products ($(C_6H_{11})_2$, $C_6H_{11}\cdot C_5H_9$) show a bias towards C_5 groups, the olefins show a bias towards C_6 groups; the yield of cyclohexene at low concentrations of cyclohexane is more than twice the maximum predicted by the "mixture law". These results confirm earlier isotopic work which showed a higher reactivity of cyclohexane-d_{12} in cyclohexane-d_{12} – cyclopentane mixtures relative to that in cyclohexane-d_{12} – cyclohexane. The results also confirm the preferential change of identity of cyclohexyl radicals to cyclopentyl radicals, which leads to a predominance of C_5 groups in the dimer.

Can. J. Chem. Downloaded from www.nrcresearchpress.com by 210.87.254.42 on 09/05/12
For personal use only.

INTRODUCTION

An alkane solvent can have a large effect on the radiolytic reactivity of other alkane solutes. This effect was first observed in alkane solutions of cyclohexane-d_{12} (C_6D_{12}) where the changes in reactivity were detected through the variation in the D_2 and HD content of the radiolytic hydrogen (1). For example, the yield of D_2 from a dilute solution of C_6D_{12} in cyclopentane is about five times greater than that from a comparable solution of C_6D_{12} in cyclohexane. We called these variations in reactivity deviations from the "mixture law" and concluded that they could only be explained by a physical mechanism, such as energy transfer or charge transfer from the alkane solvent to the cyclohexane-d_{12}.

One would expect that the high yields of D_2 and HD from solutions of C_6D_{12} in cyclopentane would be associated with high yields of the liquid products, cyclohexane-d_{10}, and the dimers $(C_6D_{11})_2$ and $C_6D_{11}\cdot C_5H_9$. By analogy one would also expect high yields of products containing C_6 groups in mixtures of undeuterated cyclohexane and cyclopentane. This last expectation was not, however, in agreement with the results of Muccini and Schuler (2), who studied the dimeric products formed in the radiolysis of cyclohexane–cyclopentane mixtures and found a greater yield of the dimers containing C_5 groups. The composition of the dimer was a function of the dose rate, the bias towards C_5 groups being more pronounced at low dose rates.

In iodine solutions Muccini and Schuler found that the yields of cyclohexyl iodide and cyclopentyl iodide were linear functions of the composition. From this they concluded that the initial yields of C_5 and C_6 radicals were, respectively, proportional to the electron fractions of cyclopentane and cyclohexane. The high yield of C_5 groups in the dimer was then explained by the change of identity reactions

$$C_6H_{11}\cdot + C_5H_{10} \rightarrow C_6H_{12} + C_5H_9\cdot \quad [1]$$

$$C_5H_9\cdot + C_6H_{12} \rightarrow C_5H_{10} + C_6H_{11}\cdot \quad [2]$$

If the rate constants for these reactions differed, k_1 being greater than k_2, then the steady state radical distribution would contain a greater fraction of $C_5H_9\cdot$ radicals. This would be shown in the composition of the dimers.

[1]*Issued as A.E.C.L. No. 1754.*

The dimer yields measured by Muccini and Schuler are not, in themselves, in conflict with our isotopic experiments since, if C_6 radicals were predominant in the initial decomposition, the change of identity reaction could still lead to a predominance of C_5 radicals if the radical lifetimes were long enough. "Mixture law" deviations should, however, be detectable in liquid products which do not have free-radical precursors. Cyclohexene is such a product; some is formed by the molecular detachment of hydrogen (3):

$$C_6H_{12} \longrightarrow\!\!\!\!\!\sim\!\!\!\!\!\rightarrow C_6H_{10} + H_2 \qquad [3]$$

Accordingly, we measured the yields and isotopic composition of all liquid products, olefins, and dimers in the three binary systems C_6D_{12}–C_6H_{12}, C_6D_{12}–C_5H_{10}, and C_6H_{12}–C_5H_{10}. The results confirm both the "mixture law" deviations predicted from our isotopic experiments and the change of identity reaction postulated by Muccini and Schuler.

In some other studies (4) we have found that "mixture law" deviations which appear in a mixture of two hydrocarbons are changed by the addition of solutes, e.g. benzene, carbon tetrachloride, cyclohexene, and iodine. Specifically, the partial yields of D_2 and HD, G_1(D) and g(HD), for cyclohexane-d_{12} in cyclopentane are 1.6 and 10.0, respectively. In 10^{-2} M iodine solution they are reduced to 1.16 and 6.50, respectively. In our opinion, experiments with additives introduce further complications to the "mixture law" deviations in hydrocarbon mixtures. For this reason, we set aside Muccini and Schuler's measurements on iodine solutions.

EXPERIMENTAL PROCEDURES

Materials

Cyclohexane (Fisher Scientific Spectranalyzed) and cyclohexane-d_{12} (Merck) were used as received. Cyclopentane (Phillips Research Grade) was passed through a column of silica gel, activated by heating to 150° C under vacuum, to remove cyclopentene.

Sample Preparation and Irradiation

The techniques of sample preparation, dosimetry, and gas analysis have been described previously (1). The irradiations were all carried out at a dose rate of $\sim 2\times10^{22}$ ev/l. hr to a total dose of $\sim 4\times10^{22}$ ev/l.

Analysis of Liquid Products

Cyclohexene and cyclohexene-d_{10} in C_6H_{12}–C_6D_{12} mixtures were separated by preparative gas–liquid chromatography. A 400-λ sample of the irradiated mixture was injected onto a 12-ft column packed with 28% ethylene glycol saturated with $AgNO_3$ on firebrick. At 40° C the retention time of the olefins was 40 minutes. The effluent was passed through a magnesium perchlorate trap to remove moisture and the olefin fraction was condensed at liquid nitrogen temperature. The ratio C_6D_{10}/C_6H_{10} was determined from the ratio of peaks at m/e = 92 and 82 measured on a Consolidated 21–130 mass spectrometer.

For the analysis of dimers $(C_6H_{11})_2$ and $C_6H_{11}\cdot C_6D_{11}$ in C_6H_{12}–C_6D_{12} mixtures, 20 ml of irradiated solution was concentrated to 4 ml by distillation. About 2 ml of the concentrate was injected 200 λ at a time onto a column packed with 0.1% Apiezon-L grease on glass beads. The column was initially at room temperature. After all the cyclohexane was eluted, the column temperature was raised slowly; the dimer was eluted at a column temperature of about 120° C, trapped at liquid nitrogen temperature, and analyzed mass spectrometrically. The ratio of peaks at m/e equal to 177 and 166 gave the ratio of $C_6H_{11}\cdot C_6D_{11}$ to $(C_6H_{11})_2$ in the product.

Cyclopentene in cyclohexane–cyclopentane mixtures was analyzed by infrared spectrophotometry on a Perkin–Elmer Model 21 spectrometer using the absorption band at 695 cm^{-1}. The techniques have been described earlier (5). Cyclohexene was measured by gas–liquid chromatography using a 12-ft column packed with 17% 1,2,3-tris(2-cyanoethoxy)propane on acid-washed firebrick. Dimer fractions were separated on a 12-ft column packed with 20% O.S. 124 (a polyphenyl ether) on "Columpack". The relative sensitivities of the hydrogen flame detector to the C_{10}, C_{11}, and C_{12} hydrocarbons were assumed to be in the ratio of their carbon numbers. This assumption was found to be correct experimentally. At low concentrations of cyclohexane the dimers were concentrated by distillation to increase the sensitivity of the analysis.

DISCUSSION

In this discussion we shall be more interested in the initial slope of the plot of a G-value as a function of concentration rather than in the G-value itself. This slope might be called

Can. J. Chem. Downloaded from www.nrcresearchpress.com by 210.87.254.42 on 09/05/12
For personal use only.

a "partial yield", one which is calculated on the basis of the energy absorbed by one component of a mixture. The partial yield of a product P_A, $g(P_A)$, derived from component A of a mixture is given by:

$$g(P_A) = \text{molecules } P_A/100 \text{ ev absorbed in component A.}$$

In our earlier paper (1) we used the mole fraction as the parameter which determines the partitioning of energy in a mixture. However, recent experiments in the gas phase carried out in this laboratory (6) have convinced us that, for mixtures of alkanes, the electron fraction is a more suitable parameter and we shall use it in this paper. Values of the partial yields, obtained from the initial slopes of yields shown in Figs. 1–4, are given in Table I.

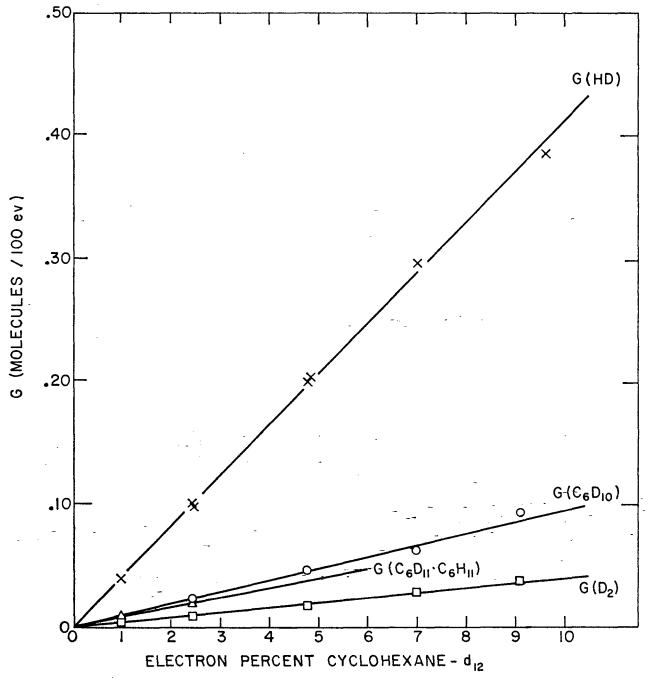

FIG. 1. Yields of deuterated products in mixtures of cyclohexane-d_{12} and cyclohexane.

TABLE I

Partial yields of products* in alkane mixtures

	Cyclohexane–cyclohexane-d_{12}	Cyclopentane–cyclohexane-d_{12}	Cyclopentane–cyclohexane	Pure cyclohexane†
$g(D_2)$‡	0.35	1.6	—	—
g(HD)	4.0	10.0	—	—
$g(C_6D_{10})$	0.9	2.6	—	—
$g(C_6H_{10})$	—	—	8.9	3.3
$g(C_6)$ in dimer	0.8§	1.9	2.5	3.9

*In this table the partial yield is G(product)/electron fraction of cyclohexane or cyclohexane-d_{12} in the mixture.
†These are the initial yields determined by Dyne and Stone (7).
‡$g(D_2)$ is identical with G_1(D) used in earlier papers (1).
§This is the value for C_6D_{11} radicals in $C_6D_{11}\cdot C_6H_{11}$.

Can. J. Chem. Downloaded from www.nrcresearchpress.com by 210.87.254.42 on 09/05/12
For personal use only.

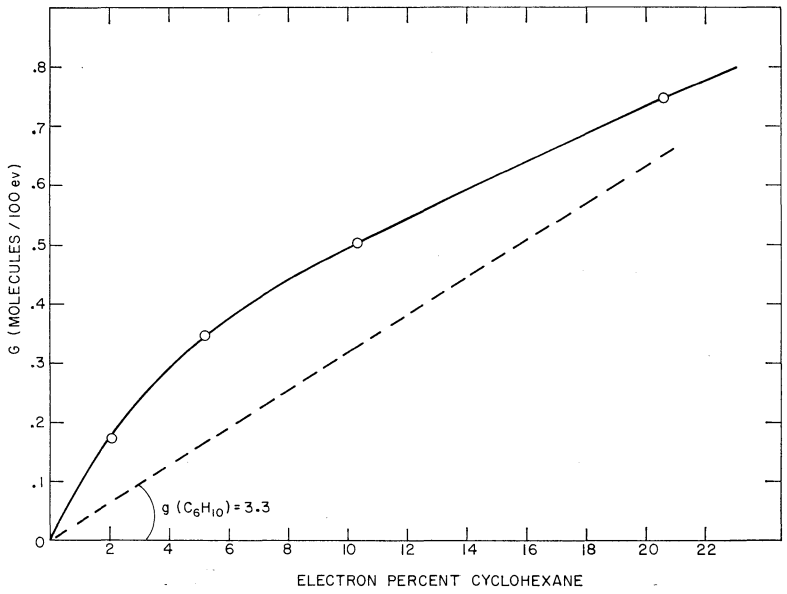

FIG. 2. Yield of cyclohexene in mixtures of cyclohexane and cyclopentane. The broken line corresponds to $g(C_6H_{10}) = 3.3$, the yield of cyclohexene in pure cyclohexane.

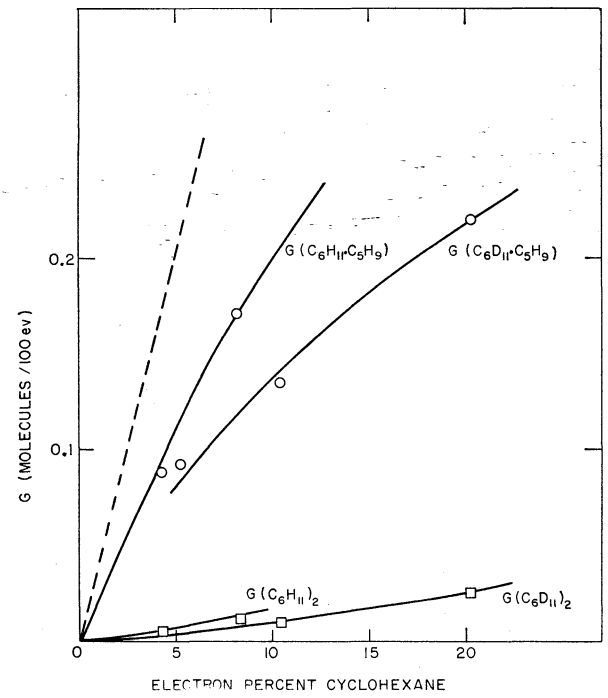

FIG. 3. Yields of dimers in cyclohexane–cyclopentane and deuterated cyclohexane–cyclopentane mixtures. The broken line corresponds to $g(C_6H_{11}) = 1.95$, the yield of bicyclohexyl in pure cyclohexane.

Can. J. Chem. Downloaded from www.nrcresearchpress.com by 210.87.254.42 on 09/05/12
For personal use only.

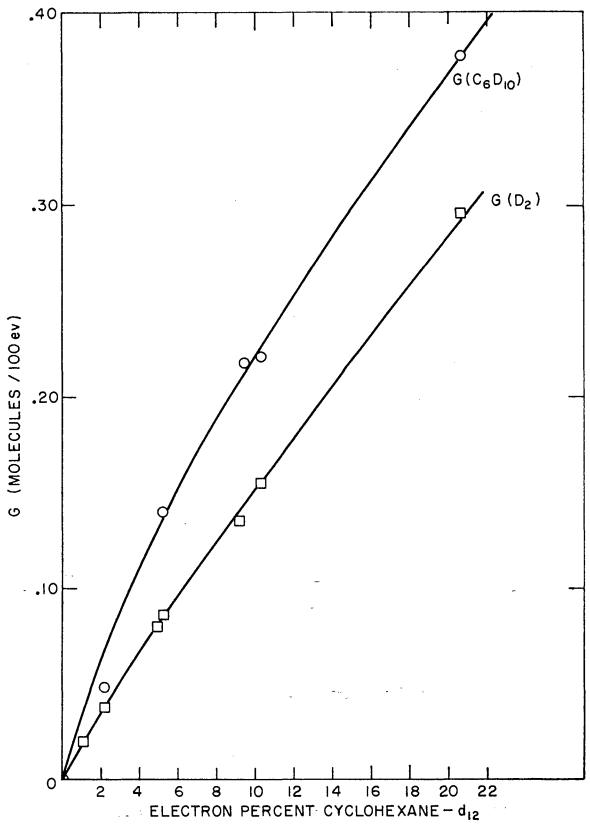

FIG. 4. Yield of deuterated cyclohexene and D_2 in mixtures of cyclohexane-d_{12} and cyclopentane.

The Change of Identity Reaction

The yield of the isotopically substituted bicyclohexyl $C_6H_{11}\cdot C_6D_{11}$ in C_6H_{12}–C_6D_{12} mixtures provides further evidence for the change of identity reactions suggested by Muccini and Schuler. Since every HD molecule is formed together with a C_6D_{11} residue, the expectation, if no disproportionation occurred, is that $g(HD)$ would be equal to $g(C_6H_{11}\cdot C_6D_{11})$. As can be seen from Table I and Fig. 1, $g(HD)$ is more than four times greater than $g(C_6H_{11}\cdot C_6D_{11})$ and is also greater than the sum of $g(C_6H_{11}\cdot C_6D_{11})$ and $g(C_6D_{10})$. The missing C_6D_{11} residues can only be present as $C_6D_{11}H$, which would be formed by the change of identity reaction

$$C_6D_{11}\cdot + C_6H_{12} \rightarrow C_6D_{11}H + C_6H_{11}\cdot$$

We have obtained partial confirmation of this reaction by isotopic analysis of irradiated C_6D_{12}–C_6H_{12} mixtures and found that $C_6D_{11}H$ is detectable. This analysis could, however, only be performed on highly irradiated mixtures, and direct comparison with the yields measured at low doses is not significant.

Analogous results are found in the C_6D_{12}–C_5H_{10} mixtures; $g(HD)$ is, in this system, about five times greater than $g(C_6)$ in the dimer.

"Mixture Law" Deviations

The qualitative expectations outlined in the introduction are borne out in the yields

Can. J. Chem. Downloaded from www.nrcresearchpress.com by 210.87.254.42 on 09/05/12
For personal use only.

of olefins. In Fig. 2, we see that $g(C_6H_{10})$ in cyclohexane–cyclopentane mixtures is initially much greater than it is in pure cyclohexane. In Fig. 4, we see first that, for cyclohexane-d_{12}–cyclopentane mixtures, the yield of deuterium is matched by the yield of C_6D_{10} and, second, that $g(C_6D_{10})$ is nearly three times greater than $g(C_6D_{10})$ in C_6D_{12}–C_6H_{12} mixtures. In addition, there is a similar difference of a factor greater than 2 for $G(C_6)$ in these two mixtures (Table I).

These simple observations require, however, more detailed discussion. Suppose that mixtures of cyclohexane and cyclopentane obeyed the "mixture law". If cyclohexene were produced only by molecular detachment, its yield would be a linear function of composition such that $g(C_6H_{10})$ would be 3.3, which is the cyclohexene yield in pure cyclohexane (7). If, on the other hand, cyclohexene were formed only by the disproportionation

$$C_6H_{11}\cdot + C_5H_9\cdot \rightarrow C_6H_{10} + C_5H_{10}$$

the initial value of $g(C_6H_{10})$ would be less than 3.3 because some of the disproportionating radicals would give cyclopentene:

$$C_6H_{11}\cdot + C_5H_9\cdot \rightarrow C_6H_{12} + C_5H_8$$

The plot of $G(C_6H_{10})$ vs. C_6H_{12} concentration would be concave upwards due to the increasing probability of the disproportionation of two $C_6H_{11}\cdot$ radicals (necessarily giving cyclohexene) which occurs at high cyclohexane concentrations. The change of identity reaction which removes $C_6H_{11}\cdot$ radicals from the system will also reduce the initial value of $g(C_6H_{10})$ below the limiting value of 3.3. The initial value of $g(C_6H_{10})$ will also be less than 3.3 if cyclohexene is formed by both molecular elimination and disproportionation.

The observed yields of cyclohexene in C_6H_{12}–C_5H_{10} mixtures do not follow either of these predictions. In Fig. 2, we see that $g(C_6H_{10})$ is initially more than twice the "expected" value shown by the broken line which corresponds to $g(C_6H_{10}) = 3.3$. This yield is concave downwards, showing, presumably, that the deviations from the "mixture law" are smaller at higher C_6H_{12} concentrations. By contrast, the yield of C_6 dimers (Fig. 3) is, in agreement with Muccini and Schuler, less than that predicted by the "mixture law".

An observation, of minor importance, which requires comment is the difference between the yields of C_6D_{10} and D_2 in both systems containing cyclohexane-d_{12}. Since $g(C_6D_{10}) > g(D_2)$, it follows that cyclohexene is being formed by some process other than the molecular detachment of deuterium. In cyclopentane solutions $g(C_6D_{10}) - g(D_2) = 1.0$.

This process could be the disproportionation

$$C_6D_{11}\cdot + C_5H_9\cdot \rightarrow C_6D_{10} + C_5H_9D,$$

which would be matched by an approximately equal number of disproportionations giving cyclopentene. The total yield of disproportionating $C_6D_{11}\cdot$ radicals is therefore about 2, which is very close to the number combining to give $C_6D_{11}\cdot C_5H_9$ (1.9). If the disproportionation is forming C_6D_{10} then the probabilities of disproportionation and combination must be approximately equal.

Two other processes which could lead to this extra yield of C_6D_{10} are (1) a dissociation to give deuterium atoms which would react to give HD:

$$C_6D_{12} \rightsquigarrow C_6D_{10} + 2D$$

and (2) molecular detachment of HD from the isotopic impurity $C_6D_{11}H$, which is present in a concentration of about 6%. We have already noted (8) that the yield of HD from 'pure' deuterated cyclohexane is inordinately high. It is possible therefore that, in mixtures, $C_6D_{11}H$ shows a reactivity much in excess of that expected from its electron fraction.

Can. J. Chem. Downloaded from www.nrcresearchpress.com by 210.87.254.42 on 09/05/12
For personal use only.

The difference between $g(C_6D_{10})$ in C_6D_{12}–C_5H_{10} mixtures (2.6) and $g(C_6H_{10})$ in C_6H_{12}–C_5H_{10} mixtures establishes the existence of a large isotope effect in the probability of molecular detachment and, possibly, in the process which leads to these "mixture law" deviations. Skurat (9), using our isotopic techniques, found similar large isotope effects in the yields of hydrogen formed by molecular detachment in the radiolysis of polyethylene and deuteropolyethylene.

ACKNOWLEDGMENT

It is a pleasure to acknowledge both the helpful advice on gas chromatographic techniques and the critical comments on this paper that we received from Dr. J. A. Stone.

REFERENCES

1. P. J. Dyne and J. Denhartog. Can. J. Chem. **40**, 1616 (1962).
2. G. A. Muccini and R. H. Schuler. J. Phys. Chem. **64**, 1435 (1960).
3. P. J. Dyne. J. Phys. Chem. **66**, 767 (1962).
4. P. J. Dyne and J. Denhartog. Unpublished work.
5. P. J. Dyne and J. W. Fletcher. Can. J. Chem. **38**, 851 (1960).
6. P. J. Dyne and D. R. Smith. Unpublished work.
7. P. J. Dyne and J. A. Stone. Can. J. Chem. **39**, 2381 (1961).
8. P. J. Dyne and W. M. Jenkinson. Can. J. Chem. **40**, 1446 (1961).
9. V. E. Skurat. Dokl. Akad. Nauk, SSSR, **141**, 161 (1961).

Can. J. Chem. Downloaded from www.nrcresearchpress.com by 210.87.254.42 on 09/05/12
For personal use only.

PREPARATION, THIN LAYER CHROMATOGRAPHY, AND ULTRAVIOLET SPECTRA OF SOME O-BENZYL DERIVATIVES OF D-GLUCOSE[1]

M. E. TATE[2] AND C. T. BISHOP
Division of Applied Biology, National Research Council, Ottawa, Canada
Received January 10, 1963

ABSTRACT

A new method for benzylation of carbohydrates has been developed which facilitated complete substitution of hydroxyl groups in one of the compounds prepared. Thin layer chromatography provides a good criterion of purity and is also a preparative method for separation of identifiable amounts of *O*-benzyl derivatives of carbohydrates. The number of benzyl groups in a compound can be determined by ultraviolet absorption spectroscopy. The following compounds were prepared, some of which have not been reported previously: benzyl-2,3,4,6-tetra-*O*-benzyl-α-D-glucoside; benzyl 2,3,4,6-tetra-*O*-benzyl-β-D-glucoside; methyl 2,3,4,6-tetra-*O*-benzyl-α-D-glucoside; 2,3,4,6-tetra-*O*-benzyl-α-D-glucose; 1-*O*-(*p*-nitrobenzoyl)-2,3,4,6-tetra-*O*-benzyl-α-D-glucose; octa-*O*-benzyl sucrose; 3,5-di-*O*-benzyl-1,2-*O*-cyclohexylidene-α-D-xylose.

Can. J. Chem. Downloaded from www.nrcresearchpress.com by 210.87.254.6 on 09/05/12
For personal use only.

The value of the benzyl group in syntheses of carbohydrate derivatives has been recognized by chemists for many years and the subject has been reviewed by McCloskey (1). More extensive use of poly-*O*-benzyl derivatives of carbohydrates has been somewhat limited undoubtedly because many of them are not crystalline at room temperature and therefore of uncertain purity. Nevertheless, a number of important compounds have been prepared from these amorphous products (2, 3, 4). The success of thin layer chromatography in separating carbohydrate acetates (5) prompted the present study to see if the same method would be useful as a criterion of homogeneity for poly-*O*-benzyl derivatives of carbohydrates. The ultraviolet absorption properties of these *O*-benzyl derivatives were also examined and found to provide a method of analysis for *O*-benzyl groups.

The compounds used in this investigation may be considered as derivatives of 2,3,4,6-tetra-*O*-benzyl-D-glucose in which substituents at the anomeric carbon were α-*O*-benzyl; β-*O*-benzyl; α-*O*-methyl; α-hydroxyl; α-*O*-(*p*-nitrobenzoyl); and α-*O*-(1,3,4,6-tetra-*O*-benzyl-β-D-fructofuranosyl), i.e. octa-*O*-benzyl sucrose.

Separations were obtained on thin layers of silica gel G by development with light petroleum containing 3–5% of methanol. As with the benzene–methanol solvent system used for carbohydrate acetates (5) the mobilities of the various components were strongly dependent upon the concentration of methanol. These two solvent systems are complementary in that they give a wide range of solvent polarity.

Figure 1 shows the separation of the fully benzylated glucoses and the resolution that can be obtained in this series with various substituents at the anomeric carbon atom. The large differences in mobilities between fully substituted derivatives and those containing a free hydroxyl group clearly indicate that thin layer chromatography is an ideal method for following reactions which involve formation of ether, ester, or acetal groups. This feature was emphasized in the attempted benzylation of benzyl 2,3,4,6-tetra-*O*-acetyl-α-D-glucoside by the usual benzyl chloride – powdered potassium hydroxide procedure (1). Thin layer chromatography of the crude reaction mixture showed a yield of only 33% of the expected benzyl 2,3,4,6-tetra-*O*-benzyl-α-D-glucoside and some 60% of a product corresponding to a tetra-*O*-benzyl glucose derivative. All attempts to force the benzylation

[1]*Issued as N.R.C. No. 7390.*
[2]*National Research Council Postdoctoral Fellow 1960–1962.*

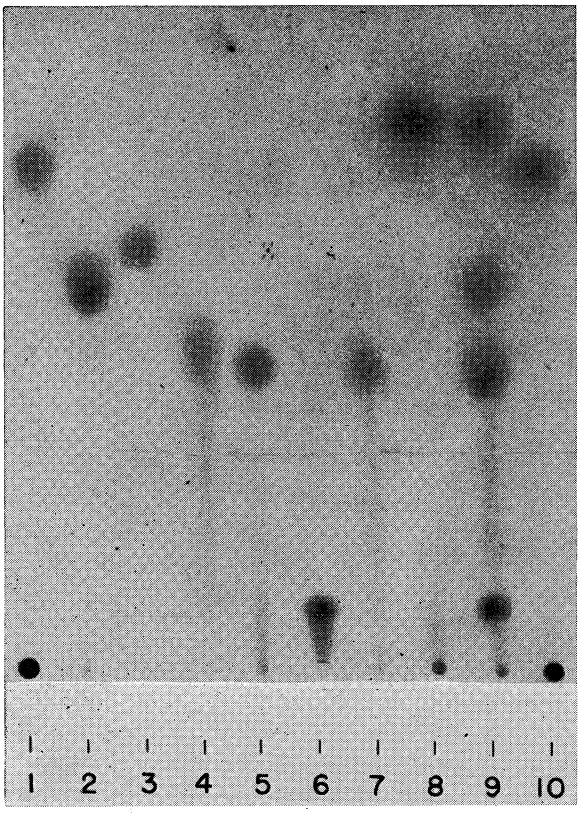

FIG. 1. Thin layer chromatogram of some D-glucose benzyl ethers.
Adsorbent, silica gel G; solvent, light petroleum (b.p. 65–110° C) containing 5% (v/v) of methanol; single ascending development to 14.7 cm.
Components in decreasing order of mobility:

1, 10. (Marker dyes) Sudan III, methyl orange
2. I
3. II
4. V
5. III
6. IV
7. VI
8. Dibenzyl ether, impurity
9. Compounds 8, 2, 4, 5, and 6

to completion by raising the temperature or extending the time of reaction were unsuccessful and led to excessive formation of dibenzyl ether. However, the tetra-*O*-benzyl glucose derivative was smoothly benzylated by benzyl chloride and sodium hydride at 130° C to give a 90% yield of crystalline benzyl 2,3,4,6-tetra-*O*-benzyl-α-D-glucoside. This method of benzylation, which does not appear to have been applied to carbohydrates before, was based upon an observation by Cristol, Ragsdale, and Meek (6) that benzyl chloride does not react with sodium hydride at temperatures up to 170° C. The use of sodium hydride also prevents the formation of dibenzyl ether, which is a major by-product in other methods of benzylation. The new method forms a useful adjunct to the older procedures (1) and is especially valuable for the benzylation of hindered hydroxyl groups. The preparation of methyl 2,3,4,6-tetra-*O*-benzyl-α-D-glucoside as described in the experimental section is an example of benzylation by the benzyl chloride – sodium hydride procedure.

The key compound 2,3,4,6-tetra-*O*-benzyl-α-D-glucose was prepared by hydrolysis of

Can. J. Chem. Downloaded from www.nrcresearchpress.com by 210.87.254.6 on 09/05/12
For personal use only.

its methyl glycoside (3) but in much better yield by hydrolysis of the corresponding benzyl glycoside. The acetate of 2,3,4,6-tetra-*O*-benzyl-α-D-glucose was not crystalline; however, a crystalline *p*-nitrobenzoate was obtained. Octa-*O*-benzyl sucrose was prepared by benzylation of sucrose with benzyl bromide, silver oxide, and barium oxide (7), the product being isolated by a procedure previously described (2) and purified for analysis by preparative thin layer chromatography. Benzylation of 1,2-*O*-cyclohexylidene-α-D-xylofuranose to the 3,5-di-*O*-benzyl derivative provided another compound to test the spectrophotometric estimation of *O*-benzyl groups as described below.

It was apparent in this work that some method for determining the number of *O*-benzyl groups in a compound would be very valuable, just as the methoxyl determination has been so useful in the chemistry of methylated carbohydrates. The early work on benzylated carbohydrates utilized the hydriodic acid fission of ethers, as used for methoxyl estimation, for determining benzyl groups (8). However, that method involves isolation of the lachrymatory benzyl iodide and is rendered invalid by the presence of a methoxyl group in the compound being analyzed. The ultraviolet absorption spectrum of the benzyl group has been used as the basis of a spectrophotometric method for the estimation of benzyl penicillin (9). Accordingly, the ultraviolet spectra of a number of crystalline *O*-benzyl derivatives of carbohydrates were examined to see if the method could be used for quantitative estimation of *O*-benzyl broups in these compounds.

With one exception, all the *O*-benzyl derivatives examined so far have shown an $\epsilon_{258.5}$ value per benzyl group of 186±2. The single exception was benzyl 2,3,4,6-tetra-*O*-acetyl-β-D-glucoside, which, in ethanol, gives a spectrum with no clear maximum at 258.5 mμ. In cyclohexane this maximum is revealed but the $\epsilon_{258.5}$ value (245) per benzyl group is much greater than those for the other compounds. Those benzyl derivatives which gave the $\epsilon_{258.5}$ value per benzyl group of 186±2 all exhibited a pronounced minimum in the vicinity of 230–240 mμ; unless this minimum is present estimates of benzyl groups from $\epsilon_{258.5}$ are likely to be in error. The spectra obtained are in agreement with that recorded (10) for benzyl alcohol, which also gives an $\epsilon_{258.5}$ value of 185. The validity of Beer's law was established for benzyl 2,3,4,6-tetra-*O*-benzyl-α-D-glucoside over the concentration range 0.02–0.12% and the constancy of the $\epsilon_{258.5}$ value per benzyl group in other compounds with varying degrees of *O*-benzyl substitution indicated its validity for them as well, over the range of concentration used.

The successful application of ultraviolet spectroscopy for estimating *O*-benzyl groups in amorphous compounds is largely dependent on the purity of those compounds. Thin layer chromatography is the method of choice for purification because the samples isolated from a single plate are more than sufficient for spectroscopic analysis. In turn, the ultraviolet spectra provide useful information about the degree of substitution in the compounds isolated and the methods therefore mutually enhance the value of each other.

EXPERIMENTAL

Thin Layer Chromatography

Glass plates (20×20×0.3 cm) were coated with silica gel G* or with silica gel G containing 1% (w/w) of fluorescent zinc silicate.† The plates were prepared and samples were applied to them as previously described (5). The dyes Sudan III and methyl orange were used as markers and plates were developed with light petroleum (b.p. 65–110° C) – methanol mixtures containing 3–5% (v/v) of methanol. As with the carbohydrate acetates (5) the methanol content of the solvent was varied, within the above limits, depending on the compounds being separated. The separation shown in Fig. 1 was obtained with a single

Research Specialties Co., 200 South Garrard Blvd., Richmond, Calif., U.S.A.
†*ZA2, S104 fluorescent green, A. D. Mackay Inc., 198 Broadway, New York 38, N.Y., U.S.A.*

Can. J. Chem. Downloaded from www.nrcresearchpress.com by 210.87.254.6 on 09/05/12
For personal use only.

ascending development (solvent front 14.7 cm) in 40 minutes using light petroleum (b.p. 65–110° C) containing 5% (v/v) of methanol. Fresh solvent was made up each day because of gradual depletion of the methanol content by adsorption onto the silicic acid.

Detection

Reaction of the components on the plates with iodine vapor was the most convenient and sensitive method of detection for routine work. A saturated atmosphere of iodine vapor was obtained by keeping 3–5 g of iodine crystals in the bottom of a covered glass jar. The thin layer chromatograms were dried in a current of air from a fan and were then placed in the tank containing the iodine. The compounds on the chromatograms became visible in a few minutes and the spots reached their maximum intensity after 30 minutes. This method will clearly detect 0.4 μg of benzyl 2,3,4,6-tetra-*O*-benzyl-α-D-glucoside. The chromatograms can be covered with clean glass plates for ease of handling or tracing. For non-destructive detection the plates were prepared from the fluorescent silica gel G described above; the chromatograms, developed and dried, were then examined under a suitable shortwave source of ultraviolet light (Mineralight S. L. 2537). Factors involved in the selection of fluorescent materials and light sources have been examined by Sease (11); the technique has been applied to thin layer chromatography by Kirchner *et al.* (12). The sensitivity of this method of detection for benzyl 2,3,4,6-tetra-*O*-benzyl-α-D-glucoside was 4 μg but obviously the level of detection will vary with the molar extinction coefficient (ϵ) of the compound being detected. In general, the iodine vapor technique was used for analytical work and the ultraviolet method for semimicro preparative plates.

Semimicro Preparative Separation

Plates were prepared as described for the analytical separations and the *O*-benzyl derivatives were applied as contiguous spots to give 30–100 mg per 20-cm plate. Fluorescent silica gel G was used and the plates were developed with light petroleum (b.p. 65–110° C) containing 5% (v/v) of methanol. The developed plates were dried in air and the zones were detected in ultraviolet light as dark areas on a fluorescent yellow background. The zones were outlined with a scalpel and scraped from the plate for elution of the separate components. This technique was described in detail for thin layer chromatography of carbohydrate acetates (5). In the majority of separations elution of the zone scrapings with chloroform yielded analytically pure samples. Products recovered for analysis were dried at 60° C in a high vacuum (0.01 mm of mercury) for 18 hours.

Preparation of O-Benzyl Derivatives

I. Benzyl 2,3,4,6-Tetra-O-benzyl-α-D-glucoside

Benzyl 2,3,4,6-tetra-*O*-acetyl-α-D-glucoside (1.0 g (13, 14); $E^{1\%}_{1\,cm}$ = 4.2 at 258.5 mμ, $\epsilon_{max/benzyl\,group}$ = 184) was benzylated by benzyl chloride (8.0 ml) and powdered potassium hydroxide (3.0 g) (1). The product was a colorless sirup (1.5 g), $[\alpha]_D^{25}$ +66.4 (*c*, 3% in chloroform). Thin layer chromatography of this sirup showed the presence of dibenzyl ether and two other products: A (R_f 0.33) and B (R_f 0.09); Sudan III had R_f 0.51. Pure samples of products A (32.2 mg) and B (48.0 mg) were obtained by preparative thin layer chromatography of a portion of the sirup.

Product A crystallized when triturated with methanol (1 ml). The crystals were filtered and washed with methanol (2×0.5 ml) to give benzyl 2,3,4,6-tetra-*O*-benzyl-α-D-glucoside I (17.8 mg) as colorless needles with a melting point of 93.5–94.5° C unchanged on recrystallization from the same solvent. Anal.: Calc. for $C_{41}H_{42}O_6$: C, 78.07%; H, 6.71%. Found: C, 77.84%; H, 6.92%. $[\alpha]_D^{28}$ +55.8° (*c*, 1.63% in chloroform). $E^{1\%}_{1\,cm}$ = 14.8 at 258.5 mμ; $\epsilon_{max/benzyl\,group}$ = 187.

Product B could not be induced to crystallize but analysis showed that it was a tetra-*O*-benzyl derivative of glucose. Anal.: Calc. for $C_{34}H_{36}O_6$: C, 75.53%; H, 6.71%. Found: C, 75.63%; H, 6.81%. $[\alpha]_D^{24}$ +90.8° (*c*, 1.42% in chloroform). Benzylation of this sirupy tetra-*O*-benzyl derivative (50 mg) by sodium hydride and benzyl chloride, as described below for methyl α-D-glucopyranoside, yielded crude benzyl 2,3,4,6-tetra-*O*-benzyl-α-D-glucoside, m.p. 91–93° C (53 mg, 91%); one recrystallization from methanol provided a pure product, m.p. 93.5–94.5° C (41 mg, 70%).

Overall yields in the benzylation were 33% of benzyl 2,3,4,6-tetra-*O*-benzyl-α-D-glucoside and 60% of the tetra-*O*-benzyl derivative. The unresolved mixture in methanol solution gave a further 270 mg of benzyl 2,3,4,6-tetra-*O*-benzyl-α-D-glucoside when seeded with crystals of the pure product obtained by thin layer chromatography.

II. Benzyl 2,3,4,6-Tetra-O-benzyl-β-D-glucoside

Benzyl 2,3,4,6-tetra-*O*-acetyl-β-D-glucoside (0.44 g (13); $E^{1\%}_{1\,cm}$ = 5.6 at 258.5 mμ, $\epsilon_{max/benzyl\,group}$ = 245) was benzylated with powdered potassium hydroxide (1.5 g) and benzyl chloride (5 ml) as described above. The oily product (0.6 g) crystallized partially when triturated with methanol at 0° C. The crystals were washed with methanol (2×0.5 ml) and dried; m.p. 79–81° C, 209 mg, 33%. Thin layer chromatography revealed trace quantities of a slower-moving component. Recrystallization from methanol (5 ml) provided pure benzyl 2,3,4,6-tetra-*O*-benzyl-β-D-glucoside, m.p. 83–84° C, $[\alpha]_D^{25}$ −14.9° (*c*, 1.48% in chloroform); reported (8), m.p. 83.5° C. Anal.: Calc. for $C_{41}H_{42}O_6$: C, 78.07%; H, 6.71%. Found: C, 77.90%; H, 6.50%. $E^{1\%}_{1\,cm}$ at 258.5 mμ = 14.8; $\epsilon_{max/benzyl\,group}$ = 187.

Can. J. Chem. Downloaded from www.nrcresearchpress.com by 210.87.254.6 on 09/05/12
For personal use only.

III. Methyl 2,3,4,6-Tetra-O-benzyl-α-D-glucoside

This compound has been reported by Schmidt *et al.* (3), who prepared it by benzylation of methyl α-D-glucopyranoside with powdered potassium hydroxide and benzyl chloride. However, the specific rotation reported is not in agreement with that found in the present work and the only analytical value cited was methoxyl content. In the present study methoxyl analysis of these compounds was found to be unreliable and gave consistently high values, probably due to interference by the *O*-benzyl groups.

A mixture of methyl α-D-glucopyranoside (5 g, finely powdered), benzyl chloride (125 ml), and sodium hydride (11 g) was stirred magnetically under anhydrous conditions for 3 hours at 125–130° C. During the strongly exothermic reaction the mixture became thick and gelatinous and then changed to a thin slurry as the reaction reached completion. The progress of the reaction was followed by thin layer chromatography, which showed that benzylation was virtually complete after 3 hours. The reaction mixture was centrifuged, the supernatant liquor was decanted, and the residue was washed with benzene (4×50 ml) by centrifugation and decantation. The excess of sodium hydride was destroyed by adding the solid residue to a large volume of ethanol. The combined benzene supernatant liquors were steam-distilled until the distillate was clear and the oily residue was extracted with chloroform (4×50 ml). The extract was dried by passage through a wad of cotton and evaporated to give a yellow sirup (22.0 g). This product was sufficiently pure for the preparation of 2,3,4,6-tetra-*O*-benzyl-D-glucose as described below. A small aliquot was purified by preparative thin layer chromatography to give methyl 2,3,4,6-tetra-*O*-benzyl-α-D-glucoside as a colorless sirup, $[\alpha]_D^{25}$ +18.7° (*c*, 1.5% in chloroform); reported (3), $[\alpha]_D^{25}$ +32.2 (*c*, 5% in chloroform). Anal.: Calc. for $C_{35}H_{38}O_6$: C, 75.79%; H, 6.91%. Found: C, 75.67%; H, 7.00%. λ_{max} 258.5 mμ; calc. $E^{1\%}_{1\,cm}$ = 13.4, found $E^{1\%}_{1\,cm}$ = 13.4; $\epsilon_{max/benzyl\,group}$ = 186.

IV. 2,3,4,6-Tetra-O-benzyl-α-D-glucose

(a) Hydrolysis of methyl 2,3,4,6-tetra-O-benzyl-α-D-glucoside.—The method of Schmidt *et al.* (3) was modified to give an improved overall yield. Crude methyl 2,3,4,6-tetra-*O*-benzyl-α-D-glucoside (21.7 g) was dissolved in glacial acetic acid (400 ml) and the solution was heated to 90° C on a steam bath. Sulphuric acid (108 ml, 2 *N*) was added and the heating was continued for 2 hours. Thin layer chromatography showed that considerable amounts of starting product were still present. A further portion (84 ml) of 2 *N* sulphuric acid was added and the solution was heated for 18 hours, after which thin layer chromatography showed that none of the initial product remained. The hydrolyzate was poured into water (3.5 l.) whereupon a yellow oil was precipitated which gradually solidified. The solid was isolated by filtration and washed with cold methanol to give colorless crystals of 2,3,4,6-tetra-*O*-benzyl-α-D-glucose (5.0 g, 35%), m.p. 146–149° C. Recrystallization of this product from methanol (160 ml) yielded needles having a melting point of 150–151° C and $[\alpha]_D^{24}$ +20.7 (*c*, 2.47% in chloroform); reported (3), m.p. 148° C, $[\alpha]_D^{20}$ +21.2° (*c*, 3.5% in chloroform). Total yield of pure product recovered from the recrystallization was 4.2 g, 30%.

(b) Hydrolysis of benzyl 2,3,4,6-tetra-O-benzyl-α-D-glucoside.—Compound I (2.0 g) was dissolved in hot, 90% acetic acid (60 ml) and to the solution was added 2 *N* sulphuric acid (16 ml). The solution was heated on a steam bath for 3 hours and then a second portion (12 ml) of 2 *N* sulphuric acid was added. The reaction was heated for a further 3 hours, after which hydrolysis was shown to be complete by thin layer chromatography. The hydrolyzate was poured into boiling water (900 ml) whereupon the product crystallized. The crystals were isolated by filtration and washed with cold methanol (2×4 ml) to give colorless needles (1.0 g), m.p. 142–145° C. Recrystallization from methanol yielded 2,3,4,6-tetra-*O*-benzyl-α-D-glucose (0.81 g, 47%), m.p. 150–151° C, $[\alpha]_D^{24}$ +20.7° (*c*, 2.5% in chloroform). $E^{1\%}_{1\,cm}$ = 13.8 at 258.5 mμ, $\epsilon_{max/benzyl\,group}$ = 186. The 1-*O*-(*p*-nitrobenzoyl)-2,3,4,6-tetra-*O*-benzyl-α-D-glucose (V) was prepared by heating IV with *p*-nitrobenzoyl chloride in anhydrous pyridine and after recrystallization from ethanol had m.p. 126–127° C and $[\alpha]_D^{26}$ +72.3° (*c*, 2.13% in chloroform). Anal.: Calc. for $C_{41}H_{39}O_9N$: C, 71.39%; H, 5.70%. Found: C, 71.43%; H, 5.40%. The high positive rotation of this derivative suggests assignment of the α-D-configuration. Catalytic de-*O*-acylation of V gave a 74% yield of Compound IV, m.p. 147–149° C raised to 150–151° C by two recrystallizations from methanol.

V. 1,3,4,6-Tetra-O-benzyl-β-D-fructosyl-2,3,4,6-tetra-O-benzyl-α-D-glucoside (Octa-O-benzyl Sucrose)

Sucrose (0.5 g) was benzylated in dimethylformamide (5 ml) by benzyl bromide (5 ml), silver oxide (5 g), and barium oxide (2.5 g) (7). Examination of the product (1.2 g) by thin layer chromatography showed the presence of two components, one of which was dibenzyl ether. Preparative thin layer chromatography of a small portion of the crude sirup yielded the second constituent, octa-*O*-benzyl sucrose, as a colorless sirup, $[\alpha]_D^{26}$ +31.6° (*c*, 1.65% in chloroform). Anal.: Calc. for $C_{68}H_{70}O_{11}$: C, 76.81%; H, 6.64%. Found: C, 76.30%; H, 6.67%. λ_{max} 258.5 mμ; calc. $E^{1\%}_{1\,cm}$ = 14.0, found $E^{1\%}_{1\,cm}$ = 14.2; $\epsilon_{max/benzyl\,group}$ = 188. The crude product could be purified on a larger scale by dissolution of the sirup in hot absolute ethanol (25 ml), which was then allowed to cool to room temperature (2). The oily product, precipitated from the cooled solution, was washed by decantation and was then dried to a yellow sirup (0.45 g, 29%).

VI. 3,5-Di-O-benzyl-1,2-O-cyclohexylidene-α-D-xylose

1,2-*O*-Cyclohexylidene-α-D-xylofuranose (6.9 g), m.p. 86–87° C, $[\alpha]_D^{25}$ −6.2° (*c*, 2.0% in methanol) (15), was benzylated by benzyl chloride (75 ml) and powdered potassium hydroxide (22.0 g) (1). The product crystallized when nucleated with seed crystals obtained by trituration of a small portion of the oil with *n*-hexane. Recrystallization from *n*-hexane (30 ml) yielded 3,5-di-*O*-benzyl-1,2-*O*-cyclohexylidene-α-D-xylose

Can. J. Chem. Downloaded from www.nrcresearchpress.com by 210.87.254.6 on 09/05/12
For personal use only.

as colorless needles (10.7 g, 87%); m.p. 91–92° C, $[\alpha]_D^{27}$ −31.3° (*c*, 1.64% in chloroform). Anal.: Calc. for $C_{25}H_{30}O_5$: C, 73.14%; H, 7.37%. Found: C, 73.13%; H, 7.37%. $E^{1\%}_{1\,cm}$ = 9.1 at 258.5 mμ, $\epsilon_{max/benzyl\,group}$ = 186.

Ultraviolet Spectroscopy

The spectra reported in this work were measured with a Cary recording spectrophotometer Model 11M using 1-cm quartz cells. The solvent used was 95% ethanol except for benzyl 2,3,4,6-tetra-*O*-acetyl-β-D-glucoside, which gave a satisfactory spectrum only in cyclohexane. A spectrum of benzyl 2,3,4,6-tetra-*O*-benzyl-α-D-glucoside in cyclohexane showed no significant difference in $\epsilon_{258.5}$ to that obtained in 95% ethanol. The $E^{1\%}_{1\,cm}$ at 258.5 mμ for benzyl 2,3,4,6-tetra-*O*-benzyl-α-D-glucoside in 95% ethanol varied from 15.0–14.8 over the concentration range 0.02–0.12%, indicating the validity of Beer's law within the reproducibility (2–3%) of the method. The $E^{1\%}_{1\,cm}$ values, cited for the compounds prepared, are of importance as a method of characterization (16). The values may be calculated for any benzylated compound from:

$$E^{1\%}_{1\,cm} = \frac{\epsilon \times 10}{\text{Mol. Wt.}}.$$

As shown here $\epsilon_{258.5} = n \times 186 \pm 2$ where n is the number of benzyl groups in the molecule; hence $E^{1\%}_{1\,cm} = 1860n/\text{Mol. Wt.}$ This value for all benzylated compounds should lie between 0 and 18.8 (the value of $E^{1\%}_{1\,cm}$ for dibenzyl ether) if there is no interference from other chromophores.

REFERENCES

1. C. M. McCloskey. Advan. Carbohydrate Chem. **12**, 137 (1957).
2. C. E. Ballou and L. I. Pizer. J. Am. Chem. Soc. **82**, 3333 (1960).
3. O. T. Schmidt, T. Auer, and H. Schmadel. Ber. **93**, 556 (1960).
4. R. Barker and H. G. Fletcher. J. Org. Chem. **26**, 4605 (1961).
5. M. E. Tate and C. T. Bishop. Can. J. Chem. **40**, 1043 (1962).
6. S. J. Cristol, J. W. Ragsdale, and J. S. Meek. J. Am. Chem. Soc. **71**, 1863 (1949).
7. R. Kuhn, I. Low, and H. Trischmann. Ber. **90**, 203 (1957).
8. G. Zemplen, Z. Csuros, and S. Angyal. Ber. **70**, 1848 (1937).
9. G. B. Levy, D. Shaw, E. S. Parkinson, and D. Fergus. Anal. Chem. **20**, 1159 (1948).
10. T. W. Campbell, S. Linden, S. Godshalk, and W. G. Young. J. Am. Chem. Soc. **69**, 880 (1947).
11. J. W. Sease. J. Am. Chem. Soc. **70**, 3630 (1948).
12. J. G. Kirchner, J. M. Miller, and G. J. Kellner. Anal. Chem. **23**, 420 (1951).
13. E. V. Piel and C. B. Purves. J. Am. Chem. Soc. **61**, 2978 (1939).
14. B. Lindberg. Acta Chem. Scand. **2**, 426 (1948).
15. V. F. Kazimirova and K. V. Levitskaya. Zh. Obshch. Khim. **30**, 723 (1960). *Translation by* Consultants Bureau Enterprises Inc., New York. J. Gen. Chem. USSR, **30**, 742 (1960).
16. A. E. Gillam and E. S. Stern. Electronic absorption spectroscopy. Edward Arnold Ltd., London. 1954. p. 7.

Can. J. Chem. Downloaded from www.nrcresearchpress.com by 210.87.254.6 on 09/05/12
For personal use only.

THE PREPARATION AND REACTIONS OF SOME SIMPLE 2,8-DISUBSTITUTED PURINES AND RELATED DERIVATIVES

ARTHUR F. LEWIS, ALDEN G. BEAMAN, AND ROLAND K. ROBINS
Department of Chemistry, Arizona State University, Tempe, Arizona, U.S.A.
Received February 25, 1963

ABSTRACT

Several previously unknown, simple 2,8-disubstituted purines have been prepared. The readily available (see H. Ballweg, Ann. **649**, 114 (1961); and A. G. Beaman and R. K. Robins, J. Appl. Chem. (London), **12**, 432 (1962)) 2,8-dichloropurine proved to be a most valuable synthetic intermediate in this work. The chemical reactivity of 2,8-dichloropurine toward nucleophilic substitution has been studied.

INTRODUCTION

The 2,6-disubstituted purines have long been known and have been thoroughly investigated (1). A systematic study of the chemistry of various 6,8-disubstituted purines has likewise been made (2); however, no such investigation of 2,8-disubstituted purines has been undertaken, although about eighteen 2,8-disubstituted purines* have been described by an almost equally large number of investigators. The purpose of the present investigation was to prepare as many as possible of the remaining unknown 2,8-disubstituted purines having relatively simple substituents.

The method of introducing an 8-amino group by fusion of a 4,5-diaminopyrimidine with guanidine (2) was further investigated in the hope of applying it to the synthesis of the unknown 2-substituted-8-aminopurines. As a consequence of this investigation, 8-amino-6-purinethiol was prepared in large quantity and dethiated with Raney nickel to give an efficient new synthesis of the difficultly accessible 8-aminopurine (4(*a*)). Fusion of guanidine with 4,5-diamino-2-hydroxypyrimidine (I) (4(*b*)) gave 8-amino-2-hydroxypurine (II). Fusion of 4,5-diamino-2-pyrimidinethiol (4(*c*)) with guanidine failed to give

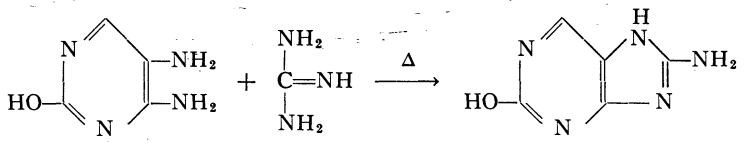

I II

8-amino-2-purinethiol. 2,4,5-Triaminopyrimidine was prepared by dethiation of 6-methylthio-2,4,5-triaminopyrimidine (5) with Raney nickel. This method proved to be superior to the preparation of 2,4,5-triaminopyrimidine from 2,4-diamino-5-nitropyrimidine (6). Fusion of this triamine with guanidine failed to give 2,8-diaminopurine (IV), which was prepared by dethiation of 2,8-diamino-6-purinethiol (III) (7) with Raney nickel. Fusion

**The known 2,8-disubstituted purines are: 2,8-dihydroxypurine (3(a, b)), 2-hydroxy-8-purinethiol (3(c)), 8-hydroxy-2-purinethiol (3(e)), 2,8-purinedithiol (3(f, h)), 2-hydroxy-8-methylthiopurine (3(e)), 8-hydroxy-2-methylthiopurine (3(e)), 2,8-bis(methylthio)purine (3(f)), 2-amino-8-hydroxypurine (3(b, d)), 2-hydroxy-8-methylaminopurine (3(c)), 2-amino-8-phenylpurine (3(g)), 8-hydroxy-2-methylsulphonylpurine (3(f)), 8-hydroxy-2-methylpurine (3(b)), 2,8-dichloropurine (3(i, j)), 2-chloro-8-hydroxypurine (3(j)), 8-chloro-2-methylthiopurine (3(e)), 2,8-dibromopurine (3(h)), 2-bromo-8-hydroxypurine (3(h)), and 2-hydroxy-8-methylpurine (3(k)).*

Can. J. Chem. Downloaded from www.nrcresearchpress.com by 210.87.254.105 on 09/05/12
For personal use only.

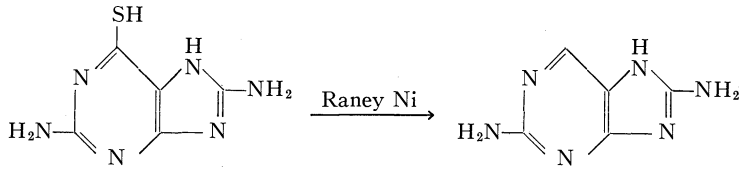

III IV

of 2,4,5-triaminopyrimidine with thiourea was successful and gave 2-amino-8-purinethiol. Treatment of 2,4,5-triaminopyrimidine with phosgene afforded a new route to 2-amino-8-hydroxypurine.

The recently described 2,8-dichloropurine (IX) (3(*i*, *j*)) proved to be a versatile intermediate for the synthesis of several inaccessible 2,8-disubstituted purines. When treated with thiourea in refluxing *n*-propanol, 2,8-dichloropurine (IX) gave a monochloromonothiopurine which was identical with 2-chloro-8-purinethiol (VIII) prepared from 2-chloro-4,5-diaminopyrimidine (V) (8) and carbon disulphide.

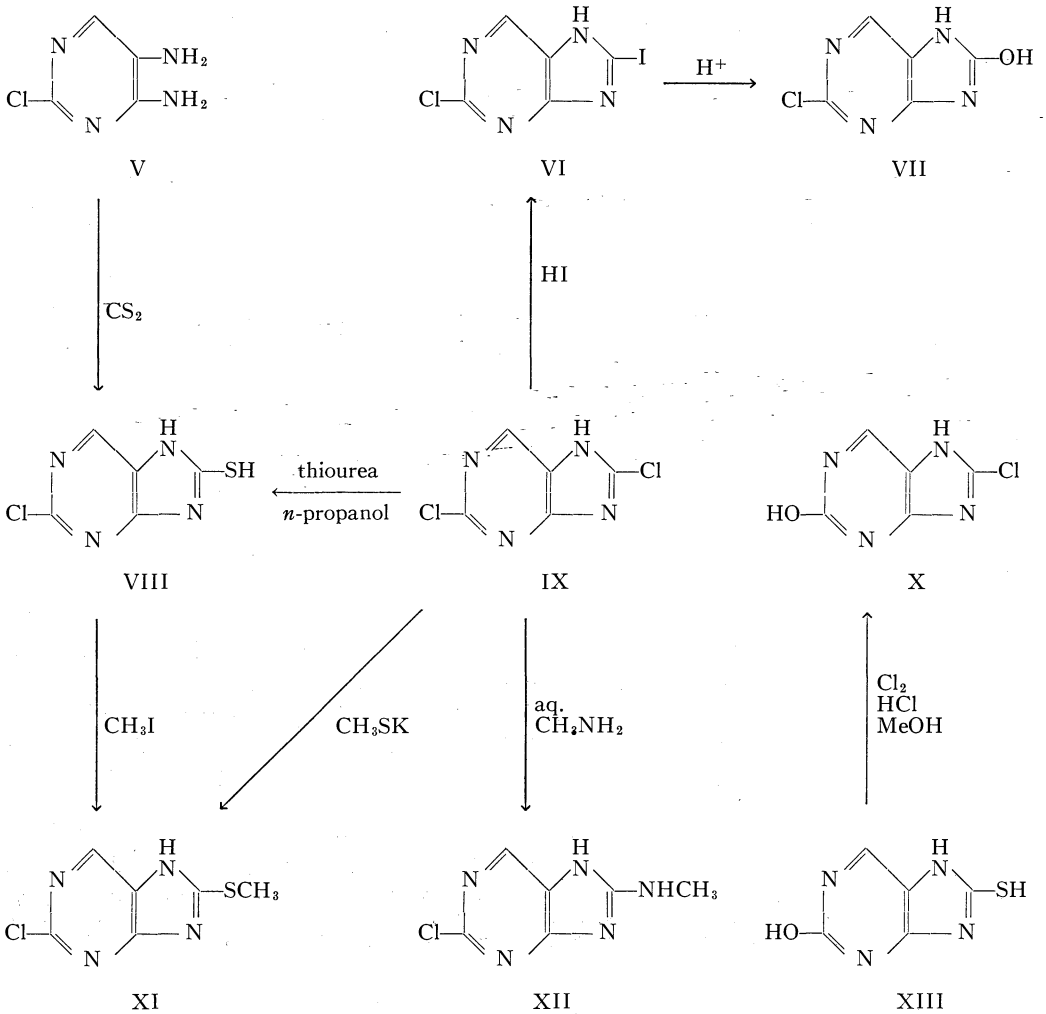

V VI VII

VIII IX X

XI XII XIII

Can. J. Chem. Downloaded from www.nrcresearchpress.com by 210.87.254.105 on 09/05/12
For personal use only.

Upon treatment with hydriodic acid, 2,8-dichloropurine (IX) gave 2-chloro-8-iodopurine (VI), the structure of which was proved by acid hydrolysis to the known 2-chloro-8-hydroxypurine (VII) (3(*j*)). With warm aqueous methylamine 2,8-dichloropurine gave 2-chloro-8-methylaminopurine (XII), the structure of which was proved by treatment with palladium-on-charcoal in the presence of hydrogen to give the known 8-methylaminopurine (4).

With potassium methylmercaptide, IX gave a compound which was identical with 2-chloro-8-methylthiopurine (XI) obtained by methylation of 2-chloro-8-purinethiol (VIII). Refluxing 2,8-dichloropurine with an excess of sodium methoxide in methanol gave 2,8-dimethoxypurine.

When 2-hydroxy-8-purinethiol (XIII) (3(*c*)) was treated with chlorine gas in methanol plus aqueous hydrochloric acid, 8-chloro-2-hydroxypurine (X) was formed.

In the cases studied with 2,8-dichloropurine (IX), nucleophilic attack occurred at position 8 before position 2 when preferential nucleophilic displacement could be accomplished. This is interesting since 2,6,8-trichloropurine (9–11) and 6,8-dichloropurine (2) usually exhibit nucleophilic displacement first in the pyrimidine ring (position 6). These experimental observations, however, are in accord with the electron density calculations of Mason (12) and Pullman (13) which predict that nucleophilic attack should occur more readily at positions 8 and 6 than at position 2.

The mechanism for acid hydrolysis of a 2,8-dihalogenated purine has been proposed as involving protonation in the imidazole ring (3(*j*)) and resulting in the 2-halogenated 8-hydroxypurine. This mechanism receives further support from the study of the acid hydrolysis of 2-chloro-8-iodopurine (VI).

The ultraviolet absorption spectra of several of the 2,8-disubstituted purines are given in Table I.

EXPERIMENTAL

2,8-Diaminopurine (IV)

2,8-Diamino-6-purinethiol (III) (7) (36 g) was dissolved in a mixture of 4 liters of water plus 2.7 liters of conc. aqueous ammonia at 70°. With vigorous stirring 175 g of water-wet Raney nickel was added, and the mixture was boiled briskly and stirred for 1.5 hours. The nickel was filtered hot and washed with boiling water, and the combined filtrate was evaporated to 500 ml under reduced pressure. A small amount of slimy residue was removed by filtration, and the filtrate was further evaporated to 100 ml and refrigerated to give 24 g of crude 2,8-diaminopurine. An additional 7 g was obtained by evaporating the filtrate to dryness. The crude product was recrystallized from boiling water (7 parts) with the aid of charcoal to give colorless crystals, m.p. 296°. Calc. for $C_5H_6N_6$: C, 40.0; H, 4.0. Found: C, 39.4; H, 4.1. A sample was recrystallized from boiling 10% sulphuric acid to give a white solid, m.p. 300° decomp. Calc. for $C_5H_6N_6 \cdot H_2SO_4 \cdot \frac{1}{2}H_2O$: C, 23.4; H, 3.5; N, 32.7. Found: C, 23.6; H, 3.6; N, 32.7.

2-Chloro-8-iodopurine (VI)

2,8-Dichloropurine (IX) (3(*j*)) (2 g) was added slowly to 25 ml of 47% hydriodic acid at −10° with stirring. After the mixture was stirred for 1.5 hours at 0°, the solid was filtered, suspended in 30 ml of water, the pH adjusted to 5–6, and the slurry refrigerated. The solid was collected and suspended in hot water, and enough ammonia added to effect solution. The solution was treated with decolorizing charcoal and filtered, and the filtrate was adjusted to pH 5 with acetic acid and cooled. The resulting solid was recrystallized from water and ethanol to give colorless 2-chloro-8-iodopurine (1 g, 34%), m.p. 238–240°. Calc. for C_5H_2ClIN: C, 21.4; H, 0.7; N, 20.0; total halogen, 58.0. Found: C, 21.6; H, 0.8; N, 20.0; total halogen, 58.3.

8-Chloro-2-hydroxypurine (X)

2-Hydroxy-8-purinethiol (XIII) (3(*c*)) (5 g) was added to a mixture of 10 ml of methanol plus 30 ml of conc. aqueous hydrochloric acid at −20°. With stirring, chlorine gas was bubbled through the solution at −10 to −5°. The solid dissolved and another solid precipitated from solution. After about 12 minutes the reaction was complete. The mixture was poured on 150 g of ice with stirring; the pH was adjusted

Can. J. Chem. Downloaded from www.nrcresearchpress.com by 210.87.254.105 on 09/05/12
For personal use only.

TABLE I

Ultraviolet absorption spectra of some 2,8-disubstituted purines

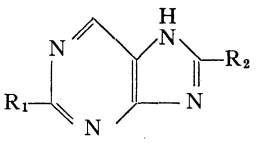

		pH 1		pH 11	
R_1	R_2	λ_{max}, mμ	ε	λ_{max}, mμ	ε
NH_2	NH_2	225.5	29,400	225–229*	16,300
		268	2,660	310	9,750
		312	6,000		
Cl	I	284.5	22,000	287.5	20,800
OH	Cl	267	4,850	266	7,100
		317	8,070	312	8,300
NH_2	SH	256	22,300	237	14,600
		338	18,950	329	18,900
Cl	SH	237.5	9,960	232	12,800
		316	26,600	320	22,400
Cl	SCH_3	227	11,200	229	13,100
		296.5	15,700	295.5	15,600
Cl	$NHCH_3$	239	5,200	221.5	13,900
		287	15,400	304	15,000
OCH_3	OCH_3	255	6,450		
		287	9,720	288	10,800
OH	NH_2	255	4,000	226	19,300
		317	8,440	267	5,060
				312	4,200
SCH_3	SCH_3†	239–246*	11,700	248	22,400
		264	23,100		
		282–290*	13,800	320	16,300
		327	11,200		

*Inflection.
†Correction of data previously published, ref. 3(*f*).

to 1.5–2 with conc. aqueous ammonia, and the mixture was refrigerated for an hour. The crude 8-chloro-2-hydroxypurine was collected, washed with ice water, and dried to yield 2.6 g (51%). A sample was recrystallized from water and ethanol. Calc. for $C_5H_3ClN_4O$: C, 35.3; H, 1.8; N, 32.9. Found: C, 35.4; H, 1.5; N, 33.0.

8-Aminopurine

8-Amino-6-purinethiol* (20 g) was dissolved in 1 liter of distilled water plus 200 ml of conc. aqueous ammonia solution. Neutral water-wet Raney nickel (200 g) was added, and the mixture was refluxed with stirring for 2.25 hours. The nickel was filtered and washed with a little hot water, and the filtrate plus wash was boiled until no odor of ammonia could be detected. The light yellow 8-aminopurine, which formed on refrigeration, weighed 8 g. An additional 1 g (total yield 56%) was obtained by concentrating the filtrate to 100 ml. A sample was purified by precipitation from solution in dilute ammonia with acetic acid (pH 7). Calc. for $C_5H_5N_5$: C, 44.4; H, 3.7; N, 51.8. Found: C, 44.6; H, 4.0; N, 52.1.

2,4,5-Triaminopyrimidine Sulphate

A mixture of 33 g of 6-methylthio-2,4,5-triaminopyridine (5), 500 ml of distilled water, 300 ml of conc.

**A much better yield of 8-amino-6-purinethiol was obtained than previously reported (2) by fusion of 4,5-diamino-6-pyrimidinethiol with guanidine for 10 hours at 180–200°.*

Can. J. Chem. Downloaded from www.nrcresearchpress.com by 210.87.254.105 on 09/05/12
For personal use only.

aqueous ammonia solution, and 200 g of neutral water-wet Raney nickel was refluxed for 7 hours with vigorous mechanical stirring. The nickel was filtered and washed with hot water. The filtrate plus wash was boiled until there was no longer any ammonia odor (volume about 400 ml). The hot solution was acidified to pH 5 with sulphuric acid and cooled overnight. The yield of light-colored sulphate salt was 29 g (82%). Calc. for $C_4H_7N_5 \cdot \frac{1}{2}H_2SO_4 \cdot \frac{1}{2}H_2O$: C, 26.2; H, 4.9; N, 38.2; H_2O, 4.9. Found: C, 26.3; H, 5.2; N, 38.0; H_2O, 4.9 (Karl Fischer).

2-Amino-8-purinethiol

2,4,5-Triaminopyrimidine sulphate (5 g) and thiourea (15 g) were fused at 160–180° for 30 minutes. The cake was dissolved in 400 ml of hot 1 *N* potassium hydroxide solution and treated with charcoal. The filtrate was acidified (pH 2–3) with sulphuric acid and cooled to give 6 g of crude material. This product was dissolved in hot, dilute ammonia (charcoal) and precipitated with sulphuric acid (pH 7) to give a yellow product. Calc. for $C_5H_5N_5S$: C, 35.9; H, 3.0; N, 41.9. Found: C, 35.9; H, 3.0; N, 41.6.

2-Chloro-8-purinethiol (VIII)

Method (A).—2,8-Dichloropurine (IX) (3(*j*)) (1.0 g) was added to a solution of 0.40 g of thiourea in 30 ml of *n*-propanol. The solution was refluxed for 1 hour, and a yellow precipitate gradually formed. After refrigeration the product was collected, washed with water and acetone, and dried to yield 0.7 g of VIII. The product had an ultraviolet absorption spectrum identical with that of 2-chloro-8-purinethiol (VIII) prepared by method (B).

Method (B).—2-Chloro-4,5-diaminopyrimidine (V) (8) (5 g) was added to a mixture of 85 ml of pyridine and 20 ml of carbon disulphide, and the solution was refluxed for 3 hours. The cold solution was acidified to pH 1 with hydrochloric acid and cooled. The crude 2-chloro-8-purinethiol (VIII) was collected, washed with water and acetone, and dried to yield 2.7 g (42%). This material was further purified by reprecipitation from warm (50°) dilute ammonia with acetic acid (pH 6). Calc. for $C_5H_3ClN_4S$: C, 32.2; H, 1.6; N, 30.0 Found: C, 32.2; H, 1.6; N, 30.3.

2-Chloro-8-methylaminopurine (XII)

2,8-Dichloropurine (IX) (5 g) was dissolved in 150 ml of 40% methylamine solution. The solution was heated on the steam bath for 2 hours. An additional 100 ml of methylamine solution was added and the solution evaporated to dryness on the steam bath. The residue was dissolved in hot, dilute hydrochloric acid, treated with charcoal, and filtered, and the pH of the filtrate was adjusted to 7 with dilute potassium hydroxide. After refrigeration overnight, the light yellow product was filtered, washed with water and ethanol, and dried to yield 0.9 g. Calc. for $C_6H_6ClN_5$: C, 39.4; H, 3.3; N, 38.2. Found: C, 39.4; H, 3.6; N, 38.3.

8-Methylaminopurine

2-Chloro-8-methylaminopurine (XII, 0.5 g) was dissolved in a solution of 0.4 g of sodium hydroxide in 100 ml of water. Then 0.5 g of 10% palladium-on-charcoal was added and the mixture shaken for 3 hours under 45 lb/sq. in. pressure of hydrogen. The catalyst was filtered, and the filtrate was treated with charcoal, neutralized, and concentrated to 50 ml. The ultraviolet absorption spectrum of this solution was identical with that recorded by Albert and Brown (4) for 8-methylaminopurine.

2-Chloro-8-methylthiopurine (XI)

Method (A).—2-Chloro-8-purinethiol (VIII, 0.9 g) was dissolved in 10 ml of 1 *N* potassium hydroxide solution. Methyl iodide (3 ml) was added and the mixture stirred at room temperature for 1.5 hours. The solution was neutralized and cooled overnight to yield a yellow product, which was filtered, washed with water and acetone, and dried. The filtrate was extracted with ethyl ether and the ether evaporated to yield additional product. The total yield was 0.7 g (72%). A sample was recrystallized from methanol and water. Calc. for $C_6H_5ClN_4S$: C, 36.0; H, 2.5; N, 28.0. Found: C, 36.1; H, 2.8; N, 28.0.

Method (B).—2,8-Dichloropurine (IX, 2 g) was dissolved in a solution of 8 g of potassium hydroxide in 50 ml of water containing 10 ml of methanethiol. The solution was heated on a steam bath for 30 minutes and cooled; an additional 10 ml of methanethiol was added and the mixture heated for an additional hour. The solution was neutralized with glacial acetic acid and cooled overnight. The white solid which precipitated was filtered, washed with water and acetone, and dried to yield 0.25 g. The filtrate was extracted with ethyl ether and the ether evaporated to give 0.5 g of additional material. The product had ultraviolet and infrared absorption spectra identical with those of the 2-chloro-8-methylthiopurine (XI) prepared by method (A).

2,8-Dimethoxypurine

2,8-Dichloropurine (IX, 5 g) was added to a solution of 6 g of sodium in 150 ml of methanol. The solution was refluxed for 2.5 hours and evaporated to dryness on the steam bath. The residue was dissolved in water (100 ml), and the solution was neutralized with hydrochloric acid and cooled overnight. The product was filtered, washed with water and acetone, and dried to yield 2.6 g (54%). A sample was further purified by dissolving the product in hot, dilute aqueous ammonia. The solution was then treated with charcoal

Can. J. Chem. Downloaded from www.nrcresearchpress.com by 210.87.254.105 on 09/05/12
For personal use only.

and filtered and the excess ammonia boiled away. The product then crystallized from the solution. Calc. for $C_7H_8N_4O_2$: C, 46.7; H, 4.4; N, 31.1. Found: C, 46.7; H, 4.7; N, 30.7.

2-Amino-8-hydroxypurine

2,4,5-Triaminopyrimidine sulphate (10 g) was dissolved in 100 ml of 2 *N* sodium hydroxide solution. Phosgene was bubbled through the solution, with stirring, for 45 minutes. Small amounts of 6 *N* sodium hydroxide solution were added as needed to maintain a basic solution (pH > 10). After this 45-minute period the phosgene addition was continued until the pH of the solution was approximately 7–8. The solution was then stirred for 0.5 hour without addition of phosgene, neutralized with aqueous hydrochloric acid, and cooled for several hours. The tan-colored solid was filtered, washed with water and acetone, and dried to yield 8 g. The product was dissolved in hot, dilute aqueous ammonia solution and precipitated with conc. hydrochloric acid (pH 6–7) to yield 4.5 g (55%). Calc. for $C_5H_5N_5O$: C, 39.7; H, 3.3. Found: C, 39.6; H, 3.6.

8-Amino-2-hydroxypurine Sulphate (II)

Guanidine hydrochloride (25.6 g) (85%) was converted to guanidine (2). 4,5-Diamino-2-hydroxypyrimidine sulphate (I) (4(*b*)) (10 g) was added, and the mixture was heated in a metal bath at 160–180° for 7.5 hours. The hard, black cake was dissolved in 500 ml of hot 1 *N* potassium hydroxide solution, treated with charcoal, and filtered and the filtrate acidified with acetic acid (pH 5). Upon refrigeration a light-colored product was obtained; it was filtered, washed with water and acetone, and dried to yield 5.5 g. The product was reprecipitated from dilute, aqueous ammonia with conc. sulphuric acid (pH 5–6) and then recrystallized from water to yield 2.0 g. The product was then extracted with methanol to remove a small amount of soluble impurity and finally recrystallized from water containing a little sulphuric acid to give 1.8 g. Calc. for $C_5H_5N_5O \cdot \frac{1}{2}H_2SO_4$: C, 30.0; H, 3.0. Found: C, 29.9; H, 3.8.

2-Chloro-8-hydroxypurine (VII)

2-Chloro-8-iodopurine (VI, 0.1 g) was dissolved in 30 ml of 1 *N* hydrochloric acid. The solution was refluxed for 20 minutes, cooled, neutralized with ammonia, and concentrated to a small volume. Upon refrigeration a white solid formed which possessed an ultraviolet absorption spectrum identical with that of 2-chloro-8-hydroxypurine (3(*j*)). The two compounds possessed the same R_f values in three solvent systems.

ACKNOWLEDGMENT

We gratefully acknowledge the support of research grants CY-4008(C3) and CY-4008(C4) from the National Cancer Institute of the National Institutes of Health, Public Health Service, Bethesda, Maryland.

REFERENCES

1. R. K. Robins. The purines and related ring systems. *In* Heterocyclic compounds. Vol. 8. *Edited by* R. C. Elderfield. John Wiley & Sons, Inc., New York, N.Y. In preparation.
2. R. K. Robins. J. Am. Chem. Soc. **80**, 6671 (1958).
3. (*a*) C. O. Johns. Am. Chem. J. **45**, 79 (1911).
   (*b*) A. Dornow and E. Hinz. Chem. Ber. **91**, 1834 (1958).
   (*c*) C. O. Johns. J. Biol. Chem. **21**, 319 (1915).
   (*d*) D. J. Brown. J. Appl. Chem. (London), **9**, 203 (1959).
   (*e*) C. W. Noell and R. K. Robins. J. Org. Chem. **24**, 320 (1959).
   (*f*) C. W. Noell and R. K. Robins. J. Am. Chem. Soc. **81**, 5997 (1959).
   (*g*) E. A. Falco, G. B. Elion, E. Burgi, and G. H. Hitchings. J. Am. Chem. Soc. **74**, 4897 (1952).
   (*h*) A. G. Beaman, J. F. Gerster, and R. K. Robins. J. Org. Chem. **27**, 986 (1962).
   (*i*) H. Ballweg. Ann. **649**, 114 (1961).
   (*j*) A. G. Beaman and R. K. Robins. J. Appl. Chem. (London), **12**, 432 (1962).
   (*k*) F. Bergmann and M. Tamari. J. Chem. Soc. 4468 (1961).
4. (*a*) A. Albert and D. J. Brown. J. Chem. Soc. 2060 (1954).
   (*b*) A. Kalmus and F. Bergmann. J. Chem. Soc. 760 (1961).
   (*c*) D. J. Brown. J. Appl. Chem. (London), **2**, 239 (1952).
5. G. D. Daves, Jr., C. W. Noell, R. K. Robins, H. C. Koppel, and A. G. Beaman. J. Am. Chem. Soc. **82**, 2633 (1960).
6. D. J. Brown. J. Appl. Chem. (London), **7**, 109 (1957).
7. J. W. Jones and R. K. Robins. J. Am. Chem. Soc. **82**, 3773 (1960).
8. A. Albert, D. J. Brown, and G. Cheeseman. J. Chem. Soc. 482 (1951).
9. E. Fischer. Ber. **30**, 2226 (1897).
10. R. K. Robins and B. E. Christensen. J. Am. Chem. Soc. **74**, 3624 (1952).
11. S. R. Breshears, S. S. Wang, S. G. Bechtolt, and B. E. Christensen. J. Am. Chem. Soc. **81**, 3789 (1959).
12. S. F. Mason. *In* The chemistry and biology of purines. A Ciba Foundation symposium. *Edited by* Wolstenholme and O'Connor. Little, Brown and Co., Boston, Mass. 1957. p. 72.
13. B. Pullman. J. Chem. Soc. 1621 (1959).

Can. J. Chem. Downloaded from www.nrcresearchpress.com by 210.87.254.105 on 09/05/12
For personal use only.

BEHAVIOR OF THE HETERO-RING IN γ-PHENYL-$\Delta^{\beta,\gamma}$-BUTENOLIDE DERIVATIVES TOWARD HYDRAZINES. ACID REARRANGEMENT OF 4-PHENYLAZO-2-PHENYLOXAZOLIN-5-ONE

AHMED MUSTAFA, SAMIR A. KHATTAB, AND WAFIA ASKER
Chemistry Department, Faculty of Science, Cairo University, Cairo, Egypt, U.A.R.

Received October 29, 1963

ABSTRACT

The substituted pyridazinones 3-phenyl- and 1,3-diphenyl-5-benzylidene-1,4,5,6-tetrahydropyridazinone-6 have been prepared from α-phenacylcinnamic acid hydrazide and α-phenacylcinnamic acid phenylhydrazone, respectively. The dipyridazinone 5,5-di(3-phenyl-1,4,5,6-tetrahydro)pyridazinone-6 was prepared from the dilactone IV, isolated as a side product in the synthesis of lactone VI.

Rearrangement of 4-phenylazo-2-phenyloxazolin-5-one now has been found to proceed also in the presence of acidic reagents.

α-Benzylidene-γ-phenyl-$\Delta^{\beta,\gamma}$-butenolide* (I) has been reported to undergo ring opening upon treatment with aqueous base, with methanol under both acidic and basic conditions (1, 2) and with benzylamine (1) to form α-phenacylcinnamic acid (II*a*), its methyl ester (II*b*), and its benzylamide derivative (II*e*) respectively.

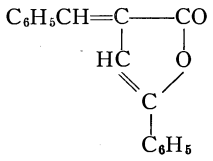

I

$C_6H_5CH{=}C(CH_2{-}COC_6H_5)COR$

II*a*, R = OH
b, R = OCH_3
c, R = $NHNH_2$
d, R = $NHNHC_6H_5$
e, R = $NHCH_2C_6H_5$

This investigation was undertaken with a view to study the behavior of the hetero-ring in compound I toward the action of hydrazines. Treatment of compound I with hydrazine hydrate effected ring opening with the formation of α-phenacylcinnamic acid hydrazide (II*c*). The latter compound underwent ring closure upon treatment with hydrochloric acid – acetic acid mixture or with aqueous sodium hydroxide solution with the formation of 3-phenyl-5-benzylidene-1,4,5,6-tetrahydropyridazinone-6 (III*a*) (or its tautomer).

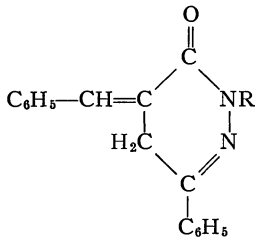

III*a*, R = H
b, R = C_6H_5

The proposed structure for the hydrazide II*c* finds support from the fact that this compound was readily obtained via treatment of methyl α-phenacylcinnamate (II*b*) with

**This nomenclature is after that used by Filler (1).*

Can. J. Chem. Downloaded from www.nrcresearchpress.com by 210.87.254.105 on 09/05/12
For personal use only.

hydrazine hydrate. Compound III*a* was also found to be identical with an authentic specimen prepared after Thiele (2).

When the dilactone IV was treated with hydrazine hydrate, 5,5′-di(3-phenyl-1,4,5,6-tetrahydro)pyridazinone-6 (V) (or its possible tautomer) was isolated, but not the corresponding acyclic hydrazide.

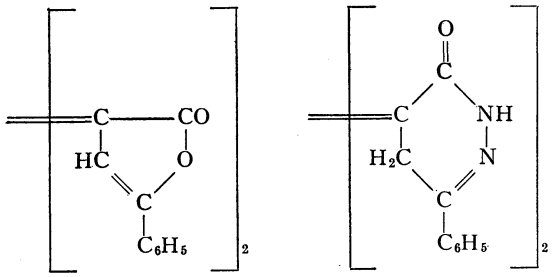

IV V

α-Phenacylcinnamic acid (II*a*), upon treatment with phenylhydrazine, gave the corresponding phenylhydrazone derivative. When the latter compound was treated with hot sodium hydroxide solution, it underwent ring closure with the formation of 1,3-diphenyl-5-benzylidene-1,4,5,6-tetrahydropyridazinone-6 (III*b*). The assigned structure for the latter compound finds support from its identity with a sample obtained via the condensation of 1,3-diphenyl-1,4,5,6-tetrahydropyridazinone-6 with benzaldehyde (3).

Phenylhydrazine was found to react with compound I, not to form the phenylhydrazone derivative of α-phenacylcinnamic acid but to give a colorless product believed to be α-phenacylcinnamic acid phenylhydrazide (II*d*).

Dieckmann described the preparation of α-phenylazo-γ-phenyl-$\Delta^{\beta,\gamma}$-butenolide (VI*a*) by coupling of γ-phenyl-$\Delta^{\beta,\gamma}$-butenolide with benzenediazonium chloride (4). We have succeeded in preparing a number of α-arylazo-γ-phenyl-$\Delta^{\beta,\gamma}$-butenolides, VI*a–d*, after the procedure described by Sawdey (5) for the preparation of 4-phenylazo-2-phenyloxazolin-5-one (VII) using β-benzoylpropionic acid for hippuric acid. Work-up of the filtrate of

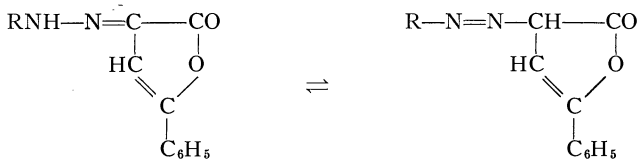

VI*a*, R = C_6H_5
b, R = C_6H_4—CH_3 (*p*)
c, R = C_6H_4—Cl (*m*)
d, R = C_6H_4—Cl (*p*)

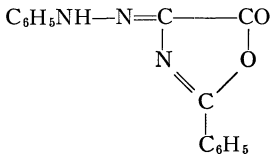

VII

the reaction mixture, after separation of the reaction products VI*a–d*, gave dark red crystals identical with the dilactone IV (6, 7).

Can. J. Chem. Downloaded from www.nrcresearchpress.com by 210.87.254.105 on 09/05/12
For personal use only.

While the rearrangement of 4-phenyl-azo-2-phenyloxazolin-5-one (VII) and its carbon analogue α-phenylazo-γ-phenyl-$\Delta^{\beta,\gamma}$-butenolide (VI*a*) was in progress in this laboratory (8), Browne and Polya (9, 10) reported the rearrangement of compound VII in the presence of basic reagents, a fact which prompts us to record our findings. Results in our hands confirm the findings of the latter authors, but we would like to report that the rearrangement of compound VII to 1,5-diphenyl-1,2,4-triazole-3-carboxylic acid hydrazide (VIII*c*) with hydrazine hydrate can be brought about in the absence of solvent. Hydrolysis of the hydrazide VIII*c* to the corresponding 1,5-diphenyl-1,2,4-triazole-3-carboxylic acid (VIII*a*) is readily effected by the action of hydrochloric acid – acetic acid mixture.

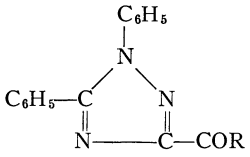

VIII*a*, R = OH
b, R = OCH_3
c, R = $NHNH_2$

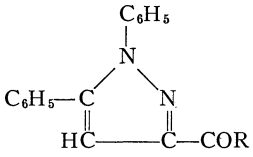

IX*a*, R = OH
b, R = OC_2H_5
c, R = $NHNH_2$

We would like also to record that, though the latter authors reported that the rearrangement of compound VII did not occur in solutions acid to litmus, in our hands treatment of this compound with hydrochloric acid – acetic acid mixture yielded the triazole acid VIII*a* in a yield similar to that obtained by alkali rearrangement (5).

The carbon analogue VI*a* underwent rearrangement by action of alcoholic alkali or hydrochloric acid – acetic acid mixture to give the corresponding 1,5-diphenylpyrazole-3-carboxylic acid (IX*a*) (4). The ethyl ester IX*b*, now obtained from the corresponding acid IX*a*, reacts with hydrazine hydrate to give 1,5-diphenylpyrazole-3-carboxylic acid hydrazide (IX*c*).

EXPERIMENTAL

All melting points are uncorrected.

Action of Hydrazine Hydrate

(a) On α-Benzylidene-γ-phenyl-$\Delta^{\beta,\gamma}$-butenolide (I)

Hydrazine hydrate (4 ml, 80%) was added to compound I (0.5 g) and the reaction mixture was allowed to stand at room temperature for half an hour with occasional shaking. The yellow color of compound I was completely discharged with the formation of a colorless deposit of α-phenacylcinnamic acid hydrazine (II*c*). It was collected, washed thoroughly with water, and upon crystallization from ethanol, gave colorless crystals, m.p. 185° (decomp.). Yield, ca. 53%.

Anal. Calc. for $C_{17}H_{16}N_2O_2$: C, 72.85; H, 5.71; N, 10.00. Found: C, 73.07; H, 5.93; N, 9.95.

It gave a red color with concentrated sulphuric acid and was found insoluble in cold aqueous sodium carbonate solution (1%). The infrared spectrum* showed well-defined absorption bands at 1650 cm^{-1} characteristic of the —CONH— group (11) and at 1700 cm^{-1} characteristic of the $—COC_6H_5$ group.

The hydrazide II*c* could also be obtained from methyl α-phenacylcinnamate (II*b*) and hydrazine hydrate in 80% yield when the reaction mixture was allowed to stand for 48 hours under the experimental conditions described above.

(b) On Dilactone IV

The reaction was carried out as for compound I and the mixture was left for 2 weeks. The product, 5,5′-di(3-phenyl-1,4,5,6-tetrahydro)pyridazinone-6 (V), was crystallized from acetic acid as colorless crystals (65% yield), m.p. >350°.

Anal. Calc. for $C_{20}H_{16}N_4O_2$: C, 69.76; H, 4.65; N, 16.27. Found: C, 69.87; H, 4.85; N, 16.19.

**The infrared spectra were produced on a Perkin–Elmer Infracord model 137B and the samples were examined in Nujol solution.*

Can. J. Chem. Downloaded from www.nrcresearchpress.com by 210.87.254.105 on 09/05/12
For personal use only.

Ring Closure of Hydrazide IIc

Method (a)

A mixture of glacial acetic acid (7 ml), hydrochloric acid (3.5 ml), and hydrazide II*c* (0.5 g) was refluxed for 1 hour. The cooled reaction mixture was poured into ice-cold water, and the precipitate so obtained was collected and washed thoroughly with water. It gave colorless crystals of 3-phenyl-5-benzylidene-1,4,5,6-tetrahydropyridazinone-6 (III*a*) from ethanol, m.p. 177°. Yield, ca. 43%.

Anal. Calc. for $C_{17}H_{14}N_2O$: C, 77.86; H, 5.34; N, 10.68. Found: C, 77.56; H, 5.46; N, 10.87.

Compound III*a* was proved to be identical with an authentic specimen prepared after Thiele (2) (mixed m.p. determination and identical infrared spectrum).

Method (b)

Aqueous sodium hydroxide solution (10 ml, 4%) was added to hydrazide II*c* (0.3 g) and the reaction mixture was refluxed for half an hour. It was then allowed to cool, diluted with water, and acidified with hydrochloric acid. The precipitated solid was collected, washed with water, and crystallized from ethanol to give colorless crystals of compound III*a*. Yield, ca. 35%.

Action of Phenylhydrazine

(a) On α-Phenacylcinnamic Acid (IIa)

Freshly distilled phenylhydrazine (3.0 g) was added to a suspension of the acid II*a* (3.0 g) in absolute ethanol (30 ml). The reaction mixture was refluxed for 5 hours. On evaporation of the solvent, an oily residue was obtained which after trituration with hot petroleum ether (b.p. 70–80°) was solidified to a pale yellow solid. Upon two crystallizations from the same solvent, it gave almost colorless crystals, m.p. 101° (slight decomp.); yield, 50%; identified as the phenylhydrazone derivative of the acid II*a*.

Anal. Calc. for $C_{23}H_{20}N_2O_2$: N, 7.86. Found: N, 7.66.

When a mixture of the above phenylhydrazone derivative (0.5 g), sodium hydroxide solution (20 ml, 4%), and ethanol (10 ml) was refluxed for 1 hour, it gave upon cooling a colorless deposit of 1,3-diphenyl-5-benzylidene-1,4,5,6-tetrahydropyridazinone-6 (III*b*). The latter was collected, washed with water, and crystallized from ethanol as colorless crystals, m.p. 124°. Yield, ca. 53%.

Anal. Calc. for $C_{23}H_{18}N_2O$: C, 81.65; H, 5.32; N, 8.28. Found: C, 81.61; H, 5.38; N, 8.28.

The product III*b* was found to be identical (m.p. and mixed m.p. determination, infrared spectral comparison, and color with concentrated sulphuric acid) with a sample obtained via the condensation of 1,3-diphenyl-1,4,5,6-tetrahydropyridazinone-6 with benzaldehyde (3).

(b) On α-Benzylidene-γ-phenyl-$\Delta^{\beta,\gamma}$-butenolide (I)

Phenylhydrazine (0.4 g) was added to a suspension of compound I (1.0 g) in absolute ethanol (30 ml). The reaction mixture was refluxed for 5 hours and then the solvent was evaporated. The oily product so obtained was solidified on trituration with cold ether or petroleum ether and was crystallized from ethanol to give colorless crystals of α-phenacylcinnamic acid phenylhydrazide (II*d*), m.p. 207° (decomp.). Yield, ca. 28%.

Anal. Calc. for $C_{23}H_{20}N_2O_2$: C, 77.52; H, 5.61; N, 7.86. Found: C, 77.41; H, 5.58; N, 8.01.

It gave a yellowish red color with concentrated sulphuric acid and was found to be insoluble in cold sodium carbonate solution (1%). The infrared spectrum showed well-defined absorption bands at 1650 cm^{-1} characteristic of the —CONH— group (11) and at 1700 cm^{-1} characteristic of the $—COC_6H_5$ group.

Preparation of α-Arylazo-γ-phenyl-$\Delta^{\beta,\gamma}$-butenolides (VIa–d)

The following exemplifies the procedure: To a solution of freshly distilled aniline (3.7 g) in glacial acetic acid (15 ml) was added hydrochloric acid (8 ml), then while the mixture was being cooled in ice and stirred, isoamyl nitrite (8 g) was added dropwise. To the diazonium mixture was added freshly fused sodium acetate (6.0 g). β-Benzoylpropionic acid (10.0 g) was added to acetic anhydride (40 ml) and the mixture was refluxed for 3 hours then allowed to cool to room temperature. This solution was added dropwise, with stirring and cooling in ice, to the diazonium mixture. The reaction mixture was allowed to stand overnight and the precipitated solid was collected, washed with water several times, and crystallized from a large volume of acetic acid.

The arylazo derivatives VI*a–d* (listed in Table I) ranged in color from brownish yellow to deep brown and were found to be sparingly soluble in common organic solvents. They showed an absorption maximum at 350 mμ, which was attributed to the arylhydrazone group (12).

α-Phenylazo-γ-phenyl-$\Delta^{\beta,\gamma}$-butenolide (VI*a*) was proved to be identical with an authentic specimen prepared after Dieckmann (4) (mixed m.p. determination and infrared spectral comparisons).

The mother liquors, after filtration of the products VI*a–d*, gave upon concentration and trituration with ether a dark red solid which was crystallized from xylene or acetic acid as dark red crystals of the dilactone IV in a yield which varied from 5–10%.

Anal. Calc. for $C_{20}H_{12}O_4$: C, 75.94; H, 3.79. Found: C, 75.84; H, 4.02.

The dilactone IV was identical with an authentic specimen prepared after Rogert and Ritter (6).

Can. J. Chem. Downloaded from www.nrcresearchpress.com by 210.87.254.105 on 09/05/12
For personal use only.

Can. J. Chem. Downloaded from www.nrcresearchpress.com by 210.87.254.105 on 09/05/12
For personal use only.

TABLE I

The arylazo derivatives (VI*a–d*)

Arylazo derivative	M.p. (°C)	Yield (%)	Color with conc. H_2SO_4	Formula	Carbon (%)		Hydrogen (%)		Nitrogen (%)		Chlorine (%)	
					Calc.	Found	Calc.	Found	Calc.	Found	Calc.	Found
VI*a*	227 (decomp.)	45	Violet	$C_{16}H_{12}N_2O_2$	72.73	72.45	4.54	4.63	10.61	10.53	—	—
VI*b*	222 (decomp.)	40	Dark brown	$C_{17}H_{14}N_2O_2$	73.38	73.88	5.03	5.11	10.07	10.20	—	—
VI*c*	238 (decomp.)	37	Deep violet	$C_{16}H_{11}ClN_2O_2$	64.32	64.37	3.68	3.84	9.38	9.08	11.89	12.12
VI*d*	252 (decomp.)	41	Deep violet	$C_{16}H_{11}ClN_2O_2$	64.32	64.57	3.68	3.77	9.38	9.68	11.89	11.57

Formation of 1,5-Diphenyl-,1,2,4-triazole-3-carboxylic Acid Hydrazide (VIIIc)

(a) From 4-Phenylazo-2-phenyloxazolin-5-one (VII)

Hydrazine hydrate (5 ml) was added to a suspension of compound VII (1.0 g) in ethanol (30 ml). On shaking the reaction mixture for 15 minutes at room temperature, the orange color of compound VII disappeared with the formation of a colorless deposit. It was allowed to stand overnight, poured into water, and the precipitated solid was collected, washed with water, and crystallized from ethanol or chlorobenzene as colorless crystals of the hydrazide VIII*c*, m.p. 185°. Yield, ca. 42%.

Anal. Calc. for $C_{15}H_{13}N_5O$: C, 64.51; H, 4.65; N, 25.08. Found: C, 64.33; H, 4.84; N, 25.21.

The hydrazide VIII*c* could also be obtained in an almost quantitative yield when a suspension of compound VII (0.6 g) in hydrazine hydrate (10 ml) was allowed to stand for 6 weeks at room temperature.

(b) From 1,5-Diphenyl-3-carbomethoxy-1,2,4-triazole (VIIIb)

Compound VIII*c* was obtained either by allowing a suspension of the ester VIII*b* (0.3 g) in hydrazine hydrate (3 ml) to stand at room temperature for 4 weeks (yield was ca. 60%) or by heating the same suspension on the direct flame until the ester dissolved in the medium and then continuing the heating on a boiling-water bath for 15 hours. Yield, ca. 33%.

Hydrolysis of 1,5-Diphenyl-1,2,4-triazole-3-carboxylic Acid Hydrazide (VIIIc)

The hydrazide VIII*c* (0.5 g) was treated with a mixture of glacial acetic acid (15 ml) and hydrochloric acid (20 ml). The reaction mixture was refluxed for 3 hours, cooled, and poured into water. The solid so obtained was collected, washed with water, and crystallized from benzene as colorless crystals of 1,5-diphenyl-1,2,4-triazole-3-carboxylic acid (VIII*a*), m.p. 181° (decomp.), not depressed when admixed with an authentic specimen prepared after Sawdey (5). Yield, ca. 63%.

Action of Hydrochloric Acid – Acetic Acid Mixture on 4-Phenylazo-2-phenyloxazolin-5-one (VII)

Compound VII (2.0 g) was treated with a mixture of glacial acetic acid (40 ml) and hydrochloric acid (60 ml) and the reaction mixture was refluxed for 5 hours. Working up of the reaction product as above gave the acid VIII*a*. Yield, ca. 80%.

Preparation of 1,5-Diphenyl-3-carbethoxypyrazole (IXb)

To 1,5-diphenylpyrazole-3-carboxylic acid (IX*a*) (1.0 g) was added absolute ethanol (25 ml) and concentrated sulphuric acid (0.5 ml) and the reaction mixture was refluxed on a boiling-water bath for 5 hours. It was cooled, poured into ice-cold sodium carbonate solution (100 ml, 0.5%) and the solid obtained was collected, washed with water, and crystallized from dilute ethanol (1:1) as colorless crystals of the ethyl ester IX*b*, m.p. 90° not depressed when admixed with an authentic specimen (13, 14). Yield, ca. 77%.

Formation of 1,5-Diphenylpyrazole-3-carboxylic Acid Hydrazide (IXc) from the Ethyl Ester IXb

Method (a)

The ester IX*b* (1.0 g) was heated with hydrazine hydrate (5.5 ml) on a boiling-water bath for half an hour, then absolute ethanol (20 ml) was added to the reaction mixture, which was then refluxed for 3 hours. It was allowed to cool and then poured into water. The hydrazide IX*c* was collected, washed with water, and upon crystallization from ethanol, colorless crystals were obtained, m.p. 174°. Yield, ca. 63%.

Anal. Calc. for $C_{16}H_{14}N_4O$: C, 69.06; H, 5.03; N, 20.14. Found: C, 69.16; H, 5.27; N, 20.25.

Method (b)

The same hydrazide could also be obtained in a similar yield as above when a mixture of the ester IX*b* (1.0 g) and hydrazine hydrate (6 ml) was allowed to stand at room temperature for 1 week.

REFERENCES

1. R. Filler and L. M. Hebron. J. Am. Chem. Soc. **81**, 391 (1959).
2. J. Thiele. Ann. **306**, 162 (1899).
3. A. Mustafa, A. H. Harhash, and co-workers. Unpublished work.
4. W. Dieckmann. Ber. **47**, 1439 (1914).
5. G. W. Sawdey. J. Am. Chem. Soc. **79**, 1955 (1957).
6. M. T. Rogert and J. J. Ritter. J. Am. Chem. Soc. **46**, 2871 (1924).
7. von M. Kugel. Ann. **299**, 50 (1898).
8. W. Asker and Z. El-Agroudi. J. Org. Chem. **26**, 1440 (1961).
9. E. J. Browne and J. B. Polya. Chem. Ind. (London), 1086 (1960).
10. E. J. Browne and J. B. Polya. J. Chem. Soc. 575 (1962).
11. B. I. R. Nicolaus, L. Mariani, G. Gallo, and E. Testa. J. Org. Chem. **26**, 2253 (1961).
12. R. H. Wiley and C. H. Jarboe. J. Am. Chem. Soc. **77**, 405 (1955).
13. C. Beyer and L. Claisen. Ber. **20**, 2185 (1887).
14. A. Bischler. Ber. **25**, 3143 (1892).

Can. J. Chem. Downloaded from www.nrcresearchpress.com by 210.87.254.105 on 09/05/12
For personal use only.

THE THERMAL DECOMPOSITION OF PERACETIC ACID IN THE VAPOR PHASE[1, 2, 3]

C. SCHMIDT AND A. H. SEHON
Department of Chemistry, McGill University, Montreal, Que.

Received June 28, 1962

ABSTRACT

The thermal decomposition of peracetic acid in a stream of toluene was studied over the temperature range 127–360° C. The main products of the reaction were CO_2, CH_3COOH, C_2H_6, CH_4, HCHO, O_2, and traces of CO. Dibenzyl was also formed.

The overall decomposition of peracetic acid was partly heterogeneous and was represented by the two parallel primary reactions

$$CH_3CO_2—OH \rightarrow CH_3CO_2 + OH \rightarrow CH_3 + CO_2 + OH \quad \text{(i)}$$

$$CH_3CO_2—OH \rightarrow CH_3COOH + \tfrac{1}{2}O_2. \quad \text{(ii)}$$

The dissociation energy of the O—O bond in peracetic acid was estimated to be 30–34 kcal/mole.

INTRODUCTION

The importance of hydroxyl radical reactions in oxidation processes of hydrocarbons is now widely accepted but very few studies have been made on the kinetics of the reactions between these radicals and different hydrocarbons. This is due in part to the lack of a suitable source of hydroxyl radicals. Several methods have been used to produce the radicals, e.g. electric discharge through water vapor (1), electron transfer reactions in aqueous solution (2), and the thermal and photochemical decomposition of hydrogen peroxide (3) and alkyl hydroperoxide (4), but all of these methods have many disadvantages.

It was considered possible that peracetic acid might be a convenient source of hydroxyl radicals both in the gas phase and in solution, the radicals being formed by the sequence of reactions

$$CH_3COOOH \rightarrow CH_3CO_2 + OH \rightarrow CH_3 + CO_2 + OH.$$

If the decomposition took place by this mechanism the rate of formation of hydroxyl radicals could readily be followed by measuring the rate of production of carbon dioxide.

In the present study the mechanism of the decomposition of peracetic acid was investigated in the gas phase using the "toluene-carrier technique" (5). It was also hoped that this study would lead to the evaluation of the O—O bond dissociation energy, $D(CH_3 \cdot CO_2—OH)$.

EXPERIMENTAL

Materials

Peracetic Acid

The primary difficulty in the preparation of peracetic acid is the extremely explosive nature of the compound. This hazard can be minimized by preparing small quantities of about 1 g and by maintaining the compound in solution at all times apart from two stages in its preparation.

The peracetic acid was prepared by the method of Egerton *et al.* (6), which yielded a product free from

[1]*This work was supported in part by a grant from the Petroleum Research Fund administered by the American Chemical Society; grateful acknowledgment is hereby made to the donors of said fund. The authors wish to thank also the National Research Council of Canada for continued financial assistance, and to Imperial Oil Ltd., Canada, for a grant-in-aid.*

[2]*Presented at the 141st Meeting of the American Chemical Society, Washington, D.C., March 1962.*

[3]*Taken in part from the thesis submitted by C. Schmidt in partial fulfillment of the requirements for the M.Sc. degree, McGill University, 1960.*

Can. J. Chem. Downloaded from www.nrcresearchpress.com by 210.87.254.42 on 09/05/12
For personal use only.

acetic acid. The method consisted of perhydrolysis of the mixed anhydride of acetic and boric acid, prepared according to the procedure of Pictet (7), with 98% hydrogen peroxide, which was kindly supplied by the Becco Chemical Div., Buffalo, N.Y. The peracetic acid was separated from solid boric acid by distillation at room temperature and at a pressure of 10–12 mm Hg. The peracetic acid obtained in this manner was only 90% pure. The solution was frozen at −3° C, the crystals were filtered off and were shown to contain 98% peracetic acid. On redistillation of the melted crystals at a pressure of 10–12 mm Hg and at 18° C at least 99% pure peracetic acid was obtained.

The purity of the peracetic acid solution was established by titration of solutions of peracetic acid in 1:1 isopropanol–water solution using potassium hydroxide for the determination of total acid and sodium thiosulphate for the iodometric determination of "free" oxygen (8). If the results obtained with the two methods agreed within 1–2% it was assumed that the peracetic acid was free from acetic acid. Since hydrogen peroxide could have interfered with these methods its absence was always ascertained by titrating the solution at 0° C with permanganate in the presence of sulphuric acid and manganous sulphate, under which conditions peracetic acid is not titrated. The peracetic acid was also shown to be free of diacetyl peroxide.

The peracetic acid prepared by this method was found to be stable for periods of over 1–2 months when kept in the freezing compartment of an ordinary refrigerator. At room temperature pure peracetic acid underwent slow decomposition, e.g. about 9% decomposed during 19 hours. However, solutions of about 4% peracetic acid in toluene were shown to be stable at room temperature for periods of the order of 24 hours.

Toluene

Nitration grade toluene was generously supplied by the Gulf Oil Corporation, Pittsburgh, Pa. It was dried over anhydrous calcium sulphate and then distilled.

Methods

The vapor phase decomposition of peracetic acid was studied using a conventional apparatus as employed in the "toluene-carrier method" (5, 9). A pyrex reaction vessel was used in the temperature range 432–561° K. The total pressure in the reaction vessel was changed from 2.2 to 14 mm Hg and the ratio of toluene to peracetic acid was varied from 50 to 340. The time of reaction was limited to 0.28–0.78 second. The effect of the surface on the reaction was established by packing the reaction vessel with pyrex glass wool, which increased the surface-to-volume ratio by a factor of 20.

In general, 200 to 500 μmoles of peracetic acid was passed in a stream of toluene through the reaction vessel for periods of up to 20 minutes. To establish a mass balance for the reaction at different temperatures and to determine the condensable products which may have been formed in small amounts, special experiments were done under identical conditions using larger amounts of reactants over periods of time up to 4 hours.

The products which were non-condensable at −190° C, i.e. carbon monoxide, methane, and oxygen, were analyzed for carbon monoxide by combustion over copper oxide at 350° C and for methane by combustion over a hot platinum wire in the presence of a known excess of oxygen. The amount of oxygen collected at −190° C was calculated as the difference between the total amount of non-condensable gases and the sum of the amounts of methane and carbon monoxide. The products condensing at −190° C were analyzed for carbon dioxide and ethane as described previously (9). The contents of the trap maintained at −78° C were analyzed for "free oxygen" and total acid by titration with thiosulphate and hydroxide solutions as described above. The amount of undecomposed peracetic acid and the amount of acetic acid formed were calculated from these data. Formaldehyde which condensed also in this trap was determined with chromotropic acid according to the method of Stone (10). No hydrogen peroxide, diacetyl peroxide, methyl alcohol, or phenol were detected amongst the reaction products.

RESULTS

The main products of the reaction were carbon dioxide, acetic acid, ethane, methane, oxygen, and formaldehyde. Small amounts of dibenzyl were produced, the amounts increasing with temperature. The presence of ethylbenzene in the contents of the trap at −78° C was confirmed by vapor phase chromatography.[4] Minute quantities of carbon monoxide were formed, and these only at higher temperatures.

The overall rate of decomposition of peracetic acid was calculated from the amount of peracetic acid recovered, and was found to be first order with respect to peracetic acid. As shown in Table I, the first-order rate constant for the overall decomposition, k_0, was independent of the partial pressures of peracetic acid and toluene at any given temperature. However, as can be seen in Table II, the first-order rate constant k_0 was somewhat time dependent.

[4]*We should like to thank Dr. T. Vrbaski for the chromatographic analyses.*

Can. J. Chem. Downloaded from www.nrcresearchpress.com by 210.87.254.42 on 09/05/12
For personal use only.

TABLE I

Expt. No.	Temperature (°K)	$[PA]_0$ (μmole)	Fraction of decomposition	Pressure of peracetic acid $\times 10^2$ (mm Hg)	Pressure of toluene (mm Hg)	Time of contact (sec)	k_0 (sec^{-1})
21	432	512	0.31	3.75	12.05	0.29	1.29
22	432	512	0.32	3.64	12.50	0.28	1.41
23	432	512	0.31	3.54	11.90	0.28	1.35
24	432	1056	0.32	1.64	12.00	0.28	1.38
25	433	1550	0.36	11.40	12.35	0.31	1.40
26	433	3220	0.35	22.70	12.40	0.29	1.46
27	433	3220	0.33	22.70	13.05	0.32	1.28
35	561	912	0.92	7.45	13.21	0.30	8.41
36	561	912	0.92	7.40	14.31	0.33	7.65
37	561	912	0.92	8.33	8.21	0.31	8.18
38	561	912	0.92	8.90	4.53	0.32	8.28
39	561	480	0.92	4.80	13.71	0.29	8.66

TABLE II

Expt. No.	Temperature (°K)	Partial pressure of peracetic acid $\times 10^2$ (mm Hg)	Partial pressure of toluene (mm Hg)	Fraction of decomposition	Time of contact (sec)	k_0 (sec^{-1})
23	432	3.54	11.90	0.31	0.28	1.37
34	433	23.70	21.10	0.34	0.31	1.36
32	432	4.33	13.45	0.51	0.72	0.99
33	433	4.50	14.06	0.50	0.79	0.88

The effect of the surface of the reaction vessel on k_0 was studied only at 432° K and 516° K. At the lower temperature the rate of decomposition in the packed reaction vessel was about 50% higher than that in the unpacked reaction vessel, as shown in Table III. At 561° K there was an increase in the rate of the reaction but this could not be determined precisely. The results of the analyses obtained for most of the products are given in Table IV, and the ratios of some of these products are given in Table V.

TABLE III

Expt. No.*	Temperature (°K)	Partial pressure of peracetic acid $\times 10^2$ (mm Hg)	Partial pressure of toluene (mm Hg)	Time of contact (sec)	Fraction of decomposition	k_0 (sec^{-1})
23	432	3.54	11.90	0.28	0.31	1.35
24	432	7.64	12.00	0.28	0.32	1.38
44P	433	7.93	13.21	0.31	0.48	2.12
45P	433	6.68	12.90	0.28	0.49	2.38
46P	433	6.15	11.50	0.28	0.49	2.40
35	561	7.45	13.21	0.30	0.92	8.41
36	561	7.40	14.31	0.33	0.92	7.65
42P	562	4.57	13.07	0.31	1.00	†
43P	563	4.77	13.20	0.31	1.00	†

*The experiments marked by letter P refer to experiments done in the packed reaction vessel.
†No rate constants were calculated for these experiments since complete decomposition had occurred. However, these results indicate that at this temperature the rate of reaction was enhanced in the packed reaction vessel.

Can. J. Chem. Downloaded from www.nrcresearchpress.com by 210.87.254.42 on 09/05/12
For personal use only.

Can. J. Chem. Downloaded from www.nrcresearchpress.com by 210.87.254.42 on 09/05/12
For personal use only.

TABLE IV

Expt. No.*	Temp. (°K)	Time of reaction (sec)	Peracetic acid Initial (μmole)	Peracetic acid Consumed (μmole)	CO_2 (μmole)	C_2H_6 (μmole)	Acetic acid (μmole)	CH_4 (μmole)	O_2 (μmole)	$\frac{CO_2 + \text{acetic acid}}{\text{Peracetic acid consumed}}$
21	432	0.29	512	159	63	14	77	0	3	0.88
22	432	0.28	512	165	59	14	79	0	3	0.83
23	432	0.28	512	161	61	14	77	0	3	0.86
24	432	0.28	1056	341	130	30	160	0	7	0.85
28	432	0.37	512	184	76	18	92	0	3	0.90
32	432	0.72	557	284	82	18	185	0	3	0.94
33	432	0.79	557	280	81	19	173	0	3	0.91
34	432	0.30	3240	1100	335	84	590	0	23	0.84
44P	432	0.31	480	231	37	8	171	0	9	0.90
45P	432	0.28	480	233	36	9	172	0	9	0.90
46P	432	0.28	480	238	37	8	174	0	9	0.90
17	456	0.57	302	196	76	16	110	0	1.5	0.95
18	500	0.52	302	272	113	24	140	0	1.2	0.92
19	513	0.45	302	278	108	21	146	0	20	0.91
20	551	0.50	302	296	159	29	124	0	25	0.96
35	562	0.30	912	839	460	71	379	15	83	1.00
36	562	0.33	912	839	448	75	383	16	76	0.96
42P	562	0.31	480	480	130	26	331	3	84	0.96
43P	562	0.31	480	480	126	26	330	3	88	0.95
									Amount HCHO (μmole)	
A	433	0.38	14.4×10^3	5.3×10^3			2.2×10^3		0.85×10^3	
31	433	0.93	14.4×10^3	8.7×10^3			6.1×10^3		0.94×10^3	
B	433	0.32	24.1×10^3	12.3×10^3			9.1×10^3		0.89×10^3	
C	561	0.34	15.3×10^3	14.1×10^3			7.4×10^3		4.0×10^3	

*Only the experiments marked by the letter P were performed with the packed reaction vessel.

TABLE V

Expt. No.*	Temperature (°K)	$\frac{2(C_2H_6 + CH_4)}{CO_2}$	$\frac{CH_2O}{CO_2}$	$\frac{2(C_2H_6 + CH_4) + CH_2O}{CO_2}$
A	433	0.47	0.39	0.86
B	433	0.48	0.47	0.95
C	561	0.41	0.53	0.94

*The conditions in experiments A, B, C were identical with those of experiments 28, 45P, 36 respectively, given in Table IV.

DISCUSSION

The main products of the reaction and the kinetic features of the overall decomposition of peracetic acid in an excess of toluene may be accounted for by the following set of reactions:[5]

$$CH_3COOOH \longrightarrow CH_3CO_2 + OH \quad [i]$$

$$CH_3CO_2 \longrightarrow CH_3 + CO_2 \quad [ii]$$

$$2CH_3 \longrightarrow C_2H_6 \quad [iii]$$

$$CH_3 + \phi CH_3 \longrightarrow CH_4 + \phi CH_2 \quad [iv]$$

$$OH + \phi CH_3 \longrightarrow H_2O + \phi CH_2 \quad [v]$$

$$CH_3 + \phi CH_2 \longrightarrow \phi CH_2CH_3 \quad [vi]$$

$$2\phi CH_2 \longrightarrow \phi CH_2CH_2\phi \quad [vii]$$

$$CH_3COOOH \xrightarrow{\text{wall}} CH_3COOH + \tfrac{1}{2}O_2 \quad [viii]$$

$$CH_3 + O_2 \longrightarrow CH_3O_2 \longrightarrow HCHO + OH. \quad [ix]$$

The results of Table IV demonstrate that the amount of peracetic acid decomposed was almost equal to the sum of carbon dioxide and acetic acid formed. Therefore, steps [i] and [viii] in the above scheme are considered to be simultaneous reactions responsible for the decomposition of peracetic acid. If the methyl radicals produced in reaction [ii] were removed only by reactions [iii], [iv], and [vi] one would expect that the ratio $2(C_2H_6+CH_4)/CO_2$ should be equal to unity. However, the results of Table V indicate that this ratio varied between 0.4 and 0.5, and this would suggest, therefore, that the methyl radicals must have disappeared by reactions leading to products other than methane and ethane. As stated previously, formaldehyde was found amongst the products. The formation of formaldehyde may be explained by the extremely rapid reaction [ix] between methyl radicals and molecular oxygen as postulated by Vanpee and Fally (11). As shown in Table V the amount of formaldehyde formed accounted almost completely for the loss of methyl radicals, i.e. the ratio $[2(C_2H_6+CH_4)+HCHO]/CO_2$ was only slightly smaller than unity.

The absence of hydrogen peroxide, and of methanol and phenol, from the reaction products excludes the possibility that the hydroxyl radicals were removed by the dimerization reaction

$$2OH \rightarrow H_2O_2$$

or by the metathetical reactions

$$\phi CH_3 + OH \rightarrow \phi OH + CH_3$$

$$\phi CH_3 + OH \rightarrow \phi + CH_3OH.$$

[5]*The symbol ϕ represents* C_6H_5.

Can. J. Chem. Downloaded from www.nrcresearchpress.com by 210.87.254.42 on 09/05/12
For personal use only.

Therefore, it would appear that most, if not all, hydroxyl radicals formed in reactions [i] and [ix] were removed by reaction [v] with toluene to form water. However, because of the great technical difficulties required to establish a water-free apparatus, no attempt was made to determine the amount of water formed in the decomposition. A similar hydrogen abstraction reaction was postulated by Kirk and Knox (4) to account for the removal of hydroxyl radicals in the presence of benzene. Since $D(\phi CH_2—H)$ is smaller than $D(\phi—H)$, it is reasonable to expect that the reaction of hydroxyl radicals with toluene would occur even more readily than that with benzene. Thus, benzyl radicals would have been produced not only in reaction [iv] but also in reaction [v], and in consequence considerably more methyl radicals could have been removed in reaction [vi] to give ethyl benzene. This may explain the fact that the ratio $[2(C_2H_6+CH_4)+HCHO]/CO_2$ was always smaller than unity. The participation of reaction [vi] was demonstrated also previously in systems leading to the formation of methyl radicals in the presence of toluene (9). The reason for methyl radicals not being removed exclusively by reaction [iv] is that the activation energy of this reaction is greater than 8 kcal/mole (9), and obviously reaction [iv] will be relatively less favorable at the lower temperatures used in these experiments.

The formation of dibenzyl is considered further evidence that the decomposition of peracetic acid involved free radicals. Carbon monoxide was formed in amounts not exceeding 1% of the amount of peracetic acid consumed and hence was ignored in the reaction scheme.

It is evident from the results listed in Table III that the pyrolysis of peracetic acid was heterogeneous. The ratio of acetic acid to carbon dioxide was larger in the packed reaction vessel, which was taken as proof for reaction [viii] occurring primarily on the surface of the reaction vessel.

All the experimental data are, therefore, consistent with the decomposition of peracetic acid proceeding by the two simultaneous reactions [i] and [viii], the first producing free radicals and the latter leading to the formation of acetic acid and oxygen on the walls of the reaction vessel.

In spite of the fact that the overall first-order rate constant k_0 was somewhat dependent on the time of the reaction, it was felt that the rate of decomposition could be represented to a good approximation by the expression

$$-\frac{d[PA]}{dt} = k_0[PA] = (k_1+k_2)[PA], \qquad [1]$$

where k_1 and k_2 represent the rate constants of reactions [i] and [viii] respectively, and [PA] refers to the peracetic acid concentration. The values of the rate constant k_1 were calculated as a function of the carbon dioxide formed, using the equation

$$k_1 = \frac{[CO_2]}{[PA]_0} k_0(1-e^{-k_0 t})^{-1}. \qquad [2]$$

In view of the complicated nature of the decomposition, the values obtained for k_1 were not considered to be sufficiently accurate to justify the calculation of the activation energy of reaction [i] from the temperature dependence of k_1. However, as was shown by Szwarc (12), an approximate value for the activation energy may be computed by assuming a reasonable value for the frequency factor in the Arrhenius equation. From a survey of the literature (3, 4) it would appear that a reasonable value of the frequency factor of reactions involving the dissociation of oxygen–oxygen bonds would be 10^{14} sec^{-1}. Using

Can. J. Chem. Downloaded from www.nrcresearchpress.com by 210.87.254.42 on 09/05/12
For personal use only.

this frequency factor and the values obtained for k_1 at the higher temperatures, where the contribution of the heterogeneous mode of decomposition was smaller, a value of 30–34 kcal/mole was estimated for the activation energy of reaction [i]. On the basis of the usual assumption that the reverse reaction involving the recombination of free radicals has no activation energy, this activation energy can be identified tentatively with the dissociation energy of the O—O bond in peracetic acid. This value seems reasonable when compared with the values of D(O—O) in hydrogen peroxide and diacetyl peroxide, which are 48.5 kcal/mole and 30 kcal/mole, respectively (13).

REFERENCES

1. L. E. Avramenko and P. V. Lorentso. Dokl. Akad. Nauk SSSR, **67**, 867 (1949).
2. J. H. Baxendale, M. G. Evans, and G. S. Park. Trans. Faraday Soc. **42**, 155 (1946).
3. D. E. Hoare, J. B. Protheroe, and A. D. Walsh. Trans. Faraday Soc. **55**, 436 (1959).
4. A. D. Kirk and J. H. Knox. Trans. Faraday Soc. **56**, 1 (1960).
5. M. Szwarc, B. N. Ghosh, and A. H. Sehon. J. Chem. Phys. **18**, 1142 (1950).
6. A. C. Egerton, W. Emte, and G. J. Minkoff. Discussions Faraday Soc. **10**, 278 (1951).
7. C. Pictet. Ber. **39**, 2219 (1903).
8. J. D'Ans and A. Kneip. Ber. **48**, 1136 (1915).
9. M. Back and A. H. Sehon. Can. J. Chem. **38**, 1261 (1960).
10. K. G. Stone. Determination of organic compounds. McGraw-Hill, New York. 1956.
11. M. Vanpee and G. Fally. Bull. Soc. Chim. Belges, **61**, 474 (1952).
12. M. Szwarc. Chem. Rev. **47**, 75 (1950).
13. A. H. Sehon and M. Szwarc. Ann. Rev. Phys. Chem. **8**, 439 (1957).

Can. J. Chem. Downloaded from www.nrcresearchpress.com by 210.87.254.42 on 09/05/12
For personal use only.

Can. J. Chem. Downloaded from www.nrcresearchpress.com by 210.87.254.42 on 09/05/12
For personal use only.

THE THERMAL DECOMPOSITION OF PERACETIC ACID IN AROMATIC SOLVENTS[1, 2]

F. W. EVANS[3] AND A. H. SEHON
Department of Chemistry, McGill University, Montreal, Que.

Received December 17, 1962

ABSTRACT

The thermal decomposition of peracetic acid in toluene, benzene, and *p*-xylene was studied over the temperature range 75–95° C. The main products of decomposition were found to be CH_4, CO_2, CH_3COOH; small amounts of methanol, phenols, and polymeric compounds were also detected.

The rate of the overall decomposition was first order with respect to peracetic acid, and the results could be explained by postulating the participation of the two simultaneous reactions:

$$CH_3COOOH \xrightarrow{k_1} CH_3CO_2 + OH \rightarrow CH_3 + CO_2 + OH \qquad (1)$$

$$CH_3COOOH + RH \xrightarrow{k_2} CH_3COOH + \text{"RHO"}. \qquad (2)$$

The rate constant of reaction (1) was independent of the solvent, whereas k_2 was dependent on the solvent. The ratio k_2/k_1 was about 10.

INTRODUCTION

The thermal decomposition of many peroxy compounds in organic solvents has been studied but very little information is available concerning the decompositions of peroxy acids. The reactions of these latter compounds with olefins leading to the formation of epoxides are well understood (1), but reactions involving peracids with other organic compounds are only now receiving attention. The results of these recent studies are, however, confusing, and several different mechanisms have been reported for the decomposition reactions of peracids. Thus, the decomposition of perbenzoic acid in benzene (2) was accounted for by a first-order free-radical reaction involving the dissociation of the O—O bond; however, this decomposition followed a different mechanism in 1-butanol solution.

Similarly, various reaction mechanisms have been postulated for the decomposition of perlauric acid in solution (3, 4). According to Swern *et al.* (3) the decomposition of perlauric acid in benzene involved primarily the formation of oxygen and lauric acid, and possibly a small amount of free radicals. However, Letort *et al.* (4) suggested that the initial step in the decomposition of perlauric acid might involve the dissociation of the O—O bond, and that the subsequent step resulted in the decarboxylation of the corresponding free radical.

The pyrolysis of peracetic acid in the vapor phase had been studied previously in this laboratory (5, 6), and was found to involve two simultaneous reactions: (i) a free-radical homogeneous reaction, and (ii) a heterogeneous reaction. Since the solvation effects in hydrocarbon solution may be expected to be quite small, it was anticipated that the rate of the free-radical reaction in solution should be of the same order of magnitude as that

[1]*This work was in part presented in the Division of Petroleum Chemistry, at the 141st Meeting of the American Chemical Society, Washington, D.C., 1962.*

[2]*The work was supported in part by the Petroleum Research Fund administered by the American Chemical Society, and grateful acknowledgment is hereby made to the donors of the said fund. The authors wish to thank also the National Research Council of Canada for continued financial assistance, and to Imperial Oil Ltd., Canada, for a grant-in-aid.*

[3]*Present address: Central Research Laboratory, Allied Chemical Corp., Morristown, N.J.*

in the vapor phase. Hence, in the present investigation the thermal decomposition of peracetic acid was studied in some aromatic solvents.

EXPERIMENTAL

Materials

The peracetic acid was prepared essentially according to the method described previously (5, 6), i.e. by the addition of 99% hydrogen peroxide to the mixed anhydride of acetic acid and boric acid. The peracetic acid was separated from the reaction mixture by distillation at room temperature and at 2–5 mm Hg pressure, the middle fraction being collected in a trap at −196° C. This product was then immediately dissolved in six times its volume of toluene and purified by crystallization from this solution in the apparatus shown in Fig. 1. The toluene solution was placed in the left-hand arm, which was equipped with a sintered-glass

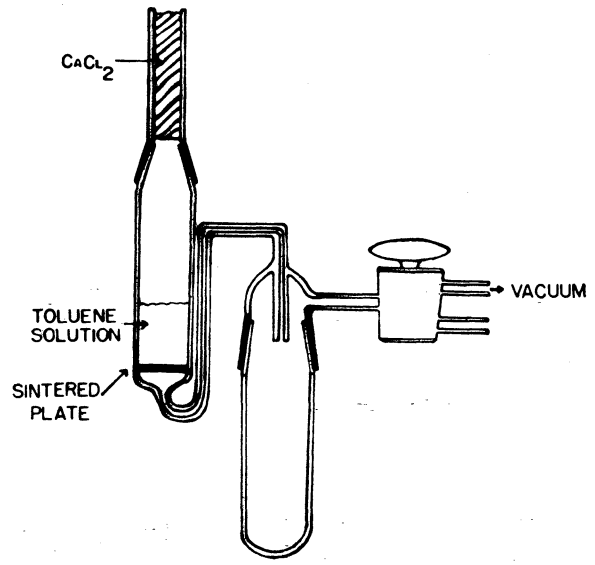

FIG. 1. Apparatus for recrystallization of peracetic acid.

disk, and cooled to −78° C. At this temperature the peracetic acid crystallized out of the solution and the supernatant was drawn off by suction, leaving the peracetic acid on the glass disk. The crystals were dissolved in pure toluene and the crystallization process was repeated. Finally, a stream of dry air was drawn over the crystals to remove the last traces of toluene. The desired solution was then made by the addition of an appropriate solvent onto the glass disk. This method was less dangerous than the method described previously (6), as the peracidic acid was never handled in the pure, solid state, but only in solution.

The purity of the product was determined by iodometric and acidimetric titrations (6); it was shown to be free of acetic acid, hydrogen peroxide, or diacetyl peroxide, and to be at least 98% pure peracetic acid.

The other reagents used in this study were commercial samples. Nitration grade toluene was generously supplied by Gulf Oil Corporation, Pittsburgh, Pa., and was dried over anhydrous calcium sulphate and then distilled. A.R. grade benzene (Mallinckrodt Chemical Works) was dried with sodium wire and distilled. *p*-Xylene (highest purity grade, Eastman Kodak Co.) was dried over sodium and then distilled; a sample of this material was found to be free from other xylenes on analysis by gas chromatography.

Methods

Known amounts of peracetic acid were dissolved in each of the appropriate solvents as described above, and the solutions were transferred into 50-cc glass reaction vessels sealed onto a high-vacuum manifold. Each of the reaction vessels was also equipped with a "break-seal". To remove all of the dissolved air, the solutions in the reaction vessels were degassed and the reaction vessels were then sealed off. The peracetic acid was decomposed by placing the reaction vessels in a thermostated water bath controlled to ±0.05° C. The decomposition was stopped after the desired period of time by removing the reaction vessel from the thermostat and placing it in a "dry-ice" bath. Five to eight solutions could be heated simultaneously and, in general, each reaction vessel was heated for a different period of time. The products of each reaction mixture were determined independently by the methods described below.

Can. J. Chem. Downloaded from www.nrcresearchpress.com by 210.87.254.42 on 09/05/12
For personal use only.

Each of the reaction vessels was connected through the "break-seal" to an apparatus designed for the analysis of small gas samples. The gaseous products of the reaction were separated and measured on a high-vacuum system by distillation of the reaction mixture through a series of traps maintained at −78° C, −117° C, and −196° C. The gases which were non-condensable at −196° C were collected by means of a Toepler pump into a calibrated volume. They were shown to contain only methane by mass spectrometric analysis. The products condensing at −196° C were measured in the same way as the methane by warming this trap to −78° C; the mass spectrometric analysis of these gases showed that they consisted of only carbon dioxide, i.e. no ethane was found amongst the reaction products.

The remainder of the products, together with the unchanged reactants, was collected in the trap maintained at −117° C. These were always analyzed for peracetic acid and for total acid by titration with sodium thiosulphate and potassium hydroxide solutions, respectively (6). The presence of acetic acid amongst the reaction products was shown by the gas chromatographic analysis of a sample of the products, which had been separated by distillation on a "Nestr" spinning-band column. The identity of the acetic acid so separated was further confirmed by infrared spectrum analysis. The other acidic materials present in the toluene solution were concentrated, tested with Millons reagent (7), and shown to contain small amounts of phenolic materials. One other product of the reaction was a dark polymeric material. This was isolated by carrying out the decomposition of peracetic acid to completion and distilling off the other products and the solvent. This polymeric material was soluble in dilute aqueous alkaline solution and in carbon tetrachloride. The infrared spectrum of this latter solution showed broad peaks at 1166, 1260, 1458, 1497, 1602, 1695, 1726, 2920, 2960, and 3030 cm^{-1}.

RESULTS AND DISCUSSION

The products of the decomposition of peracetic acid in toluene, benzene, or *p*-xylene were found to be methane, carbon dioxide, acetic acid, phenolic compounds, and a polymeric material. In general, only the first three products were determined, in addition to the amount of undecomposed peracetic acid. The results of a typical reaction are shown in Table I.

TABLE I

Reaction time (min)	CH_4 (μmole)	CO_2 (μmole)	$\frac{CH_4}{CO_2}$	Peracetic acid remaining (μmole)	Acetic acid (μmole)	Total acid remaining (μmole)	Total acid remaining plus CO_2 (μmole)
60	1.47	1.86	0.82	140	17	157	159
120	1.77	2.40	0.74	128	29	157	159
180	2.30	3.14	0.73	114	38	152	155
240	3.61	5.50	9.66	99	63	162	167
300	3.50	4.80	0.73	89	70	159	164
360	4.08	4.95	0.83	82	77	159	164

From these data the following rate constants were calculated at 85° C: $k_0 = 3.22\times10^{-5}$ sec^{-1}, $k_1 = 0.21\times10^{-5}$ sec^{-1}, and $k_2 = 3.01\times10^{-5}$ sec^{-1}

NOTE: Each sample contained initially 162 μmoles peracetic acid in 7 ml toluene.

It was found that the rate of the overall decomposition was first order with respect to peracetic acid (Fig. 2), and that the amount of peracetic acid decomposed was equal to

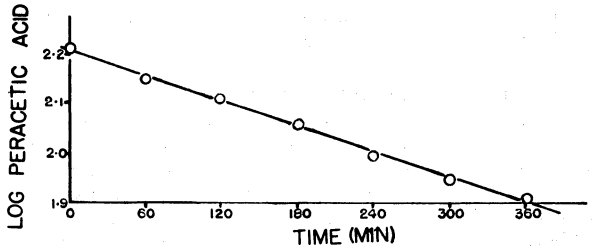

FIG. 2. Kinetics of the overall decomposition of peracetic acid.

Can. J. Chem. Downloaded from www.nrcresearchpress.com by 210.87.254.42 on 09/05/12
For personal use only.

the amount of acetic acid plus carbon dioxide formed within the uncertainties of the analytical determinations. With this limitation in mind, these results could be explained by postulating that the decomposition of peracetic acid involved the two simultaneous reactions

$$CH_3COOOH \xrightarrow{k_1} CH_3CO_2 + OH \rightarrow CH_3 + CO_2 + OH \quad [1]$$

$$CH_3COOOH + RH \xrightarrow{k_2} CH_3COOH + \text{"RHO"} \quad [2]$$

and that the rates of these reactions were measured by the rates of formation of carbon dioxide and acetic acid. The rate constants were calculated using the relations

$$k_0 = k_1 + k_2$$

$$k_1 = \frac{[CO_2]}{[PA]_0} k_0(1-e^{-k_0 t})^{-1}$$

$$k_2 = \frac{[HA]}{[PA]_0} k_0(1-e^{-k_0 t})^{-1},$$

where k_0 is the overall rate constant for the decomposition of peracetic acid, $[CO_2]$ and [HA] are the amounts of carbon dioxide and acetic acid formed, respectively, in time t from an initial amount of peracetic acid $[PA]_0$.

As is evident from Fig. 3, the kinetics of the decomposition of peracetic acid could be

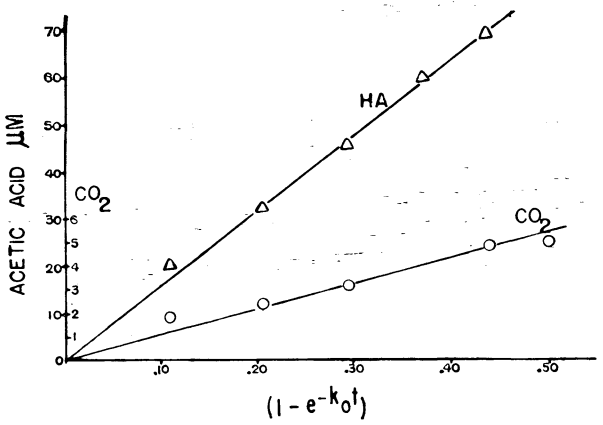

FIG. 3. Kinetics of the formation of acetic acid and carbon dioxide.

represented by this mechanism. The values of k_0, k_1, and k_2 were determined for different reaction mixtures in the three solvents at 85° C, and in the range 75–95° C for toluene solutions. From the results listed in Table II, the following conclusions can be drawn:

(i) the decomposition was first order with respect to peracetic acid,

(ii) the rate constant for reaction [1], i.e. k_1, was independent of the solvent,

(iii) the rate constant k_2 was dependent on the solvent, increasing with increasing methyl substitution of the benzene ring.

Reaction [1] was found to be independent of the solvent. It was assumed to involve the dissociation of the O—O bond and the formation of hydroxyl and acetyl radicals, and that subsequently the latter radicals decomposed to give a methyl radical and a molecule

Can. J. Chem. Downloaded from www.nrcresearchpress.com by 210.87.254.42 on 09/05/12
For personal use only.

TABLE II

The effect of temperature and solvent on the rate of decomposition of peracetic acid

Solvent	Temp. (°C)	Peracetic acid concentration (M)	$\frac{CH_4}{CO_2}$	10^5k_0 (sec^{-1})	10^5k_1 (sec^{-1})	10^5k_2 (sec^{-1})
Toluene	74.9	0.014	0.88	1.19	0.14	1.05
"	74.9	0.015	—	1.20	—	—
"	85.0	(0.007, 0.039)	0.64	3.52	0.32	3.20
"	85.0	0.023	0.72	3.22	0.21	3.01
"	94.8	0.014	0.76	7.08	0.69	6.39
"	95.0	(0.008, 0.030)	0.77	8.4	0.73	7.7
Benzene	85.0	0.024	0.16	1.43	0.31	1.12
"	85.0	0.019	0.11	1.72	0.38	1.34
p-Xylene	85.0	0.015	0.80	7.88	0.32	7.6

of carbon dioxide. In accordance with other free radical reactions in solution (8), it was considered that some of the methyl and hydroxyl radicals would combine together before escaping from the solvent cage to form methanol. For this reason a sample of the reaction products was analyzed by gas chromatography and indeed small amounts of methanol were detected.

The hydroxyl and methyl radicals which escape from the solvent would be expected to react with the solvent molecules. Methyl radicals react with aromatic compounds by abstraction of a hydrogen atom to form methane, or by addition onto the benzene ring. If all the methyl radicals react to form methane, then, according to reaction [1], one would expect the ratio of CH_4/CO_2 to be unity. However, from the results listed in Table II, it can be seen that this ratio was only of the order of 0.8 in toluene and *p*-xylene. Therefore, it follows that some of the methyl radicals were removed either by reaction with hydroxyl radicals to give methanol, or by addition to the solvent molecules. It has been demonstrated in the decomposition of diacetyl peroxide in toluene (9) that methyl radicals react with the solvent only by a hydrogen abstraction reaction. Therefore, by analogy, in the decomposition of peracetic acid in toluene and *p*-xylene, the addition of methyl radicals to the solvent may be excluded, and it is concluded that about 20% of the methyl radicals formed in these solvents react with hydroxyl radicals to form methanol. The presence of methanol amongst the products of the reaction was proved, but because of the small amounts of methanol formed, these were not determined quantitatively. From the results of Table II, it is evident that the ratio of CH_4/CO_2 in benzene was very much lower than in the other two solvents and this might be accounted for by the disappearance of a large proportion of the methyl radicals by addition onto the benzene molecules. This explanation is supported by similar results obtained in the decomposition of diacetyl peroxide in benzene (9).

Some of the hydroxyl radicals produced in reaction [1] react with methyl radicals to form methanol. The others would be expected to react with the solvent to form water or phenols. Because of technical difficulties, the small amounts of water which might have been produced were not determined. On the other hand, phenols were detected amongst the products of the reaction and were determined spectrophotometrically in a few experiments as the corresponding nitrosophenol derivatives (10). From these analyses it was estimated that the amounts of phenols formed were in excess of the amounts of hydroxyl radicals produced in reaction [1], and hence it is concluded that some, if not all, of the phenols were produced in reaction [2].

The decomposition of peracetic acid leading to the formation of acetic acid necessitates

Can. J. Chem. Downloaded from www.nrcresearchpress.com by 210.87.254.42 on 09/05/12
For personal use only.

the loss of oxygen from the reactant. In the study of the pyrolysis of peracetic acid in the vapor phase (6), it was shown that molecular oxygen was formed primarily by a heterogeneous reaction and that it was almost completely removed by reaction with methyl radicals to give formaldehyde. By contrast, in solution no detectable amounts of oxygen or of formaldehyde were produced, and it is concluded that no molecular oxygen was formed. The rate of reaction [2] was found to depend on the solvent, which indicates that peracetic acid reacted directly with the solvent molecules to form some intermediate "oxygenated" compound, denoted here as "RHO", which led to formation of phenols and polymeric materials. It is interesting to note that these products are very similar to those obtained by Cvetanović *et al.* (11) in the direct oxidation of these compounds by oxygen atoms.

The rate of reaction [2] was measured by the rate of formation of acetic acid. A comparison of the rate constants k_1 and k_2 given in Table II indicates that reaction [2] was about 10 times as fast as reaction [1] under the experimental conditions used. It is of interest to compare the decomposition of peracetic acid with that of perlauric acid (3) under similar conditions. In both cases the decomposition proceeds by two simultaneous reactions, i.e. a free-radical reaction of only secondary importance, and the main reaction leading to the formation of either acetic or lauric acid, respectively. The mechanisms of these latter reactions are, however, quite different: no oxygen was formed in the decomposition of peracetic acid and it was concluded that this peracid reacted with solvent; by contrast, the main products of the decomposition of perlauric acid were lauric acid and oxygen.

The rate of reaction [1], i.e. of the free-radical reaction, was measured in toluene at three temperatures, and in benzene and *p*-xylene at one temperature, 85° C. The concentration of peracetic acid in toluene was varied within the range 0.007–0.023 M and the time of the reaction was varied from 20 to 420 minutes. From the values of k_1, the activation energy of reaction [1] was calculated as 31.5–33.0 kcal/mole, on the assumption that the frequency factor in the Arrhenius equation was 10^{14} sec^{-1} (6). This value agrees with the value of 30–34 kcal/mole calculated for the activation energy of the same reaction in the gas phase and may be identified with the O—O bond dissociation energy in peracetic acid, i.e. $D(CH_3COO—OH)$. This value is slightly higher than the oxygen–oxygen bond dissociation energy in diacetyl peroxide of 29.5 kcal/mole (12), and lower than that for the same bond in hydrogen peroxide, i.e. $D(HO—OH) = 48$ kcal/mole (13).

REFERENCES

1. D. Swern. J. Am. Chem. Soc. **69**, 1692 (1947).
2. S. R. Cohen and J. O. Edwards. J. Phys. Chem. **64**, 1086 (1960).
3. W. E. Parker, L. P. Witnauer, and D. Swern. J. Am. Chem. Soc. **80**, 323 (1958).
4. D. Letort, C. Paquot, and J. Sorba. Bull. Soc. Chim. France, 1385 (1959).
5. C. Schmidt. M.Sc. Thesis, McGill University, Montreal, Que. 1960.
6. C. Schmidt and A. H. Sehon. Can. J. Chem. This issue.
7. F. Feigl. Spot tests in organic analysis. Elsevier Publishing Co., Amsterdam. 1960.
8. L. Herk, M. Feld, and M. Szwarc. J. Am. Chem. Soc. **83**, 2998 (1961).
9. M. Levy and M. Szwarc. J. Am. Chem. Soc. **76**, 5981 (1954).
10. K. G. Stone. Determination of organic compounds. McGraw-Hill Book Co., Inc. 1956.
11. G. R. H. Jones and R. J. Cvetanović. Can. J. Chem. **39**, 2444 (1961). G. Boocock and R. J. Cvetanović. Can. J. Chem. **39**, 2436 (1961).
12. A. Rembaum and M. Szwarc. J. Am. Chem. Soc. **76**, 5975 (1954).
13. P. A. Giguere and I. D. Liu. Can. J. Chem. **35**, 283 (1957).

Can. J. Chem. Downloaded from www.nrcresearchpress.com by 210.87.254.42 on 09/05/12
For personal use only.

Can. J. Chem. Downloaded from www.nrcresearchpress.com by 210.87.254.6 on 09/05/12
For personal use only.

NOTES

OCCURRENCE OF THE ρ PHASE AMONG CHALKOGENIDES

OSVALD KNOP

In a previous communication (1) the existence of a number of π phases of the type Co_8MS_8 has been reported and attention drawn to the relative paucity of occurrence of the π phase. This is noteworthy, as the somewhat analogous spinels, which are also based on a cubic close-packed structure of oxygen or sulphur with the metal atoms in tetrahedral or octahedral coordination, are much more widely distributed.

In an attempt to extend the number of known π phases several sulphides of the overall composition M_9S_8 (M = Ru, Rh, Pd, Ir; Ag) were prepared by dry synthesis from very pure elements. Although a cubic phase of the alleged composition Rh_9S_8 had been reported previously and its symmetry described as primitive rather than face-centered cubic (2, 3), its preparation was repeated in view of the unsatisfactory past experience with other chalkogenides of unusual stoichiometries whose formulae and structures had been assigned by analogy with better-studied compounds. Seven compositions were prepared in all, but none of them contained a π phase. Instead, the primitive cubic symmetry of "Rh_9S_8" has been confirmed and another, presumably isostructural, phase has been found in a preparation containing Rh and Pd. These phases will be referred to as ρ phases for brevity. In the following, the intended formulae (in square brackets) and the results of a phase analysis are given. Filtered Cu K radiation was used throughout ($\lambda\alpha_1$ = 1.54050 Å).

[Ru_9S_8]: A mixture of Ru and RuS_2, the latter with $a_0 = 5.6100\pm7$ Å. This value corresponds to the $C2$ phase saturated with Ru and is, to our knowledge, the most accurate value so far reported for a well-defined RuS_2.

[Rh_9S_8]: Pure cubic pattern with no systematic absences and no foreign lines present. The same phase, ρ(Rh,S), as described previously must thus have been obtained; $a_0 = 9.9103\pm23$ Å.

[Pd_9S_8]: Although the existence of an intermediate body-centered cubic phase $Pd_{2.2}S$ has been described (4), a mixture of Pd_4S and PdS was found in this preparation, presumably because of the relatively short annealing time or too high annealing temperature. The identification of PdS was not completely certain because of the poor quality of the diffraction lines.

[Ir_9S_8]: Ir + ?; the unidentified phase was neither π nor ρ.

[Rh_8PdS_8]: Pattern of a homogeneous ρ phase was found with $a_0 = 9.9301\pm21$ Å.

[Rh_8AgS_8]: ρ + ?; $a_0 = 9.9115\pm19$ Å. It is doubtful that silver was accommodated in the ρ structure to any extent. The second phase was presumably a Ag_2S polymorph, but the quality of the lines made it difficult to establish its identity.

[$Ru_{4.5}Pd_{4.5}S_8$]: Ru + $C2$ + ? The $C2$ phase had $a_0 = 5.6100\pm11$ Å and must have been RuS_2, possibly with some Pd substitution.

The ρ phase has thus been found only in three preparations, and it is likely that only *two* distinct phases were present, ρ(Rh,S) and $\rho(Rh_8PdS_8)$. In addition to these there exists ρ(Pd,Se) (4, 5). As for the true composition and structure of ρ(Rh,S), Stubbles (2) concluded from his equilibration studies that its composition was nearer Rh_8S_7 than Rh_9S_8,

and that the phase had a narrow homogeneity range and only a small degree of intrinsic disorder. The difficulty concerning the correct formula seems to have been resolved recently by Geller (6), who obtained the crystal structure of the phase and found by crystallographic argument that the true primitive formula should be $Rh_{17}S_{15}$. Since our experimental work was done before the publication of Geller's results, we had been unaware of the correct formula and therefore selected the compositions Rh_8PdS_8 and Rh_8AgS_8 on the assumption that the coordination situation in ρ(Rh,S) was similar to that in π(Co,S). Since this now has been shown not to be the case, nothing can be said at present about the nature of the Pd substitution in the ρ(Rh,S) structure, apart perhaps from a speculation that the palladium atoms would tend to prefer square planar coordination and thus might locate in the 3(*d*) sites of the *Pm3m* structure proposed by Geller. Ibrahim (7) prepared, in this laboratory, as early as 1957 a number of compositions of the type π(Co,Rh,S) and these are now being examined in the light of the tetrahedral, octahedral, and square planar coordination preferences.

Financial support by the National Research Council of Canada is hereby gratefully acknowledged.

1. O. KNOP. Chem. Ind. (London), 739 (1962).
2. J. R. STUBBLES. Personal communication.
3. B. T. MATTHIAS and S. GELLER. J. Phys. Chem. Solids, **4**, 318 (1958).
4. F. GRØNVOLD and E. RØST. Acta Chem. Scand. **10**, 1620 (1956).
5. S. GELLER. Acta Cryst. **15**, 713 (1962).
6. S. GELLER. Acta Cryst. **15**, 1198 (1962).
7. M. A. IBRAHIM and O. KNOP. Unpublished work.

RECEIVED MARCH 1, 1963.
SOLID STATE CHEMISTRY GROUP,
DEPARTMENT OF CHEMICAL ENGINEERING,
NOVA SCOTIA TECHNICAL COLLEGE,
HALIFAX, NOVA SCOTIA.

Can. J. Chem. Downloaded from www.nrcresearchpress.com by 210.87.254.6 on 09/05/12
For personal use only.

MONOFLUOROSUCCINIC ACID[1]

F. H. DEAN AND F. L. M. PATTISON

Monofluorosuccinic acid, $HOOCCH_2CHFCOOH$, is an interesting compound from a biochemical standpoint, because it is one of the few remaining monofluorinated members of the tricarboxylic acid cycle which has not yet been authenticated; as such, its action on the enzymes of the cycle would be significant in the general study of poisoning by organic fluorine compounds.

Mention has been made of this acid on several occasions. Martius (2), in 1949, reported experiments using monofluorosuccinic acid; he thanked Professor Theilacker for a gift of the acid, but no details of its preparation have appeared in the literature. In 1953, Gitter, Blank, and Bergmann (3) stated that the sodium salt is non-toxic, but gave no indication of the source nor of the method of preparation of the material tested. In 1956, Bergmann and Szinai (4) reported the preparation of an impure sample of diethyl monofluorosuccinate by reaction of the enolate of ethyl fluoroacetate with ethyl bromoacetate;

[1]*First reported at the Second International Symposium on Fluorine Chemistry, Estes Park, Colorado, July 17–20, 1962 (1).*

and that the phase had a narrow homogeneity range and only a small degree of intrinsic disorder. The difficulty concerning the correct formula seems to have been resolved recently by Geller (6), who obtained the crystal structure of the phase and found by crystallographic argument that the true primitive formula should be $Rh_{17}S_{15}$. Since our experimental work was done before the publication of Geller's results, we had been unaware of the correct formula and therefore selected the compositions Rh_8PdS_8 and Rh_8AgS_8 on the assumption that the coordination situation in ρ(Rh,S) was similar to that in π(Co,S). Since this now has been shown not to be the case, nothing can be said at present about the nature of the Pd substitution in the ρ(Rh,S) structure, apart perhaps from a speculation that the palladium atoms would tend to prefer square planar coordination and thus might locate in the 3(*d*) sites of the *Pm3m* structure proposed by Geller. Ibrahim (7) prepared, in this laboratory, as early as 1957 a number of compositions of the type π(Co,Rh,S) and these are now being examined in the light of the tetrahedral, octahedral, and square planar coordination preferences.

Financial support by the National Research Council of Canada is hereby gratefully acknowledged.

1. O. KNOP. Chem. Ind. (London), 739 (1962).
2. J. R. STUBBLES. Personal communication.
3. B. T. MATTHIAS and S. GELLER. J. Phys. Chem. Solids, **4**, 318 (1958).
4. F. GRØNVOLD and E. RØST. Acta Chem. Scand. **10**, 1620 (1956).
5. S. GELLER. Acta Cryst. **15**, 713 (1962).
6. S. GELLER. Acta Cryst. **15**, 1198 (1962).
7. M. A. IBRAHIM and O. KNOP. Unpublished work.

RECEIVED MARCH 1, 1963.
SOLID STATE CHEMISTRY GROUP,
DEPARTMENT OF CHEMICAL ENGINEERING,
NOVA SCOTIA TECHNICAL COLLEGE,
HALIFAX, NOVA SCOTIA.

Can. J. Chem. Downloaded from www.nrcresearchpress.com by 210.87.254.5 on 09/05/12
For personal use only.

MONOFLUOROSUCCINIC ACID[1]

F. H. DEAN AND F. L. M. PATTISON

Monofluorosuccinic acid, $HOOCCH_2CHFCOOH$, is an interesting compound from a biochemical standpoint, because it is one of the few remaining monofluorinated members of the tricarboxylic acid cycle which has not yet been authenticated; as such, its action on the enzymes of the cycle would be significant in the general study of poisoning by organic fluorine compounds.

Mention has been made of this acid on several occasions. Martius (2), in 1949, reported experiments using monofluorosuccinic acid; he thanked Professor Theilacker for a gift of the acid, but no details of its preparation have appeared in the literature. In 1953, Gitter, Blank, and Bergmann (3) stated that the sodium salt is non-toxic, but gave no indication of the source nor of the method of preparation of the material tested. In 1956, Bergmann and Szinai (4) reported the preparation of an impure sample of diethyl monofluorosuccinate by reaction of the enolate of ethyl fluoroacetate with ethyl bromoacetate;

[1]*First reported at the Second International Symposium on Fluorine Chemistry, Estes Park, Colorado, July 17–20, 1962 (1).*

the analysis was in error, and the authors stated that the ester could not be obtained in a pure condition. Hydrolysis of this crude material did not yield the free acid by the procedures used. Finally, Peters (5), a year later, called attention to the unconfirmed results of Martius and questioned the identity of the test sample, "as several others (personal communication) have not been successful in preparing monofluorosuccinic acid".

We now wish to report the preparation of this acid from diethyl succinate by the following route:

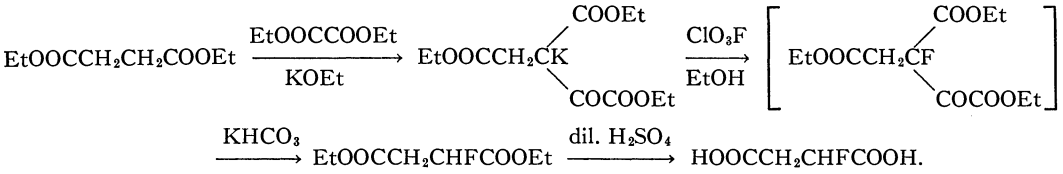

The method involves the addition of the ethoxalyl grouping, which in turn promotes fluorination (6) by perchloryl fluoride. The strongly electronegative character of the fluorine atom thus introduced greatly facilitates the alkaline cleavage of the resulting non-enolizable β-keto-ester. Under the very mild reaction conditions, beta-elimination of hydrogen fluoride becomes negligible. In short, the activating ethoxalyl grouping is preferentially removed. The overall yield of diethyl monofluorosuccinate, based on the potassium enolate of triethyl oxalylsuccinate, was 73%; the acid hydrolysis of this ester to monofluorosuccinic acid proceeded in 67% yield.

The intermediate ester, triethyl α-fluoro-α-oxalylsuccinate, could not be purified by distillation, even at 0.05 mm pressure, because of ready decarbonylation. Under these conditions, diethyl α-fluoro-α-carbethoxysuccinate was formed in 77.5% yield:

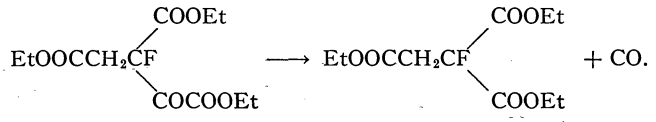

Monofluorosuccinic acid and its diethyl ester were found to be non-toxic to mice by intraperitoneal injection in propylene glycol ($LD_{50} > 107$ mg/kg). The acid is being examined in other laboratories for its biochemical properties.

EXPERIMENTAL

Melting points (uncorrected) were determined on a Kofler hot stage, and densities with a Fisher–Davidson gravitometer. The nuclear magnetic resonance spectrum was obtained with a Varian DP-60 spectrometer. Infrared spectra were obtained with a Beckman IR-7 infrared spectrophotometer (in the case of diethyl monofluorosuccinate) or with an IR-5 (in the case of monofluorosuccinic acid and diethyl α-fluoro-α-carbethoxysuccinate). The perchloryl fluoride was purchased from the Technical Division of Pennsalt Chemicals Corporation, Philadelphia 18, Pa.

Potassium Enolate of Triethyl Oxalylsuccinate

The potassium enolate was prepared by the standard procedure (7) with two modifications: (*a*) the work was carried out in a nitrogen atmosphere; and (*b*) the freshly cut potassium was not washed with ether. By this means, the formation of potassium hydroxide and carbonate was reduced. Diethyl succinate was freshly redistilled through a 23-plate spinning band column (b.p. 97° at 8 mm, n_D^{25} 1.4185, d_4^{20} 1.035). Diethyl oxalate was similarly purified (b.p. 76° at 10 mm, n_D^{25} 1.4090, d_4^{20} 1.075). The super-dry ethanol was stored over Linde molecular sieves, Type 5A. The enolate was washed with dry ether and placed in a P_2O_5 vacuum desiccator for 15 hours at 0.5 mm. Yield: 91–97%, as a light yellow, friable solid.

Diethyl Monofluorosuccinate

A 500-ml three-necked flask was equipped with a stirring magnet, a gas-inlet tube with a fritted-glass gas disperser, a drying tube filled with indicating Drierite, and a −50° to +50° thermometer secured by

Can. J. Chem. Downloaded from www.nrcresearchpress.com by 210.87.254.5 on 09/05/12
For personal use only.

gum-rubber tubing to a ground-glass holder. After the flask had been flushed with dry nitrogen, dry potassium enolate (23.6 g, 75.5 mmoles) was introduced, followed by super-dry ethanol (300 ml). To the mixture was added 2 ml of bromthymol blue (0.05% in absolute ethanol) and dry reagent-grade potassium bicarbonate (1.75 g, 17.5 mmoles). Dry nitrogen was passed through the mixture, which was stirred and cooled in an ice bath. When the temperature was steady at 4°, the perchloryl fluoride cylinder was attached to the gas disperser by gum-rubber tubing[2] and wired on securely. Perchloryl fluoride gas was then introduced until the temperature had risen to 8–10°. The gas flow was then stopped until the temperature had again fallen to 4°, when it was resumed. In this manner, 10.7 g (104.3 mmoles) of perchloryl fluoride were added over a 1-hour period, the actual duration of gas inflow being 21 minutes. As the perchloryl fluoride is being added, the original deep-green color lightens due to the formation of potassium chlorate; the end of the reaction is readily determined by a color change from green to yellow and by a fall in temperature on the addition of more perchloryl fluoride. The gas cylinder was then detached, an additional quantity (10.2 g, 102 mmoles) of potassium bicarbonate was added, the ice bath was removed, and the mixture was stirred at room temperature (20 hours). The flask was flushed with nitrogen to remove any unreacted perchloryl fluoride, water (800 ml) was added, and the solution was thoroughly extracted with ether. The combined ether extracts were washed with water and dried over magnesium sulphate. The ether was removed on a water bath and the alcohol at aspirator pressure. The residue was then distilled through a 6-in. Vigreux column under oil-pump pressure. Two main fractions were obtained: (*a*) diethyl oxalate (4.15 g), b.p. 72° at 9 mm to 62° at 2.75 mm, n_D^{25} 1.4092–1.4090; and (*b*) diethyl monofluorosuccinate (15.0 g), b.p. 75° at 2.75 mm to 72° at 0.25 mm, n_D^{25} 1.4135–1.4133. The first fraction, on redistillation through a spinning-band column, gave 3.23 g of pure diethyl oxalate, b.p. 72° at 8 mm, n_D^{25} 1.4087, d_4^{20} 1.076, the infrared spectrum of which was identical in all respects with that of a sample of the pure ester.[3] Redistillation of the second fraction, which contained about 8% of diethyl maleate (ultraviolet analysis), through the spinning-band column gave pure diethyl monofluorosuccinate (10.6 g, 73%) as a stable, colorless liquid, b.p. 72° at 1 mm, n_D^{25} 1.4125, d_4^{20} 1.142, MR_D 41.98 cc/mole; estimated 42.19 cc/mole. (Gitter, Blank, and Bergmann (3) report b.p. 70–71° at 0.8 mm, n_D^{23} 1.4240, d_4^{23} 1.1090, MR_D 44.23 cc/mole.) *Principal infrared bands* (3% solution in CCl_4), cm^{-1}: 1769.5 (C═O) s, 1746.5 (C═O) s, 1372.8 (CH_3) s, 1286.0 (C—O) s, 1264.0 m, 1179.5 (C—O) s, 1097.0 (C—F) s, 1051.2 m, 1028.5 s. *Nuclear magnetic resonance spectrum* (27.7% w/v in CCl_4 using tetramethylsilane as internal standard): chemical shifts (τ), coupling constants (c/s). Two CH_3CH_2O: 8.69 τ, 8.73 τ (*t*); 5.78 τ, 5.85 τ (*q*); J_{HH} 7.0 c/s. CH_2: 7.17 τ; J_{HH} 5.9 c/s; J_{HF} 23.3 c/s. CHF: 4.85 τ; J_{HH} 5.9 c/s; J_{HF} 47.6 c/s. The ester showed only weak end-absorption in the *ultraviolet*, ϵ_{220} 100.5 in 95% ethanol, indicating the absence of diethyl maleate (ϵ_{220} 6380); cf. diethyl succinate, ϵ_{220} 118. Anal. Calc. for $C_8H_{13}FO_4$: C, 49.99; H, 6.82; F, 9.89. Found: C, 50.16; H, 6.75; F, 9.77.

Monofluorosuccinic Acid

Pure diethyl monofluorosuccinate (3.3 g, 17.1 mmoles) and 5% sulphuric acid (20 ml) were heated under reflux at 110° for 30 minutes, that is, until the mixture appeared to be homogeneous. The cooled solution was extracted once with 35–60° petroleum ether, to remove any unchanged ester, and then was subjected to continuous ether extraction for 38 hours; no further acid was obtained after a further 24 hours of extraction. The extract was dried (magnesium sulphate), filtered, and concentrated using a Rinco rotary evaporator. The addition of benzene (5 ml) and removal of residual ether by boiling induced the acid to crystallize (1.33 g), m.p. 140–147°. Concentration of the mother liquors gave a further quantity (193 mg) of the crude acid. The petroleum ether extract gave 90 mg of unchanged ester. Yield of crude acid (1.523 g) based on ester consumed: 67%. It is important that any residual ester be removed and that the ether solution be dry to avoid difficulties in the initial crystallization of the acid. The acid may be recrystallized from benzene–ether, or, better, from hot ethyl acetate. An analytical sample is conveniently obtained by sublimation at 105° (0.3 mm) as a colorless, crystalline solid, m.p. 144–145°; positive fluorine test. The infrared spectrum in acetonitrile showed a band at 1747 cm^{-1} (C═O) with a shoulder on the high-frequency side; cf. succinic acid, 1744 cm^{-1}. Ultraviolet absorption spectrum in 95% ethanol (1-mm cells): λ_{max} 198 mμ, ϵ_{max} 130 (cf. maleic acid: λ_{max} 203 mμ, ϵ_{max} 14,900). Anal. Calc. for $C_4H_5FO_4$: C, 35.30; H, 3.70. Found: C, 35.48; H, 3.72.

Diethyl α-Fluoro-α-carbethoxysuccinate

Attempted distillation of the crude intermediate triethyl α-fluoro-α-oxalylsuccinate at 160–200° (0.05 mm) yielded the decarbonylated ester (77.5%). Redistillation gave a colorless liquid, b.p. 107–109° at 0.55 mm, n_D^{25} 1.4264. The infrared spectrum in CCl_4 showed bands at 1745 (C═O) and 1095 (C—F) cm^{-1}. Anal. Calc. for $C_{11}H_{17}FO_6$: C, 49.99; H, 6.49. Found: C, 50.13; H, 6.64.

ACKNOWLEDGMENTS

We wish to express our indebtedness to Canadian Industries Limited, Montreal, for the award of a Fellowship (F. H. D.); to the National Research Council for financial

[2]*Rubber containing carbon black may explode in contact with perchloryl fluoride.*

[3]*The formation of diethyl oxalate in this process may be explained by solvolytic cleavage of the intermediate triethyl α-fluoro-α-oxalylsuccinate.*

Can. J. Chem. Downloaded from www.nrcresearchpress.com by 210.87.254.5 on 09/05/12
For personal use only.

support; to Dr. J. B. Stothers for help with the nuclear magnetic resonance spectrum; and to Dr. M. K. McPhail and Dr. C. A. deCandole, Suffield Experimental Station, Ralston, Alberta, for determining the toxicity of monofluorosuccinic acid and its ester.

1. R. L. BUCHANAN, F. H. DEAN, and F. L. M. PATTISON. Preprints, Second International Symposium on Fluorine Chemistry, Estes Park, Colorado. 1962. p. 385.
2. C. MARTIUS. Ann. **561**, 227 (1949).
3. S. GITTER, I. BLANK, and E. D. BERGMANN. Koninkl. Ned. Akad. Wetenschap. Proc. Ser. C, **56**, 427 (1953).
4. E. D. BERGMANN and S. SZINAI. J. Chem. Soc. 1521 (1956).
5. R. A. PETERS. Advances in enzymology and related subjects of biochemistry. Vol. XVIII. Interscience Publishers, Inc., New York, N.Y. 1957. p. 120.
6. C. E. INMAN, R. E. OESTERLING, and E. A. TYCZKOWSKI. J. Am. Chem. Soc. **80**, 6533 (1958).
7. L. FRIEDMAN and E. KOSOWER. Organic syntheses. Coll. Vol. III. John Wiley and Sons, Inc., New York, N.Y. 1955. p. 510.

RECEIVED MARCH 4, 1963.
DEPARTMENT OF CHEMISTRY,
UNIVERSITY OF WESTERN ONTARIO,
LONDON, ONTARIO.

Can. J. Chem. Downloaded from www.nrcresearchpress.com by 210.87.254.5 on 09/05/12
For personal use only.

THE RATIO OF THE INDEPENDENT FORMATION CROSS SECTIONS OF THE ISOMERIC STATES OF Cs^{134} IN THE PROTON-INDUCED FISSION OF URANIUM[1]

J. H. DAVIES[2] AND L. YAFFE

Both Cs^{134m} (2.9 hr) and Cs^{134g} (2.1 yr) are formed in the proton-induced fission of uranium. The 2.9-hr metastable state is a primary product shielded by stable Xe^{134} and Ba^{134}. The 2.1-yr ground state is formed both as a primary product and from the decay of the metastable state by isomeric transition.

This nuclide provides one of the rare instances where the independent formation cross sections of a pair of isomers produced in fission can be conveniently measured.

In the course of work on the nuclear charge dispersion in the fission of natural uranium by high-energy protons (1), data were collected on the independent yields of cesium isotopes. This enabled us to calculate the ratio of the formation cross sections of the Cs^{134} isomers at a number of incident proton energies. Details of the separations and measurements are provided in the former work (1).

The β-activity of the cesium fraction, purified radiochemically, was measured by means of an end-window gas-flow proportional counter. The decay curves were resolved cleanly into three components, 32-min Cs^{138}, 2.9-hr Cs^{134}, and 12.9-day Cs^{136}, with a long-lived, low-activity tail. The γ-spectrum of this sample revealed two photopeaks attributable to Cs^{134} (2.1 yr) and Cs^{137} (30 yr) after the decay of Cs^{136}. Both the Cs^{134m} and the Cs^{134} activities were measured relative to that of Cs^{136} from the β- and γ-ray measurements respectively. The independent yield of Cs^{134g} was obtained by difference between the two measurements. The method of calculation of the formation cross sections and the correction factors used are given in the charge dispersion paper (1).

The ratio of the isomeric cross sections as a function of incident proton energy is shown in Fig. 1. It is apparent that the high-spin metastable state (8−) is always favored in this

[1]*Financial support received from the United States Air Force under Grant No. 62–64, monitored by The Air Force Office of Scientific Research of the Office of Aerospace Research.*
[2]*Present address: General Electric Company, Vallecitos Atomic Laboratory, Pleasanton, California, U.S.A.*

support; to Dr. J. B. Stothers for help with the nuclear magnetic resonance spectrum; and to Dr. M. K. McPhail and Dr. C. A. deCandole, Suffield Experimental Station, Ralston, Alberta, for determining the toxicity of monofluorosuccinic acid and its ester.

1. R. L. BUCHANAN, F. H. DEAN, and F. L. M. PATTISON. Preprints, Second International Symposium on Fluorine Chemistry, Estes Park, Colorado. 1962. p. 385.
2. C. MARTIUS. Ann. **561**, 227 (1949).
3. S. GITTER, I. BLANK, and E. D. BERGMANN. Koninkl. Ned. Akad. Wetenschap. Proc. Ser. C, **56**, 427 (1953).
4. E. D. BERGMANN and S. SZINAI. J. Chem. Soc. 1521 (1956).
5. R. A. PETERS. Advances in enzymology and related subjects of biochemistry. Vol. XVIII. Interscience Publishers, Inc., New York, N.Y. 1957. p. 120.
6. C. E. INMAN, R. E. OESTERLING, and E. A. TYCZKOWSKI. J. Am. Chem. Soc. **80**, 6533 (1958).
7. L. FRIEDMAN and E. KOSOWER. Organic syntheses. Coll. Vol. III. John Wiley and Sons, Inc., New York, N.Y. 1955. p. 510.

RECEIVED MARCH 4, 1963.
DEPARTMENT OF CHEMISTRY,
UNIVERSITY OF WESTERN ONTARIO,
LONDON, ONTARIO.

Can. J. Chem. Downloaded from www.nrcresearchpress.com by 210.87.254.105 on 09/05/12
For personal use only.

THE RATIO OF THE INDEPENDENT FORMATION CROSS SECTIONS OF THE ISOMERIC STATES OF Cs^{134} IN THE PROTON-INDUCED FISSION OF URANIUM[1]

J. H. DAVIES[2] AND L. YAFFE

Both Cs^{134m} (2.9 hr) and Cs^{134g} (2.1 yr) are formed in the proton-induced fission of uranium. The 2.9-hr metastable state is a primary product shielded by stable Xe^{134} and Ba^{134}. The 2.1-yr ground state is formed both as a primary product and from the decay of the metastable state by isomeric transition.

This nuclide provides one of the rare instances where the independent formation cross sections of a pair of isomers produced in fission can be conveniently measured.

In the course of work on the nuclear charge dispersion in the fission of natural uranium by high-energy protons (1), data were collected on the independent yields of cesium isotopes. This enabled us to calculate the ratio of the formation cross sections of the Cs^{134} isomers at a number of incident proton energies. Details of the separations and measurements are provided in the former work (1).

The β-activity of the cesium fraction, purified radiochemically, was measured by means of an end-window gas-flow proportional counter. The decay curves were resolved cleanly into three components, 32-min Cs^{138}, 2.9-hr Cs^{134}, and 12.9-day Cs^{136}, with a long-lived, low-activity tail. The γ-spectrum of this sample revealed two photopeaks attributable to Cs^{134} (2.1 yr) and Cs^{137} (30 yr) after the decay of Cs^{136}. Both the Cs^{134m} and the Cs^{134} activities were measured relative to that of Cs^{136} from the β- and γ-ray measurements respectively. The independent yield of Cs^{134g} was obtained by difference between the two measurements. The method of calculation of the formation cross sections and the correction factors used are given in the charge dispersion paper (1).

The ratio of the isomeric cross sections as a function of incident proton energy is shown in Fig. 1. It is apparent that the high-spin metastable state (8−) is always favored in this

[1]*Financial support received from the United States Air Force under Grant No. 62–64, monitored by The Air Force Office of Scientific Research of the Office of Aerospace Research.*
[2]*Present address: General Electric Company, Vallecitos Atomic Laboratory, Pleasanton, California, U.S.A.*

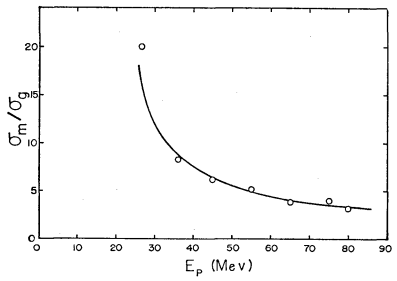

FIG. 1. Ratio of formation cross sections of the metastable and ground states of Cs^{134} as a function of proton bombarding energy.

energy range, and is formed almost exclusively at the lower energies. However, the low-spin ground state (4+) becomes increasingly favored with increasing excitation energy. This is not in agreement with the conclusions of Bailey (2), who reasoned that, since high-energy fission is a high angular momentum process, the low-spin isomer ought to be less favored at higher energies.

1. J. H. DAVIES and L. YAFFE. Can. J. Phys. In Press.
2. S. M. BAILEY. Ph.D. Thesis, University of California, Berkeley, Calif., U.S.A. 1959.

RECEIVED FEBRUARY 21, 1963.
RADIOCHEMISTRY LABORATORY,
DEPARTMENT OF CHEMISTRY,
MCGILL UNIVERSITY,
MONTREAL, QUE.

6-O-METHANESULPHONYL-D-GALACTOSE

D. L. MITCHELL

Acid hydrolysis of the *O*-isopropylidene groups of 1,2:3,4-di-*O*-isopropylidene-6-*O*-toluene-*p*-sulphonyl-D-galactose with retention of the 6-*O*-toluene-*p*-sulphonyl ester offers little difficulty and the product, 6-*O*-toluene-*p*-sulphonyl-D-galactose, has been described as a crystalline solid (1). Because the methanesulphonyl ester of a primary alcohol is more easily hydrolyzed by acid than the corresponding toluene-*p*-sulphonyl ester, and because the liberated methanesulphonic acid renders the reaction autocatalytic, selective removal of the *O*-isopropylidene groups of 1,2:3,4-di-*O*-isopropylidene-6-*O*-methanesulphonyl-D-galactose has offered greater difficulty and the product, 6-*O*-methanesulphonyl-D-galactose, has hitherto been obtained only as a syrup although two crystalline thioacetal derivatives have been reported (2).

Hydrolysis conditions are now described for the preparation of 6-*O*-methanesulphonyl-D-galactose as a crystalline compound. The product was the α-anomer since an aqueous solution mutarotated to a less positive equilibrium value. Chromatographic examination of the equilibrium solution revealed the absence of possible dehydration products, thus confirming that the rotational change originated from a mutarotation and not from the formation of 3,6-*O*-anhydro-D-galactose or other products. Acetonation of the crystalline

Can. J. Chem. Downloaded from www.nrcresearchpress.com by 210.87.254.105 on 09/05/12
For personal use only.

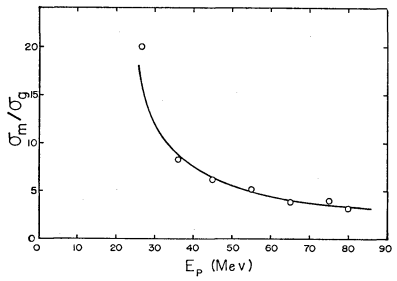

FIG. 1. Ratio of formation cross sections of the metastable and ground states of Cs^{134} as a function of proton bombarding energy.

energy range, and is formed almost exclusively at the lower energies. However, the low-spin ground state (4+) becomes increasingly favored with increasing excitation energy. This is not in agreement with the conclusions of Bailey (2), who reasoned that, since high-energy fission is a high angular momentum process, the low-spin isomer ought to be less favored at higher energies.

1. J. H. DAVIES and L. YAFFE. Can. J. Phys. In Press.
2. S. M. BAILEY. Ph.D. Thesis, University of California, Berkeley, Calif., U.S.A. 1959.

RECEIVED FEBRUARY 21, 1963.
RADIOCHEMISTRY LABORATORY,
DEPARTMENT OF CHEMISTRY,
MCGILL UNIVERSITY,
MONTREAL, QUE.

6-O-METHANESULPHONYL-D-GALACTOSE

D. L. MITCHELL

Acid hydrolysis of the *O*-isopropylidene groups of 1,2:3,4-di-*O*-isopropylidene-6-*O*-toluene-*p*-sulphonyl-D-galactose with retention of the 6-*O*-toluene-*p*-sulphonyl ester offers little difficulty and the product, 6-*O*-toluene-*p*-sulphonyl-D-galactose, has been described as a crystalline solid (1). Because the methanesulphonyl ester of a primary alcohol is more easily hydrolyzed by acid than the corresponding toluene-*p*-sulphonyl ester, and because the liberated methanesulphonic acid renders the reaction autocatalytic, selective removal of the *O*-isopropylidene groups of 1,2:3,4-di-*O*-isopropylidene-6-*O*-methanesulphonyl-D-galactose has offered greater difficulty and the product, 6-*O*-methanesulphonyl-D-galactose, has hitherto been obtained only as a syrup although two crystalline thioacetal derivatives have been reported (2).

Hydrolysis conditions are now described for the preparation of 6-*O*-methanesulphonyl-D-galactose as a crystalline compound. The product was the α-anomer since an aqueous solution mutarotated to a less positive equilibrium value. Chromatographic examination of the equilibrium solution revealed the absence of possible dehydration products, thus confirming that the rotational change originated from a mutarotation and not from the formation of 3,6-*O*-anhydro-D-galactose or other products. Acetonation of the crystalline

Can. J. Chem. Downloaded from www.nrcresearchpress.com by 210.87.254.5 on 09/05/12
For personal use only.

mono-*O*-methanesulphonyl-D-galactose regenerated the starting material, 1,2:3,4-di-*O*-isopropylidene-6-*O*-methanesulphonyl-D-galactose, and the location of the methanesulphonyl ester at the primary alcohol (carbon 6) was therefore confirmed. Quantitative periodate oxidation of the crystalline ester also gave data consistent with that expected for an aldohexopyranose substituted at the primary alcohol. Similar results were also obtained for the periodate oxidation of crystalline 6-*O*-toluene-*p*-sulphonyl-D-galactose.

Attempts to form the 2,5-dichlorophenylhydrazone and the *N*-benzylphenylhydrazone derivatives by the usual method of gentle warming of an alcoholic solution of the substituted hydrazine and 6-*O*-methanesulphonyl-D-galactose gave crystalline products that contained no sulphur. Analyses corresponded to those of anhydrohexose phenylhydrazones and the products have been tentatively identified as 3,6-*O*-anhydro-D-galactose 2,5-dichlorophenylhydrazone and 3,6-*O*-anhydro-D-galactose *N*-benzylphenylhydrazone respectively. Under refluxing conditions during the attempted formation of the phenylosazone, loss of the 6-*O*-methanesulphonyl group occurred and an anhydrohexose phenylosazone was isolated, which was most likely 3,6-*O*-anhydro-D-*lyxo*-hexose phenylosazone.

When a lower reaction temperature was employed (i.e. reaction at room temperature for several days), the expected hydrazone derivatives were obtained without the anhydro compound being simultaneously formed. Several new substituted hydrazone derivatives of 6-*O*-(methanesulphonyl- and toluene-*p*-sulphonyl-)D-galactose have been described in Table III.

EXPERIMENTAL

For paper chromatographic examination, the following solvent system was used (v:v): ethyl acetate – acetic acid – water (9:2:2). 1,2:3,4-Di-*O*-isopropylidene-D-galactose was prepared in 66% yield by a procedure adapted from the preparation of 1,2:5,6-di-*O*-isopropylidene-D-glucose (3). $[\alpha]_D^{20}$ −54.1° (*c*, 1.0, chloroform) (lit. $[\alpha]_D^{24}$ −54.7° (4)).

The above compound was methanesulphonated in 85% yield, by the usual method employing methanesulphonyl chloride and pyridine. The product, obtained as a solid when the reaction mixture was poured into ice-cold water, had m.p. 122–123° C and $[\alpha]_D^{24}$ −63.4° (*c*, 1.7, chloroform) after several recrystallizations from methanol (lit. m.p. 122° C and $[\alpha]_D^{20}$ −62° (chloroform) (5)).

6-O-Methanesulphonyl-D-galactose

1,2:3,4-Di-*O*-isopropylidene-6-*O*-methanesulphonyl-D-galactose (46.2 g) was dissolved in ethanol (200 ml), water (200 ml), and 2 *N* sulphuric acid (20 ml) and the solution was heated to 80° C for 3 hours. The cooled solution (0° C) was neutralized on columns of Amberlite IR-45 (acetate) and IR-120 (H) ion exchange resins and the eluate was concentrated under reduced pressure to a small volume (50 ml). Some of the starting material (ca. 1 g) separated and was recovered. The mother liquors were concentrated to a syrup which was repeatedly dissolved in a small volume of ethanol and reconcentrated to remove traces of water. The syrup was dissolved in acetone (50 ml), warmed slightly, and light petroleum (b.p. 60–80° C) was added to incipient turbidity. Storage at 4° C for 4 days induced crystallization (rosettes, 14.6 g, 42%). Recrystallization from ethanol–water (25:1) gave fine needles of m.p. 124–125° C, $[\alpha]_D^{23}$ 83.9° (13 minutes) → 55.2° (3.5 hours) → 52.8° (constant value) (*c*, 0.9, water), and a R_f 0.45 and R_{Rh} 1.06. Anal. Calc. for $C_7H_{14}O_8S$: C, 32.7; H, 5.5; S, 12.4. Found: C, 32.6; H, 5.5; S, 12.4. Syrupy 6-*O*-methanesulphonyl-D-galactose, obtained by using the hydrolysis conditions (dilute acetic acid) described by Stacey (2), crystallized after nucleation with the above crystalline specimen.

The above hydrolysis conditions were found to be too mild for the preparation of the corresponding 6-*O*-toluene-*p*-sulphonyl-D-galactose and a modified procedure was adopted. A solution of 1,2:3,4-di-*O*-isopropylidene-6-*O*-toluene-*p*-sulphonyl-D-galactose (20 g) in ethanol (140 ml), water (60 ml), and dilute sulphuric acid (2 *N*, 25 ml) was heated to 80° C for 4 hours. Using the above isolation procedure, 31% yield of 6-*O*-toluene-*p*-sulphonyl-D-galactose was obtained, m.p. 133–134° C and $[\alpha]_D^{23}$ 32.8° → 46.7° (24 hours) (*c*, 1.22, water).

Periodate Oxidation Experiments

Periodate oxidation at room temperature of samples (38.7 mg, 1.5×10^{-4} mole) with sodium metaperiodate solution (12×10^{-4} mole in 25 ml) under unbuffered and buffered conditions is described in Tables I and II.

Re-formation of 1,2:3,4-Di-O-isopropylidene-6-O-methanesulphonyl-D-galactose

A solution of 6-*O*-methanesulphonyl-D-galactose (110 mg) in acetone (20 ml) containing concentrated

Can. J. Chem. Downloaded from www.nrcresearchpress.com by 210.87.254.5 on 09/05/12
For personal use only.

TABLE I

Periodate oxidation of 6-*O*-methanesulphonyl-D-galactose

Determination	pH	Time (min) 5	10	20	30	60	120	180		
Uptake*	U	3.72	3.74	—	3.76	3.78	—	—	3.93 (210 min)	3.99 (21 hr)
Uptake	3.7	3.08	3.10	3.46	—	3.87	3.89	3.94	3.52 (40 min)	
Titratable acid†	U	2.6	2.7	2.9	3.1	3.8	—	—	3.8 (7.5 hr)	3.9 (17 hr)
Formaldehyde‡	U	—	—	—	—	—	—	—	Nil (21 hr)	

*Reference 9.
†An end point using the screened methyl red indicator was taken.
‡Reference 10.

TABLE II

Periodate oxidation of 6-*O*-toluene-*p*-sulphonyl-D-galactose

Determination	pH	Time (min) 10	30	60	90	21 hr	24 hr	
Uptake	U	—	2.21	—	2.63	3.83	4.13 (constant)	
Titratable acid	U	1.17	2.17	2.50	—	—	3.75	3.96 (40 hr)
Formaldehyde	U	—	—	—	—	—	Trace	

sulphuric acid (1 drop) was stored for 24 hours at room temperature. After neutralization (barium carbonate) and filtration from the inorganic salts, the solution was concentrated to a crystalline mass. This material was recrystallized from methanol and had a melting point of 121–122° C which was not depressed upon admixture with an authentic specimen of 1,2:3,4-di-*O*-isopropylidene-6-*O*-methanesulphonyl-D-galactose. The derived product possessed an infrared absorption spectrum identical with that of the authentic specimen. Both comparisons using solid material (potassium bromide disk) and chloroform solutions were employed.

6-O-Methanesulphonyl-D-galactose 2,5-Dichlorophenylhydrazone

A suspension of 6-*O*-methanesulphonyl-D-galactose (0.20 g) and 2,5-dichlorophenylhydrazine (0.17 g) in dry methanol was stored in a stoppered flask at room temperature. After 24 hours, the reactants formed a solution, which was stored for a further 24 hours. Concentration under reduced pressure afforded a solid which was recrystallized from a small volume of ethanol, m.p. 143–145° C, $[\alpha]_D^{23}$ +30° (*c*, 0.53, pyridine) (Table III).

The preparations of 6-*O*-methanesulphonyl-D-galactose *N*-benzylphenylhydrazone, and 6-*O*-toluene-*p*-sulphonyl-D-galactose 2,5-dichlorophenylhydrazone were also carried out by the above method (Table III) (6).

6-O-Methanesulphonyl-D-galactose 2,4-Dinitrophenylhydrazone

The 2,4-dinitrophenylhydrazones were prepared by mixing a warm alcoholic solution of the D-galactose sulphonyl ester with an excess of Brady's reagent. After 30 minutes' reaction, the precipitate was collected by centrifugation and repeatedly washed with ether. The physical constants are reported in Table III.

(?) 3,6-O-Anhydro-D-galactose N-Benzylphenylhydrazone

A solution of 6-*O*-methanesulphonyl-D-galactose (0.24 g) and *N*-benzylphenylhydrazine (0.50 g) in methanol (5 ml) was cautiously warmed to ca. 45–50° C intermittently for 1 hour and stored for a further 48 hours. Concentration to dryness afforded a crystalline solid that was repeatedly triturated with cold (−10° C) ether followed by hexane–ether solutions. A portion was recrystallized from ethanol to give white needles of m.p. 155–156° and $[\alpha]_D^{23}$ −22° (12 hours) (*c*, 1.2, pyridine). Anal. Calc. for $C_{19}H_{22}N_2O$: C, 66.7; H, 6.5; N, 8.2; S, nil. Found: C, 67.3; H, 6.5; N, 8.1; S, nil.

(?) 3,6-O-Anhydro-D-galactose 2,5-Dichlorophenylhydrazone

A solution of 6-*O*-methanesulphonyl-D-galactose (0.050 g) and 2,5-dichlorophenylhydrazine (0.040 g) in

Can. J. Chem. Downloaded from www.nrcresearchpress.com by 210.87.254.5 on 09/05/12
For personal use only.

Can. J. Chem. Downloaded from www.nrcresearchpress.com by 210.87.254.5 on 09/05/12
For personal use only.

TABLE III

Hydrazone derivatives of 6-*O*-(methanesulphonyl- and toluene-*p*-sulphonyl-)D-galactose

Hydrazone	Ester	M.p.* (°C)	$[\alpha]_D^{23}$ †	Formula	C		H		N		S	
					Calc.	Found	Calc.	Found	Calc.	Found	Calc.	Found
2,5-Dichlorophenyl	6-*O*-Methanesulphonyl	143–145	30°	$C_{13}H_{18}Cl_2N_2O_7S$	37.4	37.7	4.4	4.5	6.7	6.3		
2,4-Dinitrophenyl	6-*O*-Methanesulphonyl	148–150	—	$C_{13}H_{18}N_4O_{11}S$	35.8	35.6	4.4	4.1			7.3	7.9
N-Benzylphenyl	6-*O*-Methanesulphonyl	124–126	7.7°	$C_{20}H_{26}N_2O_7S$	54.8	54.8	6.0	6.2	6.4	6.5		
2,5-Dichlorophenyl	6-*O*-Toluene-*p*-sulphonyl	131–133	17.6° 8.8° (12 hr)	$C_{19}H_{22}Cl_2N_2O_7S$	46.2	46.5	4.5	4.6	5.7	5.5	6.5	6.5
2,4-Dinitrophenyl	6-*O*-Toluene-*p*-sulphonyl	148–150	—	$C_{19}H_{22}N_4O_{11}S$	44.4	44.4	4.3	4.4	10.9	10.5		

*All samples melted with decomposition.
†All observations were carried out in pyridine solutions.

methanol (5 ml) was heated to 80° C for 2 hours. The solution was concentrated to a crystalline mass which was repeatedly triturated with cold ether to yield pale yellow flakes (0.025 g) of m.p. 191–193° C (preliminary shrinking). Anal. Calc. for $C_{12}H_{14}Cl_2N_2O_4$: N, 8.7; S, nil. Found: N, 9.0; S, nil.

3,6-O-Anhydro-D-lyxo-*hexose Phenylosazone*

Attempts to prepare the phenylosazone of 6-*O*-methanesulphonyl-D-galactose using phenylhydrazine and acetate-buffered aqueous acetic acid with warming of the solution to 80° C gave a product of m.p. 203–205° C. Anal. Calc. for $C_{18}H_{20}N_4O_3$: N, 16.5. Found: N, 17.1 (lit. 3,6-*O*-anhydro-D-galactose phenylosazone, m.p. 203–204.5° C (7) and m.p. 117° C (8)).

ACKNOWLEDGMENTS

The author wishes to thank the Central Research Grants Committee, Makerere University College, for a maintenance grant and also the Royal Military College of Canada, Kingston, Ontario, for a gift of chemicals. For valuable assistance in the laboratory he wishes to thank Mr. E. S. P. Wasula-Kyasi and Mr. E. S. Gapfakubaho.

1. H. Ohle and H. Thiel. Ber. **66**, 525 (1933).
2. A. B. Foster, W. G. Overend, M. Stacey, and L. F. Wiggins. J. Chem. Soc. 2542 (1949).
3. C. L. Mehltretter, B. H. Alexander, R. L. Mellies, and C. E. Rist. J. Am. Chem. Soc. **73**, 2424 (1951).
4. K. Freudenberg and R. M. Hixon. Ber. **56**, 2119 (1923).
5. B. Helferich, H. Dressler, and R. Griebel. J. Prakt. Chem. **153**, 285 (1939).
6. E. B. Rauch and D. Lipkin. J. Org. Chem. **27**, 403 (1962).
7. A. L. Clingman, J. R. Nunn, and A. M. Stephen. J. Chem. Soc. 197 (1957).
8. T. J. Painter. Can. J. Chem. **38**, 112 (1960).
9. G. Nellmüller and E. Vasseur. Arkiv. Kemi, **5**, 235 (1953).
10. J. F. O'Dea and R. A. Gibbons. Biochem. J. **55**, 580 (1953).

Received February 18, 1963.
Department of Chemistry,
Makerere University College,
Kampala, Uganda.

DETERMINATION OF RELATIVE SIGNS OF COUPLING CONSTANTS IN QUINOLINE BY NUCLEAR MAGNETIC DOUBLE RESONANCE

W. G. Paterson* and G. Bigam

A great deal of interest has been generated recently by the discovery (1–3) that the relative signs of n.m.r. coupling constants could be determined by double-irradiation experiments. The present note describes double-resonance measurements on quinoline which yield the relative signs of the coupling constants in the heterocyclic ring. In a recent paper (4) on 2-amino-3-picoline, it was claimed that the single-resonance spectrum indicated that J_{AX} and J_{BX} were of the same sign, although details of the calculations were not given. Assuming that both coupling constants were positive, it was then shown

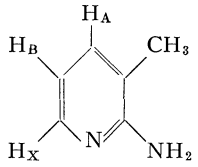

2-Amino-3-picoline

**Present address: Central Research Laboratories, Minnesota Mining and Manufacturing Co., St. Paul, Minn., U.S.A.*

Can. J. Chem. Downloaded from www.nrcresearchpress.com by 210.87.254.5 on 09/05/12
For personal use only.

methanol (5 ml) was heated to 80° C for 2 hours. The solution was concentrated to a crystalline mass which was repeatedly triturated with cold ether to yield pale yellow flakes (0.025 g) of m.p. 191–193° C (preliminary shrinking). Anal. Calc. for $C_{12}H_{14}Cl_2N_2O_4$: N, 8.7; S, nil. Found: N, 9.0; S, nil.

3,6-O-Anhydro-D-lyxo-*hexose Phenylosazone*

Attempts to prepare the phenylosazone of 6-*O*-methanesulphonyl-D-galactose using phenylhydrazine and acetate-buffered aqueous acetic acid with warming of the solution to 80° C gave a product of m.p. 203–205° C. Anal. Calc. for $C_{18}H_{20}N_4O_3$: N, 16.5. Found: N, 17.1 (lit. 3,6-*O*-anhydro-D-galactose phenylosazone, m.p. 203–204.5° C (7) and m.p. 117° C (8)).

ACKNOWLEDGMENTS

The author wishes to thank the Central Research Grants Committee, Makerere University College, for a maintenance grant and also the Royal Military College of Canada, Kingston, Ontario, for a gift of chemicals. For valuable assistance in the laboratory he wishes to thank Mr. E. S. P. Wasula-Kyasi and Mr. E. S. Gapfakubaho.

1. H. Ohle and H. Thiel. Ber. **66**, 525 (1933).
2. A. B. Foster, W. G. Overend, M. Stacey, and L. F. Wiggins. J. Chem. Soc. 2542 (1949).
3. C. L. Mehltretter, B. H. Alexander, R. L. Mellies, and C. E. Rist. J. Am. Chem. Soc. **73**, 2424 (1951).
4. K. Freudenberg and R. M. Hixon. Ber. **56**, 2119 (1923).
5. B. Helferich, H. Dressler, and R. Griebel. J. Prakt. Chem. **153**, 285 (1939).
6. E. B. Rauch and D. Lipkin. J. Org. Chem. **27**, 403 (1962).
7. A. L. Clingman, J. R. Nunn, and A. M. Stephen. J. Chem. Soc. 197 (1957).
8. T. J. Painter. Can. J. Chem. **38**, 112 (1960).
9. G. Nellmüller and E. Vasseur. Arkiv. Kemi, **5**, 235 (1953).
10. J. F. O'Dea and R. A. Gibbons. Biochem. J. **55**, 580 (1953).

Received February 18, 1963.
Department of Chemistry,
Makerere University College,
Kampala, Uganda.

DETERMINATION OF RELATIVE SIGNS OF COUPLING CONSTANTS IN QUINOLINE BY NUCLEAR MAGNETIC DOUBLE RESONANCE

W. G. Paterson* and G. Bigam

A great deal of interest has been generated recently by the discovery (1–3) that the relative signs of n.m.r. coupling constants could be determined by double-irradiation experiments. The present note describes double-resonance measurements on quinoline which yield the relative signs of the coupling constants in the heterocyclic ring. In a recent paper (4) on 2-amino-3-picoline, it was claimed that the single-resonance spectrum indicated that J_{AX} and J_{BX} were of the same sign, although details of the calculations were not given. Assuming that both coupling constants were positive, it was then shown

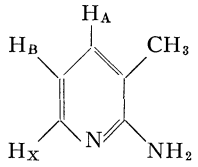

2-Amino-3-picoline

**Present address: Central Research Laboratories, Minnesota Mining and Manufacturing Co., St. Paul, Minn., U.S.A.*

Can. J. Chem. Downloaded from www.nrcresearchpress.com by 210.87.254.105 on 09/05/12
For personal use only.

by nuclear magnetic double resonance that J_{AB} was also positive. The fact that the chemical shifts in 2-amino-3-picoline are quite large compared to the coupling constants renders the intensities of the transitions quite insensitive to the relative signs of J_{AX} and J_{BX}. Furthermore, since proton A is also coupled to the methyl protons, 2-amino-3-picoline is a rather unsuitable compound, and it is therefore desirable that the relative signs of the coupling constants in pyridine derivatives be verified by a different approach.

The n.m.r. spectrum of the protons in the heterocyclic ring of quinoline at 100 Mc/s is almost first order, and the relative signs of the coupling constants may be determined by the method of Freeman (3). The single-resonance spectrum of the protons in the heterocyclic ring of quinoline at 100 Mc/s is shown in Fig. 1 along with a calculated spectrum

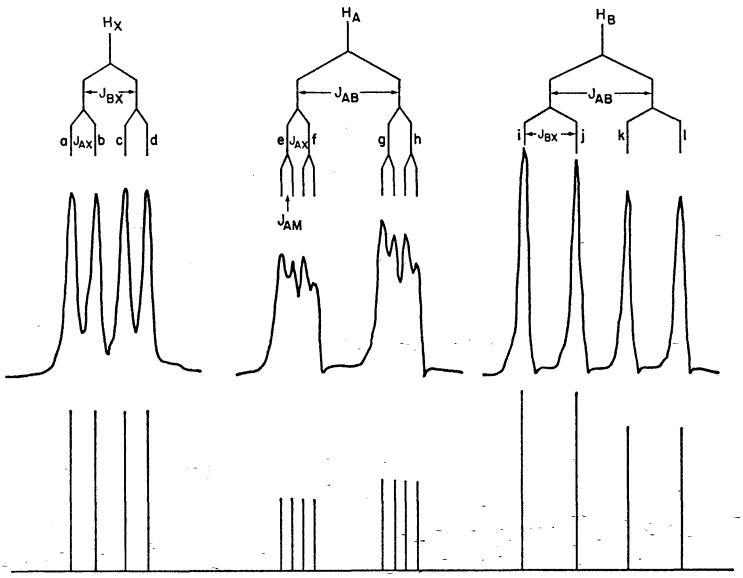

FIG. 1. The observed and calculated n.m.r. spectrum of quinoline at 100 Mc/s. The small inter-ring coupling J_{AM} was treated as a first-order perturbation. All coupling constants are assumed to be positive. The magnetic field increases from left to right.

for the heterocyclic ring based on an ABX approximation (5, Chap. 6). The n.m.r. parameters are listed in Table I. The nuclei are labeled as shown below. The calculated intensities for (i) all J's positive and (ii) with J_{AX} negative were identical within experimental error.

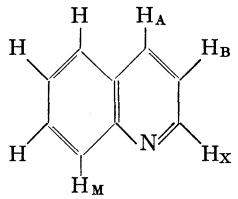

Irradiation with a moderately weak r.f. field at a frequency $\frac{1}{2}(a+c)$ in the X spectrum should collapse lines i and j in the B spectrum to a single line if J_{AB} and J_{AX} are of the same sign, or collapse lines k and l if they are of opposite sign. Analogous arguments apply to irradiation at a frequency $\frac{1}{2}(b+d)$. The possibilities are summarized in Table II. Typical experimental traces are shown in Fig. 2. It is clear that collapse of the signals is

Can. J. Chem. Downloaded from www.nrcresearchpress.com by 210.87.254.105 on 09/05/12
For personal use only.

TABLE I

Nuclear magnetic resonance parameters for the heterocyclic ring in quinoline (c.p.s.)

	$\nu_B-\nu_A$	$\nu_B-\nu_X$	J_{AB}	J_{AX}	J_{BX}	J_{AM}
Present work	73.2±0.2	195.2±0.2	8.3±0.1	1.8±0.1	4.2±0.1	0.9±0.1
Schaefer (6)	—	—	8.5±0.3	1.8±0.2	4.1±0.2	1.0±0.2
Pople, Schneider, and Bernstein (5, p. 268)	—	—	7.3	—	5.0	—

TABLE II

Separations between r.f. fields H_1 and H_2 required for determination of relative signs of J_{AB} and J_{AX}

	Location in spectrum of H_2	Separation (c.p.s.) between H_1 and H_2 required for collapse of:	
		i and j	k and l
Like signs	$\frac{1}{2}(a+c)$	191.8	—
	$\frac{1}{2}(b+d)$	—	198.5
Opposite signs	$\frac{1}{2}(a+c)$	—	200.2
	$\frac{1}{2}(b+d)$	190.1	—

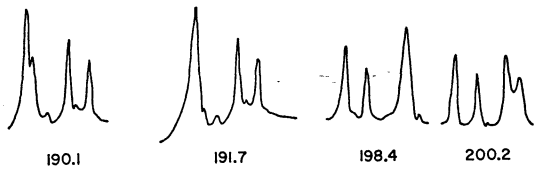

FIG. 2. The double-resonance spectra of nucleus B in quinoline observed for different frequencies of the decoupling r.f. field H_2. The separations in c.p.s. between the r.f. fields H_1 and H_2 are shown below the spectra. The magnetic field increases from left to right.

more complete when a decoupling frequency is used which corresponds to like signs for J_{AB} and J_{AX}.

Similarly, irradiation at a frequency $\frac{1}{2}(a+b)$ in the X spectrum should collapse lines e and f in the A spectrum (leaving a closely spaced doublet due to J_{AM}) if J_{AB} and J_{BX} are of like sign or collapse lines g and h if they are of opposite sign. Analogous considerations apply to irradiation at a frequency $\frac{1}{2}(c+d)$. A summary of the possibilities is given in Table III. Experimental spectra are shown in Fig. 3. Optimum collapse of the signals was obtained for the experimental arrangement which corresponded to like signs for J_{AB} and J_{BX}.

TABLE III

Separations between r.f. fields H_1 and H_2 required for determination of relative signs of J_{AB} and J_{BX}

	Location in spectrum of H_2	Separation (c.p.s.) between H_1 and H_2 required for collapse of:	
		e and f	g and h
Like signs	$\frac{1}{2}(a+b)$	119.9	—
	$\frac{1}{2}(c+d)$	—	124.1
Opposite signs	$\frac{1}{2}(a+b)$	—	128.3
	$\frac{1}{2}(c+d)$	115.7	—

Can. J. Chem. Downloaded from www.nrcresearchpress.com by 210.87.254.105 on 09/05/12
For personal use only.

FIG. 3. The double-resonance spectra of nucleus A in quinoline observed for different frequencies of the decoupling r.f. field H_2. The separations in c.p.s. between the r.f. fields H_1 and H_2 are shown below the spectra. The magnetic field increases from left to right.

It may be concluded that all three coupling constants in the heterocyclic ring of quinoline have the same sign, in agreement with the results of Rao and Baldeschwieler (4) for 2-amino-3-picoline.

EXPERIMENTAL

The n.m.r. spectra were obtained with a Varian high-resolution spectrometer operating at 100 Mc/s. The spectra were calibrated by the usual side-band method (7), using a Hewlett–Packard Model 200AB audio-oscillator and a Hewlett–Packard Model 521C frequency counter. The double-resonance experiments were carried out as described by Johnson (8). With the center-band signal phased out, the first modulation side band H_1 of the V3521 Integrator is used to record the n.m.r. spectrum while a second, stronger side band, H_2, provided by an audio-oscillator, is applied to the system under investigation such that $|\omega_2-\omega_1|$ is equal to the separation necessary to do the double-resonance experiment. The output of the oscillator is quite critical (3). The ratios of the chemical shifts to the coupling constants in the present instances were sufficiently large that corrections to the modulation frequency were unnecessary (9). The frequency of the first modulation side band of the Integrator varied slightly from day to day and was checked before each experiment. As a check on the method, the results reported by Freeman (3) for *trans*-crotonaldehyde were repeated and duplicated.

Quinoline (synthetic grade) was obtained from Matheson, Coleman, and Bell and degassed by the nitrogen bubbling technique prior to the n.m.r. measurements.

ACKNOWLEDGMENT

The financial support of the National Research Council is gratefully acknowledged.

1. D. F. EVANS and J. P. MAHER. Proc. Chem. Soc. 208 (1961).
2. R. FREEMAN and D. H. WHIFFEN. Mol. Phys. **4**, 321 (1961).
3. R. FREEMAN. Mol. Phys. **4**, 385 (1961).
4. B. D. N. RAO and J. D. BALDESCHWIELER. J. Chem. Phys. **37**, 2473 (1962).
5. J. A. POPLE, W. G. SCHNEIDER, and H. J. BERNSTEIN. High-resolution nuclear magnetic resonance. McGraw-Hill Book Co., Inc., New York. 1959.
6. T. SCHAEFER. Can. J. Chem. **39**, 1864 (1961).
7. J. T. ARNOLD and M. E. PACKARD. J. Chem. Phys. **19**, 1608 (1951).
8. L. F. JOHNSON. Varian Associates Publication No. 87-100-082. Palo Alto, California. August, 1962.
9. D. W. TURNER. J. Chem. Soc. 847 (1962).

RECEIVED MARCH 1, 1963.
DEPARTMENT OF CHEMISTRY,
UNIVERSITY OF ALBERTA,
EDMONTON, ALBERTA.

Can. J. Chem. Downloaded from www.nrcresearchpress.com by 210.87.254.105 on 09/05/12
For personal use only.

SELF-CONDENSATION OF METHYL PROPIOLATE

ERNEST WENKERT, K. A. H. ADAMS, AND CURTIS L. LEICHT

When during the course of a study of alkaloid synthesis methyl propiolate was observed to undergo a chemical change in the presence of a tertiary amine, this unusual reaction was investigated. Exposure of a benzene solution of the ester to triethylamine, N-methylpyrrolidine, or N-methylpiperidine for a short period of time gave good yields of a dimer. Elemental, infrared, ultraviolet, and proton magnetic resonance analysis of the product

FIG. 3. The double-resonance spectra of nucleus A in quinoline observed for different frequencies of the decoupling r.f. field H_2. The separations in c.p.s. between the r.f. fields H_1 and H_2 are shown below the spectra. The magnetic field increases from left to right.

It may be concluded that all three coupling constants in the heterocyclic ring of quinoline have the same sign, in agreement with the results of Rao and Baldeschwieler (4) for 2-amino-3-picoline.

EXPERIMENTAL

The n.m.r. spectra were obtained with a Varian high-resolution spectrometer operating at 100 Mc/s. The spectra were calibrated by the usual side-band method (7), using a Hewlett–Packard Model 200AB audio-oscillator and a Hewlett–Packard Model 521C frequency counter. The double-resonance experiments were carried out as described by Johnson (8). With the center-band signal phased out, the first modulation side band H_1 of the V3521 Integrator is used to record the n.m.r. spectrum while a second, stronger side band, H_2, provided by an audio-oscillator, is applied to the system under investigation such that $|\omega_2-\omega_1|$ is equal to the separation necessary to do the double-resonance experiment. The output of the oscillator is quite critical (3). The ratios of the chemical shifts to the coupling constants in the present instances were sufficiently large that corrections to the modulation frequency were unnecessary (9). The frequency of the first modulation side band of the Integrator varied slightly from day to day and was checked before each experiment. As a check on the method, the results reported by Freeman (3) for *trans*-crotonaldehyde were repeated and duplicated.

Quinoline (synthetic grade) was obtained from Matheson, Coleman, and Bell and degassed by the nitrogen bubbling technique prior to the n.m.r. measurements.

ACKNOWLEDGMENT

The financial support of the National Research Council is gratefully acknowledged.

1. D. F. EVANS and J. P. MAHER. Proc. Chem. Soc. 208 (1961).
2. R. FREEMAN and D. H. WHIFFEN. Mol. Phys. **4**, 321 (1961).
3. R. FREEMAN. Mol. Phys. **4**, 385 (1961).
4. B. D. N. RAO and J. D. BALDESCHWIELER. J. Chem. Phys. **37**, 2473 (1962).
5. J. A. POPLE, W. G. SCHNEIDER, and H. J. BERNSTEIN. High-resolution nuclear magnetic resonance. McGraw-Hill Book Co., Inc., New York. 1959.
6. T. SCHAEFER. Can. J. Chem. **39**, 1864 (1961).
7. J. T. ARNOLD and M. E. PACKARD. J. Chem. Phys. **19**, 1608 (1951).
8. L. F. JOHNSON. Varian Associates Publication No. 87-100-082. Palo Alto, California. August, 1962.
9. D. W. TURNER. J. Chem. Soc. 847 (1962).

RECEIVED MARCH 1, 1963.
DEPARTMENT OF CHEMISTRY,
UNIVERSITY OF ALBERTA,
EDMONTON, ALBERTA.

Can. J. Chem. Downloaded from www.nrcresearchpress.com by 210.87.254.6 on 09/05/12
For personal use only.

SELF-CONDENSATION OF METHYL PROPIOLATE

ERNEST WENKERT, K. A. H. ADAMS, AND CURTIS L. LEICHT

When during the course of a study of alkaloid synthesis methyl propiolate was observed to undergo a chemical change in the presence of a tertiary amine, this unusual reaction was investigated. Exposure of a benzene solution of the ester to triethylamine, N-methylpyrrolidine, or N-methylpiperidine for a short period of time gave good yields of a dimer. Elemental, infrared, ultraviolet, and proton magnetic resonance analysis of the product

as well as its conversion to dimethyl adipate on catalytic hydrogenation revealed the compound to be dimethyl *trans*-but-1-ene-3-ine-1,4-dicarboxylate (I) (1, 2). In some reactions a side product was formed. Its analyses as well as its transformation to dimethyl β-oxy-bis-propionate (3) on catalytic hydrogenation showed it to be dimethyl *trans*-β-oxy-bis-acrylate (II). Since this product reflected intervention of water in the reaction, its yield was expected, and then shown to increase on deliberate addition of water to the reaction medium.

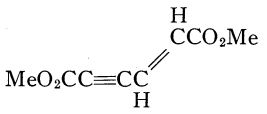

I

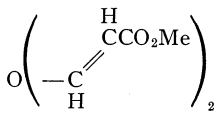

II

Whereas the hydrogen abstraction (4, 5) and the Michael addition (6) processes responsible for the formation of I have known precedents, the present case represents an interesting example of a combination of these reactions of the same propiolyl system and appears to be a high-yielding variation of the dimerization of acetylenes to en-ines under the influence of cuprous salts and acid (2, 7). Unfortunately there seems to be a subtle competition between the dimerization and polymerization of the conjugated ethynylcarbonyl substrate, as an unsuccessful attempt to bring about the dimerization of methyl ethinyl ketone illustrated.

EXPERIMENTAL

All melting points were observed on a Kofler microscope hot stage. Ultraviolet spectra were run on 95% ethanol solutions on a Cary model 12 spectrophotometer, while infrared spectra were obtained on a Perkin–Elmer model 21 spectrophotometer. Proton magnetic resonance spectra were measured on deuterochloroform solutions with tetramethylsilane as internal standard on a Varian A-60 spectrometer.

Dimethyl trans-But-1-ene-3-ine-1,4-dicarboxylate (I)

A cooled solution of 0.5 g of N-methylpiperidine in 5 ml of dry benzene was added over a 20-minute period to a cold solution of 500 mg of methyl propiolate in 5 ml of dry benzene and the mixture was stirred for 1.5 hours over nitrogen while being kept cold. Evaporation of the brown solution left a brown solid, 451 mg. Its extraction with hot hexane, evaporation of the extract, and sublimation of the residue yielded 440 mg (88%) of the diester I, m.p. 53–54° (lit. (1) m.p. 53°; (2) 57°); μ (KBr) C≡C 4.47 (m), C=O 5.81 (s), C=C 6.14 (m); λ_{max} 245 mμ (log ϵ 4.17), 254 mμ (log ϵ 4.22), and 267 mμ (log ϵ 4.08); δ two one-proton doublets 6.87 p.p.m. (J = 16 c.p.s.), 6.46 p.p.m. (J = 16 c.p.s.), two three-proton singlets 3.83 p.p.m., 3.81 p.p.m.

Anal. Calc. for $C_8H_8O_4$: C, 57.14; H, 4.80. Found: C, 57.09; H, 4.70.

Addition of some water to the hot methanol extract of the residue of the above hexane extraction induced the separation of a small quantity of solid whose gas-phase chromatographic retention time was identical with that of II (*vide infra*).

The use of N-methylpyrrolidine led to similar results, while triethylamine gave only 30–40% yields of I accompanied by black polymer, presumably polypropiolate.

Hydrogenation of a methanolic solution of I, 21 mg, and 10 mg of palladium–charcoal at atmospheric pressure and room temperature yielded 20 mg of dimethyl adipate, identified by comparison of the product's infrared and p.m.r. spectra and gas-phase chromatography retention time with those of an authentic sample.

Dimethyl trans-β-Oxy-bis-acrylate (II)

A cooled solution of 0.21 ml of N-methylpyrrolidine in 5 ml of benzene saturated with water was added over a 20-minute interval to a cold solution of 400 mg of methyl propiolate in 6 ml of benzene saturated with water and the mixture was stirred for 1.5 hours over nitrogen while being kept cold. After filtration of the resultant precipitate the mixture was evaporated and the residue extracted repeatedly with hot hexane. Evaporation of the extract and crystallization of the residual solid from ethyl acetate and from aqueous methanol gave 212 mg (45%) of white needles of the diester II, m.p. 158–159°; μ (KBr) C=O 5.82 (s), C=C 6.11 (s); λ_{max} 253 mμ (log ϵ 4.49); δ two two-proton doublets 7.67 p.p.m. (J = 12 c.p.s.), 5.71 p.p.m. (J = 12 c.p.s.), six-proton singlet, 3.79 p.p.m.

Anal. Calc. for $C_8H_{10}O_5$: C, 51.61; H, 5.41. Found: C, 51.81; H, 5.51.

The use of N-methylpiperidine led to higher yields (60–70%). Neither reaction mixture revealed any detectable amounts of ester I.

Can. J. Chem. Downloaded from www.nrcresearchpress.com by 210.87.254.6 on 09/05/12
For personal use only.

Hydrogenation of a methanolic solution of 53 mg of II and 20 mg of palladium–charcoal at atmospheric pressure and room temperature yielded 51 mg of dimethyl β-oxy-bis-propionate, identified by comparison of the product's infrared and p.m.r. spectra and gas-phase chromatographic behavior with those of an authentic sample (3).

ACKNOWLEDGMENT

The authors are indebted to the U.S. Public Health Service for support by grant MY-5815.

1. I. HEILBRON, E. R. H. JONES, and F. SONDHEIMER. J. Chem. Soc. 604 (1949).
2. L. SKATTEBOL. Acta Chem. Scand. **13**, 198 (1959).
3. I. N. NAZAROV, G. A. SHVEKHGEIMER, and V. A. RUDENKO. J. Gen. Chem. USSR. **24**, 329 (1954).
4. A. BHATI. J. Org. Chem. **27**, 2135 (1962) and references cited therein.
5. E. H. INGOLD. J. Chem. Soc. **127**, 1199 (1925).
6. J. L. SIMONSON. J. Chem. Soc. **97**, 1910 (1910).
7. R. F. GARWOOD, E. OSKAY, and B. C. L. WEEDON. Chem. Ind. (London), 1684 (1962).

RECEIVED FEBRUARY 21, 1963.
DEPARTMENT OF CHEMISTRY,
INDIANA UNIVERSITY,
BLOOMINGTON, INDIANA, U.S.A.

Can. J. Chem. Downloaded from www.nrcresearchpress.com by 210.87.254.6 on 09/05/12
For personal use only.

THE KINETICS OF THE TRIBUTYLAMINE-CATALYZED REACTION OF PHENYL ISOCYANATE WITH 1-BUTANETHIOL IN VARIOUS SOLVENTS

YOSHIO IWAKURA AND HISAO OKADA

In a previous paper (1), we reported the kinetics of the tertiary-amine-catalyzed reaction of organic isocyanate with thiols, and discussed the kinetic scheme of this reaction. In the present work, the kinetics of the tributylamine-catalyzed reaction of phenyl isocyanate with 1-butanethiol was studied in detail in various solvents at 25–45°.

The catalytic coefficients of the tributylamine-catalyzed reaction of phenyl isocyanate with 1-butanethiol in various solvents at 25° are summarized in Table I. The dielectric constants of the solvents are also listed in Table I, and compared with the catalytic coefficients. The reaction rate is found to depend generally upon the dielectric constant of the solvent, but a definite relationship between the dielectric constant of the solvent and the catalytic coefficient cannot be found. If the solvents are classified as aromatic or aliphatic, the aromatic solvents have higher reactivity, e.g., cyclohexane < toluene < benzene; ethyl acetate < ethyl benzoate.

In solvents with high-valued dielectric constants (more than about 10), such as 1,2-dichloroethane, cyclohexanone, acetone, and nitrobenzene, the reaction rate is not applicable to ordinary second-order kinetics, and deviates downwards from the plot of the ordinary second-order reaction rate equation according to the increase of the conversion.* In the case of these highly polar solvents, the rate constant was calculated on the initial reaction, and listed in Table I.

The dependency of the catalytic coefficient upon the reaction temperature was studied

Dyer et al. (2(b)) have reported that the reaction rate of the tertiary-amine-catalyzed reaction between phenyl isocyanate and thiols deviated upwards from the plot of the ordinary second-order kinetics in the solvents examined, e.g. toluene, butyl acetate, nitrobenzene, and acetonitrile. Further, they have suggested the following overall rate equation on the tertiary-amine-catalyzed reaction of phenyl isocyanate with thiols:

$$k_e = k_0 + k_b[\text{base}] + k_p[\text{product}] + k_{bp}[\text{base}][\text{product}], \qquad [1]$$

where k_e is the experimental second-order rate constant, k_b, k_p, and k_{bp} are the catalytic rate constant for the base, product, and base–product catalyzed reaction, respectively.

Hydrogenation of a methanolic solution of 53 mg of II and 20 mg of palladium–charcoal at atmospheric pressure and room temperature yielded 51 mg of dimethyl β-oxy-bis-propionate, identified by comparison of the product's infrared and p.m.r. spectra and gas-phase chromatographic behavior with those of an authentic sample (3).

ACKNOWLEDGMENT

The authors are indebted to the U.S. Public Health Service for support by grant MY-5815.

1. I. HEILBRON, E. R. H. JONES, and F. SONDHEIMER. J. Chem. Soc. 604 (1949).
2. L. SKATTEBOL. Acta Chem. Scand. **13**, 198 (1959).
3. I. N. NAZAROV, G. A. SHVEKHGEIMER, and V. A. RUDENKO. J. Gen. Chem. USSR. **24**, 329 (1954).
4. A. BHATI. J. Org. Chem. **27**, 2135 (1962) and references cited therein.
5. E. H. INGOLD. J. Chem. Soc. **127**, 1199 (1925).
6. J. L. SIMONSON. J. Chem. Soc. **97**, 1910 (1910).
7. R. F. GARWOOD, E. OSKAY, and B. C. L. WEEDON. Chem. Ind. (London), 1684 (1962).

RECEIVED FEBRUARY 21, 1963.
DEPARTMENT OF CHEMISTRY,
INDIANA UNIVERSITY,
BLOOMINGTON, INDIANA, U.S.A.

THE KINETICS OF THE TRIBUTYLAMINE-CATALYZED REACTION OF PHENYL ISOCYANATE WITH 1-BUTANETHIOL IN VARIOUS SOLVENTS

YOSHIO IWAKURA AND HISAO OKADA

In a previous paper (1), we reported the kinetics of the tertiary-amine-catalyzed reaction of organic isocyanate with thiols, and discussed the kinetic scheme of this reaction. In the present work, the kinetics of the tributylamine-catalyzed reaction of phenyl isocyanate with 1-butanethiol was studied in detail in various solvents at 25–45°.

The catalytic coefficients of the tributylamine-catalyzed reaction of phenyl isocyanate with 1-butanethiol in various solvents at 25° are summarized in Table I. The dielectric constants of the solvents are also listed in Table I, and compared with the catalytic coefficients. The reaction rate is found to depend generally upon the dielectric constant of the solvent, but a definite relationship between the dielectric constant of the solvent and the catalytic coefficient cannot be found. If the solvents are classified as aromatic or aliphatic, the aromatic solvents have higher reactivity, e.g., cyclohexane < toluene < benzene; ethyl acetate < ethyl benzoate.

In solvents with high-valued dielectric constants (more than about 10), such as 1,2-dichloroethane, cyclohexanone, acetone, and nitrobenzene, the reaction rate is not applicable to ordinary second-order kinetics, and deviates downwards from the plot of the ordinary second-order reaction rate equation according to the increase of the conversion.* In the case of these highly polar solvents, the rate constant was calculated on the initial reaction, and listed in Table I.

The dependency of the catalytic coefficient upon the reaction temperature was studied

Dyer et al. (2(b)) have reported that the reaction rate of the tertiary-amine-catalyzed reaction between phenyl isocyanate and thiols deviated upwards from the plot of the ordinary second-order kinetics in the solvents examined, e.g. toluene, butyl acetate, nitrobenzene, and acetonitrile. Further, they have suggested the following overall rate equation on the tertiary-amine-catalyzed reaction of phenyl isocyanate with thiols:

$$k_e = k_0 + k_b[\text{base}] + k_p[\text{product}] + k_{bp}[\text{base}][\text{product}], \qquad [1]$$

where k_e is the experimental second-order rate constant, k_b, k_p, and k_{bp} are the catalytic rate constant for the base, product, and base–product catalyzed reaction, respectively.

TABLE I

The reaction of phenyl isocyanate with 1-butanethiol in the presence of tributylamine in various solvents at 25° *

Solvent	Concn. of tributylamine (mole/liter)	Dielectric constant at 25° †	Catalytic coefficient‡ (liter²/mole² min)
Hydrocarbons			
Cyclohexane	0.01–0.02	2.220	0.195
Toluene	0.0025–0.0050	2.379	19.1
Benzene	0.0025–0.0050	2.274	37.1
Halogenated hydrocarbons			
1-Chlorobutane	0.0025–0.0050	7.39§	52.0
1,2-Dichloroethane	0.000625	10.36	982
Chlorobenzene	0.00125–0.00250	5.621	155
o-Dichlorobenzene	0.00125–0.00500	9.93	173
Ethers			
Dibutyl ether	0.0050–0.0100	3.06	3.26
Tetrahydrofuran	0.00375–0.00750	7.39	64.0
p-Dioxane	0.00125–0.00500	2.209	77.6
Anisole	0.00125–0.00500	4.33	265
Ketones			
Cyclohexanone	0.00125–0.00250	18.3	383
Acetone	0.000125–0.000250	20.7	2375
Esters			
Ethyl acetate	0.00125–0.00250	6.02	114.4
Ethyl benzoate	0.00125–0.00250	5.98	242.3
Nitro compound			
Nitrobenzene	0.00060–0.00125	34.82	2160

*Initial concentration of phenyl isocyanate and 1-butanethiol: $[C_6H_5NCO] = [n\text{-}C_4H_9SH] = 0.2500$ mole/liter in toluene, benzene, chlorobenzene, *p*-dioxane, and anisole; 0.1250 mole/liter in the other solvents.
†Quoted from A. Weissberger, Organic Solvents, Interscience Publishers Inc., New York, 1955, pp. 270–274; and Landolt-Börnstein, Zahlenwerte und Funktionen aus Physik, Chemie, Astronomie, Geophysik, Technik, II, Band 6, 1959.
‡Average value of the results in two or three different tributylamine concentrations.
§Value at 20°.

in several solvents at 25°, 35°, and 45°. The apparent energies of activation and log A were calculated by the Arrhenius equation, and are listed in Table II.

TABLE II

The dependency of the catalytic coefficients upon reaction temperature in the tributylamine-catalyzed reaction of phenyl isocyanate with 1-butanethiol in several solvents

Solvent	Catalytic coefficient (liter²/mole² min) 25°	35°	45°	Apparent energies of activation (kcal/mole)	log A (A in liter²/mole² min)
p-Dioxane	77.6	72.0	58.7	−2.6±0.8	−0.02±0.53
Benzene	37.0	34.1	29.1	−2.3±0.5	−0.11±0.34
Toluene	19.1	19.3	16.8	−1.2±0.8	0.04±0.57
Anisole	265	176	199	−2.8±2.8	0.35±2.01
Chlorobenzene	155	145	143	−0.8±0.3	1.62±0.20
Tetrahydrofuran	64.0	57.3	55.6	−1.3±0.4	0.82±0.29
o-Dichlorobenzene	173	155	141	−1.9±0.2	0.81±0.12

In benzene solution, the apparent activation energy of the tributylamine-catalyzed reaction of phenyl isocyanate with 1-butanethiol is −2.3 kcal/mole, as shown in Table II. On the other hand, it is 2.7 kcal/mole for the reaction with 1-butanol (both 0.250 mole/liter) (log A = −0.48, A in liter²/mole² min) (3). Therefore, if the reaction mechanism suggested previously (1) is simplified as shown in equations [2] and [3], and the activation

energy of k_3, and k_4, is expressed as E_3, and E_4, respectively, E_3 is nearly equal to $E_4-5.0$ kcal/mole.

$$R—N=C=O + R_3N \underset{k_2}{\overset{k_1}{\rightleftharpoons}} \left(\begin{matrix} R—N=C=O \\ \vdots \\ NR_3 \end{matrix} \right) \text{(complex)} \qquad [2]$$

$$\text{complex} + R—SH \xrightarrow{k_3} R—NHC(=O)S—R + R_3N \qquad [3]$$

$$\text{complex} + R—OH \xrightarrow{k_4} R—NHC(=O)O—R + R_3N \qquad [4]$$

EXPERIMENTAL

Procedure

The detailed kinetic method has been described previously (1). As shown in Table III, reproducibility of the experiments was good and agreement of duplicate runs was within ±2%.

TABLE III

Reproducibility of the tributylamine-catalyzed reaction of phenyl isocyanate with 1-butanethiol
(Initial concentration: [C_6H_5NCO] = [n-C_4H_9SH] = 0.2500 mole/liter)

Solvent	Reaction temperature (±0.02°)	Concn. of tributylamine (mole/liter)	Second-order rate constant (liter/mole min)	Catalytic coefficient (liter²/mole² min)
p-Dioxane	35	0.004827	0.349 ±0.003	72.3
		0.002413	0.176 ±0.002	72.8
		0.002525	0.179 ±0.002	71.0
Benzene	35	0.005115	0.178 ±0.002	34.7
		0.002557	0.0870±0.0008	34.0
		0.002462	0.0827±0.0009	33.6
Benzene	45	0.005380	0.162 ±0.003	30.1
		0.002690	0.0764±0.0008	28.4
		0.005517	0.160 ±0.002	28.9
		0.002758	0.0802±0.0008	29.1

Materials

The solvents used were purified carefully in the usual manner (4).

Cyclohexane was passed through a 1-m, 20 mm i.d. column packed with silica gel to remove a small amount of benzene contained in the commercial reagent, and distilled from sodium. Tetrahydrofuran was well shaken with a paste of ferrous sulphate and a small amount of concentrated sulphuric acid to remove the peroxide. It was neutralized with sodium hydroxide and dried over calcium chloride, and then boiled under reflux with sodium and distilled from the sodium. Cyclohexanone was shaken with a 5% solution of potassium bichromate in sulphuric acid, and washed with water and fractionally distilled twice under reduced pressure. The main portion of the distillate was dried over sodium sulphate and distilled under reduced pressure. Acetone was thoroughly shaken with a small amount of powdered potassium permanganate and allowed to stand for 4 days. After being distilled, the product was dried over potassium carbonate and distilled. Ethyl benzoate was synthesized from benzoic acid and ethanol, and distilled under reduced pressure.

1. Y. IWAKURA and H. OKADA. Can. J. Chem. **38**, 2418 (1960).
2. (*a*) E. DYER and J. F. GLENN. J. Am. Chem. Soc. **79**, 366 (1957).
   (*b*) E. DYER, J. F. GLENN, and E. G. LENDRAT. J. Org. Chem. **26**, 2919 (1961).
3. Y. IWAKURA and H. OKADA. Bull. Tokyo Inst. Technol. In press.
4. (*a*) L. F. FIESER. Experiments in organic chemistry. D. C. Heath & Co., New York. 1955.
   (*b*) T. KUWATA. Yoozai (Solvents). Maruzen Co. Ltd., Tokyo. 1947.
   (*c*) A. WEISSBERGER. Organic solvents. Interscience Publishers Inc., New York. 1955.

RECEIVED OCTOBER 23, 1962.
RESEARCH LABORATORY OF RESOURCES UTILIZATION,
TOKYO INSTITUTE OF TECHNOLOGY,
OOKAYAMA, MEGURO-KU,
TOKYO, JAPAN.

PRESSURE EFFECT AND MECHANISM IN ACID CATALYSIS XIII. HYDROLYSIS OF METHYL α-D-GLUCOPYRANOSIDE[1]

R. J. WITHEY[2] AND E. WHALLEY

The rate of the acid-catalyzed hydrolysis of methyl α-D-glucopyranoside in concentrated acid (1) has been interpreted to indicate both that the slow step is unimolecular (1) and probably that it is bimolecular (2). There is little doubt now that the Zucker–Hammett hypothesis, on which the first suggestion was based, is invalid, and there are enough exceptions (1, 3) to Bunnett's (2) criterion for it to be unreliable. Because the volume of activation can distinguish between the unimolecular and bimolecular slow steps in acid catalysis (4) we have measured the effect of pressures up to 3 kbar on the rate of hydrolysis.

EXPERIMENTAL METHODS AND RESULTS

The methyl α-D-glucopyranoside was a commercial sample having $[\alpha]_D^{22}$ +157.8°, and this was unchanged after recrystallization three times from ethanol. Reagent grade perchloric acid, 0.518 *M* at room temperature and pressure, was used as catalyst, and about 3 g of the glucoside in 100 cm³ of acid solution was used in each run. The optical rotation, which was measured in a 4-dm 5-cm³ polarimeter tube, changed by about 6° during each run. A Rudolph model 70 polarimeter which was reproducible to 0.01° was used. The pressure techniques have been described previously (5).

About six samples were obtained for each run. Good values of the final rotation could not be obtained at 100° due to slight coloring which occurred during the long times required, but which was inappreciable during the 10 hours or so required for a run. The final rotation was therefore obtained by hydrolyzing the glucoside in 2.6 *M* perchloric acid at 100° C for 3 hours. It agreed within the experimental error with the value calculated from the reported rotation of the products.

The first-order rate constants k_1, and the second-order rate constants k_a for which the concentration of acid was corrected for thermal expansion and compression as if it were pure water (6), are summarized in Table I. The rate constant at ordinary pressure is reasonably consistent with those reported for lower temperatures (1, 7).*

TABLE I

Rate constants for the acid-catalyzed hydrolysis of methyl α-D-glucopyranoside in 0.518 *M* (at room temperature and pressure) perchloric acid at 100.00° C

p/bar	$10^6 k_1$/sec^{-1}	$10^6 k_a$/l. mole^{-1} sec^{-1}
1	166	334
1000	148	286
2000	128	239
2000	129	241
3000	114	207

[1]*Issued as N.R.C. No. 7355.*

[2]*N.R.C. Postdoctoral Fellow 1960–1962.*

**A reviewer has suggested that side reactions of D-glucose, such as acid reversion and formation of anhydrides, may affect the apparent rate constants. The maximum extent (S. Peat, W. J. Whelan, T. E. Edwards, and O. Owen, J. Chem. Soc. 586 (1958), and earlier work referred to there) of these reactions under our conditions is less than 1% at atmospheric pressure and it is unlikely to be much greater under pressure. They will therefore have no great effect on our rate constants. The fact that the reaction is accurately first order and that the rotation of the fully hydrolyzed solution agrees within experimental error with that calculated from the initial concentration and rotation of methyl α-D-glucopyranoside and the specific rotation of α-D-glucose confirms this.*

Can. J. Chem. Downloaded from www.nrcresearchpress.com by 210.87.254.42 on 09/05/12
For personal use only.

The volume of activation $\Delta V^{\neq}$, calculated from the usual relation

$$\partial \ln k_a/\partial p = -\Delta V^{\neq}/RT,$$

where R is the gas constant and T the temperature, is $5.1 \pm \sim 0.5$ cm^3 mole^{-1} at 100° C.

DISCUSSION

The volume of activation of $5.1 \pm \sim 0.7$ cm^3 mole^{-1} indicates that the mechanism is unimolecular, i.e. if G represents methyl α-D-glucopyranoside, then if the first step is assumed to be

$$H_3O^+ + G \rightleftharpoons H_2O + GH^+, \text{ equilibrium,}$$

the second step is

$$GH^+ \xrightarrow{\text{slow}} \text{products.}$$

Further details of the slow step are uncertain (1). The entropy of activation, which is reported (7) to be 13.8 cal deg^{-1} mole^{-1}, is consistent with the unimolecular mechanism (4).

Bunnett (2) has recently suggested a modification of the Zucker–Hammett hypothesis and from it suggested that methyl α-D-glucopyranoside hydrolyzes by a bimolecular mechanism. The evidence from the volume of activation disagrees with this suggestion.

1. C. A. Bunton, T. A. Lewis, D. R. Llewellyn, and C. A. Vernon. J. Chem. Soc. 4419 (1955).
2. J. F. Bunnett. J. Am. Chem. Soc. **83**, 4956 (1961).
3. A. R. Osborn and E. Whalley. Can. J. Chem. **39**, 597 (1961). R. J. Withey and E. Whalley. Can. J. Chem. **41**, 546 (1963).
4. E. Whalley. Trans. Faraday Soc. **55**, 798 (1959) and later papers.
5. J. Koskikallio and E. Whalley. Trans. Faraday Soc. **55**, 809 (1959). A. R. Osborn and E. Whalley. Can. J. Chem. **39**, 1094 (1961).
6. P. W. Bridgman. Proc. Am. Acad. Arts Sci. **66**, 185 (1931).
7. C. Armour, C. A. Bunton, S. Patai, L. H. Selman, and C. A. Vernon. J. Chem. Soc. 412 (1961).

Received October 12, 1962.
Division of Applied Chemistry,
National Research Council,
Ottawa, Canada.

PROTON RESONANCE SPECTRA OF VINYL-METALLIC COMPOUNDS
PART II. HEXAVINYLDIGERMANE

S. Cawley and S. S. Danyluk

Considerable interest has centered recently on the dependence of cis, trans, and gem coupling constants for vinyl compounds upon the electronegativity of the substituent group. Schaefer (1) has reported a linear correlation of J_{cis}, J_{trans}, J_{gem} and their sum with electronegativities of the substituent group for a wide range of vinyl compounds. Similar correlations have also been observed independently by Waugh and Castellano (2) and Banwell and Sheppard (3). The significance of correlations of this type in sorting out unacceptable values for coupling constants in the analysis of proton resonance spectra is readily apparent. For example, Castellano and Waugh (4) recently utilized the constancy of $J_{cis}+J_{trans}+J_{gem}$ as a criterion for rejection of spectral assignments for tetravinylsilane which yielded spacings whose sum was significantly different from 38.2 c/s.

Can. J. Chem. Downloaded from www.nrcresearchpress.com by 210.87.254.42 on 09/05/12
For personal use only.

The volume of activation $\Delta V^{\neq}$, calculated from the usual relation

$$\partial \ln k_a/\partial p = -\Delta V^{\neq}/RT,$$

where R is the gas constant and T the temperature, is $5.1 \pm \sim 0.5$ cm^3 mole^{-1} at 100° C.

DISCUSSION

The volume of activation of $5.1 \pm \sim 0.7$ cm^3 mole^{-1} indicates that the mechanism is unimolecular, i.e. if G represents methyl α-D-glucopyranoside, then if the first step is assumed to be

$$H_3O^+ + G \rightleftharpoons H_2O + GH^+, \text{ equilibrium,}$$

the second step is

$$GH^+ \xrightarrow{\text{slow}} \text{products.}$$

Further details of the slow step are uncertain (1). The entropy of activation, which is reported (7) to be 13.8 cal deg^{-1} mole^{-1}, is consistent with the unimolecular mechanism (4).

Bunnett (2) has recently suggested a modification of the Zucker–Hammett hypothesis and from it suggested that methyl α-D-glucopyranoside hydrolyzes by a bimolecular mechanism. The evidence from the volume of activation disagrees with this suggestion.

1. C. A. Bunton, T. A. Lewis, D. R. Llewellyn, and C. A. Vernon. J. Chem. Soc. 4419 (1955).
2. J. F. Bunnett. J. Am. Chem. Soc. **83**, 4956 (1961).
3. A. R. Osborn and E. Whalley. Can. J. Chem. **39**, 597 (1961). R. J. Withey and E. Whalley. Can. J. Chem. **41**, 546 (1963).
4. E. Whalley. Trans. Faraday Soc. **55**, 798 (1959) and later papers.
5. J. Koskikallio and E. Whalley. Trans. Faraday Soc. **55**, 809 (1959). A. R. Osborn and E. Whalley. Can. J. Chem. **39**, 1094 (1961).
6. P. W. Bridgman. Proc. Am. Acad. Arts Sci. **66**, 185 (1931).
7. C. Armour, C. A. Bunton, S. Patai, L. H. Selman, and C. A. Vernon. J. Chem. Soc. 412 (1961).

Received October 12, 1962.
Division of Applied Chemistry,
National Research Council,
Ottawa, Canada.

PROTON RESONANCE SPECTRA OF VINYL-METALLIC COMPOUNDS
PART II. HEXAVINYLDIGERMANE

S. Cawley and S. S. Danyluk

Considerable interest has centered recently on the dependence of cis, trans, and gem coupling constants for vinyl compounds upon the electronegativity of the substituent group. Schaefer (1) has reported a linear correlation of J_{cis}, J_{trans}, J_{gem} and their sum with electronegativities of the substituent group for a wide range of vinyl compounds. Similar correlations have also been observed independently by Waugh and Castellano (2) and Banwell and Sheppard (3). The significance of correlations of this type in sorting out unacceptable values for coupling constants in the analysis of proton resonance spectra is readily apparent. For example, Castellano and Waugh (4) recently utilized the constancy of $J_{cis}+J_{trans}+J_{gem}$ as a criterion for rejection of spectral assignments for tetravinylsilane which yielded spacings whose sum was significantly different from 38.2 c/s.

Can. J. Chem. Downloaded from www.nrcresearchpress.com by 210.87.254.40 on 09/05/12
For personal use only.

Relatively few proton resonance measurements have been reported for vinyl-metallic compounds and the coupling constants for several vinyl-metallics (5) included in Schaefer's correlations are open to question (6). Since electronegativities for many of the metals fall in the range 1.5 to 2.0 additional data for compounds of this type would provide a further test of the empirical correlations. In particular, no spectra have been published for vinylgermanes and in this note we wish to report the proton resonance spectrum, coupling constants, and chemical shifts for hexavinyldigermane.

Spectra were measured with a Varian A-60 spectrometer at room temperature (23±1° C) with a drop of tetramethylsilane serving as internal reference. A commercial sample of hexavinyldigermane (Metallomer Labs, Maynard, Mass.) was used without further purification. A small amount of vinyl impurity (estimated as less than 5%) was noted. Spectra were measured for the neat compound and for 5 vol% solutions in carbon tetrachloride, acetone, and acetonitrile. No detectable changes were observed for the vinyl protons in these solvents and only a very slight change, amounting to shifts of 1 c/s, was noted for the strong peaks when the concentration was varied from 0 to 100% in acetone.

Figure 1 shows the spectrum for hexavinyldigermane in acetone (10%) and indicates a

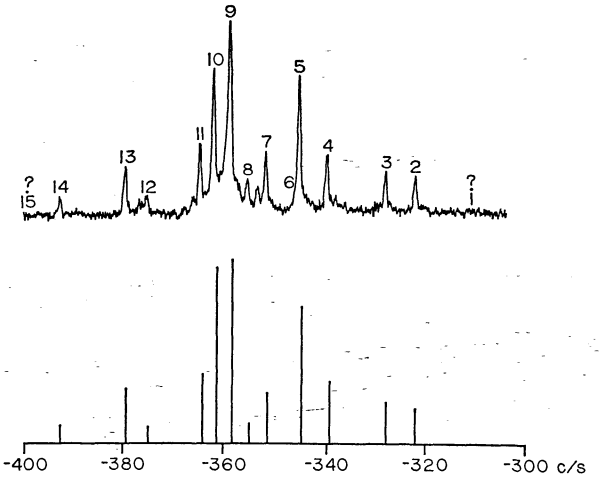

FIG. 1. Observed and calculated proton resonance spectrum for 10 vol% hexavinyldigermane in acetone (relative to tetramethylsilane as internal standard).

partially collapsed ABC pattern for the vinyl protons. A summary of the chemical shifts and coupling constants is given in Table I along with a comparison of observed and calculated frequencies. The structural parameters were computed by an iterative procedure* and are precise to ±0.001 p.p.m. for δ's and ±0.08 c/s for the J's. Very good agreement is obtained between calculated and observed frequencies—the latter representing the mean value of five spectra. Similar agreement is noted for the intensities (Fig. 1) except for the peaks at −361.35 and −358.12 c/s. The discrepancies can be attributed to vinyl impurities present in the hexavinyldigermane. A satisfactory fit of the spectrum could not be obtained if the peaks at 352.5 and 376.0 c/s were incorporated in the calculations and these are therefore ascribed to impurities.

The magnitudes of the coupling constants are almost identical, within experimental error, with those observed for tetravinylgermane and triphenylvinylgermane (7). Both

*The authors are indebted to Dr. J. D. Swalen for providing the computer program.

Can. J. Chem. Downloaded from www.nrcresearchpress.com by 210.87.254.40 on 09/05/12
For personal use only.

TABLE I

N.M.R. structural parameters for hexavinyldigermane

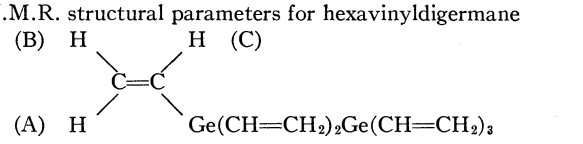

Line		Frequency	
		Obs.	Calc.
1	Combination line	—	310.93
2		321.10	321.08
3		327.02	326.99
4		338.52	338.42
5		344.26	344.34
6		—	345.59
7		351.60	351.50
8	Combination line	354.47	354.49
9		358.58	358.65
10		361.53	361.65
11		364.51	364.56
12		374.86	374.71
13		379.06	378.99
14		392.04	392.06
15	Combination line	—	399.22

$J_{AB} = 2.93 \pm 0.08$ c/s $\quad \delta_A = -335.56 \pm 0.10$ c/s

$J_{AC} = 20.07 \pm 0.09$ c/s $\quad \delta_B = -357.46 \pm 0.10$ c/s

$J_{BC} = 13.32 \pm 0.09$ c/s $\quad \delta_C = -371.61 \pm 0.10$ c/s

J_{gem}, 2.93 ± 0.08 c/s, and the sum of the three coupling constants, 36.32 ± 0.09 c/s, for hexavinyldigermane are significantly lower than the corresponding values for the vinyl-silanes, 3.6 to 3.9 c/s (7, 8) and 38.8 c/s (4, 8) respectively. This decrease in the sum of the J's parallels the slight increase in electronegativity in going from Si ($E_n = 1.90$) to Ge ($E_n = 2.00$) (9). A good fit of both J_{gem} and $J_{gem} + J_{cis} + J_{trans}$ to Schaefer's empirical correlations (1) is noted for hexavinyldigermane. This provides a further check on the correctness of the three coupling constants obtained in the numerical analysis.

The chemical shifts are all considerably lower than those for alkenes (10) and vary in the same order as observed for vinyl-silanes (8) and other vinyl-germanes (7), i.e., $\alpha <$ trans $<$ cis.* The insensitivity of the shifts to polar solvents (acetone, acetonitrile) indicates that the shielding is not due to any permanent electric field within the molecules as has been proposed for alkenes (10). Nor is it possible to attribute the low-field shifts to inductive interaction of the trigonal C atom with the Ge since the lower electronegativity of Ge would lead to shifts in the opposite direction. Similar low-field shifts (relative to alkenes) for substituted vinyl-silanes (8) have been attributed qualitatively to $d_\pi - p_\pi$ interaction between Si and the trigonal C. Although an analogous interaction is possible in hexavinyldigermane further work is required to sort out the magnitude of this contribution.

ACKNOWLEDGMENTS

The financial assistance of the National Research Council of Canada and the Advisory Committee on Scientific Research at the University of Toronto is gratefully acknowledged. The authors are also indebted to the Institute of Computer Science, University of Toronto, for use of the IBM 7090 computer.

*Here 'cis' and 'trans' refer to the proton position relative to Ge.

Can. J. Chem. Downloaded from www.nrcresearchpress.com by 210.87.254.40 on 09/05/12
For personal use only.

1. T. SCHAEFER. Can. J. Chem. **40**, 1 (1962).
2. J. S. WAUGH and S. CASTELLANO. J. Chem. Phys. **35**, 1900 (1961).
3. C. N. BANWELL and N. SHEPPARD. Mol. Phys. **3**, 350 (1960).
4. S. CASTELLANO and J. S. WAUGH. J. Chem. Phys. **37**, 1951 (1962).
5. W. BRÜGEL, TH. ANKEL, and F. KRÜCKEBERG. Z. Electrochem. **64**, 1121 (1960).
6. S. CAWLEY and S. S. DANYLUK. Unpublished results.
7. S. CAWLEY and S. S. DANYLUK. J. Chem. Phys. In press.
8. R. T. HOBGOOD, J. H. GOLDSTEIN, and G. S. REDDY. J. Chem. Phys. **35**, 2038 (1961).
9. A. L. ALLRED and E. G. ROCHOW. J. Inorg. Nucl. Chem. **5**, 269 (1958).
10. A. A. BOTHNER-BY and C. NAAR-COLIN. J. Am. Chem. Soc. **83**, 231 (1961).

RECEIVED MARCH 7, 1963.
DEPARTMENT OF CHEMISTRY,
UNIVERSITY OF TORONTO,
TORONTO, ONTARIO.

Can. J. Chem. Downloaded from www.nrcresearchpress.com by 210.87.254.40 on 09/05/12
For personal use only.

SYMMETRIZATION OF SPIN FUNCTIONS FOR THREE EQUIVALENT SPIN 1/2 NUCLEI BY MEANS OF THE POINT GROUP C_3

T. SCHAEFER AND F. HRUSKA

As is well known, group theoretical methods are very useful in simplifying calculations involving the diagonalization of operator matrices. The analyses of high-resolution nuclear magnetic resonance spectra are no exception (1). Whenever the spin system under consideration is symmetrical, additional factoring of the Hamiltonian will occur if the zero-order spin functions are chosen properly. Often the correct spin functions can be obtained by simple considerations. In general, it is necessary to apply the group theory which allows one to form linear combinations of product spin functions which are basic functions for irreducible representations of the group to which the spin system belongs. The Hamiltonian matrix then factors because the matrix elements of the type $\langle\psi_m|\mathcal{H}|\psi_n\rangle$ are zero unless ψ_m and ψ_n are both basis functions for the same irreducible representation (2, 3).

As pointed out, for instance by Corio, the point groups required in n.m.r. spectroscopy are usually simpler than those needed for the same molecule in other connections (4). He takes as an example three equivalent nuclei (the protons in a methyl group, for instance) and shows that the group C_{3v} will do, although in considering the normal vibrational modes the correct group would be D_{3h}. One might use D_{3h} but the calculations would involve much more work since D_{3h} has twice as many elements as C_{3v}. We show here that the use of the rotation group C_3, with only three elements, will suffice to derive the basis functions of proper symmetry for three magnetically equivalent nuclei of spin 1/2.

There are $2^3 = 8$ basic spin product functions $\alpha\alpha\alpha$, $\alpha\alpha\beta$, $\alpha\beta\alpha$, $\beta\alpha\alpha$, $\beta\beta\alpha$, $\beta\alpha\beta$, $\alpha\beta\beta$, and $\beta\beta\beta$. α and β are defined by $I_z\alpha = (1/2)\alpha$ and $I_z\beta = (-1/2)\beta$ where I_z is the z-component of the nuclear spin angular momentum vector operator I. These functions are eigenfunctions of the operator $F_z = I_z(1)+I_z(2)+I_z(3)$ which commutes with the Hamiltonian operator (1).

If the three spins are considered to lie at the corners of an equilateral triangle with a 3-fold symmetry axis through its center then the effect of the three symmetry operations of the group C_3 on the basis functions is as shown in Table I. E is the identity operator, C_3 is a counterclockwise rotation by $2\pi/3 = 120°$, and C_3^2 is a clockwise rotation by the same amount. Note that the functions have been blocked into groups with the same eigenvalue of F_z. There is, of course, no mixing between the different blocks. Notice also that

1. T. SCHAEFER. Can. J. Chem. **40**, 1 (1962).
2. J. S. WAUGH and S. CASTELLANO. J. Chem. Phys. **35**, 1900 (1961).
3. C. N. BANWELL and N. SHEPPARD. Mol. Phys. **3**, 350 (1960).
4. S. CASTELLANO and J. S. WAUGH. J. Chem. Phys. **37**, 1951 (1962).
5. W. BRÜGEL, TH. ANKEL, and F. KRÜCKEBERG. Z. Electrochem. **64**, 1121 (1960).
6. S. CAWLEY and S. S. DANYLUK. Unpublished results.
7. S. CAWLEY and S. S. DANYLUK. J. Chem. Phys. In press.
8. R. T. HOBGOOD, J. H. GOLDSTEIN, and G. S. REDDY. J. Chem. Phys. **35**, 2038 (1961).
9. A. L. ALLRED and E. G. ROCHOW. J. Inorg. Nucl. Chem. **5**, 269 (1958).
10. A. A. BOTHNER-BY and C. NAAR-COLIN. J. Am. Chem. Soc. **83**, 231 (1961).

RECEIVED MARCH 7, 1963.
DEPARTMENT OF CHEMISTRY,
UNIVERSITY OF TORONTO,
TORONTO, ONTARIO.

Can. J. Chem. Downloaded from www.nrcresearchpress.com by 210.87.254.105 on 09/05/12
For personal use only.

SYMMETRIZATION OF SPIN FUNCTIONS FOR THREE EQUIVALENT SPIN 1/2 NUCLEI BY MEANS OF THE POINT GROUP C_3

T. SCHAEFER AND F. HRUSKA

As is well known, group theoretical methods are very useful in simplifying calculations involving the diagonalization of operator matrices. The analyses of high-resolution nuclear magnetic resonance spectra are no exception (1). Whenever the spin system under consideration is symmetrical, additional factoring of the Hamiltonian will occur if the zero-order spin functions are chosen properly. Often the correct spin functions can be obtained by simple considerations. In general, it is necessary to apply the group theory which allows one to form linear combinations of product spin functions which are basic functions for irreducible representations of the group to which the spin system belongs. The Hamiltonian matrix then factors because the matrix elements of the type $\langle\psi_m|\mathcal{H}|\psi_n\rangle$ are zero unless ψ_m and ψ_n are both basis functions for the same irreducible representation (2, 3).

As pointed out, for instance by Corio, the point groups required in n.m.r. spectroscopy are usually simpler than those needed for the same molecule in other connections (4). He takes as an example three equivalent nuclei (the protons in a methyl group, for instance) and shows that the group C_{3v} will do, although in considering the normal vibrational modes the correct group would be D_{3h}. One might use D_{3h} but the calculations would involve much more work since D_{3h} has twice as many elements as C_{3v}. We show here that the use of the rotation group C_3, with only three elements, will suffice to derive the basis functions of proper symmetry for three magnetically equivalent nuclei of spin 1/2.

There are $2^3 = 8$ basic spin product functions $\alpha\alpha\alpha$, $\alpha\alpha\beta$, $\alpha\beta\alpha$, $\beta\alpha\alpha$, $\beta\beta\alpha$, $\beta\alpha\beta$, $\alpha\beta\beta$, and $\beta\beta\beta$. α and β are defined by $I_z\alpha = (1/2)\alpha$ and $I_z\beta = (-1/2)\beta$ where I_z is the z-component of the nuclear spin angular momentum vector operator I. These functions are eigenfunctions of the operator $F_z = I_z(1)+I_z(2)+I_z(3)$ which commutes with the Hamiltonian operator (1).

If the three spins are considered to lie at the corners of an equilateral triangle with a 3-fold symmetry axis through its center then the effect of the three symmetry operations of the group C_3 on the basis functions is as shown in Table I. E is the identity operator, C_3 is a counterclockwise rotation by $2\pi/3 = 120°$, and C_3^2 is a clockwise rotation by the same amount. Note that the functions have been blocked into groups with the same eigenvalue of F_z. There is, of course, no mixing between the different blocks. Notice also that

TABLE I

Transformation properties of product spin functions for three spins 1/2 under the C_3 point group

$(F_z)_n$	ψ_n (1, 2, 3)	E	C_3	C_3^2
3/2	1. $\alpha\alpha\alpha$	$\alpha\alpha\alpha$	$\alpha\alpha\alpha$	$\alpha\alpha\alpha$
1/2	2. $\alpha\alpha\beta$	$\alpha\alpha\beta$	$\beta\alpha\alpha$	$\alpha\beta\alpha$
	3. $\alpha\beta\alpha$	$\alpha\beta\alpha$	$\alpha\alpha\beta$	$\beta\alpha\alpha$
	4. $\beta\alpha\alpha$	$\beta\alpha\alpha$	$\alpha\beta\alpha$	$\alpha\alpha\beta$
−1/2	5. $\beta\beta\alpha$	$\beta\beta\alpha$	$\alpha\beta\beta$	$\beta\alpha\beta$
	6. $\beta\alpha\beta$	$\beta\alpha\beta$	$\beta\beta\alpha$	$\alpha\beta\beta$
	7. $\alpha\beta\beta$	$\alpha\beta\beta$	$\beta\alpha\beta$	$\beta\beta\alpha$
−3/2	8. $\beta\beta\beta$	$\beta\beta\beta$	$\beta\beta\beta$	$\beta\beta\beta$

the symmetry operators convert a function in one of the blocks into another function in the same block.

It follows that we need to apply symmetry principles only to the two blocks containing three functions each in our effort to further factor the Hamiltonian matrix. Consider the three functions ψ_2, ψ_3, and ψ_4. They clearly form a basis for a reducible representation of the group C_3 (they do not form a basis for a representation of the group C_{3v}). The reducible representation consists of the three transformation matrixes

$$\begin{pmatrix}1&0&0\\0&1&0\\0&0&1\end{pmatrix} \quad \begin{pmatrix}0&0&1\\1&0&0\\0&1&0\end{pmatrix} \quad \begin{pmatrix}0&1&0\\0&0&1\\1&0&0\end{pmatrix}$$

which are associated to the operators E, C_3, and C_3^2 respectively. It is easily checked that these matrices have the same multiplication table as the symmetry operators and therefore they are a faithful, actually the regular, representation of the group.

Since the order of the group is three, it follows that this representation can be reduced to three one-dimensional irreducible representations. The reduction by means of similarity transformations is carried out by standard methods and the three irreducible representations are found to be Γ_1, Γ_2, and Γ_3:

	C_3	C_3	C_3^2
Γ_1	1	1	1
Γ_2	1	w	w^2
Γ_3	1	w^2	w

where $w = \exp(2\pi i/3)$, $w^2 = \exp(-2\pi i/3)$, $i = \sqrt{-1}$, $1+w+w^2 = 0$.

This is, of course, the character table for the group C_3. It follows (3) that the three normalized linear combinations of ψ_2, ψ_3, and ψ_4 belonging to the three irreducible representations are

$$\psi(\Gamma_1) = \frac{1}{\sqrt{3}}(\alpha\alpha\beta+\alpha\beta\alpha+\beta\alpha\alpha)$$

$$\psi(\Gamma_2) = \frac{1}{\sqrt{3}}(\alpha\alpha\beta+w\alpha\beta\alpha+w^2\beta\alpha\alpha)$$

$$\psi(\Gamma_3) = \frac{1}{\sqrt{3}}(\alpha\alpha\beta+w^2\alpha\beta\alpha+w\beta\alpha\alpha).$$

Can. J. Chem. Downloaded from www.nrcresearchpress.com by 210.87.254.105 on 09/05/12
For personal use only.

The last two functions are accidentally degenerate as can easily be checked in the usual way (1). This degeneracy is not required by the dimensionality of the representations but is a consequence of time reversal (5). These functions do not have the same form as those derived by Corio (4) and McConnell *et al.* (6). Because of the degeneracy, however, linear combinations of the two functions are also acceptable. We find

$$\frac{1}{\sqrt{2}}\{\psi(\Gamma_2)+\psi(\Gamma_3)\} = \frac{1}{\sqrt{6}}(2\alpha\alpha\beta-\alpha\beta\alpha-\beta\alpha\alpha)$$

and

$$\frac{1}{\sqrt{2}i}\{\psi(\Gamma_2)-\psi(\Gamma_3)\} = \frac{1}{\sqrt{2}}(\alpha\beta\alpha-\beta\alpha\alpha).$$

These functions have the same form as those normally used and are also degenerate.

The same procedure can be applied to the functions ψ_5, ψ_6, and ψ_7 to find the proper symmetry combinations, although they can now be found by analogy to ψ_2, ψ_3, and ψ_4. The present approach is considerably shorter than that involving the group C_{3v}. The simplification arises by considering separately those starting spin functions with the same eigenvalue of F_z.

1. J. A. Pople, W. G. Schneider, and H. J. Bernstein. High resolution nuclear magnetic resonance. McGraw-Hill Book Co., Inc., New York. 1959. Chap. 6.
2. E. B. Wilson. J. Chem. Phys. **27**, 60 (1957).
3. E. B. Wilson, J. C. Decius, and P. C. Cross. Molecular vibrations. McGraw-Hill Book Co., Inc., New York. 1955.
4. P. L. Corio. Chem. Rev. **60**, 363 (1960).
5. J. C. Slater. Quantum theory of molecules and solids. Vol. 1. McGraw-Hill Book Co., Inc., New York. 1963. Appendix 12.
6. H. M. McConnell, A. D. McLean, and C. A. Reilly. J. Chem. Phys. **23**, 1152 (1955).

Received March 4, 1963.
Department of Chemistry,
University of Manitoba,
Winnipeg, Manitoba.

Can. J. Chem. Downloaded from www.nrcresearchpress.com by 210.87.254.105 on 09/05/12
For personal use only.

Canadian Journal of Chemistry

Issued by THE NATIONAL RESEARCH COUNCIL OF CANADA

VOLUME 41 AUGUST 1963 NUMBER 8

Can. J. Chem. Downloaded from www.nrcresearchpress.com by 210.87.254.40 on 09/05/12
For personal use only.

TEMPERATURE AND SOLVENT EFFECTS ON THE PROTON MAGNETIC RESONANCE SPECTRUM OF BIS(2,2-DICHLOROCYCLOPROPYL) ETHER

H. M. HUTTON[1] AND T. SCHAEFER

Department of Chemistry, University of Manitoba, Winnipeg, Manitoba

Received March 22, 1963

ABSTRACT

The proton magnetic resonance spectrum of bis(2,2-dichlorocyclopropyl) ether consists of two partially overlapping ABX spectra due to the meso and *d,l* isomers. A study of the temperature dependence of the spectra in different solvents demonstrates the existence of complex formation with benzene. It is found that for the most abundant isomer the heat of formation of the complex is -1700 ± 100 cal/mole, the entropy of formation is -6.2 ± 0.3 e.u. The association shifts are 52 ± 2 c.p.s., 64 ± 5 c.p.s., and 88 ± 5 c.p.s. at 60 Mc/s for the three protons situated at different points in the molecule.

INTRODUCTION

The proton magnetic resonance spectrum of bis(2,2-dichlorocyclopropyl) ether (I) consists of two slightly shifted ABX spectra arising from the meso and *d,l* isomers.* The shifts

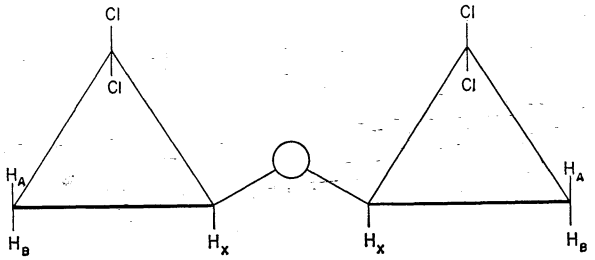

I

of the three protons in each ABX spectrum relative to one another and to an internal tetramethylsilane (TMS) reference depend markedly on solvent and temperature. We have examined our experimental data in terms of internal rotation effects, effective inversion of the oxygen atom, and association effects. It appears that the latter is consistent with experiment.

EXPERIMENTAL

The spectra were recorded on a Varian V4302 DP 60 Mc/s spectrometer. A sample of about 0.1 g of bis(2,2-dichlorocyclopropyl) ether (1) was obtained from Dr. Bernard T. Gillis. The spectra were taken at room temperature in carbon tetrachloride, benzene, carbon disulphide, and in a series of mixed solvents of benzene and carbon disulphide. Measurements were made with benzene as solvent over a temperature range of +18° C to +138° C using a temperature probe built by Mr. G. Ensell.

[1]*Holder of a C.I.L. Fellowship, 1962–1963.*

**We thank Dr. B. T. Gillis for pointing this out to us.*

Since carbon disulphide offers a wide liquid range for temperature studies the spectrum was studied from −85° C to +101° C in this solvent. The solution with the mixed solvent 0.59 mole fraction carbon disulphide and 0.41 mole fraction benzene was also observed from +18° C to +132° C. The solutions were prepared by dilution with 0.5 ml of reagent grade solvent and represent an ether concentration of about 8 mole% in benzene, 7 mole% in carbon tetrachloride, and 5 mole% in carbon disulphide. The ether was isolated by evaporation of the solvent from each solution and used again. Tetramethylsilane was the internal reference in all solutions. Other solvents such as cyclohexane and *n*-hexane, useful for the comparison of chemical shifts, were not used because of the interference of their proton resonances in the region of interest.

The results represent an average of 10 calibrated spectra for those taken at room temperature and of 6 to 8 spectra at other temperatures. Spectra were taken with an increasing and decreasing magnetic field sweep.

Temperatures were measured with a precalibrated Varian G-11A recorder using a thermocouple placed near the sample in the exit stream of the spinning and heating gas. The temperature control was approximately ±1° C over the period of time necessary to run the calibrated spectra.

RESULTS

Figure 1 shows the proton resonance spectrum in benzene at room temperature and

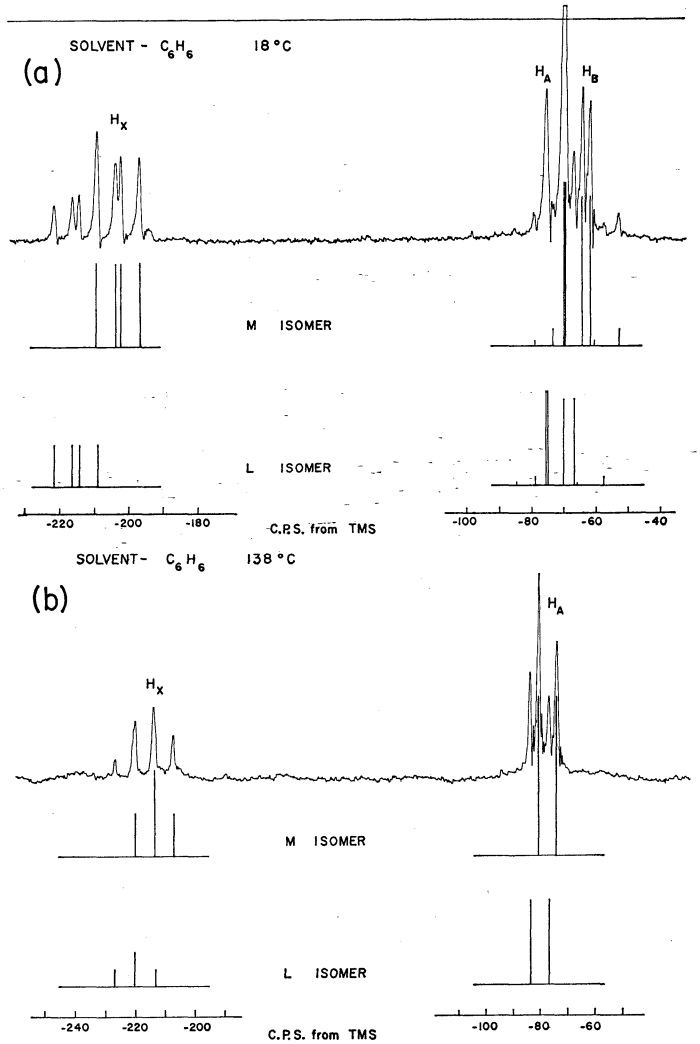

FIG. 1. Proton magnetic resonance spectrum at 60 Mc/s of bis(2,2-dichlorocyclopropyl) ether in benzene (*a*) at 18° C and (*b*) at 138° C; calibration is with respect to internal TMS.

Can. J. Chem. Downloaded from www.nrcresearchpress.com by 210.87.254.40 on 09/05/12
For personal use only.

at 138° C. From the relative intensities of the two ABX spectra one isomer (M) is seen to be about twice as abundant as the other isomer (L). The former is probably the meso isomer (2) although there is no way of deciding this from the spectrum.

The chemical shifts relative to internal TMS and the proton coupling constants are given in Tables I, II, and III. Graphs of the chemical shifts as a function of temperature in benzene and in a mixed benzene – carbon disulphide solution are shown in Figs. 2 and 3. Figure 4 shows the chemical shifts of the protons of the M isomer as a function

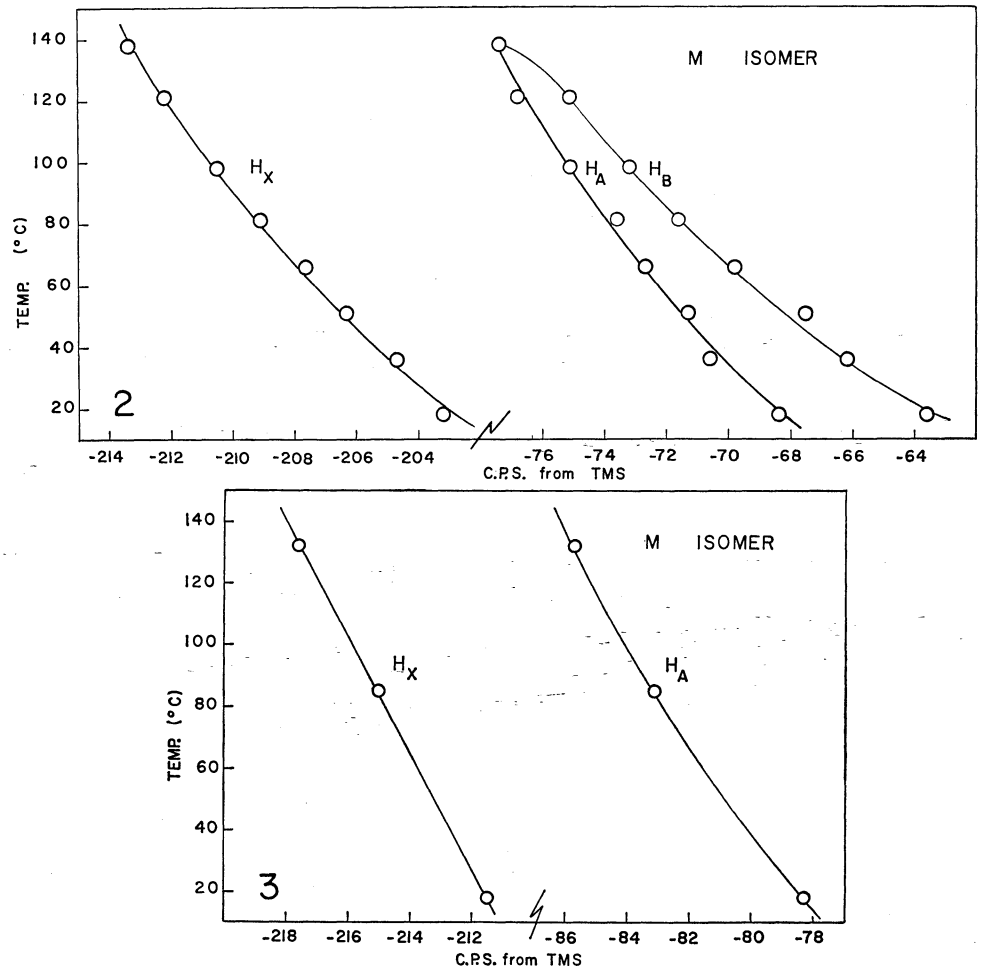

FIG. 2. Plot of proton resonance shifts of bis(2,2-dichlorocyclopropyl) ether in benzene (in c.p.s. at 60 Mc/s) against temperature; calibration is with respect to internal TMS.

FIG. 3. Plot of proton resonance shifts of bis(2,2-dichlorocyclopropyl) ether in 0.41 mole fraction benzene + 0.59 mole fraction carbon disulphide (in c.p.s. at 60 Mc/s) against temperature; calibration is with respect to internal TMS.

of the benzene concentration in the mixed solvent system. The shifts of the protons in the L isomer could not always be obtained with any accuracy because of overlapping peaks.

For the benzene solution the shift between the benzene peaks and the TMS peaks

Can. J. Chem. Downloaded from www.nrcresearchpress.com by 210.87.254.40 on 09/05/12
For personal use only.

Can. J. Chem. Downloaded from www.nrcresearchpress.com by 210.87.254.40 on 09/05/12
For personal use only.

TABLE I

Coupling constants and proton chemical shifts in c.p.s. in benzene solution

	M isomer						L isomer					
Temp (°C)	J_{gem}	J_{cis}	J_{trans}	ν_A*	ν_B*	ν_X*	J_{cis}	J_{trans}	ν_A*	ν_B*	ν_X*
18	−8.88±0.12	8.19	4.65	68.4	63.6	203.2	—	—	—	—	216.0
36	−8.96±0.12	7.89	4.85	70.6	66.2	204.7	—	—	—	—	216.5
51	−8.97±0.10	7.90	4.82	71.3	67.5	206.3	—	—	—	—	217.1
66	−8.88±0.09	8.22	4.60	72.7	69.8	207.6	8.76	4.45	76.9	73.7	217.6
81	−8.91±0.10	8.53	4.42	73.6	71.6	209.1	8.39	4.74	78.1	75.2	218.4
98	−8.92†	8.40	4.58	75.1	73.2	210.5	8.60	4.73	78.5	76.6	219.0
121	−8.92†	8.13	4.76	76.8	75.1	212.2	8.52	4.86	79.9	78.1	219.6
138	—	$(J_{cis}+J_{trans})/2 = 6.53$			77.4	213.3	$(J_{cis}+J_{trans})/2 = 6.57$		80.2		220.2
Average	−8.92	8.18	4.67				8.57	4.70			

*At 60 Mc/s to low field of TMS as internal reference.
†Average value of J_{gem} used for the analysis.

Can. J. Chem. Downloaded from www.nrcresearchpress.com by 210.87.254.40 on 09/05/12
For personal use only.

TABLE II

Coupling constants and proton chemical shifts in c.p.s. in carbon disulphide solution

	M isomer						L isomer
Temp (°C)	J_{gem}	J_{cis}	J_{trans}	ν_A*	ν_B*	ν_X*	J_{gem}
101	−8.57±0.17	7.38	5.39	95.0	101.2	226.2	−8.57±0.17
91	−8.53±0.17	7.28	5.54	94.8	101.0	225.9	−8.53±0.17
69	−8.51±0.21	7.34	5.58	95.3	101.5	226.1	−8.51±0.21
46	−8.53±0.08	7.49	5.42	95.4	101.6	226.1	−8.53±0.08
18	−8.53±0.08	7.66	5.27	95.9	101.8	226.2	−8.59±0.11
5	−8.69±0.09	7.75	4.95	96.3	102.1	226.1	−8.76±0.08
−16	−8.65±0.13	7.75	4.86	96.6	102.5	226.3	−8.75±0.11
−32	−8.62±0.12	7.89	4.71	97.0	102.9	226.2	−8.71±0.13
−38	−8.64±0.12	7.83	4.83	97.3	103.1	226.4	−8.69±0.12
−49	−8.68±0.10	7.96	4.88	97.5	103.3	226.5	−8.82±0.12
−61	−8.64±0.10	8.16	4.52	98.0	103.8	226.4	−8.73±0.11
−85	−8.81±0.14	7.74	4.72	97.6	103.4	226.6	−8.81±0.14
Average	−8.62	7.69	5.06				−8.67

*At 60 Mc/s to low field of TMS as internal reference.

Can. J. Chem. Downloaded from www.nrcresearchpress.com by 210.87.254.40 on 09/05/12
For personal use only.

TABLE III

Coupling constants and proton chemical shifts in c.p.s.

Solvent	Temp (°C)	M isomer						L isomer					
		J_{gem}	J_{cis} J_{trans} or $(J_{cis}+J_{trans})/2$		ν_A*	ν_B*	ν_X*	J_{gem}	J_{cis} J_{trans} or $(J_{cis}+J_{trans})/2$		ν_A*	ν_B*	ν_X*
CCl_4	18	−8.88±0.18	7.99	5.16	98.2	104.0	216.6	−8.95±0.14	—	—	—	—	—
0.97 mole fr. CS_2 0.03 mole fr. C_6H_6	18	−8.56±0.11	7.42	5.44	91.2	95.7	222.1	−8.62±0.16	8.27	5.01	88.8	95.4	229.5
0.92 mole fr. CS_2 0.08 mole fr. C_6H_6	18	−8.54±0.12	6.89	5.75	86.6	90.4	217.4	−8.67±0.11	8.06	5.14	87.4	92.6	225.7
0.59 mole fr. CS_2 0.41 mole fr. C_6H_6	18	—	6.45±0.13		78.3		211.5	—	6.57±0.14		81.6		222.5
0.59 mole fr. CS_2 0.41 mole fr. C_6H_6	85	—	6.50±0.09		83.1		215.0	—	6.63±0.16		88.8		—
0.59 mole fr. CS_2 0.41 mole fr. C_6H_6	132	—	6.49±0.07		85.7		217.6	—	—		—		—

*At 60 Mc/s to low field of TMS as internal reference.

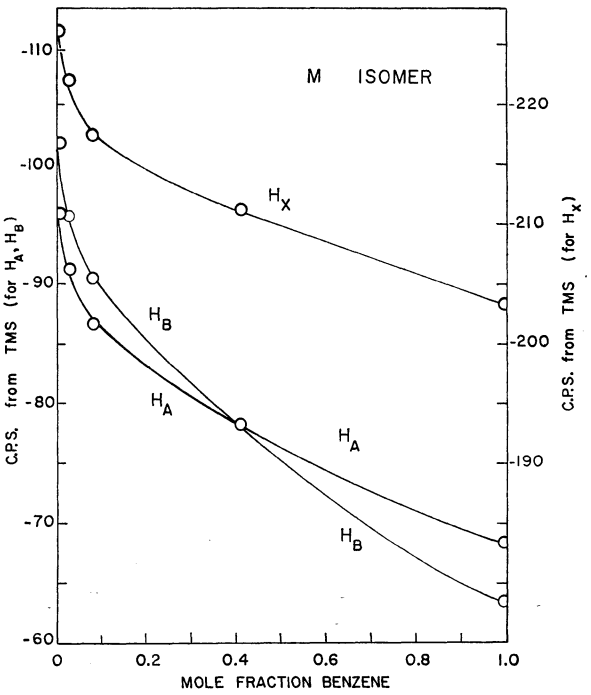

FIG. 4. Plot of proton resonance shifts of bis(2,2-dichlorocyclopropyl) ether in mixed benzene – carbon disulphide (in c.p.s. at 60 Mc/s) against mole fraction benzene at 18° C; calibration is with respect to internal TMS.

was 430.4±0.1 c.p.s. at 18° C and 431.0±0.2 c.p.s. at 102° C. For the mixed solvent (Fig. 3) these shifts were 429.1±0.1 c.p.s. at 18° C and 429.6±0.1 c.p.s. at 145° C.

DISCUSSION

(a) Coupling Constants

From a series of measurements (3–6) we are almost certain that geminal proton coupling constants in cyclopropane derivatives are negative. The vicinal couplings are then positive with the trans smaller than the cis (7–9). The labelling in Fig. 1 and in the other figures and tables assumes this relationship and that the B proton resonates at a higher field than the A proton in benzene solution.

From the tables we then have that for isomer M: $J_{AB} = J_{gem} = -8.7_7 \pm 0.25$ c.p.s.; $J_{AX}+J_{BX} = 12.8\pm0.2$ c.p.s. with $J_{AX} = J_{trans} = 5.0\pm0.5$ c.p.s. and $J_{BX} = J_{cis} = 7.8 \pm0.5$ c.p.s. For the L isomer: $J_{AB} = J_{gem} = -8.7\pm0.2$ c.p.s.; $J_{AX}+J_{BX} = 13.0\pm0.2$ c.p.s. with $J_{AX} = J_{trans} = 4.8\pm0.5$ c.p.s. and $J_{BX} = J_{cis} = 8.2\pm0.5$ c.p.s. The individual errors in J_{AX} and J_{BX} are considerably larger than in their sum because of the way in which these quantities depend on peak separations (10). For those solutions where the shift between A and B protons was zero the average of J_{AX} and J_{BX} could be determined quite accurately and was equal to half the sums given above, within experimental error. Also, within error, the couplings are independent of solvent and temperature.

(b) Chemical Shifts and Internal Rotational Effects

The internal rotational motions of the molecules about the carbon – oxygen bonds is indicated schematically in II, where R represents the substituted cyclopropyl group.

Can. J. Chem. Downloaded from www.nrcresearchpress.com by 210.87.254.40 on 09/05/12
For personal use only.

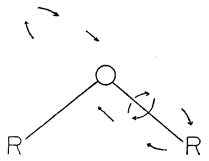

II

From Dreiding models it appears unlikely that rotations about these bonds will result in an averaging process such that the shifts of the A and B protons will become identical. This hypothesis is supported by the shift behavior of these two protons as a function of temperature in carbon disulphide and in benzene. The dielectric constants of these two solvents are almost identical and the population of the various rotational isomers should have the same temperature dependence in the two solvents. As can be seen in the tables this is not the case at all. The same objection can be levelled against a more complex motion consisting of combined rotation and an effective inversion of the oxygen atom.

(c) Chemical Shifts and Association in Benzene

Association between benzene and polar molecules has been investigated for relatively simple molecules by a number of workers (11–14). Such an association usually results in a high-field shift of the solute protons due to the disk-shaped molecules of the diamagnetically anisotropic benzene (13). A temperature increase should break up the association and result in a shift to low field of the solute proton peaks. This is exactly what we find. If the A and B protons have different association shifts, as is reasonable, the high-temperature shift equivalence must be looked upon as accidental.

The temperature dependence of the shifts in carbon disulphide is consistent with very weak association between the rod-shaped diamagnetically anisotropic carbon disulphide molecules and the solute. Such an association results in a low-field shift (13) and as the temperature increases a high-field shift is predicted. This we find, although it is small (1–3 c.p.s.) and therefore consistent with very weak association.

In this discussion we have ignored dispersion (van der Waals) effects and density effects. However, the use of an internal reference minimizes these effects. Reaction field effects (15) should be almost the same in both carbon disulphide and in benzene. The excess shifts we observe therefore can be put down to specific interactions with the solvent. The negligible change with temperature of the benzene peaks relative to the TMS peaks indicates no drastic change in packing of molecules which do not specifically interact.

We postulate that the complex formation between the ether and the benzene can be represented by

$$\text{A—H} + \text{B} \rightleftarrows \text{A—H}\cdots\text{B}$$

with an equilibrium constant

$$K = \frac{[\text{A—H}\cdots\text{B}]}{[\text{A—H}][\text{B}]} = \exp\left(\frac{\Delta S}{R}\right)\exp\left(\frac{-\Delta H}{RT}\right),$$

where [A—H] is the concentration of the ether, [B] is the concentration of the benzene, and [A—H- - -B] is the concentration of the complex. ΔS is the entropy of formation and ΔH the heat of formation of the complex. If we write K in units of mole fraction and assume our shifts to differ by a negligible amount from those of an infinitely dilute solution, the benzene concentration becomes unity.

Can. J. Chem. Downloaded from www.nrcresearchpress.com by 210.87.254.40 on 09/05/12
For personal use only.

Then

$$[1] \qquad \frac{p}{1-p} = \frac{[\text{A—H - - - B}]}{[\text{A—H}]} = \exp\left(\frac{\Delta S}{R}\right)\exp\left(\frac{-\Delta H}{RT}\right),$$

where p is the fraction of the ether in the complex form. The measured shift of the solute protons δ is the weighted mean of the shift of the unassociated solute δu and that in the complex δc. We have

$$[2] \qquad \delta = p\delta c + (1-p)\delta u.$$

From equations [1] and [2] we can find δ as a function of ΔH, ΔS, δc, δu, and the known temperature.

Following Abraham (14) we argue that at a high temperature, where $\Delta H \ll kT$, all the solute protons will be in the unassociated form. In this state the shift from internal TMS will be due to the different chemical nature of the solute and reference and to the reaction field of the benzene. Since carbon disulphide and benzene have almost the same dielectric constant we can take the high-temperature shift in carbon disulphide as the unassociated shift δu (we have ignored any small effects due to slight differences in dispersion forces). The high-temperature shift in carbon disulphide was taken in order to eliminate association effects with this solvent as far as possible. This effect is very small since we find at most a 3 c.p.s. shift with respect to internal TMS over a 200° C range (Table II).

At low temperatures, $\Delta H \gg kT$, all the solute molecules will be associated with the benzene and the shift will now be δu plus that due to complex formation. We take δu to be the origin and measure all chemical shifts from it.

Then it follows that $\delta = p\delta c$ and that

$$[3] \qquad \delta = \delta c\left\{1 + \exp\left(\frac{-\Delta S}{R}\right)\exp\left(\frac{\Delta H}{RT}\right)\right\}^{-1},$$

which is the equation given by Abraham (14). δ is now a function of three unknowns only.

We apply equation [3] to the most abundant isomer M where the individual proton shifts are most reliable. δu is taken from Table II. The experimental points in Fig. 2 can be fitted with the following values for the parameters within the error limits given:

Proton	δu (c.p.s.)	δc (c.p.s.)	ΔH (cal)	ΔS (e.u.)
H_X	−226.2	52±2	−1700±50	−6.2±0.1
H_B	−101.2	88±5	−1700±100	−6.2±0.2
H_A	− 95.0	64±5	−1700±100	−6.2±0.3

The values are reasonable in that ΔH and ΔS are the same for all three protons while δc is different. δc depends on the structure of the complex and may therefore very well be different for protons situated at different positions in the solute molecule.

CONCLUSIONS

Hydrogen bonding has been postulated to explain interactions of methyl iodide and iodoform with toluene (14) and of chloroform with mesitylene (11). Whether the interaction we have found for this ether with benzene can be similarly explained is open to speculation. We feel that an association such that the benzene molecules tend to avoid

Can. J. Chem. Downloaded from www.nrcresearchpress.com by 210.87.254.40 on 09/05/12
For personal use only.

electron-rich centers (oxygen and chlorine) is probably just as reasonable if not preferable (16). H_X would then be expected to have the smallest association shift and this we find. It is interesting to note that the dilution shifts of protons A and B in the mixed solvent (Fig. 4) have a ratio $H_A/H_B = 0.71$ while the ratio of the association shifts is 0.73. Since the former are measured against internal TMS they should also be a measure of the association dependence of the proton shifts.

ACKNOWLEDGMENTS

We are grateful to Dr. B. T. Gillis for the gift of the last 0.1 g of his ether and for his comments. The helpful discussions with many colleagues were very useful. H. M. H. would like to thank Canadian Industries Limited for fellowship support. This work was supported by the National Research Council.

REFERENCES

1. B. T. GILLIS and K. F. SCHIMMEL. J. Org. Chem. **27**, 1071 (1962).
2. E. L. ELIEL. Stereochemistry of carbon compounds. McGraw-Hill, New York. 1962. p. 138.
3. H. M. HUTTON and T. SCHAEFER. Can. J. Chem. **41**, 1623 (1963).
4. K. WIBERG. Private communication.
5. J. I. MUSHER. Private communication.
6. P. C. LAUTERBUR and R. J. KURLAND. J. Am. Chem. Soc. **84**, 3405 (1962).
7. H. M. HUTTON and T. SCHAEFER. Can. J. Chem. **40**, 875 (1962).
8. J. D. GRAHAM and M. T. ROGERS. J. Am. Chem. Soc. **84**, 2249 (1962).
9. H. M. HUTTON and T. SCHAEFER. Can. J. Chem. **41**, 684 (1963).
10. J. A. POPLE, W. G. SCHNEIDER, and H. J. BERNSTEIN. High resolution nuclear magnetic resonance. McGraw-Hill, New York. 1959.
11. L. W. REEVES and W. G. SCHNEIDER. Can. J. Chem. **35**, 251 (1957).
12. J. V. HATTON and R. E. RICHARDS. Mol. Phys. **3**, 253 (1960); Trans. Faraday Soc. **57**, 28 (1961). J. V. HATTON and W. G. SCHNEIDER. Can. J. Chem. **40**, 1285 (1962). R. E. KLINCK and J. B. STOTHERS. Can. J. Chem. **40**, 2329 (1962). W. G. SCHNEIDER. J. Phys. Chem. **66**, 2653 (1962).
13. A. D. BUCKINGHAM, T. SCHAEFER, and W. G. SCHNEIDER. J. Chem. Phys. **32**, 1227 (1960).
14. R. J. ABRAHAM. Mol. Phys. **4**, 369 (1961).
15. A. D. BUCKINGHAM. Can. J. Chem. **38**, 300 (1960).
16. T. SCHAEFER. Can. J. Chem. **39**, 1864 (1961).

Can. J. Chem. Downloaded from www.nrcresearchpress.com by 210.87.254.40 on 09/05/12
For personal use only.

HEATS OF VAPORIZATION OF A SERIES OF ALIPHATIC ALCOHOLS

K. G. McCurdy and K. J. Laidler
Department of Chemistry, University of Ottawa, Ottawa, Ontario
Received February 22, 1963

ABSTRACT

Heats of vaporization of 14 alcohols, having from one to five carbon atoms, have been determined in a Calvet microcalorimeter, using a special technique. The method consisted of allowing the alcohol to vaporize into a vacuum, the heat required for the vaporization being provided by passing a current through a resistance wire which was immersed in oil in a U-tube surrounded by the alcohol. The additivity scheme previously devised by Laidler for heats of formation and related properties was applied to the results, and the agreement with experiment was within a few tenths of a percent.

INTRODUCTION

A considerable amount of experimental work has been done on heats of combustion of compounds in the liquid and solid states, but relatively little accurate work has been done on heats of vaporization. Such heats are required for the conversion of heats for the liquid state into heats relating to the gaseous state. It was therefore decided to adapt the Calvet microcalorimeter for the determination of such heats of vaporization, and a special technique for this purpose has been developed. It was considered of particular interest to attempt to interpret the heats of vaporization in terms of additivity schemes, such as the one previously developed by Laidler (1). The work was done on a homologous series of aliphatic alcohols.

EXPERIMENTAL

Materials

The alcohols used were Fisher certified reagents. They were dried by refluxing over freshly ignited calcium oxide for 4 hours, followed by fractionation through a 40-cm column packed with short lengths of 4-mm glass tubing. Only the middle fractions were retained.

Calorimetry

The heats of vaporization were measured at 25° C using a differential microcalorimeter of the Calvet type, described in previous papers from this laboratory (2, 3). The apparatus for carrying out the vaporization, shown in Fig. 1, consists of a U-tube which contains the purified alcohol. This tube, after being loaded with the appropriate amount of alcohol, was sealed directly to a vacuum line. It was then subjected to freeze-drying to remove air that had become dissolved during loading. The U-tube was then evacuated to a pressure of approximately 0.5 mm, with the alcohol frozen in liquid air. The U-tube was then sealed off from the vacuum line by collapsing the walls of the tube.

The receiver consisted of a calibrated glass bulb of approximately 5-ml capacity connected to the U-tube by means of a calibrated capillary tube. The U-tube was placed in the calorimeter, and when it and the calorimeter had attained thermal equilibrium the distillation was started by raising a Dewar vessel of coolant on the receiving end of the U-tube. This was done by means of a raising and lowering device controlled from the exterior of the calorimeter cabin. The coolant consisted of liquid air, dry ice – acetone, or iced water, according to circumstances.

The heat required to cause vaporization was compensated for by the application of a potential across a resistance wire immersed in an oil bath, which was encased in glass and was surrounded by the alcohol. An electric timing device was used to record the duration of the passage of the current; the current was passed for 100 to 200 minutes, depending on the vapor pressure and the coolant. It was possible, by means of the elevating device, to control the rate of evaporation so that it would closely match the rate of heat delivered by the coil; in this way the amount of heat measured in the calorimeter was kept to a minimum, and the accuracy of the measurements was thereby greatly increased. The rates of evaporation ranged from about 2×10^{-4} mole/min to 5×10^{-4} mole/min.

When sufficient alcohol had been vaporized, so that the surface of the liquid was in the calibrated capillary tube, the coolant was lowered sufficiently to stop vaporization but only to such an extent that the alcohol

Can. J. Chem. Downloaded from www.nrcresearchpress.com by 210.87.254.6 on 09/05/12
For personal use only.

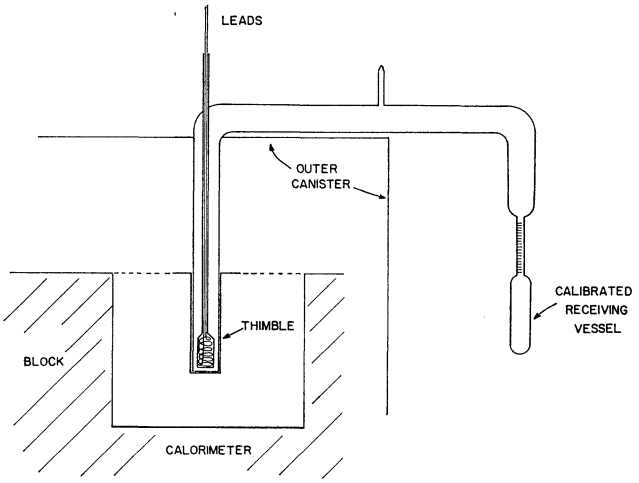

FIG. 1. Apparatus for the measurement of heats of vaporization of liquids in the microcalorimeter (schematic, not drawn to scale).

in the receiver did not distill back into the U-tube. The heater was then turned off and the calorimeter allowed to come back to thermal equilibrium. During this period part of the alcohol in the calorimeter was vaporized, with the result that the conditions in the U-tube were the same as the initial conditions. The coolant was then further lowered and the alcohol in the receiver allowed to return to 25° C; this was done in the thermostatted cabin, the temperature of which was controlled to 0.1° C. The volume was then recorded, and from a knowledge of its density it was then possible to calculate the weight of alcohol distilled.

The conditions were always adjusted so that there was a positive amount of heat evolved, indicated by a positive area on the record. This area was reproduced by passing an electric current through the resistance in the cell for a known period of time. This excess heat was usually less than 1% of the total heat absorbed in the vaporization process.

Experiments with the U-tube empty and evacuated showed that there was negligible conduction of heat along the U-tube when the coolant was placed around the receiver. Experiments in which the amount of alcohol in the U-tube was varied showed no effect on the calculated heat of vaporization, indicating that there was negligible heat loss from the tube. Experiments in which the rate of vaporization was varied, by using a different coolant and varying the potential across the resistance, gave results in good agreement with one another. This indicates negligible entrainment of liquid during the vaporization.

RESULTS

A typical set of measurements is given in Table I and the final results obtained are summarized in Table II. An estimate of the overall accuracy of the heat determinations may be arrived at as follows. The error in the measurement of time can be ignored as being much smaller (<1 in 10,000) than the other errors. An average current was 0.0750 amp, and the uncertainty in this is 0.0001 amp. The total resistance was 73.675

TABLE I

Typical experiment in the measurement of heats of vaporization of the alcohols

Electrical input (cal)	Moles of C_2H_5OH vaporized	Electrical heat in excess (cal)	Heat of vaporization (cal/mole)
911.3	0.0902	0.20	10,101
914.8	0.0908	0.26	10,070
903.5	0.0894	0.32	10,103

Can. J. Chem. Downloaded from www.nrcresearchpress.com by 210.87.254.6 on 09/05/12
For personal use only.

TABLE II

Summary of experimental heats of vaporization and the calculated heats of vaporization by the additivity scheme

Compound	Bonds	B.p. (°C)	Density at 25° (12) (g/ml)	Heat of vaporization (cal/mole) Obs.	Calc.	No. of expts.	Standard deviation
CH_3OH	$3P+A^1$	64.5	0.7866	9,010	9,010	3	±12
CH_3CH_2OH	$3P+2S+A^1$	78.2	0.7851	10,090	10,070	3	±10
$CH_3CH_2CH_2OH$	$3P+4S+A^1$	96.5	0.8001	11,130	11,130	3	±12
$(CH_3)_2CHOH$	$6P+T+A^2$	82	0.7810	10,520	10,530	3	±11
$CH_3(CH_2)_3OH$	$3P+6S+A^1$	117	0.8059	12,190	12,190	3	±10
$(CH_3)_2CHCH_2OH$	$6P+2S+T+A^1$	107	0.7979	11,910	11,890	4	± 6
$CH_3CH_2(CH_3)CHOH$	$6P+2S+T+A^2$	119.8	0.8025	11,590	11,590	4	±27
$(CH_3)_3COH$	$9P+A^3$	82	0.7810	10,720	10,710	4	±19
$(CH_3)_2CH(CH_2)_2OH$	$6P+4S+T+A^1$	131	0.8054	12,980	12,950	2	± 1.9
$CH_3CH_2(CH_3)CHCH_2OH$	$6P+4S+T+A^1$	127.5	0.8110	12,920	12,950	2	±16
$CH_3(CH_2)_2(CH_3)CHOH$	$6P+4S+T+A^2$	119.3	0.8052	12,670	12,650	2	±10
$(CH_3CH_2)_2CHOH$	$6P+4S+T+A^2$	115	0.8150	12,650	12,650	3	± 7
$(CH_3)_2CH(CH_3)CHOH$	$9P+2T+A^2$	112	0.8150	12,350	12,350	3	±15
$CH_3CH_2(CH_3)_2COH$	$9P+2S+A^3$	101.4	0.8069	11,750	11,760	3	±10

ohms, and the uncertainty in this is about 0.010 ohms. These figures lead to an uncertainty of 2.9 cal in the electrical heat, or of 0.3%. The volume vaporized was approximately 5 ml, and the uncertainty 0.01 ml or 0.2%. The heat of vaporization per mole is the ratio of a measured heat to the volume, and this leads to an overall uncertainty of 0.5%.

The calculated heats of vaporization were obtained by the use of an additivity scheme of the same kind as previously given (1) for heat of formation. The contributions for the various bonds, obtained on the IBM 650 computer by the method of least squares, are as follows:

P	(primary C—H bond)	606 cal/mole
S	(secondary C—H bond)	530 cal/mole
T	(tertiary C—H bond)	0 cal/mole
A^1	(C—O—H, in which C is primary)	7196 cal/mole
A^2	(C—O—H, in which C is secondary)	6894 cal/mole
A^3	(C—O—H, in which C is tertiary)	5250 cal/mole

There is no contribution for a C—C bond.

DISCUSSION

The standard deviations of the experimental heats of vaporization are in all cases less than 0.3%, and in most cases are 0.1 to 0.2%. The technique employed therefore seems to provide a very reliable method of measuring the heats of vaporization.

The values obtained for methanol, ethanol, and *n*-propanol may be compared with the values given by Green (4), which are 9,070±10, 10,180±20, and 11,360±10 cal/mole respectively. For higher members of this straight-chain series of aliphatic alcohols Green suggests the same increment per CH_2 unit for the heat of vaporization as is found per CH_2 unit in the straight-chain aliphatic hydrocarbon series. This value is 1200±50 cal/mole per CH_2 unit; our value for the CH_2 unit increment is 1060 cal/mole.

Parks and Barton (5) obtained values for the heats of vaporization of *i*-propyl alcohol and *t*-butyl alcohol at 25° C from vapor pressure measurements; application of the

Can. J. Chem. Downloaded from www.nrcresearchpress.com by 210.87.254.6 on 09/05/12
For personal use only.

Clausius–Clapeyron equation gives the values 10,600±150 and 10,900±200 cal/mole respectively, in good agreement with our experimental values.

Two methods most frequently employed in the calculation of the heat of vaporization at one temperature from the heat of vaporization at another temperature are due to Su (6) and Watson (7). These two methods have been applied to the data of Mathews (8), Ingle and Cody (9), Williamson and Harrison (10), and Weltner and Pitzer (11); the critical constants from the "International Critical Tables" (12) were used. The resulting values for the heats of vaporization at 25° C are shown in Tables III and IV.

TABLE III

Calculated heats of vaporization at 25° C (cal/mole)

Data of:	Mathews		Cody	
Method of:	Su	Watson	Su	Watson
CH_3OH	9,070	9,100	9,310	9,350
C_2H_5OH	10,240	10,310	10,510	10,590
n-C_3H_7OH	—	—	11,220	11,330
i-C_3H_7OH	10,700	10,770	10,490	10,550
n-C_4H_9OH	12,130	12,340	11,970	12,180
i-C_4H_9OH	11,780	12,020	—	—
s-C_4H_9OH	11,290	11,490	—	—

TABLE IV

Calculated heats of vaporization at 25° C

Temperature of measurement	Calculated value at 25° C	
	Su	Watson
Data of Weltner and Pitzer (11) for methanol		
40	8,970	9,010
55	8,980	9,090
65	9,080	9,130
Data of Williamson and Harrison (10) for n-propanol		
60	11,310	11,420
73	11,310	11,390
81	11,300	11,420
Data of Williamson and Harrison (10) for i-propanol		
51	10,800	10,810
70	10,790	10,840
80	10,690	10,380

Pitzer and Williamson have determined the heats of vaporization of certain aliphatic alcohols at several temperatures. Results of the application of the method of Su and Watson to their data are given in Table IV.

For the lower-boiling aliphatic alcohols both temperature-dependent relationships predict heats of vaporization which are too high. The data of Pitzer lead to a value in better agreement with our value when the temperature of the measurement is closer to 25° C, that is, when the amount of correction is small. This is not the case with the data of Williamson and Harrison, where the predicted heat of vaporization is too high for both n-propyl and i-propyl alcohol, and the predicted value at 25° C is independent of the temperature of the measurement. For the higher-boiling alcohols both approximation methods give values that are too low. Adjustment of the exponent in Watson's equation allows one to fit different members of the series, but one cannot predict the heats of vaporization of a number of aliphatic alcohols using a constant exponent.

Can. J. Chem. Downloaded from www.nrcresearchpress.com by 210.87.254.6 on 09/05/12
For personal use only.

The agreement between our observed and calculated heats is very satisfactory, and is usually well within the standard deviation. This can be taken as confirming the accuracy of the measurements, and shows that the additivity scheme is as good as can be developed on the basis of the present experimental results.

Strictly speaking, an additivity scheme in terms of atoms or groups, rather than of bonds, would be preferable in the case of heats of vaporization. Simple atom schemes can, however, be shown to be equivalent to bond schemes. The use of the present bond scheme has the practical advantage that it is equivalent to the scheme used for heats of formation (1), so that gases and liquids can be treated in a uniform manner.

REFERENCES

1. K. J. LAIDLER. Can. J. Chem. **34**, 626 (1956).
2. H. M. PAPEE, W. J. CANADY, and K. J. LAIDLER. Can. J. Chem. **34**, 1677 (1956).
3. W. J. CANADY, H. M. PAPEE, and K. J. LAIDLER. Trans. Faraday Soc. **54**, 502 (1958).
4. J. H. S. GREEN. J. Appl. Chem. (London), **11**, 397 (1961).
5. G. S. PARKS and B. BARTON. J. Am. Chem. Soc. **50**, 24 (1928).
6. G.-J. SU. Ind. Eng. Chem. **38**, 923 (1946).
7. K. M. WATSON. Ind. Eng. Chem. **23**, 360 (1931).
8. J. H. MATHEWS. J. Am. Chem. Soc. **48**, 562 (1926).
9. J. D. INGLE and H. P. CODY. J. Phys. Chem. **42**, 397 (1938).
10. D. WILLIAMSON and R. H. HARRISON. J. Chem. Phys. **26**, 1409 (1957).
11. W. WELTNER and K. S. PITZER. J. Am. Chem. Soc. **73**, 2606 (1951).
12. INTERNATIONAL CRITICAL TABLES. Vol. III. McGraw-Hill Publishing Co. 1928.

Can. J. Chem. Downloaded from www.nrcresearchpress.com by 210.87.254.6 on 09/05/12
For personal use only.

THE INTERACTION OF HYDRAZINE WITH BORON AND ALUMINUM HALIDES[1]

W. G. PATERSON[2] AND M. ONYSZCHUK
Inorganic Chemistry Laboratory, McGill University, Montreal, Que.
Received February 26, 1963

ABSTRACT

The interaction of boron halides BX_3 (where X is Cl or Br) or aluminum halides Al_2X_6 (where X is Cl, Br, or I) with hydrazine is characterized by the elimination of hydrogen halide and the formation of substances with boron– (or aluminum–) nitrogen linkages. The hydrogen halide appears in the products as hydrazine hydrohalide, which can be separated by a hydrazine washing technique, leaving a polymeric material with empirical formula MN_4H_5 (where M is Al or B). A reaction scheme is proposed and possible structures of this polymeric product are discussed.

INTRODUCTION

Hydrazine, like ammonia, is an electron-pair donor capable of forming coordination compounds with borane (1–3), boron trifluoride (4), and trimethylborane (5). Ammonia reacts with the other boron trihalides, BCl_3 (6, 7), BBr_3 (6), and BI_3 (8), without yielding stable adducts, but forming ammonium halide and boron amide or imide instead, by condensation reactions. Hydrazine might be expected to give similar condensation products. The experiments reported in this paper were made to examine this possibility. Since ammonia forms a series of addition compounds with aluminum trihalides (9, 10), it was also particularly interesting to determine the nature of the interaction between hydrazine and aluminum trihalides.

RESULTS AND DISCUSSION

Boron trichloride reacted with excess hydrazine in a vacuum, yielding a product in which the ratio of trichloride to hydrazine was 1:4. This suggests that the overall reaction was:

$$BCl_3 + 4N_2H_4 \rightarrow (NH_2NH)_2BCl + 2N_2H_4 \cdot HCl.$$

In tetrahydrofuran solution, however, the combining ratio was 1:6, suggesting the reaction

$$BCl_3 + 6N_2H_4 \rightarrow (NH_2NH)_3B + 3N_2H_4 \cdot HCl.$$

The products from both reactions did not have definite melting points and their infrared spectra contained bands characteristic of hydrazine hydrochloride (11) in addition to bands which could not be unambiguously assigned. Attempts were made to separate the product mixtures by fractional sublimation; these were unsuccessful due to simultaneous thermal decomposition.

Although hydrazine hydrochloride is insoluble in all dry hydrocarbon solvents, it is appreciably soluble in anhydrous hydrazine. Accordingly, the 1:4 product mixture was extracted with hydrazine until the extracts gave negative tests for chloride ion. The remaining insoluble substance, after being dried in a vacuum, contained B, N, and H, but no Cl. Reproducible analyses were obtained for B but not for N and H. The boron

[1]*Financial assistance for this work was obtained from the Defence Research Board of Canada, under Grant Number 9530-20, Project D46-95-30-20.*
[2]*Holder of National Research Council Studentships, 1957–1959. Present address: Department of Chemistry, University of Alberta, Edmonton, Alberta.*

Can. J. Chem. Downloaded from www.nrcresearchpress.com by 210.87.254.5 on 09/05/12
For personal use only.

value indicates that the substance contains 4 g-atoms of N per g-atom of boron. The most likely empirical formula, as suggested by the reaction scheme to be proposed, appears to be BN_4H_5, although other formulas containing less H cannot be ruled out because analyses for H were not reproducible. The substance did not melt or decompose when it was heated to 300°, and its infrared spectrum consisted of broad unresolved bands with centers at frequencies characteristic of N—H and B—N stretching vibrations. These properties strongly suggest that it is polymeric, but this could not be confirmed by molecular weight measurements because of its insolubility. The same substance was also ultimately obtained from the interaction of boron tribromide with excess hydrazine. The aluminum analogue, AlN_4H_5, was isolated from the reaction of hydrazine with aluminum chloride, bromide, or iodide.

We suggest that boron trichloride and tribromide and aluminum trichloride, tribromide, and triiodide each react with hydrazine initially to produce an unstable 1:1 molecular adduct. This adduct splits out hydrogen halide, which immediately forms hydrazine hydrohalide. The dihalohydrazinoborane (or alane), I, produced simultaneously reacts further with hydrazine, yielding more hydrazine hydrohalide and halodihydrazinoborane (or alane), II. The latter ultimately forms trihydrazinoborane (or alane), III, the analogue of boron amide, $B(NH_2)_3$. The overall reaction is depicted in the following scheme in which X is Cl or Br when M is B, and X is Cl, Br, or I when M is Al:

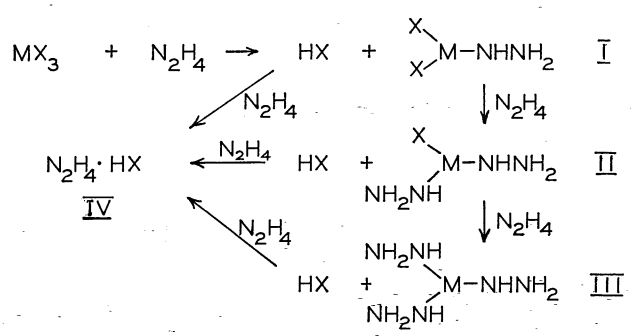

However, there was no evidence for the formation of the intermediates I, II, and III.

The above condensation reactions are similar to those briefly reported by Nöth (12) for the interaction of organoboron halides (R_3BCl) or borazenes (R_2BNR') with hydrazines, producing hydrazinoboranes and such condensation products as $R_2BNH—NHBH_2$, $R_2BNH—NHR'$, $R_2BNH—BR_2'$, and $B(NHNR_2')_3$. The details of this work have not yet been described. More recently, Holliday *et al.* (13) reported that diborontetrachloride reacts with hydrazine in a 1:5 mole ratio, which they attribute to:

$$B_2Cl_4 + 5N_2H_4 \rightarrow 4N_2H_5Cl + B_2N_2.$$

We could not isolate trihydrazino-borane and -alane, (III), presumably because they undergo rapid intermolecular condensation when dried in a vacuum at room temperature, producing hydrazine and substances with empirical composition MH_4N_5 (V), as represented by:

$$n\mathrm{M(NHNH_2)_3} \rightarrow (\mathrm{MN_4H_5})_n + n\mathrm{N_2H_4}.$$

V

Substance V cannot be a double-bonded simple molecule (VI), a six-membered ring (VII), or a zwitterion (VIII) because these structures are not compatible with the

Can. J. Chem. Downloaded from www.nrcresearchpress.com by 210.87.254.5 on 09/05/12
For personal use only.

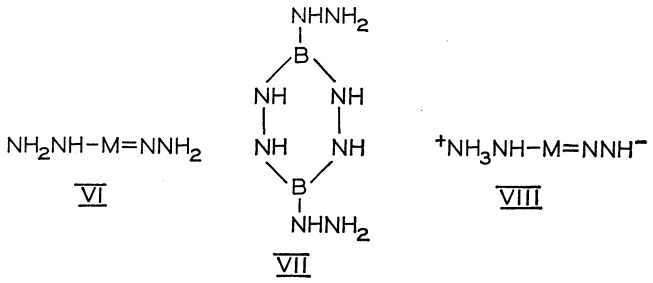

following observed properties: insoluble, non-volatile, high melting point, broad and unresolved infrared absorption bands. These properties indicate that V is probably a highly condensed polymer. One possible structure is:

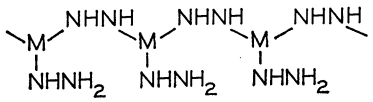

in which nitrogen and boron (or aluminum) atoms are trivalent. Polymeric structures containing trivalent Al and N have been proposed by Fetter and Bartocha (14) for the Al—N polymers formed in the reactions of methylhydrazines with trimethylaluminum or trimethylaluminum–trimethylamine. Similar bonding is proposed by the same authors for the polymeric substance $[—Al(C_2H_5)—N(C_2H_5)—]_n$ produced when $(C_2H_5)_2Al—N(CH_3)_2$ is heated at 80° C (15).

It seems more likely that B and Al attain their maximum covalency of 4 in polymeric compounds (16–19). Thus, Laubengayer *et al.* (18) found that pyrolysis of 1:1 amine – aluminum alkyl or amine – alkyl aluminum chloride additioncom pounds yields Al—N polymers for which they postulate structures assuming tetrahedral bonding of Al and N. Similar bonding in MH_4H_5 might result in the following structural pattern:

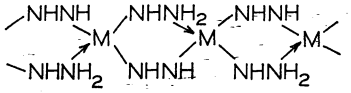

With the object of obtaining further information about B—N and Al—N polymers, we are now investigating the interaction of monomethyl- and N,N-dimethyl-hydrazine with boron and aluminum halides. These reactions might produce methyl analogues of MN_4H_5 which might be soluble in organic solvents and hence more amenable to structural determinations than the MN_4H_5 substances.

EXPERIMENTAL

The experimental techniques have been described previously (4, 5). Reagent grade samples of aluminum chloride, bromide, and iodide were used without purification. Boron trichloride and tribromide were purified by low-temperature distillations in a vacuum. Anhydrous hydrazine was prepared by refluxing the 95+% material over sodium hydroxide flakes, followed by distillation. The fraction boiling at 111–112° was used; it was 100±0.2% pure by the iodate method (20).

Reaction of Boron Trichloride with Hydrazine

(a) In the Absence of a Solvent

When BCl_3 (11.90 mmoles) and N_2H_4 (94 mmoles) were condensed together at liquid air temperature and then warmed slowly to 25°, a very vigorous exothermic reaction produced a white solid which dissolved almost completely in the excess hydrazine. The direct reaction of the two materials should be done with small quantities, otherwise there is a considerable risk of explosion. The solid contained BCl_3 and N_2H_4 in a mole ratio of 1:4. (Found: N_2H_4, 51.4, 52.5%. Calc. for $BCl_3N_8H_{16}$: N_2H_4, 52.3%.)

Can. J. Chem. Downloaded from www.nrcresearchpress.com by 210.87.254.5 on 09/05/12
For personal use only.

(b) In Tetrahydrofuran Solution

The interaction of N_2H_4 (310 mmoles) with BCl_3 (46.8 mmoles) in anhydrous tetrahydrofuran (250 ml) at 25° yielded a pale yellow tacky solid which became white and crystalline after it was washed several times with anhydrous diethyl ether. This substance contained BCl_3 and N_2H_4 in a mole ratio of 1:6. (Found: Cl, 38.7, 38.6%. Calc. for $BCl_3N_{12}H_{24}$: Cl, 38.9%.) It dissolved in water, giving a neutral solution, but was insoluble in boiling pyridine. A comparison of its infrared spectrum with that of hydrazine monohydrochloride revealed that the latter was one of the principal constituents of the product.

An attempt to separate the product into its components by fractional sublimation was unsuccessful. A sample of the product, heated at 160–165° in a vacuum, gave N_2H_4, $N_2H_4 \cdot HCl$, and an unidentified non-volatile residue containing hydrazine (found: 50.6, 50.7%), chlorine (13.2, 13.6%), and boron.

The reaction product $BCl_3N_{12}H_{24}$ was extracted 21 times with anhydrous N_2H_4 in a nitrogen-filled "dry-box". The extracts were separated from the solid each time by centrifugation. The residual material, a white solid, after being dried in a vacuum at 25°, contained 15.61% boron and no chlorine. This suggested that the substance contained 4 g-atoms of nitrogen per g-atom of boron, i.e. 80.8% nitrogen. The remaining few percent were presumed to be hydrogen. The most reasonable empirical formula appeared to be BN_4H_5 (calc. B, 15.05%). This substance did not melt when heated to 300°. It was soluble in water, giving an alkaline solution. Its infrared spectrum contained strong and very broad bands centered at 3350 (N—H stretching), 1620 (N—H deformation), 1330 (B—N stretching), 1050 (NH_2 wagging), and 700 cm^{-1} (unassigned).

Reaction of Boron Tribromide with Hydrazine

The reaction of BBr_3 (0.104 mole) with N_2H_4 (1.25 moles) in tetrahydrofuran (250 ml) gave a product composed of BBr_3 and N_2H_4 in a 1:6 mole ratio. (Found: Br, 53.9%. Calc. for $BBr_3N_{12}H_{24}$: Br, 54.2%.) This product was extracted 12 times with N_2H_4, leaving a white solid residue which contained 15.31% boron and no bromine. (Calc. for BN_4H_5: B, 15.05%.) Its infrared spectrum was identical with that of the corresponding product obtained from the reaction of BCl_3 with N_2H_4.

Reaction of Aluminum Chloride with Hydrazine

Aluminum chloride (16.5 mmoles) and hydrazine (150 mmoles) reacted at 25° in a 1:4 mole ratio, producing a white solid. (Found: N_2H_4, 51.8%; Cl, 39.2%. Calc. for $AlCl_3N_8H_{16}$: N_2H_4, 49.1%; Cl, 40.7%.) The same product was obtained when the reaction was done in carbon tetrachloride suspension. (Found: Al, 10.09, 10.14%; Cl, 39.8, 39.2%. Calc. for $AlCl_3N_8H_{16}$: Al, 10.33%; Cl, 40.7%.)

When a sample of $AlCl_3N_8H_{16}$ (1.002 g) was heated in a vacuum at 160–170° until the evolution of volatile material had ceased, the only volatile materials were hydrazine monohydrochloride (0.109 g; found: m.p. 91°, required for N_2H_5Cl: m.p. 89°) and hydrazine (0.220 g). The non-volatile residue (0.613 g) contained aluminum (15.4%), chlorine (50.2%), nitrogen, and hydrogen; analyses for the last two could not be obtained. Extraction of a sample of $AlCl_3N_8H_{16}$ 11 times with hydrazine at 25° gave a white solid containing aluminum (30.4, 30.7%) and hydrogen, but no chlorine. Its empirical formula was thought to be AlN_4H_5 (calc. Al, 30.7%). This substance did not melt when heated to 350° in a sealed tube. It dissolved readily in nitric and hydrochloric acids and only slightly in hydrazine. Water partly hydrolyzed the substance, yielding an alkaline solution. Its infrared spectrum contained broad unresolved bands centered at 3450 (N—H stretching), 1630 (N—H deformation), 1480 (N—H deformation), 1385 (N—H rocking), 1200 (N—H wagging), and 750 cm^{-1} (Al—N stretching).

Reaction of Aluminum Bromide and Iodide with Hydrazine

Hydrazine (250 mmoles) and aluminum bromide (44 mmoles) in CCl_4 (300 ml) yielded a white precipitate which, after being dried and then extracted with N_2H_4 10 times, contained aluminum (31.5%) but no bromine. This substance was the same as that obtained by the same method from the reaction of $AlCl_3$ with N_2H_4, i.e. AlN_4H_5 (calc. Al, 30.7%). Similar results were obtained for the reaction of aluminum iodide (21 mmoles) with hydrazine (220 mmoles) in diethyl ether (250 ml). The product contained aluminum, nitrogen, hydrogen, and no iodine. (Found: Al, 31.4. Calc. for AlN_4H_5: Al, 30.7%.)

ACKNOWLEDGMENTS

We are grateful for financial assistance from The Defence Research Board and for two Studentships (to W. G. P.) from The National Research Council.

REFERENCES

1. H. J. Emeléus and F. G. A. Stone. J. Chem. Soc. 840 (1951).
2. M. J. Steindler and H. I. Schlesinger. J. Am. Chem. Soc. **75**, 756 (1953).
3. J. Goubeau and E. Ricker. Z. Anorg. Allgem. Chem. **310**, 123 (1961).
4. W. G. Paterson and M. Onyszchuk. Can. J. Chem. **39**, 986 (1961).
5. W. G. Paterson and M. Onyszchuk. Can. J. Chem. **39**, 2324 (1961).
6. A. Joannis. Compt. Rend. **135**, 1106 (1902); **139**, 364 (1904).

Can. J. Chem. Downloaded from www.nrcresearchpress.com by 210.87.254.5 on 09/05/12
For personal use only.

7. P. A. TIERNEY. Abstracts of Papers, 141st Meeting of the American Chemical Society, Washington. Division of Inorganic Chemistry. 1962. p. 4M.
8. W. J. MCDOWELL and C. W. KEENAN. J. Am. Chem. Soc. **78**, 2069 (1956).
9. W. KLEMM and E. TANKE. Z. Anorg. Allgem. Chem. **200**, 343 (1931).
10. W. KLEMM, E. CLAUSEN, and U. H. JACOBI. Z. Anorg. Allgem. Chem. **200**, 367 (1931).
11. J. C. DECIUS and D. P. PEARSON. J. Am. Chem. Soc. **75**, 2436 (1953).
12. H. NÖTH. Abstracts of the XVIIth International Congress of Pure and Applied Chemistry, Munich. 1959. p. 44.
13. A. K. HOLLIDAY, F. J. MARSDEN, and A. G. MASSEY. J. Chem. Soc. 3348 (1961).
14. N. R. FETTER and B. BARTOCHA. Can. J. Chem. **39**, 2001 (1961).
15. N. R. FETTER and B. BARTOCHA. Can. J. Chem. **40**, 342 (1961).
16. A. W. LAUBENGAYER, J. D. SMITH, and G. G. EHRLICH. J. Am. Chem. Soc. **83**, 542 (1961).
17. A. W. LAUBENGAYER. *In* Inorganic polymers. Chem. Soc. (London), Spec. Publ. **15**, 78 (1961).
18. A. W. LAUBENGAYER, K. WADE, and G. LENGNICK. Inorg. Chem. **1**, 632 (1962).
19. J. I. JONES and W. S. MCDONALD. Proc. Chem. Soc. 366 (1962).
20. L. F. AUDRIETH and B. A. OGG. The chemistry of hydrazine. John Wiley and Sons, Inc., New York. 1951. p. 157.

Can. J. Chem. Downloaded from www.nrcresearchpress.com by 210.87.254.5 on 09/05/12
For personal use only.

THE SYNTHESIS OF 3-HEXULOSES

PART II. DERIVATIVES OF 1-DEOXY-L-*arabo*-3-HEXULOSE (SYN. 6-DEOXY-L-*lyxo*-4-HEXULOSE)

J. W. BIRD AND J. K. N. JONES
Department of Chemistry, Queen's University, Kingston, Ontario

Received March 18, 1963

ABSTRACT

Oxidation of 1,3:2,5-di-*O*-methylene-L-rhamnitol yielded 2,5:4,6-di-*O*-methylene-1-deoxy-L-*arabo*-3-hexulose, which was characterized as its 2,5-dichlorophenylhydrazone and by reduction to derivatives of L-rhamnitol and of 6-deoxy-L-talitol. Oxidation of 2,5-*O*-methylene-L-rhamnitol 1-benzoate yielded a syrupy 3,4-diketose which was characterized as the crystalline quinoxaline derivative. Attempts to convert 1,2:4,5-di-*O*-isopropylidene-D-mannitol 6-benzoate to a ketose were unsuccessful.

Can. J. Chem. Downloaded from www.nrcresearchpress.com by 210.87.254.40 on 09/05/12
For personal use only.

INTRODUCTION

The chemistry of the 3-ketose sugars has attracted attention during recent years because of their possible formation as intermediates in the breakdown of sugars (1); because a 3-pentulose derivative is postulated as an intermediate in the fixation of carbon dioxide during photosynthesis (2); and because of their potential value as intermediates in the synthesis of branched-chain sugars (3) and amino sugars (4). The first 3-hexulose was prepared by oxidation of L-fucitol with *Acetobacter suboxydans* to yield 1-deoxy-D-*xylo*-3-hexulose (Richtmyer *et al.* (5)). The first chemical synthesis of a 3-hexulose, from L-ascorbic acid, was described in Part I of this series (6). Oxidation of sugar alcohols to 3-hexuloses has been achieved by Sugihara and Yuen (7), who oxidized an isopropylidenated D-mannitol to a D-*lyxo*-3-hexulose derivative, and by Yuen and Sugihara (8), who oxidized a substituted D,L-galactitol and isolated from the product a crystalline *xylo*-3-hexulose. Stoodley (9) oxidized ribitol with mercuric acetate and obtained *erythro*-3-pentulose. A crystalline 3-heptulose was prepared by Schaeffer (10), who oxidized a branched-chain octose with periodate. The present work describes the preparation of 1-deoxy-L-*arabo*-3-hexulose derivatives from L-rhamnitol. This ketose is valuable as a possible intermediate in the preparation of L-streptose and other branched-chain sugars (11).

L-Rhamnitol condenses with formaldehyde in the presence of an acid catalyst to yield 1,3:2,5-di-*O*-methylene-L-rhamnitol (I) (12). This compound possesses a hydroxyl grouping on C_4 which is readily oxidized by chromium trioxide in glacial acetic acid – benzene (13) mixture to yield the crystalline ketose derivative 2,5:4,6-di-*O*-methylene-1-deoxy-L-*arabo*-3-hexulose (II), which gave a crystalline 2,5-dichlorophenylhydrazone. The ketose was readily reduced by sodium borohydride to yield the original di-*O*-methylene derivative and 1,3:2,5-di-*O*-methylene-6-deoxy-L-talitol. The latter material was produced in 55% yield when the reduction was carried out in absolute methanol solution (14) by addition of a methanolic sodium borohydride solution stabilized by sodium methoxide. The identification of the 6-deoxy-L-talitol was confirmed by its rate of movement on paper chromatographs and by comparing the retention time of the derived acetate with that of an authentic specimen on gas–liquid chromatograms (15).

Acetolysis of 1,3:2,5-di-*O*-methylene-L-rhamnitol followed by saponification of the product yielded 2,5-*O*-methylene-L-rhamnitol (12), which formed a 1-benzoate derivative. This compound, which possesses hydroxyl groups on C_3 and C_4, is readily oxidized

to a syrupy α-diketo compound (III) which with *O*-phenylenediamine yielded a quinoxaline compound (IV). Attempts to convert the α-diketo derivative to a streptosonic acid (11) analogue by a benzilic acid type rearrangement did not lead to the isolation of any identifiable products but tests indicated an α-hydroxycarboxylic acid was present.

It is likely that the hydroxyl group on C_4 of di-*O*-methylene-L-rhamnitol is oxidized easily because it is present in a relatively strain-free seven-membered ring in which the hydroxyl group is readily accessible. The oxidation of the axial 3-hydroxyl group in 2,4-*O*-methylene-xylitol 1,5-dibenzoates has been successfully achieved by Sera (16)but the oxidation of the equatorial 3-hydroxyl group on the corresponding ribitol derivative is difficult (unpublished results). It was considered likely that an isolated exocylic hydroxyl group would be more easily oxidized. To test this hypothesis 1,2:4,5-di-*O*-isopropylidene-D-mannitol 6-benzoate (17, 18) was prepared and submitted to oxidation. Unfortunately, no 3-hexulose derivative could be isolated from this reaction, perhaps because of the benzoate group on C_6 with which the hydroxyl group on C_3 may form a hydrogen bond. The 1,2:4,5-di-*O*-isopropylidene-D-mannitol gave a crystalline dibenzoate which on hydrolysis yielded the 1,4-di-*O*-benzoyl D-mannitol. This material was oxidized by periodate to a 2,5-di-*O*-benzoyl D-arabinose which is a potentially useful intermediate in the synthesis of disaccharides.

EXPERIMENTAL

All evaporations were carried out under reduced pressure and below 50°. Optical rotations were measured at 22±2°. Qualitative chromatography was carried out using the descending method (19) on Whatman No. 1 filter paper in the following solvents system (v/v): (A) butan-1-ol/ethanol/water, 3:1:1; (B) butan-1-ol/pyridine/water, 10:3:3; (C) ethyl acetate/acetic acid/formic acid/water, 18:3:1:4.

Ketoses were detected on paper chromatograms by the orcinol – trichloroacetic acid spray reagent (20) or with the *p*-anisidine hydrochloride spray reagent (21). Non-reducing compounds were detected by either the alkaline silver nitrate spray reagent (22) or by the ceric spray reagent (23). Rates of movement are quoted relative to L-rhamnose (R_{Rh}). Infrared spectra were measured using a Perkin–Elmer model 21 spectrophotometer or a Beckman IR-5B machine, as a 6% (w/v) chloroform solution or as a dispersion (0.8%) in a potassium bromide pellet. Ultraviolet spectra were measured using a Beckman DK-1 recording spectrometer.

2,5:4,6-Di-O-methylene-1-deoxy-L-arabo-3-hexulose (Cf. Ref. 13)

To a solution of 1,3:2,5-di-*O*-methylene-L-rhamnitol (12) (8.42 g) in benzene (160 ml) was added a hot solution of chromium trioxide (5.0 g, 1.1 mole equiv) in glacial acetic acid (440 ml) and water (4.44 ml). The mixture was heated at 85° for 40 minutes under reflux. The resultant solution was evaporated to a dark green syrup, which was dissolved in chloroform (200 ml). The solution was extracted with portions of cold *N* potassium carbonate solution until no further color was removed (1800 ml). Each extract was counterextracted with chloroform and the chloroform extracts were combined, washed with water, and dried (Na_2SO_4). Evaporation of the chloroform solution yielded the ketose (II) (5.64 g, 67%), which after recrystallization from ethanol had m.p. 151–152° and $[\alpha]_D$ +3.3° (*c*, 1.0, $CHCl_3$). The infrared spectrum showed a strong C=O stretching band at 1720 (approx.) cm^{-1}. The ketose gave a weak reaction with *p*-anisidine hydrochloride spray but a strong response to the alkaline silver nitrate spray. It gave a positive test for a ketose, a positive Molisch test, and reduced cold Fehling's solution. It had R_{Rh} 2.0 in solvent A and showed an absorption in the ultraviolet in aqueous solution at 297 mμ. Analysis: Calc. for $C_8H_{12}O_6$: C, 51.1%; H, 6.4%. Found: C, 50.9%; H, 6.45%.

When the ketose (0.225 g) was heated with 2,5-dichlorophenylhydrazine (0.23 g) in methanol (10 ml) a pale yellow crystalline hydrazone was produced. This, after three recrystallizations from ethyl acetate – chloroform, had m.p. 221° and $[\alpha]_D$ −154° (*c*, 1.0 in $CHCl_3$). Analysis: Calc. for $C_{14}H_{16}O_4Cl_2N_2$: C, 48.4%; H, 4.65%; Cl, 20.4%; N, 8.1%. Found: C, 48.2%; H, 4.7%; Cl, 20.7%; N, 8.1%.

Reduction of the Ketose

Reduction of the ketose with sodium borohydride yielded a mixture of the 1,3:2,5-di-*O*-methylene derivatives of L-rhamnitol and of L-talitol, the relative proportions of which were determined by the reaction conditions. Experimental details of a typical reduction are given below.

The ketose (II) (0.05 g) in 50% methanol (10 ml) was reduced by the dropwise addition at 0° of a sodium borohydride solution in 50% methanol (0.19 g, 10 ml). After 13 hours acetone was added to destroy excess borohydride, and sodium ions were removed from solution (IR-120 H resin). The acidic reaction mixture

Can. J. Chem. Downloaded from www.nrcresearchpress.com by 210.87.254.40 on 09/05/12
For personal use only.

was evaporated to dryness and boric acid was removed by distillation of methanol from the residues. The solid was then hydrolyzed by hot *N* hydrochloric acid (10 ml) and the cooled solution was deionized (Duolite A-4 OH) and concentrated to a syrup, which was acetylated (pyridine, acetic anhydride, 1 ml of each). The acetylated product was analyzed by gas–liquid chromatography. It contained L-rhamnitol and 6-deoxy-L-talitol acetates in the approximate ratio of 2 to 1. When the reaction was repeated, but substituting 50% ethanol for 50% methanol, the ratio of L-rhamnitol to 6-deoxy-L-talitol was 85:15.

When the reduction was carried out in absolute methanol plus sodium methoxide a much greater proportion of the 6-deoxy-L-talitol derivative was produced which could be isolated in a crystalline form. A typical experiment is given below.

1,3:2,5-Di-O-methylene-6-deoxy-L-talitol

2,5:4,6-Di-*O*-methylene-1-deoxy-L-*arabo*-3-hexulose (II) (0.87 g) in absolute methanol (15 ml) was reduced at 0° by the addition of sodium borohydride (0.9 g) in sodium methoxide solution (6 ml, 0.33 *N*); after 19 hours the product was isolated as described above. The crystals were recrystallized from acetone–petrol (b.p. 35–60°) and were obtained in 53% yield (0.46 g). The product had m.p. 122°, depressed to 96–97° on admixture with the L-rhamnitol derivative, and $[\alpha]_D$ +78° (*c*, 0.86 in $CHCl_3$). The infrared spectra of the L-rhamnitol and 6-deoxy-L-talitol derivative were different. Analysis: Calc. for $C_8H_{14}O_5$: C, 50.5%; H, 7.4%. Found: C, 50.5%; H, 7.4%. On hydrolysis (*N* HCl) the 2,5:4,6-di-*O*-methylene-6-deoxy-L-talitol yielded the syrupy sugar which was not separable from authentic material on paper chromatograms and the acetate was indistinguishable from an authentic specimen in the gas–liquid chromatographic apparatus.

1-Deoxy-L-arabo-*3-hexulose*

Attempts to prepare the sugar from the dimethylene compound either by acidic hydrolysis or by acetolysis were unsuccessful. In a typical experiment the di-*O*-methylene ketose (0.1 g) was hydrolyzed with *N* hydrochloric acid (20 ml) for 1 hour at 100°. Chromatographic analysis of the product showed the presence of seven components of R_{Rh} 0.33, 0.78, 1.02, 1.2, 1.95, 2.15, and 2.58. All except the component at R_{Rh} 1.02 gave a yellow color with the *p*-anisidine hydrochloride reagent. No crystalline derivative could be isolated.

Acetolysis Experiments

To the ketose derivative (II) (2 g) in 5 ml of a mixture of acetic acid (7.5 ml) and acetic anhydride (17.5 ml) was added 5.5 ml of an ice-cold acetolyzing mixture composed of sulphuric acid (1 ml), acetic anhydride (35 ml) and acetic acid (15 ml). The ketose derivative (II) dissolved at once and the solution gradually developed a violet color. After 1 hour it was poured onto ice and the mixture became green in color. The product was isolated by chloroform extraction in the usual way. Concentration of the chloroform extract yielded a syrup which did not crystallize. Two components were detected chromatographically (solvent A) with R_{Rh} 1.6 (positive test with alkaline silver nitrate) and R_{Rh} 1.78 (positive test with *p*-anisidine hydrochloride spray). Catalytic saponification (Zemplen) yielded a syrupy mixture which contained a major component at R_{Rh} 2.32 (solvent A).

2,5-O-Methylene-L-rhamnitol 1-Benzoate

To 2,5-*O*-methylene-L-rhamnitol (12) (4.4 g) in dry pyridine (20 ml) at 0° was added benzoyl chloride (3.15 ml, 1.1 mole equiv) dropwise during 5 minutes. After 20 hours at 21° the solution was poured onto ice (35 g). The product was extracted with chloroform in the usual way. Evaporation of the solvent left a crystalline residue which was recrystallized from acetone–petrol (b.p. 36–60°). Yield 4.4 g of m.p. 102° and $[\alpha]_D$ +69° (*c*, 1.0 in $CHCl_3$). Analysis: Calc. for $C_{14}H_{18}O_6$: C, 59.6%; H, 6.4%. Found: C, 59.3%; H, 6.3%.

Oxidation of 2,5-O-Methylene-L-rhamnitol 1-Benzoate to 2,5-O-Methylene-6-deoxy-L-threo-3,4-hexulodiose 1-Benzoate

The benzoate (0.86 g) in a mixture of benzene (15 ml), acetic acid (61 ml), and water (0.61 ml) was oxidized with chromium trioxide (0.67 g, 2.2 mole equiv). The mixture was heated at 80° for 35 minutes and the product (III, 0.39 g) was isolated as a yellow syrup by the procedure described above. Infrared examination of the syrup showed the absence of OH groups and a slight shift in the wavelength of the C=O stretching hand.

Characterization of the Oxidation Product

The syrupy diketose (0.1 g) was dissolved in ethanol (3 ml) and the solution was added to a solution of *O*-phenylenediamine (0.1 g) in ethanol (3 ml). The mixture was heated at 75° for 20 minutes and cooled. The resulting buff-colored crystals were collected and recrystallized from ethanol. The small needle-like crystals (50 mg) had m.p. 149°. Analysis: Calc. for $C_{20}H_{18}O_4N_2$: C, 68.6%; H, 5.2%; N, 8.0%. Found: C, 68.4%; H, 5.1%; N, 8.3%. The syrupy diketo compound (III, 0.804 g) was mixed with water (10 ml) and sodium hydroxide (4 ml, *N*); to aid solution methanol (7 ml) was added. After 2¼ hours the solution had become deep orange in color. After a further 5 minutes at 80° the cooled solution was extracted with chloroform to remove methyl benzoate. The residual aqueous layer was deionized (Amberlite IR-120 H) and the lemon yellow effluent was evaporated to yield a crystalline solid, identified as benzoic acid, m.p. 120°. The residual syrup gave tests for an α-hydroxy acid ($FeCl_3$) and showed absorption in the infrared

Can. J. Chem. Downloaded from www.nrcresearchpress.com by 210.87.254.40 on 09/05/12
For personal use only.

characteristic of a hydroxy carboxylic acid. Attempts to prepare a crystalline methyl ester by refluxing the syrup with methanolic hydrogen chloride were unsuccessful.

Derivatives of 1,2:4,5-Di-O-isopropylidene-D-mannitol

2,3:5,6-Di-*O*-isopropylidene-D-mannose was synthesized by the method of Van Grunenberg *et al.* (24). The product (5 g) was reduced by adding its solution in aqueous methanol to an ice-cold, stirred solution of sodium borohydride (5 g) in water (150 ml). (Note: If the order of addition is reversed very poor yields are obtained.) After 24 hours the solution gave a negative Molisch test for hexoses and excess of borohydride was destroyed by the addition of acetone (150 ml). The solution was evaporated and the residue was extracted with ether. The product was recrystallized with difficulty from ether–petrol. It had m.p. 50° (literature 52° (17)) and was obtained in a yield of 3.5 g. When the reduction was made with lithium aluminum hydride a similar yield was obtained.

1-O-Benzoyl 2,3:5,6-Di-O-isopropylidene-D-mannitol

A solution of 1,2:4,5-di-*O*-isopropylidene-D-mannitol (2.3 g) in dry pyridine (15 ml) was cooled at 0° and to it benzoyl chloride (1.1 ml) was added dropwise and with stirring and cooling during 15 minutes. After 24 hours at 20° the mixture was poured onto ice and the solution was extracted with ether. The extracts were washed successively with *N* hydrochloric acid, sodium bicarbonate solution, and water and then dried (Na_2SO_4). Evaporation of the ether left a syrup which rapidly crystallized. The product (2.03 g) was crystallized from ethanol and had m.p. 109°, $[\alpha]_D$ +6° (*c*, 2.5 $CHCl_3$). Analysis: Calc. for $C_{19}H_{26}O_7$: C, 62.3%; H, 7.15%. Found: C, 62.2%; H, 6.8%.

1-O-Benzoyl D-Mannitol

The 1-*O*-benzoyl 2,3:5,6-di-*O*-isopropylidene-D-mannitol (6.5 g) was dissolved in 30% acetic acid (10 ml) and the solution was heated at 86° for 15 minutes. Evaporation of the solution yielded crystalline 1-*O*-benzoyl D-mannitol (0.221 g) of m.p. 178°. Analysis: Calc. for $C_{13}H_{18}O_7$: C, 54.5%; H, 6.3%. Found: C, 54.15%; H, 6.3%. On prolonged oxidation this product consumed 5.15 mole of periodate and produced 1.05 mole of formaldehyde and 3.4 mole of formic acid per mole. Theory requires the formation of 1 mole of formaldehyde and 3 moles of formic acid per mole. The high results are due to overoxidation.

1,4-Di-O-benzoyl 2,3:5,6-Di-O-isopropylidene-D-mannitol

To dry 1,2:4,5-di-*O*-isopropylidene-D-mannitol (2 g) dissolved in dry pyridine (20 ml) was added benzoyl chloride (6 ml) with stirring at 0° during 40 minutes. The product was isolated in the usual way by extraction with ether. Evaporation of the ether yielded the 1,4-di-*O*-benzoyl derivative (3.01 g) of m.p. 136° and $[\alpha]_D$ −34° (*c*, 2.5 $CHCl_3$) after recrystallization from ethanol. Analysis: Calc. for $C_{26}H_{30}O_8$: C, 66.4%; H, 6.4%. Found: C, 66.1%; H, 6.4%.

1,4-Di-O-benzoyl D-Mannitol

Acetic acid (40%, 10 ml) was added to 1,4-di-*O*-benzoyl 2,3:5,6-di-*O*-isopropylidene-D-mannitol (1.0 g) and the mixture was heated at 85° for 30 minutes. Because the compound had not all dissolved 50% acetic acid (10 ml) was added and the solution was heated for a further 30 minutes. The solution was cooled, unchanged material (0.179 g) was collected by filtration, and the filtrate was evaporated to an oil which solidified. It had m.p. 111° and $[\alpha]_D$ −12° (*c*, 1.0 acetone) and was difficult to recrystallize. Analysis: Calc. for $C_{20}H_{22}O_8$: C, 61.5%; H, 5.7%. Found: C, 61.2%; H, 5.8%.

Periodate Oxidation

The product gave the following yields of formaldehyde (A) uptake of periodate (B) in moles per mole at the times indicated. (A): 0.94 (0.17 hr); 0.98 (0.67 hr); 0.98 (2.67 hr); and 0.98 (20.17 hr). (B): 0.91 (0.27 hr); 1.33 (1.15 hr); 1.39 (2.8 hr); 1.47 (8.5 hr); and 1.75 (22.5 hr). Attempts to oxidize 2,3:5,6-di-*O*-isopropylidene-D-mannitol 1-benzoate with chromium trioxide in pyridine or in glacial acetic acid led to recovery of starting material.

ACKNOWLEDGMENTS

The authors thank the National Research Council for a grant (N.R.C. T-19) which made this work possible.

REFERENCES

1. J. C. Sowden. Advan. Carbohydrate Chem. **12**, 68 (1957).
2. A. T. Wilson and M. Calvin. J. Am. Chem. Soc. **77**, 5948 (1955).
3. J. S. Burton, W. G. Overend, and N. R. Williams. Chem. Ind. (London), 175 (1961).
4. O. Theander. Acta Chem. Scand. **12**, 1883 (1958).
5. N. K. Richtmyer, L. C. Stewart, and C. S. Hudson. J. Am. Chem. Soc. **72**, 4934 (1950).
6. J. K. N. Jones. J. Am. Chem. Soc. **78**, 2855 (1956).
7. J. M. Sugihara and G. U. Yuen. J. Am. Chem. Soc. **79**, 5780 (1957).
8. G. U. Yuen and J. M. Sugihara. J. Org. Chem. **26**, 1958 (1961).

Can. J. Chem. Downloaded from www.nrcresearchpress.com by 210.87.254.40 on 09/05/12
For personal use only.

9. R. J. STOODLEY. Can. J. Chem. **39**, 2593 (1961).
10. R. SCHAEFFER. J. Am. Chem. Soc. **81**, 2838 (1959).
11. R. U. LEMIEUX and M. L. WOLFROM. Advan. Carbohydrate Chem. **3**, 362 (1948).
12. W. T. HASKINS, R. M. HANN, and C. S. HUDSON. J. Am. Chem. Soc. **67**, 1800 (1945).
13. D. H. RAMMLER and C. A. DEKKER. J. Org. Chem. **26**, 4615 (1961).
14. R. E. DAVIS and J. A. GOTTBRATH. J. Am. Chem. Soc. **84**, 895 (1962).
15. S. W. GUNNER, J. K. N. JONES, and M. B. PERRY. Can. J. Chem. **39**, 1892 (1961).
16. A. SERA. Bull. Chem. Soc. Japan, **35**, 2033 (1962).
17. L. S. BOGGS. Abstracts, 136th Meeting of the American Chemical Society. 1958. 6D-17.
18. H. ENDRES and M. OPPELT. Ber. **91**, 478 (1958).
19. S. M. PARTRIDGE. Biochem. J. **42**, 238 (1948).
20. R. KLEVSTRAND and A. NORDAL. Acta Chem. Scand. **4**, 1320 (1950).
21. L. HOUGH, J. K. N. JONES, and W. H. WADMAN. J. Chem. Soc. 1702 (1950).
22. W. E. TREVELYN, D. P. PROCTER, and J. S. HARRISON. Nature, **166**, 444 (1950).
23. J. W. BIRD. Can. J. Chem. **40**, 1716 (1962).
24. H. VANGRUNENBERG, C. BREDT, and W. FREUDENBERG. J. Am. Chem. Soc. **60**, 1507 (1938).

Can. J. Chem. Downloaded from www.nrcresearchpress.com by 210.87.254.40 on 09/05/12
For personal use only.

THE Co^{60} γ-RADIOLYSIS OF AQUEOUS CYSTINE SOLUTIONS

I. THE EFFECT OF CHLORIDE ION ON THE AMMONIA YIELD[1]

W. A. ARMSTRONG AND D. W. GRANT
Defence Research Chemical Laboratories, Ottawa, Canada

Received March 19, 1963

ABSTRACT

Sodium chloride has been found to increase the ammonia yield from Co^{60} γ-irradiated cystine in 0.02 M H_2SO_4. The effect is attributed to the participation of chlorine atoms, which deaminate the amino acid to a greater extent than hydroxyl radicals. The ratio of the rate constants $k_{OH + cystine}/k_{OH + Cl^-}$ is determined to be 24 in 0.02 M H_2SO_4.

INTRODUCTION

A paper chromatographic study of the products from the Co^{60} γ-radiolysis of aqueous 3×10^{-4} M cystine solutions revealed that the type of product formed was sensitive to the presence of chloride ions (1). In particular hydrochloric acid appeared to favor the production of cysteine and an unidentified compound, while sulphuric acid appeared to favor the production of cysteic acid and cystine disulphoxide. The results suggested that hydroxyl radicals and chlorine atoms formed through the reaction

$$OH + H^+ + Cl^- \rightarrow H_2O + Cl \qquad [1]$$

degrade cystine by different mechanisms. The ammonia yields from Co^{60} γ-irradiated cystine solutions were determined to see if the deamination process is sensitive to chloride ion concentration.

EXPERIMENTAL

Materials

L-Cystine was M.A. grade from Mann Research Laboratories ($[\alpha] = -216°$ in 1 M HCl). All other chemicals were reagent or analytical grade. All solutions were made using triply distilled water, the second distillation being from alkaline $KMnO_4$ and the final distillation from dilute H_2SO_4.

Irradiations

All irradiations were carried out in Pyrex vessels which had been cleaned using chromic acid, repeatedly rinsed with triply distilled water, and given a final steaming-out with steam from boiling alkaline $KMnO_4$. The γ-ray source was a nominal 200 c of cobalt-60, housed at the bottom of a water-filled well. The radiation doses received by the cystine solutions were determined using the Fricke dosimeter (2) assuming $G(Fe(III))$ to be 15.5 and the ferric ion extinction coefficient to be 2196 at 25° C for the 304 mμ band (3). Air-saturated solutions and degassed solutions were irradiated at dose rates of about 3.5×10^{16} ev/ml min and 4.5×10^{16} ev/ml min respectively.

Deaeration of Solutions

Solutions were degassed in a high-vacuum system ($<10^{-5}$ mm Hg) using the usual method of repeated cycles of freezing, pumping, and thawing. The vessels were flame-sealed while the solutions were frozen.

Ammonia Analysis

Ammonia was determined by a method based on its reaction with hypochlorite and phenol to give a colored indophenol. It is noteworthy that aliphatic amines do not undergo this reaction (4). Numerous methods based on this reaction have been described previously (4, 5). However, all those investigated suffered from a lack of reproducibility, color instability, or unacceptably high "blanks". The procedure adopted combines what are considered the best features of the methods of Bolleter, Bushman, and Tidwell (4) and Scheurer and Smith (5). The color is developed rapidly and is stable for at least 1 hour. As the color intensity depends to some extent on the age of the reagents, ammonia concentrations in irradiated samples were determined by a direct comparison of the optical densities of the indophenol produced from these

[1]*Issued as D.R.C.L. Report No. 407.*

Can. J. Chem. Downloaded from www.nrcresearchpress.com by 210.87.254.105 on 09/05/12
For personal use only.

solutions and suitable standard ammonium chloride solutions. In order to obtain low "blank" readings it was found essential to use water distilled from dilute H_2SO_4 for the preparation of all solutions, and to absorb the ammonia, liberated on steam distillation, in water rather than in boric acid as is usually recommended. The detailed procedure is outlined below.

To a 25.0-ml aliquot of irradiated solution was added 0.5 g MgO. The ammonia was removed by a 5-minute steam distillation, absorbed in water, and the distillate made up to 25 ml with water. Three aliquots of unirradiated cystine solution, two containing different standard concentrations of ammonium chloride (in the range 10^{-5}–1.4×10^{-4} M), were similarly treated. To 10.0 ml of each distillate was added 1.0 ml of saturated chlorine water prepared by bubbling chlorine into ice-cold water until solid chlorine hydrate formed. After 5 minutes 1.0 ml of 8% aqueous phenol and 0.05 ml of 0.003 M manganous chloride solution were added. Five minutes later 0.5 ml of 2 M NaOH was added and the color allowed to develop for about 10 minutes. The optical density of each colored solution was measured at 627 mμ. The ammonia concentration in the irradiated solution was taken as the mean of the results obtained using the two "standards". The concentration of "standards" always approximated to the ammonia concentrations in irradiated solutions within a factor of two.

RESULTS AND DISCUSSION

The deamination of 3×10^{-4} M and 10^{-3} M cystine solutions is sensitive to chloride ions since the initial yields of ammonia are increased four- to five-fold when the acid is changed from 0.02 M H_2SO_4 to 0.04 M HCl (Fig. 1). There is also a pH effect since the

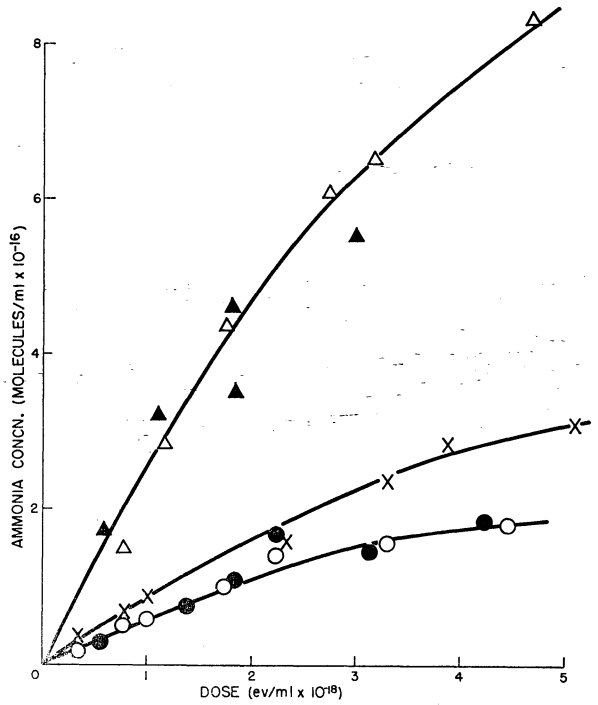

FIG. 1. Ammonia production in irradiated aerated cystine solutions. ○ 3×10^{-4} M in 0.02 M H_2SO_4; ● 10^{-3} M in 0.02 M H_2SO_4; × 3×10^{-4} M, no added acid; △ 3×10^{-4} M in 0.04 M HCl; ▲ 10^{-3} M in 0.04 M HCl.

initial ammonia yield is greater in solutions without added acid than in 0.02 M H_2SO_4 solutions of the amino acid (Fig. 1). The chloride ion effect was examined in more detail in 3×10^{-4} M cystine – 0.02 M H_2SO_4 solutions with sodium chloride concentrations varying from 10^{-3} to 0.25 M. The results (Fig. 2) show that $G_0(NH_3)$, the initial ammonia yield, increases from 0.8 to 2.75 as the chloride ion concentration is increased from

Can. J. Chem. Downloaded from www.nrcresearchpress.com by 210.87.254.105 on 09/05/12
For personal use only.

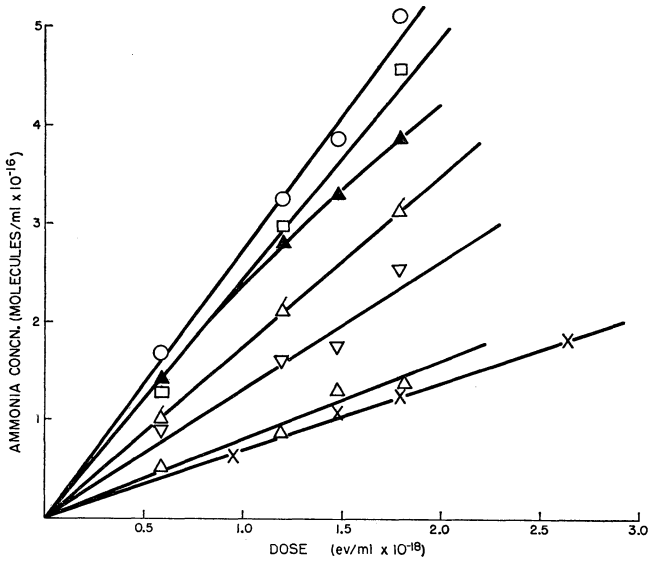

FIG. 2. Effect of sodium chloride on ammonia production in irradiated aerated 3×10^{-4} M cystine solutions. × 4×10^{-2} M NaCl, no added acid; △ 10^{-3} M NaCl – 0.02 M H_2SO_4; ▽ 5×10^{-3} M NaCl – 0.02 M H_2SO_4; △ 10^{-2} M NaCl – 0.02 M H_2SO_4; ▲ 4×10^{-2} M NaCl – 0.02 M H_2SO_4; □ 0.25 M NaCl – 0.02 M H_2SO_4; ○ 0.1 M NaCl – 0.02 M H_2SO_4.

10^{-3} to 10^{-1} M. A further increase in chloride ion concentration to 0.25 M reduced $G_0(NH_3)$ to 2.5.

The actual number of radicals available for deamination would actually tend to increase with increasing chloride ion concentration, since chloride ions have been shown (6) to scavenge hydroxyl radical precursors of the "molecular" hydrogen peroxide yield. The magnitude of this effect has not been determined at the acid concentration used in the present research. However, from Sworski's data (6) at pH 2 and in 0.8 N H_2SO_4 solutions, it is probable that even in 0.1 M sodium chloride the actual increase in radicals from this effect would not exceed 0.3 radical per 100 ev. Therefore, the magnitude of the increase in $G_0(NH_3)$ induced by chloride ions (Fig. 2) cannot be explained on the basis of a scavenging of "molecular" hydrogen peroxide precursors.

The chloride ion effect can be explained qualitatively on the basis of reactions [1], [2], and [3] if it is assumed that chlorine atoms deaminate cystine (RSSR) to a greater

$$RSSR + OH \rightarrow \text{ammonia} + \ldots \quad [2]$$

$$RSSR + Cl \rightarrow \text{ammonia} + \ldots \quad [3]$$

extent than hydroxyl radicals. Thus with sodium chloride concentrations $\geqslant 0.10$ M, it is assumed that virtually all hydroxyl radicals are scavenged by chloride ions to produce chlorine atoms (via reaction [1]), which degrade cystine predominantly in deamination reactions. In the absence of chloride ions hydroxyl radicals are scavenged by cystine and lower ammonia yields result. At intermediate chloride ion concentrations cystine and chloride ions compete for hydroxyl radicals. The slight decrease in $G_0(NH_3)$ when the sodium chloride concentration exceeds 0.1 M (Fig. 2) is not understood, since a small increase is to be expected on the basis of increased scavenging of hydroxyl radical precursors of "molecular" hydrogen peroxide. The low ammonia yield ($G_0(NH_3) = 0.7$) in aqueous cystine solutions (pH 4.1) containing 0.04 M sodium chloride (Fig. 2) supports

Can. J. Chem. Downloaded from www.nrcresearchpress.com by 210.87.254.105 on 09/05/12
For personal use only.

the view already expressed (7) that chloride ions are inefficient scavengers of hydroxyl radicals at pH > 4 possibly because the reaction

$$OH + Cl^- \rightarrow OH^- + Cl \qquad [4]$$

is endothermic.

The effect of solution deaeration prior to irradiation is seen to produce little or no change in the initial ammonia yields in the case of cystine solutions containing 5×10^{-3} *M* NaCl and 0.04 *M* HCl (C and D curves, Fig. 3), but produces a significant decrease in

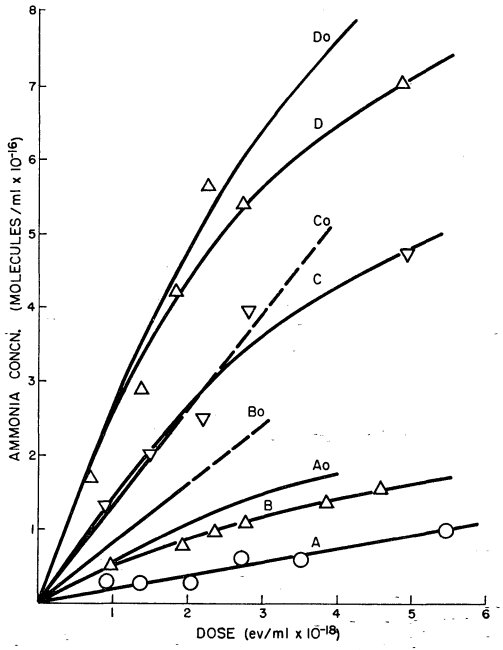

FIG. 3. Effect of deaeration on ammonia production in irradiated 3×10^{-4} *M* cystine – 0.02 *M* H_2SO_4 solutions. A deaerated, no added NaCl; A_0 aerated, no added NaCl. B deaerated, 10^{-3} *M* NaCl; B_0 aerated, 10^{-3} *M* NaCl. C deaerated, 5×10^{-3} *M* NaCl; C_0 aerated, 5×10^{-3} *M* NaCl. D deaerated, 4×10^{-2} *M* NaCl; D_0 aerated, 4×10^{-2} *M* NaCl.

the initial yields from solutions containing 10^{-3} *M* NaCl or no sodium chloride (B and A curves, Fig. 3). Deaeration of 3×10^{-4} *M* cystine solutions (pH 4.1) prior to irradiation was found (not shown) to produce a fractional decrease in the initial ammonia yield similar to that noted for 3×10^{-4} *M* cystine in 0.02 *M* sulphuric acid. These results in deaerated solutions suggest that the actual *mechanism* of deamination of cystine by chlorine atoms and hydroxyl radicals is different, the former process being oxygen independent and the latter process oxygen dependent.

Hydrogen peroxide is normally produced in irradiated aerated aqueous solutions via the reactions

$$H_2O \xrightarrow{\sim} H_2O_2,\ H_2,\ OH,\ H \qquad [5]$$

$$H + O_2 \longrightarrow HO_2 \qquad [6]$$

$$HO_2 + HO_2 \longrightarrow H_2O_2 + O_2. \qquad [7]$$

For aerated unbuffered 3×10^{-4} *M* cystine solutions the initial hydrogen peroxide yield

Can. J. Chem. Downloaded from www.nrcresearchpress.com by 210.87.254.105 on 09/05/12
For personal use only.

is 2.0 (8). Hydrogen peroxide can compete with cystine and chloride ions for radicals according to the reactions

$$Cl + H_2O_2 \rightarrow HO_2 + HCl \quad [8]$$

$$OH + H_2O_2 \rightarrow HO_2 + H_2O. \quad [9]$$

Although HO_2 radicals could conceivably participate in deamination reactions it is generally recognized (9, 10) that they are relatively unreactive, particularly toward saturated organic substances.

The Determination of the Rate Constant Ratio k_2/k_1

The ratio of the rate constants for reactions [2] and [1], i.e. k_2/k_1 may be determined from the data of Fig. 2 if the change in ammonia yield with chloride ion concentration is due solely to competition between reactions [1] and [2] for hydroxyl radicals. The participation, if any, of the HO_2 radical in deamination reactions is not likely to affect the treatment given below, since the initial ammonia yield due to this radical would presumably be a constant independent of chloride ion concentration. With regard to reaction [8], its effect on the ammonia yield is determined by $k_8[H_2O_2]/k_3[RSSR]$, which again is virtually independent of the chloride ion concentration. However, reaction [9] merits further consideration because in principle it can compete with reactions [1] and [2] for hydroxyl radicals. From the treatment of Schwarz (11) it may be deduced that the rate constant ratio $k_{OH + Br^-}/k_{OH + Cl^-}$ is approximately 40 at pH 2, and is therefore presumably about 10 in 0.02 *M* H_2SO_4. Since the experiments of Hummel and Allen (12) and Rabani and Stein (13) yield the rate consant ratios $k_{OH + Br^-}/k_{OH + EtOH} = 0.6$ and $k_{OH + EtOH}/k_{OH + H_2O_2} = 9.2$, it follows that $k_{OH + H_2O_2}/k_{OH + Cl^-} \simeq 2$ in 0.02 *M* H_2SO_4. Consequently, since $[Cl^-] \gg [H_2O_2]$ at low doses, reaction [9] cannot compete effectively with reaction [1] or presumably for that matter with reaction [2].

The initial ammonia yield is given by

$$G_0(NH_3) = \begin{bmatrix}\text{fraction of OH radicals} \\ \text{scavenged by } Cl^-\end{bmatrix} G_{max} + \begin{bmatrix}\text{fraction of OH radicals} \\ \text{scavenged by RSSR}\end{bmatrix} G_{min},$$

where G_{max} is the maximum initial ammonia yield observed, i.e. when all OH radicals are scavenged by Cl^-, and G_{min} is the minimum initial ammonia yield, i.e. when all OH radicals are scavenged by cystine.

$$G_0(NH_3) = \frac{k_1[Cl^-]\cdot G_{max}}{k_1[Cl^-]+k_2[RSSR]} + \left[1 - \frac{k_1[Cl^-]}{k_1[Cl^-]+k_2[RSSR]}\right]\cdot G_{min}$$

$$= \frac{G_{max}}{1 + \dfrac{k_2[RSSR]}{k_1[Cl^-]}} + G_{min} - \frac{G_{min}}{1 + \dfrac{k_2[RSSR]}{k_1[Cl^-]}} \quad [A]$$

The ratio k_2/k_1 may be determined using equation [A] provided the initial ammonia yields (Fig. 2) are corrected for "molecular" precursor scavenging by chloride ions. It may be assumed that hydroxyl radical scavenging within "spurs" by chloride ions results in a chlorine atom and a hydroxyl radical which diffuse out into the body of the solution. Each chlorine atom can be assumed to produce approximately one molecule of ammonia by reaction with cystine since $G_{max} \simeq G_{OH}$, and each hydroxyl radical is assumed to be scavenged by either cystine or chloride ions. When the hydroxyl radical is scavenged by cystine it is assumed that approximately 0.2 molecule of ammonia results, since $G_{min} \simeq 0.2G_{max}$. The ammonia yield due to scavenging within "spurs" is then given by

Can. J. Chem. Downloaded from www.nrcresearchpress.com by 210.87.254.105 on 09/05/12
For personal use only.

$$\Delta G(NH_3) = \Delta G_{H_2O_2} + \Delta G_{H_2O_2} \times f + \Delta G_{H_2O_2} \times 0.2(1-f), \quad [B]$$

where $\Delta G_{H_2O_2}$ is the decrease in the "molecular" peroxide yield produced by chloride ions (6) and f is the fraction of OH radicals diffusing out of "spurs" which are scavenged by chloride ions, i.e.

$$\frac{k_1[Cl^-]}{k_1[Cl^-]+k_2[RSSR]}.$$

The corrected initial ammonia yields $G(NH_3)_{corr}$ (Table I) were obtained by means of equation [B] using Sworski's data (6) for $\Delta G_{H_2O_2}$ and a value of 24 for k_2/k_1. The values

TABLE I

Calculated values for the rate constant ratio k_2/k_1 in 0.02 M H_2SO_4

[NaCl] (M)	$G_0(NH_3)$ (aerated)	$G_0(NH_3)_{corr}$	k_2/k_1
—	0.5_5 (G_{min})		
10^{-3}	0.8_0	0.7_7	26
5×10^{-3}	1.3_5	1.2_9	27
10^{-2}	1.7_5	1.6_6	25
4×10^{-2}	2.4_5	2.2_8	17
10^{-1}	2.7_5	2.5_0 (G_{max})	

thus derived for k_2/k_1 are listed in Table I. Since cystine reacts approximately 24 times as fast as chloride ions with hydroxyl radicals, it must be presumed to scavenge hydroxyl radicals from the "spurs" at a correspondingly faster rate than chloride ions. However, since the amino acid concentration was fixed at 3×10^{-4} M throughout the competition kinetic study, this scavenging effect will not change the values calculated for k_2/k_1.

CONCLUSION

Two points appear noteworthy. This paper demonstrates clearly that results obtained using amino acid hydrochlorides in hydrochloric acid are not necessarily comparable with results obtained either in sulphuric acid or in the absence of added acid. The results reported previously (1) and in the present paper suggest that chlorine atoms preferentially attack cystine at the amino group leading to deamination, while hydroxyl radicals preferentially attack cystine at the disulphide bond leading to the formation of cysteic acid in oxygenated solutions. Experiments are in progress to identify deaminated products in irradiated hydrochloric acid and sulphuric acid solutions of cystine in order to elucidate the mechanism of the different deamination processes.

REFERENCES

1. D. W. Grant, S. N. Mason, and M. A. Link. Nature, **192**, 352 (1961).
2. J. Weiss, A. O. Allen, and H. A. Schwarz. Proc. 1st Intern. Conf. Peaceful Uses At. Energy, Geneva, 1955, **14**, 179 (1956).
3. K. Scharf and R. M. Lee. Radiation Res. **16**, 115 (1962).
4. W. T. Bolleter, C. J. Bushmann, and P. W. Tidwell. Anal. Chem. **33**, 592 (1961).
5. P. G. Scheurer and F. Smith. Anal. Chem. **27**, 1616 (1955).
6. T. J. Sworski. Radiation Res. **2**, 26 (1955).
7. A. O. Allen, C. J. Hochanadel, J. A. Ghormley, and T. W. Davis. J. Phys. Chem. **56**, 575 (1952).
8. W. A. Armstrong. Unpublished work.
9. W. M. Garrison. Ann. Rev. Phys. Chem. **8**, 129 (1957).
10. G. Scholes and J. Weiss. Radiation Res. Supp. **1**, 177 (1959).
11. H. A. Schwarz. J. Am. Chem. Soc. **77**, 4960 (1955).
12. A. Hummel and A. O. Allen. Radiation Res. **17**, 302 (1962).
13. J. Rabani and G. Stein. Trans. Faraday Soc. **58**, 2150 (1962).

Can. J. Chem. Downloaded from www.nrcresearchpress.com by 210.87.254.105 on 09/05/12
For personal use only.

OCCURRENCE OF *trans*-9-*trans*-12-OCTADECADIENOIC ACID AS A SEED OIL COMPONENT[1,2]

MARY J. CHISHOLM AND C. Y. HOPKINS
Division of Pure Chemistry, National Research Council, Ottawa, Canada

Received March 29, 1963

ABSTRACT

trans-9-*trans*-12-Octadecadienoic acid was found to be a component of the glyceride oil of the seeds of *Chilopsis linearis* (Cav.) Sweet. It was isolated by fractional crystallization of the acids at low temperatures and removal of conjugated acids as their adducts with maleic anhydride. Identification was made by absorption spectra and by preparation of derivatives and degradative products. The acid is estimated to constitute about 15% of the total fatty acids of the oil. Linoleic acid was also identified.

Can. J. Chem. Downloaded from www.nrcresearchpress.com by 210.87.254.105 on 09/05/12
For personal use only.

The occurrence of one or more positional isomers of linoleic acid in natural oils and fats has been suspected for a long time but was established only recently by the isolation of 10,12-octadecadienoic acid from a seed oil (1, 2). It has been considered less likely that geometric isomers of linoleic acid would be found in seeds since nearly all monoene and diene fatty acids of vegetable oils so far discovered have had the cis configuration. However, in the present work, examination of the seed oil of *Chilopsis linearis* provided infrared spectral evidence for the presence of a fatty acid containing isolated trans double bonds. It proved to be a geometric isomer of linoleic acid.

The freshly extracted oil had infrared absorption at 986 cm^{-1}, mainly due to the conjugated triene acid component, *trans,trans,cis*-9,11,13-octadecatrienoic acid (2). The subsidiary peak at 960 cm^{-1}, however, was more intense than would be expected for a trans–trans–cis acid. The conjugated trans–trans diene acid also known to be present (2) would not contribute to the absorption in the 960 cm^{-1} region. It was presumed, therefore, that part of this absorption must be due to an isolated trans linkage. This was confirmed by fractional crystallization of the mixed fatty acids at low temperatures, which effected a substantial separation of the various components. Three fractions were shown by infrared spectra (Fig. 1) to consist of concentrates of conjugated diene acid (F21), isolated trans-unsaturated acid (F22), and conjugated triene acid (F23).

Fraction F22 was crystallized further until free of conjugated triene acid but it continued to retain a little conjugated diene acid. It was found that the conjugated diene acid could be removed as its adduct with maleic anhydride. This treatment left the acid with isolated trans bonds unchanged. The latter acid melted when pure at 26.5–27.0° and was free of conjugated material as determined by ultraviolet absorption. Its infrared spectrum, max. 963 cm^{-1}, also showed the absence of conjugated diene and triene linkages since there was no peak or shoulder in the region of 986 cm^{-1} (Fig. 2). The intensity of the peak at 963 cm^{-1} was approximately double that of the same peak in the spectrum of elaidic acid; hence the substance must contain two isolated trans double bonds.

Hydrogenation of the acid resulted in the absorption of 2 moles of hydrogen and formation of stearic acid. Oxidative splitting of the acid gave two fragments identified by gas chromatography as hexanoic and azelaic acids, showing that the diene grouping is 9,12. These reactions, along with the spectral data, established the structure and configuration of the substance as *trans*-9-*trans*-12-octadecadienoic acid. To confirm its

[1]*Issued as N.R.C. No. 7401.*
[2]*Presented before the Chemical Institute of Canada, at Toronto, June 6–8, 1963.*

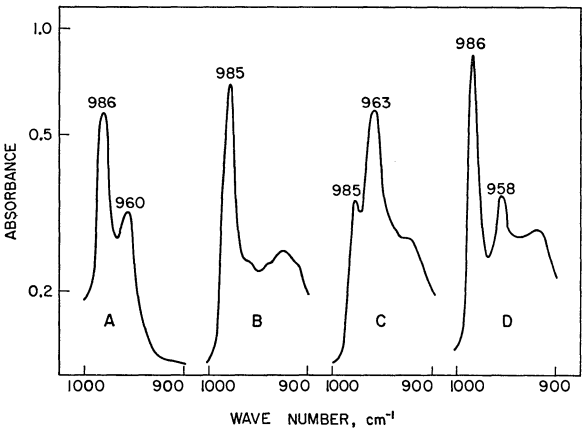

FIG. 1. Infrared absorption at 900–1000 cm^{-1}. A, chilopsis oil. B, fatty acids fraction F21, mainly trans–trans conjugated diene. C, fraction F22, mainly trans–trans non-conjugated diene. D, fraction F23, mainly trans–trans–cis conjugated triene.

identity an authentic sample was prepared by stereomutation of linoleic acid to the trans–trans form (linelaidic acid). This substance and the chilopsis acid had the same melting point and mixed melting point. The *p*-phenylphenacyl esters were also identical. The natural acid was converted by alkaline permanganate to di-*threo*-9,10,12,13-tetrahydroxystearic acid, m.p. 148°, and this was identical with an authentic sample.

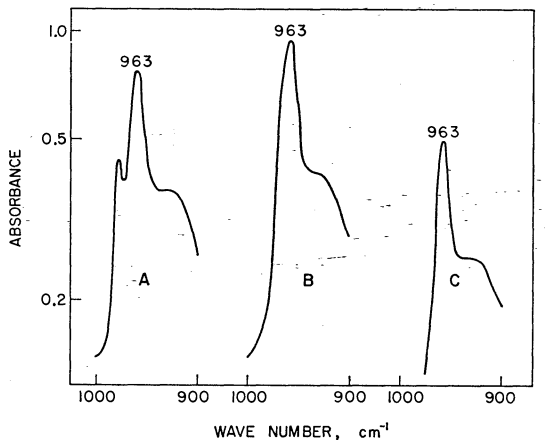

FIG. 2. Infrared absorption at 900–1000 cm^{-1}. A, fatty acids fraction, mainly trans–trans non-conjugated diene. B, pure *trans*-9-*trans*-12-octadecadienoic acid from chilopsis oil. C, *trans*-9-octadecenoic (elaidic) acid.

The most soluble fraction of the fatty acids of the oil (F4) was examined (as methyl esters) by gas chromatography. The emergence time of the major constituent was identical with that of methyl linoleate. Its identity as linoleate was confirmed by oxidizing a part of fraction F4 by alkaline permanganate. The product was the expected di-*erythro*-9,10,12,13-tetrahydroxystearic acid, m.p. 173–174°.

EXPERIMENTAL

Ultraviolet absorption measurements were made in cyclohexane solution with a Beckman DU spectrophotometer. Infrared spectra were determined in carbon disulphide in a Perkin–Elmer Model 21 spectrophotometer with sodium chloride prism. Melting points were determined in capillary tubes and are corrected. Petroleum ether refers to the fraction of b.p. 30–60°.

Can. J. Chem. Downloaded from www.nrcresearchpress.com by 210.87.254.105 on 09/05/12
For personal use only.

Chilopsis Seed Oil

Seed of *C. linearis* (Cav.) Sweet was obtained from a reliable commercial source. It was ground and extracted by stirring with petroleum ether at 25°. The solvent was removed at 25–30° in a current of nitrogen. The oil had iodine value 149, refractive index 1.4923 at 25°, and 1.3% of free fatty acid as oleic. Ultraviolet absorption maxima were at 233, 263, 272, and 283 mμ; infrared maxima were at 960 s and 986 vs cm^{-1}.

Isolation of trans-9-trans-12-Octadecadienoic Acid

The oil (54 g) was hydrolyzed at 25° by allowing it to stand for 18 hours with 6% ethanolic sodium hydroxide under nitrogen. The unsaponifiable matter was removed by extraction with petroleum ether. The fatty acids were collected in petroleum ether and the solvent was removed under reduced pressure at 25° in a current of nitrogen. The acids (47 g) were dissolved in acetone (20 ml/g) and the solution was cooled stepwise to −15, −50, and −70°. Fatty acid crystals were collected at each stage and their infrared spectra were taken (Table I).

TABLE I

Crystallization of acids of chilopsis oil

Fraction	Crystallizing temp., °C	Yield, g	Main component, as shown by infrared absorption
F1	−15	2.6	Saturated acids
F2	−50	17.8	Acid with isolated trans bonds
F3	−70	12.5	Conjugated triene acid
F4	(Filtrate)	11.3	Ordinary cis-unsaturated acids
F2 recrystallized:			
F21	−19	3.7	Conjugated trans–trans diene
F22	−40	7.1	Isolated trans–trans diene
F23	(Filtrate)	6.7	Conjugated trans–trans–cis triene
F22 recrystallized:			
F221	−20	3.4	Isolated trans–trans diene
F222	−45	2.6	Isolated trans–trans diene

Fractions F221 and F222 were mainly isolated trans–trans diene acid. The ultraviolet spectra showed that they were free of conjugated triene acid but there was 27% of conjugated diene acid in F221 and 11% in F222. Fraction F222 (2.6 g) was treated with maleic anhydride in benzene (3) to form the adduct of the conjugated acid. The benzene was evaporated in a current of nitrogen and the residue was leached with pentane. The pentane solution, cooled to −20°, yielded 1.96 g of *trans*-9-*trans*-12-octadecadienoic acid, m.p. 26.5–27.0°, n_D^{27} 1.4655; (lit. m.p., 25° (4), 27.8–28.4° (5); n_D^{27} 1.4641 (4)). The melting point was unchanged in admixture with linelaidic acid prepared by stereomutation of pure linoleic acid with Poutet's reagent (6) or with selenium. The ultraviolet spectrum had no peaks in the regions 233 mμ or 272 mμ and the content of conjugated acids was calculated to be less than 0.3%. The infrared spectrum had ν_{max} 963 vs cm^{-1} and no other peaks in the region 900–1000 cm^{-1} except the carboxyl peak at 930 cm^{-1} (Fig. 2). The intensity of the peak at 963 cm^{-1} was approximately twice that of pure elaidic acid, determined under the same conditions.

Linelaidic acid, prepared by the usual stereomutation of linoleic acid with selenium, was found by ultraviolet absorption to contain about 16% of conjugated acids. They were removed by adduction with maleic anhydride. It was necessary to start with linoleic acid entirely free from oleic acid, otherwise the product was contaminated with elaidic acid, which is very difficult to remove by crystallization.

The amount of *trans*-9-*trans*-12-octadecadienoic acid isolated initially was 4% of the total fatty acids of chilopsis oil. More was obtained by working up other fractions, especially fraction F221. The intensity of the infrared peak at 963 cm^{-1} for fractions containing little or no conjugated triene gives an indication of their content of the *trans*-9-*trans*-12 acid. Taking these into account and allowing for losses in crystallization, it is estimated that the oil contains about 15% of this acid.

Hydrogenation and Oxidative Splitting

The diene acid (0.12 g) was hydrogenated in ethanol with Adams catalyst. It absorbed 2 moles of hydrogen. The resulting solution was concentrated and cooled, giving stearic acid, m.p. and mixed m.p. 68.5–69.5°.

A portion of the diene acid (0.14 g) was subjected to oxidative splitting by permanganate–periodate (7). The acidic products were recovered and esterified by our usual procedure (8) and the methyl esters were examined by gas chromatography. Large peaks corresponding to hexanoate and azelate were observed. There were no other peaks of significant area.

p-Phenylphenacyl Ester

The diene acid (0.2 g) was treated with 2-bromo-4′-phenylacetophenone by the ordinary method (9). The product, crystallized from ethanol and then from acetone, was *p*-phenylphenacyl-*trans*-9-*trans*-12-

Can. J. Chem. Downloaded from www.nrcresearchpress.com by 210.87.254.105 on 09/05/12
For personal use only.

octadecadienoate, m.p. 51.5–52.5°. The melting point was unchanged in admixture with an authentic sample prepared from linelaidic acid. Anal. Calc. for $C_{32}H_{42}O_3$: C, 80.97; H, 8.92. Found: C, 80.86; H, 8.94. The melting point of 73–75° reported by earlier workers (10) is considered to be incorrect. Their sample, prepared from linelaidic acid, was not characterized by analysis.

p-Phenylphenacylelaidate was prepared and analyzed. It melted at 71.5–72.5° (lit. 72–73° (10)). Anal. Calc. for $C_{32}H_{44}O_3$: C, 80.61; H, 9.30. Found: C, 80.67; H, 9.12.

Tetrahydroxy Derivative

The diene acid (1.0 g) was oxidized by alkaline permanganate (11) for 20 minutes at 10° and the product was crystallized twice from ethanol, giving the higher-melting racemic form of di-*threo*-9,10,12,13-tetrahydroxystearic acid, m.p. 148°. The melting point was unchanged in admixture with an authentic sample of the acid prepared from pure linelaidic acid.

Linoleic Acid

Fraction F4 (see Table I), containing the most soluble acids from the oil, was freed from conjugated diene and triene acids by treating it twice with maleic anhydride in benzene and discarding the adducts. Two grams of the remaining acids, which were soluble in petroleum ether, was oxidized by alkaline permanganate for 10 minutes at 7°. The crude product was washed with hot ethyl acetate, crystallized from ethanol, and washed successively with ethyl acetate and acetone. The product was pure di-*erythro*-9,10,12,13-tetrahydroxystearic acid, m.p. 173–174°, alone and mixed with an authentic sample.

DISCUSSION

Although most unsaturated fatty acids in seed oils occur in the cis form, exceptions are known. Until recently, all of the exceptions were acids which had one or two trans bonds in a conjugated system, e.g. α-eleostearic acid. In 1962, however, Bagby and co-workers (12) reported the occurrence of two acids having a trans bond but not having conjugated unsaturation. They were *trans*-5-octadecenoic acid and *trans*-5-*cis*-9-*cis*-12-octadecatrienoic acid, both found in the seed oil of *Thalictrum polycarpum*.

The present work describes the occurrence of an acid containing two non-conjugated trans bonds, viz. *trans*-9-*trans*-12-octadecadienoic acid. It is notable that this acid and *trans*-10-*trans*-12-octadecadienoic acid (2) are the only two isomers of linoleic acid known so far to occur in seed oils and that both are found in the oil of *C. linearis*, along with linoleic acid itself. Hilditch has pointed out (13) that seeds containing conjugated triene acid (eleostearic) do not seem to synthesize the corresponding non-conjugated acid, linolenic. It is evident that this apparent incompatibility does not extend to the diene acids since chilopsis oil is shown to have both conjugated and non-conjugated octadecadienoic acids.

The *trans*-9-*trans*-12-acid is considered to be a natural component of the glycerides and not an artefact, for the following reasons. The seed showed no evidence of deterioration. The oil was freshly extracted and had a normal content of free fatty acid, 1.3%. The infrared spectrum of the oil showed the presence of isolated trans unsaturation when examined immediately after extraction. Furthermore, the oil and its acids were handled under very mild conditions throughout the work. The estimated content of *trans*-9-*trans*-12-octadecadienoic acid is about 15% of the total fatty acids, hence most or all of it must have been in combination in the glycerides.

A rough calculation of the composition of the total fatty acids of the oil, based mainly on the spectral analysis of the various fractions, gives the following percentages: saturated acids, 5; *trans*-10-*trans*-12-octadecadienoic, 12; *trans*-9-*trans*-12-octadecadienoic, 15; *trans*-9-*trans*-11-*cis*-13-octadecatrienoic, 25; linoleic, 25; undetermined, 18.

ACKNOWLEDGMENTS

The authors are indebted to Mr. R. Lauzon and Mrs. M. A. MacKenzie for determination of infrared spectra and to Mr. H. Seguin for the microanalyses.

Can. J. Chem. Downloaded from www.nrcresearchpress.com by 210.87.254.105 on 09/05/12
For personal use only.

REFERENCES

1. C. Y. Hopkins and M. J. Chisholm. Chem. Ind. (London), 2064 (1962).
2. C. Y. Hopkins and M. J. Chisholm. J. Am. Oil Chemists' Soc. In press.
3. C. Y. Hopkins and M. J. Chisholm. J. Chem. Soc. 573 (1962).
4. M. de Gaudemaris and P. Arnaud. Bull. Soc. Chim. France, 315 (1962).
5. C. Litchfield, A. F. Isbell, and R. Reiser. J. Am. Oil Chemists' Soc. **39**, 330 (1962).
6. H. N. Griffiths and T. P. Hilditch. J. Chem. Soc. 2315 (1932).
7. R. U. Lemieux and E. von Rudloff. Can. J. Chem. **33**, 1701 (1955).
8. M. J. Chisholm and C. Y. Hopkins. Can. J. Chem. **38**, 805 (1960).
9. M. J. Chisholm and C. Y. Hopkins. J. Org. Chem. **27**, 3137 (1962).
10. J. P. Kass, J. Nichols, and G. O. Burr. J. Am. Chem. Soc. **64**, 1061 (1942).
11. A. Lapworth and E. N. Mottram. J. Chem. Soc. **127**, 1628 (1925).
12. M. O. Bagby, C. R. Smith, Jr., K. L. Mikolajczak, and I. A. Wolff. Biochemistry, **1**, 632 (1962).
13. T. P. Hilditch. Chemical constitution of natural fats. 3rd ed. Chapman and Hall, Ltd. London. 1956. p. 202.

Can. J. Chem. Downloaded from www.nrcresearchpress.com by 210.87.254.105 on 09/05/12
For personal use only.

THE STRUCTURE OF "METACHLORAL" (2,4,6,8-TETRAKIS-(TRICHLOROMETHYL)-1,3,5,7-TETROXACANE), A NEW CYCLIC TETRAMER OF CHLORAL

MÁXIMO BARÓN, O. BRIEUX DE MANDIROLA,[1] AND J. F. WESTERKAMP[2]
Laboratorio de Investigaciones, Atanor S.A.M., Munro, F.C.N.G.B., Argentina
Received November 21, 1962

ABSTRACT

The structure of metachloral is established by n.m.r., infrared, and dipole moment studies.

INTRODUCTION

It has been previously reported (1) that treatment of chloral hydrate with cold concentrated sulphuric acid gives a polymeric compound, hitherto unreported in the literature, shown to be a cyclic tetramer of formula I. Eight-membered rings of this type (with

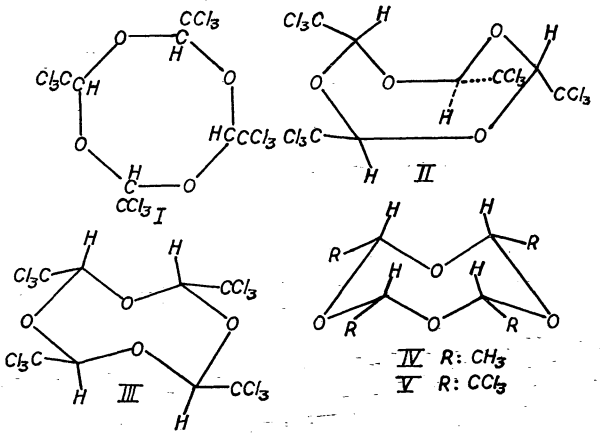

four carbon and four oxygen symmetrically distributed atoms) are very rare. Staudinger (2) isolated 1,3,5,7-tetroxacane but did not study its structure. Pauling and Carpenter (3), continuing previous work by Hassel and Marks (4), established the structure of metaldehyde (2,4,6,8-tetrakis-(methyl)-1,3,5,7-tetroxacane), IV, by means of X-ray diffraction, finding it to be in the crown conformation with four axial protons and four equatorial methyl groups (C_{4v} symmetry).

More recently much work has been reported on cycloöctane and its derivatives by Allinger and co-workers (5), Chiurdoglu (6), and Bellis and Slowinski (7), the general conclusion being that cycloöctane seems to exist in only one conformation: the crown (that is also the case of metaldehyde). It is therefore reasonable to expect a similar situation for the tetramer under study and evidence is now provided in support of conformational structure V. Nuclear magnetic resonance and infrared spectra were obtained and the dipole moment in solution was measured.

[1]*Comisión Nacional de Energía Atómica, Buenos Aires, Argentina.*
[2]*Facultad de Ciencias Exactas y Naturales, Buenos Aires, Argentina.*

Can. J. Chem. Downloaded from www.nrcresearchpress.com by 210.87.254.5 on 09/05/12
For personal use only.

Can. J. Chem. Downloaded from www.nrcresearchpress.com by 210.87.254.5 on 09/05/12
For personal use only.

RESULTS AND DISCUSSION

For eight-membered rings in general, there are basically three conformational structures: boat (II), chair (III), and crown (IV). In the present case only those will be considered where the protons are either directly or closely axial, since others are much less likely on steric grounds. These three possibilities have the following symmetries: C_2, the boat (II); C_i, the chair (III), and C_{4v}, the crown (V).

The proton magnetic resonance spectrum in deuterated chloroform shows only one signal at 359 c.p.s. (δ: 5.98 p.p.m. with reference to tetramethylsilane). The four protons are therefore structurally equivalent. This could correspond to structures III or V, both with four equatorial trichloromethyl groups. The four hydrogen atoms, although axial in each case, would be distributed with reference to the equatorial plane as follows: two above and two below in the chair (III) and all four above in the crown (V). The boat conformation (II) may then be ruled out since its protons would not be structurally equivalent and the n.m.r. spectrum could not show only one signal.

The dipole moments of the two remaining possibilities (III and V) were calculated by vector addition. For the chair conformer (III), with C_i symmetry (center of inversion), it is evident that $\mu = 0.0$ D regardless of the bond moment chosen. As for the crown conformer (V), using the values 0.2, 0.9 (8), and 1.57 (9) for the C—H, C—O, and C—Cl bond moments in preference to others reported in the literature, because of their usefulness in the study of the related parachlorals (10), a $\mu = 3.2$ D was obtained. The calculation was made by adding the four vectors at each carbon atom 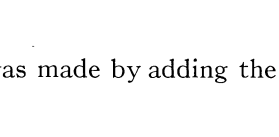 and projecting the resultant vector on the fourfold axis.

The experimental value 1.40 ± 0.1 D is therefore too far removed from both calculated values to be comparable with them. However, it does indicate the existence of a dipole moment for the crown that cannot be expected in the case of the chair conformer, due to the presence of a center of symmetry. Consequently both n.m.r. and dipole moment results tend to point towards the crown conformation as the most probable of the three.

Additional evidence was obtained by establishing the molecular symmetry from the infrared spectra. In C_2, C_i, and C_{4v} symmetries, the frequencies corresponding to the normal modes of vibration may be expected in the 3500–400 cm^{-1} region and can be divided into C—H and skeletal. At a first approximation the trichloromethyl group may be considered as a single mass R (11). Thus the molecule would consist of 16 particles and there would be 42 normal vibrations: 12 C—H, 24 skeletal, 4 R—C, and 2 torsion vibrations of the ring.

For the C—H vibrations (stretching (ν), bending (δ), and wagging (γ)) it is convenient to use the following internal coordinates: four C—H, four R—C—H angles, and four H—C out-of-plane vibration angles. As for the skeletal vibrations 24 internal coordinates were used: 8 stretching (ν) C—O, 8 bending (δ) of the rings' internal angles (4 C—O—C and four O—C—O), and 8 bending (δ') of the H—C—O angle.

In the case of the crown conformer, the characters for these vibrations are represented, according to Wilson (12), by

$$\text{(C—H)} \qquad \Gamma = 2A_1+A_2+2B_1+B_2+3E$$
$$\text{(skeletal)} \qquad \Gamma = 4A_1+2A_2+3B_1+3B_2+6E.$$

There are 12 (C—H) frequencies, of which 8 are infrared active: $2A_1+3E$. Five bands

should then be expected in the spectrum, since the E vibrations are degenerate. Of the 24 skeletal vibrations only 16 are infrared active: $4A_1+6E$. Therefore 10 bands may be expected in the spectrum, making a total of 15 bands for the C—H and skeletal vibrations only.

In the case of the chair and boat conformers, through similar reasoning (12) the characters of the C—H and skeletal vibrations are represented by

$$\Gamma \text{ (chair, } C_i) = 18A_g+18A_u, \text{ where the 18 } A_g \text{ are infrared active;}$$
$$\Gamma \text{ (boat, } C_2) = 18A+18B, \text{ with all 36 infrared active.}$$

Since the spectrum shows only 24 bands, it is evident that the boat conformation can be definitely discarded in favor of a choice between the chair and the crown. In both cases it would appear possible to assign all active fundamental frequencies and still have bands left to be assigned to the remaining vibrations (C—C, C—Cl, etc.). As can be seen in Table I the 15 bands expected for the crown are readily identified and

TABLE I

Band assignment

Wave number (cm^{-1}) and strength		Assignment	Type	Wave number (cm^{-1}) and strength		Assignment	Type
2880	Medium	ν(C—H)	A_1	1000	Medium	C—C	
2840	Weak	ν(C—H)	E	970	Medium	Skeletal	
1380	Strong	δ(R—C—H)	A_1	890	V. weak	Perhaps C—C	
1340*	Medium	δ(R—C—H)	E	850	V. strong	Skeletal	
1320	Strong	δ(R—C—H)	E	812	V. strong	Skeletal	E
1162	V. strong	Skeletal		805*	Medium	Skeletal	E
1140	V. strong	Skeletal		720	Strong	ν(C—Cl)	Asym.
1090	Medium	Skeletal		670	Strong	ν(C—Cl)	Sym.
1070	Medium	(H—C—H′) "wagging"	E	638	Strong	Skeletal	
				591	Strong	Skeletal	
1045	Weak	Probably harmonic of 554 cm^{-1}		554	Strong	Skeletal	
				481	Weak	δ(C—Cl_2)	
1020	Strong	Skeletal		458	Weak	δ(C—Cl_2)	

*These bands disappear in solution, indicating that they very likely correspond to a degenerate vibration and that there are probably two molecules per unit cell (see refs. 10 and 13).

the two remaining, which are somewhat doubtful (1045 and 890 cm^{-1}), are too weak to be safely included among the fundamentals. On the other hand if the chair conformation is postulated with 9 C—H (3 stretching (ν), 3 bending (δ), and 3 wagging (γ)) and 9 skeletal vibrations, and the 2 above-mentioned bands are included among the fundamentals, there would still be 1 band missing of the calculated 18. This absence occurs in the well-known stretching region where only two (2880 and 2840 cm^{-1}) instead of three bands appear in the spectrum.

Furthermore, the fact that two of the bands appearing in the solid (1340 and 890 cm^{-1}) disappear in solution could be explained through the existence of degenerate vibrations. This was found to be the case when there is more than one molecule per unit cell (13), as was also suggested by Novak and Whalley (10) for α-parachloral and confirmed by Abeledo and co-workers (14) through X-ray diffraction. Thus if the existence of degenerate vibrations is accepted, C_i and C_2 symmetries can be ruled out since none would appear in either case.

Summing up, the boat conformation can be rejected on the basis of n.m.r. evidence and the large difference between the number of expected active fundamentals and that actually observed in the spectrum. The chair conformation, although more acceptable

Can. J. Chem. Downloaded from www.nrcresearchpress.com by 210.87.254.5 on 09/05/12
For personal use only.

regarding the number of vibrations despite a difference that cannot be readily explained (absence of a band in the stretching region and existence of degenerate vibrations), must also be rejected since it requires the absence of a dipole moment. Therefore the crown conformation (V) is the only one consistent with all the experimental results, and bands can be assigned as follows: the 5 C—H vibrations are very likely those near 2880, 2840, 1380, 1320, and 1070 cm^{-1} (the lines at 1340 cm^{-1} could be a splitting of the E type bending vibration at 1320 cm^{-1}) and the 10 bands appearing near 1162, 1140, 1090, 1020, 970, 850, 812, 638, 591, and 554 cm^{-1} would be those expected for the skeletal vibrations (11, 15, 16).

Finally, it should be said that the determination of symmetry based principally on the stretching (ν) and bending (δ) modes of CH groups is justified in this case since the corresponding bands appear in a region where other fundamentals are not expected, as also happens with the parachlorals (10).

After a suggestion of Whalley (17) the trivial name metachloral is proposed for the tetramer here described, since it would be in accordance with the name metaldehyde for the tetramer of acetaldehyde (which it resembles closely). And also because the same author proposed (18) to call the linear polymers of chloral "polychlorals".

EXPERIMENTAL

Preparation of the Tetramer (1, 19)

Chloral hydrate (400 g) was mixed with 2000 g sulphuric acid (d: 1.84) at room temperature and shaken till completely dissolved. After 3–4 days a white solid separated, which was filtered, washed with hot water, and extracted with ethanol (100 ml/50 g) in a Soxhlet apparatus. On cooling, small white needles separated (occasionally mixed with the larger chloralide crystals), which when recrystallized from absolute ethanol gave 2.0 g (0.5% yield) of m.p. 219–220° C (corr.). Anal.: Calc. for (CCl_3CHO): C, 16.28; H, 0.68; Cl, 72.17. Found: C, 16.43; H, 0.73; Cl, 71.78. M.W. (Rast): Calc. for $(CCl_3CHO)_4$: 589.5. Found: 614; 616; 571 (average 600.3).

Nuclear magnetic resonance spectrum.—The n.m.r. spectrum was determined by Varian Associates on a Model A-60 spectrometer operating at 60 Mc. The sample was dissolved in deuterated chloroform, tetramethylsilane being used as internal reference.

Infrared spectra.—The compound was examined in KBr pressings in a model 221 P & E spectrophotometer from 4000 to 400 cm^{-1}.

Dipole moment.—The dipole moment was determined in benzene solutions at 25° using the Cole–Gross bridge and a test cell (20) consisting of three coaxial nickel cylinders in a glass jacket (Table II).

TABLE II

Measurements in benzene

w	ϵ_{12}	d_{12}
0.00211	2.275	0.8746
0.00334	2.276	0.8749
0.00466	2.276	0.8749
0.00597	2.277	0.8759
0.00827	2.278	0.8771
$\epsilon_1 = 2.274$; $d_1 = 0.8733$; $\mu = 1.40 \pm 0.1$ D		

For the dilute solutions studied, both the density change Δd and the dielectric constant increment $\Delta\epsilon$ were linear functions of the weight fraction of solute w, within experimental error. The best value of $\Delta\epsilon/w$ and of $\Delta d/w$ were used to calculate the solute polarization P_2, and the dipole moment μ, by the relation (21)

$$P_2 = \frac{3}{(\epsilon_1+2)^2}\left(\frac{M_2}{d_1}\right)\left(\frac{\Delta\epsilon_{12}}{w}\right) - \left(\frac{\epsilon_1-1}{\epsilon_1+2}\right)\left(\frac{M_2}{d_1}\right)\left(\frac{1}{d_1}\right)\left(\frac{\Delta d_{12}}{w}\right) + \left(\frac{\epsilon_1-1}{\epsilon_1+2}\right)\left(\frac{M_2}{d_1}\right)$$

and

$$\mu = 0.0127\sqrt{\{(P_2 - P_{e2})T\}},$$

Can. J. Chem. Downloaded from www.nrcresearchpress.com by 210.87.254.5 on 09/05/12
For personal use only.

where 1 and 2 refer to solvent and solute respectively, M is molecular weight, T absolute temperature, and $P_{e2} = 101.88$ electronic polarization, calculated from bond refractivity values, with no approximation being made for the atomic polarization (usually less than 5% of P_{e2}).

ACKNOWLEDGMENTS

The authors wish to thank the Argentine Atomic Energy Commission (C.N.E.A.) for allowing one of them (O. B. M.) to use its facilities to carry out part of this work; the Argentine National Research Council for partial support of the work; Dr. Hans Schumacher (Universidad Nacional de La Plata) for some of the infrared spectra; and Mr. Richard Nealey (Brown University, R.I.) for the determination of the dipole moment. They also wish to offer their thanks to Dr. R. A. Labriola (this department) for helpful discussions, to Professors J. F. Bunnett and M. R. Nace (Brown University, R.I.) for their kind cooperation, and to Dr. E. Whalley (National Research Council, Canada) for commenting on the manuscript.

REFERENCES

1. M. Barón. Nature, **192**, 258 (1961).
2. H. Staudinger and M. Lüthy. Helv. Chim. Acta, **8**, 65 (1925).
3. L. Pauling and D. C. Carpenter. J. Am. Chem. Soc. **57**, 1274 (1936).
4. O. Hassel and H. Mark. Z. Physik. Chem. **111**, 357 (1924).
5. N. Allinger *et al.* J. Am. Chem. Soc. **81**, 5727 (1959); **83**, 1664 (1961).
6. G. Chiurdoglu *et al.* Chem. Ind. (London), 1453 (1959).
7. H. E. Bellis and E. J. Slowinski, Jr. Spectrochim. Acta, **15**, 1103 (1959).
8. A. A. Maryott and S. F. Acree. J. Res. Natl. Bur. Std. **33**, 73 (1948).
9. C. P. Smyth. Dielectric behaviour and structure. McGraw-Hill Book Co., New York, N.Y. 1955. p. 293.
10. A. Novak and E. Whalley. Can. J. Chem. **36**, 1116 (1958).
11. H. Gerding and J. Lecomte. Rec. Trav. Chim. **58**, 614 (1939).
12. E. B. Wilson, J. C. Decius, and P. C. Cross. Molecular vibrations. McGraw-Hill Book Co., Inc., New York, N.Y. 1955. pp. 102–113.
13. D. F. Horning. J. Chem. Phys. **6**, 1063 (1948).
14. M. J. de Abeledo, M. R. de Benyacar, and E. Galloni. Acta Cryst. **15**, 618 (1962).
15. L. J. Bellamy. Ultrarot Spectrum and Chemische Konstitution. Verlag v. Dr. Dietrich Steinkopff, Darmstadt. 1955. p. 250.
16. A. Stair and J. Rud Nielsen. J. Chem. Phys. **27**, 402 (1957).
17. E. Whalley. Personal communication.
18. A. Novak and E. Whalley. Trans. Faraday Soc. **55**, 1490 (1950).
19. F. D. Chattaway and E. G. Kellet. J. Chem. Soc. 2709 (1928).
20. R. H. Cole and P. M. Gross. Rev. Sci. Instr. **20**, 252 (1949).
21. H. A. Pohl, M. E. Hobbs, and P. M. Gross. Ann. N.Y. Acad. Sci. **40**, Art. 5, 390 (1940).

Can. J. Chem. Downloaded from www.nrcresearchpress.com by 210.87.254.5 on 09/05/12
For personal use only.

SYNTHESIS OF L-ARABINOSE-5-C^{14}

R. K. HULYALKAR AND J. K. N. JONES
Department of Chemistry, Queen's University, Kingston, Ontario
Received March 21, 1963

ABSTRACT

L-Arabinose-5-C^{14} was synthesized by the following route: D-xylose → D-gulono-1,4-lactone-1-C^{14} → 2,3:5,6-di-*O*-isopropylidene-D-gulono-1,4-lactone-1-C^{14} → 2,3-*O*-isopropylidene-D-gulono-1,4-lactone-1-C^{14} → 3,4-*O*-isopropylidene-2,5-L-arabino-urono-lactone-5-C^{14} → methyl-α,β-L-arabinofuranosido-methyl uronate-5-C^{14} → methyl-α,β-L-arabinofuranoside-5-C^{14} → L-arabinopyranose-5-C^{14}. The overall radiochemical yield of L-arabinose-5-C^{14} was about 14% based on $KC^{14}N$ used in the first step. The structures of the isopropylidene derivatives of D-gulono-lactone have been clarified.

INTRODUCTION

C^{14}-Labeled sugars have attained a great importance in recent years due to their extensive application in studies of chemical and especially biochemical reaction mechanisms. Uniformly labeled sugars are made available by biological syntheses (1, 2, 3). General synthetic methods applicable to C_1 labeling include the nitromethane (4) and cyanohydrin (5) syntheses. No general synthetic method is available for the preparation of sugars with specific labeling in positions other than C_1.

L-Arabinose, a biologically important sugar, is found in many polysaccharides of bacterial and plant origin. L-Arabinose-1-C^{14} has been made in yields of about 3% (6) by the nitromethane synthesis and the corresponding D-arabinose-1-C^{14} was prepared in yields of about 30% (7) by the cyanohydrin synthesis. D-Arabinose-5-C^{14} is known (8), but L-arabinose-5-C^{14} is not known. The present paper describes the synthesis of this sugar. The reaction sequence employed is shown in the accompanying scheme, where C* represents C^{14}.

RESULTS

The following method was first standardized with nonradioactive materials to attain the optimum experimental conditions. It was shown by Isbell and co-workers (9) that the ratio of epimers obtained in the cyanohydrin synthesis varied with the pH of the reaction mixture. In the present synthesis sodium acetate was used as a buffer to obtain larger yields of the D-*gulo* epimer from D-xylose. Hydrolysis of the resulting cyanohydrins was carried out at a relatively low temperature according to the conditions of Isbell and co-workers (9). The deionized hydrolyzate was concentrated in the presence of acetic acid and a trace of hydrochloric acid to effect lactonization. The crystalline D-gulono-1,4-lactone-1-C^{14} (II) was obtained from D-xylose (I) in 43% radiochemical yield based on the activity of $KC^{14}N$ used. 2,3:5,6-Di-*O*-isopropylidene-D-gulono-1,4-lactone-1-C^{14} (III) was obtained in about 69% radiochemical yield from D-gulono-1,4-lactone-1-C^{14}. 2,3-*O*-Isopropylidene-D-gulono-1,4-lactone-1-C^{14} (IV) was obtained in 83% radiochemical yield from 2,3:5,6-di-*O*-isopropylidene-D-gulono-1,4-lactone-1-C^{14} by treatment with 88% acetic acid at 35°. Its identity was proved by periodate oxidation and estimation of the formaldehyde (10) produced. In the hydrolyzate small quantities of D-gulono-1,4-lactone-1-C^{14} and unchanged starting material were also present. The hydrolyzate was concentrated and the residue was extracted with benzene, which removed the unhydrolyzed di-*O*-isopropylidene derivative. The residue was then extracted with

Can. J. Chem. Downloaded from www.nrcresearchpress.com by 210.87.254.42 on 09/05/12
For personal use only.

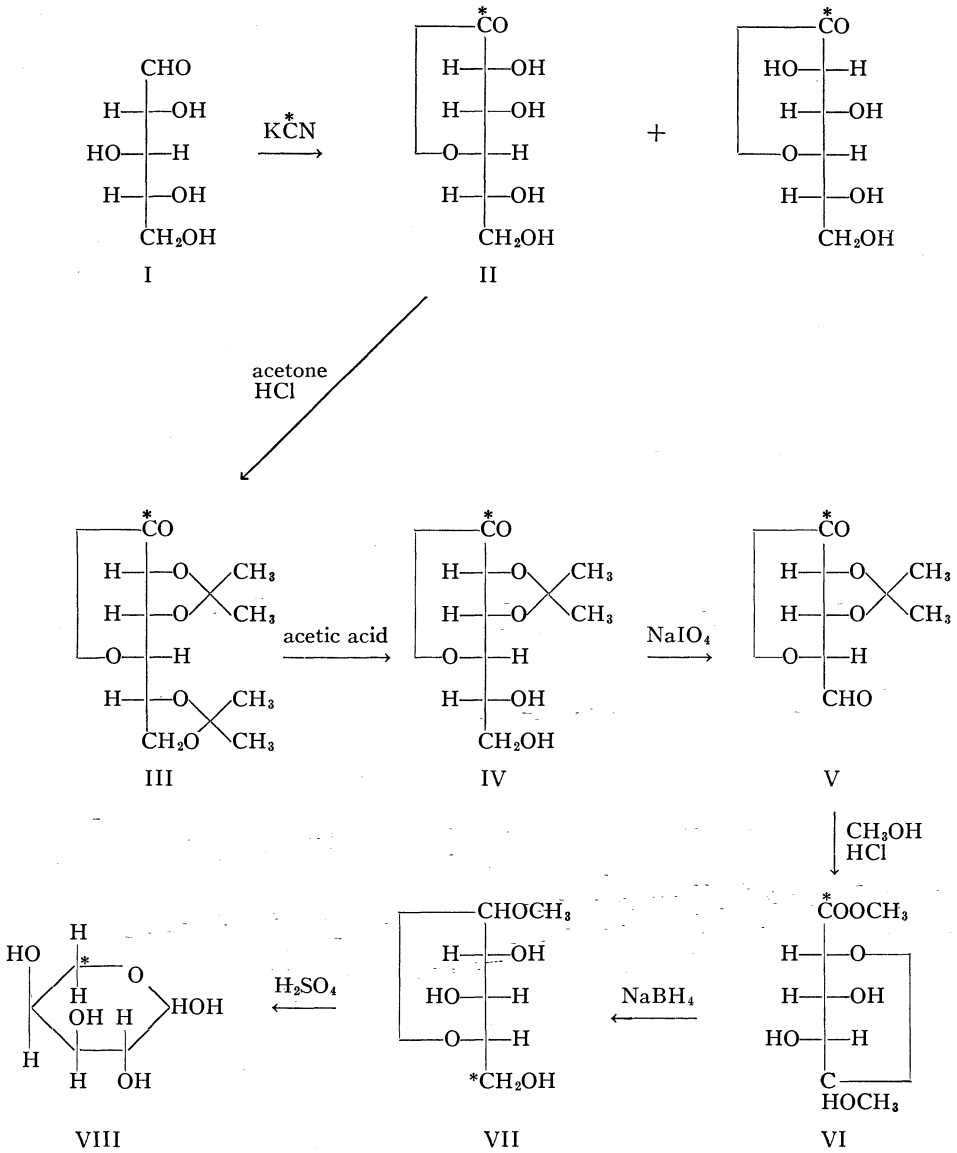

a mixture of acetone – ethyl acetate (50:50), which dissolved 2,3-*O*-isopropylidene-D-gulono-1,4-lactone-1-C^{14}, leaving the insoluble D-gulono-1,4-lactone-1-C^{14}. The acetone – ethyl acetate extracts were evaporated to dryness and the residue was recrystallized from ethyl acetate.

The 2,3-*O*-isopropylidene-D-gulono-1,4-lactone-1-C^{14} was oxidized with 1 mole of sodium periodate and the reaction mixture was evaporated to dryness at room temperature. The residue was repeatedly extracted with chloroform. The chloroform extracts were dried and evaporated to a syrup which did not crystallize. The syrupy 3,4-*O*-isopropylidene-2,5-L-arabino-urono-lactone-5-C^{14} (V) was converted to the syrupy methyl-α,β-L-arabinofuranosido-methyl uronate-5-C^{14} (VI), which was reduced to the corresponding methyl-α,β-L-arabinofuranoside-5-C^{14} (VII) with sodium borohydride. The mild

Can. J. Chem. Downloaded from www.nrcresearchpress.com by 210.87.254.42 on 09/05/12
For personal use only.

experimental conditions under which sodium borohydride reduces sugars (11) and sugar acid lactones (12, 13) are admirably suited for the reduction of the alkali-sensitive methyl-α,β-L-arabinofuranosido-methyl uronate-5-C^{14}. L-Arabinose-5-C^{14} (VIII) was finally obtained by the hydrolysis of methyl-α,β-L-arabinofuranoside-5-C^{14}. The carrier method was used at each stage to increase the radiochemical yields. The overall radiochemical yield of L-arabinose-5-C^{14} was about 14% based on $KC^{14}N$ used in the first step.

The activity in C_5 of L-arabinose-5-C^{14} was determined by the preparation of formaldehyde dimedon from the formaldehyde produced by the periodate oxidation of L-arabinose-5-C^{14} and comparison of its specific activity with that of L-arabinose-5-C^{14}. It was found that all the activity was in C_5.

L-Arabinose-5-C^{14} should be a useful starting material for the preparation of L-rhamnose-6-C^{14} via the following intermediates: L-arabinose-5-C^{14} → L-mannose-6-C^{14} → L-rhamnose-6-C^{14}. L-Galactose-2-C^{14} might also be made by the following intermediates: methyl α,β-L-arabinofuranosido-methyl uronate-5-C^{14} → L-arabinofurano-uronic acid-5 C^{14} → L-lyxono-lactone-1-C^{14} → L-lyxose-1-C^{14} → L-galactose-2-C^{14}.

It was observed that when different catalysts were used to prepare the isopropylidene derivatives of D-gulono-1,4-lactone, different yields of isopropylidene derivatives were obtained. With sulphuric acid, zinc chloride, and hydrochloric acid 2,3:5,6-di-*O*-isopropylidene-D-gulono-1,4-lactone was obtained in yields of 53%, 34%, and 70% respectively. When anhydrous copper sulphate was used as a catalyst, 5,6-*O*-isopropylidene-D-gulono-1,4-lactone (10%) and 2,3:5,6-di-*O*-isopropylidene-D-gulono-1,4-lactone (25%) were obtained. Iwadare (14) has isolated 5,6-*O*-isopropylidene-D-gulono-1,4-lactone from the reaction mixture using hydrogen chloride as a catalyst. Mitchell (15) has also reported 5,6-*O*-isopropylidene-D-gulono-1,4-lactone but with different constants. In the present work the structures of these isopropylidene derivatives were clarified by the study of periodate oxidation results. The di-*O*-isopropylidene derivative did not consume any periodate. The 2,3-*O*-isopropylidene-D-gulono-1,4-lactone consumed 2 moles of sodium periodate, liberating 1 mole each of formic acid and formaldehyde. The 5,6-*O*-isopropylidene-D-gulono-1,4-lactone consumed 3 moles of sodium periodate and liberated no formaldehyde.

EXPERIMENTAL

Melting points were determined on a Kofler hot stage and are uncorrected. Optical rotations were measured at 22±3°. Solutions were concentrated under reduced pressure below 50°. Paper chromatography was carried out by the descending method on Whatman No. 1 filter paper using the following solvent systems (v/v): (*a*) ethyl acetate, acetic acid, formic acid, water (18:3:1:4); (*b*) butan-1-ol, pyridine, benzene, water (10:6:2:6). Sugars were located on chromatograms with *p*-anisidine hydrochloride (16) or alkaline silver nitrate (17) sprays.

Determination of Radioactivity

Dilute solutions of sugar samples were plated on aluminum plates and counted at infinite thinness in a proportional methane gas flow counter and the activities were converted into microcuries (μc) assumingly 50% counting efficiency.

D-*Gulono-1,4-lactone-1-*C^{14}

An ice-cold solution of D-xylose (0.3 g) in water (15 ml) was added to a solution of $KC^{14}N$ (140 mg; 450 μc) and sodium acetate (205 mg) in water (15 ml) at 0°. The solution was kept at 0° for 3 hours and then at 5° for 5 days. Sodium hydroxide solution (5 ml, 2 *N*) was added to it and the solution was heated at 65° with aeration for 12 hours. The solution was passed through IR 120 (H^+) resin and the eluate was collected until its activity was no more than that of the background. The eluate was concentrated to a syrup with the addition of a trace of hydrochloric acid. The syrup was dissolved in methanol (20 ml), treated with activated charcoal, filtered, and concentrated to about 2 ml. A few drops of ethyl acetate were added and the solution kept at 0°. The crystals of D-gulono-1,4-lactone-1-C^{14} were collected by filtration after 24 hours. Further crops of crystalline D-gulono-1,4-lactone-1-C^{14} were obtained by using the carrier method. The results are recorded in Table I. The total radiochemical yield of D-gulono-1,4-lactone-1-C^{14}

Can. J. Chem. Downloaded from www.nrcresearchpress.com by 210.87.254.42 on 09/05/12
For personal use only.

TABLE I

Yields of D-gulono-1,4-lactone-1-C^{14} and their activities

Fraction	Wt. of carrier added (mg)	Wt. of D-gulono-1,4-lactone recovered (mg)	Total activity (μc)
I	Nil	95	115.00
II	200	215	50.20
III	200	215	12.34
IV	200	210	9.53
V	200	205	5.90
		940	192.97

was 43% based on KC^{14}N used. The D-gulono-1,4-lactone-1-C^{14} was found to be chromatographically pure and to have R_f values indistinguishable from those of an authentic sample in solvents *a* and *b*; m.p. 181–182°; $[\alpha]_D$ −53° (*c*, 2.7 in water).

Experiments with Unlabeled Compounds

Isopropylidene Derivatives of D-*gulono-1,4-lactone**

Four experiments were carried out to obtain the isopropylidene derivatives of D-gulono-1,4-lactone using (1) hydrochloric acid (1.2%), (2) sulphuric acid (3%), (3) zinc chloride (4%), and (4) a suspension of anhydrous copper sulphate in acetone as catalysts. The results are recorded in Table II.

TABLE II

Yields of isopropylidene derivatives obtained by using hydrochloric acid, sulphuric acid, zinc chloride, and anhydrous copper sulphate

Catalyst used	Di-*O*-isopropylidene-D-gulono-1,4-lactone yield (%)	5,6-Isopropylidene-D-gulono-1,4-lactone yield (%)	M.p. (°C)	$[\alpha]_D$ (deg)
Hydrochloric acid (1.2%)	70	—	153–154	−64 (in acetone)
Sulphuric acid (3%)	53	—	153–154	−64 (in acetone)
Anhydrous zinc chloride (40%)	34	—	153–154	−64 (in acetone)
Anhydrous copper sulphate suspension (10%)	25		153–154	−64 (in acetone)
		10	168–170	−21 (in acetone)

*The Structure of 2,3-O-Isopropylidene-*D-*gulono-1,4-lactone*

2,3-*O*-Isopropylidene-D-gulono-1,4-lactone was prepared from non-radioactive materials. It had m.p. 142–143°, $[\alpha]_D$ −76° (*c*, 2.7 in acetone). Analysis: Calc. for $C_9H_{14}O_6$: C, 49.5%; H, 6.4%. Found: C, 49.4%; H, 6.4%.

*Periodate Oxidation of 2,3-O-Isopropylidene-*D-*gulono-1,4-lactone*

2,3-*O*-Isopropylidene-D-gulono-1,4-lactone (8 mg) was dissolved in water (49 ml), and sodium metaperiodate solution (1 ml, 0.3 *M*) was added to it. The solution was stored at room temperature in the dark. Samples (5 ml) were removed at intervals for the determination of periodate uptake (18) and for formic acid production (19). Formaldehyde (10) was determined on 1-ml aliquots. The results are recorded in Table III.

*Periodate Oxidation of 5,6-O-Isopropylidene-*D-*gulono-1,4-lactone*

5,6-*O*-Isopropylidene-D-gulono-1,4-lactone (8 mg) was dissolved in phosphate buffer pH 8 (49 ml), and

**Experimental details for the preparation of these derivatives are given in the text.*

Can. J. Chem. Downloaded from www.nrcresearchpress.com by 210.87.254.42 on 09/05/12
For personal use only.

TABLE III

Periodate oxidation of 2,3-*O*-isopropylidene-D-gulono-1,4-lactone

Time (hr)	Periodate uptake (moles/mole)	Formic acid production (moles/mole)	Formaldehyde production (moles/mole)
0.5	0.91	0.10	0.90
1	1.50	0.71	0.98
2	1.76	0.86	0.99
3	2.10	1.01	1.01
5	2.15	1.05	1.05
15	2.15	1.05	1.05

sodium periodate (1 ml, 0.3 *M*) was added to it. The periodate uptake and the formaldehyde production were determined as before. The results are recorded in Table IV.

TABLE IV

Periodate oxidation of 5,6-*O*-isopropylidene-D-gulono-1,4-lactone

Time (hr)	Periodate uptake (moles/mole)	Formaldehyde production (moles/mole)
0.25	1.8	No formaldehyde production
0.50	2.05	
1	2.59	
2	2.95	
3	3.00 constant	

2,3:5,6-Di-O-isopropylidene-D-gulono-1,4-lactone-1-C^{14}

D-Gulono-1,4-lactone-1-C^{14} (930 mg) was stirred with acetone (50 ml) containing hydrogen chloride (1.2%) for 18 hours at room temperature, when a clear solution was obtained. The acid was neutralized with solid potassium carbonate and filtered. The filtrate was concentrated to dryness and the residue was recrystallized from alcohol–petrol (b.p. 40–60°). The carrier method was employed to obtain further crops of crystals. The yields and the activities of the products with m.p. 152–153° and $[\alpha]_D$ −64° (*c*, 2.8 in acetone) (14) are recorded in Table V. The total radiochemical yield of 2,3:5,6-di-*O*-isopropylidene-D-gulono-1,4-lactone-1-C^{14} is 69%, based on the activity of D-gulono-1,4-lactone-1-C^{14}.

TABLE V

Yields of 2,3:5,6-di-*O*-isopropylidene-D-gulono-1,4-lactone-1-C^{14} and their activities

Fraction	Wt. of carrier added (mg)	Wt. of di-*O*-isopropylidene-D-gulono-1,4-lactone recovered (mg)	Total activity (μc)
I	Nil	801	108.10
II	500	478	11.26
III	400	440	7.20
IV	400	373	4.05
V	400	467	3.61
		2559	134.22

2,3-O-Isopropylidene-D-gulono-1,4-lactone-1-C^{14}

2,3:5,6-Di-*O*-isopropylidene D-gulono-1,4-lactone-1-C^{14} (2.554 g) was dissolved in glacial acetic acid (16 ml) at 45° and to this solution water (2.25 ml) was added drop by drop with stirring; the solution was then kept at 35° for 20 hours, and evaporated to dryness at 30°. The residue was dissolved in absolute alcohol (15 ml) and again evaporated to dryness. After two more evaporations with ethanol as above,

Can. J. Chem. Downloaded from www.nrcresearchpress.com by 210.87.254.42 on 09/05/12
For personal use only.

the residue was extracted with benzene three times to remove the unhydrolyzed di-*O*-isopropylidene derivative. The residue was then extracted with acetone – ethyl acetate mixture (50:50). The insoluble residue (27 mg) was found to be D-gulono-1,4-lactone-1-C^{14} of m.p. 181–182° and $[\alpha]_D$ −53° (*c*, 2 in water). The benzene extract gave the di-*O*-isopropylidene derivative (195 mg). On recrystallization it had m.p. 151–153° and $[\alpha]_D$ −64° (*c*, 2.5 in acetone). This product was further treated with acetic acid as above and the ethyl acetate – acetone (50:50) extract was added to the main extract. The ethyl acetate – acetone (50:50) extracts were evaporated to dryness and the residue was recrystallized from ethyl acetate. The carrier method was employed to increase the radiochemical yield as shown in Table VI. The total radiochemical yield of 2,3-*O*-isopropylidene-D-gulono-1,4-lactone-1-C^{14} of m.p. 142–143° and $[\alpha]_D$ −76.5° (*c*, 2.8 in acetone) was 82.5%.

TABLE VI

Yields of fractions of 2,3-*O*-isopropylidene-D-gulono-1,4-lactone-1-C^{14} and their activities

Fraction	Wt. of carrier (mg)	Wt. of 2,3-*O*-isopropylidene-D-gulono-1,4-lactone-1-C^{14} (g)	Total activity (μc)
I	Nil	1.801	107.2
II	200	0.185	3.6
		1.986	110.8

L-Arabinose-5-C^{14}

2,3-*O*-Isopropylidene-D-gulono-1,4-lactone-1-C^{14} (1.985 g) was dissolved in water (50 ml) and a molar equivalent of a solution of sodium periodate (1.95 g) in water (25 ml) was added to it. The solution was kept at room temperature for 1½ hours and then evaporated to dryness at 30°. To the residue anhydrous sodium sulphate (2 g) was added, and the solid was extracted repeatedly with chloroform. The chloroform extracts were concentrated to a syrup which did not crystallize. The syrup was refluxed at 90° with methanolic hydrogen chloride (66 ml, 1%) for 24 hours. The cooled solution was deionized by passing it through Duolite A4 (OH^-) resin (moistened with methanol) at 5°. The eluate was concentrated to a syrup which was dissolved in methanol (50 ml), and a solution of sodium borohydride (1 g) in water (5 ml) was added drop by drop to it under stirring at 0° during 5 minutes. The solution was stirred at 0° for 2 hours and then at room temperature for 12 hours. Resin IR 120 (H^+) was added to the solution and the suspension was stirred for 1 hour to destroy the excess of sodium borohydride and to remove the sodium ions. The resin was removed by filtration and washed well with water. The filtrate and the washings were evaporated to a white residue, which was dissolved in methanol, and the solution reconcentrated. After three evaporations with methanol a clear syrup was obtained (1.6 g) which did not crystallize. The syrupy methyl-α,β-L-arabinofuranoside-5-C^{14} was hydrolyzed with sulphuric acid (15 ml, 0.8 *N*) at 90° for 3 hours. The hydrolyzate was deionized by passing it through Duolite A4 (OH^-) resin, and concentrated to a syrup (1.4 g). Chromatographic examination of the syrup showed the presence of L-arabinose mainly, with a trace of faster-moving substance in solvent systems *a* and *b*. The autoradiogram of the above syrup showed the presence of traces of two faster-moving components besides L-arabinose-5-C^{14} as a main product. L-Arabinose-5-C^{14} was crystallized from the syrup by dissolving it in a small quantity of methanol and adding a few drops of 2-propanol. Three crops of crystals were isolated as follows:

Crop	Yields (mg)	Total activity (μc)
I	640	
II	60	53.9
III	35	
	735	

The three crops of crystals of L-arabinose-5-C^{14} were combined and recrystallized from methanol–isopropanol (710 mg, 53.6 μc). The product had m.p. 158° and $[\alpha]_D$ +105° (*c*, 3.1 in water). L-Arabinose-5-C^{14} (490 mg, 9.9 μc) was further recrystallized from the residues after addition of 500 mg of carrier.

L-Arabinose-5-C^{14} p-Nitrophenylhydrazone from the Residues

The residue left after removal of the crystalline L-arabinose-5-C^{14} was dissolved in methanol (20 ml)

Can. J. Chem. Downloaded from www.nrcresearchpress.com by 210.87.254.42 on 09/05/12
For personal use only.

and a methanolic solution (20 ml) of *p*-nitrophenylhydrazine (200 mg) was added to it and the solution was refluxed at 90° for 2 hours. The solution was concentrated to about 5 ml and ethyl acetate was added to it drop by drop until a slight turbidity was observed. The solution was kept at 5° and the crystals of L-arabinose-5-C^{14} *p*-nitrophenylhydrazone were collected after 20 hours (120 mg, 1.26 μc). The product had m.p. 179–180°. The mixed melting point with an authentic sample was not depressed. The total radiochemical yield was 14.4% based on the activity of $KC^{14}N$ used in the first step.

Determination of C^{14} in C_5 of L-Arabinose-5-C^{14}

L-Arabinose-5-C^{14} (2.5 mg) was dissolved in water (1 ml), and a solution of sodium periodate (18 mg) in 0.5 *N* sodium carbonate solution (1 ml) was added to it. After the solution had been kept at room temperature for 3 hours barium acetate (80 mg) solution in water (1 ml) was added. The precipitated barium salts were removed by filtration and washed with water (3 ml). To the combined filtrate, acetic acid (0.1 ml) and dimedon solution in alcohol (1 ml, 1%) were added. The formaldehyde dimedon was collected by filtration after 20 hours and was recrystallized from aqueous alcohol (3.8 mg). It had m.p. 189–190° with a specific activity of 0.892 μc/mmole C. The specific activity of L-arabinose-5-C^{14} was 0.940 μc/mmole C. Thus the specific activity (μc/mmole C) of formaldehyde dimedon amounted to 95% of that of L-arabinose-5-C^{14}.

The filtrate left after removal of the formaldehyde dimedon was acidified with sulphuric acid, and formic acid was distilled from it. The formic acid in the distillate was ozidized with mercuric acetate (20) to carbon dioxide, which was precipitated as barium carbonate by absorbing it in alkaline barium chloride. The barium carbonate thus obtained was found to be completely non-radioactive, which proved that radioactivity was only in C_5.

ACKNOWLEDGMENTS

The authors are indebted to Dr. C. D. Nelson of the Department of Biology for allowing them to use the counting apparatus. One of us (R. K. Hulyalkar) thanks Queen's University for a "Notman Teaching Fellowship". We thank the National Research Council of Canada for a grant (N.R.C. T-19) which made this work possible.

REFERENCES

1. L. G. Livingston and G. Medes. J. Gen. Physiol. **31**, 75 (1947).
2. S. Arnoff, A. Benson, W. Z. Hassid, and M. Calvin. Science, **105**, 644 (1947).
3. E. W. Putman, W. Z. Hassid, G. Krotkov, and H. A. Barker. J. Biol. Chem. **173**, 785 (1948).
4. J. C. Sowden. Science, **109**, 229 (1949); J. Biol. Chem. **180**, 55 (1949).
5. D. E. Koshland, Jr. and F. H. Westheimer. J. Am. Chem. Soc. **71**, 1139 (1949); J. Am. Chem. Soc. **72**, 3383 (1950).
6. D. A. Rappaport and W. Z. Hassid. J. Am. Chem. Soc. **73**, 5524 (1951).
7. H. L. Frush and H. S. Isbell. J. Res. Natl. Bur. Std. **51**, 307 (1953).
8. H. L. Frush and H. S. Isbell. J. Res. Natl. Bur. Std. **51**, 167 (1953).
9. H. S. Isbell, J. V. Karabinos, M. L. Frush, N. B. Holt, A. Schwebel, and T. T. Galkowski. J. Res. Natl. Bur. Std. **48**, 163 (1952).
10. J. F. O'Dea and R. A. Gibbons. Biochem. J. **55**, 580 (1953).
11. M. Abdel-Akher, J. K. Hamilton, and F. Smith. J. Am. Chem. Soc. **73**, 4691 (1951).
12. M. L. Wolfrom and H. B. Wood. J. Am. Chem. Soc. **73**, 2933 (1951).
13. J. C. Sowden. J. Am. Chem. Soc. **74**, 4377 (1952).
14. K. Iwadare. Bull. Chem. Soc. Japan, **18**, 226 (1943).
15. D. L. Mitchell. Ph.D. Thesis, Queen's University, Kingston, Ont. 1959.
16. L. Hough, J. K. N. Jones, and W. H. Wadman. J. Chem. Soc. 4799 (1956).
17. W. E. Trevelyan, D. P. Proctor, and J. S. Harrison. Nature, **166**, 444 (1950).
18. G. Neumuller and E. Vasseur. Arkiv Kemi, **5**, 235 (1953).
19. P. Andrews, L. Hough, and J. K. N. Jones. J. Chem. Soc. 806 (1956).
20. M. D. Wieke and B. Jacobs. Ind. Eng. Chem. Anal. Ed. **8**, 44 (1936).

Can. J. Chem. Downloaded from www.nrcresearchpress.com by 210.87.254.42 on 09/05/12
For personal use only.

THE BUTYLLITHIUM-INITIATED POLYMERIZATION OF METHYL METHACRYLATE

PART II. MOLECULAR WEIGHT DISTRIBUTIONS[1, 2, 3]

B. J. COTTAM,[4] D. M. WILES, AND S. BYWATER
Division of Applied Chemistry, National Research Council, Ottawa, Canada

Received April 4, 1963

ABSTRACT

Samples of poly(methyl methacrylate) have been made in toluene solution at −30° C with *n*-butyllithium initiator. Different monomer and initiator concentrations were used to obtain products of different overall molecular weights; polymerization times were varied to achieve partial as well as complete polymerization. The polymer samples were divided into fractions which were examined as to molecular weight and microstructure. It was found that the whole polymers have unusually wide molecular weight distributions which can be attributed to a combination of two narrower distributions, one of which occurs at a low and the other at a higher molecular weight region. This "double peak" phenomenon was observed for polymers at lower conversions as well as for polymers representing complete conversion of monomer. Proton magnetic resonance measurements showed that the degree of isotacticity of various fractions of a whole polymer is not the same at all molecular weights.

In one case a second portion of monomer was polymerized after the complete polymerization of a first portion. Comparison of the molecular weight distribution before and after the second addition of methyl methacrylate indicated that polymer chains in all molecular weight regions, above a very low minimum value, are capable of further addition of monomer.

Can. J. Chem. Downloaded from www.nrcresearchpress.com by 210.87.254.105 on 09/05/12
For personal use only.

INTRODUCTION

It has been reported that the anionic polymerization of methyl methacrylate results in polymers with unusually wide molecular weight distributions. A variety of organometallic initiators has been used, including Grignard reagents and organolithium compounds. Many different $\bar{M}_w/\bar{M}_n$ ratios have been found, the values depending to a large extent on whether all or only part of the product is considered as well as on polymerization conditions. Glusker and co-workers (1) accounted for a wide molecular weight range on the basis of variable rates of polymerization, caused by the changing configuration of the growing polymer molecules. Weakley *et al.* (2) suggested that the broad molecular weight distribution could be explained in terms of a combination of two much narrower distributions, produced by simultaneously occurring mechanisms. Nevertheless, no systematic study of the effect of polymerization conditions on the molecular weight distribution of the entire product has been published.

This paper describes a study of the fractionation of a number of polymers prepared by the *n*-butyllithium initiation of methyl methacrylate in toluene at −30° C. The molecular weights of the fractions have been measured and weight distribution diagrams have been derived. The tacticity of many of the fractions has been measured.

EXPERIMENTAL

Poly(methyl methacrylate) samples were prepared in a scaled-up version of the apparatus described in Part I (3). Variations in monomer and initiator concentrations and in the degree of conversion provided samples of different overall molecular weight. The quantities used in this work were sufficiently large that approximately 10 g of material were available for a precipitation fractionation.

The organic liquids used during the fractionation and characterization experiments were reagent grade wherever possible.

[1] *Issued as N.R.C. No. 7421.*
[2] *Paper presented at the Eleventh Canadian High Polymer Forum, Windsor, Ontario, September 5–7, 1962.*
[3] *For Part I, see reference 3.*
[4] *National Research Council of Canada Postdoctoral Fellow 1961–1963.*

Preliminary work indicated that not all of the petroleum-ether-soluble product (3) was separated from insoluble polymer during the original precipitation of the reaction mixture. Hence the soluble portion was recombined with the insoluble polymer prior to each fractionation. It was convenient to dissolve the polymer in a minimum amount of chloroform and then to dilute to the required concentration with acetone. The concentrations used were, in general, approximately 5% in chloroform diluted to 0.5% by the addition of acetone. The fractionations were carried out at 25° C by slowly adding petroleum ether (boiling range 30–80° C) to the solution, with vigorous stirring, until the mixture became cloudy. The temperature was raised to 40° C to redissolve the fraction, then lowered very slowly to 25° C, and the fraction was separated by centrifugation. Each fraction was dissolved in chloroform, precipitated in petroleum ether, and dried in a vacuum desiccator operating at 50° C. The polymer was normally separated into 8–10 fractions and all but the smaller ones were subsequently refractionated.

The molecular weights of the fractions of molecular weight above 20,000 were derived from their viscosities measured in chloroform solution at 25° C, with Cannon–Ubbelohde dilution viscometers having negligible kinetic energy corrections. The viscosity – molecular weight relationship used was

$$[\eta] = 6.48\times10^{-5}M^{0.78},$$

deduced from some of the results of Schulz *et al.* (4), Bischoff and Desreux (5), and Chinai *et al.* (6) and from light scattering measurements made in these laboratories (7) on both normal and highly isotactic polymers.

The molecular weights of fractions less than 2×10^4 were estimated with an ultracentrifuge using the short column, sedimentation equilibrium method. A Spinco model E ultracentrifuge equipped with phase plate Schlieren optics and a rotor temperature control unit was used to examine 1% solutions of the fractions in butyl chloride at 36° C.

The number-average molecular weights of the precipitant-soluble products and a few of the products of slightly higher molecular weight were measured using a Mechrolab vapor pressure osmometer.

The microstructure of a selected number of fractions in chloroform solution was examined with a proton magnetic resonance apparatus under conditions similar to those described by Bovey and Tiers (8). The amounts of the three types of sequences were calculated from measurements of relative areas of the peaks in the spectra due to α-methyl protons.

RESULTS

Two series of polymers were fractionated, one prepared using a low monomer/initiator ratio (0.125 M/7.6 mM; series A) and the other using a higher monomer/initiator ratio (0.25 M/3.85 mM; series B). Series A consisted of two samples. The first (G9) was prepared by terminating the reaction after 100% conversion and the second (G5) was prepared by terminating the reaction after the addition and polymerization of a second equal portion of monomer, following the complete polymerization of a first portion. A third sample (G1; monomer/initiator, 0.25 M/7.6 mM) has been included with this series in order that the effect of the initial monomer/initiator ratio on the molecular weight distribution may be seen. Series B consisted of three samples prepared by terminating reactions after conversions of 100% (G6), 31.4% (G8), and 17.8% (G10).

The integral weight distribution values were determined from the fractionation results using the relationship

$$W_j = \sum_{i=j-1} w_i + \tfrac{1}{2}w_j,$$

where W_j is the integral weight and w_j the weight of the jth fraction. The results for the two series are shown in Figs. 1 and 2.

The differential weight distributions, w_x, obtained by graphical determination of the gradient at chosen points on the integral curves, are illustrated in Figs. 3 and 4.

The fractions of linkages that are isotactic (p_1), have been calculated from the amounts of the three types of sequences, according to the method of Braun *et al.* (9) and are plotted as a function of molecular weight in Fig. 5.

Butyllithium analyses were made in systems in the presence and absence of monomer, under the conditions used for the polymerizations. Methanol was added to react with residual butyllithium and the reaction products were examined by gas chromatography.

Can. J. Chem. Downloaded from www.nrcresearchpress.com by 210.87.254.105 on 09/05/12
For personal use only.

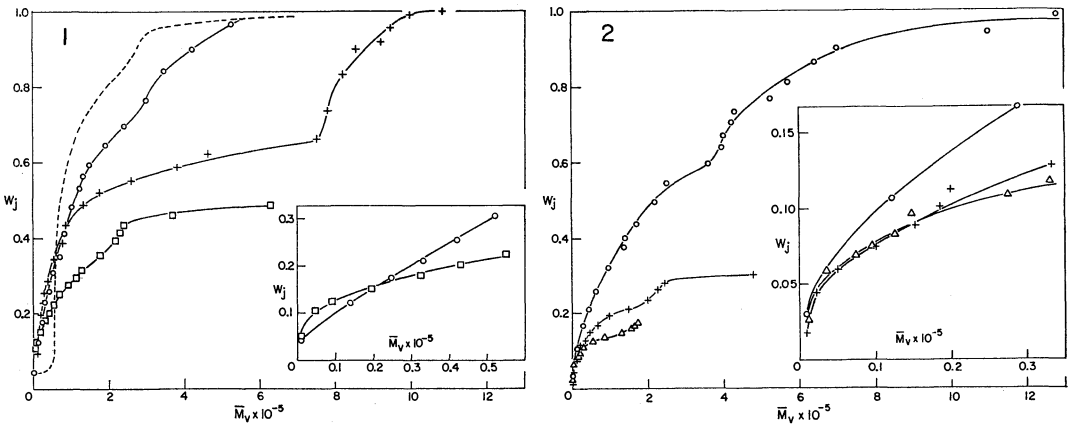

Fig. 1. Integral weight distributions for series A polymers, [BuLi] = 7.6 mM: (□) G9 [MMA] = 0.125 M; (○) G5 [MMA] = 0.125 M + 0.125 M, double addition; (+) G1 [MMA] = 0.25 M; (---) calculated from G9 assuming equal reactivity of chains during polymerization of second portion of monomer (cf. G5).

Fig. 2. Integral weight distributions for series B polymers, [BuLi] = 3.85 mM, [MMA] = 0.25 M: (○) G6 100% conversion; (+) G8 31.4% conversion; (△) G10 17.8% conversion.

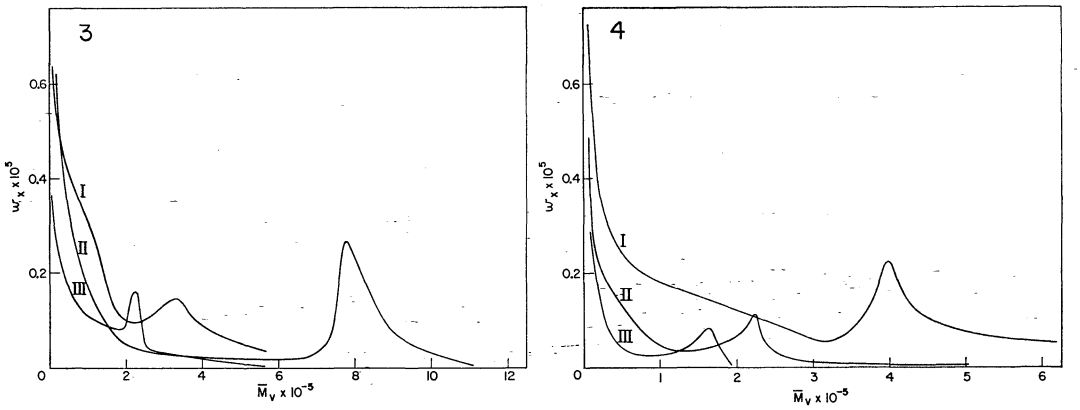

Fig. 3. Differential weight distributions for series A polymers, [BuLi] = 7.6 mM: (I) G5 [MMA] = 0.125 M + 0.125 M, double addition; (II) G1 [MMA] = 0.25 M; (III) G9 [MMA] = 0.125 M.

Fig. 4. Differential weight distributions for series B polymers, [BuLi] = 3.85 mM, [MMA] = 0.25 M: (I) G6 100% conversion; (II) G8 31.4% conversion; (III) G10 17.8% conversion.

In the absence of monomer the expected amount of butane was found. In the presence of monomer, no butane could be detected after only a few seconds of reaction, indicating that butyllithium reacts very rapidly with the nonomer.

DISCUSSION

Several interesting points emerge from the molecular weight distribution and n.m.r. results presented above. If it is assumed that each mole of product corresponds to 1 mole of butyllithium then quantitative recovery of all the added initiator was never obtained. The accuracy of this calculation is almost entirely dependent on the measurement of the yield and molecular weight of the final petroleum-ether-soluble product, which accounts for 85–90% of the chains counted.

Can. J. Chem. Downloaded from www.nrcresearchpress.com by 210.87.254.105 on 09/05/12
For personal use only.

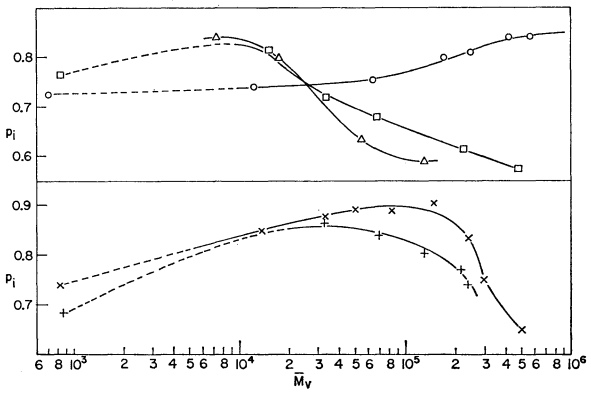

FIG. 5. Isotacticity of fractions. Series A polymers, [BuLi] = 7.6 mM: (+) G9 [MMA] = 0.125 M; (×) G5 [MMA] = 0.125 M + 0.125 M, double addition. Series B polymers, [BuLi] = 3.85 mM: [MMA] = 0.25 M; (○) G6 100% conversion; (□) G8 31.4% conversion; (△) G10 17.8% conversion.

The three experiments of series B carried out by interruption of a normal reaction process showed that at 17.8% conversion (G10) only 40% of the initiator was recovered as products but at 100% conversion (G6) over 70% was accounted for. The difference is due to an apparent increase in the number of chains in the petroleum-ether-soluble fraction. The most plausible explanation for this result is that some very low molecular weight material is lost in the drying procedure on isolation of the polymer from interrupted experiments, and that in the later stages of reaction, some of this material of very low molecular weight grows to produce material of low but now recoverable molecular weight.

A moderate chain deficiency still existed, however, at complete conversion (G6) in series B. Similarly in the two experiments of series A (G9 and G5) only about 40% of the added initiator could be accounted for. The soluble product changed neither in amount nor in measured molecular weight on the addition of the second portion of monomer and is presumed to be almost entirely inactive towards further addition of monomer at the end of a normal reaction period. Thus, in addition to the possibility of loss of very low molecular weight material through evaporation, it seems likely that some of the chain deficiencies observed at complete conversion for both series result from an attack of butyllithium on the ester function of the monomer.

Butyllithium reacts completely in less than 10 seconds to form petroleum-ether-soluble product and after only 2 minutes some insoluble polymer is formed. The broad molecular weight distributions reported by other workers for other anionic initiators appear in the present system. In addition to the petroleum-ether-soluble product, there seem, at less than 20% conversion, to be two distinct bands of insoluble polymer. This peculiar distribution continues to exist during a normal polymerization process and persists during the complete conversion of an added second portion of monomer. In series B, the $\bar{M}_w/\bar{M}_n$ ratio of the petroleum-ether-insoluble polymer stays relatively constant at about 4.6 in the three experiments, whereas it should decrease during polymerization if all the chains are equally reactive. There must be a wide variation in reactivity of different polymer chains in the first few minutes of reaction to produce this wide distribution and some of the difference persists even in later reaction stages where the higher molecular weight material seems to be still adding monomer at a faster rate. In series A, the effect can be seen more clearly. The addition of an extra portion of monomer at the end of a normal polymerization has shifted the distribution bodily even at very low molecular weights.

Can. J. Chem. Downloaded from www.nrcresearchpress.com by 210.87.254.105 on 09/05/12
For personal use only.

Polymer originally of molecular weight between 40,000 and 200,000 has added uniformly about 400 monomer units since a good fit to the final curve (G5) can be obtained by this assumption. However, the high molecular weight band seems to be adding monomer at about twice this rate and polymer originally below a molecular weight of 40,000 at a somewhat lower rate. The $\bar{M}_w/\bar{M}_n$ ratio has, however, decreased during the polymerization of this second portion of monomer but not as much as expected for a uniform growth rate. An integral weight distribution curve, the broken line shown in Fig. 1, has been calculated from G9 on the assumption that all chains are equally reactive during the polymerization of the second portion of monomer. The difference between this curve and the actual one observed (G5) is obviously greater than any probable experimental error.

Previous kinetic evidence (3) had indicated that in the later reaction stages a steady concentration of reactive ends is present. This steady concentration is, however, mainly determined by the large number of chains in the low molecular weight range, as they account for most of the monomer added. Nevertheless, there seem to be persistent differences in intrinsic reactivity between chains of different molecular weight.

The very large differences between the molecular weight distributions for G5 and G1 (Figs. 1 and 3) show that the initial monomer/initiator ratio is much more important than the overall ratio in determining the nature of the product. Not only is the viscosity average molecular weight higher for G1 but, also, the distribution of molecular weights, although of the same general type as G5, is not related in any simple way.

The tacticity measurements produce rather surprising results. In series B (varying conversion) it can be seen that below 32% conversion the more rapidly growing chains have a markedly lower isotactic content. The highest isotactic content occurs in the chains found in the molecular weight range 10,000–20,000. Nevertheless, even the petroleum-ether-soluble fraction of very low molecular weight has an appreciable content of isotactic sequences. Its inability to add additional monomer does not seem likely to be caused by a failure to achieve a favorable (i.e., isotactic) configuration as suggested by Glusker *et al.* (1). At complete conversion the dependence of tacticity on molecular weight has changed completely, since the highest molecular weight material is now the most highly isotactic. Kinetic evidence (3) had indicated that a more rapid monomer consumption was attained after 32% conversion (G8). This reaction period must therefore be associated with a change in the environment of the polymer chains since the high molecular weight chains now add with a very high isotactic probability.

In series A, experiment G9 shows that at slightly different initial monomer and initiator concentrations, even at complete conversion, the intermediate range of molecular weights has the highest isotacticity. It seems reasonable to suppose that this is the result of lower isotacticity at higher molecular weight in the early stages of reaction and that later in the reaction there has been a phase of growth of higher isotacticity, which has not been sufficient to radically change the initial molecular weight – tacticity dependence. Addition of a second portion of monomer (G5) has changed the relationship to a minor extent in that the middle ranges of molecular weight have gained in isotacticity whilst the extremes have changed little.

It seems that the polymer molecules must be divided into several species. The distinct band of material soluble in petroleum ether must be considered entirely or almost entirely inactive after complete conversion and may possibly correspond to material which has cyclized at low molecular weights (1, 10). In addition there are at least two bands of polymer where the chains are still active and probably are of different intrinsic reactivity. The difference in reactivity starts at a very early stage in the reaction, persists to complete

Can. J. Chem. Downloaded from www.nrcresearchpress.com by 210.87.254.105 on 09/05/12
For personal use only.

polymerization and even during the subsequent polymerization of further monomer. It seems also that the two reaction stages as measured kinetically (3), namely a period of slow growth followed by a period of rapid growth, correspond to changes in environment at the polymer chain ends, since at the same time there is a sharp increase in isotacticity. The exact nature of the reactive ends cannot be stated unequivocally but it is known (11) that, in the case of styrene, association of the reactive end groups with tetrahydrofuran does produce differences in reactivity which depend on the number of polar molecules associated with the growing end. In the present case, polar or charged species (e.g., lithium methoxide) can be formed in the reaction directly by side reaction of butyllithium with the monomer (12), or later during propagation (1, 10, 13). Their formation during initiation would also help to explain the apparent loss of initiator molecules in the reaction. It is therefore suggested that, in addition to the normal uncomplexed ion-pair form, the structures of the reactive ends of the polymer chains could exist in the form of normal ion pairs complexed with one or even more molecules of methoxide. These complexed ion pairs could presumably react at different rates and with different probabilities of isotactic placement.

ACKNOWLEDGMENTS

The authors are grateful to Dr. S. Brownstein for the proton magnetic resonance measurements, to Dr. J. M. G. Cowie for light scattering and ultracentrifuge measurements, and to Dr. D. J. Worsfold for helpful discussions.

REFERENCES

1. D. L. Glusker, I. Lysloff, and E. Stiles. J. Polymer Sci. **49**, 315 (1961).
2. T. J. R. Weakley, R. J. P. Williams, and J. D. Wilson. J. Chem. Soc. 3963 (1960).
3. D. M. Wiles and S. Bywater. Polymer, **3**, 175 (1962).
4. G. Meyerhoff and G. V. Schulz. Makromol. Chem. **7**, 294 (1951). H.-J. Cantow and G. V. Schulz. Z. Physik. Chem. (Frankfurt), **1**, 365 (1954).
5. J. Bischoff and V. Desreux. Bull. Soc. Chim. Belges, **61**, 10 (1952).
6. S. N. Chinai, J. D. Matlack, A. L. Resnick, and R. J. Samuels. J. Polymer Sci. **17**, 391 (1955).
7. S. Bywater, B. J. Cottam, J. M. G. Cowie, and D. M. Wiles. Unpublished results.
8. F. A. Bovey and G. V. D. Tiers. J. Polymer Sci. **44**, 173 (1960).
9. D. Braun, M. Herner, U. Johnsen, and W. Kern. Makromol. Chem. **51**, 15 (1962).
10. W. E. Goode, F. H. Owens, and W. L. Myers. J. Polymer Sci. **47**, 75 (1960).
11. S. Bywater and D. J. Worsfold. Can. J. Chem. **40**, 1564 (1962).
12. S. Bywater. Pure Appl. Chem. **4**, 319 (1962).
13. P. Rempp, V. I. Volkov, J. Parrod, and Ch. Sadron. Bull. Soc. Chim. France, 919 (1960).

Can. J. Chem. Downloaded from www.nrcresearchpress.com by 210.87.254.105 on 09/05/12
For personal use only.

THE THERMAL DECOMPOSITION OF TETRAMETHYLTETRAZENE AND TETRAETHYLTETRAZENE[1]

B. G. GOWENLOCK,[2] P. PRITCHARD JONES,[3] AND D. R. SNELLING[4]
Department of Chemistry, University of Birmingham, Birmingham, England

Received April 11, 1963

ABSTRACT

The thermal decompositions of tetramethyltetrazene (TMT) and tetraethyltetrazene (TET) have been studied using a flow system. It is shown that both the decompositions occur at, or above, the limiting pressure for unimolecularity, and Arrhenius parameters for both decompositions are obtained. The decomposition mechanism is discussed in relation to the Arrhenius parameters and theories of three-fragment decompositions. Preliminary values of some kinetic parameters for some reactions of dialkylamino radicals are presented.

INTRODUCTION

The thermal decomposition of tetraalkyltetrazenes may take place either by the two-stage mechanism [1], [2]:

$$R_2N{-}N{=}N{-}NR_2 \rightarrow R_2N + \cdot N{=}N{-}NR_2 \quad \text{(slow)} \qquad [1]$$

$$\cdot N{=}N{-}NR_2 \rightarrow N_2 + R_2N \quad \text{(fast)} \qquad [2]$$

or by a three-fragment decomposition, i.e. simultaneous splitting, [3], of the two dialkylamino radicals:

$$R_2N{-}N{=}N{-}NR_2 \rightarrow R_2N + N_2 + R_2N. \qquad [3]$$

Thermochemical data for these routes have been given (1) and discussed together with the data for the analogous azoalkanes (2). We have reported elsewhere (3) the results of a preliminary study for the flow pyrolysis of TMT, and have related this to the gas phase static measurements by Watson and Waring (4), and the single value for the decomposition in cumene solution (5).

EXPERIMENTAL

I. Materials

TMT was prepared from an ethereal solution of *unsym*-dimethylhydrazine by oxidation using either mercuric oxide (6) or silver oxide (7). After filtration, drying, and removal of the bulk of the ether, the product was fractionally distilled *in vacuo* and further purified by bulb-to-bulb distillation. The purity of the product was established by gas–liquid chromatography (GLC) and by production of a reproducible mass spectrometric cracking pattern. TET was prepared and purified in similar manner: the *unsym*-diethylhydrazine was unavailable commercially and was synthesized from diethylnitrosamine by reduction. Carrier gases were purified as described by Billinge and Gowenlock (8). Other materials used for confirmation of products were tetramethylhydrazine (TMH), dimethylnitrosamine (DMN), diethylnitrosamine (DEN), diethylamine (DEA), diethylmethylamine (DEMA), 1,3,5-triethylhexahydro-*s*-triazine (ET), ethylethylideneamine (EEA), and tetraethylhydrazine (TEH). TMH was a gift of Dr. B. J. Aylett, DEA was commercially available, DMN and DEN were prepared from nitrosation of the corresponding amine, DEMA was prepared by reductive methylation (9), ET was prepared from condensation of formaldehyde with ethylamine (10), EEA from reaction of acetaldehyde with ethylamine (11), and TEH was obtained from fractional distillation of the products of a TET pyrolysis run. It is possible that the TEH may not be completely pure and this would be reflected in wider error limits of the ratios of products for any run. The only detailed preparation of the pure compound (12) was not attempted.

II. Apparatus

A conventional flow apparatus (8) was employed. TMT or TET was entrained by passing a stream of carrier gas over a pool of the liquid maintained at constant temperature in a cylindrical vessel. The amounts of permanent gases resulting from thermal decomposition were measured by pressure measurement in a

[1]*Presented in part at the 18th International Congress of Pure and Applied Chemistry, Montreal, August 1961.*
[2]*Visiting Scientist, N.R.C., 1963.*
[3]*Present address: Department of Chemistry, The Technical College, Nottingham, England.*
[4]*Present address: Department of Chemistry, University of Toronto, Toronto 5, Ontario.*

Can. J. Chem. Downloaded from www.nrcresearchpress.com by 210.87.254.6 on 09/05/12
For personal use only.

known volume: these gases could also be toeplered into small tubes for mass spectrometric analysis. Samples of the pyrolysis products were taken from the trap system and subjected to mass spectrometric and gas–liquid chromatographic analyses. Internal standards were run with each set of GLC analyses. Unless stated, the GLC systems used were those given elsewhere (13). A Cary 14 recording spectrophotometer was used to obtain optical densities of TET–DEN mixtures. The two reaction vessels employed were of different shape and reaction zone volume. One had a volume of about 110 cc and constant diameter throughout the reaction zone, the other had a volume of about 75 cc and the diameter increased by a factor of 50% in the center of the reaction zone. A reaction vessel of dimensions identical with those of the first was constructed and packed regularly with silica fibers: the surface/volume ratio was thereby increased by a factor of 10.

RESULTS

I. TMT

Residence times were calculated assuming the ideal gas law to be obeyed by all substances within the reaction zone. The velocity constants were calculated from the first-order equation, the throughput of TMT being obtained by weighing, and the amount of decomposition from (*a*) the quantity of nitrogen produced (carrier gases CO_2, SF_6, and some runs without carrier gas), or (*b*) GLC estimation of TMH formed and TMT undecomposed (carrier gas N_2, and some runs without carrier gas), or (*c*) mass spectrometric analysis of TMH formed and TMT undecomposed (carrier gas CO_2). GLC and mass spectrometric calibrations were carried out with samples of pure material. When the mixed carrier gas, NO–CO_2, was employed, the fraction of decomposition was estimated from GLC analysis of the liquid products using a 20-ft column packed with firebrick coated with 10% Apiezon L, and operated at 120°. The liquid products were DMN, TMH, and TMT. Peak area ratios of standard mixtures were employed and compared with those of the products so that the ratios DMN:TMT and DMN:TMH could be obtained, and hence the percentage decomposition calculated. Carrier gas throughput was measured by the change in pressure in a known volume at a measured temperature.

The first-order velocity constants were independent of carrier gas, and presence of nitric oxide. Alteration of reaction vessel, packing of reaction vessel, variation of total pressure in reaction vessel (6–12 mm), TMT pressure (by a factor of up to 50), contact time (0.5–3 sec) produced no alteration in velocity constants within the limits of reproducibility (±5%) of these values. The temperature variation of the rate constants is shown in Fig. 1, and in Fig. 2 the results of other workers (4, 5) are compared with the extrapolated best straight line of Fig. 1. Figure 2 is thus a representation of the figure in our preliminary communication (3) with the static technique velocity constants (4) corrected to their true value by multiplication by 2.303[2] (14). The agreement is enheartening. Our best straight line gives $\log_{10}(A) = 14.4 \pm 0.5$ and $E_{act} = 36.1 \pm 1.0$ kcal/mole: these values lie within the wider error limits of the preliminary results ($\log_{10}(A) = 13.8 \pm 1.7$, $E_{act} = 34.5 \pm 3.0$ kcal/mole) (3). The temperature range was 193–266° C (preliminary study (3) 204–244° C).

In a large number of the runs qualitative analyses of the products were made using GLC and mass spectrometry. Over the temperature range 193–260° C the only products (in the absence of nitric oxide) were TMH and nitrogen. In the range 260–266° C two further peaks appeared in the GLC trace: subsequent trapping and mass spectrometry were employed and these served to identify the compounds trimethylamine and tetramethylmethylenediamine. This identification was confirmed by GLC analyses of the pure compounds. Discussion of the formation of these compounds is given elsewhere (13).

II. TET

For the cases of CO_2 and SF_6 carrier gases combined with unpacked reaction vessels the method is identical with that used for TMT decomposition. When the packed reaction

Can. J. Chem. Downloaded from www.nrcresearchpress.com by 210.87.254.6 on 09/05/12
For personal use only.

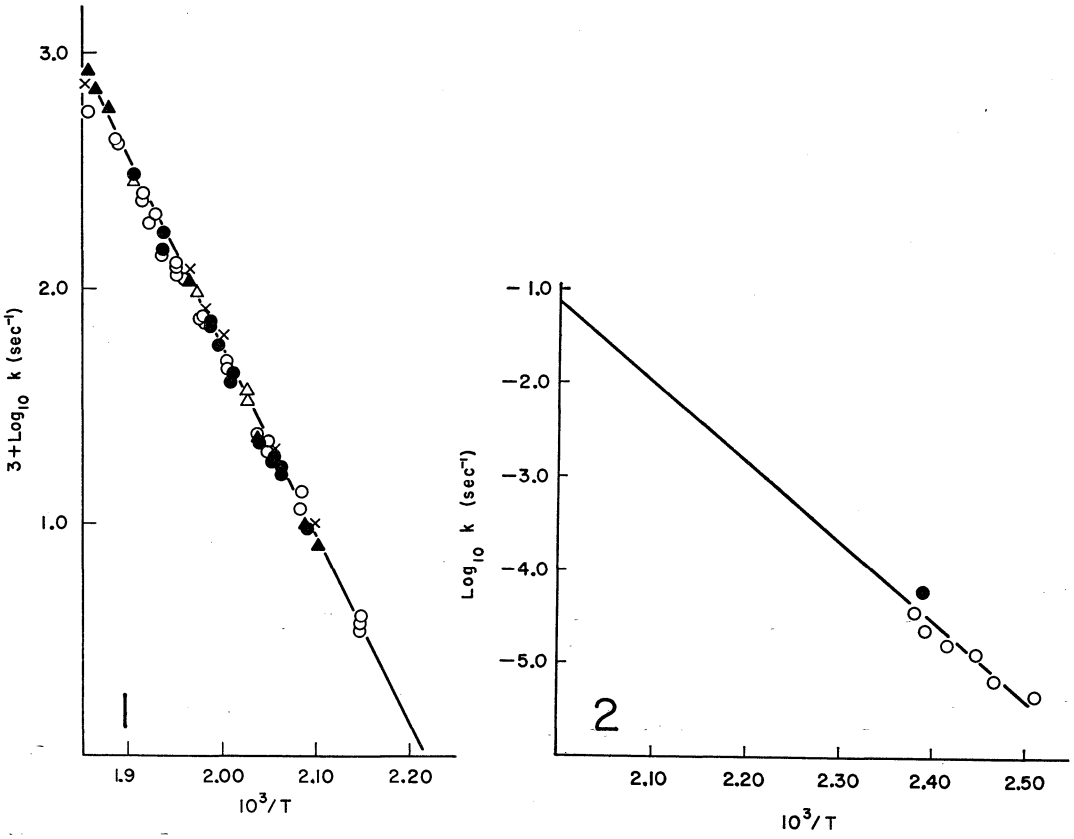

FIG. 1. Arrhenius plot for the thermal decomposition of TMT. ○ CO_2, ● SF_6, △ CO_2 + NO, ▲ pure TMT, × packed reaction vessel. Many of the points are coincident and cannot be distinguished.
FIG. 2. Comparison of our best straight line for TMT with results of other investigators. ○ references 4, 14, ● reference 5.

vessel (CO_2 carrier gas) was used, the permanent gas sample contained small quantities of methane and ethane. The following modification was employed: the reaction products were passed through three traps cooled respectively to −160°, −183°, and −210° C. The last trap removed ethane, and the proportions of methane and nitrogen present in the permanent gases were determined by mass spectrometry. Ethane was determined by vaporization into a known volume, carbon dioxide was removed from the contents of the −183° cooled trap by absorption (8) and the contents of this and of the −160° cooled trap were mixed with a known volume of ether and analyzed by GLC. Identification of the products was first made by mass spectrometry, the cracking patterns compared with the pure compounds, and the GLC analyses then confirmed by measurement of relative retention times of the pure compounds for which relative molar responses had also been obtained. Compounds present included DEA, DEMA, ET (small amounts), TEH, EEA, and two other unidentified materials.

Product analysis for runs using the mixed carrier gas (CO_2–NO) was confined to spectrophotometric analysis of the liquid products (previously condensed out at −160° C) at 350 mμ, where the molar extinction coefficients are 89.4 (DEN) (literature value (15) 90) and 0.82 (TET), and at 283.5 mμ, where they are 45 (DEN) and 7850 (TET). Comparison of the percentage decomposition based on DEN:undecomposed TET with that

Can. J. Chem. Downloaded from www.nrcresearchpress.com by 210.87.254.6 on 09/05/12
For personal use only.

based on nitrogen produced gave good agreement and suggests that no other products were formed. The contents of the trap cooled to −183° were treated to remove CO_2 (8) and no remainder was observed.

First-order velocity constants were independent of carrier gas and unaltered by nitric oxide. Alteration of reaction vessel, packing af reaction vessel, and variation of total pressure in the reaction vessel (9–29 mm), TET pressure (up to a factor of 15), and contact time (0.6–4.2 sec) produced no alteration within the limits of reproducibility (±5%) of these values. The temperature variation of velocity constants is shown in Fig. 3. Our best

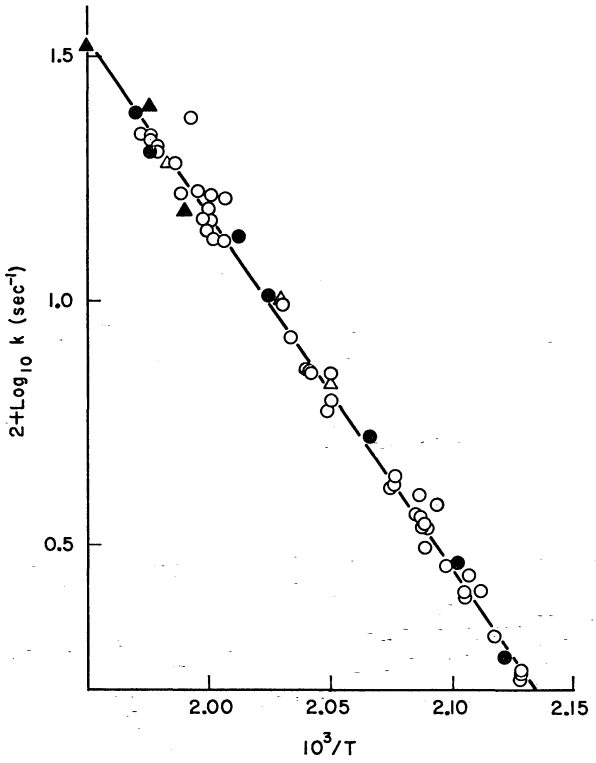

FIG. 3. Arrhenius plot for the thermal decomposition of TET. ○ CO_2, ● SF_6, △ CO_2 + NO, ▲ packed reaction vessel.

straight line gives $\log_{10}(A) = 13.7 \pm 0.9$ and $E_{act} = 33.0 \pm 2.0$ kcal/mole. The temperature range for the majority of the runs is 198–235° C and the estimated error limits are wider than those for TMT in consequence of this smaller temperature range.

DISCUSSION

For both the tetrazenes, the invariance of the velocity constants at any fixed temperature with changes in total pressure, carrier gas, and partial pressure of reactant is evidence that the decomposition is being studied at or above the limiting pressure for unimolecularity. The pressure of TMT is, in almost every case, greater than 0.1 mm, which has been shown (16) to be the limiting pressure for azoisopropane. It would be expected that TMT would have a limiting pressure at or slightly below that for azoisopropane. The evidence from nitric oxide addition shows that the decomposition is non-chain, and the packing of the reaction vessel indicates that the primary decomposition reaction is

Can. J. Chem. Downloaded from www.nrcresearchpress.com by 210.87.254.6 on 09/05/12
For personal use only.

predominantly homogeneous. As we have emphasized elsewhere (13) there are heterogeneous contributions to the radical reactions at higher temperatures and discussion of this problem is postponed until further results are available.

Batten (17) has emphasized the importance of avoiding channelling of the reaction vessel by the streaming gas in flow systems where the flow is laminar. These considerations are of particular importance when considerable changes in reaction vessel diameter take place within the heated reaction zone. The good agreement in our velocity constants for both the tetrazenes when differently shaped reaction vessels are used is good evidence for the absence of channelling. The changes in reaction vessel diameter (and hence in linear flow rate) within our reaction vessels are much less than in those used by Batten. A further feature which diminishes channelling is the centrally mounted thermocouple tube which penetrates along the whole length of the reaction vessel. This was absent in Batten's first study (17) but later work (18) indicates that the flow patterns are modified by this insertion. In addition, we employ only a short calming length prior to entry to the heated zone and entry to this calming length is tangential. These considerations indicate that there will be only a smaller tendency to channelling in our system.

We have drawn attention (2) to the pattern of thermochemical parameters for three azoalkanes and TMT, namely $E_{act} > D_1 > D_1+D_2$ (where D_1 and D_2 are the respective endothermicities of reactions [1] and [2], i.e. first and second bond dissociation energies to the azo group). It seems probable that this will be general for azoalkanes and tetraalkyltetrazenes. The similarity of thermochemical pattern is an argument in favor of proposing identical decomposition mechanisms for azoalkanes and tetrazenes. In Fig. 4 we give a simplified picture of the energy surfaces for decomposition of these molecules, the numerical values for azomethane (2, 19) being used to illustrate the general case. This

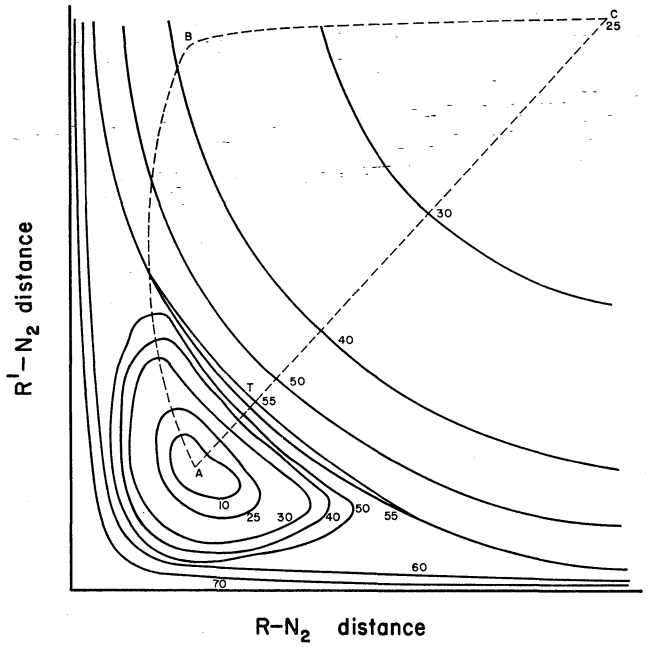

FIG. 4. Contour map for the thermal decomposition of an azocompound R′—N=N—R. Path AC corresponds to three-fragment decomposition, path ABC corresponds to two-fragment decomposition, T indicates the transition state, and the numbers indicate the energy values (in kcal/mole) for R and R′ = CH_3.

Can. J. Chem. Downloaded from www.nrcresearchpress.com by 210.87.254.6 on 09/05/12
For personal use only.

figure corrects that used by Steel and Laidler (20) and may be compared with those given by Szwarc (21). There is a marked difference between this energy surface and that for mercury dialkyls (22) because the fragment HgR decomposes endothermically in contrast to the exothermic decomposition of N_2R. It has been suggested (23) that there is an essential similarity in the decomposition mechanisms for azocompounds, ketones, and mercury dialkyls, and that all these molecules can be represented by R_2M, M being a divalent/zerovalent group. However, this classification ignores the different symmetry classes of the molecules and the different thermochemical patterns. The former of these will obviously be important if the reason for high-frequency factors be the contribution of more than one vibrational mode to the decomposition coordinate. Pritchard (24) has shown that more vibrational modes can participate in the three-fragment decomposition mechanism for mercury dialkyls than in the two-fragment mechanism. Hence, *in this case*, the multiple critical oscillator explanation of high-frequency factors is consistent with a three-fragment decomposition. However, the symmetry of an azocompound is different, and the number of vibrational modes contributing to the two-fragment decomposition is the same as the number contributing to the three-fragment decomposition. Hence, we cannot use the value of the frequency factor in this case as a diagnostic test of the number of fragments produces in the primary decomposition reaction. This contrasts with our previous assumption (2, 25). We suggest that azoalkanes and tetraalkyltetrazenes will decompose by a three-fragment mechanism and that the governing factor lies in the common thermochemical pattern. The values of the frequency factors ("high" for azoalkanes and "normal" for tetrazenes (25)) are not therefore relevant to our choice of most probable decomposition path. The relevant data are given in Table I. In these

TABLE I

Thermochemical patterns and Arrhenius parameters for the gas phase decomposition of R—N=N—R

R	$\log_{10}(A)$ (sec^{-1})	E_{act} (kcal/mole)	D_1 (kcal/mole)	D_1+D_2 (kcal/mole)	Ref.
CH_3	17.3	55.4	$\leqslant 36$	21	2, 19
C_2H_5	15.7	48.5	$\leqslant 38$	16	2, 26
i-C_3H_7	13.8,* 18.1	40.9,* 51.9	$\leqslant 33$	15	2, 16, 27
n-C_4H_9	17.1	51.8	—	—	28
i-C_4H_9	16.2	49.2	—	—	28
s-C_4H_9	17.3	48.2	—	—	28
t-C_4H_9	17.4, 16.3	43.4, 42.8	—	—	28, 29
$(CH_3)_2N$	14.4	36.1	16.5	2.3	1, 2, this paper
$(C_2H_5)_2N$	13.7	33.0	—	—	This paper

*It has been noted (30, 31) that Ramsperger's values are probably too low.

pyrolyses, the exothermic decomposition of N_2R is probably effected in one vibration. Consequently there appears to be little or no meaning in the concept of a two-fragment decomposition. For azoalkanes, where "high" (25) frequency factors occur, we consider the best available explanation to be that of a "softening" of vibrations in the activated complex (20). This implies little softening for the tetrazenes, and we suggest tentatively that this is related to the lower energy barrier. Such a suggestion is supported by the available data for the decomposition of 1,4-dimethyl-1,4-diphenyltetrazene in hydrocarbon solvents (log $(A) = 14.7$, $E = 33.0$ kcal/mole (5); log $(A) = 14.2$, $E = 31.6$ kcal/mole (32)) and of dibenzylhyponitrite in a range of solvents (log $(A) = 12.6$, $E = 23.6$ kcal/mole (32); log $(A) = 13$–14, $E = 24.0$–25.4 kcal/mole (33)), where the activation

Can. J. Chem. Downloaded from www.nrcresearchpress.com by 210.87.254.6 on 09/05/12
For personal use only.

energy is less than that for the compounds listed in Table I and, in general, the frequency factors also are lower.

We have summarized elsewhere (13) our evidence for the reactions of dimethyl- and diethyl-amino radicals. We shall therefore only discuss modifications and extensions to that discussion. A direct value for the recombination rate of amino radicals has recently become available (34). If we assume that the rates of recombination of amino and dimethylamino radicals are equal, and use our relative yields of TMH and DMN together with the average concentration of nitric oxide in the reaction vessel, we can obtain a value of $k_4 = 3 \pm 1 \times 10^7$ l./mole sec, i.e. a steric factor of approximately 10^{-4}. This assumes that reaction [4] is bimolecular. If this reaction is, in fact, termolecular as is the case for the

$$(CH_3)_2N + NO \rightarrow (CH_3)_2NNO \qquad [4]$$

corresponding reaction [5], then the steric factor reflects the termolecularity. It seems

$$CH_3 + NO + M \rightarrow CH_3NO + M \qquad [5]$$

less likely that this termolecularity should occur under our reaction conditions, as the resultant DMN contains more atoms than nitrosomethane. If the reverse reaction of [4] is in the region of falloff from unimolecularity at these pressures, then reaction [4] is presumably termolecular. Studies of DMN decomposition (35) are in progress, but surface effects complicate the interpretation of results.

Reactions [6]–[12] represent some probable reactions of diethylamino radicals and products derived therefrom. The presence of TEH, DEA, EEA, ET, DEMA, and ethane

$$2(C_2H_5)_2N \rightarrow (C_2H_5)_2NN(C_2H_5)_2 \qquad [6]$$

$$2(C_2H_5)_2N \rightarrow (C_2H_5)_2NH + C_2H_5N{=}CHCH_3 \qquad [7]$$

$$(C_2H_5)_2N \rightarrow C_2H_5N{=}CH_2 + CH_3 \qquad [8]$$

$$3C_2H_5N{=}CH_2 \rightarrow (C_2H_5N{=}CH_2)_3 \qquad [9]$$

$$(C_2H_5)_2N + CH_3 \rightarrow (C_2H_5)_2NCH_3 \qquad [10]$$

$$CH_3 + CH_3 \rightarrow C_2H_6 \qquad [11]$$

$$(C_2H_5)_2N + CH_3 \rightarrow C_2H_5N{=}CHCH_3 + CH_4 \qquad [12]$$

in the reaction products could be accounted for by reactions [6]–[11], and reaction [12] represents a route for methane production which does not necessitate a metathesis with TET and subsequent chain reaction. Approximate ratios of some of the products have been obtained from GLC, and some product ratios at 254° C are given in Table II. If we

TABLE II

Product ratios in TET pyrolysis at 254° C

	C_2H_6	DEMA	EEA	DEA	TEH
Packed reaction vessel	0.3	1.8	2.5	3.8	1
Empty reaction vessel	*	1.4	1.6	3.2	1

*Not estimated.

use our product ratios to calculate $k_{10}/(k_{11}k_6)^{1/2}$ values (36), then the results fall within the range 2–3.3. If the more accurate ratio $(k_{10}+k_{12})/k_{11}^{1/2}(k_6+k_7)^{1/2}$ (37) be used, then the results fall within the range 1.1–2.2. We emphasize that these results are not absolute, and claim only that the agreement with the established trend for alkyl radicals is encouraging. No other semiquantitative data for substituted amino radicals have yet been published. The reaction scheme [6]–[12] is not complete: other unidentified products

Can. J. Chem. Downloaded from www.nrcresearchpress.com by 210.87.254.6 on 09/05/12
For personal use only.

have been obtained in small quantity and in general DEA is in excess of EEA. In contrast to dimethylamino radicals (13), disproportionation is preferred to dimerization. Further investigations are proceeding.

ACKNOWLEDGMENTS

We wish to thank the Department of Scientific and Industrial Research for a maintenance grant (P. P. J.) and the University of Birmingham for a research scholarship (D. R. S.). We are also indebted to Dr. J. R. Majer for mass spectrometric analyses, Dr. B. J. Aylett for a gift of pure tetramethylhydrazine, and Dr. J. K. Brown for helpful discussions.

REFERENCES

1. B. G. Gowenlock, P. Pritchard Jones, and J. R. Majer. Trans. Faraday Soc. **57**, 23 (1961).
2. B. G. Gowenlock, J. R. Majer, and D. R. Snelling. Trans. Faraday Soc. **58**, 670 (1962).
3. B. G. Gowenlock and P. Pritchard Jones. Chem. Ind. (London), 557 (1960).
4. J. S. Watson and A. J. Waring. Can. J. Chem. **38**, 290 (1960).
5. B. L. Erusalimskii, B. A. Dolgoplosk, and A. P. Kavuchenko. Zh. Obshch. Khim. **27**, 267 (1957).
6. W. E. Bull, J. A. Seaton, and L. F. Audrieth. J. Am. Chem. Soc. **80**, 2516 (1958).
7. E. Renouf. Ber. **13**, 2169 (1880).
8. B. H. M. Billinge and B. G. Gowenlock. Trans. Faraday Soc. **59**, 690 (1963).
9. M. L. Moore. Org. Reactions, **5**, 301 (1947).
10. J. Graymore. J. Chem. Soc. **125**, 2283 (1924).
11. L. Henry. Compt. Rend. **120**, 837 (1895).
12. O. Westphal and M. Eucken. Ber. **76**, 1137 (1943).
13. B. G. Gowenlock and D. R. Snelling. Advan. Chem. Ser. No. 36, 150 (1962).
14. A. J. Waring. Private communication.
15. R. N. Haszeldine and J. Jander. J. Chem. Soc. 691 (1954).
16. T. A. Whatley. Dissertation Abstr. **21**, 3652 (1961).
17. J. J. Batten. Australian J. Appl. Sci. **12**, 11 (1961).
18. J. J. Batten. Private communication.
19. W. Forst and O. K. Rice. Can. J. Chem. **41**, 562 (1963).
20. C. Steel and K. J. Laidler. J. Chem. Phys. **34**, 1827 (1961).
21. M. Szwarc. *In* Peroxide reaction mechanisms. *Edited by* J. O. Edwards. Interscience Press, New York. 1960. p. 153.
22. H. V. Carter, E. I. Chappell, and E. Warhurst. J. Chem. Soc. 106 (1956).
23. D. Clark and H. O. Pritchard. J. Chem. Soc. 2136 (1956).
24. H. O. Pritchard. J. Chem. Phys. **25**, 267 (1956).
25. B. G. Gowenlock. Quart. Rev. (London), **14**, 133 (1960).
26. W. D. Clark, D. F. Swinehart, and R. D. McCoy. Abstracts of Papers, 132nd Meeting of the American Chemical Society, New York, N.Y. 1957. p. 47S.
27. H. C. Ramsperger. J. Am. Chem. Soc. **50**, 714 (1928).
28. A. V. Blackham and N. L. Eatough. Abstracts of Papers, 140th Meeting of the American Chemical Society, Chicago, Ill. 1961. p. 70Q.
29. J. B. Levy and B. K. W. Copeland. J. Am. Chem. Soc. **82**, 5314 (1960).
30. S. G. Cohen, R. Zand, and C. Steel. J. Am. Chem. Soc. **83**, 2895 (1961).
31. E. Leventhal, C. R. Simonds, and C. Steel. Can. J. Chem. **40**, 930 (1962).
32. J. C. McGowan and T. Powell. Rec. Trav. Chim. **81**, 1061 (1962).
33. S. K. Ho and J. B. DeSousa. J. Chem. Soc. 1788 (1961).
34. M. H. Hanes and E. J. Bair. J. Chem. Phys. **38**, 672 (1963).
35. B. G. Gowenlock and R. M. Haynes. Unpublished observations.
36. A. F. Trotman-Dickenson. Ann. Rept. Progr. Chem. (Chem. Soc. London), **55**, 36 (1959).
37. A. R. Blake, J. F. Henderson, and K. O. Kutschke. Can. J. Chem. **39**, 1920 (1961).

Can. J. Chem. Downloaded from www.nrcresearchpress.com by 210.87.254.6 on 09/05/12
For personal use only.

THE ALKALOIDS OF EUPATORIUM MACULATUM L.[1]

Y. TSUDA[2] AND LÉO MARION
Division of Pure Chemistry, National Research Council, Ottawa, Canada

Received April 10, 1963

ABSTRACT

The root of *Eupatorium maculatum* L. has been examined and found to contain at least four alkaloids. The major base was found to be echinatine, while the second one in importance has been identified as the non-esterified trachelanthamidine. The remaining two alkaloids are probably also of the pyrrolizidine type, but their structures could not be determined due to paucity of material.

Can. J. Chem. Downloaded from www.nrcresearchpress.com by 210.87.254.40 on 09/05/12
For personal use only.

Pyrrolizidine alkaloids are known to cause chronic poisoning associated with haemorrhage in the liver which forms the starting point for cirrhosis (1). Some species of *Eupatorium* (Compositae) have been suspected to cause liver damage in stock and this prompted a search for alkaloids in *Eupatorium maculatum* L., a plant which is widely distributed in Canada.[3] The root has yielded a number of water-soluble bases. Chromatography of the hydrochlorides of the crude bases on cellulose powder effected the separation of four distinct alkaloids.

Base A was obtained as a colorless gum by passing the methanolic solution of its hydrochloride through a column of amberlite IRA-401-OH. It could not be induced to crystallize, but it formed a crystalline picrolonate, $C_{15}H_{25}O_5N.C_{10}H_8O_5N_4$, m.p. 212–214°, and a methopicrate, $C_{16}H_{28}O_5N.C_6H_2O_7N_3$, m.p. 153–155°. An attempt to distill the base *in vacuo* caused pyrolysis, and a substance sublimed which proved to be a carboxylic acid ($C_7H_{14}O_4$) containing three C—CH_3 groups (infrared and n.m.r. spectra). This acid, which was obtained in better yield by the pyrolysis of base A hydrochloride, had properties that corresponded closely to those of viridifloric acid (II) (2, 3, 4), and a direct comparison with an authentic sample kindly sent by Dr. C. C. J. Culvenor proved the identity of the two acids.

The formation of an acid on pyrolysis together with the empirical formula of base A led to the assumption that it was an esterified pyrrolizidine base, and this was confirmed by its saponification, which gave rise to viridifloric acid (II) and a necine, $C_8H_{13}O_2N$ (III), m.p. 116.5–118°. On acetylation the necine produced a diacetyl derivative and hence contained two hydroxyl groups.

The base A when hydrogenated catalytically absorbed 1 mole of hydrogen and underwent hydrogenolysis with the addition of a second mole of hydrogen. The products of the reaction were viridifloric acid and a base, $C_8H_{15}ON$, isolated as its picrate, m.p. 198–200°. The hydrogenolyzed base had properties which coincided with those of hydroxyheliotridane (IV) reported in the literature (5).

These results strongly indicated that the necine III might be identical with heliotridine, and base A with echinatine (I). Indeed the necine and base A picrolonate respectively proved to be identical by direct comparison with authentic specimens of heliotridine and echinatine picrolonate kindly supplied by Dr. C. C. J. Culvenor. Echinatine was first isolated from *Rindera echinata* (Boraginacae) by Men'shikov and Denisova (6), and the

[1]*Issued as N.R.C. No. 7397.*
[2]*National Research Council of Canada Postdoctoral Fellow.*
[3]*The plant was collected by Mr. J. N. Chabot, Division des Cultures Spéciales, Ministère de l'Agriculture, Québec, and we acknowledge our indebtedness to him.*

structure of heliotridine was established by Men'shikov and Kuzovkov (7) and Warren and Klemperer (8).

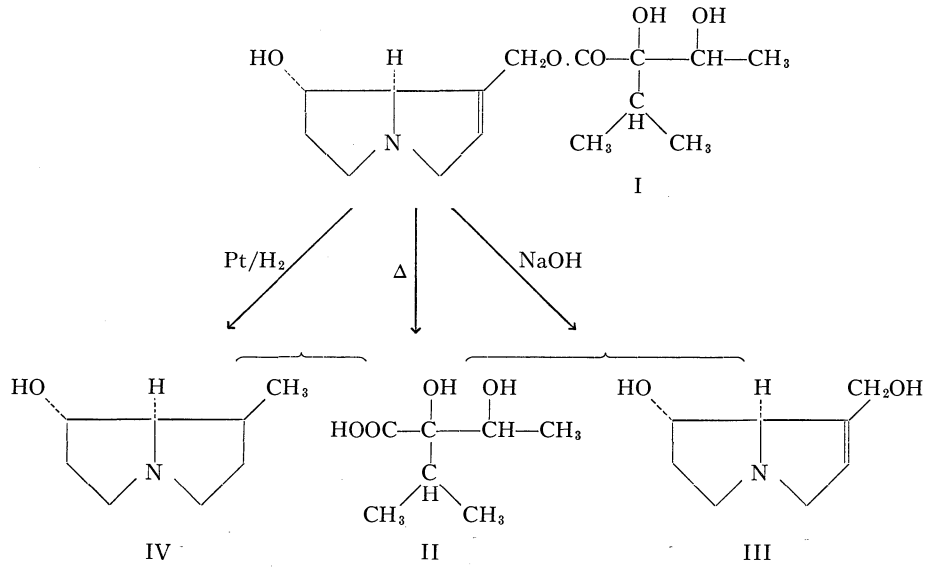

A second alkaloid (base B) was obtained in smaller quantity than echinatine. It could not be induced to crystallize but formed crystalline salts, i.e., a hydrochloride, a picrate, and a picrolonate. From the analysis of the salts its empirical formula was $C_8H_{15}ON$. The properties of the three salts were in agreement with those of the corresponding salts of trachelanthamidine (V) (9). The optical rotation of base B, $[\alpha]_D$ $-13.8°$, was approximate-

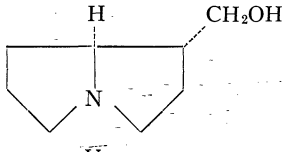

V

ly the same as that of trachelanthamidine, $[\alpha]_D$ $-12.9°$, and its n.m.r. spectrum contained no signal for an olefinic proton, but showed a doublet (δ 6.5, $J \sim 6$ c/s) indicative of the CH_2 in the grouping CH—CH_2—O—. Trachelanthamidine was originally obtained as the necine of trachelanthamine (9, 10). Since the ester alkaloid echinatine was isolated from the plant under the same conditions without undergoing hydrolysis, it is probable that trachelanthamidine is not an artifact and exists as such in the plant. Hence trachelanthamidine and its enantiomorph laburnine (11) are the only two simple pyrrolizidine alkaloids found so far to occur in nature as non-esters, although the latter has never been reported as part of an ester alkaloid.

The third alkaloid, base C, obtained as the crystalline picrate, $C_9H_{13}O_3N.C_6H_3O_7N_3$, and the fourth, base D, also isolated as the picrate, $C_8H_{13}ON.C_6H_3O_7N_3$, were present in quantities too small to permit their structural investigation. Neither base C nor base D picrate showed carbonyl absorption in the infrared.

EXPERIMENTAL

The ground root of *Eupatorium maculatum* was extracted with methanol and the concentrated extract worked up as usual into a basic, an acid, and a neutral fraction.

Can. J. Chem. Downloaded from www.nrcresearchpress.com by 210.87.254.40 on 09/05/12
For personal use only.

The strong base fraction (16 g), which on a paper chromatogram appeared to contain more than four components, was dissolved in methylene chloride (300 ml) and shaken with three portions of 7% sulphuric acid each of 100 ml. The organic layer yielded a neutral brown gum (6 g). The combined acidic extract was filtered, neutralized by the addition of ammonia to the point (pH 5) of turbidity, and extracted with two portions of 200 ml of ether (extract A). More ammonia was added to the aqueous solution (to pH 9) which was again extracted first with three portions of 200 ml of ether (extract B) and then repeatedly with methylene chloride (extract C). The aqueous solution still gave a strong test with Meyer's reagent. It was neutralized with acetic acid and sulphuric acid added to pH 3 followed by the addition of a saturated solution of ammonium reineckate until precipitation was complete. The precipitated reineckate was filtered, washed with water, and dried in air, 13.5 g.

Extract A on evaporation left a slightly yellow oil, 0.12 g. Extract B yielded a yellow oil, 0.54 g, and extract C a brown gum, 1.83 g.

The reineckate (13.5 g) was dissolved in acetone (100 ml), the solution filtered, and the insoluble material (0.7 g) washed with acetone (50 ml). To the combined filtrate previously diluted with acetone (350 ml) and water (100 ml) a hot saturated aqueous solution of silver sulphate (6 g) was added and the precipitate removed by filtration. A solution of barium chloride was added to the filtrate and the precipitate removed by centrifugation. The cleared solution was evaporated to dryness under reduced pressure at 40–50°, the residue extracted with absolute ethanol, and the extract evaporated to dryness. The residue was treated twice more as above. Evaporation of the final extract left a greenish, gummy hydrochloride (6 g). Paper partition chromatography on Whatman No. 1 filter paper with butanol – acetic acid – water (10:1:4) revealed the hydrochloride to be a mixture of at least three components (R_f 0.51, 0.31, 0.11). The same mixture of hydrochlorides was also obtained directly by passing the solution of the reineckate through a column of Amberlite IRA-401-Cl.

The greenish gummy hydrochloride (ca. 7 g) was dissolved in methanol (50 ml), thoroughly mixed with cellulose powder (50 g), and dried *in vacuo* for 2 days. This was placed on the top of a cellulose powder (600 g) column (6×56 cm) and developed and eluted with butanol – acetic acid – water (10:1:4). The eluate (3.3 l.) was collected in 32 fractions, and the column was washed with methanol (1 l.—fraction 33). Fractions 1–6 (1 l.) yielded 0.28 g of neutral product which was discarded. Fractions 10–18 (500 ml) gave base A hydrochloride (5.4 g) which on standing for several weeks crystallized as colorless elongated prisms, but failed to recrystallize because of its hygroscopic nature (R_f 0.50). Base A was also obtained from extract C (above).

Fractions 21–25 (500 ml) yielded base B hydrochloride (0.32 g, R_f 0.32). Fractions 28–31 (500 ml) on evaporation left a mixture of hydrochlorides (0.21 g) from which base C was isolated as the picrate. The methanol eluate (fraction 33) also yielded a mixture of hydrochlorides (0.34 g) from which a fourth alkaloid, base D, was isolated as the picrate.

Echinatine (Base A)

Base A hydrochloride was dissolved in methanol and passed through a column of Amberlite IRA-401-OH. Evaporation of the solution left the free base as a colorless gum which gave only one spot on a paper chromatogram. The homogeneity of the base was also confirmed by chromatography over alumina (grade III) since each fraction of the eluate yielded a base having an infrared spectrum identical with that of the original base. The pure amorphous base A has pK_a 8.2 measured in aqueous solution. Its n.m.r. spectrum in chloroform indicates the presence of —$CH(CH_3)_2$ (two doublets corresponding to six protons centered at δ 0.9) and —$CH(OH)CH_3$ (δ 1.27; J = 7 c/s) groups and one olefinic proton, while the infrared spectrum (in $CHCl_3$) shows a band at 1720 cm^{-1} attributable to an ester carbonyl.

The perchlorate and picrate of base A failed to crystallize but the picrolonate crystallized from ethanol as yellow prisms, m.p. 212–214°, ν_{max} 1730 cm^{-1} (in nujol mull). For echinatine picrolonate the literature (6) gives m.p. 206°. An authentic sample of echinatine picrolonate, kindly sent by Dr. C. C. J. Culvenor, had the same melting point either alone or in admixture with base A picrolonate and both salts had superimposable infrared spectra. Found: C, 53.49; H, 5.81; N, 12.31. Calc. for $C_{15}H_{25}O_5N.C_{10}H_8O_5N_4$: C, 53.28; H, 5.90; N, 12.43%.

Echinatine (base A) was also characterized as the methopicrate. Base A liberated from 90 mg of the hydrochloride was kept overnight at room temperature in benzene (5 ml) and methyl iodide (1 ml). The methiodide separated as a gum which after decantation of the solvent was dissolved in water and the solution poured into a saturated aqueous solution of sodium picrate. The solution was concentrated to half volume by heating to 40° under reduced pressure. On cooling, the methopicrate crystallized. After recrystallization from water it consisted of yellow needles, m.p. 153–155°, ν_{max} (nujol mull) 1707 cm^{-1}. Found: C, 48.29; H, 5.48; N, 10.54. Calc. for $C_{16}H_{28}O_5N.C_6H_2O_7N_3$: C, 48.71; H, 5.57; N, 10.33%.

Pyrolysis of Echinatine (Base A)

When echinatine (60 mg) was heated in a vacuum (10^{-3} mm) pyrolysis took place and two fractions distilled over, a sublimate at 110°, 3 mg, and a pale yellow glass at 120–170°. The sublimate was resublimed at 90–95° under 5×10^{-4} mm. It consisted of an acid crystallizing as colorless needles, m.p. 130–131°. The same acid was obtained in better yield in the pyrolysis of the base hydrochloride (9 mg acid from 44 mg salt) and also from the saponification of the base, as well as in its hydrogenolysis.

Can. J. Chem. Downloaded from www.nrcresearchpress.com by 210.87.254.40 on 09/05/12
For personal use only.

Can. J. Chem. Downloaded from www.nrcresearchpress.com by 210.87.254.40 on 09/05/12
For personal use only.

Hydrolysis of Echinatine (Base A)

Base A hydrochloride (0.835 g) was added to 10% aqueous sodium hydroxide (20 ml) and heated on the steam bath for 2 hours. The cooled solution was then passed through a column of Amberlite IR-120-H (1.5×20 cm) and the column washed with water (500 ml). The eluate (combined with the washings) was evaporated to dryness under reduced pressure. There was left a crystalline acid (0.419 g) which was dissolved in boiling ether. The solution was filtered and evaporated to dryness. The residue consisted of colorless needles; it was recrystallized from chloroform, from which it separated as colorless needles of pure viridifloric acid, 0.381 g, m.p. 119–121°.[4] The literature (2) reports m.p. 121°. The acid, which was identical with that obtained in the pyrolysis of the base, had the same melting point either alone or in admixture with an authentic sample of viridifloric acid kindly supplied by Dr. C. C. J. Culvenor and both had superimposable infrared spectra. Found: C, 51.82; H, 8.62. Calc. for $C_7H_{14}O_4$: C, 51.84; H, 8.70%.

The Amberlite column from which the acid had been eluted was further eluted with 10% hydrochloric acid (500 ml), and the eluate was evaporated to dryness under reduced pressure. The residue was heated with absolute ethanol, and the filtered solution was evaporated to dryness. This residue was treated twice more as above. It finally consisted of a gummy hydrochloride which was dissolved in methanol and the solution passed through a column (1.5×20 cm) of Amberlite IRA-401-OH. The column was washed with methanol (300 ml) and the combined eluate and washings evaporated to dryness. The residue (0.362 g) crystallized on standing. It was purified by distillation, b.p. 115° (air bath) at 0.3 mm, and crystallized from acetone, from which it separated as colorless prisms, m.p. 116–118°, $[\alpha]_D$ +30.4° (*c*, 2.5 in EtOH). Heliotridine (12) has m.p. 116.5–118°, $[\alpha]_D$ +31° (in MeOH). Found: C, 61.89; H, 8.37; N, 9.20. Calc. for $C_8H_{13}O_2N$: C, 61.91; H, 8.44; N, 9.03%. The infrared spectrum of the base was superimposable on that of an authentic specimen of heliotridine kindly supplied by Dr. C. C. J. Culvenor. The melting points of the two were identical either alone or in admixture.

The hydrolytic base (heliotridine) formed a picrate which was recrystallized from ethanol–ether, from which it separated as yellow needles, m.p. 104–105°. Found: C, 43.66; H, 4.27; N, 14.51. Calc. for $C_8H_{13}O_2N.C_6H_3O_7N_3$: C, 43.75; H, 4.20; N, 14.58%.

Diacetylheliotridine

Heliotridine (20 mg) in acetic anhydride (2 ml) was heated on a steam bath for 2 hours and the reaction mixture evaporated to dryness *in vacuo*. The residue was dissolved in water, the solution filtered, and the filtrate evaporated to dryness. There was left a pale yellow oil (25 mg) which was dissolved in the minimum quantity of water and to the solution was added a saturated aqueous solution of picric acid. Diacetylheliotridine picrate precipitated; it was crystallized from ethanol, from which it separated in yellow needles, m.p. 129–130°. Found: C, 46.33; H, 4.39; N, 11.98. Calc. for $C_{12}H_{17}O_4N.C_6H_3O_7N_3$: C, 46.15; H, 4.30; N, 11.96%. Infrared in nujol mull: 1732 cm^{-1}. Nuclear magnetic resonance in chloroform: δ 7.78 and 7.79, indicative of two acetyl groups.

Hydrogenolysis of Echinatine

Echinatine (base A) hydrochloride (800 mg) in acetic acid (7 ml) and ethanol (17 ml) was shaken with Adams' catalyst (75 mg) in the presence of hydrogen at room temperature for 4 hours. The catalyst was filtered off and the filtrate evaporated to dryness under reduced pressure. The residue dissolved in water was passed through a column (1.5×25 cm) of Amberlite IR-120-H and the column washed with water (500 ml). Evaporation of the filtrate left a residue of viridifloric acid (374 mg), m.p. 120–122°, either alone or in admixture with an authentic sample.

The Amberlite column was further washed with 15% hydrochloric acid (600 ml). These washings, on evaporation, left a residual hydrochloride (330 mg) which was dissolved in a small volume of water. The solution was made strongly basic with sodium hydroxide and extracted several times with ether. Evaporation of the extract, previously dried over sodium carbonate, left a residual oil (300 mg) which was distilled, b.p. 125° (air bath) at 10 mm, wt. of distillate 250 mg, $[\alpha]_D$ −10.6° (*c*, 1.8 in EtOH). For hydroxyheliotridane the literature (5) gives $[\alpha]_D$ −14.5° in water. Hydroxyheliotridane formed a picrate which crystallized from ethanol as yellow needles, m.p. 198–200°. The literature (5) gives m.p. 196°. Found: C, 45.73; H, 4.90; N, 15.83. Calc. for $C_8H_{15}ON.C_6H_3O_7N_3$: C, 45.40; H, 4.90; N, 15.13%.

Base B (Trachelanthamidine)

Base B hydrochloride (320 mg) mentioned above consisted of greenish crystals. It was purified by being dissolved in ethanol–acetone and chromatographed on a column of acid alumina.[5] The pure trachelanthamidine hydrochloride thus obtained crystallized from methanol – ethyl acetate as colorless elongated prisms, m.p. 114–115° (lit. (9), m.p. 110–112°). The salt, which was hygroscopic, was dried at 60°, 0.03 mm, prior to analysis. Found: C, 54.73; H, 8.73. The sample used for nitrogen analysis was kept overnight after

[4] *Viridifloric acid seems to occur in dimorphic forms since it sometimes has the higher melting point. It has been described as having m.p. 117–119° and* $[\alpha]_D$ *0° (3), but also with m.p. 127.5° and* $[\alpha]_D$ *+1.8° (4). The racemate has m.p. 150° (4).*

[5] *Woelm alumina (grade I) suspended in 2 N hydrochloric acid was heated with stirring on the steam bath for 2 hours, filtered, thoroughly washed with water until the washings were only faintly acid, and dried for 10 hours at 110°.*

drying and had become solvated. Found: N, 6.74. Calc. for $C_8H_{15}ON.HCl$: C, 54.49; H, 9.08; N, 7.88%. For $C_8H_{15}ON.HCl.H_2O$: N, 7.16 and for the dihydrate: N, 6.56%.

The hydrochloride, dissolved in methanol, was passed through a column of Amberlite IRA-401-OH and the column washed with methanol. The combined solution and washings was evaporated to dryness and the residual trachelanthamidine distilled: colorless oil, b.p. 60–65° (air bath) at 7×10^{-2} mm, $[\alpha]_D$ −13.8° (*c*, 1.28 in 95% EtOH) (lit. (9), $[\alpha]_D$ −12.9°). The n.m.r. spectrum in D_2O contains a doublet (δ 6.5, J = 6 c/s) but no signal corresponding to an olefinic proton.

The base formed a picrate which crystallized from ethyl acetate – ether as yellow needles, m.p. 178–179° (lit (9), m.p. 174°). Found: C, 45.50; H, 4.88; N, 14.71. Calc. for $C_8H_{15}ON.C_6H_3O_7N_3$: C, 45.40; H, 4.90; N, 15.13%. The picrolonate prepared in ether solution and crystallized from methanol consisted of yellow prisms, m.p. 182–183° (lit. (9), m.p. 182°).

Base C

The brown gum (mixture of hydrochlorides) obtained from fractions 28–31 was dissolved in methanol and chromatographed on a column of acid alumina. The almost colorless solid obtained from the eluate was redissolved in methanol and the solution passed through a column of Amberlite IRA-401-OH. Evaporation of the eluate yielded the gummy free base, which was treated with picric acid. The picrate, after several crystallizations from ethanol, consisted of yellow prisms, m.p. 194–195°. Found: C, 44.47; H, 4.07; N, 13.46. Calc. for $C_9H_{13}O_3N.C_6H_3O_7N_3$: C, 43.69; H, 3.91; N, 13.59%.

Base D

Fraction 33 of the eluate from the original chromatogram of the crude base left on evaporation a residue of base hydrochlorides which was contaminated with inorganic salts. It was washed repeatedly with methanol and the combined methanol extract passed through a column of Amberlite IRA-401-OH. The eluate was evaporated to dryness under reduced pressure, the residue dissolved in water, and the filtered solution evaporated to dryness. The residue (52 mg) was dissolved in methanol and poured into a saturated solution of picric acid in methanol. The precipitated picrate was crystallized first from acetone and then from methanol, from which it separated as yellow needles, m.p. 165–167°. Found: C, 45.52; H, 4.22; N, 14.75. Calc. for $C_8H_{13}ON.C_6H_3O_7N_3$: C, 45.65; H, 4.38; N, 15.21%.

ACKNOWLEDGMENTS

We wish to express our thanks to Dr. C. C. J. Culvenor, C.S.I.R.O., Melbourne, for his kindness in sending authentic specimens; also to acknowledge our indebtedness to Mr. M. Lesage for the n.m.r. spectra, to Mr. R. Lauzon for the infrared spectra, and to Mr. H. Seguin for the microanalyses.

REFERENCES

1. A. R. Cushny. J. Pharmacol. Exptl. Therap. **2**, 531 (1910–11).
2. G. P. Men'shikov. J. Gen. Chem. USSR, **18**, 1736 (1948).
3. L. J. Dry and F. L. Warren. J. Chem. Soc. 3445 (1952).
4. R. A. Adams and B. L. Duuren. J. Am. Chem. Soc. **74**, 5349 (1952).
5. G. P. Men'shikov. Ber. **68**, 1051 (1935).
6. G. P. Men'shikov and S. O. Denisova. Sb. Statei Obshch. Khim. Akad. Nauk SSSR, **2**, 1458 (1953).
7. G. P. Men'shikov and A. D. Kuzovkov. J. Gen. Chem. USSR, **19**, 1702 (1949).
8. F. L. Warren and M. E. von Klemperer. J. Chem. Soc. 4574 (1958).
9. G. P. Men'shikov and G. M. Borodina. J. Gen. Chem. USSR, **15**, 225 (1945).
10. G. P. Men'shikov and G. M. Borodina. J. Gen. Chem. USSR, **11**, 209 (1941).
11. F. Galinovsky, H. Goldberger, and M. Pohm. Monatsh, **80**, 550 (1949).
12. G. P. Men'shikov. Ber. **65**, 974 (1932).

Can. J. Chem. Downloaded from www.nrcresearchpress.com by 210.87.254.40 on 09/05/12
For personal use only.

DERIVATIVES OF DEHYDROABIETIC AND PODOCARPIC ACIDS

ERNEST WENKERT,[1,2] PETER BEAK,[1] RICHARD W. J. CARNEY,[1,2] JAMES W. CHAMBERLIN,[1]
DAVID B. R. JOHNSTON,[2] C. DEANE ROTH,[1] AND AKIRA TAHARA[1]

Departments of Chemistry, Iowa State University, Ames, Iowa, U.S.A., and Indiana University, Bloomington, Indiana, U.S.A.

Received March 4, 1963

ABSTRACT

The lithium aluminum hydride reduction of nitriles in the aromatic resin acid series to aldimines and the conversion of the products to other derivatives are described. The effect of the stereochemistry of the nitriles on the rate of reduction is noted. The transformation of dehydroabietane into a dehydro product is indicated. The syntheses of a desoxydecarboxy-5,6-dehydro-7-keto derivative of podocarpic acid and its optical antipode are discussed. The stereochemistry of hydrogenation of 5,6-dehydro derivatives of podocarpic acid is reported. The effect of a 7-keto group on the rate of hydrolysis of methyl esters of aromatic resin acids is illustrated. The reactions of 6-bromo-7-keto derivatives of methyl podocarpate with bases are portrayed.

Can. J. Chem. Downloaded from www.nrcresearchpress.com by 210.87.254.42 on 09/05/12
For personal use only.

Throughout our continuing studies directed toward the total synthesis of diterpenic natural substances (1) tangential chemical problems of synthetic and/or mechanistic interest have arisen and drawn our attention. The present communication constitutes a description of our experiences with a variety of these subjects.

Reduction of Nitriles

In connection with our total synthesis of *d*-podocarpic acid (I*a*) (2) a fair quantity of desoxypodocarpic acid enantiomer (II*a*) was needed. Whereas its nitrile (II*b*) could be prepared in a few steps from dehydroabietonitrile (I*b*) (3), it had not been hydrolyzed to the acid (II*a*). It could be anticipated that such hydrolysis would take place only with extreme difficulty in view of the highly sterically hindered, axial nature of the nitrile group (and, more importantly, of the intermediate amide function). Furthermore, the last step in the reaction sequence leading to the nitrile II*b*, hydrogenation of the enol acetate III*a*, had afforded low yields of II*b* and had generated mostly the acetoxynitrile (II*c*). While the latter had been converted into II*b*, the resultant circuitous route represented an extra obstacle in a large-scale preparation of the desired acid II*a*. However, this impediment now has been overcome by the discovery of the fact that the use of an excessive amount of palladium–charcoal catalyst in the hydrogenation of III*a* changed the ratio of the products II*b* and II*c* heavily in favor of the former.

When preliminary experiments corroborated the predicted resistance of the nitrile II*b* to hydrolysis, an alternate route for its conversion into the acid II*a* was investigated. It was reasoned that a controlled hydride reduction of the nitrile might lead to an aldimine whose acid hydrolysis to an aldehyde and subsequent oxidation would yield the desired acid. While lithium aluminum hydride reduction of nitriles is known to produce amines, reactions with lithium triethoxyaluminum hydride have been shown recently to stop at the imine stage and thus serve as a method of preparation of aldehydes (4). However, the steric environment of the nitrile function of II*b* seemed to preclude the need of a special hydride. As a consequence, II*b* was reduced with lithium aluminum hydride and the product hydrolyzed with aqueous acid (2). Permanganate oxidation of the resultant aldehyde (II*d*) yielded the acid II*a* (2).

[1]*Iowa State University.*
[2]*Indiana University.*

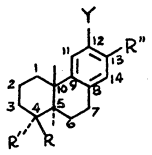

Ia, R = CO_2H, R′ = Me, R″ = H, Y = OH
b, R = Me, R′ = CN, R″ = *i*-Pro, Y = H
c, R = Me, R′ = CHO, R″ = *i*-Pro, Y = H
d, R = Me, R′ = CH_2NH_2, R″ = *i*-Pro, Y = H
e, R = R′ = Me, R″ = *i*-Pro, Y = H
f, R = R′ = Me, R″ = C(Me)=CH_2, Y = H
g, R = R′ = Me, R″ = C(OH)Me_2, Y = H
h, R = R′ = Me, R″ = CO_2H, Y = H
i, R = R′ = Me, R″ = CO_2Me, Y = H
j, R = CO_2Me, R′ = Me, R″ = H, Y = OAc
k, R = CO_2Me, R′ = Me, R″ = H, Y = OH
l, R = Me, R′ = CO_2Me, R″ = *i*-Pro, Y = H
m, R = CO_2Me, R′ = Me, R″ = Y = H
n, R = Me, R′ = CO_2Me, R″ = Y = H
o, R = CO_2Me, R′ = Me, R″ = H, Y = OMe

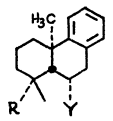

IIa, R = CO_2H, Y = H
b, R = CN, Y = H
c, R = CN, Y = OAc
d, R = CHO, Y = H
e, R = $CONHNH_2$, Y = H
f, R = CN, Y = OH
g, R = CN, Y = ONO
h, R = CH_2NH_2, Y = H
i, R = CO_2Me, Y = H

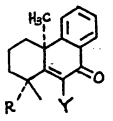

IIIa, R = CN, Y = OAc
b, R = Y = H
c, R = CN, Y = H
d, R = CO_2Me, Y = H

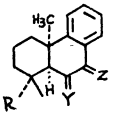

IVa, R = CN, Y = Z = H_2
b, R = CHO, Y = Z = H_2
c, R = CH_2NH_2, Y = Z = H_2
d, R = Me, Y = Z = H_2
e, R = CN, Y = H_2, Z = O
f, R = CN, Y = Z = O
g, R = CO_2Me, Y = H_2, Z = O

The above nitrile reduction was shown recently to be of importance in the steroid field (5, 6) and in the synthesis of nimbiol (7). Extension of this reduction to the equatorial nitrile I*b* and the conformationally flexible cyano compound IV*a* led to the desired aldehydes, I*c* and IV*b*, respectively. However, in these cases only control over the amount of reducing agent or over the length of reaction time prevented the formation of appreciable quantities of amines (I*d* and IV*c*, respectively). The striking contrast in the reactivity of the nitriles was revealed most sharply in the aldehyde–amine ratios of products of reductions under identical conditions (refluxing of a tetrahydrofuran solution of the nitrile and three-quarters of a mole of lithium aluminum hydride for 1 hour) and work-up. The axial nitrile II*b* yielded a 10:1 ratio, while that for I*b* and IV*a* was 1:1. Nevertheless, carefully controlled reduction of dehydroabietonitrile (I*b*), followed by Wolff–Kishner reduction of the intermediate aldehyde (I*c*), has led to a high (70%) overall yield of dehydroabietane (I*e*).[3] Similarly, a Wolff–Kishner reduction of the aldehyde IV*b* afforded the hydrocarbon IV*d* needed in another study. When during preliminary experiments designed to produce IV*b* the lithium aluminum hydride reductions were carried out in ether and followed by mild acid hydrolyses, a weakly basic solid constituted the sole isolable product. While its full characterization proved not to be feasible, its infrared spectrum supported an imine structure. Since the mere mixing of aldehyde IV*b* and amine IV*c* in ether solution led to the same compound, it appears to be the aldimine derived

[3]*Mr. D. P. Strike perfected the large-scale preparation of this substance.*

Can. J. Chem. Downloaded from www.nrcresearchpress.com by 210.87.254.42 on 09/05/12
For personal use only.

from these substances. This unusual result is reminiscent of a similar experience in the steroid field (5, 6).

In view of the recently aroused interest in the total synthesis of diterpene alkaloids (8–11) it is noteworthy that the readily obtainable compounds of structure II represent the absolute configuration of the natural bases. As a consequence, two substances have been converted into nitrogenous compounds which, in principle, are within one or two steps of construction of the all-important piperidine ring of the diterpene alkaloids. Treatment of desoxypodocarpic acid enantiomer (II*a*) with thionyl chloride and thereafter with hydrazine yielded II*e*. Irradiation of the acyl azide related to II*e* would be of interest (8, 11). Base hydrolysis of the ester II*c* yielded the hydroxynitrile II*f*. Treatment of the latter with nitrosyl chloride gave a nitrite (II*g*) whose Barton rearrangement (12) would be worthy of study.

Dehydroabietane Derivatives

In connection with our need for the dehydroabietane derivative I*f* the following chemical operations were performed. Chromic acid oxidation (1, 13, 14) of dehydroabietane (I*e*) yielded a mixture of ketoacetate V*a* and diketone V*b*. Wolff–Kishner reduction and simultaneous hydrolysis of the former produced the carbinol I*g*, whose alternate synthesis from the second oxidation product (V*b*) proceeded as follows. Treatment of the diketone with iodine and pyridine (14), followed by alkaline hydrolysis, gave a keto acid which was characterized as its methyl ester (V*c*) and which could be converted to the acid I*h* upon Wolff–Kishner reduction. Reaction of the methyl ester (I*i*) of the latter with methyl magnesium iodide yielded carbinol I*g*. Dehydration of the alcohol with phosphorous oxychloride transformed it into the olefin I*f*.

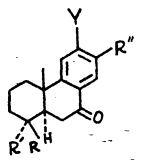

V*a*, R = R′ = Me, R″ = C(OAc)Me$_2$, Y = H
b, R = R′ = Me, R″ = Ac, Y = H
c, R = R′ = Me, R″ = CO_2Me, Y = H
d, R = CO_2Me, R′ = Me, R″ = H, Y = OAc
e, R = CO_2Me, R′ = Me, R″ = Y = H
f, R = Me, R′ = CO_2Me, R″ = *i*-Pro, Y = H
g, R = CO_2Me, R′ = Me, R″ = H, Y = OMe
h, R = CO_2Me, R′ = Me, R″ = H, Y = OH

Ring-B Oxidized Derivatives of Dehydroabietic and Podocarpic Acids

(*a*) As part of their proof of the structures of the products of aluminum-chloride-induced deisopropylation of dehydroabietic acid Ohta and Ohmori (15) converted the substances into ketone III*b* and its antipode (VI*a*). These compounds were of interest since they seemed to offer a reasonable opportunity of entry into the unsubstituted ring A of the diterpene system. An alternate method of preparation was devised. 5-Iso-7-ketodesoxypodocarponitrile enantiomer (IV*e*) (3) and methyl O-acetyl-7-ketopodocarpate (V*d*), prepared by the chromic acid oxidation (3) of methyl O-acetylpodocarpate (I*j*) (16), served as model compounds.

Compounds IV*e* and V*d* were exposed to selenium dioxide oxidation, a reaction which has been shown recently to convert 7-keto compounds to their 5,6-dehydro derivatives (1, 17). While the A/B cis compound (IV*e*) yielded a mixture of unsaturated ketone

Can. J. Chem. Downloaded from www.nrcresearchpress.com by 210.87.254.42 on 09/05/12
For personal use only.

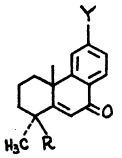

VI*a*, R = Y = H
b, R = CO_2Me, Y = OAc
c, R = CO_2Me, Y = H
d, R = CO_2Me, Y = OH
e, R = H, Y = OH
f, R = CO_2Me, Y = OMe

(III*c*) and α-diketone (IV*f*) (3), the trans system (V*d*) gave only the desired unsaturated ketone (VI*b*). This result is reminiscent of the difference of reactivity of stereochemically diverse diterpenic structures toward chromic acid oxidation (3). The low yield of III*c* and its lack of reaction in a subsequent attempt of hydrolysis of its cyano group led to the abandonment of this representative of the podocarpic acid enantiomer series in favor of its ester (III*d*), previously prepared by Ohta (15). Conversely, success in the podocarpic series led to the application of the method of oxidation to methyl 7-ketodesoxypodocarpate (V*e*) (3). This yielded the unsaturated ketone VI*c*, the antipode of III*d*. Whereas the latter had been converted to III*b* by alkali treatment, it was of interest to ascertain whether esters of this type are susceptible to dealkylation and thereafter to decarboxylation by the elegant new procedure of demethylation of methyl esters by lithium iodide – collidine treatment (18, 19). Indeed, exposure of III*d*, VI*c*, and VI*d* (*vide infra*) to these reagents yielded decarbomethoxylated products III*b*, VI*a*, and VI*e*, respectively.

(*b*) While the catalytic hydrogenation of 5,6-dehydro derivatives of dehydroabietic acid has led consistently to A/B trans compounds (20), little is known about the steric course of hydrogenation of similarly constituted podocarpic acid derivatives. For this reason the hydrogenation of VI*d* and its 7-desoxy derivative (VII*a*) came under scrutiny. The latter was synthesized from the former compound. The unsaturated ketone VI*d* was converted into its ethylene thioketal (VII*b*) by standard means. While Raney-nickel-induced desulphurization of the latter led to methyl podocarpate (I*k*), its treatment with deactivated Raney nickel yielded the desired 5,6-dehydro product VII*a*. Unfortunately this substance was exceedingly air-sensitive and could not be fully characterized. Hydrogenation of VI*d* and VII*a* produced the A/B trans methyl podocarpate (I*k*).

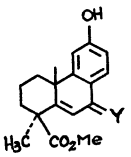

VII*a*, Y = H_2
b, Y = $(SCH_2)_2$

(*c*) Incidental observations during our studies of the chemistry of dehydroabietic and podocarpic acids over the span of several years have suggested that the rates of saponification of their difficultly hydrolyzable esters were affected by ring B substituents. While sterically properly oriented C(5) or C(6) substituents could be expected to exert some influence on the reactivity of the proximate (C4)-carboxylic esters, little effect would be predicted from C(7) substituents in rigid A/B trans ring systems. Since, as a consequence, the C(7) derivatives appeared as the most interesting compounds, it was decided to set

Can. J. Chem. Downloaded from www.nrcresearchpress.com by 210.87.254.42 on 09/05/12
For personal use only.

up a qualitative, comparative study of the speed of alkaline hydrolysis of four representative substances—methyl dehydroabietate (I*l*), its 7-keto derivative (V*f*), methyl desoxypodocarpate (I*m*), and its 7-keto compound (V*e*). Solutions of 80 mg of each of these esters and 0.6 ml of 10% potassium hydroxide in 4 ml of ethylene glycol were refluxed for 4 hours. After standard work-up the acid products as well as the unreacted neutral esters were identified by their characteristic infrared spectra. While 49% of methyl dehydroabietate (I*l*) had undergone hydrolysis (100% total recovery), its 7-keto compound (V*f*) was hydrolyzed in 99% yield (93% total recovery). Similarly, whereas methyl desoxypodocarpate (I*m*) was converted to its acid in only 5% of yield (100% total recovery), its 7-keto derivative (V*e*) was transformed to 22% acid (94% total recovery). Thus it appears that the 7-keto function has a striking effect on the reactivity of C(4) esters. This long-range phenomenon represents an example of conformational transmission, an effect investigated recently by Barton (21).

(*d*) Prior to our use of selenium dioxide oxidation as the last step of the preparation of 5,6-dehydro-7-keto compounds (VI) (*vide supra*) some of these substances had been synthesized by bromination of 7-keto compounds and base-induced dehydrobromination of the resultant 6-bromo-7-ketones. Thus Ohta and Ohmori (15) had prepared the unsaturated ketones III*d* and VIII by bromination of methyl 5-iso-7-ketodesoxypodocarpate enantiomer (IV*g*) and methyl 7-ketodeisopropyldehydroabietate (I*n*), respectively, and hydrogen bromide elimination of the bromoketones in pyridine solutions of silver nitrate, while we had synthesized a podocarpic acid derivative (VI) by a similar scheme but with the use of sodium methoxide as dehydrobromination agent. Since our results appeared inconsistent with the reported action of collidine on methyl 6-bromo-7-keto-O-methylpodocarpate (IX*a*) (22), a general study of the behavior of bromoketones in the podocarpic acid series toward bases was undertaken.

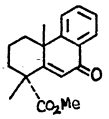

VIII

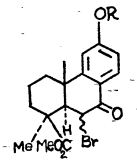

IX*a*, R = Me
b, R = OAc
c, R = OH

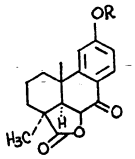

X*a*, R = Me
b, R = OAc
c, R = OH

Chromic acid oxidation of methyl O-methylpodocarpate (I*o*) and methyl O-acetylpodocarpate (I*j*) yielded the 7-keto compounds V*g* (22) and V*d*, respectively. Mild acid or base treatments or, to some extent, even absorption chromatography of the acetates V*d* and IX*b* produced the phenols V*h* and IX*c*, respectively. Bromination of the ketones led to the 6-bromo derivatives IX*a* (22) and IX*b*, respectively. Sodium methoxide treatment of the bromoketones resulted in the formation of unsaturated ketones. Thus IX*a* was transformed into VI*f*, while IX*b* and IX*c* gave VI*d*. The two enones VI*d* and VI*f* were interrelated by the conversion of phenol VI*d* to compound VI*f* by alkylation with methyl sulphate and base. Collidine treatment of the bromoketones led to mixtures of unsaturated ketones and ketolactones. The bromo derivative IX*a* led to the lactone X*a*, as reported (22), as well as ketone VI*f*; compound IX*b* yielded X*b* and VI*b*; and bromoketophenol IX*c* gave VI*d* and an oily lactone (X*c*) which on acetylation afforded crystalline acetate X*b*.

Can. J. Chem. Downloaded from www.nrcresearchpress.com by 210.87.254.42 on 09/05/12
For personal use only.

Can. J. Chem. Downloaded from www.nrcresearchpress.com by 210.87.254.42 on 09/05/12
For personal use only.

Interpretation of the unusual dehydrobromination results depends on the stereochemistry of the bromoketones IX to some extent. While the orientation of the bromine atom in these compounds cannot be considered as fully established, all available evidence points to an α-configuration. An equatorial conformation and, hence, α-configuration are indicated by the spectral properties of the 7-keto function. The 17 cm^{-1} shift to higher frequency in the infrared carbonyl absorption of the bromo compound IX*b* as compared to the ketone (V*d*) and the bathochromic shift of only 5 mμ in the ultraviolet absorption maximum of IX*b* from that of V*d* are in agreement with the general understanding of the spectral behavior of equatorial α-bromoketones (23, 24) and with the properties of a recently described β-bromo-α-tetralone (25), a simple model of IX*b*. Finally, a priori consideration of the mode of formation of compounds of structure IX also is in favor of a 6α-bromo orientation. The customary axial approach of the brominating agent to the 6,7-enol would be expected to be highly unfavorable because of strong steric interference by the axial substituents at C(4) and C(10). Furthermore, while equatorial approach of the reacting species toward the enol is less favored normally because of insufficient π-orbital overlap in the transition state, it is reasonable in the present cases since only slight bond distortions would permit full overlap with the enols in the fairly planar rings B.

If a 6α-bromo configuration be assumed for all compounds IX, their sodium-methoxide-induced dehydrobrominations appear to take a cis course. While bimolecular cis elimination and ionization of the bromide followed by proton loss represent possible reaction paths, some type of inversion at C(6), permitting a trans elimination to take place, seems more likely. Three routes of inversion of the C(6) leaving group are apparent: (*a*) base-induced isomerization of C(6)—H; (*b*) methoxide attack on the 7-keto function and bromide displacement by the resultant hemiketal anion leading to a 7α-methoxy-6β,7β-epoxide (XI); (*c*) bromide displacement by the aromatic ring leading to a cyclopropanone intermediate (XII) (particularly in the case of compounds IX*b* and IX*c*). However, a fourth and most probable reaction path for the elimination is suggested by the conformation of lactones X in the collidine reactions. The transition state (XIII) of the first step of the lactonization requires the creation of a part bond between C(6) and the C(4) methyl ester's oxygen, oriented trans diaxially with respect to C(5)—H. Consequently, a merged nucleophilic substitution – elimination (23) can be envisaged wherein transition state XIII turns to elimination product VI or to displacement intermediate XIV, which, in turn, produces the lactones X by demethylation by the base or, conceivably, leads to VI by trans elimination.[4] The difference of the steric requirements of the bases for proton abstraction may be a major factor in the dissimilar behavior of sodium methoxide and collidine in the elimination reactions.

The possible aryl participation in the bromide extrusion process and the consequent intermediacy of XII in the reaction led to a search for the interesting Favorskii rearrangement product XV among the products of the reaction of IX*b* with sodium methoxide. Along with the aforementioned product VI*d* an oily substance could be isolated in less than 1% yield from large-scale reactions. While its infrared and ultraviolet spectra were in accord with structure XV, its lack of ready availability prevented its full characterization. Sodium methoxide treatment of the model substance XVI*a* yielded merely the non-Favorskii product XVI*b* (24, 25).

[4]*Part structures XIII and XIV depict the carbonyl oxygen of the methyl esters as the intramolecular nucleophile responsible for the bromide displacement. However, in the absence of more revealing data no preference of these structures over those portraying the involvement of the ether oxygen of the esters in the displacement can be made at this time.*

Can. J. Chem. Downloaded from www.nrcresearchpress.com by 210.87.254.42 on 09/05/12
For personal use only.

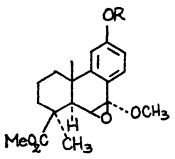

XI

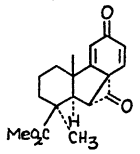

XII

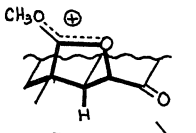

XIV

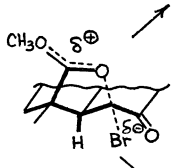

XIII

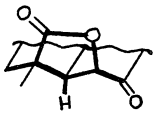

X

VI

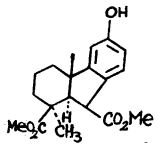

XV

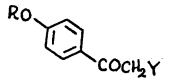

XVI*a*, R = Ac, Y = Cl
b, R = H, Y = OMe

EXPERIMENTAL

All melting points were observed on a Kofler microscope hot-stage. Ultraviolet spectra were run on 95% ethanol solutions on a Cary model 12 spectrophotometer. Infrared spectra were taken on chloroform solutions, unless noted otherwise, on a Perkin–Elmer model 21 spectrophotometer. Optical rotations were measured on chloroform solutions, unless stated differently, in a O. C. Rudolph polarimeter.

Derivatives of Desoxypodocarpic Acid Enantiomer (IIa)

Chromic acid oxidation of 5-isodesoxypodocarponitrile enantiomer (IV*a*) according to our previous procedure (3) gave improved yields (up to 35%) of the 6,7-diketone IV*f*. A mixture of 2.36 g of its enolacetate (III*a*) prepared as previously (3), 1.2 ml of conc. sulphuric acid, and 1.6 g of 10% palladium–charcoal in 120 ml of ethyl acetate was shaken for 8 hours under 10 lb of hydrogen. Then the catalyst was filtered, the solvent evaporated, water added, and the mixture extracted with ether. The extract was washed with saturated sodium bicarbonate solution and with water and was dried over anhydrous magnesium sulphate. Evaporation of the solvent yielded 1.82 g of residue. Alumina chromatography of 3.20 g of the crude product from several hydrogenations and elution with hexane gave 2.05 g of desoxypodocarponitrile enantiomer (II*b*), m.p. 87–88° (3). Further elution with 4:1 hexane–ether yielded 455 mg of 6β-acetoxydesoxypodocarponitrile enantiomer (II*c*), m.p. 117–118° (3).

A mixture of 600 mg of II*b* and 65 mg of lithium aluminum hydride in 40 ml of anhydrous tetrahydrofuran was refluxed for 1 hour. Water was added and the solvent mixture removed under reduced pressure. A mixture of the residue and 30 ml of 10% hydrochloric acid was refluxed for 4 hours, then cooled and extracted with ether. The extract was washed with water, dried over magnesium sulphate, and evaporated. Crystallization of the residue, 549 mg, from methanol yielded pure desoxypodocarpal enantiomer (II*d*), m.p. 91–94°; $[\alpha]_D^{22}$ −86.1° (EtOH); μ (in CCl_4) 3.71 (w, C—H), 5.82 (s, C=O). Anal. Calc. for $C_{17}H_{22}O$: C, 84.25; H, 9.15. Found: C, 84.18; H, 8.69.

The aqueous solution from which the aldehyde had been extracted was made basic and extracted with ether. Drying of the extract over magnesium sulphate, evaporation and distillation of the residue, 52 mg, gave desoxypodocarpyl amine enantiomer (II*h*), b.p. ca. 95° at 0.7 mm; $[\alpha]_D^{22}$ −7.8° (*c*, 3.0, EtOH). Anal. Calc. for $C_{17}H_{25}N$: C, 83.89; H, 10.35; N, 5.76. Found: C, 83.63; H, 10.54; N, 6.04.

A solution of 325 mg of potassium permanganate in 15 ml of water was added with stirring over a 5-hour period to a solution of 500 mg of II*d* in 15 ml of acetone. After the addition of sodium sulphite for the destruction of the excess permanganate as well as aqueous hydrochloric acid the solution was extracted with ether. The organic solution was extracted with 10% sodium hydroxide solution, the aqueous solution acidified and extracted with ether once again. Drying (sodium sulphate) of the extract, evaporation of the solvent, and crystallization of the residue yielded 501 mg of acidic product. Recrystallization from aqueous methanol gave desoxypodocarpic acid enantiomer (II*a*), m.p. 194–195.5°; $[\alpha]_D^{24}$ −141.0° (EtOH);[5] μ (in CCl_4) 5.75 (s) and 5.89 (w) (both C=O). Anal. Calc for $C_{17}H_{22}O_2$: C, 79.03; H, 8.58. Found: C, 79.33; H, 8.62.

An ether solution of 42.5 mg of II*a* and excess diazomethane was left 1 hour at room temperature. Upon addition of acetic acid the solution was washed with 10% sodium carbonate solution and with water and was dried (sodium sulphate). Evaporation of the solvent gave 45.3 mg of solid which on crystallization from aqueous methanol yielded crystalline platelets of methyl desoxypodocarpate enantiomer (II*i*), m.p. 140–141°; $[\alpha]_D^{25}$ −149.4° (EtOH); μ (in CCl_4) 5.77 (s, C=O). Anal. Calc. for $C_{18}H_{24}O_2$: C, 79.37; H, 8.88. Found: C, 79.62; H, 9.13.

A solution of 50 mg of II*a*, 1 ml of thionyl chloride, and 2 drops of pyridine was left standing at room temperature for 2 hours. The solution was evaporated under reduced pressure, the residue dissolved in 10 ml of ether, and 0.3 ml of 95% hydrazine hydrate in 10 ml of absolute ethanol was added at 0°. The mixture was shaken for 5 minutes, poured into water, and extracted with ether. Drying (magnesium sulphate) of the extract and evaporation of the solvent yielded 52 mg of a solid, m.p. 162–168°. Crystallization from ethyl acetate and sublimation afforded desoxypodocarpic hydrazide enantiomer (II*e*), m.p. 169–170°; $[\alpha]_D^{22}$ −127.8° (*c*, 0.80, EtOH); μ 2.91 (m), 3.04 (w, NH), 6.03 (s), 6.16 (s, C=O). Anal. Calc. for $C_{17}H_{24}ON_2$: C, 74.96; H, 8.88; N, 10.29. Found: C, 74.77; H, 8.68; N, 10.26.

A solution of 1.00 g of 6β-acetoxypodocarponitrile enantiomer (II*c*) and 50 ml of 10% sodium hydroxide in 100 ml of ethanol was stirred for 19 hours at room temperature under nitrogen. The solvent was removed under reduced pressure, water was added, and the mixture extracted with ether. The extract was washed with water, dried (magnesium sulphate), and evaporated. Crystallization of the residue, 843 mg, from ethyl acetate – chloroform gave 6β-hydroxypodocarponitrile enantiomer (II*f*), m.p. 204–205°; $[\alpha]_D^{23}$ −32.1° (*c*, 1.11); μ (Nujol) 2.88 (m, OH), 4.51 (m, C≡N). Anal. Calc. for $C_{17}H_{21}ON$: C, 79.96; H, 8.29; N, 5.49. Found: C, 80.15; H, 8.44; N, 5.36.

Nitrosyl chloride gas was bubbled through a stirred solution of 100 mg of II*f* in 15 ml of dry pyridine at −20° to −30°. When the solution appeared to have a persistent reddish brown color, water was added and the crystalline precipitate filtered and washed with water. Crystallization of the solid, 108 mg, from methylene chloride – hexane yielded 6β-hydroxypodocarponitrile nitrite enantiomer (II*g*), m.p. 189–191°; $[\alpha]_D^{23}$ −26.6° (*c*, 1.07); μ (Nujol) 4.50 (w, C≡N), 6.06 (s, N=O). Anal. Calc. for $C_{17}H_{20}O_2N_2$: C, 71.80; H, 7.09; N, 9.85. Found: C, 72.09; H, 7.34; N, 10.03.

Derivatives of 5-Isodesoxypodocarponitrile Enantiomer (IVα*)*

A lithium aluminum hydride reduction of 600 mg of IV*a* and a follow-up acid treatment were carried out in exactly the manner described for II*b* (*vide supra*). The crude products were 277 mg of aldehyde and 291 mg of amine. Distillation gave 5-isodesoxypodocarpal enantiomer (IV*b*), b.p. 85° at 0.7 mm; $[\alpha]_D^{22}$ 1.8° (*c*, 1.60, EtOH); μ 3.70 (w, C—H), 5.82 (s, C=O). Anal. Calc. for $C_{17}H_{22}O$: C, 84.25; H, 9.40. Found: C, 83.78; H, 9.40.

Crystallization of its 2,4-dinitrophenylhydrazone from ethanol gave needles, m.p. 203–204°. Anal. Calc. for $C_{23}H_{26}O_4N_4$: C, 65.38; H, 6.20; N, 13.26. Found: C, 65.56; H, 6.19; N, 13.13.

Crystallization of the basic product of the hydride reduction from ether yielded 5-isodesoxypodocarpyl amine (IV*c*), m.p. 80–81°; $[\alpha]_D^{22}$ 3.4° (*c*, 1.33, EtOH); μ 2.90 (m, NH). Anal. Calc. for $C_{17}H_{25}N$: C, 83.89; H, 10.35; N, 5.76. Found: C, 83.88; H, 10.52; N, 5.63.

A mixture of 502 mg of IV*a* and 25 mg of lithium aluminum hydride in 20 ml of ether was stirred at room temperature for 20 minutes. Water was added cautiously until hydrogen evolution had ceased and concentrated hydrochloric acid was added until the mixture was of pH < 1. After vigorous stirring for 20 minutes the ether layer was removed and the aqueous solution extracted three times with ether. The combined extracts were washed with 10% hydrochloric acid solution and with water and dried (magnesium sulphate). Solvent removal, chromatography of the crystalline residue (181 mg) on 3 g of silica, and elution with 9:1 hexane–ether yielded 150 mg of starting nitrile (IV*a*). Further elution gave only 24 mg of a mixture which was not investigated any further. The aqueous acid solution of reaction products was basified and extracted with ether. The extract was washed with minimum amounts of water, dried (magnesium sulphate), and evaporated. Upon standing, the residual oil, 297 mg, turned partly crystalline. Washing with small quantities

[5]*The optical rotation of desoxypodocarpic acid (I, R = CO_2H, R′ = Me, R″ = Y = H), the antipode of II*a*, has been recorded (16) erroneously as 40.8° (EtOH). It actually was observed as 140.8°.*

Can. J. Chem. Downloaded from www.nrcresearchpress.com by 210.87.254.42 on 09/05/12
For personal use only.

of cold ether and ether–hexane mixtures freed the crystals from surrounding oil. Crystallization of the solid from ether, in which it was quite soluble, gave a crystalline product, m.p. 136–140° (moistening at 127°); μ (Nujol) no OH, NH, CN, or CHO absorption bands, 6.02 (s, C=N). Standing out of contact with ether changed the crystalline imine to an oil, while crystallization from methanol or aqueous methanol led to gels. Gradient elution chromatography of 110 mg of the compound on 3 g of silica (250 ml of solvent changing from hexane to 1:1 hexane–ether, collected in 20-ml fractions) converted the imine to 50 mg of IV*b* and 48 mg of IV*c*. A mixture of 14 mg of aldehyde IV*b* and 14 mg of amine IV*c* was heated on a steam bath for 3 minutes and then triturated with ether and left standing for 18 hours. Evaporation of the solvent and seeding with a crystal of imine led to 17 mg of crystalline solid. Additional quantities of product were obtained upon washing of the residual oil with ether and hexane. The product had an infrared spectrum (Nujol) identical with that of the above imine.

A solution of 216 mg of IV*b* and 3 ml of hydrazine in 5 ml of anhydrous ethylene glycol was heated at 140° for 1 hour. Potassium hydroxide pellets, 2 g, were added to the cooled solution, whereupon the mixture was kept at 200° for 4 hours. Water was added and the mixture extracted with ether. The extract was washed with 10% hydrochloric acid and with water and dried (magnesium sulphate). Evaporation of the solvent and distillation of the oily residue, 153 mg, yielded 5-isodesoxypodocarpane enantiomer (IV*d*), b.p. 70° at 0.7 mm, m.p. 47–50° (lit. (15) m.p. 53–54°). Anal. Calc. for $C_{17}H_{24}$: C, 89.41; H, 10.59. Found: C, 89.48; H, 10.61.

Derivatives of Dehydroabietane (Ie)

Exposure of a tetrahydrofuran solution of 600 mg of dehydroabietonitrile (I*b*) to lithium aluminum hydride reduction in the manner described above yielded 262 mg of dehydroabietal (I*c*), m.p. 90–91° (lit. (7, 26) oil), and 317 mg of dehydroabietyl amine (I*d*), b.p. ca. 130° at 2.5 mm (lit. (27) b.p. ca. 250° at 12 mm, m.p. 41°).

Lithium aluminum hydride, 1.25 g, was added in small portions over a period of 2 minutes to a stirred cold solution of 25.0 g of nitrile I*b* in 250 ml of ether. After the mixture had been stirred for 10 minutes, during which time a white precipitate had formed, the excess hydride was decomposed by the dropwise addition of water, 50 ml of 5% hydrochloric acid solution was added and then enough concentrated hydrochloric acid was added until the mixture was acidic. Thereupon the mixture was stirred for a half hour, the layers separated, and the ether solution washed with 5% hydrochloric acid and with water and dried over magnesium sulphate. Evaporation of the solvent gave 24.9 g of oily aldehyde (I*c*). A mixture of the latter and 100 g of 95% hydrazine in 300 ml of diethylene glycol was refluxed for 6 hours. Excess hydrazine was removed by distillation when the solution was heated up to 200°. After 150 g of potassium hydroxide had been dissolved in the cooled solution, the mixture was refluxed for 3 hours. One liter of water was added and the mixture extracted with ether. The extract was washed with water, dried (magnesium sulphate), and evaporated. A hexane (100 ml) solution of the residual oil, 22.0 g, was passed through 100 g of alumina and eluted with 500 ml of hexane. Evaporation of the eluates yielded 17.4 g of dehydroabietane (I*e*), m.p. 38–42° (lit. (26) m.p. 41–44°), which required no further purification for the subsequent reactions.

Chromium trioxide, 15 g, was added over a 7-hour period to a solution of 10 g of dehydroabietane in 100 ml of acetic acid and 80 ml of acetic anhydride kept at 20–25°. After being stirred at room temperature for 18 hours the mixture was poured onto 320 g of ice and 8 g of sodium acetate and stirred for 2 hours. The preciptated gum as well as the decanted solution were extracted with ether and the combined extracts washed with water and dried (magnesium sulphate). Evaporation of the solvent, chromatography of the residue on alumina and elution with hexane yielded 6.7 g of non-crystalline ketoacetate V*a* (μ 5.78 (s), 5.95 (s, C=O)). Elution with 9:1 hexane–benzene gave 2.4 g of an oil which crystallized on standing. Crystallization from methanol yielded 7-keto-13-acetyldeisopropyldehydroabietane (V*b*), m.p. 143–145°; $[\alpha]_D^{25}$ 31.8° (*c*, 1.33); μ 5.95 (s, C=O). Anal. Calc. for $C_{19}H_{24}O_2$: C, 80.24; H, 8.51. Found: C, 80.22; H, 8.16.

A solution of 4.0 g of the ketoacetate V*a* and 50 ml of hydrazine in 100 ml of diethylene glycol was heated at 100° for 1.5 hours. After 30 g of potassium hydroxide had been added to the cooled solution, the mixture was heated to 200° and then refluxed for 4 hours. Water was added to the cooled solution and the latter extracted with ether. The extract was washed with water and with dilute hydrochloric acid and dried (magnesium sulphate). Evaporation gave 3.2 g of an oil which crystallized on trituration with hexane. Crystallization from hexane afforded the carbinol I*g*, m.p. 99–100°; $[\alpha]_D^{27}$ 52.5° (*c*, 1.70). Anal. Calc. for $C_{20}H_{30}O$: C, 83.86; H, 10.56. Found: C, 83.69; H, 10.47.

A solution of 5.0 g of diketone V*b* and 4.5 g of iodine in 100 ml of pyridine was refluxed for 3 hours and left standing for 18 hours. Water was added and the mixture extracted with chloroform. The extract was washed with 2 *N* hydrochloric acid and saturated brine solution. The solvent was evaporated, 45 ml of 10% sodium hydroxide solution and 100 ml of ethanol were added to the residue, and the mixture was refluxed for 3 hours. Much of the ethanol was distilled and the solution made acidic and extracted with ether. The extract was washed, dried (magnesium sulphate), and evaporated. Crystallization of the residue, 3.2 g, from methanol and sublimation yielded a keto acid, m.p. 222–223°; $[\alpha]_D^{23}$ 41.0° (*c*, 0.21). Anal. Calc. for $C_{18}H_{22}O_3$: C, 75.49; H, 7.74. Found: C, 75.39; H, 7.48.

Diazomethane treatment of 100 mg of this keto acid in 10 ml of ether led to 100 mg of product. Crystallization of the latter from methanol yielded 7-keto-13-carbomethoxydeisopropyldehydroabietane (V*c*), m.p. 105–107°; $[\alpha]_D^{23}$ 10.7° (*c*, 1.08); μ 5.81 (s), 5.95 (s, C=O), 6.21 (s, C=C).

Can. J. Chem. Downloaded from www.nrcresearchpress.com by 210.87.254.42 on 09/05/12
For personal use only.

Wolff–Kishner reduction of the keto acid was carried out in the manner described above. Sublimation of the product gave acid I*h*, m.p. 215–218° (softening at 113–115°); $[\alpha]_D^{23}$ 25.9° (*c*, 0.39); μ 5.82 (s, C=O). Diazomethane treatment of this acid and sublimation of the product yielded 13-carbomethoxydeisopropyldehydroabietane (I*i*), m.p. 110–111°; $[\alpha]_D^{23}$ 56.4° (*c*, 1.35). Anal. Calc. for $C_{19}H_{26}O_2$: C, 79.68; H, 9.15. Found: C, 79.40; H, 9.29.

The ester I*i*, 25 mg, was dissolved in a Grignard solution, prepared from 85 mg of magnesium and 0.5 ml of methyl iodide in 50 ml of tetrahydrofuran and the mixture refluxed for 4 hours. Aqueous ammonium chloride was added and the mixture extracted with ether. The extract was dried (magnesium sulphate) and evaporated. Crystallization of the residue from hexane yielded the carbinol I*g*, m.p., m.m.p. 99–100°; infrared spectrum identical with that of an authentic sample (*vide supra*).

A solution of 1.6 g of alcohol I*g* and 2 ml of phosphorous oxychloride in 15 ml of dry pyridine was left standing for 18 hours. Water was added and the solution acidified with dilute hydrochloric acid and extracted with ether. The extract was washed with water and saturated brine solution and dried over magnesium sulphate. Evaporation left 0.65 g of an oil whose passage through alumina and distillation yielded the olefin I*f*, b.p. 105° at 3 mm. Anal. Calc. for $C_{20}H_{28}$: C, 89.49; H, 10.51. Found: C, 89.54; H, 10.45.

Unsaturated Ketones III, VIa, VIc, and VIe

A solution of 400 mg of 5-iso-7-ketodesoxypodocarponitrile enantiomer (IV*e*) (3) and 1.50 g of freshly sublimed selenium dioxide in 35 ml of acetic acid and 5 ml of water was refluxed for 2 hours. After filtration through Celite and removal of the solvent under reduced pressure water was added and the mixture extracted with ether. The extract was dried (magnesium sulphate) and evaporated. Addition of hexane–benzene yielded 97 mg of yellow crystals identical in all respects with authentic 5-iso-6,7-diketodesoxypodocarponitrile enantiomer (IV*f*) (3). Chromatography of the mother liquor on alumina and elution with 9:1 hexane–ether gave 150 mg of crystalline solid whose crystallization from benzene–hexane and sublimation yielded 5,6-dehydro-7-ketodesoxypodocarponitrile enantiomer (III*c*), m.p. 213–214°; $[\alpha]_D^{23}$ −112.9° (*c*, 1.24); μ 4.49 (w, C≡N), 6.03 (s, C=O), 6.23 (m, C=C). Anal. Calc. for $C_{17}H_{17}ON$: C, 81.24; H, 6.82; N, 5.57. Found: C, 81.20; H, 6.90; N, 5.50.

A similar oxidation of 2.8 g of V*e* (3) with 5.0 g of selenium dioxide, 80 ml of acetic acid, and water for 6 hours yielded 2.8 g of solid product whose crystallization from methanol yielded methyl 5,6-dehydro-7-ketodesoxypodocarpate (VI*c*), m.p. 146–147° (lit. (15), its optical antipode, m.p. 147–148°); $[\alpha]_D^{23}$ 164.9° (*c*, 0.69); μ 5.81 (s), 6.03 (s, C=O), 6.24 (m, C=C). Anal. Calc. for $C_{18}H_{20}O_3$: C, 76.03; H, 7.09. Found: C, 75.76; H, 7.21.

Oxidation of 12.0 g of I*j* (16) with 14.0 g of chromic acid in 210 ml of acetic acid and 50 ml of water according to a published procedure (3) led to an oil whose benzene solution was passed through an alumina column (slow chromatography led to partly deacetylated product). Evaporation of the filtrate and crystallizations of the residue, 12.9 g, from hexane–benzene and aqueous methanol yielded methyl *O*-acetyl-7-ketopodocarpate (V*d*), m.p. 132–136°; $[\alpha]_D^{25}$ 70.0°; μ 5.68 (s), 5.81 (s), 5.96 (s, C=O), 6.23 (m, C=C); λ_{max} 255 mμ (log ϵ 4.22), λ_{min} 227 mμ (log ϵ 3.88). Anal. Calc. for $C_{20}H_{24}O_5$: C, 69.75; H, 7.02. Found: C, 69.39; H, 6.97.

Oxidation of 200 mg of V*d* with 680 mg of selenium dioxide in 20 ml of acetic acid in the manner described above yielded an oil which on crystallization from aqueous methanol gave 130 mg of solid, m.p. 130–144°. Several recrystallizations from aqueous methanol afforded methyl O-acetyl-5,6-dehydro-7-ketopodocarpate (VI*b*), m.p. 143–146°; $[\alpha]_D^{25}$ 147°; μ 5.68 (s), 6.03 (s, C=O), 6.23 (m, C=C); λ_{max} 255 mμ (log ϵ 4.20), $\lambda_{shoulder}$ 274 mμ (log ϵ 4.10), λ_{min} 222 mμ (log ϵ 3.90). Anal. Calc. for $C_{20}H_{22}O_5$: C, 70.20; H, 6.44. Found: C, 70.22; H, 6.52.

A solution of 2.00 g of VI*c* and 5 g of anhydrous lithium iodide in 60 ml of dry collidine was refluxed for 10 hours under nitrogen. Water was added to the cooled solution and the latter extracted with ether. The extract was washed with 10% hydrochloric acid and with water and dried over magnesium sulphate. Removal of the solvent under reduced pressure left 1.59 g of solid which on sublimation afforded ketone VI*a*, m.p. 119–120° (lit. (15) m.p. 120–121°); $[\alpha]_D^{23}$ 54.7° (*c*, 0.51). Anal. Calc. for $C_{16}H_{18}O$: C, 84.91; H, 8.02. Found: C, 85.19; H, 8.43.

Similar decarbomethoxylation of III*d* (15), the optical antipode of VI*c*, yielded III*b* (15), m.p. 119–120°, the enantiomer of VI*a*.

Similar treatment of 790 mg of VI*d* (*vide infra*) produced a brown solid, the passage of whose chloroform–methanol solution through an alumina column gave 200 mg of pale yellow crystals. Several crystallizations from aqueous methanol and sublimation yielded colorless platelets of ketone VI*e*, m.p. 234–237° (change to needles at 200°); $[\alpha]_D^{25}$ 115.0°; μ 3.10 (m, broad, OH), 6.08 (s, C=O), 6.28 (m), 6.35 (m, C=C); λ_{max} at 242 mμ and 301 mμ. Anal. Calc. for $C_{16}H_{18}O_2$: C, 79.35; H, 7.44. Found: C, 79.05; H, 7.96.

Hydrogenation of Compounds VII

A mixture of 300 mg of ketoester IV*d* in 6 ml of glacial acetic acid and 0.3 ml of ethanedithiol in 0.6 ml of boron trifluoride etherate was left standing at room temperature for 48 hours. Then water was added and the precipitated solid, 272 mg, m.p. 234–239°, crystallized several times from aqueous methanol. This yielded the ketal VII*b*, m.p. 237–241° (decomp.); $[\alpha]_D^{20}$ 128.5°; μ 2.80 (w), 3.02 (w, broad, OH), 5.82 (s, C=O), 6.05 (w), 6.18 (m), 6.22 (m, C=C); $\lambda_{shoulder}$ 231 mμ (log ϵ 4.35) and 282 mμ (log ϵ 3.74). Anal. Calc. for $C_{20}H_{24}O_3S_2$: C, 63.79; H, 6.38. Found: C, 63.39; H, 6.34.

Can. J. Chem. Downloaded from www.nrcresearchpress.com by 210.87.254.42 on 09/05/12
For personal use only.

Can. J. Chem. Downloaded from www.nrcresearchpress.com by 210.87.254.42 on 09/05/12
For personal use only.

A mixture of 19 mg of the ketal VII*b* and 0.2 g of W-2 Raney nickel in 4 ml of absolute ethanol was refluxed for 6 hours. The solvent was removed under vacuum, the residue extracted with chloroform, and the extract dried over sodium sulphate. Evaporation of the solvent and two crystallizations of the crystalline solid from aqueous methanol yielded methyl podocarpate (I*k*), m.p., m.m.p. 209–211°; infrared spectrum identical with that of an authentic sample.

A mixture of 59 mg of thioketal VII*b* and 0.6 g of W-2 Raney nickel in 10 ml of acetone was refluxed for 2 hours. The catalyst was filtered through Celite and the filtrate evaporated under reduced pressure. The yellow residual oil was unstable to air, changing to a deep red liquid, and resisted all attempts at crystallization. Presumably VIII*a*, μ 2.80 (w), 3.00 (w, broad, OH), 5.82 (s, C=O), 6.10 (w), 6.23 (m, C=C); $\lambda_{shoulder}$ 231 mμ (log ϵ 4.34), 256 mμ (log ϵ 4.10), 280 mμ (log ϵ 3.91), it was used for subsequent reduction without further purification. The difference of these spectral data as well as $[\alpha]_D^{25}$ 108° from the physical constants of the $\Delta^{6,7}$ derivative of methyl podocarpate (m.p. 172–176°; $[\alpha]_D^{20}$ −75°; μ 2.78 (w), 2.97 (w, broad, OH), 5.82 (s, C=O), 6.23 (m), 6.36 (w, C=C); λ_{max} 270 mμ (log ϵ 4.30), λ_{min} 241 mμ (log ϵ 3.94)) (24) showed the oil to be the $\Delta^{5,6}$ derivative (VII*a*) (cf. also the difference between the physical data for ferruginol and its $\Delta^{6,7}$ derivative (28)). The oil was hydrogenated (2 drops of conc. sulphuric acid and 10 mg of palladium–charcoal in 5 ml of ethyl acetate). The reaction ceased after a ca. 1 mole hydrogen uptake and the yellow color had disappeared. The catalyst was filtered and the solution washed with 5% sodium bicarbonate and saturated brine solution and dried over sodium sulphate. Evaporation of the solvent yielded 40 mg of methyl podocarpate (I*k*), m.p., m.m.p. 207–209° after crystallization from aqueous methanol; infrared and ultraviolet spectra identical with those of an authentic sample. A similar hydrogenation of 76 mg of VI*d* (50 mg of palladium–charcoal and 8 ml of ethanol) yielded 61 mg of methyl podocarpate (I*k*).

Bromoketones IX

Chromic acid oxidation of 1.00 g of methyl O-methylpodocarpate (I*o*) according to the procedure of the Bible patent (22) yielded 906 mg of crystalline product, m.p. 117–123°. Crystallization from aqueous ethanol gave methyl O-methyl-7-ketopodocarpate (V*g*), m.p. 121–123° (crystal change at 108–110°); $[\alpha]_D^{25}$ 79°; μ 5.84 (s), 6.03 (s, C=O), 6.28 (s), 6.40 (s, C=C); λ_{max} 226 mμ (log ϵ 4.42), 276 mμ (log ϵ 4.32), λ_{min} 243 mμ (log ϵ 3.89). Anal. Calc. for $C_{19}H_{24}O_4$: C, 72.15; H, 7.60. Found: C, 72.36; H, 7.60.

Bromination of 732 mg of V*g* according to the procedure in the Bible patent (22) produced 861 mg of solid, m.p. 118–122°, whose crystallization from aqueous methanol yielded methyl 6-bromo-7-keto-O-methylpodocarpate (IX*a*), m.p. 123–126°; $[\alpha]_D^{25}$ 87°; μ 5.80 (s), 5.97 (s, C=O), 6.25 (s), 6.35 (m, C=C); λ_{max} 231 mμ (log ϵ 4.49), 291 mμ (log ϵ 4.18).

Chromic acid oxidation of 12.0 g of methyl O-acetylpodocarpate (I*j*) by our previous general procedure (3) yielded a crude product whose benzene solution was passed rapidly through an alumina column and then evaporated. Crystallization of the residual solid, 12.9 g, from aqueous methanol and benzene–hexane yielded methyl O-acetyl-7-ketopodocarpate (V*d*), m.p. 136–138°; $[\alpha]_D^{25}$ 70°; μ 5.69 (s), 5.83 (s), 5.98 (s, C=O), 6.25 (m), 6.35 (w, C=C); λ_{max} 225 mμ (log ϵ 4.20), λ_{min} 228 mμ (log ϵ 3.89). Anal. Calc. for $C_{20}H_{24}O_5$: C, 69.75; H, 7.02. Found: C, 69.93; H, 7.01.

Slower chromatography of the reaction mixture of the oxidation or the following hydrolysis procedure led to ketophenol V*h*. A solution of 100 mg of the diester V*d*, 10 ml of 5% sodium hydroxide solution, and 1 ml of ethanol was stirred at room temperature for 3 hours. After the addition of 10 ml of saturated brine solution and enough conc. hydrochloric acid to bring the solution to pH 2 the latter was extracted with chloroform. The extract was washed with brine solution and dried over magnesium sulphate. Evaporation of the solvent and crystallization of the residual oil from aqueous methanol yielded 75 mg of solid, m.p. 220–238°. Recrystallizations afforded methyl 7-ketopodocarpate (V*h*), m.p. 237–241°; $[\alpha]_D^{25}$ 53°; μ 2.79 (w), 3.05 (m, broad, OH), 5.82 (s), 6.01 (s, C=O), 6.22 (s), 6.27 (s), 6.35 (s, C=C); λ_{max} 229 mμ; (log ϵ 4.52), 282 mμ (log ϵ 4.32), λ_{min} 245 mμ (log ϵ 4.12). Anal. Calc. for $C_{18}H_{22}O_4$: C, 71.52; H, 7.28. Found: C, 71.23; H, 7.20.

A solution of 2.9 g of bromine in 10 ml of glacial acetic acid was added dropwise to a stirred solution of 2.00 g of the diester V*d* and 2 drops of 15% hydrobromic acid in 10 ml of glacial acetic acid. The mixture was maintained at room temperature for 10 minutes and then evaporated under reduced pressure. Crystallization of the residual oil from methanol produced 1.97 g of solid, m.p. 120–125°, whose recrystallizations led to methyl 6-bromo-7-keto-O-acetylpodocarpate (IX*b*), m.p. 130–132°; $[\alpha]_D^{25}$ 59°; μ 5.69 (s), 5.82 (s), 5.92 (s, C=O), 6.24 (s), 6.35 (w, C=C); λ_{max} 260 mμ (log ϵ 3.92), λ_{min} 236 mμ (log ϵ 3.70). Anal. Calc. for $C_{20}H_{23}O_5Br$: C, 56.74; H, 5.48; Br, 18.88. Found: C, 57.11; H, 5.67; Br, 18.65.

A solution of 200 mg of the diester IX*b* in 5 ml of absolute ethanol, into which dry hydrogen chloride gas had been bubbled, was refluxed for 2 hours, and then evaporated under reduced pressure. Crystallization of the residue from aqueous methanol yielded 158 mg of solid, m.p. 193–200° (decomp.), whose recrystallization from methanol afforded methyl 6-bromo-7-ketopodocarpate (IX*c*), m.p. 200–204° (decomp.); $[\alpha]_D^{25}$ 61°; μ 2.80 (w), 2.08 (w, broad, OH), 5.82 (s), 5.96 (s, C=O), 6.22 (s), 6.26 (s), 6.35 (s, C=C); λ_{max} 234 mμ (log ϵ 3.91), 300 mμ (log ϵ 4.01), λ_{min} 254 mμ (log ϵ 3.14). Anal. Calc. for $C_{18}H_{21}O_4Br$: C, 56.71; H, 5.51. Found: C, 56.46; H, 5.72.

The same bromo compound was the product, 380 mg, of the reaction of a solution of 435 mg of IX*b* in 10 ml of conc. sulphuric acid for 4 hours at room temperature. Furthermore, it was the product, 265 mg, of the reaction of 500 mg of IX*b* in 5 ml of absolute methanol with sodium methoxide, 35 mg of sodium in 5 ml of absolute methanol, for 1 minute.

Unsaturated Ketones VIb, VId, and VIf

A solution of 3.00 g of bromoketone IX*b* in 10 ml of anhydrous methanol, in which 0.38 g of sodium had been dissolved, was refluxed for 5 hours. After the addition of 30 ml of saturated brine solution and 1.5 ml of conc. hydrochloric acid the mixture was extracted with chloroform. The extract was washed with saturated brine, dried over sodium sulphate, and evaporated. Crystallization of the residue from aqueous methanol gave 1.90 g of a solid, m.p. 205–215°, whose recrystallizations and sublimation led to methyl 5,6-dehydro-7-ketopodocarpate (VI*d*), m.p. 223–224°; $[\alpha]_D^{25}$ 143°; μ 2.85 (w), 3.15 (w, broad, OH), 5.82 (s), 6.12 (s, C=O), 6.31 (s), 6.39 (s, C=C); λ_{max} 242 mμ (log ϵ 4.27), 308 mμ (log ϵ 4.10), λ_{min} 269 mμ (log ϵ 3.60). Anal. Calc. for $C_{18}H_{20}O_4$: C, 71.98; H, 6.71. Found: C, 72.00; H, 6.67.

A solution of 200 mg of phenol VI*d* and 100 mg of sodium acetate in 5 ml of acetic anhydride was refluxed for 2 hours. The solution was concentrated under reduced pressure, 10 ml of water was added, and the mixture extracted with chloroform. The extract was washed with water, dried over sodium sulphate, and evaporated. Crystallization of the residue from aqueous methanol gave 211 mg of solid, m.p. 143–146°, whose recrystallization afforded methyl 5,6-dehydro-7-keto-O-acetylpodocarpate (VI*b*), m.p. 143–146°; $[\alpha]_D^{25}$ 147°; μ 5.70 (s), 5.81 (s), 6.06 (s, C=O), 6.24 (s, C=C); λ_{max} 255 mμ (log ϵ 4.20), $\lambda_{shoulder}$ 273 mμ (log ϵ 4.10), λ_{min} 222 mμ (log ϵ 3.90). Anal. Calc. for $C_{20}H_{22}O_5$: C, 70.20; H, 6.44. Found: 70.22; H, 6.52.

A solution of 200 mg of the phenol VI*d*, 0.1 ml of dimethyl sulphate, and 52 mg of sodium hydroxide in 3 ml of 50% aqueous ethanol was heated at 120° for 20 minutes. Water was added and the mixture extracted with ether. The extract was dried over magnesium sulphate and evaporated. The residue, 89 mg, was crystallized from benzene–hexane. Recrystallization of the product, m.p. 169–174°, and sublimation led to methyl 5,6-dehydro-7-keto-O-methylpodocarpate (VI*f*), m.p. 173–175°; $[\alpha]_D^{25}$ 153°; μ 5.80 (s), 6.08 (s, C=O), 6.25 (s), 6.35 (w, C=C); λ_{max} 235 mμ (log ϵ 4.45), 302 mμ (log ϵ 4.18), λ_{min} 270 mμ (log ϵ 4.01). Anal. Calc. for $C_{19}H_{22}O_4$: C, 72.50; H, 7.01. Found: C, 72.63; H, 7.11.

When a reaction between 261 mg of bromoketone IX*a* and sodium methoxide (20 mg of sodium in 5 ml of absolute methanol) was carried out and worked up in the manner described for the dehydrobromination of IX*b* (*vide supra*), there was produced 175 mg of crystallized product, m.p. 170–175°, whose recrystallization from aqueous methanol led to VI*f*, m.p. 173–175°, undifferentiable from the sample above.

Lactones X

A solution of 396 mg of bromoketone IX*b* in 3 ml of collidine was refluxed for 2 hours. Water, 14 ml, and conc. hydrochloric acid (up to pH 2) were added and the mixture extracted with chloroform. The extract was washed with saturated brine solution, dried over sodium sulphate, and evaporated. The residual oil, 383 mg, was chromatographed on a 4:1 Bentonite–Celite (6 g) column. Elution with carbon tetrachloride – benzene yielded 169 mg of solid whose crystallization from aqueous methanol led to VI*b*, m.p., m.m.p. 141–145°; spectra identical with those of the above sample. Further elution with benzene–chloroform gave 131 mg of solid whose crystallizations from aqueous methanol resulted in needles of 6β-hydroxy-7-keto-O-acetylpodocarpic lactone (X*b*), m.p. 161–164°; $[\alpha]_D^{25}$ 84°; μ 5.60 (s), 5.90 (s, C=O), 6.24 (s, C=C); λ_{max} 260 mμ (log ϵ 4.00), λ_{min} 232 mμ (log ϵ 3.29). Anal. Calc. for $C_{19}H_{20}O_5$: C, 69.51; H, 6.10. Found: C, 69.63; H, 6.50.

Treatment of 265 mg of bromoketone IX*c* in identical manner, chromatography of the oily reaction product, 250 mg, and elution with carbon tetrachloride – benzene, benzene, and benzene–chloroform yielded 80 mg of crude VI*d*, while elution with 2:1 benzene–chloroform and chloroform gave 150 mg of oily lactone X*c* (μ, 2.80 (w), 3.05 (w, broad, OH), 5.60 (s), 5.92 (s, C=O), 6.25 (s), 6.35 (m, C=C); λ_{max} 233 mμ (log ϵ 3.94), 299 mμ (log ϵ 4.10), λ_{min} 250 mμ (log ϵ 2.75)) which could not be induced to crystallize. Acetylation of the latter with acetic anhydride and sodium acetate afforded crystalline lactone acetate X*b*, m.p., m.m.p. 161–164°; spectra identical with those of the above sample.

Treatment of 310 mg of bromoketone IX*a* in the same manner and elution of a chromatogram of the reaction products with carbon tetrachloride and with chloroform yielded 110 mg of a solid whose crystallization from aqueous methanol afforded keto ester VI*f*, m.p., m.m.p. 171–173°; spectra identical with those of the above sample. The later chloroform eluates contained 110 mg of a solid whose crystallizations from aqueous methanol gave methyl 6β-hydroxy-7-keto-O-methylpodocarpic lactone X*a*, m.p. 195–197.5° (lit. (22) m.p. 198–200.5°); $[\alpha]_D^{25}$ 89°; μ 5.61 (s), 5.95 (s, C=O), 6.25 (s), 6.38 (m, C=C); λ_{max} 230 mμ (log ϵ 3.96), 291 mμ (log ϵ 4.12), λ_{min} 245 mμ (log ϵ 3.01). Anal. Calc. for $C_{18}H_{20}O_4$: C, 72.00; H, 6.67. Found: C, 72.15; H, 6.66.

ACKNOWLEDGMENTS

The authors are indebted to the National Science Foundation, U.S.A., and to the Ciba Pharmaceutical Company (Summit, New Jersey, U.S.A.) for research grants in support of this work, to Drs. W. Hoehn and R. Burtner (G. D. Searle and Co.) and T. F. Sanderson (Hercules Powder Co.) for gifts of the natural products starting materials and to Messrs. H. Cole, R. Eliason, D. Glover, J. D. McChesney, and C. L. Leicht and Mrs. R. Sklar for technical assistance. P. B., R. W. J. C., and C. D. R. are indebted to the U.S. Department of Health, Education and Welfare for predoctoral Public Health Service fellowships.

Can. J. Chem. Downloaded from www.nrcresearchpress.com by 210.87.254.42 on 09/05/12
For personal use only.

REFERENCES

1. E. WENKERT, R. W. J. CARNEY, and C. KANEKO. J. Am. Chem. Soc. **83**, 4440 (1961) and preceding references.
2. E. WENKERT and A. TAHARA. J. Am. Chem. Soc. **82**, 3229 (1960).
3. E. WENKERT and B. G. JACKSON. J. Am. Chem. Soc. **80**, 211 (1958).
4. H. C. BROWN, C. J. SHOAF, and C. P. GARG. Tetrahedron Letters, No. 3, 9 (1959).
5. W. NAGATA, S. HIRAI, H. ITAZAKI, and K. TAKEDA. Ann. **641**, 196 (1961).
6. W. NAGATA. Tetrahedron, **13**, 287 (1961).
7. E. WENKERT, V. I. STENBERG, and P. BEAK. J. Am. Chem. Soc. **83**, 2320 (1961).
8. J. W. APSIMON and O. E. EDWARDS. Can. J. Chem. **40**, 896 (1962).
9. I. IWAI, A. OGISO, and B. SHIMIZU. Chem. Ind. (London), 1288 (1962).
10. J. A. FINDLAY, W. A. HENRY, T. G. JAIN, Z. VALENTA, K. WIESNER, and C. M. WONG. Tetrahedron Letters, No. 19, 869 (1962).
11. W. L. MEYER and A. S. LEVINSON. Proc. Chem. Soc. 15 (1963).
12. A. L. NUSSBAUM and C. H. ROBINSON. Tetrahedron, **17**, 35 (1961).
13. T. F. SANDERSON (to Hercules Powder Co.). U.S. Patents 2,750,367 and 2,750,368.
14. M. OHTA. Pharm. Bull. (Tokyo), **4**, 273 (1956).
15. M. OHTA and L. OHMORI. Pharm. Bull. (Tokyo), **5**, 96 (1957).
16. E. WENKERT and B. G. JACKSON. J. Am. Chem. Soc. **80**, 217 (1958).
17. R. DULOU and G. DEFAYE-DUCHATEAU. Compt. Rend. **250**, 1288 (1960).
18. E. TASCHNER and B. LIBEREK. Roczniki Chem. **30**, 323 (1956).
19. F. ELSINGER, J. SCHREIBER, and A. ESCHENMOSER. Helv. Chim. Acta, **43**, 113 (1960).
20. G. STORK and J. W. SCHULENBERG. J. Am. Chem. Soc. **84**, 284 (1962).
21. D. H. R. BARTON and G. A. MORRISON. *In* Progress in the chemistry of organic natural products. Vol. 19. Springer Verlag, Vienna, Austria. 1961. p. 217.
22. R. H. BIBLE and M. GROVE (to G. D. Searle and Co.). U.S. Patent No. 2,753,357.
23. S. WINSTEIN, D. DARWISH, and N. HOLNESS. J. Am. Chem. Soc. **78**, 2915 (1956).
24. C. D. ROTH. Unpublished observation.
25. J. C. ANDERSON and C. B. REESE. Tetrahedron Letters, No. 1, 1 (1962).
26. W. P. CAMPBELL and D. TODD. J. Am. Chem. Soc. **64**, 928 (1942).
27. A. ZVENJNIEKS. Svensk Kem. Tidskr. **66**, 316 (1954).
28. J. B-SON BREDENBERG. Acta Chem. Scand. **11**, 932 (1957).

Can. J. Chem. Downloaded from www.nrcresearchpress.com by 210.87.254.42 on 09/05/12
For personal use only.

ULTRAVIOLET IRRADIATION OF PYRIMIDINE DERIVATIVES

IV. ANIONIC EFFECTS ON THE PHOTOLYSIS OF CYTOSINE AND O-METHYLCYTOSINE

A. M. MOORE[1]

Biology Branch, Atomic Energy of Canada Limited, Chalk River, Ontario

Received March 8, 1963

Can. J. Chem. Downloaded from www.nrcresearchpress.com by 210.87.254.5 on 09/05/12
For personal use only.

ABSTRACT

The course of the photochemical reactions involved in the photolysis of O-methylcytosine is strongly affected by the presence of various anions. Similar anionic effects were noted during the photolysis of cytosine but the products of this reaction appeared to be less suitable for further investigation. Ultraviolet irradiation of O-methylcytosine in water leads to destruction of the characteristic absorption bands, while irradiation in phosphate leads to the production of a new compound with marked absorption at 300 mμ, and irradiation in pyrophosphate, glycerophosphate, citrate, or cacodylate leads to the production of compounds with marked absorption at 274 mμ. The phosphate-dependent photolysis of O-methylcytosine has been studied in some detail and the product has been isolated and purified. Apparently the $H_2PO_4^-$ ion acts as a catalyst in a reaction which involves the loss of 1 mole of ammonia and the addition of 2 moles of water to O-methylcytosine.

RESULTS

Recent investigations of the chemical effects of ultraviolet light on pyrimidine derivatives have disclosed three types of reaction, namely, (*a*) nucleophilic addition of water, ethanol, or hydrogen cyanide at the 5,6-double bond (1–5), (*b*) dimerization by addition at the same double bond (6), and (*c*) ring cleavage (7). All three were encountered in studies of derivatives of uracil and thymine, in which the products of the photochemical reaction have been isolated and identified. Derivatives of cytosine have previously proved less satisfactory as subjects of investigation, the immediate products of irradiation being so unstable as to make their isolation very difficult. Spectrophotometric and other evidence in the case of cytidine and cytidylic acid indicate that addition of water to the 5,6-double bond is probably the main reaction occurring on irradiation of buffered, neutral, aqueous solutions (4). However, some anomalies have been observed. Wang (8) has reported that the product of irradiation of cytosine in water reverts spontaneously to cytosine on standing, but that the reaction is largely irreversible when a neutral buffer (nature unspecified) is used as solvent.

This observation was confirmed in the present investigation. The spectrophotometric results also provided some indication that the course of the photochemical reaction with cytosine was influenced by the nature of the anions present in the solution during irradiation (Fig. 1). However, some of the products appeared to be unstable. Earlier work in this laboratory (3) had shown that it was easier to isolate and identify the products of irradiation of 1,3-dimethyluracil than of uracil itself. Further, Shugar and Wierzchowski (9) had reported that irradiation of O-methylcytosine gave stable products with a characteristic absorption spectrum. For these reasons, O-methylcytosine (2-methoxy-4-aminopyrimidine; MAP) was selected for study in the hope that it might prove more tractable than cytosine itself.

The course of the reaction induced in MAP by ultraviolet light (253.7 mμ) was strongly influenced by the anionic constituents of the medium. When the compound was irradiated

[1]*Deceased. All communications should be forwarded to D. K. Myers, Biology and Health Physics Division, Atomic Energy of Canada Limited.*

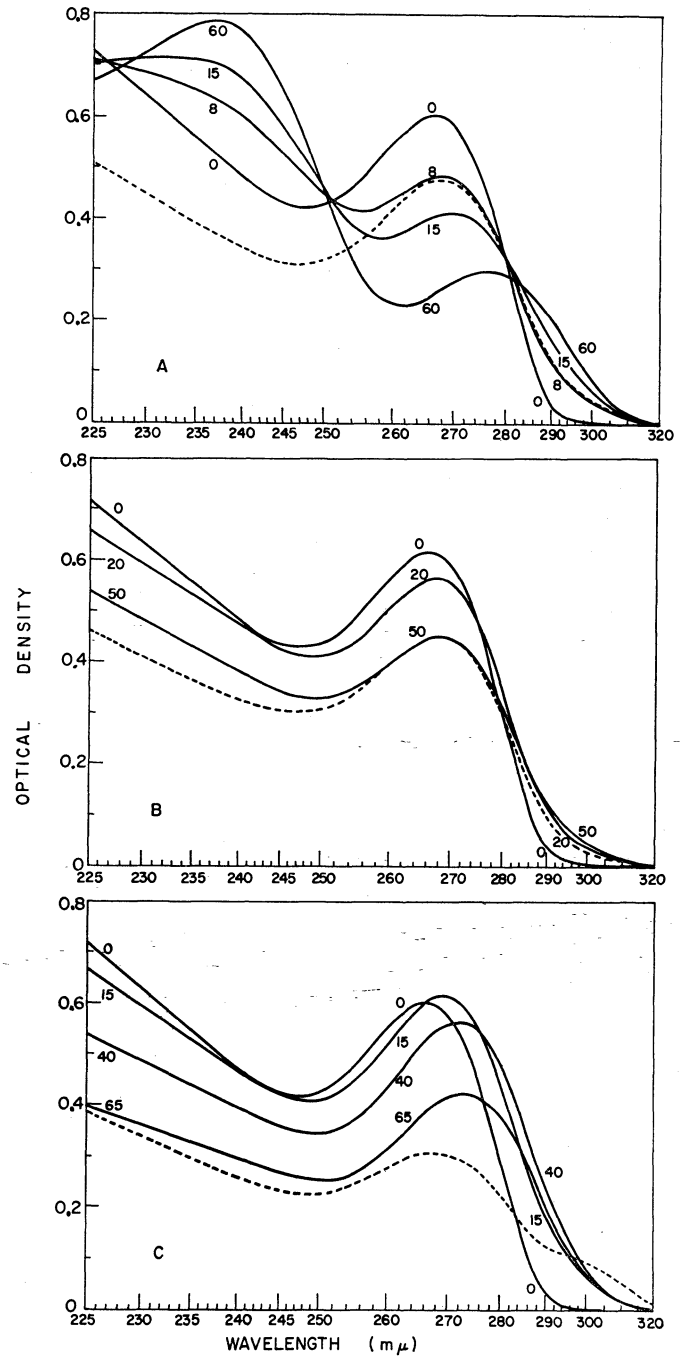

FIG. 1. Spectrophotometric changes during ultraviolet irradiation of cytosine. (A) 10^{-4} *M* cytosine in water at pH 7.0, after irradiation for 0, 8, 15, and 60 minutes. The broken line represents the spectrum of the last sample (60 minutes' irradiation) after storage at room temperature for 20 hours. (B) 10^{-4} *M* cytosine in 0.05 *M* pyrophosphate buffer pH 7.0, after irradiation for 0, 20, and 50 minutes. The broken line represents the spectrum of the last sample (50 minutes' irradiation) after storage at room temperature for 20 hours. (C) 10^{-4} *M* cytosine in 0.05 *M* phosphate buffer pH 7.0, after irradiation for 0, 15, 40, and 65 minutes. The broken line represents the spectrum of the last sample (65 minutes' irradiation) after storage at room temperature for 20 hours. All irradiations were carried out at room temperature in the apparatus described in reference 3.

Can. J. Chem. Downloaded from www.nrcresearchpress.com by 210.87.254.5 on 09/05/12
For personal use only.

in water at pH 7, the spectral change was characterized by a disappearance of the absorption maximum at 270 mμ, together with a general decrease in absorbance at all wavelengths between 210 and 286 mμ, and the transient appearance of a small shoulder above 286 mμ (Fig. 2). The same result was observed when MAP was irradiated at pH 7 in sodium

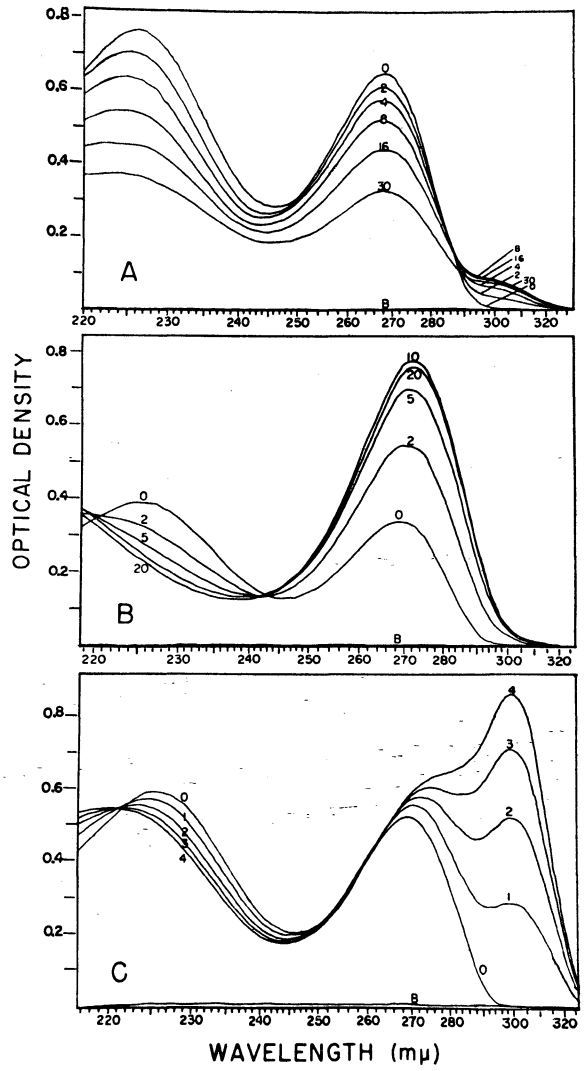

FIG. 2. Spectrophotometric changes during ultraviolet irradiation of 2-methoxy-4-aminopyrimidine (MAP). (A) 1×10^{-4} *M* MAP in water at pH 7.0 after irradiation for 0, 2, 4, 8, 16, and 30 minutes. (B) 0.5×10^{-4} *M* MAP in 0.05 *M* pyrophosphate buffer pH 7.0, after irradiation for 0, 2, 5, 10, and 20 minutes. (C) 0.77×10^{-4} *M* MAP in 0.05 *M* phosphate buffer pH 7.0, after irradiation for 0, 1, 2, 3, and 4 minutes. The concentrations of MAP were chosen for convenience of presentation. All irradiations were carried out at room temperature in the apparatus described in reference 3.

chloride or sodium sulphate solutions (0.05 *M*). These changes were not reversed by heating or on standing at room temperature, in contrast to the hydration reaction which occurs during irradiation of uracil, cytosine, or N-substituted cytosine derivatives such as cytidine and cytidylic acid.

Can. J. Chem. Downloaded from www.nrcresearchpress.com by 210.87.254.5 on 09/05/12
For personal use only.

A second pattern was observed when MAP was irradiated in pyrophosphate buffer at pH 7. Here the original absorption peak of MAP increased in optical density to more than twice the initial value, while the position of the peak shifted from 270 to 274 mμ (Fig. 2). The effects of several other anions (citrate, glycerophosphate, phosphite, cacodylate) were superficially similar to those of pyrophosphate.

In phosphate buffer at pH 7, however, a third type of reaction occurred. This resulted in the appearance of a new absorption maximum at 300 mμ with an increased optical density (Fig. 2). The only other anion that showed this effect was arsenate, which is similar to phosphate in structure and properties. However, arsenate was less efficient in producing the 300 mμ absorption band and it appeared to share some of the properties of pyrophosphate because a mixture of products with absorption maxima at 274 mμ and at 300 mμ was obtained.

The phosphate-dependent reaction appears to be a new type of photodecomposition in the pyrimidine series. In their review of the photochemistry of nucleic acids (9), Shugar and Wierzchowski noted that irradiation of MAP in phosphate buffer at pH 7 gave rise to a product with a new absorption band near 300 mμ, and that under similar conditions the spectrum of 2-ethyluracil showed an analogous shift in the absorption peak to longer wavelengths. They did not remark, however, that this reaction was obtained only in the presence of phosphate.

Paper chromatography of the photolytic products from MAP in solutions of various buffers provided further evidence for a specific effect of phosphate in directing the course of the reaction. Four products were identified; the anion present during irradiation of MAP appeared to determine which particular product was formed predominantly (Table I).

TABLE I

Paper chromatography of the products from the ultraviolet irradiation of MAP in various buffers

Buffer during irradiation	(A) Butanol–water R_f: 0.26	0.47	0.55	0.83	(B) Butanol – water – acetic acid R_f: 0.28	0.36	0.73
Pyrophosphate	++	++	+	−	++	+	++
Cacodylate	++	++	(+)	−	++	+	++
Arsenate	+	+	+	+	+	+	++
Phosphate	+	−	(+)	+++	+	−	+++

NOTE: Spots were located on the paper chromatograms by the ultraviolet print method. All R_f values are approximate and varied over a range of 0.05 from one experiment to another. The R_f of MAP in solvent A was 0.74 and in solvent B 0.48. The spot at R_f 0.73 in solvent B appears to represent two different compounds which exhibited similar mobilities in this solvent (see text).

The specific effect of phosphate on the photolysis of MAP appeared to be of particular interest and was studied in more detail. As the concentration of phosphate was increased, the rate of formation of the 300 mμ product approached a maximum, with half the maximal rate being reached at approximately 0.007 *M* phosphate (Fig. 3). The type of curve obtained is reminiscent of the dissociation curve for a complex between two ions or molecules (e.g. phosphate and MAP, or phosphate and an intermediate product) when the concentration of one of the ions is altered. However, the presence of phosphate had no measurable effect on the absorption spectrum of MAP itself. Continuous-flow experiments also failed to demonstrate measurable amounts of other products with ultraviolet absorption during the irradiation of MAP in phosphate buffer.

The yield of product with an absorption maximum at 300 mμ was strongly influenced

Can. J. Chem. Downloaded from www.nrcresearchpress.com by 210.87.254.5 on 09/05/12
For personal use only.

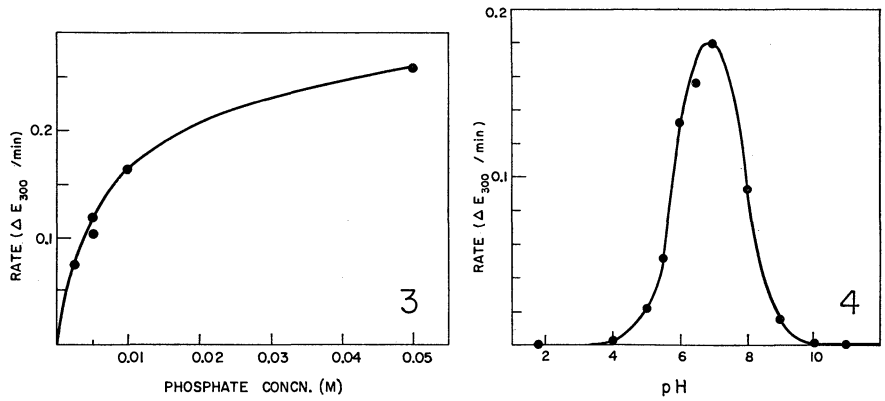

FIG. 3. Effect of phosphate concentration on the initial rate of formation of the 300 mμ product during ultraviolet irradiation of 10^{-4} *M* MAP in aqueous solution at pH 7.0. The rate is expressed as increase in optical density at 300 mμ per minute.

FIG. 4. Effect of pH on the initial rate of formation of the 300 mμ product during ultraviolet irradiation of 10^{-4} *M* MAP in 0.05 *M* phosphate. The rate is expressed as increase in optical density at 300 mμ per minute.

by the pH of the solution during irradiation (Fig. 4). Maximum rate of formation was found near pH 6.8–7.0. Since the p*K* of the second hydrogen of phosphoric acid is known to be 7.2, and the p*K* of the amino group of MAP was found by experiment to be 5.5, one might predict an optimum pH of 6.35 for a reaction involving these two molecules if the rate of reaction was determined by the relative concentrations of undissociated and dissociated ions. A more rigorous mathematical treatment, based on one model for the reaction (see below), introduces a correction factor to allow for competing reactions, which brings the theoretical value for optimum pH up to 6.8. The variation of yield with pH could not be explained by destruction of the product in slightly acid or alkaline solutions. These results (Fig. 4) suggest, therefore, that the reacting species are the unionized amino form of MAP and the singly ionized form ($H_2PO_4^-$) of phosphate.

The product with absorption maximum at 300 mμ did not contain phosphorus, nor was there any phosphorus in the other minor products formed during irradiation of MAP in phosphate. This was demonstrated by paper chromatography of MAP solutions after irradiation in the presence of phosphate labelled with radioactive P-32; no radioactivity was detected in any of the ultraviolet-absorbing spots on the chromatogram. Further, the 300 mμ peak did not appear when phosphate was added immediately after irradiation to an irradiated solution of MAP in water, showing that phosphate did not react with some long-lived irradiation product. The 300 mμ product was itself destroyed by further irradiation with ultraviolet light; however, its rate of destruction was essentially the same in the presence and absence of phosphate, thus demonstrating that the role of phosphate was not the stabilization of the 300 mμ product. We are thus left with the conclusion that phosphate acts as a catalyst in the photolysis of MAP to the 300 mμ product by some reaction mechanism as yet unknown.

Identification of the 300 mμ Product

Fifty-milligram quantities of this product were prepared by irradiation of large volumes of MAP solution containing phosphate in a specially designed apparatus, followed by subsequent chromatography of the products on a cation-exchange resin. The 300 mμ product was extracted from the eluate with chloroform and recrystallized from ethyl

Can. J. Chem. Downloaded from www.nrcresearchpress.com by 210.87.254.5 on 09/05/12
For personal use only.

acetate – hexane. The pure material was a faintly yellow, crystalline solid which melted at 153.5° C, had a molecular weight of 144, and analyzed for $C_5H_8N_2O_3$. This empirical formula suggests that in the photolysis of MAP ($C_5H_7N_3O$), one molecule of ammonia is lost and two molecules of water are added.

Three alternative structures were considered; these are indicated below in the same configuration as MAP. All three structures could, in their enol forms, exhibit the system of conjugated double bonds which is necessary to account for the high extinction coefficient (24.4×10^3) of the purified product at 300 mμ.

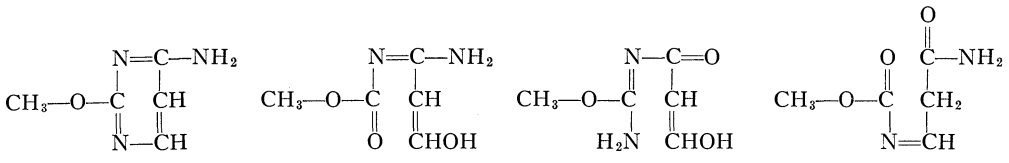

MAP I II III

The production of ammonia during irradiation of MAP in phosphate solution was verified by two separate methods (see below). The presence of one methoxyl group in the purified product was also verified. The absorption peak at 300 mμ was suppressed by treatment with hydrogen cyanide, permanganate, or semicarbazide, indicating the presence of an aldehyde group. The compound reacted readily both with bromine and with iodine, but these reactions appeared to be of a complex nature. Infrared spectra gave evidence of the presence of primary amino, hydroxyl, and carbonyl groups in the purified product. The free amino group appeared to have a pK of 3.5, as compared with the pK of 5.5 for the amino group of MAP.

The cumulative evidence suggests that the correct structure of the purified product is represented by compound I, which, in the enol form, might be designated as N-carbomethoxy-β-hydroxyacrylamidine. This conclusion remains to be proved by synthesis of compound I.

EXPERIMENTAL

2-Methoxy-4-aminopyrimidine (MAP)

MAP was synthesized according to Hilbert *et al.* (10, 11) and purified by repeated recrystallization from hot water; m.p. 170–171° C; lit. m.p. 170° (10), 174° (11). The 2,4-dichloropyrimidine used in this synthesis was prepared from uracil by two methods (10, 12). MAP was also purchased from Applied Science Laboratories, Inc., State College, Pa.; m.p. 164–167° C. All melting points were determined with a Fisher–Johns heated-stage apparatus.

The ultraviolet spectrum of an aqueous solution of MAP at pH 7.0, either in water or phosphate buffer, exhibited two maxima at 270 mμ and 225 mμ, with an intervening minimum of absorption at 245 mμ (Fig. 2). The molecular extinction coefficient was 6820 at 270 mμ and 7510 at 225 mμ. At the same pH, cytosine itself exhibited a single absorption maximum at 267 mμ (Fig. 1) with an extinction coefficient of 6130 (13). The values given above for MAP are slightly different from those reported by Shugar and Wierzchowski (9), but both the identity of the compound and the position of the absorption maxima have been carefully checked in the present experiments.

The addition of alkali had no effect on the spectrum of MAP, while the repeated addition of 10-μl portions of 0.01 N HCl to 3 ml of 10^{-4} M MAP in water resulted in a series of spectral curves with isosbestic points at 268.5, 224, and 217.5 mμ. At pH 4.5, the absorption maxima were at 259 and 229.5 mμ, with the absorption minimum at 242 mμ. The pK of the primary amino group can be calculated from a plot of these spectral changes as a function of pH (cf. ref. 13); the average value from four experiments was 5.6. Two experiments, in which a 10^{-2} M solution of MAP was titrated directly with acid, provided pK values of 5.4 and 5.5. An average pK of 5.5 has been used in mathematical calculations.

Ultraviolet Irradiation

In most experiments, solutions of MAP or of cytosine in water or in appropriate buffers were irradiated in the apparatus previously described (3) using low-pressure mercury-vapor lamps as the light source. A

Can. J. Chem. Downloaded from www.nrcresearchpress.com by 210.87.254.5 on 09/05/12
For personal use only.

0.1 *M* KBr solution was circulated through the jacket of the double-walled quartz sample chamber in order to filter out ultraviolet radiation of wavelengths below 230 mμ, and maintain a constant temperature. The wavelength of the incident radiation was preponderantly 253.7 mμ. Irradiated samples were withdrawn at various periods of time and their ultraviolet absorption spectra determined with a Beckman DK-2 recording spectrophotometer. In experiments on irradiation at different pH values (Fig. 4), the samples were neutralized before the spectra were recorded. During irradiation of MAP in 0.05 *M* phosphate at pH 7, the rate of formation of the 300 mμ product was found to be independent of MAP concentration over the range 10^{-4} to 2×10^{-3} *M*, indicating that most of the incident light was being absorbed under the experimental conditions (Table II).

TABLE II

Effect of MAP concentration on the initial rate of the photochemical reaction in 0.05 *M* phosphate buffer at pH 7.0

MAP concentration (*M*)	Rate of formation of 300 mμ product (ΔE_{300}/min)	MAP concentration (*M*)	Rate of formation of 300 mμ product (ΔE_{300}/min)
2×10^{-3}	0.260±0.037 (3)	1×10^{-4}	0.253±0.019 (8)
1×10^{-3}	0.277±0.026 (12)	5×10^{-5}	0.163±0.024 (3)
5×10^{-4}	0.270±0.050 (2)		

NOTE: Average values are given together with the standard error of the mean followed by the number of determinations in parentheses. The differences between the average rates are not statistically significant until the concentration of MAP is decreased to 5×10^{-5} *M*.

Quantum yields were measured in a modification of the same apparatus (3) using a smaller-diameter quartz chamber insert fitted with a mechanical stirrer to provide continuous mixing during irradiation. Using values of 0.0013 for 10^{-4} *M* cytosine and 0.037 for 10^{-2} *M* uridylic acid as standards (1), the quantum yield for disappearance of the absorption maximum at 270 mμ during irradiation of 10^{-4} *M* MAP in water proved to be 0.00065, while the quantum yield for formation of the 300 mμ peak during irradiation of 10^{-4} *M* MAP in 0.05–0.2 *M* phosphate at pH 7 was 0.0017. The initial rate of increase in optical density at 300 mμ during irradiation of MAP in water at pH 7 was approximately 100 times slower than the corresponding rate in phosphate buffer.

In order to look for spectrophotometric evidence of short-lived intermediates during the photolysis of MAP in phosphate buffer, a special apparatus was designed by which the MAP solution was continuously circulated from the irradiation chamber to the spectrophotometer and back again. By this means, the time between irradiation and spectrophotometric recording was reduced from several minutes to a few seconds. However, the spectra showed no evidence of ultraviolet-absorbing compounds other than those detected in previous experiments. A record of change in absorption at 300 mμ with time of irradiation also failed to show any appreciable lag between the time that irradiation was started and the time that the absorption at 300 mμ began to increase. These experiments indicate that (*a*) short-lived intermediates in the reaction mixture must be present in very low concentrations, (*b*) their half-lives are considerably less than a few seconds, or (*c*) their spectra are very similar to the spectra of MAP or the 300 mμ product.

Paper Chromatography

Solutions containing 10^{-3} *M* MAP in 0.05 *M* buffer (phosphate, pyrophosphate, arsenate, or cacodylate) at pH 7.0 were irradiated for 90–120 minutes. Ten-milliliter samples of the irradiated solutions were evaporated to dryness under a stream of air at room temperature and the residue redissolved in 1 ml water. Small amounts (20 to 50 μl) were applied to Whatman No. 1 paper, using 20 μl of 10^{-2} *M* MAP as a reference spot on each chromatogram. The chromatograms were developed for 6–16 hours with an ascending solvent consisting either of (A) butanol saturated with water, or (B) 9 volumes of butanol saturated with water plus 1 volume of glacial acetic acid. The chromatograms were subsequently dried in air and ultraviolet-absorbing spots located by the ultraviolet print method of Markham and Smith (14). R_f values were measured on the ultraviolet prints in the usual manner (Table I).

In some experiments, small portions of the chromatogram, corresponding to the ultraviolet-absorbing spots, were cut out and eluted with 4 ml of phosphate buffer. The ultraviolet spectrum of the eluates could then be recorded. In this way, it was possible to show that the products with R_f 0.26 and 0.47 in solvent A both exhibited absorption maxima in the region of 272–274 mμ, while the product with R_f 0.83 in solvent A exhibited an absorption maximum at 300 mμ. One of the above products, possibly the one with R_f 0.26, acquired a much higher mobility in solvent B and travelled with approximately the same R_f as the 300 mμ product in solvent B. Thus the product with R_f 0.73 in solvent B exhibited maximum absorption at 274 mμ when irradiation had been carried out in pyrophosphate buffer, but exhibited maximum absorption at 300 mμ when irradiation had been carried out in orthophosphate. The absorption spectrum of the product with R_f 0.55 in solvent A could not be properly defined owing to the small amounts of material present, but appeared to have a maximum near 269 mμ.

Can. J. Chem. Downloaded from www.nrcresearchpress.com by 210.87.254.5 on 09/05/12
For personal use only.

Formation of Ammonia

Ammonia was measured first by distillation at room temperature from irradiated solutions of MAP. Air was drawn through an acid trap containing 0.1 N H_2SO_4, then into an irradiated MAP solution to which an equal volume of saturated K_2CO_3 had been added, and finally into a solution of 2% boric acid. The amount of ammonia carried over into the boric acid was determined by titration with standard HCl. No ammonia was detected in MAP solutions prior to irradiation; after irradiation of MAP in 0.05 M phosphate, approximately 1 mole of ammonia was recovered per mole of MAP lost during the irradiation. Since the K_2CO_3 had no effect on the ultraviolet spectrum of the irradiated solution at room temperature, it seems probable that this ammonia must have been liberated during the irradiation.

A second method for determination of ammonia was based on determination of optical density at 420 mμ after addition of Nessler's reagent (15). On irradiation of 10^{-3} M MAP in 0.05 M phosphate at pH 7, a linear 1:1 molar relationship between ammonia production and formation of the 300 mμ product was found during the first 30 minutes of irradiation. Further irradiation resulted in a molar excess of ammonia over 300 mμ product, presumably because this product was susceptible to photodecomposition during prolonged irradiation.

Isolation of the 300 mμ Product

An apparatus was constructed whereby MAP solution from a reservoir was sprayed onto the top of two vertical glass plates and allowed to run down the surface of these plates, past a vertical bank of 10 mercury-vapor lamps, to the reservoir again. Using this apparatus, 1 liter of 10^{-3} M MAP in 0.05 M phosphate buffer pH 7.0 was irradiated for 6 hours at 5° C; this length of time provided a maximum yield of the 300 mμ product under these experimental conditions. The irradiated solution was acidified to pH 4.5–4.6 with concentrated HCl and applied under suction to an ion-exchange column (Dowex 50 W-X 8, Na form; column 4×9 cm). The column was washed under suction with 1 liter of water acidified to pH 4.5 with acetic acid and then with another liter of the same solution by gravity feed. These washings contained unchanged MAP and other ultraviolet-absorbing materials but none of the 300 mμ product; the pH of this solution, it might be noted, was below the pK of MAP (4.5) but greater than the pK of the 300 mμ product (3.5; see below). When the eluate was free of ultraviolet-absorbing materials, a solution of 1 M NaCl – sodium acetate buffer at pH 4.5 was applied to the column. The 300 mμ product was eluted almost immediately and was usually collected in a volume of 1 liter. This eluate was neutralized to pH 7 and extracted four to six times with an equal volume of chloroform (the partition coefficient of the product in a chloroform/water system being 1.12). The combined chloroform extracts were evaporated *in vacuo* almost to dryness and the last few milliliters of solvent were removed under a stream of air at room temperature.

The product was dissolved in 15 ml of boiling ethyl acetate and the resulting solution was allowed to cool to room temperature, at which point a few crystals formed. Hexane was added to opalescence and crystallization was allowed to continue. The crystals were washed twice with hexane and dried in a vacuum desiccator over P_2O_5 to eliminate residual water. The weight of crystalline material was usually 35–50 mg, representing a 25–35% yield of product from the original amount of MAP. After repeated recrystallization, the melting point of the product was 153.5° C.

Properties of the 300 mμ Product

Elementary analysis was carried out at National Research Council, Ottawa, through the kindness of Dr. Léo Marion. Found: C 41.49%, H 5.43%, N 19.38%, O (by difference) 33.70%. Calculated for $C_5H_8N_2O_3$: C 41.67%, H 5.56%, N 19.44%, O 33.33%. The molecular weight for a monomer of this elementary composition should be 144. *Molecular weight* was estimated from the decrease in vapor pressure of a solvent caused by the presence of a known amount of compound, using a Mechrolab Model 301 osmometer for this determination and 1,3-dimethyluracil as standard. The molecular weight of the 300 mμ product was found to be 144 (individual measurements 145.8 and 143.3).

The ultraviolet spectrum at pH 7.0 exhibited a maximum in absorption at 300 mμ with a molecular extinction coefficient (ϵ) of 24,400, and a second maximum at 212 mμ with an extinction coefficient of 8,300 (Fig. 5). The molecular extinction at 300 mμ was 3.6 times the molecular extinction of MAP at 270 mμ but was of the same order of magnitude as that observed with compounds such as 2,4-hexadienal (16) or 2,4-hexadienoic acid (17). The spectrum of the purified product in chloroform solution was essentially identical with that in a neutral aqueous solution.

The position and height of the absorption peak at 300 mμ were not appreciably altered by the addition of alkali, but this peak disappeared in acid without the appearance of a new peak anywhere in the region 220–330 mμ (Fig. 5). The effect of acid on the absorption spectrum was reversible on neutralizing the solution. Determination of the pK from the change in spectrum with pH gave a value of 3.5.

Ultraviolet irradiation of a 2.5×10^{-5} M solution of the purified 300 mμ compound resulted in a rapid destruction of the compound, the absorption maxima at 300 mμ and at 212 mμ both being extinguished. The average time for 50% destruction of a 2×10^{-5} M solution was 10 minutes in water at pH 7 and 8 minutes in 0.05 M phosphate at pH 7. The rate of destruction at pH 9 was similar to that at pH 7, while one experiment at pH 5 suggested a slower rate. By way of comparison it might be noted that approximately 1.2 minutes were required for the production of a 1.25×10^{-5} M concentration of 300 mμ compound during the irradiation of 10^{-4} M MAP in 0.05 M phosphate pH 7 under the same experimental conditions.

Can. J. Chem. Downloaded from www.nrcresearchpress.com by 210.87.254.5 on 09/05/12
For personal use only.

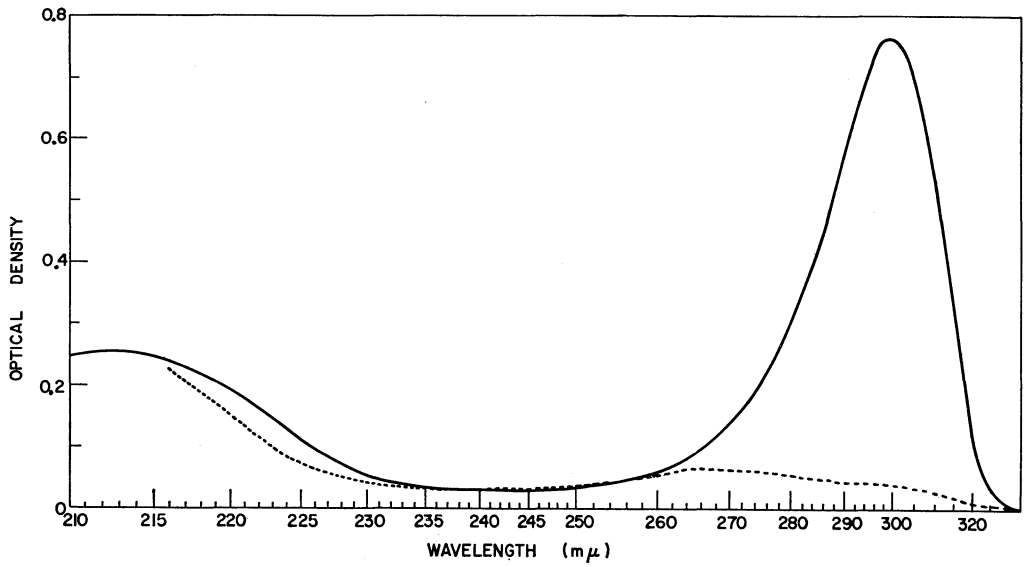

FIG. 5. The ultraviolet absorption spectrum of a 3.1×10^{-5} *M* solution of the purified 300 mμ product. The solid line represents the spectrum at pH 7 while the broken line represents the spectrum at pH 2.

Stability of the 300 mμ product in aqueous solution was limited. The absorption at 300 mμ disappeared with a half-life of 35 hours on standing at room temperature (20–22° C) in 0.05 *M* phosphate buffer at pH 7.0, and was extinguished when the same solution was heated to 100° C for 20 minutes. The stability at room temperature was not appreciably affected by exposure to visible light. Heating the compound in 0.01 *N* HCl at 100° C for 5 minutes resulted, after neutralization of the solution, in the disappearance of the absorption maximum at 300 mμ and the formation of a new maximum at 283 mμ. Preliminary experiments indicated the loss of one molecule of ammonia in hot acid solutions. Heating the compound in 0.1 *N* NaOH at 100° C for 20 minutes resulted in complete loss of ultraviolet absorption bands, with the transient appearance of a small absorption maximum near 280 mμ after shorter periods of heating.

Methoxyl content was determined by a slight modification of the method described by Clark (18), using vanillin as a standard and nitrogen as the carrier gas. Found: 21.76 and 21.63%. Calculated (for one methoxyl per 144 g): 21.53%.

The presence of an aldehyde group in the 300 mμ product was suggested by a number of observations. Reaction with hydrogen cyanide was followed spectrophotometrically. The maximum at 300 mμ decreased by approximately 40% within 20 minutes after addition of 0.017 *M* NaCN to a 2.5×10^{-5} *M* solution of the compound in 0.05 *M* phosphate.

Reaction with $KMnO_4$ was measured titrimetrically. Five milliliters of 10^{-3} *M* MAP in 0.05 *M* phosphate was irradiated for 60 minutes, then acidified with 1 ml 1 *N* H_2SO_4, warmed to 60° C, and titrated with 0.01 *N* $KMnO_4$. The irradiated solution reacted with 1.03 equivalents of permanganate, whereas the MAP solution before irradiation failed to react. Reaction with permanganate eliminated the absorption peak at 300 mμ.

The addition of 0.01 *M* semicarbazide (neutralized) to a dilute solution of impure 300 mμ product in 1 *M* sodium acetate resulted in complete disappearance of the 300 mμ absorption peak within 15–30 minutes. The semicarbazone derivative was obtained by reaction of 10 mg of purified product with excess semicarbazide, followed by evaporation of the solvent and recrystallization of the product from ethyl acetate – hexane; m.p. 90° C. No reaction of semicarbazide with MAP was observed.

A reaction with 2,4-dinitrophenylhydrazine was demonstrated by spraying this compound onto a paper chromatogram of irradiated MAP (developed with butanol–water saturated with SO_2). When the chromatogram was subsequently exposed to ammonia vapor, the 300 mμ product showed up as a dark brown spot.

Bromination was followed spectrophotometrically as in previous investigations (19). Successive additions of 10-μl samples of Br_2–H_2O, containing approximately 2.5×10^{-3} *M* bromine, were mixed with solutions containing known amounts of MAP or the 300 mμ product (3×10^{-5}–8×10^{-5} *M*) and the ultraviolet absorption spectra were recorded after each addition. The exact concentration of bromine was calculated from its optical density at 390 mμ in 0.1 *N* HCl, the molecular extinction coefficient being 175.

Bromination of MAP resulted in the formation of a new absorption maximum at 282 mμ, the optical density at this wavelength being slightly smaller than the optical density of the original MAP solution at

Can. J. Chem. Downloaded from www.nrcresearchpress.com by 210.87.254.5 on 09/05/12
For personal use only.

270 mμ. Slightly more than 1 mole of bromine per mole of MAP was required to complete this reaction. Since the bromo-MAP still exhibited a strong ultraviolet absorption band, it seems probable that the overall reactions led to the substitution of one bromine atom for hydrogen on carbon-5 of the pyrimidine ring, in much the same manner as demonstrated previously with uracil derivatives following bromination and heating (19).

Bromination of the 300 mμ product from irradiated MAP eliminated the absorption peak at 300 mμ. An unstable intermediate with maximum absorption at 320 mμ appeared during the reaction, but ultimately only an absorption peak at 241 mμ (with approximately one-third the original optical density at 300 mμ) remained. The total reaction consumed on the average 2.3 moles of bromine per mole of 300 mμ product. Irradiation of bromo-MAP in 0.05 *M* phosphate did not lead to formation of the same product but simply to disappearance of the absorption maximum at 282 mμ. Treatment of the 300 mμ compound with iodine–water produced much the same effect as with bromine–water; the 300 mμ peak disappeared with transient formation of a labile compound absorbing near 320 mμ and finally of a compound with maximum absorption at 224 mμ. These results suggest that the reactions with bromine and iodine might involve oxidation of the aldehyde group as well as addition to a double bond.

Infrared spectra were determined on a Perkin–Elmer infrared recording spectrophotometer Model 21 (NaCl prism) through the courtesy of W. M. Thurston. In most experiments, 0.5–0.6 mg of test compound was dissolved in 1 ml chloroform, mixed with 200 mg of KCl, dried, and pressed into disks at 12,000 p.s.i. for 10 minutes; these disks were then used for recording the infrared spectrum of the test compound in its solid state (Fig. 6). Both MAP and the 300 mμ product were deuterated by refluxing 0.5–0.6 mg of compound either with 0.5 ml of D_2O (99.7% isotopic purity; supplied by Development Chemistry Branch, Atomic Energy of Canada Limited) or with 0.5 ml of CH_3OD (Merck, Sharpe and Dohme Limited, Montreal) for 40–60 minutes. The compounds were then dried, mixed with chloroform and 200 mg of KCl, redried, and pressed into disks as described above. The infrared spectra of the deuterated compounds (Fig. 6) proved to be essentially identical with either D_2O or CH_3OD as deuterium source.

The infrared spectrum of MAP exhibited two absorption bands due to the —NH_2 group at 3.00 and 3.16 μ. Following deuteration, these bands shifted to 3.97 and 4.29 μ; similar results have been reported for cytosine and cytidine (20). Another absorption maximum at 6.05 μ, which shifted to 6.7 μ following deuteration, was also presumed to represent the —N—H bond (21). The series of five major absorption bands in the region between 6.3 and 7.6 μ are similar to those reported for 2-methoxypyrimidine but have not been further characterized.

The infrared spectrum of the purified 300 mμ product exhibited a similar absorption band at 6.03 μ, which shifted to 6.7 μ following deuteration. However, the corresponding absorption maxima at 2.95 and 3.14 μ for the undeuterated compound were no longer symmetrical. The increase in relative absorption at 2.95 μ may have been due to superposition of hydroxyl and amino bands; this is suggested by the fact that this band split into two components at 4.0 and 3.94 μ following deuteration. The series of overlapping absorption bands in the region between 3.3 and 3.8 μ shifted to 4.5–4.9 μ following deuteration; this shift may indicate that some of the —C—H bonds in the 300 mμ product exchanged readily with deuterium whereas a similar exchange did not occur in MAP (Fig. 6). The 300 mμ compound also exhibited an absorption band at 5.78 μ, representing a carbonyl group, which was not present in the infrared spectrum of MAP. A strong absorption band at 8.1 μ was tentatively assigned to a C—O ester linkage (21).

A hydrochloride of the 300 mμ compound was made by passing dry HCl through 1 ml of chloroform containing 0.5 mg of compound, followed by drying, mixing with KCl, and pressing into a disk as described above. The amino absorption bands at 2.95 and 3.14 μ were shifted to 3.4 and 3.5 μ, in the same manner as described for other amines (21), leaving a broad low peak at 3.0 μ. The absorption maxima at 5.74, 6.04, and 8.2 μ were scarcely altered by conversion of the compound to its hydrochloride.

The infrared spectra appeared to be consistent with structures I or II as indicated in the text above. If the absorption maximum at 8.1 μ were due to C—O ester linkage (21), the spectrum would indicate structure I. It might be noted that the infrared spectrum of crude samples of MAP that had been irradiated in phosphate buffer did not exhibit any unusual characteristics except for a small absorption peak at 4.55 μ. This absorption peak suggests the presence of a triple bond, either C≡N or C≡C, in one of the by-products of the photolytic reaction.

Nuclear magnetic resonance spectra were determined by W. G. Schneider, Division of Pure Chemistry, National Research Council, Ottawa, using $CDCl_3$ and CH_3OD as solvents. The data confirmed the presence of amino and methoxyl groups in the 300 mμ compound as well as in MAP. The spectrum of the 300 mμ product exhibited an additional low-field signal which was probably due to a hydroxyl group.

Mass spectrum was determined by J. A. Stone, Research Chemistry Branch, Atomic Energy of Canada Limited, Chalk River. In the mass spectrometer, a sample of crystalline material was exposed to an electron beam *in vacuo*; the mass and relative amount of the ionized fragments of the molecule were measured. The major peaks appeared at masses 14, 15, 16, 17, 28, 29, 31, 32, 43, and 44 with three minor peaks at masses 61, 70, and 73. On comparing the possible atomic composition of these fragments (22) with the proposed structures, it appeared probable that mass 17 must represent OH, mass 31 a methoxyl group, mass 43 either CHNO or C_2H_3O (e.g. —CH=CHOH), mass 61 either $C_2H_5O_2$ or CHO_3 (which could be formed if the carbonyl group of structure I were hydrogen bonded to the hydroxyl group), while the only probable

Can. J. Chem. Downloaded from www.nrcresearchpress.com by 210.87.254.5 on 09/05/12
For personal use only.

Can. J. Chem. Downloaded from www.nrcresearchpress.com by 210.87.254.5 on 09/05/12
For personal use only.

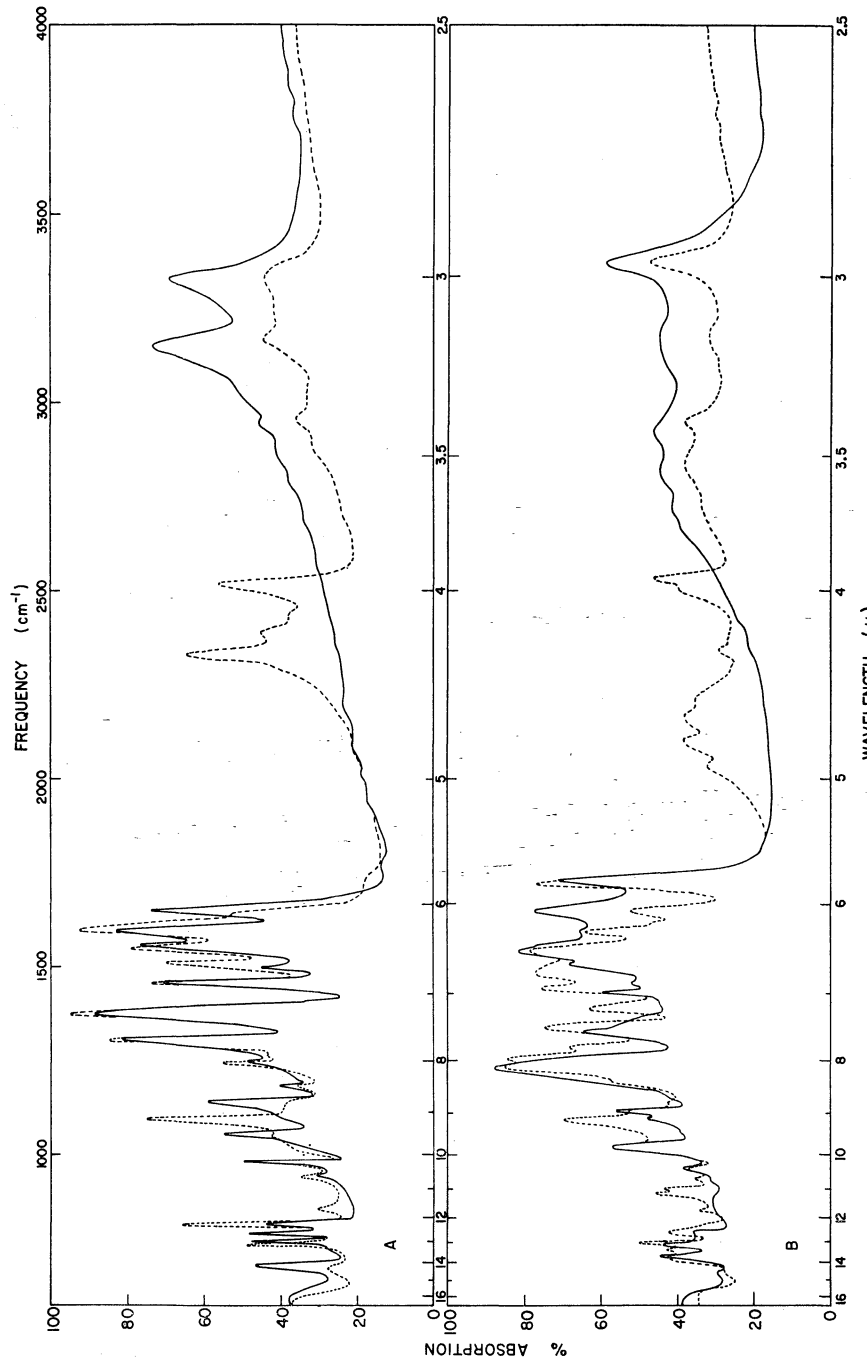

FIG. 6. Infrared spectra of MAP and of the 300 mμ product in the solid state. (A) Solid line: 0.28% MAP in a KCl disk. Broken line: approximately 0.3% deuterated MAP, formed by refluxing MAP with CH_3OD. Similar results were obtained after refluxing with D_2O. (B) Solid line: 0.25% purified 300 mμ product in a KCl disk. Broken line: approximately 0.25% deuterated product, formed by refluxing with CH_3OD.

fragment of mass 73 was $C_2H_3NO_2$ (e.g. CH_3—O—CO—N=). These fragments appear to be consistent with structure I.

Calculation of Optimum pH

Consider the hypothetical reactions

$$M + h\nu \xrightarrow{k_1} M^*$$

$$M^* + H_2O \xrightarrow{k_2} M, L, K, \text{etc.}$$

$$M^* + P \xrightarrow{k_3} MP^* \xrightarrow{k_4} Z + P$$

where M represents MAP; M* represents activated MAP after absorption of a quantum of ultraviolet light; P represents inorganic phosphate; MP* represents some undefined complex between activated MAP and phosphate (perhaps only two molecules in collision); Z represents the 300 mμ product; while L, K, etc. are by-products. Square brackets are used below to indicate molar concentrations. Using the conventional equation (23) for rate of formation of M* where I_o = incident intensity of ultraviolet radiation at 254 mμ; $D_M = \epsilon_M[M]$ = optical density of M in the solution at 254 mμ; and D = total optical density of M plus L plus K, etc.; then

[1] $$d[M^*]/dt = \text{rate of formation of } M^* - \text{rate of breakdown to other products} - \text{rate of formation of } MP^*$$
$$= k_1 I_o \frac{D_M}{D}(1 - 10^{-D}) - k_2[M^*] - k_3[M^*][P].$$

Assuming equilibrium conditions, where $d[M^*]/dt = 0$ and $d[MP^*]/dt = 0$, then

[2] $$[M^*] = \frac{k_1 I_0 D_M (1-10^{-D})}{D(k_2+k_3[P])} = \frac{A[M]}{k_2+k_3[P]}$$

where $A = k_1 I_o \epsilon_M (1-10^{-D})/D$. Since the optical density D at 254 mμ is relatively constant during irradiation of MAP in phosphate buffer (Fig. 2) and equal to D_M at zero time, A can be taken as a constant in any given experiment. From one experiment to another, A will depend on light intensity, on the concentration of MAP at zero time, and also on pH since ϵ_M varies with pH.

Under the same equilibrium conditions, the rate of formation of Z can be written as

[3] $$R = k_4[MP^*] = k_3[M^*][P]$$
$$= \frac{k_3 A[M][P]}{k_2+k_3[P]}.$$

This equation indicates that R will equal half the maximal rate when $[P] = k_2/k_3$ in experiments where [P] is varied while other experimental conditions are constant. Thus the data of Fig. 3 would indicate $k_2/k_3 = 0.007$ M.

The effect of variation in [M] on the rate will be determined by the factor $A[M]$ in equation [3]. If we substitute $D = D_M$ at zero time and consider the initial rate of reaction where [M] is approximately equal to $[M]_0$, the only important variable left in $A[M]$ is the factor $(1-10^{-D})$. This factor has a value of 0.8 when D is 0.7 and approaches 1 as D is increased to infinity. Since ϵ_M at 254 mμ is 3500 and the depth of solution in the irradiation chamber is 1.7 cm (3), a 1.2×10^{-4} M solution of MAP should provide an optical density of 0.7 at pH 7. Thus the initial rate of the reaction should be almost independent (within 20%) of $[M]_0$ when $[M]_0$ is equal to or greater than 1.2×10^{-4} M MAP at pH 7. This agrees with the experimental results; the measured rate appeared to be relatively independent of $[M]_0$ down to 1×10^{-4} M MAP and only decreased appreciably (35%) on going from 1×10^{-4} to 0.5×10^{-4} M MAP (Table II).

The effect of decrease in pH on factor A will be an increase in D_M and thus an increase in $(1-10^{-D})$. The optical density of MAP solutions at 254 mμ is almost exactly doubled when the pH is decreased from neutrality to pH 4. However, this change cannot account for the observed variations in rate between pH 7 and pH 6 (Fig. 4). First, the increase in D_M between pH 7 and pH 6 is relatively small; secondly, even a doubling in D_M due to pH changes will have little effect on the initial rate when the rate is independent of $[M]_0$ as described above.

Equation [3] can be modified to allow for the effect of pH on ionization of MAP and phosphate by introducing the fractional dissociation factors:

X_M = fraction of MAP in unionized amino form,
X_P = fraction of phosphate in doubly ionized form,

where $\log (1-X)/X = pK - pH$ for both compounds. Assuming that only the free amino form of MAP (X_M) and the singly ionized phosphate ion ($1-X_P$) are reactive (see Fig. 4), then equation [3] becomes

[4] $$R = \frac{k_3 A[M]X_M[P](1-X_P)}{k_2+k_3[P](1-X_P)}.$$

Can. J. Chem. Downloaded from www.nrcresearchpress.com by 210.87.254.5 on 09/05/12
For personal use only.

This equation can be used directly for the calculation of relative rates at different pH values by inserting the appropriate theoretical values for X_M and X_P. The equation can also be solved for optimum pH by differentiating with respect to $[H^+]$, using the expressions

$$X_M = \frac{K_M}{K_M+[H^+]},$$

$$(1-X_P) = \frac{[H^+]}{[H^+]+K_P},$$

$$\frac{dX_M}{d[H^+]} = \frac{K_M}{(K_M+[H^+])^2},$$

and

$$\frac{d(1-X_P)}{d[H^+]} = \frac{K_P}{(K_P+[H^+])^2}.$$

Putting $dR/d[H^+] = 0$ at the optimum pH, the differential of equation [4] can be simplified down to

$$\frac{1}{[H^+]^2} = \frac{1}{K_P K_M}\frac{(k_2+k_3[P])}{k_2}$$

or

[5] $$pH_{opt} = \frac{(pK_P+pK_M)}{2} + \frac{1}{2}\frac{\log\,(k_2+k_3[P])}{k_2}.$$

Inserting the values $pK_P = 7.2$, $pK_M = 5.5$, $k_2/k_3 = 0.007$ M, and $[P] = 0.05$ M as in the experiments shown in Fig. 4, then $pH_{opt} = 6.35+0.46 = 6.8$. This value is close to the experimentally determined value for optimum pH (Fig. 4). The calculation is based on the measured value of k_2/k_3 at a single pH (Fig. 3) close to the optimum pH. The value of k_2/k_3 may well vary with pH but examination of equation [5] shows that moderate changes in this ratio will not alter the calculated value for optimum pH greatly; variations in the ratio k_2/k_3 with pH can therefore be ignored for the present calculation of the approximate optimum pH value.

ACKNOWLEDGMENTS

After Dr. Moore's death, the manuscript of this paper was prepared from his notes and submitted for publication by G. C. Butler and D. K. Myers, with the assistance of Mrs. Catherine A. Vivian. Mrs. Vivian, P. E. Spencer, and Miss Joan N. Smith assisted Dr. Moore in the experiments described. A preliminary report of these experiments was presented to the Radiation Research Society on May 22, 1962 (24).

REFERENCES

1. A. M. Moore and C. H. Thomson. *In* Progress in radiobiology. *Edited by* J. S. Mitchell, B. E. Holmes, and C. L. Smith. Oliver and Boyd, Edinburgh. 1956. p. 75.
2. S. Y. Wang, M. Apicella, and B. R. Stone. J. Am. Chem. Soc. **78**, 4180 (1956).
3. A. M. Moore and C. H. Thomson. Can. J. Chem. **35**, 163 (1957).
4. K. L. Wierzchowski and D. Shugar. Biochim. Biophys. Acta, **25**, 355 (1957).
5. A. M. Moore. Can. J. Chem. **37**, 1281 (1959).
6. R. Beukers and W. Berends. Biochim. Biophys. Acta, **41**, 550 (1960).
7. S. Y. Wang. J. Am. Chem. Soc. **80**, 6199 (1958).
8. S. Y. Wang. Nature, **184**, 184 (1959).
9. D. Shugar and K. L. Wierzchowski. Polska Akad. Nauk, Postepy Biochem. **4**, Supplement, 243 (1958).
10. G. E. Hilbert and T. B. Johnson. J. Am. Chem. Soc. **52**, 1152 (1930).
11. G. E. Hilbert. J. Am. Chem. Soc. **56**, 190 (1934).
12. M. P. V. Boarland and J. F. W. McOmie. J. Chem. Soc. 1220 (1951).
13. G. H. Beaven, E. R. Holiday, and E. A. Johnson. *In* The nucleic acids. Vol. I. *Edited by* E. Chargaff and J. N. Davidson. Academic Press, Inc., New York. 1955. p. 493.
14. R. Markham and J. D. Smith. Biochem. J. **45**, 294 (1949).
15. P. B. Hawk, B. L. Oser, and W. H. Summerson. Practical physiological chemistry. 12th ed. The Blakiston Co., Philadelphia. 1947. p. 818.
16. E. R. Blout and M. Fields. J. Am. Chem. Soc. **70**, 190 (1948).
17. J. L. H. Allan, E. R. H. Jones, and M. C. Whiting. J. Chem. Soc. 1866 (1955).
18. S. J. Clark. Quantitative methods of organic microanalysis. Butterworths Scientific Publishing Co., London. 1956. p. 161.

Can. J. Chem. Downloaded from www.nrcresearchpress.com by 210.87.254.5 on 09/05/12
For personal use only.

19. A. M. MOORE and S. M. ANDERSON. Can. J. Chem. **37**, 590 (1959).
20. C. L. ANGELL. J. Chem. Soc. 504 (1961).
21. L. J. BELLAMY. The infra-red spectra of complex molecules. John Wiley and Sons, Inc., New York. 1958.
22. J. BEYNON. Mass spectrometry and its application to organic chemistry. Elsevier Publishing Co., Amsterdam. 1960.
23. J. L. ROSENBERG. *In* Physical techniques in biological research. Vol. I. *Edited by* G. Oster and A. W. Pollister. Academic Press, Inc., New York. 1955. p. 1.
24. A. M. MOORE. Radiation Res. **16**, 610 (1962).

Can. J. Chem. Downloaded from www.nrcresearchpress.com by 210.87.254.5 on 09/05/12
For personal use only.

NEUTRON-DEFICIENT ISOTOPES OF LANTHANUM— La^{127}, La^{128}, La^{129}, La^{130}, and La^{131} [1]

L. YAFFE

Radiochemistry Laboratory, Department of Chemistry, McGill University, Montreal, Que.

AND

J. M. ALEXANDER AND E. K. HYDE

Lawrence Radiation Laboratory, University of California, Berkeley, Calif., U.S.A.

Received March 20, 1963

ABSTRACT

La^{127}, La^{128}, La^{129}, and La^{131} were produced by the reaction of C^{12} ions with antimony. Half-lives of 3.5±0.5, 4.6±0.6, 8.6±1.8, and 56±3 min respectively, were obtained from the observed growth of the respective barium daughters. The half-life for Ba^{128} was found to be 2.43±0.05 days. La^{129} and La^{130} were produced and identified by the reactions $Ba^{130}(p,2n)$ and $Ba^{130}(p,n)$ respectively, carried out with targets enriched in Ba^{130}. In the proton bombardments half-lives of 10.0±0.5 min and 8.7±0.1 min were found for La^{129} and La^{130} respectively.

The identification of La^{128} and La^{130}, with half-lives of 6.5±1.0 and 9.0±1.0 min respectively, was recently made by Sheline, Sikkeland, and Chanda (1). In their work lanthanum was radiochemically separated from various targets bombarded at the Berkeley Heavy Ion Linear Accelerator (HILAC). The tentative mass assignment of La^{128} was made on the basis of cross bombardments. The assignment of the observed activity to La^{130} was made on the basis of the occurrence of a very strong 356±4 kev gamma ray presumed to be identical with the 359 kev gamma ray observed in the Coulomb excitation of Ba^{130}.

It was felt that verification of the mass assignment of La^{128} could be made by a 'milking' experiment in which the growth of the well-known 2.4-day Ba^{128} daughter (2) was measured. La^{127} and La^{129} were unknown when these experiments were begun, and the same type of experiments was expected to establish their assignments by the growth of the Cs^{127} granddaughter (3) and the 2.5-hr Ba^{129} daughter (4) respectively. The mass assignment of La^{131} has been made only on the basis of a rough mass spectrometric separation (5) without any genetic verification. The mass assignment could be confirmed by a similar 'milking' experiment to observe the growth of the 12-day Ba^{131} daughter (6). It was also decided that a study of the reactions $Ba^{130}(p,n)La^{130}$ and $Ba^{130}(p,2n)La^{129}$ with targets of naturally occurring barium, and of barium enriched in Ba^{130}, would help to confirm the La^{130} mass assignment of Sheline *et al.* (1) and to cross-check the La^{129} assignment made by the HILAC irradiations.

While this work was in progress, Preiss, Strudler, and Wolfgang of Yale University were kind enough to make available to us their recent results on La^{127}, La^{128}, and La^{129}. A comparison between the two sets of data is included later under Results.

EXPERIMENTAL

(a) La^{131} (Experiment 1)

A thick target of antimony powder (99.999% pure), packaged in 0.00025-in. foil, was fastened to the target holder of the HILAC and irradiated with C^{12} ions of incident energy of 124 Mev in order to induce the reaction $Sb^{123}(C^{12},4n)La^{131}$. The irradiated antimony powder was dissolved in hot aqua regia containing 5 mg La carrier. Ba and Cs carriers (1 mg each) were added. Lanthanum fluoride was precipitated by the addition of

[1]*Work supported by the U.S. Atomic Energy Commission.*

Can. J. Chem. Downloaded from www.nrcresearchpress.com by 210.87.254.40 on 09/05/12
For personal use only.

concentrated hydrofluoric acid. The precipitate was centrifuged, and dissolved in 2 ml of a mixture of saturated boric acid and hydrochloric acid. Lanthanum hydroxide was then precipitated by the addition of concentrated ammonia. The precipitate was dissolved in 6 *M* hydrochloric acid, following which the fluoride was again precipitated, dissolved, and converted to the hydroxide. The final precipitate of lanthanum hydroxide was dissolved in 6 *M* hydrochloric acid and an accurately determined amount (~10 mg) of Ba carrier added. After a period of about 1 hour had elapsed, barium chloride was precipitated by bubbling gaseous hydrogen chloride into the ice-cold solution.

This barium chloride was separated and set aside as the first daughter-fraction. An additional, accurately measured amount of barium carrier was added to the supernatant solution. After 1 hour this solution was chilled and resaturated with hydrogen chloride. The precipitate of barium chloride was set aside as daughter-fraction 2. This process was repeated until six daughter-fractions were removed at 1-hour intervals.

An auxiliary experiment with La^{140} tracer, carried out under identical conditions, showed that less than $\frac{1}{2}\%$ of the lanthanum is coprecipitated with barium chloride under these conditions.

The barium daughter-fractions were purified by double reprecipitations as barium chloride and a final precipitation as barium nitrate from ice-cold fuming nitric acid. Cs and La carriers were present during the chloride reprecipitations, while Cs alone was present during the precipitation of barium nitrate. The chemical yield was determined by weighing the final barium nitrate precipitate.

The activity of the barium samples was measured by a scintillation counter consisting of a 3 in.×3 in. sodium iodide crystal coupled to a 400-channel pulse-height analyzer. The photopeak intensity of the 373 kev gamma ray (8), characteristic of Ba^{131}, was compared for the various samples.

(b) La^{129} and La^{130} (Experiments 5 and 6)

Irradiations of naturally occurring barium and of barium enriched in Ba^{130} (130-fold enrichment) as barium nitrate were made in the circulating beam of the McGill University proton synchrocyclotron. The barium nitrate was placed in thin aluminum tubing and clamped to the target holder on the cyclotron probe. This probe was placed at radii corresponding to 12 Mev and 20 Mev protons—roughly the calculated peaks of the (p,n) and $(p,2n)$ excitation functions, respectively.

After bombardment the barium nitrate was dissolved in dilute hydrochloric acid containing La carrier. The solution was boiled with a few milligrams of ammonium carbonate (to remove C^{11} as CO_2) and then lanthanum hydroxide was precipitated with ammonia. The precipitate was dissolved, reprecipitated, washed, and redissolved. The activity was measured with a 3 in.×3 in. sodium iodide crystal coupled to a 100-channel pulse-height analyzer.

(c) La^{127}, La^{128}, La^{129}

(1) Procedure Used in Experiments 2 and 3

Antimony powder was irradiated with C^{12} ions in the Berkeley HILAC. After bombardment the target was dissolved in hot aqua regia, La and Ba carriers were added, and barium chloride was precipitated by bubbling gaseous hydrogen chloride into the ice-cold solution. This precipitate was discarded. After 2 or 3 minutes a known amount of barium carrier was added to the solution and a barium chloride precipitate was centrifuged out and removed exactly 4 minutes after the initial 'clean-up' precipitation. Fresh barium was added in order to form a second daughter-fraction 4 minutes later. This process was repeated at 4-minute intervals until eight daughter-fractions were obtained.

Each of the eight daughter-fractions was purified by reprecipitation of the barium, first as the chloride then as the nitrate. Chemical yields were determined by weighing barium nitrate. The beta activity in these samples was measured in a proportional counter through a 0.005-in. aluminum absorber.

(2) Procedure Used in Experiment 4

The antimony target was dissolved in hot aqua regia, and lanthanum carrier precipitated as the fluoride. The precipitate was dissolved in saturated boric acid solution and lanthanum hydroxide precipitated in the presence of barium holdback carrier. The hydroxide was dissolved in hydrochloric acid, reprecipitated, and redissolved in hydrochloric acid containing an accurately known amount of barium carrier. After an interval of exactly 8 minutes lanthanum hydroxide was precipitated and separated by centrifugation. The supernatant solution was set aside as the first Ba–Cs daughter-fraction. The lanthanum hydroxide was dissolved in hydrochloric acid and fresh barium carrier was added. After exactly 8 minutes lanthanum hydroxide was again precipitated and a second daughter-fraction set aside. The procedure was repeated until eight daughter-fractions had been separated. The Ba–Cs fractions were individually evaporated with aqua regia to destroy NH_4^+, which would interfere with the later separation of cesium, then taken up in hydrochloric acid. After about 2 hours the solution was cooled, then gaseous hydrogen chloride bubbled in. The barium chloride was washed, recentrifuged, and mounted on filter paper for activity measurements.

Preliminary tests of this procedure with Ba^{140} tracer showed that only 3% of barium activity was removed from the solution with the lanthanum hydroxide precipitate.

Cesium granddaughter activity was isolated from the mother liquor of the barium chloride precipitation in the following way (9). Two drops of 0.4 *M* solution of silicotungstic acid was added and the ice-cold solution saturated with gaseous hydrochloric acid. Free silicotungstic acid was precipitated out, carrying with it the carrier-free cesium activity. The precipitate was separated by centrifugation and dissolved in

Can. J. Chem. Downloaded from www.nrcresearchpress.com by 210.87.254.40 on 09/05/12
For personal use only.

water. The cesium was adsorbed on a short column of Dowex-50 cation resin to separate it from the silicotungstic acid carrier. The column was washed with water, after which the cesium was eluted with dilute hydrochloric acid and evaporated on a platinum plate which was mounted for activity measurements. Chemical yields were not measured but repeated preliminary test runs with Cs^{137} tracer showed that the recovery was consistently 85–90%.

(d) Activity Measurements

The activity of all barium samples from the HILAC bombardments, except those specifically designed to measure Ba^{131}, was measured by a series of intercalibrated end-window gas flow proportional β^- counters through aluminum absorbers (32.4 mg/cm²) which cut out any contribution of conversion electrons from the cesium daughters. The thickness of the samples was so nearly uniform that no self-absorption corrections were necessary. The relative activity of the cesium samples was measured by an integral gamma counter (sodium iodide) biased to record all events above the 60 kev level. The gamma activity of the lanthanum samples resulting from the cyclotron experiments was measured by a sodium iodide crystal coupled to a 100-channel pulse-height analyzer. As described previously, the 373 kev gamma rays from the Ba^{131} samples were measured by a 3 in.×3 in. sodium iodide crystal coupled to a 400-channel pulse-height analyzer.

RESULTS

Experiment 1 performed by the procedure outlined in (*a*) above was designed to confirm properties of La^{131}. The activity measurements of the barium daughter-fractions showed that the areas of the 373 kev photopeak decreased with time with the 12-day half-life expected for Ba^{131}. The half-life of the parent La^{131} was shown to be 56±3 min, in good agreement with the value of 58 min found previously by a direct determination (5). The decay curve of the parent found from various 'milkings' is shown in Fig. 1.

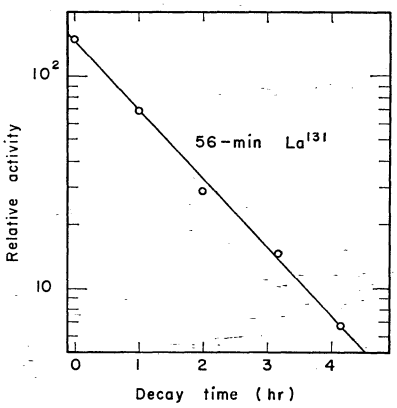

FIG. 1. Decay of La^{131} obtained by successive 'milkings' of Ba^{131}.

Experiments 2 and 3 were carried out according to procedure (*c*1) and experiment 4 according to procedure (*c*2). The decay curves of the activity in the barium daughter-fraction in all three experiments could be resolved cleanly into two components attributable to Ba^{128} and Ba^{129}. The presence of the 3 Mev β^--radiation from the 3.5-min Cs^{128} daughter (2) of Ba^{128} was confirmed by an aluminum absorption measurement. The half-life of Ba^{129} was found to be 2.20±0.05 hr from the analysis of 14 of our decay curves. Arbman and Haller (10) report two isomeric states in Ba^{129}—a β^+-form decaying with a half-life of 2.61±0.02 hr and various conversion electrons with half-lives between 2.00± 0.10 and 2.37±0.08 hr. We made no detailed examination to determine whether our Ba^{129} activity was a mixture of isomers.

The 2.4-day component of Ba^{128} was seen in every barium fraction. The best value of this half-life was determined from one sample which was followed for 22 days after the decay of Ba^{129}. This one-component decay curve gave a value of 2.43±0.05 days for the half-life of Ba^{128}.

Can. J. Chem. Downloaded from www.nrcresearchpress.com by 210.87.254.40 on 09/05/12
For personal use only.

When the resolution of the barium decay curves was complete, the amounts of Ba^{128} and Ba^{129} in each sample at the time of the separation from the lanthanum parent was plotted against the time of the separation. Suitable corrections were made for chemical yield. Since the growth times were identical, this method of plotting reveals the decay of the La^{128} and La^{129} parents. The data points are shown in Fig. 2, and the half-life values are listed in Table I.

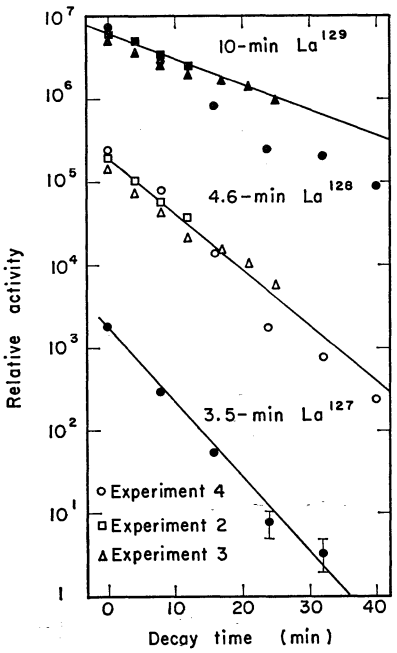

FIG. 2. Decay of La^{127}, La^{128}, and La^{129} obtained by successive 'milkings' of the daughters.

TABLE I

Summary of experimental results

Expt.	Growth time (min)	No. separations	Half-lives (min)				
			La^{127}	La^{128}	La^{129}	La^{130}	La^{131}
$Sb+C^{12}$							
1	60	5					56±3
2	4	4		4.5	9.4		
3	4	7		5.4	10.6		
4	8	6	3.5	3.8	5.8		
$Ba^{130}+p$							
5, 6					10.0±0.5	8.7±0.1	
		Best values	3.5	4.6±0.6	10.0±0.5	8.7±0.1	56±3

In experiment 4 the decay curves obtained for the cesium granddaughter fractions were easy to resolve into 6.2-hr-Cs^{127} and 32-hr-Cs^{129} components. The relative amount of Cs^{127} and Cs^{129} at the time of separation is plotted in Fig. 2. Those plots correspond to a half-life of 3.5 min and 5.8 min for La^{127} and La^{129}, respectively.

In experiment 5 barium was bombarded with 12 Mev protons to maximize the yield of La^{130} produced by the $Ba^{130}(p,n)La^{130}$ reaction. Measurements with a 3 in.×3 in.

Can. J. Chem. Downloaded from www.nrcresearchpress.com by 210.87.254.40 on 09/05/12
For personal use only.

sodium iodide scintillation crystal spectrometer showed a prominent 360 kev gamma ray decaying cleanly with a half-life of 8.7±0.1 min to a background 1 part in 10^4 of the initial counting rate. The amount of this gamma ray present in the lanthanum fraction from the targets enriched in Ba^{130} was higher by the ratio of the Ba^{130} content in both targets. This establishes the correctness of the mass assignment of Sheline *et al.* (1).

In experiment 6 barium targets were bombarded with 20 Mev protons to maximize the reaction $Ba^{130}(p,2n)La^{129}$. The decay curves of X-ray and 511 kev annihilation radiation were measured. The assignment of a 10-min activity to La^{129} was consistent with the Ba^{130} content of the samples irradiated. The 110 kev and 511 kev radiation decayed with half-lives of 10.0 and 10.5 min, respectively, into a 2.6-hr background. The shape of the composite curve and the relative amounts of 10-min and 2.6-hr activity were consistent with the decay of 10.0-min La^{129} into 2.6-hr Ba^{129}. The X-ray activity decayed initially with a 9.4-min slope which later lengthened to 4.75 hr. This longer-lived activity is probably a mixture of La^{132} and La^{133} produced from higher-mass barium isotopes in the target.

All results are summarized in Table I. 'Best' values are quoted in the last line. Our values for the half-lives of La^{127}, La^{128}, and La^{129}, determined by 'milking' experiments, agree quite well with those of Preiss *et al.* (7), who obtained values of 3.8±0.5, 4.2±0.5, and 7.2±0.5 min respectively. The most accurate determination of the half-life of La^{129} (10.0±0.5 minutes) was obtained from direct observation of La^{129} produced by the reaction Ba^{130}(20 Mev $p,2n$)La^{130}. Our results are also close to those of Sheline *et al.* (1), who obtained half-lives of 6.5±1.0 and 9.0±1.0 min, for La^{128} and La^{130} respectively.

ACKNOWLEDGMENTS

One of us (L. Y.) wishes to express his sincere appreciation to Professor I. Perlman and the members of the Chemistry Department, Lawrence Radiation Laboratory, University of California at Berkeley, for their hospitality during the summer of 1962. The authors wish to express their appreciation to Dr. R. E. Bell, Director, Radiation Laboratory, McGill University, for his ready cooperation in making the cyclotron facilities available. They also thank the HILAC crew for their able assistance, and R. S. Tilbury for assisting with the chemical separations in those experiments dealing with proton bombardments.

REFERENCES

1. R. K. Sheline, T. Sikkeland, and R. N. Chanda. Phys. Rev. Letters, **7**, C517 (1961).
2. R. W. Fink and E. O. Wiig. Phys. Rev. **91**, 194 (1953).
3. H. B. Mathur and E. K. Hyde. Phys. Rev. **95**, 708 (1954).
4. W. Henkes. Phys. Rev. **113**, 863 (1959).
5. M. M. Gransden and W. S. Boyle. Phys. Rev. **82**, 447 (1951).
6. H. W. Wright, E. I. Wyatt, S. A. Reynolds, W. S. Lyon, and T. H. Handley. Nucl. Sci. Eng. **2**, 427 (1957).
7. I. L. Preiss, P. M. Strudler, and R. Wolfgang. Phys. Rev. **129**, 1284 (1963).
8. Nuclear Data Sheets. Natl. Acad. Sci. Natl. Res. Council (U.S. Government Printing Office, Washington, D.C.). 1961.
9. E. K. Hyde. J. Am. Chem. Soc. **74**, 4181 (1952).
10. E. Arbman and I. B. Haller. Nucl. Phys. **22**, 341 (1961).

Can. J. Chem. Downloaded from www.nrcresearchpress.com by 210.87.254.40 on 09/05/12
For personal use only.

A STUDY OF $Cd^{115m,g}$ FORMED IN THE FISSION OF NATURAL URANIUM BY PROTONS OF ENERGIES 8 TO 60 MEV[1]

R. S. TILBURY[2] AND L. YAFFE
Radiochemistry Laboratory, Department of Chemistry, McGill University, Montreal, Que.
Received April 10, 1963

ABSTRACT

Excitation functions have been measured for the formation of Cd^{115m}, Cd^{115g}, and Ag^{115g} produced in the fission of natural uranium induced by protons of energies 8 to 60 Mev. The isomer yield ratio for $Cd^{115m,g}$ was found to increase with increasing proton bombarding energy over the range 20 to 60 Mev in contrast to the published results for the deuteron fission of uranium, for which a minimum was found.

INTRODUCTION

High-energy fission studies leading to nuclear isomers have been mostly concerned with the yields of Cd^{115m} and Cd^{115g}. Hicks and Gilbert (1) measured the ratio of isomer cross sections σ_m/σ_g, for the deuteron fission of U^{238} from 50 to 150 Mev, whilst Sharp and Pappas (2) measured the same ratio for deuterons of energy 10 to 25 Mev. Their combined results show a striking minimum at 25 to 50 Mev in the energy dependence of σ_m/σ_g. Unfortunately the energy range at which this minimum occurs is inaccessible to the present deuteron accelerators, lying above the range of the C.F. cyclotrons and below that at which large F.M. machines can be operated conveniently. Sharp and Pappas suggested that it would be of interest to see whether a similar minimum is obtained in proton fission with one of the 10–100 Mev proton cyclotrons which can bridge the energy gap. Munzel (3) has since measured $Cd^{115m,g}$ isomer yield ratios for the α-particle fission of U^{238} over the energy range 25 to 45 Mev and reports a less pronounced minimum.

We have examined the reaction $U^{238}(p,f)Cd^{115m,g}$ using the McGill synchrocyclotron to provide protons of energies between 8 and 60 Mev. At the same time, by including a monitor for the proton beam in the target assembly, it was possible to measure the formation cross sections of Cd^{115m}, Cd^{115g}, and that of the precursor Ag^{115g}.

The decay scheme of the mass 115 fission product chain was taken to be:

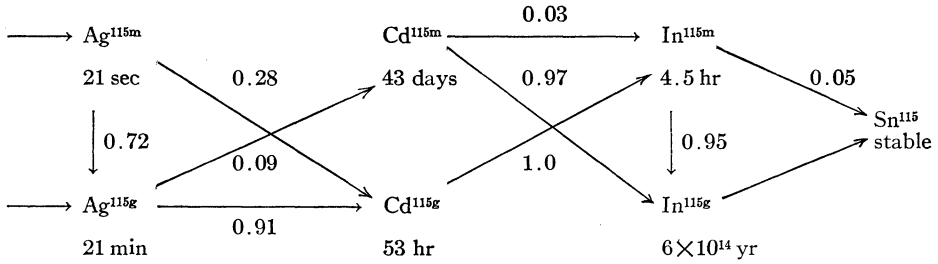

This is identical with the decay scheme used by Sharp and Pappas and is reproduced here for easy reference. By separating cadmium from silver as soon as possible after bombardment (about 20 minutes was required in the present work) it is possible to correct for the amount of $Cd^{115m \text{ and } g}$ which has grown in from Ag^{115g} during the bombardment and

[1]*This work received financial assistance from the National Research Council of Canada.*
[2]*Holder of an International Nickel Company of Canada Fellowship. Present address: Union Carbide Nuclear Co., Tuxedo, N.Y., U.S.A.*

Can. J. Chem. Downloaded from www.nrcresearchpress.com by 210.87.254.40 on 09/05/12
For personal use only.

subsequent decay. Ag^{115m} is too short lived to allow a correction to be made for it. On the basis of the above decay scheme, equations have been derived for the formation cross sections of $Cd^{115m \text{ and } g}$ and for Ag^{115g}, and from these an equation for the isomer yield ratio for $Cd^{115m,g}$:

$$\frac{\sigma_m^i}{\sigma_g^*} = \frac{\lambda_g}{\lambda_m} \frac{[A_1 Y_o - A_3 Y_a F']}{[A_2 Y_o - A_4 Y_a F']}$$

where σ_m^i is the cross section for the independent formation of Cd^{115m},

σ_g^* is the cross section for the independent formation of Cd^{115g} + 0.28 of the cross section for the cumulative formation of Ag^{115m}, σ^c,

λ_m and λ_g are the decay constants,

A_1 and A_2 are the activities due to Cd^{115m} and Cd^{115g} respectively at end of bombardment in the organic phase of the separation process,

A_3 and A_4 are the activities due to Cd^{115m} and Cd^{115g} respectively in the aqueous phase of the separation process,

Y_o and Y_a are the chemical yield factors for cadmium in the organic and aqueous phases respectively of the separation of silver from cadmium, and

$$F' = \frac{1-[e^{-\lambda t_2} - e^{-\lambda(t_1+t_2)}]}{[e^{-\lambda t_2} - e^{-\lambda(t_1+t_2)}]}$$

where t_1 and t_2 are the times of bombardment and separation respectively, and λ is the decay constant for 21-min Ag^{115g}.

Sharp and Pappas obtained a λt_1 term in place of 1, due to slightly different approximations in the simplification, but this makes only a minor difference in the calculated isomer yield ratios.

EXPERIMENTAL

The target consisted of three foils of natural uranium (0.0006 in. thick) placed beside two foils of copper monitor (0.002 in. thick) in the cyclotron target holder. The leading edge was carefully aligned and the target irradiated in the circulating beam of the McGill synchrocyclotron for about 30 minutes.

After bombardment the first 1/4 in. of the leading edge was cut off, the first copper foil was used as a monitor, and the middle uranium foil as target. The other foils served to protect the monitor and target foils from contamination by recoil atoms. The extra foils did not significantly degrade the energy of the proton beam.

As soon as possible after bombardment the middle uranium foil was dissolved in 12 *N* hydrochloric acid, to which a drop of hydrogen peroxide solution had been added. Cadmium was extracted from this solution, and the remaining four foils were later weighed in order to ascertain the weights of target and monitor.

The procedure for the chemical separation of cadmium was taken from Sharp and Pappas (2) with certain modifications. The method depends on the extraction of cadmium dithizonate into chloroform solution from strongly basic solution. Sandell (4) lists tellurium as one of the metals reacting with dithizone. Te^{132} (78 hr) and Te^{129m} (33 days) would interfere with the resolution of 53-hr Cd^{115g} and 43-day Cd^{115m}. In addition to the carriers added by Sharp and Pappas, tellurium carrier was added. Examination of separated samples on a gamma-ray spectrometer showed the gamma-ray peaks of Te^{132} present in those extractions in which Te carrier had not been added, while only the photon peaks due to Cd^{115} were observed with the modified procedure.

The β^--activity of the cadmium samples was measured with a $4\pi\beta$ proportional counter (5). Corrections were applied for absorption in the source and source mount, and for coincidence loss. Cd^{115g} decays to In^{115m} which is in transient equilibrium, and In^{115m} decays 5.5% by β^--emission to Sn^{115} and 94.5% by a 335 kev isomeric transition to the ground state. The 335 kev gamma ray is largely internally converted with a total conversion coefficient of 0.90±0.06 (6). The energies of these conversion electrons are sufficiently great (~300 kev) to be efficiently detected in the 4π counter. It was calculated that the 53-hour counting rate must be divided by 1.55 to correct for the betas due to In^{115m}.

The branching ratio of the decay of Ag^{115g} to Cd^{115m} and Cd^{115g} was checked by measuring the Cd^{115} activities, since all the Cd^{115} occurring in the aqueous phase should be due to the decay of Ag^{115g} alone if the

Can. J. Chem. Downloaded from www.nrcresearchpress.com by 210.87.254.40 on 09/05/12
For personal use only.

chemical separation of cadmium from silver had been adequate. The results found agreed with the branching ratios of 9% and 91% determined by Wahl and Bonner (7). This also provided a check on the efficiency of the separation procedure for each run.

The reaction used to monitor the proton beam was $Cu^{65}(p,pn)Cu^{64}$, and the cross-section data were those of Meghir (8). After bombardment, the copper foil was dissolved and copper separated by ion exchange, using a method due to Kraus and Moore (9) in the presence of suitable holdback carriers. The 12.8-hr Cu^{64} activity was measured by means of its positron annihilation radiation, using a calibrated gamma-ray spectrometer.

Chemical yields were determined spectrophotometrically, cadmium by dithizone in chloroform (10), and copper by diethyldithiocarbamate, extracting the complex into isoamyl alcohol (11).

RESULTS AND DISCUSSION

Table I shows the cross-section values obtained in this work. Figures 1, 2, and 3 show these results plotted graphically, together with the estimated experimental errors. At 15 Mev no Cd^{115m} was detected and at 8 Mev neither Cd^{115m} nor Cd^{115g} was detected.

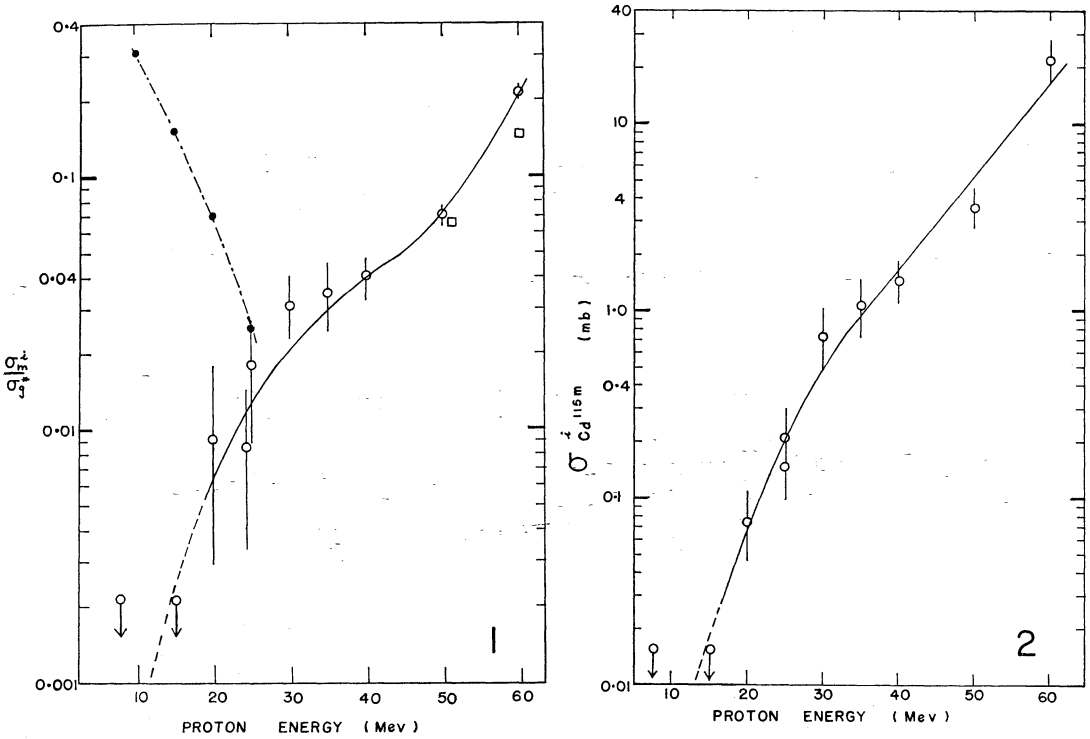

FIG. 1. Variation of σ_m^i/σ_g^* with proton bombarding energy for the reaction $U^{238}(p,f)Cd^{115m,g}$, where $\sigma_g^* = \sigma^i_{Cd^{115g}} + 0.28\sigma^c_{Ag^{115m}}$. ○ = this work; ● = Sharp and Pappas (2); □ = Hicks and Gilbert (1).

FIG. 2. Excitation function for the reaction $U^{238}(p,f)Cd^{115m}$.

The isomer yield ratio for $Cd^{115m,g}$ was found to increase from the lowest energy at which both Cd^{115m} and Cd^{115g} were detected to the highest proton energy used. No minimum in the curve was detected, in contrast to that shown in the deuteron fission of uranium. At 50 and 60 Mev the isomer yield ratios found in this work agree reasonably well with those of Hicks and Gilbert (1). The results of Sharp and Pappas for deuteron bombardments do not agree with the present results for proton bombardments at low energies. The reason for this may possibly be due to slight tellurium contamination in

Can. J. Chem. Downloaded from www.nrcresearchpress.com by 210.87.254.40 on 09/05/12
For personal use only.

Can. J. Chem. Downloaded from www.nrcresearchpress.com by 210.87.254.40 on 09/05/12
For personal use only.

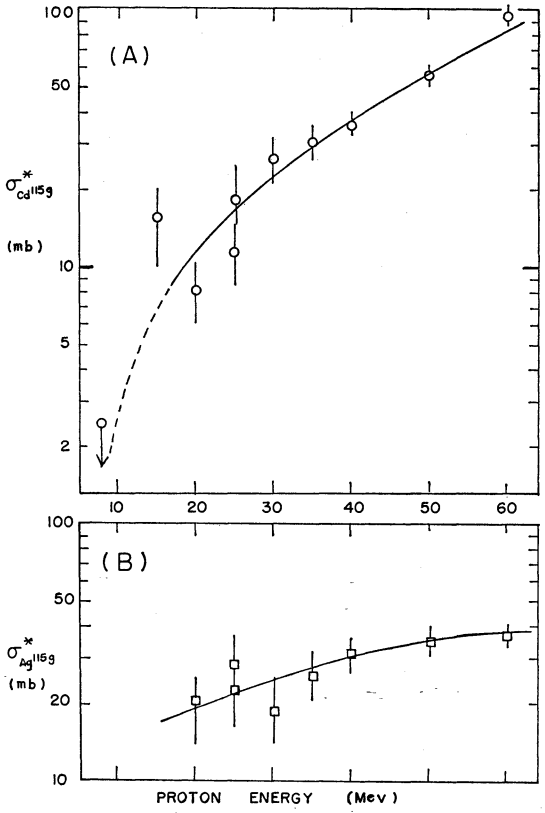

FIG. 3. Excitation functions for the reactions (A) $U^{238}(p,f)Cd^{115g}$, where $\sigma^*_{Cd^{115g}} = \sigma^i_{Cd^{115g}} + 0.28\sigma^c_{Ag^{115m}}$; (B) $U^{238}(p,f)Ag^{115g}$, where $\sigma^*_{Ag^{115g}} = \sigma^c_{Ag^{115g}} + 0.72\sigma^c_{Ag^{115m}}$.

TABLE I

Cross sections for $U^{238}(p,f)Cd^{115m,g}$, Ag^{115g}

Energy (Mev)	$\sigma_{Cu^{64}}$ (10) (mb)	$\sigma^i_{Cd^{115m}}$ (mb)	$\sigma^*_{Cd^{115g}}$ (mb)	$\frac{\sigma^i_{Cd^{115m}}}{\sigma^*_{Cd^{115g}}}$	$\sigma^*_{Ag^{115g}}$ (mb)
15	60	—	16	—	—
20	345	0.075	8.1	0.009	20
25	365	0.15	18	0.008	22
25	365	0.21	11	0.018	29
30	315	0.83	27	0.031	19
35	280	1.1	31	0.035	24
40	260	1.4	36	0.040	31
50	225	3.5	56	0.062	35
60	195	22	96	0.23	36

NOTE: $\sigma^*_{Cd^{115g}} = \sigma^i_{Cd^{115g}} + 0.28\sigma^c_{Ag^{115m}}$,
$\sigma^*_{Ag^{115g}} = \sigma^c_{Ag^{115g}} + 0.72\sigma^c_{Ag^{115m}}$.

their separation of cadmium as discussed previously. Te^{129} and Te^{132} have high fission yields in low-energy fission of uranium, whilst Cd^{115} occurs at the valley. Thus, at low energies, slight contamination with tellurium would have a large effect on the measurement of cadmium.

This difference in experimental observation between the proton and deuteron reactions at low energies would not be expected on the basis of different nuclear mechanisms. Oppenheimer-Phillips reactions do occur with deuterons at low energies, but this would merely tend to lower the threshold energy of the fission reaction. It may be that the deuteron, having a greater nuclear spin than the proton, brings in a relatively larger amount of angular momentum at low energies, but it is difficult to see why this should decrease and then start to increase above 30 Mev.

Although the cross-section values of Cd^{115m} are independent, those of the ground-state isomer are not, since they include 28% of the cumulative yield of Ag^{115m}. It has been shown that, at thermal energies, Z_p, the most probable nuclear charge, is about 3 charge units removed from stability. As the bombarding energy increases, however, Z_p moves towards stability (12, 13, 14). In the mass 115 chain, $_{47}Ag^{115}$ will be the most probable species formed directly in the fission process, at low energies, with relatively large yields of $_{46}Pd^{115}$ and $_{48}Cd^{115}$. As the bombarding energy increases, $_{48}Cd^{115}$ will be the favored product, so that at energies about 25 Mev most of the Cd^{115g} will be formed independently. Above 25 Mev, then, since the σ_m^1/σ_g^* ratio for $Cd^{115m,g}$ increases with increasing energy, the higher the bombarding energy the more is the high-spin state favored compared with the low-spin state, in agreement with what might be expected from the conclusion that high-energy fission is a high angular momentum process. Davies and Yaffe (15), however, have recently found, in the case of the Cs^{134} isomers, that increasing bombarding energy decreases the yield of the high-spin isomer, adding to the complexity of the situation.

ACKNOWLEDGMENTS

The authors wish to thank Dr. R. E. Bell and Mr. R. H. Mills for their cooperation during the cyclotron bombardments, and Mr. D. M. Marsden for his help in elucidating some of the chemical separation difficulties. One of us (R. S. T.) thanks the International Nickel Company of Canada Limited for a Fellowship from 1960–1963.

REFERENCES

1. H. G. Hicks and R. S. Gilbert. Phys. Rev. **100**, 1286 (1955).
2. R. A. Sharp and A. C. Pappas. J. Inorg. Nucl. Chem. **10**, 179 (1959).
3. H. Munzel. Nukleonik, **3**, 58 (1961).
4. E. B. Sandell. Colorimetric metal analysis. 3rd ed. Interscience, Inc., New York. 1959. p. 141.
5. B. D. Pate and L. Yaffe. Can. J. Chem. **33**, 15, 610, 929, 1656 (1955); **34**, 265 (1956).
6. I. V. Estulin and E. N. Moiseeva. Soviet Phys. JETP (Eng. Transl.), **1**, 463 (1955).
7. A. C. Wahl and N. A. Bonner. Phys. Rev. **85**, 520 (1952).
8. S. Meghir. Ph.D. Thesis, McGill University, Montreal, Que. 1962.
9. K. A. Kraus and G. E. Moore. J. Am. Chem. Soc. **75**, 1460 (1953).
10. E. G. Sandell. Colorimetric metal analysis. 3rd ed. Interscience, Inc., New York. 1959. p. 354.
11. T. D. Price and R. E. Telford. Analytical chemistry of the Manhattan project. *Edited by* C. J. Rodden. McGraw-Hill Co., New York. 1950. p. 404.
12. B. D. Pate, J. S. Foster, and L. Yaffe. Can. J. Chem. **36**, 1691 (1958).
13. J. H. Davies and L. Yaffe. Can. J. Phys. **41**, 762 (1963).
14. G. Friedlander, L. Friedman, B. Gordon, and L. Yaffe. Phys. Rev. **129**, 1809 (1953).
15. J. H. Davies and L. Yaffe. Can. J. Chem. **41**, 1836 (1963).

Can. J. Chem. Downloaded from www.nrcresearchpress.com by 210.87.254.40 on 09/05/12
For personal use only.

Can. J. Chem. Downloaded from www.nrcresearchpress.com by 210.87.254.6 on 09/05/12
For personal use only.

PHENYLLITHIUM–PYRIDINE ADDUCT AS A REDUCING AGENT FOR KETONES

R. A. ABRAMOVITCH AND B. VIG
Department of Chemistry, University of Saskatchewan, Saskatoon, Saskatchewan
Received March 19, 1963

ABSTRACT

The reduction of ketones to the corresponding alcohols using 1,2-dihydro-2-phenylpyridyllithium has been studied. Benzophenone is reduced more readily than is acetophenone, which in turn is more readily reduced than cyclohexanone. It is suggested that the by-product formed in the reduction of benzophenone is 4-diphenylhydroxymethyl-2-phenylpyridine.

The reaction of phenyllithium with pyridine and substituted pyridines has been studied extensively in these laboratories (1–4). The reaction is thought to proceed in two stages: the first is the addition leading to the formation of 1,2-dihydro-2-phenylpyridyllithium, which has been formulated either as I*a* or I*b*; this, on heating, splits off lithium hydride to give 2-phenylpyridine (II). Alternatively, it may be treated with water and the 1,2-dihydro-2-phenylpyridine formed oxidized *in situ* to II. It occurred to us that the adduct I might well behave as a selective reducing agent and it was proposed to examine the possibility of reducing a number of ketones making use of this intermediate. While this work was in progress Lansbury and Peterson (5) reported the results of their interesting work carried out using the adduct III formed between pyridine and lithium aluminum hydride, a reagent similar in many ways to the one used in the present work.

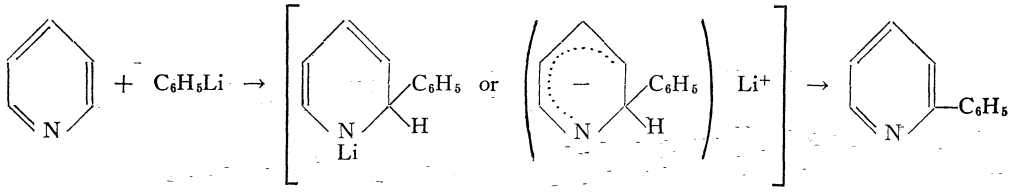

I*a* I*b* II

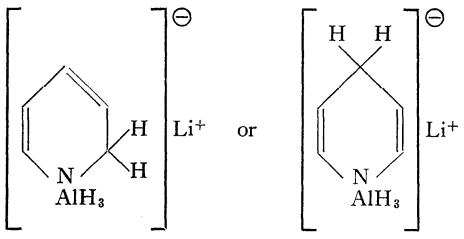

III

Dihydropyridines play an important role in biological oxidation–reduction systems and many dihydropyridine derivatives have been reported to reduce a variety of substances non-enzymically: nitro groups (6, 7), olefinic double bonds (7, 8), ketones (9), keto acids (10), quinones (7, 11), and other functional groups. The reduction of hexachloroacetone proceeds readily to give a reasonably good yield (53–60%) of the alcohol (9), but chloral only gives a 3% yield of 2,2,2-trichloroethanol with 1-benzyl-1,4-dihydronicotinamide.

Acetone is not reduced by this reagent (9) whereas alloxan is reduced rapidly by 1-methyl or 1-*n*-propyl-1,4-dihydronicotinamide (12).

The reduction of benzophenone by the intermediate I in pyridine–ether solution was investigated in detail. A solution of phenyllithium was prepared in the usual manner and added to a solution of a large excess of pyridine in ether. To this was added the benzophenone and the products worked up by column chromatography. The yield of benzhydrol varied according to the amount of phenyllithium used relative to that of benzophenone, maximal yields being obtained when the molar ratio of I to benzophenone was 2 (Table I). Yields were lowered appreciably if pyridine was not used in excess. A

TABLE I

Reduction of benzophenone with I

Molar proportion benzophenone/I*	1:1	2:1	3:1
Yield of benzhydrol (%)	20	64	23
Yield of by-product A (%)	Not determined	10	12.5

*Assuming that one equivalent of I is present for every equivalent of phenyllithium used. This is undoubtedly not the case since I undergoes polymerization quite readily (13).

by-product (A) was also obtained in these reactions. The by-product A had the molecular formula $C_{24}H_{19}ON$. It formed a hydrochloride only with difficulty (it was not extracted easily from ether solution with dilute acid), but readily gave a picrate. The infrared spectrum of A indicated the presence of a hydroxyl group, but no —NH— group. Bands characteristic of a monosubstituted phenyl group were also present. Attempts to prepare an acetyl derivative were unsuccessful, suggesting that the hydroxyl group may be tertiary. The compound could not be reduced catalytically at room temperature and pressure. On the basis of these observations, and taking into account the nature of the reactants, two plausible structures for A are 2-diphenylhydroxymethyl-6-phenylpyridine (IV) and 4-diphenylhydroxymethyl-2-phenylpyridine (V). An attempt was made to synthesize IV by

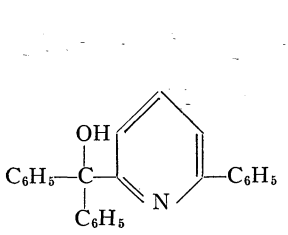

IV

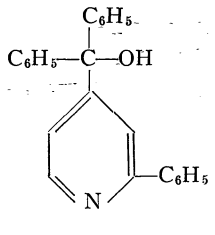

V

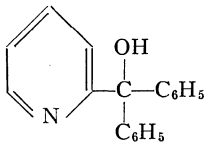

VI

the action of phenyllithium on diphenyl-2-pyridylmethanol (VI) (prepared by the action of 2-pyridyllithium on benzophenone): only starting material was recovered. 2-Bromo-6-phenylpyridine was obtained from 2-phenylpyridine via 2-amino-6-phenylpyridine (14). Reaction of 2-lithio-6-phenylpyridine with benzophenone gave the required tertiary alcohol (IV), which was different from the by-product A. That A probably has structure V was confirmed by the comparison of its n.m.r. spectrum (measured on a solution of the compound in carbon tetrachloride, at an oscillator frequency of 60 Mc/s and with tetramethylsilane as an internal standard) with that of authentic IV. The latter exhibited no peaks characteristic of a pyridine α-proton; instead, a multiplet centered at 484 c.p.s. was observed and is attributed to H_γ of the pyridine ring (1, 15). On the other hand, A exhibited a single-proton doublet centered at 524 c.p.s., which is characteristic of an H_α

Can. J. Chem. Downloaded from www.nrcresearchpress.com by 210.87.254.6 on 09/05/12
For personal use only.

proton in a pyridine ring (1, 15) and is consistent with the proposed structure (V). This by-product could arise in one of two ways: (i) by direct nucleophilic attack of benzophenone by intermediate I*b*, or (ii) by the reaction of I*a* with benzophenone to give an unstable dihydropyridine derivative (VII), which can then undergo a molecular rearrangement followed by dehydrogenation, or dehydrogenation followed by rearrangement, the

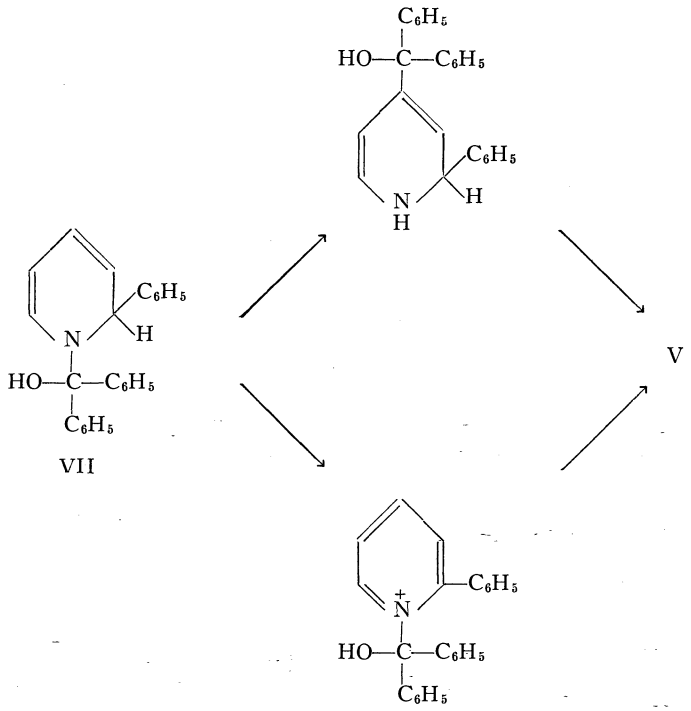

latter being similar in character to the Ladenburg rearrangement of 1-alkylpyridinium salts (16). It is not possible at this stage to distinguish between these two alternatives.

The reduction of acetophenone was investigated next. Using a 2:1 molar ratio of phenyllithium to acetophenone a low yield (14.5%) of α-phenylethanol was obtained, which could not be improved upon by varying the reaction conditions. Though a number of by-products could be isolated in a crude state by column chromatography of the reaction products none could be purified sufficiently for analysis. The reduction of cyclohexanone was also investigated: gas-chromatographic analysis of the reaction products indicated the formation of cyclohexanol in 6.5% yield. It would, therefore, appear that diaryl ketones are more readily reduced by I than are either arylalkyl or dialkyl ketones. The same conclusion was reached when the reducing agent used was III (5).

In a preliminary run in which I was used to reduce nitrobenzene no aniline could be detected gas chromatographically. An orange product was formed whose retention time was identical with that of azobenzene. A small amount of this product was collected but its infrared spectrum was different from that of azobenzene. It was not investigated further at this time.

EXPERIMENTAL

Melting points are uncorrected. Infrared spectra were measured on a Perkin–Elmer Model 21 spectrometer equipped with sodium chloride optics, and n.m.r. spectra on a Varian A60 instrument.

Can. J. Chem. Downloaded from www.nrcresearchpress.com by 210.87.254.6 on 09/05/12
For personal use only.

Reduction of Benzophenone

The general procedure used to carry out this reaction will be described for the case in which the phenyllithium:benzophenone ratio is 2.

A solution of phenyllithium in dry ether was prepared from bromobenzene and lithium under nitrogen according to a standard procedure (3). The normality of the phenyllithium solution was determined by titration with standard hydrochloric acid solution. An ethereal solution of phenyllithium (0.018 mole, 50 ml) was added to a cooled solution of pyridine (18 g) in dry ether (20 ml) under dry, oxygen-free nitrogen at such a rate that the temperature of the mixture did not rise. A solution of benzophenone (1.6 g, 0.009 mole) in dry ether (12 ml) was now added dropwise and stirring continued at room temperature under nitrogen for another 12 hours. The reaction mixture was decomposed with dilute hydrochloric acid (which removed unchanged pyridine and the 2-phenylpyridine which was formed), the ether layer washed repeatedly with water and evaporated. The residue was chromatographed on a column of alumina. Elution with benzene – light petroleum (b.p. 40–60°) (1:1 v/v) and then with benzene gave benzhydrol (1.02 g), m.p. 63°, undepressed on admixture with an authentic sample (the infrared spectra of product and authentic sample were identical). Elution with ether:benzene (1:1 v/v) gave *4-diphenylhydroxymethyl-2-phenylpyridine* (0.300 g), m.p. 156–157° (after recrystallization from dilute ethanol). (Calc. for $C_{24}H_{19}ON$: C, 85.43; H, 5.68; N, 4.15; M.W., 337. Found: C, 85.60; H, 5.95; N, 4.32; M.W. (osmometer), 343.) The *picrate* was recrystallized from benzene and had m.p. 190–191°. (Calc. for $C_{24}H_{19}ON,C_6H_3O_7N_3$: C, 63.60; H, 3.91. Found: C, 63.43; H, 3.91.)

Reduction of Acetophenone

An ethereal solution (80 ml) of phenyllithium (0.049 mole) was added to a solution of pyridine (30 g) in dry ether as described above. A solution of acetophenone (2.95 g, 0.024 mole) in dry ether was then added and the mixture worked up as for benzophenone. Evaporation of the ether extract gave a mixture of products, which was distilled up to 150° at 20 mm to give a mixture of unreacted acetophenone and of α-phenylethanol (1.54 g). This was analyzed by gas chromatography on a 6-ft×1/4-in. column packed with silicone nitrile (17%) on Chromosorb W (80–100 mesh). The column temperature was 80° and the helium inlet pressure 40 p.s.i. Two peaks corresponding to acetophenone and α-phenylethanol were observed. The yield of α-phenylethanol was 14.5% based on the amount of acetophenone used (not taking into account the recovered acetophenone).

Reduction of Cyclohexanone

This was carried out as for the reduction of acetophenone using phenyllithium (0.030 mole) and cyclocyclohexanone (0.015 mole), and the gas-chromatographic analysis performed as above. The yield of cyclohexanol (not taking into account recovered cyclohexanone) was 6.5%.

Diphenyl-2-pyridylmethanol

2-Bromopyridine (3.16 g) in dry ether (20 ml) was added dropwise with stirring to a solution of *n*-butyllithium (0.03 mole) in dry ether (30 ml) under nitrogen at −62° over a period of 1 hour and the mixture stirred for another 30 minutes. A solution of benzophenone (3.64 g) in dry ether (15 ml) was added during 10 minutes while the temperature was kept at −62°. Stirring at this temperature was continued for a further hour after which the temperature was allowed to rise to room temperature. The mixture was treated with dilute hydrochloric acid, the ether layer removed, and the aqueous acid layer extracted with ether. The acid layer was neutralized with sodium bicarbonate, extracted with ether, the ether dried (Na_2SO_4) and evaporated to give *diphenyl-2-pyridylmethanol* (3.0 g), m.p. 105° after recrystallization from methanol. (Calc. for $C_{18}H_{15}ON$: C, 82.73; H, 5.79. Found: C, 82.57; H, 5.68.)

A number of attempts were made to phenylate this alcohol with phenyllithium in various molar proportions (including a large excess of phenyllithium). In all cases, unchanged carbinol was recovered. The failure of this reaction to occur might be due to the formation of an insoluble O-Li salt with the starting material.

2-Diphenylhydroxymethyl-6-phenylpyridine

A solution of 2-lithio-6-phenylpyridine was prepared as described above for 2-pyridyllithium using 2-bromo-6-phenylpyridine (1 g, 0.0043 mole) in dry ether (15 ml) and *n*-butyllithium (0.005 mole) in dry ether (30 ml). To this solution was added benzophenone (0.80 g) in dry ether (10 ml) and the reaction mixture worked up as above to give a crude product (2.58 g) which was purified by chromatography on a column of alumina (70 g). Elution with benzene – light petroleum (b.p. 40–60°) (1:4 v/v) gave *2-diphenylhydroxymethyl-6-phenylpyridine* (0.535 g), m.p. 135–136° after recrystallization from ethanol. (Calc. for $C_{24}H_{19}ON$: C, 85.43; H, 5.60. Found: C, 84.97; H, 5.68.) The infrared spectrum of this compound was different from that of by-product A.

ACKNOWLEDGMENT

The authors are grateful to the National Research Council for financial support of this work.

Can. J. Chem. Downloaded from www.nrcresearchpress.com by 210.87.254.6 on 09/05/12
For personal use only.

REFERENCES

1. R. A. Abramovitch, Giam Choo-Seng, and A. D. Notation. Can. J. Chem. **38**, 761 (1960).
2. R. A. Abramovitch and A. D. Notation. Can. J. Chem. **38**, 1445 (1960).
3. R. A. Abramovitch and Choo-Seng Giam. Can. J. Chem. **40**, 213 (1962).
4. R. A. Abramovitch, K. S. Ahmed, and Choo-Seng Giam. Can. J. Chem. **41**, 1752 (1963).
5. P. T. Lansbury and J. O. Peterson. J. Am. Chem. Soc. **83**, 3537 (1961); **84**, 1756 (1962).
6. D. C. Dittmer and J. M. Kolyer. J. Org. Chem. **27**, 56 (1962).
7. E. A. Braude, J. Hannah, and R. Linstead. J. Chem. Soc. 3249, 3257, 3268 (1960).
8. B. E. Norcross, P. E. Klinedinst, Jr., and F. H. Westheimer. J. Am. Chem. Soc. **84**, 797 (1962).
9. D. C. Dittmer, L. J. Steffa, J. R. Potoski, and R. A. Fouty. Tetrahedron Letters No. 22, 827 (1961).
10. R. Abeles and F. H. Westheimer. J. Am. Chem. Soc. **80**, 5459 (1958). K. Wallenfels and D. Hofmann. Tetrahedron Letters, No. 15, 10 (1959).
11. H. Kühnis, W. Traber, and P. Karrer. Helv. Chim. Acta, **40**, 751 (1957). K. Wallenfels and M. Gellrich. Ann. **621**, 149 (1959).
12. D. Mauzerall and F. H. Westheimer. J. Am. Chem. Soc. **77**, 2261 (1955).
13. R. A. Abramovitch and Choo-Seng Giam. To be published.
14. F. H. Case and T. J. Kasper. J. Am. Chem. Soc. **78**, 5842 (1956).
15. L. M. Jackman. Applications of nuclear magnetic resonance spectroscopy to organic chemistry. Pergamon Press, New York. 1959.
16. A. Ladenburg. Ann. **247**, 1 (1888).

Can. J. Chem. Downloaded from www.nrcresearchpress.com by 210.87.254.6 on 09/05/12
For personal use only.

CATALYTIC HYDRODESULPHURIZATION OF THIOPHENE

IV. THE METHYLTHIOPHENES[1, 2]

P. DESIKAN[3] AND C. H. AMBERG
Division of Applied Chemistry, National Research Council, Ottawa, Canada

Received March 28, 1963

ABSTRACT

The hydrodesulphurization of 2- and 3-methylthiophene was studied over a sulphided, alumina-supported cobalt molybdate catalyst in a microreactor permitting the use of both pulse and steady-state flow techniques. The higher rates obtained with the 3-isomer were interpreted in terms of involvement of the α-carbon. The results were found to conform to the predominant reaction sequence proposed earlier for thiophene: C—S bond fission followed by diene and monoolefin formation and complete saturation. Some ancillary experiments on the hydrogenation of C_5-olefins were reported.

Can. J. Chem. Downloaded from www.nrcresearchpress.com by 210.87.254.42 on 09/05/12
For personal use only.

INTRODUCTION

In three previous publications from this laboratory (1–3) studies of the hydrodesulphurization of thiophene on a commercial cobalt molybdate catalyst and a sulphided chromia catalyst were described. By making use of the microreactor technique it was possible to examine the adsorption–desorption behavior of reactants and products on the surface of these catalysts under reaction conditions. It was argued that the rate-determining step in the reaction was either hydrogen chemisorption or a surface reaction. No thiolane or mercaptans were found among the products and it was demonstrated that ring hydrogenation was not the initial step; the latter was more likely to be C—S bond fission. Though butadiene was identified only in the products from reactions over chromia, it was assumed to have been an intermediate also with the cobalt molybdate catalyst. This has since been verified in this laboratory by infrared transmission studies of the catalyst during the reaction (4). An excess of 1-butene over the amount expected from the isomerization equilibrium in the vapor phase was noted over chromia catalyst (1). It was shown to be the initial isomer formed in a later investigation by Vernon and Richardson (5), who studied the effects of varying the amount of cobalt promoter on the activity of molybdenum sulphide catalysts for thiophene hydrogenolysis. The experiments of Kirsch *et al.* (6, 7) with cobalt molybdate catalysts are in good agreement with those of the present series in several respects, notably in their consistency with the concept of a dual function catalyst.

In extending the use of the microcatalytic reactor to the desulphurization of the methylthiophenes it was hoped to examine the effect of the methyl group in different positions on the behavior of the thiophene ring in the reaction and thus to throw further light on the detailed mechanism of hydrogenolysis. The hydrogenation and isomerization reactions of the resulting C_5-olefin products were also expected to be of interest.

EXPERIMENTAL

Essentially the same apparatus was used as in the earlier work. Variations in feed rate were effected by adjustment of the temperature of the methylthiophenes in a liquid saturator.

The commercial cobalt molybdate catalyst (Girdler G 35A, 32–65 mesh) previously described (1) was

[1]*Issued as N.R.C. No. 7432.*
[2]*For Parts I–III, see references 1–3.*
[3]*National Research Council Postdoctoral Fellow 1961–1963.*

employed in beds of 0.47 g, 1.0 g, and 5.4 g, the smallest weight being used in all the single-shot runs to avoid the long pulse delays otherwise encountered. The catalyst was again stabilized with thiophene carried in a stream of hydrogen at 400°. This sulphiding process was repeated for occasional reconditioning.

Chromatographic and mass-spectrometric estimates of impurities contained in the thiophenes used yielded the following approximate results. Thiophene (Eastman) contained 1% benzene as its major impurity, 0.1% CS_2, 0.02–0.04% methyl ethyl ketone, and two unknown species of similar concentration; with 2-methylthiophene (Aldrich) no impurity bands were detectable, the lowest limit being ~0.01%; 3-methylthiophene (Aldrich) contained 0.9% 2-methylthiophene as its only detectable impurity. All three were used as received in continuous-flow experiments, but were purified by preparative gas chromatography for the single-shot and adsorption runs. The hydrocarbons employed were all Phillips research grade. Hydrogen from a cylinder was passed through a palladium catalyst and drying column to remove oxygen and water.

Most of the hydrocarbon analysis was carried out using a 25-ft propylene carbonate column (30% w/w on 30- to 48-mesh Chromosorb, in copper tubing). Satisfactory resolution of all C_5-isomers was obtained except for *trans*-2-pentene and 2-methyl-1-butene, which had identical retention times. Since hydrogenolysis of 2-methylthiophene gives rise predominantly to normal hydrocarbons and hydrogenolysis of 3-methylthiophene to branched hydrocarbons, i.e. without the occurrence of appreciable skeletal isomerization (Table I), this was not important. Nevertheless, it was possible by a series of successive approximations to estimate the concentration of the minor component of the olefin band in a given case on the basis of the above consideration and utilizing further product distribution data given in Table I. A 6-ft tricresyl phosphate column (40% w/w on 35- to 60-mesh Chromosorb, in glass tubing) was used at 70–90° in the determination of temperature coefficients and as a check on the percentage conversion calculated from results with the propylene carbonate column.

TABLE I

Product distribution from 2- and 3-methylthiophene (2MT and 3MT)
(0.47-g catalyst; 2-μl shots; H_2 flow 50 cc/min; reactor in series with 25-ft propylene carbonate column)

	Temperature, °C:							
	277		305		345		362	
	2MT	3MT	2MT	3MT	2MT	3MT	2MT	3MT
Rate, μmole C_5 per g cat. per sec	7	13	12	22	18	30	25	41
Total C_5, mole% of feed	8.9	16.5	15.5	27.0	22.3	36.7	31.0	50.8
Saturates, mole% in C_5	23.8	15.2	26.4	15.2	26.8	15.2	30.2	21.5
Pentane, mole % of feed	2.1	0.0	3.5	0.2	5.1	0.4	7.9	1.1
Isopentane, "	0.0	2.5	0.6	4.1	0.9	5.6	1.5	10.9
1-Pentene, "	0.6	0.0	1.4	0.0	2.0	0.0	2.1	0.6
cis-2-Pentene, "	1.7	0.0	2.3	0.3	3.4	0.4	4.5	0.9
trans-2-Pentene, "	1.8	0.0	4.4	0.6	6.0	0.8	8.0	1.7
2-Methyl-1-butene, "	0.8	4.0	0.9	5.0	1.4	9.5	1.8	9.2
2-Methyl-2-butene, "	1.9	10.0	2.4	15.9	3.5	18.8	4.6	24.0
3-Methyl-1-butene, "	0.0	0.0	0.0	0.9	0.0	1.2	0.6	2.4

RESULTS AND DISCUSSION

As in the case of thiophene (1) no evidence was obtained of mercaptan or thiolane intermediates among the products. Dienes could likewise not be identified. The distribution of the products for 2-μl shots on a 0.47-g catalyst bed is shown in Table I at four different temperatures. From the table, the following conclusions can be drawn. Under the same conditions, 3-methylthiophene undergoes higher conversion than 2-methylthiophene, the activity ratio being approximately constant in the temperature range 277 to 362°, in which diffusion is not rate controlling.

The percentage of saturates in the products is always greater for 2-methylthiophene than for the 3-methyl compound. This conforms to the observation of Gaschke, Spector, and Heinemann (8) that the rate of hydrogenation of 2-pentene on a cobalt molybdate alumina catalyst is faster than that of 2-methyl-2-butene. Furthermore, there is a general tendency favoring isomerization to branched rather than normal hydrocarbons. Thus, the

Can. J. Chem. Downloaded from www.nrcresearchpress.com by 210.87.254.42 on 09/05/12
For personal use only.

percentage of skeletal rearrangement of the (branched) products of hydrogenolysis of 3-methylthiophene varies from 0 to 10% in the temperature range examined, while it remained fairly constant at about 40% for the (normal) products from the 2-isomer. Both the preferential hydrogenation of normal olefins and their tendency to isomerize to branched olefins can be rationalized if acid sites are responsible for the reactions. There is reason to believe such to be the case. A few experiments in this laboratory using cobalt molybdate catalysts containing varying amounts of sodium (deposited from aqueous sodium carbonate) showed that both hydrogenolysis and olefin hydrogenation were suppressed by the alkali. The different sites, or the different functions of the same type of site, were also shown to be selectively poisoned by H_2S (1, 7). From other investigations in cracking and isomerization (9) it is reasonable to deduce that the carbonium ion from a normal olefin is more reactive and can either isomerize to a branched carbonium ion or hydrogenate to form a saturated hydrocarbon. The branched carbonium ion is more stable and gives the branched olefin without skeletal rearrangement.

The effect of sample size on conversion is similar to that found for thiophene and is demonstrated in Fig. 1. The C_5 analysis for the experiments at 414° (diffusion-controlled

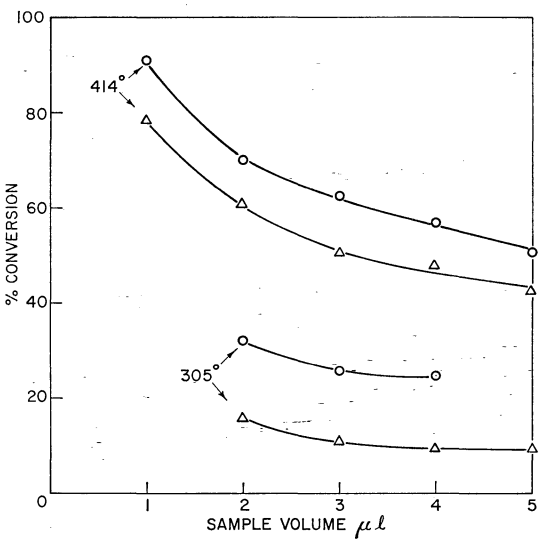

FIG. 1. The effect of sample size on conversion of the methylthiophenes on 0.47-g catalyst. △ 2-methylthiophene, ○ 3-methylthiophene.

region) was made using the tricresyl phosphate column and for those at 305° the propylene carbonate column. The effect is sufficiently marked to demonstrate that, as before (1), steady-state conditions are to be preferred for strict quantitative measurements (see e.g. Table II).

Figure 2(*a*) shows the preferential hydrogenation of 1-pentene over 2-methyl-1-butene. Hydrogenation experiments were carried out with 2-μl samples of the olefins in the absence of thiophene and H_2S, and once again the normal olefin was found to be hydrogenated to a greater extent. Also, skeletal rearrangement favored the formation of branched olefins, as indicated by Fig. 2(*b*).

In order to determine temperature coefficients of the rates of hydrogenolysis for thiophene and its homologues, continuous-flow experiments were carried out in the

Can. J. Chem. Downloaded from www.nrcresearchpress.com by 210.87.254.42 on 09/05/12
For personal use only.

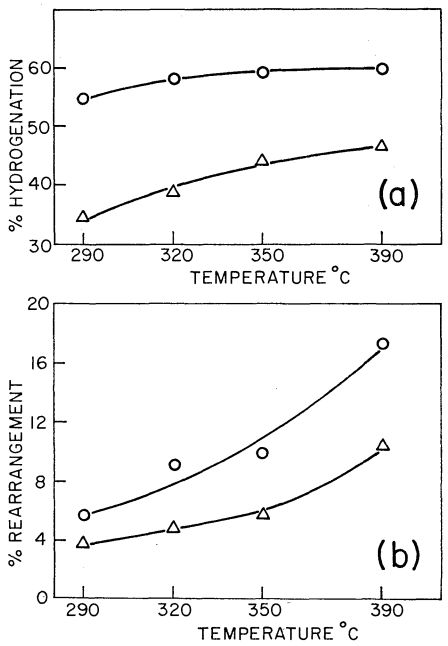

FIG. 2. Hydrogenation of 1-pentene and 2-methyl-1-butene on 0.47-g catalyst. (*a*) Percent hydrogenation. (*b*) Percent skeletal rearrangement. ○ 1-pentene, △ 2-methyl-1-butene.

temperature range 165 to 230° C on a 1.0-g catalyst bed and the results are presented in Table II. The reaction rates shown are interpolated from the rectilinear plots of log

TABLE II

Desulphurization rates over 1.0-g catalyst
(Feed rate: 55 cc/min. H_2 containing 1.67, 1.09, and 1.00 mole% of thiophene, 2-, and 3-methylthiophene (2MT and 3MT) respectively; continuous flow)

Temperature, °C	Rate, μmoles converted per g cat. per sec		
	Thiophene	2MT	3MT
170	0.8	1.1	2.7
180	1.5	1.7	4.2
190	2.8	2.7	6.7
200	4.9	4.1	10.0
210	8.7	6.1	15.6
225	18.8	10.7	27.8
E, kcal/mole	24.4±1.6	18.3±1.8	18.8±1.7

conversion vs. reciprocal temperature, which were obtained by the method of least squares; slopes and hence temperature coefficients (apparent activation energies *E*) were computed at the 95% confidence level. The energy value for thiophene proved to be the same, within experimental accuracy, as that for a 5.4-g catalyst bed and similarly agreed with that quoted in an ealier publication (1). Changing the flow and hence the feed rate did not alter the value appreciably.

It can be seen from Table II that there is little difference in the temperature coefficients of hydrogenolysis for the two methylthiophenes, in contrast to the much higher value for

Can. J. Chem. Downloaded from www.nrcresearchpress.com by 210.87.254.42 on 09/05/12
For personal use only.

thiophene. On the other hand the conversion of 3-methylthiophene is consistently more than double that of the 2-isomer. Thiophene reacts at rates similar to those of 2-methylthiophene at the lower temperatures and tends to approach its 3-methyl homologue in activity at higher temperatures.

An explanation for the higher rates of conversion of 3-methylthiophene compared to the 2-methyl compound has to be consistent with the behavior of thiophene. If hydrogen chemisorption were to be the only rate-determining step, changes in the structure of the other reactant such as introduction of a methyl group in the aromatic ring or change of its position would not affect the rates and energies of activation significantly. That the slow step could be the adsorption of the thiophene would also seem to be ruled out. Heats of adsorption of thiophene and the methylthiophenes were measured by the peak delay technique (1–3) on the 1-g catalyst sample in the range of reaction temperatures, and were found to be 8.7 ± 0.5 kcal/mole for thiophene and 11.0 ± 1.2 kcal/mole for each of the two methylthiophenes. If these are the heats of chemisorption, then the difference in the activities of the two methylthiophenes cannot be explained on the basis of differences in adsorption energy.

It is very likely then that the slow step is a surface reaction such as C—S bond fission on the catalyst surface. The surface species involved in the fission should be different for thiophene and the methylthiophenes, and different again for 2- and 3-methylthiophene. This makes it unlikely that the slowly reacting surface species is bonded to the catalyst surface through a π-bond to the aromatic ring, although the latter might be a precursor in the reaction sequence. A π-complex of this type between chromium tricarbonyl and thiophene has been characterized, for instance, by Fischer and Öfele (10). The electron density at the α-carbon atom is most probably the determining factor. The combined inductive and hyperconjugative effects of the methyl group in the 3-position can enrich the α-carbon atom of the 3-methylthiophene and impart to it greater affinity for a proton or an acidic surface site. If the α-hydrogen atom is replaced by a methyl group, however, the hyperconjugation would oppose the interaction of the aromatic double bond with the sulphur atom. There would still remain a smaller activation of the unsubstituted α-carbon. The thiophene molecule without any localizing substituent effects should then require higher activation for the C—S bond scission. The difference in activity of the 2- and 3-methylthiophenes is not reflected in their apparent activation energies possibly because of the limited accuracy of the measurements. Thus by assuming the "compensation effect" to be operative it can be estimated that a variation in rates by a factor of 2 will result in activation energy changes of the same magnitude as the uncertainty in the measured E values.

It is of interest to consider possible gas-phase intermediates. By analogy with thiophene itself, it is reasonable to expect C_5-dienes to be intermediates in the reaction of the methyl thiophenes over cobalt molybdate catalyst. A few shot runs with n-pentadienes and isoprene in a stream of hydrogen showed that, if they were initially formed in the hydrogenolysis, they would be hydrogenated too fast to be detected among the products under the conditions used. On the other hand using alumina alone, dienes were positively identified among the hydrogenolysis products arising from both thiophene and the methylthiophenes. A highly pure and acidic alumina was prepared for this purpose by the method of Pines (11) (conversions were less than 2% at 300–400° C). The insignificant departure from gas phase equilibrium (9) among the pentene and also the methylbutene isomers in the reaction products unfortunately precluded identification of the initial monoolefin formed from either of the two methylthiophenes. Previously, 1-butene had been so

Can. J. Chem. Downloaded from www.nrcresearchpress.com by 210.87.254.42 on 09/05/12
For personal use only.

identified in the case of thiophene itself (1). Cyclic intermediates with partial or complete saturation of the aromatic double bonds have apparently no place in the thiophene hydrogenolysis scheme. Desulphurization of dihydro- and tetrahydro-thiophene is being investigated and the results, to be published later, indicate the reaction pattern to be quite different. Also, the differences between the activities of thiophene and its immediate homologues depend on the retention of the thiophene double bonds before the rate-determining step, which, in turn, is consistent with a mechanism involving the α-carbon atom.

ACKNOWLEDGMENTS

The authors are grateful to M. Bednas for purification of the methylthiophenes by preparative gas chromatography.

REFERENCES

1. P. J. Owens and C. H. Amberg. Advan. Chem. Ser. **33**, 182 (1961).
2. P. J. Owens and C. H. Amberg. Can. J. Chem. **40**, 941 (1962).
3. P. J. Owens and C. H. Amberg. Can. J. Chem. **40**, 947 (1962).
4. R. A. Siddiqui and C. H. Amberg. To be published.
5. L. W. Vernon and J. T. Richardson. Abstracts of the 142nd Meeting of the American Chemical Society, Division of Colloid and Surface Chemistry, Atlantic City, N.J. Sept. 9–14, 1962. p. 71.
6. F. W. Kirsch, H. Shalit, and H. Heinemann. Ind. Eng. Chem. **51**, 1379 (1959).
7. F. W. Kirsch and S. E. Shull. Ind. Eng. Chem. Prod. Res. Develop. **2**, 48 (1963).
8. M. Gaschke, M. Spector, and H. Heinemann. Actes Congr. Intern. Catalyse, 2e, Paris, 1960, **1**, 1017 (1961).
9. F. E. Condon. *In* Catalysis. Vol. 6. P. H. Emmett (*Editor*). Reinhold, New York, 1958. p. 43.
10. E. O. Fischer and K. Öfele. Chem. Ber. **91**, 2395 (1958).
11. H. Pines and W. O. Haag. J. Am. Chem. Soc. **82**, 2471 (1960).

Can. J. Chem. Downloaded from www.nrcresearchpress.com by 210.87.254.42 on 09/05/12
For personal use only.

THE EXISTENCE OF THE FLEXIBLE CONFORMATION IN SIX-MEMBERED RINGS

F. LAUTENSCHLAEGER AND GEORGE F WRIGHT
Department of Chemistry, University of Toronto, Toronto, Ontario
Received March 11, 1963

ABSTRACT

From consideration of electrical polarization and nuclear magnetic resonance measurements, 1,4-dimethylenecyclohexane and its exo-tetramethyl and tetraphenyl analogues have been assigned the flexible ring conformation, as have also 1,4-dithiane and *cis*-1,4-dithiane-1,4-dioxide. However, the magnitudes of the moments indicate that uniform flexibility is not prevalent, the stretched form being predominant. In contrast to these flexible forms the conformation of dithiane monoxide is thought to be chair and that of 2,5-diphenyl-1,4-dithiin a fixed boat.

Can. J. Chem. Downloaded from www.nrcresearchpress.com by 210.87.254.6 on 09/05/12
For personal use only.

Evidence is accumulating to show that the Sachse-Mohr chair conformation for six-membered rings is not universal (1), and in some instances is less likely than the so-called "flexible" form of conformation (2). It has been shown by Kumler and Huitric (3) that the electric dipole moments of α-halogenocyclohexanones are best explained by some contributions from flexible forms. Correlation of dipole moments with nuclear magnetic resonance spectra of N,N′-disubstituted piperazine seems to show that these substances are entirely in the flexible form. Indeed the moment of 1,4-cyclohexanedione (μ = 1.3 D) (4), which has been interpreted in terms of an equilibrium mixture of cis and trans forms (boat and chair in the conformational sense), might better be included among substances in which a dynamic structure (flexible form) is operative. At least this is our interpretation of the fact that only one peak is found in the n.m.r. spectrum of this substance, whereas rigid-boat and chair conformations both ought to display distinctive axial and equatorial hydrogen resonance if they persist longer than 0.01–0.02 second.

The carbonyl groups in the cyclohexanones and cyclohexanedione would contribute 120° angularity to the six-membered rings of which they are a part in consequence of their sp^2 bond distribution.

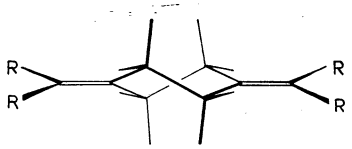

I

It seems to be worthwhile to examine analogues with this structural feature so we have synthesized 1,4-dimethylenecyclohexane (I, R = H), its exo-tetramethyl homologue (I, R = CH_3), and have included the already known 1,4-bis-diphenylmethylidene-cyclohexane (5) (I, R = C_6H_5). Structure I depicts these molecules in the non-boat (the stretched) mode of the flexible six-membered ring.

The preparation of 1,4-dimethylenecyclohexane, II, by pyrolysis of the 1,4-diacetoxy-methylcyclohexane, II, has been effected according to Bailey's method (6) for synthesis of the 1,2-structural isomer. Bailey's recommended use of the primary rather than the tertiary dialcohol minimizes the isomers which are ring unsaturated but it cannot prevent dehydrogenation and hydrogen redistribution. Notwithstanding a low yield of acetic acid

(61%) at a pyrolysis temperature of 500°, this temperature has been chosen in order to minimize the formation of xylene and other aromatic hydrocarbons.

Although the complexity of the crude product precludes separation of the ring-unsaturated isomers of 1,4-dimethylenecyclohexane (I, R = H), the presence of the conjugated isomers is readily discernible because I is transparent throughout the ultraviolet range to 215 mμ. Moreover the conjugated diene impurities can be removed by use of diethyl azodicarboxylate, with which they form Diels–Alder complexes. The fortuitous boiling point (122°) of I makes separation from toluene and xylene by fractional distillation a relatively simple operation. If 1,4-dimethyl-2,5- or -1,4-hexadienes were present in the system they have escaped detection by us.

Except for a tendency toward slow polymerization, which might be expected in view of similarity with isobutylene, the purified substance is stable under neutral conditions, especially in absence of oxygen. Upon ozonization only formaldehyde and 1,4-cyclohexanedione can be isolated. On the other hand extensive isomerization occurs upon treatment with acid; among the isomer products the thermodynamically more stable 1,4-dimethyl-1,3-hexadiene has been identified by its ozonization product, acetonylacetone.

The infrared spectrum of 1,4-dimethylenecyclohexane contains all the expected absorptions of the exo unsaturation. The CH_2-hydrogen out-of-plane deformation is indicated strongly by the absorption at 893 cm^{-1} and, weakly, by what is probably its overtone at 1780 cm^{-1}. The C—H stretching of the double bonds is indicated at about 3080 cm^{-1}; the in-plane deformation is displaced to 1405 cm^{-1} from its expected position at 1420-1410 cm^{-1}, and the C=C stretch is strong at 1660 cm^{-1}.

It is of interest that this exocyclic unsaturation behaves typically toward iodine according to the spectral behavior reported by Long and Neuzil (7) for unsymmetrically disubstituted alkenes since only a single peak at 293 mμ is observed when 1,4-dimethylenecyclohexane is treated with iodine. Thus it would seem that the double bonds in 1,4-dimethylenecyclohexane are of themselves quite normal.

The exo unsaturation of 1,4-dimethylenecyclohexane can be preserved during bromine addition and elimination under conditions (exclusion of peroxides by diphenylamine) where the radical reaction is at least not excluded. Only one tetrabromide has been found in the product, indicating to us that an equilibrium mixture of chair and boat conformations is less likely than either a chair or a flexible conformation alone.

On the other hand methoxymercuration leads to two geometric isomers, approximately in equal amount. In view of the stereospecificity of this addition with simple alkenes the formation of two isomers, especially where one is not preponderant, is less to be expected from a chair conformation than from the flexible form since the median shape of this latter is essentially colinear with respect to alkene groups. It is of interest that the reversal of oxymercuration when it is accomplished with concentrated hydrochloric acid regenerates pure 1,4-dimethylenecyclohexane, thus indicating that the process is molecular rather than ionic.

In respect of nuclear magnetic resonance 1,4-dimethylenecyclohexane behaves like 1,4-cyclohexanedione in favor of a flexible conformation. Only two peaks are observed from an undiluted sample at 25°. The peak at 20 c.p.s. must represent the methylidene hydrogens because the area enclosed by it is half of that to be attributed to the ring methylene hydrogens which occurs at 107 c.p.s. in a 60 Mc field. We have been unsuccessful in the attempts to split this absorption into axial and equatorial hydrogen resonance by lowering the temperature of a solution in carbon disulphide to −120°.

Can. J. Chem. Downloaded from www.nrcresearchpress.com by 210.87.254.6 on 09/05/12
For personal use only.

A similar study has been made with 1,4-diisopropylidenecyclohexane (I, R = CH_3) which we have prepared via the *cis*-1,4-glycol from methyl chloride Grignard reagent and diethyl 1,4-cyclohexanedicarboxylate (mainly cis). Mild acid treatment converts the cis glycol to trans with loss, whereas stronger treatment dehydrates it cleanly to the exo dialkene. This structure has been demonstrated by ozonization to acetone and 1,4-cyclohexanedione. Like its lower homologue it is ultraviolet-transparent down to 210 mμ and only one tetrabromide is obtained from it.

It is to be expected that this substance would show only two absorptions by n.m.r., and in fact in carbon disulphide one peak at 130 c.p.s. with area corresponding to the methyl hydrogens and the other peak of larger area at 97 c.p.s. have been observed. The hope that the latter peak would split when the temperature was lowered has not been realized because no suitable solvent has been found for the examination at low temperatures.

Equally unsuccessful has been the attempt to discover axial and equatorial absorption for 1,4-bis-diphenylmethylidenecyclohexane. This substance is so insoluble in appropriate organic solvents that its n.m.r. spectrum (40 Mc) can only be obtained in tetrachloroethane at 130°. The spectrum at this temperature consists of one peak at −53 c.p.s. characteristic of phenyl hydrogens and the other at +137 c.p.s. characteristic of the ring methylene hydrogens, both relative to the solvent. At room temperature tetrachloroethane has a peak 239 c.p.s. (at 40 Mc) below tetramethylsilane.

Because strongly polar groups are absent in these exo-unsaturated cyclohexanes the electrical polarizations are relatively meaningless but they have been studied. Firstly, the distortion polarizations have been determined when possible. Since 1,4-dimethylenecyclohexane is a liquid at room temperature the electric polarization (P_E) at optical frequencies has been used; likewise with dimethyl sulphoxide to be discussed later. The distortion polarizations ($P_D = P_E + P_A$) of the remainder (the solids) have been determined by the wafer technique (8, 9) and are listed among others in Table I together with

TABLE I

Distortion polarization measurements

Substance	d_4^{20}	ϵ	P_{E+A}	Mol. refraction		
				Eisenlohr	Vogel C_{ali}	Vogel C_{ar}
1,4-Dimethylenecyclohexane	0.821	1.4717*	36.9*	36.0	36.2	
Bis-isopropylidenecyclohexane	1.025	2.70	58.0	54.5	54.8	
Bis-diphenylmethylidenecyclohexane	1.159	2.64	126	132	134	
2,5-Diphenyl-1,4-dithiin	1.363	3.038	79.5	70.0	72.4	71.6
1,4-Dithiane	1.376	2.682	31.4	31.0	34.4	
1,4-Dithiane monoxide	1.433	2.825	35.9		34.3	
trans-1,4-Dithiane-1,4-dioxide	1.516	2.992	40.0		34.1	
cis-1,4-Dithiane-1,4-dioxide	1.537	3.094	40.6		34.1	

*Actually n_D^{20} and P_E for this liquid.

values calculated by the summation of atom (Eisenlohr) or bond (Vogel) polarizabilities. Only three items in the table warrant comment. It may be seen that additive MR_D for bis-1,4-diphenylmethylidenecyclohexane is appreciably higher than the P_D values obtained from the dielectric constant of wafers and absurdly so, as will be shown by comparison with total polarization of bis-diphenylmethylidenecyclohexane solutions. This discrepancy conforms with earlier studies (10) and it leads us to prefer the wafer

Can. J. Chem. Downloaded from www.nrcresearchpress.com by 210.87.254.6 on 09/05/12
For personal use only.

technique for evaluation of P_D. This preference applies to a second item, P_D for dithiane. In this instance the agreement with additive polarizability by the Eisenlohr calculation is good, although inconsistent with the Vogel bond additivity.

The third item for comment in Table I is 2,5-diphenyldithiin, because the distortion polarization determined by dielectric constant is 8.1 cc higher than the average of the summation values for MR_D despite the presence of the phenyl groups which would be expected to cause P_D to be lower than MR_D by summation of atom or bond polarizabilities. One must presume in this instance that an appreciable exhaltation in electronic polarization (P_E) is operative, a situation not unexpected in view of the divinyl sulphide linkage in this substance.

The dipole moments and data from which they are derived are shown for the substances of this report in Table II. As would be expected from resemblance to isobutylene and tetramethylethylene the moments of dimethylenecyclohexane and diisopropylidenecyclohexane are indistinguishable from zero at our present precision. However, a small moment may be attributed to bis-diphenylmethylidenecyclohexane on the basis of the measured distortion polarization. The use of MR_D by summation would lead to an absurd result. But the assignment of flexible conformation to these exo-unsaturated cyclohexanes depends not upon the moment but upon the absence of axial–equatorial peaks in the n.m.r. spectra.

In earlier publications from this laboratory the flexibility of several six-membered ring systems has been attributed entirely on geometrical grounds to the 120° ring angles contributed by carbonyl or nitramino (11) linkages as a consequence of their sp_2 hybridization. To be sure, the same type of flexible conformation is required for explanation of the appreciable moments of 1,4-diphenyl- (12) and 1,4-dimethyl-piperazines (8) in which tertiary amino groups are involved in the ring. But the 110–111° R—N—R angle of amines is an extreme form of the group which is oscillating with inversion. The flexibility of the diphenyl- or dimethyl-piperazine may then be attributed to the 120° ring angles which amino nitrogen must contribute in the planar median of the oscillation if it is assumed that the nitrogen atom oscillation is approximate to that of conformational oscillation in a flexible ring. Since the oscillation rate of the flexible ring must be 10^3–10^4 c.p.s. and that of the substituted amino group will be less than 10^7 c.p.s. the assumption of an effective 120° angles is not unreasonable, especially since one frequency might be expected to "lock in" to the other.

The question arises whether the flexible conformation is likely in absence of sp_2 angularity. An answer may be provided by consideration of 1,4-dithiacyclohexanes since information about bond lengths and bond angles of 1,4-dithiane (13) and *trans*-1,4-dithiane-1,4-dioxide (14) is available. Although these data are based on diffraction studies which specify chair conformations in the crystalline state it may be assumed that they will be applicable if the substances exist in solution as flexible forms.

The dipole moments of the 1,4-dithiacyclohexanes and their oxides are listed in Table II. The apparent moment of 1,4-dithiane (μ = 0.51–0.56 D) is small but the precision of the determination of P_D (Fig. 1) and of total polarization (P_T, Fig. 2) in benzene solution from 20 to 40° C indicates that this moment is real and is temperature dependent. The existence of the meagre moment is not surprising in view of the comparable value (0.3–0.4 D) which has been found for the analogous dioxane (15, p. 299).

However, this low moment cannot be explained either by a chair or a completely flexible conformation in view of the observed moment of dimethyl sulphide (15, p. 303). On the other hand the low moment can be rationalized in terms of a limited flexibility in

Can. J. Chem. Downloaded from www.nrcresearchpress.com by 210.87.254.6 on 09/05/12
For personal use only.

Can. J. Chem. Downloaded from www.nrcresearchpress.com by 210.87.254.6 on 09/05/12
For personal use only.

TABLE II

Orientation polarization measurements

Substance	Solvent	Temp. (°C)	$\delta\epsilon/\delta\omega$	$\delta\bar{V}/\delta\omega$	ϵ extrap.	ϵ solvent	V extrap.	V solvent	P_T (cc)	MR_D addv.	P_D	μ (D)
(1) 1,4-Dimethylenecyclohexane	Benzene	20	−0.10	0.087	2.2825	2.2826	1.13791	1.13808	37.6	36.0	36.9*	0–0.1
	Benzene	30	−0.09	0.084	2.2620	2.2623	1.15186	1.15190	37.7	36.0	36.9*	0–0.1
	Benzene	40	−0.08	0.082	2.2421	2.2422	1.16626	1.16624	38.0	36.0	36.9*	0–0.1
(2) Bis-isopropylidenecyclohexane	CCl_4	20	0.22	+0.512	2.2384	2.22384	0.62695	0.62694	58.4	54.7	58.0	0
(3) Bis-diphenylmethylidene-cyclohexane	CS_2	20	0.02	+0.098	2.6455	2.6456	0.78128	0.79130	129.4	133.0	126	0.4
(4) 2,5-Diphenyldithiin	Benzene	20	1.66	0.360	2.2829	2.2830	1.13830	1.13830	145.3	71.4	79.5	1.77
(5) 1,4-Dithiane	Dioxane	20	0.40	0.135	2.2245	2.2246	0.96740	0.96740	36.8			0.51
	Dioxane	30	0.40	0.126	2.2061	2.2062	0.97838	0.97838	37.4	32.6	31.4	0.54
	Dioxane	40	0.38	0.118	2.1818	2.1818	0.98987	0.98987	37.5			0.56
(6) *trans*-1,4-Dithiane-1,4-dioxide, m.p. 280°	Dioxane	40	0.90	0.50	2.1918	2.1920	0.98990	0.98990	44.3		40.0	0.4
(7) *cis*-1,4-Dithiane-1,4-dioxide, m.p. 257°	Dioxane	40	17.4	0.46	2.1918	2.1920	0.98992	0.98990	469.7		40.6	4.66
(8) 1,4-Dithiane-1-monoxide	Dioxane	40	9.50	0.31	2.1918	2.1920	0.98991	0.98990	244.7		35.9	3.25
(9) Dimethyl sulphoxide	Benzene	20	21.81	0.260	2.2830	2.2840	1.13800	1.13808	337.5		20.1*	3.88

*Calculated from refractive index and density.

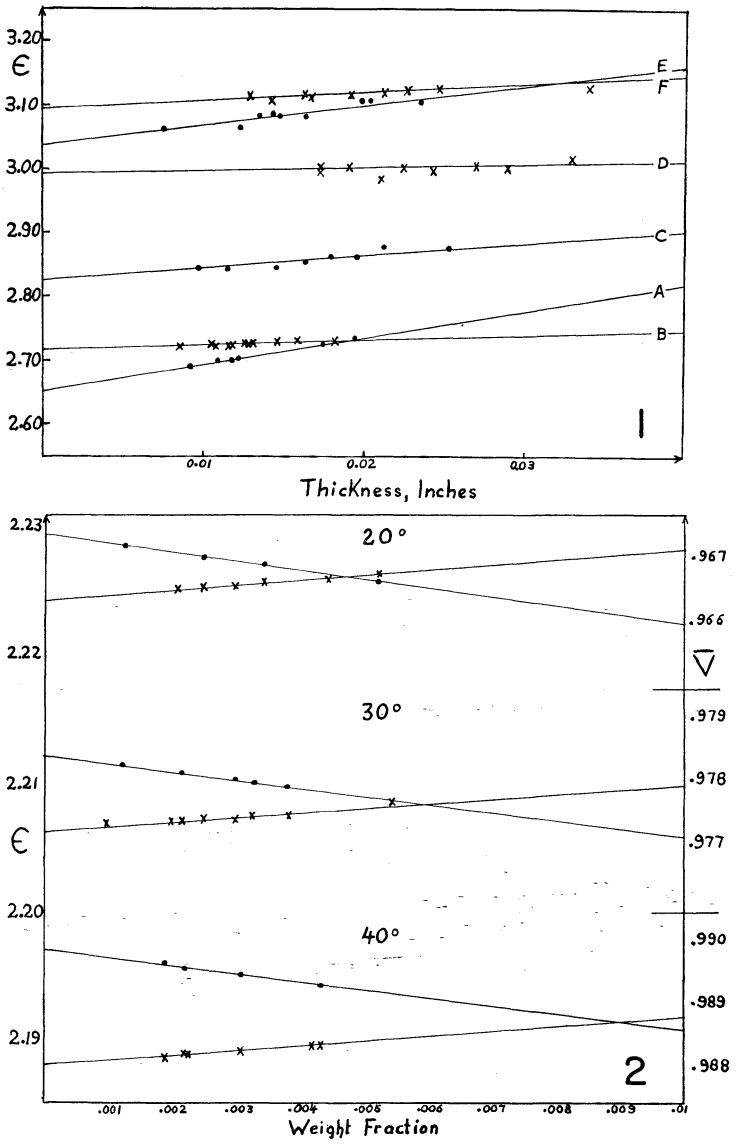

FIG. 1. Extrapolation of dielectric constants of solids. A: 1,4-Dithiane; B: 1,4-bis-diphenylmethylidene-cyclohexane; C: 1,4-dithiane monoxide; D: *trans*-1,4-dithiane dioxide; E: 2,5-diphenyldithiin; F: *cis*-1,4-dithiane dioxide.

FIG. 2. Extrapolations of dielectric constant (ϵ) and specific volume ($\bar{V}$) for dioxane solutions (weight fraction) of 1,4-dithiane.

which the molecule is largely in the "stretched" modes (II). In this connection it should be noted that unlike the isocyclic cyclohexane there will be two possibilities of "stretched" mode in dithiane of which the one where the hetero atoms tend toward the median positions should be more probable than the one where carbon rather than the sulphur occupies this median position. That is to say, II*a* is more probable than II*b*. Since the moment of II*a* would essentially be zero one must postulate on this basis that dithiane is flexible with an unequal conformational distribution favoring II*a*.

Can. J. Chem. Downloaded from www.nrcresearchpress.com by 210.87.254.6 on 09/05/12
For personal use only.

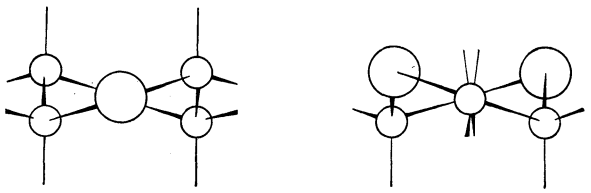

IIa IIb

Flexibility involving a frequency greater than the reading rate of an n.m.r. measurement is indicated by a single proton absorption for dithiane at room temperature. Confirmation of this evidence would be afforded if the flexible oscillation could be decreased at low temperature to an extent that it would be slower than the 116 c.p.s. downfield which Dr. S. S. Danyluk of this department has found at room temperature. When he cooled a 5% solution of dithiane to −120° in the 1:1 volume mixture of thionyl chloride – carbon disulphide (f.p. ca. −140°) he did not observe a splitting of the proton absorption band, but the marked broadening of this line toward virtual disappearance against the background at −120° is a strong indication of the complex spectrum to be expected at a relatively low oscillation rate. On balance of evidence the flexible form of dithiane is favored.

A contrasting rigidity in a six-membered ring is shown by the moment (Table II) of 2,5-diphenyldithiin. There is no possibility of a flexible form of this 1,4-dithiadiene; it must exist as a chair or boat. The observed moment (1.8 D) shows that the molecule has boat shape. If comparison with the moment of ethylene sulphide is valid (15, p. 299) the ethylene linkages in diphenyldithiin are not significantly distorted.

According to the X-ray diffraction analysis of March the C—S—C bond angle in 1,4-dithiane is 93°. This wide divergence from the 120° angle, which heretofore has seemed to characterize the flexible ring conformation, actually does not preclude flexibility. It is evident from geometry that the carbon atom in the ring is properly spaced for flexible behavior because of the greater bond length of C—S (1.81 Å) over that of C—C (1.51 Å) or C—N (1.46 Å) in exo-unsaturated cyclohexanes or piperazines. The equivalent angle in terms of the latter types would be about 115°.

According to Shearer the C—S—C bond angle in *trans*-1,4-dithiane-1,4-dioxide is 98°, which with the C—S bond length of 1.81 Å is practically equivalent to the 120° angle in exo-unsaturated cyclohexanes or piperazines. Therefore, on geometric grounds the flexible conformation is not excluded for dithiane dioxides in solutions, even though Shearer considers the trans isomers to be of chair conformation in the crystal.

It should be stressed that flexibility if it exists in the dithiane oxides is a consequence of favorable geometry due to the long C—S—C bond and not to inversion-oscillation which is characteristic of the C—N—C linkage. This is obvious in the fact that amines cannot be isolated as enantiomeric individuals because of inversion whereas the sulphoxides are configurationally stable.

In order to make a conformational evaluation from electric moment data the moment angle must be correlated with bond angle. In a substance such as 1,4-dimethylpiperazine the moment must evidently arise between the nitrogen nucleus and the non-bonded electrons of this atom. We presume that the non-bonded electrons in sulphoxides contribute little to the moment. If the contribution were appreciable the moments of *cis*- and *trans*-dithiane dioxides would not be so different as Table II shows them to be. The principal contribution must be due to the polar S→O linkage and we assume that its

Can. J. Chem. Downloaded from www.nrcresearchpress.com by 210.87.254.6 on 09/05/12
For personal use only.

bond angle is approximately the same as the moment angle. The C—S→O bond angle has been specified as 107° by Shearer so the $=C_2=S\rightarrow O$ bond angle may be taken as 110°.

If dimethyl sulphoxide of moment 3.88 D is compared with 1,4-dithiane-1-oxide it is evident that the cyclic compound cannot exist in the flexible conformation because the mean value of the moments calculated for the extreme conformers would exceed the moment of dimethyl sulphoxide in benzene. Actually the observed moment of dithiane monoxide (in dioxane, which tends to enhance the apparent moment in benzene) is 0.63 D lower than that of dimethyl sulphoxide. This moment could be due only to a rigid "stretched form" or to a chair form, and the latter is energetically more probable.

Thus the chair conformation is assigned to the monoxide but a different situation may exist in the case of dioxides. Assuming that the bond angle $=C_2=S\rightarrow O$ and the moment angle are identically 110° the moment of the trans dioxide ought to be zero while the cis isomer ought to have a moment of 6.36 D.

The observed moment for the trans isomers apparently is 0.4 D, but this value is too low to be significant. Great precision and accuracy are necessary in order to attach any meaning to an apparent moment less than 0.5 D, and the trans dioxide because of its low solubility therefore is precluded. Because of this low solubility we have been unable to determine the n.m.r. spectrum in a suitable medium. Therefore it seems best to leave the question of *trans*-dithiane dioxide conformation in abeyance.

On the other hand the cis isomer is amenable for consideration. Clearly with an observed moment of 4.66 D *cis*-1,4-dithiane-1,4-dioxide cannot exist in a fixed chair conformation which should have a moment of 6.36 D. Alternatively with postulation of a flexible ring a calculation by the method of Hazebroek and Oosterhoff (2) has been made. If the observed moment of dimethyl sulphoxide is used as the group moment for $=C_2=S\rightarrow O$ (as before) then at a moment angle of 110° the μ of the cis isomer may vary from 0 to 7.36 D. The upper limit is sterically improbable because it represents the extreme boat form in which the oxygen atoms would overlap. The moment will therefore be comprised of three other "boat" aspects plus the stretched forms which are intermediate. The resultant is approximate to the observed moment of 4.66 D on the basis of equal contributions. While this assumption is unwarranted it does give reasonable agreement which is impossible for the chair conformation. Consequently the dynamic structure of limited flexibility is assigned to *cis*-1,4-dithiane-1,4-dioxide.

EXPERIMENTAL[1]

1,4-Dimethylenecyclohexane

Into the top of a quartz tube 600×30 mm packed with 0.2–1.0 cm² Vycor chips in the region 140 mm to 440 mm from the top and heated externally to show a temperature of 510° to a centrally located thermocouple was added at a rate of 100 g/hr a total of 1040 g (4.56 mole) of a cis–trans mixture of 1,4-bis-acetoxymethylcyclohexane. During this time a 50 cc/min stream of dry 99.8% nitrogen was passed downward through the pyrolysis tube and the dry, ice-chilled receiver which was connected to it. The top of the chip bed acted as a vaporizer for the diacetate.

A solution of the pyrolyzate in ether was water-washed to remove acetic acid (336 g, 61% according to titration) then dried by means of magnesium sulphate and distilled, finally through a Vigreux column at 20 mm Hg pressure to give 265 g, b.p. 28–75°. The chilled residue yielded 111 g, m.p. 65–72°, chiefly unchanged diacetate. The remainder was discarded.

The distillate, b.p. 28–75°, was fractionated through a 40-plate helix-packed column (r.r. 20:1 at 750 mm) to give a series of fractions which were complex according to gas chromatography; only toluene and xylene were identified besides the principal fraction (103 g, n_D^{20} 1.4727, boiling at 122–123°, 750 mm). This crude 1,4-dimethylenecyclohexane, m.p. −32° to −27°, absorbed slightly (E_{max}, 87) at 230 mμ so it was treated with 50-mg portions of diethyl azodicarboxylate until the color of the latter persisted for 8 hours. The volatile fraction was removed under reduced pressure and then was distilled at 750 mm, yield 90.5 g, b.p.

[1]*Melting points have been checked against reliable standards.*

Can. J. Chem. Downloaded from www.nrcresearchpress.com by 210.87.254.6 on 09/05/12
For personal use only.

121–122°, n_D^{20} 1.4717, d_4^{20} 0.821, capillary m.p. −28 to −26.5°. This pure material (single peak, retention time 16 minutes by gas chromatography on 20% carbowax firebrick) was transparent down to 215 mμ in methanol. Anal. Calc. for C_8H_{12}: C, 88.9; H, 11.2. Found: C, 88.9; H, 11.0. The infrared absorptions in carbon tetrachloride in cm^{-1} (E_{max}) are 3075 (54), 2930 (118), 2840 (73), 1780 (19), 1655 (100), 1440 (79), 1400 (34), 1315 (36), 1180 (25), 1160 (49), 980 (21), 893 (402), 692 (105) in carbon tetrachloride. An additional peak at 785 (54) was found in carbon disulphide or in an undiluted sample but no further absorption out to 300 cm^{-1}. Slight differences from the spectrum in carbon tetrachloride were found for the neat sample, i.e. 2940 vs. 2930, 1455 (new, shoulder), 1165 vs. 1160, 982 vs. 980, and 888 vs. 893.

The nuclear magnetic resonance spectrum (60 Mc) of an undiluted sample showed two simple peaks. The peak characteristics of the four methylene hydrogens at 20 c.p.s. included half of the area under the peak at 107 c.p.s. characteristic of the eight ring hydrogens. Neither peak showed any tendency toward splitting when the temperature of a carbon disulphide solution was lowered to −120° C.

Bis-1,4-bromomethyl-1,4-bromocyclohexane

To a solution of 10.8 g (0.1 mole) of 1,4-dimethylenecyclohexane in 100 ml of diethyl ether and 2 ml of amyl alcohol containing 10 mg of diphenylamine (to favor homopolar addition) was added bromine at −40° C until the color was permanent. After solvent evaporation the product was crystallized from commercial hexane – diethyl ether (2:1) to give 29.8 g (69%), m.p. 134–135°. Anal. Calc. for $C_8H_{12}Br_4$: C, 22.5; H, 2.83. Found: C, 22.4; H, 2.78.

This tetrabromide (12.8 g, 0.03 mole) was dissolved in 200 ml of dry diethyl ether and stirred under nitrogen with 1.5 g (0.062 g-atom) of Grignard-quality magnesium plus a grain of iodine for 10 minutes and then was refluxed for 1 hour. The supernatant phase, waterwashed and magnesium sulphate dried, was distilled, finally at 121°, yield 1.3 g (40%) with negligible residue. This 1,4-dimethylenecyclohexane was transparent down to 215 mμ and gave a single gas chromatograph peak. Addition of bromine as described above gave a 62% yield of tetrabromide, m.p. 133.5–135°, not depressed by admixture with the original.

1,4-Cyclohexanedione

A solution of 0.546 g (0.005 mole) of 1,4-dimethylenecyclohexane in 20 ml of carbon tetrachloride was saturated with 5% ozonized oxygen at −10°. After vacuum evaporation of the solvent the residue was heated with powdered zinc and water at 90° for 90 minutes and then was steam-distilled. The distillate, treated with dimedone, gave the formaldehyde derivative, 0.885 g (30%), m.p. 188–189°.

The steam distillation residue was exhaustively extracted with petroleum ether (b.p. 40–60°). Evaporation of this extract left 0.22 g (39%) of 1,4-cyclohexanedione, m.p. 74°. After three sublimations the melting point, 78.4°, was not depressed by admixture with an authentic sample. The 2,4-dinitrophenylhydrazone melted at 237° (lit 240°).

The n.m.r. spectrum of a methylene dichloride solution of the cyclohexanedione showed only a single peak for all ring hydrogens at 88 c.p.s.

Bis-1,4-chloromercurimethyl-1,4-methoxycyclohexane

To a stirred suspension of 63.6 g (0.2 mole) of crystallized mercuric acetate in 400 ml of pure methanol was added 10.8 g (0.1 mole) of 1,4-dimethylenecyclohexane at room temperature. After 35 minutes the suspension showed a negative test for mercuric ion and was cooled to 0° and poured into a stirred solution of 12.2 g (0.21 mole) of sodium chloride in 400 ml of water. After 20 minutes the precipitate was filtered and washed with a little cold methanol, yield 63 g (98%). This crude product was extracted with 4 liters of boiling chloroform, leaving 15.7 g, m.p. 196–200°. Vacuum evaporation of the extract gave a first fraction (12.0 g, m.p. 170–190° (decomp.)) and then a second (32.5 g, m.p. 166–180° (decomp.)). Crystallization with recombination from hot acetone, chloroform, methanol, and dioxane separated the mercurial into its two geoisomers; A, 21 g, decomp. 217°, slightly soluble in hot chloroform, fairly soluble only in hot dioxane. Anal. Calc. for $C_{10}H_{18}O_2Hg_2Cl_2$: C, 18.7; H, 2.87. Found: C, 18.7; H, 3.01. The infrared spectrum in potassium bromide (cm^{-1}) is 2950 (s), 2900 (s), 1460 (shld., m), 1450 (shld., m), 1443 (m), 1425 (m), 1405 (m), 1360 (m), 1312 (w), 1280 (m), 1243 (s), 1193 (w), 1166 (w), 1145 (m), 1110 (s) ,1090 (s), 1075 (shld., s), 1063 (s), 1042 (shld.), 963 (w), 912 (m), 886 (m), 860 (s), 763 (w), 755 (w), 709 (w). Geoisomer B, 24 g, decomp. 193°, is soluble in cold dioxane and easily soluble in hot methanol or chloroform. Anal. Calc. for $C_{10}H_{18}O_2Hg_2Cl_2$: C, 18.7; H, 2.87. Found: C, 18.8; H, 3.07. The infrared spectrum in potassium bromide (cm^{-1}) is 2940 (s), 2840 (shld., m), 1460 (shld., m), 1450 (m), 1430 (m), 1405 (m), 1360 (w), 1340 (w), 1318 (w), 1275 (m), 1255 (m), 1185 (shld., m), 1140 (s), 1060 (s), 1025 (m), 970 (m), 943 (w), 904 (m), 865 (m), 746 (s), 703 (w), 663 (w).

When 18 g of geoisomer A (0.028 mole, decomp. 216°) was suspended in 30 ml of pure *n*-hexane and stirred vigorously with 4.8 ml (0.06 mole) of conc. hydrochloric acid for 5 minutes a residue was still undissolved. However, the hexane layer was separated, washed with water, dried with magnesium sulphate, and distilled to give a slight first fraction boiling up to 121° and then 1.6 g (53%) b.p. 121–122°. The distillation residue weighed 0.6 g (20% also calculated as dimethylenecyclohexane), was unsaturated, and showed ultraviolet peaks at 271, 260, and 253 mμ. The 1.6-g portion, n_D^{20} 1.4721, melted at −28° to −26.5°, m.m.p. not depressed with 1,4-dimethylenecyclohexane. The aqueous layer on treatment with alkali gave 11.5 g (95%) of mercuric oxide.

Can. J. Chem. Downloaded from www.nrcresearchpress.com by 210.87.254.6 on 09/05/12
For personal use only.

Polymerization of 1,4-Dimethylenecyclohexane

(a) By Ultraviolet (Broad Peak at 360 mμ)

When the pure substance in a soft glass tube at +35° was irradiated for 14 days a yellow coating developed on the wall. The remaining liquid, distilled, contained 47% of unchanged dimethylenecyclohexane and also 16% (calc. as monomer) non-volatile syrup insoluble in methanol, benzene, and carbon tetrachloride with infrared spectrum (KBr pellet) in cm^{-1}: 3075 (vw), 2950 (s), 2850 (m), 1720 (s), 1658 (m), 1435 (s), 1165 (s), 887 (m). The solid material on the wall (12%) is a hard thermoplastic insoluble in carbon tetrachloride, methanol, benzene, and hexane with infrared spectrum in cm^{-1}: 2950 (s), 1720 (s), 1640 (s), 1440 (s), 1165 (s), 887 (s).

(b) By Benzoyl Peroxide

A 20% solution of dimethylenecyclohexane in dry benzene was refluxed for 3 days while 0.5 wt% portions of benzoyl peroxide were added at 10-hour intervals. The entire volatile portion was vacuum evaporated to a syrup which was washed with alkali and with water and dried at 100° (10 mm). The remainder (9%) is thermoplastic and soluble in carbon tetrachloride. The infrared spectrum, KBr pellet, in cm^{-1}, is 2950 (s), 1630 (m), 1443 (m), 1265 (s), 887 (w), 785 (m), 710 (m).

(c) By Aluminum Chloride

A violent reaction occurred when 1 g of the exo diene was treated with 0.5 g of freshly ground aluminum chloride. The carbon tetrachloride extract when washed with water and precipitated by 10-fold dilution with methanol gave 0.3 g of a brown thermoplastic solid, infrared absorption in KBr (cm^{-1}): 2950 (s), 2325 (w), 1620 (s), 1450 (s), 1370 (m), 785 (s), 740 (m). After the aluminum chloride was washed from the carbon tetrachloride insoluble residue there remained 0.2 g of a brown thermoplastic solid. By contrast no reaction of the exo diene occurred when it was treated with a solution of aluminum chloride in carbon tetrachloride.

Aromatization of 1,4-Dimethylenecyclohexane

When a 4.3 g of the exo diene was carried by nitrogen (25 cc/min) through a 15 mm dia. Vycor chip bed 5 cm long at 700–750° C the recovered material (70 wt%) was a mixture of benzene, toluene, and xylene in ratio 1:2:1 according to retention times on a carbowax–celite column at 140°. The collected fractions were identified by their ultraviolet and infrared spectra.

Isomerization of 1,4-Dimethylenecyclohexane

A solution of 7.7 g (0.07 mole) of the exo diene in 100 ml of peroxide-free dioxane plus 0.6 ml of 66 wt% aqueous sulphuric acid was refluxed for 3 hours and let stand for 8 hours more. The ethyl ether extract of the water-diluted system, washed acid free and dried by means of magnesium sulphate, was found to distill as follows: 1 g, 126–133° C; 2 g, 133–135° C (n_D^{20} 1.4745); 0.7 g, 135–136° C (n_D^{20} 1.4730); 2 g, 136–140° C; 0.2 g, 140–141° C; residue 0.7 g. All fractions showed olefinic unsaturation.

A solution of 0.54 g (0.005 mole as 1,4-dimethyl-1,3-cyclohexanediene) of the fraction b.p. 135–136° in 15 ml of absolute ethanol was treated with 6% ozonized oxygen at −40° to saturation and then at −10°, again to saturation. Then the system was treated with aqueous sodium borohydride until oxidizing agents were absent. The solution was acidified with dilute sulphuric acid, then treated with an acid solution of 2,4-dinitrophenylhydrazine. After 2 hours the precipitate was filtered off, 0.45 g after washing with ethanol, m.p. 235–245°, and was crystallized from *p*-xylene, 0.3 g (13%), m.p. 254–256°. A mixture melting point with the derivative of acetonylacetone (m.p. 257°) was not depressed, thus indicating the presence originally of 1,4-dimethyl-1,3-cyclohexadiene.

cis-1,4-Bis-isopropylolcyclohexane

To a magnesium-free methyl chloride Grignard reagent prepared from 2.1 g-atom of the metal in 1200 ml of diethyl ether (yield 69% by titration) was added 60 g (0.3 mole) of dimethyl 1,4-cyclohexanedicarboxylate (largely cis isomer, m.p. 0°) in 60 ml of diethyl ether at a rate sufficient to maintain reflux with the vessel being ice-cooled (1 hour). After 20 minutes of subsequent reflux the cooled system was poured into cold, stirred, saturated aqueous ammonium chloride. After 10 hours the system was filtered to remove scum and both the residue and the aqueous phase of the filtrate were extracted with diethyl ether. All of the ethereal portions, dried with magnesium sulphate, were evaporated, leaving a magma from which was filtered 32 g (49%) of the glycol, m.p. 110–112°. Crystallization from benzene – carbon tetrachloride (1:2 by volume) raised the melting point to 115.5–116.5°. Anal. Calc. for $C_{12}H_{24}O_2$: C, 72.0; H, 12.1. Found: C, 72.1; H, 12.1. The infrared spectrum (KBr pellet) in cm^{-1} is 3320 (s), 2975 (s), 2950 (s), 2860 (m), 1450 (m), 1445 (m), 1365 (s), 1355 (s), 1295 (w), 1230 (m), 1220 (m), 1155 (s), 1125 (s), 1105 (w), 945 (w), 935 (w), 912 (w), 898 (w), 872 (w), 830 (w), 808 (w), 780 (w); in chloroform solution 3550 (m), 3425 (m), 2940 (s), 2850 (s), 1460 (m), 1440 (m), 1380 (s), 1360 (s), 1320 (m), 1155 (s), 1125 (s), 940 (m), 905 (s), 870 (w), 840 (w).

trans-1,4-Bis-isopropylolcyclohexane

The cis glycol (4 g, 0.02 mole) was heated for 40 minutes with 8 g of anhydrous copper(II) sulphate at 130°. The system was then extracted with cold carbon tetrachloride to remove dehydration products, and subsequently with the same solvent hot. When the hot extract was cooled 0.8 g (20%) of trans isomer, m.p. 157–158°, crystallized out. Anal. Calc. for $C_{12}H_{24}O_2$: C, 72.0; H, 12.1. Found: C, 72.0; H, 12.1. The infrared spectrum (KBr pellet) showed absorption peaks at 2975 (s), 2950 (s), 2860 (m), 1445 (m), 1370 (s), 1360 (s),

Can. J. Chem. Downloaded from www.nrcresearchpress.com by 210.87.254.6 on 09/05/12
For personal use only.

1305 (w), 1240 (m), 1225 (m), 1160 (m), 1130 (s), 1120 (s), 945 (s), 915 (s), 872 (m), 783 (w); in chloroform solution 3550 (w), 3400 (w), 2900 (s), 2850 (s), 1460 (m), 1440 (m), 1370 (s), 1360 (s), 1320 (w), 1285 (w), 1135 (s), 938 (w), 908 (s), 868 (w).

1,4-Bis-isopropylidenecyclohexane

The substance may be dehydrated over alumina at 300° but better yields were obtained using formic acid. A solution of 10 g of the cis diol (0.05 mole) in 5 ml of formic acid was heated at 90–100° until a second phase separated after 5 minutes. The non-aqueous layer in diethyl ether was water-washed until it was neutral. Vacuum evaporation of the ether left 7.3 g (90% calc. as diene) which was dissolved in 5 ml acetone. Needles separated at −80° C, 2.1 g (26%), m.p. 70–71° C, which upon crystallization from acetone, methanol and subsequent sublimation melted at 78.5–79.5° C. Anal. Calc. for $C_{12}H_{20}$: C, 87.7; H, 12.3. Found: C, 87.6; H, 12.4. This 1,4-bis-isopropylidenecyclohexane forms a tetrabromide, m.p. 205–206°, after crystallization from commercial hexane. Anal. Calc. for $C_{12}H_{20}Br_4$: C, 29.8; H, 4.17. Found: C, 29.2; H, 3.76. The 1,4-diene is transparent in the ultraviolet down to 210 mμ but absorbs strongly at shorter wavelengths. The infrared spectrum (KBr pellet) in cm^{-1} is 2930, 2850 (s), 28 (s), 1615 (w), 1430 (s), 1370 (shld., m), 1360 (s), 1195 (s), 1115 (w), 1095 (w), 970 (w), 720 (w).

The mother liquors from crystallization of the diene contained 5.6 g, b.p. 83–115° (10 mm). This oil absorbs at 281, 250, and 243 mμ and it slowly polymerizes.

1,4-Bis-diphenylmethylidenecyclohexane

To a magnesium-free Grignard reagent prepared from 1 mole of bromobenzene in 385 ml of diethyl ether was added a solution of 30 g (0.015 mole) of dimethyl 1,4-cyclohexanedicarboxylate (chiefly cis) in 60 ml of ether during 1 hour. After 20 minutes of subsequent reflux the system was poured into 300 ml of glacial acetic acid. After the addition of 2 ml of hydrochloric acid the solution was boiled for 5 minutes, cooled, and filtered, 23.4 g (91%). This diene was crystallized from dioxane (150 ml/g), m.p. 257–259°. It is also soluble in hot benzene, toluene, and carbon tetrachloride but is almost insoluble in methanol or ethanol. A dioxane solution absorbs in the ultraviolet at 246 mμ (E_{max} 27,000) comparable with the absorption by benzophenone at 250 mμ. The infrared spectrum (cm^{-1}, KBr pellet) is 3040 (m), 2950 (m), 2855 (m), 2825 (m), 1620 (w), 1590 (m), 1475 (s), 1460 (w), 1430 (s), 1210 (m), 1070 (m), 1030 (w), 995 (w), 980 (m), 915 (w), 880 (w), 765 (s), 755 (s), 730 (s), 697 (vs), 673 (w).

The substance shows strong green fluorescence in ultraviolet light but becomes permanently yellow after this irradiation. In carbon tetrachloride solution aerated with oxygen under ultraviolet irradiation the yellow color appears within 2 hours. The melting point of the recovered solid has decreased to 248–254°. In absence of light, ozonization in carbon tetrachloride does not produce a color change; the ozonide yields benzophenone (42%).

Electrical Measurements

The dielectric constants of the crystalline substances were determined by the method previously described (8, 9). The results of Table I have been calculated from the extrapolations shown in Fig. 1. All wafers were prepared from the pure compounds except in the case of bis-diphenylmethylidenecyclohexane, where it was necessary to use 2% of polyethylene wax in order to effect consolidation. The dielectric constant was corrected for this dilution. The specific volumes and dielectric constants of solutions, from which the total polarizations and moments of the dithiane oxides of Table II are calculated, are shown in Fig. 3.

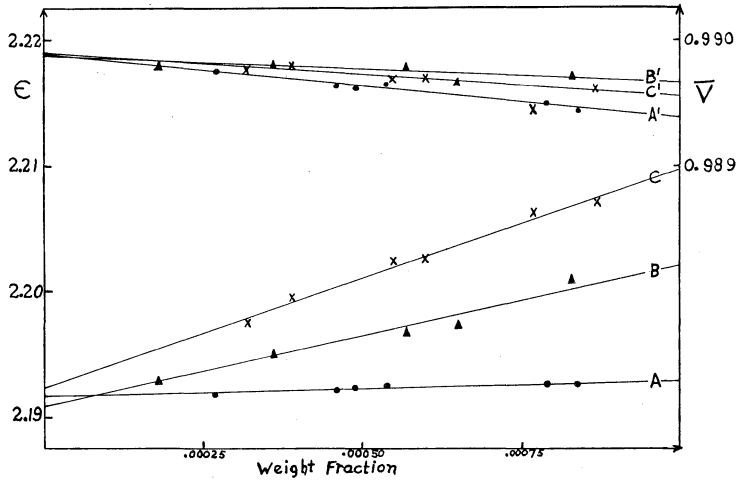

FIG. 3. Extrapolations of dielectric constant (ϵ) and specific volume ($\bar{V}$). A, A′: *trans*-1,4-Dithiane-1,4-dioxide; B, B′: dithiane monoxide; C, C′: *cis*-1,4-dithiane-1,4-dioxide.

Can. J. Chem. Downloaded from www.nrcresearchpress.com by 210.87.254.6 on 09/05/12
For personal use only.

ACKNOWLEDGMENTS

The authors are grateful to the National Research Council for financial aid and to the Tennessee Eastman Company for ample supplies of materials.

REFERENCES

1. W. KWESTROO, F. A. MEIJER, and E. HAVINGA. Rec. Trav. Chim. **73**, 717 (1954).
2. P. HAZEBROEK and L. J. OOSTERHOFF. Discussions Faraday Soc. **10**, 87 (1951).
3. W. D. KUMLER and A. C. HUITRIC. J. Am. Chem. Soc. **78**, 3369 (1956).
4. C. G. LEFÈVRE and R. J. W. LEFÈVRE. J. Chem. Soc. 1696 (1935); 3549 (1956).
5. G. WITTIG and H. POOK. Ber. Sect. B, **70**, 2485 (1937).
6. W. J. BAILEY and H. R. GOLDEN. J. Am. Chem. Soc. **75**, 4780 (1953).
7. D. R. LONG and R. W. NEUZIL. Anal. Chem. **27**, 1110 (1955).
8. M. V. GEORGE and G. F WRIGHT. Can. J. Chem. **36**, 189 (1958).
9. H. SAWATZKY and G. F WRIGHT. Can. J. Chem. **36**, 1555 (1958).
10. C. C. MEREDITH and G. F WRIGHT. Can. J. Chem. **38**, 1177 (1960).
11. M. V. GEORGE and G. F WRIGHT. J. Am. Chem. Soc. **80**, 1200 (1958).
12. J. R. PARTINGTON. Advanced treatise on physical chemistry. Vol. 5. Longmans, Green & Co. 1954. p. 538.
13. R. E. MARCH. Acta Cryst. **8**, 420 (1955).
14. H. M. M. SHEARER. J. Chem. Soc. 1394 (1959).
15. C. P. SMYTH. Dielectric behavior and structure. McGraw-Hill. 1955.

Can. J. Chem. Downloaded from www.nrcresearchpress.com by 210.87.254.6 on 09/05/12
For personal use only.

KINETICS AND MECHANISMS OF THE PYROLYSIS OF DIMETHYL ETHER

I. THE UNINHIBITED REACTION

D. J. McKenney and K. J. Laidler
Department of Chemistry, University of Ottawa, Ottawa, Canada

Received February 26, 1963

ABSTRACT

An experimental study has been made of the thermal decomposition of dimethyl ether, the temperature range being 500 to 550° C and the pressure range 100 to 700 mm Hg. A considerable surface effect was noted, and the results were not very reproducible. The reaction was of the three-halves order and the rate constant could be expressed as $2.98\times10^{14}e^{-54,900/RT}$ $cc^{1/2}$ $mole^{-1/2}$ sec^{-1}. On the basis of the results obtained in the presence of hydrogen sulphide (D. J. McKenney and K. J. Laidler. Can. J. Chem. **41**, 2009 (1963)) it is concluded that the initiating step, the dissociation of CH_3OCH_3 into CH_3O and CH_3, is in its second-order region. In order for the overall order to be three-halves the main terminating step must be either of the type $\beta\beta M$ or $\beta\mu$. The concentrations of the various radicals, and the rates of the various chain-ending steps, are calculated from known or estimated kinetic parameters for the elementary processes. It is concluded that the predominant chain-ending step is probably $CH_3 + CH_3 + M \rightarrow C_2H_6 + N$, but that there may be a significant contribution from $CH_3 + CHO + M \rightarrow CH_3CHO + M$ and from $CH_3 + CH_2OCH_3 + M \rightarrow C_2H_5OCH_3 + M$.

INTRODUCTION

During recent years determinations have been made of the kinetic parameters for a large number of the elementary processes that occur in organic pyrolyses. As a result there has been a revival of interest in the problem of establishing the overall mechanisms for such reactions, and in confirming them quantitatively. Recent work of this kind in these laboratories has been concerned with the thermal decompositions of propylene (1), ethane (2), propane (3), and butane (4). In all cases it has been found that the reactions occur predominantly by free-radical mechanisms, the molecular mechanisms being of minor importance. In the cases of ethane and propane it was concluded that under the experimental conditions the initiating unimolecular dissociation of the reactant molecule was in its low-pressure second-order region; with the larger butane molecule, on the other hand, the initial reaction is first order. It is of considerable interest to come to a conclusion about this matter for other decomposing substances, and the present investigation is concerned with the pyrolysis of dimethyl ether. For this substance the evidence as to the order of the initiating step comes from an investigation of the reaction in the presence of hydrogen sulphide, and is discussed in Part III of this series. The present paper describes an experimental study of the uninhibited dimethyl ether decomposition, and considers in some detail the nature of the chain-ending steps.

A number of previous investigations have been made of the dimethyl ether pyrolysis, and the results may be referred to briefly. The reaction was first studied by Askey and Hinshelwood (5), who concluded it to be first order with respect to the ether. The formation of products could be represented by the equation

$$CH_3OCH_3 \rightarrow CH_4 + CH_2O \rightarrow CH_4 + CO + H_2.$$

The formaldehyde builds up in the system and its concentration goes through a maximum when the reaction is about half complete. Later workers (6–11) found a great deal of evidence indicating that the decomposition was a chain reaction and could be described by a mechanism of the Rice–Herzfeld (12) type.

Can. J. Chem. Downloaded from www.nrcresearchpress.com by 210.87.254.6 on 09/05/12
For personal use only.

Benson (13) analyzed existing data and found that the reaction was three-halves order with respect to ether. Benson and Jain (14) confirmed the three-halves order relative to ether and obtained a rate constant of $k = 1.3\times10^{15}\ e^{-55,600/RT}$ cc$^{1/2}$ mole$^{-1/2}$ sec^{-1}. They found very little effect of added inert gas. The decomposition mechanism postulated by these authors involved first-order initiation, and termination involving two β radicals. They assumed that the CH_3OCH_2 radical is an important chain breaker and that the reaction

$$CH_3OCH_2 \rightarrow CH_2O + CH_3$$

is in its second-order region. Anderson and Benson (15) confirmed the presence of $CH_3OC_2H_5$ and $CH_3OCH_2CH_2OCH_3$ in the products of the pyrolysis. Their results also indicate that the reaction

$$CH_3 + CH_3OCH_2 \rightarrow CH_3OCH_2CH_3$$

is an important termination step.

Imai and Toyama (16) recently decomposed dimethyl ether in the temperature range of 360 to 440° C, and found that the rate constant could be represented as

$$k = 1.45\times10^{15}e^{-54,500/RT}\ \text{cc}^{1/2}\ \text{mole}^{-1/2}\ \text{sec}^{-1}.$$

This is in good agreement with that obtained by Benson and Jain (14).

EXPERIMENTAL

The apparatus and experimental procedure were essentially as described previously (1). Reactions were carried out in a quartz cylindrical tube of about 250-cc volume with a "dead space" of approximately 4 cc. The temperature was controlled to about 0.2° C by means of a Thermo Electric controller which was activated by means of a thermocouple in the copper furnace block. Another thermocouple in the reaction vessel was used to measure the temperature on a Thermo Electric Mini-Mite potentiometer.

Prior to a run the reaction vessel was pumped down to approximately 10 μ; this small residual pressure had no detectable effect on the rates. The pressure change as a function of time was recorded automatically by a Beckman photopen recorder in conjunction with a quartz spiral gauge, as described by Laidler and Wojciechowski (1). A pressure change of 18.6 mm Hg in the reaction vessel resulted in a deflection of 1 inch on the recorder. Pressures measured by means of the spiral gauge arrangement could be measured to $\pm$0.6 mm Hg.

RESULTS

The decomposition of dimethyl ether was studied in the temperature range of 500 to 550° C, and over a pressure range of approximately 100 to 700 mm Hg. A typical pressure–time curve for the reaction is shown as curve A of Fig. 1. Rates were calculated from the slopes of the pressure–time curves at the inflection point. The reaction was found to be three-halves order with respect to dimethyl ether over the complete range of pressure and temperature. It proved very difficult to obtain reproducible results, since the uninhibited reaction appeared to be influenced to a great extent by the condition of the surface of the reaction vessel. Greater reproducibility could be obtained after the surface had been exposed to nitric oxide either alone or mixed with ether. Enough reproducible data were accumulated by first treating the surface in this way, in order to verify the results of previous workers (14, 16). An Arrhenius plot of the data is shown in Fig. 2. Most of the points shown are the average of many and the approximate deviations are indicated (for the point at 500° C ($1/T\times10^3 = 1.294$) only a single value was obtained). The activation energy was 54.9 kcal mole^{-1}.

Because inflection-point rates were used rather than initial rates (rates at the inflection point were more reproducible), it was necessary to correlate the pressure change with the

Can. J. Chem. Downloaded from www.nrcresearchpress.com by 210.87.254.6 on 09/05/12
For personal use only.

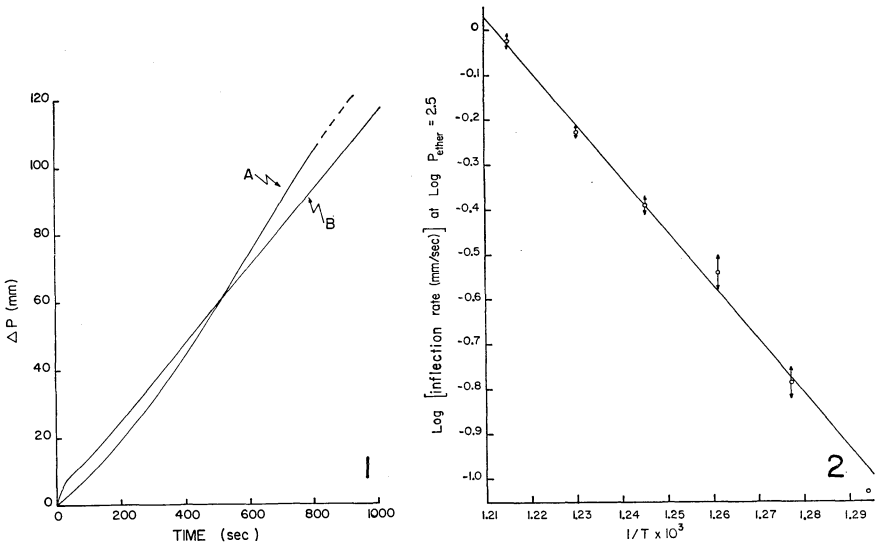

FIG. 1. Curve A: A typical pressure–time curve for the pyrolysis of dimethyl ether; this is a tracing of an actual record obtained at 520° C and at an initial pressure of 197 mm. Curve B: A pressure–time curve showing the effect of 0.4 mm of oxygen on the pyrolysis of dimethyl ether. All other conditions are the same as those for curve A.

FIG. 2. Arrhenius plot for the pyrolysis of dimethyl ether.

rate of disappearance of ether at decompositions of 20 to 30%. The data of Benson and Jain (14) were utilized for this purpose. Figure 1 of their paper is a plot of $\Delta CH_2O/\Delta CH_3OCH_3$ as a function of percentage decomposition. The overall reaction is represented by

$$\underset{(1-x)}{CH_3OCH_3} \rightarrow \underset{(x-y)}{CH_2O} + \underset{(x)}{CH_4} + \underset{(y)}{H_2} + \underset{(y)}{CO}$$

Benson and Jain have plotted $1-y/x$ against x. The change in pressure Δp, i.e. $x+y$, can thus be calculated from their data, and this can now be plotted against x. One can therefore obtain a plot of $\Delta p/p$ versus $\Delta E/p$, where ΔE is the change in partial pressure of ether. The experimental Δp can be calculated from the pressure–time curves obtained in the present work, and the corresponding value of ΔE can be estimated graphically. In all cases $\Delta E/\Delta p = 0.70 \pm 0.02$. The three-halves-order rate constant was therefore multiplied by 0.70, yielding

$$k = 2.98 \times 10^{14} e^{-54900/RT} \text{ cc}^{1/2} \text{ mole}^{-1/2} \text{ sec}^{-1}.$$

The activation energy is in good agreement with the values obtained by previous workers, and quoted above. The frequency factor and rates are, however, significantly lower than those obtained previously. This may be because our technique has minimized the surface-catalyzed reaction.

The shape of the pressure–time curve was found to be altered considerably by the addition of a small quantity (~0.2%) of oxygen. The initial rate of decomposition appeared to be greatly enhanced by the presence of oxygen, which in turn seems to be used up rapidly as suggested by the shape of the pressure–time curve shown in Fig. 1,

Can. J. Chem. Downloaded from www.nrcresearchpress.com by 210.87.254.6 on 09/05/12
For personal use only.

curve B. These effects differ somewhat from those reported by Benson and Jain (14), who state that the reaction is relatively insensitive to surface effects and to small amounts of added oxygen. Professor Benson has, however, informed us that he and Jain did observe an initial effect of oxygen, which was rapidly consumed; there therefore seems to be agreement on this point.

The uninhibited decomposition of dimethyl ether exhibits a well-defined induction period, which is particularly evident at lower pressures. Figure 3 shows that this induction

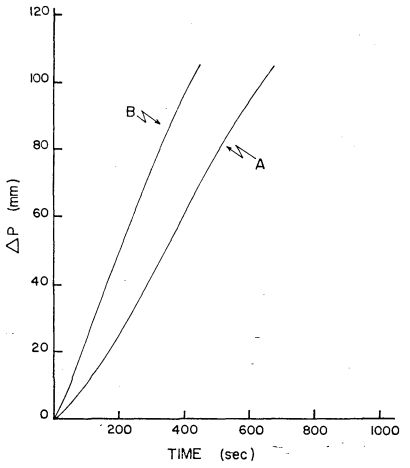

FIG. 3. Pressure–time curves for the ether decomposition at 540° C and an initial pressure of 122 mm. Curve A is for the reaction in the absence of formaldehyde; curve B for the reaction in the presence of 24 mm of formaldehyde.

period can be considerably shortened, and probably eliminated completely, by the addition of suitable amounts of formaldehyde. The formaldehyde also considerably increases the rate of the decomposition. An increase in rate on the addition of formaldehyde was also reported by Benson and Jain (14).

DISCUSSION

It is convenient to base a discussion of the mechanism of the dimethyl ether pyrolysis on that proposed by Benson and Jain (14):*

$$CH_3OCH_3 \rightarrow CH_3 + CH_3O \quad [1]$$

$$CH_3 + CH_3OCH_3 \rightarrow CH_4 + CH_2OCH_3 \quad [2]$$

$$M + CH_2OCH_3 \rightarrow CH_2O + CH_3 + M \quad [3a]$$

$$CH_3O \rightarrow CH_2O + H \quad [4]$$

$$H + CH_3OCH_3 \rightarrow H_2 + CH_2OCH_3 \quad [5]$$

$$CH_3 + CH_2OCH_3 \rightarrow CH_3CH_2OCH_3. \quad [6]$$

The main features of this scheme are that the initiation reaction [1] is first order, that the decomposition of the radical (reaction [3a]) is in its second-order region, and that the main termination process involves CH_3 and CH_3OCH_2. If reaction [3a] is second order the radical CH_3OCH_2 is a β radical, as is CH_3. The termination is thus of the $\beta\beta$ type,

*The letter a in an equation number (e.g. [3a]) is used to emphasize the fact that the reaction is in its low-pressure region.

Can. J. Chem. Downloaded from www.nrcresearchpress.com by 210.87.254.6 on 09/05/12
For personal use only.

and this together with first-order initiation gives rise to three-halves-order kinetics. Following the terminology of Laidler, Sagert, and Wojciechowski (3) this mechanism may be denoted by $^1\beta\beta_{3/2}$, the initial superscript indicating the order of the initiation process, and the subscript 3/2 denoting the overall order.

It may be noted that three-halves-order overall kinetics are also obtained if the orders of reactions [1] and [3a] are reversed; i.e. if the reactions are

$$M + CH_3OCH_3 \rightarrow CH_3 + CH_2O + M \qquad [1a]$$

$$CH_2OCH_3 \rightarrow CH_2O + CH_3. \qquad [3]$$

Initiation is now second order and CH_2OCH_3 is a μ radical; this again gives rise to three-halves-order kinetics ($^2\beta\mu_{3/2}$).

Benson and Jain's main reason for preferring the $^1\beta\beta_{3/2}$ scheme is that the apparent first-order frequency factor for reaction [3], as calculated by Trotman-Dickenson (17) from the results of Marcus, Darwent, and Steacie (18), is $\sim 10^{10}$ sec^{-1}; this is much too low to be a true frequency factor for a unimolecular dissociation involving no change of multiplicity. An apparent way out of the difficulty is to suggest that the reaction is really in its second-order region. It might also be urged in favor of the Benson–Jain scheme that if the dissociation of CH_3OCH_3 were second order that of CH_2OCH_3 would be second order *a fortiori*, in view of its lower activation energy and smaller number of degrees of freedom.

Further consideration, however, reveals that these arguments are not as convincing as they appear at first sight. Thus the analytical methods on which the experimental results of Marcus *et al.* are based are not very reliable, and involved measuring amounts of CH_2O, CO, and 'dimer' ($CH_3OCH_2CH_2OCH_3$) produced from the radical CH_2OCH_3. It seems very possible that some of what was reported as 'dimer' was actually polymerized formaldehyde, since formaldehyde is known to polymerize readily under similar analytical conditions (19). This would have a very serious effect on the experimental results, and the frequency factor and activation energy for reaction [3] therefore cannot be relied upon.

Secondly, there is a precedent for suggesting that reaction [3] is second order and reaction [1] first order, since a similar situation exists in the ethane pyrolysis; the evidence (2) there seems conclusive that the dissociation of C_2H_6 is first order and that of C_2H_5 second order. Two explanations may tentatively be put forward to explain this apparently paradoxical result:

(1) The number of effective degrees of freedom may be larger in the radical (C_2H_5 or CH_2OCH_3) than in the corresponding molecule (C_2H_6 or CH_3OCH_3) because of less symmetry (cf. Laidler and Wojciechowski (20)).

(2) When a radical decomposes in the presence of a very large excess of its parent molecule there may exist an abnormally effective mechanism for energy transfer, involving atom abstraction. Some support for this interpretation is provided by the conclusion of Purnell and Quinn (21) that the ethyl radical decomposition is not in its first-order region when it is in the presence of butane and in the absence of the parent molecule ethane.

On the basis of these arguments there remains no valid objection to concluding that the reaction is of the type $^2\beta\mu_{3/2}$. Very strong evidence that the initiating reaction is in fact in its second-order region has been obtained from a study of the reaction in the presence of hydrogen sulphide, and is described in detail in Part III. This evidence excludes the Benson–Jain $^1\beta\beta_{3/2}$ mechanism. It is consistent with a mechanism in which the chain-ending step involves the recombination of two β radicals, in the low-pressure region ($^2\beta\beta M_{3/2}$), and also with a $^2\beta\mu_{3/2}$ mechanism. These are the only two possibilities if

Can. J. Chem. Downloaded from www.nrcresearchpress.com by 210.87.254.6 on 09/05/12
For personal use only.

initiation is second order. One can at once eliminate the second of these two possibilities by the fact that the reaction shows only a very slight effect of inert gases (14); the ${}^2\beta\mu_{3/2}$ mechanism would predict a substantial positive inert gas effect, since inert gases will increase the rate of initiation but will have no effect on the rate of termination. With a ${}^2\beta\beta M_{3/2}$ mechanism, on the other hand, no strong inert gas effect is to be expected, since both initiation and termination will be affected by the addition of inert gas, and the two effects will approximately cancel.

Chain-ending Steps

Initially, before any formaldehyde has decomposed, the radicals present in the system are CH_3, CH_3O, CH_2OCH_3, and H; only CH_3 and CH_2OCH_3 are involved in chain-propagating steps, and their concentrations are very much greater than those of the other two radicals. The CH_3 radical is certainly a β radical, and CH_2OCH_3 may be either β or μ and may indeed play both roles. The following chain-ending steps are therefore possible:

$$CH_3 + CH_3 + M \rightarrow C_2H_6 + M \quad [7]$$

$$CH_3 + CH_2OCH_3 + M \rightarrow CH_3CH_2OCH_3 + M \quad [8]$$

$$2CH_2OCH_3 + M \rightarrow CH_3OCH_2CH_2OCH_3 + M. \quad [9]$$

A decision between these possibilities can be made by carrying out calculations of the concentrations of the radicals, and finding out which chain-ending steps will occur with greatest velocity. Such calculations lead to the conclusion that reaction [7] occurs somewhat more rapidly than either of the other processes ([8] and [9]). The overall reaction mechanism is therefore concluded to be, for the most part,

$$M + CH_3OCH_3 \rightarrow CH_3 + CH_3O + M \quad [1a]$$

$$CH_3 + CH_3OCH_3 \rightarrow CH_4 + CH_2OCH_3 \quad [2]$$

$$CH_2OCH_3 \rightarrow CH_2O + CH_3 \quad [3]$$

$$M + CH_3O \rightarrow CH_2O + H + M \quad [4]$$

$$H + CH_3OCH_3 \rightarrow H_2 + CH_2OCH_3 \quad [5]$$

$$CH_3 + CH_3 + M \rightarrow C_2H_6 + M. \quad [7]$$

It should be noted that reaction [4] is almost certainly in its second-order region, but this has no effect on the overall behavior. As discussed earlier, it is not certain whether reaction [3] is first order or second order, and this again makes no difference as far as the overall order is concerned.

Application of the steady-state treatment to the above mechanism gives rise to the following approximate expressions for the radical concentrations:

$$[CH_3] = \left(\frac{2k_{1a}}{k_7}\right)^{1/2} [CH_3OCH_3]^{1/2} \quad [i]$$

$$[CH_2OCH_3] = \frac{k_2}{k_3}\left(\frac{2k_{1a}}{k_7}\right)^{1/2} [CH_3OCH_3]^{3/2}. \quad [ii]$$

The overall rate is given by

$$v = k_2\left(\frac{2k_{1a}}{k_7}\right)^{1/2} [CH_3OCH_3]^{3/2}. \quad [iii]$$

Values of frequency factors and activation energies for the various elementary processes are given in Table I, which refers to a temperature of 800° K. The use of these values in

Can. J. Chem. Downloaded from www.nrcresearchpress.com by 210.87.254.6 on 09/05/12
For personal use only.

TABLE I

Kinetic parameters

Reaction	Frequency factor (sec^{-1}, cc $mole^{-1}$ sec^{-1}, or cc^2 $mole^{-2}$ sec^{-1})	Activation energy (kcal $mole^{-1}$)	Rate constant at 800° K (sec^{-1}, cc $mole^{-1}$ sec^{-1}, or cc^2 $mole^{-2}$ sec^{-1})	Reference
[1a]	1×10^{18}	74.0	5.8×10^{-3}	Estimated (see Appendix)
[2]	3×10^{11}	9.5	7.8×10^{8}	Trotman-Dickenson and Steacie (22)
[3]	7×10^{10}	19.0	4.6×10^{5}	Marcus, Darwent, and Steacie (18); Trotman-Dickenson (17)
[7]	7×10^{14}	−13.5	3.5×10^{18}	Estimated (see Appendix)

the expressions for the radical concentrations leads to the conclusion that the concentrations at 800° K, and with [M] taken as 10^{-5} moles cc^{-1}, are as follows:

$$[CH_3] = 1.8\times10^{-13} \text{ moles } cc^{-1}; \quad [CH_2OCH_3] = 3.1\times10^{-15} \text{ moles } cc^{-1}.$$

The methyl radical is therefore predominant, and reaction [7] is therefore concluded to be the main chain-ending step. One cannot, however, exclude the possibility that reactions [8] and [9] also play a small role in the process. It may be noted that the value of 10^{-5} taken for [M] corresponds to the upper range of the pressures employed (~500 mm Hg); at lower pressures the methyl radicals are predominant *a fortiori*.

Except at the very beginning of the reaction there will be significant amounts of the formyl radical HCO, which arises from the decomposition of the formaldehyde produced as an intermediate. In a personal communication Professor S. W. Benson has suggested to us that for the main part of the reaction the principal chain-ending step is

$$CH_3 + HCO \rightarrow CH_4 + CO. \qquad [10]$$

According to Professor Benson this reaction will occur more rapidly than reaction [7] except at the very beginning of reaction. We are unable, however, to agree with this suggestion, for two main reasons. In the first place, our work with hydrogen sulphide (Part III) leads unequivocally to the conclusion that the initial dissociation of dimethyl ether is, under our experimental conditions, in its second-order region. This being so, reaction [10], being of the type $\beta\beta$, leads to second-order kinetics, in disagreement with experiment; only with a first-order initiation process does this lead to the correct three-halves-order kinetics. In the second place, our calculations of radical concentrations and rates lead us to the conclusion that reaction [7] actually occurs considerably more rapidly than reaction [10]. We calculate the third-order rate constant for reaction [7] to be, at 800° K, 3.5×10^{18} cc^2 $mole^{-2}$ sec^{-1} so that, with the concentration of M taken as 10^{-6}, the rate of reaction [7] can be expressed as

$$v_7 = 3.5\times10^{12}[CH_3]^2.$$

The concentration of CHO radicals is calculated to be somewhat less than that of CH_3, but for the purpose of the present estimate it will be assumed that the concentrations are the same. Since reaction [10] is a hydrogen atom abstraction reaction its frequency factor is expected to be about 10^{11} cc $mole^{-1}$ sec^{-1} and its activation energy will be at least 5 kcal $mole^{-1}$. On this basis we calculate that the rate of reaction [10] would be, at 800° K,

$$v = 4.3\times10^{9}[CH_3][CHO].$$

Can. J. Chem. Downloaded from www.nrcresearchpress.com by 210.87.254.6 on 09/05/12
For personal use only.

Even with equal CH_3 and CHO concentrations the rate of reaction [10] is therefore considerably less than that of reaction [7]. It is to be noted that the high rate of reaction [7] is due to the fact that the complex formed from two methyl radicals has a very long life, so that the third-body recombination process occurs almost as rapidly as the second-order reaction with no activation energy.

The calculations do not, however, exclude the possibility that the recombination reaction

$$CH_3 + CHO + M \rightarrow CH_3CHO + M \qquad [11]$$

plays a significant role in the reaction. Our conclusion is, in fact, that chain ending may occur by reactions [7], [8], [9], and [11], with [7] being most important.

The Overall Reaction

As a check on the proposed mechanism, with [7] as the chain-ending step, calculations may be made of the absolute rate, frequency factor, and activation energy of the reaction on the basis of the mechanism. Using the parameters given in Table I the calculated overall values are

$$k = 0.045 \text{ cc}^{1/2} \text{ mole}^{-1/2} \text{ sec}^{-1}$$
$$A = 1.6 \times 10^{13} \text{ cc}^2 \text{ mole}^{-2} \text{ sec}^{-1}$$
$$E = 53.3 \text{ kcal mole}^{-1}.$$

The calculated rate constant is less than the experimental value (0.27 $\text{cc}^{1/2}$ $\text{mole}^{-1/2}$ sec^{-1}), as is the frequency factor, but the activation energy is in good agreement with the experimental value of 54.9 kcal mole^{-1}. The error undoubtedly lies in the rather long extrapolations required to calculate the low-pressure rate constants for the initiation and termination steps.

Can. J. Chem. Downloaded from www.nrcresearchpress.com by 210.87.254.6 on 09/05/12
For personal use only.

ACKNOWLEDGMENTS

The authors are indebted to Professor S. W. Benson for valuable suggestions, and for informing them of the results of unpublished work on this reaction in his laboratories. They are grateful to the National Research Council and the Petroleum Research Fund for grants in support of their work.

APPENDIX

The basis for the values given in Table I for reactions [1a] and [7] is as follows. Gill and Laidler's analysis (23) of the data for the recombination of methyl radicals and for the reverse reaction,

$$2CH_3 + M \underset{k_{-7}}{\overset{k_7}{\rightleftharpoons}} C_2H_6 + M,$$

led to the following rate constants at 200° C:

$$k_7 = 3 \times 10^{20} \text{ cc}^2 \text{ mole}^{-2} \text{ sec}^{-1}$$
$$= 1.67 \times 10^{17} e^{8000/RT} \text{ cc}^2 \text{ mole}^{-2} \text{ sec}^{-1}$$
$$k_{-7} = 3 \times 10^{-16} \text{ cc mole}^{-1} \text{ sec}^{-1}$$
$$= 1.5 \times 10^{20} e^{-77{,}000/RT} \text{ cc mole}^{-1} \text{ sec}^{-1}.$$

On the assumption that the temperature dependence of these rate constants is given by

the Hinshelwood formula, with $s = 9$ and $E_0 = 85$ kcal mole^{-1} as used by Gill and Laidler (23), the corresponding values at 800° K are:

$$k_7 = 3.5\times10^{18} \text{ cc}^2 \text{ mole}^{-2} \text{ sec}^{-1}$$
$$= 7.0\times10^{14}e^{13,500/RT} \text{ cc}^2 \text{ mole}^{-2} \text{ sec}^{-1}$$
$$k_{-7} = 5\times10^{-2} \text{ cc mole}^{-1} \text{ sec}^{-1}$$
$$= 2.0\times10^{18}e^{-71,500/RT} \text{ cc mole}^{-1} \text{ sec}^{-1}.$$

The parameters for k_7 are those given in Table I.

For the dissociation of CH_3OCH_3 in its second-order region we have assumed the same frequency factor as for the dissociation of ethane, namely 2×10^{18} cc mole^{-1} sec^{-1}. The low-pressure activation energy (74.0 kcal) was obtained by subtracting $8.5RT$ from 87 kcal, which is supposed to be the high-pressure value (24). It is quite possible that the value of 81 kcal reported by Rice and Johnston (6) actually corresponds to the fallen-off region, in which case their activation energy is too low.

In view of the rather long extrapolations involved (from 200° C to 800° K) there may well be considerable error in the estimated values for reactions [1a] and [7]. The present estimates seem, however, to be the best that can be made with the data available.

The parameters given in Table I for reaction [3] are also doubtful, as was noted in the main text.

REFERENCES

1. K. J. Laidler and B. W. Wojciechowski. Proc. Roy. Soc. (London), Ser. A, **259**, 257 (1960).
2. K. J. Laidler and B. W. Wojciechowski. Proc. Roy. Soc. (London), Ser. A, **260**, 91 (1961).
3. K. J. Laidler, N. H. Sagert, and B. W. Wojciechowski. Proc. Roy. Soc. (London), Ser. A, **270**, 242 (1962).
4. N. H. Sagert and K. J. Laidler. Can. J. Chem. **41**, 838, 848 (1963).
5. P. J. Askey and C. N. Hinshelwood. Proc. Roy. Soc. (London), Ser. A, **115**, 215 (1927).
6. F. O. Rice and W. R. S. Johnston. J. Am. Chem. Soc. **56**, 214 (1934).
7. R. N. Pease. J. Am. Chem. Soc. **59**, 425 (1937).
8. L. A. K. Staveley and C. N. Hinshelwood. Nature, **137**, 29 (1936).
9. L. A. K. Staveley and C. N. Hinshelwood. Proc. Roy. Soc. (London), Ser. A, **154**, 335 (1936).
10. L. A. K. Staveley and C. N. Hinshelwood. Proc. Roy. Soc. (London), Ser. A, **159**, 192 (1937).
11. F. P. Lossing, K. U. Ingold, and A. W. Tickner. Disc. Faraday Soc. **14**, 34 (1953).
12. F. O. Rice and K. F. Herzfeld. J. Am. Chem. Soc. **56**, 284 (1934).
13. S. W. Benson. J. Chem. Phys. **25**, 27 (1956).
14. S. W. Benson and D. V. S. Jain. J. Chem. Phys. **31**, 1008 (1959).
15. K. H. Anderson and S. W. Benson. J. Chem. Phys. **36**, 2320 (1962).
16. N. Imai and O. Toyama. Bull. Chem. Soc. Japan, **34**, 328 (1961).
17. A. F. Trotman-Dickenson. J. Chem. Phys. **19**, 261 (1951).
18. R. A. Marcus, B. de B. Darwent, and E. W. R. Steacie. J. Chem. Phys. **16**, 987 (1948).
19. R. L. Strong and K. O. Kutschke. Can. J. Chem. **37**, 1456 (1959).
20. K. J. Laidler and B. W. Wojciechowski. Chem. Soc. (London), Spec. Publ. **16**, 37 (1962).
21. J. H. Purnell and C. P. Quinn. Proc. Roy. Soc. (London), Ser. A, **270**, 267 (1962).
22. A. F. Trotman-Dickenson and E. W. R. Steacie. J. Chem. Phys. **19**, 329 (1951).
23. E. K. Gill and K. J. Laidler. Proc. Roy. Soc. (London), Ser. A, **250**, 121 (1959).
24. E. C. Baughan, M. G. Evans, and M. Polanyi. Trans. Faraday Soc. **37**, 377 (1941).

Can. J. Chem. Downloaded from www.nrcresearchpress.com by 210.87.254.6 on 09/05/12
For personal use only.

KINETICS AND MECHANISMS OF THE PYROLYSIS OF DIMETHYL ETHER

II. THE REACTION INHIBITED BY NITRIC OXIDE AND PROPYLENE

D. J. McKenney, B. W. Wojciechowski, and K. J. Laidler
Department of Chemistry, University of Ottawa, Ottawa, Canada

Received October 22, 1962

ABSTRACT

The thermal decomposition of dimethyl ether, inhibited by nitric oxide and by propylene, was studied in the temperature range of 500 to 600° C. About 1.5 mm of nitric oxide gave maximal inhibition, the rate then being approximately 8% of the uninhibited rate. With propylene, approximately 70 mm gave maximal inhibition, the rate being slightly higher than that using nitric oxide (~12.5% of the uninhibited rate). In both cases the degree of inhibition was independent of the ether pressure. In the maximally inhibited regions both reactions are three-halves order with respect to ether pressure. As the pressure of nitric oxide was increased beyond 10–15 mm, the overall rate increased, and in this region the reaction is first order with respect to both nitric oxide and ether. A 50:50 mixture of CH_3OCH_3 and CD_3OCD_3, with enough NO to ensure maximum inhibition, was pyrolyzed. Even at very low percentage decomposition the CD_3H/CD_4 ratio was approximately the same as that in the uninhibited decomposition, proving that the inhibited reaction is largely a chain process. Detailed inhibition mechanisms are proposed in which the inhibitor is involved both in initiation and termination reactions.

Can. J. Chem. Downloaded from www.nrcresearchpress.com by 210.87.254.5 on 09/05/12
For personal use only.

INTRODUCTION

Previous publications from this laboratory (1–6) have provided evidence for the view that maximally inhibited reactions proceed not by molecular mechanisms but by processes in which the inhibitor is involved both in initiation and in termination. Detailed mechanisms have now been worked out for the decompositions of ethane (4), propane (5), butane (6), and other substances, and a specific scheme has been proposed for the dimethyl ether decomposition (1). The present paper is concerned with an experimental study of the effects of nitric oxide and propylene on the decomposition of dimethyl ether, and with the formulation of reaction mechanisms. The mechanism previously proposed (1) has been found to require some revision.

A considerable amount of previous experimental work has been done on the inhibited dimethyl ether decomposition. The reaction inhibited by nitric oxide was first studied by Staveley and Hinshelwood (7), who found that the rate is very considerably reduced by small amounts of nitric oxide, and that a limiting rate is reached with nitric oxide pressures between about 0.5 mm and 12 mm. They reported an activation energy of 62 kcal $mole^{-1}$ for the maximally inhibited reaction, which they considered to be a molecular reaction. Gay and Travers (8) found, from a study of the products of the inhibited decomposition, that introduction of an increased quantity of nitric oxide into the reaction led to an increased amount of carbon monoxide in the products.

Thompson and Meisner (9) studied the absorption spectra of the products of the retarded decomposition of dimethyl ether, and found that during the course of the reaction the NO lines disappeared and that NH_3 lines appeared; they suggested the formation of formaldoxime (CH_2=NOH). A frozen mixture of the products gave a positive test for the nitroso group.

Recently Imai and Toyama (10) have studied the effect of nitric oxide on the pyrolysis of dimethyl ether. They found that the rate was first decreased by small amounts of nitric oxide, but that it increased linearly as larger quantities of nitric oxide were added. In this

accelerated region the order was unity with respect to both nitric oxide and ether. These authors suggested that the inhibited decomposition is a molecular process, and that large quantities of nitric oxide catalyze the molecular decomposition.

EXPERIMENTAL

The apparatus and methods were essentially the same as described previously (3; see also Part I). All gases used were research grade and were used without further purification except for the usual trap-to-trap distillation. In order to ensure complete mixing of the ether and inhibitor, and hence to eliminate any errors due to variation in reactant composition, the experimental procedure was as follows. A measured quantity of purified dimethyl ether was condensed on a cold finger in a 1-liter spherical flask. Only one stopcock was attached to this mixing vessel, and the connecting tubing was kept to a minimum. A known quantity of the inhibitor was then admitted to the mixing vessel, which contained the frozen ether. After all of the inhibitor was condensed, the stopcock was closed and the cold finger allowed to warm to room temperature. The warm gases were allowed to mix for about 15 minutes before being admitted to the reaction vessel.

Rates were calculated from the slopes of the pressure–time curves at the initial point and at the inflection point. The data obtained were fully reproducible.

The isotopic mixing experiments were carried out using equal amounts of CH_3OCH_3 and CD_3OCD_3. For the inhibited decomposition sufficient nitric oxide was added to ensure maximum inhibition. The reaction temperature was 550°, and the extent of the reaction varied from approximately 1 to 20%. The CD_3H/CD_4 ratio was determined by means of a mass spectrometer using samples from liquid-nitrogen non-condensable fractions of the reacted mixture.

Some runs were carried out at 500° C using mixtures containing approximately 10% CD_4, 90% dimethyl ether, and 0–1% nitric oxide (enough for maximum inhibition).

RESULTS

Isotopic Mixing

Table I summarizes the results obtained using 1:1 mixtures of CD_3OCD_3 and CH_3OCH_3.

TABLE I

Isotopic mixing experiments

Expt. No.	CH_3OCH_3 pressure (mm)	NO pressure (mm)	CD_4 pressure (mm)	Total pressure increase (mm)	Approx. % decomp.	Ratio CD_3H/CD_4 in products
1	314	0	0	141	22.2	2.44
2	312	0	0	96	15.4	2.53
3	311	0	0	58	9.3	2.52
4	308	0	0	35	5.7	2.51
5	305	0	0	18	3	2.44
6	299	5.5	0	115	19.2	2.41
7	294	5.4	0	39	6.6	2.48
8	296	5.4	0	23	4.2	2.47
9	297	5.5	0	13	2.2	2.46
10	297	5.5	0	10	1.7	2.44
11	297	5.5	0	4	0.7	2.39
12	436	0	43	105	12.1	0.03
13	427	4.5	46	18	2.1	0.0
14	428	4.5	51	6	0.7	0.03
15	422	4.7	50	3	0.4	0.03

NOTE: For experiments No. 1 to 11 inclusive the reaction temperature was 550° C, and for the remaining experiments the temperature was 500° C.

The average CD_3H/CD_4 ratio was 2.49±0.04 for the uninhibited runs and 2.44±0.03 for the inhibited runs. The extent of decomposition was determined from pressure measurements, and the methane ratios determined mass spectrometrically. The results from mixtures of ~10% CD_4 and ~90% CH_3OCH_3 in the absence of NO, and in the presence of ~1% NO (sufficient for maximal inhibition), are also shown in Table I.

Can. J. Chem. Downloaded from www.nrcresearchpress.com by 210.87.254.5 on 09/05/12
For personal use only.

The Overall Kinetics of the Reaction Inhibited by Nitric Oxide

Preliminary experiments were carried out to determine the quantity of nitric oxide required to reduce the rate of decomposition of dimethyl ether to a minimum. The results are summarized in Fig. 1. The curve shows that the relative rate drops sharply to a minimum with the addition of about 1.5 mm of nitric oxide. Further addition of nitric oxide

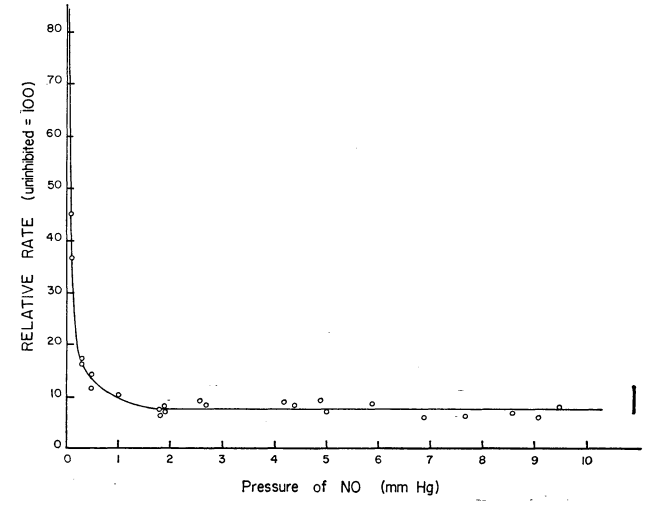

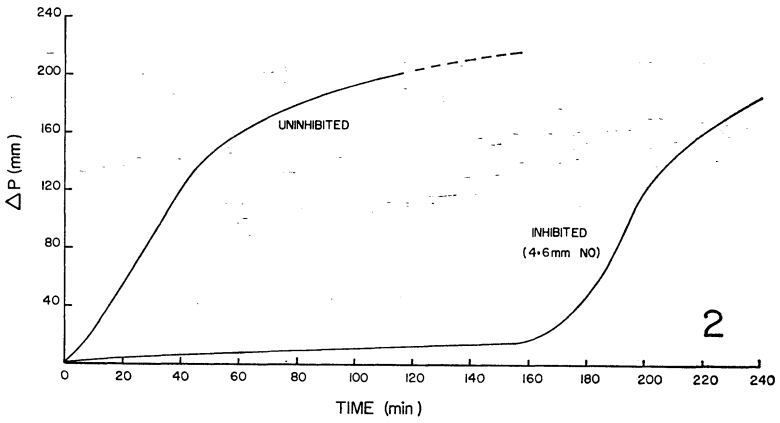

FIG. 1. Relative rate (uninhibited rate = 100) against nitric oxide pressure, at 520° C.
FIG. 2. Typical pressure–time curves for the uninhibited reaction and for the reaction maximally inhibited by nitric oxide, at 520° C. The initial ether pressure was 126 mm in each case.

has no effect on the rate until an amount greater than 10 mm has been added, and the rate then increases linearly with increasing nitric oxide pressure. Figure 1 also shows that no matter what pressure of ether was used the same minimum rate is obtained relative to the rate of the uninhibited reaction; ether pressures varying from 130 mm to 479 mm were used to obtain the points lying along the flat portion of the curve. Nitric oxide pressures between 2 mm and 10 mm were used in subsequent investigations of the maximally inhibited reaction.

Can. J. Chem. Downloaded from www.nrcresearchpress.com by 210.87.254.5 on 09/05/12
For personal use only.

Figure 2 shows a typical pressure–time curve for the maximally inhibited decomposition and a similar curve for the uninhibited reaction. The ether pressure was the same (126 mm) in both cases. The curve for the inhibited reaction initially is completely different in shape from that of the uninhibited reaction. However, after a certain "inhibition time" the rate of the inhibited reaction increases and approaches that of the uninhibited reaction. This is apparently due to the fact that the nitric oxide has been used up.

Figure 3 shows plots of the logarithm of the initial rate versus the logarithm of the ether

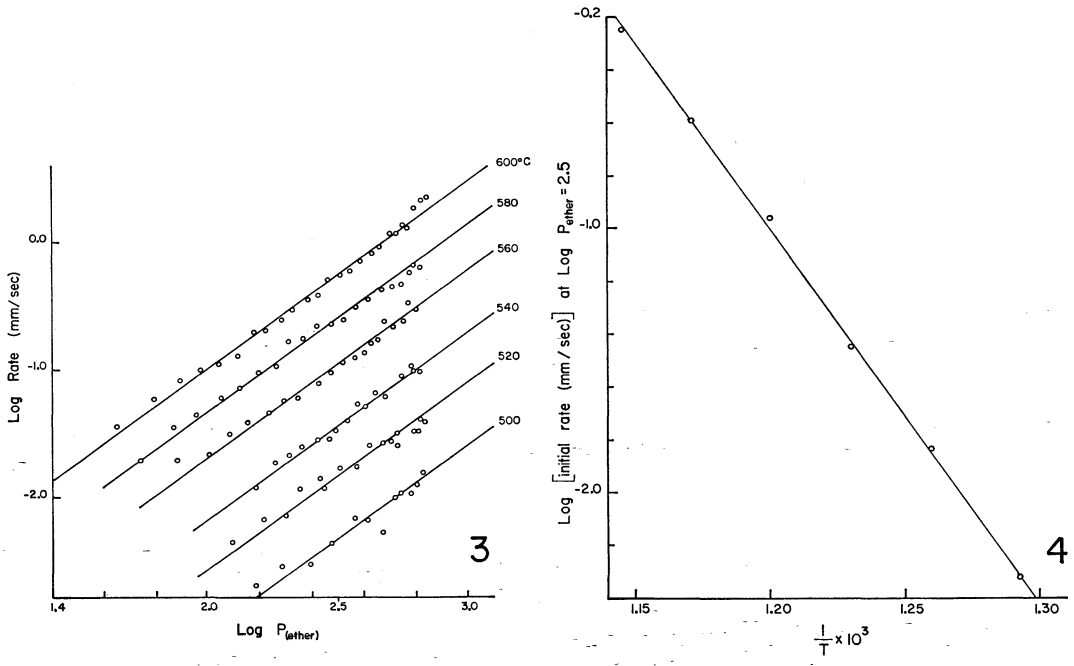

FIG. 3. Double logarithmic plots of initial rate against ether pressure, for the maximally inhibited reaction at various temperatures. The lines have slopes of 1.5.
FIG. 4. Arrhenius plot for the reaction maximally inhibited by nitric oxide.

pressure. About 5 mm of nitric oxide were used in all cases. The lines drawn have slopes of 1.5 at all temperatures. The initial rates become increasingly more difficult to measure as the temperature is lowered; the accuracy is therefore not as good at the lower temperatures, and the points become more scattered.

The activation energy, obtained from the Arrhenius plot shown in Fig. 4, was 64.6 kcal mole^{-1}. This is in satisfactory agreement with the activation energy of 62 kcal reported by Staveley and Hinshelwood (7). The three-halves-order rate constant may be expressed as

$$k = 1.2\times10^{16}e^{-64{,}600/RT}\ \text{cc}^{1/2}\ \text{mole}^{-1/2}\ \text{sec}^{-1}.$$

The effect on the "inhibition time" with varying amounts of nitric oxide is shown in Fig. 5. As the pressure of nitric oxide is increased the time required to reach the rate corresponding to the uninhibited rate steadily increases. More time is evidently required for the consumption of larger quantities of nitric oxide. The curves also demonstrate how the initial rate increases with large quantities (i.e. ~10 mm) of nitric oxide.

Can. J. Chem. Downloaded from www.nrcresearchpress.com by 210.87.254.5 on 09/05/12
For personal use only.

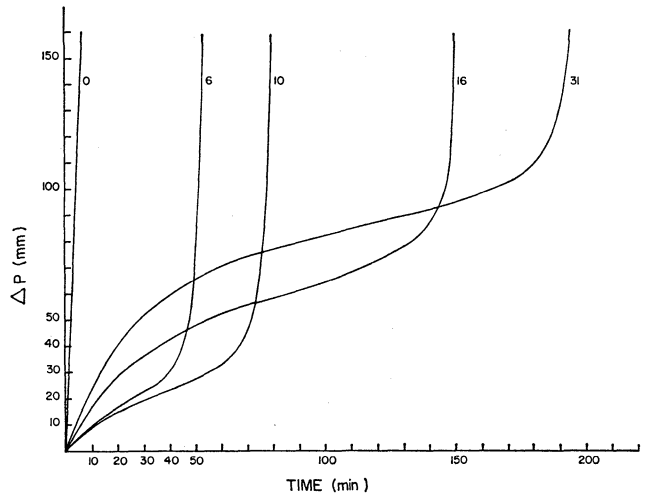

FIG. 5. Pressure–time curves for various pressures (mm Hg) of nitric oxide, which are indicated on the curves; the ether pressures were 470–485 mm, and the temperature 520° C.

The Reaction Accelerated by Nitric Oxide

Some runs were carried out using high pressures of nitric oxide. Figure 6 shows a plot of the logarithm of the initial rate against the logarithm of the pressure of nitric oxide.

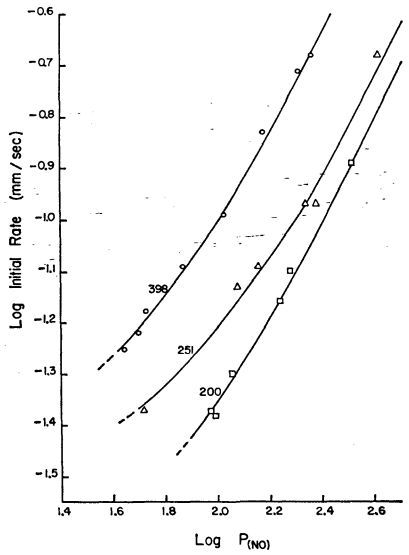

FIG. 6. Double logarithmic plot of initial rate against nitric oxide pressure, for the accelerated reaction using three different pressures of dimethyl ether, which are indicated on the curves.

The curves corresponding to different ether pressures all show some curvature at low nitric oxide pressures, but tend to linearity as the nitric oxide pressure is increased. The slopes of the linear portions of the curves are all unity. In the maximally inhibited region the order is obviously zero with respect to nitric oxide. The curvature therefore shows the gradual shift to first order in nitric oxide as the nitric oxide pressure is increased. In

Can. J. Chem. Downloaded from www.nrcresearchpress.com by 210.87.254.5 on 09/05/12
For personal use only.

subsequent studies in this region where the decomposition is sensitized by high pressures of nitric oxide, care was taken to ensure that at least 250 mm of nitric oxide (corresponding to log $P_{NO} = 2.4$ in Fig. 6) was used.

Rates were determined for the accelerated reaction for pressures of dimethyl ether varying from approximately 75 mm to 425 mm Hg, and over the temperature range from 510 to 570° C. As will be shown in the discussion, the overall rate expression for the inhibition by nitric oxide can be expressed by

$$v = k[CH_3OCH_3][NO] + k'[CH_3OCH_3]^{3/2}.$$

In the accelerated region, i.e. when [NO] is very large, the first term in the expression predominates and the reaction is first order with respect to both ether and nitric oxide; this was shown experimentally. To avoid the tedious procedure of maintaining a constant nitric oxide pressure, while studying the change in rate with variation of ether pressure, the logarithm of the rate minus the logarithm of the nitric oxide pressure was plotted against the logarithm of the ether pressure. Figure 7 shows the results of such plots. The

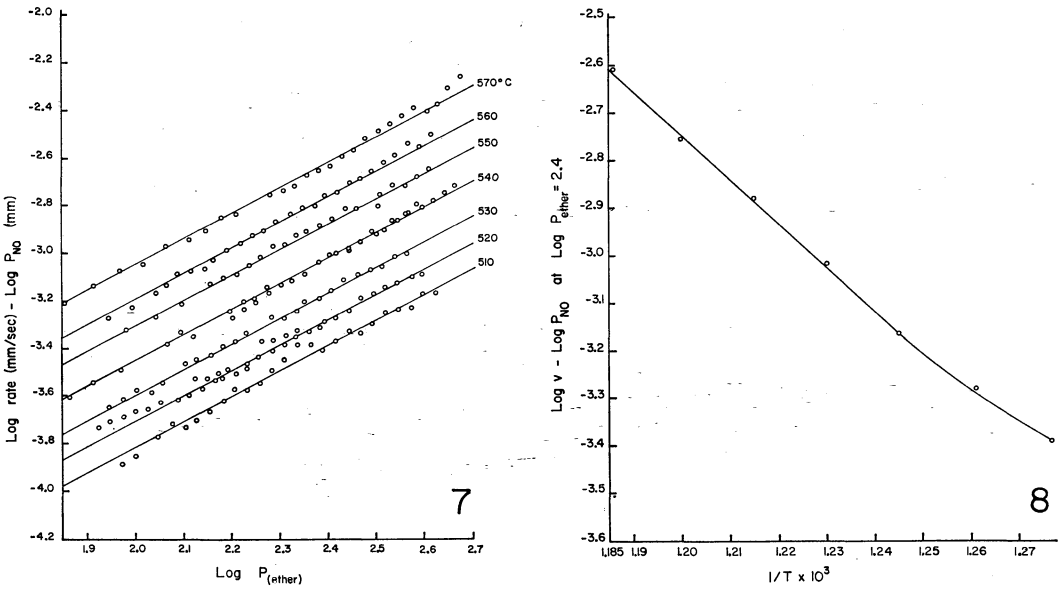

FIG. 7. Double logarithmic plots of initial rate against ether pressure, for the accelerated reaction.
FIG. 8. Arrhenius plot for the reaction accelerated by nitric oxide.

lines drawn all have slopes of approximately unity. The fact that the slopes are all slightly greater than unity (~1.1) shows that the second term in the above expression is not completely negligible even at nitric oxide pressures as high as 250 to 450 mm.

An Arrehenius plot of the data is shown in Fig. 8. The line drawn shows some curvature at the low temperatures, but is linear for temperatures above 530° C. The activation energy calculated from a least-squares treatment of the linear portion of the curve was found to be 43.5 kcal mole^{-1}, and the frequency factor was 9.6×10^{13} cc mole^{-1} sec^{-1}. This is an approximation to the true Arrhenius factor since, as was pointed out, the slopes of the curves of log v − log P_{NO} against log P_{ether} were slightly greater than unity. An approximate second-order rate expression can be written as $k \approx 1 \times 10^{14} e^{-43{,}400/RT}$ cc mole^{-1} sec^{-1}.

Can. J. Chem. Downloaded from www.nrcresearchpress.com by 210.87.254.5 on 09/05/12
For personal use only.

The Reaction Inhibited by Propylene

The inhibition curve showing the variation of relative rate with pressure of propylene is compared in Fig. 9 with the corresponding curve using nitric oxide as the inhibitor.

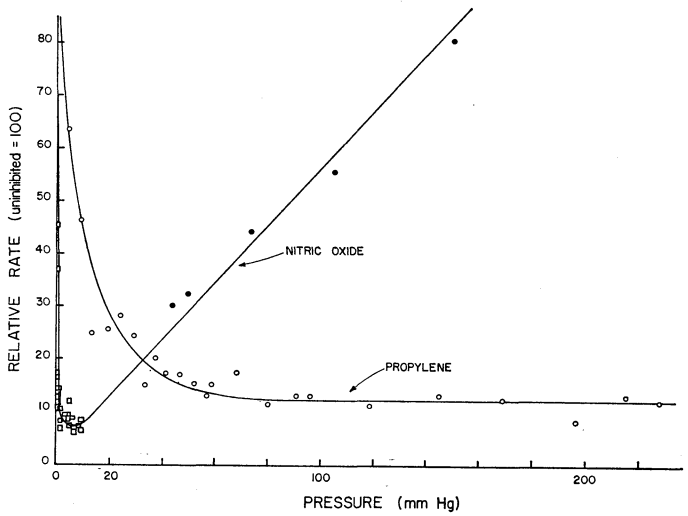

FIG. 9. Relative rate (uninhibited rate = 100) against propylene and nitric oxide pressures, at 520° C. The filled circles indicate an initial ether pressure of 398 mm. Points along the flat portions were obtained for various pressures of dimethyl ether.

About 70 mm of C_3H_6 is required at 520° to give a limiting rate. The relative rate in the maximally inhibited region is independent of ether pressure, as was also found in the case of inhibition by nitric oxide. In this case ether pressures varying from 168 mm to 513 mm are plotted along the flat portion; the variation was always well within the experimental error. The amount of propylene required to attain a limiting rate varied slightly with temperature. However, even at the highest temperature studied about 85 mm of propylene was found to be sufficient for maximal inhibition. The propylene inhibition curve differs in shape from the inhibition curve for nitric oxide in the region studied. Even pressures of propylene of about 200 mm failed to increase the rate of the decomposition, whereas pressures greater than 10–15 mm of nitric oxide produced a pronounced increase in rate. Care was taken in subsequent experiments in the fully inhibited region to maintain the propylene pressure at greater than 90 mm.

A typical pressure–time curve for the maximally inhibited reaction is shown in Fig. 10. The shape of the curve indicates that the system reaches equilibrium before an appreciable quantity of propylene is used up. The pressure–time relation for propylene therefore does not show the same behavior as does that for nitric oxide; this can be seen by comparing Fig. 10 with Fig. 2. The small quantity of nitric oxide necessary for maximal inhibition can be consumed before equilibrium is established between the ether and its products, but since much larger quantities of propylene must be used, a very long time would be required for all of the propylene to be used up, and the system comes to equilibrium before this can happen.

Figure 11 shows plots of the logarithm of the inflection-point rate against the logarithm of the ether pressure, at temperatures between 520 and 600° C. The inflection-point rates

Can. J. Chem. Downloaded from www.nrcresearchpress.com by 210.87.254.5 on 09/05/12
For personal use only.

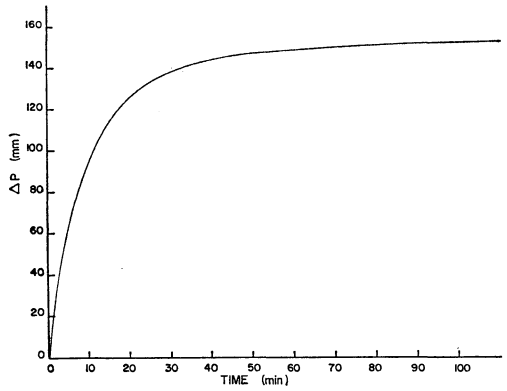

FIG. 10. A typical pressure–time curve for the reaction maximally inhibited by propylene; the initial ether pressure was 94 mm, and the temperature 600° C.

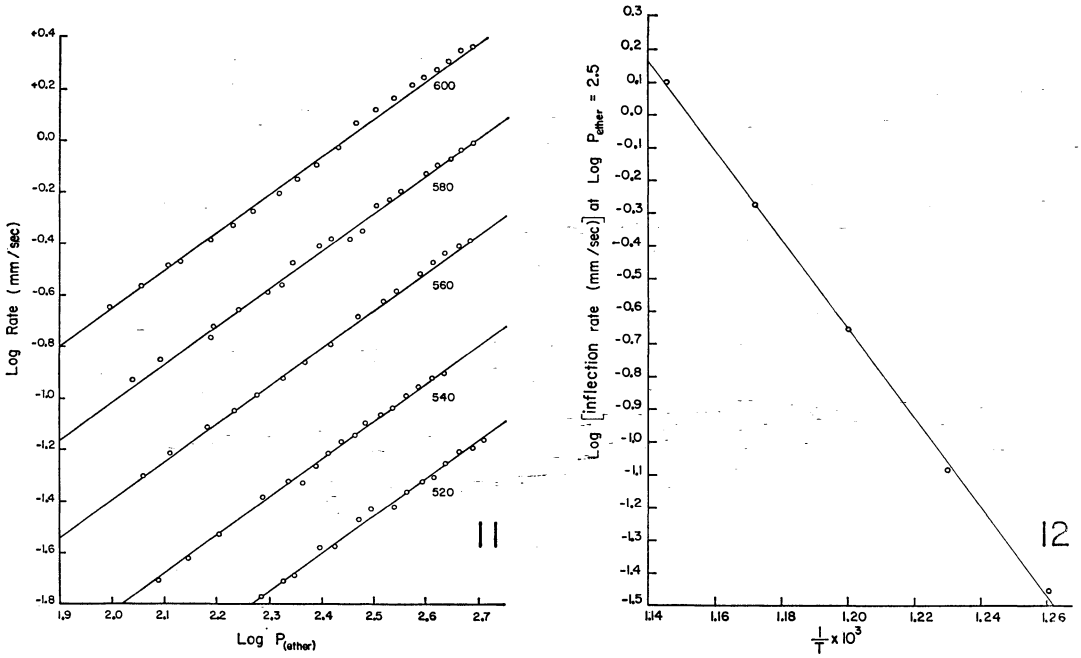

FIG. 11. Double logarithmic plots of inflection-point rate against ether pressure, for the reaction maximally inhibited by propylene.

FIG. 12. Arrhenius plot for the reaction maximally inhibited by propylene.

were used in this case because initial rates could not be measured very accurately especially at the higher temperatures.

The order, determined from the slopes of the lines in Fig. 11, was three-halves over the complete temperature and pressure ranges studied.

Figure 12 shows the Arrhenius plot for this system. The line drawn is the best fit determined by a least-squares treatment. The activation energy is 61.7 kcal mole^{-1} and the rate constant can be expressed as

$$k = 4.6\times10^{15}e^{-61{,}700/RT}\ \text{cc}^{1/2}\ \text{mole}^{-1/2}\ \text{sec}^{-1}.$$

Can. J. Chem. Downloaded from www.nrcresearchpress.com by 210.87.254.5 on 09/05/12
For personal use only.

DISCUSSION

Isotopic Mixing

Since the CD_3H/CD_4 ratio for the inhibited reaction is approximately the same as that for the uninhibited reaction (see Table I) it can be concluded that in the region of maximum inhibition the reaction is almost entirely a chain process. The suggestion made by previous workers (7, 10) that the inhibited reaction is entirely molecular must therefore be considered invalid for the dimethyl ether pyrolysis. The very low value obtained for the CD_3H/CD_4 ratio, in the case of CD_4, CH_3OCH_3, and NO mixtures, indicates that secondary processes are unimportant under these experimental conditions.

The Reaction Fully Inhibited by Nitric Oxide

The participation of nitric oxide in the initiation reaction in the dimethyl ether decomposition has been suggested by Wojciechowski and Laidler (1). Experimentally (see Fig. 2) nitric oxide effectively removes the induction period that is present in the uninhibited decomposition, and this suggests a direct reaction between NO and dimethyl ether. Initiation could therefore occur by either

$$CH_3OCH_3 + NO \rightarrow HNO + CH_3OCH_2 \qquad [1n]$$

or

$$CH_3OCH_3 + NO \rightarrow CH_3ONO + CH_3. \qquad [1n']$$

As far as the energetics of these reactions are concerned reaction [1n'] is favored. Reaction [1n] is endothermic by about 43 kcal (assuming $D(CH_3OCH_2—H)$ to be approximately 92 kcal $mole^{-1}$ as discussed later), while [1n'] is endothermic by about 39 kcal $mole^{-1}$. On the other hand [1n'] is a displacement reaction, while [1n] is an abstraction reaction and would probably be favored on steric grounds. Both reactions give similar rate expressions in the overall scheme, as will be shown below; for convenience it will be assumed that initiation is by [1n].

If reaction [1n] is the correct initiation reaction, the HNO will dissociate to produce H and NO. In hydrocarbon systems in which H atoms are present in large concentrations the reverse step also occurs. However in the decomposition of ether the hydrogen-atom concentration is quite low since the CH_3 radical is the principal chain carrier. The concentration of HNO is therefore low; the HNO largely dissociates and an equilibrium is established between CH_3, NO, CH_3NO, and CH_2NOH:

$$HNO \rightarrow H + NO$$

$$CH_3 + NO \rightleftarrows CH_3NO \rightleftarrows CH_2NOH.$$

If on the other hand reaction [1n'] is the correct one, the CH_3ONO can react with CH_3 radicals, as was shown by Jest and Phillips (11), as follows:

$$CH_3 + CH_3ONO \rightarrow CH_3NO + CH_3O.$$

The same equilibria as above would then be established.

The overall order being three-halves, the chain-ending steps must involve reaction between a β radical and either HNO or CH_3NO, of which the latter is present in much larger amounts. Isomerization of CH_3NO to $CH_2{=}NOH$ is known to occur (12), and the latter probably reacts with CH_3 more rapidly than does CH_3NO, since the process $CH_3 + CH_3NO \rightarrow C_2H_6 + NO$ probably involves a fairly high activation energy (see Appendix). The chain-ending step is therefore best written as

$$CH_3 + CH_2NOH \rightarrow CH_3CH_2—NOH \rightarrow C_2H_6 + NO.$$

Can. J. Chem. Downloaded from www.nrcresearchpress.com by 210.87.254.5 on 09/05/12
For personal use only.

This reaction is quite exothermic and can probably occur with no activation energy. The disappearance of nitric oxide is accounted for by the breakdown of CH_2NOH.

The mechanism to which these considerations leads is:*

$$CH_3OCH_3 + NO \rightarrow HNO + CH_2OCH_3 \qquad [1n]$$

$$CH_2OCH_3 \rightarrow CH_2O + CH_3 \qquad [3]$$

$$CH_3 + CH_3OCH_3 \rightarrow CH_4 + CH_2OCH_3 \qquad [2]$$

$$M + HNO \rightarrow H + NO + M \qquad [11]$$

$$H + CH_3OCH_3 \rightarrow H_2 + CH_2OCH_3 \qquad [5]$$

$$M + CH_3 + NO \underset{[-12]}{\overset{[12]}{\rightleftharpoons}} CH_3NO + M$$

$$CH_3NO \underset{[-13]}{\overset{[13]}{\rightleftharpoons}} CH_2NOH \rightarrow \text{products (HCN, etc.)}$$

$$CH_3 + CH_2NOH \rightarrow CH_3CH_2NOH \rightarrow C_2H_6 + NO. \qquad [15]$$

Application of the conventional steady-state treatment yields the following expressions for the radical concentrations:

$$[H] = \frac{k_{1n}}{k_5}[NO]$$

$$[HNO] = \frac{k_{1n}}{k_{11}}[NO]$$

$$[CH_2NOH] = \left(\frac{k_{1n}k_{12}k_{13}}{k_{-12}k_{-13}k_{15}}\right)^{1/2}[CH_3OCH_3]^{1/2}[NO]$$

$$[CH_3NO] = \left(\frac{k_{1n}k_{12}k_{-13}}{k_{-12}k_{13}k_{15}}\right)^{1/2}[CH_3OCH_3]^{1/2}[NO] + \frac{k_{1n}}{k_{13}}[CH_3OCH_3][NO]$$

$$[CH_3] = \left(\frac{k_{1n}k_{-12}k_{-13}}{k_{12}k_{13}k_{15}}\right)^{1/2}[CH_3OCH_3]^{1/2}$$

$$[CH_3OCH_2] = \frac{k_2}{k_3}\left(\frac{k_{1n}k_{-12}k_{-13}}{k_{12}k_{13}k_{15}}\right)^{1/2}[CH_3OCH_3]^{3/2} + \frac{2k_{1n}}{k_3}[CH_3OCH_3][NO].$$

The rate is given by

$$-\frac{d[CH_3OCH_3]}{dt} = 2k_{1n}[CH_3OCH_3][NO] + k_2\left(\frac{k_{1n}k_{-12}k_{-13}}{k_{12}k_{13}k_{15}}\right)^{1/2}[CH_3OCH_3]^{3/2}.$$

At low NO concentrations the first term can be neglected in comparison to the second term, and the rate expression then predicts three-halves-order kinetics with respect to ether. However, when the nitric oxide concentration is large the first term can no longer be neglected and in fact the rate becomes first order with respect to both NO and ether concentration. This is in agreement with the experimental facts.

A calculation can be made to determine whether CH_3 radicals or CH_3OCH_2 radicals are present in greater amounts:

$$\frac{[CH_3]}{[CH_3OCH_2]} = \frac{k_3}{k_2}\frac{1}{[CH_3OCH_3]}.$$

The reactions have been numbered so as to be consistent with Part I.

Can. J. Chem. Downloaded from www.nrcresearchpress.com by 210.87.254.5 on 09/05/12
For personal use only.

Use of the kinetic parameters listed in Table II, and with $[CH_3OCH_3]$ equal to 10^{-5} mole

TABLE II

Kinetic parameters for inhibition by nitric oxide

Reaction	Frequency factor (sec^{-1} or cc mole^{-1} sec^{-1})	Activation energy (kcal mole^{-1})	k at 800° K (sec^{-1} or cc mole^{-1} sec^{-1})	Reference
[1n]	1×10^{14}	43.4	1.3×10^{2}	See text
[2]	3×10^{11}	9.5	7.8×10^{8}	See Part I
[13]	7×10^{10}	19.0	4.6×10^{5}	See Part I
[11]*	2.1×10^{16}	48.0	1.6×10^{3}	Laidler, Sagert, and Wojciechowski (5)
[12]*	1×10^{11}	0	1×10^{11}	Ref. 13
[−12]*	1×10^{15}	50	21	A from ref. 14 and E estimated (see Appendix)
[13]	1×10^{13}	40	1.2×10^{2}	Ref. 15
[−13]	1×10^{13}	55	9.1×10^{-3}	Estimated (see Appendix)
[15]	1×10^{10}	0	1×10^{10}	Assumed

*The values given relate to the high-pressure region.

cc^{-1}, gives rise to, at 600° C,

$$\frac{[CH_3]}{[CH_3OCH_2]} = 59.$$

Consequently the CH_3 radical should be involved in termination rather than the CH_3OCH_2 radical.

The activation energy for the maximally inhibited reaction predicted by the mechanism is:

$$E = E_2+\tfrac{1}{2}(E_{1n}+E_{-12}+E_{-13}-E_{13}-E_{15}).$$

Agreement with the experimental value of 64.6 kcal mole^{-1} is obtained if a value of 64.8 kcal is taken for $E_{-12}+E_{-13}-E_{12}-E_{13}$. The significance of this value is that it implies that formaldoxime, CH_2NOH, is 64.8 kcal more stable than $CH_3 + NO$. This is a reasonable conclusion; further discussion is to be found in the Appendix.

The predicted frequency factor is

$$A = A_2\left(\frac{A_{1n}A_{12}A_{-13}}{A_{12}A_{13}A_{15}}\right)^{1/2} = 3\times10^{15}\ \text{cc}^{1/2}\,\text{mole}^{-1/2}\,\text{sec}^{-1}.$$

This is in satisfactory agreement with the experimental value of 1.2×10^{16} ml$^{1/2}$ mole$^{-1/2}$ sec^{-1}.

The Reaction Accelerated by Nitric Oxide

When large quantities of nitric oxide are used the rate of decomposition of dimethyl ether is considerably enhanced. The reaction has been found to be first order with respect to both NO and CH_3OCH_3 in this region. This result is predicted by the mechanism given above for the fully inhibited reaction. As the quantity of NO is increased the first term in the overall rate expression (i.e. $2k_{1n}[CH_3OCH_3][NO]$) predominates. Thus the ratio of the two terms is given by

$$\frac{\text{term 1}}{\text{term 2}} = \frac{2k_{1n}[CH_3OCH_3][NO]}{k_2\left(\frac{k_{1n}k_{-12}k_{-13}}{k_{12}k_{13}k_{15}}\right)^{1/2}[CH_3OCH_3]^{3/2}}.$$

Can. J. Chem. Downloaded from www.nrcresearchpress.com by 210.87.254.5 on 09/05/12
For personal use only.

This ratio is found to be approximately 73 after substitution of the values for the rate constants and the values $[NO] = [CH_3OCH_3] = 10^{-5}$ mole cc^{-1}. If $2k_{1n}[CH_3OCH_3][NO]$ is the dominant term when [NO] is large, a second-order rate constant can be calculated which corresponds to k_{1n}. The calculated second-order rate constant from Fig. 8 is given by

$$k_{1n} = 1 \times 10^{14} e^{-43{,}400/RT} \text{ cc mole}^{-1} \text{ sec}^{-1}.$$

The abstraction of a hydrogen atom from dimethyl ether by nitric oxide therefore has an activation energy of 43.4 kcal mole^{-1}, and the frequency factor is, to a good approximation, 1×10^{14} cc mole^{-1} sec^{-1}. The reason for the approximation is explained above. Using the value of 48.6 kcal for D(H—NO) (16), and the activation energy of 43.4 kcal determined above, an estimate of 92.0 kcal mole^{-1} for $D(CH_3OCH_2—H)$ can be made.

It is well established that increased quantities of nitric oxide increase the proportion of carbon monoxide in the products (8). This is also true in the decomposition of acetaldehyde (17) and diethyl ether (18). This result has previously been explained as being due to oxidation reactions, but it can be explained by the mechanism postulated above. Carbon monoxide is a major product in the decomposition of formaldehyde, which itself is one of the major products in the ether decomposition. From the mechanism postulated above the rate of formation of formaldehyde is given by

$$\frac{d[CH_2O]}{dt} = k_3[CH_3OCH_2]$$

$$= 2k_{1n}[CH_3OCH_3][NO] + k_2\left(\frac{k_{1n}k_{-12}k_{-13}}{k_{12}k_{13}k_{15}}\right)^{1/2}[CH_3OCH_3]^{3/2}.$$

The rate expression thus includes a term involving [NO], and therefore the proportion of formaldehyde (and hence of CO) should increase with increasing amounts of nitric oxide. On the other hand, the rate of formation of methane is not increased by adding nitric oxide, since

$$\frac{d[CH_4]}{dt} = k_2[CH_3][CH_3OCH_3]$$

$$= k_2\left(\frac{k_{1n}k_{-12}k_{-13}}{k_{12}k_{13}k_{15}}\right)^{1/2}[CH_3OCH_3]^{3/2},$$

which does not contain a term involving [NO].

The Reaction Fully Inhibited by Propylene

An analogous mechanism can be written for inhibition by propylene by assuming that the allyl radical (C_3H_5) is capable of abstracting hydrogen atoms and is therefore the counterpart of NO in the previous scheme. That C_3H_5 can abstract hydrogen atoms is well established experimentally (3, 19–22). Consequently, following the dissociation of propylene,

$$C_3H_6 \rightarrow C_3H_5 + H, \qquad [16]$$

the initiation reaction may be written as

$$CH_3OCH_3 + C_3H_5 \rightarrow C_3H_6 + CH_3OCH_2. \qquad [1p]$$

Experimentally there is an appreciable induction period in the propylene-inhibited reactions. This is required since an appreciable concentration of C_3H_5 radicals must first be formed. In the nitric oxide case the nitric oxide can abstract hydrogen atoms immediately and consequently there is no appreciable induction period.

Can. J. Chem. Downloaded from www.nrcresearchpress.com by 210.87.254.5 on 09/05/12
For personal use only.

The overall mechanism for the propylene-inhibited decomposition may therefore be written as:

$$CH_3OCH_3 + C_3H_5 \rightarrow C_3H_6 + CH_3OCH_2 \quad [1p]$$

$$CH_3OCH_2 \rightarrow CH_2O + CH_3 \quad [3]$$

$$CH_3 + CH_3OCH_3 \rightarrow CH_4 + CH_3OCH_2 \quad [2]$$

$$C_3H_6 \rightarrow C_3H_5 + H \quad [16]$$

$$H + CH_3OCH_3 \rightarrow H_2 + CH_3OCH_2 \quad [5]$$

$$CH_3 + C_3H_6 \rightarrow CH_4 + C_3H_5 \quad [17]$$

$$CH_3 + C_3H_5 \rightarrow CH_4 + H_2C{=}C{=}CH_2. \quad [18]$$

The steady-state treatment yields the following expressions for the radical concentrations:

$$[H] = \frac{k_{16}[C_3H_6]}{k_5[CH_3OCH_3]}$$

$$[CH_3] = \left(\frac{k_{1p}k_{16}}{k_{15}k_{17}}\right)^{1/2}[CH_3OCH_3]^{1/2}$$

$$[CH_3OCH_2] = \frac{k_{16}}{k_3}[C_3H_6] + \frac{k_{17}}{k_3}\left(\frac{k_{1p}k_{16}}{k_{18}k_{17}}\right)^{1/2}[CH_3OCH_3]^{1/2}[C_3H_6] + \frac{k_2}{k_3}\left(\frac{k_{1p}k_{16}}{k_{18}k_{17}}\right)^{1/2}[CH_3OCH_3]^{3/2}$$

$$[C_3H_5] = \left(\frac{k_{16}k_{17}}{k_{18}k_{1p}}\right)^{1/2}\frac{[C_3H_6]}{[CH_3OCH_3]^{1/2}}.$$

The overall rate is

$$v = -\frac{d[CH_3OCH_3]}{dt} = \left(\frac{k_{1p}k_{16}k_{17}}{k_{18}}\right)^{1/2}[C_3H_6][CH_3OCH_3]^{1/2} + k_{16}[C_3H_6] + k_2\left(\frac{k_{1p}k_{16}}{k_{18}k_{17}}\right)^{1/2}[CH_3OCH_3]^{3/2}.$$

The second term in this expression is negligible in comparison to the third term. The ratio of the third term to the first term is, using the values in Tables II and III, and with $[CH_3OCH_3] = [C_3H_6]$,

$$\frac{\text{term 3}}{\text{term 1}} = \frac{k_2}{k_{17}}\frac{[CH_3OCH_3]}{[C_3H_6]} = 2 \text{ at } 800^\circ \text{ K}.$$

Consequently the third term will predominate and the overall order is predicted to be three-halves with respect to ether, in agreement with experiment.

TABLE III

Kinetic parameters for inhibition by propylene

Reaction	Frequency factor (sec^{-1} or cc mole^{-1} sec^{-1})	Activation energy (kcal mole^{-1})	k at 800° K (sec^{-1} or cc mole^{-1} sec^{-1})	Reference
[1p]	1.0×10^{12}	38.0	4.1	Estimated
[16]	1.0×10^{15}	78.0	4.7×10^{-7}	Estimated from Szwarc (23)
[17]	5.2×10^{10}	7.7	4.1×10^{8}	Trotman-Dickenson and Steacie (24)
[18]	1.0×10^{10}	3.0	1.5×10^{9}	Estimated

Can. J. Chem. Downloaded from www.nrcresearchpress.com by 210.87.254.5 on 09/05/12
For personal use only.

Reaction [18] shows that the allyl radical is used up in forming stable products. As pointed out above one cannot observe by direct pressure measurement when all of the C_3H_5 has been consumed, as is possible with NO, because a thermodynamic equilibrium is presumably established long before the very large quantity of allyl radicals has disappeared by reaction [18]. The propylene constitutes a reservoir supplying C_3H_5 radicals to the system by reaction [16].

The predicted activation energy is

$$E = E_2+\tfrac{1}{2}(E_{1p}+E_{16}-E_{17}-E_{18})$$
$$= 62.2 \text{ kcal mole}^{-1},$$

in good agreement with the experimental value of 61.7 kcal mole^{-1}.

The predicted frequency factor is given by

$$A = A_2\left(\frac{A_{1p}A_{16}}{A_{17}A_{18}}\right)^{1/2} = 4.2\times10^{14} \text{ cc}^{1/2} \text{ mole}^{-1/2} \text{ sec}^{-1}$$

whereas the experimental value is

$$A = 4.6\times10^{15} \text{ ml}^{1/2} \text{ mole}^{-1/2} \text{ sec}^{-1}.$$

The agreement is quite satisfactory in view of the uncertainties in the individual frequency factors.

Induction Period

The induction period in the uninhibited reactions is associated with a gradual increase in rate at the beginning of the reaction; this results in the familiar S-shaped pressure–time curves. This type of curve was observed in the uninhibited reaction (see Part I), in the reaction inhibited by propylene, and in the reaction accelerated by large quantities of nitric oxide. In the latter case an induction period was evident only at low pressures and temperatures. The situation is quite different in the case of the reaction fully inhibited by nitric oxide. Here there is no evidence of any induction period at high pressures and temperatures. However, as the pressures and temperature are lowered there is a pronounced time lag before there is any pressure change in the reaction vessel. Thus the pressure–time curve exhibits a flat portion initially, followed by a sudden increase; Fig. 13 shows this effect.

The S-shaped curves can perhaps be explained by assuming a gradual approach to steady-state conditions. For the nitric oxide inhibited reaction the shape of the pressure–

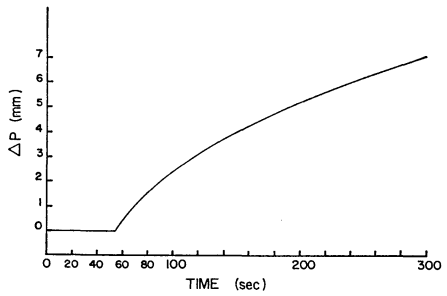

FIG. 13. Typical pressure–time curve for the reaction maximally inhibited by nitric oxide, particularly at low pressures and temperatures; this curve was obtained at 520° with an ether pressure of 591 mm and a nitric oxide pressure of 4.8 mm.

Can. J. Chem. Downloaded from www.nrcresearchpress.com by 210.87.254.5 on 09/05/12
For personal use only.

time curve suggests that there is a time delay before any ether decomposes, after which the reaction proceeds in the manner described above.

ACKNOWLEDGMENTS

The authors are grateful to Dr. F. P. Lossing of the National Research Council, for the mass spectrometric analyses, and to Drs. Margaret Back and W. A. Bryce for valuable suggestions.

The work was supported in part by a grant from the National Research Council, and in part by a grant from the Petroleum Research Fund.

APPENDIX

Figure 14 summarizes our conclusions with regard to the thermochemistry of processes related to the species HNO and CH_3NO. The main evidence for these values is as follows.

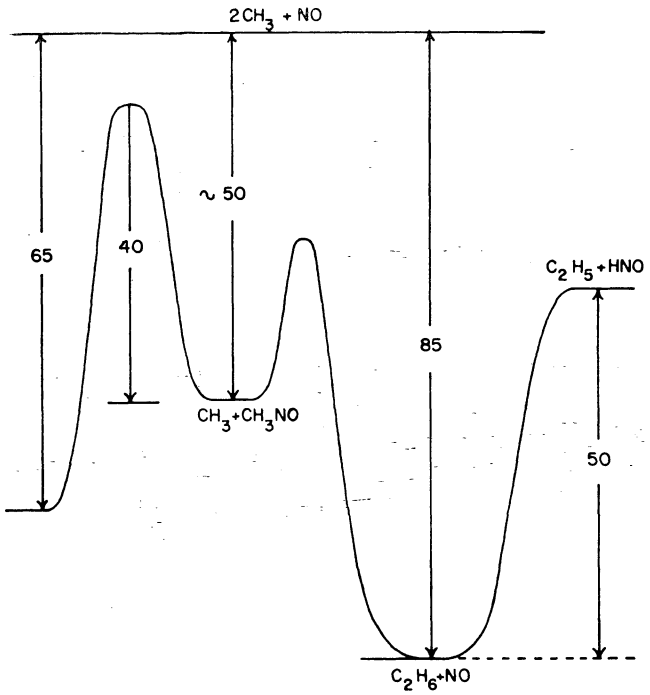

FIG. 14. Schematic energy-level diagram for the processes related to the species CH_3NO, CH_2NOH, C_2H_6, and HNO.

On the basis of their study of the ethane pyrolysis Laidler and Wojciechowski (4) concluded that the process $C_2H_6 + NO \rightleftarrows C_2H_5 + HNO$ is endothermic by 50 kcal $mole^{-1}$ and that the back reaction has no activation energy. The level of $2CH_3 + NO$ is higher than that of $C_2H_6 + NO$ by 85 kcal, the dissociation energy of the C—C bond in ethane.

The level of CH_3NO below that of $CH_3 + NO$ is not known with any certainty. Gray (25) has obtained a value of 57 kcal for $D(CH_3—NO_2)$, and Gowenlock, Trotman, and Batt (12) suggested that the value of $D(CH_3—NO)$ should be approximately the same. Gowenlock (26) now, however, favors a lower value, of about 30 kcal, on the grounds that the CH_3—NO dissociation energy should be about 15 kcal weaker than that of

Can. J. Chem. Downloaded from www.nrcresearchpress.com by 210.87.254.5 on 09/05/12
For personal use only.

H—NO. The dissociation of HNO, however, involves a predissociation (as may also that of CH_3NO), so that the evidence is not reliable. In Fig. 14 the value is about 50 kcal; the actual value has no bearing on the kinetics of the reaction. Ree, Yang, and Eyring (27), in a recent discussion of reactions inhibited by nitric oxide, have concluded that the value may be as high as 69.7 kcal mole^{-1}.

Since reaction between NO and C_2H_6 apparently gives $C_2H_5 + HNO$ (4) and not $CH_3 + CH_3NO$ it is postulated that there is a potential-energy barrier between $C_2H_6 + NO$ and $CH_3 + CH_3NO$, as shown in the diagram.

Batt and Gowenlock (15) have shown that CH_3NO isomerizes into formaldoxime, CH_2=NOH, with an activation energy of about 40 kcal mole^{-1}. The results of the present work indicate that the level of CH_2=NOH + CH_3 is 65 kcal below that of $CH_3 + CH_3 + NO$, and therefore significantly below that of $CH_3 + CH_3NO$. This is not unreasonable. Formaldoxime is expected to be a much more effective scavenger of radicals than is CH_3NO, and chain ending is therefore postulated to be

$$CH_3 + CH_2{=}NOH \rightarrow CH_3CH_2{-}NOH \rightarrow C_2H_6 + NO.$$

The breakdown of CH_2NOH accounts for the disappearance of nitric oxide in this reaction, in contrast to the situation with certain hydrocarbon decompositions (e.g. ethane, ref. 4), where CH_2NOH is not formed in significant amounts.

REFERENCES

1. B. W. Wojciechowski and K. J. Laidler. Can. J. Chem. **38**, 1027 (1960).
2. K. J. Laidler and B. W. Wojciechowski. Trans. Faraday Soc. **59**, 369 (1963).
3. K. J. Laidler and B. W. Wojciechowski. Proc. Roy. Soc. (London), Ser. A, **259**, 257 (1960).
4. K. J. Laidler and B. W. Wojciechowski. Proc. Roy. Soc. (London), Ser. A, **260**, 103 (1961).
5. K. J. Laidler, N. H. Sagert, and B. W. Wojciechowski. Proc. Roy. Soc. (London), Ser. A, **270**, 254 (1962).
6. N. H. Sagert and K. J. Laidler. Can. J. Chem. **41**, 838, 848 (1963).
7. L. A. K. Staveley and C. N. Hinshelwood. Proc. Roy. Soc. (London), Ser. A, **159**, 192 (1937).
8. P. F. Gay and M. W. Travers. Nature, **138**, 546 (1936).
9. H. W. Thompson and M. Meisner. Nature, **139**, 1018 (1937).
10. N. Imai and O. Toyama. Bull. Chem. Soc. Japan, **35**, 860 (1962).
11. B. Jest and L. Phillips. Proc. Chem. Soc. 73 (1960).
12. B. G. Gowenlock, J. Trotman, and L. Batt. Chem. Soc. (London), Spec. Publ. **10**, 75 (1957).
13. W. A. Bryce and K. U. Ingold. J. Chem. Phys. **23**, 1968 (1955).
14. A. F. Trotman-Dickenson. Gas kinetics. Butterworths Scientific Publications, London. 1955. p. 125.
15. L. Batt and B. G. Gowenlock. Trans. Faraday Soc. **56**, 682 (1960).
16. M. A. A. Clyne and B. A. Thrush. Trans. Faraday Soc. **57**, 1305 (1961).
17. F. H. Verhoek. Trans. Faraday Soc. **31**, 1533 (1935).
18. G. R. Freeman and C. J. Danby. Proc. Roy. Soc. (London), Ser. A, **245**, 68 (1958).
19. J. R. McNesby and A. S. Gordon. J. Chem. Phys. **31**, 853 (1959).
20. A. S. Gordon, S. R. Smith, and J. R. McNesby. J. Am. Chem. Soc. **81**, 5059 (1959).
21. W. A. Bryce and D. J. Ruzicka. Can. J. Chem. **38**, 835 (1960).
22. D. J. Ruzicka and W. A. Bryce. Can. J. Chem. **38**, 827 (1960).
23. M. Szwarc. J. Chem. Phys. **17**, 284 (1949).
24. A. F. Trotman-Dickenson and E. W. R. Steacie. J. Chem. Phys. **19**, 329 (1951).
25. P. Gray. Trans. Faraday Soc. **51**, 1367, 1489 (1955); **52**, 344 (1956).
26. B. G. Gowenlock. Discussions Faraday Soc. **33**, 287 (1962).
27. T. Ree, K. Yang, and H. Eyring. Trans. Faraday Soc. **58**, 2375 (1962).

Can. J. Chem. Downloaded from www.nrcresearchpress.com by 210.87.254.5 on 09/05/12
For personal use only.

KINETICS AND MECHANISMS OF THE PYROLYSIS OF DIMETHYL ETHER

III. THE REACTION ACCELERATED BY HYDROGEN SULPHIDE

D. J. McKenney and K. J. Laidler
Department of Chemistry, University of Ottawa, Ottawa, Canada
Received November 23, 1962

ABSTRACT

The thermal decomposition of dimethyl ether in the presence of hydrogen sulphide was studied in the temperature range of 480 to 530° C, and over the pressure range of 5 to 500 mm of Hg. For a given pressure of dimethyl ether the rate of decomposition increased with the addition of increasing quantities of hydrogen sulphide, reaching a plateau after approximately 30% H_2S had been added. The relative rate of decomposition then remained constant until more than 50% H_2S had been added. Further increase in the hydrogen sulphide concentration produced a linear increase in the relative rate. In the region between 30 and 50% added H_2S, the decomposition of dimethyl ether was three-halves order with respect to ether pressure, and zero order with respect to hydrogen sulphide pressure. In this region the three-halves-order rate constant can be expressed by $k = 1.06\times10^{14}e^{-53,200/RT}$ $cc^{1/2}$ $mole^{-1/2}$ sec^{-1}. In the region beyond 50% added H_2S, the reaction was first order with respect to dimethyl ether, and one-half order with respect to hydrogen sulphide. In this region the three-halves-order rate constant is given by $k = 4.98\times10^{14}e^{-52,500/RT}$ $cc^{1/2}$ $mole^{-1/2}$ sec^{-1}. The experimental facts are shown to be consistent with a mechanism involving hydrosulphide radicals as the principal chain carriers. These HS radicals are produced mainly from the reaction of methyl radicals with hydrogen sulphide. The work leads to a value of 85.6 kcal for the dissociation energy of H_2S into H + SH.

INTRODUCTION

A number of workers (1–7) have suggested that thiyl radicals (RS) are more reactive than alkyl radicals. Thus thiols generally accelerate free-radical reactions involving saturated aldehydes; this has been shown to be the case in the liquid phase (1), in photodecomposition reactions in the gas phase (2, 3) and in thermal decompositions in the gas phase (4–7). Birrell and co-workers (2) observed that various thiols (H_2S, CH_3SH, C_2H_5SH, etc.) catalyzed the photodecomposition of acetaldehyde, and in most cases the thiols increased the rate of the decomposition. The rates increased to a plateau with the addition of thiol and remained constant over a range of concentrations. When the thiol concentration was about three-quarters of the acetaldehyde concentration the relative rate (ratio of catalyzed to uncatalyzed rate) increased further. Hydrogen sulphide was found to be the most effective catalyst, and the catalytic effect decreased with increasing complexity of the thiol. The mechanism proposed for catalysis by methanethiol involved the chain transfer reaction

$$CH_3 + CH_3SH \rightarrow CH_3S + CH_4$$

followed by

$$CH_3S + CH_3CHO \rightarrow CH_3SH + CH_3 + CO$$

and termination by

$$2CH_3S \rightarrow CH_3SSCH_3.$$

Such a simple mechanism could not, however, explain the effects observed for other thiols.

More recently Imai and Toyama have postulated mechanisms to explain the acceleration by hydrogen sulphide and methanethiol of the decomposition of acetaldehyde (4, 5, 7). The effect of hydrogen sulphide on the decomposition of dimethyl ether was also studied (6). These workers suggest that the catalytic effect of hydrogen sulphide is

Can. J. Chem. Downloaded from www.nrcresearchpress.com by 210.87.254.5 on 09/05/12
For personal use only.

essentially due to reaction of methyl radicals with hydrogen sulphide, with the production of hydrosulphide (SH) radicals which in turn abstract hydrogen atoms from the substrate. These reactions are suggested to be faster than the reaction between methyl radicals and the substrate. For the thermal decomposition of dimethyl ether in the presence of hydrogen sulphide the rate increased with increasing concentration of hydrogen sulphide and reached a limit where further addition of hydrogen sulphide had no effect. The maximum amount of hydrogen sulphide which was added was approximately 67%, and the reactions were carried out over the temperature range of 360 to 440° C. The mechanism suggested for the reaction in the presence of sufficient hydrogen sulphide to ensure "limiting" acceleration was as follows:*

$$CH_3OCH_3 \rightarrow CH_3 + CH_3O \quad [1]$$

$$CH_3O + H_2S \rightarrow CH_3OH + HS \quad [24]$$

$$CH_3 + H_2S \rightarrow CH_4 + HS \quad [21]$$

$$CH_3OCH_3 + HS \rightarrow H_2S + CH_3OCH_2 \quad [20]$$

$$CH_3OCH_2 \rightarrow CH_2O + CH_3 \quad [3]$$

$$HS + HS \rightarrow \text{products.} \quad [23]$$

The rate equation to which this mechanism leads is

$$-\frac{d[CH_3OCH_3]}{dt} = \frac{d[CH_4]}{dt} = k_{20}\left(\frac{k_1}{k_{23}}\right)^{1/2}[CH_3OCH_3]^{3/2}$$

and a three-halves-order dependence on ether concentration was obtained experimentally. The results led to a rate constant of $k = 1.82\times10^{15}e^{-51,800/RT}$ cc$^{1/2}$ mole$^{-1/2}$ sec^{-1}.

In the light of recent work (Part II) in this laboratory on the action of inhibitors on the thermal decomposition of dimethyl ether, it was thought that a mechanism similar to inhibition mechanisms could be applied to the reaction accelerated by hydrogen sulphide. It also seemed necessary to extend the experimental investigation to higher temperatures and higher pressures of H_2S. The fact that there was an increase in relative rate at very high pressures of H_2S (>50% added H_2S) indicated that the mechanism postulated by Imai and Toyama (6) is not sufficient to describe the reaction completely.

EXPERIMENTAL

The apparatus used was essentially the same as described previously (8; see also Part I of this series). The dimethyl ether and hydrogen sulphide were 99.5% pure, and were used after three trap-to-trap distillations. The reactants were mixed thoroughly prior to a run, the procedure described earlier (Part II) being employed.

The reaction vessel was a cylindrical quartz tube of about 250-ml volume. A Thermo Electronic controller, activated by means of a thermocouple in the copper furnace block, maintained the temperature constant to about ±0.2° C. The temperature was measured by means of a thermocouple in the reaction vessel and a Thermo Electric Mini-Mite potentiometer.

Before each run the reaction vessel was pumped down to less than 10 μ. This small residual pressure had no detectable effect on the rates. A Beckman photopen recorder in conjunction with a quartz spiral gauge automatically recorded the pressure change as a function of time. The details of this arrangement have been described by Laidler and Wojciechowski (8).

Rates were calculated from the slopes of the pressure–time curves at the inflection point, and the results were found to be fully reproducible over the entire range of pressure and temperature. The induction period for the reaction in the presence of H_2S was generally quite short, so that the inflection point occurred in all cases at less than 10% decomposition. The rates can therefore be considered to be initial rates to a very close approximation.

**The numbering is written so as to be consistent with the mechanism postulated below, as well as with the numbering in Parts I and II of this series.*

Can. J. Chem. Downloaded from www.nrcresearchpress.com by 210.87.254.5 on 09/05/12
For personal use only.

RESULTS

Preliminary experiments were carried out with hydrogen sulphide alone in the reaction vessel at 600° C. It was found that the total pressure decreased by approximately 1% to a limit. This slight pressure change is insignificant compared to the pressure change for the decomposition of dimethyl ether in the presence of H_2S, and was therefore ignored.

In order to verify the experimental results of previous workers (6) the rate of decomposition of dimethyl ether was measured for various added amounts of hydrogen sulphide. A plot of relative rate (i.e., the rate in the presence of H_2S divided by the rate in the absence of H_2S) is shown in Fig. 1. The curves drawn have been calculated from Fig. 2,

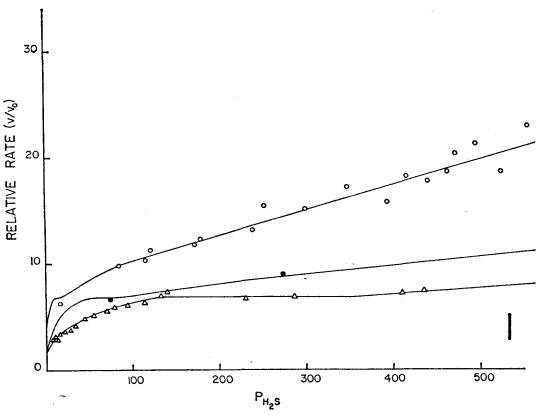

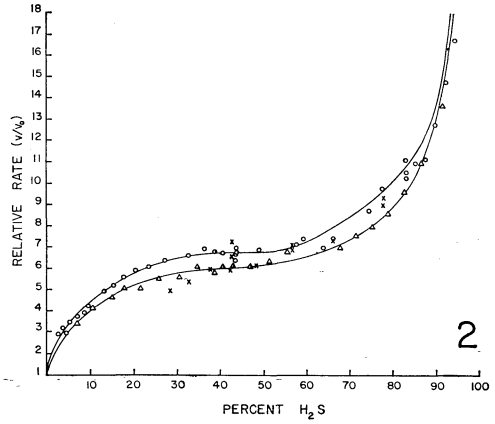

FIG. 1. Relative rate (v/v_0) against pressure of hydrogen sulphide for three different pressures of ether: △ 300 mm, ● 100 mm, and ○ 20 mm of ether. The solid lines have been calculated from Fig. 2.

FIG. 2. Relative rate (v/v_0) against the percentage of hydrogen sulphide for three different temperatures: △ 530° C, ○ 520° C, and × 480° C.

to be considered later. For a given pressure of ether the relative rate increases to a plateau with an increasing concentration of hydrogen sulphide. In this region the order with respect to hydrogen sulphide is obviously zero. As still greater quantities of H_2S are added the relative rate increases linearly. It is apparent from the curves shown in Fig. 1 that the length of the plateau depends on the pressure of ether; the lower the ether pressure, the shorter the plateau. This suggests that the effects depend only on the *proportion* of H_2S relative to ether, rather than on the absolute amount of H_2S. This result differs from that found in the nitric oxide inhibited decomposition of dimethyl ether (Part II). A plot of relative rate against the percentage of hydrogen sulphide (Fig. 2) shows this dependence more clearly. Points were determined at three different temperatures—480, 520, and 530° C. Within the experimental error, the plateau occurs at approximately the same relative rate in all cases, although there appears to be a slight increase with decreasing temperature, i.e. the plateau seems to be higher for the low temperatures.

Kinetic measurements were carried out with about 40% added H_2S, and with about 75 to 99% added H_2S. Hydrogen sulphide in the amount of 40% was sufficient to ensure "limiting" acceleration (independent of H_2S), while over 75% H_2S ensured that the reaction was in the region dependent on the percentage of hydrogen sulphide.

A typical pressure–time curve is shown in Fig. 3. Curve A is an actual tracing of the record obtained for the decomposition of 90 mm of dimethyl ether in the absence of H_2S. Curve B is a similar tracing showing the decomposition of 85 mm of dimethyl ether

Can. J. Chem. Downloaded from www.nrcresearchpress.com by 210.87.254.5 on 09/05/12
For personal use only.

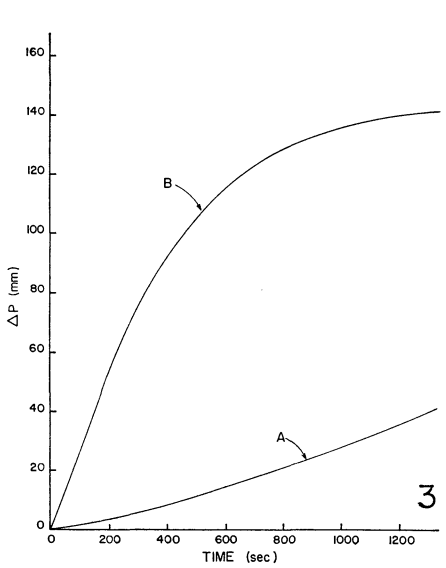

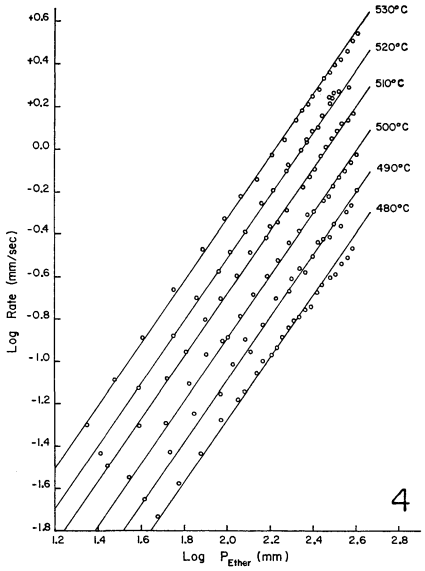

FIG. 3. Typical pressure–time curves. Curve A is a tracing of the record obtained for the decomposition of 90 mm of ether in the absence of hydrogen sulphide. Curve B is a similar tracing showing the decomposition of 85 mm of ether in the presence of 475 mm of H_2S. The temperature in both cases was 510° C.

FIG. 4. Double logarithmic plot of inflection rate against ether pressure for various temperatures. The lines all have slopes of 1.5. These curves were determined for the decomposition in the presence of about 40% H_2S (i.e. the plateau region).

in the presence of 475 mm of H_2S. Both runs were carried out at 510° C. The accelerating effect of the added H_2S is readily seen.

Figure 4 shows plots of the logarithm of the rate against the logarithm of the ether pressure, for the reaction in the plateau region where about 40% H_2S was added. All of the lines have slopes of 1.5. The corresponding Arrhenius curve is shown in Fig. 5.

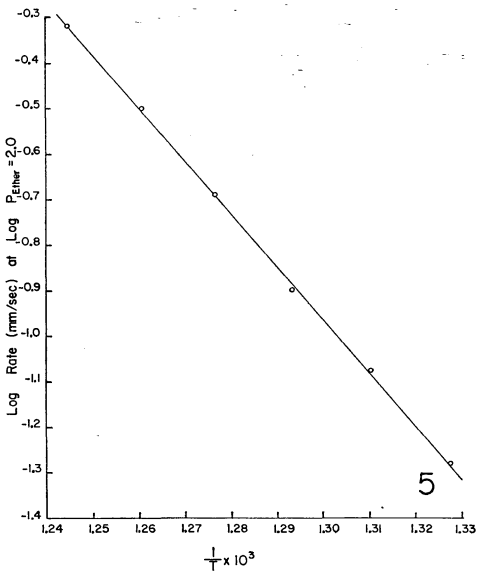

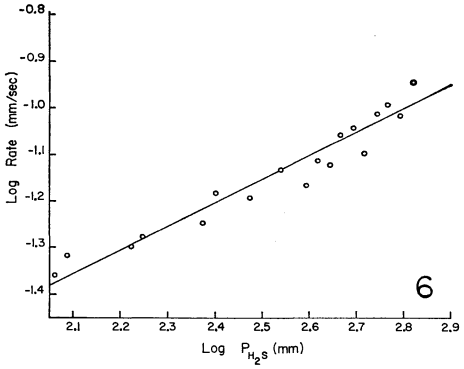

FIG. 5. Arrhenius plot for the decomposition in the presence of about 40% H_2S (i.e. the plateau region).

FIG. 6. Double logarithmic plot of inflection rate against pressure of hydrogen sulphide at 520° C. The ether pressure was constant at about 20 mm. The slope of the line is 0.5.

Can. J. Chem. Downloaded from www.nrcresearchpress.com by 210.87.254.5 on 09/05/12
For personal use only.

The three-halves-order rate constant may be expressed as $k = 1.06\times10^{14}e^{-53,200/RT}$ cc$^{1/2}$ mole$^{-1/2}$ sec^{-1}. This is to be compared with $k = 1.82\times10^{15}e^{-51,800/RT}$ cc$^{1/2}$ mole$^{-1/2}$ sec^{-1} obtained by Imai and Toyama (6).

The kinetic measurements made with 75 to 99% H_2S are shown in Figs. 6, 7, and 8. Figure 6 is a double logarithmic plot of rate against pressure of hydrogen sulphide, for a

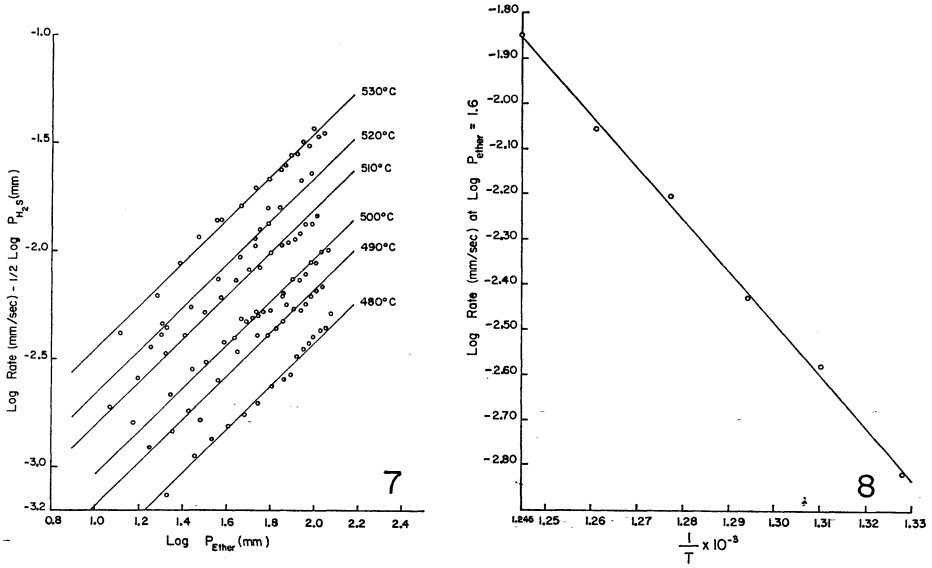

FIG. 7. Double logarithmic plot of inflection rate against ether pressure for various temperatures. The lines all have slopes of 1.5. These curves were determined for the decomposition in the presence of 75–99% H_2S.

FIG. 8. Arrhenius plot for the decomposition in the presence of 75–99% H_2S.

constant (~20 mm) pressure of dimethyl ether. The line drawn has a slope of 0.5, showing that the order with respect to H_2S pressure is one-half in the region of very high percentages of H_2S. The logarithm of the rate minus one-half the logarithm of the hydrogen sulphide pressure is plotted against the logarithm of the ether pressure in Fig. 7. A plot of this kind enabled the dependence on ether pressure to be determined, without the tedious task of holding the H_2S pressure constant. All of the lines drawn in Fig. 7 have slopes of unity. The corresponding Arrhenius plot is shown in Fig. 8. The calculated activation energy for the reaction accelerated by very high percentages of hydrogen sulphide is 52.5 kcal mole^{-1}. The rate constant may be expressed by $k = 4.98\times10^{14}$ $e^{-52,500/RT}$ cc$^{1/2}$ mole$^{-1/2}$ sec^{-1}.

DISCUSSION

The fact that the rate of decomposition of dimethyl ether in the presence of hydrogen sulphide relative to the rate in the absence of hydrogen sulphide depends on the proportion of H_2S to ether (see Figs. 1 and 2) suggests that competitive reactions are involved in the process. At these temperatures it is well known that dimethyl ether decomposes to form methyl and methoxy radicals. Hydrosulphide radicals are almost certainly formed from the decomposition of hydrogen sulphide. This is suggested by the fact that there is a slight decrease in pressure when H_2S alone is present in the reaction vessel at 600° C. The thermal decomposition of hydrogen sulphide has in fact been studied in the temperature range employed in this research (9). The evidence suggests that the decomposition

Can. J. Chem. Downloaded from www.nrcresearchpress.com by 210.87.254.5 on 09/05/12
For personal use only.

proceeds mainly by heterogeneous processes at temperatures below 600° C. The radical HS would probably be formed in large quantities, and can also be produced from reactions such as

$$CH_3 + H_2S \rightarrow CH_4 + HS.$$

Consequently, during the decomposition of dimethyl ether in the presence of hydrogen sulphide, there should be a plentiful supply of hydrosulphide radicals. These could initiate the ether decomposition by abstraction of a hydrogen atom,

$$CH_3OCH_3 + HS \rightarrow H_2S + CH_3OCH_2.$$

The overall rate expression for the thermal decomposition of pure dimethyl ether is of the form (Part I and ref. 10)

$$v_0 = k[CH_3OCH_3]^{3/2}.$$

The shape of the curves shown in Figs. 1 and 2 suggests the following relationships:

$$v = k'[H_2S]^n[CH_3OCH_3]^m + k''[CH_3OCH_3]^{3/2}$$

or

$$\frac{v}{v_0} = \frac{k'[H_2S]^n[CH_3OCH_3]^m + k''[CH_3OCH_3]^{3/2}}{k[CH_3OCH_3]^{3/2}}.$$

This reduces to

$$\frac{v}{v_0} = \frac{k'}{k}\frac{[H_2S]^n}{[CH_3OCH_3]^{3/2-m}} + \frac{k''}{k}.$$

Thus on a plot of relative rate (v/v_0) against the percentage of hydrogen sulphide a plateau would be observed when the proportion of H_2S to CH_3OCH_3 is small and k''/k is the dominant term. However, as the ratio of H_2S to CH_3OCH_3 becomes larger the relative rate should then increase with increasing percentage of hydrogen sulphide.

The rate expression for the reaction in the presence of H_2S should therefore involve two terms—one predicting three-halves-order behavior with respect to dimethyl ether and no dependence on hydrogen sulphide, the second predicting dependence with respect to both hydrogen sulphide and dimethyl ether. Figures 6, 7, and 8 show that the order is one-half in H_2S and first in CH_3OCH_3, i.e. $n = 1/2$ and $m = 1$, for the reaction with high percentages of H_2S.

The mechanism to which these considerations lead can be written as:

$$M + CH_3OCH_3 \rightarrow CH_3 + CH_3O + M \quad [1a]$$

$$M + H_2S \rightarrow H + HS + M \quad [19]$$

$$H + CH_3OCH_3 \rightarrow H_2 + CH_3OCH_2 \quad [5]$$

$$HS + CH_3OCH_3 \rightarrow H_2S + CH_3OCH_2 \quad [20]$$

$$CH_3OCH_2 \rightarrow CH_2O + CH_3 \quad [3]$$

$$CH_3 + H_2S \rightarrow CH_4 + HS \quad [21]$$

$$M + CH_3O \rightarrow CH_2O + H + M \quad [4]$$

$$HS + HS \underset{[-22]}{\overset{[22]}{\rightleftharpoons}} H_2S + S$$

$$M + HS + HS \rightarrow H_2S_2 + M \quad [23a]$$

Can. J. Chem. Downloaded from www.nrcresearchpress.com by 210.87.254.5 on 09/05/12
For personal use only.

Can. J. Chem. Downloaded from www.nrcresearchpress.com by 210.87.254.5 on 09/05/12
For personal use only.

where M represents a third body. Application of the conventional steady-state approximation yields for the radical concentrations:

$$[HS] = \left(\frac{2k_{19}}{k_{23a}}\right)^{1/2}[H_2S]^{1/2} + \left(\frac{2k_{1a}}{k_{23a}}\right)^{1/2}[CH_3OCH_3]^{1/2}$$

$$[CH_3O] = \frac{k_{1a}}{k_4}[CH_3OCH_3]$$

$$[H] = \frac{k_{19}}{k_5} + \frac{k_{1a}}{k_5}[CH_3OCH_3]$$

$$[CH_3OCH_2] = \frac{k_{20}}{k_3}\left(\frac{2k_{19}}{k_{23a}}\right)^{1/2}[CH_3OCH_3][H_2S]^{1/2} + \frac{k_{20}}{k_3}\left(\frac{2k_{1a}}{k_{23a}}\right)^{1/2}[CH_3OCH_3]^{3/2} + \frac{k_{1a}}{k_3}[CH_3OCH_3][M] + \frac{k_{19}}{k_3}[H_2S][M]$$

$$[CH_3] = \frac{k_{1a}}{k_{21}}\frac{[CH_3OCH_3][M]}{[H_2S]} + \frac{k_{20}}{k_{21}}\left(\frac{2k_{19}}{k_{23a}}\right)^{1/2}\frac{[CH_3OCH_3]}{[H_2S]^{1/2}} + \frac{k_{1a}}{k_{21}}\frac{[CH_3OCH_3]}{[H_2S]} + \frac{k_{20}}{k_{21}}\left(\frac{2k_{1a}}{k_{23a}}\right)^{1/2}\frac{[CH_3OCH_3]^{3/2}}{[H_2S]} + \frac{k_{19}}{k_{21}}[M].$$

The rate is given by

$$v = 2k_{1a}[CH_3OCH_3][M] + k_{20}\left(\frac{2k_{19}}{k_{23a}}\right)^{1/2}[H_2S]^{1/2}[CH_3OCH_3] + k_{20}\left(\frac{2k_{1a}}{k_{23a}}\right)^{1/2}[CH_3OCH_3]^{3/2} + k_{19}[H_2S][M].$$

The first and fourth terms in this expression are small in comparison to the second and third terms, and hence may be neglected. The rate can therefore be written as

$$v = k_{20}\left(\frac{2k_{19}}{k_{23a}}\right)^{1/2}[H_2S]^{1/2}[CH_3OCH_3] + k_{20}\left(\frac{2k_{1a}}{k_{23a}}\right)^{1/2}[CH_3OCH_3]^{3/2}.$$

A crude estimate of the percentage of H_2S at which the change in order takes place can be made using the values for k_{1a} and k_{19} from Table I. The ratio of the first to the second term is

$$\left(\frac{k_{19}}{k_{1a}}\right)^{1/2}\frac{[H_2S]^{1/2}}{[CH_3OCH_3]^{1/2}} = 0.1103 \times \frac{[H_2S]^{1/2}}{[CH_3OCH_3]^{1/2}}.$$

This expression becomes greater than unity when the ratio $[H_2S]/[CH_3OCH_3]$ becomes greater than 9.1. Thus the first term in the rate expression predominates when the pressure of hydrogen sulphide exceeds 90%. The transition actually takes place with about 50–70% H_2S. The agreement is therefore quite satisfactory in view of the uncertainties in the rate constants. Consequently, to describe the rate for the plateau region the following expression can be written:

$$v = k_{20}\left(\frac{2k_{1a}}{k_{23a}}\right)^{1/2}[CH_3OCH_3]^{3/2}.$$

This expression is identical with that postulated by Imai and Toyama (6). The reason

TABLE I

Kinetic parameters

Reaction	Frequency factor (sec^{-1}, cc $mole^{-1}$ sec^{-1}, or cc^2 $mole^{-2}$ sec^{-1})	Activation energy (kcal $mole^{-1}$)	k at 800° K (sec^{-1}, cc $mole^{-1}$ sec^{-1}, or cc^2 $mole^{-2}$ sec^{-1})	Reference
[1a]	1×10^{18}	74.0	5.8×10^{-3}	See Part I
[19]	1×10^{18}	81.0	7.0×10^{-5}	Estimated (see footnote)
[20]	1×10^{12}	13.0	2.8×10^{8}	Assumed
[3]	7×10^{10}	19.0	4.6×10^{5}	See Part I
[21]	2.5×10^{11}	2.6	1.9×10^{10}	Imai and Toyama (11)
[23a]	1×10^{14}	−5.6	2.9×10^{12}	Estimated (see footnote)
[2]	3×10^{11}	9.5	7.8×10^{8}	See Part I
[7]	7×10^{14}	−13.5	3.5×10^{18}	See Part I

NOTE: The values for reactions [19] and [23a] were calculated in the same manner as in the Appendix of Part I. Four effective degrees of freedom were assumed for HS + SH, by analogy with hydrogen peroxide, and three effective degrees of freedom were taken for $M + H_2S \rightarrow H + HS + M$.

for this is that reaction [19] is unimportant until large relative quantities of hydrogen sulphide are used. Thus with the neglect of reactions [19] and [5], the mechanism is essentially the same as that postulated by Imai and Toyama (6). The reaction in this region is therefore predicted to be three-halves order with respect to ether, in agreement with experiment. The predicted activation energy is given by $E = E_{20}+\frac{1}{2}(E_{1a}-E_{23a})$. Substitution of the appropriate values given in Table I yields $E = 52.8$ kcal $mole^{-1}$, in good agreement with the experimental value of 53.2 kcal $mole^{-1}$. The predicted frequency factor is $A = A_{20}(2A_{1a}/A_{23a})^{1/2} = 1.0\times10^{14}$ $cc^{1/2}$ $mole^{-1/2}$ sec^{-1}. This is also in good agreement with the experimental value of 1.06×10^{14} $cc^{1/2}$ $mole^{-1/2}$ sec^{-1}.

In the region of high percentages of H_2S the rate is given by

$$v = k_{20}\left(\frac{2k_{19}}{k_{23a}}\right)^{1/2}[H_2S]^{1/2}[CH_3OCH_3].$$

Experimentally the reaction is one-half order with respect to hydrogen sulphide and first order with respect to dimethyl ether in this region, in agreement with this rate expression. The predicted activation energy is $E = E_{20}+\frac{1}{2}(E_{19}-E_{23a}) = 56.3$ kcal $mole^{-1}$, in fair agreement with the experimental value of 52.5 kcal $mole^{-1}$. The predicted frequency factor is $A = A_{20}(2A_{19}/A_{23a})^{1/2} = 1.0\times10^{14}$ $cc^{1/2}$ $mole^{-1/2}$ sec^{-1}, whereas the experimental value is $A = 4.98\times10^{14}$ $cc^{1/2}$ $mole^{-1/2}$ sec^{-1}.

The Termination Reaction

Darwent and Roberts (9) concluded, from a study the photolysis of H_2S, that about 13% of the HS radicals disappeared by the reaction $2HS \rightarrow S_2 + H_2$ while about 87% reacted by the process $2HS \rightarrow H_2S + S$ followed by $2S + M \rightarrow S_2 + M$.

In view of this evidence, the equilibrium process

$$HS + HS \underset{[-22]}{\overset{[22]}{\rightleftharpoons}} H_2S + S$$

has been included in the mechanism. The small quantity of S atoms produced may react with H_2S as shown or with CH_3OCH_3:

$$CH_3OCH_3 + S \rightarrow HS + CH_3OCH_2. \qquad [24]$$

It is suggested that reaction [−22] is faster than [24], and hence [24] can be ignored.

Can. J. Chem. Downloaded from www.nrcresearchpress.com by 210.87.254.5 on 09/05/12
For personal use only.

The concentration of HS radicals is large in this system and their combination will give rise to H_2S_2. This reaction will require a third body under these experimental conditions.

The Initiation Reaction

An important conclusion arises from this study with regard to the order of the initiation reaction: the dissociation of the ether molecule into the radicals CH_3 and CH_3O. Consideration of the steady-state equations shows that the only apparent way to obtain the correct pressure dependence in both H_2S and CH_3OCH_3 is by having the initiation in its low-pressure second-order region. This observation is important with reference to the mechanism of the uninhibited reaction, as discussed in Part I.

The Dissociation Energy of Hydrogen Sulphide

The present work provides a method of estimating the dissociation energy (D(H—SH)) of hydrogen sulphide. The difference between the activation energies for the reaction in the plateau region and the region of high H_2S percentages is given from the overall rate expression as

$$\begin{aligned}\Delta E &= [E_{20}+\tfrac{1}{2}(E_{1a}-E_{23a})]-[E_{20}+\tfrac{1}{2}(E_{19}-E_{23a})]\\ &= \tfrac{1}{2}[E_{1a}-E_{19}].\end{aligned}$$

The experimental difference is 0.7 kcal mole^{-1}. Since E_{1a} is known (Part I) E_{19} can be calculated as, at high pressures,

$$E_{19} = E_{1a}-2\Delta E = 85.6 \text{ kcal mole}^{-1}.$$

Previous work has led to conflicting values for this dissociation energy; values varying from 81 to 95 kcal mole^{-1} have been reported (12). Johns and Ramsay (13) recently determined the dissociation energy of the hydrosulphide radical and obtained D(H—S) = 81.4±2.9 kcal mole^{-1}. This can be used to calculate a value for D(H—SH), since the heats of formation of S, H, and H_2S are known (14). For the process SH → S + H,

$$\begin{aligned}D(\text{S—H}) &= \Delta H_f^0(\text{S})+\Delta H_f^0(\text{H})-\Delta H_f^0(\text{SH})\\ 81.4 &= 53.23+52.09-\Delta H_f^0(\text{SH}),\end{aligned}$$

whence

$$\Delta H_f^0(\text{SH}) = 23.9 \text{ kcal mole}^{-1}.$$

For $H_2S \rightarrow H + SH$

$$\begin{aligned}D(\text{H—SH}) &= \Delta H_f^0(\text{H})+\Delta H_f^0(\text{SH})-\Delta H_f^0(\text{H}_2\text{S})\\ &= 52.09+23.9-(-4.82)\\ &= 80.9 \text{ kcal mole}^{-1}.\end{aligned}$$

Cottrell (12) favors a more recent value of 57 kcal mole^{-1} for ΔH_f^0(S), and Ansdell and Page (15) support this value on the basis of their determination of the electron affinity of the sulphur atom. This value yields D(H—SH) = 84.65 kcal mole, in good agreement with our value. On the other hand, Mackle and McClean (16) prefer a value of 35.2 kcal mole^{-1} for ΔH_f^0(HS), which was determined from a calorimetric study of benzyl mercaptan. This yields D(H—SH) = 92 kcal mole^{-1}. Palmer and Lossing (17) recently determined $\Delta H_f^0(\text{HS}) \leqslant 33.7$ by mass spectrometric techniques, and this leads to an estimate

Can. J. Chem. Downloaded from www.nrcresearchpress.com by 210.87.254.5 on 09/05/12
For personal use only.

of $D(H—SH) \leqslant 90.6$ kcal mole^{-1}. The value is therefore still in doubt, but our value of 85.6 kcal mole^{-1} calculated from the difference in activation energies supports the lower values. Admittedly the experimental errors involved in this estimation are large. The value of 85.6 kcal mole^{-1} was taken for the calculations considered above.

The Effect of Temperature on the Relative Rate

The main features of the thermal decomposition of dimethyl ether can be represented by the following scheme (see Part I):

$$M + CH_3OCH_3 \rightarrow CH_3 + CH_3O + M \quad [1a]$$

$$CH_3 + CH_3OCH_3 \rightarrow CH_4 + CH_3OCH_2 \quad [2]$$

$$CH_3OCH_2 \rightarrow CH_2O + CH_3 \quad [3]$$

$$M + CH_3O \rightarrow CH_2O + H + M \quad [4]$$

$$H + CH_3OCH_3 \rightarrow H_2 + CH_3OCH_2 \quad [5]$$

$$M + CH_3 + CH_3 \rightarrow C_2H_6 + M. \quad [7]$$

The overall rate expression derived by means of the usual steady-state approximation is given by

$$v_0 = k_2\left(\frac{2k_{1a}}{k_7}\right)^{1/2}[CH_3OCH_3]^{3/2}.$$

It was shown above that the rate expression for the reaction in the plateau region (~30 to 50% added H_2S) can be written as

$$v = k_{20}\left(\frac{2k_{1a}}{k_{23a}}\right)^{1/2}[CH_3OCH_3]^{3/2}.$$

The relative rate is therefore

$$\frac{v}{v_0} = \frac{k_{20}\left(\frac{2k_{1a}}{k_{23a}}\right)^{1/2}[CH_3OCH_3]^{3/2}}{k_2\left(\frac{2k_{1a}}{k_7}\right)^{1/2}[CH_3OCH_3]^{3/2}},$$

which reduces to

$$\frac{v}{v_0} = \frac{k_{20}}{k_2}\left(\frac{k_7}{k_{23a}}\right)^{1/2}.$$

The predicted activation energy for the relative rate in this region is therefore

$$E = E_{20} - E_2 + \tfrac{1}{2}(E_7 - E_{23a}).$$

Substitution of the appropriate values from Table I yields $E = -0.45$ kcal mole^{-1}. This is in good agreement with the experimental value determined by subtracting the activation energy for the reaction in the absence of H_2S from the activation energy for the reaction in the presence of 40% H_2S, i.e. $53.2 - 54.9 = -1.7$ kcal mole^{-1}. This explains why the relative rate seems to increase with decreasing temperature. The fact that -1.7 is so small is indicated from Fig. 2, which shows that the curves for the three temperatures fall very close to one another.

Similarly for the region using high percentages of hydrogen sulphide the relative rate is given by

$$\frac{v}{v_0} = \frac{k_{20}}{k_2}\left(\frac{k_{19}k_7}{k_{1a}k_{23a}}\right)^{1/2}\frac{[H_2S]^{1/2}}{[CH_3OCH_3]^{1/2}}.$$

Can. J. Chem. Downloaded from www.nrcresearchpress.com by 210.87.254.5 on 09/05/12
For personal use only.

The activation energy for the relative rate is predicted to be

$$E = E_{20} - E_2 + \tfrac{1}{2}(E_{19} + E_7 - E_{1a} - E_{23a})$$
$$= 3.85 \text{ kcal mole}^{-1}.$$

This is in fair agreement with the experimental value of -2.4 kcal mole^{-1}, considering the uncertainties in the individual activation energies.

ACKNOWLEDGMENTS

The authors are indebted to Dr. B. W. Wojciechowski for valuable suggestions. The work was supported by grants from the National Research Council and the Petroleum Research Fund.

REFERENCES

1. K. E. J. Barrett and W. A. Waters. Discussions Faraday Soc. **14**, 221 (1953).
2. R. N. Birrell, R. F. Smith, A. F. Trotman-Dickenson, and H. Wilkie. J. Chem. Soc. 2807 (1957).
3. J. A. Kerr and A. F. Trotman-Dickenson. J. Chem. Soc. 3322 (1957).
4. N. Imai and O. Toyama. Bull. Chem. Soc. Japan, **33**, 1120 (1960).
5. N. Imai, Y. Yoshida, and O. Toyama. Bull. Chem. Soc. Japan, **35**, 752, 759 (1962).
6. N. Imai and O. Toyama. Bull. Chem. Soc. Japan, **34**, 328 (1961).
7. N. Imai and O. Toyama. Bull. Chem. Soc. Japan, **33**, 1408 (1960).
8. K. J. Laidler and B. W. Wojciechowski. Proc. Roy. Soc. (London), Ser. A, **259**, 257 (1960).
9. B. De B. Darwent and R. Roberts. Proc. Roy. Soc. (London), Ser. A, **216**, 344 (1953).
10. S. W. Benson and D. V. S. Jain. J. Chem. Phys. **31**, 1008 (1959).
11. N. Imai and O. Toyama. Bull. Chem. Soc. Japan, **33**, 652 (1960).
12. T. L. Cottrell. The strengths of chemical bonds. Butterworths Scientific Publications, London. 1958. p. 188.
13. J. W. C. Johns and D. A. Ramsay. Can. J. Phys. **39**, 210 (1961).
14. Selected Values of Chemical Thermodynamic Properties. Natl. Bur. Std. (U.S.), Circr. 500. 1952.
15. D. A. Ansdell and F. M. Page. Trans. Faraday Soc. **58**, 1084 (1962).
16. H. Mackle and R. T. B. McClean. Trans. Faraday Soc. **58**, 895 (1962).
17. F. Palmer and F. P. Lossing. J. Am. Chem. Soc. **84**, 4661 (1962).

Can. J. Chem. Downloaded from www.nrcresearchpress.com by 210.87.254.5 on 09/05/12
For personal use only.

THE METAL-CATALYZED AUTOXIDATION OF TETRALIN

I. INTRODUCTION. THE COBALT-CATALYZED AUTOXIDATION IN ACETIC ACID[1]

Y. KAMIYA,[2] S. BEATON,[3] A. LAFORTUNE, AND K. U. INGOLD
Division of Applied Chemistry, National Research Council, Ottawa, Canada

Received April 23, 1963

ABSTRACT

The catalytic effect of transition metal salts on the rate of autoxidation of organic substances reaches a constant value at some critical catalyst concentration. Three possible explanations of this phenomena are critically examined. The cobalt acetate catalyzed autoxidation of tetralin in acetic acid has been reinvestigated and the limiting rate of oxidation at high cobalt concentrations has been shown to be due to the production of a steady-state concentration of hydroperoxide. The present results are in fair agreement with the experimental work of Woodward and Mesrobian (J. Am. Chem. Soc. **75**, 6189 (1953)) and are in excellent agreement with theoretical predictions.

Can. J. Chem. Downloaded from www.nrcresearchpress.com by 210.87.254.40 on 09/05/12
For personal use only.

INTRODUCTION

Although it has been known for many years that trace amounts of the salts of heavy metals, particularly transition metals, generally increase the rates of autoxidation of organic substances many details of the processes involved are still not fully understood (1, 2). In particular, it has frequently been observed, both in polar (3, 4) and non-polar (5–8) media, that the catalytic effect of metal salts reaches a constant value at some critical concentration, further increases in the concentration of the metal salt having no further effect on the rate. Three explanations have been advanced to explain this phenomena.

1. The Catalyst Produces a Steady-State Concentration of Hydroperoxide

Only this explanation has received experimental support, which has been provided by Woodward and Mesrobian (3) in their very fine work on the cobaltous acetate catalyzed oxidation of tetralin in acetic acid. Their work confirmed a suggestion made by Tobolsky in 1948 (9) that the limiting rate of oxidation is reached when the rate of formation of hydroperoxide is equal to its rate of decomposition to free radicals by the catalyst. This theory was presented in greater detail and was backed up with experimental results on the photochemically induced oxidation of rubber by Tobolsky, Metz, and Mesrobian in 1950 (10). Since the results obtained in this and the following paper are in good agreement with this theory it will be discussed in some detail and, so far as is possible, we shall use the same nomenclature as Woodward and Mesrobian to facilitate comparison of the two sets of data.

The kinetic scheme is represented by:

$$\mathrm{ROOH} + n\mathrm{CoAc_2} \xrightarrow{k_1'} \text{radical} \xrightarrow{\mathrm{RH}} \mathrm{R}^{\bullet} \qquad [1D]$$

$$\mathrm{R}^{\bullet} + \mathrm{O_2} \xrightarrow{k_2} \mathrm{RO_2}^{\bullet} \qquad [2D]$$

$$\mathrm{RO_2}^{\bullet} + \mathrm{RH} \xrightarrow{k_3} \mathrm{ROOH} + \mathrm{R}^{\bullet} \qquad [3D]$$

$$\mathrm{RO_2}^{\bullet} + \mathrm{RO_2}^{\bullet} \xrightarrow{k_6} \text{inactive products} + \mathrm{O_2}. \qquad [4D]$$

[1]*Issued as N.R.C. No. 7440.*
[2]*N.R.C. Postdoctoral Fellow 1962–1963.*
[3]*N.R.C. Summer Student 1962.*

The cobalt catalyst cycles continuously between its divalent and trivalent state by reacting with hydroperoxide and producing free radicals at each step. The reactions can be represented by:

$$ROOH + Co^{2+} \rightarrow RO^{\bullet} + HO^{-} + Co^{3+} \quad [1B]$$

$$ROOH + Co^{3+} \rightarrow RO_2^{\bullet} + H^{+} + Co^{2+} \quad [1C]$$

so that, under steady-state conditions,

$$k_{1B}[Co^{2+}] = k_{1C}[Co^{3+}] = \tfrac{1}{2}k_1'[Co].$$

When the rate of hydroperoxide decomposition is negligible compared with its rate of formation, the overall rate of oxidation is given by

$$\frac{-d[O_2]}{dt} = k_3\left(\frac{k_1'}{2k_6}\right)^{1/2}[RH][ROOH]^{1/2}[CoAc_2]^{n/2}. \quad [2]$$

As the hydroperoxide concentration increases with time its rate of decomposition will eventually equal its rate of formation. This steady-state concentration is given by

$$[ROOH]_\infty = \frac{k_3^2[RH]^2}{2k_1'k_6[CoAc_2]^n} \quad [3]$$

and, therefore, the maximum rate of oxidation is given by

$$\left(\frac{-d[O_2]}{dt}\right)_\infty = \frac{k_3^2[RH]^2}{2k_6}. \quad [4]$$

In actual fact, this derivation of equation [3] and [4] is oversimplified since no account is taken of the $RO^{\bullet}$ radicals produced in reaction [1B] nor of the oxygen evolved in reaction [4D]. Both reactions are, of course, of major importance in the limiting-rate region where every molecule of hydroperoxide decomposed produces only one new molecule of hydroperoxide. In this region, a more complete kinetic treatment including the reactions

$$RO^{\bullet} + RH \rightarrow R^{\bullet} + ROH \quad [3E]$$

and

$$RO^{\bullet} + RO^{\bullet} \rightarrow \text{inactive products} \quad [4E]$$

in addition to reactions [1B], [1C], [2D], [3D], and [4D] also gives equations [3] and [4] provided $k_{3E}^2[RH]^2 \gg 4k_1'k_{4E}[Co][ROOH]_\infty$. Moreover, this derivation shows that two molecules of oxygen oxidize three molecules of tetralin in the limiting-rate region, i.e. $(d[RH]/dt)/(-d[O_2]/dt)_\infty = 1.5$, and also shows that the rate of decomposition of hydroperoxides is equal to the rate of oxidation, i.e. $k_1'[Co][ROOH]_\infty = (-d[O_2]/dt)_\infty$.

Equations [3] and [4] were apparently verified experimentally by Woodward and Mesrobian. That is, it was shown that the rate of oxidation reached a constant value at, or above, a cobalt acetate concentration of 2.0×10^{-3} mole/l. However, our own results indicate that the true maximum rate is not achieved until the cobalt acetate concentration is more than 5.0×10^{-2} mole/l. The steady-state hydroperoxide concentration was shown to be proportional to the square of the cobalt acetate concentration from 1.0×10^{-3} to 4.0×10^{-3} mole/l. $[CoAc_2]$, i.e. $n = 2$ in equation [3], suggesting that the active catalyst is a dimer. At a cobalt acetate concentration of 2×10^{-3} mole/l., $[ROOH]_\infty$ was also shown to be proportional to the square of the tetralin concentration in the range 0.2 to 1.8

Can. J. Chem. Downloaded from www.nrcresearchpress.com by 210.87.254.40 on 09/05/12
For personal use only.

mole/l. [RH]. The oxidation rate at 2.0×10^{-3} mole/l. [$CoAc_2$] was also stated to be proportional to the square of the tetralin concentration, but this might be a misprint. That is, this relationship is shown in Fig. 3 of Woodward and Mesrobian's paper and the order is given as 1.93, but actual measurement of the graph shows that the order is nearer 1.73, although it might be as high as 1.8. However, we have shown that at the true maximum rate the order is indeed 2.0 with respect to tetralin, as required by equation [4].

The theoretical limiting rate of oxidation can be obtained experimentally in the absence of cobalt acetate by measuring the rate of oxidation in the presence of a free-radical initiator such as 2,2′-azo-bis-isobutyronitrile (AIBN) or benzoyl peroxide. Again following Woodward and Mesrobian's kinetic scheme, we have,

$$\text{initiator} \xrightarrow{k_7} 2R'^{\bullet} \xrightarrow{RH} 2R^{\bullet}. \qquad [1A]$$

Hence,

$$\frac{-d[O_2]}{dt} = k_3\left(\frac{2e_1k_7}{2k_6}\right)^{1/2}[RH][\text{initiator}]^{1/2}; \qquad [1]$$

therefore,

$$\frac{\left(\frac{-d[O_2]}{dt}\right)^2}{2e_1k_7[\text{initiator}]} = \frac{k_3^2[RH]^2}{2k_6}, \qquad [7]$$

where e_1, the efficiency of initiation, was taken to have its maximum value of 1.0. With this assumption, which is by no means correct (see below), the theoretical limiting rate obtained with AIBN and benzoyl peroxide was in fairly good agreement with the measured rate at a cobalt acetate concentration of 2.0×10^{-3} mole/l.

Woodward and Mesrobian also showed that the rate of tetralin hydroperoxide decomposition by cobalt acetate in equimolar mixtures of benzene and acetic acid was roughly first order in hydroperoxide and was *approximately* proportional to the square of the cobalt concentration, i.e.,

$$\frac{-d[ROOH]}{dt} = k_1'[ROOH][CoAc_2]^2. \qquad [5]$$

In actual fact, this decomposition appears to be quite complicated and, in addition, its rate shows a strong solvent dependence (see later). However, these authors compared the value of k_1' determined by direct measurement under nitrogen in a 1:4 tetralin – acetic acid mixture (i.e. 40 $l^2/mole^2$ sec) with the value calculated from the ratio of equation [4] to equation [3], i.e.

$$\frac{\left(\frac{-d[O_2]}{dt}\right)_\infty}{[ROOH]_\infty} = k_1'[CoAc_2]^n. \qquad [6]$$

Their comparison is given in their Table IV for a tetralin concentration of 1.84 mole/l. and a cobalt acetate concentration of 2.0×10^{-3} mole/l. Although the agreement in k_1' appears to be fairly good some mistakes have apparently been made in this table. From the data given in their numerous figures it can readily be calculated that the table should

Can. J. Chem. Downloaded from www.nrcresearchpress.com by 210.87.254.40 on 09/05/12
For personal use only.

read as follows, where the numbers in parenthesis are the numbers given by Woodward and Mesrobian:

$(-d[O_2]/dt)_\infty$, mole/l. sec	$[ROOH]_\infty$, mole/l.	k_1' (calc.), $l^2/mole^2$ sec	k_1' (obs.), $l^2/mole^2$ sec
2.93×10^{-5}	~0.25	29.3*	†
(2.93×10^{-5})	(0.140)	(52)	(40)

*At $[ROOH]_\infty = 0.140$ mole/l., $(-d[O_2]/dt)_\infty = 1.5\times10^{-5}$ mole/l. sec, giving $k_1' = 26.8$ $l^2/mole^2$ sec.
†k_1' obtained from the data given at 2.0×10^{-3} mole/l. [$CoAc_2$] in the equimolar benzene – acetic acid mixture is 210 $l^2/mole^2$ sec.

In spite of the errors which seem to have slipped into Woodward and Mesrobian's calculations the agreement between their results and Tobolsky's theory is sufficiently close to confirm its major premise. Our own work has largely confirmed their data and, moreover, where our results differ they give an even better agreement with the theoretical predictions.

It should perhaps be added that Denisov and Emanuel (2) have pointed out that rather similar kinetic expressions can be obtained by including the catalyzed decomposition of hydroperoxides to non-radical products or by including a radical-induced hydroperoxide decomposition plus the formation of a new radical by the reaction of a peroxy radical with the catalyst. However, neither of these kinetic treatments predicts the agreement that is actually found between the measured maximum rate and the theoretical limiting rate.

2. Micelle Formation by the Catalyst

In hydrocarbon media metal salts of organic acids are normally associated into micelles (7) except at very low concentrations. Once the critical micelle concentration has been passed further increases in catalyst will tend to cause an increase in the size and number of micelles rather than an increase in the amount of catalyst in true solution. If the micelles are inactive catalysts the rate of oxidation will therefore reach a maximum value at the critical micelle concentration. This has been suggested by various authors (2, 7), but it seems probable that the catalyst in micelle form should have some activity and the rate of oxidation should therefore show a slow increase as the catalyst concentration is increased rather than reaching a true maximum. However, most transition metal salts are not very soluble in non-polar media at low temperatures and a comparatively inactive catalyst might therefore be too insoluble for its concentration in true solution or in micelles ever to rise to a value where the rate of hydroperoxide decomposition equalled the rate of the propagation reaction. In this way, an apparent steady limiting rate could be obtained. This cause of limiting rates is more likely to occur at low temperatures than at high temperatures where the catalyst would be more soluble.

3. Chain Termination by the Catalyst

In 1946, on the basis of a study of the cupric, ferric, and cobaltous stearate catalyzed oxidations of tetralin and stearic acid, George *et al.* (6) suggested the the metal catalysts both initiate and terminate free-radical chains. They represented the rate of oxidation by

$$R_m = \frac{(a+dm)}{(b+em)} \cdot p,$$

where a and b are the initiation and termination rates in the thermal oxidation, d and e are the rates of initiation and termination for unit catalyst concentration, p is the propagation

Can. J. Chem. Downloaded from www.nrcresearchpress.com by 210.87.254.40 on 09/05/12
For personal use only.

rate, and m the catalyst concentration. On this very simple basis it is obvious that the rate will be independent of the catalyst concentration when dm and em are much greater than a and b. More sophisticated kinetic treatments of chain termination by the catalyst indicate that the true rate expression is far more complicated than this simple derivation suggests (1). Moreover, it has been pointed out (2) that, at the high oxidation rates normally involved with metal catalysts, the peroxy radical concentration will be large and therefore the normal bimolecular termination reaction between two peroxy radicals is intrinsically more probable than a reaction between a peroxy radical and the catalyst.

In spite of these arguments, Kropf (8), has preferred to interpret his results on the copper, cobalt, nickel, and vanadium phthalocyanine catalyzed oxidation of cumene and some other alkyl benzenes in terms of this mechanism. Tobolsky's theory of limiting rates was dismissed without serious consideration mainly because there was an almost quantitative production of cumene hydroperoxide at temperatures below 105° C when copper phthalocyanin was used as the catalyst. It was therefore concluded that chain initiation did not occur primarily by reactions [1B] or [1C] and for this reason the limiting rate of oxidation could not be due to the formation of a steady-state concentration of hydroperoxide. However, the limiting rates of oxidation were obtained by extrapolation, to infinite catalyst concentrations, of the measured rates at two to four catalyst concentrations only, rather than by increasing the catalyst concentration until the limiting rate was achieved. The catalyst concentrations were in the range 7×10^{-4} to 5×10^{-3} mole/l. and if the chain length is fairly long in this concentration range hydroperoxide could form the major oxidation product. The Tobolsky theoretical limiting rate of oxidation at 60° C can be calculated from the data of Blanchard (11) on the AIBN-catalyzed oxidation of cumene by means of equation [7]. It is found to be about 5.4×10^{-4} mole/l. sec. At this temperature the rates of oxidation at infinite catalyst concentration can be calculated from Kopf's data to be 7.3×10^{-4} (Co), 2.6×10^{-4} (Ni), 4.7×10^{-5} (Cu), and 7.5×10^{-6} mole/l. sec (V). Considering the method by which the limiting rates were obtained these values strongly suggest that Tobolsky's theories are applicable to this system with cobalt phthalocyanine and, quite probably, also with nickel phthalocyanine.

In the liquid phase free radicals are never completely "free", that is, their reactivity is modified by the surrounding medium, decreasing reactivity with change of solvent being associated with the increasing stability of a radical–solvent complex. Recent work has shown that in both polar and non-polar solvents free radicals are even less "free" in the presence of heavy metals (1). For example, the decomposition of hydroperoxides and peroxides in the presence of heavy metals, particularly copper, yields radicals which are much less reactive than those obtained by thermal decomposition since they show a much greater stereospecificity in their subsequent reactions than do thermally produced radicals (1). As a result of the stabilization of peroxy radicals by metal salts the rate of chain propagation may be expected to decrease. The rate of chain termination might either increase or decrease. In general, the decrease in the rate of propagation more than outweighs any decrease in the rate of termination (12, 13) although the opposite effect has also been observed in the cobalt-catalyzed oxidation of cumene (14).* Since theory predicts a limiting rate equal to $k_3^2[RH]^2/2k_6$ and since both k_3 and k_6 will change if the radicals are complexed with the metal catalyst the measured limiting rate might be either larger or smaller† than the theoretical value depending on the relative influence of the catalyst on

*This result may possibly explain the fact that Kropf's limiting rate for the cobalt-catalyzed oxidation of cumene is larger than the theoretical value.

†In Part II of this series, it is shown that the measured limiting rate will also be smaller than the theoretical value if the catalyst decomposes some of the hydroperoxide to non-radical products.

Can. J. Chem. Downloaded from www.nrcresearchpress.com by 210.87.254.40 on 09/05/12
For personal use only.

k_3 and k_6. This means that different metal catalysts could give different limiting rates even though the cause of the limiting rate is in all cases due to the production of a steady-state hydroperoxide concentration. The absolute value of a measured limiting rate is therefore not a criterion of the validity of Tobolsky's theory, the only sure criterion being a dependence of the limiting rate of oxidation on $[RH]^2$ and an agreement between k_1' measured directly and indirectly when this is possible. The limiting rates of oxidation of cumene obtained by Kropf for copper and even vanadium phthalocyanine do not, therefore, disprove the Tobolsky theory of limiting rates for these metals.

It is clear from the foregoing discussion that only the first theory of limiting rates has been properly confirmed and then only with the metal cobalt and under rather unusual oxidation conditions. That is, it has only been confirmed in a highly polar solvent in which both the catalyst and hydrocarbon are fully soluble up to quite high concentrations so that, even though polar media are known to reduce the efficiency of metal catalysts (15), solubilities do not affect the kinetics. As a preliminary to a study of the effect of high concentrations of various metal catalysts on oxidation rates in non-polar media we have repeated the work of Woodward and Mesrobian on the cobaltous acetate catalyzed oxidation of tetralin in acetic acid. The second paper in this series deals with the cobalt catalyzed oxidation of undiluted tetralin (16).

EXPERIMENTAL

The purification of tetralin and the oxygen absorption apparatus have been described previously (17). All the experiments described in this work were done at 50° C. The cell cleaning procedure was that of Chalk and Smith (18) with the addition of a final heating of the cell to the softening point of glass in a stream of dry air. Tetralin hydroperoxide was prepared and analyzed by the method of Woodward and Mesrobian (3). It was stored at −10° C. Acetic anhydride (1% by volume) was added to freshly opened bottles of glacial acetic acid 24 hours before use (3). Anhydrous cobaltous acetate was prepared by dehydrating the tetrahydrate and 2,2′ azo-bis-isobutyronitrile (AIBN) was carefully recrystallized from ethyl alcohol at tempratures below 40° C.

RESULTS AND DISCUSSIONS

Determination of the Theoretical Maximum Rate of Autoxidation

Measurements of the rate of nitrogen evolution from AIBN dissolved in tetralin under oxygen-free helium at 50° C gave

$$k_7 = 2.33\times10^{-6}\ \text{sec}^{-1},$$

in good agreement with previous work in benzene (19), toluene (19), and styrene (20). The efficiency of chain initiation by AIBN was calculated in the usual manner (20) by measuring the induction period produced in the AIBN-catalyzed oxidation of tetralin by a known concentration of the free-radical inhibitor 2,6 di-*tert*-butyl-4-methylphenol (BMP). It was found that the efficiency $e_1 = 0.65$, in good agreement with the value found in several other hydrocarbons (20). Measurements of the rate of oxidation of tetralin at several AIBN concentrations yield the relation

$$\frac{-d[O_2]}{dt} = 5.5\times10^{-5}[\text{AIBN}]^{1/2}\ \text{mole/l. sec}$$

at 50° C after correcting for the nitrogen evolution by the AIBN. From equation [7], the theoretical limiting rate of the metal-catalyzed oxidation of tetralin at 50° C is given by

$$\frac{k_3^2[RH]^2}{2k_6} = \frac{(5.5\times10^{-5})^2}{2\times0.65\times2.33\times10^{-6}} = 1.0\times10^{-3}\ \text{mole/l. sec.}$$

Can. J. Chem. Downloaded from www.nrcresearchpress.com by 210.87.254.40 on 09/05/12
For personal use only.

Oxygen Absorption and Hydroperoxide Formation

The absorption of oxygen and the buildup of hydroperoxide to a steady concentration in a typical experiment are shown in Fig. 1. At a given tetralin concentration the maximum rate of oxidation is independent of the cobalt acetate concentration in the range 5.0×10^{-2} to 1.0 mole/l. Within this range of catalyst concentrations the rate is exactly proportional to the square of the tetralin concentration from 0.4 to 4.0 mole/l. as required by equation [4]. Extrapolation of these measured maximum rates to obtain the maximum rate of oxidation of pure tetralin gives a value of $1.00\pm(0.05)\times10^{-3}$ mole/l. sec, in perfect agreement with the theoretical limiting rate. This agreement by itself provides convincing evidence of the validity of Tobolsky's theory of limiting rates. This limiting rate can be compared with the value of 3.3×10^{-4} mole/l. sec which is obtained by a linear extrapolation of Woodward and Mesrobian's data at a cobalt acetate concentration of 2.0×10^{-3} mole/l.

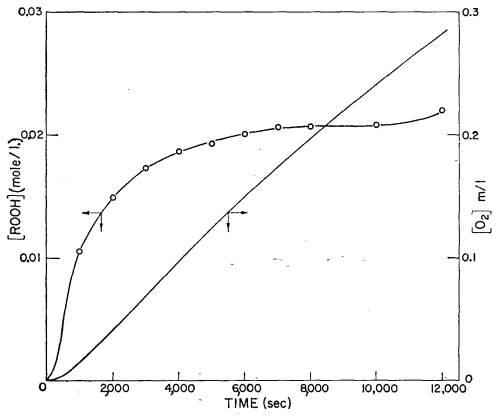

FIG. 1. Oxygen absorption and hydroperoxide formation during the oxidation of 1.22 mole/l. of tetralin in acetic acid catalyzed by 6.0×10^{-3} mole/l. of cobalt acetate.

At high catalyst concentrations the decrease in rate after the maximum fairly closely follows the oxygen consumption with a square dependence on the unconsumed tetralin. That is, the measured rate divided by the square of the tetralin concentration is approximately constant from the maximum-rate region up to at least a 20% consumption of the tetralin, provided it is assumed that two molecules of oxygen oxidize three molecules of tetralin. This provides an independent check on the reaction order with respect to [RH] in the limiting-rate region, and, furthermore, proves that cobalt is a true catalyst in this system, i.e., it is not deactivated in the reaction.

The induction period, defined as the intercept of the extrapolated maximum rate on the time axis, is about 1 minute at high cobalt concentrations. At lower cobalt concentrations the induction period increases remarkably and, at a given cobalt concentration, it increases with increasing dilution of the tetralin, i.e. with increasing dilution of the hydroperoxide which is initially present in the tetralin (normally about 10^{-3} mole/l.). At cobalt concentrations below 10^{-3} mole/l. it is necessary to add hydroperoxide at the start of the reaction in order to reach the maximum rate in a reasonable length of time. At a given tetralin concentration the reaction order with respect to tetralin decreases with decreasing cobalt concentration, probably to its limiting value of 1.0 defined by equation [2]. At a given cobalt concentration this reaction order tends to increase to its limiting value of 2.0

Can. J. Chem. Downloaded from www.nrcresearchpress.com by 210.87.254.40 on 09/05/12
For personal use only.

(as defined by equation [4]) with decreasing tetralin concentration.* For example, with 10^{-2} mole/l. [Co] the rate is equal to the limiting rate at tetralin concentrations below 1.9 mole/l. (i.e. rate $\propto$ [RH]^2 in this region), but at a tetralin concentration of 3.67 mole/l. the rate is only 1.9×10^{-4} mole/l. sec compared with a limiting rate of 2.5×10^{-4} mole/l. sec. Therefore, the rate of oxidation of pure tetralin cannot be obtained by extrapolation except in the region of the limiting rate where the order in [RH] is constant. The oxidation rates found in this work at 2×10^{-3} mole/l. [Co] are about 50% greater than those reported by Woodward and Mesrobian.

Oxidation rates were measured over a range of cobalt acetate concentrations from 10^{-4} to 1.0 mole/l. For example, the following rates in mole/l. sec$\times10^4$ were obtained at a tetralin concentration of 3.67 mole/l., the cobalt concentration in mole/l. being given in parentheses: 2.5 (1.0, 10^{-1}, 5×10^{-2}), 1.9 (10^{-2}), 1.3 (10^{-3}), 0.20 (10^{-4}). At this tetralin concentration limiting-rate effects become comparatively unimportant below 10^{-3} mole/l. [Co] and the rate of oxidation becomes almost first order in cobalt. Therefore, $n = 2$ in equation [2] and the reaction chains are initiated by a cobalt acetate dimer.

It can be seen from Fig. 1 that the hydroperoxide concentration rises to a steady value during the cobalt-catalyzed oxidation of tetralin in acetic acid. The steady-state concentration of hydroperoxide obtained in this experiment, i.e., $[ROOH]_\infty = 0.021$ mole/l. at [Co] $= 6\times10^{-3}$ mole/l., [RH] = 1.22 mole/l., and $[ROOH]_0 = 2\times10^{-4}$ mole/l., is in excellent agreement with the value obtained by extrapolation of Woodward and Mesrobian's data at lower cobalt concentrations. An "initial rate" method was used by these authors to measure $[ROOH]_\infty$. That is, given amounts of the pure hydroperoxide were added to the other reagents previously placed in the reaction vessel. Reaction conditions identical with those used in oxygen absorption measurements were maintained but instead of recording oxygen uptake two aliquots of the reaction mixture were taken for hydroperoxide determination. The first aliquot, removed immediately after the addition of the hydroperoxide, served to establish $[ROOH]_0$ and the added hydroperoxide concentration was varied until this quantity became identical with the hydroperoxide concentration found in the second aliquot, which was removed at a later fixed time interval. This constant hydroperoxide concentration was taken to represent $[ROOH]_\infty$. These authors pointed out that the advantage of this technique is that the change in tetralin concentration during reaction is negligibly small and also any products of peroxide decomposition or tetralin oxidation which may impart an inhibiting effect to the reaction are held to a minimum.

The decomposition of tetralin hydroperoxide in benzene – acetic acid mixtures is a very complex reaction (see following section). After elucidating some of its complexities we realized that the simple dependence of $[ROOH]_\infty$ on [RH]^2 predicted by equation [3] and reported by Woodward and Mesrobian could not be an accurate representation of the kinetics during oxidation. Using Woodward and Mesrobian's method of determining $[ROOH]_\infty$ by varying $[ROOH]_0$, but removing several aliquots of the reaction mixture at varying time intervals to ensure that the true $[ROOH]_\infty$ was obtained, the variation of $[ROOH]_\infty$ with [RH] was measured at a cobalt concentration of 6×10^{-3} mole/l. The data are given in Table I and it is found that instead of $[ROOH]_\infty$ being proportional to [RH]^2 it is proportional to [RH]^2[AcH]^2, where [AcH] represents the acetic acid concentration. This relationship is in agreement with our results for the cobalt acetate catalyzed decomposition of the hydroperoxide in benzene – acetic acid mixtures. It should be noted, moreover, that the value of $[ROOH]_\infty$ determined by this technique is significantly lower

See following paper for a full discussion of the influence of limiting-rate effects on reaction order.

Can. J. Chem. Downloaded from www.nrcresearchpress.com by 210.87.254.40 on 09/05/12
For personal use only.

than the value found when the hydroperoxide concentration is allowed to build up to its steady-state value during the oxidation, probably because a significant portion of the tetralin is oxidized at this point. For example, at [RH] = 1.22 mole/l. and [Co] = 6×10^{-3} mole/l., $[ROOH]_\infty$ = 0.0120 mole/l. by the initial method (Table I) but equals 0.021 mole/l. by the continuous oxidation method (Fig. 1). At the highest tetralin concentration (3.67 mole/l.) the hydroperoxide concentration is only constant for about 700 seconds and thereafter starts to increase, possibly because of a deactivation of the catalyst at this tetralin concentration (see following paper). At the other three tetralin concentrations the hydroperoxide concentration is constant for more than 3000 seconds.

TABLE I

Dependence of $[ROOH]_\infty$ on [RH] and [AcH] at a cobalt concentration of 6×10^{-3} mole/l.

[RH], mole/l.	[AcH], mole/l.	$[ROOH]_\infty$, mole/l.	$\frac{[ROOH]_\infty}{[RH]^2}$, l./mole	$\frac{[ROOH]_\infty}{[RH]^2[AcH]^2}\times10^5$, $l^3/mole^3$
0.668	15.88	0.0044	0.00986	3.91
1.224	14.56	0.0120	0.00801	3.79
1.836	13.10	0.0220	0.00653	3.81
3.673	8.735	0.0395	0.00293	3.84

NOTE: [RH] represents tetralin concentration and [AcH] acetic acid concentration.

The variation of $[ROOH]_\infty$ with [Co] at a tetralin concentration of 1.22 mole/l. is shown in Fig. 2. Over a range of cobalt concentrations from 1.0×10^{-3} to 8.0×10^{-3} mole/l.,

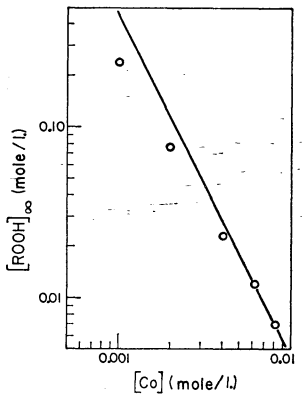

FIG. 2. Dependence of $[ROOH]_\infty$ on cobalt acetate concentration for 1.22 mole/l. of tetralin in acetic acid. The line drawn on the figure has a slope of 2.0.

$[ROOH]_\infty$ is approximately proportional to $[Co]^{-1.7}$ but the experimental points show some curvature and at cobalt concentrations above 6×10^{-3} mole/l., $[ROOH]_\infty$ appears to become approximately inversely proportional to the square of the cobalt concentration. The line that has been drawn in Fig. 2 has this limiting slope of 2.0. As the cobalt concentration is reduced, $[ROOH]_\infty$ becomes inversely proportional to a lesser power of the cobalt concentration. This effect is apparently due to the occurrence of a radical-induced decomposition of the hydroperoxide, a reaction which also causes the measured rate constant for the cobalt-catalyzed decomposition of tetralin hydroperoxide to increase as the cobalt concentration is decreased (see following section). It might be added that the

Can. J. Chem. Downloaded from www.nrcresearchpress.com by 210.87.254.40 on 09/05/12
For personal use only.

determination of $[ROOH]_\infty$ at cobalt concentrations below 2×10^{-3} mole/l. is very time consuming since the rate of change of hydroperoxide concentration becomes very small. A great many experiments are therefore necessary to ensure that the initially added hydroperoxide concentration is very close to $[ROOH]_\infty$ and that at least two of the initial concentrations bracket $[ROOH]_\infty$ within $\pm10\%$.

It seems reasonable to assume that most of the cobalt acetate and most of the hydroperoxide will be associated with molecules of acetic acid in this system even in quite dilute acetic acid solutions. Making the further assumption that the catalytically active dimer of cobalt acetate contains one less molecule of acetic acid than the monomer and that this dimer reacts only with free hydroperoxide we can write

$$2(CoAc_2AcH) \rightleftarrows ((CoAc_2)_2AcH) + AcH \qquad [a]$$

$$(ROOHAcH) \rightleftarrows ROOH + AcH \qquad [b]$$

$$(CoAc_2)_2AcH + ROOH \rightarrow \text{radical} \qquad [1]$$

$$\text{radical} + RH \rightarrow ROOH + \text{radical} \qquad [3]$$

$$\text{radical} + ROOH \rightarrow \text{radical} \qquad [i]$$

$$\text{radical} + \text{radical} \rightarrow \text{inactive products.} \qquad [6]$$

This reaction scheme is only intended to be illustrative and not in any way exclusive of other similar reaction schemes. For example, the rate-controlling chain-initiation step could equally well involve a trivalent cobalt dimer or charged dimer without in any way affecting the resultant kinetics. Replacing $(CoAc_2AcH)$ by Co on the assumption that all the monomeric cobalt acetate is associated with acetic acid and applying the usual stationary-state approximation, we obtain

$$[\text{radical}] = \left(\frac{k_1K_aK_b}{2k_6}\right)^{1/2}\frac{[Co]}{[AcH]}[ROOHAcH]^{1/2}.$$

The steady-state concentration of hydroperoxide is given by

$$\frac{-d[ROOH]}{dt} = \frac{-d[ROOHAcH]}{dt} = 0 = \frac{k_1K_aK_b[Co]^2[ROOHAcH]_\infty}{[AcH]^2}$$
$$+ k_i\left(\frac{k_1K_aK_b}{2k_6}\right)^{1/2}K_b\frac{[Co]}{[AcH]^2}[ROOHAcH]_\infty^{3/2} - k_3\left(\frac{k_1K_aK_b}{2k_6}\right)^{1/2}\frac{[Co]}{[AcH]}[RH][ROOHAcH]_\infty^{1/2}.$$

This quadratic expression simplifies to

$$[ROOHAcH]_\infty = \frac{k_3^2[RH]^2[AcH]^2}{2k_6k_1K_aK_b[Co]^2} \qquad [3']$$

at high cobalt concentrations, provided $[Co]^2 \gg (2k_ik_3[RH][AcH])/(k_1k_6K_a)$. Under these conditions the induced decomposition becomes unimportant compared with the direct cobalt-catalyzed decomposition. The measured steady-state concentration of hydroperoxide corresponds to $[ROOHAcH]_\infty$ and is described by equation [3′] at cobalt concentrations of 6×10^{-3} mole/l. and higher (see Table I and Fig. 2).* In the cobalt con-

**An expression similar to equation [3′] is also obtained if it is assumed that either the hydroperoxide is not associated with acetic acid, or that the associated hydroperoxide reacts with the active cobalt dimer, provided the concentration of this dimer is inversely proportional to the square of the acetic acid concentration, e.g.*

$$2(CoAc_2AcH) \rightleftarrows (CoAc_2)_2 + 2AcH.$$

However, in this case the kinetics derived for the cobalt-catalyzed decomposition of the hydroperoxide do not fit the observed results in acetic acid – benzene mixtures quite as well as the kinetics derived from the equations outlined above.

Can. J. Chem. Downloaded from www.nrcresearchpress.com by 210.87.254.40 on 09/05/12
For personal use only.

centration range where this equation applies, the limiting rate of oxidation will be achieved and is given by

$$\left(\frac{-d[O_2]}{dt}\right)_\infty = \frac{k_3^2[RH]^2}{2k_6} \qquad [4]$$

as is found experimentally. At lower cobalt concentrations, $[ROOHAcH]_\infty$ will become inversely proportional to a power of the cobalt concentration which will decrease from its maximum value of 2.0 as the cobalt concentration is reduced (see Fig. 2). Under these conditions, there is, of course, too low a concentration of cobalt acetate for the oxidation rate to reach its limiting value. Moreover, at these low cobalt concentrations the maximum rate of oxidation appears to be unaffected by the initial hydroperoxide concentration. This suggests that reaction [1] occurs by way of an intermediate complex, as has already been suggested by several workers (6, 18, 21, 22, 23), i.e.

$$(CoAc_2)_2AcH + ROOH \rightleftarrows ((CoAc_2)_2AcHROOH) \xrightarrow{k_1} \text{radical.}$$

Dividing equation [4] by equation [3′] we obtain

$$\left(\frac{-d[O_2]}{dt}\right)_\infty \Big/ [ROOHAcH]_\infty = \frac{k_1K_aK_b[Co]^2}{[AcH]^2}. \qquad [6']$$

At a cobalt concentration of 6×10^{-3} mole/l. and a tetralin concentration of 1.224 mole/l., $[ROOHAcH]_\infty = 0.0120$ mole/l. (Table I). At this tetralin concentration the limiting rate of oxidation is 2.8×10^{-5} mole/l. sec and because the tetralin is fairly dilute this rate is achieved with 6×10^{-3} mole/l. [Co].* Substituting these values into equation [6′] we obtain

$$k_1K_aK_b = 13{,}740 \text{ sec}^{-1}.$$

Hydroperoxide Decomposition

In our study of the cobalt acetate catalyzed decomposition of tetralin hydroperoxide in acetic acid – benzene mixtures we first repeated Woodward and Mesrobian's experiment with $[ROOH]_0 = 0.04$ mole/l. and $[CoAc_2] = 2.0\times10^{-3}$ mole/l. in a 1:1 by volume acetic acid – benzene solution. Half-lives of 690 and 730 sec were obtained in two experiments. These values are in fair agreement with a value of about 820 sec which can be read from Fig. 6 in Woodward and Mesrobian's paper for the same $[ROOH]_0$ and $[CoAc_2]$ in an equimolar acetic acid – benzene solution. Assuming that the active catalyst is dimeric, the rate constant for hydroperoxide decomposition would be

$$k_1' = \frac{\log_e 2.0}{710\times(2\times10^{-3})^2} = 244 \text{ l}^2/\text{mole}^2 \text{ sec},$$

which is in very poor agreement with the values obtained indirectly from the limiting rate of oxidation and $[ROOH]_\infty$; e.g. from equation [6], at $[CoAc_2] = 6\times10^{-3}$ mole/l., $[RH] = 1.224$ mole/l.,

$$k_1' = \frac{2.8\times10^{-5}}{0.012\times(6\times10^{-3})^2} = 64.8 \text{ l}^2/\text{mole}^2 \text{ sec}.$$

However, further experiments soon showed that not only was the decomposition not exactly second order in cobalt and first order in hydroperoxide but that its rate decreased very noticeably as the ratio of acetic acid to benzene in the solvent was increased. It was

**At higher tetralin concentrations the limiting rate is not achieved at this cobalt concentration.*

Can. J. Chem. Downloaded from www.nrcresearchpress.com by 210.87.254.40 on 09/05/12
For personal use only.

found, in fact, that at a given [Co] and $[ROOH]_0$ the rate was inversely proportional to the square of the acetic acid concentration.

In all the solvent mixtures studied the cobalt-catalyzed decomposition of the hydroperoxide is only pseudo first order in hydroperoxide. That is, a plot of log ($[ROOH]/[ROOH]_0$) against time is only linear until about 50% of the peroxide has been decomposed, thereafter the rate of decomposition decreases. Moreover, in a given solvent at a fixed cobalt concentration the initial rate of hydroperoxide decomposition decreases as $[ROOH]_0$ is decreased. Changes in rate of this type have been observed during the decomposition of many peroxides and they are known to be due to the occurrence of a radical-induced decomposition of the peroxide, that is, the changes are due to reaction [*i*]. The theoretical rate of peroxide decomposition obtained from reactions [*a*], [*b*], [1], [*i*], and [6] is given by

$$\frac{-d[ROOH]}{dt} = \frac{k_1K_aK_b[Co]^2[ROOH]}{[AcH]^2} + k_i\left(\frac{k_1K_aK_b}{2k_6}\right)^{1/2}K_b\frac{[Co]}{[AcH]^2}[ROOH]^{3/2}.$$

Therefore,

$$\frac{-d[ROOH]}{dt}\frac{[AcH]^2}{[Co]^2[ROOH]} = k_1K_aK_b + k_iK_b\left(\frac{k_1K_aK_b}{2k_6}\right)^{1/2}\frac{[ROOH]^{1/2}}{[Co]}$$

and a plot of the left-hand side of this equation against $[ROOH]^{1/2}/[Co]$ should give a straight line with an intercept equal to $k_1K_aK_b$ and a slope of $k_iK_b(k_1K_aK_b/2k_6)^{1/2}$. The results obtained in several benzene – acetic acid mixtures and in pure acetic acid are shown plotted in this manner in Fig. 3. A straight line through the experimental points is consistent with an intercept of 13,740 sec^{-1} as required for the value of $k_1K_aK_b$ obtained from the limiting rate and $[ROOHAcH]_\infty$ at a cobalt concentration of 6×10^{-3} mole/l. The points cover a range of cobalt concentrations from 5×10^{-4} to 6×10^{-3} mole/l., a range of $[ROOH]_0$ from 0.01 to 0.08 mole/l., and an acetic acid to benzene ratio from 1:3 by volume to pure acetic acid. The scatter of the points is probably due mainly to experimental error but the possibility that other reactions affecting the decomposition rate are also occurring cannot be excluded. In particular, the results suggest that some of the hydroperoxide may be present as a reactive hydroperoxide dimer.

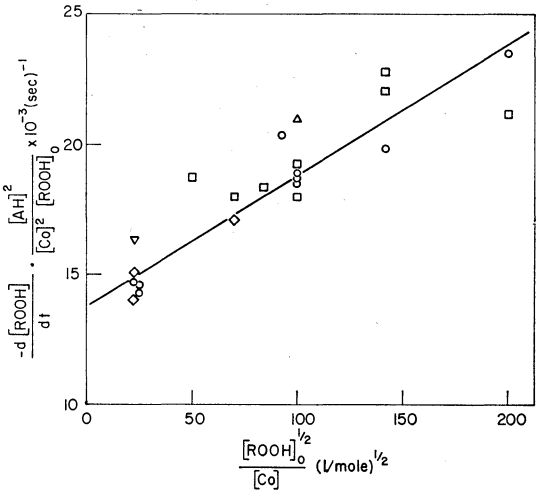

FIG. 3. The measured rate constant for the cobalt acetate catalyzed decomposition of tetralin hydroperoxide in acetic acid – benzene mixtures plotted against $[ROOH]_0^{1/2}/[Co]$. Solvents: ◇ pure acetic acid; ▽ 5:1 by volume acetic acid – benzene; ○ 3:1; □ 1:1; and △ 1:3.

Can. J. Chem. Downloaded from www.nrcresearchpress.com by 210.87.254.40 on 09/05/12
For personal use only.

The contribution of the radical-induced decomposition of the hydroperoxide to the measured rate constant should be eliminated by the addition of a free-radical inhibitor in sufficient concentration to pick up all the radicals before they have a chance to react with the hydroperoxide (24). It is, of course, essential that the inhibitor does not catalyze the decomposition of the hydroperoxide, and the highly hindered phenol 2,6-di-*tert*-butyl-4-methylphenol (BMP) generally appears to satisfy this requirement (24). Peroxide decomposition rates were therefore measured in the presence of 0.2 mole/l. [BMP] with various concentrations of cobalt and hydroperoxide in several different benzene – acetic acid mixtures. The measured rate constants, i.e. $(-d[\mathrm{ROOH}]/dt)([\mathrm{AcH}]^2/[\mathrm{Co}]^2[\mathrm{ROOH}])$, were independent of $[\mathrm{ROOH}]_0$ as was expected, but they were all less than 13,740 sec^{-1} and they decreased as the cobalt concentration was increased from 5×10^{-4} to 6×10^{-3} mole/l. (see Fig. 4). Extrapolation of the data to zero cobalt concentration gives the required rate constant of 13,740 sec^{-1}, which suggests that in the presence of the inhibitor the measured rate constant should be either of the form $k_1K_aK_b-f[\mathrm{Co}]$ or possibly $k_1K_aK_b/(1+f[\mathrm{Co}])$. This aspect of the decomposition was not studied in detail, but the observed kinetics might possibly result from a cobalt-catalyzed oxidation of a product of the inhibitor–radical reaction to re-form hydroperoxide.

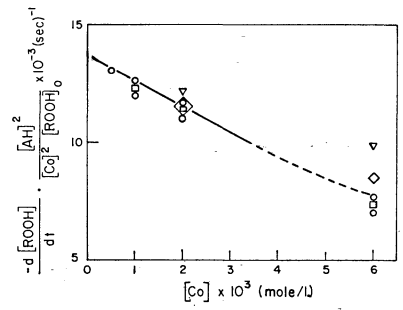

FIG. 4. The measured rate constant for the cobalt acetate catalyzed decomposition of tetralin hydroperoxide in acetic acid – benzene mixtures in the presence of 0.2 mole/l. of 2,6-di-*tert*-butyl-4-methylphenol plotted against the cobalt concentration. Solvents: ◇ pure acetic acid; ▽ 5:1 by volume acetic acid – benzene; ○ 3:1; □ 1:1.

In conclusion, the present results afford a striking confirmation of Tobolsky's steady-state theory. That is, the limiting rate of the cobalt-catalyzed oxidation of tetralin in acetic acid is achieved when the rate of formation of hydroperoxide in the propagation step becomes equal to its rate of decomposition to free radicals by the catalyst.

REFERENCES

1. K. U. INGOLD. Lipids and their oxidation. *Edited by* H. W. Schultz and E. A. Day. Avi Publishing Co., Inc., Westport, Conn. 1962. Chap. 5.
2. E. T. DENISOV and N. M. EMANUEL. Usp. Khim. **29**, 1409 (1960).
3. A. E. WOODWARD and R. B. MESROBIAN. J. Am. Chem. Soc. **75**, 6189 (1953).
4. C. E. H. BAWN. Discussions Faraday Soc. **14**, 181 (1953).
5. P. GEORGE and A. ROBERTSON. Trans. Faraday Soc. **42**, 217 (1946).
6. P. GEORGE, E. K. RIDEAL, and A. ROBERTSON. Proc. Roy. Soc. (London), Ser. A, **185**, 288 (1946).
7. J. H. T. BROOK and J. B. MATTHEWS. Discussions Faraday Soc. **10**, 298 (1951).
8. H. KROPF. Ann. **637**, 73, 93, 111 (1960); Erdoel Kohle, **15**, 78 (1962); Tetrahedron Letters, No. 13, 577 (1962).
9. A. V. TOBOLSKY. India Rubber World, **118**, 363 (1948).
10. A. V. TOBOLSKY, D. J. METZ, and R. B. MESROBIAN. J. Am. Chem. Soc. **72**, 1942 (1950).
11. H. S. BLANCHARD. J. Am. Chem. Soc. **81**, 4548 (1959).
12. M. S. KHARASCH and A. FONO. J. Org. Chem. **24**, 72, 606 (1959).
13. J. K. KOCHI and F. F. RUST. J. Am. Chem. Soc. **83**, 2017 (1961).

Can. J. Chem. Downloaded from www.nrcresearchpress.com by 210.87.254.40 on 09/05/12
For personal use only.

14. H. S. BLANCHARD. J. Am. Chem. Soc. **82**, 2014 (1960).
15. N. URI. Nature, **177**, 1177 (1956).
16. Y. KAMIYA, S. BEATON, A. LAFORTUNE, and K. U. INGOLD. Can. J. Chem. This issue.
17. K. U. INGOLD. Can. J. Chem. **34**, 600 (1956).
18. A. J. CHALK and A. H. SMITH. Trans. Faraday Soc. **53**, 1214, 1235 (1957).
19. J. P. VAN HOOK and A. V. TOBOLSKY. J. Am. Chem. Soc. **80**, 779 (1958).
20. J. A. HOWARD and K. U. INGOLD. Can. J. Chem. **40**, 1851 (1962).
21. M. H. DEAN and G. SKIRROW. Trans. Faraday Soc. **54**, 849 (1958).
22. D. BENSON and L. H. SUTCLIFFE. Trans. Faraday Soc. **55**, 2107 (1959).
23. H. BERGER and A. F. BICKEL. Trans. Faraday Soc. **57**, 1325 (1961).
24. K. U. INGOLD. J. Phys. Chem. **64**, 1636 (1960).

Can. J. Chem. Downloaded from www.nrcresearchpress.com by 210.87.254.40 on 09/05/12
For personal use only.

THE METAL-CATALYZED AUTOXIDATION OF TETRALIN

II. THE COBALT-CATALYZED AUTOXIDATION OF UNDILUTED TETRALIN AND OF TETRALIN IN CHLOROBENZENE[1]

Y. KAMIYA,[2] S. BEATON,[3] A. LAFORTUNE, AND K. U. INGOLD
Division of Applied Chemistry, National Research Council, Ottawa, Canada

Received April 23, 1963

ABSTRACT

The catalysis of the autoxidation of tetralin by the cobalt salts of 10 organic acids has been examined at 50° C over a concentration range from 2×10^{-6} to 1.0 mole/l. of cobalt. The measured rate of oxidation reaches a limiting value at cobalt concentrations above 2×10^{-2} mole/l., which is about half the expected limiting rate. The cobalt salt catalysts are deactivated during the oxidation, probably in the initiation reaction with hydroperoxide, each cobalt atom being capable of decomposing about 100 molecules of hydroperoxide. Upon correcting the measured limiting rate for cobalt deactivation and for the amount of tetralin consumed at the point where the rate reaches a maximum value an extrapolated limiting rate about equal to the expected value is obtained. Although no steady concentration of hydroperoxide occurs during the oxidation the results suggest that the limiting rate of oxidation is basically due to the same phenomena that produce a limiting rate for the cobalt-catalyzed autoxidation of tetralin in acetic acid (Y. Kamiya *et al.* Can. J. Chem. **41**, 2020 (1963)).

Can. J. Chem. Downloaded from www.nrcresearchpress.com by 210.87.254.40 on 09/05/12
For personal use only.

INTRODUCTION

In the preceding paper (1), it has been shown that the limiting rate of the cobalt-catalyzed autoxidation of tetralin in acetic acid is in agreement with theoretical predictions (2, 3, 4). Although the reaction appears to be a lot more complicated in the absence of acetic acid, the same theory still gives a very satisfactory explanation for the experimental results.

EXPERIMENTAL

The catalytic effects of the cobalt salts of the following acids were examined: acetic, hexanoic, octanoic, decanoic, myristic, stearic, behenic, pivalic, *p*-toluic, and 12-hydroxystearic. These salts were prepared by the method of Heaton and Uri (5), the concentration of the reactants being increased for the more water soluble salts. The salts were dehydrated by heating to 60° C or more under a high vacuum and were stored under vacuum in the dark to prevent their autoxidation. In general, for experiments with cobalt concentrations of 10^{-2} mole/l. and greater the cobalt salt was weighed directly into the cell, which was then evacuated and heated to 60–90° C for half an hour before it was cooled and the tetralin was added. At lower concentrations the cobalt salt was dissolved in a benzene – ethyl alcohol mixture, an aliquot of this solution was added to the cell, the solvent was removed under vacuum, and this was followed by heating under vacuum as for the solid samples. During the course of this work it was found that these cobalt salt solutions deteriorated very rapidly unless oxygen was rigidly excluded from the solvents. This continued loss of catalytic activity was overcome by making a fresh solution for each experiment.

Reagent grade chlorobenzene was used as a solvent to study the cobalt-catalyzed decomposition of tetralin hydroperoxide since this compound appears to act merely as an inert diluent in the oxidation experiments, although it appears that the cobalt salts are rather less soluble in chlorobenzene than in tetralin. The following procedure was employed: 15 ml of chlorobenzene, previously warmed to 50° C, was added to a cell containing a known amount of the dried cobalt salt. After half a minute, 5 ml of a tetralin hydroperoxide solution ($\sim4.0\times10^{-2}$ mole/l.), previously warmed to 50° C, was added with vigorous shaking of the reaction flask and the first sample was removed for hydroperoxide determination (4) after 10 seconds. Subsequent samples were taken at time intervals dependent on the rate of reaction. Hydroperoxide concentrations were also followed during autoxidations by withdrawing samples for titration at appropriate time intervals.

α-Tetralol was prepared by the sodium borohydride reduction of α-tetralone (Eastman).

[1]*Issued as N.R.C. No. 7442.*
[2]*N.R.C. Postdoctoral Fellow 1962–1963.*
[3]*N.R.C. Summer Student 1962.*

RESULTS AND DISCUSSION

Oxygen Absorption

The effect on the rate of autoxidation of tetralin at 50° C of the 10 cobalt salts listed in the experimental section was examined over a range of cobalt concentrations from 2.0×10^{-6} to 1.0×10^{-1} mole/l. In addition, the decanoate and stearate were examined up to 1.0 mole/l. As normally used, the tetralin contained about 10^{-3} mole/l. of hydroperoxide. Some typical oxidation curves are shown in Figs. 1, 2, and 3. In general, the curves are sigmoidal in shape and, with the exception of the acetate, the maximum rate was found to be virtually independent of the anion over the entire concentration range. The $\log_{10}$ of the measured maximum rate (ρ_m) has been plotted as the solid curve against $\log_{10}$ [Co] in Fig. 4. Over the main part of the graph, i.e. from 2.5×10^{-5} to 1.0×10^{-1} mole/l. [Co], the majority of the experimental points lie within 10–20% of the curve. It can be seen that at cobalt concentrations between 2.0×10^{-2} and 1.0×10^{-1} mole/l., ρ_m reaches a limit of about 5.3×10^{-4} mole/l. sec, which is just over half the theoretical limit of 1.0×10^{-3} mole/l. sec (1).

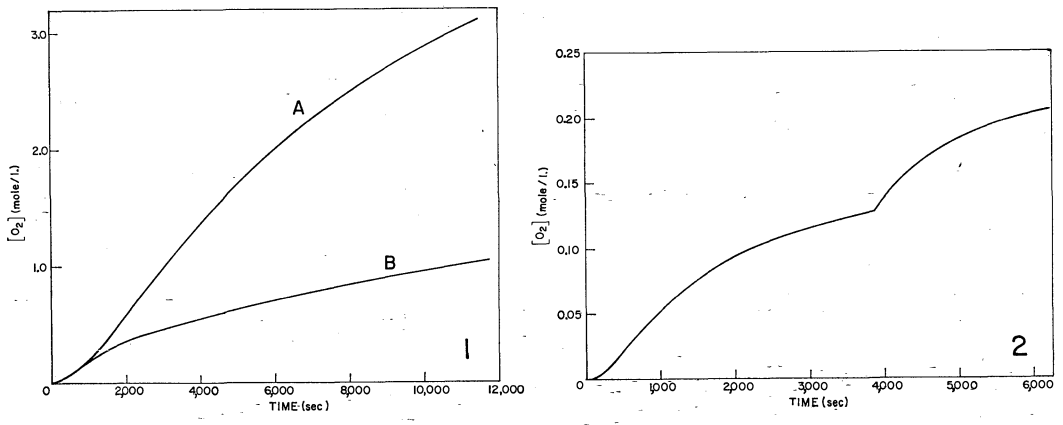

FIG. 1. Oxygen absorption by tetralin. A. Cobalt decanoate at 5.1×10^{-2} mole/l. B. Cobalt decanoate at 9.7×10^{-4} mole/l.

FIG. 2. Oxygen absorption by tetralin at a cobalt decanoate concentration of 1.0×10^{-4} mole/l. A fresh sample of cobalt decanoate at the same concentration was added at 3900 seconds.

In contrast to ρ_m, the induction period (which was defined as the intercept of the extrapolated maximum rate on the time axis) shows a noticeable dependence on the anion which appears to be connected with the solubility of the cobalt salt. That is, the more soluble cobalt salts (pivalate, *p*-toluate, octanoate, and decanoate) gave induction periods of between 100 and 300 seconds at cobalt concentrations below 3×10^{-3} mole/l. The less soluble salts (acetate, stearate, behenate, and 12-hydroxystearate) gave induction periods of about 500 to 1000 seconds while the hexanoate and myristate fall between these two groups. From 5×10^{-3} to 10^{-1} mole/l. [Co] the induction period changes to between 700 and 1000 seconds for all the salts except the acetate, where it is much longer.

One of the most interesting features of the oxidation curves shown in Figs. 1, 2, and 3 which helps to explain several aspects of the overall reaction is the way the rate decreases after reaching its maximum value at lower extents of oxidation the lower the cobalt concentration. This decrease in rate after the maximum is due to deactivation of the catalyst at low concentrations of cobalt and to the oxidation of a significant fraction of the tetralin

Can. J. Chem. Downloaded from www.nrcresearchpress.com by 210.87.254.40 on 09/05/12
For personal use only.

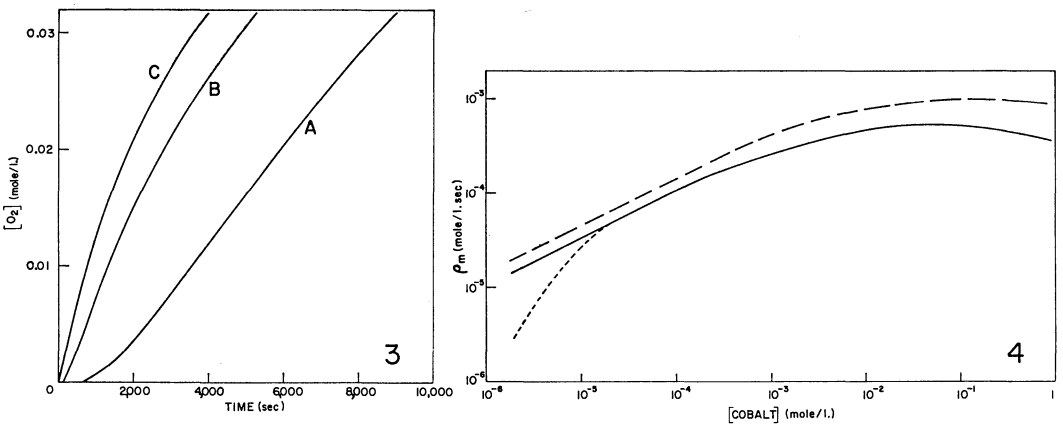

FIG. 3. Oxygen absorption by tetralin at a cobalt toluate concentration of 3×10^{-6} mole/l. A. No detectable hydroperoxide at the beginning of the reaction. B. $[ROOH]_0 = 1.0\times10^{-3}$ mole/l. C. $[ROOH]_0 = 3.2\times10^{-2}$ mole/l. and 1.0×10^{-1} mole/l.

FIG. 4. The variation in the maximum rate of oxidation of tetralin (solid curve) and the extrapolated maximum rate (broken curve) with cobalt concentration.

at high concentrations. The fact that the cobalt is deactivated during the oxidation is shown conclusively in Fig. 2. In this experiment, tetralin was oxidized in the presence of 10^{-4} mole/l. of cobalt decanoate until the rate had fallen to a small fraction of its maximum value. A portion of this oxidized tetralin was transferred to a new cell containing an amount of cobalt decanoate sufficient to give a fresh 10^{-4} mole/l. solution. The initial rate of oxidation, even after allowance is made for the residual rate due to the first sample of cobalt decanoate, is within 10–15% of the original maximum rate. However, the second oxidation curve is not exactly superposable upon the first since its rate decreases slightly more rapidly. Metal catalyst deactivation has also been observed by previous workers during the catalyzed autoxidation of *n*-decane (6), ethylbenzene (7), and cumene (8).

The results suggested that the deactivation of the cobalt was dependent on the amount of oxygen absorbed and this was confirmed by plotting the amount of oxygen absorbed when the rate has fallen to half its maximum value (i.e. $\log_{10}[O_2]\rho_{m/2}$) against $\log_{10}[Co]$ (Fig. 5). The points for all the cobalt salts examined in the present work fell very close (greatest deviation 20%) to a single straight line of slope 0.5 over a range of cobalt concentrations from 2.5×10^{-5} to 1.3×10^{-2} mole/l. and they are therefore not shown in the figure. The equation describing this line is

$$[O_2]\rho_{m/2} = 12.8[Co]^{1/2} \text{ mole/l.} \qquad [8]$$

The initial decrease of the rate from its maximum value generally occurs between one half and one third of $[O_2]\rho_{m/2}$.

Since the deactivation process is half order in cobalt it suggests that the initiation reaction is first order in cobalt and that the cobalt is occasionally deactivated in either the initiation or termination reaction. Alternatively, the cobalt might be deactivated by a product of these reactions. That is, assuming the rate-determining initiation process is either

$$ROOH + CoA_2 \rightarrow RO^{\cdot} + CoA_2OH \qquad [1a]$$

or

$$ROOH + CoA_2OH \rightarrow RO_2^{\cdot} + CoA_2 + H_2O, \qquad [1b]$$

Can. J. Chem. Downloaded from www.nrcresearchpress.com by 210.87.254.40 on 09/05/12
For personal use only.

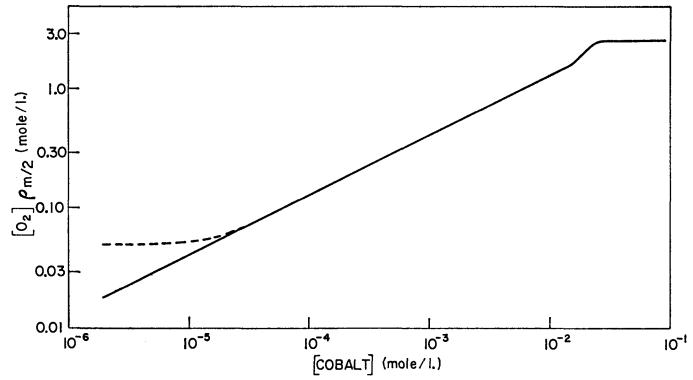

FIG. 5. Amount of oxygen absorbed when the rate reaches half its maximum value as a function of the initial cobalt concentration.

then, using the same nomenclature as in Part I (1), under stationary-state conditions,

$$\frac{-d[O_2]}{dt} = k_3\left(\frac{k_1[Co]}{2k_6}\right)^{1/2}[RH][ROOH]^{1/2}, \qquad [2a]$$

where A represents the anion attached to the cobalt and n in equation [2] (1) is equal to 1.0. Therefore, if the cobalt concentration is decreased by a factor m, the amount of intiation and termination also decreases by the same factor but the rate decreases by a factor of $m^{1/2}$. If unit concentration of cobalt requires x units of initiation or termination for the rate to reach half its maximum value, than $1/m$ units of cobalt will only require x/m units of initiation or termination. Since the rate is decreased by $(1/m)^{1/2}$, for the same amount of oxygen consumed there will have been $x/m^{1/2}$ effectively deactivating initiation or termination steps. Therefore, x/m effectively deactivating steps will occur when the oxygen absorbed is $(1/m)^{1/2}$ of the amount required at unit cobalt concentration. That is, to reach a given degree of deactivation of the cobalt requires an amount of oxygen proportional to the square root of the initial cobalt concentration.

Deactivation in the termination process might occur in two different ways. Firstly, by the reaction sequence (9)

$$RO_2^{\bullet} + RO_2^{\bullet} \rightarrow \alpha\text{-tetralone} + \alpha\text{-tetralol} + O_2 \qquad [4d]$$

$$CoA_2 + \begin{cases}\alpha\text{-tetralone}\\ \alpha\text{-tetralol}\end{cases} \rightarrow \text{inactive cobalt} \qquad [4e]$$

and, secondly, directly in the termination reaction

$$CoA_2 + RO_2^{\bullet} + RO_2^{\bullet} \rightarrow \text{inactive cobalt} + \text{inactive products.} \qquad [4f]$$

The first possibility can be discarded since the addition of 10^{-1} mole/l. of α-tetralone and α-tetralol to a reaction catalyzed by 10^{-4} mole/l. of cobalt had virtually no effect on the maximum rate of oxidation.* The second alternative cannot be completely discarded but seems improbable in view of the fact that there is good agreement between the extrapolated maximum rate and the theoretical limiting rate (see below). Moreover, the fact that the extrapolated maximum rate is independent of [Co] at high concentration indicates that reaction [4f] and similar reactions, e.g.

$$CoA_2 + RO_2^{\bullet} \rightarrow \text{inactive cobalt} + \text{inactive products,} \qquad [4g]$$

**The induction period was, however, increased by a factor of about 5 with α-tetralol but this is probably due to the production of some phenolic material from impurities in the α-tetralone during its reduction.*

Can. J. Chem. Downloaded from www.nrcresearchpress.com by 210.87.254.40 on 09/05/12
For personal use only.

Can. J. Chem. Downloaded from www.nrcresearchpress.com by 210.87.254.40 on 09/05/12
For personal use only.

can play no more than a minor part in the oxidation. It must therefore be concluded that deactivation occurs in the initiation process and again there are two possibilities. Water is produced in reaction [1*b*] and there is no doubt that water has a slight inhibiting effect on the reaction at low cobalt concentrations. For example, in one experiment at 5×10^{-5} mole/l. [Co] the rate was reduced by a factor of 5 by the addition of 10% by volume of water (6.1 mole/l.) and in a second experiment at 4×10^{-5} mole/l. [Co] the rate was reduced by a factor of 7 by the addition of 0.2 mole/l. of water.* The inhibiting effect of water is probably due to its addition to the coordination shell of the cobalt (i.e. to hydration of the cobalt salt) which will greatly reduce the ease with which a molecule of hydroperoxide can approach the cobalt in order to react with it. In fact, it is likely that a coordinated water molecule has to be replaced by a hydroperoxide molecule before reaction can occur. The large amounts of water added to the present system therefore probably represent the limiting inhibiting effect of water in this system. It is, therefore, not surprising to find that at 1.3×10^{-2} mole/l. [Co] (where ρ_m is independent of [Co]) 25% by volume of water has no effect on the maximum rate. The magnitude of the inhibiting effect of water is sufficiently large that water cannot be ruled out as a major cause of catalyst deactivation. However, the second alternative by which cobalt is deactivated during the initiation reaction appears to give a more satisfactory explanation of the results. The following reaction scheme, leading to the formation of insoluble basic salts and hydroxides of cobalt, is suggested:

$$\mathrm{ROOH} + \mathrm{CoA_2OH} \rightarrow \mathrm{CoAOH}\downarrow + \mathrm{AH} + \mathrm{RO_2}^{\bullet} \qquad [1c]$$

$$\mathrm{ROOH} + \mathrm{CoAOH} \rightarrow \mathrm{CoA(OH)_2}\downarrow + \mathrm{RO}_{\bullet} \qquad [1d]$$

$$\mathrm{ROOH} + \mathrm{CoA(OH)_2} \rightarrow \mathrm{Co(OH)_2}\downarrow + \mathrm{AH} + \mathrm{RO_2}^{\bullet} \qquad [1e]$$

$$\mathrm{ROOH} + \mathrm{Co(OH)_2} \rightarrow \mathrm{Co(OH)_3}\downarrow + \mathrm{RO}^{\bullet}. \qquad [1f]$$

Reactions [1*c*] and [1*e*] must occasionally replace reaction [1*b*].

The cobalt is undoubtedly precipitated during the reaction since a very fine black or brownish-black precipitate is always produced during extensive oxidation at intermediate cobalt concentrations. In one experiment, the precipitate produced by the oxidation for 8 hours of a liter of tetralin containing 514 mg of cobalt myristate (i.e., 10^{-3} mole/l.) was examined. It weighed 171 mg and contained about 25% cobalt by weight (determined both by ignition and by reprecipitation from solution with sodium anthranilate). Because of its very small particle size it is probable that not all the precipitate was collected and, therefore, not less than 73% of the cobalt was precipitated. X-Ray examination in a focusing camera using monochromatic Cu K_α radiation showed that the precipitate was completely amorphous and its infrared spectrum in a nujol mull contained only the broad bands corresponding to hydrogen-bonded hydroxyl groups.

Organic acids are produced by this deactivation scheme and they apparently have a small accelerating effect on the oxidation rate at low cobalt concentrations (e.g., at 10^{-4} mole/l. [Co] the rate was increased by a factor of 2–3 on the addition of 7×10^{-2} mole/l. of decanoic acid) but they have no effect on the limiting rate. This catalytic activity may be partly due to a decrease in the efficiency of catalyst deactivation (11). However, it is probably mainly due to an increase in the rate of the cobalt-catalyzed decomposition of

**Michaels (10) has studied the cobalt naphthenate catalyzed oxidation of tetralin at 70° C by an induction period method in which, after allowing 15 minutes for the system to reach equilibrium, the amount of oxygen consumed in 1 hour was measured. At 9.5×10^{-6} mole/l. [Co] he reported that the rate of oxidation was inversely proportional to $[H_2O]^{0.11}$ over a range of water concentrations from 5.5×10^{-3} to 5.5×10^{-2} mole/l. Although in this work it does not appear to have been realized that the catalyst was probably deactivated during the oxidation, the order might possibly have been closer to 0.5 if water were mainly responsible for deactivation.*

hydroperoxide since 10^{-1} mole/l. of decanoic acid increased the rate of decomposition of tetralin hydroperoxide (10^{-2} mole/l., catalyzed by 2×10^{-3} mole/l. [Co]) by a factor of about 5. In this respect, therefore, decanoic acid appears to function somewhat differently to acetic acid since the latter decreases the rate of the cobalt–hydroperoxide reaction. The water produced during oxidation probably causes a relatively slight inhibition of the reaction and it may account for the fact that there was a slightly more rapid decrease in rate in the second stage of the experiment shown in Fig. 2. This deactivation scheme may also, in part, account for the fact that porphin complexes of heavy metals appear to be more powerful catalysts of autoxidation than the corresponding heavy metal soaps at very low concentrations (12, 13) since it is possible that the complexed metal will be less susceptible to deactivation than the uncomplexed metal in the soaps. However, deactivation does occur with some complexed metal catalysts since cobalt phthalocyanine is deactivated during the autoxidation of cumene (14). The absence of cobalt deactivation in acetic acid as a solvent (1) is also to be expected since any cobalt oxide or hydroxide which is formed will be immediately reconverted to cobalt acetate.

Equation [8] is obeyed from 1.3×10^{-2} to 2.5×10^{-5} mole/l. [Co] for the tetralin as normally used, and is obeyed down to 2×10^{-6} mole/l. [Co] in the presence of a sufficiently large initial concentration of hydroperoxide (see below). Over this range of cobalt concentrations the measured maximum rate of oxidation is very roughly proportional to the square root of the initial cobalt concentration as predicted by equation [2*a*] (see Fig. 4). It therefore follows that approximately 75% of the cobalt will have been deactivated when the rate falls to half its maximum value or, more accurately, 75% of the cobalt which is still present in the region of the maximum rate. This will, of course, be more than 75% of the initial cobalt since our results indicate that the cobalt is deactivated throughout the entire oxidation. When the rate falls to half this value again, i.e. to $0.25\rho_m$, then 75% of the remaining 25% will have been deactivated and this should require the further absorption of half the amount of oxygen required to give the half maximum rate. That is, all the cobalt should be deactivated when the oxygen absorption equals $2[O_2]\rho_{m/2}$ and further oxidation should cease at this point. A plot of the measured rate (ρ) divided by ρ_m against absorbed $[O_2]/[O_2]\rho_{m/2}$ should therefore give a straight line of slope -0.5, intercepting the ρ/ρ_m axis at 1.0 and the $[O_2]/[O_2]\rho_{m/2}$ axis at 2.0. When plots of this kind are made (see Fig. 6 for a typical example) they give a rather poor fit to the predicted relation. That is, between 10^{-5} and 10^{-2} mole/l. [Co] the plots are horizontal to a value of $[O_2]/[O_2]\rho_{m/2} = 0.4\sim0.6$ (corresponding to the linear maximum-rate region), they then decrease more rapidly than predicted and finally tail off more slowly than expected, generally at about 15–30% of ρ_m. The residual thermal reaction initiated by the non-catalyzed decomposition of hydroperoxide contributes very little to this tailing since 1.5×10^{-1} mole/l. [ROOH] gives a rate of less than 10^{-6} mole/l. sec in the absence of cobalt. Instead, the tailing is due to the fact that the cobalt is not totally deactivated but is merely altered to a much less active form. This was shown by an experiment in which cobaltous oxide was ground to pass through a 400-mesh screen: 10^{-1} mole/l. of this oxide gave a maximum rate of oxidation which was about 14% of that obtained with a cobalt soap. This finding that even an insoluble cobalt compound has some catalytic activity is in agreement with the results of Chalk and Smith (15) on the copper sulphate catalyzed oxidation of cyclohexene. These authors showed that the catalytic activity of the solid was proportional to its surface area. The tailing in Fig. 6 suggests that the finely divided cobalt precipitate formed at first slowly agglomerates into larger particles.

The main portion of the ρ/ρ_m against $[O_2]/[O_2]\rho_{m/2}$ plots can be most readily explained

Can. J. Chem. Downloaded from www.nrcresearchpress.com by 210.87.254.40 on 09/05/12
For personal use only.

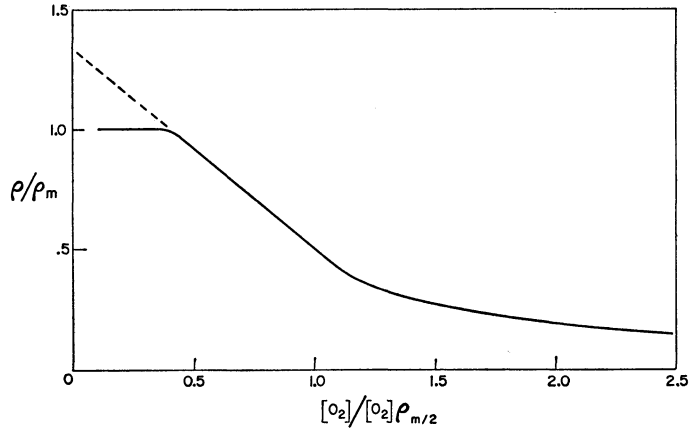

FIG. 6. The oxidation rate as a function of the amount of oxygen absorbed at a cobalt decanoate concentration of 9.7×10^{-5} mole/l.

on the assumption that the cobalt is being deactivated throughout the oxidation since it seems improbable that no cobalt will have been deactivated until the rate starts to fall below its maximum value. That is, a certain fraction of the initial cobalt will have been deactivated by the time the rate reaches its maximum value and more will be deactivated while the maximum rate is maintained. At cobalt concentrations where the active cobalt becomes completely dissolved by the time the maximum rate is reached the true maximum rate will be obtained by extrapolating the sloping linear region in Fig. 6 to zero oxygen absorption (broken line). Extrapolated maximum rates obtained by this method, after applying one or two other corrections the importance of which depend on the cobalt concentration (see below), are shown as the broken curve in Fig. 4. These extrapolated maximum rates are also independent of the anion. It can be seen by comparison of the two curves that this correction amounts to about 40% at low cobalt concentrations where this is the only correction factor of importance.

The second correction that must be made to ρ_m arises from the fact that at high cobalt concentrations an appreciable fraction of the tetralin has been consumed while the rate is still at its maximum value (see Fig. 1). According to equation [4], i.e. (1, 4),

$$\left(\frac{-d[O_2]}{dt}\right)_\infty = \frac{k_3^2[RH]^2}{2k_6}, \qquad [4]$$

the limiting theoretical rate should be proportional to $[RH]^2$. This has been confirmed both directly and indirectly. In the direct determination the tetralin was diluted with chlorobenzene, which appears to be chemically inert in this system, and ρ_m was measured at four tetralin concentrations with 1.0×10^{-2} and 2.0×10^{-2} mole/l. [Co]. In both cases ρ_m is proportional to $[RH]^2$ for mixtures containing more than about 50% tetralin (see Fig. 7). The small increase in order with more dilute tetralin solutions is probably due to a lower solubility of the catalyst in chlorobenzene than in tetralin. That is, insufficient cobalt is dissolved by the dilute mixtures for them to give a measured limiting rate directly comparable with the more concentrated tetralin solutions. The reaction order was also derived indirectly from the fact that at cobalt concentrations above 1.3×10^{-2} mole/l. equation [8] is no longer obeyed. It is found instead that from 1.3×10^{-2} to 2.5×10^{-2} mole/l. [Co], $[O_2]\rho_{m/2}$ increases more rapidly than expected but that it then levels off at

Can. J. Chem. Downloaded from www.nrcresearchpress.com by 210.87.254.40 on 09/05/12
For personal use only.

about 2.4 mole/l. (see Fig. 5). Assuming one molecule of oxygen oxidizes one molecule of tetralin* this levelling off corresponds to a tetralin consumption of 32.7% and, therefore, to a calculated rate = $(0.673)^2\rho_m = 0.453\rho_m$. The slight discrepancy from the expected value of 0.50 is due both to inaccuracies in this assumption and to the oxidation of some of the tetralin before the maximum rate is reached (see Fig. 1). The sharp increase in $[O_2]_{\rho_{m/2}}$ from 1.3×10^{-2} to 2.5×10^{-2} mole/l. [Co] is probably due to the fact that the rate is independent of the cobalt concentration in this region for which reason appreciably more than 75% of the cobalt must be deactivated before the rate falls to half its maximum value.

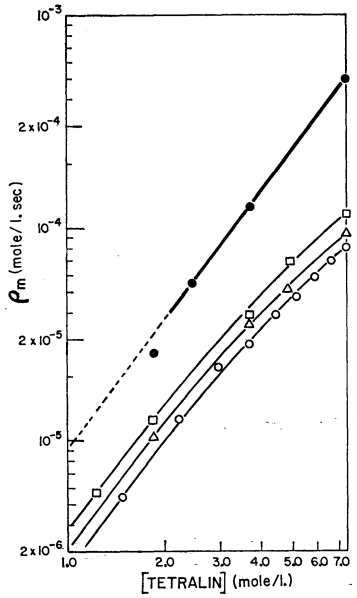

FIG. 7. The maximum rate of oxidation as a function of tetralin concentration. Key: ● [Co] = 1.0×10^{-2} mole/l. and 2.0×10^{-2} mole/l.; □ [Co] = 7.9×10^{-5} mole/l., $[ROOH]_0 = 4.6\times10^{-3}$ mole/l.; △ [Co] = 4.9×10^{-5} mole/l., $[ROOH]_0 = 1.0\times10^{-3}$ mole/l.; ○ [Co] = 2.4×10^{-5} mole/l., $[ROOH]_0 = 2.0\times10^{-2}$ mole/l.

The correction for tetralin consumption is of major importance in obtaining the true maximum rate at cobalt concentrations above 10^{-3} mole/l. It must, of course, be applied before the correction relating to cobalt deactivation.† Moreover, in the limiting-rate region the correction must be based on the assumption that two molecules of oxygen oxidize three molecules of tetralin (1), i.e. $(d[RH]/dt)/(-d[O_2]/dt) = r = 1.5$. The magnitude of this correction factor is about 6% at 10^{-3} mole/l. [Co] ($r = 1.0$), 45% at 10^{-2} and 10^{-1} mole/l. [Co] ($r = 1.5$, or 30% if $r = 1.0$), and as high as 135% ($r = 1.5$) for finely divided cobalt acetate at 10^{-1} mole/l. (see below). The importance of this factor can be further illustrated by reference to curve A in Fig. 1. The rate appears to drop below the maximum value at $[O_2] = 0.9$ mole/l. at which point the correction factor = 1.45 for $r = 1.5$ (i.e. extrapolated rate = $1.45\rho_m$); at $[O_2] = 1.9$ mole/l. the rate has dropped 46% but the corrected rate is still 1.45 times ρ_m; at $[O_2] = 3.0$ mole/l. the rate has dropped 64% but the corrected rate is still 1.16 ρ_m.

**In the region of the maximum rate this assumption is incorrect since two molecules of oxygen oxidize three molecules of tetralin (1). However, once the rate starts to decrease from its maximum value the amount of hydroperoxide formed increases rapidly (see Fig. 8). The chain length is, therefore, no longer unity and this assumption will not be too inaccurate for fairly extensive oxidation.*

†*The correction for cobalt deactivation becomes negligible above 5×10^{-2} mole/l.* [Co].

Can. J. Chem. Downloaded from www.nrcresearchpress.com by 210.87.254.40 on 09/05/12
For personal use only.

One further correction has been applied at cobalt concentrations above 3×10^{-2} mole/l. to make allowance for the dilution of the tetralin by the catalyst. The magnitude of this correction naturally depends on the molecular weight of the acid with which the cobalt is combined. As an example, this correction is about 6.5% with 10^{-1} mole/l. of cobalt stearate and is proportionately larger at higher concentrations.

After applying all the necessary correction factors, the extrapolated maximum rate for all the cobalt salts examined in this work is $(1.0\pm0.1)\times10^{-3}$ mole/l. sec in the range from 10^{-2} to 10^{-1} mole/l. [Co], which is in gratifying agreement with the predicted limiting rate of 1.0×10^{-3} mole/l. sec (1). The fact that the measured limiting rate is only about half of its theoretical value is, in all probability, basically due to the low solubility in tetralin of all the cobalt catalysts studied in this work. The oxygen-containing reaction products help to solubilize the cobalt catalysts and the tetralin must therefore be oxidized to a significant extent in order to dissolve sufficient catalyst to give a high oxidation rate. However, in the course of solubilizing the catalyst some of it is destroyed and also the tetralin concentration is decreased. Correction of the measured limiting rate for these two effects gives an extrapolated limiting rate in very satisfactory agreement with the theoretical value. It is obvious that with a less active metal catalyst than cobalt the measured rate at the highest practical catalyst concentrations could be very much less than the theoretical limiting value. Incidentally, the agreement between extrapolated and theoretical rates with cobalt catalysts indicates that any reaction between the cobalt catalyst and the hydroperoxide to give non-radical products (rate constant k_1*) must be unimportant compared with the reaction giving free radicals (rate constant k_1). That is, the inclusion of such a reaction in the kinetic scheme leads to the prediction that the measured limiting rate will be smaller than the theoretical value, i.e., it predicts that

$$\left(\frac{-d[O_2]}{dt}\right)_\infty = \frac{k_3^2[RH]^2}{2k_6}\frac{k_1}{k_1+k_1^*}. \qquad [4a]$$

The theories of Tobolsky (2, 3) give a very satisfactory explanation of our data. It would appear that none of the following factors have any appreciable effect on the measured limiting rate: (i) the solubility (within reasonable limits) of the cobalt salt; (ii) the mild steric protection afforded to the cobalt atom in cobalt pivalate; (iii) minor changes in the oxidation–reduction potential of the cobalt caused by the various anions. However, it should be added that solubilities may play a minor role in determining the rate in the range from 5×10^{-4} to 5×10^{-3} mole/l. [Co] since the extrapolated ρ_m values for the less soluble salts fall slightly, although perhaps not significantly, below the curve shown in Fig. 4. If this effect is real, it suggests that cobalt is micelle form has only a slightly lower catalytic activity than free cobalt, which seems rather unlikely. On the other hand, the variation in the amount of hydroperoxide produced at a given extent of oxidation shows a smaller dependence on the cobalt concentration than would be expected in the range 1.0×10^{-2} to 4.0×10^{-2} mole/l. [Co] (see following section). This suggests that above 10^{-2} mole/l. [Co] the effective concentration of even the more soluble cobalt salts increases rather slowly with increasing catalyst concentration.

It is convenient at this point to consider the efficiency of the cobalt deactivation process. At cobalt concentrations where the limiting rate of oxidation is achieved the reaction chain length must be very close to unity, i.e., one molecule of hydroperoxide is decomposed for each molecule of oxygen absorbed (1). The maximum concentration of cobalt at which $\rho_{m/2}$ is reached because of cobalt deactivation rather than because of tetralin consumption is 2.5×10^{-2} mole/l. [Co]. For the measured rate to fall to half the measured maximum

Can. J. Chem. Downloaded from www.nrcresearchpress.com by 210.87.254.40 on 09/05/12
For personal use only.

rate it can be seen from Fig. 4 that the amount of cobalt remaining at this point will be 10^{-3} mole/l. Therefore, from Fig. 5, 2.4 mole/l. $[O_2]$ deactivated $2.5\times10^{-2}-1.0\times10^{-3} = 2.4\times10^{-2}$ mole/l. of cobalt. Assuming unit chain length over the whole of this concentration range 2.4×10^{-2} mole/l. cobalt is deactivated by reaction with 2.4 mole/l. of hydroperoxide. That is, each atom of cobalt is capable, on average, of decomposing 100 molecules of hydroperoxide.

As has already been mentioned, ρ_m for cobalt acetate is somewhat smaller than that for the other cobalt salts apparently because of its low solubility in unoxidized tetralin. It is considerably more soluble in oxidized tetralin (like the other cobalt salts) and therefore tends not to exert its full catalytic effect until a rather large amount of oxygen has been absorbed and therefore a rather large amount of cobalt acetate has been deactivated. This effect showed up very noticeably at 10^{-1} mole/l. $[CoAc_2]$ where ρ_m was found to depend on the state of subdivision of the solid. A maximum rate of 4.4×10^{-4} mole/l. sec (which is still 20% below ρ_m for the other salts at this concentration) was only obtained by grinding the hydrated salt to pass through a 400-mesh screen and then dehydrating it rapidly under vacuum to increase further its state of subdivision. Even with these steps, the induction period was about 5000 seconds and the maximum rate was not reached until 1.7 mole/l. $[O_2]$ was absorbed, corresponding to a correction factor of 2.35 and an extrapolated ρ_m of $1.0_3\times10^{-3}$ mole/l. sec.

Although the results obtained with cobalt decanoate and stearate at concentrations above 10^{-1} mole/l. were markedly different only these two salts were examined since it is not clear how much significance should be attached to the results in view of the pasty consistency of such mixtures. The curves shown in Fig. 4 represent the results obtained with cobalt stearate. The measured rates with cobalt decanoate follow these curves up to a concentration of 0.40 mole/l., but at 0.48 mole/l., less than 0.10 mole/l. $[O_2]$ was absorbed in 15,000 seconds to give an induction period $\geqslant$ 5,200 seconds and $\rho_m \geqslant 1.0\times10^{-5}$ mole/l. sec. Similar very sudden increases in induction periods at high catalyst concentration have been reported previously for the copper stearate catalyzed oxidation of *n*-decane at catalyst concentrations of 0.6 mole% (16). This phenomena of a "critical catalyst concentration" was attributed to chain termination by the catalyst (16). The difference in the behavior of cobalt stearate and decanoate suggests that, in addition to the metal, the anion plays a very important role in this phenomena.

In the initial work the maximum rates obtained at catalyst concentrations of less than 2.5×10^{-5} mole/l. [Co] were rather irreproducible and consistently fell well below the rate expected on the assumption that it should be proportional to $[Co]^{1/2}$, and the overall oxidation rate curve appeared to have the form

$$\frac{-d[O_2]}{dt} = \frac{a[Co]}{b+c[Co]}.$$

Furthermore, $[O_2]\rho_{m/2}$ levelled off at about 0.05 mole/l. at low cobalt concentrations. The broken curves in Figs. 4 and 5 represent these results which were obtained with tetralin containing an initial hydroperoxide concentration $[ROOH]_0$ of 10^{-3} mole/l. At cobalt concentrations above 2.5×10^{-5} mole/l., ρ_m does not alter as $[ROOH]_0$ is varied from 10^{-3} to 2.0×10^{-1} mole/l., although the induction period is reduced slightly at the higher initial peroxide levels. However, if the tetralin is carefully freed from hydroperoxide by passing it through alumina in the complete absence of oxygen ($[ROOH]_0 < 10^{-6}$ mole/l.) the induction period is significantly increased and, at cobalt concentrations below 5×10^{-3} mole/l., ρ_m is decreased. For example, at a cobalt toluate concentration of 1.7×10^{-4}

Can. J. Chem. Downloaded from www.nrcresearchpress.com by 210.87.254.40 on 09/05/12
For personal use only.

mole/l., ρ_m was reduced by a factor of 4 and the induction period was increased by a similar factor. Moreover, the maximum rate was not reached until 0.05 mole/l. $[O_2]$ had been absorbed whereas with the normal tetralin, ρ_m was reached after the absorption of 0.01∼ 0.02 mole/l. $[O_2]$. This suggested that, provided the cobalt concentration was above 2.5×10^{-5} mole/l., the normal tetralin contained sufficient hydroperoxide for ρ_m to be reached before a significant fraction of the cobalt was deactivated, but that below this cobalt concentration it would be necessary to add hydroperoxide to the tetralin to obtain the true maximum rate only slightly affected by cobalt deactivation. In order to compare rates obtained at low cobalt concentrations with the values at higher concentrations it was therefore necessary to add hydroperoxide before the start of the reaction. A typical series of experiments at 3×10^{-6} mole/l. [Co] is shown in Fig. 3. In the absence of initial hydroperoxide it is obvious that the cobalt is in a rather inactive form by the time the maximum rate is reached. At the two highest initial hydroperoxide concentrations (3×10^{-2} and 1.0×10^{-1} mole/l.) the oxidation curves are identical and ρ_m occurs at the very beginning of the reaction (i.e., the cobalt is immediately and completely soluble at this concentration). Moreover, this value of ρ_m agrees perfectly with the value predicted from the rate data at higher cobalt concentrations on the assumption that $\rho_m \propto [Co]^{1/2}$. In addition, $\rho_{m/2}$ is now reached at, or even slightly before, the oxygen absorption predicted by a similar extrapolation, i.e. the continuation of the straight line in Fig. 5. At these very low cobalt concentrations it is rather difficult to estimate the extrapolated maximum rate since a not insignificant fraction of the cobalt will have been deactivated before any measurements can be made. However, within the limits of error, the extrapolated ρ_m values also depend on $[Co]^{1/2}$. That is, provided allowance is made for cobalt deactivation, the curves in Fig. 4 show that ρ_m and the extrapolated ρ_m depend on $[Co]^{1/2}$ from 2×10^{-6} to 1.0×10^{-3} mole/l. [Co], in agreement with the dependence predicted by equation [2*a*]. This means that chain initiation in this system is first order in cobalt and chain termination is bimolecular in peroxy radicals.

The importance of catalyst deactivation in determining kinetics in this and in other similar systems cannot be overemphasized. Errors are particularly likely to arise when kinetics are determined by an induction period method. Several cases where unusual kinetics have been reported in the literature can readily be explained on the basis of catalyst deactivation. For example, Michaels (10) has reported that the rate of oxidation of tetralin at 70° C catalyzed by cobalt naphthenate is proportional to $[Co]^{0.6}$. His experimental technique was to measure the decrease in oxygen pressure over the tetralin that occurred in 1 hour, but after first allowing 15 minutes for the system to reach equilibrium. The oxidation that occurs during this equilibrium period and the consequent deactivation of the cobalt will naturally tend to give a somewhat higher order than the true one (see e.g., broken curve in Fig. 4). Michaels also reports that the reaction is inhibited by added hydroperoxide and therefore, following a suggestion of Uri (12), suggests that the main initiation reaction is

$$Co^{2+} + O_2 \rightarrow Co^{2+}O_2^{\cdot}. \qquad [9]$$

However, with a 15-minute equilibrium period, particularly at 70° C, it is clear from Fig. 3 that in the presence of added hydroperoxide the reaction will be largely over before any measurements are made. That is, the effective cobalt concentration after 15 minutes will be much smaller if hydroperoxide is added initially than if the hydroperoxide is absent. This is bound to cause an *apparent* inhibition of the reaction by added hydroperoxide.

Can. J. Chem. Downloaded from www.nrcresearchpress.com by 210.87.254.40 on 09/05/12
For personal use only.

The importance of catalyst deactivation has also, perhaps, been overlooked in the work of Heaton and Uri (5) on the cobalt stearate catalyzed oxidation of 0.10 *M* linoleic acid in benzene and cyclohexane at 37° C. The kinetics in this case were determined by measuring the hydroperoxide concentration in solution after a fixed time interval. These authors report that from 4×10^{-5} to 2×10^{-4} mole/l. [Co] the rate is proportional to [Co], but their experimental points from which this conclusion is derived show a curvature which is not dissimilar to that shown by the broken line in Fig. 4. As we have shown, this apparent increase in order with decreasing cobalt concentration at low initial hydroperoxide levels is due to catalyst deactivation. This effect possibly occurs at higher cobalt concentrations in the work of Heatin and Uri since great precautions were taken to remove all hydroperoxides from their starting materials. Heaton and Uri also report some very unusual kinetic results at cobalt concentrations below 4×10^{-5} mole/l. In these experiments, the solvents containing the catalyst were aerated by bubbling air through them prior to the oxidation reaction. As has already been mentioned, it has been found in the present work that the activity of cobalt salt catalysts in benzene solution decreases very rapidly unless oxygen is excluded from the solvent, so these results could also perhaps be due to catalyst deactivation. Moreover, the conclusion of these authors that reaction [9], or some modification of this reaction, is responsible for the kinetic peculiarities at low cobalt concentrations is contrary to our own finding that ρ_m is independent of the oxygen pressure (from 300 to 760 mm) over our entire cobalt concentration range. One further point is that the absence of any measurable catalytic effect at [Co] $< 10^{-6}$ mole/l. has led Uri (5, 12) to conclude that the so-called residual thermal reaction in the absence of initial hydroperoxide in many organic substances is initiated by trace metal contaminants by way of reaction [9]. However, in view of the very small amounts of absorbed oxygen which would probably be required to deactivate such contaminants unless they are present in a form which cannot be deactivated, and in view of the work of Russell (17) and Denisov (18) on the initiating reactions

$$RH + O_2 \rightarrow R^{\cdot} + HO_2^{\cdot} \qquad [10]$$

and

$$2RH + O_2 \rightarrow 2R^{\cdot} + H_2O_2, \qquad [11]$$

we can see no evidence to support this conclusion. The recent work of Privett and Blank (19) on the initial stages of the autoxidation of the methyl esters of unsaturated fatty acids also throws considerable doubt on the importance of reaction [9] as a chain-starting process.

Many other examples exist in the literature of metal-catalyzed autoxidations where rather complex reactions have been suggested on what appears to us to be an inadequate kinetic foundation. We should like to suggest that such reactions be treated with considerable reserve until they have withstood the test of more rigorous examination.

The observation that the initial hydroperoxide concentration only affects ρ_m up to a certain limiting concentration implies, of necessity, that the rate-controlling chain-initiation reaction between cobalt and hydroperoxide is not a simple bimolecular reaction. Instead, the rate-controlling step must involve the slow decomposition of a rapidly formed complex. In non-polar media most workers are agreed that reaction [1*a*] is much faster than reaction [1*b*]. Moreover, visual observation of our own system shows the green color of trivalent cobalt once oxidation commences. It is therefore probable that the rate-controlling initiation reaction can be written:

$$ROOH + CoA_2OH \underset{\text{fast}}{\rightleftharpoons} [ROOHCoA_2OH] \xrightarrow[\text{slow}]{} RO_2^{\cdot} + CoA_2 + H_2O. \qquad [1b']$$

Can. J. Chem. Downloaded from www.nrcresearchpress.com by 210.87.254.40 on 09/05/12
For personal use only.

The conclusion that chain initiation occurs by way of an intermediate complex is in agreement with similar conclusions reached by other workers (15, 20).

At sufficiently low initial hydroperoxide concentrations reaction [1b'] implies that the rate of oxidation should be proportional to $[ROOH]^{1/2}$. Although, at low cobalt concentrations, the initial rates of oxidation are not inconsistent with this relationship, it could not be properly verified because hydroperoxide is the major oxidation product and also because of the necessity of correcting for cobalt deactivation during the oxidation.

According to equation [2a], ρ_m should be proportional to [RH] provided limiting-rate effects do not come into play. One of the most interesting features of metal-catalyzed autoxidations uncovered in this work is the discovery that limiting-rate effects become very important in determining reaction order with respect to [RH] even at quite low cobalt concentrations. The reason for this can be illustrated by reference to Fig. 7. The heavy line represents the limiting rate obtained with 1×10^{-2} and 2×10^{-2} mole/l. [Co] as a function of [RH] in chlorobenzene. As already described, this line has a slope of 2.0 for fairly concentrated tetralin solutions and no rate can ever lie above this line. As the cobalt concentration is decreased, the rate in pure tetralin will decrease, but any decrease in reaction order can only occur over a rather limited range of tetralin concentration, after which the order must increase towards 2.0 as [RH] is further decreased. This means that there should be a family of curves which approach the limiting rate line at sufficiently low [RH], the detailed shape of each curve depending on the cobalt concentration. The expected family of curves was obtained at three cobalt concentrations and is shown in Fig. 7. The true reaction order in [RH] must be obtained from the limiting slope at low cobalt and high tetralin concentrations. The measured limiting slope is about 1.35–1.4 at the lowest cobalt concentration at which ρ_m could be measured with reasonable accuracy over a range of tetralin concentrations without the difficulties associated with catalyst deactivation, i.e. $[Co] = 2.4\times10^{-5}$ mole/l. and $[ROOH]_0 = 2\times10^{-2}$ mole/l. The question therefore arises as to whether limiting-rate effects are still influencing the reaction order even at this low cobalt concentration and, if they are not responsible for the reaction order, then the question arises as to whether the order is really 1.5 or whether it lies between 1.0 and 1.5 for some other reason. It is not possible to answer these questions on the basis of Fig. 7 alone. However, if ρ_m is proportional to $[RH]^{1.5}$ it implies that the complex formed in reaction [1b'] is decomposed to radicals by reaction with a molecule of tetralin (cf. the ferric ion – hydrogen peroxide catalyzed oxidation of ethyl alcohol (21)) and if the order is between 1.0 and 1.5 it suggests that this reaction is in competition with the unimolecular decomposition of the complex. Solution of the appropriate kinetic equations shows that the expression for the limiting rate of oxidation is unaffected (i.e., it is still given by equation [4]) but that in the first case,

$$[ROOH]_\infty = \frac{k_3^2[RH]}{2k_6K k_1'[Co]}, \qquad [3a]$$

and in the second case,

$$[ROOH]_\infty = \frac{k_3^2[RH]^2}{2k_6K[Co](k_1'+k_1''[RH])}, \qquad [3b]$$

where it has been assumed there is an equilibrium constant (K) for the complex and k_1' is the rate constant for its unimolecular decomposition. k_1'' is the rate constant for the reaction

$$[ROOHCoA_2OH] + RH \rightarrow \text{radicals}. \qquad [1b'']$$

Can. J. Chem. Downloaded from www.nrcresearchpress.com by 210.87.254.40 on 09/05/12
For personal use only.

If limiting-rate effects are responsible for the observed reaction order, then

$$[\mathrm{ROOH}]_\infty = \frac{k_3^2[\mathrm{RH}]^2}{2k_6Kk_1'[\mathrm{Co}]}. \qquad [3]$$

In spite of the difficulty of measuring $[\mathrm{ROOH}]_\infty$ with any precision in this system (see following section) it appears that, with chlorobenzene as the diluent, the measured hydroperoxide concentration at a given extent of oxidation is proportional to the square of the tetralin concentration at low cobalt concentrations ($\sim 5\times10^{-3}$ mole/l.). At higher cobalt concentrations the apparent order decreases but this seems to be due to a lower solubility of the catalyst in tetralin–chlorobenzene mixtures compared with that in pure tetralin. It must therefore be concluded that $[\mathrm{ROOH}]_\infty$ can be best represented by equation [3] and that reaction [1b''] is probably unimportant compared with the unimolecular decomposition of the catalyst–hydroperoxide complex. The measured dependence of the oxidation rate on [RH] is therefore still influenced by limiting-rate effects even at a cobalt concentration of 2.4×10^{-5} mole/l. Incidentally, decomposition of the complex by reaction with a second molecule of hydroperoxide (cf. refs. 22, 23) (rate constant k_1''') also leads to the same expression for the limiting rate of oxidation but in this case,

$$[\mathrm{ROOH}]_\infty = \frac{k_3[\mathrm{RH}]}{(2k_6Kk_1''')^{1/2}[\mathrm{Co}]^{1/2}}, \qquad [3c]$$

which does not describe the dependence of $[\mathrm{ROOH}]_\infty$ on [RH] nor on [Co] in the concentration region where the cobalt salts are soluble (see following section). In a similar way, analysis of the kinetics indicates that initiation is not due to a reaction between two of the complexes.

It should perhaps be pointed out that although a reaction order of 1.5 with respect to [RH] might appear to be accounted for at low cobalt concentrations by the slow reaction

$$\mathrm{CoA_2OH} + \mathrm{RH} \rightarrow \mathrm{CoA_2} + \mathrm{H_2O} + \mathrm{R}^\bullet \qquad [12]$$

the inclusion of this reaction at high cobalt concentrations precludes the occurrence of a limiting rate of oxidation equal to the theoretical value calculated on the basis of the Tobolsky theory. That is, at low cobalt and high hydroperoxide concentrations reaction [12] could be rate determining, with reaction [1a] becoming rate controlling as the hydroperoxide concentration is reduced. To account for the limiting rate of oxidation equalling the theoretical value one is forced to conclude that reaction [1a] is also rate determining at high cobalt concentrations. However, at high cobalt concentrations the addition of large amounts of hydroperoxide at the start of the reaction merely reduces the induction period very slightly (presumably by helping to solubilize the catalyst) but has no effect on the maximum rate. This is true even when more than sufficient hydroperoxide is added to convert all the cobalt to the trivalent state (see Fig. 8). This leads to the conclusion that at high cobalt concentrations reaction [1a] is rate controlling irrespective of the hydroperoxide concentration, a result diametrically opposed to the conclusion that was drawn at low cobalt concentrations. Reaction [12] can therefore play no important role in the oxidation.

In view of the shapes of the curves in Fig. 7 it is obvious that considerable caution should be exercised in deducing reaction mechanisms on the basis of incomplete kinetic analysis. That is, for any substrate and solvent in which the rate of a metal-catalyzed autoxidation is really first order with respect to the substrate the apparent reaction order over a limited concentration range will lie between 1.0 and 2.0. In particular, at low

Can. J. Chem. Downloaded from www.nrcresearchpress.com by 210.87.254.40 on 09/05/12
For personal use only.

[RH] or comparatively high [catalyst] an apparent order of 1.5 might be obtained. Such an order could lead to the incorrect conclusion that the substrate was involved in the rate-controlling initiation reaction. This conclusion has in fact been drawn by several authors (24, 25) but the kinetic basis appears to be rather weak in much of the work. The initiating reaction generally proposed to account for these kinetics is

$$M^{(n+1)+} + RH \rightarrow M^{n+} + H^+ + R^\cdot \qquad [12a]$$

leading to an oxidation rate proportional to $[M]^{1/2}[RH]^{3/2}$. While there is no doubt that this reaction can occur with a variety of substrates and metal catalysts in aqueous media (24) it appears less probable in non-polar media. An example which may possibly illustrate this effect is contained in the work of Heaton and Uri referred to previously (5). Their experimental evidence for reaction [12] was obtained at an initial hydroperoxide concentration of 0.10 mole/l. and a cobalt stearate concentration of 10^{-4} mole/l. over a range of linoleic acid concentrations from 0.05 to 0.4 mole/l. in benzene. The experimental rates indicate an average order of 1.5 in [RH] but they show a considerable curvature in the direction to be expected if limiting-rate phenomena are coming into play. Their data could therefore be accounted for either by reaction [12], or by reaction [1*b*′] if limiting-rate effects are coming into play, or by reaction [1*b*″], and no definite choice can be made between these three possibilities. This discussion of reaction [12] is not intended to imply that it never occurs in non-polar media since some of the extensive data collected by Denisov and Emanuel in their review article (25) indicate that aldehydes and possibly some other very readily oxidized substances may undergo such a reaction at elevated temperatures. However, at low temperatures, kinetic evidence alone which has been obtained over a small range of substrate concentration should not be taken as giving unequivocal proof that reaction [12] is the rate-determining initiation process.

Hydroperoxide Formation

The formation of tetralin hydroperoxide during the cobalt-catalyzed (1.9×10^{-2} mole/l. [Co]) oxidation of tetralin containing an initial concentration of 1.0×10^{-3} and 4.1×10^{-2} mole/l. [ROOH] is shown in Fig. 8. It can be seen that within a comparatively short time the hydroperoxide concentration at a given extent of oxidation is independent of its initial concentration. The hydroperoxide concentration increases fairly steadily throughout the region of the steady maximum rate of oxidation and then starts to increase more rapidly as the oxidation rate decreases because a large fraction of the cobalt has been deactivated at this point. There is no truly steady concentration of hydroperoxide (i.e. no $[ROOH]_\infty$) such as occurs in acetic acid as the solvent (1). This is apparently due both to the continuous deactivation of the cobalt and to the fact that, even with the more soluble cobalt salts, not all the cobalt will dissolve in the tetralin at this high cobalt concentration until some oxidation has occurred. That is, the oxygen-containing products of the reaction help to solubilize the cobalt salt. It is extremely difficult to correct for these two factors so that it is not really possible to obtain $[ROOH]_\infty$ in this system. However, at the same cobalt concentration it should be permissible to compare hydroperoxide concentrations for different tetralin concentrations in chlorobenzene by measuring [ROOH] at the same extent of oxidation of the tetralin and therefore at the same extent of cobalt deactivation. This was first done with 2×10^{-2} mole/l. [Co] in pure tetralin and in a 50% and a 25% by volume solution of tetralin in chlorobenzene. It was found that the measured [ROOH] depended on a power of the tetralin concentration lying between 1.0 and 2.0, in apparent agreement with equation [3*b*]. However, the measured order not only increased during

Can. J. Chem. Downloaded from www.nrcresearchpress.com by 210.87.254.40 on 09/05/12
For personal use only.

the oxidation but also increased as the tetralin concentration was increased. That is, with 25% tetralin and 50% tetralin, respectively, the measured orders with respect to undiluted tetralin increased from 1.15 and 1.3 at a 2% oxidation of the tetralin to 1.5 and 1.9 at 16% oxidation. It has already been mentioned that the cobalt catalysts appear to be more soluble in tetralin than in tetralin–chlorobenzene mixtures since measured oxidation rates at high cobalt concentrations decrease more rapidly than expected as the tetralin concentration in chlorobenzene is reduced, i.e. the apparent order in [RH] increases (see Fig. 7). The catalyst solubility will also affect the hydroperoxide concentration in tetralin–chlorobenzene mixtures. That is, since there is relatively less catalyst in solution the more dilute the tetralin is, the measured hydroperoxide concentration does not decrease as rapidly as expected as the tetralin concentration is reduced. The correct dependence of [ROOH] on [RH] is therefore given under conditions where comparable amounts of catalyst are dissolved in the system. The approach to a limiting order of 2.0 as the oxidation proceeds and the catalyst becomes solubilized by the products together with the increase in order at a given extent of oxidation as the tetralin concentration is increased (i.e. the opposite of the effect predicted by equation [3*b*]) both suggest that under strictly comparable conditions [ROOH] would be proportional $[RH]^2$ as required by equation [3]. This conclusion was verified at a lower cobalt concentration where catalyst solubility effects are greatly reduced. That is, with 5×10^{-3} mole/l. [Co] it was found that the hydroperoxide concentration at a given extent of oxidation was exactly proportional to $[RH]^2$ over almost the entire course of the oxidation (i.e. from 0.5% to 12% tetralin consumption) for a range of tetralin concentrations from pure tetralin to a 60% by volume solution of tetralin in chlorobenzene. The complex formed by reaction of the cobalt with hydroperoxide therefore undergoes a first-order decomposition and, at sufficiently low [Co] and high [RH], the rate of oxidation should become directly proportional to [RH].

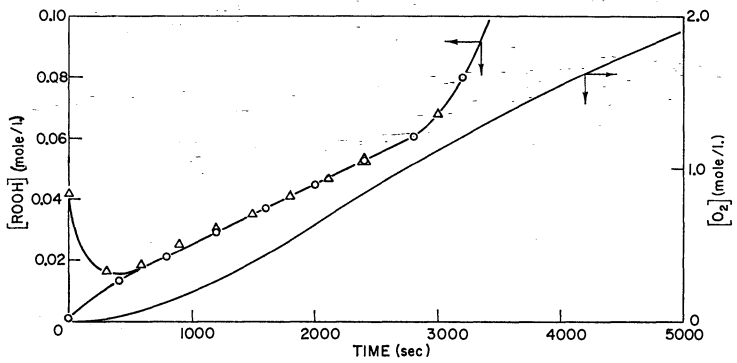

FIG. 8. Oxygen absorption and hydroperoxide formation at a cobalt decanoate concentration of 1.9×10^{-2} mole/l. Key: ○ $[ROOH]_0 = 1.0\times10^{-3}$ mole/l.; △ $[ROOH]_0 = 4.1\times10^{-2}$ mole/l.

At a given extent of oxidation the amount of active cobalt remaining in the system, although not necessarily in solution, can be very roughly calculated from equation [8] (see previous section). By comparing measured hydroperoxide concentrations at extents of oxidation where the same fraction of the cobalt should have been deactivated it appears that the hydroperoxide concentration decreases rather more slowly than expected at cobalt (decanoate) concentrations above 1.0×10^{-2} mole/l. (cf. [ROOH] at 1500 seconds in Figs. 8 and 9). This suggests that the effective cobalt concentration in solution increases rather

Can. J. Chem. Downloaded from www.nrcresearchpress.com by 210.87.254.40 on 09/05/12
For personal use only.

slowly with increasing cobalt concentration in this range. However, at cobalt concentrations below 10^{-2} mole/l. (and at the same relative extents of cobalt deactivation) [ROOH] becomes roughly inversely proportional to the initial cobalt concentration as required by equation [3]. The measured hydroperoxide concentrations can be roughly corrected to allow for cobalt deactivation during an oxidation and when this is done the increase in [ROOH] during an oxidation is greatly reduced, as can be seen in Fig. 9. This figure shows the measured [ROOH] during the oxidation of undiluted tetralin containing 5.0×10^{-3} and 9.0×10^{-3} mole/l. of cobalt decanoate and the calculated [ROOH] based on equation [8], i.e., based on the assumption that with 5×10^{-3} mole/l. [Co], $12.8(5\times10^{-3})^{1/2} = 0.91$ mole/l. [O_2] deactivates $0.75\times5\times10^{-3} = 3.75\times10^{-3}$ mole/l. [Co] and with 9×10^{-3} mole/l. [Co], 1.2 mole/l. [O_2] deactivates 6.8×10^{-3} mole/l. [Co]. Although the corrected [ROOH] still does not reach a true steady state it is not too far from one in the region of the maximum rate of oxidation (~1500 seconds). At cobalt concentrations below 1.0×10^{-2} mole/l. the corrected hydroperoxide concentration in the region of the maximum rate can perhaps be used as a very approximate measure of the steady-state hydroperoxide concentration which should exist were it not for the low solubility of the catalyst at the beginning of the reaction and its continuous deactivation during the reaction. That is, taking $[ROOH]_\infty \approx 0.07$ mole/l. at 5×10^{-3} mole/l. [Co], we can calculate the rate constant for chain initiation by cobalt in pure tetralin from equation [6] (1), using, of course, the extrapolated limiting rate of oxidation since this also allows for cobalt deactivation, i.e.

$$\left(\frac{-d[O_2]}{dt}\right)_\infty \Big/ [ROOH]_\infty = k[Co]. \qquad [6]$$

Therefore,

$$k \approx \frac{1.0\times10^{-3}}{7\times10^{-2}\times5\times10^{-3}} \approx 2.9 \text{ l./mole sec},$$

where k is either Kk_1' or k_1' depending on whether the complex in reaction [1b'] is formed by a reversible or irreversible process.

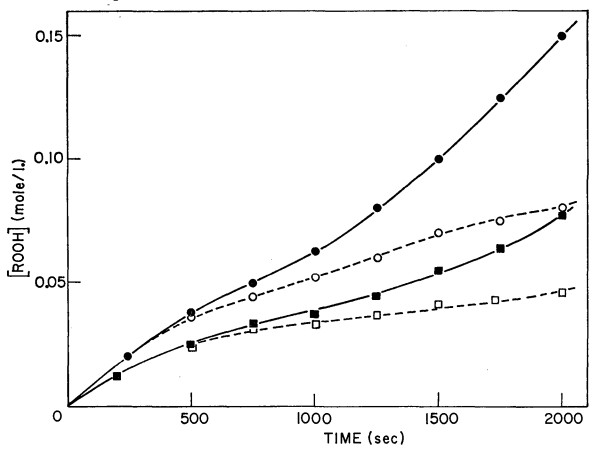

FIG. 9. The formation of hydroperoxide during the oxidation of tetralin. Key: Measured hydroperoxide at [Co] = 9.0×10^{-3} mole/l. (■), and at [Co] = 5.0×10^{-3} mole/l. (●); calculated hydroperoxide corrected for cobalt deactivation given by □ and ○.

Can. J. Chem. Downloaded from www.nrcresearchpress.com by 210.87.254.40 on 09/05/12
For personal use only.

Hydroperoxide Decomposition

The measurement of the rate of the cobalt-catalyzed decomposition of tetralin hydroperoxide in chlorobenzene solution is complicated by the deactivation of the cobalt and this reaction was not studied in as much detail as the decomposition in the benzene – acetic acid mixtures (1). The reaction is much faster in chlorobenzene than in the mixture containing acetic acid possibly because the cobalt is not very strongly associated with the solvent, and hydroperoxide molecules therefore have ready access to the cobalt. At a given [Co] and $[ROOH]_0$ the reaction is pseudo first order in hydroperoxide for a limited extent of decomposition but the measured rate constant increases with increasing concentration of peroxide and with decreasing concentration of cobalt. This increase in rate constant is probably not due to a reaction that is bimolecular in peroxide since the addition of the free-radical inhibitor, 2,6-di-*tert*-butyl-4-methylphenol (BMP), greatly reduces the variation in the measured rate constant. This implies that in the uninhibited reaction a radical-induced decomposition, [*i*], is superposed on the main decomposition reaction, i.e.,

$$\text{radical} + \text{ROOH} \rightarrow \text{radical} + \text{products.} \qquad [i]$$

The rate of hydroperoxide decomposition is therefore given by

$$\frac{-d[\text{ROOH}]}{dt} = Kk_1'[\text{Co}][\text{ROOH}] + k_i[\text{ROOH}]\left(\frac{Kk_1'[\text{Co}][\text{ROOH}]}{2k_6'}\right)^{1/2},$$

where k_6' is the rate constant for the self-termination of the radicals produced in the decomposition. The induced decomposition and cobalt deactivation were kept to a minimum by working with as large a cobalt concentration and as small an initial hydroperoxide concentration as was practical. With $[ROOH]_0 = 10^{-2}$ mole/l. the apparent rate constants were 9.4, 8.8, 8.0, and 7.2 l./mole sec at cobalt concentrations of 2.5, 3.5, 5.5, and 10.0×10^{-4} mole/l. When these values are plotted against $1/[\text{Co}]^{1/2}$ an excellent straight line is obtained with an intercept of 5.0 l./mole sec at infinite cobalt concentration which should correspond to the complete suppression of the induced chain decomposition, i.e., it should represent Kk_1' in chlorobenzene. This value is in satisfactory agreement with the value of 2.9 l./mole sec obtained in tetralin from the limiting rate of oxidation and $[ROOH]_\infty$ when the difficulties associated with the determination of the rate constant in the two systems are considered.

At the same initial hydroperoxide concentration the rate constant becomes very difficult to measure at cobalt concentrations below 2.5×10^{-4} mole/l. owing to the fact that a significant fraction of the cobalt is deactivated when comparatively little of the peroxide has been decomposed. The first-order plots of peroxide decomposition therefore show a very marked curvature and since it is not possible to obtain the initial rate accurately the measured rate constant may appear to decrease rather than increase as the cobalt concentration is reduced. This phenomenon may perhaps account for the greater than first order dependence on [Co] which has been reported by Dyer *et al.* (26) for the cobaltous 2-ethylhexanoate catalyzed decomposition of tetralin hydroperoxide in xylene at comparatively low cobalt concentrations ($\sim0.5\times10^{-4}$ to 1.0×10^{-4} mole/l.). That is, the reported order was about 2.0 at 25.5° C (cf., however, reference 27) and about 1.5 at 50.5° C.*

Under conditions where the initial hydroperoxide concentration is large relative to the cobalt concentration the rate of hydroperoxide decomposition rapidly drops to almost

**At 50.5° C the measured rate constant at 1.07×10^{-4} mole/l. [Co] was 77×10^{-5} sec^{-1}, i.e., 7.2 l./mole sec, which is in fairly good agreement with the value of 11.7 l./mole sec obtained by extrapolation from our own data at higher cobalt concentrations (where deactivation is less important and the rate can be more accurately measured).*

Can. J. Chem. Downloaded from www.nrcresearchpress.com by 210.87.254.40 on 09/05/12
For personal use only.

zero. For example, with 10^{-4} mole/l. [Co] and 4×10^{-2} mole/l. $[ROOH]_0$ the reaction ceases after 30% of the hydroperoxide has been decomposed. In chlorobenzene, each cobalt salt molecule is therefore capable of decomposing about 120 molecules of hydroperoxide, which is in fairly good agreement with the value of 100 calculated from equation [8] at high cobalt concentrations in tetralin.

The true rate constant for the catalyzed decomposition of the hydroperoxide was also obtained by suppressing the induced decomposition by the addition of the inhibitor BMP. With 10^{-2} mole/l. $[ROOH]_0$ and 10^{-3} mole/l. [Co] the measured rate constants in the presence of 1.2×10^{-2}, 2.4×10^{-2}, and 3.6×10^{-2} mole/l. [BMP] were 5.6, 5.2, and 5.1 l./mole sec respectively. Extrapolation to infinite BMP concentration where the induced decomposition should be completely eliminated gives a true rate constant of 4.8 l./mole sec, in good agreement with the value of 5.0 l./mole sec obtained by extrapolation to infinite cobalt concentration.

SUMMARY AND CONCLUSIONS

The extrapolated limiting rate of the cobalt-catalyzed oxidation of undiluted tetralin is in good agreement with the theoretical value even though there is no steady-state concentration of hydroperoxide formed during the oxidation. Upon dilution with chlorobenzene the limiting rate of oxidation shows the expected dependence on the square of the tetralin concentration provided the tetralin is not too dilute. Cobalt salt catalysts are deactivated during the oxidation, probably in the chain-initiation process, each atom of cobalt being able to decompose about 100 molecules of hydroperoxide. The rate of oxidation at low cobalt concentrations shows the expected dependence on the square root of the cobalt concentration, chain initiation most probably occurring by the unimolecular decomposition of a cobalt–hydroperoxide complex. There is no evidence for initiation by either a direct reaction of trivalent cobalt with the substrate or by a reaction of divalent cobalt with oxygen.

ACKNOWLEDGMENT

The authors wish to express their thanks to Dr. I. E. Puddington for his continued advice and encouragement throughout the course of this work.

REFERENCES.

1. Y. Kamiya, S. Beaton, A. Lafortune, and K. U. Ingold. Can. J. Chem. This issue.
2. A. V. Tobolsky. India Rubber World, **118**, 363 (1948).
3. A. V. Tobolsky, D. J. Metz, and R. B. Mesrobian. J. Am. Chem. Soc. **72**, 1942 (1950).
4. A. E. Woodward and R. B. Mesrobian. J. Am. Chem. Soc. **75**, 6189 (1953).
5. F. W. Heaton and N. Uri. J. Lipid Res. **2**, 152 (1961).
6. D. G. Knorre, Z. K. Maizus, and N. M. Emanuel. Zh. Fiz. Khim. **29**, 710 (1955).
7. R. F. Vasil'ev, Z. G. Kozlova, and L. G. Chuchukina. Izv. Akad. Nauk SSSR, Otd. Khim. Nauk, 1337 (1960).
8. B. V. Erofeev and T. I. Soroko. Zh. Prikl. Khim. **33**, 903 (1960).
9. G. A. Russell. J. Am. Chem. Soc. **79**, 3871 (1957).
10. N. Michaels. Univ. Microfilms. University of Michigan, Ann Arbor, Mich. Order No. 61–5525.
11. N. G. Ariko and B. V. Erofeev. Sb. Nauchn. Rabot, Inst. Fiz. Organ. Khim. Akad. Nauk Belorussk. S.S.R. 155 (1960).
12. N. Uri. Nature, **177**, 1177 (1956).
13. N. Uri. Essential Fatty Acids. Interscience Publishers Inc., New York. 1958.
14. H. Kropf. Ann. **637**, 73 (1960).
15. A. J. Chalk and J. F. Smith. Trans. Faraday Soc. **53**, 1214 (1957).
16. D. G. Knorre, L. G. Chuchukina, and N. M. Emanuel. Zh. Fiz. Khim. **33**, 877 (1959).
17. G. A. Russell. J. Am. Chem. Soc. **78**, 1041 (1956).
18. E. T. Denisov. Dokl. Akad. Nauk S.S.S.R. **130**, 1055 (1960).
19. O. S. Privett and M. L. Blank. J. Am. Oil Chemists' Soc. **39**, 465 (1962).
20. P. George, E. K. Rideal, and A. Robertson. Proc. Roy. Soc. (London), Ser. A, **185**, 288 (1946).

Can. J. Chem. Downloaded from www.nrcresearchpress.com by 210.87.254.40 on 09/05/12
For personal use only.

21. M. L. KREMER. Nature, **184**, 720 (1959).
22. M. L. KREMER and G. STEIN. Trans. Faraday Soc. **55**, 959 (1959).
23. M. L. KREMER. Trans. Faraday Soc. **58**, 702 (1962).
24. K. U. INGOLD. Lipids and their oxidation. *Edited by* H. W. Schultz and E. A. Day. Avi Publishing Co., Inc., Westport, Conn. 1962. Chap. 5.
25. E. T. DENISOV and N. M. EMANUEL. Usp. Khim. **29**, 1409 (1960).
26. E. DYER, K. R. CARLE, and D. E. WEIMAN. J. Org. Chem. **23**, 1464 (1958).
27. A. ROBERTSON and W. A. WATERS. J. Chem. Soc. 1578 (1948).

Downloaded from www.nrcresearchpress.com by 210.87.254.40 on 09/05/12
For personal use only.

IONIZATION AND DISSOCIATION OF FORMATE ESTERS BY ELECTRON IMPACT

D. VAN RAALTE AND A. G. HARRISON[1]
Department of Chemistry, University of Toronto, Toronto, Ontario
Received March 19, 1963

ABSTRACT

The mass spectra of methyl formate-*d*, ethyl formate-*d*, and isopropyl formate-*d* are compared with the mass spectra of the undeuterated compounds. By use of the deuterium labelling and appearance potential studies the dissociation reactions leading to a number of the oxygen-containing ions have been elucidated. The proton affinity of formic acid is estimated to be 157 kcal/mole from the appearance potential of the $HC(OH)_2^+$ ion in the mass spectra of ethyl formate and isopropyl formate.

INTRODUCTION

A survey of the mass spectra of aliphatic esters by Sharkey and co-workers (1) has established the main dissociation reactions on electron impact and has pointed out a number of important rearrangement processes. Beynon *et al.* (2) have extended this work by using high-resolution mass spectrometry to determine the empirical formulae of the ions formed. Some information on the energetics and mechanism of ion formation has been obtained by King and Long (3) in a detailed study of C^{13}-labelled methyl formate and methyl acetate, while more recently Godbole and Kebarle (4) have studied some of the rearrangement processes in various deuterated ethyl and isopropyl acetates and ethyl formate. The present paper reports the mass spectra of methyl formate-*d*, ethyl formate-*d*, and isopropyl formate-*d*. The use of deuterium labelling combined with appearance potential studies has permitted the elucidation of the mechanism of a number of the important rearrangement processes.

EXPERIMENTAL

The mass spectra were obtained with an Associated Electrical Industries MS-2 mass spectrometer. The operating conditions were 50 v electron energy, 20 μa ionizing current, and 3 v repeller ($\sim$7 v/cm field strength). The appearance potentials were determined as previously described (5) using xenon as the calibrating gas.

The deuterated compounds were obtained from Merck, Sharp and Dohme of Canada. The isotopic purity was checked by low-energy analysis as will be discussed below. The mass spectra showed no other detectable impurities. The unlabelled methyl and ethyl formates were commercial samples which were distilled before use. The isopropyl formate was prepared by standard methods and purified by distillation.

RESULTS AND DISCUSSION

The major peaks in the mass spectra of the deuterated and undetuerated esters are presented in Table I. The intensities are expressed as percentage of the total ion yield and ion currents less than 0.5% have not been listed unless they are of special interest. The spectra have all been corrected for C^{13} isotope contribution and in the case of methyl formate-*d* for 0.5% undeuterated methyl formate as determined by low-energy analysis. Low-energy analysis of ethyl formate-*d* and isopropyl formate-*d* showed less than 1% isotopic impurity in each case; no correction for this has been made. The isotopic analysis of the isopropyl formate was carried out in the mass 45–46 region due to the low intensity of the parent ion.

[1]*Alfred P. Sloan Research Fellow 1962–1964.*

Can. J. Chem. Downloaded from www.nrcresearchpress.com by 210.87.254.40 on 09/05/12
For personal use only.

TABLE I

Mass spectra of formate esters*

m/e	$HCOOCH_3$	$DCOOCH_3$	$HCOOC_2H_5$	$DCOOC_2H_5$	$HCOOCH(CH_3)_2$	$DCOOCH(CH_3)_2$
14	1.00	0.94	0.95	0.77	0.37	0.32
15	7.44	6.30	2.48	1.81	2.52	1.97
16			0.06	0.53	0.07	0.48
19			1.22	0.29	1.89	0.34
20				1.16		1.86
26			3.36	3.06	0.62	0.64
27			11.95	11.09	7.86	7.47
28	3.06	2.80	17.31	20.30	0.61	0.94
29	18.50	6.52	16.62	10.19	4.70	1.75
30	2.14	13.09	1.10	6.06	0.08	2.47
31	36.52	5.18	23.17	1.12	1.05	0.32
32	15.90	34.58		24.08		1.62
33		15.00				
39					4.30	4.36
40					0.90	0.95
41			0.21	0.34	10.11	9.85
42			0.61	0.61	12.28	12.34
43			2.82	2.06	11.96	10.85
44	0.64	0.40	0.46	1.15	0.46	1.30
45	0.59	0.11	8.41	2.94	29.43	0.53
46		0.19	0.22	5.32		29.43
47			1.86		2.00	
48				2.16		1.95
56			0.74	0.39		
57				0.60		
59	0.26	0.19	0.44		1.64	
60	13.68	0.04		0.26		1.50
61		14.10				
73			0.35	0.08	5.43	
74			2.04	0.25		5.20
75				2.12		
87					0.11	
88					0.14	0.02
89						0.19

*Intensities expressed as percentage of total ion yield.

Table II lists the appearance potentials of some of the more important ions for the three esters. In general, the agreement with previously published results is within experimental error.

Of particular interest in the mass spectra are the oxygen-containing ions at masses* 73, 59, 47, 45, 31, and 19, and their counterparts in the deuterated isomers. These ions can be divided into two classes, those which are formed by direct dissociation and those which are formed by a rearrangement reaction.

Ions Formed by Direct Dissociation

(a) Loss of H

The small ion current at mass 73 (loss of deuterium) in ethyl formate-*d* indicates that loss of the formyl hydrogen occurs to a significant extent in ethyl formate. The mass spectrum of $HCO_2CD_2CH_3$ showed (4) a much larger loss of H than can be accounted for by loss of the formyl hydrogen. Since Godbole and Kebarle (4) also observed loss of deuterium, it is apparent that all hydrogens are lost to some extent from ethyl formate.

**Since doubly charged ions are not discussed, the mass-to-charge ratio will be referred to as the mass throughout.*

Can. J. Chem. Downloaded from www.nrcresearchpress.com by 210.87.254.40 on 09/05/12
For personal use only.

TABLE II
Appearance potentials in formate esters

Compound	*m/e*	Appearance potential (v±0.1 v) This work	Literature
$HCOOCH_3$	60	11.12	11.1 (3)
	32	11.53	11.5 (3)
	31	12.35	12.4 (3)
$HCOOC_2H_5$	74	10.70	10.5 (3), 10.79 (4)
	47	11.60	11.64 (3), 11.73 (4)
	45	11.55	11.7 (3)
	31	12.02	12.2 (3), 12.44 (4)
$DCOOC_2H_5$	46	12.33	12.15 (7)
	45	11.55	
$HCOOCH(CH_3)_2$	47	10.87	
	45	11.53	
	31	13.45	
$DCOOCH(CH_3)_2$	32	13.53	

The mass 59 ion of methyl formate corresponds to loss of hydrogen. The observation of both mass 59 (loss of D) and mass 60 (loss of H) in the mass spectrum of methyl formate-*d* indicates that both the formyl and the methyl hydrogens are lost, with loss of the methyl hydrogen accounting for approximately 20% of the ion current. The observation of loss of the methyl hydrogen is in contrast to the results of Renaud and Leitch (6), who concluded, from the mass spectrum of $HCOOCD_3$, that only the formyl hydrogen was lost. It should be noted, however, that their reported spectra gave mass 63/mass 62 = 0.0456 for $HCOOCD_3$ compared to mass 60/mass 59 = 0.0186 for $HCOOCH_3$. This suggests an appreciable impurity of $HCOOCD_2H$ in the $HCOOCD_3$ and makes interpretation of the results difficult.

(b) Loss of CH_3

The mass 73 ion in isopropyl formate corresponds to loss of CH_3. The observation of this ion at mass 74 in the deuterated compound indicates that the formyl hydrogen is retained. It is probable that the methyl is lost without isotopic mixing.

The mass 59 ion of ethyl formate has been shown (2) to have the empirical formula $C_2H_3O_2^+$, formed by loss of CH_3. In $DCOOC_2H_5$ this ion is observed at mass 60, while in $HCOOCD_2CH_3$ the ion is observed (4) at mass 61. These results indicate the structure $HCOOCH_2^+$, the methyl group being lost without isotopic mixing.

(c) Formation of $C_2H_5O^+$ from Ethyl Formate

High-resolution work by Beynon *et al.* (2) has shown that the mass 45 ion in ethyl formate has the empirical formula $C_2H_5O^+$ with negligible contribution from HCO_2^+.

Both masses 45 and 46 are found in the mass spectrum of ethyl formate-*d*. The former must be $C_2H_5O^+$, consisting of the original ethoxy group of the ester, while the latter ion, incorporating the formyl hydrogen, is presumably the $DOCHCH_3^+$ ion. The relative intensities indicate that in ethyl formate approximately 65% of the mass 45 ion is a rearrangement ion incorporating the formyl hydrogen. Godbole and Kebarle (4) observed both $CH_3CD_2O^+$ and CH_3CDOH^+ in the mass spectrum of $HCOOCD_2CH_3$. From the relative intensities they assigned, one calculates 43% retention of the two deuteriums. This is significantly higher than the 35% retention of the total ethoxy group calculated in the present work and suggests that some of the mass 45 ion may be formed by loss of one of the methyl hydrogens with transfer of the formyl hydrogen.

Can. J. Chem. Downloaded from www.nrcresearchpress.com by 210.87.254.40 on 09/05/12
For personal use only.

The appearance potential of mass 45 ($C_2H_5O^+$) in the ethyl formate-*d* is in agreement with *A*(mass 45) = 11.55 ev. in the undeuterated compound. Using ΔH_f(ethyl formate) = −88 kcal/mole (7) this appearance potential leads to $\Delta H_f(C_2H_5O^+)$ = 152 kcal/mole assuming H + CO as the neutral fragments and 178 kcal/mole assuming HCO as the neutral fragment. The lower value is only slightly higher than $\Delta H_f(CH_3CHOH^+)$ = 145 kcal/mole, obtained from appearance potential studies of the simple alcohols (8, 9). Although no reliable value for $\Delta H_f(C_2H_5O^+)$ has been established, both the values 152 and 178 kcal/mole are too low by comparison with $\Delta H_f(CH_3O^+)$ = 212 kcal/mole (7). It appears likely that the ion has rearranged to the more stable carbinyl structure and is formed with H + CO as the neutral fragments.

Ions Formed by Rearrangement

A number of the major rearrangement reactions which occur can be represented by the following general reaction first suggested by King and Long (3):

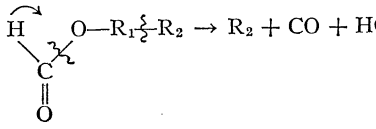

$$\rightarrow R_2 + CO + HOR_1^+. \qquad [1]$$

The main driving force for this rearrangement is undoubtedly the stability of the CO produced and the stability of the hydroxycarbinyl ion.

(a) Loss of H + CO (R_2 = H)

The loss of H + CO from isopropyl formate leads to the formation of mass 59, which has been shown (2) to have the empirical formula $C_3H_7O^+$. In isopropyl formate-*d* this ion has moved to mass 60, indicating retention of the formyl hydrogen. The ion is thus not the original isopropoxy group of the ester but is a rearrangement ion formed by reaction [1], the hydrogen lost probably being the tertiary hydrogen of the isopropyl group.

As discussed above the large intensity at mass 46 in ethyl formate-*d* indicates approximately 65% retention of the formyl hydrogen in formation of the $C_2H_5O^+$ ion. The ion probably has the structure $HOCHCH_3^+$ formed by rearrangement reaction [1].

A(CH_3CHOD^+) from ethyl formate-*d* is in agreement with *A*(mass 46) reported by Bernecker and Long (7). The appearance potential leads to $\Delta H_f(CH_3CHOD^+)$ = 162 kcal/mole assuming the neutral fragments H + CO. This is considerably higher than the best value for this ion and implies the presence of excess energy in the rearrangement process.

The mass 31 ion in methyl formate has been postulated (3) to be the original methoxy group formed with HCO as the neutral fragment. The large intensity at mass 32 in methyl formate-*d* indicates that the major fraction of this ion incorporates the formyl hydrogen and is thus the CH_2OH^+ ion formed by reaction [1] with H + CO as neutral fragments. Comparison of the mass 32 intensity in $DCOOCH_3$ with the mass 31 intensity in $HCOOCH_3$ indicates 95% formyl hydrogen retention neglecting any isotope effects.

The appearance potential of mass 31 from methyl formate leads to $\Delta H_f(CH_2OH^+)$ = 176±3 kcal/mole, using $\Delta H_f(HCOOCH_3)$ = −83.7 kcal/mole (7) and assuming H + CO as the neutral fragments. This is in reasonable agreement with $\Delta H_f(CH_2OH^+)$ = 180±3 kcal/mole obtained from simple alcohols (8, 9).

(b) Loss of CH_3 + CO (R_2 = CH_3)

Mass 45 in isopropyl formate corresponds to loss of CH_3 + CO. In isopropyl formate-*d* this ion has moved quantitatively to mass 46, indicating retention of the formyl hydrogen. The ion is thus formed by rearrangement reaction [1] with R_2 = CH_3.

Can. J. Chem. Downloaded from www.nrcresearchpress.com by 210.87.254.40 on 09/05/12
For personal use only.

The appearance potential of CH_3CHOH^+ from isopropyl formate leads to $\Delta H_f(CH_3CHOH^+) = 163$ kcal/mole using ΔH_f(isopropyl formate) $= -97$ kcal/mole as estimated from the heats of formation of other formate esters. Again this is considerably higher than the best estimates for this ion and implies the involvement of excess energy in the rearrangement process.

The mass 31 in ethyl formate has moved to mass 32 in $DCOOC_2H_5$. This result, in conjunction with the observation of the ion at mass 33 in $HCOOCD_2CH_3$ (4), clearly shows retention of the formyl hydrogen and loss of the terminal methyl group without isotopic mixing in the rearrangement reaction. The appearance potential of mass 31 from ethyl formate obtained in the present work is slightly lower than that obtained previously and leads to $\Delta H_f(CH_2OH^+) = 183 \pm 3$ kcal/mole, in reasonable agreement with the best value of 180 kcal/mole (8, 9).

(c) Formation of Mass 31 from Isopropyl Formate

In contrast to the above results, the rearrangement to form mass 31 in isopropyl formate follows a somewhat different mechanism. As shown in Table I the ion has moved to mass 32 in isopropyl formate-*d*, indicating retention of the formyl hydrogen. The most reasonable mechanism for formation of this ion is through the mass 59 ($(CH_3)_2COH^+$) as follows:

$$HCOOCH(CH_3)_2^+ \rightarrow H + CO + HOC(CH_3)_2^+ \rightarrow C_2H_4 + HOCH_2^+. \qquad [2]$$

Deuterium labelling (11) has shown that formation of mass 31 from isopropyl alcohol occurs with retention of the hydroxyl hydrogen and complete loss of the tertiary hydrogen, while recent work in this laboratory (9) indicates that the reaction proceeds through the mass 59 intermediate as indicated by the above mechanism and in agreement with the labelling evidence.

The appearance potential of CH_2OH^+ from isopropyl formate was found to be 13.45 ev compared to 13.53 ev for $A(CH_2OD^+)$ from isopropyl formate-*d*. The average value, 13.49 ± 0.1 ev, leads to $\Delta H_f(CH_2OH^+) = 177 \pm 3$ kcal/mole assuming the above mechanism. Considering the possible errors in the estimation of the heat of formation of the ester this is in satisfactory agreement with the best value of 180 kcal/mole. This result affords further support for the mechanism of formation proposed.

It is apparent from the above results that mass 31 in methyl formate and in ethyl formate, mass 46 in ethyl formate-*d*, and masses 45 and 59 in isopropyl formate arise by similar rearrangement reactions represented by the general reaction [1]. Three possibilities must be considered when discussing the time sequence by which the reaction occurs. These are:

(*a*) CO leaves first;

(*b*) R_2 leaves first;

(*c*) concerted rearrangement in which R_2 and CO leave simultaneously.

Sequence (*a*) should lead to significant ion currents for the corresponding alcohol ions in the case of methyl and ethyl formates. For methyl formate a significant ion current for CH_3OH^+ is observed. Subsequent loss of $R_2 = H$ would be consistent with the labelling results, since the mass spectra of deuterated methanols show predominantly methyl hydrogen loss (9, 10). The mass 31 intensity in methyl formate is greater than might be expected from decomposition of the methanol ion and it is probable that one or both of sequences (*b*) and (*c*) contribute.

The absence of the $CH_3CH_2OH^+$ ion in the spectrum ethyl formate would argue against the occurrence of reaction [1] by sequence (*a*) in this case. For the formation of

Can. J. Chem. Downloaded from www.nrcresearchpress.com by 210.87.254.40 on 09/05/12
For personal use only.

CH_2OH^+ from ethyl formate the observation (4) of a metastable form at mass 16.3 corresponding to the transition

$$HCOOCH_2^+ (59) \rightarrow CH_2OH^+ (31) + CO (28); m^* = \frac{31^2}{59} = 16.3 \quad [3]$$

indicates for this ion a significant occurrence of the rearrangement [1] by a time sequence in which R_2 is lost first. For the other cases the present results do not permit decisions as to the time sequence of the rearrangement.

Mass 19

The mass spectra of ethyl formate and isopropyl formate both show significant ion currents at mass 19 corresponding to the hydronium ion. For both esters the spectra of the deuterated isomers show that the major part of this ion incorporates the formyl hydrogen. The energetics and mechanism of hydronium ion formation in esters and alcohols will be discussed in a further communication.

Proton Affinity of Formic Acid

The mass sepctra of ethyl and isopropyl formates show significant ion currents at mass 47 which must correspond to a protonated formic acid molecule. The spectra of the deuterated molecules show that this ion incorporates the formyl hydrogen. The three reported appearance potentials for $HC(OH)_2^+$ from ethyl formate (Table II) agree within experimental error. The average value, 11.66±0.1 ev, leads to $\Delta H_f(HC(OH)_2^+) = 115\pm3$ kcal/mole assuming C_2H_3 ($\Delta H_f = 65$ kcal/mole (7)) as the neutral fragment. $A(HC(OH)_2^+) = 10.87\pm0.1$ ev from isopropyl formate leads to $\Delta H_f(HC(OH)_2^+) = 122\pm3$ kcal/mole assuming C_3H_5 ($\Delta H_f = 30$ kcal/mole (7)) as the neutral fragment. This mechanism is similar to that proposed by McLafferty and Hamming (12) for the similar rearrangement in isobutyl esters. Although the agreement of the two estimates is barely within experimental error the results suggest that $\Delta H_f(HC(OH)_2^+) = 118$ kcal/mole is not in serious error. Combination of this value with $\Delta H_f(HCOOH) = -90$ kcal/mole and $\Delta H_f(H^+) = 365$ kcal/mole (7) leads to 157 kcal/mole for the proton affinity of formic acid in the gas phase. This is substantially less than the estimate of 177 kcal/mole by Godbole and Kebarle (4) for the proton affinity of acetic acid, but is not unexpected in view of the stabilizing effect of the methyl group compared to hydrogen.

ACKNOWLEDGMENTS

The authors are indebted to the Advisory Committee on Scientific Research, University of Toronto, and the National Research Council of Canada for financial support.

REFERENCES

1. A. G. Sharkey, J. L. Shultz, and R. A. Friedel. Anal. Chem. **31**, 87 (1959).
2. J. H. Beynon, R. A. Saunders, and A. E. Williams. Anal. Chem. **33**, 221 (1961).
3. A. B. King and F. A. Long. J. Chem. Phys. **29**, 374 (1958).
4. E. W. Godbole and P. Kebarle. Trans. Faraday Soc. **58**, 1897 (1962).
5. A. G. Harrison and T. W. Shannon. Can. J. Chem. **40**, 1730 (1962).
6. R. Renaud and L. C. Leitch. Can. J. Chem. **34**, 179 (1956).
7. R. R. Bernecker and F. A. Long. J. Phys. Chem. **65**, 1565 (1961).
8. L. Friedman, F. A. Long, and M. Wolfsberg. J. Chem. Phys. **27**, 613 (1957).
9. D. Van Raalte and A. G. Harrison. To be published.
10. J. H. Baxendale and R. G. Sedgwick. Trans. Faraday Soc. **57**, 2157 (1961).
11. L. Friedman and J. Turkevich. J. Am. Chem. Soc. **74**, 1666 (1952).
12. F. W. McLafferty and M. C. Hamming. Chem. Ind. (London), 1366 (1958).

Can. J. Chem. Downloaded from www.nrcresearchpress.com by 210.87.254.40 on 09/05/12
For personal use only.

INTENSITIES OF EMISSION LINES IN FLAMES OF METAL HALIDES WITH ACTIVE NITROGEN

L. F. PHILLIPS
Chemistry Department, University of Canterbury, Christchurch, New Zealand
Received April 3, 1963

ABSTRACT

The intensities of spectral lines emitted by flames of a number of metal halides with active nitrogen have been found to vary as the square of the nitrogen atom concentration. When the total energy required for simultaneous dissociation of the halide and excitation of the metal atom is less than about 200 kcal/mole the energy transfer process is too efficient to be attributed to the termolecular reaction of a halide molecule with a pair of nitrogen atoms. The observations are consistent with the hypothesis that in this case energy is transferred to the halide molecule during collision with a nitrogen molecule in the $^5\Sigma_g^+$ state. Possible excitation mechanisms are discussed for less intense lines which would require up to 276 kcal/mole for simultaneous dissociation and excitation.

INTRODUCTION

In a previous communication (1) it was shown that in flames of thallous halides with active nitrogen the intensity of the 5350 Å thallium line is proportional to the first power of the halide concentration and to the square of the nitrogen atom concentration. The rate of the overall reaction, calculated from the absolute intensity of the 5350 Å line and also from the rate of consumption of halide, was approximately 2×10^{-29} cm^{6}molecule^{-2}sec^{-1}, whereas the largest value to be expected for a termolecular reaction is about 10^{-31} cm^{6}molecule^{-2}sec^{-1} (2).

Thallium lines were observed photographically down to 3230 Å, for which the energy required in the case of TlF is 221 kcal/mole. The results were discussed in terms of the transfer of energy to the halide during a collision with an electronically excited nitrogen molecule (equation [1]), the excited molecule being produced during nitrogen atom recombination. In the steady state the concentration of N_2^* is proportional to the square of the nitrogen atom concentration. It was suggested that the excited molecule involved was in the $^5\Sigma_g^+$ state, since the amount of energy required appeared to be too great to be provided by other metastable species.

$$N_2^* + TlX \rightarrow Tl^* + X + N_2 \qquad [1]$$

In the present paper the intensity measurements are extended to all of the thallium lines and to flames of active nitrogen with some halides of other metals. For all of the emission lines the intensity varies as the square of the nitrogen atom concentration, proportionality to the halide concentration also being observed over the range of partial pressures used. The lines may be divided into three classes, depending on whether the total energy required to dissociate the halide and excite the metal atom is less than about 200 kcal/mole, between 200 and 225 kcal/mole, or greater than 225 kcal/mole. For lines in the first class the efficiency is in general too high for the termolecular mechanism [2]

$$N + N + MX_n \rightarrow N_2 + M^* + nX \qquad [2]$$

X = halogen atom, M = metal atom of valency n

and the arguments of the previous paper (1) may be applied, leading to the conclusion that energy is probably transferred from a nitrogen molecule in the $^5\Sigma_g^+$ state. For lines

Can. J. Chem. Downloaded from www.nrcresearchpress.com by 210.87.254.105 on 09/05/12
For personal use only.

in the second class either of these mechanisms may operate. For lines in the third class both mechanisms may be ruled out on energetic grounds, while a termolecular mechanism involving one ground state and one excited nitrogen atom may be eliminated on grounds of efficiency because of the small proportion of excited atoms in discharged nitrogen (3). There are two other alternatives for this case, one involving a higher metastable state of N_2 and the other using consecutive excitation processes similar to [1] or [2] to overcome the high energy requirement. Of these alternatives the latter is favored since it leads more readily to a dependence of intensity on the square of the atom concentration.

This work is essentially a continuation of the series of observations of Strutt (4) on flames supported by active nitrogen, with the advantage that in the intervening 50 years a reasonably complete theory of active nitrogen has developed (5). In the current theory most of the activity of discharged nitrogen is attributed to the presence of ground-state nitrogen atoms; however, the role of metastable nitrogen molecules has been stressed by a number of investigators (6–9, 1). Mulliken (10) has listed most of the known or predicted states of N_2, together with their theoretical dissociation products and important spectroscopic constants, including the known or predicted energy of the ground vibrational level. Table I, selected from Mulliken's data, contains those states which are expected to be metastable or long lived. As pointed out by Kenty (11), a state may be slightly above another to which transition is allowed yet have a long lifetime because of smallness of the factor ν^3 in the expression for the transition probability. Where a state is expected to be long lived for this reason the nearby state to which a transition is allowed is given in the right-hand column of Table I. As in Mulliken's table, square brackets indicate predicted states or values, parentheses indicate doubtful values.

TABLE I

Long-lived electronic states of N_2

State	Energy ($v = 0$), kcal/mole	D^0, kcal/mole	Dissociation products	Allowed transition
$X^1\Sigma_g^+$	0	225	$^4S+^4S$	—
$A^3\Sigma_u^+$	142	83	$^4S+^4S$	—
$[^3\Delta_u]$	[172]	[107]	$^4S+^2D$	$\rightarrow B^3\Pi_g$ at 170 kcal
$a^1\Pi_g$	196	138	$^2D+^2D$	—
$a'^1\Sigma_u^-$	(202)	(132)	$^2D+^2D$	$\rightarrow a^1\Pi_g$ at 196 kcal
$^5\Sigma_g^+$	(222)	(3)	$^4S+^4S$	—
$[^1\Sigma_g^+]$	[(280)]	[(182)]	$^4S+(s^2p^2.3S)^4P$	$\rightarrow [^1\Pi_u]$ at [(279)] kcal
(Possibly other states, of high multiplicity, above this)				

EXPERIMENTAL

The reaction vessel and flow system were as previously described (1) except that an improved heating jacket enabled the reaction vessel to be heated to 550° C. This higher temperature was necessary for flames with sodium iodide, a temperature of 400±10° C being used with the other halides. The reaction vessel consisted of a length of 34 mm o.d. quartz tubing having one end window at right angles to the length of the tube and two parallel side windows. In the present work photometric observations were made through the side windows. Active nitrogen from a microwave discharge was pumped through the reaction tube with a linear velocity of 1.2 m/sec at 3.0 mm Hg, the majority of the experiments being carried out at this pressure. Metal halides were carried from a small, independently heated oven by a stream of argon, and entered the reaction vessel through a 0.2 mm jet at the end of a 3 mm o.d. quartz tube. This jet could be moved over a range of 6 cm along the axis of the reaction vessel. Nitrogen atom flows were determined by visual titration with nitric oxide (12). Typical partial pressures of atomic nitrogen and metal halide were 0.05 mm and 0.0005 mm respectively.

Thallous halides were as used previously. The other halides were A.R. grade or else the best reagent grade available. The process of vacuum sublimation involved in producing a flame appeared to be sufficient to eliminate the effects of most impurities, especially since the greatest source of this kind of error would be

Can. J. Chem. Downloaded from www.nrcresearchpress.com by 210.87.254.105 on 09/05/12
For personal use only.

the presence in the reaction vessel of traces of halides from previous experiments. Prolonged cleaning of the vessel with 20% hydrofluoric acid was not sufficient to entirely free the walls of metals or metal halides. Measurements were carried out in an order which would minimize the effect of this contamination; for example TlF was studied before TlI, the intensity of emission at all wavelengths being greater for the latter. In every case the background intensity was measured with the argon flow cut off and a suitable correction applied.

Photometric measurements were carried out using a Hilger medium quartz spectrograph fitted with an E720 scanning unit and a 1P28 photomultiplier. The output of the photomultiplier was taken to a 0–250 μa meter through a cathode follower. The variation of photometer sensitivity with wavelength was determined from the response to a tungsten strip filament lamp of known temperature and emissivity (13).

RESULTS

The four thallous halides, lead (II) chloride, bromide, and iodide, cuprous iodide, and sodium iodide were studied. The spectral features observed were thallium lines at 5350, 3776, 3530, 3519, and 3230 Å, lead lines at 4058, 3683, and 3639 Å and visible bands of PbX, copper lines at 3247 and 3274 Å with visible bands of CuI, and sodium lines at 5890, 5896, and 3302 Å with the respective halides. Flames of this sort have often been used as sources of MX bands for spectroscopy (14). Flames of sodium and thallous halides were short and tended to be spherical at low halide flows. Those of the other halides were much more elongated and sometimes extended well beyond the heated portion of the flow system. This suggests that the reactions leading to consumption of the latter halides are comparatively slow, and perhaps proceed in stages. Dark-colored deposits, similar to those noticed previously with thallous halides, were formed in cool parts of the reaction system with all of the halides except sodium iodide, where a white deposit was formed. Hydrofluoric acid removed the metallic appearance of the deposits, leaving solids which were similar to the original halides and which could be removed with hot water.

The effect of variation of nitrogen atom concentration on the intensity of the emission lines is shown in Fig. 1. All of the observed lines vary in intensity as the square of the nitrogen atom concentration. The MX bands that appeared with halides of lead and copper were superimposed on some moderately intense afterglow emission; however it was noticed that the total intensity varied more slowly than $[N]^2$. Since the intensity of the afterglow alone is proportional to $[N]^2$ (8) this suggests that the MX-band intensity depends on a lower power of the nitrogen atom concentration.

For the measurements of Fig. 1 the power supplied to the discharge was varied, the atom concentration at each power level being determined by NO titration in absence of halide. The end point of the titration is difficult to locate at high temperatures, apparently because of reduced efficiency of the light-emitting reactions, so the calibrations of power level in terms of atom concentration were carried out near room temperature. The amount of nitric oxide required to extinguish the halide flame at the high temperature was invariably the same as that required to titrate the nitrogen atoms at the low temperature.

In order to determine the relative efficiencies of the various excitation processes the intensities of emission lines were measured for each flame under as nearly the same conditions as possible. Observations were made at 2 cm from the halide inlet jet and the intensities were corrected to the same partial pressures of halide and atomic nitrogen. The same argon flow (12.1 μmoles/sec), nitrogen flow (265 μmoles/sec), total pressure (3.0 mm Hg), and temperature ($400\pm10°$ C) were used in every case except that of sodium iodide where the temperature was 550° C.

The results of the intensity measurements, normalized to a value of 200 for the rate of production of Tl($7.^2S_{\frac{1}{2}}$) atoms from TlI, are given in Table II. On this scale the nominal upper limit for the rate of a termolecular reaction is unity and emission lines which have

Can. J. Chem. Downloaded from www.nrcresearchpress.com by 210.87.254.105 on 09/05/12
For personal use only.

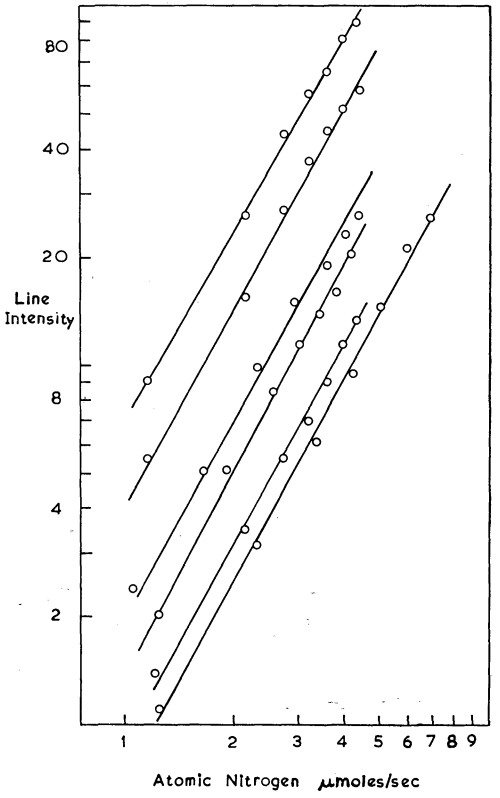

FIG. 1. Variation of intensity of metallic emission lines with atomic nitrogen flow. Molecular nitrogen flow rate 265 moles/sec. Total pressure 3.0 mm Hg. Description of graphs, reading from top to bottom: Tl 5350 Å, from TlCl; Na 5893 Å, NaCl; Pb 3683 Å, PbI_2; Tl 3230 Å, TlF; Cu 3247 Å, CuI; Pb 4058 Å, $PbCl_2$. Intensities in arbitrary units.

relative intensities which exceed this by an order of magnitude are almost certainly excited by a different kind of process. Also listed in Table II are the excitation energies E of the emission lines (15) and the dissociation energies D of the halides (16, 17). For lead halides the energies for dissociation into atoms at 400° C were calculated from a thermodynamic cycle using data from Lewis, Randall, Pitzer, and Brewer (18). These dissociation energies will be slightly high because heats of fusion of the halides were neglected and heats of vaporization were calculated directly from vapor pressure data (19) without allowance for the possible presence of polymeric species in the vapor. The results are entered in Table II in order of increasing $D+E$.

DISCUSSION

The results in Table II show a steady trend with increasing value of the sum $(D+E)$, the only marked exception being found with cuprous iodide. It is well known that in this case the vapor contains a large proportion of dimer Cu_2I_2 and extrapolation of the vapor pressures of the two species (19) indicates that at 400° C the ratio of dimer to monomer is of the order of 100, which is sufficient to explain the low intensity.

The criterion that the intensity in Table II should be more than about 10 for a process to be too efficient to be accounted for by the termolecular mechanism [2] leads to an

Can. J. Chem. Downloaded from www.nrcresearchpress.com by 210.87.254.105 on 09/05/12
For personal use only.

TABLE II

Relative intensities of metal lines at same partial pressure of halide

Atomic line	E, kcal/mole	Halide	D, kcal/mole	$D+E$	Intensity
5890–5896 Å Na	48.7	NaI	70	119	50
3776–5350 Å Tl	75.5	TlI	68	144	200
3247–3274 Å Cu	88	CuI	69	157	0.45
3776–5350 Å Tl	75.5	TlCl	89	165	131
3519–3530 Å Tl	104	TlI	68	172	35
3230 Å Tl	111	TlI	68	179	13
3776–5350 Å Tl	75.5	TlF	110	186	45
3519–3530 Å Tl	104	TlCl	89	193	23
3230 Å Tl	111	TlCl	89	200	8.1
3519–3530 Å Tl	104	TlF	110	214	3.5
3230 Å Tl	111	TlF	110	221	0.17
3683 Å Pb	100	PbI_2	125	225	0.84
4058 Å Pb	101	PbI_2	125	226	1.8
4058 Å Pb	101	$PbBr_2$	152	253	0.32
3683 Å Pb	100	$PbCl_2$	175	275	0.16
4058 Å Pb	101	$PbCl_2$	175	276	0.34

NOTE: E = excitation energy of atomic line, D = dissociation energy of halide (at 0° K for all except lead halides, where they are calculated for 400° C; see text).

approximate lower limit for this mechanism at $D+E = 200$ kcal/mole. There is no theoretical reason to expect a lower limit for process [2]; however, it is still not possible to rule out mechanism [2] for $D+E$ greater than 200 kcal. This is not necessarily an upper limit for the bimolecular process [1], and there is nothing to imply that the same mechanism does not operate over the whole range of $D+E$ below 222 kcal/mole. Apart from the $^5\Sigma_g^+$ state the only metastable states of N_2 which might be present in appreciable concentrations and which could supply 200 kcal/mole are the a and a' states (Table I). With both of these states the available energy is on the low side, and a further point against them is that the $^5\Sigma_g^+$ state is probably required to be their precursor if they are to be formed from ground-state atoms. Unfortunately little is known about the relevant crossing probabilities, but the strength of the Lewis–Rayleigh afterglow suggests that most $^5\Sigma_g^+$ molecules prefer to cross into the B state. The observed quenching of the afterglow in the presence of metal halides also favors the choice of $^5\Sigma_g^+$ as the state of the excited N_2 in equation [1].

With lead halides the energy required for simultaneous dissociation and excitation of the emission lines is equal to or greater than 225 kcal/mole, which is the maximum which can be supplied by recombination of ground-state nitrogen atoms. Another kind of mechanism is therefore required. As mentioned in the introduction, a termolecular reaction of the halide with one ground state and one excited nitrogen atom would not be efficient enough to account for the observed intensities because of the small proportion of excited atoms in active nitrogen (3). It is also difficult to see how this mechanism could lead to a dependence of intensity on the square of the (ground-state) nitrogen atom concentration. In this respect the results of Fig. 1 were surprising because it had been anticipated that with lead halides the intensity would vary as some higher power of the atom concentration. The bimolecular mechanism [1] might explain the observations if the excited nitrogen molecule were in the predicted $^1\Sigma_g^+$ state, but here again it is difficult to see how a dependence on $[N]^2$ could arise. The only remaining possibility is that of excitation by consecutive energy transfer steps. This mechanism can lead to a dependence of intensity

Can. J. Chem. Downloaded from www.nrcresearchpress.com by 210.87.254.105 on 09/05/12
For personal use only.

on $[N]^2$, as is shown below, taking lead chloride as an example. In this mechanism the

$$PbCl_2 + N_2^* \rightarrow PbCl^* + Cl + N_2 \quad [3]$$

$$PbCl^* + N_2^* \rightarrow Pb^* + Cl + N_2 \quad [4]$$

$$PbCl^* + N_2 \rightarrow PbCl + N_2 \quad [5]$$

$$PbCl^* \rightarrow PbCl + h\nu \quad [6]$$

$$PbCl + N_2^* \rightarrow Pb^* + Cl + N_2 \quad [7]$$

$$Pb^* \rightarrow Pb + h\nu' \quad [8]$$

part of N_2^* could equally well be taken by a pair of uncombined nitrogen atoms. Recombination of PbCl and Cl has been neglected because of the low halide partial pressure, while quenching of excited lead atoms should be negligible because of their short lifetime (ca. 10^{-8} sec). Halogen atoms are expected to be removed at the walls of the reaction vessel (20). At the steady state

$$[PbCl^*] = k_3[PbCl_2][N_2^*]/(k_4[N_2^*]+k_5(N_2]+k_6) \quad [9]$$

$$[PbCl] = (k_5[N_2]+k_6)[PbCl^*]/k_7[N_2^*] \quad [10]$$

$$[Pb^*] = k_3[PbCl_2][N_2^*]/k_8. \quad [11]$$

The intensity of PbCl emission bands is given by $k_6[PbCl^*]$. The observation that the intensity of these bands varies more slowly than $[N]^2$ suggests that $k_4[N_2^*]$ is comparable in magnitude with the other terms in the denominator of equation [9]. The total intensity of Pb lines is given by $k_8[Pb^*]$ and is equal to the rate of the primary process [3] when recombination and quenching of Pb* are not taken into account. It is probable that in the present experiments a completely stationary state was not reached in the short time spent by the reactants in the reaction vessel, since it was found that the Pb-line intensity increased steadily with increasing distance from the halide inlet jet.

A similar consecutive excitation mechanism for thallium halides is ruled out by the observation of finite spherical flames at low halide flows. Thallium nitride is unknown and thallium metal has been found as a reaction product (1), so from the fact that no Tl emission occurs in the region immediately following the flame, where both thallium and active nitrogen are certainly present, it follows that the efficiency of excitation of metallic thallium by active nitrogen under the conditions of the present experiments is very low. This conclusion was tested by mixing thallium vapor with active nitrogen in a simple reaction vessel which had a fixed inlet jet and a single end window and which was able to be taken to temperatures approaching 1000° C. At a cherry red heat (ca. 800° C) the vapor pressure of the metal is similar to that of thallous iodide at 400° C. The emission at 5350 Å with the metal at this temperature was less than 1% of that which was observed in a subsequent experiment with the iodide at 400° C. The behavior of lead should be similar to that of thallium in this respect, and in the mechanism just given no allowance is made for the possibility of excitation of lead atoms by N_2^*.

ACKNOWLEDGMENTS

The author is grateful to the New Zealand University Research Grants Committee for financial support and to Mr. C. G. Freeman for assistance with many of the measurements. In addition it is a pleasure to acknowledge the contribution of discussions and correspondence with Dr. A. N. Wright of McGill University to both this and the previous paper.

Can. J. Chem. Downloaded from www.nrcresearchpress.com by 210.87.254.105 on 09/05/12
For personal use only.

REFERENCES

1. L. F. PHILLIPS. Can. J. Chem. **41**, 732 (1963).
2. S. W. BENSON. The foundations of chemical kinetics. McGraw-Hill, New York. 1960.
3. Y. TANAKA, A. JURSA, and F. LEBLANC. The threshold of space. *Edited by* M. Zelikoff. Pergamon Press, New York. 1957. p. 89.
4. STRUTT (Lord Rayleigh). Proc. Roy. Soc. Ser. A, **85**, 219 (1911); **86**, 56 (1911); **88**, 539 (1913); **91**, 303 (1915).
5. K. R. JENNINGS and J. W. LINNETT. Quart. Rev. (London), **12**, 116 (1958).
6. A. N. WRIGHT, R. L. NELSON, and C. A. WINKLER. Can. J. Chem. **40**, 1082 (1962).
7. C. KENTY. J. Chem. Phys. **35**, 2267 (1961).
8. A. N. WRIGHT and C. A. WINKLER. J. Phys. Chem. **67**, 172 (1963).
9. K. D. BAYES. Can. J. Chem. **39**, 1074 (1961).
10. R. S. MULLIKEN. The threshold of space. *Edited by* M. Zelikoff. Pergamon Press, New York. 1957. p. 169.
11. C. KENTY. J. Chem. Phys. **37**, 1567 (1962).
12. F. KAUFMAN and J. R. KELSO. J. Chem. Phys. **27**, 1209 (1957).
13. J. C. DEVOS. Thesis, Amsterdam. 1956.
14. R. W. B. PEARSE and A. G. GAYDON. The identification of molecular spectra. Chapman and Hall, London. 1950.
15. C. E. MOORE. Natl. Bur. Std. (U.S.), Circ. 467, Vol. I (1949); Vol. II (1952); Vol. III (1958).
16. E. M. BULEWICZ, L. F. PHILLIPS, and T. M. SUGDEN. Trans. Faraday Soc. **57**, 921 (1961).
17. A. G. GAYDON. Dissociation energies. Chapman and Hall, London. 1953.
18. G. N. LEWIS, M. RANDALL, K. S. PITZER, and L. BREWER. Thermodynamics. McGraw-Hill, New York. 1961.
19. LLANDOLT-BÖRNSTEIN. Tabellen. Zweiter Band, Teil 2, Bandteil *a*. Springer-Verlag, Berlin. 1960. p. 49.
20. E. A. OGRYZLO. Can. J. Chem. **39**, 2556 (1961).

Can. J. Chem. Downloaded from www.nrcresearchpress.com by 210.87.254.105 on 09/05/12
For personal use only.

DETERMINATION OF α OR β SUBSTITUTION OF THE INDOLE NUCLEUS BY NUCLEAR MAGNETIC RESONANCE[1]

R. V. JARDINE AND R. K. BROWN
Department of Chemistry, University of Alberta, Edmonton, Alberta
Received April 5, 1963

ABSTRACT

Marked differences in chemical shift of the signal for the α proton in indole and substituted indoles occur when spectra are obtained in non-polar and polar solvents. In contrast, using polar and non-polar solvents, only small differences are observed in the chemical shift of the signal for the β proton in indoles. The utility of the solvent effect on the chemical shift to distinguish between α and β substitution of the indole nucleus is pointed out.

INTRODUCTION

Witkop *et al.* (1) have shown that nuclear magnetic resonance can be used to determine substitution at the *alpha* or *beta* position of the indole nucleus. In carbon tetrachloride or deuterochloroform solution the signal for the α protons of indole, N-methylindole, skatole, and tryptamine was at the respective τ value (referred to the internal standard, tetramethylsilane) of 3.32 (triplet), 3.18 (doublet), 3.20 (poorly resolved doublet), and 3.08 (doublet). The β proton signal in indole, N-methylindole, and 2-methylindole was at a τ value of 3.62 (triplet), 3.52 (doublet), and 3.87 (broad single peak) respectively. Thus the β proton gave a signal at higher field than that found for the α proton, the difference in chemical shift for these two protons lying between 0.3 and 0.8 τ units. The signals for the α and β protons were quite clearly discernible, well separated, and at higher field than those for the remaining protons in the indole nucleus, except for the case of quebrachamine, whose signal for the α proton was buried in the more complicated absorption due to the aromatic ring protons in the region approximately between 2 and 3 τ.

We have had occasion to determine whether the α or β position of certain indole nuclei was substituted by groups other than alkyl, and hence turned to n.m.r. for assistance in this problem. When groups more electronegative than alkyl substituents were introduced into the α position, the signal for the remaining β proton, normally found well isolated at about 3.5 to 3.9 τ (1), occurred considerably farther downfield, at approximately 2.8 to 3.2 τ, in the region where the α proton absorption is shown to occur in indole and 3-alkylated indoles (3.08–3.32 τ). Hence, observation of a signal in this region is not conclusive proof that the β, rather than the α, position has been substituted.

Among the factors listed by Roberts (2) which affect the extent of chemical shift of protons is that due to solvent. It occurred to us that, because of the obvious difference in electron environment at the α and β protons, change in solvent from one of non-polar character to one of highly polar character might affect one of the protons (α or β) to a greater extent than it did the other. Hence solvent shift or lack of solvent shift might be used as a means to determine whether we were dealing with the α- or β-substituted indole nucleus.

Accordingly a number of indole derivatives were synthesized in which substitution at the α or β position was known. These, along with indole itself, were subjected to n.m.r. analyses on a 60 Mc Varian spectrometer using a variety of solvents. Tetramethylsilane

[1]*Taken from the thesis of R. V. Jardine to be submitted to the Faculty of Graduate Studies at the University of Alberta as part of the requirements for the degree of Doctor of Philosophy.*

was used as an internal standard and all values were expressed on the τ scale (3). To aid in determining the position of the α and β proton resonance signals, use was made of the fact that the doublet or multiplet, caused by spin–spin coupling between the proton on the nitrogen atom and the α or β proton, collapses to a singlet or to a simpler system when the >N—H is converted to >N—D (1). Where the complexity of signals for the aromatic protons interfered, the greater resolving power of the 100 Mc Varian spectrometer (HR-100) was found to be helpful in locating α or β proton resonance signals. The results of the analyses are shown in Table I.

RESULTS AND DISCUSSION

The signal for the β proton in either indole or 2-methylindole is quite well discernible in all the seven solvents employed. Its position, ranging from 3.52 τ to 3.71 τ ($\Delta\tau = 0.19$) for indole and 3.86 τ to 4.10 τ ($\Delta\tau = 0.24$) for 2-methylindole, lies well beyond and at higher field than the absorption peaks of the aromatic protons (2.0 τ to 3.0 τ). There is a slight downfield shift of the signal in polar solvents as compared with its position in non-polar solvents.

The signal for the α proton of indole is found between 2.70 and 3.46 τ, a range ($\Delta\tau$) of 0.76 τ units, whereas for 3-methylindole the signal is found between 2.94 and 3.65 τ, over a range ($\Delta\tau$) of 0.71 τ units.

It is clearly seen that the signal position of the α proton in the indole nucleus is influenced to a much greater extent by the nature of the solvent than is that of the β proton. In more polar or more basic solvents, the chemical shift of the α proton is sufficient to place it in the region assigned to the aromatic proton absorption. In some solvents (acetone, dimethylsulphoxide, dioxane, and triethylamine) the assignment of the signal for the α proton of indole was not certain and hence is tentative, as indicated by the values in parentheses in Table I. However, from the simplification of multiplets caused by the conversion of >N—H to >N—D, and with the aid of high-resolution spectra, it was quite definitely ascertained that the α proton signal must lie *below* certain τ values as indicated in the table. In only one solvent, acetone, was a similar ambiguity found for the signal position of the α proton in 3-*methyl*indole.

It is of interest to note that the methyl group in both 2- and 3-methylindole caused greater shielding of the β *and* α protons than that found for indole itself, as indicated by the shift to higher field of the signals for these protons in the alkylated indoles. This is apparent in both cases only when one *compares the spectra obtained in the same solvent.* Witkop *et al.* (1) have noted the greater shielding effect on the β proton in 2-methylindole caused by the introduction of the methyl substituent, but their data indicate that a similar increased shielding of the α proton is not found in 3-methylindole. In fact the α proton in *3-methylindole* was found to give a signal at 3.20 τ while the α proton of *indole* absorbed at 3.32 τ. However, their use of CCl_4 as solvent for indole but $CDCl_3$ for the methylindole accounts for this inconsistency. From our observations it is now clear that the more polar solvent, $CDCl_3$, will cause a significantly greater decrease in shielding for the α proton than for the β proton in indole and any increase in shielding due to the methyl substituent is not sufficient to compensate for the large downfield shift of the α proton signal due to the solvent effect.

Substitution of the α or β proton of indole by an electron-withdrawing group such as acetyl, carbonyl, carbethoxy, and benzoyl shifts the absorption of the remaining β or α

TABLE I

The effect of change of solvent on the position of the resonance signals for the α or β protons in β- or α-substituted indoles

Compound	Position of the signals for the α and β protons in the solvents (τ)							Overall $\Delta\tau$
	CCl_4	$CDCl_3$	Acetone	Dimethyl sulphoxide	Dioxane	CS_2	$(C_2H_5)_3N$	
Indole[1] (α proton)	3.46 a	3.26 a	<2.75 (2.72 b*)	<2.71 (2.6 to 2.7)	<2.89 (2.84 b*)	3.45 a	<3.12 (2.80 b*)	0.76
Indole[1] (β proton)	3.66 a	3.59 a	3.52 b	3.53 b	3.52 b	3.71 a	3.57 b	0.19
3-Methylindole[1] (α proton)	3.65 b*	3.39 b*	⩽3.0 (3.0)	2.94 b*	3.13 b*	3.63 b*	3.25 b*	0.71
2-Methylindole[1] (β proton)	4.06 b*	3.95 b	3.86 b*	3.88 b*	3.88 b*	4.10 b*	3.93 b*	0.24
Ethyl indole-3-carboxylate[2] (α proton)	Insol.	2.15 c 2.21 c	1.97 c 2.01 c	1.88 d	2.07 c 2.12 c	Insol.	2.22 d	0.25
Ethyl indole-2-carboxylate[3] (β proton)	Insol.	2.77 b*	2.78 b*	2.80 b*	2.80 b*	Insol.	(2.80)	0.03
3-Acetylindole[4] (α proton)	Insol.	Insol.	1.80 c* 1.83 c*	1.66 d	Insol.	Insol.	Insol.	0.17
Indole 3-carboxylic acid[6] (α proton)	Insol.	Insol.	Insol.	1.82 c 1.86 c	Insol.	Insol.	Insol.	
Indole 2-carboxylic acid[5] (β proton)	Insol.	Insol.	2.77 c 2.80 c	2.80 c 2.82 c	2.72 c* 2.76 c*	Insol.	Insol.	0.08
3-Benzoylindole[7] (α proton)	Insol.	Insol.	Insol.	(2.0)	Insol.	Insol.	Insol.	
2-Benzoylindole[8] (β proton)	Insol.	(2.54 b*)	(2.3)	?	?	?	?	
3-Bromoindole[8] (α proton)	Insol.	2.96 c 3.00 c	2.56 c 2.59 c	(2.42 c*)	2.76 c 2.78 c	3.10 c 3.15 c	2.93 c 2.96 c	0.54
β, β'-Diindolyldisulphide[9] (α proton)	Insol.	Insol.	2.80 c 2.83 c	2.62 c 2.66 c	2.86 c 2.90 c	Insol.	—	0.18

NOTE: A question mark indicates that no assignment could be made. The symbol < indicates that the signals for the α or β protons were certainly less than the values given. Figures in parentheses are tentative assignments. a — triplet; b — multiplet; c — doublet; d — singlet; the asterisk indicates poorly resolved signals. The term "insol." indicates either insoluble or insufficiently soluble to obtain an n.m.r. spectrum.

[1]Eastman White label.
R. K. Brown and R. A. Garrison. J. Am. Chem. Soc. **77**, 3839 (1953).
[2]See Experimental.
[3]Chem. Abstr. **5**, 2638 (1911).
[4]Reference 5.
[5]Obtained from the hydrolysis of ethyl indole-3-carboxylate; cf. R. Majima and M. Kotake. Ber. **63**, 2237 (1930).
[6]W. C. Anthony. J. Org. Chem. **25**, 2079 (1960).
[7]R. Weissgerber. Ber. **46**, 652 (1913).
[8]M. S. Grant and H. R. Snyder. J. Am. Chem. Soc. **82**, 2742 (1960).

proton as much as 0.7 to 1.2 τ units downfield from the corresponding position of the signals of indole itself. Here again one must compare spectra of compounds in the same solvent. A greater shift occurs for the α than for the β proton: The $\Delta\tau$ ranges from 0.95 to 1.2 for the α proton as compared with 0.7 to 1.1 for the β proton. Thus, for ethyl indole-3-carboxylate, the α proton signal in $CDCl_3$ is a doublet at 2.15 and 2.21 τ, while that of the α proton in 3-methylindole and indole in the same solvent occurs at 3.39 τ and 3.26 τ respectively. On the other hand, for ethyl indole-2-carboxylate, the β proton signal is found at 2.80 τ in dioxane solution while in the same solvent, the β proton signal for 2-methylindole and indole is at 3.88 τ and 3.52 τ respectively.

For compounds in which the β proton was replaced by either sulphur or halogen, the deshielding effect on the α proton due to these substituents was less than that found for the carbonyl compounds.

In dimethylsulphoxide, for the two compounds ethyl indole-3-carboxylate and 3-acetylindole it was noted that the normally expected doublet for the α proton, due to spin–spin coupling with the proton on the adjacent nitrogen atom, did *not* occur. Instead, a sharply defined singlet was observed at 1.88 τ and 1.66 τ respectively. Deuteration produced an unchanged singlet at the same position. The carboxylate exhibited the same phenomenon in triethylamine. The insolubility of the 3-acetylindole in triethylamine thwarted attempts to detect a similar observation. In other solvents (e.g. acetone and dioxane) doublets due to spin–spin coupling were clearly shown. When the spectral grade acetone solvent was treated with a small amount of water or dilute hydrochloric acid, 3-acetylindole still showed a doublet, unchanged; for the α proton. In reagent pyridine the spectrum of 3-acetylindole gave a closely spaced doublet at 1.75 τ which collapsed to a singlet when the compound was deuterated.

We have assigned the α proton absorption of 3-acetylindole to the doublet appearing at 1.80 and 1.83 τ on the basis of the collapse of this doublet to a singlet in the N-deuterated compound. Additional evidence to support the assignment was obtained from the fact that this signal disappeared completely when the α hydrogen was substituted by a methyl group.

From the data in Table I it is clear that the greater solvent dependence of the chemical shift of the α proton as compared with that of the β proton is a useful means of determining or corroborating α or β substitution in the indole nucleus. The limited solubility or the insolubility of the compounds in some of the solvents normally employed for n.m.r. spectra determinations restricts the utility somewhat. However, considering a *pair of solvents* such as acetone and dimethylsulphoxide, in which most of the compounds are soluble, the position of the β proton signal is nearly the same in either solvent, with a maximum difference of 0.03 τ. But for the α proton, a difference in signal position of 0.08 to 0.17 τ occurs. A larger difference in the chemical shift for the α proton is found when one compares signal position in a non-polar or slightly polar solvent ($CDCl_3$) and highly polar solvent (acetone or dimethylsulphoxide).

It is of interest to note that the signal position for the proton attached to the nitrogen atom of the indole ring is influenced even more strongly by the solvent employed than is the α proton. Table II summarizes the information obtained.

Where the signals are clearly discernible they are found generally to be broad, but less so in dimethylsulphoxide.

In non-polar, or relatively non-polar solvents (CCl_4, $CDCl_3$, CS_2), the N—H signals of indole and alkylated indoles are buried in the complex absorption due to the aromatic protons, roughly in the region 2.9 to 3.1 τ. Approximate locations of the signal are given

TABLE II

The effect of solvent on the position of the resonance signal for the proton on the nitrogen atom of indole and substituted indoles

	Position of the signal for the N—H proton in the solvents (τ)						
	CCl_4	$CDCl_3$	Acetone	Dimethyl sulphoxide	Dioxane	CS_2	$(C_2H_5)_3N$
Indole	(3.0)	(2.9)	0.00	−1.01	+0.48	(3.1)	−0.08
2-Methylindole	(3.1)	(3.0)	+0.33	−0.82	+0.84	(3.1)	+0.08
3-Methylindole	(3.1)	(2.9)	+0.48	−0.69	+0.91	(3.1)	−0.59
Ethyl indole-2-carboxylate	Insol.	+0.44	−0.79	−1.87	−0.51	Insol.	?
3-Bromoindole	Insol.	(2.8)	−0.61	−1.46	+0.22	(2.9)	−1.01
β,β′-Diindolyldisulphide	Insol.	Insol.	−0.46	−1.54	+0.13	Insol.	Insol.
3-Benzoylindole	Insol.	Insol.	Insol.	−2.00	Insol.	Insol.	Insol.
2-Benzoylindole	Insol.	+0.08	−1.06	?	?	?	?
3-Acetylindole	Insol.	Insol.	Insol.	−1.92	Insol.	Insol.	Insol.
3-Acetyl-2-methylindole	—	—	—	−1.8	—	—	—

NOTE: Figures in parentheses are approximate locations of the signals. The term "insol." means that the compound was either insoluble or insufficiently soluble for satisfactory n.m.r. analysis. A question mark indicates that the signal for the N—H proton could not be detected.

by the figure in parentheses, and are obtained from the decrease in integrated areas for the N-deuterated compounds. The disappearance of the signal upon N-methylation, in the case of indole, supports the assignment of this signal to the N—H proton. Electronegative substituents in the α or β positions cause a pronounced downfield shift also.

Polar solvents and those which associate with the indole compound (i.e. ethers) cause a larger chemical shift to lower field in the order dimethylsulphoxide > triethylamine > acetone > dioxane.

EXPERIMENTAL

Nuclear magnetic resonance spectra were obtained at a temperature of 40° using a Varian A-60 spectrometer. Wherever possible the concentration employed was that obtained by dissolving 100 mg of the substance in 0.35 to 0.40 ml of spectral grade solvent. In a few cases (diindolyl disulphide in dioxane, indole-2-carboxylic acid in dioxane, 3-acetylindole in actone, and ethyl indole-2-carboxylate in $CDCl_3$ and in $(C_2H_5)_3N$) saturated solutions were used unavoidably. High-resolution spectra, using a Varian HR-100 spectrometer, were obtained at 29.2° with solutions containing 20 mg of solute in 0.40 ml of the respective solvent.

Deuteration

General Procedure

The following general procedure was employed in all deuterations. About 120 mg of the indole compound was dissolved in 8 ml of reagent acetone and then 2 ml of D_2O (99.7%) was added. The resulting solution was freed of solvent in a rotary evaporator under vacuum. This treatment was repeated two or three times. Final drying was carried out in a desiccator over P_2O_5. Care was taken to protect the solutions from direct light.

The extent of deuteration was determined by infrared spectrometry and by n.m.r. Disappearance of the >N—H peak between 3100 and 3500 cm^{-1} in the infrared and the appearance of a new peak due to >N—D at a frequency of about 0.75 of that of the >N—H stretching gave a measure of the amount of deuteration. N-Deuteration was more rapid for the indoles containing electronegative substituents in the α or β positions. For indole and 2-substituted indoles, considerable deuteration occurred at the β position, as detected by the lower integrated area for β proton signal in the N-deuterated compounds.

*De*deuteration, both at the nitrogen atom and at the β carbon, occurred readily when the compounds were dissolved in 95% ethanol and the solvent evaporated.

N-Deutero-3-bromoindole.—Since 3-bromoindole (5) decomposes spontaneously when its solution is completely freed of solvent, the following procedure was employed. A quantity of 3-bromoindole (4) (5.0 g, 0.025 mole) was treated with 2 ml of D_2O (99.7%). The solution was concentrated at room temperature under vacuum by rotary evaporator almost to dryness, then acetone and D_2O added again and the process repeated. The concentrated solution now was poured into 100 ml of *n*-heptane to which 5 g of anhydrous

magnesium sulphate was then added. After addition of decolorizing charcoal, the mixture was stirred vigorously and heated to the boiling point. As long as the 3-bromoindole was *in solution* it could be heated above its normal decomposition temperature (67°) with no ill effect. The boiling solution was quickly filtered into a *cooled* receiver. Cooling is essential since 3-bromoindole deposited at a temperature close to or above its decomposition point will spontaneously decompose. The N-deutero-3-bromoindole crystallized as plates in a yield of 80%, melting at 65–66° (decomp.).

N,β-Dideuteroindole.—A solution of indole (11.7 g, 0.1 mole) in ether (50 ml) was added slowly to an ether solution of 0.2 mole of ethyl magnesium iodide (from 4.8 g, 0.2 mole, of magnesium and 31.2 g, 0.2 mole, of ethyl iodide in 250 ml of ether). When reaction was complete the solution, protected from moisture, was cooled to 0° and then stirred rapidly while 10 ml of D_2O (99.7%) in 50 ml of anhydrous tetrahydrofuran was added dropwise. When addition was complete, the solution was refluxed overnight. The cooled mixture was then filtered rapidly to minimize admission of water since this causes rapid *de*deuteration. The solvent was then removed completely by rotary evaporator under vacuum. Sufficient hot *n*-heptane was then added to dissolve the indole which had precipitated. The resulting clear solution was dried ($MgSO_4$) and filtered. When the solution was cooled and allowed to stand overnight the dideuteroindole separated. The solid was quickly isolated by filtration, and dried under nitrogen in a desiccator. Yield, 6 g (51%). The n.m.r. analysis indicated that the β position was deuterated approximately to the extent of 50%. Infrared analysis showed that the nitrogen atom was deuterated approximately to the extent of 50%.

2-Benzoylindole

Thionyl chloride (22 ml) was slowly added to 12.3 g (0.075 mole) of solid, powdered indole-2-carboxylic acid (6). When the initial vigorous reaction had subsided, the mixture was heated for 20 minutes on a steam bath. Excess thionyl chloride was removed under vacuum. The solid product was taken up in 50 ml of dioxane and the solution then slowly added to 50 g (0.19 mole) of diphenyl cadmium (7) dissolved in 300 ml of benzene. The reaction mixture was then heated under reflux for 12 hours. The cooled solution was poured slowly, with stirring, onto 2 kg of ice, while sufficient acetic acid was added to maintain approximately a pH of 7 (hydrion paper). The benzene layer was separated and treated with ether to precipitate the 2-benzoylindole. The crude precipitate was extracted with pentane for 24 hours in a Soxhlet apparatus. The pentane extract was freed from solvent and the residue crystallized from a mixture of ethanol and water. There was obtained 5.4 g (32%) of colorless needles melting at 146–148°. The infrared spectrum in $CHCl_3$ showed N—H stretching at 3452 cm^{-1}, bonded N—H at 3325 cm^{-1}, and carbonyl stretching at 1625 cm^{-1}.

Anal. Calculated for $C_{15}H_{11}NO$: C, 81.45; H, 4.88; N, 6.33; O, 7.24. Found: C, 81.19; H, 5.37; N, 6.36; O, 7.21.

3-Acetyl-2-methylindole

The procedure for the preparation of this compound as described in the literature (8) failed to give satisfactory results. Accordingly the following method was devised. A solution of 4 g (0.033 mole) of 2-methylindole (9) in ether was added slowly to ethyl magnesium iodide (from 1.6 g, 0.067 mole, of magnesium metal and 9.6 g, 0.065 mole, of ethyl iodide) in 100 ml of ether. When addition was complete, the resulting solution was cooled to 0° and then 2.6 g (0.033 mole) of acetyl chloride in 10 ml of ether was added dropwise so that the temperature of the mixture remained below 5°. Then the mixture, continually stirred, was allowed to come to room temperature overnight. The contents of the reaction vessel was poured onto ice (200 g) along with sufficient acetic acid to react with the magnesium hydroxide produced. The precipitated 3-acetyl-2-methylindole was removed by filtration and crystallized from aqueous ethanol to yield 3.2 g (56.5%) of pure product melting sharply at 204° (lit., 195–196° (8)). An n.m.r. spectrum in dimethylformamide indicated acetyl methyl at 7.44 τ, α-methyl buried in the signal due to solvent at about 7.08 τ, and a broad signal at −2.24 τ due to N—H. In pyridine the respective τ values for acetyl methyl and α-methyl were clearly separated and discernible at 7.34, 7.22. Infrared spectra in halo oil showed N—H stretching at 3082 cm^{-1}, and carbonyl absorption at 1605 cm^{-1}.

Ethyl Indole-2-carboxylate

A solution of indole-2-carboxylic acid (5.0 g, 0.31 mole) (6) in 50 ml of anhydrous ethyl alcohol, saturated with anhydrous hydrogen chloride, was allowed to stand overnight. The mixture was poured into water and made slightly basic with dilute caustic soda. The cold, basified solution was twice extracted with 100-ml portions of ether. Removal of the ether and crystallization of the residue from aqueous ethanol gave long needles melting at 125°. Lit., 125–126° (10). Yield, 74.5%. Infrared spectra in nujol showed N—H stretching at 3310 cm^{-1} and carbonyl absorption at 1685 cm^{-1}.

ACKNOWLEDGMENTS

The authors wish to thank the National Research Council of Canada for financial assistance throughout the course of this work. Grateful acknowledgment is made to Dr. W. G. Paterson of this department for advice and comments.

REFERENCES

1. L. A. COHEN, J. W. DALY, H. KNY, and B. WITKOP. J. Am. Chem. Soc. **82**, 2184 (1960).
2. J. D. ROBERTS. Nuclear magnetic resonance. McGraw-Hill Book Co., Inc., New York. 1959. pp. 21–25.
3. G. V. D. TIERS. J. Phys. Chem. **62**, 1151 (1958).
4. L. M. JACKMANN. Applications of nuclear magnetic resonance spectroscopy in organic chemistry. Pergamon Press, New York. 1959. pp. 26–28.
5. R. WEISSGERBER. Ber. **46**, 652 (1913).
6. W. O. KERMACK, W. H. PERKIN, JR., and R. ROBINSON. J. Chem. Soc. **119**, 1625 (1921).
7. D. A. SHIRLEY. Organic reactions. Vol. 8. John Wiley and Sons, Inc., New York. 1954. p. 28.
8. O. R. JACKSON. Ber. **14**, 880 (1881).
9. E. FISCHER. Ann. **236**, 126 (1886).
10. S. GABRIEL, W. GERHARD, and R. WALTER. Ber. **56**, 1027 (1923).

THE SULPHUR–OXYGEN BOND IN SULPHURYL AND THIONYL COMPOUNDS: CORRELATION OF STRETCHING FREQUENCIES AND FORCE CONSTANTS WITH BOND LENGTHS, BOND ANGLES, AND BOND ORDERS

R. J. GILLESPIE
Department of Chemistry, McMaster University, Hamilton, Ontario
AND
E. A. ROBINSON
Department of Chemistry, University of Toronto, Toronto, Ontario
Received March 28, 1963

ABSTRACT

It is shown that the bond length of an SO bond and the bond angle of an SO_2 group may be very satisfactorily correlated with the SO stretching frequency. The bond-length – stretching-frequency relationship is used to predict some bond lengths that have not been measured and the OSO angles in some sulphuryl compounds are also calculated. The problem of defining and measuring the bond order of sulphur–oxygen bonds is discussed. It is shown that there is a linear relationship between the force constant and the bond order and a non-linear relationship between the bond length and the bond order.

INTRODUCTION

The nature of the SO bond in $XYSO_2$ and XYSO molecules has long been a subject of controversy. Classically the structures of molecules such as $SOCl_2$ and H_2SO_4 were written with double bonds between sulphur and oxygen (I and II). In order to make the electronic

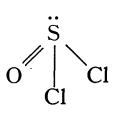
I

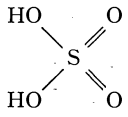
II

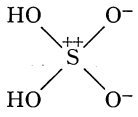
III

configuration of sulphur in these compounds conform to his octet rule Lewis (1) suggested that they should be written with single bonds only (III). Such structures were accepted for many years and, indeed, are still widely used.

However the bond lengths of SO bonds (2) and the angle in the SO_2 group (3) provide strong support for the double-bond structures. By analogy with the familiar σ–π description of multiple bonds between carbon atoms, double bonding in SO bonds has been described in terms of π-bonds formed between oxygen $2p$ orbitals and $3d_{x^2-y^2}$ and $3d_{z^2}$ orbitals on sulphur (4–8). Recently Cruickshank (9) has given a detailed discussion of this type of description of the sulphur–oxygen double bond.

We expect that SO bonds will in general be intermediate between IV and V. The former is meant to indicate two completely covalent bonds in which both electron pairs forming

IV

V

the bond are equally shared and hence neither atom has any resultant charge. This would necessitate that the other atoms attached to sulphur had electronegativities sufficiently

Can. J. Chem. Downloaded from www.nrcresearchpress.com by 210.87.254.42 on 09/05/12
For personal use only.

great to raise the effective electronegativity of sulphur to that of oxygen. This situation is probably approached in SO_2F_2 and SOF_4. With decreasing electronegativity of the attached groups the double bond becomes polar and the electron pairs are no longer shared equally between the S and O atoms. If a double bond is described in terms of σ- and π-components it is generally assumed for C=C and C=O bonds that the π-bond is more polarizable than the σ-bond. It seems reasonable to assume that this is also the case for SO bonds and that therefore the greater part of the polarity may be ascribed to the π-bond (5). There will, of course, be an accompanying but smaller change in the polarity of the σ-bond; we assume that to a first approximation this does not vary independently of the bond order. In the limiting case, where the π-bond electron pair resides essentially wholly in a p-orbital on oxygen, structure V is obtained. If we define the bond order simply as the average number of electron pairs available per bond IV has a bond order of two and V has a bond order of unity. Evidently the situation in real molecules may be reasonably well described as being intermediate between IV and V and the bond order increases while the bond polarity simultaneously decreases with increasing electronegativity of the ligands.

Cruickshank (9) assumes that whenever oxygen ligands are attached to sulphur both the $3d_{z^2}$ and the $3d_{x^2-y^2}$ orbitals of sulphur are fully utilized in double bonding and thus he ascribes bond orders of 1.5 to the sulphate ion and 2.0 to $XYSO_2$ compounds in general. He further assumes that there is a linear relationship between bond length and bond order determined by the single bond length of 1.69 Å deduced from the Schomaker–Stevenson equation (10) and the observed length of 1.49 Å for the sulphate ion. However, there is no theoretical justification for the Schomaker–Stevenson rule or for the linear relationship between bond length and bond order, which in any case seems unlikely, since for carbon–carbon bonds, for example, this relationship is certainly non-linear (11). Cruickshank's linear relationship predicts an improbably short bond length of 1.30 Å for a bond order of 2.0. The observed length of 1.43 Å for dimethyl sulphone (12) implies a very low bond order and is ascribed by Cruickshank to "the smaller electronegativity of the group R than of oxygen, and to the asymmetry of the σ-bonding about sulphur so that the effective nuclear charge, $Z_{eff}(3d)$, for the $3d$ orbitals is lowered with loss of bonding strength". However, this cannot be the case for SO_2F_2, where the bond length is 1.405 Å (13) and the bond order of the SO bond order must surely be close to 2.0. This is confirmed by the arguments given in this paper and it is also shown that the bond-order – bond-length relationship is very probably not linear.

It is the purpose of this paper to present the experimental evidence for some definite correlations between the various different properties of SO bonds. On the basis of the correlations an attempt is made to estimate SO bond orders.

CORRELATION OF STRETCHING FREQUENCIES WITH BOND LENGTHS AND BOND ANGLES

Recently one of us showed (14) that the linear correlation between the symmetric and asymmetric stretching frequencies of the sulphuryl group that was first demonstrated by Bellamy and Williams (15) is valid for a large number of sulphuryl compounds and that it also applies to the anions XSO_3^- and SO_4^{2-}. It was noted that the frequencies of these stretching vibrations increase with increasing electronegativity of the groups X and Y in the sulphones. Thus the highest observed frequencies (1270 and 1502 cm^{-1}) are found for SO_2F_2 while the lowest (980 and 1104 cm^{-1}) are those of the sulphate ion. Similarly in the case of the sulphoxides X_2SO the highest SO stretching frequency is observed for SOF_2

Can. J. Chem. Downloaded from www.nrcresearchpress.com by 210.87.254.42 on 09/05/12
For personal use only.

(1308 cm^{-1}). In the case of SOF_4 (16) the SO stretching frequency of 1379 cm^{-1} is higher than that in SOF_2, which is consistent with the presence of two additional highly electronegative ligands. Since increasing the electronegativity of the groups X and Y should increase the order of the SO bond, it seems reasonable to assume that there is a correlation between the bond order and stretching frequency and to suppose that the stretching frequency may be used as a measure of the bond order. Thus SO_2F_2 has the highest bond order and the SO_4^{2-} ion the lowest bond order of the sulphuryl compounds considered. The bond orders for molecules with intermediate frequencies must lie between these limits.

In order to find SO bonds with orders smaller than that of the sulphate ion it is necessary to consider molecules which have formally single bonds between sulphur and oxygen, such as the RO—S bonds in sulphates of the type $(RO)_2SO_2$. However, in such cases the mass of the R group will in general introduce the complication that it will not be possible to make a satisfactory assignment of an observed vibrational frequency to the S—O bond alone, and if this is attempted as Simon and Kriegsmann have done (17) the observed frequency will depend on the mass of R. However, there is one case where the mass of R is unimportant, namely when R is hydrogen, and it is reasonable to suppose that the small increase in mass produced by the hydrogen atom has a relatively unimportant effect on the frequency compared with changes in the SO bond order. Some confirmation of this supposition is provided by the fact that the $S(OH)_2$ symmetric and asymmetric stretching frequencies (910 and 976 cm^{-1}) for H_2SO_4 (18) fit the straight-line correlation previously established for the SO_2 symmetric and asymmetric stretching frequencies. These frequencies indicate that the order of these bonds is lower than that of the S—O bonds in the sulphate ion.

It is interesting to note that although the S—O bond in a sulphoxide could be formally regarded as a triple bond formed by the use of both the $d_{x^2-y^2}$ and d_{z^2} sulphur orbitals the vibrational frequencies 1308 cm^{-1} and 1109 cm^{-1} for dimethyl sulphoxide show that the bond order is somewhat less than that in the sulphuryl compounds with the same ligands. This may be ascribed to an effect of the lone pair of electrons on sulphur in reducing its electronegativity.

Since the lengths of SO bonds are presumably also related to their bond order there would be expected to be a correlation of bond length with stretching frequency. That such a correlation does indeed exist was first demonstrated by Barnard, Fabian, and Koch (19), who showed that for seven compounds there is a general increase of stretching frequency with decrease of bond length. We have found that the correlation can be extended to include many more compounds, including both neutral molecules and ions, and S—OH as well as S—O frequencies. For sulphuryl compounds Barnard, Fabian, and Koch (19) used the mean of the symmetric and asymmetric stretching frequencies as a measure of the frequency that the SO vibration would have in the absence of coupling between the two SO bonds. A similar procedure has been used by Simon and Kriegsmann (17) in their discussion of the force constants of sulphuryl compounds. Barnard, Fabian, and Koch justified the approximation by showing that for the sulphur dioxide molecule a bond stretching force constant of 9.86×10^5 dynes cm^{-1} is obtained on the basis of this method while a value of 9.97×10^5 dynes cm^{-1} is obtained by rigorous methods (20). Lehmann (21) has recently pointed out that the assumption of a simple valence-force field leads to the result that for a linear AB_2 molecule the stretching frequency of the AB group is the root mean square of the symmetric and asymmetric stretching frequencies. For most purposes the arithmetic mean is a good approximation for the root mean square. Lehmann has shown that this "average rule" is also a good approximation for the A—B stretching

Can. J. Chem. Downloaded from www.nrcresearchpress.com by 210.87.254.42 on 09/05/12
For personal use only.

frequency of an angular AB_2 group if the bending force constant is small, if the symmetric stretching frequency is appreciably larger than the bending frequency, and if the coupling of the AB_2 group with the rest of the molecule is small. Lehmann also shows that for an AB_x group where the asymmetric stretch has a degeneracy $(x-1)$ the average rule becomes

$$[1] \qquad \nu_{AB} = (1/x)[\nu_{sym}+(x-1)\nu_{asym}].$$

The "average rule" has also been shown by Bernstein to be a very good approximation in the special case of X—H bonds (22). SO stretching frequencies ν_{SO} were obtained from the experimental data by means of equation [1].

The available data which is collected in Table I and Fig. 1 shows that there is a reasonably good correlation between bond length and stretching frequency. The frequencies are

TABLE I

Bond lengths and stretching frequencies for SO bonds

Molecule	r_{SO}	Method[2]	ν_s (cm^{-1})	ν_{as} (cm^{-1})	ν_{SO}[3] (cm^{-1})
S_3O_9	1.40	X[4]	1231 1270	1489[20] 1515	1376
SO_2F_2	1.405±0.003	m.w.[5]	1269	1502[21]	1385
SOF_2	1.412±0.001	m.w.[6]	1308	—[21]	1308
$SO_2(OH)_2$	1.425±0.01	X[7]	1195	1368[22]	1280
SO_2Cl_2	1.43±0.02	e.d.[8]	1182	1414[21]	1298
$(CH_3)_2SO_2$	1.43±0.02	e.d.[9]	1143	1310[23]	1227
SO_2	1.43±0.01	m.w.[10]	1151	1361[24]	1259
SO_3	1.43±0.02	e.d.[8]	1070	1390[20]	1230
$S_2O_6^{2-}$	1.43	X[11]	1092 1000	1206[25] 1235	1162
$S_2O_7^{2-}$	1.437±0.004	X[12]	1065 1095	1253[24] 1276	1203
$NH_2\cdot SO_3^-$	1.44±0.03	X[13]	1059	1202[24]	1154
$SOCl_2$	1.45±0.02	e.d.[8]	1229	—[21]	1229
$NH(SO_3)^{2-}$	1.45	X[15]	1082 1024	1222[24] 1260	1178
$EtO\cdot SO_3^-$	1.46	X[14]	1063	1221[24]	1168
$CH_2(SO_3)_2^{2-}$	1.461±0.005	X[12]	1042	1183[24]	1159
$HO\cdot SO_3^-$	1.47±0.015	X[16]	1040	1200[22]	1147
$(CH_3)_2SO$	1.47±0.03	e.d.[17]	1109	—[26]	1109
SO_4^{2-}	1.49	X[18]	986	1090[27]	1062
$SO_2(OH)_2$	1.535±0.015[1]	X[7]	910	968[22]	968[29]
$HO\cdot SO_3^-$	1.56[1]	X[16]	895	—[22]	923[29]
SO_3^{2-}	1.39	X[19]	737	807[28]	784

[1]S—O(H).
[2]m.w. ≡ microwave spectroscopy, e.d. ≡ electron diffraction, X ≡ X-ray diffraction.
[3]Calculated from ν_s and ν_{as} by equation [1].
[4]R. Westrik and C. H. MacGillavry. Rec. Trav. Chim. **60**, 794 (1941).
[5]D. R. Lide, D. E. Mann, and R. M. Fristrom. J. Chem. Phys. **26**, 734 (1954).
[6]R. C. Ferguson. J. Am. Chem. Soc. **76**, 850 (1954).
[7]R. Pascard. Compt. Rend. **240**, 2162 (1955).
[8]K. J. Palmer. J. Am. Chem. Soc. **60**, 2360 (1938).
[9]R. E. Rundle. Dissertation, Calif. Inst. Techn., Pasadena, Calif. (1941).
[10]D. Kivelson. J. Chem. Phys. **22**, 904 (1954).
[11]S. Martinez. Acta Cryst. **9**, 145 (1956). E. Stanley. Acta Cryst. **9**, 897 (1956).
[12]H. R. Lynton and M. R. Truter. J. Chem. Soc. 5112 (1960).
[13]G. A. Jeffrey and H. P. Stadler. J. Chem. Soc. 1467 (1951).
[14]J. A. J. Jarvis. Acta Cryst. **6**, 327 (1953).
[15]D. W. J. Cruickshank (9).
[16]L. H. Loopstra and C. H. MacGillavry. Acta Cryst. **11**, 349 (1958).
[17]O. Bastiansen and H. Viervoll. Acta Chem. Scand. **2**, 702 (1948).
[18]M. Atozi and R. E. Rundle. J. Chem. Phys. **29**, 1306 (1958).
[19]W. H. Zachariasen and H. E. Buckley. Phys. Rev. **37**, 1295 (1931).
[20]R. J. Gillespie and E. A. Robinson. Can. J. Chem. **39**, 2189 (1961).
[21]R. J. Gillespie and E. A. Robinson. Can. J. Chem. **39**, 2171 (1961).
[22]R. J. Gillespie and E. A. Robinson (18).
[23]E. A. Robinson and S. K. Hall. Unpublished experiments.
[24]E. A. Robinson (14).
[25]W. G. Palmer. J. Chem. Soc. 1552 (1961).
[26]W. D. Horrocks and F. A. Cotton (24).
[27]G. Herzberg. Molecular spectra and molecular structure. Vol. II. Van Nostrand, New York. 1944. p. 167.
[28]F. A. Miller and C. H. Wilkins. Anal. Chem. **24**, 1253 (1952).
[29]Corrected for mass of OH group.

Can. J. Chem. Downloaded from www.nrcresearchpress.com by 210.87.254.42 on 09/05/12
For personal use only.

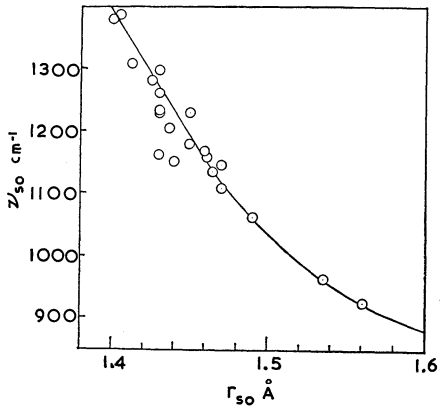

FIG. 1. Correlation of SO stretching frequencies with bond lengths.

in general more accurate than the bond lengths and the scatter of the points is in most cases not greater than ±0.02 Å, which is approximately the experimental error in many of the bond-length determinations. The SO bond length given for the sulphite ion is evidently incorrect and would merit reinvestigation. The SO bond length in sulphamide is probably also somewhat in error. It is possible to use this stretching-frequency – bond-length correlation to predict SO bond lengths in molecules where these have not been measured, to a probable accuracy of ±0.02 Å. Some examples are given in Table II.

TABLE II

Some calculated SO bond lengths and bond orders, and SO_2 bond angles

Molecule	ν_s (cm^{-1})[1]	ν_{as} (cm^{-1})[1]	ν_{SO}[2]	r_{SO} (Å)	$\widehat{OSO}$ (deg)[3] (a)	$\widehat{OSO}$ (deg)[3] (b)	n
SOF_4	1379	—	1379	1.40	—	—	2.00
$FOSO_2F$	1248	1501	1375	1.40	123	123	2.00
$S_2O_5F_2$	1255	1490	1373	1.40	120	122	2.00
$S_2O_6F_2$	1246	1495	1370	1.40	122	123	1.99
CF_3SO_2F	1239	1463	1351	1.41	119	121	1.97
$CH_3O\cdot SO_2F$	1235	1465	1350	1.41	120	121	1.97
SO_2FBr	1228	1460	1344	1.41	122	121	1.96
SO_2FCl	1224	1455	1340	1.41	122	121	1.95
CF_3SO_2Cl	1239	1439	1339	1.41	116	121	1.95
$FSO_2\cdot OH$	1230	1445	1338	1.41	118	121	1.95
$S_2O_5Cl_2$	1209	1444	1327	1.42	122	120	1.92
$(CH_2)_4SO_2$	1224	1412	1318	1.42	115	120	1.91
$ClSO_2\cdot OH$	1209	1408	1309	1.42	117	119	1.89
CH_3SO_2F	1210	1401	1306	1.42	115	119	1.88
CCl_3SO_2Cl	1183	1404	1294	1.42	120	119	1.86
CH_3SO_2Cl	1175	1370	1273	1.43	117	118	1.82
CH_3SO_2OH	1174	1354	1264	1.43	115	117	1.81
FSO_3^-	1080	1225	1154	1.47	112	113	1.67
$ClSO_3^-$	1054	1209	1132	1.48	114	112	1.60
$CF_3SO_3^-$	1030	1225	1128	1.48	120	112	1.59
$N(SO_3)_3^{3-}$	1064	1175	1120	1.48	108	111	1.58
$CH_3SO_3^-$	1065	1167	1118	1.48	106	111	1.58
SO_3^{2-}	737	807	784	1.65	98	96	1.13

[1]Data taken from references 14, 16, and 25 and from R. J. Gillespie and E. A. Robinson, Can. J. Chem., **39**, 2171 (1961).
[2]Calculated from equation [1].
[3](*a*) Calculated from equation [2]; (*b*) interpolated from Fig. 2.

Can. J. Chem. Downloaded from www.nrcresearchpress.com by 210.87.254.42 on 09/05/12
For personal use only.

With increasing bond order the electron density in the SO bonds increases, hence the repulsion between the SO bonds in the SO_2 group will increase and the bond angle should increase accordingly (23). Although the data available on bond angles (Table III) is

TABLE III

Comparison of calculated and observed SO_2 bond angles

Molecule	ν_s (cm^{-1})	ν_{as} (cm^{-1})	ν_{SO} (cm^{-1})	$\widehat{OSO}_{calc}$ (deg)	$\widehat{OSO}_{obs}$ (deg)
H_2SO_4[1]	910	968	939	109	108
SO_4^{2-}	980	1104	1062	110	110
$CH_2(SO_3)_2^{2-}$	1042	1183	1159	113	112
$NH_2SO_3^-$	1059	1202	1154	111	112
$S_2O_7^{2-}$	1065 1095	1253 1276	1203	114	116
$(NH_2)_2SO_2$	1163	1350	1256	119.4	116
SO_2	1150	1334	1259	120	116
H_2SO_4	1195	1368	1260	116	114
SO_2Cl_2	1182	1414	1298	119.8	122
$(SO_3)_3$	1231 1270	1489 1515	1376	120	122
SO_2F_2	1269	1501	1385	124	120

[1]$S(OH)_2$ group.

rather scanty and not always very accurate Fig. 2 shows that there does appear to be an approximately linear correlation between the bond angle and the SO stretching frequency.

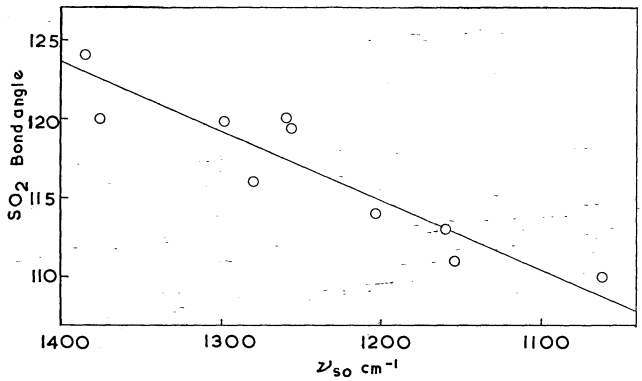

FIG. 2. Correlation of SO stretching frequencies with bond angles.

By making use of the approximations involved in Lehmann's "average rule", namely that the bending force constant, d, is much smaller than the stretching force constant, k, and that the symmetric stretching frequency is appreciably larger than the bending frequency the following relation between the bond angle 2α and the SO stretching frequencies can be obtained for SO_2 groups:

$$[2] \qquad \nu_{sym}/\nu_{asym} = [(1 + \cos^2 \alpha)/(1 + \sin^2 \alpha)]^{\frac{1}{2}}.$$

A comparison is made in Table III of bond angles predicted in this way from the stretching frequencies and the experimentally determined values. The agreement is rather better than might have been expected in view of the approximations involved. Table II gives some predicted OSO bond angles in some species where this angle has not been measured, obtained both by interpolation from Fig. 2 and from equation [2].

Can. J. Chem. Downloaded from www.nrcresearchpress.com by 210.87.254.42 on 09/05/12
For personal use only.

Can. J. Chem. Downloaded from www.nrcresearchpress.com by 210.87.254.42 on 09/05/12
For personal use only.

FORCE CONSTANTS

Reasonably rigorous calculations of force constant have been made for only a few of the molecules we are considering (24, 25, 26), and in many cases they cannot be made at present because complete assignments have not been given for the vibrational spectra and the bond angles and bond lengths have not been measured. However, if it is assumed that there is negligible coupling between the vibrations of the SO_2 or SO group and the other vibrations of the molecule then an approximate value for the force constant of the SO bond may be obtained by treating the SO group as a simple diatomic molecule and the SO_2 group as a simple triatomic molecule. An SO_2 group can also be treated as a diatomic SO group if the appropriate SO stretching frequency is first calculated using Lehmann's average rule (17). Hence we have

$$[3] \qquad k_{SO} = \frac{5.889\nu_{SO}^2 \times 10^{-2}}{(1/m_S + 1/m_O)} = 0.6282\nu_{SO}^2,$$

where m_S and m_O are the atomic weights of sulphur and oxygen, respectively. Values of the stretching force constants obtained from equation [3] and those of other workers are shown in Table IV. The general agreement between our approximate force constants and

TABLE IV

Stretching force constants and bond orders for SO bonds

	10^5k[1]					
Molecule	(*a*)	(*b*)	(*c*)	(*d*)	(*e*)	*n*
SOF_4[2]	11.74	—	—	—	—	2.00
S_3O_9	11.89	12.15	—	—	—	2.00
SO_2F_2	12.05	12.04	11.27	12.0	11.28	2.00
SO_2FBr	11.35	11.38	—	—	—	1.96
SO_2FCl	11.28	11.30	—	—	—	1.95
SOF_2	10.95	—	10.33	10.8	11.0	1.91
SO_2Cl_2	10.58	10.75	10.29	10.5	10.61	1.87
H_2SO_4	10.29	10.26	—	—	—	1.84
SO_2	9.96	9.97	—	9.9	—	1.81
$SO_2(NH_2)_2$	9.92	9.81	—	—	—	1.80
$SO_2(CH_3)_2$	9.48	9.40	—	—	—	1.77
SO_3	9.50	10.40	10.32	9.7	10.79	1.75
$SOCl_2$	9.49	—	9.30	9.4	9.69	1.75
$S_2O_7^{2-}$	9.09	8.85	—	—	—	1.71
FSO_3^-	8.70	8.65	—	—	—	1.67
$NH(SO_3)_2^{2-}$	8.70	8.51	—	—	—	1.67
$EtO \cdot SO_3^-$	8.57	8.24	—	—	—	1.65
$S_2O_6^{2-}$	8.48	8.24	7.84	8.4	—	1.64
$CH_2(SO_3)_2^{2-}$	8.44	—	—	—	—	1.64
$NH_2SO_3^-$	8.36	8.03	—	—	—	1.63
HSO_4^-	8.26	—	—	—	—	1.62
$EtSO_3^-$	8.09	7.69	—	—	—	1.60
$(CH_3)_2SO$	7.72	—	—	7.0	6.54	1.56
SO_4^{2-}	7.08	6.72	6.52	6.9	9.07	1.50
H_2SO_4	5.89	5.57	—	—	—	1.35
HSO_4^-	5.35	—	—	—	—	1.29
SO_3^{2-}	3.86	3.95	—	—	—	1.13

[1](*a*) Treated as an SO group; (*b*) treated as an SO_2 group; (*c*) Siebert (26); (*d*) Simon and Kriegsmann (17); (*e*) Hunt and Wilson (24), Horrocks and Cotton (25), Herzberg (G. Herzberg. Molecular spectra and molecular structure. Vol. II. Van Nostrand, New York. 1944. p. 167).

[2]See also J. Mol. Spectry. **10**, 115 (1963).

the limited number of more precise values provides some justification for our use of these approximate force constants.

Figure 3 shows that there is a linear relationship between log k_{SO} and log r_{SO}, where k_{SO} and r_{SO} are the stretching force constant and bond length, respectively, which may

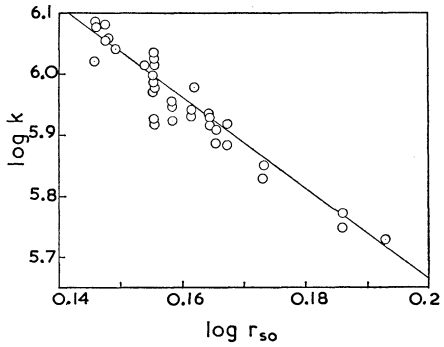

FIG. 3. Linear relation between log k and log r_{SO}.

be expressed by the equation

[4] $$\log k_{SO} = -7.41 \log r_{SO} + 7.15$$

or

$$k_{SO} r_{SO}^{7.4} = 1.41 \times 10^7,$$

where r_{SO} is in angstroms and k_{SO} in dynes cm^{-1}. This relation is of the general form

$$kr^n = C$$

which was suggested by Linnett (27) as being the best general relation between force constant and bond length. This is a modified form of the relation $kr^6 = C$ originally proposed by Douglas-Clark (28).

If we substitute for k_{SO} in terms of ν_{SO} in equation [2] we obtain the expression

[5] $$\log \nu_{SO} = -3.7 \log r_{SO} + 3.68$$

or

$$\nu_{SO} r_{SO}^{3.7} = 4.79 \times 10^3.$$

The line determined by this equation is shown in Fig. 1.

BOND ORDERS

In order to determine the relationship between the bond properties we have been discussing and bond orders it is necessary to know the bond orders in at least two and preferably several molecules containing SO bonds. An apparently obvious method would be to calculate the lengths of SO single and double bonds from tables of covalent radii. For the SO single bond Pauling's covalent radii (29, p. 224) give a value of 1.70 Å while the Schomaker–Stevenson rule (10) gives 1.69 Å. For a double bond Pauling's covalent radii give 1.49 Å and the Schomaker–Stevenson rule 1.47 Å. In fact no compound is known in which the S—O bond is as long as the predicted single-bond values. The longest bonds that have been found are 1.66 Å in SF_5OOSF_5 (30); 1.645 Å for the SOS bridge bonds in the $S_2O_7^{--}$ ion (32), and 1.64 Å in SF_5OF (31) and the bridge bonds in $HS_2O_7^-$ (33) and SO_3 polymer (34). It is reasonable that the longest SO bonds are formed in these molecules

Can. J. Chem. Downloaded from www.nrcresearchpress.com by 210.87.254.42 on 09/05/12
For personal use only.

since the sulphur 3*d* orbitals normally used for double bonding with oxygen are largely used up in forming single bonds to fluorine or double bonds to other oxygen atoms. However, even for these long SO bonds there is evidence that there is a small amount of delocalization of oxygen lone-pair electrons into the partially available $3d_{x^2-y^2}$ or $3d_{z^2}$ orbitals or possibly into the other *d* orbitals which form considerably weaker π-bonds (9, 35). Hence these bonds may be expected to be slightly shorter than a true single bond, and it seems reasonable to take the value of 1.70 Å as the bond length of an SO single bond. The predicted double bond lengths are, however, much less satisfactory since many SO bonds are known with lengths shorter than either of the above values and there is no reason to assume that the bond orders are considerably greater than two. It can only be concluded that either the double-bond radii are incorrect or that the simple additivity rule and the Schomaker–Stevenson rule are invalid for the SO double bond. The Pauling single-bond radii are reasonably satisfactory as they are derived from a large number of experimental determinations of bond lengths but the values of the double-bond radii are based on many fewer experimental data and the additivity relationship has not been so well tested. Hence these double-bond radii may not be correct. The shortest observed SO bond lengths* are 1.405 Å in SO_2F_2 (12), 1.412 Å in SOF_2 (36), and 1.40 Å in S_3O_9 (33). These short SO bonds are also the strongest as measured by the stretching frequencies and force constants and it seems reasonable to make the assumption that they have an order of two. In view of the high electronegativity of fluorine it is unlikely that bonds of a higher order than those in SO_2F_2 and SOF_4 will be found. Unfortunately the bond length in SOF_4 is not known but the SO stretching frequency in this molecule is very close to that in SO_2F_2, suggesting that the bond length will be close to 1.40 Å. Since replacement of an oxygen in SO_2F_2 by two fluorines in SOF_4 fails to raise the value of SO stretching frequency we assume that in both of these molecules the effective electronegativity of sulphur is large enough to achieve essentially complete double-bond formation. Extrapolation of the log k – log r and ν_{SO}–r plots in Figs. 3 and 1 then gives $\nu = 655$ cm^{-1} and $k = 2.7\times10$ dynes cm^{-1} for a single bond and $\nu = 1385$ cm^{-1} and $k = 11.7$ dynes cm^{-1} for a double bond.

In order to determine the form of the relationship between force constant and bond order it is necessary to have at least one and preferably several additional pairs of force-constant and bond-order values. Assuming that fluorine substituents on sulphur cause the SO bond order to achieve its maximum value of 2.0, as in SOF_2 and SOF_4, it seems reasonable to assume that in the fluorosulphate ion, FSO_3^-, the bond order of the SO bonds has the maximum possible value of 1.67. In the case of anions of the general formula XSO_3^- the SO stretching frequencies are all close to the SO stretching frequency of FSO_3^-. Hence the bond orders in anions of the type XSO_3^- are all very close to the maximum theoretical value of 1.67, suggesting that the group X has a much smaller effect on the SO stretching frequency than in $XYSO_2$ compounds. This may be attributed to the effect of the negative charge. Using the force constant for FSO_3^- and a bond order of 1.67 together with the values for SO single and double bonds given above it may be seen in Fig. 4 that they exhibit a linear relationship. It is interesting to note that the force-constant – bond-order relationship is also linear for C—C single, double, and triple bonds (39). Some confirmation of this linear relationship for SO bonds is provided by the force constant for the SO_4^{2-} ion, which, if a bond order of 1.5 is assumed, fits the straight line relationship well. Because of the high negative charge of the sulphate ion we consider that the electronegativities of

**Although equally short bonds are also reported for $SO_2(NH_2)_2$ (37) and SO_3^{2-} (38) these are quite inconsistent with the other properties of these bonds and they must be considered to be of doubtful accuracy.*

Can. J. Chem. Downloaded from www.nrcresearchpress.com by 210.87.254.42 on 09/05/12
For personal use only.

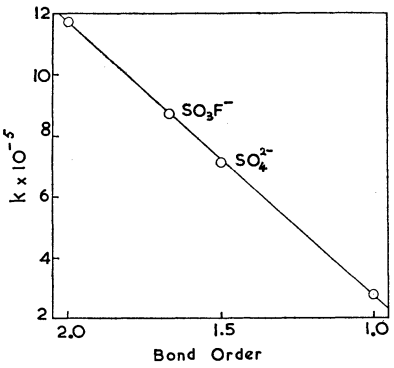

FIG. 4. Linear relation between bond order and force constant.

the groups attached to sulphur will be even less important in determining the bond order than was found to be the case for the anions XSO_3^- and thus the bond order of 1.5 is reasonable for the sulphate ion. The straight line in Fig. 4 is determined by the equation

$$n = 1.11\times10^{-6}k+0.7, \qquad [6]$$

where n is the bond order.

This equation may now be used in conjunction with equation [4] to obtain the relationship between bond length and bond order:

$$n_{SO} = \frac{15.65}{r_{SO}^{7.4}}+0.7. \qquad [7]$$

This curve is plotted in Fig. 5 and is not a straight line as Cruickshank assumed (9), but has a shape similar to the corresponding curve for C—C bonds (11).

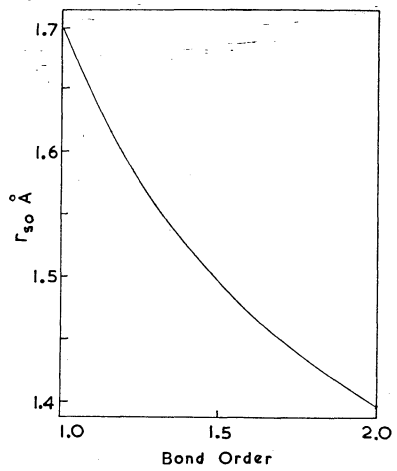

FIG. 5. Bond-length – bond-order relationship.

Pauling and Coulson (29, p. 236; 40) have deduced the following general expression for the length r_n of a bond of order n intermediate between a single and double bond, where r_1

Can. J. Chem. Downloaded from www.nrcresearchpress.com by 210.87.254.42 on 09/05/12
For personal use only.

[8] $$r_n = r_1 - \frac{r_1 - r_2}{1 + \left(\frac{2-n}{n-1}\right)\frac{k_1}{k_2}}.$$

and r_2 are the single and double bond lengths and k_1 and k_2 the corresponding force constants. On the basis of the SO single- and double-bond distances and the bond length in the sulphate ion ($n = 1.5; r = 1.49$ Å), equation [8] becomes

[9] $$r_n = 1.70 - \frac{0.30}{1+0.46\left(\frac{2-n}{n-1}\right)}$$

for SO bonds. Bond lengths calculated from both equations [7] and [9] agree exactly to two decimal places. This would appear to lend some support to our choice of single- and double-bond lengths given above.

Bond orders interpolated from Fig. 4 for most of the compounds for which data is available are given in Table IV.

ACKNOWLEDGMENTS

We thank the Directorate of Chemical Sciences, United States Air Force Office of Scientific Research, and the National Research Council of Canada for generous financial assistance.

REFERENCES

1. G. N. Lewis. Valence and the structure of atoms and molecules. The Chemical Catalog Company, New York. 1923.
2. A. F. Wells. Structural inorganic chemistry. 3rd ed. Oxford University Press. 1962. p. 434.
3. R. J. Gillespie. J. Chem. Educ. **40**, 295 (1963).
4. L. Pauling. J. Phys. Chem. **56**, 361 (1952).
5. W. Moffitt. Proc. Roy. Soc. (London), Ser. A, **200**, 409 (1950).
6. H. H. Jaffe. J. Phys. Chem. **58**, 185 (1954).
7. D. P. Craig et al. J. Chem. Soc. 332 (1954).
8. C. C. Price and S. Oae. Sulfur bonding. The Ronald Press Co., New York. 1962.
9. D. W. J. Cruickshank. J. Chem. Soc. 5486 (1961).
10. V. Schomaker and D. P. Stevenson. J. Am. Chem. Soc. **63**, 37 (1941).
11. C. A. Coulson. Valence. 2nd ed. Oxford University Press. 1961. p. 270.
12. R. E. Rundle. Private communication quoted by P. W. Allen and L. E. Sutton in Acta Cryst., **3**, 46 (1950).
13. D. R. Lide, D. E. Mann, and R. M. Fristrom. J. Chem. Phys. **26**, 734 (1957).
14. E. A. Robinson. Can. J. Chem. **39**, 247 (1961).
15. L. J. Bellamy and R. L. Williams. J. Chem. Soc. 863 (1957).
16. P. L. Goggin, H. L. Roberts, and L. A. Woodward. Trans. Faraday Soc. **57**, 1877 (1961).
17. A. Simon and H. Kriegsmann. Z. Physik. Chem. **204**, 369 (1955).
18. R. J. Gillespie and E. A. Robinson. Can. J. Chem. **40**, 644 (1962).
19. D. Barnard, J. M. Fabian, and H. P. Koch. J. Chem. Soc. 2422 (1949).
20. G. B. B. M. Sutherland and W. G. Penney. Proc. Roy. Soc. (London), Ser. A, **156**, 654 (1936).
21. W. J. Lehmann. J. Mol. Spectry. **7**, 261 (1961).
22. H. J. Bernstein. Spectrochim. Acta, **18**, 161 (1962).
23. R. J. Gillespie. J. Am. Chem. Soc. **82**, 5978 (1960).
24. G. R. Hunt and M. K. Wilson. Spectrochim. Acta, **18**, 959 (1962).
25. W. D. Horrocks and F. A. Cotton. Spectrochim. Acta, **16**, 358 (1960); **17**, 134 (1961).
26. H. Siebert. Z. Anorg. Chem. **275**, 210 (1954).
27. J. W. Linnett. Quart. Rev. Chem. Soc. **1**, 73 (1947).
28. C. H. Douglas-Clark. Phil. Mag. **18**, 459 (1934); **22**, 1137 (1936).
29. L. Pauling. The nature of the chemical bond. 3rd ed. Cornell University Press. 1960.
30. R. B. Harvey and S. H. Bauer. J. Am. Chem. Soc. **76**, 859 (1954).
31. H. Lynton and M. R. Truter. J. Chem. Soc. 5112 (1960).
32. R. Westrick and C. H. MacGillavry. Acta Cryst. **7**, 764 (1954).
33. J. W. M. Steeman and C. H. MacGillavry. Acta Cryst. **7**, 402 (1954).
34. R. A. Crawford, F. B. Dudley, and K. Hedberg. J. Am. Chem. Soc. **81**, 5287 (1959).

Can. J. Chem. Downloaded from www.nrcresearchpress.com by 210.87.254.42 on 09/05/12
For personal use only.

35. R. J. GILLESPIE and E. A. ROBINSON. Spectrochim. Acta, **19**, 741 (1963).
36. R. C. FERGUSON. J. Am. Chem. Soc. **76**, 850 (1954).
37. K. N. TRUEBLOOD and S. W. MAYER. Acta Cryst. **9**, 628 (1956).
38. W. H. ZACHARAISEN and H. E. BUCKLEY. Phys. Rev. **37**, 1295 (1931).
39. H. SIEBERT. Z. Anorg. Chem. **273**, 170 (1953).
40. C. A. COULSON. Proc. Roy. Soc. (London), Ser. A, **168**, 413 (1939); **207**, 306 (1951).

Can. J. Chem. Downloaded from www.nrcresearchpress.com by 210.87.254.42 on 09/05/12
For personal use only.

REACTIONS OF PHENYL-SUBSTITUTED HETEROCYCLIC COMPOUNDS

III. FREE-RADICAL PHENYLATION OF 1-PHENYLPYRAZOLE[1]

BRIAN M. LYNCH[2]

Departments of Chemistry, Memorial University of Newfoundland, St. John's, Newfoundland, and St. Francis Xavier University, Antigonish, Nova Scotia

AND

MISBAHUL AIN KHAN[3]

Department of Chemistry, Memorial University of Newfoundland, St. John's, Newfoundland

Received January 29, 1963

ABSTRACT

Phenyl radicals furnished by benzoyl peroxide attack both rings of 1-phenylpyrazole, and the orientation of substitution has been examined using gas–liquid partition chromatography. Substitution occurs at all positions of the phenyl ring, although predominantly at the ortho positions, while attack in the pyrazole ring is confined to the 3-position. The results are in agreement with the suggestion that the *free valence* at a given position is a major factor in determining the orientation of free-radical phenylation of 1-phenylpyrazole, but in conflict with predictions from resonance theory.

In earlier papers of this series (1, 2), we have examined some electrophilic substitutions of N-phenylazoles. The present work is concerned with the attack of free radicals on 1-phenylpyrazole (I), where the phenyl and benzoate radicals liberated by benzoyl peroxide

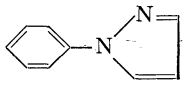

I

effect nuclear substitution. Reactions were carried out by allowing benzoyl peroxide to decompose in 20% solution in 1-phenylpyrazole at 80° C, and the products were separated and isolated using standard procedures (3, 4). The yields obtained in the various experiments are listed in Table I.

1-Phenylpyrazole behaves typically towards benzoyl peroxide, in that the predominant reaction paths are the nuclear phenylation and benzoyloxylation reactions, i.e.,

$$(Ph\cdot CO_2)_2 + X\cdot H \begin{cases} Ph\cdot CO_2H + CO_2 + Ph\cdot X \\ Ph\cdot CO_2H + Ph\cdot CO_2\cdot X \end{cases} \qquad (X = C_9H_7N_2)$$

Since the molar yields of free benzoic acid are appreciably higher than the combined yields of substitution products, it is possible that some direct N-oxidation of 1-phenylpyrazole by benzoyl peroxide occurs (compare the pyridine – benzoyl peroxide system (5)).

The distribution of products is fairly similar to that observed in the reactions of benzoyl peroxide with biphenyl (6), although the benzoyloxylation:phenylation ratio (an index of reactivity towards radical attack (3)) is somewhat higher for 1-phenylpyrazole.

[1]*For Part II, see reference 2. This study was supported by a grant from the National Research Council. A preliminary report was given at the 45th Annual Conference of the Chemical Institute of Canada, Edmonton, Alberta, May 27–30, 1962. Abstracted in part from a thesis presented by M. A. Khan in partial fulfillment of the requirements for the degree of Master of Science, Memorial University of Newfoundland.*

[2]*Correspondence should be addressed to this author at the Department of Chemistry, St. Francis Xavier University, Antigonish, Nova Scotia.*

[3]*Graduate Research Assistant, 1961–1962. Present address: Florida State University, Tallahassee, Florida, U.S.A.*

Can. J. Chem. Downloaded from www.nrcresearchpress.com by 210.87.254.40 on 09/05/12
For personal use only.

TABLE I

Products formed by reaction of benzoyl peroxide with 1-phenylpyrazole

	Expt. No.			
	1	2	3	4
Reactants (g)				
$(Ph \cdot CO_2)_2$	20	20	16	10
1-Phenylpyrazole	100	100	80	50
Products* (g)				
Carbon dioxide	—	—	1.73 (0.60)	1.10 (0.61)
Free benzoic acid	10.40 (1.03)	10.80 (1.07)	7.40 (0.92)	5.00 (0.99)
Phenylation products	8.10† (0.45)	8.10 (0.45)	6.85 (0.47)	4.00 (0.44)
Phenolic fraction‡	1.50 (0.11)	1.60 (0.12)	1.10 (0.10)	—
Benzoic acid from hydrolysis	2.30 (0.23)	2.21 (0.22)	1.20 (0.15)	—

*Quantities in parentheses are yields in mole/mole benzoyl peroxide.
†Anal. Calc. for $C_{15}H_{12}N_2$: C, 81.80; H, 5.50; N, 12.72%. Found: C, 81.86; H, 5.48; N, 12.97%.
‡Calculated as hydroxy-1-phenylpyrazoles.

Phenylations are usually unselective processes (for reviews listing isomer ratios, see Augood and Williams (7) and Williams (8)), and we expected that each of the six possible phenylated 1-phenylpyrazoles would be present in the reaction products. Consequently, authentic samples of each isomer were prepared as follows: 1,3- and 1,5-diphenylpyrazoles by previously reported cyclizations (9, 10); and 1,4-diphenylpyrazole, 1-*o*-, 1-*m*-, and 1-*p*-biphenylylpyrazoles from the appropriate nitro-1-phenylpyrazoles (by reduction, diazotization, and Gomberg arylation (cf. Khan *et al.* (2))). The latter two biphenylylpyrazoles were also synthesized using the standard cyclization of the appropriate substituted hydrazine and 1,1,3,3-tetramethoxypropane (11). Attempted cyclization using *o*-hydrazinobiphenyl gave carbazole and biphenyl, with no evidence for the formation of 1-*o*-biphenylylpyrazole: this reaction, which is reminiscent of a Fischer indole cyclization, is under further study.

The mixtures of phenylation products from the various experiments were examined by gas–liquid partition chromatography, and the presence of 1,3-diphenylpyrazole and the three 1-biphenylylpyrazoles was established by comparison of the retention times observed for the components of the reaction mixtures with those of authentic samples of the various isomers. The ratios of these isomers in the phenylation products were evaluated by direct comparison of the peak areas found for the various isomers, after it was established that the response of the detector to corresponding quantities of each of the isomers was identical. The results are shown in Table II. The infrared spectra of the phenylation products isolated from the various experiments were consistent with the results from the gas–liquid partition chromatography, as bands diagnostic of each of the three 1-biphenylylpyrazoles and 1,3-diphenylpyrazole were observed, while absorption was absent at frequencies noted in the spectra of authentic samples of 1,4- and 1,5-diphenylpyrazoles.

Unusual features of the isomer distribution are the marked preference for ortho substitution in the phenyl ring, the apparently selective attack of the 3-position in the pyrazole ring, and the consequence that the total phenylation is greater in the phenyl ring than in the pyrazole ring. The high ortho:para ratio, and the isomer distribution for phenylation

Can. J. Chem. Downloaded from www.nrcresearchpress.com by 210.87.254.40 on 09/05/12
For personal use only.

TABLE II

Percentages of isomers in the phenylation of 1-phenylpyrazole*

	Site of substitution			
	Phenyl ring			Pyrazole ring
Expt. No.	Ortho	Meta	Para	3-
1	54 (77)	6 (9)	10 (14)	30
2	58 (82)	5 (7)	8 (11)	29
3	58 (83)	3 (4)	9 (13)	30
4	55 (77.5)	6 (8.5)	10 (14)	29

*Quantities in parentheses refer to substitution in the phenyl ring only.

in the phenyl ring of 1-phenylpyrazole, appear quite similar to results observed for free-radical substitution of other molecules with substituent groups having unshared $2p$ electron pairs (i.e., +T substituents): this is illustrated by Table III, where isomer percentages in the phenylation, methylation, and phenoxymethylation of anisole, the

TABLE III

Percentages of isomers in free-radical substitution of molecules with +T substituents

Substrate	Reaction	Temp. (°C)	Isomer percentages			Ref. No.
			Ortho	Meta	Para	
1-Phenylpyrazole (mean values for substitution in the phenyl ring)	Phenylation	80	80	7	13	Present work
Anisole	Phenylation	154	77	10	13	4
		80	70	14	16	12
	Methylation	140	74	15	11	13
	Phenoxymethylation	140	70	21	9	14
Phenetole	Phenylation	100	67	18	15	15
Pyridine N-oxide*	Phenylation	181	79	8	13	16
		131	76	8	16	16

*Isomer percentages refer to 2-, 3-, and 4-substitution.

phenylation of phenetole, and the phenylation of pyridine N-oxide are compared with the corresponding quantities for attack on the phenyl ring of 1-phenylpyrazole. Preferred ortho, para orientation in free-radical substitution of benzenoid compounds is often rationalized in terms of the additional resonance stabilization of the σ-complexes formed by attack ortho or para to a substituent, as a result of delocalization of the unpaired electron into the substituent group (8, 17–20): such stabilization cannot be important for the σ-complex formed by attack meta to a substituent. However, it does not appear to have been realized that interaction with an unpaired electron cannot involve delocalization onto the key atom of the substituent if the substituent is a +T group derived from a first-row element. For such a substituent, depicted as Y in structures II*a–d* and III*a–d*,* interaction must involve unpairing of $2p$ electrons, and generation of an electron pair at the carbon atom carrying the substituent: this electron pair is then subject to delocalization, as indicated in structures II*b–d* and III*b–d*. Although this type of electron delocalization might appear novel, it is closely analogous to the delocalization occurring in the

**In the structures II through VII, lines (—) adjacent to atoms (the lines may be horizontal, vertical, or at 45°) denote unshared electron pairs.*

Can. J. Chem. Downloaded from www.nrcresearchpress.com by 210.87.254.40 on 09/05/12
For personal use only.

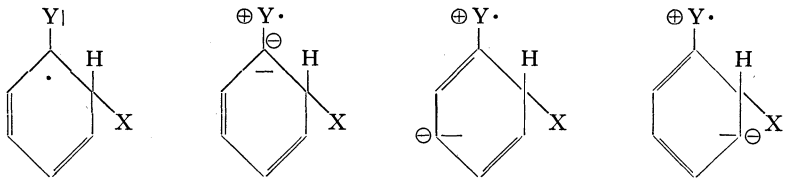

IIa IIb IIc IId

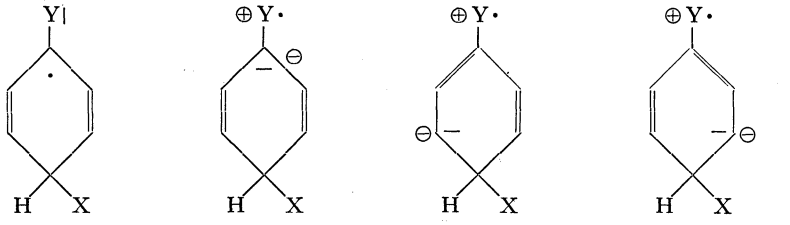

IIIa IIIb IIIc IIId

diphenylpicrylhydrazyl radical, where the five-line pattern noted in the hyperfine structure of the electron paramagnetic resonance spectrum shows conclusively that the odd electron is shared equally between the two central nitrogen atoms (cf. ref. 20(*a*)).

Other treatments of the effects of +T substituents have suggested contributing structures such as IV*b* for the σ-complex IV*a* formed by attack para to the methoxy substituent

IVa IVb

of anisole (19–21), but since contributing structures with more than eight electrons in the outer shells of first-row elements would involve use of high-energy 3*d* orbitals, we consider that structures of type IV*b* should be disregarded. Even if structures of types II*b–d* and III*b–d* are assumed to be important in determining the relative stabilities of the σ-complexes formed from ortho, para, or meta attack, and if the relative stabilities are taken to determine the orientation of the final substitution products, interpretation on this basis is at best qualitative, and offers no explanation for the high ortho:para ratios, since there are no obvious differences in energy between the type II and type III structures. In other words, treatment based on resonance theory gives no quantitative account of the results listed in Table III.

Furthermore, it is doubtful whether the relative stabilities of the various σ-complexes can be regarded as controlling orientation, since the minor differences in the relative reactivities of different positions of substituted benzenes, and the absence of appreciable steric effects, indicate that the transition states for phenylations involve weak bonding of the phenyl radical to the carbon atom being attacked, with this atom still partly conjugated with the residual molecule (cf. refs. 4, 22). The σ-complexes are better regarded as reaction intermediates, persisting long enough to dimerize under favorable circumstances (23, 24).

These considerations of the suggested nature of the transition states indicate that quantities characteristic of the isolated reactant molecules (such as the free valence

Can. J. Chem. Downloaded from www.nrcresearchpress.com by 210.87.254.40 on 09/05/12
For personal use only.

(25–27) at a given position) might be more relevant in discussions of orientation. There is, in fact, remarkable agreement between the orientations calculated for free-radical substitution in aniline and phenol, where the partial rate factors are deduced from the appropriate free valences (Sandorfy (28)), and the isomer percentages listed in Table III. The partial rate factors are related to the free valences by the expression

$$ {}^{X}_{H}k_r = \exp\,(34{,}000({}^{X}F_r - 0.398)/RT), $$

where ${}^{X}_{H}k_r$ is the partial rate factor for position r of a benzene derivative C_6H_5X, ${}^{X}F_r$ is the free valence at position r, 0.398 is the free valence for a benzene position, and T is the temperature (see Augood and Williams (7), Williams (8)). The calculated orientations for a temperature of 80° C are summarized in Table IV, together with the appropriate

TABLE IV

Free valences, partial rate factors, and predicted orientation of free-radical substitution in phenol and aniline

Phenol				Aniline			
Position	${}^{X}F_r$	${}^{X}_{H}k_r$	Isomer percentage	Position	${}^{X}F_r$	${}^{X}_{H}k_r$	Isomer percentage
Ortho	0.422	3.20	66.7	Ortho	0.431	4.95	72.3
Meta	0.395	0.86	17.9	Meta	0.396	0.91	13.3
Para	0.406	1.47	15.4	Para	0.412	1.97	14.4

free valences and partial rate factors. It is apparent that aniline and phenol may be regarded as satisfactory models for prediction of the orientation of radical substitution in the phenyl ring of N-phenylpyrazole and in anisole, phenetole, and pyridine N-oxide respectively.

The predominant 3-phenylation in the pyrazole ring is in direct conflict with qualitative predictions from resonance theory. If the σ-complexes (V*a*, VI*a*, VII*a*) for phenyl radical

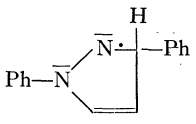

V*a*

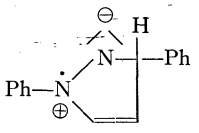

V*b*

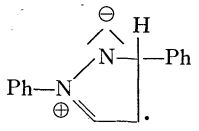

V*c*

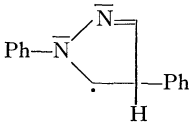

VI*a*

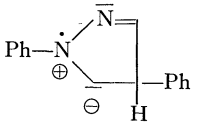

VI*b*

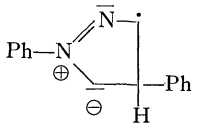

VI*c*

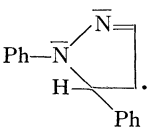

VII*a*

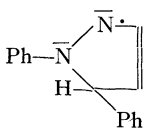

VII*b*

Can. J. Chem. Downloaded from www.nrcresearchpress.com by 210.87.254.40 on 09/05/12
For personal use only.

attack at the 3-, 4-, and 5-positions are compared, it is apparent that delocalization of the unpaired electron in the σ-complexes for 3- or 4-substitution must involve charge separation (compare the contributing structures V*b*, V*c*, VI*b*, VI*c*), while uncharged contributing structures (VII*a* $\leftrightarrow$ VII*b*) can be written for the σ-complex for 5-substitution. If the relative stabilities of the σ-complexes govern the yields of phenylation products, then these should lie in the order $5 > 3 > 4$, since charged contributing structures are generally of higher energy than uncharged ones, while contributing structures with a negative charge on nitrogen (e.g., V*b*) should be more stable than those with a negative charge on carbon (e.g., VI*b*).

In view of the successful correlation of the orientation of substitution in the phenyl ring of 1-phenylpyrazole with the free valences at the ring carbons in aniline (which is regarded as a suitable model for 1-phenylpyrazole because of the +T character of the amino group, and its possession of an identical key atom in the substituent), it appeared possible that a similar correlation might be found between the free valences at the various positions of *pyrazole* and the orientation of substitution in the pyrazole ring of 1-phenylpyrazole. The relevant free valences, calculated from recently published π-bond orders for pyrazole (29), are: (position, free valence) 3-, 0.440; 4-, 0.286; 5-, 0.393. The predicted order of reactivity towards radicals is therefore 3- $\gg$ 5- $\gg$ 4-, and is consistent with the observed orientation in the pyrazole ring of 1-phenylpyrazole. The observed preponderance of substitution in the phenyl ring can be attributed to the low free valences at the 4- and 5-positions of the pyrazole ring.

Reservations have been expressed about the validity of the assumption that free valence can be regarded as an index of reactivity towards free radicals, particularly for non-alternant hydrocarbons, heteroaromatic compounds, and substituted benzenes (8, 26, 27). The main justification of the use we have made of this assumption in the present study is its success in predicting the orientation of substitution in each ring. In view of the approximations inherent in regarding aniline and pyrazole as suitable models for the two rings of 1-phenylpyrazole, and in neglecting inter-ring conjugation, the agreement with experiment is remarkably good. Since the approach we have adopted can be used to predict the orientation of substitution of other phenyl-substituted heterocycles by free radicals, we have initiated studies of free-radical substitution in 1-phenylpyrrole, 1-phenylimidazole, and 2-phenyl-1,2,3,2H-triazole, in order to test these predictions.

The nuclear benzoyloxylation products (isolated as mixed hydroxy-1-phenylpyrazoles after saponification in the standard isolation procedure (3, 4)) were examined briefly. The mixtures of hydroxy compounds were methylated, and their infrared spectra were compared with those of authentic samples of 1-*o*- and 1-*p*-methoxyphenylpyrazole: marked resemblances were evident (see Experimental), indicating that the pattern of benzoyloxylation qualitatively resembles that of phenylation. However, no attempt was made to evaluate accurate isomer ratios, or to establish the occurrence of benzoyloxylation in the pyrazole ring.

In the course of this work, we recorded the ultraviolet spectra of the various phenylated 1-phenylpyrazoles, and noted that the wavelengths of maximum absorption and the molecular extinction coefficients of correspondingly substituted arylbenzenes and arylpyrazoles resembled one another closely. This is shown in Table V (the data for the arylbenzenes are taken from the compilations by Kamlet (30) and Ungnade (31)). Resemblances between the electronic spectra of arylbenzenes and analogously substituted heterocycles, or between correspondingly substituted derivatives of different heterocyclic

Can. J. Chem. Downloaded from www.nrcresearchpress.com by 210.87.254.40 on 09/05/12
For personal use only.

TABLE V

Ultraviolet spectra of arylbenzenes and arylpyrazoles

Arylbenzene	λ_{max} (mμ)	log ε	Arylpyrazole	λ_{max} (mμ)	log ε
Biphenyl	249	4.23	1-Phenylpyrazole	252	4.13
o-Terphenyl	233	4.40	1-*o*-Biphenylylpyrazole	233	4.35
m-Terphenyl	246	4.58	1,5-Diphenylpyrazole	240	4.18
p-Terphenyl	276	4.51	1-*m*-Biphenylylpyrazole	250	4.38
			1-*p*-Biphenylylpyrazole	280	4.50
			1,4-Diphenylpyrazole	262	4.28
			1,3-Diphenylpyrazole	280	4.46
				285 sh	4.44

aromatic compounds, can be of obvious assistance in assignments of structure (for an example, see Lynch and Chan (1)).

EXPERIMENTAL

General

Analyses are by the Schwarzkopf Microanalytical Laboratory, Woodside, N.Y., U.S.A. Melting points were observed using a Fisher–Johns apparatus and are uncorrected. Infrared spectra were recorded using a Unicam SP100 spectrophotometer equipped with an SP130 grating accessory. Unless noted otherwise, samples were examined using the potassium chloride disk technique. Ultraviolet spectra were recorded in 95% ethanol using a Beckman DK-2A spectrophotometer. A Beckman GC-2A gas chromatograph, with a Beckman No. 70008 column (Apiezon "L" on C-22 firebrick), helium as carrier gas (flow rate, 70 ml/min), and a column temperature of 220° C, was used for the gas–liquid partition chromatography.

Starting Materials

Benzoyl peroxide was purified by repeated precipitation from chloroform solution by methanol, and had minimum purity 98% (iodometric estimations). 1-Phenylpyrazole, m.p. 11°, b.p. 246°, n_D^{25} 1.5957, was prepared by reaction of phenylhydrazine hydrochloride with 1,1,3,3-tetramethoxypropane in ethanol solution (2, 11).

Reference Samples

(a) Phenylated 1-Phenylpyrazoles

1,3-Diphenylpyrazole, m.p. 84° (lit. 84°), and 1,5-diphenylpyrazole, m.p. 55° (lit. 55–56°), were prepared by cyclization of hydroxymethyleneacetophenone with phenylhydrazine (9, 10). 1,4-Diphenylpyrazole, m.p. 97° (lit. 97°) (anal. calc. for $C_{15}H_{12}N_2$: C, 81.80; H, 5.50%; found: C, 81.72; H, 5.50%); 1-*o*-biphenylylpyrazole, b.p. 208° at 20 mm (anal. calc. for $C_{15}H_{12}N_2$: N, 12.72%; found: N, 13.03%); 1-*m*-biphenylylpyrazole, b.p. 205° at 20 mm (anal. found: C, 81.84; H, 5.72%); and 1-*p*-biphenylylpyrazole, m.p. 126° (lit. 126°), were prepared from the appropriate nitro-substituted 1-phenylpyrazoles by reduction to the corresponding amines with tin and hydrochloric acid, followed by diazotization and reaction of the buffered diazonium salt solutions with benzene (Gomberg arylation). Full details of this method have been given (2) for the synthesis of 1-*p*-biphenylylpyrazole. Overall yields from 10-g quantities of the respective nitro-1-phenylpyrazoles were 32, 33, 32, and 52%. 1-*m*-Biphenylylpyrazole and 1-*p*-biphenylylpyrazole are also available in good yields by cyclization of the appropriate hydrazinobiphenyls (prepared by diazotization of the appropriate aminobiphenyl, followed by reduction with stannous chloride (32)) with 1,1,3,3-tetramethoxypropane. However, when *o*-hydrazinobiphenyl (5 g) and 1,1,3,3-tetramethoxypropane (5 g) were heated under reflux in 3 *N* ethanolic hydrochloric acid (100 ml), carbazole (1 g), m.p. and mixed m.p. 246°, and biphenyl (1 g), m.p. and mixed m.p. 70°, were the only products obtained.

(b) 1-Methoxyphenylpyrazoles

1-*o*-Methoxyphenylpyrazole, b.p. 280°, n_D^{25} 1.5883 (anal. calc. for $C_{10}H_{10}N_2O$: C, 68.95; H, 5.79%; found: C, 69.15; H, 5.98%), was prepared from *o*-methoxyphenylhydrazine and 1,1,3,3-tetramethoxypropane (2, 11). 1-*p*-Methoxyphenylpyrazole, m.p. 33–35°, b.p. 130° at 5 mm (lit. b.p. 138–142° at 0.5 mm (33)) (anal. found: C, 69.00; H, 5.42%), was obtained as follows: 1-*p*-aminophenylpyrazole (8.5 g), m.p. 45° (lit. 45°), was diazotized in 3 *N* hydrochloric acid at 5°, and the resulting solution was boiled with excess of water until the evolution of nitrogen ceased. The phenolic material was recovered by standard methods, and methylated with dimethyl sulphate – sodium hydroxide; distillation yielded 1-*p*-methoxyphenylpyrazole (1.84 g).

General Procedure for Reactions

Benzoyl peroxide and 1-phenylpyrazole were heated together at 80° C as indicated in Table I. The various products were separated and isolated following previously outlined procedures (3, 4).

Can. J. Chem. Downloaded from www.nrcresearchpress.com by 210.87.254.40 on 09/05/12
For personal use only.

Examination of Reaction Products—Phenylated Fractions

(a) Gas–Liquid Partition Chromatography

Retention times for the various isomeric phenyl-substituted 1-phenylpyrazoles were established with authentic samples of each compound, using the standardized operating conditions noted above. Trial experiments using ethyl ether or acetone as solvents for the compounds, and sample volumes from 0.02–0.05 ml, showed that the peak areas were directly proportional to the amounts of each isomeric compound taken, and that the molar response of the detector was identical for all of the isomers. The following retention times were observed: 1-*m*-biphenylylpyrazole, 6.70 min; 1-*o*-biphenylylpyrazole, 8.20 min; 1,3-diphenylpyrazole, 9.80 min; 1,5-diphenylpyrazole, 12.00 min; 1,4-diphenylpyrazole, 12.60 min; 1-*p*-biphenylylpyrazole, 15.00 min. Preliminary examination of the mixtures of phenylation products from expts. 1–4 failed to reveal any evidence for the presence of 1,4- or 1,5-diphenylpyrazole, although peaks were observed at the characteristic retention times of each of the other four isomers. By addition of varying amounts of 1,4- and 1,5-diphenylpyrazole to samples of the reaction products, and examination of the resulting peak areas, it was estimated that the lower limit of detection was 3% of either of these isomers. Detailed comparisons of the peak areas corresponding to the four isomers detected in the phenylation products gave the results summarized in Table II. The identification of the various peaks was checked by making artificial additions of each isomer to separate samples of the experimental reaction mixtures, when increments in the areas of the appropriate peaks were observed.

(b) Infrared Spectra

The infrared spectra of capillary films of the various phenylated fractions from Expts. 1–4 were recorded, and showed no absorption bands other than those assignable to the 1-biphenylylpyrazoles or to 1,3-diphenylpyrazole: thus, the results are consistent with those from the gas–liquid partition chromatography. However, the spectra of the various 1-biphenylylpyrazoles and 1,*x*-diphenylpyrazoles resemble one another closely: only in the 650–1000 cm^{-1} regions are bands present which allow qualitative identification of a single isomer in a mixture of several, and many bands in this region are common to more than one isomer. Typical spectra of reaction mixtures showed the following medium or strong bands in this region (letters in parentheses following the frequency (cm^{-1}) and intensity (m or s) of an absorption band indicate that bands at this frequency are observed in the spectra of a pure isomer, as follows: A, B, C: 1-*o*-, 1-*m*-, and 1-*p*-biphenylylpyrazoles; D, E, F: 1,3-, 1,4-, and 1,5-diphenylpyrazoles): 660 m (ABC), 680 m (AB), 690 s (DEF), 702 vs (ABCDEF), 755 vs (DEF), 760 vs (ABCE), 790 m (B), 840 m (C), 887 m (ABC), 920 m (C), 940 s (ABCD), 955 s (D). Strong absorption bands noted at 804, 867, 904, and 960 cm^{-1} for 1,4-diphenylpyrazole, and at 674, 765, 834, 880, 925, and 960 cm^{-1} for 1,5-diphenylpyrazole, were absent from the spectra of the mixtures of phenylation products from the various experiments. Full details of the spectra of the isomeric phenyl-substituted 1-phenylpyrazoles are available on request.

(c) Direct Isolation by Adsorption Chromatography

When samples of reaction mixtures were chromatographed on alumina using benzene as eluant, 1-*p*-biphenylylpyrazole was the most readily eluted material, in agreement with the suggestion that the order of elution in a series of isomeric compounds follows the reverse order of dipole moments (34). Fair agreement (within ±10%) was found between the quantities of 1-*p*-biphenylylpyrazole isolated directly from the reaction mixtures and the amounts calculated from the gas–liquid partition chromatography.

Examination of Reaction Products—Hydroxyphenylpyrazole Fractions

These mixtures were methylated with dimethyl sulphate – sodium hydroxide, and the infrared spectra were recorded and compared with those of authentic 1-*o*- and 1-*p*-methoxyphenylpyrazole. Of 20 strong bands observed between 650 and 1600 cm^{-1} in the spectra of the methylated hydroxyphenylpyrazole fractions, all are found in the spectra of one or other of the authentic 1-methoxyphenylpyrazoles. Full details of these spectra are available on request.

ACKNOWLEDGMENTS

We thank the National Research Council for generous support through Operating and Major Equipment Grants, and Misses D. A. Chalker and J. Murphy for skilled technical assistance in spectrophotometry.

REFERENCES

1. B. M. Lynch and T. Chan. Can. J. Chem. **41**, 274 (1963).
2. M. A. Khan, B. M. Lynch, and Y-Y. Hung. Can. J. Chem. **41**, 1540 (1963).
3. B. M. Lynch and K. H. Pausacker. Australian J. Chem. **10**, 165 (1957).
4. B. M. Lynch and R. B. Moore. Can. J. Chem. **40**, 1461 (1962).
5. K. H. Pausacker. Australian J. Chem. **11**, 200 (1958).
6. M. Karelsky and K. H. Pausacker. Australian J. Chem. **11**, 39 (1958).
7. D. R. Augood and G. H. Williams. Chem. Rev. **57**, 123 (1957).
8. G. H. Williams. Homolytic aromatic substitution. Pergamon Press, London. 1960.

Can. J. Chem. Downloaded from www.nrcresearchpress.com by 210.87.254.40 on 09/05/12
For personal use only.

9. K. v. AUWERS and H. MAUSS. Ann. **452**, 182 (1927).
10. L. PANIZZI and E. MONTI. Gazz. Chim. Ital. **77**, 556 (1947).
11. I. L. FINAR and R. J. HURLOCK. J. Chem. Soc. 3024 (1957).
12. R. T. MORRISON, J. CAZES, N. SAMKOFF, and C. A. HOWE. J. Am. Chem. Soc. **84**, 4152 (1962).
13. B. R. COWLEY, R. O. C. NORMAN, and W. A. WATERS. J. Chem. Soc. 1799 (1959).
14. H. B. HENBEST, J. A. W. REID, and C. J. M. STIRLING. J. Chem. Soc. 5239 (1961).
15. B. M. LYNCH and J. D. HALLIDAY. To be published. (For a preliminary account, see 7th Report of Research under the Sponsorship of the Petroleum Research Fund, American Chemical Society, Washington, 1963.)
16. L. K. DYALL and K. H. PAUSACKER. J. Chem. Soc. 18 (1961).
17. C. WALLING. Free radicals in solution. John Wiley and Sons, Inc., New York. 1957. p. 485.
18. J. HINE. Physical organic chemistry. 2nd ed. McGraw-Hill Book Co., Inc., New York. 1962. p. 470.
19. E. S. GOULD. Mechanism and structure in organic chemistry. Henry Holt and Co., New York. 1959. p. 723.
20. C. S. RONDESTVEDT and H. S. BLANCHARD. J. Org. Chem. **21**, 229 (1956).
20 (*a*). C. A. HUTCHISON, R. C. PASTOR, and A. G. KOWALSKY. J. Chem. Phys. **20**, 534 (1952).
21. E. S. GOULD. Mechanism and structure in organic chemistry. Henry Holt and Co., New York. 1959. p. 675.
22. H. WEINGARTEN. J. Org. Chem. **26**, 730 (1961).
23. B. M. LYNCH and K. H. PAUSACKER. Australian J. Chem. **10**, 40 (1957).
24. D. F. DETAR and R. A. J. LONG. J. Am. Chem. Soc. **80**, 4742 (1958).
25. B. PULLMAN and A. PULLMAN. Progress in organic chemistry. Vol. 4. Butterworths Scientific Publications, London. 1958. p. 31.
26. F. H. BURKITT, C. A. COULSON, and H. C. LONGUET-HIGGINS. Trans. Faraday Soc. **47**, 553 (1951).
27. R. D. BROWN. Quart. Rev. (London), **6**, 63 (1952).
28. C. SANDORFY. Bull. Soc. Chim. France, **16**, 615 (1949).
29. H. HAMANO and H. F. HAMEKA. Tetrahedron, **18**, 985 (1962).
30. M. J. KAMLET (*Editor*). Organic electronic spectral data. Vol. I. Interscience Publishers, Inc., New York. 1960.
31. H. E. UNGNADE (*Editor*). Organic electronic spectral data. Vol. II. Interscience Publishers, Inc., New York. 1960.
32. W. J. HICKINBOTTOM. Reactions of organic compounds. Longmans, Green, and Co., London. 1946. p. 355.
33. J. D. KENDALL and G. E. DUFFIN. Brit. Patent No. 797,144 (June 25, 1958).
34. E. R. WARD and W. H. POESCHE. J. Chem. Soc. 2825 (1961).

Can. J. Chem. Downloaded from www.nrcresearchpress.com by 210.87.254.40 on 09/05/12
For personal use only.

Can. J. Chem. Downloaded from www.nrcresearchpress.com by 210.87.254.6 on 09/05/12
For personal use only.

NOTES

GAS CHROMATOGRAPHIC SEPARATION OF DEUTERIUM-SUBSTITUTED OLEFINS BY UNSTABLE COMPLEX FORMATION[1]

R. J. Cvetanović, F. J. Duncan,[2] and W. E. Falconer

The increasing use of deuterium-substituted hydrocarbons in gas kinetic investigations creates an important need for methods of analysis of small amounts of the deuterated reaction products. Wilzbach and Riesz (1) first indicated the possibility of separating extensively isotopically substituted hydrocarbons by gas–liquid chromatography in 1957. Falconer and Cvetanović (2) separated fully and partially deuterated hydrocarbon isomers from each other and from their non-deuterated counterparts by partition chromatography using a non-polar column for which retention times increase linearly with boiling points. This method proved suitable only for the heavier hydrocarbon gases; *n*-butane, *n*-butane-d_{10} was the lowest-boiling pair that could be separated under the conditions used. Techniques to extend the range of separations to include the low-boiling hydrocarbons are badly needed.

Columns prepared from silver nitrate – ethylene glycol solutions on firebrick have been found to be particularly selective for olefins (3), and Muhs and Weiss (4) have related the equilibrium complexing constants calculated from the retention times for a large number of olefins to steric and strain characteristics of the olefins. The retention times of olefins on silver nitrate – ethylene glycol – firebrick columns are also strongly affected by deuterium substitution.

EXPERIMENTAL

Saturated silver nitrate – ethylene glycol solution was prepared by stirring an excess of finely ground silver nitrate together with ethylene glycol at ~40° C, and decanting the supernatant liquid after the mixture had stood overnight at room temperature. Two column packings were made: (1) 17 ml of saturated solution mixed with 100 ml (39 g) 30/60 mesh firebrick (Johns-Manville Chromosorb P), and (2) 5 ml of saturated solution mixed with 100 ml of the same firebrick. After thorough mixing, both packings appeared dry and flowed easily. Packings (1) and (2) were loaded respectively into 16- to 48-ft lengths of 4 mm I.D. and 2.5 mm I.D. Pyrex tubing.

Samples (~1 μmole) were flushed onto the columns from a U-shaped bypass injector. Helium was used as carrier gas, and linear flows were 2–3 cm sec^{-1}. Detection was with a Gow-Mac thermal conductivity cell for the 4-mm columns, and with a flame ionization detector for the 2.5-mm columns. A 10:1 bypass system was inserted between the injection system and the column when the narrower columns were used, to reduce the effective injection time.

The deuterated olefins used were obtained as follows: ethylene-d_4 and *cis*-2-butene-d_8, kindly supplied by Dr. L. C. Leitch of these laboratories; *cis*- and *trans*-ethylene-d_2 and propylene-d_6, commercial samples from Merck, Sharp and Dohme, Ltd; *trans*-2-butene-d_8, produced by the mercury-photosensitized isomerization (5) of *cis*-2-butene-d_8; *cis*- and *trans*-2-pentene-d_8, 2-methyl-2-butene-d_8, and 3-methyl-1-butene-d_8, produced by the reaction of non-deuterated triplet methylene (6) with *cis*-2-butene-d_8.

RESULTS

Figure 1 shows the separation of propylene-d_0, propylene-d_6 and of ethylene-d_0, ethylene-d_2, ethylene-d_4 on a 40-ft, 2.5 mm I.D. silver nitrate – ethylene glycol – firebrick column (packing (2)) at −16° C. This column was most effective for this separation. Although the column performance did not depend critically on operating parameters, slight improvements in separation were observed upon lowering the column temperature.

[1]*Issued as N.R.C. No. 7403.*

[2]*National Research Council Postdoctoral Fellow 1961–1963.*

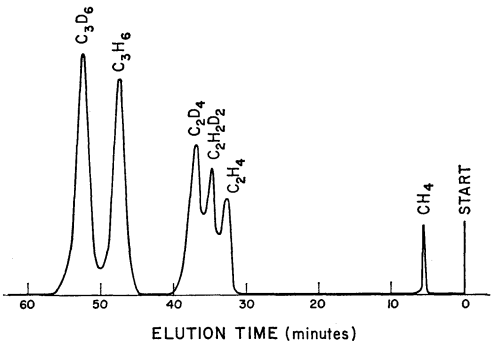

FIG. 1. Separation of ethylene and propylene isomers on a 40-ft silver nitrate – ethylene glycol column at −16° C.

For this reason, and because retention times were more convenient, most measurements were made below room temperature. Column efficiencies per unit length were similar for both types of columns used, and were not affected greatly by temperature change. Efficiencies increased markedly from ~50 theoretical plates per foot for short retention times (e.g. *trans*-2-butene, ethylene) to ~150 plates per foot for long retention times (e.g. *cis*-2-pentene). For a given retention time, the longer, more lightly loaded columns gave better peak resolution than shorter columns, with more stationary phase per gram of firebrick. The former are therefore recommended for analytical applications.

The adjusted retention times of deuterated olefins relative to their light isomers ($r_{H,L}$) are given for various temperatures in Table I. These values are independent of the column

TABLE I

Retention times for deuterated olefins, relative to their light isomers, at various temperatures

	−16±3° C	1±1° C	23±1° C	58±1° C
Ethylene-1,2-d_2	1.07_5	1.07		
Ethylene-d_4	1.15	1.14	1.11_5	1.09
Propylene-d_6	1.12	1.11	1.08	
trans-2-Butene-d_8	1.11	1.09		
cis-2-Butene-d_8	1.10	1.08		
2-Methyl-2-butene-d_8	1.10	1.07		
3-Methyl-1-butene-d_8	1.11	1.10		
trans-2-Pentene-d_8	1.10	1.08_5		
cis-2-Pentene-d_8	1.08	1.07		

used for their measurement. They show a slight increase with decreasing temperature, but the significance of this trend is questionable since the change is of the same order as the error in measurement.

DISCUSSION

Silver–olefin complexing provides a gas chromatographic technique of general applicability for the separation of olefin isomers differing only in the extent of deuterium (and no doubt tritium) substitution. The application is particularly interesting because it permits the separation of ethylene and propylene isomers which have not been resolved by partition methods. The increase in $r_{H,L}$ observed on going from 2-butene-d_8 to propylene-d_6 to ethylene-d_4 suggests that deuterium substitution at the double bond has the greatest effect. That the contributions from substitution elsewhere in the molecule are smaller but not negligible can be seen by a comparison of the $r_{H,L}$ values for 2-butene-d_8 and ethylene-d_2.

Can. J. Chem. Downloaded from www.nrcresearchpress.com by 210.87.254.6 on 09/05/12
For personal use only.

It is noteworthy that the isotope effect observed here is in the direction *opposite* to that for a conventional stationary phase in partition chromatography (1, 2). The isotope effects on the silver–olefin equilibrium complexing constant are still larger than those listed in Table I for the overall effect on relative retention times, since the partition coefficient of the olefin in ethylene glycol, which is probably lowered by deuterium substitution (2), affects the overall retention time (4).

Attempts to obtain greater resolution by preparing high-resolution capillary columns by coating polyethylene, nylon, or stainless steel narrow bore tubing with either saturated silver nitrate – ethylene glycol solution or silver nitrate – ethylene glycol solution diluted with water have so far been unsuccessful.

1. K. E. Wilzbach and P. Riesz. Science, **126**, 748 (1957).
2. W. E. Falconer and R. J. Cvetanović. Anal. Chem. **34**, 1064 (1962).
3. M. E. Bednas and D. S. Russell. Can. J. Chem. **36**, 1272 (1958).
4. M. A. Muhs and F. T. Weiss. J. Am. Chem. Soc. **84**, 4697 (1962).
5. R. J. Cvetanović, H. E. Gunning, and E. W. R. Steacie. J. Chem. Phys. **31**, 573 (1959).
6. F. J. Duncan and R. J. Cvetanović. J. Am. Chem. Soc. **84**, 3593 (1962).

Received March 1, 1963.
Division of Applied Chemistry,
National Research Council,
Ottawa, Canada.

Can. J. Chem. Downloaded from www.nrcresearchpress.com by 210.87.254.6 on 09/05/12
For personal use only.

1(7),4(8)-*p*-MENTHADIENE

B. M. Mitzner, E. T. Theimer, and S. Lemberg

1(7),4(8)-*p*-Menthadiene (I) has not been reported previously, neither as found in nature[1] nor as a synthetic compound.

We have observed that when gamma-terpinyl acetate (II) is pyrolyzed at 400° C, it eliminates acetic acid to form I and terpinolene (III), presumably by the usual concerted mechanism involving IV*a* and IV*b*.

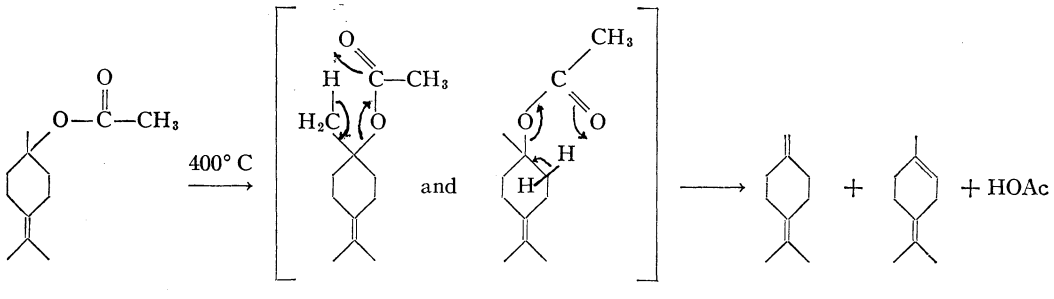

II IV*a* IV*b* I III

Nuclear magnetic resonance and infrared analyses support the structure of the 1(7),4(8)-*p*-menthadiene, I. The n.m.r. spectrum of I indicates the following (in tau values, tetramethylsilane, $\tau = 10.00$):

[1]*A terpene called crithmene has been obtained from Oil of Samphire, and assigned structure I (1). The same hydrocarbon was later isolated by other workers from French Oil of Samphire (2). Subsequently, a new hydrocarbon (called moslene) was isolated from the essential oil Mosla Japonica Maxim, and assigned structure I (3). It has been conclusively shown that crithmene and moslene are, in fact, gamma-terpinene (4).*

It is noteworthy that the isotope effect observed here is in the direction *opposite* to that for a conventional stationary phase in partition chromatography (1, 2). The isotope effects on the silver–olefin equilibrium complexing constant are still larger than those listed in Table I for the overall effect on relative retention times, since the partition coefficient of the olefin in ethylene glycol, which is probably lowered by deuterium substitution (2), affects the overall retention time (4).

Attempts to obtain greater resolution by preparing high-resolution capillary columns by coating polyethylene, nylon, or stainless steel narrow bore tubing with either saturated silver nitrate – ethylene glycol solution or silver nitrate – ethylene glycol solution diluted with water have so far been unsuccessful.

1. K. E. Wilzbach and P. Riesz. Science, **126**, 748 (1957).
2. W. E. Falconer and R. J. Cvetanović. Anal. Chem. **34**, 1064 (1962).
3. M. E. Bednas and D. S. Russell. Can. J. Chem. **36**, 1272 (1958).
4. M. A. Muhs and F. T. Weiss. J. Am. Chem. Soc. **84**, 4697 (1962).
5. R. J. Cvetanović, H. E. Gunning, and E. W. R. Steacie. J. Chem. Phys. **31**, 573 (1959).
6. F. J. Duncan and R. J. Cvetanović. J. Am. Chem. Soc. **84**, 3593 (1962).

Received March 1, 1963.
Division of Applied Chemistry,
National Research Council,
Ottawa, Canada.

Can. J. Chem. Downloaded from www.nrcresearchpress.com by 210.87.254.6 on 09/05/12
For personal use only.

1(7),4(8)-*p*-MENTHADIENE

B. M. Mitzner, E. T. Theimer, and S. Lemberg

1(7),4(8)-*p*-Menthadiene (I) has not been reported previously, neither as found in nature[1] nor as a synthetic compound.

We have observed that when gamma-terpinyl acetate (II) is pyrolyzed at 400° C, it eliminates acetic acid to form I and terpinolene (III), presumably by the usual concerted mechanism involving IV*a* and IV*b*.

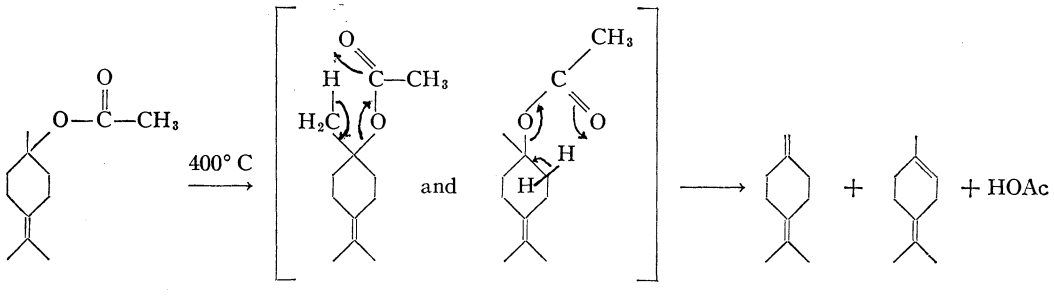

II IV*a* IV*b* I III

Nuclear magnetic resonance and infrared analyses support the structure of the 1(7),4(8)-*p*-menthadiene, I. The n.m.r. spectrum of I indicates the following (in tau values, tetramethylsilane, $\tau = 10.00$):

[1]*A terpene called crithmene has been obtained from Oil of Samphire, and assigned structure I (1). The same hydrocarbon was later isolated by other workers from French Oil of Samphire (2). Subsequently, a new hydrocarbon (called moslene) was isolated from the essential oil Mosla Japonica Maxim, and assigned structure I (3). It has been conclusively shown that crithmene and moslene are, in fact, gamma-terpinene (4).*

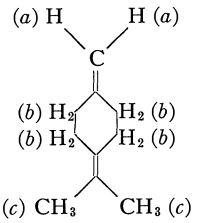

(*a*) τ = 5.41, singlet, 2 hydrogens
(*b*) τ = 7.82, allylic methylene, singlet, 8 hydrogens
(*c*) τ = 8.30, singlet, 6 hydrogens

The following are the pertinent n.m.r. signals of the compound: $\tau = 8.30$, $(CH_3)_2C{=}C$; 7.82, allylic methylene; 5.41, $>C{=}CH_2$. It is interesting to note that all the allylic methylenes give rise to one sharp signal at 7.82.

The infrared spectrum of the 1(7),4(8)-*p*-menthadiene is characterized by a strong absorption at 886 cm^{-1} due to the $>C{=}CH_2$ group; this absorption is also found in 1(7)-*p*-menthene.[2] A medium intensity band is present at 1237 cm^{-1} which we attribute to the $R_1R_1C{=}CR_2R_2$ configuration. The same absorption is present in 4(8)-*p*-menthene.[2] The absence of the *gem*-dimethyl split (ca. 1375 cm^{-1} and 1385 cm^{-1}), which is also absent in 4(8)-*p*-menthene, supports the proposed structure.

The terpinolene (III) was identical with that of authentic terpinolene isolated from a natural source[3] by the congruency of the n.m.r. and infrared spectra.

EXPERIMENTAL

Terpinyl acetate[4] is a mixture of alpha-, beta-, and gamma-terpinyl acetate. A vapor-phase chromatogram of this material (obtained on a 10 ft×1/4 in. O.D.×3/16 in. I.D. copper column packed with 20% Reoplex 400 on 60- to 80-mesh silane-treated celite at a column temperature of 140° C and an inlet pressure of 30 p.s.i. helium with a flow rate of 55 ml/min) yielded an excellent separation of the beta isomer and only a slight separation of the gamma isomer, actually appearing as a shoulder on the front of the alpha-terpinyl acetate peak. (If the alpha-terpinyl acetate can be considered to have a retention volume of 1.0, then the relative retention volume of beta-terpinyl acetate is 0.64 and that of gamma-terpinyl acetate is 0.95.) Therefore, the front side of the alpha-terpinyl acetate peak was trapped on a preparative unit to concentrate the gamma isomer. (The preparative unit contained a 1/2 in. O.D.×7/16 in. I.D. copper column 9 ft long and packed with 20% Reoplex 400 on 60- to 80-mesh silane-treated celite at 150° C. An inlet pressure of 20 p.s.i. helium was used and a flow of 175 ml/min was obtained.) Ten grams of material was obtained by means of 30 repeated trappings using 1-ml samples. The starting material contained 15% gamma- and 12% beta-terpinyl acetate. The first trapping contained approximately 35% of the gamma isomer and the beta isomer was completely eliminated. The 10 grams of material was retrapped, again using 1-ml samples, yielding 3 g of gamma-terpinyl acetate which was 65% pure. The structures of the alpha-terpinyl acetate and gamma-terpinyl acetate were confirmed by n.m.r. analysis.[5] This was then passed through a 1-ft×1/8 in. O.D.×2/32

[2]*The infrared spectra of 1(7)-p-menthene, 4(8)-p-menthene, and 1(7),4(8)-p-menthadiene have been reported (5).*

[3]*Sample of terpinolene from pure stump oil was generously supplied by the Hercules Chemical Co., Wilmington, Delaware.*

[4]*Prepared by the acetylation of commercial terpineol, a mixture of the alpha, beta, and gamma isomers.*

[5]*The proof of the structures of the gamma and alpha isomers is based primarily on n.m.r. analysis. Briefly, the assignments are made as follows: An olefinic ring proton appearing at τ = 4.68 p.p.m. is attributed to the alpha isomer. This signal is then correlated quantitatively with the acetoxy methyl group, τ = 8.07 p.p.m., of the gamma isomer; the acetoxy methyl group of the alpha isomer appears at slightly higher fields, τ = 8.12 p.p.m., thus making these measurements possible. Moreover, the ratio of the acetoxy methyl group signals corresponds to the ratio of the two peaks, gamma and alpha, obtained via v.p.c. measurements. The methyls on a double bond, τ = 8.38 p.p.m., are attributed to the methyls of the isopropylidene and the ring methyl on the double bond, but the chemical shifts here are identical and allow no distinction between the isomeric species. In view of the fact that a mixture is being analyzed, the authors are aware that the structures cannot be assigned unequivocally; however, the compounds resulting from the pyrolysis have been isolated pure and their structures established with certainty (which indirectly supports the structure of gamma-terpinyl acetate and of alpha-terpinyl acetate).*

Can. J. Chem. Downloaded from www.nrcresearchpress.com by 210.87.254.6 on 09/05/12
For personal use only.

in. I.D. stainless steel tube heated to 400° C, at a flow rate of approximately 1 ml/min, a small flow of nitrogen being used as the carrier. The pyrolyzate (2 g) was separated into its components on a preparative v.p.c. unit using a 3/8 in. O.D.×5/16 in. I.D. copper column packed with 20% Reoplex 400 on 60- to 80-mesh silane-treated celite at a temperature of 110° C and an inlet pressure of 20 p.s.i. helium with a flow rate of 90 ml/min. In this way, the 1(7),4(8)-*p*-menthadiene and terpinolene were easily separable; the former, which eluted first, was pure by v.p.c. analysis. Since the pyrolysis products of alpha-terpinyl acetate (which was present to the extent of 35% in the pyrolyzed material) are terpinolene and dipentene, it was not possible to obtain a quantitative ratio of the pyrolysis products of the gamma-terpinyl acetate.[6]

1. L. Francesconi and E. Sernagiotto. Gazz. Chim. Ital. **43**, 608 (1913).
2. M. Delepine and G. de Belsunce. Bull. Soc. Chim. France, **23**, 34 (1918).
3. Y. Murayama. J. Pharm. Soc. Japan, No. 475, 769 (1921).
4. F. Richter and W. Wolf. Chem. Ber. **60**, 477 (1927).
5. B. M. Mitzner and S. K. Freeman. Applied Spectry. To be published.

Received November 15, 1962.
Research Laboratories,
International Flavors & Fragrances Inc.,
Union Beach, N.J., U.S.A.

[6]*The pyrolyzate components elute in the following order in the gas chromatographic columns previously described: dipentene, 1(7),4(8)-p-menthadiene, followed by terpinolene. If dipentene is considered to have a retention volume of 1.0, then 1(7),4(8)-p-menthadiene has a relative retention volume of 1.20 and terpinolene has a relative retention volume of 1.55 when using a Reoplex 400 column.*

THE PHOTOLYSIS OF SOME α-SUBSTITUTED CYCLOHEXANONES[1]

H. G. Ferguson, P. de Mayo, F. L. M. Pattison, and T. Tabata

The photolysis of cyclohexanones in alcoholic solution to give, by cleavage, saturated esters is well known. It occurred to us that the cleavage of α-fluorocyclohexanones might provide a route to fluoro esters. To this end 2-fluoro-, 2-fluoro-4-methyl-, and 2-fluoro-3,5-dimethyl-cyclohexanone were prepared and photolyzed in methanol.

Vapor phase chromatography revealed that methyl 6-fluorohexanoate was indeed produced in the photolysis of 2-fluorocyclohexanone, but in insignificant yield. No trace of the 2-fluoro ester, available by another route in these laboratories, could be detected. An ester, presumably ω-substituted because of the ester carbonyl frequency (~1740 cm^{-1}), was similarly obtained in small yield from the 3,5- and 4-methyl derivatives.

The photolysis of 2-formyloxycyclohexanone was also investigated. In an inert solvent this could proceed, in principle, by ejection of the formyloxy group, or by a cyclic process involving γ-hydrogen (1, 2) abstraction. Since the latter would result in the formation of carbon dioxide, the two steps formylation and irradiation might have provided a useful procedure for the conversion of ketols to ketones. Irradiation of 2-formyloxycyclohexanone did give cyclohexanone, but in yields (up to 30%) inferior to those obtained by other methods available for the reduction of the ketol.

EXPERIMENTAL

The α-Fluorocyclohexanones (Method of Kissman, Small, and Weiss (3))

(*a*) A mixture of cyclohexanone (49.7 g) and diethyl oxalate (63 g) was added at 10° to a solution of sodium

[1]*This work was supported in part by a grant (No. 2020–29) from the Defence Research Board of Canada. We wish to thank Mr. F. H. Dean for help in preparing the α-fluorocyclohexanones.*

Can. J. Chem. Downloaded from www.nrcresearchpress.com by 210.87.254.6 on 09/05/12
For personal use only.

in. I.D. stainless steel tube heated to 400° C, at a flow rate of approximately 1 ml/min, a small flow of nitrogen being used as the carrier. The pyrolyzate (2 g) was separated into its components on a preparative v.p.c. unit using a 3/8 in. O.D.×5/16 in. I.D. copper column packed with 20% Reoplex 400 on 60- to 80-mesh silane-treated celite at a temperature of 110° C and an inlet pressure of 20 p.s.i. helium with a flow rate of 90 ml/min. In this way, the 1(7),4(8)-*p*-menthadiene and terpinolene were easily separable; the former, which eluted first, was pure by v.p.c. analysis. Since the pyrolysis products of alpha-terpinyl acetate (which was present to the extent of 35% in the pyrolyzed material) are terpinolene and dipentene, it was not possible to obtain a quantitative ratio of the pyrolysis products of the gamma-terpinyl acetate.[6]

1. L. Francesconi and E. Sernagiotto. Gazz. Chim. Ital. **43**, 608 (1913).
2. M. Delepine and G. de Belsunce. Bull. Soc. Chim. France, **23**, 34 (1918).
3. Y. Murayama. J. Pharm. Soc. Japan, No. 475, 769 (1921).
4. F. Richter and W. Wolf. Chem. Ber. **60**, 477 (1927).
5. B. M. Mitzner and S. K. Freeman. Applied Spectry. To be published.

Received November 15, 1962.
Research Laboratories,
International Flavors & Fragrances Inc.,
Union Beach, N.J., U.S.A.

[6]*The pyrolyzate components elute in the following order in the gas chromatographic columns previously described: dipentene, 1(7),4(8)-p-menthadiene, followed by terpinolene. If dipentene is considered to have a retention volume of 1.0, then 1(7),4(8)-p-menthadiene has a relative retention volume of 1.20 and terpinolene has a relative retention volume of 1.55 when using a Reoplex 400 column.*

THE PHOTOLYSIS OF SOME α-SUBSTITUTED CYCLOHEXANONES[1]

H. G. Ferguson, P. de Mayo, F. L. M. Pattison, and T. Tabata

The photolysis of cyclohexanones in alcoholic solution to give, by cleavage, saturated esters is well known. It occurred to us that the cleavage of α-fluorocyclohexanones might provide a route to fluoro esters. To this end 2-fluoro-, 2-fluoro-4-methyl-, and 2-fluoro-3,5-dimethyl-cyclohexanone were prepared and photolyzed in methanol.

Vapor phase chromatography revealed that methyl 6-fluorohexanoate was indeed produced in the photolysis of 2-fluorocyclohexanone, but in insignificant yield. No trace of the 2-fluoro ester, available by another route in these laboratories, could be detected. An ester, presumably ω-substituted because of the ester carbonyl frequency (~1740 cm^{-1}), was similarly obtained in small yield from the 3,5- and 4-methyl derivatives.

The photolysis of 2-formyloxycyclohexanone was also investigated. In an inert solvent this could proceed, in principle, by ejection of the formyloxy group, or by a cyclic process involving γ-hydrogen (1, 2) abstraction. Since the latter would result in the formation of carbon dioxide, the two steps formylation and irradiation might have provided a useful procedure for the conversion of ketols to ketones. Irradiation of 2-formyloxycyclohexanone did give cyclohexanone, but in yields (up to 30%) inferior to those obtained by other methods available for the reduction of the ketol.

EXPERIMENTAL

The α-Fluorocyclohexanones (Method of Kissman, Small, and Weiss (3))

(*a*) A mixture of cyclohexanone (49.7 g) and diethyl oxalate (63 g) was added at 10° to a solution of sodium

[1]*This work was supported in part by a grant (No. 2020–29) from the Defence Research Board of Canada. We wish to thank Mr. F. H. Dean for help in preparing the α-fluorocyclohexanones.*

Can. J. Chem. Downloaded from www.nrcresearchpress.com by 210.87.254.5 on 09/05/12
For personal use only.

ethoxide (from 11.5 g sodium) in absolute ethanol (150 ml). After 1 hour at this temperature and 6 hours at room temperature, dimethylformamide (100 ml) was added and the mixture cooled to 10°. After displacement of oxygen in the system by nitrogen, perchloryl fluoride (55 g) was bubbled in. After standing overnight at room temperature, the product was isolated, dissolved in aqueous ethanol (80%; 350 ml) containing potassium acetate (196 g), and refluxed for 4 hours. Isolation of the product in the usual way gave 2-fluorocyclohexanone, 7.2 g (12%), b.p. 71–72° at 13 mm, n_D^{25} 1.4422 (lit. (4): b.p. 83–83.5° at 20 mm, n_D^{25} 1.4432); 2,4-dinitrophenylhydrazone m.p. 138–141° (lit. (4): m.p. 139–140°).

(*b*) 2-Fluoro-3,5-dimethylcyclohexanone was prepared from the appropriate ketone by the above method. The final product was purified by V.P.C. on 12-ft diethylene glycol succinate columns and was obtained in 12% overall yield, b.p. 62–63° at 2.3 mm, n_D^{25} 1.4401, d_4^{20} 1.070. Calc. for $C_8H_{13}FO$: C, 66.63; H, 9.08. Found: C, 66.73; H, 8.95%. The 2,4-dinitrophenylhydrazone had m.p. 186–189°. Calc. for $C_{14}H_{17}FN_4O_4$: C, 51.85; H, 5.29; N, 17.28. Found: C, 52.02; H, 5.34; N, 17.41%.

(*c*) 2-Fluoro-4-methylcyclohexanone was obtained similarly in 12% yield, b.p. 75–76° at 5 mm, n_D^{25} 1.4386, d_4^{20} 1.054. Calc. for $C_7H_{11}FO$: C, 64.57; H, 8.52. Found: C, 64.64; H, 8.67%. The 2,4-dinitrophenylhydrazone had m.p. 135–139°. Calc. for $C_{13}H_{15}FN_4O_4$: C, 50.32; H, 4.87; N, 18.06. Found: C, 50.55; H, 5.15; N, 18.20%.

2-Formyloxycyclohexanone

To a solution of 2-hydroxycyclohexanone (5.04 g) in monoglyme (85 ml) and pyridine (30 ml) was added 8–9 ml formyl fluoride (5) and the mixture left at −70° for 40 hours and at 0° for 30 minutes. After filtration the product was isolated with ether in the usual way. The crude formate was filtered through a silica gel column and the material eluted with ether – light petroleum (1:9) and distilled to give the ester, b.p. 78° at 0.8 mm, n_D^{25} 1.4643, ν_{max} 1738, 1717 cm^{-1}. Calc. for $C_7H_{10}O_3$: C, 59.14; H, 7.09. Found: C, 59.11; H, 7.19%.

Irradiations

(a) 2-Fluorocyclohexanone

The ketone (5 g) in methanol (170 ml) was irradiated in a quartz immersion apparatus (6) with an 80-w medium-pressure lamp for 20 hours. The neutral material, isolated with ether, was distilled (12 mm). Analysis of the distillate on a 17% 3/8-in.×10-ft diethylene glycol succinate column on firebrick at 145° (He at 25 p.s.i.) revealed the presence of methyl 6-fluorohexanoate (retention time = 8.3 minutes). A portion was isolated by the same procedure and identified by comparison of retention time, infrared spectrum, and refractive index with an authentic specimen.

(b) 2-Fluoro-3,5-dimethylcyclohexanone

Irradiation of this ketone as described for 2-fluorocyclohexanone gave, on similar isolation, methyl 6-fluoro-3,5-dimethylhexanoate, n_D^{25} 1.4171, ν_{max} 1741, 1012 cm^{-1}. Calc. for $C_9H_{17}FO_2$: C, 61.34; H, 9.73. Found: C, 61.25; H, 9.82%. The FCH_2— group appeared as a pair of doublets centered at 250 c.p.s.* (from TMS) with $J_{HF} \sim 47$ and $J_{HH} \sim 7$ c.p.s.

(c) 2-Fluoro-4-methylcyclohexanone

Irradiation of this ketone and isolation as described above gave methyl 6-fluoro-4-methylhexanoate, n_D^{25} 1.4141, ν_{max} 1741, 996 cm^{-1}. Calc. for $C_8H_{15}FO_2$: C, 59.24; H, 9.32. Found: C, 59.53; H, 9.48%.

The Irradiation of 2-Formyloxycyclohexanone

A 0.5% solution of the ester in cyclohexane was placed in a vycor flask and irradiated with an 80-w medium-pressure mercury lamp for 5 hours. The yield of cyclohexanone was estimated by V.P.C. on a 20-ft 20% carbowax column by calibration with standard solutions. Isolation of a portion of the ketone and conversion to the 2,4-dinitrophenylhydrazone gave material identical in melting point and infrared spectrum with an authentic specimen; the mixed melting point gave no depression.

1. V. Brunet and W. A. Noyes. Bull. Soc. Chim. France, 21 (1958).
2. R. Srinivasan. J. Am. Chem. Soc. **84**, 2475 (1962).
3. H. M. Kissman, A. M. Small, and M. J. Weiss. J. Am. Chem. Soc. **82**, 2312 (1960).
4. S. Nakanishi, K-I. Morita, and E. V. Jensen. J. Am. Chem. Soc. **81**, 5259 (1959).
5. G. A. Olah and S. J. Kuhn. J. Am. Chem. Soc. **82**, 2380 (1960).
6. P. de Mayo. Advances in organic chemistry. Vol. 2. Interscience Pub. Co., 1960. p. 370.

Received April 8, 1963.
Department of Chemistry,
University of Western Ontario,
London, Ontario.

*In CCl_4 using a Varian DP-60 spectrometer. The authors wish to thank Mr. R. E. Klinck for this determination.

Can. J. Chem. Downloaded from www.nrcresearchpress.com by 210.87.254.5 on 09/05/12
For personal use only.

DERIVATIVES OF MONOGERMANE
PART III. INFRARED SPECTRA OF THREE DIHALOGERMANES

T. N. Srivastava,* J. E. Griffiths,† and M. Onyszchuk

In an earlier publication (1) we reported the vibration–rotation spectra of germyl fluoride and bromide. The infrared spectra of dihalogermanes have not yet been described, although there is much information about the spectra of dihalosilanes (2–4) and dihalomethanes (5). We now report the infrared spectra of difluoro-, dichloro-, and dibromogermane in the 4000–650 cm^{-1} range and compare them with those of the corresponding dihalosilanes.

EXPERIMENTAL

Difluoro-, dichloro- and dibromo-germane were obtained in low yield (10–20%) as by-products in the preparation of the corresponding monohalogermanes (6–8). Crude samples were purified by fractional distillation in vacuum until tensimetrically pure. Vapor pressures (v.p.) and molecular weights (M) were: (i) for GeH_2F_2: v.p. 18.6 mm at 0°, M 112.8 (calc. 112.6); (ii) for GeH_2Cl_2: v.p. 29.0 mm at 0°, M 146.0 (calc. 145.6); (iii) for GeH_2Br_2: v.p. 6.2 mm at 0°, M 233.5 (calc. 234.4). An attempt to prepare diiodogermane was unsuccessful because the compound appears to be too unstable at room temperature to be isolated in the pure form (7).‡

Spectra (Fig. 1) were recorded in the range 4000–650 cm^{-1} by a Perkin–Elmer Model 21 spectrometer

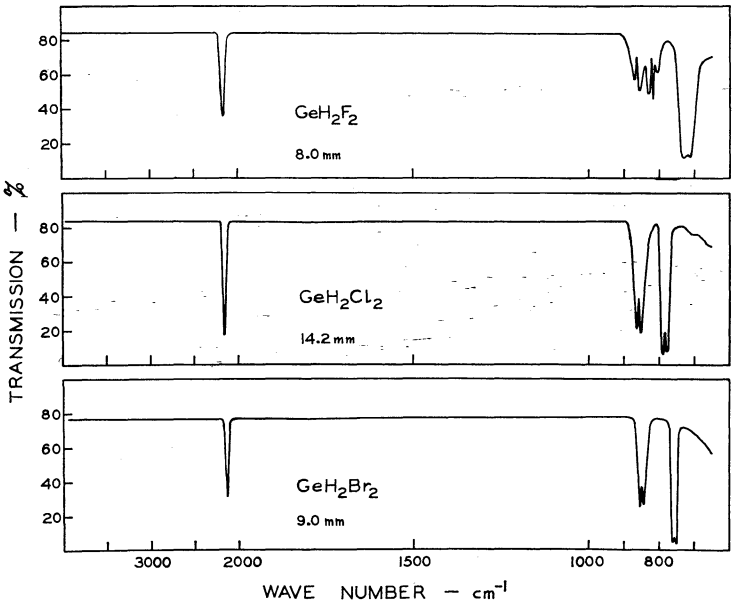

Fig. 1. Vapor-phase infrared spectra of difluoro-, dichloro-, and dibromo-germane.

equipped with a sodium chloride prism. The instrument was calibrated using water vapor and polystyrene. Measurements were made on compounds in the gas phase in a glass cell of 10-cm length and 5-cm diameter

Holder of an N.R.C. Postdoctoral Research Fellowship at McGill University, 1959–1961; on leave from the Department of Chemistry, University of Lucknow, Lucknow, India.

†Holder of N.R.C. Studentships, 1956–1958. Present address: Bell Telephone Laboratories, Incorporated, Murray Hill, N.J., U.S.A.

‡S. Sujishi has claimed the preparation of mono- and di-iodogermane (Abstracts of the XVIIth International Congress of Pure and Applied Chemistry, Munich. 1959. p. 53); the details of this work have not yet been published.

Can. J. Chem. Downloaded from www.nrcresearchpress.com by 210.87.254.42 on 09/05/12
For personal use only.

with 5 mm thick sodium chloride end-plates. The frequency assignments given in Table I are based on those previously reported for dihalosilanes (2–4). The wave numbers reported are accurate to ± 3 cm^{-1} in the range 2000–650 cm^{-1}, and to ± 10 cm^{-1} above 2000 cm^{-1}.

TABLE I

Infrared vibration frequencies (cm^{-1}) of dihalogermanes

GeH_2F_2	GeH_2Cl_2	GeH_2Br_2	Assignment
2175, s	2150, s	2130, s	$\nu_1(a_1)$ GeH_2 stretching
2175, s	2150, s	2130, s	$\nu_6(b_1)$ GeH_2 stretching
870, *R*, m	862, *R*, s	853, *R*, s	
(863), *Q*, m	(856), *Q*	(848), *Q*	$\nu_2(a_1)$ GeH_2 bending
855, *P*, m	850, *P*, s	844, *P*, s	
828, *R*, m	788, *R*, s	760, *R*, s	
815, *Q*, m	(780), *Q*	(756), *Q*	$\nu_8(b_2)$ GeH_2 wagging
805, *P*, m	773, *P*, s	752, *P*, s	
730, *R*, s			
(722), *Q*	—	—	$\nu_9(b_2)$ GeF_2 stretching
714, *P*, s			

NOTE: s = strong; m = medium.

DISCUSSION

Dihalogermanes, like dihalosilanes, belong to the symmetry group C_{2v} and hence should have nine fundamental vibrations including the torsional mode $\nu_5(a_2)$ which is forbidden in the infrared. The GeH_2 stretching vibrations, $\nu_1(a_1)$ and $\nu_6(b_1)$, are unresolved and located between 2130 and 2175 cm^{-1}. There is a gradual shift toward lower frequencies as the mass of the halogen atom increases.

The GeH_2 bending vibration, $\nu_2(a_1)$, occurs as a strong doublet in dichloro- and dibromogermane, about 90 cm^{-1} lower than the similar doublet observed in the corresponding dihalosilanes. The GeH_2 wagging vibration, $\nu_8(b_2)$, is also found as a strong doublet in GeH_2Cl_2 and GeH_2Br_2, again about 90 cm^{-1} below those in the analogous silicon compounds.

In difluorogermane the GeH_2 bending and wagging modes give five peaks of moderate intensity. These peaks may be attributed to the *P*, *Q*, and *R* branches of $\nu_2(a_1)$ and $\nu_8(b_2)$, with the *P* branch of the former overlapping slightly with the *R* branch of the latter, giving increased intensity to the bands at 855 and 828 cm^{-1}. The strong doublet centered at 722 cm^{-1} is assigned to the GeF_2 antisymmetric stretching vibration $\nu_9(b_2)$. The $GeCl_2$ and $GeBr_2$ antisymmetric stretching frequencies occurred below 650 cm^{-1}, which is the limit of spectrometer, and hence were not observed. The remaining vibrations $\nu_7(b_1)$, $\nu_3(a_1)$, and $\nu_4(a_1)$ also occurred below 650 cm^{-1}.

ACKNOWLEDGMENT

We are grateful to the National Research Council for financial assistance.

1. T. N. SRIVASTAVA, J. E. GRIFFITHS, and M. ONYSZCHUK. Can. J. Chem. **40**, 579 (1962).
2. J. A. HAWKINS and M. K. WILSON. J. Chem. Phys. **21**, 360 (1953).
3. J. A. HAWKINS, S. R. POLO, and M. K. WILSON. J. Chem. Phys. **21**, 1122 (1953).
4. D. W. MAYO, H. E. OPITZ, and J. S. PEAKE. J. Chem. Phys. **23**, 1344 (1955).
5. G. HERZBERG. Infrared and Raman spectra of polyatomic molecules. D. Van Nostrand Co., Inc., Princeton, N.J. 1945. p. 322.

Can. J. Chem. Downloaded from www.nrcresearchpress.com by 210.87.254.42 on 09/05/12
For personal use only.

6. T. N. Srivastava and M. Onyszchuk. Proc. Chem. Soc. 205 (1961).
7. L. M. Dennis and P. R. Judy. J. Am. Chem. Soc. **51**, 2321 (1929).
8. T. N. Srivastava, J. E. Griffiths, and M. Onyszchuk. Can. J. Chem. **40**, 739 (1962).

Received February 26, 1963.
Inorganic Chemistry Laboratory,
McGill University,
Montreal, Que.

Can. J. Chem. Downloaded from www.nrcresearchpress.com by 210.87.254.42 on 09/05/12
For personal use only.

ACID-CATALYZED REACTIONS OF VINYL COMPOUNDS
PART II. PRODUCTS OF THE REACTION OF VINYL ACETATE AND BENZENE

J. M. Pepper and B. P. Robinson

In Part I (1) of this series, preliminary studies were reported on the nature of the aluminum chloride catalyzed reaction of vinyl acetate and benzene. A more thorough investigation of the products of this reaction, using the molar ratio 3:1:10 respectively, has revealed that, in addition to the compounds reported previously (acetophenone, *p*-ethylacetophenone, 1,1-diphenylethane, and 9,10-dimethylanthracene), ethylbenzene, *o*-ethylacetophenone, 2,4- and 3,4-diethylacetophenone, and 1,1-diphenylethene were also produced. They have been isolated and characterized. Except for 9,10-dimethylanthracene, which was isolated and weighed (1), the yield of each product was determined by gas–liquid chromatographic analysis. These data are given in Table I.

TABLE I

Products from benzene – vinyl acetate reaction*

Compound	Yield		
	Run 1, g	Run 2, g	Percent (average)
Ethylbenzene	0.09	0.10	0.85†
Acetophenone	3.09	3.03	25.5†
o-Ethylacetophenone	0.25	0.26	1.75†
p-Ethylacetophenone	3.92	3.70	25.8†
2,4-Diethylacetophenone	0.45	0.49	5.6‡
3,4-Diethylacetophenone	Trace	Trace	
1,1-Diphenylethane	0.18	0.12	0.85†
1,1-Diphenylethene	0.47	0.59	2.95†
9,10-Dimethylanthracene	3.24	3.08	30.7‡

*Vinyl acetate (0.1 mole), benzene (1 mole), and aluminum chloride (0.3 mole).
†Assuming that 1 mole of vinyl acetate is required to produce 1 mole of product.
‡Assuming that 2 moles of vinyl acetate are required to produce 1 mole of product.

The characterization of the products, other than 9,10-dimethylanthracene, was effected as follows. The crude reaction product was distilled and the fraction boiling at 90–140° at 12 mm was collected. This distillate was separated into its components by gas–liquid chromatography, using a Beckman No. 17 449 silicone column (6 ft) at a column temperature of 220° and with a helium flow rate of 56 ml/min. By repeated injections (100-μl sample) and collections a sufficient sample of each of six of the products was obtained. These separate samples were again distilled and analyzed. The analytical data are shown in Table II.

6. T. N. Srivastava and M. Onyszchuk. Proc. Chem. Soc. 205 (1961).
7. L. M. Dennis and P. R. Judy. J. Am. Chem. Soc. **51**, 2321 (1929).
8. T. N. Srivastava, J. E. Griffiths, and M. Onyszchuk. Can. J. Chem. **40**, 739 (1962).

Received February 26, 1963.
Inorganic Chemistry Laboratory,
McGill University,
Montreal, Que.

Can. J. Chem. Downloaded from www.nrcresearchpress.com by 210.87.254.5 on 09/05/12
For personal use only.

ACID-CATALYZED REACTIONS OF VINYL COMPOUNDS
PART II. PRODUCTS OF THE REACTION OF VINYL ACETATE AND BENZENE

J. M. Pepper and B. P. Robinson

In Part I (1) of this series, preliminary studies were reported on the nature of the aluminum chloride catalyzed reaction of vinyl acetate and benzene. A more thorough investigation of the products of this reaction, using the molar ratio 3:1:10 respectively, has revealed that, in addition to the compounds reported previously (acetophenone, *p*-ethylacetophenone, 1,1-diphenylethane, and 9,10-dimethylanthracene), ethylbenzene, *o*-ethylacetophenone, 2,4- and 3,4-diethylacetophenone, and 1,1-diphenylethene were also produced. They have been isolated and characterized. Except for 9,10-dimethylanthracene, which was isolated and weighed (1), the yield of each product was determined by gas–liquid chromatographic analysis. These data are given in Table I.

TABLE I

Products from benzene – vinyl acetate reaction*

Compound	Yield		
	Run 1, g	Run 2, g	Percent (average)
Ethylbenzene	0.09	0.10	0.85†
Acetophenone	3.09	3.03	25.5†
o-Ethylacetophenone	0.25	0.26	1.75†
p-Ethylacetophenone	3.92	3.70	25.8†
2,4-Diethylacetophenone	0.45	0.49	5.6‡
3,4-Diethylacetophenone	Trace	Trace	
1,1-Diphenylethane	0.18	0.12	0.85†
1,1-Diphenylethene	0.47	0.59	2.95†
9,10-Dimethylanthracene	3.24	3.08	30.7‡

*Vinyl acetate (0.1 mole), benzene (1 mole), and aluminum chloride (0.3 mole).
†Assuming that 1 mole of vinyl acetate is required to produce 1 mole of product.
‡Assuming that 2 moles of vinyl acetate are required to produce 1 mole of product.

The characterization of the products, other than 9,10-dimethylanthracene, was effected as follows. The crude reaction product was distilled and the fraction boiling at 90–140° at 12 mm was collected. This distillate was separated into its components by gas–liquid chromatography, using a Beckman No. 17 449 silicone column (6 ft) at a column temperature of 220° and with a helium flow rate of 56 ml/min. By repeated injections (100-μl sample) and collections a sufficient sample of each of six of the products was obtained. These separate samples were again distilled and analyzed. The analytical data are shown in Table II.

TABLE II

Analytical data of products from benzene – vinyl acetate reaction*

Compound	Retention time, min	B.p., °C	Found C, %	Found H, %	Found Mol. wt.	Calculated	Calculated C, %	Calculated H, %	Calculated Mol. wt.
1	6	88, 13 mm	79.44	7.12		For C_8H_8O:	79.97	6.71	
2	9.3	100, 10 mm	80.63	8.31	150	For $C_{10}H_{12}O$:	81.04	8.16	148
3	13	120, 12 mm	80.86	7.77		For $C_{10}H_{12}O$:	81.04	8.16	
4	17.6	114, 13 mm	82.08	9.29		For $C_{12}H_{16}O$:	81.77	9.15	
4A	25								
5	27	140–144, 15 mm	92.08	7.89	185	For $C_{14}H_{14}$:	92.26	7.74	182
6	29.6	146–148, 15 mm	93.13	7.08	184	For $C_{14}H_{12}$:	93.29	6.71	180

*The compounds are numbered as they were in Table II, Part I of this series (1).

Compounds 1 and 3 had already been shown to be acetophenone and *p*-ethylacetophenone respectively (1). Compound 2 ($C_{10}H_{12}O$) gave a positive iodoform test and its infrared spectrum indicated that it was an ortho-substituted aromatic ketone. The preparation of *o*-ethylacetophenone from *o*-ethylaniline by the Beech reaction (2) and its proved identity with compound 2 confirmed the structure of compound 2.

The analysis ($C_{12}H_{16}O$) of compound 4 indicated that this compound was a diethylacetophenone. Oxidation by alkaline potassium permanganate gave an acid, m.p. 213–215°, which, by comparison with the three benzenetricarboxylic acids (obtained by the alkaline permanganate oxidation of the corresponding trimethylbenzenes), was shown to be identical with benzene-1,2,4-tricarboxylic acid. To distinguish whether compound 4 was the 2,4-, 3,4- or 2,5-diethylacetophenone, these compounds were synthesized by the Friedel–Crafts acylation reaction from *o*-, *m*-, and *p*-diethylbenzene respectively. The structure of each of these ketones was confirmed by its oxidation to the previously prepared benzene-1,2,4-tricarboxylic acid. By direct comparison, compound 4 was shown to be identical with the previously unreported 2,4-diethylacetophenone. Similarly, by a comparison of gas chromatographic retention times and infrared spectra, compound 4A was shown to be 3,4-diethylacetophenone.

Compounds 5 and 6, although previously reported (1) as constituents of the carbonyl-containing fraction, have now been shown to be hydrocarbons. By a comparison of retention times and infrared spectra, compound 5 ($C_{14}H_{14}$) was shown to be identical with an authentic sample of 1,1-diphenylethane, and compound 6 ($C_{14}H_{12}$) was shown to be identical with 1,1-diphenylethene.

The ethylbenzene reported, in Table I, as a product of the benzene – vinyl acetate reaction was detected only by the gas chromatographic study of the crude reaction product. Its identity was indicated by a comparison of its retention times with those of authentic ethylbenzene when measured under a variety of chromatographic conditions as shown in Table III.

This note describes the isolation and characterization of five compounds, namely: ethylbenzene, *o*-ethylacetophenone, 2,4- and 3,4-diethylacetophenone, and 1,1-diphenylethene, which had not been reported previously as products of the aluminum chloride interaction of benzene and vinyl acetate. The significance of the relative abundance of these and the other reported reaction products, as well as a discussion of the mechanism of their formation, will be the subject of a subsequent publication.

Can. J. Chem. Downloaded from www.nrcresearchpress.com by 210.87.254.5 on 09/05/12
For personal use only.

TABLE III

Gas–liquid chromatographic identification of ethylbenzene

Column	Temperature, °C		Helium, ml/min	Retention time, min	
	Injector	Detector		Reaction product	Authentic sample
Beckman silicone (No. 17449), 6 ft	250	235	42.5	2.1	2.1
	170	150	58.4	7.4	7.4
10% Apiezon L on Chromosorb (80–100 mesh), 6 ft	155	150	53.1	2.4	2.4
	105	90	66.7	7.7	7.7

EXPERIMENTAL

Melting points are uncorrected. The infrared spectra were measured using a Perkin–Elmer Model 21 instrument with sodium chloride optics. Gas–liquid chromatography was effected using a Beckman GC-2 chromatograph, with a thermal conductivity detector unit, and which had been modified by placing the injection system as close as possible to one end of the column and by making it more comparable electronically to the GC-2A.

Reaction of Vinyl Acetate and Benzene

To obtain the data recorded in Table I the following procedure was followed. Vinyl acetate (8.6 g, 0.1 mole) was added slowly over a period of 1 hour to a well-stirred mixture of benzene (78 g, 1.0 mole) and sublimed, anhydrous aluminum chloride (40 g, 0.3 mole) in a 200-ml 3-necked flask equipped with reflux condenser, dropping funnel, and mechanical stirrer. Both the condenser and dropping funnel were fitted with calcium chloride drying tubes. Throughout the addition, the flask was cooled in an ice bath, but after the addition was complete, the reaction mixture was refluxed for 3 hours. The complex was decomposed by its addition to a mixture of concentrated hydrochloric acid (75 ml) and crushed ice (75 g). The aqueous layer was extracted with benzene (3×25 ml), the benzene extract dried over anhydrous sodium carbonate, and the excess solvent removed to leave a brownish orange oil which crystallized on cooling. The yellow precipitate, after filtering and washing with methanol (10 ml), was dried, weighed, and recorded as 9,10-dimethylanthracene, m.p. 179–181° (reported 180–181° (3)). The filtrate and the methanol wash were combined and diluted to 25 ml with methanol. By gas–liquid chromatography, using a Beckman No. 17449 silicone column (6 ft), with a column temperature of 230° and a helium flow of 40 ml/min, and comparison of the peak areas with standard curves previously prepared from authentic samples, the abundance of each product was obtained.

To obtain the analytical samples on which the data recorded in Table II were found, a similar reaction procedure was followed with the exception that the crude reaction product, obtained from the benzene extract, was distilled and the fraction b.p. 90–140 at 12 mm was collected. From this fraction the samples of the compounds 2, 3, 4, 4A, 5, and 6 that are reported in Table II were obtained by gas–liquid chromatography.

Synthesis of Reference Compounds

o-Ethylacetophenone.—The procedure used was similar to that described by Beech (2) for the synthesis of *p*-chloroacetophenone. Condensation of the diazonium salt obtained from *o*-ethylaniline (22.0 g) with acetaldoxime (16.5 g) and subsequent hydrolysis gave *o*-ethylacetophenone (2.45 g, 9.1%), b.p. 100° at 10 mm (reported 99–103° at 13 mm (4)). Reduction using the Wolff–Kishner method (Huang–Minlon modification) gave a hydrocarbon which was identical with an authentic sample of *o*-diethylbenzene.

2,4-, 3,4-, and 2,5-Diethylacetophenones.—Into a 15-ml, three-necked flask equipped with a mechanical stirrer and with a condenser and dropping funnel each fitted with a calcium chloride guard tube was placed light petroleum (b.p. 37–49°) (5 ml) and anhydrous aluminum chloride (1.80 g, 0.0135 mole). After cooling in an ice bath, a mixture of the appropriate diethylbenzene (1.74 g, 0.013 mole) and acetyl chloride (1.10 g, 0.014 mole) was added over a period of 1 hour while the mixture was stirred vigorously. After standing overnight, this reaction mixture was added to crushed ice (10 g) and concentrated hydrochloric acid (2 ml). The required ketones were recovered from the organic phase and by ether extraction of the aqueous phase. In each case, distillation of the product, b.p. ca. 240° at 720 mm (reported for 2,5-diethylacetophenone 246–247° at 769 mm (5)), gave a colorless oil. The resulting 2,4-diethylacetophenone was found to be chromatographically pure. The 2,5- and 3,4-isomers were about 97% pure and were purified by gas–liquid chromatography followed by distillation. Calc. for $C_{12}H_{16}O$: C, 81.77; H, 9.15%. Found: for 2,4-diethylacetophenone, C, 81.88; H, 9.47%; for 3,4-diethylacetophenone, C, 81.33; H, 9.23%; and for 2,5-diethylacetophenone, C, 81.22; H, 9.66%. In two earlier reports the preparation of 3,4-diethylacetophenone had been indicated (6, 7) but few details were given.

Can. J. Chem. Downloaded from www.nrcresearchpress.com by 210.87.254.5 on 09/05/12
For personal use only.

1,1-Diphenylethane.—To a solution of 1,1-diphenylethene (5.4 g) in absolute ethanol (70 ml), sodium (5 g) was added in small portions. The resulting solution was poured into water (100 ml) and thoroughly extracted with benzene. This extract was dried over anhydrous sodium sulphate, and concentrated to a yellow liquid residue (6.1 g). Distillation of this product yielded 1,1-diphenylethane (4.1 g, 83%), b.p. 144–147° at 15 mm (reported 136–137° at 11 mm (8)). This product was chromatographically pure.

ACKNOWLEDGMENTS

Grateful acknowledgment is made of the financial assistance provided by Imperial Oil Limited. The authors wish to thank both the University of Saskatchewan and Canadian Industries Limited for the award to one of them (B. P. R.) of a Graduate Assistantship (1961–1962) and a Fellowship (1962–1963) respectively. The molecular weights were determined by Mr. E. Mazurek, National Research Council, Saskatoon.

1. J. M. Pepper, B. P. Robinson, and G. W. Schwanbeck. Can. J. Chem. **40**, 122 (1962).
2. W. F. Beech. J. Chem. Soc. 1297 (1954).
3. R. B. Sandin and R. Kitchen. J. Am. Chem. Soc. **67**, 1305 (1945).
4. B. van Zanten and W. Th. Nauta. Rec. Trav. Chim. **79**, 1211 (1960).
5. A. Klages and R. Keil. Ber. **36**, 1633 (1903).
6. I. G. Farbenind. A.-G. Ger. Patent No. 637,384 (October 29, 1936).
7. G. Baddeley. J. Chem. Soc. S229 (1949).
8. H. Gilman and B. J. Gaj. J. Am. Chem. Soc. **82**, 6326 (1960).

Received March 25, 1963.
Department of Chemistry,
University of Saskatchewan,
Saskatoon, Saskatchewan.

THE ELECTRON SPIN RESONANCE SPECTRA OF GAMMA-IRRADIATED THIOSULPHATE

R. L. Eager and D. S. Mahadevappa

In a study of the effect of Co^{60} γ rays on various alkali thiosulphates the electron spin resonance (e.s.r.) spectra of the irradiated salts has been obtained.

Reagent grade $Na_2S_2O_3.5H_2O$ was used without further purification. Crystalline anhydrous $Na_2S_2O_3$ was obtained by evaporating to dryness at 80° C (1) a saturated solution of sodium thiosulphate pentahydrate. The potassium salt $3K_2S_2O_3.5H_2O$ was obtained by dissolving the C.P. grade reagent in water followed by repeated recrystallizations from a hot solution. All three of the salts were microcrystalline.

The irradiation source was a "Gamma Cell 220 Co^{60} Irradiation Unit" manufactured by Atomic Energy of Canada Ltd. The unit provides a dose rate of 10^5 r/hr.

The e.s.r. spectra were obtained with a Varian 4500 spectrometer. Magnetic field modulation of 200 c/s was used. The magnetic field survey in the region of $g = 2.00$ was calibrated by obtaining spectra of the semiquinone ion. The g values were determined by calibration of the spectra with signals from microcrystalline diphenylpicrylhydrazyl (D.P.P.H.) included with each sample. Electron spin concentrations were measured by graphical double integrations of the recorded spectra and comparison, through a substandard of gamma-irradiated barium dichloracetate, with solutions of D.P.P.H. in benzene.

Most of the spectra were obtained with the samples at room temperature and are free of power-saturation effects. A few spectra of the three salts were also obtained at liquid nitrogen temperature. At this temperature the samples could readily be power saturated.

Can. J. Chem. Downloaded from www.nrcresearchpress.com by 210.87.254.5 on 09/05/12
For personal use only.

1,1-Diphenylethane.—To a solution of 1,1-diphenylethene (5.4 g) in absolute ethanol (70 ml), sodium (5 g) was added in small portions. The resulting solution was poured into water (100 ml) and thoroughly extracted with benzene. This extract was dried over anhydrous sodium sulphate, and concentrated to a yellow liquid residue (6.1 g). Distillation of this product yielded 1,1-diphenylethane (4.1 g, 83%), b.p. 144–147° at 15 mm (reported 136–137° at 11 mm (8)). This product was chromatographically pure.

ACKNOWLEDGMENTS

Grateful acknowledgment is made of the financial assistance provided by Imperial Oil Limited. The authors wish to thank both the University of Saskatchewan and Canadian Industries Limited for the award to one of them (B. P. R.) of a Graduate Assistantship (1961–1962) and a Fellowship (1962–1963) respectively. The molecular weights were determined by Mr. E. Mazurek, National Research Council, Saskatoon.

1. J. M. Pepper, B. P. Robinson, and G. W. Schwanbeck. Can. J. Chem. **40**, 122 (1962).
2. W. F. Beech. J. Chem. Soc. 1297 (1954).
3. R. B. Sandin and R. Kitchen. J. Am. Chem. Soc. **67**, 1305 (1945).
4. B. van Zanten and W. Th. Nauta. Rec. Trav. Chim. **79**, 1211 (1960).
5. A. Klages and R. Keil. Ber. **36**, 1633 (1903).
6. I. G. Farbenind. A.-G. Ger. Patent No. 637,384 (October 29, 1936).
7. G. Baddeley. J. Chem. Soc. S229 (1949).
8. H. Gilman and B. J. Gaj. J. Am. Chem. Soc. **82**, 6326 (1960).

Received March 25, 1963.
Department of Chemistry,
University of Saskatchewan,
Saskatoon, Saskatchewan.

Can. J. Chem. Downloaded from www.nrcresearchpress.com by 210.87.254.40 on 09/05/12
For personal use only.

THE ELECTRON SPIN RESONANCE SPECTRA OF GAMMA-IRRADIATED THIOSULPHATE

R. L. Eager and D. S. Mahadevappa

In a study of the effect of Co^{60} γ rays on various alkali thiosulphates the electron spin resonance (e.s.r.) spectra of the irradiated salts has been obtained.

Reagent grade $Na_2S_2O_3.5H_2O$ was used without further purification. Crystalline anhydrous $Na_2S_2O_3$ was obtained by evaporating to dryness at 80° C (1) a saturated solution of sodium thiosulphate pentahydrate. The potassium salt $3K_2S_2O_3.5H_2O$ was obtained by dissolving the C.P. grade reagent in water followed by repeated recrystallizations from a hot solution. All three of the salts were microcrystalline.

The irradiation source was a "Gamma Cell 220 Co^{60} Irradiation Unit" manufactured by Atomic Energy of Canada Ltd. The unit provides a dose rate of 10^5 r/hr.

The e.s.r. spectra were obtained with a Varian 4500 spectrometer. Magnetic field modulation of 200 c/s was used. The magnetic field survey in the region of $g = 2.00$ was calibrated by obtaining spectra of the semiquinone ion. The g values were determined by calibration of the spectra with signals from microcrystalline diphenylpicrylhydrazyl (D.P.P.H.) included with each sample. Electron spin concentrations were measured by graphical double integrations of the recorded spectra and comparison, through a substandard of gamma-irradiated barium dichloracetate, with solutions of D.P.P.H. in benzene.

Most of the spectra were obtained with the samples at room temperature and are free of power-saturation effects. A few spectra of the three salts were also obtained at liquid nitrogen temperature. At this temperature the samples could readily be power saturated.

The e.s.r. spectra (the first derivative of the absorption curve) for the three irradiated salts are shown in Fig. 1. The vertical line shown in each of these spectra indicates the

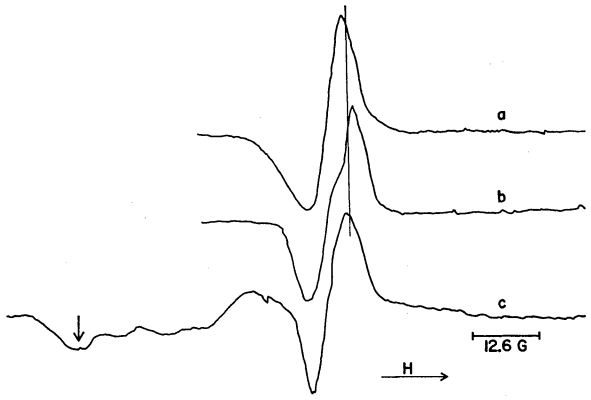

FIG. 1. Electron spin resonance spectra for samples at room temperature: (*a*) $Na_2S_2O_3.5H_2O$; (*b*) $3K_2S_2O_3.5H_2O$; (*c*) $Na_2S_2O_3$ anhydrous. The vertical line indicates the position of the D.P.P.H. spectrum. The vertical arrow is at a *g* value of 2.032. The magnetic field increases from left to right.

position of the D.P.P.H. spectrum. The magnetic field increases from left to right. The spectra for each of the salts appears to be essentially a single absorption line, except for anhydrous $Na_2S_2O_3$, where there is in addition a low-field structure. No hyperfine splitting was observed. The results for the three salts after they had been irradiated for 144 hours are given in Table I. The results are from spectra of samples which were at room tempera-

TABLE I

Electron spin resonance spectra of microcrystalline thiosulphates

Compound	Absorbed dose $\times 10^{-20}$ (ev/g)	Number of spins per gram $\times 10^{-17}$	*g* value	Line width* (gauss)
$Na_2S_2O_3$	5.94	5.9	2.006	6.6
$Na_2S_2O_3.5H_2O$	6.96	5.1	2.005	8.8
$3K_2S_2O_3.5H_2O$	6.54	4.0	2.005	9.1

*The width between the points of maximum slope, taken from the first derivative plots of the e.s.r. spectra.

ture. The electron spin concentrations were found to increase at first with an increase in absorbed dose but became almost constant for higher doses. The results shown in Table I are from samples with nearly the maximum electron spin concentrations.

The above results by themselves are not sufficient to enable an identification of the species responsible for the spectra. Gardner and Fraenkel (2) made the tentative suggestion that polyatomic free radicals in which the odd electron is primarily associated with a sulphur atom would be expected to have a *g* value of about 2.02. However, if the odd electron is in a sulphur-containing compound and is not primarily localized on a sulphur atom, the *g* value would normally be closer to the free-spin value of 2.0023. The *g* values recorded in Table I would suggest that the odd electron is not primarily on a sulphur atom.

The presence of sulphite free-radical ions, SO_3^-, in the irradiated salts would account for the products obtained when the irradiated salts are dissolved in water. Chantry *et al.* (3) have reported on the optical and e.s.r. spectra of γ-irradiated single crystals of sodium dithionate, sulphamic acid, potassium sulphamate, potassium amine sulphonate, and

Can. J. Chem. Downloaded from www.nrcresearchpress.com by 210.87.254.40 on 09/05/12
For personal use only.

potassium methane disulphonate. The e.s.r. spectra are similar for all these compounds, consisting of a single absorption line with a g value of 2.004. The authors (3) present evidence indicating that the e.s.r. spectra are due to the presence of sulphite free-radical ions. The g values found in the present work are significantly higher than the value of 2.004 reported by Chantry *et al.* Hence it would appear that if the interpretation of these authors is correct the spectra obtained in the present work are not due to sulphite free-radical ions.

Clark *et al.* (4) suggested that the SO_2^- free-radical ion was responsible for the e.s.r. spectra obtained by them from X-irradiated sodium and potassium dithionites. The spectra obtained in the present work for γ-irradiated thiosulphates are similar to those obtained by Clark *et al.* As a check, a sample of sodium dithionite was irradiated with Co^{60} γ rays. The e.s.r. spectra of the irradiated sample, at room temperature and at liquid nitrogen temperature, were obtained. At the lower temperature the sample could be readily power saturated. At both temperatures the g value of the peak was 2.005 and the line width was 10.4 gauss. The values reported by Clark *et al.* are 2.005 and 11.5 gauss, respectively.

On the basis of the similarity of the e.s.r. spectra of irradiated dithionites and thiosulphates it seems safe to tentatively assume that SO_2^- free-radical ions are produced in the gamma irradiation of thiosulphates.

The g value for the low-field shoulder of the low-field structure observed in the e.s.r. spectra of anhydrous $Na_2S_2O_3$ is 2.032. Free radicals in which the odd electron is mainly involved with the sulphur atom may be responsible for this structure (2). Low-field structures at a similar g value have been noted in the e.s.r. spectra of sulphur dissolved in oleum (5) and of chilled sulphur vapor (6). Such a conclusion is consistent with the observation that colloidal sulphur is formed when gamma-irradiated thiosulphates are dissolved in water.

ACKNOWLEDGMENT

The authors gratefully acknowledge financial assistance from the National Research Council of Canada in the form of a research grant.

1. J. W. MELLOR. A comprehensive treatise on inorganic and theoretical chemistry. Vol. 10. Longmans, Green and Co., London. 1930. p. 520.
2. D. M. GARDNER and G. K. FRAENKEL. J. Am. Chem. Soc. **78**, 3279 (1956).
3. G. W. CHANTRY, A. HORSFIELD, J. R. MORTON, J. R. ROWLANDS, and D. H. WHIFFEN. Mol. Phys. **5**, 232 (1962).
4. H. C. CLARK, A. HORSFIELD, and M. C. R. SYMONS. J. Chem. Soc. 7 (1961).
5. D. J. E. INGRAM and M. C. R. SYMONS. J. Chem. Soc. 2437 (1957).
6. H. E. RADFORD and F. O. RICE. J. Chem. Phys. **33**, 774 (1960).

RECEIVED APRIL 17, 1963.
DEPARTMENT OF CHEMISTRY AND CHEMICAL ENGINEERING,
UNIVERSITY OF SASKATCHEWAN,
SASKATOON, SASKATCHEWAN.

PREPARATION OF ANTIDOTES FOR ANTICHOLINESTERASE POISONING
II. TERTIARY AND QUATERNARY SALTS OF PARPANIT AND PARPANIT ANALOGUES*

R. A. B. BANNARD, J. H. PARKKARI, AND I. W. COLEMAN

In connection with a study of the analogues of Parpanit (2-diethylaminoethyl 1-phenylcyclopentanecarboxylate hydrochloride) as cholinolytics for treatment of Sarin poisoning

*Issued as D.R.C.L. Report No. 411.

Can. J. Chem. Downloaded from www.nrcresearchpress.com by 210.87.254.40 on 09/05/12
For personal use only.

potassium methane disulphonate. The e.s.r. spectra are similar for all these compounds, consisting of a single absorption line with a g value of 2.004. The authors (3) present evidence indicating that the e.s.r. spectra are due to the presence of sulphite free-radical ions. The g values found in the present work are significantly higher than the value of 2.004 reported by Chantry *et al.* Hence it would appear that if the interpretation of these authors is correct the spectra obtained in the present work are not due to sulphite free-radical ions.

Clark *et al.* (4) suggested that the SO_2^- free-radical ion was responsible for the e.s.r. spectra obtained by them from X-irradiated sodium and potassium dithionites. The spectra obtained in the present work for γ-irradiated thiosulphates are similar to those obtained by Clark *et al.* As a check, a sample of sodium dithionite was irradiated with Co^{60} γ rays. The e.s.r. spectra of the irradiated sample, at room temperature and at liquid nitrogen temperature, were obtained. At the lower temperature the sample could be readily power saturated. At both temperatures the g value of the peak was 2.005 and the line width was 10.4 gauss. The values reported by Clark *et al.* are 2.005 and 11.5 gauss, respectively.

On the basis of the similarity of the e.s.r. spectra of irradiated dithionites and thiosulphates it seems safe to tentatively assume that SO_2^- free-radical ions are produced in the gamma irradiation of thiosulphates.

The g value for the low-field shoulder of the low-field structure observed in the e.s.r. spectra of anhydrous $Na_2S_2O_3$ is 2.032. Free radicals in which the odd electron is mainly involved with the sulphur atom may be responsible for this structure (2). Low-field structures at a similar g value have been noted in the e.s.r. spectra of sulphur dissolved in oleum (5) and of chilled sulphur vapor (6). Such a conclusion is consistent with the observation that colloidal sulphur is formed when gamma-irradiated thiosulphates are dissolved in water.

ACKNOWLEDGMENT

The authors gratefully acknowledge financial assistance from the National Research Council of Canada in the form of a research grant.

1. J. W. MELLOR. A comprehensive treatise on inorganic and theoretical chemistry. Vol. 10. Longmans, Green and Co., London. 1930. p. 520.
2. D. M. GARDNER and G. K. FRAENKEL. J. Am. Chem. Soc. **78**, 3279 (1956).
3. G. W. CHANTRY, A. HORSFIELD, J. R. MORTON, J. R. ROWLANDS, and D. H. WHIFFEN. Mol. Phys. **5**, 232 (1962).
4. H. C. CLARK, A. HORSFIELD, and M. C. R. SYMONS. J. Chem. Soc. 7 (1961).
5. D. J. E. INGRAM and M. C. R. SYMONS. J. Chem. Soc. 2437 (1957).
6. H. E. RADFORD and F. O. RICE. J. Chem. Phys. **33**, 774 (1960).

RECEIVED APRIL 17, 1963.
DEPARTMENT OF CHEMISTRY AND CHEMICAL ENGINEERING,
UNIVERSITY OF SASKATCHEWAN,
SASKATOON, SASKATCHEWAN.

PREPARATION OF ANTIDOTES FOR ANTICHOLINESTERASE POISONING
II. TERTIARY AND QUATERNARY SALTS OF PARPANIT AND PARPANIT ANALOGUES*

R. A. B. BANNARD, J. H. PARKKARI, AND I. W. COLEMAN

In connection with a study of the analogues of Parpanit (2-diethylaminoethyl 1-phenylcyclopentanecarboxylate hydrochloride) as cholinolytics for treatment of Sarin poisoning

*Issued as D.R.C.L. Report No. 411.

Can. J. Chem. Downloaded from www.nrcresearchpress.com by 210.87.254.5 on 09/05/12
For personal use only.

(1, 2) it became necessary to obtain a variety of salts of this compound as well as a series of quaternary derivatives of it and certain other cholinolytics. The preparation of the compounds required is described herein.

2-Diethylaminoethyl 1-phenylcyclopentanecarboxylate nitrate, bromide, and methanesulphonate were prepared from the hydrochloride by ion exchange using Amberlite IRA-400 resin in the appropriate anionic form (see Table I). Attempts to obtain the sulphate in the same manner, by metathesis of Parpanit with silver sulphate, or by interaction of the free base with sulphuric acid, led instead to good yields of the bisulphate, due presumably to a solubility effect.

For preparation of anionic variants of a given quarternary ammonium salt, most workers still appear to prefer the more classical metathetical reactions to ion exchange (3–10). However, it seemed to us that the latter procedure had much to recommend it in the present application from the standpoint of manipulative convenience and ease of purification, since only small quantities of the compounds were required. Accordingly, the Parpanit quaternary salts shown in Table II were prepared from the methiodide by ion exchange. Parpanit methylacetate, methylcitrate, methyllactate, and methyltartrate were not obtained as crystalline salts from the methiodide by ion exchange or by metathesis with the appropriate silver salt.

For preparation of quaternary ammonium salts from tertiary bases, only two basic methods are in common use. These are, interaction of the neat dry halide and base, and treatment of the base with a halide in the presence of a dry solvent. Although the first of these is commonly used to prepare methiodides as derivatives for characterization of amines (11), the second has recently been used with increasing frequency for synthesis of alkyl, benzyl, and substituted benzyl quarternary ammonium salts (3–5, 7, 10, 12–21). Both methods have been conducted at room temperature (14, 16, 19), at the reflux temperature of the halide (21) or solvent (4, 5, 7, 12, 14–18, 20), or in sealed vessels at elevated temperatures (3, 13, 16, 18–20). The solvent which has been used most frequently is benzene (7, 12, 16–18), but ethanol (4, 10, 13, 16), ether (5, 7, 14), methyl ethyl ketone (3, 4, 20), methanol (13, 15), nitromethane (10, 20), acetone (19), and chloroform (22) have also been employed. For preparation of Parpanit methobromide and methiodide and the quaternary salts given in Tables III, IV, and V it was necessary to use a variety of conditions, details of which are given in the Experimental section.

Interaction of Parpanit free base with excess isopropyl bromide at 130° in a sealed tube furnished Parpanit hydrobromide in 66% yield, due presumably to unfavorable competition between the substitution reaction and an elimination reaction which leads to dehydrohalogenation of the alkyl halide (4, 10, 23). Attempts to increase the S_N to E ratio by operating at low base concentration (0.1 *M*), low temperature (0°), and in polar solvents (acetonitrile) (23) failed to yield Parpanit isopropylbromide. This substance was, however, obtained in 38% yield by the action of ethyl bromide on 2-isopropylethylaminoethyl 1-phenylcyclopentanecarboxylate (24).

EXPERIMENTAL*†

Preparation of Parpanit Tertiary Salts by Ion Exchange

The method used for preparation of 2-diethylaminoethyl 1-phenylcyclopentanecarboxylate hydrogen nitrate is typical. A 2% aqueous solution of 2-diethylaminoethyl 1-phenylcyclopentanecarboxylate hydrochloride (3.26 g, 10 meq) was passed through Amberlite IRA-400 resin (50 ml, 50 meq) in the nitrate form, followed by water (500 ml). The eluate was evaporated to dryness *in vacuo* and the residue was dried at

**All melting points are uncorrected.*

†Microanalyses by J. G. Helie of these laboratories.

Can. J. Chem. Downloaded from www.nrcresearchpress.com by 210.87.254.5 on 09/05/12
For personal use only.

Can. J. Chem. Downloaded from www.nrcresearchpress.com by 210.87.254.5 on 09/05/12
For personal use only.

TABLE I

Parpanit tertiary salts

Anion	Empirical formula	Solvent for recrystallization	M.p. (°C)	% yield	Analysis (%)	C	H	N	S	Br
Bisulphate	$C_{18}H_{29}NO_6S$	Ethanol–ether	100–100.5	74	Calc.	55.79	7.54	3.62	8.27	
					Found	55.62	7.55	3.52	8.00	
Bromide	$C_{18}H_{28}NO_2Br$	Acetone	139.5–140	84	Calc.	58.37	7.62	3.78		21.58
					Found	58.24	7.47	3.60		21.65
Methane-sulphonate*	$C_{19}H_{31}NO_5S$	Benzene–ether	54–55	65	Calc.	59.19	8.11	3.63		
					Found	59.30	7.96	3.64		
Nitrate	$C_{18}H_{28}N_2O_5$	Ethanol–ether	105–105.5	87	Calc.	61.34	8.01	7.95		
					Found	61.56	8.21	7.76		

*Very hygroscopic.

TABLE II

Parpanit methyl quaternary ammonium salts

Anion	Empirical formula	Method§	Solvent for recrystallization	M.p. (°C)	% yield	Analysis (%)	C	H	N	S	Halogen
Bromide	$C_{19}H_{30}NO_2Br$	A	Acetone–ether	117–117.5	89	Calc.	59.37	7.87	3.64		20.79
						Found	59.51	7.80	3.61		20.67
Chloride* †	$C_{19}H_{30}NO_2Cl$	C	Acetone–ether	113–113.5	41	Calc.	67.13	8.90	4.12		10.43
						Found	67.07	8.74	3.96		10.41
Iodide‡	$C_{19}H_{30}NO_2I$	B	Acetone–ether	139–140	96	Calc.	52.90	7.01	3.25		29.42
						Found	53.21	6.97	3.09		29.54
Methane-sulphonate	$C_{20}H_{33}NO_5S$	C	Acetone–ether	98.5–99.5	80	Calc.	60.12	8.33	3.51	8.02	
						Found	60.01	8.05	3.33	8.23	
Nitrate	$C_{19}H_{30}N_2O_5$	C	Ethanol–ether	106.5–107	87	Calc.	62.27	8.25	7.65		
						Found	62.33	8.07	7.37		
Sulphate	$C_{38}H_{60}N_2O_8S \cdot 1.5H_2O$	C	Acetone–ether	99–100	46	Calc.	62.35	8.68	3.83	4.37	
						Found	62.60	8.80	3.79	4.60	

*Very hygroscopic.
†Reported in Swiss Patent No. 246,134 without physical constants (28).
‡M.p. 136° (25).
§See Experimental.

Can. J. Chem. Downloaded from www.nrcresearchpress.com by 210.87.254.5 on 09/05/12
For personal use only.

TABLE III

Methyl quaternary ammonium salts of miscellaneous spasmolytics

Compound	Empirical formula	Method§	M.p.‖ (°C)	% yield	Analysis (%)					
						C	H	N	S	Br
Atropine methonitrate*	$C_{18}H_{26}N_2O_6$	C	161–163	93	Calc.	59.00	7.15	7.64		
					Found	59.28	6.97	7.73		
Atropine methylmethane-sulphonate	$C_{19}H_{29}NO_6S$	C	112–113	35	Calc.	57.12	7.32	3.51	8.02	
					Found	57.12	7.07	3.36	7.91	
Phenergan methobromide	$C_{18}H_{23}N_2BrS$	A	245–246	92	Calc.	56.98	6.11			21.07
					Found	56.82	5.89			21.29
Trasentin methobromide†	$C_{21}H_{28}O_2NBr$	A	104–105.5	79	Calc.	62.06	6.94	3.45		19.67
					Found	61.80	6.90	3.18		19.64
Trasentin 6H methobromide‡	$C_{21}H_{34}O_2NBr$	A	181–182	93	Calc.	61.16	8.31	3.40		19.38
					Found	61.35	8.13	3.41		19.42

*M.p. 163° (29).
†M.p. 106–107° (22).
‡M.p. 174–179° (30).
§See Experimental.
‖After recrystallization from ethanol–ether.

Can. J. Chem. Downloaded from www.nrcresearchpress.com by 210.87.254.5 on 09/05/12
For personal use only.

TABLE IV

Parpanit quaternary ammonium halides

Quaternary compound	Empirical formula	Method‡	M.p. (°C)	% yield	Analysis (%)				
						C	H	N	Halogen
Ethobromide	$C_{20}H_{32}NO_2Br$	D	150–150.5§	78	Calc.	60.29	8.10	3.52	20.06
					Found	60.11	8.09	3.43	20.11
n-Propylbromide*	$C_{21}H_{34}NO_2Br$	D	123.5–124.5	76	Calc.	61.16	8.31	3.40	19.38
					Found	61.11	8.44	3.45	19.62
Isopropylbromide†	$C_{21}H_{34}NO_2Br$	D	128–129	38	Calc.	61.16	8.31	3.40	19.38
					Found	61.04	8.23	3.23	19.66
n-Butylbromide	$C_{22}H_{36}NO_2Br$	D	121–122	66	Calc.	61.96	8.51	3.28	18.74
					Found	61.96	8.51	3.04	18.84
n-Hexylbromide	$C_{24}H_{40}NO_2Br$	D	122–123	37	Calc.	63.42	8.87	3.08	17.58
					Found	63.16	8.85	2.96	17.51
Benzylbromide	$C_{25}H_{34}NO_2Br$	E	108.5–109	64	Calc.	65.21	7.44	3.04	17.36
					Found	65.19	7.39	3.11	17.28
Benzylchloride	$C_{25}H_{34}NO_2Cl$	F	129.5–130	52	Calc.	72.18	8.24	3.37	8.52
					Found	72.25	8.30	3.36	8.51
p-Phenylbenzyl-bromide	$C_{31}H_{38}NO_2Br$	G	157–157.5	84	Calc.	69.39	7.14	2.61	14.90
					Found	69.23	7.17	2.58	14.77

*M.p. 150–152° (26).
†Starting material 2-isopropylethylaminoethyl 1-phenylcyclopentanecarboxylate (24).
‡See Experimental.
§All but the isopropylbromide (acetone) and *p*-phenylbenzylbromide (ethanol–ether) recrystallized from acetone–ether.

TABLE V

Methobromides of Parpanit analogues

1-Phenylcyclopentane-carboxylate methobromide*	Empirical formula	Solvent for recrystalli-zation	M.p. (°C)	% yield	Analysis (%)				
						C	H	N	Br
2-Ethyl-2-fluoroethyl-aminoethyl	$C_{19}H_{29}NO_2BrF$	Acetone–ether	93.5–94.5	80	Calc.	56.71	7.26	3.48	
					Found	56.41	7.36	3.31	
2-Ethyl-2-isopropyl-aminoethyl	$C_{20}H_{32}NO_2Br$	*n*-Propanol–ether	154.5–155.5	64	Calc.	60.29	8.10	3.52	20.06
					Found	60.53	8.14	3.43	20.10
2-Diisopropylaminoethyl	$C_{21}H_{34}NO_2Br$	*n*-Propanol–ether	176.5–177	21	Calc.	61.16	8.31	3.40	19.38
					Found	60.90	8.28	3.35	19.49
2-Piperidinoethyl	$C_{19}H_{28}NO_2Br$	Acetone–ether	136.5–137	81	Calc.	59.68	7.38	3.66	20.90
					Found	59.46	7.35	3.59	21.02
2-Pyrrolidinoethyl	$C_{20}H_{30}NO_2Br$	Ethanol–ether	183–183.5	78	Calc.	60.60	7.63	3.53	20.16
					Found	60.85	7.52	3.35	20.20

Method H described in Experimental used throughout.

0.001 mm pressure. Two recrystallizations from ethanol–ether gave 3.05 g (86.7%) of Parpanit nitrate as colorless needles, m.p. 105–105.5°.

Preparation of Quaternary Ammonium Salts of Parpanit

Method A: Parpanit Methobromide

Parpanit (1.00 g, 0.00307 mole), dissolved in water (25 ml), was neutralized with 10% aqueous sodium hydroxide and extracted with ether (4×25 ml). The extract was dried over magnesium sulphate and filtered. Removal of the ether *in vacuo* followed by drying at 0.001 mm pressure gave 0.840 g (94.7%) of 2-diethylaminoethyl 1-phenylcyclopentanecarboxylate as a colorless mobile oil. The flask was fitted with a dry-ice condenser, and methyl bromide (10 ml, 17 g, 0.18 mole) was added. A precipitate began to form almost immediately. After 2 hours the excess methyl bromide was allowed to evaporate and the residue was dried at 0.001 mm pressure. Two recrystallizations from acetone–ether gave 1.05 g (89.0%) of Parpanit methobromide as colorless flakes, m.p. 117–117.5°.

Method B: Parpanit Methiodide

Parpanit (5.00 g, 0.0153 mole) was converted to the free base as described in Method A. The free base was dissolved in acetone (50 ml), methyl iodide (10 ml, 23 g, 0.16 mole) was added, and the solution was heated under reflux with stirring for 30 minutes. Removal of volatiles *in vacuo* followed by two recrystallizations from acetone–ether gave 6.34 g (96.0%) of Parpanit methiodide as colorless needles, m.p. 139–140°. Mndzhoyan *et al.* (25) report m.p. 136°.

Method C: Preparation of Parpanit Methyl Quaternary Ammonium Salts by Ion Exchange

The procedure followed was identical with that given for conversion of Parpanit to the nitrate salt except that Parpanit methiodide was used as starting material. Yields are given in Table II.

Method D: Parpanit n-Alkylbromides

The preparation of Parpanit ethobromide is typical. Parpanit (1.00 g, 0.00307 mole) was converted to the free base as described in Method A. The free base was heated in a sealed tube for 16 hours at 100° with ethyl bromide (5.0 g, 0.046 mole) which had been freshly dried over phosphorus pentoxide. The precipitate was removed from the tube by dissolving it in acetone, the solvents were removed *in vacuo*, and the solid residue was twice recrystallized from acetone–ether, yielding 0.95 g (78%) of Parpanit ethobromide as colorless needles, m.p. 150–150.5°. Van Campen and Tilford (26) report m.p. 150–152°. When the reactants were merely heated under reflux for 48 hours, a 25% yield was obtained.

Method E: Parpanit Benzylbromide

A mixture of Parpanit free base (0.87 g, 0.0030 mole) and freshly distilled and dried benzyl bromide (0.77 g, 0.0045 mole) was kept at room temperature for 24 hours. Anhydrous ether (25 ml) was added and the resultant precipitate was collected by filtration. Two recrystallizations from acetone–ether gave 0.88 g (64.0%) of Parpanit benzylbromide as colorless needles, m.p. 108–108.5°. When the reaction was conducted in ether as solvent under otherwise identical conditions, the yield decreased to 4%. The use of benzene as solvent, when the same proportions of reactants were heated under reflux for 2 hours, gave only a 12% yield.

Method F: Parpanit Benzylchloride

A mixture of Parpanit free base (0.87 g, 0.0030 mole) and freshly distilled and dried benzyl chloride (0.57 g, 0.0045 mole) was kept at 110° for 24 hours. Anhydrous ether (25 ml) was added, causing separation of an oil which crystallized on standing. The solid was recrystallized twice from acetone–ether, yielding 0.65 g (52.0%) of Parpanit benzylchloride as colorless needles, m.p. 129.5–130°.

Method G: Parpanit p-Phenylbenzylbromide

A mixture of Parpanit free base (1.26 g, 0.0044 mole), *p*-phenylbenzylbromide (2.20 g, 0.0088 mole) (prepared according to the method of Zervas and Dilaris (27)), and anhydrous ether (50 ml) was heated under gentle reflux for 3 days. Removal of the solvent *in vacuo* followed by two recrystallizations of the oily residue from ethanol–ether gave 1.98 g (84.5%) of Parpanit *p*-phenylbenzylbromide as colorless needles, m.p. 157–157.5°. The yield was reduced to 37% when the period of reflux was shortened to 16 hours.

Preparation of Methobromides of Parpanit Analogues

Method H: 2-Isopropylethylaminoethyl 1-Phenylcyclopentanecarboxylate Methobromide

2-Isopropylethylaminoethyl 1-phenylcyclopentanecarboxylate hydrochloride (24) (1.70 g, 0.0050 mole) was converted to the free base (1.49 g, 97.4%) by the procedure described in Method A. A mixture of the latter, methyl bromide (10 ml, 17 g, 0.18 mole), and acetone (25 ml) in a flask fitted with a dry-ice condenser was magnetically stirred for 1 hour under reflux. Removal of the excess halide *in vacuo* followed by three recrystallizations from *n*-propanol–ether gave 1.27 g (64.0%) of 2-isopropylethylaminoethyl 1-phenylcyclopentanecarboxylate methobromide as colorless needles, m.p. 154.5–155.5°.

ACKNOWLEDGMENTS

We are indebted to Geigy Pharmaceuticals Ltd., Montreal, for kindly providing the Parpanit used in preparation of the Parpanit tertiary and quaternary salts, and to Miss Anne Fairhurst for technical assistance.

Can. J. Chem. Downloaded from www.nrcresearchpress.com by 210.87.254.5 on 09/05/12
For personal use only.

1. I. W. COLEMAN, P. E. LITTLE, and R. A. B. BANNARD. Can. J. Biochem. Physiol. **40**, 815 (1962).
2. I. W. COLEMAN, P. E. LITTLE, and R. A. B. BANNARD. Can. J. Biochem. Physiol. **40**, 827 (1962).
3. R. A. ROBINSON. J. Org. Chem. **16**, 1911 (1951).
4. P. A. S. SMITH and S. FRANK. J. Am. Chem. Soc. **74**, 509 (1952).
5. S. B. COAN and D. PAPA. J. Org. Chem. **20**, 774 (1955).
6. W. F. COCKBURN and A. F. MCKAY. J. Am. Chem. Soc. **77**, 397 (1955).
7. A. C. COPE, N. A. LEBEL, H.-H. LEE, and W. R. MOORE. J. Am. Chem. Soc. **79**, 4720 (1957).
8. R. M. LEMMON, P. K. GORDON, M. A. PARSONS, and F. MAZZETTI. J. Am. Chem. Soc. **80**, 2730 (1958).
9. R. MCMULLAN and G. A. JEFFREY. J. Chem. Phys. **31**, 1231 (1959).
10. D. V. BANTHORPE, E. D. HUGHES, and SIR C. K. INGOLD. J. Chem. Soc. 4054 (1960).
11. R. L. SHRINER, R. C. FUSON, and D. Y. CURTIN. The systematic identification of organic compounds. 4th ed. John Wiley and Sons Inc., New York. 1956. p. 228.
12. L. SPIALTER and J. A. PAPPALARDO. J. Org. Chem. **22**, 840 (1957).
13. G. WITTIG and R. POLSTER. Ann. **599**, 13 (1956).
14. M. S. KHARASCH, G. H. WILLIAMS, and W. NUDENBERG. J. Org. Chem. **20**, 937 (1955).
15. C. R. HAUSER and A. WEINHEIMER. J. Am. Chem. Soc. **76**, 1264 (1954).
16. S. W. CANTOR and C. R. HAUSER. J. Am. Chem. Soc. **73**, 4122 (1951).
17. C. S. MARVEL, E. W. SCOTT, and K. L. AMSTUTZ. J. Am. Chem. Soc. **51**, 3638 (1929).
18. J. F. KERWIN, G. C. HALL, E. MACKO, R. A. MCLEAN, E. J. FELLOWS, and G. E. ULLOT. J. Am. Chem. Soc. **73**, 5681 (1951).
19. K. NADOR and L. GYERMEK. Acta Chim. Acad. Sci. Hung. **3**, 95 (1952).
20. R. A. ROBINSON (to G. D. Searle and Co.). U.S. Patent No. 2,692,285 (Oct. 19, 1954); Chem. Abstr. **49**, 4243b (1955).
21. K. VON AUWERS and W. MAUSS. Ber. Sect. B, **61**, 2411 (1928).
22. J. W. CUSIC and R. A. ROBINSON. J. Org. Chem. **16**, 1921 (1951).
23. E. S. GOULD. Structure and mechanism in organic chemistry. Holt, Rinehart, and Winston Inc., New York. 1959. Chap. 12.
24. R. A. B. BANNARD, J. H. PARKKARI, and I. W. COLEMAN. Can. J. Chem. **40**, 1909 (1962).
25. A. L. MNDZHOYAN, G. T. TATEVOSYAN, and S. G. ALBALYAN. Dokl. Akad. Nauk Arm. SSR, **27**, 93 (1958); Chem. Abstr. **53**, 18,904c (1959).
26. M. G. VAN CAMPEN and C. H. TILFORD (to Wm. S. Merrell Co.). U.S. Patent No. 2,474,796 (June 28, 1949); Chem. Abstr. **44**, 3017h (1950).
27. L. ZERVAS and I. DILARIS. J. Am. Chem. Soc. **77**, 5355 (1955).
28. J. R. GEIGY A.-C. Swiss Patent No. 246,134 (Sept. 16, 1947); Chem. Abstr. **43**, 5796h (1949).
29. THE MERCK INDEX. 6th ed. Merck and Co., Rahway, N.J. 1952. p. 107.
30. SOC. POUR L'IND. CHIM. À BÂLE. Swiss Patent No. 215,775 (Nov. 1, 1941); Chem. Abstr. **42**, 3777a. (1948).

RECEIVED FEBRUARY 26, 1963.
DEFENCE RESEARCH CHEMICAL LABORATORIES,
OTTAWA, ONTARIO.

Can. J. Chem. Downloaded from www.nrcresearchpress.com by 210.87.254.5 on 09/05/12
For personal use only.

NUCLEAR SPIN–SPIN COUPLING IN C^{13}-ENRICHED ACETYLENE, ETHYLENE, AND ETHANE

D. M. GRAHAM AND C. E. HOLLOWAY

The application of Ramsay's theory of nuclear spin–spin coupling (1) has been limited by lack of knowledge of the coupling constants of simple molecules where, because of symmetry, the effect of nuclear spin coupling does not appear in the transition energies. H^2 substitution has been used to circumvent the symmetry selection rules. However this technique may lead to complicated spectra, particularly when several nuclei are present, due to the greater multiplicity of energy levels arising from the spin of the deuteron. In many cases C^{13} substitution should be preferable in spite of greater synthetic difficulties since this may allow the determination of H^1–H^1 as well as C^{13}–H^1 and C^{13}–C^{13} coupling parameters. Such information should afford and indeed has afforded an additional means for evaluating different approaches for calculation of molecular wave functions.

1. I. W. COLEMAN, P. E. LITTLE, and R. A. B. BANNARD. Can. J. Biochem. Physiol. **40**, 815 (1962).
2. I. W. COLEMAN, P. E. LITTLE, and R. A. B. BANNARD. Can. J. Biochem. Physiol. **40**, 827 (1962).
3. R. A. ROBINSON. J. Org. Chem. **16**, 1911 (1951).
4. P. A. S. SMITH and S. FRANK. J. Am. Chem. Soc. **74**, 509 (1952).
5. S. B. COAN and D. PAPA. J. Org. Chem. **20**, 774 (1955).
6. W. F. COCKBURN and A. F. MCKAY. J. Am. Chem. Soc. **77**, 397 (1955).
7. A. C. COPE, N. A. LEBEL, H.-H. LEE, and W. R. MOORE. J. Am. Chem. Soc. **79**, 4720 (1957).
8. R. M. LEMMON, P. K. GORDON, M. A. PARSONS, and F. MAZZETTI. J. Am. Chem. Soc. **80**, 2730 (1958).
9. R. MCMULLAN and G. A. JEFFREY. J. Chem. Phys. **31**, 1231 (1959).
10. D. V. BANTHORPE, E. D. HUGHES, and SIR C. K. INGOLD. J. Chem. Soc. 4054 (1960).
11. R. L. SHRINER, R. C. FUSON, and D. Y. CURTIN. The systematic identification of organic compounds. 4th ed. John Wiley and Sons Inc., New York. 1956. p. 228.
12. L. SPIALTER and J. A. PAPPALARDO. J. Org. Chem. **22**, 840 (1957).
13. G. WITTIG and R. POLSTER. Ann. **599**, 13 (1956).
14. M. S. KHARASCH, G. H. WILLIAMS, and W. NUDENBERG. J. Org. Chem. **20**, 937 (1955).
15. C. R. HAUSER and A. WEINHEIMER. J. Am. Chem. Soc. **76**, 1264 (1954).
16. S. W. CANTOR and C. R. HAUSER. J. Am. Chem. Soc. **73**, 4122 (1951).
17. C. S. MARVEL, E. W. SCOTT, and K. L. AMSTUTZ. J. Am. Chem. Soc. **51**, 3638 (1929).
18. J. F. KERWIN, G. C. HALL, E. MACKO, R. A. MCLEAN, E. J. FELLOWS, and G. E. ULLOT. J. Am. Chem. Soc. **73**, 5681 (1951).
19. K. NADOR and L. GYERMEK. Acta Chim. Acad. Sci. Hung. **3**, 95 (1952).
20. R. A. ROBINSON (to G. D. Searle and Co.). U.S. Patent No. 2,692,285 (Oct. 19, 1954); Chem. Abstr. **49**, 4243b (1955).
21. K. VON AUWERS and W. MAUSS. Ber. Sect. B, **61**, 2411 (1928).
22. J. W. CUSIC and R. A. ROBINSON. J. Org. Chem. **16**, 1921 (1951).
23. E. S. GOULD. Structure and mechanism in organic chemistry. Holt, Rinehart, and Winston Inc., New York. 1959. Chap. 12.
24. R. A. B. BANNARD, J. H. PARKKARI, and I. W. COLEMAN. Can. J. Chem. **40**, 1909 (1962).
25. A. L. MNDZHOYAN, G. T. TATEVOSYAN, and S. G. ALBALYAN. Dokl. Akad. Nauk Arm. SSR, **27**, 93 (1958); Chem. Abstr. **53**, 18,904c (1959).
26. M. G. VAN CAMPEN and C. H. TILFORD (to Wm. S. Merrell Co.). U.S. Patent No. 2,474,796 (June 28, 1949); Chem. Abstr. **44**, 3017h (1950).
27. L. ZERVAS and I. DILARIS. J. Am. Chem. Soc. **77**, 5355 (1955).
28. J. R. GEIGY A.-C. Swiss Patent No. 246,134 (Sept. 16, 1947); Chem. Abstr. **43**, 5796h (1949).
29. THE MERCK INDEX. 6th ed. Merck and Co., Rahway, N.J. 1952. p. 107.
30. SOC. POUR L'IND. CHIM. À BÂLE. Swiss Patent No. 215,775 (Nov. 1, 1941); Chem. Abstr. **42**, 3777a. (1948).

RECEIVED FEBRUARY 26, 1963.
DEFENCE RESEARCH CHEMICAL LABORATORIES,
OTTAWA, ONTARIO.

Can. J. Chem. Downloaded from www.nrcresearchpress.com by 210.87.254.5 on 09/05/12
For personal use only.

NUCLEAR SPIN–SPIN COUPLING IN C^{13}-ENRICHED ACETYLENE, ETHYLENE, AND ETHANE

D. M. GRAHAM AND C. E. HOLLOWAY

The application of Ramsay's theory of nuclear spin–spin coupling (1) has been limited by lack of knowledge of the coupling constants of simple molecules where, because of symmetry, the effect of nuclear spin coupling does not appear in the transition energies. H^2 substitution has been used to circumvent the symmetry selection rules. However this technique may lead to complicated spectra, particularly when several nuclei are present, due to the greater multiplicity of energy levels arising from the spin of the deuteron. In many cases C^{13} substitution should be preferable in spite of greater synthetic difficulties since this may allow the determination of H^1–H^1 as well as C^{13}–H^1 and C^{13}–C^{13} coupling parameters. Such information should afford and indeed has afforded an additional means for evaluating different approaches for calculation of molecular wave functions.

EXPERIMENTAL

Acetylene was prepared from C^{13}-enriched barium carbonate (59.7%) by reduction to the carbide with excess calcium followed by reaction with water. Ethylene was obtained by reduction of the acetylene with chromous chloride. Reduction of ethylene by hydrogen on palladium – barium carbonate catalyst gave enriched ethane.

Proton spectra were obtained with a Varian V 4302 spectrometer at 60 Mc; carbon spectra at 15.1 Mc. All measurements were made on pure liquid samples at −70° C. The peak positions were measured by the audio side-band technique, and the modulation frequency was determined by a Hewlett–Packard 522 B frequency counter. By varying the audio-modulation frequency as the spectrum was scanned a side band of one of the stronger lines could be used to provide a base-line frequency calibration. In the case of ethylene and acetylene averaging a number of such spectra gave line positions to ±0.1 c/s in most cases. With ethane, however, field instability increased the average deviation to ±0.5 c/s. In all cases, the position of certain lines which were critical in the analysis of the spectrum was determined to better than ±0.1 c/s by the wiggle-beat method or by a combination of these two techniques.

To a certain extent for ethylene and particularly with ethane the C^{13} spectrum was more useful than the proton spectrum since the line spacings were greater and hence the lines were more readily resolved and their positions could be determined more precisely.

RESULTS

The enriched compounds prepared are actually mixtures of species containing zero, one, and two C^{13} atoms. Resolution of the spectra into contributions from each isotopically substituted species was aided by observations on the "C^{13}-satellite" spectra of the unenriched compounds. The resulting proton and carbon spectra were analyzed as follows.

Acetylene (Fig. 1).—The spectrum is obviously a superposition of an ABX pattern due to $HCC^{13}H$ and an A_2X_2 pattern arising from $HC^{13}C^{13}H$. Calculation of the spin-coupling

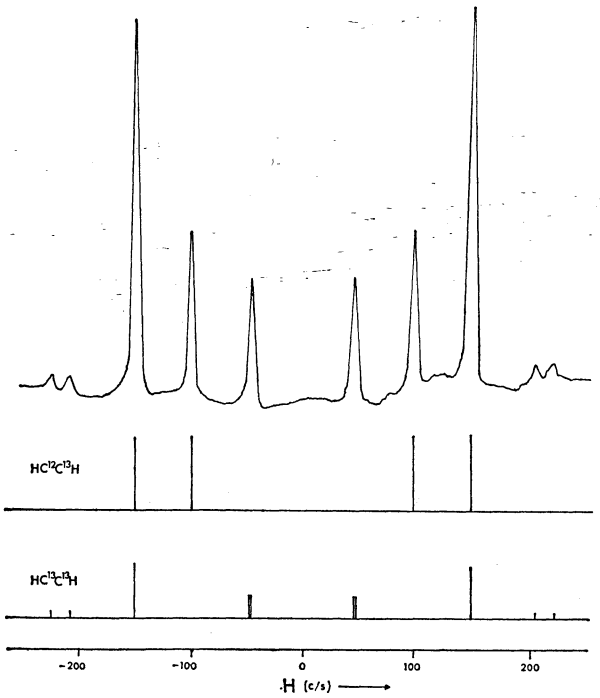

FIG. 1. Observed and calculated C^{13} n.m.r. spectra of enriched acetylene.

constants was readily carried out using the published energy levels and transitions for these spin systems (2).

Can. J. Chem. Downloaded from www.nrcresearchpress.com by 210.87.254.5 on 09/05/12
For personal use only.

Ethylene (Fig. 2).—The lines in the spectrum resulting from the mono-enriched species were obtained in terms of an A_4X system using spin functions of C_2 symmetry. The transitions arising from the other species were obtained from an A_4X_2 analysis using spin functions of D_2 symmetry. Separation of the lines due to each species in the observed spectra was aided by the chemical shift due to isotopic substitution; $\delta_{HC^{13}} - \delta_{HC^{12}} = 0.0102 \pm 0.003$ p.p.m.; $\delta_{C^{13}C^{12}} - \delta_{C^{13}C^{13}} = 0.30 \pm 0.001$ p.p.m. It proved possible using both the H^1 and C^{13} spectra to obtain directly all the coupling constants except that between the gem protons and the carbon–carbon coupling. Here it was necessary to solve 4×4 secular determinants and to determine the constants by successive approximations.

Ethane (Fig. 3).—The $H_3C^{13}C^{12}H_3$ spectrum was calculated using a set of spin functions formed from the carbon spin function and the product of two sets of D_3 symmetry spin functions corresponding to the two groups of three equivalent protons. The symmetry of the resulting functions was assigned by the application of standard group theory operations and rules (3). Further simplification of the secular equation was obtained by taking linear combinations of wave functions within each symmetry group which were degenerate as a result of free internal rotation of the methyl groups. A similar procedure was used for the $H_3C^{13}C^{13}H_3$ transitions; in this case carbon spin functions of C_2 symmetry were used. The only parameter that could be obtained directly from the spectra was the sum of the long- and short-range C^{13}–H^1 coupling constants. The remaining constants were obtained by an iterative procedure. Since the protons within each methyl group are equivalent, the gem coupling constant could not be obtained.

The results obtained are summarized in Table I. Shortly before completion of this work the results of a similar study became available (4). Since this work was based on proton

TABLE I

Spin–spin coupling constants (c/s)
(Results from other work are given in parentheses)

	J_{CC}	J_{CH} (short)	J_{CH} (long)	J_{HH}		
Acetylene						
	170.6 (171.6)*	248.7 (249.0)*	49.7 (49.3)*		9.8 (9.55)* (9.1±2.0)§	
Ethylene				Gem	Cis	Trans
	67.2† (67.6)*	156.2 (156.4)*	−2.4 (−2.4)*	2.3 (2.5)* (2.0)‡	11.5 (11.7)* (11.4)‡	19.1 (19.1)* (18.8)‡
Ethane						
	34.6† (34.4)*	125.0 (125.3)*	−4.8 (−4.5)*		8.0 (8.0)*	

*From proton resonance spectra of C^{13}-enriched compounds (4).
†The authors of ref. 4 have pointed out in a private communication that the observed C^{13} spectrum of ethylene can arise only if the C—C and H—H coupling constants have the same sign, thus confirming their deduction that the contact term is dominant in J_{CC}. We have recently shown that this is also the case for ethane.
‡From proton "C^{13}-satellite" spectrum (6).
§From deuteration (7).

spectra and the work reported here was primarily (but not entirely) based on C^{13} resonance measurements, the excellent agreement obtained independently tends to confirm the spectral analyses. This is particularly important for ethylene and ethane where the large number of possible transitions presented a formidable problem in arriving at a reasonable and unique assignment.

Can. J. Chem. Downloaded from www.nrcresearchpress.com by 210.87.254.5 on 09/05/12
For personal use only.

Can. J. Chem. Downloaded from www.nrcresearchpress.com by 210.87.254.5 on 09/05/12
For personal use only.

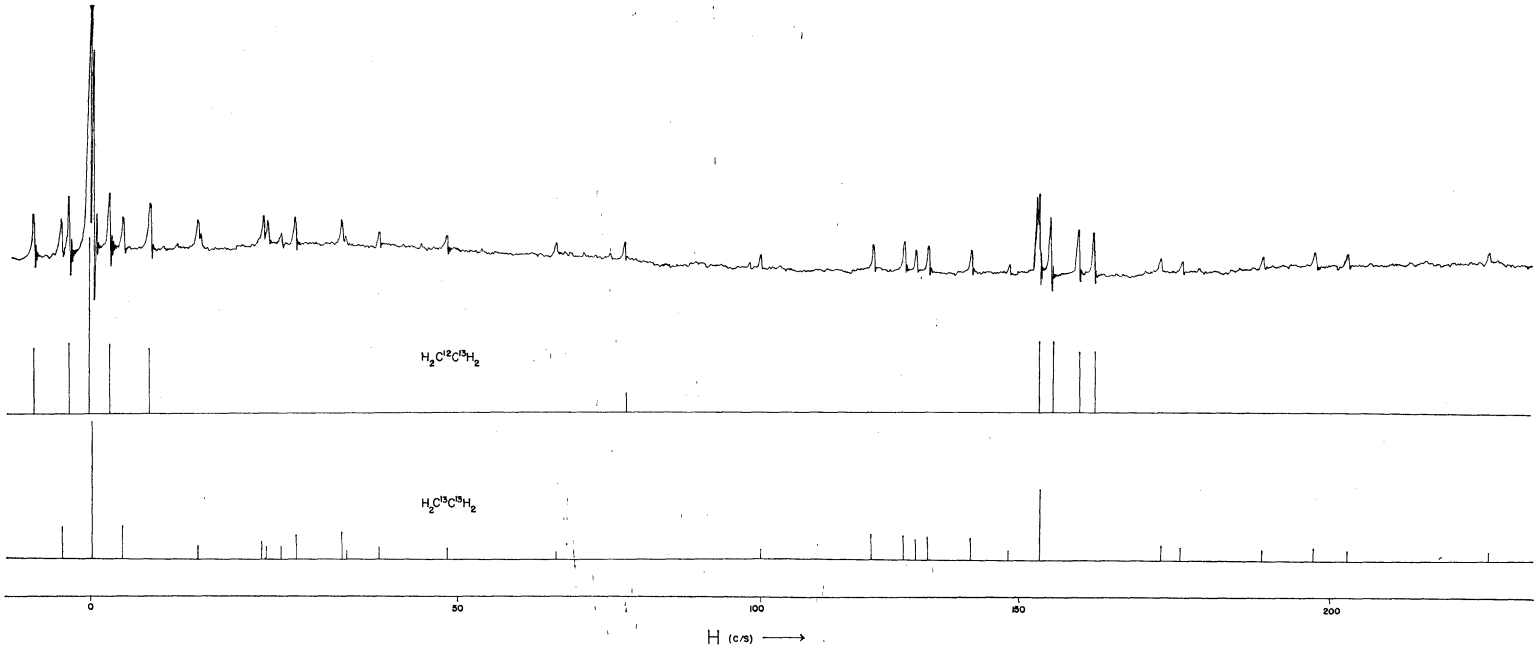

FIG. 2. Observed and calculated C^{13} n.m.r. spectra of enriched ethylene.

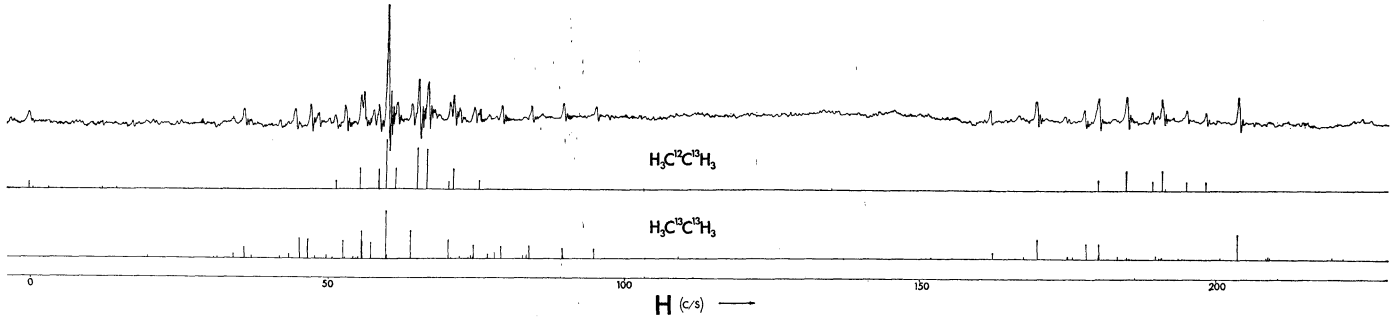

FIG. 3. Observed and calculated C^{13} n.m.r. spectra of enriched ethane.

The data also provide additional verification of the linear relation between C^{13}–H^1 short-range coupling constants and the fractional *s*-character of the C—H bond (ρ_{CH}) (5). Making the reasonable assumption that the hybridization in acetylene is pure *sp*, the relation is $\rho_{CH} = 0.201 J_{CH}$. This gives 0.315 and 0.251 for the fractional *s*-character in ethylene and ethane, respectively, consistent with the bond angles and lengths reported for these molecules.

The carbon–carbon coupling constants also appear to follow a similar trend. Extension of the argument of reference 5 to carbon–carbon coupling predicts a linear dependence of J_{CC} on the square of the fractional *s*-character. The experimental values do not fit such a relation and it appears probable that the simple picture used is not applicable to carbon–carbon coupling in general, and also that there may be appreciable contributions to J_{CC} from π electrons in the unsaturated compounds. Further work is in progress which it is hoped will resolve this problem.

ACKNOWLEDGMENT

The authors gratefully acknowledge financial support from the National Research Council of Canada.

1. N. F. RAMSEY. Phys. Rev. **91**, 303 (1953).
2. J. A. POPLE, W. G. SCHNEIDER, and H. J. BERNSTEIN. High resolution nuclear magnetic resonance. McGraw-Hill Inc., New York. 1959. Chap. 6.
3. E. B. WILSON, JR., J. C. DECIUS, and P. C. CROSS. Molecular vibrations. McGraw-Hill Inc., New York. 1955.
4. R. M. LYNDEN-BELL and N. SHEPPARD. Proc. Roy. Soc. (London), Ser. A, **269**, 385 (1962).
5. N. MULLER and D. E. PRITCHARD. J. Chem. Phys. **31**, 768, 1471 (1959).
6. G. S. REDDY and J. H. GOLDSTEIN. J. Mol. Spectry. **8**, 475 (1962).
7. M. KARPLUS and D. H. ANDERSON. J. Chem. Phys. **27**, 597 (1957).

RECEIVED OCTOBER 25, 1962.
DEPARTMENT OF CHEMISTRY,
UNIVERSITY OF WESTERN ONTARIO,
LONDON, ONTARIO.

Can. J. Chem. Downloaded from www.nrcresearchpress.com by 210.87.254.5 on 09/05/12
For personal use only.

SOLVOLYSIS IN LIGHT AND HEAVY WATER
V. EFFECT OF DIOXANE ON THE SOLVENT ISOTOPE EFFECT WITH *t*-BUTYL CHLORIDE[1]

WM. G. CRAIG,[2] LEO HAKKA,[2] P. M. LAUGHTON, AND R. E. ROBERTSON[3]

In paper I of this series (1), we reported data for the solvolytic rate ratio k_{D_2O}/k_{H_2O} for a few alkyl halides, including *t*-butyl chloride. This part of the work was motivated by a paper of Swain, Cardinaud, and Ketley (2) which reported a large difference in the ratio between methyl halides and *t*-butyl chloride. Our work essentially confirmed their data for the latter, but changed the values for the former. Dr. Swain has since informed us that redetermination of the methyl halide values in his laboratories confirmed our results.

[1]*Issued as N.R.C. No. 7456.*
[2]*Summer undergraduate research assistant, Carleton University, 1962; made possible by a grant in aid of research from the National Research Council to P. M. Laughton.*
[3]*Division of Pure Chemistry, National Research Council, Ottawa.*

The data also provide additional verification of the linear relation between C^{13}–H^1 short-range coupling constants and the fractional *s*-character of the C—H bond (ρ_{CH}) (5). Making the reasonable assumption that the hybridization in acetylene is pure *sp*, the relation is $\rho_{CH} = 0.201 J_{CH}$. This gives 0.315 and 0.251 for the fractional *s*-character in ethylene and ethane, respectively, consistent with the bond angles and lengths reported for these molecules.

The carbon–carbon coupling constants also appear to follow a similar trend. Extension of the argument of reference 5 to carbon–carbon coupling predicts a linear dependence of J_{CC} on the square of the fractional *s*-character. The experimental values do not fit such a relation and it appears probable that the simple picture used is not applicable to carbon–carbon coupling in general, and also that there may be appreciable contributions to J_{CC} from π electrons in the unsaturated compounds. Further work is in progress which it is hoped will resolve this problem.

ACKNOWLEDGMENT

The authors gratefully acknowledge financial support from the National Research Council of Canada.

1. N. F. RAMSEY. Phys. Rev. **91**, 303 (1953).
2. J. A. POPLE, W. G. SCHNEIDER, and H. J. BERNSTEIN. High resolution nuclear magnetic resonance. McGraw-Hill Inc., New York. 1959. Chap. 6.
3. E. B. WILSON, JR., J. C. DECIUS, and P. C. CROSS. Molecular vibrations. McGraw-Hill Inc., New York. 1955.
4. R. M. LYNDEN-BELL and N. SHEPPARD. Proc. Roy. Soc. (London), Ser. A, **269**, 385 (1962).
5. N. MULLER and D. E. PRITCHARD. J. Chem. Phys. **31**, 768, 1471 (1959).
6. G. S. REDDY and J. H. GOLDSTEIN. J. Mol. Spectry. **8**, 475 (1962).
7. M. KARPLUS and D. H. ANDERSON. J. Chem. Phys. **27**, 597 (1957).

RECEIVED OCTOBER 25, 1962.
DEPARTMENT OF CHEMISTRY,
UNIVERSITY OF WESTERN ONTARIO,
LONDON, ONTARIO.

Can. J. Chem. Downloaded from www.nrcresearchpress.com by 210.87.254.5 on 09/05/12
For personal use only.

SOLVOLYSIS IN LIGHT AND HEAVY WATER
V. EFFECT OF DIOXANE ON THE SOLVENT ISOTOPE EFFECT WITH *t*-BUTYL CHLORIDE[1]

WM. G. CRAIG,[2] LEO HAKKA,[2] P. M. LAUGHTON, AND R. E. ROBERTSON[3]

In paper I of this series (1), we reported data for the solvolytic rate ratio k_{D_2O}/k_{H_2O} for a few alkyl halides, including *t*-butyl chloride. This part of the work was motivated by a paper of Swain, Cardinaud, and Ketley (2) which reported a large difference in the ratio between methyl halides and *t*-butyl chloride. Our work essentially confirmed their data for the latter, but changed the values for the former. Dr. Swain has since informed us that redetermination of the methyl halide values in his laboratories confirmed our results.

[1]*Issued as N.R.C. No. 7456.*
[2]*Summer undergraduate research assistant, Carleton University, 1962; made possible by a grant in aid of research from the National Research Council to P. M. Laughton.*
[3]*Division of Pure Chemistry, National Research Council, Ottawa.*

Since that time, our view of the origin of this solvent effect in water has been developed in a series of papers both on k_{D_2O}/k_{H_2O} (3–6) and in extensive work by one of us (R. E. R.) on the apparent heat capacity of solvolysis, $\Delta C_p^{\ddagger}$ (7). Central to our interpretation is the concept that water forms a solvation shell of the gas-hydrate type about the initial-state substrate (8). This solvation shell undergoes rearrangement near the reaction site in the activation process. The slight differences in the work required to rearrange the initial-state solvation shell in the two solvents (H_2O and D_2O) provide the source of the difference in the solvolysis rates in the two media. As might have been anticipated, these differences closely parallel comparable differences which have been observed where some physical test involves the disruption of the water structure in the two media (9).

Just as the viscosity of water is reduced by an increase in temperature, the *difference* in viscosity between light and heavy water is reduced proportionately. Similarly, the addition of a hydrogen-bonding solvent such as dioxane will modify the structure of bulk water and particularly the solution properties, which are among the more striking consequences of water structure. The gas-hydrate type of initial-state solvation shell characteristic of aqueous solution of neutral molecules will, as a consequence of this modification, be modified toward a less organized structure in the solvent mixture. There should be a corresponding reduction in the work to break down this structure in the activation process and hence a reduction in the difference due to isotopic substitution (6).

It was therefore a source of continuing concern for us that Swain, Cardinaud, and Ketley (2) reported no perceptible change in k_{D_2O}/k_{H_2O} from 10% to 80% dioxane solution. We decided to re-examine this system, choosing a dioxane mole fraction between 0.1 and 0.2 because of evidence from many sources that aqueous solvolytic parameters go through maxima or minima in this region (10).

EXPERIMENTAL

Rate determinations were made using a conductometric method (11). Concentration resistance relationships were determined empirically with a precision rod displacement titrimeter (one counter unit = 8.33×10^{-4} ml (12) with a precision of this order for 1-ml displacement). The reactions were studied in stirred cells of 80-ml volume with shiny platinum electrodes and a cell constant of approximately 0.1. The cells were filled under dry nitrogen and the substrate was introduced through a serum cap and silicone plug mounted on a 10/30 standard taper joint. Temperature control was ±0.003° C as indicated by a platinum resistance thermometer.

Dioxane was purified by the method of Vogel (13), distilled in a 5-ft Vigreux column under nitrogen, and subjected to partial freezing, n_D^{25} 1.4213, single VPC peak. When distilled with a 2-ft saddle-packed column from sodium, it was found to be strongly basic. Conductivity water was boiled under nitrogen before use. Liquid transfers were carried out in glass and Teflon systems under dry nitrogen, the dioxane by weight, the conductivity water by volume. The solvent was 40 vol% water or D_2O, 60% dioxane (86.77 mole% water), n_D^{25} 1.3750 and 1.3700, respectively. The *t*-butyl chloride was a center cut from Eastman Kodak white label material. Convenient aliquots were 0.1 ml of solution made up from 5 μl of substrate in 1 ml of solvent.

Rates were calculated by the Guggenheim method, resistance readings being converted to counter readings corrected for volume change in the titration calibration, which preceded the kinetic study.

RESULTS

At 20.099°, replicate values for the rate of hydrolysis of *t*-butyl chloride in 60 vol% dioxane in light water were 4.64×10^{-4} and 4.62×10^{-4} sec^{-1}, and at 20.106°, 4.66×10^{-4} sec^{-1}. The corresponding values at 20.106° when D_2O replaced H_2O were 4.53×10^{-4} and 4.36×10^{-4} sec^{-1} with slight scatter. These results indicate a ratio k_{D_2O}/k_{H_2O} of 0.94–0.97. Our best value in the pure waters is 0.70 at 4°, which, when extrapolated to 20° according to the temperature correlations of papers III and IV (4, 6), would change to 0.73–0.75. Thus, even if the scatter of our values in heavy water conceals a systematic error of as

Can. J. Chem. Downloaded from www.nrcresearchpress.com by 210.87.254.5 on 09/05/12
For personal use only.

much as 5%, the ratio has still changed substantially toward unity on diluting water with dioxane, conforming to our expectations.

One of us (P. M. L.) wishes to acknowledge the hospitality of Dr. A. Streitwieser, Jr., of the University of California at Berkeley, where this note was written during a sabbatical leave from Carleton University. The technical assistance of Mr. B. R. Weston of the National Research Council in constructing and troubleshooting the conductance bridge was invaluable.

1. P. M. LAUGHTON and R. E. ROBERTSON. Can. J. Chem. **34**, 1714 (1956).
2. C. G. SWAIN, R. CARDINAUD, and A. D. KETLEY. J. Am. Chem. Soc. **77**, 934 (1955).
3. P. M. LAUGHTON and R. E. ROBERTSON. Can. J. Chem. **37**, 1491 (1959).
4. R. E. ROBERTSON and P. M. LAUGHTON. Can. J. Chem. **35**, 1319 (1957).
5. P. M. LAUGHTON and R. E. ROBERTSON. Can. J. Chem. **39**, 2155 (1961).
6. R. L. HEPPOLETTE and R. E. ROBERTSON. J. Am. Chem. Soc. **83**, 1834 (1961).
7. R. E. ROBERTSON. Suomen Kemistilehti, A, **33**, 63 (1960).
8. D. N. GLEW. J. Phys. Chem. **66**, 605 (1961).
9. R. C. HARDAY and R. L. COTTINGTON. J. Res. Natl. Bur. Std. **42**, 573 (1949).
10. J. B. HYNE. J. Am. Chem. Soc. **82**, 5129 (1960).
11. L. HAKKA, A. QUEEN, and R. E. ROBERTSON. To be published.
12. R. E. ROBERTSON. Unpublished work.
13. A. I. VOGEL. A text book of practical organic chemistry. Longmans, Green and Co., 1951.

RECEIVED APRIL 10, 1963.
DIVISION OF PURE CHEMISTRY,
NATIONAL RESEARCH COUNCIL,
OTTAWA, CANADA,
AND
DEPARTMENT OF CHEMISTRY,
CARLETON UNIVERSITY,
OTTAWA, CANADA.

Can. J. Chem. Downloaded from www.nrcresearchpress.com by 210.87.254.5 on 09/05/12
For personal use only.

TRITIATION OF AROMATICS BY HTO-PROMOTED ALUMINUM CHLORIDE

CONSTANŢA MĂNTESCU AND ALEXANDRU T. BALABAN

In the search for a better tritiation agent for aromatics we investigated the action of tritiated water on derivatives of benzene and pyridine in the presence of aluminum chloride. As known (1) water-promoted aluminum chloride contains the complex acid $H[AlCl_3OH]$, one of the strongest Brönsted acids, which is able to abstract hydride ions from alkanes and thus to cause isomerization (2).

Benzene and pyridine derivatives were selected for investigation; in order to find out the limitations of the method, compounds less reactive than benzene were tested. The reaction consisted of the addition of 0.05 mole tritiated water (specific activity 3.96×10^9 disintegrations sec^{-1} $mole^{-1}$) to a stirred mixture of aromatic (0.1–0.3 mole) and 0.1 mole anhydrous aluminum chloride. In some cases methylene chloride was used as solvent. Temperatures up to 100° and reaction times up to 12 hours were employed. After completion of the reaction the mixture was poured into ice water and the product was purified by repeated washing with water, drying, and distillation.

Pyridines were purified by strong alkalinization of the hydrolyzed reaction mixture, extraction with ether, repeated washing with concentrated alkali, drying, and distillation.

After counting, the products were again washed, dried, distilled, and counted, in order to verify if all activity due to water had been removed.

Activities were determined (3) by introducing from a vacuum line the labeled products

much as 5%, the ratio has still changed substantially toward unity on diluting water with dioxane, conforming to our expectations.

One of us (P. M. L.) wishes to acknowledge the hospitality of Dr. A. Streitwieser, Jr., of the University of California at Berkeley, where this note was written during a sabbatical leave from Carleton University. The technical assistance of Mr. B. R. Weston of the National Research Council in constructing and troubleshooting the conductance bridge was invaluable.

1. P. M. LAUGHTON and R. E. ROBERTSON. Can. J. Chem. **34**, 1714 (1956).
2. C. G. SWAIN, R. CARDINAUD, and A. D. KETLEY. J. Am. Chem. Soc. **77**, 934 (1955).
3. P. M. LAUGHTON and R. E. ROBERTSON. Can. J. Chem. **37**, 1491 (1959).
4. R. E. ROBERTSON and P. M. LAUGHTON. Can. J. Chem. **35**, 1319 (1957).
5. P. M. LAUGHTON and R. E. ROBERTSON. Can. J. Chem. **39**, 2155 (1961).
6. R. L. HEPPOLETTE and R. E. ROBERTSON. J. Am. Chem. Soc. **83**, 1834 (1961).
7. R. E. ROBERTSON. Suomen Kemistilehti, A, **33**, 63 (1960).
8. D. N. GLEW. J. Phys. Chem. **66**, 605 (1961).
9. R. C. HARDAY and R. L. COTTINGTON. J. Res. Natl. Bur. Std. **42**, 573 (1949).
10. J. B. HYNE. J. Am. Chem. Soc. **82**, 5129 (1960).
11. L. HAKKA, A. QUEEN, and R. E. ROBERTSON. To be published.
12. R. E. ROBERTSON. Unpublished work.
13. A. I. VOGEL. A text book of practical organic chemistry. Longmans, Green and Co., 1951.

RECEIVED APRIL 10, 1963.
DIVISION OF PURE CHEMISTRY,
NATIONAL RESEARCH COUNCIL,
OTTAWA, CANADA,
AND
DEPARTMENT OF CHEMISTRY,
CARLETON UNIVERSITY,
OTTAWA, CANADA.

TRITIATION OF AROMATICS BY HTO-PROMOTED ALUMINUM CHLORIDE

CONSTANŢA MĂNTESCU AND ALEXANDRU T. BALABAN

In the search for a better tritiation agent for aromatics we investigated the action of tritiated water on derivatives of benzene and pyridine in the presence of aluminum chloride. As known (1) water-promoted aluminum chloride contains the complex acid $H[AlCl_3OH]$, one of the strongest Brönsted acids, which is able to abstract hydride ions from alkanes and thus to cause isomerization (2).

Benzene and pyridine derivatives were selected for investigation; in order to find out the limitations of the method, compounds less reactive than benzene were tested. The reaction consisted of the addition of 0.05 mole tritiated water (specific activity 3.96×10^9 disintegrations sec^{-1} $mole^{-1}$) to a stirred mixture of aromatic (0.1–0.3 mole) and 0.1 mole anhydrous aluminum chloride. In some cases methylene chloride was used as solvent. Temperatures up to 100° and reaction times up to 12 hours were employed. After completion of the reaction the mixture was poured into ice water and the product was purified by repeated washing with water, drying, and distillation.

Pyridines were purified by strong alkalinization of the hydrolyzed reaction mixture, extraction with ether, repeated washing with concentrated alkali, drying, and distillation.

After counting, the products were again washed, dried, distilled, and counted, in order to verify if all activity due to water had been removed.

Activities were determined (3) by introducing from a vacuum line the labeled products

Can. J. Chem. Downloaded from www.nrcresearchpress.com by 210.87.254.6 on 09/05/12
For personal use only.

as quenching agents admixed with ethanol in known amounts into two compensated Geiger–Müller counters of identical characteristics except their lengths.

Results are presented in Table I. As it may be seen, although the specific activities

TABLE I

Tritiation of aromatics by 0.05 mole HTO (3.96×10^9 disintegrations sec^{-1} $mole^{-1}$) in the presence of 0.1 mole $AlCl_3$

Aromatic		CH_2Cl_2, ml	Temp., °C	Time, hr	Specific activity, disintegrations sec^{-1} $mole^{-1}$
Compound	Moles				
Benzene	0.1	—	25	0.5 1 1.5	2.2×10^9 4.5×10^9 6.7×10^9
Fluorobenzene	0.1	—	86	3	1.85×10^9
Chlorobenzene	0.1	—	100	3	3.6×10^8
2,4,6-Collidine	0.1	20	41–42	3 7	7.5×10^6 1×10^7
2,6-Lutidine	0.1	20	41–42	7	4.8×10^6
Pyridine	0.1	25	41–42	12	5×10^5
Nitrobenzene	0.15	25	41–42	12	8×10^4
2,6-Di-*t*-butyl-4-picoline	0.1	20	41–42	3 7	2.5×10^7 4×10^7

obtained refer neither to comparable conditions nor to equilibrium composition (excepting benzene which reaches equilibrium in 1.5 hours), they reflect the order of decreasing reactivity towards electrophilic substitution: benzene ~ fluorobenzene > chlorobenzene > 2,4,6-collidine > 2,6-lutidine > pyridine > nitrobenzene.

Other tritiated acids that were used as electrophilic tritiation agents, namely sulphuric acid (4, 5), trifluoroacetic acid (6), and the recently described complex acid $T[F_3BOPO_3H_2]$ (7), give lower reaction rates, since they are weaker acids. In order to be able to make a comparison with published rate constants, the tritiation of benzene by THO-promoted aluminum chloride was investigated at 25°. The first-order rate constant is 10 times larger than that in the presence of $T[F_3BOPO_3H_2]$ (7) and 2000 times larger than that in the presence of $THSO_4$ (4). Moreover, the present method allows the tritiation of pyridine, while tritiated sulphuric acid is unable to tritiate pyridine even at 200° C during 40 hours (5).

The tritiation of 2,6-di-*t*-butyl-4-picoline (8) is the most rapid of all pyridines studied, despite the fact that the substitution in position 3 is retarded by an ortho effect due to the *t*-butyl group; this is explained by the fact that, unlike all other pyridines, this compound is not protonated (9) and is therefore substituted as a pyridine more easily than as a pyridinium salt.

1. J. A. Miliotis. Compt. Rend. **245**, 1314 (1957).
2. C. D. Nenitzescu, M. Avram, and E. Sliam. Bull. Soc. Chim. France, 1266 (1955).
3. C. Mănțescu and M. Fiti. Acad. Rep. Populare Romine, Studii Cercetări Fiz. **11**, 788 (1960).
4. S. Olsson. Arkiv Kemi, **14**, 85 (1959).
5. A. R. Katritzky and B. J. Ridgewell. Proc. Chem. Soc. 114 (1962).
6. B. Aliprandi and F. Cacace. Ann. Chim. (Rome), **51**, 397 (1961).
7. P. M. Yavorsky and E. Gorin. J. Am. Chem. Soc. **84**, 1071 (1962).
8. A. T. Balaban and C. D. Nenitzescu. Ann. **625**, 74 (1959).
9. H. C. Brown and B. Kanner. J. Am. Chem. Soc. **77**, 1723 (1955).

Received April 22, 1963.
Institute of Atomic Physics,
Bucharest, Rumania.

Can. J. Chem. Downloaded from www.nrcresearchpress.com by 210.87.254.6 on 09/05/12
For personal use only.

Canadian Journal of Chemistry

Issued by The National Research Council of Canada

VOLUME 41 SEPTEMBER 1963 NUMBER 9

Can. J. Chem. Downloaded from www.nrcresearchpress.com by 210.87.254.5 on 09/05/12
For personal use only.

HIGH-YIELD SYNTHESES OF N-MONO- AND N,N-DI-SUBSTITUTED UREAS AND THIOUREAS FROM SILICON PSEUDOHALIDES

Roy G. Neville[1] and John J. McGee

Department of Chemistry, Aerospace Corporation, El Segundo, California, U.S.A.

Received March 22, 1963

ABSTRACT

This study demonstrates that N-mono- and N,N-di-substituted ureas and thioureas may expediently be synthesized, in essentially theoretical yield, by reacting primary or secondary aliphatic, alicyclic, aralkyl, aromatic, and heterocyclic amines with silicon tetraisocyanate or tetraisothiocyanate, or the corresponding methyl-substituted analogues. The method fails with aromatic amines possessing bulky (e.g. phenyl, bromo), or strongly electronegative (e.g. trifluoromethyl), substituents in the 2-, or 2,6-positions of the aromatic nucleus. Data on several new substituted ureas and thioureas are reported, and improved preparative procedures for the silicon pseudohalides are described.

It has long been known that organic isocyanates and isothiocyanates react readily with primary and secondary aliphatic and aromatic amines to produce substituted ureas and thioureas. Indeed, these reactions are commonly employed to characterize amines and to prepare urea derivatives (1, 2). Despite the large amount of literature available on compounds containing the carbon–isocyanate and carbon–isothiocyanate groups, very few studies have been published on the reactions of amines with compounds containing the silicon–isocyanate (Si–NCO) and silicon–isothiocyanate (Si–NCS) groups.

In 1951, Anderson (3) reported that silicon tetraisocyanate and several alkyl- and arylsilicon mono-, di-, and tri-isocyanates and isothiocyanates react readily with aniline, but the products resulting from these reactions were not characterized. Later, O'Brien (4) showed that trimethylsilicon isocyanate in benzene solution reacts with *n*-, *i*-, *s*-, and *t*-butylamines to produce butylureas. In 1958, Neville (5) demonstrated that silicon tetraisocyanate and isocyanates of empirical formula $R_xSi(NCO)_{4-x}$ (R = Me, Ph; x = 0, 1, 2, 3) reacted alone or in benzene solution with allylamine, diallylamine, aniline, benzylamine, and *o*- and *p*-toluidines to produce essentially theoretical yields of the corresponding N-mono- or N,N-di-substituted ureas. In every case the isocyanates and amines reacted in stoichiometric proportions and intermediate silylureas were not isolated. That these reactions do, in fact, involve silylurea intermediates was shown by Goubeau and Heubach (6), who reacted aniline and several secondary aliphatic amines with methylsilicon isocyanates, $Me_xSi(NCO)_{4-x}$ (x = 0, 1, 2, 3), in petroleum ether.* The silylureas isolated

[1]*All inquiries, including requests for reprints, should be addressed to this author.*

**It is significant that these workers specifically state that trimethylsilicon isocyanate does* not *react with aniline. In the present study we found that trimethylsilicon isocyanate reacts readily with aniline to produce phenylurea upon hydrolysis of the trimethylsilylurea intermediate.*

were extremely readily hydrolyzed by moisture to a silicon-containing moiety and a substituted urea:

$$4RR'NH + Si(NCO)_4 \rightarrow Si(NHCONRR')_4 \xrightarrow{2H_2O} 4H_2NCONRR' + SiO_2.$$

The extreme reactivity of the readily prepared silicon tetraisocyanate and tetraisothiocyanate with amines, coupled with the essentially theoretical yields of ureas obtained upon hydrolysis of the products, prompted us to investigate the scope and limitations of these reactions to ascertain whether they might furnish a preparatively useful general synthetic method for N-mono- and N,N-di-substituted ureas and thioureas. Usually, substituted ureas and thioureas of this type are prepared by reacting an amine hydrochloride in *aqueous* solution with cyanic or thiocyanic acid (7). An alternative procedure is the reaction of ammonia with the rather inaccessible dialkyl- or diaryl-carbamyl chlorides (1). The obvious advantage of silicon tetraisocyanate and tetraisothiocyanate (and their methylsilicon analogues) is that these reagents are very soluble in benzene, chloroform, and many other non-prototropic solvents in which amines are also soluble. Reaction is thus carried out in a homogeneous medium and the urea and thiourea products, which are insoluble in the solvent, immediately precipitate. Since essentially theoretical yields (usually $>95\%$) are obtained there are no organic by-products, and the gelatinous silica remaining is easily separated by filtration.

Silicon Isocyanates and Isothiocyanates

Silicon tetraisocyanate (8) and methylsilicon isocyanates (9) were prepared in 75–90% yields by reacting the appropriate chlorosilanes with dry silver cyanate in anhydrous benzene. Forbes and Anderson (8, 9) state that lead cyanate reacts with chlorosilanes to produce low yields of silicon isocyanates. We have found that lead cyanate, when *freshly* prepared and dried, consistently gives 52–71% yields of the silicon isocyanates and can, therefore, advantageously replace the more expensive silver cyanate.

Silicon tetraisothiocyanate (10) and the three methylsilicon isothiocyanates (11) were prepared in 80–86% yields by reaction of the corresponding chlorosilanes with freshly prepared, anhydrous silver thiocyanate or ammonium thiocyanate (12) in anhydrous benzene. Although the use of silver thiocyanate has been found to produce approximately 5% higher yields, ammonium thiocyanate gives purer silicon isothiocyanates.

Reactions with Amines

To determine the scope and limitations of this novel procedure approximately 60 primary and secondary amines, of widely differing structure, were reacted with silicon tetraisocyanate and tetraisothiocyanate, and in certain cases with methylsilicon isocyanates and isothiocyanates. In the aliphatic series unbranched- and branched-chain alkyl and alkenyl, and certain alicyclic, amines were investigated. In the aromatic series representative aryl, aralkyl, and heterocyclic amines were studied.

In all cases aliphatic unbranched- and branched-chain primary and secondary amines were found to react very readily, and usually exothermically, with silicon tetraisocyanate and tetraisothiocyanate. Methylsilicon isocyanates and isothiocyanates behaved similarly. In almost all cases the urea or thiourea derivative rapidly crystallized (1–2 minutes) in essentially 100% yield on cooling the solution to room temperature. To ensure that the silylurea intermediates were completely hydrolyzed, the products were dissolved in dilute isopropyl alcohol and refluxed for a few minutes. Gelatinous silica was easily removed by filtering the hot solution through a sintered-glass funnel containing Celite, and the urea or thiourea derivative was obtained by evaporating the filtrate. Alicyclic amines

406705

Can. J. Chem. Downloaded from www.nrcresearchpress.com by 210.87.254.5 on 09/05/12
For personal use only.

(e.g. cyclohexylamine) reacted very readily and exothermically. In the case of a few short-chain aliphatic amines (e.g. diallylamine, cyclopropylamine) some difficulty was experienced in isolating a high (>90%) yield of the urea or thiourea. This difficulty was possibly due to tenacious occlusion of the urea or thiourea derivative by the gelatinous silica. Most aliphatic amines investigated could be quantitatively converted to the corresponding urea or thiourea derivative in 5–10 minutes and the entire preparation of the purified product could be completed within 1 hour. The method is greatly superior to earlier published procedures (employing *aqueous* cyanic or thiocyanic acids) in that it is simple, rapid, and produces high yields.

Primary aromatic amines (e.g. aniline, toluidines, naphthylamines) and aralkylamines (e.g. benzylamine) reacted exothermically, or occasionally without noticeable exotherm, in benzene or chloroform solution to produce essentially theoretical yields of urea and thiourea derivatives. Heterocyclic primary amines (e.g. 2-aminopyridine) behaved similarly. Secondary aromatic amines (e.g. N-methylaniline, N-ethylaniline) reacted slowly with silicon tetraisocyanate, or tetraisothiocyanate, and required longer reflux periods (1–2 hours) depending upon the amine. Diphenylamine, for example, yielded N,N-diphenylurea in theoretical yield only after refluxing for 4 hours with silicon tetraisocyanate. In the case of silicon tetraisothiocyanate a 6-hour reflux period was required to produce a theoretical yield of N,N-diphenylthiourea.

To determine the effect of steric hindrance on the reactivity of arylamines with silicon tetraisocyanate, or tetraisothiocyanate, a series of 2-mono-, 2,4-di-, and 2,4,6-tri-substituted amines was studied. Although 2-chloro-, 2-bromo-, and 2-iodo-anilines readily yielded the 2-halophenylureas or thioureas, 2-fluoroaniline reacted slowly to produce 2-fluorophenyl derivatives. 2,6-Dibromoaniline was extremely slow to react with silicon tetraisocyanate and, under the experimental conditions employed, a pure derivative could not be isolated. Both 2,6-dimethylphenylurea and 2,6-dimethylphenylthiourea were readily obtained from 2,6-dimethylaniline, but 2-trifluoromethylaniline was totally unreactive. 2-Nitroaniline and 2-methoxyaniline yielded the corresponding urea and thiourea derivatives without difficulty.

In general, theoretical yields were readily obtainable from anilines substituted in the ortho or diortho positions, provided that the substituents were not too bulky (e.g. C_6H_5 groups), or that they deactivated the amino group by inductive withdrawal of electrons as in the case of 2-trifluoromethylaniline.

The reactivities of amines with silicon tetraisocyanate or tetraisothiocyanate and their methylsilicon analogues may be summarized as follows:

$$RNH_2 > R_2NH > ArNH_2 \gg ArNHR \gg Ar_2NH$$

(R = alkyl, aralkyl; Ar = aryl)

In the course of this investigation, several new compounds were prepared. These, and the other compounds synthesized, are listed in Tables I, II, and III.

Silicon tetraisocyanate and tetraisothiocyanate were reacted with ethylenediamine and *o*- and *p*-phenylenediamines to demonstrate that the method can be extended to synthesize diureas and dithioureas, although the preparation of these compounds was not studied in detail.

Ureas and thioureas were characterized by their melting point, Kjeldahl nitrogen analysis, and infrared spectra. The following infrared absorption characteristics were observed: NH stretching at 3390–3470 cm^{-1}; NH_2 vibration at 3180–3370 cm^{-1}; NH_2

Can. J. Chem. Downloaded from www.nrcresearchpress.com by 210.87.254.5 on 09/05/12
For personal use only.

TABLE I

N-Mono- and N,N-di-substituted ureas ($RR'NCONH_2$)

R	R′	M.p., °C*	Ref.
Allyl	H	85	14
Allyl	Allyl	64	15
N-Propyl	N-Propyl	76	14
n-Butyl	H	96	14
i-Butyl	H	141	16
s-Butyl	H	170	14
t-Butyl	H	179 decomp.	14
Cyclopropyl	H	123	17
Cyclohexyl	H	195	18
Cyclohexyl	Cyclohexyl	247	19
Benzyl	H	148	14
Benzyl	Benzyl	125	14
Phenyl	H	147	14
Phenyl	Phenyl	189	14
2-Fluorophenyl	H	175	(*a*)
3-Fluorophenyl	H	149	(*b*)
4-Fluorophenyl	H	179	20
2-Chlorophenyl	H	152	14
2-Bromophenyl	H	202	14
3-Bromophenyl	H	165	14
4-Bromophenyl	H	227	1
2-Iodophenyl	H	198	21
2-Nitrophenyl	H	186	14
2-Methoxyphenyl	H	162	22
4-Methoxyphenyl	H	168	23
o-Tolyl	H	191	14
m-Tolyl	H	143	14
p-Tolyl	H	182	14
2,4-Dimethylphenyl	H	207	24
2,5-Dimethylphenyl	H	209	22
2,6-Dimethylphenyl	H	>300	25
2,4,6-Trimethylphenyl	H	>300	26
2-Biphenylyl	H	157	27
1-Naphthyl	H	215	14
3-Methyl-2-pyridyl	H	193	(*c*)
3-Quinolinyl	H	228	(*d*)
N-(2-Benzothiazolyl)	H	>350	28
Piperidyl	—	125	29

NOTE: New compounds: (*a*) Calc. for $C_7H_7FN_2O$: N, 18.17. Found: N, 18.20. (*b*) Calc. for $C_7H_7FN_2O$: N, 18.17. Found: N, 18.39. (*c*) Calc. for $C_7H_9N_3O$: N, 27.80. Found: N, 28.38. (*d*) Calc. for $C_{10}H_9N_3O$: N, 22.45. Found: N, 21.96.
*Melting points are uncorrected.

deformation (for aliphatic side chains) at 1600–1645 cm^{-1}; phenyl absorption at 1600–1615 cm^{-1}; $\rangle C{=}O$ absorption at 1636–1662 cm^{-1}; and $\rangle C{=}S$ absorption at 1075–1098 cm^{-1} (13).

EXPERIMENTAL

Silicon Isocyanates

These compounds were synthesized by employing modifications of the procedures of Forbes and Anderson (8, 9).

The synthesis of silicon tetraisocyanate is typical. Freshly prepared, dry, finely powdered silver cyanate (660 g; 4.4 moles; 10% theoretical excess) was stirred with anhydrous (sodium dried) benzene (800 ml). Silicon tetrachloride (170 g; 1.0 mole) was added, dropwise, over a 45-minute period, to the rapidly agitated suspension. As the reaction was strongly exothermic, the temperature was maintained below 45° by immersing the flask in ice water. The vigorously stirred suspension was heated at gentle reflux for 3 hours, then cooled to room temperature. After the mixture was filtered, the silver salts were washed with five 70-ml aliquots of anhydrous benzene, pressed, and drained. The benzene was distilled at atmospheric pressure, and the fraction of the residue boiling at 185–189° was collected. Upon redistilling, using a 50-cm Vigreux

Can. J. Chem. Downloaded from www.nrcresearchpress.com by 210.87.254.5 on 09/05/12
For personal use only.

TABLE II

N-Mono- and N,N-di-substituted thioureas ($RR'NCSNH_2$)

R	R′	M.p., °C*	Ref.
Ethyl	Ethyl	102	30
Allyl	H	78	14
n-Butyl	H	79	14
t-Butyl	H	165	14
Cyclohexyl	H	162	18
Phenyl	H	154	14
Phenyl	Methyl	107	14
Phenyl	Phenyl	212	31
2-Fluorophenyl	H	145	(*a*)
4-Fluorophenyl	H	163	32
2,5-Dimethylphenyl	H	135	33
2,6-Dimethylphenyl	H	202	30
2,4,6-Trimethylphenyl	H	220	33
Benzyl	H	165	14
Benzyl	Benzyl	139	14
1-Naphthyl	H	198	14
2,6-Dimethylmorpholinyl	H	166	(*b*)
3-Methyl-2-pyridyl	H	115	(*c*)

NOTE: New compounds: (*a*) Calc. for $C_7H_7FN_2S$: N, 16.46. Found: N, 16.52. (*b*) Calc. for $C_7H_{14}N_2OS$: N, 16.08. Found: N, 15.92. (*c*) Calc. for $C_7H_9N_3S$: N, 25.13. Found: N, 24.98.

*Melting points are uncorrected.

TABLE III

Diureas and dithioureas

Name	Structure	M.p., °C*	Ref.
Ethylene-1,2-diurea	$CH_2NHCONH_2$ | $CH_2NHCONH_2$	194–196	34
Ethylene-1,2-dithiourea	$CH_2NHCSNH_2$ | $CH_2NHCSNH_2$	202	35
o-Phenylenediurea	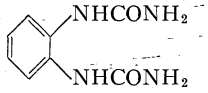	290	36
p-Phenylenedithiourea	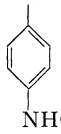	218	37

*Melting points are uncorrected.

column, 167 g (85.3%) of colorless liquid silicon tetraisocyanate, b.p. 185.6°, was obtained. This compound was stored in the refrigerator, where it froze to colorless crystals, m.p. 26°.

When dry, finely powdered lead cyanate (642 g; 2.2 moles; 10% theoretical excess) was employed in the above procedure, the yield of silicon tetraisocyanate was 121 g (61.8%).

The three methylsilicon isocyanates (9) were similarly prepared from the appropriate methylchlorosilanes and silver cyanate. Approximately 30% lower yields of these compounds were obtained when lead cyanate was employed. The boiling points and yields (by the silver and lead cyanate methods, respectively) were: trimethylsilicon isocyanate, b.p. 91.0° (91%, 71%); dimethylsilicon diisocyanate, b.p. 139.2° (84%, 52%); methylsilicon triisocyanate, b.p. 170.8° (88%, 60%).

Silicon tetraisocyanate and the three methylsilicon isocyanates were stored in tightly stoppered bottles to prevent hydrolysis (by atmospheric moisture) to gelatinous silica and cyanic acid. When sealed in glass ampoules these isocyanates could be stored indefinitely.

Can. J. Chem. Downloaded from www.nrcresearchpress.com by 210.87.254.5 on 09/05/12
For personal use only.

Can. J. Chem. Downloaded from www.nrcresearchpress.com by 210.87.254.5 on 09/05/12
For personal use only.

Silicon Isothiocyanates

These compounds were synthesized by employing modifications of previously published (10–12) procedures. Although silver thiocyanate gave approximately 5% higher yields, the resulting products were less pure than those obtained using ammonium thiocyanate.

The preparation of silicon tetraisothiocyanate is typical of the procedure employed to obtain the purest isothiocyanates.

Finely powdered ammonium thiocyanate (190 g; 2.5 moles; 25% theoretical excess) was stirred with anhydrous benzene (800 ml). Silicon tetrachloride (85 g; 0.5 mole) was added, over a 5-minute period, to the rapidly stirred suspension. The mixture was refluxed, with stirring, for 3 hours, cooled to 70°, and filtered through a coarse-grade sintered-glass funnel. After the solids were washed with hot benzene until the characteristic odor of the isothiocyanate could no longer be detected, the combined filtrates were distilled to a residual volume of approximately 200 ml. The hot contents of the flask were immediately transferred to a 400-ml beaker, and the flask was rinsed with 30 ml of benzene. When cold, the crystalline silicon tetraisothiocyanate was *rapidly* filtered through a coarse-grade sintered-glass funnel, washed with a few milliliters of cold benzene, pressed, and drained. Silicon tetraisothiocyanate was thus obtained as 112 g (86%) of colorless crystals, m.p. 144°. An additional 10 g of less pure isothiocyanate was obtained by evaporating the mother liquor to dryness in a rotary evaporator.

When silver thiocyanate was employed, the silicon tetraisothiocyanate obtained was bright yellow.

The three methylsilicon isothiocyanates were prepared using the appropriate methylchlorosilanes and a 25% theoretical excess of ammonium thiocyanate. The following data were obtained: trimethylsilicon isothiocyanate, b.p. 143–143.5° at 760 mm (80%); dimethylsilicon diisothiocyanate, b.p. 64° at 1.0 mm (86%); methylsilicon triisothiocyanate, m.p. 72.5° (83%).

All the silicon isothiocyanates were rapidly hydrolyzed to gelatinous silica and thiocyanic acid on contact with moist air or water. They could be stored without change in tightly stoppered glass bottles or sealed ampoules.

N-Mono- and N,N-Di-substituted Ureas and Thioureas

The following typical synthetic procedure was employed, although in certain instances more solvent was required to dissolve the amine.

A solution of the primary or secondary amine (0.04 mole)* in anhydrous (sodium dried) benzene (10 ml) was added, dropwise, to a solution of silicon tetraisocyanate (1.96 g; 0.01 mole)† in benzene (60 ml). As the addition of many amines resulted in a strongly exothermic reaction, it was occasionally necessary to cool the reaction flask in ice water. The mixture was then heated at reflux for 15–30 minutes, after which the benzene was removed on the steam bath or rotary evaporator. Dilute isopropyl alcohol (45 ml *i*-PrOH: 5 ml H_2O) was added to the residue, the mixture refluxed for 15–30 minutes, then filtered hot through a coarse-grade sintered-glass funnel. The gelatinous silica was washed with two 15-ml aliquots of acetone, and the combined filtrates evaporated on the steam bath or rotary evaporator. The crude product was then recrystallized twice from isopropyl alcohol. To obtain pure ureas or thioureas from certain of the aromatic amines, it was necessary to employ activated charcoal during their recrystallization from alcohol. Using this procedure essentially theoretical (97–100%) yields of the ureas and thioureas were obtained.

The compounds listed in Tables I, II, and III were prepared by this procedure, and analyzed correctly for nitrogen.

It should be noted that no reaction occurred when attempts were made to react silicon tetraisocyanate, or tetraisothiocyanate, with the following amines: 2-trifluoromethylaniline, 2,6-dibromoaniline, and diisobutylamine.

Large-scale Preparations

This general synthetic procedure was employed to prepare large amounts (0.4 *M*) of the following compounds (yields in parentheses): *t*-butylurea (95%), cyclohexylurea (97%), benzylurea (96%), phenylurea (95%), N-(2-benzothiazolyl)urea (95%), *t*-butylthiourea (98%), dibenzylthiourea (95%), 2,6-dimethylphenylthiourea (99%), and 2,4,6-trimethylphenylthiourea (99%). The following preparations are typical.

Benzylurea.—A solution of benzylamine (42.8 g, 0.4 mole) in 100 ml anhydrous benzene was added to a mechanically stirred solution of silicon tetraisocyanate (19.6 g, 0.1 mole) in benzene (150 ml). The mixture was heated at reflux for 0.5 hour, the benzene removed using a rotary evaporator, dilute isopropyl alcohol (200 ml; i.e. 180 ml *i*-PrOH:20 ml H_2O) added, and the mixture refluxed a further 0.5 hour. The hot mixture was filtered through a coarse-grade sintered-glass funnel containing a 0.5-inch layer of Celite. After the gelatinous silica was washed with acetone and the solvents evaporated the crude benzylurea (57.6 g; 96%) was recrystallized from isopropyl alcohol as pearly white platelets, m.p. 148°. Anal.: Calc. for $C_8H_{10}N_2O$: N, 18.65. Found: N, 18.88.

2,4,6-Trimethylphenylthiourea.—Silicon tetraisothiocyanate (26.0 g; 0.10 mole) was finely ground under anhydrous benzene (100 ml) and rapidly added to a well-stirred solution of 2,4,6-trimethylaniline (54.0 g;

**Only 0.02 mole of a diamine is required.*

†When silicon tetraisothiocyanate was used in this procedure, 2.60 g (0.01 mole) was triturated under benzene and quickly transferred to the flask.

0.4 mole) in benzene (100 ml). The procedure was then exactly the same as that employed in the preparation of benzylurea. The yield of white acicular crystals was 76.8 g (99%), m.p. 220°. Anal.: Calc. for $C_{10}H_{14}N_2S$: N, 14.57. Found N, 14.38.

REFERENCES

1. R. B. WAGNER and H. D. ZOOK. Synthetic organic chemistry. John Wiley and Sons, Inc., New York. 1961. pp. 645–648.
2. N. V. SIDGWICK. The organic chemistry of nitrogen. Clarendon Press, Oxford. 1945. p. 332.
3. H. H. ANDERSON. J. Am. Chem. Soc. **73**, 2351 (1951).
4. J. F. O'BRIEN. WADC (Wright Air Develop. Center), Tech. Rept. 57–503 (1957).
5. R. G. NEVILLE. J. Org. Chem. **23**, 937 (1958).
6. J. GOUBEAU and E. HEUBACH. Ber. **93**, 1117 (1960).
7. F. KURZER. Org. Syn. **31**, 21 (1951).
8. G. S. FORBES and H. H. ANDERSON. J. Am. Chem. Soc. **62**, 761 (1940).
9. G. S. FORBES and H. H. ANDERSON. J. Am. Chem. Soc. **70**, 1222 (1948).
10. P. MIGUEL. Bull. Soc. Chim. France, **28**, 103 (1877); Ann. Chim. Phys. **11**, 289 (1877). J. E. REYNOLDS. J. Chem. Soc. **89**, 397 (1906).
11. H. H. ANDERSON. J. Am. Chem. Soc. **69**, 3049 (1947); **72**, 193, 196, 2761 (1950); **75**, 1576 (1953).
12. M. G. VORONKOV and B. N. DOLGOV. Soviet research in organo-silicon chemistry 1949–56. Part II. English Translation. Consultants Bureau, Inc., New York. pp. 344–347.
13. J. BOIVIN and P. BOIVIN. Can. J. Chem. **32**, 561 (1954). R. MECKE and R. MECKE. Chem. Ber. **89**, 343 (1956). L. J. BELLAMY. The infra-red spectra of complex molecules. John Wiley and Sons, New York. 1958. p. 223.
14. I. HEILBRON and H. M. BUNBURY. Dictionary of organic compounds. Oxford University Press, New York. 1953.
15. T. MUKAIYAMA, S. OHISHI, and H. TAKAMURA. Bull. Chem. Soc. Japan, **27**, 416 (1954).
16. F. VON BRUCHHAUSEN and H. HOFFMANN. Ber. **74B**, 1584 (1941).
17. V. P. GOL'MOV. J. Gen. Chem. (USSR) (Engl. Transl.), **5**, 1562 (1935).
18. A. SKITA and H. ROLFES. Ber. **53B**, 1242 (1920).
19. G. FOUQUE. Ann. Chim. (Rome), **15**, 291 (1921).
20. U.S. Patent No. 2,787,574 (1957).
21. R. DOHT. Monatsh. **25**, 943 (1904).
22. C. M. DESAI and M. N. DESAI. J. Indian Chem. Soc. **26**, 249 (1949).
23. R. D. COGHILL and T. B. JOHNSON. J. Am. Chem. Soc. **47**, 184 (1925).
24. R. WALTHER and S. WLODKOWSKI. J. Prakt. Chem. **59**, 276 (1899).
25. R. DAHLBOM and L. E. ÖSTERBERG. Acta Chem. Scand. **9**, 1553 (1955).
26. J. PACKER, J. VAUGHAN, and T. W. WATTS. J. Chem. Soc. 2654 (1952).
27. G. T. MORGAN and L. P. WALLS. J. Chem. Soc. 2225 (1932).
28. R. H. WILEY and A. J. HART. J. Org. Chem. **18**, 1368 (1953).
29. E. E. SLOSSON. Am. Chem. J. **29**, 302 (1903).
30. F. KURZER and P. M. SANDERSON. J. Chem. Soc. 4461 (1957).
31. A. E. DIXON and J. TAYLOR. J. Chem. Soc. **93**, 684 (1908).
32. U.S. Patent No. 2,061,243 (1937).
33. G. M. DYSON and R. F. HUNTER. J. Soc. Chem. Ind. **45**, 81 (1926).
34. T. L. DAVIS and K. C. BLANCHARD. J. Am. Chem. Soc. **51**, 1790 (1929).
35. S. TAKAGI, H. TANAKA, M. YAHO, and K. MACHIDA. Chem. Pharm. Bull. (Tokyo), **7**, 206 (1959).
36. G. PELLIZZARI. Gazz. Chim. Ital. **49**, 23 (1919).
37. E. LELLMAN. Ann. **221**, 1 (1883).

Can. J. Chem. Downloaded from www.nrcresearchpress.com by 210.87.254.5 on 09/05/12
For personal use only.

COORDINATION COMPLEXES OF GROUP (IV) HALIDES

PREPARATION AND INFRARED SPECTRA OF COORDINATION COMPOUNDS OF TITANIUM TETRACHLORIDE, TITANIUM TETRABROMIDE, ZIRCONIUM TETRACHLORIDE, AND TIN TETRACHLORIDE WITH α,ω-DINITRILES AS LIGANDS[1]

SUMER CHAND JAIN AND ROLAND RIVEST
Department of Chemistry, University of Montreal, Montreal, Que.

Received March 25, 1963

ABSTRACT

Coordination complexes between dinitriles of dicarboxylic acids and tetrahalides of titanium, zirconium, or tin have been prepared. The analytical results and the infrared spectra indicate that on working under different experimental conditions three types of compounds are obtained: $2MX_4.L—L$, $MX_4.L—L$, and $MX_4.2L—L$ where MX_4 is a Lewis acid and L—L a bidentate ligand. The compounds $2MX_4.L—L$ are explained by the formation of halogen bridging between the two metal atoms. The compounds $MX_4.L—L$ are considered to be either coordination polymers or chelates of variable ring size and the compounds $MX_4.2L—L$, ordinary addition compounds where no chelation takes place because of the mutual interaction of the two CN groups in a dinitrile of a short chain length.

INTRODUCTION

The compounds $TiCl_4$, $TiBr_4$, $ZrCl_4$, and $SnCl_4$ are all strong Lewis acids. The reactions of $TiCl_4$ with donor molecules have been summarized in a review paper (1). Very little work has been published on the reactions of nitriles with the above mentioned Lewis acids. Emeléus and Rao (2) reported that $TiCl_4$ reacted with two mononitrile molecules to give the 1:2 addition compound. Physicochemical measurements carried out on benzene solutions of these addition compounds (3) led to the conclusion that in dilute solution the 1:2 complexes are dissociated into the 1:1 complexes and the free nitriles. Coerver and Curran (4), reporting on the infrared absorption of the C≡N group in addition compounds, indicated that coordination involving the nitrile group could be evidenced by infrared spectra measurements because of the positive shift of the C≡N stretching frequency on addition-compound formation. It has been recently established (5) that halogen bridging is possible in multinuclear complexes of titanium tetrachloride.

The present work was undertaken to study the possibility of chelate formation and halogen bridging, when dinitriles of increasing chain length react with $TiCl_4$, $TiBr_4$, $ZrCl_4$, and $SnCl_4$. With a short carbon chain the possible interaction between the two CN groups was expected to reduce the donor ability of the second CN group involved in coordination. In such cases compounds of the general formulae $MX_4.2L—L$ are expected.

EXPERIMENTAL

Material and Manipulations

Reagent grade titanium tetrachloride was purified by the method of Gilchrist (6) and the middle fraction of the distillate used in complex formation. Tin tetrachloride was purified by the method patented by Pittsburg Plate Glass Company (7). Commercial zirconium tetrachloride was sublimed in nitrogen atmosphere at 200° C. The compound so obtained was a white powder. Titanium tetrabromide was purified by distilling the commercial product at low pressure. The dinitriles were obtained from Fisher Scientific Company and used as such. The solvents used were purified and made anhydrous by suitable methods. The experimental methods and the methods of analysis for metal and halogens are essentially the same as described previously (8, 9). All the analytical results are included in Table I. The setup used to prepare the complexes was the same as the one used in previous experiments (10).

[1]*Presented at the XXXth Congrès de l'Association Canadienne Française pour l'Avancement des Sciences, Montréal, Nov. 3, 1962.*

Can. J. Chem. Downloaded from www.nrcresearchpress.com by 210.87.254.5 on 09/05/12
For personal use only.

The spectrophotometric measurements were carried out on a Perkin–Elmer Infrared spectrophotometer, model 21, using sodium chloride prism in nujol mulls.

The molecular weights of the complexes were determined by cryoscopic method using anhydrous acetic acid as solvent.

Preparation of the Complexes

The preparation of these complexes was performed in methylene chloride. Three types of compound were prepared. The $MX_4.L$—L compounds were prepared with solutions of the reactants in 1:1 molar ratio.

TABLE I

Complex	Analytical results, found and calculated (%) Metal	Halogen	M.p. (°C)	Infrared spectra results (cm^{-1}) ν_C*	ν_N†	$\Delta\nu$
$TiCl_4NCCH_2CN$	18.47	54.12	150 D‡	2320	2278	42
	18.72	55.42				
$TiCl_42NCCH_2CN$	14.94	44.40	115 D	2330	2278	52
	14.88	44.04				
$TiCl_4NC(CH_2)_2CN$	17.60	51.50	200 D	2315	2262	53
	17.75	52.54				
$2TiCl_4NC(CH_2)_2CN$	21.07	61.50	190 D	2318	2262	56
	20.84	61.70				
$TiCl_4NC(CH_2)_3CN$	16.64	49.10	215 D	2310	2254	56
	16.87	49.97				
$TiCl_4NC(CH_2)_4CN$	15.75	45.65	215 D	2300	2245	55
	16.08	47.60				
$2TiCl_4NC(CH_2)_4CN$	19.60	58.01	190 D	2301	2245	56
	19.65	58.15				
$TiCl_4NC(CH_2)_5CN$	15.50	44.85	200 D	2299	2244	55
	15.36	45.45				
$TiCl_4NC(CH_2)_8CN$	13.70	39.60	162–163	2300	2244	56
	13.52	40.06				
$2TiCl_4NC(CH_2)_8CN$	17.30	50.45	134–136	2300	2244	56
	17.62	52.15				
$TiBr_4NCCH_2CN$	10.93	71.50	160 D	2320	2278	42
	11.04	73.68				
$TiBr_4NC(CH_2)_2CN$	10.80	70.06	150 D	2315	2262	53
	10.71	71.48				
$TiBr_4NC(CH_2)_3CN$	10.18	67.70	130 D	2310	2254	56
	10.38	69.21				
$TiBr_4NC(CH_2)_4CN$	9.97	65.20	160 D	2300	2245	55
	10.07	67.17				
$TiBr_4NC(CH_2)_5CN$	9.82	63.43	135 D	2298	2244	54
	9.78	65.27				
$TiBr_4NC(CH_2)_8CN$	8.92	58.10	114–115	2295	2244	51
	9.01	60.10				
$ZrCl_42NCCH_2CN$	24.89	36.40	170 D	2315	2278	37
	24.98	38.83				
$ZrCl_4NC(CH_2)_4CN$	27.31	39.47	200 D	2295	2244	51
	26.73	41.55				
$ZrCl_4NC(CH_2)_8CN$	23.41	34.57	170–172 D	2295	2244	51
	22.96	35.69				
$SnCl_42NCCH_2CH$	29.0	35.90	80–82	2290	2278	12
	30.24	36.11				
$SnCl_4NC(CH_2)_2CN$	33.55	41.46	158–160 D	2300	2262	38
	34.86	41.62				
$SnCl_4NC(CH_2)_3CN$	32.17	39.62	150–151	2297	2254	43
	33.47	39.98				
$SnCl_4NC(CH_2)_4CN$	31.20	39.15	168–169	2296	2245	51
	32.20	38.46				
$SnCl_4NC(CH_2)_5CN$	31.46	36.80	148–149	2295	2244	51
	31.02	37.03				
$SnCl_4NC(CH_2)_8CN$	27.80	33.60	120–121	2294	2244	50
	27.95	33.38				
$TiCl_4CH_3CN$	20.61	61.03	180–181	2290	2250	40
	20.75	61.43				

*ν_C: CN stretching frequency in the compound.
†ν_N: CN stretching frequency in the pure nitrile.
‡D: decomposed by turning black without melting.

Can. J. Chem. Downloaded from www.nrcresearchpress.com by 210.87.254.5 on 09/05/12
For personal use only.

In all cases powders were obtained which were washed with dry methylene chloride and dried in vacuum at room temperature. The $TiCl_4$ complexes yielded yellow powders; $TiBr_4$, dark red powders; and $SnCl_4$, white powders. Zirconium tetrachloride being insoluble in common solvents, its complexes were prepared by adding excess dinitrile to a suspension of zirconium tetrachloride in the same solvent and the reaction allowed to proceed for about a week. The excess ligand could then be washed out and the white precipitates so obtained dried under vacuum as usual. The $2MX_4.L$—L complexes could be obtained only with $TiCl_4$, and were prepared by adding a dinitrile solution to an excess of the Lewis acid. The yellow powders so obtained were filtered on a sintered-glass filter, washed with the solvent, and dried under vacuum. The $MX_4.2L$—L complexes were obtained only with malononitrile when reacted either with titanium tetrachloride, tin tetrachloride, or zirconium tetrachloride.

The $TiCl_4.2CN—CH_2—CN$ complex is obtained when excess malononitrile is reacted with $TiCl_4$ in solution. The yellow powder is then washed and dried as usual. The $SnCl_4.2CNCH_2CN$ crystalline white compound is always obtained even if the reactants are made to react in a 1:1 molar ratio.

The results of elementary analysis and of infrared spectra measurements are included in Table I.

INFRARED SPECTRA AND STRUCTURAL DISCUSSION

The infrared absorption frequencies of the pure dinitriles and their complexes are included in Table I and illustrated in Fig. 1. As it was observed by Coerver and Curran

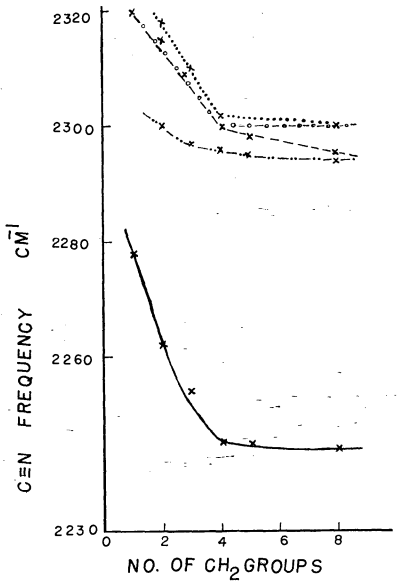

FIG. 1. Variation of the C≡N stretching frequency with respect to the number of CH_2 groups in the dinitrile: ··· 2:1 $TiCl_4NC(CH_2)_nCN$ compounds; o– 1:1 $TiCl_4NC(CH_2)_nCN$ compounds; – – 1:1 $TiBr_4$-$NC(CH_2)_nCN$ compounds; –·· 1:1 $SnCl_4NC(CH_2)_nCN$ compounds; — pure dinitriles.

(4), Kharitonov, Chiang, and Babaeva (11), as a result of complex formation the C≡N stretching frequency increases instead of decreases as in the complexes of carbonyl donors (12). The fact that coordination in nitrile complexes takes place through the nitrogen atom and not through the triple bond of CN group has been confirmed by X-ray examination (13, 14). In all the dinitrile complexes an increase in —C≡N stretching frequency varying from 12 to 56 cm^{-1} has been observed. This suggests that the shift of free electron pair from nitrogen atom of CN group towards metal ion would decrease the mutual repulsion and favor an increase in electron density between the carbon and the nitrogen of the triple bond. The above discussion explains the reason for an increase in —C≡N stretching frequency on coordination.

Can. J. Chem. Downloaded from www.nrcresearchpress.com by 210.87.254.5 on 09/05/12
For personal use only.

In Fig. 1 is represented the —C≡N stretching frequencies of the pure dinitriles as a function of the number of CH_2 groups in the chain. The decrease in —C≡N stretching frequency with increase in chain length shows that with short chain length one C≡N group markedly influences the spectroscopic and chemical behavior of the second C≡N group in the same molecule. But as the chain length increases this mutual influence fades away and in the later members of the series the two C≡N groups in the molecule coordinate independently without influencing each other. This can be observed from the plots of C≡N stretching frequencies of the complexes as a function of CH_2 groups (Fig. 1). The shape of the curves is similar to the pure dinitrile one.

In Fig. 2 the shift in C≡N stretching frequencies has been plotted as a function of the number of CH_2 groups in the dinitrile complexes of the 1:1 composition. From these

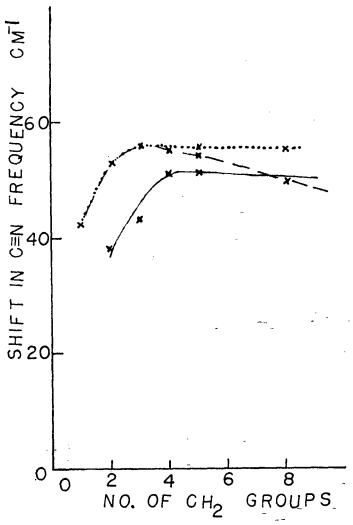

FIG. 2. Variation of the bathochrome effect as a function of the number of CH_2 groups in the dinitrile: ··· 1:1 $TiCl_4NC(CH_2)_nCN$ compounds; – – 1:1 $TiBr_4NC(CH_2)_nCN$ compounds; — 1:1 $SnCl_4NC(CH_2)_nCN$ compounds.

results it is observed that after the number of CH_2 group reaches three and four the curve becomes almost flat, showing that after the chain has reached a certain length, the interaction between the two CN of the same dinitrile is small. From previous experience (8) it seems that if these 1:1 complexes were chelates of variable ring size, it should be evident from the curves of Fig. 2. The fact that compounds of the 1:1 composition are obtained with malononitrile and succinonitrile where ring closure, on the same titanium atom, is almost impossible due to rigid nature of C—C≡N group led us to believe that at least for these specific cases we have polynuclear complexes, which could be cyclic dimers, trimers, or linear coordination polymers.

The formation of $MX_4.2L$—L complex with malononitrile with one CH_2 group is favored where one CN group is coordinated, leaving another C≡N group free. This interpretation is further supported by the infrared spectra of such complexes, where both the shifted peak due to coordination and the unshifted original peak are obtained (Fig. 3).

In the complexes $2MX_4.L$—L we assume that the two metal ions are held together through halogen bridging (Fig. 4).

Can. J. Chem. Downloaded from www.nrcresearchpress.com by 210.87.254.5 on 09/05/12
For personal use only.

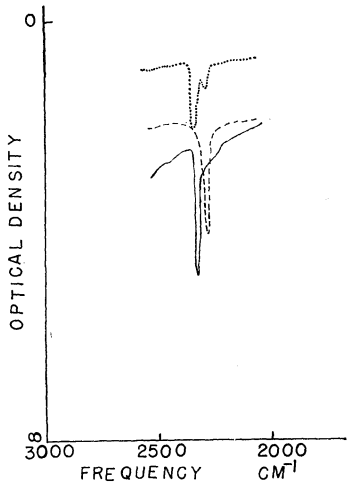

FIG. 3. Infrared spectra of the malononitrile complexes with $TiCl_4$: ···1:2 $TiCl_4NCCH_2CN$ compounds; — 1:1 $TiCl_4NCCH_2CN$ compounds; – – pure $NCCH_2CN$.

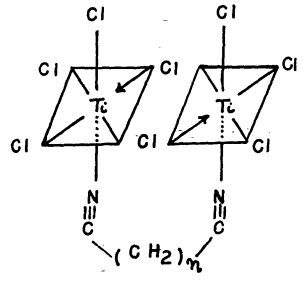

FIG. 4. Chloride bridging in $2TiCl_4NC(CH_2)_nCN$ compounds.

An attempt to determine the molecular weight of these compounds was made. The 1:1 $TiCl_4$, $TiBr_4$, and $SnCl_4$ complexes gave yellow, dark red, and colorless solutions respectively in dry acetic acid. The infrared spectra of some of these solutions indicated that there was dissociation leading to some uncoordinated C≡N group. The amount of dissociation was found to increase with dilution. Conductivity measurements on these solutions indicate about 100-fold increase in conductivity of the solutions as compared to the conductivity of the pure solvent. The increase in conductivity shows that ionization is not very important. The dissociation effect is much harder to assess since the infrared absorption of C≡N frequency is much more intense when this group is coordinated. We have attempted to recover the complex from the solution by evaporating the solvent and observed the formation of a white precipitate the analysis of which confirms the composition $TiCl_2(CH_3COO)_2$.

The molecular weight determinations by cryoscopy on these solutions are included in Table II. They were found to be about half that of the theoretical values. It is to be noticed that the molecular weight found increased with concentration and this is in conformity with the dissociation hypothesis. The fact that the acetate complex mentioned above is very slightly soluble in CH_3COOH and the fact that the observed molecular weight depends upon the dinitrile used strongly suggest that if the complexes are polymers they are probably decomposed by the very polar solvent.

Can. J. Chem. Downloaded from www.nrcresearchpress.com by 210.87.254.5 on 09/05/12
For personal use only.

TABLE II

Complex	Molal concentration	Molecular weight	
		Obtained	Calculated
$TiCl_4NCCH_2CN$	0.0838	126.7	255.8
	0.1026	138.7	
$TiCl_4NC(CH_2)_5CN$	0.0756	167.2	311.9
	0.1289	191.6	
$TiCl_4NC(CH_2)_4CN$	0.0388	128.7	297.88
$TiBr_4NC(CH_2)_5CN$	0.0764	251.8	489.73
$SnCl_4NC(CH_2)_5CN$	0.0881	234.6	382.7

CONCLUSION

From the previous discussion one can draw the following conclusions:

(1) The interaction of Lewis acids with dinitriles can lead to two main types of compounds: $MX_4.L—L$ and $2MX_4.L—L$.

(2) The compounds $2MX_4.L—L$ cannot be polymeric in nature, but can be best explained by assuming halogen bridging between the two titanium atoms of the binuclear complex. It is also possible that in these compounds titanium exhibits a coordination number of 5. To prove this we have prepared the compound $TiCl_4.CH_3CN$, which is very stable and can even be sublimed under low pressure without decomposition. The infrared spectrum of this last complex does not indicate that the triple bond is involved in coordination since the CN stretching frequency is increased by about 40 cm^{-1} through coordination. Attempts to determine the molecular weight of this compound have failed due to the lack of suitable solvents. So there are only two possibilities left for this compound, it is either a single addition compound where the titanium atom has a coordination number of 5, or it is a dinuclear complex where halogen bridging takes place.

(3) The compounds $MX_4.L—L$ can be either coordination polymers or chelated complexes. We have no definite experimental evidence to prove any one of these two possibilities. However, the observations made on solutions in dry acetic acid would give a slight indication that in solutions we are not dealing with coordination polymers.

ACKNOWLEDGMENT

The authors gratefully acknowledge the continued financial support from the National Research Council of Canada.

SOMMAIRE

Des complexes de coordination entre les dinitriles dérivés des acides α,ω-dicarboxyliques et des tétrahalogénures de titane, de zirconium ou d'étain ont été préparés. Les résultats analytiques et les spectres infrarouges montrent que suivant les conditions expérimentales, on peut obtenir les trois sortes de composés suivants: $2MX_4.L—L$, $MX_4.L—L$ et $MX_4.2L—L$ où MX_4 est un acide de Lewis et L—L un ligand bidentate. On explique la formation des composés $2MX_4.L—L$ par la présence de ponts halogénés entre les deux atomes de métal. On considère que les composés $MX_4.L—L$ sont ou bien des polymères de coordination ou des chélates de dimension variable et les composés $MX_4.2L—L$ des composés d'addition ordinaire où il n'y a pas chelation, à cause de l'interaction mutuelle des deux groupes CN du même dinitrile.

REFERENCES

1. I. Shiihara, W. T. Schwartz, Jr., and H. W. Post. Chem. Rev. **61**, 1 (1961).
2. H. J. Emeléus and G. S. Rao. J. Chem. Soc. 4245 (1958).

Can. J. Chem. Downloaded from www.nrcresearchpress.com by 210.87.254.5 on 09/05/12
For personal use only.

3. H. ULICH, E. HERTEL, and W. NESPITAL. Z. Physik. Chem. Ser. B, **17**, 21 (1931).
4. H. J. COERVER and C. CURRAN. J. Am. Chem. Soc. **80**, 3522 (1958).
5. R. RIVEST. Can. J. Chem. **40** (1962).
6. W. S. CLABAUGH, R. T. LESLIES, and R. GILCHRIST. J. Res. Natl. Bur. Std. **55**, 261 (1955).
7. PITTSBURG PLATE GLASS CO. Brit. Patent No. 600,0038 (1948).
8. E. RIVET, R. AUBIN, and R. RIVEST. Can. J. Chem. **39**, 2343 (1961).
9. J. ARCHAMBAULT and R. RIVEST. Can. J. Chem. **36**, 1461 (1958).
10. J. ARCHAMBAULT and R. RIVEST. Can. J. Chem. **38**, 1331 (1960).
11. Y. Y. KHARITONOV, N. C. CHIANG, and A. V. BABAEVA. Russian J. Inorg. Chem. **7**, 9 (1962).
12. S. C. JAIN and ROLAND RIVEST. Can. J. Chem. **40**, 2243 (1962).
13. J. R. HOLDEN and N. C. BAENZIGER. Acta Cryst. **9**, 194 (1956).
14. J. L. HOARD, T. B. OWEN, and O. N. SALON. Acta Cryst. **3**, 130 (1950).

Can. J. Chem. Downloaded from www.nrcresearchpress.com by 210.87.254.5 on 09/05/12
For personal use only.

THERMAL DECOMPOSITION OF MOLECULAR COMPLEXES

II. β-QUINOL CLATHRATES

H. G. McAdie

Department of Physical Chemistry, Ontario Research Foundation, Toronto, Ontario

Received March 1, 1963

ABSTRACT

The β-quinol clathrates of nitrogen, carbon dioxide, methanol, and methyl cyanide decompose at temperatures well below the melting point of the host quinol lattice. The accompanying endothermal effect is broad, indicating that the decomposition occurs gradually over a considerable temperature range. The clathrate decomposition was verified by measurement of the gas evolved. The enthalpy change accompanying decomposition correlates closely with the energy of interaction of the guest molecule with the β-quinol lattice, and the decomposition of the clathrate is suggested to occur by a lattice distortion mechanism in which the size and shape of the guest molecule are important.

Can. J. Chem. Downloaded from www.nrcresearchpress.com by 210.87.254.105 on 09/05/12
For personal use only.

The formation of three dimensionally closed networks of quinol molecules, capable of containing individual molecules of a variety of relatively small species, was first elucidated by the structural work of Powell and collaborators (1). The cavities produced within the quinol network are capable of a limited deformation to accept certain molecules having non-spherical symmetry, and generally not all cavities are filled with guest molecules, the vacancies being stabilized by neighboring units.

Unlike some other types of inclusion compounds, the guest molecules are completely enclosed by the host clathrate lattice. At room temperature interactions between the guest molecules and the quinol network contribute to the overall stability of the clathrate (2), the heat of formation increasing linearly with the fraction of available cavities filled.

Since the quinol cavities can only be filled during their formation, it was of interest to determine whether the guest molecules remained trapped until the melting point of the quinol cage was reached, or whether a process prior to melting was responsible for the thermal decomposition of these materials. Isothermal studies (3) have indicated that clathrates have a measurable decomposition pressure at temperatures well below the melting point of quinol. The evident reversibility of the process

$$\text{clathrate (s)} \rightarrow \text{quinol (s)} + \text{guest (g)}$$

implies reference to the β-modification of the quinol lattice and an increasing ease of interchange between a guest molecule in the cavity and one in the surroundings as temperature increases.

EXPERIMENTAL

Samples of the quinol clathrates of carbon dioxide and nitrogen were obtained from the National Lead Company. Clathrates of methanol and methyl cyanide were prepared by slow crystallization from warm solutions of quinol in these solvents. α-Quinol was recrystallized from distilled water and dried over P_2O_5. γ-Quinol was prepared by sublimation of α-quinol under vacuum at about 160° C.

The fraction of filled cavities in the clathrates was determined by dissolving known weights in ethanol, evaporating the solvent under vacuum at room temperature, and measuring the weight loss. The lattice structures were confirmed by Debye–Scherrer powder patterns obtained using Cu $K\alpha$ radiation with a nickel filter.

For differential thermal analysis, −100-mesh samples were diluted to 20% by weight in ignited α-alumina. Differential thermograms were obtained with an apparatus described earlier (4), having provision

for purging the furnace by a controlled stream of a desired gas. Temperatures were calibrated against the fusion endotherm of a National Bureau of Standards calorimetric sample of benzoic acid. Thermograms were obtained at heating rates of 1.2 and 3.0° C min^{-1}.

In a separate series of experiments samples of undiluted clathrates were placed in a small bulb of known volume attached to a mercury manometer. The sample was heated at 1° C min^{-1} and the pressure within the system continuously measured. After correcting for the air present in the system the results were calculated as the fraction of available guest molecules liberated at a given temperature.

RESULTS

The thermograms of α- and γ-quinol obtained at 3.0° C min^{-1} are shown in Fig. 1. Corrected fusion peak temperatures for these two modifications were found to be 172.7

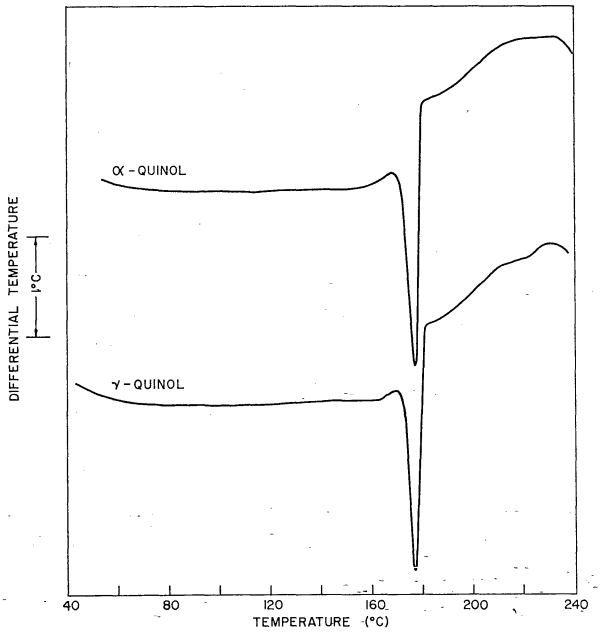

FIG. 1. Differential thermograms of non-clathrate forms of quinol.

and 172.4° C respectively. No transitions were observed below approximately 155° C, where a drift in the base line commenced, interrupted by the sharp quinol fusion peak and followed by a marked displacement of the base line. The initial base-line drift appeared to be slightly less in the case of the γ-quinol. The displacement of the base line is attributed to decomposition of the quinol on melting, forming gaseous products (5) which alter the specific heat of the sample with respect to the reference. No attempt was made to determine these decomposition products, but even under inert atmospheres the samples were found to be completely charred at 200° C. The formation of gaseous decomposition products was also indicated in the case of α-quinol by an increase in pressure beginning at about 150° C.

The base-line displacement was characteristic also of all the clathrates, thus being independent of the original crystal modification of the quinol. It was also found to be unaffected by the nature of the furnace atmosphere, the same effect being noted in carbon dioxide, nitrogen, or argon atmospheres as well as in air. It appears, therefore, that quinol begins to degrade near its melting point, the fusion endotherm being superimposed upon this degradation.

Can. J. Chem. Downloaded from www.nrcresearchpress.com by 210.87.254.105 on 09/05/12
For personal use only.

Thermograms of the clathrates, also obtained at 3.0° C min^{-1}, appear in Fig. 2. The quinol fusion peak temperatures for the range of clathrates studied was found to be

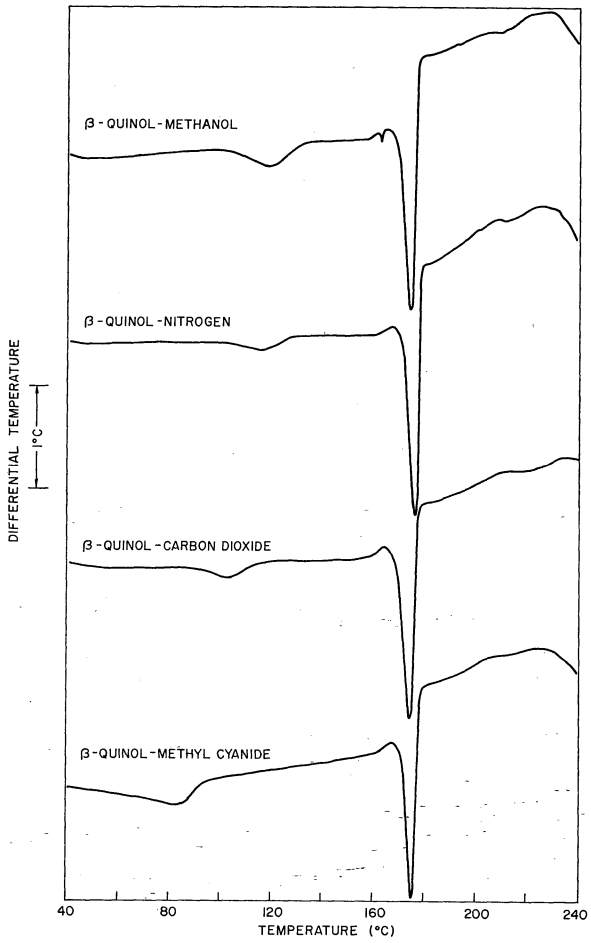

FIG. 2. Differential thermograms of quinol clathrates.

172.0±0.5° C. Changing the furnace atmosphere from one of air to one of the pure guest species (in the cases of the nitrogen and carbon dioxide clathrates) tended to sharpen the quinol fusion endotherm slightly without altering its peak temperature.

Clathrate thermograms also exhibited a broad shallow endotherm at temperatures considerably below the fusion temperature of the host quinol lattice. This endotherm was somewhat more accentuated when obtained at 3° C min^{-1} than at 1.2° C min^{-1}. The gas evolution curves, obtained at 1.2° C min^{-1} and shown in Fig. 3, indicate that these low-temperature endotherms correspond to the decomposition of the clathrate, and a further estimate of the decomposition temperature could be obtained by extrapolating the linear portions of these curves to the temperature axis. The results obtained are compared with the peak temperatures of the decomposition endotherms in Table I.

To estimate the enthalpy change associated with the decomposition endotherm, comparison was made of the areas under this endotherm and under the quinol fusion endotherm. Because of the base-line displacement, it was difficult to define the latter accurately;

Can. J. Chem. Downloaded from www.nrcresearchpress.com by 210.87.254.105 on 09/05/12
For personal use only.

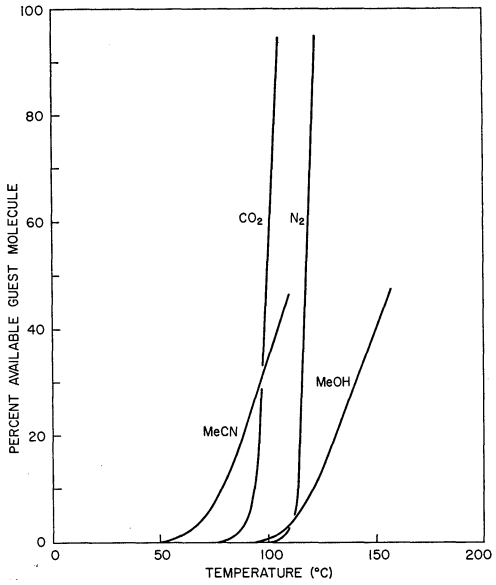

FIG. 3. Gas evolution accompanying thermal decomposition of quinol clathrates.

TABLE I

Decomposition temperatures of quinol clathrates (°C)

Guest	DTA	Gas evolution
MeOH	116.5	113.0
N_2	114.5	115.5
CO_2	101.0	94.5
MeCN	80.0	73.0

however, an estimate was made based on the construction of Berg (6). The heat of decomposition of the clathrate having all available cavities filled can be calculated from the relation

$$\Delta H_d = (3/x) \cdot (a_C/a_Q) \cdot \Delta H_f,$$

where

ΔH_d = heat of clathrate decomposition (kcal mole^{-1} guest),
x = fraction of available cavities filled,
a_C = area of clathrate decomposition endotherm,
a_Q = area of quinol fusion endotherm,
ΔH_f = heat of fusion (kcal mole^{-1} quinol) (7).

The theoretical composition of a clathrate is 3 moles quinol per mole guest (1), so that the ratio $3/x$ is equivalent to the actual molar ratio prevailing in the experimental sample. Table II compares the data obtained in this way with reported values for heat of decomposition (2).

The various modifications of quinol were confirmed by Debye–Scherrer powder patterns, the results agreeing with accepted values (8). The principal differences between these structures, first reported by Caspari (9, 10) and subsequently modified by Powell

Can. J. Chem. Downloaded from www.nrcresearchpress.com by 210.87.254.105 on 09/05/12
For personal use only.

TABLE II

Heats of decomposition of quinol clathrates
(kcal mole^{-1} guest)

Guest	Found	Literature (2)
N_2	+ 5.8	+ 5.8
MeOH	+10.0	+11.0
CO_2	+13.3	—
MeCN	+ 7.5	—

TABLE III

Crystalline modifications of quinol

		Found			Accepted (6)		
α-Quinol (from water)	*d*-Spacing (Å)	4.12	3.22	4.40	4.11	3.21	4.41
	Intensity	100	100	70	100	100	65
β-Quinol (from methanol)	*d*-Spacing (Å)	3.88	4.39	4.81	3.89	4.40	4.80
	Intensity	100	60	40	100	60	30
β-Quinol–nitrogen	*d*-Spacing (Å)	3.87	4.38	4.80	—	—	—
	Intensity	100	60	40	—	—	—
β-Quinol – carbon dioxide	*d*-Spacing (Å)	3.90	4.41	4.78	—	—	—
	Intensity	100	60	40	—	—	—
β-Quinol – methyl cyanide	*d*-Spacing (Å)	4.01	4.64	3.28	—	—	—
	Intensity	100	80	80	—	—	—

(1), are indicated by their *d*-spacings in Table III. Clathrates of most species exhibited *d*-spacings very similar to those shown for β-quinol from methanol. However, the methyl cyanide clathrate appeared to have *d*-spacings considerably different from any other clathrate lattice examined, or any other modification of quinol. This may be associated with the considerable distortion of the quinol lattice necessary to accommodate this essentially linear guest molecule.

Diffraction patterns of the γ-quinol indicated this material to be metastable and to revert to the α-modification on storage.

DISCUSSION

The crystalline modifications of quinol behave similarly on heating, there being no sharp transitions between room temperature and the melting point. Once formed, each lattice appears to be stable, although the clathrate modification (β-quinol) is capable of sufficient distortion or rearrangement to permit the trapped guest molecules to evolve. Since it is not presently possible to undertake an X-ray examination of the quinol lattice remaining following the clathrate decomposition, it is uncertain whether loss of the guest molecules is accompanied by a change in quinol lattice, say from β- to α-quinol. The enthalpy change between these two modifications is only 0.17 kcal mole^{-1} (2).

At 25° C the energy of interaction of guest molecules with the β-quinol lattice, corresponding to the process

$$\text{clathrate (s)} = \beta\text{-quinol (s)} + \text{guest (g)},$$

has been determined (2), and the results compare well with heats of decomposition determined from the differential thermograms (Table II). Thus, energetically the quinol clathrates evidently decompose according to the process stated above. The range of values for the heats of decomposition may be ascribed to differences in dipole–dipole

Can. J. Chem. Downloaded from www.nrcresearchpress.com by 210.87.254.105 on 09/05/12
For personal use only.

interactions between the guest and the β-quinol lattice. These are absent in the case of the nitrogen clathrate, but increase with the polarizability of guest molecules containing C—O, O—H, and C—N bonds. The result is that the interaction of the guest molecule with the β-quinol lattice exceeds the mutual interactions of the pure species in its liquid or solid state (2), i.e. more energy is required to remove a single molecule from the clathrate cavity than to remove it from its own crystal lattice.

The symmetry of the guest molecule plays an important part in the thermal decomposition of its clathrate. Of the species examined, nitrogen is easily accommodated without distortion of the β-quinol network. Methanol, carbon dioxide, and methyl cyanide, in this order, progressively extended the cavity along the *c*-direction (11), with corresponding decrease in the *a*-direction. This reduces the possible rotation of the guest molecule within the cavity (12, 13) and the strain introduced into the lattice appears to cause these clathrates to decompose at progressively lower temperatures, suggesting that the mechanism responsible for the thermal decomposition of quinol clathrates is basically one of lattice distortion. At a suitable temperature the lattice may possess sufficient thermal motion between the two interpenetrating quinol networks to allow distortion of the cavity, perhaps producing a bottleneck type of opening through which the guest molecule can escape. Such distortion would occur gradually and continuously with temperature rather than at some discrete temperature. The existence of initial distortion due to the presence of a non-spherical guest molecule would facilitate this process, causing the clathrate to decompose at a lower temperature.

Reduction of the ambient pressure causes the clathrates to decompose at lower temperatures and the effect of pressure is not the same for each clathrate (14). This is to be expected if the reversible nature (3) of the decomposition process

$$\text{clathrate (s)} \rightarrow \beta\text{-quinol (s)} + \text{guest (g)}$$

is correct. Such reversibility may better be understood in terms of a distortion of the β-quinol lattice to the extent that the guest molecule may pass between the cavity and the surroundings. Since vacant normal cavities can be stabilized by their occupied neighbors, it is suggested that distorted cavities may also be stabilized due to the long-range interpenetration of the two quinol networks. Thus a cavity once distorted sufficiently to allow the guest to escape would remain so, permitting the re-entry required by a truly reversible process.

In general, the heats of decomposition increase with the size of the guest molecule, although methyl cyanide again appears to be somewhat anomalous. Since the diffraction pattern of this clathrate is markedly different from the others, it is possible that the distortion inherent in this material has altered the interaction of these molecules with the quinol network. It is further interesting that the gas evolution curves for nitrogen and carbon dioxide are similar and quite steep, while those for methyl cyanide and methanol have a similar but much lower slope. This could be interpreted as due to the guest molecule having to escape through a bottleneck opening in the cavity wall, the relatively large methyl group in each case requiring more time to diffuse through. It appears that clathrates of guest molecules having roughly similar size and shape tend to decompose at the same rate, so that the overall decomposition characteristics are determined by the extent of initial distortion of the lattice by the guest molecule and the size and shape of this guest, which determines the extent of further distortion required and the rate of eventual decomposition.

Can. J. Chem. Downloaded from www.nrcresearchpress.com by 210.87.254.105 on 09/05/12
For personal use only.

One further endothermal effect was observed only in the case of the methanol clathrate. This occurred just prior to the quinol fusion endotherm (Fig. 1) and was quite sharp, although small in magnitude. Since the clathrate is decomposed by this temperature, the magnitude of this endotherm suggests it could be associated with a transition in the quinol lattice from the β- to the α-modification, although this could not be detected in any other clathrate or quinol modification examined.

A more detailed examination of the quinol lattice structure following clathrate decomposition, and of the gas evolution characteristics during thermal decomposition, is expected to resolve some of these interesting features.

ACKNOWLEDGMENTS

This research was carried out under a research grant to the Ontario Research Foundation from the Province of Ontario, received through the Department of Economics and Development.

The author wishes to thank the National Lead Company for making available samples of the nitrogen and carbon dioxide clathrates, and Messrs. G. C. Cranton and D. Cobb for their technical assistance.

REFERENCES

1. H. M. POWELL. J. Chem. Soc. 61 (1948).
2. D. F. EVANS and R. E. RICHARDS. Proc. Roy. Soc. (London), Ser. A, **223**, 238 (1954).
3. W. F. K. WYNNE-JONES and A. R. ANDERSON. Compt. Rend. Réunion Chim. Phys., 2e, Paris, 1952. p. 246.
4. H. G. MCADIE. Can. J. Chem. **40**, 2195 (1962).
5. A. HAGEMANN. Z. Physik. Chem. **42**, 355 (1929).
6. L. G. BERG. Compt. Rend. Acad. Sci. URSS, **49**, 648 (1945).
7. D. H. ANDREWS, G. LYNN, and J. JOHNSTON. J. Am. Chem. Soc. **48**, 1274 (1926).
8. AMERICAN SOCIETY for Testing Materials Index to X-Ray Powder Data File. 1962.
9. W. A. CASPARI. J. Chem. Soc. 2944 (1926).
10. W. A. CASPARI. J. Chem. Soc. 1093 (1927).
11. D. E. PALIN and H. M. POWELL. J. Chem. Soc. 815 (1948).
12. J. S. DRYDEN. Trans. Faraday Soc. **49**, 1333 (1953).
13. L. A. K. STAVELEY. J. Phys. Chem. Solids, **18**, 46 (1961).
14. M. GILFORD and S. GORDON. U.S. Dept. Commerce, Office Tech. Serv. PB Rept. 145517. 1960.

Can. J. Chem. Downloaded from www.nrcresearchpress.com by 210.87.254.105 on 09/05/12
For personal use only.

THERMAL DECOMPOSITION OF MOLECULAR COMPLEXES

III. UREA INCLUSION COMPOUNDS OF MONOSUBSTITUTED ALIPHATIC SERIES[1]

H. G. McAdie

Department of Physical Chemistry, Ontario Research Foundation, Toronto, Ontario

Received April 24, 1963

ABSTRACT

Examination of the thermal decomposition of urea inclusion compounds has been extended to complexes of the even-numbered members of the following aliphatic series: *n*-alcohols, *n*-alkylamines, *n*-alkyl bromides, and *n*-carboxylic acids. The decomposition has been studied primarily by differential thermal analysis and an attempt made to correlate the observed decomposition temperatures and heats of decomposition with the particular guest species. The decomposition mechanism appears to involve acquisition of sufficient energy by the guest molecule to permit its diffusion from the canal, the decomposition temperature being related to the activation energy required for this diffusion process.

Can. J. Chem. Downloaded from www.nrcresearchpress.com by 210.87.254.6 on 09/05/12
For personal use only.

Many of the urea–*n*-paraffin inclusion compounds have been shown to endothermally decompose below the melting point of urea, with a concurrent change in the crystal lattice of urea and loss in weight (1). Energetically, the decomposition involves the process

$$\text{complex (s)} = \text{urea (s)} + \text{guest (liq.)}$$

and it was suggested that this decomposition was similar to the fusion of the pure long-chain species. For the complex to decompose, the guest molecule must achieve a certain level of vibrational–rotational energy before it is sufficiently mobile to escape the canal. In the case of complexes stable up to the melting point, the host urea cage simply melts, liberating the entrapped guest molecule.

It was of interest to extend these studies to urea inclusion compounds of other even-numbered, long-chain series, having one terminal group different from hydrogen. The stability of the complex should be influenced by the size of this group and its ability to associate with other guest molecules either through dipole–dipole interaction or through hydrogen bonding. The present work describes the thermal decomposition of complexes having as guest molecules the even-numbered *n*-alcohols, *n*-carboxylic acids, *n*-alkylamines, and *n*-alkyl bromides. In these cases a maximum of two guest molecules can be mutually associated within the urea canal, while it is hoped a future paper will report the extension of this work to some α,ω-disubstituted long-chain guest molecules in which the number of guest molecules consecutively associated within the canal may be higher.

EXPERIMENTAL

Preparation of the various inclusion compounds was by methods described previously (1). All guest materials were Eastman white label grade or equivalent, while other materials were reagent grade. The presence of the hexagonal urea complex lattice was confirmed in each case by Debye–Scherrer powder patterns obtained using Cu $K\alpha$ radiation with a nickel filter.

Differential thermograms of the complexes were obtained by the method described earlier (1), except that samples were ground to pass only a 100-mesh screen prior to dilution with ignited α-alumina. Visual microscopy was not found to yield reproducible decomposition temperature data and was not used to any extent. Thermogravimetric analysis was carried out on the urea–*n*-alcohol series of complexes only, because of the high decomposition temperatures found.

[1]*Presented in part at the 144th Meeting of the American Chemical Society, Los Angeles, California, March–April, 1963.*

RESULTS

Differential Thermal Analysis

The differential thermograms of the various series of complexes are shown in Figs. 1 to 4, inclusive. In all cases a low-temperature endotherm was observed, corresponding

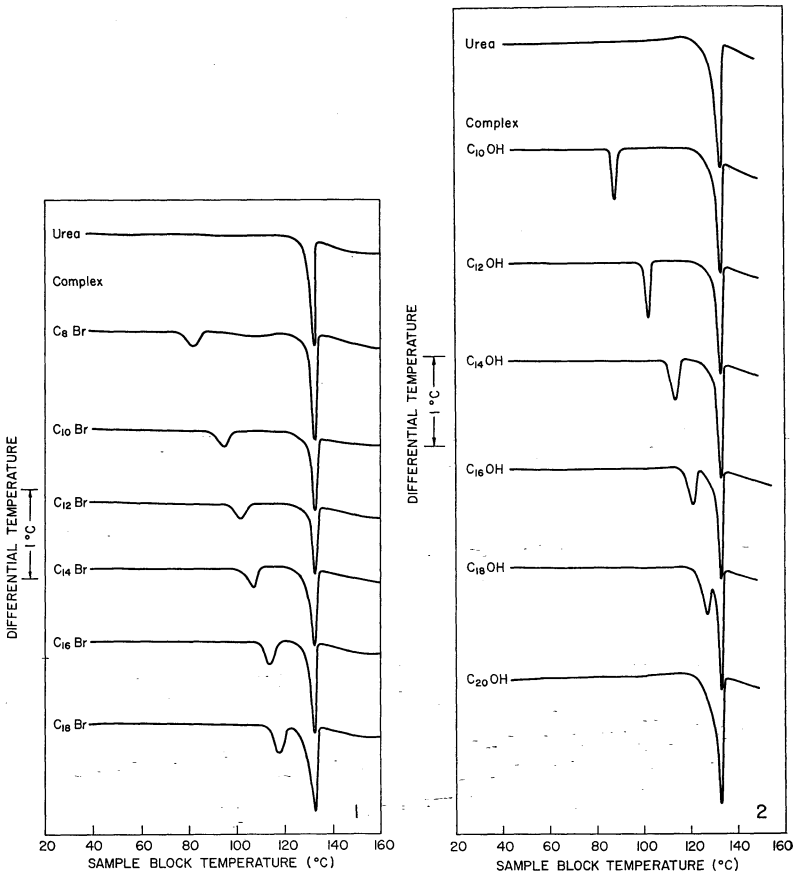

FIG. 1. Differential thermograms of urea–*n*-alkyl bromide complexes.
FIG. 2. Differential thermograms of urea–*n*-alcohol complexes.

to the complex decomposition, which progressed steadily towards the urea fusion endotherm as the carbon chain length of the guest molecule increased. The urea fusion endotherm allowed each system to be internally calibrated with respect to temperature and to the enthalpy change equivalence of peak area.

Complexes of the *n*-alcohols (Fig. 2) and the *n*-carboxylic acids (Fig. 3) decompose over a narrower temperature range than those of the other series studied, although the point of incipient decomposition is less well defined in the case of the *n*-carboxylic acid complexes. Thermograms of the *n*-alkylamine complexes (Fig. 4) exhibit an exotherm immediately following the urea fusion endotherm. This is attributed to the reaction of the molten urea with the liquid *n*-alkylamine liberated at a lower temperature, producing substituted ureas (2). The decyl- and dodecyl-amine complexes give only traces of this exotherm since these guest molecules volatilize more readily in the interval between

Can. J. Chem. Downloaded from www.nrcresearchpress.com by 210.87.254.6 on 09/05/12
For personal use only.

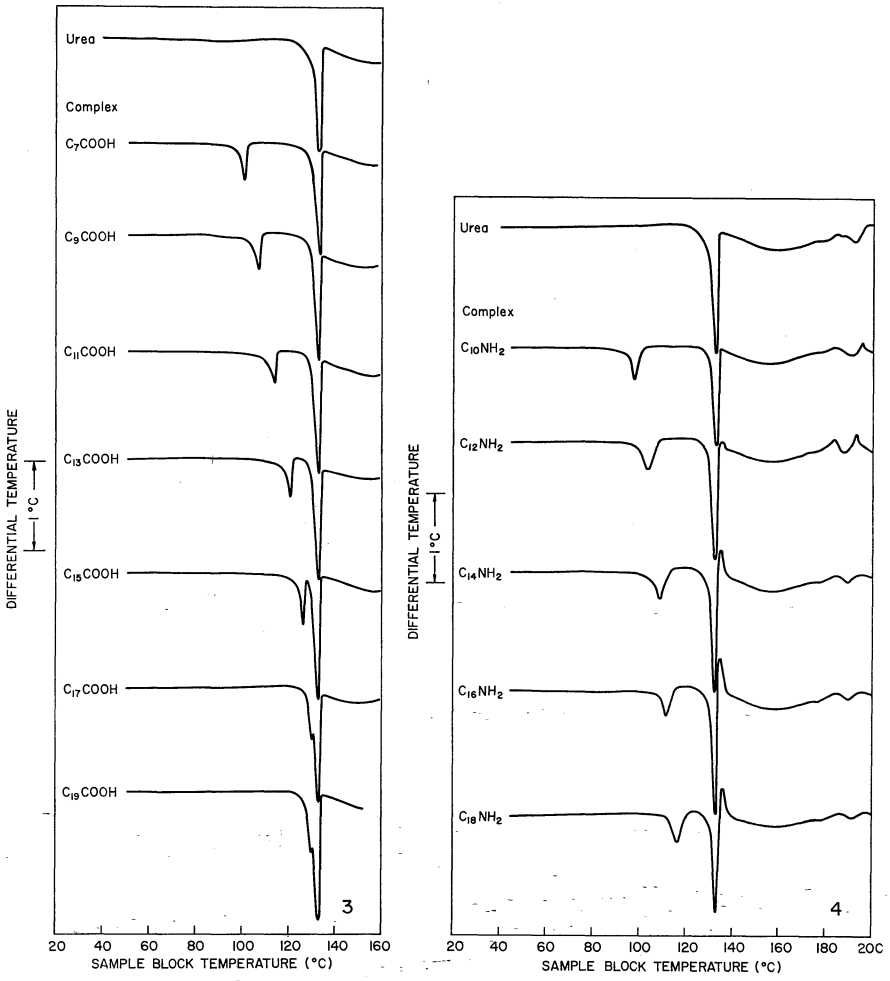

FIG. 3. Differential thermograms of urea–*n*-carboxylic acid complexes.
FIG. 4. Differential thermograms of urea–*n*-alkylamine complexes.

complex decomposition and urea fusion. There was some evidence of further reactions between 160° and 200° C, but no attempt was made to investigate these further.

The decomposition temperatures of the various complexes are given in Table I as the peak temperature of the decomposition endotherms corrected to a value of 132.7° C for

TABLE I
Decomposition temperatures of urea inclusion compounds (°C)

Carbon chain length	Guest				
	n-Paraffin	*n*-Alkyl bromide	*n*-Alcohol	*n*-Alkylamine	*n*-Carboxylic acid
10	82.4	92.4	87.2	100.0	107.6
12	92.5	102.1	102.7	109.3	114.3
14	102.4	108.1	113.6	119.2	120.8
16	108.4	113.5	121.7	125.7	127.2
18	113.9	117.5	127.1	129.0	130.5
20	117.9	—	129.4	—	131.8

Can. J. Chem. Downloaded from www.nrcresearchpress.com by 210.87.254.6 on 09/05/12
For personal use only.

the peak of the urea fusion endotherm. This is a procedural decomposition temperature corresponding to about 50–80% of decomposition, depending upon the reaction rate, but in a given system it is more reproducible than incipient temperatures defined in a variety of ways. Further, by calibrating over a reasonably short temperature interval with another, known peak temperature, the influence of heating rate upon peak temperature is substantially reduced. Redetermined data for the urea–*n*-paraffin complexes are included and correlate satisfactorily with earlier measurements (1).

Enthalpy changes accompanying the decomposition process were calculated from peak areas by the method previously used (1) and are given in Table II. In all cases, these

TABLE II

Enthalpy of decomposition of urea inclusion compounds (kcal mole^{-1} guest)

Carbon chain length	Guest				
	n-Paraffin	*n*-Alkyl bromide	*n*-Alcohol	*n*-Alkylamine	*n*-Carboxylic acid
10	+11.3	+9.6	+9.4	+11.9	+12.6
12	13.8	12.8	12.1	14.7	16.3
14	16.6	16.5	15.0	16.6	20.5
16	19.5	20.7	18.4	19.0	25.2
18	22.6	25.3	22.0	22.7	—
20	26.0	—	—	—	—

enthalpy changes increased linearly with carbon chain length and compared favorably with those obtained from equilibrium data (3, 4) for the process

$$\text{complex (s)} = \text{urea (s)} + \text{guest (liq.)}.$$

No such data were available in the literature for the urea–*n*-alkylamine complexes, which decompose at temperatures intermediate to complexes of the *n*-alcohols and *n*-carboxylic acids. Experimental heats of decomposition were generally slightly lower than heats of reaction for the above process, due to the presence of coprecipitated urea.

Thermogravimetric Analysis

The loss in weight following decomposition of the urea–*n*-alcohol complexes is shown in Fig. 5. Decompositions in excess of 100% correspond to thermal degradation of the urea which begins to show a detectable weight loss at about 125° C. Since the decomposition temperatures of all the complexes examined were greater than those for the urea–*n*-paraffin complexes (1), it was impractical to carry out extensive thermogravimetric analysis because of the poor resolution of the two-stage decomposition process. As seen from Fig. 5 only complexes of the two shorter chain length *n*-alcohols could be so resolved.

DISCUSSION

It is convenient to divide the complexes studied into two groups, one in which the end-group influence may be predominantly related to size and the other where intermolecular association between successive guest molecules is the principal feature. Neither group can be completely exclusive of the other and in each case comparison will be made with the urea–*n*-paraffin complexes as reference.

Group I

The *n*-alkyl bromides were selected as representative of a large terminal group which could be readily accommodated within the hexagonal urea canal. Comparison of this series

Can. J. Chem. Downloaded from www.nrcresearchpress.com by 210.87.254.6 on 09/05/12
For personal use only.

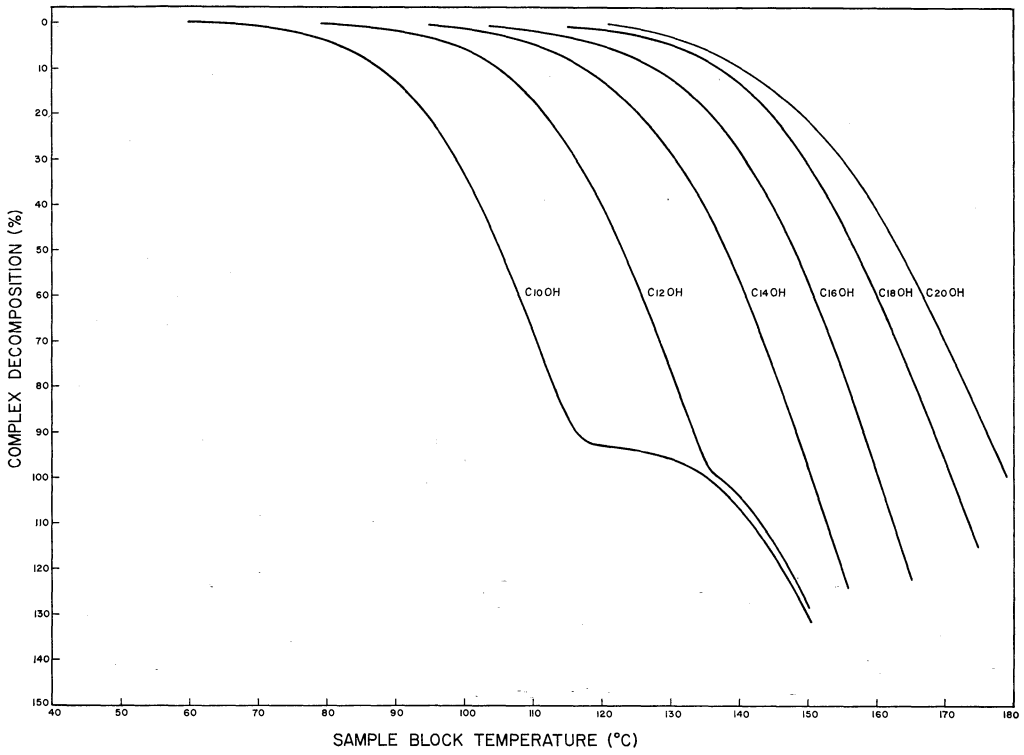

FIG. 5. Thermogravimetric analysis curves for urea–*n*-alcohol complexes.

of complexes with those of the *n*-paraffins is displayed in Fig. 6. The *n*-alkyl bromide complexes decompose at higher temperatures than the *n*-paraffin complexes, although the two pure species melt at virtually the same temperature (5, 6). Evidently the volume of a terminal bromine atom, compared to a terminal hydrogen atom, has increased the stability of the complex by occupying a larger portion of the available canal cross section. Calculation of the increase in effective area occupied suggests that there may be a limited strain introduced into the canal walls adjacent to the bromine atom.

The greater molecular volume of the *n*-alkyl bromides is reflected in an increased ratio of urea to guest (3, 4, 7, 8) compared with *n*-paraffin complexes of the same chain length. If the only difference were due to replacement of a hydrogen by a bromine, it would be expected that the reported comparative molar ratios should increase in parallel fashion with carbon chain length. However, this is not the case, the molar ratio of urea:bromide increases faster than that of urea:paraffin. This divergence of molar ratios appears to be a peculiarity of complexes in which the guest molecule has a cross section close to, or slightly greater than, the available canal cross section (4) and may be associated with the longitudinal packing of the guest molecules within the canal. Since the C—Br bond is at an appreciable angle to the axis of the carbon chain, dielectric evidence (9, 10) suggests that this grouping may occupy preferred sections of the canal where the potential energy of stable sites and the strain induced into the canal walls are at a minimum. The C—Br bond is likely directed towards one of the corners of the hexagonal canal with the polar groups located in planes normal to the longitudinal axis containing the oxygen

Can. J. Chem. Downloaded from www.nrcresearchpress.com by 210.87.254.6 on 09/05/12
For personal use only.

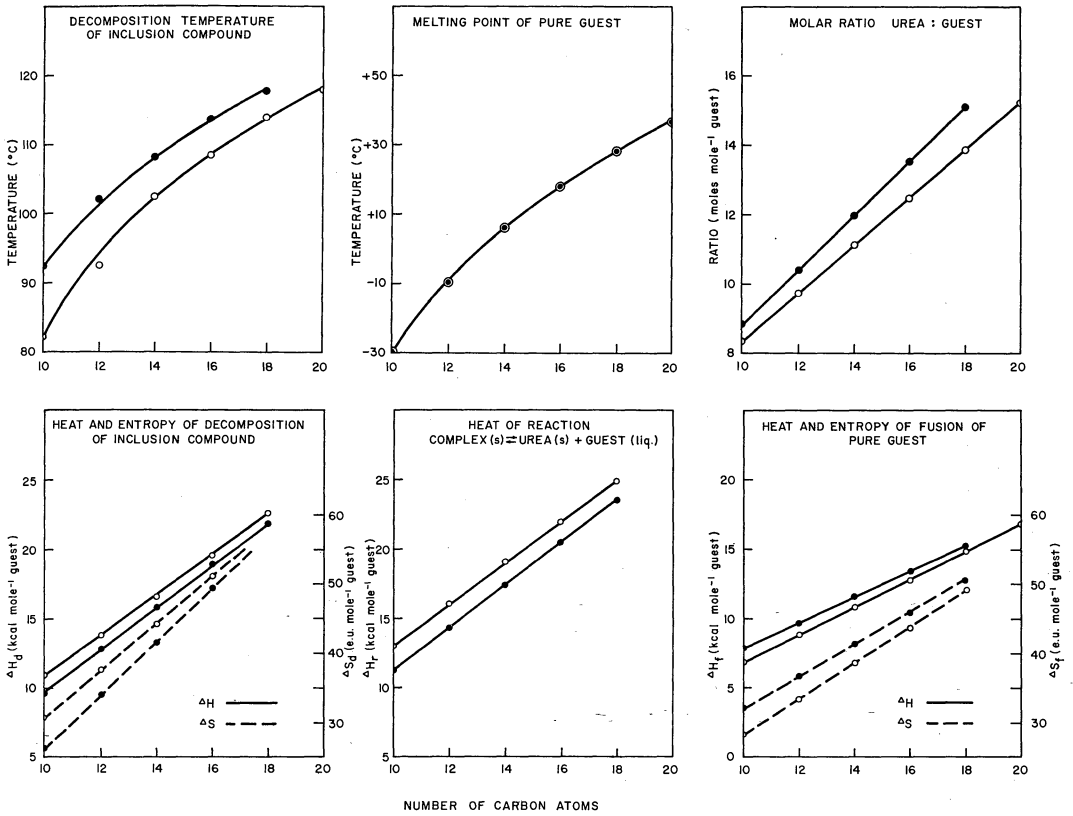

FIG. 6. Comparisons of the *n*-paraffin (○) and *n*-alkyl bromide (●) systems.

atoms of urea molecules. The introduction of such preferred locations for guest molecules within the canal would affect the regularity with which guest molecules could be accommodated.

Considering the energetics of the two systems, the heats and entropies of fusion of the pure guest species converge (5, 11). The heats and entropies of decomposition of their complexes also converge, but in opposite array, the *n*-paraffin complexes absorbing more energy on decomposition and undergoing a larger entropy change than those of the *n*-alkyl bromides. The same features are shown in the heats of reaction calculated from equilibrium data in the literature (3, 4).

The melting of a long-chain species is generally associated with increased rotation of the molecule (12, 13) and it appears that the same holds true for the decomposition of the complex. Nuclear magnetic resonance (14) and infrared (15) evidence have shown the long chains to be capable of considerable motion within the canal, including restricted rotation as well as other possible modes. Since the urea lattice is capable of slight expansion with temperature (10) it is suggested that at the decomposition temperature the overall energy of the chain becomes adequate to render it sufficiently mobile to diffuse out of the canal. This does not necessarily mean there has to be complete dynamic rotation of all guest molecules, but rather that these have acquired sufficient energy of rotational vibration to permit frequent passage over the potential barriers situated at 60° intervals around the canal (9) and now have required a translational component along the axis of the canal.

Can. J. Chem. Downloaded from www.nrcresearchpress.com by 210.87.254.6 on 09/05/12
For personal use only.

Energetically the decomposition follows a process which yields the guest molecule in the liquid state, as expected since the decomposition temperatures of the complexes all lie above the melting points of the pure guest species, and accounts for the heat of decomposition of the *n*-alkyl bromide complexes being less than that for the corresponding *n*-paraffin complexes. Dielectric evidence (9) indicates that in the liquid state more association of the *n*-alkyl bromides is possible than in the urea canal. Therefore, when the *n*-alkyl bromide chains are liberated from the canal and aggregate into the liquid state there should be an energy *release* not present when the *n*-paraffin chains undergo the same process. This energy release, corresponding to an increased dipole association among the *n*-alkyl bromide molecules, and superimposed upon the energy absorption required to place these guest molecules in an adequately mobile state within the canal, results in an experimental heat of decomposition below that for the *n*-paraffin complexes.

Once the guest molecule is sufficiently mobile, there is still the problem of its removal from the canal. This may occur by a diffusion mechanism and as such would have an activation energy associated with it. It would then be expected that the size of the bromine atom would result in a higher activation energy for diffusion of this species from the canal. Since the complex does not decompose until a given section of the canal is vacant, this results in the *n*-alkyl bromide complexes decomposing at higher temperatures than the *n*-paraffin complexes.

At present it has not been feasible to estimate activation energies for the diffusion of long-chain molecules from the urea canal. Although under certain circumstances it is possible to estimate such data from the results of both DTA and TGA experiments, neither of these techniques, as presently applied, uniquely measures the diffusion process. If activation energies are based upon DTA endotherms, they will refer to the energy absorption process which consists to a large measure in changes in the N—H···O bond lengths in urea involved in the transition from the hexagonal to the tetragonal lattice (8, 16). If activation energies are based upon TGA weight loss data, they will be associated with the ultimate volatilization of the long-chain molecule *after* it has escaped the canal and aggregated into the liquid state. If the long-chain molecules escaped the canal and volatilized immediately, higher overall heats of reaction should have been found.

Group II

This group represents guest molecules which are capable of extensive intermolecular association through the formation of hydrogen bonds, and includes complexes of the *n*-alcohols, *n*-carboxylic acids, and *n*-alkylamines. In their urea complexes, it is known that the *n*-carboxylic acids exist as dimers within the canal so that the molecules lie alternately head-to-head and tail-to-tail (17), terminal methyl group interactions alternating with hydrogen-bonded carboxyl groups. It is probable that the *n*-alcohols and *n*-alkylamines may also exist to a large extent in this alternating arrangement within the canal. The possibility of ring-type polymers involving the guest molecules is precluded by the spatial characteristics of the hexagonal urea lattice.

Since the capacity for hydrogen-bond formation involving urea molecules is satisfied within the hexagonal lattice structure by sets of two different N—H···O bonds (8), it is unlikely that there will be any further hydrogen-bond formation between guest molecules and the walls of the urea canal. It is possible, however, that some dipole interactions may exist in the case of polar guest molecules, although the general freedom of guest molecules indicated by dielectric (9), n.m.r. (14), and spectroscopic (15) evidence suggests that the extent of such additional association would be slight.

Can. J. Chem. Downloaded from www.nrcresearchpress.com by 210.87.254.6 on 09/05/12
For personal use only.

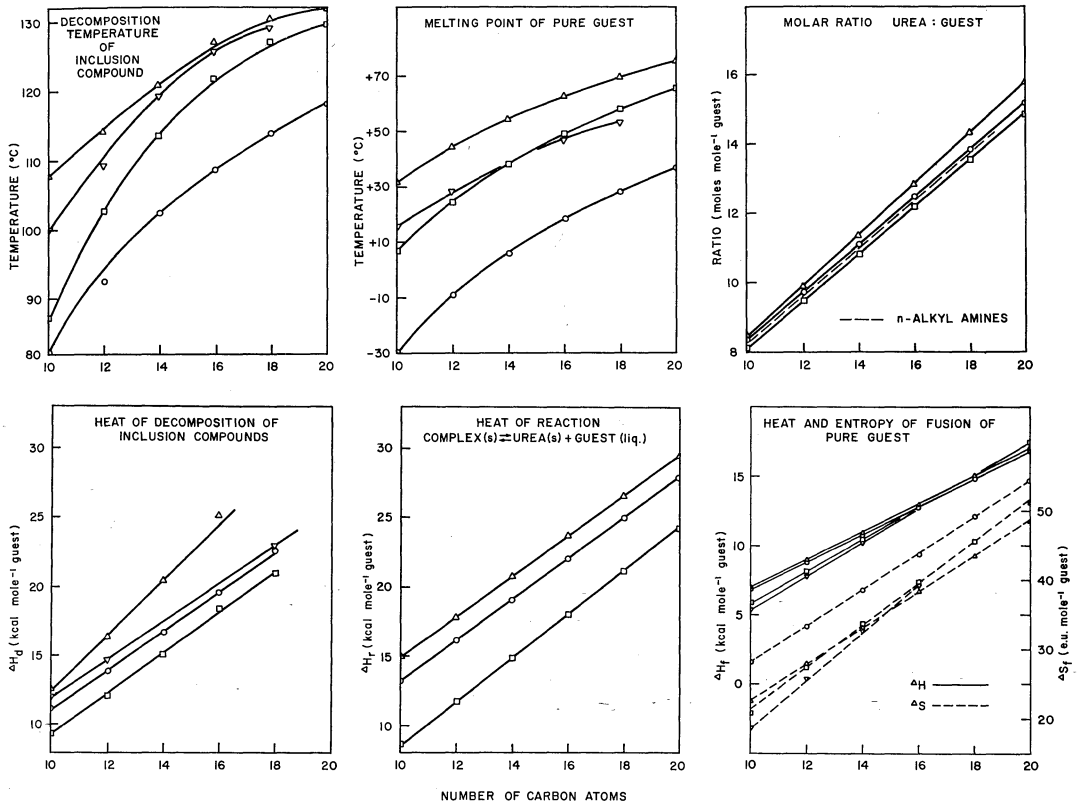

FIG. 7. Comparisons of the *n*-paraffin (○), *n*-alcohol (□) *n*-alkylamine (▽), and *n*-carboxylic acid (△) systems.

Comparison of these three systems with the *n*-paraffins, Fig. 7, shows that their complexes progressively increase in thermal stability with carbon chain length and, for a given carbon chain length, in the order paraffin < alcohol < amine < acid. For comparison, the *n*-alkyl bromide complexes decompose at temperatures intermediate to those of the *n*-paraffins and *n*-alcohols. The melting points (17) of the pure guest species, for a given carbon chain length, increase in the same order as the decomposition temperatures of their complexes except for the *n*-alkylamines, which cross the *n*-alcohols at about C_{14}. It therefore appears that many of the molecular properties responsible for the sequence of melting points in the pure solids may be retained within the urea canal.

Literature data for the molar ratios of urea to guest (3, 4, 7, 8) show this ratio to be greatest in the case of the urea–*n*-carboxylic acid complexes due to the size of the hydrogen-bonded dimer produced. While a similar association of the *n*-alcohols and *n*-alkylamines within the canal will not markedly affect the overall cross section of the guest at this point, the carboxyl group dimer, being somewhat larger than the available canal diameter, produces a "bump" in the middle of each long-chain pair. This causes the *n*-carboxylic acids to behave somewhat like the *n*-alkyl bromides and show a molar ratio which diverges from other series. The effect is not so marked in this case, however, since there is effectively only one bulky group per two molecules, rather than one for each molecule. Again, it appears to be a matter of accommodating this bulky group at positions where the strain induced into the canal wall and the potential energy of the site are minimal.

Can. J. Chem. Downloaded from www.nrcresearchpress.com by 210.87.254.6 on 09/05/12
For personal use only.

Since no data were available for the urea–*n*-alkylamine complexes, the molar ratio in this case was calculated from the measurement of molecular models, assuming the alternate terminal NH_2 groups participate in an N—H···N bond with its counterpart on the succeeding guest molecule.

All complexes studied decompose according to the same energetic process, viz.

$$\text{complex (s)} = \text{urea (s)} + \text{guest (liq.)},$$

although the values for heats of decomposition obtained from thermograms are not as well separated as the heats of reaction reported in the literature (4). There are no equilibrium data for the urea–*n*-alkylamine complexes which appear to have energies of decomposition, as determined from thermograms, close to those for the urea–*n*-paraffin complexes of the same chain length.

The heats of decomposition of the urea–*n*-alcohol complexes are lower than those of any other series. Infrared studies (18) have shown that long-chain alcohols decrease in hydrogen bonding on passing from the solid to the liquid state. In the crystal lattice each OH group participates in two O—H···O bonds (19) so that in the pure liquid the average number of hydrogen bonds per *n*-alcohol molecule must be somewhat less than two. In the case of the urea–*n*-alcohol complexes, the dimensions of the canal constrain the guest molecules to form not more than one hydrogen bond per two molecules. Thus, when the *n*-alcohol molecules are liberated from the canal and aggregate into the liquid state, there may be expected to be an *increase* in intermolecular hydrogen bonding, relative to the condition of these molecules in the urea canal, with a consequent release of energy. This energy release, superimposed upon the energy absorption accompanying the decomposition process, would result in a net experimental energy change lower than that for the corresponding *n*-paraffin complexes.

Because the literature appears to be lacking in adequate heat of fusion data for the *n*-alcohols and *n*-alkylamines, estimations of these were made from solubility data (20, 21) assuming solutions of these materials in chloroform to be approximately ideal. More extensive data were available for the *n*-paraffins (5) and the *n*-carboxylic acids (22, 23, 24).

Heats and entropies of fusion of the *n*-carboxylic acids indicate that these materials behave similarly to the *n*-paraffins on melting, the lower entropy of fusion for the acids indicating the melt is less disordered than that of the *n*-paraffins. Until better thermodynamic data are available for the *n*-alcohols only speculation can be made about the position of heats and entropies of fusion of these materials relative to the *n*-paraffins. Since *n*-alcohols undergo some hydrogen-bond rupture on melting, this would be expected to raise the heat of fusion. However, in the liquid *n*-alcohol there exists a long-range order which results in less change in the orientation of the carbon chains relative to the solid state, thereby producing lower values for the heats and entropies of fusion. As the carbon chain length increases, the slopes of these curves suggest that the effect of this long-range ordering diminishes somewhat. A similar situation may occur in the case of the *n*-alkylamines, although the hydrogen bonds involved are weaker and the long-range order in the liquid state somewhat less than that for the *n*-alcohols.

The above considerations appear to be consistent with the mechanism for complex decomposition presented earlier. The decomposition temperature of the complex is determined by the temperature at which the guest molecule becomes sufficiently mobile to pass frequently over the potential barriers in the canal, and possesses sufficient activation energy for the translational diffusion out of the canal. The larger the end group, or the stronger its interaction with a succeeding guest molecule, the higher will be the energy

Can. J. Chem. Downloaded from www.nrcresearchpress.com by 210.87.254.6 on 09/05/12
For personal use only.

requirement for the guest molecule to achieve adequate freedom within the canal. However, because of differences in the relative association in the canal and in the pure liquid guest, the measured overall energy changes may not lie in the same order as the decomposition temperatures.

Once the guest molecule has departed a section of the canal and is not replaced by another guest molecule, the hexagonal urea lattice collapses and reverts to the tetragonal form. By this means the complexes decompose from the "inside out". Where guest molecules are sufficiently large that the complex is stable up to the melting point of urea, the host cage melts away from the trapped guest thus decomposing from the "outside in".

ACKNOWLEDGMENTS

The author wishes to acknowledge the assistance of Mr. G. C. Cranton. The work was carried out under a research grant to the Ontario Research Foundation from the Province of Ontario received through the Department of Economics and Development.

REFERENCES

1. H. G. McAdie. Can. J. Chem. **40**, 2195 (1962).
2. T. L. David and H. W. Underwood, Jr. J. Am. Chem. Soc. **44**, 2595 (1922).
3. O. Redlich, C. M. Gable, A. K. Dunlop, and R. W. Millar. J. Am. Chem. Soc. **72**, 4153 (1950).
4. E. Terres and S. Nath Sur. Brennstoff-Chem. **38**, 7 (1957).
5. F. D. Rossini, K. S. Pitzer, R. L. Arnett, R. M. Brown, and G. C. Pimentel. Selected values of physical and thermodynamic properties of hydrocarbons and related compounds. Carnegie Press, Pittsburgh, Pa. 1953.
6. Manufacturing Chemists' Association Research Project on the Properties of Chemical Compounds, Vol. I. Carnegie Press, Pittsburgh, Pa. 1961.
7. W. Schlenk, Jr. Ann. **565**, 204 (1949).
8. A. E. Smith. Acta Cryst. **5**, 224 (1952).
9. R. J. Meakins. Trans. Faraday Soc. **51**, 953 (1955).
10. J. J. Lauritzen, Jr. J. Chem. Phys. **28**, 118 (1958).
11. Beilsteins Handbuch der Organischen Chemie, Springer Verlag. 1941.
12. A. M. King and W. E. Garner. J. Chem. Soc. 1368 (1936).
13. R. H. Aranow, L. Witten, and D. H. Andrews. J. Phys. Chem. **62**, 812 (1958).
14. D. F. R. Gilson and C. A. McDowell. Mol. Phys. **4**, 125 (1961).
15. R. A. Durie and R. J. Harrisson. Spectrochim. Acta, **18**, 1505 (1962).
16. H. G. McAdie and G. B. Frost. Can. J. Chem. **36**, 635 (1958).
17. L. C. Fetterley. Thesis, University of Washington, Seattle, Wash. 1950.
18. D. Chapman. Proc. Colloq. Spectry. Intern. 6th Amsterdam, 1957. p. 609.
19. S. Abrahamsson, G. Larsson, and E. v. Sydow. Acta Cryst. **13**, 770 (1960).
20. C. W. Hoerr, H. J. Harwood, and A. W. Ralston. J. Org. Chem. **9**, 267 (1944).
21. A. W. Ralston, C. W. Hoerr, W. O. Pool, and H. J. Harwood. J. Org. Chem. **9**, 102 (1944).
22. W. E. Garner and K. Randall. J. Chem. Soc. 881 (1924).
23. W. E. Garner, F. C. Madden, and J. E. Rushbrooke. J. Chem. Soc. 2600 (1926).
24. K. Stratton and J. R. Partington. Phil. Mag. **48**, 1085 (1924).

Can. J. Chem. Downloaded from www.nrcresearchpress.com by 210.87.254.6 on 09/05/12
For personal use only.

THE CARBONYL-STRETCHING VIBRATION OF ARYLALIPHATIC ESTERS

KEITH BOWDEN,[1] N. B. CHAPMAN, AND J. SHORTER
Chemistry Department, The University, Hull, England
Received April 1, 1963

ABSTRACT

The infrared spectra in the carbonyl-stretching region of certain arylaliphatic esters, RCOOMe, have been examined. The stretching frequencies and absorption intensities are presented and are discussed in terms of polar and α-mass effects and the occurrence of conformational isomers.

INTRODUCTION

As carbonyl vibrations are considered rarely to be perturbed by coupling with other vibrations, the corresponding absorption band and its variation with structure has been widely studied. Several factors may affect this vibration, of which the most important, for the present work, are polar, α-mass, and steric effects.

Thompson and his co-workers (1) have suggested that the force constant is primarily determined by the relative contributions of the canonical structures I, II, III, and IV to the structure of the carbonyl group. The relative importance of these structures is

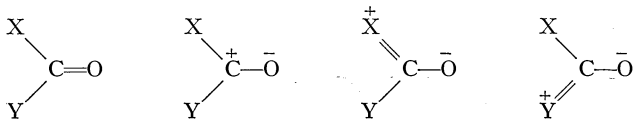

I II III IV

determined by the ability of X and Y either to interact with the carbonyl bond (cf. III and IV), or to alter the relative contributions of I and II by an electrostatic effect (i.e. inductive or direct field). Since the value of the frequency indicates the energy needed to produce a dipolar state, a reduction in the part played by structures II, III, and IV will increase the frequency.

The effect on the frequency of increasing the mass of α-substituents is significant for small masses but reaches a limit for group X or Y in XYC=O with higher masses (e.g., Halford (2) considers the effects to be constant above about 27 atomic weight units for X or Y). Substitution of deuterium for α-hydrogen atoms in esters or ketones has been found to give fairly large α-mass effects (3).

A reduction in the X—C—Y intervalency angle in X—CO—Y will increase the frequency as has been observed for the carbonyl vibrations of strained ring ketones (4, cf. ref. 2). In the absence of any change in the steric environment of the motion, successful correlations have been obtained of the carbonyl frequencies of substituted ethyl benzoates and acetophenones with substituent constants of the Hammett type (5). Similar correlations involving the carbonyl-stretching frequencies of substituted aliphatic esters and ketones have been made with varying success. Correlations of doubtful value for intensities, due to the narrow range of intensities covered and the small number of substituents involved (6), have also been attempted.

A number of investigators have observed the splitting of the carbonyl bands of ketones

[1]*Present address: Department of Chemistry, University of British Columbia, Vancouver 8, British Columbia.*

Can. J. Chem. Downloaded from www.nrcresearchpress.com by 210.87.254.40 on 09/05/12
For personal use only.

and esters. Possible explanations of this phenomenon are the occurrence of rotational isomers (7), Fermi resonance (8), and a solvation effect (9). Fermi resonance can be discounted in normal cases, as the effect of solvent, temperature, and concentration change is not that expected. However, the occurrence of Fermi resonance in five-membered ring ketones has been suggested (8). The solvation effect cannot easily explain the occurrence of splitting in such solvents as cyclohexane. Rotational isomers are considered to be the cause in most known cases. Brown (10, 17) has examined the spectra of a number of substituted ethyl acetates (in carbon tetrachloride) and has attempted to explain the integrated absorption coefficients and the vibrational frequencies of the carbonyl groups by reference to Taft's polar substituent constants (11) and the existence of conformational isomers.

EXPERIMENTAL

(a) Preparation of Esters

The preparation of the esters has been described elsewhere (12); their purity was determined by vapor phase chromatography. No significant impurity was found in any samples of esters subsequently used for measurements.

(b) Infrared Spectra

The carbonyl-stretching vibrations of the esters were examined by use of a Unicam S.P. 100 double-beam infrared recording spectrophotometer, operating with a nitrogen atmosphere. A 0.55-cm cell was used and the cell-well temperature was 30±1°. The calibration was checked by using a solution of acetone in carbon tetrachloride (band at 1719 cm^{-1}). The bands were normally scanned at 8 cm^{-1} min^{-1}. "Analar" carbon tetrachloride or cyclohexane (Hopkin and Williams, Ltd., "Spectrosol" grade) was used as the solvent and the solutions were approximately 0.01 *M*. At least two independent measurements were made on each ester.

The values of ν_{max} (wave number at the absorption maximum), the apparent molecular extinction coefficients at the maximum, the partial band widths, and the apparent integrated absorption intensities were determined. Intensities were measured from a solvent–solvent base line superimposed on the record of the absorption of the solution (determined with solvent in reference beam). Peaks were symmetrical unless otherwise stated.

The absorption curves were integrated graphically using an "Allbrit" planimeter to give the apparent integrated absorption intensities, A^a. The integration interval chosen was 50 cm^{-1} on each side of the peak maximum, or, in the case of split peaks, from 45 cm^{-1} on the low-frequency side of the lower-frequency peak to 45 cm^{-1} on the high-frequency side of the higher-frequency peak. Approximation formulae (13) can be used to give $A^a = 2.303 N E^a_{max}$, where N is a function of the partial band widths, such that $N = \pi\Delta\nu_{\frac{1}{2}}/2$, $\pi\Delta\nu_{\frac{1}{4}}/2\sqrt{3}$, or $\pi\Delta\nu_{\frac{1}{8}}/2\sqrt{7}$, where $\Delta\nu_x$ is the partial band width at $x \times$ the optical density. In using these formulae it is assumed that symmetrical absorption curves of a Lorentz shape are involved. Mean values obtained from them were about 5% higher than the values obtained by the graphical method.

EXPERIMENTAL RESULTS

The apparent integrated absorption intensities, apparent molecular extinction coefficients, the partial band widths, and values of ν_{max} are shown in Table I. The accuracy of the measurements is considered to be ±1 cm^{-1} in the wave number (relative to the standard); ±0.5 cm^{-1} in the partial band widths; ±1.5% in the apparent molecular extinction coefficient; and ±2.0% in the apparent integrated absorption coefficient.

DISCUSSION

(a) Stretching Frequencies

The factors which may affect the carbonyl-stretching vibration frequency are shown in Table II. The values of ν_{max} in Table I are conveniently discussed by reference to a plot of ν_{max} (carbon tetrachloride solutions) against the values of the Taft polar substituent constant σ^* obtained previously (12) (Fig. 1).

The band splitting observed for ester 7, methyl fluorene-9-carboxylate, suggests the occurrence of two conformers. (The abnormally great band spreading for esters 2, 4, 5,

Can. J. Chem. Downloaded from www.nrcresearchpress.com by 210.87.254.40 on 09/05/12
For personal use only.

TABLE I

Carbonyl-stretching vibrations of esters in carbon tetrachloride

Ester	ν_{max} (cm^{-1})	Apparent molecular extinction coefficient E^a_{max} (l. $mole^{-1}$ cm^{-1})	Apparent integrated absorption intensity $10^4 A^a$ (l. $mole^{-1}$ cm^{-2})	Partial band widths (cm^{-1}) $\Delta\nu_{\frac{1}{2}}$	$\Delta\nu_{\frac{1}{4}}$	$\Delta\nu_{\frac{1}{8}}$
1. Methyl acetate[a]	1751	640	2.92	14	22.5	31.5
2. Methyl phenylacetate	1747	455	2.81	19	30	44.5
3. Methyl diphenylacetate	1749	515	2.49	15.5	24.5	34.5
4. Methyl 2,2-diphenylpropionate	1738.5	450	2.62	19	29	39
5. Methyl 2,2-diphenylbutyrate	1737.5	450	2.65	19	29.5	39.5
6. Methyl triphenylacetate	1740	565	2.67	15	24	33
7. Methyl fluorene-9-carboxylate	1750, 1739	$\alpha_1/\alpha_2 = 1.00$[c]	2.68	—	—	—
Methyl fluorene-9-carboxylate[b]	1754, 1742	$\alpha_1/\alpha_2 = 1.19$[c]	2.54	—	—	—
8. Methyl 9-methylfluorene-9-carboxylate	1735.5	585	3.36	16.5	27	36
9. Methyl 9-ethylfluorene-9-carboxylate	1734.5	625	3.15	15.5	25.5	35.5
10. Methyl 9-isopropylfluorene-9-carboxylate	1733.5	535	2.78[d]	18	28	37
11. Methyl 9-*t*-butylfluorene-9-carboxylate	1733	535	2.51	14.5	24	33.5
12. Methyl 9-phenylfluorene-9-carboxylate	1740.5	590	2.52	14	22	30
13. Methyl 9,10-dihydroanthracene-9-carboxylate	1744	485	2.61[d]	18.5	28.5	40
Methyl 9,10-dihydroanthracene-9-carboxylate[b]	1748.5	565	2.22	12	20	29

[a]Previous workers give ν_{max} as 1748 to 1751 cm^{-1} (3, 7, 16) and A^a as 2.2 units (16).
[b]In cyclohexane.
[c]Ratio of optical density of the high- (α_1) to the low- (α_2) frequency band.
[d]Unsymmetrical peak.

TABLE II

Factors affecting the carbonyl-stretching frequency

Factor	Effect on ν_{max}
Increase in α-mass (X or Y)	Decreases
Steric compression of carbonyl bond	Increases
Increase in the angle X—C—Y	Decreases
Polar effects: electron withdrawing	Increases
electron releasing	Decreases

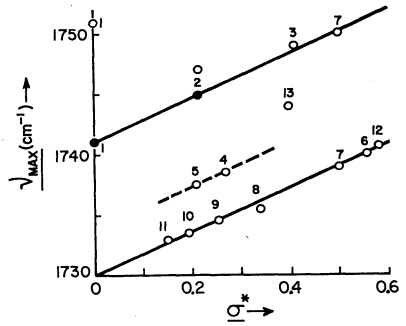

FIG. 1. Relation between Taft's polar substituents σ^* and carbonyl-stretching frequency for the esters. (Esters 1 and 2 are also shown with α-mass correction.)

Can. J. Chem. Downloaded from www.nrcresearchpress.com by 210.87.254.40 on 09/05/12
For personal use only.

10, and 13 and asymmetry of the band for esters 10 and 13 indicate the occurrence of 'hidden' conformers.) The most likely conformations for these are shown below, with

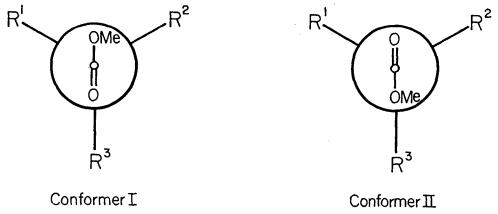

R^1 and R^2 together denoting the fluorene system, and R^3 = H. The higher value of ν_{max} may be attributed to conformer II. Steric interaction between the methoxyl group and the fluorene system in conformer I will be greater than that between carbonyl–oxygen and the fluorene system in II, because of the greater steric requirements of the methoxy group. In conformer I the 'X·CO·Y' angle (see above p. 2154) will therefore be greater than that in conformer II, and so II will have the higher value of ν_{max} (4).

For esters 8 to 12 there is good correlation between ν_{max} and σ^*, and the lower value for ester 7 lies on the same line. These esters apparently occur as conformer I and the effect of structure upon ν_{max} is due to the polar effect of the 9-substituent. The slope of the line (a 'reaction constant', ρ^*, see ref. 11) is 18.0, and this agrees fairly well with values of 19.6 to 19.9 found for similar series of compounds in previous studies (6). The 'X·CO·Y' angle is constant in the series, since the steric environment of the methoxyl group does not alter, and it appears that even with the largest 9-substituents there is no effect on ν_{max} due to compression of the carbonyl group. Variations in 'α-mass' are not significant in the series since the systems are very massive (see below). When the hydrogen atom in the 9-position is replaced by an alkyl or a phenyl group the interaction between these and the methoxyl group in conformer II is evidently so great that this conformer does not occur to an appreciable extent.

Ester 6, methyl triphenylacetate, gives ν_{max} lying on the line discussed above and therefore exists as conformer I with all R's = Ph. In this conformer steric interaction of the methoxy group with the phenyl substituents will be minimal. If the interaction of carbonyl–oxygen with the phenyl group R^3 is significant, however, rotation of the ester group will occur so as to separate these two slightly. The 'X·CO·Y' angle must be about the same in conformer I of ester 6 as in ester 7 to 12.

In esters 4 and 5 steric interactions involving the methoxyl group should be minimal in conformer I, with R^1 = R^3 = Ph, and R^2 = Me or Et, although appreciable interaction between carbonyl–oxygen and phenyl might twist the ester group to bring the methoxyl group slightly closer to R^2. At all events, steric interaction involving the methoxyl group should be less than in the main series already discussed, leading to a decrease in the 'X·CO·Y' angle, and to an increase in ν_{max} relative to the main series, as actually found.

Since ν_{max} for ester 3, methyl diphenylacetate, is close to the higher value for ester 7, it is likely that ester 3 exists as conformer II, with R^1 = R^2 = Ph, and R^3 = H. For ester 1 conformer I would be expected, with all R's = H. In ester 2 interaction between the phenyl group and carbonyl–oxygen may be relatively important. Analogy with halogeno- and cyano-acetic esters (10, 14) suggests conformer I with R^1 = Ph and R^2 = R^3 = H. Dipole interaction which is dominant in halogeno- and cyano-esters

Can. J. Chem. Downloaded from www.nrcresearchpress.com by 210.87.254.40 on 09/05/12
For personal use only.

should be less important in methyl phenylacetate. However, conformer I with R^1 = Ph and R^2 = R^3 = H (giving less interaction involving the methoxy group) appears also sterically more probable. In esters 1, 2, and 3 the methoxy group is thus involved in little steric interaction, as in conformer II of ester 7. The 'X·CO·Y' angle in these esters should be approximately constant, but the effect of polar substituents on ν_{max} should be observed. The figure shows a line drawn through the points for esters 3 and 7, and parallel to that for the main series. The point for ester 1 is well off the line, and that for 2 is slightly displaced. This is doubtless due to the smaller 'α-mass' of esters 1 and 2 leading to an increase in ν_{max}.

Like ester 7, ester 13 might be expected to occur in both conformers I and II, where R^1 and R^2 together denote the dihydro-anthracene system and R^3 = H. The band is wide and asymmetric, and may be an unresolved doublet with an apparent value of ν_{max} at a frequency intermediate between those characteristic of the conformers.

The factors influencing ν_{max} can now be tentatively evaluated. In Table III estimates of the relative contributions of α-mass and polar effects to the change in ν_{max} (relative

TABLE III

Ester RCO_2Me[a] R	σ^*	$\Delta\nu_{max}$ (cm^{-1}) Polar effect[b]	α-Mass effect	Steric effect[c]	Observed	Conformer present[a] Type	R^1	R^2	R^3
1. Me	0.0	0.0	0.0	0.0	0.0	I	H	H	H
2. $PhCH_2$	0.215	4.0	− 8.0	0.0	− 4.0	I	Ph	H	H
3. Ph_2CH	0.405	7.5	−10.0	+ 0.5	− 2.0	II	Ph	Ph	H
4. Ph_2CMe	0.270	5.0	−10.0	− 7.5	−12.5	I	Ph	Ph	Me
5. Ph_2CEt	0.210	4.0	−10.0	− 7.5	−13.5	I	Ph	Ph	Et
6. Ph_3C	0.560	10.0	−10.0	−11.0	−11.0	I	Ph	Ph	Ph
7. FlCH−	0.500	9.0	−10.0	0.0	− 1.0	II		Fl	H
	0.500	9.0	−10.0	−11.0	−12.0	I		Fl	H
8. FlCMe	0.320	6.0	−10.0	−11.5	−15.5	I		Fl	Me
9. FlCEt	0.255	4.5	−10.0	−11.0	−16.5	I		Fl	Et
10. $FlCPr^i$	0.195	3.5	−10.0	−11.0	−17.5	I		Fl	Pr^i
11. $FlCBu^t$	0.150	3.0	−10.0	−11.0	−18.0	I		Fl	Bu^t
12. FlCPh	0.585	10.5	−10.0	−11.0	−10.5	I		Fl	Ph
13. AnCh	0.400	7.0	−10.0	− 4.0	− 7.0	I & II?		An	H

[a]Fl = 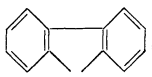 , An = 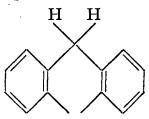

[b]The reaction constant, ρ^*, is equal to 18.0.
[c]Obtained by difference.

to methyl acetate) are given. The polar effect is calculated by use of σ^* values and the above value of ρ^*. It is assumed that for esters 3 and 7 (conformer II) there is no steric contribution, so that the α-mass effect may be evaluated by subtracting the polar contribution from the observed ν_{max}. The α-mass effect thus found for ester 7 (conformer II) is assumed to apply to all the esters except 2. The estimates are reasonable in the light of pertinent data (2, 3). The steric effect is now calculated by difference.

(b) Intensities

The electronic ground state of a carbonyl compound has contributions from the canonical structures I, II, III, and IV. When the carbonyl carbon–oxygen bond distance increases, the ionic structure becomes more important. Carbonyl stretching is therefore an electron-demanding process and will be assisted by electron-releasing and hindered

Can. J. Chem. Downloaded from www.nrcresearchpress.com by 210.87.254.40 on 09/05/12
For personal use only.

by electron-withdrawing substituents. The intensity (A) varies linearly with $(\partial\mu/\partial r)^2$ and will fall for electron-withdrawing substituents (16).

Attempts have been made to correlate the intensities by use of the following alternative relations (6, 15) which are similar to those of Hammett and Taft:

$$A/A_0 \quad \text{or} \quad \log(A/A_0) \quad \text{or} \quad A^{1/2}/A_0{}^{1/2} = \rho\sigma \quad \text{or} \quad \rho^*\sigma^*.$$

The results obtained in this study give a very poor correlation with the Taft polar substituent constants. The only reasonably meaningful correlation is that using $A^{1/2}/A_0{}^{1/2}$. The results, with the exception of those for esters 8, 9, and 11, give ρ^* equal to -0.150 and A_0 equal to 1.68_5. The correlation coefficient is 0.764, a very low value. However, the correlation is as good as that found by other workers (6, 15) for similar series. The four alkyl fluorene esters show in fact a regression of opposite sign to that expected. Brown, in a recent study (17), concludes that the steric size and conformation, rather than the polar effect, is of greatest importance in determining the carbonyl intensity. In the series of substituted fluorene esters studied there does appear to be a steady decrease in intensity with size of the substituent group.

ACKNOWLEDGMENTS

The authors are indebted to Dr. C. W. Gray and Mrs. D. Strickland for making the measurements and Dr. T. L. Brown for helpful suggestions.

REFERENCES

1. E. J. Hartwell, R. E. Richards, and H. W. Thompson. J. Chem. Soc. 1436 (1948).
2. J. O. Halford. J. Chem. Phys. **24**, 830 (1956).
3. B. Nolin and R. N. Jones. Can. J. Chem. **34**, 1382, 1392 (1956).
4. R. N. Jones and C. Sandorfy. *In* Technique of organic chemistry. Vol. IX. *Edited by* W. West. Interscience Publishers, Inc., New York. 1956. Chap. 4. p. 485.
5. R. N. Jones, W. F. Forbes, and W. A. Mueller. Can. J. Chem. **35**, 504 (1957). P. J. Krueger and H. W. Thompson. Proc. Roy. Soc. (London), Ser. A, **250**, 22 (1959).
6. C. N. R. Rao and R. Venkataraghavan. Can. J. Chem. **39**, 1757 (1961).
7. R. N. Jones and E. Spinner. Can. J. Chem. **36**, 1020 (1958). M. L. Josien and R. Callas. Compt. Rend. **240**, 1641 (1955).
8. R. N. Jones, C. L. Angell, T. Ito, and R. J. D. Smith. Can. J. Chem. **37**, 2007 (1959).
9. T. V. Yakovleva, A. G. Maslennikova, and A. A. Petrov. Opt. Spectry. (USSR) (Engl. Transl.), **10**, 64 (1961).
10. T. L. Brown. J. Am. Chem. Soc. **80**, 3513 (1958).
11. R. W. Taft. *In* Steric effects in organic chemistry. *Edited by* M. S. Newman. John Wiley and Sons, Inc., New York. 1956. Chap. 13.
12. K. Bowden, N. B. Chapman, and J. Shorter. To be published.
13. A. Cabana and C. Sandorfy. Spectrochim. Acta, **16**, 335 (1960).
14. L. J. Bellamy and R. L. Williams. J. Chem. Soc. 4294 (1957).
15. L. Gutjahr. Spectrochim. Acta, **16**, 1209 (1960).
16. G. M. Barrow. J. Chem. Phys. **21**, 2008 (1953).
17. T. L. Brown. Spectrochim. Acta, **18**, 1615 (1962).

Can. J. Chem. Downloaded from www.nrcresearchpress.com by 210.87.254.40 on 09/05/12
For personal use only.

THE NEAR-ULTRAVIOLET SPECTRA OF SOME 9-ALKYLPHENANTHRENES

F. A. L. ANET
Chemistry Department, University of Ottawa, Ottawa, Canada
AND
P. M. G. BAVIN
Smith Kline & French Laboratories Ltd., Welwyn Garden City, England
Received March 25, 1963

ABSTRACT

The ultraviolet spectra are reported of a series of 9-alkylphenanthrenes. The bathochromic shifts relative to phenanthrene of the longest-wavelength (α) band are not explicable in terms of hyperconjugation. It is suggested that the band envelope is influenced by the rotameric forms of the alkyl substituents.

Can. J. Chem. Downloaded from www.nrcresearchpress.com by 210.87.254.5 on 09/05/12
For personal use only.

The effect of alkyl substituents upon the near-ultraviolet spectra of polycyclic aromatic hydrocarbons is not fully understood (see ref. 1), and few systematic studies have been made. Theoretical studies have shown that in alternant hydrocarbons such substitution can lead only to bathochromic shifts, provided that strong steric effects are absent (2,3). In non-alternant hydrocarbons the shifts may be either bathochromic or hypsochromic, depending on the position of substitution (3). These results were obtained by treating the inductive and hyperconjugative effects separately but additively, and agree with experiment for some methylated azulenes and fulvenes. Similar results have been obtained using Hückel's method (4, 5).

The near-ultraviolet spectra of benzene, toluene, ethylbenzene, *i*-propylbenzene, and *t*-butylbenzene have been measured in the vapor phase and in solution (6). The results were interpreted as showing that the spectral shifts relative to benzene were due to the differing hyperconjugative powers of the alkyl groups (6; 7, pp. 667–675).

We now report the near-ultraviolet spectra of the following 9-alkylphenanthrenes: methyl, ethyl, propyl, *i*-propyl, butyl, *s*-butyl, *i*-butyl, *t*-butyl, *t*-amyl, benzyl, cyclopentyl, cyclohexyl. Comparison of the spectra, summarized in Table I, has revealed certain interesting regularities.

The spectrum of phenanthrene has been reported by several authors (8, 9, 10; see also footnote, page 230, ref. 11) and has recently been discussed in some detail (12). The low extinction coefficients and high resolution of the longest-wavelength band system (α-band (13) or series III band (14)), little improved at $-170°$ (8; cf. $-100°$ (12)), suggest that it has its origin in a single electronic transition. Since in addition the extinction coefficients are only slightly affected by overlap with neighboring band systems, we have confined our discussion to the α-band system.

The shifts of the longest-wavelength peak relative to phenanthrene follow the usual order (6) for the methyl, ethyl, *i*-propyl, and *t*-butyl substituents. The data for the other substituents show that the shifts are not explicable in terms of relative hyperconjugative powers alone, a view previously expressed in more general terms by Jones (1) for alkyl-substituted polycyclic aromatic hydrocarbons, and more forcibly by Dewar (15, p. 79).

Variations of the extinction coefficients revealed in Table I are of greatest interest. The spectra are divisible into two groups. In the first, the α-band shows six peaks, with

Can. J. Chem. Downloaded from www.nrcresearchpress.com by 210.87.254.5 on 09/05/12
For personal use only.

TABLE I

Substituent														
Hydrogen	Wavelength (mμ)	346.2	338.9	330.4	323.1	315.4	309.0	292.9	281	274			251	246
	log ε	2.44	2.39	2.49	2.41	2.37	2.29	4.10	3.99	4.09			4.83	4.72
Methyl	Wavelength (mμ)	349.0	340.7	332.9	325.2	317.5	310.6	296.1	284.3	275.5	269.2		252.5	246.8
	log ε	2.69	2.44	2.65	2.44	2.46	2.36	4.11	4.04	4.16	4.21		4.81	4.72
Ethyl	Wavelength (mμ)	349.0	340.3	332.6	325.1	317.2		296.5	284.7	273.3	269.5		252	246
	log ε	2.60	2.41	1.60	2.42	2.44		4.05	3.99	4.12	4.20		4.80	4.71
Propyl	Wavelength (mμ)	348.7	340.2	332.8	325.2	317.2								
	log ε	2.54	2.27	2.53	2.34	2.36					N.R.			
i-Propyl	Wavelength (mμ)	348.6	340.3	332.4	325.2	317.3		296.4	284.5	276.4	269.4		252.5	246
	log ε	2.56	2.40	2.57	2.41	2.42		4.04	3.97	4.09	4.17		4.77	4.70
Butyl	Wavelength (mμ)	248.9	240.3	332.7	325.2	317.4					N.R.			
	log ε	2.54	2.33	2.53	2.34	2.37								
s-Butyl	Wavelength (mμ)	349.2	340.7	333.0	325.4	317.8					N.R.			
	log ε	2.54	2.40	2.56	2.42	2.44								
i-Butyl	Wavelength (mμ)	349.2	340.7	332.9	325.5	317.8					N.R.			
	log ε	2.55	2.33	2.52	2.33	2.36								
t-Butyl	Wavelength (mμ)	347.7	339.5	331.7	324.3	316.8	309.9	295.7	284	276.2	268		252.5	246
	log ε	2.68	2.47	2.66	2.47	2.46	2.37	4.16	4.05	4.20	4.18		4.88	4.65
t-Amyl	Wavelength (mμ)	348.2	339.8	332.0	324.8	317.2	310.3	296.3	284.5	276.7	269.5		252.5	246
	log ε	2.64	2.45	2.63	2.45	2.44	2.37	4.11	3.96	4.16	4.17		4.81	4.71
Benzyl	Wavelength (mμ)	348.2	339.8	332.0	324.3	316.8		296.5	284.2	275.5	268.7		253	246.5
	log ε	2.57	2.43	2.58	2.43	2.44		4.09	4.01	4.12	4.19		4.81	4.70
Cyclopentyl	Wavelength (mμ)	347.8	339.8	332.1	324.7	316.9					N.R.			
	log ε	2.55	2.36	2.54	2.36	2.38								
Cyclohexyl	Wavelength (mμ)	348.0	339.9	331.9	324.7	317.0					N.R.			
	log ε	2.57	2.40	2.58	2.41	2.43								
9,10-Dimethyl	Wavelength (mμ)	352.7		336.5	328.3	320.8		298.7	286.6	277.8	270.8	268.2	254.6	248.5
	log ε	2.74		2.77	2.56	2.63		4.12	4.18	4.31	4.41	4.40	4.86	4.74

NOTE: N.R., not recorded.

the first and third particularly well resolved. Phenanthrene and the methyl, *t*-butyl, and *t*-amyl derivatives belong to this group. The second group shows only five peaks in the α-band, the first and third being broader and having lower extinction coefficients. Differences between the two groups are well illustrated in Fig. 1 by the spectra of $M/500$

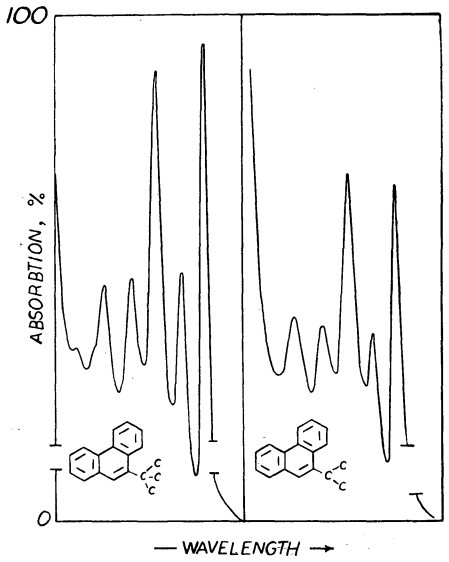

FIG. 1. Spectra of $M/500$ solutions of 9-*t*-butylphenanthrene and 9-*i*-propylphenanthrene in ethanol

solutions of 9-*i*-propyl- and 9-*t*-butyl-phenanthrenes in ethanol. Contrary to the view expressed elsewhere (16, p. 326) the 9-monoalkylphenanthrenes retain fine structure in the α-band.

We can explain our results in terms of the symmetry of the alkyl group about the axis of the bond joining it to the ring system. Methyl and *t*-butyl and, to a first approximation, *t*-amyl have trigonal symmetry so that only a single rotamer, I (18), exists in each case.

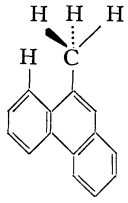

I

The other alkyl groups are less symmetrical so that at least two rotamers can exist. Since the corresponding bands of the rotamers in any one compound would not be expected to coincide exactly, a slight broadening should be observed (cf. refs. 17, 19).

EXPERIMENTAL

The alkylphenanthrenes were prepared either by heating the 9-alkyl-9-fluorenylmethanol with phosphorus pentoxide under xylene (method A (20), where references are given to earlier work) or by decomposing the tosylate in formic acid (method B (20)). 9-Methyl-, -ethyl-, -*i*-propyl-, -*t*-butyl-, and -benzyl-phenanthrenes were available from earlier work (20).

Can. J. Chem. Downloaded from www.nrcresearchpress.com by 210.87.254.5 on 09/05/12
For personal use only.

9-t-Amylphenanthrene (Method B)

Methyl 9-t-amylfluorene-9-carboxylate crystallized as needles (76%) from methanol, m.p. 56–57°. Found: C, 81.81; H, 7.40. Calc. for $C_{20}H_{22}O_2$: C, 81.60; H, 7.53%. The *acid* formed colorless needles from benzene–hexane, m.p. 200–204° with decomposition. Neutralization equivalent found: 277; calc.: 280. *9-t-Amyl-9-fluorenylmethanol* separated from hexane as colorless needles (91%), m.p. 104–106°. Found: C, 86.56; H, 7.63. Calc. for $C_{19}H_{20}O$: C, 86.32; H, 7.63%. The tosylate crystallized from benzene, slightly yellow prisms, m.p. 105–118° varying with the rate of heating, with decomposition to 9-*t*-amylphenanthrene.

9-t-Amylphenanthrene crystallized from methanol as lustrous plates, more rarely as prisms, m.p. 87–88°. Found: C, 92.05; H, 8.17. Calc. for $C_{19}H_{20}$: C, 91.88; H, 8.12%.

9-s-Butylphenanthrene (Methods A and B)

Methyl 9-*s*-butylfluorene-9-carboxylate (20), carefully purified by repeated crystallization, was reduced ($LiAlH_4$) and the alcohol esterified with tosyl chloride. Neither the alcohol nor the tosylate could be induced to crystallize.

9-*s*-Butylphenanthrene was obtained as an oil by either of the methods A or B. After distillation at 4 mm from sodium, the *1,3,5-trinitrobenzene adduct* was prepared as bright yellow needles from methanol, m.p. 124–125°. Found: C, 63.78; H, 4.25; N, 9.81. Calc. for $C_{24}H_{21}N_3O_6$: C, 64.42; H, 4.73; N, 9.39%. Decomposition of the adduct by passing its solution in hexane through a column of activated alumina gave the pure hydrocarbon as a colorless oil, which has not crystallized. Found, after redistillation: C, 92.44; H, 7.63. Calc. for $C_{18}H_{18}$: C, 92.26; H, 7.74%. The ultraviolet spectrum was not changed by further attempts at purification through adducts with trinitrobenzene or picric acid.

9-i-Butylphenanthrene (Method B)

Methyl 9-i-butylfluorene-9-carboxylate formed colorless prisms from methanol (71%), m.p. 67–69°. Found: C, 81.42; H, 7.18. Calc. for $C_{19}H_{20}O_2$: C, 81.39; H, 7.19%. Reduction ($LiAlH_4$) and esterification gave the *tosylate*, colorless needles from hexane, m.p. 104–105°. Found: C, 74.12; H, 6.40. Calc. for $C_{25}H_{26}O_3S$: C, 73.86; H, 6.45%. 9-*i*-Butylphenanthrene formed colorless needles from acetone–methanol, m.p. 98–99° (lit. m.p. 96–97° (21)).

9-n-Butylphenanthrene (Method B)

Methyl 9-butylfluorene-9-carboxylate (20), purified by distillation at 0.1 mm and subsequent crystallization from methanol, was reduced ($LiAlH_4$) and esterified to give the *tosylate*, prisms from hexane, m.p. 104–105°, depressed when mixed with the *i*-butyl isomer. Found: C, 74.12; H, 6.46.

9-Butylphenanthrene crystallized from acetone–methanol as colorless needles, m.p. 78–79° (lit. m.p. 78.5–79.0° (22); 80–81° (23)).

9-n-Propylphenanthrene (Method A)

Methyl 9-propylfluorene-9-carboxylate (20) was converted via the alcohol to 9-propylphenanthrene, which crystallized as lustrous plates from methanol, m.p. 62–63° (lit. m.p. 59° (22); 57–58° (23); 58.5–59.5° (24)). The picrate separated as orange needles from methanol, m.p. 94–95° (lit. m.p. 95.5–96.0° (24); 98–99° (23)).

9-Cyclopentylphenanthrene (Method A)

Methyl 9-cyclopentylfluorene-9-carboxylate (25) was converted through the alcohol to 9-cyclopentylphenanthrene, colorless needles from methanol, m.p. 125–126°. Lit. m.p. 124–125.5° (25).

9-Cyclohexylphenanthrene (Method A)

Methyl 9-cyclohexylfluorene-9-carboxylate (20) was converted through the alcohol to 9-cyclohexylphenanthrene, colorless prisms from methanol, m.p. 113–114°. Found: C, 92.05; H, 7.96. Calc. for $C_{20}H_{20}$: C, 92.26; H, 7.74% (lit. m.p. 112–113° (27)).

A sample of phenanthrene was purified by treatment with maleic anhydride (11, 28), spectroscopic examination confirming the absence of anthracene (9).

The spectra were taken with a Beckmann DK-2 recording spectrophotometer. Solutions were initially *M*/500 in ethanol, secondary solutions being prepared by volume dilution. Estimated errors are ± 0.2 mμ for the α-band, $\pm 5\%$ for ϵ_{max} values.

ACKNOWLEDGMENTS

P. M. G. Bavin is indebted to the National Research Council of Canada for a Postdoctoral Fellowship (1954–1956) at The University of Ottawa. Miss E. V. Eggington (Smith Kline & French Laboratories Ltd.) recorded some of the spectra. Dr. Cammille Sandorfy kindly read the manuscript at an early stage.

REFERENCES

1. R. N. Jones. Chem. Rev. **32**, 1 (1943).
2. M. J. S. Dewar. J. Chem. Soc. 2329 (1950).

Can. J. Chem. Downloaded from www.nrcresearchpress.com by 210.87.254.5 on 09/05/12
For personal use only.

3. H. C. LONGUETT-HIGGINS and R. G. SOWDEN. J. Chem. Soc., 1404 (1952).
4. B. PULLMANN, M. MAYOT, and G. BERTHIER. J. Chem. Phys. **18**, 257 (1950).
5. D. PETERS. J. Chem. Soc. 646 (1951).
6. F. A. MATSEN, W. W. ROBERTSON, and R. L. CHUOKE. Chem. Rev. **41**, 273 (1947).
7. F. A. MATSEN. *In* Technique of organic chemistry. Vol. IX. *Edited by* A. Weissberger. Interscience Publishers Inc., New York. 1956. Part II.
8. E. CLAR. Spectrochim. Acta, **4**, 116 (1950).
9. F. P. HAZLETT, R. B. HANAN, and J. H. WELLS. Anal. Chem. **22**, 1132 (1950).
10. W. V. MAYNEORD and E. M. F. ROE. Proc. Roy. Soc. (London), Ser. A, **158**, 634 (1937).
11. D. P. CRAIG. Rev. Pure Appl. Chem. **3**, 230 (1953).
12. R. N. JONES and E. SPINNER. Spectrochim. Acta, **16**, 1060 (1960).
13. E. CLAR. Aromatische Kohlenwasserstoffe. Verlag von Julius Springer, Berlin. 1952.
14. G. M. BADGER, R. S. PEARCE, and R. PETTIT. J. Chem. Soc. 3199 (1951).
15. M. J. S. DEWAR. Hyperconjugation. Ronald Press Co., New York. 1962.
16. H. H. JAFFE and M. ORCHIN. Theory and applications of ultra-violet spectroscopy. John Wiley and Sons, Inc., New York. 1962.
17. J. J. SHIPMAN, V. L. FOLT, and S. KRIMM. Spectrochim. Acta, **18**, 1603 (1962).
18. M. S. NEWMAN. J. Chem. Educ. **32**, 344 (1955).
19. W. J. JONES and N. SHEPPARD. Proc. Chem. Soc. 420 (1961).
20. F. A. L. ANET and P. M. G. BAVIN. Can. J. Chem. **34**, 991 (1956).
21. C. K. BRADSHER and W. J. JACKSON. J. Am. Chem. Soc. **76**, 734, 4140 (1954).
22. G. B. BACHMANN and R. I. HOAGLIN. J. Am. Chem. Soc. **63**, 621 (1941).
23. C. K. BRADSHER and S. T. AMORE. J. Am. Chem. Soc. **63**, 493 (1941).
24. W. E. BACHMANN and M. W. CRONYN. J. Org. Chem. **8**, 456 (1943).
25. P. M. G. BAVIN. Can. J. Chem. **39**, 2035 (1961).
26. W. E. BACHMANN and L. H. KLEMM. J. Am. Chem. Soc. **72**, 4911 (1950).
27. N. G. RULE and W. J. HICKINBOTTAM. J. Chem. Soc. 2517 (1959).
28. P. M. G. BAVIN and M. J. S. DEWAR. J. Chem. Soc. 164 (1956).

Can. J. Chem. Downloaded from www.nrcresearchpress.com by 210.87.254.5 on 09/05/12
For personal use only.

THE HEARTWOOD EXTRACTIVES OF PINUS BANKSIANA LAMB.[1]

E. VON RUDLOFF AND A. SATO[2]
National Research Council of Canada, Prairie Regional Laboratory, Saskatoon, Saskatchewan
Received April 22, 1963

ABSTRACT

The heartwood of jack pine was analyzed by various chromatographic techniques and countercurrent distribution. The major components were found to be isopimaric, abietic, dehydroabietic, and neoabietic acids, as well as glycerides of oleic, linoleic, and linolenic acids. Smaller amounts of pimaric, sandaracopimaric, myristic, palmitic, stearic, palmitoleic, and four unidentified acids were recorded, as well as fatty acid esters of β-sitosterol, α-terpineol, and four unidentified volatile alcohols. Of the phenols, pinocembrin, pinobanksin, and pinosylvin monomethyl ether predominated. Pinosylvin was isolated and several minor constituents including lignan-like compounds were detected in the acetone extract. The methanol extract was composed mainly of polymeric lignan-like fractions. From one of these a trimer, $C_{60}H_{66}O_{24}$, m.p. 186–188° C, $[\alpha]_D$ +3.2°, was isolated. The small amount of steam-volatile material consisted mainly of α- and β-pinene, benzoic acid, and α-terpineol. Traces of methyl benzoate, camphene, limonene, β-phellandrene, *cis-p*-menthan-8-ol, and nine unidentified trace components were recorded.

INTRODUCTION

Jack pine (*Pinus banksiana* Lamb.) is a medium- to large-sized conifer found from Nova Scotia to northern British Columbia and the MacKenzie River valley (1). This pine is used extensively in the lumber industry and in Kraft pulping. In 1931 Hibbert and Phillips (2) made a thorough study of the resins found in green and seasoned jack pine wood and reported the presence of abietic, pimaric, oleic, and linoleic acids as well as smaller amounts of linolenic acid, saturated fatty acids, resenes, phytosterol, and α-pinene. More recently, Buchanan *et al.* (3) confirmed that oleic and linoleic acids are the major fatty acids, and found, in addition to the above, small amounts of lignoceric acid, these fatty acids occurring mainly as triglycerides. Erdtman (4) isolated from the heartwood the two flavanones pinocembrin and pinobanksin and the hydroxystilbene pinosylvin monomethyl ether. Lindstedt and Misiorny (5) confirmed the presence of these three polyphenols by paper chromatography and found also pinosylvin and three unidentified minor constituents. Haagen-Smit *et al.* (6) investigated the volatile oil from the oleoresin of jack pine and reported the major constituents to be *dl*- and *l*-α-pinene (ca. 85%) and *l*-β-pinene (ca. 10%).

These various studies have shown that the composition of the wood extractives of jack pine is very complex and that separation into individual components or groups of related compounds by the conventional techniques is very tedious and only partially successful. Furthermore, procedures which involve heating in alkaline or acidic media undoubtedly lead to some isomerization and polymerization (2). No complete analysis of the heartwood extractives with more modern techniques appears to have been published. In the present study an attempt was made to obtain as comprehensive as possible an analysis by employing countercurrent distribution (7) and chromatographic techniques.

The heartwood was milled and extracted first with acetone and then with methanol. These extracts were analyzed as shown in the flow sheet (Fig. 1). In a separate experiment the steam-volatile components (0.05%) were recovered and analyzed by gas–liquid chromatography (GLC) (8, 9). The major components were found to be α- and β-pinene,

[1]*Issued as N.R.C. No. 7445.*
[2]*National Research Council of Canada Postdoctoral Fellow, 1961–1963.*

Can. J. Chem. Downloaded from www.nrcresearchpress.com by 210.87.254.40 on 09/05/12
For personal use only.

Can. J. Chem. Downloaded from www.nrcresearchpress.com by 210.87.254.40 on 09/05/12
For personal use only.

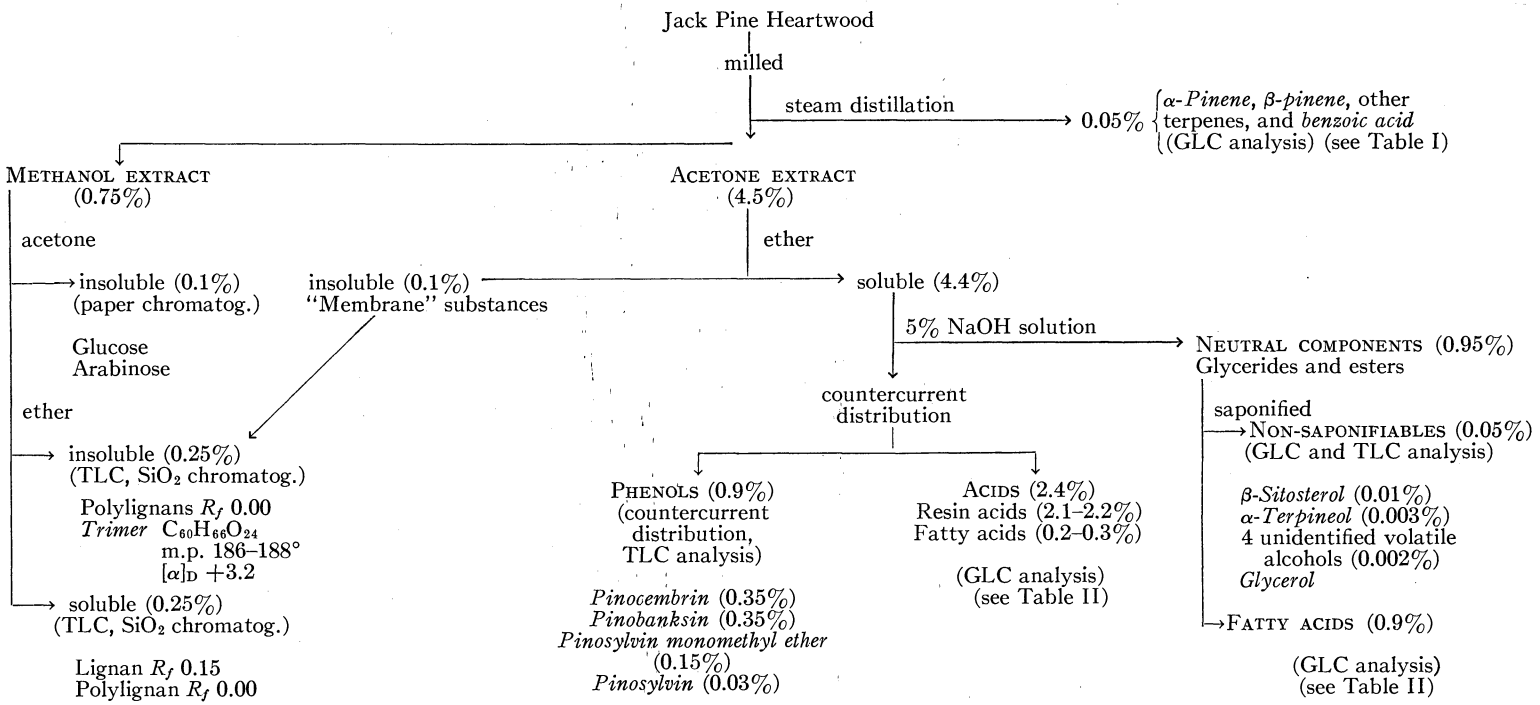

FIG. 1. Fractionation scheme for the wood extractives of jack pine.

confirming the findings of Haagen-Smit *et al.* (6). Thus, jack pine could be used for turpentine production, although the yield is low. In addition to the pinenes, smaller amounts of α-terpineol and benzoic acid were isolated, and camphene, limonene, β-phellandrene, *cis*-*p*-menthan-8-ol, and methyl benzoate were tentatively identified by retention characteristics (see Table I). Nine unidentified trace components were also

TABLE I

Composition of steam-volatile fraction from jack pine wood

Compound	Percent	RRT*
(*a*) Hydrocarbons†		
α-Pinene	46	0.29
(Camphene)	2	0.42
β-Pinene	28	0.55
(? Myrcene)	1	0.78
(Limonene)	1	1.00
(β-Phellandrene)	1	1.05
(? γ-Terpinene)	Trace	1.43
Unidentified	Trace	1.70
(*b*) Oxygenated‡		
Unidentified	0.5	0.90
Unidentified	1.5	1.05
(*cis*-*p*-Menthan-8-ol)	2	1.33
Unidentified	1.5	1.65
Unidentified	3	1.86
Unidentified	3	2.06
α-Terpineol	7.5	2.24
Unidentified	2	2.47
(Methyl benzoate)	Trace	1.57
(*c*) After treatment with diazomethane		
Methyl benzoate	10	1.57

NOTE: Names in parentheses refer to compounds identified by retention times only.
*RRT = relative retention time on 6 ft×1/4 in. polyethylene glycol column (PEG 20 M).
†Hydrocarbons at 65° C (limonene = 1.00).
‡Oxygenated monoterpenes at 120° C (camphor = 1.00).

recorded in the monoterpene range, but α-terpinyl acetate, propionate, or sesquiterpenoid constituents were not detected.

The acetone-soluble portion (4.5%) of the wood was divided into petrol- and ether-soluble material. Only a small amount (see Fig. 1) was insoluble in these two solvents (so-called "membrane" substances (4)). Initially, fractionation into neutral, phenolic, and acidic constituents was attempted by extraction with aqueous alkali of different strength. However, the separation into distinct groups of compounds was incomplete, and the material was, therefore, divided only into neutral and total acidic material. The neutral components were almost exclusively esters, and after saponification β-sitosterol, α-terpineol, four unidentified steam-volatile alcohols, and a mixture of long-chain fatty acids were isolated (see Fig. 1). Glycerol, the major non-saponifiable constituent, was identified by GLC as the triacetate. The fatty acid mixture was analyzed qualitatively and quantitatively by GLC (10) after conversion to the methyl esters. The quantitative data (see Table II) confirm that oleic and linoleic acids are the major acidic constituents of the glycerides (3), but appreciable amounts of linolenic acid were also recorded. Lignoceric acid was not detected; instead a number of minor acids, including three unidentified ones, were recorded in the C_{14} to C_{20} range. When an aliquot of the neutral material was chromatographed on a column of silicic acid, a partial separation of the triglycerides from the β-sitosteryl esters was obtained, some of the latter being obtained as waxy material melting in the 65 to 80° range (see Experimental).

Can. J. Chem. Downloaded from www.nrcresearchpress.com by 210.87.254.40 on 09/05/12
For personal use only.

TABLE II

Composition of the resin and fatty acid mixtures and relative retention times (methyl arachidate = 1.00) of methyl esters on various GLC columns

Methyl ester	Composition		Relative retention times			
			GLC column:*			
	Combined acids (%)	Free acids (%)	A	B	C	D
Benzoate	—	—	0.015	—	—	—
Laurate	—	—	0.04	—	—	—
Myristate	Trace	—	0.13	—	0.16	0.13
Palmitate	4	—	0.20	0.20	0.30	0.25
Palmitoleate	Trace	—	0.185	0.24	0.32	0.29
Unidentified	Trace	1	0.27	—	—	—
Stearate	2	—	0.45	0.46	0.50	0.50
Oleate	27	3	0.41	0.49	0.58	0.525
Linoleate	38	2	0.37	0.53	0.63	0.62
Linolenate	22	1.5	0.34	0.55	0.68	0.75
Unidentified	Trace	—	0.53	—	—	—
Unidentified	5	—	0.72	—	—	—
Behenate	—	—	2.30	—	—	2.01
Lignocerate	0	—	4.75	—	—	3.98
Arachidate (? Palustrate)	0 —}	0.5	1.00	1.00	1.00	1.00
Pimarate	—	4	0.81	0.93	0.71	1.27
Sandaracopimarate	—	2	0.87	0.99	0.80	1.53
Isopimarate	—	33	1.06	1.30	0.94	2.02
Levopimarate	—	0	1.20	1.83	1.28	1.96
Dehydroabietate	—	15	1.20	1.80	1.29	3.14
Abietate	—	24	1.50	2.04	1.50	3.14
Neoabietate	—	11	1.76	—	—	3.80

*A: Apiezon N (5% on Anakrom ABS 60–70 mesh) at 210° C. B: Neopentyl glycol adipate polyester (1% on Chromosorb W 60–80 mesh) at 190° C. C: QF-1 fluorinated silicone polymer (5% on Anakrom ABS) at 185° C. D: Polyethylene glycol 20 M (3% on Anakrom ABS) at 190° C.

Initially the phenolic (and acidic) fractions were analyzed by paper chromatography, using Lindstedt's technique (5, 11). However, it was found that the material from jack pine streaked and that R_f values fluctuated excessively. Employing different solvent systems did not give improved results and thin-layer chromatography (TLC) (12) was investigated. Using silica gel G and chloroform – acetic acid (9:1) or toluene–dioxane–water (1:1:1) satisfactory separation and well-defined spots were obtained with a variety of polyphenols, acids, and lignans (see Table III). R_f values were reproducible within narrow limits when measured relative to a reference compound (e.g. chrysin). This technique also gave satisfactory results for the analysis of the phenolic heartwood constituents of jack pine (cf. Fig. 2). However, resin and fatty acids were not resolved sufficiently. Since methyl esters of fatty acids are conveniently and accurately analyzed by GLC (cf. e.g. ref. 10), this technique was employed for identification and estimation of acidic constituents. Hudy (13) has reported satisfactory separation of the methyl esters of a number of resin acids using Apiezon N and polyester GLC columns. However, the use of temperatures of 225° C and higher resulted in a partial isomerization of methyl levopimarate and palustrate to methyl abietate and dehydroabietate. In the present study, other liquid phases were investigated, and by employing a higher ratio of solid support to liquid phase, operating temperatures were reduced sufficiently to reduce isomerization to a negligibly small amount. Relative retention times (RRT) were measured with respect to methyl arachidate (see Table II), which was also used as internal standard for the quantitative data. The results obtained show the major acidic constituents to be isopimaric

Can. J. Chem. Downloaded from www.nrcresearchpress.com by 210.87.254.40 on 09/05/12
For personal use only.

TABLE III

R_f values of lignans, polyphenols, β-sitosterol, and some acids on thin-layer chromatograms*

Compound	Chloroform – acetic acid (9:1 v/v)	Toluene–dioxane–water (1:1:1)	Color with acidic $KMnO_4$ reagent
Polylignan (unknown 1)	0.00	0.00	Brown
Olivil	0.05	0.06	Violet-brown
Isolariciresinol	0.09	0.11	Pink
Secoisolariciresinol	0.10	0.17	Brown
Unknown 2	0.15	0.21	Brown
Lariciresinol	0.18	0.23	Brown
Unknown 3	0.32	0.42	Brown
Pinosylvin	0.37	0.46	Brown
α-Conidendrin	0.49	0.38	Pink
Pinoresinol	0.49	0.42	Grey-brown
Unknown 4	0.50	0.46	Brown
Pinobanksin	0.56	0.59	Yellow
Chrysin	0.57	0.61	Yellow
Unknown 5	0.60	0.50	Brown
Pinocembrin	0.68	0.69	Yellow
Pinosylvin monomethyl ether	0.71	0.72	Yellow-brown
β-Sitosterol	0.76	0.56	Brown
Abietic acid	0.82	0.68	Brown
Stearic acid	0.83		Weak
Oleic acid	0.85	0.51	Light yellow
Pinostrobin	0.84	0.64	Yellow
Pinosylvin dimethyl ether	0.86	0.67	Yellow-brown
Benzoic acid	0.86		None

*Thirty minutes ascending, on silica gel G (250 μ thick).

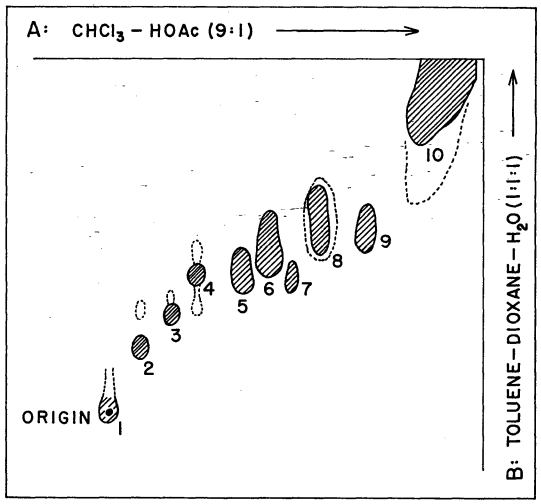

FIG. 2. Two-dimensional thin-layer chromatogram of phenolic and acidic jack pine heartwood extractives.
1. Unknown 1 (polylignan)
2. Unknown 2 (lignan R_f 0.15)
3. Unknown 3
4. Pinosylvin
5. Unknown 4
6. Pinobanksin
7. Unknown 5
8. Pinocembrin
9. Pinosylvin monomethyl ether
10. Resin acids etc.

and abietic acids, with lesser amounts of dehydroabietic, neoabietic, pimaric, sandaracopimaric, and unsaturated fatty acids also being recorded (see Table II). A fairly large

Can. J. Chem. Downloaded from www.nrcresearchpress.com by 210.87.254.40 on 09/05/12
For personal use only.

peak of RRT 1.00 was also recorded, and, since no arachidic acid was detected in the mixture of acids from the triglycerides, this component could be palustric acid (13).

Countercurrent distribution (7) was found to be a suitable method for separating the phenolic components from resin and fatty acids. The major phenolic constituents were fractionated sufficiently to permit estimation and isolation when 200 transfers were employed. Pinocembrin and pinobanksin were found to be the major polyphenols, smaller amounts of pinosylvin monomethyl ether and pinosylvin also being isolated (see Fig. 1). TLC indicated that five other minor constituents were present. Of these, two (R_f 0.00 and 0.15) were lignan-like constituents found in larger amounts in the methanol extract (see below). No pinosylvin dimethyl ether, dihydropinosylvins, or chrysin was detected. These findings are in good agreement with the work of Erdtman (4) and Lindstedt and Misiorny (5). The unidentified compound F described by the latter authors may have been benzoic acid, but their compounds D and E could not be correlated with any of the above minor components. The ether-insoluble portion of the acetone extract ("membrane" substances) had R_f 0.00 (TLC) and was very similar to the major fraction obtained from the methanol extract.

The methanol extract (0.75%) was divided into ether-soluble and -insoluble material. The former was chromatographed on silicic acid and elution with chloroform gave a trace of the compound with R_f 0.15. Its infrared spectrum was very similar to that of lariciresinol (R_f 0.18), but the melting point (135.5–137° C) and molecular weight (573) differed from those of this lignan. Elution of the chromatogram with more polar solvents did not yield other crystalline components. All fractions appeared to contain lignan-like material of higher molecular weight. The ether-insoluble portion was taken up in hot acetone and the insoluble carbohydrate material was filtered off. Paper chromatography of the latter gave spots corresponding to glucose and arabinose. Erdtman (14) reported arabinose to be a constituent of jack pine and other pine species. The acetone-soluble portion was fractionated by crystallization and column chromatography, when several sharp-melting, amorphous fractions were obtained. One of these (m.p. 164–165° C, R_f 0.00) gave on recrystallization a small amount of a polylignan, $C_{60}H_{66}O_{24}$, m.p. 186–188° C, $[\alpha]_D$ +3.2°, λ_{max}^{MeOH} 281 mμ, which had an infrared spectrum resembling very closely that of lariciresinol. Acetylation gave an acetate, m.p. 101–102.5° C, $[\alpha]_D$ −1.0°, but methylation gave intractable material. It is noteworthy that the oxygen content of this polylignan is 4 atoms per phenylpropanoid unit as compared with 3 in lignans of the lariciresinol type. Recently Freudenberg (15), in discussing a soluble oligomeric lignan-like material which Brauns (16) found in spruce wood (native lignin), pointed out that alcoholic solvents may react with lignin during isolation and that alcohols or sugars may add to dehydration polymerizates during lignin formation. Similarly, the higher oxygen content of the polylignan isolated in the present study suggests that the material may be the product of the addition of methanol to a reactive lignan-like compound. Two other fractions having similar properties, but with melting points of 124–125° C and 148–151° C, were also isolated. The nature and the source of these polylignans will be investigated further.

Benzoic acid and its methyl ester are not considered to be typical pine heartwood extractives (14). It is possible that these are artefacts, produced for example by oxidative degradation of the pinosylvins or flavanones. From a crude sample of pinobanksin, which had been standing several months, benzoic acid was isolated. However, benzoic acid was found in the steam-volatile fraction, and if it is a degradation product, it must have been produced during the milling or steam distillation of the wood.

Can. J. Chem. Downloaded from www.nrcresearchpress.com by 210.87.254.40 on 09/05/12
For personal use only.

EXPERIMENTAL

Melting points were determined with a Leitz hot-stage microscope. Countercurrent distribution was carried out with a modified 100-tube E.C. Apparatus Co. instrument (20-ml volume lower phase, 5- to 30-ml variable upper phase for each tube). Gas–liquid chromatograms were obtained with an instrument of conventional design (10), having a thermal conductivity cell as detector and using helium as carrier gas. A 1-mv Honeywell recorder was used with a chart speed of 0.5 in./min. Columns were made of 6 ft×1/4 in. (6 mm) O.D. copper or stainless steel tubing. The liquid phase was applied to the solid support (Chromosorb W 60–80 mesh) by means of the tray method in the ratio of 1 to 6, unless otherwise stated. Individual fractions were collected at the heated outlet in glass traps which were externally cooled. Infrared spectra were recorded with a Perkin–Elmer Model 21 double-beam spectrophotometer, liquids being mounted as films between sodium chloride plates and solids as KBr disks. Molecular weights were determined by means of a Mechrolab Model 301 osmometer.

Paper-partition Chromatography (PPC)

Initially, Lindstedt's technique (5, 11) was used for the separation of phenols. However, it was found that with benzene–ligroin–methanol (50:50:1 v/v) saturated with water as solvent R_f values fluctuated and spots streaked frequently even when the paper (Whatman No. 4) was allowed to equilibrate with the solvent in the chamber for 8 hours. R_f values (measured at the top of the spot) for pinosylvin, its monomethyl ether, pinobanksin, pinocembrin, and chrysin varied from 0.08 to 0.15, 0.71 to 0.84, 0.13 to 0.21, 0.35 to 0.44, and 0.15 to 0.25 respectively in different runs. The spray reagent was diazotized benzidene and ultraviolet fluorescence or absorption was also used. With some of the phenolic fractions from jack pine heartwood extractives excessive streaking was obtained. Other solvent systems, including *n*-butanol – acetic acid – water (4:1:1.8), chloroform – acetic acid – water (13:6:1), benzene–ligroin–methanol (5:5:1), and benzene–ligroin–acetic acid – methanol – water (5:5:1:1:5, upper phase), were tried without marked improvement.

Sugars were chromatographed on Whatman No. 1 paper using *n*-butanol – acetic acid – water (4:1:5, upper phase) and *n*-butanol–pyridine–water (3:3:1) as solvent and aniline phthalate as spray reagent. The R_f values for glucose, arabinose, and xylose were 0.12 and 0.16, 0.18 and 0.21, and 0.19 and 0.27 respectively.

Thin-layer Chromatography (TLC)

To solve the above difficulties with phenolic constituents TLC according to Stahl (12) was tried. Well-defined spots and good resolution were obtained on silica gel G (Merck, Darmstadt, Germany) and either chloroform – acetic acid (9:1) or toluene–dioxane–water (1:1:1, upper phase) as developing solvent. Phenolic compounds were detected by use of ultraviolet light, diazotized benzidene, or $FeCl_3$–$K_3Fe(CN)_6$ (1% aqueous solutions, 1:1) spray. Equally good separation was obtained with some lignans and the technique could also be used for the detection of resin acids, fatty acids, β-sitosterol, and benzoic acid. The spray reagents used were: 0.1 *M* $KMnO_4$ and 10% H_2SO_4 (1:3, heated 5 minutes at 105° C), rhodamine B (0.05% in 10% aqueous acetone), and antimony trichloride (0.05% in chloroform). The glass plates were 5×20 cm or 13×13 cm in dimension, the support was applied in about 250-μ thickness and development time was about 30 minutes, when the solvent had travelled about 10 cm. R_f values for individual compounds varied by about 0.05 unit between different runs, but when measured with respect to a reference compound (e.g. chrysin) they were constant to within ±0.02 unit. The R_f values of lignans, polyphenols, some acids, and β-sitosterol, as well as those of the unidentified components of the jack pine heartwood extractives, are shown in Table III. A two-dimensional chromatogram obtained with phenolic and acidic components from the jack pine wood extract is shown in Fig. 2.

Gas–Liquid Chromatography (GLC)

Steam-volatile components were analyzed by the GLC technique described by one of us for the analysis of terpenes (8) and essential oils (9, 17). Monoterpene hydrocarbons were analyzed at 65° C (flow rate 120 ml/min) on polyethylene glycol 20 M (PEG 20 M) and adipate polyester (APEG, NGA) columns. Relative retention times (RRT) were measured with respect to limonene. Oxygenated monoterpenes and methyl benzoate were chromatographed on the same columns at 120° C and RRT values were measured with respect to camphor. When separation was incomplete, analysis was also carried out on ethylene glycol bis(propionitrile) or QF-1 fluorinated silicone polymer columns. The percentage composition was obtained by the triangulation method, the error being ±(1–3)% for large- to medium-sized peaks and ±(3–10)% for medium- to small-sized ones.

Free fatty acids were methylated with freshly prepared diazomethane and the resulting methyl esters were analyzed by GLC at 160–190° C on Apiezon N (5% on Anakrom ABS, 60–70 mesh), QF-1 (5% on Anakrom ABS 60–70 mesh), neopentyl glycol adipate polyester (NGA, 1% on Chromosorb W, 60–80 mesh), and polyethylene glycol (PEG 20 M, 3% on Anakrom 60–70 mesh) columns. Resin acids were similarly methylated, but in the presence of some methanol in order to ensure complete esterification. A mixture of abietic acid (48%) and arachidic acid (52%) methylated in this manner gave peaks (at 185° to 210° C) which had corresponding areas (±(2–3)%) on the Apiezon N, QF-1, and SE-30 columns. On the polyester and

Can. J. Chem. Downloaded from www.nrcresearchpress.com by 210.87.254.40 on 09/05/12
For personal use only.

polyethylene glycol columns the area of the peak recorded for methyl abietate was 5 to 15% smaller than the theoretical value. Therefore, all quantitative data were calculated from data recorded on the former columns. For methyl esters of fatty acids correction factors for acids of different chain length were required. Taking methyl arachidate as 1.00, the factors for stearate, oleate, linoleate, and palmitate were 0.95, 0.96, 0.96, and 0.90 (±0.02) respectively. All retention times were measured with respect to methyl arachidate and the various RRT values obtained are shown in Table II.

Extraction of the Wood and Preliminary Fractionation

The logs of jack pine wood came from the Candle Lake district of Northern Saskatchewan.* The bark and sapwood was removed and the heartwood was milled in a hammer and a Wiley mill. The air-dried wood (5.0 kg) was extracted with acetone (15 liters) in a Soxhlet extractor for 30 to 36 hours. Excess solvent was removed by evaporation *in vacuo* on a rotatory evaporator. The residual wood meal was extracted similarly with methanol.

The brown, viscous residue from the acetone extract (226 g, 4.5%) was poured with stirring into petrol (b.p. 40–60° C; 2 liters), and after decantation of the petrol solution and washing with fresh solvent (2×250 ml), the insoluble residue (80 g, 35.4%) was taken up in a minimum of acetone and poured similarly into ether (2 liters). The ethereal solution was filtered to remove the insoluble precipitate ("membrane" substances, 4.3 g, 1.9%).

When small aliquots of the petrol and ether solutions were extracted successively with saturated sodium bicarbonate, 5% sodium carbonate, and 5% sodium hydroxide solution, the separation into neutral, phenolic, and acidic components was incomplete (TLC analysis). The insoluble resin acid salt layer (4), after acidification and chromatography on silicic acid gave a number of fractions with sharp melting points (0.5 to 1.5° spread) in the 70 to 90° C range. Subsequent analysis showed these to be mixed crystals of resin acids, fatty acids, and esters (see also below). A trace (1.5 mg) of a white, crystalline compound, m.p. 199.5–200° C, was isolated from the first fraction eluted with chloroform. The infrared spectrum had strong adsorption bands at 3400, 1730, 1268, 1200, 1080, 1065, and 700 (triplet) cm^{-1} and medium-intensity ones at 1600, 1508, 1453, 1023, 968, 880, 800, and 752 cm^{-1}, indicating that the compound may be an aromatic ester having free hydroxyl groups. This compound was not isolated again by the techniques described below.

In subsequent work the petrol- and ether-soluble material was extracted exhaustively with aqueous sodium hydroxide solution to remove all acidic and phenolic components. The ether layer was washed with water, dried (Na_2SO_4), and evaporated to dryness to give the neutral constituents (47.8 g, 21.2%; 15.2% from the petrol-soluble portion). The aqueous alkaline solutions and washings were combined, acidified, and extracted with ether to give the combined acidic and phenolic constituents (171.2 g, 75.7%; 46.3% from the petrol-soluble portion).

Steam-volatile Components

Fresh wood meal (200 g) was steam-distilled for 2 hours and the distillate was extracted with ether. After drying, the solvent was evaporated on a steam bath, using a small flask having a long neck. The residual oil (0.10 g, 0.05%) contained about 3% ether and had n_D^{25} 1.4680, $[\alpha]_D$ −18.2° (*c*, 1.2, $CHCl_3$). Aliquots (1–10 μl) were analyzed by GLC for monoterpenes as described above. The average composition is shown in Table I. The identity of α-pinene, β-pinene, and α-terpineol was confirmed by isolation and comparison of infrared spectra. The optical rotation of both pinene fractions was negative.

GLC analysis at higher temperatures (120–180° C) showed no peaks corresponding to α-terpinyl acetate or propionate, nor were any peaks in the sesquiterpene range recorded. When the steam-volatile product was treated with diazomethane a substantial peak (about 10%) corresponding to methyl benzoate (RRT 1.57) was observed. The presence of free benzoic acid was confirmed when steam distillation of the acidic portion of the wood extract gave crystalline benzoic acid, m.p. 117.5–120° C, which was undepressed on admixture with an authentic sample (m.p. 120–121° C). Steam distillation of the neutral portion of the acetone extract gave a very small amount of an oil similar in composition to the one obtained by direct steam distillation of the wood.

Countercurrent Distribution

An aliquot of the acetone extract (4.0 g) was distributed equally between the first four tubes of the apparatus, using 70% aqueous ethanol equilibrated with petrol (b.p. 60–70° C) as lower and upper phase (20 ml each per tube). After applying 100 transfers, the contents of each tube were withdrawn, the solvent evaporated, and the residual material weighed. By plotting weight against tube number the distribution curve was obtained. Tubes 0 to 25 contained about 20% of the extract, which was distributed in two overlapping peaks. Tubes 26 to 68 were practically devoid of material, whereas tubes 69 to 95 contained the balance of the extract. From tubes 79 and 82 crystalline material of m.p. 87–88° C and 73–74° C was obtained. The infrared spectra resembled those of β-sitosteryl esters, with free acids as contaminants. Removal of the acidic material (resin acids, GLC analysis) gave waxy ester fractions, m.p. 70–74° and 67–72° C respectively, which were saponified. β-Sitosterol, m.p. 135–137° C (TLC R_f 0.76), was isolated from the non-saponifiable portion, whereas GLC analysis showed the saponifiable portion to contain a mixture of C_{18}

**Identified and supplied by Dr. W. B. Denyer, Department of Forest Pathology, Forestry Department, Saskatoon.*

Can. J. Chem. Downloaded from www.nrcresearchpress.com by 210.87.254.40 on 09/05/12
For personal use only.

fatty acids (see also below). TLC analysis of the material in tubes 0 to 25 showed it to be composed of pinocembrin, pinobanksin, pinosylvin monomethyl ether, and several unidentified phenolic components.

From this experiment it was concluded that a fairly low number of transfers would suffice to separate the phenolic constituents completely from resin acids and neutral components, but that a very high number of transfers would be required to obtain fractionation into individual components. Since the neutral and acidic components were analyzed more conveniently by other techniques, only the phenolic constituents were fractionated by this means (see below).

Neutral Components

The infrared spectrum of the neutral portion indicated that it was composed mainly of esters. An aliquot (20 g) was saponified by heating under reflux with sodium hydroxide solution (5% in 80% aqueous ethanol) for 2 hours. After diluting with water, the non-saponifiables (0.2 g) were extracted with ether. GLC analysis showed the presence of five volatile components with RRT (camphor = 1.00, PEG 20 M column at 120° C) values of 0.88, 1.31, 1.90, 2.08, and 2.24 in the area ratios of 2:5:1:1:24. These RRT values correspond to those of some of the oxygenated terpenes found in the steam-volatile fraction (Table I). The component with RRT 2.24 was isolated and its infrared spectrum agreed in all respects with that of α-terpineol. The peak at RRT 1.31 may correspond to *cis*-*p*-menthan-8-ol. TLC analysis showed the non-volatile component to be β-sitosterol (R_f 0.76). The non-saponifiable material was steam-distilled and the volatiles were extracted with ether. On concentrating the ether solution a small amount of crystalline β-sitosterol, m.p. 136–137° C, was obtained. The soluble material was fractionated by GLC and the major component with RRT 2.24 was isolated pure in small amounts. The infrared spectrum agreed with that of α-terpineol in all respects. From the non-volatile portion (0.12 g) crystalline β-sitosterol, m.p. 135–136° C, $[\alpha]_D^{25}$ −24.2° (*c*, 2.5, $CHCl_3$), was obtained after recrystallization from ethanol. TLC analysis gave a single spot of R_f 0.76. The acidic components (17 g) were recovered from the saponification mixture in the usual manner. After methylation with diazomethane these were analyzed by GLC. The average composition is shown in Table II. The residual aqueous solution was deionized by treatment with ion-exchange resin and evaporated to a sirupy residue (3 g). An aliquot was acetylated and the ether-soluble product was analyzed by GLC (PEG 20 M column at 160° C), when a peak corresponding to glycerol triacetate, RRT 7.07 (camphor = 1.00), was recorded.

An aliquot (1.0 g) of the neutral portion was chromatographed on a column of silicic acid (25 g). Elution with chloroform gave two waxy fractions (mg amounts) having m.p. 67–72° C and 78.5–82° C respectively. The infrared spectra resembled that of β-sitosteryl stearate. Saponification gave β-sitosterol (TLC R_f 0.75) and a mixture of oleic, linoleic, and stearic acids (GLC).

Acidic Constituents (77.6%)

The total acidic material was fractionated into phenolic and acidic components by countercurrent distribution. Applying 50 transfers with 75% aqueous ethanol–petrol (b.p. 60–70° C) as solvent pair, an aliquot (5 g) was resolved into phenols (1.3 g; tubes 0 to 18) and resin and fatty acids (3.6 g; tubes 26 to 49).

Aliquots of the free acids were taken up in a mixture of ether and methanol (1:1) and were methylated with excess diazomethane solution. The average composition of the mixture of methyl esters as determined by GLC analysis is shown in Table II.

The phenolic material was analyzed by two-dimensional TLC (see Fig. 2). This, together with earlier paper chromatograms, showed that the major components were most likely pinocembrin, pinobanksin, and pinosylvin monomethyl ether. Spots corresponding to pinosylvin and five unidentified minor components were also detected (see Table III). To obtain an estimate of the relative amounts and to isolate pure components, an aliquot (5 g) was fractionated in a 200-transfer countercurrent experiment, using 75% aqueous ethanol–petrol (b.p. 60–70° C) as solvent pair. The distribution curve showed two main peaks with maxima at tube 6 (K = 0.031) and tube 18 (K = 0.099) respectively, and shoulders at tubes 2, 9, and 28. Calculation of theoretical curves (7) gave values of about 35% for the two major components, about 20% for that giving a shoulder at tube 28, and about 3% each for the other two components. Using TLC, these were tentatively identified as pinobanksin, pinocembrin, pinosylvin monomethyl ether, pinosylvin, and an unknown respectively. From tubes 5 to 7, pinobanksin, m.p. 177–180° C (from ethanol), $[\alpha]_D^{25}$ −6.4° (*c*, 1.1, MeOH), was obtained; from tubes 16 to 20, pinocembrin, m.p. 203.5–204° C, $[\alpha]_D^{25}$ −16.9° (*c*, 1.0, $CHCl_3$); and from tubes 27 to 30, pinosylvin monomethyl ether, m.p. 112.5–114° C. When pinobanksin was crystallized from aqueous solvents, it was obtained as the monohydrate, m.p. 174.5° C. Found: C, 61.60; H, 4.75%. Calculated for $C_{15}H_{12}O_5 \cdot H_2O$: C, 62.10; H, 4.86%. Pinosylvin was obtained as mixed crystals with pinobanksin from tubes 1 to 3, m.p. 156–170° C. Column chromatography on silicic acid gave practically pure pinosylvin, m.p. 154–156° C. The identity of each compound was confirmed by mixed melting points and comparison of infrared spectra. Attempts to obtain the unidentified components (cf. Fig. 2) in the crystalline state failed, and it was not possible to obtain crude products which were free from the above major constituents. It is noteworthy that crude fractions of pinobanksin gave crystalline benzoic acid (sublimed at the top of test tubes) on standing for several months in the cold.

Ether-insoluble Material (1.9%)

The ether-insoluble portion of the acetone extract was a brown, amorphous material having R_f 0.0 (TLC). Using acetic acid – hydrochloric acid – water (30:3:1 v/v) as developing solvent a single spot of R_f 0.77 was

Can. J. Chem. Downloaded from www.nrcresearchpress.com by 210.87.254.40 on 09/05/12
For personal use only.

obtained, which gave an orange-brown color with diazotized benzidene. The infared spectrum of the crude material was similar to that of the material R_f 0.0 (TLC) obtained from the methanol extract (see below).

Methanol Extract

The residue (9.0 g) from the methanol extract (0.75%) was extracted with ether and the ether-soluble portion (4.0 g) was fractionated by column chromatography on silicic acid. Elution with chloroform gave a very small amount (8 mg) of an amorphous compound, m.p. 135.5–137° C, having an infrared spectrum similar to that of lariciresinol (m.p. 169.5–170.5° C). The R_f value (TLC) was 0.15, i.e. that of unknown 2 (Fig. 2), which is close to that of lariciresinol (R_f 0.18). However, the molecular weight was found to be 573, which is about 1.6 times that of lariciresinol. Further elution of the chromatogram with more polar solvents did not produce fractions of sharp melting points.

The ether-insoluble portion (5.0 g) was taken up in hot acetone and the mixture was filtered hot. The insoluble residue (1.0 g) was taken up in water and analyzed by paper chromatography. Two spots, corresponding in R_f values (see above) to glucose and arabinose, were detected. The acetone solution was allowed to cool slowly overnight, when an amorphous precipitate, m.p. 164–165° C, was obtained. Recrystallization from ethanol gave a microcrystalline powder, compound A (61 mg), m.p. 186–188° C, λ_{max}^{MeOH} 281 mμ, $[\alpha]^{23}_D$ +3.2° (*c*, 1.2, dioxane). The infrared spectrum was similar to that of lariciresinol, but the R_f value (TLC) was 0.0. Found: C, 61.03; H, 5.65; CH_3O, 17.39%; mol. wt., 1167. Calculated for $C_{60}H_{66}O_{24}$: C, 61.53; H, 5.68; CH_3O, 15.3%; mol. wt., 1171.4. Acetylation with acetic anhydride in the presence of sodium acetate gave a compound, m.p. 101.5–102.5° C, $[\alpha]_D^{25}$ −1.0° (*c*, 1.0, acetone). Found: C, 61.84; H, 5.64; CH_3O, 11.42; AcO, 26.83%; mol. wt., 1558. Calculated for decaacetate: C, 60.8; H, 4.84; CH_3O, 11.4; AcO, 25.9%; mol. wt., 1581.41. Calculated for nonaacetate: C, 59.3; H, 4.91; CH_3O, 11.7; AcO, 26.6%; mol. wt., 1540.38. Methylation with dimethyl sulphate gave intractable, viscous material. Treatment with diazomethane gave an amorphous compound of mol. wt. 1460. The parent compound gave a single spot of R_f 0.86 on TLC analysis, using acetic acid – hydrochloric acid – water (30:3:1) as solvent. The acetone-soluble (cold) portion was chromatographed on silicic acid (30 g), eluting successively with ether, chloroform, 2-butanone, and methanol. Elution with 2-butanone gave an amorphous material (240 mg), compound B, m.p. 124–125° C, after precipitation with water from a solution in dioxane. Elution with 2-butanone–methanol (1:1) gave another amorphous fraction, compound C, m.p. 148–151° C, $[\alpha]_D$ +3.2° (*c*, 1, dioxane). Both compounds had R_f values of 0.0 (TLC) and had infrared spectra similar to those of compound A and lariciresinol.

ACKNOWLEDGMENTS

We wish to thank Dr. W. B. Denyer for procuring the jack pine wood, Professor H. Erdtman for samples of pine polyphenols, Professor K. Freudenberg for samples of lignans, and Dr. E. O. Edwards and the Hercules Powder Co., Wilmington, U.S.A., for samples of resin acids. Microanalyses were carried out by Mr. M. Mazurek and infrared spectra were recorded by Mr. W. C. Haid. The technical assistance of Mr. M. Granat is also gratefully acknowledged.

REFERENCES

1. Canadian Department of Forestry. Native trees of Canada. 6th ed. Queen's Printer, Ottawa. 1961. p. 16.
2. H. Hibbert and J. B. Phillips. Can. J. Res. **4**, 1 (1931).
3. M. A. Buchanan, R. V. Sinnett, and J. A. Jappe. Tappi, **42**, 578 (1959).
4. H. Erdtman. Svensk. Kem. Tidn. **56**, 95 (1946).
5. G. Lindstedt and A. Misiorny. Acta Chem. Scand. **5**, 121 (1951).
6. A. J. Haagen-Smit, C. T. Redemann, T. H. Wang, and N. T. Mirov. J. Am. Pharm. Assoc. **39**, 260 (1950).
7. L. C. Craig, D. Craig, and E. G. Scheibel. *In* Technique of organic chemistry. Vol. III, Part I. *Edited by* A. Weissberger. Interscience Publishers Inc., New York. 1950. p. 286.
8. E. von Rudloff. Can. J. Chem. **39**, 1190, 1200 (1961).
9. E. von Rudloff. Phytochemistry, **1**, 195 (1962).
10. B. M. Craig and N. L. Murty. J. Am. Oil Chemists' Soc. **36**, 1124 (1959).
11. G. Lindstedt. Acta Chem. Scand. **4**, 448 (1950).
12. E. Stahl. Z. Anal. Chem. **181**, 303 (1961).
13. J. A. Hudy. Anal. Chem. **31**, 1754 (1959).
14. H. Erdtman. *In* Progress in organic chemistry. Vol. 1. *Edited by* J. W. Cook. Butterworths Scientific Publications, London. 1952. pp. 22–63.
15. K. Freudenberg. *In* Fortschritte der Chemie organischer Naturstoffe. *Edited by* L. Zechmeister. Springer-Verlag, Wien. 1962. p. 41.
16. F. E. Brauns. J. Am. Chem. Soc. **61**, 2124 (1939).
17. E. von Rudloff. Tappi, **45**, 181 (1962).

Can. J. Chem. Downloaded from www.nrcresearchpress.com by 210.87.254.40 on 09/05/12
For personal use only.

ISOTOPE EFFECTS IN X-RAY-IRRADIATED ACIDIFIED H_2O–D_2O SOLUTIONS

CHAVA LIFSHITZ[1]
Department of Physical Chemistry, The Hebrew University of Jerusalem, Israel
Received February 13, 1963

ABSTRACT

H_2O–D_2O mixtures containing 0.1–1 *N* H_2SO_4 were irradiated by 200-kv X rays. The molecular isotope effect, $\alpha_M = (H/D)_{H_2}/(H/D)_{H_2O}$, was determined from experiments on KBr solutions. The atomic isotope effect, $\alpha_A = (H/D)_H/(H/D)_{H_2O}$, was determined from experiments on ethanol solutions. At 96% D_2O, $\alpha_A = 3.7\pm0.5$ and $\alpha_M = 4.0\pm0.2$. The isotope effects are discussed in connection with the radiation-chemical reaction $H_3O^+ + eH_2O \rightarrow H + 2H_2O$. The connection between the atomic and molecular hydrogen is discussed. It is concluded that the relation between the observed atomic and molecular isotope effects is *not* contrary to a hydrogen atom recombination reaction leading to the molecular product. Isotope effects due to the oxidation of Fe^{+2} ions by hydrogen atoms in acid solutions were measured and the mechanism of this reaction is discussed.

INTRODUCTION

The primary chemical act taking place when aqueous solutions are subjected to ionizing radiations is represented schematically as follows:

$$H_2O \rightarrow H, OH, H_2, H_2O_2. \qquad [1]$$

When suitable solutes are present (e.g. methanol, $Fe^{+2}(H^+)$), the hydrogen atoms lead to further hydrogen molecule production, in addition to the molecular hydrogen produced by the primary chemical reaction [1].

When H_2O–D_2O mixtures are irradiated, the hydrogen atoms and molecules formed via [1] are enriched with light hydrogen with respect to the water (1–5). A study of the dependence of these isotope effects on various factors, such as type of solute, deuterium concentration of the water, etc., is important for the understanding of the mechanism of formation of the primary products as well as the secondary reactions between the reactive intermediates formed (e.g. hydrogen atoms) and the solutes present. Such a study is of particular interest, since none of the mechanisms which were proposed for the radiation-chemical decomposition of water was found consistent with all the observed isotope effects (4–6).

The present paper presents results on the isotopic enrichment of hydrogen gas evolved from irradiated acidified solutions of various solutes, in particular, KBr, $FeSO_4$, and ethanol. The dependence of the isotope effects on the deuterium concentration of the solution is presented. The results obtained are compared with existing data, and possible reaction mechanisms leading to the observed isotope effects are discussed.

EXPERIMENTAL

Air-free solutions were irradiated with 200-kv X rays and the isotopic composition of the gas was determined mass spectrometrically. The detailed experimental procedure was described in a previous paper (7).

RESULTS

The Molecular Isotope Effect

The effect of solute concentration and deuterium content of the water on $\alpha_M = (H/D)_{H_2}/(H/D)_{H_2O}$ was examined for two basically different types of solute: (*a*) non-oxidizing solutes and (*b*) oxidizing solutes.

[1]*Present address: Department of Chemistry, Cornell University, Ithaca, New York.*

Can. J. Chem. Downloaded from www.nrcresearchpress.com by 210.87.254.40 on 09/05/12
For personal use only.

(*a*) Acidified aqueous solutions of KBr and KI of various D_2O concentrations were irradiated and the isotopic composition of the hydrogen evolved was determined. The Br^- ion was chosen as a solute in a principal series of experiments carried out to determine the molecular isotope effect, since it is an efficient hydroxyl radical scavenger yet does not react with hydrogen atoms. In these experiments one thus gets the full molecular hydrogen yield, via [1], and this molecular hydrogen is protected from further attack of OH by the Br^- (8). The isotopic separation observed is then the initial separation characteristic of the molecular product and unaffected by secondary reactions.

Values of α_M in the presence of various solutes at low deuterium concentrations were compared, in order to examine the dependence of α_M on the type of solute. The radiation-chemical behavior of I^- was found to be slightly different from that of Br^- (9, p. 108). α_M values obtained from KBr and KI solutions of low deuterium concentration are presented in Table I. The hydrogen yields in these experiments are equal, within the experimental error. (The molecular yield, in terms of the number of hydrogen molecules formed per 100 ev absorbed, is $G_M = 0.7 \pm 0.1$.)

TABLE I

α_M at low deuterium concentrations (0.8 N H_2SO_4)

% D in solution	Solute	α_M
2.95	—	2.0_5
2.1	1×10^{-4} M KBr	2.2_6
1.0	1×10^{-4} M KBr	1.9_8
1.0	1×10^{-2} M KBr	1.9_7
3.0	1×10^{-2} M $CuSO_4$; 7×10^{-4} M $FeSO_4$	2.2_0
1.0	1×10^{-2} M KI	2.0_5
1.0	5×10^{-1} M KI	2.1_5

From the experiments on 1% D_2O solutions of KBr (Table I) one observes that α_M is independent of KBr concentration. The addition of 10^{-4} M KBr to a solution containing no KBr increases α_M slightly, but any concentration change beyond that has no effect.

The dependence of α_M on the deuterium content of acidified KBr solutions is presented in Fig. 1. An increase in α_M is observed with increasing deuterium concentration. α_M in

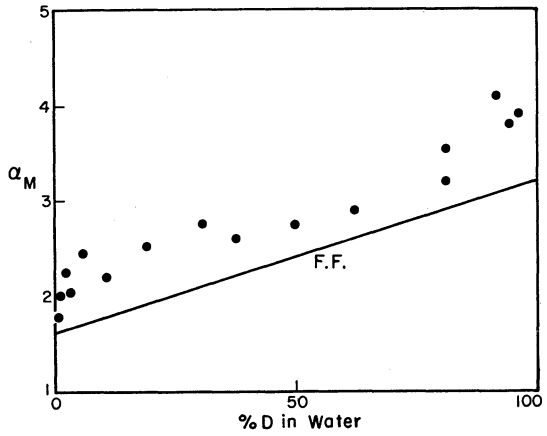

FIG. 1. α_M dependence on deuterium concentration. Experimental results from 10^{-4} M KBr, 0.8 N H_2SO_4 solutions. Curve F.F. is the computed isotopic enrichment of H_3O^+ from ref. 4.

Can. J. Chem. Downloaded from www.nrcresearchpress.com by 210.87.254.40 on 09/05/12
For personal use only.

Fig. 1 shows an additional upward trend at high deuterium concentrations. Several experiments were carried out on 99.8% D_2O solutions. Great care was taken not to contaminate the D_2O with light hydrogen. The results obtained are summarized in Table II. Since

TABLE II

α_M values at 99.8% D_2O (neutral solutions)

% D	Solute	$(HD/D_2)_{gas}$	α_M
96.5	1×10^{-2} *M* KBr		3.6 (7)
97.0	1×10^{-1} *M* KNO_2		4.3 (7)
99.8	1×10^{-3} *M* KBr	0.020	5.0
99.8	2×10^{-2} *M* KBr	0.025	6.1
99.8	5×10^{-3} *M* KNO_2	0.017	4.3
99.8	5×10^{-2} *M* KNO_2	0.200	45.5
99.8	2×10^{-1} *M* KNO_2	0.060	14.5
Standard (99.8% D in the gas)		0.004	

these experiments were carried out on neutral solutions, we included two of our previous results (7) on lower D_2O concentrations in neutral solutions. The ratio of HD to D_2 in the gas evolved from 99.8% irradiated D_2O solutions, as well as the HD-to-D_2 ratio for the standard (99.8%) gas used, is presented in Table II. No $m/e = 2$ was observed in these mass spectrometric measurements, beyond that due to the background and to the D^+ contribution. HD/D_2 values are thus the true values for the gas originating in these highly concentrated D_2O solutions. It should be emphasized, however, that a minute H_2O contamination, of the irradiated water, may lead to values of α_M considerably higher than the true values in this concentration region. (For example, if the irradiated water is 99.7% D_2O instead of 99.8%, D/H is not 500 but 330 and α_M observed is greater than the true value by a *factor* of 1.5, since the value 500 was used in the computation.) The α_M values for 99.8% D_2O should thus be treated with some caution. Nevertheless, some genuine further increase in α_M is believed to occur at high deuterium concentrations.

(*b*) Acidified aqueous solutions of Cu^{+2} and Ce^{+4} of various D_2O concentrations were irradiated and the isotopic composition of the hydrogen evolved was determined. Oxidizing solutes are capable of reacting with hydrogen atoms and affecting the molecular yield (9). Oxidizing solutes may thus affect α_M. α_M at low Cu^{+2} concentration and low D_2O content is included in Table I. It is seen that, under limiting low solute concentrations, α_M is independent of the type of the solute.

Figure 2 shows the dependence of α_M on $CuSO_4$ concentration for 0.1 *N* H_2SO_4. Contrary to the behavior found for non-oxidizing solutes (Table I), a marked decrease in α_M is observed when the $CuSO_4$ concentration is increased. A similar decrease in α_M was found for neutral solutions of NO_3^- containing 10^{-3} *M* KBr and 1.5–2% D_2O. α_M decreased upon increasing the NO_3^- concentration as follows:

NO_3^- concn., *M*	1.1×10^{-3}	1.1×10^{-2}	1.1×10^{-1}	8.8×10^{-1}
α_M	1.8_0	1.6_3	1.2_9	$1._0$

The increase of α_M with deuterium concentration observed for KBr in Fig. 1 was also observed in experiments with oxidizing solutes. The pair Cu^{+2}/Fe^{+2} ($[Cu^{+2}] > [Fe^{+2}]$) was previously studied at 84.5% D and in 0.1 *N* H_2SO_4 (2). Additional experiments were carried out with these ions at 0.8 *N* H_2SO_4 and high deuterium concentrations and the

Can. J. Chem. Downloaded from www.nrcresearchpress.com by 210.87.254.40 on 09/05/12
For personal use only.

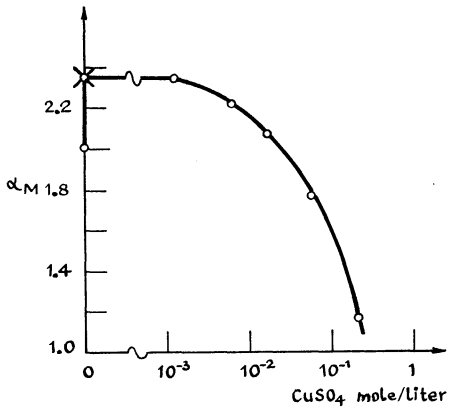

FIG. 2. α_M dependence on $CuSO_4$ concentration (3% D_2O, 0.1 N H_2SO_4); the crossed point contains 10^{-4} M KBr.

TABLE III

The dependence of α_M on deuterium concentration (0.8 N H_2SO_4)

% D	Solute	α_M	Reference
0.9	2×10^{-3} M $Ce(NH_4)_2(SO_4)_3$	1.94	1, 10
74.0	"	2.5	This work
92.5	"	4.3	"
34.0	1×10^{-2} M $CuSO_4$; 7×10^{-4} M $FeSO_4$	2.7	"
84.5	" (0.1 N H_2SO_4)	3.2	2
97.0	1×10^{-2} M $CuSO_4$; 7×10^{-4} M $FeSO_4$	4.3_8	This work

results are given in Table III. Ce^{+4} was also among the ions studied previously at low deuterium concentrations and in 0.8 N H_2SO_4 (1, 10). Further results at higher deuterium concentrations are also included in Table III. Previously published values on Cu^{+2}/Fe^{+2} and Ce^{+4} are given for comparison. The increase in α_M with increasing deuterium concentrations is also observed in neutral solutions of oxidizing solutes as is seen from the experiments with NO_2^- (Table II and ref. 7).

The Atomic Isotope Effect

The enrichment in light hydrogen, of the hydrogen atoms produced in reaction [1], was studied using mainly ethanol solutions. When a suitable organic solute is present in the irradiated water, the hydrogen atoms formed by reaction [1] react with it to abstract a further hydrogen atom and form molecular hydrogen. The isotopic composition of the evolved hydrogen gas was studied by us, in order to determine $\alpha_A = (H/D_{atoms}/(H/D)_{water}$, in this system. If the abstracted hydrogen atoms have a known isotopic composition, then the isotopic composition of the atoms, formed from the water, can be computed. (Contribution from the molecular product, via [1], to the total hydrogen yield has to be taken into account.) When ethanol is dissolved in water its hydroxylic hydrogen exchanges with the water. It has been shown that the hydroxylic hydrogen is not attacked, however, by hydrogen atoms and that the main abstraction reaction occurs at the α-hydrogen of the ethanol (11, 12). The hydrogen atoms of the ethanol, participating in the reaction, are thus of a known isotopic composition. Furthermore, although electron transfer from an alcohol molecule to H_2^+ at acid pH's was suggested to occur in photochemical systems

Can. J. Chem. Downloaded from www.nrcresearchpress.com by 210.87.254.40 on 09/05/12
For personal use only.

(13), no evidence for this reaction could be found in the present case (14). The composition of the hydrogen atoms from irradiated H_2O–D_2O mixtures containing ethanol is thus directly obtained from the composition of the hydrogen molecules, since the abstracted hydrogen atoms are all light. Similarly, in formic acid, the hydrogen atoms react with the hydrogen attached to the carbon (15) and since these do not exchange with the water, they are also light hydrogens only.

α_A was determined at low deuterium concentrations on 0.1 N and 0.8 N H_2SO_4 solutions of ethanol and formic acid and the results are given in Table IV. The method for calcu-

TABLE IV

α_A in acidified solutions of low deuterium concentrations

% D	Solute	G (hydrogen)	$(D/H)_{gas}$	α_A
0.8 N H_2SO_4				
1.0	1.7×10^{-3} M ethanol	4.1_0	$2.0_2\times10^{-3}$	$3._4$
1.0	3.5×10^{-2} M ethanol	4.3_0	$2.1_7\times10^{-3}$	$3._0$
2.25	1×10^{-2} M HCOOH	3.9_5	$5.5_8\times10^{-3}$	$2._6$
1.0	1×10^{-1} M HCOOH	4.1_0	$2.5_8\times10^{-3}$	$2._4$
0.1 N H_2SO_4				
2.8	1.7×10^{-2} M ethanol	4.3_0	$5.6_5\times10^{-3}$	$3._4$
3.35	1×10^{-2} M HCOOH	3.3_0	$6.8_9\times10^{-3}$	$3._9$*
3.9	1×10^{-1} M HCOOH	3.7_5	$9.8_0\times10^{-3}$	$2._7$

*The total hydrogen yield in this experiment is quite low. This is characteristic for relatively low concentrations of carboxylic acids in acid solutions (16) and the interpretation of $(D/H)_{gas}$ in terms of the given α_A may be incorrect.

lating α_A from the isotopic results, as well as the notations used in Table IV, was explained in a previous paper (7). α_M values, needed for computing α_A, were taken from the KBr experiments.

The values for α_A obtained from the ethanol experiments are slightly higher than those from the formic acid experiments (Table IV). It is doubtful whether any significance should be attached to this, since the relative arbitrariness in the choice of the value of the molecular yield used for computing α_A introduces a considerable uncertainty into the results (7), at low deuterium concentrations. α_A at low deuterium concentrations in acid solution is thus 3.0 ± 0.5. Previous results for α_A at low deuterium concentrations are from experiments on neutral solutions and are as follows: 2.7 (4), 2.4 (5), and 3.1 (7).

The dependence of α_A on the deuterium concentration of the water was studied using 0.1 N H_2SO_4 and 1 N H_2SO_4 solutions of ethanol in water. The results are given in Table V. Notations used are as in reference 7. G_M denotes the molecular hydrogen yield. Since at high deuterium concentrations there is no contribution to $G(H_2)$ from the molecular product, one can compute α_A directly from α_M without assuming any value for G_M; in fact G_M is computed at the same time. α_A and G_M values in experiments 3–9 of Table V were computed as previously explained (7). α_M values used for the calculations of Table V are from the KBr experiments (Fig. 1). If the deuterium concentration is low, as in experiments 10–13, so that there is a contribution to $G(H_2)$ from the molecular product, the computation of α_A is based on assumed values for both α_M and G_M. α_A values given in experiments 10–13 were computed using the G_M values given in parentheses. These G_M values are obtained by simple interpolation from G_M values in the pure solvents. G_M values computed in experiments 6–9 (Table V) are higher than the ones computed for experiments 3–5, since the ethanol concentration is lower. In experiments 1 and 2 the concentration of ethanol is comparable to that of experiments 6–9, yet $G(D_2)$ is lower

Can. J. Chem. Downloaded from www.nrcresearchpress.com by 210.87.254.40 on 09/05/12
For personal use only.

TABLE V

The dependence of α_A on deuterium concentration

Expt. No.	% D	H_2SO_4 (N)	Ethanol (M)	G (hydrogen)	$G(H_2)$	$G(HD)$	$G(D_2)$	$(D/H)_{gas}$	α_A	G_M
1	99.7	0.1	3.57×10^{-3}	4.3_7	0.1_0	3.5_8	0.6_9			
2	99.7	0.1	1.4×10^{-3}	4.2_1	0.0_9	3.4_7	0.6_5			
3	97.5	0.1	1.2×10^{-1}	4.4_7	0.3_3	3.7_5	0.3_9		3.6	0.4_9
4	96.5	0.1	8.8×10^{-1}	5.0_1	0.5_5	4.1_3	0.3_3		3.7	0.4_4
5	95.4	0.1	1.1×10^{-1}	4.5_1	0.5_5	3.5_8	0.3_8		3.4	0.5_5
6	94.5	0.1	1.3×10^{-3}	4.3_7	0.5_9	3.2_5	0.5_3		4.2	0.8_6
7	94.0	0.1	1.4×10^{-3} $+5\times10^{-4}$ KBr	4.1_9	0.6_5	2.9_2	0.6_2		4.0	1.0_0
8	96.0	0.96	1.75×10^{-3}	4.5_4	0.4_5	3.4_9	0.6_0		3.3	0.8_4
9	90.0	0.96	1.75×10^{-3}	4.4_1	0.8_9	3.1_1	0.4_1		3.1	0.9_4
10	72.0	0.88	1.75×10^{-3}	4.4_8				$3.6_4\times10^{-1}$	2.8	(0.6)
11	50.1	0.1	1.0×10^{-1}	4.4_0				$1.6_6\times10^{-1}$	3.0	(0.6)
12	46.5	0.1	1.3×10^{-3}	4.0_6				$1.5_5\times10^{-1}$	3.0	(0.7)
13	37.0	0.92	1.75×10^{-3}	3.9_4				$1.1_5\times10^{-1}$	2.8	(0.7)

than G_M of experiments 6–9. The possibility exists that even at the very high deuterium concentrations employed in experiments 1 and 2 there is a contribution to HD from the molecular product.

The value of α_A obtained at high deuterium concentrations is thus 3.7 ± 0.5. Previous values for α_A at similar D_2O concentrations are: 4.1 in acid solution (2) and 4.3 for the "residual" yield in neutral solution (7) or 1.6 for the total yield in neutral solution (5). The present values for α_A are higher than α_M at low deuterium concentrations and lower than α_M at high deuterium concentrations. At 50% D α_M and α_A are approximately equal.

Isotope Effects in Secondary Reactions

Solutions of 10^{-2} M $FeSO_4$, 0.8 N H_2SO_4 were studied. The isotopic composition of hydrogen gas evolved from H_2O–D_2O mixtures was determined. Cr^{+2} was run once at low deuterium concentration for comparison with the Fe^{+2}. Both of these ions give high hydrogen yields (equal to the "atomic" plus "molecular" yields) and $\alpha = (H/D)_{gas}/(H/D)_{water}$ for 1% D_2O was 3.53 from Fe^{+2} and 3.71 from Cr^{+2}. When Cu^{+2} is added to ferrous solutions the hydrogen yield is decreased. Figure 3 presents the dependence of α upon the total

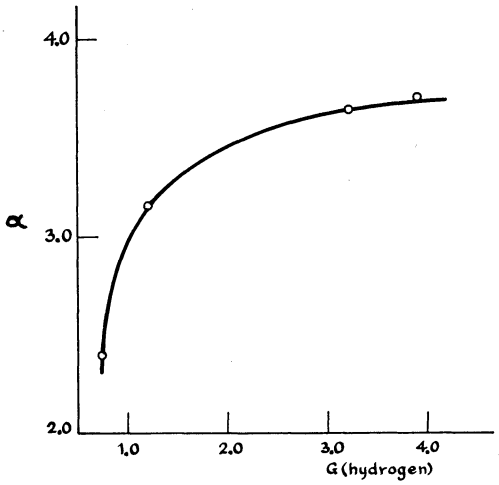

FIG. 3. α dependence on hydrogen yield from 0.8 N H_2SO_4 solutions of varying Cu^{+2}/Fe^{+2} ratios and 3% D_2O.

Can. J. Chem. Downloaded from www.nrcresearchpress.com by 210.87.254.40 on 09/05/12
For personal use only.

hydrogen yield as the ratio $[Cu^{+2}]/[Fe^{+2}]$ is varied at constant low deuterium concentration of the solution. Similar concentration effects were observed on a 34% D_2O solution, where α changes from 2.7 to 3.05 and 3.95 as the yield changes from the molecular one (no Fe^{+2} present) to $G = 0.93$ and $G = 4.25$, respectively.

Various deuterium concentrations were studied in the $FeSO_4$ case and the dependence of α on deuterium concentration is presented in Table VI. Several initial Fe^{+3} ion yields

TABLE VI

Isotope effects in acidified $FeSO_4$ solutions

% D	G (hydrogen)	$G(Fe^{+3})_{initial}$	α	$\alpha_{Fe^{++}}$
2.3	3.95	8.7_0	3.6_2	$4._0$
4.6	3.8_5		3.8_5	
12.4	4.4_0		3.9_5	
20.0	3.9_0	8.7_0	4.0_4	
39.1	4.2_5		3.9_3	
49.5	4.2_5	9.2_5	3.9_5	
60.0	4.3_0		3.9_5	
71.3	4.3_0		4.0_0	
90.0	4.2_5		4.1_5	
93.5	4.1_0		4.3_5	
98.8	4.2_5	9.3_5	4.8_5	$4._5$

are presented. These were measured on analogous experiments given low total doses. To determine the isotopic composition of the gas, one needs relatively high conversions and the hydrogen yields presented are the ones measured at the end of the total irradiation period. Both hydrogen and Fe^{+3} yields exhibit the expected increase of hydrogen *atom* yield (light + heavy) with increasing deuterium concentration. The initial Fe^{+3} yield is a measure of the initial hydrogen yield, atomic plus molecular, since $G(Fe^{+3}) = 2G(\text{hydrogen})$ in this system (9, p. 36). The contribution of the molecular yield to the total hydrogen yield is minor and the increase observed in $G(Fe^{+3})$ reflects the increase in the atomic yield. $\alpha_{Fe^{+2}}$ are computed values obtained when the contribution of the molecular product via [1] with its α_M is subtracted, in the usual manner (2).

DISCUSSION

Isotope effects encountered in water radiolysis are incompatible with the simple Samuel–Magee model (17). In addition to the isotopic separations observed in irradiated H_2O–D_2O mixtures, another type of effect occurs, namely the radical and molecular yields are different in light and heavy water (2, 5, 18–20); $G(D)$ in D_2O is larger than $G(H)$ in H_2O, while G_{D_2} is smaller than G_{H_2}. A broader initial distribution of D atoms in D_2O was suggested, in order to explain this phenomenon (21). However, previous attempts to reconcile this suggestion with the observation $\alpha_A > \alpha_M$ (at low deuterium concentrations) were unsuccessful (4).

Contributions from isotopic exchange reactions and diffusion processes to the observed isotope effects in H_2O–D_2O mixtures have been discussed previously (3). It was concluded that any contribution from isotopic exchange reactions (e.g. between hydrogen atoms and hydrogen molecules, water molecules, etc.) to the observed isotope effects is ruled out, since these are too slow to compete with hydrogen atom recombination. Diffusion processes of the hydrogen atoms cannot contribute to the isotopic separation either, since any difference in atomic diffusion rates out of the spurs is counterbalanced by the difference in rates of the diffusion-controlled atom recombination reactions (3). Thus, any difference between α_M and α_A reflects a difference in the mechanisms of production

Can. J. Chem. Downloaded from www.nrcresearchpress.com by 210.87.254.40 on 09/05/12
For personal use only.

of the molecular and atomic species. Furthermore, any variation of solute concentration should have no effect upon α_A or α_M, unless more than one radiation-chemical process is operative. α_A was found by Baxendale and Hughes to be independent of solute (methanol) concentration in the concentration range of 0.2–1 *M* (2).

In the following discussion we will try to explain the observed isotope effects, taking into account the effects on *yields* as well. We will also attempt to explain observed differences between α_A and α_M as well as effects of solute concentration on α_M.

α_A and the Mechanism of Hydrogen Atom Formation in Acid Solutions

It has been shown recently (22–24) that most or all of the reducing species are formed in water radiolysis as aquated electrons. Reaction [1] has to be modified, therefore, in the following way:

$$H_2O \rightarrow e^-_{aq}, OH, H_2, H_2O_2. \qquad [1']$$

The aquated electrons are transformed in acid solution to hydrogen atoms by the reaction (22–24)

$$H_3O^+ + e^-_{aq} \rightarrow H + H_2O. \qquad [2]$$

It has been shown that reaction [2] may give rise to $\alpha_A > 2$ at $\sim$100% D (4) and indeed the experimental results of Baxendale and Hughes (2) in this direction are verified by our results (Table V). It should be pointed out, here, that the value of α_A is not proof for the occurrence of [2]; it is possible that another reaction could be found leading to the observed α_A. What this rather means is that α_A is *compatible* with [2], while it is not so with several other reactions which have been proposed previously for the mechanism of hydrogen atom formation. (For a discussion of this point see references 4 and 7.)

Another question is whether reaction [2] is compatible with the observation $G(D), D_2O > G(H), H_2O$. It has been suggested that, as a result of the greater relaxation time of D_2O compared to that of H_2O, electrons are trapped and react with water farther away from the positive ion in D_2O than in H_2O (21) and this causes the observed difference in atomic and molecular yields. It is now suggested that the electron in acid solution does not react with H_2O but with H_3O^+ (reaction [2]). Yet, since reaction [2] occurs with aquated electrons (22), the position at which the electrons are trapped still determines the degree of recombination reactions versus reactions with the solute. It is important to note, however, in this connection, that $G(D)/G(H)$ is larger in neutral than in acid solutions (5), a result which suggests that trapping of the unaquated electron by H_3O^+ occurs in strongly acid solutions and suppresses this isotope effect. On the other hand solutes such as H_2SO_4 decrease the relaxation time of water. This decrease is a linear function of solute concentration.* If the decrease in the relaxation time D_2O due to the addition of sulphuric acid is greater than the similar effect in H_2O, this may provide a more plausible explanation for the reduced isotope effects on the yields in acid solution.* Until further data are available for D_2O this question must be left open. The "residual" atomic yield in neutral solutions, obtained when electron scavengers are present, is smaller in D_2O than in H_2O (7), showing that the major part of the "residual" yield is due to a track reaction, the contribution of which is smaller in D_2O than in H_2O.

α_M and the Mechanism of Production of Hydrogen Molecules

Since α_M and α_A were found to have different values for the same initial deuterium concentration, it was suggested that the mechanisms of production of the atomic and

*J. B. Hasted, D. M. Ritson, and C. H. Collie. J. Chem. Phys. **16**, 1 (1948). This point was suggested by the referee.*

Can. J. Chem. Downloaded from www.nrcresearchpress.com by 210.87.254.40 on 09/05/12
For personal use only.

molecular products are different (2, 4). On the other hand, from independent experiments on the dependence of the molecular hydrogen yield upon solute concentration, it was believed that most or all of the molecular product is due to hydrogen atom recombination (9, p. 63). In this connection let us observe first of all that the difference between α_M and α_A at any deuterium concentration is much smaller than the previously observed difference. Secondly, the molecular product may be due to a recombination of hydrogen atoms, but of such atoms formed by a mechanism different than the ones reacting with the solute. Reaction [2] itself may be viewed in either of two ways—either as an acid-catalyzed reaction of the electron with a water molecule:

$$eH_2O + H_3O^+ \rightarrow H\cdots OH^- + H^+\cdots H_2O \rightarrow H + 2H_2O \qquad [2']$$

or as a capture of the electron by the H_3O^+:

$$H_3O^+ + e(e^- \text{ or } e_{aq}^-) \rightarrow H + H_2O. \qquad [2'']$$

The captured electron in [2''] may be a thermalized *un*aquated electron, although such an electron cannot react with H_2O to give a hydrogen atom (24). However, for the electron to be unaquated in reaction [2''] there has to be a very high local concentration of H_3O^+ in the track, so that this reaction can compete effectively with the process of aquating the electron.

Although [2'] and [2''] both lead to hydrogen atoms by reaction of the electron with H_3O^+, they involve quite different isotope effects.

It has been suggested lately that the molecular yield is due to a recombination reaction of aquated electrons (25), according to

$$e_{aq}^- + e_{aq}^- \rightarrow H_2 + 2OH^-. \qquad [3]$$

The dependence of the molecular yield on scavenger concentration may in some cases be explained better by a scavenging of the electrons (2, 26). Recent experiments with C_2H_5OD in D_2O at pH 13, utilizing pulse techniques, establish that the product of the bimolecular reaction of two aquated electrons is a molecule of hydrogen (27(*a*)).

If the molecular product is formed from hydrogen atoms via H_3O^+ (reaction [2]), the isotopic enrichment will be, in part, due to the enrichment of H_3O^+ relative to the water. If it is formed via e_{aq}^-, the isotopic enrichment of the latter is involved. The curve F.F. in Fig. 1 represents the isotopic enrichment of H_3O^+ with respect to the water, as computed by Fiquet-Fayard (4). No attempt has yet been made to compute the isotopic enrichment of e_{aq}^-. The experimental results for α_M and its dependence on deuterium concentration follow the similar behavior of the "residual" atomic yield in neutral solutions (7). We suggest that they have similar origins and that the molecular yield is formed mainly by hydrogen atom recombination, the atoms being formed by the track reaction [2]. (The aquated electron has been shown to disappear even in neutral water, containing no added solute, by more than one process (27(*b*)).) Scavengers may reduce the molecular yield either by preventing reaction [2], i.e. reacting with the electrons prior to their being transformed into hydrogen atoms, or by preventing the recombination reaction

$$H + H \rightarrow H_2. \qquad [4]$$

There may be some contribution to the molecular yield from reaction [3] and this may cause the difference between α_A and α_M.

As is seen from the experiments on Cu^{+2} in Fig. 2 and on NO_3^-, α_M itself is not uniform. Since the concentration of the solute should have no effect on α_M, if only one process contributes to the molecular yield, the dependence observed must be due to the occurrence

Can. J. Chem. Downloaded from www.nrcresearchpress.com by 210.87.254.40 on 09/05/12
For personal use only.

of more than one process. From the dependence of the molecular hydrogen yield on NO_3^- concentration, it was concluded that two processes lead to the molecular product (28). These may be [2] (followed by [4]) and [3]. The occurrence of another process was considered recently (25(*b*)):

$$H_2O^* \rightarrow H + OH \qquad [5]$$

(where H_2O^* is an excited water molecule) followed by [4]. Reactions [2] and [3] can lead to α_M values larger than 2 at high deuterium concentrations, as is observed, but reaction [5] cannot. (This is in the line of the usual statistical argument (4, 7).) Reaction [5] cannot be, therefore, a major process leading to the molecular product. Increased solute concentrations can affect α_M without affecting the hydrogen yield very much, by providing an alternative route for hydrogen molecule production. For example, one explanation given for the track effects of doubly and triply charged metal ions was electron capture. The excited metal ions formed in this way can react with water to give hydrogen atoms (2). The hydrogen atoms thus formed may then recombine via [4] as usual.

In the previous section we have seen that since the deuterium atom has a greater chance of escaping recombination reactions in pure D_2O than the hydrogen atom has in pure H_2O, $G(D) > G(H)$. The question which arises, in connection with the relation of the molecular to the atomic product, is whether the deuterium atom has a greater chance of escaping recombination reactions in an H_2O–D_2O *mixture* than the hydrogen atom has. This has been suggested, so that if the molecular product is due to hydrogen atom recombination, one should always have $\alpha_M > \alpha_A$, which is contrary to what is observed at low deuterium concentrations (4). We do believe that the hydrogen molecules are formed by atomic recombination, but according to the present picture, the chance of escaping recombination is determined by the distance at which the electron is trapped. This distance depends upon the deuterium concentration of the water, so that in a mixture of light and heavy water the *total* hydrogen atom yield (light and heavy) is intermediate between the yields in pure light or pure heavy water. (This agrees with the observed trend, Table VI.) The competition is between recombination reactions and reactions with the solute and one gets less recombination the higher the D_2O content is, since the hydrogen atom distribution, light or heavy, is wider (depending upon where the electron was trapped). Nevertheless, the separation is always in favor of light hydrogen and, observing that $\alpha_M \leqslant \alpha_A$, is not contrary to hydrogen atom recombination.

Some additional effects are observed at high deuterium concentrations (Tables II and V). In a previous paper (11) we have observed a decrease in D_2 yield for irradiated ethanol–D_2O solutions as H_2SO_4 increased from 0.1 *N* to 0.8 *N*. Since the sulphuric acid in these experiments was H_2SO_4 rather than D_2SO_4, this change in acid concentration involved a slight decrease in deuterium concentration of the solution. Thus, the decrease in D_2 may not be due to a genuine decrease in molecular yield, but rather to a considerably higher α_M value in this concentration region, where part of the molecular yield is in the form of HD. Isotope effects in highly concentrated irradiated D_2O solutions were measured previously. Some measurements utilizing the e.s.r. technique were carried out on irradiated ice containing D_2O at 4.2° K (29–31). Careful analysis of the results showed that no isotope effect is observed for 50% and 80% D_2O; however, D_2O ice containing trace amounts of HDO (0.2%) exhibits a very large isotope effect in favor of H atom production (31). The authors suggest a model of delocalization of electronic energy, where the HDO acts as a defect in the solid, which is strongly coupled by hydrogen bonding. They suggest that trace amounts of HDO in H_2O should act similarly. Our results on α_M (Fig. 1) show that there is a further *decrease* of α_M in solutions of very low D_2O concentrations. The

Can. J. Chem. Downloaded from www.nrcresearchpress.com by 210.87.254.40 on 09/05/12
For personal use only.

overall dependence of α on deuterium concentration of the liquid may thus be due to a superposition of the effects observed in ice at limiting ($\sim$0% and $\sim$100%) deuterium concentrations (since the liquid water is also hydrogen bonded to some extent) over the general dependence of α on the deuterium concentration of the liquid. The effects at limiting concentrations may be due to electron transfer, rather than energy transfer. Since these large effects at $\sim$100% D were not observed in liquid water previously (5), when hydrogen was the only solute in the irradiated water, it seems worthwhile to study further the isotope effect at high deuterium concentrations.

Isotope Effects in Secondary Reactions

The ion Fe^{+2} was studied at first in order to obtain α_A (1). Later it was shown that $\alpha_{Fe^{+2}}$ obtained is not α_A (2), since the hydrogen formed in [6]:

$$Fe^{+2} + H^+ + H \rightarrow Fe^{+3} + H_2, \qquad [6]$$

originates partly in the H atoms (with their characteristic isotopic separation) and in part in H^+ (with another characteristic isotopic separation). $\alpha_{Fe^{+2}}$ is the isotopic enrichment of H_2 formed via [6], with respect to the irradiated water.

Two mechanisms are kinetically possible for the oxidation of Fe^{+2} by H (32, 33):

$$H + H^+ \rightleftharpoons H_2^+;\ H_2^+ + Fe^{+2} \rightarrow H_2 + Fe^{+3} \qquad [6']$$

$$H + Fe^{+2} \rightleftharpoons H\cdots Fe^{+2};\ H\cdots Fe^{+2} + H^+ \rightarrow H_2 + Fe^{+3}. \qquad [6'']$$

Reaction [6] takes place in the photochemical oxidation of Fe^{+2} as well and isotope effects in that system have been measured recently for low deuterium concentrations (34). The numerical results are very similar to our radiation-chemical results for α_A as well as for $\alpha_{Fe^{+2}}$. Since α_A is known, one can compute the enrichment of H^+ in reaction [6] from the observed $\alpha_{Fe^{+2}}$ (this means going in a reverse order to that taken by Fiquet-Fayard (4)). This was done for low deuterium concentrations in the photochemical system (34), and the isotopic enrichment of H^+ in the oxidation reaction [6] was calculated to be $\alpha_{H^+} = 5 \pm 0.5$. Since this is a relatively high separation, it was decided that this reflects the isotopic enrichment of H_3O^+ so that the mechanism for reaction [6] is the hydride formation reaction [6''].

If we take α_A to be 3.0 at low deuterium concentrations and 3.5 at high ones, we calculate from our results for $\alpha_{Fe^{+2}}$ (4.0 and 4.5, respectively) that α_{H^+} is $6._0$ and $5._5$ for low and high deuterium concentrations. The value at high deuterium concentrations points indeed to mechanism [6'']. In H_2^+ (which is the species involved in mechanism [6']) the enrichment of the proton is that of the bare H^+, although H_2^+ is probably hydrated; at the time of reaction with Fe^{+2} the H^+ is bound to an H atom and only that H can go over to the H_2 which is formed. On the other hand, the proton in mechanism [6''] involves the enrichment of H_3O^+ (34) and any of the three hydrogen atoms of H_3O^+ can eventually be incorporated into the H_2. If we make use of the computed isotopic enrichment of H_3O^+ ($\alpha_{H_3O^+}$) at low and at high deuterium concentrations (ref. 4 and Fig. 1), 1.66 and 3.2 respectively, α'_{H^+} is computed, according to (where α'_{H^+} is the corrected separation factor S'_{ox} of ref. 34)

$$\alpha'_{H^+} \cdot \alpha_{H_3O^+} = \alpha_{H^+}. \qquad [I]$$

We find α'_{H^+} equal to $3._6$ and $1._7$ at low and high deuterium concentrations, respectively. Equation [I] is valid only if the different H_3O^+ isotopic species (e.g. H_3O^+ and H_2DO^+, at low deuterium concentrations) react with the ferrous hydride at the same rate. If this is so, then fractionation will occur owing to the different rates at which D and H escape the isotopic H_3O^+ in the activated complex. Let the relative rates at which H and

Can. J. Chem. Downloaded from www.nrcresearchpress.com by 210.87.254.40 on 09/05/12
For personal use only.

D escape such an activated complex be k_H/k_D. Taking into account statistical factors, such as having two H atoms to one D atom in H_2DO^+ (4), we compute k_H/k_D to be equal to 4.9 and 2.6 at low and high deuterium concentrations, respectively. Since these two values are not equal, the model and/or experiment need further refinement. The computed k_H/k_D cannot be compared for the time being with the relative rates of oxidation of Fe^{+2} in light and heavy water, which was found to be 2.4 (2).

CONCLUSIONS

Isotope effects in acidified H_2O–D_2O mixtures are compatible with the radiation-chemical reaction $H_3O^+ + e^-_{aq} \rightarrow H + H_2O$. The molecular product is formed by hydrogen atom recombination. The lowering effect that high Cu^{+2} concentrations have on α_M is due to the interaction of Cu^{+2} with the electron, which forms a different path for hydrogen atom formation.

ACKNOWLEDGMENTS

This research was sponsored by the Israel Atomic Energy Commission. The author wishes to thank Professors G. Stein and E. D. Bergmann for their continued interest in this work. The author also thanks Mrs. V. Fishoff at the Isotope Department of the Weizman Institute, Rehovoth, for carrying out most of the mass spectrometric measurements and Dr. C. M. Stevens, Argonne National Laboratory, for the measurements at 99.8% D.

REFERENCES

1. P. Kelly, T. Rigg, and J. Weiss. Nature, **173**, 1130 (1954).
2. J. H. Baxendale and G. Hughes. Z. Physik Chem. (Frankfurt), **14**, 323 (1958).
3. P. J. Dyne and J. H. Kennedy. Can. J. Chem. **36**, 1528 (1958).
4. F. Fiquet-Fayard. J. Chim. Phys. **57**, 467 (1960).
5. P. J. Dyne, J. W. Fletcher, W. M. Jenkinson, and L. P. Roy. Can. J. Chem. **39**, 933 (1961).
6. A. O. Allen. *In* The chemical and biological action of radiations. Vol. V. *Edited by* M. Haissinsky. Academic Press. 1961. p. 9.
7. C. Lifshitz. Can. J. Chem. **40**, 1903 (1962).
8. E. R. Johnson and A. O. Allen. J. Am. Chem. Soc. **74**, 4147 (1952).
9. A. O. Allen. The radiation chemistry of water and aqueous solutions. D. Van Nostrand Co. 1961.
10. P. Kelly, T. Rigg, and J. Weiss. Chem. Ind. (London), 1291 (1954).
11. C. Lifshitz and G. Stein. J. Chem. Soc. 3706 (1962).
12. I. A. Taub and L. M. Dorfman. J. Am. Chem. Soc. **84**, 4053 (1962).
13. E. Collinson, F. S. Dainton, and M. A. Malati. Trans. Faraday Soc. **55**, 2096 (1959).
14. C. Lifshitz and G. Stein. To be published.
15. J. H. Baxendale and D. Smithies. Z. Physik Chem. (Frankfurt), **7**, 242 (1956).
16. E. Hayon and J. Weiss. J. Chem. Soc. 5091 (1960).
17. A. H. Samuel and J. L. Magee. J. Chem. Phys. **21**, 1080 (1953).
18. H. A. Mahlman and J. W. Boyle. J. Am. Chem. Soc. **80**, 773 (1958).
19. T. J. Hardwick. J. Chem. Phys. **31**, 226 (1959).
20. F. S. Dainton. Radiation Res. Suppl. 1, 1 (1959).
21. D. A. Armstrong, E. Collinson, and F. S. Dainton. Trans. Faraday Soc. **55**, 1375 (1959).
22. G. Czapski and H. A. Schwarz. J. Phys. Chem. **66**, 471 (1962).
23. G. Czapski and A. O. Allen. J. Phys. Chem. **66**, 262 (1962).
24. E. J. Hart and J. W. Boag. J. Am. Chem. Soc. **84**, 4090 (1962).
25. (*a*) A. Hummel and A. O. Allen. Radiation Res. **17**, 302 (1962).
(*b*) E. Hayon. Nature, **194**, 737 (1962).
26. H. A. Schwarz. Private communication. December 1961.
27. (*a*) I. A. Taub and L. M. Dorfman. J. Am. Chem. Soc. To be published.
(*b*) J. P. Keene. Nature **197**, 47 (1963).
28. H. A. Mahlman. J. Chem. Phys. **32**, 601 (1960).
29. S. Siegel, J. M. Flournoy, and D. H. Baum. J. Chem. Phys. **34**, 1782 (1961).
30. H. N. Rexroad and W. Gordy. Phys. Rev. **125**, 242 (1962).
31. H. S. Judeikis, J. M. Flournoy, and S. Siegel. J. Chem. Phys. **37**, 2272 (1962).
32. G. Chapski and G. Stein. J. Phys. Chem. **63**, 850 (1959).
33. J. Halpern, G. Czapski, J. Jortner, and G. Stein. Nature, **186**, 629 (1960).
34. J. Jortner and G. Stein. J. Phys. Chem. **66**, 2200 (1962).

Can. J. Chem. Downloaded from www.nrcresearchpress.com by 210.87.254.40 on 09/05/12
For personal use only.

REACTION MECHANISM STUDIES

1. THE DIAXIAL → DIEQUATORIAL REARRANGEMENT OF BROMOHYDRIN SULPHONATE ESTERS[1]

J. F. KING, R. G. PEWS,[2] AND R. A. SIMMONS
Department of Chemistry, University of Western Ontario, London, Ontario

Received April 24, 1963

ABSTRACT

3α-Bromocholestan-2β-yl *p*-toluenesulphonate on heating in solution rearranges to an equilibrium mixture in which the diequatorial isomer, 2α-bromocholestan-3β-yl *p*-toluenesulphonate, predominates. 2β-Bromocholestan-3α-yl *p*-toluenesulphonate and the corresponding diaxial benzenesulphonate and *p*-nitrobenzenesulphonate rearrange analogously. These are the first examples of the diaxial → diequatorial rearrangement with sulphonic esters. Replacement of the para methyl group of 2β-bromocholestan-3α-yl *p*-toluenesulphonate by more electrophilic substituents is accompanied by an increase in the rate of rearrangement. It is concluded that in the transition state the bromine atom is positively charged and the sulphonate group negatively charged relative to the starting material.

Can. J. Chem. Downloaded from www.nrcresearchpress.com by 210.87.254.40 on 09/05/12
For personal use only.

The diaxial → diequatorial rearrangement (1), illustrated in the general case by I ⇌ II, has been shown to proceed readily with dihalides (e.g. I*a*) (2, 3) and halohydrin carboxylic esters (I*b*) (4). As part of a study of the relation between rearrangement, solvolysis, and reduction of 1,2-dihalides and related compounds, we became interested in the possibility of a diaxial → diequatorial rearrangement of bromohydrin sulphonates.

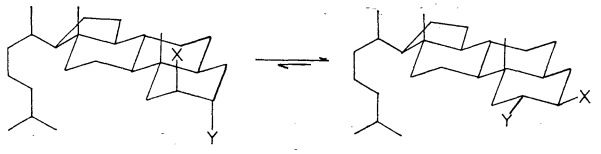

I II

(a) X,Y = Br

(b) X = Br, Y = O-C-R

(c) X = OSO_2—C$_6$H$_4$—CH_3, Y = Br

(d) X = Br, Y = OSO_2—C$_6$H$_4$—CH_3

(e) X = Br, Y = OSO_2—C$_6$H$_5$

(f) X = Br, Y = OSO_2—C$_6$H$_4$—NO_2

We chose as substrates for initial work the two diaxial bromohydrin *p*-toluenesulphonates (tosylates) I*c* and I*d*. Preliminary experiments indicated that when heated in the melt, I*d* decomposed, yielding no readily identified products, but further investigation showed that when heated in a high-boiling solvent, I*c* and I*d* underwent mutarotation without extensive decomposition. A triglyme (triethylene glycol dimethyl ether) solution of 3α-bromocholestan-2β-yl tosylate (I*c*, diaxial) on heating for 16 hours or more at 135° showed a change in specific rotation from +50° to 0°. The major product was identified

[1]*Presented at the 45th Annual Meeting of the Chemical Institute of Canada, Edmonton, Alberta, May 1962.*
[2]*Holder of a National Research Council Studentship 1962–1963 and a Dow Chemical of Canada Limited Postgraduate Fellowship, 1961–1962.*

Can. J. Chem. Downloaded from www.nrcresearchpress.com by 210.87.254.40 on 09/05/12
For personal use only.

as the diequatorial isomer, 2α-bromocholestan-3β-yl tosylate (II*c*), by comparison with a sample prepared from 2α-bromocholestan-3β-ol (5, 6). The specific rotation of the diequatorial compound (II*c*) on similar heating changed from $-27°$ to $-12°$. The equilibrium mixture is estimated (see Experimental) to consist of $85\pm8\%$ of the diequatorial compound (II*c*) and $15\pm8\%$ of the diaxial isomer (I*c*). In addition an uncharacterized, dextrorotatory, probably olefinic material which separates into at least three components on thin-layer chromatography was also formed in these pyrolyses.

The other diaxial bromohydrin tosylate (I*d*) also mutarotated on heating in triglyme. The product proved difficult to purify by recrystallization because of a strong tendency to form gels. An authentic sample of the diequatorial compound (II*d*) was prepared from the corresponding alcohol, 3β-bromocholestan-2α-ol, the latter compound being obtained by acid hydrolysis of the acetate (II*b*, R = CH_3) (4). The tosylate so obtained also yielded gels on attempted crystallization but a few precipitations from petroleum ether gave a white powder which gave satisfactory elemental analyses. Comparison of infrared spectra and behavior on thin-layer chromatography clearly established that II*d* is the major product of the pyrolysis of I*d*; the equilibrium mixture of I*d* and II*d* is estimated to contain $95\pm5\%$ of the diequatorial isomer (II*d*).

In previous studies of the rearrangement of dibromides (7) and bromohydrin carboxylic esters (4) it was concluded that there is, in general, separation of charge in the transition states of these reactions. These conclusions may be summarized by representing the midpoint of each reaction (i.e. the species in which the migrating groups are bonded as strongly to one carbon as to the other) by structures III and IV. In addition, Grob and Winstein (7) have suggested that as the reaction is carried out in various solvents the magnitude of "δ" in III may vary with the ionizing power of the solvent.

For the rearrangement of the bromohydrin tosylates three such half-way species are conceivable: V, VI, and VII, the last being the special case in which $\delta = 0$ (compared with

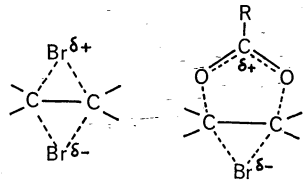

III IV

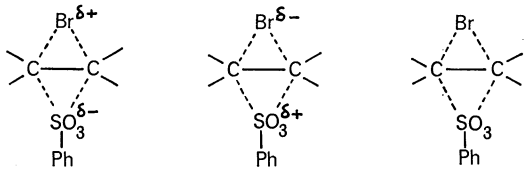

V VI VII

starting material). Species V would seem the most likely of these, both on (*a*) general considerations of the relative reactivities of bromine and tosyl functions as leaving groups and as neighboring groups in heterolyses, and on (*b*) the specific example of the

reaction of *trans*-2-bromocyclohexyl tosylate with concentrated hydrobromic acid. In the latter case the product is *trans*-1,2-dibromocyclohexane, formed, apparently, via the bromonium ion (8); this reaction and the present rearrangement, however, are carried out in media of greatly different ionizing power and acidity. To provide direct evidence to decide between the possibilities V, VI, and VII we have studied the effect of para substituents on the rate of rearrangement. As can be seen from Table I, the benzenesulphonate (I*e*) rearranges nearly twice as fast as the tosylate (I*d*), in triglyme at 135°. The *p*-nitrobenzenesulphonate (I*f*) was not sufficiently soluble in triglyme for rate studies, but in phenetole at 99° the rearrangement of I*f* is about 20 times as fast as that of the tosylate under the same conditions. These results clearly exclude either VI or VII and are only compatible with a reaction proceeding through a transition state in which there is separation of charge in the sense of V.

TABLE I

Rates of rearrangement of diaxial cholestanyl bromohydrin sulphonates

Compound	Solvent	Temp. (°C)	$k \times 10^6$	k/k_{Id} (under same conditions)*
3α-Bromocholestan-2β-yl tosylate (I*c*)	Triglyme	135	45±5	0.38
2β-Bromocholestan-3α-yl tosylate (I*d*)	Triglyme	135	120±15	1.00
2β-Bromocholestan-3α-yl tosylate (I*d*)	Phenetole	99	5.6±0.3	1.00
2β-Bromocholestan-3α-yl benzenesulphonate (I*e*)	Triglyme	135	220±30	1.8
2β-Bromocholestan-3α-yl benzenesulphonate (I*e*)	Phenetole	99	(6±1)†	1
2β-Bromocholestan-3α-yl *p*-nitrobenzenesulphonate (I*f*)	Phenetole	99	130±20	23

*Rate relative to that of I*d* under identical conditions.
†Average value from three measurements only.

It is interesting to contrast these conclusions with those from the study of carboxylic esters (4). Though it might appear contradictory to propose that the bromine is negatively charged in one case and positively charged in the other, such behavior is well established in, respectively, unimolecular solvolysis of alkyl bromides and reactions involving participation of bromine in solvolysis at a neighboring carbon. The studies on carboxylic and sulphonic esters of bromohydrins, by showing that bromine may be either positively or negatively charged in the transition state of a diaxial → diequatorial rearrangement, agree with the proposal (7) that the rearrangement of *dibromides* takes place through a species in which one bromine is positively and the other negatively charged.

EXPERIMENTAL

Unless otherwise stated optical rotations refer to chloroform solutions at room temperature. Melting points were determined on a Kofler block and are uncorrected. Infrared spectra were obtained using Beckman IR-5 or IR-7 spectrophotometers equipped with sodium chloride optics; all values quoted for the infrared maxima positions were determined with the IR-7 instrument. Petroleum ether refers to the fraction of boiling range 35–60°. Thin-layer chromatography was carried out using Camag Kieselgel D5; unless otherwise specified the developing solvent was petroleum ether – benzene (1:1).

For the pyrolyses, commercial triglyme (triethylene glycol dimethyl ether) supplied under the designation Ansul Ether 161 by Ansul Chemical Company, Marinette, Wis., U.S.A., was heated at 140–150° in a nitrogen atmosphere with sodium and benzophenone until the dark purple color of the benzophenone

Can. J. Chem. Downloaded from www.nrcresearchpress.com by 210.87.254.40 on 09/05/12
For personal use only.

ketyl was produced. The triglyme was then distilled under reduced pressure. It was tested for peroxides before use; if these were found to be present the triglyme was redistilled from lithium aluminum hydride. The phenetole used in the rate measurements was obtained by distilling B.D.H. Analar grade from lithium aluminum hydride.

Rate Measurements

The rearrangements were carried out either in sealed Pyrex ampoules or in a test tube with a standard taper male joint in the middle and a female joint at the top, as previously described (4). The sample was weighed into the tube and a measured volume of solvent added. The tube was then flushed with nitrogen, closed, and, if necessary, warmed to dissolve the compound. The tube was then inserted into a three-necked flask containing a refluxing liquid so that the portion of the tube which contained the solution was well heated by the vapor of the liquid. Ethylbenzene was the refluxing liquid for the experiments at 135±1° and water for those at 99±1°. The extent of reaction was determined by quickly cooling the solution and determining the optical rotation. The rate constants in Table I were calculated from the half-life estimated graphically from a plot of 5 to 10 values of $\log \alpha-\alpha_{eq}/\alpha_0-\alpha_{eq}$ vs. reaction time (α is the measured specific rotation after a certain reaction time, α_0 the specific rotation of the starting material, and α_{eq} the specific rotation of the equilibrium mixture—see Table II and accompanying text).

Determination of the Composition of the Pyrolytic Equilibrium Mixtures

Table II summarizes much of the data on the pyrolyses. In addition the following separate experiments were carried out.

TABLE II

Pyrolytic equilibration experiments

Reaction	Starting material	Solvent	Temp. (°C)	Time (hr)	$[\alpha]_D$ of diaxial isomer (I)	$[\alpha]_D$ of di-equational isomer (II)	$[\alpha]_D$ of pyrolysis product	α_{eq}	Estimated % of II at equilibrium
Ic ⇌ IIc	Ic	Triglyme	135	25	+50	−26	0		
			135	16			0		
			135	25			−2		
	IIc		135	25			−14	(−15)*	85±8 (see text)
			135	36			−11		
			135	16			−11		
			135	16			−10		
			175	1			−12		
Id ⇌ IId	Id	Triglyme	175	3.5	+49	−26	−24		
			175	5.5			−23		
			135	12			−23	−23	95±5
			135	15			−21		
		Phenetole	135	24	+54.5		−30		
			135	24			−28	−29	
Ie ⇌ IIe	Ie	Triglyme	135	3.0	+51	−23	−15		
			135	6.0			−17	−16	90±5
		Phenetole	100	64	+47	−27	−17		
			100	71			−18	−17.5	88±5
If ⇌ IIf	If	Phenetole	100	4.5	+49	−38	−26		
			100	6.5			−29	−27.5	88±5

*Calculated from the estimated percentage of IIc and Ic in the equilibrium mixture.

(a) 3α-Bromocholestan-2β-yl Tosylate (Ic) ⇌ 2α-Bromocholestan-3β-yl Tosylate (IIc)

Compound Ic (22 mg) was heated at 135° for 25 hours in triglyme (1 ml). The reaction product ($[\alpha]_D$ −2°) was poured into ether and the ether layer washed six times with water, dried with sodium sulphate, and the solvent evaporated. Recrystallization from ether–methanol gave white crystals melting at 135–165°; the infrared spectra of this material and pure 2α-bromocholestan-3β-yl tosylate (IIc) were identical.

As can be seen from Table II the rotation of the reaction mixtures from Ic and IIc differ by about 10°. Thin-layer chromatography, however, showed that the product from either Ic or IIc contained Ic and IIc in apparently identical proportions. In a comparison with mixtures of known content the relative intensities of the spots due to Ic and IIc were indistinguishable from those containing either 85% IIc and 15% Ic or 90% IIc and 10% Ic. Thin-layer chromatography (using either petroleum ether – benzene, 1:1, or petroleum ether alone) also showed that, in addition to Ic and IIc, the pyrolysis products contained a

Can. J. Chem. Downloaded from www.nrcresearchpress.com by 210.87.254.40 on 09/05/12
For personal use only.

small amount of other material which appeared as three spots (two were only partially resolved) near the solvent front. The three spots were distinctly more intense in the product of pyrolysis of I*c*, though the identical spots were nonetheless present in the product of the pyrolysis of II*c*; in the pyrolysis product from I*c* the two partially resolved spots appeared, when taken together, to be more intense than that due to I*c* itself. Pyrolysis of II*c* (400 mg) at 180° for 2 hours in triglyme, followed by extraction as above, gave a product which on chromatography on alumina (Woelm Grade III basic) yielded a material (25 mg) eluted rapidly with petroleum ether. The remaining fractions (total 386 mg) were found to consist of II*c* mixed with a little I*c*. The 25 mg eluted first with petroleum ether showed three intense spots on thin-layer chromatography (with petroleum ether) corresponding exactly to those from the crude products. This material had a specific rotation of +45° and in the infrared spectrum did not show the characteristic tosylate bands at 1185 and 1175 cm^{-1} but did show bands at 3030, 700, and 665 cm^{-1}, suggesting the presence of olefinic hydrogen.

The infrared spectra (IR-7) of the pyrolysis products from I*c* and II*c* were virtually identical and were indistinguishable from that of a mixture containing 90% II*c* and 10% I*c*. The spectrum of pure II*c* showed distinct differences from those of the pyrolysis products or the 90:10 mixture, in particular the latter all showed a small but distinct peak at 862 cm^{-1} which is absent in that of II*c* but present as a moderately strong band in the spectrum of pure I*c*.

The polarimetric, chromatographic, and infrared data, taken together, lead to the estimate that the equilibrium mixture of I*c* and II*c* contains 85±8% of II*c*.

(b) 2β-Bromocholestan-3α-yl Tosylate (Id) ⇌ 3β-Bromocholestan-2α-yl Tosylate (IId)

Workup, as in part (*a*), of the product of pyrolysis of I*d* gave a material whose infrared spectrum was virtually superimposable on that of an authentic sample of II*d* (see below). Thin-layer chromatography, however, showed the presence of a little I*d* (estimated by comparison with mixtures of known content to amount to less than 1/10 of the amount of II*d*) and also a small proportion of fast-moving decomposition products. From the chromatographic and polarimetric data the equilibrium mixture is estimated to contain 95±5% of II*d*.

(c) Other Equilibria

The pyrolysis products of one run each from I*e* (in both triglyme and phenetole) and I*f* (in phenetole) were worked up by pouring into water and extracting with chloroform. The extracts were washed with water, dried over sodium sulphate, and the solvent evaporated. The infrared spectrum in each case clearly showed the product to consist principally of the diequatorial isomers.

3α-Bromocholestan-2β-ol

The following procedure was found to be more convenient than that of Alt and Barton (3). A solution of N-bromosuccinimide (1.50 g) in ethylene glycol dimethyl ether (150 ml) was added slowly to a solution of cholest-2-ene (3.0 g) in a mixture of ethylene glycol dimethyl ether (300 ml) and 0.5 *N* aqueous perchloric acid (20 ml). The reaction mixture was allowed to stand at room temperature for 2 hours and was then poured into water and extracted with ether. The ether extract was washed with dilute potassium bicarbonate solution and water and dried with sodium sulphate, and the solvent evaporated. The crude product was dissolved in petroleum ether and poured onto a column of silica gel (50 g, BDH "for chromatographic adsorption"). Elution with petroleum ether gave cholest-2-ene (500 mg), elution with benzene gave 3α-bromocholestan-2β-ol (2.5 g), m.p. 130–132°, $[\alpha]_D$ +59°, identified by comparison of its infrared spectrum, melting point, and optical rotation with those of an authentic sample prepared as previously described (3).

2β-Bromocholestan-3α-ol

This compound was prepared from cholestan-2α,3α-epoxide as described by Alt and Barton (3); m.p. 115–118°, $[\alpha]_D$ +44°; reported m.p. 115–118°, $[\alpha]_D$ +44°.

2α-Bromocholestan-3β-ol

This compound was prepared by reduction of 2α-bromocholestan-3-one with sodium borohydride as previously described (5, 6); m.p. 113°, $[\alpha]_D$ +12°; reported m.p. 113–114°, $[\alpha]_D$ +12°.

3β-Bromocholestan-2α-yl Acetate

This compound was prepared by diaxial → diequatorial rearrangement of 2β-bromocholestan-3α-yl acetate as previously described (4): m.p. 117–119°, $[\alpha]_D$ −20°; reported m.p. 118–119°, $[\alpha]_D$ −22°.

3β-Bromocholestan-2α-ol

A suspension of 3β-bromocholestan-2α-yl acetate (1.10 g) in a mixture of methanol (90 ml) and 70% perchloric acid (2 ml) was stirred for 36 hours. The mixture was then poured into water and extracted with ether, the extract washed with dilute potassium bicarbonate solution and water and dried with sodium sulphate, and the solvent evaporated. Recrystallization of the crude product from ether–methanol gave 3β-bromocholestan-2α-ol (886 mg), m.p. 102–103°, $[\alpha]_D$ +17°. Calculated for $C_{27}H_{47}OBr$: C, 69.35%; H, 10.13%; Br, 17.09%. Found: C, 69.51%; H, 9.92%; Br, 17.02%.

Can. J. Chem. Downloaded from www.nrcresearchpress.com by 210.87.254.40 on 09/05/12
For personal use only.

Preparation of the Sulphonate Esters

About 1 to 2 equivalents of the sulphonyl chloride was added to a solution of the alcohol in about 5 to 10 times its weight of dry pyridine and the mixture allowed to stand for 3 to 5 days. It was then poured into ether or chloroform and washed with dilute potassium bicarbonate solution, dilute sulphuric acid and water, respectively. The organic layer was then dried and evaporated and the product recrystallized (or precipitated).

3α-Bromocholestan-2β-yl p-Toluenesulphonate (Ic)

Recrystallized four times from acetone, m.p. 174–177°, $[\alpha]_D$ +49°. Calculated for $C_{34}H_{53}O_3SBr$: C, 65.68%; H, 8.59%; S, 5.16%; Br, 12.85%. Found: C, 65.61%; H, 8.59%; S, 5.15%; Br, 12.81%. Infrared maxima below 1400 cm^{-1} (0.1 mm, CCl_4 solution): 1377 (s), 1188 (s), 1177 (s), 1096 (m), 966 (w), 922 (m), 905 (m), 896 (m), 880 (m), 862 (m), 674 (m).

2β-Bromocholestan-3α-yl p-Toluenesulphonate (Id)

M.p. 168–170°, $[\alpha]_D$ +49°; reported m.p. 168–170°, $[\alpha]_D$ +49° (4). Infrared maxima below 1400 cm^{-1} (0.1 mm CCl_4 solution): 1377 (s), 1188 (s), 1178 (s), 1095 (m), 967 (m), 944 (w), 912 (m), 900 (s), 892 (s), 867 (m), 848 (w), 825 (w), 817 (w), 716 (m), 673 (m).

2β-Bromocholestan-3α-yl Benzenesulphonate (Ie)

Recrystallized four times from acetone, m.p. 159–161°, $[\alpha]_D$ +59°. Calculated for $C_{33}H_{51}O_3SBr$: C, 65.23%; H, 8.40%; S, 5.24%; Br, 13.16%. Found: C, 65.46%; H, 8.43%; S, 5.15%; Br, 13.14%. Infrared maxima below 1400 cm^{-1} (0.1 mm, $CHCl_3$ solution): 1377 (s), 1185 (s), 1175 (m), 1094 (m), 966 (m), 943 (w), 912 (m), 900 (s), 891 (s), 865 (w), 822 (w), 686 (m), 665 (m).

2β-Bromocholestan-3α-yl p-Nitrobenzenesulphonate (If)

Recrystallized four times from chloroform–methanol, fine white needles, m.p. 159–161°, $[\alpha]_D$ +47°. (The recrystallization was apparently accompanied by rearrangement. Attempts to obtain a second crop yielded only a gelatinous precipitate.) Calculated for $C_{33}H_{50}O_5NSBr$: C, 60.68%; H, 7.72%; S, 4.97%. Found: C, 60.30%; H, 7.76%; S, 4.77%. Infrared maximum at 1536 cm^{-1} (vs) and the following maxima below 1400 cm^{-1} (0.1 mm, $CHCl_3$ solution): 1378 (s), 1366 (m), 1350 (s), 1313 (w), 1184 (s), 1044 (m), 1013 (w), 964 (w), 898 (s), 852 (m), 820 (w), 685 (w).

2α-Bromocholestan-3β-yl p-Toluenesulphonate (IIc)

Recrystallized five times from ether–methanol, $[\alpha]_D$ −38.5°, apparently dimorphous: partly melts around 135° then resolidifies slowly finally melting at 165°. Calculated for $C_{34}H_{53}O_3SBr$: C, 65.68%; H, 8.59%; S, 5.16%; Br, 12.85%. Found: C, 65.64%; H, 8.20%; S, 5.23%; Br, 12.85%. Infrared maxima below 1400 cm^{-1} (0.1 mm, CCl_4 solution): 1374 (s), 1188 (s), 1177 (s), 1096 (m), 990 (m), 955 (s), 922 (m), 902 (m), 841 (s), 830 (m), 717 (w), 685 (m), 669 (m).

3β-Bromocholestan-2α-yl p-Toluenesulphonate (IId)

Precipitated three times from petroleum ether, apparent m.p. 134–138°, $[\alpha]_D$ −28.5°. Calculated for $C_{34}H_{53}O_3SBr$: C, 65.68%; H, 8.59%; S, 5.16%. Found: C, 65.97%; H, 8.44%; S, 4.89%. Infrared maxima below 1400 cm^{-1} (0.1 mm, CCl_4 solution): 1376 (s), 1191 (s), 1180 (s), 1098 (m), 988 (w), 968 (s), 947 (m), 933 (m), 916 (s), 848 (s), 824 (w), 716 (w), 672 (m).

3β-Bromocholestan-2α-yl Benzenesulphonate (IIe)

Precipitated three times from petroleum ether, apparent m.p. 133–135°, $[\alpha]_D$ −20.4°. Calculated for $C_{33}H_{51}O_3SBr$: C, 65.23%; H, 8.40%; S, 5.24%. Found: C, 64.70%; H, 8.47%; S, 5.25%. Infrared maxima below 1400 cm^{-1} (0.1 mm, $CHCl_3$ solution): 1385 (s), 1187 (s), 1177 (s), 1156 (m), 1098 (m), 988 (w), 968 (s), 948 (m), 933 (m), 848 (s), 820 (m), 719 (m), 685 (m), 666 (w).

3β-Bromocholestan-2α-yl p-Nitrobenzenesulphonate (IIf)

Precipitated three times from petroleum ether, apparent m.p. 187–189° (decomp.), $[\alpha]_D$ −39.5°. Calculated for $C_{33}H_{50}O_5NSBr$: C, 60.68%; H, 7.72%; S, 4.97%. Found: C, 60.84%; H, 7.49%; S, 5.12%. Infrared maximum at 1540 cm^{-1} (vs) and the following maxima below at 1400 cm^{-1} (0.1 mm, $CHCl_3$): 1386 (s), 1353 (s), 1318 (m), 1189 (s), 1179 (s), 1097 (m), 1082 (w), 1014 (w), 989 (w), 962 (m), 941 (s), 917 (w), 856 (s), 849 (s), 820 (m), 685 (m).

ACKNOWLEDGMENTS

We thank Dow Chemical of Canada Limited for a scholarship, the National Research Council of Canada for a scholarship and grants-in-aid, and Research Corporation for a Frederick Gardner Cottrell grant-in-aid.

Can. J. Chem. Downloaded from www.nrcresearchpress.com by 210.87.254.40 on 09/05/12
For personal use only.

REFERENCES

1. D. H. R. BARTON. *In* Theoretical organic chemistry papers presented to the Kekulé Symposium. Butterworths, London. 1959. p. 127.
2. D. H. R. BARTON and E. MILLER. J. Am. Chem. Soc. **72**, 1066 (1950).
3. G. H. ALT and D. H. R. BARTON. J. Chem. Soc. 4284 (1954).
4. D. H. R. BARTON and J. F. KING. J. Chem. Soc. 4398 (1958).
5. E. J. COREY. J. Am. Chem. Soc. **75**, 4832 (1953).
6. L. F. FIESER and W.-Y. HUANG. J. Am. Chem. Soc. **75**, 4837 (1953).
7. C. A. GROB and S. WINSTEIN. Helv. Chim. Acta, **35**, 782 (1952).
8. S. WINSTEIN. J. Am. Chem. Soc. **64**, 2792 (1942).

Can. J. Chem. Downloaded from www.nrcresearchpress.com by 210.87.254.40 on 09/05/12
For personal use only.

INTERACTION OF VANADIUM WITH PROTONS OF ENERGIES UP TO 84 MEV[1]

S. HONTZEAS[2] AND L. YAFFE

Radiochemistry Laboratory, Department of Chemistry, McGill University, Montreal, Que.

Received March 25, 1963

ABSTRACT

Radiochemical techniques have been used to determine absolute excitation functions for 17 nuclides formed as spallation products from the irradiation of vanadium by protons of energy up to 84 Mev. The shape of the excitation functions and classical threshold calculations showed evidence of contribution of heavy-particle emission in the reactions of the type $(p,3pxn)$, $(p,5pxn)$, and $(p,7pxn)$. The Barr method for analysis of the cross-section distribution was modified and applied at 60 and 80 Mev bombarding energies. The experimentally measured cross sections for 16 nuclides at 60 and 80 Mev bombarding energies were fitted to the four-parameter Rudstam equation $\sigma(A,Z) = \exp\ [PA-Q-R(Z-SA)^2]$. Comparison of the results obtained at 8 Mev bombarding energy with the predictions of the weak and strong absorption models showed better agreement with the predictions obtained by using the surface absorption Fernbach–Bjorklund potential.

INTRODUCTION

The study of nuclear reactions initiated by various particles incident on different target nuclei is one of the experimental approaches to the elucidation of nuclear structure. Because of the present condition of theories of nuclear structure, it is desirable to study a simple system. Vanadium may be considered such a system, since it is virtually a monoisotopic element (99.75% V^{51}, 0.25% V^{50}). In addition, it belongs to the range of medium-weight elements where there is no severe Coulomb barrier. The energy range studied in this paper bridges the low-energy region where simple reactions are treated by the compound nucleus theory and the high-energy region where nuclear transparency becomes important.

In the present work, absolute excitation functions for protons of energy up to 84 Mev incident on vanadium have been measured by radiochemical techniques. These results are compared with those obtained by other workers (1–6) in this and other energy ranges.

EXPERIMENTAL METHODS

(a) Targets and Irradiations

All the bombardments were done in the circulating beam of the McGill synchrocyclotron. The target materials were vanadium foils of normal isotopic composition (0.002 in.) obtained from the Electrometallurgical Co., Toronto, Ontario. Spectrographic analysis of the foils showed the following impurities to be present: Al, 0.02%; Ba, 0.02%; Ca, 0.04%; Fe, 0.01%; Zn, 0.04%. The following reactions were used to monitor the proton beam—$Cu^{63}(p,n)Zn^{63}$ at proton energies less than 16 Mev and $Cu^{65}(p,pn)Cu^{64}$ at higher energies. Ghoshal's (7) values were used for the former reaction while Meadows' values (8), corrected by Meghir (9), were taken for the latter reaction. The copper foils (0.002 in.) were carefully aligned with the vanadium at the leading edge since this part of the target intercepted most of the beam.

At the end of the irradiation, the first 1/8 in. of the leading edge of the foil stack was cut off and used. Initially three foils of copper and two of vanadium were used in the foil stack. The degradation of the beam was estimated using the values of Sternheimer (10). Usually the degradation of the beam was less than the energy spread of the McGill cyclotron (±2 Mev) and the degradation has been neglected (except in one case). In the later bombardments, one foil of copper and one of vanadium were used as targets for bombarding energies up to 30 Mev. At higher bombarding energies two vanadium foils (the first vanadium foil acting as guard foil to prevent contamination of the second target foil by the copper spallation products) were used.

[1]*This work received financial assistance from the National Research Council of Canada.*

[2]*Present address: Department of Chemistry, Massachusetts Institute of Technology, Cambridge 39, Mass., U.S.A.*

Can. J. Chem. Downloaded from www.nrcresearchpress.com by 210.87.254.6 on 09/05/12
For personal use only.

This arrangement was reasonable since it has been shown (11) that, in the range of the McGill cyclotron (up to 90 Mev), recoil losses in the monitor copper foil (0.002 in.) were negligible.

(b) Chemical Separations

The number of elements to be separated depended upon the energies at which a particular bombardment was made. The separation and purification procedures for the different elements are given below.

(1) Chlorine (12)

The vanadium target was transferred to a microdistillation apparatus and dissolved in dilute nitric acid containing 5 mg of Cl^- carrier. The target solution was boiled to distill the hydrochloric acid into a receiver containing a few drops of nitric acid and sufficient silver nitrate to precipitate the Cl^- as silver chloride. The precipitate was removed by centrifugation, washed with dilute nitric acid and then dissolved in 5 *N* ammonia. The solution was scavenged with ferric hydroxide, acidified with nitric acid, and more silver nitrate was added to complete the precipitation. The chemical yield (50–60%) was determined gravimetrically.

(2) Chromium–Vanadium

The vanadium target was dissolved in dilute nitric acid containing 5 mg of chromium carrier, and the hydroxides were precipitated with ammonia and ammonium chloride. The precipitate was washed with dilute ammonia and then boiled with 1 *N* sodium hydroxide and hydrogen peroxide. The supernate (chromates–vanadates) was evaporated to remove peroxide, neutralized, and dissolved in 0.1 *M* hydrochloric and 0.1 *M* oxalic acids. The solution was then passed through a column of Dowex-1 (×10, 100–200 mesh) anion exchange resin which had been previously washed with the hydrochloric–oxalic eluant. The chromium was eluted initially while vanadium was later eluted with a mixture of 0.4 *M* hydrochloric and 0.1 *M* oxalic acids. The chromium chemical yield (50–80%) was determined colorimetrically by diphenylcarbohydrazide (13). The peroxide method (13) was used for the colorimetric determination of the chemical yield of vanadium (40–50%).

(3) Titanium–Scandium

The vanadium target was dissolved in dilute nitric acid containing 4 mg of titanium and 5 mg of scandium carriers, and the solution was made ammoniacal. The precipitate was washed twice with dilute ammonia and then boiled with 1 *N* sodium hydroxide and hydrogen peroxide. The precipitate was washed, dissolved in hydrochloric acid, and more vanadium carrier, sodium hydroxide, and hydrogen peroxide were added. The precipitate was boiled, centrifuged, washed, and dissolved in 0.4 *M* hydrochloric acid. After complete dissolution an equal volume of 0.1 *M* oxalic acid was added and the solution passed through a Dowex-1 (×10, 100–200 mesh) anion exchange resin column which had been washed with 0.4 *M* hydrochloric acid and 0.1 *M* oxalic acid. Scandium appeared at the beginning (14) and titanium was eluted with 0.4 *M* hydrochloric acid. The chemical yields were determined colorimetrically (13) for both titanium and scandium (30–50%).

(4) Potassium–Calcium

The vanadium target was dissolved in dilute nitric acid containing 5 mg K^+ and 5 mg Ca^{++} carriers. Iron scavenger was added, the solution made ammoniacal, and the supernate again scavenged with a ferric hydroxide precipitation, evaporated, and ammonia and hydrogen peroxide added. The solution was boiled to remove peroxide and passed through a cation exchange column (D-50, ×12, 200–400 mesh) in NH_4^+ form. The column was washed with 10 ml of water, and potassium and calcium were eluted with 2.2 *N* hydrochloric acid. The acidic solution was concentrated, made ammoniacal, and calcium oxalate precipitated with ammonium oxalate. The precipitate was washed with a solution containing ammonium oxalate and then dissolved in dilute nitric acid. The calcium yield (10–20%) was determined by direct EDTA titration (15) with phthaleincomplexone indicator. The potassium yield (20–30%) was determined gravimetrically by the cobaltinitrite method (16).

(5) Copper

The copper monitor foil was dissolved in nitric acid, the solution evaporated and redissolved in hydrochloric acid (4.5 *M*) and passed through a D-1 anion exchange column previously washed with 4.5 *M* hydrochloric acid. Elution with 4.5 *M* hydrochloric acid removed nickel and cobalt impurities. The copper was eluted with 1.5 *M* hydrochloric acid (17). The chemical yield (50–90%) was determined colorimetrically with diethyldithiocarbamate (17) by a modified procedure (18).

(c) Activity Measurements

The gamma activity of the samples was measured by a 3 in.×3 in. NaI(Tl) crystal in conjunction with a 100-channel pulse-height analyzer. Background radiation was reduced by placing the crystal and photomultiplier tube assembly inside a cylinder of lead 1½ in. thick. Fluorescent X rays from the lead were attenuated by lining the lead shielding with 1/4 in. of iron and 1/8 in. of lucite.

The radioactive nuclides were identified by means of their half-lives and gamma-ray energies. These half-lives were usually obtained graphically from the decay curves, but a few half-life determinations were made using the method of least squares. The gamma-ray energies were determined from a calibration curve obtained by measuring well-known gamma energies of long-lived standards (Na^{22}, Cs^{137}, Co^{60}, etc.). Sc^{43}

Can. J. Chem. Downloaded from www.nrcresearchpress.com by 210.87.254.6 on 09/05/12
For personal use only.

and Sc^{44} have identical half-lives and the mixture of their activities was analyzed by measuring the 511-kev annihilation photopeak common to both and obtaining an independent determination of the disintegration rate of Sc^{44} from its 1.16-Mev γ ray which is in 100% abundance. Sc^{44} may be formed independently or from the decay of the 2.4-day Sc^{44m} isomer. The decay of Sc^{44m} was determined by measuring the distinctive 270-kev γ ray. The independent yield of Sc^{44} was corrected for the isomer contribution.

EXPERIMENTAL RESULTS

(a) Calculations

The observed gamma emission rate was converted to a disintegration rate, $D_\gamma{}^0$, by using the equation

$$[1] \qquad D_\gamma{}^0 = N_\gamma{}^0 \cdot \frac{1+\alpha_T}{R} \cdot \frac{1}{Y} \cdot \frac{1}{F},$$

where $N_\gamma{}^0$ = the absolute photon emission rate; α_T = total internal conversion coefficient; R = branching ratio; Y = chemical yield; and F = dilution factor. Since the energy degradation was negligible in general, the target was assumed to be thin. The independent cross section for the formation of shielded nuclides was calculated by the equation

$$[2] \qquad \sigma_x = \sigma_m \frac{A_m}{A_t} \cdot \frac{W_t}{W_m} \cdot \frac{B_m}{B_t} \cdot \frac{D_x{}^0}{D_m{}^0} \cdot \frac{(1-e^{-\lambda_m T})}{(1-e^{-\lambda_x T})}.$$

The subscripts m and t refer to the monitor and target respectively; σ = cross section; A = natural abundance; W = atomic weight; B = weight used, $D_x{}^0$ and $D_m{}^0$ = disintegration rates of the nuclide under consideration and monitor at end of bombardment, respectively; and λ = decay constant. For unshielded nuclides, a correction for the contribution from the parent was applied, if the parent half-life was known. Where the parent contribution was not known, the cross sections are reported as cumulative.

(b) Estimation of the Error (Standard Deviation) of the Cross-Section Calculation

Equation [2] may be written in the form

$$[3] \qquad \sigma_x = \sigma_m \cdot K_n \cdot \frac{D_x{}^0}{D_m{}^0} \cdot \frac{f(t_m)}{f(t_x)}.$$

$K_n = (A_m/A_t) \cdot (W_t/W_m) \cdot (B_m/B_t)$, where t and m refer to vanadium target and copper monitor respectively, and $f(t_m) = 1-e^{-\lambda_m T}$ and $f(t_x) = 1-e^{-\lambda_x T}$. Since the errors associated with the different terms in equation [3] are independent, the standard deviation of σ_x is obtained by taking the square root of the sum of the squares of the standard deviations of the different terms for the yield of each nuclide. The standard deviation of σ_m was taken as $\pm 13.5\%$ as reported by Meghir (9).

A probable error of $\pm 1\%$ was assigned to the terms K_n, $f(t_m)$, and $f(t_x)$ respectively. The error associated with the term $D_m{}^0$ was found experimentally to be $\pm 13.5\%$. For $D_x{}^0$, the error for each nuclide was: $\pm 11.5\%$ for Cr^{51}, Cr^{49}, Cr^{48}, Ti^{45}, Sc^{47}, Sc^{46}, Sc^{44m}; $\pm 7\%$ for V^{48}; $\pm 16.3\%$ for V^{46}; $\pm 29\%$ for Sc^{43}, Sc^{44}, Ca^{47}; and $\pm 23.6\%$ for Cl^{34m}, Cl^{38}, Cl^{39}, K^{42}, K^{43}.

However, the errors shown in the following figures do not include the errors in the measurement of the absolute cross section of the monitor, but only those present in this series of experiments. The errors thus associated with the absolute value of the various nuclides are as follows: $\pm 17.5\%$ for Cr^{51}, Cr^{49}, Cr^{48}, Ti^{45}, Sc^{47}, Sc^{46}, Sc^{44m}; $\pm 15\%$ for V^{48}; $\pm 21\%$ for V^{47}; $\pm 32\%$ for Ca^{47}, Sc^{44}, Sc^{43}; and $\pm 27\%$ for Cl^{39}, Cl^{38}, Cl^{34m}, K^{43}, K^{42}.

Can. J. Chem. Downloaded from www.nrcresearchpress.com by 210.87.254.6 on 09/05/12
For personal use only.

RESULTS AND DISCUSSION

The nuclides which were identified and measured are given in Table I. The yield is characterized as independent when the measured nuclides are shielded by stable or relatively long-lived isobars. Cr^{51}, for our purposes, may be considered as shielded since its parent nuclide, Mn^{51}, cannot be formed by the proton bombardment of vanadium. The same applies for Cl^{38} since the parent, S^{38}, is not formed in the energy range of interest. The yield of Sc^{47} is characterized as independent since the parent, Ca^{47}, is formed in very low yield and only above bombarding energies of 50 Mev. In the case of V^{48}, the parent, Cr^{48}, was measured and the yield corrected for the parent contribution. The yields were characterized as cumulative when the short half-life of the parent made its contribution difficult to determine. The experimentally determined values of the formation cross sections are given in Tables II and III.

The excitation functions obtained are given in Figs. 1–5 inclusive. The spread in the bombarding energy (~2 Mev) is indicated in the excitation function graphs by horizontal

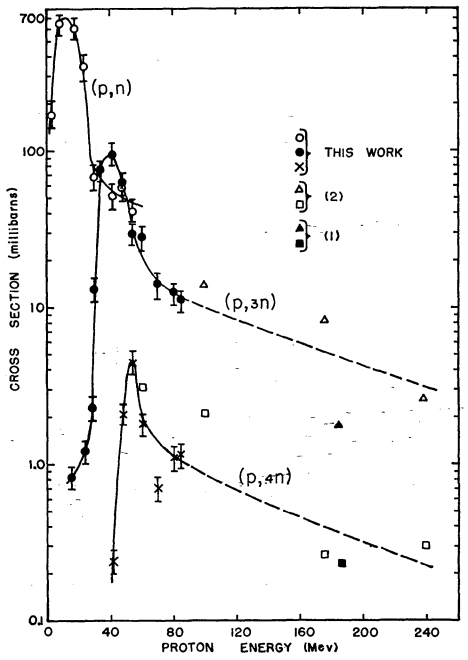

FIG. 1. Excitation functions for (p,xn) reactions.

bars through the experimental points. The vertical bars are the standard deviations estimated in this experiment. The results of other workers (1–6) are also plotted where feasible for purposes of comparison. In general, the agreement between the results obtained in this work and other authors is satisfactory.

(a) Qualitative Analysis

(1) (p,xn) Reactions (Fig. 1)

In the (p,n) reaction, the rapid rise above the threshold to a maximum yield, followed by a rapid decline as other reactions begin to compete, can be accounted for by compound nucleus theory. The yield of this reaction does not fall to a negligible value but tails off

Can. J. Chem. Downloaded from www.nrcresearchpress.com by 210.87.254.6 on 09/05/12
For personal use only.

Can. J. Chem. Downloaded from www.nrcresearchpress.com by 210.87.254.6 on 09/05/12
For personal use only.

TABLE I

Decay characteristics of nuclides studied in this work

Nuclide	Type of decay	Half-life		Half-periods over which measurement took place	Energy of γ ray used for identification (Mev)	Abundance (%)	Internal conversion coefficient (α_T)	Type of yields†
		Literature*	This work					
Cr^{51}	K	28 d (19)	27.82±0.2 d	2–6	0.320	9	1.5×10^{-3}	I
Cr^{49}	β^+	42 m (19)	42.3±0.09 m	2–6	0.090	30	6×10^{-2}	I
					0.511	93		
Cr^{48}	K	23 h	22.96±0.03 h	2–5	0.310	100	6×10^{-3}	I
					0.117			
V^{48}	β^+	16.18 d	16.26±0.05 d	4–6	0.986			
					0.511	55		I
V^{47}	β^+	31.1 m	32 m	2–5	0.511	97		C
Ti^{45}	β^+, K	3.08 h	3.19±0.07 h	3–7	0.511	85		C
Sc^{48}	β^-	1.83 d	1.80 d	3–4	1.314	100	7×10^{-5}	I
Sc^{47}	β^-	3.4 d	3.38±0.09 d	3–6	0.160	66	3.6×10^{-3}	I
Sc^{46}	β^-	84 d	84±0.9 d	1.5–3	0.887	100	1.6×10^{-4}	I
Sc^{44m}	e^-	2.44 d	2.4 d	3–8	0.270	100	1.39×10^{-1}	I
Sc^{44}	β^+	3.92 h	4 h	3–6	0.511	91.5		
					1.160	100	6.3×10^{-3}	I
Sc^{43}	β^+	3.92 h	4 h	3–6	0.511	88		C
Ca^{47}	β^-	4.7 d	4.3 d	2	0.480			
					0.830			
K^{43}	β^-	22.4 h	21.75±0.5 h	3–4	0.614	81	2×10^{-4}	I
K^{42}	β^-	12.5 h	12.28±0.7 h	3–7	1.530	100	10^{-5}	I
Cl^{39}	β^-	56.0 m	58 m	3	0.246	51	1.6×10^{-3}	I
Cl^{38}	β^-	38 m	38 m	3–5	1.600	100	1.26×10^{-5}	I
					2.150	100	1.36×10^{-5}	I
Cl^{34m}	β^+	32.4 m	34 m	3–5	0.511	60		I
					2.15	100		

*All values other than those with a reference number were obtained from Nuclear Data Sheets, National Academy of Sciences, National Research Council (U.S. Government Printing Office, Washington, D.C.).

†I = independent yield; C = cumulative yield.

Can. J. Chem. Downloaded from www.nrcresearchpress.com by 210.87.254.6 on 09/05/12
For personal use only.

TABLE II

Cross sections (millibarn)

Bombarding energy (Mev)	Cr^{51} (p,n)	Cr^{49} $(p,3n)$	Cr^{48} $(p,4n)$	V^{48} $(p,p3n)$	V^{47} $(p,p4n)$	Ti^{45} $(p,2p5n)$	Sc^{48} $(p,3pn)$	Sc^{47} $(p,3p2n)$	Sc^{46} $(p,3p3n)$
3	169	—	—	—	—	—	—	—	—
8	647	—	—	—	—	—	—	—	—
17	—	0.8	—	—	—	—	—	—	—
18	603	—	—	—	—	—	—	—	—
24	349	1.2	—	—	—	—	—	1.20	—
28	—	2.3	—	—	—	—	—	—	—
30	67	13.1	—	0.3	—	—	—	—	—
35	—	77.0	—	—	—	—	—	10.8	—
36	—	—	—	—	—	—	—	16.0	6.7
42	51	97.3	0.2	16.8	2.5	0.08	—	21.0	39.3
48	58	61.8	2.1	37.0	2.2	0.7	—	5.3	24.4
54	41	29.7	4.5	86.5	4.7	3.2	0.6	7.4	28.9
60	—	28.9	1.8	79.8	14.1	5.7	0.6	3.6	7.8
70	—	14.7	0.7	88.8	23.3	4.4	0.9	6.8	11.1
80	—	12.8	1.1	54.5	24.1	4.0	1.3	14.3	20.8
84	—	11.1	1.1	47.0	23.9	4.8	—	16.6	—

TABLE III

Cross sections (millibarn)

Bombarding energy (Mev)	Sc^{44m} $(p,3p5n)$	Sc^{44} $(p,3p5n)$	Sc^{43} $(p,3p6n)$	Ca^{47} $(p,4pn)$	K^{43} $(p,5p4n)$	K^{42} $(p,5p5n)$	Cl^{39} $(p,7p6n)$	Cl^{38} $(p,7p7n)$	Cl^{34} $(p,7p11n)$
24	0.04	—	0.02	—	—	—	—	—	—
30	0.04	—	—	—	—	—	—	—	—
48	0.07	—	0.2	—	0.07	—	—	—	—
54	0.6	—	0.8	—	—	—	—	—	—
60	1.6	0.9	2.2	0.07	0.7	0.4	0.0007	0.002	0.003
70	5.3	4.8	4.2	—	—	—	0.003	0.002	0.004
80	8.0	6.5	8.9	—	0.7	0.3	0.007	0.005	0.005
84	—	—	—	0.2	0.9	0.4	0.02	0.025	0.007

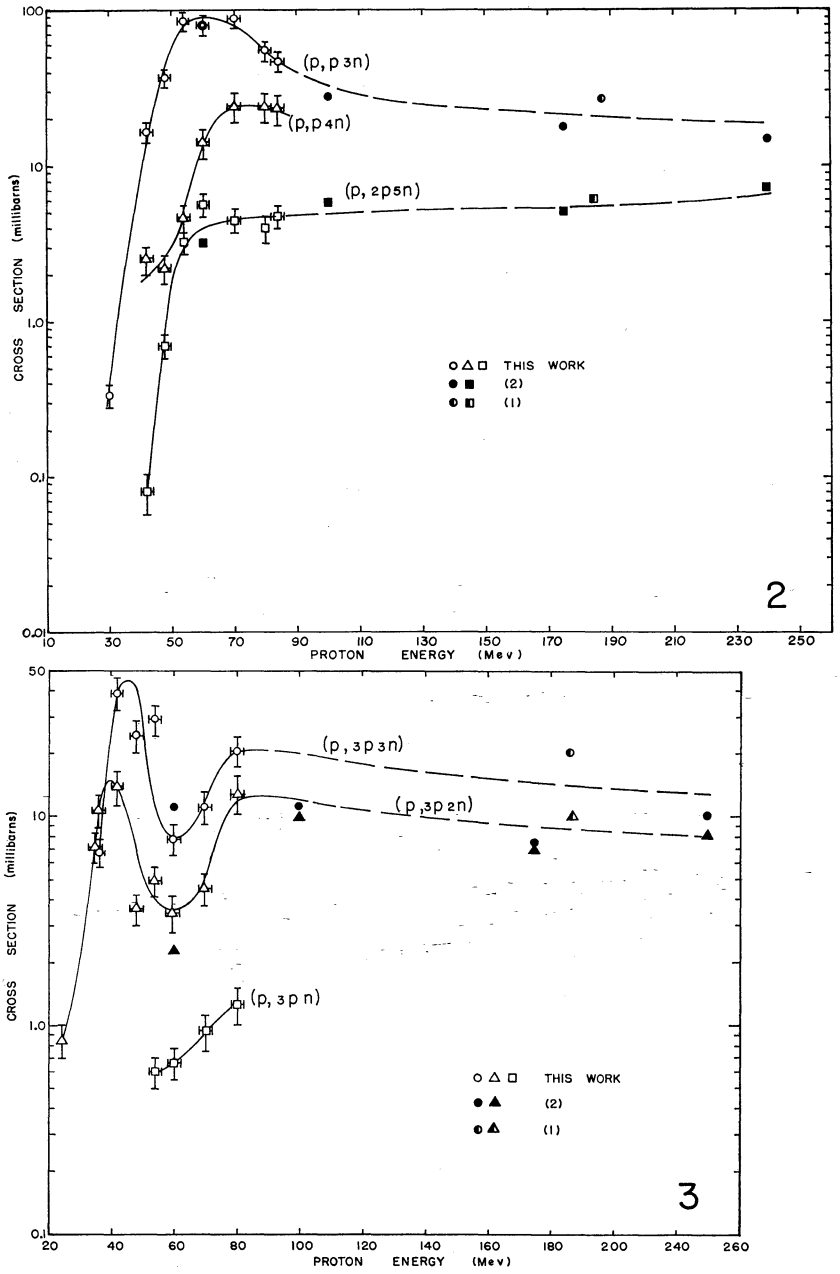

FIG. 2. Excitation functions for (p,pxn) and $(p,2pxn)$ reactions.
FIG. 3. Excitation functions for $(p,3pxn)$ reactions.

at higher bombarding energies, indicating that the knock-on cascade mechanism is of importance here. The excitation functions of the $(p,3n)$ and $(p,4n)$ reactions show the same general shape with the difference that the knock-on mechanism predominates at higher energies. The unusually low yield for the $(p,4n)$ reaction can be explained by assuming a low-level density (20) for even–even Cr^{48}.

Can. J. Chem. Downloaded from www.nrcresearchpress.com by 210.87.254.6 on 09/05/12
For personal use only.

Can. J. Chem. Downloaded from www.nrcresearchpress.com by 210.87.254.6 on 09/05/12
For personal use only.

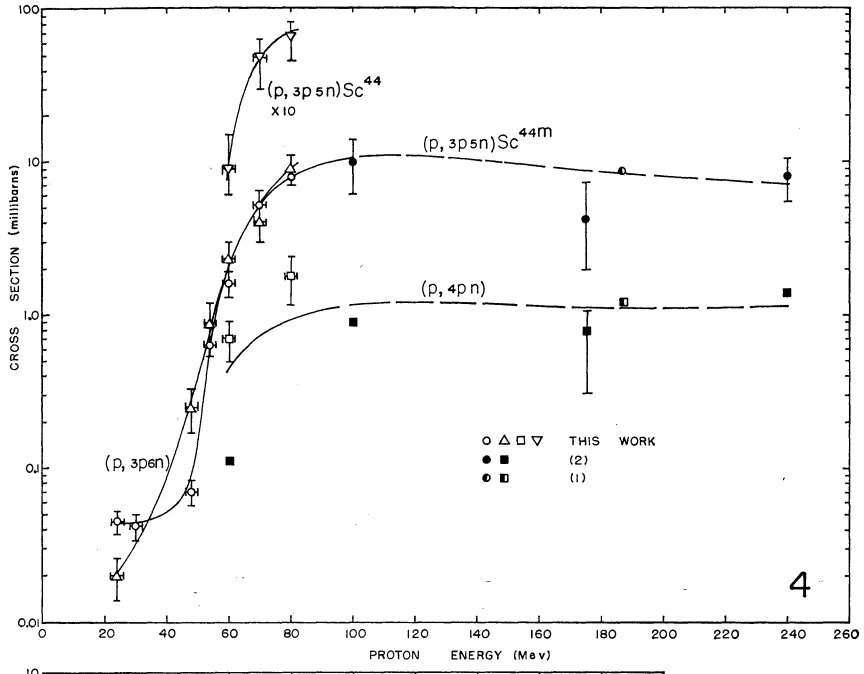

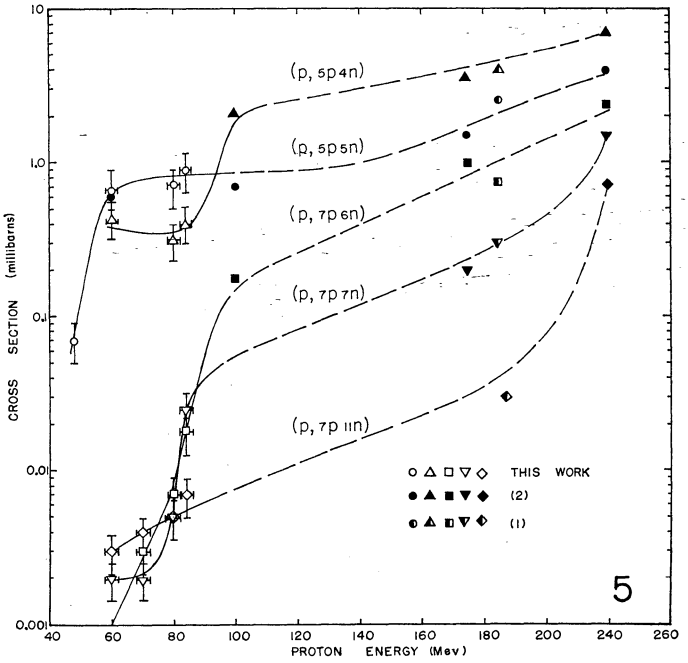

FIG. 4. Excitation functions for $(p,3pxn)$ and $(p,4pn)$ reactions.
FIG. 5. Excitation functions for $(p,5pxn)$ and $(p,7pxn)$ reactions.

(2) (p,pxn) Reactions (Fig. 2)

The excitation functions of these reactions show the same general characteristics as the $(p,3n)$ and $(p,4n)$ excitation functions. Comparison of the $(p,4n)$ and $(p,p3n)$ reactions

indicates that the relative yield of the $(p,4n)$ reaction may be explained according to the statistical model by virtue of the position of Cr^{48} and V^{48} with respect to the valley of the stability (Fig. 6). The sharp decrease in yield as the distance from the stable valley

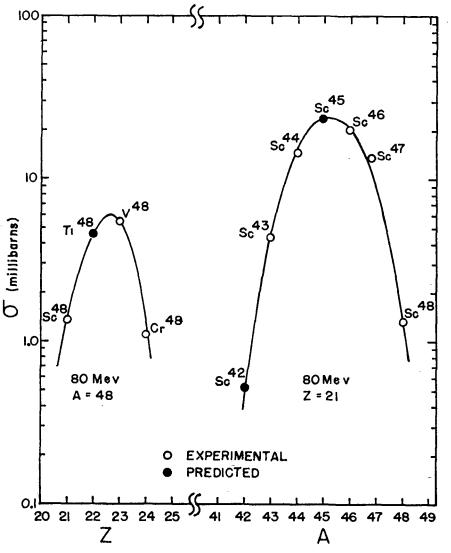

FIG. 6. Formation cross sections of isobars of $A = 48$ and isotopes of $Z = 21$ at 80 Mev.

increases is strong evidence for the importance of the evaporation mechanism which favors de-excitation modes leading towards the stable valley (21). The low value of the ratio of the $(p,4n)/(p,p3n)$ yields suggests that, if sufficient energy is available for four-particle emission, the proton is favored to be among the particles emitted.

(3) (p,2pxn) Reactions (Fig. 2)

The only reaction of this type observed is the $(p,2p5n)$ reaction. The shape of the excitation function supports the Serber mechanism.

(4) (p,3pxn) Reactions (Figs. 3 and 4)

For the reactions (except for $x = 2, 3$) the excitation functions increase monotonically up to the highest bombarding energy available at the McGill cyclotron.

The low yield of the $(p,3pn)$ reaction to produce Sc^{48} may be explained by its position with respect to the stability valley (Fig. 6). When energy is available for single-particle emission (3 protons, 1 neutron) the ratios of the $(p,4n)/(p,3pn)$ and $(p,p3n)/(p,3pn)$ reactions suggest that Sc^{48} is formed mainly by an evaporation process in the energy region of interest. This can be ascertained from Table IV.

TABLE IV

Ratio of formation cross sections

	60 Mev	80 Mev
$\frac{p,4n}{p,3pn} = \frac{Cr^{48}\text{ (even–even)}}{Sc^{48}\text{ (odd–odd)}}$	3.0	0.85
$\frac{p,p3n}{p,3pn} = \frac{V^{48}\text{ (odd–odd)}}{Sc^{48}\text{ (odd–odd)}}$	133	42.5

Can. J. Chem. Downloaded from www.nrcresearchpress.com by 210.87.254.6 on 09/05/12
For personal use only.

The shapes of the $(p,3p2n)$ and $(p,3p3n)$ excitation functions show that many of the reactions observed cannot possibly be due to single-particle emission only.

Table V lists $-Q$ values obtained, using the Seeger (22) semiempirical mass formula, for a number of possible mechanisms for the formation of the nuclides Sc^{43}, Sc^{44}, Sc^{46}, etc.

TABLE V

Threshold calculations

Product nuclide	Reaction mechanism	$-Q$ (Mev)	Product nuclide	Reaction mechanism	$-Q$ (Mev)
Sc^{43}	$V^{51}(p,Li^8n)$	35.70	Sc^{44}	$V^{51}(p,Li^7n)$	28.40
	(p,Li^72n)	37.70		(p,Li^8)	26.50
	(p,Li^63n)	48.10		(p,Li^62n)	35.60
	$(p,\alpha p4n)$	48.50		$(p,d\alpha 2n)$	37.00
	$(p,\alpha d3n)$	46.20		$(p,\alpha p3n)$	39.20
	(p,H^3He^33n)	60.0		(p,He^3p4n)	59.50
	$(p,2pd5n)$	74.00		(p,H^3He^32n)	57.10
	$(p,2dp4n)$	71.80		$(p,3d2n)$	60.50
	(p,H^32p4n)	65.6		$(p,2pd4n)$	62.50
	$(p,3p6n)$	76.10	Sc^{46}	$V^{51}(p,Li^6)$	16.00
Sc^{47}	$V^{51}(p,\alpha p)$	9.05		$(p,\alpha d)$	17.40
	(p,He^3d)	27.10		$(p,\alpha pn)$	19.60
	(p,H^32p)	28.60		(p,H^3He^3)	31.40
	$(p,2dp)$	32.50		(p,H^32pn)	39.10
	$(p,d2pn)$	34.80		$(p,2dpn)$	43.00
	$(p,3p2n)$	36.95		$(p,d2p2n)$	45.20
Cl^{34}	$V^{51}(p,7p11n)$	156		$(p,3p3n)$	48.00
	$(p,2\alpha Li^73n)$	62	Cl^{38}	$V^{51}(p,C^{13}n)$	26.35
	$(p,2\alpha Li^64n)$	72.5		$(p,3\alpha pn)$	36.80
	$(p,dC^{13}3n)$	53.60		$(p,7p7n)$	115.50
	$(p,3\alpha p5n)$	72.80			
	(p,Be^9Li^63n)	62.05	Cl^{34}	$Ca^{40}(p,\alpha He^3)$	18.70
	(p,Be^8Li^64n)	69.10		(p,Li^6p)	19.30
	$(p,N^{17}n)$	45.80		$(p,4p3n)$	57.84*
					49.20†

*Obtained from measured isotopic mass of Ca^{40} and calculated mass of Cl^{34m}.
†Obtained from calculated masses of Ca^{40} and Cl^{34m}.

In the case of formation of Sc^{47}, $(p,3p2n)$ reaction, all possible mechanisms are listed. Only $(p,\alpha p)$, (p,td), and $(p,t2p)$ mechanisms can explain the yield below 30 Mev. A mixture of these mechanisms contributes to the yield over most of the excitation curve. From other experimental evidence (23–25) it is known that alpha particles are produced in high yield in reactions of this type and that protons, deuterons, and tritons are also emitted. Therefore it is probable that the first maximum in the Sc^{47} excitation function represents a large contribution from α-particle emission, while the second maximum is probably due to the emission of protons, deuterons, and tritons.

The $(p,3p3n)$ excitation function shows the same characteristics as that of the $(p,3p2n)$. The only difference is that the yield of Sc^{46} (odd–odd) is significantly greater than that of Sc^{47} (odd–even). Energetic considerations indicate that only the first five mechanisms (Table V) could explain the yield of $(p,3p3n)$ reaction below 40 Mev. The higher yield of Sc^{46} compared with Sc^{47}, in spite of the fact that the reaction leading to the formation of Sc^{47} might be expected to be more probable than the reaction leading to the formation of Sc^{46}, can be explained by assuming that the odd–odd nuclide Sc^{46} has a higher-level density than odd–even Sc^{47}, in agreement with the statistical model. The odd–odd, odd–even, even–even effect is shown in Table VI. The $(p,3p3n)$ excitation function could also be explained on the same grounds as the $(p,3p2n)$ excitation function. Excitation functions

Can. J. Chem. Downloaded from www.nrcresearchpress.com by 210.87.254.6 on 09/05/12
For personal use only.

TABLE VI
Odd–even effects

Type of reaction	Cross-section ratio at curve maximum	Cross-section ratio at 84 Mev
$\frac{(p,4n)}{(p,p3n)} = \frac{(E–E)}{(O–O)}$	$\frac{4.2}{80} = 0.05$	$\frac{1.1}{47} = 0.02$
$\frac{(p,p4n)}{(p,3p2n)} = \frac{(O–E)}{(O–E)}$	$\frac{27}{15} = 1.8$	$\frac{24}{16.6} = 1.45$

showing two maxima in the energy range of interest and of the same type have previously been observed in spallation studies of Cu (20) and Co (26) by protons.

The excitation functions of Sc^{43}, Sc^{44}, and Sc^{44m} also provide evidence for multiple-charged-particle emission. The high-spin state of Sc^{44m} is formed far below 60 Mev bombarding energy, while the low-spin ground-state Sc^{44} only begins to be formed in measurable amounts at 60 Mev.

The yield ratios at different bombarding energies indicate that the high-spin state is favored (Table VII). The result may be explained by assuming that the residual nucleus

TABLE VII
Yield differences of Sc^{44m} and Sc^{44} at various bombarding energies

Bombarding energy (Mev)	Sc^{44m} cross section (millibarn)	Total angular momentum J ($\hbar$)	Sc^{44} cross section (millibarn)	Total angular momentum J ($\hbar$)	Ratio $\frac{Sc^{44m}}{Sc^{44}}$
24	0.04	6, 7	—	2, 3	—
48	0.07		—		—
60	1.60		0.90	—	1.78
70	5.30		4.80		1.10
80	8.00		6.50		1.23

formed from a fast process (cascade) containing a large amount of excitation energy has a high spin and may tend to retain this state while it de-excites by evaporation preferentially forming the high-spin state of the isomeric pair.

(5) (p,4pxn) Reactions (Fig. 4)

Ca^{45} was observed but, because of the very low count rate and the high self-absorption (due to the separation chemistry) in the 4π counting, the results were discarded and no cross-section calculations were performed. The yield of Ca^{47} is depressed, as was expected, due to shell effects ($Z = 20$).

(6) (p,5pxn) Reactions (Fig. 5)

The examination of the $(p,5pxn)$ ($x = 4, 5$) excitation functions leads to the following considerations. The energetics of these reactions would predict that the $(p,5p4n)$ reaction is more favored than that of $(p,5p5n)$. The latter leads to the formation of K^{42} ((O–O) type) (high-level density) while the $(p,5p4n)$ leads to the formation of odd–even K^{43}. The de-excitation mode, according to the evaporation model, suggests that K^{42} should have a higher yield than K^{43} because of its position with respect to the stability valley. The data show that the yield of K^{42} is significantly lower than the yield of K^{43} up to 80 Mev bombarding energy. On the other hand, the energetics suggest that the K^{43} yield at 48 Mev

Can. J. Chem. Downloaded from www.nrcresearchpress.com by 210.87.254.6 on 09/05/12
For personal use only.

cannot be explained by single-particle emission but only under the assumption of multiple-charged-particle emission.

(7) (p,7pxn) Reactions (Fig. 5)

The production of complex particles like Li^8, Be^8, etc. has been found (27–32) mostly at very high excitation energies. The reaction mechanism for the production of these particles was first investigated by Camerini *et al.* (33) and since then in more detail (34, 35). Multiple-charged-particle emission (statistical model) in general is militated against by high barriers and $-Q$ values, but, on the other hand, is favored by statistical factors (36).

The $(p,7p11n)$ reaction leads to the production of Cl^{34m}. The threshold for this reaction is above 150 Mev. Cl^{34m} was at first identified at 60 Mev bombarding energy. Spectrographic analysis of the vanadium target has shown calcium impurities of the order of 0.04%. This is the only impurity which could produce chlorine by reaction with protons (Ca^{40}, 97.01%). If Cl^{34m} were indeed being produced by reactions on calcium, one would have expected the appearance of Cl^{34m} at lower energies, as indicated in Table V. It is energetically possible for it to have been produced by a reaction like $(p,N^{17}n)$.

(b) Cross-Section Distribution and Application of a General Cross-Section Equation

Spallation studies on medium-weight elements at very high energies (37, 38) have shown that:

(i) the independent yields across an isobar or an element are largest in the region of the stable isotopes and fall rapidly on the wings of those isolines;

(ii) along isodiapheric lines, originating at the various isotopes of the target element, the measured cross sections seem to vary in a smooth manner.

Since there are not enough measurable cross sections across any of the isobars below the vanadium target, the Barr (38) method was first applied to scandium isotopes in a slightly modified manner. Figure 6(*b*) shows the distribution of scandium isotopes at 80 Mev. The cross-section distribution, within experimental error, followed the assumed shape. The cross sections for three scandium isotopes (Sc^{44}, Sc^{46}, Sc^{48}) ((O–O) type) were fitted to an equation of the form

$$\ln \sigma = aA^2+bA+c, \quad [4]$$

where σ = measured cross section of the isotope in millibarns; A = mass number for that isotope.

The parameters a, b, c were determined and the cross sections for the nuclides of the (O–E) type were calculated and compared with the predicted values (80 Mev bombarding energy, Sc^{47}, predicted/measured = 0.55; Sc^{43}, predicted/measured = 0.86). The quantity $-b/2a$ was calculated. This corresponds to the most probable A for a given Z. It was assumed that the quantity $-b/2a$ for each element of interest should fall on the line defined by the origin and the value $-b/2a$ for scandium. The assumption was tested by predicting measured cross sections for the elements potassium and chlorine, from the isodiapheric lines. The values of $-b/2a$ for K and Cl indeed fall on the assumed straight line (Fig. 7). The ratios for K^{43} and Cl^{39} respectively are not of course very satisfactory because of the previously mentioned discrepancy due to multiple-charged-particle emission for K^{43}.

The measured cross sections for the elements Cl, K, Ca, Sc, Ti, V, and Cr were determined in this way as long as there was one measured cross section for the element under consideration. Three yields for each mass number were fitted to an equation of the form

$$\ln \sigma = aZ^2+bZ+c, \quad [5]$$

Can. J. Chem. Downloaded from www.nrcresearchpress.com by 210.87.254.6 on 09/05/12
For personal use only.

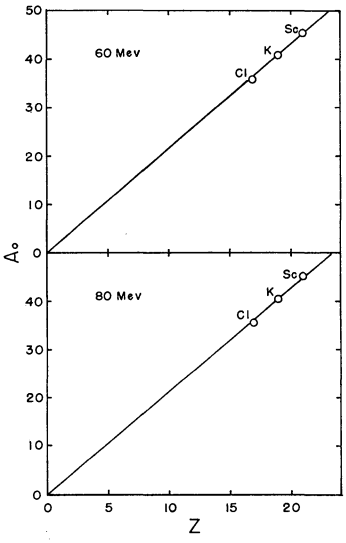

FIG. 7. Most probable maximum number for a given Z at 60 and 80 Mev.

where Z is the atomic number of the isotope with cross section σ. The validity of the parabolic distribution was therefore tested. The parameter a remained essentially constant. A plot of the most probable Z for a given A was made (Fig. 8) from the value $-b/2a$. The cross section for each mass number was summed and Fig. 9 was constructed for 60

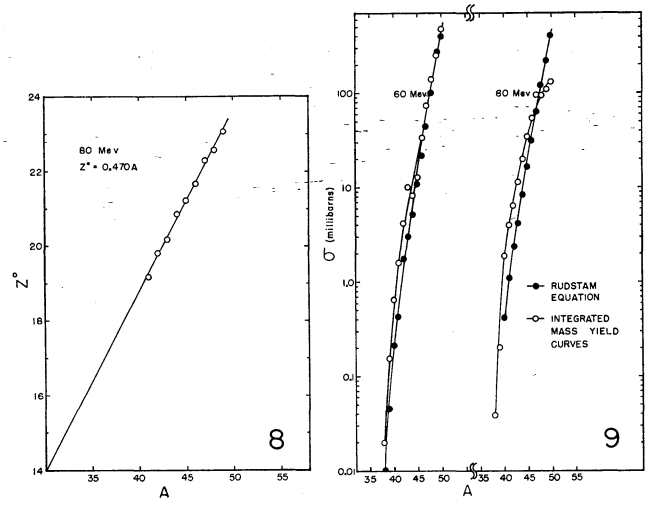

FIG. 8. Most probable Z for a given A at 80 Mev.
FIG. 9. Comparison of integrated maximum yield curves with values predicted by Rudstam at 60 and 80 Mev.

and 80 Mev respectively. The overall shape of the curves suggested that the relationship may be approximated by the four-parameter Rudstam equation (1). The slope of the curves in Fig. 8 represents the parameter S in the Rudstam equation:

$$\sigma(A,Z) = \exp\,[P-Q-R(Z-SA)^2]. \qquad [6]$$

Can. J. Chem. Downloaded from www.nrcresearchpress.com by 210.87.254.6 on 09/05/12
For personal use only.

The parameters P, Q, R were obtained by fitting the data for the nuclide measured to equation [7] by the method of least squares. The values obtained are consistent with the systematics for the parameters established by Rudstam (37). Table VIII gives the comparison of the cross sections calculated from equation [7] with those actually measured for the nuclides of interest.

TABLE VIII

Comparison of calculated and measured cross sections

Nuclide	Cross section measured (millibarn) 60 Mev	80 Mev	Cross section calculated (millibarn) $\ln \sigma = PA-Q-R(Z-SA)^2$ 60 Mev	80 Mev
Cr^{49}	28.90	12.80	30.0	23.8
Cr^{48}	1.80	1.10	2.9	4.80
V^{48}	79.80	54.50	41.10	61.30
V^{47}	14.15	24.10	8.20	14.20
Ti^{45}	5.70	4.00	2.25	4.60
Sc^{48}	0.65	1.35	1.10	1.90
Sc^{47}	3.6	14.3	3.65	6.50
Sc^{46}	7.80	20.85	6.30	15.70
$Sc^{44\ \&\ 44m}$	2.50	14.50	2.55	5.70
Sc^{43}	2.20	8.90	0.60	1.50
Ca^{47}	0.07	0.18	0.028	0.06
K^{43}	0.68	0.72	0.130	0.145
K^{42}	0.43	0.32	0.27	0.76
Cl^{39}	0.0007	0.007	0.0046	0.02
Cl^{38}	0.002	0.005	0.011	0.017
Cl^{34}	0.003	0.005	0.0005	0.003
	148.2	157.6	99.08	140.99
			$e^{\pm 1.009} = 2.71$	$e^{\pm 0.946} = 2.57$

Figure 10 is a graphical representation of the data. The root mean squares, m, of the differences between the experimental and calculated logarithms of the cross sections were

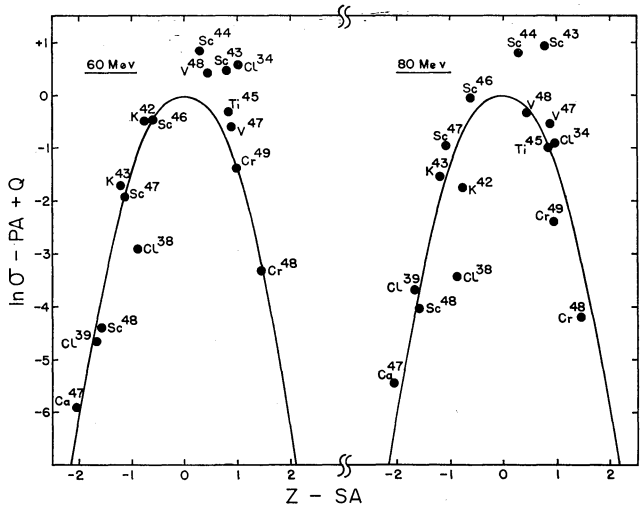

FIG. 10. Graphical representation of a chart between values predicted for individual nuclides by the Rudstam equation and those obtained experimentally.

Can. J. Chem. Downloaded from www.nrcresearchpress.com by 210.87.254.6 on 09/05/12
For personal use only.

found to be 0.849 and 0.887 at 60 and 80 Mev bombarding energies respectively. The expression $e^{\pm m} = 2.327$ and 2.427, for 60 and 80 Mev respectively, gives the average ratio between the experimental and calculated cross sections. However, the empirical equation is more useful when it covers as wide a range of mass numbers as possible.

(c) Quantitative Analysis of Experimental Results at 8 Mev Bombarding Energy

To compare reaction cross sections with the optical model, the quantities $\sigma(p,n)$, $\sigma(p,\gamma)$, $[\sigma(p,p')+\sigma(p,\alpha)]$, and σ_{ce} (compound elastic scattering) must be added. The quantity $\sigma(p,n)$ was determined experimentally in this work (647 millibarns). The other quantities were taken from the literature (6), giving a total of 799 millibarns for total absorption cross section. The theoretical (Fig. 11) (surface and volume) absorption curves were

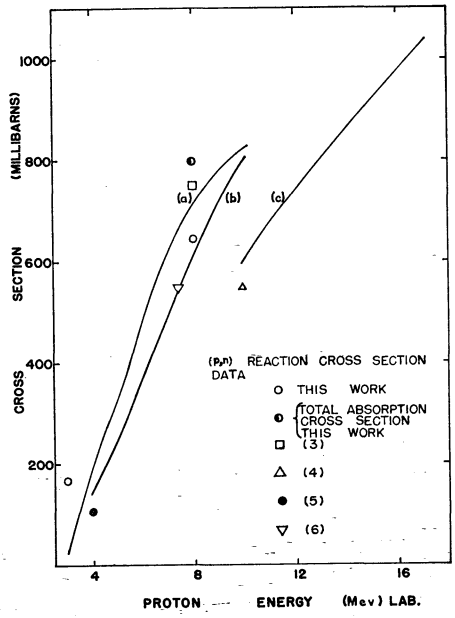

FIG. 11. Agreement between theoretical and experimental cross sections at 4 and 8 Mev bombarding energies: (*a*) strong absorption model; (*b*) weak absorption model (surface absorption Fernbach–Bjorklund potential); (*c*) weak absorption model (volume absorption Woods–Saxon potential).

derived using the results of Fernbach and Bjorklund (39), Albert (40), and Melkanoff *et al.* (41). The value $r_0 = 1.36\times10^{-13}$ was obtained using the equation $\pi R^2 = \pi(r_0\times 10^{-13}\times A/3)^2 = 799$ millibarns. The results rather support the surface absorption model. The strong absorption model curve was obtained using Shapiro's (42) approximation for the calculation of compound nucleus formation. The best value of r_0 for the fit (1.5×10^{-13}) was used for the calculations. However, this is misleading since the calculations based on the strong absorption model assume that at this bombarding energy there is one de-excitation channel (p,n) in the compound nucleus sense, and the theory does not take into account the quantities $\sigma(p,\gamma)$, $[\sigma(p,p')+\sigma(p,\alpha)]$, and σ_{ce}.

ACKNOWLEDGMENTS

We wish to express our gratitude to Professor R. E. Bell, Director of the Radiation Laboratory, McGill University, for his kind cooperation in making the cyclotron readily available to us.

Can. J. Chem. Downloaded from www.nrcresearchpress.com by 210.87.254.6 on 09/05/12
For personal use only.

REFERENCES

1. S. G. Rudstam. Phil. Mag. **7**, 44, 1131 (1953).
2. C. G. Heininger and E. O. Wiig. Phys. Rev. **101**, 1074 (1956).
3. S. Tanaka and M. Furucawa. J. Phys. Soc. of Japan, **14**, 1269 (1959).
4. V. Meyer and N. M. Hintz. Proceedings of the International Conference on Nuclear Structure, Kingston, Canada. 1960. p. 231.
5. B. Lobkowicz and P. Marnier. Helv. Phys. Acta, **34**, 85 (1961).
6. B. W. Shore, N. S. Wall, and J. W. Irvine, Jr. Phys. Rev. **123**, 276 (1961).
7. S. N. Ghoshal. Phys. Rev. **80**, 939 (1950).
8. J. W. Meadows. Phys. Rev. **91**, 885 (1953).
9. S. Meghir. Ph.D. Thesis, McGill University, Montreal, Que. 1962.
10. R. M. Sternheimer. Phys. Rev. **111**, 137 (1959).
11. L. R. Chervu. Ph.D. Thesis, McGill University, Montreal, Que. 1962.
12. R. E. Batzel, D. R. Miller, and G. T. Seaborg. Phys. Rev. **84**, 671 (1951).
13. E. B. Sandell. Colorimetric determination of traces of metals. 3rd ed. Interscience Publishers, Inc., New York. 1959.
14. R. I. Walter. J. Inorg. Nucl. Chem. **6**, 58 (1958).
15. F. J. Welcher. The analytical uses of ethylenediamine tetracetic acid. D. van Nostrand Co., Inc., New York. Reprinted 1958.
16. F. P. Treadwell and W. T. Hall. Analytical chemistry. Vol. 2. 7th ed. J. Wiley and Sons, New York. 1928.
17. C. J. Rodden. Analytical chemistry of the Manhattan project. 5th ed. McGraw-Hill Book Co., New York. 1950.
18. G. V. S. Rayudu. Ph.D. Thesis, McGill University, Montreal, Que. 1961.
19. Handbook of Physics. American Institute of Physics. 1958.
20. J. W. Meadows. Phys. Rev. **98**, 744 (1955).
21. G. Friedlander and J. W. Kennedy. Nuclear and radiochemistry. J. Wiley and Sons, New York. 1955.
22. P. A. Seeger. Nucl. Phys. **25**, 1 (1961).
23. J. Hadley and N. York. Phys. Rev. **80**, 345 (1950).
24. P. W. Waniek and T. Ohtsuka. Phys. Rev. **89**, 1307 (1953).
25. R. W. Deutsch. Phys. Rev. **90**, 499 (1953); **97**, 1110 (1955).
26. R. A. Sharp, R. N. Diamond, and G. Wilkinson. Phys. Rev. **101**, 1493 (1956).
27. B. A. Munir. Phil. Mag. **1**, 345 (1956).
28. S. Nakagawa, E. Tamai, and S. Nomoto. Nuovo Cimento, **9**, 780 (1958).
29. D. H. Perkins. Proc. Roy. Soc. (London), Ser. A, **203**, 399 (1950).
30. S. O. C. Sörensen. Phil. Mag. **42**, 188 (1951).
31. E. Baker, G. Friedlander, and J. Hudis. Phys. Rev. **112**, 1319 (1958).
32. D. V. Lozhkin and H. A. Perfilov. Soviet Phys. JETP (English Transl.), **4**, 790 (1957).
33. U. Camerini, W. O. Lock, and D. H. Perkins. Progress in cosmic ray physics. Amsterdam-North Holland Publishing Co. 1952.
34. J. Hudis and J. M. Miller. Phys. Rev. **112**, 1322 (1958).
35. I. Dostrovsky, Z. Fraenkel, and P. Rabinowitz. Phys. Rev. **118**, 791 (1960).
36. T. Ericson. Phil. Mag. Suppl. **9**, No. 36, 425 (1960).
37. S. G. Rudstam. Thesis, Uppsala University, Uppsala, Sweden. 1956.
38. D. W. Barr. Ph.D. Thesis, University of California, Berkeley, Calif. 1957.
39. S. Fernbach and F. Bjorklund. Phys. Rev. **109**, 1295 (1958).
40. R. P. Albert. Phys. Rev. **115**, 925 (1959).
41. N. A. Melkanoff, J. Nodvik, D. S. Saxon, and R. D. Woods. Phys. Rev. **106**, 793 (1957).
42. M. M. Shapiro. Phys. Rev. **90**, 171 (1953).

Can. J. Chem. Downloaded from www.nrcresearchpress.com by 210.87.254.6 on 09/05/12
For personal use only.

AUTOMATIC ADIABATIC SOLUTION CALORIMETER USING THERMISTORS

LAWRENCE BENJAMIN
The Procter and Gamble Company, Miami Valley Laboratories, Cincinnati, Ohio, U.S.A.
Received February 27, 1963

ABSTRACT

A calorimeter is described, of capacity 40–50 ml, which is suitable for the investigation of solutions between 0° C and 70° C. Temperatures are measured to better than 0.0001° C using thermistors and the latter are also used to provide automatic adiabatic control. A novel mechanism is used for opening sample cells and the associated heat effect can be measured with a precision of 0.01 cal or better. Stirring of the calorimeter is achieved by continuous rocking of the vessel through 180°. The performance of the calorimeter is illustrated by results obtained for the heat of solution of NaCl at 25° C.

Can. J. Chem. Downloaded from www.nrcresearchpress.com by 210.87.254.105 on 09/05/12
For personal use only.

I. INTRODUCTION

An accurate study of enthalpy changes occurring in dilute solutions, where the amount of heat to be measured is of the order of a calorie, is difficult to carry out. The calorimeter to be described is intended for use in such studies with aqueous surfactant systems. Since solution of these materials is not always rapid, an adiabatic instrument is to be preferred in the experiments. Thermistor bridge circuits are used for temperature measurement and adiabatic control, stirring of the calorimeter being achieved by continuous rocking through 180°.

One of the limitations to the accuracy attainable in the measurement of small heat changes is the reproducibility of the blank heat change occurring on opening an empty sample cell, q_b. Factors associated with the magnitude of q_b have been discussed in some detail (1) together with a number of general features pertaining to the design of solution calorimeters. A novel breaking mechanism is employed in the present instrument which enables an accurate allowance for q_b to be made in solution and dilution experiments.

After a description of the calorimeter is given, its use is illustrated by results obtained for the heat of solution of sodium chloride in water at 25° C. (The calorimeter is designed and constructed to operate over a considerable temperature range. Heat capacity determinations using water have been successfully carried out up to 70° C with no apparent loss of accuracy.)

II. CALORIMETER DESCRIPTION

In some respects the calorimeter is similar to those described by Benson and co-workers (1, 2) but uses an immersed submarine mounted in a thermostat bath to contain the calorimeter vessel, in a manner similar to that employed by Gunn (3). The assembly is shown schematically in Fig. 1 while Fig. 2 shows a photograph of the polished stainless steel calorimeter vessel suspended by nylon loops and light springs in a cradle made of 1/16 in. mild steel rods. A nine-pin connector collects the leads from the vessel components and fits a socket sealed in the cap of the glass submarine with an epoxy resin. The submarine is constructed from freeze-drying flasks (Virtis, 500 ml) and can be evacuated using the stopcock shown. A bright aluminum coating is applied to its inside surfaces in order to reduce heat transfer by radiation. The flexible nature of the cradle allows it to

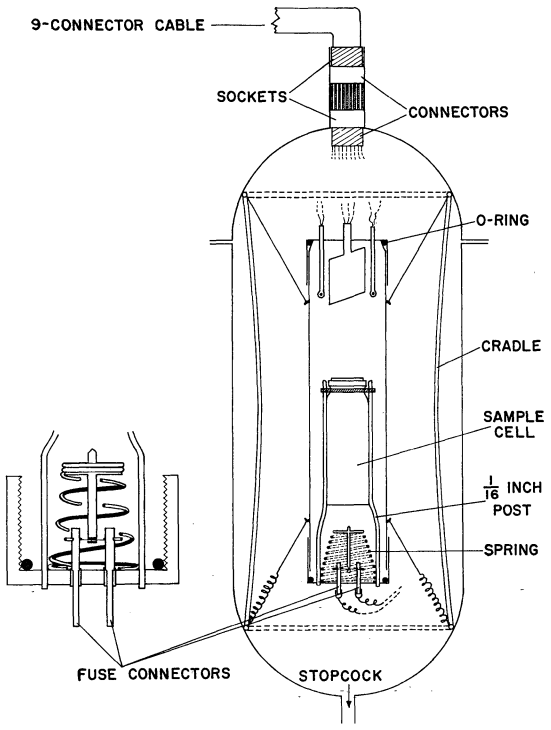

FIG. 1. Diagram of calorimeter assembly.

be held rigidly in the submarine when the cap is in position, the parts of the cradle coming in contact with the glass being covered with tape or coated with Tygon (see Fig. 2).

Stainless steel is used for all metal parts of the calorimeter vessel, which consists of a 1 in. diameter tube, 4 in. long, sealed by caps tightening on neoprene O-rings. Fairly loose threads are used on the caps and no pressure is therefore developed during sealing. The capacity of the vessel is approximately 50 ml. Epoxy resin is used to seal two thermistors (for temperature measurement and control) and a heater in the top cap and fuse connectors in the lower cap, silver solder being preferred for holding the 1/16 in. diameter posts in position. The solder is only required on the outside of the cap, however, and does not come into contact with the vessel contents. The heater consists of approximately 100-ohm manganin wire, 40 gauge, wound non-inductively on a mica form attached to a porcelain tube, together with a similar length of 38-gauge copper wire on the form to act as a heat trap. A third lead for potential measurements is attached just as the leads leave the vessel. Following a thin coating of epoxy resin, the heater is plated with copper and then gold. Since the electrical insulation of this heater deteriorated with use, as had also been found with epoxy-resin coatings, a final layer of a heat-curing epoxy resin (Hysol 4102) was applied to the gold. This has given quite satisfactory insulation during subsequent use.

Sample cells are made from standard female tapered joints (12/30) by grinding away most of the taper and cutting the attached tube to the required length. This cut end is ground flat and sealed with a 15 mm diameter cover glass, 0.006 in. thick, attached with the Hysol resin. Sealing of the tubes can be achieved using tapered Teflon stoppers or

Can. J. Chem. Downloaded from www.nrcresearchpress.com by 210.87.254.105 on 09/05/12
For personal use only.

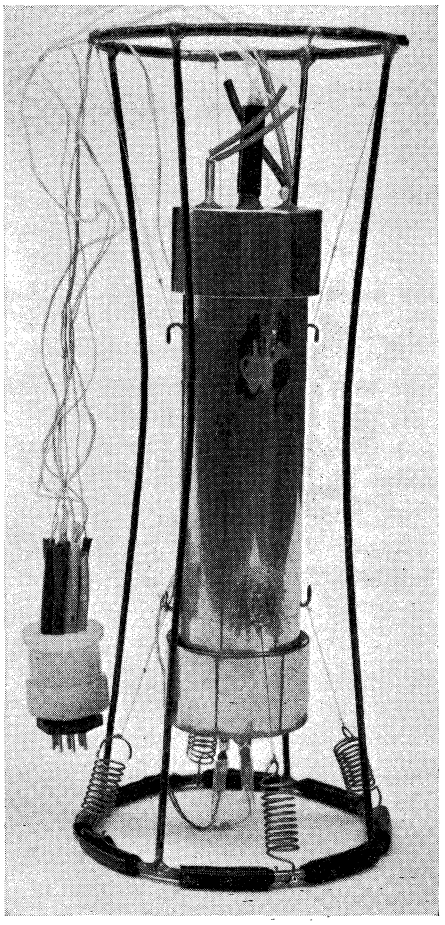

FIG. 2. Calorimeter vessel in flexible cradle.

quite conveniently with sections of neoprene stoppers. The sample cells are aligned with the supporting rods along two grooves in their sides. The coil spring (0.035 in. diam. wire) is held in compression by the 0.003 in. diameter stainless steel wire across the fuse connectors. Short plugs fitting tapered holes in the connectors keep the fuse wire in position and the cutting point is thus held about 1/4 in. from the cover glass. Larger-diameter copper leads (28 gauge) are used for making connection to the fuse to minimize the total resistance, the latter being 1 ohm. One of the fuse connectors is connected to the negative terminal of a 6-v storage battery which serves as the apparatus ground. A push-button switch allows opening of the sample cell by applying 6 v to the fuse wire when the latter is above the liquid level. It is not necessary to interrupt the rocking action to carry out this operation. Two calorimeter vessels are used, differing only in the volume of their sample cells, one being 2 ml and the other 5 ml.

The submarine, held in a metal clamp around its center, is attached by a set screw to a shaft passing through a graphitized-nylon bearing in the side of a temperature-controlled bath. The latter is kept as small as is possible yet allowing room for rotation of the submarine: the capacity of the bath is 35 l. A circulating pump provides rapid stirring and the bath can be heated electrically or cooled by passing cold tap water through an

Can. J. Chem. Downloaded from www.nrcresearchpress.com by 210.87.254.105 on 09/05/12
For personal use only.

immersed copper coil; the flow of cold water is controlled by a solenoid-operated valve and a reducing valve. The bath is well insulated with Styrofoam to allow use of the calorimeter at elevated temperatures. Figure 3 shows a photograph of the external features of the calorimeter.

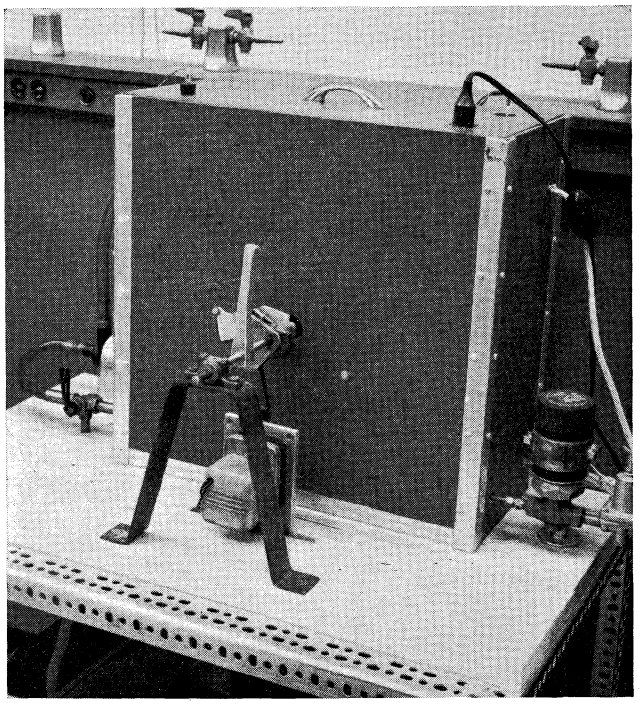

FIG. 3. External features of calorimeter showing rocking mechanism and bath.

A shielded nine-connector cable is soldered to a socket (female) which fits a connector sealed in the exit tube of the submarine cap (Fig. 1). It is necessary to minimize movement at the connection and this is achieved by fairly tight fitting of the socket in the glass tube. Also, the cable is bent at 90° just above the socket and the elbow made rigid up to the connector using epoxy resin. Rubber tubing is used to enclose the cable from its point of entry to the bath (through a metal tube in the wall) up to the glass tube of the submarine cap. This flexible connecting cable forms one coil adjacent to the side of the bath and is supported in its upper portion by very light springs. In this way the cable is kept clear of the submarine, rocking of which produces negligible strain on the electrical connections to the vessel.

Continuous rocking of the submarine through 180° is achieved using a rack and pinion movement (see Fig. 3). A brass arm attached to the shaft of a 7 r.p.m. motor is connected to the end of the rack, the point of connection describing a circle of diameter equal to half the circumference of the pinion. The latter is rigidly attached to the rotation shaft with a set screw but the brass mount, in which the rack moves linked to the pinion, is free to rotate about the shaft. The resulting motion is smooth and reliable, giving a slight dwell period at the vertical positions of the submarine. In this way good stirring of the calorimeter contents by the enclosed air bubble is obtained. Manual rotation can be readily accomplished by releasing the pinion set screw.

Can. J. Chem. Downloaded from www.nrcresearchpress.com by 210.87.254.105 on 09/05/12
For personal use only.

Electrical circuits connected with the instrument are shown schematically in Fig. 4. During electrical calibration of the calorimeter the current flowing through the heater

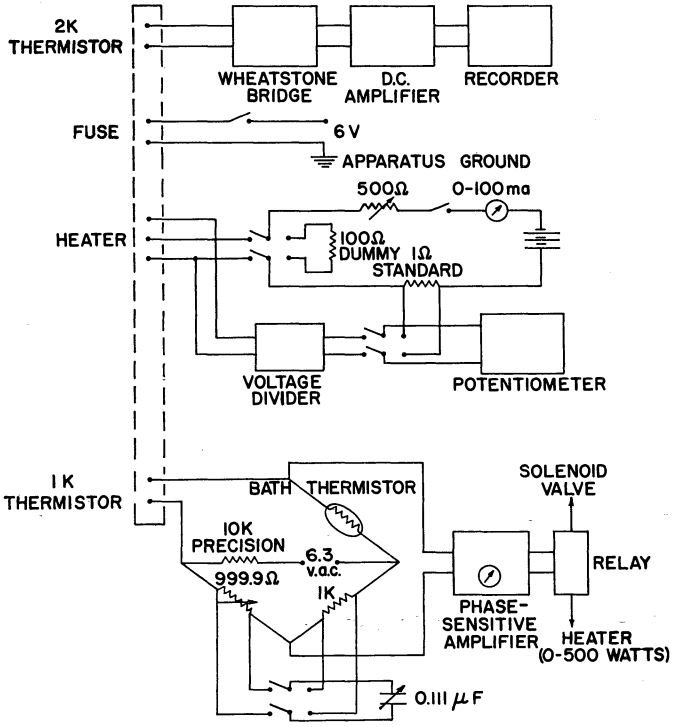

FIG. 4. Schematic diagram of electrical connections in the calorimeter.

and the e.m.f. applied across it are measured using a potentiometer (Honeywell–Rubicon Model 2781) and standard resistance in series with the heater. Five- or ten-minute heating periods are usually used and are timed to 0.02 second with an electric clock, the clutch of which is ganged with the heater circuit switch. The accuracy of timing using line frequency in this way has been checked by using a counter working in conjunction with an accurate crystal-controlled oscillator. The maximum difference in time interval recorded by the timer and by the counter, over a large number of heating periods, has been 0.01% and in the majority of cases agreement has been as good as the clock-reading error will allow. Current and e.m.f. readings are steady to better than 0.001% during a heating period, in which 20–50 cal are supplied to the vessel. Successive heat-capacity determinations usually agree within 0.05%. All calorimeter components are in a laboratory maintained at a constant temperature (±0.5° C) and 40% humidity. A regulated power supply is used for operating the calorimeter.

III. TEMPERATURE MEASUREMENT AND CONTROL

Temperature measurement is achieved by measuring the resistance of one of the thermistors (Veco A 60, approximately 2000 ohms at 25° C) with a Wheatstone bridge (Gray Instrument Co., E-1005 A) the off-balance signal from which is amplified and recorded (Leeds and Northrup microvolt amplifier 9835-B, Speedomax G Recorder, 1 mv full scale). Full scale of the recorder corresponds to 0.008° C with the sensitivity range

Can. J. Chem. Downloaded from www.nrcresearchpress.com by 210.87.254.105 on 09/05/12
For personal use only.

usually used. Under these conditions, electronic noise is negligible whereas a trace variation, synchronous with rocking of the vessel, is present. The width of the trace thus obtained is 0.1–0.2 μv (1–2% of recorder scale) and is regular. Some of this synchronous variation is no doubt due to motion of part of the measuring circuit in the earth's magnetic field and its magnitude can be greatly increased by a number of factors, such as loose-fitting connectors or poor electrical insulation of the heater. Periodic variation of the temperature of the medium adjacent to the thermistor will also occur during rocking because of its power dissipation, but this is minimized by applying as low a voltage as possible to the Wheatstone bridge; in the present case 0.2 v is used.

The thermistor is calibrated by finding its resistance at a number of points between 0 and 50° C using a calibrated thermometer (NBS certificate). Least-squares analysis of the data using a computer gives the constants in the equation

$$R_T = R_0 e^{\beta(1/T - 1/T_0)}, \quad [1]$$

where R_0 is the resistance at a standard temperature T_0, for which 298.15° K is chosen. Subsequent conversion of resistance values to temperatures is straightforward but requires the use of seven-figure logarithms to obtain values accurate to 0.00001° C. If a computer is not available, temperature changes, ΔT, can often be more readily computed using a differentiated form of equation [1]:

$$\frac{dR_T}{dT} = -R_T\beta\left[\frac{1}{T_0^2} + \frac{2}{\beta T_0}\ln\frac{R_T}{R_0} + \frac{1}{\beta^2}\left(\ln\frac{R_T}{R_0}\right)^2\right] \quad [2]$$

and

$$\Delta T \simeq \frac{\Delta R}{dR_T/dT} \text{ (using mean } R_T\text{)}. \quad [3]$$

These equations are accurately and readily applied to small temperature changes in the vicinity of T_0 since only the first term in eqn. [2] is then significant. The error introduced by ignoring the second term, roughly proportional to ΔT, is about 0.4% per degree ΔT, and a correction using the second term is not difficult to apply for greater precision (the third term can be ignored). Long-term drift rates in thermistor resistance values, following thermal shock, have recently been studied (4). The results are very pertinent to the use of thermistors in accurate calorimetry studies.

Automatic adiabatic control in the calorimeter is achieved using a circuit described by Cleland and Harding (5). Two thermistors, one in the calorimeter vessel and one in the bath, form arms of a resistance bridge, the other arms being a precision 1K resistance and a 4-dial decade resistance (cf. Fig. 4). A variable capacitance (3-dial decade) can also be connected in parallel to either of the resistance arms and allows good balancing of the bridge to be achieved without the care otherwise needed in mounting thermistors (5). The thermistors used (Veco 31A16, approximately 1000 ohms at 25° C) are chosen so that the ratio of their resistance is almost independent of temperature. In order to reduce power dissipation by the vessel thermistor, only 0.27 v A.C. is applied to the bridge and for this reason an extra amplification stage has been added to the original circuit together with a meter to record the amplified signal. The circuit is stable and actuates the solenoid valve and bath heater, giving a uniform sawtooth temperature control ($\pm$0.01° C). The bath temperature is monitored using another thermistor bridge circuit and recorder. Adiabatic conditions are maintained for all reasonable rates of temperature variation, exceptions being dealt with as outlined later.

Can. J. Chem. Downloaded from www.nrcresearchpress.com by 210.87.254.105 on 09/05/12
For personal use only.

IV. EXPERIMENTAL PROCEDURE

Before loading the calorimeter vessel, the contents are cooled below the desired temperature of solution or dilution. A partial vacuum is created in the submarine, heat transfer only being affected by a factor of 3 by the presence or absence of air around the vessel (1); under these conditions K, the thermal leakage modulus, is approximately 0.01° C per minute per °C head for a vessel having a heat capacity of 65 cal/°C and compares with values for similar calorimeters (1, 2). Unless a high vacuum can be continually maintained in the submarine, such as by installing another flexible connection, it is thought best to use only a partial vacuum in order to minimize desorption effects which might otherwise occur.

The calorimeter is brought to a steady state at the required temperature by heating the vessel and by finding the control bridge setting which then keeps the vessel virtually adiabatic. This setting is constant for a particular vessel and varies only slightly with the contents, except when the latter are poor thermal conductors. The calorimeter temperature is rarely exactly constant but varies linearly with time, the drift rate being usually less than 0.0001° C per minute. A regular variation of the vessel temperature, synchronous with the bath on–off cycle (about 1 minute), is just discernible (±about 0.00001° C).

After approximately 15 minutes of steady-state behavior, the sample cell is opened and the amplifier sensitivity reduced. For endothermic or exothermic changes, ice or hot water, respectively, is added to the bath at such a rate as to keep the bath and vessel temperatures nearly equal as indicated by the control circuit meter. This is only necessary during the initial rapid temperature change and the circuit is able to take over control again after some 10–20 seconds. Approximately 15 minutes after the heat change a steady state is again reached and, after adjusting the setting of the Wheatstone bridge, a linear drift rate, usually of a slightly different slope, is recorded. After a further period of time, sufficient for temperature-trace extrapolation, a heating period is carried out during which the calorimeter is kept adiabatic automatically. The recorder chart is calibrated in terms of resistance by obtaining a suitable shift of trace on altering the Wheatstone bridge setting.

Extrapolation of the temperature trace to the 'time of half-heating' allows estimation of ΔT. This value is usually found accurately since there is little change in drift rate before and after a heat change. With heating periods the 'time of half-heating' is well defined and most solution and dilution processes are virtually instantaneous.

V. THE HEAT ASSOCIATED WITH OPENING SAMPLE CELLS

The ultimate accuracy of the calorimeter, when measuring small heat changes, is limited by the reproducibility with which the blank heat change accompanying the opening of sample cells, q_b, can be measured. One of the main sources of variation in such values has been the heat change involved in fracture of glass cells (see reference 1), but in the method described this variation is minimized by using standard cover glasses, very thin, which are almost completely shattered and removed every time during breaking.

In a series of experiments using water in the vessels, q_b was found to be 0.032±0.003 cal (heating) and 0.006±0.007 cal (cooling) for the 2-ml and 5-ml cells, respectively. When the cells contained water prior to opening, the respective values of q_b were 0.046 cal and 0.035 cal (both heating). The differences for each cell when empty and when containing water correspond closely to the values calculated for the heat of evaporation from 40% to 100% relative humidity. The greater variation of q_b values for the larger cell is consistent with variations of room humidity. With sufficient information regarding the

Can. J. Chem. Downloaded from www.nrcresearchpress.com by 210.87.254.105 on 09/05/12
For personal use only.

humidity at the time of loading and the vapor pressure of solutions it is therefore possible to make accurate allowance for q_b.

VI. THE HEAT OF SOLUTION OF SODIUM CHLORIDE AT 25° C

In order to assess the performance of the calorimeter, the integral heat of solution of sodium chloride in water was found in the concentration range 0.02 to 0.7 molal and the values compared with those found by other investigators as summarized in reference 1.

The water used for these studies was distilled and then passed through an ion-exchange column (Illco-way research model). No attempt was made to remove dissolved gases. The sodium chloride used was Baker Analyzed reagent (100.0% assay) which was dried at 110° C and stored in a desiccator over P_2O_5. The particle size was ~1 mm and should therefore exhibit negligible surface energy effects. The salt was considered sufficiently pure from its batch analysis to be used without further purification.

Only the small (2 ml) sample cell was used and 48 ml of water was weighed into the vessel. Weights were corrected to vacuum and results stated in terms of the defined calorie (4.1840 absolute joules). The vapor space in the vessel above the solution was approximately 5 ml and errors due to the heat effect associated with changes in water vapor pressure on solution were negligible. Solution was effected near 25.0° C and heat-capacity data of aqueous sodium chloride (6), water, and sodium chloride (7) were used to correct for small deviations from this temperature. Heat changes measured in these runs varied from 0.8 to 35 cal.

Results are shown in Table I. They are found to agree well with the smoothed values given by Benson and Benson (1) together with the heat of dilution data of Robinson below

TABLE I

The heat of solution of sodium chloride in water at 25.0° C

Molality	ΔH_S (cals/mole)	% deviation from smoothed values (1, 8, 9)	Molality	ΔH_S (cals/mole)	% deviation from smoothed values (1, 8, 9)
0.0188	971.9	−0.22	0.1040	1005.0	−0.35
0.0214	968.0	−0.89	0.2035	1013.2	−0.31
0.0270	978.1	−0.38	0.2706	1014.0	+0.12
0.0303	984.7	+0.04	0.3515	1002.7	−0.09
0.0304	978.0	−0.61	0.3590	1004.6	+0.19
0.0310	978.7	−0.58	0.3626	1003.7	+0.14
0.0429	986.0	−0.55	0.3770	1000.1	−0.03
0.0444	996.4	+0.27	0.3774	1001.9	+0.15
0.0508	1000.6	+0.52	0.3795	1000.8	+0.07
0.0518	998.5	+0.27	0.5327	979.3	−0.01
0.0601	1005.2	+0.62	0.7198	951.8	+0.06
0.0656	1002.3	+0.15			

0.05 molal (8), summarized by Harned and Owen (9). Percentage deviations of the present results from these smoothed data are shown in Table I and it can be seen that agreement is almost exact above 0.1 molal with a mean deviation of the results equal to ±0.1%. Below 0.1 molal the results fall slightly lower (0.1% mean) than the smoothed values and agree within themselves to ±0.4%. The performance of the calorimeter, as judged by these results, is considered to be quite satisfactory and compares well with other adiabatic solution calorimeters (cf. Fig. 4, ref. 1) particularly in view of the relatively small volume of solution required. The reproducibility of q_b allows reasonable precision to be maintained in the measurement of small heat changes of the order of a calorie or less.

Can. J. Chem. Downloaded from www.nrcresearchpress.com by 210.87.254.105 on 09/05/12
For personal use only.

ACKNOWLEDGMENTS

The author is grateful for the assistance of Messrs G. McNeil and N. E. Gilman during design, construction, and operation of the calorimeter and for the advice and encouragement of Dr. W. L. Courchene and other colleagues in these laboratories.

REFERENCES

1. G. C. Benson and G. W. Benson. Rev. Sci. Instr. **26**, 477 (1955).
2. G. C. Benson, E. D. Goddard, and C. A. J. Hoeve. Rev. Sci. Instr. **27**, 725 (1956).
3. S. R. Gunn. Rev. Sci. Instr. **29**, 377 (1958).
4. J. H. Swartz and R. Raspet. Nature, **190**, 875 (1961).
5. W. W. Cleland and R. S. Harding. Rev. Sci. Instr. **28**, 696 (1957).
6. S. G. Lipsett, F. M. G. Johnson, and O. Maass. J. Am. Chem. Soc. **49**, 1940 (1927).
7. Handbook of chemistry and physics. 43rd ed. Chemical Rubber Publishing Co., Cleveland, Ohio. 1961. pp. 2297, 2309.
8. A. L. Robinson. J. Am. Chem. Soc. **54**, 1311 (1932).
9. H. S. Harned and B. B. Owen. The physical chemistry of electrolytic solutions. 3rd ed. Reinhold Publishing Corporation, New York. 1958. p. 333.

Can. J. Chem. Downloaded from www.nrcresearchpress.com by 210.87.254.105 on 09/05/12
For personal use only.

SPECTROPHOTOMETRIC STUDY OF XANTHATE AND DIXANTHOGEN SOLUTIONS

A. POMIANOWSKI[1] AND J. LEJA
Department of Mining and Metallurgy, University of Alberta, Edmonton, Alberta

Received March 29, 1963

ABSTRACT

Xanthate solutions of pH 6–10, prepared from "aged" potassium ethyl xanthate crystals, KEtX, were investigated spectrophotometrically in the region 190–400 mμ and showed coexistence of xanthate ions, EtX^-, dixanthogen, $(EtX)_2$, and carbon disulphide, CS_2. Optical density measurements on the spectra of dixanthogen solutions led to the evaluation of: molar absorptivities of dixanthogen at wavelengths corresponding to the two main bands in the xanthate ion spectrum, i.e. at 301 mμ—6130 liter/mole cm, and at 226 mμ—18,400 liter/mole cm; the solubility of dixanthogen, ca. 1.3×10^{-5} mole/liter; and the equilibrium constant, $k = 3\times10^{10}$, of the reaction $2(EtX)_2 + 4OH^- \rightarrow 4EtX^- + 2H_2O + O_2$, for solutions saturated with air at atmospheric pressure. Simultaneous reactions leading to decomposition of xanthate and/or dixanthogen species to alcohol and carbon disulphide have been detected by a strong band at 206.5 mμ due to CS_2 (with an estimated molar absorptivity of the order of 60,000–70,000 liter/mole cm).

The behavior of xanthates in solution (particularly their dissociation, decomposition on acidification, and oxidation) has been the subject of numerous investigations. Yet, owing to the complexity of the xanthate systems, many aspects have not been clarified. In the recent papers of Majima (1, 2) the relevant literature is reviewed and new data are presented (based on ultraviolet spectrophotometry) concerning the dissociation, decomposition, and stability constants of alkyl xanthates from methyl to amyl, and lead, nickel, and cobalt xanthate complexes. Solubilities of numerous metal xanthates have been correlated in great detail by Sheka and Kriss (3) while Wronski (4) discusses the effects of increased pH in xanthate solutions.

In investigating the kinetics of xanthate adsorption from mixed solutions containing quaternary ammonium compounds the use of ultraviolet spectrophotometric analyses of these mixed solutions necessitated a preliminary study of various products of xanthate decomposition. The most probable reactions involved in the decomposition of xanthate solutions are hydrolysis and formation of xanthic acid, [1]; decomposition to alcohol and CS_2, [2]; and oxidation to dixanthogen, [3]:

$$\begin{aligned} &ROCS_2^-K^+ + H_2O \rightarrow ROCS_2H + K^+OH^- \\ &ROCS_2^-K^+ + H^+Cl^- \rightarrow ROCS_2H + K^+Cl^- \end{aligned} \qquad [1]$$

$$\begin{aligned} &ROCS_2^-K^+ + H^+Cl^- \rightarrow ROH + CS_2 + K^+Cl^- \\ &ROCS_2H + H_2O \rightarrow ROH + CS_2 + K^+OH^- \end{aligned} \qquad [2]$$

$$2(ROCS_2^-K^+) + H_2O + \tfrac{1}{2}O_2 \rightarrow (ROCS_2)_2 + 2(K^+OH^-). \qquad [3]$$

Of these reactions, the production of xanthic acid and the subsequent decomposition to alcohol and CS_2, particularly in low pH regions, have been most recently studied by Iwasaki and Cooke (6), Klein *et al.* (7), and Majima (1). The oxidation to dixanthogen has been considered irreversible and of little interest, particularly since tests with O_2 bubbled through xanthate solutions indicated this to be a slow reaction (Iwasaki and Cooke (6), Rao and Patel (8)); dixanthogen itself has been considered insoluble in water and no analytical method appears to be available for accurate determination of small quantities of dixanthogen.

[1]*On leave from the Institute of Physical Chemistry, Polish Academy of Sciences, Krakow, Poland.*

Can. J. Chem. Downloaded from www.nrcresearchpress.com by 210.87.254.42 on 09/05/12
For personal use only.

Klein *et al.* (7) recorded the infrared and ultraviolet spectra of xanthic acid, and evaluated the absorptivity of its pronounced absorption band at 270 mμ as 10,670 liter/mole cm, and at 301 mμ (the major band of xanthate anion) as 117 liter/mole cm. However, in their work on fast decomposition of xanthate in acid solutions only the region 310–260 mμ was scanned.

EXPERIMENTAL

Ultraviolet spectra in the region 190–400 mμ were recorded on a Perkin–Elmer 350 spectrophotometer, using 10 mm path length quartz cells for 10^{-5}–10^{-4} *M* solutions, and 0.8 mm path length microcells for 10^{-4}–2×10^{-3} *M* solutions.

Xanthate compounds (potassium salts of ethyl, butyl, hexyl, and nonyl xanthates) were prepared by the standard method of reacting the corresponding alcohols with KOH, treating the alcoholates with CS_2, and doubly recrystallizing the xanthates from acetone solutions. Their purity (over 99%) was checked by titration with iodine and by comparison of their infrared spectra with those obtained previously (5) on samples analyzed microchemically for individual elements. Ethyl dixanthogen was prepared by oxidation of potassium ethyl xanthate solutions with iodine, extraction of dixanthogen with ether, and evaporation of ether.

Aqueous solutions were prepared using water distilled once in presence of air; when necessary, the pH was adjusted using $Na_2CO_3.9H_2O$, $KHCO_3$, or NaOH.

RESULTS AND INTERPRETATION

The ultraviolet absorption spectra of freshly recrystallized potassium ethyl xanthate (KEtX) are given in Fig. 1. They show two strong maxima, at 301 mμ and 226 mμ, an

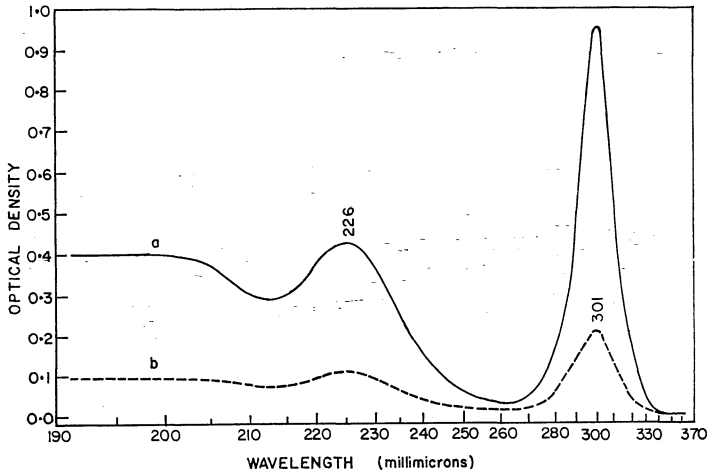

FIG. 1. Ultraviolet spectra of solutions of pure potassium ethyl xanthate (KEtX): (*a*) 1×10^{-4} mole/liter; (*b*) 2.3×10^{-5} mole/liter.

absorption plateau below approximately 200 mμ, and a very weak band at 380 mμ appearing only in concentrated solutions. Two deep minima are observed at 264 mμ and 213 mμ.

The applicability of Beer's law was established for KEtX concentrations of 3×10^{-5}–1.5×10^{-3} *M* solutions, Fig. 2, with the average molar absorptivities (extinction coefficients) equal to ϵ_{226} = 8,920 liter/mole cm and ϵ_{301} = 17,750 liter/mole cm (compared to ϵ_{226} = 8,780 and ϵ_{301} = 17,460 given by Majima (1)). The ratio of optical densities was d_{226}/d_{301} = 0.504 with an average deviation of ±0.005.

It was observed, however, that the optical densities in the region below approximately 280 mμ were affected by the length of the storage period since recrystallization of the

Can. J. Chem. Downloaded from www.nrcresearchpress.com by 210.87.254.42 on 09/05/12
For personal use only.

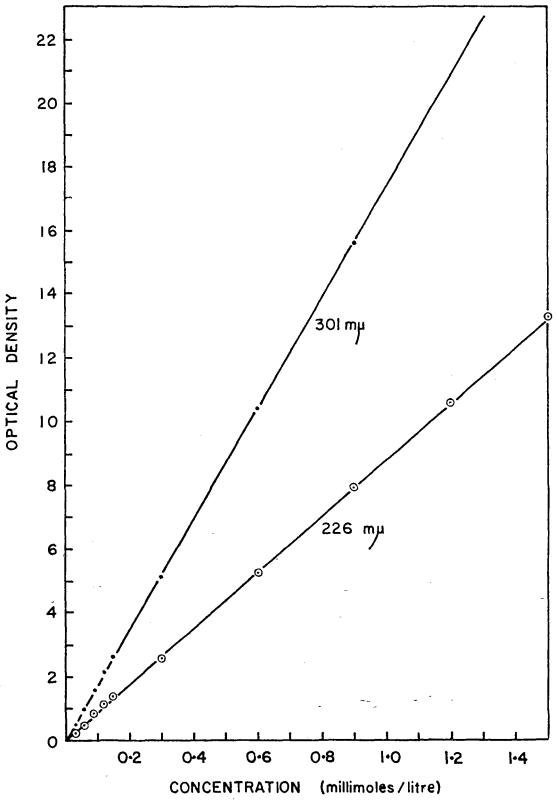

FIG. 2. Optical density vs. concentration of pure KEtX.

solid xanthate, and also by the method of preparation of the solutions. Spectra of dilute solutions (10^{-5}–10^{-4} M) obtained by dissolution of the required quantity of finely crystalline potassium ethyl xanthate (which was stored for prolonged time in dark) showed higher optical densities in the region below 280 mμ than the solutions obtained by dilution of 10^{-2} M stock solution or those obtained by dissolution of freshly recrystallized solid xanthate. The appearance of this "background" in the spectrum, chiefly responsible for an increase in the optical density of the 226 mμ maximum, resulted in the observed variations in the ratio of optical densities d_{226}/d_{301} ranging from 0.49–0.53. A more detailed investigation of xanthate solutions, and decomposition products, was undertaken with the view of uncovering the cause of this "background".

(a) Xanthic Acid

Comparison of several spectra obtained from solutions stored for several days or prepared from "aged" solid xanthates with the spectra of freshly recrystallized xanthates indicated that xanthic acid formation, with its pronounced maximum at 270 mμ, was not likely to be the primary cause of the general "background" at lower wavelengths. A spectrum of xanthic acid extracted by chloroform from acidified xanthate solution is shown in Fig. 3.

(b) Carbon Disulphide

At 22° C the solubility of CS_2 in water is given as 2.2 g/liter (9); because of its very

Can. J. Chem. Downloaded from www.nrcresearchpress.com by 210.87.254.42 on 09/05/12
For personal use only.

high absorptivity below about 380 mμ, CS_2 is not used as a solvent in ultraviolet spectrophotometry. The spectrum of a CS_2 solution (containing 3 ml of water saturated with CS_2 and diluted to 1000 ml) is shown in Fig. 3. Accepting the above figure for CS_2 solubility,

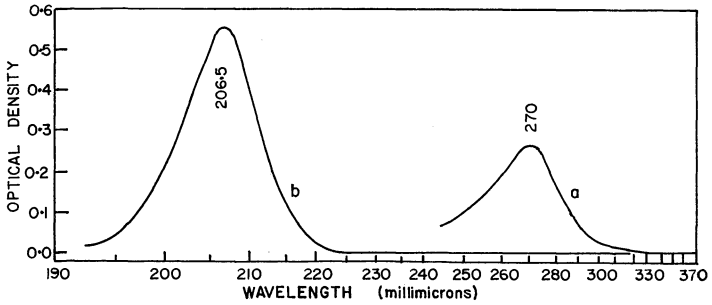

FIG. 3. Ultraviolet spectra of: (*a*) ethyl xanthic acid (EtXH) in chloroform extract from acidified KEtX solution; (*b*) carbon disulphide in water (3 ml of CS_2 saturated aqueous solution diluted to 1 liter).

the absorptivity at 206.5 mμ was estimated to be 60,000–70,000 liter/mole cm. Owing to high vapor pressure of CS_2 (400 mm Hg at 28° C) it easily volatilizes out of solution unless the cell is tightly corked.

(c) Dixanthogen

Ethyl dixanthogen was shaken with distilled water to obtain saturated solution, and its spectrum recorded; also, dixanthogen was dissolved in various solvents (chloroform, ethyl alcohol, ethyl ether) to determine its absorption bands. The spectra are shown in Fig. 4. It is seen that two wide absorption bands are present between 280–300 mμ and

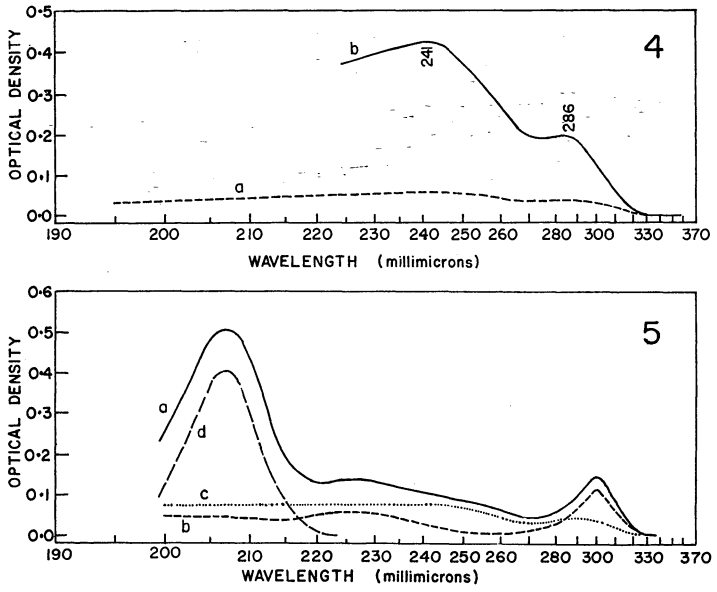

FIG. 4. Ultraviolet spectra of ethyl dixanthogen $(EtX)_2$: (*a*) freshly prepared aqueous solution in distilled water; (*b*) 4.1×10^{-5} mole/liter solution in ethyl ether.

FIG. 5. Sequence of ultraviolet spectra indicating the products of dixanthogen decomposition: (*a*) saturated dixanthogen solution (after prolonged contact of dixanthogen with distilled water); (*b*) xanthate solution—equivalent to the difference of (*a*) and (*c*); (*c*) freshly prepared dixanthogen solution; (*d*) CS_2 solution—difference of (*a*), (*b*), and (*c*).

Can. J. Chem. Downloaded from www.nrcresearchpress.com by 210.87.254.42 on 09/05/12
For personal use only.

220–250 mμ which, for the 4.1×10^{-5} *M* solutions of dixanthogen in ethyl ether, are more clearly defined at 286 mμ and 241 mμ. It is clear from these spectra that any formation of dixanthogen in xanthate solutions raises the optical densities of xanthate spectra at 301, 226, and below 200 mμ.

When distilled water (final pH 5.9–6.1) was kept in contact with dixanthogen (in well-stoppered flasks) for several days, the resultant spectrum, curve *a* in Fig. 5, indicated the presence of all three species: xanthate ion (301 mμ band), dixanthogen (~240 mμ band), and carbon disulphide (206.5 mμ). It was found that a stationary state was reached in this solution only after 15–20 days.

When the supernatant water (in a duplicate experiment) was decanted and centrifuged, then treated with NaOH to pH ~10, the sequence of spectra obtained after 15 minutes at 22° C, and after 2 hours at 40° C, showed a gradual transition of dixanthogen to xanthate with the concurrent appearance of CS_2, Fig. 6.

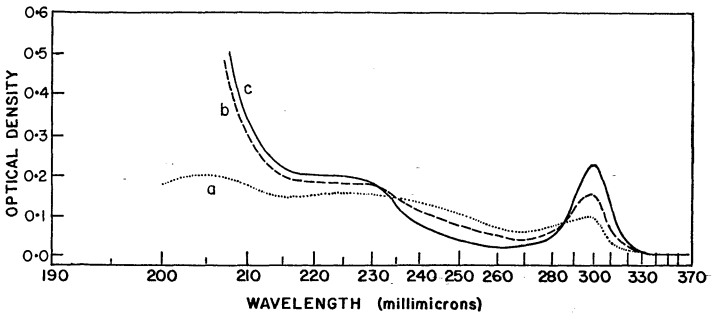

FIG. 6. Changes with time in the ultraviolet spectrum of ethyl dixanthogen aqueous solution at pH 10: (*a*) initial spectrum of aqueous dixanthogen (shaken with distilled water at pH 6, allowed to stand several hours in order to settle the suspension); (*b*) spectrum taken 15 minutes (at 22° C) after the addition of NaOH to raise the pH of solution (*a*) to pH 10; (*c*) the same solution as (*b*) after 2 hours at 40° C.

The reactions involved are:

$$2(EtX)_2 + 4OH^- + 4K^+ \rightarrow 4EtX^- + 2H_2O + O_2 + 4K^+; \quad [4]$$

which is the reverse reaction to [3], i.e. oxidation of xanthate in solution; and the simultaneous decomposition of either xanthate ions, or dixanthogen:

$$EtX^- + K^+ + H_2O \rightarrow EtOH + CS_2 + KOH \quad [5]$$

$$(EtX)_2 + H_2O \rightarrow 2EtOH + 2CS_2 + 2OH^-. \quad [6]$$

The stoichiometric overall reaction is, therefore,

$$2(EtX)_2 + 2OH^- + 2K^+ \rightarrow 2EtX^- + 2EtOH + 2CS_2 + 2K^+ + O_2. \quad [7]$$

The increase in the optical densities below 280 mμ observed in the spectra of solutions prepared from aged potassium ethyl xanthate was ascribed to the oxidation taking place on the surface of the solid xanthate, resulting in dixanthogen and carbonate:

$$2KEtX + \tfrac{1}{2}O_2 + CO_2 \rightarrow (EtX)_2 + K_2CO_3. \quad [8]$$

An attempt was made to obtain qualitative evidence for the existence of dixanthogen and carbonate on the surfaces of aged crystals, using infrared spectroscopy of mulls in hexachlorobutadiene. The band at ~1450 cm^{-1}, shown by all carbonates (10), was, however, masked by the C—H deformation band of the hydrocarbon radical in the xanthate. A weak band at ~1260 cm^{-1} indicated the presence of dixanthogen (5) on the surface of crystals.

Can. J. Chem. Downloaded from www.nrcresearchpress.com by 210.87.254.42 on 09/05/12
For personal use only.

A solution of aged xanthate had its pH raised to 8.5 by $KHCO_3$ and was kept for 19 hours at 85° F. The spectra obtained from the initial and the final states of this solution, Fig. 7, show an increase in optical density at 301 mμ due to the formation of EtX^- anion

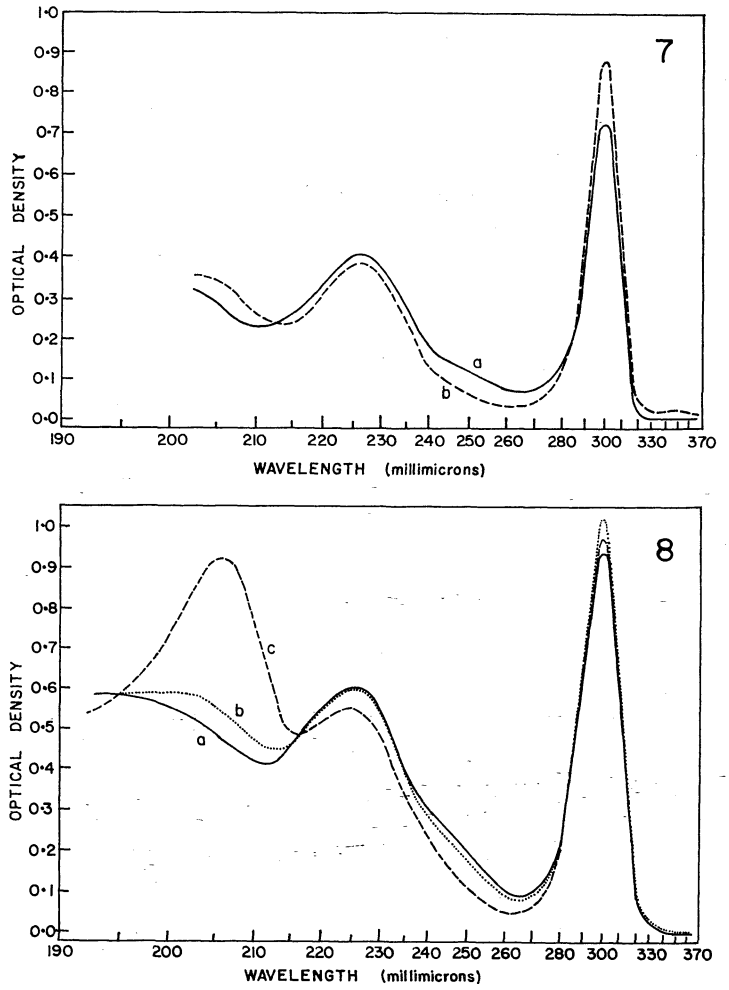

FIG. 7. Decomposition in xanthate solution: (*a*) the ultraviolet spectrum of pure potassium ethyl xanthate solution, ca. 0.9×10^{-4} mole/liter, freshly prepared in water of pH 8.5; (*b*) the same as (*a*) after 19 hours at 85° F.

FIG. 8. Ultraviolet spectra of 1.1×10^{-4} mole/liter ethyl xanthate solution at pH 6, kept in closed cell at 98° F for (*a*) 0 hours, (*b*) 7 hours, (*c*) 24 hours.

from dixanthogen decomposition, a reduction in optical densities in the range 216–280 mμ due to disappearance of some dixanthogen, and an increase in optical densities below 216 mμ caused by the formation of CS_2. Even freshly made ethyl xanthate solution of pH 6, kept at 98° F in a well-stoppered flask, indicated a progressive decomposition of dixanthogen initially present on the surface of the aged solid xanthate, Fig. 8. The sequence of changes in optical densities at 301 mμ, i.e. an increase after 7 hours followed by a decrease after 24 hours, may be significant and may indicate that, under the conditions of the experiment, the decomposition of dixanthogen to xanthate (shown by reaction [4]) is faster than the decomposition to carbon disulphide and alcohol.

Can. J. Chem. Downloaded from www.nrcresearchpress.com by 210.87.254.42 on 09/05/12
For personal use only.

Using spectra of solutions contaminated by dixanthogen (reaction [8]), the measured optical densities were compared with those obtained on freshly recrystallized xanthate (Fig. 2) to evaluate the absorptivities of dixanthogen at 226 and 301 mμ (the major bands in the spectrum of pure xanthate solution); for this, an assumption was made that the ratio of absorptivities for dixanthogen is $\epsilon^{D}_{301} = \frac{1}{3}\epsilon^{D}_{226}$. This assumption is supported by the relative optical density measurements:

$$\frac{d_{226}}{d_{301}} = \sim 3 \text{ for water solutions of dixanthogen,}$$
$$\sim 3.2 \text{ for ethyl alcohol solutions of dixanthogen,}$$
$$\sim 2.8 \text{ for methyl alcohol solutions of dixanthogen,}$$
$$\sim 3.1 \text{ for ethyl ether solutions of dixanthogen.}$$

The calculation is given in the Appendix. The absorptivities of dixanthogen at 301 and 226 mμ thus evaluated were then used to calculate the solubility of dixanthogen in water (using spectra of appropriate solutions) and the equilibrium constant of reaction [4] (see Appendix). The results are listed in Table I with data from literature.

TABLE I
Summary of spectrophotometric data for dixanthogen and related compounds

	Wavelength, mμ	ε, liter/mole cm	Solubility, mole/liter (at 22° C)
Ethyl dixanthogen	226	18,300	1.3×10^{-5}
	301	6,100	
Ethyl xanthate ion	226	8,920	(~1–2)
	301	17,750	
Ethyl xanthic acid (6)	270	10,670	(Unstable, the monomolecular decomposition rate constant was determined to be 4.3 min^{-1})
	(301)	(117)	
Carbon disulphide (9)	206.5	>60,000	(ca. 3×10^{-2})

It was also of interest to study spectrophotometrically the standard method of titration of xanthate solution with iodine, according to the accepted reaction

$$I_3^- + 2EtX^- \rightarrow (EtX)_2 + 3I^-. \qquad [9]$$

At concentrations of iodine used (0.1 *M* in 2.5 *M* KI) the spectra of aqueous iodine solutions are free from maxima down to 250 mμ. (At higher concentration, two weak maxima at 355 mμ and 288 mμ appear.) Below 250 mμ, two strong iodide maxima at 226.5 mμ and 193.5 mμ make it practically impossible to interpret spectra of xanthates in this region.

When a dilute solution of potassium ethyl xanthate is titrated with iodine, a progressive lowering of optical density at 301 mμ is obtained with the appearance of an isosbestic point at 278 mμ for 5.2×10^{-5} *M* EtX^-.

The isosbestic point is shifted during the titration with I_2 towards the 301 mμ maximum of xanthate ion, as shown schematically in Fig. 9. This "shift in isosbestic point" is due to the formation of one molecule of dixanthogen from two ions of xanthate, hence the xanthate concentration falls off twice as fast as the dixanthogen concentration increases.

If the initial xanthate concentration used for titration is high, so that the dixanthogen formed on oxidation exceeds the solubility, the solution becomes opalescent as a result of formation of dixanthogen emulsion. Departures in optical density readings become evident, as shown in Fig. 10, where the points represent the actual readings and the line

Can. J. Chem. Downloaded from www.nrcresearchpress.com by 210.87.254.42 on 09/05/12
For personal use only.

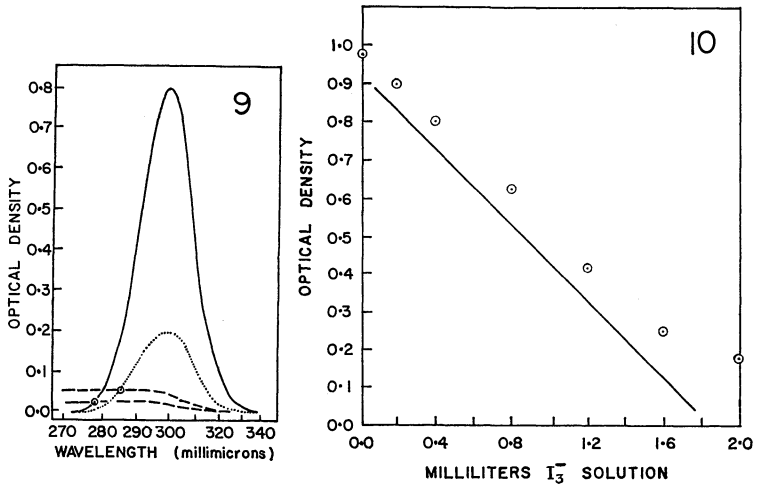

FIG. 9. "Shift in the isosbestic point" during conversion of ethyl xanthate to dixanthogen, on titration with iodine solution (schematic).

FIG. 10. Optical density at 301 mμ on 20 ml solution of "aged" ethyl xanthate titrated with iodine solution, 5.56×10^{-4} N I_3^-.

represents the theoretical optical densities of xanthate ions alone, based on stoichiometry of reaction.

DISCUSSION

The evidence obtained from spectrophotometric measurements on xanthate solutions containing dixanthogen shows not only the instability of dixanthogen but also the existence of other concurrent reactions. In order to describe an aqueous xanthate solution at a given pH, temperature, and pressure, at least the following six reactions have to be taken into consideration:

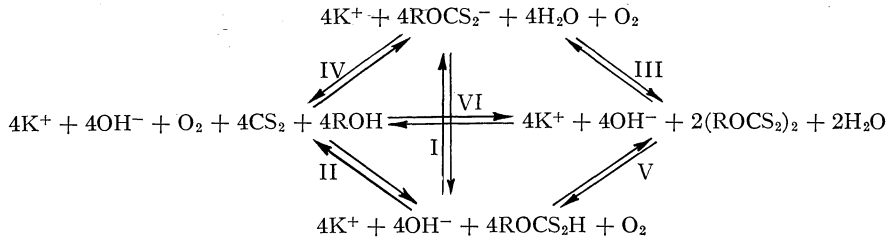

Of these reactions I, II, and III have been long recognized and studied, but both II and III have been generally considered irreversible, yielding CS_2 and dixanthogen, respectively. Spectra presented above show the reversibility of reaction III, and the appearance of the CS_2 band indicates the occurrence of either the reaction VI, IV, or II. Reaction IV is that employed in the standard method of xanthate production and its reversibility is not unexpected. The occurrence of xanthic acid in solutions of pH 6–10 has not been substantiated in this spectrophotometric work but it does not mean that reactions I, II, or V do not take place. Accepting the equilibrium constant derived by Iwasaki and Cooke (6) for reaction I, $K = ([EtX^-][H^+])/[EtXH] \simeq 2\times10^{-2}$, and applying it to pH 6 with activity of H^+ equal to concentration, the concentration of xanthic acid present in 10^{-5} M

Can. J. Chem. Downloaded from www.nrcresearchpress.com by 210.87.254.42 on 09/05/12
For personal use only.

solution of xanthate ions is found to be of the order of

$$[EtXH] = \frac{[EtX^-][H^+]}{K} \simeq \frac{10^{-5} \cdot 10^{-6}}{2 \cdot 10^{-2}} = \frac{1}{2} \cdot 10^{-9}\ M.$$

Using the molar absorptivity derived by Klein *et al.* (7), the optical density change expected from this concentration of xanthic acid would be $\Delta d_{270} = 10{,}670 \times 5 \times 10^{-10} = 5.3 \times 10^{-6}$, i.e. well outside the possibility of detection even when using a 10 cm optical path length cell.

Similarly, other reactions resulting in the formation of sulphides and trithiocarbonates, investigated by Klauditz (11) in highly alkaline xanthate solutions, may also be involved in the overall scheme of xanthate reactions, but could not be detected spectrophotometrically under the conditions employed.

The intermediate equilibrium constant for reaction [4], viz., $k = [EtX^-]^2/([OH^-]^2 \times [(EtX)_2]) \simeq 3.3 \times 10^{10}$ (see Appendix), evaluated from spectrophotometric measurements of dixanthogen solutions, can be used to calculate the approximate concentrations of ethyl dixanthogen in xanthate solution of different concentrations and at different pH (see Table II). It is seen that solutions of ethyl xanthate become saturated with respect

TABLE II

Approximate concentrations of ethyl dixanthogen, mole/liter, in equilibrium with xanthate ions at different pH values

	[EtX⁻], mole/liter			
pH	10^{-3}	10^{-4}	10^{-5}	10^{-6}
5				(3×10^{-5})
6			(3×10^{-5})	3×10^{-7}
7		(3×10^{-5})	3×10^{-7}	3×10^{-9}
8	(3×10^{-5})	3×10^{-7}	3×10^{-9}	3×10^{-11}
9	3×10^{-7}	3×10^{-9}	3×10^{-11}	3×10^{-13}
10	3×10^{-9}	3×10^{-11}	3×10^{-13}	3×10^{-15}
11	3×10^{-11}	3×10^{-13}	3×10^{-15}	3×10^{-17}
12	3×10^{-13}	3×10^{-15}	3×10^{-17}	3×10^{-19}

to ethyl dixanthogen at different pH values depending on the concentration of xanthate ion; for 10^{-3}, 10^{-4}, 10^{-5}, 10^{-6} M concentrations of xanthate ions in solutions, the saturation points are respectively just above pH 8, 7, 6, and 5.

For pH values lower than these saturation points the solutions exposed to air are supersaturated by dixanthogen, the excess of which forms an emulsion (or lenses at the air/water interface).

Figures in parentheses denote amounts of dixanthogen in excess of its saturation, ca. 1.3×10^{-5} M. Under the conditions of pH lower than the saturation pH, there is no tendency of the excess dixanthogen to be converted to xanthate since the equilibrium values (in parentheses) exceed the solubility value. However, if an excess of dixanthogen is initially present at a higher pH (where equilibrium values in Table II are smaller than the solubility), then the reaction of converting dixanthogen to xanthate takes place until the concentration of dixanthogen is reduced to the equilibrium value.

Using the constant K obtained by Iwasaki and Cooke (6), $K = ([EtX^-][H^+])/[EtXH] \simeq 2 \times 10^{-2}$, and the intermediate equilibrium constant k obtained in this work, $k = [EtX^-]^2/([OH^-]^2[(EtX)_2]) \simeq 3.3 \times 10^{10}$, together with $[OH^-][H^+] = 10^{-14}$, the ratio of dixanthogen to xanthic acid present in xanthate solutions at different pH values and

Can. J. Chem. Downloaded from www.nrcresearchpress.com by 210.87.254.42 on 09/05/12
For personal use only.

different concentrations of xanthate ions (in solutions saturated with air at 1 atm pressure) can be expressed by:

$$\frac{[(EtX)_2]}{[EtXH]} = \frac{1}{k}\cdot\frac{[EtX^-]^2}{[OH^-]^2}\cdot\frac{K}{[EtX^-][H^+]} \simeq 6\times10^{15}[EtX^-][H^+].$$

It appears therefore that for the normal conditions employed in most flotation systems (10^{-5}–10^{-4} M xanthate solutions, pH 8–11) the concentration of dixanthogen is always greater than that of xanthic acid; in slightly alkaline xanthate solutions it is greater by several orders of magnitude. This would suggest that, in agreement with Cook's (12, 13) arguments for the adsorption of neutral molecules and Nixon's (14) deductions presented during discussion of hydrolytic adsorption, the active species in adsorption from xanthate solutions is the dissolved dixanthogen rather than xanthic acid. Infrared and ultraviolet spectrophotometric evidence, accumulated respectively by Poling (15) and Pomianowski (16), fully supports this supposition and will be published later.

It is significant that the ratio of dixanthogen to xanthic acid, derived above, reproduces the critical pH/concentration curves obtained by Wark and Cox (17) for various minerals and collectors; it has been pointed out by Barsky (18) that for each of these curves $[EtX^-][H^+]$ = constant.

ACKNOWLEDGMENTS

Grateful acknowledgment is made to the National Research Council for financial support of this work. The authors also wish to thank Miss Jean Begg for the preparations of xanthates used, and Mr. Colin Duncan for valuable assistance.

REFERENCES

1. H. Majima. Sci. Rep. Res. Inst., Tohoku Univ., Ser. A, **13**, 183 (1961).
2. H. Majima. Sci. Rep. Res. Inst., Tohoku Univ., Ser. A, **13**, 433 (1961).
3. Z. A. Sheka and J. Kriss. Proceedings, Investigations on Chemistry of Solutions and Complexes. Ukrain. Acad. Sci. 135 (1959).
4. M. Wronski. Roczniki Chem. **33**, 1071 (1959).
5. L. H. Little, G. W. Poling, and J. Leja. Can. J. Chem. **39**, 745 (1961).
6. (*a*) I. Iwasaki and S. R. B. Cooke. J. Am. Chem. Soc. **80**, 285 (1958).
   (*b*) I. Iwasaki and S. R. B. Cooke. J. Phys. Chem. **63**, 1321 (1959).
7. E. Klein, J. K. Bosarge, and J. Norman. J. Phys. Chem. **64**, 1666 (1960).
8. S. R. Rao and C. C. Patel. J. Mines, Metals and Fuels, **8**, 9 (1960).
9. Handbook of Chemistry and Physics. Chem. Rubber Publ. Co. 1962. p. 910.
10. F. A. Miller and C. H. Wilkins. Anal. Chem. **24**, 1253 (1952).
11. W. Klauditz. Chem. Abstr. **33**, 8401 (1939).
12. M. A. Cook and J. C. Nixon. J. Phys. Chem. **54**, 445 (1950).
13. M. A. Cook and M. E. Wadsworth. 2nd International Congress on Surface Chemistry. Vol. III. Butterworths. 1957. p. 228.
14. J. C. Nixon. 2nd International Congress on Surface Chemistry. Vol. III. Butterworths. 1957. p. 369.
15. G. W. Poling. Ph.D. Thesis, University of Alberta, Edmonton, Alta. 1963.
16. A. Pomianowski and J. Leja. To be published.
17. I. W. Wark and A. B. Cox. Trans. Am. Inst. Mining Met. Engrs. **112**, 189 (1934).
18. G. Barsky. Trans. Am. Inst. Mining Engrs. **112**, 236 (1934).

APPENDIX

Optical densities of pure xanthate solutions were compared with optical densities of xanthate solutions contaminated with dixanthogen in order to calculate the solubility of dixanthogen and the equilibrium constant of the reaction

$$2(EtX)_2 + 4OH^- \rightarrow 4EtX^- + 2H_2O + O_2. \qquad [3] \text{ or } [4]$$

$$K' = \frac{[EtX^-]^4[H_2O]^2[O_2]}{[OH^-]^4[(EtX)_2]^2} = k^2[H_2O]^2[O_2],$$

Can. J. Chem. Downloaded from www.nrcresearchpress.com by 210.87.254.42 on 09/05/12
For personal use only.

where $k = [EtX^-]^2/([OH^-]^2[(EtX)_2])$ is an intermediate constant for solutions saturated with O_2 from the air under 1 atm total pressure.

(a) Evaluation of Dixanthogen Absorptivities

Pure KEtX (12.08 mg) dissolved in 1 liter would give 7.53×10^{-5} M solution, with optical densities $d_{301} = 1.34$ and $d_{226} = 0.67$, the absorptivities being $\epsilon_{301} = 17750$ liter/mole cm and $\epsilon_{226} = 8920$ liter/mole cm. The spectrum of 12.08 mg of "aged" KEtX dissolved in 1 liter showed the optical densities $d_{301} = 0.990$ and $d_{226} = 0.645$.

Assuming the applicability of Beer's law to the mixtures of xanthate ions and dixanthogen:

$$d_{301} = \epsilon^{X}_{301}\cdot C_X + \epsilon^{D}_{301}\cdot C_D = 0.990 \qquad [A]$$

and

$$d_{226} = \epsilon^{X}_{226}\cdot C_X + \epsilon^{D}_{226}\cdot C_D = 0.645, \qquad [B]$$

where X denotes xanthate ion and D dixanthogen. Using the ratio

$$\frac{d^{D}_{226}}{d^{D}_{301}} = 3 = \frac{\epsilon^{D}_{226}}{\epsilon^{D}_{301}} \qquad [C]$$

and substituting other known data to the above equations [A] and [B], the actual concentration C_X of xanthate ions was calculated.

The difference in the amounts of xanthate used and determined, $12.08-8.40 = 3.68$ mg, was due to the products of surface oxidation:

$$2KEtX + \tfrac{1}{2}O_2 + CO_2 \rightarrow (EtX)_2 + K_2CO_3 \qquad [7]$$

$$2\times160.3 + 16 + 44 \qquad 242.4 + 138.2$$

giving $(3.68\times10^{-3})/380.6 = 9.7\times10^{-6}$ M dixanthogen concentration. Substituting the evaluated concentrations, $C_D = 9.7\times10^{-6}$ M and $C_X = 5.24\times10^{-5}$ M, into eqn. [B] the absorptivities $\epsilon^{D}_{226} = 18{,}300$ liter/mole cm and $\epsilon^{D}_{301} = 6{,}100$ liter/mole cm (from eqn. [C]) were obtained.

(b) Evaluation of Dixanthogen Solubility and Equilibrium Constant k

Several spectra were recorded of distilled water, immediately after shaking with dixanthogen, after prolonged contact (in well-stoppered flasks) with a dixanthogen layer, and after additions of alkalies to establish equilibrium conditions between EtX^- ions and $(EtX)_2$. Interpretation of the spectrum recorded after prolonged contact with dixanthogen at 22° C, which indicated only negligible amount of CS_2 produced, led to the evaluation of dixanthogen solubility and equilibrium constant k:

$$\text{pH} = 6.0,\ [OH^-] = 10^{-8}\ \text{mole/liter}$$
$$d_{301} = 0.195 = 17{,}750C_X + 6{,}100C_D\ \text{(measured)}$$
$$d_{226} = 0.295 = 8{,}920C_X + 18{,}300C_D\ \text{(measured)};$$

hence

$$C_X = 7.0\times10^{-6}\ M$$

and

$$C_D = 1.3\times10^{-5}\ M.$$

Can. J. Chem. Downloaded from www.nrcresearchpress.com by 210.87.254.42 on 09/05/12
For personal use only.

These two values correspond to 3.3×10^{-5} M of total EtX^- concentration, and the measurements at the "shifting isosbestic point" confirmed that the total concentration was between the limits

$$3\times10^{-5} < (C_X \text{ total}) < 4\times10^{-5} \text{ mole/liter.}$$

The value of $C_D = 1.3\times10^{-5}$ M was accepted as the solubility of dixanthogen in water at pH 6 and 22° C. The optical density d^D_{301} at saturation point of dixanthogen alone was, therefore,

$$d^D_{301} = 6100\times1.3\times10^{-5} = 0.079.$$

Using the above data, the intermediate equilibrium constant was obtained:

$$k = \frac{[EtX^-]^2}{[OH^-]^2[(EtX)_2]} = 3.3\times10^{10}.$$

(c) Titration of Xanthate Solution with Iodine

In titration with I_3^-, when the dixanthogen saturation point is exceeded, the concentration of xanthate cannot be directly evaluated from

$$C_X\cdot\epsilon^X_{301}+1.3\times10^{-5}\epsilon^D_{301} = 17{,}750\ C_X+0.079 = d_{301} \text{ (measured)} \qquad [D]$$

because of the unknown effect of emulsion. However, before the point of saturation is reached, the concentrations of xanthate and dixanthogen can be evaluated from

$$C_X\cdot\epsilon^X_{301} + \left(\frac{C^0_X}{2} - \frac{C_X}{2}\right)\epsilon^D_{301} = d_{301} \text{ (measured)},$$

where C^0_X is the initial concentration of pure xanthate.

The results of titration of a 20-ml xanthate solution with 5.56×10^{-4} N solution of I_3^- are given in Table III. The figures in parentheses have been calculated using eqn. [D];

TABLE III

Results of titration with I_3^- solution

	I_3^- solution added, ml						
	0	0.2	0.4	0.8	1.2	1.6	2.0
Measured d_{301}	0.990	0.905	0.802	0.640	0.427	0.270	0.172
Calculated C_X, 10^{-5} M	5.2	4.65	(4.05)	(3.15)	(1.96)	(1.07)	(0.5)
Calculated C_D, 10^{-5} M	0.95	1.28	Saturated solutions				

Fig. 10 shows the departure of measured optical densities from those for the residual concentration of pure xanthate ions, based on stoichiometry of the reaction.

Can. J. Chem. Downloaded from www.nrcresearchpress.com by 210.87.254.42 on 09/05/12
For personal use only.

A SYNTHESIS OF 3,3,3-TRICHLORO-1,2-EPOXYPROPANE FROM THE TETRAHALOPROPANE DERIVED FROM A CARBON TETRAHALIDE AND ETHYLENE[1]

WILKINS REEVE AND LEONARD W. FINE
Chemistry Department, University of Maryland, College Park, Maryland, U.S.A.

Received April 2, 1963

ABSTRACT

A study has been made of the reactions involving the addition of bromotrichloromethane to ethylene to give 3-bromo-1,1,1-trichloropropane, subsequent dehydrohalogenation of this to 3,3,3-trichloro-1-propene, and the isomerization of the latter to 1,1,3-trichloro-1-propene; the experimental conditions have been improved so that the minimum yield obtained in any one step is 78%. The 1,1,3-trichloro-1-propene is converted to a chlorohydrin in 36% yield by reaction with *tert*-butyl hypochlorite, and the chlorohydrin is converted in 61% yield to 3,3,3-trichloro-1,2-epoxypropane by treatment with base. The reaction of 3,3,3-trichloro-1-propene with methoxide ion to form 1,1-dichloro-3-methoxy-1-propene provides another example of an S_N2' reaction.

A convenient synthesis of 3,3,3-trichloro-1,2-epoxypropane was desired to make the compound available in relatively large amounts for another synthetic program. It had previously been prepared on a small scale by the reaction of diazomethane with chloral (1).

The synthesis which was developed involved the addition of carbon tetrachloride or bromotrichloromethane to ethylene to form the tetrahalopropane, which was then dehydrohalogenated and the resulting olefin isomerized and then converted to the epoxide via the chlorohydrin. Some of the reactions have been reported on previously, but significant improvements have been worked out for these steps and much new information has been developed.

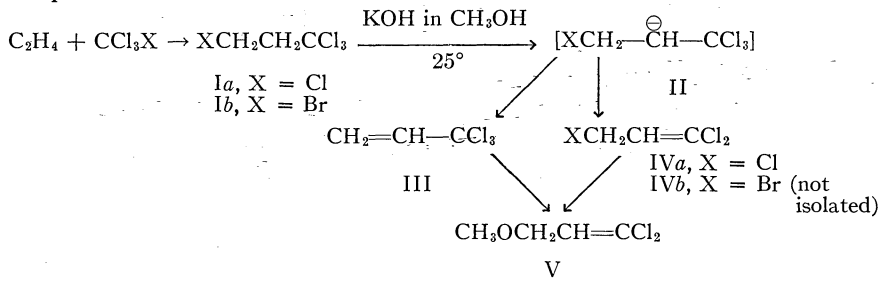

Reaction of Carbon Tetrachloride with Ethylene

The addition of carbon tetrachloride to ethylene has been reported previously (2), but in our hands the reaction was quite unsatisfactory when carried out batchwise according to the published directions. A steel reaction vessel fitted with a glass liner was used and the latter was filled one eighth full with carbon tetrachloride. Ethylene was fed in at 7–10 atm pressure. At 80° and with 0.8% benzoyl peroxide as the free-radical initiator, about 11% of the theoretical yield was the most that could be obtained in one run, although this corresponded to a yield of 25% when allowance was made for the recovered carbon tetrachloride. As has been reported previously (2(*a*)), telomers were produced in addition to the desired product.

[1]*This investigation was supported in part by a Predoctoral Fellowship to L. W. F. from the Division of General Medical Studies, United States Public Health Service.*

Can. J. Chem. Downloaded from www.nrcresearchpress.com by 210.87.254.5 on 09/05/12
For personal use only.

A series of peroxides was studied, and it was found that *tert*-butyl perbenzoate was superior to benzoyl peroxide for this reaction when equal amounts of catalysts were used. The optimum conditions involved using 2.4% of *tert*-butyl perbenzoate; the yield was then 28% before allowing for recovered carbon tetrachloride. The results are summarized in Table I.

TABLE I

The reaction of ethylene with carbon tetrachloride and with bromotrichloromethane

	Catalyst	
	Benzoyl peroxide	*t*-Butyl perbenzoate
Conditions		
Reaction temperature, °C	80	115
Pressure of ethylene, atm	7 to 10	7 to 10
Volume of glass liner, ml	1125	1125
Volume of starting CCl_3X, ml	125	125
With CCl_4		
Moles catalyst/mole CCl_4	0.0048*	0.0192
Yield of 1:1 adduct, %	11	28
Yield of telomers, %	10	25
Recovered CCl_4, %	56	34
With $CBrCl_3$		
Moles catalyst/mole $CBrCl_3$	0.0048	0.0048
Yield of 1:1 adduct, %	78	78
Yield of telomers, %	0	0
Recovered $CBrCl_3$, %	4	6

*In larger runs, it was found that increasing the amount of catalyst did not increase the yield.

Peroxides which were less effective than the above included lauroyl peroxide, hydroxyheptyl peroxide, and *tert*-butyl hydroperoxide. All of the peroxides were used at reaction temperatures (70 to 130°) which corresponded to a half-life of 3 hours for the pure catalyst when decomposed thermally by heating alone in benzene at the given temperature (3).

Reaction of Bromotrichloromethane with Ethylene

As shown in Table I, bromotrichloromethane adds to ethylene to give a 78% yield of the 1:1 adduct with either benzoyl peroxide or *tert*-butyl perbenzoate as catalysts.* No telomers were formed and very little of the bromotrichloromethane was unreacted. Haszeldine previously observed that this addition reaction using benzoyl peroxide would occur in 60% yield (2(*d*)), and the reaction has also been reported to occur in unstated or lower yields by others (4). This provides an excellent example of a chain-transfer reaction, [1], taking precedence over the chain-propagation reaction, [2], observed with carbon

$$\cdot CH_2CH_2CCl_3 + BrCCl_3 \rightarrow BrCH_2CH_2CCl_3 + \cdot CCl_3 \quad [1]$$

$$\cdot CH_2CH_2CCl_3 + CH_2{=}CH_2 \rightarrow \cdot CH_2CH_2CH_2CH_2CCl_3 \quad [2]$$

tetrachloride because of the greater lability of the carbon–bromine bond in bromotrichloromethane as compared with the carbon–chlorine bond in carbon tetrachloride.

It was observed that the amount of catalyst required depended on the relative volumes of the gas and liquid phases inside of the glass liner. When the liner was filled 17% (50% more than the volume specified in Table I), the concentration of the *tert*-butyl perbenzoate catalyst had to be doubled in order to obtain a 78% yield.

The addition of bromotrichloromethane to ethylene at 120° and 50 atm pressure in the absence of peroxides has been used successfully by others as a preparative method. However, Elser and Saure (H. Elser and S. Saure. Angew Chem. **74, 253 (1962)) have recently reported the occurrence of a violent explosion under these conditions.*

Can. J. Chem. Downloaded from www.nrcresearchpress.com by 210.87.254.5 on 09/05/12
For personal use only.

Dehydrohalogenation of the Tetrahalopropanes

The base-catalyzed dehydrohalogenation of 1,1,1,3-tetrachloropropane has been previously studied and both of the olefins III and IV*a* have been reported to be obtained in yields of 31 and 12% (5), 50 and 30% (6), and 57 and 30% (2(*d*)) respectively. The dehydrohalogenation of 3-bromo-1,1,1-trichloropropane has been reported to give 57% of olefin III (7).

From the theoretical standpoint, this dehydrohalogenation of the 1,1,1,3-tetrachloropropane is of considerable interest since the intermediate carbanion II should be capable of forming either of the two olefins, III or IV. The conformation of the tetrahalopropane required for the formation of olefin III is given in Fig. 1. This conformation might be

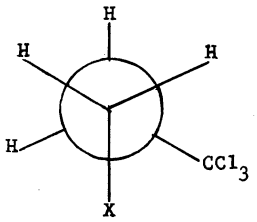

FIG. 1.

considered to be unlikely due to both steric interaction and dipole–dipole repulsion of the groups in this skew configuration. Therefore, formation of olefin III might be considered less likely than formation of olefin IV. The formation of the latter involves no steric problems and the developing double bond would have considerable resonance stabilization from the two vinylic chlorine atoms. Despite these considerations, the results in Table II show that the trichloromethyl group is so inert that the major reaction product is olefin III.

TABLE II

Percentage yields of products in dehydrohalogenation reaction*

Products	From $ClCH_2CH_2CCl_3$	From $BrCH_2CH_2CCl_3$
$CH_2{=}CHCCl_3$ (III)	55	80
$XCH_2CH{=}CCl_2$ (IV)	24	0
$CH_3OCH_2CH{=}CCl_2$ (V)	11	14

*Twofold excess of potassium hydroxide in methanol solvent at 25° for 90 minutes.

Our results are based on vapor phase chromatographic analysis of the reaction products before distillation, whereas the results of earlier workers are based on careful fractional distillation. It is now apparent that some isomerization of olefin III to olefin IV can occur under distillation conditions. Our procedure differed from the others also in that a twofold excess of methanolic potassium hydroxide was employed at 25° and the reaction was carried out in 90 minutes. Earlier workers used ethanolic potassium hydroxide at temperatures from 0 to 25°, base concentrations from 0 to 30% in excess of theory, and reaction times up to 6 hours.

The increased amount of olefin III formed from the 3-bromo-1,1,1-trichloropropane is in accord with the known much greater tendency of alkyl bromides relative to alkyl chlorides to undergo an elimination reaction rather than a substitution reaction (8). It is probable that a small amount of 3-bromo-1,1-dichloro-1-propene (IV*b*) is also formed and

Can. J. Chem. Downloaded from www.nrcresearchpress.com by 210.87.254.5 on 09/05/12
For personal use only.

is converted completely to the unsaturated ether V. This unsaturated ether can be formed either by an S_N2 attack of methoxide ion on olefin IV or by an S_N2' attack of methoxide ion on olefin III. To determine which is the more likely route, separate portions of each of the pure olefins were reacted with potassium hydroxide in methanol at 80° and the reaction rates were determined semiquantitatively by withdrawing samples at various time intervals and analyzing for the ratio of olefin to unsaturated ether by vapor phase chromatography. At 80°, 1,1,3-trichloro-1-propene (IV*a*) was converted to the unsaturated ether (V) approximately six times as rapidly as was 3,3,3-trichloro-1-propene (III). If this same ratio of S_N2 to S_N2' attack holds at 25°, and if allowance is made for olefin III being present in larger amounts than olefin IV, then it would appear that approximately 20% of the unsaturated ether V arises by an S_N2' attack of methoxide ion on olefin III and the balance by an S_N2 attack of methoxide ion on olefin IV.

Isomerization of Olefin III to Olefin IV

This reaction has been previously studied (6) and shown to occur even at 0° with an acid catalyst but in relatively poor yield (2(*d*), 9); at 140° it occurs in 74% yield with no catalyst (2(*d*)). In the present work, a 95% yield was obtained by heating olefin III at 150° for 5 hours under pressure.

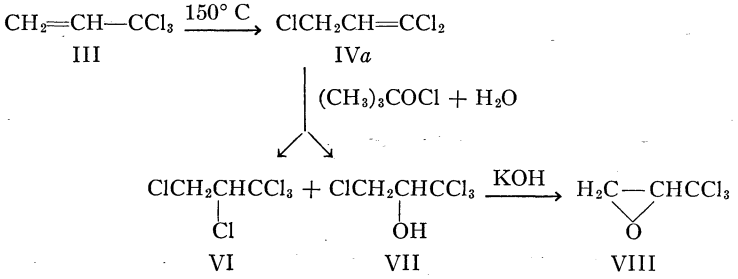

Formation of Chlorohydrin

The chlorohydrin 1,1,1,3-tetrachloro-2-propanol (VII) was first prepared by Meerwein by means of a Meerwein–Ponndorf reduction of tetrachloroacetone (10). Later Shelton and Lee prepared it in unstated yield from olefin IV*a* and hypochlorous acid (11). In the present work, it was prepared by reacting olefin IV*a* with a twofold excess of *tert*-butyl hypochlorite in 10% aqueous acetic acid. The chlorohydrin was obtained in 36% yield and 1,1,1,2,3-pentachloropropane (VI) was obtained in 42% yield. These were separated by distillation, but the purity of the chlorohydrin so obtained was estimated to be about 90% based on vapor phase chromatographic analyses; also the chlorine analysis was 4% high.

Formation of Epoxide

Chlorohydrin VII was converted to the epoxide VIII, 3,3,3-trichloro-1,2-epoxypropane, in 61% yield by "titrating" the chlorohydrin with slightly less than the theoretical amount of alcoholic potassium hydroxide solution at 25° to 35° in the presence of phenolphthalein indicator.

Attempts to synthesize the epoxide directly from olefin III and peracetic acid, perbenzoic acid, or *tert*-butyl hydroperoxide were unsuccessful.

EXPERIMENTAL

All melting and boiling points are corrected. Analyses are by Dr. Franz J. Kasler. The infrared spectra were determined on a Beckman IR-5. The liquids were measured as a film between sodium chloride plates.

Can. J. Chem. Downloaded from www.nrcresearchpress.com by 210.87.254.5 on 09/05/12
For personal use only.

3-Bromo-1,1,1-trichloropropane (Ib)

The apparatus used was a rocking-type steel autoclave (1640-ml volume) fitted with a glass liner (1125-ml inner volume). In the glass liner were placed 125 ml (1.3 moles) of freshly distilled bromotrichloromethane and 1.5 g (0.0062 mole) of dibenzoyl peroxide. The autoclave was flushed thoroughly with ethylene, the ethylene pressure raised to 100 lb/sq. in., and the autoclave then rocked and heated to the initiation temperature of 115°, at which point the pressure began to drop. Each time the pressure fell to 100 lb/sq. in., the autoclave was recharged to 175 lb/sq. in. The rate of pressure change was slow at first, reached a maximum, and then gradually tapered off with about 3 hours' reaction time required. Distillation yielded 230 g (78% yield) of 3-bromo-1,1,1-trichloropropane, b.p. 78–80° at 26 mm, n_D^{26} 1.5125. The physical constants are in agreement with the literature values (4(*a*)).

Dehydrohalogenation of 3-Bromo-1,1,1-trichloropropane

Over a 30-minute period, 56 g (1 mole) of potassium hydroxide dissolved in 130 ml of methanol was added with mechanical stirring to 112 g (0.5 mole) of 3-bromo-1,1,1-trichloropropane. The temperature was maintained at 25° with an ice-water bath. Stirring was continued for 1 hour, the reaction mixture then poured into 300 ml of cold water, the organic layer washed once with water, dried over anhydrous magnesium sulphate, and then distilled through a modified Widmer column. There was obtained 57 g (80% yield) of *1,1,1-trichloro-1-propene*, b.p. 100–100.5° at 760 mm, n_D^{25} 1.4684. The physical constants are in agreement with the literature values (5). Infrared spectrum, ν_{max}: 1890 (vinyl overtone), 1630 ($\rangle C{=}C\langle$ weak), 1410, 1125, 970, 945, and 813–770 cm^{-1}.

There was also obtained 12 g (14% yield) of *1,1-dichloro-3-methoxy-1-propene* (V), b.p. 132–133° at 760 mm. For preparative purposes, the preferred synthesis of this involved treating 1,1,3-trichloro-1-propene (IV*a*) according to the above procedure, but with refluxing at approximately 80° for 6 hours after the methanolic potassium hydroxide had been added to the reaction mixture. The yield was 80% of the theoretical. Infrared spectrum, ν_{max}: 2975, 2875, 1625, 1450, 1370, 1360, 1285, 1225, 1185, 1150, 1115–1065, 980–960, 912, 878–863, and 825 cm^{-1}. Anal Calc. for $C_4H_6Cl_2O$: C, 34.08; H, 4.29. Found: C, 34.25; H, 4.47.

1,1,3-Trichloro-1-propene (IVa)

Freshly distilled 3,3,3-trichloro-1-propene (146 g, 1.0 mole) was placed in the glass liner in the autoclave and heated for 5 hours at 150°. Shaking was not necessary. After cooling overnight, there was obtained on distillation 139 g (95% yield) of 1,1,3-trichloro-1-propene, b.p. 130–131° at 760 mm. The physical constants were in agreement with the literature values (6(*a*)). Infrared spectrum, ν_{max}: 3025, 2930, 1725, 1690, 1605, 1475, 1285, 1245, 1175, 1070, 945, 880–815, 740, and 695–675 cm^{-1}.

1,1,1,3-Tetrachloro-2-propanol (VII)

In a 500-ml 3-necked flask, equipped with a Hershberg stirrer and a thermometer, were placed 15 g (0.1 mole) of 1,1,3-trichloro-1-propene, 24 g of glacial acetic acid, and 250 ml of water. To this, 22 g (0.2 mole) of *tert*-butyl hypochlorite (12) was added dropwise over a 20-minute period with the temperature of the reaction mixture being maintained at 0°. After another 30 minutes, the reaction mixture was allowed to warm up to room temperature and was stirred for an additional 2 hours. The aqueous layer was separated and extracted with chloroform, the chloroform combined with the organic layer, washed once with water, dried, and distilled through a modified Widmer column. There was obtained 7 g (36% yield) of *1,1,1,3-tetrachloro-2-propanol* (VII), b.p. 98–100° at 17 mm, n_D^{25} 1.5165. Reported values are: b.p. 87–90° at 14 mm and n_D^{20} 1.5145 (10). Analysis by v.p.c. indicated the material to be 90% pure. Anal Calc. for $C_3H_4Cl_4O$: C, 18.21; H, 2.03. Found: C, 18.48; H, 2.20.

There was also obtained 12% of unreacted starting material, and 9 g (42% yield) of *1,1,1,2,3-pentachloropropane (VI)*, b.p. 81–83° at 17 mm, identified by analysis and by comparison with an authentic sample.

3,3,3-Trichloro-1,2-epoxypropane (VIII)

In a 250-ml 3-necked flask equipped with a dropping funnel, Hershberg stirrer, and a thermometer was placed 20 g (0.1 mole) of 1,1,1,3-tetrachloro-2-propanol. One milliliter of phenolphthalein indicator solution was added and a 1 *N* methanolic (or ethanolic) potassium hydroxide solution was introduced dropwise at such a rate that the reaction mixture never became highly colored. The temperature was maintained at 25 to 35°. Two to three hours were required for 80% of the stoichiometric amount of base to be added, at which point the reaction was stopped by adding 200 ml of water and separating the layers. The organic layer was washed twice with water, dried over anhydrous magnesium sulphate, and distilled. There was obtained 10 g (61% yield, based on the chlorohydrin), b.p. 47–49° at 17 mm, n_D^{26} 1.4783. Literature values are b.p. 39–40° at 11 mm and n_D^{25} 1.4768 (13). An authentic research sample from an industrial source had a boiling point of 147–149° at 760 mm, n_D^{25} 1.4768.

Infrared spectrum of the 10-g sample, ν_{max}: 3065, 3010, 2920, 1475, 1385, 1270, 1155, 1140, 1105, 1075, 955, 885, 848, and 830–770 cm^{-1}. Anal Calc. for $C_3H_3Cl_3O$: C, 22.32; H, 1.87; Cl, 65.90. Found: C, 22.10; H, 1.81; Cl, 66.15.

Can. J. Chem. Downloaded from www.nrcresearchpress.com by 210.87.254.5 on 09/05/12
For personal use only.

ACKNOWLEDGMENTS

We wish to express our appreciation to Drs. Ellis Lippincott and Francis Powell for their assistance in obtaining and interpreting the infrared spectra. The financial support provided by the National Institutes of Health is deeply appreciated.

REFERENCES

1. F. ARNDT and B. EISTERT. Ber. **61**, 1118 (1928).
2. (*a*) R. M. JOYCE, W. E. HANFORD, and J. HARMON. J. Am. Chem. Soc. **70**, 2529 (1948).
   (*b*) IMPERIAL CHEMICAL INDUSTRIES LTD. Brit. Patent No. 581, 899 (Oct. 26, 1946); Chem. Abstr. **41**, 3477 (1947).
   (*c*) A. N. NESMEYANOV *et al.* Chem. Tech. (Berlin), **9**, 139 (1957); Chem. Abstr. **51**, 15,407 (1957).
   (*d*) R. N. HASZELDINE. J. Chem. Soc. 3371 (1953).
3. D. F. DOEHNERT and O. L. MAGELI. Ann. Tech. Management Conf., Reinforced Plastics Div., Soc. Plastics Ind. **13**, 1 (1958); Chem. Abstr. **53**, 18,534 (1959).
4. (*a*) M. S. KHARASCH, O. REINMUTH, and W. H. URRY. J. Am. Chem. Soc. **69**, 1105 (1947).
   (*b*) E. M. HODNETT and A. M. SCHNITZER. Proc. Oklahoma Acad. Sci. **32**, 94 (1951).
   (*c*) J. R. SHELTON and L. H. LEE. J. Org. Chem. **23**, 1876 (1958).
5. E. C. LADD and S. D. SHINKLE. U.S. Patent No. 2,561,516 (July 24, 1951); Chem. Abstr. **46**, 2561 (1952).
6. (*a*) A. N. NESMEYANOV, R. KH. FREIDLINA, and V. I. FIRSTOV. Doklady Akad. Nauk SSSR, **78**, 717 (1951); Chem. Abstr. **46**, 1957 (1952).
   (*b*) A. N. NESMEYANOV, V. N. KOST, L. J. ZAKHARKIN, and R. KH. FREIDLINA. Bull. Acad. Sci. USSR, Div. Chem. Sci. (English Transl.), 415 (1960).
7. W. A. SKINNER, E. BISHOP, D. TIESZEN, and J. D. JOHNSON. Ind. Eng. Chem. **51**, 1359 (1959).
8. J. N. NEF. Ann. **309**, 136 (1899).
9. UNITED STATES RUBBER CO. Brit. Patent No. 660,475 (Nov. 7, 1951); Chem. Abstr. **46**, 9575 (1952).
10. H. MEERWEIN, B. V. BOCK, BR. KIRSCHNICK, W. LENZ, and A. MIGGE. J. Prakt. Chem. **147**, 211 (1936).
11. J. R. SHELTON and L. H. LEE. J. Org. Chem. **24**, 1271 (1959).
12. W. E. HANBY and H. M. RYDON. J. Chem. Soc. 114 (1946).
13. H. GILMAN and R. K. ABBOTT, JR. J. Org. Chem. **8**, 224 (1943).

Can. J. Chem. Downloaded from www.nrcresearchpress.com by 210.87.254.5 on 09/05/12
For personal use only.

X-RAY DIFFRACTION DATA FOR AMMONIUM TETRATHIOTUNGSTATE

R. W. MOONEY AND C. W. W. HOFFMAN

Sylvania Electric Products Inc., Chemical and Metallurgical Division, Towanda, Pennsylvania, U.S.A.

Received May 9, 1963

ABSTRACT

The tetrathiotungstate salt of ammonia has been prepared. Zero-layer Weissenberg photographs have been used to establish that this material is orthorhombic with $a = 9.62_3$ Å, $b = 12.40_6$ Å, and $c = 7.05_5$ Å with space group $Pn2_1a$—C_{2v}^9 or $Pnma$—D_{2h}^{16}. The data have been used to index the Debye–Scherrer pattern.

INTRODUCTION

The preparation of ammonium thiotungstate, $(NH_4)_2WS_4$, has been known for about a hundred years (1). The preparation given by Corleis (2) yields substantially pure, crystalline $(NH_4)_2WS_4$. In 1885, Vater (3), from geometrical considerations, obtained the axial ratios $a:b:c = 0.7783:1:0.5675$. He described the crystal habit as rhombic bipyramidal, consistent with orthorhombic symmetry. Recently, Bernard and Tridot (4, 5) prepared some of the alkali and ammonium thiotungstates and studied the solutions spectrophotometrically. They observed three thiotungstate ions: $WO_2S_2^{2-}$, WOS_3^{2-}, and WS_4^{2-}, in solution, obtained successively by gassing tungstate solutions.

EXPERIMENTAL

Ammonium tetrathiotungstate, $(NH_4)_2WS_4$, was prepared in this laboratory by prolonged gassing of an ammonium tungstate solution with H_2S. $(NH_4)_2WS_4$ crystallized as orange, translucent crystals. These crystals showed a platy hexagonal habit. Cursory microscopic examination revealed, however, that these plates were usually elongated in what later was designated the *c*-direction. In addition, one pair of the opposite angles (the *c*-apices) was found to be very close to 60°. The other two pairs were found to be close to 59° and 61°. The chemical analysis of the crystals was: Found: W, 52.99%; S, 37.41%; NH_3, 9.6%. Theoretical, $(NH_4)_2WS_4$: W, 52.80%; S, 36.84%; NH_3, 9.78%. At room temperature, $(NH_4)_2WS_4$ is fairly stable but has a slight odor of H_2S; very slow decomposition may be taking place. At high temperatures, in air, it reacts, forming H_2S, NH_3, SO_2, and WO_3. Spectrographic qualitative analysis of the WO_3 obtained from firing showed 0.01% Mo and Si, and 0.001% Fe and Mg. The density obtained by ordinary pycnometric means was 2.71 g cm^{-3}.

Ni-filtered Cu $K\alpha$ ($\lambda = 1.5418$ Å) radiation was used to obtain zero-layer Weissenberg photographs taken about each of the three axes. The equi-inclination method was used to obtain the $h1l$ reflections. Inspection of the reciprocal lattice nets for each zone of reflection showed that the unit cell was orthorhombic with the approximate dimensions: $a = 9.6$ Å, $b = 12.4$ Å, and $c = 7.0$ Å. The $0kl$ reciprocal lattice net showed almost perfect hexagonal symmetry as a result of the absence of all reflections with $k+l = 2n+1$. A back reflection Laue photograph taken along the same *a*-axis also showed near-perfect 6-fold symmetry superimposed upon two mirror planes at right angles to each other. The Laue group must, however, be *mmm*. Twinning was observed parallel to the *b*-axis.

The unit cell dimensions were determined from high-order reflections on the single-crystal rotation photographs, tungsten ($a_0 = 3.1648$ Å) being used to correct for film shrinkage. The layer line photographs were then used to index the Debye–Scherrer pattern to a 2θ of 35° ($d = 2.50$ Å) as given in Table I.

RESULTS AND DISCUSSION

Extrapolation of single-crystal data to $2\theta = 180°$ refined the cell dimensions to: $a = 9.62_3 \pm 0.005$ Å, $b = 12.40_6 \pm 0.005$ Å, and $c = 7.05_5 \pm 0.005$ Å. Based on these figures, the ratio $b:c$ is very close to $\sqrt{3}$, namely 1.758, and with the absence of the $0kl$ reflections for which $k+l = 2n+1$ accounts for the near-hexagonal symmetry of the $0kl$ reciprocal lattice net. The cell dimensions lead to $a:b:c = 0.7757:1:0.5687$ ratios in excellent agreement with those of Vater. (Also, using Vater's ratios, the ratio $b:c$ is 1.762.)

Can. J. Chem. Downloaded from www.nrcresearchpress.com by 210.87.254.42 on 09/05/12
For personal use only.

TABLE I

X-Ray powder data for ammonium tetrathiotungstate

I	d_{obs}	d_{calc}	hkl
vs	6.18	6.20	020
m	6.10	6.13	011
vs	5.20	5.21	120
vs	5.16	5.17	111
vs	4.81	4.81	200
m	3.79	3.79	211
		3.80	220
s	3.55	3.57	031
m	3.51	3.53	002
m	3.33	3.35	221
vw	3.19	3.20	112
vs	3.08	3.11	310
		3.10	040
w	3.05	3.07	022
m	2.94	2.95	140
w	2.93	2.92	122
m	2.85	2.85	320
s	2.84	2.84	202
w	2.76	2.77	212
vw	2.60	2.61	240
w	2.58	2.59	132
vw	2.53	2.54	330

The volume of the unit cell is 842.2 Å^3. Assuming four $(NH_4)_2WS_4$ units per unit cell, the calculated density is 2.75 g cm^{-3}, in satisfactory agreement with the experimental figure of 2.71 g cm^{-3}. The tetramolecular unit cell is consistent with the space group discussed below.

Lack of systematic absences in the $h1l$ reciprocal lattice net indicated a primitive unit cell. No systematic absences occurred in the $hk0$ zone. However, the systematic absence of $h0l$ when h was odd and of $0kl$ when $k+l$ was odd indicated the space group was either $Pn2_1a$—C_{2v}^9 or $Pnma$—D_{2h}^{16}. Vater's early observations, although unconfirmed in this work, support the latter space group. However, without more detailed information from a complete structure analysis the choice of a unique space group is unreliable.

In spite of the lack of definitive data, certain speculations concerning the structure of $(NH_4)_2WS_4$ are possible. There are two common structure types (6) having the A_2BX_4 stoichiometry that display a tetramolecular unit cell with pseudohexagonal orthorhombic symmetry, namely chrysoberyl (Al_2BeO_4) and the room-temperature form of potassium sulphate (K_2SO_4). Both of these compounds have the more probable space group $Pnma$—D_{2h}^{16}. The relative ratios of the unit cell dimensions of $(NH_4)_2WS_4$, K_2SO_4, and Al_2BeO_4 are: 0.776:1:0.569, 0.742:1:0.573, and 0.583:1:0.471, respectively. This tends to favor the isomorphism of $(NH_4)_2WS_4$ and K_2SO_4. However, such data by themselves are insufficient to establish an isomorphic relationship.

ACKNOWLEDGMENTS

The authors are indebted to V. Chiola and C. D. Vanderpool for the preparation of $(NH_4)_2WS_4$ crystals and to I. L. Ericson for the chemical analyses.

REFERENCES

1. J. W. MELLOR. A comprehensive treatise on inorganic and theoretical chemistry. Longmans, Green and Co., London. 1922.

Can. J. Chem. Downloaded from www.nrcresearchpress.com by 210.87.254.42 on 09/05/12
For personal use only.

2. E. CORLEIS. Liebigs Ann. Chem. **232**, 257 (1886).
3. H. VATER. Z. Kryst. **10**, 392 (1885).
4. J. C. BERNARD and G. TRIDOT. Bull. Soc. Chim. France, **1961**, 810 (1961).
5. J. C. BERNARD and G. TRIDOT. Bull. Soc. Chim. France, **1961**, 813 (1961).
6. R. W. G. WYCKOFF. Crystal structures. Interscience Publishers, Inc., New York. 1948.

Can. J. Chem. Downloaded from www.nrcresearchpress.com by 210.87.254.42 on 09/05/12
For personal use only.

CONTRIBUTION CONCERNING THE PROBLEM OF THE INTRAMOLECULAR HYDROGEN BONDS IN ORTHO HALOPHENOLS

HENRIETTE BOURASSA-BATAILLE, P. SAUVAGEAU, AND C. SANDORFY
Département de Chimie, Université de Montréal, Montréal, Qué.
Received April 1, 1963

ABSTRACT

The infrared spectra of the four ortho halophenols were measured in carbon tetrachloride solutions containing variable amounts of ether. The integrated intensities of the stretching band corresponding to the intermolecularly hydrogen-bonded OH groups were determined and plotted against ether concentration. From the curves obtained in this manner it was possible to deduce the relative strengths of the *intra*molecular hydrogen bonds which are present in these molecules. They are, in order of increasing strength: F < I < Br < Cl. This result is compared to others, published in the literature, obtained using alternative methods.

INTRODUCTION

Ortho-substituted phenol derivatives have received a great deal of attention in recent years (1–9). In particular the nature of the intramolecular hydrogen bond in the ortho halophenols has been the subject of many publications since Wulf, Liddel, and Hendricks (10) found that these molecules have two OH stretching bands in the infrared; and since Pauling (11) suggested that for these compounds cis and trans isomers are possible, the cis isomer being stabilized by hydrogen bonding. Ferguson (12) pointed out that in this case the energies of the hydrogen bonds may not vary proportionally with the frequency shifts of the infrared OH stretching bands, because the hydrogen bonds must be bent to a large extent.

The shifts increase in the natural order of the halogens, F < Cl < Br < I, giving the impression that iodine forms the strongest hydrogen bond in this series. The following data were measured in this laboratory (13), but, of course, these bands were known long before.

	Free OH (trans)	Bonded OH (cis)
o-Fluorophenol	—	3591
o-Chlorophenol	3608	3545
o-Bromophenol	3604	3522
o-Iodophenol	3600	3499
Phenol	3610.5	—

If the frequency shifts were proportional to the hydrogen bond energies, it would be expected that the trans/cis ratio would decrease in the same order. This is, however, not so. Baker (1) and Baker and Kaeding (2) measured the integrated absorption intensities of the trans and cis bands for the four compounds; and also for 2,4,6-trisubstituted phenols with two different halogens in the 2 and 6 positions, where two bonded bands appear: they concluded from the relative intensities of the bands that the strength of the hydrogen bonds increases in the order I < F < Br < Cl, with chlorine giving the strongest hydrogen bond.

More recently Allan and Reeves (14) measured the nuclear magnetic resonance spectra of the *o*-halophenols. They determined equilibrium constants for the cis–trans conversion,

Can. J. Chem. Downloaded from www.nrcresearchpress.com by 210.87.254.40 on 09/05/12
For personal use only.

and from their temperature dependence they calculated ΔH, the heat of formation of the hydrogen bonds. They obtained:

	ΔH, cal/mole
o-Chlorophenol	2.356
o-Bromophenol	2.141
o-Iodophenol	1.651

Chlorine again gave the strongest hydrogen bond. For *o*-fluorophenol they concluded that no hydrogen bond formation takes place.

The dipole moments of the cis and trans forms are very different: this led Richards and Walker (15) to determine the trans/cis ratios by dipole moment measurements. The order was dependent on the solvent, but in CCl_4 it was $I > F > Cl = Br$, essentially the same as the order found by Baker and Kaeding.

The above-mentioned infrared studies suffer from the implicit assumption that the relative intrinsic intensity of the trans and cis bands remains the same for all the *o*-halophenols. The n.m.r. work of Allan and Reeves is free of this drawback, but their conclusion concerning *o*-fluorophenol does not seem to be well founded (see below). Those results of Richards and Walker which were obtained in CCl_4 are also somewhat uncertain, according to these authors themselves, because their calculations involve small differences of low dipole moments.

The present work is an attempt to supply additional infrared evidence concerning the order of the hydrogen bond energies of the ortho halophenols.

OUTLINE OF THE WORK

The intramolecular hydrogen bonds in ortho halophenols are relatively weak. Therefore, if we put a strong proton acceptor into the solution we might expect that the intramolecular hydrogen bonds will be broken in order to give rise to stronger intermolecular bonds. One such case has been described by Bellamy and Hallam (16), who examined the infrared spectra of pyrrole – pyrrole complexes in the presence of strongly associating solvent molecules; and Pople, Schneider, and Bernstein mention similar observations made with n.m.r. spectra (9, p. 412).

In our investigation we prepared dilute solutions of the *o*-halophenols in CCl_4 at a concentration (0.0189 *M*) where intermolecular hydrogen bonding is negligible, and then solutions in CCl_4 containing diethyl ether in concentrations varying from 0 to about 9 *M*. The intensity of the sharp "intramolecular" bands diminishes gradually and then disappears as the ether concentration increases; and at the same time a broad band appears at 3300 cm^{-1}, the integrated intensity of which increases gradually, indicating the formation of intermolecular hydrogen bonds.

We plotted curves of integrated intensities of the intermolecular bands against ether concentration. If a para or meta halophenol is used as solute the curve rises rapidly to reach a plateau at moderate ether concentrations. But for an ortho halophenol the rising is much slower, showing that the equilibrium is much less in favor of intermolecular bonds in the reaction: intramolecularly bonded *o*-halophenol + ether $\rightleftarrows$ intermolecularly bonded *o*-halophenol to ether (cf. ref. 17). Figure 1 illustrates this situation in the case of *o*-chlorophenol, the other three *o*-halophenols yielding similar sets of curves. On Fig. 2 the ortho curves are collected together.

Can. J. Chem. Downloaded from www.nrcresearchpress.com by 210.87.254.40 on 09/05/12
For personal use only.

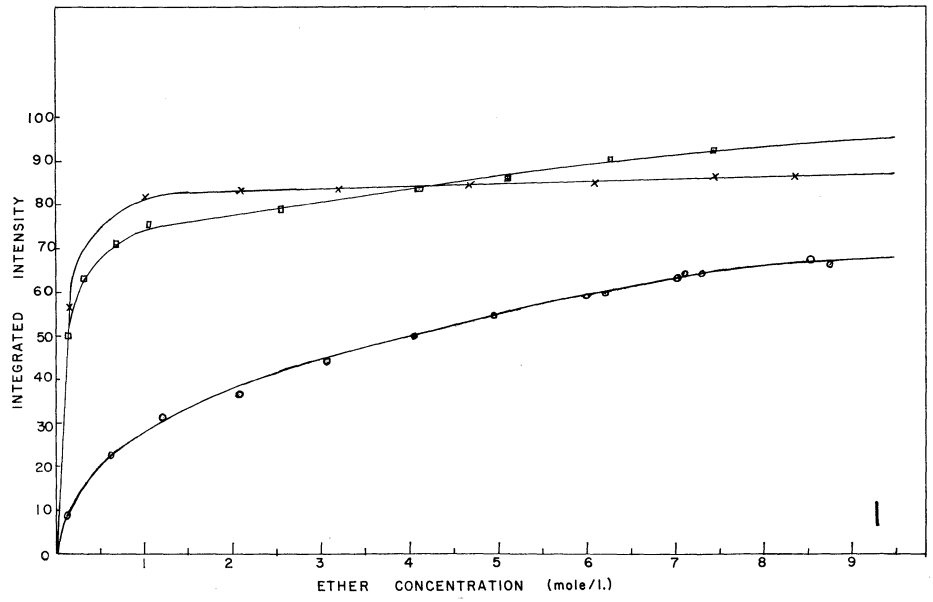

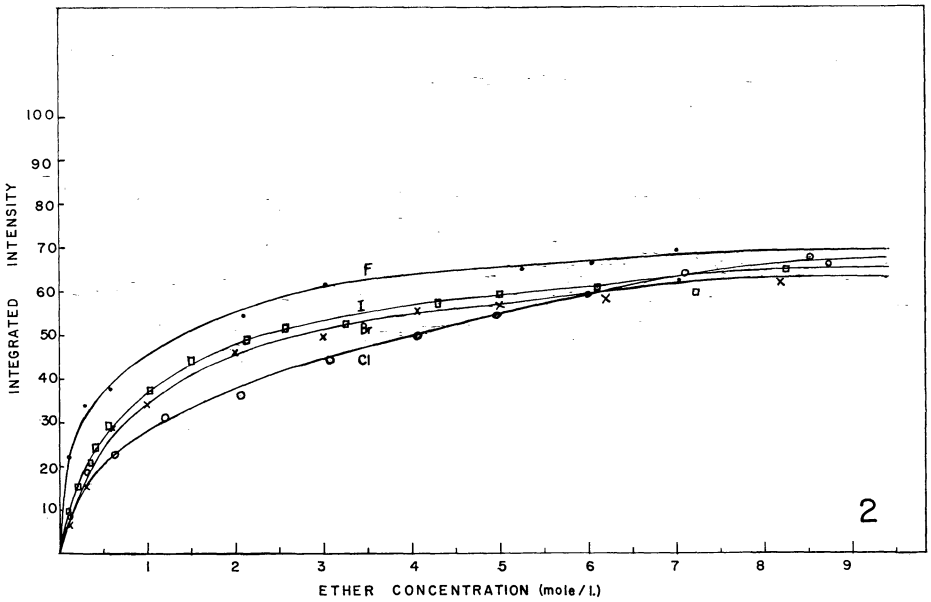

FIG. 1. Intensities (in arbitrary units) vs. ether concentration for *o*-chlorophenol (○), *m*-chlorophenol (×), and *p*-chlorophenol (□).
FIG. 2. Intensities (in arbitrary units) vs. ether concentration for *o*-chlorophenol (○), *o*-bromophenol (×), *o*-iodophenol (□), and *o*-fluorophenol (●).

Only the intermolecular band was used because the intensity of the intramolecular band is influenced too much by overlap with the other bands.

EXPERIMENTAL

The purity of the compounds is a rather important factor in spectroscopic studies of the halophenols, as has been emphasized by Rossmy, Lüttke, and Mecke (18). Our samples were reagent or highest purity

Can. J. Chem. Downloaded from www.nrcresearchpress.com by 210.87.254.40 on 09/05/12
For personal use only.

grade commercial products; and we further purified them by vacuum distillation, sublimation in vacuum, or chromatographic methods according to the cases. We cannot claim that our compounds were of the same high degree of purity as those of Baker (1), but we calculated that they would have to contain a rather unreasonably high amount of phenol, the most probable impurity, in order to impair our conclusions.

A Perkin–Elmer model 21 spectrometer was used, mounted with a sodium chloride prism. For the lowest ether concentrations 1-mm cells were used, for the rest 0.1-mm cells. Ether absorbs heavily from 3100 cm^{-1} and, therefore, the parts of our curves above 5 M have to be interpreted with caution: no conclusions will be drawn from the occasional crossing between curves encountered at high ether concentrations.

The area under the intermolecular OH band was planimetered out between the center of the band ± 150 cm^{-1}. Since the center of these broad bands was always very close to 3300 cm^{-1}, and since their shapes were all very similar, we believe we have obtained reliable relative intensities. No attempt was made, however, to compute absolute intensities, and so the results are given in arbitrary units.

Although all the work was conducted in an entirely quantitative manner, only qualitative conclusions will be drawn from the results.

DISCUSSION

It may be inferred from the curves of Fig. 2 that the order of increasing intramolecular hydrogen bond strength is F < I < Br < Cl. Drawing this conclusion would, however, imply the supposition that the intrinsic intensity of the intermolecular band is the same for all four compounds. This may appear to be so since the frequency of the center of the band is in all cases very close to 3300 cm^{-1}, as far as it is possible to tell in view of its broadness. But, if this were really true, the intensity versus ether concentration curves of Fig. 2 should all attain the same height at high ether concentrations, when all the OH groups are intermolecularly bonded. But clearly this is not the case, and the differences may be great enough to affect our conclusions. In fact, if hydrogen bonding were the only important factor in determining the intensity of the intermolecular band at high ether concentrations, even the ortho, meta, and para curves should eventually reach a plateau of the same height. Figure 1 shows clearly that the electronic structure of the proton-donor molecule has a great influence on the intensity of the bands, even though it hardly affects their frequency.

The slope of the curves is, however, independent of the intrinsic intensities of the bands. Therefore we computed the change in ether concentration, $\Delta_{I'-I''}$, needed to raise the intensity from I' to I'' for all four molecules at a number of places that we considered to be the meaningful parts of the curves, say from about 0.2 to 4.5 mole/liter; I' and I'' are measured on the same arbitrary scale as used in Figs. 1 and 2. Here is a typical example:

	$\Delta_{(35-55)}$
Cl	3.43
Br	2.75
I	2.53
F	1.58

In every case the sequence turned out to be F < I < Br < Cl, which is actually the same as what would follow from a simple consideration of the order of the curves of Fig. 2.

This is the same order as the one found by Allan and Reeves (14), but differs by one inversion (F ↔ I) from the order given by Baker and Kaeding (2). According to our results Cl is further apart from the others than found by previous authors, but this may be due partly to some phenol impurity, phenol being more difficult to eliminate from *o*-chlorophenol than from the other three *o*-halophenols (1). In computing our results the trans isomers were disregarded since they could only influence the slope at very low ether concentrations, as can easily be shown by using trans/cis ratios which are certainly higher than the true ones.

Can. J. Chem. Downloaded from www.nrcresearchpress.com by 210.87.254.40 on 09/05/12
For personal use only.

o-Fluorophenol deserves some special comment. According to Baker and Kaeding there is an intramolecular hydrogen bond in this molecule, but according to Allan and Reeves there is not. We should like to support the opinion of the former authors since for *o*-, *m*-, and *p*-fluorophenol we obtained a set of curves similar to those shown on Fig. 1, even though the ortho curve runs closer to the meta and para curves than for the ortho halophenols. This means that the *o*-fluorophenol band at 3591 cm^{-1} is either entirely due to an intramolecularly bonded OH group and the trans band is too weak to show up or that the trans band is too close to the cis band and melted into it (see ref. 19). Actually this band is appreciably more intense and somewhat broader than the free OH bands of the other halophenols, although it is not unusually assymetrical. For example:

	A	h, cm^{-1}
o-Fluorophenol	8.64	24.1
m-Fluorophenol	6.28	18.6
p-Fluorophenol	5.97	17.1

A is the integrated intensity in absolute units multiplied by 10^7 and h is the half width (20).

We believe that F < I < Br < Cl is the reliable order of increasing hydrogen bond energies in the ortho halophenols. Nothing emerges from our work, however, to explain this order. The interorbital repulsion theory of Baker and Kaeding offers the only comprehensive explanation available, and it probably goes as far as might be hoped for from qualitative arguments. For a more thorough treatment we shall likely have to wait until the next stage in the development of quantum chemistry.

ACKNOWLEDGMENTS

We are grateful for financial support from the National Research Council of Canada and from the Petroleum Research Fund of the American Chemical Society.

Our thanks are due to Miss Ton-Nu-Thi-Nga for help in carrying out the experimental work.

We are indebted to Mr. David Davies for correcting the English of our manuscript.

REFERENCES

1. A. W. Baker. J. Am. Chem. Soc. **80**, 3598 (1958).
2. A. W. Baker and W. W. Kaeding. J. Am. Chem. Soc. **81**, 5904 (1959).
3. K. U. Ingold. Can. J. Chem. **38**, 1092 (1960).
4. K. U. Ingold. Can. J. Chem. **40**, 111 (1962).
5. L. J. Bellamy and R. L. Williams. Proc. Roy. Soc. (London), Ser. A, **254**, 119 (1960).
6. L. J. Bellamy, G. Eglinton, and J. F. Morman. J. Chem. Soc. 4762 (1961).
7. I. Brown, G. Eglinton, and M. Martin-Smith. Spectrochim. Acta, **18**, 1593 (1962).
8. P. J. Krueger and W. H. Thompson. Proc. Roy. Soc. (London), Ser. A, **250**, 22 (1959).
9. J. A. Pople, W. G. Schneider, and H. J. Bernstein. High-resolution nuclear magnetic resonance. McGraw-Hill Book Co., New York. 1959. pp. 260, 412.
10. O. R. Wulf, U. Liddel, and S. B. Hendricks. J. Am. Chem. Soc. **58**, 2287 (1936).
11. L. Pauling. J. Am. Chem. Soc. **58**, 94 (1936).
12. L. N. Ferguson. Electron structures of organic molecules. Constable, London. 1952. p. 267.
13. A. Cabana, J. L. Patenaude, C. Sandorfy, and P. M. G. Bavin. J. Phys. Chem. **64**, 1941 (1960).
14. E. A. Allan and L. W. Reeves. J. Phys. Chem. **66**, 613 (1962).
15. J. H. Richards and S. Walker. Trans. Faraday Soc. **57**, 412 (1961).
16. L. J. Bellamy and H. E. Hallam. Trans. Faraday Soc. **55**, 220 (1959).
17. C. M. Huggins, G. C. Pimentel, and J. N. Shoolery. J. Phys. Chem. **60**, 1311 (1956).
18. G. Rossmy, W. Lüttke, and R. Mecke. J. Chem. Phys. **21**, 1606 (1953).
19. K. U. Ingold and D. R. Taylor. Can. J. Chem. **39**, 471, 481 (1961).
20. A. Cabana and C. Sandorfy. Spectrochim. Acta, **16**, 335 (1960); and unpublished work.

Can. J. Chem. Downloaded from www.nrcresearchpress.com by 210.87.254.40 on 09/05/12
For personal use only.

REACTIONS OF CARBOHYDRATE DERIVATIVES DURING GAS–LIQUID CHROMATOGRAPHY[1]

C. T. BISHOP, F. P. COOPER, AND R. K. MURRAY[2]
Division of Applied Biology, National Research Council, Ottawa, Canada
Received May 10, 1963

ABSTRACT

The following reactions have been shown to occur during gas–liquid chromatography of carbohydrate derivatives: (*a*) deamidation, (*b*) change in size of the sugar ring, (*c*) rearrangement of acetal or ketal groups, (*d*) degradative rearrangement of acetylated amino sugars. The results emphasize that stability of a compound under conditions used in gas–liquid chromatography is a necessary prerequisite to the application of that technique; the precautions that should be followed to determine stability are indicated.

Can. J. Chem. Downloaded from www.nrcresearchpress.com by 210.87.254.42 on 09/05/12
For personal use only.

The polyhydroxylated carbohydrates are not sufficiently volatile for gas–liquid chromatography and must be converted into stable, volatile derivatives for the successful application of this method of separation. Derivatives that are sufficiently volatile include *O*-methyl ethers (1-4), *O*-acetyl esters (5–7), acetals and ketals (2, 8, 9), and *O*-trimethylsilyl ethers (10–12); through use of these derivatives gas–liquid chromatography has been applied to a number of problems in the chemistry of carbohydrates (13). Although much attention has been given to the search for easily prepared carbohydrate derivatives of sufficient volatility for gas–liquid chromatography, the stabilities of these drivatives under the conditions used have not been critically assessed in most instances. Column temperatures required for gas–liquid chromatography of carbohydrate derivatives range from 150° C to 250° C depending upon the compounds being examined and the injection port is usually kept at a temperature some 60° C higher than the column. Oxidative and hydrolytic processes are probably not operative, or are held to a minimum, in the atmosphere of inert gas (helium, argon, nitrogen) used as a mobile phase. However, among the various classes of organic compounds, carbohydrate derivatives are noted for their lability at high temperatures and for undergoing complex rearrangements under a variety of conditions. The possibility that a carbohydrate derivative may be modified during gas–liquid chromatography should not, therefore, be overlooked.

The present investigation draws attention to this possibility by describing four general types of modification that can occur during gas–liquid chromatography of carbohydrate derivatives. It also indicates those classes of derivatives for which caution should be observed in interpreting results of gas–liquid chromatography and describes methods for determining when modification has occurred. The four general types of modification are (*a*) deamidation, (*b*) change in size of the sugar ring, (*c*) rearrangement of acetal or ketal groups, (*d*) degradative rearrangement of *O*-acetyl esters of amino sugars.

The first modification was illustrated by the behavior of 2,3,5-tri-*O*-methyl-L-arabonamide and 2,3,5-tri-*O*-methyl-D-galactonamide during gas–liquid chromatography. Each amide yielded only ammonia, which emerged with the solvent peak, and the corresponding lactone. The lactones were identified by comparison of their retention volumes (R_v) with those of authentic samples and, after collection from the effluent gas stream, by the melting points of their mixtures with previously characterized specimens.

[1]*Issued as N.R.C. No. 7465.*
[2]*Guest worker, May–September 1962. Present address: Department of Biochemistry, University of Toronto, Toronto, Ont.*

Can. J. Chem. Downloaded from www.nrcresearchpress.com by 210.87.254.42 on 09/05/12
For personal use only.

The change in size of the sugar ring was demonstrated by conversion of methyl 3,6-anhydro-α-D-mannopyranoside to methyl 3,6-anhydro-α-D-mannofuranoside. The pyranoside derivative gave four components on gas–liquid chromatography, the major one (75%) being identified as the corresponding furanoside by its R_v value and, after collection from the effluent gas stream, by the melting point of its mixture with an authentic sample. Methyl 3,6-anhydro-α-D-mannofuranoside showed only one component on gas–liquid chromatography and was recovered unchanged from the effluent gas stream. Identities of the other components arising from methyl 3,6-anhydro-α-D-mannopyranoside could not be established; when recovered from the effluent none of them proved to be the initial compound. These may have been caused by other rearrangements such as anomerization or ring cleavage, or they may have been present as impurities in the methyl 3,6-anhydro-α-D-mannopyranoside. Although the latter had the reported physical properties no other criterion of purity was available.

Rearrangements of acetal and ketal groups were found with the benzylidene glycerols and with di-*O*-isopropylidene-D-mannitols. The mixture of benzylidene glycerols obtained by acid-catalyzed condensation of glycerol with benzyldehyde showed four components on gas–liquid chromatography. These were undoubtedly the cis and trans isomers of 1,2-*O*- and 1,3-*O*-benzylidene glycerol. The four components were collected individually from the effluent gas stream and chromatographed again as a check on their purity. Three of the single components each gave the same four peaks found on the original chromatogram but in varying amounts, showing that equilibrium conditions were not established. The fourth component could be rechromatographed without change and was identified as the stable *cis*-1,3-*O*-benzylidene glycerol. Both 1,2:3,4-di-*O*-isopropylidene-D-mannitol and 1,2:5,6-di-*O*-isopropylidene-D-mannitol were well-characterized, crystalline specimens. Each isomer gave a single peak on gas–liquid chromatography but the retention volumes did not differ greatly and collection of the material from the effluent gas stream gave products with depressed melting points. The di-*O*-acetates of each di-*O*-isopropylidene-D-mannitol showed single peaks with widely differing retention volumes on gas–liquid chromatography and the products were recovered unchanged from the effluent gas stream. The products with depressed melting points, obtained by gas–liquid chromatography of the 1,2:3,4-di-*O*- and 1,2:5,6-di-*O*-isopropylidene-D-mannitols, were therefore acetylated and examined separately by gas–liquid chromatography. The results showed that the 1,2:3,4-di-*O*-isopropylidene-D-mannitol yielded 2% of the 1,2:5,6-di-*O*-isopropylidene isomer and two unknown products (1.5% and 0.5%) on gas–liquid chromatography; 96% of the initial product was recovered unchanged. The 1,2:5,6-di-*O*-isopropylidene-D-mannitol yielded 13% of the 1,2:3,4-di-*O*-isopropylidene isomer and two unknown products (3% and 8%) having the same R_v values as those obtained from the 1,2:3,4-di-*O*-isopropylidene-D-mannitol; 76% of the initial product was recovered unchanged. Identities of the two unknown products could not be established because of a paucity of material but their retention volumes indicated that they were probably di-*O*-isopropylidene hexitols.

An example of the degradative rearrangement of *O*-acetyl esters of amino sugars was obtained in attempts to find a derivative of 2-amino-2-deoxy-D-glucose (glucosamine) that was suitable for gas–liquid chromatography. Gas–liquid chromatography of *N*-acetyl-D-glucosamine tetraacetate (α- or β-anomer) yielded two products that were eluted at different temperatures. The faster-moving component was crystalline, m.p. 80–81° C, $[\alpha]_D^{27}$ −0.6° (*c*, 1.7% in methanol), and was obtained in yields of about 7%. It constituted about 50% of the volatile products. Analyses of the compound indicated the following

composition, $C_{10}H_{11(12)}O_4N$, which included two acetyl groups. Infrared spectroscopy indicated the presence of a C=N grouping, probably in an oxazoline ring. Nuclear magnetic resonance spectroscopy indicated that the following groupings were probably present: 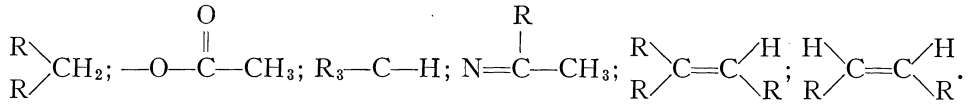 .

The compound decomposed when warmed with acid or base and readily took up bromine. Although further work is required to establish the structure of this product it must be an unsaturated compound, probably containing an oxazoline ring, and quite possibly is a variant of the following structure:

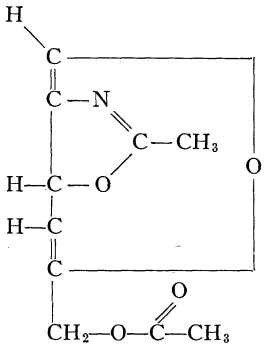

The same two products were obtained from fully acetylated D-galactosamine (α, β mixture). The compound eluted at the higher temperature was not examined further except to show that it was not a fully acetylated hexosamine and therefore must have been another product of degradation.

The results described here could have been caused by the high temperatures of the columns or injection port; by the types of liquid phases or inert supports or any pretreatment of the latter; by the tubing used for the column; by the solvent used for injection of the sample; and no doubt by other parameters as well. No attempts were made to vary any of these parameters in order to reduce or increase the extent of any of the changes described. The conditions used were those normally employed for gas–liquid chromatography of carbohydrate derivatives and the results indicate that considerable modification can occur.

Obviously, amide groups must be regarded as unstable under conditions of gas–liquid chromatography. Similarly, the size of a glycoside ring may be changed in a molecule where that change is structurally favorable and is not forbidden by substituent groups. Acetal and ketal groups may undergo rearrangement on gas–liquid chromatography but it appears that such rearrangement can be prevented by prior substitution of all available hydroxyl groups. Thus, the two di-*O*-isopropylidene-D-mannitols were partially rearranged but their diacetates were completely stable. These three modifications can be anticipated or prevented and hence should not cause much difficulty in the application of gas–liquid chromatography. However, the degradation of *N*-acetyl-D-glucosamine tetraacetate not only showed that compound to be unsuitable for gas–liquid chromatography but raised a question about the propriety of using any *O*-acetyl derivatives for that purpose. Although the structure of the degradation product has not been established completely it is clear that double bonds were formed, most likely by elimination of the elements of acetic acid.

Can. J. Chem. Downloaded from www.nrcresearchpress.com by 210.87.254.42 on 09/05/12
For personal use only.

The effect of the *N*-acetyl group on this elimination is not clear but a similar degradation has been observed with the acetylated aminols, 2-acetamido-2-deoxy-D-glucitol pentaacetate and 2-acetamido-2-deoxy-D-galactitol pentaacetate; mixtures of these two derivatives on gas–liquid chromatography gave highly variable quantitative results that could be accounted for only by a random degradation of the products on the column (14). It may be that the higher temperature required for the gas–liquid chromatography of these amino sugar derivatives is alone responsible for the degradation because good quantitative separations of sugar alcohol acetates have been obtained at lower temperatures (5). However, the same workers have pointed out that *O*-acetyl esters must be injected directly onto the column packing to prevent decomposition of the samples and that discontinuities in the column packings should be avoided for satisfactory results (6).

Obviously, the utmost caution should be used when gas–liquid chromatography is applied to the separation of carbohydrate derivatives. It is essential that compounds be stable under the conditions used if erroneous results are to be avoided. A simple test that will show whether or not any compound is suitable for gas–liquid chromatography is its recovery, unchanged, from the effluent gas stream. Indeed, positive identification of a compound separated by gas–liquid chromatography can be achieved only by its recovery from the effluent gas and determination of its physical constants. The possibility that some products on a chromatogram are artifacts arising from another component can be checked by the collection and reinjection of each separated component in the mixture. The occurrence of partial decomposition of a compound can be detected by quantitative estimations of its mixtures with another compound that is known to be stable under the conditions used. Gas–liquid chromatography can be used safely to separate any derivatives that meet these checks satisfactorily.

EXPERIMENTAL

The following conditions were common to all gas–liquid chromatography experiments described below: apparatus—F and M model 500; column—1/4-inch coiled copper tubing; flow rate—60 ml helium/min; injection port temperature—265° C; detector—thermal conductivity cell.

Deamidation

2,3,5-Tri-*O*-methyl-L-arabonamide (15), m.p. 134–136° C, $[\alpha]_D^{26}$ +20° (*c*, 0.5% in ethanol), was dissolved in 95% ethanol for injection into the chromatogram through a silicone rubber septum by means of a Hamilton syringe. The column temperature was 200° C; the packing was 10% neopentyl glycol succinate polyester on Gas Chrom Z, 100–120 mesh; column length was 8 ft. Only one component was shown on the chromatogram and it had the same R_v value as 2,3,5-tri-*O*-methyl-L-arabonolactone. Samples were injected repeatedly (six to seven times 0.04 ml of a 10% solution) to provide enough of the single component for characterization. The product was collected for the effluent gas stream in a straight glass tube fitted to the outlet port through a silicone rubber *O*-ring. The sirupy product crystallized when cooled and had m.p. 25–26° C, unchanged on admixture with 2,3,5-tri-*O*-methyl-L-arabonolactone (16) having m.p. 27° C and $[\alpha]_D^{26}$ −26° equilibrium (*c*, 0.6% in water).

Gas–liquid chromatography of 2,3,5-tri-*O*-methyl-D-galactonamide (17), m.p. 143–144° C, $[\alpha]_D^{26}$ +5° (*c*, 2% in water), under exactly the same conditions also yielded only one component. It was identified, after collection from the effluent gas stream, as 2,3,5-tri-*O*-methyl-D-galactonolactone (17), m.p. 83–84° C, unchanged on admixture with a sample prepared according to Alexander *et al.* (18) which had m.p. 83–84° C and $[\alpha]_D^{23}$ −38°, 5 minutes (*c*, 1.44% in water).

Moist indicator paper, held at the outlet port, showed a strong basic reaction during emergence of the solvent peak for each of the foregoing samples. This reaction was not observed when solvent alone was passed through the chromatograph.

Change in Size of Sugar Ring

Methyl 3,6-anhydro-α-D-mannopyranoside (19) was prepared according to Foster *et al.* (20) and had m.p. 130–131° C and $[\alpha]_D^{20}$ +97° (*c*, 0.7% in water) in excellent agreement with the reported (19, 20) values. This compound, injected as a solution in ethanol, showed four components on the gas–liquid chromatogram. Except for a higher column temperature (225° C) the conditions of chromatography were exactly the same as those described for the deamidation. The major component (75% of the mixture) crystallized after being

Can. J. Chem. Downloaded from www.nrcresearchpress.com by 210.87.254.42 on 09/05/12
For personal use only.

collected from the effluent gas and had m.p. 84–85° C, unchanged on admixture with methyl 3,6-anhydro-α-D-mannofuranoside (19) having m.p. 84–85° C and $[\alpha]_D^{26}$ +157° (*c*, 3.06% in water), in agreement with reported values. The other three products were present in about equal quantities (each about 8% of the mixture) and none of them was the initial compound. Only one of those three products crystallized; its melting point of 102–103° C indicated that it might be methyl 3,6-anhydro-β-D-mannopyranoside but there was insufficient material to confirm this. Methyl 3,6-anhydro-α-D-mannofuranoside showed only one peak on gas–liquid chromatography and was recovered unchanged from the effluent gas stream.

Acetal and Ketal Migration

A mixture of benzylidene glycerols was prepared according to Baggett *et al.* (21) and examined by gas–liquid chromatography under the following conditions: column—8 ft, 20% Carbowax 20M on Gas Chrom A, 100–150 mesh, 250° C. Four components were revealed with relative retention volumes of 1.00, 1.07, 1.21, and 1.81. The most mobile component (R_v = 1.00) crystallized when collected from the effluent gas and had m.p. 84.5–85° C unchanged on admixture with an authentic sample of *cis*-1,3-*O*-benzylidene glycerol (m.p. 84–85° C) prepared as described previously (21). On rechromatography the *cis*-1,3-*O*-benzylidene glycerol gave only one peak and was recovered unchanged from the effluent gas. Each of the other three components gave all four peaks when rechromatographed.

1,2:3,4:5,6-Tri-*O*-isopropylidene-D-mannitol, m.p. 70° C, was prepared as described by Wiggins (22); 1,2:5,6-di-*O*-isopropylidene-D-mannitol (23), m.p. 123–124° C, was obtained as a water-soluble by-product from preparation of the tri-*O*-isopropylidene derivative; 1,2:3,4-di-*O*-isopropylidene-D-mannitol, m.p. 37° C, was prepared by partial hydrolysis of the tri-*O*-isopropylidene derivative (22).

The di-*O*-isopropylidene-D-mannitols were examined by gas–liquid chromatography using an 8-ft column of 20% QF-1 on Chromosorb-W, 100–120 mesh, at 225° C. Each di-*O*-isopropylidene derivative gave a single peak with similar retention volumes and the products, collected from the effluent gas stream, showed depressed melting points. These products were acetylated separately in pyridine – acetic anhydride and the acetates were examined by gas–liquid chromatography. The material from 1,2:3,4-di-*O*-isopropylidene-D-mannitol showed four components with retention volumes relative to tri-*O*-isopropylidene-D-mannitol of 2.87 (1.5%), 3.47 (96%), 3.79 (0.5%), and 4.06 (2.0%). The material from 1,2:5,6-di-*O*-isopropylidene-D-mannitol yielded products with the same R_v values in yields of 3%, 13%, 8%, and 76% respectively. The product with R_v 3.47 was characterized as 1,2:3,4-di-*O*-isopropylidene-D-mannitol 5,6-diacetate by isolation of 1,2:3,4-di-*O*-isopropylidene-D-mannitol, m.p. 37° C, after deacetylation with barium methoxide. The product with R_v 4.06 crystallized when collected from the effluent gas and did not depress the melting point of 1,2:5,6-di-*O*-isopropylidene-D-mannitol 3,4-diacetate (23), m.p. 123° C. Products with R_v 2.87 and 3.79 were not identified. Each of the known di-*O*-isopropylidene-D-mannitol diacetates gave only one peak when examined separately by gas–liquid chromatography and each was recovered unchanged from the effluent gas stream.

Degradation of Acetylated Amino Sugars

2-Acetamido-2-deoxy-1,3,4,6-tetra-*O*-acetyl-α-D-glucose (24), m.p. 133–134° C, $[\alpha]_D^{25}$ +84° (*c*, 1.21% in chloroform), was examined by gas–liquid chromatography under the same conditions used for the acetals and ketals. One product emerged when the column was maintained at 225° C, and a second product appeared when the column temperature was raised to 270° C. The same two products were obtained from gas–liquid chromatography of the β-anomer, of the mixture from acetylation of *N*-acetyl-D-glucosamine in pyridine – acetic anhydride, and of the mixture from acetylation of *N*-acetyl-D-galactosamine by the same procedure.

The first product crystallized when collected from the effluent gas, m.p. 80–81° C, $[\alpha]_D^{27}$ −0.6° (*c*, 1.7% in methanol). Anal: Calc. for $C_{10}H_{11}O_4N$: C, 57.4%; H, 5.27%; N, 6.70%; for $C_{10}H_{12}O_4N$: C, 57.2%; H, 5.72%; N, 6.67%. Found: C, 56.8%; H, 5.54%; N, 6.50%. Analysis for *O*-acetyl showed the presence of two such groups: 40.95%, calc. 41.1%.

The infrared spectrum in potassium bromide showed the following absorption bands, (S)—strong, (M) medium, (W)—weak; frequencies (cm^{-1}): 3420 (M), 3140 (W), 2930 (W), 1733 (S), 1695 (S), 1655 (S), 1592 (W), 1555 (M), 1412 (M), 1377 (S), 1332 (M), 1305 (M), 1267 (M), 1255 (S), 1185 (W), 1105 (S), 1050 (S), 987 (M), 977 (W), 907 (M), 860 (M), 835 (W), 792 (M), 720 (M), 633 (W). The band at 1695 cm^{-1} was attributed to the C=N bond in an oxazoline ring (25).

τ values	Tentative assignment	τ values	Tentative assignment
8.59 (1H)	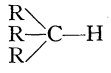	5.14 (2H)	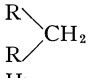
7.82 (3H)	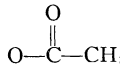	3.20, 2.93, 2.61, 2.34 (2H, quartet)	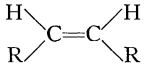
7.52 (3H)	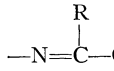	2.23 (1H)	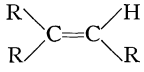

Can. J. Chem. Downloaded from www.nrcresearchpress.com by 210.87.254.42 on 09/05/12
For personal use only.

The 60 Mc/s nuclear magnetic resonance spectrum, measured on a Varian A 60 spectrometer, had peaks at the τ values given in the table, for which the tentative assignments shown were made.

The unknown compound readily decolorized a solution of bromine in carbon tetrachloride and yielded black tars in warm acid or alkali. It readily reduced Fehling's solution in the cold and gave negative tests with ninhydrin and Elson–Morgan reagents.

The second compound, obtained when the column temperature was raised to 270° C, has not been examined. However, it failed to crystallize when seeded with any of the initial products and therefore could not be any of the fully acetylated hexosamines.

ACKNOWLEDGMENTS

The authors wish to thank Dr. O. E. Edwards and Dr. L. D. Hall for their assistance in determining and interpreting the nuclear magnetic resonance spectrum. Dr. P. E. Gardner, Industrial Cellulose Research Ltd., Hawkesbury, Ont., prepared the methyl 3,6-anhydro-D-mannosides in this laboratory in connection with another project. One of the authors (R. K. M.) gratefully acknowledges a grant from the National Research Council of Canada.

REFERENCES

1. A. G. McInnes, D. H. Ball, F. P. Cooper, and C. T. Bishop. J. Chromatog. **1**, 556 (1958).
2. H. W. Kircher. Anal. Chem. **32**, 1103 (1960).
3. C. T. Bishop and F. P. Cooper. Can. J. Chem. **38**, 388 (1960).
4. M. Gee and H. G. Walker. Anal. Chem. **34**, 650 (1962).
5. S. W. Gunner, J. K. N. Jones, and M. B. Perry. Chem. Ind. (London), 255 (1961).
6. S. W. Gunner, J. K. N. Jones, and M. B. Perry. Can. J. Chem. **39**, 1892 (1961).
7. R. J. Ferrier. Chem. Ind. (London), 831 (1961).
8. E. J. Hedgley, O. Meresz, W. G. Overend, and R. Rennie. Chem. Ind. (London), 938 (1960).
9. H. G. Jones, J. K. N. Jones, and M. B. Perry. Can. J. Chem. **40**, 1559 (1962).
10. E. J. Hedgley and W. G. Overend. Chem. Ind. (London), 378 (1960).
11. R. J. Ferrier. Tetrahedron, **18**, 1149 (1962).
12. R. Bentley, C. C. Sweeley, M. Makita, and W. W. Wells. Biochem. Biophys. Res. Commun. **11**, 14 (1963).
13. C. T. Bishop. Methods Biochem. Analy. **10**, 1 (1962).
14. M. B. Perry. Private communication.
15. E. L. Hirst and J. K. N. Jones. J. Chem. Soc. 506 (1946).
16. F. Smith. J. Chem. Soc. 744 (1939).
17. S. P. Luckett and F. Smith. J. Chem. 1114 (1940).
18. B. H. Alexander, R. J. Dimler and C. L. Mehltretter. J. Am. Chem. Soc. **73**, 4658 (1951).
19. F. Valentin. Collection Czech. Chem. Commun. **6**, 354 (1934).
20. A. B. Foster, W. G. Overend, M. Stacey, and G. Vaughan. J. Chem. Soc. 3367 (1954).
21. N. Baggett, J. S. Brimacombe, A. B. Foster, M. Stacey, and D. H. Whiffen. J. Chem. Soc. 2574 (1960).
22. L. F. Wiggins. J. Chem. Soc. 13 (1946).
23. L. Vargha. Ber. **66**, 1394 (1933).
24. C. A. Lobry De Bruyn and W. Alberda van Ekenstein. Rec. Trav. Chim. **18**, 77 (1899).
25. K. Eichenberger, E. Ganz, and J. Druey. Helv. Chim. Acta, **38**, 284 (1955).

Can. J. Chem. Downloaded from www.nrcresearchpress.com by 210.87.254.42 on 09/05/12
For personal use only.

THE ELECTRON DENSITY DISTRIBUTIONS IN HYDRIDE MOLECULES

III. HYDROGEN FLUORIDE[1]

R. F. W. BADER[2] AND G. A. JONES[3]

Department of Chemistry, University of Ottawa, Ottawa, Canada

Received April 2, 1963

ABSTRACT

An electron density distribution is determined for the hydrogen fluoride molecule in its equilibrium configuration by requiring the distribution to predict the correct dipole moment and to exert forces on the nuclei equal and opposite to the nuclear forces of repulsion. The ability of the density function to give good estimates of the expectation values of other one-electron operators is found to be satisfactory. It is shown that an electron population analysis of the orbital densities, when interpreted in terms of the electronic forces which these densities exert on the nuclei, is of value in the understanding of chemical binding.

Can. J. Chem. Downloaded from www.nrcresearchpress.com by 210.87.254.5 on 09/05/12
For personal use only.

INTRODUCTION

In two previous papers (1, 2) we have given the electron density distributions for the equilibrium configuration of the water and ammonia molecules as determined by the requirement that the densities exert forces on the nuclei which are equal and opposite to the nuclear forces of repulsion. In each case the general characteristics, e.g., hybridization and bond polarity, of the densities so obtained are in good agreement with the results obtained from S.C.F. calculations. In addition, the densities determined by the requirement of zero resultant forces provide expectation values for the one-electron operators which are in as good, or better, agreement with experiment as the values predicted by wave functions obtained from S.C.F. calculations. This points to the main reason for carrying out such calculations. It was felt that a reliable picture of the one-electron density could be readily obtained by requiring the distribution to reproduce a property which is itself determined directly by the one-electron density, i.e., the forces on the nuclei. The wave function derived from a variational calculation is obtained by minimizing the energy with respect to the second-order density distribution. Therefore, the resulting one-electron density is not necessarily the best possible one obtainable from the given basis set of orbitals. This was elegantly demonstrated by Mukherji and Karplus in their use of a constrained wave function for hydrogen fluoride (3).

In the present paper we determine the electron density distribution for the hydrogen fluoride molecule by requiring that it balance the forces on the hydrogen and fluorine nuclei and, in addition, give the observed dipole moment. It is worth noting that the criteria of zero resultant forces fixes the electric field due to the density in the region of each nucleus while the requirement of reproducing the observed dipole moment governs the overall disposition of the density in the molecule. The present results substantiate the previous ones in that good estimates are obtained by this method for those molecular properties which depend on the density. In addition, however, we wish to illustrate the advantage gained in the understanding and interpretation of the binding in molecules (4). Since the molecular forces are determined by the one-electron density, their discussion is rigorously carried out in terms of classical electrostatics, thus affording an excellent medium in which to interpret the nature of the binding in a molecule.

[1]*Abstracted from the thesis submitted by G. A. Jones in partial fulfillment of the requirements for the degree of Doctor of Philosophy.*

[2]*Present address: Department of Chemistry, McMaster University, Hamilton, Ontario.*

[3]*Recipient of a Commonwealth Scholarship.*

The Determination of the Density Distribution

The electron density is obtained in terms of the single determinantal L.C.A.O. M.O. approximation. The basis set includes $1s$, $2s$, and $2p$ atomic orbitals on fluorine (denoted by s_o, s, and p respectively) and a $1s$ orbital on hydrogen (denoted by h). The set is later extended to include d orbitals on the fluorine atom. The orbitals are assigned the orbital exponents determined by Ransil (5) in a S.C.F. calculation for the hydrogen fluoride molecule. By using these values (termed the B.L.M.O. set) a meaningful comparison of the S.C.F. and the present results may be made. The molecular orbitals written in the equivalent orbital form are: the fluorine atom inner shell orbital

$$\phi_o = c_o s_o + c_1 s + c_2 p,$$

the bond orbital

$$\phi_b = \lambda[\cos \epsilon_b\, s + \sin \epsilon_b\, p + c_3 s_o] + \mu h_o,$$

and three doubly occupied lone pair orbitals which we write as one sigma lone pair orbital along the bond axis and two π orbitals

$$\phi_l = \cos \epsilon_l\, s - \sin \epsilon_l\, p$$
$$\phi_\pi = p_\pi.$$

These latter three orbitals may of course be combined to give three equivalent lone pair orbitals. The angle the equivalent lone pair orbitals make with the bond axis will be determined by the relative amount of $2s$ and $2p$ in the ϕ_l orbital.* The symbols h_o and s in the above expressions denote orbitals orthogonal to the s_o orbital of fluorine.

The orbitals embody three independent parameters: ϵ_b, the bond hybridization parameter, ϵ_l, the corresponding parameter for the lone pair orbital, and the polarity factor λ/μ. These three variables are fixed by requiring the density to balance the two nuclear forces and duplicate the dipole moment. The remaining orbital coefficients are uniquely determined by the orthogonality conditions which are listed in the Appendix. The values of the parameters which satisfy the three conditions are given in Table I together with the

TABLE I

Parameters for the electrostatic and S.C.F. molecular orbitals for HF

	ϵ_b	ϵ_l	λ/μ	Force on H (a.u.)*	Force on F (a.u.)	Dipole moment (D)
Electrostatic method	112°46′	−6°0′	1.6845	−0.004	0.000	1.82
S.C.F. (4)	100°23′	6°41′	1.377	−0.084	−2.944	1.44

*A negative force is one in the same direction as the force of nuclear repulsion.

values of the same parameters obtained from the transformed S.C.F. calculation of Ransil (5).†

These parameters succinctly characterize the density distribution. The value of ϵ_l for the electrostatic density indicates that the sigma lone pair orbital is 99% $2s$ and 1% $2p$

For example, when $\epsilon_l = 0$, the equivalent lone pair orbitals are sp^2 hybrids in a plane perpendicular to the bond axis through the fluorine nucleus, and when $\epsilon_l = 30°$, the orbitals are sp^3 hybrids which project out behind the fluorine nucleus symmetrically placed around the bond axis at an angle of 70°32′ with this axis.

†*Equivalent orbitals are obtained from the 2σ and 3σ symmetry orbitals of Ransil by an orthogonal transformation which yields one orbital with no hydrogen contribution (the lone pair) and another containing all of the hydrogen contribution (the bond orbital). This results in a unique set of orbitals.*

Can. J. Chem. Downloaded from www.nrcresearchpress.com by 210.87.254.5 on 09/05/12
For personal use only.

in character. Since ϵ_l is negative, the small amount of $2p$ character present actually projects density towards the hydrogen atom rather than away from it. This gives three equivalent lone pair orbitals of almost sp^2 character (1.00 part $2s$, 2.03 parts $2p$) which make an angle of 86° with the bond axis, and are directed towards the H atom. Conceivably, the sigma lone pair orbital could possess an orbital character of either $2s$ or $2p$ or any intermediate hybrid. As previously pointed out (1) only the limiting $2s$ form for this orbital will result in a balanced force on either the fluorine or hydrogen nuclei. Any lone pair s–p hybridization on the fluorine atom in the conventional direction results in a large force on the fluorine nucleus in a direction away from the hydrogen. This same s–p polarization removes density from the binding region and places it behind the fluorine nucleus, thus resulting in a greatly decreased shielding with respect to the hydrogen nucleus. Of the two possible limiting forms $2s$ and $2p$, the lone pair will become a $2s$ orbital and the bond orbital will then be primarily $2p$ in character. This form for the bond orbital exerts a much larger binding force than does the $2s$ form (1). Similar results were obtained for the water and ammonia molecules, both of which were predicted to possess lone pair orbitals with the maximum possible amount of $2s$ character.

To reach the limiting $2s$ form for the lone pair orbital orthogonality restrictions require the introduction of negative $2s$ character into the bond orbital, i.e., $\epsilon_b > 90°$. In the water and ammonia molecules the amount of negative $2s$ character so introduced was reduced to a minimum by delocalization of the hydrogen $1s$ orbitals. No such mechanism is possible in the case of hydrogen fluoride and consequently a larger percentage (actually 15%) of negative $2s$ character must be included in the bond orbital. It is interesting, however, that the nuclear force on hydrogen can still be balanced in spite of the density removed from the binding region by this adverse polarization of the fluorine density. Such is not the case for water and ammonia, where the forces on hydrogen cannot be balanced for large negative values of $\cos \epsilon_b$. Thus, where delocalization is possible, it is found to be essential, and where not possible, not necessary in order to achieve electrostatic equilibrium. Actually the slight projection of the sigma lone pair orbital towards the hydrogen atom in hydrogen fluoride compensates for the reverse polarization in the bond orbital.

A large bond polarity λ/μ is necessary to meet the observed dipole moment. There is a small positive atomic dipole contribution from the reverse hybridization in the bond orbital but the major contribution to the dipole moment is due to removal of charge from hydrogen (small μ) to the fluorine (large λ). This again is similar to the previous results for water and ammonia where the dipole was found to be due almost entirely to the bond polarity. A density contour map of the electron density for hydrogen fluoride by the electrostatic method is shown in Fig. 1.

The general features exhibited by the S.C.F. density distribution are similar to those found from the electrostatic approach. Lone pair hybridization is unimportant (although the small amount of hybridization, $\epsilon_l = 6°41'$, predicted by the S.C.F. function has a very adverse effect on the forces). The bond orbital contains 3% negative $2s$ character. Polarity is significantly smaller, as reflected in the low value of the predicted dipole moment.

Duncan and Pople (15) determined density distributions for the hydrogen fluoride, water, and ammonia molecules by requiring the density to duplicate only the observed dipole moment. In all three cases their results predicted a large degree of hybridization for the lone pair electrons (approaching overall sp^3 hybridization in all three molecules). We have previously shown (1, 2) these results to be untenable for water and ammonia,

Can. J. Chem. Downloaded from www.nrcresearchpress.com by 210.87.254.5 on 09/05/12
For personal use only.

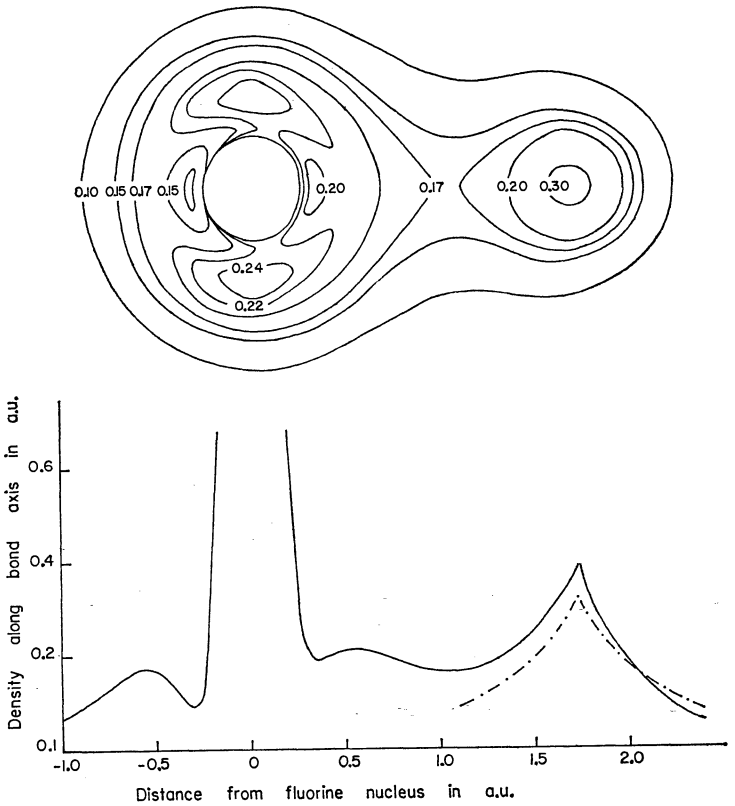

FIG. 1. The upper diagram gives lines of constant density in a plane through the hydrogen fluoride molecule, as determined by the electrostatic method. Only the valence orbital contributions are shown. The concentration of the lone pair electrons in p_π orbitals and in the $2s$ orbital leads to a pileup of density in the plane through fluorine perpendicular to the bond axis and an effective "hole" behind the fluorine nucleus. The lone pair density is concentrated toward the hydrogen nucleus, where it can exert a binding force on both nuclei.

Below the contour map is a graph showing the variation in electron density along the bond axis. The dotted line is the density distribution in an isolated hydrogen atom. It can be seen that the increased orbital exponent of the h orbital in the molecule tends to counteract the effect of a high bond polarity, so that the peak height at the proton is hardly changed on bond formation.

where such lone pair hybridization results in enormous forces of repulsion on all of the atoms in the molecule. The failure of their method in these two cases was due to their relating the degree of hybridization to bond geometry (i.e., not allowing for bent bonds or delocalization). In their treatment of hydrogen fluoride they exclude the possibility arrived at in this paper of three equivalent lone pair orbitals projected in a plane perpendicular to the bond axis through the fluorine nucleus (sp^2 hybridization). They do this on the grounds that such hybridization would of necessity lead to negative λ/μ values, i.e., correspond to an antibonding bond orbital. This is not a consequence, however, if one allows for negative values of cos ϵ_b as in the present treatment or as found in the S.C.F. wave function. (This can be seen from their equation number 4.2.) The distribution favored by Duncan and Pople has three lone pair orbitals of approximately sp^3 hybridization projected out behind the fluorine nucleus. This distribution results in large unbalanced forces of repulsion on both the hydrogen and fluorine nuclei. For the sp^3 case, the final force on the proton is -1 a.u. and on the fluorine nucleus is -13 a.u. These figures should be compared with those in Table I.

Can. J. Chem. Downloaded from www.nrcresearchpress.com by 210.87.254.5 on 09/05/12
For personal use only.

The electrostatic density distribution predicted for hydrogen fluoride agrees with the rule previously proposed (1): "in hydride molecules which possess at least one lone pair of electrons the bond orbitals will be primarily of p character and the lone pair orbitals will contain close to the maximum possible amount of s character". The "maximum possible amount of s character" corresponds in each case to the lone pair density being symmetrically placed with respect to a plane passing through the heavy nucleus and perpendicular to the main symmetry axis: sp^2 orbitals in HF, sp orbitals in H_2O, and an s orbital in NH_3. These forms for the orbitals do not exert any force on the heavy nucleus, and in addition they provide the maximum possible screening of the heavy nucleus from the protons. Any increase in p character from these lower limits displaces charge from the hydrogen side to the remote side of the F, O, and N nuclei and results in large imbalanced forces on both the hydrogen and heavy-atom nuclei.

It is always found that it is necessary to introduce inner shell polarization to an appreciable extent to balance the nuclear force of repulsion on the heavy atom in the hydride molecules with lone pair electrons. This polarization is brought about by including a $2p$ contribution in the inner shell orbital. In the present calculation the coefficient determining the amount of $2p$ so introduced (c_2) has a value of 0.069653.* This is larger than that predicted by variational calculations but it must be pointed out that the S.C.F. results for H_2O, NH_3, and HF all predict a resultant force on the heavy atom approximately equal to the full nuclear force of repulsion. Such a large discrepancy denotes a serious lack of flexibility in the basis orbitals chosen for the S.C.F. calculations. Because of the $1/r_i^2$ dependence of the forces, any inadequacy of the wave function in regions close to a heavy nucleus is emphasized more than in an energy calculation. The large value of c_2 found necessary for electrostatic equilibrium could be markedly reduced if an orbital which permitted polarization of the $1s$ density close to the heavy nucleus was included in the basis set. A good choice for such an orbital would be a "Kp" orbital, i.e. one of the form $\cos\theta\, e^{-\alpha r}$. Since this orbital, unlike the $2p$, has no pre-exponential radial dependence it peaks at the nucleus and, therefore, provides a much larger polarization and hence larger force than the same amount of $2p$. The present results and those for water and ammonia (1, 2) suggest that the inclusion of such an orbital will be necessary for obtaining wave functions from S.C.F. calculations which satisfy the criterion of electrostatic equilibrium.

Another form of polarization not represented in the basis set is that of $2p$ with $3d$. To be most effective these should be "shrunken" $3d$ orbitals, of the same radius as the $2p$ orbitals. In order to investigate the effect of $3d$ polarization by the present method it is necessary to ignore inner shell polarization as we have only three restraining conditions available. It is found that invoking $3d$ polarization cannot of itself enable the system to attain electrostatic equilibrium. The d_π or d_σ polarization removes density from the outermost regions of the fluorine atom and concentrates it in the region between the nuclei. This displaced density increases the force on the hydrogen nucleus as well as the force on fluorine. Regardless of the values assigned to the other parameters the amount of $3d$ polarization necessary to balance the force on fluorine always results in too large a force on the proton. On the other hand, inner shell polarization can be introduced to balance the force on fluorine without greatly changing the force on the proton and thus the system can attain electrostatic equilibrium. This is due to the fact that inner shell polarization displaces charge close to the fluorine nucleus rather than moving it into the overlap

*We previously reported values of c_2 for the water and ammonia molecules about a factor of 10 less than the present value. This is due to our neglect of the overlap between the heavy atom 1s orbital and the hydrogen 1s orbital. When this overlap is taken into consideration the c_2 values are comparable to that obtained for HF but the remaining parameters in the H_2O and NH_3 densities remain unchanged.

Can. J. Chem. Downloaded from www.nrcresearchpress.com by 210.87.254.5 on 09/05/12
For personal use only.

region. In a fuller treatment using this extended basis set, the $3d$ orbitals may provide part of the shielding obtained by negative lone pair hybridization in the present treatment. Sternheimer (6) has calculated the electric field at various nuclei in atoms and ions when they are subject to an external perturbing field. He concluded that inner shell polarization was very important for the alkali atoms (7), but in the negative fluoride ion (8) he found that the largest contribution to the electric field came from a p–d type perturbation. In the latter treatment the inner shell was approximated by a Slater $1s$ orbital as opposed to the Hartree-Fock orbitals employed for the valence electrons. Sternheimer estimated an error of $\pm 20\%$ in the inner shell contribution as a result (8), but since this contribution was small compared to those of the s–p, p–s, or p–d perturbations, the final result was not affected. It seems therefore that $3d$ polarization is much more important in the diffuse negative ion than in the neutral fluorine atom taking part in bond formation.

A Force Analysis of the Wave Functions for HF

An investigation of the forces exerted by an electron density distribution provides insight into the nature of molecular binding (4). When the L.C.A.O. approach is used in the construction of molecular orbitals the resulting density expression will consist of a sum of products of atomic orbitals of the form $c_i c_j \phi_{i\alpha}\phi_{j\beta}$ where c_i and c_j are the orbital coefficients and ϕ_i and ϕ_j denote the type of orbital ($1s$, $2s$, etc.) situated on nucleus α or β. We thus obtain the three basic electron populations, the atomic population terms $\phi_{i\alpha}\phi_{j\alpha}$ or $\phi_{i\beta}\phi_{j\beta}$ and the overlap population $\phi_{i\alpha}\phi_{j\beta}$. Each of these three electron populations gives rise to its own distinct contribution to the force acting on a particular nucleus.

Atomic Force

The atomic force is the force exerted on nucleus α by the density $\phi_{i\alpha}\phi_{j\alpha}$. If $\phi_{i\alpha}\phi_{j\alpha}$ possesses a center of symmetry, then this density will not exert a force on nucleus α. However, the introduction of any asymmetry, due to hybridization or polarization, gives rise to a force on nucleus α. Consequently the atomic force term is sensitive to the degree of charge polarization on a nucleus.

Penetration Force

The penetration force is the force exerted on nucleus α by the atomic charge density situated entirely on another nucleus, $\phi_{i\beta}\phi_{j\beta}$. It is a measure of the electronic shielding of nucleus β from nucleus α and the amount of this shielding is determined by the extent to which nucleus α penetrates the density around β. When $\phi_{i\beta}\phi_{j\beta}$ possesses spherical symmetry the penetration force has a particularly simple physical interpretation. It can be shown from a well-known theorem of electrostatics that the total force exerted on α by a spherical charge density on β is simply the force that would be exerted by that density contained within a sphere of radius d (the bond length) if all this charge was situated at nucleus β. Thus the penetration force due to spherical orbitals is numerically equal to the number of electrons contained in a sphere of radius equal to the bond length, all divided by d^2. As d decreases, a smaller fraction of the electrons is contained in the smaller sphere and nucleus β is less shielded from nucleus α. The density of tightly held inner shell electrons lies completely within the sphere defined by the bond length and thus they effectively screen an equal number of nuclear charges. The more diffuse valence shell electrons do not. The electron density in a p_σ orbital on β, since it places charge along the bond axis, exerts a shielding force greater than the same amount of density spherically disposed. Electrons in p_π orbitals, on the other hand, are less effective than s electrons at shielding since their density is principally directed perpendicular to the bond axis. As would be

Can. J. Chem. Downloaded from www.nrcresearchpress.com by 210.87.254.5 on 09/05/12
For personal use only.

anticipated a closed shell in which all the orbitals have the same orbital exponent, i.e. a $ns^2np_\sigma^2np_\pi^4$, acts as a spherical distribution and the force is simply eight times that of a single electron in an ns atomic orbital.

Overlap Force

The overlap force is the force on nucleus α due to the density $\phi_{i\alpha}\phi_{j\beta}$ resulting from the overlap of the two atomic orbitals. This force term is a sensitive measure of the binding power of a molecular orbital. The binding is not simply proportional to the extent of overlap, of equal importance is where this density is placed. Thus a $2s1s$ overlap is larger than is a $2p1s$ overlap, but the latter is much more effective at binding since more of the overlap charge density is placed along the bond axis, where it exerts the maximum force.

We shall illustrate the advantages of a force analysis by applying the method to Ransil's S.C.F. results for hydrogen fluoride. We consider the forces exerted on the hydrogen atom first. The forces due to the atomic and overlap populations for each of the symmetry orbitals are given in Table II. Since the atomic density on hydrogen possesses spherical

TABLE II

Forces on the proton in HF (S.C.F. density) in a.u. of $(1/d^2)$

Orbital	Penetration force P_H	Overlap force O_H	Electronic force	Nuclear repulsion	Net force
1σ	2.00	0.00	2.00	−2.00	0.00
2σ	1.77	0.38	2.15	−2.00	+0.15
3σ	0.97	0.57	1.54	−1.00	+0.54
π	3.07	0.00	3.07	−4.00	−0.93
Total	7.81	0.95	8.76	−9.00	−0.24

symmetry ($1s$ orbital) there are no atomic force contributions in this case. Great simplification is achieved by omitting the factor $1/d^2$ from the numerical values of the forces. The nuclear repulsion is then simply $-Z_FZ_H = -9$. The sum of the electronic forces must equal minus this same number to attain electrostatic equilibrium. In the case of the separated atoms where there is no penetration each electron shields one unit of nuclear charge and the net force is zero.* We therefore break up the total nuclear repulsion of -9 into contributions for each orbital as determined by the shielding each orbital would exert in the case of the separated atoms. Consider the 1σ orbital. This orbital is made up almost entirely from the $1s$ orbital on fluorine. The pair of electrons in this orbital is very tightly held by the fluorine nucleus as is evidenced by the fact that the penetration force equals simply 2.000. Thus these two electrons effectively shield 2 units of positive charge on the fluorine nucleus from the hydrogen nucleus. The overlap force term in this case is insignificant and the net force due to this orbital and its share of the nuclear charge is zero. That is, in the separated atoms or in the molecule the inner shell orbital on fluorine simply acts to shield two units of nuclear charge, exerting no resultant force on the hydrogen nucleus. This is termed a *nonbinding* orbital in accordance with the definition previously proposed (4).

In the limit of separated atoms the 2σ orbital becomes the doubly occupied $2s$ orbital on fluorine and so is again assigned two units of the nuclear repulsion. The penetration of this charge density by the proton is much greater than in the 1σ case as evidenced by

**There would be a small quadrupole force operative due to the fact that fluorine does not have a closed-shell structure.*

Can. J. Chem. Downloaded from www.nrcresearchpress.com by 210.87.254.5 on 09/05/12
For personal use only.

the value for $P_H(2\sigma)$ being less than 2. However, this loss is offset by the gain in force due to the density transferred to the overlap region. The net force is +0.15, which thus makes the 2σ orbital a *net-binding* orbital. The fluorine contribution to the 3σ orbital in the limit of separated atoms becomes a singly occupied $2p$ orbital. Thus it is assigned a corresponding nuclear repulsion of −1 unit. The molecular orbital of course contains two electrons, but of these one is gained from the hydrogen in bond formation. Thus the penetration for the 3σ orbital is to be measured against −1 and due to the large p character of this orbital it is seen to approach this limiting value quite closely. In addition, there is a large overlap force which points to this orbital as being the main source of the binding of the proton in the hydrogen fluoride molecule. An analysis of the 2σ and 3σ orbitals in terms of Mulliken's method of overlap populations (9) leads to the opposite conclusion. In such an analysis the bonding character of an orbital is related to the magnitude of the overlap population irrespective of where this overlap density is placed. The $2s$ orbital of fluorine, which is the main constituent of 2σ, has a larger numerical overlap with hydrogen than does the $2p_\sigma$ orbital found primarily in the 3σ orbital. Thus the 2σ orbital is found to have the highest overlap population and is thus rated as being the most strongly bonding orbital. As was pointed out in the discussion of the overlap forces, the $2p_\sigma$ overlap, while numerically less than the $2s$ overlap, concentrates the overlap density along the bond axis, where it exerts a much greater force on the proton than does the $2s$ overlap density. Thus the force analysis which relates the strength of binding not to the density itself but to the actual force exerted by the density leads to the conclusion that the 3σ orbital is the orbital principally responsible for binding the proton in the hydrogen fluoride molecule. The 3σ orbital is again a net-binding orbital, as the resultant force is one which draws the two nuclei together.

The degenerate p_π orbitals have no overlap with the hydrogen and are thus restricted to a penetration force. Out of the four units of nuclear charge they shield in the separated atoms, only approximately three of these are shielded at the equilibrium bond length. These orbitals thus give a net force of −1, which tends to push the two nuclei apart. The p_π orbitals are, therefore, net *antibinding*. Since Ransil's wave function does not predict a zero resultant force for the hydrogen nucleus the total electronic force does not equal the total nuclear force in this case as can be seen from the totals given in the last row of the table. The totals of the separate force contributions are of some interest. The density in the overlap population exerts 11% of the total electronic force which binds the proton in HF. The other 89% of the binding is due entirely to the density on the fluorine nucleus. It should be recalled that at infinite separation $P_H = 9.00$ and $O_H = 0.00$. Thus in forming the molecule the proton penetrates the fluorine atom density to the extent that effectively only 7.8 of the nuclear charges are screened but there is an accompanying transfer of density to the binding region which gives rise to the overlap forces and thus to the formation of a stable molecule. Table III gives the corresponding breakdown for the forces on hydrogen obtained in terms of equivalent orbitals by the electrostatic method. If Ransil's orbitals are transformed into equivalent orbitals, the 2σ and 3σ orbitals become the ϕ_l and ϕ_b orbitals. The ϕ_o and p_π orbitals give almost identical results in the two cases (the p_π's exactly so). Thus to compare the densities we may compare the sum of the contributions of ϕ_b and ϕ_l with those from 2σ and 3σ. The electrostatic density is seen to predict a greater shielding of the fluorine nucleus, actually giving a result of 3.21, which is greater than the 3 units of nuclear charge associated with these two orbitals in the separated atoms. This is obtained by a large λ/μ value, removing charge from hydrogen and placing it on the fluorine atom in the bonding orbital, and by

Can. J. Chem. Downloaded from www.nrcresearchpress.com by 210.87.254.5 on 09/05/12
For personal use only.

TABLE III

Forces on the proton in HF (electrostatic density)

Orbital	P_H	O_H	Electronic force	Nuclear force	Net force
ϕ_o	2.02	0.00	2.02	−2.00	+0.02
ϕ_b	1.10	0.70	1.80	−1.00	+0.80
ϕ_l	2.11	0.00	2.11	−2.00	+0.11
ϕ_π	3.07	0.00	3.07	−4.00	−0.93
Total	8.30	0.70	9.00	−9.00	0.00

having a negative ϵ_l for the lone pair which removes charge from behind the fluorine nucleus and places it on the side facing the proton. The total overlap force is actually less in the electrostatic case, but the total electronic force is now large enough to achieve electrostatic equilibrium.

In Table IV we give the breakdown of the forces operating on the fluorine nucleus for

TABLE IV

Forces on the fluorine nucleus in HF (in units of $9/d^2$ a.u.)

Orbital	A_F	O_F	P_F	Electronic force
		Electrostatic density		
ϕ_o	2.565	0.000	0.000	2.565
ϕ_b	−4.105	1.393	0.386	−2.326
ϕ_l	0.761	0.000	0.000	0.761
Total	−0.779	1.393	0.386	1.000
		S.C.F. density		
1σ	0.078	−0.004	0.000	0.074
ϕ_b	−1.395	1.656	0.483	0.744
ϕ_l	−0.800	0.000	0.000	−0.800
Total	−2.117	1.652	0.483	0.018

both the electrostatic and S.C.F. densities. As previously stated, the S.C.F. calculation falls far short of predicting a zero resultant force on the fluorine nucleus. The principal reason for this is the large negative atomic force due to the *sp* hybridization in the sigma lone pair orbital. In the electrostatic calculation this atomic force term is of positive sign (due to the negative value for ϵ_l). These figures illustrate the great sensitivity of the force on a heavy nucleus to atomic polarization of the charge density. Any hybridization must be proposed with care as it results in exceedingly large forces acting on the nucleus in question.

The Calculation of the Molecular Properties Determined by the One-electron Density

Many of the moments of hydrogen fluoride which can be compared to observed properties of the molecule have been calculated by Karplus and Lipscomb and co-workers (10–13). They found that wave functions which gave reasonable estimates of energies did not necessarily yield good estimates of these properties. A method of "constrained" variation calculations was suggested by Karplus and Mukherji (3). In this approach it was required that integrals of certain operators agreed with the known values for the corresponding properties. It was hoped that the resultant increase in energy would be more than

Can. J. Chem. Downloaded from www.nrcresearchpress.com by 210.87.254.5 on 09/05/12
For personal use only.

compensated for by an increase in the accuracy with which other one-electron operator functions could be calculated. The method was applied to hydrogen fluoride, by modifying the 'best limited' wave function obtained by Ransil. Karplus and Mukherji chose as constraining functions the dipole moment and the electric field gradient at the deuteron in DF. They found that the diamagnetic and paramagnetic contributions to the susceptibility were in better agreement with experiment; the calculated diamagnetic proton shielding constant decreased, but no accurate measurement is available for comparison; the force on the hydrogen nucleus approached closer to zero, but the force on fluorine increased. The significance of their results is clear: for the first time it has been demonstrated that, starting with a given set of basis orbitals, that wave function which gives the best energy does not necessarily predict the best values of all other properties.

It was concluded from the anomalous value predicted for the force on the fluorine nucleus that "considerably greater distortion of the fluorine atom wave function than that permitted by limitations in the basis set appears to be required". However, the inner shell orbital was left unchanged in the constrained treatment on the grounds that a variation of its coefficients would result in a large increase in energy and only a small change in the dipole moment and field gradient. The present calculations indicate that the force on fluorine would greatly improve if such a variation was included.

It is possible to compare three wave functions using the same basis set of orbitals but derived under the following criteria:

(i) the minimum energy criterion of the variation method (Ransil);

(ii) the same, with the additional requirements that $\langle P_2/r_D^3 \rangle$ and $\langle P_1 r \rangle$ give the correct values (Karplus and Mukherji);

(iii) the criterion of electrostatic equilibrium, which requires $\langle P_1/r_H^2 \rangle$ and $\langle P_1/r_F^2 \rangle$ to be correct, with the dipole moment criterion of $\langle P_1 r \rangle$.

The properties calculated from these functions are listed in Table V. Two densities are given for the electrostatic method to illustrate how the properties change with lone pair hybridization. On transforming the constrained function it is found that $\epsilon_1 = 8.5°$ compared to 0° and $-6°$ for the best electrostatic densities. These latter three functions all have the correct dipole moment and therefore the same polarity of $\sim$1.6, compared to a λ/μ of 1.38 for the Ransil function.

Forces and Deuteron Quadrupole Coupling Constant

The forces for the electrostatic case are equal to or close to zero since they were used to fix the densities. The difference between the forces predicted by the other two functions can be explained in terms of the parameters describing them. Since more lone pair hybridization is predicted by the constrained function than by Ransil's, the force on fluorine increases. However, the force on hydrogen is more sensitive to the change of polarity than to this small increase in ϵ_1 and it consequently improves. The reason for this unfavorable change in the lone pair hybridization in the constrained function can be found in the criterion of meeting the deuteron quadrupole coupling constant.

Kolker and Karplus (12) have discussed the contribution to this constant from different atomic orbitals on fluorine in relation to the corresponding nuclear contributions. They found that the 1*s* electrons exactly shield their share of charge while the $2p_\pi$ electrons only shield about two-thirds of the corresponding nuclear charge. Thus both the field and the field gradient at the nuclei, as measured by the forces and the quadrupole coupling constants respectively, are sensitive to the same parameters. The same factors tend to increase or decrease the electronic contribution to both the field and the field gradient

Can. J. Chem. Downloaded from www.nrcresearchpress.com by 210.87.254.5 on 09/05/12
For personal use only.

Can. J. Chem. Downloaded from www.nrcresearchpress.com by 210.87.254.5 on 09/05/12
For personal use only.

TABLE V

Properties of hydrogen fluoride

Property	S.C.F. calculation*	Constrained calculation	Electrostatic calculations $\epsilon_1 = 0°$	Electrostatic calculations $\epsilon_1 = -6°$	Experiment
Dissociation energy (ev)	2.56	2.44	—	—	6.06±0.2†
Dipole moment (D)	1.44	1.82	1.82	1.82	1.820±0.003‡
Diamagnetic susceptibility $\times 10^6$ (e.m.u./mole)§	−9.585	−9.329	−9.200	−9.112	−9.2
Proton shielding constant $\times 10^5$‖	3.11	3.01	2.98	2.97	—
Deuteron quadrupole coupling constant (kc/sec)¶	372.2	339.9	306.0	284.0	340±40
Force on fluorine (a.u.)**	−2.944	−3.099	0.000	0.000	0
Force on hydrogen (a.u.)	−0.084	−0.044	−0.018	−0.004	0

*Apart from the deuteron quadrupole coupling constant, all moment results listed for the constrained function and for Ransil's function have been checked by an independent evaluation of integrals.

†J. W. C. Jones and R. F. Barrow. Proc. Roy. Soc. (London), Ser. A, **251**, 504 (1959).

‡R. Weiss. Abstracts of 6th Brookhaven Conference on Molecular Beams, June, 1962.

§The diamagnetic contribution was calculated from the fluorine nucleus as origin. R. P. Hurst, M. Karplus, and T. P. Das, J. Chem. Phys., **36**, 2786 (1962), calculated the corresponding paramagnetic term from the results of M. R. Baker, C. H. Anderson, J. Pinkerton, and N. F. Ramsey, Bull. Am. Phys. Soc., **6**, 19 (1961), on the rotational magnetic moment of HF. The total susceptibility was measured by P. Ehrlich, Z. Anorg. Allgem. Chem., **249**, 219 (1942). Combining these leads to the "experimental" value quoted.

‖The paramagnetic part of the shielding constant is −79.6±0.5 p.p.m. as determined by S. I. Chan and T. P. Das, J. Chem. Phys., **37**, 1527 (1962), from the spin rotational constants measured by N. F. Ramsay, Am. Scientist, **49**, 509 (1961). The proton was taken as the origin for the diamagnetic part.

¶Q_D was taken as 2.82×10^{-27} cm² (J. P. Auffray. Phys. Rev. Letters, **6**, 120 (1961)). The experimental determination of the coupling constant of DF was made by H. M. Nelson, J. A. Leavitt, M. R. Baker, and N. F. Ramsey, Phys. Rev., **122**, 856 (1961).

**The result for the force on fluorine for Ransil's function was slightly in error in the work of Karplus and Mukherji (3). The authors agree with the present value.

at the proton. As the lone pair hybridization decreases (other factors being equal) both these quantities decrease. At $\epsilon_1 = 8.5°$ the calculated coupling constant reproduces the experimental value, but the force on hydrogen is too large; at $\epsilon_1 = -6°$ the force on hydrogen is correct, but the calculated coupling constant is lower than the experimental value. The chosen value of the deuteron quadrupole coupling constant is subject to experimental error and the calculated value is subject to an uncertainty in Q_D (12). Thus the deuteron quadrupole coupling constant would seem to be a less reliable criterion of the density distribution than that of electrostatic equilibrium.

Diamagnetic Susceptibility

The diamagnetic contribution to the susceptibility of hydrogen fluoride (χ_d) is determined by $\langle r_F^2 \rangle$ and therefore by the density in the region of the proton, where r_F is large. Changes in hybridization of the fluorine atom would have little effect on this property. The factors which determine the density at the hydrogen nucleus are the polarity and the orbital exponent of the $1s$(H) orbital. A low polarity and a small orbital exponent both increase this density and, as a result, χ_d. The first effect is illustrated by the results in Table V. Both the constrained function and the electrostatic functions have the correct dipole moment and give very good estimates of χ_d. The S.C.F. density has a low polarity, as shown by the dipole moment, and predicts too large a value for χ_d. It can be concluded from these susceptibility calculations that the electrostatic function with $\epsilon_1 = 0$ gives the best representation of the density at hydrogen. However, the lack of an error estimate for the experimental determination detracts from the significance of the agreement with this particular point.

Proton Shielding Constant

No accurate measurement of the proton chemical shift of gaseous hydrogen fluoride is available, due to experimental difficulties (12). The shielding constant of gaseous methane is 3.01×10^{-5} and that of unassociated hydrogen fluoride is within 2 p.p.m. of this value. The results given in Table V indicate that the chemical shift is very small relative to methane. Perhaps this is the reason for the failure of Schneider and co-workers (14) to observe a signal due to gaseous HF relative to methane. Again the constrained density and electrostatic densities give very similar results while the S.C.F. density predicts a larger value. The latter can be attributed to the low polarity predicted by the straight energy calculation. Since the shielding constant measures the amount of density right at the nucleus, while the susceptibility is determined by that density in the general region of the proton, it is less sensitive to polarity than it is to choice of orbital exponent.

Dipole Moment

The importance of the dipole moment in determining molecular properties is apparent from these results, particularly if they are compared to those calculated from the simple "Slater atom" and "best atom" orbitals (11, 12) which predict very low dipole moments. A wave function predicting the correct dipole moment for which the hydrogen orbital exponent has been optimized might be expected to always yield good estimates of the diamagnetic susceptibility and proton-shielding constant. The field and field gradient are more sensitive than these properties to the details of the electron distribution on each nucleus, but still need an accurate estimate of the polarity to yield the correct results.

The calculations of the molecular properties support our thesis that the forces and dipole moment provide a good test of the overall density distribution. A density satisfying these criteria will also yield good estimates of the other one-electron properties discussed above.

Can. J. Chem. Downloaded from www.nrcresearchpress.com by 210.87.254.5 on 09/05/12
For personal use only.

ACKNOWLEDGMENTS

We wish to thank the Computing Centre at the University of Ottawa for their assistance and machine time on the I.B.M. 650 used in these calculations. We are also grateful to Mr. Peter Sefton for his mathematical assistance and to Professor Martin Karplus for the integrals used in the calculation of the deuteron quadrupole coupling constant.

APPENDIX

The requirement of orthogonality between the orbitals gives rise to three orthogonality conditions. In these, S_2 and S_3 are the overlaps of h_o with the s and p orbitals on fluorine.

Bond – lone pair condition:

$$[1] \qquad \tan \epsilon_1 = \frac{\lambda/\mu \cos \epsilon_b + S_2}{\lambda/\mu \sin \epsilon_b + S_3}.$$

Bond – inner orbital condition:

$$[2] \qquad \lambda[c_1 \cos \epsilon_b + c_2 \sin \epsilon_b + c_o c_3] + \mu[c_1 S_2 + c_2 S_3] = 0.$$

Lone pair – inner orbital condition:

$$[3] \qquad c_1 \cos \epsilon_1 - c_2 \sin \epsilon_1 = 0.$$

Normalizations of the inner orbital and bond orbital yield the additional equations

$$[4] \qquad c_o^2 + c_1^2 + c_2^2 = 1$$

and

$$[5] \qquad \lambda^2[1 + c_3^2] + \mu^2 + 2\lambda\mu[\cos \epsilon_b S_2 + \sin \epsilon_b S_3] = 1.$$

The limiting case of no inner shell polarization occurs when $c_2 = 0$. It follows from equations [2], [3], and [4] that $c_3 = c_1 = 0$ and $c_o = 1$. This set of orbitals was used by Duncan and Pople (15) in their calculations on hydrogen fluoride, with the difference that h was not orthogonal to the inner shell s_o orbital. As a result the overlap integrals were defined differently in the expression they gave for the bond orthogonality with an equivalent lone pair orbital.

Machine computation was employed to calculate the parameters and the resulting forces and dipole moment. The three variable parameters chosen for input data were ϵ_1, λ/μ, and c_3; then the above equations sufficed to find the remaining parameters. In order to solve for ϵ_b, the sin and cos terms in equation [2] were expressed in terms of tan $(\epsilon_b/2)$.

Integrals

All of the force integrals were obtained from analytical expressions listed in ref. 16. They are given in units of $1/d^2$ and therefore have to be divided by 3.00329 to obtain the absolute values. The symbols s' and h refer to Slater $2s$ and $1s$ orbitals on fluorine and on hydrogen respectively. In the overlap force integrals $O(\phi_\alpha,\phi_\beta)$ refers to the force on nucleus α.

Overlap integrals

$S(s_o,s') = 0.2332215$ $S(h,s_o) = 0.0487047$ $S(h,s') = 0.438805$
$S(h,p_\sigma) = 0.334687$

Can. J. Chem. Downloaded from www.nrcresearchpress.com by 210.87.254.5 on 09/05/12
For personal use only.

Force integrals

$P(h,h) = 0.833308$	$P(s_o,s_o) = 1.000000$	$P(s',s') = 0.939979$
$P(p_\sigma,p_\sigma) = 1.269856$	$P(p_\pi,p_\pi) = 0.767683$	$P(s',s_o) = 0.233209$
$P(s',p_\sigma) = 0.541784$	$P(s_o,p_\sigma) = 0.0588034$	$P(s_o,d_\sigma) = 0.00824764$
$P(d_\sigma,d_\sigma) = 1.235793$	$P(d_\sigma,p_\sigma) = 0.684819$	$P(d_\sigma,s') = 0.365623$
$P(d_\pi,d_\pi) = 0.647067$	$P(d_\pi,p_\pi) = 0.254032$	
$A(s_o,p_\sigma) = 9.255707$	$A(s',p_\sigma) = 3.939211$	$A(s,p) = 1.831075$
$A(d_\sigma,p_\sigma) = 1.881810$	$A(d_\pi,p_\pi) = 1.577357$	
$O(s_o,h) = 0.275440$	$O(s',h) = 0.487701$	$O(p,h) = 1.178331$
$O(h,s_o) = 0.0549793$	$O(h,s') = 0.593065$	$O(h,p) = 0.734855$
$O(h,d_\sigma) = 0.662681$	$O(d_\sigma,h) = 0.772126$	

Orbital Coefficients

For the electrostatic density with $\epsilon_1 = -6°$ the orbital coefficients are

$$\phi_o = 0.999304s_o - 0.0075187s' + 0.0695626p$$
$$\phi_b = -0.0138658s_o - 0.315884s' + 0.747854p + 0.481459h$$
$$\phi_1 = -0.238521s_o + 1.022725s' + 0.104528p.$$

REFERENCES

1. R. F. W. Bader and G. A. Jones. Can. J. Chem. **41**, 586 (1963).
2. R. F. W. Bader and G. A. Jones. J. Chem. Phys. **38**, 2791 (1963).
3. A. Mukherji and M. Karplus. J. Chem. Phys. **38**, 44 (1963).
4. R. F. W. Bader and G. A. Jones. Can. J. Chem. **39**, 1253 (1961).
5. B. J. Ransil. Rev. Mod. Phys. **32**, 245 (1960).
6. R. M. Sternheimer. Phys. Rev. **96**, 951 (1954).
7. R. M. Sternheimer. Phys. Rev. **127**, 1220 (1962).
8. R. M. Sternheimer. Phys. Rev. **115**, 1198 (1959).
9. R. S. Mulliken. J. Chem. Phys. **36**, 3428 (1962).
10. T. P. Das and M. Karplus. J. Chem. Phys. **36**, 2275 (1962).
11. R. P. Hurst, M. Karplus, and T. P. Das. J. Chem. Phys. **36**, 2786 (1962).
12. H. J. Kolker and M. Karplus. J. Chem. Phys. **36**, 960 (1962).
13. C. W. Kern and W. N. Lipscomb. J. Chem. Phys. **37**, 260 (1962).
14. W. G. Schneider, H. J. Bernstein, and J. A. Pople. J. Chem. Phys. **28**, 601 (1958).
15. A. B. F. Duncan and J. A. Pople. Trans. Faraday Soc. **49**, 217 (1953).
16. C. A. Coulson. Proc. Cambridge Phil. Soc. **38**, 210 (1942).

Can. J. Chem. Downloaded from www.nrcresearchpress.com by 210.87.254.5 on 09/05/12
For personal use only.

A NEW SYNTHETIC APPROACH TO THE BENZO[*c*]PHENANTHRIDINE SYSTEM: INTERNUCLEAR CYCLIZATION ONTO A PYRIDINE RING

R. A. ABRAMOVITCH AND G. TERTZAKIAN[1]
Department of Chemistry, University of Saskatchewan, Saskatoon, Saskatchewan
Received April 5, 1963

ABSTRACT

Benzo[*c*]phenanthridine has been synthesized in low overall yield by the Pschorr cyclization of *trans*-α-(4-isoquinolyl)-*o*-aminocinnamic acid. The condensation of 4-isoquinolylacetonitrile with *o*-nitrobenzaldehyde gave the *cis*-cinnamonitrile. The preparation of a number of intermediates is described.

Can. J. Chem. Downloaded from www.nrcresearchpress.com by 210.87.254.40 on 09/05/12
For personal use only.

The benzo[*c*]phenanthridine ring system (I) is found in a number of alkaloids such as chelidonine, chelerythrine, and sanguinarine (1). A number of these and their derivatives have been synthesized (2–4) starting from an alicyclic system, the nitrogen-containing ring being built up in the course of the synthesis. Current interest in chelerythrine (III) stems from its synergistic effect in enhancing the cancer chemotherapeutic action of colchicinamide (5). It was decided to develop a more flexible synthesis of the ring system which would permit the introduction of various substituents into the nucleus, and to use the Pschorr cyclization to achieve this end.

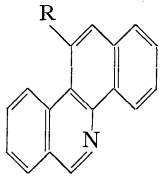

I, R = H
II, R = CO_2H

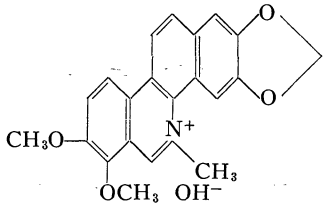

III

There have been a number of attempts made to apply a Pschorr type of ring closure to the synthesis of this ring system (6–8) but these failed in each case. The diazotization and subsequent decomposition of 2-amino-*N*-methylbenzo-1′-naphthalide (IV) was studied in detail by Hey and Turpin (9). No benzophenanthridone was formed, the only identifiable product being benzo-1-naphthalide, which results from the demethylation and deamination of IV. In the present work the cyclization of *trans*-α-(4-isoquinolyl)-*o*-aminocinnamic acid (V) to II, which would involve an internuclear attack onto a pyridine ring, has been studied.

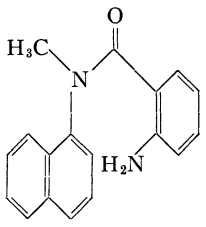

IV

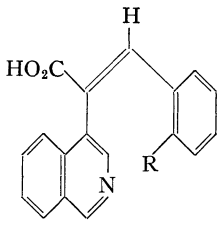

V, R = NH_2
VI, R = NO_2

[1]*Present address: Prairie Regional Laboratory, National Research Council, Saskatoon, Sask.*

Can. J. Chem. Downloaded from www.nrcresearchpress.com by 210.87.254.40 on 09/05/12
For personal use only.

It had been suggested (10) that the pyridine ring is more difficult to attack than a benzene ring in such reactions, a conclusion based on the fact that poor yields had been obtained in two examples studied (11, 12). It was shown, however, that under suitable conditions excellent yields of cyclized products resulting from attack onto a pyridine ring may be obtained (13). Another example of such a cyclization has been reported more recently (14). There seemed, therefore, to be no reason to suppose that the cyclization of V would not take place, provided the necessary amine having the right geometry could be prepared.

The route chosen initially for the preparation of V was the straightforward one involving the Perkin condensation of *o*-nitrobenzaldehyde with 4-isoquinolylacetic acid (VII) (15). Various attempts were made to prepare VII or its ethyl ester or anilide via an Arndt-Eistert homologation of isoquinoline-4-carboxylic acid. Though an acid chloride hydrochloride could be readily obtained from the latter and treatment of this with an excess of diazomethane gave a yellow crude diazoketone in no case could any of the required rearrangement products be obtained. This may be due to the fact that the acid chloride hydrochloride is insoluble in ether and is used in the form of a suspension. It could have been, then, that a coating of diazoketone was formed which prevented further reaction with the diazomethane. On the other hand, the infrared spectrum of the solid yellow product exhibited bands characteristic of a diazo group (2115 cm^{-1}) but not of the starting acid chloride hydrochloride. In any event, this route to the acetic acid had to be abandoned. An attempt was made to condense 4-bromoisoquinoline or its *N*-oxide with diethyl sodiomalonate under a variety of conditions: in no case did any reaction take place.

4-Isoquinolyl methyl ketone (VIII) could be prepared (in 20% yield) in one step from 4-aminoisoquinoline using the Beech reaction (16). This is a more convenient procedure than that which requires the preparation of the β-ketoester from ethyl isoquinoline 4-carboxylate followed by ketonic hydrolysis (17): the overall yields are of the same order of magnitude but many more steps are required in the latter procedure. When the methyl ketone (VIII) was subjected to a Willgerodt reaction only a low yield (9%) of ethyl 4-isoquinolylacetate was obtained. Other approaches were therefore investigated. Ethyl isoquinoline 4-carboxylate was reduced to the alcohol (IX) with lithium aluminum hydride and the latter oxidized to the corresponding aldehyde (X) with manganese dioxide in benzene. Various attempts were made to condense X with *o*-nitrophenylacetic acid but without success. Though condensation with oxindole took place no pure product could be obtained. A very low yield of 5-(4′-isoquinolylidene)-2-phenyloxazolone was obtained from the reaction of X with hippuric acid, so that this route was also not pursued further.

4-Isoquinolylmethanol (IX) was converted into its hydrochloride, which, with thionyl chloride, gave 4-chloromethylisoquinoline hydrochloride. The latter gave moderate yields of 4-isoquinolylacetonitrile (XI) when treated with sodium cyanide in either aqueous ethanol (18) or dimethyl sulphoxide (19). The moderate to low yields are probably due to a certain amount of polymerization of the free 4-chloromethylisoquinoline formed

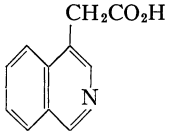

VII

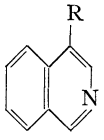

VIII, R = CO—CH_3
IX, R = CH_2OH
X, R = CHO

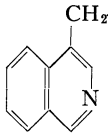

XI

Can. J. Chem. Downloaded from www.nrcresearchpress.com by 210.87.254.40 on 09/05/12
For personal use only.

when its hydrochloride reacted with the basic sodium cyanide. The yields reported for the analogous synthesis of 3-pyridylacetonitrile are also not high (18, 20). The condensation of 4-isoquinolylacetonitrile with *o*-nitrobenzaldehyde in acetic anhydride in the presence of triethylamine gave the α-(4-isoquinolyl)-*o*-nitrocinnamonitrile, of unknown geometry, in good yield. Catalytic reduction of this led to absorption of two molar equivalents of hydrogen and the formation of a product, $C_{18}H_{13}N_3O$, m.p. 261°, in quantitative yield. The same substance was obtained when the cinnamonitrile was reduced with hydrazine and Raney nickel. This product was soluble in acid but not in base; it effervesced on attempted diazotization and the resulting solution did not give a coupling product with alkaline β-naphthol. It was unaffected by prolonged boiling with acid or with base. The absence of a cyano group was confirmed by the fact that no band was present in the infrared at about 2200 cm^{-1}; the bands observed at 3350 and 1625 cm^{-1} were attributed to N—H and C=N groups respectively. The reduction product gave a positive test for *N*-oxides (21), and on further reduction with stannous chloride in acetic acid saturated with hydrogen chloride, or on heating with ferrous oxalate (22), gave a primary amine, $C_{18}H_{13}N_3$, m.p. 253° (positive carbylamine test). The cinnamonitrile has, therefore, the undesired cis configuration (XII) and, on reduction, gives the amine oxide (XIII). Deoxygenation of this gives 2-amino-3-(4′-isoquinolyl)quinoline (XIV). That diazotization of the 2-amino group does not take place normally is now understandable. This sequence of reactions is not exceptional since Pschorr and Wolfe (23) found that reduction of the product (XV) of condensation of phenylacetonitrile and *o*-nitrobenzaldehyde gave

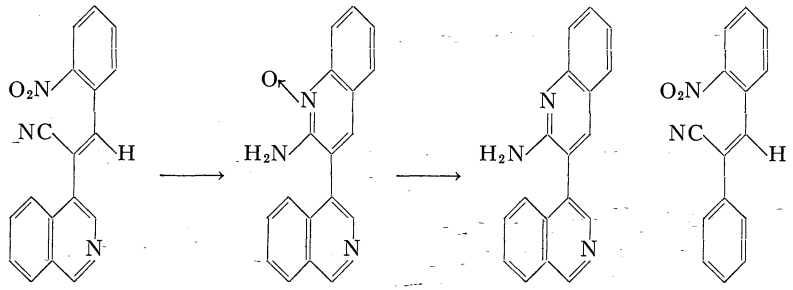

XII XIII XIV XV

2-amino-3-phenylquinoline; XV must thus also have the cis configuration. An attempt was made to isomerize XII to the trans form by irradiating its benzene solution in a quartz vessel with ultraviolet light. No isomerization appeared to take place.

The most convenient method for the conversion of the nitrile (XI) to the required acid (VII) was to hydrolyze XI to the amide, which, on treatment with nitrous acid, gave VII in good yield. Lower yields were obtained by ethanolysis or complete hydrolysis of XI. Condensation of VII with *o*-nitrobenzaldehyde gave the expected *trans*-cinnamic acid (VI), which was reduced to the amine (V) with ferrous sulphate and ammonia. Diazotization and cyclization in the presence of copper powder gave the expected benzo[*c*]phenanthridine-11-carboxylic acid (II) in 50% yield. The crude acid was readily decarboxylated to benzo[*c*]phenanthridine. The overall yield of I from 4-bromoisoquinoline was of the order of 1%, though the individual steps gave yields of at least 50%. Had the Arndt-Eistert reaction given the required acid this synthetic sequence would have been rendered much more attractive. The method should still be useful for the synthesis of substituted benzo[*c*]phenanthridines which may not be readily available using the Bailey–Robinson approach.

EXPERIMENTAL

Melting points are uncorrected. Infrared spectra were recorded on a Perkin–Elmer Model 21 spectrophotometer using sodium chloride optics. The main peaks only are reported. Unless otherwise specified, light petroleum refers to the fraction boiling between 36° and 48°, which was purified by stirring with concentrated sulphuric acid followed by distillation.

Attempted Arndt-Eistert Reactions

Isoquinoline 4-carboxylic acid (24) (3 g) was dissolved in warm ethanol (50 ml) and hydrogen chloride bubbled through the solution for 1 hour. The hydrochloride (3.6 g), m.p. 310°, was filtered, washed with absolute ethanol, dried, and boiled under reflux with thionyl chloride (12 ml) for 1½ hours. Benzene (30 ml) was added to the reaction mixture to precipitate isoquinoline 4-carboxylic acid chloride hydrochloride (3.8 g), m.p. > 310°. The solid was washed with dry benzene and dried. Infrared spectrum (KBr disk): 1745 (s), 1710 (s), 1580 (m), 1360 (m), 1225 (m), 1055 (m), 790 (w), 777 (w), and 745 cm^{-1} (m).

The acid chloride hydrochloride (1 g) was suspended in anhydrous ether (50 ml) and the suspension gradually added, with vigorous stirring, to a solution of diazomethane (from 4 g of *N*-nitroso-*N*-methylurea) in ether (50 ml) cooled to 5°. Nitrogen was evolved and initially some of the acid chloride dissolved, but most of the added solid turned yellow. The mixture was stirred for a further hour, the ether evaporated, and the yellow diazoketone used directly in the next step. Infrared spectrum (KBr disk): 2990 (m), 2115 (m), 1730 (m), 1685 (s), 1618 (s), 1465 (s), 1125 (m), 877 (m), and 760 cm^{-1} (m). The above diazoketone in ethanol (60 ml) was stirred and treated with a slurry of silver oxide (from 600 mg of silver nitrate) in ethanol (30 ml). The mixture was stirred at 60–70° for 4 hours, and then boiled under reflux for 1 hour. A silver mirror formed on the walls of the flask and the solution turned brown. The solvent was filtered and evaporated and the brown amorphous residue (0.50 g) extracted with benzene (0.15 g was insoluble). The solution was chromatographed on a column of alumina (30 g) but no pure product could be isolated. Similar intractable amorphous solids were obtained when, for instance, aqueous dioxane containing aniline was used to decompose the diazoketone.

4-Bromoisoquinoline 2-Oxide

A solution of 4-bromoisoquinoline (5 g) in acetic acid (10 ml) containing hydrogen peroxide (30%, 3 ml) was heated at 60–70° for 4 hours, a further amount of hydrogen peroxide (3 ml) was added, and heating continued for another 15 hours. The solution was evaporated under vacuum and the residue dissolved in chloroform (10 ml) and boiled under reflux with an excess of solid sodium carbonate for 30 minutes. The suspension was filtered, the solid washed with chloroform, and the combined filtrates evaporated to dryness. Ethyl acetate (0.5 ml) was added; when the sides of the flask were scratched with a glass rod nearly white crystals of *4-bromoisoquinoline 2-oxide* (0.5 g) separated which, after recrystallization from ethanol, had m.p. 182–183°. (Calc. for C_9H_6NOBr: C, 48.22; H, 2.68. Found: C, 48.47; H, 2.63.) Infrared spectrum (Nujol mull): 1597 (m), 1470 (m), 1355 (s), 1177 (s), 1130 (s), 765 (m), and 755 cm^{-1} (m). Evaporation of the ethyl acetate mother liquor gave 4-bromoisoquinoline (4.5 g) as a pale yellow oil which crystallized on standing and had m.p. 38–39°.

4-Isoquinolyl Methyl Ketone

Ice (6 g) was added with stirring to a solution of 4-aminoisoquinoline (2 g) in concentrated hydrochloric acid (4.5 ml) and water (4 ml) at 0–5°. To this was slowly added a solution of sodium nitrite (1 g) in water (2 ml) and the resulting deep red suspension neutralized to Congo red by the addition of sodium acetate (2 g) in water (3 ml). The diazonium salt solution was slowly introduced under the surface of a cold (10–15°) solution of acetaldoxime (1.3 g), copper sulphate (0.7 g), and sodium sulphite (0.055 g) in water (10 ml), with stirring. A solution of sodium acetate (9 g) in water (10 ml) was added and stirring was continued at room temperature for 1 hour, during which time nitrogen was evolved. The resulting suspension was acidified with enough hydrochloric acid to dissolve all the solid material. The red solution was boiled under reflux for 3 hours, cooled, basified with aqueous ammonia, and extracted with ether. The dried (Na_2SO_4) ether extract was evaporated and the brown tarry residue (0.88 g) dissolved in benzene and chromatographed on a column of alumina (60 g). Elution with benzene gave 4-isoquinolyl methyl ketone (0.40 g), m.p. 70–72°. Padbury and Lindwall (17) give m.p. 70–71° for this ketone.

Ethyl 4-Isoquinolylacetate (by the Willgerodt Reaction)

4-Isoquinolyl methyl ketone (0.189 g), sulphur (0.035 g), and morpholine (0.415 g) were boiled under reflux for 15 hours. Ethanolic sodium hydroxide (5%) (2 ml) was added to the black solution, which was boiled under reflux for a further 73 hours. The reaction mixture was poured into water (5 ml), the solution evaporated to about one third of its original volume under reduced pressure, water (5 ml) added, the solution saturated with salt and extracted with ether. The aqueous layer was taken almost to dryness, the dark oil remaining was treated with hydrochloric acid, and the mixture evaporated to dryness. The resulting light brown solid was warmed with absolute ethanol, filtered from any sodium chloride, and the filtrate poured into ether. A light brown flocculent precipitate which separated was filtered and dissolved in absolute ethanol

Can. J. Chem. Downloaded from www.nrcresearchpress.com by 210.87.254.40 on 09/05/12
For personal use only.

saturated with dry hydrogen chloride, and the solution boiled under reflux overnight. It was poured into a saturated aqueous solution of sodium chloride, the solution basified with ammonia and extracted with ether. The dried (Na_2SO_4) ether extract was evaporated to give a brown gum which was sublimed at 100° at 15 mm. Colorless needles (0.020 g), m.p. 60–62°, of *ethyl 4-isoquinolylacetate* were obtained which, on recrystallization from light petroleum, had m.p. 62.5°. (Calc. for $C_{13}H_{13}NO_2$: C, 72.54; H, 6.09. Found: C, 72.33; H, 6.34.) Infrared spectrum (film): 1725 (s), 1627 (m), 1512 (m), 1299 (m), 1205 (s), 1115 (m), 800 (w), and 765 cm^{-1} (m).

4-Isoquinolylmethanol

Ethyl 4-isoquinoline carboxylate (7.9 g) in anhydrous ether (125 ml) was added dropwise to a stirred suspension of lithium aluminum hydride (1.9 g) in dry ether (250 ml) at 0°. The mixture was stirred for 1 hour and water (40 ml) added carefully. Carbon dioxide was bubbled through the mixture for 10 minutes, the ether layer removed, and the pasty aqueous phase washed with ether (5×100 ml). The combined ether layers were dried (Na_2SO_4) and evaporated to give an oil (5.6 g) which, on trituration with a small amount of ether, gave *4-isoquinolylmethanol* (4.3 g). Recrystallization from ether gave colorless crystals, m.p. 93–94°. (Calc. for $C_{10}H_9NO$: C, 75.45; H, 5.70. Found: C, 75.38; H, 5.84.) Infrared spectrum (Nujol mull): 3170 (s) (br), 1640 (m), 1475 (m), 1100 (s), 785 (w), and 755 cm^{-1} (m).

4-Formylisoquinoline

A solution of 4-isoquinolylmethanol (0.46 g) in benzene (100 ml) was shaken with activated manganese dioxide (1 g) (25) for 16 hours at room temperature, the mixture filtered and evaporated to dryness to give the aldehyde (0.40 g) as a white solid, m.p. 103.5–104.5°. (Calc. for $C_{10}H_7NO$: C, 76.42; H, 4.49. Found: C, 76.59; H, 4.69.) Angyal, Penman, and Warwick report m.p. 103° for 4-formylisoquinoline (26).

5-(4'-Isoquinolylidene)-2-phenyloxazolone

4-Formylisoquinoline (0.052 g), hippuric acid (0.060 g), fused sodium acetate (0.025 g), and acetic anhydride (0.153 g) were heated together at 140–145° for 15 minutes. Water (10 ml) was added to the hot melt, the brown solid was filtered and recrystallized from benzene to give the *azlactone* (0.009 g) as green hair-like crystals, m.p. 251–252°. (Calc. for $C_{19}H_{12}N_2O_2$: C, 75.99; H, 4.03. Found: C, 76.33; H, 4.60.)

4-Chloromethylisoquinoline Hydrochloride

4-Isoquinolylmethanol (4.3 g) in benzene (70 ml) was treated with dry hydrogen chloride gas and the solid hydrochloride which precipitated (4.63 g) was filtered, washed with benzene, and dried. It was then boiled under reflux with thionyl chloride (13 ml) for 1 hour. Benzene (35 ml) was added to the cold mixture and the white solid which precipitated was filtered, washed with benzene, and dried to give *4-chloromethylisoquinoline hydrochloride* (4.76 g), m.p. 225° (decomp.). (Calc. for $C_{10}H_8NCl,HCl$: C, 56.10; H, 4.25. Found: C, 56.18; H, 3.89.) Infrared spectrum (KBr disk): 2310 (s) (br), 2070 (s), 1645 (m), 1615 (m), 1375 (m), 1240 (m), 865 (m), 785 (s), and 755 cm^{-1} (m).

4-Isoquinolylacetonitrile

(i) Using aqueous ethanol as solvent.—4-Chloromethylisoquinoline hydrochloride (4.3 g) in 50% aqueous ethanol (30 ml) was added dropwise to a stirred, boiling solution of sodium cyanide (7 g) in water (12 ml) and ethanol (80 ml) over a period of 30 minutes. The resulting brown mixture was stirred and boiled under reflux for a further 40 minutes, evaporated to dryness under reduced pressure, and the black oily residue extracted with ether (6×70 ml). The dried (Na_2SO_4) ether extract was evaporated and the residual brown oil (3 g), which partially crystallized on cooling, was dissolved in benzene and chromatographed on a column of alumina (200 g). A mixture of benzene – light petroleum (2:1 v/v) eluted *4-isoquinolylacetonitrile* (1.45 g), m.p. 108–110°, which, on recrystallization from benzene – light petroleum (b.p. 60–80°), had m.p. 109–110°. (Calc. for $C_{11}H_8N_2$: C, 78.55; H, 4.79. Found: C, 78.54; H, 4.87.) Infrared spectrum (KBr disk): 2250 (w), 1625 (m), 1592 (m), 1391 (s), 870 (m), 780 (m), and 741 cm^{-1} (s).

(ii) Using dimethyl sulphoxide as solvent.—A suspension of 4-chloromethylisoquinoline hydrochloride (12 g) in dimethyl sulphoxide (110 ml) was added over 30 minutes to a stirred solution of sodium cyanide (6.2 g) in dimethyl sulphoxide (50 ml) at room temperature. The solution was stirred for 2½ hours, poured into water (1 l.), and the suspension extracted with ether (5×100 ml). The combined ether extracts were washed with water (3×100 ml), dried (Na_2SO_4), and evaporated to give a brown oil (8.9 g) which crystallized partly on standing. A small amount of ether was added, and the crystals of the nitrile (4.7 g), m.p. 107–109°, thus obtained were filtered and washed with a little ether.

cis-α-(4-Isoquinolyl)-o-nitrocinnamonitrile

4-Isoquinolylacetonitrile (1 g) and *o*-nitrobenzaldehyde (0.92 g) in acetic anhydride (12 ml) containing triethylamine (1.5 ml) were heated on a steam bath overnight and the reaction mixture cooled, when the *cis-cinnamonitrile* separated. Ether (1 ml) was added to the mixture and the solid (1.6 g) filtered, washed with a small amount of ether, and recrystallized from ethanol to give the pure product, m.p. 177–178°. (Calc. for $C_{18}H_{11}N_3O_2$: C, 71.75; H, 3.68. Found: C, 71.50; H, 3.78.) Infrared spectrum (KBr disk): 2220 (w), 1623 (w), 1570 (w), 1515 (s), 1355 (s), 907 (w), 850 (w), 780 (m), 755 (m), and 720 cm^{-1} (m).

Can. J. Chem. Downloaded from www.nrcresearchpress.com by 210.87.254.40 on 09/05/12
For personal use only.

2-Amino-3-(4'-isoquinolyl)quinoline 1-Oxide

cis-α-(4-Isoquinolyl)-*o*-nitrocinnamonitrile (0.20 g) in ethyl acetate (70 ml) was hydrogenated at room temperature and pressure over 10% palladium–charcoal (0.05 g) for 24 hours. Two equivalents of hydrogen were absorbed. The deep yellow solution was filtered and evaporated to give *2-amino-3-(4'-isoquinolyl)-quinoline 1-oxide* (0.185 g), m.p. 248–250° (decomp.), which, after recrystallization from acetone, had m.p. 260–261°. (Calc. for $C_{18}H_{13}N_3O$: C, 75.24; H, 4.56; N, 14.63. Found: C, 75.25, 75.20; H, 4.68, 4.56; N, 14.37.) Infrared spectrum (KBr disk): 3300 (s) (br), 1625 (s), 1590 (m), 1395 (m), 1360 (m), 753 (m), and 743 cm^{-1} (m).

2-Amino-3-(4'-isoquinolyl)quinoline

(i) 2-Amino-3-(4'-isoquinolyl)quinoline 1-oxide (0.10 g) was treated with a solution of stannous chloride in acetic acid saturated with dry hydrogen chloride (27) (2 ml) and the resulting solution boiled under reflux for 18 hours. Water (10 ml) was then added, the solution made alkaline with 40% aqueous potassium hydroxide and extracted with chloroform (3×15 ml), and the extracts dried (Na_2SO_4) and evaporated to give a waxy solid (0.085 g). Recrystallization from ethanol afforded the *amine* (0.055 g), m.p. 252–253.5°, as pale yellow crystals. (Calc. for $C_{18}H_{13}N_3$: C, 79.68; H, 4.83. Found: C, 79.28; H, 5.12.) Infrared spectrum (KBr disk): 3350 (s) (br), 1647 (s), 1613 (m), 1435 (s), 757 (s), and 745 cm^{-1} (s).

(ii) The *N*-oxide (0.10 g), ferrous oxalate dihydrate (0.11 g), and granulated lead (2 g) were mixed and heated at 330° for 20 minutes under air condenser to give 2-amino-3-(4'-isoquinolyl)quinoline (0.009 g), m.p. 250–253°, undepressed on admixture with a sample obtained as above.

Ethyl 4-Isoquinolylacetate (from the Nitrile)

4-Isoquinolylacetonitrile (0.10 g) was dissolved in a mixture of anhydrous ethanol (0.7 ml) and concentrated sulphuric acid (0.7 ml) and the solution boiled under reflux for 3 hours. The resulting dark brown solution was poured into ice and water, made alkaline by the careful addition of ammonia, and the precipitated ester (0.070 g), m.p. 62–64°, filtered. The melting point was undepressed on admixture with a sample prepared by the Willgerodt reaction, and the infrared spectra of the compounds were identical.

4-Isoquinolylacetamide

4-Isoquinolylacetonitrile (0.50 g) was dissolved in concentrated sulphuric acid (3 ml) and the solution kept at room temperature for 17 hours, poured into water, and made just basic with 20% aqueous sodium hydroxide solution. The solid (0.475 g), m.p. 219–220°, which precipitated was recrystallized from water to give *4-isoquinolylacetamide* as fine white needles, m.p. 232–232.5°. (Calc. for $C_{11}H_{10}N_2O$: C, 70.95; H, 5.41. Found: C, 70.75; H, 5.42.) Infrared spectrum (KBr disk): 3470 (s), 1628 (m), 1400 (m), 1256 (m), 790 (m), and 758 cm^{-1} (m).

4-Isoquinolylacetic Acid Hydrochloride

The amide (0.31 g) in 6 *N* hydrochloric acid (10 ml) was treated with a large excess of sodium nitrite in water and the solution kept at room temperature overnight, when *4-isoquinolylacetic acid hydrochloride* (0.32 g) separated as colorless rods. These were recrystallized from absolute ethanol and had m.p. 241–243° (decomp.). (Calc. for $C_{11}H_9NO_2,HCl$: C, 59.06; H, 4.47. Found: C, 59.09; H, 4.71.) Infrared spectrum (KBr disk): 3000 (s) (br), 2680 (s) (br), 2020 (w), 1723 (s), 1650 (m), 1378 (s), 1175 (s), and 788 cm^{-1} (s).

trans-α-(4-Isoquinolyl)-o-nitrocinnamic Acid

4-Isoquinolylacetic acid hydrochloride (1.41 g) and *o*-nitrobenzaldehyde (0.97 g) were boiled under reflux with acetic anhydride (16 ml) containing triethylamine (14 ml) and anhydrous sodium acetate (0.4 g) for 35 minutes. The mixture was poured into water (80 ml), heated, and filtered to remove some tarry material and the filtrate kept in the refrigerator overnight, when *trans-α-(4-isoquinolyl)-o-nitrocinnamic acid* (1.14 g) separated as orange-yellow crystals. Recrystallization from methanol gave the pure acid, m.p. 246–247°. (Calc. for $C_{18}H_{12}N_2O_4$: C, 67.50; H, 3.78. Found: C, 67.78; H, 3.98.) Infrared spectrum (KBr disk): 3400 (m) (br), 2400 (w) (br), 1700 (m), 1526 (s), 1316 (s), 1295 (m), 785 (m), and 752 cm^{-1} (m).

trans-α-(4-Isoquinolyl)-o-aminocinnamic Acid

trans-α-(4-Isoquinolyl)-*o*-nitrocinnamic acid (1 g) was dissolved in hot aqueous ammonia and the solution added to a rapidly stirred and boiling solution of ferrous sulphate (6 g) in water (17 ml). The reaction mixture was stirred for a further 10 minutes while ammonia was added to it to maintain it basic. It was then filtered, neutralized with acetic acid, and kept in the refrigerator for 3 hours, when the *amino acid* (0.40 g) separated as a yellow solid. This was recrystallized from ethanol and had m.p. 279–281° (decomp.). (Calc. for $C_{18}H_{14}N_2O_2$: C, 74.47; H, 4.86. Found: C, 74.02; H, 5.03.) Infrared spectrum (Nujol mull): 2400 (w) (br), 1685 (m), 1620 (m), 1460 (s), 1378 (m), 1256 (s), and 751 cm^{-1} (m).

Benzo[c]phenanthridine

trans-α-(4-Isoquinolyl)-*o*-aminocinnamic acid (0.250 g) in 5% hydrochloric acid (10 ml) was diazotized with a solution of sodium nitrite (0.070 g) in water (5 ml), the temperature being kept below 1°. The excess nitrous acid was decomposed by the addition of urea, and Gattermann copper powder (0.25 g) added to the mixture, which was stirred at room temperature for 5 hours. The mixture was made just acid with acetic

Can. J. Chem. Downloaded from www.nrcresearchpress.com by 210.87.254.40 on 09/05/12
For personal use only.

acid, filtered, and the solid extracted with methanol in a Soxhlet extractor for 15 hours. The methanol solution was evaporated to dryness and the brown solid residue washed with a little cold methanol to give what is presumed to be benzo[*c*]phenanthridine-11-carboxylic acid (0.120 g), m.p. 270–272° (decomp.), as a nearly white solid. Several attempts to recrystallize this solid to obtain an analysis specimen were unsuccessful. Infrared spectrum (KBr disk): 3400 (s) (br), 1700 (s), 1620 (s), 1450 (m), 1285 (s), 1230 (s), 760 (s), and 730 cm^{-1} (m).

The acid (0.050 g) was dissolved in purified quinoline (5 drops), copper powder (0.010 g) was added, and the suspension was heated under reflux (metal bath). After the initial vigorous evolution of gas had subsided heating was continued for a further 10 minutes, water (1.5 ml) was added, and the quinoline removed by steam distillation. The residue was extracted with ether, the ether dried (Na_2SO_4) and evaporated to give a brown oil (0.033 g) which solidified on cooling. This was chromatographed through a column of alumina (7 g); elution with benzene – light petroleum (1:3 v/v) gave benzo[*c*]phenanthridine (0.020 g), m.p. 135–135.5° (after recrystallization from aqueous ethanol). (Calc. for $C_{17}H_{11}N$: C, 89.05; H, 4.84. Found: C, 89.02; H, 5.09.) λ_{max} 265, 312, 343, 361 mμ; $10^{-3} \times \epsilon$ 80.5, 8.75, 5.60, 6.72 (in $CHCl_3$). Infrared spectrum (KBr disk): 1625 (m), 1270 (m), 824 (m), 798 (s), 760 (s), and 681 cm^{-1} (s). Whaley and Meadow (28) give m.p. 135° for benzo[*c*]phenanthridine.

ACKNOWLEDGMENTS

This work was carried out during the tenure (1960–1961) (by G. T.) of a University of Saskatchewan Graduate Assistantship and of a C.I.L. Fellowship (1961–1962). Financial support for this work by the National Research Council is also gratefully acknowledged.

REFERENCES

1. R. H. F. Manske and H. L. Holmes. The Alkaloids. Vol. IV. Academic Press Inc., New York. 1954. p. 253; Vol. VII. 1960. p. 430.
2. A. S. Bailey, R. Robinson, and R. S. Staunton. J. Chem. Soc. 2277 (1950). A. S. Bailey and C. R. Worthing. J. Chem. Soc. 4535 (1956).
3. K. W. Gopinath, T. R. Govindachari, P. C. Parthasarathy, and N. Viswanathan. J. Chem. Soc. 4012 (1959). K. W. Gopinath, T. R. Govindachari, and N. Viswanathan. Tetrahedron, **14**, 322 (1961).
4. H. R. Arthur and Y. L. Ng. J. Chem. Soc. 4010 (1959).
5. A. L. Bluhm. Dissertation Abstr. **20**, 880 (1959).
6. T. Richardson, R. Robinson, and E. Seijo. J. Chem. Soc. 835 (1937).
7. C. R. Noller, R. O. Denyes, J. W. Gates, and W. L. Wasley. J. Am. Chem. Soc. **59**, 2079 (1937).
8. H. S. Forrest, R. D. Haworth, A. R. Pinder, and T. S. Stevens. J. Chem. Soc. 1311 (1949).
9. D. H. Hey and D. G. Turpin. J. Chem. Soc. 2471 (1954).
10. H. Plieninger and M. Schach von Wittenau. Ber. **91**, 1905 (1958).
11. D. H. Hey and J. M. Osbond. J. Chem. Soc. 3164 (1949).
12. R. A. Abramovitch, D. H. Hey, and R. D. Mulley. J. Chem. Soc. 4263 (1954).
13. R. A. Abramovitch. Can. J. Chem. **38**, 2273 (1960).
14. W. Hertz and D. R. K. Murty. J. Org. Chem. **26**, 418 (1961).
15. P. H. Leake. Chem. Rev. **56**, 27 (1956).
16. W. F. Beech. J. Chem. Soc. 1297 (1954).
17. J. J. Padbury and H. G. Lindwall. J. Am. Chem. Soc. **67**, 1268 (1945). C. F. Koelsch. J. Org. Chem. **10**, 34 (1945).
18. S. Okuda and M. M. Robison. J. Am. Chem. Soc. **81**, 742 (1959).
19. L. Friedman and H. Schechter. J. Org. Chem. **25**, 877 (1960).
20. H. S. Mosher and J. E. Tossieri. J. Am. Chem. Soc. **73**, 4925 (1951).
21. N. A. Coates and A. R. Katritzky. J. Org. Chem. **24**, 1836 (1959).
22. R. A. Abramovitch and K. A. H. Adams. Can. J. Chem. **39**, 2516 (1961).
23. R. Pschorr and H. Wolfe. Ber. **32**, 3402 (1899).
24. F. W. Bergstrom and J. H. Rodda. J. Am. Chem. Soc. **62**, 3030 (1940).
25. M. Harfeist, A. Bavely, and W. A. Lazier. J. Org. Chem. **19**, 1608 (1954).
26. S. J. Angyal, D. R. Penman, and G. P. Warwick. J. Chem. Soc. 1740 (1953).
27. J. Thiele and O. Dimroth. Ann. **305**, 114 (1899).
28. W. M. Whaley and M. Meadow. J. Org. Chem. **19**, 661 (1954).

Can. J. Chem. Downloaded from www.nrcresearchpress.com by 210.87.254.40 on 09/05/12
For personal use only.

INTERBRANCH SEQUENCES IN THE WHEAT ARABINO-XYLAN

SELECTIVE ENZYMOLYSIS STUDIES[1]

H. R. GOLDSCHMID[2] AND A. S. PERLIN

National Research Council of Canada, Prairie Regional Laboratory, Saskatoon, Saskatchewan

Received May 2, 1963

ABSTRACT

A *Streptomyces* xylanase degrades the soluble arabino-xylan of wheat with formation of polymeric fragments and several oligosaccharides. The overall data, together with information about the spatial requirements of the xylanase, show that (*a*) the arabino-xylan molecules are constituted predominantly of highly branched regions in which isolated and paired L-arabinosyl branches are separated by single D-xylosyl units; (*b*) at unequal intervals (averaging 20–25 main-chain units) this type of sequence is interrupted by "open regions" of at least two to five unbranched D-xylosyl units; and (*c*) infrequently, an L-arabinosyl branch is removed from other branches at either side by at least two D-xylosyl units.

A new tetrasaccharide isolated from the enzymic digest is shown to be *O*-α-L-arabinofuranosyl-(1 → 3)-*O*-[β-D-xylopyranosyl-(1 → 4)]-*O*-β-D-xylopyranosyl-(1 → 4)-D-xylose.

The soluble pentosans of wheat flour (1–6) comprise a group of closely related polysaccharides containing a linear chain of (1 → 4)-linked β-D-xylopyranosyl units to which L-arabinofuranosyl branches are appended by (1 → 2)- and (1 → 3)-bonds. The branches occur most frequently on isolated or on two consecutive D-xylosyl units (6), and a high proportion of these units contains two L-arabinosyl branches. Additional information about the structure of the arabino-xylans has now been obtained through enzymic degradation studies.

An enzyme preparation obtained from *Streptomyces* QMB 814 (7)* was found to partially degrade the pentosans. This preparation shows strong cellulolytic activity but, according to Reese (8), also contains a xylanase component. Chromatographic examination of the digest showed the presence of only traces of arabinose and xylose, but substantial quantities of at least five oligosaccharides. About 60% of the substrate was accounted for as a polymeric residue having an average molecular size less than one-tenth that of the original pentosan, which showed that most of the molecules had been degraded at least partially by the enzyme. The oligosaccharide mixture was chromatographed first on charcoal and then on cellulose, affording five fractions in a combined yield of about 15%. Two major oligosaccharides were the (1 → 4)-β-linked xylobiose (I) and xylotriose (II), each being characterized as the derived β-acetate. The three additional oligosaccharides (III, IV, and V) were amorphous and yielded both arabinose and xylose on acid hydrolysis; from their chromatographic mobilities they appeared to be tetra-, penta-, and hexa-saccharide components, respectively.

Of these latter mixed oligosaccharides, III has been examined in some detail. It was found to contain arabinose and xylose in a ratio of 1:3 and to have a molecular weight close to that of a tetrasaccharide. When hydrolyzed partially III yielded xylotriose, which was characterized as the β-octaacetate. On oxidation with lead tetraacetate – potassium acetate, III consumed 5 moles of oxidant and produced 2 moles of formic acid at the same rate as for xylotriose (9). Therefore, the tetrasaccharide consists of a unit of

[1]*Issued as N.R.C. No. 7499.*

[2]*National Research Council of Canada Postdoctoral Fellow, 1958–1960.*

**The authors are grateful to Dr. E. T. Reese, who, by supplying the enzyme preparations, made these studies possible.*

Can. J. Chem. Downloaded from www.nrcresearchpress.com by 210.87.254.42 on 09/05/12
For personal use only.

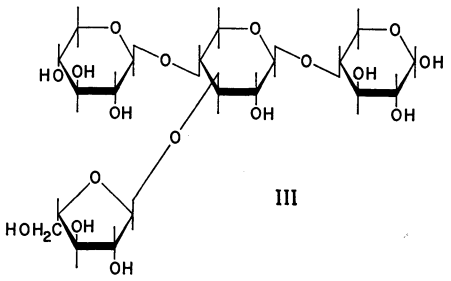

III

xylotriose and the L-arabinofuranosyl unit is attached to the central D-xylosyl unit through position 2 or 3. A crystalline decaacetate (VI) was prepared from III, and the purified sample (VII) obtained by deacetylation of VI showed the same properties on partial hydrolysis and lead tetraacetate oxidation as did crude III.

Information about the point of attachment of the L-arabinosyl unit was obtained by degrading the tetrasaccharide with alkali. Xylotriose itself is degraded readily, unit by unit, from the reducing end of the molecule (10). However, if a branch is introduced at position 2 of the central xylosyl unit the erosion process should be interrupted with three-quarters of the molecule intact (11), whereas more extensive degradation should result if the branch is at position 3 (11, 12). When VII was treated with dilute lime water (10), its rate of decomposition was close to that for xylotriose. This behavior is indicative, therefore, of a (1 → 3)-bond between the L-arabinosyl branch and the central D-xylosyl unit of the tetrasaccharide, and hence favors the structure represented by formula III. Such a product is consistent with the fact that the parent polysaccharide on methylation and hydrolysis yields 2-*O*-methyl-D-xylose (2, 4). Also it provides direct evidence that single (2), isolated (6) L-arabinofuranosyl units are to be found attached to the main xylan chain.

The specific rotation of III and of acetate VI, when compared with rotatory data for pertinent reference compounds (Table I), indicates that the L-arabinofuranosyl unit

TABLE I

Rotatory values for arabinose-xylose oligosaccharides and related compounds

Compound	$[\alpha]_D$	M_D
1. Xylotriose	− 46.9 (21)	−19,420
2. Methyl α-L-arabinofuranoside	−135°	−22,150
3. Methyl β-L-arabinofuranoside	+118° (22)	+19,350
Calc. for arabinose-xylose tetrasaccharide IV		
with α-L-arabinosyl unit (M_D 1 + 2)		−41,570
with β-L-arabinosyl unit (M_D 1 + 3)		−70
4. Arabinose-xylose tetrasaccharide III	− 75°	−41,100
5. β-Xylotriose octaacetate	− 85° (21)	−63,750
6. Compound 2 triacetate	− 76°	−22,000
7. Compound 3 triacetate	—	+19,350*
Calc. for tetrasaccharide acetate VI		
with α-L-arabinosyl unit (M_D 5 + 6)		−85,750
with β-L-arabinosyl unit (M_D 5 + 7)		−44,400
8. Tetrasaccharide acetate VI	− 85°	−82,200
9. Xylobiose	− 26°	−7,330
Calc. for arabinose-xylose trisaccharide		
with α-L-arabinosyl unit (M_D 9 + 2)		−29,480
with β-L-arabinosyl unit (M_D 9 + 3)		+12,020
10. Arabinose-xylose trisaccharide (14, 15)	− 19°	−7,990

*Assumed to be the same as or close to that of compound 3.

Can. J. Chem. Downloaded from www.nrcresearchpress.com by 210.87.254.42 on 09/05/12
For personal use only.

possesses the α-(1,2-*trans*)-configuration. This assignment agrees with conclusions reached recently by Marchessault (13), who examined the rotatory power of several arabino xylans including the wheat flour pentosans. Based on Marchessault's data, the calculated molecular rotation for III is 36,600, whereas the found value is 41,000. However, rotational data in this series are not always clearly indicative of configuration. Thus, a trisaccharide consisting of an L-arabinofuranosyl unit linked 3′ to a xylobiose unit (14, 15) has a molecular rotation which deviates about equally from values calculated to allow either for an α- or a β-L-arabinosyl branch (Table I, compound 10).

Since xylobiose and xylotriose are produced by the enzyme, but only traces of arabinose released, it is clear that these oligosaccharides represent interbranch segments of the xylan main chain. In fact, such segments are even larger than indicated by the dimensions of the oligosaccharides themselves, as shown by the recent finding (16) that the xylan chain is cleaved only when there are at least two unbranched β-D-xylosyl units in sequence. This follows from the fact that the polymeric residues (as well as the known oligosaccharide products) contain reducing and non-reducing end-units that are devoid of L-arabinosyl branches (16). Hence, a structure such as VIII appears subject to hydrolysis (broken

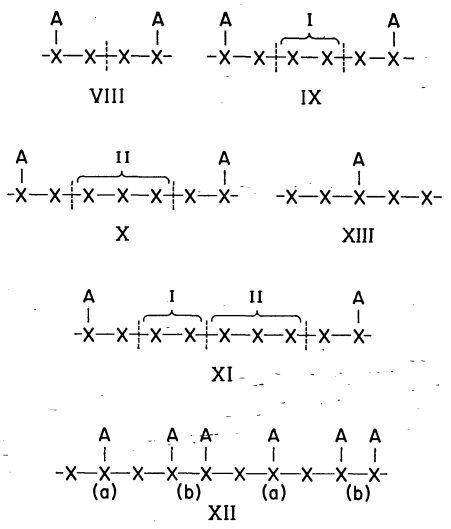

line) and the formation of xylobiose I can be envisioned from a sequence such as IX which involves a minimum of four interbranch xylosyl units. Similarly, at least five such units (as in X) are required for release of xylotriose II. The interbranch regions sometimes may be large enough, e.g., as in XI, to afford more than one oligosaccharide molecule or a large oligosaccharide which subsequently is degraded to I or II. However, the ready solubility of the arabino-xylan, when contrasted with the low solubility of xylans containing relatively low proportions of arabinosyl branches (2), suggests that few molecules are likely to have interbranch regions much larger than depicted in XI.

The incidence of branching in the pentosan is sufficiently high—i.e., two out of five D-xylosyl units contain L-arabinosyl branches (2)—that if the isolated and paired branches were distributed in a completely uniform fashion, there would be no sequence of four or more consecutive unbranched D-xylosyl units present from which D-xylose oligosaccharides could be derived. Since, however, the yield of I and II corresponds to about 13% of the xylan component of the polysaccharide, branching in the latter must deviate substantially from a uniform type of arrangement. About 22% of the xylan component is accounted

Can. J. Chem. Downloaded from www.nrcresearchpress.com by 210.87.254.42 on 09/05/12
For personal use only.

for by these oligosaccharides, by adjusting their yield to allow for two additional D-xylosyl units per segment (as in structures IX and X). Consequently, almost all of the arabinosyl branches are to be found concentrated in regions of the pentosan that involve barely three-quarters of the xylan chain. In these regions, therefore, about four in seven D-xylosyl units must be branched,* as compared with a figure of two in five for the overall molecule, and hence the distance between the isolated and paired branch points rarely can exceed one xylosyl unit. Since the minimum spatial requirement for enzymic hydrolysis is two adjacent unbranched D-xylosyl units (16), it is understandable that these highly branched regions of the polysaccharide are immune to attack by the *Streptomyces* enzyme.

The data available from the current and earlier studies now provide rather detailed information about the structure of the arabino-xylan. The molecules may be represented predominantly by XII, in which the incidence of branching is high (many of the D-xylosyl units even contain two branches): sometimes isolated D-xylosyl units serve as branch points (*a*), sometimes two (and less frequently more than two) consecutive branched units (*b*) occur between single unbranched units. At unequal intervals, averaging 20–25 units (average D.P. of the polymeric fragments), this type of sequence (XII) is interrupted by "open regions" in which at least two to five unbranched D-xylosyl units are found (as in VIII, IX, and X). An additional type of sequence is represented by the formation of tetrasaccharide III, in which an occasional arabinosyl branch is removed from other branches at either side by at least two D-xylosyl units (as in XIII). The relative distribution of these sequence types is not known. However, it was found earlier (1, 2) that the arabino-xylans comprise a series of polymers in which the arabinose-xylose ratio varies substantially. Therefore, some molecules probably contain a relatively large proportion of the highly branched type of sequence XII whereas others contain more "open regions".

EXPERIMENTAL

Melting points are corrected. Specific rotations were measured at 25±2°.

Evaporations were carried out *in vacuo* at 40–50° C.

Paper chromatography was carried out with Whatman No. 1 or 3 MM paper using ethyl acetate – pyridine – water (100:40:30) as solvent.

Pentose was estimated colorimetrically by the orcinol – ferric chloride reaction (17).

Preparation of Arabino-xylan

The procedure was essentially that described earlier (1): crude water-soluble pentosan (43.0 g) was acetylated in formamide with acetic anhydride and pyridine; the acetone-soluble fraction of the derived acetate was precipitated fractionally from acetone with ligroin. Each fraction was examined by deacetylation and acid hydrolysis, and those fractions containing arabinose and xylose predominantly were combined and again fractionally precipitated. A major final fraction (8.6 g) containing the two pentose sugars almost exclusively was deacetylated catalytically with sodium methoxide in boiling methanol, for use in the enzymolysis experiments.

Enzymic Degradation of Arabino-xylan

In preliminary experiments the arabino-xylan was incubated in water at 45° C with varying proportions of the *Streptomyces* enzyme preparation (7), ratios being varied from 27:1 to 3:1. Approximately the same degree of hydrolysis (copper-reducing power (18)) was reached within 24 hours' reaction time with each digest in which the substrate–enzyme ratio was 10:1 or less.

Arabino-xylan (4.74 g) in water (500 ml) was treated at 45° C with the enzyme preparation (470 mg) for 29 hours. The digest was then heated on the steam bath to inactivate the enzyme and the solution was concentrated to a volume of 60 ml.

Polymeric Fragments

Ethanol was added slowly with stirring to the digest concentrate, yielding, first, a brown precipitate which appeared to consist mostly of enzymic material (this fraction was not examined further). Further

**This increased incidence of branching is evident in the polymeric residues from a relatively high arabinose content and low periodate uptake.*

Can. J. Chem. Downloaded from www.nrcresearchpress.com by 210.87.254.42 on 09/05/12
For personal use only.

increments of alcohol caused precipitation of three additional fractions (1, 2, and 3), each of which was centrifuged off. The supernatant solution was concentrated to a volume of 30 ml, and ethanol again added, yielding two more precipitated fractions (4 and 5). Yields of these five fractions were as follows: 1, 0.31 g; 2, 0.37 g; 3, 0.87 g; 4, 0.85 g; 5, 0.56 g. (Total yield, 62%.) In a separate experiment (16), these polymeric fragments were recovered in a total yield of 60% as two fractions (1A and 2A), the addition of alcohol to the digest concentrate in this experiment being less gradual.

The degree of polymerization of fractions 3, 4, 1A, and 2A, as estimated by copper-reducing power, was 22, 12, 28 and 15, respectively. The derived acetates of fractions 1A and 2A have molecular weights of 5100 and 2700, respectively (16).

Fractions 2, 5, 1A, and 2A, when hydrolyzed with 0.1 *N* sulphuric acid, each yielded arabinose and xylose; the arabinose:xylose ratios estimated by quantitative paper chromatography were 1.1, 0.7, 1.0, and 0.7, respectively. (In the original pentosan this ratio is about 0.6 (1, 2).)

On oxidation with excess sodium metaperiodate at 12° C fractions 1A, 2A, and 3 consumed 0.69, 0.77, and 0.71 mole of periodate per mole, respectively (18 hours' reaction time; constant value during succeeding 24 hours); the corresponding estimates of formic acid produced were 0.064, 0.115, and 0.084 mole per mole, making for corrected periodate uptake values of 0.63, 0.65, and 0.63 mole per mole, respectively. (The uptake of periodate by the original pentosan is about 0.7 mole per mole (2).)

Isolation of Oligosaccharides

The mother liquor remaining after precipitation of polymeric fragment fractions 1–5 was concentrated to a syrup (2.47 g) which was chromatographed on a column of coconut charcoal (19), aqueous ethanol solutions of 5, 10, 20, 30, and 40% ethanol being used successively as eluants. Oligosaccharide components contained in these eluates (detected by paper chromatography) were purified further by preparative chromatography on 3 MM paper sheets. This sequence of isolation steps afforded the following oligosaccharides in a chromatographically pure condition (listed in order of decreasing chromatographic mobility): xylobiose, 0.18; xylotriose, 0.16 g; oligosaccharide III, 0.19 g; oligosaccharide IV, 0.14 g; oligosaccharide V, 0.12 g.

Purification of Oligosaccharides

Each of the above oligosaccharides was acetylated with acetic anhydride, using anhydrous sodium acetate, on the steam bath for 2 hours. The derived products were isolated by precipitation with ice water and crystalline materials were recrystallized from ethanol, affording: *β-xylobiose hexaacetate*, m.p. 154–155° C, identity confirmed by X-ray powder diagram; *β-xylotriose octaacetate*, m.p. 106–108° C, identity confirmed by X-ray powder diagram; *oligosaccharide III decaacetate (VI)*, m.p. 179–180° C, $[\alpha]_D$ −85° (*c*, 1, chloroform); calculated for $C_{40}H_{54}O_{27}$: C, 49.69%; H, 5.63%; found: C, 49.64%; H, 5.73%. The acetates of oligosaccharides IV and V were syrupy products. Oligosaccharide V acetate was found by silicic acid column chromatography to contain at least two components.

Characterization of Oligosaccharide III

(*a*) The amorphous solid, $[\alpha]_D$ −75° (*c*, 1, water), was found by oxidation with alkaline hypoiodite (using xylotriose as standard) to have an equiv. wt. of 514 (pentose tetrasaccharide requires 546). A solution containing 37 γ of pentose was treated with excess of sodium borohydride for 4 hours, and then found to contain 28 γ of pentose; the latter value, being 75% of the original pentose value, agrees with formulation of III as a tetrasaccharide.

(*b*) The tetrasaccharide (2 mg) was hydrolyzed on the steam bath with 0.2 *N* sulphuric acid (0.2 ml) in a sealed tube for 15 hours, the hydrolyzate was neutralized with Dowex-1 (bicarbonate form). Arabinose and xylose were detected by paper chromatography and, by elution from the chromatograms, these sugars were estimated colorimetrically to be present in a ratio of 1 to 3.

(*c*) A solution of the tetrasaccharide (85 mg) in 0.05 *N* sulphuric acid (2 ml) was heated on the steam bath for 35 minutes, then neutralized with Dowex-1 (bicarbonate form). Arabinose and xylotriose were detected in the hydrolyzate by paper chromatography, and the latter product (47 mg) was isolated by use of 3 MM paper sheets and characterized as the derived acetate, m.p. 108–110° C; the X-ray powder diagram was indistinguishable from that of β-xylotriose octaacetate.

(*d*) The tetrasaccharide was oxidized with lead tetraacetate – potassium acetate in 90% acetic acid under conditions described elsewhere (9). In 5.5 hours' reaction time the consumption of lead tetraacetate was 6.5 moles per mole and the yield of formic acid (CO_2) was 1.8 moles per mole. Structure III requires 7.0 moles of lead tetraacetate and 2.0 moles of formic acid per mole. In a simultaneous oxidation of xylotriose, 5.7 moles of lead tetraacetate were consumed and 1.9 moles of formic acid released (requires 6.0 and 2.0 moles per mole, respectively). Both the tetrasaccharide and xylotriose released 1 mole of acid rapidly (15 minutes' reaction time) and the second mole slowly, chracteristic of oligosaccharides of the (1 → 4)-xylobiose series (9).

(*e*) The acetylated tetrasaccharide (VI) (1.9 mg) in methanol (0.4 ml) was treated with excess sodium methoxide for 6 hours. Acetic acid was added, the solvent evaporated off at room temperature, and the deacetylated product (VII) treated with lead tetraacetate – potassium acetate in 90% acetic acid. The consumption of lead tetraacetate, measured spectrophotometrically (20), reached a constant value of 6.5 moles per mole in 5–6 hours' reaction time (structure III requires 7.0 moles per mole). On partial acid hydrolysis, as in section *c*, VII yielded xylotriose and arabinose (paper chromatographic evidence).

Can. J. Chem. Downloaded from www.nrcresearchpress.com by 210.87.254.42 on 09/05/12
For personal use only.

(*f*) Acetate VI and xylotriose octaacetate were each (2-mg samples) deacetylated with sodium methoxide, the solutions were neutralized with carbon dioxide and concentrated *in vacuo*. Each product was taken up in 0.04 *N* lime water (previously saturated with oxygen-free nitrogen), and at intervals the pentose content

	% pentose remaining	
Time (hr)	Tetrasaccharide VII	Xylotriose
0	100	100
21	55.0	65.6
46	32.3 (30.2)*	37.6 (39.0)*
90	21.2 (20.6)*	27.6
190	15.9	24.9 (19.1)*

*Duplicate experiment.

was estimated: Comparative values given (10) for xylotriose based on the production of acidic products in 0.04 *N* lime water are as follows (% oligosaccharide undegraded (hours)): 56 (25); 36 (48); 25 (73); 13 (120).

ACKNOWLEDGMENTS

The authors are most grateful to Dr. E. T. Reese for a generous supply of *Streptomyces* QMB 814 enzyme. They also thank Mrs. J. Nuttall and Miss M. Gates for technical assistance. Microanalyses were performed by Mr. M. Mazurek and X-ray powder diagrams were prepared by Mr. W. C. Haid.

REFERENCES

1. A. S. PERLIN. Cereal Chem. **28**, 370 (1951).
2. A. S. PERLIN. Cereal Chem. **28**, 383 (1951).
3. F. J. SIMPSON. Can. J. Microbiol. **1**, 131 (1954).
4. R. MONTGOMERY and F. SMITH. J. Am. Chem. Soc. **77**, 3325 (1955).
5. B. H. HOWARD. Biochem. J. **67**, 643 (1957).
6. C. M. EWALD and A. S. PERLIN. Can. J. Chem. **37**, 1254 (1959).
7. E. T. REESE, E. SMAKULA, and A. S. PERLIN. Arch. Biochem. Biophys. **85**, 171 (1959).
8. E. T. REESE. Unpublished data.
9. A. S. PERLIN and A. R. LANSDOWNE. Can. J. Chem. **34**, 451 (1956).
10. R. L. WHISTLER and W. M. CORBETT. J. Am. Chem. Soc. **78**, 1003 (1956).
11. R. L. WHISTLER and J. N. BEMILLER. Advan. Carbohydrate Chem. **13**, 289 (1958).
12. G. O. ASPINALL, C. T. GREENWOOD, and R. J. STURGEON. J. Chem. Soc. 3667 (1961).
13. R. H. MARCHESSAULT. Private communication.
13.(*a*) R. H. MARCHESSAULT, H. HOLAVA, and T. E. TIMELL. Can. J. Chem. **41**, 1612 (1963).
14. C. T. BISHOP. J. Am. Chem. Soc. **78**, 2840 (1956).
15. G. O. ASPINALL, I. M. CAIRNCROSS, R. J. STURGEON, and K. C. B. WILKIE. J. Chem. Soc. 3881 (1960).
16. A. S. PERLIN and E. T. REESE. Can. J. Biochem. Physiol. **41**, 1842 (1963).
17. W. MEIJBAUM. Hoppe-Seylers Z. Physiol. Chem. **258**, 117 (1939).
18. M. SOMOGYI. J. Biol. Chem. **160**, 61 (1945).
19. F. W. BARTH and T. E. TIMELL. Can. J. Chem. **36**, 1321 (1958).
20. A. S. PERLIN and S. SUZUKI. Can. J. Chem. **40**, 1226 (1962).
21. R. L. WHISTLER and C. C. TU. J. Am. Chem. Soc. **74**, 3609 (1952).
22. I. AUGESTAD and E. BERNER. Acta Chem. Scand. **8**, 251 (1954).

Can. J. Chem. Downloaded from www.nrcresearchpress.com by 210.87.254.42 on 09/05/12
For personal use only.

A GLUCAN PRODUCED BY CLAVICEPS PURPUREA[1]

A. S. PERLIN AND W. A. TABER
National Research Council of Canada, Prairie Regional Laboratory, Saskatoon, Saskatchewan
Received May 23, 1963

ABSTRACT

A glucan is produced by pure cultures of *Claviceps purpurea* (Fr.) Tul., PRL 1980, and its formation appears to be related to the accumulation of other shunt products such as ergot alkaloids, polyols, and trehalose. The glucan consists of β-D-glucopyranosyl units, most of which constitute a (1 → 3)-linked main chain. Other units are attached as branches to units of the main chain by (1 → 6)-linkages and are distributed in a relatively uniform arrangement along the length of the polymer. The glucan is resistant to attack by an endo type of laminarinase but is degraded vigorously by one of the exo type, yielding D-glucose and gentiobiose.

Can. J. Chem. Downloaded from www.nrcresearchpress.com by 210.87.254.40 on 09/05/12
For personal use only.

In attempting to relate the physiology of certain strains of *Claviceps purpurea* to production of ergot alkaloids, changes in content of mycelial and filtrate constituents of high- and low-alkaloid-producing cultures are being studied (1, 2). Alkaloid is produced in vitro when the media lack requirements for maximum cell growth (1) but do not simultaneously cause a noticeable inhibition of respiration (2). These imbalanced culturing conditions also influence markedly the formation and cellular accumulation of other shunt products (3) such as polyols, trehalose, and nucleotides (2).

When grown on a medium rich in D-glucose and phosphate, *Claviceps purpurea* (Fr.) Tul., PRL 1980, produces only traces of ergot alkaloid, but the cultures become unusually viscous, and addition of one-half to one volume of ethanol to the culture filtrate yields a fibrous polysaccharide (I). During earlier stages of growth (3–6 days) a substantial amount of polysaccharide (II) is associated intimately with the mycelium, from which it has been extracted with trichloroacetic acid, but none appears to be present in the mycelium of 7- to 8-day-old cultures. The polysaccharides from both sources are found to be closely related in structure, and hence I may not be elaborated by the fungus as an extracellular product but possibly is excreted into the medium as the mycelium ages. This loss of mycelial polysaccharide does not appear to be due to disintegration of cells for there is a commensurate drop in trehalose content but not in total polyol and dry weight (2), which suggests that a selective transport or utilization of carbohydrate reserves occurs within the culture. Under conditions that favor the production of more alkaloid the organism produces less polysaccharide, virtually all of which is present in the filtrate throughout the growth period. This polysaccharide shows characteristics notably different from those of I, and requires further examination. The present paper deals mainly with the structure of I isolated from filtrates of 8-day cultures.

Isolated polysaccharide I is water insoluble, but it dissolves readily in dilute alkali and remains in solution when excess acid is added. Gradual addition of ethanol to such a solution has afforded several fractions of the polymer, but no structural variations between these fractions have been detected. D-Glucose appears to be the sole sugar component of I, as shown by acid hydrolysis and other data reported below and, since solutions of the polymer in alkali are levorotatory, a predominance of β-D-glucosidic linkages is indicated.

On treatment with sodium metaperiodate the glucan consumed 0.6 mole of oxidant

[1]*Issued as N.R.C. No. 7489.*

per anhydroglucose unit, glycol cleavage resulting in the release of 0.25 mole of acid per unit. Hence virtually all of the oxidation was confined to about 25% of residues that contain a 1,2,3-triol grouping, i.e., to end-units and/or to 6-substituted D-glucopyranosyl units. The remaining three-quarters of the polymer appeared, therefore, to be linked by (1 → 3)-bonds. Accordingly, treatment of the oxidized material with hot phenylhydrazine acetate (4) afforded in high yield a polymeric product (III) virtually immune to further oxidation by periodate. This product, which was insoluble even in 1 *N* alkali, was obtained also by reducing the oxidized polysaccharide and then subjecting the derived polyol to partial acid hydrolysis (5). These results show the presence in I of a central chain of (probably several hundred, based on the low periodate uptake) 3-substituted D-glucopyranosyl units, and also suggest that the oxidizable units occur as end groups.

The presence of a high proportion of end groups in the polysaccharide is demonstrated more clearly by methylation data. Unfortunately, the glucan proved highly resistant to complete methylation and the derived ether was poorly soluble, making for a low recovery of methylated product. However, acid methanolysis of the polymeric methyl ether afforded a mixture of glucosides which, from gas–liquid phase chromatographic analysis, consisted of a tetra-, a tri-, and a di-methyl derivative. The yield of the tetramethyl glucoside was about 17%, showing that most of the formic acid liberated by periodate oxidation had been derived from end groups. The trimethyl fraction, constituting about 60% of the mixture, gave 2,4,6-tri-*O*-methyl D-glucose on acid hydrolysis, thus confirming that the 3-linked D-glucopyranosyl unit is the dominant structural type in the glucan. Units comprising the branch points are of this same type but are linked to other units also through position 6, the dimethyl ether derived from such units being the 2,4-isomer.

Although the glucan contains many 3-substituted β-D-glucopyranosyl units it is attacked in solution to only a small extent by the "*endo*-laminarinase" of *Rhizopus arrhizus* QM 1032 (6). However, *Basidiomycete* QM 866 "*exo*-laminarinase" (6) was found to degrade the polysaccharide (even as a suspension) rapidly and extensively, yielding D-glucose and the disaccharide gentiobiose. These products were formed in a ratio of 3:2 and accounted for 80% of the glucan. Isolation of gentiobiose confirms the methylation evidence that (1 → 6)-β-D-glucosyl linkages are present in the polymer, and the strong affinity of the β-D-glucosidase for the glucan provides a further indication that all (or nearly all) of the remaining glycosidic bonds possess the β-D-configuration. Polymeric product III, from which the end groups have been removed selectively, also is hydrolyzed by the exo enzyme but with production of glucose only, a clear indication that in glucan I the end groups constitute non-reducing end-units of the gentiobiosyl structures.

The *exo*-laminarinase provided a highly useful means for structural comparison of various samples of the glucan. Thus, polysaccharide II, extracted from the *Claviceps* mycelium, was found in this way to be closely similar to I since it was degraded readily by the enzyme to glucose and gentiobiose. Similarly, subfractions of I obtained by fractional precipitation each yielded glucose and gentiobiose in about the same ratio, which indicated strongly that any difference between fractions is mainly one of molecular size.

The overall data are consistent with a structure for the glucan represented by formula I. There is a main chain of (1 → 3)-linked β-D-glucopyranosyl units (Glp), and single β-D-glucopyranosyl units are attached as branches to (on the average) about every fourth unit of this main chain through (1 → 6)-linkages. The *Claviceps* glucan is thus closely related structurally to a new type of glucan described recently by Smith (7) that is produced by an unidentified fungus; however, this latter polysaccharide is more highly branched and readily soluble in water.

Can. J. Chem. Downloaded from www.nrcresearchpress.com by 210.87.254.40 on 09/05/12
For personal use only.

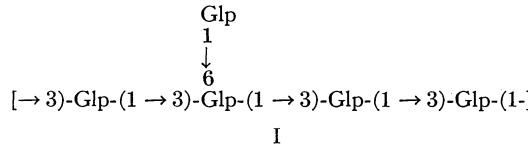

I

As noted above, the *Rhizopus endo*-laminarinase effects very limited degradation of glucan I, as compared with its activity on laminarin. A similar comparison with polymer III was not possible because of the marked insolubility* of this material; however, a suspension of III was slowly degraded by the enzyme whereas there was no evidence of attack on I in suspension. These observations suggest, therefore, that the branch units in I limit accessibility of the enzyme to most of the 3-substituted β-D-glucosyl units of the main chain, and hence that branching is distributed along the length of the polymer in such a way that relatively few large interbranch regions are to be found.

EXPERIMENTAL

Melting points are corrected. Optical rotations were measured at 25±2°. Concentration of solutions was carried out *in vacuo* at 40–45° C.

Paper chromatography was carried out using as solvents (A) ethyl acetate – pyridine – water (10:4:3) or (B) butanol–ethanol–water (40:11:15). Gas–liquid phase chromatography was carried out with a temperature-programmed unit over the range 60–200° C using an 8 ft×3/16 in. column of phthalate – ethylene glycol polyester (9) on C-22 activated firebrick (ratio 4.5:1); helium flow rate 70 cc/min.

Formation of Polysaccharide by Claviceps purpurea PRL 1980

The medium consisted of D-glucose (65 g), D-mannitol (65 g), succinic acid (7.2 g), potassium dihydrogen phosphate (2 g), and various other salts per liter (1, 2); the pH of the medium was adjusted to 5.2 with ammonia. A washed and homogenized vegetative inoculum was added and the cultures were shaken at 24° C. At various intervals the mycelium was filtered off with suction on Whatman No. 2 paper and washed on the filter with water. The lyophilized mycelium was then extracted successively with cold and hot 5% trichloroacetic acid solution (TCA). Ethanol was added to each of these extracts and to the culture filtrate to promote turbidity, and the precipitates obtained were recovered by filtration, washed with ethanol and acetone, and dried *in vacuo*. The relative amounts of polysaccharide isolated from these three different sources are indicated by the following crude yields obtained from a series of cultures (mg/flask).

	Age of culture (days)					
	3	4	5	6	7	8
Filtrate	60	132	189	161	140	115
Cold TCA extract	26	50	53	46	0	0
Hot TCA extract	23	42	40	41	0	0

Each of the materials extracted by TCA at 5 days was readily degraded by *Basidiomycete* QM 866 *exo*-laminarinase (see below), yielding glucose and gentiobiose in a ratio of about 1:1 (paper chromatographic evidence).

Polysaccharide I

Polysaccharide I used for the detailed structural studies was obtained from clear filtrates of 8-day-old cultures by precipitation with one-half to one volume of ethanol. The highly gelatinous flocculus was centrifuged off, washed several times each with 50% aqueous ethanol and water, then it was suspended in water, and lyophilized. In a typical experiment 1.0 g of colorless, fibrous material was isolated from 1 liter of culture. Found: C, 41.3%; H, 6.5%; N, 1.1%; ash, 3.3%. Calculated for $C_6H_{10}O_5$: C, 44.4%; H, 6.2%. $[\alpha]_D$ −4° (*c*, 1 in 1 *N* NaOH).

The polysaccharide (0.1 g) in 1 *N* sulphuric acid (10 ml) was heated in a sealed tube on the steam bath for 18 hours. The hydrolyzate, which contained a small quantity of a gelatinous sediment, was neutralized and, on paper chromatographic examination, found to contain only glucose.

**This observed decrease in solubility associated with conversion of a branched to a linear polymer is thus similar to the effect found with the soluble arabino-xylan of wheat (8), i.e., removal of the* L-*arabinosyl branches of this latter polysaccharide yields an insoluble linear xylan.*

Can. J. Chem. Downloaded from www.nrcresearchpress.com by 210.87.254.40 on 09/05/12
For personal use only.

Polysaccharide I (0.20 g) was dissolved in 1 *N* sodium hydroxide (20 ml), the solution was acidified with acetic acid, and then ethanol was added slowly with good stirring, four precipitated fractions being collected with increasing alcohol concentration: 1, 25 mg; 2, 140 mg; 3, 35 mg; 4, 40 mg.

Each fraction was hydrolyzed readily by *Streptomyces* QM 806 laminarinase at 45° C, a paper chromatogram of the hydrolyzates indicating that each yielded glucose and gentiobioise in about the same proportion as unfractionated glucan I.

Periodate Oxidation of I

The glucan (32 mg) was suspended in a solution of sodium metaperiodate (83 mg, 10 ml) in the absence of light; stirred magnetically, the suspension was stored first for 5 hours at 25° C and then at 12° C. Periodate uptake measured iodometrically was as follows (moles/mole (hour)): 0.43 (1), 0.54 (5), 0.61 (92); at 92 hours the yield of formic acid was 0.24 mole/mole.

Glucan I (0.30 g) was treated with sodium metaperiodate (0.65 g in 25 ml water) as above for 72 hours. Excess ethylene glycol was added, the sediment was centrifuged off and washed with 50% acetic acid until it gave a negative test for iodate, then it was suspended in water, and lyophilized (wt., 0.28 g).

Partially-degraded Glucan (III)

(*a*) Periodate-oxidized I (0.15 g) was treated according to Barry (4) with phenylhydrazine (1 ml) and acetic acid (1.2 ml) in 50% ethanol (10 ml) under reflux for 6 hours. A highly swollen gel was obtained, centrifuged off, washed thoroughly with 50% ethanol, and then heated under reflux in this solvent for 5 hours with benzaldehyde (1 ml) and benzoic acid (0.2 g) (10). The pale yellow flocculus was centrifuged off, washed thoroughly with ethanol and ether, and dried *in vacuo* (wt., 0.10 g).

(*b*) Periodate-oxidized I (0.30 g) was added with vigorous stirring to sodium borohydride (0.15 g) in water (10 ml). After 6 hours, acetic acid (50 ml) was added, the precipitate was centrifuged off, washed with 50% ethanol, and suspended in 0.1 *N* sulphuric acid (5). After 18 hours, the precipitate was washed with water and lyophilized (wt., 0.16 g).

Prepared by procedure (*a*) or (*b*), degraded polymer III was found to consume only trace quantities of sodium metaperiodate. Both preparations, suspended in water at 45° C, were degraded by the *exo*-laminarinase (6), yielding glucose, and by *Rhizopus arrhizus* QM 1032 *endo*-laminarinase (6), yielding glucose and laminaribiose (paper chromatographic evidence).

Methylation of I

To a solution of glucan I (0.20 g) in 10% potassium hydroxide (20 ml) dimethyl sulphate (2 ml) was added slowly with good stirring. After 18 hours the solution was neutralized with sulphuric acid, concentrated to a slurry, 20 ml of the alkali was again added, and a second methylation carried out. The slurry obtained from this reaction mixture was dialyzed to remove salts, and a precipitate which formed in the dialysis sac was centrifuged off, and lyophilized. Dimethylformamide (20 ml) (11)was added to the methylation product, together with methyl iodide (10 ml) and silver oxide (4 g), and the mixture was shaken for 18 hours. The suspension was filtered, the solids were extracted several times with hot acetone, and the combined extracts and filtrate were concentrated. Yield, 0.14 g. After a second methylation with methyl iodide, the filtrate contained only a few milligrams of material, and the acetone extract, 60 mg of product (A). Therefore, the solids were suspended in sodium cyanide solution and dialyzed against water, more sodium cyanide being added periodically until no more silver oxide appeared to remain. The final, neutral, suspension contained in the dialysis membrane was lyophilized. Yield, 50 mg (B).

Methanolysis and Hydrolysis Products of Methylated I

Methylation products A and B were treated with 1% methanolic hydrogen chloride in sealed tubes on the steam bath for 18 hours. The methanolysates were neutralized with ethereal diazomethane, concentrated, and the syrupy residues examined by gas–liquid phase chromatography. Both products showed the presence of six components, the relative emergence times of which corresponded to those reported (12) for α- and β-anomers of a tetra-, a tri-, and a di-*O*-methyl methyl hexoside. Triangulation of the peaks obtained gave the following percentage compositions (anomeric percentages in parentheses).

	Fraction A	Fraction B
Tetra-	17.1 (4.4, 12.7)	16.8 (4.9, 11.9)
Tri-	64.6 (18.4, 46.2)	59.2 (15.8, 43.4)
Di-	18.3 (5.6, 12.7)	23.9 (7.4, 16.5)

The glycoside mixtures were hydrolyzed with 1 *N* sulphuric acid, and examination of the neutral hydrolyzates by paper chromatography indicated that each contained a tetra-, a tri-, and a di-*O*-methyl ether constituent, together with a trace proportion of a monomethyl component.

The hydrolyzates of A and B were combined and the sugar mixture was chromatographed on Whatman 3 MM paper (solvent B). Extraction of the trimethyl component from the paper afforded a solid product

Can. J. Chem. Downloaded from www.nrcresearchpress.com by 210.87.254.40 on 09/05/12
For personal use only.

which, after recrystallization from ether, had m.p. 119–121° C, undepressed by admixture with 2,4,6-tri-*O*-methyl-D-glucose.

The dimethyl component was a syrup. It did not react readily with lead tetraacetate in acetic acid, showing that position 2 was substituted (13). After reduction with sodium borohydride, formaldehyde was produced when the product was oxidized with lead tetraacetate – potassium acetate in 90% acetic acid, and chromatographic examination of the oxidation mixture indicated the presence of a material having characteristics consistent with those of a di-*O*-methyl pentose. These properties tentatively identify the D-glucose ether as the 2,4-di-*O*-methyl derivative.

Enzymic Degradation of Glucan I

Glucan I (0.20 g) was suspended in water (20 ml) at 35° C, and *Basidiomycete* QM 866 *exo*-laminarinase preparation (50 mg) (6) was added with stirring. In 1 hour most of the polysaccharide appeared to have been brought into solution, the digest was then stored at 40° C for 18 hours, and finally it was heated on the steam bath for 1 hour. Paper chromatographic examination of the digest showed the presence of glucose (strong), a disaccharide (strong), and probably a trisaccharide (trace). The solution was concentrated to a volume of 3–4 ml, several volumes of ethanol were added, and precipitated material was recovered (wt., 60 mg). A concentrate of the supernatant solution was chromatographed on Whatman 3 MM paper (solvent A). Elution of the appropriate zones yielded: (*a*) α-D-Glucose [95 mg); crystallized from water–methanol–ethanol, m.p. 144–146° C; $[\alpha]_D$ 52.0° (*c*, 1.8 in water, equilibrium value). (*b*) α-Gentiobiose (64 mg); crystallized from aqueous methanol, m.p. 90–92° C; $[\alpha]_D$ 8.9° (*c*, 1.4 in water, equilibrium value); the X-ray powder diagram was indistinguishable from that of an authentic specimen containing methanol of crystallization. Calculated for $C_{12}H_{22}O_{11}.2CH_3OH$: C, 41.38%; H, 7.44%. Found: C, 41.67%; H, 7.53%.

ACKNOWLEDGMENTS

The authors gratefully acknowledge the generosity of Dr. E. T. Reese, who provided preparations of laminarinase-type enzymes. They also thank D. Mansfield and Miss M. Gates for valuable technical assistance and L. Hoffman for carrying out gas–liquid phase chromatographic analyses. Microanalyses were performed by M. Mazurek.

REFERENCES

1. W. A. TABER and L. C. VINING. Can. J. Microbiol. **9**, 1 (1963).
2. W. A. TABER. Bacteriol. Proc. 23 (1963).
3. J. W. FOSTER. Chemical activities of the fungi. Academic Press, New York. 1949. p. 164.
4. V. C. BARRY. Nature, **152**, 537 (1943).
5. I. J. GOLDSTEIN, G. W. HAY, B. A. LEWIS, and F. SMITH. Abstracts, 135th Meeting of the American Chemical Society, Boston, Mass. 1959. p. 30.
6. E. T. REESE and M. MANDELS. Can. J. Microbiol. **5**, 173 (1959).
7. F. SMITH. International Symposium on Carbohydrate Chemistry, Birmingham, July 1962. p. 16.
7. (*a*) J. JOHNSON, S. KIRKWOOD, A. MISOKI, T. E. NELSON, J. V. SCALETTI, and F. SMITH. Chem. Ind. (London), 820 (1963).
8. A. S. PERLIN. Cereal Chem. **28**, 382 (1951).
9. B. M. CRAIG. Chem. Ind. (London), 1442 (1960).
10. C. M. EWALD and A. S. PERLIN. Can. J. Chem. **37**, 1254 (1959).
11. R. KUHN, H. TRISCHMANN, and I. LOW. Angew. Chem. **67**, 32 (1955).
12. C. T. BISHOP. Methods Biochem. Analy. **10**, 1 (1962).
13. A. J. CHARLSON and A. S. PERLIN. Can. J. Chem. **34**, 1200 (1956).

Can. J. Chem. Downloaded from www.nrcresearchpress.com by 210.87.254.40 on 09/05/12
For personal use only.

BACK-SCATTERING AND SELF-ABSORPTION OF β^--PARTICLES[1]

M. S. LAFLEUR
Radiochemistry Laboratory, Department of Chemistry, McGill University, Montreal, Que.
AND
S. KAHANA AND T. F. MORRIS
Department of Physics, McGill University, Montreal, Que.
AND
L. YAFFE
Radiochemistry Laboratory, Department of Chemistry, McGill University, Montreal, Que.
Received January 21, 1963

Can. J. Chem. Downloaded from www.nrcresearchpress.com by 210.87.254.42 on 09/05/12
For personal use only.

ABSTRACT

The self-absorption of the β^--radiation from S^{35} and P^{32} has been studied in various compounds. The function derived by Gora and Hickey has been shown to fit the data. The back-scattering of the β^--radiation from P^{32} by various elements and compounds has been examined and a semiempirical treatment used to suggest an effective atomic number for back-scattering by compounds.

INTRODUCTION

There have been many experimental studies dealing with the phenomenon of scattering and absorption of β^--radiation in counters of various geometrical efficiencies. These have been made to try to describe these processes adequately and to use the data obtained to transform measured counting rates into accurately known disintegration rates.

The theoretical description of scattering and absorption of β^--radiation is difficult because of the continuous distribution of β^--particle energies and the complexity of the scattering process. It is known that, when β^--particles interact with matter, they are scattered by elastic collision with atomic nuclei and lose energy by inelastic collision with atomic electrons. Absorption is due to the combined effects of scattering and energy loss.

In this paper we have studied the problems of self-absorption and back-scattering with counters of geometrical efficiencies of 2π steradians and less.

(a) Self-absorption

Self-absorption, the absorption of radiation in the material of the source itself, is the limiting factor in accurate disintegration-rate determinations where the sample is mounted in solid form. The absorption of β^--radiation is described approximately by the exponential law

$$A = A_0 e^{-\mu x}, \quad [1]$$

where A is the activity observed when radiation from a source of activity A_0 has passed through material of thickness x cm. The absorption coefficient, μ, in cm^{-1}, can be related to the density, d, in mg cm^{-3}, of the absorber and the end-point energy E_0 of the β^--emitter by equations of which the following (1) is typical:

$$\mu = 0.022 d E_0^{-1.33}. \quad [2]$$

Many self-absorption relations have been based on the approximate exponential

[1]*This work received financial assistance from the National Research Council of Canada.*

absorption as shown in equation [1]. The general approach has been to consider the absorption of radiation emitted from a point in the source, then to sum up the contribution from all possible points. Early self-absorption studies (2–6) were made with counters of very low geometrical efficiency. The electrons were assumed to travel normal to the source and the problem was reduced to a one-dimensional type. Equation [1] was integrated over the sample thickness from $x = 0$ to $x = a$ and the following relation obtained:

$$A = \frac{A_0}{\mu a}(1-e^{-\mu a}). \qquad [3]$$

It was pointed out (6, 7) that, for thin samples of superficial density less than 1 mg/cm^2, self-scattering is a very important factor. In subsequent publications (8–10) equations were derived which took this effect into account.

Objections to the simple self-absorption relation expressed in equation [3] were also raised as self-absorption was studied with counters subtending larger solid angles. Elliot and co-workers (11–14) showed that, from very thin layers, radiation is emitted isotropically, while from thicker layers the intensity observed at an angle θ to the normal approaches a cos θ relationship.

According to these results, the activity observed at an angle θ is written

$$A_\theta = \frac{A_0 \cos\theta}{\mu a}(1-e^{-\mu a/\cos\theta}),$$

which reduces to the experimental cosine distribution at large values of a.

Gora and Hickey (15) measured self-absorption in a flow-type counter. They assumed isotropic distribution and integrated both over sample thickness from $x = 0$ to $x = a$ and over the angles from $\theta = 0$ to $\theta = \pi/2$ to obtain

$$\frac{A}{A_0} = \tfrac{1}{2}\left[\frac{1-e^{-\mu a}}{\mu a} + e^{-\mu a} + \mu a Ei(-\mu a)\right]. \qquad [4]$$

$Ei(-\mu a)$ is the exponential integral of $(-\mu a)$. Gora and Hickey found that the simple relation described by equation [3] held only if the value of μ was varied with the geometrical efficiency of the counter.

Roalsvig and Haslam (16) later derived a similar equation. They irradiated disks of Cu, Zn, Ni, Mo, and polystyrene of thicknesses ranging from ten to several hundred milligrams per square centimetre. They found that equation [4] fitted their experimental results very well for $\mu/d = 0.0119E_0^{-1.83}$.

Hendler (17) studied the self-absorption of C^{14} and found that a hyperbolic function described the situation over the range of investigation. Katz (18) then showed that the hyperbolic function did not fit his data and Massini (19) pointed out that possibly the effect of the counting arrangement used by Hendler led to the hyperbolic function.

Self-absorption in counters of geometrical efficiencies of 2π steradians and less still poses many problems. (The problem of self-absorption in a 4π counting geometry has been intensively investigated by Yaffe and co-workers (20, 21) and Campion and co-workers (22–25).) Most experimental work has concerned itself with the study of self-absorption of a particular β^--emitting nuclide in source material of a particular composition. In the present work the composition of the source, the energy of the β^--emitter, and the geometrical efficiency of the counter have all been varied.

(b) Back-scattering

The main features of back-scattering observed in counters of less than 2π geometry

Can. J. Chem. Downloaded from www.nrcresearchpress.com by 210.87.254.42 on 09/05/12
For personal use only.

have been well examined (26, 27) so that the effects of varying the energy of the β^--emitter, the atomic number, and mass thickness of the back-scatterer are known.

An important experimental fact about back-scattering is that the extent of back-scattering increases with the thickness of the backing material to a fixed value. The fixed value defines a condition termed 'saturation back-scattering'. For elements, the saturation back-scattering is a function of atomic number. For compounds, it has been suggested that the saturation back-scattering value obtained might characterize an 'effective' atomic number.

Various experimenters have defined an 'atomic number' for compounds purely empirically to suit their particular experimental data.

Glendenin and Solomon (28) proposed an average atomic number $\bar{Z}$ to explain their back-scattering results:

$$\bar{Z} = \frac{N_1Z_1+N_2Z_2+\ldots N_nZ_n}{N_1+N_2+\ldots N_n},$$

where $Z_1 \ldots Z_n$ are the atomic numbers of the various elements in the compound and $N_1 \ldots N_n$ are the numbers of atoms of each in the formula.

Perlman and Friedlander (29) used another definition of an average atomic number for their self-absorption studies:

$$\bar{Z}^{\frac{1}{2}} = \frac{N_1A_1Z_1^{\frac{1}{2}}+N_2A_2Z_2^{\frac{1}{2}}+\ldots}{N_1A_1+N_2A_2+\ldots} = \frac{\sum_i N_iA_iZ_i^{\frac{1}{2}}}{\sum_i N_iA_i},$$

where A_i is the atomic weight of the element defined by atomic number Z_i. This is the form these authors use, although it is referred to as $\bar{Z}^{\frac{1}{2}}$ in their paper.

Saldick and Allen (30), in studying the oxidation of ferrous sulphate in acid solution by high-energy cathode rays, suggested an effective atomic number, $\bar{Z}_E$:

[5] $$\bar{Z}_E = \sum_i [(\text{electron density})_i Z_i].$$

Their formula is a special case of the more general formula of Henriksen and Baarli (31):

[6] $$\bar{Z}_{E_1} = \sum_i [(\text{electron density})_i Z_i^x]^{1/x}.$$

Müller (32) defined an empirical effective atomic number, $\bar{Z}_{E_2}$, to explain his data for the back-scattering of β^--radiation by compounds:

[7] $$\bar{Z}_{E_2} = \sum_i [(\text{weight fraction})_i Z_i] = \frac{\sum_i N_iA_iZ_i}{\sum_i N_iA_i},$$

where the effective atomic number is the sum of each atomic number multiplied by the weight fraction of that atom present in the compound.

Danguy and Quivy (33) studied the back-scattering of electrons by solutions and alloys and found that their results could be fitted by Müller's effective atomic number.

Gray *et al.* (34) calculated effective atomic numbers according to equations [5], [6], and [7], and correlation was completed with observed back-scatter intensities. Müller's effective atomic number (equation [7]) showed the poorest correlation, with marked

Can. J. Chem. Downloaded from www.nrcresearchpress.com by 210.87.254.42 on 09/05/12
For personal use only.

scatter on the points. The results using equation [5] were much better. The best results were obtained using equation [6] for effective atomic number with a value of $x = 0.93$.

In this paper the back-scattering due to compounds has been investigated in order to check the various formulations with regard to effective atomic number.

EXPERIMENTAL

(a) Self-absorption

Two β^--emitters were studied, S^{35} ($E_0 = 0.167$ Mev) and P^{32} (1.71 Mev). The self-absorption of the β^--radiation was measured by varying the composition of the sources and varying the solid angle subtended by the counter at the sources.

Sources containing P^{32} were prepared by precipitating the orthophosphates of Ca, Cu, Ba, and Pb from a stock solution of orthophosphoric acid containing a fixed ratio of the active P^{32} to the inactive P^{31} isotope. Similarly, sources containing S^{35} were prepared by precipitating the sulphates of Ba, Sr, and Pb from a stock solution of sulphuric acid containing a fixed ratio of S^{35} to inactive sulphur isotopes. Aliquots of varying size of the precipitated salts (orthophosphate or sulphate) in slurry form were transferred to aluminum planchettes of standard dimensions. To ensure uniform distribution over the area of the planchette, the slurry was stirred before evaporation to dryness. Acetone was found to be a convenient slurrying agent for the unhydrated salts, while water was used for the hydrated salts.

Sources of varying thicknesses and constant area were thus prepared and weighed. The superficial density of the sources ranged from 0.05 to 35.0 mg/cm^2. The activity of the sources was measured with a 2π proportional counter and in two positions below an end-window gas-flow proportional counter. This gave results in geometrical efficiencies of 4%, 20%, and 50%. The aluminum planchettes, used as source mounts, were of sufficient thickness to ensure saturation back-scattering from the aluminum for all sources.

(b) Back-scattering

Inorganic compounds were used as backing material in powder form. The powder, finely ground, was contained in cylindrical metal boxes of sufficient depth to ensure saturation back-scattering.

Elements were also used as backing material to provide a standard curve of back-scattering vs. atomic number. The elements were in either foil or powder form.

The high-energy β^--emitter, P^{32}, was used as source material. To obtain a point source, 100 microliters of P^{32} solution of high specific activity was pipetted on to VYNS film and allowed to evaporate. The VYNS film, of superficial density 10 μg/cm^2, was then placed over the circular hole of an aluminum tray designed to fit as a shelf in the end-window counter. The backing material was cemented into position closely behind the source. Care was taken in all cases to keep the distance from the source to the backing constant. The activity of the samples was measured by the end-window counter in a geometrical efficiency of 20%.

RESULTS

(a) Self-absorption

Experimental self-absorption curves were obtained in the conventional manner by plotting the logarithm of the 'apparent' specific activity (measured activity per milligram of compound) versus the superficial density (mg/cm^2). The results of measurements in geometrical efficiencies of 50%, 20%, and 4% were normalized to the 50% position and were found to be superimposable.

In Fig. 1 is shown the self-absorption results for the phosphate sources. The points represent the experimental data. The difference in the self-absorption of the betas of P^{32} in phosphates of various densities is clearly shown. In Fig. 2 the self-absorption data for the sulphate sources are shown. Again the effect of density is clearly evident for the various sulphate sources.

The data have been fitted to the Gora and Hickey (15) function for a value of $\mu a = 0.022 d a E_0^{-1.33}$ (equation [2]). In Figs. 1 and 2 the solid lines represent the curves thus calculated. The agreement between the experimental and calculated results is very good for all the data. The error in each experimental point is estimated to be $\pm 5\%$. This includes non-uniformity of samples, statistical fluctuations in activity measurements, and weighing of samples. No correction has been made for the back-scattered radiation. The back-scatterer was the same for all sources, and the effect due to it was treated as a constant.

Can. J. Chem. Downloaded from www.nrcresearchpress.com by 210.87.254.42 on 09/05/12
For personal use only.

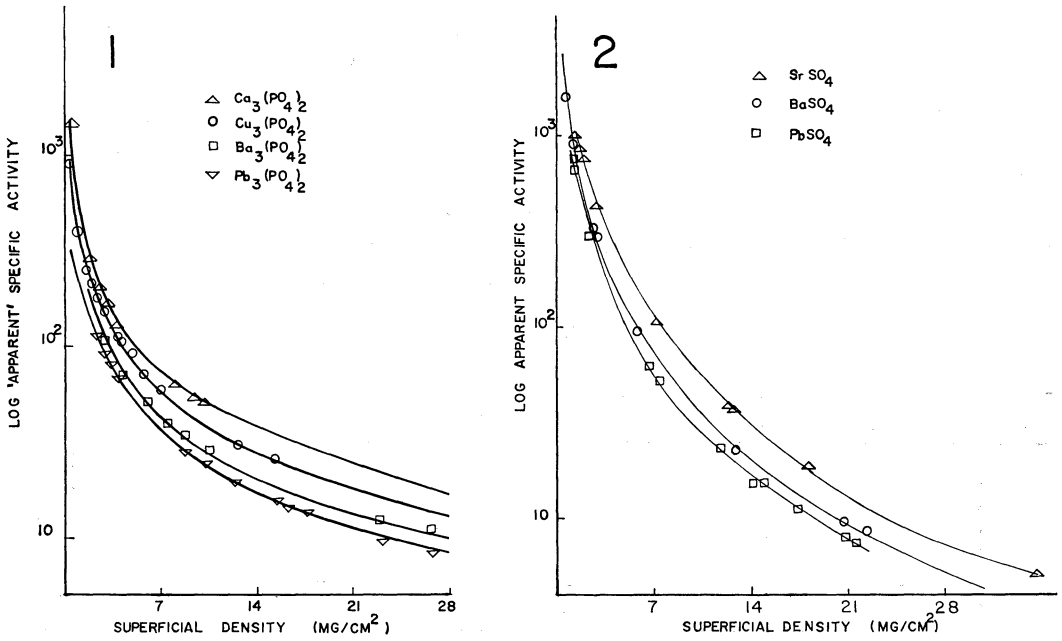

FIG. 1. Self-absorption of P^{32} by various phosphates.
FIG. 2. Self-absorption of S^{35} by various sulphates.

A further test of this function has been made by Meghir (35),* who studied the self-absorption of C^{11} in barium carbonate in a 4π counter which is essentially two 2π counters. The results are shown in Fig. 3. The triangles represent the self-absorption data for C^{11} in

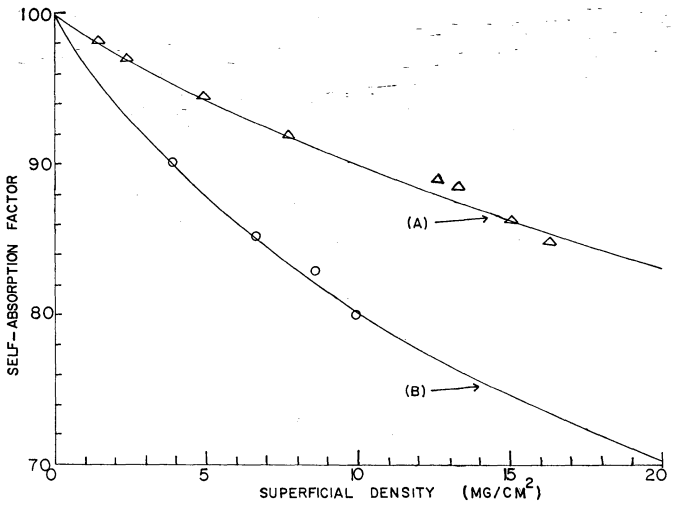

FIG. 3. Test of Gora and Hickey function: △ C^{11} in $BaCO_3$. The triangles represent the data obtained by Meghir (35). The solid line represents the curve obtained from the self-absorption expression. ○ Self-absorption of C^{11} in polystyrene (36). The solid curve was obtained by Meghir using the appropriate density corrections.

We are grateful to Dr. S. Meghir of this laboratory for kindly allowing us to use his results.

Can. J. Chem. Downloaded from www.nrcresearchpress.com by 210.87.254.42 on 09/05/12
For personal use only.

barium carbonate. The solid curve (A) is again obtained from the Gora and Hickey function. Crandall *et al.* (36) studied the self-absorption of C^{11} in polystyrene. Their data are shown by open circles, and Meghir obtained the curve (B) shown by use of the above function with the appropriate density correction.

Back-scattering

The effective atomic number, $\bar{Z}_{E_1}$, of each compound used was calculated from equation [6] with $x = 1$. The empirical effective atomic number, $\bar{Z}_{E_2}$, of Müller (equation [7]) was also calculated. The materials used as back-scatterers and their 'atomic numbers' are given in Table I. It is seen that the two formulae for effective Z give virtually the same

TABLE I

Effective atomic number of elements and compounds used as back-scatterers

Back-scatterer	$\bar{Z}_{E_1}$	$\bar{Z}_{E_2}$	Back-scatterer	$\bar{Z}_{E_1}$	$\bar{Z}_{E_2}$
C	6.00	6.00	Ni	28.00	28.00
BeO	6.67	6.56	Cu	29.00	29.00
NaF	10.10	10.09	KI	44.03	44.99
Mg	12.00	12.00	Ag	47.00	47.00
KCN	13.94	14.02	$Pb(NO_3)_2$	50.04	54.37
CaO	16.57	16.58	$PbCl_2$	60.45	65.43
KCl	18.05	18.05	Pb	82.00	82.00
ZnO	25.37	25.67			

result for low 'atomic numbers'. However, at high 'atomic numbers' there is a significant difference.

In Fig. 4 saturation back-scattering is plotted versus $\bar{Z}_{E_1}$. It is seen that a smooth curve may be drawn through all the points representing both elements and compounds. In Fig. 5 saturation back-scattering is plotted versus Müller's $\bar{Z}_{E_2}$. A smooth curve may be drawn through the points representing elements and the points representing compounds of low 'atomic number'. The points representing compounds of high 'atomic number' fall below the curve.

We were not able to reproduce the points of inflection found by Müller corresponding to atomic numbers of the rare gas configurations. Indeed, it seemed possible to redraw the Müller data without these points of inflection, especially since the rare gases were not used as back-scatterers in his experiments.

It is possible from a crude one-dimensional model* to suggest an 'effective atomic number' for back-scattering by compounds. This is shown in Fig. 6. The β-source is located at $x = 0$ on the x-axis. The activity of the source is $2a_0$. It is assumed that the shape of the β-spectrum and the angular distribution pattern of the β-radiation are virtually unchanged by passage through and absorption in the source. The absorption is assumed to be nearly exponential.

In Fig. 6(A), when there is no reflector, the measured activity is a_0, as only the activity in the negative direction reaches the counter. When there is a reflector, as in Fig. 6(B), the measured activity is the sum of the activity emitted in the negative direction plus the activity reflected back from the positive direction, i.e. a_0+b_0. The reflector is imagined to be infinite in length in order to describe the case of saturation back-scattering.

R, the reflection coefficient, is equal to the product of the number of scatterers and the cross section for back-scattering. For elements of low atomic number the screening of the

**A somewhat similar treatment has been given by G. L. Brownell (Preliminary Report No. 8, Nuclear Science Series, National Research Council, Washington, 1950), but to the authors' knowledge never published elsewhere.*

Can. J. Chem. Downloaded from www.nrcresearchpress.com by 210.87.254.42 on 09/05/12
For personal use only.

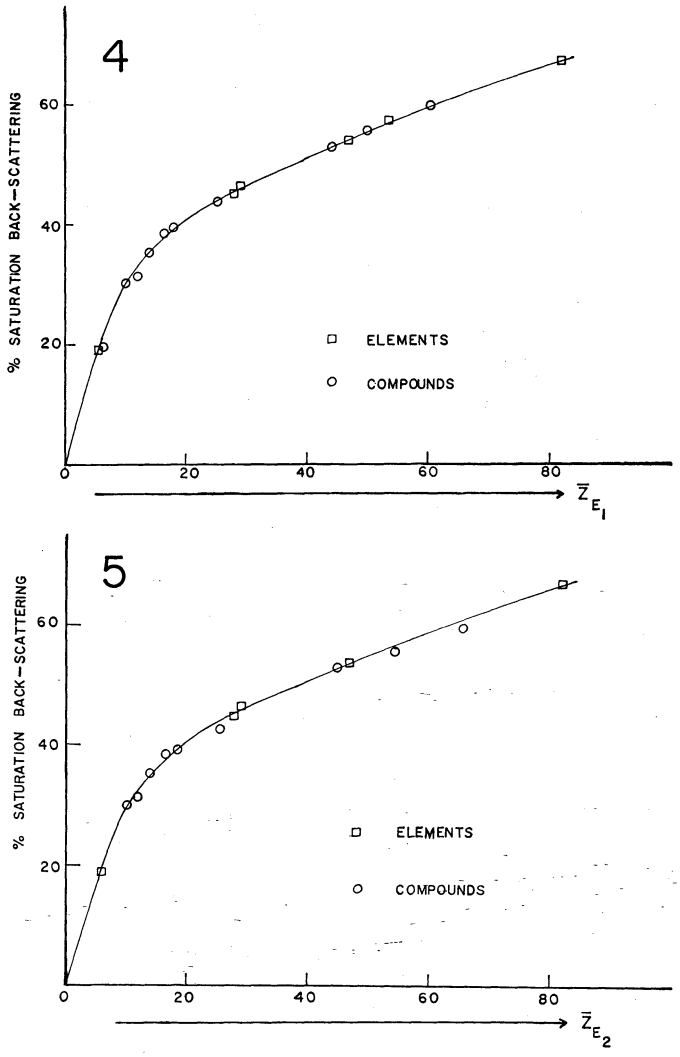

FIG. 4. Effective atomic number for saturation back-scattering using formula of Henriksen and Baarli (31).

FIG. 5. Effective atomic number for saturation back-scattering using formula of Müller (32).

nucleus can be ignored, Rutherford scattering applies, and

$$R \propto NZ^2,$$

where Z = nuclear charge and N = number of nuclei per unit length.

Let ϵdx represent the fractional number of electrons that fall below the detection threshold in the length dx. The loss coefficient, ϵ, will depend principally on small angle scattering by the electrons and thus, for elements,

$$\epsilon \propto NZ.$$

If one considers a point, x, in the one-dimensional reflector, the number of beta particles moving in the positive direction is

$$a(x) = a_0 e^{-\mu x}$$

Can. J. Chem. Downloaded from www.nrcresearchpress.com by 210.87.254.42 on 09/05/12
For personal use only.

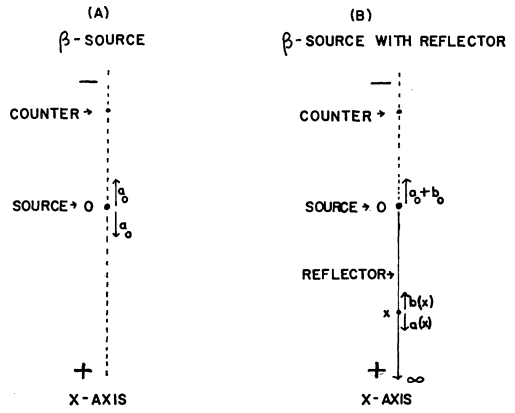

FIG. 6. One-dimensional representation of back-scattering.

and the number moving in the negative direction is

$$b(x) = b_0 e^{-\mu x}.$$

To determine $b(x)$ in terms of $a(x)$, one considers the number of beta particles moving in the positive direction at a distance dx from x. Then $a(x+dx)$ will be the sum of the number transmitted from x and the number reflected from x.

$$a(x+dx) = a(x)-(R+\epsilon)a(x)dx+Rb(x)dx$$

$$\frac{da}{dx} = -(R+\epsilon)a(x)+Rb(x)$$

$$-\mu a_0 e^{-\mu x} = -(R+\epsilon)a_0 e^{-\mu x}+Rb(x)$$

and

$$b(x) = \left\{\frac{(R+\epsilon)-\mu}{R}\right\}a_0 e^{-\mu x}.$$

To find μ in terms of R and ϵ, one considers the number of beta particles moving in the negative direction at $x-dx$.

$$b(x-dx) = b(x)-(R+\epsilon)b(x)dx+Ra(x)dx$$

$$-\frac{db}{dx} = -(R+\epsilon)b(x)+Ra(x).$$

Then

$$\mu\left\{\frac{(R+\epsilon)-\mu}{R}\right\}a_0 e^{-\mu x} = -(R+\epsilon)\left\{\frac{(R+\epsilon)-\mu}{R}\right\}a_0 e^{-\mu x} + Ra_0 e^{-\mu x}$$

and

$$\mu = \sqrt{[(R+\epsilon)^2-R^2]}.$$

Hence $b(x)$ may be expressed

$$b(x) = \left\{\frac{(R+\epsilon)-\sqrt{[(R+\epsilon)^2-R^2]}}{R}\right\}a_0 e^{-\mu x}.$$

Can. J. Chem. Downloaded from www.nrcresearchpress.com by 210.87.254.42 on 09/05/12
For personal use only.

At $x = 0$

$$b(x) = b_0 = \left\{\frac{(R+\epsilon)-\sqrt{[(R+\epsilon)^2-R^2]}}{R}\right\}a_0.$$

The efficiency of reflection, η, is then

$$\eta = \frac{b_0}{a_0} = 1 + \frac{\epsilon}{R} - \sqrt{\left[\left(1 + \frac{\epsilon}{R}\right)^2 - 1\right]}.$$

The percentage back-scattering is given by the efficiency

$$\left\{\left(a_0 + \frac{b_0}{a_0}\right) - a_0\right\} \times 100$$

$$= \frac{b_0}{a_0} \times 100.$$

Therefore back-scattering depends on the ratio ϵ/R. This suggests an effective Z for compounds. For a compound, the reflection coefficient is given by

$$R \propto N_1Z_1^2 + N_2Z_2^2 + \ldots N_nZ_n^2,$$

where $N_1 \ldots N_n$ represent the particle densities and $Z_1 \ldots Z_n$ the atomic numbers of elements $1 \ldots n$.

The loss coefficient is given by

$$\epsilon \propto N_1Z_1 + \ldots N_nZ_n.$$

Therefore

$$\frac{\epsilon}{R} \propto \frac{N_1Z_1 + \ldots N_nZ_n}{N_1Z_1^2 + \ldots N_nZ_n^2}.$$

This indicates an effective Z as given in equation [6]:

$$\frac{N_1Z_1^2 + N_2Z_2^2 + \ldots N_nZ_n^2}{N_1Z_1 + \ldots N_nZ_n} = \bar{Z}_{E1}.$$

The reflection coefficient may be written

$$\eta = 1 + \frac{\gamma}{\bar{Z}_{E1}} - \sqrt{\left[\left(1 + \frac{\gamma}{\bar{Z}_{E1}}\right)^2 - 1\right]},$$

where γ is some constant of proportionality. Let $S = 1 + \gamma/\bar{Z}_{E1}$, then

$$\eta = S - \sqrt{[S^2 - 1]}.$$

Therefore $S = (1+\eta^2)/2\eta$ and

$$\frac{\gamma}{\bar{Z}_{E1}} = \frac{(1-\eta)^2}{2\eta}$$

$$\bar{Z}_{E1} = 2\gamma\frac{\eta}{(1-\eta)^2}.$$

The plot of $\bar{Z}_{E1}$ should yield a straight line.

In Fig. 7, curve (A) shows a plot of $\eta/(1-\eta)^2$ vs. $\bar{Z}_{E1}$. However, for $\bar{Z}_{E1} > 60$, the results are anomalously high. For high values of Z the inner shells will screen the nucleus and

Can. J. Chem. Downloaded from www.nrcresearchpress.com by 210.87.254.42 on 09/05/12
For personal use only.

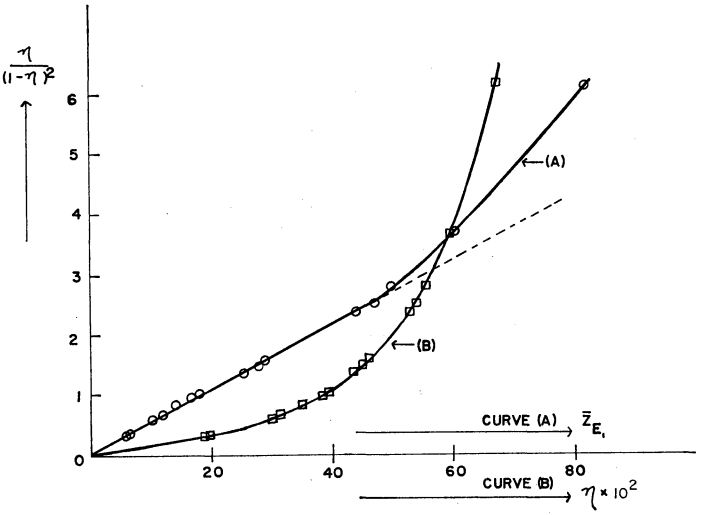

FIG. 7. (A) Plot of $\eta/(1-\eta)^2$ vs. $\bar{Z}_{E_1}$. (B) Plot of $\eta/(1-\eta)^2$ vs. η.

reduce the effective value of Z^2 in R. Only the loosely bound electrons will contribute to ϵ and hence the value of Z in ϵ is reduced as well. The first effect will tend to reduce the reflection coefficient, the second to increase it. In curve (B) of Fig. 7 it is seen that the ratio $\eta/(1-\eta)^2$ increases for high η, indicating that the second effect is the more important.

REFERENCES

1. R. D. EVANS. The science and engineering of nuclear power. Addison-Wesley, Cambridge, Mass. 1947. p. 53.
2. W. D. ARMSTRONG and J. SCHUBERT. Anal. Chem. **20**, 270 (1948).
3. E. BRODA, W. E. GRUMMITT, J. GUÉRON, L. KOWARSKI, and G. WILKINSON. Proc. London Phys. Soc. **60**, 460 (1948).
4. F. C. HENRIQUES, JR., G. B. KISTIAKOWSKY, C. MARGNETTI, and W. G. SCHNEIDER. Ind. Eng. Chem., Anal. Ed. **18**, 349 (1946).
5. F. C. HENRIQUES, JR. and C. MARGNETTI. Ind. Eng. Chem., Anal. Ed. **18**, 415 (1946).
6. A. K. SOLOMON, R. G. GOULD, and C. B. ANFINSEN. Phys. Rev. **72**, 1097 (1947).
7. R. H. HENDRICKS, L. C. BRYNER, M. D. THOMAS, and J. O. IVIE. J. Phys. Chem. **47**, 469 (1943).
8. R. G. BAKER and L. KATZ. Nucleonics, **11**, 14 (1953).
9. C. H. COLLIE, P. F. D. SHAW, and H. J. GALE. Proc. London Phys. Soc., **63A**, 282 (1950).
10. W. E. NERVIK and P. C. STEVENSON. Nucleonics, **10**, 18 (1952).
11. N. ELLIOT, D. W. ENGELKEMEIR, and W. RUBINSON. National Nuclear Energy Series. Div. IV. Vol. 9. McGraw-Hill. 1951. Paper 1.
12. N. ELLIOT and E. SHAPIRO. National Nuclear Energy Series. Div. IV. Vol. 9. McGraw-Hill. 1951. Paper 2.
13. D. W. ENGELKEMEIR, J. A. SEILER, E. P. STEINBERG, and L. WINSBERG. National Nuclear Energy Series. Div. IV. Vol. 9. McGraw-Hill. 1951. Paper 4.
14. T. B. NOVEY and N. ELLIOT. National Nuclear Energy Series. Div. IV. Vol. 9. McGraw-Hill. 1951. Paper 3.
15. E. K. GORA and F. C. HICKEY. Anal. Chem. **26**, 1158 (1954).
16. J. P. ROALSVIG and R. N. H. HASLAM. Can. J. Phys. **37**, 499 (1959).
17. R. W. HENDLER. Science, **130**, 772 (1959).
18. J. KATZ. Science, **131**, 1886 (1960).
19. P. MASSINI. Science, **133**, 877 (1961).
20. B. D. PATE and L. YAFFE. Can. J. Chem. **34**, 265 (1956).
21. L. YAFFE and J. B. FISHMAN. International Atomic Energy Agency, Vienna, 1960. p. 185.
22. P. J. CAMPION, J. G. V. TAYLOR, and J. S. MERRITT. Intern. J. Appl. Radiation Isotopes, **8**, 8 (1960).
23. J. S. MERRITT, J. G. V. TAYLOR, W. F. MERRITT, and P. J. CAMPION. Anal. Chem. **32**, 310 (1960).
24. P. J. CAMPION, J. G. V. TAYLOR, and J. S. MERRITT. International Atomic Energy Agency, Vienna, 1960. p. 227.
25. J. S. MERRITT, J. G. V. TAYLOR, and P. J. CAMPION. Can. J. Chem. **37**, 1109 (1959).
26. L. YAFFE and K. M. JUSTUS. J. Chem. Soc. S341 (1949).
27. B. P. BURTT. Nucleonics, **5**, 28 (1949).

Can. J. Chem. Downloaded from www.nrcresearchpress.com by 210.87.254.42 on 09/05/12
For personal use only.

28. L. E. GLENDENIN and A. K. SOLOMON. Science, **112**, 623 (1950).
29. M. L. PERLMAN and G. FRIEDLANDER. Phys. Rev. **74**, 442 (1948).
30. J. SALDICK and A. O. ALLEN. J. Chem. Phys. **22**, 438 (1954).
31. T. HENRIKSEN and J. BAARLI. J. Radiation Res. **6**, 415 (1957).
32. R. H. MÜLLER. Anal. Chem. **29**, 969 (1957).
33. L. DANGUY and R. QUIVY. J. Phys. Radium, **17**, 320 (1956).
34. P. R. GRAY, D. H. CLAREY, and W. H. BEAMER. Anal. Chem. **32**, 582 (1960).
35. S. MEGHIR. Ph.D. Thesis, McGill University, Montreal, Que. 1962.
36. W. E. CRANDALL, G. P. MILLBURN, R. V. PYLE, and W. BIRNBAUM. Phys. Rev. **101**, 329 (1956).

Can. J. Chem. Downloaded from www.nrcresearchpress.com by 210.87.254.42 on 09/05/12
For personal use only.

Can. J. Chem. Downloaded from www.nrcresearchpress.com by 210.87.254.42 on 09/05/12
For personal use only.

HETEROCYCLIC STEROIDS

II. PREPARATION AND N.M.R. SPECTRA OF 17,17-DIALKYL-13(14)-UNSATURATED STEROIDS[1]

E. CASPI[2] AND D. M. PIATAK
Worcester Foundation for Experimental Biology, Shrewsbury, Massachusetts, U.S.A.

Received May 6, 1963

ABSTRACT

A series of 17,17-dialkyl-13(14)-unsaturated steroids was prepared via the Wagner–Meerwein rearrangement. Some of the steroids were synthesized with an isoxazole ring or a pyrazole ring attached to ring A. The n.m.r. spectra of the compounds prepared are discussed.

During investigations on steroidal isoxazoles (1) 17β-acetoxyandrost-4-eno[2,3*d*]isoxazole (I) and 17,17-dimethyl-18-norandrosta-4,13(14)-dieno[2,3*d*]isoxazole (III) were found to have tumor-inhibiting properties when assayed by the method of Abe *et al.* (2). Further biological data disclosed that the 17β-acetoxyisoxazole I had 1/5 of the androgenic activity of testosterone, while the 17,17-dimethylisoxazole III was devoid of accompanying activity. In order to explore these observations, several steroidal analogues were prepared. In addition, the n.m.r. spectra of the compounds are discussed.

Preparation of 17,17-dimethyl-18-norandrosta-4,13(14)-dien-3-one (VI), 2α,17,17-trimethyl-18-nor-5α-androst-13(14)-en-3-one (IX), 17β-methyl-17α-ethyl-18-norestra-4,13-(14)-dien-3-one (VII), and 17,17-dimethyl-9α-fluoro-11β-hydroxy-18-norandrosta-4,13-(14)-dien-3-one (VIII) involved simple Wagner–Meerwein rearrangement of the

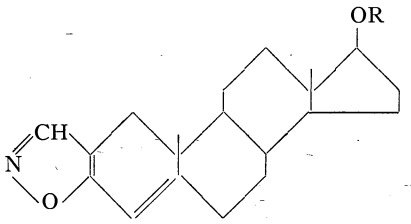

I: R = Ac
II: R = CH_3

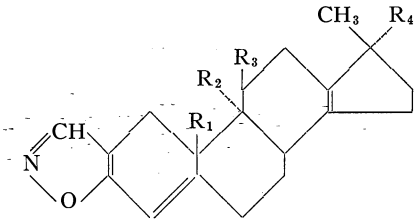

III: R_1 = CH_3; R_2 = H; R_3 = H; R_4 = CH_3
IV: R_1 = H; R_2 = H; R_3 = H; R_4 = CH_2CH_3
V: R_1 = CH_3; R_2 = F; R_3 = OH; R_4 = CH_3

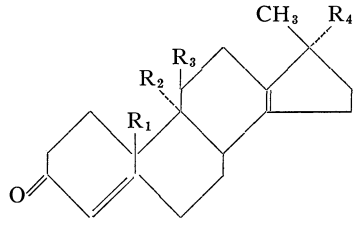

VI: R_1 = CH_3; R_2 = H; R_3 = H; R_4 = CH_3
VII: R_1 = H; R_2 = H; R_3 = H; R_4 = CH_2CH_3
VIII: R_1 = CH_3; R_2 = F; R_3 = OH; R_4 = CH_3

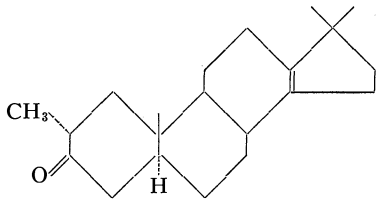

IX

[1]*This work was supported by Grant A-5326 from the U.S. Public Health Service.*
[2]*Recipient of a Public Health Service Research Career Program Award CA-K3-16614 from National Cancer Institute.*

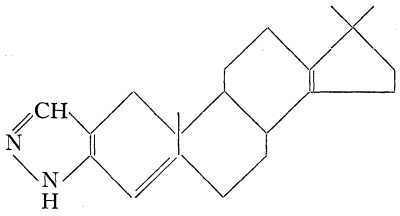

X

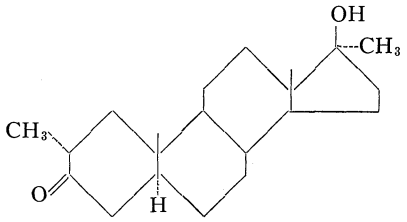

XI

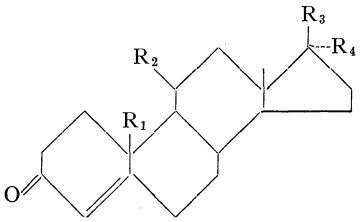

XII: $R_1 = CH_3$; $R_2 = H$; $R_3 = OH$; $R_4 = CH_3$
XIII: $R_1 = CH_3$; $R_2 = H$; $R_3 = OAc$; $R_4 = H$
XIV: $R_1 = CH_3$; $R_2 = OH$; $R_3 = OH$; $R_4 = CH_3$
XV: $R_1 = H$; $R_2 = H$; $R_3 = OH$; $R_4 = CH_2CH_3$

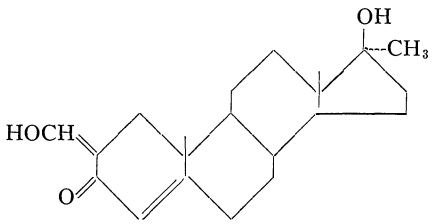

XVI

corresponding 17β-hydroxy-17α-alkylandrostanes. Structural assignments were based primarily on elemental analysis and n.m.r. spectroscopy.

Confirmation of the α orientation of the 2-methyl group of IX was established by its optical rotary dispersion curve, which was identical in shape with that of 17β-hydroxy-2α-methyl-5α-androstan-3-one; their magnitudes of molar rotation were also the same. Stereochemistry of the migrating methyls was rationalized on mechanistic grounds as being β, since Wagner–Meerwein rearrangements are known to proceed with "retention" of configuration (3).

The steroidal pyrazole 17,17-dimethyl-18-norandrosta-4,13(14)-dieno[3,2*c*]pyrazole (X) was conveniently prepared by refluxing hydrazine hydrate with 2-hydroxymethylene-17,17-dimethyl-18-norandrosta-4,13(14)-dien-3-one in ethanol according to the procedure of Clinton *et al.* (4). The compound gave the correct analysis, a λ_{max}^{MeOH} 260 mμ, and characteristic infrared bands at 1675, 1630, and 1560 cm^{-1} (4).

The isoxazoles were obtained as described previously (1) by refluxing the corresponding 2-hydroxymethylene steroids in glacial acetic acid with hydroxylamine hydrochloride. The 17β-methyl-17α-ethyl-18-norestra-4,13(14)-dieno[2,3*d*]isoxazole (IV) was prepared from 17β-methyl-17α-ethyl-18-norestra-4,13(14)-dien-3-one (VII); the fluoroisoxazole V, from 11β,17β-dihydroxy-9α-fluoro-17α-methylandrost-4-en-3-one (4); and the 17β-methoxy isoxazole II, from 17β-methoxyandrost-4-en-3-one (5). Concomitant Wagner–Meerwein rearrangement occurred with isoxazole formation in the preparation of V. Identification of the isoxazoles was made by elemental analyses and ultraviolet, infrared, and n.m.r. spectroscopy.

Certain pertinent n.m.r. bands are listed in Table I. In compounds with a 17,17-dialkyl group, i.e. III to X, the methyl at 17 (or 17-*gem*-dimethyl) is observed at τ = 9.00–9.05, quite significantly shifted upfield from the tertiary 17α-methyl in 17β-hydroxy-17α-alkyl compounds, XI, XII, and XVI. This shift (+0.3 p.p.m.) is consistent with the expected downfield shift (7) of tertiary alkyl moieties when an oxygen function is added to the

Can. J. Chem. Downloaded from www.nrcresearchpress.com by 210.87.254.42 on 09/05/12
For personal use only.

TABLE I

Summary of n.m.r. bands*

Compound	Methyls C-19	Methyls C-18†	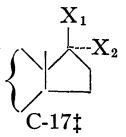 C-17‡	C-4 proton	C-2 group
I	8.97	9.15	—	3.81	1.99§
II	8.98	9.19	$X_1 = OCH_3 = 6.53$	3.84	1.97§
III	9.03	—	$X_1 = X_2 = CH_3 = 9.03$	3.80	1.98§
IV	—	—	$X_1 = CH_3 = 9.03$		
			$X_2 = Et = 9.25$ ($J = 6.7$ c.p.s.)	3.78	2.04§
V	8.68	—	$X_1 = X_2 = CH_3 = 9.00$	3.72	1.93§
VI	8.83	—	$X_1 = X_2 = 9.05$	4.25	—
VII	—	—	$X_1 = CH_3 = 9.04$		
			$X_2 = Et = 9.27$ ($J = 6.7$ c.p.s.)	4.14	—
VIII	8.48	—	$X_1 = X_2 = CH_3 = 9.02$	4.18	—
IX	8.95	—	$X_1 = X_2 = CH_3 = 9.04$	—	8.98‖ ($J = 8.5$ c.p.s.)
X	9.08	—	$X_1 = X_2 = 9.04$	3.79	
X¶	9.05	—	$X_1 = X_2 = 9.00$	3.72	1.93,** 2.54††
XI	8.92	9.13	$X_1 = OH$		
			$X_2 = CH_3 = 8.79$	—	9.01‖ ($J = 5.5$ c.p.s.)
XII	8.82	9.10	$X_1 = OH$		
			$X_2 = CH_3 = 8.82$	4.29	—
XIII	8.81	9.17	—	4.28	—
XIV	8.53	8.84	$X_1 = OH$		
			$X_2 = CH_3 = 8.84$	4.32	—
XV	—	9.08	$X_2 = CH_2CH_3 = 9.02$ ($J = 7$ c.p.s.)	4.18	—
XVI	8.96	9.09	$X_1 = OH$		
			$X_2 = CH_3 = 8.78$	4.21	2.64‡‡

*Spectra taken on $CDCl_3$ solutions unless otherwise noted. Results expressed in τ units as described previously (1).
†If no C-18 value is given, the compound has a 13(14)-double bond.
‡Values are given only for methyl groups.
§Proton on 3′-carbon of isoxazole ring.
‖Protons on C-2α-methyl.
¶CD_3OD solution.
**Proton on 5′-carbon of pyrazole ring.
††Proton on 2′-nitrogen of pyrazole ring.
‡‡Proton on carbon of hydroxymethylene at C-2.

carbon bearing the alkyl moiety. The *secondary methyl* of the ethyl moiety in the *gem*-dialkyl compounds IV and VII shows an analogous upfield shift. The structure of compounds containing the 17,17-dialkyl-13(14)-ene moiety was deduced from this upfield shift, the disappearance of an 18-methyl band, and the absence of a band ($\tau \approx 4$) attributable to a vinyl proton at other than C-4.

Of interest is the variation in chemical shift for the C-19 methyl group brought about by substitution of a hydroxymethylene at C-2 or a hydroxy function at C-11. An upfield shift of ca. +0.2 p.p.m. is seen in the instance where the C-2 position is substituted by hydroxymethylene, e.g. XII to XVI. This upfield shift of +0.2 p.p.m. is also evident when an isoxazole or pyrazole ring is formed at the C-2, C-3 positions, e.g. XIII to I, VI to III, VIII to V, and VI to X. The 11β-hydroxyl causes the known downfield shift (8) of the 19-methyl (−0.3 p.p.m.) as evidenced in the shift from $\tau = 8.8$ to $\tau = 8.5$ for XIV to XII and for VI to VIII and in the shift from $\tau = 9.0$ to $\tau = 8.7$ for III to V. The 9α-fluorine does not appear to have a pronounced influence on the 19-methyl. These chemical shifts are additive as illustrated with the value for the 19-methyl of VI ($\tau = 8.83$). By adding the upfield shift of +0.2 p.p.m. for substitution at C-2 and the downfield shift of −0.3 p.p.m. for substitution at C-11, the figure arrived at ($\tau = 8.73$) is in fair agreement with the value for V ($\tau = 8.68$).

The chemical shift of the vinylic proton at C-4 varies significantly with substitution

Can. J. Chem. Downloaded from www.nrcresearchpress.com by 210.87.254.42 on 09/05/12
For personal use only.

Can. J. Chem. Downloaded from www.nrcresearchpress.com by 210.87.254.42 on 09/05/12
For personal use only.

TABLE II

Summary of physical data of compounds prepared

Compound	M.p. (°C)	Yield (%)	λ_{max}	ϵ	Infrared (cm^{-1})			Calc. (%)			Found (%)		
								C	H	N	C	H	N
II	102–105	59.1	285	10,500	1,625	1,590	1,100	77.02	8.93	4.28	77.21	8.85	4.35
IV	94–98	14.8	286	11,000	1,635	1,615		81.51	8.80	4.53	81.53	8.83	4.92
V	206–211	53.3	283	11,000	3,390	1,635	1,610	73.44	7.63		73.68	7.91	
VI	66–70	100	240	16,500	1,670	1,610		84.45	9.92		84.26	9.97	
VII	83–85	100	250	16,800	1,665	1,615		84.45	9.92		84.60	9.79	
VIII	205–207	72.4	238	17,500	3,360	1,660	1,615	75.43	8.55		75.55	8.60	
IX	118–121	64.7	—	—	1,710			83.94	10.73		83.68	10.86	
X	191–195	23.4	260	10,500	3,270	1,675	1,630	81.77	9.15	9.08	81.74	9.03	9.13
					1,560								

at C-2 and C-3, while little effect is observed by substitution at C-9 and C-11. A pronounced downfield shift of −0.4 p.p.m. is brought about by the formation of an isoxazole or pyrazole ring at the C-2, C-3 positions, as seen by comparing VI to VIII and XVI with I to II and III to V.

In the case of the attached heterocyclic rings the proton on the carbon at the 3′-position of the isoxazole ring or at the 5′-position of the pyrazole ring exhibits a value of τ = 1.9–2.0. These chemical shifts seem to be characteristic for the —N=CH—C= grouping.

Preliminary biological evaluation indicated that there was no consistent enhancement of antitumor activity for the compounds prepared. A full report will be published in a later communication.

EXPERIMENTAL*

Preparation of 17,17-Dialkyl-3-ketones VI, VII, VIII, and IX

To a solution of the 17β-hydroxy-17α-alkylsteroid (1.00 g) in glacial acetic acid (15 ml) was added glacial acetic acid saturated with hydrogen chloride (1.0 ml). The solution was then heated at reflux for 10 minutes. The solution was cooled, water added, and most of the acetic acid removed *in vacuo*. The steroids were recovered with ether, washed with saturated sodium bicarbonate solution, then water, dried, and concentrated *in vacuo*. The compounds crystallized readily upon trituration with methanol. (See Table II for analytical results.)

17,17-Dimethyl-18-norandrosta-4,13(14)-dieno[3,2c]pyrazole (X)

The 2-hydroxymethylene derivative of I was prepared via the sodium hydride procedure of Weisenborn *et al.* (6).

A solution of the obtained 2-hydroxymethylene compound (4.42 g) and hydrazine hydrate (85%; 1.7 g) in 100 ml ethanol was heated at reflux for 4 hours. The solvent was removed *in vacuo*. Chromatography of the reaction mixture on silica followed by recrystallization from acetone gave pure 17,17-dimethyl-18-norandrosta-4,13(14)-dieno[3,2*c*]pyrazole. (See Table II for analytical results.)

Preparation of Isoxazoles

The isoxazole steroids were prepared from 2-hydroxymethylene derivatives and hydroxylamine hydrochloride in glacial acetic acid, exactly as described in our previous communication (1).

ACKNOWLEDGMENT

The steroids used in this study were provided by Cancer Chemotherapy National Service Center, National Cancer Institute, U.S. Public Health Service.

REFERENCES

1. E. Caspi and D. M. Piatak. Chem. Ind. (London), 1984 (1962).
2. O. Abe, E. Herranen, and R. I. Dorfman. Proc. Soc. Exptl. Biol. Med. **111**, 706 (1962).
3. M. Uskokovic, M. Gut, and R. I. Dorfman. J. Am. Chem. Soc. **82**, 3668 (1960).
4. R. O. Clinton, A. J. Manson, F. W. Stonner, H. C. Neumann, R. G. Christiansen, R. L. Clarke, J. H. Ackerman, D. F. Page, J. W. Dean, W. B. Dickinson, and C. Carabateas. J. Am. Chem. Soc. **83**, 1478 (1961).
5. M. Neeman, M. C. Caserio, J. D. Roberts, and W. S. Johnson. Tetrahedron, **6**, 36 (1959).
6. F. L. Weisenborn, D. C. Remy, and T. L. Jacobs. J. Am. Chem. Soc. **76**, 552 (1959).
7. L. M. Jackman. Applications of nuclear magnetic resonance spectroscopy in organic chemistry. Pergamon Press, London. 1959. p. 53.
8. R. F. Zürcher. Helv. Chim. Acta, **44**, 1380 (1961).

**Melting points were taken on a micro hot stage and are corrected. Elemental analyses were provided by Dr. A. Schöeller, Kronach, Germany. Ultraviolet spectra were recorded with a Cary Model 14 spectrometer. Infrared spectra were taken on KBr blotters with a Perkin–Elmer Model 237 spectrometer.*

Can. J. Chem. Downloaded from www.nrcresearchpress.com by 210.87.254.42 on 09/05/12
For personal use only.

THE SYNTHESIS OF ALKYLPHOSPHONOUS DICHLORIDES FROM ALUMINUM CHLORIDE – PHOSPHORUS TRICHLORIDE – ALKYL CHLORIDE COMPLEXES[1]

B. J. PERRY, J. B. REESOR, AND J. L. FERRON[2]
Suffield Experimental Station, Ralston, Alberta
Received March 8, 1963

ABSTRACT

In 1957, a new method for the synthesis of methylphosphonous dichloride, in high yield, by the reduction of the aluminum chloride – phosphorus trichloride – methyl chloride complex in diethyl phthalate solution by finely powdered antimony, was developed. That this is a general method for the synthesis of the more volatile alkylphosphonous dichlorides was demonstrated by the preparation, in good yield, of a series of compounds from the aluminum chloride – phosphorus trichloride complexes formed from ethyl chloride, *n*-propyl chloride, *i*-propyl chloride, *n*-butyl chloride, and *s*-butyl chloride. As expected, isomerization occurred in the case of the normal alkyl chlorides.

Can. J. Chem. Downloaded from www.nrcresearchpress.com by 210.87.254.40 on 09/05/12
For personal use only.

In the period 1956–1957, a requirement arose for the synthesis of P^{32}-labelled organophosphorus compounds, of high specific activity, from methylphosphonous dichloride. A literature survey at this time revealed no simple methods for the preparation which were suitable and 'safe' for use in a radioactive synthesis involving multicurie sources of P^{32}.

A new method for the preparation of methylphosphonous dichloride was developed, therefore, which appears to have general application for the synthesis of alkylphosphonous dichloride (1), although the present discussion is restricted to those more volatile than antimony trichloride because of the recovery techniques employed.

In 1958, Komkov *et al.* (2) reported a similar synthesis. Their method appeared not to be as suitable for use in the radioactive synthesis of methylphosphonous dichloride as the method described herein, because the reduction reaction proceeded violently at times, even with close control, the manipulative techniques were more complex, and the yields somewhat lower.

The synthesis of 'sarin', isopropyl methylphosphonofluoridate, labelled P^{32}, has been described (3). Methylphosphonic dichloride, the basic intermediate in this synthesis, was prepared from the aluminum chloride – phosphorus trichloride – methyl chloride complex by solution in diethyl phthalate followed by treatment with gaseous sulphur dioxide.

$$[CH_3PCl_3]^+[AlCl_4]^- \xrightarrow[\text{phthalate}]{\text{diethyl}} CH_3PCl_4 + [DEP][AlCl_3]$$
$$\downarrow SO_2$$
$$CH_3POCl_2 + SOCl_2$$

While methylphosphonic tetrachloride was never isolated from the reaction mixture, its presence is clearly demonstrated by the subsequent reaction with sulphur dioxide, since neither the complex itself, nor its solution in solvents which do not form a complex with aluminum chloride, reacts with sulphur dioxide. It appeared likely, therefore, that

[1]*Issued as Suffield Technical Paper No. 189, D.R.B. Project No. D52-20-20-27. Permission to publish this work is gratefully acknowledged.*
[2]*Present address: Collège Militaire Royal, St. Jean, Que.*

reduction of methylphosphonic tetrachloride might be a route to methylphosphonous dichloride.

$$[CH_3PCl_3]^+[AlCl_4]^- \xrightarrow[\text{phthalate}]{\text{diethyl}} CH_3PCl_4 + [DEP][AlCl_3]$$

$$CH_3PCl_4 \xrightarrow{\text{reduction}} CH_3PCl_2$$

In the synthesis of sarin, labelled P^{32}, granular antimony is used in the first step, to reduce phosphorus pentachloride to phosphorus trichloride. The addition of finely powdered antimony (250 mesh) to an efficiently stirred solution of the aluminum chloride – phosphorus trichloride – methyl chloride complex in diethyl phthalate results in a smooth, strongly exothermic reaction, which, on completion, gives a 90% yield of redistilled methylphosphonous dichloride (yield based on phosphorus trichloride).

That this is a general method for the synthesis of alkylphosphonous dichlorides was demonstrated by the preparation of the compounds listed in Table I from the aluminum

TABLE I

Products obtained by antimony reduction of aluminum chloride – phosphorus trichloride – alkyl chloride complexes in diethyl phthalate solution

RCl in complex	Product	Crude yield (%)	Redistilled yield (%)	Redistilled product	
				B.p. (°C/mm Hg)	Refractive index (n_D/°C)
CH_3Cl	CH_3PCl_2	93	90*	78–79/700	
C_2H_5Cl	$C_2H_5PCl_2$	90	83*	64/150	
n-C_3H_7Cl	*i*-$C_3H_7PCl_2$	85	61†	88–88.5/199–203	1.4868/25
i-C_3H_7Cl	*i*-$C_3H_7PCl_2$	86	67†	88/202	1.4870/25.4
n-C_4H_9Cl	*s*-$C_4H_9PCl_2$	94	85*	70/40	1.4909/25
s-C_4H_9Cl	*s*-$C_4H_9PCl_2$	56	40*	62–62.5/28	1.4908/25
s-C_4H_9Cl	*s*-$C_4H_9PCl_2$	78		68/37	

*Fractionated through a Vigreux column.
†Carefully fractionated through a Todd column (16 theoretical plates).

chloride – phosphorus trichloride complexes formed with ethyl chloride, *n*-propyl chloride, *i*-propyl chloride, *n*-butyl chloride, and *s*-butyl chloride.

The identities of the products from the methyl and ethyl chloride complexes were confirmed by addition of sulphur to give methylphosphonothionic dichloride and ethylphosphonothionic dichloride respectively.

It will be noted that the products obtained from the complexes formed from *n*-propyl and *i*-propyl chlorides have the same boiling point, refractive index, and, it was found, identical infrared spectra, i.e., they are the same compound. The product was confirmed to be isopropylphosphonous dichloride by oxidation to isopropylphosphonic dichloride. It is of interest to note that unlike methylphosphonous dichloride and ethylphosphonous dichloride, isopropylphosphonous dichloride does not add sulphur even on being heated to 100° C with anhydrous aluminum chloride as a catalyst.

Products obtained from the complexes formed from *n*-butyl and *s*-butyl chlorides are also identical. The nature of the product was confirmed as *s*-butylphosphonous dichloride by its conversion to the *s*-butylphosphonic dichloride.

The results obtained are to be expected since, under the reaction conditions, the *n*-alkyl chlorides will be isomerized to the *s*-alkyl chlorides (4, 5). The results also parallel those of Kinnear and Perren (6), who showed that the complexes from the *n*-alkyl and *s*-alkyl chlorides gave only *s*-alkylphosphonic dichloride on treatment with water.

Can. J. Chem. Downloaded from www.nrcresearchpress.com by 210.87.254.40 on 09/05/12
For personal use only.

In our investigation, the products have been recovered by direct distillation from the reaction mixture. Thus, while the reaction described would appear to have a fairly general application, other separation techniques would have to be employed for those compounds less volatile than antimony trichloride and/or diethyl phthalate.

EXPERIMENTAL

The reduction reactions are very exothermic and cooling is required to keep the temperature below 75° C. At higher temperatures the reaction mixture slowly decomposes to give ethyl chloride from the diethyl phthalate, which reduces the yield of desired product. Good yields are also dependent on the complete formation of the aluminum chloride – phosphorus trichloride – alkyl chloride complex.

The apparatus used was similar to that described (3) for the synthesis of P^{32}-labelled methylphosphonic dichloride from the complex. It differed in that no hot-air jacket was required on the inlet tube to the crude product receiver and the column was fitted with a Whitmore-Lux type, total reflux, variable takeoff head.

Methylphosphonous Dichloride

The complex from aluminum chloride (200 g, 1.5 mole), phosphorus trichloride (137.5 g, 1 mole), and methyl chloride (50.5 g, 1 mole) was prepared by the method previously described (3). This complex was dissolved with external cooling in diethyl phthalate (600 ml) and the solution thoroughly degassed at 2 mm and at a temperature of 75° C. The solution was rapidly cooled to 30° C, efficiently stirred, and finely powdered antimony (250 mesh, 81.2 g, 0.667 mole) added. The temperature rose slowly at first and then more rapidly; external cooling was used at this stage to maintain the temperature at approximately 55° C. The reaction appeared to be complete in 35 minutes, when most of the antimony had disappeared and a fine white precipitate had formed (presumed to be antimony trichloride). The product was flashed from the mixture at 10 mm pressure and a temperature of 75° C into the crude product receiver, cooled in dry ice – acetone. The product was then distilled to give methylphosphonous dichloride (109 g, 93%; b.p. 77–79° C at 700 mm) and fractionated to give a very small forerun and methylphosphonous dichloride (105.5 g, 90%; b.p. 78–79° C at 700 mm).

Methylphosphonothionic Dichloride

Methylphosphonous dichloride (196.4 g, 1.68 mole), prepared in the manner described above, and anhydrous aluminum chloride (1.5 g) were introduced into a three-necked reaction flask, fitted with a condenser, thermometer, and magnetic stirring bar, under an atmosphere of dry nitrogen. Dried granular sulphur (53.8 g, 1.68 mole) was added in small portions with external water cooling, in amounts sufficient to keep the reaction temperature at 60–65° C. Addition took 50 minutes, the cooling bath was removed, and the reaction mixture heated to 85° C for 5 minutes. The product, methylphosphonothionic dichloride, was recovered by fractional distillation under reduced pressure (244.5 g, 98%; b.p. 68–69° C at 35 mm; n_D^{27} 1.5468). Physical constants (7): b.p. 40° C at 5 mm; n_D^{25} 1.5473.

Ethylphosphonous Dichloride

Ethyl chloride (74.2 g, 1.15 mole), aluminum chloride (133.3 g, 1.0 mole), and phosphorus trichloride (137.5 g, 1.0 mole) were shaken in a sealed pressure bottle at room temperature. After 2 hours the reaction mixture had liquefied and then solidified. Reaction was completed by heating the mixture to 100° C for 1 hour. The product was powdered in a dry box under an atmosphere of dry nitrogen, added to the 'complex' reaction flask, and dissolved in diethyl phthalate (600 ml) with external cooling (temperature rose to 35° C). The solution was degassed at 2 mm and a temperature of 55° C and then cooled to room temperature. Finely powdered antimony (250 mesh, 81.2 g, 0.667 mole) was then added to the efficiently stirred mixture. The temperature began to rise immediately and when it had reached 65° C (5 minutes) the reaction flask was externally cooled with an ice–water mixture. The temperature rose to 75° C and then slowly fell. Reaction appeared complete in 30 minutes and the crude product was flashed from the mixture at 75° C and 10 mm into the crude product receiver, cooled in dry ice – acetone. The crude product was fractionated to give ethylphosphonous dichloride (108.6 g, 83%; b.p. 64° C at 150 mm).

Ethylphosphonothionic Dichloride

Dried granular sulphur (26.1 g, 0.815 mole) was added to ethylphosphonous dichloride (107 g, 0.815 mole), prepared above, in a similar manner to the preparation of methylphosphonothionic dichloride. The sulphur addition reaction was slower but proceeded smoothly at a temperature of 90° C. Cooling was used to keep the temperature between 90 and 110° C and the reaction was finally heated to 110° C for 30 minutes, after all the sulphur had been added to the reaction mixture. The product was recovered by fractional distillation under reduced pressure to give 116.5 g, 87.6%; b.p. 52° C at 6 mm; $n_D^{27.5}$ 1.5390. Physical constants (7): b.p. 47–48° C at 3 mm; n_D^{25} 1.5406. The infrared spectrum agreed with that of a reference sample.

Isopropylphosphonous Dichloride

(a) From Isopropyl Chloride

Isopropyl chloride (78.5 g, 1 mole) was added dropwise to an efficiently stirred mixture of anhydrous aluminum chloride (133.3 g, 1 mole) and phosphorus trichloride (137.5 g, 1 mole) in the complex reaction

Can. J. Chem. Downloaded from www.nrcresearchpress.com by 210.87.254.40 on 09/05/12
For personal use only.

flask. The reaction was strongly exothermic and required external cooling in dry ice – acetone to keep the temperature at 35° C. After addition of approximately two thirds of the isopropyl chloride the reaction mixture solidified. After methylene chloride (100 ml) was added, the remainder of the isopropyl chloride was added dropwise to the stirred reaction mixture which was then heated to reflux for 1 hour. Diethyl phthalate (600 ml) was added very slowly, with external cooling, to the stirred reaction mixture, the solution degassed at 75° C and 2 mm and cooled to room temperature. Finely powdered antimony (250 mesh, 81.2 g, 0.667 mole) was added to the well-stirred solution, using external water cooling. Rapid reaction took place and the temperature reached 68° C. The reaction mixture was finally heated to 75° C for 15 minutes and the crude product recovered in the normal way. Distillation gave the product (124.3 g, 85.8%; b.p. 63° C at 76 mm, 69° C at 80 mm). This product was carefully fractionated through a Todd column to give isopropylphosphonous dichloride (97. 8 g, 67.4%; b.p. 88° C at 202 mm; $n_D^{25.4}$ 1.4870).

(b) From n-Propyl Chloride

By the same procedure as used in (*a*) above, *n*-propyl chloride (78.5 g, 1.0 mole) gave the same product (123 g, 85%; b.p. 58° C at 64 mm, 62.5° C at 80 mm). Careful fractionation through a Todd column gave 88.7 g, 61.2%; b.p. 88–88.5° C at 199–203 mm; n_D^{25} 1.4868. The infrared spectra of the products from (*a*) and (*b*) were identical.

Isopropylphosphonic Dichloride

Isopropylphosphonous dichloride (from (*b*) above) (68.4 g, 0.47 mole) was weighted into a 200-ml three-necked flask fitted with a condenser, thermometer, gas inlet tube, and magnetic stirring bar. A slow stream of dry oxygen was passed through the stirred liquid and external water cooling used to maintain the temperature at 35° C in the early stages. Oxygenation was continued for 8 hours, by which time the temperature of the reaction mixture had dropped to room temperature. The reaction product was fractionated through a Todd column to give isopropylphosphonic dichloride (45.5 g, 60%; b.p. 37° C at 1.5 mm, 60° C at 5.6 mm, 85° C at 28 mm; n_D^{25} 1.4647). Physical constants: b.p. 35.3° C at 1.5 mm (6); b.p. 60° C at 6 mm (7).

s-Butylphosphonous Dichloride

The same method as for the preparation of isopropylphosphonous dichloride was used. *s*-Butyl chloride (92.5 g, 1 mole) gave *s*-butylphosphonous dichloride (89 g, 56%; b.p. 68° C at 37 mm). Fractionation through a Vigreux column gave 63.7 g, 40%; b.p. 62–62.5° C at 28 mm; n_D^{25} 1.4908. A repeat reaction gave 123.5 g, 77.6%; b.p. 68° C at 37 mm. *n*-Butyl chloride (92.5 g, 1 mole) gave the same product (149.2 g, 93.7%; b.p. 72–73° C at 45 mm). Fractionation through a Vigreux column gave 135 g, 85%; b.p. 70° C at 40 mm; n_D^{25} 1.4909. The infrared spectra of the products from *n*-butyl and *s*-butyl chlorides were identical.

s-Butylphosphonic Dichloride

The same method as for the preparation of isopropylphosphonic dichloride was used. Starting with 25.0 g, 0.16 mole of *s*-butylphosphonous dichloride, a yield of 16.9 g (62%) of *s*-butylphosphonic dichloride was obtained (b.p. 56° C at 2 mm; n_D^{25} 1.4700). Physical constant (6): b.p. 57° C at 2 mm.

ACKNOWLEDGMENTS

The technical assistance of Mr. S. G. Gibbens and Mr. R. F. Silver is gratefully acknowledged.

REFERENCES

1. J. L. Ferron, B. J. Perry, and J. B. Reesor. Nature, **188**, 227 (1960).
2. J. P. Komkov, K. V. Karavanov, and S. Z. Ivin. J. Gen. Chem. USSR. **28**, 2992 (1958).
3. J. B. Reesor, B. J. Perry, and E. Sherlock. Can. J. Chem. **38**, 1416 (1960).
4. C. C. Price. Organic reactions. Vol. III. John Wiley and Sons Inc., New York. 1949. p. 6.
5. C. C. Price. Chem. Rev. **29**, 37 (1941).
6. A. M. Kinnear and E. A. Perren. J. Chem. Soc. 3437 (1952).
7. A. H. Ford-Moore (deceased). Private communication.

Can. J. Chem. Downloaded from www.nrcresearchpress.com by 210.87.254.40 on 09/05/12
For personal use only.

THE FORCES OPERATIVE IN HOMONUCLEAR DIATOMIC MOLECULES

RICHARD F. W. BADER[1]
Department of Chemistry, University of Ottawa, Ottawa, Canada
Received May 24, 1963

ABSTRACT

The electron densities obtained from the S.C.F. wave functions determined by Ransil for some first-row homonuclear diatomic molecules are tested through a calculation of the forces acting on the nuclei. None of the density functions (for Li_2, Be_2, C_2, N_2, and F_2) give the required condition of electrostatic equilibrium, the departure from a nonzero force increasing with increasing nuclear charge. Adverse atomic polarizations are shown to be primarily responsible for these results, and in particular for the surprising result that the density in the $3\sigma_g$ orbital of N_2 and F_2 actually exerts a force tending to separate the molecule into atoms.

Can. J. Chem. Downloaded from www.nrcresearchpress.com by 210.87.254.40 on 09/05/12
For personal use only.

I. INTRODUCTION

The forces exerted on the nuclei in a number of first-row diatomic molecules are calculated from the wave functions determined by Ransil (1). Our reasons for doing this are as follows. The wave functions obtained by Ransil employ only a minimal basis set and represent one of the simplest approximations to the Hartree-Fock solutions for these molecules. While the dissociation energies predicted by these functions are disappointingly low it is important to test these same wave functions against other observable properties in order to determine their overall reliability. For example, it is conceivable that the distribution of the electron density as obtained from these wave functions may not be too far removed from a satisfactory one even though the energy eigenvalue is incorrect. This is possible due to the differing sensitivity of various properties to the radial and angular characteristics of the wave function. A sensitive test of the overall density distribution is provided by a calculation of the forces operative on a nucleus in a molecule. The electronic forces are determined by a one-electron operator $\langle P_1/r_i^2 \rangle$ and hence by the one-electron density distribution (2). Hall (3) has shown that wave functions determined by the self-consistent field procedure (such as the ones considered in this paper) are "stable" to one-electron operators, and in particular, that these wave functions will satisfy the exact Hellmann–Feynman theorem for the calculation of the electronic forces. In addition, a discussion of the orbital contributions to the forces gives an insight into the nature of the binding in these molecules and, it is hoped, may also indicate the manner in which the original basis set is most seriously lacking.

II. CALCULATIONS AND RESULTS

The forces were calculated for the wave functions termed the "best limited L.C.A.O.–M.O." set (1). These are sets of molecular orbitals, constructed from the inner shell and valence atomic orbitals only, in which the orbital exponents have been optimized with respect to the molecular energy by a variational procedure. The electron density ρ is given by

$$\rho = 2 \sum_i \phi_i \phi_i^*,$$

where the ϕ_i are doubly occupied orthonormal molecular orbitals, (orbitals of π symmetry are considered as two doubly occupied ones). The electronic force on nucleus α

[1]*Present address: Department of Chemistry, McMaster University, Hamilton, Ontario.*

along the bond axis is given by

$$F_{\alpha e} = Z_\alpha \int (\cos\theta_i/r_i^2)\rho\, d\tau,$$

where Z_α is the nuclear charge of atom α. Since the density is given by a sum of orbital contributions, the total electronic force may be broken up in a similar manner as follows. Both the nuclear and electronic forces involve a common factor of Z_α/R^2, where R is the internuclear distance. Thus the total force on nucleus α can be conveniently written (4) as

$$F_\alpha = \frac{Z_\alpha}{R^2} \sum_i (f_i - 1), \qquad [1]$$

where the f_i are the electronic forces due to each doubly occupied molecular orbital with the factor Z_α/R^2 removed. For closed-shell homonuclear diatomic molecules within the single determinantal approximation the number of such doubly occupied orbitals is equal to Z_α (counting each completely filled π orbital twice) and thus summing over i in equation [1] gives simply

$$F_\alpha = \frac{Z_\alpha}{R^2} \sum_i f_i - \frac{Z_\alpha^2}{R^2} = F_{\alpha e} + F_{\alpha n}.$$

When R refers to the equilibrium bond length $F_{\alpha e} = -F_{\alpha n}$ and the resultant force must equal zero. At this point of electrostatic equilibrium $\sum_i f_i = Z_\alpha$.* Formulation [1] brings out clearly the physical interpretation to be given to the electronic forces due to each of the molecular orbitals (4). At infinite internuclear separations each electron will shield one unit of nuclear charge and thus in the limit of large values for R, each f_i value will approach unity and the total force between the two atoms will be zero. A pair of electrons which are tightly bound in an inner shell orbital will continue to shield one unit of charge on each nucleus as R decreases and also give an f_i value of unity, i.e., even on molecule formation the inner shell electrons are not effectively penetrated by the approaching nucleus and their f_i value remains constant from $R = \infty$ to $R = R_e$. The resultant force $f_i - 1$ due to the presence of such electrons is zero and the orbital is termed a *nonbinding*† orbital. The f_i value of a bonding orbital exceeds unity as R decreases due to the accumulation of charge in the binding region between the nuclei. Such an orbital thus has an $f_i - 1$ value greater than zero, indicating that its density is distributed so as to exert a binding force on the nuclei in excess of the associated nuclear repulsive force. Such an orbital is termed a *net-binding* orbital. An antibonding combination of atomic orbitals leads to a decrease in the f_i value as R decreases and thus to an $f_i - 1$ value which is negative. Orbitals possessing such negative values are termed net *antibinding* as they lead to a net force of repulsion on the nuclei, tending to separate the molecule into atoms. Thus the value of f_i relative to unity indicates immediately whether or not the electrons in the corresponding orbital are distributed in such a way as to simply shield an equivalent number of nuclear charges, whether they contribute to the binding by exerting a force pulling the two nuclei together, or whether their presence leads to a net force of repulsion tending to separate the molecule into atoms.

The f_i values and the total resultant forces for the lowest $^1\Sigma_g^+$ states of the molecules

*This is another reason why the force provides a good observable by which to test the electron density function. A knowledge of the equilibrium bond length which is often accurately known allows one to determine the "experimental" value for $F_{\alpha e}$ with greater accuracy than is possible for many other molecular properties.

†In accordance with a suggestion made by T. Berlin, J. Chem. Phys., **19**, 214 (1951), we use the term binding when referring to forces and reserve the term bonding for the usual interpretation in terms of energy.

Can. J. Chem. Downloaded from www.nrcresearchpress.com by 210.87.254.40 on 09/05/12
For personal use only.

Li_2, Be_2, C_2, N_2, and F_2 at their equilibrium internuclear separations are given in Table I.

In no case do the densities calculated by Ransil for these molecules lead to a zero resultant force on the nuclei. For Li_2 the electronic force is too large, and in the remaining cases the electronic force is not large enough to counterbalance the nuclear force of repulsion. The error in the resultant force is seen to increase as the nuclear charge increases. This result is to be expected as the forces possess a $1/r_i^2$ radial dependence which causes their value to be sensitive to the nature of the wave function in regions close to the nucleus. This sensitivity increases, due to the contraction of the charge density, as Z_α increases. The results for the forces on the Be, C, N, and F nuclei parallel those found for the heavy nuclei in HF (5), H_2O (6), and NH_3 (7) as calculated from S.C.F. wave functions. In these three hydride molecules the force on hydrogen was close to zero but the resultant force on the heavy nucleus was in each case close to the entire nuclear force of repulsion. While the errors in the present results are much smaller in magnitude than the total nuclear forces of repulsion, the two sets of values are nevertheless very similar. The forces on the F and N nuclei in HF and NH_3 (and hence the resultant electric fields at the F and N nuclei) were found to be of the same order of magnitude as those found in F_2 and N_2, the values of the forces being -2.94 and -2.05 a.u. respectively. The results indicate that the S.C.F. densities, particuarlly for the C_2, N_2, and F_2 molecules, are only fair approximations to the distributions required for electrostatic equilibrium. The reasons for these nonzero resultant forces are best determined through a consideration of the orbital contributions to the forces. In order to facilitate this discussion and that of the binding in these molecules in terms of the atomic orbital contributions to the electron density, we give in Table II a more detailed breakdown of the orbital forces in the N_2 molecule.

The atomic, penetration, and overlap forces arise from the three possible types of atomic and overlap population densities.* *Atomic force*: the force exerted on a nucleus due to the polarization (e.g., $2s$–$2p$ hybridization) of the atomic charge density situated on that nucleus. *Penetration force*: the force exerted on a nucleus by the atomic charge density situated entirely on another nucleus. It is a measure of the electronic shielding of one nucleus from the other and the amount of this shielding is determined by the extent to which one nucleus penetrates the charge density surrounding the second nucleus. *Overlap force*: the force on a nucleus due to the density resulting from the overlap of atomic orbitals situated on two different nuclei. This force term is a sensitive measure of the binding power of a molecular orbital. The binding is not simply proportional to the magnitude of the overlap which determines the amount of density transferred on molecule formation. Of equal importance is where the density is placed and this is quantitatively measured by the overlap force.

In all five cases the f_i values for the $1\sigma_g$ and $1\sigma_u$ orbitals (which are primarily comprised of the $1s$ orbitals) are very close to unity. These orbitals are, therefore, nonbinding as their density simply shields an equivalent number of nuclear charges. This shielding is evident from the results for these two orbitals in N_2 in Table II where the penetration forces are seen to be close to unity and the atomic and overlap forces are very small.

The $2\sigma_g$ orbital exerts a strong binding force on the nuclei, the net force $(f(2\sigma_g)-1)$ being actually greater than unity in all cases except that of Li_2. The overriding contribution to $f(2\sigma_g)$ in all the cases but that of F_2 is from the overlap density, a result which

*For a fuller discussion of the force contributions and a similar force analysis of the S.C.F. results for hydrogen fluoride see reference 5.

Can. J. Chem. Downloaded from www.nrcresearchpress.com by 210.87.254.40 on 09/05/12
For personal use only.

Can. J. Chem. Downloaded from www.nrcresearchpress.com by 210.87.254.40 on 09/05/12
For personal use only.

TABLE I

The forces and their orbital contributions*

	$f(1\sigma_g)$	$f(1\sigma_u)$	$f(2\sigma_g)$	$f(2\sigma_u)$	$f(1\pi_u)$†	$f(3\sigma_g)$	$f(1\pi_g)$†	$\sum_i f_i$	Z_α	F_α‡ (in a.u.)
Li_2	1.0171	1.0296	1.6064					3.6531	3	0.07679
Be_2	1.0397	1.1123	2.1075	−0.5775				3.6822	4	−0.08902
C_2	1.0406	1.0923	2.1997	−0.7375	0.9262			5.4475	6	−0.6016
N_2	1.0667	1.1256	2.6327	−0.6482	0.9550	−0.2722		5.8146	7	−1.940
F_2	0.9948	1.0726	2.6155	−0.3868	1.0347	−0.3376	0.7621	7.5521	9	−1.814

*A negative force is one in the same direction as the force of nuclear repulsion. The resultant force F_α is in atomic units (e^2/a_0^2). To change an f_i value into atomic units multiply the value by Z_α/R^2.

†These values are for a two-electron density. They must be doubled to obtain the total electronic force.

‡For comparison, the forces on the Li and N nuclei when the internuclear separations in the Li_2 and N_2 molecules are increased by 0.1 Å are 0.0031 and 0.28 a.u. respectively.

TABLE II

Force contributions from the atomic and overlap densities in N_2

Molecular orbital	$1\sigma_g$	$1\sigma_u$	$2\sigma_g$	$2\sigma_u$	$1\pi_u$	$3\sigma_g$
Atomic force	0.0540	0.1514	0.1902	−1.2406	0.0000	−1.6916
Penetration force	0.9987	1.0052	0.8187	0.8445	0.5613	0.6492
Overlap force	0.0140	−0.0309	1.6238	−0.2521	0.3937	0.7702
Total orbital force (f_i)	1.0667	1.1256	2.6327	−0.6482	0.9550	−0.2722
Orbital energy in a.u. (1)	−15.647	−15.644	− 1.421	−0.7137	−0.5454	−0.5555

indicates that this orbital is the one primarily responsible for the binding in these molecules. The detailed results for N_2 in Table II show that a great deal of charge is transferred to the binding region between the nuclei in the formation of this molecular orbital. Unlike the $2\sigma_u$ and $3\sigma_g$ orbitals, the atomic force contribution is relatively small for $2\sigma_g$.

The $2\sigma_u$ orbital is not only net antibinding but is actually antibinding (i.e., $f(2\sigma_u)$ is itself negative). The main reason for the strongly antibinding nature of this orbital is the unfavorable direction of the atomic polarization on each nucleus arising from the $2s$–$2p$ hybridization. This hybridization removes charge from the binding region and concentrates it behind each nucleus. The density which is transferred in the formation of this molecular orbital is also concentrated primarily in the antibinding regions as the overlap force contribution is negative. It seems somewhat surprising that the $2\sigma_u$ orbital should be so strongly antibinding, although it is interesting to note that in the N_2 and F_2 molecules where the $2\sigma_g$ and $2\sigma_u$ orbitals are not the uppermost ones, the sum of their f_i values is approximately two. This indicates that when considered together the 2σ orbitals are quite similar to the 1σ pair in that they simply shield two units of nuclear charge, the strong net binding of $2\sigma_g$ just cancelling the net antibinding of $2\sigma_u$.

The most surprising result is the strongly antibinding character of the $3\sigma_g$ orbital which is occupied in both the N_2 and F_2 molecules. Since it is an orbital of σ_g symmetry it is assumed to be a bonding one (its orbital energy is negative) but the force analysis indicates that the density is so disposed as to pull the nuclei away from one another. In both N_2 and F_2 the force due to the overlap density in this orbital is binding, as one would expect for a σ_g orbital. Indeed in F_2 the overlap force contribution is larger for this orbital than for any other in the molecule. However, there is a large negative atomic force term due to the unfavorable $2s$–$2p$ hybridization which negates the overlap force. The net result is that the density in the $3\sigma_g$ orbital exerts a large force tending to separate the two nuclei. The unfavorable $2s$–$2p$ hybridization undoubtedly is of the kind termed "forced hybridization" by Mulliken (8), i.e., hybridization necessary to retain orthogonality to the $1\sigma_g$ and $2\sigma_g$ orbitals. A more flexible basis set of orbitals should be capable of yielding a $3\sigma_g$ orbital which concentrates charge in the binding region without the necessity of introducing unfavorable atomic polarizations to maintain the necessary orthogonalities. For example, it would be of interest to examine the "double-zeta" wave function for the nitrogen molecule (9) in a similar fashion and see if one of the major changes is as suggested here, i.e., a large overlap force but with a smaller amount of $2s$–$2p$ hybridization.

Table I indicates that the density in the $1\pi_u$ orbital in C_2, N_2, and F_2 can be roughly described as nonbinding. The density approximately shields its share of the nuclear charge. The overlap between π atomic orbitals can be appreciable (of the same order of magnitude as the $2s$ atomic orbital overlap) but the density which is transferred because of this overlap is placed above and below the internuclear axis where it is not as effective at binding the nuclei. (Compare the overlap force contributions in Table II for the $2\sigma_g$ orbital, which is principally $2s$, with the corresponding contribution from the $1\pi_u$ orbital.) In addition, the π atomic orbitals offer poor shielding of the nuclei (compare the penetration contributions to $2\sigma_g$ and $1\pi_u$ in Table II). The combination of these two effects leads to very small net-binding or net-antibinding forces for these orbitals. Any polarization of the π orbitals, say d_π–p_π, can increase the amount of density in the binding region and increase the binding of these orbitals.

All but one of the integrals required to calculate the forces were determined by machine computation (I.B.M. 650) from programs derived from the analytical expressions for

Can. J. Chem. Downloaded from www.nrcresearchpress.com by 210.87.254.40 on 09/05/12
For personal use only.

these integrals (10, 11). The integral determining the force on atom α due to the overlap of a $2p$ atomic orbital on α with a $2s$ orbital on another atom (with a different orbital exponent) was evaluated by the method of Barnett and Coulson (12).

ACKNOWLEDGMENTS

We are very indebted to Miss O. Boshko for writing the programs for the force integrals and obtaining their numerical values and also to the Computing Centre at the University of Ottawa for machine time. We are grateful to Dr. G. A. Jones for helpful discussions and to Mrs. P. Bader and Mrs. H. Weinberg for checking the numerical results.

REFERENCES

1. B. J. Ransil. Rev. Mod. Phys. **32**, 245 (1960).
2. R. P. Feynmann. Phys. Rev. **56**, 340 (1939).
3. G. G. Hall. Phil. Mag. **6**, 249 (1961).
4. R. F. W. Bader and G. A. Jones. Can. J. Chem. **39**, 1253 (1961).
5. R. F. W. Bader and G. A. Jones. Can. J. Chem. This issue.
6. R. F. W. Bader and G. A. Jones. Can. J. Chem. **41**, 586 (1963).
7. R. F. W. Bader and G. A. Jones. J. Chem. Phys. **38**, 2791 (1963).
8. R. S. Mulliken. J. Chem. Phys. **19**, 912 (1951).
9. J. W. Richardson. Rev. Mod. Phys. **32**, 461 (1960).
10. R. F. W. Bader. Can. J. Chem. **40**, 2140 (1962).
11. C. A. Coulson. Proc. Cambridge Phil. Soc. **38**, 210 (1942).
12. M. P. Barnett and C. A. Coulson. Phil. Trans. Roy. Soc. London, Ser. A, **243**, 221 (1951).

Can. J. Chem. Downloaded from www.nrcresearchpress.com by 210.87.254.40 on 09/05/12
For personal use only.

A REINVESTIGATION OF THE RANGE OF Na^{24} IONS OF KEV ENERGIES IN ALUMINUM[1]

M. McCargo,[2] F. Brown, and J. A. Davies
Research Chemistry Branch, Atomic Energy of Canada Limited, Chalk River, Ontario

Received May 3, 1963

ABSTRACT

The range of Na^{24} in aluminum has been reinvestigated in the energy region 1.0–100 kev, using an isotopically separated beam of Na^{24}. Below 10 kev, the results differ significantly from our earlier data in which a much larger integrated flux of alkali metal ions (Na^{23} + Na^{24}) was required. Above 10 kev the discrepancy between the two sets of data disappears. The recent theoretical treatment of Oen, Holmes, and Robinson is found to be in quite reasonable agreement with the median ranges ($\overrightarrow{R_m}$) obtained in the present work, particularly if an allowance for the electronic stopping contribution at the higher energies is included.

INTRODUCTION

The range of radioactive alkali metal ions of kev energies in aluminum has previously been investigated at these laboratories (1, 2). The ions were produced by a linear accelerator without a mass-separation stage and hence a rather large integrated beam current was needed in order to inject into the target a sufficient number of radioactive atoms for subsequent analysis.

Recent work (3) has shown that, unless the integrated flux is extremely small, the penetration depth of the incident beam can decrease significantly during the bombardment. For example, in the case of 30 kev Xe ions, an integrated flux of $\sim 10^{16}$ ions/cm^2 was found to reduce the penetration depth of the incident beam by almost a factor of 2. A similar effect was observed also with Ar^{41} ions in aluminum. The existence of such a marked "saturation effect" for inert gas ions in aluminum suggests that some of our earlier measurements of alkali metal ions be reinvestigated to determine whether or not the observed data had been influenced significantly by the rather large integrated currents used. In this earlier work, the integrated beam current striking the target was about 5 microcoulombs (3×10^{13} ions) for Cs^+ bombardments, and as much as 100 microcoulombs (6×10^{14} ions) for Na^+. The actual bombarded area in each run was not recorded, but autoradiography of several targets suggested an approximate value of 0.1 cm^2. The corresponding integrated fluxes, therefore, must have been approximately 3×10^{14} Cs^+/cm^2 and 6×10^{15} Na^+/cm^2. The latter value is large enough to have exerted a possibly significant effect on the range distribution at the lower energies.

Consequently, the range of Na^{24} ions in aluminum has been reinvestigated over the energy region 1.0–100 kev. An electromagnetic isotope separator has been used to provide a beam of monoenergetic, isotopically separated Na^{24} ions, thereby enabling the integrated flux to be reduced to a negligibly small level ($\sim 10^{11}$ atoms/cm^2).

EXPERIMENTAL

In brief, the experimental technique consists of three stages: (i) bombardment of a highly polished aluminum target with a beam of radioactive ions of chosen energy; (ii) removal of successive thin layers of aluminum by a two-step process of anodic oxidation and stripping; and (iii) measurement of the residual radioactivity in the target after each layer is removed.

[1]*Issued as A.E.C.L. No. 1795.*
[2]*N.R.C. Postdoctoral Fellow, 1961–1963.*

Can. J. Chem. Downloaded from www.nrcresearchpress.com by 210.87.254.5 on 09/05/12
For personal use only.

The anodizing, stripping, and counting procedures have been described fully in an earlier paper (4), as has also the bombardment technique (5).

The radioactive isotope Na^{24} was prepared by neutron irradiation of Na_2CO_3 in the NRU reactor.

RESULTS AND DISCUSSION

Integral range distribution curves at each of the incident ion energies studied are illustrated in Fig. 1. Two distribution curves obtained in the earlier work (2) have been

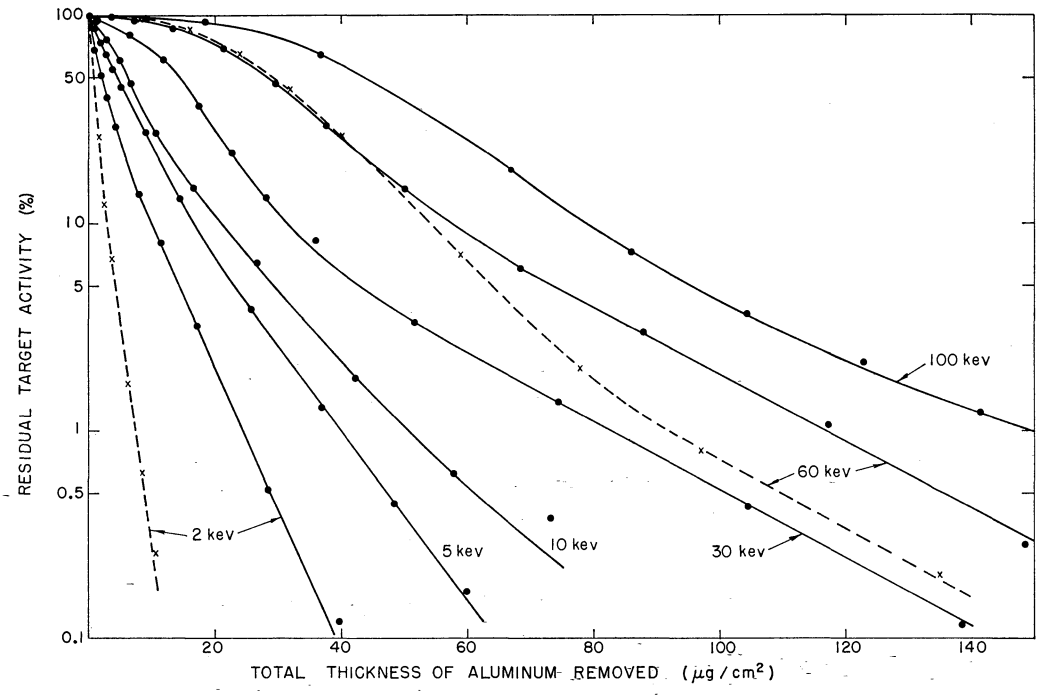

FIG. 1. Integral range distributions of Na^{24} ions in aluminum: ● new data, using trace bombardments; × previous work (2).

included for comparison. Again, as in the previous experiments, we observe a point of inflection followed by an approximately exponential tail. The significance of this tail has been discussed recently by Robinson and Oen (6). In general, the qualitative features of the distribution are the same as those observed with the larger integrated flux, except that at the lower energies the range distribution for trace bombardments is shifted significantly to larger penetration depths. This shift can be seen more clearly in Table I.

The symbol (→) signifies that the measured value is the projected range perpendicular to the target surface (i.e. the penetration depth), and *not* the total distance travelled by the projectile. It is evident that below about 10 kev the integrated flux used in the earlier work was sufficiently large to reduce significantly the measured penetration depth. At higher energies, as one might expect, the flux effect becomes smaller; and above 10 kev the two sets of data agree within the experimental reproducibility of ±6%.

COMPARISON WITH THEORY

Recently, Oen, Robinson, and Holmes (7) have developed a Monte Carlo technique for calculating the range of atomic projectiles in solids, based on an exponentially screened

Can. J. Chem. Downloaded from www.nrcresearchpress.com by 210.87.254.5 on 09/05/12
For personal use only.

TABLE I

Range of Na^{24} in aluminum ($\mu g/cm^2$)

E (kev)	'Most probable' range $\overrightarrow{R_p}$ (a)	(b)	Median range $\overrightarrow{R_m}$ (a)	(b)	Mean range $\overrightarrow{R}$ (a)	(b)	Half-thickness of "tail" $X_{1/2}$ (a)	(b)
1.0	—	—	0.5±0.2	1.8±0.2	0.6±0.2	3.1	0.7±0.1	3.3
2.0	0.7±0.3	1.0±0.3	1.1±0.2	2.6±0.2	1.3±0.2	4.4	1.6	3.5
5.0	1.6±0.4	2.6	3.0	5.1	3.9	7.7	3.6	7.5
10.5	3.9	4.3	6.2	7.2	8.0	10.0	8.3	8.6
30	13.1	14	15.0	14.2	19.8	17.8	15.5	18.0
60	26	24	29.5	28.0	32.4	32.8	16	19.0
100	—	42	—	44	—	49	—	—

NOTE: (a) Previous work (2)—using a mixture of Na^{23} and Na^{24}. (b) Present data—using a trace bombardment of Na^{24}. Except where otherwise stated, the estimated experimental error is ±10% for $\overrightarrow{R_p}$, and ±6% for $\overrightarrow{R_m}$, $\overrightarrow{R}$, and $X_{1/2}$.

coulomb, or "Bohr", potential for the atomic scattering process, and ignoring any contribution from electronic stopping. Using this treatment, they have computed the range of Na^{24} in Al as a function of energy, and have compared their predicted curve with our previous experimental values (ref. 7, Fig. 11).

In Fig. 2, we have extended their comparison to include the more accurate experimental

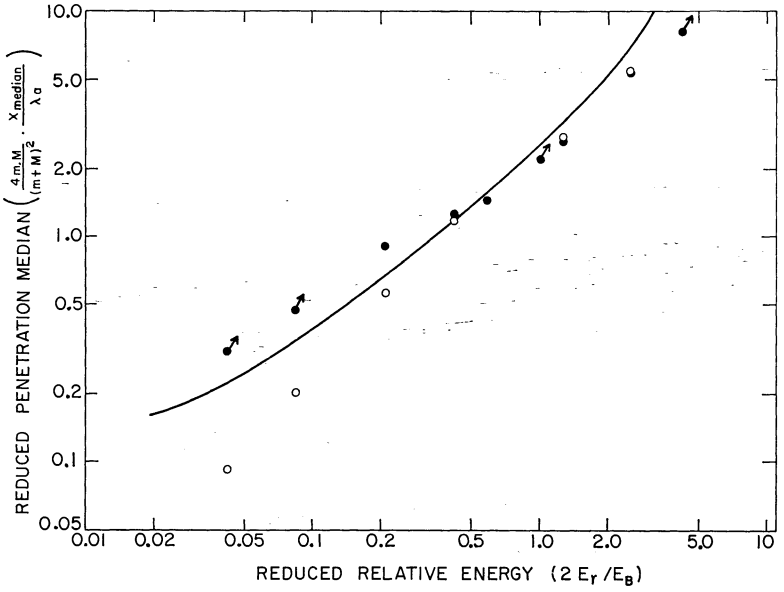

FIG. 2. Comparison of experimental data for Na^{24} in aluminum with the theoretical curve of Oen *et al.* (see ref. 7, Fig. 11): ● new data, using trace bombardments; ○ previous work (2).

data obtained in the present work. The screening distance a_B used by Oen *et al.* is not necessarily the Bohr value, but includes a factor k which is introduced by them as an adjustable parameter to permit a closer fit of the experimental results to the theoretical curve. The points in Fig. 2 have been calculated from the experimental data, using the Bohr value of the screening distance (i.e. $k = 1.0$). The effect of using a "screening length" 10% greater than the Bohr value (i.e. $k = 1.1$) is illustrated by an arrow on some of the

Can. J. Chem. Downloaded from www.nrcresearchpress.com by 210.87.254.5 on 09/05/12
For personal use only.

points. The matching between theory and experiment for $k = 1.0$ is quite good, particularly at the lower energies. Above 30 kev, the experimental points fall somewhat below the predicted curve, a fact which can reasonably be attributed to the increased importance of electronic stopping. It can be seen that the appreciable discrepancy noted previously (7) at low energy was due mainly to the large integrated flux used in the earlier experimental work. There is no significant improvement in using $k = 1.1$, and we conclude that for Na in Al the Bohr screening distance is a reasonable approximation.

An alternative theoretical treatment of the atomic stopping process, based on a Thomas–Fermi potential, has been developed by Lindhard and Scharff (8), who obtain by analytical methods a range-energy expression in the form of a universal curve relating a reduced range parameter ρ and a reduced energy parameter ϵ. In a more recent communication, Lindhard (9) has modified his treatment to take account of the important contribution of electronic stopping at higher energies. The range predicted by the Lindhard theory is the total path length, not the experimentally measured projected range ($\rightarrow$) perpendicular to the target surface. Lindhard therefore has derived a suitable formula (ref. 8, eqn. 5) for converting projected ranges into total path lengths, thereby enabling comparison between experiment and theory.

The results of such a comparison for Na^{24} in Al are illustrated in Fig. 3. The experi-

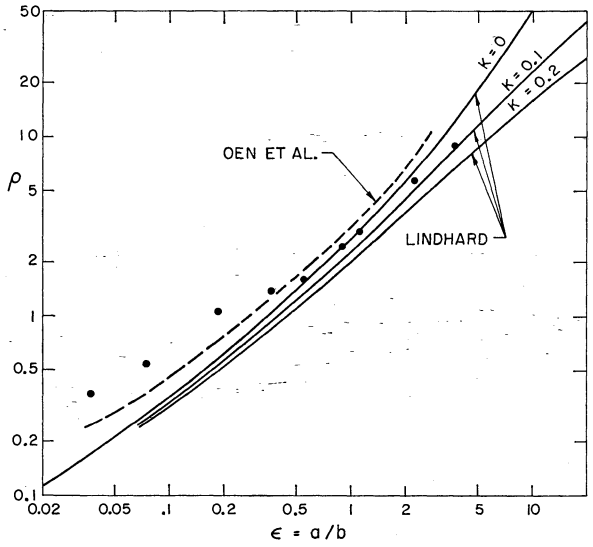

FIG. 3. Comparison of the new experimental data, using trace bombardments, with various theoretical curves. For the definition of ρ and ϵ, see reference 8. The appropriate value of Lindhard's electronic stopping parameter K, for Na^{24} in aluminum, is 0.15.

mental points were obtained from the $\overrightarrow{R_m}$ values in Table I, multiplied by the appropriate path length conversion factor 1.38. The $K = 0$ curve is the universal range-energy expression derived by Lindhard and Scharff for nuclear stopping alone. When electronic stopping is included, a series of theoretical curves is obtained, each one characterized by an electronic stopping parameter K. At low energies, these curves all approach the $K = 0$ curve. For Na^{24} in Al, the appropriate K value is 0.15.* The theoretical curve of Oen *et al.* (see Fig. 2) has also been included for comparison.

**The expression for K, given by Lindhard (9), is*

$$K = \xi_e \cdot \frac{0.0793 Z_1^{1/2} Z_2^{1/2}}{(Z_1^{2/3}+Z_2^{2/3})^{3/4}} \cdot \frac{(A_1+A_2)^{3/2}}{A_1^{3/2} A_2^{1/2}}$$

where A and Z are the mass and atomic numbers, the subscripts 1 and 2 refer to the projectile and target atom, and $\xi_e \simeq Z_1^{1/6}$.

Can. J. Chem. Downloaded from www.nrcresearchpress.com by 210.87.254.5 on 09/05/12
For personal use only.

Both theoretical treatments are in quite reasonable accord with the experimental data obtained in the present work. Oen's treatment gives somewhat better agreement than Lindhard's at lower energies where electronic stopping is negligible; at higher energies, however, the Lindhard treatment accounts quite satisfactorily for the increasing importance of electronic stopping. A similar agreement with the Lindhard theory has been observed recently with various inert gas ions in aluminum (5, 10) and in other solids (11).

In the above comparisons with theory, $\vec{R}_m$ values have been used in preference to $\vec{R}$ in order to minimize the contribution of the penetrating "tail" in the range distribution. Robinson and Oen (6) suggest that the "tail" is caused by a channeling effect in the crystal lattice, an explanation which has recently been verified experimentally in these laboratories (12). Since the theoretical treatments are based on a random distribution of atoms in the solid, they are evidently applicable only to that portion of the beam which has not become channeled. Consequently, $\vec{R}_m$ is a more appropriate quantity than $\vec{R}$ for comparison with theory.

With the newly discovered importance (12) of crystal-lattice effects on the range of atomic projectiles, it is obvious that future experimental work should be carried out either in amorphous solids or in single crystals of known orientation.

ACKNOWLEDGMENTS

It is a pleasure to acknowledge the invaluable help of G. A. Sims in all this experimental work, and the assistance of J. C. Tole and R. L. Cushing in carrying out the ion bombardments.

REFERENCES

1. J. A. Davies, J. D. McIntyre, R. L. Cushing, and M. Lounsbury. Can. J. Chem. **38**, 1535 (1960).
2. J. A. Davies and G. A. Sims. Can. J. Chem. **39**, 601 (1961).
3. F. Brown and J. A. Davies. Can. J. Phys. **41**, 844 (1963).
4. J. A. Davies, J. Friesen, and J. D. McIntyre. Can. J. Chem. **38**, 1526 (1960).
5. J. A. Davies, F. Brown, and M. McCargo. Can. J. Phys. **41**, 829 (1963).
6. M. T. Robinson and O. S. Oen. Appl. Phys. Letters, **2**, 30 (1963).
7. O. S. Oen, D. K. Holmes, and M. T. Robinson. J. Appl. Phys. **34**, 302 (1963).
8. J. Lindhard and M. Scharff. Phys. Rev. **124**, 128 (1961).
9. J. Lindhard. Private communication. Unpublished paper presented at the Physics of the Electromagnetic Separation Method Conference, Paris, 1962.
10. I. Bergström, J. A. Davies, B. Domeij, and J. Uhler. Arkiv Fysik. **24**, 377, 389 (1963).
11. D. Powers and W. Whaling. Phys. Rev. **126**, 61 (1962).
12. G. R. Piercy, F. Brown, J. A. Davies, and M. McCargo. Phys. Rev. Letters, **10**, 399 (1963).

Can. J. Chem. Downloaded from www.nrcresearchpress.com by 210.87.254.5 on 09/05/12
For personal use only.

NEUTRAL EXTRACELLULAR GLUCAN OF PULLULARIA PULLULANS (DE BARY) BERKHOUT[1]

W. SOWA,[2] A. C. BLACKWOOD,[3] AND G. A. ADAMS
Division of Applied Biology, National Research Council, Ottawa, Canada
Received May 9, 1963

ABSTRACT

A neutral extracellular glucan ($[\alpha]_D^{23}$ +189°) was produced in 12% yield by *Pullularia pullulans* (de Bary) Berkhout grown on a glucose substrate. A single symmetrical peak on free-boundary electrophoresis in borate and acetate buffers was evidence of homogeneity. Infrared spectroscopy showed that the predominant glucoside linkages were $\alpha(1 \rightarrow 4)$ and $\alpha(1 \rightarrow 6)$ with a small proportion of $\alpha(1 \rightarrow 3)$. Graded acid hydrolysis under conditions of minimum reversion yields glucose, maltose, isomaltose, nigerose, panose, and isomaltotriose. In addition, a trisaccharide, *O*-α-D-glucopyranosyl-$(1 \rightarrow 4)$-*O*-α-D-glucopyranosyl-$(1 \rightarrow 6)$-D-glucopyranose, was isolated. Another trisaccharide was isolated and tentatively identified as *O*-α-D-glucopyranosyl-$(1 \rightarrow 4)$-*O*-[α-D-glucopyranosyl-$(1 \rightarrow 6)$]-D-glucose and hence a small degree of branching may occur in the molecule. The present study has confirmed previous observations that the main linkages are $\alpha(1 \rightarrow 4)$ and $\alpha(1 \rightarrow 6)$ and has provided unequivocal proof of the presence of $\alpha(1 \rightarrow 3)$ linkages. Periodate oxidation studies confirmed the foregoing structural features and showed that the glucan was linked $\alpha(1 \rightarrow 4)$, 65%; $\alpha(1 \rightarrow 6)$, 29%; and $\alpha(1 \rightarrow 3)$, 6%.

The yeast-like fungus *Pullularia pullulans* produces a mixture of glucose-containing extracellular polysaccharides (1). It has been shown (2, 3) that one of the polysaccharides formed by the fungus from glucose as the carbon source is a linear glucan ("pullulan") having $[\alpha]_D$ +192° and composed of approximately 300 α-D-glucopyranose units linked $(1 \rightarrow 4)$ and $(1 \rightarrow 6)$ in the ratio 3:2. Bouveng *et al.* (4) have examined the polysaccharides produced by *Pullularia pullulans* from various sugar substrates, and have found that a sucrose medium yielded a linear glucan having $[\alpha]_D$ +190° and consisting of more than 250 units linked $\alpha(1 \rightarrow 4)$ and $\alpha(1 \rightarrow 6)$ in the ratio 2:1. A small amount (1–2%) of glucose remaining after periodate oxidation of the polysaccharide suggested that $(1 \rightarrow 3)$ linkages might be present, although this was not supported by methylation data. No evidence for the presence of $(1 \rightarrow 3)$ linkages in the polysaccharide produced from glucose was reported in earlier work (2, 3).

The present publication reports the results obtained from partial acid hydrolysis and from periodate oxidation of the glucan produced by *Pullularia pullulans* grown on glucose.

The growth conditions of the organism and the method of recovery used for the preparation of the polysaccharide in the present work favored isolation of the water-soluble glucan to the exclusion of the more insoluble jelly-like polysaccharide which adheres to the mycelium (1). The polysaccharide showed a single symmetrical peak on electrophoresis in borate and acetate buffers, gave no precipitate with Cetavlon, and showed no carboxyl absorption in its infrared spectrum. This evidence showed that the polysaccharide was homogeneous and contained no acid groups. Bouveng *et al.* (4) found that yields of polysaccharide were increased and that formation of uronic acid and other hexose units was diminished when the organism was grown on glucose rather than other sugar substrate (except for sucrose).

Infrared spectroscopy of the polysaccharide showed strong absorption at 850 cm^{-1},

[1]*Issued as N.R.C. No. 7490.*
[2]*National Research Council Postdoctoral Fellow 1961–1963. Present address: Ontario Research Foundation, Toronto 5, Ontario.*
[3]*Professor of Agricultural Bacteriology, MacDonald College, Montreal, Que.*

characteristic of α-D-glucopyranose units (5). Absorption at 755 cm^{-1} and from 915 cm^{-1} to 930 cm^{-1} indicated that the predominant linkages were $\alpha(1 \rightarrow 4)$ and $\alpha(1 \rightarrow 6)$. The presence of $\alpha(1 \rightarrow 3)$ linkages was indicated by a small amount of absorption at 790 cm^{-1}; glucopyranose units linked in this manner absorb at 793 ± 3 cm^{-1} (5). Glucose was the only sugar detectable in acid hydrolyzates of the polysaccharide by both paper and gas–liquid partition chromatographic techniques.

The polysaccharide was partially hydrolyzed under conditions which, in studies of amylopectin (6) and glycogen (7), have been shown to produce minimum reversion. The sugars so obtained were separated by paper chromatography and paper electrophoresis. The results are shown in Table I.

TABLE I

Products from partial hydrolysis of glucan

Sugar	Yield (wt% based on glucan)
D-Glucose	20.2
Maltose (4-*O*-(α-D-glucopyranosyl)-D-glucopyranose)	4.4
Isomaltose (6-*O*-(α-D-glucopyranosyl)-D-glucopyranose)	11.2
Nigerose (3-*O*-(α-D-glucopyranosyl)-D-glucopyranose)	1.4
Isomaltotriose (*O*-α-D-glucopyranosyl-(1 → 6)-*O*-α-D-glucopyranosyl-(1 → 6)-D-glucopyranose)	3.3
Panose (*O*-α-D-glucopyranosyl-(1 → 6)-*O*-α-D-glucopyranosyl-(1 → 4)-D-glucopyranose)	4.3
Oligosaccharide A (*O*-α-D-glucopyranosyl-(1 → 4)-*O*-α-D-glucopyranosyl-(1 → 6)-D-glucopyranose)	2.5
Oligosaccharide B (*O*-α-D-glucopyranosyl-(1 → 4)-*O*-[α-D-glucopyranosyl-(1 → 6)]-D-glucose)	0.9

Glucose, maltose, isomaltose, nigerose, and panose were obtained in crystalline form or were characterized by the preparation of crystalline derivatives. Isomaltotriose was identified on the basis of its chromatographic properties, specific optical rotation, and products of partial hydrolysis. Oligosaccharide A was a trisaccharide having a high M_G value in borate buffer, indicative of a reducing end group linked through positions 3 or 6 (8). Infrared spectroscopy showed that it contained both $\alpha(1 \rightarrow 4)$ and $\alpha(1 \rightarrow 6)$ linkages. The products of partial hydrolysis of the reduced trisaccharide were isomaltitol, maltose, glucose, and sorbitol. The absence of maltitol on paper chromatography or paper electrophoresis showed that the C_4 of the reducing end group was not substituted. On the basis of this evidence the oligosaccharide was identified as *O*-α-D-glucopyranosyl-(1 → 4)-*O*-α-D-glucopyranosyl-(1 → 6)-D-glucopyranose. Oligosaccharide B was obtained in small yield (0.9%), and from its R_G value (Table II) appeared to be a trisaccharide. Its infrared spectrum showed that it contained both $\alpha(1 \rightarrow 4)$ and $\alpha(1 \rightarrow 6)$ linkages, although it was not obtained completely free of glucose, isomaltose, and a trace of panose. Since it was not maltotriose, isomaltotriose, panose, or oligosaccharide A it was tentatively identified as *O*-α-D-glucopyranosyl-(1 → 4)-*O*-[α-D-glucopyranosyl-1(1 → 6)]-D-glucose, which would result from branching in the polysaccharide. The M_G value (0.50) was higher than expected for an oligosaccharide substituted at position 4 of the reducing unit (8). There is

TABLE II

Chromatography of glucose trisaccharides

Trisaccharide	$R_{Glucose}$ in solvent system			
	A (26 hr)	B (48 hr)	C (65 hr)	E (65 hr)
Panose	0.41	0.27	0.21	0.27
Isomaltotriose	0.38	0.22	0.21	0.28
Oligosaccharide A	0.28	0.16	0.17	0.22
Oligosaccharide B	0.42	0.24	0.27	0.32
Maltotriose	0.50		0.27	

some evidence for branching in the glucan from the work of Wallenfels *et al.* (3), who detected 2,3-di-*O*-methyl-D-glucose after methylation and hydrolysis of "pullulan".

The polysaccharide consumed 1.23 moles of periodate and released 0.29 mole of formic acid per anhydroglucose unit. These results indicate that 29% of the linkages were (1 → 6), 65% were (1 → 4), and 6% were (1 → 3). The 29% of (1 → 6) linkages is based on the assumption that the molecule has only a small amount of branching (as indicated by the small proportion of oligosaccharide B) and that there are few end groups in the molecule.

The periodate-oxidized glucan yielded glucose after reduction and hydrolysis, indicating that some units in the polysaccharide were substituted through C_3 or doubly substituted at positions 2 and 4. The formation of glycerol and erythritol during these reactions provided additional evidence for (1 → 4) and (1 → 6) linkages in the polysaccharide.

The present study has confirmed previous observations that the main linkages are $\alpha(1 \rightarrow 4)$ and $\alpha(1 \rightarrow 6)$, the former predominating (2–4). Previous conclusions were based on methylation and paper chromatographic data while in the present investigation isomaltose and panose have been isolated and identified. Maltotriose was not recoverable due to the lability of the $\alpha(1 \rightarrow 4)$ linkages under the hydrolytic conditions used.

The glucan produced by *Pullularia pullulans* from glucose under the present experimental conditions differs from "pullulan" by having $\alpha(1 \rightarrow 3)$ linkages and also by having a ratio of (1 → 4) to (1 → 6) linkages of 2.2 to 1 instead of 3 to 2. In this latter respect it resembles more closely the glucan produced from a sucrose substrate and having a linkage ratio of 2 to 1 (4).

Unequivocal evidence for the presence of $\alpha(1 \rightarrow 3)$ linkages in the glucan has been provided by the isolation of the crystalline acetate of nigerose. Hydrolytic conditions were such as to preclude its formation by reversion in the amounts isolated. Additional supporting evidence for the existence of $\alpha(1 \rightarrow 3)$ linkages in the polysaccharide was provided by infrared examination and also by the finding of intact glucose residues after prolonged periodate oxidation. Although Bouveng *et al.* (4) suggested that (1 → 3) linkages might be present in the *Pullularia* glucan, they were unable to find supporting evidence in methylation studies. Bender *et al.* (2) and Wallenfels *et al.* (3) found evidence for only $\alpha(1 \rightarrow 4)$ and $\alpha(1 \rightarrow 6)$ linkages in their polysaccharide from *Pullularia pullulans*.

EXPERIMENTAL

Paper chromatograms were run by the descending method at room temperature on Whatman No. 1 paper using the following solvent systems (v/v): (A) butan-1-ol, pyridine, water—6:4:3; (B) ethyl acetate, pyridine, water—10:4:3; (C) propan-1-ol, ethyl acetate, water—7:1:2; (D) butan-1-ol, ethanol, water—3:1:1; (E) ethyl acetate, acetic acid, formic acid, water—18:3:1:4.

Paper electrophoresis was carried out on Whatman 3 MM paper in 0.1 *M* sodium tetraborate buffer at 550 v and 50 ma for 3–4 hours.

Sugars on the chromatograms were detected by *p*-anisidine hydrochloride (9), silver nitrate – sodium hydroxide (10), or benzidine – trichloroacetic acid (11) reagents.

Evaporations were carried out under reduced pressure at a bath temperature of 40° or less. Solutions were deionized with Amberlite IR 120 (H^+) and Duolite A 4 (OH^-) resins.

Preparation of Pullularia pullulans Polysaccharide

The microorganism was grown in a medium having the following composition per liter of distilled water: 20 g glucose, 0.1 g yeast extract, 1.0 g asparagine, 1.0 g K_2HPO_4, 0.5 g $MgSO_4$, 10 γ thiamine. In addition the medium for the inoculum contained 0.5% cystein. The cultures were grown at 25° C with continuous shaking in 2-liter flasks each containing 750 ml of medium. After 5 days' growth the cultures were centrifuged and the polysaccharide was isolated from the supernatant liquid by precipitation with acetone in a Waring blendor. The crude polysaccharide was purified by reprecipitation from aqueous solution once with acetone and once with ethanol. The purified product was recovered in 12% yield (based on the glucose in the medium) by freeze-drying.

General Properties of the Polysaccharide

The purified polysaccharide had $[\alpha]_D^{23}$ +189° (*c* 0.91 in water), ash 0.46%, nitrogen nil, phosphate nil.

Examination of the polysaccharide by moving-boundary electrophoresis in 0.05 *M* sodium tetraborate buffer using a Spinco Model H Tiselius-type apparatus showed a single moving peak and also a non-moving peak due to borate. In acetate buffer, pH 5 and ionic strength 0.1, there was a single, large, stationary peak along with a barely visible trace of a moving peak. The moving peak later disappeared due to diffusion.

When an aqueous solution of "Cetavlon" (cetyl trimethyl ammonium bromide) (10%, w/v) was added to twice its volume of a solution of the polysaccharide in water (1%, w/v), no precipitate was formed.

The polysaccharide (10 mg) was hydrolyzed in *N* sulphuric acid (2 ml) at 100° C for 7 hours. The cooled solution was deionized, concentrated to a sirup, and examined by paper chromatography in solvent systems (A), (D), and (E). Only glucose was detectable with the *p*-anisidine hydrochloride and the silver nitrate – sodium hydroxide reagents respectively. The syrup (10.7 mg) was acetylated in pyridine (0.1 ml) and acetic anhydride (0.1 ml) at room temperature for 18 hours. The reaction mixture (12) was examined by gas–liquid partition chromatography using an F and M chromatograph with an 8-ft column of DC QF-1 (13% by weight, Dow Corning fluorosilicone) on Chromosorb W, 100–120 mesh, at 225° C. The helium flow rate was ca. 80 ml/min. Only two peaks corresponding to α- and β-glucopyranose pentaacetates were observed.

The infrared spectrum of the polysaccharide in potassium bromide disks showed strong absorption at 850 cm^{-1}, 755 cm^{-1}, and from 915 cm^{-1} to 930 cm^{-1}. There was also a very small amount of absorption at 790 cm^{-1}.

Partial Hydrolysis of the Polysaccharide

The glucan (10.0 g) was added to refluxing hydrochloric acid (0.1 *N*, 2.5 l.) (7). After 2 hours, the hydrolysis was stopped by pouring the solution into ice and water and the hydrolyzate was deionized and concentrated to a syrup (10.2 g). A preliminary experiment had established that under these conditions of hydrolysis the specific optical rotation changed from $[\alpha]_D^{27}$ +190° (*c* 0.4 in 0.1 *N* hydrochloric acid) after 1/2 hour to $[\alpha]_D^{27}$ +56° (*c* 0.4 in 0.1 *N* hydrochloric acid) after 8 hours. The maximum amount of oligosaccharides (chromatographic examination) was formed after 2–4 hours ($[\alpha]_D^{26}$ ca. +125° (*c* 0.4 in 0.1 *N* hydrochloric acid)).

Initial fractionation of an aliquot of the hydrolyzate (4.8 g) was obtained by chromatography on sheets of Whatman 3 MM paper using solvent system (A). The following fractions were obtained: glucose (958 mg), maltose (208 mg), isomaltose (529 mg), and a trisaccharide fraction (402 mg). Paper electrophoresis of the latter fraction showed that it was composed of two major trisaccharide components and a third very minor component (oligosaccharide B). The two major trisaccharides, panose (74 mg) and isomaltotriose (58 mg), were obtained by extraction of the appropriate areas of the electrophoretograms with water. The aqueous solutions were deionized and then distilled repeatedly with methanol to remove borate. By paper chromatography of the remainder of the acid hydrolyzate (5.1 g) on sheets of Whatman 3 MM paper in solvent system (C), three additional oligosaccharides were obtained, nigerose (70 mg), oligosaccharide A (126 mg), and oligosaccharide B (46 mg).

Characterization of the Sugars

D-*Glucose*

The sugar having the same R_G as glucose was crystallized from methanol. After recrystallization from methanol, it melted at 140–146° C, undepressed by admixture with α-D-glucopyranose and had $[\alpha]_D^{21}$ +94° → +51° (*c* 2.3 in water).

Maltose

The sugar corresponding to maltose on chromatograms crystallized from a syrup. It had m.p. 118–120° C and $[\alpha]_D^{19}$ +115° → +128° (*c* 0.97 in water). Paper chromatographic examination of the crystalline maltose showed that traces of other oligosaccharides were present. A portion of the syrup (25 mg) was acetylated with acetic anhydride (1 ml) containing sodium acetate (15 mg) by refluxing the mixture for 1 hour. The

cooled solution was poured into ice water (50 ml) and extracted with chloroform (3×20 ml). The chloroform extract was washed with saturated sodium bicarbonate solution, dried with anhydrous sodium sulphate, and evaporated to a syrup. The β-maltose octaacetate was crystallized twice from ethanol, m.p. and mixed m.p. 157–158° C.

Isomaltose

The isolated sugar which was chromatographically indistinguishable from isomaltose was acetylated with sodium acetate and acetic anhydride. The acetate, after isolation, crystallized from ethanol. After two recrystallizations from ethanol, the crystals had $[\alpha]_D^{23}$ +97.7 (*c* 1.8 in chloroform) and m.p. 143–144° C. The mixed melting point with β-isomaltose octaacetate was undepressed.

Panose

An oligosaccharide having M_G 0.33 in borate buffer was obtained from the trisaccharide fraction. It crystallized from ethanol–water after seeding the solution with authentic panose. After recrystallization from methanol–water, it had m.p. and mixed m.p. 220° (decomp.) and $[\alpha]_D^{23}$ +160° → +150° (*c* 3.3 in water).

Isomaltotriose

The oligosaccharide isolated from the trisaccharide fraction by electrophoresis and having M_G 0.65 in borate buffer had $[\alpha]_D^{23}$ +137° (*c* 2.55 in water). Reported values for isomaltotriose range from +128° to +145° (7, 13–16). In solvent (A), the oligosaccharide had $R_{Glucose}$ 0.37–0.39; Myrbäck and Willstaedt record $R_{Glucose}$ 0.368 for isomaltotriose (17). An aliquot of the syrup (3–5 mg) was partially hydrolyzed with 0.5 *N* hydrochloric acid (1 ml) in a sealed tube at 100° for 45 minutes. The solution was deionized and concentrated to a syrup. The only products of hydrolysis detectable with silver nitrate – sodium hydroxide after paper chromatography in solvent (A) were isomaltose and glucose.

Nigerose

A small amount of sugar having M_G 0.71 in borate buffer and $R_{Maltose}$ 1.28 in solvent (C) was recovered from the hydrolyzate. Ough reports $R_{Maltose}$ 1.27 for nigerose in this solvent system (18). A portion of the syrup (30 mg) was acetylated with sodium acetate and acetic anhydride as described earlier. The β-nigerose octaacetate, which did not crystallize from ethanol, was freed from a small amount of β-glucose pentaacetate by thin-layer chromatography of the syrup on silica gel G (19). A solution of the mixture in chloroform was applied to two plates (20 cm×20 cm) which were run (2×45 minutes) in benzene containing methanol (4%, v/v). The disaccharide was made visible by spraying the plates with water. The powder obtained from the appropriate areas of the plates was eluted with methanol–chloroform (1:1) to yield β-nigerose octaacetate. After two crystallizations from ethanol, it had $[\alpha]_D^{25}$ +79° (*c* 0.19 in chloroform) and m.p. 150–152°. The mixed melting point with an authentic sample was undepressed.

Oligosaccharide A

Oligosaccharide A (amorphous) had $[\alpha]_D$ +128° (*c* 2.92 in water). Its molecular weight, determined in methanol by vapor pressure osmometry,* was 500 and its degree of polymerization, determined by the method of Peat, Whelan, and Roberts (20), was 2.8. It was different from panose, isomaltotriose, and maltotriose on paper chromatography in several solvent systems (Table II). In borate buffer, M_G 0.64 was indicative of a 1 → 3 or 1 → 6 linkage at the reducing end. The infrared absorption in potassium bromide at 915 cm^{-1}, 845 cm^{-1}, and 763 cm^{-1} was consistent with the presence of both α(1 → 4) and α(1 → 6) linkages. Oligosaccharide A (8 mg) was reduced with sodium borohydride (8 mg) in water (2 ml) for 3½ hours at room temperature. The solution was made slightly acidic with dilute acetic acid, deionized, and distilled to dryness with methanol several times to yield the reduced trisaccharide (6 mg). This was partially hydrolyzed in refluxing hydrochloric acid (0.1 *N*, 1.5 ml) for 15 minutes. The solution was passed through Duolite A4 resin and concentrated to a syrup. Paper chromatography in solvent systems (B) and (E) and detection with the silver nitrate reagent showed that the products were unhydrolyzed reduced trisaccharide, maltose, isomaltitol, glucose, and sorbitol. After electrophoresis in sodium molybdate buffer at pH 5 (21) and detection with the silver nitrate reagent, four spots were observed having $M_{Sorbitol} < 0.1$ (maltose), 0.6 (unhydrolyzed reduced A), 0.7 (isomaltitol), and 1.0 (sorbitol).

Oligosaccharide B

Oligosaccharide B was obtained as a syrup which contained small amounts of glucose, isomaltose, and a trace of panose as impurities. Its R_G in several solvent systems (Table II) was similar to that of a glucose trisaccharide. In borate buffer it had M_G 0.50. Infrared spectra of the oligosaccharide in potassium bromide and in Nujol were very similar to the spectra of amorphous panose, indicating the presence of α(1 → 4) and α(1 → 6) linkages. The oligosaccharide was converted to its β-acetate but this could not be obtained crystalline. On thin-layer chromatograms (19) the acetate travelled more slowly than β-maltotriose hendecaacetate.

Oxidation of the Polysaccharide with Periodate

The polysaccharide (0.5003 g) was oxidized in 0.018 *M* sodium periodate solution in a volumetric flask (500 ml) which was kept in the dark at room temperature (25–27° C). Aliquots (5 ml) were removed at

**Mechrolab Vapour Pressure Osmometer, model 301A, Fisher Scientific Company.*

intervals for estimation of periodate and formic acid. The periodate consumption was determined by adding an aliquot to a solution of potassium iodide (10% w/v, 5 ml) and phosphate buffer (pH 6.98, 50 ml) (22). The iodine which was liberated was titrated with 0.0101 *N* sodium thiosulphate solution using starch as indicator. The formic acid produced by oxidation was determined by titration with standard alkali. An aliquot was added to ethylene glycol (0.5 ml) to destroy unreacted periodate and after 30 minutes, the formic acid was titrated with 0.0100 *N* sodium hydroxide solution using methyl red as indicator. Periodate consumed and formic acid produced are shown in Table III. Extrapolation of a plot of these results to

TABLE III

Periodate oxidation of polysaccharide

Time (hr)	8	28	73	121	168
Moles IO_4/AGU	1.046	1.152	1.236	1.274	1.303
Moles HCO_2H/AGU	0.183	0.258	0.288	0.326	0.340

zero time showed that 1.23 moles of periodate was consumed and 0.29 mole of formic acid was released per anhydroglucose unit.

After 168 hours of oxidation, 300 ml was withdrawn from the reaction mixture and iodate and periodate were precipitated by the addition of lead acetate (0.2 *M*). After filtration and deionization of the solution the polyaldehyde was recovered by freeze-drying. This product was reduced in water (40 ml) with sodium borohydride (300 mg) for 3 hours at room temperature. The solution was then acidified with dilute acetic acid, deionized, and distilled several times with methanol. The polyalcohol (158 mg) was recovered by freeze-drying.

A sample of the polyalcohol (16 mg) was hydrolyzed in *N* sulphuric acid (2 ml) at 100° C for 7 hours. The solution was deionized, concentrated, and examined by paper chromatography in solvent system (D). The silver nitrate – sodium hydroxide reagent showed the presence of glycerol, erythritol, and a trace of glucose.

REFERENCES

1. B. Bernier. Can. J. Microbiol. **4**, 195 (1958).
2. H. Bender, J. Lehmann, and K. Wallenfels. Biochim. Biophys. Acta, **36**, 309 (1959).
3. K. Wallenfels, H. Bender, G. Keilich, and G. Bechtler. Angew. Chem. **73**, 245 (1961).
4. H. O. Bouveng, H. Kiessling, B. Lindberg, and J. McKay. Acta Chem. Scand. **16**, 615 (1962).
5. S. A. Barker, E. J. Bourne, M. Stacey, and D. H. Whiffen. J. Chem. Soc. 171 (1954).
6. A. Thompson, M. L. Wolfrom, and E. J. Quinn. J. Am. Chem. Soc. **75**, 3003 (1953).
7. M. L. Wolfrom and A. Thompson. J. Am. Chem. Soc. **79**, 4212 (1957).
8. A. B. Foster. Advan. Carbohydrate Chem. **12**, 81 (1957).
9. L. Hough, J. K. N. Jones, and W. H. Wadman. J. Chem. Soc. 1702 (1950).
10. W. E. Trevelyan, D. P. Procter, and J. S. Harrison. Nature, **166**, 444 (1950).
11. J. S. D. Bacon and J. Edelman. Biochem. J. **48**, 114 (1951).
12. S. W. Gunner, J. K. N. Jones, and M. B. Perry. Can. J. Chem. **39**, 1892 (1961).
13. M. L. Wolfrom and A. Thompson. J. Am. Chem. Soc. **78**, 4182 (1956).
14. A. Sato, Y. Ito, and H. Ono. Chem. Ind. (London), 301 (1962).
15. A. Jeanes, C. A. Wilham, R. W. Jones, H. M. Tsuchiya, and C. E. Rist. J. Am. Chem. Soc. **75**, 5911 (1953).
16. S. A. Barker, E. J. Bourne, A. E. James, W. B. Neely, and M. Stacey. J. Chem. Soc. 2096 (1955).
17. K. Myrbäck and E. Willstaedt. Arkiv Kemi, **6**, 417 (1953).
18. L. D. Ough. Anal. Chem. **34**, 660 (1962).
19. M. E. Tate and C. T. Bishop. Can. J. Chem. **40**, 1043 (1962).
20. S. Peat, W. J. Whelan, and J. G. Roberts. J. Chem. Soc. 2258 (1956).
21. E. J. Bourne, D. H. Hutson, H. Weigel. Chem. Ind. (London), 1047 (1959); J. Chem. Soc. 4252 (1960).
22. G. Neumuller and E. Vasseur. Arkiv Kemi, **5**, 235 (1953).

Can. J. Chem. Downloaded from www.nrcresearchpress.com by 210.87.254.5 on 09/05/12
For personal use only.

STERIC EFFECTS IN AROMATIC CARBONYL COMPOUNDS

I. BASICITIES AND ULTRAVIOLET SPECTRA

KEITH YATES AND BRIAN F. SCOTT
Department of Chemistry, University of Toronto, Toronto, Ontario

Received April 1, 1963

ABSTRACT

The basicities of eight *o*-methyl and *o*-dimethyl carbonyl compounds have been determined by spectrophotometric methods in aqueous sulphuric acid. The basicities of a further 19 compounds of the same class have been recalculated from literature data using a recently determined H_0 scale of acidity. The effects of ortho substitution on the base strength have been found to increase with the steric requirements of the group attached to the carbonyl carbon.

The ultraviolet intensities of 18 of the above compounds have either been freshly determined or carefully redetermined. The mean interplanar angle θ between carbonyl and phenyl groups has been obtained for both base and conjugate acid forms using the relationship $\epsilon/\epsilon_{planar} \simeq \cos^2\theta$.

For the conjugate acids of the *o*-methyl derivatives a linear relation exists between $\epsilon/\epsilon_{planar}$ and the steric effect on basicity. This is discussed in terms of inhibition of resonance in the cations. No similar relation exists for the *o*-dimethyl derivatives. Steric effects on basicity in the latter are discussed in terms of steric inhibition of solvation of the cations.

INTRODUCTION

The failure of the Hammett equation to correlate the reactivities of ortho-substituted aromatic compounds is well known, and is due to steric interactions between reacting group and ortho substituent (1). The ionization of aromatic carbonyl compounds in strong acids illustrates this. Although the basicities of meta- and para-substituted compounds of this class (where X = H, CH_3, OH, NH_2) have been shown (2–5) to obey

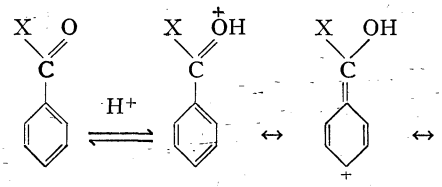

I II

linear free-energy relationships of the Hammett type, the *basicities* of ortho-substituted benzoic acids, for example, do not (6). Although modified forms of the Hammett equation (7) have been used with success for some of the reactions of ortho-substituted benzene derivatives, this particular class of ionization is not amenable to this type of treatment (6), due to the greater possibilities for resonance stabilization in II than in I. This is presumably even more true for diortho-substituted bases. The bulk of the *o*-methyl groups forces the protonated carbonyl group out of the plane of the aromatic ring and hence raises the energy of the cation with respect to the neutral molecule, in which resonance effects are of much less importance.

In addition to this steric inhibition of resonance by ortho groups, there are to be considered steric inhibition of solvation (which will also be more important in the cation than in the neutral molecule), the electronic effect of the substituents, and the possibility of specific interactions such as hydrogen bonding.

We have attempted to study only the first two of the above effects on the ionization of this type of base. For this purpose we have investigated the base strengths and ultraviolet spectra of a series of *o*-methyl- and *o*-dimethyl-substituted benzaldehydes, benzoic acids, acetophenones, benzamides, and benzophenones. For the basicity determinations we have used modified forms of the general Hammett technique in aqueous sulphuric acid (3), using recently determined H_0 values based on a uniform set of indicators (8), and have recalculated previous data (2, 3, 4, 9) where necessary. *o*-Methyl substituents were chosen since their interactions approximate closely to bulk steric effects. Specific interactions should be small for these groups, and their electronic effects can reasonably be assessed from the effects of *p*-methyl substituents.

We have also estimated the steric inhibition of coplanarity (and hence of π-orbital overlap) between the carbonyl group and phenyl ring from ultraviolet spectral data. This approach has also been used by Wepster to estimate inhibition of resonance in *p*-nitroaniline type bases (10).

EXPERIMENTAL

Reagents

Commercially available benzaldehydes were purified by vacuum distillation using a small positive pressure of nitrogen. Commercially available acetophenones, benzoic acids, and benzamides were purified by recrystallization or vacuum distillation. Diazotization of 2,6-dimethylaniline, followed by the standard Sandmeyer procedure with cuprous cyanide, gave the nitrile, which was then hydrolyzed in hot 85% H_2SO_4 to give 2,6-dimethylbenzamide. M.p. 139–139.5° C, lit. m.p. 139° C (11). Several attempts to hydrolyze this amide further failed to give 2,6-dimethylbenzoic acid. 2-Methylbenzophenone was prepared from *o*-toluyl chloride and benzene by the standard Friedel–Crafts method. B.p. 89° C at 0.6 mm, lit. b.p. 168° C at 12 mm (12). Calc. for $C_{14}H_{12}O$: C, 85.6; H, 6.12. Found: C, 84.9; H, 6.20.

Sulphuric acid solutions ranging from 0.001 *N* to 98% by weight were prepared from Fisher C.P. Reagent grade sulphuric acid (95% min.) and Fisher Reagent Fuming (30%) sulphuric acid. Concentrations were determined by titrating weighed samples with standard base. The H_0 values of these acids were obtained by interpolation from a composite curve constructed using the values given by Paul and Long (13) for the range 0–60% acid, and the values recently determined by Jorgenson and Hartter (8) for the range 60–98% acid.

Measurement of Ultraviolet Spectra

All spectra were measured on a Bausch and Lomb Spectronic 505 Recording Spectrophotometer, using 1-cm quartz cells and a thermostatically controlled cell-block at 25±0.05° C. Solutions of the bases in the various sulphuric acids were prepared essentially as described previously (3) using a Hamilton syringe and Chaney adaptor to measure out stock solutions of organic compounds. All spectra in strongly acid solutions were repeated with time to check for possible decomposition. In the case of 2,4,6-trimethylacetophenone it was necessary to record spectra as rapidly as possible after mixing (about 2 minutes) and repeat the measurements at intervals. Spectra were then obtained by extrapolation back to zero time. In all other cases, spectra were measured as rapidly as possible after mixing with acid.

Determination of pK_{BH^+} Values

These were obtained by the spectrophotometric method essentially as described previously (3). In cases of low solubility of the organic compound in the more dilute sulphuric acids, a modification similar to that described by Stewart and Granger (6) was used. To test for possible acylium ion formation, solutions of 2,6-dimethyl- and 2,4,6-trimethyl-benzamide in 95% acid were poured into ice water several minutes after mixing. The original amides were recovered almost quantitatively from these solutions, showing that these compounds ionize in the region studied by simple proton addition, as do the other carbonyl bases.

Calculation of pK_{BH^+}

The basicity constants of all compounds except the benzamides were obtained from the spectral data by the "linear" modification of the method of Davis and Geissman (14) previously described by Stewart and Granger (6). If the bases are behaving as typical Hammett indicators, plots of $\log\{(D_{BH^+}-D)/(D-D_B)\}$ (Stewart's notation (6)) against H_0 should be linear with unit slope and intercepts equal to pK_{BH^+}. Since in all cases good linear plots were obtained with slopes in the range 0.90–1.05 it was felt that Stewart's method of correcting for medium effects was adequate and that the ionizations of these compounds were following the H_0 function sufficiently closely for the purposes of the present investigation. (Also this method is considerably less laborious than the one applied to the benzamides.)

Can. J. Chem. Downloaded from www.nrcresearchpress.com by 210.87.254.5 on 09/05/12
For personal use only.

The treatment of the data for 2,4,6-trimethylacetophenone was somewhat different to the above. In addition to the fact that this compound decomposes fairly rapidly in sulphuric acid (15), the neutral base absorbs only weakly ($\epsilon_B < 2000$). Therefore the above "linear" method was applied to data obtained at one wavelength only, the wavelength of maximum absorption of the conjugate acid, 320 mμ. The function $\log\{(\epsilon_{BH^+} - \epsilon)/(\epsilon - \epsilon_B)\}$ was plotted against H_0, where ϵ_{BH^+} refers to the measured extinction in 95% acid, ϵ_B to the value in 46% acid, and ϵ to values obtained in intermediate acids. The spectrum in each of 16 different sulphuric acids was recorded and extrapolated as described. This was repeated on two fresh samples of ketone in each acid, and an average of three extrapolated values taken. Although the points on the log plot showed scattering, especially in the more concentrated acids where decomposition is rapid, a least mean squares treatment gave a correlation coefficient of 0.97, with a slope of 0.93 and intercept −7.4. It is felt that this pK_{BH^+} is as accurate as can reasonably be expected, and is more reliable than the earlier estimate of −8.4 (−7.9 on the old H_0 scale) made by Schubert and Latourette (15) on the basis of measurements in only three different sulphuric acid concentrations.

It has recently been shown that the H_0 function is not strictly applicable to the ionization of benzamides (16), but that these bases are probably following some related acidity function. A method was described for estimating pK_{BH^+} for these bases, using the modified equation

$$H_0 = pK_{BH^+} - n \log \frac{BH^+}{B},$$

where n is not unity as in the Hammett relation (13). This method has been used exclusively to obtain pK_{BH^+} for the benzamides. A typical fit of experimental data to a line calculated using the above equation with $n = 1.59$ and $pK_{BH^+} = -2.10$ is shown for mesitamide in Fig. 1. The corresponding change of extinction

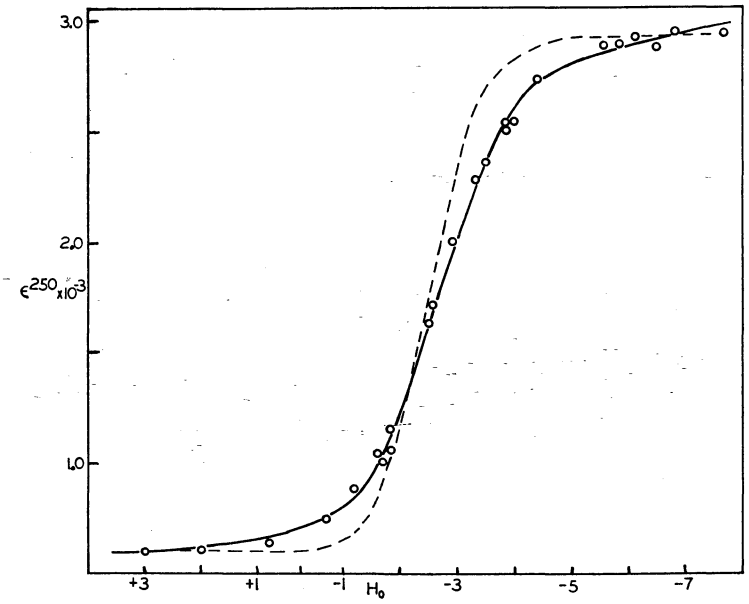

FIG. 1. Mesitamide: change in ϵ at 250 mμ with H_0. Circles are experimental points. Solid line calculated from $H_0 = pK_{BH^+} - 1.59 \log [BH^+]/[B]$ as in ref. 16. Broken line calculated for a Hammett base with pK_{BH^+} obtained as in ref. 6.

with acidity expected for a Hammett base ($n = 1$) is shown for comparison. It is felt that this method gives more accurate relative pK_{BH^+} values for the amides, although the absolute values may be subject to uncertainty because the bases do not follow H_0 precisely.

Recalculation of Previously Reported pK_{BH^+} Values

In order to compare the above pK_{BH^+} values with previously reported results it was necessary to convert the latter to the acidity scale used to define pK_{BH^+} in the present work. The reason for choosing the new values of H_0 obtained by Jorgenson and Hartter in the region 60–98% was that this scale was established with a uniform set of structurally similar indicators, using modern spectrophotometric techniques. Further it was shown by the above authors (8) that plots of $\log [BH]^+/[B]$ against percentage of H_2SO_4 were more closely parallel for successive indicators than those obtained with the original Hammett indicators (13, 17).

The procedure used to convert the old pK_{BH^+} values was simply to take the reported sulphuric acid

Can. J. Chem. Downloaded from www.nrcresearchpress.com by 210.87.254.5 on 09/05/12
For personal use only.

concentration corresponding to 50% ionization, based on the old scale (13), and read the corresponding value directly off a plot of the new H_0 values against concentration.

To test the validity of this procedure, the spectra of benzoic acid, whose ionization range approximately covers the region of divergence of the two scales, were freshly determined in 50–95% H_2SO_4. Treatment of this data using the new H_0 values resulted in a pK_{BH^+} of −7.60, compared with −7. 58 obtained by converting the reported value of −7.18 (6) by the interpolation method.

RESULTS AND DISCUSSION

Steric Effects on Base Strength

The experimental pK_{BH^+} values for the *o*-methyl- and *o*-dimethyl-substituted carbonyl bases are listed in Table I, together with data for the unsubstituted and *p*-methyl

TABLE I

Basicity constants and steric effects

Type	Substituent	$-pK^{exptl}_{BH^+}$	$-pK^{calc}_{BH^+}$	Steric effect $(pK^{exptl}_{BH^+}-pK^{calc}_{BH^+})$
Benzaldehydes	Hydrogen	7.47*		
X = H	*o*-Methyl	6.78*	6.56	0.18
	p-Methyl	6.56*		
	2,4,6-Trimethyl	5.00†	4.74	0.26
Benzoic acids	Hydrogen	7.60‡		
X = OH	*o*-Methyl	7.51*	7.27	0.24
	p-Methyl	7.27*		
	2,4,6-Trimethyl	7.25§	6.61	0.64
Acetophenones	Hydrogen	6.36*		
X = CH_3	*o*-Methyl	6.13*	5.57	0.56
	2,4,5-Trimethyl	5.11	4.62	0.49
	m-Methyl	6.20*		
	p-Methyl	5.57*		
	2,6-Dimethyl	8.32	4.88	3.54
	2,4,6-Trimethyl	7.4	3.99	3.4
Benzamides	Hydrogen	2.15		
X = NH_2	*o*-Methyl	2.24	1.81	0.43
	p-Methyl	1.81		
	2,6-Dimethyl	2.42	1.25	1.17
	2,4,6-Trimethyl	2.10	0.80	1.30
Benzophenones	Hydrogen	6.41‖		
X = C_6H_5	*o*-Methyl	6.72	6.09	0.63
	p-Methyl	6.09‖		
	p-*t*-Butyl	6.86‖		
	2,6-Dimethyl	6.36‖	5.77	1.09
	2,4,6-Trimethyl	6.59‖	5.45	0.91
	2,6-Dimethyl-4-*t*-butyl	6.21‖	5.57	1.02

*Taken from refs. 2, 3, 4 and corrected to new H_0 scale in ref. 8.
†Redetermined by present method. A previously reported value for this compound is −4.7 (26), giving a corrected value of −4.8.
‡The value determined in the present work agrees with corrected value from ref. 6 within the experimental error.
§Taken from ref. 25 and corrected to H_0 scale in ref. 8.
‖Taken from ref. 9 and corrected to H_0 scale in ref. 8.

derivatives ($pK_{BH^+} = H_0 + \log [BH^+]/[B]$). The calculated pK_{BH^+} values listed for those bases with methyl groups in ortho positions are values to be expected for these compounds in the absence of steric effects. These have been obtained by assuming that the total electronic effect of a methyl group in the ortho position is the same as that in the para position, and that substituent effects are additive (18).

The difference $(pK^{exptl}_{BH^+}-pK^{calc}_{BH^+})$ has then been taken as a measure of the steric effect on the basicity. It can be seen that in every case the steric effect of one ortho group is positive, i.e. base weakening, and increases with the size of the group X in the order $H < OH < NH_2 < CH_3 < C_6H_5$, qualitatively as expected. In order to compare these

Can. J. Chem. Downloaded from www.nrcresearchpress.com by 210.87.254.5 on 09/05/12
For personal use only.

effects on a more quantitative basis, allowance should be made for the fact that the ionization behavior of each type of base has a different sensitivity to total electronic effects. This will be discussed later. In two cases, the *o*-methyl derivative is actually weaker than the unsubstituted base, despite the base-strengthening electronic effect of a methyl group. These effects on basicity arise in part from steric inhibition of coplanarity between the carbonyl group and ring, the resulting loss of resonance stabilization energy being more serious in the conjugate acid than in the free base. Two possible preferred planar conformations can be written for these conjugate acids:

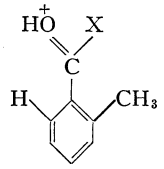

III

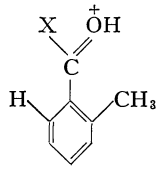

IV

Contributing structures showing charge delocalization have been omitted since the possibilities for π-orbital overlap are somewhat different in each type of base. Structure III is presumably the preferred conformation only in the case of *o*-tolualdehyde (X = H), where the steric interactions are between ortho methyl and aldehyde hydrogen, and between ortho hydrogen and the hydroxyl group. Since neither of these should be large it is not surprising that the magnitude of the steric effect is not much greater than the experimental uncertainty in pK_{BH^+}. In all other cases, structure IV will be preferred. In this case the *o*-methyl–hydroxyl repulsion will be common to all four bases, *differences* in steric effects arising mainly from the repulsion of X by the ortho hydrogen. The effect of the first of these repulsions can be estimated roughly from the steric effect for *o*-toluic acid, where the protonated carboxyl group is symmetrical, and hence III and IV are

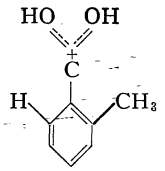

equivalent. The total steric effects in *o*-methylacetophenone, 2,4,5-trimethylacetophenone, and *o*-toluamide are larger, as would be expected. The reason the decrease in basicity is not much larger than these in *o*-methylbenzophenone, where X is a bulky phenyl group, is due to the fact that at least one of the aromatic rings can easily adopt a coplanar arrangement with the protonated carbonyl group, and thus provide resonance stabilization of the cation. There is evidence that the predominant effect of single ortho groups in carbonyl type bases is steric inhibition of resonance in the conjugate acid (6). It will be noted that these effects are not large, ranging from 0.18–0.63 pK units.

If we consider now the steric effects of two *o*-methyl groups, then all five types of base have the same "planar" conformation as given below. Therefore differences in steric

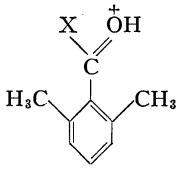

Can. J. Chem. Downloaded from www.nrcresearchpress.com by 210.87.254.5 on 09/05/12
For personal use only.

effects are again largely determined by the interaction of the group X with an ortho substituent. Since the latter is now the more bulky methyl group, changes in base strength are more pronounced. This is shown by the data in Table I, the effects again being qualitatively in agreement with the size of X, except for X = C_6H_5, where the effect is not expected to be very large, for the reasons discussed earlier. The effects are not large where X = H or OH, but are particularly striking where X = CH_3 or NH_2. The base 2,4,6-trimethylacetophenone is several thousand times weaker than would be predicted if only the base-strengthening electronic effects of the three methyl groups were considered, and is actually weaker than acetophenone itself by a factor of 10. (This has been pointed out before (2) but the earlier quantitative estimate of the steric effect was based on a pK_{BH^+} value for 2,4,6-trimethylacetophenone which we believe to be less reliable than the present one.) Where X = NH_2, the steric effects are also large, resulting in basicities more than 10 times lower than expected on the basis of substituent electronic effects alone, two independent estimates of the effect agreeing to 0.13 unit. Although steric effects are apparently more pronounced in the ketones than the amides it must be remembered that the latter are less sensitive to the effects of overlap with the π-orbitals of the ring. This is due to the appreciable resonance stabilization within the protonated carboxamide group itself as shown by the very high basicity of amides compared to other types of carbonyl base (5). A study of molecular models shows that if all atoms in the carboxamide group are to be essentially coplanar in order to achieve this internal resonance stabilization, the coplanarity of phenyl and side chain is more difficult to achieve in the amide than in the ketone. In the latter, the ketone methyl group can be rotated to minimize repulsions with the *o*-methyl group whereas in the amides rotation about the C—N bond is appreciably restricted (19), resulting in a tendency to twist the whole group out of the plane of the benzene ring.

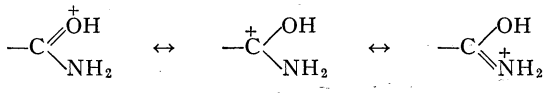

Ultraviolet Spectra and Interplanar Angles

The spectral data for the neutral and protonated forms of the carbonyl bases discussed above are listed in Table II. The values of λ_{max} and ϵ_{max} are mainly those determined in the present work, since it was felt that for purposes of calculation these would be more self-consistent than a collection of data from various sources, obtained by different experimental techniques and in non-standard sulphuric acid concentrations. (In the cases of two *o*-dimethyl derivatives, however, values of ϵ_B and ϵ_{BH^+} have been taken from the literature and used to calculate further data.) The values of λ_{max} for both B and BH^+ are in close agreement with literature values, where available, but the values of ϵ_B and ϵ_{BH^+} are in several cases appreciably different from previously reported values. The ϵ values reported herein are the mean values of up to six independent determinations, with a *maximum* deviation from the means of $\pm 2\%$.

The above extinction coefficient data were used to calculate mean interplanar angles between the carbonyl group and benzene ring in both the free bases and their conjugate acids. This was done using the approximate relation $\epsilon/\epsilon_{planar} \approx \cos^2\theta$ (20), where ϵ_{planar} is the extinction coefficient to be expected in a system which can easily adopt a uniplanar arrangement and θ is the mean angle of twist between the carbonyl group and aromatic ring in a sterically hindered compound having an extinction coefficient ϵ. This method has been described by Braude (20) and has been used with success both by Braude and

Can. J. Chem. Downloaded from www.nrcresearchpress.com by 210.87.254.5 on 09/05/12
For personal use only.

TABLE II

Ultraviolet absorption and mean interplanar angles

Compound	Neutral bases*				Conjugate acids†		
	λ_{max}	ϵ^{B}_{max}	f	θ_B, deg	λ_{max}	$\epsilon^{BH^+}_{max}$	θ_{BH^+}, deg
Benzaldehyde	251	12,100		0	295	23,100	0
p-Methyl	264	12,000	0.254	0	313	20,000	0
o-Methyl	260	11,700	0.252	9	303	19,300	10
2,4,6-Trimethyl	273	12,900		0	324	30,200	0
Benzoic acid	233	9,800		0	261	15,500	0
p-Methyl	243	13,600	0.287	0	277	19,100	0
o-Methyl	234	7,900	0.181	41	265	15,100	27
2,4,6-Trimethyl‡	240	3,200		65	282	20,000§	
Acetophenone	251	11,500		0	290	21,400	0
m-Methyl‖	252	7,600		0	300	15,100	0
p-Methyl	260	14,900	0.283	0	312	23,800	0
o-Methyl	249	8,500	0.187	41	297	17,400	31
2,4,5-Trimethyl	252	6,100		49	317	14,100	33
2,6-Dimethyl¶					310	7,200	58
2,4,6-Trimethyl	260	1,700		74	322	12,300	49
Benzamide					253	11,500	0
p-Methyl					259	14,500	0
o-Methyl**					243	6,100	50
2,6-Dimethyl**					240	2,100	70
2,4,6-Trimethyl**					247	2,800	68

*Spectra of base forms measured in 46–47% H_2SO_4.
†Spectra of conjugate acids measured in 95–96% H_2SO_4, except amides which are fully protonated in 59% H_2SO_4.
‡Data for this compound taken from ref. 25.
§Absorption spectrum partly due to presence of acylium ion.
‖Data for this compound taken from ref. 3.
¶Data for this compound taken from ref. 15.
**These amides have no clearly defined absorption maxima in the base form.

co-workers (21), who obtained results in good agreement with angles of twist calculated from dipole moment measurements, and by Wepster (10), who investigated steric effects in aniline type bases. We have taken ϵ for the *p*-methyl isomers to be ϵ_{planar} and thus calculated θ values for the *o*-methyl isomers. This is reasonable since the cross-sectional areas of the two molecules are the same and the electronic effects of *o*- and *p*-methyl groups are approximately equal. The angles θ_B and θ_{BH^+} for the two forms of each base are also listed in Table II. Strictly speaking, the oscillator strength f, and not ϵ, should be used to estimate angle of twist (10) but difficulties arise in estimating f for these compounds since the type of electronic transition studied, $\pi \rightarrow \pi^*$, is overlapped to some extent by the weaker $n \rightarrow \pi^*$ band, and in some cases by the more intense bands occurring in the 200 mμ region. This is not too serious in the more dilute acid solutions and an approximate separation of the three bands can be achieved. This was done for the spectra in 46% H_2SO_4 and oscillator strengths obtained from the relation $f = 4.32 \times 10^9 \int \epsilon d\nu$. These are given in Table II. The six values which could be obtained are linearly related to the corresponding ϵ values; therefore ϵ values, which are easier to obtain, were used throughout to calculate angles of twist.

Turning to the spectra of the 2,6-dimethyl and 2,4,6-trimethyl derivatives, values of θ can only be calculated if the assumption is made that each ortho or para substituent causes an equal increment in ϵ for the parent compound. In this way ϵ_{planar} can be estimated from ϵ values for the unsubstituted and para-substituted derivatives. That this assumption is not strictly valid is shown by the fact that ϵ_{planar} calculated for 2,4,6-trimethylbenzaldehyde is actually *lower* than the observed ϵ value in any given solution.

Can. J. Chem. Downloaded from www.nrcresearchpress.com by 210.87.254.5 on 09/05/12
For personal use only.

In this case θ was assumed to be effectively zero. This is supported by the results of dipole moment studies (20). In view of these considerations, the estimates of $\epsilon/\epsilon_{planar}$ and hence θ for the *o*-dimethyl-substituted compounds are somewhat less quantitative than those for the *o*-methyl compounds, where the assumptions involved are more reasonable.

It can be seen from Table II that the calculated mean interplanar angle between carbonyl and aromatic ring increases with size of the group X attached to the carbonyl carbon, and also with the number of *o*-methyl groups, as would be expected. This is true of both the B and BH^+ forms, although in general the conjugate acids have lower values of θ than their corresponding bases, presumably due to the extra stabilization to be gained from delocalization of charge into the ring.

A study of molecular models and projection diagrams shows that Braude's explanation of the decrease in θ in terms of reduced possibilities for coplanarity is a reasonable one (20). In the case of 2,4,6-trimethylacetophenone, for example, a molecular model shows that coplanarity must be very difficult to achieve, resulting in a very low population of uniplanar molecules. This is reflected in the ϵ value of 1700, which is extremely low for the allowed benzoyl $\pi \rightarrow \pi^*$ transition which normally has $\epsilon > 10^4$.

Relationship of Base Strength and Ultraviolet Intensities

If the major effect of ortho substitution on base strength is steric inhibition of resonance between the protonated carbonyl group and benzene ring, as suggested by Stewart and Granger (6), there should be a correlation between ΔpK_{BH^+} ($= pK^{calc}_{BH^+} - pK^{exptl}_{BH^+}$) and ϵ_{BH^+}. Such a correlation has been found by Wepster (10) between the basicities and ultraviolet intensities of *p*-nitroanilines. This was attributed to steric inhibition of resonance of the nitro group with the ring.

In the present case, where different classes of carbonyl base are being considered, each series has a different sensitivity to overall electronic effects, as measured by the Hammett ρ value. Therefore in order to compare the magnitudes of steric effects on a more nearly equal basis, the ΔpK_{BH^+} values should be divided by ρ. The pK_{BH^+} values for benzaldehydes (2), acetophenones (3), and benzoic acids (4) have previously been found to obey the modified Hammett equation $\log (K_{BH^+}/K^0_{BH^+}) = \rho\sigma^+$ (22) with a high degree of precision. Thus ρ values based on σ^+ rather than σ have been recalculated in accordance with the H_0 scale used in the present paper and are given in Table III. The pK_{BH^+} values

TABLE III

Hammett rho values for the ionizations of carbonyl bases

Class	r	n	ρ	Ref.
Benzaldehydes	0.995	7	2.30	2
Benzoic acids	0.979	17	1.20	4
Acetophenones	0.981	15	2.41	3
Benzamides		9	0.91	16
Benzophenones		4	~2	9

of the benzamides have previously been reported to follow σ more closely than σ^+, and this was proposed as evidence for N-protonation of the carboxamide group (5). However, it now seems certain that amides protonate on oxygen (23), and in fact more recent determinations of pK_{BH^+} for substituted benzamides (16) show that pK_{BH^+} correlates reasonably well with σ^+ ($r = 0.914$) as compared to σ ($r = 0.911$). While it is now generally recognized that the σ^+ scale of substituent effects is not necessarily applicable to all systems in which a positively charged group is conjugated with a benzene ring, all compounds

Can. J. Chem. Downloaded from www.nrcresearchpress.com by 210.87.254.5 on 09/05/12
For personal use only.

studied in the present work do protonate predominantly on oxygen and hence direct conjugation with the ring is possible in each case. For this reason ρ for the benzamides has been estimated from a plot of pK_{BH^+} versus pK_{BH^+} for the acetophenones. Thus all ρ values in Table III are essentially values relative to ρ for the acetophenones, and are based on the same solvent system and the same experimental approach. In this way the steric effects as measured by $\Delta pK_{BH^+}/\rho$ should be accurate relative to each other, even if their absolute values are subject to some uncertainty.

The plot of $\Delta pK_{BH^+}/\rho$ for the *o*-methyl-substituted derivatives against $\epsilon/\epsilon_{planar}$ for the corresponding conjugate acids in Fig. 2 shows a good linear relationship. Since $\epsilon/\epsilon_{planar}$

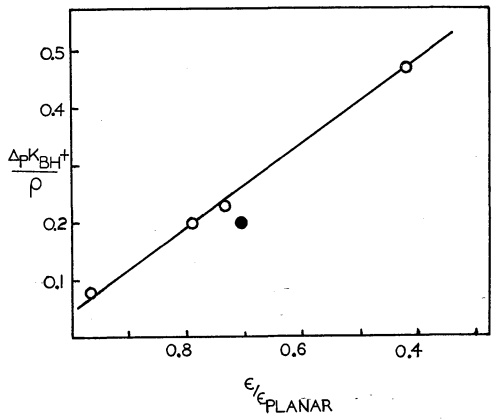

FIG. 2. Relation between steric effect on base strength and on ultraviolet intensity. Open circles, 2-methyl derivatives. Solid circle, 2,4,5-trimethylacetophenone.

$\approx \cos^2\theta$, and the overlap between the two π-electron systems is reduced by an amount proportional to $\cos^2\theta$ (24), this linear relationship is evidence that steric inhibition of resonance in the conjugate acid is the predominant steric effect when one *o*-methyl group is present, and supports the conclusion reached earlier by Stewart and Granger (6).

However, no such simple relationship exists for the *o*-dimethyl-substituted compounds. All the $\Delta pK_{BH^+}/\rho$ values in Table IV are greater than would be predicted by the simple

TABLE IV

Steric effects on base strength and ultraviolet intensity

	Benz-aldehydes	Benzoic acids	Aceto-phenones	Benz-amides
o-Methyl derivatives				
$\Delta pK_{BH^+}/\rho$	0.08	0.20	0.23	0.47
			0.20 (2,4,5-)	
$\epsilon/\epsilon_{planar}$	0.965	0.790	0.731	0.420
			0.703 (2,4,5-)	
o-Dimethyl derivatives				
$\Delta pK_{BH^+}/\rho$	0.11	0.53	1.47 (2,6-)	1.29 (2,6-)
			1.41 (2,4,6-)	1.43 (2,4,6-)
Estimated value*	0.04	0.27	0.57	0.70
			0.47	0.68
$\epsilon/\epsilon_{planar}$	ca. 1	0.689†	0.277	0.120
			0.421	0.137

*From $\epsilon/\epsilon_{planar}$ and relationship in Fig. 2.
†Spectrum complicated due to acylium ion formation.

Can. J. Chem. Downloaded from www.nrcresearchpress.com by 210.87.254.5 on 09/05/12
For personal use only.

relationship shown in Fig. 2; therefore some other base-weakening steric effect must be operating in addition to steric inhibition of resonance. The magnitude of this effect is small in the case of 2,4,6-trimethylbenzyldehyde and mesitoic acid, although in the latter case the interpretation of $\epsilon/\epsilon_{planar}$ in terms of interplanar angles is complicated by appreciable mesitoylium ion formation (25). In the 2,6- and 2,4,6-substituted acetophenones and benzamides, however, the effect is much larger. If the line in Fig. 2 is extrapolated and used to estimate steric effects based on $\epsilon/\epsilon_{planar}$ for these compounds, the values obtained are much smaller than those observed, as shown in Table IV. This additional steric effect can reasonably be explained by steric inhibition of solvation of the conjugate acid forms in the following way. With only one *o*-methyl substituent present, the carbonyl group is twisted out of plane by about 30° or less, so that some charge delocalization by resonance is still possible. Thus the effective size of the cation is large and one *o*-methyl group cannot effectively hinder the approach of solvent molecules. In this case steric inhibition of resonance is the predominant base-weakening effect. Where two *o*-methyl substituents are present, the angle of twist is larger, especially where the group X is CH_3 or NH_2 (θ = 50–60° in the ketones and 70° in the amides). Thus overlap and resultant charge delocalization into the ring are drastically reduced, and the effective size of the cation is smaller. Therefore solvent stabilization is more important. In addition there are now two *o*-methyl groups to block the approach of solvent molecules. This is illustrated by the projection diagram for 2,6-dimethylacetophenone where the positive charge is shown residing effectively on the carbonyl group. Thus for large angles of twist there is a cumula-

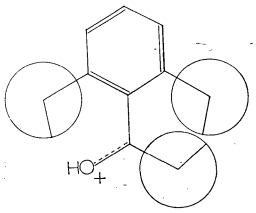

tive effect. As steric inhibition of resonance is increased, steric inhibition of solvation becomes more serious as the charge is more localized, and is comparable to if not greater in magnitude than inhibition of resonance where the group attached to the carbonyl is NH_2 or CH_3. It can be estimated roughly that this additional loss of stabilization amounts to about 3 kcal in the ketone, and 1 kcal in the amide, conjugate acids. The reason this is smaller in the amides is presumably due to the fact that appreciable charge delocalization within the protonated carboxamide group results in a larger effective cation size, in which solvation effects are of less importance and which is also more difficult for the methyl groups to block.

The benzophenones have not been included in the above discussion. In similarly substituted ArCOX molecules where the group X is also phenyl, the values of ϵ cannot be as simply interpreted in terms of angle of twist since the unsubstituted phenyl ring X can easily assume coplanarity with the carbonyl group, resulting in a high absorption intensity.

ACKNOWLEDGMENT

The financial support of the National Research Council is gratefully acknowledged.

REFERENCES

1. L. P. HAMMETT. Physical organic chemistry. McGraw-Hill Book Co., New York. 1940. Chap. 7.
2. K. YATES and R. STEWART. Can. J. Chem. **37**, 664 (1959).
3. R. STEWART and K. YATES. J. Am. Chem. Soc. **80**, 6355 (1958).

Can. J. Chem. Downloaded from www.nrcresearchpress.com by 210.87.254.5 on 09/05/12
For personal use only.

4. R. STEWART and K. YATES. J. Am. Chem. Soc. **82**, 4059 (1960).
5. J. T. EDWARD, H. S. CHANG, K. YATES, and R. STEWART. Can. J. Chem. **38**, 1518 (1960).
6. R. STEWART and M. R. GRANGER. Can. J. Chem. **39**, 2508 (1961).
7. R. W. TAFT, JR. *In* Steric effects in organic chemistry. *Edited by* M. J. Newman. John Wiley and Sons Inc., New York. 1956. Chap. 13. A. C. FARTHING and B. NAM. *In* Steric effects in conjugated systems. *Edited by* G. W. Gray. Butterworths, London. 1958. Chap. 11.
8. M. J. JORGENSON and D. R. HARTTER. J. Am. Chem. Soc. **85**, 878 (1963).
9. A. FISCHER, B. A. GRIGOR, J. PACKER, and J. VAUGHAN. J. Am. Chem. Soc. **83**, 4208 (1961).
10. B. M. WEPSTER. Rec. Trav. Chim. **76**, 335 (1957). B. M. WEPSTER. *In* Steric effects in conjugated systems. *Edited by* G. W. Gray. Butterworths, London. 1958. Chap. 3.
11. G. BERGER and S. C. J. OLIVIER. Rec. Trav. Chim. **46**, 600 (1927).
12. A. W. SMITH. Ber. **24**, 4047 (1891).
13. M. A. PAUL and F. A. LONG. Chem. Rev. **57**, 1 (1957).
14. C. T. DAVIS and T. A. GEISSMAN. J. Am. Chem. Soc. **76**, 3507 (1954).
15. W. M. SCHUBERT and H. K. LATOURETTE. J. Am. Chem. Soc. **74**, 1829 (1952).
16. A. R. KATRITZKY, A. J. WARING, and K. YATES. Tetrahedron, **19**, 465 (1963).
17. L. P. HAMMETT and A. J. DEYRUP. J. Am. Chem. Soc. **54**, 2721 (1932).
18. H. H. JAFFE. Chem. Rev. **53**, 191 (1953).
19. J. D. ROBERTS. Nuclear magnetic resonance. McGraw-Hill Book Co., New York. 1959. p. 70.
20. E. A. BRAUDE. *In* Determination of organic structure by physical methods. *Edited by* E. A. Braude and F. C. Nachod. Academic Press, New York. 1955. Chap. 4.
21. E. A. BRAUDE and F. SONDHEIMER. J. Chem. Soc. 3754 (1955).
22. H. C. BROWN and Y. OKAMOTO. J. Am. Chem. Soc. **79**, 1913 (1957). N. C. DENO and W. L. EVANS. J. Am. Chem. Soc. **79**, 5804 (1957).
23. G. FRAENKEL and C. NIEMANN. Proc. Natl. Acad. Sci. U.S. **44**, 688 (1958). A. BERGER, A. LOEWENSTEIN, and S. MEIBOOM. J. Am. Chem. Soc. **81**, 62 (1959). A. R. KATRITZKY and R. A. Y. JONES. Chem. Ind. (London), 722 (1961). R. J. GILLESPIE and T. BIRCHALL. Can. J. Chem. **41**, 148 (1963).
24. C. A. COULSON. Conference on quantum mechanical methods in valence theory. U.S. Government Printing Office. 1951. p. 47.
25. H. HOSOYA and S. NAGAKURA. Spectrochim. Acta, **17**, 324 (1961).
26. W. M. SCHUBERT and R. E. ZAHLER. J. Am. Chem. Soc. **76**, 1 (1954).

Can. J. Chem. Downloaded from www.nrcresearchpress.com by 210.87.254.5 on 09/05/12
For personal use only.

CYCLOHEXANE COMPOUNDS

IV. NUCLEAR MAGNETIC RESONANCE SPECTRA OF SOME DERIVATIVES OF THE STEREOISOMERIC 3-AMINO-1,2-CYCLOHEXANEDIOLS[1]

F. A. L. ANET
Department of Chemistry, University of Ottawa, Ottawa, Ontario
AND
R. A. B. BANNARD
Defence Research Chemical Laboratories, Ottawa, Ontario
AND
L. D. HALL
Department of Chemistry, University of Ottawa, Ottawa, Ontario

Received April 29, 1963

ABSTRACT

The n.m.r. spectra of 1α-methoxy-2β-hydroxy-3α-aminocyclohexane, 1α-methoxy-2α-hydroxy-3β-aminocyclohexane, their N-acetyl and O,N-diacetyl derivatives, ethoxy analogues, and 3α-amino-1α,2β-cyclohexanediol and 3β-amino-1α,2α-cyclohexanediol triacetates were measured in chloroform solution. From the chemical shifts of the O- and/or N-acetyl methyl protons it was possible to assign conformations to all the substituted derivatives and in most cases the assignments thus made were confirmed by first-order analysis of the multiplet pattern from the methine protons. In all cases, the conformations found were those predicted on simple conformational grounds and no evidence for a conformational equilibrium at room temperature was obtained from the coupling constants. In general, the coupling constants for the methine protons followed the pattern predicted by the Karplus equation. Acetylation of the 1α-alkoxy-2α-hydroxy-3β-aminocyclohexanes with acetic anhydride gave both the O,N-diacetyl derivative and the O,N,N-triacetyl derivative.

In an earlier paper (1) a chemical proof of structure for the 3-amino-1,2-cyclohexanediols I and II was given, from which the structures of the corresponding 1-alkoxy-2-hydroxy-3-aminocyclohexanes III and IV (R = CH_3 or C_2H_5) and 1-alkoxy-2,3-epoxy-

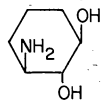

I

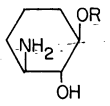

III

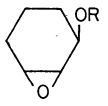

V

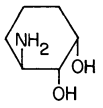

II

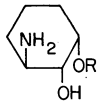

IV

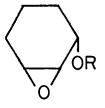

VI

cyclohexanes V and VI (R = CH_3 or C_2H_5) used as intermediates in their synthesis were deduced. Although the stereochemical configurations of compounds I–IV were thus established, their conformations were not, and it was of interest to verify that the conformations were in fact those predicted on the basis of simple conformational principles (2, 3); i.e.

[1]*Issued as D.R.C.L. Report No. 415.*

Can. J. Chem. Downloaded from www.nrcresearchpress.com by 210.87.254.40 on 09/05/12
For personal use only.

e,e,e for I and III and a,e,e, for II and IV (cf. ref. 9). The usefulness of n.m.r. spectroscopy for elucidation of the configuration and conformation of cyclohexane compounds was first demonstrated by Lemieux, Kullnig, and Moir (4) using the 1,3-dimethoxy-2-acetoxycyclohexanes which were obtained from the oxides V and VI (R = CH_3) by methanolysis followed by acetylation. The method was subsequently extended by Lemieux and coworkers (5) to the determination of the structures of other compounds containing six-membered rings, notably penta- and hexa-pyranose carbohydrate derivatives, and has gained widespread use in recent years for the solution of such structural problems (6–9). Recently, Richardson and McLaughlan (9) assigned structures to some 3-amino-3,6-dideoxyhexapyranose derivatives on the basis of their n.m.r. spectra, and observed chemical shifts for the protons of acetoxyl, acetamido, and methoxyl groups which were apparently characteristic of their conformations. It therefore seemed of interest to examine the n.m.r. spectra of similar derivatives of compounds I to IV to demonstrate whether the chemical shifts referred to above apply to the cyclohexane series with equal facility. The structures of the compounds examined in this connection are given in Chart I.

CHART I

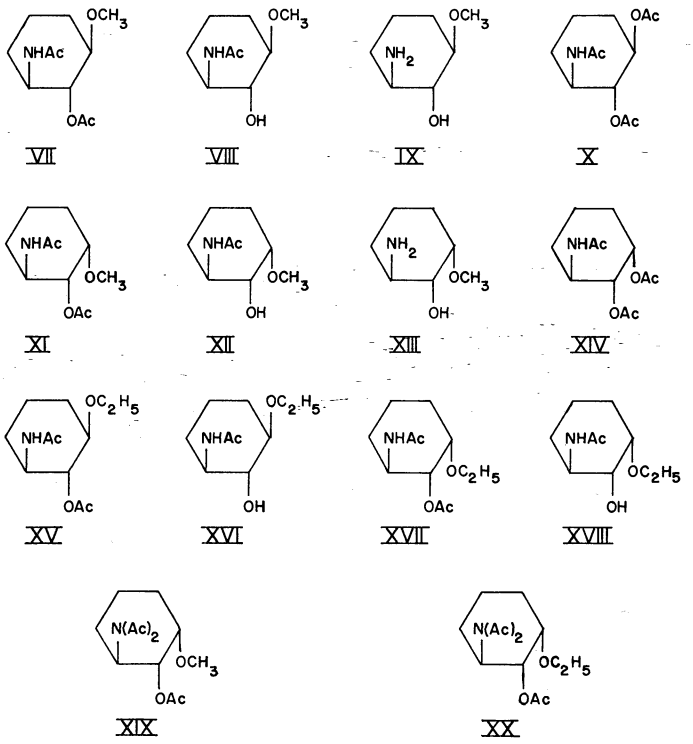

Interpretation of the spectra was generally straightforward and was facilitated, in cases in which the compounds contained unsubstituted hydroxyl or amino hydrogens, by equilibration with deuterium oxide. Since the unsubstituted aminoalcohols are basic, a single sharp peak was observed for the NH_2/OH protons. In no case was it possible to analyze the complex pattern due to the methylene ring hydrogens, but the downfield shift of the methine ring hydrogens caused by the adjacent substituents made it possible for the signals

Can. J. Chem. Downloaded from www.nrcresearchpress.com by 210.87.254.40 on 09/05/12
For personal use only.

Can. J. Chem. Downloaded from www.nrcresearchpress.com by 210.87.254.40 on 09/05/12
For personal use only.

TABLE I

Chemical shifts (τ-values)

Compound	$OMe_{(1)}$	$OAc_{(1)}$	$OAc_{(2)}$	$NAc_{(3)}$	H_1	H_2	H_3	NHAc†	$NH_2 + OH$†	OH†	$(CH_2)_3$
VII	6.62	—	7.93	8.09	6.79	5.30	6.05	3.91	—	—	7.87–8.97
VIII	6.59	—	—	8.01	6.8*	6.8*	6.29	3.35	—	6.29	8.04–9.22
IX	6.59	—	—	—	7.07 ⟷		7.66	—	7.45	—	7.66–9.05
X	—	7.98	7.95	8.07	5.14	5.14	5.98	3.98	—	—	8.29–8.83
XI	6.63	—	7.90	8.08	6.39	5.29	5.61	4.20	—	—	7.86–9.24
XII	6.64	—	—	8.02	6.38	6.6*	5.99	3.87	—	6.80	8.29–9.46
XIII	6.66	—	—	—	6.38	6.82	7.15	—	7.92	—	8.13–9.28
XIV	—	7.90	7.97	8.04	4.60	5.18	5.67	4.28	—	—	8.03–8.79
XV	6.37; 8.84§	—	7.92	8.08	6.64	5.26	5.99	3.91	—	—	7.87–8.77
XVI	6.34; 8.79§	—	—	8.00	6.8*	6.8*	6.30	3.50	—	6.49	7.82–9.04
XVII	6.41; 8.81§	—	7.90	8.07	6.25	5.23	5.65	4.11	—	—	7.58–8.97
XVIII	6.47; 8.83§	—	—	8.02	6.33	6.3*	6.07	3.83	—	7.07	7.85–9.05
XIX	6.66	—	7.99	7.66‡	6.22	4.51	5.81	—	—	—	7.78–8.57
XX	6.43; 8.84§	—	7.97	7.64‡	6.10	4.55	5.76	—	—	—	7.85–8.77

*Estimated.
†Confirmed by deuteration.
‡For $N(Ac)_2$.
§For OCH_2CH_3.

due to these protons to be analyzed. The chemical shifts and coupling constants obtained by first-order analysis of the spectra are shown in Tables I and II respectively. In the

TABLE II

Coupling constants (c.p.s.)

Compound	$J_{1,2}$	$J_{2,3}$	$J_{3,4a}$	$J_{3,4e}$
VII	9.1	9.1	—	—
XI	2.3	10.4	—	—
XIII	2.9	9.1	9.1	4.1
XIV	2.8	10.7	—	—
XV	8.8	8.8	—	—
XVII	2.5	10.5	—	—
XIX	2.8	10.6	11.0	3.5
XX	3.0	10.7	10.7	3.9

following discussion reference will be made only to the methoxy derivatives and the 3-amino-1,2-cyclohexanediol triacetates, since the ethoxy compounds gave essentially the same results and hence served only to confirm the conclusions reached for the methoxy series. The only noteworthy point observed in the ethoxy series was the increased multiplicity of the signal of the methylene protons of the ethoxy group, which is to be expected because of the molecular asymmetry (10).

Inspection of the chemical shifts observed for the acetoxy and acetamido methyl protons indicated in all cases that the substituents had the expected conformations. Thus, 1α-methoxy-2α-acetoxy-3β-acetamidocyclohexane (XI) showed an acetoxy methyl resonance at τ 7.90 and an acetamido methyl resonance at τ 8.08. Since both values are consistent with those found by Richardson and McLaughlan (9) for equatorially oriented substituents, compound XI probably has the conformation XI*a*. Comparison of the τ-values

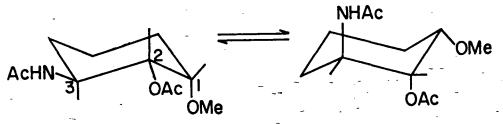

XIa XIb

for the methoxy methyl protons showed that there is little difference between axial (6.64$\pm$0.01) and equatorial (6.60$\pm$0.01) values, so that these resonances are not indicative of conformation in these derivatives.

In several compounds (VII, XI, XIII, XIV, XV, XVII, XIX, and XX) the methine ring hydrogens (H_1, H_2, and H_3) gave separate multiplets from which the first-order coupling constants were obtained. A complete analysis of these spectra was not necessary because of the large chemical shift of the methine protons from the methylene protons and accordingly, the three methine ring hydrogens were analyzed as an ABC-system.* The coupling constants thus obtained were virtually identical with those obtained from the splittings of the H_2 multiplet. Attempts to remove the coupling between the methine and methylene protons by field sweep double irradiation were unsuccessful presumably due to the rather large spread of the methylene resonance. The coupling constants from the acetylated compounds clearly establish the correctness of the conformations assigned on the basis of substituent resonances. Furthermore, the values observed for the unsubstituted compound XIII showed for the first time that it also has the expected conformation.

It is, however, difficult to rationalize the precise values found for the coupling constants

**Using an I.B.M. Model 650 computer and a program devised by Dr. R. R. Fraser and Miss O. Boshko.*

Can. J. Chem. Downloaded from www.nrcresearchpress.com by 210.87.254.40 on 09/05/12
For personal use only.

or indeed to explain why such a wide range of values should be obtained for axial:axial and axial:equatorial couplings. Karplus (11) derived by quantum mechanical analysis an equation for the relationship between the coupling constant (J) of two hydrogens and their dihedral angle (ϕ),

$$J = J_0 \cos^2 \phi - C,$$

where J_0 and C are constants. When this equation was derived there was sufficient experimental evidence (12) to show that the coupling constants varied slightly with the electronegativity of the substituents and recent work has shown that although the $\cos^2 \phi$ term adequately describes the relationship (13) it is necessary to modify either the J_0 (13, 14) or the C term (15). If it is assumed that the largest coupling constants observed correspond to protons on adjacent carbon atoms which are truly diaxial (i.e. the dihedral angle between them is 180°) it still remains to explain the smaller values observed for other compounds which should possess identical conformations. The smaller coupling constants could arise because of an equilibrium between two conformations, because the dihedral angle between axially oriented protons on adjacent carbon atoms is less than 180°, or because of some hitherto unrecognized effect of the substituent at C_1 on the axially unsymmetrical acetoxyl and acetamido groups which is reflected in a modification of the coupling constant in question.

If there were an equilibrium between conformers XI*a* and XI*b* and the rate of interconversion was rapid, the observed coupling constants would be the weighted mean of the couplings from each conformer and would thus have a smaller value than expected. Although such a conformational inversion would be energetically unfavorable, it might be stabilized by the occurrence of hydrogen bonding. Some suggestive evidence for this comes from the fact that in this series of compounds the small a:a coupling constants are observed in two out of three cases (compounds VII and XV) when the C_1 substituent is cis with respect to the acetamido function. When these groups are trans, however, the a:a coupling $J_{2,3}$ is with one exception (compound XIII) 10.5±0.1 c.p.s. Accordingly, the spectrum of compound VII was measured in acetic acid, which would probably prevent intramolecular hydrogen bonding between the 1,3-substituents. The a:a coupling constant $J_{2,3}$ was increased thereby only from 9.1 to 9.4 c.p.s., which is hardly significant. It is therefore concluded that conformational inversion at room temperature is an improbable explanation for the low $J_{2,3}$ values observed.

Although some slight distortion of the ring might result from a change in configuration of the substituent at C_1 with a consequent small distortion of the dihedral angle between the axially oriented protons at C_2 and C_3, the magnitude of the effect on $J_{2,3}$ seems too large to be caused by such a mechanism. Hence, it is tentatively suggested that the variations in a:a coupling constants reported here and elsewhere (8, 16) owe their origin in part to modification of the orientation of the axially unsymmetrical substituents attached to the carbon atoms bearing the protons in question, by a change in configuration of another unsymmetrical substituent located on an adjacent carbon atom. In view of the few examples available, however, it is not possible to decide unequivocally at present whether such a substituent effect is responsible for the low a:a coupling constants and further work to elaborate this point is planned.

Comparison of the different chemical shifts for H_1, H_2, and H_3 enables a limited number of substituent effects to be assigned. Thus, the equatorial H_1 shows a downfield shift of ca. 0.4 p.p.m. compared with the axial H_1, which agrees well with values recorded elsewhere (17, p. 116). Acetylation of the hydroxy substituent at C_2 causes H_2 to shift to low field by 1.5 p.p.m., which is slightly more than usual (ref. 17, p. 55). Acetylation of the

Can. J. Chem. Downloaded from www.nrcresearchpress.com by 210.87.254.40 on 09/05/12
For personal use only.

primary amino function at C_3 shifts H_3 downfield by 1.2 p.p.m. Acetylation of the hydroxyl group also causes shifts in the resonance of the N-Ac (+0.06 p.p.m.), NH (+0.4 p.p.m.), and H_3 (−0.33 p.p.m.) protons which must be due to the diamagnetic anisotropy of the acetoxy carbonyl function.

Acetylation of IX and III (R = C_2H_5) with acetic anhydride under reflux gave the O,N-diacetyl derivatives VII and XV in 74% and 70% yield respectively. Acetylation of the N-acetyl derivative XII or the aminoalcohol IV (R = C_2H_5), however, under identical conditions, furnished the crystalline O,N-diacetyl derivatives XI and XVII in yields of only 50% and 48% respectively, but gave in addition the corresponding liquid O,N,N-triacetyl derivatives XIX and XX in 48% and 37% yield respectively.

The structures of the latter compounds were deduced from their elemental analyses and their n.m.r. and infrared spectra. The main points of difference between the n.m.r. spectra of the O,N,N-triacetyl and O,N-diacetyl derivatives are shown in Figs. 1 and 2

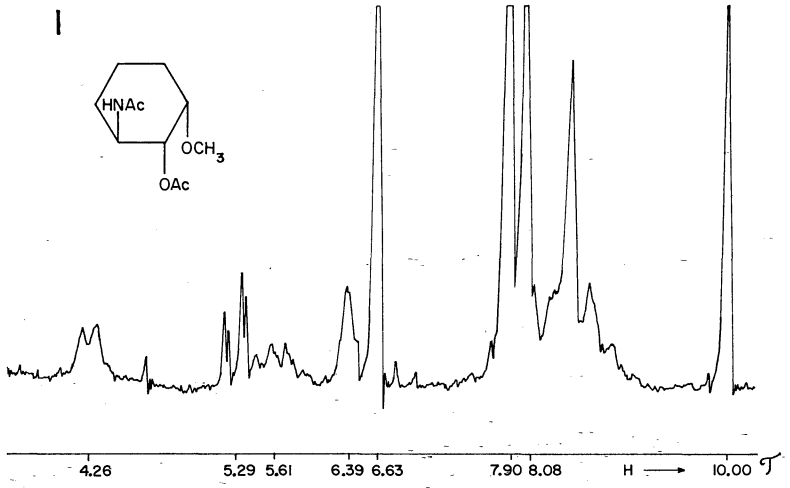

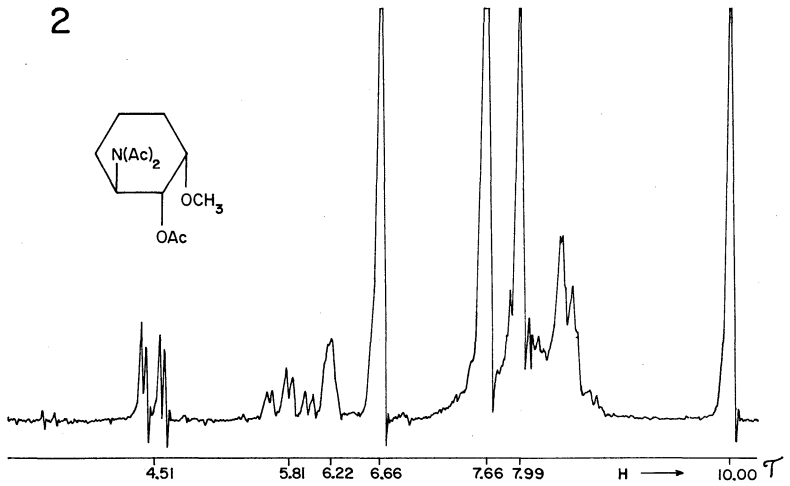

FIG. 1. The n.m.r. spectrum of 1α-methoxy-2α-acetoxy-3β-acetylaminocyclohexane (XI).
FIG. 2. The n.m.r. spectrum of 1α-methoxy-2α-acetoxy-3β-diacetylaminocyclohexane (XIX).

Can. J. Chem. Downloaded from www.nrcresearchpress.com by 210.87.254.40 on 09/05/12
For personal use only.

for the methoxy compounds XIX and XI. The doublet at τ 4.20 in the spectrum of the O,N-diacetyl derivative XI which had been assigned to the NH proton was not observed in compound XIX. Furthermore, no signal corresponding to N-acetyl protons at τ 8.08 was observed for the latter, which instead showed a resonance at τ 7.66 equivalent to two methyl groups which was assigned to a di-N-acetyl function. On these grounds XIX was assigned the O,N,N-triacetyl structure. The n.m.r. spectra of the corresponding ethoxy derivatives XVII and XX were entirely analogous.

The structural assignment made on the basis of the n.m.r. spectra of compounds XI and XIX was confirmed by measurement of their infrared spectra in carbon tetrachloride solution. Compound XI showed prominent bands at 3410 cm^{-1} (N—H, non-bonded), 3320 cm^{-1} (N—H, bonded), 1722 cm^{-1} (C=O, ester), 1683 cm^{-1} (C=O, amide I), 1233 cm^{-1} (C—O, acetate), and 1500 cm^{-1} (amide II) (18). The ester carbonyl and amide I absorptions were of equal intensity. Compound XIX, on the other hand, showed no N—H or amide II absorption but gave prominent bands at 1743 cm^{-1} (C=O, ester), 1700 cm^{-1} (C=O, amide I), and 1225 cm^{-1} (C—O, acetate). The intensity of the amide I absorption was considerably greater than that of the ester carbonyl and the observed shift in frequency of the amide I band from 1683 cm^{-1} in XI to 1700 cm^{-1} in XIX is in agreement with the tertiary amide structure, since Richards and Thompson observed that substitution of an amide nitrogen with an electrophilic group produces a shift to higher frequency (19). The infrared spectra of XVII and XX were analogous to those of XI and XIX respectively.

EXPERIMENTAL* †

The proton magnetic resonance spectra were measured on a Varian V-4302 spectrometer operating at 60 Mc/sec, using a Varian V-4352 integrator for base-line stabilization. All solutions were 10% w/v in chloroform and were calibrated with reference to internal tetramethylsilane by the usual side-band technique.

Infrared spectra were measured in carbon tetrachloride (0.05 *M*) using a Perkin–Elmer Model 21 double-beam recording spectrometer.

The preparation of all the compounds used herein except VII, XI, XV, XVII, XIX, and XX was described previously by Bannard and Hawkins (1).

1α-Methoxy-2β-acetoxy-3α-acetylaminocyclohexane (VII)

1α-Methoxy-2β-hydroxy-3α-aminocyclohexane (IX) (1) (0.290 g, 0.002 mole) was heated under reflux for 1 hour with acetic anhydride (5 ml) in an apparatus protected from entry of moisture. The excess acetic anhydride was removed from the cooled solution by distillation *in vacuo* (0.001 mm) at room temperature. The crystalline residue was recrystallized from acetone, yielding 340 mg (74.2%) of colorless needles, m.p. 168–169°. Calc. for $C_{11}H_{19}O_4N$: C, 57.62; H, 8.35; N, 6.11%. Found: C, 57.89; H, 8.36; N, 6.30%.

1α-Methoxy-2α-acetoxy-3β-acetylaminocyclohexane (XI) and 1α-Methoxy-2α-acetoxy-3β-diacetylaminocyclohexane (XIX)

1α-Methoxy-2α-hydroxy-3β-acetylaminocyclohexane (XII) (1) (0.374 g, 0.002 mole) was acetylated under the conditions described above. Removal of the excess anhydride *in vacuo* left a pale brown oil which did not crystallize on standing. The material was transferred to a four-bulb Späth tube and heated in an air bath at 79–84° at 0.03 mm pressure. A colorless distillate collected in the second bulb, leaving a viscous brown oil in the first bulb. The latter material crystallized on standing overnight. The distillation process was repeated from bulb 2 to bulb 3 at an air bath temperature of 79–81° and finally from bulb 3 to bulb 4 at 74–76°. The crops of crystals remaining in bulbs 1 to 3 were collected and recrystallized from anhydrous ether, yielding 230 mg (50.2%) of 1α-methoxy-2α-acetoxy-3β-acetylaminocyclohexane (XI) as colorless feathery needles, m.p. 138–140°. Calc. for $C_{11}H_{19}O_4N$: C, 57.62; H, 8.35; N, 6.11%. Found: C, 57.60; H, 8.37; N, 5.95%. This compound sublimed slowly under the conditions used for final distillation of the oil fraction, 258 mg (47.6%), which proved to be pure 1α-methoxy-2α-acetoxy-3β-diacetylaminocyclohexane (XIX). Calc. for $C_{13}H_{21}O_5N$: N, 5.16; acetyl, 46.50%. Found: N, 5.17; acetyl, 46.45%.

1α-Ethoxy-2β-acetoxy-3α-acetylaminocyclohexane (XV)

1α-Ethoxy-2β-hydroxy-3α-aminocyclohexane (III, R = C_2H_5) (0.318 g, 0.002 mole) on acetylation under the conditions described for the preparation of VII yielded 336 mg (69.1%) of 1α-ethoxy-2β-acetoxy-3α-acetylaminocyclohexane (XV) as colorless needles, m.p. 167–169°, after recrystallization from 95% ethanol. Calc. for $C_{12}H_{21}O_4N$: C, 59.24; H, 8.70; N, 5.76%. Found: C, 59.41; H, 8.83; N, 5.78%.

**All melting points are uncorrected.*

†*Microanalyses are by Mr. J. G. Helie of Defence Research Chemical Laboratories.*

Can. J. Chem. Downloaded from www.nrcresearchpress.com by 210.87.254.40 on 09/05/12
For personal use only.

1α-Ethoxy-2α-acetoxy-3β-acetylaminocyclohexane (XVII) and 1α-Ethoxy-2α-acetoxy-3β-diacetylaminocyclohexane (XX)

Acetylation of 1α-ethoxy-2α-hydroxy-3β-aminocyclohexane (IV, R = C_2H_5) (0.335 g, 0.0021 mole) under the same conditions as described for the preparation of XI and XIX gave 244 mg (47.6%) of 1α-ethoxy-2α-acetoxy-3β-acetylaminocyclohexane (XVII) as colorless needles, m.p. 113.5–114.5° after recrystallization from anhydrous ether. Calc. for $C_{12}H_{21}O_4N$: C, 59.24; H, 8.70; N, 5.76%. Found: C, 59.16; H, 8.78; N, 5.86%. The oil fraction, 1α-ethoxy-2α-acetoxy-3β-diacetylaminocyclohexane (XX), 223 mg (37.2%), was recovered in the same manner as its lower homologue. Calc. for $C_{14}H_{23}O_5N$: N, 4.91; acetyl, 45.25%. Found: N, 4.76; acetyl, 44.93%.

ACKNOWLEDGMENTS

The authors are indebted to Dr. R. N. Jones and Mr. R. Lauzon, Division of Pure Chemistry, National Research Council, Ottawa, for recording the infrared spectra. One of us (R. A. B. B.) wishes to thank the Defence Research Board of Canada for granting him leave of absence to participate in this work.

REFERENCES

1. R. A. B. Bannard and L. R. Hawkins. Can. J. Chem. **36**, 1241 (1958).
2. D. H. R. Barton. J. Chem. Soc. 1027 (1953).
3. D. H. R. Barton and R. C. Cookson. Quart. Rev. (London), **10**, 44 (1956).
4. R. U. Lemieux, R. K. Kullnig, and R. Y. Moir. J. Am. Chem. Soc. **80**, 2237 (1958).
5. R. U. Lemieux, R. K. Kullnig, H. J. Bernstein, and W. G. Schneider. J. Am. Chem. Soc. **80**, 6098 (1958).
6. G. E. McCasland, S. Furuta, L. F. Johnson, and J. N. Schoolery. J. Am. Chem. Soc. **83**, 2335 (1961).
7. L. D. Hall, L. Hough, K. A. McLaughlan, and K. Pachler. Chem. Ind. (London), 1465 (1962).
8. L. D. Hall. Unpublished results.
9. A. C. Richardson and K. A. McLaughlan. J. Chem. Soc. 2499 (1962).
10. J. D. Roberts. Nuclear magnetic resonance, applications to organic chemistry. McGraw-Hill Book Co., Inc., New York. 1959. p. 58.
11. M. Karplus. J. Chem. Phys. **30**, 11 (1959).
12. R. E. Glick and A. A. Bothner-By. J. Chem. Phys. **25**, 362 (1956).
13. R. J. Abraham and K. A. McLaughlan. Mol. Phys. **5**, 513 (1962).
14. R. J. Abraham, L. D. Hall, L. Hough, and K. A. McLaughlan. J. Chem. Soc. 3699 (1962).
15. R. U. Lemieux, J. D. Stevens, and R. R. Fraser. Can. J. Chem. **40**, 1955 (1962).
16. F. A. L. Anet. J. Am. Chem. Soc. **84**, 1053 (1962).
17. L. M. Jackman. Application of nuclear magnetic resonance spectroscopy in organic chemistry. Pergamon Press, London. 1959. p. 116.
18. L. J. Bellamy. The infra-red spectra of complex molecules. 2nd ed. Methuen Co. Ltd., London. 1958. Chap. 12.
19. R. E. Richards and H. W. Thompson. J. Chem. Soc. 1248 (1947).

Can. J. Chem. Downloaded from www.nrcresearchpress.com by 210.87.254.40 on 09/05/12
For personal use only.

RING-PROTON CHEMICAL SHIFTS OF SOME SUBSTITUTED ANILINES IN CARBON TETRACHLORIDE AND TRIFLUOROACETIC ACID

W. F. Reynolds and T. Schaefer
Department of Chemistry, University of Manitoba, Winnipeg, Manitoba
Received April 26, 1963

ABSTRACT

The chemical shifts of the ring-proton spectra of a series of substituted anilines are reported relative to internal benzene in the solvents carbon tetrachloride and trifluoroacetic acid. The substituent parameters in cyclohexane derived by Martin can be used together with our parameters for the para-fluoro and -ammonio (NH_3^+) groups to demonstrate additivity of the substituent effects in both carbon tetrachloride and trifluoroacetic acid. The somewhat puzzling ring-proton shifts in the latter solvent are attributed to counterion effects arising from a juxtaposition of the two centers of charge. Steric hindrance to π-overlap of the amino group with the ring is demonstrated in certain cases and a parallel behavior is found between the ring-proton shifts and the electronic spectra of these molecules.

INTRODUCTION

Differences in shielding between ring protons in substituted benzenes have been discussed in terms of additive substituent effects (1–3); Hammett sigma constants (1–6); electric field effects due to substituents (2, 3, 4, 6, 7); magnetic anisotropy of the substituents (3, 4); and of special solvent effects (8).

In the course of a study of the exchange of amino protons in substituted anilines we have measured the ring-proton shifts in a number of ring- and N-substituted anilines in CCl_4 and trifluoroacetic acid (TFA). We establish the minimum amount of alkyl substitution in the ortho position necessary for the observation of steric effects on the chemical shifts of the ring protons in anilines. We give a qualitative interpretation of the ring-proton shifts in TFA and establish additivity relationships in this solvent.

EXPERIMENTAL

The ring-proton resonance spectra of 5 mole% solutions of the anilines in CCl_4 and TFA were measured at 60 Mc/s on a Varian DP-60 spectrometer. The internal reference was benzene and peak separations were measured by standard techniques. A small amount of the anhydride was added to the TFA solutions to react with any water present. The compounds were mostly reagent grade chemicals but a few others were used as well.

RESULTS

In Carbon Tetrachloride

In Table I the shifts for the ring protons of various anilines are given in p.p.m. relative to internal benzene. For aniline and its N-substituted derivatives the shifts in CCl_4 result from an approximate analysis. The spectra were actually of the type A_2B_2C (9). However, at 60 Mc/s the relative shifts were fairly large and we estimate that the shifts are accurate to 0.05 p.p.m. For aniline and N,N-dimethylaniline a comparison with the definitive deuteration experiments of Spiesecke and Schneider confirms this estimate (4). In those cases in Table I where shifts are given to three significant figures they were arrived at by an exact analysis. Because methyl groups couple to ortho protons (10, 11) and because methyl groups shift the resonances by small amounts (see below), the asymmetrically methyl-substituted anilines gave spectra which could be analyzed with some confidence. We feel their shifts are accurate to 0.05 p.p.m.

Can. J. Chem. Downloaded from www.nrcresearchpress.com by 210.87.254.105 on 09/05/12
For personal use only.

Can. J. Chem. Downloaded from www.nrcresearchpress.com by 210.87.254.105 on 09/05/12
For personal use only.

TABLE I

Chemical shifts in p.p.m. relative to internal benzene of the ring protons in substituted anilines in 5 mole% solutions in carbon tetrachloride and trifluoroacetic acid

	Chemical shift*								
	CCl_4 solution			CF_3COOH solution			CCl_4–CF_3COOH		
Substituent	Ortho	Meta	Para	Ortho	Meta	Para	Ortho	Meta	Para
1. 4-NH_2	0.897	0.897	—	−0.550	−0.550	—	1.447	1.447	—
2. 4-OCH_3	0.825	0.677	—	−0.072	+0.232	—	0.897	0.445	—
3. 4-NO_2		Insoluble		−0.585	−1.232	—			
4. 4-CH_3	0.897	0.460	—	−0.10	−0.10	—	0.997	0.560	—
5. 4-CH_3, N-CH_3	0.860	0.390	—	−0.15	−0.15	—	1.010	0.540	—
6. 4-I	0.882	−0.097	—	−0.042	−0.705	—	0.924	0.608	—
7. 4-Br	0.817	0.112	—	−0.167	−0.483	—	0.984	0.595	—
8. 4-Cl	0.772	0.227	—	−0.267	−0.267	—	1.039	0.494	—
9. 4-F	0.773	0.487	—	−0.293	−0.030	—	1.066	0.517	—
9*a*. 4-CN		Insoluble		−0.414	−0.574				
10. 3,5-Di-CH_3	1.1	—	1.0	0.2	—	0.05	0.9	—	0.95
11. 2,6-Di-CH_3	—	0.47 (0.483)	0.77 (0.787) Ref. 5	—	−0.02	−0.02	—	0.49	0.79
12. 2,3-Di-CH_3	0.90	0.52	0.80	0.03	0.03	0.03	0.87	0.49	0.77
13. 2,4-Di-CH_3	0.90	0.5	—	0.02	0.02	—	0.88	0.48	—
14. 2,5-Di-CH_3	0.95	0.5	0.9	−0.05	−0.05	−0.05	1.0	0.55	0.95
15. 3,4-Di-CH_3	1.0	0.5	—	0.0	0.0		1.0	0.5	—
16. 3-CH_3	1.0	0.4	0.8	−0.1	−0.1	−0.1	1.1	0.5	0.9
17. 2-CH_3	0.8	0.4	0.7	−0.2	−0.2	−0.2	1.0	0.6	0.9
18. H	0.8	0.2	0.6_5	−0.3	−0.3	−0.3	1.1	0.5	0.9_5
19. N-CH_3	0.8	0.2	0.7	−0.3	−0.3	−0.3	1.1	0.5	1.0
20. N-CH_3, 2-CH_3	0.8	0.3	0.7_5	−0.2	−0.2	−0.2	1.0	0.5	0.9_5
21. N-Di-CH_3	0.6	0.1	0.7	−0.4	−0.4	−0.4	1.0	0.5	1.1
22. N-Di-CH_3, 2-CH_3	0.3_5	0.3	0.4	−0.3	−0.3	−0.3	0.6	0.6	0.6
23. N-C_2H_5	0.7	0.2	0.7	−0.4	−0.4	−0.4	1.1	0.6	1.1
24. N-Di-C_2H_5	0.7	0.2	0.7	−0.4	−0.4	−0.4	1.1	0.6	1.1
25. N-C_2H_5, CH_3	0.7	0.2	0.7	−0.4	−0.4	−0.4	1.1	0.6	1.1
26. N-(n-C_3H_7)$_2$	0.7	0.2	0.8	−0.3	−0.3	−0.3	1.0	0.5	1.1
27. N-(n-C_4H_9)	0.8	0.2	0.7	−0.3	−0.3	−0.3	1.1	0.5	1.0
28. N-C_6H_5	0.3	0.1	0.2	−0.3	−0.3	−0.3	0.6	0.4	0.5
29. N-C_6H_5, CH_3	0.1	0.0	0.0	−0.3	−0.3	−0.3	0.4	0.3	0.3

*The ring protons are labelled relative to the amino group.

The amino protons had broad resonance peaks at 3 to 4 p.p.m. from benzene, indicating proton exchange between nitrogen atoms (12) or quadrupole relaxation of the nitrogen nuclei at a rate rapid enough to broaden the hydrogen peaks (13).

In Trifluoroacetic Acid

The collapse of the ring-proton spectrum of aniline in acetic acid was first observed by Isobe *et al.* (14) and by Schneider (15). The collapse is not quite complete for N-substituted anilines when the substituents are larger than methyl. For ring-substituted anilines the relative shifts between ring protons are dominated by the substituents other than the ammonio (NH_3^+) group. (The very broad ammonio-proton resonances occurred at 1 to 1.5 p.p.m. to low field from benzene.) The anilines are protonated* in TFA since the N-alkyl groups always showed coupling of 5.2 to 5.6 c/s with an extra proton as expected for the proper anilinium ion. For example, N-methylaniline gave a methylt riplet peak with a measured splitting of 5.5 ± 0.1 c/s. This agrees with the structure $C_6H_5NH_2^+(CH_3)$. Hence, at 5 mole%, the lifetime of the ion at room temperatures exceeds 0.03 second. The exchange rate is a function of both temperature and concentration and is the subject of investigation in our laboratory.

DISCUSSION

The Para-substituted Anilines

The very careful work of Martin (3) on the ring-proton shifts of para-substituted benzenes at infinite dilution in cyclohexane shows that deviations from additivity of the substituent effects amount to 0.1 p.p.m. Using Martin's shielding parameters we can reproduce our observed shifts in CCl_4 with a mean deviation of 0.05 p.p.m. Part of this deviation is no doubt due to our use of 5 mole% solutions. We do not give the tabular values here since they only serve to establish the relative accuracy of our measurements. Martin's shielding parameters agree well with the chemical shifts of monosubstituted benzenes found by Spiesecke and Schneider (4). The substituent effects appear to be the result of several superimposed effects, presumably dominated by the polarization of the benzene π-electron system. We do not discuss them further here since they are fully discussed in a forthcoming paper by Martin (16).

We can account for the ring proton shifts in TFA by assigning a shielding parameter to the ammonio group of -0.30 p.p.m. for both the meta and ortho positions. This is the shift to low field from benzene of the broad peak of aniline in TFA (compound 18 in Table I).† Table II compares the predicted and observed shifts using Martin's substituent parameters in cyclohexane and $\delta_{m,p}(NH_3^+) = -0.30$ p.p.m. (see footnote in Table II). The mean deviation is less than 0.05 p.p.m.

Proton Shifts of Aniline in Trifluoroacetic Acid

It is not obvious why the ring-proton resonance of aniline in TFA should be a single broad peak, indicating a shielding difference of not more than about 0.1 p.p.m. Given that π-overlap with the ring is destroyed by protonation, an isolated anilinium ion should still show differences in shielding at the various ring positions of many c/s. This follows from a simple calculation involving the field due to a monopole. The use of Buckingham's equation (7) predicts shifts of -1.11 p.p.m., -0.49 p.p.m., and -0.38 p.p.m. relative to benzene for the ortho, meta, and para protons respectively. These predicted shifts would

Even anilines with strongly electron-withdrawing substituents are protonated at low concentrations in TFA, although, of course, the exchange rate will be higher.

†*The width of the peak would allow a shift between protons of as much as 0.1 p.p.m. if the usual magnitudes of ring-proton coupling constants are assumed.*

Can. J. Chem. Downloaded from www.nrcresearchpress.com by 210.87.254.105 on 09/05/12
For personal use only.

TABLE II
Predicted and observed shifts in p.p.m. of ring protons of para-substituted anilines in trifluoroacetic acid relative to benzene

	Chemical shift†			
	Predicted		Observed	
Substituent*	Ortho	Meta	Ortho	Meta
H	−0.30	−0.30	−0.3	−0.3
CH_3	−0.193	−0.117	−0.1	−0.1
F	−0.300	−0.020	−0.29	−0.03
Cl	−0.235	−0.300	−0.27	−0.27
Br	−0.166	−0.459	−0.17	−0.48
I	−0.035	−0.663	−0.04	−0.70
OCH_3	−0.182	+0.177	−0.07	+0.23
NO_2	−0.455	−1.255	−0.58	−1.23
CN	−0.400	−0.577	−0.41	−0.57
NH_3^+	−0.60	−0.60	−0.55	−0.55

*Martin's substituent parameters are used together with $\delta_o^F = 0.280$ p.p.m., $\delta_m^F = 0.000$ p.p.m., and $\delta_o^{NH_3^+} = -0.30$ p.p.m.
†Ring protons are labelled relative to the amino group.

be modified somewhat by reaction field effects in solution (7). The fact that Martin's substituent parameters, derived from measurements in cyclohexane, could be used in Table II also indicates some other explanation for the observed effects of the ammonio group.

In this connection the studies of Fraenkel appear to resolve the dilemma (17). By means of n.m.r. techniques he has shown that anilinium salts in various solvents exist as intimate ion pairs *with the two centers of charge juxtaposed.* The anion–cation exchange is fast on an n.m.r. time scale. At the high solute concentrations used here such a result is to be expected. It thus appears that the effect of the ammonio group at the different ring positions is counteracted by the trifluoroacetate anion. If the ortho and meta positions were in a symmetrical environment with respect to the anion there would be no coalescence effect such as we observe in aniline.* There is still a net shift to low field of 0.3 p.p.m. which can probably be put down to an incomplete neutralization of the effect of theNH_3^+ group by the anion.

Methyl-substituted Anilines

Using Martin's substituent parameters for the methyl group the observed shifts in CCl_4 (compounds 10–17 in Table I) can be predicted to within a mean deviation of 0.07 p.p.m. Our measured shifts are little more reliable than this. However, the effect of a methyl group is also only about three times this deviation and the actual shifts are therefore dominated by the amino group.

In TFA the mean deviation between observed and predicted shifts in Table III is 0.04 p.p.m. We have assumed the substituent parameter to be −0.30 p.p.m. for the ammonio group at all positions. The agreement is certainly within experimental error at all three positions.

Steric Effects

It is natural to assume that the shifts of the ring protons of aniline itself in CCl_4 approximately reflect the overlap of the amino group with the π-orbitals of the ring. Spiesecke

It is only a coincidence that the n.m.r. spectra and electronic spectra of both benzene and the anilinium ions are very similar. In the case of electronic spectra the inductive effect of a substituent shifts the ground and excited states about equally and in the same direction (18). Therefore the inductive effect produces little change in the position or intensity of the benzene bands. Anilinium salts have electronic spectra virtually superimposable on the benzene spectrum (19, p. 248), a strong argument for no conjugation or *hyperconjugation of the* NH_3^+ *group with the ring. In this connection see a recent calculation by Bishop and Craig (20).*

Can. J. Chem. Downloaded from www.nrcresearchpress.com by 210.87.254.105 on 09/05/12
For personal use only.

TABLE III

Predicted and observed ring-proton shifts in p.p.m. of methyl-substituted anilines in trifluoroacetic acid relative to internal benzene

	Chemical shift*					
	Predicted			Observed		
Substituents	Ortho	Meta	Para	Ortho	Meta	Para
2,6-Di-CH_3	—	0.04	−0.08	—	−0.02	−0.02
3,5-Di-CH_3	0.04	—	0.07	0.2	—	0.05
2,3-Di-CH_3	−0.03	−0.03	−0.01	0.03	0.03	0.03
2,4-Di-CH_3	−0.08	(−0.04) (−0.06)	—	0.02	0.02	
2,5-Di-CH_3	−0.01	−0.01	−0.01	−0.05	−0.05	−0.05
3,4-Di-CH_3	(−0.03) (−0.01)	−0.01	—	0.0	0.0	—
2-CH_3	−0.19	(−0.14) (−0.12)	−0.19	−0.2	−0.2	−0.2
3-CH_3	(−0.14) (−0.12)	−0.19	−0.12	−0.1	−0.1	−0.1

*Ring protons are labelled relative to the ammonio group.

and Schneider (4) found a good correlation of the para shifts with the appropriate Hammett sigma constants in a series of monosubstituted benzenes. At other positions such a correlation was poor, presumably mainly due to magnetic anisotropy effects of the substituents. (Our shifts also show a poor correlation at meta and ortho positions with the sigma constants, although we do not give the graphs here.)

Although the shifts for compounds 19–22 in Table I are not known very accurately it is clear that a noticeable steric effect arises only when a methyl group is substituted ortho to the N,N-dimethyl group. When substituted ortho to the N-methyl group a methyl group does not appear to have a noticeable effect. Fraser has found a steric effect on the shifts when two methyl groups are substituted ortho to the N-methyl group (5).

In unsubstituted N,N-dimethylaniline, the nitrogen valences are probably nearly planar at about 120° to each other (19, p. 409). Steric effects twist the dimethylamino group out of the plane of the ring and the nitrogen valences become increasingly more pyramidal: the lone-pair electrons gain *s* character. When the angle of twist is 90° the nitrogen valences are pyramidal. Appreciable deviation from planarity is required before the interaction with the ring is reduced significantly since the overlap follows a $\cos^2\theta$ law.

The behavior found in the shifts closely parallels that of the electronic spectra (19, pp. 410–413; 20). The parent aniline has only a small alteration of its electronic spectrum due to ortho substituents, the spectrum of N-methylaniline is slightly affected, while the spectrum of N,N-dimethylaniline is strongly affected by ortho-methyl groups. The angle of twist inferred from the data is 50° for 2-methyl-N,N-dimethylaniline and 68° for 2,6-dimethyl-N,N-dimethylaniline if the intensities of the *C*-band are used, assuming planarity for the unsubstituted compound. Subtraction of the substituent parameters for the methyl groups from the observed shifts for the two compounds (compound 22 in Table I and reference 5) leaves 0.5 p.p.m. as the decrease in the para shift in both cases due to steric hindrance. On a $\cos^2\theta$ basis this would mean an angle of twist of $\cos^2\theta = 0.2/0.7 =$ (observed shift/expected shift in the absence of hindrance). This gives $\theta = 57°$ in both cases.* It is doubtful whether this number is to be taken seriously but investigation of a series of likely compounds is perhaps indicated.

**We have assumed that the para shift caused by the amino group is entirely mesomeric, an assumption which receives support from other work (4).*

Can. J. Chem. Downloaded from www.nrcresearchpress.com by 210.87.254.105 on 09/05/12
For personal use only.

In N-phenylaniline (compound 28 in Table I) the lone pair now overlaps with two rings and, naively, one might expect a twofold decrease in shielding, as is roughly true. The addition of a methyl group to the nitrogen (compound 29) causes crowding and, we conclude from the shift, decreases overlap almost to zero or to an sp^3 configuration at the nitrogen.

NOTE ADDED IN PROOF

A further calculation of the effect of the ammonio group on chemical shift has yielded results more consistent with experimental measurements. It was assumed that the charge on the group (4.8×10^{-10} e.s.u.) was distributed equally on the three protons. The field due to this charge was calculated for two possible positions of the ammonio group: (*a*) with one proton in the plane of the ring, adjacent to the ortho and meta protons under consideration; (*b*) with one proton in the plane of the ring opposite to the ortho and meta protons. The two positions have an equivalent effect on the para proton. The net result of this calculation is the consideration of the effect of a charge averaged over six possible positions. This should represent a close approximation to integration over all possible positions.

The components of the field along the bond axes of the different protons were precisely calculated. However, the complete calculation of the resultant of the total field acting at the proton was only carried out for the ortho protons since it is complex and tedious. The total field acting at the meta and para positions was approximated by assuming that the total charge was concentrated at the center of the circle circumscribed by the ammonio protons. Since the meta and para protons are relatively far removed from the ammonio group, this assumption should introduce only a very slight error.

The results of the calculation are given in Table IV. If Buckingham's equation (7) is

TABLE IV

Calculation of the field effect due to the ammonio group

Position	$10^{-5}E_z$ (e.s.u.)	$10^{-11}E^2$ (e.s.u.^{2})	$-2\times10^{-12}E_z-10^{-18}E^2$ (p.p.m.)	$-2\times10^{-12}E_z-0.25\times10^{-18}E^2$ (p.p.m.)
Ortho	1.15	2.77	−0.51	−0.30
Meta	1.44	0.35	−0.32	−0.30
Para	1.39	0.20	−0.29	−0.28

used in unmodified form, agreement with experiment is better than for the calculation outlined in the previous text, but still not particularly good. It is interesting to note that the estimated effect of E_z is now least at the ortho position. This suggests that if the coefficient of E^2 in Buckingham's equation is too high, then a lower value of the coefficient may give much better agreement. As seen in column 5 of Table IV, predicted shifts agree, within experimental error, with those determined experimentally if one assumes a value of 0.25×10^{-18} for the coefficient of the E^2 term.

ACKNOWLEDGMENTS

We are grateful to Dr. J. Martin for a copy of his thesis, to Dr. G. Fraenkel for information on his experiments with aniline salts, and to the National Research Council for financial support.

Can. J. Chem. Downloaded from www.nrcresearchpress.com by 210.87.254.105 on 09/05/12
For personal use only.

REFERENCES

1. P. DIEHL. Helv. Chim. Acta, **44**, 829 (1961).
2. P. DIEHL. Helv. Chim. Acta, **45**, 568 (1962).
3. J. MARTIN. Thesis, Columbia University, New York, N.Y. 1962.
4. H. SPIESECKE and W. G. SCHNEIDER. J. Chem. Phys. **35**, 731 (1961).
5. R. R. FRASER. Can. J. Chem. **38**, 2226 (1960).
6. W. G. PATERSON and N. R. TIPMAN. Can. J. Chem. **40**, 2122 (1962).
7. A. D. BUCKINGHAM. Can. J. Chem. **38**, 300 (1960).
8. W. G. SCHNEIDER. J. Phys. Chem. **66**, 2653 (1962).
9. H. J. BERNSTEIN, J. A. POPLE, and W. G. SCHNEIDER. Can. J. Chem. **35**, 65 (1957).
10. T. SCHAEFER and W. G. SCHNEIDER. J. Chem. Phys. **32**, 1218 (1960).
11. B. D. NAGESWARA RAO and J. D. BALDESCHWIELER. J. Chem. Phys. **37**, 2473 (1962).
12. J. T. ARNOLD. Phys. Rev. **102**, 136 (1956).
13. J. A. POPLE. Mol. Phys. **1**, 168 (1958).
14. T. ISOBE, T. IKENOVE, and G. HAZATO. J. Chem. Phys. **30**, 1371 (1959).
15. W. G. SCHNEIDER. Private communication. 1959.
16. J. MARTIN and B. P. DAILEY. J. Chem. Phys. In press. 1963.
17. G. FRAENKEL. Abstracts, Summer Symposium on High-Resolution NMR Spectroscopy, Boulder, Colorado. 1962.
18. A. STREITWIESER. Molecular orbital theory. John Wiley and Sons, Inc., New York. 1961. p. 230.
19. H. H. JAFFÉ and M. ORCHIN. Theory and applications of ultraviolet spectroscopy. John Wiley and Sons, Inc., New York. 1962.
20. D. M. BISHOP and D. P. CRAIG. Mol. Phys. **6**, 139 (1963).

Can. J. Chem. Downloaded from www.nrcresearchpress.com by 210.87.254.105 on 09/05/12
For personal use only.

CONSTITUTION OF THE HEMICELLULOSE FROM MESTA FIBER (HIBISCUS CANNABINUS)

S. K. SEN

Department of Chemistry, Technological Research Laboratories, Indian Central Jute Committee, Calcutta, India

Received February 19, 1963

Can. J. Chem. Downloaded from www.nrcresearchpress.com by 210.87.254.5 on 09/05/12
For personal use only.

ABSTRACT

The chlorite holocellulose of mesta fiber (*Hibiscus cannabinus*) was extracted with alkaline solutions of successively increasing concentration and finally with alkaline borate solution. Hemicellulose fractions (I–IV) were thus obtained. Analytical data are recorded for each fraction.

Partial acid hydrolysis of the mesta hemicellulose gave 2-O-(4-O-methyl-α-D-glucopyranosyl uronic acid)-D-xylopyranose. Methanolysis and hydrolysis of the fully methylated hemicellulose (fraction II) gave a mixture of 3-O-methyl-D-xylose, 2,3-di-O-methyl-D-xylose, 2,3,4-tri-O-methyl-D-xylose, and 2-O-(2,3,4-tri-O-methyl-α-D-glucopyranosyl uronic acid)-3-O-methyl-D-xylopyranose in the approximate molar ratio of 1.6:34:1:6.4. The number-average molecular weight of the methylated polysaccharide was 18,400±500 (degree of polymerization, 110±3). The number-average molecular weight of the original hemicellulose (fraction II) was found to be 23,000±500 (degree of polymerization, 164±3). On the basis of this and other evidences it is suggested that the polysaccharide is composed of chains of 144 (1 → 4)-linked β-D-xylopyranose residues having approximately every seventh residue carrying a terminal 4-O-methyl-α-D-glucuronic acid residue linked through position 2. A small degree of branching in the backbone of D-xylose is indicated.

Mesta is a bast fiber which grows extensively in India and also in some parts of Eastern Asia. It is used as a substitute for jute.

In the present investigation an attempt has been made to fractionate the total carbohydrate constituents of mesta fiber. The chemical constitution of the main hemicellulose fraction has been studied in some detail.

Defatted mesta fiber was delignified by treatment with dilute sodium chlorite solution (1). The resulting holocellulose was extracted successively with 2% sodium carbonate solution, 4% sodium hydroxide solution, 10% sodium hydroxide solution, and finally with 16% sodium hydroxide solution containing 4% boric acid (2). This led to the isolation of four hemicellulose fractions (I–IV). Fraction II was purified further with Fehling's solution (3) to give fraction IIA.

Partial acid hydrolysis of mesta hemicellulose gave xylose and a main acidic component, identified as 2-O-(4-O-methyl-α-D-glucopyranosyluronic acid)-D-xylopyranose.

The hemicellulose (fraction II) was converted into its fully methylated derivative, which on hydrolysis gave 2,3,4-tri-O-methyl-D-xylose, 2,3-di-O-methyl-D-xylose, 3-O-methyl-D-xylose, and partially methylated aldobiouronic acid in the approximate molar ratio of 1.0:34.0:1.6:6.4. The methyl ester methyl glycoside of the partially methylated aldobiouronic acid was reduced with lithium aluminum hydride (4). Hydrolysis of the reduced product yielded 2,3,4-tri-O-methyl-D-glucose, identified as its aniline derivative, and 3-O-methyl-D-xylose, characterized by ionophoresis and also as its aniline derivative.

DISCUSSION

The large quantity of 2,3-di-O-methyl-D-xylose obtained, in conjunction with the negative rotations of the original and methylated hemicellulose indicated that the xylose residues in the backbone of the hemicellulose molecule were linked together by β-(1 → 4)-glycosidic bonds. The fact that the partly methylated aldobiouronic acid was unsubstituted

at C_4 of the xylose moiety together with the absence of any 3,4-di-O-methyl-D-xylose in the neutral portion of the hydrolyzate of the methylated hemicellulose showed that the xylose residues were attached directly to the (1 → 4)-linked xylan framework. The constitution of the aldobiouronic acid showed that the side chains were composed of (1 → 2)-linked 4-O-methyl-α-D-glucuronic acid residues. The data from methylation study of the mesta hemicellulose showed the presence of approximately seven xylose residues for each 4-O-methyl glucuronic acid residue. This has been corroborated by the equivalent weight and uronic anhydride content of the fraction IIA hemicellulose.

The number-average molecular weight of the methylated polysaccharide, as determined by osmometry, was found to be 18,400±500 (D.P., 110±3). Since methylation indicated the presence of two non-reducing xylose end groups for a molecule of this size, there was on the average one branch in the main chain of xylose residues. For the original polysaccharide there would be two such branch points. The amount of formic acid liberated by periodate oxidation of the polysaccharide suggested a few branches in the molecule. The presence of mainly 3-O-methyl xylose in the hydrolysis product of the methylated polysaccharide indicated that the branch points involve (1 → 2)-linkages. The slightly higher proportion of 3-O-methyl xylose probably arises from partial hydrolysis of the partially methylated aldobiouronic acid or incomplete methylation of hemicellulose or demethylation during hydrolysis.

On the basis of these results the annexed partial structure for the hemicellulose from mesta fiber indicates the main features of the molecule.

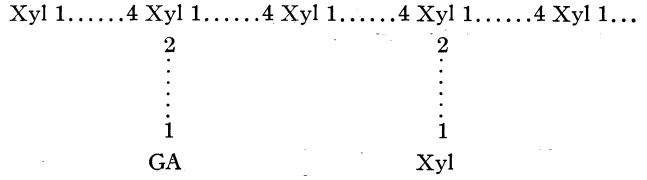

Xyl = D-xylopyranose, GA = 4-O-methyl-α-D-glucuronic acid

Consumption of 6.6 moles of periodate per 7 sugar residues of the polymer is in fair agreement with the above simplified structure.

The structure of the main fraction of the mesta hemicellulose thus appears to be identical with that of jute (5) or roselle hemicelluloses (6); it is also similar to that of flax hemicellulose (7).

EXPERIMENTAL

All specific rotations are equilibrium values unless otherwise stated. Evaporations were carried out under diminished pressure at 40–45° C (bath temperature).

Paper chromatograms were run by the descending method using the following solvent systems (v/v): (A) butan-1-ol – ethanol – water (40:11:19); (B) butan-1-ol – pyridine – water (10:3:3); (C) ethyl acetate – acetic acid – formic acid – water (18:3:1:4); (D) ethyl acetate – acetic acid – water (9:2:2); (E) butan-2-one, two-thirds saturated with water containing 1% of ammonia; and (F) benzene–ethanol–water (169:47:15; upper layer). A saturated solution of aniline oxalate (8) in water was used as the spray reagent. Paper ionophoresis was in borate buffer at pH 10.

Composition of the Fiber

The composition of the mesta fiber, analyzed by standard methods (9), was: alpha-cellulose 60.04, xylan 14.82, lignin (after Schwalbe) 10.11, uronic anhydride 3.87, acetyl 4.82, nitrogen 0.19, fat and wax 0.62, ash 0.69, residues of galactose 0.65, glucose 64.31, mannose 0.70, arabinose 1.24, xylose 12.35, and rhamnose 0.79%.

Isolation and Purification of the Hemicellulose Fractions

The mesta fiber was cut into small pieces and exhaustively extracted with an azeotropic mixture of

Can. J. Chem. Downloaded from www.nrcresearchpress.com by 210.87.254.5 on 09/05/12
For personal use only.

ethanol–benzene (1:2; w/w). The defatted fiber was delignified by the sodium chlorite method (1) to give holocellulose (yield 90.38; lignin (Schwalbe's) 3.65 and acetyl 4.13%).

Holocellulose (437.6 g) was extracted successively with 10 parts of 2% sodium carbonate solution, 4% sodium hydroxide solution, 10% sodium hydroxide solution, and finally with 16% sodium hydroxide solution containing 4% boric acid for 48, 2, 2, and 72 hours respectively. Hemicellulose fractions (I–IV) were isolated from the extracts as described in the case of jute hemicellulose (10). Hemicellulose fraction I was light brown in color due to the presence of lignin, which was removed by treatment with sodium chlorite in hot methanol (11). Hemicellulose fraction II (5 g) was purified by three precipitations with Fehling's solution according to the method of Chanda *et al.* (3) to give hemicellulose fraction IIA (3.95 g). The analytical data on the hemicellulose fractions are given in Table I. Samples of hemicellulose fractions, alpha-cellulose (prepared

TABLE I

Analytical data of fractions of hemicellulose

Fraction	Yield,* %	Xylan, %	Uronic anhydride, %	Methoxyl, %	Equiv. wt.	$[\alpha]_D^{30}$ (*N* NaOH)
I	1.09	40.47	42.10	2.86	460	−14.58°
II	9.25	71.95	16.08	3.75	1152	−69.98°
IIA	—	77.33	16.19	3.09	1100	−61.65°
III	5.31	72.49	16.77	3.78	1185	−69.95°
IV	1.24	56.65	14.34	3.28	1277	−75.80°

*On the basis of oven-dry fiber.

from mesta holocellulose), and cellulose residue left after extraction of hemicellulose fractions were hydrolyzed according to the method of Saeman *et al.* (12) and the neutral sugars in the hydrolyzates were estimated by filter paper chromatography (13) using solvent systems B and D. The proportions of neutral sugars present are summarized in Table II.

TABLE II

Fraction	Galactose	Glucose	Mannose	Arabinose	Xylose	Rhamnose
I	3.68	2.58	—	3.63	88.24	3.12
II	1.45	0.86	—	1.23	95.11	1.33
IIA	—	0.57	—	—	98.79	0.66
III	0.77	2.86	0.17	—	93.74	0.91
IV	0.38	6.39	8.53	—	83.80	0.85
Cellulose residue	—	98.64	0.35	—	1.02	—
Alpha-cellulose	—	94.14	0.33	—	5.53	—

Isolation and Identification of Aldobiouronic Acid

Aldobiouronic acid was isolated by partial acid hydrolysis of the hemicellulose (mixtures of fraction II and III. 50 g) as described for jute hemicellulose (5). Chromatography of the product in solvent C showed the presence of a main component with R_{xyl} 0.85. A portion of the acidic syrup (5.43 g) was separated on a cellulose column (72×4.5 cm) (14) using solvent D into a main portion of aldobiouronic acid and a trace of xylose, which was removed by chromatographic separation on filter sheets with solvent B. The pure aldobiouronic acid was extracted from the appropriate strips with water, treated with Amberlite IR-120 (H), concentrated, and dried to a powder (1.52 g). It had $[\alpha]_D^{32}$ +96.56° (*c*, 1.07 in water). Anal. Calc. for $C_{12}H_{20}O_{11}$: equiv. wt., 340; OMe, 9.1%. Found: equiv. wt., 337.5; OMe, 9.25%. The acetate derivative (15) had m.p. 201° C, $[\alpha]_D^{25}$ +99.6° (*c*, 0.6 in chloroform). Anal. Calc. for $C_{22}H_{32}O_{15}$: OMe, 17.3%. Found: OMe, 17.02%. A portion of the aldobiouronic acid (480 mg) was converted to the methyl ester methyl glycoside, which on reduction with lithium aluminum hydride in dry tetrahydrofuran (4) followed by hydrolysis and chromatographic separation on filter sheets yielded D-xylose having m.p. and mixed m.p. 144° C, $[\alpha]_D^{30}$ +18° (*c*, 1.5 in water), and 4-O-methyl-D-glucose having $[\alpha]_D^{27}$ +60.5° (*c*, 1.1 in water). The xylose dibenzylidine dimethyl acetal derivative (16) had m.p. and mixed m.p. 210° C and $[\alpha]_D^{27}$ −11.7° (*c*, 1.5 in chloroform). The derived 4-O-methyl-D-glucosazone had m.p. and mixed m.p. 159–160° C. Anal. Calc. for $C_{19}H_{24}O_4N_4$: OMe, 8.3%; N, 15.0%. Found: OMe, 8.6%; N, 15.4%.

Another portion of the aldobiouronic acid (762 mg) was converted to the fully methylated disaccharide (497 mg) by the usual method. Hydrolysis of the fully methylated disaccharide (432 mg) yielded a syrup which was separated by paper chromatography using solvent A into fractions *a* and *b*. Fraction *a* (156 mg) was 2,3,4,6-tetra-O-methyl-D-glucose having m.p. and mixed m.p. 86–88° C, $[\alpha]_D^{32}$ +83.6° (*c*, 1.6 in water).

Can. J. Chem. Downloaded from www.nrcresearchpress.com by 210.87.254.5 on 09/05/12
For personal use only.

Anal. Calc. for $C_{10}H_{20}O_6$: OMe, 52.5%. Found: OMe, 52.1%. The anilide of 2,3,4,6-tetra-O-methyl-D-glucose had m.p. and mixed m.p. 126–127° C, $[\alpha]_D^{27}$ +210° (*c*, 0.5 in acetone). Anal. Calc. for $C_{16}H_{25}O_5N$: OMe, 39.87%; N, 4.5%. Found: OMe, 39.4%; N, 4.1%. Fraction *b* (81.8 mg) was obtained as a syrup. Chromatography with solvent F and ionophoresis showed only 3,4-di-O-methyl-D-xylose, $[\alpha]_D^{32}$ +23.22° (*c*, 0.81 in water). Anal. Calc. for $C_7H_{14}O_5$: OMe, 34.8%. Found: OMe, 34.5%. The derived anilide had m.p. and mixed m.p. 113–114° C.

Methylation of the Hemicellulose

Hemicellulose (fraction II, 19.2 g) was methylated by successive addition of dimethyl sulphate and sodium hydroxide and finally with methyl iodide and silver oxide to yield a fully methylated derivative (19.8 g), $[\alpha]_D^{30}$ −42.4° (*c*, 1.1 in chloroform) (found: OMe, 39.1%). The infrared spectrum of the product indicated complete substitution. The methylated hemicellulose (10.8 g) was fractionated by treatment with a mixture of boiling chloroform – light petroleum ether (b.p. 60–65° C) to yield a main fraction (10.1 g) soluble in chloroform – petroleum ether (3:7). It had $[\alpha]_D^{31}$ −40.9° (*c*, 0.95 in chloroform) (found: OMe, 38.91%).

Hydrolysis of the Methylated Hemicellulose and Separation of Methylated Sugars

The methylated hemicellulose (5.19 g) was hydrolyzed with methanolic hydrochloric acid and then with aqueous hydrochloric acid in the usual way. Evaporation after neutralization with silver carbonate yielded a syrup (5.41 g) which was treated (in aqueous solution) with barium carbonate. The mixture of methylated sugars was fractionated on a column (90×4.5 cm) of powdered cellulose with solvent E to give three fractions, and elution of the column with water afterwards yielded a fourth fraction which was treated with Amberlite resin IR-120 (H) to remove barium ion.

Fraction I.—Chromatography of the sugar (111.9 mg) in solvent A showed that it corresponded to an authentic sample of 2,3,4-tri-O-methyl-D-xylose. The syrup crystallized partially on standing. Recrystallization from diethyl ether containing a small amount of petroleum ether yielded crystals of 2,3,4-tri-O-methyl-D-xylose having m.p. and mixed m.p. 89–90° C, $[\alpha]_D^{30}$ +19.8° (*c*, 0.54 in water). Anal. Calc. for $C_8H_{16}O_5$: OMe, 48.4%. Found: OMe, 48.1%.

Fraction II.—The syrup (3.528 g) crystallized when seeded with 2,3-di-O-methyl-D-xylose. Recrystallization from diethyl ether yielded crystals having m.p. and mixed m.p. 91–92° C, $[\alpha]_D^{24}$ −12.86° (6 minutes) → +23.6° (53 minutes constant) (*c*, 1.86 in water). Anal. Calc. for $C_7H_{14}O_5$: OMe, 34.8%. Found: OMe, 34.3%. The crystalline aniline derivative, recrystallized twice from ethyl acetate, had m.p. and mixed m.p. 123–124° C, $[\alpha]_D^{24}$ +181.6° (*c*, 0.4 in ethyl acetate). Anal. Calc. for $C_{13}H_{19}O_4N$: OMe, 24.5%; N, 5.5%. Found: OMe, 24.3%; N, 5.7%.

Fraction III.—The syrup (153 mg), $[\alpha]_D^{24}$ +16.1° (*c*, 0.9 in water), could not be crystallized. Paper ionophoresis of the syrup showed the presence of 3-O-methyl-D-xylose together with a trace of 2-O-methyl-D-xylose. Anal. Calc. for $C_6H_{12}O_5$: OMe, 18.9%. Found: OMe, 18.4%.

Fraction IV.—The syrup (1.425 g) was found to be a partially methylated aldobiouronic acid. Reduction and hydrolysis of the methyl ester methyl glycoside followed by chromatography on filter sheets with solvent A gave two fractions, *a* and *b*. Fraction *a*, obtained as a syrup (128.8 mg), was identified as 3-O-methyl-D-xylose by paper electrophoresis. It had $[\alpha]_D^{31}$ +16.3° (*c*, 1.28 in water). Anal. Calc. for $C_6H_{12}O_5$: OMe, 18.9%. Found: OMe, 18.5%. The aniline derivative had m.p. 135° C, $[\alpha]_D^{30}$ +81.28° (*c*, 0.54 in ethyl acetate). Anal. Calc. for $C_{12}H_{17}O_4N$: OMe, 12.97%; N, 5.86%. Found: OMe, 12.5%; N, 5.57%. Fraction *b* (143 mg), identified as 2,3,4-tri-O-methyl-D-glucose, had $[\alpha]_D^{32}$ +67.8° (*c*, 1.43 in water). Anal. Calc. for $C_9H_{18}O_6$: OMe, 41.9%. Found: OMe, 41.6%. The aniline derivative had m.p. and mixed m.p. 144–145° C. Anal. Calc. for $C_{15}H_{23}O_5N$: OMe, 31.3%. Found: OMe, 31.7%.

Quantitative Estimation of O-Methyl Xyloses

The mixture of neutral O-methyl xyloses from the hydrolysis product of methylated hemicellulose was separated by filter paper chromatography using solvent A. The appropriate strips were eluted with water and component sugars were estimated by alkaline hypoiodite method (3) using sodium hydroxide – phosphate buffer (pH 11.4). The molar ratio between mono-, di-, and tri-O-methyl-D-xyloses from duplicate experiments was 1.5:33.8:1.

Periodate Oxidation of the Hemicelluloses

Hemicellulose fractions II and III (0.99 g) in water (59.9 ml) were oxidized by 0.3 *M* sodium metaperiodate solution (29.3 ml) in the dark at 10–15° C. Analyses for periodate consumption according to the arsenite method of Fleury and Lange (17) were made at 24-hour intervals. The oxidation was essentially complete after 289 hours with the consumption of 0.81 mole of periodate per mole of anhydropentose unit in both the cases.

The sodium salts of hemicellulose fractions II and III (0.89 g), in water (60 ml) containing potassium chloride (5 g), were oxidized with 0.3 *M* sodium metaperiodate (30 ml) in the dark at 10–12° C. The formic acid released was estimated by the procedure of Halsall, Hirst, and Jones (18), which showed that 1 mole of formic acid was produced from 3800 g of the hemicellulose in both the cases.

Determination of the Molecular Weights

The number-average molecular weight of hemicellulose fraction II was determined by measuring the

Can. J. Chem. Downloaded from www.nrcresearchpress.com by 210.87.254.5 on 09/05/12
For personal use only.

osmotic pressure of a solution of its sodium salt in 0.4 *M* sodium chloride. The measurements were made by the static method at 35±0.02° with the Hellfritz osmometer (19). The membrane was du Pont's Gel cellophane 600 P.T. The molecular weight of the methylated hemicellulose was determined in butyl acetate solution using "Ultrazellafilteraller feinst" membrane supplied by Membranfiltergesellschaft, Göttingen. The osmotic height was measured for different concentrations of the polysaccharide and the values $\Delta h/C$, the reduced osmotic pressure, were linearly extrapolated to zero concentrations. The results are summarized in Table III.

TABLE III

Osmometry data

Hemicellulose			Methylated hemicellulose		
C*	Δh†	$\Delta h/C$	C	Δh	$\Delta h/C$
4.50	4.84	1.075	6.44	11.03	1.71
3.80	4.11	1.080	4.64	7.72	1.66
3.00	3.21	1.070	3.90	6.51	1.67
2.30	2.58	1.120	3.00	4.98	1.66
1.80	1.96	1.090	2.20	3.67	1.67
			1.50	2.45	1.63

*Concentration in g/l.
†Osmotic height in cm solvent.

ACKNOWLEDGMENTS

The author is much indebted to Dr. P. C. Das Gupta for helpful discussions throughout the course of this investigation. He is also grateful to Dr. P. B. Sarkar, Director, for his kind advice and encouragement.

REFERENCES

1. H. Chattopadhyay and P. B. Sarkar. Proc. Natl. Inst. Sci. India, **12**, 23 (1946).
2. J. K. N. Jones, L. E. Wise, and J. T. Jappe. Tappi, **39**, 139 (1956).
3. S. K. Chanda, E. L. Hirst, J. K. N. Jones, and E. G. V. Percival. J. Chem. Soc. 1289 (1950).
4. M. Abdel-Akher and F. Smith. Nature, **166**, 1037 (1950). B. Lythgoe and S. Trippett. J. Chem. Soc. 1983 (1950).
5. G. O. Aspinall and P. C. Das Gupta. J. Chem. Soc. 3627 (1958).
6. P. C. Das Gupta. J. Chem. Soc. 5262 (1961).
7. J. D. Geerdes and F. Smith. J. Am. Chem. Soc. **77**, 3569, 3572 (1955).
8. R. H. Horrocks and G. B. Manning. Lancet, **256**, 1042 (1949).
9. P. C. Das Gupta. J. Sci. Ind. Res. India, **21D**, 79 (1962).
10. P. B. Sarkar, A. K. Mazumdar, and K. B. Pal. Textile Res. J. **22**, 529 (1952).
11. S. C. Rogers, R. L. Mitchell, and G. J. Ritter. Anal. Chem. **19**, 1029 (1947).
12. J. F. Saeman, W. E. Moore, R. L. Mitchell, and M. A. Millett. Tappi, **37**, 336 (1954).
13. A. E. Flood, E. L. Hirst, and J. K. N. Jones. J. Chem. Soc. 1679 (1948).
14. L. Hough, J. K. N. Jones, and W. H. Wadman. J. Chem. Soc. 2511 (1949). R. L. Whistler, H. E. Conrad, and L. Hough. J. Am. Chem. Soc. **76**, 1668 (1954).
15. T. E. Timell. Can. J. Chem. **37**, 827 (1959).
16. L. J. Breddy and J. K. N. Jones. J. Chem. Soc. 738 (1945).
17. P. P. Fleury and J. Lange. J. Pharm. Chim. **17**, 107 (1933).
18. T. G. Halsall, E. L. Hirst, and J. K. N. Jones. J. Chem. Soc. 1399, 1427 (1947).
19. H. Hellfritz. Makromol. Chem. **7**, 184 (1951).

Can. J. Chem. Downloaded from www.nrcresearchpress.com by 210.87.254.5 on 09/05/12
For personal use only.

DIBENZOYLSILANES AND SUBSTITUTED BENZOYLSILANES

A. G. Brook and G. J. D. Peddle[1]
Department of Chemistry, University of Toronto, Toronto, Ontario
Received April 23, 1963

ABSTRACT

A number of silicon-substituted benzoylsilanes have been prepared. These all showed identical carbonyl infrared stretching wavelengths, and were all yellow, having essentially identical ultraviolet absorption spectra. Hence it is concluded that the spectral properties of benzoylsilanes are insensitive to the nature of the groups attached to silicon, even when these could provide d_π–p_π bonding.

Can. J. Chem. Downloaded from www.nrcresearchpress.com by 210.87.254.42 on 09/05/12
For personal use only.

It has previously been reported that benzoylsilanes (α-silylketones) have anomalous infrared and ultraviolet spectra, compared with their carbon analogues. Not only is the carbonyl-stretching vibration at considerably longer wavelength (6.18 μ, 1618 cm^{-1}) than in usual carbonyl compounds, but the long wavelength (carbonyl) ultraviolet absorption band falls in the visible region at about 403–417 mμ, so that all benzoylsilanes are yellow, regardless of whether phenyl or methyl groups are attached to silicon.

It seems reasonable to assume that the available *d* orbitals of silicon play some role in these spectral phenomena. West (2) has observed that d_π–p_π bonding can occur between silicon and adjacent atoms possessing unshared electrons such as halogen and oxygen, and that as the number of groups available for such bonding increases, the strength of the d_π–p_π bonds decreases. If d_π–p_π bonding with the carbonyl group is associated with the spectral behavior of the acylsilanes, then if alternative and perhaps stronger d_π–p_π bonding with some other group becomes possible, it might be anticipated that the spectral behavior of the ketone would revert toward that of a normal ketone. In order to see if this concept was valid attempts have been made to synthesize a number of substituted benzoylsilanes. These were of three main types: (*a*) hydroxy- and methoxy-benzoylsilanes, I; (*b*) halogenobenzylbenzoylsilanes, II; (*c*) dibenzoylsilanes, III.

$PhCOSiPh_2(OR)$	$PhCOSiPh_2CXYPh$	$PhCOSiR_2COPh$
I	II	III
(*a*) R = H	(*a*) X = H, Y = Cl	(*a*) R = Ph
(*b*) R = Me	(*b*) X = H, Y = Br	(*b*) R = Me
	(*c*) X = Cl, Y = Br	
	(*d*) X = Y = Br	

The synthesis of these compounds followed, in general, previously reported routes (1, 3). However, acylsilanes, with the possible exception of benzoyltriphenylsilane, are not particularly stable, hydrolyzing rapidly on exposure to air, benzaldehyde being formed. Most of the benzoylsilanes reported herein were exceptionally unstable.

The hydroxy- and methoxy-benzoylsilanes were synthesized as indicated by the following sequence of reactions:

[1]*Woodrow Wilson Fellow*, 1959–1960.

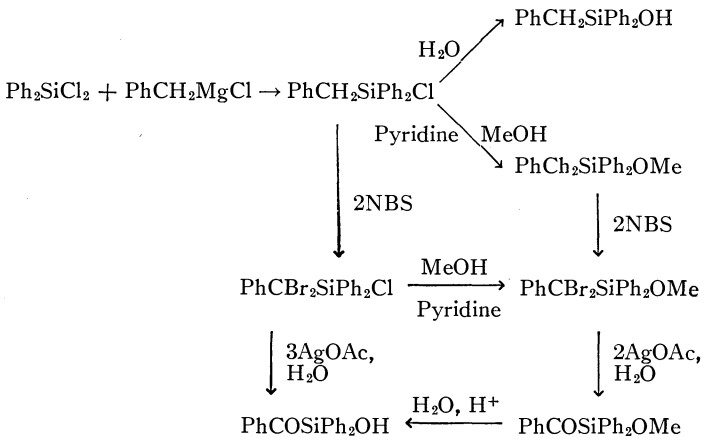

All of these reactions occurred readily and in good yield with the exception of the hydrolysis of dibromobenzyldiphenylmethoxysilane. Under all conditions used the methoxy group also hydrolyzed readily, giving the hydroxysilane or a mixture of the hydroxy- and methoxy-silanes, which were separated only with difficulty.

The synthesis of the dibenzoylsilanes caused particular difficulty, largely due to their instability. They and the various halobenzylbenzoylsilanes were prepared by the following routes:

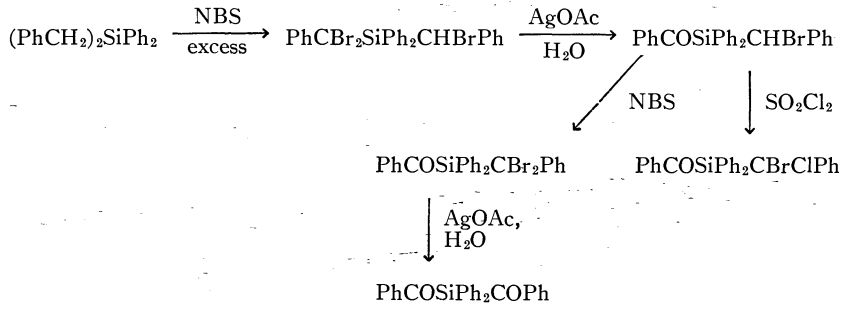

Dibenzyldiphenylsilane resisted tetrabromination with N-bromosuccinimide even in refluxing tetrachlorethylene, probably because of steric hindrance, and only a tribromo derivative could be isolated. Hence hydrolysis of the tribromide to a bromoketone, followed by further halogenation, toward which the ketone was not very stable, had to be employed. Hydrolysis of this dibromoketone gave very low yields of an extremely unstable compound, which appeared to be dibenzoyldiphenylsilane (see below).

Attempts to prepare the related dibenzoyldimethylsilane were made by an analogous route, except that tetrabromination with N-bromosuccinimide was successful. Hydrolysis with silver acetate – water gave a yellow oil which, however, decomposed to colorless products during attempted distillation, or during chromatography on silica gel or silicic acid columns. The major decomposition products isolated were benzaldehyde and/or benzoic acid, formed by hydrolysis and oxidation, and benzoin. The formation of this latter product may be explained as arising from rearrangement of the dibenzoyl compound, by a route analogous to that found for monobenzoylsilanes (4, 5), as illustrated below:

Can. J. Chem. Downloaded from www.nrcresearchpress.com by 210.87.254.42 on 09/05/12
For personal use only.

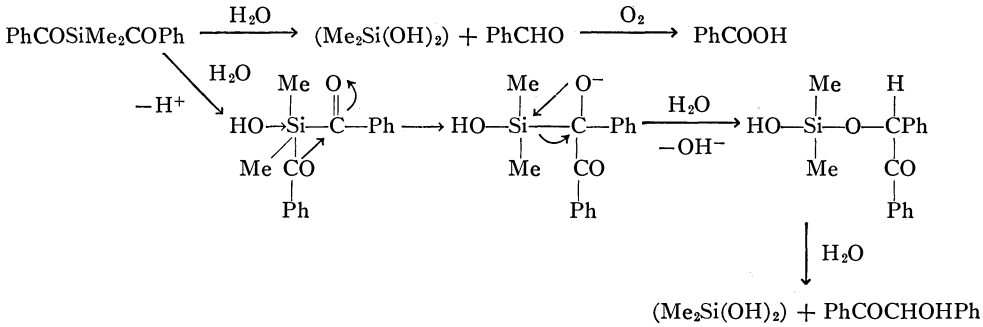

The ultraviolet spectra and carbonyl-stretching region of the infrared spectra for the new benzoylsilanes are reported in Table I together with the data for benzoylmethyldiphenylsilane (1) as reference compound. It is evident that in these compounds the carbonyl-stretching vibration is insensitive to the substituents attached to silicon, as was

TABLE I

Infrared and ultraviolet absorption data for benzoylsilanes

Compound	Infrared (C=O), μ	Ultraviolet (π–π^*) λ_{max}, mμ	Carbonyl group λ_{max}, mμ	
$PhCOSiPh_2OH$	6.19	257 (ϵ, 16,900)	[a]	415 (ϵ, 318)
$PhCOSiPh_2OMe$	6.19		405–415[b]	
$PhCOSiPh_2CHBrPh$	6.18	260 (ϵ, 16,800)	403 (s) (ϵ, 244)	417 (ϵ, 292)
$PhCOSiPh_2CBr_2Ph$	6.18	259 (ϵ, 18,600)	405 (s) (ϵ, 233)	416 (ϵ, 265)
$PhCOSiPh_2CHClPh$	6.18			
$PhCOSiPh_2CBrClPh$	6.18			
$PhCOSiPh_2COPh$	6.18, 5.97	258 (ϵ, 24,100)	405 (s) (ϵ, 233)	416 (ϵ, 244)
$PhCOSiMe_2Ph$	6.18	255 (ϵ, 13,900)	403 (s) (ϵ, 200)	415 (ϵ, 216)

NOTE: (s) = shoulder.
[a]Unresolved shoulder at about 405 mμ.
[b]Extinction coefficient not determined since compound contaminated with small amount of benzoyldiphenylsilanol, as shown by infrared spectrum.

observed previously (1). The ultraviolet spectra also conform closely to those found earlier for methyl- or phenyl-benzoylsilanes, with no significant change occurring in position for either the π–π^* or for the long wavelength (carbonyl) band. These results indicate that if d_π–p_π bonding is occurring between silicon and the adjacent oxygen or halogen atoms in these molecules, it has little effect on the silicon–carbonyl interaction which causes the anomalous spectral behavior.

The spectra of dibenzoyldiphenylsilane are worthy of comment. Since the compound was too unstable to be analyzed it is necessary to establish that impurities are not responsible for any of the prominent absorption bands. The most probable impurities, based on our experience, are benzaldehyde, benzoic acid, benzoin, and silanols. That these were not present in significant concentrations is evident from the absence of absorption bands at 2.8–3.0 μ (OH) or in the 3.7 μ (CHO) region.

The intensity of the π–π^* band of the compound (ϵ 24,100) relative to benzoyldiphenylmethylsilane (ϵ 13,900) indicates the presence of two benzoyl groups, although the long wavelength (carbonyl) band has an extinction coefficient little greater than that of the monobenzoylsilane. At the same time, the infrared shows two strong carbonyl bands at 5.97 and 6.18 μ. These may be due to two non-equivalent carbonyl groups, due to differences in the interaction with silicon or to conformational effects (6). Alternatively the two

Can. J. Chem. Downloaded from www.nrcresearchpress.com by 210.87.254.42 on 09/05/12
For personal use only.

carbonyl bands may be due to equivalent carbonyl groups undergoing vibrational coupling with each other to produce two bands, as has been observed with other dicarbonyl compounds (7). It does not seem possible at this time to decide whether both carbonyl groups of dibenzoyldiphenylsilane interact identically with the silicon atom, or whether one is a typical α-silyl ketone and the other acts as a "normal" ketone type of carbonyl group.

EXPERIMENTAL

All reactions involving organometallics were carried out under a dry oxygen-free nitrogen atmosphere. Infrared spectra were taken in CCl_4 on a Beckman IR5 instrument calibrated against polystyrene; ultraviolet spectra were taken in ethanol.

A. Benzyldiphenylchlorosilane and its Derivatives

Benzyldiphenylchlorosilane

To 104 g (0.41 mole) of diphenyldichlorosilane in 250 ml of ether was added dropwise 0.41 mole of 1.65 *N* benzylmagnesium chloride. After the mixture had been stirred overnight a negative Gilman color test I (8) was obtained. To the suspension was added 1 l. of petroleum ether (b.p. 60–70°) and the mixture was filtered. After removal of the solvents the material was distilled at 190–194° at 0.6 mm to give 85 g (67%) of benzyldiphenylchlorosilane, n_D^{25} 1.6078 Anal. Calc. for $C_{19}H_{17}SiCl$: Si, 9.07. Found: Si, 9.12.

α,α-Dibromobenzyldiphenylchlorosilane

To 20.0 g (0.65 mole) of benzyldiphenylchlorosilane in 150 ml of carbon tetrachloride was added 25.0 g (0.14 mole) of N-bromosuccinimide and a few small lumps of benzoyl peroxide. The mixture was refluxed for 16 hours, cooled, and the succinimide filtered off. Evaporation of the filtrate to dryness gave a yellow oil which was crystallized twice from hexane to give 15.75 g (52%) of α,α-dibromobenzyldiphenylchlorosilane, m.p. 79–81°. Anal. Calc. for $C_{19}H_{15}SiClBr_2$: C, 48.8; H, 3.22. Found: C, 48.8; H, 3.29.

Benzoyldiphenylsilanol

To 5.0 g (0.0107 mole) of dibromobenzyldiphenylchlorosilane in 50 ml acetone and 7 ml of water was added at 0° (ice-water bath) 7.1 g (0.032 mole) of silver trifluoroacetate in 110 ml of benzene. A pale yellow color and grey precipitate formed immediately. The ice bath was removed once addition was complete and the mixture was stirred for 2 hours. The silver bromide was filtered off, about 1 l. of water was added, and the mixture was extracted with benzene. The benzene layers were back-extracted with water, dilute sodium bicarbonate, and then water. After the benzene layer was dried over sodium sulphate the solvents were removed under reduced pressure to yield a yellow oil, which was recrystallized from hexane–cyclohexane to give 2.13 g (65%) of bright yellow benzoyldiphenylsilanol, m.p. 97–99°. Anal. Calc. for $C_{19}H_{16}SiO_2$: C, 75.0; H, 5.28. Found: C, 74.5; H, 5.22. The solid became a sticky mass in a few days with a strong odor of benzaldehyde.

Benzyldiphenylmethoxysilane

To 15 g (0.048 mole) of benzyldiphenylchlorosilane in 80 ml of methanol was added 5 ml of pyridine. The reaction mixture became hot. After 15 minutes the reaction mixture was drowned in water and extracted with benzene. The dried benzene layer on distillation gave 10 g (70%) of benzyldiphenylmethoxysilane, b.p. 159–161° at 0.28 mm, n_D^{25} 1.5932.

Benzyldiphenylsilanol

To 1 l. of ice and water containing 5 ml of conc. ammonium hydroxide was added slowly with vigorous stirring 10 g (0.032 mole) of benzyldiphenylchlorosilane in 100 ml of ether. After 0.5 hour the ether layer was removed, dried over sodium sulphate, and the solvent removed under reduced pressure to give 9.4 g of a white solid, m.p. 46–49°. Recrystallization from petroleum ether (b.p. 60–70°) gave 7.2 g (77%) of benzyldiphenylsilanol, m.p. 51.5–53°. Anal. Calc. for $C_{19}H_{18}SiO$: C, 78.5; H, 6.23. Found: C, 78.4; H, 6.22.

α,α-Dibromobenzyldiphenylmethoxysilane

(a) From dibromobenzyldiphenylchlorosilane.—To 5.0 g (0.011 mole) of the dibromobenzyl compound in 15 ml of methanol and 25 ml of benzene was added 0.9 ml (0.012 mole) of pyridine. After 18 hours the reaction was drowned in water and ether-extracted. The combined organic layers were dried with sodium sulphate, and removal of the solvents under reduced pressure gave 4.02 g (81%) of α,α-dibromobenzyldiphenylmethoxysilane, m.p. 79–82°, which on recrystallization from hexane had m.p. 80–82°. Anal. Calc. for $C_{20}H_{18}SiOBr_2$: C, 52.0; H, 3.91. Found: C, 52.7; H, 3.91.

(b) From Benzyldiphenylmethoxysilane.—A solution of 3.0 g (0.01 mole) of benzyldiphenylmethoxysilane in 50 ml of carbon tetrachloride was refluxed 5.5 hours with 3.56 g (0.02 mole) of N-bromosuccinimide and a few small lumps of benzoyl peroxide. On cooling and filtering of the succinimide, the filtrate was evaporated to dryness to yield a viscous oil. Crystallization from hexane gave 3.48 g (72%) of α,α-dibromobenzyldiphenylmethoxysilane, m.p. 79–81°, identified by mixed melting point with the material described above. Their infrared spectra were identical.

Can. J. Chem. Downloaded from www.nrcresearchpress.com by 210.87.254.42 on 09/05/12
For personal use only.

Attempted Preparation of Benzoyldiphenylmethoxysilane

To 4.62 g (0.01 mole) of α,α-dibromobenzyldiphenylmethoxysilane in 100 ml of acetone and 50 ml of benzene was added 3.4 g (0.02 mole) of silver acetate and 5 ml of water. The mixture was stirred overnight in the dark. The yellow solution was filtered from the silver bromide, drowned in water, and extracted into ether. Removal of the ether gave an oily yellow solid whose infrared spectrum showed the presence of strong Si—OMe absorption at 9.2 μ and only very weak OH absorption in the 2.7–2.8 μ region. The carbonyl absorption occurred at 6.19 μ. Attempts to purify the material by crystallization from hexane or by chromatography on alumina failed, and the odor of benzaldehyde soon became apparent. Subsequent repetitions of this experiment, with changes in solvent or of time of hydrolysis, failed to yield pure benzoyldiphenylmethoxysilane. When the silver acetate was replaced by silver trifluoroacetate, the major product was benzoyldiphenylsilanol, m.p. 97–99°, identified by mixed melting point.

B. Dibenzyldiphenylsilane and its Derivatives.

The polyhalogenated derivatives of this compound, most of which served as precursors for the preparations of ketones through hydrolysis with silver acetate, were prepared by conventional methods such as are described in Section A. Hence only a few typical preparations will be described in detail—the properties of the various additional compounds are summarized in Table II.

TABLE II
Organosilicon compounds

Compound	M.p., °C	Yield, %
$PhCH_2SiPh_2CHClPh$	159 decomp.	26[a]
$PhCBr_2SiPh_2CHClPh$	140 decomp.	86[b]
$PhCOSiPh_2CHClPh$	100–101	62[c]
$PhCOSiPh_2CBrClPh$	118–120	47[d]

[a]Indicated are solvents of recrystallization and analysis, petroleum ether (b.p. 60–70°) – CCl_4.
[b]EtOH. Calc. for $C_{26}H_{21}SiBr_2Cl$: Si, 5.04. Found: Si, 4.99.
[c]EtOH–EtOAc. Calc. for $C_{26}H_{21}SiClO$: C, 75.6; H, 5.17. Found: C, 74.7; H, 5.13.
[d]EtOH–EtOAc. Calc. for $C_{26}H_{20}SiBrClO$: Si, 5.70. Found: Si, 5.60.

α,α,α'-Tribromodibenzyldiphenylsilane

Dibenzyldiphenylsilane was prepared from diphenyldichlorosilane and benzylmagnesium chloride in 61% yield, m.p. 60.5–61°, reported (9) 61°. A mixture of 36.4 g (0.1 mole) of dibenzyldiphenylsilane and 80 g (0.45 mole) of N-bromosuccinimide in 300 ml of carbon tetrachloride was refluxed for 44 hours with occasional small additions of benzoyl peroxide. After cooling and removal of 51.8 g (91%) of succinimide, the filtrate was concentrated under vacuum. Addition of petroleum ether gave 47 g (79%) of α,α,α'-tribromobenzyldiphenylsilane, m.p. 129–130°, which after several recrystallizations melted at 145–149°.

Attempts to further brominate the tribromide with N-bromosuccinimide in carbon tetrachloride, in tetrachloroethylene, or in a mixture of these solvents, over various time intervals, gave mainly recovered tribromide, and no tetrabromide could be isolated.

Benzoyl-α-bromobenzyldiphenylsilane

A mixture of 15 g (0.025 mole) of α,α,α'-tribromodibenzyldiphenylsilane and 14.9 g (0.089 mole) of silver acetate in 150 ml of ethanol, 120 ml of acetone, and 60 ml of water was stirred in the dark for 41 hours. The silver bromide was filtered off, water was added to the filtrate, and the material was extracted with ether several times. The ether layers, after being dried over sodium sulphate, were concentrated under reduced pressure, and the resulting yellow oil was crystallized from ethanol – ethyl acetate to give 5.1 g (64%) of yellow benzoyl-α-bromobenzyldiphenylsilane, m.p. 90–92°. Anal. Calc. for $C_{26}H_{21}SiOBr$: C, 68.4; H, 4.60. Found: 68.4, H, 4.67.

α,α,α'-Tribromo-α'-chlorodibenzyldiphenylsilane

A solution of 6.18 g (0.011 mole) of α,α,α'-tribromodibenzyldiphenylsilane and 1.62 g (0.012 mole) of sulphuryl chloride in 50 ml of chlorobenzene was refluxed for 2.5 hours with a trace of added benzoyl peroxide. Red fumes, presumably bromine, were evolved during the reaction. The solvent was removed under reduced pressure and the resulting oil was crystallized from ethyl acetate – ethanol to give 4.17 g (58%) of α,α,α'-tribromo-α'-chlorodibenzyldiphenylsilane, m.p. 125–140°, which on recrystallization melted at 125–127°. The crystals turned orange-brown on standing. Anal. Calc. for $C_{26}H_{20}SiBr_3Cl$: Si, 4.42. Found: Si, 4.47, 4.59.

α,α-Dibromobenzylbenzoyldiphenylsilane

A solution of 0.68 g (0.0015 mole) of α-bromobenzylbenzoyldiphenylsilane in 10 ml of carbon tetrachloride and 0.23 g (0.0013 mole) of N-bromosuccinimide was refluxed for 1 hour with a trace of benzoyl peroxide. After removal of the succinimide and the solvent the yellow oil was chromatographed on a 6-in. silica gel column, and eluted with benzene. The yellow eluate, after removal of the solvent and crystallization from

Can. J. Chem. Downloaded from www.nrcresearchpress.com by 210.87.254.42 on 09/05/12
For personal use only.

ethyl acetate – ethanol – petroleum ether (b.p. 40–60°), gave 0.35 g (44%) of yellow α,α-dibromobenzylbenzoyldiphenylsilane, m.p. 107–109°. After 5 days marked decomposition had occurred, although the product was stored in sealed containers. Similar runs on a larger scale gave yields from 0–45%—in general better yields were obtained from smaller runs. Anal. Calc. for $C_{26}H_{20}SiBr_2O$: C, 58.2; H, 3.76. Found: C, 59.6; H, 3.95.

Dibenzoyldiphenylsilane

A solution of 0.3 g (0.0005 mole) of dibromobenzylbenzoyldiphenylsilane in 3 ml of acetone, 12 ml of ethanol, 5 ml of benzene, and 0.2 ml of water was stirred in the dark for 7 hours with 0.3 g (0.0018 mole) of silver acetate. The silver salts were filtered off and the yellow filtrate was added to ether, washed with water, and dried with sodium sulphate; the ether was then removed under vacuum and the yellow oil was chromatographed on an 8-in. silica gel column, using benzene as eluant. Two yellow bands appeared on the column, the first eluted giving a positive test for halogen. This was isolated and shown to be recovered dibromobenzylbenzoyldiphenylsilane, 0.25 g (83%) after crystallization from petroleum ether (b.p. 60–70°), m.p. 107–109°. The second yellow fraction eluted was an oil which failed to crystallize when treated with a variety of solvents. It gave a negative test for halogen, and identification as dibenzoyldiphenylsilane, 0.02 g (9%), is based on the infrared and ultraviolet spectra (see discussion section). The compound decomposed rapidly on standing, even in a nitrogen atmosphere, liberating the odor of benzaldehyde.

Runs similar to the above, but without the use of acetone during the "hydrolysis", gave after chromatography on silicic acid dibenzoyldiphenylsilane in yields up to 40%.

Dibenzyldimethylsilane

To a solution of 26.4 g (0.20 mole) of dimethyldichlorosilane in 400 ml of toluene was added 0.41 mole of benzylmagnesium chloride in 300 ml of ether. The ether was distilled off and the mixture was refluxed at 100° for 21 hours. After filtration of the magnesium salts the solvents were removed under reduced pressure and the resulting oil was crystallized from ethanol to give 47 g (96%) of dibenzyldimethylsilane, m.p. 56–58°. Anal. Calc. for $C_{16}H_{20}Si$: C, 79.93; H, 8.39. Found: C, 80.21; H, 8.23.

$\alpha,\alpha,\alpha',\alpha'$-Tetrabromodibenzyldimethylsilane

Bromination of 10 g (0.042 mole) of dibenzyldimethylsilane in 150 ml of carbon tetrachloride with 30 g (0.17 mole) of N-bromosuccinimide at reflux with an added trace of benzoyl peroxide over 6 hours gave, after removal of the succinimide and solvents, and crystallization from ethyl acetate, 21.8 g (94%) of $\alpha,\alpha,\alpha',\alpha'$-tetrabromodibenzyldimethylsilane, m.p. 122–125°. Anal. Calc. for $C_{16}H_{16}SiBr_4$: C, 34.54; H, 2.90. Found: C, 34.90; H, 3.16.

Hydrolysis of Tetrabromodibenzyldimethylsilane

A solution of 5.0 g (0.009 mole) of the above tetrabromide in 20 ml ethanol, 30 ml of benzene, and 1 ml of water was treated with 6.01 g (0.036 mole) of silver acetate. An immediate exothermic reaction occurred, a dark precipitate formed, and the solution became yellow. The mixture was stirred for 3 hours in the dark. The silver salts, 6.6 g (98%), were filtered off, ether was added, and the ether layer was washed with water and dried over sodium sulphate; the ether was removed to give 2.8 g of yellow oil.

Attempts to crystallize the oil, which smelt strongly of benzaldehyde, from a variety of solvents failed. Attempted distillation at 0.06 mm failed when the material decomposed, turning black at 125°. If the oil was left in contact with air, it decomposed, turning black and forming solid from which benzoin, m.p. 134–136°, identified by mixed melting point, could be isolated in 25% yield.

Attempts to purify the oil by chromatography on silica gel, silicic acid, or alumina also failed. While two yellow bands were separated on the column, only one yellow band (benzoyldibromobenzyldimethylsilane?), which contained halogen and smelled strongly of benzaldehyde, could be eluted; the second faded to colorless on the column before it could be eluted.

Attempted hydrolysis using silver nitrate instead of silver acetate gave essentially quantitative yields of silver bromide, but only pale yellow oils, together with up to 70% yields of benzoic acid, m.p. 120–121°, could be obtained, indicating that considerable hydrolysis and oxidation had occurred.

ACKNOWLEDGMENT

This research was supported in part by a grant from the National Research Council.

REFERENCES

1. A. G. Brook, M. A. Quigley, G. J. D. Peddle, N. V. Schwartz, and C. M. Warner. J. Am. Chem. Soc. **82**, 5102 (1960).
2. R. West, L. S. Whatley, and K. J. Lake. J. Am. Chem. Soc. **83**, 761 (1961).
3. A. G. Brook. J. Am. Chem. Soc. **79**, 4373 (1957).
4. A. G. Brook. J. Org. Chem. **25**, 11072 (1960).
5. A. G. Brook and N. V. Schwartz. J. Org. Chem. **27**, 2311 (1962).
6. J. B. Rogan and D. J. Ellis. J. Org. Chem. **26**, 5232 (1961).
7. R. A. Abramovitch. Can. J. Chem. **37**, 361 (1959).
8. H. Gilman and F. Schulze. J. Am. Chem. Soc. **47**, 2002 (1925).
9. M. Mainthal *et al.* J. Am. Chem. Soc. **76**, 6392 (1954).

Can. J. Chem. Downloaded from www.nrcresearchpress.com by 210.87.254.42 on 09/05/12
For personal use only.

STRUCTURAL RELATIONSHIPS OF EXTRACELLULAR POLYSACCHARIDES FROM PHYTOPATHOGENIC XANTHOMONAS SPP.

PART II. X. HYACINTHI, X. TRANSLUCENS, AND X. MACULOFOLIIGARDENIAE[1]

P. A. J. GORIN AND J. F. T. SPENCER
National Research Council of Canada, Prairie Regional Laboratory, Saskatoon, Saskatchewan

Received May 6, 1963

ABSTRACT

The extracellular polysaccharide formed from *Xanthomonas hyacinthi* is shown to be a branched polymer containing glucuronic acid, mannose, and glucose. Acid and enzymic hydrolysis show the presence of β-D-Glp 1 → 4 D-Man and the 4-unit sequence β-D-GlpA 1 → 2 D-Manp 1 → 3 β-D-Glp 1 → 4 D-Gl. Examination by the methylation technique showed the presence of a considerable proportion of 2-linked mannopyranose units. The spectrum of methyl glycosides formed from this polysaccharide and those from *Xanthomonas maculofoliigardeniae* and *Xanthomonas translucens* are similar, and in terms of sugar linkages differentiate them from that of *Xanthomonas stewartii*, which contains glucuronic acid, glucose, and galactose.

Can. J. Chem. Downloaded from www.nrcresearchpress.com by 210.87.254.42 on 09/05/12
For personal use only.

The extracellular polysaccharides from phytopathogenic *Xanthomonas* spp. appear to have several structural features in common. In general they contain glucuronic acid, glucose, and mannose (1–4), and in the species so far examined 4,6-carboxyethylidene groups (5). These properties distinguish the organisms from *Xanthomonas stewartii*, which yields a polysaccharide containing glucuronic acid, glucose, and galactose (3). In this paper the *Xanthomonas hyacinthi* polysaccharide is examined in detail. Two other polysaccharides produced by *Xanthomonas translucens* and *Xanthomonas maculofoliigardeniae* were examined by the methylation technique in order to find whether there are any basic differences in fine structure.

The polysaccharide from *X. hyacinthi* was examined for structural details using chemical and enzymic hydrolysis techniques. The polysaccharide contained 1 acidic function for every 7 sugar units. Hydrolysis with aqueous acid yielded a series of acidic oligosaccharides, the number of units in a sequence being assumed from their paper chromatographic behavior rather than their neutral equivalents, which were too high for accurate measurement. These appeared to be a di-, tri-, and tetra-saccharide and were isolated chromatographically and characterized. The disaccharide was shown to be 2-*O*-β-D-glucuronopyranosyl-D-mannose, identified by its hydrolysis products, lead tetraacetate oxidation characteristics, and by its crystalline hepta-*O*-methyl methyl ester. The trisaccharide, which consisted of glucuronic acid, mannose, and glucose, appeared to be closely related to that isolated from the polysaccharides of *Xanthomonas campestris* (6) and *Xanthomonas oryzae* (4). On treatment with lead tetraacetate, nearly one mole of oxidant was consumed per mole of trisaccharide, which resulted in oxidation of the glucose unit. The product, on hydrolysis, yielded arabinose, or arabitol when the oxidation product was first reduced with sodium borohydride. Since the trisaccharide gave 2-*O*-β-D-glucuronopyranosyl-D-mannose on hydrolysis the mannose unit must be attached to the 3-position of glucose (7) (structure I). Methylation followed by hydrolysis gave a little tetra-*O*-methylhexose and no dimethylhexose, indicating the presence of some hexopyranosyl-2-*O*-β-D-glucuronopyranosyl-D-mannose also. The tetrasaccharide which gave the aldobiouronic acid

[1]*Issued as N.R.C. No. 7482.*

and glucose on acid hydrolysis offered further information on the polysaccharide structure. Under milder acidic conditions it yielded a little material which chromatographed with the aldotriouronic acid. Lead tetraacetate oxidation characteristics indicated a 1,4 reducing end-unit (7), suggesting it had structure II.

Partial degradation of the polysaccharide with acid followed by enzymolysis of the fragments with an enzyme preparation, S157B, containing cellulase, kindly supplied by Dr. E. Reese, gave in low yield cellobiose, characterized as its β-octaacetate and glucose, thus indicating that some glucose units linked 1,4-β are present in the polysaccharide. Information on the source of the liberated cellobiose and glucose was obtained by enzymolysis of the aldotetraouronic acid. This material yielded glucose and the aldobiouronic acid, thus indicating that the enzyme had a wide range of enzymic attack. Evidently it can attack the 1,4-β glucose-to-glucose unit at the reducing end and the 1,3 mannose-to-glucose unit (Fig. 1). Possibly, the absence of cellobiose is due to the presence of a β-glucosidase in the enzyme preparation. Acetolysis of the acetate of *X. hyacinthi* polysaccharide gave material which, after deacetylation and chromatography, was shown to

β-D-GlpA 1 → 2 D-Manp 1 → 3 D-Gl (I)
↓ acid or enzyme S157B
β-D-GlpA 1 → 2 D-Man + Glucose
↑ enzyme S157B
β-D-GlpA 1 → D-Manp 1 → 3 β-D-Glp 1 → 4 D-Gl (II)

FIG. 1.

contain 4-*O*-β-D-glucopyranosyl-D-mannose, characterized by its lead tetraacetate oxidation characteristics and acid hydrolysis products before and after sodium borohydride reduction.

Periodate oxidation of the *X. hyacinthi* polysaccharide followed by sodium borohydride reduction and then acid hydrolysis gave glucose, glycerol, and erythritol. A similar result was also obtained using the *X. maculofoliigardeniae* and *X. translucens* polysaccharides. These results are consistent with the finding that 1,4-linked and 1,3-linked glucose and 1,2-linked mannose units are present in the oligosaccharides formed on partial hydrolysis.

The ratios of glucose to mannose and the specific rotations of the three polysaccharides showed variation and are recorded in Table I. A greater degree of structural difference

TABLE I

Neutral sugar components formed on acid hydrolysis of polysaccharides

Polysaccharide source	Glucose	Mannose	Specific rotation of polysaccharides
X. hyacinthi	1	0.78	−5°
X. translucens	1	0.90	−12°
X. maculofoliigardeniae	1	0.95	−35°

was found when the linkage sites on the majority of the neutral sugars units were determined by methylation, followed by methanolysis of the methylated products. The fragments, thus formed, were compared quantitatively by gas phase chromatography. Although complications were possible due to the presence of carboxyethylidene groups, the gas chromatograms gave a characteristic spectrum of products in which only the

Can. J. Chem. Downloaded from www.nrcresearchpress.com by 210.87.254.42 on 09/05/12
For personal use only.

proportions showed variation. The presence of methyl tetra-*O*-methyl-glycosides showed that the polysaccharides are non-linear. The relative amounts of methyl tetra-*O*-methyl-glucoside and -mannoside showed great variation from one polysaccharide to another. However, whether these differences are due to the presence of 4,6-carboxyethylidene groups is not clear at this stage. Less information could be obtained on the identity of the methyl tri-*O*-methyl glycosidic fragments since in this region many different glycosides co-chromatograph. The presence of methyl 3,4,6-tri-*O*-methyl-D-mannose and methyl 2,3,6-tri-*O*-methyl-D-glucose was assumed by reference to the periodate oxidation results and the partial hydrolytic studies. In the di-*O*-methyl series the presence of methyl 2,6-di-*O*-methyl-D-glucoside was also assumed. The ratios of these glycosides by peak area were not reproducible from one column packing to another. The packing used with the greatest response for methyl tri-*O*-methyl- compared with methyl tetra-*O*-methyl-hexosides was the fully methylated hydroxyethyl cellulose WP-09 of Kircher (8). Comparison in terms of peak areas of the proportions of *O*-methyl glycosidic fragments is made in Table II.

TABLE II

Neutral glycosides formed on methanolysis of methylated polysaccharides in terms of gas chromatographic peak areas

Methyl glycoside	Source of methylated polysaccharide		
	X. hyacinthi	*X. translucens*	*X. maculofoliigardeniae*
2,3,4,6-Tetra-*O*-methyl-D-mannose	3.8	4.6	2.3
2,3,4,6-Tetra-*O*-methyl-D-glucose	2.1	7.9	3.8
3,4,6-Tri-*O*-methyl-D-mannose*	10 (10)	10 (10)	10 (10)
2,3,6-Tri-*O*-methyl-D-glucose*	8.4 (7.6)	9.7 (8.7)	10 (9.0)
3,4-Di-*O*-methyl-D-mannose?	0.5	0.8	0.7
Unknown	1.1	2.8	2.8
2,6-Di-*O*-methyl-D-glucose	3.1	2.7	4.4

*The figures in parentheses are the molar ratios of the methyl glycosides after a calibration correction has been made.

EXPERIMENTAL

Evaporations were carried out under reduced pressure and specific rotations measured at 25° C. The organisms used were *X. hyacinthi* (ATCC 12612), *X. maculofoliigardeniae* (ATCC 10201), and *X. translucens* (ATCC 10722). These were grown on media identical with that used for *Corynebacterium* spp. (9).

Estimation of Hexoses in Xanthomonas Spp. Polysaccharides

The polysaccharides (1.0 g samples) were heated overnight at 100° C in 2 *N* sulphuric acid (20 ml). The solutions were neutralized ($BaCO_3$), filtered, and evaporated to sirups. The neutral components with the exception of traces of rhamnose, which was also present, were estimated colorimetrically with the benzidine reagent after strip separation on paper chromatograms (10). The mannose–glucose ratios are recorded in Table I. In addition the neutral equivalent of *X. hyacinthi* polysaccharide was shown to be 1050.

Partial Acid Hydrolysis of X. hyacinthi Polysaccharide

The polysaccharide (35 g) was heated on a steam bath for 6 hours in *N* sulphuric acid. The solution was neutralized ($BaCO_3$), filtered, and treated with Amberlite IR 120. Acidic material was removed with Dowex-1 (bicarbonate form), which was filtered off. Treatment with 5% aqueous formic acid (2 liters) eluted the uronic acids and evaporation of the solution yielded 11.6 g of solids. The material was fractionated on a cellulose column using ethyl acetate – acetic acid – water (9:4:4 v/v) as solvent. The aldobiouronic acid (1.7 g) was isolated and hydrolyzed overnight with 6 *N* sulphuric acid at 100° C to yield glucuronic acid and mannose. The material was resistant to lead tetraacetate oxidation and was therefore linked 1,2 (7). A portion (0.22 g) was methylated by the dimethyl sulphate – sodium hydroxide method. Extraction of the acidified solution yielded partly methylated material (0.17 g). This was refluxed in methyl iodide (10 ml) and three daily additions of silver oxide (0.50 g) were made. The solution was filtered and evaporated to a

Can. J. Chem. Downloaded from www.nrcresearchpress.com by 210.87.254.42 on 09/05/12
For personal use only.

crust (0.16 g). Extraction with hot hexane followed by evaporation to a small volume allowed crystals to separate on cooling. Recrystallization from ether–hexane yielded methyl 2-*O*-[methyl(2,3,4-tri-*O*-methyl-β-D-glucuronosyl]-3,4,6-tri-*O*-methyl-D-mannoside with m.p. 141° C (11). Calculated for $C_{20}H_{36}O_{12}$: C, 51.3%; H, 7.75%. Found: C, 51.15%; H, 7.8%.

(i) Characterization of the Aldotriouronic Acid

The aldotriouronic acid (0.46 g), $[\alpha]_D$ +15° (*c*, 1.0, H_2O), was eluted next and on hydrolysis with *N* sulphuric acid at 100° C overnight gave the above aldobiouronic acid, glucose, and a trace of mannose. A few milligrams in water (0.1 ml) was treated with sodium borohydride (5 mg) for 18 hours. Acetic acid was then added, followed by Amberlite IR 120. Filtration and evaporation gave a solid which was dissolved in methanol, which was then evaporated. Two more evaporations gave the reduced aldotriouronic acid. Hydrolysis with *N* sulphuric acid on a steam bath overnight yielded the aldobiouronic acid, and only traces of mannose and glucose, thus indicating that the aldotriouronic acid has a glucose reducing end-unit. Lead tetraacetate oxidation of the aldotriouronic acid resulted in 0.7, 0.8, and 0.9 mole of oxidant being consumed after 3, 10, and 20 minutes, respectively, suggesting mainly a 3-linked glucose reducing end-unit. The 3-linkage was confirmed since hydrolysis of the oxidized sugar with aqueous oxalic acid resulted in the production of arabinose. Sodium borohydride reduction of the oxidized sugar followed by acid hydrolysis yielded arabitol, with only traces of other polyols.

Methylation of the aldotriouronic acid by means of the same procedure as used for the aldobiouronic acid gave a fully methylated product. On hydrolysis with *N* sulphuric acid at 100° C overnight it yielded, in addition to acidic material and tri-*O*-methylhexose, a trace of tetra-*O*-methylhexose. No di-*O*-methylhexose was formed.

(ii) Characterization of Aldotetraouronic Acid

The next material eluted from the cellulose column appeared to be an aldotetraouronic acid with $[\alpha]_D$ +17° (*c*, 0.5, H_2O). Acid hydrolysis with *N* sulphuric acid at 100° C overnight gave an aldobiouronic acid, a trace of mannose, and a greater proportion of glucose than that formed on hydrolysis of the aldotriouronic acid. Hydrolysis for 2 hours under the same conditions yielded a trace of material which co-chromatographed with the aldotriouronic acid. Sodium borohydride reduction followed by acidic hydrolysis of the aldotetraouronic acid showed that the non-reducing end-group was glucose. On treatment with lead tetraacetate 0.7, 1.1, and 1.5 moles were consumed after 3, 10, and 25 minutes respectively, thus indicating mainly a 1,4-linked reducing group.

Enzymic Hydrolysis of Partially Degraded X. hyacinthi Polysaccharide

The polysaccharide (20 g) was heated on a steam bath in 0.1 *N* sulphuric acid (500 ml) for 3 days. The solution was no longer viscous and was neutralized ($BaCO_3$), filtered, and evaporated to a small volume. This procedure gave free mannose with only traces of glucose. Acidic material was then precipitated by addition of the aqueous solution to methanol. A portion (2.3 g) of the isolated solid (9.5 g) was dissolved in water and treated with Amberlite IR 120. After filtration and partial evaporation to 20 ml the pH was brought to 6 with sodium bicarbonate. Enzyme preparation S157B (100 mg) was added and the solution kept at 45° C for 16 hours. Cellobiose (31 mg) and glucose (21 mg) were liberated and isolated on Whatman No. 3 paper sheets using ethyl acetate – pyridine – water (10:4:3 v/v) as solvent and the disaccharide was converted to β-octaacetyl cellobiose by the hot acetic anhydride – sodium acetate method. Two recrystallizations of the product from ethanol gave crystals with m.p. 194–195° C that gave an X-ray diffraction pattern identical with that of authentic material.

Enzymic hydrolysis of the aldotrio- and aldotetrao-uronic acids under identical conditions gave 2-*O*-β-D-glucuronopyranosyl-D-mannose and -glucose, identified chromatographically.

Acetolysis of X. hyacinthi Polysaccharide

The acetate of the polysaccharide was formed by the action of dimethylformamide – pyridine – acetic anhydride, and isolated by precipitation from excess water. The acetate (10 g) was dissolved in acetic anhydride (100 ml) containing sulphuric acid (9 ml) and the solution kept at 35° C for 24 hours. It was then added to ice water and after destruction of acetic anhydride was complete the solution was extracted with chloroform, which was evaporated. The residue was redissolved in chloroform (200 ml), and methanol (100 ml) containing sodium (0.50 g) was added. After 30 hours the solution was extracted with water, which was evaporated to give a sirup. This was shown to consist mainly of mannose and an aldobiouronic acid on paper chromatograms in the ethyl acetate – acetic acid – water (9:2:2 v/v) solvent. In addition a disaccharide slightly faster than the acid could be detected with the *p*-anisidine hydrochloride spray (12). This (230 mg) was isolated by chromatography on a cellulose column using acetone–water (5:1 v/v) as solvent. Hydrolysis with *N* sulphuric acid overnight showed it consisted of glucose and mannose. The reducing end was shown to be mannose since only glucose remained on sodium borohydride reduction followed by acid hydrolysis. The disaccharide consumed 0.74, 1.14, and 1.57 moles of lead tetraacetate after 3, 10, and 30 minutes, respectively and was therefore linked 1,4. Its specific rotation, +15° (*c*, 0.6, H_2O), agrees with that (+12°) noted by Bergmann and Schotte (13) for 4-*O*-β-D-glucopyranosyl-D-mannose.

Can. J. Chem. Downloaded from www.nrcresearchpress.com by 210.87.254.42 on 09/05/12
For personal use only.

Periodate Oxidation of Polysaccharides

This was carried out by shaking the polysaccharide (1%) in a 5 *M* excess of periodic acid in water. After a week the acid was neutralized with barium carbonate, the solution was filtered, and sodium borohydride was added. Excess reagent was destroyed after a day and borate was removed. Hydrolysis of the modified polysaccharide was carried out with *N* sulphuric acid at 100° C overnight. The hydrolysis products were identified on paper chromatograms as glucose, erythritol, and glycerol.

Methylation and Methanolysis of Polysaccharides

The polysaccharides were methylated as in Part I of this series (3), first with the dimethyl sulphate – sodium hydroxide reagent. After three methylations the partly methylated polysaccharides became insoluble in water and these were isolated and fully methylated by the Kuhn procedure (14). The products were first partially methanolyzed with 5% methanolic hydrogen chloride overnight and then neutralized (Ag_2CO_3), filtered, and evaporated. The products were hydrolyzed to the free sugars in *N* H_2SO_4, heated at 100° C for 18 hours. The hydrolyzates were then neutralized ($BaCO_3$), filtered, and evaporated. Conversion to the methyl glycosides was carried out by refluxing in 5% methanolic hydrogen chloride for 18 hours. The samples obtained after neutralization (Ag_2CO_3) and evaporation were then analyzed by gas phase chromatography.

Gas Phase Chromatography of Methyl Glycosidic Fragments

Gas phase chromatography was carried out at 210° C using a 6-ft phthalate – ethylene glycol on Celite (1:4.5) column (15) in order to obtain good resolution of trimethyl and tetramethyl glycosides. For comparison of di-, tri-, and tetra-*O*-methyl glycosides a 4-ft column consisting of 30% fully methylated hydroxyethyl cellulose WP-09 (Union Carbide Chemicals Co.) on Gas-Chrom P (60–80 mesh) was used at 190° C and 220° C (8). The detectors used were of the hot-wire type and helium was the carrier gas.

In order to make calculations of the relative amounts the following equilibrium ratios of methyl glucosidic anomers were used, the former figures corresponding to the material with the greater retention time: methyl 2,3,4,6-tetra-*O*-methyl- (66:34); methyl 2,3,6-tri-*O*-methyl- (71:29); and methyl 2,6-di-*O*-methyl-glucoside (70:30). Methyl 3,4,6-tri-*O*-methyl- and methyl 2,3,4,6-tetra-*O*-methyl-mannoside gave single peaks on chromatography.

The methyl glycosidic standards used in comparisons of retention times in the glucose series were 2,3,4,6-, 2,3,4-, 2,3,6-, 2,4,6-, 3,4,6-, and 2,6-. In the mannose series 2,3,4,6-, 3,4,6-, 2,3,4-, 2,3,6-, 2,4,6-, and 3,4- were used. The gas chromatograms had peak areas as recorded in Table II.

ACKNOWLEDGMENTS

The authors wish to thank Mrs. S. F. Hector and Mr. N. Gardner for technical assistance and Mr. M. Mazurek for carrying out elemental analysis. Our thanks are due to Dr. E. Reese for supplying a sample of enzyme preparation S157B.

REFERENCES

1. S. M. Lesley and R. N. Hochster. Can. J. Biochem. Physiol. **37**, 513 (1959).
2. A. Jeanes, J. E. Pittsley, and F. R. Senti. J. Appl. Polymer Sci. **5**, 519 (1961).
3. P. A. J. Gorin and J. F. T. Spencer. Can. J. Chem. **34**, 2282 (1961).
4. A. Misaki, S. Kirkwood, J. V. Scaletti, and F. Smith. Can. J. Chem. **40**, 2204 (1962).
5. J. H. Sloneker and D. G. Orentas. Nature, **194**, 478 (1962).
6. J. H. Sloneker and A. Jeanes. Can. J. Chem. **40**, 2066 (1962).
7. A. J. Charlson and A. S. Perlin. Can. J. Chem. **34**, 1200 (1956).
8. H. W. Kircher. Anal. Chem. **32**, 1103 (1960).
9. P. A. J. Gorin and J. F. T. Spencer. Can. J. Chem. **39**, 2275 (1961).
10. J. K. N. Jones and J. B. Pridham. Biochem. J. **58**, 288 (1954).
11. F. Smith and A. M. Stephen. J. Chem. Soc. 4892 (1960).
12. L. Hough, J. K. N. Jones, and W. H. Wadman. J. Chem. Soc. 1702 (1950).
13. M. Bergmann and H. Schotte. Ber. **54**, 1564 (1921).
14. R. Kuhn, H. Trischmann, and I. Low. Angew Chem. **67**, 32 (1955).
15. B. M. Craig. Chem. Ind. (London), 1442 (1960).

Can. J. Chem. Downloaded from www.nrcresearchpress.com by 210.87.254.42 on 09/05/12
For personal use only.

Can. J. Chem. Downloaded from www.nrcresearchpress.com by 210.87.254.105 on 09/05/12
For personal use only.

EXTRACTIVES FROM POPULUS TREMULOIDES HEARTWOOD

THE TRITERPENE ALCOHOLS[1]

R. A. ABRAMOVITCH AND R. G. MICETICH
Department of Chemistry, University of Saskatchewan, Saskatoon, Saskatchewan

Received May 3, 1963

ABSTRACT

The 'unsaturated alcohol fraction' from *P. tremuloides* heartwood (R. A. Abramovitch, R. G. Micetich, and S. J. Smith, Tappi, **46**, 37 (1963)) has been found to contain α- and β-amyrin, butyrospermol, 24-methylenecycloartanol, lupeol, and α-amyrenonol. Some aspects of the infrared and n.m.r. spectra of these compounds are discussed and the suggestion is made that the tritisterols and orysterols may actually be $C_{31}H_{52}O$ triterpenes containing a cyclopropane ring.

The extractives from aspen poplar (*Populus tremuloides*) heartwood have been investigated systematically and separated into a number of fractions (1). The structure of a crystalline steroidal ketone, tremulone, has been established and confirmed by a partial synthesis (2). The present paper is concerned with the resolution and the characterization of the individual components of the 'unsaturated alcohol fraction' (1).

The 'unsaturated alcohol fraction' was obtained as a yellow waxy solid (20% by weight of the unsaponifiable fraction which, in turn, constitutes 0.4% by weight of the dry wood) of indefinite melting point, which could not be resolved into its components by chromatography. Resolution into at least eight components was finally achieved by acetylation followed by alumina column chromatography and fractional crystallization of the mixture of acetates. Table I summarizes the results obtained.

TABLE I

Column chromatography of the 'unsaturated alcohol' acetates

Fraction No.	Eluant	Product	Wt% of total acetates
1*	Light petroleum (b.p. 60–65°)	Acetates IIA, IIB, III	45
2	Benzene – light petroleum (1:9)	Acetate IV	7
3	Benzene – light petroleum (1:4)	Acetate I	19
4	Ether – light petroleum (1:1)	Ketoacetate I	12
5	Ether	Ketoacetate II	15
6	Ether–methanol (1:1)	Alcohol ketoacetate	2

*Fraction No. 1 was resolved into its three component acetates by fractional crystallization from ethanol.

Acetate IIA

This was the least soluble of the three fractions and had m.p. 238–240°, $[\alpha]_D^{22}$ +85.5° (chloroform). It analyzed for $C_{32}H_{52}O_2$. Deacetylation gave the alcohol, m.p. 200–201°, $[\alpha]_D^{22}$ +102° (chloroform). These values are in good agreement with those reported for β-amyrin acetate and β-amyrin, respectively (3, 4). The n.m.r. spectrum of the acetate also agreed with this formulation: a triplet centered at 4.72 τ (C_{12} olefinic proton), a triplet centered at 5.46 τ (J 7.5 c.p.s.) (axial C_3 proton), a strong band at 8.0 τ (acetate C—CH_3), and three strong signals, characteristic of the amyrins (5), were observed at 8.87, 9.01, and 9.12 τ. A direct comparison with an authentic sample of β-amyrin acetate finally confirmed the assignment.

[1]*Presented at the First Canadian Wood Chemistry Symposium, Toronto, September 4–6, 1963.*

Can. J. Chem. Downloaded from www.nrcresearchpress.com by 210.87.254.105 on 09/05/12
For personal use only.

dihydro acetate (16). Taking all these results into consideration led to the assumption that acetate I was probably the acetate of 24-methylenecycloartanol (I). This triterpenoid ($C_{31}H_{52}O$) has been isolated from rice bran oil (17), and more recently from the wood of *Tristania conferta* R. Br and *Angophora subvelutina* F. Muell (18). The proposed structure of acetate I was confirmed by its ozonolysis. Apart from formaldehyde, a ketone was obtained which, on Wolff–Kishner reduction followed by acetylation, gave cycloartanyl acetate, indistinguishable from an authentic sample obtained by the catalytic reduction of cycloartenyl acetate. At that time, samples of 24-methylenecycloartanyl acetate and the alcohol became available through the courtesy of Dr. G. Ohta, and proved to be identical with acetate I and the corresponding alcohol, respectively.

A comparison of the optical rotations and melting points of the known monohydroxy triterpenoids containing a cyclopropane ring and their acetates with those reported for the tritisterols and orysterols (Table II) is of interest. These "sterols" of reported composition $C_{30}H_{50}O$ were isolated from wheat germ oil and rice germ oil, and are supposed

TABLE II

Physical constants of the tritisterols and orysterols (19) and triterpenes containing a cyclopropane ring

Compound	Alcohol		Acetate	
	M.p. (°C)	$[\alpha]_D$ (deg)	M.p. (°C)	$[\alpha]_D$ (deg)
α-Tritisterol	114–115	+54.3	107–108	+70.4
β-Tritisterol	70–97	+49.2	—	+55.5
α-Orysterol	121–122	+49	—	—
β-Orysterol	113–114	+51.3	104	—
γ-Orysterol	119–120	+51.9	111.5	+59.4
Cycloartenol (20)	99	+48–54	119–120	+59
Cycloeucalenol (21)	138–139	+45	110	+63
Cyclolaudenol (22)	125	+46	120–121	+55
24-Methylenecycloartanol (17)	121–122	+43	116–117	+54

to be related to the tetracyclic triterpenes. It would seem likely, however, that they are, in fact, $C_{31}H_{52}O$ triterpenoids with cyclopropane rings and may well be impure samples of known compounds of this series.

Ketoacetate I

This compound, $C_{32}H_{50}O_3$, had m.p. 280° (decomp.), and $[\alpha]_D^{22}$ +94° (chloroform). It exhibited bands at 1745 cm^{-1} (acetate) and 1668 cm^{-1} (α,β-unsaturated ketone) in the infrared. Hydrolysis gave a ketoalcohol, $C_{30}H_{48}O_2$, m.p. 206°, $[\alpha]_D^{22}$ +98.6° (chloroform), λ_{max}^{EtOH} 250 mμ, which, on chromic acid oxidation, gave a diketone (bands at 1710 and 1665 cm^{-1}), m.p. 197–198°, $[\alpha]_D^{22}$ +136° (chloroform). This indicates that the alcohol group must be present either in a six-membered ring or in a side chain. The above data are consistent with ketoacetate I being α-amyrenonyl acetate and the corresponding alcohol α-amyrenonol (II) (23). The n.m.r. spectrum of ketoacetate I would support such a formulation. A sharp single-proton peak at 4.58 τ is assigned to the C_{12} olefinic proton, a triplet centered at 5.57 τ (J 13 c.p.s.) to the axial C_3 proton,* and a strong signal at 8.04 τ to the acetate C—CH_3. There are also three signals of increasing strength

**For other triterpenes the splitting constant for the axial C_3 proton is about 7 c.p.s. (β-amyrin, J = 7.5 c.p.s.; butyrospermyl acetate, J = 6.5 c.p.s.). The larger splitting constant observed here might be a reflection of the slight ring distortion caused by the presence of a carbonyl function at C_{11}.*

Can. J. Chem. Downloaded from www.nrcresearchpress.com by 210.87.254.105 on 09/05/12
For personal use only.

at 8.72, 8.88, and 9.17 τ, respectively, which seems to be characteristic of triterpenes of the amyrane and lupane series. That the alcohol was indeed α-amyrenonol was established by its catalytic reduction over platinum oxide in acetic acid, followed by acetylation to give α-amyrin acetate (24).

The question arises, as in the case of tremulone (2), as to whether α-amyrenonol is present in the plant as such, or whether it is an artifact resulting from the oxidation of α-amyrin. This cannot be answered at this time. It may be significant that the keto group in both cases arises through the oxidation of the methylene group adjacent to the double bond.

Fractions 5 and 6

The infrared spectrum of fraction 5 indicated the presence of an unsaturated ketoacetate while fraction 6 gave, in addition, bands characteristic of a hydroxyl group. The latter may arise by partial deacetylation on the column, or may be due to a tertiary hydroxyl group. These fractions were obtained as waxes which could not be recrystallized and were not examined further at this time.

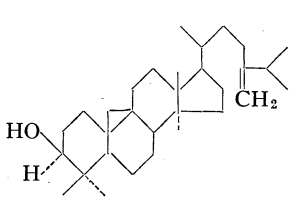

I

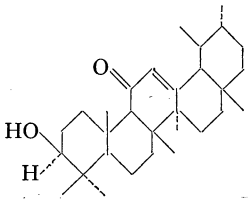

II

EXPERIMENTAL

Melting points are uncorrected. Infrared spectra were measured on a Perkin–Elmer Model 21 spectrometer on potassium bromide disks of the compounds. Nuclear magnetic resonance spectra were recorded on a Varian A60 instrument using carbon tetrachloride solutions of the compounds and tetramethylsilane as internal standard, and with an oscillator frequency of 60 Mc/sec. Chromatographic alumina Type H was used. The light petroleum used had b.p. 60–65° and was free of unsaturation.

Resolution of the Unsaturated Alcohol Acetates

The crude unsaturated alcohol fraction (1) (0.617 g) was boiled under reflux with acetic anhydride (10 ml) and pyridine (5 ml) for 3 hours, and the solution evaporated to dryness under vacuum to give a brown wax (0.620 g). This was dissolved in the minimum amount of light petroleum and chromatographed on a column of alumina (ca. 50–80 times the weight of the acetates) and developed as outlined in Table I. Fractions of 250 ml each were collected and the progress of the chromatography followed by the weight, appearance, and infrared spectrum of each fraction. Fraction 1 was a sandy white solid whose infrared spectrum did not show any strong bands at 885 cm^{-1}. Fraction 2 was a solid and exhibited an intense band at 885 cm^{-1}. Fraction 3 was a wax whose infrared spectrum differed appreciably from that of fraction 2, but which also exhibited a strong band at 885 cm^{-1}. Fraction 4 was a light yellow wax with bands at 1745 and 1668 cm^{-1} in the infrared, but no strong band at 885 cm^{-1}. Fraction 5 was a red wax, while fraction 6 showed strong hydroxyl absorption in the infrared.

Fraction 1, m.p. ca. 200°, was fractionally crystallized from 95% ethanol. The least soluble fraction was acetate IIA, the next acetate IIB, the most soluble acetate III.

Acetate IIA—β-Amyrin Acetate

After repeated recrystallization from 95% ethanol, it had m.p. 238–240°, $[\alpha]_D^{22}$ +85.5° (chloroform). Its melting point and infrared and n.m.r. spectra were identical with those of an authentic sample of β-amyrin acetate; the melting point of this compound was undepressed on admixture with the authentic sample. (Calc. for $C_{32}H_{52}O_2$: C, 81.99; H, 11.18. Found: C, 82.04; H, 11.07.)

Acetate IIA (0.100 g) was boiled under reflux with 4% ethanolic potassium hydroxide (10 ml) for 3 hours, the cooled mixture filtered through a short column of alumina, and the solvent evaporated. The residue was recrystallized from light petroleum to give β-amyrin, m.p. 200–201°, $[\alpha]_D^{22}$ +102° (chloroform). The reported (3) constants for β-amyrin are: m.p. 199–200°, $[\alpha]_D$ +99.8° (benzene).

Can. J. Chem. Downloaded from www.nrcresearchpress.com by 210.87.254.105 on 09/05/12
For personal use only.

Acetate IIB—α-Amyrin Acetate

This crystallized from 95% ethanol in needles, m.p. 223°, $[\alpha]_D^{22}$ +79° (chloroform), identical (mixed melting point and infrared spectrum) with authentic α-amyrin acetate.

Acetate III—Butyrospermyl Acetate

This crystallized from 95% ethanol in needles, m.p. 143–144°, $[\alpha]_D^{22}$ +3.5° (chloroform). (Calc. for $C_{32}H_{50}O_2$: C, 81.99; H, 11.18. Found: C, 81.54; H, 11.33.) Heilbron, Jones, and Robins (25) give m.p. 146.5–147.5°, $[\alpha]_D^{20}$ +11±2° for butyrospermyl acetate.

Butyrospermyl Benzoate

Acetate III (0.050 g) was boiled under reflux with 3% methanolic potassium hydroxide (5 ml) for 3 hours. The cooled solution was filtered through a short column of alumina and the methanol removed on a steam bath. The residual wax (0.038 g) was heated with benzoyl chloride (1 ml) and pyridine (1 ml) on a steam bath for 3 hours and then kept at room temperature overnight. Water was added, the mixture extracted with chloroform, the chloroform layer washed in succession with dilute sulphuric acid, water, dilute sodium hydroxide, and water, and dried ($MgSO_4$). The chloroform was evaporated and the residue recrystallized from a chloroform–methanol mixture to give butyrospermyl benzoate (0.010 g), m.p. 128°, undepressed on admixture with an authentic sample.

Acetate IV—Lupeol Acetate

Repeated recrystallization of fraction 2 from methanol gave lupeol acetate, m.p. 218–219°, $[\alpha]_D^{22}$ +47.8° (chloroform), identical in all respects with an authentic sample.

Acetate I—24-Methylenecycloartanyl Acetate

Repeated recrystallization of fraction 3 from ethanol gave the pure acetate, m.p. 114–115°, $[\alpha]_D^{22}$ +53.4° (chloroform), identical with an authentic sample. (Calc. for $C_{33}H_{54}O_2$: C, 82.09; H, 11.27; mol. wt., 483. Found: C, 81.90, 82.35; H, 11.26, 11.13; mol. wt. (osmometer), 493.)

24-Methylenecycloartanol

Acetate I (0.100 g) was boiled under reflux with 3% methanolic potassium hydroxide (10 ml) for 3 hours, water (10 ml) was added, and the methanol removed in a stream of warm air. Crystals which separated from the cooled solution were recrystallized from aqueous methanol and were obtained as flakes (0.070 g), m.p. 120–121°, $[\alpha]_D^{22}$ +43.1° (chloroform), identical with authentic 24-methylenecycloartanol. (Calc. for $C_{31}H_{52}O$: C, 84.48; H, 11.89; mol. wt., 441. Found: C, 84.17; H, 11.72; mol. wt. (osmometer), 448.)

24-Methylcycloartanyl Acetate

This (m.p. 122°, $[\alpha]_D^{22}$ +54.8° (chloroform)) was obtained by the reduction of acetate I in ethanol over 10% palladium–charcoal. Ohta (17) gives m.p. 123–124°, $[\alpha]_D$ +54.5° for this compound.

Cycloartanyl Acetate

Acetate I (0.125 g) in ethyl acetate (20 ml) was ozonized at −78°, Adams' catalyst (0.060 g) was added, and the reaction product hydrogenated at 0°. Formaldehyde was detected with chromotropic acid. The filtered solution was evaporated and the residual 24-ketocycloartanyl acetate (0.070 g) recrystallized from ethanol. It had m.p. 119°. Ohta (17) gives m.p. 121–123° for this ketone. The ketone was subjected to a Wolff–Kishner reduction using the procedure outlined previously (2) and the product acetylated to give cycloartanyl acetate (0.025 g), m.p. 132–133°, identical with an authentic sample. The latter was obtained by the catalytic reduction of cycloartenyl acetate.

Ketoacetate I—α-Amyrenonyl Acetate

Repeated recrystallization of fraction 4 from an ether–methanol mixture gave the acetate, m.p. 280° (decomp.), $[\alpha]_D^{22}$ +94° (chloroform). (Calc. for $C_{32}H_{50}O_3$: C, 79.62; H, 10.44. Found: C, 79.61, 79.65; H, 10.54, 10.37.) Spring and Vickerstaff (23) give m.p. 278° for α-amyrenonyl acetate. Deacetylation as described above for 24-methylenecycloartanyl acetate gave α-amyrenonol, m.p. 206°, $[\alpha]_D^{22}$ +98.6° (chloroform), λ_{max}^{EtOH} 250 mμ. (Calc. for $C_{30}H_{48}O_2$: C, 81.76; H, 10.98; mol. wt., 441. Found: C, 81.67; H, 10.85; mol. wt. (osmometer), 430.) Spring and Vickerstaff (23) give m.p. 208°, $[\alpha]_D^{20}$ +108.6° (benzene), λ_{max}^{EtOH} 250 mμ for α-amyrenonol. α-Amyrenonol (0.065 g) in glacial acetic acid (2 ml) was hydrogenated at atmospheric pressure and room temperature. Uptake of hydrogen was very slow. The filtered solution was diluted with water and extracted with chloroform. The chloroform layer was washed with water, dried ($MgSO_4$), and the solvent evaporated. The residue was acetylated and the product recrystallized from ethanol to give α-amyrin acetate (0.030 g), m.p. 225°, identical with an authentic sample.

α-Amyrendione

The alcohol (0.050 g) obtained by the deacetylation of ketoacetate I was dissolved in glacial acetic acid (5 ml) and a solution of chromic anhydride (0.020 g) in acetic acid (5 ml) and water (0.5 ml) was added slowly with stirring. The mixture was kept overnight at room temperature, diluted with water, and extracted with benzene. The benzene extract was washed with water, filtered through a short column of alumina, and the benzene evaporated. The residue was recrystallized from aqueous methanol and was obtained as

Can. J. Chem. Downloaded from www.nrcresearchpress.com by 210.87.254.105 on 09/05/12
For personal use only.

fine needles (0.030 g), m.p. 197–198°, $[\alpha]_D^{22}$ +136° (chloroform). The values reported (23) for α-amyrendione are: m.p. 193°, $[\alpha]_D^{20}$ +141° (chloroform).

ACKNOWLEDGMENTS

This work was carried out during the tenure (by R. G. M.) of a National Research Council Studentship, and was supported financially by a grant from the Saskatchewan Research Council. The authors wish to thank Dr. P. de Mayo for samples of the α- and β-amyrin acetates and of butyrospermyl benzoate, and Dr. G. Ohta for samples of 24-methylenecycloartanol and its acetate, and of cycloartenyl acetate.

REFERENCES

1. R. A. Abramovitch, R. G. Micetich, and S. J. Smith. Tappi, **46**, 37 (1963).
2. R. A. Abramovitch and R. G. Micetich. Can. J. Chem. **40**, 2017 (1962).
3. I. M. Heilbron and H. M. Bunbury. Dictionary of organic compounds. Vol. I. Eyre and Spottiswoode, London. 1953. p. 158.
4. J. Simonsen and W. C. J. Ross. The terpenes. Vol. IV. The University Press, Cambridge. 1957. p. 116, 170.
5. G. G. Allan. Chem. Ind. (London), 529 (1958).
6. I. L. Allsop, A. R. H. Cole, D. E. White, and R. L. S. Willix. J. Chem. Soc. 4868 (1956).
7. G. Snatzke, F. Lampert, and R. Tschesche. Tetrahedron, **18**, 1417 (1962).
8. D. S. Irvine, W. Lawrie, A. S. McNab, and F. S. Spring. J. Chem. Soc. 2029 (1956).
9. M. C. Dawson, T. G. Halsall, E. R. H. Jones, G. D. Meakins, and P. C. Phillips. Chem. Ind. (London), 918 (1955). M. C. Dawson, T. G. Halsall, E. R. H. Jones, and P. A. Robins. J. Chem. Soc. 586 (1953).
10. R. E. Glick, R. O. Mumma, and M. Shamma. Chem. Ind. (London), 1092 (1959); J. Org. Chem. **27**, 4512 (1962).
11. R. O. Mumma. Dissertation Abstr. **21**, 2485 (1961).
12. H. Conroy. *In* Advances in organic chemistry. Vol. II. Interscience Publishers, Inc., New York. 1960. p. 289.
13. R. McCrindle and C. Djerassi. Chem. Ind. (London), 1311 (1961).
14. K. S. Brown and S. M. Kupchan. J. Am. Chem. Soc. **84**, 4590 (1962).
15. G. V. Pigivlenskii and A. I. Konokotina. Zh. Obshch. Khim. **31**, 2410 (1961); Chem. Abstr. **56**, 1075a (1962).
16. W. H. Washburn and M. J. Mahoney. J. Am. Chem. Soc. **80**, 505 (1958).
17. G. Ohta and M. Shimizu. Chem. Pharm. Bull. (Tokyo), **6**, 325 (1958). G. Ohta. Chem. Pharm. Bull. (Tokyo), **8**, 5, 9 (1960).
18. E. Ritchie, D. Snape, and W. C. Taylor. Australian J. Chem. **14**, 471 (1961). E. Ritchie and W. C. Taylor. Australian J. Chem. **14**, 473 (1961).
19. P. Karrer, H. Salomon, and H. Fritzsche. Helv. Chim. Acta, **20**, 1422 (1937). A. R. Todd, F. Bergel, H. Waldmann, and T. S. Work. Biochem. J. **31**, 2247 (1937).
20. D. H. R. Barton, J. E. Page, and E. W. Warnhoff. J. Chem. Soc. 2715 (1954). H. R. Bentley, J. A. Henry, D. S. Irvine, and F. S. Spring. J. Chem. Soc. 3673 (1953). D. S. Irvine, J. A. Henry, and F. S. Spring. J. Chem. Soc. 1316 (1955).
21. J. S. G. Cox, F. E. King, and T. J. King. J. Chem. Soc. 1384 (1956); 514 (1959).
22. H. R. Bentley, J. A. Henry, D. S. Irvine, D. Mukerji, and F. S. Spring. J. Chem. Soc. 596 (1955). J. A. Henry, D. S. Irvine, and F. S. Spring. J. Chem. Soc. 1607 (1955).
23. F. S. Spring and T. Vickerstaff. J. Chem. Soc. 650, 1859 (1934); 249 (1937).
24. L. Ruzicka, H. Leuenberger, and H. Schellenberg. Helv. Chim. Acta, **20**, 1278 (1937).
25. I. M. Heilbron, E. R. H. Jones, and P. A. Robins. J. Chem. Soc. 444 (1949).

Can. J. Chem. Downloaded from www.nrcresearchpress.com by 210.87.254.105 on 09/05/12
For personal use only.

REARRANGEMENT STUDIES WITH C^{14}

XV. ETHYL-2-C^{14} IODIDE FROM THE IRRADIATION OF ETHYL-1-C^{14} IODIDE WITH COBALT-60 GAMMA RAYS

I. S. BHARDWAJ[1] AND C. C. LEE

Department of Chemistry, University of Saskatchewan, Saskatoon, Saskatchewan

Received March 20, 1963

ABSTRACT

Irradiation of ethyl-1-C^{14} iodide gave ethyl-2-C^{14} iodide with G_r of 0.27–0.28 for samples that were either deaerated or not deaerated. Addition of 1% by weight of iodine before irradiation decreased the extent of rearrangement to nearly zero. The occurrence of 1,2-hydrogen shifts in ethyl radicals outside of the spurs, which may be susceptible to scavenger action, is suggested as a possible path which would lead to the ethyl-2-C^{14} iodide.

Can. J. Chem. Downloaded from www.nrcresearchpress.com by 210.87.254.40 on 09/05/12
For personal use only.

The irradiation of 2% aqueous solutions of ethanol-1-C^{14} with Co^{60} γ-rays was found to give ethanol-2-C^{14} with a G value of about 0.04 (1). A similar study on the irradiation of liquid 2-phenylethyl-1-C^{14} iodide gave 2-phenylethyl-2-C^{14} iodide with a G value of about 0.5 (2). A possible explanation for these isotope position rearrangements may be the occurrence of 1,2-shifts in the free radicals produced during irradiation. Adloff and Ricq (3) have also reported that following Co^{60} γ-irradiation of an aqueous solution of benzoic acid-1-C^{14}, rearrangement of the C^{14} to the aromatic ring was observed with a G value of 0.01. The possible involvement of an intermediate cycloheptatrienyl radical or tropylium ion was suggested. On the other hand, irradiation of toluene-α-C^{14} with a 3-Mev electron beam gave bibenzyl with essentially no activity in the rings, indicating that benzyl radical formation did not proceed through a symmetrical tropylium ion (4). The present paper deals with another application of C^{14} as label in the study of isotope position rearrangements induced by γ-irradiation.

RESULTS AND DISCUSSION

Two-milliliter samples of ethyl-1-C^{14} iodide,* either not deaerated, or deaerated by several cycles of freezing, evacuating, and thawing, were sealed in Pyrex tubes and irradiated at room temperature in fixed positions near a 50-c Co^{60} source. Two of the deaerated samples also contained 1% by weight of added iodine. Radiation dosages were measured in roentgens by a Farmer–Baldwin "substandard" X-ray dosimeter, model Mk II.† Using a conversion factor of 1 r equals 0.975 rad for water (5) and correcting for the difference in electron density between ethyl iodide and water, the dose rates were about 55,000 rads/hr for ethyl iodide. Allowance was also made for the decay of Co^{60} in calculating the total absorbed dosage. After irradiation for various periods up to a maximum of about 4.5 months (175 million rads or 10.9×10^{21} ev/g), the samples were worked up for rearrangement to ethyl-2-C^{14} iodide.

The ethyl iodide was converted to the corresponding Grignard reagent and then treated with oxygen to give ethanol which, in turn, was reacted with iodine and sodium hydroxide to give iodoform. The activity of the iodoform thus gave a measure of the C^{14} content in the C-2 position. Such a degradation on freshly obtained ethyl-1-C^{14} iodide

[1]*Holder of a National Research Council of Canada Studentship, 1962–1963.*
**Supplied by New England Nuclear Corp., Boston, Mass.*
†*Supplied by The Baldwin Instrument Co., Dartford, Kent, England.*

or on ethyl-1-C^{14} iodide that had been stored for several months without γ-irradiation resulted in essentially inactive iodoform. After sufficient extents of irradiation, active iodoform was obtained. The results are summarized in Table I. As basis for calculation,

TABLE I

Rearrangement after irradiation of ethyl-1-C^{14} iodide

Sample	Absorbed dosage (10^{21} ev/g)	Activity* (mμc/mmole)		Rearrangement to ethyl-2-C^{14} iodide	
		Anilide†	CHI_3	%	G_r
	0	2000	0±0.4	0±0.02	
Deaerated	3.60	"	5.2	0.26	0.28
"	7.90	"	11.2	0.56	0.27
"	10.90	"	16.0	0.80	0.28
Not deaerated	3.77	"	5.1	0.26	0.27
"	7.90	"	10.9	0.55	0.27
Deaerated + 1%I_2	4.65	3500	1.6	0.05	
"	5.80	"	1.4	0.04	

*C^{14} activity in millimicrocuries per millimole of sample was assayed as CO_2 gas with a vibrating reed electrometer.
†Propionanilide derived from ethyl-1-C^{14} iodide before irradiation.

the activity of the ethyl-1-C^{14} iodide before irradiation was measured as the anilide derivative, prepared from reaction of ethyl-1-C^{14}-magnesium iodide with phenylisocyanate (6). From the activities of the iodoform and the anilide, the percentage rearrangement to ethyl-2-C^{14} iodide and values for G_r, the number of molecules rearranged per 100 ev absorbed, were calculated and included in Table I.

It can be seen from Table I that the extent of rearrangement increases with increasing radiation dosage. The rearrangement yield, expressed as G_r, is remarkably constant at 0.27–0.28 for both the deaerated and not deaerated samples. The absence of observable effects of dissolved air on rearrangement yields possibly may be explained by assuming that during the prolonged irradiation of the samples, all dissolved oxygen would have been used up in the initial stages of irradiation before the occurrence of measurable extents of rearrangement. Addition of 1% iodine to the samples before irradiation, however, decreased the extent of rearrangement to a very low level. Rearrangements of less than 0.1% may be considered to have only marginal significance since under the conditions of the C^{14} assays an observed activity of only twice that of background for a 20-mg iodoform sample would be equivalent to about 0.1% rearrangement. The observed activities of the iodoform derived from the iodine-containing samples were of the order of background. The fact that, of the two iodine-containing samples, the more highly irradiated one even gave slightly less active iodoform would suggest that the 0.04–0.05% rearrangement calculated for these samples may not be of great significance. It may, therefore, be concluded that the presence of 1% iodine, added before irradiation, could cut the rearrangement down to nearly zero.

The radiolysis of liquid ethyl iodide has been extensively investigated. More recent studies (7–10) have summarized the earlier work and have paid special attention to the possible mechanistic pathways of the radiolysis. The chief products from γ-irradiation of liquid ethyl iodide have been shown to be iodine, ethylene, and ethane, with smaller amounts of hydrogen iodide and *n*-butane, and with acetylene, methane, and hydrogen as minor products (10). The presence of thermalized ethyl radicals was demonstrated by exchange with I^{131} during irradiation (7, 8, 11). However, since iodine, either added before irradiation or produced during irradiation, did not completely scavenge all free radicals,

Can. J. Chem. Downloaded from www.nrcresearchpress.com by 210.87.254.40 on 09/05/12
For personal use only.

parts of the products of radiolysis of liquid ethyl iodide must arise from reactions between "hot" radicals within the spurs (7–10). A comprehensive diffusion-controlled mechanism has recently been suggested by Gilles, Williams, and Hamill (10).

Since ethylene and hydrogen iodide are among the products of radiolysis, one might argue that the formation of ethyl-2-C^{14} iodide from irradiation of ethyl-1-C^{14} iodide arose from addition of hydrogen iodide to C^{14}-labeled ethylene. However, the amounts of ethylene and hydrogen iodide produced were not greatly decreased when ethyl iodide was irradiated in the presence of added iodine (10). The present finding that iodine added before irradiation practically eliminated the rearrangement to ethyl-2-C^{14} iodide suggests, therefore, that reaction between hydrogen iodide and C^{14}-labeled ethylene, both of which would be present among the products, may not be the most probable route of the rearrangement. On the other hand, reaction between ethylene and hydrogen iodide might proceed in steps similar to those postulated by McCauley, Hamill, and Williams (12) in explaining the formation of isopropyl iodide during photolysis of *n*-propyl iodide:

$$C_2H_4 + I\cdot \rightarrow C_2H_4I\cdot$$
$$C_2H_4I\cdot + HI \rightarrow C_2H_5I + I\cdot$$

It could then be argued that added iodine would interfere with the second step, giving rise to ethylene iodide instead of ethyl iodide. Thus an overall addition of hydrogen iodide to labeled ethylene to give ethyl-1-C^{14} and -2-C^{14} iodide cannot be excluded absolutely. However, it should be pointed out that in the analogous study on γ-induced rearrangement of 2-phenylethyl-1-C^{14} iodide to 2-phenylethyl-2-C^{14} iodide (2), addition of hydrogen iodide to labeled styrene cannot be the reaction path since such an addition would lead to either unchanged 2-phenylethyl-1-C^{14} iodide or structurally rearranged 1-phenylethyl-2-C^{14} iodide, but not to the isotopically rearranged 2-phenylethyl-2-C^{14} iodide.

The occurrence of 1,2-hydrogen shifts remains as a possible explanation for the observed rearrangement. Again, since added iodine effectively reduced the extent of rearrangement to nearly zero, and since hot radicals or the first binary encounters within the spurs may be immune to interference by added scavenger (7, 10), the observed rearrangement likely involved thermalized ethyl radicals outside of the spurs. Recombination of the rearranged radical with iodine would give ethyl-2-C^{14} iodide:

$$CH_3C^{14}H_2\cdot \rightarrow \cdot CH_2C^{14}H_3$$
$$C^{14}H_3CH_2\cdot + I_2 \rightarrow C^{14}H_3CH_2I + I\cdot$$

With iodine added before irradiation, thermal radicals may be scavenged before hydrogen shifts can take place. The fact that G_r for this rearrangement is greater than that for the corresponding irradiation of aqueous ethanol-1-C^{14} (1) is reasonable as ethyl radicals would be more readily formed from ethyl iodide. The G value for the rearrangement to 2-phenylethyl-2-C^{14} iodide from irradiation of 2-phenylethyl-1-C^{14} iodide (2) is greater than that of the present system. This may be regarded as indicative of more facile 1,2-phenyl shifts than 1,2-hydrogen shifts as have been observed in carbonium ion reactions (13–15).

EXPERIMENTAL

Propionanilide

Ethyl-1-C^{14} iodide (1.0 ml) was converted to the Grignard reagent and then treated with phenylisocyanate according to an established procedure (6) to give propionanilide, m.p. 103–104° C (lit. (6) m.p. 104–104.5° C). It was repeatedly crystallized until its specific activity was essentially constant.

Can. J. Chem. Downloaded from www.nrcresearchpress.com by 210.87.254.40 on 09/05/12
For personal use only.

Degradation of Ethyl Iodide

Before or after irradiation, the active ethyl iodide was converted to ethylmagnesium iodide in anhydrous ether. The solution was cooled in an ice bath and oxygen was bubbled through for 12 hours. The resulting complex was decomposed by dilute sulphuric acid and the solution was then fractionated through a helix-packed column. After removal of most of the ether, the distillate, boiling above 60° C, and containing both ethanol and water, was used directly for conversion to iodoform.

Preliminary trials showed that the weight of iodoform obtainable from the haloform reaction with ethanol was rather low. High yields of iodoform were reported in the literature only when a rather elaborate electrochemical oxidation procedure was used (16). However, the following method, worked out by D. G. Lee (1, 17), gave sufficiently high yields (about 25%) for the present purpose.

In a 500-ml three-necked flask fitted with magnetic stirrer, reflux condenser, and two dropping funnels were placed the aqueous ethanol distillate and a buffer solution consisting of 3.25 g boric acid, 2.94 g potassium hydroxide, and 105 ml distilled water (16). With the temperature maintained at about 50° C by a heating mantle and with constant stirring, 50 ml of 10% sodium hydroxide solution was added dropwise through one funnel and a solution of iodine and potassium iodide (50 g iodine, 100 g potassium iodide in 400 ml water) was added through the second funnel. About 3 hours was required for the addition of the sodium hydroxide. The addition of the iodine – potassium iodide solution was carried out more slowly and continued until the dark iodine color remained undischarged. This required up to 48 hours, during which time up to 150 ml of the iodine – potassium iodide solution was consumed. The iodoform precipitated during the course of the reaction was collected and recrystallized about six times to give a sample with essentially constant specific activity, melting at 118–118.5° C (lit. (18) m.p. 119° C).

ACKNOWLEDGMENT

We wish to thank Mr. John Dyck of the Prairie Regional Laboratory, National Research Council of Canada, for carrying out the C^{14} assays. The financial support given by the National Research Council of Canada is also gratefully acknowledged.

REFERENCES

1. C. C. Lee and D. G. Lee. Can. J. Chem. **38**, 2315 (1960).
2. C. C. Lee, D. G. Lee, and I. S. Bhardwaj. Radiation Res. **17**, 536 (1962).
3. J.-P. Adloff and M. Ricq. Compt. Rend. **254**, 1417 (1962).
4. L. H. Gale, B. E. Gordon, G. Steinberg, and C. D. Wagner. J. Phys. Chem. **66**, 1538 (1962).
5. R. J. Woods and J. W. T. Spinks. Can. J. Chem. **35**, 1475 (1957).
6. H. W. Underwood, Jr. and J. C. Gale. J. Am. Chem. Soc. **56**, 2117 (1934).
7. R. H. Schuler and R. C. Petry. J. Am. Chem. Soc. **78**, 3954 (1956).
8. E. O. Hornig and J. E. Willard. J. Am. Chem. Soc. **79**, 2429 (1957).
9. R. J. Hanrahan and J. E. Willard. J. Am. Chem. Soc. **79**, 2434 (1957).
10. H. A. Gillis, R. R. Williams, Jr., and W. H. Hamill. J. Am. Chem. Soc. **83**, 17 (1961).
11. L. H. Gevantman and R. R. Williams, Jr. J. Phys. Chem. **56**, 569 (1952).
12. C. E. McCauley, W. H. Hamill, and R. R. Williams, Jr. J. Am. Chem. Soc. **76**, 6263 (1954).
13. J. D. Roberts and J. A. Yancey. J. Am. Chem. Soc. **74**, 5943 (1952).
14. J. D. Roberts and C. M. Regan. J. Am. Chem. Soc. **75**, 2069 (1953).
15. C. C. Lee and J. W. T. Spinks. Can. J. Chem. **31**, 761 (1953).
16. F. L. J. Sixma and H. Hendriks. Rec. Trav. Chim. **75**, 169 (1956).
17. D. G. Lee. M.A. Thesis, University of Saskatchewan, Saskatoon, Saskatchewan. 1960.
18. R. L. Shriner and R. C. Fuson. The systematic identification of organic compounds. 3rd ed. John Wiley and Sons Inc., New York. 1948. p. 258.

Can. J. Chem. Downloaded from www.nrcresearchpress.com by 210.87.254.40 on 09/05/12
For personal use only.

THE OXIDATION OF FERROUS SULPHATE BY Co^{60} γ-RADIATION[1]

E. ONAT,[2] R. L. HAINES, AND I. H. S. HENDERSON
Defence Research Chemical Laboratories, Ottawa, Ontario

Received May 10, 1963

ABSTRACT

An investigation of the Co^{60} γ-oxidation of ferrous sulphate in the range 0.015 to 0.15 *M* in 1.0 *N*, 5.0 *N*, and 10.0 *N* sulphuric acid solutions shows that although the yields obtained were invariably higher than those predicted from the concentration ratios of ferrous ion to dissolved oxygen, no evidence was obtained to confirm the very high yields reported by Proskurnin and co-workers. The increase in yield observed has been attributed to interference with the "primary" hydrogen yield by a mechanism involving electron or hydrogen atom capture by a ferrous ion – oxygen complex.

INTRODUCTION

The oxidation of millimolar ferrous ion in 0.8 *N* sulphuric acid has been investigated extensively and the yields of ferric ion well established as 15.6 ferric ions per 100 ev absorbed in air-saturated solution (1) and as 8.2 ferric ions per 100 ev absorbed in oxygen-free solution (2, 3). Proskurnin, Orekhov, and Chernova (4), investigating this reaction at higher concentrations of ferrous ion, sulphuric acid, and oxygen, reported yields up to 60 ferric ions per 100 ev absorbed.

Miller (5), Johnson (6), and Le Bail *et al.* (7) attempted to verify the work of Proskurnin but found no increase in yield at the higher concentrations. Le Bail (7), however, found that the yield was enhanced in the presence of traces of benzene, metallic platinum, and stainless steel. Chernova, Orekhov, and Proskurnin (8) reported later that the reason the above workers did not find evidence of an enhanced yield was because, under high oxygen pressure, a compound of iron was formed that was not determined either at a wavelength of 304 mμ as ferric ion or by titration as ferrous ion. These authors ascribed the appearance of an unidentified absorption band at 250 mμ to such a compound.

The work reported here was undertaken as part of an investigation of the feasibility of the conversion of radiation energy into electrical energy through an electrochemical system, in which it is obviously desirable to utilize the maximum fraction of radiation energy to yield electrochemically active products. Attempts were made to confirm and extend Proskurnin's work, with a view to determining whether conditions could be found under which there would be a substantial increase in the yield of oxidation products.

EXPERIMENTAL

All irradiations were carried out using Co^{60} γ-radiation at dose rates of 2.5×10^{17}, 6.2×10^{17}, or 8.4×10^{18} ev/ml hr from sources of approximately 400 and 1200 c, or from a well source of approximately 200 c. Dose rates were determined by means of the Fricke dosimeter with millimolar ferrous sulphate and sodium chloride in 0.8 *N* sulphuric acid, using the value 15.6 ferric ions produced per 100 ev absorbed. All irradiations were carried out in borosilicate glass containers which had been preirradiated in contact with sulphuric acid solutions in order to remove traces of organic impurities. At the two lower dose rates, solutions were irradiated in open test tubes containing approximately 75 ml of sample. Irradiations under water using the well source at the highest dose rates employed were carried out in sealed ampoules containing 4.0 ml of sample or in a sealed annular cell containing 30.0 ml of sample.

Irradiations were carried out under air and under 1 and 5 atm of oxygen. The initial ferrous ion concentration was varied from 0.015 to 0.15 g-ions/liter in 1.0 *N*, 5.0 *N*, and 10.0 *N* sulphuric acid. Total dose

[1]*Issued as Defence Research Chemical Laboratories Report No. 416.*

[2]*Lt. Col. E. Onat, Army of the Republic of Turkey; Canadian Defence Research Fellow, 1961–1962. Present address: Ozel Silahlar S. Md., M.S.B. ARGE Bsk. Ligi, Ankara, Turkey.*

Can. J. Chem. Downloaded from www.nrcresearchpress.com by 210.87.254.105 on 09/05/12
For personal use only.

Can. J. Chem. Downloaded from www.nrcresearchpress.com by 210.87.254.105 on 09/05/12
For personal use only.

was varied from 1.0×10^{17} ev/ml to 2.5×10^{18} ev/ml. In experiments carried out under 1 atm oxygen, the solutions were kept saturated by bubbling oxygen through the solution at flow rates of 60–300 ml/min. For experiments at 5.0 atm, the glass irradiation vessels were placed in a thin-walled (0.030 in.) steel bomb which could be maintained at the desired pressure for some time prior to and during irradiation. Solutions were prepared using triply distilled water and reagent grade sulphuric acid. For solutions of ferrous ion less than 2.0×10^{-2} *M*, Merck Reagent Grade salts were employed without purification. In order to reduce the blank from ferric ion in solutions of ferrous ion greater than 2.0×10^{-2} *M*, it was found necessary to subject the stock solutions to a preliminary electrolysis under argon between platinum electrodes at a current of a few milliamperes for at least 2 weeks, with frequent replacement of anolyte by siphoning partially purified solution through the salt bridge. In general, the ratio of ferric ion to ferrous ion concentration was maintained at a value less than 1.0×10^{-4}. The reduced ferrous sulphate stock solution was stored in the dark under argon.

Ferric ion was determined using a Cary recording spectrophotometer model 14 PM, at a wavelength of 304 mμ (9). Before analysis, the irradiated solutions were brought to the temperature of the cell compartment in a constant-temperature bath. Calibration curves were plotted for ferric ion absorption at 304 mμ in 1.0 *N*, 5.0 *N*, and 10.0 *N* solutions of sulphuric acid. Values of extinction coefficients relative to those obtained with 0.8 *N* H_2SO_4 were 0.98, 1.015, and 1.297 at 1.0 *N*, 5.0 *N*, and 10.0 *N* sulphuric acid, in excellent agreement with those reported by Boyle and Mahlman (10). The data of Scharf and Lee (11) were used to evaluate the extinction coefficient in 0.8 *N* H_2SO_4 at 24.2°, the temperature at which the cell compartment was thermostated.

In some experiments the radiolytically produced ferric ion was determined indirectly by titration of the ferrous ion solutions with 2×10^{-3} *N* potassium permanganate before and after irradiation as well as by the direct spectrophotometric method. Titrimetric end points were determined potentiometrically using the procedure outlined by Kolthoff and Sandell (12). Although the precision of the method was inherently low because of the low percentage conversion, it was used to check the suggestion of Chernova *et al.* (8) that total iron was not accounted for as the sum of ferrous ion determined by titration and ferric ion determined spectrophotometrically.

Oxidation of Ferrous Ion By Molecular Oxygen

Preliminary investigations indicated that ferrous ion was oxidized rapidly by molecular oxygen, particularly at the higher concentrations of ferrous ion employed. The results obtained here followed the kinetic dependence reported by Lamb and Elder (13) for oxygen oxidation of solutions of ferrous ion in sulphuric acid solution, and by George (14) for the oxidation reaction in perchloric acid solution, namely,

$$\frac{d[Fe^{2+}]}{dt} = -k[Fe^{2+}]^2[O_2].$$

The data for the ferric ion yield in 5 *N* sulphuric acid saturated with oxygen at 1 atm are shown plotted against the square of ferrous ion concentration in Fig. 1. The yield was independent of oxygen flow rate in

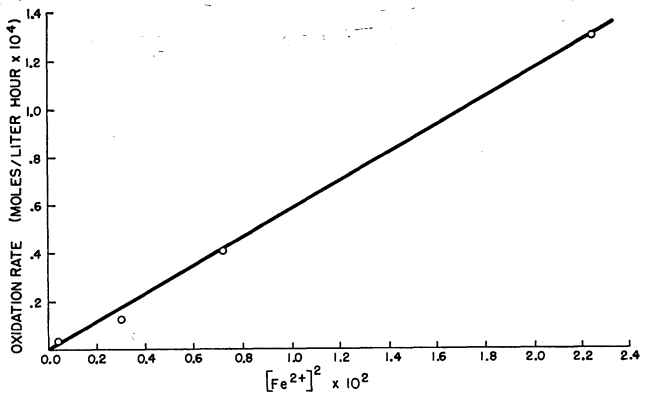

FIG. 1. Rate of oxidation of ferric ion by molecular oxygen at 25° C in 5.0 *N* H_2SO_4 under 1.0 atm O_2 vs. square of initial concentration of ferrous ion.

the range 60 ml/min to 300 ml/min. The experiments at pressures of 5 atm oxygen showed less consistency because of the time required for the solutions to equilibrate with the gas, and the difficulty of maintaining a standard temperature. However, the observed ratio of the rate of ferric ion production under 5 atm and 1 atm pressure was approximately 5:1. The oxidation rate increased with increasing acid concentration in the

range 1–10 N H_2SO_4. The rate of production of ferric ion from 0.1 M ferrous ion in 5.0 N sulphuric acid at 1 atm oxygen was found to be 5.8×10^{-5} mole Fe^{3+} per liter per hour at 24° C.

Blank corrections for ferric ion produced as a result of "dark" reaction between ferrous ion and molecular oxygen were made by using, as reference solutions in the spectrophotometer, solutions which had been subjected to the same oxygen pressures for the same time as the irradiated solutions. As noted above, this procedure was not entirely satisfactory for experiments at an oxygen pressure of 5.0 atm, but the results obtained under these conditions were consistent within experimental scatter with the other data reported here. In the absence of confirmation of the very high yields reported by Proskurnin *et al.* (4, 8) the experiments were not repeated.

EXPERIMENTAL RESULTS

In general it was found that the concentration of ferric ion increased linearly with dose up to a total dose of at least 2.0×10^{18} ev/ml. However, in air-saturated solutions of 5.0 N and 10.0 N sulphuric acid, in which the oxygen solubility was appreciably less than that in 1.0 N sulphuric acid, a falloff in yield was sometimes observed for doses in excess of 1.2×10^{18} ev/ml. Ferric ion yields reported below were evaluated either from the initial slopes of ferric ion vs. dose curves, or, when preliminary experiment had established linearity of yield with dose, from the equation

$$G_{Fe^{3+}} = \frac{15.6(\text{O.D.})_s\,\epsilon_f\,t_f\,(\text{e.d.})_f}{(\text{O.D.})_f\,\epsilon_s\,t_s\,(\text{e.d.})_s},$$

where $(\text{O.D.})_s$ was the observed 304 mμ optical density for the sample after an irradiation time t_s, $(\text{O.D.})_f$ the optical density for the Fricke solution after irradiation time t_f at the same position, ϵ_f/ϵ_s the ratio of the 304 mμ extinction coefficients and $(\text{e.d.})_f/(\text{e.d.})_s$ the ratio of calculated electron densities for the two solutions.

The data for experiments carried out under air are shown in Fig. 2 as number of ferric

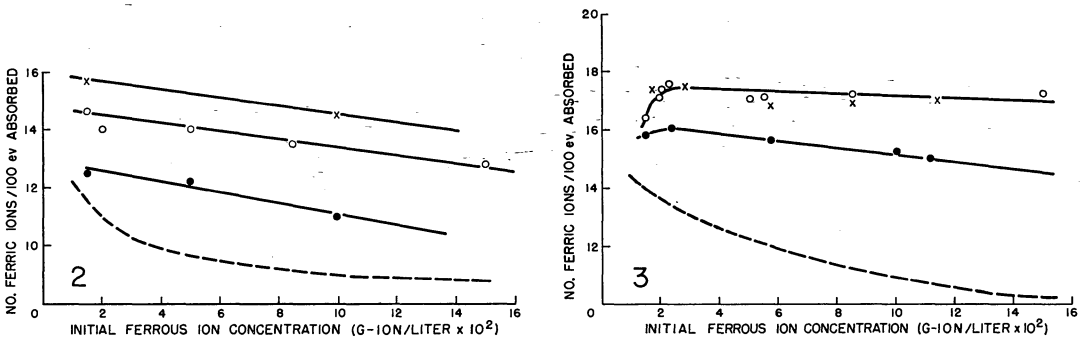

FIG. 2. Plot of $G_{Fe^{3+}}$ as a function of initial ferrous ion concentration under air. Dose rate 6.2×10^{17} ev/ml hr. × 1 N H_2SO_4; ○ 5 N H_2SO_4; ● 10 N H_2SO_4. Broken line, $G_{Fe^{3+}}$ in air-saturated, 10.0 N sulphuric acid calculated from the equation of Allen and Rothschild (3).

FIG. 3. Plot of $G_{Fe^{3+}}$ as function of initial ferrous ion concentration under O_2 at 1 atm. Dose rates, 2.5×10^{17}, 6.2×10^{17}, 7.4×10^{18} ev/ml hr. × 1 N H_2SO_4; ○ 5 N H_2SO_4; ● 10 N H_2SO_4. Broken line, $G_{Fe^{3+}}$ in 10.0 N sulphuric acid under oxygen at 1.0 atm calculated from the equation of Allen and Rothschild (3).

ions produced per 100 ev absorbed ($G_{Fe^{3+}}$) plotted against initial ferrous ion concentration for the three acid concentrations employed. The dose rate for this series of experiments was approximately 6.2×10^{17} ev/ml hr. Figure 3 shows similar plots for solutions saturated with oxygen at 1.0 atm pressure at dose rates of approximately 6.2×10^{17} ev/ml hr and 7.4×10^{18} ev/ml hr. Since no dependence of yield on dose rate was observed, no identification of dose rates is shown on the curves. In one series of experiments with 0.02 M

Can. J. Chem. Downloaded from www.nrcresearchpress.com by 210.87.254.105 on 09/05/12
For personal use only.

ferrous ion in 5.0 N sulphuric acid, parallel determinations of ferric ion were made spectrophotometrically and indirectly by determination of ferrous ion consumed by potentiometric titration, since it had been reported that yields determined from ferrous consumption were approximately four times as high as spectrophotometric values (8). The results of individual experiments are given in Table I. Because the titration method required

TABLE I

Comparison of ferric ion yields obtained spectrophotometrically and by titration

Initial Fe^{2+}, mole/l.	O_2 press., atm	Acid concn., N	Dose rate, ev/ml hr	Total dose, ev	Fe^{3+}, mole/l. (titra.)	Fe^{3+}, mole/l. (spect.)	$G_{Fe^{3+}}$ (titra.)	$G_{Fe^{3+}}$ (spect.)
1.922×10^{-2}	1	5	7.4×10^{18}	2.66×10^{18}	8.12×10^{-4}	8.52×10^{-4}	16.4	17.2
					8.17×10^{-4}		16.5	
1.926×10^{-2}	1	5	7.4×10^{18}	3.55×10^{18}	1.085×10^{-3}		16.4	17.1
						1.134×10^{-3}		
					1.075×10^{-3}		16.3	
					1.045×10^{-3}		15.8	
						Average	16.1	17.2
1.53×10^{-2}	5	10	6.2×10^{17}	1.83×10^{18}	6.62×10^{-4}	6.08×10^{-4}	17.3	15.9
1.53×10^{-2}	5	10	6.2×10^{17}	1.87×10^{18}	6.87×10^{-4}	6.18×10^{-4}	17.6	15.9
						Average	17.5	15.9

the determination of the difference between two relatively large numbers, much less reliance could be placed on this analysis than the spectrophotometric method. However, the agreement observed is such as to preclude the possibility of a difference as great as that reported previously (8).

At the higher concentrations of ferrous ion employed, the initial concentration of ferric ion approached 10^{-4} M or higher, particularly in experiments carried out under an oxygen pressure of 5.0 atm. Therefore it was desirable to determine the influence of initial ferric ion concentration on the yield to permit an estimate of the relative importance of ferric ion reduction by hydrogen atoms. In this experiment, the initial ferric ion concentration was varied from 0.3% to 11.9% of the total iron concentration of 0.0227 M in 5.0 N sulphuric acid. The solutions were saturated with oxygen at 1.0 atm. The results, given in Table II, showed no dependence of yield on initial ferric ion concentration. Several

TABLE II

Effect of relative ferric ion concentration on yield
(Total iron concentration 2.27×10^{-2} M, 1.0 N H_2SO_4;
Fricke dose rate 7.4×10^{18} ev/ml hr)

Initial Fe^{3+}, % of total iron	Fe^{3+} produced, mole/l.	$G_{Fe^{3+}}$
0.3	5.21×10^{-4}	17.8
2.04	5.20×10^{-4}	17.8
4.17	5.11×10^{-4}	17.4
11.9	5.20×10^{-4}	17.8

experiments, not reported separately, indicated no change of yield when ferrous ammonium sulphate was substituted for ferrous sulphate.

The data for individual experiments in which the solutions were saturated with oxygen at 5.0 atm are given in Table III in order to provide an indication of the reproducibility

Can. J. Chem. Downloaded from www.nrcresearchpress.com by 210.87.254.105 on 09/05/12
For personal use only.

TABLE III

Ferric ion yields under an oxygen pressure of 5.0 atm

1 N H_2SO_4		5 N H_2SO_4		10 N H_2SO_4	
Initial Fe^{2+}, mole/l.	$G_{Fe^{3+}}$	Initial Fe^{2+}, mole/l.	$G_{Fe^{3+}}$	Initial Fe^{2+}, mole/l.	$G_{Fe^{3+}}$
		0.03	18.6	0.015	15.9
0.015	19.2	0.03	18.4	0.05	22.5
		0.05	18.5		
0.015	19.1	0.05	17.6	0.05	19.4
0.05	19.4	0.05	17.8		
		0.05	20.7		
		0.015	16.1		
		0.10	15.2		

obtained under these conditions. In these runs the analytical error was increased because the blank correction for ferric ion produced by dark reaction was large, in some instances substantially larger than the radiation yield.

DISCUSSION

Examination of the experimental data of the present work indicates that there were two opposing effects which modified the yield. The first of these, which tends to increase the yield to values in excess of 15.6 ferric ions per 100 ev absorbed, is revealed most clearly in the data obtained at an oxygen pressure of 1.0 atm in 1.0 and 5.0 N sulphuric acid with ferrous ion concentrations 0.015 M and greater and in the data obtained at 5.0 atm oxygen pressure. As noted below, there is evidence that this effect was present in all ferrous ion solutions greater than 0.015 M in the present work, but that its influence was masked in part by the second effect, namely the dependence of yield on the ferrous ion/oxygen concentration ratio. This dependence was investigated in detail by Allen and Rothschild (3) for solutions of ferrous ion up to 0.002 M in 0.8 N sulphuric acid at a variety of oxygen partial pressures in which excellent agreement was observed with the equation

$$G_{Fe^{3+}} = 8.2 + \frac{7.35}{1 + \dfrac{K_5[Fe^{2+}]}{K_3[O_2]}}. \qquad [a]$$

The k's are rate constants for reactions in the sequence below, which very satisfactorily describes the radiolytic ferrous ion oxidation for solute concentrations in the ranges indicated:

$$H_2O_2 + 2Fe^{2+} = 2Fe^{3+} + 2OH^- \qquad [1]$$

$$OH + Fe^{2+} = Fe^{3+} + OH^- \qquad [2]$$

$$H + O_2 = HO_2 \qquad [3]$$

$$HO_2 + H^+ + Fe^{2+} = Fe^{3+} + H_2O_2 \qquad [4]$$

$$H + H^+ + Fe^{2+} = H_2 + Fe^{3+} \qquad [5]$$

$$Fe^{3+} + H = Fe^{2+} + H^+. \qquad [6]$$

Modifying equation [a] to include variation of hydrogen ion activity in order to permit a test of the applicability of the equations to the present results, we obtain

$$G_{Fe^{3+}} = 8.2 + \frac{7.35}{1 + \dfrac{k_5[Fe^{2+}][H_3O^+]_c}{k_3[O_2][H_3O^+]_{0.8}}}, \qquad [b]$$

Can. J. Chem. Downloaded from www.nrcresearchpress.com by 210.87.254.105 on 09/05/12
For personal use only.

where $[H_3O^+]_c/[H_3O^+]_{0.8}$ is the ratio of hydrogen ion concentrations in sulphuric acid of concentrations c and 0.8 N, respectively, while the value of k_5/k_3 was taken as 1/1200 in 0.8 N sulphuric acid (3). The results showing lack of dependence of yield on initial ferric ion concentration in the present concentration range (Table II) indicated the validity of neglecting equation [6] in this derivation. Oxygen concentrations in 1.0 N, 5.0 N, and 10.0 N sulphuric acid at 25° C relative to that in 0.8 N sulphuric acid were calculated from the data presented by Seidell (15) to be 0.89, 0.63, and 0.48 respectively. (As noted below, the possibility of complexing between oxygen and ferrous ion could modify the oxygen solubility, particularly at the higher ferrous ion concentrations, but in the absence of experimental confirmation, the above values were assumed.) Estimates of hydrogen ion concentrations in the sulphuric acid solutions employed were made from the Raman spectral data of Young *et al.* (16) using the equation $C_{H^+} = C_{HSO_4^-} + 2C_{SO_4^{2-}}$. The concentration ratios obtained were 1.00:1.25:6.51:12.89 for 0.8 N, 1.0 N, 5.0 N, and 10.0 N solutions, respectively.

Calculated values of $G_{Fe^{3+}}$ using equation [*b*] are compared with interpolated values from the curves of Figs. 2 and 3 in Table IV for two ferrous ion concentrations in each

TABLE IV

Comparison of experimental yields with those calculated from the equation of Allen and Rothschild (3) for two initial ferrous ion concentrations

Fe^{2+}, mole/l.	O_2, atm	H_2SO_4, N	$\frac{[Fe^{2+}][H_3O^+]_c}{1200[O_2][H_3O^+]_{0.8}}$	$G_{Fe^{3+}}$ (calc)	$G_{Fe^{3+}}$ (exptl) (interpolated)
0.03	0.21	1	0.135	14.7	15.5
0.1	0.21	1	0.451	13.3	14.5
0.03	1.0	1	0.027	15.4	17.5
0.1	1.0	1	0.090	14.9	17.2
0.03	5.0	1	0.0054	15.5	(19)
0.1	5.0	1	0.018	15.4	(19)
0.03	0.21	5	0.444	13.3	14.3
0.1	0.21	5	1.479	11.0	13.3
0.03	1.0	5	0.0885	15.0	17.5
0.1	1.0	5	0.295	14.0	17.2
0.03	5.0	5	0.018	15.4	18.4
0.1	5.0	5	0.059	15.1	15.2
0.03	0.21	10	4.34	9.6	12.4
0.1	0.21	10	14.5	8.7	11.0
0.03	1.0	10	0.867	12.1	16.0
0.1	1.0	10	2.89	10.1	15.2
0.03	5.0	10	0.173	14.4	—
0.1	5.0	10	0.578	12.8	—

sulphuric acid concentration and oxygen pressure employed, and compared graphically for 10.0 N sulphuric acid solutions in Figs. 2 and 3. For each concentration, equation [*b*] leads to lower $G_{Fe^{3+}}$ values than those determined experimentally.

That the experimental yields are higher than those calculated from equation [*b*] coupled with the observation of yields as high as 17.6 ions per 100 ev in 1.0 N and 5.0 N sulphuric acid saturated with oxygen at 1.0 atm, with comparable results at 5.0 atm, suggests the occurrence here of reactions not significant at concentrations of ferrous ion less than 0.01 M. It is suggested that there is a sufficiently high concentration of a complex such as FeO_2^{2+} at the higher concentrations of ferrous ion to interfere with intratrack formation of molecular hydrogen by atom combination or by neutralization of a hydrogen-molecule ion by a free electron. The overall reaction,

$$FeO_2^{2+} + e^- + 2H^+ \rightarrow Fe^{3+} + H_2O_2, \qquad [7]$$

Can. J. Chem. Downloaded from www.nrcresearchpress.com by 210.87.254.105 on 09/05/12
For personal use only.

would lead to a maximum enhancement of the ferric ion yield of $6G_{H_2}$ where G_{H_2} is the "primary" hydrogen yield in millimolar ferrous ion in 0.8 N sulphuric acid, that is to approximately 2.5+15.6 or 18.1. Evidence for the existence of a complex such as FeO_2^{2+} has been inferred from the kinetics of ferrous ion oxidation by molecular oxygen (14). Chernova, Orekhov, and Proskurnin (8) suggested that the appearance of a band at about 250 mμ was due to such a complex. In order to check this latter possibility, a spectrum was recorded from 210 mμ to 330 mμ on a solution of 0.052 M ferrous ion in 5.0 N sulphuric acid solution having a ferric ion concentration less than 1.0×10^{-6} M and this was compared with spectra obtained on samples of the same solution (*a*) after exposure to oxygen at 5.0 atm for 19 hours and (*b*) after addition of sufficient 30% hydrogen peroxide to produce as much ferric ion as had been produced in the sample exposed to oxygen (4.40×10^{-4} M Fe^{3+}). No evidence was obtained for a band attributable to a complex between ferrous ion and oxygen in the region of 250 mμ, the major band being that due to ferric ion at 220 mμ (11). These results do not, however, preclude the possibility of complexing between ferrous ion and oxygen.*

CONCLUSIONS

The results of the present work confirm those of other workers, (5–7) who have attempted to reproduce the very high ferric ion yields reported by Proskurnin, Orekhov, and Chernova (4, 8). The sources of the discrepancy have not been determined, but may be associated with experimental details not duplicated in the present work. The suggestion offered to explain the occurrence of these high yields (G = 60 ferric ions/100 ev absorbed), namely that there exists a discrepancy between titrimetric and spectrophotometric determination of ferric ion (8), was also not confirmed in the present work.

When the ferrous ion concentration was increased to values in excess of 0.015 M, two opposing effects were noted. The first of these, a decrease in the ferric ion yield with increasing ratio of ferrous ion to oxygen concentration, was in qualitative agreement with the data of Allen and Rothschild (3). The second effect, which tended to increase the yield, has been tentatively attributed to electron capture by a ferrous ion – oxygen complex, thus decreasing the formation of "primary" molecular hydrogen, leading to an enhancement of the ferric yield by a maximum of $6G_{H_2\ prim} = 2.5$.

ACKNOWLEDGMENTS

The authors gratefully acknowledge many helpful discussions with Dr. D. W. Grant and Dr. J. R. Coleman of the Defence Research Chemical Laboratories.

REFERENCES

1. C. J. Hochanadel and J. A. Ghormley. J. Chem. Phys. **21**, 880 (1953).
2. N. F. Barr and C. G. King. J. Am. Chem. Soc. **76**, 5565 (1954); **78**, 303 (1956).
3. A. O. Allen and W. G. Rothschild. Radiation Res. **7**, 591 (1957).
4. M. A. Proskurnin, V. D. Orekhov, and A. I. Chernova. Sb. Rabot po Radiatsionnoi Khim. Akad. Nauk SSSR, 79 (1955); Symp. Radiation Chem. Moscow, 63 (1955) (English Transl.).
5. N. Miller. J. Chim. Phys. **52**, 644 (1955).
6. E. Johnson. J. Chim. Phys. **52**, 644 (1955).
7. H. LeBail and J. Sutton. J. Chim. Phys. **53**, 430 (1956).
8. A. I. Chernova, V. D. Orekhov, and M. A. Proskurnin. Trudy 1-go Vsesoyez. Soveshch. po Radiatsionnoi Khim., Akad. Nauk SSSR Otdel. Khim. Nauk, Moscow, 55 (1957) (pub. 1958).
9. T. J. Hardwick. Can. J. Chem. **30**, 17 (1952).
10. J. W. Boyle and H. A. Mahlman. Radiation Res. **16**, 416 (1962).

**A weak absorption band, tentatively attributed to a complex between ferrous ion and sulphate in the absence of oxygen, was observed at 240 mμ. Extinction coefficients at this wavelength were approximately 18.0 liter/mole in 5.0 N sulphuric acid and 8.0 liter/mole in 1.0 N sulphuric acid.*

Can. J. Chem. Downloaded from www.nrcresearchpress.com by 210.87.254.105 on 09/05/12
For personal use only.

11. K. SCHARF and R. M. LEE. Radiation Res. **16**, 115 (1962).
12. I. M. KOLTHOFF and E. B. SANDELL. Textbook of quantitative inorganic analysis. Macmillan 1953.
13. A. B. LAMB and L. W. ELDER, JR. J. Am. Chem. Soc. **53**, 137 (1931).
14. P. GEORGE. J. Chem. Soc. 4349 (1954).
15. A. SEIDELL. Solubilities on inorganic and metal organic compounds. Vol. I. 3rd ed. D. Van Nostrand Company Inc., 1940.
16. T. F. YOUNG, L. F. MARANVILLE, and H. M. SMITH. *In* The structure of electrolytic solutions. *Edited by* W. J. Hamer. John Wiley and Sons, Inc., New York. 1959. p. 35.

Can. J. Chem. Downloaded from www.nrcresearchpress.com by 210.87.254.105 on 09/05/12
For personal use only.

NOTES

REACTIONS OF PHENYL-SUBSTITUTED HETEROCYCLIC COMPOUNDS
IV. BROMINATION OF 2-PHENYL-1,2,3,2H-TRIAZOLE

BRIAN M. LYNCH

Addition of silver sulphate to a solution of bromine in concentrated sulphuric acid produces a highly reactive electrophilic brominating species, which is probably $AgBr_2^+$ (cf. Arotsky and Symons (1)). In previous work (2), we have used this combination of reagents to effect selective para bromination of 1-phenylpyrazole (which probably reacts in the form of its conjugate acid under the reaction conditions).

The present note reports the application of this bromination technique to 2-phenyl-1,2,3,2H-triazole (I), where 2-*p*-bromophenyl-1,2,3,2H-triazole (II), m.p. 113°, is obtained. Apparently, the highly reactive "positive bromine" overcomes the deactivating influence of the electron-attracting triazole ring (cf. ref. 3), even under circumstances where this influence may be enhanced as a result of protonation in the strongly acidic reaction medium.

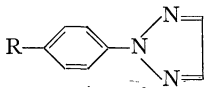

I: R = H
II: R = Br
III: R = NO_2

The proton magnetic resonance spectrum of the bromination product of I offered a particularly simple proof of structure II: it showed a typical A_2B_2 pattern centered at a τ value of 2.25 for the four protons of the *p*-bromophenyl group, and a single line at τ 2.25 for the two equivalent protons of the triazole ring. Analysis of the A_2B_2 pattern assuming that $J_{AB}' = 0$ and $J_A = J_B$ (cf. Richards and Schaefer (4)) gave $J_{AB} = 9.4$ c/s, and an A–B chemical shift separation of 0.39 τ. Since the triazolyl group in derivatives of I is known to be strongly electron attracting (3), it is presumed that the protons ortho to the triazole ring would have the lower τ values in the absence of spin–spin coupling, and on this basis it is possible to deduce τ 2.05_5 for the protons ortho to the triazole ring, and τ 2.44_5 for the protons ortho to the bromine atom. If we assume, following Pople, Schneider, and Bernstein (5), that the chemical shift of a proton in a 1-X, 4-Y benzene will be X_o+Y_m at the 2-position, and X_m+Y_o at the 3-position (X_o, X_m and Y_o, Y_m are the chemical shifts of the ortho and meta protons in the monosubstituted benzenes C_6H_5X and C_6H_5Y), and also that the chemical shifts of the protons influenced by the triazolyl group are similar to those under the corresponding influence of a nitro group (supporting evidence for this assumption is presented below), these τ values appear reasonable.

The τ value 2.25, observed for the protons of the triazole ring in II, is consistent with the positions noted for the proton resonances in other five-membered nitrogen heterocyclic compounds. Thus, Reddy, Hobgood, and Goldstein (6) found τ 2.30 and 2.86 for the 2- and 4(5)-protons of imidazole, while Moore and Whittaker (7) found τ 1.77 for the ring proton of 2-ethyltetrazole.

The product II was found to be identical with a sample of the bromophenyl-1,2,3,2H-triazole, m.p. 113–114°, prepared previously (8) by treatment of glyoxal bisphenylhydrazone with bromine in aqueous suspension. This reaction presumably involves initial para bromination of the bisphenylhydrazone, followed by oxidative cyclization, since bromine in aqueous suspension has no effect on I; although the structure of the product obtained previously (8) was not proved by an unambiguous synthesis, it could be subject to little doubt in view of the demonstrated generality of the initial para bromination of the bisarylhydrazones of glucose and glyoxal before their oxidative cyclization to triazoles (cf. ref. 8).

The product II was also obtained via a Sandmeyer reaction from 2-*p*-nitrophenyl-1,2,3,2H-triazole (III). The structure III was assigned recently (9) to the mononitration product of I, and the correlation of the bromo- and nitro-phenyl-1,2,3,2H-triazoles confirms the assignment of structure III.

More direct confirmation of the structure III for the mononitration product of I was provided by its proton magnetic resonance spectrum. Two signals, at τ 1.70 (four protons) and 2.10 (two protons), were observed. The higher-field absorption is assigned to the triazole ring protons, deshielded from the value noted for the compound II by the electron-attracting *p*-nitrophenyl group, while the four-proton signal is assigned to the protons of the nitrophenyl group. It is suggested that the chemical shifts induced by the nitro and triazolyl substituents are of closely similar magnitudes, thus leading to virtual equivalance of all four protons in the nitrophenyl group of III (the four-proton signal showed barely resolvable fine structure, revealed as an asymmetric triplet (separation, ca. 1 c/s) by adjustment of sweep width).

It is evident that measurements of proton magnetic resonance spectra offer simple and convenient alternatives to classical syntheses in proving the structures of derivatives of phenyl-substituted heterocyclic compounds.

EXPERIMENTAL

Melting points are uncorrected. The microanalysis was by the Schwarzkopf Microanalytical Laboratory, Woodside, N.Y., U.S.A.

2-p-Bromophenyl-1,2,3,2H-triazole (II)

(a) By Direct Bromination

2-Phenyl-1,2,3,2H-triazole (I) (3 g) was dissolved in sulphuric acid (*d* 1.84, 45 ml), and bromine (1 ml) was added dropwise. Finely powdered silver sulphate (8 g) was added, and the mixture was stirred vigorously for 3 hours. Silver bromide was filtered off and the filtrate was poured onto ice. The resulting precipitate was extracted with hot benzene, and the benzene extract deposited large plates, m.p. 112°, on slow evaporation. Crystallization of this crude material from methanol yielded needles of 2-*p*-bromophenyl-1,2,3,2H-triazole (II) (3.1 g), m.p. 113°, identical (mixed m.p.) with a sample prepared by the action of bromine on glyoxal bisphenylhydrazone (cf. ref. 8). Anal. Calc. for $C_8H_6BrN_3$: C, 42.88; H, 2.70%. Found: C, 43.06; H, 2.72%.

(b) Via a Sandmeyer Reaction

2-*p*-Aminophenyl-1,2,3,2H-triazole hydrochloride (1.6 g) (from reduction of 2-*p*-nitrophenyl-1,2,3,2H-triazole (III) with tin and hydrochloric acid) was dissolved in 6 *N* sulphuric acid (9 ml) and cooled to 0°, diazotized with sodium nitrite (0.7 g) in water (2 ml), and kept at 5° for 30 minutes. The solution of the diazonium salt was added to a boiling solution of cuprous bromide (8 g) in hydrobromic acid (48%, 60 ml). Steam distillation afforded 2-*p*-bromophenyl-1,2,3,2H-triazole, which was collected and crystallized from methanol, yielding needles (0.5 g), m.p. 113°, identical (mixed m.p.) with the product obtained in (*a*) above.

Proton Magnetic Resonance Spectra

The spectra were measured on a Varian A-60 Analytical n.m.r. spectrometer operating at 60 Mc/s. The samples were examined as solutions in deuterochloroform with tetramethylsilane as internal reference. Copies of the spectra are available on request.

ACKNOWLEDGMENTS

I thank the National Research Council of Canada for a grant in support of this work, Dr. A. G. McInnes and Mr. D. G. Smith (Atlantic Regional Laboratory, National Research Council, Halifax) for the measurements of proton magnetic resonance spectra, Dr. H. El Khadem (University of Alexandria) for his courtesy in carrying out a mixed melting point determination, and Miss Y. Hung for technical assistance.

1. J. Arotsky and M. C. R. Symons. Quart. Rev. (London), **16**, 282 (1962).
2. M. A. Khan, B. M. Lynch, and Y. Hung. Can. J. Chem. **41**, 1540 (1963).
3. H. El Khadem. J. Chem. Soc. 3146 (1961).
4. R. E. Richards and T. P. Schaefer. Trans. Faraday Soc. **54**, 1280 (1958).
5. J. A. Pople, W. G. Schneider, and H. J. Bernstein. High resolution nuclear magnetic resonance. McGraw-Hill Book Co. Inc., New York. 1959. p. 262.
6. G. S. Reddy, R. T. Hobgood, and J. H. Goldstein. J. Am. Chem. Soc. **84**, 336 (1962).
7. D. W. Moore and A. G. Whittaker. J. Am. Chem. Soc. **82**, 5007 (1960).
8. H. El Khadem, Z. M. El-Shafei, and Y. S. Mohammed. J. Chem. Soc. 3993 (1960).
9. B. M. Lynch and T. Chan. Can. J. Chem. **41**, 274 (1963).

Received April 22, 1963.
Department of Chemistry,
St. Francis Xavier University,
Antigonish, Nova Scotia.

THE SYNTHESIS OF 5-O-β-D-GLUCOPYRANOSYL-D-XYLOSE AND 3,5-DI-O-β-D-GLUCOPYRANOSYL-D-XYLOSE

J. K. N. Jones and P. E. Reid

In continuation of a program (1) of synthesizing oligosaccharides which may occur as components of polysaccharides we have investigated the products of the condensation of 2,3,4,6-tetra-*O*-acetyl-α-D-glucopyranosyl bromide (4.18 moles) with 1,2-*O*-isopropylidene-D-xylofuranose (1 mole) under standard Koenigs–Knorr conditions (2). This condensation would be expected to yield a mixture of 5-*O*-β-D-glucopyranosyl-D-xylose, 3-*O*-β-D-glucopyranosyl-D-xylose, and 3,5-di-*O*-β-D-glucopyranosyl-D-xylose. After removal of the blocking groups the mixture of monosaccharides and oligosaccharides was fractionated by chromatography on a charcoal column followed by chromatography on an ion exchange resin (3) and where necessary on sheets of Whatman 3 mm paper. These techniques yielded two chromatographically pure oligosaccharide fractions.

Fraction I (5-O-β-D-Glucopyranosyl-D-xylose)

This fraction was obtained as a crisp, white, hygroscopic glass. Chromatographic examination of the hydrolyzate of the fraction indicated the presence of glucose and xylose only. Hydrolysis of the methyl ether of the fraction and fractionation of the resulting mixture of methylated sugars yielded 2,3,4,6-tetra-*O*-methyl-D-glucose and 2,3-di-*O*-methyl-D-xylose. Thus fraction I is either 5-*O*-β-D-glucopyranosyl-D-xylose or 4-*O*-β-D-glucopyranosyl-D-xylose but is not 3-*O*-β-D-glucopyranosyl-D-xylose.

The disaccharide and the reduced disaccharide obtained by reduction with sodium borohydride were oxidized with sodium metaperiodate at 23±2° under unbuffered conditions. The results obtained were plotted graphically and the flattened portions of the curves were extrapolated to zero time. The values obtained indicate that the disaccharide consumed 4.2 moles of sodium metaperiodate and released 3.0 moles of formic

ACKNOWLEDGMENTS

I thank the National Research Council of Canada for a grant in support of this work, Dr. A. G. McInnes and Mr. D. G. Smith (Atlantic Regional Laboratory, National Research Council, Halifax) for the measurements of proton magnetic resonance spectra, Dr. H. El Khadem (University of Alexandria) for his courtesy in carrying out a mixed melting point determination, and Miss Y. Hung for technical assistance.

1. J. Arotsky and M. C. R. Symons. Quart. Rev. (London), **16**, 282 (1962).
2. M. A. Khan, B. M. Lynch, and Y. Hung. Can. J. Chem. **41**, 1540 (1963).
3. H. El Khadem. J. Chem. Soc. 3146 (1961).
4. R. E. Richards and T. P. Schaefer. Trans. Faraday Soc. **54**, 1280 (1958).
5. J. A. Pople, W. G. Schneider, and H. J. Bernstein. High resolution nuclear magnetic resonance. McGraw-Hill Book Co. Inc., New York. 1959. p. 262.
6. G. S. Reddy, R. T. Hobgood, and J. H. Goldstein. J. Am. Chem. Soc. **84**, 336 (1962).
7. D. W. Moore and A. G. Whittaker. J. Am. Chem. Soc. **82**, 5007 (1960).
8. H. El Khadem, Z. M. El-Shafei, and Y. S. Mohammed. J. Chem. Soc. 3993 (1960).
9. B. M. Lynch and T. Chan. Can. J. Chem. **41**, 274 (1963).

Received April 22, 1963.
Department of Chemistry,
St. Francis Xavier University,
Antigonish, Nova Scotia.

Can. J. Chem. Downloaded from www.nrcresearchpress.com by 210.87.254.40 on 09/05/12
For personal use only.

THE SYNTHESIS OF 5-O-β-D-GLUCOPYRANOSYL-D-XYLOSE AND 3,5-DI-O-β-D-GLUCOPYRANOSYL-D-XYLOSE

J. K. N. Jones and P. E. Reid

In continuation of a program (1) of synthesizing oligosaccharides which may occur as components of polysaccharides we have investigated the products of the condensation of 2,3,4,6-tetra-*O*-acetyl-α-D-glucopyranosyl bromide (4.18 moles) with 1,2-*O*-isopropylidene-D-xylofuranose (1 mole) under standard Koenigs–Knorr conditions (2). This condensation would be expected to yield a mixture of 5-*O*-β-D-glucopyranosyl-D-xylose, 3-*O*-β-D-glucopyranosyl-D-xylose, and 3,5-di-*O*-β-D-glucopyranosyl-D-xylose. After removal of the blocking groups the mixture of monosaccharides and oligosaccharides was fractionated by chromatography on a charcoal column followed by chromatography on an ion exchange resin (3) and where necessary on sheets of Whatman 3 mm paper. These techniques yielded two chromatographically pure oligosaccharide fractions.

Fraction I (5-O-β-D-Glucopyranosyl-D-xylose)

This fraction was obtained as a crisp, white, hygroscopic glass. Chromatographic examination of the hydrolyzate of the fraction indicated the presence of glucose and xylose only. Hydrolysis of the methyl ether of the fraction and fractionation of the resulting mixture of methylated sugars yielded 2,3,4,6-tetra-*O*-methyl-D-glucose and 2,3-di-*O*-methyl-D-xylose. Thus fraction I is either 5-*O*-β-D-glucopyranosyl-D-xylose or 4-*O*-β-D-glucopyranosyl-D-xylose but is not 3-*O*-β-D-glucopyranosyl-D-xylose.

The disaccharide and the reduced disaccharide obtained by reduction with sodium borohydride were oxidized with sodium metaperiodate at 23±2° under unbuffered conditions. The results obtained were plotted graphically and the flattened portions of the curves were extrapolated to zero time. The values obtained indicate that the disaccharide consumed 4.2 moles of sodium metaperiodate and released 3.0 moles of formic

acid per mole of disaccharide and the reduced disaccharide consumed 4.9 moles of sodium metaperiodate and released 2.78 moles of formic acid per mole of reduced disaccharide. In both cases overoxidation was negligible.

The results obtained from the reduced disaccharide are consistent with those expected theoretically from reduced 5-*O*-β-D-glucopyranosyl-D-xylose (1) but would not be expected to result from the periodate oxidation of reduced 4-*O*-β-D-glucopyranosyl-D-xylose or 3-*O*-β-D-glucopyranosyl-D-xylose.

The periodate oxidation of 5-*O*-β-D-glucopyranosyl-D-xylose (1) would be expected to result in a rapid consumption of 4 moles of sodium metaperiodate and a release of 2 moles of formic acid per mole of disaccharide followed by a slow consumption of 1 mole of periodate and a release of 2 moles of formic acid, this latter depending on the rate of hydrolysis of the intermediate formyl ester. The periodate oxidation of 4-*O*-β-D-glucopyranosyl-D-xylose (1) would be expected to result in an uptake of 4 moles of sodium metaperiodate and a release of 2 moles of formic acid per mole of disaccharide followed by a slow release of 1 mole of formic acid due to the hydrolysis of a formyl ester and the formation of an intermediate stable to further oxidation.

The results obtained are difficult to interpret. The curve for periodate consumption followed that expected for 5-*O*-β-D-glucopyranosyl-D-xylose but the curve for formic acid release did not show a break at the expected point. The periodate oxidation of the disaccharide thus rules out the possibility of a $1 \rightarrow 4$ linkage and also a $1 \rightarrow 3$ linkage but does not unequivocally prove the presence of a $1 \rightarrow 5$ linkage. In view of this uncertainty the disaccharide phenylosazone was subjected to oxidation with sodium metaperiodate. Hough, Powell, and Woods (4) have shown that pentose disaccharides containing $1 \rightarrow 5$, $1 \rightarrow 4$, and $1 \rightarrow 3$ linkages may be distinguished by the periodate oxidation of their phenylosazones. Thus, on the basis of the results of Hough, Powell, and Wood (4) it would be expected that 5-*O*-β-D-glucopyranosyl-D-xylose phenylosazone on periodate oxidation would yield mesoxaldehyde bis-1,2-phenylhydrazone whilst the phenylosazone of 4-*O*-β-D- or 3-*O*-β-D-glucopyranosyl-D-xylose would not.

Periodate oxidation of the disaccharide phenylosazone yielded mesoxaldehyde bis-1,2-phenylhydrazone, indicating a $1 \rightarrow 5$ linkage. On the basis of the evidence discussed above fraction I was identified as 5-*O*-β-D-glucopyranosyl-D-xylose.

Fraction II (3,5-Di-O-β-D-glucopyranosyl-D-xylose)

Fraction II was obtained as a crisp, white, hygroscopic glass. Chromatographic examination of the partial hydrolyzate of the fraction indicated the presence of components chromatographically identical with glucose, xylose, and 5-*O*- and 3-*O*-β-D-glucopyranosyl-D-xylose.

The reducing oligosaccharide and the reduced oligosaccharide obtained after reduction with sodium borohydride were oxidized with sodium metaperiodate at $23 \pm 2°$ under unbuffered conditions. The results obtained (calculated for a trisaccharide) were plotted graphically and the flattened portions of the curves were extrapolated to zero time. The reducing oligosaccharide consumed 4.85 moles of sodium metaperiodate per mole oligosaccharide and released 1.85 moles of formic acid per mole oligosaccharide followed by a slow release of formic acid. The reduced trisaccharide consumed 4.7 moles of sodium metaperiodate and released 1.85 moles of formic acid per mole of oligosaccharide.

The theoretical results expected from the periodate oxidation of a trisaccharide composed of 2 moles of glucose attached glycosidically to a single xylose residue which has a free C_1 position are shown in Table I. The theoretical results expected from the periodate

Can. J. Chem. Downloaded from www.nrcresearchpress.com by 210.87.254.40 on 09/05/12
For personal use only.

oxidation of a trisaccharide composed of two molecules of glucose attached glycosidically to a single xylose residue which has been reduced to a pentitol are shown in Table II. Comparison of the results of the periodate oxidation of fraction II with the theoretical results shown in Tables I and II, coupled with the results of the partial hydrolysis of fraction II, indicates that the compound is probably *3,5-di-O-β-*D*-glucopyranosyl-*D*-xylose.*

TABLE I

Periodate oxidation of reducing trisaccharide (unbuffered conditions)

Linkage	Moles of periodate consumed/mole trisaccharide	Moles of formic acid released/mole trisaccharide	Moles of formic acid/mole trisaccharide as formyl ester	Overoxidation expected
1 → 2 1 → 3 pyranose	4	2	0	No
1 → 2 1 → 4	4	2	0	No
1 → 2 1 → 5	4	2	0	No
1 → 3 1 → 4	5	2	1	No
1 → 3 1 → 5	5	2	1	No

TABLE II

Periodate oxidation of reduced trisaccharide (unbuffered conditions)

Linkage	Moles of periodate consumed/mole of reduced trisaccharide	Moles of formic acid released/mole of reduced trisaccharide	Overoxidation expected
1 → 2 1 → 5	5	2	No
1 → 2 1 → 3	5	2	No
1 → 2 1 → 4	4	2	No
1 → 3 1 → 4	5	2	No
1 → 3 1 → 5	5	2	No

EXPERIMENTAL

Optical rotations were measured at 23±2°. Solutions were concentrated under reduced pressure at 50° or less. The following solvent systems were used to separate sugars on paper chromatograms: (*a*) ethyl acetate, acetic acid, water (9:2:2); (*b*) ethyl acetate, acetic acid, formic acid, water (18:3:1:4); (*c*) butan-1-ol, ethanol, water, (3:1:1); (*d*) butan-1-ol, pyridine, water (5:3:2) (all v/v). Reducing sugars were detected with the *p*-anisidine spray (5) and non-reducing sugars were detected by the alkaline silver nitrate spray (6). Rates of movement of sugars on paper chromatograms are quoted relative to the rate of movement of D-galactose (R_{gal}).

Periodate Oxidation

The periodate oxidations of the di- and tri-saccharides and of their non-reducing derivatives obtained after sodium borohydride reduction were carried out on accurately weighed samples (ca. 20 mg) with 0.3 *M* sodium metaperiodate (2 ml) made up to 50 ml with distilled water. The reactions were carried out in the dark at room temperature. Aliquots (2 ml) were withdrawn for analysis. The periodate consumption was estimated by the method of Neumuller and Vasseur (7) and the formic acid that was released by the method of Andrews *et al.* (8).

Can. J. Chem. Downloaded from www.nrcresearchpress.com by 210.87.254.40 on 09/05/12
For personal use only.

Fraction B.—Chromatographic examination in solvent (*b*) indicated the presence of 2,3,4,6-tetra-*O*-methyl-D-glucose and 2,3-di-*O*-methyl-D-xylose plus traces of other components.

Fraction C.—This was chromatographically identical with 2,3-di-*O*-methyl-D-xylose in solvents (*b*) and (*c*) and was definitely separated from 2,4-di-*O*-methyl-D-xylose. It yielded *N*-phenyl 2,3-di-*O*-methyl-D-xylosylamine, m.p. and mixed m.p. 118–123°, $[\alpha]_D$ +189° (*c*, 0.65 in ethyl acetate).

Reduction of Disaccharide

The disaccharide (0.39 g) in water (11 ml) was treated with sodium borohydride (0.116 g) for 18 hours, sodium borohydride (0.162 g) was added, and the solution was allowed to stand for 24 hours. A large excess of acetone was added (ca. 10 ml) and after 3 hours the solution was diluted with water, passed through a small bed of Amberlite IR120 (H form) ion exchange resin, concentrated to a syrup, and codistilled with methanol three times. The syrup ran as a single component in solvent (*b*). It gave a positive reaction with the silver nitrate spray but not with the *p*-anisidine spray reagent. It had $[\alpha]_D$ −19° (*c*, 2.7 in water).

Periodate Oxidation of Disaccharide

The results are quoted as moles of periodate consumed and moles of formic acid produced per mole at stated time intervals at room temperature: 1.92, 1.40 (10 minutes); 2.08, 1.44 (20 minutes); 2.38, 1.84 (60 minutes); 3.13, 2.24 (120 minutes); 3.42, 2.5 (180 minutes); 3.68, 2.75 (240 minutes); 4.1, 3.12 (420 minutes); 4.32, 3.32 (720 minutes); 4.42, 3.73 (1740 minutes).

Periodate Oxidation of Reduced Disaccharide

The results are quoted as moles of periodate consumed and formic acid released at time intervals stated at room temperature: 2.45, 1.67 (10 minutes); 2.6, 1.78 (20 minutes); 2.98, 1.89 (60 minutes); 3.28, 2.03 (120 minutes); 3.52, 2.18 (180 minutes); 3.82, 2.28 (240 minutes); 4.1, 2.46 (360 minutes); 4.4, 2.5 (630 minutes); 4.95, 2.78 (1440 minutes); 5.05, 2.78 (2880 minutes).

Periodate Oxidation of Disaccharide Phenylosazone

The disaccharide phenylosazone (0.1 g) in 50% aqueous ethanol was oxidized with sodium metaperiodate as described by Hough, Powell, and Woods (4). After 10 minutes a yellow precipitate separated and was removed by filtration. The precipitate was washed well with water and recrystallized twice from aqueous ethanol to give orange needles, m.p. and mixed m.p. with authentic mesoxaldehyde bis-1,2-phenylhydrazone (prepared from glucosazone) 198–200°. The compound had absorption spectra in the ultraviolet and visible ranges identical with those of authentic mesoxaldehyde bis-1,2-phenylhydrazone.

Fraction II (3,5-Di-O-β-D-glucopyranosyl-D-xylose)

The compound was a crisp, white, hygroscopic glass easily soluble in methanol and water; R_{gal} 0.16, solvent (*b*); R_{gal} 0.070, solvent (*c*); $[\alpha]_D$ −30° (*c*, 0.1 in water).

Partial Hydrolysis of Fraction II

A small sample of the fraction was heated with 0.1 *N* hydrochloric acid at 100° and samples were taken at intervals. Chromatographic examination in solvent (*d*) indicated the presence of components chromatographically identical with D-glucose, D-xylose, 5-*O*-β-D-glucopyranosyl-D-xylose, and 3-*O*-β-D-glucopyranosyl-D-xylose.

Reduction of Fraction II

The fraction was reduced with sodium borohydride as described for the disaccharide. The product was a crisp, white glass, $[\alpha]_D$ −17.4° (*c*, 0.54 in water).

Periodate Oxidation of Fraction II

The results are quoted as moles of periodate consumed and moles of formic acid released per mole (calculated for trisaccharide) at stated time intervals at room temperature: 2.08, 0.59 (15 minutes); 2.64, 0.82 (45 minutes); 3.5, 1.17 (90 minutes); 3.9, 1.63 (180 minutes); 4.42, 1.87 (300 minutes); 4.67, 1.98 (410 minutes); 4.87, 2.1 (680 minutes); 4.95, 2.5 (1500 minutes).

Periodate Oxidation of Reduced Fraction II

The results are quoted as moles of periodate and formic acid released per mole (calculated for reduced trisaccharide) at stated time intervals at room temperature: 1.93, 0.81 (15 minutes); 3.12, 1.26 (45 minutes); 3.6, 1.45 (90 minutes); 4.07, 1.72 (180 minutes); 4.33, 1.89 (300 minutes); 4.7, 1.89 (420 minutes); 4.94, 1.99 (1680 minutes).

ACKNOWLEDGMENTS

The authors thank the National Research Council for a grant (NRC T-19). One of us, P. E. R., wishes to thank the National Research Council for the award of a studentship.

1. J. K. N. Jones and P. Reid. Can. J. Chem. **38**, 944 (1960).
2. W. Koenigs and E. Knorr. Ber. **34**, 957 (1901).
3. J. K. N. Jones and R. A. Wall. Can. J. Chem. **38**, 2285, 2290 (1960).
4. L. Hough, D. B. Powell, and B. M. Woods. J. Chem. Soc. 4799 (1956).
5. L. Hough, J. K. N. Jones, and W. H. Wadman. J. Chem. Soc. 1702 (1950).

Can. J. Chem. Downloaded from www.nrcresearchpress.com by 210.87.254.40 on 09/05/12
For personal use only.

The periodate oxidation of the disaccharide osazone was carried out in 50% aqueous ethanol (v/v) by the method of Hough, Powell, and Woods (4) and an oxidation of glucosazone was carried out concurrently by the same method.

Condensation of 1,2-O-Isopropylidene-D-xylofuranose and 2,3,4,6-Tetra-O-acetyl-α-D-glucopyranosyl Bromide

1,2-*O*-Isopropylidene-D-xylofuranose (14.9 g) (prepared by the method of Levene and Raymond (9)) was dissolved in ethanol-free dry chloroform (200 ml) and was shaken in the dark with argentous oxide (102 g), drierite (100 g), iodine (2 g), and glass beads (3-mm diameter, 100 g) for ½ hour. 2,3,4,6-Tetra-*O*-acetyl-α-D-glucopyranosyl bromide (145 g) (prepared by the method of Barzai-Martos and Korosy (10)) in ethanol-free dry chloroform (400 ml) was added and the mixture was shaken for 7 days. The solution was filtered, the residue washed with chloroform, and the filtrate and washings were concentrated to a syrup. The syrup was dissolved in chloroform and deacetylated by the addition of sodium methoxide at 0° C. The solution was concentrated to a syrup, dissolved in water, passed through a small bed of Amberlite IRA-400 (OH form) ion exchange resin, and concentrated to a syrup (70.4 g).

The syrup was dissolved in water (150 ml), an aliquot (14 ml) was taken and diluted to 28 ml, and barium hydroxide (1 g) was added. The solution was heated at 80–90° for 2 hours, barium hydroxide (1 g) was added, and heating continued for 1 hour. The solution was neutralized with solid carbon dioxide, filtered and the filtrate was passed through beds of Amberlite IR120 (H form) and IRA-400 (OH form) ion exchange resins. The eluate was concentrated to a syrup (2.76 g) and heated at 100° with 0.1 *N* sulphuric acid for 1½ hours. The solution was neutralized with barium carbonate, filtered, passed through a small bed of Amberlite IR120 (H form) resin, and concentrated to a syrup (2.21 g). Chromatographic examination in solvent (*a*) indicated the presence of glucose, xylose, and at least two oligosaccharides. The remainder of the solution was treated with barium hydroxide (30 g) for 6 hours at 70° and was recovered as described above. The process was repeated using barium hydroxide (10 g). The syrup so obtained (36 g) was treated with 0.1 *N* sulphuric acid as described above (yield 23.1 g).

The resultant syrupy product was dissolved in water and fractionated on a column of charcoal (Darco-G-60). The column was eluted with water and then with increasing concentrations of aqueous ethanol up to 10% v/v. Fractions containing oligosaccharides were fractionated on a column of Dowex 50WX2 200–400 mesh, Li^+ salt ion exchange resin (95×1.8 cm) (3) and where necessary the fractions obtained were refractionated on sheets of Whatman 3 mm paper by development in solvent (*a*) or (*b*). By these means two chromatographically pure fractions were obtained.

Fraction I (5-O-β-D-Glucopyranosyl-D-xylose)

The compound was obtained as a crisp, white, hygroscopic glass easily soluble in water and methanol. R_{gal} 0.74, solvent (*b*); R_{gal} 0.5, solvent (*c*). $[\alpha]_D$ −2.6° (*c*, 2.82 in water). Calc. for $C_{11}H_{20}O_{10}$: C, 42.3%; H, 6.4%. Found: C, 42.4%, 42.3%; H, 6.6%, 6.5%.

Hydrolysis of Disaccharide

The disaccharide was hydrolyzed with sulphuric acid (*N*) for 9 hours at 100°. The hydrolyzate was neutralized with barium carbonate, filtered and the filtrate was concentrated to a syrup. Chromatographic examination of the syrup in solvent (*b*) indicated the presence of glucose and xylose only.

Preparation of Disaccharide Phenylosazone

Disaccharide (0.2 g), sodium acetate (0.115 g), acetic acid (0.15 g), freshly distilled phenylhydrazine (0.24 g), and water (4 ml) were heated in a boiling-water bath for 30 minutes and allowed to cool. The precipitate was recovered by centrifugation, washed three times with ice-cold dilute acetic acid and three times with ice water. After recrystallization from aqueous methanol it had m.p. 211–213° (decomp.), mixed m.p. glucosazone 188–203 (decomp.). Calc. for $C_{23}H_{30}N_4O_8$: C, 56.3%; H, 6.19%; N, 11.4%. Found: C, 56.6%; H, 6.4%; N, 11.2%.

Methylation of Disaccharide

The disaccharide (0.39 g) was methylated with dimethyl sulphate and sodium hydroxide. The syrup obtained partially crystallized. The crystals were recrystallized from ether and then ether/light petroleum (b.p. 40–60°) to give white needles, m.p. 104–105°, $[\alpha]_D$ +56.6° (*c*, 0.5 in methanol). Calc. for $C_{18}H_{34}O_{10}$: C, 52.6%; H, 8.3%; OCH_3, 52.9%. Found: C, 52.2%; H, 8.2%; OCH_3, 51.9%. Hydrolysis of a small portion of the crystalline material with 85% formic acid for 9 hours at 100° and chromatography of the syrup (in solvent (*c*)) obtained after removal of the formic acid by distillation indicated the presence of 2,3-di-*O*-methyl-D-xylose and 2,3,4,6-tetra-*O*-methyl-D-glucose.

The disaccharide methyl ether (0.3 g, mixture of crystals and syrup) was hydrolyzed with 50% formic acid for 5 hours at 80° and with 70% formic acid at 100° for 8 hours. The solution was concentrated to a syrup and codistilled with water three times. The syrup was dissolved in water, deionized by passage through small beds of Amberlite IR120 (H form) and Dowex-A4 (OH form) ion exchange resins and concentrated to a syrup. The syrup was dissolved in butanol/light petroleum (b.p. 100–120°) and fractionated on a cellulose column (120×0.5 cm).

Fraction A.—This fraction was chromatographically identical with 2,3,4,6-tetra-*O*-methyl-D-glucose in solvent (*c*). It crystallized spontaneously, m.p. and mixed m.p. with authentic 2,3,4,6-tetra-*O*-methyl-D-glucose 83–85°, $[\alpha]_D$ +70° (25 minutes) → +78° (equilibrium) (*c*, 0.9 in water).

Can. J. Chem. Downloaded from www.nrcresearchpress.com by 210.87.254.40 on 09/05/12
For personal use only.

6. W. E. TREVELYAN, D. D. PROCTOR, and J. S. HARRISON. Nature, **166**, 444 (1950).
7. G. NEUMULLER and E. VASSEUR. Arkiv Kemi, **2**, 235 (1953).
8. P. ANDREWS, L. HOUGH, and J. K. N. JONES. J. Chem. Soc. 806 (1954).
9. P. A. LEVENE and A. L. RAYMOND. J. Biol. Chem. **102**, 331 (1933).
10. M. BARZAI-MARTOS and F. KOROSY. Nature, **165**, 369 (1950).

RECEIVED MAY 2, 1963.
DEPARTMENT OF CHEMISTRY,
QUEEN'S UNIVERSITY,
KINGSTON, ONTARIO.

Can. J. Chem. Downloaded from www.nrcresearchpress.com by 210.87.254.40 on 09/05/12
For personal use only.

THE STRUCTURE OF HYDRANGIN

K. H. PALMER

An extract of the roots and rhizomes of the small tree *Hydrangea arborescens* Linn. indigenous to the Eastern United States was used by the Cherokee Indians as a cure for urinary calculi and cystitis (1). Although early workers (1, 2) reported the isolation of an alkaloid, Bondurat (3) and later Schroeter (4) isolated a crystalline "glucoside", m.p. 236°, named hydrangin.

A methanolic extract of the milled roots and rhizomes yielded on concentration 3% of crude hydrangin (m.p. 225–228°), which on recrystallization or, better, vacuum sublimation (200°, 0.01 mm), gave pure hydrangin, m.p. 229°. Only sublimed samples of the material gave consistent analytical results and analyzed for $C_9H_6O_3$. A saturated chloroform solution had an infrared spectrum consistent with aromatic ring (1593 cm^{-1}), unsaturated carbonyl group (1709 cm^{-1} and 1688 cm^{-1}), and a strongly bonded hydroxyl group (envelope 3300 cm^{-1}). The ultraviolet absorption maxima (2033, 3290, 3784 Å; log ϵ, 4.42, 3.98, 3.79) showed in alkaline solution a bathochromic shift and intensity changes (2110, 2325, 3816 Å; log ϵ, 4.68, 4.31, 4.66) characteristic of phenolic compounds (5). Hydrangin failed to show the bathochromic shift in a buffered boric acid solution characteristic of *o*-diphenols (6). The formation of a monoacetylhydrangin m.p. 142° (ν_{max} 1777 cm^{-1}) confirmed the presence of a single phenolic group.

All the above data were consistent with either a monohydroxychromone or hydroxycoumarin. The latter alternative was preferred since all simple coumarins have an ultraviolet absorption minimum from 2600 to 2650 Å, whilst chromones show appreciable absorption in this region (7). The insolubility of hydrangin precluded the characteristic frequency shifts in the infrared maxima, observed in polar and non-polar solvents, of lactone systems (8). Simple model coumarins in acetonitrile solution showed an absorption maximum at 1739 ± 5 cm^{-1}; both hydrangin and acetylhydrangin have a maximum at 1739 cm^{-1}. The bathochromic shift in the ultraviolet absorption maxima and the absence of a maximal absorbance between 2800 and 3250 Å (7) of hydrangin suggested that the hydroxyl group was present on the aromatic ring. A negative Gibb's test (9), given by phenols with a free para position, indicated that hydrangin was either a 6- or 7-hydroxycoumarin. Umbelliferone (7-hydroxycoumarin) was synthesized (10) and found to be identical in all respects with hydrangin. Further processing of the mother liquors yielded an additional 1% of umbelliferone.

EXPERIMENTAL

Ultraviolet spectra were determined in 95% ethanol (log ϵ_{max} in parentheses) using a Unicam SP700 spectrophotometer; the infrared spectra were obtained using a Perkin–Elmer DB21 instrument. Melting points are corrected and were determined on a Kofler micro hot stage.

6. W. E. TREVELYAN, D. D. PROCTOR, and J. S. HARRISON. Nature, **166**, 444 (1950).
7. G. NEUMULLER and E. VASSEUR. Arkiv Kemi, **2**, 235 (1953).
8. P. ANDREWS, L. HOUGH, and J. K. N. JONES. J. Chem. Soc. 806 (1954).
9. P. A. LEVENE and A. L. RAYMOND. J. Biol. Chem. **102**, 331 (1933).
10. M. BARZAI-MARTOS and F. KOROSY. Nature, **165**, 369 (1950).

RECEIVED MAY 2, 1963.
DEPARTMENT OF CHEMISTRY,
QUEEN'S UNIVERSITY,
KINGSTON, ONTARIO.

Can. J. Chem. Downloaded from www.nrcresearchpress.com by 210.87.254.105 on 09/05/12
For personal use only.

THE STRUCTURE OF HYDRANGIN

K. H. PALMER

An extract of the roots and rhizomes of the small tree *Hydrangea arborescens* Linn. indigenous to the Eastern United States was used by the Cherokee Indians as a cure for urinary calculi and cystitis (1). Although early workers (1, 2) reported the isolation of an alkaloid, Bondurat (3) and later Schroeter (4) isolated a crystalline "glucoside", m.p. 236°, named hydrangin.

A methanolic extract of the milled roots and rhizomes yielded on concentration 3% of crude hydrangin (m.p. 225–228°), which on recrystallization or, better, vacuum sublimation (200°, 0.01 mm), gave pure hydrangin, m.p. 229°. Only sublimed samples of the material gave consistent analytical results and analyzed for $C_9H_6O_3$. A saturated chloroform solution had an infrared spectrum consistent with aromatic ring (1593 cm^{-1}), unsaturated carbonyl group (1709 cm^{-1} and 1688 cm^{-1}), and a strongly bonded hydroxyl group (envelope 3300 cm^{-1}). The ultraviolet absorption maxima (2033, 3290, 3784 Å; log ϵ, 4.42, 3.98, 3.79) showed in alkaline solution a bathochromic shift and intensity changes (2110, 2325, 3816 Å; log ϵ, 4.68, 4.31, 4.66) characteristic of phenolic compounds (5). Hydrangin failed to show the bathochromic shift in a buffered boric acid solution characteristic of *o*-diphenols (6). The formation of a monoacetylhydrangin m.p. 142° (ν_{max} 1777 cm^{-1}) confirmed the presence of a single phenolic group.

All the above data were consistent with either a monohydroxychromone or hydroxycoumarin. The latter alternative was preferred since all simple coumarins have an ultraviolet absorption minimum from 2600 to 2650 Å, whilst chromones show appreciable absorption in this region (7). The insolubility of hydrangin precluded the characteristic frequency shifts in the infrared maxima, observed in polar and non-polar solvents, of lactone systems (8). Simple model coumarins in acetonitrile solution showed an absorption maximum at 1739±5 cm^{-1}; both hydrangin and acetylhydrangin have a maximum at 1739 cm^{-1}. The bathochromic shift in the ultraviolet absorption maxima and the absence of a maximal absorbance between 2800 and 3250 Å (7) of hydrangin suggested that the hydroxyl group was present on the aromatic ring. A negative Gibb's test (9), given by phenols with a free para position, indicated that hydrangin was either a 6- or 7-hydroxycoumarin. Umbelliferone (7-hydroxycoumarin) was synthesized (10) and found to be identical in all respects with hydrangin. Further processing of the mother liquors yielded an additional 1% of umbelliferone.

EXPERIMENTAL

Ultraviolet spectra were determined in 95% ethanol (log ϵ_{max} in parentheses) using a Unicam SP700 spectrophotometer; the infrared spectra were obtained using a Perkin–Elmer DB21 instrument. Melting points are corrected and were determined on a Kofler micro hot stage.

Can. J. Chem. Downloaded from www.nrcresearchpress.com by 210.87.254.105 on 09/05/12
For personal use only.

The Extraction of Hydrangea arborescens

A 1-kg quantity of roots and rhizomes of *H. arborescens* Linn., obtained from the S. B. Penick Co., was finely ground and extracted by the cold percolation method—first by heptane then by methanol. The methanol extract was concentrated *in vacuo*, when 30 g of a brown crystalline solid (I), m.p. 225–228°, separated and was collected by filtration. On further evaporation of the mother liquors, an additional 10 g of deep brown crystalline material (II), m.p. 213–220°, was precipitated from the syrupy dark brown liquor. To the mother liquor was added 100 ml of 1 *N* sodium hydroxide solution. The resulting solution was extracted with chloroform; the aqueous liquors were made neutral and extracted with a chloroform/methanol (4:1) mixture.

The initial chloroform extract was evaporated to dryness *in vacuo* and to a portion of the resultant syrup dilute sulphuric acid was added; the acid extract failed to give a positive test for alkaloids with either Meyers or Dragendorff's reagent. An acetic acid extract of the syrup similarly gave a negative test for alkaloids.

The chloroform/methanol extract gave on evaporation a deep yellow syrup (3 g), which did not contain appreciable amounts of hydrangin. The crude hydrangin (I) was recrystallized from methanol, when faintly colored needles, m.p. 225–228°, were obtained (2.80 g). Sublimation of this material at 165–200° (at 0.01 mm Hg) gave colorless needles, m.p. 229°. λ_{max}: 2033 Å (4.42), 3290 Å (3.98), 3784 Å (3.79); λ_{min}: 2646 Å. In alkaline solution, λ_{max}: 2110 Å (4.68), 2325 Å (4.31), 3816 Å (4.66); λ_{min}: 2899 Å. ν_{max} (Nujol mull): 3300 cm^{-1} (bonded hydroxyl); 1709 cm^{-1}, 1688 cm^{-1} (carbonyl); 1593 cm^{-1}, 1515 cm^{-1}, 1485 cm^{-1} (aromatic ring); (CH_3CN solution): 3400 cm^{-1} (bonded hydroxyl); 1739 cm^{-1} (carbonyl); (saturated $CHCl_3$ solution): 3200 cm^{-1} (bonded hydroxyl); 1717 cm^{-1}, 1682 cm^{-1} (carbonyl). Calculated for $C_9H_6O_3$: C, 66.7; H, 3.7. Found: C, 66.7, 66.68; H, 3.65, 3.7. Gibb's test with 2,6-dibromoquinone chlorimide did not give the blue color which is indicative of a phenol with a free para position.

Acetylhydrangin

Hydrangin (0.500 g) was dissolved in 5 ml of pyridine, 1 ml of acetic anhydride added, the whole refluxed for 1 hour, the pyridine and excess acetic anhydride were removed *in vacuo*, and the resultant pale yellow syrup dissolved in chloroform and washed with saturated aqueous solution of sodium bicarbonate, followed by water. The dried chloroform solution was evaporated *in vacuo* to give a pale yellow froth (0.6104 g) which crystallized from methanol to give colorless needles, m.p. 142°; yield 0.55 g.

Calculated for $C_{11}H_8O_4$: C, 64.69; H, 3.95. Found: C, 64.70, 64.72; H, 4.00, 3.99. ν_{max} (Nujol mull): 1777 cm^{-1} (O-acetylaromatic); 1754 cm^{-1} (carbonyl); 1625 cm^{-1} (aromatic ring).

Model coumarin infrared spectra—only the ν_{max} for the 1800–1650 cm^{-1} range are reported in Table I. All the compounds listed were recrystallized from methanol to constant melting points.

TABLE I

	ν_{max}, cm^{-1}				
		Solvents used:			
Compound	Nujol mull	CH_3OH	$CHCl_3$	CCl_4	CS_2
Coumarin	1716	1739	1760 1733	1760 1748	1778 1762
7-Hydroxycoumarin	1716	1739	1761 1733	—	—
7-Methoxycoumarin	1709	1739	1760 1735	1759 1749	1779 1760
Tromexan ethylacetate*	1730	1739 1666	—	—	—
Warfarin†	1680	1739	—	—	—
Sintrom‡	1709	1739	—	—	—

*Tromexan brand of 3,3′-carboxymethylene-bis-(4-hydroxycoumarin) ethyl ester.
†Warfarin is 3α-phenyl-β-acetylethyl-4-hydroxycoumarin.
‡Sintrom brand of 3(α-p-nitrophenyl-β-acetylethyl)-4-hydroxycoumarin.

7-Hydroxycoumarin

7-Hydroxycoumarin was synthesized and crystallized from methanol, then sublimed at 170° at 0.01 mm; m.p. 229°, literature 227–228° (10). Calculated for $C_9H_6O_3$: C, 66.66; H, 3.70. Found: C, 66.70; H, 3.71. ν_{max} and λ_{max} identical in all respects with hydrangin.

1. S. W. Butler. N.Y. Med. Reptr. 44 (1850); 393, 426 (1854); 115 (1885). *Cited in* United States dispensatory. Vol. 15. Lippincott, Philadelphia. 1886. p. 1665.
2. J. Baur. Am. J. Pharm. 157 (1881).
3. C. S. Bondurat. Am. J. Pharm. 122 (1887).
4. H. M. J. Schroeter. Am. J. Pharm. 117 (1889).

5. H. W. LEMON. J. Am. Chem. Soc. **69**, 2998 (1947). T. W. CAMPBELL and G. M. COPPINGER. J. Am. Chem. Soc. **73**, 2709 (1951).
6. L. JURD. Arch. Biochem. Biophys. **63**, 376 (1956).
7. KALYANANMAY SEN and P. BAGCHI. J. Org. Chem. **24**, 316 (1959).
8. R. N. JONES, C. L. ANGELL, T. ITO, and R. J. D. SMITH. Can. J. Chem. **37**, 2007 (1959).
9. J. R. CANNON, G. K. HUGHES, E. RITCHIE, and W. C. TAYLOR. Australian J. Chem. **6**, 86 (1953).
10. R. ADAMS (*Editor-in-Chief*). Organic reactions. Vol. I. John Wiley & Sons. 1953. p. 20.

RECEIVED APRIL 26, 1963.
FACULTY OF PHARMACY,
UNIVERSITY OF ALBERTA,
EDMONTON, ALBERTA.

Can. J. Chem. Downloaded from www.nrcresearchpress.com by 210.87.254.105 on 09/05/12
For personal use only.

SYNTHESIS OF DEUTERIATED METHYL BENZOATES AND DIMETHYL PHTHALATES[1]

R. PHILLIPS AND L. C. LEITCH

As part of an investigation (1) of the infrared spectra of carbonyl compounds, the deuteriated methyl benzoates and dimethyl phthalates shown below were synthesized:

$C_6H_5CO_2CD_3$	$C_6H_4(CO_2CD_3)_2$
$C_6D_5CO_2CH_3$	$C_6D_4(CO_2CH_3)_2$
$C_6D_5CO_2CD_3$	$C_6D_4(CO_2CD_3)_2$

For reasons stated in previous communications on deuterated esters (2, 3) the required compounds were prepared from the silver salts and methyl or trideuteriomethyl iodide rather than by esterification. Silver phthalate was more conveniently prepared from aqueous solutions of the ammonium salt and silver nitrate than from the acid and silver carbonate as described by Ekeley and Banta (4). The methyl esters were formed in moderate yield when a suspension of the silver salt was stirred in an ether solution of methyl iodide for a day. Deuterated benzoic and phthalic acids were prepared by the platinum-catalyzed exchange of potassium benzoate and phthalate in deuterium oxide (5). The deuterium content of the compounds was determined by the method of Jones and MacKenzie (6).

EXPERIMENTAL

Tetradeuteriophthalic Acid

Phthalic acid (8.3 g; 0.05 mole) was stirred in 100 ml of water and neutralized by the addition of 20% aqueous potassium carbonate. The neutral or slightly alkaline solution was evaporated to dryness under reduced pressure. The residue was dissolved in 40 ml of 99.5% deuterium oxide and the solution was poured into a tube which contained 0.1 g of platinum oxide, and which was constricted at the top near the joint. A stream of deuterium was bubbled through for a minute or two to reduce the oxide to platinum and then the tube was evacuated on the vacuum line, sealed, and heated for 72 hours in a rocking furnace at 130°. At the end of this period, the contents of the tube were poured into a flask for removal of the solvent under reduced pressure. The residue was heated with a second 40-ml portion of deuterium oxide as before. The residue from the second exchange was taken up in 100 ml of water and the solution was acidified with hydrochloric acid. It was filtered hot with the aid of carbon black. On cooling the filtrate, deuteriophthalic acid crystallized out. It was filtered off, washed with a little ice-cold water, and dried. Yield: 7.0 g.

Silver Phthalate

Phthalic acid (1.7 g; 0.01 mole) was mixed with 10 ml of water in a beaker and neutralized with ammonium hydroxide. The solution was heated on the steam bath until free of excess ammonia and diluted with water to about 75 ml. A solution of 4.0 g of silver nitrate in 25 ml of water was then added with stirring. The precipitate of monosilver salt which first formed redissolved. Further addition of silver nitrate solution precipitated the disilver salt, which was filtered off, washed once with water, then with acetone, and dried. The yield was nearly quantitative.

Silver Tetradeuteriophthalate

The deuterated silver phthalate was prepared in the same manner from tetradeuteriophthalic acid.

[1]*Issued as N.R.C. No. 7471.*

5. H. W. LEMON. J. Am. Chem. Soc. **69**, 2998 (1947). T. W. CAMPBELL and G. M. COPPINGER. J. Am. Chem. Soc. **73**, 2709 (1951).
6. L. JURD. Arch. Biochem. Biophys. **63**, 376 (1956).
7. KALYANANMAY SEN and P. BAGCHI. J. Org. Chem. **24**, 316 (1959).
8. R. N. JONES, C. L. ANGELL, T. ITO, and R. J. D. SMITH. Can. J. Chem. **37**, 2007 (1959).
9. J. R. CANNON, G. K. HUGHES, E. RITCHIE, and W. C. TAYLOR. Australian J. Chem. **6**, 86 (1953).
10. R. ADAMS (*Editor-in-Chief*). Organic reactions. Vol. I. John Wiley & Sons. 1953. p. 20.

RECEIVED APRIL 26, 1963.
FACULTY OF PHARMACY,
UNIVERSITY OF ALBERTA,
EDMONTON, ALBERTA.

Can. J. Chem. Downloaded from www.nrcresearchpress.com by 210.87.254.40 on 09/05/12
For personal use only.

SYNTHESIS OF DEUTERIATED METHYL BENZOATES AND DIMETHYL PHTHALATES[1]

R. PHILLIPS AND L. C. LEITCH

As part of an investigation (1) of the infrared spectra of carbonyl compounds, the deuteriated methyl benzoates and dimethyl phthalates shown below were synthesized:

$C_6H_5CO_2CD_3$	$C_6H_4(CO_2CD_3)_2$
$C_6D_5CO_2CH_3$	$C_6D_4(CO_2CH_3)_2$
$C_6D_5CO_2CD_3$	$C_6D_4(CO_2CD_3)_2$

For reasons stated in previous communications on deuterated esters (2, 3) the required compounds were prepared from the silver salts and methyl or trideuteriomethyl iodide rather than by esterification. Silver phthalate was more conveniently prepared from aqueous solutions of the ammonium salt and silver nitrate than from the acid and silver carbonate as described by Ekeley and Banta (4). The methyl esters were formed in moderate yield when a suspension of the silver salt was stirred in an ether solution of methyl iodide for a day. Deuterated benzoic and phthalic acids were prepared by the platinum-catalyzed exchange of potassium benzoate and phthalate in deuterium oxide (5). The deuterium content of the compounds was determined by the method of Jones and MacKenzie (6).

EXPERIMENTAL

Tetradeuteriophthalic Acid

Phthalic acid (8.3 g; 0.05 mole) was stirred in 100 ml of water and neutralized by the addition of 20% aqueous potassium carbonate. The neutral or slightly alkaline solution was evaporated to dryness under reduced pressure. The residue was dissolved in 40 ml of 99.5% deuterium oxide and the solution was poured into a tube which contained 0.1 g of platinum oxide, and which was constricted at the top near the joint. A stream of deuterium was bubbled through for a minute or two to reduce the oxide to platinum and then the tube was evacuated on the vacuum line, sealed, and heated for 72 hours in a rocking furnace at 130°. At the end of this period, the contents of the tube were poured into a flask for removal of the solvent under reduced pressure. The residue was heated with a second 40-ml portion of deuterium oxide as before. The residue from the second exchange was taken up in 100 ml of water and the solution was acidified with hydrochloric acid. It was filtered hot with the aid of carbon black. On cooling the filtrate, deuteriophthalic acid crystallized out. It was filtered off, washed with a little ice-cold water, and dried. Yield: 7.0 g.

Silver Phthalate

Phthalic acid (1.7 g; 0.01 mole) was mixed with 10 ml of water in a beaker and neutralized with ammonium hydroxide. The solution was heated on the steam bath until free of excess ammonia and diluted with water to about 75 ml. A solution of 4.0 g of silver nitrate in 25 ml of water was then added with stirring. The precipitate of monosilver salt which first formed redissolved. Further addition of silver nitrate solution precipitated the disilver salt, which was filtered off, washed once with water, then with acetone, and dried. The yield was nearly quantitative.

Silver Tetradeuteriophthalate

The deuterated silver phthalate was prepared in the same manner from tetradeuteriophthalic acid.

[1]*Issued as N.R.C. No. 7471.*

Di(trideuteriomethyl) Phthalate

Silver phthalate (3.78 g; 0.01 mole) was pulverized in a mortar and added to 50 ml of anhydrous ether in which had been dissolved 1.5 ml of trideuteriomethyl iodide. The mixture was stirred under a reflux condenser for 24 hours. The yellow precipitate of silver iodide was filtered off and washed with ether. The ether solution and washings were largely evaporated on the steam bath and the residue was purified by distillation from a Späth bulb in an air bath at 90–100° under 0.1 mm pressure. Yield: 1.5 g (72%), n_D^{20} 1.5122. For ordinary dimethyl phthalate, n_D^{20} is 1.5140. Calc. for $C_{10}H_4D_6O_4$: D, 6.00. Found: D, 6.06.

Dimethyl Tetradeuteriophthalate

This ester was prepared as described above for the methyl-labelled ester, n_D^{20} 1.5132. Calc. for $C_{10}H_6D_4O_4$: D, 4.00. Found: D, 3.99.

Di(trideuteriomethyl) Tetradeuteriophthalate

The totally deuterated ester was also prepared as described above, n_D^{20} 1.5119. Calc. for $C_{10}D_{10}O_4$: D, 10.00. Found: D, 10.24.

Pentadeuteriobenzoic Acid

Sodium benzoate (14.2 g, 0.1 mole) was exchanged as described by Brown and Garnett (5). The yield of deuterated benzoic acid was quantitative.

Methyl Pentadeuteriobenzoate

A suspension of 8.0 g (0.034 mole) of pulverized silver pentadeuteriobenzoate was stirred under reflux for 24 hours with 250 ml of absolute ether and 7.0 g of methyl iodide. The silver iodide was filtered off and washed with ether. The filtrate was evaporated on the steam bath and the residue of methyl pentadeuteriobenzoate was purified by distillation in a Späth bulb. Yield: 4.0 g (82%), n_D^{20} 1.5140. For normal methyl benzoate, n_D^{20} is 1.5160. Calc. for $C_8H_3D_5O_2$: D, 5.00. Found: D, 4.83.

Trideuteriomethyl Benzoate

This compound was prepared in the same manner as the above compound from trideuteriomethyl iodide and silver benzoate. The yield of product, n_D^{20} 1.5150, was 75%. Calc. for $C_8H_5D_3O_2$: D, 3.00. Found: D, 3.00.

Trideuteriomethyl Pentadeuteriobenzoate

The compound was similarly prepared from trideuteriomethyl iodide and silver pentadeuteriobenzoate. The yield of product, n_D^{20} 1.5142, was 75%. Calc. for $C_8D_8O_2$: D, 8.00. Found: D, 7.92.

ACKNOWLEDGMENT

The authors are indebted to Dr. R. N. Jones and Mrs. M. A. MacKenzie of these laboratories for the deuterium analyses.

1. R. N. Jones and J. B. Di Giorgio. Unpublished work.
2. M. E. Isabelle and L. C. Leitch. Can. J. Chem. **36**, 440 (1958).
3. B. Nolin. Can. J. Chem. **31**, 1257 (1953).
4. J. B. Ekeley and C. Banta. J. Am. Chem. Soc. **39**, 764 (1917).
5. W. G. Brown and J. L. Garnett. J. Am. Chem. Soc. **80**, 5272 (1958).
6. R. N. Jones and M. A. MacKenzie. Talanta, **7**, 124 (1960).

Received May 3, 1963.
Division of Pure Chemistry,
National Research Council,
Ottawa, Canada.

SYNTHESES INVOLVING IMIDOGEN INTERMEDIATES: PHENANTHRIDINES AND BENZO[c]PHENANTHRIDINES[1]

R. A. Abramovitch, D. Newman, and G. Tertzakian

It has been suggested (1, 2) that the reaction of certain aromatic nitro compounds with ferrous oxalate involves the formation of imidogen intermediates[2] which could be either

[1]*Preliminary communication: ref. 1.*

[2]*These have also been called azene or nitrene intermediates. Both of these names are now considered unsuitable. Imidogen is used by Chemical Abstracts (Index). We wish to thank Drs. R. L. Shriner and R. S. Cahn for their advice on this matter.*

Can. J. Chem. Downloaded from www.nrcresearchpress.com by 210.87.254.40 on 09/05/12
For personal use only.

Di(trideuteriomethyl) Phthalate

Silver phthalate (3.78 g; 0.01 mole) was pulverized in a mortar and added to 50 ml of anhydrous ether in which had been dissolved 1.5 ml of trideuteriomethyl iodide. The mixture was stirred under a reflux condenser for 24 hours. The yellow precipitate of silver iodide was filtered off and washed with ether. The ether solution and washings were largely evaporated on the steam bath and the residue was purified by distillation from a Späth bulb in an air bath at 90–100° under 0.1 mm pressure. Yield: 1.5 g (72%), n_D^{20} 1.5122. For ordinary dimethyl phthalate, n_D^{20} is 1.5140. Calc. for $C_{10}H_4D_6O_4$: D, 6.00. Found: D, 6.06.

Dimethyl Tetradeuteriophthalate

This ester was prepared as described above for the methyl-labelled ester, n_D^{20} 1.5132. Calc. for $C_{10}H_6D_4O_4$: D, 4.00. Found: D, 3.99.

Di(trideuteriomethyl) Tetradeuteriophthalate

The totally deuterated ester was also prepared as described above, n_D^{20} 1.5119. Calc. for $C_{10}D_{10}O_4$: D, 10.00. Found: D, 10.24.

Pentadeuteriobenzoic Acid

Sodium benzoate (14.2 g, 0.1 mole) was exchanged as described by Brown and Garnett (5). The yield of deuterated benzoic acid was quantitative.

Methyl Pentadeuteriobenzoate

A suspension of 8.0 g (0.034 mole) of pulverized silver pentadeuteriobenzoate was stirred under reflux for 24 hours with 250 ml of absolute ether and 7.0 g of methyl iodide. The silver iodide was filtered off and washed with ether. The filtrate was evaporated on the steam bath and the residue of methyl pentadeuteriobenzoate was purified by distillation in a Späth bulb. Yield: 4.0 g (82%), n_D^{20} 1.5140. For normal methyl benzoate, n_D^{20} is 1.5160. Calc. for $C_8H_3D_5O_2$: D, 5.00. Found: D, 4.83.

Trideuteriomethyl Benzoate

This compound was prepared in the same manner as the above compound from trideuteriomethyl iodide and silver benzoate. The yield of product, n_D^{20} 1.5150, was 75%. Calc. for $C_8H_5D_3O_2$: D, 3.00. Found: D, 3.00.

Trideuteriomethyl Pentadeuteriobenzoate

The compound was similarly prepared from trideuteriomethyl iodide and silver pentadeuteriobenzoate. The yield of product, n_D^{20} 1.5142, was 75%. Calc. for $C_8D_8O_2$: D, 8.00. Found: D, 7.92.

ACKNOWLEDGMENT

The authors are indebted to Dr. R. N. Jones and Mrs. M. A. MacKenzie of these laboratories for the deuterium analyses.

1. R. N. Jones and J. B. Di Giorgio. Unpublished work.
2. M. E. Isabelle and L. C. Leitch. Can. J. Chem. **36**, 440 (1958).
3. B. Nolin. Can. J. Chem. **31**, 1257 (1953).
4. J. B. Ekeley and C. Banta. J. Am. Chem. Soc. **39**, 764 (1917).
5. W. G. Brown and J. L. Garnett. J. Am. Chem. Soc. **80**, 5272 (1958).
6. R. N. Jones and M. A. MacKenzie. Talanta, **7**, 124 (1960).

Received May 3, 1963.
Division of Pure Chemistry,
National Research Council,
Ottawa, Canada.

SYNTHESES INVOLVING IMIDOGEN INTERMEDIATES: PHENANTHRIDINES AND BENZO[c]PHENANTHRIDINES[1]

R. A. Abramovitch, D. Newman, and G. Tertzakian

It has been suggested (1, 2) that the reaction of certain aromatic nitro compounds with ferrous oxalate involves the formation of imidogen intermediates[2] which could be either

[1]*Preliminary communication: ref. 1.*

[2]*These have also been called azene or nitrene intermediates. Both of these names are now considered unsuitable. Imidogen is used by Chemical Abstracts (Index). We wish to thank Drs. R. L. Shriner and R. S. Cahn for their advice on this matter.*

Can. J. Chem. Downloaded from www.nrcresearchpress.com by 210.87.254.5 on 09/05/12
For personal use only.

in the triplet or singlet state: these intermediates then undergo further reactions leading to the observed products. Arguments in favor of the triplet state for imidogen intermediates obtained by the thermal decomposition of azides have been put forward by Smolinsky (3) and by Walker and Waters (4). Support for the mechanism of the ferrous oxalate reaction has come from studies on the deoxygenation of aromatic *C*-nitroso compounds by triethyl phosphite (5).

From the thermal decomposition of 2′-azido-2,4,6-trimethylbiphenyl in hexadecane solution Smolinsky (6) obtained 8,10-dimethylphenanthridine (II) as the major product, some amine (III) (arising from hydrogen abstraction from the solvent and the dihydrophenanthridine formed initially), and a small amount of 2,4,9-trimethylcarbazole. The action of ferrous oxalate dihydrate on 2′-nitro-2,4,6-trimethylbiphenyl (I) at 300° in the absence of solvent has now been studied. The amine (III) (27.4%) and phenanthridine (II) (22.6%) were isolated, but no carbazole. The amine cannot, therefore, arise exclusively from the dihydrophenanthridine formed initially by insertion of the imidogen intermediate

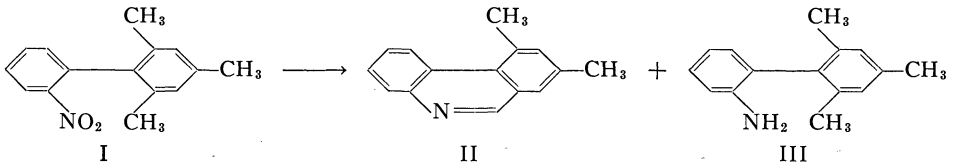

into an adjacent side-chain methyl group. The unlikely possibility that III could have arisen by hydrogen abstraction from the water of hydration of the oxalate by the imidogen intermediate was eliminated by the use of anhydrous ferrous oxalate: the proportion of II to III was practically unchanged. Hydrogen abstraction by the imidogen intermediate must, therefore, have taken place from methyl groups *in another molecule* (much intractable tar was formed in these reactions and yields of products were low) somewhat more readily than intramolecularly. This can be rationalized if it is assumed that (i) the reaction is taking place at the surface of the ferrous oxalate (or its decomposition products e.g. FeO), and (ii) that the molecules, the two rings of which are non-coplanar, tend to orient themselves at the oxalate surface such that the nitro group of one molecule may be close in space to the methyl group of another. Some supporting evidence for the first assumption was obtained as follows: anhydrous ferrous oxalate was boiled under reflux with hexadecane (internal temperature 290°), when very little decomposition occurred, even after prolonged heating. On the other hand, when I was added brisk decomposition of the oxalate occurred at about 250°. It therefore seems as though the decomposition of the ferrous oxalate is assisted by the nitro compound adsorbed on its surface and in turn this causes the imino intermediate to be formed. When a solution of I in hexadecane was heated with ferrous oxalate the amine (III) (42.1%) and phenanthridine (II) (14.8%) were obtained. In this case, hydrogen abstraction from the solvent is also possible.

It was attractive to attempt to extend this synthesis of the phenanthridine ring system to the formation of the interesting benzo[*c*]phenanthridine nucleus, found in nature in a number of alkaloids (7). A new synthetic route to this type of compound, which involves an internuclear cyclization of the Pschorr type (8), suffers from the disadvantage that it involves a relatively large number of steps and that the overall yield of product is low. The required 2-mesityl-1-nitronaphthalene (V) was readily obtained by a Gomberg–Hey reaction of 1-nitronaphthalene-2-diazonium sulphate (IV) with mesitylene. The use of the diazonium chloride led to complications (9) and did not result in the formation of the required product. When the nitro compound (V) was heated with triethyl phosphite (10) no cyclized product could be isolated and only starting material was recovered. The nitro

Can. J. Chem. Downloaded from www.nrcresearchpress.com by 210.87.254.5 on 09/05/12
For personal use only.

compound was heated with ferrous oxalate at 300°, and the ether-soluble products chromatographed on a column of alumina to give 8,10-dimethylbenzo[*c*]phenanthridine (VI) (20%) and 1-amino-2-mesitylnaphthalene (VII) (10%). The structure of VI was established by its elementary analysis and the fact that its ultraviolet absorption spectrum was very similar to that of benzo[*c*]phenanthridine (8) (Fig. 1). Reduction of 2-mesityl-1-nitronaphthalene with hydrazine hydrate in the presence of palladium–charcoal yielded the

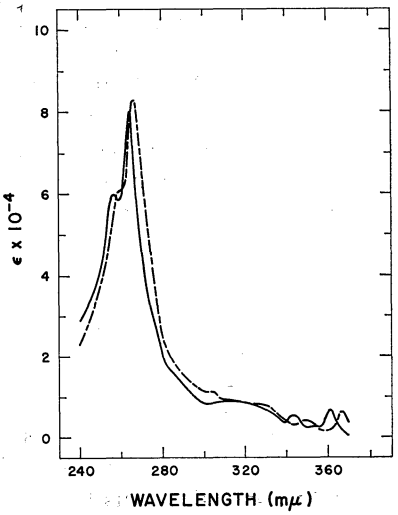

FIG. 1. Ultraviolet absorption spectrum of benzo[*c*]phenanthridine (—) and 8,10-dimethylbenzo[*c*]-phenanthridine (- — -).

primary amine whose infrared spectrum was identical with that of the amine isolated from the ferrous oxalate reaction. The method seems to be a promising one, but might be limited by the availability of the required substituted nitro compounds.

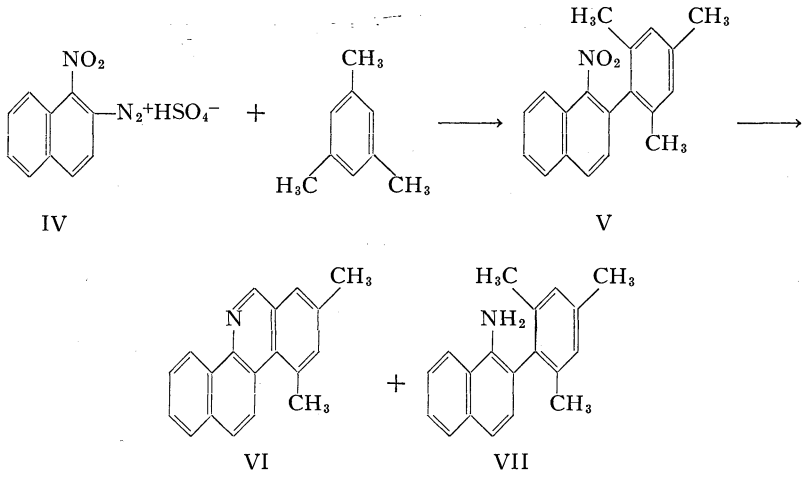

EXPERIMENTAL

Melting points are uncorrected. Ultraviolet spectra were measured on a Cary Model 14 spectrometer, and infrared spectra on a Perkin–Elmer Model 21 instrument using sodium chloride optics. The alumina used in the column chromatographies was Peter Spence, Type H (100–200 mesh).

Can. J. Chem. Downloaded from www.nrcresearchpress.com by 210.87.254.5 on 09/05/12
For personal use only.

Reaction of 2′-Nitro-2,4,6-trimethylbiphenyl with Ferrous Oxalate

(a) Using Anhydrous Ferrous Oxalate

2′-Nitro-2,4,6-trimethylbiphenyl (11) (1.5 g), anhydrous ferrous oxalate (2.5 g; prepared by heating the dihydrate in mineral oil (12)), and granulated lead (12 g) were heated under air condenser in a metal bath at 240° (internal temperature), when a reaction set in. The temperature was slowly raised to 300°, the mixture then cooled and extracted with ether, and the dried ($MgSO_4$) ether extract evaporated to give a brown oil (0.723 g). This was chromatographed on a column of alumina. Elution with light petroleum (b.p. 60–80°) gave first 2′-amino-2,4,6-trimethylbiphenyl (0.362 g) whose infrared spectrum was identical with that of an authentic sample (prepared by the reduction of the nitro compound with hydrazine hydrate and Raney nickel). Further elution with light petroleum gave 8,10-dimethylphenanthridine (0.298 g), m.p. 149–150°, undepressed on admixture with an authentic sample (kindly supplied by Dr. G. Smolinsky). The infrared spectra of both samples were identical. Similar results were obtained using hydrated ferrous oxalate.

(b) In n-Hexadecane Solution using Anhydrous Ferrous Oxalate

In a preliminary experiment it was shown that heating anhydrous ferrous oxalate with *n*-hexadecane at 290° led to almost no decomposition of the oxalate. Even at 340° most of the oxalate had not begun to decompose despite the fact that it turned darker.

The nitro compound (1.4 g) and anhydrous ferrous oxalate (3 g) in *n*-hexadecane (10 ml) were stirred and heated under air condenser. At about 250° a vigorous reaction occurred, the temperature was slowly raised to 300° and maintained there for 20 minutes. The mixture was cooled and extracted with ether, the solvent evaporated, and the residue chromatographed on a column of alumina (70 g). Elution with light petroleum gave first *n*-hexadecane, followed by 2′-amino-2,4,6-trimethylbiphenyl (0.510 g) and then 8,10-dimethylphenanthridine (0.170 g), which were identified as before.

2-Mesityl-1-nitronaphthalene

2-Amino-1-nitronaphthalene (1.88 g) in concentrated sulphuric acid (2.5 ml) and water (30 ml) was heated on a steam bath for 15 minutes, the suspension of the sulphate cooled to 0–5°, and a solution of sodium nitrite (2 g) in water (5 ml) slowly added with stirring. At the completion of the diazotization mesitylene (25 ml) was added followed by 20% aqueous sodium hydroxide. The strongly basic mixture was stirred vigorously at 0–5° for 2 hours, at room temperature for 19 hours, and finally at 80° for 1 hour. The organic layer was separated, the aqueous layer extracted with two small portions of mesitylene and the combined mesitylene layers dried (Na_2SO_4) and the solvent distilled under vacuum. The residual dark brown oil was distilled under reduced pressure and a fraction (0.81 g), b.p. 182–192° at 0.6 mm, collected and chromatographed on a column of alumina (60 g). Elution with light petroleum (b.p. 36–48°) gave *2-mesityl-1-nitronaphthalene* (0.416 g) as pale yellow crystals, m.p. 127.5–128°. Several recrystallizations from light petroleum (b.p. 60–70°) raised the melting point to 130–130.5°. (Calc. for $C_{19}H_{17}NO_2$: C, 78.33; H, 5.88. Found: C, 78.62; H, 6.11.) Infrared spectrum (KBr disk): 1623 (m), 1535 (s), 1380 (s), 1340 (s), 820 (m), and 742 cm^{-1} (s).

1-Amino-2-mesitylnaphthalene

A solution of 2-mesityl-1-nitronaphthalene (0.100 g) in ethanol (10 ml) was boiled under reflux for 20 minutes in the presence of hydrazine hydrate (98–100%, 1 ml) and 10% palladium–charcoal (0.050 g). The resulting solution was filtered and evaporated to yield *1-amino-2-mesitylnaphthalene* (0.087 g) as an almost colorless wax which could not be recrystallized. Infrared spectrum (liquid film): 3460 (s) (br), 1596 (m), 1400 (m), 790 (s), and 752 cm^{-1} (s). Schotten–Baumann benzoylation of the amine followed by chloroform extraction of the product gave a brown gum (0.055 g) which was chromatographed on alumina (8 g). Elution with benzene gave the *N-benzoyl derivative* (0.030 g) which, on recrystallization from light petroleum (60–80°), had m.p. 179–180°. (Calc. for $C_{26}H_{23}NO$: C, 85.45; H, 6.34. Found: C, 85.58; H, 6.32.) Infrared spectrum (Nujol mull): 3310 (m), 1645 (s), 1512 (s), 1277 (m), 815 (w), and 740 cm^{-1} (m).

Reaction of 2-Mesityl-1-nitronaphthalene with Ferrous Oxalate

2-Mesityl-1-nitronaphthalene (0.60 g) was thoroughly mixed with ferrous oxalate dihydrate (0.80 g) and finely granulated lead (8 g) and heated under air condenser at 340° (bath temperature) for 15 minutes. The cooled product was extracted with ether, the solvent removed, and the brown gum (0.240 g) thus obtained chromatographed on a column of alumina (17 g). Elution with light petroleum (b.p. 36–48°) gave *8,10-dimethyl-benzo[c]phenanthridine* (0.102 g) which, on recrystallization from absolute ethanol, had m.p. 130°. (Calc. for $C_{19}H_{15}N$: C, 88.68; H, 5.88. Found: C, 88.56; H, 6.18.) Infrared spectrum (Nujol mull): 1615 (s), 1403 (s), 1278 (m), 850 (w), 800 (s), and 735 cm^{-1} (m). Elution with light petroleum – benzene (3:1 v/v) gave 1-amino-2-mesitylnaphthalene (0.050 g) as a colorless oil, the infrared spectrum of which was identical with that of the authentic specimen prepared above.

ACKNOWLEDGMENTS

This work was carried out during the tenure (by G. T.) of a C.I.L. Fellowship and with the financial support of the National Research Council. The authors are also grateful to Dr. G. Smolinsky for a sample of 8,10-dimethylphenanthridine.

Can. J. Chem. Downloaded from www.nrcresearchpress.com by 210.87.254.5 on 09/05/12
For personal use only.

1. R. A. ABRAMOVITCH, Y. AHMAD, and D. NEWMAN. Tetrahedron Letters, No. 21, 752 (1961).
2. R. A. ABRAMOVITCH and K. A. H. ADAMS. Can. J. Chem. **39**, 2516 (1961).
3. G. SMOLINSKY. J. Am. Chem. Soc. **83**, 2489 (1961).
4. P. WALKER and W. A. WATERS. J. Chem. Soc. 1632 (1962).
5. P. J. BUNYAN and J. I. G. CADOGAN. J. Chem. Soc. 42 (1963).
6. G. SMOLINSKY. J. Am. Chem. Soc. **82**, 4717 (1960).
7. R. H. F. MANSKE and H. L. HOLMES. The Alkaloids. Vol. IV. Academic Press Inc., New York. 1954. p. 253; Vol. VII. 1960. p. 430.
8. R. A. ABRAMOVITCH and G. TERTZAKIAN. Can. J. Chem. This issue.
9. G. T. MORGAN. J. Chem. Soc. 1376 (1902). L. SIHLBORN. Acta Chem. Scand. **5**, 872 (1951).
10. J. I. G. CADOGAN and M. CAMERON-WOOD. Proc. Chem. Soc. 361 (1962).
11. J. ELKS, J. W. HAWORTH, and D. H. HEY. J. Chem. Soc. 1284 (1940).
12. H. C. WATERMAN and D. L. VIVIAN. J. Org. Chem. **14**, 289 (1949).

RECEIVED APRIL 16, 1963.
DEPARTMENT OF CHEMISTRY,
UNIVERSITY OF SASKATCHEWAN,
SASKATOON, SASK.

Can. J. Chem. Downloaded from www.nrcresearchpress.com by 210.87.254.5 on 09/05/12
For personal use only.

THE STRUCTURAL SIGNIFICANCE OF GLYCERALDEHYDE AND GLYCOLLIC ALDEHYDE IN POLYSACCHARIDE DEGRADATIONS AND THEIR RECOVERY AND IDENTIFICATION AS THE REDUCED ANALOGUES[1]

A. M. UNRAU

In the early application of periodate oxidation (1) of sugars, the so-called dialdehydes were converted to the corresponding dicarboxylic acids (2) because of the relative instability of the aldehyde. A much more convenient approach involved the reduction of the dialdehyde with sodium borohydride (3, 4, 5), and the acetal system thus generated could easily be hydrolyzed with acid to yield its characteristic components. This procedure has been extensively used by Smith *et al.* in their investigations on the nature of the trihydric alcohols resulting from degradations of disaccharides (6) and degradations of a variety of polysaccharides. In recent years the same school (7) has developed an improved degradative scheme which has been subsequently used to great advantage in structural investigations of very complex synthetic polysaccharides (8) and natural polysaccharides (9). Application of a sequence of this newer procedure has indicated that polysaccharides such as mesquite gum (10) and a galactan from *Centrosema* (11) have an internal matrix the structure of which is more complex than was first anticipated.

In these investigations, usually little attention is paid to the glycollic aldehyde which is invariably formed in the reaction sequence. This is due chiefly to the lability of this compound and not because of its insignificance as a structural entity. Another possible product which may be encountered is glyceraldehyde which could arise from a 1,2-linkage. This fragment will be lost in the usual procedure due to its lability and thermal instability. Both of these compounds can, however, be easily recovered as the reduced derivatives, namely glycerol and ethylene glycol, by the incorporation of a few additional reactions in the general sequence.

In the event that 1,2-linkages are suspected in a polysaccharide, the glyceraldehyde released after the mild acid cleavage of the acetal systems can be readily transformed to the corresponding glyceric acid by bromine oxidation. Glycollic aldehyde present would also be transformed to the corresponding acid and both could be removed from the neutral

[1]*Contribution No. 76 from the Department of Plant Science, University of Manitoba, Winnipeg 19, Manitoba.*

1. R. A. ABRAMOVITCH, Y. AHMAD, and D. NEWMAN. Tetrahedron Letters, No. 21, 752 (1961).
2. R. A. ABRAMOVITCH and K. A. H. ADAMS. Can. J. Chem. **39**, 2516 (1961).
3. G. SMOLINSKY. J. Am. Chem. Soc. **83**, 2489 (1961).
4. P. WALKER and W. A. WATERS. J. Chem. Soc. 1632 (1962).
5. P. J. BUNYAN and J. I. G. CADOGAN. J. Chem. Soc. 42 (1963).
6. G. SMOLINSKY. J. Am. Chem. Soc. **82**, 4717 (1960).
7. R. H. F. MANSKE and H. L. HOLMES. The Alkaloids. Vol. IV. Academic Press Inc., New York. 1954. p. 253; Vol. VII. 1960. p. 430.
8. R. A. ABRAMOVITCH and G. TERTZAKIAN. Can. J. Chem. This issue.
9. G. T. MORGAN. J. Chem. Soc. 1376 (1902). L. SIHLBORN. Acta Chem. Scand. **5**, 872 (1951).
10. J. I. G. CADOGAN and M. CAMERON-WOOD. Proc. Chem. Soc. 361 (1962).
11. J. ELKS, J. W. HAWORTH, and D. H. HEY. J. Chem. Soc. 1284 (1940).
12. H. C. WATERMAN and D. L. VIVIAN. J. Org. Chem. **14**, 289 (1949).

RECEIVED APRIL 16, 1963.
DEPARTMENT OF CHEMISTRY,
UNIVERSITY OF SASKATCHEWAN,
SASKATOON, SASK.

Can. J. Chem. Downloaded from www.nrcresearchpress.com by 210.87.254.42 on 09/05/12
For personal use only.

THE STRUCTURAL SIGNIFICANCE OF GLYCERALDEHYDE AND GLYCOLLIC ALDEHYDE IN POLYSACCHARIDE DEGRADATIONS AND THEIR RECOVERY AND IDENTIFICATION AS THE REDUCED ANALOGUES[1]

A. M. UNRAU

In the early application of periodate oxidation (1) of sugars, the so-called dialdehydes were converted to the corresponding dicarboxylic acids (2) because of the relative instability of the aldehyde. A much more convenient approach involved the reduction of the dialdehyde with sodium borohydride (3, 4, 5), and the acetal system thus generated could easily be hydrolyzed with acid to yield its characteristic components. This procedure has been extensively used by Smith *et al.* in their investigations on the nature of the trihydric alcohols resulting from degradations of disaccharides (6) and degradations of a variety of polysaccharides. In recent years the same school (7) has developed an improved degradative scheme which has been subsequently used to great advantage in structural investigations of very complex synthetic polysaccharides (8) and natural polysaccharides (9). Application of a sequence of this newer procedure has indicated that polysaccharides such as mesquite gum (10) and a galactan from *Centrosema* (11) have an internal matrix the structure of which is more complex than was first anticipated.

In these investigations, usually little attention is paid to the glycollic aldehyde which is invariably formed in the reaction sequence. This is due chiefly to the lability of this compound and not because of its insignificance as a structural entity. Another possible product which may be encountered is glyceraldehyde which could arise from a 1,2-linkage. This fragment will be lost in the usual procedure due to its lability and thermal instability. Both of these compounds can, however, be easily recovered as the reduced derivatives, namely glycerol and ethylene glycol, by the incorporation of a few additional reactions in the general sequence.

In the event that 1,2-linkages are suspected in a polysaccharide, the glyceraldehyde released after the mild acid cleavage of the acetal systems can be readily transformed to the corresponding glyceric acid by bromine oxidation. Glycollic aldehyde present would also be transformed to the corresponding acid and both could be removed from the neutral

[1]*Contribution No. 76 from the Department of Plant Science, University of Manitoba, Winnipeg 19, Manitoba.*

components through the use of anion exchange resin. The acids can then be eluted with base, the free acid regenerated through the use of cation exchange resin, and the acids heated under high vacuum to yield a mixture of dimeric lactones. Reduction of the lactones (12) with potassium borohydride yields the corresponding alcohols, which can easily be separated and identified as characteristic crystalline derivatives. This approach has in part been used to some advantage in structural studies on mesquite gum (10), acidic xylans (9), and a synthetic xylan.

An alternative procedure involves the second introduction of reducing agent after the mild acid cleavage of the acetal systems. In this way, glycollic aldehyde will be reduced directly to ethylene glycol, and any glyceraldehyde or free sugars will be transformed to the corresponding alcohols.

The suggested reaction sequences were easily tested using model systems. For an example of a 1,2-linkage, 1,2-monoacetone-D-galactose and D-mannose 1,2-orthoacetate were chosen. These compounds were readily prepared following published (13, 14, 15) procedures. Periodate oxidation, in which one mole of oxidant was consumed per mole of each hexose derivative, gave the dialdehydes, which were reduced to the corresponding alcohols with sodium borohydride. To prevent the possible loss of the substituents on C_1 and C_2 during the oxidation, the solutions were buffered to pH 7.2–7.5. Acid hydrolysis of the alcohols released glycerol (from C_4, C_5, and C_6) and D-glyceraldehyde from the D-galactose derivative and L-glyceraldehyde from D-mannose 1,2-orthoacetate. Addition of bromine oxidized the aldehydes to the respective glyceric acids. Chromatographic examination of the mixtures indicated the presence of glycerol and an acidic substance corresponding to glyceric acid. These compounds were present in a 1:1 molar ratio as determined by the periodate – chromotropic acid procedure (17, 18). The carboxylic acids were separated from glycerol by use of ion exchange resins. The glyceric acids were again regenerated and then converted to the dimeric lactones in the usual manner; reduction with potassium borohydride gave glycerol, which was identified chromatographically and as the crystalline *p*-nitrobenzoate.

Glycollic aldehyde arises upon periodate oxidation followed by reduction (BH_4) from pentose and hexose units in which the C_2- and C_3-hydroxyls are not substituted. This two-carbon fragment was easily recovered as the reduced analogue, ethylene glycol, by two routes using starch as a model substrate. Starch was degraded according to the Smith procedure (7). After the mild acid hydrolysis of the polyalcohol, the solution was neutralized and reducing agent (KBH_4) added to reduce glycollic aldehyde to ethylene glycol. The reaction mixture was worked up in the usual manner and erythritol, glycerol, and ethylene glycol identified as the crystalline *p*-nitrobenzoates. The ratio of erythritol and glycerol to ethylene glycol was 1:1 as theoretically required.

In the event that 1,2-linkages are suspected and bromine is introduced into the reaction mixture after the mild acid hydrolysis step, glycollic acid thus generated can be adsorbed on anion exchange resin. This reaction sequence was carried out using starch as the model substrate. Upon elution of the acid from the anion exchange resin with alkali and regeneration of the free acid with cation exchange resin, the residue was heated at 80–90° C under high vacuum to effect lactonization. The product was reduced with borohydride, and ethylene glycol was eventually recovered and characterized as the crystalline *p*-nitrobenzoate.

EXPERIMENTAL

Paper chromatographic separations were carried out using the descending technique. For routine qualitative and quantitative procedures, Whatman No. 1 paper sheets were used while Whatman No. 3 MM was

Can. J. Chem. Downloaded from www.nrcresearchpress.com by 210.87.254.42 on 09/05/12
For personal use only.

employed for resolution of larger quantities of mixtures. The following three solvent systems were used: A, ethyl acetate – acetic acid – water (8:2:2); B, ethyl acetate – pyridine – water (9:2:1); and C, *n*-butanol – acetic acid – water (12:5:3). Tollens solution and *p*-anisidine–trichloroacetate solution were used for detection of non-reducing and reducing components, respectively.

Specific rotations quoted are equilibrium values. Melting points quoted are uncorrected. Unless otherwise stated, evaporations were carried out under reduced pressure at a bath temperature of 38–45° C.

*Preparation of 1,2-Isopropylidene-*D*-galactose*

This compound was prepared according to the procedures outlined by Levene and Meyer (13) and Svanberg and Sjoberg (14) with only slight modifications. The syrupy product which presumably already contained some monoacetone-galactose was dissolved in ethyl acetate containing concentrated nitric acid (16) and the solution heated for a short interval (just to boiling). The solution was cooled and upon addition of petroleum ether, 1,2-monoacetone-D-galactose crystallized which after recrystallization had m.p. 156–157° C, $[\alpha]_D^{25}$ −10.8° in ethanol (*c*, 3.0).

*Periodate Oxidation of 1,2-Monoacetone-*D*-galactose*

To a quantity (4.1 g) of the compound in alkaline (pH 7.5) phosphate buffer (200 ml), $[\alpha]_D^{25}$ −9.9°, was added a 50% molar excess of sodium periodate. A slightly alkaline buffer was used to prevent any hydrolysis of the 1,2-isopropylidene group. After the observed rotation became constant ($[\alpha]_D^{20}$ −2.9° of the dialdehyde) periodate and iodate were precipitated by addition of barium chloride. To the filtrate was added potassium borohydride and the solution kept at room temperature for 24 hours. The specific rotation changed to a constant value of 3.1°. The acetal was hydrolyzed in dilute acid to yield glycerol from C_4, C_5, and C_6 and D-glyceraldehyde from C_1, C_2, and C_3. The change in rotation ($[\alpha]_D^{25}$ 0.12° → 0.21°) indicated the liberation of D-glyceraldehyde, $[\alpha]_D^{25}$ 14° (*c*, 1.5 in water).

Bromine Oxidation

To the above mixture was added bromine at 1-hour intervals, in the presence of barium carbonate, to transform D-glyceraldehyde to the corresponding carboxylic acid. The completion of this reaction was assumed from the change in the specific rotation to that approximating D-glyceric acid (barium salt), $[\alpha]_D^{25}$ 21.3° (*c*, 1.5 in water). Upon acidification, the specific rotation changed to 14°. The solution was evaporated, the mixture of glycerol and D-glyceric acid extracted with alcohol (95%), and the molar ratio as determined chromatographically using the periodate – chromotropic acid procedure (7, 18) found to be 1:1 as theoretically expected. The two components were separated by means of ion exchange resin columns. The neutral eluate was evaporated to a syrupy residue which when chromatographed was found to contain glycerol. Treatment of the dry residue with *p*-nitrobenzoyl chloride (10% molar excess) in pyridine (4 ml) in the usual manner gave tri-*p*-nitrobenzoylglycerol, m.p. and mixed m.p. 194–195° C.

Reduction of D*-Glyceric Acid to Glycerol*

Glyceric acid was eluted from the anion exchange resin with 1 *N* NaOH, and the free acid regenerated by treatment of the alkaline solution with cation exchange resin. The solution was evaporated to near dryness and chromatographic examination revealed one component corresponding to glyceric acid. Water was removed by drying under high vacuum. The residue was heated for 2 hours at 70° C under vacuum to effect lactone formation (presumably the dimeric lactone forms since this is more likely, from stereochemical considerations, than a beta-lactone) and the product dissolved in water containing potassium borohydride. After 24 hours, the solution was evaporated to dryness, methanolic hydrogen chloride added, which upon evaporation removes borate. An aqueous solution of the residue was deionized and the final syrupy product chromatographed. Only glycerol was detected. The dry residue upon treatment with *p*-nitrobenzoyl chloride gave glycerol tri-*p*-nitrobenzoate, m.p. and mixed m.p. 194–195° C.

Periodate Degradation of D*-Mannose 1,2-(Methyl orthoacetate)*

This compound was prepared according to the general procedure described by Isbell (16). A quantity (3.2 g) of the 1,2-orthoacetate was obtained by alkaline deacetylation of 3,4,6-triacetyl-D-mannose 1,2-orthoacetate. The orthoacetate was treated with sodium periodate in an alkaline medium (pH 7.4–7.6) to prevent loss of the orthoacetate substituent. After the consumption of one molecular equivalent of periodate, the dialdehyde was reduced with sodium borohydride in the usual manner. The product was hydrolyzed with mineral acid to yield glycerol (from C_4, C_5, and C_6) and L-glyceraldehyde (from C_1, C_2, and C_3). The specific rotation, considering only the optically active component, was −13.2°, indicating a good yield of the aldehyde. The mixture was treated with bromine and barium carbonate as described previously to yield barium L-glycerate, $[\alpha]_D^{25}$ −19.8° (*c*, 2.1 in water). Acidification gave the free acid, $[\alpha]_D^{25}$ −13.6° (*c*, 1.9 in water). Glycerol and L-glyceric acid were found to be present in a 1:1 molar ratio as deduced by paper chromatography and appropriate application of the periodate – chromotropic acid reagent. The two components were quantitatively separated as described before. Glycerol was identified as the tri-*p*-nitrobenzoate, m.p. and mixed m.p. 194–195° C. Lactonization of the acid and reduction of the lactone with borohydride gave glycerol, which was identified as the solid *p*-nitrobenzoate.

Can. J. Chem. Downloaded from www.nrcresearchpress.com by 210.87.254.42 on 09/05/12
For personal use only.

Isolation of Glycollic Acid from Periodate-degraded Starch

Soluble starch, 2.0 g, in water (100 ml) was oxidized with periodic acid in the usual manner. After no further periodate was consumed, the solution was neutralized with barium carbonate and filtered. The polyaldehyde was reduced with potassium borohydride followed by mild acid hydrolysis. The mixture was further treated with bromine to oxidize glycollic aldehyde to the corresponding carboxylic acid. The solution was finally neutralized ($PbCO_3$), evaporated to dryness, borate removed, and an aqueous solution of the residue deionized. The neutral effluent was shown to contain erythritol, glycerol, and a trace of glucosyl-erythritol as deduced from hydrolysis of this component and the resulting equimolar ratio of glucose and erythritol. Glycollic acid was eluted from the anion exchange resin with dilute alkali and the free acid regenerated. The solution was evaporated and the residue heated (80° C) under high vacuum. Because of the possible volatility of the lactonized product, a cold finger apparatus was used. The product was reduced with potassium borohydride and the reaction mixture worked up in the usual manner. Ethylene glycol was identified chromatographically and as the di-*p*-nitrobenzoate, m.p. and mixed m.p. 145–146° C. As theoretically required, the molecular proportion of ethylene glycol was approximately equivalent to the combined molecular proportions of glycerol and erythritol.

Borohydride Reduction of Starch Polyalcohol Hydrolyzate

A quantity of starch (2 g) which had been treated with periodate, borohydride, and hydrolyzed with weak acid (7) in that order was re-treated with potassium borohydride to reduce glycollic aldehyde to ethylene glycol. Jayme and Satre (19) used a similar but somewhat less satisfactory procedure to characterize glycollic aldehyde. The mixture was worked up in the usual manner. The oily residue was chromatographed and found to contain erythritol, glycerol, and ethylene glycol. The relative molar quantity of each was determined by the periodate – chromotropic acid procedure (17, 18) and the combined molar quantity of glycerol and erythritol was equivalent to the molar quantity of ethylene glycol as theoretically required. The components were separated by paper chromatography and each compound further identified as the solid *p*-nitrobenzoate: ethylene glycol *p*-nitrobenzoate had m.p. and mixed m.p. 144–145° C, glycerol *p*-nitrobenzoate had m.p. and mixed m.p. 194–196° C, and erythritol *p*-nitrobenzoate had m.p. and mixed m.p. 249–252° C.

ACKNOWLEDGMENT

The continued financial support of the National Research Council, Ottawa, Canada, is gratefully acknowledged.

1. L. Malaprade. Bull. Soc. Chem. **43**, 683 (1928); Compt. Rend. **186**, 382 (1928).
2. E. L. Jackson and C. S. Hudson. J. Am. Chem. Soc. **58**, 378 (1936).
3. F. Smith and J. W. VanCleve. J. Am. Chem. Soc. **77**, 3091 (1955).
4. F. Smith. Proceedings of the 115th Meeting of the American Chemical Society, San Francisco, Calif. 1949.
5. M. Abdel-Akher, J. E. Cadotte, B. A. Lewis, R. Montgomery, G. Smith, and J. W. VanCleve. Nature, **171**, 474 (1953).
6. M. Abdel-Akher, F. Smith, and D. R. Spriestersbach. J. Chem. Soc. 3637 (1952).
7. I. J. Goldstein, G. W. Hay, B. A. Lewis, and F. Smith. Abstracts, 135th Meeting of the American Chemical Society, Boston, Mass. 1959. 3D.
8. A. M. Unrau and G. G. S. Dutton. Can. J. Chem. **40**, 1196, 1479, 2101 (1962).
9. A. M. Unrau and G. G. S. Dutton. Can. J. Chem. **40**, 348 (1962).
10. A. M. Unrau and G. G. S. Dutton. Unpublished results.
11. A. M. Unrau. Unpublished results.
12. M. L. Wolfrom and H. B. Wood. J. Am. Chem. Soc. **73**, 2933 (1951).
13. P. A. Levene and G. M. Meyer. J. Biol. Chem. **64**, 473 (1925).
14. O. Svanberg and K. Sjoberg. Ber. **56**, 863 (1923).
15. H. S. Isbell. J. Res. Natl. Bur. Std. **7**, 1115 (1931).
16. H. W. Coles, L. D. Goodhue, and R. M. Hixon. J. Am. Chem. Soc. **51**, 523 (1929).
17. M. Lambert and A. C. Neish. Can. J. Res. **28B**, 83 (1950).
18. A. M. Unrau and F. Smith. Chem. Ind. (London), 330 (1957).
19. G. Jayme and M. Satre. Ber. **77**, 248 (1944).

Received March 18, 1963.
Department of Plant Science,
University of Manitoba,
Winnipeg 19, Manitoba.

THE DIMER OF BROMOTRIFLUOROETHYLENE

W. R. Cullen and Pritam Singh

Park, Holler, and Lacher (1) have briefly reported that dimerization of bromotrifluoroethylene takes place at 210° in the presence of the polymerization inhibitor Terpene-B.

Can. J. Chem. Downloaded from www.nrcresearchpress.com by 210.87.254.42 on 09/05/12
For personal use only.

Isolation of Glycollic Acid from Periodate-degraded Starch

Soluble starch, 2.0 g, in water (100 ml) was oxidized with periodic acid in the usual manner. After no further periodate was consumed, the solution was neutralized with barium carbonate and filtered. The polyaldehyde was reduced with potassium borohydride followed by mild acid hydrolysis. The mixture was further treated with bromine to oxidize glycollic aldehyde to the corresponding carboxylic acid. The solution was finally neutralized ($PbCO_3$), evaporated to dryness, borate removed, and an aqueous solution of the residue deionized. The neutral effluent was shown to contain erythritol, glycerol, and a trace of glucosyl-erythritol as deduced from hydrolysis of this component and the resulting equimolar ratio of glucose and erythritol. Glycollic acid was eluted from the anion exchange resin with dilute alkali and the free acid regenerated. The solution was evaporated and the residue heated (80° C) under high vacuum. Because of the possible volatility of the lactonized product, a cold finger apparatus was used. The product was reduced with potassium borohydride and the reaction mixture worked up in the usual manner. Ethylene glycol was identified chromatographically and as the di-*p*-nitrobenzoate, m.p. and mixed m.p. 145–146° C. As theoretically required, the molecular proportion of ethylene glycol was approximately equivalent to the combined molecular proportions of glycerol and erythritol.

Borohydride Reduction of Starch Polyalcohol Hydrolyzate

A quantity of starch (2 g) which had been treated with periodate, borohydride, and hydrolyzed with weak acid (7) in that order was re-treated with potassium borohydride to reduce glycollic aldehyde to ethylene glycol. Jayme and Satre (19) used a similar but somewhat less satisfactory procedure to characterize glycollic aldehyde. The mixture was worked up in the usual manner. The oily residue was chromatographed and found to contain erythritol, glycerol, and ethylene glycol. The relative molar quantity of each was determined by the periodate – chromotropic acid procedure (17, 18) and the combined molar quantity of glycerol and erythritol was equivalent to the molar quantity of ethylene glycol as theoretically required. The components were separated by paper chromatography and each compound further identified as the solid *p*-nitrobenzoate: ethylene glycol *p*-nitrobenzoate had m.p. and mixed m.p. 144–145° C, glycerol *p*-nitrobenzoate had m.p. and mixed m.p. 194–196° C, and erythritol *p*-nitrobenzoate had m.p. and mixed m.p. 249–252° C.

ACKNOWLEDGMENT

The continued financial support of the National Research Council, Ottawa, Canada, is gratefully acknowledged.

1. L. Malaprade. Bull. Soc. Chem. **43**, 683 (1928); Compt. Rend. **186**, 382 (1928).
2. E. L. Jackson and C. S. Hudson. J. Am. Chem. Soc. **58**, 378 (1936).
3. F. Smith and J. W. VanCleve. J. Am. Chem. Soc. **77**, 3091 (1955).
4. F. Smith. Proceedings of the 115th Meeting of the American Chemical Society, San Francisco, Calif. 1949.
5. M. Abdel-Akher, J. E. Cadotte, B. A. Lewis, R. Montgomery, G. Smith, and J. W. VanCleve. Nature, **171**, 474 (1953).
6. M. Abdel-Akher, F. Smith, and D. R. Spriestersbach. J. Chem. Soc. 3637 (1952).
7. I. J. Goldstein, G. W. Hay, B. A. Lewis, and F. Smith. Abstracts, 135th Meeting of the American Chemical Society, Boston, Mass. 1959. 3D.
8. A. M. Unrau and G. G. S. Dutton. Can. J. Chem. **40**, 1196, 1479, 2101 (1962).
9. A. M. Unrau and G. G. S. Dutton. Can. J. Chem. **40**, 348 (1962).
10. A. M. Unrau and G. G. S. Dutton. Unpublished results.
11. A. M. Unrau. Unpublished results.
12. M. L. Wolfrom and H. B. Wood. J. Am. Chem. Soc. **73**, 2933 (1951).
13. P. A. Levene and G. M. Meyer. J. Biol. Chem. **64**, 473 (1925).
14. O. Svanberg and K. Sjoberg. Ber. **56**, 863 (1923).
15. H. S. Isbell. J. Res. Natl. Bur. Std. **7**, 1115 (1931).
16. H. W. Coles, L. D. Goodhue, and R. M. Hixon. J. Am. Chem. Soc. **51**, 523 (1929).
17. M. Lambert and A. C. Neish. Can. J. Res. **28B**, 83 (1950).
18. A. M. Unrau and F. Smith. Chem. Ind. (London), 330 (1957).
19. G. Jayme and M. Satre. Ber. **77**, 248 (1944).

Received March 18, 1963.
Department of Plant Science,
University of Manitoba,
Winnipeg 19, Manitoba.

THE DIMER OF BROMOTRIFLUOROETHYLENE

W. R. Cullen and Pritam Singh

Park, Holler, and Lacher (1) have briefly reported that dimerization of bromotrifluoroethylene takes place at 210° in the presence of the polymerization inhibitor Terpene-B.

Can. J. Chem. Downloaded from www.nrcresearchpress.com by 210.87.254.105 on 09/05/12
For personal use only.

They suggested that the dimer is 1,2-dibromohexafluorocyclobutane since debromination gives hexafluorocyclobutene. They also suggested that their product was an approximately 50:50 mixture of the cis and trans forms. During the course of a study of the reactions of bromotrifluoroethylene with compounds containing As—As and P—P bonds (2) a product of molecular formula $C_4F_6Br_2$ was often obtained; therefore, it was decided to investigate further the preparation and structure of this compound.

It has now been found that dimerization of bromotrifluoroethylene occurs under quite mild conditions, giving a product which can be debrominated to give hexafluorocyclobutene. The infrared spectrum of this product is very similar to that of the product obtained by the bromination of hexafluorocyclobutene. However, extra bands are present in the spectrum of the dimer. Both these spectra are similar to that of the cyclic dimer of chlorotrifluoroethylene. The retention times of the dimer and the bromination product are identical on a dinonylphthalate column at 100°.

The ^{19}F n.m.r. spectrum of the bromination product (Fig. 1(*a*)) shows an AB quartet

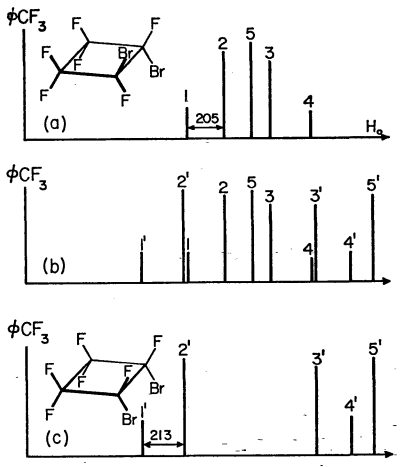

FIG. 1.

(lines 1–4) and an absorption due to one other nonequivalent fluorine (line 5). This pattern would be expected from a pure isomer of 1,2-dibromohexafluorocyclobutane, the two adjacent equivalent CF_2 groups giving rise to the AB pattern and the other absorption being due to the two equivalent fluorines on the two adjacent CFBr groups (3). The coupling constant for the AB system, 205 cycles/sec, is of the same order as that found for similarly fluorinated cyclobutanes (3). The ^{19}F n.m.r. spectrum of the dimer is shown in Fig. 1(*b*), and if the bands corresponding to those in Fig. 1(*a*) are removed then the spectrum of Fig. 1(*c*) remains. This last spectrum is again what would be expected from a pure isomer of 1,2-dibromohexafluorocyclobutane, consisting of an AB pattern (lines 1′, 2′, 3′, 4′) (coupling constant 213 cycles/sec) and one other line (line 5′).

Bromination of hexafluorocyclobutene would be expected to give predominantly the trans isomer and since only one isomer appears to be present this must be the trans form. Consequently the spectrum of Fig. 1(*c*) is that of the cis isomer.

These results strongly indicate that the dimer of bromotrifluoroethylene is a mixture of *cis*- and *trans*-1,2-dibromohexafluorocyclobutane. The relative amounts of the isomers are given by the relative intensities of lines 5 and 5′ (Fig. 1(*b*)). The proportion is therefore approximately 60% cis and 40% trans.

Can. J. Chem. Downloaded from www.nrcresearchpress.com by 210.87.254.105 on 09/05/12
For personal use only.

EXPERIMENTAL

Volatile reagents and products were manipulated in a vacuum system. Infrared spectra were recorded on a Perkin–Elmer model 421 instrument. Nuclear magnetic resonance spectra were determined on neat liquids using a Varian spectrometer operating at 40 Mc/sec.

Dimerization of Bromotrifluoroethylene

In a typical experiment 17.4 g of bromotrifluoroethylene was heated in a sealed tube (50 ml) for 6 days at 100°. Unchanged monomer (12.5 g) was recovered. The reaction products were an involatile polymer (0.90 g), which remained in the tube, and 3.8 g of a volatile fraction, which condensed in a trap cooled to −78°. This fraction was purified by v.p.c. (dinonylphthalate on firebrick at 100°) and found to contain ca. 70% of the expected dimer (found: mol. wt., 323; calc.: mol. wt., 322). The infrared spectrum showed the following absorption bands (vapor): 1375 (s), 1278 (s), 1230 (vs), 1172 (vw), 1072 (vw), 1047 (vw), 1016 (w), 996 (w), 963 (w), 941 (w), 866 (s), 836 (s), 797 (w), 759 (w), 724 (w) cm^{-1}. The ^{19}F n.m.r. spectrum (Fig. 1(*b*)) had absorption at 1667, 1872, 1880, 2082, 2199, 2249, 2460, 2487, 2703, 2855 cycles/sec to the high-field side of an internal benzotrifluoride reference.

In further experiments it was found that irradiation of the monomer for 5 hours in thick-walled Pyrex tubes using a 100-w ultraviolet lamp produced very little polymer (3%) and no dimer. Dimerization by heating at 100° was slow, e.g. 2% dimer and 1% polymer after 18 hours, but at higher temperatures the rate was faster, e.g. 45% dimer and 40% polymer after 48 hours at 150°.

Debromination of the Dimer

When the dimer (2.338 g), benzonitrile (5 ml), and zinc dust (2.0 g) were shaken at 20° for 4 hours, hexafluorocyclobutene (0.788 g; 67% yield) was obtained which was identified by its molecular weight of 163 (calc.: mol. wt., 162) and by its infrared spectrum.

Bromination of Hexafluorocyclobutene

The butene (16.6 g) and bromine (16.6 g) in a sealed tube were irradiated with a 100-w ultraviolet lamp for 8 hours (4). The crude 1,2-dibromohexafluorocyclobutane so obtained distilled at 96–97° (760 mm) (lit. value, 96–97° (4)) and was purified by v.p.c. The major component of the distillate (ca. 90%) had the same retention time on the dinonylphthalate column (100°) as did the dimer. The infrared spectrum of the bromination product showed the following absorption bands (vapor): 1375 (s), 1276 (s), 1230 (vs), 1193 (w), 1171 (w), 1071 (vw), 1046 (w), 996 (s), 946 (w), 846 (w), 840 (s), 759 (s), 636 (w) cm^{-1}. The ^{19}F n.m.r. spectrum (Fig. 1(*a*)) had absorption at 1877, 2082, 2199, 2249, 2460 cycles/sec to the high-field side of an internal benzotrifluoride reference.

ACKNOWLEDGMENTS

The authors wish to acknowledge financial assistance from the National Research Council of Canada. They are also indebted to Dr. L. W. Reeves for assistance in obtaining and interpreting the n.m.r. data.

1. J. D. Park, H. V. Holler, and J. R. Lacher. J. Org. Chem. **25**, 990 (1960).
2. W. R. Cullen and N. K. Hota. To be published.
3. J. A. Pople, W. G. Schneider, and H. J. Bernstein. High resolution nuclear magnetic resonance. McGraw-Hill. 1959.
4. M. W. Buxton, D. W. Ingram, F. Smith, M. Stacey, and J. C. Tatlow. J. Chem. Soc. 3830 (1952).

Received April 11, 1963.
Department of Chemistry,
University of British Columbia,
Vancouver, British Columbia.

THE PREPARATION OF 3-BROMOINDOLE

K. Piers, C. Meimaroglou, R. V. Jardine, and R. K. Brown

The few reports in the literature describing attempts at the direct halogenation of indole in the pyrrole ring, with bromine, chlorine, or iodine (1–3), indicate that a vigorous reaction does indeed occur. However, only in the case of iodination, and then only in

Can. J. Chem. Downloaded from www.nrcresearchpress.com by 210.87.254.105 on 09/05/12
For personal use only.

EXPERIMENTAL

Volatile reagents and products were manipulated in a vacuum system. Infrared spectra were recorded on a Perkin–Elmer model 421 instrument. Nuclear magnetic resonance spectra were determined on neat liquids using a Varian spectrometer operating at 40 Mc/sec.

Dimerization of Bromotrifluoroethylene

In a typical experiment 17.4 g of bromotrifluoroethylene was heated in a sealed tube (50 ml) for 6 days at 100°. Unchanged monomer (12.5 g) was recovered. The reaction products were an involatile polymer (0.90 g), which remained in the tube, and 3.8 g of a volatile fraction, which condensed in a trap cooled to −78°. This fraction was purified by v.p.c. (dinonylphthalate on firebrick at 100°) and found to contain ca. 70% of the expected dimer (found: mol. wt., 323; calc.: mol. wt., 322). The infrared spectrum showed the following absorption bands (vapor): 1375 (s), 1278 (s), 1230 (vs), 1172 (vw), 1072 (vw), 1047 (vw), 1016 (w), 996 (w), 963 (w), 941 (w), 866 (s), 836 (s), 797 (w), 759 (w), 724 (w) cm^{-1}. The ^{19}F n.m.r. spectrum (Fig. 1(*b*)) had absorption at 1667, 1872, 1880, 2082, 2199, 2249, 2460, 2487, 2703, 2855 cycles/sec to the high-field side of an internal benzotrifluoride reference.

In further experiments it was found that irradiation of the monomer for 5 hours in thick-walled Pyrex tubes using a 100-w ultraviolet lamp produced very little polymer (3%) and no dimer. Dimerization by heating at 100° was slow, e.g. 2% dimer and 1% polymer after 18 hours, but at higher temperatures the rate was faster, e.g. 45% dimer and 40% polymer after 48 hours at 150°.

Debromination of the Dimer

When the dimer (2.338 g), benzonitrile (5 ml), and zinc dust (2.0 g) were shaken at 20° for 4 hours, hexafluorocyclobutene (0.788 g; 67% yield) was obtained which was identified by its molecular weight of 163 (calc.: mol. wt., 162) and by its infrared spectrum.

Bromination of Hexafluorocyclobutene

The butene (16.6 g) and bromine (16.6 g) in a sealed tube were irradiated with a 100-w ultraviolet lamp for 8 hours (4). The crude 1,2-dibromohexafluorocyclobutane so obtained distilled at 96–97° (760 mm) (lit. value, 96–97° (4)) and was purified by v.p.c. The major component of the distillate (ca. 90%) had the same retention time on the dinonylphthalate column (100°) as did the dimer. The infrared spectrum of the bromination product showed the following absorption bands (vapor): 1375 (s), 1276 (s), 1230 (vs), 1193 (w), 1171 (w), 1071 (vw), 1046 (w), 996 (s), 946 (w), 846 (w), 840 (s), 759 (s), 636 (w) cm^{-1}. The ^{19}F n.m.r. spectrum (Fig. 1(*a*)) had absorption at 1877, 2082, 2199, 2249, 2460 cycles/sec to the high-field side of an internal benzotrifluoride reference.

ACKNOWLEDGMENTS

The authors wish to acknowledge financial assistance from the National Research Council of Canada. They are also indebted to Dr. L. W. Reeves for assistance in obtaining and interpreting the n.m.r. data.

1. J. D. Park, H. V. Holler, and J. R. Lacher. J. Org. Chem. **25**, 990 (1960).
2. W. R. Cullen and N. K. Hota. To be published.
3. J. A. Pople, W. G. Schneider, and H. J. Bernstein. High resolution nuclear magnetic resonance. McGraw-Hill. 1959.
4. M. W. Buxton, D. W. Ingram, F. Smith, M. Stacey, and J. C. Tatlow. J. Chem. Soc. 3830 (1952).

Received April 11, 1963.
Department of Chemistry,
University of British Columbia,
Vancouver, British Columbia.

THE PREPARATION OF 3-BROMOINDOLE

K. Piers, C. Meimaroglou, R. V. Jardine, and R. K. Brown

The few reports in the literature describing attempts at the direct halogenation of indole in the pyrrole ring, with bromine, chlorine, or iodine (1–3), indicate that a vigorous reaction does indeed occur. However, only in the case of iodination, and then only in

Can. J. Chem. Downloaded from www.nrcresearchpress.com by 210.87.254.40 on 09/05/12
For personal use only.

dilute aqueous solution, has the isolation of a monohaloindole (3-iodoindole) been successful (1, 2). The reaction of chlorine and bromine with indole is reported to yield "a mixture of higher substitution products" (3) which apparently could not be resolved.

A more successful route to 3-bromo- and 3-chloro-indole, devised by Weissgerber (3), involved the action of halogens on N-benzoylindole. Sulphuryl chloride has been reported to convert indole to 3-chloroindole or to 2,3-dichloroindole depending upon the amount of halogenating agent used (4). Buu-Hoï (5) found that the reaction of N-bromosuccinimide with N-benzoylindole gave a reasonably good yield of 3-bromo-N-benzoylindole which could readily be hydrolyzed to 3-bromoindole (3). More recently Yanovskaya (6) reported that in dioxane solution at 0° the action of dioxane dibromide on indole gave a 60% yield of 3-bromoindole.

Certain work in progress in this laboratory required a considerable quantity of 3-bromoindole. Although Weissgerber's procedure gave reasonably good results and produced 3-bromoindole from indole in an overall yield of about 45% (3), this route is time consuming. Accordingly, the preparation of the haloindole was attempted following the procedure reported by Yanovskaya (6). However, in our hands, the reaction in purified dioxane solvent (7, p. 284) gave only a very small amount of material, which spontaneously decomposed on attempts at its purification, in the manner characteristic of 3-bromoindole. The temperature of the reaction solvent could not be reduced to 0°, as reported, since the solvent and contents solidified below 8°. Hence we carried out the bromination at 8–10°, but otherwise as described (6). The same procedure, modified by the addition of a small amount of diethyl ether as diluent for the dioxane to permit attainment of 0° reaction temperature gave the same "tarry" material as before and little or no 3-bromoindole.

In the above reactions it was noted that hydrogen bromide evolved from the solution, especially near the end of the bromination reaction. Since Weissgerber found that 3-bromoindole decomposed readily when impure, or when in the presence of strong mineral acids, it was felt that some means of neutralizing or removing the acid would improve the reaction. The solvent pyridine proved to be the answer to the problem. When the halogenation was carried out using pyridine as solvent, indole could be converted to 3-bromoindole with dioxane dibromide in 48% yield. Use of pyridinium bromide perbromide as halogenating agent and pyridine as solvent and carrying the reaction out at 0–2° increased the yield of pure 3-bromoindole to at least 64%.

EXPERIMENTAL

To a solution of 4.0 g (0.034 mole) of indole in 40 ml of reagent pyridine cooled to 0–2°, was added slowly 10.8 g (0.034 mole) of pyridinium bromide perbromide (7, p. 65) dissolved in 30 ml of pyridine. The rate of addition was such that the temperature of the reaction mixture did not rise above 2°. When addition was complete, the solution was poured into cold ether and the resulting mixture freed from insoluble material by filtration. The cold ether solution was washed several times with cold dilute aqueous hydrochloric acid to remove the pyridine. The residual ether solution of the haloindole was then washed first with cold dilute aqueous sodium hydroxide, then with water. The dried ether solution ($MgSO_4$) was freed from ether and the residue crystallized from *n*-heptane and decolorized with charcoal if necessary. Yield, 4.3 g (64%) of pure 3-bromoindole melting at 65–66° (decomp.).

When dioxane dibromide was used as brominating agent in pyridine solution the same procedure gave 3-bromoindole in 48% yield.

In the recrystallization procedure, it is important not to heat the solution above 60° since 3-bromoindole, which deposits in the flask, begins to decompose at 65°. 3-Bromoindole may be kept satisfactorily if placed under a solvent such as pentane and stored at −20°. Otherwise even very pure material undergoes slow decomposition.

ACKNOWLEDGMENT

The authors wish to thank the National Research Council for financial assistance throughout the course of this work.

Can. J. Chem. Downloaded from www.nrcresearchpress.com by 210.87.254.40 on 09/05/12
For personal use only.

1. A. Oswald. Z. Physiol. Chem. **73**, 128 (1911).
2. H. Pauly and K. Gundermann. Ber. **41**, 4001 (1908).
3. R. Weissgerber. Ber. **46**, 652 (1913).
4. G. Mazzara and A. Borgo. Centralblatt, 854 (1906).
5. Ng.Ph. Buu-Hoï. Ann. **556**, 1 (1944).
6. L. A. Yanovskaya. Dokl. Akad. Nauk SSSR, **71**, 693 (1950); Chem. Abstr. **44**, 8354 (1950).
7. L. F. Fieser. Experiments in organic chemistry. 3rd ed. D. C. Heath and Co., Boston. 1955.

Received April 1, 1963.
Department of Chemistry,
University of Alberta,
Edmonton, Alberta.

Can. J. Chem. Downloaded from www.nrcresearchpress.com by 210.87.254.40 on 09/05/12
For personal use only.

Canadian Journal of Chemistry

Issued by THE NATIONAL RESEARCH COUNCIL OF CANADA

VOLUME 41 OCTOBER 1963 NUMBER 10

BORATE COMPLEXING BY FIVE-MEMBERED-RING *vic*-DIOLS

VAPOR PRESSURE EQUILIBRIUM AND N.M.R. SPECTRAL OBSERVATIONS[1]

M. MAZUREK AND A. S. PERLIN

National Research Council of Canada, Prairie Regional Laboratory, Saskatoon, Saskatchewan

Received May 27, 1963

ABSTRACT

Thermometric measurement of vapor pressure equilibria in reaction mixtures containing borate ion and *cis*-3,4-dihydroxytetrahydrofuran (I) or D-glucose 5,6-carbonate (II) indicate that complexing involves at least three different equilibria. Borate complexing by I is characterized by a gross change in n.m.r. spectral characteristics, most striking being a strong overall decoupling effect. Alterations in the spectrum of II and of 5-*O*-methyl D-glucose in the presence of borate, when compared with those of D-glucose, suggest that complex formation by the latter sugar proceeds with a pyranose-to-furanose interconversion. The O—C—C—O dihedral angle, within the range 0° to about 40°, does not appear to be a factor determining the stability of borate complexes. Crystalline spirane-type complexes of I, II, and of D-threose have been prepared, illustrating the usefulness of borate complexing for the isolation of some furanose sugars and derivatives.

Solutions of alkali tetraborates are found by thermometric vapor pressure measurements to behave as equimolecular mixtures of alkali borate and boric acid.

The reaction of boric acid and borate salts with diols has for long provided a highly useful means for examining stereochemical and structural problems (1–3). Borate–polyol systems frequently involve complicated equilibria between several types of compounds (1, 4–6), i.e., cyclic esters (I) and ionized, strongly acidic complexes in which one boron

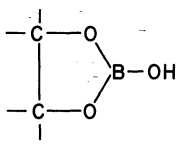

I

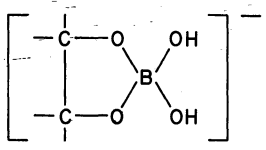

II

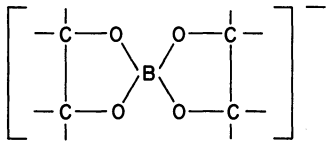

III

atom is associated with one (II) or two (III) molecules of a diol. A different kind of complex, also strongly acidic, is the "tridentate" type formed by cyclitols that contain a

[1]*Issued as N.R.C. No. 7487.*

Can. J. Chem. Downloaded from www.nrcresearchpress.com by 210.87.254.40 on 09/05/12
For personal use only.

cis-cis-1,3,5-triol grouping, in which the hydroxyl groups are axially-oriented by bonding to the central tetrahedral boron atom (3). Several methods have been used for examining borate-complexing reactions: conductivity, pH, and cryoscopic measurements and, especially with carbohydrates, polarimetry (6) and ionophoresis (2, 3). In the current study, some new data have been obtained by thermometric measurement of vapor pressure equilibria* (7) in borate–diol systems and by proton magnetic resonance (n.m.r.) spectroscopy, attention being centered on 5-membered-ring compounds containing a *cis*-1,2-glycol group.

Cryoscopic data indicate that alkali tetraborates in water dissociate to form borate ion and boric acid in equimolecular proportion (8, 9). Thermometric values for solutions of potassium or sodium tetraborate (Experimental, Fig. 5) accord with this view in that at high dilution approximately six particles per mole appear to be present,† corresponding to:

$$K_2B_4O_7 + H_2O = 2K^+ + 2BO_2^- + 2HBO_2. \qquad [1]$$

In concentrated solutions the apparent molarity decreases, possibly due to the existence of $B_4O_7^{--}$ under these conditions (9). The behavior of tetraborate solutions on addition of acid or alkali agrees with that expected from equation [1]. Acid results in the formation of more boric acid, the vapor pressure properties of which are those of a monomeric, undissociated molecule, and the overall number of particles is decreased proportionately (equation [2]). On addition of alkali, water is formed (but is not detected in the presence of the solvent), again with a decrease in total particles (equation [3]).

$$\underset{(4\text{ particles})}{K^+BO_2^- + H^+Cl^-} = \underset{(3\text{ particles})}{K^+Cl^- + HBO_2} \qquad [2]$$

$$\underset{(3\text{ particles})}{HBO_2 + Na^+OH^-} = \underset{(2\text{ particles})}{Na^+BO_2^- + H_2O} \qquad [3]$$

Thermometric measurements of reactions between boric acid and several polyols are characterized by negligibly small values of $\Delta\Delta R$, whereas alkali borates give large $\Delta\Delta R$ values with the same polyols (10). According to the considerations of the previous paragraph, therefore, the thermometric estimation of complexing between a diol and tetraborate can be related to the two borate ions present rather than to the total number of species containing boron. This molar relationship has been adopted as a basis for cryoscopic (11) and polarimetric measurements (6) on sugar–tetraborate reactions and appears to be valid also for the present purposes.

When erythritan (*cis*-3,4-dihydroxytetrahydrofuran (IV)) is treated with increasing proportions of potassium tetraborate there is a sharp initial rise in $\Delta\Delta R$. Equilibrium then appears to be maintained at a maximum level over a broad range, and finally a moderate decrease in $\Delta\Delta R$ is observed (Fig. 1). Such characteristics correspond closely to those expected from theoretical considerations. As has been pointed out (4, 6) a low proportion of borate favors formation of a spirane complex (III), whereas with additional borate present the equilibrium should be shifted towards formation of a type II complex and, in lesser amount, of an ester (I). Hence, the extensive complexing observed at the outset is consistent with formation of III (equation [4]; D = diol) since the maximum $\Delta\Delta R$ value

$$2D + K^+B^- = K^+[DBD]^- \text{ (III)} \qquad [4]$$

is reached when the proportion of diol to borate ion is 2:1 (diol:tetraborate = 0.1 M:0.025

**The vapor pressure difference (heat of vaporization) between the aqueous solution and water is measured thermometrically as a function of electrical resistance (ΔR). The deviation from the sum of individual ΔR values for diol and borate when the two components are admixed is $\Delta\Delta R$; i.e., $\Delta\Delta R = (\Delta R_{diol} + \Delta R_{borate}) - \Delta R_{diol+borate}$.*

†For simplicity, the hydration of metaboric acid or metaborate ion is not considered in these equations.

Can. J. Chem. Downloaded from www.nrcresearchpress.com by 210.87.254.40 on 09/05/12
For personal use only.

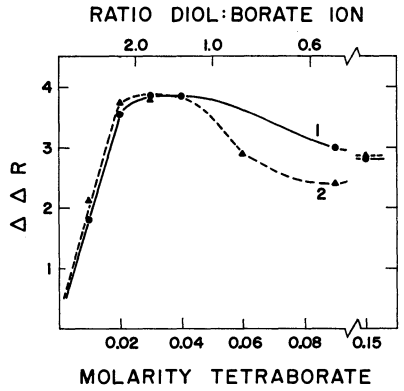

FIG. 1. Thermometric measurement of vapor pressure equilibria in solutions containing potassium tetraborate and (1) *cis*-3,4-dihydroxytetrahydrofuran, (2) D-glucose 5,6-carbonate. $\Delta\Delta R$ values for the latter derivative at tetraborate concentrations greater than 0.05 *M* decrease with time, possibly due to instability of the carbonate group at high pH.

M). At this point the apparent degree of complexing is 70% of that expected for quantitative formation of III but, due to the attendant drop in pH (to 7.8), the $\Delta\Delta R$ value probably should be about 10% greater (the $\Delta\Delta R$ value for the potassium tetraborate solution is lowered by about this amount when the pH is adjusted to 7.8).* Since the interconversion of III to a 1:1 complex (equation [5]) involves no overall change in the total number of

$$K^+[DBD]^- \text{ (III)} + K^+B^- = 2K^+[BD]^- \text{ (II)} \qquad [5]$$

particles present, it could account for the levelling-off effect (Fig. 1) as the diol:borate ion ratio approaches 1:1. Formation of an unionized species (I) then could lead to decreasing $\Delta\Delta R$ values (or a low overall $\Delta\Delta R$ value) since this reaction would be accompanied by an increase in the number of effective particles, but without change in the amounts of complexed borate and diol (equation [6]). Alternatively, the complexes may be less stable at

$$K^+[BD]^- \text{ (II)} = BD \text{ (I)} + K^+OH^- \qquad [6]$$

the relatively high pH of the more concentrated borate solutions, making for the observed decrease in $\Delta\Delta R$. In any event, the increased alkalinity has a bearing on these relationships, as shown by the fact that the addition of potassium hydroxide instead of more potassium tetraborate to a solution in which the diol:borate ratio is 1:1 causes a drop in $\Delta\Delta R$.

A crystalline erythritan–borate complex (V) of the spirane type has been prepared using conditions recommended by Vermaas (4), but derivatives corresponding to I and II have not been isolated from the reaction mixtures. The potassium salt of V was not entirely suitable for combustion analysis but the ammonium salt proved more satisfactory for this purpose. These salts were found thermometrically to be dissociated completely in water and partially in ethanol. The n.m.r. spectrum for V (Fig. 2B) is markedly different from that of erythritan itself (Fig. 2A) and shows a moderate paramagnetic shift for the 3- and 4-protons, associated with esterification of the hydroxyl groups in α-position (12, 13). Most striking in the spectrum of the complex is the fact that signals for the 2,2′- (and 5,5′-) protons constitute essentially an AB pattern, whereas these protons in the parent

**Erythritan and boric acid together (molar ratio of 2:1) show no significant change in $\Delta\Delta R$, but on addition of 1 mole of potassium hydroxide the same value for $\Delta\Delta R$ is obtained as above, when the diol–tetraborate molar ratio is 0.1:0.025. Hence the boric acid component of tetraborate does not influence the stoichiometry of the thermometric measurement.*

Can. J. Chem. Downloaded from www.nrcresearchpress.com by 210.87.254.40 on 09/05/12
For personal use only.

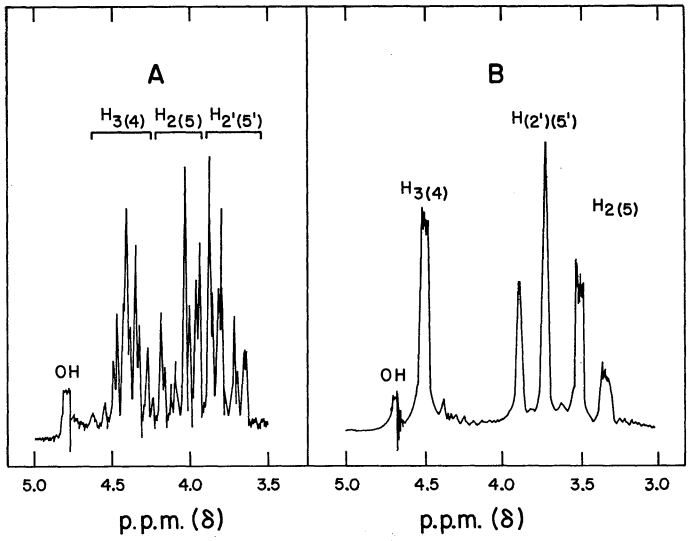

FIG. 2. Proton magnetic resonance spectrum of (A) *cis*-3,4-dihydroxytetrahydrofuran in deuterium oxide; (B) ammonium salt of *cis*-3,4-dihydroxytetrahydrofuran – borate spirane complex (V) in deuterium oxide (the potassium salt of V gives the same spectrum).

compound are coupled with protons 3 and 4 as the AB part of an ABX spectrum.* Also, it is probable that the relative chemical shifts for the AB protons are reversed by complex formation. Thus, of the two quartets comprising the four-proton signal at about 4.0 p.p.m. (Fig. 2A) that at lower field (4.1 p.p.m.) shows stronger splitting due to coupling with $H_{3(4)}$ and is ascribed to $H_{2(5)}$ (14). In Fig. 2B, however, the signal for $H_{2(5)}$ appears to be at relatively higher field since only the doublet at 3.4 p.p.m. shows evidence for coupling with $H_{3(4)}$. The large change in spin coupling constants J_{AX} and J_{BX} produced by complexing presumably can be ascribed chiefly to introduction of the anisotropic boron atom, but might be enhanced by conformational changes in the erythritan moiety.

The plot for complex formation between tetraborate and D-glucose 5,6-carbonate (VI), an example of a furanose sugar, is closely similar to that for erythritan (Fig. 1), and hence the same equilibrium relationships must apply. Complexing by this sugar appears feasible only at the 1,2-hydroxy-hemiacetal group of the α-anomer, which is made more clearly evident by changes in the n.m.r. spectrum of VI when borate is introduced (Fig. 3). Signals attributable to the α- and β-anomeric protons (which show an anomeric ratio at equilibrium of approximately 1:1) are found to be replaced as complexing occurs by the one-proton signal at lower field, the large coupling constant for the latter being consistent with a 1,2-*cis*-configuration for the complex (15). A crystalline ammonium salt of a borate complex of VI has been prepared and also found to contain 2 moles of the sugar per mole of borate. Incidentally, this spirane complex is unusual in that it contains a remarkably large number (six) of 5-membered heterocyclic rings.

The chemical shift for the anomeric proton of the D-glucose–carbonate complex (5.85 p.p.m.), and its coupling constant (3.8 c.p.s.) are close to those recorded for the anomeric proton of D-glucose in borax solution (13). The overall complexing behavior of D-glucose (Fig. 4) differs from that of the 5,6-carbonate derivative but, by analogy with acetonide

**As kindly pointed out by Dr. H. J. Bernstein, the erythritan spectrum should be classified more strictly as of the ABX–XBA type.*

Can. J. Chem. Downloaded from www.nrcresearchpress.com by 210.87.254.40 on 09/05/12
For personal use only.

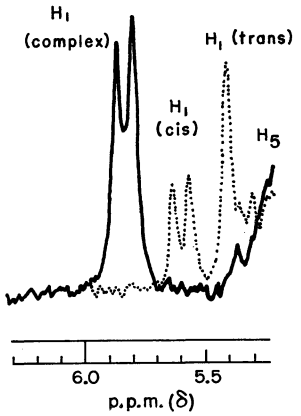

FIG. 3. Partial proton magnetic resonance spectrum of D-glucose 5,6-carbonate (dotted line) in deuterium oxide (cis and trans refer to the α- and β-(1,2-*cis* and -*trans*)-anomers, respectively), and of the ammonium salt of D-glucose 5,6-carbonate – borate spirane complex (solid line) in deuterium oxide.

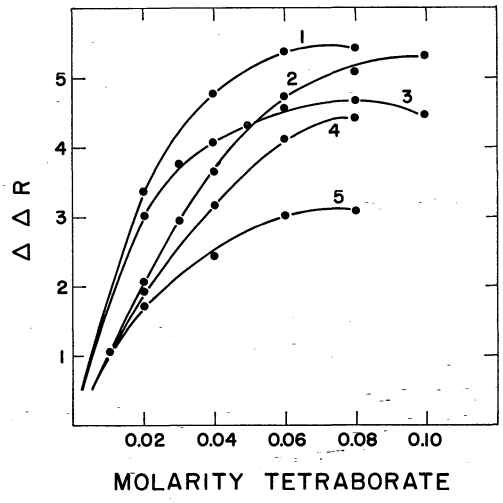

FIG. 4. Thermometric measurement of vapor pressure equilibria in solutions containing potassium tetraborate and (1) L-sorbose, (2) D-glucose, (3) D-fructose, (4) D-arabinose, and (5) D-mannose.

formation, it is possible that D-glucopyranose yields an α-D-furanose form of the 1,2-cyclic borate. Strong support for this surmise is found in the close similarities observed between the n.m.r. spectra for D-glucose and 5-*O*-methyl D-glucofuranose in tetraborate solution. Thus, the chemical shifts for H_1, H_2, and H_3 are at 5.9, 4.5, and 4.3 p.p.m., respectively, in both spectra, and the same values are found in both for J_{12} (3.8 c.p.s.) and J_{23} (<0.5 c.p.s.). By contrast, 4-substituted D-glucose derivatives—cellobiose and 4,6-*O*-ethylidene-D-glucopyranose—exhibit small and different kinds of spectral changes in the presence of borate, most noticeable being the absence of any effect on their anomeric proton signals. These pyranose derivatives also have relatively low electrophoretic mobility in borax (2) and give $\Delta\Delta R$ values only 20–25% of those for D-glucose and its 5-*O*-methyl, 3,5-di-*O*-methyl, and 5,6-carbonate derivatives. Hence the present data point to the likelihood that a furanose form is involved in the reaction of D-glucose with borate ions, while providing no support for the assumption (13) that the pyranose structure is retained

Can. J. Chem. Downloaded from www.nrcresearchpress.com by 210.87.254.40 on 09/05/12
For personal use only.

in the complex. Also, they support the conclusion of Boeseken (1) that D-glucofuranose contributes importantly to the conductivity of D-glucose – boric acid solutions.

A decrease in ring size during complex formation may well take place with other sugars. Thus the effect of borate on the n.m.r. spectrum of D-xylose (13) and on the vapor pressure equilibrium of D-arabinose (Fig. 4) is strikingly similar to its effect on the corresponding properties of D-glucose. The thermometric plot for D-fructose– and L-sorbose–borate (Fig. 4) closely duplicate that for the 5-membered-ring diols at the outset, consistent with formation initially of a furanose–spirane complex. With all of these sugars, in contrast to erythritan and D-glucose carbonate, the $\Delta\Delta R$ values do not go through a maximum at a $\Delta\Delta R$ of about 4, but this difference is due likely to additional reaction by borate with other free diol groupings present in the 1,2-complexes (see refs. 2 and 6). A somewhat different type of behavior is shown by D-mannose (Fig. 4) in that there is no marked change in the region characteristic of a 2:1 complex, but a constant $\Delta\Delta R$ value is obtained at a sugar: borate ratio of 1:1. The low degree of complexing observed for mannose is in accord with its relatively small electrophoretic mobility in borax (2).

Crystalline borate complexes of several diols have been prepared (4, 5) although, aside from those of the ester type, few have been reported in the sugar series (6). As shown with erythritan and D-glucose carbonate, complexes of the spirane type are easily obtained and might prove useful in the isolation and purification of furanose sugars and their derivatives. This possibility is illustrated further in the preparation of an ammonium borate complex of D-threose. Since the tetrose itself is not crystalline the borate salt offers the advantage of a derivative from which the free sugar can be regenerated under mild conditions, e.g., by use of ion-exchange resins. The n.m.r. spectral changes in signals for the anomeric proton observed during formation of this complex are virtually the same as shown in Fig. 4, the anomeric mixture being apparently converted entirely to the 1,2-*cis*-form. The spin-coupling constant J_{12} for the crystalline product is the same as that for the glucofuranose derivative and, as observed with erythritan, complexing markedly decreases splitting of the signals for the methylene protons.

The preferred conformation of 1,2-cyclic acetals and ketals appears to be one in which puckering of the ring makes for a dihedral angle of 35–45° between the two C—O bonds (15, 16). Chelates formed by the tetrahedral borate ion and *vic*-diols would be expected to adopt a similar type of energetically favorable conformation. It may be noted, therefore, that the spin-coupling constant J_{12} (3.8 c.p.s.) for the complex of D-glucofuranose 5,6-carbonate or of 5-*O*-methyl D-glucofuranose is the same as that reported for 1,2-*O*-isopropylidene-D-glucofuranose (15). Since, however, the relationship between coupling constant and dihedral angle (17) is influenced by the chemical nature of a compound (16), the actual size of the angle could be somewhat different in these two types of derivatives. A value of 45° given by the Karplus curve (17) probably is close to the true angle for the acetonide (15, 16) but may be slightly high for the borate, since 1,2-*cis*-cyclohexanediol reacts only weakly with borax (2, 3) yet its C—O bonds define an angle of 50° without the introduction of noticeable strain (18). A dihedral angle substantially smaller than that of the O—C_1—C_2—O grouping in the D-glucose products characterizes the complex formed between methyl β-D-erythroside and potassium tetraborate, as shown by a relatively large spin-coupling constant for J_{23} of 6.2 c.p.s. Since there is no reason to expect that the fused 5-membered rings of this latter complex are planar, the observed value of J probably represents a dihedral angle not too far removed from the 30° value given by the Karplus curve. However, complexing also can take place readily with a diol in which the hydroxyl groups are virtually eclipsed: camphane-2-*exo*,3-*exo*-diol, in which the two C—O bonds

Can. J. Chem. Downloaded from www.nrcresearchpress.com by 210.87.254.40 on 09/05/12
For personal use only.

define an angle close to 0° (19, 20), gives approximately the same $\Delta\Delta R$ value (3.8 at a diol:borate ratio 2:1) as do methyl β-D-erythroside and D-glucose 5,6-carbonate. Hence the dihedral angle of the O—C—C—O grouping, within the range 0° to about 40°, does not appear to be a factor determining the stability of borate complexes.

The adverse influence of steric factors such as non-bonded interaction with groups close to the diol group is seen in the lower degree of complexing by methyl α-D-erythrofuranoside, as compared with that reported above for the β-(1,2-*trans*)-anomer ($\Delta\Delta R$ 2.87 vs. 3.93). This greater instability, associated with the larger number of 1,2-*cis*-interactions in the α-D-glycoside, is reflected more markedly in the behavior of D-erythrose and of 5-*O*-methyl D-mannofuranose (21). In these compounds there appears to be the possibility for complexing at the 1,2-position of the *cis*-anomer and also with the 2,3-*cis*-diol group. The n.m.r. spectrum of each sugar indicates that the 1,2-*trans*-anomer greatly predominates in solution. Displacement of the equilibrium towards formation of a 1,2-*cis*-complex, as found with D-threose and the D-glucofuranose derivatives, involves more unfavorable interactions than when the 2,3-complex is formed. Changes produced by borate on the n.m.r. spectra of these sugars show, accordingly, that although considerable complexing must occur, little can involve the C_1-hydroxyl since signals for the anomeric protons are not shifted to lower field.

EXPERIMENTAL

Proton magnetic resonance spectra were prepared with a Varian A-60 high-resolution spectrometer. Deuterium oxide was used as solvent and tetramethylsilane as external standard.

Measurement of Vapor Pressure Equilibrium

A thermoelectric "osmometer" (Mechrolab Inc., Mountain View, California) was used. Measurements were made with an aqueous probe at 37° C, the procedure being that used for determination of molecular weight. The solution was stored in a syringe mounted in the chamber, a drop of it was applied to the appropriate thermistor bead, and a drop of water to the other bead. Changes in resistance (ΔR) were noted at 3 minutes' equilibration time, the molarity was then obtained by reference to a plot of ΔR vs. molarity, prepared under the same conditions with standard solutions.

A typical estimate of the degree of borate complexing is given by the following data for erythritan and potassium tetraborate:

	ΔR		ΔR
0.1 *M* erythritan	5.37	0.1 *M* erythritan	5.37
0.02 *M* borate	6.42	0.04 *M* borate	11.83
Calc. for 1:1 mixture	11.79		17.20
Found	8.23		13.36
$\Delta\Delta R$ =	3.56		3.84

The calculated value for complete complexing is ΔR 5.37, i.e., the found ΔR value for a 0.1 *M* solution of an undissociated compound.

Some Properties of Potassium Tetraborate Solutions

The apparent molarity of potassium tetraborate solutions of varying concentration is given in Fig. 5.

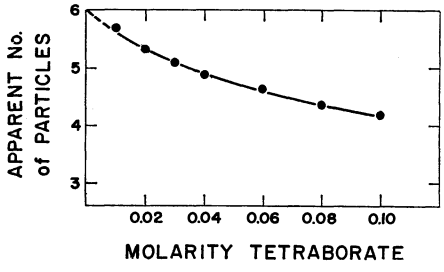

FIG. 5. Thermometric measurement of vapor pressure equilibria in solutions of potassium tetraborate.

Can. J. Chem. Downloaded from www.nrcresearchpress.com by 210.87.254.40 on 09/05/12
For personal use only.

A change in ΔR equivalent to an overall decrease of approximately one particle in solution is found on addition of hydrochloric acid or sodium hydroxide to potassium tetraborate solution (the ΔR values for solutions of the acid and base themselves are approximately twice those for equimolar solutions of un-ionized compounds):

ΔR of 1:1 mixture with the borate solution

	ΔR	Calc.	Found	$\Delta\Delta R$
0.02 *M* borate	6.06			
0.01 *M* HCl	1.05	7.11	6.58	0.53
0.02 *M* HCl	2.09	8.15	7.22	0.93
0.01 *M* NaOH	1.03	7.09	6.57	0.52
0.02 *M* NaOH	2.06	8.12	7.09	1.03

Erythritan – Potassium Borate Complex (V)

Erythritan (660 mg; freshly distilled) and potassium tetraborate tetrahydrate (493 mg) were dissolved in water (1 ml), ethanol (3 ml) was added, and the solution stored at 3° C. After 18 hours the solid product was collected and washed twice each with ethanol and ether and dried *in vacuo*. Yield, 250 mg; highly birefringent needles. Calculated for $C_8H_{12}O_6KB$: C, 37.18%; H, 4.76%; K, 15.39%; mol. wt., 254 (unionized), 127 (ionized). Found: C, 34.17%; H, 4.75%; K, 15.29%; mol. wt. (osmometric), 118 in water.

Erythritan – Ammonium Borate Complex

Prepared as above for V from erythritan (528 mg) and ammonium tetraborate tetrahydrate (340 mg). Yield, 215 mg. Calculated for $C_8H_{16}NB.H_2O$: C, 38.27%; H, 7.23%; N, 5.58%. Found: C, 38.32%; H, 6.94%; N, 5.75%. A dihydrate was formed when the sample was equilibrated to atmospheric moisture for 3 hours. Calculated for $C_8H_{16}O_6NB.2H_2O$: C, 35.71%; H, 7.49%; N, 5.21%; mol. wt., 269 (unionized), 135 (ionized). Found: C, 35.34%; H, 7.35%; N, 5.02%; mol. wt., 126 in water (171 in ethanol).

D-*Glucose 5,6-Carbonate – Ammonium Borate Complex*

Prepared as for V from D-glucose 5,6-carbonate (1.13 g) and ammonium tetraborate tetrahydrate, $[\alpha]_D$ −10.0° (*c*, 2 water). Yield, 570 mg. Calculated for $C_{14}H_{20}O_{14}NB.3H_2O$: C, 34.23%; H, 5.34%; N, 2.85%; mol. wt., 491 (unionized), 246 (ionized). Found: C, 34.39%; H, 5.35%; N, 2.75%; mol. wt., 239 in water (450 in ethanol).

D-*Threose – Ammonium Borate Complex*

To a solution of D-threose (1.8 ml containing about 1.0 g of the sugar) was added ammonium tetraborate tetrahydrate. Ethanol (6 ml) was added and the solution was stored at 3° C, affording crystalline material (0.52 g); $[\alpha]_D$ −49.5° (*c*, 2 water). Calculated for $C_8H_{16}O_8NB.\frac{1}{2}H_2O$: C, 35.05%; H, 6.25%; N, 5.11%. Found: C, 34.86%; H, 6.16%; N, 5.04%.

The D-threose starting material, prepared via lead tetraacetate oxidation of D-galactose, contains several percent of D-lyxose (22). Treatment of the isolated complex with Amberlite-IR 120 followed by paper chromatographic examination showed that all but a trace of the pentose component had been removed.

ACKNOWLEDGMENT

Nuclear magnetic resonance spectra were measured at the University of Saskatchewan, through the kind cooperation of Professor K. J. McCallum.

REFERENCES

1. J. Böeseken. Advan. Carbohydrate Chem. **4**, 189 (1949).
2. A. B. Foster. Advan. Carbohydrate Chem. **12**, 81 (1957).
3. S. J. Angyal and D. J. McHugh. J. Chem. Soc. 1423 (1957).
4. N. Vermaas. Rec. Trav. Chim. **51**, 67 (1932).
5. P. H. Hermans. Z. Anorg. Allgem. Chem. **142**, 83 (1925).
6. H. S. Isbell, J. F. Brewster, N. B. Holt, and H. L. Frush. J. Res. Natl. Bur. Std. **40**, 129 (1948).
7. A. P. Brady, H. Huff, and J. W. McBain. J. Phys. Colloid Chem. **55**, 304 (1951).
8. L. Kahlenberg and O. Schreiner. Z. Physik. Chem. (Leipzig), **20**, 547 (1896).
9. A. Kesans, S. Vimba, and E. Svarcs. Latvijas PSR Zinatnu Akad. Vestis, 127 (1955); Chem. Abstr. **50**, 14420f (1956).
10. M. Mazurek and A. S. Perlin. Biochem. Biophys. Res. Commun. **6**, 314 (1961).
11. M. Levy. J. Biol. Chem. **84**, 763 (1929).
12. L. M. Jackman. Applications of nuclear magnetic resonance spectroscopy in organic chemistry. Pergamon Press, London. 1959. p. 55.
13. R. W. Lenz and J. P. Heeschen. J. Polymer Sci. **51**, 247 (1961).
14. H. J. Bernstein, J. A. Pople, and W. G. Schneider. Can. J. Chem. **35**, 65 (1957).

Can. J. Chem. Downloaded from www.nrcresearchpress.com by 210.87.254.40 on 09/05/12
For personal use only.

15. R. J. ABRAHAM, K. A. MCLAUCHLAN, L. D. HALL, and L. HOUGH. Chem. Ind. (London), 213 (1962).
16. R. U. LEMIEUX, J. D. STEVENS, and R. R. FRASER. Can. J. Chem. **40**, 1955 (1962).
17. M. KARPLUS. J. Chem. Phys. **30**, 11 (1959).
18. L. P. KUHN. J. Am. Chem. Soc. **76**, 4323 (1954).
19. S. J. ANGYAL and R. J. YOUNG. J. Am. Chem. Soc. **81**, 5467 (1960).
20. F. A. L. ANET. Can. J. Chem. **39**, 2262 (1961).
21. A. S. PERLIN. Unpublished preparation.
22. A. S. PERLIN and C. BRICE. Can. J. Chem. **34**, 541 (1956).

Can. J. Chem. Downloaded from www.nrcresearchpress.com by 210.87.254.40 on 09/05/12
For personal use only.

FREE RADICALS BY MASS SPECTROMETRY

XXXI. H-ATOM AND D-ATOM REMOVAL IN THE MERCURY-PHOTOSENSITIZED DECOMPOSITION OF ISOBUTANE AND DEUTEROISOBUTANES[1]

T. F. PALMER[2] AND F. P. LOSSING
Division of Pure Chemistry, National Research Council, Ottawa, Canada
Received May 2, 1963

ABSTRACT

In the reaction of isobutane with Hg^3P_1 atoms, cleavage of the tertiary C—H bond is about seven times as frequent as cleavage of a primary C—H bond. This ratio is greatly changed by deuterium substitution in the tertiary position. Cleavage of the tertiary C—D bond in $(CH_3)_3CD$ occurs only about 0.6 times as frequently as cleavage of a primary C—H bond. In $(CD_3)_3CH$, no cleavage of a primary C—D bond could be detected, and only the tertiary H-atom is removed.

INTRODUCTION

The reaction of Hg^3P_1 atoms with isobutane has been the subject of a number of investigations, both as to the quenching cross section (1, 2) and the nature of the primary dissociation step (3, 4). This work, and its relation to the general question of the mercury-photosensitized reactions of other paraffins has recently been reviewed (5) and will not be discussed here in any detail. As for other paraffins, the primary dissociation in isobutane appears to involve only C—H bonds, but it is not clear whether the H-atom removed in this reaction is uniquely the tertiary H-atom, or whether removal of a primary H-atom occurs concurrently. Recent work on the quenching cross sections of deuterated propanes shows that the primary interactions of Hg^3P_1 with propane occurs mainly at the secondary C—H bonds (2), but the actual bond cleavage may occur at either position in a ratio not far from unity (6, 7). Taking account of the number of primary and secondary hydrogens available, it appears that secondary bond rupture is favored by a significant factor. In the present work an attempt has been made to determine the relative frequencies of bond rupture in isobutane, which contains only primary and tertiary C—H bonds.

In the course of this work, some experiments were carried out on deuteroisobutane. In agreement with recent findings of other workers (6, 7) substitution of D for H is found to have a large effect on the frequency of bond rupture.

EXPERIMENTAL

The Hg^3P_1-photosensitized reactions were carried out in a flow system coupled to a mass spectrometer, using the techniques previously described (8, 9). Although butyl radicals could be detected in the reaction when low-energy ionizing electrons were used, no identification of these as *t*-butyl or isobutyl could be made. Analysis of the ratio of *t*-butyl radicals to isobutyl radicals by means of the relative amounts of the three possible dimerization products proved not to be feasible. Owing to the small amount of radicals formed initially and to an appreciable loss of these by secondary reactions with excited mercury atoms or, more probably, with H-atoms (6), the quantity of octanes was extremely small. The mass spectra of the three possible octanes, moreover, in the region free from interference by isobutane (i.e. above mass 58) consists of peaks of low intensity. Above mass 57, for example, the spectra of 2,2,4-trimethylpentane and 2,2,3,3-tetramethylbutane have no peaks with intensities greater than 6% of the base (most intense) peak. The solution to this analytical problem therefore rested on the "trapping" of the butyl radicals with an excess of CD_3 radicals produced from the Hg-photosensitized decomposition of $Hg(CD_3)_2$ added to the reaction

[1]*Issued as N.R.C. No. 7488.*
[2]*National Research Council Postdoctoral Fellow, 1960–1962. Present address: U.K. Atomic Energy Authority, Harwell, England.*

Can. J. Chem. Downloaded from www.nrcresearchpress.com by 210.87.254.105 on 09/05/12
For personal use only.

stream (9). With such an excess, the reactions of the butyl radicals were reduced to the four combination and disproportionation reactions

$$(CH_3)_3C + CD_3 \xrightarrow{k_1} (CH_3)_3CCD_3 \quad [1]$$

$$\xrightarrow{k_2} CD_3H + \text{isobutene} \quad [2]$$

$$(CH_3)_2CHCH_2 + CD_3 \xrightarrow{k_3} (CH_3)_2CHCH_2CD_3 \quad [3]$$

$$\xrightarrow{k_4} CD_3H + \text{isobutene}. \quad [4]$$

Assuming all other reactions of butyl radicals to be swamped by these reactions, the quantities of *t*-butyl and isobutyl radicals can be estimated from the yields of neopentane-d_3 and isopentane-d_3, and the disproportionation to combination ratios k_2/k_1 and k_4/k_3. The analysis of the pentanes was carried out using the mass-60 peak ($(CH_3)_2{}^+CCD_3$) for neopentane-d_3 and the mass-75 peak (parent ion) for isopentane-d_3. The mass spectral sensitivity coefficient for neopentane-d_3 was measured using a sample of the pure compound. No standard sample of isopentane-d_3 was available, so the sensitivity coefficient was taken to be the same as that of undeuterated isopentane. Since the comparison involves only parent ions, this assumption introduces little error.

Samples of the deuterated species, isobutane-d_1, isobutane-d_9, neopentane-d_3, and $Hg(CD_3)_2$ were obtained from Merck and Co., Montreal. A sample of neopentane-d_9 was prepared by the Grignard reaction from $(CD_3)_3Cl$ (97%, Merck and Company), followed by purification by VPC on a squalane–celite column at 45° C. The neopentane-d_9 was found to have an isotopic purity of 96%.

The sample of isobutane-d_9 contained about 5% of isobutene-d_8. This was removed by passing it through the squalane column at room temperature.

RESULTS AND DISCUSSION

The results obtained by the addition of increasing amounts of $Hg(CD_3)_2$ to the reaction stream carrying a partial pressure of 7 μ of isobutane are shown in Fig. 1. The yield of

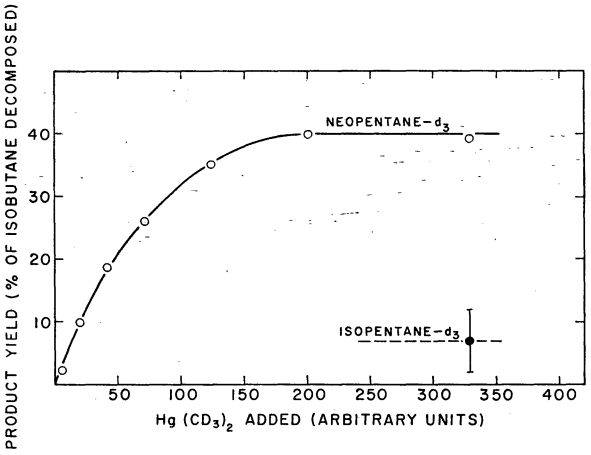

FIG. 1. Limiting yields of neopentane and isopentane formed by adding an excess of CD_3 radicals to the reaction stream containing Hg^3P_1 atoms and $(CH_3)_3CH$.

neopentane-d_3 (per isobutane decomposed) increased rapidly with added $Hg(CD_3)_2$ and levelled off at about 40%. The limiting yield of isopentane-d_3 was extremely small, amounting to about 7% with an estimated accuracy of ±5%. This yield is shown as a single point in Fig. 1 at the highest pressure of $Hg(CD_3)_2$. With lower amounts of $Hg(CD_3)_2$ the mass-75 peak was barely detectable. Taking $k_2/k_1 = 0.9$ (10, 11), the maximum yield of neopentane-d_3, 40%, corresponds to a 76% yield of *t*-butyl radicals. The disproportionation-to-combination ratio k_4/k_3 is not known, but by comparison with the

Can. J. Chem. Downloaded from www.nrcresearchpress.com by 210.87.254.105 on 09/05/12
For personal use only.

ratios for $CH_3 + n\text{-}C_4H_7$ and $CH_3 + t\text{-}C_4H_7$, a value of 0.5 seems reasonable. Taking $k_4/k_3 = 0.5$, the yield of isopentane-d_3 ($7\pm5\%$) corresponds to a yield of 11% for isobutyl radicals, with a rather large uncertainty. These values give an overall yield of $87\pm10\%$. On the assumption that the missing $13\pm10\%$ is distributed proportionately between *t*-butyl and isobutyl radicals, these results show that in the primary dissociation tertiary C—H bond cleavage accounts for about 87% of the total reaction, and is therefore about seven times as frequent as cleavage of a primary C—H bond. Owing to the uncertainties in the isopentane-d_3 yield and in the ratio k_4/k_3, the ratio of tertiary/primary cleavage could be as low as 4 or as high as 10.

Deuteroisobutanes

A possibility not considered in the foregoing discussion is that of an isomerization of isobutyl radicals to *t*-butyl radicals. This point was investigated using isobutane-d_1, $(CH_3)_3CD$. If an isobutyl radical formed from this species isomerizes to *t*-butyl and combines with CD_3, the neopentane formed would be -d_4. No neopentane-d_4 was detected in this experiment, and the possibility of a significant amount of isomerization in this system at 55° C can be ruled out.

The introduction of a D-atom in the tertiary position, however, caused a large change in the ratio of initial bond rupture, as can be seen from Fig. 2. The major combination

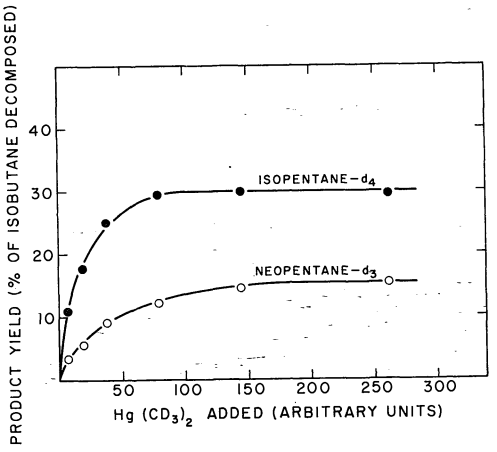

FIG. 2. Limiting yields of neopentane and isopentane formed by adding an excess of CD_3 radicals to the reaction stream containing Hg^3P_1 atoms and $(CH_3)_3CD$.

product on the addition of CD_3 is isopentane, rather than neopentane as in Fig. 1. For $(CH_3)_3CD$, the two dissociation reactions are

$$(CH_3)_3CD + Hg^* \rightarrow (CH_3)_3C + D + Hg \quad [5]$$

$$\rightarrow (CH_3)_2CDCH_2 + H + Hg. \quad [6]$$

Addition of CD_3 radicals to the stream gives the combination and disproportionation reactions [1] and [2] for *t*-butyl as before, and reactions [7] and [8] for isobutyl

$$(CH_3)_2CDCH_2 + CD_3 \xrightarrow{k_7} (CH_3)_2CDCH_2CD_3 \quad [7]$$

$$\xrightarrow{k_8} CD_4 + \text{isobutene}. \quad [8]$$

Taking $k_2/k_1 = 0.9$, the limiting yield of 15% of neopentane-d_3 corresponds to a yield of

Can. J. Chem. Downloaded from www.nrcresearchpress.com by 210.87.254.105 on 09/05/12
For personal use only.

29% for *t*-butyl radical formation. Assuming $k_8/k_7 = k_4/k_3 \approx 0.5$, the limiting yield of isopentane (30%) corresponds to a yield of 45% for isobutyl radicals. The total yield in this case is about 74%. The ratio of tertiary to primary bond rupture for $(CH_3)_3CD$ is therefore about 0.6, as compared to about 7 for $(CH_3)_3CH$.

With such a large factor favoring C—H bond cleavage over C—D bond cleavage, one might expect that the decomposition of isobutane-d_9 $(CD_3)_3CH$ would be almost entirely by a tertiary C—H rupture. Figure 3 shows the yield of neopentane-d_9 obtained by

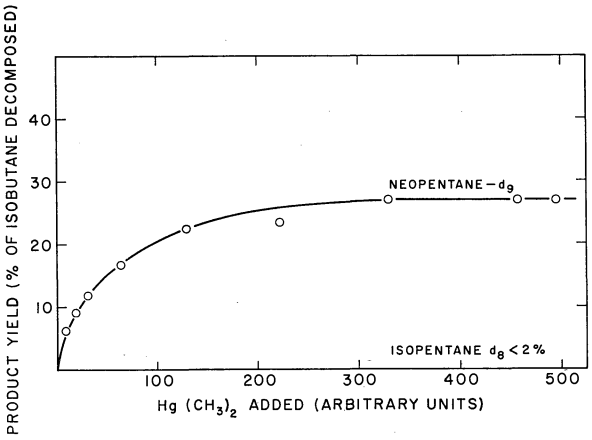

FIG. 3. Limiting yields of neopentane and isopentane formed by adding an excess of CH_3 radicals to the reaction stream containing Hg^3P_1 atoms and $(CD_3)_3CH$.

reacting $(CD_3)_3CH$ with Hg* in the presence of increasing amounts of $Hg(CH_3)_2$. Any isopentane-d_8 that may have been formed was below the limit of detection, i.e., less than 2%. The yield of neopentane-d_9 rose with increasing $Hg(CH_3)_2$, and levelled off at 27%. This is much less than the limiting yield of neopentane-d_3 from $(CH_3)_3CH$ (Fig. 1), even though no evidence for isobutyl radical formation could be found. Unless the total yield in this case is much lower for some unknown reason, it would appear that the disproportionation-to-combination ratio for $CH_3 + (CD_3)_3C$ must be much greater than for $CD_3 + (CH_3)_3C$. Owing to this uncertainty, a reliable upper limit for the yield of isobutyl radicals from $(CD_3)_3CH$ cannot be obtained from these results. However, since the isopentane yield was less than 2% it can be estimated that the ratio of tertiary to primary cleavage is probably greater than 20.

The large effect of deuterium substitution on the frequency of bond rupture in isobutane is similar to that reported recently for propane (6, 7). The ratios of secondary to primary bond cleavage in $(CH_3)_2CH_2$ and $(CH_3)_2CD_2$ were 1.2 and 0.2 (6) (1.38 and 0.3 (7)). In the present work the ratios for tertiary to primary bond cleavage in $(CH_3)_3CH$ and $(CH_3)_3CD$, 7 and 0.6, exhibit a change which is about the same or possibly a little larger. The overall effect on the secondary C—H bond in propane has been defined by Gunning *et al.* (7) as

$$[k_i(\mathrm{H})/k_i(\mathrm{D})] = [\sigma_Q^2(\mathrm{H})/\sigma_Q^2(\mathrm{D})] \times [\%(i\text{-pr})_H/\%(i\text{-pr})_D].$$

For $(CH_3)_2CH_2$ and $(CH_3)_2CD_2$, the secondary bond effect was found to be 18. Defining a tertiary bond effect in the same way

$$[k_t(\mathrm{H})/k_t(\mathrm{D})] = [\sigma_Q^2(\mathrm{H})/\sigma_Q^2(\mathrm{D})] \times [\%(t\text{-bu})_H/\%(t\text{-bu})_D]$$

Can. J. Chem. Downloaded from www.nrcresearchpress.com by 210.87.254.105 on 09/05/12
For personal use only.

and using the quenching cross sections measured by Gunning *et al.* (7), the ratios for t-C—H and t-C—D bond rupture found in this work give $k_t(H)/k_t(D)$ for isobutane to be $[4.8/0.44]\times[87/39] = 24$.

REFERENCES

1. B. DE B. DARWENT. J. Chem. Phys. **18**, 1532 (1950).
2. Y. ROUSSEAU and H. E. GUNNING. Can. J. Chem. **41**, 465 (1963).
3. B. DE B. DARWENT. J. Phys. Chem. **49**, 150 (1945).
4. S. BYWATER and E. W. R. STEACIE. J. Chem. Phys. **19**, 172 (1951).
5. R. J. CVETANOVIĆ. Mercury photosensitized reactions. *In* Progress in reaction kinetics. Vol. 2. *Edited by* G. Porter. Pergamon, London. 1963.
6. P. KEBARLE and M. AVRAHAMI. Can. J. Chem. **41**, 335, 347 (1963).
7. Y. ROUSSEAU, G. N. C. WOODALL, and H. E. GUNNING. J. Chem. Phys. **37**, 2722 (1962).
8. F. P. LOSSING, D. G. H. MARSDEN, and J. B. FARMER. Can. J. Chem. **34**, 701 (1956).
9. J. COLLIN and F. P. LOSSING. Can. J. Chem. **35**, 778 (1957).
10. G. R. MACMILLAN. J. Am. Chem. Soc. **82**, 2422 (1960).
11. A. R. BLAKE, J. F. HENDERSON, and K. O. KUTSCHKE. Can. J. Chem. **39**, 1920 (1961).

Can. J. Chem. Downloaded from www.nrcresearchpress.com by 210.87.254.105 on 09/05/12
For personal use only.

REPLACEMENT REACTIONS IN THE QUINIC ACID SERIES[1,2]

P. A. J. GORIN

National Research Council of Canada, Prairie Regional Laboratory, Saskatoon, Saskatchewan

Received March 8, 1963

ABSTRACT

The action on D-quinic acid of hot 95% acetic acid containing mineral acid gave, after complete acetylation, 1,4,5-tri-*O*-acetyl-epi-quinide consisting of approximately equal portions of the (−)- and (±)-isomers, and tetra-*O*-acetyl-scyllo-quinic acid. The stereochemistry of the products and their derived free polyols were determined by nuclear magnetic resonance (n.m.r.) spectroscopy and synthesis.

Elimination of the tosyloxy group in 5-tosyl-epi-quinicol was shown to take place readily in aqueous acetic acid with participation of the primary carbinol group to give an anhydro quinicol derivative and epi-quinicol.

Can. J. Chem. Downloaded from www.nrcresearchpress.com by 210.87.254.40 on 09/05/12
For personal use only.

It has been shown (1) that certain inositols can be converted to partly acetylated stereoisomers by refluxing with 95% acetic acid – mineral acid. Inversion takes place most readily when one hydroxyl group in a six-membered ring has an adjacent *cis*-hydroxyl on one side and a *trans*-hydroxyl on the other. Such an arrangement is common in the more readily available inositols, *O*-methylinositols, quercitols, and cyclohexanetetrols. Reactions involving these materials have been evaluated, both from a preparative point of view and as a means of calculating non-bonded interaction energies in six-membered rings (2).

D-Quinic acid, by virtue of the orientation of its hydroxyl groups, should also undergo modification to yield partly acetylated derivatives of its optically active stereoisomer. Accordingly, quinic acid was treated for several days in refluxing 95% acetic acid containing 1.5% sulphuric acid. Gas phase chromatographic examination of the product after complete acetylation followed by treatment with diazomethane indicated that at least five materials were present. The reaction when followed by this method showed that equilibrium was not reached in 93 hours at which time carbonization in the medium was considerable. Because of this consideration and the complexity of the mixture the system does not lend itself to the calculation of non-bonded interaction energies, but only to the preparation of new isomeric quinic acid derivatives.

The reaction product obtained after 100 hours was acetylated with acetic anhydride to give a mixture containing 45% lactone and 55% free acid. Two chemically distinguishable compounds were isolated by fractional crystallization. One of these, obtained in 5% yield, was an optically inactive stereoisomer of tetra-*O*-acetyl-D-quinic acid, indicating that the reaction was not as stereospecific as with hexasubstituted cyclitols. The other product was isolated in 17% yield and shown to be an optically active γ-lactone triacetate with an empirical formula of $C_{13}H_{16}O_8$ (I). On fractional crystallization this product ($[\alpha]_D$ −61°) gave two materials, chemically the same, as indicated by their identical n.m.r. spectra, but having different specific rotations (−119° and 0°). The rotation of the optically active substance differed markedly from the D-quinic acid analogue (3) and although there are several structures possible for the active lactone only one (I) arising by inversion of the substituent at C-4 is possible. All other active lactones would be racemized in the equilibrium mixture on re-formation from the corresponding acid.

[1]*Issued as N.R.C. No. 7501.*

[2]*This work was carried out in part in the Department of Organic Chemistry, University of New South Wales, Sydney, Australia.*

Fletcher and Hedgeley (4) have shown that an acetate group bounded by *cis*- and *trans*-acetoxy neighbors in inositols can be inverted, with concomitant deacetylation, by the action of liquid hydrogen fluoride. In the present investigation this reagent, however, did not yield the lactone triacetate (I) readily from quinic acid. Starting with tetra-*O*-acetyl-D-quinic acid, a mixture of γ-lactones was obtained. Acetylation of this with acetic anhydride in pyridine yielded the highly crystalline optically active lactone triacetate, but only in 1% yield.

The lactone triacetate (I) prepared by the 95% acetic acid – sulphuric acid method could be reduced to a polyol using sodium borohydride. This polyol (IV) could be prepared definitively by treating the polyol pentaacetate (5) (III), derived from D-quinic acid, with liquid hydrogen fluoride. Chromatography yielded the required material which was characterized as its di-*O*-isopropylidene derivative. A similar type of reaction could be effected by treating the polyol with the 95% acetic acid reagent. However, the yield of desired product was poor probably due to simultaneous oxidation.

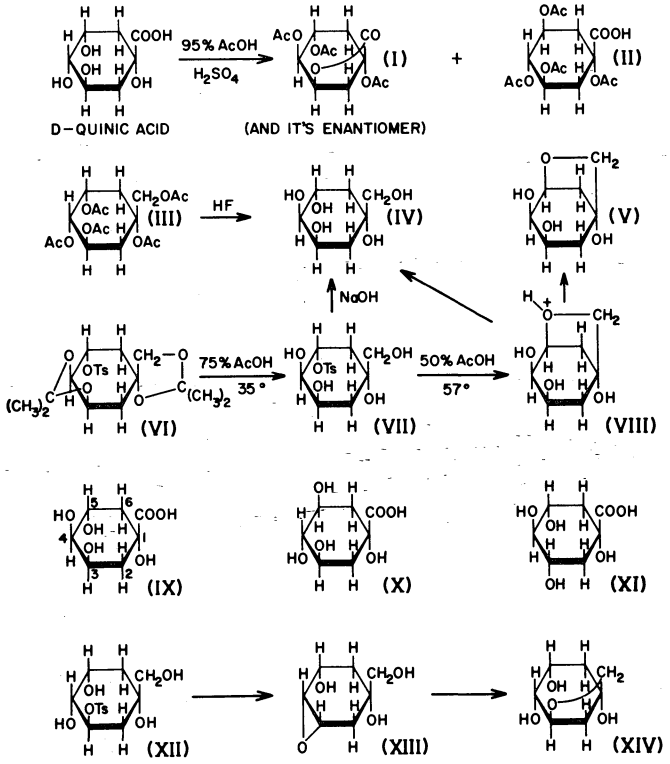

It should be noted that stereoisomers of quinic acid have not been previously obtained and named. Maquenne's nomenclature systems for cyclitols (6) is available and this can be modified in order to cover systematically the quinic acids and their derived alcohols. On the other hand, it is proposed that the three new quinic acids, described presently, be called epi-(−)-quinic acid (XI), epi-(±)-quinic acid, and scyllo-quinic acid (X). Although there are many types of compounds having somewhat similar names, it should not be confusing to call the corresponding alcohols epi-quinicol and scyllo-quinicol, respectively. The acids are numbered in the same way as in quinic acid (as depicted in IX) and the derived alcohols too, except that the hydroxymethyl carbon atom is called C-2′.

Can. J. Chem. Downloaded from www.nrcresearchpress.com by 210.87.254.40 on 09/05/12
For personal use only.

Can. J. Chem. Downloaded from www.nrcresearchpress.com by 210.87.254.40 on 09/05/12
For personal use only.

As mentioned previously one crystalline product obtained from quinic acid was an optically inactive isomer of tetra-*O*-acetyl-D-quinic acid which is believed to be tetra-*O*-acetyl-scyllo-quinic acid (II). This material, on examination by n.m.r. spectroscopy, gave two acetoxy proton signals, the greater at 2.06 p.p.m. and the other, one third in magnitude, at 2.22 p.p.m. Tetra-*O*-acetyl-D-quinic acid gave three signals at 2.07, 2.11, and 2.18 p.p.m. in the ratio of 2:1:1, respectively. The signal at 2.07 p.p.m. clearly corresponds to the equatorial acetoxy protons at C-4 and C-5 (7). It seems likely that the signal at 2.11 p.p.m. is from the C-3 acetoxy protons and the one at 2.18 p.p.m. arises from the C-1 acetoxy protons.* By analogy the signals in tetra-*O*-acetyl-scyllo-quinic acid would correspond to equatorial acetoxy protons at C-3, C-4, and C-5 (2.06 p.p.m.) and C-1 acetoxy protons (2.22 p.p.m.). Lithium aluminum hydride reduction of tetra-*O*-acetyl-scyllo-quinic acid methyl ester gave scyllo-quinicol and this was readily converted to its 2′,3,4,5-tetraacetate, the tertiary hydroxyl group remaining unacetylated. The n.m.r. spectrum of this material was in accord with that assigned to its acidic precursor since signals at 2.05 p.p.m. and 2.11 p.p.m. were obtained in the ratio 3:1. These should correspond to the protons of the equatorial 3-, 4-, and 5-acetoxyls and those of the primary acetoxyl respectively.

Synthesis of scyllo-quinicol was possible by two methods. It was isolated, in 3% yield, from the sodium borohydride reduction of crude quinide, that is, material obtained by lactonizing D-quinic acid at 210° C. These lactonizing conditions are milder than those of Hesse (8), who used 220–250° C and produced 'inactive quinide', as it was named by later workers. Evidently isomerization of the quinic acid or its derived lactone took place under these conditions and it would not be surprising if further examination of the crude mixture showed that other materials in the quinic series were present.

Attempts to improve the low yield were made by hydrogenolyzing D-quinicol at 165° C with copper chromite. This procedure, which can cause isomerization (9, 10) to yield all-*trans* methyl β-glucopyranoside starting from isomeric methyl β-hexopyranosides (11), gave scyllo-quinicol in only 2% yield. Increasing the temperature to 180° C gave mainly tetrols instead of quinicols and from the mixture one unidentified tetrol was isolated in a crystalline state.

Since a more definitive synthesis of scyllo-quinicol was required an alternative route was attempted. Reduction of crude 1,4,5-tri-*O*-acetyl-epi-quinide ($[\alpha]_D$ −61°) with sodium borohydride yielded epi-quinicol (IV), which was converted to its di-*O*-isopropylidene derivative with acetone – sulphuric acid. Tosylation gave 5-tosyl-2′,1:3,4-di-*O*-isopropylidene-epi-quinicol (VI) which proved to be racemic, and could be hydrolyzed to 5-tosyl-epi-quinicol (VII) with 75% acetic acid at 35° C. However, treatment of this substance with hot aqueous alkali gave mainly epi-quinicol (IV) and only a trace of material corresponding with scyllo-quinicol on a paper chromatogram.

The above n.m.r. and synthetic data therefore suggest that scyllo-quinic acid has either structure X or XI, with a preference for the former. Although the action of 95% acetic acid – mineral acid on D-quinic acid does not bring about equilibrium, the kinetic data obtained shows that, on extrapolation, it is unlikely that partly acetylated D-quinic acid or its racemate would ever predominate over the scyllo isomer. The formation of XI rather than X in such proportions would therefore not be likely in view of the higher free energy of the former.

At 57° C in 50% acetic acid further reaction of 5-tosyl-epi-quinicol took place, the

**Examination of tetra-O-acetyl-epi-quinic acid gave one signal only at 2.17 p.p.m., presumably due to time averaging.*

tosyloxy group being eliminated by rearward attack of the C-2′-hydroxymethyl group to yield a 2′,5-anhydro quinicol (V). From this a monoisopropylidene derivative and a triacetate could be prepared. The remainder of the product consisted of epi-quinicol (IV). This reaction appears to involve an oxonium ion intermediate (VIII) which can decompose via two separate routes. The participation of a hydroxyl group is rare, one of the very few unequivocal examples being the ring closure of tetramethylene chlorhydrin to yield tetrahydrofuran in water at 70° C (12).

The participation of the primary hydroxyl group of compounds in this series in alkaline elimination reactions can also be demonstrated. Treatment of 3-tosyl-D-quinicol (XII) with sodium methoxide and following of the reaction chromatographically showed the presence of an intermediate 1,2-epoxide (XIII) which rearranged to give 2′,3-anhydro-D-quinicol (XIV), a more rapid conversion occurring when aqueous alkali was used. These reactions bear a resemblance to the conversion of 4,1′6′-tri-*O*-tosylsucrose pentaacetate to 3,6-anhydro-α-D-galactopyranosyl-1,4:3,6-dianhydro-β-D-fructose using sodium ethoxide (13). In this case, an epoxide migration took place prior to formation of the 3,6-anhydro ring in the pyranose moiety.

EXPERIMENTAL

Solutions were evaporated under reduced pressure and specific rotations measured at 25° C.

Reaction of D-Quinic Acid with 95% Acetic Acid – Sulphuric Acid

A 1% solution of quinic acid in 95% acetic acid containing sulphuric acid (1.5% by volume) was refluxed. At appropriate intervals aliquots were withdrawn and added to excess pyridine – acetic anhydride (1:1). After a day at 40° C the solutions were added to excess dilute sulphuric acid and left until destruction of acetic anhydride was complete. Extraction with chloroform followed by evaporation yielded the acetate mixtures, which were treated in methanol with ethereal diazomethane. Gas chromatographic examination was carried out at 210° C on a 4-ft column of 2% LAC-IR-296 on Chromosorb W 80/100 mesh (14) using helium as carrier gas. The results (in %) are listed below:

Emergence order of acetates	Time (hr)					
	1	2.25	10.25	30	60	93
1 (Unknown)			2	4	8	14
2 (Tetra-*O*-acetyl-scyllo-quinic acid methyl ester)	6	10	17	31	32	25
3 (1,4,5-Tri-*O*-acetyl-D-quinide and tetra-*O*-acetyl-epi-quinic acid methyl ester)	16	25	34	20	16	16
4 (Tetra-*O*-acetyl-D-quinic acid methyl ester)	68	50	23	19	16	15
5 (1,4,5-Tri-*O*-acetyl-epi-quinide)	12	16	22	25	28	29

Preparation of Isomeric Quinic Acid Derivatives

In a typical run, D-quinic acid (10 g) was refluxed in 95% acetic acid (500 ml) containing sulphuric acid (7.5 ml) for 100 hours. After the mixture was cooled, acetic anhydride (500 ml) was added, the temperature not being allowed to rise above 50° C, and after 18 hours the acetylation mixture was added to excess ice water. The mixture was extracted twice with chloroform, washed once with water, dried ($MgSO_4$), filtered, and evaporated to a syrup which crystallized.

Crystallization was completed by addition of a little ether to yield a substance which was recrystallized twice from ethyl acetate – ether. It (2.72 g) had m.p. 176–178° C and $[\alpha]_D$ −61° (*c*, 2,2, $CHCl_3$). In the infrared there were two absorption bands at 1750 cm^{-1} corresponding to acetate carbonyls and a single peak at 1795 cm^{-1} due to a γ-lactone carbonyl of a quinic acid isomer (1,4,5-tri-*O*-acetyl-epi-quinide (I)). Calculated for $C_{13}H_{16}O_8$: C, 52.0%; H, 5.3%. Found: C, 51.65%; H, 5.0%.

Fractional crystallizations from chloroform – ethyl acetate yielded the (−)-isomer with m.p. 209–210° C and $[\alpha]_D$ −119° (*c*, 1.0, $CHCl_3$). The mother liquors contained the racemic isomer with m.p. 182–183° C. The n.m.r. spectra of these substances were identical.

After removal of the above lactone derivatives the mother liquors yielded more crystals from ether. Two further recrystallizations from ether yielded optically inactive tetra-*O*-acetyl-scyllo-quinic acid (II)

Can. J. Chem. Downloaded from www.nrcresearchpress.com by 210.87.254.40 on 09/05/12
For personal use only.

(0.92 g) with m.p. 198–200° C. It absorbed in the infrared at 1750 cm^{-1} (acetate carbonyl) and 1720 cm^{-1} (carboxyl carbonyl). Nuclear magnetic resonance spectroscopy in chloroform showed two proton signals, one at 2.22 p.p.m. corresponding to one acetate and the other at 2.06 p.p.m. to three acetate groups. Calculated for $C_{15}H_{20}O_{10}$: C, 50.0%; H, 5.6%. Found: C, 50.0%; H, 5.6%. Authentic tetra-*O*-acetyl-D-quinic acid gave three signals at 2.07, 2.11, and 2.18 p.p.m. in the ratio 2:1:1 respectively.

The crude mixture obtained above from D-quinic acid was fractionated on a silicic acid column. Lactones were eluted with chloroform and free acids with acetone. By a gravimetric estimation the mixture consisted of 45% lactone triacetates and 55% acid tetraacetates.

1,4,5-Tri-O-acetyl-epi-(−)-quinide (I) from Tetra-O-acetyl-D-quinic Acid using Hydrogen Fluoride

Liquid hydrogen fluoride (20 ml) was added to an ice-cooled polythene vessel containing tetra-*O*-acetyl-D-quinic acid (7.5 g). After the mixture had been left at 25° C overnight it was added to pyridine (100 ml) containing acetic anhydride (50 ml) and kept at 50° C for 6 hours. The acetylated products were isolated by addition to ice-cold 5% sulphuric acid (2 liters) and extraction with chloroform. The acetates, consisting entirely of γ-lactones with infrared absorption at 1800 cm^{-1}, were dissolved in ether (50 ml) and kept in the refrigerator for a week. The crystals which formed were recrystallized from ethyl acetate. The triacetyl-epi-quinide (80 mg) had m.p. and mixed m.p. 208° C and $[\alpha]_D$ −112° (*c*, 1.0, $CHCl_3$). Calculated for $C_{13}H_{16}O_8$: C, 52.0%; H, 5.3%. Found: C, 52.1%; H, 5.3%.

epi-(−)-Quinicol (IV) from Penta-O-acetyl-D-quinicol (III) using Hydrogen Fluoride

By a procedure similar to that described above, penta-*O*-acetyl-D-quinicol (2.00 g) was converted with hydrogen fluoride to a mixture of isomeric quinicol acetates (1.80 g). These were deacetylated in 0.1 *N* sodium methoxide (25 ml) and the resulting mixture of polyols was partially resolved by cellulose column chromatography using *n*-butanol one quarter saturated with water as solvent. The first compound eluted was epi-(−)-quinicol (211 mg) with $[\alpha]_D$ −3° (*c*, 4.1, MeOH). It was characterized by refluxing a 100-mg sample in acetone (15 ml) containing sulphuric acid (0.1 ml) for 3 hours. After neutralization (Na_2CO_3), filtration, and evaporation 2′,1:3,4-di-*O*-isopropylidene-epi-(−)-quinicol was obtained and recrystallized twice from hexane. It (37 mg) had m.p. and mixed m.p. 119–120° C and was identical with authentic material obtained from 1,4,5-tri-*O*-acetyl-epi-(−)-quinide by the method described later in this section. Calculated for $C_{13}H_{22}O_5$: C, 60.4%; H, 8.6%. Found: C, 60.3%; H, 8.5%.

scyllo-Quinicol and Derivatives from Tetra-O-acetyl-scyllo-quinic Acid (II)

Tetra-*O*-acetyl-scyllo-quinic acid was treated in methanol with an excess of ethereal diazomethane. On evaporation the methyl ester crystallized and after two recrystallizations from methanol had m.p. 145–148° C. Calculated for $C_{16}H_{22}O_{10}$: C, 51.3%; H, 5.9%. Found: C, 51.2%; H, 5.9%.

Crude methyl ester obtained from the free acid (1.3 g) was added in ether (25 ml) to refluxing ether (50 mg) which contained lithium aluminum hydride (1.5 g). After 1 hour ethyl acetate was added, followed by acetic acid, and the solution evaporated to dryness. Aqueous sodium hydroxide was added and the mixture heated at 100° C for 1 hour and the resulting suspension was treated with mixed-bed resin and filtered. Evaporation yielded a syrup (0.72 g), from which scyllo-quinicol could be isolated by crystallization. Two recrystallizations from methanol–ethanol gave 176 mg with m.p. 184–186° C. Calculated for $C_7H_{14}O_5$: C, 47.2%; H, 7.9%. Found: C, 47.0%; H, 7.8%.

The polyol (50 mg) was added to acetic anhydride – pyridine (1 ml:1 ml) which was heated at 100° C for 1 hour and the solvent then evaporated. Two recrystallizations from ether–hexane gave 2′,3,4,5-tetra-*O*-acetyl-scyllo-quinicol with m.p. 113–114° C. Calculated for $C_{15}H_{22}O_9$: C, 52.2%; H, 6.4%. Found: C, 52.0%; H, 6.3%. Examination of the acetate protons by n.m.r. spectroscopy in chloroform showed three protons at 2.11 p.p.m. and nine protons at 2.05 p.p.m.

Isolation of scyllo-Quinicol by Reduction of Crude D-Quinide

In a separate experiment quinic acid (10 g) was converted to a mixture containing mainly D-quinicol by the method used for the preparation of 3-tosyl-D-quinicol which is described later. Fractionation of the polyols on a cellulose column using *n*-butanol one quarter saturated with water as solvent gave D-quinicol (4.22 g) and scyllo-quinicol (0.31 g). The latter was recrystallized twice from ethanol to give a product with m.p. and mixed m.p. 185–186° C. Calculated for $C_7H_{14}O_5$: C, 47.2%; H, 7.9%. Found: C, 47.6%; H, 7.9%.

scyllo-Quinicol Formed by Hydrogenolysis of D-Quinicol

D-Quinicol (0.95 g) was dissolved in dioxane (50 ml) containing copper chromite (0.47 g) and hydrogenated for 6 hours at 165° C under 1000 p.s.i. of hydrogen. After filtration and evaporation a portion of the product was fractionated on a cellulose column as above to yield D-quinicol (437 mg) and scyllo-quinicol (45 mg). Two crystallizations of the latter from ethanol gave material with m.p. and mixed m.p. 184–185° C. Calculated for $C_7H_{14}O_5$: C, 47.2%; H, 7.9%. Found: C, 47.2%; H, 7.95%.

Repetition of the hydrogenolysis at 180° C with 2.0 g of D-quinicol gave a complex mixture, consisting mainly of tetrols. Only one of these was isolated crystalline by cellulose chromatography using benzene–ethanol–water (200:50:1) as solvent. Two recrystallizations from ethanol gave 55 mg of material with m.p. 151–152° C. Calculated for $C_7H_{14}O_4$: C, 51.8%; H, 8.7%. Found: C, 52.0%; H, 8.7%. No further characterization studies were carried out.

Can. J. Chem. Downloaded from www.nrcresearchpress.com by 210.87.254.40 on 09/05/12
For personal use only.

epi-Quinicol (IV) and its Di-O-isopropylidene Derivative from 1,4,5-Tri-O-acetyl-epi-quinide (I)

Crude 1,4,5-tri-*O*-acetyl-epi-quinide (8.0 g) consisting of a mixture of (−)- and (±)-isomers, was deacetylated by addition of 0.1 equivalent of 0.1 *N* sodium methoxide in methanol and the solution evaporated to dryness.

The de-esterified product was dissolved in methanol (100 ml) at 0° C, sodium borohydride (3.0 g) added and the solution left in the refrigerator overnight. The polyol was isolated by the procedure described previously for the preparation of D-quinicol.

The di-*O*-isopropylidene derivative was obtained by heating the polyol under reflux for 10 minutes in acetone (50 ml) containing sulphuric acid (0.5 ml). The solution was neutralized (Na_2CO_3) and then added to a chloroform–water mixture. After shaking the mixture, the chloroform layer was washed once with water and evaporated to a syrup. This crystallized and one crystallization from *n*-hexane yielded 2′,1:3,4-di-*O*-isopropylidene-epi-quinicol (3.0 g). A further crystallization gave material with m.p. 121–122° C and $[\alpha]_D$ 0° (*c*, 1.0, $CHCl_3$). Calculated for $C_{13}H_{22}O_5$: C, 60.4%; H, 8.6%. Found: C, 60.3%; H, 8.6%.

2′,1:3,4-Di-O-isopropylidene-5-tosyl-epi-(±)-quinicol (V)

The diacetone polyol (2.01 g) was treated overnight in pyridine (4 ml) containing tosyl chloride (2.0 g). After work-up of the product the tosylate was crystallized twice from ether and had m.p. 115–116° C and $[\alpha]_D$ 0° (*c*, 2.0, $CHCl_3$). Yield, 2.74 g. Calculated for $C_{20}H_{28}O_7S$: C, 58.6%; H, 7.1%. Found: C, 58.2%; H, 6.8%.

Alkaline Hydrolysis of 5-Tosyl-epi-quinicol (VII)

The tosyl derivative (0.10 g) was dissolved in 75% acetic acid (2 ml) and the solution kept at 35° C for 3 hours. Evaporation yielded a syrup which was dissolved in 0.1 *N* sodium hydroxide (10 ml) and then heated on a steam bath for 2 hours. Deionization of the solution and evaporation gave a product which contained mainly epi-quinicol and only a trace of a substance corresponding to scyllo-quinicol on a paper chromatogram (solvent: *n*-butanol–ethanol–water, 40:11:19; spray: ammoniacal silver nitrate (15)).

Elimination of Tosyloxy Group of 5-Tosyl-epi-quinicol in 50% Acetic Acid

The tosylate (2.7 g) was heated at 57° C in 50% acetic acid (250 ml) for 6 hours. Liberated toluenesulphonic acid was removed by addition of Dowex-1, and the solution evaporated to a syrup. A portion was acetylated and examined by gas phase chromatography using 1½% LAC-IR-296 on a celite column. Peaks corresponding to epi-quinicol (18%) and anhydro quinicol (87%) derivatives were detected. Fractionation on a cellulose column using *n*-butanol one half saturated with water as solvent gave the anhydro quinicol (1.09 g) and a little epi-quinicol (0.14 g; characterized as its di-*O*-isopropylidene derivative).

The anhydro fraction gave 520 mg of crystals (V) with an indeterminate melting point greater than 165° C after two crystallizations from ethanol and $[\alpha]_D$ 0° (*c*, 1.0, H_2O). Calculated for $C_7H_{12}O_4$: C, 52.5%; H, 7.55%. Found: C, 52.2%; H, 7.45%. It was converted to its triacetate by being heated in pyridine–acetic anhydride at 100° C for an hour. The product was crystallized twice from ether–hexane and had m.p. 151–153° C. Calculated for $C_{13}H_{18}O_7$: C, 54.5%; H, 6.3%. Found: C, 54.7%; H, 6.2%.

The anhydro compound (40 mg) was dissolved in acetone (20 ml) containing 2 drops of sulphuric acid and Drierite (5 g). After 3 hours the product was isolated after neutralization with sodium carbonate and extraction with chloroform from water. Crystallization from ether–hexane gave the isopropylidene compound with m.p. 98–99° C. Calculated for $C_{10}H_{16}O_4$: C, 60.0%; H, 8.05%. Found: C, 60.1%; H, 8.2%.

Starting from 1,4,5-tri-*O*-acetyl-epi-(−)-quinide the following derivatives were prepared and their specific rotations recorded: sodium epi-(−)-quinate, $[\alpha]_D$ −27° (*c*, 1.1, dil. NaOH); epi-(−)-quinic acid, $[\alpha]_D$ −18° (*c*, 1.0, H_2O); epi-(−)-quinicol, $[\alpha]_D$ −10° (*c*, 6.6, H_2O); 2′,1:3,4-di-*O*-isopropylidene-epi(−)-quinicol, $[\alpha]_D$ −9° (*c*, 10.0, $CHCl_3$), its 5-tosyl derivative, $[\alpha]_D$ −90° (*c*, 10.0, $CHCl_3$); and the derived anhydro compound, $[\alpha]_D$ −41° (*c*, 0.8, H_2O).

2′,1:4,5-Di-O-isopropylidene-3-tosyl-D-quinicol

The product obtained by heating D-quinic acid (10 g) at 210° C for 3 hours was dissolved in methanol (100 ml) which was made alkaline with sodium methoxide, and sodium borohydride (3.0 g) added. After 18 hours the solution was acidified with acetic acid and evaporated to dryness, the residue dissolved in water and treated with Amberlite-IR 120. Boric acid was removed by repeated evaporations in methanol. The product was refluxed for 10 hours in acetone (500 ml) containing sulphuric acid (2 ml). Excess sodium carbonate was added and when neutral the solution was evaporated to a solid which was partitioned between chloroform and water. The diisopropylidene polyol obtained by evaporation of the chloroform layer gave only gummy crystals and was therefore converted directly to its more crystalline tosyl derivative.

The syrup was dissolved in pyridine (20 ml) and tosyl chloride (5.0 g) added. After 18 hours the solution was cooled and excess reagent destroyed with a little water. Addition of excess water precipitated the tosylate, which was recrystallized from ethanol and had $[\alpha]_D$ −63° (*c*, 1.0, $CHCl_3$) and m.p. 149–152° C. Calculated for $C_{20}H_{28}O_7S$: C, 58.2%; H, 6.9%. Found: C, 58.3%; H, 6.8%.

3-Tosyl-D-quinicol (XII)

The di-*O*-isopropylidene tosyl quinicol (1.63 g) was hydrolyzed by being warmed for 6 hours at 60° C in 50% acetic acid (80 ml). The solution was evaporated and two recrystallizations of the residue from ethanol

Can. J. Chem. Downloaded from www.nrcresearchpress.com by 210.87.254.40 on 09/05/12
For personal use only.

gave 3-tosyl-D-quinicol (0.81 g) with m.p. 136–138° C and $[\alpha]_D$ −51° (*c*, 1.6, MeOH). Calculated for $C_{14}H_{20}O_7S$: C, 50.6%; H, 6.1%. Found: C, 50.9%, 50.9%; H, 6.1%, 6.2%.

2′,3-Anhydro-D-quinicol (XIV) from Alkaline Elimination of 3-Tosyl-D-quinicol

3-Tosyl-D-quinicol (200 mg) was dissolved in methanol (3 ml) containing sodium (16 mg). After 3 hours at 5° C all starting material had disappeared and two new spots appeared on a paper chromatogram. On leaving the mixture overnight at room temperature the slower moving material disappeared and the solution was evaporated and deionized with mixed-bed resin. Filtration and evaporation yielded crystals which were recrystallized twice from ether containing a trace of ethanol. The 2′,3-anhydro-D-quinicol had a vague melting point greater than 160° C and $[\alpha]_D$ −20° (*c*, 1.0, H_2O). Calculated for $C_7H_{12}O_4$: C, 52.5%; H, 7.55%. Found: C, 52.5%; H, 7.6%. The above reaction was observed to take place more readily with aqueous sodium hydroxide.

ACKNOWLEDGMENTS

The author would like to thank Professor S. J. Angyal for his interest in this work. Thanks are due to Mr. M. Mazurek for carbon and hydrogen estimations and Mr. W. C. Haid for carrying out n.m.r. spectroscopic determinations.

REFERENCES

1. S. J. Angyal, P. A. J. Gorin, and M. Pitman. Proc. Chem. Soc. 337 (1962).
2. S. J. Angyal and P. A. J. Gorin. Unpublished work.
3. H. O. L. Fischer. Ber. **54**, 782 (1921).
4. L. J. Hedgeley and H. G. Fletcher, Jr. J. Am. Chem. Soc. **84**, 3726 (1962).
5. R. Grewe and E. Nolte. Ann. **575**, 1 (1951).
6. L. Maquenne. Les sucres et leurs principaux derives. Carre et Naud, Paris. 1900. p. 14.
7. R. U. Lemieux, R. K. Kullnig, H. J. Bernstein, and W. G. Schneider. J. Am. Chem. Soc. **80**, 6098 (1958).
8. O. Hesse. Ann. **110**, 333 (1859).
9. A. S. Perlin, E. von Rudloff, and A. P. Tulloch. Can. J. Chem. **36**, 921 (1958).
10. E. von Rudloff and A. P. Tulloch. Can. J. Chem. **36**, 661 (1958).
11. P. A. J. Gorin. Can. J. Chem. **38**, 641 (1960).
12. H. W. Heine, A. D. Miller, W. H. Barton, and R. W. Greiner. J. Am. Chem. Soc. **75**, 4778 (1953).
13. R. U. Lemieux and J. P. Barrette. J. Am. Chem. Soc. **80**, 2243 (1958).
14. S. J. Angyal and Z. S. Krczeminski. J. Chem. Soc. 3251 (1962).
15. S. M. Partridge. Nature, **158**, 270 (1946).

Can. J. Chem. Downloaded from www.nrcresearchpress.com by 210.87.254.40 on 09/05/12
For personal use only.

PERFLUOROALKYL ARSENICALS

PART VIII. REACTION OF ARSENIC SULPHIDES WITH PERFLUOROALKYL IODIDES

W. R. CULLEN

Department of Chemistry, University of British Columbia, Vancouver, British Columbia

Received May 10, 1963

ABSTRACT

$(CH_3)_2AsSC_2H_5$, prepared from $(CH_3)_2AsCl$ and $Pb(SC_2H_5)_2$, and $((CH_3)_2As)_2S_2$ react with R_fI at 100° to give the compounds $(CH_3)_2AsR_f$ ($R_f = CF_3$, C_3F_7). The compounds As_2S_x ($x = 2, 3$) do not react with CF_3I at 100°. $((CF_3)_2As)_2S$, prepared from $(CF_3)_2AsI$ and Ag_2S or from $(CF_3)_2AsH$ and S, reacts with Hg to give $((CF_3)_2As)_2$, decomposes at 175° to give $(CF_3)_3As$, and reacts with CF_3I at 125° to give mainly $(CF_3)_3As$. Some $(CF_3)_2AsI$ and $CF_3SAs(CF_3)_2$ is also produced from this last reaction.

Abel has reported (1) that the Si—S bond in *n*-butylthiotrimethylsilane is cleaved by *n*-butyl iodide to give iodotrimethylsilane and di-*n*-butyl sulphide:

$$(CH_3)_3SiSC_4H_9 + C_4H_9I \rightarrow (CH_3)_3SiI + (C_4H_9)_2S.$$

It was therefore of interest to determine if the reversed polarity of perfluoroalkyl iodides (2) would result in similar reactions taking place to give perfluoroalkyl silicon compounds, and preliminary studies in this laboratory indicate that this is so. However, in order to test the idea that this reaction might apply to systems other than those containing Si—S bonds a study of the reactions of some compounds containing As—S bonds has been made.

Ethylthiodimethylarsine, b.p. 150°, prepared from chlorodimethylarsine and lead mercaptide, reacts with trifluoroiodomethane and heptafluoroiodopropane at 100° to give dimethyltrifluoromethyl- and heptafluoropropyldimethyl-arsine respectively in moderate yield. In both reactions diethyl disulphide is formed so that addition of the perfluoroalkyl iodide to the As—S bond appears to take place to a considerable extent according to the following reactions:

$$(CH_3)_2AsSC_2H_5 + R_fI \rightarrow (CH_3)_2AsR_f + ISC_2H_5 \qquad (R_f = CF_3 \text{ or } C_3F_7)$$

$$2ISC_2H_5 \rightarrow C_2H_5S—SC_2H_5 + I_2.$$

Although other unidentified products are produced it is worth noting that iododimethylarsine is not formed in either reaction and that ethyltrifluoromethyl sulphide is not present in the reaction products obtained from the thioarsine and trifluoroiodomethane.

Dimethyltrifluoromethylarsine is also obtained in moderate yield from the reaction, at 100°, of trifluoroiodomethane with the compound formulated by Bunsen as cacodyl disulphide, $((CH_3)_2As)_2S_2$ (3). This compound is now known to have the structure $(CH_3)_2As(S)—S—As(CH_3)_2$ (4), thus only one As—S bond would be expected to be easily attacked by trifluoroiodomethane. An unusual feature of this reaction was the slow deposition of a colorless solid from the volatile reaction products. This solid which decomposed above 200° is provisionally identified as dimethyltrifluoromethylarsenic sulphide. The qualification arises because not enough material was available to fully characterize the compound.

Although trialkylarsines and tetramethyldiarsine react fairly readily with perfluoroalkyl iodides (5 and references cited therein, 6) arsines of the type R_2AsX (R = CH_3;

Can. J. Chem. Downloaded from www.nrcresearchpress.com by 210.87.254.105 on 09/05/12
For personal use only.

X = halogen or C_6H_5) require temperatures in excess of 100° for reaction to occur (5 and references cited therein) and it is thought that these higher-temperature reactions involve attack by perfluoroalkyl radicals. The reactivity of compounds containing $(CH_3)_2As—S$ units therefore appears to be a function of the As—S bond, and the direction of addition of the perfluoroalkyl iodide to this bond appears to be a function of the polarity of this bond.

However, not all compounds containing As—S bonds react in this way since bistrifluoromethylarsenious sulphide reacts with trifluoroiodomethane at 125° to give low yields of iodobistrifluoromethylarsine and bistrifluoromethyl(trifluoromethylthio)arsine:

$$(CF_3)_2As—S—As(CF_3)_2 + CF_3I \rightarrow (CF_3)_2AsI + CF_3SAs(CF_3)_2.$$

The major volatile product is tristrifluoromethylarsine. The sulphide itself undergoes very slow decomposition when heated to 125° but when heated to 175° tristrifluoromethylarsine and arsenic disulphide are produced. Therefore, the reaction with trifluoroiodomethane at 125° seems to take place by two different paths, the minor one being the cleavage reaction described above, and the major one being the thermal decomposition reaction to produce tristrifluoromethylarsine. This arsine could also be formed by cleavage reactions of the sort

$$(CF_3)_2As—S—As(CF_3)_2 + CF_3I \rightarrow (CF_3)_2AsCF_3 + ISAs(CF_3)_2,$$

but this would use up much more trifluoroiodomethane than is found experimentally. The thermal decomposition reaction is faster in the presence of trifluoroiodomethane, suggesting that it is being catalyzed either by the trifluoroiodomethane or the products of the cleavage reaction. The direction of the cleavage reaction may be significant since the presence of two strongly electronegative groups on the arsenic could reverse the polarity of the As—S bond.

Neither arsenic trisulphide nor disulphide react with trifluoroiodomethane at 100°. The disulphide in particular could be expected to react easily with perfluoroalkyl iodides since it appears to contain both As—S and As—As bonds (7). However, recent molecular-orbital calculations on As_4S_4 and the related molecule S_4N_4 (8) indicate that in those compounds the bonding electrons are considerably delocalized so that the reactivity of the bonds may be considerably diminished.

Bistrifluoromethylarsenious sulphide, a colorless liquid, b.p. 86° (153 mm), is prepared from iodobistrifluoromethylarsine and silver sulphide at 20°:

$$2(CF_3)_2AsI + Ag_2S \rightarrow ((CF_3)_2As)_2S + 2AgI.$$

The sulphide is stable to water at 20° but reacts quantitatively with mercury to give tetrakistrifluoromethyldiarsine:

$$((CF_3)_2As)_2S + Hg \rightarrow ((CF_3)_2As)_2 + HgS.$$

A similar reaction is known for dimethylarsenious sulphide (9). Bistrifluoromethylarsenious sulphide is also produced when bistrifluoromethylarsine and sulphur are heated to 100°. There is no reaction between the two at 20°:

$$2(CF_3)_2AsH + 2S \rightarrow ((CF_3)_2As)_2S + H_2S.$$

Dimethylarsine has been reported to react with sulphur at 20° according to the following reactions (10):

$$2(CH_3)_2AsH + 2S \rightarrow ((CH_3)_2As)_2S + H_2S$$
$$2(CH_3)_2AsH + 3S \rightarrow ((CH_3)_2As)_2S_2 + H_2S.$$

In the present investigation the second of these reactions has been repeated. The yield

Can. J. Chem. Downloaded from www.nrcresearchpress.com by 210.87.254.105 on 09/05/12
For personal use only.

of hydrogen sulphide is quantitative after 1 month and cacodyl disulphide is amongst the solid products. Cacodyl sulphide is reported to react with sulphur to give cacodyl disulphide (3) and therefore it is suggested that in both reactions of dimethylarsine with sulphur, cacodyl sulphide is first produced which, when excess sulphur is present, reacts further to give cacodyl disulphide:

$$(CH_3)_2As—S—As(CH_3)_2 + S \rightarrow (CH_3)_2As(S)—S—As(CH_3)_2.$$

On this basis the failure of bistrifluoromethylarsine to react with excess sulphur to give a disulphide would not be unexpected since disulphide formation to give a compound analogous to cacodyl disulphide would involve oxidation of one of the arsenic atoms by sulphur and the presence of the electronegative trifluoromethyl group would make this much more difficult. Thus, although trimethylarsine is easily oxidized by sulphur, tristrifluoromethylarsine does not react at 20° (11) and it has now been found that dimethyltrifluoromethylarsine does not react with sulphur at 100°.

EXPERIMENTAL

The apparatus and techniques used in this investigation were the same as have been described in previous papers in this series.

Preparation of Ethylmercaptodimethylarsine

Lead mercaptide was prepared and purified as described by Abel (1). The mercaptide (80 g) and chlorodimethylarsine (40 g) were refluxed in a nitrogen atmosphere for 4 hours. The volatile contents of the reaction flask were removed under vacuum and distilled at atmospheric pressure to give *ethylmercaptodimethylarsine*, b.p. 150° (75% yield). Anal. Found: C, 28.9; H, 6.62%, $C_4H_{11}AsS$ requires: C, 29.5; H, 6.44%. The compound was unstable to air, a white solid being slowly formed. The infrared spectrum showed the following absorption bands (liquid film): 2940 (s), 2900 (s), 2850 (sh,m), 2795 (sh,w), 1805 (vw), 1448 (s), 1425 (s), 1415 (s), 1370 (m), 1305 (vw), 1257 (s), 1050 (w), 967 (m), 895 (s), 837 (s), 825 (sh,w), 760 (m), 730 (w) cm^{-1}.

Reactions of Ethylmercaptodimethylarsine

(*a*) *With trifluoroiodomethane.*—The arsine (5.7 g) and trifluoroiodomethane (12 g) were heated to 100° for 6 days. Volatile products were taken into the vacuum system, leaving an orange liquid (0.5 g) in the tube. The infrared spectrum of this liquid showed the absence of any C—F bands. The liquid in an attempted distillation was heated to 250° in an atmosphere of nitrogen (760 mm) without decomposition. The liquid had a boiling point of 180–184° at 136 mm. Analysis gave C, 8.6; H, 1.92; As, 22.2; S, 6.30%, results which do not seem to fit any reasonable reaction product. The volatile products were separated by trap-to-trap distillation into unreacted trifluoroiodomethane, a fraction which condensed at −98° and which was identified by its infrared spectrum as dimethyltrifluoromethylarsine (3.6 g, 60% yield), and a fraction which condensed at −64°. The last fraction was distilled in a nitrogen atmosphere (760 mm) to give a few drops refluxing at 56–60° (probably dimethyltrifluoromethylarsine), otherwise it all distilled at 145–155°. This fraction, an orange liquid (1.5 g), was separated into two components by v.p.c. (dinonyl phthalate column at 140°). One component, ca. 15% of the mixture, on the evidence of its infrared spectrum contained C—F bonds, but the amount recovered did not allow characterization; the other component was identified as diethyl disulphide by means of its infrared spectrum.

(*b*) *With n-heptafluoroiodopropane.*—The arsine (6.9 g) and heptafluoroiodopropane (19.0 g) were heated to 100° for 9 days. The volatile contents of the reaction tube were taken into the vacuum system, leaving an orange oil similar to that obtained in the preceding experiment. The volatile fraction was carefully distilled at 760 mm in an atmosphere of nitrogen to give 5.8 g (51% yield) of heptafluoropropyldimethylarsine, b.p. 90–95° (lit. value 92° (6)), identified by its infrared spectrum, and a small fraction which distilled in the range 100–150°. Vapor phase chromatography (dinonyl phthalate columns at 140°) showed that this contained two main components; one of these was identified as unreacted ethylmercaptodimethylarsine by comparison of retention times, the other was identified as diethyl disulphide by its infrared spectrum and by analysis. Found: C, 39.3; H, 7.9%. Calc. for $C_4H_{10}S_2$: C, 40.2; H, 8.2%. The weight of the disulphide collected was 0.6 g.

Reaction of Cacodyl Disulphide with Trifluoroiodomethane

The sulphide was prepared by passing hydrogen sulphide through an alcoholic solution of dimethylarsinic acid (3). The sulphide (2.3 g) and trifluoroiodomethane (17.5 g) were heated to 100° for 5 days. Trifluoroiodomethane (14.3 g) was recovered. The only reaction products which were investigated were those which on

Can. J. Chem. Downloaded from www.nrcresearchpress.com by 210.87.254.105 on 09/05/12
For personal use only.

preliminary separation passed through a trap cooled to −46°. This fraction slowly deposited a small amount of a colorless solid and was set aside until this deposition had stopped. The remaining liquid on trap-to-trap distillation gave 0.9 g of dimethyltrifluoromethylarsine which was identified by its molecular weight of 168 (calc.: M, 174) and by its infrared spectrum. The white solid decomposed at temperatures above 200° and showed polymorphic changes on heating. Analysis indicated that the solid was *dimethyltrifluoromethylarsenic sulphide*. Found: C, 17.4; H, 4.9; As, 35.8; S, 15.1%. $C_3H_6AsF_3S$ requires: C, 17.5; H, 2.92; As, 36.4; S, 15.5%.

Reaction of Arsenic Sulphides with Trifluoroiodomethane

Trifluoroiodomethane (10.0 g) and arsenic disulphide (10.0 g) were heated to 100° for 7 days. No fraction less volatile than trifluoroiodomethane (9.9 g) was isolated. A similar result was obtained when trifluoroiodomethane and arsenic trisulphide were heated to 100° for 4 days.

Preparation of Bistrifluoromethylarsenious Sulphide

Iodobistrifluoromethylarsine (5 g) and freshly prepared silver sulphide (17 g) were left for 12 days at 20°. A colorless liquid (3.5 g) was obtained which condensed as a solid in a trap cooled to −46°. This fraction distilled at 86° (153 mm) in a nitrogen atmosphere and was identified as *bistrifluoromethylarsenious sulphide*. Anal. Found: C, 10.6; H, 0.0; As, 32.5; F, 50.1; S, 6.79%; M, 455 (Rast). $C_4As_2F_{12}S$ requires: C, 10.5; H, 0.0; As, 32.8; F, 49.6; S, 6.99%; M, 458. The infrared spectrum showed the following absorption bands (vapor): 2320 (vw), 1257 (vw), 1187 (vw), 1159 (vs), 1130 (vs), 1105 (vs), 1060 (sh,w), 1045 (sh,w), 730 (s) cm^{-1}.

Reactions of Bistrifluoromethylarsenious Sulphide

(*a*) *With water.*—The sulphide (0.304 g) and water (3 ml) were immiscible and did not react at 20° (20 days).

(*b*) *With mercury.*—When the sulphide (0.514 g) and mercury (60 g) were shaken at 20° for 21 days tetrakistrifluoromethyldiarsine was produced (0.476 g, 100% yield). The diarsine was identified by its infrared spectrum and its molecular weight of 430 (calc.: M, 426).

(*c*) *Pyrolysis.*—The sulphide (0.410 g) was heated to 125° for 14 days. No involatile product was formed and the infrared spectrum of the recovered sample was essentially the same as that of the starting material. When the sulphide (0.152 g) was heated to 175° for 3 days tristrifluoromethylarsine (0.084 g; found: M, 279; calc.: M, 282), of known infrared spectrum, was produced. A red-yellow crystalline solid had formed on the tube walls and an X-ray powder photograph of this solid showed the presence of arsenic disulphide. Unchanged bistrifluoromethylarsenious sulphide (0.025 g) was recovered.

(*d*) *With trifluoroiodomethane.*—Trifluoroiodomethane (6.8 g) and the sulphide (0.786 g) were heated to 125° for 8 days. A red-yellow film slowly formed on the tube walls. Trifluoroiodomethane (6.6 g) was recovered and the volatile products were identified as tristrifluoromethylarsine (0.452 g; M, 281) and an orange-yellow mixture of iodobistrifluoromethylarsine and bistrifluoromethyl(trifluoromethylthio)arsine. The iodoarsine was identified by its infrared spectrum and by its reaction with mercury to give tetrakistrifluoromethyldiarsine. The mixture of the diarsine and the thioarsine weighed 0.116 g and the components could be separated well enough by trap-to-trap distillation to enable positive identification of their infrared spectra.

Reaction of Bistrifluoromethylarsine with Sulphur

There was no reaction when the arsine (0.591 g) and sulphur (0.6 g) were left for 20 days at 20°. When the same reactants were heated to 100° for 3 days hydrogen sulphide (0.0076 g; found: M, 34.0. calc.: M, 34.0) and bistrifluoromethylarsenious sulphide (0.328 g) were isolated. Bistrifluoromethylarsine (0.260 g) was recovered. All fractions were of known infrared spectrum.

Reaction of Dimethylarsine with Sulphur

The arsine (1.928 g) and sulphur (1.2 g) were left for 1 month at 20°. Large white crystals slowly formed and hydrogen sulphide (0.300 g, 100% yield; M, 34.1) was isolated. The solid was extracted with warm alcohol and the alcohol was removed *in vacuo*. The remaining white vile smelling solid was recrystallized from ether and was identified as slightly impure cacodyl disulphide by means of its X-ray powder photograph.

Reaction of Dimethyltrifluoromethylarsine with Sulphur

The arsine (2.701 g) and sulphur (1.0 g) did not react after 3 days at 115°. Recovery of the arsine was nearly quantitative (2.665 g).

ACKNOWLEDGMENTS

The author wishes to acknowledge the financial assistance of the National Research Council of Canada. Microanalyses were performed by Mrs. A. Aldridge and Dr. Alfred Bernhardt.

Can. J. Chem. Downloaded from www.nrcresearchpress.com by 210.87.254.105 on 09/05/12
For personal use only.

REFERENCES

1. E. W. ABEL. J. Chem. Soc. 4406 (1960).
2. J. BANUS, H. J. EMELÉUS, and R. N. HASZELDINE. J. Chem. Soc. 60 (1951).
3. R. W. BUNSEN. Ann. **46**, 1 (1843).
4. N. CAMERMAN and J. TROTTER. Unpublished results.
5. W. R. CULLEN. Can. J. Chem. **40**, 426 (1962).
6. W. R. CULLEN. Can. J. Chem. **38**, 439 (1960).
7. Chem. Soc. (London), Spec. Publ. **11** (1958).
8. D. CHAPMAN and T. C. WADDINGTON. Trans. Faraday Soc. **58**, 1679 (1962).
9. R. W. BUNSEN. Ann. **42**, 14 (1842).
10. W. M. DEHN and B. B. WILCOX. Am. Chem. J. **35**, 1 (1906).
11. H. J. EMELÉUS, R. N. HASZELDINE, and E. G. WALACHEWSKI. J. Chem. Soc. 1552 (1953).

Can. J. Chem. Downloaded from www.nrcresearchpress.com by 210.87.254.105 on 09/05/12
For personal use only.

PROTON MAGNETIC RESONANCE SPECTRUM OF 1-PHENYLCYCLOPROPYLCARBOXYLIC ACID: A_2B_2 SPECTRA OF CYCLOPROPANES

H. M. HUTTON[1] AND T. SCHAEFER
Department of Chemistry, University of Manitoba, Winnipeg, Manitoba
Received May 21, 1963

ABSTRACT

A_2B_2 spectra of 1,1-disubstituted cyclopropanes have been calculated over a range of values of the spectral parameters. The sign of the geminal coupling is opposite to that of the vicinal couplings. Since this is also the case with other saturated ring systems the theoretical spectra should be useful in studies of other saturated ring systems.

The shifts and coupling constants are given for the protons in 1-phenylcyclopropylcarboxylic acid in solution in carbon disulphide, chloroform, and benzene as an example of the A_2B_2 analysis. The ring protons in 1-phenylcyclopropylcarbinol were found to be equivalent in different solvents, with insignificant coupling to the protons in the methylene and phenyl groups. A qualitative discussion of the shifts of the various protons in various solvents is given.

INTRODUCTION

The analysis of A_2B_2 spectra has been discussed in some detail (1, 2, 3), especially in regard to unsaturated ring systems (2, 3). Here we propose to discuss and illustrate with an example the probable A_2B_2 proton spectra for 1,1-disubstituted cyclopropanes. This discussion is applicable also to A_2B_2 arrangements in other fixed saturated ring systems (4, 5). From the collection of proton coupling constants in cyclopropanes (6 and references cited therein) and from spin decoupling experiments (7 and references cited therein) we know that the probable range of values is -4 to -8 c.p.s. for J_{gem}, 4 to 8 c.p.s. for J_{trans}, and 7 to 11 c.p.s. for J_{cis}, depending on the substituents. We use an approach similar to that which Martin and Dailey (2) applied to disubstituted benzenes except that we express our parameters in units of Δ, the chemical shift.

Computation of the A_2B_2 Spectra

For our systems there are four coupling constants as in I. J_A and J_B are the two cis couplings and the parameters K, L, M, N, and Δ are also defined.

I

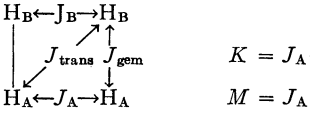

$$\Delta = \eta H_0(\sigma_B - \sigma_A)$$

$$K = J_A + J_B \qquad N = J_{gem} + J_{trans}$$

$$M = J_A - J_B \qquad L = J_{gem} - J_{trans}$$

The secular equation for this system has been repeatedly tabulated (1, 2, 3). We refer the reader to page 2595 of reference 2 for the notation and give an abbreviated set of transitions in Table I to which we will refer later. The substitution of $-L$ for L does not alter the secular equation and that of $-M$ for M merely interchanges the labeling of certain transitions, so that the signs of L and M cannot be obtained from the spectrum. The spectrum is, however, sensitive to the relative signs of K and N (3). We here define K, the sum of the two cis coupling constants, to be positive (8 and references cited therein). N may then be negative or positive and, for the spectra under consideration, we have $N < 0$ for $|J_{gem}| > |J_{trans}|$ and $N > 0$ for $|J_{gem}| < |J_{trans}|$. It is almost certain that $J_{gem} < 0$ and that $J_{trans} > 0$ (6, 7, 8) and hence we have $L < 0$, which makes it possible

[1]*C.I.L. Fellowship Holder 1962–1963.*

Can. J. Chem. Downloaded from www.nrcresearchpress.com by 210.87.254.40 on 09/05/12
For personal use only.

TABLE I

Computation of A_2B_2 spectra

Explicitly defined parameters			Solution of the 4×4 determinant
$2C_N = (\Delta^2+N^2)^{1/2}$	$\tan 2\phi = N/\Delta$		$p_m = E(mS_0^1) - H_{mm}(S_0)$ (E is the energy value and $H_{mm}(S_0)$ is the diagonal element in the representation used)
$2C_{LM\pm} = [(\Delta\pm M)^2+L^2]^{1/2}$	$\tan 2\theta_a = L/K$		
$2L_M = (L^2+M^2)^{1/2}$	$\tan 2\psi_\pm = L/(\Delta\pm M)$		

The coefficients C_{mn} of the diagonal representation are given by:
$(mS_0^1) = C_{m1}(1S_0)+C_{m2}(2S_0)+C_{m3}(3S_0)+C_{m4}(4S_0)$

Transitions in the high-field half-spectrum

Transition in c.p.s. from center of spectrum	Relative intensity	
1. $C_N+1/2N$		$1 - \sin 2\phi$
2. $\Delta+1/2N-C_N-p_1$	$[(C_{11}+C_{14})$	$\cos\phi - (C_{12}+C_{14})\sin\phi]^2$
3. $C_N-1/2N$		$1 + \sin 2\phi$
4. $\Delta-1/2N-C_N+p_2$	$[(C_{22}+C_{24})$	$\cos\phi + (C_{21}+C_{24})\sin\phi]^2$
5. C_N+K-p_3	$[(C_{32}+C_{31})$	$\cos\phi + (C_{31}+C_{34})\sin\phi]^2$
6. C_N+p_4	$[(C_{41}+C_{44})$	$\cos\phi - (C_{42}+C_{44})\sin\phi]^2$
7. C_N-p_4	$[(C_{42}+C_{44})$	$\cos\phi + (C_{41}+C_{44})\sin\phi]^2$
8. C_N-K+p_3	$[(C_{31}+C_{34})$	$\cos\phi - (C_{32}+C_{34})\sin\phi]^2$
9. $C_{LM+}+L_M$		$\sin^2(\theta_a-\psi_+)$
10. $C_{LM-}+L_M$		$\cos^2(\theta_a+\psi_-)$
11. $C_{LM+}-L_M$		$\cos^2(\theta_a-\psi_+)$
12. $C_{LM-}-L_M$		$\sin^2(\theta_a+\psi_-)$

to assign values to J_{gem} and J_{trans} from the spectrum. J_A and J_B will differ by hardly more than 1 c.p.s. in these systems (6). We therefore have no specific information as to the relative signs of L and M and we cannot distinguish between J_A and J_B from the spectra.

The eigenvalues and eigenvectors of the 4×4 determinant of the secular equation were computed on an IBM 1620. The theoretical spectra were obtained for all combinations of the parameters in units of the shift Δ:

$$K = 0.4, 0.6, 0.8, 1.0, 1.2, 1.5 \qquad M = 0, 0.01, 0.02, 0.04$$
$$L = 0.3, 0.4, 0.5, 0.6 \qquad N = -0.1, 0, 0.1, 0.2$$

These values correspond to the most probable values of the coupling constants (4, 5, 6) together with the values of Δ which would give rise to intelligible spectra. Some of the computed spectra are presented in Figs. 1 to 9. Since the spectra are symmetric about the centers, only the high-field halves are shown. Parentheses around transition 8 indicate that it now comes from the low-field proton transitions.

The Effect of the Parameters K, L, M, N

The effect of the relative signs of the coupling constants and the magnitudes and signs of the parameters K, L, M, N upon the A_2B_2 spectra has been discussed in detail by Grant *et al.* (3). The changes which occur specifically for 1,1-disubstituted cyclopropanes will be outlined.

(a) Parameter K

The K parameter does not change the positions of lines 1 and 3 nor those of the antisymmetric set of transitions 9, 10, 11, 12. It does, however, change the position of the symmetric set of transitions 5, 6, 7, 8, of line 2, and of line 4 to a small extent. Line 2, at a position of $\Delta+\frac{1}{2}N-C_N-p_1$, moves toward the outer portion of the B spectrum as K

Can. J. Chem. Downloaded from www.nrcresearchpress.com by 210.87.254.40 on 09/05/12
For personal use only.

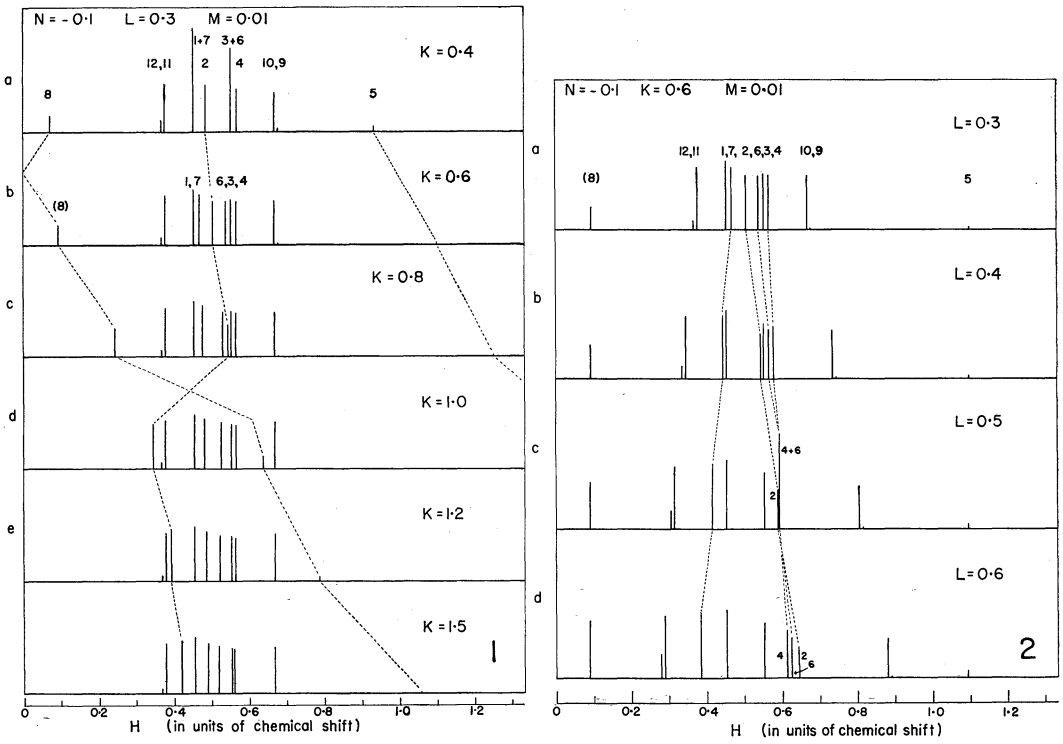

FIG. 1. The variation of the spectrum with a change in the parameter K is presented for $N = -0.1\Delta$, $L = 0.3\Delta$, and $M = 0.01\Delta$. The high-field B transitions of the symmetrical A_2B_2 spectrum are illustrated with the magnetic field in units of the chemical shift from the center of the spectrum. The parentheses around transition 8 indicate in this and all succeeding diagrams that it is an A transition overlapping the B spectrum. The intensities of transitions 5 and 9 have been doubled relative to the intensities of the other transitions. The parameters K, L, N, M are given in units of the chemical shift Δ.

FIG. 2. Starting with the spectrum presented in Fig. 1(*b*), the spectral changes due to the parameter L are shown for $N = -0.1\Delta$, $K = 0.6\Delta$, and $M = 0.01\Delta$. The changes in the spectrum when varying L from 0.3Δ to 0.6Δ for the other values of the parameter K in Fig. 1 are the same as that given here for the case of $K = 0.6\Delta$.

increases until $|K| > |-\Delta-\frac{1}{2}N|$. At this point the valve of p_1 reverses sign, bringing line 2 back into the interior of the spectrum. These changes in the spectrum can be seen in Figs. 1, 3, 5, and 7 for $L = 0.3\Delta$, $N = -0.1\Delta$, 0, 0.1Δ, 0.2Δ.

The parameter K may be approximated from the spectra as the differences $\nu_8-\nu_7 = \nu_6-\nu_5$.

(b) Parameter L

The change in the spectrum with an increase in the value of L from 0.3Δ to 0.6Δ can be seen in Figs. 2, 4, 6, and 8. Both the antisymmetrical transitions 9 through 12 and the symmetrical transitions 5 through 8 are affected by an increase in L. As L increases the difference $\nu_8-\nu_7 = \nu_6-\nu_5$ becomes less and less a reasonable approximation to the value of K. Transitions 2 and 4 also shift with an increase in L, but 1 and 3 are unaffected. When $|L| \gg |M|$, L may be obtained almost exactly from the spectrum as the difference between lines 9, 11 or 10, 12. This is very likely the case for 1,1-disubstituted cyclopropanes.

(c) Parameter N

Lines 1 to 4 are most affected by a change of N. As N decreases to zero lines 1, 3 coalesce at the chemical shift position and reverse their relative positions when N becomes negative.

Can. J. Chem. Downloaded from www.nrcresearchpress.com by 210.87.254.40 on 09/05/12
For personal use only.

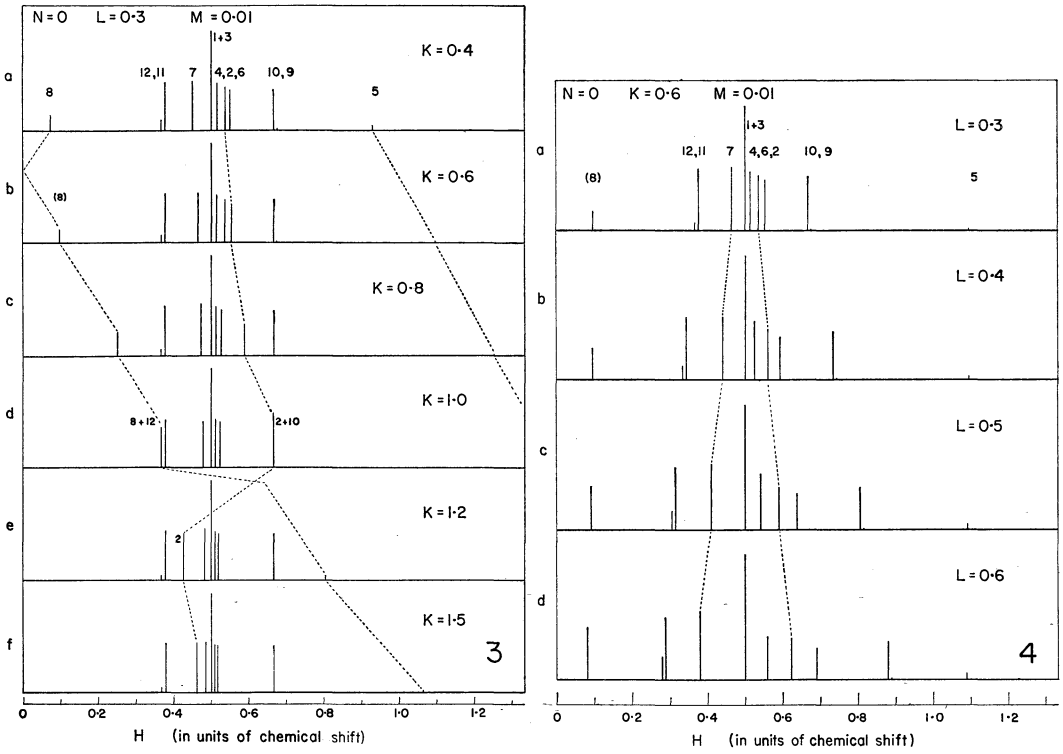

FIG. 3. The variation of the spectrum with a change in the parameter K is presented for $N = 0$, $L = 0.3\Delta$, and $M = 0.01\Delta$.

FIG. 4. Starting with the spectrum presented in Fig. 3(*b*) the spectral changes due to the parameter L are shown for $N = 0$, $K = 0.6\Delta$, and $M = 0.01\Delta$. The changes in the spectrum when varying L from 0.3Δ to 0.6Δ for the other values of the parameter K in Fig. 3 are the same as that given here for the case of $K = 0.6\Delta$.

Lines 1 and 3 are always separated by the algebraic value of N. The most important change as N goes from a positive to a negative value is that of lines 2 and 4. These two lines reverse their relative positions so that the sign of N can be distinguished from the appearance of the spectrum as shown in Figs. 1 and 5, 2 and 6. This indicates the relative signs of J_{gem} and J_{trans} in substituted cyclopropanes. The antisymmetrical transitions 9 to 12 are unaffected by a change of N. The symmetrical quartet 5 to 8 is also not significantly changed over the small range over which N has been varied.

(d) Parameter M

The M parameter affects only the positions of the antisymmetrical set 9 to 12 for any given value of L. As a first approximation the value of M may be taken as the difference between lines 9 and 10 or 11 and 12. As M increases from zero lines 11, 12, and 9, 10 separate, as Fig. 9 indicates. Since $M = J_A - J_B$ is of the order of 1 c.p.s. or less (6) the spectra presented have all been calculated assuming a small, and rather arbitrary, value of $M = 0.01\Delta$.

Analysis of Spectra

The A_2B_2 spectra for cyclopropane derivatives can be conveniently analyzed using the transition frequencies of Martin and Dailey (2) given in Table I. The use of symmetry

Can. J. Chem. Downloaded from www.nrcresearchpress.com by 210.87.254.40 on 09/05/12
For personal use only.

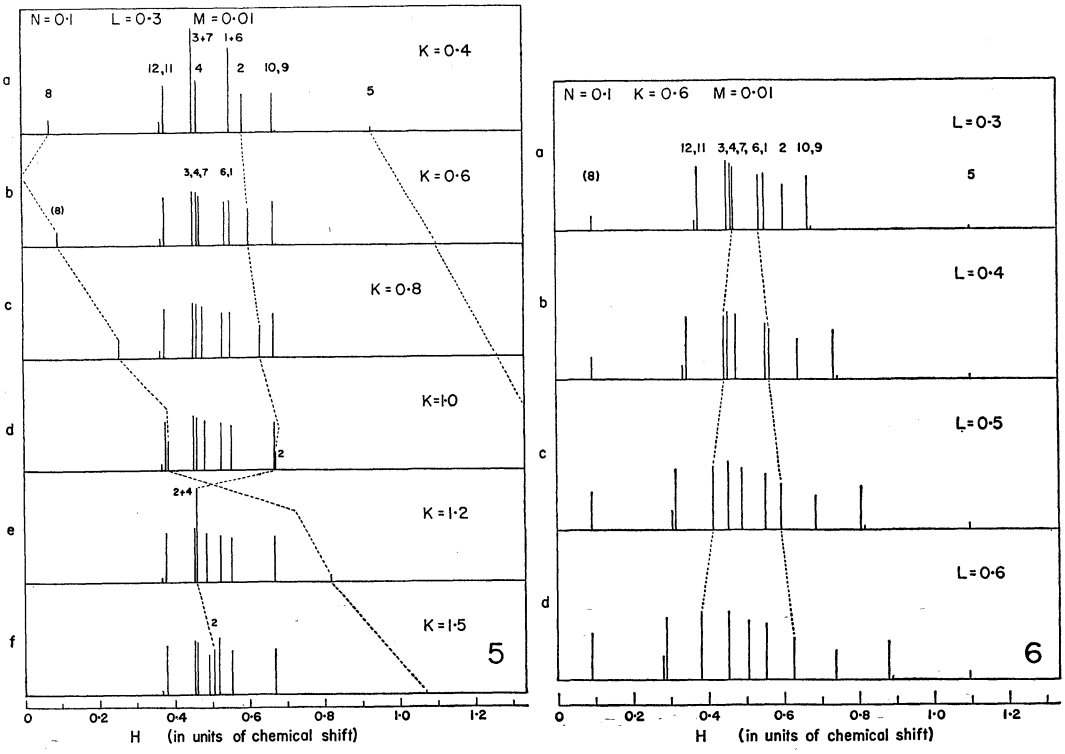

FIG. 5. The variation of the spectrum with a change in the parameter K is presented for $N = 0.1\Delta$, $L = 0.3\Delta$, and $M = 0.01\Delta$. A comparison of corresponding spectra in this diagram and Fig. 1 illustrates the spectral change for N negative $|J_{gem}| > |J_{trans}|$ and N positive $|J_{gem}| < |J_{trans}|$.

FIG. 6. Starting with the spectrum presented in Fig. 5(*b*), the spectral changes due to the parameter L are shown for $N = 0.1\Delta$, $K = 0.6\Delta$, and $M = 0.01\Delta$. Here also, a comparison with the corresponding spectra in Fig. 2 illustrates the difference for a negative and positive value of N. The changes in the spectrum when varying L from 0.3Δ to 0.6Δ for the other values of the parameter K in Fig. 5 are the same as that given here for the case of $K = 0.6\Delta$.

and of the spin operator leaves only one 4×4 determinant which cannot be solved explicitly. The transitions which arise from this subdeterminant are lines 2, 4, 5, 6, 7, 8. These lines involve the quantities p_m and C_{mn} which must be obtained from the numerical solution of the 4×4.

Since the frequencies and intensities of the remaining transitions are given explicitly in terms of the molecular parameters Δ, L, N, and M, the main problem is the identification of these lines. The value of N may be obtained from the difference of lines 1 and 3 and the chemical shift Δ from the position of either 1 or 3 with respect to the center of the spectrum. L and M may be calculated from lines 9, 10, 11, 12. When $|L| \gg |M|$, as will normally be true for these spectra, the parameter L may be obtained from $\nu_9 - \nu_{11} = \nu_{10} - \nu_{12}$. M will be approximately $\nu_9 - \nu_{10} = \nu_{11} - \nu_{12}$. These two parameters can then be adjusted to fit the experimental and theoretical spectra to within the accuracy desired.

One parameter, K, remains to be evaluated. The values obtained for Δ, N, and L are used to solve the 4×4 numerically with the method of successive approximations to find the value of K. The lines which vary the most with a change of K, lines 2 and 8, are a good means of identifying the correct value of K. If a fit between the experimental and theoretical transitions cannot be obtained using N as a positive quantity, then the calculations should be repeated for N negative.

Can. J. Chem. Downloaded from www.nrcresearchpress.com by 210.87.254.40 on 09/05/12
For personal use only.

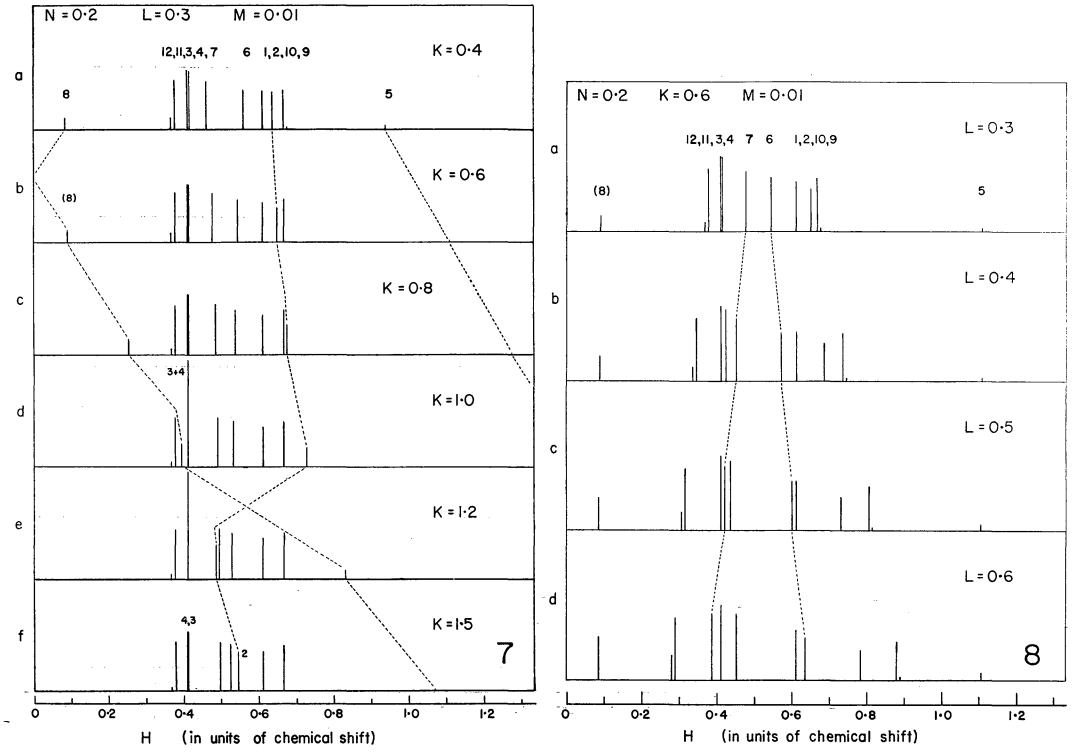

FIG. 7. The variation of the spectrum with a change in parameter K is presented for $N = 0.2\Delta$, $L = 0.3\Delta$, and $M = 0.01\Delta$.

FIG. 8. Starting with the spectrum presented in Fig. 7(*b*) the spectral changes due to the parameter L are shown for $N = 0.2\Delta$, $K = 0.6\Delta$, and $M = 0.01\Delta$. The changes in the spectrum when varying L from 0.3Δ to 0.6Δ for the other values of the parameter K in Fig. 7 are the same as that given here for the case of $K = 0.6\Delta$.

Application to 1-Phenylcyclopropylcarboxylic Acid

The values obtained for the chemical shifts with respect to internal TMS and the coupling constants for 1-phenylcyclopropylcarboxylic acid are given in Table II. Figure 10 shows the proton resonance spectrum with the calculated spectrum below. The phenyl

TABLE II

Chemical shifts and coupling constants of 1-phenylcyclopropylcarboxylic acid in c.p.s.

	Chemical shifts*								J_A†		J_B†	
Solution	H_A†	H_B†	L	N	K	M‡	J_{gem}	J_{trans}	$M =$ 0	$M =$ 0.4	$M =$ 0	$M =$ 0.4
6 mole% in CS_2	93.7	68.1	±10.89	+3.00	+19.3	±0.2	−3.89	6.89	9.6_5	9.8_5	9.6_5	9.4_5
8 mole% in C_6H_6	89.1	52.8	±10.96	+3.00	+19.4	±0.2	−3.99	6.97	9.7	9.9	9.7	9.5
7 mole% in $CHCl_3$	98.8	74.3	±10.95	+2.89	+19.4	±0.2	−4.03	6.92	9.7	9.9	9.7	9.5

*In c.p.s. at 60 Mc/s to low field from internal tetramethylsilane.
†The protons H_A, H_B and their respective coupling constants cannot be distinguished in the analysis and are designated arbitrarily.
‡Value of M could be of the order of 0 to 0.4 c.p.s.

Can. J. Chem. Downloaded from www.nrcresearchpress.com by 210.87.254.40 on 09/05/12
For personal use only.

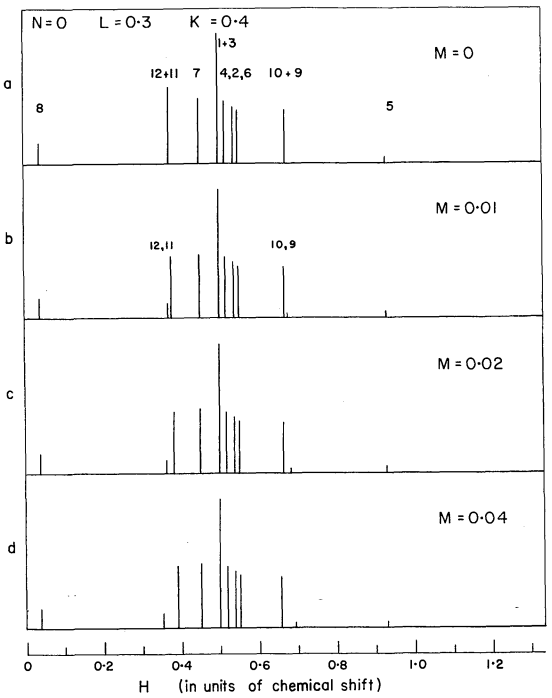

FIG. 9. The effect of the M parameter on the A_2B_2 spectrum is illustrated. The spectrum in Fig. 3(*a*) corresponds to that in (*b*) above. Since the parameter M for 1,1-disubstituted cyclopropanes appears to be small, all the spectra in Figs. 1 to 8 were calculated for $M = 0.01\Delta$. For other values of M only transitions 9, 10, 11, 12 in the preceding figures would change as illustrated above.

and carboxyl protons were approximately 440 c.p.s. and 740 c.p.s. to low field of TMS. They will not be discussed further.

The parameters give a fit of the theoretical and experimental lines to within ± 0.1 c.p.s., which is as good as the uncertainty in the measurements. The parameter M could not be evaluated since no splitting of lines 11, 12 and 9, 10 was observed. This does not necessarily indicate that $M = 0$ since there appears to be sufficient coupling of the cyclopropyl protons with the phenyl substituent to broaden the lines slightly. This could mask any splitting of up to 0.4 c.p.s. The spectrum in Fig. 10 was calculated assuming $M = 0.2$ c.p.s. Line 5 was not observed in the spectrum due to its low intensity and the broadening by the phenyl group.

The designation of protons H_A and H_B in Fig. 10 is assigned arbitrarily and could be reversed. J_A cannot be distinguished from J_B, especially since their values are very similar. From the spectrum alone J_{gem} and J_{trans} cannot be distinguished. However, we know that J_{gem} is almost certainly negative and J_{trans} positive (6, 7, 8). A satisfactory fit to the observed spectrum could only be obtained with opposite signs for J_{trans} and J_{gem}.

The Proton Spectrum of 1-Phenylcyclopropylcarbinol

This compound was expected to have an A_2B_2 spectrum but in the four solutions mentioned in Table III the ring protons were isochronous. They were not sufficiently coupled to either substituent to give an observable splitting of the single resonance peak.*

**If there were a small coupling to the ortho protons of the phenyl ring this would be obscured by an averaging effect over the other phenyl protons. This is so because the phenyl ring protons are isochronous and the coupling to the meta and para protons would be expected to be very nearly zero (10).*

Can. J. Chem. Downloaded from www.nrcresearchpress.com by 210.87.254.40 on 09/05/12
For personal use only.

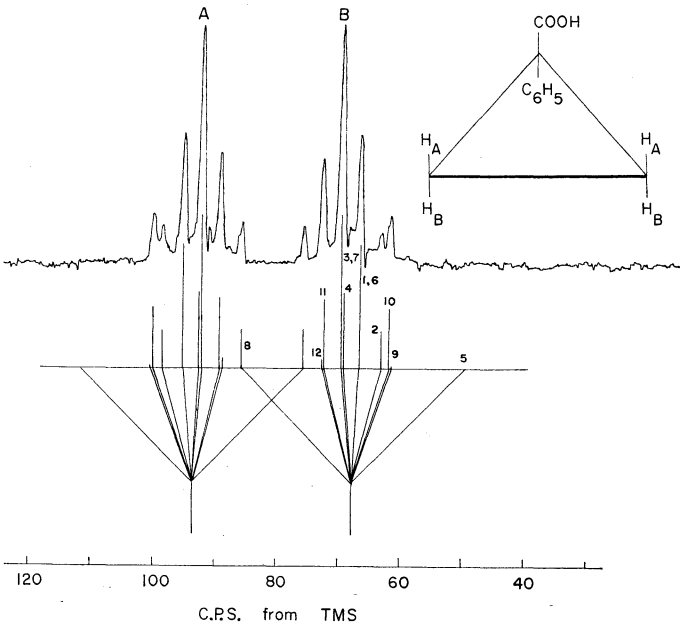

FIG. 10. Proton magnetic resonance spectrum at 60 Mc/s of 1-phenylcyclopropylcarboxylic acid, 8 mole% in benzene; calibration is to low field with respect to internal tetramethylsilane. The calculated spectrum below it illustrates the overlap of transition 8 from the B region into the A region. Protons A and B are assigned arbitrarily and cannot be distinguished from the spectrum alone. The calculated spectrum assumes J_{gem} to be of opposite sign to J_{cis} and J_{trans}.

TABLE III

Proton chemical shifts* of 1-phenylcyclopropylcarbinol in solution

Solution	Ring protons	—CH_2–	—OH	—C_6H_5
10 mole% in CS_2	39.7	200.2	186.2	427
15 mole% in CS_2	38.6	199.6	203.6	425.6
20 mole% in C_6H_6	41.1	206.3	179.1	≈400†
20 mole% $CHCl_3$	43.7	205.9	180.7	≈425†

*In c.p.s. at 60 Mc/s to low field from internal TMS.
†Phenyl resonance hidden by solvent peak.

No coupling was observed between the methylene and hydroxyl protons, indicating exchange of the hydroxyl protons at a rate sufficient to obscure the expected splitting of about 5 c.p.s. (9). The shifts of all protons relative to internal TMS are given in Table III.

The chemical shifts in the various solutions merit some discussion. The phenyl proton shifts are almost solvent independent. This is also nearly the case for the protons on the cyclopropyl ring. By way of contrast, the similarly placed protons in bis(2,2-dichlorocyclopropyl) ether show a difference of about 0.5 p.p.m. in carbon disulphide and benzene solutions (11). Relative to internal TMS the shift is to high field in benzene. In the latter case we have shown that the shift is markedly temperature dependent, indicating association effects (11). Association effects in the present case must be very small. In fact, there is a small shift to *low* field when the solvent is changed from carbon disulphide to benzene. This is also so for the methylene protons. The dielectric constants of benzene and carbon disulphide are nearly the same and reaction field effect differences must therefore be very small (16). We suggest that these very odd shifts must be a result of a peculiar packing

Can. J. Chem. Downloaded from www.nrcresearchpress.com by 210.87.254.40 on 09/05/12
For personal use only.

arrangement in solution which cannot, however, be more closely specified at present. The unexpected shifts in benzene solution are further emphasized by the almost identical shifts at the same concentration in chloroform. Further studies of the concentration and temperature dependence of these shifts are indicated.

The hydroxyl proton shifts in the two carbon disulphide solutions are reasonable since dilution would be expected to break up hydrogen bonding to other hydroxyl groups, thus causing a high-field shift (12). Again, hydrogen bonding to benzene solvent molecules is indicated since this would cause a shift to high field (13).

Ring Proton Shifts of the Acid

In Table II it can be seen that the H_B protons shift more to high field than do the H_A protons when the solvent is changed from carbon disulphide to benzene. If it could be decided which side of the cyclopropane ring is avoided by the benzene solvent molecule, a definite assignment of H_A and H_B could be made. From previous experience with benzene as a solvent (7, 14, 15) we suggest that the carboxyl group will cause a closer packing of the benzene molecules about the protons trans to it. The H_B protons as given in Table II would then be trans to the carboxyl group. A series of studies to establish preferences of this type are indicated.

Because of the magnetic anisotropy of *both* the C=O bond and the benzene ring, coupled with the possibility of rapid rotation on an n.m.r. time scale of both groups about the bonds to the cyclopropyl ring, we hesitate to speculate further on the relative shifts of the H_A and H_B protons in carbon disulphide itself. However, from Tables II and III it is clear that substitution of a carboxyl group for the hydroxymethyl group causes a large low-field shift for both H_A and H_B. *If* we attribute this to the anisotropy of the C=O bond, it may be reasonable that the protons cis to it (H_A) should be most affected. This assignment would then agree with that suggested above from benzene solvent effects.

In chloroform both protons shift to low field and since the carboxyl group may be expected to introduce a considerable dipole moment, we suggest that this is a reaction field effect (16).

EXPERIMENTAL

1-Phenylcyclopropylcarboxylic acid was studied as a 6 mole% solution in carbon disulphide, 7 mole% solution in chloroform, and as an 8 mole% solution in benzene. 1-Phenylcyclopropylcarbinol was investigated as a 20 mole% solution in benzene and chloroform and 10 mole% and 15 mole% solution in carbon disulphide. Tetramethylsilane (TMS) was used as an internal standard. Small quantities of these compounds were a gift from Dr. James W. Wilt. Their physical properties are given in his paper (17). No impurities were observable in the proton spectra.

The spectra were obtained on a Varian Associates high-resolution DP60 spectrometer. The results represent an average of 10 spectra run forward and reverse. Corresponding A and B transitions were found to be symmetrical with respect to the center of the spectrum to within ±.05 c.p.s. The possible error in each line position is not more than ±0.1 c.p.s.

ACKNOWLEDGMENTS

We are grateful to Dr. J. W. Wilt for the gift of the compounds. H. M. H. thanks Canadian Industries Limited for fellowship support. The financial assistance of the National Research Council is deeply appreciated.

REFERENCES

1. H. M. McConnell, A. D. McLean, and C. A. Reilly. J. Chem. Phys. **23**, 1152 (1955). J. A. Pople, W. G. Schneider, and H. J. Bernstein. Can. J. Chem. **35**, 1060 (1957). R. E. Richards and T. Schaefer. Trans. Faraday Soc. **54**, 1280 (1958). J. A. Pople, W. G. Schneider, and H. J. Bernstein. High resolution nuclear magnetic resonance. McGraw-Hill Book Co., Inc., New York. 1959. P. L. Cario. Chem. Rev. **60**, 363 (1960). B. Dischler and G. Englert. Z. Naturforsch. **16a**, 1180 (1961). K. B. Wiberg and B. J. Nist. Interpretation of NMR spectra. W. A. Benjamin, Inc., New York. 1962.

Can. J. Chem. Downloaded from www.nrcresearchpress.com by 210.87.254.40 on 09/05/12
For personal use only.

2. J. MARTIN and B. P. DAILEY. J. Chem. Phys. **37**, 2594 (1962).
3. D. M. GRANT, R. C. HIRST, and H. S. GUTOWSKY. J. Chem. Phys. **38**, 470 (1963).
4. H. S. GUTOWSKY and C. JUAN. J. Chem. Phys. **37**, 120 (1962).
5. E. LUSTIG. J. Chem. Phys. **37**, 2725 (1962).
6. H. M. HUTTON and T. SCHAEFER. Can. J. Chem. **41**, 684 (1963).
7. H. M. HUTTON and T. SCHAEFER. Can. J. Chem. **41**, 1623 (1963).
8. P. C. LAUTERBUR and R. J. KURLAND. J. Am. Chem. Soc. **84**, 3405 (1962).
9. J. T. ARNOLD. Phys. Rev. **102**, 136 (1956).
10. T. SCHAEFER and W. G. SCHNEIDER. Can. J. Chem. **37**, 2078 (1959).
11. H. M. HUTTON and T. SCHAEFER. Can. J. Chem. **41**, 1857 (1963).
12. U. LIDDEL and N. F. RAMSEY. J. Chem. Phys. **19**, 1608 (1951).
13. L. W. REEVES and W. G. SCHNEIDER. Can. J. Chem. **35**, 251 (1957).
14. T. SCHAEFER. Can. J. Chem. **39**, 1864 (1961).
15. W. G. SCHNEIDER. J. Phys. Chem. **66**, 2653 (1962).
16. A. D. BUCKINGHAM. Can. J. Chem. **38**, 300 (1960).
17. J. W. WILT and D. ROBERTS. J. Org. Chem. **27**, 3430 (1962).

Can. J. Chem. Downloaded from www.nrcresearchpress.com by 210.87.254.40 on 09/05/12
For personal use only.

THE CONSTITUTION OF A SYNTHETIC GLUCAN

II. METHYLATION STUDIES[1]

G. G. S. DUTTON AND A. M. UNRAU[2]

Department of Chemistry, University of British Columbia, Vancouver, British Columbia

Received April 16, 1963

ABSTRACT

After repeated and vigorous treatments, a fully methylated glucan was obtained. Hydrolysis of the methylated glucan with sulphuric acid gave tetra-, tri-, di-, and mono-*O*-methyl-D-glucoses in a 5:5:3:1 ratio. Both the furanose and pyranose tetramethyl isomers were identified. Nearly all of the possible pyranose and furanose cyclic trimethylglucoses were positively identified. An attempted resolution of the dimethylglucoses was relatively unsuccessful. The monomethylglucoses were identified by electrophoresis.

Can. J. Chem. Downloaded from www.nrcresearchpress.com by 210.87.254.42 on 09/05/12
For personal use only.

An earlier paper (1) has reported the general structural features of a synthetic glucan prepared by Mora (2). The present paper describes an investigation of the fully methylated glucan which was obtained after successive Haworth, Kuhn (3), and Purdie methylations. Several extended treatments of the partially methylated glucan (96 hours) with Purdie's reagents were required to obtain a product which had 45.35% methoxyl and showed no hydroxyl band in its infrared spectrum. The methylated glucan was soluble in petroleum ether (30–60°) containing 5% chloroform. A small quantity of insoluble material was obtained when the chloroform concentration was 3% by volume. A methylated synthetic xylan showed similar properties (4).

Hydrolysis of the methylated glucan with sulphuric acid under conditions shown to minimize demethylation (5) gave tetra-, tri-, di-, and mono-methylglucose fractions in a 4.9:5.0:2.9:1 ratio. A small quantity of glucose was present. Since the sulphuric acid hydrolysis technique (5) was used, the presence of glucose may have some structural significance.

By chromatography on a cellulose-hydrocellulose column using butanone–water azeotrope (17) the mixture of methylated sugars was resolved into four main fractions containing tetra-, tri-, di-, and mono-*O*-methyl ethers. The components within each fraction were then split into two parts by reaction with 1% methanolic hydrogen chloride at room temperature. Under these conditions all the methyl ethers carrying a free hydroxyl group on C_4 should form furanosides (designated by F) and by column chromatography should be separable from the pyranose forms of the free sugars (designated by P). It is of course to be expected that such a separation will not be clear-cut and that a portion of the sugars with free hydroxyls on C_4 may appear in the P-fractions. In the case of the tri- and di-*O*-methyl ethers a further subdivision may be achieved by taking advantage of the fact that trityl chloride will react selectively with a free C_6-hydroxyl group. Thus the trimethyl components designated 3F were separated into those which formed a trityl derivative (3FTr) and those in which the C_6-position was methylated (3F6, and similarly for the other fractions). An attempt was then made to separate chromatographically the components of each subfraction either directly or after periodate oxidation. In certain cases some insight into the composition of a subfraction was obtained by estimating the periodate

[1]*Presented at the 44th Chemical Institute of Canada Meeting in Montreal, August, 1961.*

[2]*Present address: Department of Plant Sciences, University of Manitoba, Winnipeg, Manitoba.*

consumption and formaldehyde production from a portion of the derived glucitols prepared by reduction with sodium borohydride. It is obvious that such manipulations cannot give a strictly quantitative picture but they do serve to indicate some of the main structural features of the polysaccharide. Careful attempts were made to characterize each component by crystalline derivatives but this did not prove successful in all cases. It may be mentioned that a sample of the glucoside mixture from this polysaccharide (and also from the polyxylose (4)) was subjected to vapor phase chromatography but gave a pattern that was too complex to resolve. Despite the excellent pioneer work which has been carried out on the separation of methylated methyl glycosides there is still a paucity of data on methyl furanosides. A description of the results obtained in the chemical separation of this mixture of methylated glucoses is given below.

The tetramethylglucose fraction was shown by its rotation to contain about 20% 2,3,5,6-tetra-*O*-methyl-D-glucose, the rest being the 2,3,4,6-isomer. Both isomers were identified by separation of the furanose component as the methyl glycoside from the pyranose sugar, on a cellulose column. The pyranose sugar gave the crystalline *p*-nitrobenzoate while the furanose sugar was transformed, after hydrolysis, to the corresponding gluconamide.

Part of the slowest-moving tri-*O*-methyl fraction was obtained crystalline and identified as the 2,4,6-isomer from the physical constants of the sugar and by conversion to the *N*-phenylglycosylamine. The remainder of the tri-*O*-methyl fraction was treated with methanolic hydrogen chloride at room temperature and the furanosides thus formed separated from the pyranose sugars on the column, giving two fractions designated 3F and 3P. The two fractions were then separately resolved as follows:

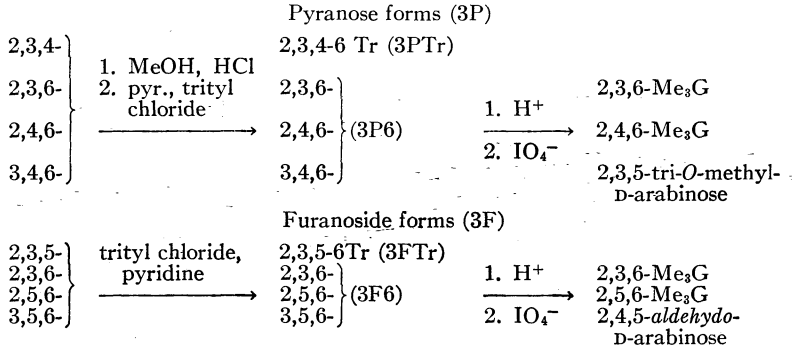

The pyranose sugars were converted to the glycosides and the mixture treated with trityl chloride, which readily gave methyl 2,3,4-tri-*O*-methyl-6-*O*-trityl-D-glucoside. The 2,3,4-tri-*O*-methyl-D-glucose was further identified by (*a*) conversion to the *N*-(*p*-nitrophenyl)-glycosylamine and (*b*) reduction ($NaBH_4$), periodate oxidation, and preparation of the 1-*p*-nitrobenzoate of the resulting 2,3,4-tri-*O*-methyl-L-xylose. The 3P6 mixture of pyranosides was hydrolyzed and oxidized with periodate to give a trimethylpentose and two unchanged trimethylglucoses. The mixture was resolved by cellulose column chromatography and the 2,3,6-tri-*O*-methyl-D-glucose converted to the crystalline 1,4-di-*p*-nitrobenzoate. The other tri-*O*-methyl-D-glucose had a rotation corresponding to that of the 2,4,6-isomer and was chromatographically identical with it. The pentose, presumed to be 2,3,5-tri-*O*-methyl-D-arabinose, was oxidized (Br_2) to the acid. The amide gave a negative Weerman test (6) and the lactone and amide had optical rotations very similar to those expected from the respective L-compounds. The amide did not crystallize, however.

Can. J. Chem. Downloaded from www.nrcresearchpress.com by 210.87.254.42 on 09/05/12
For personal use only.

From the furanoside (3F) mixture, a water-insoluble trityl derivative was obtained which was presumed to be the 6-*O*-trityl ether of methyl 2,3,5-tri-*O*-methyl-D-glucoside. The trityl group was removed and the free sugar oxidized (Br_2). The derived amide gave a negative Weerman test (6), showing that the hydroxyl on C_2 was substituted. Treatment of the lactone with phenylhydrazine gave the solid phenylhydrazide of 2,3,5-tri-*O*-methyl-D-gluconic acid. The mixture of water-soluble furanosides (2,5,6-, 2,3,6- and 3,5,6-trimethyl ethers) was hydrolyzed and treated with periodate. Three components were obtained, one presumably being 2,4,5-tri-*O*-methyl-*aldehydo*-D-arabinose and two unchanged tri-*O*-methylglucoses. The mixture was resolved by cellulose chromatography and the compounds identified as follows: 2,3,6-tri-*O*-methyl-D-glucose gave the crystalline 1,4-di-*p*-nitrobenzoate; 2,5,6-tri-*O*-methyl-D-glucose was oxidized (Br_2) and converted to the lactone. The latter gave a negative Weerman test and formed a solid phenylhydrazide; 2,4,5-tri-*O*-methyl-*aldehdyo*-D-arabinose gave a positive Schiff test. The amide of the corresponding acid gave a negative Weerman test.

An attempt was made to resolve the dimethylglucose mixture by a technique similar to that outlined for the tri-*O*-methylglucose mixture. The furanoside (2F) and pyranose (2P) mixture was separated by column chromatography as before. The components were then treated as follows:

Pyranose forms (2P)

2,4-, 3,4-, 4,6- —(1. MeOH, HCl; 2. trityl chloride, pyr.)→ 2,4-6Tr, 3,4-6Tr (2PTr), 4,6-(2P6)

2PTr —(1. H^+; 2. IO_4^-)→ 2,4-di-*O*-methyl-D-glucose; 2,3-di-*O*-methyl-D-arabinose

Furanoside forms (2F)

2,3-, 2,5-, 2,6-, 3,5-, 3,6-, 5,6- —(trityl chloride, pyridine)→ 2,6-, 3,6-, 5,6- (2F6)

2F6 —(1. H^+; 2. IO_4^-)→ 1-*O*-methylglyceraldehyde; 2,5-di-*O*-methyl-D-arabinose; 3,4-di-*O*-methyl-D-erythrose

2,3-6Tr, 2,5-6Tr, 3,5-6Tr (2FTr) —(1. H^+; 2. IO_4^-)→ 2,3-di-*O*-methyl-D-glucose; 2,5-di-*O*-methyl-D-glucose; 2,4-di-*O*-methyl-D-glucose

Considering the pyranose sugars (2P) first, component 2P6, which should have been 4,6-di-*O*-methyl-D-glucose, failed to crystallize. Electrophoresis demonstrated that the syrup was composed of two compounds in approximately equal quantities and a third substance in minor quantities. The periodate oxidation of component 2PTr showed that part of the mixture was not attacked by periodate and the R_f and M_g values suggested that this sugar was 2,4-di-*O*-methyl-D-glucose. 2,3-Di-*O*-methyl-D-arabinose was apparently present as indicated by the R_f and M_g values. Two components with R_f values of about 0.79 and 0.85, whose identities are unknown, were also present. These compounds gave a peculiar purple color when paper chromatograms were sprayed with *p*-anisidine.

Periodate oxidation of component 2F6 gave a complex mixture of products. A considerable amount of dimethyl sugar was not attacked by periodate whereas, according to the reaction scheme, none of the dimethylglucoses should have escaped periodate attack. The unchanged dimethyl fraction was shown by electrophoresis to be composed of at least three sugars. Chromatographic evidence was obtained for a faster-migrating dimethylpentose, presumably 2,5-di-*O*-methyl-D-arabinose. Several components with R_f greater than 0.75 were observed. The presence of 1-*O*-methylglyceraldehyde was shown as follows: The distillate from the periodate reaction mixture was bubbled through a solution of sodium borohydride. Chromatographic examination of the distillate gave a small amount

Can. J. Chem. Downloaded from www.nrcresearchpress.com by 210.87.254.42 on 09/05/12
For personal use only.

of Tollens-positive material. On the assumption that this material was 1-*O*-methylglycerol it consumed approximately 1 mole of periodate and gave 1 mole of formaldehyde. Demethylation gave glycerol. These results establish the identity of 1-*O*-methylglycerol, and of the possible dimethylglucoses this can only be formed by 2,6-di-*O*-methyl-D-glucose. In a similar manner, a component with R_f 0.81 gave results which corresponded to 3,4-di-*O*-methylerythritol. Of the dimethylglucoses only 5,6-di-*O*-methyl-D-glucose can furnish the corresponding 3,4-di-*O*-methyl-D-erythrose.

Whereas the general procedure outlined served quite well in the resolution of the tri-*O*-methylglucose mixture, very little success was experienced when it was applied to the di-*O*-methylglucose mixture. It is suspected that all the possible di-*O*-methylglucoses were present and a more rigorous scheme must be evolved to resolve this complex mixture satisfactorily.

The identity and ratio of the mono-*O*-methylglucoses was established by electrophoresis and paper chromatography. By the latter, no appreciable 5-*O*-methyl isomer appeared to be present. The remaining four monomethylglucoses, the 2-, 3-, 4-, and 6-*O*-methyl isomers, were present in a 3:5:1:2 ratio. A small quantity of glucose was obtained crystalline and transformed to the phenylosazone.

From these results the following conclusions may be drawn: (i) a fully methylated polysaccharide may be obtained but a much more prolonged treatment was required than is usual for the majority of natural polysaccharides; (ii) the fully methylated polysaccharide had an unusually high solubility in petroleum ether; (iii) of the terminal glucose units about 20% of them were furanose; (iv) some of the internal glucose units were also furanose but the predominant linkage appeared to be $1 \rightarrow 6$-glucopyranose although evidence for $1 \rightarrow 2$, $1 \rightarrow 3$, and $1 \rightarrow 4$ linkages were also found; (v) those sugar glycosides having a free hydroxyl group on C_6 may be readily separated from mixtures as their water-insoluble trityl ethers. In summary, it is clearly shown that the synthetic glucan is extremely highly branched and composed of a high proportion of glucofuranose units. This is in marked contrast to natural glucans but is in agreement with an earlier study of this material by periodate oxidation (1).

EXPERIMENTAL

Paper chromatographic separations were carried out using the descending technique and butanone–water azeotrope as the developing solvent. Electrophoresis was carried out in 0.1 *M* sodium borate at 1000 v. The sugars on paper chromatograms were detected by use of *p*-anisidine–trichloroacetate spray reagent.

Evaporations were carried out under reduced pressure at a bath temperature of 40–45° C. Optical rotations recorded are equilibrium values at 21±2° C. Melting points quoted are uncorrected.

Methylation of the Glucan

A sample (7.5 g) of the synthetic glucan was methylated in the usual manner with the Haworth reagents to yield a water-insoluble amorphous product. This substance was further methylated by the procedure of Kuhn (2) to give a pale yellow, amorphous glass which contained 43% methoxyl. The product was consequently treated four times with Purdie's reagents over extended intervals (96 hours each) on a steam bath to yield finally a brittle glass (8.1 g), $[\alpha]_D$ 72.5° in $CHCl_3$, 71.8° in methanol (*c*, 3.1), which showed no OH band in the infrared spectrum and contained 45.35% methoxyl (theory 45.6%). The methylated glucan was suspended in petroleum ether (30–60°), 3% (by volume) chloroform added, and the milky solution allowed to stand 12 hours. The clear solution was decanted and evaporated to yield a pale yellow amorphous glass (7.75 g).

Hydrolysis of Methylated Glucan

The methylated glucan was dissolved in 72% cold sulphuric acid to yield a thick syrup to which was added cold water to give approximately a 2 *N* H_2SO_4 solution. This solution was boiled for 10 hours, neutralized ($BaCO_3$), deionized, and evaporated to a colorless, mobile syrup. Chromatographic examination of the hydrolyzate showed the presence of tetra- (multi-colored spot suggesting the presence of furanose isomer), tri- (elongated spot), di-, and mono-*O*-methylglucoses and glucose (present in minor amount).

Can. J. Chem. Downloaded from www.nrcresearchpress.com by 210.87.254.42 on 09/05/12
For personal use only.

Cellulose Column Chromatography

The mixture was passed through a cellulose–hydrocellulose column using butanone–water azeotrope solvent in approximately 900-mg aliquots. The contents of tubes consisting of a mixture, for example of tetra- and tri-*O*-methyl sugars, were rechromatographed.

Fraction	Weight (g)	Molar ratio
4. Tetra-*O*-methyl-glucose	2.082	4.9
3. Tri-*O*-methyl-glucose	2.002	5.0
2. Di-*O*-methyl-glucose	1.078	2.9
1. Mono-*O*-methyl-glucose	0.352	1
	0.025	—

Fraction 4

The mixture showed $[\alpha]_D$ 64° (*c*, 8.1 in water). The reported rotation for 2,3,4,6-tetra-*O*-methyl-D-glucose is 84° in water (equilibrium value), while the 2,3,5,6-tetra-*O*-methyl isomer has a rotation of −11° (7). The fraction of the 2,3,5,6-tetra-*O*-methyl isomer present in the mixture is therefore about 21% or approximately 420 mg. The mixture was dissolved at room temperature in dry methanol containing 1% hydrogen chloride and the change in rotation at room temperature followed. When no further change was observed, the solution was neutralized (Ag_2CO_3), evaporated, and passed through a cellulose–hydrocellulose column. The eluate immediately appearing after the solvent front and until 2,3,4,6-tetra-*O*-methyl-D-glucose appeared was combined and evaporated to a syrup (180 mg). Hydrolysis of this non-reducing substance (20 ml 0.1 *N* H_2SO_4, 3 hours on steam bath), followed by neutralization ($BaCO_3$) of the solution and evaporation, gave a syrupy product (175 mg), $[\alpha]_D$ −9.5° (*c*, 3.5 in water), which had an R_f slightly greater than that of authentic 2,3,4,6-tetra-*O*-methyl-D-glucose. The syrup was dissolved in water and the sugar oxidized with bromine in the usual fashion. The acid was heated under vacuum to effect lactone formation and the syrupy product showed $[\alpha]_D$ 52° (*c*, 1.6 in MeOH). The lactone was dissolved in dry methanol containing ammonia, the solution left for 72 hours, and the solvent evaporated. The syrupy product, $[\alpha]$ 39.5° in water (*c*, 1.5 in water), was dissolved in acetone, ether and pet. ether (30–60°) were added, whereupon partial crystallization took place. Removal of some crystals followed by washing with cold ether and drying on a porous plate gave a substance which melted at 86–89° C; reported (7) m.p. for 2,3,5,6-tetra-*O*-methyl-D-gluconamide is 91° C.

A portion (188 mg) of the reducing sugar obtained from the above separation of the furanoside from the pyranose isomer showed $[\alpha]_D$ 74° (*c*, 1.9 in MeOH). The sugar was treated with *p*-nitrobenzoyl chloride in the usual manner to give the water-insoluble *p*-nitrobenzoate. After recrystallization from an acetone – ethyl acetate solvent mixture, the 2,3,4,6-tetra-*O*-methyl-1-*O*-*p*-nitrobenzoyl-D-glucose had m.p. 98–100° C; reported (8) melting point is 102° C.

Identification of 2,3,4- and 2,4,6-Tri-O-methyl-D-glucose

A portion (250 mg) of fraction 3 was rechromatographed on the cellulose–hydrocellulose column and the effluent collected in five distinct fractions. A small quantity (about 15 mg) of fast-migrating material was not further investigated. The second fraction (66 mg), having an R_f similar to that of 2,3,4-tri-*O*-methyl-D-glucose, showed $[\alpha]_D$ 75° (*c*, 0.7 in acetone). Treatment of the sugar with *p*-nitroaniline (9) gave needle-like crystals which upon recrystallization from an ethanol–ether solvent mixture had m.p. 221–224° C, $[\alpha]_D$ −245° (*c*, 0.1 in pyridine); reported (9) m.p. for 2,3,4-tri-*O*-methyl-*N*-(*p*-nitrophenyl)-D-glucosylamine is 224–225° C, $[\alpha]_D$ −251° in pyridine.

The slowest fraction (22.5 mg), $[\alpha]_D$ 71° (*c*, 0.3 in MeOH), crystallized upon standing. Removal of some crystals followed by washing with cold ether and drying on a porous plate gave a substance which had m.p. 116–120° C. The compound was treated with aniline to give the *N*-phenylglucosylamine, $[\alpha]_D$ −109° (*c*, 0.3 in MeOH), which had m.p. 158–160° C; reported (10) m.p. for 2,4,6-tri-*O*-methyl-*N*-phenyl-D-glucosylamine is 162–166° C, $[\alpha]_D$ −113° in MeOH.

Treatment of Fraction 3 with Methanol–HCl

The bulk (1.75 g) of fraction 3 (trimethylglucoses) was dissolved in dry methanol (25 ml) containing 1% hydrogen chloride. When no further change in rotation was observed, the solution was neutralized (Ag_2CO_3) and evaporated. The syrupy product was passed through a cellulose–hydrocellulose column. The effluent was collected as described in the separation procedure for the tetramethyl mixture. The yield of furanoside (component 3F) was about 420 mg. Hydrolysis of a small portion (60 mg) with sulphuric acid and chromatography of the hydrolyzate gave evidence for the presence of substances with R_f values of 0.74, 0.66, and 0.57. The slower-moving substance was presumed to be 2,3,6-tri-*O*-methyl-D-glucose.

Periodate Oxidation of Trimethylglucofuranose Mixture (3F)

A portion (40.7 mg or 0.1815 mmole) of the furanose mixture from the above hydrolysis was dissolved in water (20 ml), and a solution (5 ml) of sodium borohydride (25 mg) added. The reduction was allowed to proceed for 48 hours at room temperature. The solution was neutralized with acetic acid, and sodium

Can. J. Chem. Downloaded from www.nrcresearchpress.com by 210.87.254.42 on 09/05/12
For personal use only.

periodate (5 ml 0.5 *M* solution) was added. After 5- and 8-hour intervals, formaldehyde was determined (11). Formaldehyde (0.0369 mmole) would originate from 0.0369 mmole 3,5,6-tri-*O*-methyl-D-glucitol, or about 20% of the original mixture was 3,5,6-tri-*O*-methyl-D-glucose. A total of 0.1490 mmole of periodate was consumed; therefore 0.1815 − 0.1490 or 0.0325 mmole (18%) of 2,3,5-tri-*O*-methyl-D-glucose was present since the corresponding hexitol would be the only hexitol immune to periodate attack. The remainder (62%) of the mixture would be 2,3,6- or 2,5,6-tri-*O*-methyl-D-glucose or a mixture of both.

Further Resolution of Component 3F

The remainder (365 mg) of the tri-*O*-methylfuranosides was dissolved in dry pyridine (10 ml), and trityl chloride (0.5 molar equivalent) was added and the solution left at room temperature for about 48 hours. Water was added to the mixture, whereupon the insoluble tritanol and trityl derivative (3FTr) precipitated. Of the possible furanosides (2,3,5-, 2,3,6-, 2,5,6-, 3,5,6-tri-*O*-methyl), only methyl 2,3,5-tri-*O*-methyl-D-glucoside would form the water-insoluble 6-trityl derivative. The precipitate was dissolved in methanol (15 ml) containing 1% HCl and the solution boiled for 1 hour. Water (50 ml) was added and the solution boiled for an additional 2 hours to regenerate the free sugar. The solution was neutralized ($PbCO_3$), filtered, and deionized. Evaporation of the effluent gave a syrup, 22 mg, $[\alpha]_D$ 15° (*c*, 0.75 in MeOH), which had an R_f 0.59–0.61. The sugar was oxidized with bromine in the usual fashion. The acid (25 mg) gave a neutralization equivalent of 260, theoretical is 240. After the acid was heated under vacuum to effect lactone formation, a few milligrams of product was subjected to the Weerman test (6). The negative result indicated that C_2 of the sugar was substituted. To the lactone, in boiling ether, was added phenylhydrazine. The small amount of insoluble phenylhydrazide was collected, washed with ether, and after drying had m.p. 150–154° C; reported (12) m.p. for 2,3,5-tri-*O*-methyl-D-gluconophenylhydrazide is 156–157° C.

Component 3F6

From the previous experiment, the furanosides which could not form 6-*O*-trityl ethers were subjected to acid hydrolysis to give the free sugars. This mixture should now be composed of 2,3,6-, 2,5,6-, and 3,5,6-tri-*O*-methyl-D-glucoses. The syrup (300 mg) was dissolved in 0.15 *M* periodic acid (100 ml) and left at 5° C for 24 hours. The solution was neutralized ($BaCO_3$), deionized, and evaporated to a syrup. Chromatography revealed three components with R_f values of (*a*) 0.49 (2,3,6-tri-*O*-methyl-D-glucose), (*b*) 0.59 (2,5,6-tri-*O*-methyl-D-glucose), and (*c*) 0.80 (presumed to be 2,4,5-tri-*O*-methyl-*aldehydo*-D-arabinose arising from periodate cleavage of 3,5,6-tri-*O*-methyl-D-glucose). The mixture was resolved by cellulose column chromatography. *Component (a)*, 55 mg, $[\alpha]_D$ 73° (*c*, 0.5 in water), was treated with *p*-nitrobenzoyl chloride in the usual manner. The product after recrystallization from acetone–ether had m.p. 188–190° C, $[\alpha]_D$ −32° (*c*, 0.4 in $CHCl_3$); reported (13) m.p. for di-*p*-nitrobenzoate of 2,3,6-tri-*O*-methyl-D-glucose is 189–190° C, $[\alpha]_D$ −33° in $CHCl_3$. *Component (b)*, 31 mg, had $[\alpha]_D$ 12.5° (*c*, 0.6 in water), 19° (*c*, 0.6 in MeOH), and was presumed to be 2,5,6-tri-*O*-methyl-D-glucose (14). The sugar was oxidized with bromine and the acid converted to the lactone by the usual techniques. A small portion (5 mg) of the amide was subjected to the Weerman test (6). The negative result indicated that the C_2-hydroxyl was substituted. Treatment of the lactone, in boiling ether, with phenylhydrazine gave a solid which after washing with ether and pet. ether (30–60°) and drying had m.p. 157–161° C. *Component (c)*, 184 mg, showed $[\alpha]_D$ 17.5° (*c*, 1.9 in MeOH), and was presumed to be 2,4,5-tri-*O*-methyl-*aldehydo*-D-arabinose. The substance gave a positive Schiffs test. A small portion (10 mg) was oxidized and converted to the amide, which gave a negative Weerman test, indicating that the C_2-hydroxyl of the aldehydo sugar was substituted. An attempt to prepare the 2,4-dinitrophenylhydrazone failed.

Tri-O-methyl-D-glucopyranose Constituents (3P)

The tri-*O*-methylglucoses which did not form furanosides in the treatment with methanolic hydrogen chloride at room temperature (see previous section) were presumed to consist of 2,3,4-, 2,3,6-, 2,4,6-, and 3,4,6-tri-*O*-methyl-D-glucoses. The mixture (1.2 g) was boiled with methanol containing 1.5% hydrogen chloride. The product was tritylated as described before to give the water-insoluble *O*-trityl ether of methyl 2,3,4-tri-*O*-methyl-D-glucoside (3PTr) and the unreacted water-soluble methyl glycosides (3P6) of 3,4,6-, 2,3,6-, and 2,4,6-tri-*O*-methyl-D-glucoses. *Component 3PTr*, 400 mg, had $[\alpha]_D$ of detritylated free sugar 72° (*c*, 1.2 in acetone). Treatment of a portion (80 mg) of the free sugar with *p*-nitroaniline gave the corresponding 2,3,4-tri-*O*-methyl-*N* (*p*-nitrophenyl)-D-glucosylamine (9), m.p. 221–224° C, $[\alpha]_D$ −248° (*c*, 0.1 in pyridine). A portion (175 mg) of the sugar was reduced ($NaBH_4$) and the glucitol oxidized with periodic acid, whereby a syrupy pentose (110 mg), $[\alpha]_D$ −17° (*c*, 0.5 in water), was obtained. Treatment with *p*-nitrobenzoyl chloride gave 2,3,4-tri-*O*-methyl-1-*O*-*p*-nitrobenzoyl-L-xylose (8, p. 517), m.p. 134–135° C, $[\alpha]_D$ −73° (*c*, 0.4 in $CHCl_3$). The free sugar had R_f 0.79. *Component 3P6*: The water-soluble material (750 mg) from the previous tritylation experiment was presumed to be composed of methyl 2,4,6-, 3,4,6-, and 2,3,6-tri-*O*-methyl-D-glucosides. The mixture was boiled (10 hours) in *N* sulphuric acid (25 ml) and after neutralization ($BaCO_3$) a syrup (710 mg) was obtained. A small portion of this syrup was reduced ($NaBH_4$), oxidized with periodate, and the formaldehyde measured (11). The result indicated that about 15% of the original mixture was 3,4,6-tri-*O*-methyl-D-glucose. Periodate oxidation of the bulk of the syrup followed by chromatographic examination of the product (645 mg) gave evidence for three components: (*a*) R_f 0.81, presumed to be 2,3,5-tri-*O*-methyl-D-arabinose from periodate cleavage of 3,4,6-tri-*O*-methyl-D-glucose, (*b*) R_f 0.51, presumed to be 2,3,6-tri-*O*-methyl-D-glucose, and (*c*) R_f 0.46, presumed to be 2,4,6-tri-*O*-methyl-D-glucose. The mixture was resolved

Can. J. Chem. Downloaded from www.nrcresearchpress.com by 210.87.254.42 on 09/05/12
For personal use only.

on a cellulose column in the usual manner. *Component (a)*, 85.5 mg, showed $[\alpha]_D$ 38.5° (*c*, 0.8 in water), 47° (*c*, 0.8 in MeOH). The sugar was oxidized with bromine and converted to the lactone (73 mg), $[\alpha]_D$ 23° (*c*, 1.2 in water). The lactone was treated with methanolic ammonia (30 ml), left 48 hours, and the solvent evaporated. The amide (70 mg), which did not crystallize, showed $[\alpha]_D$ −20° (*c*, 1.5 in EtOH), −15° (*c*, 1.5 in water) and gave a negative Weerman test. Reported rotation of 2,3,5-tri-*O*-methyl-L-arabinolactone, −45 → −24° in water; of amide, +16° in water and +21° in EtOH (15). *Component (b)*, 229 mg, $[\alpha]_D$ 72° (*c*, 0.7 in water), was presumed to be 2,3,6-tri-*O*-methyl-D-glucose. The syrupy substance was treated with *p*-nitrobenzoyl chloride in the usual manner to give 2,3,6-tri-*O*-methyl-1,4-di-*O*-*p*-nitrobenzoyl-D-glucose (8, p. 533) which after recrystallization from acetone–ether mixture had m.p. 186–188° C, $[\alpha]_D$ −32° (*c*, 2.1 in $CHCl_3$). *Component (c)*, 126 mg, $[\alpha]_D$ 71° (*c*, 1.3 in water) was believed to be 2,4,6-tri-*O*-methyl-D-glucose. This sugar was identified previously. Treatment with *p*-nitrobenzoyl chloride gave a thick semisolid which did not crystallize.

Attempted Resolution of Di-O-methyl-D-glucoses

The mixture of di-*O*-methylglucoses was treated with methanolic hydrogen chloride as previously described and the product passed through a cellulose column to yield the furanoside fraction (component 2F) and the pyranose fraction (2P). The 2P-component (460 mg), presumed to consist of a mixture of 2,4-, 3,4-, and 4,6-di-*O*-methyl-D-glucoses, was boiled with methanolic hydrogen chloride and the methyl glycoside mixture treated with trityl chloride as described before. The water-insoluble substance was presumed to be a mixture of the methyl 6-*O*-trityl-2,4-, and 3,4-di-*O*-methyl-D-glucosides and tritanol (component 2PTr). This material was hydrolyzed to recover the free sugars and the mixture (198 mg) oxidized with periodic acid. The product, isolated in the usual manner, was tentatively shown to contain a dimethylglucose, R_f 0.21, presumed to be 2,4-di-*O*-methyl-D-glucose, a dimethylpentose, R_f 0.27, presumed to be 2,3-di-*O*-methyl-D-arabinose, and two unknown components, R_f 0.79 and 0.84. The mixture was not investigated further. The water-soluble material (213 mg) (component 2P6) recovered from the above tritylation treatment was hydrolyzed and the syrupy product (205 mg), R_f 0.22, presumed to be 4,6-di-*O*-methyl-D-glucose, analyzed by electrophoresis. Two components in apparently equal quantities were found to be present.

Attempted Resolution of Component 2F

This syrupy substance (505 mg) was treated with trityl chloride as described before to give the trityl fraction (component 2FTr, 75 mg) and the non-tritylated fraction (component 2F6, 265 mg). The two fractions were subjected to the following treatments: *Component 2F6* was unintentionally treated with periodate. Since 2,6-, 3,6-, and 5,6-di-*O*-methyl-D-glucoses were presumed to be present, the distillate from the evaporation of the neutralized ($BaCO_3$) oxidation mixture was bubbled through a solution of sodium borohydride to catch and reduce any volatile aldehyde fragments that might have been formed. The distillate was acidified, evaporated, borate removed (MeOH–HCl), and the small quantity (25 mg) of product chromatographed and found to contain one Tollens-positive substance with an R_f greater than glycerol (R_{xylose} 2.95 in EtOAc:HOAc:H_2O (8:2:2)). A portion (10 mg) of the syrup was oxidized with periodic acid (20 ml, 0.1 *M*) and after 30 and 60 minutes, 2.65 mg formaldehyde had been produced (theoretical yield 2.84 mg based on 1-*O*-methylglycerol), and 0.0881 mmole of periodate had been consumed (theoretical consumption of 1-*O*-methylglycerol is 0.0944). The remainder (15 mg) of the syrup was dissolved in 48% hydrobromic acid (3–4 ml) and refluxed on a steam bath for about 20 minutes, the solution was neutralized ($PbCO_3$), and the product (11 mg) was examined chromatographically. Glycerol was identified with a trace of faster-moving material, and the oily product was treated with *p*-nitrobenzoyl chloride to give glycerol tri-*O*-*p*-nitrobenzoate, m.p. and mixed m.p. 186–189° C. Only 2,6-di-*O*-methyl-D-glucose will furnish 1-*O*-methylglycerol upon periodate oxidation and its presence is thus established.

The non-volatile mixture from the periodate oxidation described above was chromatographed and found to contain some (major quantity) unreacted di-*O*-methylglucose (R_f 0.23), a dimethylpentose in smaller amount and presumed to be 2,5-di-*O*-methyl-D-arabinose (R_f 0.55), and at least four substances with R_f ranging from 0.70 to 0.88. This mixture was resolved chromatographically and electrophoresis of the di-*O*-methylglucose fraction showed that it was composed of two major components and one in lesser quantities. A component (13 mg) with R_f 0.79–0.81 was analyzed as described above for 1-*O*-methylglycerol. A portion (4.3 mg) of the substance upon periodate oxidation gave about 94% of the theoretical amount of formaldehyde and the periodate consumption was 96% of theory (assuming that the substance was 3,4-di-*O*-methyl-D-erythritol, which would have arisen from the periodate cleavage of 5,6-di-*O*-methyl-D-glucose). The remainder (10.7 mg) of the substance was demethylated and erythritol identified chromatographically as the major component.

Component 1

The syrupy mixture of mono-*O*-methyl-D-glucoses was shown by chromatography to contain a negligible amount of the 5-*O*-methyl isomer. Electrophoresis showed that the mixture contained 3-*O*-methyl, M_g 0.86, 6-*O*-methyl, M_g 0.78, 2-*O*-methyl, M_g 0.31, each identical with authentic material; and 4-*O*-methyl, M_g 0.24. The ratio of the sugars was determined by the phenol – sulphuric acid method (16) and found to be 5:2:3:1 respectively.

D-*Glucose*

The syrup, $[\alpha]_D$ 51° (*c*, 0.75 in water), crystallized spontaneously. After washing with ethanol, the solid

Can. J. Chem. Downloaded from www.nrcresearchpress.com by 210.87.254.42 on 09/05/12
For personal use only.

had m.p. and mixed m.p. 143–145° C. Treatment of the sugar with phenylhydrazine hydrochloride in aqueous ethanol gave D-glucose phenylosazone, m.p. and mixed m.p. 205–208° C.

ACKNOWLEDGMENTS

This investigation was supported by a research grant (RG 7652) from the Division of General Medical Sciences, Public Health Service (U.S.A.), to whom we express our thanks. We are also indebted to Miss J. Hunter for skillful technical assistance.

REFERENCES

1. G. G. S. DUTTON and A. M. UNRAU. Can. J. Chem. **40**, 1196 (1962).
2. P. T. MORA, J. W. WOOD, P. MAURY, and B. G. YOUNG. J. Am. Chem. Soc. **80**, 693 (1958).
3. R. KUHN, I. LOW, and N. TRISCHMAN. Ber. **90**, 203 (1957).
4. G. G. S. DUTTON and A. M. UNRAU. Can. J. Chem. **40**, 2105 (1962).
5. I. CROON, G. HERRSTROM, G. KULL, and B. LINDBERG. Acta Chem. Scand. **14**, 1338 (1960).
6. R. A. WEERMAN. Rec. Trav. Chim. **37**, 16 (1917).
7. E. J. BOURNE and S. PEAT. *In* Advances in carbohydrate chemistry. Vol. 5. *Edited by* C. S. Hudson and S. M. Cantor. Academic Press, New York. 1950. pp. 188, 190.
8. F. SMITH and R. MONTGOMERY. *In* Plant gums and mucilages. Reinhold, New York. 1959. p. 534.
9. J. W. VAN CLEVE, W. C. SCHAFFER, and C. E. RIST. J. Am. Chem. Soc. **78**, 4435 (1956).
10. H. GRANICHSTADTEN and E. G. V. PERCIVAL. J. Chem. Soc. 54 (1943).
11. A. M. UNRAU and F. SMITH. Chem. Ind. (London), 330 (1957).
12. (*a*) F. SMITH. J. Chem. Soc. 571 (1944).
    (*b*) R. J. DIMLER, H. A. DORIS, and G. E. HILBERT. J. Am. Chem. Soc. **68**, 1377 (1946).
13. P. A. REBERS and F. SMITH. J. Am. Chem. Soc. **76**, 6097 (1954).
14. C. T. BISHOP and J. SCHMORAK. Can. J. Chem. **34**, 845 (1956).
15. G. G. MAHER. *In* Advances in carbohydrate chemistry. Vol. 10. *Edited by* M. L. Wolfrom. Academic Press, New York. 1955. p. 264.
16. N. DUBOIS, J. K. HAMILTON, K. A. GILLES, P. A. REBERS, and F. SMITH. Anal. Chem. **28**, 350 (1956).
17. J. D. GEERDES, B. A. LEWIS, R. MONTOGOMERY, and F. SMITH. Anal. Chem. **26**, 264 (1954).

Can. J. Chem. Downloaded from www.nrcresearchpress.com by 210.87.254.42 on 09/05/12
For personal use only.

THE THEORY OF CURRENT DISTRIBUTION AND POTENTIAL PROFILE AT AN ELECTRODE OF SIGNIFICANT OHMIC RESISTANCE

B. E. CONWAY AND E. GILEADI[1]
Department of Chemistry, University of Ottawa, Ottawa, Canada

AND

H. G. OSWIN
Leesona Moos Laboratories, Lake Success Park, Community Drive, Great Neck, New York, U.S.A.

Received May 24, 1963

ABSTRACT

The problem of current distribution at an electrode of linear geometry having a significant ohmic resistance is examined for conditions where the ohmic potential drop along the electrode material is of the same order of magnitude as the metal–solution potential difference. This problem is of practical significance in primary and secondary cells at high current drains and in certain types of fuel cell electrodes. The current distribution and metal–solution potential profiles are calculated as limiting cases of a general theory. The true and apparent current–potential relations are compared theoretically.

I. INTRODUCTION

In recent years, current distribution problems in electrolysis processes have become of of renewed importance in certain applications involving high current drains in batteries, palladium hydrogen diffusion anodes operating at elevated temperatures, and in anodic electrolytic machining. General problems of current density distribution were recognized in early work on electroplating and throwing-power (1, 2) and renewed interest in this and related kinds of problems has recently been apparent (3, 4). In the above work, the inhomogeneous current density distribution is treated largely in terms of the finite resistance of the electrolyte. The corresponding problem, in which the *electrode resistance* effect is significant at high current drains, has not previously been examined, except in the case of thin-film light modulators (5) where film resistance and solution conductance effects have been simultaneously considered as a special problem. Co-conduction effects longitudinally through the solution (6) and through the double layer (7) parallel to a thin wire electrode have been considered for cases where the electrode resistance was not negligible compared with the electrolyte solution resistance. Such studies can lead to information about adsorption in the double layer (7) and the electrode potential distribution in the case of a wire in a solution with contacts at each end to an external electric circuit (6).

In the present work, we examine the general theory of current density and overpotential distribution for a thin wire or tubular diffusion electrode having significant ohmic resistance and immersed in an electrolyte with contact to the external circuit at one end; relations are also obtained for the true and apparent Tafel slope for an electrode process occurring at the wire under such conditions.

II. CALCULATION OF POTENTIAL AND CURRENT PROFILES

1. Model

We consider the model for a cylindrical electrode of length L, radius r, and specific

[1]*Present address: John Harrison Laboratory of Chemistry, University of Pennsylvania, Philadelphia 4, Pennsylvania.*

Can. J. Chem. Downloaded from www.nrcresearchpress.com by 210.87.254.42 on 09/05/12
For personal use only.

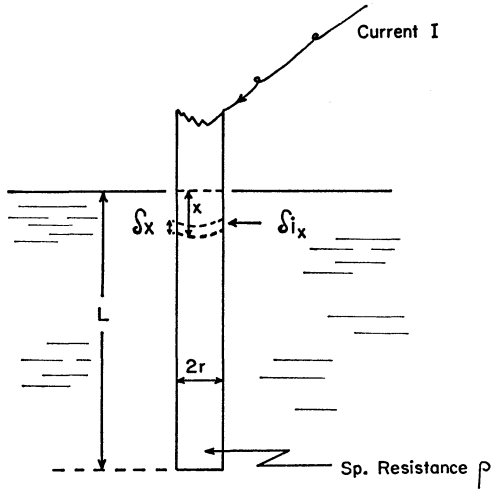

FIG. 1. Schematic diagram of the model considered in the current distribution problem at a cylindrical electrode, showing some of the quantities involved in the treatment.

resistance ρ, shown in Fig. 1. The electrode may be a thin wire or a thin tube, as in the case of palladium hydrogen diffusion anodes where significant electrode resistance can arise. An element of current di_x is regarded as passing across an element of area $2\pi r dx$ at a position x below the top of the electrode (taken as the level of immersion of the electrode in the electrolyte). The total current passing into, or out of, the electrode is written as I and the overvoltage which would determine the rate of the electrode reaction if ρ were negligible is expressed as V_0. The normal current density i passing in the absence of ohmic effects is related to the exchange current density by the Tafel equation in exponential form as

$$i = i_0 \exp [\alpha V_0 F/RT] = i_0 \exp [V_0/b].$$

We assume the current density passing at any point x along the electrode is determined by the overvoltage V_0 (arising from an impressed voltage, or from a galvanic potential difference in the case of a battery or fuel cell) less the ohmic drop ΔV_x existing at the position x down the electrode from the top. This potential drop will be determined by the current passing in the cylinder from the top to x and by the specific resistance ρ of the electrode. The current passing will not be uniform and will decrease down the electrode. At any given point, the current density will be exponentially related to the overpotential and hence the metal–solution p.d. existing at that point, i.e. to $V_0 - \Delta V_x$.

2. Formulation of Equations

At x, the element of actual anodic* current passing across an area ds equal to $2\pi r \cdot dx$ is

$$[1] \qquad di_x = i_0 \exp [\alpha(V_0 - \Delta V_x)F/RT] \cdot 2\pi r \cdot dx,$$

where i_0 is the usual exchange *current density* for the electrode process concerned and α the transfer coefficient characteristic of the rate-determining process.

The potential drop ΔV_x in the conductor is a function of length but is not simply linearly related to it since the current in the conductor is not uniform but decreases down the

**For convenience, we write the kinetic expression for an anodic reaction involving a one-electron transfer as in the H ionization case.*

Can. J. Chem. Downloaded from www.nrcresearchpress.com by 210.87.254.42 on 09/05/12
For personal use only.

cylinder. The quantity ΔV_x will hence increase with x but as some function x^n where $0 < n < 1$, and n may be a function of x.

In the element of the electrode surface of area $2\pi r \cdot dx$, at the position x, the potential drop dV down the element is given by

$$dV = i_x \rho dx/\pi r^2,$$

where i_x is the total current in the conductor crossing a plane perpendicular to the electrode axis at a position x along the electrode determined by the sum of all current elements entering the electrode from $x = L$ to the representative position $x = x$.

The total potential drop ΔV_x from the top of the electrode to x is then

[2]* $$\Delta V_x = \int_0^x dV = \frac{\rho}{\pi r^2} \int_0^x i_x \cdot dx.$$

But i_x is already the integral of di_x over the length $x = L$ to a position x which involves ΔV_x from equation [1], i.e.,

[3] $$i_x = i_o \exp\left[\frac{\alpha V_o F}{RT}\right] 2\pi r \int_x^L \exp -\left[\frac{\alpha \Delta V_x F}{RT}\right] dx$$

and ΔV_x in equation [3] is given by the integral equation [2] which itself involves i_x. The mathematical problem is thus a particularly complex one and an explicit solution is not obtainable without some simplification.

3. Linear Approximation

Equation [3] can be linearized under two conditions:

(*a*) if the current densities along the electrode do not exceed approximately 1.7 i_o (the condition for linear current – potential behavior in the basic rate expression), or

(*b*) if $\Delta V_x < RT/\alpha F$; this latter condition only obtains at moderately low c.d. or fairly low ohmic resistance of the conductor such as is the case in most practical problems.

In either case, we could write approximately for the forward (anodic) current, e.g. in H ionization,

[4] $$i_x = i_o \exp\left[\frac{\alpha V_o F}{RT}\right] 2\pi r \int_x^L \left[1 - \frac{\alpha \Delta V_x F}{RT}\right] dx$$

and the equation then becomes with [2] and $i = i_o \exp [\alpha V_o F/RT]$

[5] $$i_x = 2\pi r i \int_x^L dx - 2\pi r i \int_x^L \left[\frac{\alpha \Delta V_x F}{RT}\right] dx,$$

which can be written

[6] $$i_x = K_1 - K_2 x - K_3 \int_x^L \left[\int_0^x i_x dx\right] dx,$$

where K_1, K_2, and K_3 are constants, the significance of which follows by reference to equation [5]. We may write equation [6] conveniently in differential form as

[7] $$di_x/dx = -K_2 + K_3 \int_0^x i_x dx$$

**In this and other related equations, the term $\rho/\pi r^2$ will become $\rho/\pi(r^2 - [r-a]^2)$ for the case of a tubular electrode of radius r and annular thickness a.*

Can. J. Chem. Downloaded from www.nrcresearchpress.com by 210.87.254.42 on 09/05/12
For personal use only.

and

$$[8] \qquad d^2i_x/dx^2 = K_3 i_x = \frac{2\rho i\alpha F}{rRT} i_x.$$

4. Evaluation of ΔV_x as a Function of x and Determination of the Profile of i_x as a Function of x

The general solution of the differential equation [8] is

$$[9] \qquad i_x = A \exp(-K_3^{1/2}x) + B \exp[K_3^{1/2}x].$$

The constant B is set equal to zero since i_x must always decrease with increasing x, i.e.

$$[9a] \qquad di_x/dx = K_3^{1/2}[-A \exp(-K_3^{1/2}x) + B \exp(K_3^{1/2}x)] < 0$$

and the above inequality will be satisfied for all values of x only if $B = 0$. Also, at $x = 0$, we have

$$i_x = I = A.$$

Hence we obtain the following specific solution to the differential equation [8]:

$$[10] \qquad i_x = I \exp -(K_3^{1/2}x) = I \exp -\left(\frac{2\rho i\alpha F}{rRT}\right)^{1/2} x.$$

The current density distribution may then be obtained as

$$[11] \qquad -\frac{di_x}{ds} = -\frac{1}{2\pi r}\frac{di_x}{dx} = \frac{1}{2\pi r} K_3^{1/2} I \exp -(K_3^{1/2}x)$$

and the current density at x is

$$[11a] \qquad -\frac{di_x}{ds} = \frac{K_3^{1/2}}{2\pi r} i_x.*$$

The evaluation of ΔV_x as a function of x may then be carried out as follows. Substituting i_x from equation [10] into equation [2] we have

$$[12] \qquad \Delta V_x = \frac{\rho}{\pi r^2}\int_0^x i_x dx = \frac{\rho}{\pi r^2} I \int_0^x \exp[-K_3^{1/2}x]dx,$$

i.e.,

$$\Delta V_x = -\frac{\rho I}{\pi r^2 K_3^{1/2}}[e^{-K_3^{1/2}x} - 1] = \frac{\rho I}{\pi r^2 K_3^{1/2}}[1 - \exp(-K_3^{1/2}x)]$$

so that, upon substituting the value of K_3, we have

$$[12a] \qquad \Delta V_x = \left(\frac{\rho RT}{2\pi^2 r^3 i\alpha F}\right)^{1/2} I\left[1 - \exp\left(-\frac{2\rho i\alpha F}{rRT}\right)^{1/2} x\right].$$

We may note that i_x is the total current entering the electrode from the bottom up to a position x, while ΔV_x is the potential drop along the electrode measured from the top. Accordingly we find that i_x decreases with increasing x (equation [10]) and ΔV_x increases with increasing x (equation [12*a*]).

**The negative sign arises here on account of the manner in which i_x is defined. In any case the c.d. must have the same sign as the total current and this is satisfied above since the derivative of i_x with respect to x is negative (equation [9a]).*

Can. J. Chem. Downloaded from www.nrcresearchpress.com by 210.87.254.42 on 09/05/12
For personal use only.

III. CALCULATION OF THE APPARENT CURRENT – POTENTIAL RELATION

1. Conditions and Model

We now consider the relation between the apparent and real current – potential behavior at an electrode of length L and specific resistance ρ, as defined in Section II. The model is the same as that considered above but the electrode is regarded as divided into a large number n of segments Δx in length ($n\Delta x = L$) and Δi_j is taken as the actual current passing from a representative j'th segment into the solution.

2. Formulation of Equations

For convenience in the mathematical development, we treat the problem now in terms of summations. From the definitions above, we may write

$$\sum_{j=1}^{n} \Delta i_j = I. \tag{13}$$

If the ohmic resistance of the electrode is not negligible, conditions will be as in the previous calculation (Section II) and the current density will decrease down the electrode. Let it be assumed that each segment is small enough for the ohmic p.d. within it to be, to a *first* approximation, negligible and that the potential operative at the j'th segment depends on the potential V_0 applied to the electrode less the ohmic potential drop down the $j-1$ preceding segments, as in the previous calculation. At the middle of the first segment the current passing is taken as

$$\Delta i_1 = i_0 2\pi r \Delta x \exp [V_0/b]. \tag{14}$$

At the corresponding position in the second segment, the potential operative in determining the current will be less than V_0 by the ohmic potential drop in segment one, i.e.

$$\begin{aligned}\Delta i_2 &= i_0 2\pi r \Delta x \exp \frac{1}{b}\left[V_0 - \frac{\rho}{\pi r^2} \Delta x (I - \Delta i_1) \right] \\ &= i_0 2\pi r \Delta x \exp \frac{V_0}{b}\left[1 - \frac{\rho}{\pi r^2} \frac{\Delta x}{V_0} (I - \Delta i_1) \right].\end{aligned} \tag{15}$$

Similarly

$$\begin{aligned}\Delta i_3 &= i_0 2\pi r \Delta x \exp \frac{1}{b}\left[V_0 - \frac{\rho}{\pi r^2} \Delta x (I - \Delta i_1) - \frac{\rho}{\pi r^2} \Delta x (I - \Delta i_1 - \Delta i_2) \right] \\ &= i_0 2\pi r \Delta x \exp \frac{V_0}{b}\left[1 - \frac{\rho}{\pi r^2} \frac{\Delta x}{V_0} (2I - 2\Delta i_1 - \Delta i_2) \right]\end{aligned} \tag{16}$$

and

$$\begin{aligned}\Delta i_4 &= i_0 2\pi r \Delta x \exp \frac{1}{b}\left[V_0 - \frac{\rho}{\pi r^2} \Delta x (2I - 2\Delta i_1 - \Delta i_2) - \frac{\rho}{\pi r^2} \Delta x (I - \Delta i_1 - \Delta i_2 - \Delta i_3) \right] \\ &= i_0 2\pi r \Delta x \exp \frac{V_0}{b}\left[1 - \frac{\rho}{\pi r^2} \frac{\Delta x}{V_0} (3I - 3\Delta i_1 - 2\Delta i_2 - \Delta i_3) \right]\end{aligned} \tag{17}$$

and, in general, for the current at the j'th element

$$\begin{aligned}\Delta i_j &= i_0 2\pi r \Delta x \exp \frac{1}{b}\left[V_0 - \frac{\rho}{\pi r^2} \Delta x \{ (j-1)I - (j-1)\Delta i_1 - (j-2)\Delta i_2 \right. \\ &\qquad \left. - (j-3)\Delta i_3 - (j-k)\Delta i_k \} \right] \\ &= i_0 2\pi r \Delta x \exp \frac{V_0}{b} \exp -\left[\frac{\rho}{\pi r^2} \frac{\Delta x}{b} (j-1) I \right] \exp \frac{\rho}{\pi r^2} \frac{\Delta x}{b}\left[\sum_{k=1}^{j-1} (j-k)\Delta i_k \right].\end{aligned} \tag{18}$$

Can. J. Chem. Downloaded from www.nrcresearchpress.com by 210.87.254.42 on 09/05/12
For personal use only.

The total current is

$$I = \sum_{j=1}^{n} \Delta i_j.$$

The latter summation cannot be evaluated analytically since it is a sum of exponentials having different arguments. However, if the variation of current density along the electrode is not too large, the procedures given below can be adopted as an approximation.

Here, let it be assumed that the arithmetic mean of the current over the n elements can be approximated by the geometric mean. That is

[19] $$\frac{1}{n}\sum_{j=1}^{n} \Delta i_j = (\overset{j}{\Pi}\, \Delta i_j)^{1/n}$$

and hence

[20] $$I = n\,(\overset{j}{\Pi}\, \Delta i_j)^{1/n}.$$

Taking logarithms of the terms in equation [18] for Δi_j gives

[21] $$\ln \Delta i_j = \ln (i_0 2\pi r \Delta x) + \frac{V_0}{b} + \frac{1}{b}\left[-\frac{\rho}{\pi r^2}\Delta x(j-1)I + \frac{\rho}{\pi r^2}\Delta x \sum_{k=1}^{j-1}(j-k)\Delta i_k\right];$$

then since

[22] $$\ln [\overset{j}{\Pi}\, \Delta i_j] = \sum_{j=1}^{n} \ln [\Delta i_j]$$

we obtain

[23] $$\sum_{1}^{n} \ln \Delta i_j = n \ln (i_0 2\pi r \Delta x) + \frac{nV_0}{b} - \frac{1}{b}\frac{\rho}{\pi r^2}\Delta x I \sum_{j=1}^{n}(j-1) + \frac{\rho}{\pi r^2}\frac{\Delta x}{b}\sum_{j=1}^{n}\sum_{k=1}^{j-1}(j-k)\Delta i_k$$

or

[24] $$\frac{1}{n}\sum_{j=1}^{n} \ln \Delta i_j = \ln (i_0 2\pi r \Delta x) + \frac{V_0}{b} - \frac{1}{nb}\frac{\rho}{\pi r^2}\Delta x I \frac{n(n-1)}{2} + \frac{\rho}{\pi r^2}\frac{\Delta x}{nb}\sum_{j=1}^{n}\sum_{k=1}^{j-1}(j-k)\Delta i_k.$$

Now

$$\ln (I/n) = \ln [\overset{j}{\Pi}\, \Delta i_j]^{1/n} = \frac{1}{n}\sum_{j=1}^{n} \ln [\Delta i_j],$$

so that

$$\ln (I/n) = \text{r.h.s. of [24]}$$

or

[25] $$\frac{I}{n} = i_0 2\pi r \Delta x \exp\left[\frac{V_0}{b}\right]\exp\left[-\frac{\rho I \Delta x}{\pi r^2 b}\frac{(n-1)}{2}\right]\exp\left[\frac{\rho \Delta x}{\pi r^2 n b}\sum_{j=1}^{n}\sum_{k=1}^{j-1}(j-k)\Delta i_k\right].$$

If we make the simplification that $n-1 = n$ since n can be made arbitrarily large, and with $n\Delta x = L$, we have

[26] $$I = i_0 2\pi r L \exp\left[\frac{V_0}{b}\right]\exp\left[\frac{\rho L}{\pi r^2}\frac{I}{2b}\right]\exp\left[\frac{\rho L}{\pi r^2}\frac{1}{n^2 b}\sum_{j=1}^{n}\sum_{k=1}^{j-1}(j-k)\Delta i_k\right].$$

Can. J. Chem. Downloaded from www.nrcresearchpress.com by 210.87.254.42 on 09/05/12
For personal use only.

Since the resistance of the whole electrode is given by $\mathscr{R} = \rho L/\pi r^2$ and its total surface area is $S = 2\pi rL$, we can rewrite equation [26] as

$$[27] \qquad I = i_0 S \exp(V_0/b) \exp(-\mathscr{R}I/2b) \exp\left[\frac{\mathscr{R}}{n^2 b} \sum_{j=1}^{n} \sum_{k=1}^{j-1} (j-k)\Delta i_k\right].$$

We shall now examine the physical significance of the various terms in equation [27]. The term

$$i_0 \exp[V_0/b]$$

is obviously the value of I/S when $\rho = 0$, i.e. when no finite resistance of the electrode is considered and is the theoretically significant quantity since its value and, in particular, its variation with V_0 are characteristic of the kinetics of the electrochemical reaction occurring at the electrode. In fact, it is the purpose of these calculations to relate this "ideal" current density to the mean overall value which would be experimentally measured, viz. I/S.

The second term in equation [27], $\exp[-RI/2b]$, is effectively a correction factor which takes into account a linear potential drop along the electrode due to its ohmic resistance; the last term on the r.h.s. of equation [27] is a second-order correction factor which takes into account the departure from linearity of this potential drop arising from the exponential variation of reaction resistance with electrode potential. The double sum in the last term can be represented in tabular form as shown below:

Terms in the double sum in equation [27]

k \ j	1	2	3	4	5 ..... j
1	0	Δi_1	$2\Delta i_1$	$3\Delta i_1$	$4\Delta i_1$ ..... $(j-1)\Delta i_1$
2	0	0	Δi_2	$2\Delta i_2$	$3\Delta i_2$ ..... $(j-2)\Delta i_2$
3	0	0	0	Δi_3	$2\Delta i_3$ ..... $(j-3)\Delta i_3$
4	0	0	0	0	Δi_4 ..... $(j-4)\Delta i_4$
5	0	0	0	0	0 ..... $(j-5)\Delta i_5$
⋮					
k	0	0	0	0	0 ..... $(j-k)\Delta i_k$

Since the term involving the summation in equation [27] constitutes a second-order correction, we may make the approximation

$$[28] \qquad \Delta i_k = \Delta i_{k+1} = I/n,$$

so that the last term in equation [27] becomes

$$\exp\frac{\mathscr{R}}{b}\cdot\frac{1}{n^2} \sum_{j=1}^{n} \sum_{k=1}^{j-1} (j-k)\Delta i_k = \exp\frac{\mathscr{R}I}{b}\cdot\frac{1}{n^3} \sum_{j=1}^{n} \sum_{k=1}^{j-1} (j-k).$$

It can be shown that

$$[29] \qquad \lim_{n\to\infty}\left[\frac{1}{n^3} \sum_{j=1}^{n} \sum_{k=1}^{j-1} (j-k)\right] = 1/6,$$

so that, combining equations [27] and [29],

$$[30] \qquad I/S = i \exp\left[-\frac{\mathscr{R}I}{2b}\right] \exp\left[\frac{\mathscr{R}I}{6b}\right] = i \exp\left[-\frac{\mathscr{R}I}{3b}\right]$$

Can. J. Chem. Downloaded from www.nrcresearchpress.com by 210.87.254.42 on 09/05/12
For personal use only.

or

$$i = (I/S) \exp [\mathscr{R}I/3b]. \quad [31]$$

Equation [31] has been derived for convenience for an anodic process; it is obviously applicable generally for any electrode process since $I/b > 0$ in all cases.

Apparent Tafel Slope

The observed Tafel slope $dV/d \ln I$ will be related to the mechanistically significant Tafel slope $dV/d \ln i$ through the equation

$$dV/d \ln i = (dV/d \ln I)(d \ln I/\mathrm{d} \ln i) \quad [32]$$

from equation [31]

$$(d \ln i/d \ln I) = 1 + \frac{\mathscr{R}I}{3b}. \quad [33]$$

Hence

$$dV/d \ln i = dV/d \ln I(1+\mathscr{R}I/3b)^{-1}. \quad [34]$$

We note, therefore, that a finite electrode resistance will cause a decrease in the overall current density from that predicted by the corresponding Tafel equation: also the observed apparent Tafel slope will be larger than the real one (b in equation [34]) and will tend to increase with current density.

Since equation [34] was derived assuming that RI, although not negligible, was relatively small, the true Tafel slope can be obtained from a measured value of $dV/d \ln I$ and the known specific resistance of the electrode at a given total current I. The result can be further improved, if required, by a series of successive approximations. It is of interest to note also that the current–potential behavior at electrodes at which a given reaction is proceeding with a high value of b will be relatively less affected by electrode resistance effects than that for reactions associated with low Tafel slopes.

The above calculations have been made in order that at electrodes of significant resistance where internal ohmic potential drops are not negligible at high current densities, the true, mechanistically significant Tafel slopes can nevertheless be evaluated from the observed current-potential relation for high-load conditions, and the current-density distribution can also be calculated. We also note that, since there is a drop of potential down the electrode, significant longitudinal ionic currents may arise in the solution. Such effects will be small when the solution resistance is not too low and ρ is not high.

ACKNOWLEDGMENT

Grateful acknowledgment is made to the Defence Research Board, Department of National Defence, for support on Grant No. 5401.

REFERENCES

1. H. E. Haring and W. Blum. Trans. Amer. Electrochem. Soc. **44**, 313 (1923).
2. T. P. Hoar and J. N. Agar. Discussions Faraday Soc. **1**, 162 (1947).
3. C. W. Tobias. Papers presented at the Electrochemical Society Meeting, Boston, 1962, and at the C.I.T.C.E. meeting, Rome, 1962; J. Electrochem. Soc. In press.
4. C. Wagner. J. Electrochem. Soc. **107**, 445 (1960).
5. S. Zaromb. J. Electrochem. Soc. **109**, 912 (1962).
6. W. W. Harvey. J. Electrochem. Soc. **109**, 638 (1962).
7. G. M. Schmid and N. Hackerman. J. Electrochem. Soc. **107**, 142, 647 (1960).

Can. J. Chem. Downloaded from www.nrcresearchpress.com by 210.87.254.42 on 09/05/12
For personal use only.

THE REACTION OF METHYL RADICALS WITH METHYL ALCOHOL

T. W. SHANNON AND A. G. HARRISON
Department of Chemistry, University of Toronto, Toronto, Ontario
Received May 13, 1963

ABSTRACT

The photolysis of acetone in the presence of methyl alcohol and of methyl-d_3 alcohol has been studied between 406 and 472° K. The rates and Arrhenius parameters for the following abstraction reactions have been determined:

$$CH_3 + CH_3OH \rightarrow CH_4 + \begin{cases} CH_3O \\ HOCH_2 \end{cases} \quad [a]$$

$$CH_3 + CD_3OH \rightarrow CH_4 + CD_3O \quad [b]$$

$$\rightarrow CH_3D + CD_2OH. \quad [c]$$

At 182° C the rate of reaction [*b*] is found to be approximately four times greater than the rate of reaction [*c*].

INTRODUCTION

There now exists a large body of data on the hydrogen abstraction reactions of methyl radicals and some correlation between molecular structure and reactivity are apparent (1). In many cases, however, there is uncertainty as to which hydrogen is abstracted by the methyl radical. Although the reaction of methyl radicals with methyl alcohol has been studied (2, 3) it is not clear from the results whether the methyl or the hydroxyl hydrogen is abstracted. The present work reports a study of the reaction of methyl radicals, produced by the photolysis of acetone, with methyl-d_3 alcohol to determine the relative importance of the two possible abstraction processes.

EXPERIMENTAL

The photolyses were carried out in a cylindrical pyrex reaction vessel of 157 cc capacity maintained to ±1° C in an aluminum block furnace. Corex-D windows on the cell removed radiation below 2800 Å. The light source was a B.T.H. type ME/D 250 watt mercury discharge lamp. The light beam was roughly collimated by a quartz lens and filled the whole reaction cell. Photolyses were carried out for periods from 700 to 1200 seconds, corresponding to 2 to 3% decomposition of the acetone.

The reaction products were passed through traps at 142° K and the volatile products transferred by a Toepler pump to a calibrated gas burette and thence to sample flasks for analysis with an A.E.I. MS-2 mass spectrometer.

The acetone was Fisher spectranalyzed grade dried and distilled *in vacuo* before use. Fisher certified reagent methanol was found to contain trimethyl borate impurity. This was removed by refluxing with water followed by fractional distillation. The methyl-d_3 alcohol was obtained from Merck, Sharp and Dohme, Montreal. Mass spectrometric analysis showed hexadeuterodimethyl ether as the only impurity. This was easily removed by pumping at low temperature. Low-energy analysis showed less than 1% isotopic impurity. The CH_3OH and CD_3OH were stored in quartz containers connected to the vacuum line by metal valves.

RESULTS

Photolysis of Acetone

The main features of the photolysis of acetone are well established (4). Above 100° C the formation of the products methane and ethane can be described by the following scheme:

$$CH_3COCH_3 + h\nu \rightarrow 2CH_3 + CO \quad [1]$$

$$2CH_3 \rightarrow C_2H_6 \quad [2]$$

$$CH_3 + CH_3COCH_3 \rightarrow CH_4 + CH_2COCH_3, \quad [3]$$

Can. J. Chem. Downloaded from www.nrcresearchpress.com by 210.87.254.42 on 09/05/12
For personal use only.

leading to the following rate expression

$$R_{CH_4}/R_{C_2H_6}^{\frac{1}{2}}[Ac] = k_3/k_2^{\frac{1}{2}}. \quad [I]$$

In the present work the photolysis of acetone alone was studied between 415 and 499° K to check the accuracy of the experimental techniques and to establish values for $k_3/k_2^{\frac{1}{2}}$ pertaining to the present system. From a least squares plot the best straight line fitting the experimental data is given by the equation

$$13 + \log k_3/k_2^{\frac{1}{2}} \text{ (cc}^{\frac{1}{2}} \text{ molecule}^{-\frac{1}{2}} \text{ sec}^{-\frac{1}{2}}) = 5.80(\pm 0.05) - 2.021(\pm 0.023)10^3/T.$$

Using $k_2 = 2.2 \times 10^{13}$ cc mole^{-1} sec^{-1} (5) and $E_2 = 0$, this relationship gives log A_3 (cc mole^{-1} sec^{-1}) = 11.35±0.05 and $E_3 = 9.3 \pm 0.1$ kcal mole^{-1}. This is in satisfactory agreement with previous values of 11.5 and 9.7 (6), 11.5 and 9.6 (7), and 11.35 and 9.5 (8) for log A_3 and E_3 respectively.

Photolysis of Acetone – Methyl Alcohol Mixtures

When acetone is photolyzed in the presence of methyl alcohol the following reaction leading to methane formation must be added to the reaction scheme given above:

$$CH_3 + CH_3OH \rightarrow CH_4 + \begin{Bmatrix} CH_2OH \\ CH_3O \end{Bmatrix} \quad [4]$$

The following equation may be derived:

$$R_{CH_4}/R_{C_2H_6}^{\frac{1}{2}}[CH_3OH] = k_4/k_2^{\frac{1}{2}} + k_3/k_2^{\frac{1}{2}} \cdot [Ac]/[CH_3OH]. \quad [II]$$

Since $k_3/k_2^{\frac{1}{2}}$ is known from experiments with acetone alone $k_4/k_2^{\frac{1}{2}}$ may be determined. Photolyses of acetone – methyl alcohol mixtures were carried out in the temperature range 406 to 472° K. From a least squares analysis the best straight line fitting the experimental data is given by the equation

$$13 + \log k_4/k_2^{\frac{1}{2}} \text{ (cc}^{\frac{1}{2}} \text{ molecule}^{-\frac{1}{2}} \text{ sec}^{-\frac{1}{2}}) = 5.20(\pm 0.07) - 1.90(\pm 0.032)10^3/T,$$

leading to $E_4 = 8.7 \pm 0.2$ kcal mole^{-1} and log A_4 (cc mole^{-1} sec^{-1}) = 10.76±0.07. Phibbs and Darwent (2) obtained log $A_4 = 10.49$ and $E_4 = 8.2 \pm 0.5$ while Trotman-Dickenson and Steacie (3) obtained log $A_4 = 10.53$ and $E_4 = 8.2 \pm 0.2$. Both the A factor and the activation energy obtained in the present work are somewhat higher; however the values for k_4 at 182° C are in excellent agreement for all three studies.

Photolysis of Acetone – Methyl-d_3 Alcohol Mixtures

The following reactions are proposed to explain the formation of CH_4, CH_3D, and C_2H_6 when acetone is photolyzed in the presence of CD_3OH at temperatures above 100° C:

$$2CH_3 \rightarrow C_2H_6 \quad [2]$$

$$CH_3 + CH_3COCH_3 \rightarrow CH_4 + CH_2COCH_3 \quad [3]$$

$$CH_3 + CD_3OH \rightarrow CH_4 + CD_3O \quad [5]$$

$$CH_3 + CD_3OH \rightarrow CH_3D + CD_2OH. \quad [6]$$

From this reaction scheme the following equations may be derived:

$$R_{CH_4}/R_{C_2H_6}^{\frac{1}{2}}[Ac] = k_3/k_2^{\frac{1}{2}} + k_5/k_2^{\frac{1}{2}} \cdot [CD_3OH]/[Ac] \quad [III]$$

$$R_{CH_3D}/R_{C_2H_6}^{\frac{1}{2}}[CD_3OH] = k_6/k_2^{\frac{1}{2}} \quad [IV]$$

$$R_{CH_4}/R_{CH_3D} = k_5/k_6 + k_3/k_6[Ac]/[CD_3OH]. \quad [V]$$

Can. J. Chem. Downloaded from www.nrcresearchpress.com by 210.87.254.42 on 09/05/12
For personal use only.

The photolyses of acetone–CD_3OH mixtures were carried out at five temperatures between 427 and 477° K with the ratio of CD_3OH to acetone being varied from 0.3 to 3.0. The results are given in Table I. In addition to the expected products mass spectrometric analysis showed small amounts of products having parent masses of 33 and 19,

TABLE I

Photolysis of CH_3COCH_3 in the presence of CD_3OH

Run	Temp. (°A)	$[Ac]\times10^{-17}$ (molecules/cc)	$[CD_3OH]\times10^{-17}$ (molecules/cc)	R_{CH_4}*	R_{CH_3D}*	$R_{C_2H_6}$*	R_{CO}*	$\frac{k_6}{k_2^{\frac{1}{2}}}\times10^{13}$
3	427	15.52	31.39	1.24	0.081	2.62	3.76	0.507
4	"	17.22	18.24	1.33	0.052	3.19	4.31	0.507
5	"	31.03	16.72	2.33	0.047	4.17	6.13	0.438
6	"	26.55	17.74	2.05	0.052	3.99	5.91	0.466
7	"	11.86	35.59	0.988	0.077	2.24	2.93	0.459
8	"	35.16	18.35	2.83	0.056	4.89	6.54	0.437
27	435	25.22	20.81	2.40	0.087	3.46	5.70	0.708
28	"	30.32	19.41	3.33	0.083	4.21	7.37	0.658
29	"	17.30	33.23	1.78	0.116	2.64	4.18	0.680
30	"	28.64	17.35	3.04	0.077	4.41	7.21	0.666
32	"	10.51	32.67	1.04	0.093	1.78	2.69	0.674
21	444	14.66	14.16	1.37	0.052	2.21	3.46	0.784
22	"	18.08	14.69	1.92	0.058	2.82	4.53	0.744
24	"	29.00	11.34	3.24	0.052	3.71	6.54	0.748
33	"	26.18	15.84	3.10	0.081	3.23	5.97	0.896
34	"	15.16	30.89	1.82	0.137	2.03	3.73	0.981
35	"	11.10	33.39	1.34	0.130	1.65	2.89	0.958
9	461	15.89	16.26	2.29	0.129	2.54	4.40	1.57
10	"	29.02	16.17	4.24	0.116	3.32	6.59	1.25
11	"	15.59	31.83	2.37	0.199	2.12	4.16	1.36
12	"	23.43	17.05	3.50	0.119	2.94	5.72	1.29
13	"	10.90	35.82	1.66	0.204	1.61	2.93	1.42
14	"	28.50	12.30	4.74	0.092	3.91	7.49	1.20
15	477	14.83	16.57	2.79	0.152	2.07	4.23	2.02
16	"	25.06	16.30	5.28	1.81	2.91	7.11	2.06
17	"	23.18	11.59	4.53	0.134	2.80	6.41	2.19
18	"	14.64	28.50	2.90	0.248	1.89	4.10	2.00
19	"	9.69	27.03	1.78	0.214	1.31	2.84	2.19

*R in units of 10^{13}(molecules sec^{-1} cc^{-1}).

presumably CD_3CH_3 and CD_3H. The proportion increased with increasing temperature, reaching 5% of the $CH_4 + C_2H_6$ product at the highest temperature. These products suggest the formation of CD_3 radicals; however it was not possible to obtain concrete evidence concerning the mechanism of formation owing to the small amounts involved. In any event the formation of these products should not invalidate the kinetic scheme proposed above for the major products.

The values obtained for $k_6/k_2^{\frac{1}{2}}$ via equation [IV] (column 9, Table I) are constant, within experimental error, for each temperature. The average values are given in Table II,

TABLE II

Rate constant ratios*

Temp. (°K)	$k_6/k_2^{\frac{1}{2}}$	$k_5/k_2^{\frac{1}{2}}$	k_5/k_6	k_3/k_6	$k_{6'}/k_2^{\frac{1}{2}}$
427	0.469	2.43	3.71	24.15	2.99
435	0.677	2.90	3.57	22.03	3.74
444	0.852	4.37	2.29	23.33	4.85
461	1.35	4.25	0.38	21.04	7.45
477	2.09	5.20	3.58	15.73	10.85

*Rate constants in cc $molecule^{-1}$ sec^{-1}.

Can. J. Chem. Downloaded from www.nrcresearchpress.com by 210.87.254.42 on 09/05/12
For personal use only.

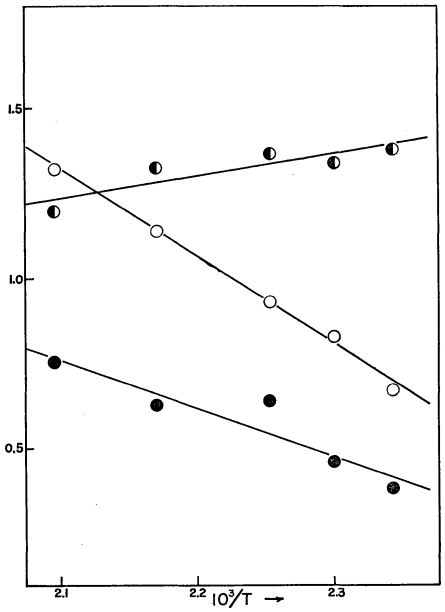

FIG. 1. Arrhenius activation energy plot: ○ 14 + log $k_6/k_2^{\frac{3}{2}}$; ● 13 + log $k_5/k_2^{\frac{3}{2}}$; ◐ log k_3/k_6.

while an Arrhenius plot of the data is shown in Fig. 1. The least squares line gives log A_6 (cc mole^{-1} sec^{-1}) = 11.25±0.28 and E_6 = 11.7±0.6 kcal mole^{-1}, using Shepp's value for k_2.

The experimental data are plotted in the form of equation [III] in Fig. 2. The intercept of the straight lines obtained should give values for $k_3/k_2^{\frac{3}{2}}$. The best straight line fitting the experimental intercepts is given by equation

$$13 + \log k_3/k_2^{\frac{3}{2}} = 5.77(\pm 0.23) - 2.017(\pm 0.10)10^3/T,$$

in excellent agreement with the equation obtained above from the photolysis of acetone alone.

From the slopes of the lines in Fig. 2 the values of $k_5/k_2^{\frac{3}{2}}$ reported in Table II are obtained. The Arrhenius plot of this data (Fig. 1) leads to log A_5 (cc mole^{-1} sec^{-1}) = 9.25 ±0.3 and E_5 = 6.4±0.7 kcal mole^{-1}.

The experimental data is plotted in the form of equation [V] in Fig. 3. The values of k_5/k_6 and k_3/k_6 obtained from the intercepts and slopes of the least squares lines are given in Table II. The values of k_5/k_6 show irregular variations and do not give a satisfactory Arrhenius plot. The amounts of CH_3D and CH_4 formed by reactions [5] and [6] are quite small and analytical errors will have a much larger effect on the intercept than the slope. The plot of log k_3/k_6 vs. $1/T$ (Fig. 1) leads to $E_6 - E_3$ = 3.0±1.0 kcal mole^{-1}. Using E_3 = 9.3 this gives E_6 = 12.3±1.1 kcal mole^{-1}, in agreement with the value of 11.7 ±0.6 kcal mole^{-1} obtained above.

DISCUSSION

The above results indicate that the reaction of methyl radicals with CH_3OH previously written as reaction [4] is the sum of two reactions:

$$CH_3 + CH_3OH \rightarrow CH_4 + CH_3O \quad [5']$$
$$\rightarrow CH_4 + HOCH_2 \quad [6']$$

Can. J. Chem. Downloaded from www.nrcresearchpress.com by 210.87.254.42 on 09/05/12
For personal use only.

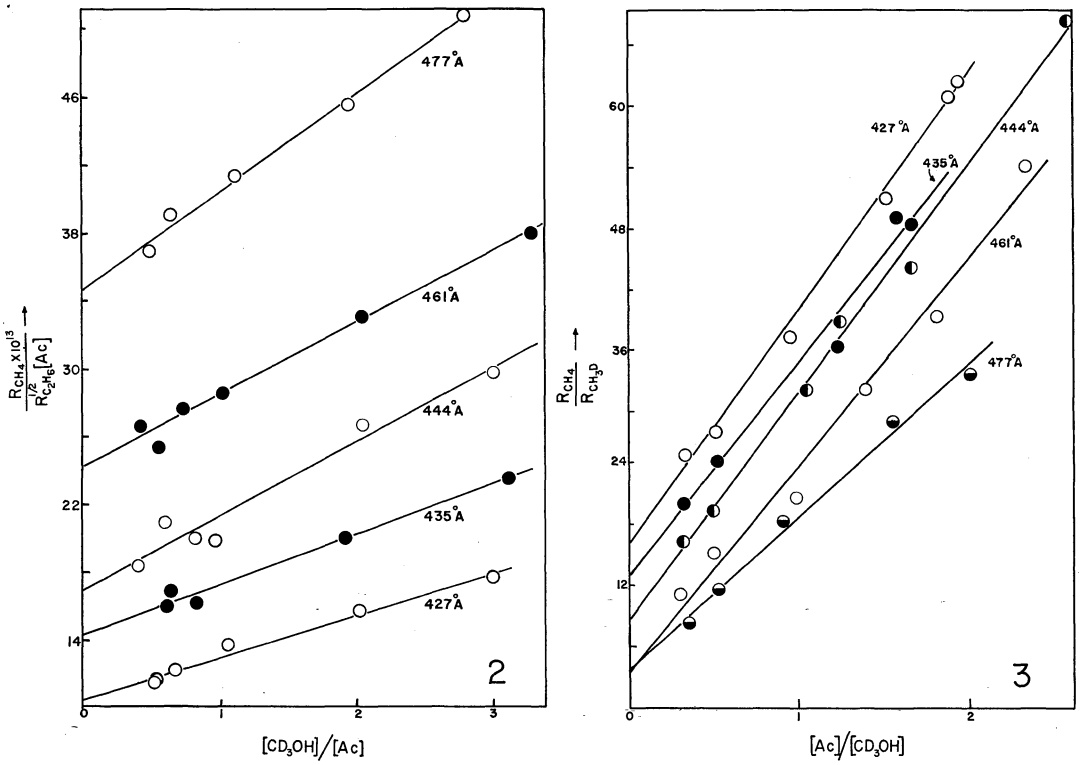

FIG. 2. Photolysis of acetone with methyl-d_3 alcohol. Experimental plot of equation [III].
FIG. 3. Photolysis of acetone with methyl-d_3 alcohol. Plot of equation [V]. (Scale for plots from 461 to 427° A raised 3 units successively.)

It follows that $k_4/k_2^{\frac{1}{2}}$ obtained above is given by the following relation:

$$k_4/k_2^{\frac{1}{2}} = k_{5'}/k_2^{\frac{1}{2}} + k_{6'}/k_2^{\frac{1}{2}}. \qquad [VI]$$

If we assume that the rate of abstraction of the hydroxyl hydrogen is independent of hydrogen–deuterium substitution of the methyl we may equate $k_{5'}/k_2^{\frac{1}{2}}$ with $k_5/k_2^{\frac{1}{2}}$ and solve equation [VI] for $k_{6'}/k_2^{\frac{1}{2}}$. The values thus obtained are recorded in Table II and are best represented by the equation

$$13 + \log k_{6'}/k_2^{\frac{1}{2}} = 5.82 - 2.28110^3/T.$$

This leads to $E_{6'} = 10.4$ kcal mole^{-1} and log $A_{6'}$ (cc mole^{-1} sec^{-1}) $= 11.38$. These values contain relatively large errors due to the accumulation of errors in the ratios from which they were calculated. The difference in activation energy for D vs. H abstraction is thus given by $E_6 - E_{6'} = 1.3$ kcal mole^{-1}. Using the stretching frequencies for C—H and C—D bonds in CH_3OH and CD_3OH, 2845 and 2094 cm^{-1} respectively (9), the difference in zero-point energies is calculated to be 1.1 kcal mole^{-1}. Rice and Vanderslice (10) have reported activation energy differences for D and H abstraction from various alkanes to be in the region 0.6 to 2.3 kcal mole^{-1} while Ausloos and Steacie (11) have reported 1.1 kcal mole^{-1} difference for abstraction from acetaldehyde. The present result therefore appears reasonable.

A summary of the rate constants and Arrhenius parameters of the reactions studied in

Can. J. Chem. Downloaded from www.nrcresearchpress.com by 210.87.254.42 on 09/05/12
For personal use only.

TABLE III
Summary of results

Reaction	E (kcal mole^{-1})	$k\times10^{-6}$ (182° C) (mole^{-1} cc sec^{-1})	$A\times10^{-11}$ (mole^{-1} cc sec^{-1})	$p\times10^{4}$
3	9.3±0.1	7.87	2.13	6.2
4	8.7±0.2	3.90	0.575	1.7
6	11.7±0.6	0.43	1.79	7.2
6′	10.4	2.4	2.4	7.2
5′ (or 5)	6.4±0.7	1.52	0.0179	0.054

the present work is given in Table III. The steric factors were calculated using collision diameters for CH_3, CH_3OH, and CH_3COCH_3 of 3.5 (3), 5.0 (2), and 5.1 Å (6) respectively. Reaction [6] was assigned the same steric factor as reaction [6′].

The outstanding feature of the present results is the low activation energy and low A factor for abstraction of the hydroxyl hydrogen. Although the A factor for methyl hydrogen abstraction is similar to that normally found for methyl radical reactions the A factor for hydroxyl hydrogen abstraction is a factor of 100 lower. Furthermore the activation energy $E_{5'}$ is quite low considering the strength of the bond being broken. Two lines of evidence can be presented which indicate that the present result is not likely to be in serious error.

$E_{5'}$ = 6.4 kcal mole^{-1} when combined with $D(CH_3O—H)$ = 100 kcal mole^{-1} (12) and $D(CH_3—H)$ = 102 kcal mole^{-1} (13) leads to E = 8.4 kcal mole^{-1} for reaction [7].

$$CH_3O + CH_4 \rightarrow CH_3OH + CH_3 \qquad [7]$$

Bercés and Trotman-Dickenson (14) have reported an activation energy of 7.1 kcal mole^{-1} for methoxy radical abstraction from ethane. Considering the difference in bond strength between methane and ethane the value calculated for E_7 appears quite reasonable. It is interesting to note that $E_{6'}$ = 10.4 kcal mole^{-1} when combined with $D(HOCH_2—H)$ = 90 kcal mole^{-1} (15) and $D(CH_3—H)$ leads to E_8 = 22 kcal mole^{-1}. Although there is

$$HOCH_2 + CH_4 \rightarrow HOCH_3 + CH_3 \qquad [8]$$

little information available on the reactions of hydroxy-methyl radicals they do not appear to be particularily reactive.

Of particular interest with regard to the present results are the results obtained by Thynne (16) for the reaction of methyl radical with CH_3NH_2. Thynne obtained log A = 11.15±0.12 and E = 9.3±0.2 kcal mole^{-1} for abstraction of the methyl hydrogen and log A = 9.34±0.34 and E = 5.26±0.66 kcal mole^{-1} for abstraction of the amino hydrogen. The general trend of the results is identical with that found for methyl alcohol. Abstraction of the methyl hydrogen, which involves the weakest bond, occurs with a relatively high activation energy and a normal A factor, while abstraction of the amino or hydroxyl hydrogen occurs with a low activation energy and a low pre-exponential factor. The reasons for the low A factors are not apparent and further work is planned to determine if this is a general phenomenon for alcohols.

While this manuscript was in preparation Cher (17) reported a study of the reaction of CD_3 radicals with methyl-d_3 alcohol in the liquid phase at 30° C. He found the rate of abstraction of the methyl deuterium to be approximately five times faster than abstraction of the hydroxyl hydrogen. This should correspond to the ratio k_6/k_5 of the present work. The results in Table III give k_6/k_5 = 0.28 at 182° C and extrapolate to k_6/k_5 = 0.06 at 30° C. This apparent discrepancy can be explained by the logical assumption that

Can. J. Chem. Downloaded from www.nrcresearchpress.com by 210.87.254.42 on 09/05/12
For personal use only.

hydrogen bonding in the liquid phase has greatly reduced the reactivity of the hydroxyl hydrogens.

ACKNOWLEDGMENTS

The authors are indebted to Dr. J. Thynne for communication of his results before publication and to the National Research Council of Canada and the Advisory Committee on Research, University of Toronto, for financial support.

REFERENCES

1. A. F. Trotman-Dickenson. Quart. Rev. (London), **7**, 198 (1953).
2. M. K. Phibbs and B. deB. Darwent. Can. J. Research, **28B**, 395 (1950).
3. A. F. Trotman-Dickenson and E. W. R. Steacie. J. Chem. Phys. **19**, 329 (1951).
4. E. W. R. Steacie. Atomic and free radical reactions. 2nd. ed. Reinhold Publishing Corp., New York. 1954.
5. A. Shepp. J. Chem. Phys. **24**, 939 (1956).
6. A. F. Trotman-Dickenson and E. W. R. Steacie. J. Chem. Phys. **18**, 1097 (1950).
7. A. J. C. Nicholson. J. Am. Chem. Soc. **73**, 3981 (1951).
8. J. C. J. Thynne and P. Gray. Trans. Faraday Soc. **58**, 2403 (1962).
9. H. D. Noether. J. Chem. Phys. **10**, 693 (1942).
10. F. O. Rice and T. A. Vanderslice. J. Am. Chem. Soc. **80**, 291 (1958).
11. P. Ausloos and E. W. R. Steacie. Can. J. Chem. **33**, 31 (1955).
12. P. Gray. Trans. Faraday Soc. **52**, 344 (1956).
13. T. L. Cottrell. The strengths of chemical bonds. 2nd ed. Butterworths, London. 1958.
14. T. Bercés and A. F. Trotman-Dickenson. J. Chem. Soc. 348 (1961).
15. E. Buckley and E. Whittle. Trans. Faraday Soc. **58**, 536 (1962).
16. J. C. J. Thynne. Personal communication.
17. M. Cher. J. Phys. Chem. **67**, 605 (1963).

Can. J. Chem. Downloaded from www.nrcresearchpress.com by 210.87.254.42 on 09/05/12
For personal use only.

DINITROPHENYL PEPTIDES

I. PREPARATION AND PROPERTIES OF SOME DINITROPHENYL GLYCYL DIPEPTIDES

J. H. LOUDFOOT AND J. E. KRUGER
Department of Chemistry, University of Manitoba, Winnipeg, Manitoba
Received February 15, 1963

ABSTRACT

Some dinitrophenyl glycyl peptides have been prepared from dipeptides and from dinitrophenyl glycyl chloride, and the products suitably characterized. Electrophoresis gave good separation of those differing by more than two carbon atoms.

Dinitrophenyl peptides prepared from protein or peptide hydrolyzates by Sanger's method (1) are usually characterized by chromatographic identification of their hydrolysis products. Where direct comparison with authentic dinitrophenyl peptides has been made, this was based only on chromatographic behavior (2, 3, 4). Comparison on the basis of other physical properties, such as melting point, specific rotation, etc., would require the synthesis of authentic dinitrophenyl peptides, preferably by several independent methods, and determination of their physical properties. Rhinesmith (5) has recently reported the synthesis of dinitrophenyl-DL-valyl peptides from dinitrophenyl-DL-valyl chloride, but did not report their physical properties or compare them with products from any other preparative method. Also, yields were calculated from spectral data, and analysis was based on chromatographic and spectral estimation of the hydrolysis products.

We have therefore undertaken a systematic study of the preparation and properties of dinitrophenyl peptides, in particular the dinitrophenyl derivatives of glycylglycine, glycyl-L-alanine, glycycl-L-valine, and glycyl-L-leucine by two procedures found to be the most suitable. Separation of these peptide derivatives from one another and from dinitrophenyl glycine by electrophoresis is also reported.

EXPERIMENTAL

Dinitrophenyl Glycine

This compound was prepared by the method of Levy and Chung (6) using sodium bicarbonate instead of sodium carbonate as condensing agent.

Dinitrophenyl Glycyl Chloride

Dinitrophenyl glycine (1 g) and thionyl chloride (10 ml) were heated 1 hour under reflux, and the excess thionyl chloride removed by distillation under vacuum. The yellow crystalline residue was heated under reflux with carefully dried benzene to complete solution; on cooling, the product crystallized as large yellow needles. Yield 1 g (92.5% theory), m.p. 129–130°. Anal. Calc. for $C_8H_6N_3O_5Cl$: C, 36.96, H 2.33, N 16.17, Cl 13.66. Found: C 37.42, H 2.62, N 15.29, Cl 12.57. The preparation of this compound was studied previously (5) but lower yields were obtained and its melting point was not reported.

Dinitrophenyl Peptides

The dinitrophenyl peptides made directly from the dipeptides and from the acid chloride were identical, and distinct from dinitrophenyl glycine, as established by mixed melting point determination. When they were made from dinitrophenyl glycyl chloride, little if any racemization occurred, and sodium hydroxide was unsuitable as acid binder.

A. From the Dipeptides

The dipeptide and 2,4-dinitrofluorobenzene (equimolar quantities) were added to 15% (w/v) sodium bicarbonate solution (8.7 ml/mmole of peptide), and the mixture stirred 2 hours at room temperature. Immediate acidification with hydrochloric acid precipitated the product as a yellow solid, which was filtered and washed with water.

Can. J. Chem. Downloaded from www.nrcresearchpress.com by 210.87.254.5 on 09/05/12
For personal use only.

B. From Dinitrophenyl Glycyl Chloride

A solution of the acid chloride (1 mmole) in dry benzene (6–8 ml) was added slowly with stirring to an ice-cold solution of the amino acid (1 mmole) in 3.5% (w/v) aqueous sodium carbonate (18 ml) during 2 hours. The stirring was continued for a further 2 hours at ice-bath temperature, whereupon the benzene layer was removed and the aqueous layer acidified with hydrochloric acid to precipitate the dinitrophenyl peptide. With all the peptides except glycyl glycine, a darker-colored impurity appeared during the initial stages of acidification, before precipitation of the product. This impurity was easily removed by careful addition of acid until no further impurity separated, followed by decantation; the remainder of the acid was then added immediately.

Dinitrophenyl Glycylglycine

The solid was recrystallized by dissolving in ethanol and adding just enough water for crystals to form, which were filtered and dried 4 hours at 104°. *Method A*—91–92% yield, m.p. 194–195°, optically inactive in 95% ethanol. *Method B*—54–55% yield, m.p. 194–195°, optically inactive in 95% ethanol. Anal. Calc. for $C_{10}H_{10}N_4O_7$: C 40.03, H 3.38, N 18.8, equiv. 298.14. Found: C 39.44, H 3.64, N 16.72, equiv. 299.4.

Dinitrophenyl Glycyl-L-alanine

Method A—Recrystallization and drying were as described for dinitrophenyl glycylglycine; 75–76% yield, m.p. 175–176.5°, $[\alpha]_D^{21}$ −23.4±2° (2.77% in 95% ethanol). *Method B*—Recrystallization had to be as described for dinitrophenyl glycyl-L-valine; drying was as for method A; yield 44–45%, m.p. 175–176.5°, $[\alpha]_D^{21}$ −23.4±2° (2.75% in 95% ethanol). Anal. Calc. for $C_{11}H_{12}N_4O_7$: C 42.31, H 3.87, N 17.98, equiv. 312.27. Found: C 41.73, H 3.77, N 18.01, equiv. 317.1.

Dinitrophenyl Glycyl-L-valine

This compound was recrystallized by dissolving in ethanol,* diluting with a large volume of water, evaporating to small bulk at room temperature,† and repeating the entire process as often as necessary to reach a constant melting point; it was dried 4 hours at 90°.

Method A—44–45% yield, m.p. 132–134°, $[\alpha]_D^{22}$ −21.2±2° (1.18% in 95% ethanol). *Method B*—44–45% yield, m.p. 131–132°, $[\alpha]_D^{22}$ −20.4±2° (1.22% in 95% ethanol). Anal. Calc. for $C_{13}H_{16}N_4O_7$: C 45.59, H 4.74, N 16.38, equiv. 340.3. Found: C 45.29, H 4.96, N 14.9, equiv. 337.0.

Dinitrophenyl Glycyl-L-leucine (Monohydrate)

Recrystallization was as for the glycyl-L-valine derivative, and it was dried overnight at room temperature over phosphorus pentoxide. *Method A*—46–47% yield, m.p. 98–100°, $[\alpha]_D^{22}$ −29.8±2° (1.01% in 95% ethanol). *Method B*—57–58% yield, m.p. 96–98°, $[\alpha]_D^{22}$ −29.1±2° (1.03° in 95% ethanol). Anal. Calc. for $C_{14}H_{20}N_4O_8$: C 45.16, H 5.41, N 15.05, equiv. 373.32. Found: C 45.82, H 5.24, N 15.11, equiv. 364.3–369.1.

Carbon, hydrogen, and nitrogen analyses were by Geller Laboratories, Bardonia, N.Y.

Electrophoresis

A Reco model E 800-2 open strip apparatus was used, at 300 v and 5 ma for 20 hours at 21°, with 0.02 *M* borate buffer (pH 9.11) and Whatman No. 1 paper, 50×20 cm. A bridge support was placed under the paper near the positive plate, to ensure that the compounds (in anionic form) would be migrating on a rising incline. The initial spots were placed near the opposite end, avoiding the part of the paper held to the cooling surface by unavoidable capillary action.

The movements of dinitrophenyl glycine and of the products, separately and in various admixtures with one another, were studied. The glycine derivative moved much further than the dipeptide derivatives, and the latter showed good separation of those differing by more than two carbon atoms. Distances moved by the dinitrophenyl derivatives of glycine, glycylglycine, glycyl-L-alanine, glycyl-L-valine, and glycyl-L-leucine were 17.5, 14, 13.2, 10.7, and 10.5 cm respectively.

ACKNOWLEDGMENT

Financial support for this work, including a Summer Assistantship (for J. E. K.), was made available by the National Research Council of Canada.

REFERENCES

1. F. SANGER. Biochem. J. **39**, 507 (1948).
2. W. A. SCHROEDER, L. M. KAY, J. LEGETTE, L. HONNER, and F. C. GREEN. J. Am. Chem. Soc. **76**, 3356 (1954).
3. W. A. SCHROEDER and J. LEGETTE. J. Am. Chem. Soc. **75**, 4612 (1953).
4. W. A. SCHROEDER and L. R. HONNER. J. Am. Chem. Soc. **75**, 4615 (1953).
5. H. S. RHINESMITH *et al.* Anal. Biochem. **4**, 284 (1962).
6. A. L. LEVY and D. CHUNG. J. Am. Chem. Soc. **77**, 2899 (1955).

**The ethanol must not be warmed.*
†Air must not be bubbled through the liquid.

Can. J. Chem. Downloaded from www.nrcresearchpress.com by 210.87.254.5 on 09/05/12
For personal use only.

THE SULPHURIC ACID SOLVENT SYSTEM

PART V. SOLUTIONS OF SOME ORGANOSILICON COMPOUNDS

R. H. FLOWERS, R. J. GILLESPIE,[1] AND E. A. ROBINSON[2]
Department of Chemistry, University College, London, England
Received May 27, 1963

ABSTRACT

The cryoscopic and conductimetric behavior of solutions of hexamethyldisiloxane, trimethylethoxysilane, dimethyldiethoxysilane, methyltriethoxysilane, and tetraphenylsilane in 100% sulphuric acid has been investigated. The measurements show that stable non-electrolytes such as $(CH_3)_3Si\cdot HSO_4$ and $(CH_3)_2Si(HSO_4)_2$ are formed from the tri- and di-alkyl compounds. Species such as $CH_3Si(HSO_4)_3$, which are presumably formed in the reaction of monoalkyl compounds, and $Si(HSO_4)_4$, which it is reasonable to suppose is the initial product from the cleavage of tetraphenylsilane, are unstable and polymerize to give polymers containing Si—O—Si bridging groups. No evidence was obtained for the formation of siliconium ions or for the formation of compounds containing silicon with a coordination number greater than four.

INTRODUCTION

The reactions of organosilicon compounds with sulphuric acid are of interest in view of the use of sulphuric acid as an equilibrating agent in the preparation of silicones (1) and in cleavage reactions of complex organosilicon compounds (2). There have consequently been several investigations of the cryoscopic behavior of organosilicon compounds (2–4), although no previous conductimetric studies have been reported.

In this paper the results of cryoscopic and conductimetric studies of solutions of hexamethyldisiloxane, trimethylethoxysilane, dimethyldiethoxysilane, methyltriethoxysilane, and tetraphenylsilane are reported. Ethyl silicate, triphenylsilanol, trinaphthylsilanol, silicon tetraacetate, and diphenylsilanediol were found to be insoluble in sulphuric acid and they reacted slowly to give gelatinous solids.

EXPERIMENTAL

Cryoscopic measurements were carried out using the Beckmann method of cryoscopy as described previously (5). Solid-stem mercury in glass thermometers which had been calibrated against a platinum resistance thermometer was used for temperature measurements. Conductivities were measured at 25° C (6). In each case addition of a small quantity of the strong base potassium sulphate to the solution of the silicon compound at the end of an experiment led to an increase in the specific conductance, showing that all the compounds ionize as bases.

Hexamethyldisiloxane, trimethylethoxysilane, dimethylethoxysilane, and methyltriethoxysilane were obtained from the Midland Silicone Company and were at least 99% pure as supplied. They were distilled through a column and the middle fraction of constant boiling point collected in each case. (Boiling points: $[(CH_3)_3Si]_2O$, 99.5°; $(CH_3)_3SiOEt$, 75–76°; $(CH_3)_2Si(OEt)_2$, 112–113°; $CH_3\cdot Si(OEt)_3$, 141–142°). Tetraphenylsilane was prepared according to the method of Gilman and Jones (7) from triphenylchlorosilane and phenyllithium. It had a melting point of 236°.

The sulphuric acid solvent was prepared from 'AnalaR' sulphuric acid and sulphur trioxide and adjusted to the composition 100% H_2SO_4 by means of its freezing point or specific conductivity (5, 6).

RESULTS

The results of the cryoscopic and conductimetric measurements are shown in Tables I, II, and III and the conductivities are compared with the conductivities of solutions of the strong base water in Fig. 1. In the case of the cryoscopic measurements corrections

[1]*Present address: McMaster University, Hamilton, Ontario.*
[2]*Present address: University of Toronto, Toronto 5, Ontario.*

Can. J. Chem. Downloaded from www.nrcresearchpress.com by 210.87.254.6 on 09/05/12
For personal use only.

TABLE I

Freezing points of solution in sulphuric acid

$m\times10^2$	F.p. (°C)	$m\times10^2$	F.p. (°C)	$m\times10^2$	F.p. (°C)
	$[(CH_3)_3Si]_2O$				
0.000	10.365	0.000	10.365		
0.173	10.350	0.208	10.345		
0.299	10.331	0.654	10.280		
1.479	10.122	1.899	10.030		
2.769	9.834	4.560	9.425		
4.221	9.388	6.673	8.918		
7.238	8.779	8.774	8.410		
9.067	8.343	10.390	8.113		
	$(CH_3)_3Si\cdot OC_2H_5$				
0.000	10.365	0.000	10.365		
0.495	10.300	0.269	10.332		
1.678	10.095	0.696	10.275		
3.442	9.736	2.018	10.037		
4.915	9.374	2.941	9.830		
6.985	8.881	4.322	9.517		
9.122	8.373	6.015	9.119		
		8.204	8.586		
		9.337	8.320		
		10.520	8.026		
	$(CH_3)_2Si(OC_2H_5)_2$				
0.000	10.365	0.000	10.365		
0.234	10.320	0.386	10.257		
0.697	10.142	1.267	9.948		
1.243	9.945	2.740	9.354		
3.503	9.017	4.061	8.796		
4.331	8.665	5.240	8.305		
5.513	8.181	5.943	8.013		
6.049	7.952				
		$CH_3\cdot Si(OC_2H_5)_3$			
0.000	10.365	0.000	10.365	0.000	10.365
0.172	10.308	0.271	10.274	0.550	10.199
0.357	10.255	0.545	10.187	1.410	9.847
0.707	10.132	1.123	9.972	2.412	9.403
1.415	9.844	1.932	9.636	3.967	8.719
2.208	9.496	2.608	9.344	5.481	8.086
3.041	9.109	3.709	8.840		
4.331	8.508	4.325	8.560		
5.075	8.149	5.025	8.250		
		5.585	7.995		
		$(C_6H_5)_4Si$			
0.000	10.365	0.000	10.365	0.000	10.365
0.011	10.353	0.383	10.206	0.085	10.320
0.325	10.260	0.838	9.994	0.598	10.087
0.844	9.990	1.119	8.848	0.991	9.869
		1.628	9.582	1.417	9.550
		2.105	9.335	2.261	9.073
		2.842	8.982*	3.081	8.590*

*The final solution in each case was slightly opaque.

for supercooling and the repression of the solvent self-dissociation by the added solute were obtained by standard methods (5, 8). Values of ν, the number of moles of solute particles (molecules and ions) produced by the reaction of 1 mole of solute, were obtained from the equation

$$\nu = \theta(1+0.002\theta)/6.12\phi m - m_d/m,$$

where θ is the freezing-point depression calculated from the freezing point of hypothetical

Can. J. Chem. Downloaded from www.nrcresearchpress.com by 210.87.254.6 on 09/05/12
For personal use only.

TABLE II

Conductivities of solutions in sulphuric acid

$m\times10^2$	$\kappa\times10^2$	$m\times10^2$	$\kappa\times10^2$
	$[(CH_3)_3Si]_2O$		
0.00	1.044	0.00	1.044
0.44	1.046	0.42	1.048
1.47	1.085	1.47	1.091
2.58	1.173	2.77	1.202
4.27	1.365	4.34	1.383
6.64	1.671	6.38	1.646
9.66	2.056	8.87	1.969
2.64	2.474	3.67	2.533
	$(CH_3)_3Si\cdot OC_2H_5$		
0.00	1.044	0.00	1.044
0.73	1.044	0.32	1.044
1.86	1.091	1.10	1.063
3.82	1.278	1.75	1.098
6.18	1.584	3.47	1.264
8.93	1.957	6.36	1.640
2.08	2.363	9.18	2.020
		12.81	2.486
		16.27	2.882
	$(CH_3)_2Si(OC_2H_5)_2$		
0.00	1.044	0.00	1.044
0.49	1.058	0.43	1.051
1.53	1.217	1.03	1.113
3.35	1.692	1.69	1.238
5.25	2.200	3.23	1.637
7.83	2.830	5.06	2.141
		7.15	2.676
		0.05	3.321
		3.42	3.947
	$(CH_3)_3Si\cdot OC_2H_5$		
0.00	1.044	0.00	1.044
1.05	1.178	0.22	1.046
2.13	1.460	0.52	1.088
3.14	1.780	0.98	1.186
4.43	2.127	1.82	1.425
6.74	2.695	3.16	1.812
		3.98	2.041
		6.55	2.681
	$(C_6H_5)_4Si$		
0.00	1.044		
0.14	1.044		
0.32	1.055		
0.53	1.079		
0.80	1.133		
1.05	1.187		
1.54	1.327		
2.36	1.581		

undissociated sulphuric acid (10.625°), m is the stoichiometric concentration of the solute, and m_d is the total concentration of the self-dissociation species. The osmotic coefficient ϕ was taken as unity: thus the ν-values obtained are only approximate as no allowance is made for non-ideality effects. Earlier workers who used slightly aqueous sulphuric acid as solvent expressed their cryoscopic results in terms of the vant'Hoff i-factor, $i = \theta/6.12m$. Values of γ, which is approximately equal to the number of moles of hydrogen sulphate ion produced by the ionization of 1 mole of solute, were obtained by comparison of the specific conductance with that of a standard electrolyte such as water (6).

Can. J. Chem. Downloaded from www.nrcresearchpress.com by 210.87.254.6 on 09/05/12
For personal use only.

TABLE III

Values of ν and γ for solutions of silicon compounds in sulphuric acid

m	F.p. (°C)	θ	ν	γ
		$[(CH_3)_3Si]_2O$		
0.01	10.210	0.405	3.98	1.00
0.02	10.000	0.615	4.01	1.00
0.03	9.779	0.836	4.09	1.00
0.04	9.542	1.073	4.10	1.00
0.05	9.292	1.323	4.13	1.00
0.06	9.045	1.570	4.13	0.98
0.07	8.797	1.818	4.12	0.97
0.08	8.550	2.065	4.12	0.96
0.10	8.052	2.563	4.11	0.95
		Mean	4.1	1.0
		$(CH_3)_3Si(OC_2H_5)$		
0.01	10.220	0.395	3.83	1.00
0.02	10.030	0.585	3.87	1.00
0.03	9.815	0.800	3.89	1.00
0.04	9.588	1.027	3.92	1.00
0.05	9.341	1.274	3.98	1.00
0.06	9.089	1.526	4.00	0.98
0.07	8.835	1.780	4.05	0.97
0.08	8.581	2.034	4.05	0.96
0.10	8.079	2.536	4.06	0.95
		Mean	4.0	1.0
		$(CH_3)_2Si(OC_2H_5)_2$		
0.015	9.861	0.754	7.29	2.00
0.020	9.662	0.953	7.25	2.00
0.025	9.446	1.169	7.27	2.00
0.030	9.229	1.386	7.27	2.00
0.035	8.920	1.695	7.26	2.00
0.040	8.785	1.830	7.26	2.00
0.050	8.341	2.274	7.25	2.00
0.060	7.898	2.717	7.25	1.98
		Mean	7.3	2.0
		$CH_3Si(OC_2H_5)_3$		
0.010	10.018	0.597	8.36	2.80
0.015	9.812	0.803	8.01	2.73
0.020	9.587	1.028	7.94	2.60
0.025	9.354	1.261	7.90	2.48
0.030	9.121	1.494	7.87	2.41
0.035	8.888	1.727	7.83	2.37
0.040	8.655	1.960	7.79	2.35
0.050	8.186	2.429	7.73	2.28
0.060	7.951	2.664	7.70	2.21
		$(C_6H_5)_4Si$		
0.005	10.150	0.465	10.81	2.70
0.010	9.861	0.754	10.86	2.70
0.015	9.561	1.054	10.67	2.65
0.020	9.249	1.366	10.63	2.60
0.025	8.939	1.676	10.55	2.55
0.030	8.630	1.985	10.30	2.53

DISCUSSION

Trialkylsilanols and Derivatives

Our cryoscopic measurements on hexamethyldisiloxane, ($\nu = 4.1$), are in agreement with those of Newman, Craig, and Garrett (4) ($i = 4.1$), and Price (3) ($i = 4.3$), who suggested that trimethylsilicon hydrogen sulphate is formed according to the equation

$$[(CH_3)_3Si]_2O + 3H_2SO_4 = 2(CH_3)_3Si\cdot HSO_4 + H_3O^+ + HSO_4^-.$$

Can. J. Chem. Downloaded from www.nrcresearchpress.com by 210.87.254.6 on 09/05/12
For personal use only.

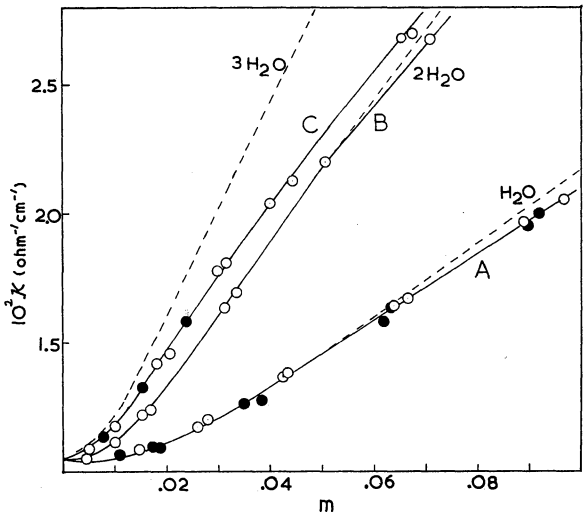

FIG. 1. Conductivities of solutions of some silicon compounds: A, ○ hexamethyldisiloxane, ● trimethylethoxysilane; B, dimethyldiethoxysilane; C, ○ methyltriethoxysilane, ● tetraphenylsilane.

Our conductivity results give $\gamma = 1.0$, which provides confirmation of this suggested reaction. It may be noted that the values of ν are slightly greater than the expected value of 4.0; this may be attributed to non-ideality of the solutions (9). The high i-factors obtained by Newman and co-workers (4) and by Price (3) can, at least partly, be accounted for in a similar manner. Also, these earlier measurements were made in sulphuric acid containing a little water and it has been shown that some non-electrolytes and weak electrolytes such as nitro compounds (10, 11) give anomalously large freezing-point depressions, probably because of a 'salting-out' effect. If, as seems probable, the alkylsilicon hydrogen sulphates behave similarly this would provide an additional reason for the high i-values. There is no evidence that the trimethylsilicon hydrogen sulphate is further ionized either to give a 'siliconium' ion $[(CH_3)_3Si]^+$ as suggested by Price (3) in order to account for his i-factors, or by acting as a weak proton acceptor. Any such additional ionization would be expected to give a conductivity somewhat greater than that of water, i.e. $\gamma > 1$. Actually the observed conductivity coincides with that of water at low concentrations of solute and is a little less than that of water at higher concentrations. This is consistent with the presence of the non-electrolyte $(CH_3)_3Si \cdot HSO_4$ since non-electrolytes are known to decrease the conductivity of sulphuric acid slightly (6, 12).

Our results for trimethylethoxysilane ($\nu = 4.0$, $\gamma = 1.0$), and those of Newman, Craig, and Garrett (4) for triethylethoxysilane ($i = 4.3$) and triethylsilanol ($i = 3.0$), can be similarly accounted for in terms of the formation of trialkyl hydrogen sulphates according to the equations

$$R_3SiOEt + 3H_2SO_4 = R_3Si \cdot HSO_4 + EtHSO_4 + H_3O^+ + HSO_4^-$$

and

$$R_3SiOH + 2H_2SO_4 = R_3Si \cdot HSO_4 + H_3O^+ + HSO_4^-.$$

Dialkylsilanols and Their Derivatives

Our results for dimethyldiethoxysilane ($\nu = 7.3$, $\gamma = 2.0$) suggest that it reacts to form dimethylsilicon di(hydrogen sulphate) according to the equation

$$(CH_3)_2Si(OEt)_2 + H_2SO_4 = (CH_3)_2Si(HSO_4)_2 + 2EtHSO_4 + 2H_3O^+ + 2HSO_4^-.$$

Can. J. Chem. Downloaded from www.nrcresearchpress.com by 210.87.254.6 on 09/05/12
For personal use only.

This is consistent with Price's i-value of 12.6 for the tetramer $[(CH_3)_2SiO]_4$ which he accounted for in terms of the reaction

$$[(CH_3)_2SiO]_4 + 12H_2SO_4 = 4(CH_3)_2Si(HSO_4)_2 + 4H_3O^+ + 4HSO_4^-.$$

The rather high values of ν and i may be attributed to non-ideality of the solutions.

Monoalkylsilanols and Their Derivatives

Methyltriethoxysilane differs from the compounds discussed above in that both ν and γ show quite a definite concentration dependence: ν decreases from 8.4 to 7.7 while γ decreases from 2.8 to 2.2 over the concentration range 0.01 to 0.06 molal. In this case values of γ were obtained by comparison of the conductivity with that of $(CH_3)_2Si(OEt)_2$ which approximately corrects for the effect on the conductivity of the non-electrolytes formed in the reaction. For the formation of methylsilicon tri(hydrogen sulphate) values of $\nu = 10$ and $\gamma = 3$ would be expected:

$$CH_3Si(OEt)_3 + 9H_2SO_4 = CH_3Si(HSO_4)_3 + 3EtHSO_4 + 3H_3O^+ + 3HSO_4^-.$$

Presumably the low observed values of ν and γ and their concentration dependence are due to polymerization of the methylsilicon tri(hydrogen sulphate). The general equation for the formation of linear polymers may be written

$$CH_3Si(OEt)_3 + (6 + 3/n)H_2SO_4 = 1/n\left[HSO_4\text{—}Si(CH_3)(SO_4H)\text{—}O\text{—}\left(Si(CH_3)(SO_4H)\text{—}O\right)_{n-2}\text{—}Si(CH_3)(SO_4H)\text{—}SO_4H\right] + 3EtHSO_4 + (2 + 1/n)H_3O^+ + (2 + 1/n)HSO_4^-$$

	n	$\nu = (7n+3)/n$	$\gamma = (2n+1)/n$
dimer	2	8.5	2.5
trimer	3	8.0	2.3
tetramer	4	7.75	2.25

It is possible that these polymers are better formulated as containing six-membered rings with bridging sulphate groups formed by elimination of sulphuric acid from the linear polymer:

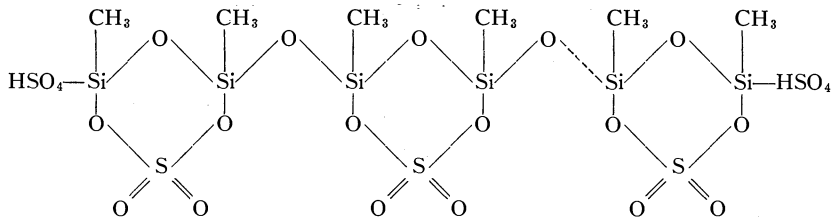

This is consistent with the structures recently proposed for complex sulphato compounds of boron (13) and arsenic (14). The formation of a mixture of these polymers would account satisfactorily for the experimental observations. The i-factors of between 8.5 and 8.0 obtained by Price (3) for the compound $[(CH_3)_3SiO]_3Si\cdot CH_3$ are consistent with the formation of the same linear polymers:

$$[(CH_3)_3SiO]_3SiCH_3 + (6 + 3/n)H_2SO_4 = 1/n\left[HSO_4\text{—}Si(CH_3)(SO_4H)\text{—}O\left(Si(CH_3)(SO_4H)\text{—}O\right)_{n-2}\text{—}Si(CH_3)(SO_4H)\text{—}SO_4H\right] + 3(CH_3)_3Si\cdot HSO_4 + (2 + 1/n)H_3O^+ + (2 + 1/n)HSO_4^-$$

Can. J. Chem. Downloaded from www.nrcresearchpress.com by 210.87.254.6 on 09/05/12
For personal use only.

for which $\nu = 7+3/n$. The formation of analogous cyclic polymers as suggested by Price (3) is not in such good agreement with the experimental results. For example,

$$CH_3Si(OEt)_3 + 6H_2SO_4 = 1/n[CH_3Si(SO_4H)O]_n + 3EtHSO_4 + 2H_3O^+ + 2HSO_4^-$$

and

$$[(CH_3)_3SiO]_3 + 6H_2SO_4 = 1/n[CH_3Si(SO_4H)O]_n + 3(CH_3)_3SiHSO_4 + 2H_3O^+ + 2HSO_4^-.$$

For the former reaction $\nu = 7+1/n$ and $\gamma = 2$ while for the latter $\nu = 7+1/n$.

The possibility of the formation of other types of polymers was also considered but no agreement with the experimental results could be obtained. For example the formation of polymers containing sulphate bridges,

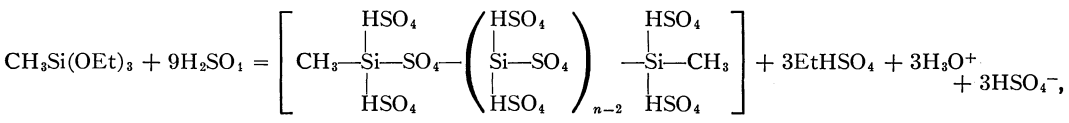

would give $\nu = 9+1/n$ and $\gamma = 3$.

Tetraphenylsilane

A cryoscopic study of this compound and also tetrabenzylsilane and hexaphenyldisiloxane has been previously carried out by Szmant, Devlin, and Brost (2). They found that their results could only be accounted for if it was assumed that complete cleavage of the Si—C bonds occurs with the formation of the corresponding arylsulphonic acid; they were able to isolate these sulphonic acids from the sulphuric acid solutions.

The cleavage of C—Si bonds is well known to be caused by a variety of both acidic and basic reagents and kinetic studies have been made of the cleavage of phenyltrimethylsilane by sulphuric acid (15). However the simple formation of $Si(HSO_4)_4$ or of the anions $Si(HSO_4)_5^-$ or $Si(HSO_4)_6^{2-}$ is not in agreement with the cryoscopic results:

$$Ph_4Si + 12H_2SO_4 = Si(HSO_4)_4 + 4PhSO_3H + 4H_3O^+ + 4HSO_4^- \quad (\nu = 13, \gamma = 4),$$

$$Ph_4Si + 12H_2SO_4 = Si(HSO_4)_5^- + 4PhSO_3H + 4H_3O^+ + 3HSO_4^- \quad (\nu = 12, \gamma = 3),$$

$$Ph_4Si + 12H_2SO_4 = Si(HSO_4)_6^{2-} + 4PhSO_3H + 4H_3O^+ + 2HSO_4^- \quad (\nu = 11, \gamma = 2).$$

Our ν values are somewhat higher than the i-values obtained by Szmant, Devlin, and Brost and unlike their values they show a definite decrease with increasing concentration. This decrease in ν and the corresponding decrease in γ with increasing concentration indicate clearly that some form of polymerization is occurring. Szmant *et al.* (2) explained their results in terms of the cyclic polymers $[Si(HSO_4)_2O]_n$ first proposed by Price (3); however, our results cannot be explained fully by either cyclic or linear polymers, mainly because neither can give a γ-value less than 3.0:

$$Ph_4Si + 9H_2SO_4 = 1/n[Si(HSO_4)_2O]_n + 4PhSO_3H + 3H_3O^+ + 3HSO_4^- \quad (\nu = 10 + 1/n, \gamma = 3.0)$$

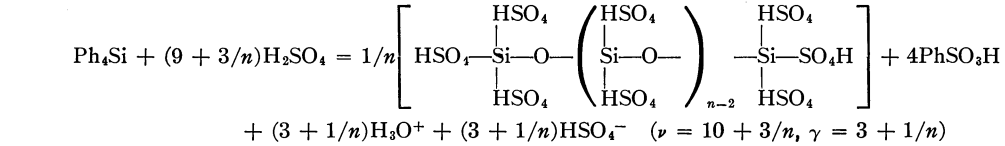

$$+ (3 + 1/n)H_3O^+ + (3 + 1/n)HSO_4^- \quad (\nu = 10 + 3/n, \gamma = 3 + 1/n)$$

The best explanation of the conductimetric results appears to be obtained by postulating the formation of a three-dimensional polymer as first proposed by Price for the related compound $Si[OSi(CH_3)_3]_4$ (3):

$$Ph_4Si + 15/2H_2SO_4 = 1/2n[Si_2(HSO_4)_2O_3]_n + 5/2H_3O^+ + 5/2HSO_4^- + 4PhSO_3H \quad (\nu = 9 + 1/2n, \gamma = 2.5)$$

Can. J. Chem. Downloaded from www.nrcresearchpress.com by 210.87.254.6 on 09/05/12
For personal use only.

The fact that the observed ν-values are a little higher than predicted can be reasonably attributed to non-ideality. Probably the predominant species at low concentrations are small cyclic polymers, which are replaced at higher concentrations by an increasing amount of the three-dimensional polymer, which eventually separates out, even from quite dilute solutions, as a gelatinous precipitate. The somewhat less accurate cryoscopic results of Szmant and co-workers (2) on tetrabenzylsilane and hexaphenyldisiloxane, and Price's results (3) on the compound $[(CH_3)_3SiO_4]Si$, can be accounted for in an exactly analogous manner.

REFERENCES

1. W. Patnode and D. F. Wilcock. J. Am. Chem. Soc. **68**, 358 (1946).
2. H. H. Szmant, O. M. Devlin, and G. A. Brost. J. Am. Chem. Soc. **73**, 3059 (1951).
3. F. P. Price. J. Am. Chem. Soc. **70**, 871 (1949).
4. M. S. Newman, R. A. Craig, and A. B. Garrett. J. Am. Chem. Soc. **71**, 869 (1949).
5. R. J. Gillespie, E. D. Hughes, and C. K. Ingold. J. Chem. Soc. 2504 (1950).
6. R. J. Gillespie and C. S. Solomons. J. Chem. Soc. 1796 (1957).
7. H. Gilman and R. G. Jones. J. Am. Chem. Soc. **63**, 1441 (1941).
8. S. J. Bass, R. J. Gillespie, and E. A. Robinson. J. Chem. Soc. 821 (1960).
9. S. J. Bass and R. J. Gillespie. J. Chem. Soc. 2804 (1959).
10. R. J. Gillespie and E. A. Robinson. J. Chem. Soc. 4233 (1957).
11. J. R. Brayford and P. A. H. Wyatt. J. Chem. Soc. 3453 (1955).
12. R. J. Gillespie and S. Wasif. J. Chem. Soc. 209 (1953).
13. R. J. Gillespie and E. A. Robinson. Can. J. Chem. **40**, 1009 (1962).
14. R. J. Gillespie and E. A. Robinson. Can. J. Chem. **41**, 450 (1963).
15. C. Eaborn. Organosilicon compounds. Butterworth, London. 1960. p. 146.

Can. J. Chem. Downloaded from www.nrcresearchpress.com by 210.87.254.6 on 09/05/12
For personal use only.

NUCLEAR MAGNETIC RESONANCE MEASUREMENTS OF PROTON EXCHANGE IN ALCOHOL–WATER SYSTEMS

PART II. n-C_3H_7OH–H_2O AND i-C_3H_7OH–H_2O[1]

W. G. PATERSON[2]

Department of Chemistry, University of Alberta, Edmonton, Alberta

Received April 4, 1963

ABSTRACT

Recent methods of analysis of exchange-broadened n.m.r. multiplets are used to make measurements of multiplet spacings and line widths in the n.m.r. spectra of n-C_3H_7OH–H_2O and i-C_3H_7OH–H_2O solutions. The data are interpreted in terms of the proton exchange reaction ROH + HOH* $\rightleftharpoons$ ROH* + HOH (R = n-C_3H_7 and i-C_3H_7) for which rate constants k = 1.7±0.3 (R = n-C_3H_7) and 0.35±0.06 (R = i-C_3H_7) l.mole^{-1} sec^{-1} at 42±1° are suggested. Possible exchange mechanisms are discussed.

INTRODUCTION

The n.m.r. spectrum of a liquid or solution may undergo striking changes if the molecules concerned are participating in rate processes. Since its discovery several years ago, interest in this phenomenon has become widespread (4). In particular, much attention has been given to intermolecular proton exchange.

Previous n.m.r. studies of proton exchange in alcohol–water solutions[3] have been confined principally to the system C_2H_5OH–H_2O, with widely varying results being reported. Qualitative measurements of proton exchange in the systems n-C_3H_7OH–H_2O and i-C_3H_7OH–H_2O appeared recently (5), and in this paper results of a more quantitative nature are presented. This paper is the second of a series dealing with proton exchange in alcohol–water systems.

EXPERIMENTAL

The n.m.r. spectra were measured on a Varian A-60 n.m.r. spectrometer operating at 60 Mc/s. Through the use of a copper–constantan thermocouple, the temperature of the solutions, in the spectrometer, was found to be 42±1°. Calibration of the instrument was achieved by the customary side-band technique (6), using a Hewlett–Packard Model 200AB audio-oscillator and a Hewlett–Packard Model 521C frequency counter. The precision in the n.m.r. measurements varied from 0.02 c.p.s. to 0.1 c.p.s. depending on signal shape. Nearly all measurements were an average of at least five determinations. Transverse relaxation times (T_2) were measured as previously described (1). The degree of resolution of the n.m.r. spectrometer was deliberately made poorer than usual in order that T_2 be governed chiefly by magnetic field inhomogeneities (7).

All glassware which was used either in the purification of materials or in the rate measurements was cleaned with the following substances in the order given, and then heated for several hours at 120°: Fisher "Sparkleen" detergent, distilled water, dilute hydrochloric acid, distilled water, dilute ammonia, distilled water. The rinsings with distilled water were done 10–20 times.

Anhydrous n-propyl alcohol was prepared from Fisher Certified Reagent Grade material by the method quoted by Fieser (8) for anhydrous ethyl alcohol. A 30 in Vigreux fractionating column and a Kjeldahl spray trap were used in the distillation, and air was excluded from the apparatus by passing a very slow stream of dried, carbon dioxide free nitrogen through it. A middle fraction was collected (n_D^{25} = 1.3832; Brunel (9) gives n_D^{25} = 1.3835). Vapor-phase chromatography indicated the presence of trace impurities only. No water peak was observed in the n.m.r. spectrum run at high recorder gain. The alcohol —OH signal was a sharp triplet with spacings which varied in different preparations from 5.14±0.04 c.p.s. to 5.16±0.05 c.p.s. (average of 10 determinations). These variations should have a negligible effect on the

[1]*For Part I, see reference 1.*

[2]*Present address: Central Research Laboratories, Minnesota Mining and Mfg. Co., St. Paul 19, Minnesota, U.S.A.*

[3]*See reference 1 for a summary.*

Can. J. Chem. Downloaded from www.nrcresearchpress.com by 210.87.254.105 on 09/05/12
For personal use only.

results quoted, since any set of measurements on *n*-propyl alcohol – water solutions was compared to the purified *n*-propyl alcohol prepared for that set.

Nichols Reagent Grade isopropyl alcohol was refluxed over calcium oxide for 4 hours in an atmosphere of dry, carbon dioxide free nitrogen, decanted into a clean flask, refluxed over sodium metal for 2 hours in a nitrogen atmosphere, and distilled as described above for *n*-propyl alcohol. The middle cut had $n_D^{25} = 1.3755$ (Brunel (9) reports 1.3749). No water peak could be detected in the n.m.r. spectrum run at high gain. The alcohol —OH signal was a sharp doublet with spacing 4.29±0.02 c.p.s. (average of 10 determinations).

Pure water was prepared in two different ways as described previously (1), by distillation from alkaline permanganate and by ion exchange. Two different preparations gave $n_D^{28} = 1.3323$ and $n_D^{25.5} = 1.3325$. Literature values (10) are $n_D^{28} = 1.3322$ and $n_D^{25.5} = 1.3325$. The pH of water thus prepared varied between 6.7 and 7.0, corresponding to $[H^+] = 2\times10^{-7}$ mole/l. or less. Alcohol–water solutions, approximately 40% v/v, gave similar pH readings. A single measurement also showed that a *n*-propyl alcohol – water solution had a very low conductivity. Identical rate plots, within experimental error, were obtained using water prepared by the two methods. The alcohol–water solutions were prepared by weight and the concentrations in moles/l. calculated from published density data (11).

All flasks and n.m.r. tubes which were used in sample preparation were flushed with dried, carbon dioxide free nitrogen before use. Since the solutions slowly leach impurities from the glass (1, 2), it was found necessary to do a given set of n.m.r. measurements on the same day that the materials were distilled.

Further experimental details are obtainable elsewhere (1, 2).

RESULTS AND DISCUSSION

The simplest interpretation of the kinetic data is obtained if it is assumed that the only reaction of kinetic significance in the alcohol–water solutions is

$$ROH + HOH^* \rightleftharpoons ROH^* + HOH, \qquad [1]$$

where R = *n*-C_3H_7 or *i*-C_3H_7. This assumption is probably valid in view of the extremely small ionic concentrations in neutral alcohol–water solutions (12, 13), and the fact that there is no observable proton exchange in the pure alcohols (see Experimental). Since the average lifetime τ_{ROH} of a hydroxyl proton on an alcohol molecule ROH before exchange with a proton on a different site (1, 12) is

$$\tau_{ROH} = \frac{[ROH]}{d[ROH]/dt} = \frac{1}{k[H_2O]}, \qquad [2]$$

where k is the rate constant for reaction [1], a plot of τ_{ROH}^{-1} vs. $[H_2O]$ should be a straight line with slope k passing through the origin. Figures 1 and 2 suggest that this is approxi-

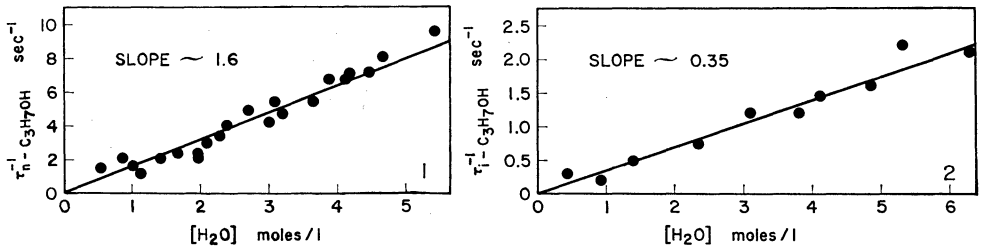

FIG. 1. Variation of $\tau_{n\text{-}C_3H_7OH}^{-1}$ with $[H_2O]$.
FIG. 2. Variation of $\tau_{i\text{-}C_3H_7OH}^{-1}$ with $[H_2O]$.

mately true. The point scatter is probably due to minute traces of impurities, to which the exchange process is very susceptible (1, 2, 12).

Since $\tau_{ROH} = \tau_{H_2O}$ for reaction [1], where τ_{H_2O} is the average lifetime of a proton on a water molecule before exchange with a proton on an alcohol molecule, a plot of $\tau_{H_2O}^{-1}$ vs. $[H_2O]$ should also be a straight line with the same slope k passing through the origin

Can. J. Chem. Downloaded from www.nrcresearchpress.com by 210.87.254.105 on 09/05/12
For personal use only.

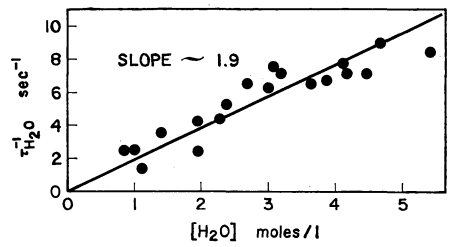

FIG. 3. Variation of $\tau^{-1}_{H_2O}$ with $[H_2O]$.

(Fig. 3). Although there is a severe point scatter, the previous observation (1) of a linear plot with zero intercept for the system ethyl alcohol – water lends support to a similar interpretation of Fig. 3. No reliable data of this nature were obtainable from the spectra of isopropyl alcohol – water solutions due to interference from the methine proton signal. It may be significant that the slope of the plot $\tau^{-1}_{H_2O}$ vs. $[H_2O]$ is slightly greater than that of τ^{-1}_{ROH} vs. $[H_2O]$ for both the systems C_2H_5OH–H_2O and n-C_3H_7OH–H_2O. However, this feature has thus far been ignored and the slopes have been averaged to obtain the apparent rate constant.

The values of $\tau^{-1}_{n\text{-}C_3H_7OH}$ and $\tau^{-1}_{i\text{-}C_3H_7OH}$ were obtained from the transverse relaxation time, T_2, and the spacings of the triplet and doublet —OH signals, respectively, using analytical methods previously discussed (1–3). Values of $\tau^{-1}_{H_2O}$ were obtained from the expression (12, 14, 15) $\tau^{-1}_{H_2O} = \pi\Delta\nu_{\frac{1}{2}} - T_2^{-1}$ where $\Delta\nu_{\frac{1}{2}}$ is the full width of the water signal at half-maximum amplitude. Typical —OH and H_2O signals are presented in Figs. 4 and 5.

The average of the slopes of Figs. 1 and 3 yields a rate constant k for reaction [1] (R = n-C_3H_7) equal to 1.7±0.3 l. mole^{-1} sec^{-1} at 42±1°. The slope of Fig. 2 yields a

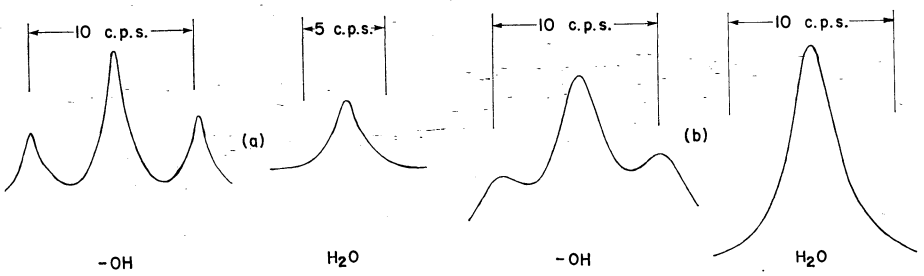

FIG. 4. Typical —OH and H_2O signals in the n.m.r. spectra of n-C_3H_7OH–H_2O solutions. (*a*) $[H_2O]$ = 1.12 moles/l.; (*b*) $[H_2O]$ = 3.89 moles/l. The —OH and H_2O signals were recorded at different recorder gain settings.

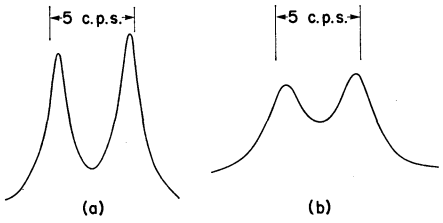

FIG. 5. Typical —OH signals in the n.m.r. spectra of i-C_3H_7OH–H_2O solutions. (*a*) $[H_2O]$ = 2.34 moles/l. (*b*) $[H_2O]$ = 6.28 moles/l.

Can. J. Chem. Downloaded from www.nrcresearchpress.com by 210.87.254.105 on 09/05/12
For personal use only.

value 0.35 ± 0.06 l. mole^{-1} sec^{-1} at $42\pm1°$ as the rate constant k for reaction [1] (R = i-C_3H_7). The errors quoted are somewhat arbitrary. A summary of the data is given in Table I. It could be argued that these rate constants are upper limits, since proton-

TABLE I

Rate constants for proton exchange in neutral alcohol–water solutions

Alcohol	k (l. mole^{-1} sec^{-1})	Temperature (°C)
C_2H_5OH	$2.7\ \pm0.4$ (1)	42 ± 1
	0.8 (12)	22 ± 2
n-C_3H_7OH	$1.7\ \pm0.3$	42 ± 1
i-C_3H_7OH	0.35 ± 0.06	42 ± 1

transfer reactions involving ionic mechanisms have very large rate constants (12), of the order of 10^6–10^8 l. mole^{-1} sec^{-1} at room temperature.

If the exchange reaction [1] is bimolecular, as suggested by the experimental data, several mechanisms are feasible. One of these (5) could involve the interaction of —OH dipoles via a four-center transition state

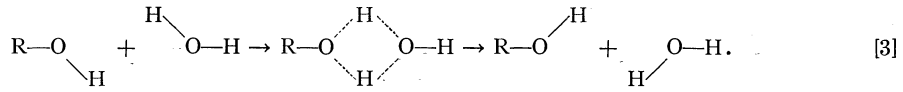

[3]

Others might involve a slow ionization reaction to a pair of ions followed by a rapid recombination reaction, e.g.,

$$ROH + H_2O \underset{\text{fast}}{\overset{\text{slow}}{\rightleftharpoons}} RO^- + H_3O^+ \qquad [4]$$

$$ROH + H_2O \underset{\text{fast}}{\overset{\text{slow}}{\rightleftharpoons}} ROH_2^+ + OH^-. \qquad [5]$$

The reverse reactions must be very fast since the recombination of H_3O^+ and OH^- ions in aqueous solution (16) has a rate constant $k = (1.4\pm0.2)\times10^{11}$ l. mole^{-1} sec^{-1}. Reactions [4] and [5] are perhaps more feasible than reaction [3] since the orientation conditions during collision are less stringent. Variable-temperature studies of the exchange rates would permit an evaluation of the entropy of activation from which one might be able to decide between the possibilities.

It has been known for a long time that water behaves as a base in ethanolic solutions (13), and if the same is true for aqueous solutions of n-propyl alcohol and i-propyl alcohol, reaction [4] is preferable to reaction [5]. On the basis of inductive effects, the relative order of acidity of the three alcohols thus far investigated is $C_2H_5OH > n$-$C_3H_7OH > i$-C_3H_7OH. If equation [4] represents the exchange mechanism, then in the three systems studied, the rates of proton exchange should be in the order C_2H_5OH–$H_2O > n$-C_3H_7OH–$H_2O > i$-C_3H_7OH–H_2O. As this was the observed order, the experimental data are therefore consistent with equation [4] rather than equation [5] as the exchange mechanism. Further, the relative extents of autoprotolysis (17) in the pure alcohols are in the same order. The pair of ions formed in reaction [4] can be envisaged as

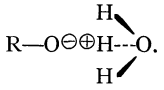

Can. J. Chem. Downloaded from www.nrcresearchpress.com by 210.87.254.105 on 09/05/12
For personal use only.

After formation of the pair of ions, the three protons become equivalent, and since any one of them may return to the alkoxide ion, proton exchange between the alcohol and water molecules is thereby effected. If the same proton returns, there is no change in the spectrum. If another proton with different spin returns, broadening of the n.m.r. signals will be observed.

It should be emphasized that the foregoing discussion of the exchange mechanism is highly speculative. Further results on other alcohol–water systems will be published shortly (18).

ACKNOWLEDGMENTS

This work was supported in part by the National Research Council of Canada, whose financial assistance is greatly appreciated. The author is indebted to Mr. R. Mermelstein, Dr. C. C. Bigelow, Dr. R. N. O'Brien, and Mr. A. Patil for assistance and advice concerning the experimental work, and to Dr. D. Darwish for helpful suggestions about the manuscript. The author also wishes to thank Mr. R. N. Swindlehurst and Mr. R. Kadlecz for careful maintenance of the n.m.r. apparatus.

REFERENCES

1. W. G. PATERSON. Can. J. Chem. **41**, 714 (1963).
2. W. G. PATERSON and R. E. RICHARDS. Trans. Faraday Soc. To be published.
3. M. TAKEDA and E. O. STEJSKAL. J. Am. Chem. Soc. **82**, 25 (1960).
4. J. A. POPLE, W. G. SCHNEIDER, and H. J. BERNSTEIN. High-resolution nuclear magnetic resonance. McGraw-Hill Book Co., Inc., New York. 1959. Chap. 10, 15.
5. G. MAVEL. Compt. rend. **250**, 1477 (1960).
6. J. T. ARNOLD and M. E. PACKARD. J. Chem. Phys. **19**, 1608 (1951).
7. VARIAN ASSOCIATES and STAFF. NMR–EPR spectroscopy. Pergamon Press, London. 1960. Chap. 9.
8. L. F. FIESER. Experiments in organic chemistry. 3rd ed. D. C. Heath and Co., Boston. 1957. p. 285.
9. R. F. BRUNEL. J. Am. Chem. Soc. **45**, 1334 (1923).
10. HANDBOOK of Chemistry and Physics. 34th ed. Chemical Rubber Publishing Co., Cleveland, Ohio. 1952. p. 2491.
11. INTERNATIONAL critical tables. McGraw-Hill Book Co., Inc., New York. Vol. III. pp. 119–120.
12. Z. LUZ, D. GILL, and S. MEIBOOM. J. Chem. Phys. **30**, 1540 (1959).
13. L. P. HAMMETT. Physical organic chemistry. McGraw-Hill Book Co., Inc., New York. 1940. pp. 256, 262.
14. H. M. MCCONNELL. J. Chem. Phys. **28**, 430 (1958).
15. H. S. GUTOWSKY, D. W. MCCALL, and C. P. SLICHTER. J. Chem. Phys. **21**, 279 (1953).
16. M. EIGEN and L. DEMAYER. Proc. Roy. Soc. (London), Ser. A, **247**, 505 (1958).
17. A. TÉZÉ and R. SCHAAL. Compt. rend. **253**, 114 (1961).
18. W. G. PATERSON and H. SPEDDING. Can. J. Chem. This issue.

Can. J. Chem. Downloaded from www.nrcresearchpress.com by 210.87.254.105 on 09/05/12
For personal use only.

NUCLEAR MAGNETIC RESONANCE MEASUREMENTS OF PROTON EXCHANGE IN ALCOHOL–WATER SYSTEMS

PART III. *n*-, *i*-, *s*-, AND *t*-C_4H_9OH–H_2O

W. G. PATERSON[1] AND H. SPEDDING
Department of Chemistry, University of Alberta, Edmonton, Alberta

Received May 24, 1963

ABSTRACT

Measurements of exchange-broadened n.m.r. signals are analyzed by recent methods to yield proton exchange rates of the reaction ROH + H*OH ⇄ ROH* + HOH, where R = *n*-, *i*-, *s*-, and *t*-C_4H_9. The rate constants suggested are 0.95 (44°), 0.90 (42°), 0.60 (46°), and 0.25 (46°) l. mole^{-1} sec^{-1}, respectively. The trend in rate constants for these four systems, and the C_2H_5OH–, *n*-C_3H_7OH–, and *i*-C_3H_7OH–H_2O systems examined in Parts I and II (W. G. Paterson, Can. J. Chem. **41**, 714, 2472 (1963)), is discussed in terms of the nature of the alkyl groups in each alcohol.

INTRODUCTION

The work described below is an extension of Parts I and II (1, 2), and is based on the same theoretical analyses (1, 3, 4) used therein. Data have now been accumulated for the eight alcohol–water systems from CH_3OH–H_2O through *t*-C_4H_9OH–H_2O. It is shown that the results form a consistent pattern when they are interpreted in terms of the inductive nature of the alkyl groups in each alcohol.

EXPERIMENTAL

Spectroscopic Measurements

The n.m.r. spectra were measured on a Varian A-60 spectrometer operating at 60 Mc/s. The temperature of the samples, in the spectrometer probe, was measured by means of a copper–constantan thermocouple. It varied between 42° and 46° over the course of the measurements; the individual temperature for each of the four alcohol–water systems is given in Table I. The customary side-band technique (5) was used to

TABLE I

System	Temp. (±1°) (°C)	Apparent rate constant *k*: τ_{ROH}^{-1}/[HOH] (l. mole^{-1} sec^{-1})	Apparent rate constant *k*: τ_{HOH}^{-1}/[HOH] (l. mole^{-1} sec^{-1})	Average *k* (l. mole^{-1} sec^{-1})
Methanol–water	Exchange too rapid to be measured by this technique*			
Ethanol–water†	42	2.5	2.9	2.7 ±0.4
n-Propanol–water‡	42	1.6	1.9	1.7 ±0.3
i-Propanol–water‡	42	0.35	—	0.35±0.06
i-Propanol–water	46	0.55	—	0.55±0.1
n-Butanol–water	44	0.95	0.95	0.95±0.2
i-Butanol–water	42	1.0	0.85	0.90±0.2
s-Butanol–water	46	0.55	0.70	0.60±0.1
t-Butanol–water	46	0.25	0.25	0.25±0.1

*Present work. Also obtained by Z. Luz, D. Gill, and S. Meiboom, J. Chem. Phys. **30**, 1540 (1959).
†Reference 1.
‡Reference 2.

calibrate the instrument for the measurement of the multiplet spacings of the pure alcohols quoted below. A Hewlett–Packard Model 200AB audio-oscillator and a Hewlett–Packard Model 521C frequency counter were used for these calibrations. The transverse relaxation time (T_2) was measured as described previously (1) from the line widths of cyclohexane and water, and was deliberately made sufficiently low to be governed

[1]*Present address: Central Research Laboratories, Minnesota Mining and Mfg. Co., St. Paul 19, Minnesota, U.S.A.*

Can. J. Chem. Downloaded from www.nrcresearchpress.com by 210.87.254.40 on 09/05/12
For personal use only.

chiefly by magnetic field inhomogeneities (6). The line widths of these two substances were checked at intervals during the measurements on each system.

For —OH triplet (*n*- and *i*-C_4H_9OH) and doublet (*s*-C_4H_9OH) signals, the lifetime τ before exchange of the hydroxyl proton was estimated from the multiplet spacing (1–4). In the case of *t*-C_4H_9OH, where the —OH signal is a singlet, this lifetime was estimated from the half band-width of the hydroxyl proton signal in the manner previously described for H_2O signals (1, 2). All spacings and half band-widths were an average of at least five determinations.

Glassware

All the glassware used in the purification of the alcohols and water and in the subsequent measurements was cleaned as described previously (2). In addition, however, the n.m.r. sample tubes were given a further conditioning treatment. Before they were used at all, and again between runs, all the tubes were filled with concentrated nitric acid (16 normal) for 10 minutes, emptied, rinsed 25 times with distilled water, dried at ~120° (for convenience), and then baked overnight at 580°. This treatment was found necessary in order to obtain reproducible and sensible results with two of the alcohols, and was therefore adopted as a standard procedure. (Some additional qualitative experiments suggested that the nitric acid cleaning might not have been necessary. The annealing, however, was essential.) All flasks and n.m.r. tubes that were used for the alcohol–water solutions were flushed beforehand with dried, carbon dioxide free nitrogen.

Materials

Water was purified by passing distilled water from the tap through a Barnstead "Bantam Demineralizer" ion-exchange column, and then bubbling carbon dioxide free nitrogen through it to remove carbon dioxide. This was one of the two methods used previously (1). The pH of water prepared in this manner corresponded to $[H^+] = (1–2)\times10^{-7}$ moles/l. Such water was always used on the same day that it was prepared.

Purified *n*-butanol was prepared from Fisher Certified Reagent Grade material by the method of Lund and Bjerrum (7). The distillation apparatus and procedure were the same as those used in Parts I and II (1, 2). The —OH signal was a sharp triplet with spacing 5.11±0.02 c.p.s.; $n_D^{25} = 1.3980$ (lit. value (8): 1.3974). No water peak was observed in the n.m.r. spectrum of any of the alcohols run at high recorder gain.

Purified *i*-butanol was prepared by refluxing Fisher Certified Reagent Grade material over small lumps of reagent grade calcium oxide for 20 hours in an apparatus protected from atmospheric moisture, and then distilling from the same calcium oxide as previously described. $n_D^{25} = 1.3947$ (lit. value (9): 1.3939). The —OH signal was a sharp triplet with spacing 5.35±0.03 c.p.s.

Purified *s*-butanol was prepared from Eastman Kodak Reagent Grade material in the manner described for *i*-butanol. $n_D^{20} = 1.3982$ (lit. value (9): 1.3978). The —OH signal was a sharp doublet with spacing 4.88±0.03 c.p.s.

Purified *t*-butanol was prepared from Eastman Kodak Reagent Grade material by the method described for *i*-butanol. $n_D^{28.5} = 1.3832$ (lit. values at 25° (9, 10): 1.3823 and 1.3845).

The alcohol–water solutions were prepared by weight, and their molar concentrations were calculated from published density data (11 or reference therein).

RESULTS AND DISCUSSION

The interpretation of the kinetic data is based on the same assumptions discussed in Parts I and II (1, 2). The influences of the various complicating factors that were discussed there, such as trace impurities and uncertainty about T_2, were also operative in the present work. The effect of the latter factor is more pronounced in the exchange rates estimated from band widths than in those based on multiplet spacings because of the nature of the calculations involved (1). Furthermore, the effect of any error in the value taken for T_2 becomes more pronounced the slower the exchange rate, because the latter is obtained as the difference between the observed half band-width and T_2^{-1}. That the approximation of the half band-width of water and cyclohexane for T_2^{-1} in all the alcohols is a reasonable one is suggested by the satisfactory agreement found in the case of *t*-butanol, the only instance where T_2^{-1} was directly obtainable on account of the hydroxyl peak being a singlet.

In all the four alcohol–water systems examined here both the hydroxyl and water signals were free from interference by overlap. The results are given in Table I and Figs. 1–8 along with new data for the systems CH_3OH–H_2O and *i*-C_3H_7OH–H_2O, as well as the

Can. J. Chem. Downloaded from www.nrcresearchpress.com by 210.87.254.40 on 09/05/12
For personal use only.

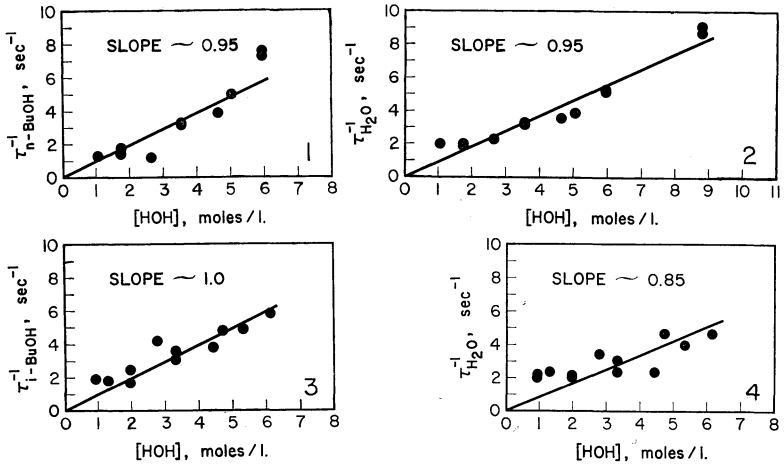

FIG. 1. Variation of $\tau^{-1}_{n\text{-}C_4H_9OH}$ with [HOH] in the system n-C_4H_9OH–H_2O.
FIG. 2. Variation of τ^{-1}_{HOH} with [HOH] in the system n-C_4H_9OH–H_2O.
FIG. 3. Variation of $\tau^{-1}_{i\text{-}C_4H_9OH}$ with [HOH] in the system i-C_4H_9OH–H_2O.
FIG. 4. Variation of τ^{-1}_{HOH} with [HOH] in the system i-C_4H_9OH–H_2O.

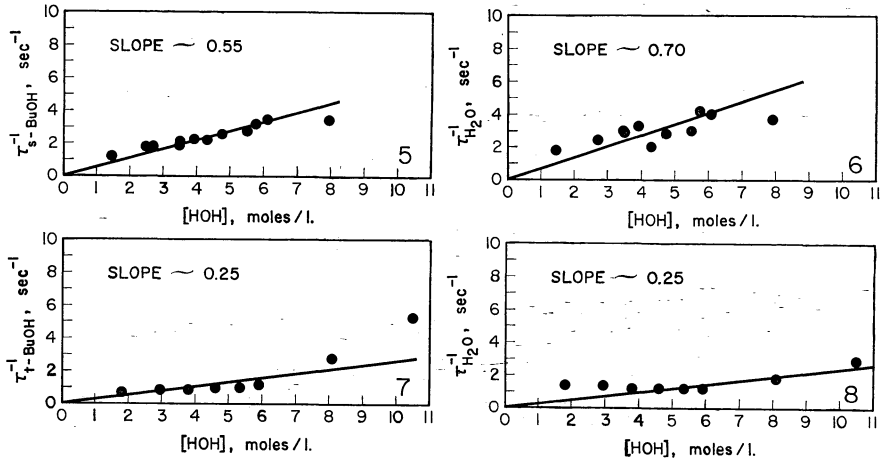

FIG. 5. Variation of $\tau^{-1}_{s\text{-}C_4H_9OH}$ with [HOH] in the system s-C_4H_9OH–H_2O.
FIG. 6. Variation of τ^{-1}_{HOH} with [HOH] in the system s-C_4H_9OH–H_2O.
FIG. 7. Variation of $\tau^{-1}_{t\text{-}C_4H_9OH}$ with [HOH] in the system t-C_4H_9OH–H_2O.
FIG. 8. Variation of τ^{-1}_{HOH} with [HOH] in the system t-C_4H_9OH–H_2O.

results obtained previously (1, 2). In the previous papers, for the systems C_2H_5OH–H_2O and n-C_3H_7OH–H_2O, $\tau^{-1}_{H_2O}/[H_2O]$ was slightly greater than $\tau^{-1}_{ROH}/[H_2O]$; no comparison was possible in the system i-C_3H_7OH–H_2O. The present results show that this difference probably has little if any significance and presumably is due to experimental error. A few measurements on solutions where the water concentration was much less than 1 mole/l showed marked deviations from the plots given in Figs. 1–8; the reason for this is not known.

The results in Table I show that substitution of a methyl group for a hydrogen atom in the alcohols studied leads to a reduction in the apparent rate constant k in every instance

Can. J. Chem. Downloaded from www.nrcresearchpress.com by 210.87.254.40 on 09/05/12
For personal use only.

but one; in the latter (i-C_3H_7OH to s-C_4H_9OH), there is no perceptible change. The effect of substitution is illustrated below. A graphical summary of all the rate data is given in

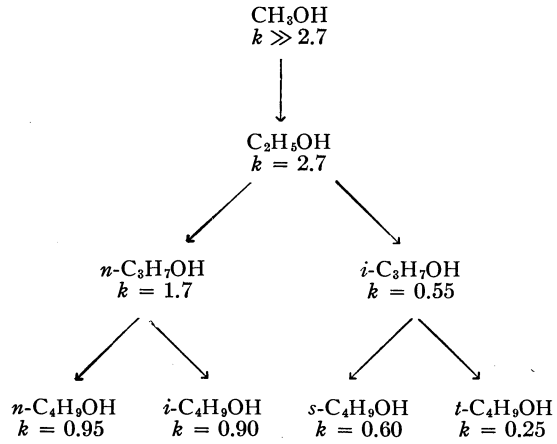

Fig. 9. The pattern is a remarkably consistent one—especially if one includes the CH_3OH–H_2O system where the apparent rate constant, given by $k = \tau^{-1}/[H_2O]$, is too great to permit an accurate evaluation by the present method.

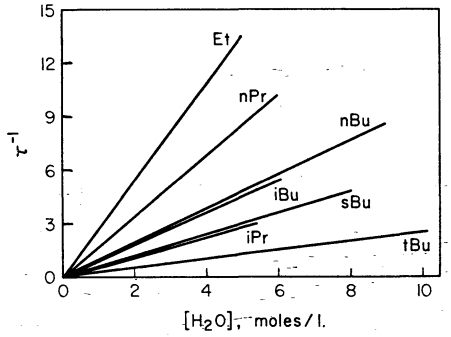

FIG. 9. Variation of τ^{-1} with $[H_2O]$ (average values) in the systems ROH–H_2O. τ is the average lifetime of a hydroxyl proton on an alcohol molecule before exchange with a water molecule.

It is tempting to ascribe the observed changes in apparent rate constant to the greater inductive (+I) effect, or greater polarizability, of the methyl group (as compared to hydrogen) retarding the reaction $ROH + H_2O \rightarrow RO^- + H_3O^+$ by rendering the loss of the alcoholic proton more difficult (2). However, there are many examples, provided by the study of the effect of structure on reactivity (12), where a similar trend would be expected but is not realized. Instead, several different trends are to be found, showing that other factors (steric hindrance, solvation, etc.), whose relative importance varies according to the reaction type involved, are also operating. In the present instance, an explanation based on steric effects and the alcohols behaving as bases ($ROH + HOH \rightleftarrows ROH_2^+ + OH^-$) is a possible alternative. It is, however, a less likely one because (*a*) ethanol is known to act as the acid in ethanol–water solutions (2), and (*b*) it is hard to see how the large changes observed along the series ethanol, n-propanol, and n-butanol could be ascribed to steric opposition, by methyl groups that are well removed from the hydroxyl group, to the acceptance of a water proton.

Can. J. Chem. Downloaded from www.nrcresearchpress.com by 210.87.254.40 on 09/05/12
For personal use only.

ACKNOWLEDGMENTS

This work was supported in part by the National Research Council of Canada, whose financial assistance is greatly appreciated. The authors also wish to thank Mr. R. Kadlecz and Mr. R. N. Swindlehurst for careful maintenance of the n.m.r. spectrometer. Helpful discussions with Dr. R. J. Crawford and Dr. D. Darwish are also acknowledged.

REFERENCES

1. W. G. Paterson. Can. J. Chem. **41**, 714 (1963).
2. W. G. Paterson. Can. J. Chem. This issue.
3. M. Takeda and E. O. Stejskal. J. Am. Chem. Soc. **82**, 25 (1960).
4. W. G. Paterson and R. E. Richards. Trans. Faraday Soc. To be published.
5. J. T. Arnold and M. E. Packard. J. Chem. Phys. **19**, 1608 (1951).
6. Varian Associates and Staff. NMR–EPR spectroscopy. Pergamon Press. 1960. Chap. 9.
7. K. B. Wiberg. Laboratory technique in organic chemistry. McGraw-Hill Book Co., Inc., New York. 1960.
8. R. F. Brunel, J. L. Crenshaw, and E. Tobin. J. Am. Chem. Soc. **43**, 561 (1921).
9. A. Weissberger. Organic solvents. 2nd ed. Interscience Publishers, Inc., New York. 1955.
10. B. B. Allen, S. P. Lingo, and W. A. Felsing. J. Phys. Chem. **43**, 425 (1939).
11. International Critical Tables. Vol. III. McGraw-Hill Book Co., Inc., New York. 1928. pp. 113–114.
12. L. P. Hammett. Physical organic chemistry. McGraw-Hill Book Co., Inc., New York. 1940. Chap. 7.

Can. J. Chem. Downloaded from www.nrcresearchpress.com by 210.87.254.40 on 09/05/12
For personal use only.

REARRANGEMENT STUDIES WITH C^{14}

XVI. REARRANGEMENTS INDUCED BY γ-IRRADIATION OF 2-PHENYLETHYL-1-C^{14} BROMIDE OR 2-*p*-METHOXYPHENYLETHYL-1-C^{14} BROMIDE

D. P. THORNHILL[1] AND C. C. LEE

Department of Chemistry, University of Saskatchewan, Saskatoon, Saskatchewan

Received April 22, 1963

ABSTRACT

Irradiation of 2-phenylethyl-1-C^{14} bromide with up to 133 million rads of Co^{60} γ-rays gave 2-phenylethyl-2-C^{14} bromide with a mean G_r of 0.30 ± 0.01. Similar studies with 2-*p*-methoxyphenylethyl-1-C^{14} bromide resulted in 2-*p*-methoxyphenylethyl-2-C^{14} bromide with a mean G_r of 0.46 ± 0.04. Monomeric, liquid organic products were found to be benzene, ethylbenzene, and styrene, or the analogous *p*-methoxy derivatives, from the irradiation of 2-phenylethyl bromide or 2-*p*-methoxyphenylethyl bromide, respectively. Possible mechanisms for the radiation-induced isotope position rearrangements are discussed.

Can. J. Chem. Downloaded from www.nrcresearchpress.com by 210.87.254.40 on 09/05/12
For personal use only.

As an extension of studies in this laboratory on the γ-irradiation-induced rearrangement of 2-phenylethyl-1-C^{14} iodide to 2-phenylethyl-2-C^{14} iodide (1) and of ethyl-1-C^{14} iodide to ethyl-2-C^{14} iodide (2), this communication reports findings on isotope position rearrangements resulting from irradiation of 2-phenylethyl-1-C^{14} bromide (I) or 2-*p*-methoxyphenylethyl-1-C^{14} bromide (II) with Co^{60} γ-rays.

The bromides, I and II, were prepared from treatment of 2-phenyl- or 2-*p*-methoxyphenyl-ethyl-1-C^{14} *p*-toluenesulphonate with lithium bromide in acetone. Such a method of preparation is expected to cause no rearrangement in the desired products (3) and this was confirmed by degradation of I and II, respectively, to essentially inactive benzoic acid and anisic acid. It is of interest to note that treatment of 2-phenylethanol-1-C^{14} with phosphorus tribromide resulted in I containing about 1.5% of the C^{14} in the C-2 position (4).

Three gram samples of I or II were irradiated at ambient temperature in the same manner as described for the irradiation of 2-phenylethyl-1-C^{14} iodide (1), with the exception that a 1000 c Co^{60} γ-cell,* instead of a 90 c unit, was used as radiation source. Under the conditions employed in these experiments, the dose rates were about 78,000 rads/hr. Irradiation was carried up to an absorbed dosage of 133 million rads. Degradation of I and II, before and after irradiation, was effected in the same way as in the study with 2-phenylethyl-1-C^{14} iodide (1). Through carbonation of the corresponding Grignard reagents, I and II were converted, respectively, to hydrocinnamic acid (III) and *p*-methoxyhydrocinnamic acid (IV). Alkaline permanganate oxidation of III and IV resulted in benzoic acid and anisic acid whose activities gave measures to the extents of rearrangement of the C^{14} from the C-1 to the C-2 positions of I and II. The results, together with the calculated G_r values, representing the number of molecules of I rearranging to 2-phenylethyl-2-C^{14} bromide, or II rearranging to 2-*p*-methoxyphenylethyl-2-C^{14} bromide, per 100 ev absorbed, are summarized in Table I.

The active benzoic acid or anisic acid derived from various irradiated samples was combined and decarboxylated by heating with soda lime. The liquid products, benzene or anisole, were found to contain no activity as expected.

[1]*Holder of a Commonwealth Scholarship, 1961–1963.*
**Supplied by Atomic Energy of Canada Ltd.*

TABLE I

Rearrangements from the irradiation of 2-phenylethyl-1-C^{14} bromide (I) or 2-*p*-methoxyphenylethyl-1-C^{14} bromide (II)

Compound irradiated	Absorbed dosage (megarads)	Compound assayed	Specific activity* (mμc/mmole)	Rearrangement %	Rearrangement G_r
I	0	$C_6H_5CH_2CH_2COOH$	200		
	0	C_6H_5COOH	0.0	0.0	—
	71.0	"	0.85	0.43	0.31
	89.5	"	1.02	0.51	0.30
	112.0	"	1.24	0.62	0.29
	133.0	"	1.50	0.75	0.29
II	0	$CH_3OC_6H_4CH_2CH_2COOH$	1270		
	0	$CH_3OC_6H_4COOH$	0.34	0.03	—
	15.3	"	2.18	0.17	0.50
	42.2	"	5.56	0.44	0.47
	63.2	"	7.86	0.62	0.44
	92.0	"	12.0	0.95	0.46
	125.5	"	15.2	1.20	0.43

*Radioactivity was measured in a liquid scintillation counter as previously described (12). Counting efficiency was determined by measuring known C^{14} standards so that specific activity in mμc/mmole may be calculated.

From Table I, it may be noted that, as in previous studies with iodides (1, 2), the extent of rearrangement increases with increasing dosage of radiation. The mean G_r value of I is 0.30±0.01, and of II is 0.46±0.04. These values may be compared with the G_r of 0.50±0.05 for the γ-induced rearrangement of 2-phenylethyl-1-C^{14} iodide to 2-phenylethyl-2-C^{14} iodide (1).

Ordinary samples of I and II, which were not labeled with C^{14}, were examined by vapor phase chromatography after irradiation. From I, the monomeric, liquid organic products were found to be benzene ethylbenzene, and styrene, with a trace of toluene. The yields are given in Table II.* Qualitatively, anisole, *p*-methoxyethylbenzene, and *p*-methoxy-

TABLE II

Monomeric, liquid organic products from radiolysis of 2-phenylethyl bromide

Absorbed dosage (megarads)	Product	Yield % by wt. in sample	Yield G
65.3	Benzene	0.10	0.19
	Ethylbenzene	0.45	0.63
	Styrene	0.40	0.57
112.0	Benzene	0.20	0.22
	Ethylbenzene	0.83	0.67
	Styrene	0.11	0.09

styrene were obtained after irradiation of II, but quantitative measurements were not carried out (see Experimental). Addition of 1 mole% of iodine to II before irradiation essentially eliminated the chromatogram peaks corresponding to these three compounds.

It may be of interest to note that in the photolysis of 2-phenylethyl bromide solutions in the glassy state at low temperature, styrene was reported as a primary product (5). In the radiolysis of liquid I, a more complex mixture of products arising from secondary processes is to be expected. The chief monomeric materials detected, ethylbenzene and

These results were obtained by I. S. Bhardwaj.

Can. J. Chem. Downloaded from www.nrcresearchpress.com by 210.87.254.40 on 09/05/12
For personal use only.

styrene, may be explained as resulting from hydrogen abstraction and disproportionation of the 2-phenylethyl radical produced during irradiation. The lower net yield of styrene at the higher absorbed dosage (Table II) is likely related to its ability to undergo further reaction, such as polymerization (6, pp. 77–85). The fact that added iodine could practically prevent the formation of *p*-methoxyethylbenzene, *p*-methoxystyrene, and anisole during irradiation of II also suggested the involvement of radicals which were scavenged by iodine, giving rise to organic iodides which were not detectable under the conditions used for the v.p.c. analyses.

Returning to the results summarized in Table I, it is evident that a net 1,2-aryl shift has occurred upon irradiation or either I or II. The exact nature of the process responsible for the observed rearrangements, however, is not clear. One might simply say that irradiation of I or II led to some excited state which collapses to give the rearranged products. On the other hand, free-radical rearrangements have been postulated as the explanation for the γ-induced isomerization of *n*-butyl to *s*-butyl, and *i*-butyl to *t*-butyl halides (7, 8). The formation of 1-phenylethyl radical in the photolyses of 2-phenylethanol in a rigid medium at low temperature was suggested as having resulted from isomerization of the 2-phenylethyl radical (5). As it is generally accepted that, with the exception of the carbon–fluorine bond, the carbon–halogen bond is ruptured preferentially during radiolysis of organic halides (6, pp. 111–116), and in view of the fact that ethylbenzene and styrene, or the *p*-methoxy analogues, were obtained as radiolysis products in the present studies, it is reasonable to assume that 2-phenylethyl or 2-*p*-methoxyphenylethyl radicals are produced during irradiation of I or II, respectively. 1,2-Aryl shifts in these radicals could then lead to the observed isotope position rearrangements.

In a recent paper, Neddenriep and Willard (9) listed a number of reasons for expecting differences in the radiolysis of alkyl iodides and bromides. Among these is that the carbon–iodine bond is weaker than the carbon–bromine bond. Although Porter and Strachan (5) have pointed out that bond dissociation energies in the liquid state are largely unknown, if the relative order of bond energies is not reversed in changing from the vapor to the liquid state for the carbon–bromine bond in I and the carbon–iodine bond in 2-phenylethyl iodide, the lower G_r in the irradiation of bromide I, as compared to the results from studies with 2-phenylethyl-1-C^{14} iodide (1), may be associated with the less ready formation of the 2-phenylethyl radical from the bromide.

The introduction of a *p*-methoxy group increased the G_r value from 0.30 for I to 0.46 for II. It is known that substitution of the *p*-hydrogen by a methoxy group enhances the migratory aptitude of the aryl group in carbonium ion processes (10–12), while in free-radical reactions, the migratory ratio of *p*-methoxyphenyl to phenyl has been reported to be 0.35 (13, 14). However, Zimmerman and Sandel (15) pointed out very recently that in organic photochemistry, the electronic distribution in the excited state may be quite unlike that of its ground-state progenitor and that there is no assurance that ground-state experience would extend to excited states. It was shown with monosubstituted benzenes that the electronic effects of substituents, such as the methoxy group, on the excited state are quite different from such effects on the ground state (15). Thus the *p*-methoxyphenyl to phenyl migratory ratio of 0.35 obtained from the decarbonylation of β-arylisovaleraldehydes (13, 14) may not necessarily hold in free-radical rearrangements induced by γ-irradiation of I and II. Upon irradiation of I or II, it is possible that excitation is followed by dissociation to 2-arylethyl radicals or formation of 2-arylethyl cations which may undergo 1,2-aryl shifts, leading eventually to isotopically rearranged I or II.

Can. J. Chem. Downloaded from www.nrcresearchpress.com by 210.87.254.40 on 09/05/12
For personal use only.

EXPERIMENTAL

Preparation of 2-Phenylethyl-1-C^{14} Bromide (I)

2-Phenylethyl-1-C^{14} *p*-toluenesulphonate (16) was treated with a 20% excess of anhydrous lithium bromide in dry acetone in a manner analogous to that described for the reaction of this sulphonate with sodium iodide in acetone (16). The yield of 2-phenylethyl-1-C^{14} bromide (I), b.p. 90° C at 9 mm (lit. (3) b.p. 110–113° C at 17 mm), was 65%. Conversion of a sample of I to the Grignard reagent followed by reaction with carbon dioxide gave a 74% yield of the solid derivative, hydrocinnamic acid (III), m.p. 48–49° C (lit. (3) m.p. 48–49° C).

Preparation of 2-p-Methoxyphenylethyl-1-C^{14} Bromide (II)

2-*p*-Methoxyphenylethanol-1-C^{14} was prepared according to the method of Lee, Newman, and Thornhill (12). This alcohol was converted to 2-*p*-methoxyphenylethyl-1-C^{14} *p*-toluenesulphonate (11) which, in turn, was treated with anhydrous lithium bromide in dry acetone to give a 79% yield of 2-*p*-methoxyphenylethyl-1-C^{14} bromide (II), b.p. 90° at 1 mm (lit. (17) b.p. 79° C at 0.5 mm). Anal. Calc. for $C_9H_{11}OBr$: C, 50.25; H, 5.15; Br, 37.15. Found: C, 50.09; H, 5.18; Br, 37.76. Reaction of the Grignard from II with carbon dioxide gave a 77% yield of *p*-methoxyhydrocinnamic acid (IV), m.p. 104–105° C (lit. (12) m.p. 104–105° C). Anal. Calc. for $C_{10}H_{12}O_3$: C, 66.70; H, 6.71. Found: C, 67.06; H, 6.85.

Irradiation

Three gram samples of I or II were placed in 4 ml glass vials, stoppered and sealed with wax, and then irradiated at room temperature in fixed positions in a gamma cell originally containing 1000 c of Co^{60}. The dose rate was determined by measuring the ferric ions formed on irradiating solutions of ferrous ammonium sulphate (18) and correcting for the difference in electron densities of the organic sample and dosimeter solution. Irradiation was continued for periods of up to about 2.5 months. Allowance was made for the decay of the Co^{60} in calculating the total absorbed dosage.

Degradation of I and II

Aliquots of the irradiated samples of I or II were converted to the corresponding Grignard reagents and treated with carbon dioxide to give hydrocinnamic acid (III) or *p*-methoxyhydrocinnamic acid (IV), respectively. Alkaline permanganate oxidation (3) of III or IV gave benzoic acid or anisic acid whose activities measured the extents of rearrangement. Similar degradations carried out on I and II before irradiation gave inactive benzoic and anisic acids.

Vapor Phase Chromatography Analyses

Ordinary, unlabeled samples of I or II were irradiated and then examined by a Beckman GC-2A chromatograph, using a column of apiezon L (25%) on firebrick. For irradiated samples of I, using a column temperature of 150° C, helium pressure of 20 p.s.i., and filament current of 200 ma, benzene, ethylbenzene, and styrene were identified and measured quantitatively after calibration with authentic compounds. Higher-boiling materials were removed by prolonged sweeping with helium while the column was maintained at 190° C. For irradiated samples of II, anisole, *p*-methoxyethylbenzene, and *p*-methoxystyrene were also identified. Because of technical difficulties arising from the requirement of higher inlet and column temperatures, irradiated samples of II were not analyzed extensively nor quantitatively.

ACKNOWLEDGMENT

The financial support given by the National Research Council of Canada is gratefully acknowledged.

REFERENCES

1. C. C. Lee, D. G. Lee, and I. S. Bhardwaj. Radiation Res. **17**, 536 (1962).
2. I. S. Bhardwaj and C. C. Lee. Can. J. Chem. **41**, 2368 (1963).
3. C. C. Lee and J. W. T. Spinks. Can. J. Chem. **32**, 1005 (1954).
4. W. B. Smith and J. D. Anderson. J. Am. Chem. Soc. **82**, 656 (1960).
5. G. Porter and E. Strachan. Trans. Faraday Soc. **54**, 1595 (1958).
6. R. O. Bolt and J. G. Carroll (*Editors*). Radiation effects on organic materials. Academic Press, New York. 1963.
7. W. S. Wilcox. Radiation Res. **10**, 112 (1959).
8. E. B. Dismukes and W. E. Wilcox. Radiation Res. **11**, 754 (1959).
9. R. J. Neddenriep and J. E. Willard. J. Phys. Chem. **65**, 1206 (1961).
10. J. D. Roberts and C. M. Regan. J. Am. Chem. Soc. **75**, 2069 (1953).
11. E. F. Jenny and S. Winstein. Helv. Chim. Acta, **41**, 807 (1958).
12. C. C. Lee, D. Newman, and D. P. Thornhill. Can. J. Chem. **41**, 620 (1963).
13. C. Rüchard. Ber. **94**, 2609 (1961).

Can. J. Chem. Downloaded from www.nrcresearchpress.com by 210.87.254.40 on 09/05/12
For personal use only.

14. C. RÜCHARD and S. EICHLER. Ber. **95**, 1921 (1962).
15. H. E. ZIMMERMAN and V. R. SANDEL. J. Am. Chem. Soc. **85**, 915 (1963).
16. C. C. LEE, G. P. SLATER, and J. W. T. SPINKS. Can. J. Chem. **35**, 1417 (1957).
17. C. H. DEPUY and D. H. FROEMSDORF. J. Am. Chem. Soc. **79**, 3710 (1957).
18. J. WEISS, A. O. ALLEN, and H. A. SCHWARZ. Proc. 1st Intern. Congr. Peaceful Uses Atomic Energy, Geneva, 1955, **14**, 169 (1956).

Can. J. Chem. Downloaded from www.nrcresearchpress.com by 210.87.254.40 on 09/05/12
For personal use only.

THE THERMAL CIS–TRANS ISOMERIZATION OF CROTONONITRILE

JAMES N. BUTLER[1] AND ROBERT D. MCALPINE
Department of Chemistry, University of British Columbia, Vancouver, British Columbia

Received May 22, 1963

ABSTRACT

The thermal cis–trans isomerization of crotononitrile has been studied in the gas phase at pressures from 0.2 to 20 mm and temperatures from 300° C to 560° C. For the equilibrium cis → trans, $\Delta H = 0.17 \pm 0.12$ kcal/mole, and $\Delta S = -0.39 \pm 0.19$ cal/mole °K. The isomerization is a homogeneous, unimolecular, reversible first-order reaction, the rate constant for the reaction cis → trans being given by

$$k_1 = 10^{11.0 \pm 1.0} e^{-51.3 \pm 3.7 \text{ kcal}/RT}.$$

The only side reaction with appreciable rate was a surface polymerization.

INTRODUCTION

The cis–trans isomerization of 2-butene (1) has been shown to be a unimolecular reaction at low pressures in the gas phase, but the cis–trans isomerization of dichloroethylene (2) appears to be a free-radical reaction. An intermediate case which might be interesting to study is dicyanoethylene, but its vapor pressure is too low to make a gas-phase study practicable. Crotononitrile, CH_3—CH=CH—CN, has an appreciable vapor pressure at room temperature, however, so a study of its cis–trans isomerization in the gas phase appeared promising.

EXPERIMENTAL

Materials

Crotononitrile was obtained from the Columbia Organic Chemical Company, Columbia, South Carolina, and was found to contain about 40% of the trans isomer and 60% of the cis isomer, together with small amounts of allyl cyanide, methacrylonitrile, and the various isocyanides. The cis and trans isomers were identified by comparison of their n.m.r. spectra with published spectra (3), and purified by gas chromatography. The purified *cis*-crotononitrile contained about 1% of trans isomer, and the purified *trans*-crotononitrile contained about 2% of the cis isomer.

Procedure

The apparatus used has been described previously (4). A sample of either *cis*- or *trans*-crotononitrile was admitted to the 100 ml reactor by expansion of its vapor from a storage vessel. When the reaction had proceeded for the desired length of time, the products were condensed into a side tube of 0.2 ml volume, and sealed off. No non-condensable products were observed.

Analysis

Analysis was performed on a Perkin–Elmer model 226 gas chromatograph using a 150 ft capillary column coated with polypropylene glycol (type R). A flame ionization detector was used. The sample tube was frozen in liquid nitrogen and broken open. Fifty microliters of ether was added immediately, and the solution was thoroughly stirred. Five to ten microliters of this solution was injected into the gas chromatograph and analyzed. Quantitative analysis was performed by measuring peak heights. Calibrations were made by analysis of known mixtures of approximately the same composition. The results of successive analyses on the same sample agreed to within ±5%.

EQUILIBRIUM

Although a detailed spectroscopic analysis of *trans*-crotononitrile has been performed (5) and the thermodynamic functions of this compound have been tabulated, no study has been made of the temperature dependence of the cis–trans ratio. Since this information

[1]*To whom all correspondence should be addressed, at TYCO Laboratories, Inc., Bear Hill, Waltham 54, Mass.*

Can. J. Chem. Downloaded from www.nrcresearchpress.com by 210.87.254.6 on 09/05/12
For personal use only.

was necessary in order to calculate the rate constants for the cis–trans isomerization, a study of the equilibrium was undertaken.

Samples of *cis*-crotononitrile, *trans*-crotononitrile, and mixtures of the two were pyrolyzed at temperatures from 300° C to 500° C. The low-temperature experiments were performed in sealed tubes with a small amount of iodine present as a catalyst (6, 7, 8). High-temperature experiments were performed in the gas phase with no catalyst present. The results are presented in Table I. Each value is the average of the results of three experiments.

TABLE I

Equilibrium data for crotononitrile

Temp. (°C)	Equilibrium cis/trans ratio
Sealed tube, I_2 catalyst	
303	1.40
362	1.39
400	1.39
455	1.35
Gas phase, no catalyst	
479	1.20
520	1.38
560	1.54

Although the high-temperature results scatter much more widely than the low-temperature results, they seem to be consistent. By fitting the more precise low-temperature data with a least-squares straight line, the following thermodynamic functions were calculated for the reaction cis → trans:

$$\Delta H = 0.17 \pm 0.12 \text{ kcal/mole}$$

$$\Delta S = -0.39 \pm 0.19 \text{ cal/mole °K.}$$

Crotononitrile is similar to difluoroethylene (8) and dichloroethylene (9, 10) in that the cis isomer is more stable than the trans isomer. For the dihaloethylenes, this results from a large positive value of ΔH, which has been attributed (11) to the high electronegativity and small size of the halogen atoms. In crotononitrile, ΔH is positive but rather small, and the stability of the cis isomer is primarily due to the negative value of ΔS.

The negative value of ΔS which has been observed in 2-butene has been explained (12) in terms of the potential barrier to hindred rotation of a methyl group. A similar explanation can be invoked for crotononitrile. In the cis isomer, with the methyl group in its low-energy conformation, the repulsion between the cyano group and the nearest two hydrogens of the methyl group is greater than that for the low-energy conformation of the trans isomer, where the two hydrogens of the methyl group interact only with a hydrogen on the other side of the double bond. In the high-energy conformation of either isomer the repulsion will be nearly the same between the single hydrogen of the methyl group and either the cyano group or the hydrogen on the other side of the double bond. The result is that the barrier to internal rotation has approximately the same maximum energy in both cis and trans isomers, but the minimum energy is higher in the cis isomer, and hence the internal rotation in the cis isomer can occur more freely. This could account for the higher entropy of the cis isomer.

Can. J. Chem. Downloaded from www.nrcresearchpress.com by 210.87.254.6 on 09/05/12
For personal use only.

KINETICS OF THE CIS–TRANS ISOMERIZATION

The kinetics of the isomerization of crotononitrile was studied in the gas phase at pressures from 0.7 to 20 mm and temperatures from 400° C to 560° C. Very little low-boiling side-reaction products were observed, although extensive charring and polymerization occurred, blackening the walls of the vessel. On the walls of the tube connecting the vessel with the vacuum system was found a red-brown tarry deposit, which apparently had such a low vapor pressure that none of it distilled into the sample tube.

This polymerization was rapid enough at 600° C to prevent equilibrium from being attained. If a sample of pure *cis*-crotononitrile was pyrolyzed for a sufficiently long time, a steady value of the cis/trans ratio was obtained, approximately 2.0, which was somewhat larger than the equilibrium value, 1.35, extrapolated from lower temperatures. Similarly, if a sample of pure *trans*-crotononitrile was pyrolyzed a steady state was reached in which the cis/trans ratio was 1.05, smaller than the extrapolated equilibrium value. Under these conditions, however, almost no side-reaction products were detected in the boiling point range from 80° C to 150° C. The competing reaction which prevented the attainment of equilibrium appeared to be polymerization. Although polymerization affected the equilibrium runs, it was unimportant at the short times used for the kinetic runs.

At lower temperatures and for shorter reaction times, however, the results showed the isomerization to be a simple reversible first-order reaction:

$$\text{cis} \underset{k_2}{\overset{k_1}{\rightleftharpoons}} \text{trans},$$

and the rate constants were calculated using the conventional integrated rate equation for this mechanism (see, for example, reference 13).

The rate constants listed in Table II were calculated from experiments at 480° C using

TABLE II

Variation of rate constant with time at 480° C

Starting material	Time (sec)		$k_1 \times 10^5$ (sec^{-1})
Cis (22 mm pressure)	100		13.7
	300		14.7
	600		16.5
	1200		12.1
	2940		15.4
	4830		13.9
	8240		13.9
		Average	14.3
Trans (11 mm pressure)	650		15.6
	1920		13.8
	5720		15.7
		Average	15.0

both *cis*- and *trans*-crotononitrile as starting materials, and varying the time of reaction by a factor of 80. No trend is apparent with either time of reaction or direction from which equilibrium is approached.

The rate constant was measured as a function of temperature from 393° C to 560° C, and the results are summarized in Table III. A least-squares straight line fitted to the

Can. J. Chem. Downloaded from www.nrcresearchpress.com by 210.87.254.6 on 09/05/12
For personal use only.

TABLE III

Temperature dependence of rate constant

Temp. (°C)	$k_1 \times 10^5$ (sec^{-1})	No. of points
Starting material cis		
392.9	0.13	3
435.5	1.52	2
444.8	2.41	1
479.4	14.2	9
519.8	95.5	4
560.8	545	3
Starting material trans		
435.2	1.17	1
479.6	15.3	4
Packed vessel, cis		
474.8	7.3	2

Arrhenius plot of this data gave the following parameters:

$$E_a = 51.3 \pm 3.7 \text{ kcal/mole}$$

$$\log A = 11.0 \pm 1.0.$$

The activation energy is lower than the 65 kcal/mole observed for 2-butene (2), and dideuteroethylene (14) but higher than the 46 kcal/mole observed for cyanostyrene (15). The fact that crotononitrile falls between the conjugated styrene system and the unconjugated ethylene system lends support to the hypothesis that conjugation in the side groups makes the activation energy for isomerization lower. The pre-exponential factor is almost exactly the same as the log $A = 11.6$ observed for cyanostyrene, and the similar entropy of activation implies that the transition state configuration in the two cases is similar.

The rate of reaction was unaffected by the addition of up to 1% of oxygen or by packing the reaction vessel with glass wool. This evidence, together with the hgh frequency factor and activation energy, suggests that the reaction is a truly homogeneous unimolecular one.

Further evidence for the unimolecular nature of this reaction is provided by the dependence of the rate constant on pressure. Figure 1 shows the rate constant as the pressure

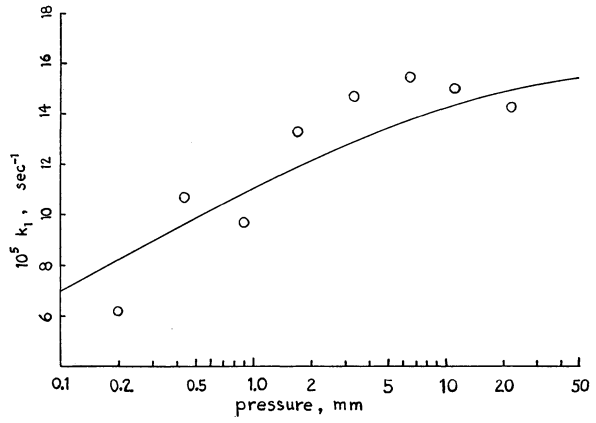

FIG. 1. Pressure dependence of rate constant.

Can. J. Chem. Downloaded from www.nrcresearchpress.com by 210.87.254.6 on 09/05/12
For personal use only.

was varied from 0.2 to 20 mm at 480° C. Although the scatter in the data is large, due principally to the method of analysis, the rate constant can be seen to decrease by about a factor of 2 over this range of pressure.

The curve in Fig. 1 was drawn using the Kassel (16) equation with the following parameters: Infinite-pressure rate constant 1.60×10^{-4} sec^{-1}, collision diameter 5.5 Å, and fall-off parameter $s = 9$. Although by analogy with 2-butene and dideutereothylene (2) we might expect s to be in the range from 15 to 25, this value is not unreasonable.

ACKNOWLEDGMENTS

The authors gratefully acknowledge the financial assistance of the National Research Council of Canada and the University of British Columbia President's Research Fund. They also thank Mr. Peter G. Norton for his assistance with the calculations.

REFERENCES

1. B. S. Rabinovitch and K. W. Michel. J. Am. Chem. Soc. **81**, 5065 (1959).
2. B. S. Rabinovitch and M. J. Hulatt. J. Chem. Phys. **27**, 592 (1957). C. Steel. J. Phys. Chem. **64**, 1588 (1960).
3. G. S. Reddy, J. H. Goldstein, and L. Mandell. J. Am. Chem. Soc. **83**, 1300 (1961).
4. J. N. Butler and G. J. Small. Can. J. Chem. This issue.
5. H. R. Wyss and H. Gunthard. Helv. Chim. Acta, **44**, 626 (1961).
6. R. E. Wood and R. G. Dickinson. J. Am. Chem. Soc. **61**, 3259 (1939).
7. R. M. Noyes, R. G. Dickinson, and V. Schomaker. J. Am. Chem. Soc. **67**, 1319 (1945).
8. N. C. Craig and E. A. Entemann. J. Am. Chem. Soc. **83**, 3047 (1961).
9. R. E. Wood and D. P. Stevenson. J. Am. Chem. Soc. **63**, 1650 (1941).
10. A. R. Olson and W. Maroney. J. Am. Chem. Soc. **56**, 1320 (1934).
11. K. S. Pitzer and J. L. Hollenberg. J. Am. Chem. Soc. **76**, 1493 (1954).
12. W. G. Dauben and K. S. Pitzer. *In* Steric effects in organic chemistry. *Edited by* M. Newman. John Wiley and Sons, Inc., New York. 1956, p. 58.
13. A. A. Frost and R. G. Pearson. Kinetics and mechanisms. 2nd ed. John Wiley and Sons, New York. 1961. p. 186.
14. J. E. Douglas, B. S. Rabinovitch, and F. S. Looney. J. Chem. Phys. **23**, 315 (1955).
15. G. B. Kistiakowsky and W. R. Smith. J. Am. Chem. Soc. **58**, 2428 (1936).
16. L. S. Kassel. Kinetics of homogeneous gas reactions. Reinhold Publishing Co., New York. 1932. E. W. Schlag, B. S. Rabinovitch, and F. W. Schneider. J. Chem. Phys. **32**, 1599 (1960).

Can. J. Chem. Downloaded from www.nrcresearchpress.com by 210.87.254.6 on 09/05/12
For personal use only.

THE THERMAL CIS–TRANS ISOMERIZATION AND DECOMPOSITION OF METHYL CROTONATE

JAMES N. BUTLER[1] AND GERALD J. SMALL
Department of Chemistry, University of British Columbia, Vancouver, British Columbia
Received May 22, 1963

ABSTRACT

Methyl crotonate undergoes a homogeneous, unimolecular cis–trans isomerization in the gas phase at temperatures from 400° C to 560° C. The rate constant for the cis → trans reaction was found to be

$$k_1 = 10^{13.2\pm0.3}e^{-57.8\pm1.5 \text{ kcal}/RT}$$

independent of pressure in the range from 0.1 mm to 10 mm. The equilibrium trans/cis ratio is approximately 4.5, independent of temperature, from 200° C to 500° C. Simultaneous free-radical reactions also occur, the most important of which are the isomerization to methyl vinylacetate, and the decomposition to give carbon dioxide and the various butene isomers. Side reactions gave carbon monoxide, methane, propylene, numerous other hydrocarbons, and various ethers.

INTRODUCTION

The cis–trans isomerization of butene-2 was for a long time thought to have an anomalously low frequency factor and activation energy, but a recent study at low pressures using gas chromatography for analysis (1) showed that both the frequency factor ($10^{13.8}$) and the activation energy (62.8 kcal) were normal. The availability in this laboratory of the cis isomer of methyl crotonate, CH_3—CH=CH—$COOCH_3$, suggested that an investigation of the cis–trans isomerization of methyl crotonate at low pressures using gas chromatography might be interesting.

Some brief experiments conducted in sealed tubes (2) indicated that methyl vinylacetate, CH_2=CH—CH_2—$COOCH_3$, was formed from methyl crotonate. Part of the purpose of this study was to investigate whether methyl vinylacetate was formed in the gas phase, and if so, by what mechanism.

EXPERIMENTAL

Materials

trans-Methyl crotonate was obtained from K and K Laboratories, Inc., New York, and purified by gas chromatography. The purified material contained approximately 0.1% of the cis isomer, and approximately 0.1% of methyl vinylacetate. *cis*-Methyl crotonate was provided by Dr. D. E. McGreer of the University of British Columbia, who prepared it by the thermal decomposition of 3-carbomethoxypyrazoline (2). The sample was purified by gas chromatography, and the purified material contained approximately 0.2% of *trans*-methyl crotonate, and approximately 3% of methyl vinylacetate.

Procedure

Experiments were conducted in a vacuum system entirely free from stopcock grease. Metal diaphragm valves (Hoke) were used, and were connected to the glass parts of the apparatus with epoxy resin cement. The reaction vessel was of 100 ml volume, and was kept at constant temperature by an electrically heated air bath. The temperature was controlled by operating the furnace from a variac and voltage-regulating transformer, and enclosing the furnace in an insulated copper drum which was cooled by tap water at 8° C circulating through coils fastened to its outside. The temperature could be maintained to within 0.5° C for periods of up to 1 hour in the temperature range from 300° C to 600° C. A sample of either *cis*- or *trans*-methyl crotonate was admitted to the reactor by expansion from a storage vessel. Normally, the pressure in the reactor was the vapor pressure of the material at room temperature: 10 to 14 mm for both the trans and cis isomers.

When the reaction had proceeded for the desired length of time, the material in the reactor was pumped

[1]*To whom all correspondence should be addressed, at TYCO Laboratories, Inc., Bear Hill, Waltham 54, Mass.*

Can. J. Chem. Downloaded from www.nrcresearchpress.com by 210.87.254.105 on 09/05/12
For personal use only.

through a trap cooled in liquid nitrogen. Normally all non-condensable gases were discarded. The condensable material was distilled into a side tube of volume 0.2 ml, and sealed off.

Routine Analysis

Analysis was performed on a Perkin–Elmer model 226 gas chromatograph, using a 50 m capillary column coated with polypropylene glycol (type R), and a flame ionization detector. The contents of the sample tube was dissolved in anhydrous ether and injected in the gas chromatograph. Peak height ratios were measured and calibrated with known mixtures of approximately the same composition. The results of successive analyses of the same sample agreed to within about ±5%.

Analysis for Side-reaction Products

In order to establish the nature and extent of the side reactions which proceeded at the same time as the cis-trans isomerization, a nearly complete separation of the products of the reaction was desirable. Under the normal conditions of analysis, only the compounds boiling in the range from 80° C to 150° C were detected.

To detect the intermediate-range compounds, the temperature of the 50 m capillary column was initially held at 0° C, and was raised during the course of the analysis to 120° C. *n*-butyl ether (b.p. 147.2–147.3° C, purified by gas chromatography) was used as a solvent, so that peaks for all the products boiling up to 145° C except CO and CO_2 (to which the detector did not respond) appeared on the chromatogram. Peaks from C_4 up were well resolved. A packed silica gel column (type J) at room temperature resolved CO, CH_4, CO_2, and C_2H_6. A tetraisobutylene column (type D) separated all the products up through the butenes except for CO and CH_4, which appeared as a single peak. A polypropylene glycol column (type R) was used to confirm the identification of the various peaks, but it did not separate propylene from allene, methylacetylene, and dimethyl ether.

EQUILIBRIUM MEASUREMENTS

Although the entropy and enthalpy changes for a number of cis–trans isomerizations have been determined, methyl crotonate is not among these. We therefore undertook a study of the temperature dependence of the equilibrium trans/cis ratio. *cis*-Methyl crotonate, *trans*-methyl crotonate, and mixtures of the two of varying composition were pyrolyzed both in the gas phase at 14 mm pressure and in sealed tubes using I_2 as a catalyst (3, 4, 5).

At temperatures above 450° C, the decomposition of methyl crotonate occurred so rapidly that if a sample of pure trans was heated, the trans/cis ratio would fall to some value which was higher than the equilibrium value, remain there for some time, and then begin to increase again. Similarly, if a sample of pure cis was heated, the trans/cis ratio would increase to a steady-state value which was less than the equilibrium value. In order to achieve equilibrium it was necessary to start with a mixture which was near the equilibrium composition and to pyrolyze it for a sufficiently short time that decomposition was not extensive. At temperatures above 500° C, the results were so irreproducible that they were discarded.

The results obtained are listed in Table I. Although the results are not very precise, the trans/cis ratio can be seen to be approximately 4.5, independent of temperature, over the temperature range from 200° C to 500° C. A least-squares fit of the data gave the following thermodynamic functions for the reaction cis → trans:

$$\Delta H^0 = -0.2 \pm 0.4 \text{ kcal/mole}$$

$$\Delta S^0 = +2.7 \pm 0.7 \text{ cal/mole °K.}$$

KINETICS OF THE CIS–TRANS ISOMERIZATION

Because of the extensive formation of side products, it was necessary to account for them in the calculation of the rate constant. The method of analysis used made measurement of product ratios more precise than measurement of the absolute amounts of products, and therefore the expression for the rate constant was cast into this form.

Can. J. Chem. Downloaded from www.nrcresearchpress.com by 210.87.254.105 on 09/05/12
For personal use only.

TABLE I

Equilibrium trans/cis ratios

Temperature (°C)	Equilibrium trans/cis ratio	Predominant isomer of starting material
Sealed tubes, I_2 catalyst		
204.8	4.88	Cis
244.0	4.98	Cis
266.8	5.20	Cis
280.0	4.58	Cis
280.0	4.20	Trans
357.0	4.40	Cis
358.5	4.44	Trans
358.5	4.02	Trans
Gas phase, 14 mm, uncatalyzed		
425.5	4.54	Trans
437.6	4.96	Trans
447.5	4.24	Trans
448.5	4.25	Trans
450.2	4.88	Cis
478.0	4.82	Cis

The mechanism followed was assumed to be a reversible first-order reaction with a parallel, irreversible side reaction:

$$\text{cis} \underset{k_2}{\overset{k_1}{\rightleftarrows}} \text{trans}$$

$$\text{cis} \rightarrow \text{side products.}$$

If the cis–trans isomerization is first order, the rate of formation of trans is

$$[1] \qquad \frac{d[T]}{dt} = k_1[C]-k_2[T],$$

where $[T]$ is the partial pressure of *trans*-methyl crotonate, and [C] is the partial pressure of *cis*-methyl crotonate. Let $[S]$ represent the partial pressure of *cis*-methyl crotonate which has formed side products, the sum of methyl vinylacetate, propylene, and butene being a good approximation. A material balance gives

$$[2] \qquad [C]+[T]+[S] = [\mathrm{C}]_0+[T]_0+[S]_0,$$

where the subscript zero indicates the partial pressures in the starting material. Substituting [2] in [1] and integrating gives

$$[3] \qquad \ln\left\{\frac{k_1([C]_0+[S]_0-[S])-k_2[T]_0}{k_1[C]-k_2[T]}\right\} = (k_1+k_2)t.$$

Introducing the equilibrium constant $[T]_{eq}/[C]_{eq} = k_1/k_2$, and approximating $[S]/[C]_0 = [S]/[C]$, [3] may be expressed entirely in terms of product ratios:

$$[4] \qquad \ln\left\{\frac{\left[\frac{k_1}{k_2}\left(1+\frac{[S]_0}{[C]_0}-\frac{[S]}{[C]}\right)-\frac{[T]_0}{[C]_0}\right]\left[1+\frac{[T]}{[C]}+\frac{[S]}{[C]}\right]}{\left[\frac{k_1}{k_2}-\frac{[T]}{[C]}\right]\left[1+\frac{[T]_0}{[C]_0}+\frac{[S]_0}{[C]_0}\right]}\right\} = (k_1+k_2)t.$$

An expression is obtained from the isomerization of *trans*-methyl crotonate, which is the same form as [4] except that $[C]$ and $[T]$, k_1 and k_2, are interchanged. The results of a

Can. J. Chem. Downloaded from www.nrcresearchpress.com by 210.87.254.105 on 09/05/12
For personal use only.

series of experiments at 10 mm pressure and 480° C, starting with pure *trans*-methyl crotonate, are listed in Table II. The calculated rate constant k_1 for the cis → trans

TABLE II

Rate constant calculated from equation [4] for varying times of reaction at 10 mm pressure, 480° C

Time (sec)	$k_1 \times 10^5$ (sec^{-1})
129	31.4
251	45.8
679	32.6
1443	34.3
4520	39.7
Average	36.8

isomerization showed no trend as the time was varied by a factor of 40. Apparently the mechanism described represents the data satisfactorily.

Addition of up to 1% oxygen or packing the vessel with glass wool had no effect on the rate of the cis–trans isomerization.

The rate constant was also found to be independent of pressure. In Table III are listed

TABLE III

Pressure dependence of rate constant for cis → trans isomerization

Pressure (mm)	$k_1 \times 10^5$ (sec^{-1})
8.95	24.4
5.22	29.4
2.90	27.2
1.71	19.3
1.57	25.9
0.77	23.0
0.75	12.9
0.48	21.2
0.22	28.2
0.21	27.9
0.11	38.4
Average	25.3

the values of k_1 obtained by pyrolyzing *trans*-methyl crotonate for approximately 10 minutes at 478° C and at pressures ranging from 11 mm down to 0.1 mm. No trend is apparent with pressure.

The number of vibrational modes in methyl crotonate is 39, and by analogy with 2-butene (1) one might expect that nearly all of these would be effective in the Slater (6) model for a unimolecular isomerization. This would imply that a unimolecular falloff in rate constant should be about 30% at a pressure of 0.01 mm, which is well below the pressure of our lowest measurement. These results indicate that the cis–trans isomerization is a truly homogeneous, unimolecular reaction.

The temperature dependence of the rate constant at 10 mm pressure was studied from 350° C to 550° C, using both *trans*-methyl crotonate and *cis*-methyl crotonate as starting material. The results are summarized in Table IV. A least-squares fit to the Arrhenius

Can. J. Chem. Downloaded from www.nrcresearchpress.com by 210.87.254.105 on 09/05/12
For personal use only.

TABLE IV

Temperature dependence of rate constant for cis – trans isomerization

Temperature (°C)	$k_1 \times 10^5$ (sec^{-1})	No. of points averaged
Trans starting material		
394.2	0.32	3
425.2	1.33	6
437.4	3.06	3
449.6	4.39	7
481.2	36.7	5
514.0	153	5
545.0	1123	1
Cis starting material		
354.2	0.0191	1
424.1	1.53	7
436.8	2.16	3
514.2	154	2
Packed vessel, *trans*		
474.0	19	2

plot of these data gave the parameters

$$E = 57.8 \pm 1.5 \text{ kcal/mole}$$

$$\log A = 13.2 \pm 0.3.$$

No curvature was detectable in the Arrhenius plot.

Examination of Table IV will show that, within the experimental errors, the same values were obtained for k_1 whether the starting material was cis or trans. This further confirms the proposed mechanism, and the value measured for the equilibrium constant.

The values of the activation energy and frequency factor are very similar to those obtained in the known unimolecular isomerization of 2-butene (1). For methyl crotonate, the frequency factor is $10^{13.2}$; for 2-butene, the frequency factor is $10^{13.78}$. Since methyl crotonate is unsymmetrical and 2-butene is symmetrical, we might expect that the frequency factor for 2-butene would be a factor of 2 larger than for methyl crotonate. This is true within the experimental errors. The activation energy for methyl crotonate is 57.8 kcal, which is only slightly lower than that for 2-butene: 62.8. This 5 kcal lowering could be rationalized by considering some conjugative effect due to the highly electronegative oxygen atoms so close to the double bond.

A compound which we might also expect to be similar to methyl crotonate in its behavior is dimethyl maleate. The thermal cis–trans isomerization of dimethyl maleate (7) was followed by freezing point depression. As was shown in the case of 2-butene (1), small amounts of side reaction can introduce systematic errors in a rate constant measured by this technique.

The frequency factor (10^5) and activation energy (26 kcal) for the isomerization of dimethyl maleate are both extremely low compared to methyl crotonate and 2-butene, even though the temperature at which a comparable rate occurs is not very much lower. Furthermore, both 2-butene and methyl crotonate show a pressure dependence of the rate constant which is consistent with nearly all the normal modes of the molecule taking part in the reaction. The pressure dependence of the rate of isomerization of dimethyl maleate, if explained by the theory of unimolecular reactions, implies that only 1 normal mode of vibration out of the possible 42 normal modes is active in the reaction.

Can. J. Chem. Downloaded from www.nrcresearchpress.com by 210.87.254.105 on 09/05/12
For personal use only.

Although we cannot conclude from these comparisons alone that the rate constant for dimethyl maleate is in error, it certainly seems reasonable that the isomerization of dimethyl maleate should be reinvestigated at low pressures using gas chromatography for analysis.

KINETICS OF THE FORMATION OF METHYL VINYLACETATE

One of the major side reactions in the thermal cis–trans isomerization of methyl crotonate is the formation of methyl vinylacetate:

$$CH_3—CH=CH—COOCH_3 \xrightarrow{k_3} CH_2=CH—CH_2—COOCH_3.$$

Unfortunately, the rate of this reaction was not nearly so reproducible as the rate of the cis–trans isomerization: variations in k_3 of a factor of 10 occurred in experiments under supposedly the same conditions. Nevertheless, some approximate results were obtained.

The formation of methyl vinylacetate appears to be first order, since the rate constant k_3 shows no noticeable trend with pressure, or with time of reaction. The rate is not affected by the addition of small amounts of oxygen or by packing the vessel with glass wool. The temperature dependence of the rate constant gave the Arrhenius expression

$$k_3 = 10^{8.7\pm1.5}e^{-43\pm5 \text{ kcal}/RT}.$$

Approximately the same values of k_3 were obtained whether the starting material was cis or trans.

The isomerization of methyl crotonate to methyl vinylacetate might appear at first to be a homogeneous unimolecular reaction. However, the large amounts of other products of free-radical decomposition, and the extreme irreproducibility of the results, imply that the reaction proceeds by a free-radical mechanism. Furthermore, the low frequency factor and activation energy imply that the mechanism is not a simple unimolecular one. An ionic reaction on the surface of the vessel is ruled out by the fact that packing the vessel does not affect the rate appreciably.

The decomposition of methyl crotonate (next section) gives a large number of free radicals, and it is conceivable that abstraction and displacement reactions occurring between these radicals and methyl crotonate result in the shift of a hydrogen atom in methyl crotonate. A possible scheme might involve a radical which is stabilized by allylic resonance (8):

$$R\cdot + CH_3—CH=CH—COOCH_3 \rightarrow RH + \cdot CH_2—CH=CH—COOCH_3$$

$$\cdot CH_2—CH=CH—COOCH_3 \leftrightarrow CH_2=CH—\dot{C}H—COOCH_3$$

$$RH + CH_2=CH—\dot{C}H—COOCH_3 \rightarrow R\cdot + CH_2=CH—CH_2—COOCH_3,$$

but experiments using isotopic tracers would be required to elucidate the mechanism more definitely.

DECOMPOSITION REACTIONS

Extensive decomposition of methyl crotonate occurs at the temperatures where the *cis–trans* isomerization proceeds at a measurable rate. A nearly complete analysis of a typical product mixture is given in Table V. In addition to the trans isomer and methyl vinylacetate, pyrolysis of *cis*-methyl crotonate gave carbon monoxide, carbon dioxide, methane, propylene, butenes, and 20 or more minor products ranging in boiling point from −30° C to over 150° C.

Can. J. Chem. Downloaded from www.nrcresearchpress.com by 210.87.254.105 on 09/05/12
For personal use only.

TABLE V

Side-reaction products in the pyrolysis of methyl crotonate*

Product	Relative amount	Product	Relative amount
cis-Methyl crotonate	400	A peak occurring near propylene, probably allene + dimethyl ether	8
trans-Methyl crotonate	100	A peak occurring near the butenes, probably methyl acetylene	5
Carbon dioxide	60	4 closely spaced peaks following the butenes, compounds boiling in the 20–30° C range	1
Carbon monoxide	30	4 closely spaced peaks, compounds boiling in the 35–45° C range, perhaps $C_3H_5OCH_3$	3
Methane	23	3 closely spaced peaks boiling in the 80–90° C range, perhaps 2,4-hexadienes	9
Methyl vinylacetate	20	7 peaks of nearly the same height, boiling in the 140–150° C range	4
Propylene	9		
trans-2-Butene	9		
cis-2-Butene	6		
1-Butene	4		
Ethane	3		
Methyl methacrylate	1		
Methanol	0.2		
1,5-Hexadiene	<0.1		

*This analysis reports the approximate amounts of the products formed when *cis*-methyl crotonate was pyrolyzed for 40 minutes at 480° C.

The decomposition of methyl crotonate to give CO_2, CO, and various hydrocarbons and ethers proceeded at a rate which was only slightly slower than the rate of cis–trans isomerization. A probable mechanism involves an initial split to give propenyl radicals:

$$CH_3—CH=CH—COOCH_3 \rightarrow CH_3—CH=CH\cdot + CO_2 + CH_3\cdot$$
$$\rightarrow CH_3—CH=CH\cdot + CO + CH_3O\cdot.$$

The recombination of propenyl and methyl radicals produces 2-butene. Isomerization of propenyl to allyl, and subsequent recombination with methyl, would give 1-butene. Propylene, allene, and methylacetylene can be formed by abstraction of hydrogen from methyl crotonate. Polymeric materials as well as the high-boiling products can be formed by addition of the various radicals to methyl crotonate.

The presence of CO in the products makes it almost certain that CH_3O radicals are present in the reaction scheme. These radicals might be expected to form methanol by abstraction of a hydrogen atom from methyl crotonate. Only a barely detectible trace of methanol was found in the products, which implies that methoxyl radicals are being consumed by some other process, possibly by addition to the double bond of methyl crotonate or recombination with other radicals. The recombination of methoxyl with allyl or propenyl radicals would give ethers of the form $C_3H_5OCH_3$, which might account for the peaks having boiling points in the 35–45° C range. If dimethyl ether were formed by recombination of methoxyl with methyl, it would appear in the same peak as propylene.

A direct unimolecular elimination of CO_2 to form butene is unlikely, since all three butene isomers were formed. Furthermore, pyrolysis of *cis*-methyl crotonate, *trans*-methyl crotonate, and methyl vinylacetate all gave roughly the same distribution of butene isomers.

The presence of allyl radicals (9, 10, 11) would be expected to give 1,5-hexadiene as a product, but no trace of this material could be found in the pyrolysis of either *cis*- or *trans*-methyl crotonate. Pyrolysis of methyl vinylacetate gave a trace (about 0.5% of products) of 1,5-hexadiene, but not nearly as much as might be expected. Apparently allyl radicals are being consumed by other reactions much more rapidly than they are being recombined with each other.

On the other hand, the appearance of three peaks of almost equal height in the correct

Can. J. Chem. Downloaded from www.nrcresearchpress.com by 210.87.254.105 on 09/05/12
For personal use only.

boiling point region implies the presence of moderate amounts of the three isomers of 2,4-hexadiene in the products. These would be formed by recombination of propenyl radicals. On such tentative evidence it is difficult to draw any definite conclusion, but it would appear that propenyl radicals recombine much more rapidly than do allyl radicals, possibly because of the resonance stabilization of allyl radicals.

A small amount of methyl methacrylate observed in the products increases by about a factor of 10 when the pyrolysis is conducted in a packed vessel, whereas the other free-radical decomposition products are formed at approximately the same rate as in the unpacked vessel. This implies that the methyl group shift occurs on the surface, probably by an ionic mechanism (12, 13).

Can. J. Chem. Downloaded from www.nrcresearchpress.com by 210.87.254.105 on 09/05/12
For personal use only.

ACKNOWLEDGMENTS

The authors gratefully acknowledge the financial support of the National Research Council of Canada, and the University of British Columbia President's Research Fund. Dr. D. E. McGreer generously provided a sample of *cis*-methyl crotonate. We also thank Dr. W. A. Bryce for his helpful advice, Mr. Robert D. McAlpine for performing a few of the equilibrium experiments, and Mr. Peter G. Norton for assisting with the calculations.

REFERENCES

1. B. S. Rabinovitch and K. W. Michel. J. Am. Chem. Soc. **81**, 5065 (1959).
2. D. E. McGreer. J. Org. Chem. **25**, 852 (1960).
3. R. G. Dickinson and H. Lotzkar. J. Am. Chem. Soc. **59**, 472 (1937).
4. R. M. Noyes, R. G. Dickinson, and V. Schomaker. J. Am. Chem. Soc. **67**, 1319 (1945).
5. N. C. Craig and E. A. Entemann. J. Am. Chem. Soc. **83**, 3047 (1961).
6. N. B. Slater. Theory of unimolecular reactions. Cornell University Press, Ithaca, N.Y. 1959.
7. M. Nelles and G. B. Kistiakowsky. J. Am. Chem. Soc. **54**, 2208 (1932).
8. W. A. Bryce and P. Kebarle. Trans. Faraday Soc. **54**, 1660 (1958).
9. W. A. Bryce and H. S. Hardiman. Can. J. Chem. **40**, 1031 (1962).
10. D. J. Ruzicka and W. A. Bryce. Can. J. Chem. **38**, 827 (1960).
11. W. A. Bryce and D. J. Ruzicka. Can. J. Chem. **38**, 835 (1960).
12. P. J. Lucchesi, D. L. Baeder, and J. P. Longwell. J. Am. Chem. Soc. **81**, 3235 (1959).
13. W. O. Haag and H. Pines. J. Am. Chem. Soc. **82**, 2488 (1960).

METHYLATION OF SUGAR DITHIOACETALS

V. D-MANNOSE DIETHYL DITHIOACETAL

G. G. S. DUTTON AND Y. TANAKA[1]

Department of Chemistry, University of British Columbia, Vancouver, British Columbia

Received June 17, 1963

ABSTRACT

Partial methylation of D-mannose diethyl dithioacetal in tetrahydrofuran with methyl iodide and silver oxide yielded 2-, 3-, and 6-*O*-methyl-D-mannose in the ratio of 12:1:1, respectively. The major component, 2-*O*-methyl-D-mannose, was characterized as the phenylhydrazone and the other isomers identified by electrophoresis. The M_g values of these mono-*O*-methyl ethers were recorded.

Can. J. Chem. Downloaded from www.nrcresearchpress.com by 210.87.254.6 on 09/05/12
For personal use only.

In Part I of this series it was demonstrated that various sugar dithioacetals could be successfully methylated in tetrahydrofuran with methyl iodide and silver oxide (1). Subsequent papers have reported the nature of the mono-*O*-methyl ethers obtained by partial methylation of the diethyl dithioacetals of L-arabinose (2), D-galactose (3), and D-xylose (4). The present paper reports the mono-*O*-methyl ethers obtained by methylation of D-mannose diethyl dithioacetal under similar conditions and is a continuation of our study on the relative reactivities of hydroxyl groups in sugar dithioacetals.

Preparation of D-mannose diethyl dithioacetal by Fischer's method (5) was found to give unreliable results since on several occasions the crude product decomposed on washing with ice water. It was found preferable to neutralize with barium carbonate and dilute with methanol whence the dithioacetal could be obtained by evaporation of the filtered solution.

The dithioacetal was shaken in tetrahydrofuran at room temperature with an appropriate amount of silver oxide and methyl iodide to give a reasonable yield of the mono-*O*-methyl ethers, after hydrolysis. The mono- and di-*O*-methyl ethers were separated from the unchanged and poly-*O*-methylated D-mannoses by chromatography in butanone–water azeotrope.

Electrophoresis in 0.05 *M* borate showed that the mixture of mono-*O*-methyl ethers contained three isomers, one of which was predominant judging from the size and intensity of the spots. These three components had M_g values of 0.38, 0.54, and 0.63, and were shown to be 2-, 3-, and 6-*O*-methyl-D-mannose, respectively, by concurrent electrophoretic examination with synthetic samples of these isomers. 2-*O*-Methyl-D-mannose gave the strongest and largest spot, and the others were weak and small. The mixture of di-*O*-methyl ethers, which might contain the 5-*O*-methyl ether, was also examined by electrophoresis but only a very slowly migrating component was detected, suggesting no 5-*O*-methyl ether was present.

The phenol – sulphuric acid method (6) of quantitative analysis on the mixture of mono-*O*-methyl-D-mannoses gave a ratio of 12:1:1 for 2-, 3-, and 6-*O*-methyl-D-mannose, respectively.

The mixture of mono-*O*-methyl-D-mannoses was separated on Whatman No. 3MM paper by electrophoresis and the area corresponding to the 2-*O*-methyl-D-mannose was extracted with water. The extract was deionized and evaporated to a sirup, which was

[1]*Present address: Department of Chemistry, Queen's University, Kingston, Ontario.*

then treated with methanol many times in order to destroy possible borate complexes (7). The residue was condensed with phenylhydrazine in warm ethanol to give the phenylhydrazone, m.p. 161–163° C.

Authentic 2-, 3-, and 6-*O*-methyl-D-mannose were prepared by reported procedures. 2-*O*-Methyl-D-mannose was synthesized by the method of Curtis and Jones (8), except that the diethyl dithioacetal was used. This ether was also prepared by the method of Aspinall and Zweifel (9). The synthesis according to their procedure showed, however, that the product was accompanied by a small amount of the 3-*O*-methyl ether.

3-*O*-Methyl-D-mannose was also prepared by the method of Aspinall and Zweifel (9). Following their procedure, methyl 4,6-*O*-ethylidene-α-D-mannopyranoside was partially *O*-nitrated in acetic anhydride, but the infrared spectrum of the product showed the bands of *O*-acetate at 5.75 and 8.13 μ as well as the bands of *O*-nitrate at 6.10 and 7.85 μ, indicating partial acetylation during the nitration. Bell and Synge (10) have successfully deacetylated methyl 2,6-di-*O*-acetyl-3,4-di-*O*-nitro-β-D-glucopyranoside in a mixture of methanol and chloroform with sodium. Application of this method on the partially acetylated product gave a sirup which showed no band of *O*-acetate in its infrared spectrum. Completion of Aspinall and Zweifel's process with this deacetylated product showed, however, that the final product was accompanied by a small amount of 2-*O*-methyl-D-mannose.

Waters, Hockett, and Hudson (11) have reported the synthesis of 6-*O*-methyl-D-mannose. Due to acetyl migration the use of this method resulted in only a very small yield of this compound, which was separated from the mixture by chromatography.

The results reported here demonstrate the preferential reactivity of the 2-position of D-mannose diethyl dithioacetal to methylation, in marked contrast to the D-galactose isomer where the 2-, 3-, and 6-position showed similar reactivity. A discussion of these and other related results is planned.

EXPERIMENTAL

All evaporations were carried out *in vacuo* at a bath temperature not exceeding 40° C. Chromatograms were run by the descending technique in butanone–water azeotrope and the same solvent was used for column separations. Electrophoretic separations were carried out in 0.05 *M* borate at 950–1050 v, 25–30 ma.

Preparation of D-*Mannose Diethyl Dithioacetal*

D-Mannose (15 g) was mixed with concentrated hydrochloric acid (15 g) in an ice-water bath. Ethane thiol (10 g) was added portionwise with vigorous shaking. After all the ethane thiol was added, the mixture was shaken mechanically for 20 minutes. The clear solution thus obtained was partially neutralized with barium carbonate, and then completely neutralized with excess barium carbonate after addition of methanol (100 ml) to the mixture. Barium chloride and excess barium carbonate were removed by filtration, and evaporation of the filtrate gave a sirupy residue which was separated from inorganic impurities by extraction with cold absolute ethanol (ca. 150 ml). The solvent was evaporated and the residue was recrystallized from ethanol–ether. Yield 14.2 g (60%). Melting point and mixed melting point with a sample prepared by Fischer's method were 132–134° C.

Methylation of D-*Mannose Diethyl Dithioacetal*

To a solution of D-mannose diethyl dithioacetal (1.00 g) in tetrahydrofuran (100 ml), silver oxide (1.50 g), Drierite (3 g), and methyl iodide (10.0 ml) were added, and the mixture was shaken mechanically at room temperature for 12 hours. After another 10.0 ml of methyl iodide was added, the mixture was shaken similarly for a further 12 hours. The mixture was filtered and the inorganic substances were washed with tetrahydrofuran (20 ml). The filtrate and washing were concentrated to a sirup, which was redissolved in chloroform (20 ml) in order to remove inorganic impurities in the sirup by filtration. A light brown sirup (1.157 g) obtained by evaporation of the filtered chloroform solution was hydrolyzed for 5 hours in a boiling mixture of ethanol (10 ml) and 2 *N* sulphuric acid (5 ml). Evaporation of the deionized hydrolyzate (Duolite A-4 resin) gave a sirup (528 mg) which showed the following spots by paper chromatography: R_f 0.34, 0.22, 0.07, and a few spots of high R_f values. The spot of R_f 0.07 was strong in its intensity and the others weak.

From the same quantities of reactants, another sirup (508 mg) of methylated D-mannoses was obtained and

Can. J. Chem. Downloaded from www.nrcresearchpress.com by 210.87.254.6 on 09/05/12
For personal use only.

paper chromatography showed the following spots: R_f 0.43, 0.29, 0.11, 0.03 and a few spots of high R_f values. The spots of R_f 0.11 and 0.03 were strong and the others weak.

These combined sirups (528+508 mg) were separated on a cellulose–hydrocellulose column (solvent flow: 10 ml/20 mins), and the component of R_f 0.07 (or R_f 0.11) was detected in tubes No. 80–200, whereas the components of R_f 0.22 and 0.35 (or R_f 0.29 and 0.43) were found in tubes No. 40–70 (10 minute fractions) but without clear separation. The yield of these fractions was 115.7 mg and 21.3 mg respectively.

Methylation using the same quantities of reactants was performed twice more, and two sirups (484 mg and 419 mg) of *O*-methyl-D-mannoses were obtained. These sirups were chromatographed together in a similar manner as described above and mixtures of mono- and di-*O*-methyl ethers (70.5 mg and 11.7 mg, respectively) were obtained.

The two fractions of mono-*O*-methyl ethers were amalgamated and treated with charcoal in hot water and an electrophoretic examination of the recovered sirup (170 mg) showed three spots, M_g 0.32 (strong), 0.48 (weak), and 0.60 (weak), which corresponded to authentic samples of 2-, 3-, and 6-*O*-methyl-D-mannose, respectively.

The two di-*O*-methyl fractions were also examined by electrophoresis under the same conditions, and one large spot (two or three components (?)) of M_g 0.14–0.15 was detected in both sirups.

The phenol – sulphuric acid method (6) was used to estimate the ratio of mono-*O*-methyl ethers in the sirupy mixture. A ratio of 12:1:1 for 2-, 3-, and 6-*O*-methyl-D-mannose was obtained.

Identification of 2-O-Methyl-D-mannose

The mixture (170 mg) of mono-*O*-methyl-D-mannoses was separated by electrophoresis (950–1050 v, 50 minutes in 0.05 *M* sodium borate solution) on three 15 cm wide Whatman No. 3MM sheets, and 2-*O*-methyl-D-mannose was located on the guide strips. The appropriate areas of the sheets were extracted with cold water (30 ml×3), the solution was deionized, and the residue obtained by evaporation of the extracts was treated with cold methanol (about 5 ml) and the solvent was then evaporated. After this treatment was repeated about 20 times, a sirupy residue (28.7 mg) of 2-*O*-methyl-D-mannose was obtained.

Absolute ethanol (2 ml) and phenylhydrazine (16.0 mg) in absolute ethanol (0.1 ml) were added to the residue and after the mixture was warmed for 20 minutes petroleum ether was added. The precipitated phenylhydrazone which was separated by centrifugation and recrystallized from ethanol – petroleum ether had m.p. 161–163° C. Admixture with synthetic 2-*O*-methyl-D-mannose phenylhydrazone showed no depression of the melting point.

Preparation of 2-O-Methyl-D-mannose

(I) The published procedure (8) was used starting with D-mannose diethyl dithioacetal, and the deionized hydrolyzate of the completely methylated di-*O*-isopropylidene dithioacetal showed by paper chromatography a strong spot (R_f 0.07) of mono-*O*-methyl-D-mannose as well as a medium spot of unchanged mannose and a series of weak spots of poly-*O*-methylated D-mannoses. The following components were detected on a paper chromatogram run for 48 hours: R_{mannose} 2.50 (strong), 1.40 (weak), and 1.00 (medium). Chromatographically and electrophoretically pure 2-*O*-methyl-D-mannose (M_g 0.38) was obtained as a sirup by chromatography on a cellulose–hydrocellulose column and it was characterized as its phenylhydrazone, m.p. 161–163° C. Lit. (8) m.p. 161–163° C.

(II) A preparation from methyl 4,6-*O*-ethylidene-α-D-mannopyranoside (1.33 g) following the method of Aspinall and Zweifel (9) gave a sirup (190 mg) of methylated mannoses with components of R_{mannose} 3.32, 2.54, and 1.00. Column separation yielded the component with R_{mannose} 2.54 (78 mg) identical with the 2-*O*-methyl-D-mannose prepared from the dithioacetal, although neither sample crystallized.

Preparation of 3-O-Methyl-D-mannose

This was prepared by the published procedure (9) except that during the nitration of methyl 4,6-*O*-ethylidene-α-D-mannopyranoside with nitric acid in acetic anhydride some acetylation also occurred. The crude product was deacetylated with sodium in methanol–chloroform before tosylation. A mixture of methylated mannoses was finally obtained which contained components with R_{mannose} 3.34 (weak), 2.50 (strong), and 1.00 (medium). Separation on Whatman 3 MM yielded a sirup of 3-*O*-methyl-D-mannose (M_g 0.54). Chromatography on paper of this sirup in butanone–water saturated with borax showed a small amount of the 2-*O*-methyl isomer as a contaminant (R_{mannose} 2.22, strong; 2.40, weak).

The sirup (14.3 mg) was dissolved in 20% acetic acid to which phenylhydrazine (26.5 mg) in absolute ethanol (0.15 ml) was added. The mixture was heated in boiling water for several hours and on cooling the osazone precipitated. After recrystallization from ethanol–water the osazone melted at 165° C (lit. (9) 165–166° C) and gave no depression with 3-*O*-methyl-D-glucose phenylosazone.

Preparation of 6-O-Methyl-D-mannose

The published procedure (11) gave a mixture of mono-*O*-methyl-D-mannoses due to acyl migration, and an electrophoretically pure sirup (M_g 0.63) was obtained by column chromatography but in very poor yield.

The pure sirup (10 mg) was dissolved in 20% acetic acid (2 ml) and was heated for 5 hours in boiling water with phenylhydrazine (20 mg) in absolute ethanol (0.11 ml) and a little sodium bisulphite. The

Can. J. Chem. Downloaded from www.nrcresearchpress.com by 210.87.254.6 on 09/05/12
For personal use only.

phenylosazone which precipitated on cooling melted at 171° C, lit. (11) m.p. 172° C, after recrystallization from ethanol–water.

Full details of the syntheses of these three mono-*O*-methyl-D-mannoses are given elsewhere (12).

ACKNOWLEDGMENTS

We are grateful to the Research Corporation for financial support and one of us (Y. T.) thanks the National Research Council for the award of a studentship.

REFERENCES

1. G. G. S. DUTTON and K. YATES. Can. J. Chem. **36**, 550 (1958).
2. G. G. S. DUTTON and Y. TANAKA. Can. J. Chem. **39**, 1797 (1961).
3. G. G. S. DUTTON and Y. TANAKA. Can. J. Chem. **40**, 1146 (1962).
4. G. G. S. DUTTON and Y. TANAKA. Can. J. Chem. **40**, 1899 (1962).
5. E. FISCHER. Ber. **27**, 673 (1894).
6. M. DUBOIS, K. A. GILLES, J. K. HAMILTON, P. A. REBERS, and F. SMITH. Anal. Chem. **28**, 350 (1956).
7. C. T. BISHOP. Can. J. Chem. **38**, 1636 (1960).
8. E. J. C. CURTIS and J. K. N. JONES. Can. J. Chem. **38**, 890 (1960).
9. G. O. ASPINALL and G. ZWEIFEL. J. Chem. Soc. 2271 (1957).
10. D. J. BELL and R. I. M. SYNGE. J. Chem. Soc. 833 (1938).
11. A. J. WATERS, R. C. HOCKETT, and C. S. HUDSON. J. Am. Chem. Soc. **61**, 1528 (1939).
12. Y. TANAKA. Ph.D. Thesis. University of British Columbia, Vancouver, B.C. October, 1961.

Can. J. Chem. Downloaded from www.nrcresearchpress.com by 210.87.254.6 on 09/05/12
For personal use only.

DIRECT CARBONYLATION OF THE BENZOPHENONE SEMICARBAZONES AND BENZOPHENONE AZINE USING DICOBALT OCTACARBONYL[1]

ALEX ROSENTHAL AND S. MILLWARD
Department of Chemistry, University of British Columbia, Vancouver, British Columbia
Received April 29, 1963

ABSTRACT

Benzophenone semicarbazone (I) reacted with carbon monoxide at about 4000 p.s.i. and at 235–245° in the presence of preformed dicobalt octacarbonyl as catalyst to yield 3-phenylphthalimidine (II), 3-phenyl-2-(N-benzhydrylcarboxamido)phthalimidine (V), N,N′-dibenzhydrylurea (VI), and N-benzhydrylurea (VII). At 200–220° substance I gave compound VII, benzophenone azine (VIII), and benzophenone 4-benzhydrylsemicarbazone (IX). When the reaction temperature was further reduced to 175–185°, compound I did not produce the carbonylation product obtained in the second experiment but only the degradation and reduction products VIII, and IX, respectively. Carbonylation of benzophenone azine at 235–245° produced 3-phenylphthalimidine, whereas that of benzophenone 4-benzhydrylsemicarbazone at the same temperature yielded 3-phenylphthalimidine and 3-phenyl-2-(N-benzhydrylcarboxamido)phthalimidine.

Independent syntheses of the last compound and of benzophenone 4-benzhydrylsemicarbazone are described.

Can. J. Chem. Downloaded from www.nrcresearchpress.com by 210.87.254.42 on 09/05/12
For personal use only.

We have previously reported the synthesis of phthalimidines and N-carboxyanilide derivatives of phthalimidines by the direct incorporation of one and two carbon monoxide units into aromatic ketoximes and phenylhydrazones, respectively (1, 2). Because the kind of products obtained was dependent on temperature, we hoped to obtain information on the mechanism of the cyclization reaction by a further study of the direct carbonylation of other substrates containing the imino group (but containing different substituents on the nitrogen).

In this paper we report the results of a study of the carbonylation of aromatic imino compounds containing the ureido (—$NHCONH_2$), ureylene (—NHCONH—), and imino groups attached to the nitrogen of the C=N group. In particular, benzophenone semicarbazone, benzophenone 4-benzhydrylsemicarbazone, and benzophenone azine were carbonylated under a variety of reaction conditions. The last substance was included in this study since it is known that benzophenone semicarbazone decomposes above its melting point to yield benzophenone azine (3).

Benzophenone semicarbazone reacted with carbon monoxide at about 4000 p.s.i. and at 235–245° in the presence of preformed dicobalt octacarbonyl to give a mixture of reduction and carbonylation products (the latter are shown in Chart I) which were separated by chromatography on alumina. Most of the product directly crystallized out of the reaction mixture as a blue crystalline material (designated as A in experimental). This material was extracted with ethanol and then chromatographed to yield N,N′-dibenzhydrylurea (VI) and 3-phenylphthalimidine (II). The structures of both of these substances were established by direct comparison with authentic samples of N,N′-dibenzhydrylurea (4) and 3-phenylphthalimidine (5).

The filtrate remaining after the removal of the blue material A was evaporated to dryness and the residue (B) then fractionated by alumina chromatography. Diphenylmethane (7% yield) and 1,1,2,2-tetraphenylethane (2%) were isolated from the residue

[1]*Presented before the XIX International Congress of Pure and Applied Chemistry at London, England, July, 1963.*

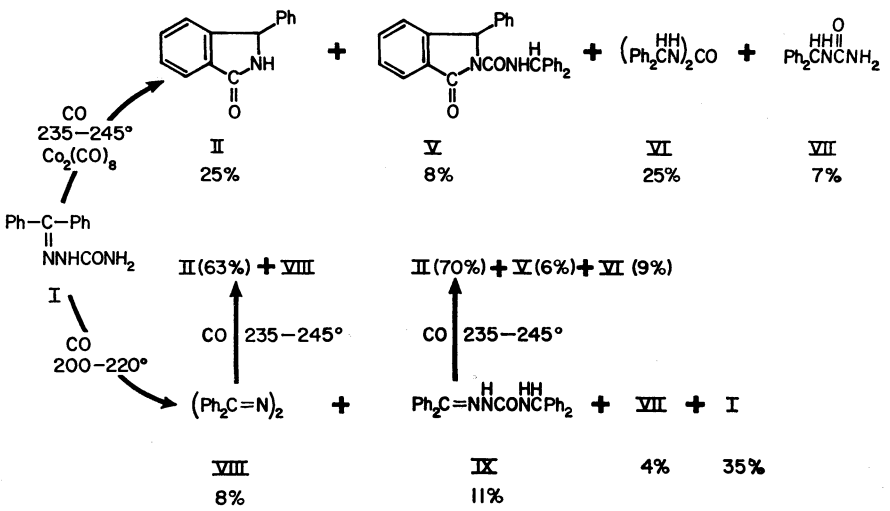

CHART I

Carbonylation of benzophenone semicarbazones and benzophenone azine

B and characterized by direct comparison (m.p. and infrared) with authentic samples of these substances. The fact that these compounds were present indicated that the high-purity carbon monoxide (containing about 0.01% hydrogen) acted as a reducing agent.

Compound V was unequivocally assigned the structure of 3-phenyl-2-(N-benzhydryl-carboxamido)phthalimidine on the following bases: (*a*) infrared analyses showed the presence of two carbonyls at 1684 and 1700 cm^{-1}, in excellent agreement with the spectrum of the previously reported N-carboxyanilide of 3-phenylphthalimidine (2); (*b*) refluxing compound V in 99% deuterium oxide gave a substance the infrared spectrum of which indicated the presence of an N—D grouping (see Experimental); (*c*) proton magnetic resonance analyses of the compound suggested a structure similar to that of 3-phenylphthalimidine-N-carboxyanilide (absorption at δ equal to 6.09 and 6.20 indicated the presence of the two benzylic hydrogens; comparison of the n.m.r. of compound V with that of 3-phenylphthalimidine-N-carboxyanilide established that the peak at 6.20 was due to the CH of the HC(Ph)=N group). The structure of V was then confirmed by direct comparison with an authentic sample of 3-phenyl-2-(N-benzhydrylcarboxamido)-phthalimidine, prepared by the condensation of 3-phenylphthalimidine with benzhydryl-isocyanate according to established procedures previously described (2, 6, 7).

Compound VII was directly compared with an authentic sample of N-benzhydrylurea (8), prepared by the condensation of benzhydrylisocyanate with ammonia, and shown to be the same.

When the reaction temperature was reduced to 175–180°, benzophenone semicarbazone did not cyclize with carbon monoxide but pyrolyzed and was reduced to yield two major products, one of which was readily characterized as benzophenone azine (VIII). This assignment of structure is in accord with that of Borsche and Merkivitz (3), who first reported that the thermal decomposition of benzophenone semicarbazone yielded benzophenone azine. On the bases of elemental, infrared, and proton magnetic resonance

Can. J. Chem. Downloaded from www.nrcresearchpress.com by 210.87.254.42 on 09/05/12
For personal use only.

studies it appeared that the second product (compound IX in Experimental) was benzophenone 4-benzhydrylsemicarbazone. Confirmation of this assignment of structure was obtained by condensing benzhydrylamine with benzophenone semicarbazone to yield ammonia and benzophenone 4-benzhydrylsemicarbazone (identical in m.p. and infrared with compound IX).

At an intermediate temperature of 200–220°, benzophenone semicarbazone afforded the same reduction products as obtained at 175–185°, and in addition N-benzhydrylurea. It is noteworthy that these reactions therefore indicate that carbonylation of the semicarbazone to yield a urea takes place between 180–220°.

Although the mechanism of formation of benzophenone 4-benzhydrylsemicarbazone from benzophenone semicarbazone is obscure, it is probable that a portion of the latter substance was reduced by the carbon monoxide via some type of hydrogen-transfer process, as envisaged by Natta, Pino, and Ercoli (9), to yield benzhydrylamine which then condensed with the remaining portion of benzophenone semicarbazone to yield compound IX.

The fact that benzophenone azine and benzophenone 4-benzhydrylsemicarbazone were present in the product of the 200-220° experiment but were not in that of the higher temperature one suggested that one or both of these substances might be the reactive intermediates in the direct ring closure reactions to yield the phthalimidines. In order to test this hypothesis, both of these substances were carbonylated at 235–245°. Benzophenone azine yielded only 3-phenylphthalimidine, whereas benzophenone 4-benzhydrylsemicarbazone afforded both 3-phenylphthalimidine and 3-phenyl-2-(N-benzhydrylcarboxamido)phthalimidine. Since some unreacted benzophenone azine remained after it had been treated with carbon monoxide at 235–245° but none was present when benzophenone semicarbazone or benzophenone 4-benzhydrylsemicarbazone was carbonylated at the same temperature for the same time one might assume that stronger complexing had occurred between the semicarbazones and the catalyst than between benzophenone azine and the catalyst which facilitated the cyclization reaction to yield the phthalimidines.

The fact that diphenylmethane and 1,1,2,2-tetraphenylethane were present in the reaction product suggests strongly that benzhydryl free radicals were produced by thermal decomposition of the azo tautomer of the semicarbazone. Evidence for a similar tautomerization of arylhydrazones has been recently noted by Connor (10). The homolytic cleavage of the azo tautomer of the semicarbazone might be expected to yield nitrogen and benzhydryl free radicals. Abstraction of hydrogen from the substrate might then be expected to yield diphenylmethane. On the other hand one might envisage that benzophenone semicarbazone might be reduced by the small quantity of hydrogen present in the gas to benzhydrylamine and the latter might then undergo hydrogenolysis to yield diphenylmethane.

EXPERIMENTAL

General Considerations

(*a*) The high-pressure equipment has been described previously (1).

(*b*) In every carbonylation experiment preformed dicobalt octacarbonyl (11) was used, and high-purity carbon monoxide supplied by the Matheson Co., East Rutherford, N.J., was added to an initial pressure of about 2100 p.s.i. at room temperature.

(*c*) The aluminum oxide (calcined) "Analar" was procured from the British Drug Houses (Canada) Ltd., Toronto 14.

(*d*) All melting points were obtained on a Leitz heating stage and are uncorrected. The infrared analyses were done on a Perkin–Elmer spectrophotometer, Model 21, using a sodium chloride crystal. Microanalyses

Can. J. Chem. Downloaded from www.nrcresearchpress.com by 210.87.254.42 on 09/05/12
For personal use only.

were done by Dr. A. Bernhardt, Mikroanalytisches Laboratorium, im Max-Planck Institut fur Kohlenforschung, Mulheim (Ruhr), Germany, and by Mrs. Aldridge of this department. The n.m.r. spectra were obtained on a Varian A-60 instrument using tetramethylsilane as the internal standard (set at $\delta = 0$).

Carbonylation of Benzophenone Semicarbazone at 235–245°

To a mixture of 10.0 g of benzophenone semicarbazone (0.04 mole) in 45 ml of dry purified benzene were added 3.0 g of preformed dicobalt octacarbonyl and 2100 p.s.i. of carbon monoxide. The mixture was heated to 235–245° (at about 4000 p.s.i.) for 150 minutes. The bomb was then cooled overnight (the pressure drop at room temperature was 40 p.s.i., equal to 0.019 mole of carbon monoxide) and vented. The vented gas contained no basic material. The reaction product consisted of 7.4 g of a blue solid (A) and a brown liquid (essentially free of catalyst) which on evaporation yielded 4.6 g of a brown solid (B).

3-Phenylphthalimidine (from Blue Solid A)

The blue solid (A) was extracted with ethanol for 24 hours in a Soxhlet apparatus, yielding 4.3 g of crystalline material. Chromatography of 0.105 g of this substance on alumina using benzene–chloroform (5:1) as developer yielded 0.019 g (10%) of N,N′-dibenzhydrylurea. Further elution of the column with chloroform afforded 0.054 g (25%) of solid which on recrystallization from ethanol had a melting point of 222–224°. The mixed melting point of the latter substance (II) and an authentic sample of 3-phenylphthalimidine (5) was 222–224°. The infrared spectra of the two compounds were identical.

Separation of Substances in Solid B

Solid B was separated into five components by thin-layer chromatography (12) on silica gel using chloroform as a developer and concentrated nitric acid – sulphuric acid as a detector.

A 2.17-g portion of material B dissolved in a minimum of benzene was chromatographed on an alumina column (133×54 mm diameter). The following developers were then added consecutively with elutions as indicated: (1) 600 ml of benzene – petroleum ether (30–60°) (1:1) eluted 0.283 g (8%) of liquid III; (2) 300 ml of benzene eluted 0.050 g (2%) of solid IV; (3) 400 ml of benzene yielded no material; (4) 600 ml of benzene eluted a trace; (5) 800 ml of benzene gave 0.328 g (8%) of solid V; (6) 1200 ml of benzene–ethanol (99:1) eluted nothing; (7) 500 ml of benzene–ethanol (98:2) yielded 0.595 g (15%) solid VI; (8) 300 ml of benzene–ethanol (98:2) gave no material; (9) 400 ml of benzene–ethanol (5:1) gave 0.312 g (7%) sirup VII.

Characterization of Fractions

Diphenylmethane (III)

Fraction III was purified by vapor phase chromatography using a silicone column at 270° C. Scratching of the liquid induced crystallization, m.p. 25°; mixed melting point with an authentic sample of diphenylmethane was 24–25°. The infrared spectrum of compound III was identical with that of an authentic sample of diphenylmethane.

1,1,2,2-Tetraphenylethane (IV)

Compound IV was recrystallized from ligroin, m.p. 215–217°. Anal. Found: C, 93.69; H, 6.40. Calc. for $C_{26}H_{22}$: C, 93.40; H, 6.64. The infrared spectrum of compound IV was identical with that of an authentic sample of 1,1,2,2-tetraphenylethane (13), prepared by the reduction of tetraphenylethylene.

3-Phenyl-2-(N-benzhydrylcarboxamido)phthalimidine (V)

Compound V was recrystallized twice from benzene – petroleum ether (b.p. 30–60°); m.p. 200–201°; mixed m.p. of compound V with an authentic sample of 3-phenyl-2-(N-benzhydrylcarboxamido)phthalimidine, 199–200°.

Infrared spectrum of compound V (KBr): 3260 (w), 3050 (w), 3020 (w), 2930 (w), 1700 (s), 1684 (s), 1607 (w), 1593 (w), 1582 (w), 1528 (s), 1493 (m), 1465 (w), 1453 (w), 1359 (m), 1340 (m), 1324 (m), 1295 (w), 1236 (m), 1201 (w), 1185 (m), 1158 (w), 1137 (m), 1090 (w), 1083 (m), 1024 (w), 894 (w), 849 (w), 770 (m), 762 (m), 750 (s), 738 (s), 727 (s), 697 (s). Nuclear magnetic resonance signals (given in δ units; spectra

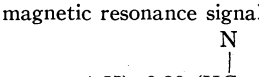

obtained in deuterated chloroform): 6.09 (HC—Ph_2, area = 1 H), 6.20 (HC—Ph, area = 1 H), 7.20 (aromatic H, area = 15 H), 7.48 (phenylphthalimidine, aromatic H, area about 4 H), 9.45 (N—H, doublet, area 1 H). Anal. Found: C, 80.8; H, 5.29; N, 6.58. Calc. for $C_{28}H_{22}N_2O_2$: C, 80.35; H, 5.30; N, 6.70.

Exchange Reaction of 3-Phenyl-2-(N-benzhydrylcarboxamido)phthalimidine with D_2O

3-Phenyl-2-(N-benzhydrylcarboxamido)phthalimidine was refluxed for 17 hours in 10 ml of D_2O containing 0.05 g of K_2CO_3. The product was obtained in the usual way. The infrared spectrum showed a strong N—D band at 2430 cm^{-1} and a lowering of the carbonyl band to 1695 cm^{-1}.

Synthesis of Authentic 3-Phenyl-2-(N-benzhydrylcarboxamido)phthalimidine

Diphenylacetic acid was first converted into diphenylacetyl chloride according to the procedure of Stollé and Wolf (7). Diphenylacetyl chloride (5.0 g), dissolved in 35 ml of acetone, was added dropwise through a separatory funnel into a well-stirred solution of sodium azide (2.9 g) in 10 ml of water at such a rate that the temperature did not exceed 15°. Stirring was continued for a further 75 minutes; then 20 ml of cold aqueous

Can. J. Chem. Downloaded from www.nrcresearchpress.com by 210.87.254.42 on 09/05/12
For personal use only.

sodium bicarbonate (10%) was added. The reaction mixture was poured into 50 ml of ice-cold water and extracted with three 40-ml portions of cold ethyl ether. The combined extract was washed with cold aqueous sodium bicarbonate (10%) and then with cold water, dried over anhydrous magnesium sulphate, filtered into 100 ml of dry benzene, and warmed to 65° for 90 minutes. Removal of the benzene *in vacuo* yielded 3.32 g (73% of theoretical) of the crude isocyanate, which was subsequently distilled at 112° and 0.08 mm Hg, n_D^{26} 1.5765. The infrared spectrum showed the characteristic strong absorption at 2270 cm^{-1} and a medium absorption at 2130 cm^{-1}. The benzhydrylisocyanate (0.48 g) was then condensed with 3-phenylphthalimidine (0.48 g) following the procedure previously described (2) to yield 0.89 g (93% of theoretical) of 3-phenyl-2-(N-benzhydrylcarboxamido)phthalimidine; m.p. 198–199°; Anal. Found: C, 80.37: H, 5.41. Calc. for $C_{28}H_{22}N_2O_2$: C, 80.35; H, 5.30.

N,N′-Dibenzhydrylurea (VI)

Compound VI was rechromatographed on alumina using benzene–chloroform (4:1). The first fraction from this column was decolorized with norite and recrystallized from ethyl acetate; m.p. 289–290°. Infrared spectrum of purified compound VI in KBr: 3290 (m), 3050 (w), 3020 (w), 2890 (w), 1623 (s), 1568 (s), 1490 (m), 1451 (m). As this spectrum suggested that compound VI was a urea, an authentic sample was prepared by allowing benzhydrylisocyanate to react with the moisture in the air. The product recrystallized from acetone had a melting point of 291–291.5°; mixed melting point of compound VI and authentic N,N′-dibenzhydrylurea, 290–291°. The literature melting point for this compound is 269–270° (4). Anal. Found: C, 82.81; H, 6.47; N, 6.95. Calc. for $C_{27}H_{24}N_2O$: C, 82.61; H, 6.16; N, 7.14.

N-Benzhydrylurea (VII)

Compound VII was recrystallized from benzene and then from hot water; m.p. 148–149°. The mixed melting point of an authentic sample of N-benzhydrylurea, prepared from benzhydrylisocyanate and ammonia, was 148–149° (literature m.p. is 143° (8)). Anal. (compound VII): Found: C, 73.89; H, 6.45; N, 12.33. Calc. for $C_{14}H_{14}N_2O$: C, 74.28; H, 6.23; N, 12.38.

Carbonylation of Benzophenone Semicarbazone at 200–220°

A 2.2-g aliquot of the product obtained from the carbonylation of benzophenone semicarbazone at 200–220° for 2.5 hours was chromatographed on alumina and yielded the following: 0.071 g of diphenylmethane (4%), 0.28 g (8%) of benzophenone azine (VIII), 0.85 g of benzophenone semicarbazone (35%), 0.45 g (11%) of a substance (IX) having a melting point of 179–181°, and 0.09 g of N-benzhydrylurea (4%).

Anal. (Compound IX): Found: C, 79.60; H, 5.67; N, 10.58; O, 4.11; mol. wt., 369 (Rast). Calc. for $C_{27}H_{23}N_3O$: C, 79.97; H, 5.72; N, 10.36; O, 3.95; mol. wt., 405. Nuclear magnetic resonance signals (deutereochloroform) of compound IX: 6.25 (HC—Ph_2, doublet, area 1 H), 6.95 (NH, area = 1 H), 7.32 (aromatic H, area = 20 H), 7.72 (NH, area = 1 H). Infrared spectrum (KBr): 3410 (m), 3150 (w), 3060 (w), 1668 (s), 1580 (m), 1495 (s), 1445 (m), 1365 (w), 1325 (w), 1230 (w), 1180 (m), 1105 (s), 1065 (m), 1025 (m), 945 (w), 910 (w), 862 (w), 835 (w), 782 (m), 753 ()s, 735 (m), 695 (s). The infrared spectrum of benzophenone semicarbazone showed peaks at 3460, 3190, and 1700 cm^{-1}.

Hydrolysis of compound IX with dilute sulphuric acid yielded benzophenone (isolated as benzophenone 2,4-dinitrophenylhydrazone).

Synthesis of Benzophenone 4-Benzhydrylsemicarbazone

A mixture of 0.38 g of benzophenone semicarbazone and 0.47 g of benzhydrylamine was heated at 120° for 4 hours. The reaction was accompanied by the evolution of ammonia. The residue was recrystalized from 25 ml of ethanol; yield, 0.47 g (74%), m.p. 179.5–180.5°; mixed melting point with compound IX was 179–180°. The infrared spectra of both compounds were the same.

Carbonylation of Benzophenone Semicarbazone at 175–180°

Similarly, 15.3 g of benzophenone semicarbazone was dissolved in chlorobenzene and treated with carbon monoxide at 175–180° for 2.5 hours. Chromatography of 3.3 g of the product on alumina yielded 0.11 g of diphenylmethane, 0.05 g of 1,1,2,2-tetraphenylethane, 1.0 g of benzophenone azine (35%), 0.75 g of substance IX (24%), and 1.4 g of unreacted starting material.

Carbonylation of Benzophenone Azine

Benzophenone azine was carbonylated at 235–245° for 2.5 hours under conditions similar to those used in the first experiment. Chromatography of the product yielded 63% of 3-phenylphthalimidine and unreacted starting material.

Carbonylation of Benzophenone 4-Benzhydrylsemicarbazone

The benzene solution obtained from the carbonylation of 0.47 g of benzophenone 4-benzhydrylsemicarbazone at 235–245° for 2.5 hours was boiled for 30 minutes to destroy the catalyst, filtered, and evaporated to dryness under vacuum. Chromatography of this residue on alumina as described previously yielded 0.044 g of diphenylmethane (11%), about 0.015 g of benzophenone (about 7%), 0.030 g of 3-phenyl-2-(N-benzhydrylcarboxamido)phthalimidine (6%), 0.04 g of N,N′-dibenzhydrylurea (9%), and 0.170 g of 3-phenylphthalimidine (70%). The yields are based on mole quantities possible from each moiety of the starting material.

Can. J. Chem. Downloaded from www.nrcresearchpress.com by 210.87.254.42 on 09/05/12
For personal use only.

ACKNOWLEDGMENT

This research was supported by a grant from the Petroleum Research Fund administered by the American Chemical Society. Grateful acknowledgment is hereby made to the donors of said fund.

REFERENCES

1. A. Rosenthal, R. F. Astbury, and A. Hubscher. J. Org. Chem. **23**, 1037 (1958).
2. A. Rosenthal and Mary R. S. Weir. Can. J. Chem. **40**, 610 (1962).
3. W. Borsche and C. Merkivitz. Ber. **37**, 3180 (1904).
4. L. W. Jones and C. D. Hurd. J. Am. Chem. Soc. **43**, 2422 (1921).
5. R. E. Rose. J. Am. Chem. Soc. **33**, 388 (1911).
6. P. F. Wiley. J. Am. Chem. Soc. **71**, 1310 (1949).
7. R. Stollé and F. Wolf. Ber. **46**, 2248 (1913).
8. R. Leuckart and E. Bach. Ber. **19**, 2128 (1886).
9. G. Natta, P. Pino, and R. Ercoli. J. Am. Chem. Soc. **74**, 4496 (1952).
10. R. O'Connor. J. Org. Chem. **26**, 4375 (1961).
11. I. Wender, H. W. Sternberg, S. Metlin, and M. Orchin. Inorg. Syn. **5**, 190 (1957).
12. E. Demolé. J. Chromatog. **1**, 24 (1958).
13. C. B. Wooster and N. W. Mitchell. J. Am. Chem. Soc. **52**, 688 (1930).

Can. J. Chem. Downloaded from www.nrcresearchpress.com by 210.87.254.42 on 09/05/12
For personal use only.

POLAROGRAPHY OF VANADIUM (II) COMPLEXES

WENDELL J. BIERMANN AND WEN-KUEI WONG
Department of Chemistry, University of Manitoba, Winnipeg, Manitoba
Received March 6, 1963

ABSTRACT

Polarograms taken in solutions of vanadium (II) perchlorate, 0.10 *N* with respect to perchloric acid and at an ionic strength of 0.20, indicate that vanadium (II) exists predominately as a dimer in the concentration region of 5 millimolar. Oxidation of one of these ions appears to make the second relatively inert towards oxidation until labilized by further oxidation of the first to vanadyl ion.

No indication of complex formation of vanadium (II) was found with sulphate, chloride, iodide, or bromide ions. The existence of fluoro and thiocyanato complexes was noted, the vanadium (II) complexes having lower formation constants than the corresponding vanadium (III) complexes.

Can. J. Chem. Downloaded from www.nrcresearchpress.com by 210.87.254.6 on 09/05/12
For personal use only.

The coordination chemistry of the lower oxidation states of vanadium should contain interesting examples of the effects of ligand field stabilization energies. As the ligand field strength increases, it would seem likely that there would be an increased stability of the complexes of divalent vanadium, as compared to corresponding complexes of trivalent vanadium. Experimental difficulties in working with these strongly reducing solutions seem to have discouraged investigation of these systems to the point that little is known about the coordination compounds of divalent vanadium (1, 2).

The absorption spectra of complexed vanadium (II) were too similar to that of the aquated species for this to be of use in investigating formation constants. Similarly the use of a metal – metal salt electrode to obtain free ligand concentrations was not possible because of reduction of the metal salt by vanadium (II) in a variety of electrodes tried.

The dropping mercury electrode has been used in vanadium (II) solutions and found, by Lingane and Meites (3, 4, 5), to be well behaved. The present work may be viewed as a continuation of these earlier investigations. As only the oxidation process can be studied in this case, it was not possible to obtain formation constants, but only to establish ratios between the formation constants of vanadium (II) and vanadium (III) for the same number of ligands.

EXPERIMENTAL

Solutions were prepared from a crystalline vanadium (II) sulphate heptahydrate. This was prepared according to the method of Jones and Colvin (6), reducing reagent grade vanadium pentoxide, suspended in concentrated sulphuric acid, by sulphur dioxide to vanadyl sulphate. This, in turn, was reduced electrolytically at a mercury cathode, using a platinum anode, to the vanadium (III) and vanadium (II) states, successively. Crystallization of the vanadium (II) sulphate was accomplished by placing the reduced solution under a layer of 95% ethyl alcohol, which, by slow diffusion, brought about the separation of well-crystallized vanadium (II) sulphate heptahydrate.

Five different batches of the divalent vanadium salt were prepared and analyzed. Sulphate was determined as barium sulphate and vanadium was precipitated with ammonium benzoate and weighed as vanadium pentoxide, following the procedure of Shemyakin (7, 8). Water was determined by difference. The following average values were obtained, the theoretical values for $VSO_4.7H_2O$ being given in parenthesis for comparison: vanadium 18.64±0.02% (18.65%), sulphate 35.14±0.03% (35.17%), water 46.23%.

The solid vanadium (II) sulphate and solutions of divalent vanadium were stored in an atmosphere of flowing oxygen-free hydrogen, and transfers of these were made in an inert atmosphere chamber filled with purified nitrogen. Standardization of vanadium (II) solutions was done by permanganate titration.

Various solid reagents employed were reagent grade chemicals, further purified by recrystallizing twice from conductivity water.

All measurements reported here were made at a constant ionic strength of 0.20 with a perchloric acid concentration of 0.10 formal. The ionic strength was adjusted to the 0.20 figure by addition of the calculated amount of 1.00 formal sodium perchlorate solution. As the possibility of forming a sulphate complex had not been eliminated prior to the investigation of the oxidation of the aquated vanadium (II) ion, these investigations were carried out in solutions containing perchlorate as the only anion. In these cases vanadium (II) sulphate was treated with an equivalent amount of barium perchlorate solution, to give a vanadium (II) perchlorate solution.

Figure 1 shows the titration-type polarographic cell used in this work. Four hundred milliliters of solution

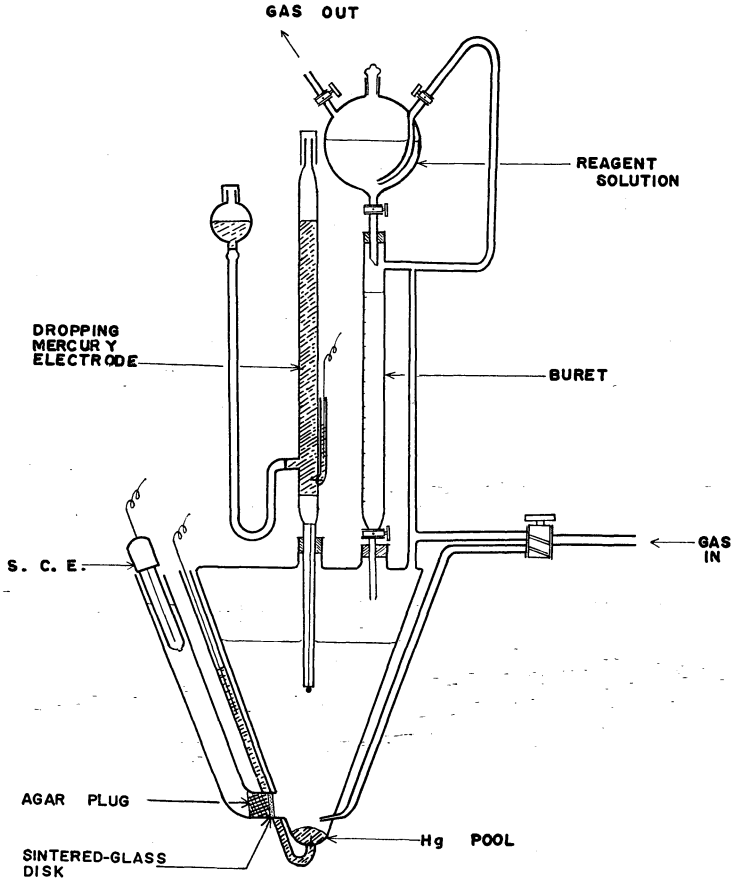

FIG. 1. Titration-type polarographic cell used in this work.

was used in this cell and the gas passed through was purified hydrogen. The applied voltage was taken from a Sargent–Heyrovsky model XII polarograph and the polarograms recorded on a Moseley X-Y recorder, using the potential drop across a precision 10,000 ohm resistor as a measure of current. A variable capacitor in parallel with the resistor was used to damp the current oscillations. The cell was thermostatted at 25.0±0.1° C.

DATA AND RESULTS

The Polarography of Vanadium (II) in 0.10 N Perchloric Acid

In Fig. 2 are shown typical polarograms obtained over a range of concentrations of vanadium (II) in 0.20 ionic strength perchlorate solution, including 0.10 *N* perchloric acid. Table I contains a series of observed half-wave potentials and diffusion currents over

Can. J. Chem. Downloaded from www.nrcresearchpress.com by 210.87.254.6 on 09/05/12
For personal use only.

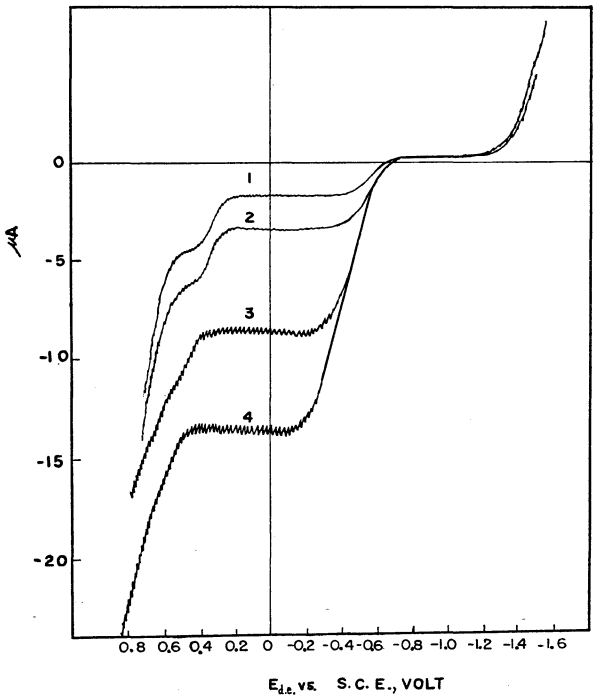

FIG. 2. Typical polarograms obtained with vanadium (II) at various concentrations. Curve 1 for [V (II)] of 0.082 mM, curve 2 for 1.62 mM, curve 3 for 3.94 mM, and curve 4 for 6.36 mM.

TABLE I

Half-wave potentials and diffusion currents of vanadium (II) sulphate in various concentrations

[V (II)] (mM)	$-E_{1/2}$ vs. S.C.E. (v)	i_d (μa)	$i_d/Cm^{2/3}t^{1/6}$	$\frac{-E_{d.e.}}{\log\left(\frac{i}{i_d-i}\right)}$ (m.v.)
0.819	0.550	1.68	1.96	84.92
1.622	0.539	3.36	1.97	87.75
2.668	0.495	5.73	2.05	129.98
3.938	0.472	8.55	2.07	126.51
4.435	0.449	9.48	2.04	128.25
4.926	0.449	10.46	2.03	130.31
5.410	0.449	11.55	2.03	129.98
5.889	0.449	12.64	2.05	131.71
6.362	0.437	13.43	2.01	134.31
7.518	0.415	15.99	2.03	138.65

a concentration range of divalent vanadium 0.80 to 7.5 mM. Also included are the calculated diffusion current constants and the slopes of $E_{d.e.}$ vs. log $(i)/(i_d-i)$ for each of these waves.

At concentrations below about 2.5 mM, the polarograms show several ill-defined steps with diffusion current constants somewhat less than the constant value reached at higher concentrations. Plots of the dropping mercury electrode potential, $E_{d.e.}$, against log $(i)/(i_d-i)$ do not give slopes capable of simple interpretation. Above 2.5 mM the test slope becomes reasonably constant and in acceptable agreement with the theoretical slope of 118.4 mv which would be predicted for a reversible, average half-electron transfer.

Can. J. Chem. Downloaded from www.nrcresearchpress.com by 210.87.254.6 on 09/05/12
For personal use only.

The explanation offered for these observations is that above 2.5 mM vanadium (II), in the solvent environment employed, the vanadium species present is a dimeric form, probably a hydrated $(V_2O)^{2+}$, which is initially oxidized by a one-electron transfer to $(V_2O)^{3+}$. Below this concentration the polynucleation process is presumably incomplete and the two waves which begin to appear are probably due to oxidation of hydrated V^{2+} and VOH^+ ions. Meites and Lingane (4), who did most of their work in 1.0 N acid, commented on the "irreversibility" at lower acid concentrations and also proposed that hydrolysis was taking place.

Above about 7 mM the behavior of the system suggests that important amounts of more complex polynuclear species are beginning to be formed.

Because of the difference in ionic strength and acidity, a comparison of the half-wave potentials found in this work with those of Lingane is not possible. Jones and Colvin (6), however, have shown that in 0.10 N sulphuric acid the half potential of the V (II) → V (III) oxidation could be expressed as $E_{1/2} = 0.2025+0.0820(C_3+C_2)$ v versus a normal hydrogen electrode, C_3 and C_2 being the molar concentrations of V (III) and V (II), respectively. Taking C_3+C_2 as 0.005 moles/liter and adding −0.246 v, a half-wave potential of −0.449 v versus the saturated calomel electrode is predicted, which is the value obtained in this work in the concentration region [V (II)] = 5 mM.

Further support of an initial oxidation process involving the loss of one electron from an entity containing two V (II) ions was obtained by titrating a solution of vanadium (II) sulphate in 0.10 N perchloric acid with 0.100 N potassium permanganate and taking polarograms at intervals during the titration. These data are tabulated in Table II, which

TABLE II

Half-wave potentials and diffusion currents of vanadium in the potassium permanganate titration

[V (II)] (mM)	[$KMnO_4$] (mM)	$(E_{1/2})_1$ (v)	$(i_d)^1_a$ (μa)	$(i_d)^1_c$ (μa)	$(E_{1/2})_2$ (v)	$(i_d)^2_c$ (μa)	$[(i_d)^1_a+(i_d)^2_c]/2$ (μa/mole) [V]
7.52	0	0.415	15.99	0.20	—	—	21.28
7.40	1.405	0.472	12.65	2.96	—	—	21.08
7.30	2.769	0.485	9.49	6.10	—	—	21.10
7.08	5.38	0.623	3.75	9.53	1.235	0.79	21.00
6.99	6.63	0.674	1.54	11.01	1.275	1.98	19.37
6.89	7.84	0.651	00.20	10.32	1.291	4.58	18.59
6.80	9.02	0.629	—	7.91	1.296	9.09	18.33
6.70	10.18	0.617	—	5.18	1.291	13.54	17.82
6.62	11.30	0.607	—	2.77	1.279	19.01	18.47
6.53	12.39	—	—	0.40	1.279	24.01	19.00
6.49	12.81	—	—	—	1.178	24.70	19.02

gives the total molarity of vanadium in terms of the concentration of V (II) placed in the titration cell and the amount of permanganate added in terms of the normality it would show if diluted to the volume of solution in the cell at that point in the titration. An anodic and cathodic diffusion current are shown for each step of the titration, computed from the wave which is characterized by a half-wave potential of about 0.5 v, these presumably being proportional to the concentrations of V (II) and V (III).

When the anodic wave has been reduced to half its original value (i.e. half the V (II) has been oxidized) a second cathodic wave with a half-wave potential of 1.2 v appears, as shown in the sixth and seventh columns of Table II. This is the same potential as reported by Jones and Colvin (6) for the process

$$VO^{2+} + 2H^+ + e = V^{3+} + H_2O,$$

Can. J. Chem. Downloaded from www.nrcresearchpress.com by 210.87.254.6 on 09/05/12
For personal use only.

which was found to be reversible. As shown in the right-hand columns of Table II, the diffusion current for this latter wave is about twice that of the first anodic wave for a given vanadium concentration, suggesting that further oxidation of the $[V_2O]^{3+}$ formed in the first step involves the formation of VO^{2+}, with simultaneous labilization and oxidation of the remaining V (II) ion, giving a net transfer of one electron per vanadium ion, as observed.

Complex Formation

As the preparation of vanadium (II) perchlorate would be unnecessary if it could be demonstrated that the sulphato complex was very weak, this possibility was examined. The half-wave potentials of 5 mM VSO_4 solutions, 0.10 formal in $HClO_4$ and with various sulphate concentrations (ionic strength kept constant at 0.20 with sodium perchlorate), were measured. These were constant at -0.449 v, indicating that no significant formation of sulphato complex takes place.

Fluoride Complex

Table III shows the variation of half-wave potential as a function of excess fluoride

TABLE III

Half-wave potential of vanadium (II) fluoride complex ion as a function of the fluoride concentration (Concentration of vanadium (II) sulphate was 0.005 to 0.0045 M)

NaF in excess (mM)	Log C_{F^-}	$-E_{1/2}$ vs. S.C.E. (v)	NaF in excess (mM)	Log C_{F^-}	$-E_{1/2}$ vs. S.C.E. (v)
3.3	−2.48	0.476	31.3	−1.50	0.518
6.6	−2.18	0.489	45.5	−1.44	0.529
9.8	−2.01	0.492	59.0	−1.23	0.530
13.0	−1.89	0.497	71.8	−1.14	0.529
16.1	−1.79	0.501	89.6	−1.05	0.532
23.7	−1.63	0.514	100.4	−0.99	0.528

ion, approximated on the assumption that a monofluoro complex is formed. The slope of a plot of the half-wave potential as a function of log C_F, where C_F is the molar concentration of free fluoride ions, is a measure of the difference of the coordination number in the lower oxidation state ("p") and in the higher oxidation state ("q") through the relationship (9, p. 218)

$$(E_{1/2})_C - (E_{1/2})_S = E_C^0 - E_S^0 - \frac{(p-q)}{a} 0.0591 \log C_X,$$

where the subscripts C and S refer to the complexed and aquated forms, respectively, C_X is the concentration of free ligand X, and a is the number of electrons transferred per vanadium ion. The slope becomes 0.00 when the fluoride ion concentration exceeds 0.045 M, indicating that $p = q$ above this concentration.

The formation constants of the oxidized and reduced forms:

$$K_{ox} = \frac{[(V_2OF_q)^{3-q}]}{[(V_2O)^{3+}][F^-]^q}$$

and

$$K_{red} = \frac{[(V_2OF_p)^{2-p}]}{[(V_2O)^{2+}][F^-]^p},$$

Can. J. Chem. Downloaded from www.nrcresearchpress.com by 210.87.254.6 on 09/05/12
For personal use only.

can be best compared in the concentration region where $p = q$ by means of the relationship (9, p. 222)

$$(E_{1/2})_C - (E_{1/2})_S = \frac{0.0591}{a} \log \frac{K_{red}}{K_{ox}} - \frac{(p-q)}{a} 0.0591 \log C_X.$$

It is found that $K_{ox}/K_{red} = 23.4$, indicating that the higher oxidation state leads to a substantially more stable fluoro complex.

Thiocyanate Complex

Table IV shows the variation of half-wave potential as a function of excess thiocyanate

TABLE IV

Half-wave potential of vanadium (II) thiocyanate complex ion as a function of the thiocyanate concentration (Concentration of vanadium (II) sulphate was 0.005 to 0.0045 *M*)

NH_4CNS in excess (m*M*)	Log C_{CNS^-}	$-E_{1/2}$ vs. S.C.E. (v)	NH_4CNS in excess (m*M*)	Log C_{CNS^-}	$-E_{1/2}$ vs. S.C.E. (v)
3.15	−2.50	0.467	43.54	−1.36	0.514
7.81	−2.11	0.478	56.43	−1.25	0.516
15.39	−1.81	0.489	68.64	−1.16	0.516
22.74	−1.64	0.494	91.11	−1.04	0.517
29.88	−1.53	0.498	120.93	−0.92	0.515
36.80	−1.43	0.503			

ion. Again, above a free ligand concentration of 0.045 *M* the coordination numbers in the two oxidation states becomes equal, and the ratio of formation constants $K_{ox}/K_{red} = 13.70$. This lowering of the ratio of formation constants is to be anticipated because of the higher field associated with the thiocyanate ion, giving additional ligand field stabilization of the lower oxidation state.

Other Halide Ions

The half-wave potential was found to be independent of the concentrations of chloride, bromide, or iodide ions, indicating that only very weak complexing could take place.

ACKNOWLEDGMENTS

One of us (W. K. W.) gratefully acknowledges the research fellowship made possible by the Frederick G. Cottrell Research Corporation. A grant from the National Research Council of Canada made it possible to obtain the equipment and materials for this work.

REFERENCES

1. KING and GARNER. J. Am. Chem. Soc. **74**, 3709 (1952).
2. G. SCHWARTZENBACH and J. SANDERA. Helv. Chim. Acta, **36**, 1089 (1953).
3. J. J. LINGANE. J. Am. Chem. Soc. **67**, 182 (1945).
4. J. J. LINGANE and L. MEITES. J. Am. Chem. Soc. **70**, 2525 (1948).
5. J. J. LINGANE and L. MEITES. J. Am. Chem. Soc. **73**, 2165 (1951).
6. JONES and COLVIN. J. Am. Chem. Soc. **66**, 1563 (1944).
7. F. M. SHEMYAKIN. Chem. Abstr. **29**, 2880 (1935).
8. F. M. SHEMYAKIN and V. F. CHAPUIGIN. J. Applied Chem. USSR (Engl. Transl.), **8**, 536 (1935).
9. I. M. KOLTHOFF and J. J. LINGANE. Polarography. Vol. I. Interscience Publishers, New York. 1952.

Can. J. Chem. Downloaded from www.nrcresearchpress.com by 210.87.254.6 on 09/05/12
For personal use only.

NUCLEAR REACTIONS INDUCED IN TANTALUM BY PROTONS OF ENERGY UP TO 84 MEV[1]

C. L. RAO[2] AND L. YAFFE
Radiochemistry Laboratory, Department of Chemistry, McGill University, Montreal, Que.
Received April 19, 1963

ABSTRACT

Nuclear reactions induced in tantalum by protons of energy up to 84 Mev have been studied and excitation functions obtained for products formed by (*p*,*xn*), (*p*,*pxn*), (*p*,2*pxn*), and (*p*,3*pxn*) reactions. Radiation characteristics of the products were redetermined. Previously unreported γ-rays with energies 90 to 1050 kev have been found for W^{176}, and 113 kev for W^{177}. A new half-life of 2.7 ± 0.1 hr for W^{176} is reported. The cross sections for the (*p*,*xn*) reactions were compared with the values predicted by Jackson's schematic model and found to be in reasonable agreement. More complex reactions are discussed in the light of current nuclear theories.

INTRODUCTION

Nuclear reactions induced by protons and other particles of kinetic energies up to a few tens of Mev in medium heavy-weight elements have been chiefly interpreted in terms of the compound nucleus (1). However, significant deviations from the predictions of this model, as observed in the large inelastic scattering cross sections and the anisotropy of the emitted particles, prompted the introduction of a direct interaction mechanism (2, 3) as an alternative to the compound nucleus mechanism. The investigation of the excitation functions of a neutron-excess nucleus with high atomic number offers a convenient method of differentiating reactions that proceed through compound nucleus formation from those reactions, like (*p*,*pn*), which take place via other non-compound-nucleus processes.

The present study pertains to the investigation of the nuclear reactions induced in tantalum by protons in the energy range 8–84 Mev. In this energy range, these reactions are not greatly complicated by fission or other exotic processes. Tantalum was chosen for this study for the following reasons:

(1) The element is available in a very pure form commercially as a foil in different thicknesses, and it is essentially monoisotopic.

(2) The detailed study of the spallation reactions in this mass region ($150 < A < 200$) and energy range (8–90 Mev) is not extensive. A literature survey is given by Miller and Hudis (4) covering the work carried out up to 1959. At higher energies nuclear reactions on tantalum have been studied, among which the studies with 340 Mev (5) and 5.7 Bev (6) protons are the most comprehensive. An extension of these data to lower energies would be informative.

(3) It was also felt desirable to investigate the gamma spectra of neutron-deficient nuclides of W, Ta, Hf, and Lu, since these are poorly identified.

Even though a large number of stable nuclides would be formed in several reactions on tantalum, which cannot be studied radiochemically, a limited comparison with the total reaction cross section, as derived from the continuum theory or from the optical model, can be obtained at a few energies.

[1]*This work received financial assistance from the National Research Council of Canada.*
[2]*Present address: Radiochemistry and Isotope Division, Atomic Energy Establishment, Trombay, Bombay, India.*

Can. J. Chem. Downloaded from www.nrcresearchpress.com by 210.87.254.105 on 09/05/12
For personal use only.

EXPERIMENTAL PROCEDURES

(a) Target Assembly

Tantalum metal, used as the target foil, was available in two thicknesses (84.3 mg/cm² and 21 mg/cm²). The thinner foil was used in the study of (*p*,*xn*) and (*p*,*pxn*) reactions and the thicker foil for the study of (*p*,2*pxn*) and (*p*,3*pxn*) reactions.* Spectrographic analysis of the tantalum foil indicated that no detectable impurities would cause any interference in the present study. The monitor foil was a 'spec pure' copper foil 0.002 in. thick obtained from Johnson, Matthey and Co. A study to determine the recoil losses in the monitor foil was made by irradiating a copper foil and a pure aluminum foil as a catcher foil at two energies, 50 Mev and 85 Mev. The recoil losses of Cu^{64} were found to be less than 0.25% of the total Cu^{64} activity at both the above energies and were therefore neglected. The recoil losses from tantalum were not measured and it was assumed that they would be negligible. Hence no guard foils were used for the monitor or target foil during irradiations.

The tantalum foils were cleaned with concentrated nitric acid and rinsed with distilled water. The copper foils were cleaned with acetone and distilled water. The two foils, each of about 2 cm² in area, were carefully aligned and fixed to the target holder in such a way that the beam of protons first struck the monitor foil. It was necessary to ensure that equal areas of the monitor and the target foils intercepted the beam. Before bombardments, the sides of the foils were trimmed with a pair of scissors and examined under a magnifying glass to make sure that the foils were uniformly cut and the leading edge was perfectly aligned. After bombardments, the foils were again sheared at about 4 mm from the leading edge, such that, after being weighed, equal areas of the target and monitor foils were processed for activity determination.

(b) Irradiations

The target holder was fixed to the probe of the McGill Synchrocyclotron and the probe set at the desired radii, thus letting the target intercept the internal circulating proton beam at various energies. The calibration curve for radial distance vs. proton energy by Kirkaldy (7) was used. Energy degradation of the proton beam at all energies at which irradiations were carried out was estimated from the range-energy values of Sternheimer (8) and was found to be negligible within the energy spread of the proton beam (~2 Mev). The irradiation period was about one hour in most of the experiments.

(c) Chemical Procedures

The elements that are expected to be formed in the spallation of Ta in the present study are W, Ta, Hf, Lu, and possibly Yb. Depending upon the energy of the bombardment, either all or some of these elements would be formed. The formation of any product formed by secondary reactions was neglected on account of the thin targets employed in this work. In copper, zinc, copper, nickel, cobalt, and iron would be formed as spallation products. It was found convenient to separate in one series of experiments throughout the energy range only Ta and W, and in another series Hf and Lu, from the spallation products of Ta. The formation of Yb was neglected. The existing chemical procedures for the separation of the spallation products of Ta (5) and Cu (9) were slightly modified to suit the present experimental conditions in order to achieve a high degree of decontamination.† Tantalum was dissolved in the minimum amount of concentrated nitric and hydrofluoric acids in the presence of W, Zr (for Hf), and La (for Lu) carriers in a platinum crucible by gently warming the mixture on a steam bath for a few minutes. Briefly, Ta was separated by extraction with diisopropylketone from the acid medium twice, and finally back-extracted from the ketone layer into 50% tartaric acid solution. Tungsten was precipitated as $CoWO_4$ followed by complexing with thiocyanate and recovery of the tungsten in ammoniacal solution. Similarly, zirconium, used as a carrier for Hf, was precipitated as barium zirconyl fluoride and later extracted with TTA in xylene and, finally, Zr(Hf) was recovered in 5 *M* hydrochloric acid. Lanthanum, used as carrier for Lu, was precipitated as fluoride and later as hydroxide, and finally recovered in 4 *M* hydrochloric acid. Copper was separated from its spallation products by suitable adaptation of anion exchange methods.

All the solutions containing the purified elements were made up to a certain volume, and an aliquot of each was pipetted into a standard screw-cap glass vial in order to measure the radiation characteristics and decay rates. Aliquots of the above solutions were analyzed spectrophotometrically for chemical yield determinations; Ta as a phenylfluorone complex (10), W as a thiocyanate complex (11), Zr (Hf) as a thoron complex (12), La (Lu) as an alizarin red S complex (11), and Cu as diethyldithiocarbamate complex (13).

(d) Beam Intensity Measurement

In order to measure the absolute cross sections, it was necessary to know the number of protons that had passed through the target foils. Copper was used as the monitor foil for the proton beam. For low-energy bombardments, the monitor reaction $Cu^{63}(p,n)Zn^{63}$ was utilized, and the cross-section values from the excitation function given by Ghoshal (14) for this reaction were used. At higher energies (above 15 Mev),

**The nomenclature used in indicating all these reactions is not intended to imply any particular reaction mechanism.*

†*A detailed account of the chemical procedures, measurement techniques, and resolution of decay curves may be found in the thesis of Lakshman Rao Chervu, McGill University, Montreal, Que., 1962.*

Can. J. Chem. Downloaded from www.nrcresearchpress.com by 210.87.254.105 on 09/05/12
For personal use only.

the reaction $Cu^{65}(p,pn)Cu^{64}$ was utilized, for which the cross-section values were obtained from Meadows (15). The cross sections for the monitors at the various energies are given in Table I.

TABLE I

Monitor cross-section values used in this work

Proton energy (Mev)	σ (millibarn)		Proton energy (Mev)	σ (millibarn)	
	Zn^{63} (14)	Cu^{64} (15)		Zn^{63} (14)	Cu^{64} (15)
8	260	—	42	—	315
12	540	—	48	—	280
18	—	155	54	—	260
24	—	520	64	—	230
30	—	440	74	—	217
36	—	360	84	—	183

(e) Activity Measurements

All the samples were measured by a calibrated 3 in.×3 in. sodium iodide crystal (16) coupled to a photomultiplier tube in conjunction with a 100-channel pulse-height analyzer. This γ-ray spectrometer was used for the measurement of the intensity of γ-rays and *K* X-rays in every sample. The energy calibration was made with a number of well-known γ-ray emitters.

(f) Treatment of Data

The areas of the prominent photopeaks were converted into photon-emission rates by applying the photopeak counting efficiency in the crystal and the resolution losses as observed on the pulse analyzer. A plot of the photon-emission rate as a function of time gave the radioactive decay curve. The *K* X-ray photopeak decay curves of the samples were graphically analyzed into several components, depending upon the energy at which the irradiation was made, in order to separate the contributions from the different isotopes of each element. In those cases where some of the decaying species had radioactive daughter species growing in the fraction after radiochemical purification, graphical analysis of the multicomponent decay curve was too difficult. If an easily observed γ-ray of known energy and abundance was emitted by the parent or its daughter, the photon-emission rate of the species was obtained without resolving the *K* X-ray decay curve for that particular nuclide. In those cases where it was not possible to follow any specific γ-ray, the *K* X-ray decay curve was analyzed for the longer-lived daughter components only, from which the parent activities were estimated.

For the calculation of the disintegration rates at the end of bombardment for each nuclide observed, the corrections applied to the photon-emission rates were the following: decay during the period between the end of bombardment and the measurement time, chemical yield of the sample and dilution factor, γ-ray and *K* X-ray abundance (17, 18) per disintegration of each nuclide detected. In the case of positron emitters, the intensity of the annihilation γ-rays was measured and a factor of 2 included in the calculation of disintegration rates to allow for the emission of two quanta.

Finally, the cross sections for the formation of the nuclide were calculated by means of the following equation:

$$\sigma_p = \sigma_m \cdot \frac{D_0^p}{D_0^m} \cdot \frac{n_m}{n_T} \cdot \frac{(1-e^{-\lambda_m t})}{(1-e^{-\lambda_p t})}$$

where σ_p and σ_m = formation cross sections of product and monitor respectively;
D_0^p and D_0^m = disintegration rates of product and monitor respectively at end of bombardment;
n_m and n_T = number of atoms of monitor and target respectively;
λ_m and λ_p = disintegration constants of monitor and product respectively;
t = time of irradiation.

In the case of those nuclides which are not shielded, if the parent half-lives and formation cross sections are known, corrections for the formation from the precursors was applied to obtain independent cross sections; when the precursor half-lives are too short that they decayed away into the daughter nuclide before any chemical separation was effected, cumulative cross sections only were given.

RESULTS

*(a) Radiation Characteristics**

(i) W^{176}

This nuclide has previously been reported only by Wilkinson (19), who assigned a half-life of 80 min to it and a γ-ray of about 1.3 Mev in energy. In the present work two

**The error in gamma-ray energy values quoted is ±5% unless otherwise indicated.*

Can. J. Chem. Downloaded from www.nrcresearchpress.com by 210.87.254.105 on 09/05/12
For personal use only.

Can. J. Chem. Downloaded from www.nrcresearchpress.com by 210.87.254.105 on 09/05/12
For personal use only.

γ-rays of energies 90 kev and 1050 kev were found attributable to W^{176}. They decayed with a half-life of 2.7±0.1 hr over four half-lives. The mass assignment was made both on the basis of excitation functions for the $Ta^{181}(p,6n)$ reaction and the observed growth of the Ta^{176} daughter (half-life 8 hr) which was consistent with having a 2.7-hr parent.

(ii) W^{177}

This nuclide was produced by the reaction $Ta^{181}(p,5n)$. It had previously been reported only by Wilkinson (19), who found a half-life of 2.17±.05 hr for it and assigned γ-rays of energies 450 and 1200 kev to it. In the present work we found γ-rays of 113, 450, and 1050 kev decaying with a half-life of 2.2±0.1 hr over five half-lives.

(iii) W^{178}, W^{179}, W^{181}

These nuclides were prepared by the $(p,4n)$, $(p,3n)$, and (p,n) reactions respectively on Ta^{181}. The half-lives found, viz. 22±0.5 days, 40±2 min, 140±2 days, agreed well with the literature values (17). The values were derived by resolution of the X-ray curves. Ta^{178} (9.3-min half-life), in secular equilibrium with W^{178}, has a prominent γ-ray at 1.35 Mev energy and 511 kev annihilation radiation due to a 2% positron branching. Both decayed with the 22-day parent half-life.

(iv) Ta^{173}

This nuclide was produced by the $(p,p8n)$ reaction on Ta^{181} and by decay of the short-lived W^{173} formed by the $(p,9n)$ reaction on Ta^{181}. The half-life for Ta^{173} was found to be 3.7 hr, in agreement with that reported by Faler and Rasmussen (20). Ta^{173} was observed by the growth of an intense photopeak due to Hf^{173} (24 hr) in the separated tantalum fraction. Harmatz *et al.* (21) have proposed a half-life of 2.5 hr for Ta^{173}. In Fig. 1 are

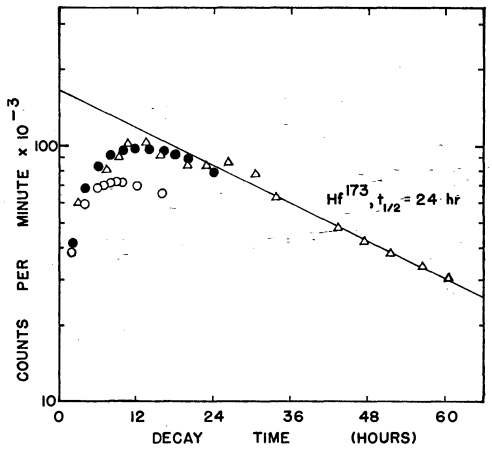

FIG. 1. Growth of 24-hr Hf^{173} from Ta^{173}: △ experimental points; ● theoretical growth curve assuming a half-life of 3.7 hr for Ta^{173}; ○ theoretical growth curve assuming a half-life of 2.5 hr for Ta^{173}.

shown the experimental data and the theoretical growth curves for both a 2.5-hr and a 3.7-hr parent feeding a 24-hr daughter. The data are consistent with the latter value.

(v) Ta^{174}

This nuclide was formed by the reaction $Ta^{181}(p,p7n)$ and by decay of short-lived W^{184} produced by the reaction $Ta^{181}(p,8n)$. The 511-kev annihilation radiation peak decayed with a half-life of 1.3±0.1 hr, in agreement with that found by Faler and Rasmussen (20).

(vi) Ta^{175}

The formation of this nuclide was recognized by the growth of the characteristic 340 kev γ-ray due to Hf^{175}. Gamma rays of energies 125, 205, 265, and 350 kev were found attributable to Ta^{175}. Due to the complexity of the spectrum, the abundance of Ta^{175} was calculated from the growth of Hf^{175}.

(vii) Ta^{176}

This is produced by decay of W^{176} and from the reaction $Ta^{181}(p,p5n)$. Gamma rays at 202, 1160, and 1700 kev were observed to decay with a half-life of 8 hr, in agreement with previous work. In all, about 60 transitions of energies up to 2 Mev (21) have been reported for this nuclide. The resolution of the decay curve yielded an 8-hr component, a mixture of Ta^{176} and Ta^{180m}, and thus no yield determinations of Ta^{176} were made.

(viii) Ta^{177}

This is produced by the decay of W^{177} and from the reaction $Ta^{181}(p,p4n)$. Resolution of the X-ray curves gave a half-life of 56 ± 1 hr for this nuclide, in good agreement with the work of Mann *et al.* (22).

(ix) Ta^{178}

This nuclide was formed by the reaction $Ta^{181}(p,p3n)$. Gamma rays of energies 213, 330, and 427 kev were found decaying with a half-life of 2.2 ± 0.1 hr. These γ-rays originate (17) mainly from the 4.8-sec Hf^{178m} state in equilibrium with Ta^{178}.

(x) Ta^{179}

This was formed from the reaction $Ta^{181}(p,p2n)$ and by decay of W^{179}. No prominent γ-rays were observed and measurements were made by resolution of the X-ray photopeak. A half-life of about 600 days (19) has been reported for Ta^{179}. Measurements made over a period of one half-life were consistent with this value.

(xi) Ta^{180m}

The formation cross section of this nuclide, produced by the reaction $Ta^{181}(p,pn)$, was measured by the X-ray photopeak. A half-life of 8.1 ± 0.1 hr was obtained, in good agreement with previous data (17). At higher energies, production of Ta^{176} made measurements in this fashion impossible.

(xii) Hf^{171}

The γ-ray spectrum of separated Hf fractions at higher energies was very complex. Gamma rays at 680, 880, and 1100 kev were found attributable to Hf^{171} as these were not found at bombarding energies where Hf^{173} alone was produced. Although the spectrum was too complex for decay-curve analysis, the decay of these peaks was consistent with a 16-hr half-life (17). The growth of the 740 kev photopeak due to the Lu^{171m} daughter (21) was used to measure the formation cross section.

(xiii) Hf^{172}

This nuclide (half-life $\sim$ 5 yr) was identified and measured with the help of the high-energy photopeaks due to Lu^{172} (6.7 day) in secular equilibrium with the parent nuclide.

(xiv) Hf^{173}

Very intense photopeaks at 120 and 300 kev decayed with a half-life of 24 ± 0.5 hr. This nuclide was observed both as a direct spallation product and, at high energies, by decay of its precursors.

(xv) Hf^{175}

The very intense 340 kev photopeak attributable to this nuclide decayed with a half-life of 70 ± 2 days. Hf^{175} was formed directly at 42 Mev proton bombarding energies.

Can. J. Chem. Downloaded from www.nrcresearchpress.com by 210.87.254.105 on 09/05/12
For personal use only.

This did not result from decay of Ta^{175} since the formation of the latter was not observed at proton energies less than 64 Mev. At these energies the production of Hf^{175} from its precursors was observed.

(xvi) Hf^{180m}

This nuclide was first observed at a proton bombarding energy of 42 Mev. Characteristic γ-rays at energies of 216, 340, 440, and 500 kev were found. The 216 kev peak decayed with a half-life of 5.5±0.1 hr, in excellent agreement with the result of Burson *et al.* (23).

(xvii) Lu^{171m}

This was identified by the characteristic photopeak (21) at 740 kev. The decay of this photopeak gave a half-life of 7.7±0.2 days, measured over a period of four half-lives, shorter than that of 8.2 days reported by Bonner *et al.* (24).

(xviii) Lu^{172}

Gamma rays at energies of 113, 180, 200, 300, 370, and 1090 kev were observed. The decay of the most intense peak was followed for seven half-lives and gave a value of 6.7±0.1 days, in very good agreement with the literature values (17).

(xix) Lu^{176m}

The decay of the 90 kev gamma peak reported (17) for this nuclide gave a half-life of 3.8 hr, in good agreement, with literature values (17).

(xx) Lu^{177}

This was detected as a very weak β^- activity observed in lutetium fraction decaying with a half-life of approximately 7 days. The gamma spectrum indicated weak peaks at 113 and 208 kev due to Lu^{177}.

(b) Experimental Cross Sections

The radiation characteristics used to determine the formation cross sections are given in Table II. The cross sections found experimentally are listed in Table III. The estimated accuracy quoted for each cross-section value is the standard deviation calculated by

TABLE II

Radiation characteristics used to determine formation cross sections of nuclides

Nuclide	Half-life	Radiation measured	Abundance (per disintegration)
W^{181}	140 days	K X-rays	0.72 (25)
W^{179}	40 min	K X-rays	1 (assumed)
W^{178}	22 days	K X-rays	1.54 (W^{178} + Ta^{178}) (6)
W^{177}	2.2 hr	K X-rays	0.87 (calc.)
W^{176}	2.7 hr	K X-rays	0.94 (calc. for Ta^{176})
Ta^{180m}	8.1 hr	K X-rays	0.66 (26)
Ta^{179}	600 days	K X-rays	0.57 (25)
Ta^{178}	2.2 hr	K X-rays	1 (17)
Ta^{177}	56 hr	K X-rays	0.87 (6)
Ta^{175}	11 hr	340 kev γ (Hf^{175})	0.86 (17)
Ta^{174}	1.3 hr	511 kev γ	0.76 (20)
Ta^{173}	3.7 hr	120 kev γ (Hf^{173})	1.1 (17)
Hf^{180m}	5.5 hr	216 kev γ	0.88 (17)
Hf^{175}	70 days	340 kev γ	0.86 (17)
Hf^{173}	24 hr	120 kev γ	1.1 (17)
Hf^{172}	5 yr	1.09 Mev γ (Lu^{172})	0.61 (17)
Hf^{171}	16 hr	740 kev γ (Lu^{171m})	1 (21)
Lu^{177}	6.7 days	β^-	1 (17)
Lu^{176m}	3.8 hr	390 kev γ	0.13 (estimated)
Lu^{172}	6.7 days	1.09 Mev γ	0.61 (17)
Lu^{171m}	7.7 days	740 kev γ	1 (21)

Can. J. Chem. Downloaded from www.nrcresearchpress.com by 210.87.254.105 on 09/05/12
For personal use only.

Can. J. Chem. Downloaded from www.nrcresearchpress.com by 210.87.254.105 on 09/05/12
For personal use only.

TABLE III

Formation cross sections

	Proton energy (Mev):													
	8	12	18	24	30	36	42	48	54	64	74	84	Type of yield	Accuracy (%)
	σ (millibarn)													
Nuclide														
W^{181}	60	98	35	47	44								I	±22
W^{179}			26	1200	920	280							I	±22
W^{178}					240	760	430	200	130	120	62	64	I	±22
W^{177}						130	550	830	650	200	110	98	I	±28
W^{176}								87	420	320	170	73	I	±28
Ta^{180m}			16	100	110	180	170						I	±22
Ta^{179}			0.5	29	74	190							I	±28
Ta^{178}						38	82	180	180				I	±28
Ta^{177}						5	120	280	270	170	180	220	I	±28
Ta^{175}										130	440	290	C	±28
Ta^{174}												300	C	±28
Ta^{173}												160	C	±28
Hf^{180m}							0.03		.05				I	±28
Hf^{175}							6		13	10	3	2	I	±28
Hf^{173}										25	21	24	I	±28
Hf^{172}											22		C	±28
Hf^{171}											3.5	21	C	±28
Lu^{177}							0.05						I	±28
Lu^{176m}							0.008		.08	0.2			I	±22
Lu^{172}										.07	1.2	3.7	I	±22
Lu^{171m}											0.3	2.6	I	±28

NOTE: I = independent yield; C = cumulative yield.

taking into account the errors in obtaining the disintegration rates and saturation factors. No allowance was made for the uncertainty in the monitor cross-section values or for that in the radiation abundance values used.

DISCUSSION

The formation cross sections presented in Table III indicate the general behavior expected in the spallation of a medium-weight element, in the energy range 8–84 Mev, namely production of neutron-deficient nuclides up to of the order of a few mass numbers below that of the target nucleus.

(a) (p,xn) Cross Sections

The individual excitation functions for the (*p,xn*) reactions, forming W isotopes, all exhibit sharp peaks separated from each other by about 12 Mev, as shown in Figs. 2–6.

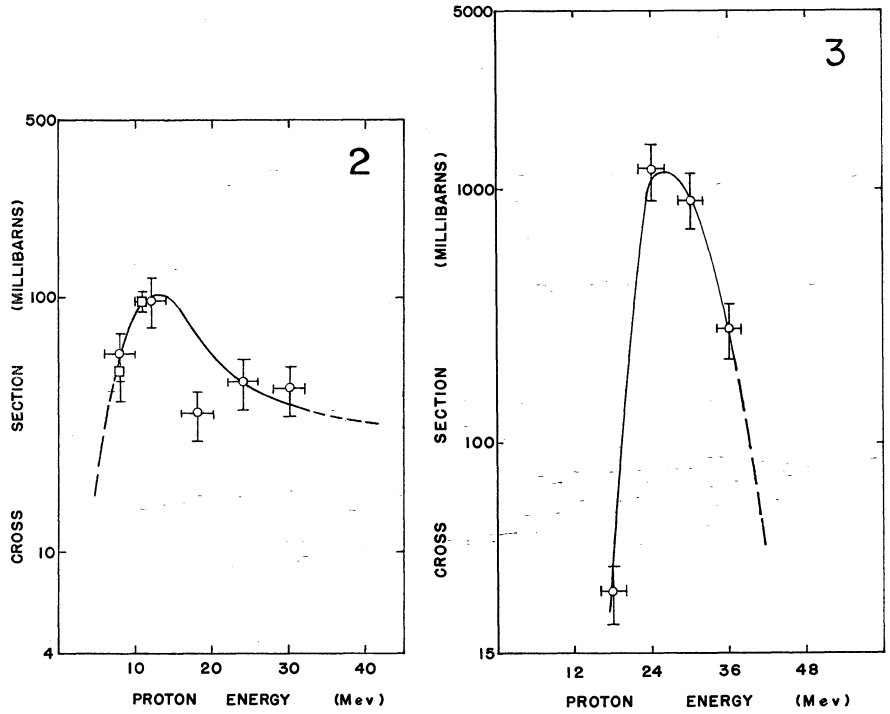

FIG. 2. Excitation function for the $Ta^{181}(p,n)W^{181}$ reaction: ○ present work; □ Hansen *et al.* (34).
FIG. 3. Excitation function for the $Ta^{181}(p,3n)W^{179}$ reaction.

These are typical of reactions proceeding at lower energies through the formation of a compound system with the subsequent decay governed by statistical considerations. The tailing off of each of these excitation functions at higher energies indicates that the nucleon–nucleon internal cascade mechanism (27) is becoming important.

In order to calculate the cross section for the (*p,xn*) reaction proceeding primarily through a compound nucleus mechanism in heavy non-fissile elements at these energies, an application of the statistical model was made by Jackson (28). He combined the Monte Carlo calculations of McManus *et al.* (29) for the prompt knock-on cascade process with a simplified evaporation model in order to calculate the excitation functions for the

Can. J. Chem. Downloaded from www.nrcresearchpress.com by 210.87.254.105 on 09/05/12
For personal use only.

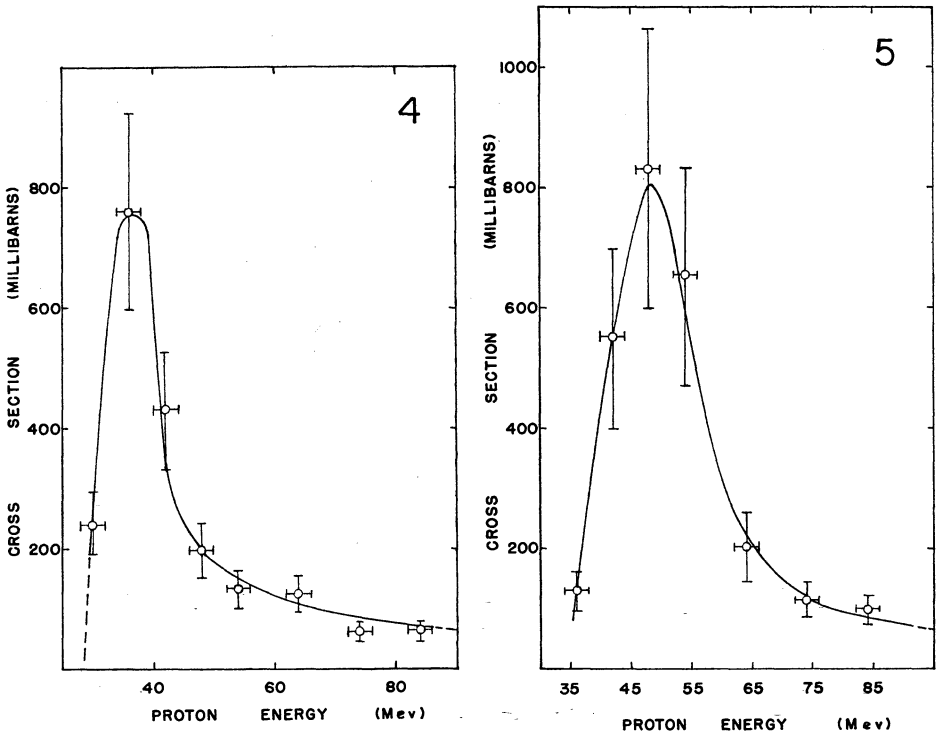

FIG. 4. Excitation function for the $Ta^{181}(p,4n)W^{178}$ reaction.
FIG. 5. Excitation function for the $Ta^{181}(p,5n)W^{177}$ reaction.

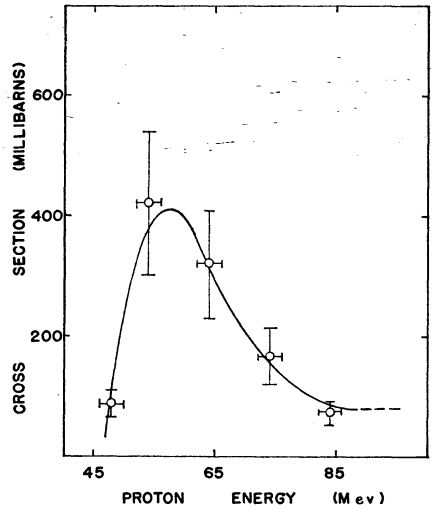

FIG. 6. Excitation function for the $Ta^{181}(p,6n)W^{176}$ reaction.

(p,xn) reaction up to 100 Mev. In the energy range up to 50 Mev, the knock-on cascade process enters as a minor correction, since the incident protons that enter the nuclear core will probably lead to compound nucleus formation. Hence the Jackson model was applied in the present work assuming only the compound nucleus mechanism.

Can. J. Chem. Downloaded from www.nrcresearchpress.com by 210.87.254.105 on 09/05/12
For personal use only.

The probability that a nucleus with initial excitation energy E will evaporate exactly x neutrons is given by:

$$P(E,x) = I(\Delta_x,2x-3)-I(\Delta_{x+1},2x-1),$$

where $I(z,n)$ is Pearson's incomplete gamma function,

$$\Delta_x = (E - \textstyle\sum_i^x B_i)/T.$$

B_i is the binding energy of the ith neutron, and Δ_x is the energy (in units of T, the nuclear temperature) above the threshold for the emission of x neutrons. The nuclear temperature is given by the relationship

$$\Delta E = \bar{B}+2T.$$

ΔE in Mev is the energy separation between the successive peaks of the (p,xn) excitation functions (12 Mev) which corresponds closely to the average energy carried off by the successive neutrons. $\bar{B}$, the average neutron binding energy, was calculated as 8.1 Mev from the neutron binding energies given by Seeger (30). A nuclear temperature of 1.95 Mev was thus deduced. The $P(E,x)$ values for several values of x were obtained from Pearson's Incomplete Gamma Function Tables (31) and individual neutron binding energies from Seeger's Mass Tables.

If the mechanism is assumed to be entirely that of compound nucleus formation, then

$$\sigma(p,xn) = \sigma_c(E_0)P(E,x),$$

where $\sigma_c(E_0)$ is the cross section for compound nucleus formation at an incident proton energy of E_0. The values of $\sigma_c(E_0)$ were calculated from the continuum theory of Shapiro (32) for a nuclear radius of $R = 1.3\times10^{-13}\ A^{1/3}$cm. The experimental and calculated excitation functions are given in Fig. 7.

As is evident from the results, the agreement is good only at some energies for all the reactions. The theoretical curves fall slightly to the right of those experimentally determined. A smaller value for the nuclear temperature would shift the predicted curves to slightly lower energies, but that alone would not give any better agreement with the experimental values. A more detailed account of the properties of the nucleus, combined with the excitation distribution appropriate to each of the prompt processes and evaporation steps, would perhaps better predict these cross-section values.

A comparison with the (p,xn) excitation functions (33) for Bi and Pb with those of Ta shows that the Ta curves are shifted to lower energies, since the incident proton binding energy is 6.6 Mev for Ta^{181} as compared to 5 Mev for Bi^{209} and 3.3 Mev for Pb^{206}. At low energies, at 8 Mev and 12 Mev, the cross section for the (p,n) reaction reported here, 60 and 98 millibarns respectively, are comparable to the values given by Hansen *et al.* (34) for the same reaction, 52 and 90 millibarns at the corresponding energies. At the highest bombarding energy, 84 Mev, the cross-section values for $(p,4n)$, $(p,5n)$, and $(p,6n)$ reactions are 64, 98, and 73 millibarns as compared to the values for these reactions at 340 Mev by Nervik and Seaborg (5), which are 65, 30, and 65 millibarns. The cross section for the $(p,6n)$ reaction product W^{176} by Nervik and Seaborg will be nearly halved in view of the new half-life of 2.7 hr reported for this nuclide in the present work as compared to the earlier value of 1.3 hr.

(b) (p,pxn), (p,2pxn), and (p,3pxn) Cross Sections

The data for the (p,pxn) reactions are shown in Figs. 8–11. The excitation functions

Can. J. Chem. Downloaded from www.nrcresearchpress.com by 210.87.254.105 on 09/05/12
For personal use only.

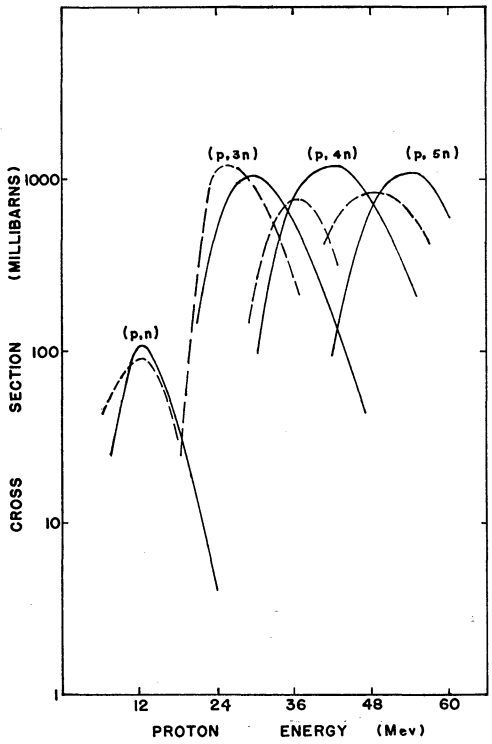

FIG. 7. Comparison of experimental excitation functions with those predicted by the Jackson model: - - - experimental; — Jackson model.

of these reactions, as well as the more complex ones, increase rapidly above the threshold. Some of these reach a maximum value and then decrease slowly with increasing energy, while others increase monotonically up to the highest bombarding energy (84 Mev). Reactions of this type are expected to have negligibly small cross sections compared with the (p,xn) cross section in medium-heavy target nuclei like Ta on the basis of statistical theory, since they are inhibited by the Coulomb barrier in both the entrance and exit channels. The experimental cross sections for these reactions are, however, quite large and the alternative mechanism proposed, that might lead to these reactions at low and medium energies, is the direct interaction (2, 3) process. The difference between the direct interaction mechanism at low energies and at high energies proposed by Serber (27) is that at low energies the knock-on process is assumed to occur with the nucleons in the surface of the target nucleus, while at higher energies direct interaction occurs in the interior of the nucleus with a sharp boundary. Internal direct processes at low energies account for only a very small fraction of the (p,$xpxn$) cross sections and hence are relatively unimportant (28, 35). Monte Carlo calculations of the cascade–evaporation phases of the high-energy interactions (35–38), based on the Serber model, assume a sharp cutoff nuclear boundary, and the cross sections predicted (26, 39) for the (p,$xpxn$) reactions at high energies are smaller than the experimental values. Further, these calculations do not take into account any interaction in the knock-on phase with the incoming particle of aggregates of nucleons and thus cascade emission of complex units as deuterons, tritons, or alphas is neglected. In the light of these remarks, the spallation yields of (p,$xpxn$) reactions on Ta are discussed below in the order of increasing complexity.

Can. J. Chem. Downloaded from www.nrcresearchpress.com by 210.87.254.105 on 09/05/12
For personal use only.

Can. J. Chem. Downloaded from www.nrcresearchpress.com by 210.87.254.105 on 09/05/12
For personal use only.

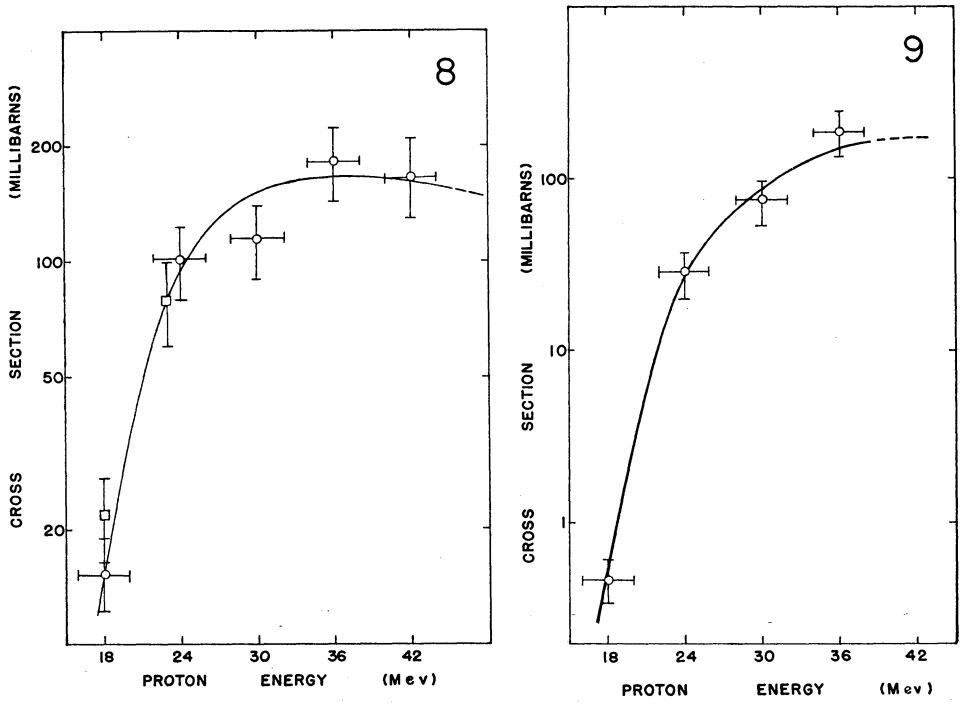

FIG. 8. Excitation function for the $Ta^{181}(p,pn)Ta^{180m}$ reaction: ○ present work; □ Cohen *et al.* (43).
FIG. 9. Excitation function for the $Ta^{181}(p,p2n)Ta^{179}$ reaction.

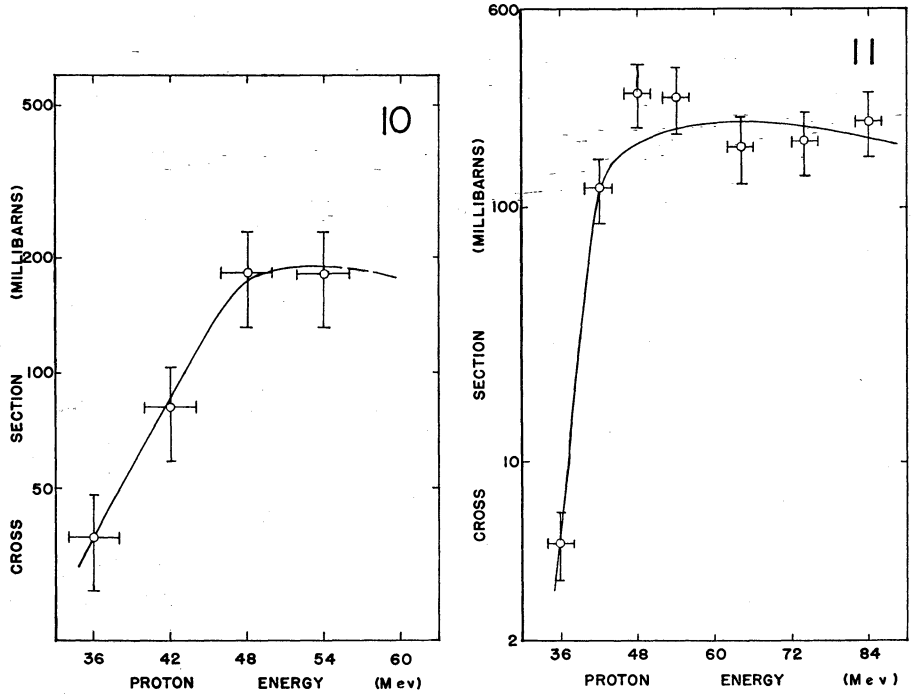

FIG. 10. Excitation function for the $Ta^{181}(p,p3n)Ta^{178}$ reaction.
FIG. 11. Excitation function for the $Ta^{181}(p,p4n)Ta^{177}$ reaction.

(i) (p,pn) and (p,2p) Cross Sections

These two reactions lead partially to isomeric states and partially to the stable ground states of Ta^{180} and Hf^{180} respectively. It is not known what percentage goes to the ground states and hence any comparison of cross sections for Ta^{180m} and Hf^{180m} indicates only the nature of the reaction paths favoring one reaction over the other. The possible mechanisms for these two reactions in this energy range are:

(*a*) direct interaction process involving collision of the incident proton with a neutron or a proton in which both collision partners escape from the nucleus;

(*b*) direct inelastic scattering of the incident proton followed by evaporation of a particle;

(*c*) for the (*p*,*pn*) reaction, the emission of deuterons by the well-known pickup process, i.e. the (*p*,*d*) reaction, which is another case of direct interaction important at low energies.

A comparison of the cross section for the (*p*,2*p*) reaction forming Hf^{180m} at 42 Mev, 0.03 millibarn, with the cross section for the (*p*,*pn*) reaction forming Ta^{180m} at the same energy, 170 millibarns, indicates how the several reaction paths favor the production of Ta^{180m} in contrast to that of Hf^{180m}. For the formation of Hf^{180m}, only mechanism (*a*) is significant. The fact that the cross sections for (*p*,2*p*) reactions below 54 Mev are extremely small is consistent with the Monte Carlo calculations (35, 36), indicating that, below about 100 Mev, absolute values of cross sections for multiple particle cascades are small. The yields for both Hf^{180m} and Ta^{180m} could not be studied up to the highest bombarding energy available. The probability for the (*p*,2*p*) reaction may increase due to an increase in the knock-on process, while the (*p*,*pn*) cross section may level off or gradually drop due to the decreasing importance of mechanism (*c*) among other factors (26, 40). The excitation function for Ta^{180m} compares well with those obtained for the same reaction on Ir^{193} reported by Grant (41) and on Au^{197} by Kavanagh and Bell (42) in the energy range where the investigations overlap. Cohen *et al.* (43) report a value of 80 millibarns at 23 Mev for the same reaction on Ta^{181}, in close agreement with the present work.

(ii) (p,p2n), (p,p3n), and (p,p4n) Cross Sections

These reactions occur by the same mechanism as discussed above. The excitation energy of the residual nucleus after the direct interaction event must be appropriate to evaporate the required number of neutrons. The pickup process, e.g. (*p*,*t*) reaction, may also contribute to these cross sections. After reaching a maximum cross-section value, the excitation functions level off or decrease slowly with increasing bombarding energy. The maximum cross-section values are about the same for all these reactions, including the previously discussed (*p*,*pn*) reaction. It may be mentioned that the Ta^{178} yield represents only a part of the Ta^{181}(*p*,*p*3*n*) cross section, so that the yields for all these reactions are quite large.

The cross-section value for the (*p*,*p*3*n*) reaction at 54 Mev, 180 millibarns, may be compared with the cross-section value of 152 millibarns reported by Nervik and Seaborg at 340 Mev (5). The cross section for Ta^{177}, formed by the (*p*,*p*4*n*) reaction at 84 Mev, is 220 millibarns and at 340 Mev, 27 millibarns, as reported by the same authors.

(iii) (p,2pxn) and (p,3pxn) Cross Sections

The direct interaction mechanism suggested for the (*p*,*pxn*) reactions involving inelastic scattering of the proton followed by particle evaporation cannot possibly account for the formation yields of the (*p*,2*pxn*) and (*p*,3*pxn*) reactions observed from 42 Mev onwards with appreciable cross sections. If the direct interaction occurs with only one particle, the residual excitation energy may be insufficient to evaporate even a number of neutrons. For example, at 42 Mev, Hf^{175} formed by (*p*,2*p*5*n*) reaction has a cross section of 6.0

Can. J. Chem. Downloaded from www.nrcresearchpress.com by 210.87.254.105 on 09/05/12
For personal use only.

millibarns and Lu^{177} produced by the $(p,3p2n)$ reaction has a value of 0.05 millibarn. The threshold energies ($-Q$ values) calculated from Seeger's mass tables (30) for formation of these nuclides, formally written as $(p,2pxn)$ and $(p,3pxn)$ reaction products, are listed in Table IV.

TABLE IV
Threshold calculations

Product nuclide	Reaction mechanism	$-Q$ (Mev)
Hf^{175}	$(p,2p5n)$	42.7
Hf^{173}	$(p,2p7n)$	58.4
Hf^{172}	$(p,2p8n)$	64.5
Hf^{171}	$(p,2p9n)$	74.6
Lu^{177}	$(p,3p2n)$	26.7
Lu^{176}	$(p,3p3n)$	34.6
Lu^{172}	$(p,3p7n)$	63.5
Lu^{171}	$(p,3p8n)$	71.0

It has been known that the (p,α) reactions in medium heavy elements proceed through direct interaction of the incoming proton with an alpha particle or by a triton pickup reaction (44, 45). This process must be assumed to occur only at the nuclear surface, instead of throughout the nuclear volume, because of the small mean free path of the α-particles in nuclear matter (46). A nucleon, in the peripheral region of the nucleus, spends a substantial fraction of its time, probably about one-third to one-half, in an 'alpha particle' as concluded by Hodgson (45) at 40 Mev and at higher energies by Ostroumov and Filov (47). The (p,α) cross section in Ta^{181} at 23 Mev is 6 millibarns (48) and it probably increases at higher energies. According to Lindner and Turkevich (39), the yields of the products of the reactions, formally written as $(p,3pxn)$, are considerably higher than predicted by the cascade–evaporation model (35, 36), and they state that such products are perhaps produced by the reaction of the $(p,\alpha pxn)$ type in which the α-particle is knocked out of the nucleus during the cascade step, since the evaporation stage seems hardly likely to provide enough charged-particle emission in heavy elements bombarded with 340 Mev proton. Similarly, at lower energies below 70 Mev, Foreman *et al.* (49) suggest that $(\alpha,xpxn)$ reactions are formed by direct interaction with complex particles emitted in preference to a series of protons and neutrons. Thus at low energies below 100 Mev, the large yields of the $(p,2pxn)$ and $(p,3pxn)$ reaction products in Ta^{181} can best be explained by direct interaction of the incoming particle with aggregates of nucleons, like H^3, He^3, He^4, He^6, Li^5, Li^6, Li^7, etc., followed by evaporation of an appropriate number of neutrons, rather than by multiple emission of particles, unless an appreciable reduction of the Coulomb barrier, proposed only at high energies of excitation (50, 51), occurs even at low excitation energies (48) permitting the evaporation of charged particles. However, it has been shown theoretically that barrier penetrability should remain roughly constant up to 30 Mev of excitation energy (52).

The $(p,2pn)$, $(p,2p2n)$, $(p,2p3n)$, and $(p,2p4n)$ reactions lead to Hf^{179}, Hf^{178}, Hf^{177}, and Hf^{176}, respectively which are stable and their yields cannot be determined radiochemically. The $(p,2p5n)$ reaction product, Hf^{175}, would probably result from a $(p,Hexn)$ reaction, with the proton–helium isotope knockout mechanism, followed by neutron evaporation at 42 Mev and above. Its isobar, Ta^{175}, formed either through the decay of W^{175} or independently through a $(p,p6n)$ reaction, was observed only at bombarding energies above 64 Mev, which might be explained on the basis that no alternative reaction paths are

Can. J. Chem. Downloaded from www.nrcresearchpress.com by 210.87.254.105 on 09/05/12
For personal use only.

available for its formation, except by neutron evaporation from an excited nucleus after proton inelastic scattering. It may also be pointed out that the two reaction products, Ta^{178} formed by the $(p,p3n)$ reaction and Hf^{175} produced by the $(p,\alpha 3n)$ reaction, were observed at about the same energy, the former at 36 Mev and the latter at 42 Mev, suggesting a similarity of the two reaction processes. The drop in the excitation function for Hf^{175} at higher energies is somewhat puzzling and further experiments alone would clarify this point. The independent yields of Hf^{173}, formed by the $(p,2p7n)$ reaction, may also be explained by the same mechanism of helium isotope surface knockout, followed by neutron evaporation. Its formation in comparable yield to that of Hf^{175} indicates a greater deposition of energy in the residual nucleus with increasing bombarding energy favoring evaporation of many neutrons, which may be one of the reasons for the gradual decrease in the yields of Hf^{175} at higher energies.

The $(p,3pxn)$ reaction products have been observed at about 42 Mev. The $(p,3p2n)$ reaction at 42 Mev, leading to Lu^{177}, has a low cross section, 0.05 millibarn, indicating the low probability even for its alternative reaction path, $(p,\alpha p)$ mechanism, in which both collision partners escape the target nucleus, as explained for the $(p,2p)$ reaction. Lu^{176} formed by a $(p,3p3n)$ reaction cannot be determined radiochemically, and the yield determined for Lu^{176m} represents only a fraction of the total yield for this reaction. The yields are low, 0.2 millibarn at 64 Mev, indicating the low probability for the reaction to occur via a $(p,\alpha d)$, $(p,\alpha pn)$, or (p,Li^5n) reaction, the last reaction being more probable than the others. Lu^{172} and Lu^{171m}, produced by $(p,3p7n)$ and $(p,3p8n)$ reactions at 84 Mev, have cross sections of 3.7 and 2.6 millibarns respectively, and they are likely to be formed by surface interaction with a lithium isotope or a helium isotope followed by particle evaporation.

A comparison of the cross-section values for the $(p,2pxn)$ and $(p,3pxn)$ reactions in Ta^{181} with those of similar reactions induced in erbium isotopes (53) and iridium isotopes (41) does show that the high yields for these reactions indeed occur in the medium heavy elements even in the energy range of present interest.

(c) The Total Reaction Cross Section

At low energies (<12 Mev) the measurement of the (p,xn) cross section gives direct information about the proton reaction cross section, since the contribution from the proton inelastic scattering cross section is negligible. Experimentally, it was found in the present study that the (p,pn) reaction did not occur at 12 Mev, in agreement with Cohen *et al.* (43), who determined a value of about 0.5 millibarn at 13.5 Mev for this reaction. Thus, at 8 Mev and 12 Mev, the total reaction cross section is the sum of the cross sections for (p,n) and $(p,2n)$ reactions, the others like (p,γ) being negligible. The experimentally determined values for the (p,n) reaction at 8 Mev and 12 Mev in this work are 60 and 98 millibarns. The $(p,2n)$ reaction leading to stable W^{180} has calculated (34) cross-section values of 6 and 400 millibarns at 8 Mev and 12 Mev respectively. Thus the total reaction cross-section values of 66 millibarns at 8 Mev and 500 millibarns at 12 Mev compare well with the values computed with the optical model using a surface absorption potential (34). The proton capture cross sections at these energies, calculated by Shapiro (32) with $R = 1.5\times10^{-13}A^{1/3}$, correspond to 60 and 470 millibarns, which also agree with the above total reaction cross-section values, again pointing out that the (p,n) interaction proceeds via the compound nucleus at these low energies and direct interaction interference is negligible.

The theoretical proton total reaction cross section at 31.5 Mev given by Melkanoff *et al.* (54) for Ta is 1830 millibarns, which may be compared with the value, 1650 ± 360

Can. J. Chem. Downloaded from www.nrcresearchpress.com by 210.87.254.105 on 09/05/12
For personal use only.

millibarns, obtained at 30 Mev in the present work. The experimental value includes the (p,p') cross section for Ta at 31 Mev (2) and also the $(p,2n)$ cross section at 30 Mev (55) for Bi^{209}. The (p,α) cross sections are not significant. A similar experimental value of 1600 millibarns was given (42) for the total reaction cross section of a medium heavy nucleus like Au^{197} or Bi^{209}. Gooding (56) reported a value of 1775 millibarns for Pb as the total proton reaction cross section at 34 Mev, obtained by beam attenuation measurements. A similar comparison cannot be extended to higher energies because of the large number of competing undetermined cross sections.

ACKNOWLEDGMENTS

The authors wish to express their appreciation to Dr. R. E. Bell for making the facilities of the Radiation Laboratory so readily available to us.

One of us (C. L. R.) wishes to express his appreciation to the Canadian Universities Foundation and to the Ministry of Scientific Research and Cultural Affairs, Government of India, under whose joint auspices a Canadian Commonwealth Scholarship was held.

REFERENCES

1. J. M. Blatt and V. F. Weisskopf. Theoretical nuclear physics. John Wiley and Sons, Inc., New York. 1952.
2. R. M. Eisberg and G. Igo. Phys. Rev. **93**, 1039 (1954).
3. N. Austern, J. T. Butler, and H. McManus. Phys. Rev. **92**, 350 (1953).
4. J. M. Miller and J. Hudis. Ann. Rev. Nucl. Sci. **9**, 159 (1959).
5. W. E. Nervik and G. T. Seaborg. Phys. Rev. **97**, 1092 (1955).
6. J. R. Grover. Phys. Rev. **126**, 1540 (1962).
7. J. S. Kirkaldy. Ph.D. Thesis, McGill University, Montreal, Que. 1953.
8. R. M. Sternheimer. Phys. Rev. **117**, 137 (1959).
9. K. A. Kraus and F. Nelson. Proc. Intern. Conf. Peaceful Uses At. Energy, Geneva, 1955, **7**, 113 (1955).
10. C. L. Luke. Anal. Chem. **31**, 904 (1959).
11. E. B. Sandell. Colorimetric determination of traces of metals. 3rd ed. Interscience Publishers, Inc., New York. 1959.
12. A. D. Horton. Anal. Chem. **25**, 1331 (1953).
13. T. D. Price and R. E. Telford. National Nuclear Energy Series. Div. VIII, Vol. 1. McGraw-Hill Book Co., Inc. New York. 1950. p. 404.
14. S. N. Ghoshal. Phys. Rev. **80**, 939 (1950).
15. J. W. Meadows. Phys. Rev. **91**, 885 (1953).
16. G. V. S. Rayudu, M. May, and G. R. Grant. Quoted in thesis of G. R. Grant, McGill University, Montreal, Que. 1961.
17. Nuclear Data Sheets. National Academy of Sciences, National Research Council (U.S. Government Printing Office, Washington, D.C.). 1959.
18. D. Strominger, J. M. Hollander, and G. T. Seaborg. Rev. Mod. Phys. **30**, 585 (1958).
19. G. Wilkinson. Phys. Rev. **80**, 495 (1950).
20. K. T. Faler and J. O. Rasmussen. Phys. Rev. **118**, 265 (1960).
21. B. Harmatz, T. H. Handley, and J. W. Mihelich. Phys. Rev. **119**, 1345 (1960).
22. L. G. Mann, R. J. Nagle, and H. I. West. Bull. Am. Phys. Soc. **2**, 231 (1957).
23. S. B. Burson, K. W. Blair, H. B. Keller, and S. Wexler. Phys. Rev. **83**, 62 (1951).
24. N. A. Bonner, W. Goishi, W. H. Hutchin, G. M. Iddings, and H. A. Tewes. Phys. Rev. **127**, 217 (1962).
25. R. C. Jopson, H. Mark, C. D. Swift, and J. H. Zenger. Phys. Rev. **124**, 157 (1961).
26. S. S. Markowitz, S. S. Rowland, and G. Friedlander. Phys. Rev. **112**, 1295 (1958).
27. R. Serber. Phys. Rev. **72**, 1114 (1947).
28. J. D. Jackson. Can. J. Phys. **34**, 767 (1956).
29. H. McManus, W. T. Sharp, and H. Gellman. Phys. Rev. **93**, 924 (1954).
30. P. A. Seeger. Nucl. Phys. **25**, 1 (1961).
31. K. Pearson. Tables of the incomplete gamma functions. Cambridge University Press, Cambridge, England. 1951.
32. M. M. Shapiro. Phys. Rev. **90**, 171 (1953).
33. R. E. Bell and H. M. Skarsgard. Can. J. Phys. **34**, 745 (1956).
34. L. F. Hansen, R. C. Jopson, H. Mark, and C. D. Swift. Nucl. Phys. **30**, 389 (1962).
35. N. Metropolis, R. Bivins, M. Storm, A. Turkevich, J. M. Miller, and G. Friedlander. Phys. Rev. **110**, 185 (1958).
36. N. Metropolis, R. Bivins, M. Storm, J. M. Miller, G. Friedlander, and A. Turkevich. Phys. Rev. **110**, 204 (1958).

Can. J. Chem. Downloaded from www.nrcresearchpress.com by 210.87.254.105 on 09/05/12
For personal use only.

37. I. DOSTROVSKY, P. RABINOWITZ, and R. BIVINS. Phys. Rev. **111**, 1659 (1958).
38. I. DOSTROVSKY, Z. FRAENKEL, and P. RABINOWITZ. Proc. Intern. Conf. Peaceful Uses At. Energy, Geneva, **15**, 1615 (1958).
39. M. LINDNER and A. TURKEVICH. Phys. Rev. **119**, 1632 (1960).
40. W. R. WARE and E. O. WIIG. Phys. Rev. **122**, 1837 (1961).
41. G. R. GRANT. Ph.D. Thesis, McGill University, Montreal, Que. 1961.
42. T. M. KAVANAGH and R. E. BELL. Can. J. Phys. **39**, 1172 (1961).
43. B. L. COHEN, E. NEWMAN, R. A. CHARPIE, and T. H. HANDLEY. Phys. Rev. **94**, 620 (1954).
44. C. B. FULMER and B. L. COHEN. Phys. Rev. **112**, 1672 (1958).
45. P. E. HODGSON. Nucl. Phys. **8**, 1 (1958).
46. W. B. CHESTON and A. E. GLASSGOLD. Phys. Rev. **106**, 1215 (1957).
47. V. I. OSTROUMOV and R. A. FILOV. J. Exptl. Theoret. Phys. (USSR), Translation, **10**, 459 (1960).
48. C. B. FULMER and C. D. GOODMAN. Phys. Rev. **117**, 1339 (1960).
49. B. M. FOREMAN, JR., W. M. GIBSON, R. A. GLASS, and G. T. SEABORG. Phys. Rev. **116**, 382 (1959).
50. K. J. LE COUTEUR. Proc. Phys. Soc. (London), A, **63**, 259 (1950); A, **65**, 718 (1952).
51. Y. FUJIMOTO and Y. YAMAGUCHI. Prog. Theoret. Phys. (Kyoto), **5**, 76 (1950).
52. A. M. LANE and K. PARKER. Nucl. Phys. **16**, 690 (1960).
53. G. V. S. RAYUDU. Ph.D. Thesis, McGill University, Montreal, Que. 1961.
54. M. A. MELKANOFF, J. S. NODVIK, D. S. SAXON, and R. D. WOODS. Phys. Rev. **106**, 793 (1957).
55. E. L. KELLEY. Univ. Calif. Radiation Lab. Rept. UCRL-1044. 1950. Unpublished.
56. T. J. GOODING. Nucl. Phys. **12**, 241 (1959).

Can. J. Chem. Downloaded from www.nrcresearchpress.com by 210.87.254.105 on 09/05/12
For personal use only.

THE SPALLATION OF IRIDIUM WITH PROTONS OF ENERGIES 9–87 MEV[1]

G. R. GRANT[2] AND L. YAFFE
Radiochemistry Laboratory, Department of Chemistry, McGill University, Montreal, Que.
Received May 8, 1963

ABSTRACT

Iridium metal has been bombarded with protons varying in energy from 8 to 87 Mev. The spallation products were radiochemically separated and decay characteristics and formation cross sections were determined. It was confirmed that both Pt^{187} and Pt^{186} have half-lives of about 3 hr, and a half-life of 13.3±0.2 days was found for Ir^{189}. An isomeric state of Ir^{186} with half-life 2.0±0.5 hr has been found. Fair agreement was obtained between excitation functions for (*p,xn*) reactions determined experimentally and those predicted by the Jackson model. The (*p,pn*) yield at 84 Mev has been compared with that calculated from Monte Carlo cascade data combined with evaporation theory and found to be too high by a factor of 4.

INTRODUCTION

The purpose of the present investigation was twofold: (*a*) to investigate half-lives and other decay characteristics of the spallation products of iridium that were observed by bombarding iridium with protons of up to ~87 Mev energy, and (*b*) to determine excitation functions for these products. The energy range covered is an interesting one since it is in this region that the mechanism of nuclear reactions is believed to change from a compound nucleus type to one which is predominantly a knock-on cascade reaction, followed by nucleon evaporation.

To date, there have been relatively few studies of a similar nature in this particular mass region, but a few notable exceptions are the following: (*p,xn*) reactions on isotopes of lead and bismuth (1) where *x* is the number of neutrons emitted, the alpha and deuteron bombardment of bismuth and lead (2), the proton bombardment of gold (3), and recently the proton bombardment of tantalum (4).

EXPERIMENTAL

(a) Preparation and Irradiation of Targets

The targets were prepared by loading approximately 10–15 mg of an intimate mixture of 'spec-pure'* iridium sponge and 'spec-pure'* copper powder (both metals were of normal isotopic abundance) into thin-walled aluminum tubing (2S purity). The target was fastened to the end of the cyclotron probe and inserted to the proper radius, depending upon the energy desired.

The reactions $Cu^{63}(p,n)Zn^{63}$ and $Cu^{65}(p,pn)Cu^{64}$ were used to monitor the proton beam intensity. There are some discrepancies in the published cross sections for both of these reactions. However, there seems to be reasonable agreement between Ghoshal (5), Linder and James (6), and Howe (7) for the former reaction and Ghoshal's results have been used for bombarding energies of less than 15 Mev. For higher proton energies, Meadows' results (8) for the $Cu^{65}(p,pn)Cu^{64}$ reaction were used. The monitor cross sections are shown in Table I.

(b) Dissolution of Target

After irradiation the target (aluminum tubing, plus copper and iridium mixture) was placed in a thick-walled pyrex combustion tube along with ~1 ml 12 *M* hydrochloric acid to dissolve the aluminum and 1 drop of 30% hydrogen peroxide to speed the solution of the copper powder. The mixture was heated gently for a few minutes to remove dissolved gases and then cooled to liquid-air temperature. About 0.04 g of sodium chlorate was added as oxidant and the end of the pyrex tube was sealed prior to placing it inside a stainless

[1]*This work received financial assistance from the National Research Council of Canada.*
[2]*Present address: Atomic Energy of Canada Limited, Whiteshell Division, Whiteshell, Manitoba.*
**Obtained from Johnson, Matthey and Mallory Limited.*

Can. J. Chem. Downloaded from www.nrcresearchpress.com by 210.87.254.42 on 09/05/12
For personal use only.

TABLE I

Monitor cross sections

Proton energy (Mev)	$\sigma_{Zn^{63}}$ (millibarn)	$\sigma_{Cu^{64}}$ (millibarn)	Proton energy (Mev)	$\sigma_{Cu^{64}}$ (millibarn)
9	370		47	280
12	520		57	250
16		110	67	230
23		510	77	210
30		420	84	190
38		330	87	190

steel pressure vessel. The steel vessel was heated for 1 hour at 300° C in a muffle furnace to dissolve the iridium sponge (9). The high internal pressure of the pyrex vessel was counterbalanced by placing a weighed amount of 'dry ice' inside the steel vessel, thus keeping breakages to a minimum.

It was found most convenient to add osmium carrier before dissolution of the iridium, while all the other necessary carriers were added after dissolution of the target. However, essentially complete removal of the spallation products from the pyrex tube was verified by means of gamma-ray spectroscopy.

(c) Chemical Separations and Chemical Yields

Depending upon the energy at which the target was irradiated, the target solution may have contained activities of a few or all of the following elements: Pt, Ir, Os, Re—from the iridium target; Zn, Cu, Ni, Co, Fe—from the copper monitor, and Al, Na, F—from the aluminum tubing.

Osmium and fluorine were distilled from an all-glass distilling apparatus (10) and collected in ice-cold 6 *N* sodium hydroxide. The osmium was then purified by slightly acidifying the distillate with hydrochloric acid and extracting the osmium tetroxide twice with carbon tetrachloride (11). The osium tetroxide was then back-extracted into 1 *N* sodium hydroxide and the osmium complexed with 1,2,3-benzotriazole (12).

The remaining elements were separated on a column of Dowex-1, using the data of Kraus and Nelson (13) as a guide. After distillation of the osmium and fluorine, the residue was made 0.5 *M* in hydrochloric acid and applied to the top of a column of Dowex-1 (100 to 200 mesh, ×8%). The diameter of the column was 5 mm and the resin bed was 6 cm deep.

Copper and its spallation products were first washed from the column by eluting with water. The monitor (Zn^{63} or Cu^{64}) was then separated from the other copper spallation products at a convenient time after the bombardment. For this purpose a second column of Dowex-1 was used following a modification of the procedure outlined by Kraus and Moore (14).

Iridium was removed from the first column by reducing the Ir(IV) to Ir(III) by passing a few milliliters of aqueous hydroquinone solution through the column and then washing it with about 15 ml 6 *M* hydrochloric acid.

About 30 ml 9 *M* hydrochloric acid was sufficient to elute the Re(VII), but it was usually contaminated with trace amounts of iridium and platinum. Therefore the Re(VII) was further purified by distilling rhenium heptoxide from a perchloric acid medium and trapping it in ice-cold 6 *N* sodium hydroxide.

Since Pt(IV) is adsorbed very strongly at all hydrochloric acid concentrations (13), about 20 ml of 35% perchloric acid was used as eluant (15).

The various samples were analyzed to determine the chemical yields in the separations after the activities had decreased substantially. The methods of analyses used were taken from the literature with some simplifications introduced because of the previous separations performed. The analytical procedures used were:

zinc—volumetric titration with ethylenediaminetetracetic acid (EDTA) (16);
copper—volumetric titration with EDTA (16) or colorimetrically with diethyldithiocarbamate (17);
platinum—colorimetrically with potassium iodide (11);
iridium—potentiometric titration with Fe(II) (18) or spectrophotometrically with EDTA (19);
osmium—gravimetrically with 1,2,3-benzotriazole (12);
rhenium—colorimetrically with thiocyanate and Sn(II) (11).

(d) Radiation Measurements

Aliquots of the separated samples were made up to 2 ml in small, glass, screw-cap vials and the gamma activity of the samples was measured with a 3 in.×3 in. NaI(Tl) crystal in conjunction with a 100-channel pulse-height analyzer. The crystal was calibrated experimentally for photopeak efficiency using several sources which had been standardized using a 4π β-proportional counter. Since the gamma-ray spectra of most of the spallation products were generally quite complicated, the sources were usually measured on a shelf no closer to the detector than about 6 cm in order to reduce summing effects.

Can. J. Chem. Downloaded from www.nrcresearchpress.com by 210.87.254.42 on 09/05/12
For personal use only.

RESULTS AND DISCUSSION

(a) Radiation Characteristics

The Pt–Ir–Os system is exceedingly complex since the half-lives of many of the nuclides are so similar and the decay schemes very complex and in some cases virtually unknown (23).

(i) Pt^{191}.—Gamma rays of 130, 355, 410, and 540 kev energies were found attributable to Pt^{191}. These decayed with a half-life of 2.9±0.2 days, measured over four half-lives.

(ii) Pt^{189}.—Two γ-rays of energies 550 and 720 kev were observed in the decay of Pt^{189}. Their intensities decayed with a half-life of 9±1 hr, somewhat shorter than the values found recently by Anderson and Ringh (20) and Albouy *et al.* (21) (11.1±0.4 and 11.5 hr respectively). The relative intensities of the 550 and 720 kev γ-rays were determined to be 100 and 56 respectively. From more recent data (22), it would appear that the 550 kev peak observed is in reality a mixture of 545 kev and 608 kev γ-rays.

(iii) Pt^{188}.—A 633 kev γ-ray was found which showed the characteristic growth and decay of a 10-day parent decaying to a 41-hr daughter, i.e. $Pt^{188} \rightarrow Ir^{188}$. This energy corresponds to one of the known energy levels in Os^{188} (23).

(iv) Pt^{187} and Pt^{186}.—Recently Malysheva *et al.* (24) reported that both Pt^{187} and Pt^{186} have half-lives of 2.2±0.5 hr. This similarity in half-lives for the two isotopes has been substantiated in the present investigation. Figure 1 shows the two excitation functions

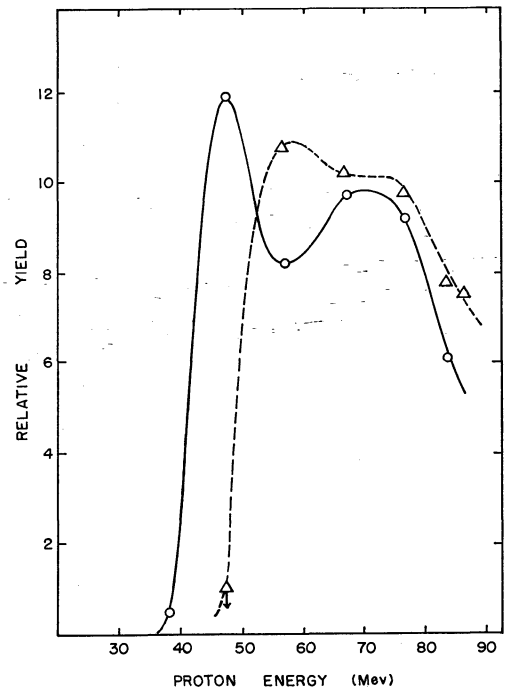

FIG. 1. Excitation functions of Pt^{187} and Pt^{186}: ○ 2100 kev γ-ray from Pt^{187}; △ 670 kev γ-ray from Pt^{186}.

found for this pair of isotopes. The solid curve is attributed to Pt^{187} on the basis of the energies at which the excitation functions $Ir^{191}(p,5n)Pt^{187}$ and $Ir^{193}(p,7n)Pt^{187}$ reach

Can. J. Chem. Downloaded from www.nrcresearchpress.com by 210.87.254.42 on 09/05/12
For personal use only.

their maxima. The formation cross sections for Pt^{187} were based on a 3.1±0.5 hr component of the γ-ray spectrum at 2.15 Mev energy. Cameron's mass formula (25) also lends support to this assignment since it predicts an available decay energy of 2.16 Mev for Pt^{187} and only 0.76 Mev for Pt^{186}. The excitation function for Pt^{186}, shown as a broken curve in Fig. 1, was based on a very broad γ-peak at 670 kev energy. This activity decayed with a half-life of 3.0±0.3 hr measured over a period of four half-lives. The yield curve is consistent with $(p,6n)$ and $(p,8n)$ reactions on Ir^{191} and Ir^{193} respectively.

(v) Ir^{192}.—This nuclide is produced independently by the reaction $Ir^{193}(p,pn)Ir^{192}$. Gamma rays of energies 140, 315, 470, 605, and 790 kev were found decaying with a half-life of 74±1.2 days (measured over two half-lives) in good agreement with that of Kastner (26).

(iv) Ir^{190m} *and* Ir^{190g}.—Gamma rays of 190, 365, and 510 kev energies were found decaying with the half-lives of both the metastable and ground state. The half-life of Ir^{190m} was found to be 3.0±0.2 hr, measured over nine half-lives, while that of the ground state was 11±1 days.

(vii) Ir^{189}.—Ir^{189} was not found as a primary spallation product. It undoubtedly was produced, but could not be resolved in the presence of the complicated spectra of Ir^{190} (with similar half-life) and Ir^{192}. Ir^{189} was, however, observed as a daughter of Pt^{189} in a separated Pt fraction. Smith and Hollander (27) have assigned a half-life of 11±2 days to Ir^{189}. We have remeasured the half-life by purifying a platinum sample and then separating the iridium daughter from this several days later. The only activity present was Ir^{189} since, under the bombardment conditions, the only radioactive platinum isotopes formed would be Pt^{191} and Pt^{189}, and Pt^{191} decays to a stable iridium isotope. A half-life of 13.3±0.2 days (measured over five half-lives) was found. This is in agreement with a recent value by Lerohl (28) of 13.3±0.1 days.

(viii) Ir^{188}.—Most of the known γ-rays of Ir^{188} were observed in both purified platinum and iridium fractions, i.e. 155, 475, 633, 830, 1200, 1440, 1700, and 2100 kev. The last three peaks appeared to be complex. In the iridium fraction Ir^{188} decayed with a half-life of 41±1 hr, while the growth and decay of Ir^{188} peaks in the platinum fractions were consistent with 41-hr Ir^{188} in equilibrium with 10-day Pt^{188}.

(ix) $Ir^{187, 186, 185}$.—These three isotopes present a situation which is very difficult to handle experimentally since they all have very similar half-lives, viz. 13 to 16 hr (29). As a result of this, and because of the complex gamma spectra, the only one of the three directly observed was 15-hr Ir^{186}. It was identified by gamma peaks at 135, 295, 630, 770, and 950 kev. These γ-ray energies for 16-hr Ir^{186} correspond closely to those reported by Diamond and Hollander (29), who also reported possible gamma rays up to 1.099 Mev in energy. In the present work, additional gamma rays of energies 1700 and 2100 kev have been observed, which are believed to follow the decay of Ir^{186}. All of the gamma rays of Ir^{186} showed a shorter-lived component of 2±0.5 hr half-life. This has been taken as evidence for the existence of a shorter-lived metastable state of Ir^{186}. It is considered unlikely that this activity could be attributed to the short-lived neutron-deficient iridium isotopes (Ir^{184}—3.2 hr, or Ir^{183}—53 min) recently reported by Diamond *et al.* (30). The 2-hr activity was first observed at a bombarding energy of 57 Mev, and it is unlikely that it was energetically possible to produce Ir^{183} or Ir^{184} at that energy. Recently Bonch-Osmolovskaya *et al.* (31) have isolated an iridium fraction from a gold target irradiated with 660 Mev protons. They observed that the γ-ray at 137 kev attributed to Ir^{186} had a shorter-lived component of 1.7±0.2 hr which they proposed belonged to an isomer of Ir^{186},

Can. J. Chem. Downloaded from www.nrcresearchpress.com by 210.87.254.42 on 09/05/12
For personal use only.

in agreement with this work. Ir^{185}, while not observed directly, was found by means of the growth of its daughter 94-day Os^{185} in a separated iridium sample.

(x) Os isotopes.—A 16-day component in the X-ray decay curve of a separated osmium sample was assigned to Os^{191}, although the characteristic 129 kev γ-ray of this nuclide was not observed due to the complexity of the spectrum in that region. Os^{185} was identified by its 645 kev γ-ray, the intensity of which decayed with a half-life of 94 days. A 382 kev γ-ray, characteristic of Os^{183}, was observed, the intensity of which decayed with half-lives of 12 and 14 hr in samples of separated osmium from bombardments at 77 and 84 Mev respectively, resulting from different admixtures of Os^{183} and Os^{183m}. Os^{182} was identified by the 510 kev γ-ray which decayed with a half-life of 20 ± 0.2 hr (over six half-lives).

(xi) Re isotopes.—Re^{181} was found in a separated rhenium fraction as evidenced by the decay of its 365 kev γ-ray. A half-life of 18 ± 1 hr was found, measured over six half-lives.

(b) Formation Cross Sections

In order to determine the cross sections of the individual spallation products, it was necessary to know the decay schemes of the nuclides concerned. For some of the nuclides observed these data are not yet available and only a lower limit to the cross section could be obtained by assuming a branching ratio of 100%.

The nuclear characteristics used to determine the formation cross sections are given in Table II and the cross sections found experimentally are shown in Table III. At the time

TABLE II

Radiation characteristics of nuclides used*

Nuclide	Half-life	Radiation, γ (kev)	Abundance (%)	Total internal conversion coefficient α_T
Pt^{191}	3 days	540	14.4 (22)	0.058 (22)
Pt^{189}	9 hr	545 608	12.8 14.9 } 27.7 (22)†	0.051 (22)
Pt^{188}	10 days → 41 hr Ir^{188}	633	28.7	0.012
Pt^{186}	3 hr	670	100 (assumed)	0 (assumed)
Ir^{192}	74 days	296 308 316	32 36 } 159 91	0.09
Ir^{190m}	3 hr	361	100	0.054
Ir^{190}	11 days	361 371 }	34.4	0.049
Ir^{188}	41 hr	633	28.7	0.012
Ir^{186}	15 hr	297	20.5‡	0.084
Ir^{185}	15 hr → 94 days Os^{185}	646	80	0.013
Os^{185}	94 days	646	80	0.013
Os^{183}	12 hr	382	87	0.013
Os^{182}	20 hr	510	100 (assumed)	0.058
Re^{181}	19 hr	365	50 (32)	0.35 (32)

*Unless otherwise indicated, pertinent data have been obtained from Nuclear Data Sheets (23).
†Abundance calculated by assuming a 60% electron capture branch to the 722 kev excited state in Ir^{189}.
‡Estimated from present measurements and published relative γ-ray intensities.

this work was being done enriched iridium isotopes were not readily available. All of the nuclides given in Table II, with the exception of Ir^{192}, could be produced by reactions on both Ir^{191} and Ir^{193}. For purposes of calculation iridium was assumed to be monoisotopic. Many of the experiments were run twice at the same energy to check reproducibility.

Can. J. Chem. Downloaded from www.nrcresearchpress.com by 210.87.254.42 on 09/05/12
For personal use only.

Can. J. Chem. Downloaded from www.nrcresearchpress.com by 210.87.254.42 on 09/05/12
For personal use only.

TABLE III

Formation cross sections: σ from Ir^{191} and Ir^{193}

Nuclide	Proton energy (Mev): 9	12	16	23	30	38	47	57	67	77	84	87	Type of yield	Error (%)
	σ (millibarn)													
Pt^{191}	12	73	32	620	460								I	±20
Pt^{189}			6.8	160	340	240	640	230	160	120	120		I	±20
Pt^{188}					49	490	250	550	290	150	130		I	±20
Pt^{186}							<50	250	230	220	190	180	I	±20
Ir^{192}			4.0	60	99	180	160	180	110	140	120		I*	±20
Ir^{190m}				0.3	2.8	10	17						I	±20
Ir^{190}				16	36	53	240	180	140	120	160		I	±20
Ir^{188}						17	66	110	180	160	200		I	±20
Ir^{186}								240	450	500	670	500	I	±20
Ir^{185}								47	180	210	210		C	±25
Os^{185}								11	33	17	37		I	±25
Os^{183}								3.3	7.1	12	31	30	C	±25
Os^{182}									5.6	7.8	9.0	13	C	±25
Re^{181}										6.9	18	14	C	±25

NOTE: I* = independent yield from Ir^{193}; I = independent yield from both Ir isotopes; C = cumulative yield.

The two results showed a spread of about 10%. The estimated error in each of the determinations was obtained from the square root of the sum of the squares of errors in the various operations which included photopeak areas (±10%), photopeak efficiency (±5%), chemical yields (±2% to ±5%), pipetting and dilution (±1%), ratio of number of atoms in monitor to target (±6%), giving overall errors of ±20% to ±25%. No allowance has been made for errors in monitor cross sections or in values chosen for the nuclear characteristics of the radiations used.

All of the (*p,xn*) reactions observed have the same general features, i.e. two peaks separated by about 20 Mev as expected from the contributions from the two isotopes of the target which are separated by two mass numbers. These are shown in Figs. 1–4

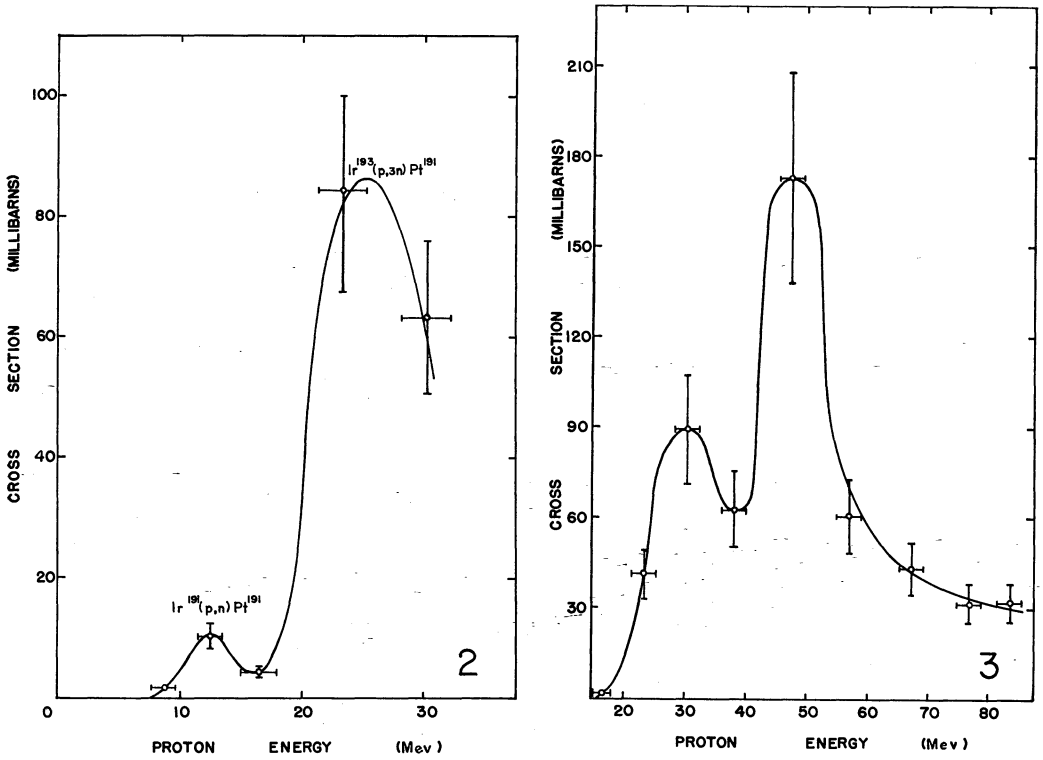

FIG. 2. Excitation functions for the reactions $Ir^{191}(p,n)Pt^{191}$ and $Ir^{193}(p,3n)Pt^{191}$.
FIG. 3. Excitation functions for the reactions $Ir^{191}(p,3n)Pt^{189}$ and $Ir^{193}(p,5n)Pt^{189}$.

inclusive. The (*p,pxn*) and (*p,2pxn*) reactions show excitation functions which increase rapidly above the threshold. Some reach a maximum value and decrease only slowly with increasing energy, while others increase monotonically to the highest bombarding energy available in the McGill synchrocyclotron. At these energies the yields of (*p,pxn*) and (*p,xn*) products are roughly equal, while those formed by (*p,2pxn*) reactions have yields roughly an order of magnitude lower. At an energy corresponding to a peak in a (*p,xn*) excitation function the yield is many times higher than that corresponding to the isobar formed by the corresponding (*p,pxn*) reaction. For example, at a bombarding energy of 38 Mev, $\sigma_{Pt^{188}}/\sigma_{Ir^{188}} \approx 30$, as shown in Fig. 4.

Can. J. Chem. Downloaded from www.nrcresearchpress.com by 210.87.254.42 on 09/05/12
For personal use only.

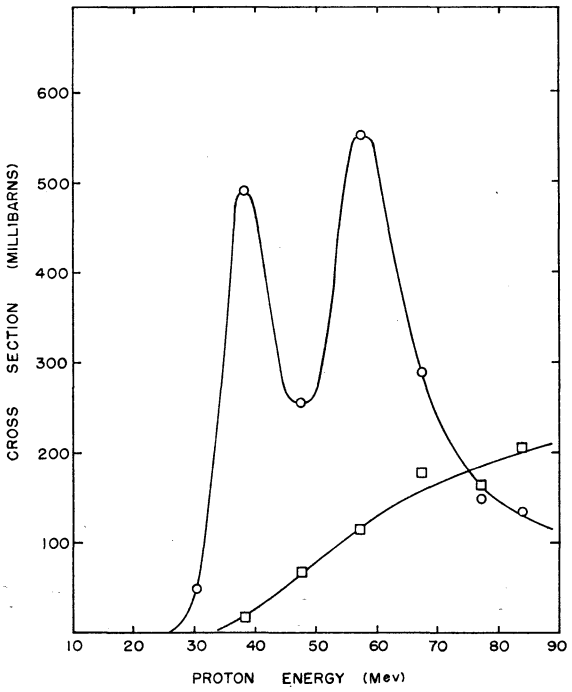

FIG. 4. Excitation functions for the production of Pt^{188} and Ir^{188}: ○ Pt^{188}; □ Ir^{188}.

The (p,xn) excitation functions show the characteristics of the two main mechanisms by which nuclear reactions in this energy range are thought to proceed. Compound nucleus formation accounts for the rapid rise above the threshold to a maximum yield followed by a rapid decrease in yield as other reactions begin to compete. However, the yields do not fall to negligible values at higher energies, showing that the knock-on reactions are making a contribution.

Even though iridium is not monoisotopic, it has been possible to compare the results of the $Ir^{191}(p,n)Pt^{191}$, $Ir^{193}(p,3n)Pt^{191}$, and $Ir^{191}(p,4n)Pt^{188}$ reactions with the model for (p,xn) reactions suggested by Jackson (33). Jackson made the assumptions that neutron emission occurred whenever energetically possible, proton evaporation was neglected, and the evaporated neutron energy spectrum was proportional to $E \exp(-E/T)$, where E is the excitation energy and T the nuclear temperature, which is taken to be constant. The cross section for a particular reaction is then given by

$$\sigma_{(p,xn)} = \sigma_c(E_0)[I(\Delta_x,2x-3) - I(\Delta_{x+1},2x-1)],$$

where

$$\Delta_x = (E - \textstyle\sum_i^x B_i)/T.$$

The term $\sigma_c(E_0)$ is the cross section for compound nucleus formation which, for our calculations, was taken from Shapiro's (34) tabulations, using a nuclear radius $r = 1.3\times10^{-13}A^{1/3}$. The term in the square brackets is the difference of two Pearson incomplete gamma functions, giving the probability for the emission of exactly x neutrons. The individual neutron binding energies, B_i, were taken from Cameron's tables (25) and a constant nuclear temperature of 1.8 Mev was used.

Can. J. Chem. Downloaded from www.nrcresearchpress.com by 210.87.254.42 on 09/05/12
For personal use only.

The calculated excitation functions for (p,n), $(p,3n)$, and $(p,4n)$ reactions on an iridium target are shown by the solid curves in Fig. 5. In order to compare some experimental yields with those predicted by the model, it was necessary to make certain assumptions.

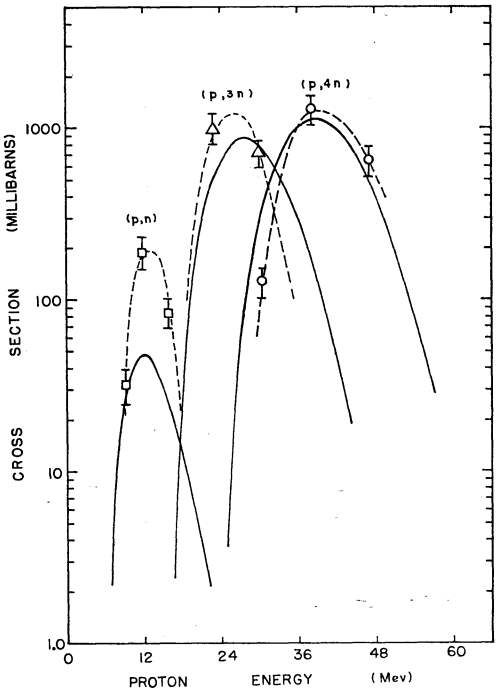

FIG. 5. Comparison of experimental excitation functions with those predicted from the Jackson model: - - - experimental; — theoretical.

In the production of Pt^{188} it has been assumed that below ~50 Mev proton energy a $(p,6n)$ reaction on Ir^{193} is negligible compared to a $(p,4n)$ reaction on Ir^{191}, and the measured cross sections below ~50 Mev were corrected for isotopic abundance of the target. Similarly, in the production of Pt^{191} we have corrected our results for the isotopic abundance of Ir^{191} and assumed the $Ir^{191}(p,n)Pt^{191}$ reaction to be predominant below ~17 Mev proton energy and the $Ir^{193}(p,3n)Pt^{191}$ reaction to be predominant above this energy.

There is fair agreement between the experimental and predicted cross sections. Use of a larger nuclear radius at low bombarding energies, as suggested by Bell and Skarsgard (1), would give better agreement with the experimental results.

In Fig. 6 is shown the excitation functions for the two Ir^{190} isomers which are formed independently. The ground state, which is the low-spin isomer in this case, is preferred in the reaction.

In this work Ir^{192} is formed by a (p,pn) reaction on Ir^{193}. The excitation function is shown in Fig. 7. The experimental cross section for this reaction was compared with that predicted from the Monte Carlo data* of Metropolis *et al.* (35) at a proton energy or 82 Mev on Bi^{209}, by combining with them the contribution from nuclear evaporation af was done by Yule and Turkevich (36). The experimental cross section was about fous times higher than that predicted by theory. A similar discrepancy has been found by other workers (35, 36, 37).

**We wish to express our appreciation to Dr. G. Friedlander, who kindly made the cascade calculations available to us.*

Can. J. Chem. Downloaded from www.nrcresearchpress.com by 210.87.254.42 on 09/05/12
For personal use only.

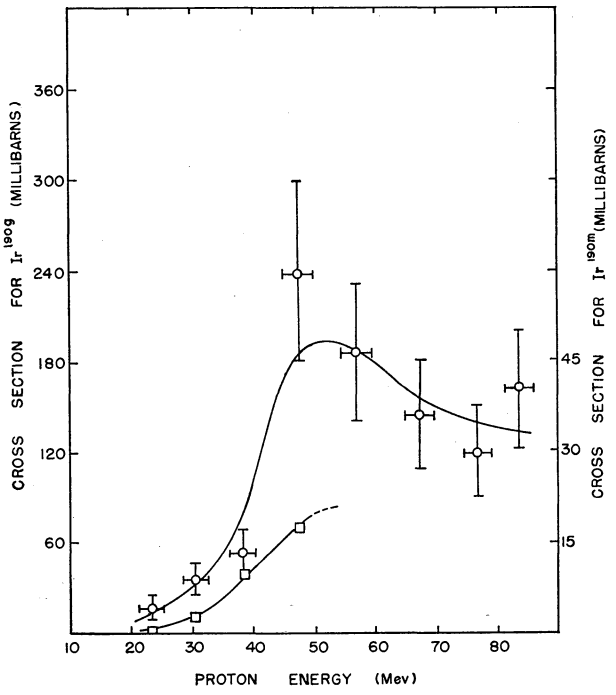

FIG. 6. Excitation functions for the production of Ir^{190g} and Ir^{190m}: ○ Ir^{190g}; □ Ir^{190m}.

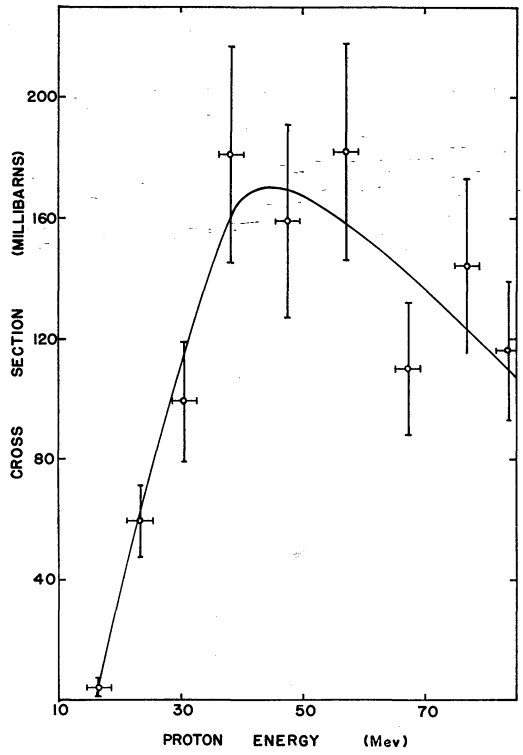

FIG. 7. Excitation function for the reaction $Ir^{193}(p,pn)Ir^{192}$.

Can. J. Chem. Downloaded from www.nrcresearchpress.com by 210.87.254.42 on 09/05/12
For personal use only.

REFERENCES

1. R. E. Bell and H. M. Skarsgard. Can. J. Phys. **34**, 745 (1956).
2. W. J. Rambler, J. Wing, D. J. Henderson, and J. R. Huizenga. Phys. Rev. **114**, 154 (1959).
3. M. Gusakow, Y. Tegoux, and R. Sergolle. Compt. Rend. **251**, 70 (1960).
4. L. R. Chervu. To be published.
5. S. N. Ghoshal. Phys. Rev. **80**, 939 (1950).
6. B. Linder and R. A. James. Phys. Rev. **114**, 322 (1959).
7. H. A. Howe. Phys. Rev. **109**, 2083 (1958).
8. J. W. Meadows. Phys. Rev. **91**, 885 (1953).
9. E. Wichers, W. G. Schlecht, and C. L. Gordon. J. Res. Natl. Bur. Std. **33**, 363 (1944).
10. R. Gilchrist and E. Wichers. J. Am. Chem. Soc. **57**, 2565 (1935).
11. E. B. Sandell. Colorimetric determination of traces of metals. 3rd ed. New York. 1959.
12. R. F. Wilson and L. J. Baye. Talanta, **1**, 351 (1958).
13. K. A. Kraus and F. Nelson. Proc. Intern. Conf. Peaceful Uses At. Energy, Geneva, 1955, **7**, 113 (1955).
14. K. A. Kraus and G. E. Moore. J. Am. Chem. Soc. **75**, 1460 (1953).
15. S. S. Berman and W. A. E. McBryde. Can. J. Chem. **36**, 835 (1958).
16. F. J. Welcher. The analytical uses of ethylenediaminetetracetic acid. Princeton, N.J. 1958.
17. T. D. Price and R. E. Telford. National Nuclear Energy Series. Div. VIII, Vol. 1. McGraw-Hill Book Co., Inc. New York. 1950. p. 408.
18. W. A. E. McBryde and M. L. Cluett. Can. J. Res. B, **28**, 788 (1950).
19. W. M. MacNevin and O. H. Kriege. Anal. Chem. **28**, 16 (1956).
20. G. Andersson and R. Ringh. Arkiv Fysik, **18**, 385 (1961).
21. G. Albouy, M. M. Gusakow, and N. Poffe. J. Phys. Radium, **21**, 751 (1960).
22. B. Harmatz, T. H. Handley, and J. W. Mihelich. Phys. Rev. **128**, 1186 (1962).
23. Nuclear Data Sheets. National Academy of Sciences, National Research Council (U.S. Government Printing Office, Washington, D.C.).
24. T. V. Malysheva, B. A. Khotin, A. K. Lavrukhina, L. N. Kryukova, and V. V. Muraveva. Izv. Akad. Nauk SSSR, Ser. Fiz. **24**, 1109 (1960).
25. A. G. W. Cameron. At. Energy Canada Ltd. Rept. CRP-690. 1957.
26. J. Kastner. Can. J. Phys. **29**, 480 (1951).
27. W. G. Smith and J. M. Hollander. Phys. Rev. **98**, 1258 (1955).
28. J. K. Lerohl. Dissertation Abstr. **23**, 661 (1962).
29. R. M. Diamond and J. M. Hollander. Nucl. Phys. **8**, 143 (1958).
30. R. M. Diamond, J. M. Hollander, D. J. Horen, and R. A. Naumann. Nucl. Phys. **25**, 248 (1961).
31. N. A. Bonch-Osmolovskaya, K. Ya. Gromov, B. S. Dzhelepov, O. E. Kraft, T. S. Malysheva, L. N. Nikitguk, B. A. Khotin, Chzhou Yue-Va, and V. G. Chumin. Izv. Akad. Nauk SSSR, Ser. Fiz. **26**, 975 (1962).
32. B. Harmatz, T. H. Handley, and J. W. Mihelich. Phys. Rev. **119**, 1345 (1960).
33. J. D. Jackson. Can. J. Phys. **34**, 767 (1956).
34. M. M. Shapiro. Phys. Rev. **90**, 171 (1953).
35. N. Metropolis, R. Bivins, M. Storm, A. Turkevich, J. M. Miller, and G. Friedlander. Phys. Rev. **110**, 185 (1958).
36. H. P. Yule and A. Turkevich. Phys. Rev. **118**, 1591 (1960).
37. S. S. Markowitz, F. S. Rowland, and G. Friedlander. Phys. Rev. **112**, 1295 (1958).

Can. J. Chem. Downloaded from www.nrcresearchpress.com by 210.87.254.42 on 09/05/12
For personal use only.

REACTIONS PRODUCED ON ERBIUM BY PROTONS OF ENERGIES BETWEEN 6 AND 87 MEV[1]

G. V. S. RAYUDU[2] AND L. YAFFE
Radiochemistry Laboratory, Department of Chemistry, McGill University, Montreal, Que.
Received May 17, 1963

ABSTRACT

Erbium was bombarded with protons of energies varying between 6 and 87 Mev. Nuclear characteristics and excitation functions were studied for isotopes of Tm, Er, Ho, and Dy, formed by various (p,xn) and $(p,xpxn)$ reactions. Bombardment of enriched Er isotopes helped elucidate some of the excitation functions. A comparison has been made of the experimental (p,xn) cross sections with those predicted by the Jackson model and reasonable agreement has been found. Holmium was bombarded with α-particles to produce the compound nucleus Tm^{169*} and the ratios $\sigma(p,n):\sigma(p,2n) = \sigma(\alpha,n):\sigma(\alpha,2n)$ were found to hold.

The aim of the present study was twofold. First, it was desired to bombard a medium heavy element with protons of energies in the region where the compound nucleus type of reaction begins to be replaced by a direct nucleon–nucleon type of interaction characteristic of higher-energy processes. Secondly, the development of rapid ion exchange processes for lanthanide separations and the recent availability of isotopically enriched lanthanides would enable the characterization of the nuclear properties of known and new radioactive nuclides in this region.

EXPERIMENTAL

(a) Targets

The targets were a mixture of 'spec-pure' erbium oxide and copper oxide which had been obtained from Johnson, Matthey and Co. The reactions $Cu^{63}(p,n)Zn^{63}$ and $Cu^{65}(p,pn)Cu^{64}$ were used to monitor the proton beam at energies below and above 13 Mev respectively. The cross sections used are those of Meadows (1), and are shown in Table I. Isotopically enriched erbium oxide was used in some of the later bombardments

TABLE I

Monitor cross-section values used

Proton energy (Mev)	$\sigma_{Zn^{63}}$ (millibarn)	$\sigma_{Cu^{64}}$ (millibarn)	Proton energy (Mev)	$\sigma_{Cu^{64}}$ (millibarn)
6	200		40	320
10	380		47	280
13	400		57	250
16		150	67	230
22		480	77	210
28		500	87	180
34		360		

to verify isotopic assignments and to clarify the assignment of excitation functions. The target and monitor were mixed mechanically. At low energies (6, 10, and 13 Mev) an atom ratio of erbium to copper of 1:1 was used, while at higher energies the atom ratio was 1:2. About 10 to 15 mg of powdered mixture was placed in a thin aluminum tube which was fastened to the probe, inserted to intercept the circulating beam of the McGill proton synchrocyclotron. Targets were irradiated for periods ranging from 15 minutes to 2 hours. The uncertainty in proton energy, due to the spread of the beam was ± 2 Mev. Slight corrections ($\sim$0.5 Mev) were made to the three lowest energy values used to correct for beam attenuation due to the sample.

[1]*This work received financial assistance from the National Research Council of Canada.*
[2]*Present address: Department of Chemistry, Carnegie Institute of Technology, Schenley Park, Pittsburgh, Pennsylvania, U.S.A. Holder of National Research Council Studentship 1960–1961.*

Can. J. Chem. Downloaded from www.nrcresearchpress.com by 210.87.254.5 on 09/05/12
For personal use only.

Several irradiations* were made with alpha particles in order to study Ho(α,xn) reactions. The targets of holmium oxide were prepared by a method developed by Dodson *et al.* (2). A known amount of holmium oxide (>99.9% pure) was dissolved in concentrated nitric acid, evaporated almost to dryness, and the holmium nitrate dissolved in a 1% zapon solution (0.4 cc zapon, obtained from Glidden Paint Co., Ohio, as syrup of aquanite, 6 cc ethyl acetate, and 28 cc of 95% ethanol). The concentration of holmium in this mixture was 6 mg/cc. A piece of aluminum foil, 6.69 mg/cm², carefully flattened, was used as the target backing. The foil was placed on a glass plate which was put on the turntable of a record player. A quantity of the mixture was painted on to the foil with a fine camel hair brush while the foil was rotating. The mixture was air-dried and then the aluminum foil dropped onto the surface of a hot plate (400° C). This process was repeated several times, the surface of the foil being carefully smoothed with lens paper and by ironing after each application. With practice, very uniform targets would be prepared in this way. Circular targets were punched out of the foil and affixed to the target holder with sufficient aluminum absorbers (3) to degrade the energy to the required values. The α-particle energy of the Cyclotron was 39.8±0.5 Mev. The integrated current was measured by a Faraday cup. Seven targets were irradiated simultaneously by the stacked-foil technique.

(b) Chemical Separations

No chemical separations were necessary for the targets irradiated at low proton energies (6–13 Mev inclusive) since the activities were readily separable by the use of a multichannel analyzer as described later. The target mixture was dissolved in concentrated hydrochloric acid, made up to a known volume, and an aliquot taken for activity measurements.

At higher proton energies the target was dissolved in a minimum amount of concentrated hydrochloric acid and then transferred to the top of a column containing Dowex 1×8 (100 mesh) anion exchange resin which had been preconditioned with concentrated hydrochloric acid. The separation was based on the work of Kraus and Moore (4). The lanthanides and nickel were eluted with concentrated hydrochloric acid, leaving copper and any other spallation products on the column. Manganese and cobalt were eluted with 4 *M* hydrochloric acid, and copper with 1.5 *M* hydrochloric acid. The copper was made up to volume and an aliquot taken for activity measurements.

To the concentrated hydrochloric acid eluate about 2 mg of nickel was added as holdback carrier, and the lanthanides were precipitated as hydroxides by the addition of 6 *M* ammonium hydroxide, leaving the nickel in solution. The combined hydroxides were washed, dissolved in hydrochloric acid, and made up to volume.

From this stock solution an aliquot was taken for activity measurements. To a further aliquot known amounts (~4 mg) of Tm, Ho, Dy, and Tb were added and this mixture, after repeated evaporation with 0.06 *M* hydrochloric acid, was carefully pipetted onto the top of a heated (87° C) column (5) of 400 mesh 12% cross-linked Dowex 50 cation exchange resin. It was found empirically that the addition of a small amount of Na^+ ion helped improve the separation of Tm and Er, so that a small amount (~0.5 mg) was added with the loading mixture. The resin had been carefully graded and preconditioned by repeated treatment with 6 *M* ammonium hydroxide, hot distilled water, hydrochloric acid, and finally stored as the ammonium form in degassed distilled water. The elutriant solution used was 0.2 *M* α-hydroxyisobutyric acid at pH = 4.1. The commercial grade of the acid was purified by repeated recrystallization from ether. The flow rate was 0.6 ml/min, and the entire separation was concluded in 70 minutes. The fractions were collected into centrifuge cones, those which were known to contain a particular element combined, the lanthanide precipitated as the hydroxide, washed, dissolved in dilute hydrochloric acid, and made to volume from which aliquots were taken for activity measurements.

No chemical separations were done on the holmium targets which had been bombarded by α-particles. The targets were separated, dissolved in 0.1 ml hydrogen peroxide and 0.5 ml concentrated hydrochloric acid, and made up to a known volume from which aliquots were taken for activity measurements.

(c) Chemical Yield Determinations

Chemical yields were determined by means of standard spectrophotometric methods. Copper was determined by means of diethyldithiocarbamate (6) and the lanthanides with Alizarin Red-S (7).

(d) Activity Measurements

Gamma-ray measurements were made using a 3 in. × 3 in. sodium iodide thallium-activated scintillation detector coupled to a 100-channel pulse-height analyzer. The energy scale was calibrated by the use of well-known γ-emitters and the geometrical efficiency in the various positions was obtained by using sources of known disintegration rate calibrated by a 4π β-proportional counter. Beta radiation was measured by a 2π-flow proportional counter.

RESULTS

(a) Radiation Characteristics

The nuclides observed and their radiation characteristics observed are discussed below.

We are grateful to Dr. J. Hudis for arranging these irradiations with the Brookhaven Cyclotron.

Can. J. Chem. Downloaded from www.nrcresearchpress.com by 210.87.254.5 on 09/05/12
For personal use only.

(i) Tm^{170}

Tm^{170}, produced by the reaction $Er^{170}(p,n)$, was found only in small amounts due to its long half-life. The decay of the 80 kev γ-ray was followed after subtracting the contribution due to 86-day Tm^{168}. The latter was produced by a $(p,3n)$ reaction on natural erbium at 30 Mev, where the (p,n) reaction cross section to produce Tm^{170} is negligibly small and products formed from reactions on other erbium isotopes are relatively short-lived. A half-life of 128 ± 10 days, measured over two half-lives, was observed, in good agreement with the values of Bonner *et al.* (8), Caldwell (9), and Ketelle (10), who obtained values of 125, 120, and 129 days respectively.

(ii) Tm^{168}

Tm^{168} was produced by the reactions $Er^{168}(p,n)Tm^{168}$ and $Er^{170}(p,3n)Tm^{168}$, and $Ho^{165}(\alpha,n)$. Gamma rays at 80, 100, 200, 270, 490, 750, 800, 1280, and 1450 kev were observed. The γ-ray energies are in accord with those measured by Kochevanov *et al.* (11) and Jacob *et al.* (12). The decay curve of the 200 kev γ-ray was followed over a period of five half-lives and gave a value of 86 ± 3 days, in good agreement with that of Wilkinson and Hicks (13), and Handley and Olson (14), who obtained values of 85 and 87 days respectively, but lower than the value of 93 days obtained by Bonner *et al.* (8).

(iii) Tm^{167}

Tm^{167} was produced by the reactions $Er^{167}(p,n)$, $Er^{168}(p,2n)$, $Er^{170}(p,4n)$, and $Ho^{165}(\alpha,2n)$. Gamma rays of energies 110, 200, 510, and 710 kev, as well as a K X-ray, were found attributable to Tm^{167}. The 200-kev X-ray was followed over a period of six half-lives to give a value of 9.6 ± 0.2 day half-life. The half-life is in good agreement with the values of Wilkinson and Hicks (13), Handley and Olson (14), and Bonner *et al.* (8), while the observed gamma peaks are in accord with those found by Narasimhaih and Pool (15).

(iv) Tm^{166}

Tm^{166} was produced by the reactions $Er^{177}(p,n)$, $Er^{167}(p,2n)$, $Er^{168}(p,3n)$, and $Er^{170}(p,5n)$. The γ-ray peaks observed at 10, 180, 800, 790, 1200, 1850, and 2050 kev agree with those published recently by Pool and Wilson (16). The decay of the 2050 kev photopeak was followed for eight half-lives and gave a value of 7.7 ± 0.1 hr, in agreement with the value of Wilkinson and Hicks (13), Michel and Templeton (17), and Wilson and Pool (16).

(v) Tm^{165}

Tm^{165} was produced by the reactions $Er^{166}(p,2n)$, $Er^{167}(p,3n)$, $Er^{168}(p,4n)$, and $Er^{170}(p,6n)$. Photopeaks were observed at 220, 300, 830, 1160, and 1380 kev, in agreement with the work of Handley and Olson (18), and Gorodinskii *et al.* (19). The half-life determined in the present work by observation of the 1160 kev photopeak over a period of six half-lives was found to be 28 ± 1.5 hr compared with values of 24.5 and 29 hr obtained by Handley and Olson, and Gorodinskii *et al.* respectively. Gamma rays at 200, 800, 1160, and 1400 kev were observed.

(vi) Tm^{164}

When this work was begun, this isotope of thulium was unknown. Tm^{164} was identified by irradiations of naturally occurring erbium and of erbium enriched in mass 164. Irradiations were of the order of 2 minutes with 7 Mev protons, and the decay of the X-ray was followed immediately without chemical separation. A half-life of 1.8 ± 0.1 min was assigned to Tm^{164}. This is in very good agreement with that found recently by Wilson and Pool (20). The existence of this isotope was also confirmed by Abdurazakov *et al.* (21), who established the existence of the decay chain

$$Yb^{164} \xrightarrow{75\text{ min}} Tm^{164} \xrightarrow{2\text{ min}} Er^{164}.$$

Can. J. Chem. Downloaded from www.nrcresearchpress.com by 210.87.254.5 on 09/05/12
For personal use only.

(vii) Tm^{163}

Tm^{163} was produced by the reaction $Er^{164}(p,2n)$ with natural erbium and erbium enriched in mass 164. The decay of the 110-kev γ-ray gave a half-life of 1.8±0.1 hr, followed over a period of four half-lives. This agrees well with the values of Harmatz *et al.* (22), who established the existence of the decay chain

$$Tm^{163} \xrightarrow{2\text{ hr}} Er^{163} \xrightarrow{75\text{ min}} Ho^{163} \xrightarrow{0.8\text{ sec}} Dy^{163},$$

and Bjørnholm *et al.* (23), who recently obtained a value of 1.8±0.1 hr.

(viii) Tm^{162}

Tm^{162} was unknown when this work commenced. Erbium, enriched in mass 162, was bombarded with 7 Mev protons for about 2 hours. The *K* X-ray curve was resolved into three components with half-lives 90±10 min; 7.7 hr, Tm^{166}; and 9.6 days, Tm^{167}. The first component has been attributed to Tm^{162}. Pool and Wilson (20) recently reported a half-life of 77 min obtained by irradiating erbium, enriched in Er^{162}, with 6 Mev protons.

(ix) Tm^{161}

This isotope was produced by a 20 Mev proton irradiation of erbium enriched in Er^{162}. The presence of Er^{161} (3.1 hr) in a separated thulium fraction indicated a half-life of 20–30 min for Tm^{161}, although the initial growth of the Er^{161} daughter was obscured by the other activities present.

(x) Er^{169}

Er^{169} was produced by the reaction $Er^{170}(p,pn)$. The half-life was obtained by following the decay of the β^--activity. A half-life of 9.0±0.1 days, measured over six half-lives, was obtained, in agreement with that of Butement's (24) value of 9 days but slightly lower than the values of Ketelle and Peacock (25) and Pavlotskaia and Lavrukhina (26) of 9.4 and 9.5 days respectively.

(xi) Er^{165}

Er^{165} was produced by the reactions $Er^{166}(p,pn)$, $Er^{167}(p,p2n)$, $Er^{168}(p,p3n)$, and $Er^{170}(p,p5n)$, and by decay from the parent Tm^{165}. The half-life was determined accurately by an auxiliary radiation to get the $Ho^{165}(p,n)$ reaction. This produced pure Er^{165}. The decay of the *K* X-ray was followed for 10 half-lives, giving a half-life of 10.4±0.1 hr, in good agreement with 10.5 hr by Grigorev *et al.* (27). In agreement with several other authors (28), no gamma rays ascribable to Er^{165} were found.

(xii) Er^{161}

Er^{161} was produced by (p,pxn) reactions on all the erbium isotopes and by decay of Tm^{161} (*vide supra*). Photopeaks were found at 200, 300, 820, 1160, 1400, 1700, and 2000 kev. The decay of the activity of the 820 kev photopeak was followed for six half-lives, giving a half-life of 3.1±0.1 hr for Er^{161}, in very good agreement with 3.01 hr by Nervik and Seaborg (29) but lower than the values given by Handley and Olson (30) and Michel and Templeton (17) of 3.6 and 3.5 hr repectively.

(xiii) Er^{160}

Er^{160} was produced by (p,pxn) reactions on all the erbium isotopes and by decay of short-lived Tm^{160}. A half-life of 29.5±0.5 hr was obtained by following the decay of the activity of the *K* X-ray, in good agreement with previously determined values (28).

(xiv) Ho^{161}

Ho^{161} was produced by $(p,xpxn)$ reactions on all the erbium isotopes and by decay of Er^{161}. The half-life obtained from the decay curve of the *K* X-ray was 2.5±0.2 hr, measured over four half-lives, in good agreement with previous values (28).

Can. J. Chem. Downloaded from www.nrcresearchpress.com by 210.87.254.5 on 09/05/12
For personal use only.

Can. J. Chem. Downloaded from www.nrcresearchpress.com by 210.87.254.5 on 09/05/12
For personal use only.

TABLE II

Radiation characteristics used*

Nuclide	Half-life	Radiation measured	Branching ratio	$1+\alpha_T$	Fluorescence yield	K X-ray per disintegration
Tm^{170}	128 days	0.084 Mev γ	0.24	5.6 (31)		
Tm^{168}	86 days	0.200 Mev γ	0.81	1.21		
Tm^{167}	9.6 days	0.200 Mev γ (15)	0.98	2.67 (32)		
Tm^{166}	7.7 hr	2.05 Mev γ	1.00 (assumed)	1.00 (assumed)		
Tm^{165}	28 hr	1.16 Mev γ	1.00 (assumed)	1.00 (assumed)		
Tm^{163}	1.8 hr	0.105 Mev γ	1.00 (assumed)	1.00 (assumed)		
Er^{169}	9 days	0.34 Mev β^-	1.00	—		
Er^{165}	10.4 hr	X-Ray	—	—	0.97	2.2
Er^{161}	3.1 hr	0.820 Mev γ	0.56	1.00 (33)		
Er^{160}	29.5 hr	X-Ray	—	—	0.97	0.82
Ho^{161}	2.5 hr	X-Ray	—	—	0.96	1.33
Ho^{160m}	5 hr	X-Ray	—	—	0.96	0.82
Dy^{159}	138 days	X-Ray	—	—	0.95	1.35
Dy^{157}	8.2 hr	0.32 Mev γ	1.00	1.00 (34)		

*Unless stated otherwise, data have been taken from present work and Nuclear Data Sheets.

Can. J. Chem. Downloaded from www.nrcresearchpress.com by 210.87.254.5 on 09/05/12
For personal use only.

TABLE III

Formation cross sections for nuclides formed in proton bombardments

Nuclide	Proton energy (Mev): 6	10	13	16	22	28	34	40	47	57	67	77	87	Type of yield	Error (%)
	σ (millibarn)														
Tm^{170}		95	170	24										I	±20
Tm^{168}		71	120	24	520	620	260							I	±15
Tm^{167}		57	180	1200	680	380	430	510	160	110	94	59	48	I	±15
Tm^{166}	0.3	9.3	25	95	99	98	54	36	47	21	22	13	13	I*	±15
Tm^{165}				1.5	1.2	8.4	8.0	9.7	6.0	3.3				I*	±15
Tm^{163}							1.6	23	29	41	34	17	0.4	I*	±15
Er^{169}				3.6	4.3	5.9	29	46	69	120	110	89	62	I	±10
Er^{165}					1.5		50	41	120	190	390	230	230	I	±15
Er^{161}							8.5		17	120	400	300	260	C	±15
Er^{160}										42	80	190	240	I	±15
Ho^{161}										45	93		80	I	±20
Ho^{160m}										3.8	17	17	25	I	±20
Dy^{159}											5.2	33	33	C	±20
Dy^{157}											1.7	5.3	7.1	C	±20
Tm^{167*}				550	1700	4.0	120							I	±20

NOTE: I = independent yield; I* = lower limit for independent yield (branching ratio assumed to be 1.00); C = cumulative yield. Tm^{167*}—obtained on the basis of enriched isotope experiments.

(xv) Ho^{160m}

Ho^{160m} was produced by (*p*,*xpxn*) reactions on all the erbium isotopes and by decay of Er^{160}. Photopeaks were observed at 87, 190, 650, 730, 890, and 970 kev. The decay of the *K* X-ray activity gave a half-life of 5±0.2 hr, measured over a period of five half-lives, in good agreement with previous values (28).

(xvi) Dy^{159}

Dy^{159} was produced in very low yield both by (*p*,*xpxn*) reactions on the erbium isotopes and by decay of Ho^{159}. The decay of the *K* X-ray activity gave a half-life of 138±5 days, measured over two half-lives, in reasonable agreement with previous values (28).

(xvii) Dy^{157}

Dy^{157} was produced by (*p*,*xpxn*) reactions on the lighter erbium isotopes as well as by decay of Ho^{157} (unknown). The half-life, found by following the decay of the 320 kev photopeak, of 8.2±0.2 hr, measured over six half-lives, is in good agreement with previous work (28).

(b) Formation Cross Sections

The radioactive characteristics used in determining the formation cross sections for the spallation products are given in Table II, and the cross sections found for the various proton bombardments are shown in Table III. In Table IV are given the formation cross sections determined in the α-bombardments.

TABLE IV

Cross sections for the reactions $Ho^{165}(\alpha,n)Tm^{168}$ and $Ho^{165}(\alpha,2n)Tm^{167}$

	Energy (Mev):						
	15	20	25	30	35	39	Error (%)
	σ(millibarn)						
(α,*n*)	6.8	39	5.6				±15
(α,2*n*)		25	480	450	110	60	±15

In general, the formation cross sections were calculated by means of the following equation:

$$\sigma_p = \sigma_m \cdot \frac{D_p^0}{D_m^0} \cdot \frac{W_{Cu}}{W_{Er}} \cdot \frac{A_{Er}}{A_{Cu}} \cdot \frac{(1-e^{-\lambda_m t})}{(1-e^{-\lambda_p t})},$$

where the subscripts p and m refer to the product and monitor respectively, and σ = cross section, D^0 = disintegration rate at end of bombardment, W_{Cu} = weight of copper monitor, W_{Er} = weight of erbium target, A_{Er}/A_{Cu} = ratio of atomic weight of erbium to copper, λ = disintegration constant, t = time of bombardment.

In the cross-section calculations of Tm^{166}, Tm^{165}, Tm^{163}, Er^{165}, Er^{163}, Er^{160}, Ho^{161}, Ho^{116m}, Dy^{159}, and Dy^{157}, the total weight of erbium recovered has been assumed to be W_{Er}. In the case of the Tm^{170} and Er^{169} calculations, the natural isotopic abundance of Er^{170} was used (14.9%) since these nuclides could be produced only by reactions on Er^{170}. For the production of Tm^{168}, the isotopic abundance of Er^{168} (29.1%) was taken as the target weight for the reactions with protons up to 16 Mev in energy, since only the (*p*,*n*) reaction was contributing. For the proton energies between 16 and 34 Mev, the target weight was considered to be that due only to Tm^{170}, since now only the (*p*,3*n*) reaction was contributing. In the Tm^{167} calculations, the weight of target has been arbitrarily taken as

Can. J. Chem. Downloaded from www.nrcresearchpress.com by 210.87.254.5 on 09/05/12
For personal use only.

66.9% of the erbium used, since only Er^{170}, Er^{168}, and Er^{177} can contribute to the production of Tm^{167}. However, two irradiations were made on erbium enriched in mass 168 at proton energies of 22 and 28 Mev. It was assumed that the Er^{167} (p,n) would not contribute at these energies and that any contribution from Er^{170} (1.5% abundance in this target) would be negligible. The weight of Er^{168} was taken as the target weight in these two experiments. Data for this $(p,2n)$ reaction at 16 and 34 Mev were obtained by solving two simultaneous equations obtained from the irradiation of natural erbium and erbium enriched in mass 168. The results are shown in the last line of Table III.

In the case of the alpha radiations, the same equation as above was used with the appropriate values for holmium inserted. Holmium is monoisotopic, so that there is no question as to what weight to use in the calculations.

The errors quoted in Tables III and IV are the standard deviations obtained by compounding the errors involved in the individual terms used to calculate the cross sections. No estimate of error in the monitor cross section is included.

DISCUSSION

The excitation functions for the (p,xn) reactions follow, at low energies, the behavior predicted by the compound nucleus theory. Several of these are shown in Figs. 1–3

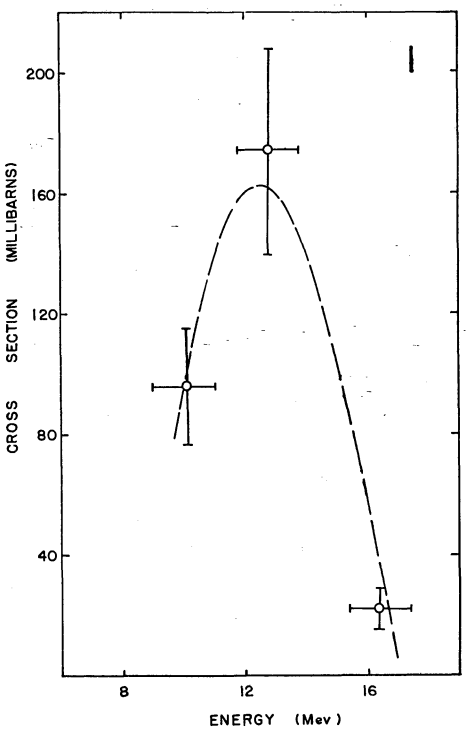

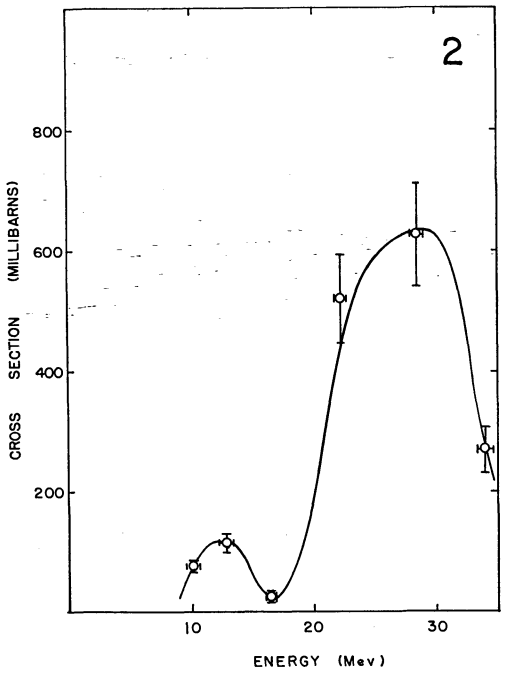

FIG. 1. Excitation function for the $Er^{170}(p,n)Tm^{170}$ reaction.
FIG. 2. Excitation functions for the $Er^{168}(p,n)Tm^{168}$ and $Er^{170}(p,3n)Tm^{168}$ reactions.

inclusive. Elucidation is made easier by virtue of the fact that Er^{168} and Er^{170} are stable and will contribute to (p,xn) reactions, but Er^{169} which is unstable will not, thus leaving a gap. The (p,pxn) reactions do not fall to zero, but show signs of levelling off. A typical

Can. J. Chem. Downloaded from www.nrcresearchpress.com by 210.87.254.5 on 09/05/12
For personal use only.

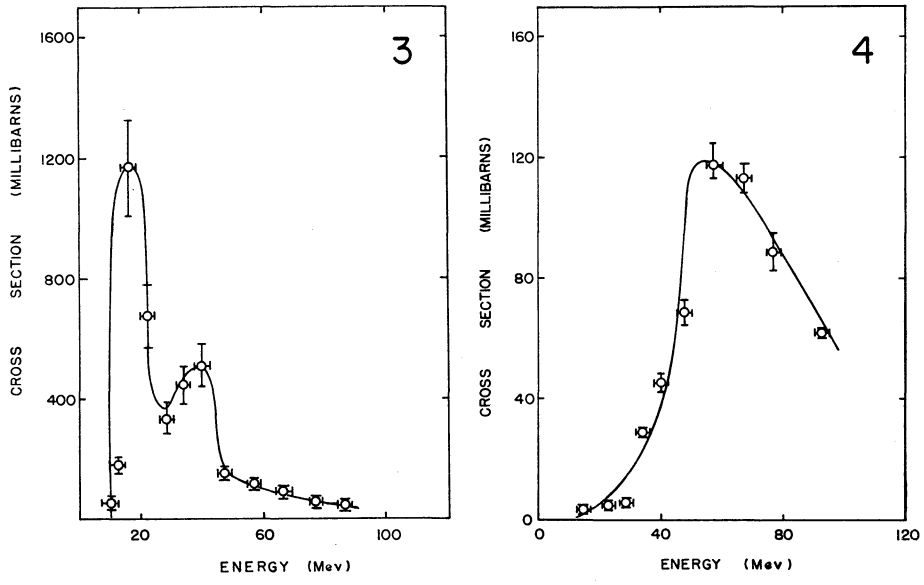

FIG. 3. Excitation functions for the $Er^{167}(p,n)Tm^{167}$, $Er^{168}(p,2n)Tm^{167}$, and $Er^{170}(p,4n)Tm^{167}$ reactions.
FIG. 4. Excitation function for the $Er^{170}(p,pn)Er^{169}$ reaction.

curve is that for the $Er^{170}(p,pn)Er^{169}$ reaction given in Fig. 4, showing that at higher energies the knock-on process is now contributing.

The cross sections of $(p,2pxn)$ reactions were found to be an order of magnitude lower than those of the corresponding (p,pxn) reactions. The former increased monotonically with energy, since it was not possible to reach the curve maxima with the cyclotron energies available.

The multi-isotopic nature of the erbium target limits the possibilities of comparison of experimentally and theoretically determined cross sections. A limited comparison can be made, however, for the reactions $Er^{170}(p,n)Tm^{170}$, $Er^{168}(p,n)Tm^{168}$, $Er^{168}(p,2n)Tm^{167}$, and $Er^{170}(p,3n)Tm^{168}$ with the theoretical (p,xn) calculations of Jackson (35). Jackson combined the Monte Carlo results of McManus *et al.* (36) for the nuclear cascade with a simplified evaporation theory in order to calculate formation cross sections. Jackson showed that the probability that a nucleus with initial excitation energy E will evaporate x neutrons is given by:

$$P(E,x) = I(\Delta_x,2x-3)-I(\Delta_{x+1},2x-1),$$

where the values of I are obtained from Pearson's incomplete gamma functions (37). The term

$$\Delta_x = \left(E - \sum_i^x B_i\right) \Big/ T,$$

where B_i is the binding energy of the ith neutron and T is the nuclear temperature. The average binding energy of the neutrons in this region was taken from Cameron's (38) tables to be 7.4 Mev. An approximate nuclear temperature, T, was calculated from the expression

$$\Delta E = \bar{B}+2T,$$

where ΔE represents the energy separation in Mev between successive peaks of (p,xn)

Can. J. Chem. Downloaded from www.nrcresearchpress.com by 210.87.254.5 on 09/05/12
For personal use only.

excitation functions (~13 Mev for $Z = 69$) and the average binding energy per nucleon, $\bar{B}$, was taken as 8.2 Mev, giving $T = 2.4$ Mev.

In the range of bombarding energies where all the interactions of the bombarding particle with the target nucleus involve the initial formation of a compound nucleus followed by neutron evaporation, the formation cross sections can be given by simple functions of the type

$$\sigma(p,xn) = \sigma_c(E_0)P(E,x),$$

where $\sigma_c(E_0)$ is the cross section for compound nucleus formation at incident energy E_0. The values of $\sigma_c(E_0)$ have been taken from Shapiro (39). His curve has been extrapolated to 50 Mev and a nuclear radius $R = 1.3\times10^{-13}A^{1/3}$ cm has been used.

The comparison between the experimental (broken) curves and the calculated (solid) curves is shown in Fig. 5. The measured cross sections for the reaction $Er^{168}(p,n)Tm^{168}$

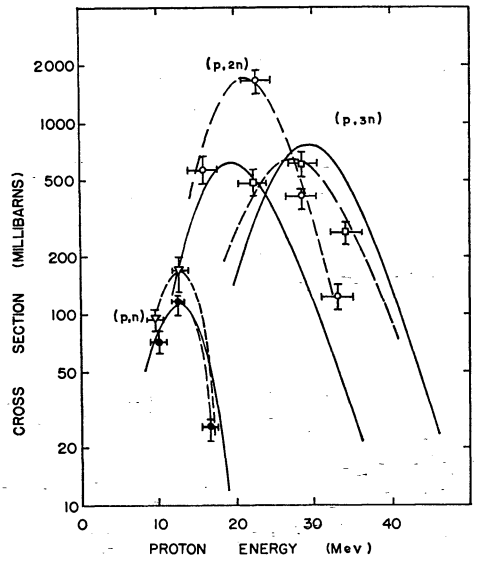

FIG. 5. Comparison of experimentally determined excitation functions with those predicted by the Jackson model: — theoretical; --- experimental; ▽ $Er^{170}(p,n)Tm^{170}$; ● $Er^{168}(p,n)Tm^{168}$; ○ $Er^{168}(p,2n)Tm^{167}$; □ $Er^{170}(p,3n)Tm^{168}$.

agreed well with the calculated values, whereas the calculated values for the reaction $Er^{170}(p,n)Tm^{170}$ were about 30% too low. In the case of the $Er^{168}(p,2n)Tm^{167}$ results, the calculated values were only about half the experimental values. The calculations for the reaction $Er^{170}(p,3n)Tm^{168}$ agreed well with the experimental values. Some of the discrepancies mentioned above may, of course, be due to uncertainties in the decay schemes used.

Yule and Turkevich calculated (p,pn) reaction cross sections at various energies by combining the cascade results with a simplified evaporation theory. For $A = 169$ they calculated a formation cross section of 30 millibarns for the (p,pn) reaction. This is to be compared with our experimental value of 60 millibarns. This type of discrepancy has been noticed by other authors (40–42) and it has been ascribed to the use of too sharp a nuclear boundary in the calculations, giving an incorrect number of low-energy depositions.

An attempt was made in the present work to check the compound nucleus mechanism

Can. J. Chem. Downloaded from www.nrcresearchpress.com by 210.87.254.5 on 09/05/12
For personal use only.

by a Ghoshal-type (44) of experiment, i.e. production of the same compound nucleus by two different nuclear reactions and comparison of the excitation functions. The reactions were the following:

$$_{67}Ho^{165} + \alpha \rightarrow {}_{69}Tm^{169*} \rightarrow Tm^{168} + {}_{0}n^{1} \qquad (a)$$
$$_{68}Er^{168} + p \rightarrow {}_{69}Tm^{169*} \rightarrow Tm^{168} + {}_{0}n^{1}$$

$$_{67}Ho^{165} + \alpha \rightarrow {}_{69}Tm^{169*} \rightarrow Tm^{167} + 2{}_{0}n^{1} \qquad (b)$$
$$_{68}Er^{168} + p \rightarrow {}_{69}Tm^{169*} \rightarrow Tm^{167} + 2{}_{0}n^{1}.$$

The ratios of the excitation functions have been calculated at the same excitation energy, which was determined in the following way. The α-bombardment energy to produce Tm^{169} is equal to the proton bombardment energy to produce Tm^{169} plus the proton binding energy (5.900 Mev) minus the α-binding energy (-0.534 Mev) (38). Thus 6.434 Mev has to be added to the proton bombarding energy to produce Tm^{169} at the same excitation energy as that produced by the alpha bombardments. (The small factor involved in changing from center-of-mass to laboratory coordinates has been neglected.) The excitation functions are plotted in Fig. 6 and the data are given in Table V.

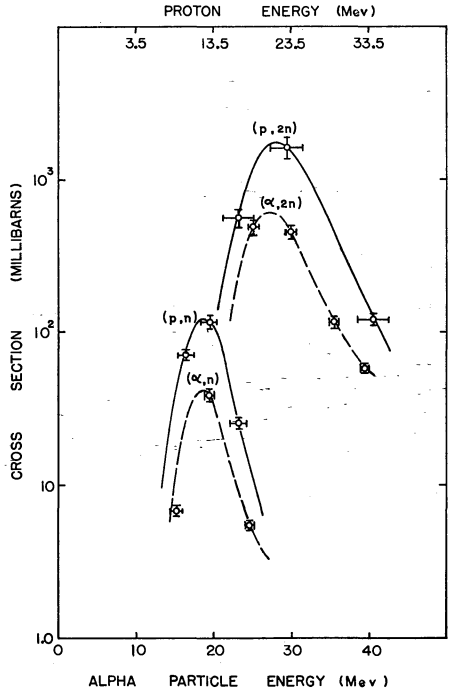

FIG. 6. Comparison of excitation functions for $Ho^{165} + \alpha$, and $Er^{168} + p$ reactions: --- $Ho^{165}(\alpha,xn)$; — $Tm^{168}(p,xn)$.

The formation cross sections for the proton reactions were interpolated from the previous excitation functions. The two excitation function sets matched when the proton energy scale was shifted by 6.5 ± 1 Mev, in good agreement with the threshold calculations. Ghoshal (44) was able to superimpose the excitation functions and observe the following ratio to hold true for the compound nucleus Zn^{64}:

$$\sigma(p,n):\sigma(p,2n):\sigma(p,pn) = \sigma(\alpha,n):\sigma(\alpha,2n):\sigma(\alpha,pn).$$

Can. J. Chem. Downloaded from www.nrcresearchpress.com by 210.87.254.5 on 09/05/12
For personal use only.

TABLE V

Ratio of cross sections for reactions induced by protons and alpha particles

Proton energy (Mev)	Alpha energy (Mev)	$\frac{\sigma(p,n)}{\sigma(\alpha,n)}$	$\frac{\sigma(p,2n)}{\sigma(\alpha,2n)}$
8.5	15	2.9	
13.5	20	2.9	
18.5	25	2.5	2.9
23.5	30		3.4
28.5	35		3.6
32.5	39		3.0

John (45) was similarly able to superimpose excitation functions for the compound nucleus Po^{210} and found the following ratio to hold true:

$$\sigma(p,2n):\sigma(p,3n):\sigma(p,4n) = \sigma(\alpha,2n):\sigma(\alpha,3n):\sigma(\alpha,4n).$$

In our experiments superimposition was not possible (again perhaps due to decay scheme difficulties) but the ratio

$$\sigma(p,n):\sigma(p,2n) = \sigma(\alpha,n):\sigma(\alpha,2n)$$

held true. Similar results have been found by Gibson (46), who studied the compound nucleus Am^{241}.

REFERENCES

1. J. W. Meadows. Phys. Rev. **91**, 885 (1953).
2. R. W. Dodson, A. C. Graves, L. Helmholtz, D. F. Hufford, R. M. Potter, and J. G. Povelites. National Nuclear Energy Series. Div. V, Vol. 3. McGraw-Hill Book Co., New York. 1952. p. 1.
3. H. Bichsel. Phys. Rev. **112**, 1089 (1958).
4. K. A. Kraus and G. E. Moore. J. Am. Chem. Soc. **75**, 1460 (1953).
5. S. G. Thompson, B. G. Harvey, G. R. Choppin, and G. T. Seaborg. J. Am. Chem. Soc. **76**, 6229 (1954).
6. T. D. Price and R. E. Telford. National Nuclear Energy Series. Div. VIII, Vol. 1. McGraw-Hill Book Co., New York. 1950. p. 419.
7. R. W. Rinehart. Anal. Chem. **26**, 1820 (1954).
8. N. A. Bonner, W. Goishi, W. H. Hutchin, G. M. Iddings, and H. A. Tewes. Phys. Rev. **127**, 217 (1962).
9. R. L. Caldwell. Phys. Rev. **78**, 407 (1950).
10. B. H. Ketelle. Oak Ridge Natl. Lab. Rept. ORNL-229. 34. 1948. Unpublished.
11. V. I. Kochevanov, R. A. Kuznetsov, A. N. Murin, V. N. Pokrovskii, and L. A. Smirnov, Izv. Akad. Nauk SSSR, Ser. Fiz. **23**, 1455 (1959).
12. K. P. Jacob, J. W. Mihelich, B. Harmatz, and T. H. Handley. Phys. Rev. **117**, 1102 (1960).
13. G. Wilkinson and H. G. Hicks. Phys. Rev. **75**, 1370 (1949).
14. T. H. Handley and E. L. Olson. Phys. Rev. **94**, 968 (1954).
15. H. Narasimhaih and M. L. Pool. Nucl. Phys. **21**, 340 (1960).
16. R. G. Wilson and M. L. Pool. Phys. Rev. **119**, 262 (1960).
17. M. C. Michel and D. H. Templeton. Phys. Rev. **93**, 1422 (1954).
18. T. H. Handley and E. L. Olson. Phys. Rev. **92**, 1260 (1953).
19. G. M. Gorodinskii, A. N. Murin, U. N. Pokrovskii, and B. K. Preobrazhenskii. Izv. Akad. Nauk SSSR, Ser. Fiz. **21**, 1004 (1957).
20. R. G. Wilson and M. L. Pool. Phys. Rev. **120**, 1827 (1960).
21. A. A. Abdurazakov, K. Gromov, B. Dalkhasuren, B. Dzelepov, I. Lovenberg, A. Murin, and I. Yutlandov. Joint Institute for Nuclear Research, Dubna, USSR, JINR-P-495. 1960.
22. B. Harmatz, T. H. Handley, and J. W. Mihelich. Phys. Rev. **114**, 1082 (1959).
23. S. Bjørnholm, H. L. Nielsen, O. B. Nielsen, G. Sidenius, O. Skilbreid, and A. Svanheden. J. Inorg. Nucl. Chem. **21**, 193 (1961).
24. F. D. S. Butement. Proc. Phys. Soc. (London), Sect. A, **64**, 395 (1951).
25. B. H. Ketelle and W. C. Peacock. Phys. Rev. **73**, 1260 (1948).
26. F. I. Pavlotskaia and A. K. Lavrukhina. Soviet Phys. JETP, **7**, 732 (1958).
27. O. I. Grigorev, B. S. Kusnetsov, N. S. Shimanskaya, and I. Ya. Yutlandov. Izv. Akad. Nauk SSSR, Ser. Fiz. **22**, 850 (1958).

Can. J. Chem. Downloaded from www.nrcresearchpress.com by 210.87.254.5 on 09/05/12
For personal use only.

28. NUCLEAR DATA SHEETS. National Academy of Sciences, National Research Council (U.S. Government Printing Office, Washington, D.C.). 1961.
29. W. E. NERVIK and G. T. SEABORG. Phys. Rev. **97**, 1092 (1955).
30. T. H. HANDLEY and E. L. OLSON. Phys. Rev. **93**, 524 (1954).
31. D. STROMINGER, J. M. HOLLANDER, and G. T. SEABORG. Rev. Mod. Phys. **30**, 585 (1958).
32. M. E. ROSE. Tables of internal conversion coefficients. North-Holland Publications, Amsterdam. 1958.
33. H. A. GRENCH and S. B. BURSON. Phys. Rev. **121**, 831 (1961).
34. K. S. TOTH and O. B. NIELSEN. Nucl. Phys. **22**, 57 (1961).
35. J. D. JACKSON. Can. J. Phys. **34**, 767 (1956).
36. H. MCMANUS, W. T. SHARP, and H. GELLMAN. Phys. Rev. **93**, 924 (1954).
37. K. PEARSON. Tables of the incomplete gamma functions. Cambridge University Press, Cambridge, England. 1951.
38. A. G. W. CAMERON. At. Energy Canada Ltd. Rept. CRP-690. 1957. Unpublished.
39. M. M. SHAPIRO. Phys. Rev. **90**, 171 (1953).
40. H. P. YULE and A. TURKEVICH. Phys. Rev. **118**, 1591 (1960).
41. P. P. STROHAL and A. A. CARETTO. Phys. Rev. **121**, 1815 (1961).
42. A. A. CARETTO and G. FRIEDLANDER. Phys. Rev. **110**, 1169 (1958).
43. S. S. MARKOWITZ, F. S. ROWLAND, and G. FRIEDLANDER. Phys. Rev. **112**, 1295 (1958).
44. S. N. GHOSHAL. Phys. Rev. **80**, 939 (1950).
45. W. JOHN. Phys. Rev. **103**, 704 (1956).
46. W. M. GIBSON. Univ. Calif. Radiation Lab. Rept. UCRL-3493. 1956. Unpublished.

Can. J. Chem. Downloaded from www.nrcresearchpress.com by 210.87.254.5 on 09/05/12
For personal use only.

TARTRATE COMPLEXES OF THE RARE-EARTH ELEMENTS

I. THE *d*-, *dl*-, AND meso-TARTRATE COMPLEXES OF Tb AND Eu[1]

P. G. MANNING[2]

Mines Branch, Department of Mines and Technical Surveys, Ottawa, Canada

Received May 21, 1963

ABSTRACT

Solvent extraction and radiotracer techniques have been applied to the study of metal – tartrate ion association in water at 25° C. Trace concentrations of the radioisotopes Tb^{160} and $Eu^{152/154}$ were equilibrated between aqueous sodium tartrate solutions and organic phases of thenoyltrifluoroacetone in toluene. The ionic strength (0.0597) and the pH (4.53) of the aqueous phase were kept constant by means of sodium perchlorate and sodium acetate.

Metal complexing with the *d*-, *dl*-, and meso isomers of the ligand was examined. For all isomers two complex species were identified with metal:ligand ratios of 1:1 and 1:2, and stability constants for both stages of ion association have been estimated. No third (1:3) complex was detected.

Metal coordination numbers and the formation of tartrate–tartrate hydrogen bridges in the 1:2 complex are discussed.

Can. J. Chem. Downloaded from www.nrcresearchpress.com by 210.87.254.6 on 09/05/12
For personal use only.

INTRODUCTION

The application of organic acids to the separation of rare earths by successive elution from ion-exchange resins has, in recent years, stimulated research into the chemistry of these elements in solutions of carboxylic acids. Data as to the nature, number, and stabilities of the complexes formed are, however, limited to the simpler α- or β-hydroxycarboxylic acids and some multidentate aminopolycarboxylic acids.

That at least two tartrate ions will associate with a single lanthanide ion is evident from the fact that the addition of the ammonium salt of the racemic acid to an aqueous solution of a rare earth gives, initially, a precipitate, which dissolves in excess of reagent (1). Mattern (2), from spectrophotometric measurements, similarly concluded that at least two stages of ion association were involved, but the experimental accuracy was such that quantitative data in the form of stability constants were unobtainable. Manning and Monk (3) used the solvent extraction – radiotracer method to show that, in solutions of racemic tartaric acid, EuL^+ and EuL_2^- are formed (where L = ligand), and the sole reported stability constants appear to be those of these workers.

Recent publications on the complex chemistry of the lanthanides have suggested that metal coordination numbers of eight are possible. Thus the synergic extraction of the lanthanides by mixtures of acidic (HX, e.g. thenoyltrifluoroacetone) and neutral (S, e.g. tributyl phosphate) extractants proceeds through the formation of the species MX_3S_2 (4–6). If the S molecules are coordinated to the metal ion, then coordination numbers of eight must be proposed, as thenoyltrifluoroacetone is a bidentate chelating agent. Sonesson (7) and Choppin and Chopoorian (8) have shown that four glycolate ions will associate with a single metal ion, but it is possible that some of the ligands are of monodentate character. Thompson and Loraas (9) explained their results on the addition of ethylenediaminediacetic acid to 1:1 lanthanide-N-hydroxyethylethylenediaminetriacetic acid chelates on the basis of coordination numbers of greater than six. As tartrate is, potentially, a tetradentate ligand, and since ML_2^- forms, a study of lanthanide–tartrate ion-pair formation could well shed light on the problem of rare-earth coordination numbers.

[1]*Crown copyright reserved.*

[2]*National Research Council of Canada Postdoctoral Fellow.*

The association of carboxylic acids, and other oxygenated organic molecules, in solution, has been attributed to the formation of intermolecular hydrogen bonds of the type O—H- - -O (10), and one of the aims of this work has been to determine whether ligand–ligand hydrogen bonds can form in the rigid structures of the higher complexes of metal carboxylates. Although the existence of such an intracomplex bridging phenomenon has not been reported in the literature, its presence should be manifested in the enhanced stability of the complexes. Tartaric acid seemed a promising complexing agent as it contains two carboxyls and two hydroxyls, groups that readily form hydrogen bonds.

EXPERIMENTAL

The *d*- and *dl*-tartaric acids were British Drug Houses Analytical Reagent. *l*-Tartaric acid was purchased from K and K Laboratories, Jamaica 33, New York. Molecular weight determinations by alkalimetry gave values within 0.2% of calculated. meso-Tartaric acid (K and K Laboratories) possessed a molecular weight of 167.5 (calculated for the monohydrate 168.1) and a melting point of 139° C (literature 140° C). The *d*- and *l*-isomers gave equal and opposite optical rotations, and synthetic *dl*-solutions were inactive. Stock solutions of sodium tartrate were prepared by 80% neutralization, with carbonate-free NaOH, of weighed amounts of the acids. Sodium perchlorate, used to maintain a constant ionic strength, was prepared and standardized as described in a previous publication (3). Thenoyltrifluoracetone (HTTA), obtained from the Fisher Scientific Company Ltd., was recrystallized from hexane, and stock solutions in thiophene-free toluene prepared by weight. Succinic and malic acids were Fisher Certified and Highest Purity reagents respectively.

pH constancy in the aqueous phase was ensured by the introduction of a 0.0040 *M* sodium acetate – acetic acid mixture, both these reagents being of Analytical Reagent grade. pH measurements of the aqueous phase were effected with an Electronic Instruments Ltd. (Richmond, England) Model 23A pH meter. This same instrument was also used in the determination of the p*K* values for the tartaric acids.

The radioisotopes were purchased from the Radiochemical Centre, Amersham, England. In all experiments the total metal concentration was $\sim 10^{-7}$ *M*; this ensured that extractant and ligand concentrations remained essentially constant. The γ-emitting isotopes were assayed using a NaI(Tl) scintillation detector coupled to a Nuclear-Chicago automatic sample changer.

Distribution measurements were performed by agitating 10.00 ml of both phases in ground-glass-stoppered Erlenmeyer flasks fitted with polytetrafluoroethylene (PTFE) sleeves. The flasks were suspended in a constant-temperature water bath (25.0±0.2° C) from the arms of a variable-amplitude wrist-action shaker. Three hours' shaking was ample for equilibration. All organic phases were pre-equilibrated.

THEORY

The distribution coefficient of a nuclide is

$$[1] \qquad K = \frac{\text{concentration of nuclide in organic phase}}{\text{concentration of nuclide in aqueous phase}}.$$

Adopting the convention of Sonesson (7), the overall (β) and successive (b) stability constants are

$$[2] \qquad \beta_n = \frac{[ML_n^{(3-2n)+}]}{[M^{3+}][L^{2-}]^n}$$

$$[3] \qquad b_n = \frac{[ML_n^{(3-2n)+}]}{[ML_{n-1}^{(5-2n)+}][L^{2-}]},$$

where M and L represent metal and ligand.

Since it is well established that lanthanide–ClO_4^- complexing in water is negligible (at least at $[ClO_4^-] \simeq 0.06$ *M*), then when $[L^{2-}] = 0$, from equation [1]

$$[4] \qquad K^o = \frac{[M(TTA)_3]_o}{\{[M^{3+}]+[MA^{2+}]+[MA_2^{+}]+\ldots\}_w},$$

where A^- represents the acetate ion, and "o" and "w" are organic and water phase species respectively.

Can. J. Chem. Downloaded from www.nrcresearchpress.com by 210.87.254.6 on 09/05/12
For personal use only.

In the presence of tartrate ion,

$$[5] \qquad K = \frac{[M(TTA)_3]_o}{\{[M^{3+}]+[MA^{2+}]+\ldots+[ML^{+}]+[ML_2^{-}]+\ldots\}_w}.$$

From equations [2], [4], and [5], it can be shown (3)

$$[6] \qquad \frac{\{(K^\circ/K)-1\}}{[L^{2-}]} = \frac{\{\beta_1+\beta_2[L^{2-}]+\beta_3[L^{2-}]^2+\ldots\}}{\{1+\beta_1'[A^-]+\beta_2'[A^-]^2+\ldots\}},$$

where β and β' are stability constants for the lanthanide–tartrate and lanthanide–acetate complexes respectively.

Since only one lanthanide–acetate complex (MA^{2+}) forms under these experimental conditions (3), putting $1+\beta_1'[A^-] = D$ we get

$$[7] \qquad \frac{D\{(K^\circ/K)-1\}}{[L^{2-}]} = \beta_1+\beta_2[L^{2-}]+\beta_3[L^{2-}]^2+\ldots.$$

D is a correction factor for metal–acetate interaction, and is constant under given experimental conditions for any one lanthanide.

It follows from equation [7] that a plot of $D\{(K^\circ/K)-1\}/[L^{2-}]$ against $[L^{2-}]$ is horizontal if only ML^+ forms (whence β_1 = intercept when $[L^{2-}] = 0$), linear with positive slope if ML^+ and ML_2^- form (whence β_1 and β_2 are intercept and slope respectively), and curved (of ever-increasing curvature) if ML_3^{3-} also forms.

Stability constants have been calculated from these plots using the least mean squares analysis.

RESULTS

The pK_1 and pK_2 values for the different tartaric acids, determined by potentiometric titration (11), are given in Table I.

TABLE I

pK values for the tartaric acids at 25° C

	Isomer		
	d-	*dl-*	Meso
pK_1	2.935	2.89	3.17
pK_2	4.21	4.09	4.68

At the pH = 4.53 employed in these experiments, much of the tartrate is present as the protonated ligand HL^-. Free-ligand concentrations, $[L^{2-}]$, have, therefore, been computed from the expression

$$[8] \qquad C_L/[L^{2-}] = 1+[H^+]f_{H^+}f_{L^{2-}}/K_2,$$

where C_L is the total sodium tartrate concentration, and f_{H^+} and $f_{L^{2-}}$ are activity coefficients calculable from the Debye–Hückel expression (12)

$$[9] \qquad -\log f = 0.509z^2\{I^{\frac{1}{2}}/(1+I^{\frac{1}{2}})\}-0.2I,$$

where z is the ionic charge and I is the ionic strength. Similar calculations have been performed to estimate $[A^-]$ for the determination of D (equation [7]). The β_1' values of Kolat and Powell (13) at $I = 0.1$ have been corrected to $I = 0.0597$ using equation [9]. Also, $pK_{HA} = 4.76$ (14). For Eu and Tb, $D = 1.436$ and 1.255 respectively.

Can. J. Chem. Downloaded from www.nrcresearchpress.com by 210.87.254.6 on 09/05/12
For personal use only.

Although a third term involving $[H^+]^2$ and K_1K_2 has been ignored in equation [8], the error introduced in $[L^{2-}]$ by so doing ($<1\%$) is much smaller than the reproducibility of the distribution coefficients ($\pm 2\%$). Also, the validity of equation [9], when used to calculate f_{H^+} and $f_{L^{2-}}$ under the present experimental conditions, must be considered. Davies (12) has shown that equation [9] is valid for 1:2 electrolytes (in the present work, HL^-) to within 2% up to $I = 0.1$. However, the aqueous phase in the present work is not pure water: it is, in fact, a mixed solvent, and activity coefficients in mixed solvents can differ appreciably from those in pure water. Manning and Monk (15) used the solvent extraction method to study cobalt–dicarboxylate complexing, and showed that the values of the parameters $\mathring{a}$ and b in the equation

$$[10] \qquad -\log f = 0.509z^2\left\{\frac{I^{\frac{1}{2}}}{1+B\mathring{a}I^{\frac{1}{2}}} - bI\right\}$$

were 4.0–4.5 and 0.15 respectively. These values agree with those of McCauley and Nancollas (16), who carried out a potentiometric examination of the same system. Also, equation [9] has been applied successfully to the analogous Eu–SO_4 system (3). We may conclude, therefore, that equations [8] and [9] are applicable to the present work.

Lanthanide–Tartrate Systems at 25° C

In Table II are listed metal distribution coefficients at different ligand concentrations.

TABLE II

$[L^{2-}]$, K_{Tb}, and K_{Eu} values
($I = 0.0597$, pH = 4.53, [HTTA] = 0.015 M)

d-Tartaric acid ($C_L/[L^{2-}] = 1.201$)				*dl*-Tartaric acid ($C_L/[L^{2-}] = 1.154$)				meso-Tartaric acid ($C_L/[L^{2-}] = 1.593$)		
$10^4[L^{2-}]$, M	K_{Tb}	K_{Tb}*	K_{Eu}	$10^4[L^{2-}]$, M	K_{Tb}	K_{Tb}†	K_{Eu}	$10^4[L^{2-}]$, M	K_{Tb}	K_{Eu}
0	3.45	3.46	1.698	0	3.02	3.46	1.52	0	3.02	1.52
2.08	1.19	1.237	0.494	2.17	1.217	1.218	0.462	1.57	0.417	0.170
2.91	0.931	0.89	0.389	3.03	0.799	0.867	0.351	2.20	0.276	0.1185
4.16	0.671	0.642	0.280	4.33	0.623	0.612	0.237	3.14	0.186	0.0728
5.00	0.517	0.498	0.213	5.20	0.492	0.512	0.182	3.77	0.148	0.0603
6.24	0.390	0.361	0.165	6.49	0.442	0.371	0.142‡	4.71	0.118	0.0440
8.33	0.272	0.257	0.1106	8.67	0.255	0.250	0.101	6.28	0.0725	0.0289
10.41	0.189	0.190	0.0791	10.83	0.190	0.165	0.0698	7.85	0.0601	0.0208
12.49	0.136	0.144	0.0603	13.00	0.1465	0.125	0.0526	9.42	0.0449	0.0165

*l-Tartaric acid.
†Synthetic *dl*-tartaric acid.
‡See text for explanation.

The *d*- and *l*-isomers were checked against each other, and a synthetic *dl*-solution against the B.D.H. racemic compound.

Plots of $\{(K^\circ/K)-1\}/[L^{2-}]$ against $[L^{2-}]$ are linear in all instances, indicating that two complexes, ML^+ and ML_2^-, are formed. Calculated values of β_1 and β_2, together with b_1:b_2 ratios, are presented in Table III. The estimated error in β_1 and β_2 is generally less than 10%.

To show that lanthanide–HL^- complexing may be ignored, a "run" was carried out with europium and *dl*-tartaric acid at a pH = 5.02, whence $C_L/[L^{2-}] = 1.050$ and $D = 1.715$. When $[L^{2-}] = 0$, $K_{Eu}^\circ = 42.0$, and when $[L^{2-}] = 6.50\times10^{-4}$ M, $K_{Eu} = 4.81$. From these figures, $D\{(K^\circ/K)\}-1/[L^{2-}] = 2.05\times10^4$. The corresponding value of $D\{(K^\circ/K)\}-1/[L^{2-}]$ at a pH = 4.53, using the information of Table II marked ‡, is 2.15×10^4. As the

Can. J. Chem. Downloaded from www.nrcresearchpress.com by 210.87.254.6 on 09/05/12
For personal use only.

TABLE III

β_1, β_2, and b_1/b_2 values for metal–tartrate complexes

	Isomer	Tb	Eu
$10^{-3}\beta_1$	*d*, *l*	8.4	11.8
$= 10^{-3}b_1$	*dl*	7.1	11.8
	dl (synth.)	7.6	
	meso	44	60
	d, *l*	11.8	15.0
$10^{-6}\beta_2$	*dl*	9.1	14.4
	dl (synth.)	13.5	
	meso	48	88
	d, *l*	1.40	1.27
$10^{-3}b_2$	*dl*	1.3	1.22
	dl (synth.)	1.78	
	meso	1.1	1.47
	d, *l*	6.0	9.3
b_1/b_2	*dl*	5.5	9.7
	dl (synth.)	4.3	
	meso	40	41

reproducibility of the distribution coefficients is $\pm 2\%$, it is evident that metal complexing by the HL^- ion is negligible.

Europium–Succinate System

The free-ligand concentrations, K, and $\{(K^\circ/K)-1\}/[\text{succinate}^=]$ values are listed in Table IV. The values of $\{(K^\circ/K)-1\}/[\text{succinate}^=]$ are constant within experimental error,

TABLE IV

Data for europium succinate
($pK_2 = 5.48$ (15), $C_L/[Succ^=] = 4.75$, $D = 1.436$)

$10^3[Succ^=]$, M	0	1.59	2.13	2.41	5.74
K_{Eu}	1.52	0.57	0.52	0.38	0.24
$10^{-3}D\{(K^\circ/K)-1\}/[Succ^=]$	—	1.5	1.3	1.8	1.3

thus indicating that $EuSucc^-$ forms. The average value of β_1 is 1.5×10^3, but this value must be considered as approximate due to the high concentration of undissociated acid.

Europium–Malate System

Table V contains the relevant ligand concentrations, K values, and $\{(K^\circ/K)-1\}/[Mal^=]$ values. Two complexes are present, and the estimated values of β_1 and β_2 are 4.5×10^3 and $1.4.10^6$ respectively, from which $b_2 = 3\times10^2$.

TABLE V

Data for europium malate
($pK_2 = 5.05$ (15), $C_L/[Mal^=] = 2.39$, $D = 1.436$)

$10^3[Mal^=]$, M	0	1.01	1.26	2.52	3.77
K_{Eu}	1.52	0.276	0.234	0.096	0.058
$10^{-3}D\{(K^\circ/K)-1\}/[Mal^=]$	—	6.4	6.25	8.4	9.6

Can. J. Chem. Downloaded from www.nrcresearchpress.com by 210.87.254.6 on 09/05/12
For personal use only.

DISCUSSION

That the hydroxyl groups of the tartrate ion coordinate to the central metal ion is readily apparent from a comparison of the β_1 values of the europium complexes of succinate (1.5×10^3), malate (4.5×10^3), and tartrate ($11.8\text{–}60\times10^3$). These figures show that β_1 increases as the number of —OH groups in the ligand increased, which suggests that both the —OH groups of the tartrate ion coordinate in the ML^+ complex. An identical trend in stabilities is exhibited by the corresponding complexes of Ca, Ba, Sr, and Co (15, 17–21).

Cozzi and Vivarelli (22) have prepared a complex tartrate of indium, to which chelate they assigned the structure (with a tetradentate tartrate)

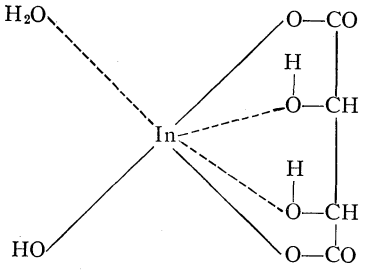

The greater stabilities of the Tb and Eu chelates of meso-tartaric acid over those of *d*- or *dl*-tartaric acid are attributable to the more favorable spatial arrangement of the hydroxyl groups of the meso-isomer. It is apparent from Fig. 1 that, unless steric crowding

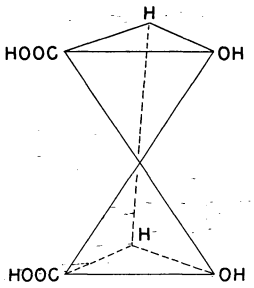

FIG. 1. Configuration of meso-tartaric acid.

around the metal ion becomes of importance, both —OH groups will bind if chelation occurs at all. It has been demonstrated for lanthanide–EDTA (ethylenediaminetetraacetic acid) complexes, that five, if not six, of the available groups coordinate to the metal ion (23, 24). It would seem that steric crowding of groups in the ML^+ complex may be insignificant.

Assuming coordination numbers of either six or eight for the rare-earth ions, the possible bonding contributions of the ligands (two tartrates and water) to the coordination number of the metal ion are shown in Table VI. For example, in scheme Y, the first tartrate to

TABLE VI

Possible bonding contributions of the ligands

Scheme	L′	L″	H_2O	Coord. No.
W	4	2	0	6
X	4	2	2	8
Y	4	3	1	8
Z	4	4	0	8

Can. J. Chem. Downloaded from www.nrcresearchpress.com by 210.87.254.6 on 09/05/12
For personal use only.

coordinate (L′) functions as a tetradentate ligand, the second (L″) as a tridentate ligand, while a molecule of water also coordinates to give a coordination number of eight. The possibility that L″ might not be tetradentate must be considered, as Betts and Dahlinger (24) suggested that the discontinuity in many of the properties of lanthanide complexes at Gd might be due to a change in configuration, e.g., in the case of EDTA, the change is one from hexa- to penta-coordination. Since, in the present work, $\beta_1(\mathrm{Eu}) > \beta_1(\mathrm{Tb})$ for all the different tartrates, it is likely that the "Gd break" effect is present in the tartrate systems also. It is unlikely, however, that the "Gd break" is a manifestation of differences in configuration, since the discontinuity is more pronounced for such simple monodentate ligands as acetate (13) and chloride (25)—where effects due to configurational differences should be at a minimum—than it is for multidentate ligands such as EDTA. Moreover, the partial molal entropies of the ion pairs, TbL′ and $\mathrm{EuL_1}'$, are approximately equal, indicating that the Eu and Tb chelates are structurally similar (26).

The relative coordinating power of L″ is reflected in the magnitude of b_1/b_2. For statistical reasons, there being fewer coordination sites available, $b_1/b_2 > 1$. On the basis of lanthanide coordination numbers of six, Bjerrum (26) has shown that for simple chelating agents, e.g. glycolate,

$$b_1:b_2:b_3 = 12:2:0.33.$$

The theoretical value of b_1/b_2 for a lanthanide glycolate would therefore be six. The average experimental value is 4.1 (7), which suggests that coordination numbers greater than six are possible. While the second glycolate ion to associate has a choice of two coordination sites out of four on the basis of a metal coordination number of six (two out of six, if eight), the choice available to L″ is limited: two from two or four from four depending on the configuration of the metal. The statistical factor demands, therefore, for lanthanide–tartrate complexes, that $b_1/b_2 \gg 4.1$ (whether the metals exert coordination numbers of six or eight). The b_1/b_2 values for the 1:2 M–*d*–*d* and M–*d*–*l* tartrate complexes of Eu and Tb range from 9.7 to 4.3, values which are incomprehensible on the basis of the Bjerrum treatment. It is apparent that a mechanism must be in operation in the second stage of ion association that confers increased stability on the ML′L″ complexes (omitting charges).

Another factor that will influence b_1/b_2 will be the number of groups of L″ coordinating to the metal ion. If neither —OH group of L″ binds, L″ is approximately equivalent to a succinate, and if one hydroxyl binds, a malate. Now b_2 (europium malate) $= 3\times10^2$, and this value gives us an upper limit to b_2 for the addition of a malate-type ion to a EuL′ complex (where L′ = meso-tartrate). Since b_1 (europium meso-tartrate) $= 60\times10^3$, then, if only one —OH group of L″ coordinates, $b_1/b_2 \simeq 200$. If neither —OH group of L″ coordinates, the value of $b_1/b_2 \gg 200$. The experimentally determined values of b_1/b_2 are 40 and 41 for Tb and Eu respectively (Table III), indicating that L″ is also of tetradentate identity. Coordination numbers of eight are, therefore, possible for the rare-earth ions.

The most striking feature of these results are the remarkably low b_1/b_2 values for the M–*d*–*d* and M–*d*–*l* complexes. The b_2 values listed in Table III show that it is more difficult for a second meso-tartrate to coordinate to Tb than it is for a *d*- or an *l*-tartrate to coordinate to a 1:1 *d*-tartrate chelate: an unexpected result considering the more favorable configuration of —OH groups in the meso-isomer. The low values of b_1/b_2 in *d*- and *dl*-tartrate systems cannot be brought about by steric hindrance, or by L′ being tetradentate and L″ being tridentate, as both these effects would lead to larger-than-expected b_1/b_2 values. Because the *d*- and *l*-isomers of tartaric acid are mirror images, a potential binding metal ion cannot distinguish between them (β_1 values Table III).

Can. J. Chem. Downloaded from www.nrcresearchpress.com by 210.87.254.6 on 09/05/12
For personal use only.

Similarly, the identical β_2 values for the M–*d*–*d* and M–*d*–*l* complexes indicate that the 1:1 *d*-tartrate chelate cannot do so either. Since the b_1/b_2 values for the meso-tartrate complexes are reconcilable with the theoretical Bjerrum treatment (27), it would seem that the enhanced β_2 values for the M–*d*–*d* and M–*d*–*l* species are linked with the orientation of the —OH groups of the tartrates. To explain these results, therefore, it is necessary to postulate tartrate–tartrate hydrogen bridging in the M–*d*–*d* and M–*d*–*l* chelates. The orientation of the active groups must, from a comparison of the stability constants listed in Table III, be identical in the metal chelates of *d*- and *dl*-tartaric acid, while the configuration of the M–meso–meso complex is such that hydrogen bridging is absent or very weak.

Three bridging models are possible, depending on the active groups involved and the nature of the hydrogen bond formed. For example, in one model O—H - - - O hydrogen bridging occurs via the —OH groups of L′ and the —OH groups of L″, while a similar type of bridge could be formed between the —OH and the —COO^- of different ligands. Another mode of orientation of L′ and L″ could induce bridging between the —OH of one ligand and C—H of the other ligand, but evidence for the existence of C—H - - - O bonds is scant (10).

Insufficient experimental data are available at the present time to warrant giving a detailed picture of the molecular configurations in the three models, but it is hoped to present a theoretical treatment to account for these results in a future publication in this series.

CONCLUSIONS

Two tartrate ions (whether *d*-, *dl*-, or meso-), functioning as tetradentate ligands, coordinate with a central lanthanide ion, conferring on the latter a coordination number of eight.

The trends in stabilities for the two stages of ion association are

$$M^{3+} + L^{2-} = ML^{+};\ \text{meso} > d = dl$$

$$ML^{+} + L^{2-} = ML_2^{-};\ \text{meso} \leqslant d = dl.$$

A suggestion has been made that ligand–ligand hydrogen bridging may be responsible for the extra stability of ML_2^- complexes of *d*- and *dl*-tartaric acid.

ACKNOWLEDGMENTS

The author wishes to thank the National Research Council of Canada for the award of a Fellowship, and Dr. G. G. Eichholz for many stimulating discussions.

REFERENCES

1. P. C. Stevenson and W. E. Nervik. The radiochemistry of the rare-earths. Natl. Acad. Sci.—Natl. Res. Council, Nucl. Sci. Ser. NAS-NS 3020. 1961. p. 64.
2. K. L. Mattern. Complex ions of lanthanum in aqueous solutions. Univ. Calif. Radiation Lab. Rept. UCRL-1407. 1951.
3. P. G. Manning and C. B. Monk. Trans. Faraday Soc. **58**, 938 (1962).
4. T. V. Healy. J. Inorg. Nucl. Chem. **19**, 314 (1961).
5. H. Irving and D. N. Edgington. J. Inorg. Nucl. Chem. **21**, 169 (1961).
6. P. G. Manning. Can. J. Chem. **41**, 658 (1963).
7. A. Sonesson. Acta Chem. Scand. **13**, 998 (1959).
8. G. R. Choppin and J. A. Chopoorian. J. Inorg. Nucl. Chem. **22**, 97 (1961).
9. L. C. Thompson and J. A. Loraas. Inorg. Chem. **2**, 89 (1963).
10. G. C. Pimental and A. L. McClellan. The hydrogen bond. Freeman, San Francisco. 1960.
11. H. T. S. Britton. Hydrogen ions. Chapman and Hall, London. 1929.
12. C. W. Davies. J. Chem. Soc. 2093 (1938).

Can. J. Chem. Downloaded from www.nrcresearchpress.com by 210.87.254.6 on 09/05/12
For personal use only.

13. R. S. KOLAT and J. E. POWELL. Inorg. Chem. **1**, 293 (1962).
14. M. LLOYD, V. WYCHERLEY, and C. B. MONK. J. Chem. Soc. 1786 (1951).
15. P. G. MANNING and C. B. MONK. Trans. Faraday Soc. **57**, 1996 (1961).
16. A. MCCAULEY and G. NANCOLLAS. J. Chem. Soc. 2215 (1961).
17. N. E. TOPP and C. W. DAVIES. J. Chem. Soc. 87 (1940).
18. J. M. PEACOCK and J. C. JAMES. J. Chem. Soc. 1371 (1949).
19. J. SCHUBERT. J. Am. Chem. Soc. **76**, 3442 (1954).
20. J. SCHUBERT and A. LINDENBAUM. J. Am. Chem. Soc. **74**, 3529 (1952).
21. J. SCHUBERT. J. Phys. Chem. **56**, 113 (1952).
22. D. COZZI and S. VIVARELLI. Z. Elektrochem. **58**, 907 (1954).
23. E. J. WHEELWRIGHT, F. H. SPEDDING, and G. SCHWARZENBACH. J. Am. Chem. Soc. **75**, 4196 (1953).
24. R. H. BETTS and O. F. DAHLINGER. Can. J. Chem. **37**, 91 (1959).
25. D. F. PEPPARD, G. W. MASON, and I. HUCHER. J. Inorg. Nucl. Chem. **24**, 881 (1962).
26. P. G. MANNING. Unpublished data.
27. J. BJERRUM. Metal ammine formation in aqueous solution. P. Haase and Son, Copenhagen. 1941.

Can. J. Chem. Downloaded from www.nrcresearchpress.com by 210.87.254.6 on 09/05/12
For personal use only.

TARTRATE COMPLEXES OF THE RARE-EARTH ELEMENTS

II. THE *dl*- AND meso-TARTRATE COMPLEXES OF La, Ce, Pm, Tm, AND Y[1]

P. G. MANNING[2]

Mines Branch, Department of Mines and Technical Surveys, Ottawa, Canada

Received June 10, 1963

ABSTRACT

The liquid–liquid distribution method has been used to measure the stability constants of the *dl*-tartrate complexes of La^{3+}, Ce^{3+}, Pm^{3+}, Tm^{3+}, and Y^{3+}, and the meso-tartrate complexes of Ce^{3+} and Tm^{3+}. Thenoyltrifluoroacetone was the organic phase extractant, and the aqueous phase, acetate buffered (pH = 4.53), was maintained at a constant ionic strength (0.0597) by means of sodium perchlorate.

The order of stabilities for the two stages of ion association are

$$M^{3+} + L^{2-} = ML^{+};\ \text{meso} > dl$$

$$ML^{+} + L^{2-} = ML_2^{-};\ \text{meso} < dl.$$

The b_1/b_2 values, where b is a stepwise stability constant defined as

$$b_n = [ML_n^{(3-2n)+}]/[ML_{n-1}^{(5-2n)+}][L^{2-}],$$

are lower (by factors of 4–8) for the *dl*-tartrates than for the meso-tartrate complexes. The b_1/b_2 ratios decrease as the ionic radius of the metal ion decreases, and for the *dl*-tartrates of Tb^{3+}, Y^{3+}, and Tm^{3+}, the b_1/b_2 values are 5.3, 5.0, and 4.3 respectively. The enhanced stabilities of the 1:2 (ML_2^-) *dl*-tartrate chelates have been interpreted in terms of ligand–ligand hydrogen bridging in the 1:2 complex.

Can. J. Chem. Downloaded from www.nrcresearchpress.com by 210.87.254.40 on 09/05/12
For personal use only.

INTRODUCTION

In Part I of this series (1), it was proposed that the enhanced stabilities of the 1:2 chelates of Tb and Eu with *d*- and *dl*-tartaric acid were attributable to ligand–ligand hydrogen bridging. In the present paper we report additional results for *dl*-tartrate complexing with La^{3+}, Ce^{3+}, Pm^{3+}, Tm^{3+}, and Y^{3+}, and also meso-tartrate complexing with Ce^{3+} and Tm^{3+}.

A qualitative account of three possible hydrogen bridging models, depending on the groups involved and the nature of the hydrogen bond formed, is presented.

EXPERIMENTAL

The experimental details are identical with those described in Part I of this series (1).

Carrier-free La^{140} was "milked" from a Ba^{140}/La^{140} fission product mixture by extraction with thenoyltrifluoroacetone (HTTA) at pH = 4.53, followed by back extraction of any traces of Ba^{140} with an aqueous phase of identical composition. The other (β-emitting) radioisotopes, of high specific activity, were purchased from the Radiochemical Centre, Amersham, England. The β-emitters were assayed using a conventional Geiger–Müller counter, and the La^{140} using a NaI(Tl) scintillation detector.

The temperature was maintained at 25.0±0.2° C.

THEORY

The distribution coefficient of a given nuclide is

$$[1] \qquad K = \frac{\text{concentration of nuclide in organic phase}}{\text{concentration of nuclide in aqueous phase}}.$$

[1]*Crown copyright reserved.*

[2]*National Research Council of Canada Postdoctoral Fellow.*

The overall (β) and stepwise (b) stability constants are

[2] $$\beta_n = [ML_n^{(3-2n)+}]/[M^{3+}][L^{2-}]^n$$

and

[3] $$b = [ML_n^{(3-2n)+}]/[ML_{n-1}^{(5-2n)+}][L^{2-}]^n.$$

The theoretical deviation of the equation,

[4] $$D\{(K^\circ/K)-1\}/[L^{2-}] = \beta_1+\beta_2[L^{2-}]+\beta_3[L^{2-}]^2+\ldots$$

has been described in greater detail in previous publications (1, 2). Here, $K^\circ = K$ when $[L^{2-}] = 0$, and D ($= 1+\beta_1'[Ac^-]$, where β_1' represents the stability constants for the 1:1 lanthanide acetate complex) is a correction factor for metal–acetate interaction. The D values, evaluated using the β_1' values of Kolat and Powell (3), are given in Table I. The

TABLE I

D values for lanthanide–acetate complexing

Metal	La	Ce	Pm	Tm	Y
D	1.177	1.210	1.287	1.176	1.159

method of calculation of free ligand concentrations has also been described previously (1).

It follows from equation [4], therefore, that a plot of $D\{(K^\circ/K)-1\}/[L^{2-}]$ against $[L^{2-}]$ is horizontal if ML^+ forms, linear with positive slope if ML^+ and ML_2^- form, and curved if ML_3^{3-} also forms.

RESULTS

In Table II are presented metal distribution coefficients at different ligand concentrations. The K values were generally reproducible to $\pm 3\%$.

For all the metals studied, and for both stereoisomeric forms of tartaric acid, plots of $D\{(K^\circ/K)-1\}/[L^{2-}]$ against $[L^{2-}]$ were linear, indicating that ML^+ and ML_2^- are formed. The estimated values of β_1, β_2, b_2, and b_1/b_2 are collected in Table III. The estimated errors in β_1 and β_2 are $\pm 10\%$. The least mean squares analysis was applied to the plots.

DISCUSSION

If the β_1 values for the Tb and Eu chelates (measured in Part I of this series, ref. 1) are included for comparison, it is observed that the spectrum of β_1 values for the lanthanide

TABLE II

$[L^{2-}]$ and K values for lanthanide tartrates

	dl-Tartaric acid					meso-Tartaric acid		
$10^4[L^{2-}]$	La	Ce	Pm	Tm	Y	$10^4[L^{2-}]$	Ce	Tm
0	1.255	8.78	3.93	2.66	2.97	0	7.78	8.34
2.17	0.550	3.96	1.291	0.597	1.205	1.57	1.786	0.698
3.03	—	3.32	1.137	0.421	—	2.20	1.227	0.516
4.33	0.351	2.29	0.948	0.246	0.651	3.14	0.947	0.316
5.20	0.304	2.00	0.707	0.201	0.496	3.77	0.803	0.255
6.49	—	1.78	0.595	0.114	0.431	4.71	0.681	0.182
8.67	0.183	1.317	0.439	0.0842	0.313	6.28	0.482	0.115
10.83	0.151	0.993	0.334	0.0528	0.210	7.85	0.390	0.0839
13.00	0.124	0.816	0.216	0.0455	0.151	9.42	0.276	0.0629

NOTE: [HTTA], M = 0.09 (La), 0.09 (Ce), 0.045 (Pm), 0.0075 (Tm), 0.015 (Y).

Can. J. Chem. Downloaded from www.nrcresearchpress.com by 210.87.254.40 on 09/05/12
For personal use only.

TABLE III

Stability constants for lanthanide tartrates

		La	Ce	Pm	Eu*	Tb*	Y	Tm
$10^{-3}\beta_1$	*dl*	5.6	6.4	9.8	11.8	8.0	6.15	12.1
	meso	—	30	—	60	44	—	51
$10^{-6}\beta_2$	*dl*	1.05	2.1	2.8	14.7	11.5	7.5	34
	meso	—	8.1	—	88	48	—	95
$10^{-3}b_2$	*dl*	0.19	0.33	0.28	1.25	1.48	1.22	2.8
	meso	—	0.27	—	1.47	1.1	—	1.9
b_1/b_2	*dl*	30	20	35	9.5	5.3	5.0	4.3
	meso	—	110	—	41	40	—	26.8

*Part I of this series (1).

tartrates (both *dl*- and meso-) conforms with the trend exhibited by rare-earth complexes generally. β_1 values increase with decreasing ionic radius from La to Eu, but at this point a discontinuity occurs, and $\beta_1(\text{Tb}) < \beta_1(\text{Eu})$. From Tb to Lu, stabilities again increase with decreasing ionic radius.

The β_1 value for the *dl*-tartrate complex of Y is close to that of Ce, giving Y a lanthanide atomic number equivalent of 58. From consideration of ionic radii (4), one would expect Y (r = 0.90 Å) to be closest in its chemical properties to Ho (r = 0.89 Å) or Dy (r = 0.91 Å), bestowing upon Y a lanthanide atomic number equivalent of 67.6. However, the b_1/b_2 values, when correlated with ionic radius, place Y between Tb and Tm (Z = 65 and 69 respectively). In its chemical properties generally, the position of Y on this atomic number scale is extremely nomadic, and in very few instances, e.g., the extraction by tributyl phosphate (5) from strong nitric acid solutions, does the lanthanide atomic number equivalent of Y equal 67.6. Usually, Y behaves as a lanthanide of $Z < 67.6$, while for ionic complexes with, e.g., acetate (3) and sulphate (6), Y cannot be placed on the atomic number scale at all, i.e., $Z < 57$. In most of its reactions, therefore, Y behaves like a rare earth of effective ionic radius greater than that of Ho or Dy, suggesting that Y retains its hydration shell to a much greater extent than do either Ho or Dy. Moreover, Schwarzenbach (7) has shown that the properties of Y are closest to those of Ho and Dy when it forms strong complexes. These complexes are generally formed by association with powerful chelating or coordinating agents, e.g., ethylenediaminetetraacetic acid or tributyl phosphate, reagents that readily displace hydration sheaths (8). The nomadic behavior of Y on the rare-earth atomic number scale could, conceivably, be due to hydration effects, Y forming, in its weaker complexes "outer sphere" ion pairs. The b_1/b_2 value for the *dl*-tartrate chelate suggests that, in the 1:2 complex, the hydration sheath has been displaced to the same degree as for Ho and Dy.

In Part I of this series (1) it was shown that the b_1/b_2 values for the *d*- and *dl*-tartrate complexes of Tb and Eu were irreconcilable with the Bjerrum statistical treatment (9), and it was concluded that a mechanism was present in the second stage of ion association whereby the stability of the ML_2^- species (hereafter denoted as ML'L'', where L' designates the first tartrate ion to coordinate, and L'' the second) was increased. The b_1/b_2 values for the corresponding meso-tartrates were greater than those for the *d*- or *dl*-complexes by factors of 4–8, indicating that the effect responsible for the increased stability of the 1:2 M–*d*–*d* (i.e., ML'L'' where L' = L'' = *d*-tartrate) and M–*d*–*l* chelates is either absent, or very weak in the 1:2 M–meso–meso complexes. The low b_1/b_2 values

Can. J. Chem. Downloaded from www.nrcresearchpress.com by 210.87.254.40 on 09/05/12
For personal use only.

(Table III) measured for the *d*- and *dl*-tartrate chelates were attributed to hydrogen bridging in the 1:2 complex.

As Table III shows, b_1/b_2 values for the 1:2 M–meso–meso species decrease with decreasing ionic radius of the central metal ion. It would seem, therefore, that either steric hindrance is negligible or that hydrogen bridging, although comparatively weak, is, nevertheless, strong enough to overcome steric obstruction.

In solutions of *dl*-tartaric acid, the species M–*d*–*d*-, M–*l*–*l*, M–*d*–*l*, and M–*l*–*d* will be formed, but the structures M–*d*–*d* and M–*l*–*l* are equivalent, as are also M–*d*–*l* and M–*l*–*d*. The equivalence in complexing power of *d*- and *dl*-tartaric acid (1) indicates that the orientation of the bridging groups of L′ relative to those of L″ must be identical in the M–*d*–*l* and M–*d*–*d* complexes.

Tartaric acid is well endowed with carboxyl and hydroxyl groups, each of which is a potential bridging site. Three bridging models have been considered, two of which are based on O—H - - - O hydrogen bridging, in the first instance via the —OH groups of L′ and L″, and in the second via the —OH of one ligand and the COO^- of the other. A third model would involve C*—H - - - O bridging via the —OH of one ligand and the C*—H of the other. C* represents an asymmetric C atom.

Model A: O—H - - - O Bridging via —OH of L′ and L″

Figures 1(*a*)–1(*c*) represent the structural configurations of *d*-, *l*-, and meso-tartaric

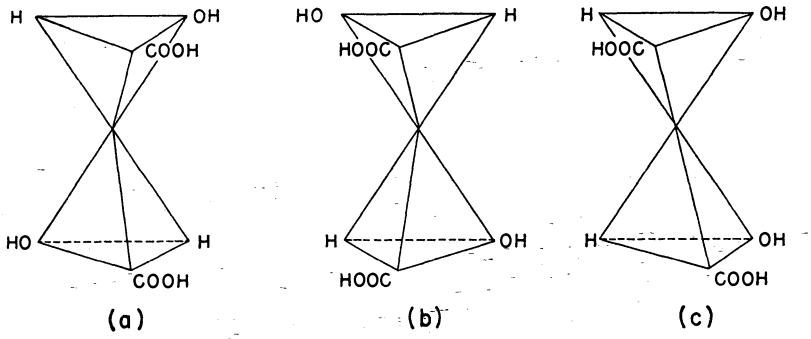

FIG. 1. Configurations of the tartaric acids: (*a*) *d*-tartaric acid; (*b*) *l*-tartaric acid; (*c*) meso-tartaric acid.

acids. For pictorial clarity the tetrahedral space formula for tartaric acid has been used.

Let us, first of all, consider metal complexing in solutions of *d*-tartaric acid, and, more specifically, the two-stage reaction (omitting ionic charges)

$$M + L' = ML'$$
$$ML' + L'' = ML'L''$$

where L′ = L″ = *d*-tartrate. Further, let us consider the probable position of the metal ion in relation to the coordinating groups of L′. Since all four groups of L′ coordinate (1), the metal ion (dotted line in Fig. 2) will be symmetrically placed relative to them. It should be stressed that this and following figures are purely diagrammatic, and serve to give a qualitative picture only. It is difficult to construct atomic models with any geometrical precision, as it is certain that some geometrical distortion of the ligands will occur on complexing. It is possible, for example, that the C*—C* bond axis will attain some curvature, the degree of which depends on how close the ions approach each other.

If we compare the b_1/b_2 values for the *d*- and *dl*-tartrates with those for meso-tartrates,

Can. J. Chem. Downloaded from www.nrcresearchpress.com by 210.87.254.40 on 09/05/12
For personal use only.

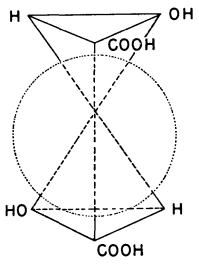

FIG. 2. Configuration of the 1:1 *d*-tartrate complex.

it is evident that hydrogen bridging occurs in the 1:2 *d*- and *dl*-tartrate complexes of all the metals studied. The strengths of the hydrogen bridges in the M–*d*–*d* and M–*d*–*l* complexes will naturally increase as the ionic radius of the metal ion decreases, thus explaining the trend in the b_1/b_2. Since La and Tm have ionic diameters of 2.16 and 1.74 Å respectively (4), it is apparent that some latitude in the geometrical dimensions of the reacting ions in Fig. 2 is permissible. Figure 2 seems a reasonable representation when we consider that C*—C*, C*—C, and C*—OH bond lengths are all of the order of 1.5 Å (10).

The next step to be considered is the addition of L″ to ML′. Rotating Fig. 1(*a*) on its base through an angle of 180° and superimposing directly on Fig. 2, it is evident that the —H and —OH attached to the C* of L′ are, respectively, immediately opposite the —OH and —H of L″. By further rotating L″ on an axis perpendicular to the plane of the paper, it is possible to align the two —OH groups of L″ with those of L′, an orientation conducive to the formation of hydrogen bridges across the M–*d*–*d* complex. Figure 3(*a*) depicts the type of structure conceived, the hydrogen bridges being depicted by arrows.

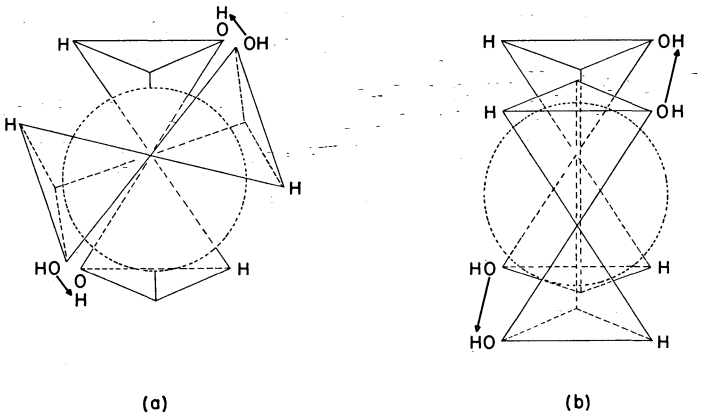

FIG. 3. (*a*) Configuration of ML′L″ (O—H - - - O bridging); L′ = L″ = *d*-tartrate. (*b*) Configuration of ML′L″ (O—H - - - O bridging); L′ = *d*-tartrate, L″ = *l*-tartrate.

Since *d*- and *dl*-tartaric acids give complexes of similar stabilities, the bridging mechanism must, perforce, be in operation in the 1:2 M–*d*–*l* complexes also. The configuration of Fig. 3(*a*) does not, however, represent the system where L′ = *d*-tartrate and L″ = *l*-tartrate, as the —OH groups would no longer be adjacent. If Fig. 1(*b*) is rotated on its base through an angle of 180° and superimposed directly on Fig. 2, the configuration for optimum hydrogen bridging is again achieved (Fig. 3(*b*)).

Can. J. Chem. Downloaded from www.nrcresearchpress.com by 210.87.254.40 on 09/05/12
For personal use only.

Model A has some disadvantages, however. Thus the O atoms of the hydroxyls are already coordinated to three other atoms, and it is reasonable to propose that steric crowding around the O atom may be sufficiently important to prevent its taking part in a hydrogen bond. Moreover, it has been assumed that L′ and L″ are able to orientate themselves, after coordination to the metal ion, in order to make the O—H - - - O bond lengths in the M–*d*–*d* and M–*d*–*l* complexes equal.

Model B: C—H - - - O Bridging*

The possibility exists that four C*—H - - - O hydrogen bridges, involving the —OH groups of L′ and the H atoms attached to the C* of L″ (and vice versa), could be formed in the ML′L″ complex. For complexes with racemic acid, if we rotate Fig. 1(*b*) (*l*-isomer) through 180° on its base and through 45° on an axis perpendicular to the plane of the paper, then superposition on Fig. 2 brings into alignment four (C*—H) hydrogen atoms and four —OH groups. The resultant complex, stabilized by four hydrogen bridges, resembles a Maltese cross (Fig. 4). Again, when L′ = L″ = *d*-tartrate, the rotation of

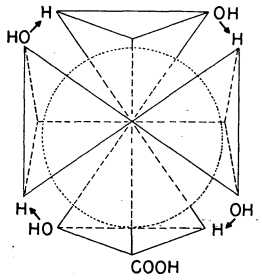

FIG. 4. Configuration of ML′L″ (C—H - - - O bridging); L′ = *d*-tartrate, L″ = *l*-tartrate.

Fig. 1(*a*) through 180° on its base and superposition on Fig. 2 could also bring about hydrogen bonding. However, in only one system, the association of chloroform with strong bases such as pyridine, has conclusive evidence been obtained that a C*—H group can function as a H-bonding acid (11). Since hydrogen bonding in the chloroform–pyridine system is facilitated by the activating influence of three Cl atoms, and since O is more electronegative than C, it would seem that C*—H - - - O bridging in the 1:2 complexes of metal tartrates is comparatively unlikely.

Model C: O—H - - - O Bridging via —OH and —COOH

A hydrogen bridging structure that seems to be the most likely is one involving the —OH groups of one ligand and the C=O of the carboxyl groups of the other ligand. Such a model has one great advantage over models A and B, in that less emphasis is placed on the relative orientation of L′ and L″. In models A and B, it was postulated that the bridging groups (—OH and C*—H) were positioned "off-center" with respect to the metal ion, and to explain the similar stabilities of the M–*d*–*d* and M–*d*–*l* complexes, it was necessary to assign fixed, but different, orientations for L′ and L″ (Figs. 3(*a*), 3(*b*), and 4). It was pointed out in Part I of this series (1) that an ML′ chelate cannot differentiate between a potential binding *d*-tartrate and an *l*-tartrate. Now a —COO^- group of L′ cannot distinguish between a *d*- or an *l*-tartrate either, since the difference would be one between identical groups being to its left and to its right. It follows, therefore, that whatever the relative orientation of L′ and L″, hydrogen bridging, through the —COO^- of L′ and the —OH of L″, will be identical in the M–*d*–*d* and M–*d*–*l* complexes.

Can. J. Chem. Downloaded from www.nrcresearchpress.com by 210.87.254.40 on 09/05/12
For personal use only.

On the basis of an electrostatic model for hydrogen bonding, one would expect that the strength of an O—H - - - O bond formed between —OH and —COOH groups would be greater than that for a similar bond formed via two —OH groups, due to the greater dipole moment of the carboxyl oxygen. Coulson (12) has pointed out, however, the absence of correlation between dipole moment and the strength of a hydrogen bond, indicating that a hydrogen bond has appreciable covalent character. According to Coulson and Danielsson (13), the degree of covalent character associated with a hydrogen bond depends on the bond length; the shorter the bond length the greater the covalency. As the hydrogen bond length is unknown in the 1:2 metal chelates, and since hydrogen bond lengths between similar groups can vary appreciably, it is not possible to presume, on the basis of dipole moments, that hydrogen bridging through the C=O group is favored.

The configurations of the M–*d*–*d* and M–*d*–*l* complexes have not been drawn diagrammatically, as model C imposes no restrictions on the relative orientations of L′ and L″. Presumably, L′ and L″ are positioned at random with respect to each other, and the extreme positions would be represented by the configurations of Figs. 3(*a*) and 4, although hydrogen bridging would occur through the —OH and —COO^- groups.

From the magnitudes of the b_1/b_2 values, bridging must be much weaker in the M–meso–meso complexes. Let us suppose that Fig. 5 represents the 1:1 meso-tartrate chelate, and let us consider the extreme ligand positions whereby hydrogen bridging in the 1:2 complex is first at a maximum, and then at a minimum. Thus the rotation of Fig. 1(*c*) through 45°, anticlockwise, on its base, and superposition of Fig. 5 brings into alignment the carboxyls

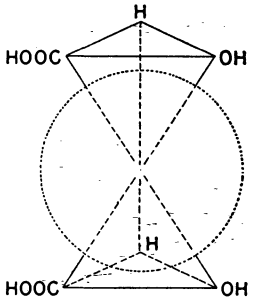

FIG. 5. Symmetrical structure of 1:1 meso-tartrate complex.

and hydroxyls of different ligands, a criterion for strong hydrogen bonding. Also, by rotating Fig. 1(*c*) through 45° clockwise, inverting end-over-end, and then superimposing on Fig. 5, it is evident that the —COO^- and —OH groups of L′ are, respectively, opposite their counterparts of L″. In this configuration, hydrogen bridging would be at a minimum. Statistically, therefore, the degree of hydrogen bridging in the M–meso–meso complexes should be of the same order of magnitude as that in the M–*d*–*d* and M–*d*–*l* chelates. The much greater b_1/b_2 values for the 1:2 meso-tartrates (indicating weaker hydrogen bridging) suggest that a model in which the two —OH and the two —COOH groups have an "equal share" of the cation is incorrect, and that an unsymmetrical configuration, as depicted in Fig. 6, might be a better representation of the 1:1 meso-tartrate chelate. The coordination of L″ to ML′ results in a "staggered" configuration (Fig. 7), in which hydrogen bridging is considerably weakened. Figure 7 indicates that the two coordinated ligands are in fixed orientation relative to each other, but if the unsymmetrical configuration of ML′ (Fig. 6) is correct, then it is conceivable that electronic distortion of the cation renders the "staggered" structure for the M–meso–meso complex the most stable.

Can. J. Chem. Downloaded from www.nrcresearchpress.com by 210.87.254.40 on 09/05/12
For personal use only.

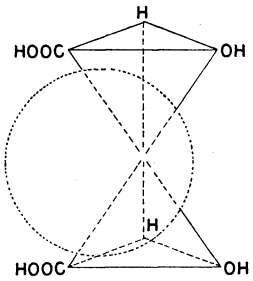

FIG. 6. Unsymmetrical structure of 1:1 meso-tartrate complex.

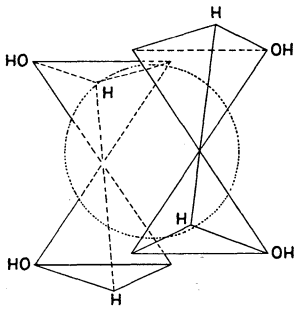

FIG. 7. Staggered configuration of ML'L''; L' = L'' = meso-tartrate.

The approximate dimensions of the 1:2 M–*d*–*d* and M–*d*–*l* complexes may be gauged from the fact that hydrogen bond lengths are normally of the order of 2.5–3 Å. Depending on the degree of geometrical distortion of the ligands, this would suggest an upper limit of about 5 Å for the "diameter" of the complex along the L'—M—L'' axis. Manning and Monk (14) showed that the mean distance of approach of Co and tartrate ions was 4.0 Å, indicating that in the M–*d*–*d* and M–*d*–*l* complexes bonding is covalent in character, or that the ions are stripped of their hydration sheaths and are in contact.

It is interesting to compare our results with those of Fronaeus (15) for complexing between Cu^{2+} and *d*- or *dl*-tartaric acids. This worker found that β_1(Cu *d*-tartrate) > β_1(Cu *dl*-tartrate), while β_2(Cu *d*-tartrate) = β_2(Cu *dl*-tartrate). Four tartrates coordinated to a single Cu^{2+}, and β_3(Cu *d*-tartrate) < β_2(Cu *d*-tartrate), indicating that structural changes, brought about by the coordination of L''', have resulted in a weaker complex.

CONCLUSION

The increased stability of the ML_2^- complexes of lanthanide ions with *d*- and *dl*-tartaric acid has been ascribed to ligand–ligand hydrogen bridging. Three different hydrogen bridging models have been described. It is proposed that O—H - - - O bridging occurs via the —COO^- groups of one ligand and the —OH groups of the other.

Some light could be shed on this problem of hydrogen bridging in metal chelates, by examining the infrared and Raman spectra of Th(tartrate)$_2$, and some work along those lines is in progress.

ACKNOWLEDGMENTS

The author wishes to express his gratitude to the National Research Council of Canada for the award of a Fellowship, and to Dr. G. G. Eichholz for many stimulating discussions.

Can. J. Chem. Downloaded from www.nrcresearchpress.com by 210.87.254.40 on 09/05/12
For personal use only.

REFERENCES

1. P. G. MANNING. Can. J. Chem. This issue.
2. P. G. MANNING and C. B. MONK. Trans. Faraday Soc. **58**, 938 (1962).
3. R. S. KOLAT and J. E. POWELL. Inorg. Chem. **1**, 293 (1962).
4. D. H. TEMPLETON and C. H. DAUBEN. J. Am. Chem. Soc. **76**, 5237 (1954).
5. D. F. PEPPARD, W. J. DRISCOLL, R. J. SIRONEN, and S. MCCARTY. J. Inorg. Nucl. Chem. **4**, 326 (1957).
6. F. H. SPEDDING and S. JAFFE. J. Am. Chem. Soc. **76**, 882 (1954).
7. F. J. WHEELWRIGHT, F. H. SPEDDING, and G. SCHWARZENBACH. J. Am. Chem. Soc. **75**, 4196 (1953).
8. T. MOELLER and T. M. HSEU. J. Inorg. Nucl. Chem. **24**, 1635 (1962).
9. J. BJERRUM. Metal ammine formation in aqueous solution. P. Haase and Son, Copenhagen. 1941.
10. F. STERN and C. A. BEEVERS. Acta Cryst. **3**, 341 (1950).
11. G. C. PIMENTEL and A. L. MCCLELLAN. The hydrogen bond. Freeman, San Francisco. 1960.
12. C. A. COULSON. Research (London), **10**, 149 (1957).
13. C. A. COULSON and U. DANIELSSON. Arkiv Fysik. **8**, 239 (1954).
14. P. G. MANNING and C. B. MONK. Trans. Faraday Soc. **57**, 1996 (1961).
15. S. FRONAEUS. Dissertation, Lund. 1948.

Can. J. Chem. Downloaded from www.nrcresearchpress.com by 210.87.254.40 on 09/05/12
For personal use only.

PROTONATED CARBONYL GROUPS

II. γ-PYRIDONE SALTS[1]

DENYS COOK

Exploratory Research Laboratory, Dow Chemical of Canada, Limited, Sarnia, Ontario

Received June 10, 1963

ABSTRACT

The salts of 1,2,6-trimethyl-4-pyridone and 1-ethyl-2,6-dimethyl-4-pyridone and mineral acids and their deuterated analogues have been prepared and their spectra recorded. The spectra are consistent with protonation at the carbonyl oxygen atom, not the nitrogen atom. Many similarities with the spectra of γ-pyrone salts (D. Cook. Can. J. Chem. **41**, 505 (1963)) have been observed. ν_{OH} varies from 2495 cm^{-1} in the HCl salt to 3470 cm^{-1} in the HPF_6 salt. The deformation mode, ν_{OH}, is much more constant in frequency and is doubled, near 1300 and 1230 cm^{-1}, probably due to correlation field splitting. A few of the more strongly hydrogen-bonded salts have torsional modes around 800 cm^{-1}.

Many of the salts can also be prepared in a hydrated form which contains the same organic cation, probably hydrogen bonded to chains of water molecules.

In one case a salt containing 2 molecules of the base to 1 of acid ($HAsF_6$) has been prepared. The spectrum contains a very broad, strong band, near 1300 cm^{-1}, probably due to the species $[B\cdots H\cdots B]^+AsF_6^-$.

INTRODUCTION

The vibrational spectra of γ-pyrones (1) and γ-pyridones (2, 3) and their complexes with Lewis acids (4, 5) have recently been recorded. The latter were consistent with the view that the donor site was the carbonyl oxygen atom. Several protonated γ-pyrones revealed interaction at the same site (6).* Though there was a wide variation in the frequency of the OH stretching vibration, ν_{OH}, depending on the nature of the anion, O—H···X⁻, the bending mode, δ_{OH}, was much more constant (±18 cm^{-1}) while the torsional mode, γ_{OH}, was not observed.

Since the γ-pyridones are structurally very similar to the γ-pyrones, and are made from them by simple reactions, it was of interest to see if the spectroscopic behavior of protonated γ-pyridones was similar to that of γ-pyrones.

Previous work on the n.m.r. spectra of γ-pyridone salts in solution led to the conclusion that oxygen protonation took place (7). However, the vibrational spectrum of 4-pyridone.HCl was interpreted on the basis of a protonated nitrogen atom (8).

RESULTS

The frequencies of the absorption bands have been abstracted from the spectra and are shown in Tables I and II for 1-ethyl-2,6-dimethyl-4-pyridone and 1,2,6-trimethyl-4-pyridone salts respectively. The bands due to the stretching vibrations of the protonating hydrogen and deuterium atoms are collected in Table III, and those due to the in-plane deformations in Table IV.

The spectrum of a representative 1-ethyl-2,6-dimethyl-4-pyridone salt is shown in Fig. 1, the solid line being that of the H_2SnCl_6 salt, the broken line being that of the deuterated salt. The 1,2,6-trimethyl-4-pyridone salts have very similar spectra except for differences in absorptions due to the nitrogen alkyl group vibrations.

[1]*Contribution No. 96.*
**Part I of the series.*

Can. J. Chem. Downloaded from www.nrcresearchpress.com by 210.87.254.40 on 09/05/12
For personal use only.

TABLE

	Cl^-		Br^-		I^-		$SiF_6^=$		ClO_4^-	
	H	D	H	D	H	D	H	D	H	D
νCH	3065w	3055w	3058m, sh	3050m, sh	3060m		3065m	3062m	3072m	3064m
νCH	3048w	3044w	3046m	3042m	3036m					
νCH_3			2978m	2980m	~2980m, sh		2995m	2995m	3002m	3002w
νCH_3	2934w	2936w	2932m	2932m			2930w	2932w	2952w	2953vw
	2721m	2100w								
	2690w	2064m								
	2641w	2047m	2890m, sh	2378m						
	2600m	2038m, sh	2860m, sh	2192m						
	2568m	1995m, sh	2835s	2170m, sh	2930s, b			2250m, sh		
νOH	2495s	1969s	2782s, b	2140s	2908s, b	2203s		2235m, b	3190s, b	2389s
	2466s	1932s	2735s	2120m, sh	2875s, sh	2180m, sh		2043w	3125m, sh	2365s, sh
		1922s	2685m, sh	1991m	2800m, sh	2160m, sh				
	2370w, sh	1880m, sh	2639m	1975m	2730m, sh	2110m				
			2599m	1965m, sh	2670w, sh					
			2574m	1929m	2570w					
			2528m	1915m, sh	2505w					
			2463m		2440w					
	1695w									
	1637s, sh	1638s	1648s, sh						1649s, sh	1646s, sh
νCC	1630s	1632s	1639s	1635s	1641s	1638s	1637s	1639s	1644s	1640s
					1638s, sh		1634s, sh	1636s, sh		
νCC	1583m	1571s	1585m	1578m, sh	1586m	1572m	1589m	1572m	1598s	1584m
	1578m, sh	1578m, sh	1564m	1570m	1580m, sh	1580m	1578m, sh	1580m, sh	1580m, sh	1579m, sh
	1560m, sh	1560m, sh		1560m, sh	1560w, sh	1560m, sh	1560w, sh	1560w, sh	1561w, sh	1560w, sh
	1511m	1509m	1509m, sh	1508w, sh	1508w, sh		1512w, sh	1507m	1515m	
	1501m	1501m	1500m	1500m, sh			1500m	1498m, sh	1500m	1508m
νCO	1477s	1478s	1474s	1473m	1497m	1488m	1480m	1480m	1480m	1480m
		1473m, sh			1460m, sh	1470m			1475m, sh	1472m, sh
	1460m	1460m	1460m, sh	1455m, sh	1450m, sh	1455m, sh	1442m	1448m	1450m	
	1440m	1440m	1438m	1430m, sh	1442m	1440m, sh			1437m	1438w
						1410w, sh				
	1370w, sh		1370w, sh	1368w, sh			1368m, sh	1368m	1376w, sh	1372w, sh
	1360m	1362m	1359m	1358m	1365w, sh	1365w, sh	1360m, sh		1366m	1363m
	1342m		1334w		1352m	1354m	1350m		1356m	1354m
							1330m, sh	1333m, sh	1330w, sh	
	1324s	1324m	1321s	1320m	1320m	1319s	1323s	1326s	1320s	1319s
δOH	1307m	1009m	1298m	998m	1282m	990m	1310m	1015m	1295m	999m
		1252w						1260w		1252w
δOH	1231w	939w	1228m	932w	1218m	926m	1240m	924m	1230m	
							1222w	1225vw		
		1188w, sh								
	1180w	1181w	1182m	1180w	1180m	1178m	1190m	1192m	1185m	1184m
δCH	1162s	1162s	1161s	1160w	1160s	1159s	1163s	1165s	1161s	1160s
	1127w	1130w	1128w	1134m	1129w	1124w	1128w	1128w		
	1088w	1088w	1088m	1088w	1084w	1083m	1075m	1078w	1088s	1088m
		1061w				1060m				
	1050w	1050w	1049m	1048m	1048w	1048m	1050w	1050m, sh		
		1041w					1038m	1042m		
νCC	1028w	1029w	1029m	1028w	1029w	1029m		1025m, sh	1030s	1028s
	980vw	982vw	983w		985m	975m			987w	
	968w	968w	967w	965w	963w	963m	958vw	962vw	976w	970w
	948vw	939w					940vw	938w	950vw	
							920m	915w	931m	930m
									925m, sh	922m, sh
δCC	894m	885m	889m	887m	895m	893m	896s	898m	885m	884m
	877s	875s	872s	872m	872m	872m	873m	876vw		
									865m	864m
γOH	862m		800m		745w					
	802w	802w					790w	792vw	803w	802w
	730w	730w							748m	730w

Can. J. Chem. Downloaded from www.nrcresearchpress.com by 210.87.254.40 on 09/05/12
For personal use only.

I

	$SnBr_6^=$		$PtCl_6^=$		$SnCl_6^=$		BF_4^-		AsF_6^-		PF_6^-	
	H	D	H	D	H	D	H	D	H	D	H	D
ν_{CH}	3054vw		3053m	3052m	3058m	3053m	3079w	3080w	3086w	3085w	3084w	3080w
ν_{CH_3}			2984w	2984w	2998w	2997w						
ν_{CH_3}			2938w	2940w	2953w	2940w	3008w	3006w	2999w	2999w	3010w, sh	3010w, sh
							2959w	2956w	2952w	2950w	3000w	3000m
			3300m, sh	2455m, sh								
			3260s, sh	2430s								
ν_{OH}	3220s, vb	2400m, b	3230s, b	2420s	3238s	2412s	3292s	2450s	3462s	2565s	3470s	2567s
		2140w		2375m, sh								
							1658m, sh	1652m, sh	1655w, sh	1657w, sh		
		1637s, sh	1637s	1639s	1636s, sh	1635s, sh	1649s, sh	1647s, sh	1650m, sh	1650m, sh		
ν_{CC}	1630s	1630s	1632s	1632s	1631s	1629s	1645s	1640s	1641s	1640s	1640s	1640s
ν_{CC}	1591s	1578m	1591s	1582m	1589m	1578m	1600s	1587m	1600s	1590m	1600s	1588s
								1578m, sh				
		1560m, sh						1565w, sh				
	1508w							1510m				
							1500m			1500w	1500w	1500 w
ν_{CO}	1490m	1490m	1494m	1493m	1492m	1492m	1482m	1480s	1480s	1480s	1480s	1478s
	1470m	1470m	1474m	1473m	1478m	1478m			1475m, sh	1478m, sh	1472m, sh	1472s, sh
	1433m	1435vw			1449m	1447m	1452m	1440m	1445m	1450m	1445m	1450m
	1422m	1420m	1436m	1438m	1440m	1435m			1436m	1435m		
		1410m, sh			1432m				1419w	1420w		
	1374w	1374w	1368m, sh	1368m, sh	1370m	1368m	1380w	1379w	1380w	1380w	1380w	1382w
	1368m	1367m	1360m	1362m	1360m	1358m	1368w	1364m, sh	1372w	1370w	1370w	1370w
	1355m	1354m					1355m	1355m	1362m	1361m	1360m	1360s
	1330m	1330m			1332w							
	1316s	1317m	1321m	1320s	1320m	1319m	1322s	1318s	1324m	1322s	1324s	1323s
δ_{OH}	1290m	994m	1292m	992m	1295m	995m	1296m	1000m	1291m	994m	1290s	996m
	1261w	1255w		1250w		1251w	1280w, sh	1270w		1255w	1232m	1255w
δ_{OH}	1221m	929m	1231m	929m	1216w	926m	1230w	930m	1220w	930m	1220m	933m
			1218w	1220vw								
	1178m	1178w	1182m	1182m	1178w	1178w	1188w	1182m	1185m	1184m	1187m	1187m
δ_{CH}	1157s	1157s	1159s	1160s	1156s	1150s	1162s	1159s	1160s	1160s	1160s	1160s
	1128vw	1130w	1126w	1122w	1122vw	1120w		1138s	1132w	1130w	1134m	1140m
	1087m	1088w	1088w	1088w	1090w	1090w	1085s	1085vs	1087w	1087w	1088w	1089m
			1078w	1078m								
	1038w	1038w	1042vw	1045w								
ν_{CC}	1027m	1025w	1030m	1030m		1040vw	1039m	1035m	1045w	1045w	1046w	1048m
			1022w	1020w	1022m	1020w	1029m	1020m	1032w	1032w	1032w	1032m
	982vw		985vw		985vw	976vw			988vw	977w	989vw	978m
	969vw	969w	964vw	968w, sh	969vw	968vw	968s	957s	965vw	965w, sh	966vw	
	940vw		942vw		942vw						945vw	
δ_{CC}	870s	869m	890m	890m	891m	890m	888m	883m	881m	880m		
			878m	877m	879m	878m	868m	863m	869m	869m		
	865m	863m	868m	865m								
γ_{OH}												
	808vw	803w	804w	804w	806w	804w	808w	801w	801w	801w		
	730w	730w	730w	730w	730w	730w	730w	730w				

Can. J. Chem. Downloaded from www.nrcresearchpress.com by 210.87.254.40 on 09/05/12
For personal use only.

Can. J. Chem. Downloaded from www.nrcresearchpress.com by 210.87.254.40 on 09/05/12
For personal use only.

TABLE II

	Cl^-		Br^-		I^-		AsF_6^-		$SbCl_6^-$		PF_6^-	
	H	D	H	D	H	D	H	D	H	D	H	D
					3108m							
	3068w	3044m, sh	3063m		3055m, sh							
	3042w	3035m	3040m		3039m, sh							
	2962m											
	2715w	2085w										
	2644w	2050w										
	2598w	2030w		2275m								
	2528m	1970m, sh	2940s	2190m, sh								
	2470m, sh	1952m	2865s, sh	2180m								
ν_{OH}	2410s	1888s	2815s, b	2142s	2988s, b	2244s	3395vs, b	2562vs	3403s	2530s	3458vs, b	2562vs
	2370s, sh	1860m, sh	2728s, sh	2010s, sh	2940s, sh	2160m						
	2355m, sh	1800w, sh	2652s	2032w	2850m, sh							
	2312m, sh		2606m	1997m	2790m, sh							
	2175w		2558s	1979m	2548w							
	1762vw		2512m	1961m	2498w							
	1744vw		2468m	1926m	2452w							
	1706w				1765vw							
	1652m, sh	1653m, sh										
	1647m, sh	1647s, sh			1656m, sh	1654m, sh	1654s, sh		1658m, sh	1656m, sh		
	1636s, sh	1637s	1655s, sh	1657s, sh	1650s, sh	1646s	1648s, sh	1651s, sh	1650m, sh	1648s, sh	1651s, sh	1652s
ν_{CC}	1630s	1632s	1648s	1649s	1642s	1636s	1638s	1644s	1640s	1640s	1644s	1648s, sh
			1638s, sh	1630s	1625m, sh	1628s, sh			1632s	1635s, sh		
ν_{CC}	1586m	1578s	1592s	1583s	1592s	1582s	1596s	1587s	1594s	1585s	1596s	1588s
	1577m, sh	1560w, sh	1560m, sh	1580s, sh	1578m, sh	1578m, sh	1578m, sh	1575m, sh	1580w, sh		1575w, sh	1575w, sh
			1552m	1550m	1560w	1558w	1560w, sh	1557w, sh			1560w	1560w, sh
	1520vw		1520vw		1515w		1518w, sh	1508w, sh	1510w	1498w	1518w	1508w
		1498m, sh	1495m, sh	1495m, sh	1492m	1490m						
ν_{CO}	1480s	1481m	1483s	1482m	1482m	1480m	1492s	1491s	1491s	1490s	1483m	1483m
							1472m, sh		1440m	1438m	1445m	1440w, sh
	1440vw	1435w	1442w		1446m	1455w	1440m	1440w	1417m	1415m	1420m	1422m
	1417m	1415w, sh	1415s	1418m	1420m	1418m	1422m	1417m				
	1402m	1409m			1396m	1400w						
	1380w		1380w	1380w	1378m	1375w	1374w		1370w	1368w		
	1361m		1365w	1365w	1368m	1361m			1340s	1335s	1366m	1367w
	1330m, sh	1340m, sh	1325s	1330s	1332s	1329s	1335s	1332s	1333m	1330m, sh	1330m	1338s
	1325s	1328s	1320s, sh		1325m, sh	1320w, sh	1325m, sh		1318m		1315m	1330s, sh
							1304m	1312w, sh	1308m	1303m	1305m	1310w, sh
δ_{OH}	1275m	1008m	1274m	1002m	1270m	992m	1265m	990m	1264m	987m	1268m	990m
δ_{OH}	1230m	930w	1230m	930m	1224m	923m	1206m	915m	1217m	913m	1220m	919m
	1180m	1180m			1185w	1182w	1180w	1176w, sh	1182w		1180m	1180m, sh
	1168s	1166s	1170s	1171s	1169s	1169s	1160s	1160s	1164s	1163s	1162s	1162s
	1110vw			1129m								1118w
	1046m	1046m			1046w	1046w	1045m	1040m, sh	1040m, sh	1039m, sh	1040m	1041m
	1036m	1036m	1039m	1035m	1037m	1034m	1036m	1030m	1032m	1031m	1030m	1031m
		1025w	1025m	1026m	1025m	1024m						
	980vw	980vw	982w	982w	985w	977vw	987w	970w	972w	968m	981w	974m
	936vw		939w	926w	938w		936w		935w	935vw		
	898m	887m	893m	893m	890m	888m	870s	875m	870s	869s		879vs
	878s	870s	865s	868m	864m	863m	863m	866m	860s	859s		
	858w											
	785vw	785vw	790m	790w		800m						

TABLE III

OH and OD stretching frequencies in 4-pyridone salts

	ν_{OH}	$\Delta\nu_{1/2}$*	ν_{OD}	$\Delta\nu_{1/2}$*	ν_{OH}/ν_{OD}
		1-Ethyl-2,6-dimethyl-4-pyridone salts			
Cl^-	2495		1969		1.27
Br^-	2782		2140	80	1.30
I^-	2908	180	2203	70	1.32
$SiF_6^=$			2235	160	
ClO_4^-	3190	180	2389	90	1.34
$SnBr_6^=$	3220	205	2400	130	1.34
$PtCl_6^=$	3230	200	2420	120	1.33
$SnCl_6^=$	3238	125	2412	75	1.34
BF_4^-	3292	110	2448	65	1.34
AsF_6^-	3462	80	2565	55	1.35
PF_6^-	3470	75	2567	60	1.35
		1,2,6-Trimethyl-4-pyridone salts			
Cl^-	2410	195	1888	110	1.28
Br^-	2815	180	2142	80	1.31
I^-	2988	120	2244	85	1.33
AsF_6^-	3395	165	2550	95	1.33
$SbCl_6^-$	3403	85	2530	50	1.35
PF_6^-	3458	95	2562	50	1.35

*Approximate band half-width. Where none is given it could not be estimated because of overlapping of multiple bands.

TABLE IV

OH and OD bending frequencies in 4-pyridone salts

	δ_{OH}	δ_{OD}	Ratio	δ_{OH}	δ_{OD}	Ratio
			1-Ethyl-2,6-dimethyl-4-pyridone salts			
Cl^-	1307	1009	1.30	1231	939	1.31
Br^-	1298	998	1.30	1228	932	1.32
I^-	1282	990	1.29	1218	926	1.32
$SiF_6^=$	1310	1015	1.29	1240	924	1.34
ClO_4^-	1295	999	1.30	1230		
$SnBr_6^=$	1290	994	1.30	1221	929	1.31
$PtCl_6^=$	1292	992	1.30	1231	929	1.33
$SnCl_6^=$	1295	995	1.30	1216	926	1.31
BF_4^-	1296	1000	1.30	1230	930	1.32
AsF_6^-	1291	994	1.30	1220	930	1.31
PF_6^-	1290	996	1.30	1220	933	1.31
			1,2,6-Trimethyl-4-pyridone salts			
Cl^-	1275	1008	1.26	1230	930	1.32
Br^-	1274	1002	1.27	1230	930	1.32
I^-	1270	992	1.28	1224	923	1.33
AsF_6^-	1265	990	1.28	1206	915	1.32
$SbCl_6^-$	1264	987	1.28	1217	913	1.33
PF_6^-	1268	990	1.28	1220	919	1.33

DISCUSSION

Anhydrous 1:1 Salts

Most of the important features in the spectra of the γ-pyrone salts (6) are duplicated in those of the γ-pyridone salts. These include the strong absorption with multiple peaks centered near 2495 cm^{-1} in the HCl salt, moving and narrowing as the anionic influence weakens to 3470 cm^{-1} in the HPF_6 salt. In the deuterated salts the expected shifts to lower frequency occur, the isotopic ratios being between 1.29 and 1.35 (see Table III).

The in-plane hydrogen-bending mode is doubled, and at a similar frequency in the

Can. J. Chem. Downloaded from www.nrcresearchpress.com by 210.87.254.40 on 09/05/12
For personal use only.

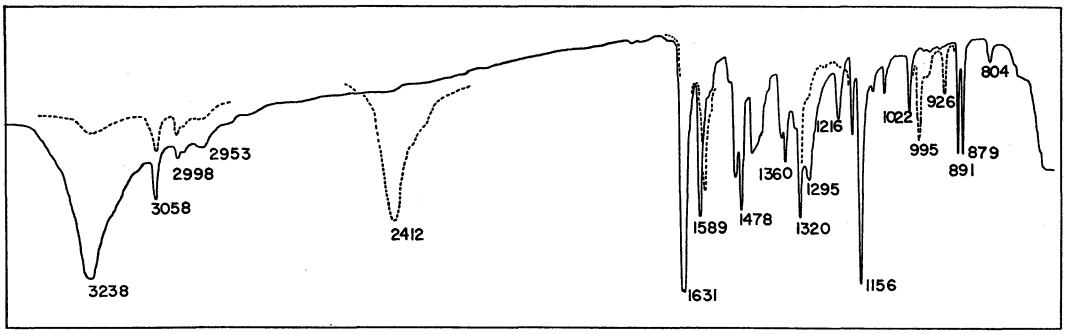

FIG. 1. Infrared spectrum of (1-ethyl-2,6-dimethyl-4-pyridone)$_2$.H_2SnCl_6, solid line; deuterated salt, broken line.

two sets of compounds. In the γ-pyridone salts there is a doublet near 1300 and 1230 cm^{-1} with slight variation in the different salts. A plot of ν_{OH} against δ_{OH} reveals a trend to higher deformation frequencies as the stretching frequency lowers. This is in keeping with the view (9) that stronger hydrogen bonds have higher δ_{OH} and lower ν_{OH}, but the plot is very scattered with a poor correlation. The higher-frequency component of the doublet is the more intense, but part of this may be due to another strong band close to it near 1320 cm^{-1}. On deuteration these bending modes give absorption bands near 1000 and 930 cm^{-1}, of comparable intensity, with isotopic ratios near 1.30.

The splitting of the in-plane hydrogen-deformation mode into two components near 1300 and 1230 cm^{-1} recalls similar doubling in γ-pyrone salts (6), which was attributed to correlation field splitting. The similarity of the splittings both in frequency and separation suggests that a very similar space group will be involved in the structural arrangements in these γ-pyridone salts. The N-alkyl groups, which constitute the sole difference between the γ-pyridones presently considered and the γ-pyrones, would be expected to play a minor part in the determination of the crystal structure, the hydrogen bond having a dominant role. Other possible causes for the doubled bending mode have been sought but none is as satisfactory as correlation field splitting. Fermi resonance of a single bending mode with an overtone or a combination tone can be discounted in view of the isotope shifts, except if a torsional mode having a constant frequency also involving an isotopic shift were involved. This again can be rejected because of the large variation in position of the torsional modes (862, 800, and 745 cm^{-1} respectively in the HCl, HBr, and HI salts of 1-ethyl-2,6-dimethyl-4-pyridone). Two distinctly different crystallographic environments could cause splitting; but as the largest and smallest values of δ_{OH} differ by 28 cm^{-1} it seems unlikely that the observed splittings (average 76 cm^{-1}) can be explained in this way.

All these bands (with the exception of those due to the torsional mode) are so similar to those in γ-pyrone salts that a strong presumption of a similar protonation site is present. Further evidence can be derived from the carbonyl and ring stretching frequencies. All the salt spectra show a very strong band at about 1630 cm^{-1}, a weaker one at about 1480 cm^{-1}, and a still weaker one near 1583 cm^{-1}. In 1-ethyl-2,6-dimethyl-4-pyridone itself these bands are at 1638, 1566, and 1547 cm^{-1} respectively. In the Lewis acid complexes (5) only one band at 1566 cm^{-1} showed any change in position, and this in a progressive manner to lower frequency as the Lewis acid strength increased. This band was assigned to the carbonyl stretching vibration. In the protonated salts the

Can. J. Chem. Downloaded from www.nrcresearchpress.com by 210.87.254.40 on 09/05/12
For personal use only.

band at 1480 cm^{-1} is to be associated with the carbonyl frequency, and the two bands at 1630 and 1580 cm^{-1} with the ring modes. Again, this behavior follows very closely that of the protonated γ-pyrones. Furthermore, the spectra of salts of 1-ethyl-2,6-dimethyl-4-thiopyridone, while showing a strong band near 1620 cm^{-1} and a weaker one near 1560 cm^{-1}, have no band near 1480 cm^{-1}, which strengthens the assignment of the protonated carbonyl group stretching vibration to the 1480 cm^{-1} band.

Evidence is thus accumulating that a protonated carbonyl group has in-plane hydrogen-bending frequencies near 1260 cm^{-1} (mean value of split components), for example, the salts of 1-ethyl-2,6-dimethyl-4-pyridone, 1261 cm^{-1}; 1,2,6-trimethyl-4-pyridone, 1246 cm^{-1}; 2,6-dimethyl-4-pyrone, 1253 cm^{-1} (6); 4-pyrone, 1273 cm^{-1} (6); N,N dicyclohexylacetamide, 1287 cm^{-1} (10); antipyrine, 1260 cm^{-1} (11). (The N,N-dicyclohexylacetamide value may be slightly affected by coupling, in that the ratio of the hydrogen and deuterium deformation frequencies is 1.18, whereas in all the other salts listed it is near 1.31.) It has been pointed out before (6) that these deformation frequencies are very different from those of protonated tertiary (sp^3) amines, which are close to 1400 cm^{-1}, for example, $(CH_3)_3N$ salts, 1420 cm^{-1} (12, 13); triphenylamine salts, 1390 cm^{-1} (13); N-alkylpiperidine salts, 1400 cm^{-1} (14); NH_4^+ salts, ν_4, 1390 cm^{-1} (15, 16). These values are so well founded that it is possible to assert with some confidence that a structure such as I is not consistent with the experimental data, while structure II is.

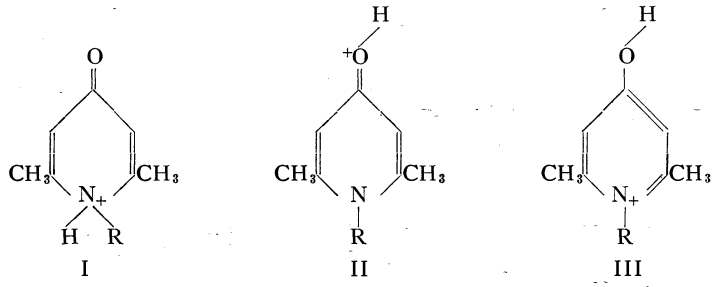

Experimental evidence is also accumulating that a protonated carbonyl group results in a carbonyl stretching frequency in the region 1400–1500 cm^{-1}, for example, the salts of 1-ethyl-2,6-dimethyl-4-pyridone, 1475 cm^{-1}; 1,2,6-trimethyl-4-pyridone, 1485 cm^{-1}; 2,6-dimethyl-4-pyrone, 1480 cm^{-1} (6); 4-pyrone, 1490 cm^{-1} (6); N,N-dicyclohexylacetamide, 1400 cm^{-1} (10). The last value may be slightly affected by coupling.

It could be suggested that since the salts with weak hydrogen bonding between the OH group and the anion have high values of ν_{OH} (close to values for phenols) III would represent a realistic description of the structure of the cation. This would neglect the rather high stretching frequency of the CO bond. At about 1480 cm^{-1} this is somewhat higher than in phenols. A CO bond distance appropriate to this stretching frequency has been derived (ref. 17 and unpublished work) of about 1.28 Å. This is a good deal smaller than the CO bond distance in some phenols, for example, 4-isopropylideneaminophenol, 1.38 Å (18), α-resorcinol, 1.35 Å (19), indicating a significant contribution from π-electron binding in the CO bond in the pyridone salts. This contribution must be sensibly constant too in all the salts considered, since the position of all bands other than those due to the OH group are remarkably constant in frequency.

Anhydrous 2:1 Salts

It is possible to prepare a salt of 1-ethyl-2,6-dimethyl-4-pyridone and $HAsF_6$ containing 2 moles of base to 1 of acid. Its spectrum is significantly different from those

Can. J. Chem. Downloaded from www.nrcresearchpress.com by 210.87.254.40 on 09/05/12
For personal use only.

of the 1:1 salts (see Fig. 2) and is characterized by lack of absorption in the region above 2500 cm^{-1}, but has a strong, broad absorption near 1300 cm^{-1}.

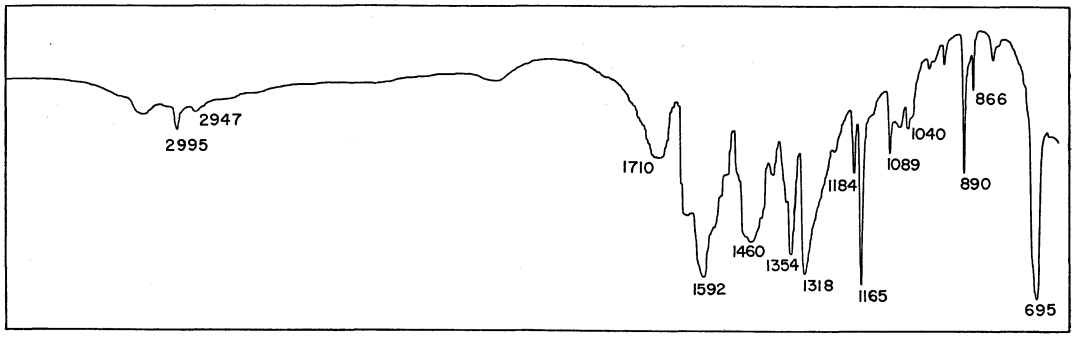

FIG. 2. Infrared spectrum of (1,2,6-trimethyl-4-pyridone)$_2$.$HAsF_6$.

Similar complex acids have been found to give anomalous 2:1 salts with pyridine-1-oxides (20), and the suggested structure was $[C_5H_5NO\cdots H\cdots ONC_5H_5]^+MX_n^-$. Other bases which have been found to give 2:1 salts are trimethylamine oxide, triethylamine oxide, 2,6-dimethyl-4-pyrone, 1-methyl-2-pyridone, and 1-methyl-2-quinolone (21).

The high intensity, low frequency, and great breadth of the bands due to the proton in these 2:1 salts are associated with very short, probably symmetrical, hydrogen bonds as was described by Albert and Badger (22) and Takei (23) for acetamide hemihydrochloride, by Kutzelnigg and Mecke for other acetamide salts (24) and some urea salts (25), and by Hadzi for salts of various oxide bases (26).

Hydrated 1:1 Salts

The hydrated salts incorporate 1 molecule of water into the lattice for each molecule of base. This alters the absorption bands above 2000 cm^{-1} but makes little difference to those below this region. In particular, the bands at 1630, 1580, and 1480 cm^{-1} are unchanged. The in-plane hydrogen-deformation vibration still gives rise to a doubled absorption near 1230 and 1300 cm^{-1}. The pyridone cation is therefore present, which makes it likely that the hydrate structure is $(BaseH)^+.X^-.H_2O$ rather than $Base.H_3O^+.X^-$. The OH stretching vibrations above 2000 cm^{-1} show some unusual splittings and are being investigated further.

EXPERIMENTAL

1-Ethyl-2,6-dimethyl-4-pyridone

This was prepared as described previously (5).

HCl Salt

The preparation has been previously described (5).

HBr Salt

A chloroform–ether solution of the anhydrous pyridone was treated with anhydrous HBr, depositing the anhydrous salt; m.p. 234–235°. Found: HBr, 34.1%. Calc. for $C_9H_{13}NO.HBr$: HBr, 34.8%.

HI Salt

The same technique was used with anhydrous ethereal HI (from aqueous HI, by shaking with ether then drying with anhydrous Na_2SO_4), giving the anhydrous salt; m.p. 208–210°. Found: HI, 45.3%. Calc. for $C_9H_{13}NO.HI$: HI, 45.8%.

Can. J. Chem. Downloaded from www.nrcresearchpress.com by 210.87.254.40 on 09/05/12
For personal use only.

H_2SiF_6 Salt

The anhydrous pyridone (0.76 g) and aqueous (30%) H_2SiF_6 (1.2 g) were mixed and the excess water removed *in vacuo*; m.p. 150–151°. Found: H_2SiF_6, 32.2%. Calc. for $(C_9H_{13}NO)_2.H_2SiF_6$: H_2SiF_6, 32.2%.

$HClO_4$ Salt

Crystals of the hydrated salt were deposited when 1.03 g of the pyridone trihydrate in 2 ml water was mixed with aqueous (60%) $HClO_4$ (0.7 g). The anhydrous salt was obtained by removal of water *in vacuo*; m.p. 208–210°. Found: $HClO_4$, 39.4%. Calc. for $C_9H_{13}NO.HClO_4$: $HClO_4$, 39.8%.

H_2SnBr_6 Salt

The pyridone HBr salt (2.32 g) in water (2 ml) gave a copious precipitate of the anhydrous salt when treated with $SnBr_4$ (3.4 g) in aqueous (48%) HBr (2 ml); m.p. 202–204°. Found: H_2SnBr_6, 67.6%. Calc. for $(C_9H_{13}NO)_2.H_2SnBr_6$: H_2SnBr_6, 66.6%.

H_2PtCl_6 Salt

Aqueous (5%) $H_2PtCl_6.6H_2O$ (15.5 g) and the pyridone HCl salt (1.2 g) on being mixed gave a clear solution which quickly precipitated out the hydrated salt; m.p. 221–222°. Found: C, 29.55%; H, 3.97%; N, 3.73%. Calc. for $(C_9H_{13}NO)_2.H_2PtCl_6.H_2O$: C, 29.27%; H, 4.09%; N, 3.79%. The anhydrous material was obtained by dehydration *in vacuo*; m.p. 218–219°. Found: H_2PtCl_6, 58.0%. Calc. for $(C_9H_{13}NO)_2.H_2PtCl_6$: H_2PtCl_6, 57.6%.

H_2SnCl_6 Salt

The pyridone HCl salt (0.94 g) in H_2O (3 ml) on being mixed with $SnCl_4$ (1.22 g) in conc. HCl (3 ml) deposited the anhydrous salt; m.p. 256–259°. Found: H_2SnCl_6, 53.5%. Calc. for $(C_9H_{13}NO)_2.H_2SnCl_6$: H_2SnCl_6, 52.5%.

HBF_4 Salt

The pyridone (1.51 g) was slurried with H_2O (1 ml), and aqueous (50%) HBF_4 (1.78 g) added, giving crystals of the hydrated salt; m.p. 68–70°. Found: C, 42.26%; H, 5.64%; N, 5.37%; HBF_4, 33.3%; H_2O, 6.83%. Calc. for $C_9H_{13}NO.HBF_4.H_2O$: C, 42.05%; H, 6.27%; N, 5.45%; HBF_4, 34.2%; H_2O, 7.01%. The water of crystallization was removed *in vacuo*, giving the anhydrous salt; m.p. 164–168°.

$HAsF_6$ Salt

The pyridone (1.51 g) slurried in H_2O (2 ml) followed by the addition of aqueous (65%) $HAsF_6$ (2.79 g) gave crystals of the 1:1 anhydrous salt after a few hours; m.p. 199–200°. Found: $HAsF_6$, 56.1%. Calc. for $C_9H_{13}NO.HAsF_6$: $HAsF_6$, 55.7%. Subsequent efforts to prepare this salt resulted only in the 2:1 salt; m.p. 183–184°. Found: C, 44.05%; H, 5.16%; N, 5.84%; As, 13.3%. Calc. for $(C_9H_{13}NO)_2.HAsF_6$: C, 43.91%; H, 5.53%; N, 5.69%; As, 15.2%. (Two crystal modifications seem to exist for this compound.)

HPF_6 Salt

The pyridone (1.51 g) and water (2 ml) were treated with aqueous (65%) HPF_6 (2.25 g). The excess water was removed *in vacuo*, giving the anhydrous salt; m.p. 165–168°. Found: C, 36.27%; H, 4.78%; N, 4.68%. Calc. for $C_9H_{13}NO.HPF_6$: C, 36.37%; H, 4.75%; N, 4.71%.

1,2,6-Trimethyl-4-pyridone

This was prepared as previously described (5).

HCl Salt

The preparation has been described previously (5).

HBr Salt

The same procedure as that used for the 1-ethyl derivative was followed, giving a compound with m.p. 272–273° (decomp.) Found: HBr, 37.0%. Calc. for $C_8H_{11}NO.HBr$: HBr, 37.1%.

HI Salt

The same procedure as that used for the 1-ethyl derivative was followed, giving a compound with m.p. 252–253°. Found: C, 35.82%; H, 4.57%; N, 5.09%; HI, 47.2%. Calc. for $C_8H_{11}NO.HI$: C, 36.24% = H, 4.56%; N, 5.28%; HI, 48.3%.

$HAsF_6$ Salt

The hydrated 1:1 salt was deposited on mixing 1.37 g of the anhydrous pyridone and 2.90 g aqueous (65%) $HAsF_6$; m.p. 124–126°. Found: As, 19.6%; H_2O, 4.79%. Calc. for $C_8H_{11}NO.HAsF_6.H_2O$: As, 21.7%; H_2O, 5.22%. The anhydrous salt was obtained by warming slightly *in vacuo*; m.p. 151° (decomp.).

$HSbCl_6$ Salt

The pyridone in $CHCl_3$ was treated with $SbCl_5$ in $CHCl_3$ saturated with HCl, resulting in a precipitate of the anhydrous salt; m.p. 239–240°. Found: C, 20.71%; H, 2.59%; N, 2.82%. Calc. for $C_8H_{11}NO.HSbCl_6$: C, 20.33%; H, 2.56%; N, 2.96%.

Can. J. Chem. Downloaded from www.nrcresearchpress.com by 210.87.254.40 on 09/05/12
For personal use only.

HPF_6 Salt

Aqueous (65%) HPF_6 (1.94 g) was added to the anhydrous pyridone (1.18 g) in warm water (14 ml). On cooling, hydrated crystals formed; m.p. 118–119°. Found: H_2O, 4.79%. Calc. for $C_8H_{11}NO.HPF_6.H_2O$: H_2O, 5.22%. The anhydrous salt was obtained by warming slightly *in vacuo*; m.p. 150–155°.

The deuterated materials were prepared by exchange with an excess of D_2O, except the DBr salts, which were made from gaseous DBr using a $CDCl_3$ solution of the pyridone. The DBr was generated from D_2O and phosphorus tribromide. The D_2O was 99.77% pure and was purchased from Atomic Energy of Canada Ltd.

All melting point measurements were made in sealed tubes and are not corrected. The metal analyses were determined by X-ray fluorescence, and the acids were estimated titrimetrically.

A Perkin–Elmer model 221 prism-grating spectrometer was used to record the spectra, from 4000 to 650 cm^{-1}, of emulsions of the finely ground solids in nujol and fluorolube. Sensitive materials, and all the deuterated compounds, were prepared *in vacuo* and subsequently handled in a dry box.

ACKNOWLEDGMENTS

The assistance of Miss C. D. Anderson in preparing many of the compounds and recording their spectra is gratefully acknowledged. The metal analyses were obtained through the kind cooperation of Mr. D. G. Barnes. Mr. K. Sketris (Dow Chemical of Canada, Limited) and Dr. L. E. Swim and associates (The Dow Chemical Company, Midland, Michigan, U.S.A.) are thanked for the microanalyses.

REFERENCES

1. A. R. KATRITZKY and R. A. JONES. Spectrochim. Acta, **17**, 64 (1961).
2. L. J. BELLAMY and P. E. ROGASCH. Spectrochim. Acta, **16**, 30 (1961).
3. A. R. KATRITZKY and R. A. JONES. J. Chem. Soc. 2947 (1960).
4. D. COOK. Can. J. Chem. **39**, 1184 (1961).
5. D. COOK. Can. J. Chem. **41**, 515 (1963).
6. D. COOK. Can. J. Chem. **41**, 505 (1963).
7. A. R. KATRITZKY and R. A. Y. JONES. Proc. Chem. Soc. 313 (1960).
8. E. SPINNER. J. Chem. Soc. 1226 (1960).
9. G. C. PIMENTEL and A. L. MCCLELLAN. The hydrogen bond. W. H. Freeman and Co., San Francisco. 1960. p. 118.
10. D. COOK. Can. J. Chem. **40**, 2362 (1962).
11. D. COOK. In preparation.
12. E. A. V. EBSWORTH and N. SHEPPARD. Spectrochim. Acta, **13**, 261 (1959).
13. R. H. NUTTALL, D. W. A. SHARP, and T. C. WADDINGTON. J. Chem. Soc. 4965 (1960).
14. D. COOK. Unpublished results.
15. F. A. MILLER and C. H. WILKINS. Anal. Chem. **24**, 1254 (1952).
16. R. C. PLUMB and D. F. HORNIG. J. Chem. Phys. **23**, 947 (1955).
17. E. M. LAYTON, R. D. KROSS, and V. A. FASSELL. J. Chem. Phys. **25**, 135 (1956).
18. D. R. HOLMES and H. M. POWELL. Acta Cryst. **6**, 256 (1953).
19. G. E. BACON and N. A. CURRY. Proc. Roy. Soc. (London), Ser. A, **235**, 552 (1956).
20. D. COOK. Chem. Ind. (London), 607 (1963).
21. D. COOK. Unpublished results.
22. W. TAKEI. Ph.D. Thesis. California Institute of Technology, Pasadena, Calif. 1957.
23. N. ALBERT and R. M. BADGER. J. Chem. Phys. **29**, 1193 (1958).
24. W. KUTZELNIGG and R. MECKE. Spectrochim. Acta, **18**, 459 (1962).
25. W. KUTZELNIGG and R. MECKE. Chem. Ber. **94**, 1706 (1961).
26. D. HADŽI. J. Chem. Soc. 5128 (1962).

Can. J. Chem. Downloaded from www.nrcresearchpress.com by 210.87.254.40 on 09/05/12
For personal use only.

ANALOGUES OF PSILOCIN AND LYSERGIC ACID DIETHYLAMIDE

I. CHLORO, NITRO, AND AMINO DERIVATIVES OF 3-SUBSTITUTED INDOLES

J. B. McKay, R. M. Parkhurst, R. M. Silverstein, and W. A. Skinner[1]

Physical and Life Sciences Divisions, Stanford Research Institute, Menlo Park, California, U.S.A.

Received June 5, 1963

ABSTRACT

A number of indole derivatives structurally related to either psilocin or lysergic acid diethylamide (LSD) were synthesized. The following structural analogues of psilocin are reported: 4-chloro-3-dimethylaminoethylindole, 4-nitro-3-dimethylaminoethylindole, 4-nitro-3-aminoethylindole, 4-amino-3-dimethylaminoethylindole, and 4-amino-3-aminoethylindole. Compounds structurally related to LSD that were synthesized are: 3-[β-carboxyethylaminoethyl]-4-nitroindole and 4-nitro-3-[N-methyl-N-(N′,N′-diethylcarboxamidoethyl)-aminoethyl]indole. Several 3,5- and 3,6-disubstituted indoles are also reported.

A number of compounds possessing the indole structure have aroused considerable interest because of their hallucinogenic reactions in man. Two of the more potent of these hallucinogens are lysergic acid diethylamide (LSD) and psilocin, 3-dimethylaminoethyl-4-hydroxyindole. Both of these compounds are 3,4-disubstituted indoles. This paper reports the synthesis of a number of 3,4-disubstituted indoles structurally related to psilocin and LSD (1). Also included are several 3,5-disubstituted indoles, used as models for synthesis, and several 3,6-disubstituted indoles which were obtained together with the 3,4-compounds from Fischer ring closures.

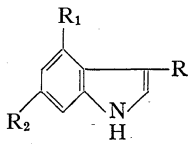

(Undesignated R-groups refer to hydrogen)

I: $R_1 = Cl$
II: $R_1 = Cl$; $R = COCOCl$
III: $R_1 = Cl$; $R = COCON(CH_3)_2$
IV: $R_1 = Cl$; $R = CH_2CH_2N(CH_3)_2$
V: $R_1 = NO_2$; $R = CH_2CH_2Cl$
VI: $R_2 = NO_2$; $R = CH_2CH_2Cl$
VII: $R_1 = NO_2$; $R = CH_2CH_2N(CH_3)_2$
VIII: $R_2 = NO_2$; $R = CH_2CH_2N(CH_3)_2$
IX: $R_1 = NO_2$; $R = CH_2CH_2NH_2$
X: $R_2 = NO_2$; $R = CH_2CH_2NH_2$
XI: $R_1 = NO_2$; $R = CH_2CH_3$
XII: $R_2 = NO_2$; $R = CH_2CH_3$
XIII: $R_1 = NO_2$; $R = CH_2CH_2NHCH_2CH_2CO_2H$
XIV: $R_2 = NO_2$; $R = CH_2CH_2NHCH_2CH_2CO_2H$
XV: $R_1 = NO_2$; $R = CH_2CH_2N(CH_3)CH_2CH_2CON(C_2H_5)_2$
XVI: $R_2 = NO_2$; $R = CH_2CH_2N(CH_3)CH_2CH_2CON(C_2H_5)_2$
XVII: $R_1 = NH_2$; $R = CH_2CH_2N(CH_3)_2$
XVIII: $R_2 = NH_2$; $R = CH_2CH_2N(CH_3)_2$
XIX: $R_2 = NH_2$; $R = CH_2CH_2NH_2$
XX: $R_1 = NH_2$; $R = CH_2CH_2NH_2$

Conditions which were suitable for reaction of indole (2) with oxalyl chloride gave virtually no product with 4-chloroindole. However, carrying out the reaction in refluxing ether solution for 15 hours yielded 4-chloro-3-indolylglyoxylchloride (II) in 73% yield. Treatment of a suspension of II in ether with dimethylamine for 6 hours gave 4-chloro-3-indolyl-N,N-dimethylglyoxamide (III) in 82% yield. Reduction of III with lithium aluminum hydride in refluxing tetrahydrofuran afforded the desired 4-chlorodimethylaminoethylindole (IV) in 97% yield. Treatment of IV with cuprous cyanide under a wide

[1]*To whom inquiries should be addressed.*

Can. J. Chem. Downloaded from www.nrcresearchpress.com by 210.87.254.40 on 09/05/12
For personal use only.

variety of conditions (3), however, failed to yield isolable amounts of 4-cyano-3-dimethylaminoethylindole.

Attempts to utilize 4-bromoindole (4) in the same reaction sequence failed owing to its low reactivity toward oxalyl chloride; steric hindrance may be partly responsible since it was later found that 5-bromoindole reacts readily with oxalyl chloride.

Fischer cyclization (5) of γ-chlorobutyraldehyde gave a mixture of 3-chloroethyl-4-nitroindole (V) and 3-chloroethyl-6-nitroindole (VI). Isomer separation by column chromatography was clean, and isomer identification by n.m.r. was straightforward. Reaction of the separated 3-chloroethyl isomers with dimethylamine yielded 3-dimethylaminoethyl-4-nitroindole (VII) and 3-dimethylaminoethyl-6-nitroindole (VIII), and reaction with ammonium hydroxide yielded 3-aminoethyl-4-nitroindole (IX) and 3-aminoethyl-6-nitroindole (X).

Model studies were carried out on the 3-nitrophenylhydrazone of butyraldehyde, closure of which yielded the readily separated isomers 3-ethyl-4-nitroindole (XI) and 3-ethyl-6-nitroindole (XII).

A brief investigation of the synthesis of γ-chlorobutyraldehyde disclosed that Rosenmund reduction (6) of commercially available γ-chlorobutyryl chloride with sulphur-quinoline poisoned palladium on barium sulphate (3) was the method of choice; the yield was 92%.

Reaction of 3-chloroethyl-4-nitroindole (V) with the sodium salt of β-alanine in aqueous ethanol for 12 days at room temperature gave 3-[β-carboxyethylaminoethyl]-4-nitroindole (XIII), isolated as the hydrochloride. Similar treatment of 3-chloroethyl-6-nitroindole (VI) gave 3-[β-carboxyethylaminoethyl]-6-nitroindole (XIV). Reaction of V with β-methylamino-N,N-diethylpropionamide (from methylamine and diethylacrylamide) gave 4-nitro-3-[N-methyl-N-(N′,N′-diethylcarboxamidoethyl)-aminoethyl]indole (XV), isolated as the picrate. Similar treatment of VI gave 6-nitro-3-[N-methyl-N-(N′,N′-diethylcarboxamidoethyl)-aminoethyl]indole (XVI), isolated as the hydrochloride. The side chain at the 3-position of compounds XIII, XIV, XV, and XVI was designed to resemble part of the molecule of LSD.

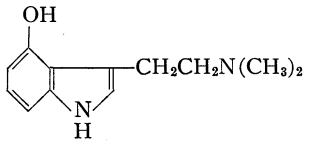

Psilocin

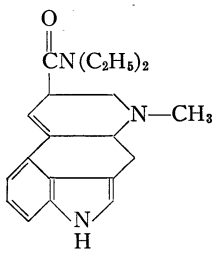

Lysergic acid diethylamide (LSD)

Reduction of the nitro group to an amino group with sodium dithionite was studied utilizing the readily prepared model compound (5), 3-ethyl-5-nitroindole. This method of reduction was successfully used for the preparation of 5-amino-3-ethylindole, 4-amino-3-dimethylaminoethylindole (XVII), 6-amino-3-dimethylaminoethylindole (XVIII), and 3-aminoethyl-6-aminoindole (XIX), but failed in the attempted preparation of 3-aminoethyl-4-aminoindole (XX). This latter compound was prepared in excellent yield by catalytic reduction of the corresponding nitro compound with platinum oxide at atmospheric pressure.

Can. J. Chem. Downloaded from www.nrcresearchpress.com by 210.87.254.40 on 09/05/12
For personal use only.

Several attempts to replace the diazotized amino group of the model compound, 5-amino-3-ethylindole, with a cyano or a mercapto group demonstrated the lack of utility of the amino compounds as intermediates.

EXPERIMENTAL

4-Chloro-3-indolyl-N,N-dimethylglyoxamide (III)

To a solution of 3.84 g (0.025 mole) of fractionally distilled 4-chloroindole (Aldrich, b.p. 144–145° at 10.5 mm, n_D^{22} 1.6272) in 20 ml ether (distilled from lithium aluminum hydride) stirred at room temperature under nitrogen was added 6.62 g (0.0521 mole) of oxalyl chloride in 30 ml dry ether. After addition, the mixture was refluxed for 15 hours. The yellow precipitate was filtered and washed with ether; it weighed 4.5 g (73%). This product was suspended in 60 ml ether, 6.5 g (0.144 mole) of anhydrous dimethylamine dissolved in 50 ml of ether was added, and the mixture was stirred for 6 hours. The ether and excess dimethylamine were removed under reduced pressure, and the residue was treated with water. This mixture was filtered and the precipitate was washed with water, then dried under reduced pressure at room temperature for 64 hours. It weighed 3.83 g (82%), m.p. 223.5–224.5° corr., λ_{max}^{Nujol} (μ) 3.25 (NH); 6.05 (C=O, keto); 6.20 (C=O, amide). Anal. Calc. for $C_{12}H_{11}ClN_2O_2$: C, 57.5; H, 4.42; Cl, 14.1; N, 11.2. Found: C, 57.8; H, 4.99; Cl, 13.9; N, 10.9.

4-Chloro-3-dimethylaminoethylindole (IV)

To a slurry of 13.00 g (0.344 mole) of $LiAlH_4$ in 150 ml of tetrahydrofuran (THF), freshly distilled from $LiAlH_4$, was added a solution of 14.2 g (0.0568 mole) of 4-chloro-3-indolyl-N,N-dimethylglyoxamide (III) in 1 liter of dry tetrahydrofuran (THF). The mixture was refluxed for 3 hours, then cooled, and 110 ml of methyl alcohol – THF 1:1 mixture was added, followed by 30 ml of saturated sodium sulphate. The mixture was concentrated under reduced pressure almost to dryness, then dissolved in 200 ml of ether. This solution was extracted three times with 20-ml portions of 5% HCl solution, dried over anhydrous sodium sulphate, and evaporated to dryness under reduced pressure. The residue of nonbasic material weighed less than 0.4 g. The combined acid extracts were made basic with cold 50% sodium hydroxide and extracted with chloroform. The combined chloroform extracts were dried over sodium sulphate and evaporated to dryness under reduced pressure. The residue of crude basic product weighed 12.25 g (97%). Repeated recrystallization from cyclohexane afforded an analytical sample, m.p. 136.5–138° corr., λ_{max}^{Nujol} (μ) 3.30 (NH); absence of C=O bands at 6.06, 6.20. Anal. Calc. for $C_{12}H_{15}ClN_2$: C, 64.7; H, 6.79; N, 12.6; Cl, 15.9. Found: C, 64.7; H, 6.75; N, 12.6; Cl, 15.9.

3-Ethyl-4- and -6-nitroindoles (XI and XII)

A solution of 10 g (0.0484 mole) of *n*-butyraldehyde-3-nitrophenylhydrazone in 200 ml of concentrated hydrochloric acid and 200 ml of benzene was stirred for 3 hours at room temperature. The benzene was replaced with fresh benzene for another 3 hours. The combined benzene fractions were washed with water, dried over sodium sulphate, and chromatographed on acid-washed Merck alumina (3×25 cm).

The first major fraction from the column, an orange crystalline solid, m.p. 109.5–112°, was found to be the 3-ethyl-4-nitroindole by its n.m.r. spectrum.

The second major fraction, yellow needles, melting at 87–89°, was found to be the 6-isomer. The overall yields were about 0.55 g (6%) and 0.18 g (2%), respectively.

The infrared absorption spectra of the 4- and 6-nitro isomers were very similar. 3-Ethyl-4-nitroindole: λ_{max}^{Nujol} (μ) 2.95 (NH); 6.63, 7.60 (NO_2); 7.91, 8.86, 9.36, 10.2, 10.4, 12.1, 12.6, 13.8. 3-Ethyl-6-nitroindole: λ_{max}^{Nujol} (μ) 2.95 (NH); 6.63, 7.65 (NO_2); 8.15, 9.05, 9.40, 11.4, 11.9, 12.3, 12.7, 13.3, 13.7.

The n.m.r. spectra made possible assignment of structures to the two isomers. 3-Ethyl-4-nitroindole: CH_3 (triplet, 8.80 τ); CH_2 (quartet, 7.15 τ); 2 H and 6 H (2.78 τ); 7 H (2.36 τ); 5 H (doublet, 2.24 τ, additional meta coupling); 1 H (1.43 τ). 3-Ethyl-6-nitroindole: CH_3 (triplet, 8.65 τ); CH_2 (quartet, 7.23 τ); 2 H (2.63 τ); 4 H (doublet, 2.40 τ); 5 H (doublet, 1.98 τ, additional meta coupling); 7 H (doublet, 1.65 τ); 1 H (1.40 τ).

3-Ethyl-4-nitroindole: λ_{max}^{EtOH} 2400 Å, ϵ = 8650; 3-ethyl-6-nitroindole: λ_{max}^{EtOH} 2525 Å, ϵ = 8930; 2680 Å, ϵ = 8530.

Anal. Calc. for $C_{10}H_{10}N_2O_2$: C, 63.1; H, 5.31; N, 14.7. Found 4-NO_2: C, 63.5; H, 5.57; N, 14.6. Found 6-NO_2: C, 62.9; H, 5.20; N, 14.7.

γ-Chlorobutyraldehyde by Rosenmund Reduction

A mixture of 153 g (1.085 moles) of γ-chorobutyryl chloride, 16 g palladium on barium sulphate catalyst, 1.66 ml of sulphur-quinoline poison (7), and 900 ml of toluene was refluxed and vigorously stirred while hydrogen was passed through; the effluent gas was bubbled through water. After 6.5 hours, the evolution of hydrogen chloride ceased. The mixture was filtered and the filtrate washed with water, sodium bicarbonate solution, and water. After drying over sodium sulphate, the toluene was removed by distillation under reduced pressure through a Vigreux column. The yield of crude product was 99.7 g (92%), b.p. 28–29° at 2.0 mm; 2,4-dinitrophenylhydrazone, m.p. 130–131°, lit. 130–131°.

Can. J. Chem. Downloaded from www.nrcresearchpress.com by 210.87.254.40 on 09/05/12
For personal use only.

γ-Chlorobutyraldehyde-3-nitrophenylhydrazone

A solution of 10 g (0.1 mole) of crude γ-chlorobutyraldehyde and 20 g (0.132 mole) of 3-nitrophenylhydrazine dissolved in a minimum amount of hot ethanol containing 10% of acetic acid was allowed to stand on the steam bath for 1 hour. The mixture was cooled, and water was added until a dark red oil started to separate out. Because attempts to crystallize this oil failed, the alcohol was evaporated *in vacuo*, the water was decanted off, and the crude oil used directly in the next step.

3-[β-Chloroethyl]-4- and -6-nitroindoles (V and VI)

A solution of 29 g of the crude 3-nitrophenylhydrazone of γ-chlorobutyraldehyde in 300 ml of concentrated hydrochloric acid and 200 ml of benzene was stirred rapidly for 3 hours. The benzene was replaced with fresh benzene, and stirring was continued for another 4 hours. The combined benzene fractions were washed with water, dried over anhydrous sodium sulphate, and evaporated *in vacuo* to about 35 ml. The solution was placed on a column of alumina (3×25 cm) and eluted with benzene. The two major fractions were 3-[β-chloroethyl]-4-nitroindole, 1.89 g (7%), and 3-[β-chloroethyl]-6-nitroindole, 2.19 g (8%). Several recrystallizations from benzene – petroleum ether gave products which melted at 134–135°, golden yellow plates, in the case of the 4-nitro, and 108–110°, canary yellow needles, in the case of the 6-nitro compound.

The infrared absorption spectra of the two isomers were similar. 3-[β-Chloroethyl]-4-nitroindole: λ_{max}^{Nujol} (μ) 3.00 (NH); 6.60, 7.60 (NO_2); 8.95, 10.03, 10.2, 12.4, 12.6, 13.7. 3-[β-Chloroethyl]-6-nitroindole: λ_{max}^{Nujol} (μ) 2.90 (NH); 6.25 (aryl); 6.55, 7.45 (NO_2); 9.10, 9.45, 11.3, 13.3, 13.7, 14.0.

3-[β-Chloroethyl]-4-nitroindole: CH_2CH_2Cl (triplet, 6.62 τ); CH_2CH_2Cl (triplet, 6.25 τ); 2 H (2.80 τ); 6 H (2.63 τ); 7 H (doublet, 2.34 τ, *m*-coupled); 5 H (doublet, 2.09 τ, *m*-coupled); 1 H (1.40 τ). 3-[β-Chloroethyl]-6-nitroindole: CH_2CH_2Cl (triplet, 6.73 τ); CH_2CH_2Cl (triplet, 6.22 τ); 2 H (2.57 τ); 4 H (doublet, 2.39 τ); 5 H (doublet with additional *m*-coupling, $J \sim 2$ c.p.s., 1.97 τ); 7 H (doublet 1.62 τ); 1 H (1.22 τ).

3-[β-Chloroethyl]-4-nitroindole: λ_{max}^{EtOH} 2375 Å, $\epsilon = 7480$. 3-[β-Chloroethyl]-6-nitroindole: λ_{max}^{EtOH} 2525 Å, $\epsilon = 8290$; 2650 Å, $\epsilon = 7900$.

Anal. Calc. for $C_{10}H_9ClN_2O_2$: C, 53.5; H, 4.04; Cl, 15.8; N, 12.5. Found 4-NO_2: C, 53.3; H, 4.26; Cl, 15.5; N, 12.4. Found 6-NO_2: C, 53.5; H, 4.28; Cl, 15.9; N, 12.5.

3-Dimethylaminoethyl-4-nitroindole (VII)

A solution of 356.8 mg (1.59 mmoles) of 3-[β-chloroethyl]-4-nitroindole in 20 ml of alcohol and 20 ml of 34.3% aqueous dimethylamine was left at room temperature for 7 days. The alcohol was removed *in vacuo*, and the orange-yellow crystalline material was filtered; the crude yield was 300 mg (81%). The material was dissolved in dilute hydrochloric acid, filtered, and precipitated with dilute sodium hydroxide. Recrystallization from alcohol–water mixtures gave orange needles melting at 115–116°. Anal. Calc. for $C_{12}H_{15}N_3O_2$: C, 61.8; H, 6.48; N, 18.0. Found: C, 61.6; H, 6.39; N, 18.3.

3-Dimethylaminoethyl-6-nitroindole (VIII)

A solution of 485.7 mg (2.16 mmoles) of 3-[β-chloroethyl]-6-nitroindole in 20 ml of ethanol was treated with aqueous dimethylamine as in the case of the 4-isomer above. The crude yield was 423 mg (85%). The recrystallized product appeared as yellow plates melting at 171.5–172.5°. Anal. Calc. for $C_{12}H_{15}N_3O_2$: C, 61.8; H, 6.48; N, 18.0. Found: C, 61.2; H, 6.47; N, 17.8.

3-Aminoethyl-4-nitroindole (IX)

A solution of 1.0 g (4.46 mmoles) of 3-[β-chloroethyl]-4-nitroindole, 50 ml of concentrated NH_4OH, and 75 ml of ethyl alcohol was kept in a stoppered flask for 10 days. The alcohol was removed under reduced pressure, and the precipitate was filtered. The crude product was dissolved in hydrochloric acid and the solution filtered with Celite. After precipitation with dilute sodium hydroxide, the product was collected and recrystallized from ethanol–water; yield, 0.587 g (64.5%), m.p. 145–147°. Anal. Calc. for $C_{10}H_{11}N_3O_2$: C, 58.5; H, 5.40; N, 20.5. Found: C, 58.0; H, 5.61; N, 20.1.

3-Aminoethyl-6-nitroindole (X)

A solution of 2.0 g (8.92 mmoles) of 3-[β-chloroethyl]-6-nitroindole, 150 ml of concentrated ammonia, and 150 ml of ethyl alcohol was kept at room temperature for 9.5 days. The solvent was evaporated under reduced pressure, and the residue was dissolved in 10% hydrochloric acid. The acid solution was filtered with Celite, made basic, and the precipitated amine was filtered and recrystallized from ethyl acetate – petroleum ether (60–110°). Yield 1.37 g (71.5%). Another recrystallization yielded an analytical sample, m.p. 185–186° (decomp.). Anal. Calc. for $C_{10}H_{11}N_3O_2$: C, 58.5; H, 5.4; N, 20.5. Found: C, 58.5; H, 5.5; N, 20.4.

3-[β-Carboxyethylaminoethyl]-4-nitroindole Hydrochloride (XIII)

A solution of 1.0 g (4.46 mmoles) of 3-[β-chloroethyl]-4-nitroindole, 0.15 mole of β-alanine sodium salt in 75 ml of water, and 75 ml of ethyl alcohol was kept in a stoppered flask at room temperature for 12 days. The solvent was removed under reduced pressure and the residue triturated with benzene. The benzene-insoluble precipitate was dissolved in water, precipitated with HCl, and the crude product was collected and recrystallized from water; yield 3-[β-carboxyethylaminoethyl]-4-nitroindole, 0.20 g (28.6%), m.p. 210°. The hygroscopic orange product was dried *in vacuo* to constant weight. Anal. Calc. for $C_{13}H_{15}ClN_3O_4$: C, 49.8; H, 5.14; Cl, 11.3; N, 13.4. Found: C, 49.8; H, 5.35; Cl, 11.3; N, 13.5.

Can. J. Chem. Downloaded from www.nrcresearchpress.com by 210.87.254.40 on 09/05/12
For personal use only.

3-[β-Carboxyethylaminoethyl]-6-nitroindole Hydrochloride (XIV)

A solution of 374 mg (1.67 mmoles) of 3-[β-chloroethyl]-6-nitroindole in 25 ml of alcohol and a solution of 0.1 mole of β-alanine sodium salt in 25 ml of water were mixed and allowed to stand at room temperature for 10 days. Evaporation of the alcohol and addition of hydrochloric acid caused the precipitation of a green solid weighing 300 mg (57%). The infrared spectrum of this material shows a strong band at 5.80 μ. The light green hydrochloride was recrystallized from water four times, dried to constant weight, m.p. 220° (decomp.). Anal. Calc. for $C_{13}H_{16}ClN_3O_4$: C, 49.8; H, 5.14; Cl, 11.3; N, 13.4. Found: C, 49.6; H, 5.84; Cl, 11.2; N, 13.3.

β-Methylamino-N,N-diethylpropionamide

To a solution of 26 g (0.84 mole) of methylamine in 80 ml of absolute ethyl alcohol was added, with cooling, 25.5 g (0.20 mole) of diethylacrylamide. The solution was allowed to stand in a freezer (−15°) for 45 hours. The solvent and excess methylamine were removed under reduced pressure, and the residue was distilled. One fraction was collected, b.p. 76–80° at 0.6 mm, n_D^{20} 1.4617. This material was redistilled through a spinning band column; one fraction of b.p. 62–63° at 0.40 mm, weight 16.6 g, n_D^{23} 1.4609 was collected. The hydrochloride was precipitated from ether with anhydrous HCl; m.p. 84.5–86°. Anal. Calc. for $C_8H_{19}ClN_2O$: C, 49.3; H, 9.84; Cl, 18.2; N, 14.4. Found: C, 49.1; H, 9.74; Cl, 17.3; N, 13.9.

6-Nitro-3-[N-methyl-N-(N',N'-diethylcarboxamidoethyl)-aminoethyl]indole (XVI)

A solution of 0.5 g (2.23 mmoles) of 3-β-chloroethyl-6-nitroindole in 3.0 ml of β-methylamino-N,N-diethylpropionamide was allowed to stand at room temperature for 10 days. The solution was poured into water, and the insoluble oil was isolated by centrifugation. The oil was dissolved in dilute acid, filtered with Celite, the solution made basic, and the product extracted into chloroform. The solution was dried ($MgSO_4$), and the solvent was removed under reduced pressure. The residue crystallized on scratching. Yield 0.67 g (87%). An analytical sample was obtained by repeated recrystallization from benzene – petroleum ether mixture; m.p. 93–94°. Anal. Calc. for $C_{18}H_{26}N_4O_3$: C, 62.4; H, 7.56; N, 16.2. Found: C, 62.3; H, 7.46; N, 16.2.

4-Nitro-3-[N-methyl-N-(N',N'-diethylcarboxamidoethyl)-aminoethyl]indole (XV)

A solution of 0.290 g (1.29 moles) of 3-[β-chloroethyl]-4-nitroindole in 6 ml of β-methylamino-N,N-diethylpropionamide was allowed to stand at room temperature for 14 days. The solution was poured into water and the oil which formed was isolated by centrifugation. The oil was dissolved in dilute hydrochloric acid, filtered, the solution made basic, and the product extracted into chloroform. The chloroform extracts were dried over anhydrous magnesium sulphate, and the solvent was removed under reduced pressure. Because the residue (0.187 g, 58%) could not be crystallized, the picrate was made. An analytical sample of the picrate was obtained by recrystallization from ethyl acetate; m.p. 205–208°. Anal. Calc. for $C_{24}H_{29}N_7O_{10}$: C, 50.1; H, 5.08; N, 17.0. Found: C, 50.0; H, 4.98; N, 16.7.

6-Amino-3-dimethylaminoethylindole (XVIII)

To a solution of 1.0 g (4.3 mmoles) of 3-dimethylaminoethyl-6-nitroindole in 75 ml of alcohol and 20 ml of *N* sodium hydroxide at 50° was added a solution of 6 g of sodium dithionite in 30 ml of 0.2 *N* sodium hydroxide. The mixture was filtered hot and the filtrate evaporated to dryness. The residue was dissolved in 5% hydrochloric acid solution, filtered, and made basic with cold 30% sodium hydroxide. The basic solution was extracted with ether, and the light purple ether solution was evaporated to dryness. The purple solid residue weighed 0.66 g (75%), m.p. 93–96°. Two sublimations at 110° at 0.1 mm gave a white crystalline product; m.p. 98–99°. Anal. Calc. for $C_{12}H_{17}N_3$: C, 70.9; H, 8.43; N, 20.7. Found: C, 70.5; H, 8.95; N, 20.5.

4-Amino-3-dimethylaminoethylindole (XVII)

To a solution of 0.52 g (2.2 mmoles) of 3-dimethylaminoethyl-4-nitroindole in 35 ml of ethyl alcohol and 10 ml of *N* sodium hydroxide at 50° was added a solution of 3 g of sodium dithionite in 15 ml of 0.2 *N* sodium hydroxide. The mixture was filtered hot and the filtrate evaporated to dryness. The residue was dissolved in acid, filtered, made basic, and extracted into ether. The residue from evaporation of the ether weighed 0.21 g (47.5%), m.p. 129–131°, and sublimed at 125–130° at 0.1 mm. The sublimate weighed 0.182 g, m.p. 130.5–131.5°. Anal. Calc. for $C_{12}H_{17}N_3$: C, 70.9; H, 8.43; N, 20.7. Found: C, 71.4; H, 7.72; N, 20.8.

3-Aminoethyl-6-aminoindole (XIX)

A solution of 3.0 g of sodium dithionite in 15 ml of 0.5 *N* sodium hydroxide solution was added to a solution of 0.50 g of 3-aminoethyl-6-nitroindole in 35 ml ethyl alcohol and 10 ml *N* sodium hydroxide solution at 50° C. The mixture was then filtered hot, and the filtrate was evaporated to dryness, 0.27 g (63.5% yield). The viscous oil residue was sublimed at 130° at 0.1 mm. The noncrystalline sublimate was partially dissolved in ether and cooled in a dry ice – acetone bath. Crystallization was induced by scratching with a glass rod. The ether was removed under reduced pressure and the residue, m.p. 102–105°, was sublimed twice at 110–120° at 0.015 mm, m.p. 105.5–107.5°. Anal. Calc. for $C_{10}H_{13}N_3$: C, 68.5; H, 7.48; N, 24.0. Found: C, 68.0; H, 7.54; N, 24.0.

Can. J. Chem. Downloaded from www.nrcresearchpress.com by 210.87.254.40 on 09/05/12
For personal use only.

3-Aminoethyl-4-aminoindole (XX)

A mixture of 0.232 g (1.13 mmole) of 3-aminoethyl-4-nitroindole, 0.0165 g (0.07 mmole) of platinum oxide, and 25 ml of absolute ethanol was stirred in an atmospheric hydrogenation apparatus. The reaction ceased after 50 minutes at 95% completion. The solution was filtered and the filtrate evaporated to dryness under reduced pressure. The oily residue was crystallized by cooling an ether solution in a dry ice – acetone bath and scratching the flask wall with a glass rod. The ether was removed under reduced pressure. The light purple product (0.18 g, 90%, m.p. 106–113°) was sublimed twice (100° at 0.01 mm, m.p. 116°). Anal. Calc. for $C_{10}H_{13}N_3$: C, 68.5; H, 7.48; N, 24.0. Found: C, 68.2; H, 7.81; N, 24.1.

ACKNOWLEDGMENT

The authors wish to express their appreciation to the United States Army Chemical Center Research and Development Command for support of this research under contract RFP-147, DA 18-108-405-CML-839.

REFERENCES

1. T. KRALT, W. J. ASMA, H. H. HAECK, and H. D. MOED. Rec. Trav. Chim. **80**, 313 (1961).
2. M. E. SPEETER and W. C. ANTHONY. J. Am. Chem. Soc. **76**, 6208 (1954). K. N. F. SHAW, A. MCMILLAN, A. G. GUDMUNDSON, and M. D. ARMSTRONG. J. Org. Chem. **23**, 1171 (1958). F. TROXLER, F. SEEMANN, and A. HOFMANN. Helv. Chim. Acta, **42**, 2073 (1959).
3. F. C. UHLE. J. Am. Chem. Soc. **71**, 761 (1949).
4. H. PLIENINGER. Chem. Ber. **88**, 370 (1955).
5. E. SHAW and D. W. WOOLEY. J. Am. Chem. Soc. **75**, 1877 (1953).
6. R. B. LOFTFIELD. J. Am. Chem. Soc. **73**, 1365 (1951).
7. E. B. HERSHBERG and J. CASON. Org. Syn. **21**, 84 (1941).

Can. J. Chem. Downloaded from www.nrcresearchpress.com by 210.87.254.40 on 09/05/12
For personal use only.

A VAPOR PRESSURE STUDY OF THE ALLOYS OF MANGANESE WITH COPPER[1]

B. F. PETERS[2] AND D. R. WILES[3]
Department of Mining and Metallurgy, University of British Columbia, Vancouver, British Columbia
Received August 15, 1960

ABSTRACT

The Knudsen effusion method has been applied in a study of the vapor pressures of manganese in equilibrium with copper–manganese alloys at high temperatures. The amount of manganese effused was determined by the use of radioactive Mn^{54}. The odd behavior noted in this system at 20–30% Mn, observed in a number of studies of various physical properties, has been observed once more in the apparent activity of manganese. Some discussion is given of the Knudsen effusion method, particularly regarding some possible sources of error.

INTRODUCTION

A number of studies have been made in recent years of the copper–manganese alloy system, and all results point to its being of great interest. A study of high-temperature magnetic susceptibilities led Myers (1) to suspect that the number of electrons contributed by manganese to the conduction band is a function of composition. Somewhat different studies by Scheil and Wachtel (2) and by Valentiner and Becker (3) of the magnetic susceptibilities at somewhat lower temperatures brought out the suggestion of short-range order. Neutron diffraction studies by Meneghetti and Sidhu (4) supported this latter view, and antiferromagnetic ordering was suggested. Specific heat studies by Kussmann and Wollenberger (5) showed ordering below 270° C.

The copper–manganese system is one of the few in which two quite dissimilar metals show solid solubility over an appreciable composition range. (The phase diagram (6) is given in Fig. 1.) The properties of the γ-phase of this system are therefore of considerable interest in throwing light on the structure of such alloys. This is especially so in view of the fact that the sizes of the copper and manganese atoms are not greatly different, so that these studies may shed some light on the effects of such factors as electronegativity and electronic structure.

This paper reports on measurements of the vapor pressures of manganese over a series of Cu–Mn alloys.

Of the two components in the copper–manganese system, manganese is known to have the higher vapor pressure and consequently this work involves a study of the partial pressures of manganese alone. Determination of this vapor pressure was done by the Knudsen effusion method (7, 8) because of its ready applicability to the determination of very low pressures.

The Knudsen equation for the calculation of vapor pressures is given as equation (I)

$$p = \frac{m}{tAf}\sqrt{\left(\frac{2\pi RT}{M}\right)}, \qquad \text{(I)}$$

where p is the pressure in dynes/cm^2, m is the weight of material of molecular weight M collected after having effused for t seconds through an orifice of area A, where f is the

[1]*Presented at the Annual Conference of the Chemical Institute of Canada, Ottawa, June 13–15, 1960. Based largely on the M.A.Sc. Thesis of B. F. P. submitted to the Department of Mining and Metallurgy, University of British Columbia, Vancouver, B.C., 1958.*
[2]*Present address: Pacific Naval Laboratories, Esquimalt, British Columbia.*
[3]*Present address: Chemistry Department, Carleton University, Ottawa, Ontario.*

Can. J. Chem. Downloaded from www.nrcresearchpress.com by 210.87.254.6 on 09/05/12
For personal use only.

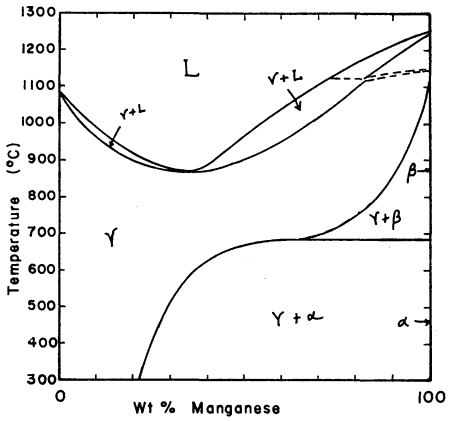

FIG. 1. Phase diagram for the copper–manganese system.

fraction of the effused material which is collected. R and T represent, as usual, the gas constant and temperature, respectively. The activity and other thermodynamic functions can be calculated by well-known methods. It is important to note that in the use of this method we must assume that (*a*) the vapor is monatomic (i.e. that $M = 54.9$) and (*b*) all atoms which strike the collecting surface remain there. These assumptions will be discussed later.

EXPERIMENTAL

The Knudsen effusion apparatus used is shown schematically in Fig. 2. The cell itself was made of molybdenum, which had been shown by McCabe and Hudson (9) not to dissolve in nor react with manganese at high temperatures. The orifice was a circular hole drilled in 0.003 in. molybdenum. The diameter of the hole was varied from about 1 to 3 mm without effect on the pressure values obtained. The furnace was of Kanthal strip wound on machined lava block.

Temperatures were measured with two chromel–alumel thermocouples inserted into the cell as shown in Fig. 2—one deep inside the cell wall, the other in a shallow hole in the bottom. The thermocouples were calibrated at the boiling point of water and at the melting point of aluminum. The temperatures given by the two thermocouples differed by about 3°, that in the shallow hole showing the lower temperature.* The effective temperature of the cell was assumed to be 1° lower than that shown by the thermocouple in the cell wall. Temperature readings were made by means of a Tinsley Type 3387B potentiometer.

Temperature control was effected by means of a control thermocouple located close to the furnace windings, and connected to a Minneapolis-Honeywell Controller, operating an on, 3/4-on furnace circuit. Variations in the temperature at equilibrium amounted to ±0.5°. The absolute error in the effective temperature is estimated to be not greater than 2° C.

The effused manganese vapor was collected on water-cooled manganese-coated aluminum disks. Precoating of the disks with manganese was found necessary to provide an unvarying surface on which to collect the vapor. The disks were arranged in a sample changing device to make possible several measurements on a given alloy without breaking the vacuum. The same device made it possible to specify accurately the time and temperature at which each sample was collected. The pressure under operating conditions was about 10^{-5} mm Hg.

The measurement of the quantity of effused manganese collected was done using radioactive manganese-54 as tracer. The radioactive manganese was obtained carrier free, in HCl solution, from Nuclear Science and Engineering Corp. Measurements were made with an end-window proportional counter, counting the conversion electrons from the 0.84 Mev γ-ray. For a single vapor pressure determination several samples were collected for different lengths of time, and intercompared to eliminate possible non-statistical errors. Agreement was generally very good among samples.

The manganese was 99.9% pure electrolytic manganese obtained from the Electromanganese Corp. of America. The copper was Fisher Reagent metal of 99.7% purity.

**This deviation persisted through a number of changes and interchanges of the thermocouples, and is thus real. It seems likely that heat was being lost from the bottom of the cell because of inadequate thermal shielding.*

Can. J. Chem. Downloaded from www.nrcresearchpress.com by 210.87.254.6 on 09/05/12
For personal use only.

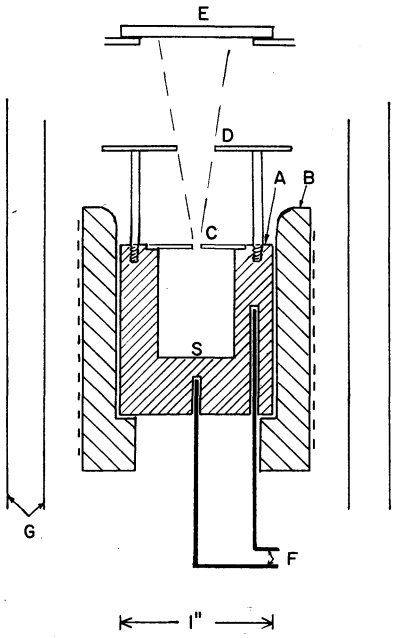

FIG. 2. Schematic diagram of the Knudsen effusion cell and the vapor collecting system.

A. Molybdenum cell	E. Collection disk
B. Lava-block furnace	F. Chromel–alumel thermocouples
C. Molybdenum orifice plate	G. Thermal shields
D. Collimator	S. Location of sample

The radioactive manganese metal, and the labelled alloys, were made in the following way: A few drops of carrier-free Mn^{54} solution were evaporated on the surface of a manganese chip, and this melted together with more, inactive, manganese by induction heating in a closed argon-filled system. The manganese melt was contained in a Norton RA84 silica crucible. The alloys were made by melting together weighed amounts of copper and radioactive manganese, using a molybdenum crucible. The melts were rapidly cooled under argon. Subsequent microscopic examination revealed no inhomogeneity. The manganese content of the alloys was determined spectrophotometrically as permanganate. The specific activity of the stock manganese was determined by using very small aliquots of a nitric acid solution of the active manganese. These were evaporated on aluminum disks similar to the vapor-collection disks. Several different-sized aliquots of the manganese solutions were used, and the observed activity was seen to be a linear function of the size of the aliquot used. The calibration curve was checked by dissolving collected manganese off a disk and analyzing this spectrophotometrically.

EVALUATION OF ERRORS

A number of sources of error were found which, although consistent throughout the experiments, tend to cast some doubt on the absolute accuracy of the values.

The orifice plate was observed visually to be somewhat cooler than the inside of the cell and some manganese was observed to condense on its under side. Using an optical pyrometer, it was estimated that the difference in temperature was about 25°. Since all discussions of the Knudsen method emphasize that the orifice must be no cooler than the rest of the cell, we feel obliged to make some comments of justification.

The extreme case—that of partial clogging of the orifice with condensed atoms—was never observed. The effect to be expected, then, is a decrease in the flux of atoms in the downward direction because of condensation of some atoms on the orifice plate. This would have some effect on the concentration of atoms on the bottom surface, and consequently on the flux of atoms moving upward toward the orifice. The magnitude of this

Can. J. Chem. Downloaded from www.nrcresearchpress.com by 210.87.254.6 on 09/05/12
For personal use only.

effect was estimated through a direct experiment (10) in which the amount of manganese condensed on the inside of the orifice plate was found to be 16% of that striking the plate. Considering that the orifice plate subtends approximately 18% of the total solid angle it may be estimated with some confidence that the error in absolute vapor pressures resulting from this effect is not more than 5%, as long as the rate of evaporation is much higher than the rate of effusion. Good agreement with the values obtained by McCabe and Hudson for pure manganese gives confidence that the evaporation rate is adequate to ensure equilibrium. For the alloys this condensation was never observed.

Oxidation was a problem in the case of pure manganese. It was observed (10) that after only a short time at high temperatures the manganese samples were coated with a loosely adherent green layer, even at the best vacuum obtained. This layer was identified from its X-ray diffraction pattern as MnO. It was found, however, that on prolonged heating this layer became very porous, spalling off to expose large areas of what appeared to be bare metal. Vapor pressure studies made on such samples showed an interesting behavior as a function of time, which tend to substantiate this last observation. These results are shown in Fig. 3.

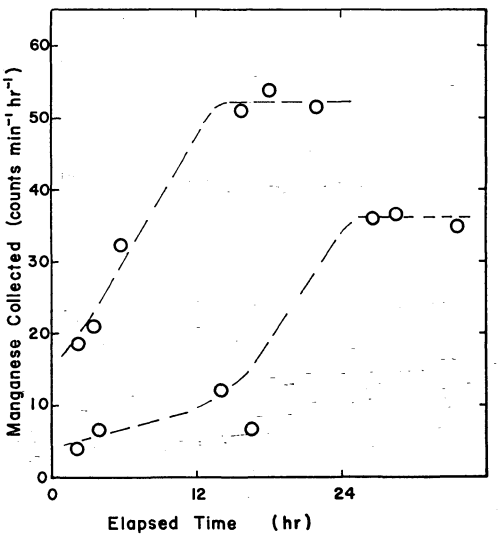

FIG. 3. Apparent vapor pressures of pure manganese measured at various times showing the effect of oxidation. Upper curve: 862° C; lower curve: 832° C.

It was concluded from these experiments that after a 'soaking' time of 20–30 hours, depending on the temperature, the manganese surface was no longer blocked by the adherent oxide layer, and the vapor pressures observed were, in fact, those of pure manganese. For this reason all experimental runs on pure manganese were made after an initial 24 hour heating period.

Collection of the effused vapor was found to be fraught with some initial difficulties. It was found that the collection efficiency varied as a function of time, when aluminum disks were used for collecting the vapor. Other substrates, e.g. silver, copper, were found to be no better. This variation is shown by curve 3 in Fig. 4. This behavior was corrected when the aluminum disks were given a thick coating of non-radioactive manganese prior to use, as is seen in curve 1 of Fig. 4. This delayed deposition was observed a long

Can. J. Chem. Downloaded from www.nrcresearchpress.com by 210.87.254.6 on 09/05/12
For personal use only.

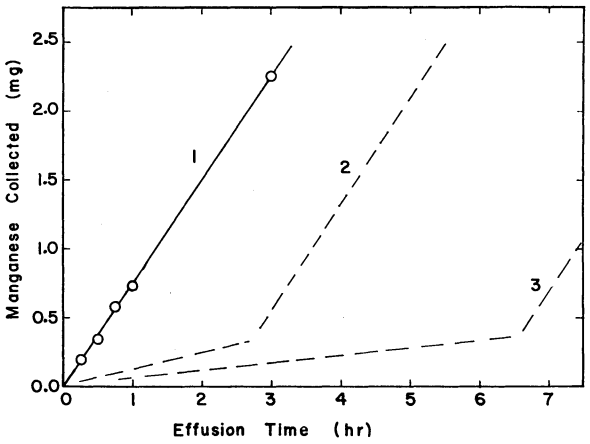

FIG. 4. Collection of manganese for various times on various substrates, showing the necessity for having clean manganese for good collection. Curve 1: disk precoated with Mn just prior to use; curve 2: disk precoated with Mn and kept in air for 72 hours before use; curve 3: clean Al disk.

time ago by Wood (11), Estermann (12), and others. It is explained as resulting from the fact that manganese atoms are held strongly only when they condense on a clean manganese surface, while when they strike any other surface, the condensation is inefficient until a manganese layer is built up. This is true even when the collecting layer is mildly oxidized manganese, as is seen in curve 2 of Fig. 4. In all experiments the aluminum collection disks were thickly coated with non-radioactive manganese prior to use and kept under high vacuum.

All experiments were done so as to collect several samples representing different exposure times. These were checked for linearity in time (as in curve 1, Fig. 4) and the rate of effusion per unit time computed from the average.

A more fundamental source of error is the assumption that the vapor is monatomic (i.e. that M in equation (I) is equal to 54.9). Although on the average the vapor is likely very nearly monatomic, there is no certainty of this. Moreover, any error arising from this assumption will be temperature dependent and lead to false values of the heat of sublimation. At any one temperature, this error would be independent of composition.*

Errors in the radioactive measurements were small and random.

An assessment of the magnitude of the errors is very difficult in this case, where many sources of non-random errors exist. By holding these errors constant, as described, the relative errors were held to a minimum, and the authors are confident that the measurements are internally consistent to within about 10%, at any temperature.

The accuracy and reproducibility of measurements made using this technique are conveniently checked by comparing the results obtained for pure manganese with those reported by McCabe and Hudson (9). The absolute values of the manganese vapor pressure are found to agree quite well. There is, however, a considerable difference between the values for the heat of sublimation, and our value of 92 kcal/mole, determined from the slope of the curve of ln P vs. $1/T$, in Fig. 5, is in poor agreement with theirs of 67 kcal/mole. Since the present work was done over such a narrow range of temperatures, we feel that our value is not reliable, and does not offer a challenge to the earlier value.

**This independence of composition would no longer be true in the case of direct evaporation from a metal surface into a vacuum.*

Can. J. Chem. Downloaded from www.nrcresearchpress.com by 210.87.254.6 on 09/05/12
For personal use only.

From this comparison, we deduce that the pressure values obtained are internally consistent, when considered at a single temperature, but that the ΔH values, while probably consistent, may not be sufficiently reliable to warrant their being used in detailed thermodynamic calculations. The discussion to follow, then, is based on the interpolated values at 820° C.

One serious uncertainty may arise in attempting to prove that the vapor collected from alloy samples reflects their true equilibrium pressure. It is possible, for example, that the extent of depletion of manganese in the surface was controlled by the rate of diffusion of manganese from the body of the sample to the surface.*

Since no regular variation in evaporation rate was ever noted as a function of either sample area or length of heating time, it seems unlikely that this deviation from equilibrium would be significant. However, it is not at present possible to rule out this possibility. and we will refer to "apparent" pressures, "apparent" activities, and so on, so as to emphasize this uncertainty.

RESULTS AND DISCUSSION

The results of measurements on the copper–manganese system are given in Table I, and plotted as a function of reciprocal temperature in Fig. 5. As explained earlier, these data will be discussed at a single temperature only—820° C—using values obtained from Fig. 5 by interpolation. The interpolated values at 820° C are given in Table II.

TABLE I

Primary vapor pressure data for manganese and copper–manganese alloys*

Alloy	Temperature (°C)	Pressure (atm×10^{-7})	Log pressure (atm)	Alloy	Temperature (°C)	Pressure (atm×10^{-7})	Log pressure (atm)
Pure Mn	818	3.43	−6.46	29.7% Mn	820	1.94	−6.71
	818	2.90	−6.54		827	2.33	−6.63
	820	2.86	−6.54		844	4.30	−6.37
	828	4.45	−6.35	25.9% Mn	822	1.39	−6.86
	834	5.30	−6.28		831	1.97	−6.71
	838	7.00	−6.15		842	2.98	−6.53
	840	7.20	−6.14	23.4% Mn	818	1.30	−6.89
	844	8.94	−6.05		829	1.49	−6.83
59% Mn	818	3.35	−6.47		835	1.69	−6.77
	831	4.57	−6.34		841	2.09	−6.68
	837	5.56	−6.25	20.0% Mn	824	1.11	−6.95
	844	8.18	−6.09		828	1.26	−6.90
40.2% Mn	818	2.20	−6.66		833	1.53	−6.82
	824	2.81	−6.55		841	1.70	−6.77
	836	4.10	−6.39		846	2.27	−6.64
	840	4.26	−6.37				
	844	5.22	−6.28				

*These data are shown graphically in Fig. 5.

The apparent pressure values at 820° C are shown in Fig. 6 as thermodynamic activities (the activity, a, is given by $a=(P/P_0)$, where P and P_0 are the pressures of manganese in equilibrium with the alloy and pure γ-manganese,† respectively). Two distinct regions are evident. Up to about 25%, there appears to be a small positive deviation of the

*We are grateful to one of the referees for pointing out this possibility.

†Conversion of standard state to γ-Mn was done using the heat of transition $\Delta H_{\beta\gamma}$ = 545 cal/mole at the transition temperature of 1374° C (13).

Can. J. Chem. Downloaded from www.nrcresearchpress.com by 210.87.254.6 on 09/05/12
For personal use only.

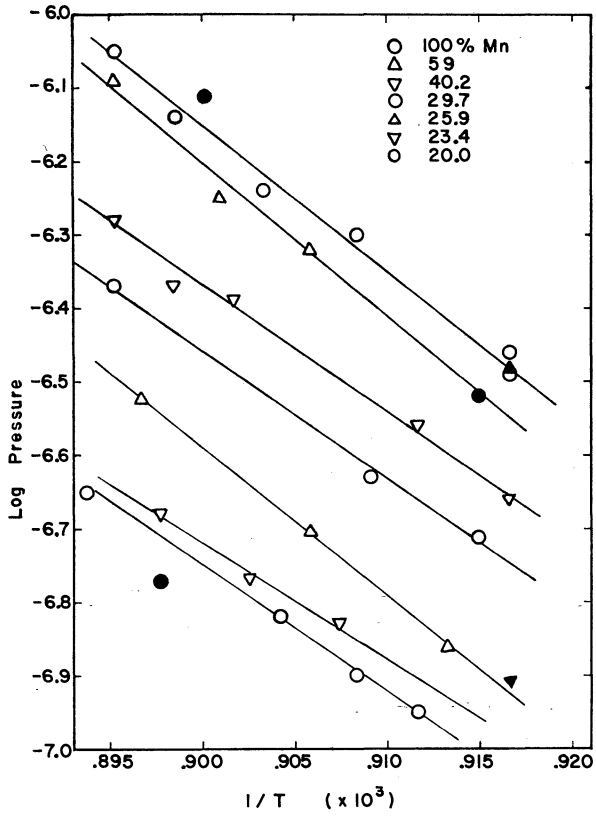

FIG. 5. Arrhenius plot of the vapor pressures of manganese over copper–manganese alloys. Solid points were ignored in fitting the lines.

TABLE II

Manganese activity data interpolated to 820° C

% Mn	Pressure×10⁷ (atm)	Activity*	Activity coefficient
20	0.92	0.27	1.33
23.4	1.04	0.30	1.30
25.9	1.19	0.34	1.32
29.7	1.79	0.51	1.73
40.2	2.21	0.64	1.59
59	2.82	0.82	1.39
100.0 (β-Mn)	3.29	0.95	0.95
100.0 (γ-Mn)		*1.00*	*1.00*

*Activity and activity coefficient data are computed as relative to γ-Mn, because the alloys studied are in the γ-phase.

activity from that to be expected from Raoult's Law. Although the data allow no conclusion to be made, one may speculate that the behavior of manganese in dilute solution in copper follows Henry's law, in which the apparent activity coefficient, though differing from unity, is constant. In the second region—from 30% up to 87%, where β-manganese forms a second phase at 820° C—the deviation from ideality is quite large, and it is clear that neither Raoult's nor Henry's law could correlate the results.

Can. J. Chem. Downloaded from www.nrcresearchpress.com by 210.87.254.6 on 09/05/12
For personal use only.

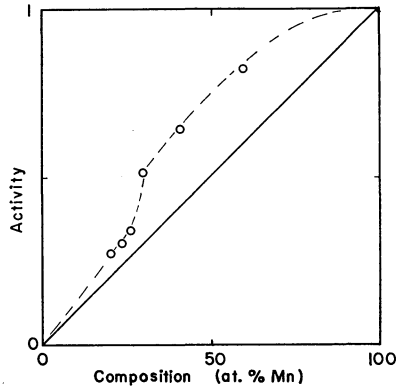

FIG. 6. Apparent activity of manganese in copper–manganese alloys at 820° C (relative to γ-Mn).

The same results are shown in Fig. 7 in the form of the apparent activity coefficients. Here the transition from the one region to the other is quite abrupt. The same data in the form of the excess free energy ($\Delta F^x = RT \ln \gamma$) fall on a very similar curve, which need not be presented here. The abruptness of the change between 26% and 29% is somewhat startling, and may well be exaggerated as it is drawn in Fig. 7.

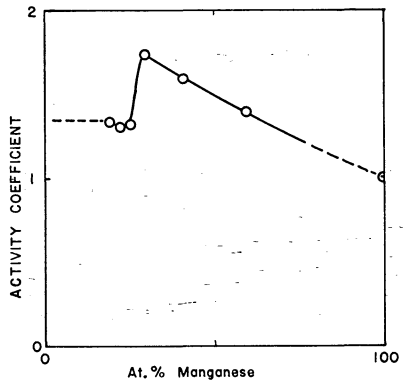

FIG. 7. Apparent activity coefficients of manganese in copper–manganese alloys at 820° C (relative to γ-Mn).

The results indicate a considerable change in the structure of the alloy—a sudden increase of the lattice spacing, an abrupt change in electronegativity difference, or perhaps a "clustering" of the manganese atoms. (It is to be noted that should the apparent vapor pressures reflect a diffusion-controlled evaporation rate, the anomalous values once more point to a marked change in the nature of the lattice.) A detailed interpretation of these data can scarcely be made without accurate heat and entropy data and, as was discussed earlier, we do not feel that our temperature range was wide enough to give the required accuracy in view of our other experimental uncertainties.

Perhaps the most significant point in the present work, to which attention is now directed, is that the observed discontinuity in the apparent activity occurs in the same region as those found in the magnetic properties. Myers' measurements (1) at 800° showed a distinct, if not sharp, break in the magnetic susceptibility at about 30 at% manganese.

Can. J. Chem. Downloaded from www.nrcresearchpress.com by 210.87.254.6 on 09/05/12
For personal use only.

Similar measurements by Scheil and Wachtel (2) on alloys quenched from 800° C to 100–200° C showed a very pronounced maximum in the magnetic susceptibility between 20% and 25% manganese. Likewise values of the magnetic susceptibility obtained at −188° C by Valentiner and Becker (4) showed a strong maximum between 20% and 30% manganese.

Although several workers (2–5) have suggested magnetic ordering as the cause of the phenomena observed, Myers' suggestion (1) of an electronic change in the alloy from a localized d^6s^1 configuration of the manganese to a delocalized d-band common to both copper and manganese seems to offer a more reasonable explanation of the present results. Indeed it may be that this valence change underlies all of the anomalies observed.

ACKNOWLEDGMENTS

The authors gratefully acknowledge the able assistance of Mr. R. G. Butters in the design and construction of the apparatus, and to the National Research Council for financial assistance. Several discussions with Dr. E. A. Flood, Dr. M. J. Dignam, and Dr. C. S. Samis have been very stimulating and helpful.

REFERENCES

1. H. P. Myers. Can. J. Phys. **34**, 527 (1956).
2. E. Scheil and E. Wachtel. Z. Metallk. **48**, 571 (1957).
3. S. Valentiner and G. Becker. Z. Physik, **80**, 735 (1935). *Quoted in* A. H. Sully. Manganese. Butterworth, London. 1955.
4. D. Meneghetti and S. S. Sidhu. Phys. Rev. **105**, 130 (1957).
5. A. Kussmann and H. J. Wollenberger. Naturwiss. **43**, 395 (1956).
6. B. M. Loring. *In* A.S.M. metals handbook. The American Society for Metals, Cleveland. 1948. p. 1198.
7. M. Knudsen. Ann. Physik, **29**, 179 (1909); also The kinetic theory of gases. Methuen. 1934.
8. R. Speiser and H. L. Johnson. Trans. Am. Soc. Metals, **42**, 283 (1950).
9. C. L. McCabe and R. G. Hudson. J. Metals, **9**, 17 (1957).
10. W. E. Mills and D. R. Wiles. Unpublished. 1959.
11. R. W. Wood. Phil. Mag. **32**, 364 (1916).
12. I. Estermann. Z. Elektrochem. **31**, 441 (1925).
13. B. F. Naylor. J. Chem. Phys. **13**, 329 (1945).

Can. J. Chem. Downloaded from www.nrcresearchpress.com by 210.87.254.6 on 09/05/12
For personal use only.

TOXIC FLUORINE COMPOUNDS

XIX. ω-FLUOROALKYNES[1]

F. L. M. PATTISON AND R. E. A. DEAR
Department of Chemistry, University of Western Ontario, London, Ontario
Received June 3, 1963

ABSTRACT

Some ω-fluoroalkynes have been prepared and shown to be valuable intermediates in the synthesis of rare long-chain ω-fluoro compounds; successful representative reactions, in all of which the C—F bond remained intact, included Grignard reactions, partial and total catalytic hydrogenation, halogenation, and miscellaneous coupling reactions.

The potential value of ω-fluoro-1-alkynes for the synthesis of unusual long-chain ω-fluoro compounds has been recognized for several years. Early work was not encouraging (2), because loss of fluorine occurred under the reaction conditions employed. More recent improvements in techniques involving acetylenic intermediates led us to re-examine the problem. In the course of the work, improved procedures for preparing ω-fluoro-1-alkynes were developed, and the importance of these compounds as intermediates was established. In illustration of their usefulness, the synthesis of two naturally occurring compounds (ω-fluoro-oleic acid and ω-fluoropalmitic acid) has already been described (1).

The preparations of the ω-fluoro-1-alkynes have been discussed (1, 2). The method of choice involves the reaction of an ω-fluoroalkyl chloride or bromide (3) with lithium acetylide stabilized as the ethylenediamine complex; the optimum reaction temperature for chlorides was 25° and for bromides 5–10°. The use of this complex obviates the need for gaseous acetylene and results in a higher yield of product. This is the only method which gives high yields of 1-alkynes directly from chlorides. Previous objections (1) to the use of alkyl chlorides, arising from the presence of unreacted chloride in the product, have been overcome by slowly warming the reaction mixture to 60° after the initial brisk reaction has ceased. This final step ensures complete reaction both of chlorides and of bromides. (Alkyl fluorides apparently do not react with the complex under the reaction conditions employed.) Yields of ω-fluoro-1-alkynes as high as 92% have thus been obtained. Physical constants are shown in Table I. The reactions which follow were undertaken to study the stability of the C—F bond under widely varying experimental conditions.

The first reactions of the ω-fluoro-1-alkynes to be studied were those involving Grignard reagents. Previous work using ethylmagnesium bromide had resulted only in fluorine-free mixtures (2). However, by using ethylmagnesium chloride under carefully controlled conditions, normal reactions occurred. The resultant Grignard reagents formed the corresponding N-α-naphthyl-ω-fluoro-2-alkynoamides with α-naphthyl isocyanate, and the corresponding ω-fluoro-2-alkynoic acids with carbon dioxide; in this work, the studies of Hollingsworth, Wotiz *et al.* (4, 5, 6) were of assistance. The first of these reactions is of value for characterizing the ω-fluoro-1-alkynes as crystalline derivatives. The second is interesting as an example of a "forced" Grignard reaction, wherein the reacting species are respectively diethylmagnesium and the di-(ω-fluoroalkynyl)magnesiums; to this end, the use of dioxane as solvent forced the Schlenk equilibrium in the desired direction.

[1]*For Part XVIII, see reference 1.*

Can. J. Chem. Downloaded from www.nrcresearchpress.com by 210.87.254.105 on 09/05/12
For personal use only.

$$F(CH_2)_nC{\equiv}CMgCl \xrightarrow{C_{10}H_7NCO} F(CH_2)_nC{\equiv}CCONHC_{10}H_7 \quad \text{(yields: 72–88\%)}$$

$$(F(CH_2)_nC{\equiv}C)_2Mg \xrightarrow{CO_2} F(CH_2)_nC{\equiv}CCOOH \quad \text{(yields: 51–95\%)}$$

Partial catalytic hydrogenation of the ω-fluoro-1-alkynes was next examined. The usual procedure, employing an alkali metal in liquid ammonia, gave fluorine-free products. However, by using hydrogen in the presence of Lindlar catalyst (7; 8, p. 200), high yields (75–86%) of the corresponding ω-fluoro-1-alkenes were obtained; uptake of hydrogen ceased abruptly after the addition of 1 mole. Oxygen-containing solvents caused total hydrogenation to the 1-fluoroalkanes; it is therefore important to use hydrocarbon solvents, such as *n*-pentane, for the reaction.

Halogenation of the acetylenic hydrogen was accomplished using sodium hypobromite, or by treating the lithium derivative with *p*-toluenesulphonyl chloride. The bromination reaction was based on the work of Straus *et al.* (9). For the lower members, the reaction proceeded well in the aqueous medium; but the low solubility of the higher members made the use of dioxane as solvent, and a higher reaction temperature, necessary for satisfactory yields. Yields of 1-bromo-ω-fluoro-1-alkynes ranged from 67–87%. The chlorination reaction was examined only in the case of 8-fluoro-1-octyne. Extending the observations of Truchet (10), who advocated the use of the sodium or potassium derivative of a 1-alkyne, we found that the preparation of the lithium derivative, using *n*-butyllithium in a hydrocarbon solvent, was more convenient, because it avoided the use of liquid ammonia; the subsequent reaction with *p*-toluenesulphonyl chloride proceeded smoothly to give 1-chloro-8-fluoro-1-octyne in an overall yield of 42%.

$$F(CH_2)_nC{\equiv}CH + NaOBr \rightarrow F(CH_2)_nC{\equiv}CBr + NaOH$$

$$F(CH_2)_6C{\equiv}CLi + CH_3C_6H_4SO_2Cl \rightarrow F(CH_2)_6C{\equiv}CCl + CH_3C_6H_4SO_2Li$$

Attempts were then made to prepare 1-fluoro-1-alkynes by reaction of metal derivatives of 1-alkynes with perchloryl fluoride. It is known that the fluorine atom in this compound displays, under appropriate conditions, electrophilic reactivity towards many types of carbanions. However, reaction of alkynyl anions, formed from 1-alkynes and *n*-butyllithium, with perchloryl fluoride gave only a low yield (16.5%) of the symmetrical diyne, $RC{\equiv}C{\cdot}C{\equiv}CR$. The reactions of alkynyl anions with various aromatic sulphonyl fluorides were equally unsuccessful in forming 1-fluoro-1-alkynes.

Of greater importance to the overall objective of preparing long-chain compounds were various coupling reactions. ω-Fluoro-1-alkynes, in the presence of lithium amide, formed *in situ* in liquid ammonia, reacted with ω-fluoroalkyl iodides to form α,ω-difluoroalkynes. ω-Chloroalkyl iodides similarly gave the corresponding α-chloro-ω-fluoroalkynes (1), which were then utilized in the synthesis of ω-fluoro-oleic and ω-fluoropalmitic acids. Yields in these simple couplings were good (65–89%). Successful couplings between the dilithium derivative of diacetylene (11) and ω-fluoroalkyl iodides have also been carried out; the former is conveniently prepared *in situ* from 1,4-dichloro-2-butyne and four equivalents of lithium amide in liquid ammonia. Overall yields fell in the range 40–50%. The diacetylene route is of value only for forming symmetrical diynes. The method of Chodkiewicz (12) was therefore employed for preparing unsymmetrical diynes; this involves the reaction of 1-alkynes with 1-bromo-1-alkynes in the presence of a cuprous salt and a primary amine. Yields were good (55–71%).

$$F(CH_2)_nC{\equiv}CLi + I(CH_2)_mF \rightarrow F(CH_2)_nC{\equiv}C(CH_2)_mF + LiI$$

$$2F(CH_2)_nI + LiC{\equiv}C{\cdot}C{\equiv}CLi \rightarrow F(CH_2)_nC{\equiv}C{\cdot}C{\equiv}C(CH_2)_nF + 2LiI$$

$$F(CH_2)_nC{\equiv}CH + BrC{\equiv}C(CH_2)_mF \rightarrow F(CH_2)_nC{\equiv}C{\cdot}C{\equiv}C(CH_2)_mF + HBr$$

Can. J. Chem. Downloaded from www.nrcresearchpress.com by 210.87.254.105 on 09/05/12
For personal use only.

Catalytic hydrogenation of the conjugated diynes using platinum gave the α,ω-difluoroalkanes in about 60% yield; ethanol was found to be a much better solvent for this than ethyl acetate. Previous preparations of α,ω-difluoroalkanes have usually involved anodic couplings, giving members containing an even number of carbon atoms. The acetylenic route is equally satisfactory for the even members, and provides a ready means of preparing the less accessible odd members.

One related reaction is of general interest. Paul and Tchelitcheff (13) have shown that dihydropyran on treatment with *n*-amylsodium forms 5-hydroxy-1-pentyne, a useful intermediate in this work. When we substituted *n*-butyllithium for *n*-amylsodium in this reaction, *trans*-1-hydroxy-4-nonene was formed in 73% yield. Thus the reaction had not followed the normal ring opening, but instead the dihydropyran had undergone addition of *n*-butyllithium followed by ether cleavage. This represents the simplest and best preparation of this unsaturated alcohol yet found.

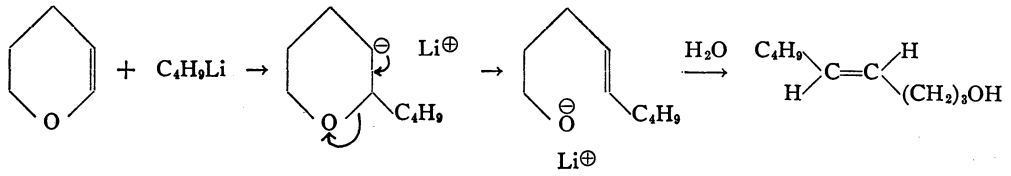

Toxicities of some representative ω-fluoroalkynes have been given in earlier reports (1, 2). The LD_{50} results listed in Table I do not add much to the current knowledge concerning the metabolism of the alkyne grouping. The two new ω-fluoro-1-alkynes conform to the toxicity pattern previously established. The results of the three ω-fluoro-2-alkynoic acids suggest that the presence of an α,β-acetylenic bond does not affect the ultimate fate of ω-fluorocarboxylic acids; that is, the unsaturation has little effect on the toxicity. Similar observations have been made previously with ω-fluoro-2-alkenoic acids, $F(CH_2)_nCH{=}CHCOOH$ (14), and with their metabolites such as ω-fluoro-β-hydroxyacids, $F(CH_2)_nCH(OH)CH_2COOH$ (15) and ω-fluoro-β-ketoacids, $F(CH_2)_nCOCH_2COOR$ (16). The alternation of toxicity in the 1-bromo-ω-fluoro-1-alkyne series is similar to, but less pronounced than that given by the ω-fluoroalkyl halide series (3). No particular trend is apparent in the α,ω-difluoro series containing non-terminal mono- and di-yne functions.

The interpretation of the results obtained with the ω-fluoro-1-alkenes remains as obscure as ever (2). The three new α,ω-difluoroalkanes gave toxicity results in line with those described in earlier work (3).

The most important conclusion from the work described in this paper is that ω-fluoro-1-alkynes may be prepared conveniently and in good yield from ω-fluoroalkyl halides (including chlorides), and that the acetylenic function undergoes further reactions, under a wide range of experimental conditions, without loss of fluorine. The ω-fluoro-1-alkynes are thus well established as important intermediates in the synthesis of biologically active aliphatic fluorine compounds.

EXPERIMENTAL

Many of the reactions described herein were followed by gas chromatography and infrared spectroscopy. Physical constants and analytical data for all new compounds are given in Table I. The preparations described below represent typical examples of each procedure; obvious variations for obtaining different members have not been included. Melting points (uncorrected) were determined on a Kofler hot stage, and densities with a Fisher-Davidson gravitometer. Infrared spectra were obtained with Beckman IR-7 and IR-5 infrared spectrophotometers. Analyses were performed by the Schwarzkopf Microanalytical Laboratory, Woodside, 77, N.Y. The presence of the ω-fluorine atom has previously been shown by nuclear magnetic

Can. J. Chem. Downloaded from www.nrcresearchpress.com by 210.87.254.105 on 09/05/12
For personal use only.

Can. J. Chem. Downloaded from www.nrcresearchpress.com by 210.87.254.105 on 09/05/12
For personal use only.

TABLE I

Physical constants, toxicities, and analytical results

Compound	Formula	Boiling point °C	Boiling point mm	n_D^{25} or m.p., °C	d_4^{20}	LD_{50} (mice, intraperitoneal), mg/kg (95% confidence limits)	Carbon, % Calc.	Carbon, % Found	Hydrogen, % Calc.	Hydrogen, % Found	Other, % Calc.	Other, % Found
5-Fluoro-1-pentyne	$F(CH_2)_3C{\equiv}CH$	75.5–76	742	1.3902	0.884	>100	69.74	70.00	8.20	8.26		
6-Fluoro-1-hexyne*	$F(CH_2)_4C{\equiv}CH$	106–106.5	742	1.4025		—¶						
7-Fluoro-1-heptyne†	$F(CH_2)_5C{\equiv}CH$	131.5–132	742	1.4106		—¶						
8-Fluoro-1-octyne‡	$F(CH_2)_6C{\equiv}CH$	82–82.5	60	1.4176		—¶						
9-Fluoro-1-nonyne§	$F(CH_2)_7C{\equiv}CH$	114	108	1.4221		—¶						
10-Fluoro-1-decyne	$F(CH_2)_8C{\equiv}CH$	81–82	10	1.4250	0.877	5.21 (2.74–9.46)	76.87	76.48	10.97	11.07		
N-α-Naphthyl-2-heptynoamide	$CH_3(CH_2)_3C{\equiv}CCONHC_{10}H_7$	—	—	118.5–119.5	—	—	81.24	81.30	6.82	6.83	N, 5.57	N, 5.60
N-α-Naphthyl-9-fluoro-2-nonynoamide	$F(CH_2)_6C{\equiv}CCONHC_{10}H_7$	—	—	80–80.5	—	—	76.74	76.74	6.78	6.85	N, 4.71	N, 4.90
N-α-Naphthyl-10-fluoro-2-decynoamide	$F(CH_2)_7C{\equiv}CCONHC_{10}H_7$	—	—	88–89.5	—	—	77.14	77.22	7.12	7.12	N, 4.50	N, 4.70
N-α-Naphthyl-11-fluoro-2-undecynoamide	$F(CH_2)_8C{\equiv}CCONHC_{10}H_7$	—	—	89.5–90	—	—	77.51	77.75	7.43	7.49	N, 4.31	N, 4.44
9-Fluoro-2-nonynoic acid	$F(CH_2)_6C{\equiv}CCOOH$	121	0.2	1.4593	1.075	>100	62.77	62.98	7.61	7.57		
10-Fluoro-2-decynoic acid	$F(CH_2)_7C{\equiv}CCOOH$	115	0.01	1.4599	1.064	ca. 7.5	64.49	64.67	8.12	8.22		
11-Fluoro-2-undecynoic acid	$F(CH_2)_8C{\equiv}CCOOH$	120–120.5	0.03	1.4602	1.056	42 (23.3–75.6)	65.97	66.16	8.56	8.74		
7-Fluoro-1-heptene	$F(CH_2)_5CH{=}CH_2$	117–117.5	742	1.3984	0.823	10–30	72.37	72.29	11.28	11.29		
8-Fluoro-1-octene	$F(CH_2)_6CH{=}CH_2$	140	742	1.4059	0.820	25–30	73.79	73.91	11.61	11.68		
9-Fluoro-1-nonene	$F(CH_2)_7CH{=}CH_2$	104	108	1.4128	0.812	11 (3.9–30.8)	74.94	75.20	11.88	12.06		
10-Fluoro-1-decene	$F(CH_2)_8CH{=}CH_2$	119	90	1.4179	0.815	41.5 (29.6–58.1)	75.89	76.16	12.10	12.07		
1-Bromo-6-fluoro-1-hexyne	$F(CH_2)_4C{\equiv}CBr$	62.5	12	1.4613	1.392	30 (17.1–52.5)**	40.25	40.47	4.50	4.55	Br, 44.63	Br, 44.61
1-Bromo-7-fluoro-1-heptyne	$F(CH_2)_5C{\equiv}CBr$	74	10	1.4630	1.334	>100	43.55	43.66	5.22	5.21	Br, 41.39	Br, 41.62
1-Bromo-8-fluoro-1-octyne	$F(CH_2)_6C{\equiv}CBr$	89	10	1.4634	1.272	39 (20.5–74.1)	46.40	46.54	5.84	5.95		
1-Bromo-9-fluoro-1-nonyne	$F(CH_2)_7C{\equiv}CBr$	102	10	1.4636	1.234	>100	48.89	48.80	6.38	6.33		
1-Bromo-10-fluoro-1-decyne	$F(CH_2)_8C{\equiv}CBr$	117	10	1.4639	1.194	25–40	51.08	51.20	6.86	6.71	Br, 33.98	Br, 34.17
1-Chloro-8-fluoro-1-octyne	$F(CH_2)_6C{\equiv}CCl$	112	55	1.4411		40–50**	59.08	59.12	7.44	7.54	Cl, 21.80	Cl, 21.81
1,12-Difluoro-6-dodecyne	$F(CH_2)_5C{\equiv}C(CH_2)_5F$	130.5–131	11	1.4356	0.948	55 (39.9–75.9)	71.25	71.40	9.97	10.15		
1,14-Difluoro-7-tetradecyne	$F(CH_2)_6C{\equiv}C(CH_2)_6F$	95–96	0.1	1.4394	0.925	35 (22.9–53.6)	73.00	73.23	10.50	10.39		
1,11-Difluoro-4,6-undecadiyne	$F(CH_2)_3C{\equiv}C\cdot C{\equiv}C(CH_2)_4F$	89	0.05	1.4816	1.006	>100	71.71	71.81	7.66	7.75		
1,12-Difluoro-5,7-dodecadiyne	$F(CH_2)_4C{\equiv}C\cdot C{\equiv}C(CH_2)_4F$	122	0.8	1.4819	0.994	20–25	72.70	72.95	8.14	8.18		
1,13-Difluoro-5,7-tridecadiyne	$F(CH_2)_4C{\equiv}C\cdot C{\equiv}C(CH_2)_5F$	99–100	0.03	1.4819	0.978	>100	73.55	73.47	8.55	8.40		
1,14-Difluoro-6,8-tetradecadiyne	$F(CH_2)_5C{\equiv}C\cdot C{\equiv}C(CH_2)_5F$	103–104	0.04	1.4815	0.955	97	74.30	74.49	8.91	9.21		
1,6-Difluorohexane‖	$F(CH_2)_6F$	126.5–127	742	1.3758		7.7 (6.21–9.55)	58.99	59.15	9.91	10.05		
1,11-Difluoroundecane	$F(CH_2)_{11}F$	108–108.5	11	1.4125	0.903	62.5	68.70	68.89	11.53	11.42		
1,13-Difluorotridecane	$F(CH_2)_{13}F$	135	12	1.4194	0.893	ca. 21	70.86	71.13	11.90	11.88		

*Lit. (2) b.p. 106–106.5° at 745 mm, n_D^{25} 1.4058.
†Lit. (2) b.p. 131–131.5° at 748 mm, n_D^{25} 1.4103.
‡Lit. (2) b.p. 77–78° at 50 mm, n_D^{25} 1.4165.
§Lit. (2) b.p. 66–66.5° at 12 mm, n_D^{25} 1.4192.
‖Isolated from the partial halogen exchange reaction of 1,6-dichlorohexane and potassium fluoride; lit. (18) b.p. 129.9°, n_D^{25} 1.3739.
¶The following toxicities of ω-fluoro-1-alkynes have been reported (2): $F(CH_2)_4C{\equiv}CH$, 5.7; $F(CH_2)_5C{\equiv}CH$, 53; $F(CH_2)_6C{\equiv}CH$, 7.5; $F(CH_2)_7C{\equiv}CH$, 79.
**For comparison, the toxicity of two 1-halo-1-alkynes was determined: $CH_3(CH_2)_3C{\equiv}CBr$, >100; $CH_3(CH_2)_3C{\equiv}CCl$, >100; this lack of toxicity does not bear out the statement that "the lower 1-chloroalkynes are extremely toxic" (Raphael (8, p. 57)).

resonance spectroscopy, and the significance of the spectra discussed (1). The lithium acetylide (stabilized as the ethylenediamine complex) and the *n*-butyllithium solution were purchased from Foote Mineral Co., Route 100, Exton, Pa. Ethylmagnesium chloride solution was purchased from Arapahoe Chemicals, Inc., Boulder, Colorado. The 1,4-dichloro-2-butyne was kindly presented by Antara Chemicals, General Aniline and Film Corporation, 435 Hudson Street, New York 14, N.Y.

ω-Fluoro-1-alkynes

Two methods for preparing the ω-fluoro-1-alkynes have already been described (1). By the sodium acetylide route in xylene–DMF were prepared 8-fluoro-1-octyne (from 6-fluorohexyl bromide in 50.0% yield) and 10-fluoro-1-decyne (from 8-fluoro-octyl bromide in 60.1% yield). By the lithium acetylide route were prepared the following: 5-fluoro-1-pentyne (from 3-fluoropropyl bromide in 21.4% yield[2]); 6-fluoro-1-hexyne (from 4-fluorobutyl chloride in 74.8% yield); 7-fluoro-1-heptyne (from 5-fluoropentyl chloride in 91.8% yield); 8-fluoro-1-octyne (from 6-fluorohexyl chloride in 76.4% yield); and 9-fluoro-1-nonyne (from 7-fluoroheptyl bromide in 76.4% yield). The optimum reaction temperature for the alkyl chlorides is 25° and for alkyl bromides 10°. It was previously noted (1) that incomplete reaction rendered chlorides unsuitable as starting materials, owing to the similarities in boiling points and refractive indices between the chlorides and resultant alkynes. By slowly warming the reaction mixture to 60°, after reaction at the initial low temperature has ceased, both chlorides and bromides may be caused to react completely. Unreacted starting material thus ceases to be a problem.

N-α-Naphthyl-9-fluoro-2-nonynoamide

Ethylmagnesium chloride (5.15 ml of 3 *M* solution; 0.0156 mole) was placed in a dry 100-ml three-necked flask fitted with a nitrogen inlet, a dropping funnel, a precision-bore stirrer, and a condenser. A nitrogen atmosphere was maintained throughout. 8-Fluoro-1-octyne (2 g, 0.0156 mole) in ether (10 ml) was added slowly with stirring. The ether refluxed and the dark brown color of the original Grignard suspension lightened considerably. When gas evolution had ceased, a solution of α-naphthyl isocyanate (2.6 g, 0.0154 mole) in dry ether (10 ml) was added slowly with stirring; fast addition results in urea formation. When refluxing had ceased, the mixture was poured onto crushed ice and extracted with ether. The extract was washed with water and dried over calcium sulphate. Removal of the ether gave the amide (3.31 g, 72.2%). Recrystallization from ether – petroleum ether, followed by drying *in vacuo* at 40°, gave the pure material.

The following were prepared similarly: *N-α-naphthyl-10-fluoro-2-decynoamide* (87.6%); *N-α-naphthyl-11-fluoro-2-undecynoamide* (75.3%); and *N-α-naphthyl-2-heptynoamide* (77.0%).

Principal infrared bands of the three fluorinated amides ($CHCl_3$, cm^{-1}): 3378 and 3257 (free N—H) w; 3049 and 2985 (aromatic C—H) w; 2933 and 2857 (aliphatic C—H) m; 2232 (C≡C) m; 1664 (C=O) s; 1524 (combination N—H and C—N) s; 1488 s; 1350 m; 1256 m; 1046 and 990 (C—F) w.

9-Fluoro-2-nonynoic Acid

Precautions were observed to exclude moisture and oxygen, as in the previous procedure; the apparatus was the same. Ethylmagnesium chloride (14.5 ml of 3 *M* solution; 0.042 mole) and dry ether (29 ml) were added to the flask, thus giving a 1 *M* solution. This was stirred and heated under reflux, and dioxane (sodium dried; 3.78 g, 0.042 mole) was added. The resulting suspension was refluxed and stirred for 5 hours. 8-Fluoro-1-octyne (5 g, 0.039 mole) was added slowly, and the mixture was stirred without heating for 1 hour. It was then poured onto a mixture of powdered dry ice (150 g) suspended in dry ether (60–70 ml), and stirred for 1 hour. The mixture was hydrolyzed with saturated ammonium chloride solution and then acidified with dilute hydrochloric acid. The ether layer was extracted with sodium carbonate solution. Removal of the ether allowed recovery of unreacted alkyne. The aqueous extract was acidified and extracted with ether. Washing, drying ($CaSO_4$), and distillation gave the acid (3.39 g, 50.5%).

The following were prepared similarly: *10-fluoro-2-decynoic acid* (94.6%) and *11-fluoro-2-undecynoic acid* (75.0%).

Principal infrared bands of the three acids (CCl_4, cm^{-1}): 3521 (free O—H) w; 3077, 2660, and 2532 (bonded O—H) m; 2941 and 2865 (C—H) s; 2242 (C≡C) s; 1689 (C=O) s; 1466 (C—H) m; 1412 and 1279 (C—O and O—H) s; 1050 and 1013 (C—F) m; 919 (O—H) m.

7-Fluoro-1-heptene

Lindlar catalyst (7, 8) (200 mg) was suspended in *n*-pentane, and 5% synthetic quinoline in *n*-pentane (1 ml) was added. Upon saturation with hydrogen at room temperature and atmospheric pressure, no noticeable uptake of hydrogen occurred. 7-Fluoro-1-heptyne (4.56 g, 0.04 mole) in *n*-pentane (20 ml) was added, and hydrogenation was started. The theoretical amount of hydrogen was absorbed in just under 3 hours, after which no further uptake was observed. The catalyst was filtered off and washed with *n*-pentane. The filtrate was washed with dilute hydrochloric acid and then with water, dried ($CaSO_4$), and distilled to give the alkene (3.56 g, 80.4%).

The following were prepared similarly: *8-fluoro-1-octene* (86.0%); *9-fluoro-1-nonene* (79.8%); and *10-fluoro-1-decene* (74.9%).

[2]*The low yield is explained by the very high volatility of the product. Suitable variations in technique would undoubtedly raise the yield to that of the other members.*

Can. J. Chem. Downloaded from www.nrcresearchpress.com by 210.87.254.105 on 09/05/12
For personal use only.

Principal infrared bands of the fluoroalkenes (CCl_4, cm^{-1}): 3067 (olefinic C—H) w; 2907 and 2857 (C—H) s; 1642 (C=C) m; 1464, 1445, and 1416 (C—H) m; 1052 and 1018 (C—F) m; 952 (olefinic C—H) m; 912 (olefinic C—H) s; 722 (C—H) w.

1-Bromo-6-fluoro-1-hexyne

Sodium hydroxide (10 *N*, 37 ml, 0.367 mole) was cooled in a flask surrounded by ice. Water (23 ml) was added, followed by dropwise addition of bromine (17.2 g, 0.108 mole). 6-Fluoro-1-hexyne (10 g, 0.100 mole) in ether (5 ml) was added with vigorous stirring. The mixture was then stirred overnight at room temperature. The heterogeneous mixture was poured into water and extracted with ether. The extracts were washed, dried ($CaSO_4$), and distilled to give the bromoalkyne (15.47 g, 86.4%).

The following were prepared similarly: *1-bromo-7-fluoro-1-heptyne* (86.6%), and *1-bromo-8-fluoro-1-octyne* (73.8%). The same procedure, but using dioxane (10 ml) in place of the ether and a temperature of 35°, gave: *1-bromo-9-fluoro-1-nonyne* (64.9%) and *1-bromo-10-fluoro-1-decyne* (86.4%). The 1-bromo-1-alkynes must all be distilled at reduced pressure to avoid decomposition.

Principal infrared bands (CCl_4, cm^{-1}): 2933 and 2865 (C—H) s; 2222 (C≡C) w; 1468 and 1433 (C—H) m; 1380 w; 1330 w; 1110 w; 1053 and 1012 (C—F) m; 722 (C—H) w.

1-Chloro-8-fluoro-1-octyne

The reaction was carried out in an atmosphere of dry nitrogen. 8-Fluoro-1-octyne (3.84 g, 0.03 mole) was dissolved in *n*-pentane (25 ml), and the solution was freed of any dissolved oxygen by refluxing in a stream of nitrogen for 15 minutes. *n*-Butyllithium (11.45 g of 15.2% w/w solution; 1.74 g C_4H_9Li; 0.0272 mole) in hexane was added slowly with stirring. The alkynyllithium separated. The mixture was warmed to ensure completion of the reaction. After no more butane was evolved, sodium-dried dioxane (5 ml) was added, thus dissolving most of the solid. *p*-Toluenesulphonyl chloride (freshly distilled and recrystallized, 5.7 g, 0.0298 mole) was added in dioxane, and the orange-yellow lithium sulphinate was deposited. The mixture was stirred for 15 minutes and then was poured onto crushed ice. Separation of the organic layer, ether extraction of the aqueous layer, washing, drying ($CaSO_4$), and distillation gave the chloroalkyne (2.05 g, 41.8%). Principal infrared bands (CCl_4, cm^{-1}): 2933 and 2857 (C—H) s; 2232 (C≡C) w; 1464 and 1431 (C—H) m; 1391 w; 1330 w; 1078 m; 1048 and 1012 (C—F) m.

Attempted Preparation of 1-Fluoro-1-octyne

1-Octynyllithium was prepared from 1-octyne (12.1 g) as described in the previous procedure. Dioxane was added to dissolve the solid and perchloryl fluoride was passed in at 0°. An exothermic reaction occurred and a white precipitate was deposited. Working up the mixture in the usual way gave only recovered 1-octyne (3.94 g) and 7,9-hexadecadiyne (1.35 g, 16.5%). A reaction analogous to the preparation of 1-chloro-8-fluoro-1-octyne, using *p*-toluenesulphonyl fluoride, gave no fluoroalkyne.

1,12-Difluoro-6-dodecyne and 1,14-Difluoro-7-tetradecyne

These were prepared in yields of 65.0% and 77.0% by the procedure described for 1-chloro-17-fluoro-8-heptadecyne (1). The infrared spectra of these two compounds were similar to those of the chlorofluoroalkynes (1), except that no C—Cl bands were present and the C—F bands were stronger.

1,12-Difluoro-5,7-dodecadiyne

Liquid ammonia (200 ml) was introduced into a 500-ml three-necked flask fitted with a stirrer, a dropping funnel, and a dry-ice condenser. Anhydrous ferric chloride (0.1 g) and small pieces of lithium (1.85 g, 0.264 g-atom) were added. At the end of 10 minutes, a grey suspension of lithium amide was present. 1,4-Dichloro-2-butyne (8.1 g, 0.066 mole) was added slowly. The ensuing dehydrochlorination was rapid and exothermic, being complete in about 1 minute. 4-Fluorobutyl iodide (3) (26.83 g, 0.132 mole) was added slowly, and the mixture was stirred for 4.5 hours. Ammonium chloride was added to neutralize any unreacted amide, and the ammonia was allowed to evaporate. The brown residue was extracted with ether, and the extracts were washed, dried ($CaSO_4$), and distilled, giving recovered 4-fluorobutyl iodide (3.16 g) and the required symmetrical diyne (4.83 g, 40.8%).

1,14-Difluoro-6,8-tetradecadiyne was prepared similarly in 47.8% yield.

1,11-Difluoro-4,6-undecadiyne

A 250-ml flask was fitted with a gas inlet tube, a dropping funnel, a stirrer, and a condenser. The flask was purged with nitrogen, and 5-fluoro-1-pentyne (2.88 g, 0.0335 mole) in absolute methanol (25 ml) was added. To this solution was added 10 ml of a 33% v/v solution of *n*-propylamine in methanol (i.e. ca. 0.06 mole of amine), cuprous chloride (70 mg), and hydroxylamine hydrochloride (0.2 g). The mixture was cooled to 0° and a methanolic solution of 1-bromo-6-fluoro-1-hexyne (6 g, 0.0335 mole) was added dropwise and with vigorous stirring. Small crystals of hydroxylamine hydrochloride were added from time to time to maintain the copper in the reduced state. The reaction was complete after about 1 hour. The copper was complexed by the addition of sodium cyanide (1 g). The mixture was diluted with water, extracted with ether, and the extracts were washed, dried ($CaSO_4$), and distilled, yielding the unsymmetrical diyne (3.36 g, 54.6%).

Can. J. Chem. Downloaded from www.nrcresearchpress.com by 210.87.254.105 on 09/05/12
For personal use only.

1,13-Difluoro-5,7-tridecadiyne was prepared similarly in 71.4% yield.

Principal infrared bands of the four diynes (CCl_4, cm^{-1}): 2933 and 2857 (C—H) s; 2257 and 2155 (C≡C?) vw; 1477, 1458, and 1431 (C—H) m; 1391 m; 1351 w; 1326 m. The next six bands must be due to C—F, because none of them are present in the nonfluorinated analogues; all are strong: 1066, 1044, 1019, 1006, 986, and 959.

1,11-Difluoroundecane

Platinum dioxide (250 mg) was reduced in ethanol to finely divided platinum black. 1,11-Difluoro-4,6-undecadiyne (1.99 g, 0.0108 mole) in ethanol was added; hydrogenation proceeded smoothly until the theoretical quantity of hydrogen had been taken up. The catalyst was removed by filtration, and the ethanol by distillation, to give the difluoroalkane (1.98 g). Distillation gave the pure material (1.33 g, 64.0%).

1,13-Difluorotridecane was prepared similarly in 53.2% yield.

trans-1-Hydroxy-4-nonene

A 500-ml flask, fitted with a gas inlet tube, a dropping funnel, a precision-bore stirrer, and a condenser, was purged with nitrogen. *n*-Butyllithium (163 g of a 15.2% w/w solution; 24.6 g C_4H_9Li; 0.385 mole) was introduced, and dihydropyran (17.7 g, 0.19 mole based on 90% purity) was added over a period of 30 minutes. The temperature rose from 26° to 34°. The mixture was heated under reflux for 3 hours and then cooled. Excess *n*-butyllithium was destroyed by the slow addition of water, with cooling. The layers were separated and the aqueous layer was extracted with ether. Drying ($CaSO_4$) and distillation yielded the product (19.8 g, 73.0%) of b.p. 209–210° and n_D^{25} 1.4465; lit. (17) b.p. 103–104° at 14 mm, n_D^{20} 1.4494. Principal infrared bands (CCl_4, cm^{-1}): 3610 (free O—H) w; 3322 (bonded O—H) m; 2959, 2924, and 2857 (C—H) s; 1468, 1458, 1439, and 1381 (C—H) m; 1058 (C—O and O—H) s; 970 (*trans*-RCH=CHR′) s.

ACKNOWLEDGMENTS

We wish to express our indebtedness to Allied Chemical Corporation, General Chemical Division, Morristown, N.J., for financial assistance; to Dr. M. K. McPhail and Dr. C. A. deCandole, Suffield Experimental Station, Ralston, Alberta, for carrying out the toxicity determinations; to Dr. O. F. Beumel, Jr., Foote Mineral Co., Exton, Pa., for helpful advice in the use of the lithium acetylide complex; and to Antara Chemicals, General Aniline and Film Corporation, 435 Hudson Street, New York 14, N.Y., for a gift of 1,4-dichloro-2-butyne.

REFERENCES

1. R. E. A. Dear and F. L. M. Pattison. J. Am. Chem. Soc. **85**, 622 (1963).
2. F. L. M. Pattison and J. J. Norman. J. Am. Chem. Soc. **79**, 2311 (1957).
3. F. L. M. Pattison and W. C. Howell. J. Org. Chem. **21**, 748 (1956).
4. L. V. Guild, C. A. Hollingsworth, D. H. McDaniel, S. K. Podder, and J. H. Wotiz. J. Org. Chem. **27**, 762 (1962).
5. R. E. Dessy, J. H. Wotiz, and C. A. Hollingsworth. J. Am. Chem. Soc. **79**, 358 (1957).
6. J. H. Wotiz, C. A. Hollingsworth, and R. E. Dessy. J. Am. Chem. Soc. **78**, 1221 (1956).
7. H. Lindlar. Helv. Chim. Acta, **35**, 446 (1952).
8. R. A. Raphael. Acetylenic compounds in organic synthesis. Butterworth Scientific Publications, London. 1955.
9. F. Straus, L. Kollek, and W. Heyn. Ber. **63**, 1868 (1930).
10. R. Truchet. Ann. Chim. (Rome), **16**, 309 (1931).
11. J. B. Armitage, E. R. H. Jones, and M. C. Whiting. J. Chem. Soc. 44 (1951).
12. W. Chodkiewicz. Ann. Chim. (Paris), **2**, 819 (1957).
13. R. Paul and S. Tchelitcheff. Bull. Soc. Chim. France, 808 (1952).
14. F. L. M. Pattison, S. B. D. Hunt, and J. B. Stothers. J. Org. Chem. **21**, 883 (1956).
15. M. S. Kharasch *et al.* Unpublished results. 1943–1945.
16. R. R. Fraser, J. E. Millington, and F. L. M. Pattison. J. Am. Chem. Soc. **79**, 1959 (1957).
17. M. F. Ansell and D. A. Thomas. J. Chem. Soc. 3302 (1957).
18. F. W. Hoffmann. J. Org. Chem. **14**, 105 (1949).

Can. J. Chem. Downloaded from www.nrcresearchpress.com by 210.87.254.105 on 09/05/12
For personal use only.

A MASS SPECTROMETRIC STUDY OF THE OXIDATION OF HYDROGEN SULPHIDE

PART I. OBSERVATION AND IDENTIFICATION OF SOME INTERMEDIATES

D. G. H. MARSDEN
Department of Chemistry, Laval University, Quebec, Que.
Received May 29, 1963

ABSTRACT

The oxidation of hydrogen sulphide has been followed mass-spectrometrically by direct sampling from a reaction vessel having a small leak. In the neighborhood of the third explosion limit, there is a period of 8–12 seconds of accelerating reaction before the explosion; during this time peaks are observed to grow, disappearing after explosion. By using $D_2S/^{16}O_2$ and $H_2S/^{18}O_2$ mixtures, it has been shown that these peaks arise from the ions H_2^+, S_2O^+, H_2SO^+, S_2^+, and $H_2S_2^+$. It is evident that the first two ions represent the intermediate formation of hydrogen and disulphur monoxide; the parents of the last three ions are discussed, and it is concluded that the most likely possibilities are H_2SO_2, S_2, and H_2S_2. Only during the explosion itself is there any evidence for SO radical.

Can. J. Chem. Downloaded from www.nrcresearchpress.com by 210.87.254.105 on 09/05/12
For personal use only.

INTRODUCTION

The oxidation of hydrogen sulphide was first studied in the 1930's. The first investigations (1–5) showed that the reaction was preceded by an induction period, was autocatalytic, and at sufficiently high pressures and temperatures led to an explosion. The explosion limit was at first thought to represent part of an explosion peninsula, but Jacovlev and Schantarovitsch (6) showed later that this limit was a third limit, the true explosion peninsula lying at considerably lower pressures, as would have been expected. Previous workers had not noticed it for two reasons; firstly, their manometers were not sufficiently sensitive, and secondly, the explosion was feeble and took place after a considerable amount of slow reaction, even in the middle of the peninsula. The induction period and autocatalytic reaction were observed in the whole press.–temp. plane; as the pressure was raised above the upper limit the induction period was shortened and the acceleration more marked, leading eventually to the third explosion limit. It appeared that the third limit was a thermal one; Frank-Kamenetskii calculated the position of this limit, and found good agreement with the experimental value, using the maximum rate of reaction during the acceleration period as a basis for the calculation of self-heating (7).

The facts that the reaction was autocatalytic, that the final products, SO_2 and water, were without influence on the kinetics, and that the maximum rate of reaction occurred at 10–15% conversion indicated that an intermediate product was formed which could give rise to degenerate branching; however, the intermediate was evidently less stable than the peroxides in hydrocarbon oxidation, since the reaction was complete in a matter of minutes.

Semenov and Emanuel (8, 9) were able to demonstrate the presence of the intermediate in the following manner. They found that if a mixture were partially reacted at a certain temperature and pressure and then transferred to a second reactor at a different temperature and pressure, the induction period in this second reactor was reduced considerably, or even eliminated, depending on the length of time the mixture had remained in the first reactor; this indicated that the intermediate survived the transfer from one reactor to another. It was then found that if, before introduction to the second reactor, the partially

reacted mixture were diluted with fresh mixture, the induction period was again lengthened, evidently due to dilution of the intermediate; it was found that there was a direct relation between induction period and dilution. They were able, thus, to use the induction period in the second reactor to measure relative concentrations of intermediate after various times of reaction in the first reactor. It was found that the intermediate was produced right from the start, i.e. even during the induction period (no pressure change), and rose to maximum concentration at the point of inflection of the pressure–time curve. Experiments also showed that the intermediate lasted for some hours at room temperature, but decayed faster in the presence of water vapor.

To identify the intermediate, Emanuel (9) took ultraviolet absorption spectra of cooled, partially reacted mixtures; new bands were observed and identified with those of Schenk's sulphur monoxide (10). In addition it was noticed that on cooling partially reacted mixtures there was an abnormal pressure decrease. Emanuel concluded that the intermediate was SO, but that on cooling it dimerized to S_2O_2; thus Schenk's sulphur monoxide as prepared and observed in ultraviolet absorption at room temperature was in fact S_2O_2. The same conclusion had also been reached earlier by Kondratiev and Kondratieva (11) for energetic reasons. The pressure decrease was then used to obtain absolute concentrations of SO; it appeared that in the early stages of reaction up to 75% of the H_2S consumed appeared as SO.

Later work by Jones (12) appeared to confirm the formula S_2O_2 at room temperature, since two infrared absorption bands were found. However, recently Myers (13, 14) has reinvestigated the compound and has shown conclusively by means of stoichiometry, molecular weight determination, mass spectrometry, and microwave spectroscopy that the correct formula is in fact S_2O, the thioanalogue of SO_2. Thus the compound prepared by Schenk, the intermediate observed by Emanuel at room temperature, and the end product observed in the flash-photolysis of H_2S/O_2 mixtures at room temperature by Norrish and Zeelenberg (15, 16) must all be considered as S_2O, disulphur monoxide.

It was therefore considered that it would be of interest to study the thermal oxidation by means of mass spectrometry in order to determine whether S_2O or SO were the important intermediate at the temperature of reaction, and to see if any other intermediates were formed. The region of the third limit was chosen, for three reasons. First, the induction period is negligible and the rate of reaction at its fastest, so that concentrations of intermediate would be expected to be relatively large. Secondly, the time scale is short, explosion taking place after 8–12 seconds; a relatively large sampling leak may be used in the reaction vessel, thus increasing sensitivity, without sensibly diminishing the pressure during the time interval of interest. Thirdly, there was the possibility of observing intermediates during the explosion itself. All experiments were carried out on stoichiometric mixtures.

EXPERIMENTAL

The mass spectrometer has recently been described in detail (17). It is essentially a 60° sector instrument with fast electrostatic scanning, having a large vacuum chamber at the source end, which holds a reaction vessel with surrounding furnace. The reaction vessel has a small leak from which the escaping gas passes directly through the ion source and is pumped away. The cylindrical reaction vessel used in this work was 40 mm in diam. and 120 mm long; the leak was 30 μ in diam., giving a leak rate of 2%/min at 100 mm pressure.

The ions are collected by an ion-electron multiplier and peaks displayed on a Tektronix 545A oscilloscope synchronized with the ion-voltage scan. The mass spectra were recorded on a Bolex H16 cinecamera, which triggered the oscilloscope so as to give one mass spectrum per frame; the time of scan was 0.01 second, and the framing rate either 8 or 7 1/2 frames per second.

Can. J. Chem. Downloaded from www.nrcresearchpress.com by 210.87.254.105 on 09/05/12
For personal use only.

Gases were obtained as follows:

Hydrogen sulphide, from a cylinder; purified by passage over iodine, ice-cold baryta solution; dried over P_2O_5, finally bulb-to-bulb distilled.

Oxygen, from a cylinder, 99.6% pure; dried over P_2O_5.

Deuterium sulphide, reaction of D_2O on freshly prepared aluminum sulphide (using degreased aluminum powder). To obtain a pure product it was necessary to degas the sulphide at 1200° C *in vacuo*; the reactants were sealed in ampoules which were broken inside an evacuated 5 *l* flask. The product was bulb-to-bulb distilled twice.

Oxygen-18, from the Weizman Institute, Israel; purity ^{18}O 98.73%, ^{17}O 0.36%, ^{16}O 0.91%, randomly distributed isotopically. Exchange with a silica surface at the temperatures used has been shown to be negligible (25).

Disulphur monoxide, prepared after Schenk (10) by passing a mixture of sulphur dioxide and sulphur vapor through a discharge tube (aluminum electrodes, 15 kv neon-sign transformer). The product was probably 50% diluted with unchanged SO_2.

Experimental Method

In the case of H_2S or D_2S mixtures with $^{16}O_2$ the gases were mixed at appropriate pressures in a large flask and the mixture expanded to a smaller flask, at a known pressure, whence it was expanded into the reaction vessel through a quick-opening lever valve; pressures were equalized in 1/4 second. All pressures were measured with a silica bourdon gauge nulled against a mercury manometer.

With the mixtures of H_2S and $^{18}O_2$ it was necessary to eliminate as much dead space as possible, in view of the small quantity available (150 cc $^{18}O_2$ at NTP). In this case, a vessel of appropriate size was glass-blown to the break-seal-equipped ampoule containing $^{18}O_2$ and filled with hydrogen sulphide to give a stoichiometric mixture at as high pressure as possible. After the seal was broken, the gases were allowed to mix for 3 days. A small Toepler pump was used to transfer the mixture to a small sampling volume attached to the bourdon gauge, from which it was expanded to the reaction vessel.

In an experimental run the reaction mixture was let into the reaction vessel and the camera started simultaneously. In certain cases the oscilloscope sensitivity was switched manually during a run (8–12 seconds) to observe rapidly changing peaks with greater precision.

In the runs with added S_2O, the discharge tube was allowed to run a few minutes while connected to the pumps. Then the evacuated reaction vessel was connected to the pump-line, allowing some S_2O to enter; after evacuating the line, the reaction mixture was then admitted to the reaction vessel, the camera being started simultaneously.

All electron energies quoted are relative and do not take into account surface potentials, etc.; where several experiments were done at different electron energies, they were done in succession, to minimize as much as possible changes in source conditions.

EXPERIMENTAL RESULTS

The third and upper explosion limits for stoichiometric mixtures found in this work are shown in Fig. 1, together with those found by Jacovlev and Schantarovitsch (6) for a

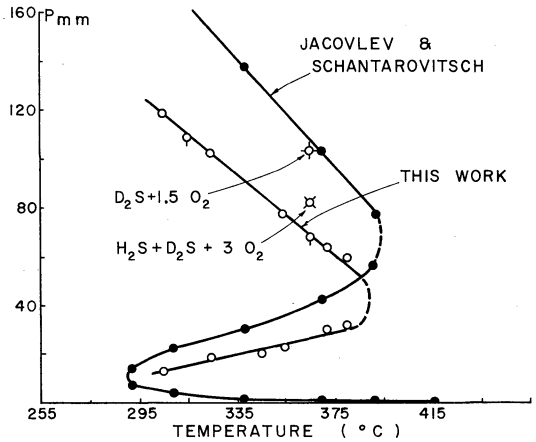

FIG. 1. Explosion limits in stoichiometric H_2S/O_2 mixtures. Points with tails represent determinations after an interval of 6 months.

Can. J. Chem. Downloaded from www.nrcresearchpress.com by 210.87.254.105 on 09/05/12
For personal use only.

vessel of the same diameter. The limits were reproducible, as shown by points taken after an interval of several months; the difference between the curves may be due to some non-uniformity in the temperature of the reaction vessel. A point on the third limit is also shown for D_2S/O_2 stoichiometric mixture, and for a 50–50 $H_2S/D_2S/O_2$ stoichiometric mixture. It is of interest to note the considerable rise in the limit.

At the third limit the explosion takes place after a period of 8–12 seconds, during which peaks at mass 18 and 64 grow right from entry of the mixture into the reaction vessel, the rate accelerating up to the moment of explosion. During this time a peak is observed to grow at mass 80, which disappears after the explosion. This peak could be due to either the ion SO_3^+ or S_2O^+. The previous work suggested that it was probably S_2O^+, since it is known (13) that S_2O has a parent peak; this was borne out also by the abnormal height of the isotopic peak, mass 82. Confirmation was obtained using $^{18}O_2$; Fig. 2 shows some

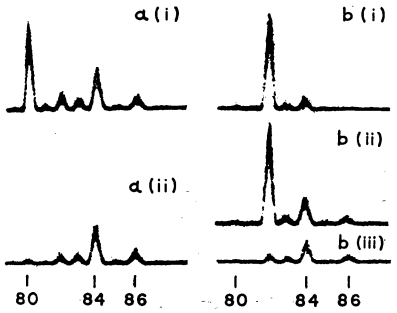

FIG. 2. Identification of S_2O: *a*(i) $H_2S/^{16}O_2$/Kr mixture just before explosion; *a*(ii) Kr alone before entry of reactants; *b*(i) $H_2S/^{18}O_2$ mixture; *b*(ii) $H_2S/^{18}O_2$/Kr mixture, both just before explosion; *b*(iii) Kr alone, before entry of reactants. Pressure, temperature: *a*, 95 mm, 340° C; *b*, 105 mm, 350° C. Electron energy 50 v.

oscilloscopic traces of these peaks, alone and in the presence of Kr as marker. It is observed that with $^{18}O_2$ the peaks are shifted to mass 82 and 84 and there is no peak at mass 86 ($^{32}S^{18}O_3^+$).

During the acceleration reaction peaks also grow at mass 2 and 48. The peak at mass 2 was shown to be due to hydrogen, since its growth was observed at electron energies too low for it to be formed as a fragment ion from H_2O or H_2S. After explosion it disappeared, while if the mixture were below the third limit it continued to grow (Fig. 3). The peak at mass 18 is necessarily due to water, but the peaks at mass 48 and 64 could arise from various species. Mass 48 was shown to be due to SO^+ and not O_3^+, since no peak at mass 54 was found using $^{18}O_2$, but the SO^+ ion could be formed in several ways: (*a*) by fragmentation of SO_2 or S_2O; (*b*) by fragmentation of some other SO-containing molecule; (*c*) by direct ionization of SO radical. Mass 64 could be SO_2^+ ion, formed from (*a*) SO_2, by direct ionization, or (*b*) some SO_2-containing species, by fragmentation; it could also be S_2^+ ion formed by (*a*) direct ionization of S_2 molecule, or (*b*) fragmentation of S_2O or some other S_2-containing species.

As noted in the introduction, Emanuel (9) considered that SO was the active intermediate and was formed in a larger amount than SO_2 at the beginning of reaction. To see if this were so, the ratio of peaks 64 to 48 was measured during the acceleration period and compared with the value after explosion, when the only species present is SO_2; the measurements were taken at various electron energies (Fig. 4). It may be seen that at

Can. J. Chem. Downloaded from www.nrcresearchpress.com by 210.87.254.105 on 09/05/12
For personal use only.

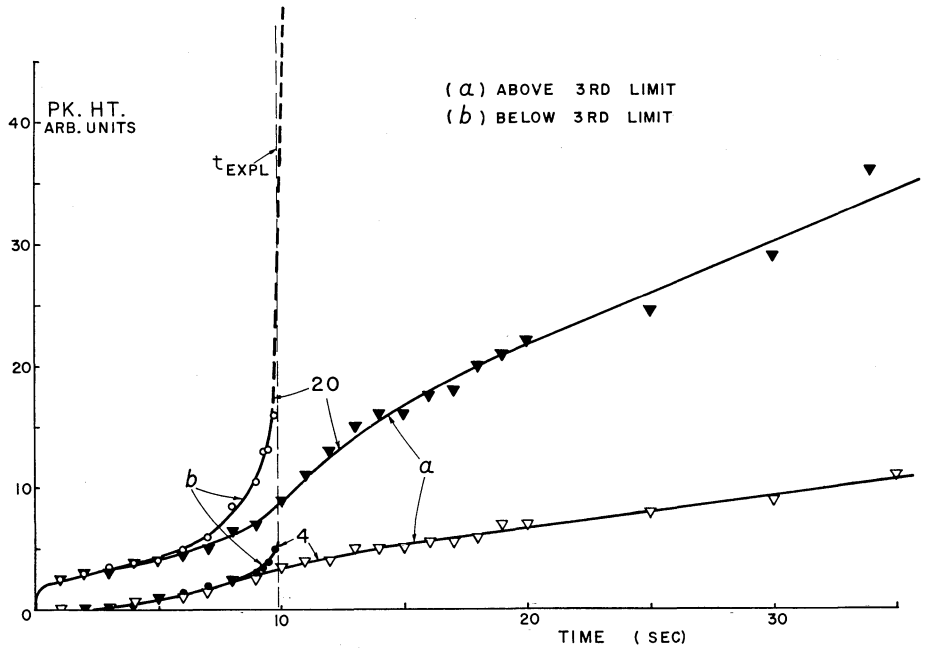

FIG. 3. Growth of hydrogen and water above and below third explosion limit. $D_2S/^{16}O_2$ mixture; temperature 364° C, pressure 110 mm and 99 mm.

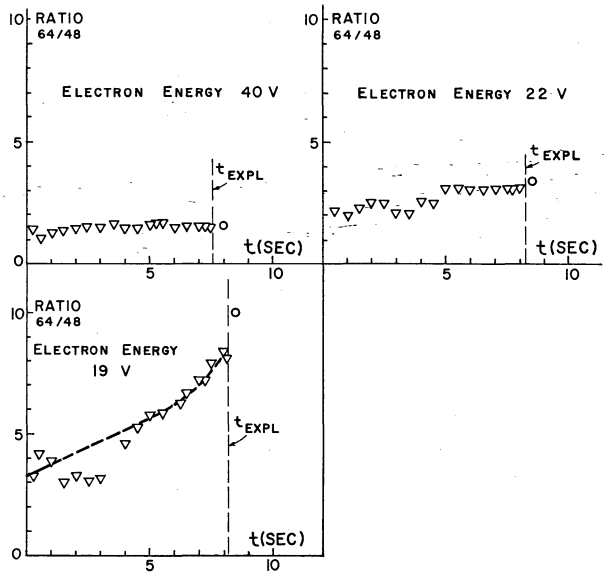

FIG. 4. Ratio of peaks 64/48 during acceleration reaction and after explosion; $D_2S/^{16}O_2$ mixture; temperature 364° C, pressure 110 mm.

40 v the ratio is effectively constant during the acceleration period and unchanged after explosion, while at the two lower electron energies, the ratio 64/48 increases during the acceleration period and is lower than the value after explosion. This might be considered as evidence that SO radical was being formed in greater quantity at the beginning of

Can. J. Chem. Downloaded from www.nrcresearchpress.com by 210.87.254.105 on 09/05/12
For personal use only.

reaction, the proportion of SO_2 increasing during the acceleration period. However, it will be noted that at corresponding times the actual value of the ratio 64/48 is bigger at lower electron energies; therefore if it is assumed that at low energies the 48 peak represents SO radical, then the 64 peak must be largely due to S_2^+ at the beginning of reaction. In fact, there is a considerable contribution from S_2^+ ion, as will be seen, but nevertheless the quantity of SO radical must be small, since there is no change in ratio at 40 v. Further experiments were made at energies below the appearance potential of SO from SO_2, as measured on a sample of SO_2 introduced into the reaction vessel. There was no evidence for any peak at mass 48 during the acceleration period. However, during the explosion itself a transient growth and decay was observed; Fig. 5 is a time exposure showing the transient taken with the mass spectrometer focused on mass 48 and the oscilloscope sweep running free, the electron energy being below A.P. $SO^+/(SO_2)$. It is of interest that the ultraviolet spectrum of SO has recently been observed in the flash-photolysis of H_2S/O_2 mixtures under adiabatic conditions (18).

It would therefore appear that SO radical is formed in very small amount, if at all, during the acceleration period. The fact that the 64/48 ratio grows during the acceleration period at low electron energies may be explained by supposing that SO^+ is being formed not only from SO_2, but also from S_2O or other intermediates. Since I.P. S_2O is undoubtedly lower than I.P. SO_2 (31), and the S—S bond weaker than the S—O bond, the contribution to mass 48 will come more and more from S_2O as the electron energy is lowered; as the reaction proceeds, 64 will grow not only from S_2^+, but also from SO_2^+ contributions, faster than 48, since, as will be seen, SO_2 grows faster than S_2O; after the explosion the ratio will be larger, since all the contribution to mass 48 is now from SO_2. At high electron energies, the increased cross section for ionization and fragmentation of SO_2 masks the effects of S_2O fragmentation, so that at 50 v SO_2 is the main contributor to peaks 48 and 64.

In observing the growth of peaks 48 and 64 at low energies, it was noted that the ^{34}S isotopic peaks at masses 50 and 66 were higher in proportion to the main peaks before the explosion than after. Since this effect was only observed at low energies, it was thought that some intermediate was being formed in small quantity at the same mass number. Fig. 6A(i and ii), recorded just before and after the explosion, show the effect at mass 50; similarly Fig. 6B(i and ii) show the effect at mass 66. Using D_2S, peaks were observed at mass 52 and 68 before the explosion, disappearing after the explosion (Fig. 6A(iii and iv); B(iii and iv)). The peak at mass 66 (68) could be due to either $H_2S_2^+$ ($D_2S_2^+$) or $H_2SO_2^+$ ($D_2SO_2^+$), while the peak at mass 50 (52) can only be ascribed to H_2SO^+ (D_2SO^+); this ion has recently been observed by Henglein (26).

To decide between these possibilities, $H_2S/^{18}O_2$ mixtures were reacted. First, it was verified that the isotopic anomaly at mass 52 ($H_2S^{18}O^+$) was still present at low electron energies. The results are shown in Fig. 7, where it may be observed that peak 52 is larger in relation to peak 50 before the explosion, *a*, than after, *b*. The large peak at mass 48, which would at first sight indicate gross contamination by ^{16}O, is in fact due to $C^{18}O_2^+$ produced by reaction with the filament; this may be inferred from the fact that it remains at almost the same height before and after the explosion, and that on raising the electron energy to 50 v after the explosion, *c*, it becomes much smaller in relation to peak 50; the purity of the oxygen-18 was confirmed by mass spectrometric analysis after the series of experiments was finished.

When the series of peaks from mass 64 to 70 was examined, indications were found that the $H_2S/^{18}O_2$ mixture that had been made up was richer than stoichiometric. First, there

Can. J. Chem. Downloaded from www.nrcresearchpress.com by 210.87.254.105 on 09/05/12
For personal use only.

Can. J. Chem. Downloaded from www.nrcresearchpress.com by 210.87.254.105 on 09/05/12
For personal use only.

PLATE I

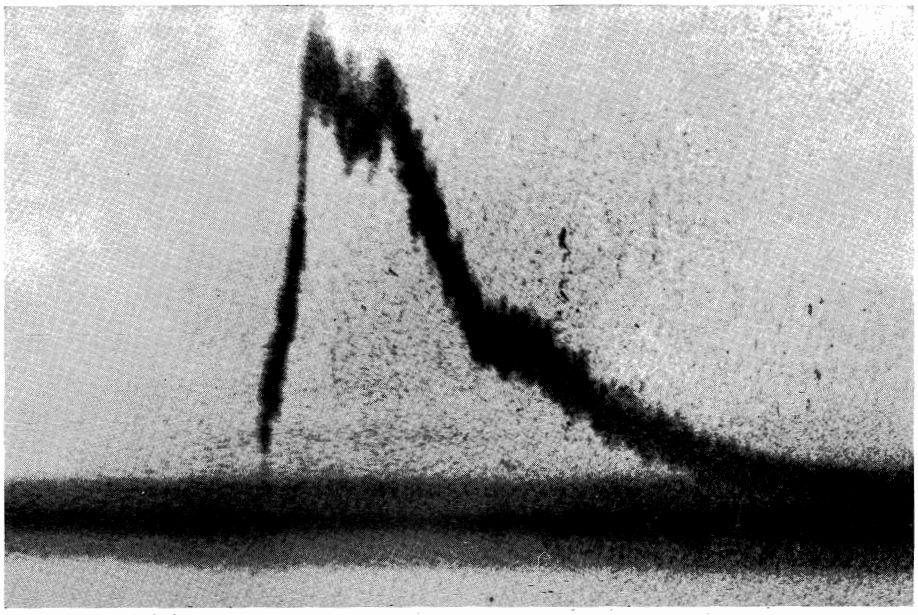

FIG. 5. Transient growth and decay of peak at mass 48 during explosion. Time scale 1/60 second. $H_2S/^{16}O_2$ mixture; pressure 95 mm, temperature 340° C; electron energy adjusted to be below A.P. $SO^+(SO_2)$.

Can. J. Chem. Downloaded from www.nrcresearchpress.com by 210.87.254.105 on 09/05/12
For personal use only.

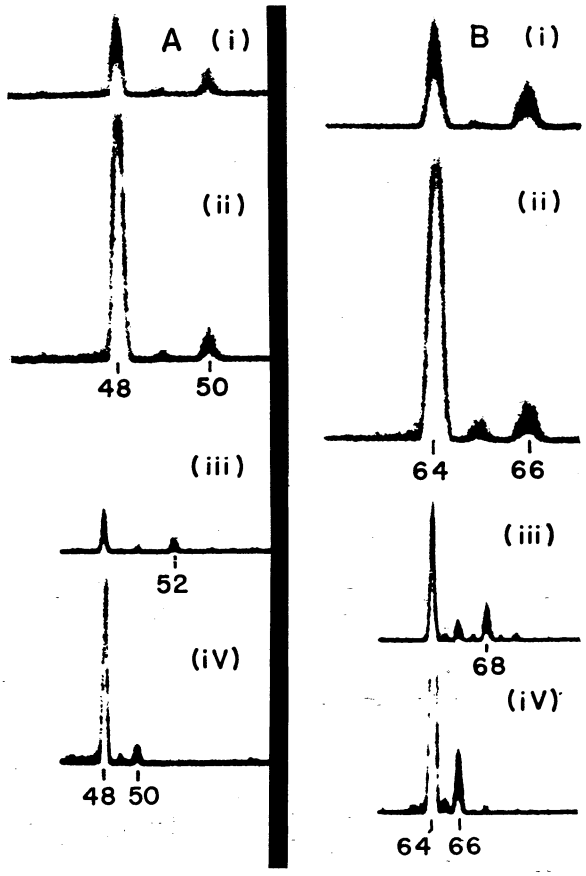

FIG. 6. A. Peaks at masses 48–52: (i) before explosion; (ii) after explosion, using $H_2S/^{16}O_2$ mixture; (iii) before explosion; (iv) after explosion, using $D_2S/^{16}O_2$ mixture. B. Peaks at masses 64–68: (i) before explosion; (ii) after explosion, using $H_2S/^{16}O_2$ mixture; (iii) before explosion; (iv) after explosion, using $H_2S/^{18}O_2$ mixture.

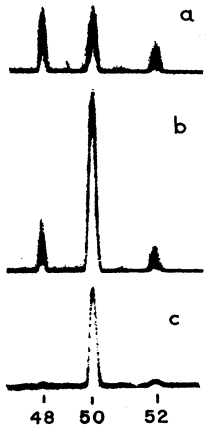

FIG. 7. Peaks at masses 48–52 using $H_2S/^{18}O_2$ mixture: *a*, before explosion; *b*, after explosion, all at low electron energy; *c*, after explosion, at 50 v electron energy (scale change of 25).

Can. J. Chem. Downloaded from www.nrcresearchpress.com by 210.87.254.105 on 09/05/12
For personal use only.

was a deposit of sulphur in a short section of cold tubing leading from the reaction vessel to its inlet valve; secondly, the peak at mass 64 after explosion was too large to be attributed to isotopic impurity in SO_2, and disappeared more slowly than the peak at mass 68 on pumping out; thirdly, a small peak at mass 82 was present after the explosion (S_2O may be synthesized by incomplete combustion of sulphur (19)). It was felt that these effects could not be accounted for by the presence of mercury vapor in the Toepler, for two reasons. Firstly, there was no such effect during trial runs with stoichiometric $H_2S/^{16}O_2$ mixtures; secondly, mercury vapor would tend to lower the sulphur content, forming hydrogen and non-volatile HgS.

Attempts were made to reduce the H_2S content by partial condensation in a capillary cold finger, and it was possible to suppress almost entirely the sulphur deposit and residual S_2O peak after explosion. It was felt that even if the mixture was still slightly richer than stoichiometric, essentially the same intermediates should be formed before the explosion, since during this time only 10–15% reaction occurred. Some oscilloscopic traces of masses 64–70 are shown in Fig. 8, *a* and *b* being taken near the beginning and end of the acceleration period respectively; *c* after explosion, all at low electron energy; *d* was taken after

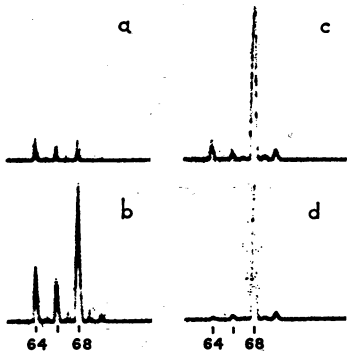

FIG. 8. Peaks at masses 64–70 using $H_2S/^{18}O_2$ mixture; *a*, at beginning of acceleration reaction; *b*, just before explosion; *c*, after explosion, all at low electron energy; *d*, after explosion at 50 v electron energy (scale change of 500).

the explosion at high electron energy. In *a* and *b* it may be observed that peaks 64, 66, and 68 are all of the same order of magnitude, 68 increasing toward the end of the acceleration period. It may be deduced immediately that the ions S_2^+, $H_2S_2^+$, and SO_2^+ are present. Mass 68 must be largely $S^{18}O_2^+$ since the contribution of $H_2\ ^{34}S^{32}S^+$ would be only 9% of the 66 peak; similarly 66 must be largely $H_2S_2^+$, since the contribution from $^{34}S^{32}S^+$ would be only 9% of the 64 peak. It is clear that peaks 64 and 66 belong to one or more intermediate compounds. The presence of sulphur after the explosion is shown also by Table I, where the experimental 50 v analysis after the explosion is compared with that expected; the 64 peak is too large, and increases at low electron energies (I.P. S_2 < I.P. SO_2).

The Effect of Added S_2O

When S_2O, produced by the discharge tube, was admitted to the reaction vessel before the reaction mixture, the period of acceleration could be reduced by one half or more, depending on the amount of S_2O produced by the discharge and the time elapsed before the reaction mixture was added; the same effect was observed by Emanuel (9). The explosion limit was unaffected. Figures 9–12 show growth of peaks 80, 64, 48, 18, 20 (D_2O^+),

Can. J. Chem. Downloaded from www.nrcresearchpress.com by 210.87.254.105 on 09/05/12
For personal use only.

TABLE I

50 v analysis of products at masses 64–70 using $H_2S/^{18}O_2$ mixture

Mass	Theoretical isotopic distribution in SO_2	Experimental distribution
64	0.1	1.4 (8 at 16 v)
65	Small	—
66	2.4	2.1*
67	0.8	0.9
68	100	100
69	0.9	1.3
70	4.4	4

*Corrected for $S^{34}S^{32}$ contribution from S_2.

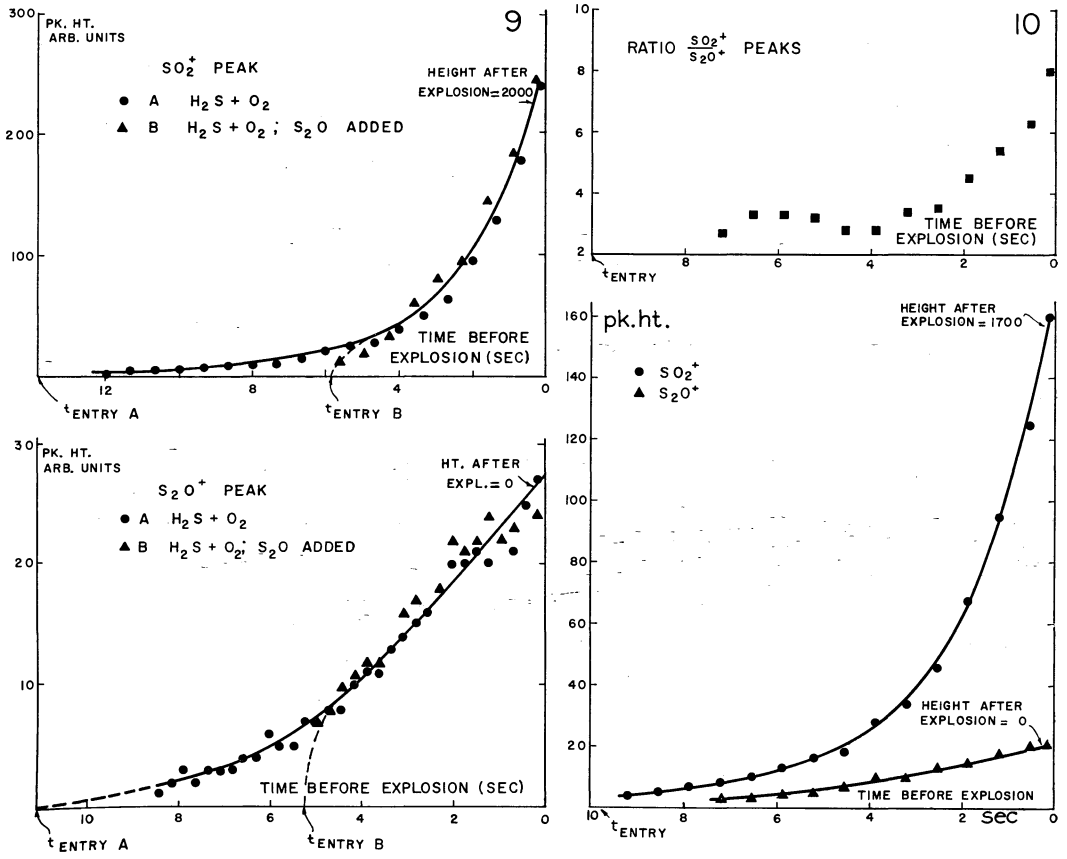

FIG. 9. Growth of SO_2 and S_2O during acceleration period, with and without added S_2O (scales are different); 50 v electron energy.

FIG. 10. Growth of SO_2 and S_2O; variation of peak height ratio with time; 50 v electron energy, same scale.

4 (D_2^+), using H_2S or D_2S/O_2 mixtures, in the presence and absence of added S_2O. The curves have been plotted against time before explosion; it is observed that the effect of added S_2O is simply to start the reaction further along the acceleration curve.

If, as discussed above, peaks 64 and 48 are due predominantly to SO_2 at 50 v electron energy, then plots of the ratios 80/64, 48/18, and 18/2 (or 20/4 in the case of D_2S)

Can. J. Chem. Downloaded from www.nrcresearchpress.com by 210.87.254.105 on 09/05/12
For personal use only.

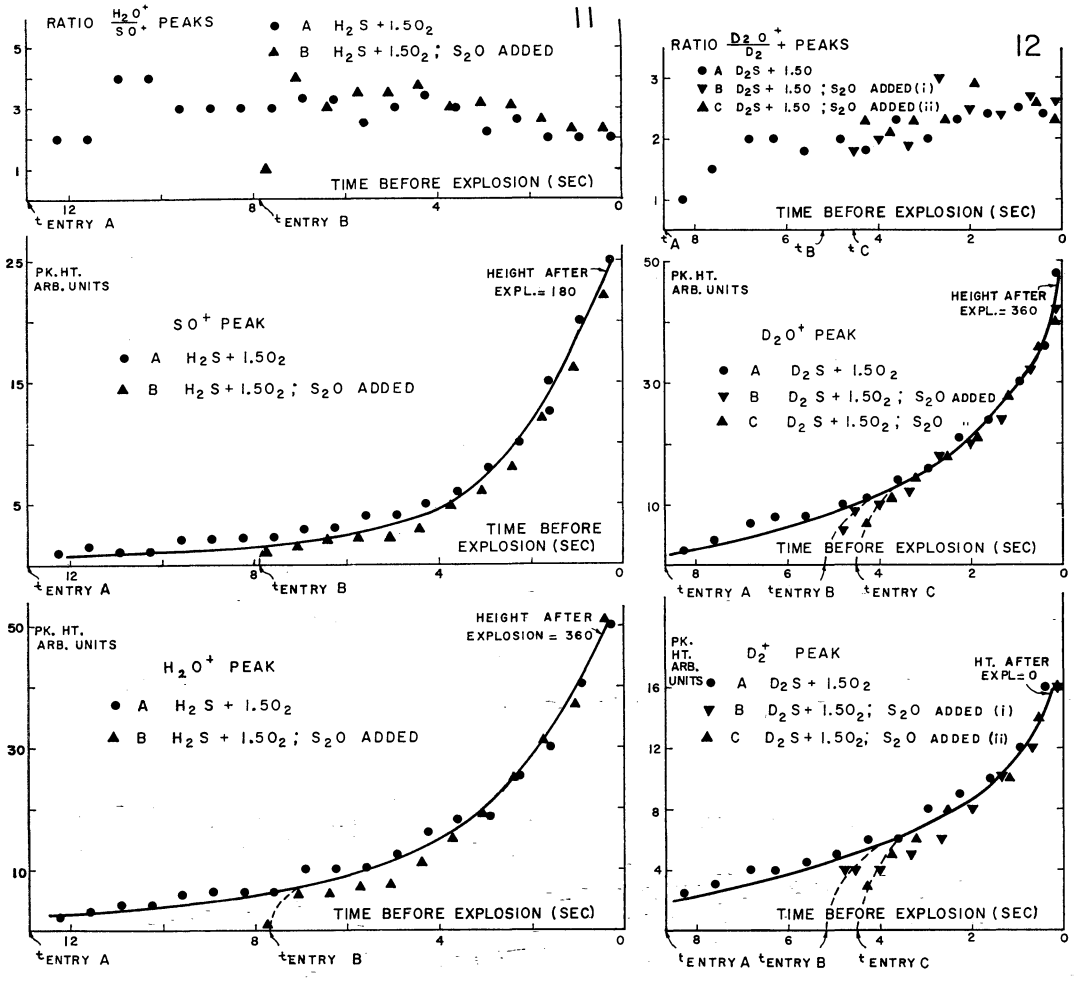

FIG. 11. Growth of SO^+ and H_2O^+ and variation of peak height ratio with time in the presence and absence of added S_2O; 50 v electron energy.

FIG. 12. Growth of D_2 and D_2O and variation of peak height ratio with time; $D_2S/^{16}O_2$ mixture, electron energy reduced sufficiently to eliminate contribution to D_2^+ peak from D_2O and D_2S.

represent the relative growth of S_2O^+, SO_2, H_2O, and H_2. However, in order that peak heights be proportional to concentrations, it is necessary that there be molecular flow through the reaction vessel leak; in the present case this is not so, for reasons of sensitivity (17), and the flow is in the transition region between molecular and viscous. Nevertheless, since only 10–20% of reaction occurs during the acceleration period, the viscosity may be assumed to be reasonably constant, so that peak heights are a fair indication of concentration.

Figures 10–12 show ratios of peaks 80/64, 48/18, and 20/4 during the acceleration period, the last two with and without added S_2O; the ratio 80/64 is also independent of added S_2O, as shown by Fig. 9. It may be seen that within the statistical scatter (largest at the beginning of the acceleration period, due to the small number of ions formed) H_2, H_2O, and SO_2 all grow at the same relative rate, while S_2O grows more slowly.

Can. J. Chem. Downloaded from www.nrcresearchpress.com by 210.87.254.105 on 09/05/12
For personal use only.

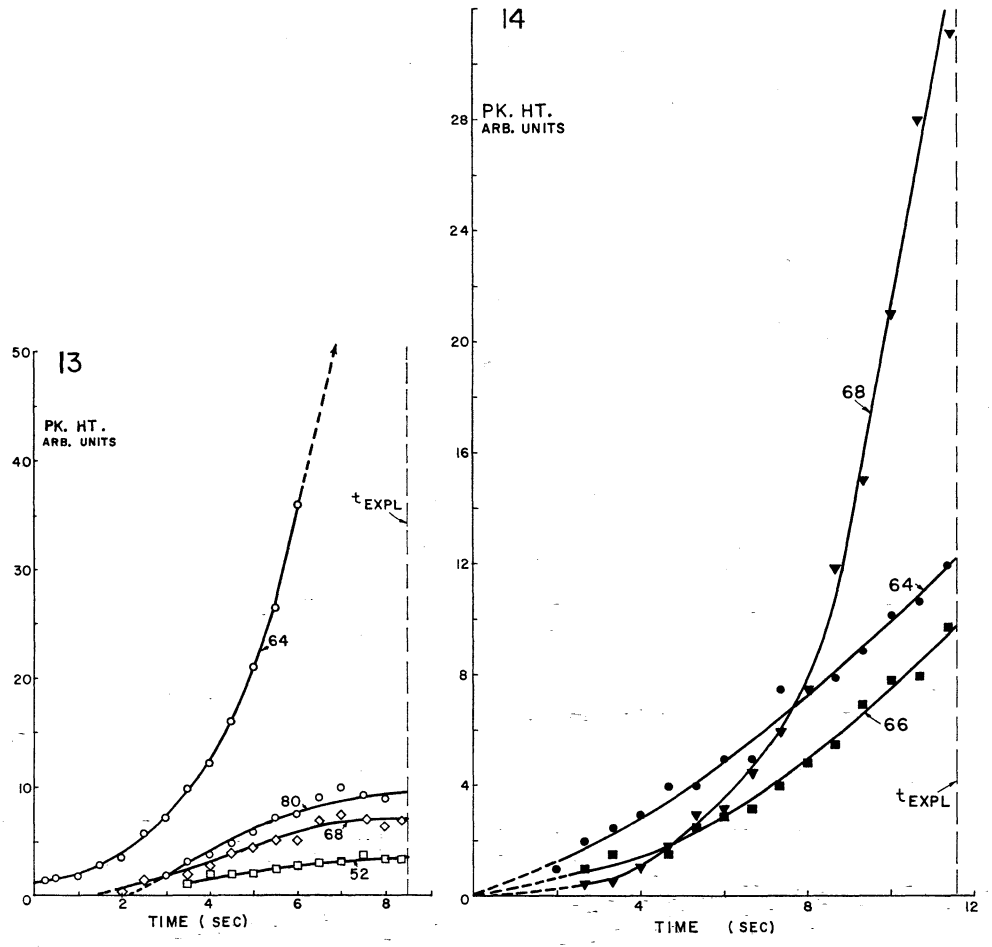

FIG. 13. Variation with time of peaks 52, 64, 68, 80; $D_2S/^{16}O_2$ mixture.
FIG. 14. Variation with time of peaks 64, 66, 68; $H_2S/^{18}O_2$ mixture; low electron energy.

Figures 13 and 14 show the growth of peaks 52, 68, 80 ($D_2S/^{16}O_2$) and the growth of peaks 64, 66, 68 ($H_2S/^{18}O_2$). It is to be noted, especially from Fig. 14, where the contribution to mass 68 can only be from SO_2^+, that peaks 52, 64, and 66, as well as peak 80, grow considerably more slowly than SO_2. Due to the smallness of the peaks it was impossible to measure with any accuracy differences between the rate of growth of peaks 50 (52), 64, 66 (68), and 80 (82); certainly no marked difference was observed.

Experiments on S_2O

Numerous experiments were carried out on reactions of S_2O, produced by the discharge tube; oxygen, H_2S or D_2S, H_2O or D_2O, H_2 or D_2, and various mixtures of these at different temperatures and pressures were added to see if the intermediates already found could be detected. Alone, i.e. at a pressure of a few mm and mixed with unchanged SO_2 from the discharge tube, S_2O is observable for several minutes at 350° C, and indefinitely at room temperature. In the presence of small quantities of oxygen it disappears faster, and above a critical pressure, immediately; the critical oxygen pressure is lower the higher the temperature, as has also been noted by Kondratiev and Kondratieva (20). No precise

Can. J. Chem. Downloaded from www.nrcresearchpress.com by 210.87.254.105 on 09/05/12
For personal use only.

measurements were made, as the efficiency of the discharge tube in producing S_2O was was variable, but it was established that S_2O was destroyed immediately if the same pressure of oxygen was added that would be present in an H_2S/O_2 mixture at the third limit. No evidence for SO radical was obtained during the decomposition in the presence of oxygen.

In the presence of D_2O vapor at 350° C, the disappearance of S_2O was somewhat faster than in its absence, but the difference was not nearly as marked as Emanuel observed at room temperature (9); he found, however, that the reaction had a negative temperature coefficient. During the decomposition, no peak was observed at mass 68 ($D_2O \rightarrow D_2S_2^+$), but a small peak appeared at mass 36, shifting to mass 34 when H_2O was used, thus indicating the formation of H_2S. Addition of H_2S had no effect on the decomposition; mixtures of $H_2O + H_2S$ or $H_2O + O_2$ produced no other intermediate substances. Further experiments were made with $SO_2/H_2(D_2)$ and $SO_2/H_2O(D_2O)$ mixtures; again no reaction occurred and no intermediates were observed.

DISCUSSION

It appears certain that the S_2O^+ ion may be identified with the compound S_2O; if S_2O_2 does exist and is present during the acceleration period, it must lack a parent peak (no other peaks being found up to mass 150). In addition, the absorption spectra observed by Emanuel and by Norrish are certainly due to S_2O; if S_2O_2 were formed during the oxidation its absorption spectrum should have been observed, in addition to that of S_2O.

The identification of the compound or compounds giving rise to the ions H_2SO^+, S_2^+, and $H_2S_2^+$ is more difficult. It is hard to imagine that a compound $H_{2+x}S_{2+y}O_z$ could exist at the temperature of experiment, since such compounds as the thio acids are relatively unstable even at room temperature. H_2S_2 is the most stable of the polysulphides (21), and the simplest molecule able to give this peak. The ion H_2SO^+, again, would be more likely to arise from a compound $H_{2+x}SO_{1+y}$ than one containing several sulphur atoms. There are no obvious compounds containing more than two hydrogen atoms, so that the simplest choice would be one of the series H_2SO_{1-5}. Of this series the only known compounds are H_2SO_4 and H_2SO_5, H_2SO_3 being probably non-existent (22). H_2SO_5 is only formed under extreme oxidizing conditions, is unstable, and therefore unlikely to be formed under the experimental conditions. If H_2SO_4 were formed, it is surprising that no peak was observed at mass 86 ($^{32}S^{18}O_3^+$) or higher; it would also have been expected that sulphuric acid would condense in the cool reaction vessel inlet and give rise to persistent residual peaks. Of the two remaining possibilities H_2SO_2 might be formulated as the unknown parent compound of (*a*) the sulphoxylates, (*b*) the sulphinic acids, or (*c*) the sulphones. From the thermal stabilities of the known examples of these compounds, formulation (*c*) would be expected to be most stable (23). It is to be noted also that this form would be isoelectronic with the ion $H_2PO_2^-$. Some inconclusive evidence for its existence lies in the reaction of hydrogen atoms with sulphur dioxide at low temperatures; it was reported (24) that the rate of consumption of H and SO_2 corresponded with the stoichiometry H_2SO_2, though the products on warming up were complex. If the compound exists, it must lack a parent peak, since no isotopic anomaly was observed at mass 70, using $^{18}O_2$.

If H_2SO^+ is the parent ion, then the analogous known compounds are the sulphenates and the sulphoxides, of which the latter are by far the more stable, though considerably less so than the sulphones (23).

The peak S_2^+ could arise (*a*) as a fragment from sulphur vapor (S_{4-8}); (*b*) as a fragment

Can. J. Chem. Downloaded from www.nrcresearchpress.com by 210.87.254.105 on 09/05/12
For personal use only.

from S_2O or H_2S_2; or (*c*) from S_2 itself. The first possibility may be ruled out, since no peaks higher than 80 were observed, while they are known to exist in the mass spectrum of sulphur vapor (27).

Case (*b*) is difficult to establish, since values of I.P. S_2 exist between 8.3 v and 11.0 v (27–31), while the only published value of I.P. H_2S_2 (10.2 v) has been obtained indirectly (30). It is impossible to choose a particular selection of these values such that the series I.P. S, S_2, H_2S, H_2S_2 falls into line with the series I.P. O, O_2, H_2O, H_2O_2, though such comparisons have been used to justify the correctness of values obtained (27, 30).

An experiment was done using $H_2S/^{18}O_2$ mixture under the same conditions as the experiment illustrated by Figs. 8 and 14, but at an electron energy 2 v lower. Peaks 64, 66, and 82 were smaller, but in the same relation to each other, while 68 was relatively considerably smaller than before, as expected, since it is known that I.P. S_2 < I.P. SO_2 (31). In addition it was observed that peak 80 always disappeared at 11–12 v indicated electron energy, using S_2O produced either during the oxidation of hydrogen sulphide or synthetically; using the values found by Hagemann (31) for I.P. S_2O and A.P. $SO^+(S_2O)$, it may be concluded that S_2^+ is unlikely to arise from S_2O. The possibility of S_2^+ arising from H_2S_2 cannot be excluded, since calculation of A.P. $S_2^+(H_2S_2)$ using $\Delta H_f(H_2S_2)$, $\Delta H_f(S_2)$, and I.P. S_2 would give A.P. $S_2^+(H_2S_2) \geqslant 9.5$–12.2 v. If the value reported (30) for I.P. H_2S_2 is correct, then it is unlikely that A.P. $S_2^+(H_2S_2)$ is less than 10.2 v, since it is unusual for $D(H—X^+)$ to be negative in value; in fact, two bonds are broken, so that A.P. $S_2^+(H_2S_2)$ would be expected to be somewhat higher.

If the true electron energy can be assumed to about 1–2 v lower than the indicated value, as a comparison of I.P. S_2O measured in this work with that obtained by Hagemann would suggest, one would expect that the ratio 64/66 should change markedly on going from 16 v to 14 v indicated electron energy, if mass 64 were a fragment from H_2S_2; in fact it did not change, suggesting that S_2^+ is not a fragment ion.

To sum up, it is clear that hydrogen is an intermediate in this reaction, and it is almost certain that the intermediate giving rise to the peak at mass 80 is S_2O; the most plausible species likely to give rise to the ions H_2SO^+, $H_2S_2^+$, and S_2^+ are H_2SO_2, H_2S_2, and S_2.

ACKNOWLEDGMENTS

The author would like to acknowledge the support of the National Research Council of Canada, and the continuing interest of Professor C. Ouellet.

REFERENCES

1. H. A. Taylor and E. M. Livinston. J. Phys. Chem. **35**, 2676 (1931).
2. H. W. Thompson and N. S. Kelland. J. Chem. Soc. 1809 (1931).
3. L. Farkas. Z. Elektrochem. **37**, 670 (1931).
4. H. W. Thompson. Nature, **127**, 629 (1931).
5. H. W. Thompson. J. Phys. Chem. **36**, 3621 (1932).
6. B. Jacovlev and P. S. Schantarovitsch. Acta Physicochim. URSS, **6**, 71 (1937).
7. D. A. Frank-Kamenetskii. Zh. Fiz. Khim. **13**, 738 (1939).
8. N. N. Semenov and N. M. Emanuel. Dokl. Akad. Nauk SSSR, **28**, 220 (1940).
9. N. M. Emanuel. Zh. Fiz. Khim. **18**, 15 (1945).
10. P. W. Schenk. Z. Anorg. Allgem. Chem. **211**, 150 (1933).
11. V. Kondratiev and E. Kondratieva. Zh. Fiz. Khim. **14**, 1528 (1940). V. Kondratiev and A. Jakovleva. Zh. Fiz. Khim. **14**, 859 (1940).
12. A. V. Jones. J. Chem. Phys. **18**, 1263 (1950).
13. R. J. Myers and D. J. Meschi. J. Am. Chem. Soc. **78**, 6220 (1957).
14. R. J. Myers and D. J. Meschi. J. Mol. Spectry. **3**, 405 (1959).
15. A. P. Zeelenberg. Seventh Combustion Symposium, 1958. Butterworths, London. 1959. p. 546.
16. R. G. W. Norrish and A. P. Zeelenberg. Proc. Roy. Soc. (London), Ser. A, **240**, 293 (1957).
17. D. G. H. Marsden. Rev. Sci. Instr. **33**, 288 (1962).
18. W. D. McGrath and J. J. McGarvey. J. Chem. Phys. **37**, 1574 (1962).

Can. J. Chem. Downloaded from www.nrcresearchpress.com by 210.87.254.105 on 09/05/12
For personal use only.

19. A. V. MURTHY. Proc. Indian Acad. Sci. **36**, 388 (1952).
20. V. KONDRATIEV and N. KONDRATIEVA. Compt. Rend. Acad. Sci. URSS, **31**, 128 (1941).
21. F. FEHER and G. WINKHAUS. Z. Anorg. Allgem. Chem. **292**, 210 (1957). F. FEHER and G. HITZEMANN. Z. Anorg. Allgem. Chem. **294**, 50 (1958).
22. P. A. GIGUÈRE and M. FALK. Can. J. Chem. **36**, 1121 (1958).
23. W. K. BUSFIELD, K. J. IVIN, H. MACKLE, and P. A. G. O'HARE. Trans. Faraday Soc. **57**, 1044 (1961). H. MACKLE and P. A. G. O'HARE. Trans. Faraday Soc. **57**, 2119 (1961).
24. K. H. GEIB and P. HARTECK. Ber. B, **66**, 1816 (1933).
25. D. A. HUTCHINSON. J. Chem. Phys. **22**, 758 (1954).
26. A. HENGLEIN. Z. Naturforsch. **17A**, 37 (1962).
27. P. BRADT, V. H. DIBELER, and F. L. MOHLER. J. Res. Natl. Bur. Std. **57**, 223 (1956).
28. H. D. SMYTH and L. P. BLEWETT. Phys. Rev. **46**, 276 (1934).
29. L. P. BLANCHARD and P. LEGOFF. Can. J. Chem. **35**, 89 (1957).
30. R. W. KISER and B. G. HOBROCK. J. Phys. Chem. **66**, 1214, 1648 (1962).
31. R. HAGEMANN. Compt. Rend. **255**, 899, 1102 (1962).

Can. J. Chem. Downloaded from www.nrcresearchpress.com by 210.87.254.105 on 09/05/12
For personal use only.

THE WATER-SOLUBLE POLYSACCHARIDES OF DERMATOPHYTES

II. A GLUCAN FROM MICROSPORUM QUINCKEANUM[1]

H. ALFES[2] AND C. T. BISHOP

Division of Applied Biology, National Research Council, Ottawa, Canada

AND

F. BLANK

The Skin and Cancer Hospital, Temple University School of Medicine, Philadelphia, Pennsylvania, U.S.A.

Received June 7, 1963

ABSTRACT

A levorotatory glucan with a minimum degree of polymerization of 36 has been isolated from the water-soluble polysaccharides of the dermatophyte *Microsporum quinckeanum*. Hydrolysis of the methylated glucan yielded the following *O*-methyl-D-glucoses: 2,3,4,6-tetra- (10.2 mole%); 2,3,4-tri- (57.7 mole%); 2,4,6-tri- (22.2 mole%); 2,4-di- (8.2 mole%); and 2-mono- (1.6 mole%). The glucan consumed 1.53 moles of periodate with production of 0.70 mole of formic acid per mole anhydroglucose. Reduction and hydrolysis of the periodate-oxidized glucan yielded glycerol, erythritol, and D-glucose in a molar ratio of 72.3:0.6:27.1. The results showed that the glucan consisted of β-D-glucopyranose units joined in straight chains by $1 \rightarrow 6$ (57%) and $1 \rightarrow 3$ (24%) linkages. Approximately 3 in every 37 glucose residues constitute branch points in the glucan with branches occurring at the C_6 and C_3 positions of the same glucose unit. The glucan bears some resemblance to the yeast glucans of *Saccharomyces cerevisiae* and *Candida albicans* but differs from them in the relative number of $1 \rightarrow 6$ and $1 \rightarrow 3$ linkages and in the degree of branching.

It has been shown (1) that water-soluble polysaccharides form an essential part of antigenic material from cultures of dermatophytes and are therefore of considerable immunochemical importance. Preliminary examination of the polysaccharides isolated from five dermatophytes indicates that each has a similar pattern of water-soluble polysaccharides, specifically, two galactomannans and a glucan. The immediate objective of this program is to determine the main structural features of these polysaccharides by periodate oxidation and methylation procedures to see if they can be related to species differences and immunological properties. More detailed structural investigations are being reserved until these relationships are clear. The first paper (2) in this series described the purification and gross structural features of a galactomannan from *Trichophyton granulosum* Sabouraud, 1909. The present publication describes the isolation and constitution of a glucan from *Microsporum quinckeanum* (Zopf) Guiart and Grigorakis, 1928.

The polysaccharides were extracted in 4.7% yield from powdered cells of *M. quinckeanum* as described previously for *T. granulosum* (2). The product was a tan-colored powder containing significant amounts of ash and nitrogen and yielding mannose, glucose, and galactose on hydrolysis. Moving-boundary electrophoresis of this material in borate buffer (3) showed the presence of three migrating components. The mixture was separated into four fractions by chromatography on diethylaminoethyl (DEAE) cellulose (4). The first fraction eluted from the column contained no nitrogen and no ash, yielded only glucose on hydrolysis, and gave a single symmetrical peak ($\mu = 3.45 \times 10^{-5}$ cm²/volt sec) on moving-boundary electrophoresis. The other three fractions were mixtures, two of them still containing some protein.

The specific rotation of the glucan changed from $-27 \pm 1°$ to $53 \pm 1.5°$ on hydrolysis,

[1]*Issued as N.R.C. No. 7514.*
Presented at the 145th Meeting of the American Chemical Society, New York, 1963.
[2]*National Research Council Postdoctoral Fellow, 1962–1963.*

Can. J. Chem. Downloaded from www.nrcresearchpress.com by 210.87.254.105 on 09/05/12
For personal use only.

indicative of a predominance of β-glycosidic linkages. Isolation of a crystalline derivative confirmed the identity of the constituent monosaccharide as glucose and showed that it was present as the D-enantiomorph. The methylated glucan had a molecular weight of 8000 (degree of polymerization, 36) as shown by osmometry; this must be regarded as a minimum because some degradation of the glucan may have occurred during methylation.

The methylated glucan (OCH_3, 44.3%) was hydrolyzed and *O*-methyl glucoses in the hydrolyzate were isolated and estimated by preparative paper chromatography and by gas–liquid chromatography of their methyl glycosides (5). Figure 1 shows the separation

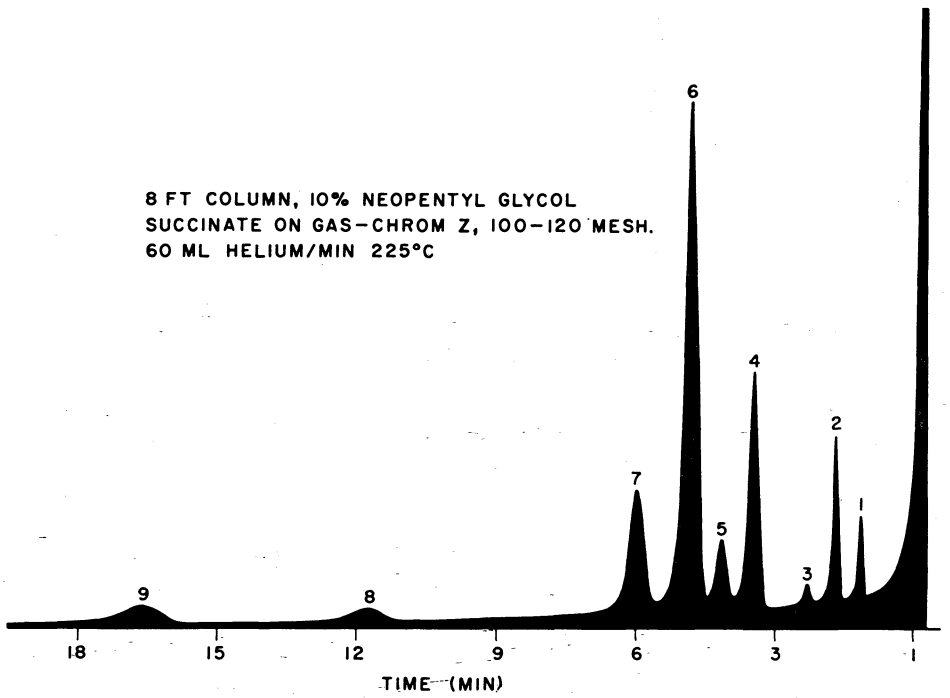

FIG. 1. Gas–liquid chromatogram of methyl *O*-methyl glucosides from methylated glucan of *M. quinckeanum*.

1. Methyl 2,3,4,6-tetra-*O*-methyl-β-D-glucoside
2. Methyl 2,3,4,6-tetra-*O*-methyl-α-D-glucoside
3. Unknown
4. Methyl 2,3,4-tri-*O*-methyl-β-D-glucoside
5. Methyl 2,4,6-tri-*O*-methyl-β-D-glucoside
6. Methyl 2,3,4-tri-*O*-methyl-α-D-glucoside
7. Methyl 2,4,6-tri-*O*-methyl-α-D-glucoside
8. Methyl 2,4-di-*O*-methyl-β-D-glucoside
9. Methyl 2,4-di-*O*-methyl-α-D-glucoside

TABLE I

Hydrolysis products from methylated glucan of *M. quinckeanum*

O-Methyl-D-glucose	Mole percent composition	
	Gas–liquid chromatography	Preparative paper chromatography
2,3,4,6-Tetra-	9.6	10.2
2,3,4-Tri-	59.4	57.7
2,4,6-Tri-	22.8	22.2
2,4-Di-	8.4	8.2
2-Mono-	—	1.6

Can. J. Chem. Downloaded from www.nrcresearchpress.com by 210.87.254.105 on 09/05/12
For personal use only.

obtained by the latter method; the separated components were identified by comparison of their retention volumes (R_v) with those of authentic samples and by isolation of crystalline derivatives after separation of the free sugars by preparative paper chromatography. Table I shows the quantitative data obtained by the two methods; the results were in excellent agreement. Preparative paper chromatography showed the presence of a small amount of 2-*O*-methyl-D-glucose which was not sufficiently volatile to be estimated in the presence of the other components by gas–liquid chromatography.

The results in Table I show that the repeating unit of the glucan is made up of the following residues in the approximate ratios shown:

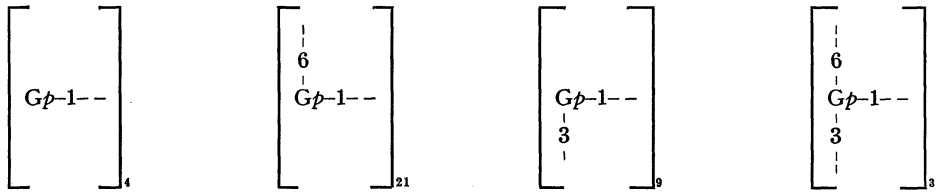

I II III IV

Thus, most of the β-D-glucopyranose units are joined in straight chains by 1 → 6 (II) and 1 → 3 (III) linkages. There are approximately three branch points in every 37 units, each branch being formed by linkages through C-6 and C-3 of a single glucose unit (IV). All chains are terminated by D-glucopyranose residues (I). In any study of polysaccharide structure by the methylation procedure the significance of 2–3% or less of a hydrolysis product is questionable because it may have arisen from incomplete methylation or from demethylation during hydrolysis. Although the 2-*O*-methyl-D-glucose (Table I) may represent a triple branch point in the glucan, the amount present (1.6%) was too small to be certain about this point.

A glucan made up of units I–IV should consume 1.35 moles of periodate with production of 0.68 mole of formic acid per anhydroglucose unit. The oxidized glucan, after reduction and hydrolysis (6), should yield glycerol and D-glucose in a ratio of 25:12. The values found were 1.53 moles of periodate and 0.70 mole of formic acid per mole anhydroglucose and a glycerol to D-glucose ratio of 25:9 in the reduced, hydrolyzed product. The periodate-oxidized, reduced glucan also yielded a small amount (0.6 mole%) of erythritol on hydrolysis. This may represent a 1 → 4 linkage in the polysaccharide but, as with the 2-*O*-methyl-D-glucose, the amount was too small to be certain of its significance. The results of periodate oxidation were thus in reasonable agreement with the main structural features deduced from the methylation data.

The structural units shown (I–IV) could be joined together in a number of ways. For example, short side chains of 1 → 3-linked units could be attached at intervals, through the C_3 positions, along a basic chain of 1 → 6-linked residues. Another possible structure could be a straight chain of 1 → 6- and 1 → 3-linked residues with single-unit side chains. Distinction between these or other possible structures requires the isolation of oligosaccharide fragments by partial hydrolysis of the periodate-oxidized, reduced glucan (7) and of the glucan itself.

The glucan from *M. quinckeanum* differs from glucans that have been isolated from other microorganisms. It is clearly distinguished by its negative rotation from the dextrorotatory bacterial dextrans (8) and from *pullulan*, a glucan from the yeast-like fungus *Pullularia pullulans* (9). In this respect it more closely resembles the levorotatory yeast

Can. J. Chem. Downloaded from www.nrcresearchpress.com by 210.87.254.105 on 09/05/12
For personal use only.

glucans isolated from *Saccharomyces cerevisiae* (10, 11) and from *Candida albicans* (12). A further similarity between these yeast glucans and that from *M. quinckeanum* is the almost exclusive occurrence of $1 \rightarrow 6$ and $1 \rightarrow 3$ linkages. Differences arise in the relative amounts of these two linkages and in the degree of branching in the polysaccharides. Thus, the glucan from *S. cerevisiae* was shown to be a linear polysaccharide in which 10–20% of the linkages were β-1 $\rightarrow$ 6, the remainder being β-1 $\rightarrow$ 3 (11). The glucan from *C. albicans* contained only β-1 $\rightarrow$ 6 linkages in the linear portions of the molecule with branches (23%) being formed by β-1 $\rightarrow$ 3 bonds (12). The glucan from *M. quinckeanum* contains both β-1 $\rightarrow$ 6 (57%) and β-1 $\rightarrow$ 3 (24%) linkages in the linear portions of the polysaccharide, and branch points, involving the same linkages, constitute only some 8% of the molecule.

EXPERIMENTAL

Paper chromatograms were run by the descending method using the following solvent systems (v/v):
(A) pyridine:ethyl acetate:water—1:2.5:2.5 (upper phase);
(B) butan-1-ol:ethanol:water—3:1:1;
(C) butan-1-ol:pyridine:water—6:4:3;
(D) butanone saturated with water.

Sugars were detected on chromatograms by the *p*-anisidine hydrochloride spray reagent (13) or by silver nitrate – sodium hydroxide sprays (14). A Tiselius-type, Spinco model H apparatus was used for moving-boundary electrophoresis in 0.05 *M* borate buffer (3). A Pye Argon Chromatograph and an F and M Model 500 Chromatograph were used for gas–liquid chromatography (5). Evaporations were done at 35–40° C under diminished pressure; melting points are corrected; specific rotations are equilibrium values unless otherwise specified. R_g values represent movement relative to 2,3,4,6-tetra-*O*-methyl-D-glucose on paper chromatograms.

Preparation of Water-soluble Polysaccharides

Microsporum quinckeanum, isolated from a scutulum of a mouse, was cultured and polysaccharides were extracted from the dried mycelium as described previously for *T. granulosum* (2). The preparation thus obtained was a light brown powder which contained 0.52% nitrogen and 4.91% ash and amounted to 4.7% of the dried mycelium. A sample (5 mg) of this preparation was hydrolyzed by *N* sulphuric acid (1.5 ml) at 97° C in a sealed tube for 12 hours. Paper chromatography of the hydrolyzate in solvent A showed the presence of mannose, glucose, and galactose. Another sample (150 mg) of the water-soluble polysaccharides was dissolved in 0.05 *M* sodium tetraborate (15 ml), equilibrated with the buffer by dialysis for 20 hours, and examined by moving-boundary electrophoresis (3). Although resolution was not complete, three components could be detected.

Isolation of Glucan

A portion (500 mg) of the mixture of water-soluble polysaccharides obtained above was resolved on a column (32×3 cm) of diethylaminoethyl (DEAE) cellulose by successive elution with 0.01 *M* sodium tetraborate, 0.05 *M* sodium tetraborate, 0.02 *N* sodium hydroxide, and 0.1 *N* sodium hydroxide (4). Fractions (20 ml each) were collected automatically every 15 minutes. Aliquots (1 ml) of each fraction were mixed with 2 ml of anthrone reagent (200 mg anthrone in 100 ml of 95% sulphuric acid) and the optical densities at 625 mμ were read on a colorimeter to give the relative amounts of polysaccharide in each fraction. The relative amounts of protein in the fractions were determined from the optical densities of the eluates at 280 mμ. Four polysaccharide fractions were eluted successively, one in each of the solutions described above. The eluates containing the first two polysaccharide fractions (eluted by 0.01 *M* and 0.05 *M* sodium tetraborate respectively) were passed over Amberlite IR-120 ion exchange resin and evaporated to dryness. Boric acid was removed from the residues by repeated addition and evaporation of methanol. Polysaccharide fractions 1 and 2 were then washed with ether and dried. The eluates containing polysaccharide fractions 3 and 4 (eluted by 0.02 *N* and 0.1 *N* sodium hydroxide respectively) were dialyzed and freeze-dried. These procedures yielded polysaccharide fractions 1 (62.4 mg); 2 (26.0 mg); 3 (270.0 mg); and 4 (41.6 mg): recovery, 400 mg, 80%. The losses were accountable in part by the 5% of each fraction of eluate used for the anthrone test and in part by the irreversible absorption of highly pigmented impurities on the DEAE cellulose. The recovered polysaccharides were ash-free, water-soluble powders. The optical densities at 280 mμ showed that fractions 3 and 4 contained protein; fractions 1 and 2 were protein free. The polysaccharide fractions yielded the following sugars on hydrolysis as revealed by paper chromatography (solvent A): 1—glucose; 2—glucose with smaller amounts of mannose and galactose; 3—mannose and galactose with a trace of glucose; 4—glucose, mannose, and galactose. Subsequent work has shown that fraction 3 could be resolved into two

Can. J. Chem. Downloaded from www.nrcresearchpress.com by 210.87.254.105 on 09/05/12
For personal use only.

galactomannans by fractional precipitation with Fehling's solution and the same procedure showed that fraction 4 was a mixture of polysaccharides. In view of these results it seemed likely that fraction 2 was a mixture of a glucan and at least one galactomannan. Fraction 1 was the only homoglycan obtained in the separation and it also showed a single, symmetrical peak on electrophoresis with a mobility, μ, equal to 3.45×10^{-5} cm²/volt sec.

The separation was repeated a sufficient number of times (12 g of crude polysaccharide on a column (29×9 cm) of DEAE cellulose, 240 g) to yield 4.5 g of polysaccharide fraction 1, the glucan on which the balance of this work was done.

Properties of Glucan

The polysaccharide had $[\alpha]_D^{26}$ $-27\pm1°$ (*c*, 1% in water) changing to $[\alpha]_D^{26}$ $+53\pm1.5°$ (*c*, 1% in *N* hydrochloric acid) after hydrolysis in *N* hydrochloric acid at 97° C for 12 hours. The hydrolyzate was neutralized (Amberlite IR-45 ion exchange resin), evaporated to dryness, and the residue was heated with *p*-nitroaniline in methanol solution for 40 minutes. The solution was cooled and the crystals which separated were recrystallized from methanol to yield N-(*p*-nitrophenyl)-D-glucopyranosylamine dihydrate (15), m.p. 183° C, $[\alpha]_D^{26}$ $-199\pm1°$ (*c*, 1% in pyridine). The minimum degree of polymerization of the glucan was 36 as determined for its methylated derivative by osmometry.

Periodate Oxidation

The glucan (200 mg, 1.235 mmoles) was dissolved in 0.02 *M* sodium periodate (200 ml). Reagent blanks were also prepared and the oxidation was allowed to proceed at 5° C in the absence of light. At intervals samples were removed for estimation of formic acid by iodometric titration and of periodate by the excess arsenite procedure (16). The results, in moles per mole anhydroglucose, were as follows:

Time (hr)	Formic	Periodate
23	0.52	0.14
47	0.70	1.52
71	0.70	1.50
95	0.69	1.56
173	0.71	1.53

After the oxidation was complete iodate and excess periodate were precipitated by addition of 0.5 *M* barium acetate and the precipitate was filtered. The filtrate was deionized by Amberlite ion exchange resins IR-120 and IR-45 and then potassium borohydride (100 mg) was added. After 48 hours the solution was neutralized with acetic acid and deionized again. The solution was then evaporated to dryness and last traces of boric acid were removed from the residue by repeated evaporation with methanol. The residue was dissolved in water (5 ml) and an aliquot (1 ml) was hydrolyzed by 2 *N* sulphuric acid at 97° C for 12 hours. Paper chromatography (solvent B) showed the presence of two components that were identical with authentic samples of glycerol and glucose run on the same paper strips. The hydrolysis products from another aliquot of the polyol were acetylated by pyridine – acetic anhydride (1:1) and the reaction mixture was examined directly by gas–liquid chromatography (5, 17). Four components were found having retention volumes corresponding to those of authentic samples of glycerol triacetate, erythritol tetraacetate, α-D-glucose pentaacetate, and β-D-glucose pentaacetate. The molar ratio of glycerol to erythritol to glucose was 72.3:0.6:27.1, as determined from the relative areas under the peaks.

Methylation of Glucan

The glucan (3.5 g) was methylated 10 times by dimethyl sulphate and 30% sodium hydroxide (18) and 5 times by silver oxide and methyl iodide (19) to yield a product (OCH_3, 42.1%) showing weak hydroxyl absorption in its infrared spectrum. One further methylation by dimethyl sulphate and powdered sodium hydroxide in tetrahydrofuran (20) yielded the fully methylated glucan; 1.8 g; $[\alpha]_D^{22}$ $-30\pm1°$ (*c*, 1.5% in chloroform); OCH_3, 44.3%, calc. 45.6%; molecular weight by osmometry, 8000.

Hydrolysis Products from Methylated Glucan

The methylated glucan (1.8 g) was hydrolyzed by sulphuric acid under the conditions described by Croon *et al.* (21) as causing minimum degradation and demethylation. The neutralized (Amberlite IR-45) hydrolyzate was evaporated to dryness and a portion of the residue was boiled under reflux for 6 hours with 2% methanolic hydrogen chloride. Acid was removed by silver carbonate and the methyl glucosides in the solution were examined by gas–liquid chromatography. The conditions used and the separation obtained are shown in Fig. 1. The quantitative data given in Table I were obtained from the areas under the peaks as measured by a planimeter. The compounds giving the individual peaks (Fig. 1) were identified by comparison of their retention volumes with those of authentic samples under the same conditions.

To confirm the identities of the *O*-methyl-D-glucoses the remainder of the hydrolyzate was fractionated by

Can. J. Chem. Downloaded from www.nrcresearchpress.com by 210.87.254.105 on 09/05/12
For personal use only.

preparative paper chromatography on Whatman 3 MM paper (solvent D) to yield the following products:

2,3,4,6-tetra-*O*-methyl-D-glucose	125 mg
2,3,4-tri-*O*-methyl-D-glucose	711 mg
2,4,6-tri-*O*-methyl-D-glucose	274 mg
2,4-di-*O*-methyl-D-glucose	101 mg
2-*O*-methyl-D-glucose	20 mg

2,3,4,6-Tetra-O-methyl-D-glucose

This product showed the same chromatographic mobility in solvents B, C, and D as an authentic sample (R_g 1.00). The compound crystallized from light petroleum (30–60° C) and was recrystallized from *n*-hexane to yield 2,3,4,6-tetra-*O*-methyl-D-glucose (21), m.p. 93–94° C, unchanged on admixture with an authentic sample, $[\alpha]_D^{24}$ +83° (*c*, 1% in water).

2,3,4-Tri-O-methyl-D-glucose

The sirupy product had R_g values of 0.88 and 0.85 in solvents B and D respectively. Anilide formation yielded a crystalline product that was recrystallized from ether to give *N*-phenyl-2,3,4-tri-*O*-methyl-D-glucosylamine (22), m.p. 145° C, $[\alpha]_D^{25}$ +70° (*c*, 1% in ethanol).

2,4,6-Tri-O-methyl-D-glucose

On paper chromatograms the compound gave the same color reaction with *p*-anisidine hydrochloride and the same R_g values (0.86 and 0.79 in solvents B and D respectively) as 2,4,6-tri-*O*-methyl-D-glucose. The sirupy product was extracted with boiling ether and the extract was evaporated to a small volume. The crystals which separated were recrystallized from ether to yield 2,4,6-tri-*O*-methyl-D-glucose (23), m.p. 122° C, $[\alpha]_D^{25}$ +71° (*c*, 1% in water).

2,4-Di-O-methyl-D-glucose

The compound from preparative paper chromatography showed the same R_g values in solvents B, C, and D, and the same color reaction with *p*-anisidine hydrochloride as 2,4-di-*O*-methyl-D-glucose. The sample was boiled under reflux with 2% methanolic hydrogen chloride for 6 hours. The anomeric methyl glycosides were then separated by gas–liquid chromatography and were collected separately from the effluent gas stream. Both glycosides crystallized in the collecting tubes and were recrystallized from ether – light petroleum (30–60° C) to yield methyl 2,4-di-*O*-methyl-α-D-glucoside (24), m.p. 79–80° C, $[\alpha]_D^{24}$+160° (*c*, 0.2% in acetone), and methyl 2,4-di-*O*-methyl-β-D-glucoside (24), m.p. 123–124° C, $[\alpha]_D^{24}$ −18° (*c*, 0.1% in acetone).

2-O-Methyl-D-glucose

The compound showed the same chromatographic behavior in solvents B and C as 2-*O*-methyl-D-glucose. Reduction by sodium borohydride followed by acetylation yielded a mono-*O*-methyl-penta-*O*-acetyl-D-glucitol which had the same retention time on gas–liquid chromatography as 2-*O*-methyl-1,3,4,5,6-penta-*O*-acetyl-D-glucitol (25). The product crystallized and had m.p. 53–54° C, unchanged on admixture with an authentic sample.

ACKNOWLEDGMENT

The authors wish to thank Mr. F. P. Cooper for assistance with the gas–liquid chromatography.

REFERENCES

1. B. Bloch, A. Labouchere, and F. Schaaf. Arch. Dermatol. and Syphilol. **148**, 413 (1925).
2. C. T. Bishop, F. Blank, and M. Hranisavljevic-Jakovljevic. Can. J. Chem. **40**, 1816 (1962).
3. D. H. Northcote. Biochem. J. **58**, 353 (1954).
4. H. Neukom, H. Deuel, W. J. Heri, and W. Kundig. Helv. Chim. Acta, **43**, 64 (1960).
5. C. T. Bishop. Methods Biochem. Analy. **10**, 1 (1962).
6. M. Abdel-Akher, J. K. Hamilton, R. Montgomery, and F. Smith. J. Am. Chem. Soc. **74**, 4970 (1952).
7. I. J. Goldstein, G. W. Hay, B. A. Lewis, and F. Smith. Abstracts, 135th Meeting of the American Chemical Society, 3D, 1959.
8. M. Stacey and S. A. Barker. Polysaccharides of micro-organisms. Oxford University Press, London. 1960.
9. H. O. Bouveng, H. Kiessling, B. Lindberg, and J. McKay. Acta Chem. Scand. **16**, 615 (1962).
10. D. J. Bell and D. H. Northcote. J. Chem. Soc. 1944 (1950).
11. S. Peat, J. R. Turvey, and J. M. Evans. J. Chem. Soc. 3868 (1958).
12. C. T. Bishop, F. Blank, and P. E. Gardner. Can. J. Chem. **38**, 869 (1960).
13. L. Hough, J. K. N. Jones, and W. H. Wadman. J. Chem. Soc. 1702 (1950).
14. W. E. Trevelyan, D. P. Procter, and J. S. Harrison. Nature **166**, 444 (1950).
15. F. Weygand, W. Perkow, and P. Kuhner. Chem. Ber. **84**, 594 (1951).
16. P. Fleury and J. Lange. J. Pharm. Chim. **17**, 107 (1933).

Can. J. Chem. Downloaded from www.nrcresearchpress.com by 210.87.254.105 on 09/05/12
For personal use only.

17. C. T. Bishop and F. P. Cooper. Can. J. Chem. **38**, 793 (1960).
18. W. N. Haworth. J. Chem. Soc. **107**, 8 (1915).
19. T. Purdie and J. C. Irvine. J. Chem. Soc. **83**, 1021 (1903).
20. E. L. Falconer and G. A. Adams. Can. J. Chem. **34**, 338 (1956).
21. J. C. Irvine and J. W. H. Oldham. J. Chem. Soc. **119**, 1744 (1921).
22. S. Peat, E. Schluchterer, and M. Stacey. J. Chem. Soc. 581 (1939).
23. W. N. Haworth and W. G. Sedgwick. J. Chem. Soc. 2573 (1926).
24. M. H. Adams, R. E. Reeves, and W. F. Goebel. J. Biol. Chem. **140**, 653 (1941).
25. C. T. Bishop and F. P. Cooper. Can. J. Chem. **38**, 388 (1960).

Can. J. Chem. Downloaded from www.nrcresearchpress.com by 210.87.254.105 on 09/05/12
For personal use only.

STUDIES WITH A PERFLUOROALKYL–SILICON COMPOUND

H. C. CLARK, J. T. KWON, AND D. WHYMAN
Department of Chemistry, University of British Columbia, Vancouver, British Columbia
Received June 3, 1963

ABSTRACT

Some detailed chemical studies are described of dimethylbis(perfluoropropyl)silane (I), prepared from *n*-perfluoropropyllithium and dimethyldichlorosilane. The hydrolytic stability of (I) towards base is described, and pyrolyses in the temperature range 185–295°, leading to the formation of dimethyldifluorosilane, $(CH_3)_2SiF_2$, and fluorocarbons, are discussed. Chlorination of (I) leads to stepwise chlorination of the CH_3 groups, and even excess chlorine does not cause cleavage. Bromine does not react with (I). The reaction of (I) with iodine and catalytic amounts of aluminum in boiling toluene causes rapid cleavage of C_3F_7 as C_3F_7I. The mechanisms of some of these reactions are discussed.

INTRODUCTION

A number of reports appear in the literature describing the preparation of perfluoroalkyl–silicon compounds. The passage of perfluoroiodoalkanes over a heated mixture of silicon and copper at 400–500° is said to produce bis(perfluoroalkyl)silicon dihalides (1), while compounds such as trifluoro(trifluoromethyl)silane, CF_3SiF_3, are reported (2) to be formed on the passage of fluorine and silicon tetrafluoride over calcium carbide at 300°. No further details of these reactions have appeared in the literature and there is some doubt as to their reliability. Compounds such as CF_3SiCl_3 and $(CF_3)_2SiCl_2$ have been described briefly by other workers (3), but details of the preparative method and of their properties have not been given. Even less information has appeared concerning the chemical behavior of perfluoroalkyl–silicon compounds, and several conflicting statements have been made. Thus, Rochow (4) has stated that CF_3 groups are cleaved from silicon by cold water, while Haszeldine and Marklow (3) contend that the CF_3—Si bonds of CF_3SiCl_3 and $(CF_3)_2SiCl_2$ are not broken on treatment with water, although reaction with dilute aqueous alkali is said to liberate fluoroform rapidly.

Diethylbis(perfluoropropyl)silane, $(C_2H_5)_2Si(C_3F_7)_2$, has been prepared (5) from methyllithium, perfluoroiodopropane, and diethyldichlorosilane. The compound is reported to be stable towards 3 *N* sulphuric acid at 100°, and towards methanolic sodium hydroxide below 75°, but other chemical properties are not described. Recently, we have shown (6) that perfluoro-*n*-propyllithium can be prepared directly from perfluoroiodopropane and lithium metal; this provides a more direct synthetic route to perfluoro-*n*-propyl derivatives and has allowed us to prepare and examine in some detail a perfluoropropyl–silicon compound.

DISCUSSION

The compound chosen for study, dimethylbis(perfluoro-*n*-propyl)silane, $(CH_3)_2Si(C_3F_7)_2$, (hereafter referred to as (I)) was prepared directly in ethereal solution from dimethyldichlorosilane and perfluoro-*n*-propyllithium:

$$(CH_3)_2SiCl_2 + 2n\text{-}C_3F_7\text{-}Li \rightarrow (CH_3)_2Si(C_3F_7)_2 + 2LiCl.$$

(I) is a colorless liquid which boils at 124° and which is stable to air and water. Treatment of (I) with 50% aqueous potassium hydroxide causes rapid cleavage of C_3F_7 as C_3F_7H. This was not quantitative under conditions which required heating at 110° for 18

Can. J. Chem. Downloaded from www.nrcresearchpress.com by 210.87.254.6 on 09/05/12
For personal use only.

hours, so that the rate of hydrolysis seems comparable to that observed for heptafluoropropyl–phosphorus compounds (7).

Decomposition of (I) was appreciable at 185°, and above 250° was almost complete. In the present investigation, the aim was to determine the general decomposition scheme and it was apparent, from the nearly quantitative formation of $(CH_3)_2SiF_2$ from each pyrolysis, that this could be represented by the equation

$$(CH_3)_2Si(C_3F_7)_2 \xrightarrow{\Delta} (CH_3)_2SiF_2 + x[(C_3F_6)].$$

Complete identification of the fluorocarbon fragments was not possible, largely because comparisons could not be made with samples from a complete set of known fluorocarbon compounds, particularly for fluorinated cycloalkane derivatives.

Our results indicate that the fluorocarbon products are largely C_3 or C_6 compounds, that some unsaturated C_3 products are formed, and that both cyclic and straight-chain C_6 compounds may also be produced. It has been proposed (8) that the thermal breakdown of polyfluoroalkyl–silicon compounds containing fluorine in the α-position occurs by an α-elimination of fluorine. Such a mechanism probably operates also for (I), again initiated by an internal nucleophilic attack on silicon by the α-fluorine atom:

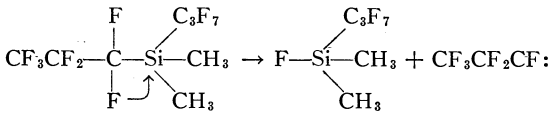

A similar second step involving the second C_3F_7 group will give the final product, $(CH_3)_2SiF_2$, in agreement with the experimental results, and two CF_3CF_2CF: radicals. The latter must undergo considerable rearrangement and dimerization (9) leading to $CF_3CF{=}CF_2$, perfluorocyclopropane, hexanes, and cyclohexanes, the latter three presumably resulting from possible formation of $\cdot CF_2CF_2CF_2\cdot$. From the infrared spectra and molecular weights of the fluorocarbon mixtures, and from the observed formation during pyrolysis of small quantities of SiF_4 and C_3F_7H, it is clear that secondary reactions are occurring which may well involve reaction of hydrocarbon groups and hydrogen abstraction. However, the evidence certainly indicates the above type of thermal decomposition leading to the formation of the difluorodimethylsilane.

In an attempt to ascertain more clearly the nature of the fluorocarbon products, a pyrolysis of (I) in the presence of tetrafluoroethylene was performed. It was hoped that any carbene such as CF_3CF_2CF: would add preferentially to the C_2F_4 to give a more readily identifiable product. However, no such addition seemed to occur and only the decomposition products of (I) seemed to be formed.

The reactions of (I) with the halogens are of considerable interest since cleavage of either methyl or perfluoropropyl groups is possible, or alternatively halogenation of the CH_3 groups may occur. Information may thus be obtained concerning the relative ease of cleavage of alkyl, and perfluoroalkyl, groups. Chlorination of (I) takes place readily although a temperature of 110° is required to complete the reaction. The major volatile product is hydrogen chloride, showing that chlorination of the CH_3 groups occurs in preference to cleavage. Reactions were carried out in which the ratio of chlorine to (I) was 1:1, 2:1, 4:1, 6:1, and 8:1. In the first case, as can be seen in Table II, 50% of (I) was recovered unchanged from the reaction, and the yield of hydrogen chloride was in accord with the equation

$$(CH_3)_2Si(C_3F_7)_2 + 2Cl_2 \rightarrow (CH_2Cl)_2Si(C_3F_7)_2 + 2HCl.$$

Can. J. Chem. Downloaded from www.nrcresearchpress.com by 210.87.254.6 on 09/05/12
For personal use only.

However, since it has been shown (10) that a Si—CH_2Cl group is more readily chlorinated than a Si—CH_3 group, it is possible that the final product is $(CH_3)(CHCl_2)Si(C_3F_7)_2$. As the ratio of chlorine to (I) is increased, further chlorination of the methyl groups occurs, till in the 6:1 case six equivalents of hydrogen chloride are released, and the remaining involatile silicon compound contains no C—H bonds. Even with excess chlorine (8:1 ratio of Cl_2:(I)), no cleavage occurs and the excess chlorine is recovered from the reaction. In all these chlorinations, side reactions also occurred but only to a small extent (approx. 5%), as evidenced by the separation of small quantities of compounds such as $CClF_3$, and CCl_2F_2. In no case was there evidence of the formation of CH_3Cl. This inability of chlorine to cleave either the CH_3 or C_3F_7 groups of (I) is in agreement with earlier observations (11, p. 126) on the cleavage of silicon–alkyl bonds.

The reaction of (I) with bromine did not lead to cleavage, or to bromination of the CH_3 group. This is also in agreement with the fact that bromine alone does not react with Si—CH_3 groups (11, p. 381).

The cleavage of silicon–alkyl bonds by iodine in the presence of aluminum iodide as catalyst is well known (11, p. 126), and in this case such a reaction provides a method of determining the relative ease of cleavage of Si—CH_3 and Si—C_3F_7 groups. The reaction of (I) with iodine and catalytic amounts of aluminum powder in refluxing toluene caused rapid cleavage of C_3F_7 as C_3F_7I. As has also been shown in other cases (11, p. 126), this

$$(CH_3)_2Si(C_3F_7)_2 + 2I_2 \rightarrow [(CH_3)_2SiI_2] + 2C_3F_7I$$

reaction is actually catalyzed by aluminum iodide which we have observed is formed by the direct reaction of iodine and aluminum in toluene. Because of its reactivity and great ease of decomposition, the diiodosilane, $(CH_3)_2SiI_2$, was not itself characterized, but it was readily shown that the reaction residue contained no C_3F_7 groups. No CH_3I was formed.

For hydrocarbon groups, the ease of cleavage falls in the order Ph $\gg$ Me $>$ Et $>$ *n*-Pr (12). Since phenyl groups are readily cleaved from silicon by bromine (11, p. 152), whereas C_3F_7 is not, it seems that a probable order of ease of cleavage, including the C_3F_7 group, is: Ph $>$ C_3F_7 $>$ Me $>$ Et $>$ *n*-Pr. It is therefore not possible to obtain perfluoropropyl–silicon halides by direct halogenation of compounds such as (I).

EXPERIMENTAL

The techniques and procedure used in the preparation of perfluoro-*n*-propyllithium have been described previously (6) and some further reactions of halides of group IIIA–VA elements with perfluoro-*n*-propyllithium will be reported elsewhere (13).

Dimethylbis(perfluoro-*n*-propyl)silane was obtained, in a typical preparation, from perfluoroiodopropane (46.3 g), lithium metal containing 2% sodium (2.4 g), and dimethylsilicon dichloride (12.9 g) in dry diethyl ether (30 ml) at −40°. Fractionation *in vacuo* of the reaction mixture followed by two distillations at 760 mm gave a final yield of 5.4 g (20%) of I, b.p. 124±1.0°, M.W. 382±10 (calc. M.W. for $(CH_3)_2Si(C_3F_7)_2$: 396). (Calc. for $C_8H_6F_{14}Si$: C, 24.3; H, 1.53; F, 67.1. Found: C, 24.8; H, 1.81; F, 65.1.) A vapor phase chromatographic examination of I, using a Beckman GC-2A gas chromatograph fitted with a dinonyl phthalate – Chromosorb column at 70°, with helium as carrier gas, showed the presence of approximately 6–7% of a more volatile impurity which presumably accounts for slight deviations in the analytical results. This parallels the results of Pierce *et al.* (5), who found that along with $(C_2H_5)_2Si(C_3F_7)_2$, the monochloro compound, $(C_2H_5)_2SiCl(C_3F_7)$, was also formed in small amounts and that the latter could not be satisfactorily purified. In the present case, therefore, the impurity was probably $(CH_3)_2SiCl(C_3F_7)$ and since the presence of such an impurity would not affect the reactions being studied, no further purification was attempted.

Hydrolysis

(I) (0.2935 g) was treated with 50% aqueous potassium hydroxide in a sealed tube at 110° for 18 hours to give 0.1594 g of C_3F_7H, identified spectroscopically. This corresponds to 79.8% hydrolysis, and oily droplets of unreacted I, which is immiscible with water, remained after the completion of the experiment.

Can. J. Chem. Downloaded from www.nrcresearchpress.com by 210.87.254.6 on 09/05/12
For personal use only.

A second experiment under the same conditions also gave approximately an 80% yield of C_3F_7H. Hydrolysis of (I) occurred readily with ethanolic potassium hydroxide but the difficulty of completely separating the C_3F_7H from ethanol prevented a quantitative measure of the degree of hydrolysis.

Pyrolysis

Samples of (I) were heated at various temperatures in the range 185–295° in sealed tubes for 20 hours. The reaction products were separated by trap-to-trap distillation in a conventional vacuum apparatus and each product was identified by measurements of its molecular weight and vapor pressure, and by its infrared spectrum. From each experiment, fractions were obtained which, in order of increasing volatility, condensed at −23°, −64°, −96°, −125°, and −196°. That at −23° was shown to be unreacted (I). The −125° fraction contained just one compound, which was identified by its infrared spectrum (14) and molecular weight (calc. 96, observed values 96–100) as difluorodimethylsilane, $(CH_3)_2SiF_2$. It is of interest that, while Kriegsmann's spectrum of $(CH_3)_2SiF_2$ shows a broad unresolved band at 900–1000 cm^{-1} due to Si—F stretching, the present spectra all showed excellent and reproducible resolution so that maxima were observed in this region at 900, 910, 937, 948, 958, and 980 cm^{-1}. The −196° fractions had molecular weights of approximately 100 and all observed infrared bands could be assigned (15) to SiF_4 and to C_3F_7H. The −64° and −96° fractions were complex mixtures; in fact, a gas chromatographic examination of a −64° fraction showed the presence of two major and two minor components. Because of the difficulty of obtaining a sufficiently wide range of known fluorinated compounds for comparison, it was not possible to identify each component of these mixtures. However, the −96° fractions gave molecular weights in the range 210–280, and their infrared spectra showed them to contain C_3 compounds such as perfluorocyclopropane and $CF_3CF{=}CF_2$, as well as compounds containing C—H bonds, in view of the weak absorptions at 2900–3000 cm^{-1}. The less volatile −64° fractions gave molecular weights in the 310–330 region, and together with their infrared spectra, this clearly indicated that fluorinated C_6 compounds were present (e.g. the major absorptions for C_6F_{14} were observed). At the higher pyrolysis temperatures (250–295°), the spectrum of this −64° fraction always showed a characteristic triplet at 1280, 1315, and 1345 cm^{-1} which occurs in a number of fluorinated cyclohexane derivatives (15, 16), and also in unsaturated C_5 and C_6 fluorocarbons (15). However, since the spectrum showed that this fraction contained no C=C group, this triplet is considered to be due to six-membered cyclic components. Since a very weak C—H absorption was observed at 2900 cm^{-1}, these components may be only partially fluorinated cyclohexanes. The effect of temperature on the approximate distribution of products between the various fractions is shown in Table I.

TABLE I

Pyrolysis experiments

Pyrolysis temp. (°C)	Wt. sample (g)	% recovered	Wt.% of products* in: −64° fraction	−96° fraction	−125° fraction	−196° fraction
185	1.564	85.0	6.6	6.5	1.3	0.2
225	0.890	18.3	23.5	28.5	26.0	1.1
255	1.183	7.0	39.7	21.0	24.7	1.8
295	0.865	3.0	21.8	43.0	25.3	1.5

*As a percentage of the total weight of material in the experiment.

In a further effort to identify some of the fluorocarbon components, all of the −96° fractions were combined and subjected to further fractionation. Most of the material was condensed at −78°, gave a molecular weight of 260±10, and had an infrared spectrum showing absorptions expected for perfluorocyclopropane, C=C groups, and C—H groups. Individual components could not be further characterized.

Reaction of (I) with C_2F_4

Tetrafluoroethylene (0.232 g, 2.32 mmole) and (I) (0.846 g, 2.13 mmole) were heated in a sealed tube for 20 hours at 255°. Fractionation of the reaction mixture gave: (I) (0.092 g) identified spectroscopically; a −64° fraction (0.164 g), M.W. 320±30, whose infrared spectrum was very similar to that of *n*-C_6F_{14} and which did not show the spectroscopic features of a cyclohexane group; a −96° fraction (0.210 g) whose infrared spectrum was identical with that of the similar fractions obtained from pyrolysis of (I); a −125° fraction (0.306 g), M.W. 110, shown spectroscopically to consist largely of $(CH_3)_2SiF_2$ together with a smaller amount of C_2F_4; and a −196° fraction (0.026 g), M.W. 110, whose spectrum clearly showed the major components to be SiF_4, C_2F_4, and C_3F_7H. In addition 0.12 g of a white, involatile residue remained in the reaction tube, this residue having an infrared spectrum showing the presence of only C—F and C—C groups. The residue was hence polymerized tetrafluoroethylene.

Can. J. Chem. Downloaded from www.nrcresearchpress.com by 210.87.254.6 on 09/05/12
For personal use only.

Chlorination

Samples of (I) were reacted with chlorine in varying molar ratios, in sealed tubes under ultraviolet irradiation. To ensure completion of the reactions, tubes were finally heated for several hours at 110°. The results are shown in Table II.

TABLE II

Chlorination reactions

Reactants				Wt. of products (g) in:				
Chlorine		(I)		−10°	−23°	−96°	−125°	−196°
g	mmole	g	mmole	fraction	fraction	fraction	fraction	fraction
0.183	2.55	1.010	2.55	0.533	0.502	0.024	0.016	0.110
0.178	2.50	0.495	1.25	0.541	0.050	0.025	0.009	0.098
0.326	4.60	0.454	1.15	0.596	—	—	0.010	0.168
0.510	7.18	0.466	1.18	0.484*	—	0.007	0.010	0.294

*Incomplete recovery due to absorption on grease.

In some reactions, a portion of (I) was recovered unchanged as a fraction which condensed at −23° and which could be identified by its vapor pressure, molecular weight, and infrared spectrum. A major product in each chlorination was a colorless liquid of very low volatility, which condensed at −10° or remained in the reaction tube. Because of the low vapor pressure, molecular weights could not readily be obtained, but infrared studies showed the $>Si(C_3F_7)_2$ portion of (I) to be present in these products, and marked changes occurred in the 700 and 800 cm^{-1} regions, which are associated with the $>Si(CH_3)_2$ group (17, pp. 336–337), and also with C—Cl linkages (17, p. 330). Moreover, as the molar ratio of (I) to chlorine was increased from 1:2 to 1:4 to 1:6, the intensity of the C—H absorption at 2900–3000 cm^{-1} decreased and was completely absent from the spectrum of the involatile colorless liquid obtained from the 1:6 reaction.

The other major product was a gas which condensed at −196° and which was identified (observed molecular weights for these fractions fell in the range 37–42) as hydrogen chloride. The infrared spectra of these fractions showed slight contamination by C_2F_4 (~2–4%), SiF_4 (~2%), and also an unknown component (<5%) which gave strong absorption at 2300 cm^{-1} and in the 1150–1350 cm^{-1} region, suggesting some type of fluorinated C≡C linkage. Minor products condensed at −96° and −125°. Those at −96° had molecular weights of the order of 125–150 and were shown spectroscopically to contain compounds such as CCl_2F_2, CH_2Cl_2, $CClF_3$, and CCl_3F. The −125° fractions gave molecular weight of 190–210 and contained C_3F_7Cl and $CF_3CF{=}CF_2$.

In none of the chlorination reactions was there any evidence of methyl chloride as a product.

In another experiment, the ratio (I):chlorine was 1:8. The products were identical with those obtained in the reactions of Table II, with the addition that 25% of the chlorine was recovered unchanged.

Reaction of (I) with Bromine

Samples of (I) with bromine in a 1:6 and 1:2 molar ratio were reacted under the same conditions as used for chlorination. In both cases, at least 95% of the bromine was recovered, together with approximately 80% of unreacted (I). Small quantities of fluorocarbons produced by the decomposition of (I) were also separated.

Reaction of (I) with Iodine

Iodine (0.625 g, 2.48 mmole) and (I) (0.454 g, 1.15 mmole) were refluxed in 20 ml of toluene, with a trace of aluminum powder. After 1 hour, only a faint iodine color remained, and refluxing was continued for a further hour to ensure complete reaction. Fractionation of the reaction mixture left a tarry, black involatile residue which fumed slightly in air and whose infrared spectrum showed the complete absence of fluorocarbon groups. The chief volatile product, condensing at −78°, was identified spectroscopically as C_3F_7I (0.450 g, 67% yield).

In a reaction in which (I) and iodine were heated in a sealed tube at 135° for 60 hours in the absence of a solvent but with a trace of aluminum powder, 50% of (I) was recovered unchanged.

ACKNOWLEDGMENT

The financial support of the U.S. Office of Naval Research is gratefully acknowledged.

Can. J. Chem. Downloaded from www.nrcresearchpress.com by 210.87.254.6 on 09/05/12
For personal use only.

REFERENCES

1. H. J. PASSINO and L. C. RUBIN. U.S. Patent No. 2,686,194; Chem. Abstr. **49**, 1363h (1955).
2. J. H. SIMONS and R. D. DUNLAP. U.S. Patent No. 2,651,651; Chem. Abstr. **48**, 10056a (1954).
3. R. N. HASZELDINE and R. J. MARKLOW. J. Chem. Soc. 962 (1956).
4. E. G. ROCHOW. Chemistry of the silicones. 2nd ed. John Wiley and Sons Inc., New York. 1951. p. 25.
5. O. R. PIERCE, E. T. MCBEE, and G. F. JUDD. J. Am. Chem. Soc. **76**, 474 (1954).
6. J. A. BEEL, H. C. CLARK, and D. WHYMAN. J. Chem. Soc. 4423 (1962).
7. H. J. EMELEUS and J. D. SMITH. J. Chem. Soc. 375 (1959).
8. R. E. BANKS and R. N. HASZELDINE. Polyfluoroalkyl derivatives of metalloids and non-metals. *In* Advances in inorganic chemistry and radiochemistry. Vol. 3. Academic Press Inc., New York. 1961.
9. R. FIELDS and R. N. HASZELDINE. Proc. Chem. Soc. 22 (1960).
10. J. L. SPEIER. J. Am. Chem. Soc. **73**, 824 (1951).
11. C. EABORN. Organosilicon compounds. Butterworths Publications Ltd., London. 1960.
12. C. EABORN. J. Chem. Soc. 2755 (1949).
13. H. C. CLARK and D. WHYMAN. To be published.
14. H. KRIEGSMANN. Z. Elektrochem. **62**, 1033 (1958).
15. D. G. WEIBLEN. *In* Fluorine chemistry. Vol. 2. *Edited by* J. H. Simons, Academic Press Inc., New York. 1954.
16. H. W. THOMPSON and R. B. TEMPLE. J. Chem. Soc. 1432 (1948).
17. L. J. BELLAMY. The infra-red spectra of complex molecules. John Wiley and Sons Inc., New York. 1958.

Can. J. Chem. Downloaded from www.nrcresearchpress.com by 210.87.254.6 on 09/05/12
For personal use only.

NUCLEAR ISOMERS $Hg^{197m,g}$, $Hg^{195m,g}$, AND $Au^{196m,g}$ FORMED BY BOMBARDMENT OF GOLD WITH PROTONS OF ENERGIES FROM 8 TO 60 MEV[1]

R. S. TILBURY[2] AND L. YAFFE

Radiochemistry Laboratory, Department of Chemistry, McGill University, Montreal, Que.

Received April 22, 1963

ABSTRACT

Gold has been bombarded with protons of energies from 8 to 60 Mev to study excitation functions and isomer yield ratios for the formation of the isomeric pairs $Hg^{197m,g}$, $Hg^{195m,g}$, and $Au^{196m,g}$. For $Hg^{197m,g}$ and $Hg^{195m,g}$, the ratio of the yield of the metastable state to that of the ground state, σ_m/σ_g, was found to increase with increasing proton bombarding energy up to 20 and 35 Mev respectively, whilst that for $Au^{196m,g}$ showed a maximum at about 40 Mev.

Can. J. Chem. Downloaded from www.nrcresearchpress.com by 210.87.254.40 on 09/05/12
For personal use only.

INTRODUCTION

The study of the formation of nuclear isomeric pairs in nuclear reactions may be used as an aid in the investigation of the mechanism of nuclear reactions. At low energies (less than about 30 Mev) nuclear reactions are believed to proceed by a compound nucleus mechanism. The compound nucleus de-excites by emission first of particles (while there is sufficient excitation energy available) to give a residual excited nucleus, and then by γ-ray emission to a product nucleus. If the product nucleus can exist in two isomeric states of definite angular momentum, the ratio of the yields for formation of the two isomers will reflect the angular momentum states of the compound residual nuclei. The yield ratio of high-spin to low-spin isomer would be expected to increase regularly with increasing bombarding energy.

Above approximately 30 Mev (for nuclear reactions in the heavy-mass region) the compound nucleus mechanism is believed to give way to a direct interaction mechanism in which not all the energy of the bombarding particle is transferred to the target nucleus. The yield ratio of high-spin to low-spin isomers might then not continue its regular increase, but would level off or even peak and decrease before coming to a steady value. Thus a change in the yield ratios might serve as a sensitive indicator as to the extent of the two types of processes.

Gold was chosen as target material, since, on bombardment with protons over the available energy range (8 to 80 Mev), it should produce cleanly three isomeric pairs with convenient half-lives. The nuclear reactions giving rise to these nuclear isomers occur over different energy ranges such that the isomer yield ratios should form a critical test of the different nuclear mechanisms operating.

EXPERIMENTAL

(a) Target Preparation

Gold powder, in a sealed aluminum tube, was used as target material. The sealed aluminum tube was a precautionary measure to ensure that no mercury would be lost by evaporation during bombardments.

Copper powder, mixed with the gold, was used to monitor the proton beam. The monitor reactions used were $Cu^{63}(p,n)Zn^{63}$ at low energies and $Cu^{65}(p,pn)Cu^{64}$ at all higher energies, and the cross sections used are shown in Table I. Those for the first reaction were taken from the work of Ghoshal (1) while those for the second are from the work of Meghir (2).

[1]*This work received financial assistance from the National Research Council of Canada.*

[2]*Holder of an International Nickel Co. of Canada Fellowship. Present address: Union Carbide Nuclear Co., Research Center, P.O. Box 324, Tuxedo, N.Y., U.S.A.*

TABLE I
Monitoring cross sections

Proton energy (Mev)	$\sigma_{Zn^{63}}$ (millibarn) (1)	$\sigma_{Cu^{64}}$ (millibarn) (2)	Proton energy (Mev)	$\sigma_{Cu^{64}}$ (millibarn) (2)
8	300		28	345
10	450		31	320
11	480		34	290
12	520		37	275
13	530		40	260
14.5	490		46	240
16		100	52	210
20		300	60	190
24		370		

For bombardments, about 10 mg of gold and 10 mg of copper powders were weighed separately into a 2S aluminum tube (about 3.5 cm long and 1/16 inch internal diameter and 0.003 inch wall thickness) which was crimped at one end. The other end of the tube was then closed and the weighed gold and copper powders thoroughly mixed by shaking. The mixing of the powders was tested previously by shaking them together in a glass tube of the same dimensions as the aluminum tube, when it was seen that the powders mixed together quite homogeneously. The aluminum tube containing the mixture was mounted in the target holder for bombardment in the circulating beam of the cyclotron.

Corrections were made for proton energy degradation by the target. The range-energy data of Sternheimer (3) were used for this correction, and it was found to be approximately 1 Mev at a proton energy of 20 Mev.

(b) Chemical Procedures

After bombardment, the aluminum tube and its contents were dissolved in aqua regia. For most runs the following chemical separations were made. Carriers of 10.0 mg Hg^{++}, about 5 mg each of Pt^{++}, Ni^{++}, Zn^{++}, Co^{+++}, and Na^{+} were added and the nitric acid destroyed by repeated evaporation with concentrated hydrochloric acid. The volume of the solution was made up to about 20 ml with concentrated hydrochloric acid and gold extracted with isoamyl acetate. The isoamyl acetate extract was washed with 6 *M* hydrochloric acid and the washing combined with the acid layer, since otherwise some copper would be extracted with the gold. The gold was back-extracted from the organic layer with water, made up to known volume with dilute hydrochloric acid, and an aliquot taken for activity measurement.

Mercury was precipitated from the aqueous phase as mercurous chloride by reduction with stannous chloride solution, and repurified by distillation as mercurous chloride. The chloride was then dissolved in aqua regia, made up to volume, and an aliquot taken for activity measurement.

The remaining solution was evaporated to about 2 ml in volume and copper separated from nickel, cobalt, zinc, and sodium by means of Dowex 1 anion exchange resin based on the method of Kraus and Moore (4). The ion exchange column, 10 cm long and 7 mm in diameter, was washed with concentrated hydrochloric acid, and the solution containing the elements to be separated, in 2 ml of concentrated hydrochloric acid, was mixed with a little of the resin and transferred to the top of the column. The column was then eluted with 1.5 *M* hydrochloric acid until the first few drops of blue solution indicated the presence of copper in the eluate. The eluate was collected until the blue copper color had almost disappeared (between 2 and 5 ml were sufficient), made up to volume, and an aliquot taken for activity measurement. The column was eluted with a further 5 ml of 1.5 *M* hydrochloric acid to remove copper completely and then eluted with water to remove zinc which could be collected and an aliquot taken for measurement, if required.

Examination of the separated samples by gamma ray spectroscopy and half-life measurements was used as a check on the radiochemical purity of the samples. In the accepted runs, the half-lives for the monitors never varied by more than 2% from the literature values.

(c) Chemical Yield Determinations

The chemical yield of each element separated was determined so that absolute cross sections could be calculated for the various nuclear reactions. All chemical yield determinations, with the exception of that for zinc, were based on standard spectrophotometric methods using a Beckman DU spectrophotometer and 1 cm Pyrex cells. Mercury was determined as mercury dithizonate in chloroform (5), gold by means of its complex ion $[AuBr_4]^-$ (6), and copper by means of the diethyldithiocarbamate complex in isoamyl alcohol (7). Zinc was determined volumetrically, using disodium ethylenediaminetetraacetic acid and eriochrome black T as the indicator (8).

(d) Activity Measurements

The 511 kev annihilation radiation was used to measure the Zn^{63} and Cu^{64} activities. A 3in.×3 in. sodium iodide (Tl activated) crystal and photomultiplier tube assembly were used as the detector. The pulses from

Can. J. Chem. Downloaded from www.nrcresearchpress.com by 210.87.254.40 on 09/05/12
For personal use only.

this were fed into a 100-channel pulse-height analyzer assembly. It was determined in auxiliary experiments that complete annihilation of the positrons from both Zn^{63} and Cu^{64} occurred in the liquid source and glass vial, so that no correction factor for this effect had to be introduced. The mercury and gold activities were also measured by the scintillation detector. Corrections for the overall detector efficiency were made to the counting data from empirical efficiency curves available in our laboratory.

(e) Calculation of Cross Sections

The cross sections for formation, σ_A, were calculated from the equation

$$[1] \qquad \sigma_A = \sigma_m \cdot \frac{D_A}{D_m} \cdot \frac{n_m}{n_A} \cdot \frac{(1-e^{-\lambda_m T})}{(1-e^{-\lambda_A T})},$$

where A refers to the product and m refers to the monitor, and σ = cross section, D = disintegration rate at end of bombardment, n = number of atoms in target, λ = disintegration constant, T = time of bombardment.

In cases where the ground-state isomer was formed by decay of the upper state, the disintegration rate, D_A, was corrected for that which had grown in during the bombardment. In general, the cumulative disintegration rate of a daughter at the end of bombardment is given by

$$[2] \qquad D_d' = D_d + \frac{D_p}{1-e^{-\lambda_p T}}\left[1 - \frac{\lambda_p e^{-\lambda_d T} - \lambda_d e^{-\lambda_p T}}{\lambda_p - \lambda_d}\right],$$

where the subscripts p and d refer to parent and daughter respectively, and D_d and D_p are the amounts formed directly. D_d can be calculated, substituted for D_A in equation [1], and the formation cross section of the independently formed daughter thus calculated.

RESULTS

(a) $Au^{197}(p,n)Hg^{197m,g}$

Photon peaks at 75 and 134 kev were observed in the γ-spectrum from the mercury fraction in the low-energy (8–20 Mev) runs. The peak at 134 kev decayed with a half-life of 24±1 hr measured over six half-lives. It is due to Hg^{197m} and occurs in 97% of the disintegrations (9). A conversion coefficient $\alpha_T = 2.1$ (9) has been used in the cross-section calculations. The peak at approximately 75 kev decayed with a half-life of 65±2 hr, measured over a period of six half-lives. The peak is a combination of the K X-ray and a 77 kev γ-ray from the first excited state of Au^{197}. It was assumed, for purposes of calculation, that 1 K X-ray corresponded to 1 disintegration of Hg^{197g}. The K X-ray fluorescence yield was taken to be 0.945 (10).

Since Hg^{197m} decays 97% by isomeric transition to Hg^{197g}, the cross section thus calculated for Hg^{197g} (σ_g*) actually represents the cross section for the independent formation of Hg^{197g} plus 0.97 of the cross section for the formation of Hg^{197m}. By making this subtraction, the cross section for the independent formation of Hg^{197g} was obtained (σ_g). The data are given in Table II and shown in Figs. 1 and 2. These results agree reasonably

TABLE II

Formation cross sections for the reactions $Au^{197}(p,n)Hg^{197m,g}$

Proton energy (Mev)	σ_m (millibarn)	σ_g* (millibarn)	σ_g (millibarn)	$\frac{\sigma_m}{\sigma_g}$
8	3.5	13	10	0.35
10	22	73	52	0.42
11	37	120	84	0.45
12	46	140	94	0.49
13	60	150	96	0.63
14.5	47	110	67	0.70
16	13	30	17	0.76
20	17	35	19	0.91

NOTE: $\sigma_g^* = \sigma_g + 0.97\,\sigma_m$.

Can. J. Chem. Downloaded from www.nrcresearchpress.com by 210.87.254.40 on 09/05/12
For personal use only.

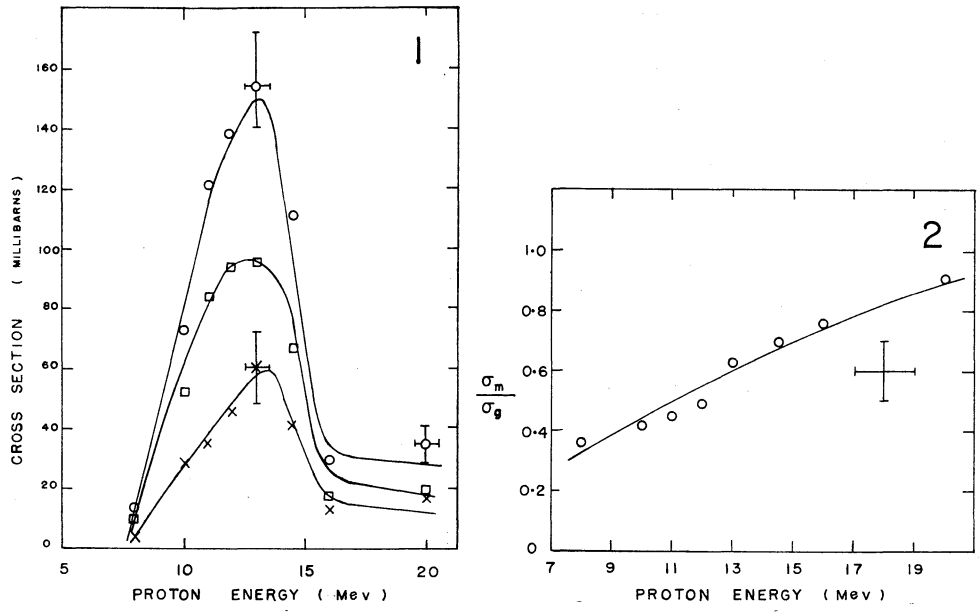

FIG. 1. Excitation functions for $Au^{197}(p,n)Hg^{197m,g}$ reactions: ○ $\sigma_{Hg^{197g}}+0.97\sigma_{Hg^{197m}}$; × $\sigma_{Hg^{197m}}$; □ $\sigma_{Hg^{197g}}$.
FIG. 2. Variation of the isomer cross-section ratios for the reactions $Au^{197}(p,n)Hg^{197m,g}$ with proton bombarding energy. The vertical and horizontal lines represent the estimated error in the isomer ratio and proton energy respectively.

well with those of Vandenbosch and Huizenga (11) up to 10 Mev, the maximum energy of their measurements, but not so well with those of Hansen *et al.* (12) at 12.7 Mev, the maximum energy of their measurements, as shown in Table III.

TABLE III

Comparison of results of formation cross sections for the reactions $Au^{197}(p,n)Hg^{197m,g}$ with those of other workers

Energy (Mev)	This work			Vandenbosch and Huizenga (11)			Hansen *et al.* (12)		
	σ_m	σ_g	σ_m/σ_g	σ_m	σ_g	σ_m/σ_g	σ_m	σ_g	σ_m/σ_g
8	3.5	10	0.35	2	8.9	0.225	12	31	0.39
10	22	52	0.42	21	66	0.32	38	52	0.73
13	60	96	0.63	—	—	—	40	25	1.6

(b) $Au^{197}(p,pn)Au^{196m,g}$

Photopeaks of 150 and 190 kev, due to Au^{196m}, were observed to decay with a half-life of 9.5±0.5 hr, measured over a period of three half-lives. Since the conversion coefficients of the γ-rays from Au^{196m} have not been measured, the disintegration rate was taken from the *K* X-ray peak, assuming one X-ray per disintegration. The half-life of the metastable state obtained from the X-ray decay curve was always slightly longer than that obtained from the γ-ray photopeaks, in conformity with observations made previously (13). At bombarding energies of 52 and 60 Mev, contributions from 39-hr Au^{194} were subtracted from the decay curve. Above a bombarding energy of 60 Mev, the formation of 17-hr Au^{193} interfered with the resolution of the curve and limited the presentation of the data.

Can. J. Chem. Downloaded from www.nrcresearchpress.com by 210.87.254.40 on 09/05/12
For personal use only.

A well-defined peak at 350 kev, due to Au^{196g}, decayed with a half-life of 6.1±0.1 days measured over six half-lives, in good agreement with recent values (9). The decay of Au^{196g} is well established and the curves of the photopeaks from three neighboring γ-rays, 333, 356, and 426 kev, were summed to obtain disintegration rates. From recent data (9), the total conversion coefficients, α_T, for the 333 kev (26.9% branching ratio), the 356 kev (66.7%), and the 426 kev (6%) peak were calculated to be 0.084, 0.063, and 0.035 respectively. The area under the composite peak was multiplied by 1.12 to allow for branching ratio and internal conversion corrections.

TABLE IV

Formation cross sections for the reactions $Au^{197}(p,pn)Au^{196m,g}$

Proton energy (Mev)	σ_m (millibarn)	σ_T (millibarn)	σ_g (millibarn)	$\frac{\sigma_m}{\sigma_g}$
24	0.60	24	23	0.026
28	5.1	104	98	0.052
31	14	138	124	0.11
34	21	170	149	0.14
37	37	191	154	0.24
40	44	191	147	0.30
46	40	180	140	0.29
52	25	170	145	0.17
60	23	159	136	0.17

In Table IV are given the experimental results for the formation of the Au^{196} isomeric pair. The cross section for formation of the ground-state isomer, σ_g, is then obtained by

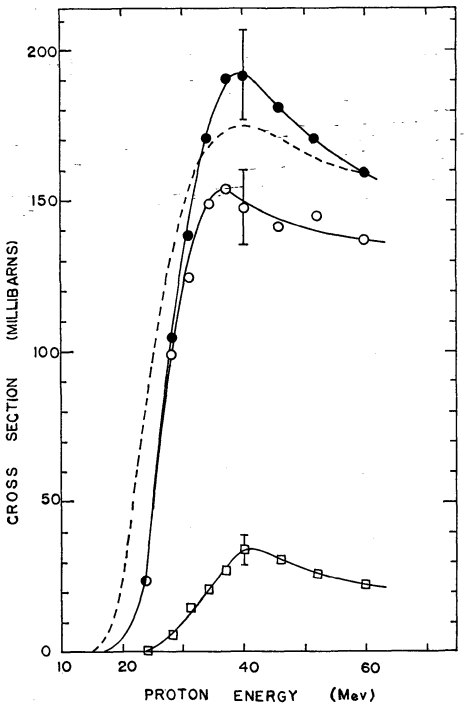

FIG. 3. Excitation functions for reactions $Au^{197}(p,pn)Au^{196m,g}$: - - - σ_T (15); ● σ_T, this work; ○ σ_g, this work; □ σ_m, this work.

Can. J. Chem. Downloaded from www.nrcresearchpress.com by 210.87.254.40 on 09/05/12
For personal use only.

subtraction from σ_T, the total cross section. The cross-section ratio, σ_m/σ_T can be obtained, using the ratio of counting rates at the end of bombardment rather than disintegration rate, so that errors in chemical yield and sampling factors do not affect the result. From $\sigma_m/\sigma_T = \sigma_m/(\sigma_m+\sigma_g)$ the ratio σ_m/σ_g can be calculated and is given in Table IV. The results are shown graphically in Figs. 3 and 4. The values of σ_T compare favorably with the values

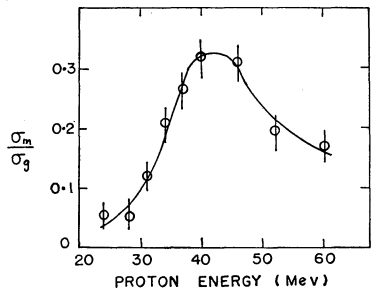

FIG. 4. Variation of isomer yield ratios with proton bombarding energy for the reactions $Au^{197}(p,pn)Au^{196m,g}$.

of the cross section for formation of Au^{196} as measured by Kavanagh and Bell (15). The displacement of the two excitation functions is about 4 Mev in terms of proton bombardment energy which may be compared with the ±2 Mev uncertainty in the proton energy.

(c) $Au^{197}(p,3n)Hg^{195m,g}$

The decay scheme of $Hg^{195m,g}$ is very complicated. The γ-ray spectrum obtained from the chemically separated and purified mercury fraction showed a prominent X-ray peak, and peaks at 185 and 260 kev which decayed with half-lives of 6.5 and 42 hr respectively. The peak at 260 kev is due to Au^{195} and occurs in 26% of the decays of Hg^{195m}. The peak at 185 kev showed a half-life (6.5 hr) far removed from the 9.5 hr associated with Hg^{195g}. The X-ray peak was nicely resolvable into three components—a long-lived tail, 40 hr, and 9.5 hr, and this peak was used to measure the counting rates of the metastable and ground states. Disintegration rates were calculated assuming a fluorescence yield of 0.945 (10) and that each disintegration yielded one X-ray. The cross-section values are given in Table V and are shown in Fig. 5. Figure 6 shows the ratio σ_m/σ_g.

TABLE V

Formation cross sections for the reactions $Au^{197}(p,3n)Hg^{195m,g}$

Proton energy (Mev)	σ_m (millibarn)	σ_g (millibarn)	$\frac{\sigma_m}{\sigma_g}$
24	140	68	2.0
28	600	270	2.2
31	750	310	2.4
34	590	150	3.9
37	340	72	4.7
40	260	—	—

ERRORS

A standard deviation of ±18% in the absolute cross sections for formation of the metastable states has been calculated. For the ground-state isomers whose disintegration

Can. J. Chem. Downloaded from www.nrcresearchpress.com by 210.87.254.40 on 09/05/12
For personal use only.

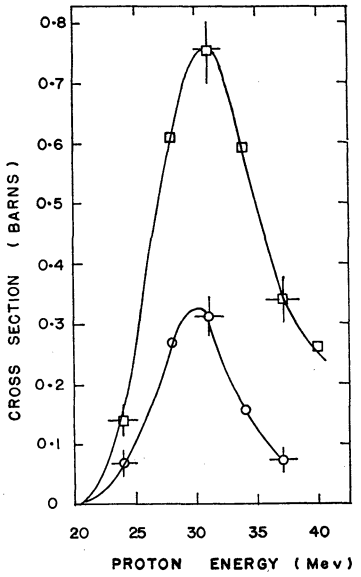

FIG. 5. Excitation functions for the reactions $Au^{197}(p,3n)Hg^{195m,g}$: □ σ_m; ○ σ_g.

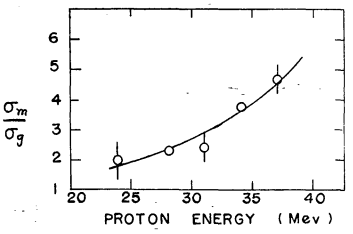

FIG. 6. Variation of isomer yield ratios with proton bombarding energy for the reactions $Au^{197}(p,3n)Hg^{195m,g}$.

rates at the end of bombardment had to be corrected for that which had grown in during the bombardment, the standard deviation in the absolute values rose to ±25%.

If the external errors are neglected, i.e. errors in the monitor cross-section values, the standard deviations in this work range between ±10% and ±16%, and these are the vertical error bars shown in the figures. The uncertainty in the proton bombarding energy (±2 Mev) is indicated by horizontal bars.

The errors involved in the calculation of the isomer cross-section ratios are smaller, since the cross section of the monitor, the chemical yield factors, and sampling factors all cancel in the expression for σ_m/σ_g. For $Hg^{197m,g}$, the standard deviation in the cross-section ratio varied between 10 and 15%, for $Au^{196m,g}$ between 10 and 20%, and for $Hg^{195m,g}$ between 7 and 15%. Due to uncertainties in the decay schemes and incomplete knowledge of the conversion coefficients, there may be systematic errors here which have not been taken into account. However, the relative values of the σ_m/σ_g values and the shape of the curves of σ_m/σ_g against energy would not be affected.

DISCUSSION

The shapes of the (p,n) and $(p,3n)$ excitation functions, as expected, show the effect of the operation of the compound nucleus mechanism. The probability for forming the

Can. J. Chem. Downloaded from www.nrcresearchpress.com by 210.87.254.40 on 09/05/12
For personal use only.

compound nucleus increases sharply above the threshold energy to a maximum at the optimum energy of the reaction, and then falls steeply as the next competing reaction becomes energetically possible.

The (p,pn) excitation functions (Fig. 3) also show a sharp initial rise as the energy of the proton beam increases above the threshold value. The excitation functions reach a maximum and fall off slowly with increasing proton energy, in contrast to those for the (p,n) and $(p,3n)$ reactions. This shape of the (p,pn) excitation functions is in agreement with the work of Bell and Kavanagh (14) and Meadows *et al.* (15) and shows that the (p,pn) reaction involves a larger percentage of direct interactions than the (p,n) or $(p,3n)$ reactions.

The isomer yield ratios for the (p,n) and $(p,3n)$ reactions increase with energy over the energy range studied, whilst the yield ratio for the (p,pn) reaction passes through a maximum at about 40 Mev. Several attempts have been made to calculate expected isomer yield ratios for low-energy nuclear reactions assuming the compound nucleus mechanism (11, 16, 17). In the present work this type of calculation is applicable only to the (p,n) reaction, since this occurs at sufficiently low energies for the compound nucleus mechanism only to apply. However, no values for the transmission coefficients for protons in gold, which are required in the calculation, are available. The calculations are very lengthy, and for these reasons have not yet been attempted.

The $(p,3n)$ and $(p,4n)$ reactions occur over too high an energy range for the above calculations to be valid, as a considerable percentage of the initial events is direct interaction in which only a fraction of the energy and angular momentum of the projectile are transferred to the compound nucleus. It is expected that direct interactions will favor the production of the isomer whose spin is closer to the target spin. This effect is noticed for the σ_m/σ_g ratios for Au^{196} where the ground-state isomer ($I = 2$) becomes favored above 40 Mev, compared to the metastable state ($I = 12$). The spin of the target Au^{197} is 3/2.

Can. J. Chem. Downloaded from www.nrcresearchpress.com by 210.87.254.40 on 09/05/12
For personal use only.

ACKNOWLEDGMENTS

The authors wish to thank Dr. R. E. Bell and Mr. R. H. Mills for their cooperation during the cyclotron irradiations. One of us (R. S. T.) thanks the International Nickel Company of Canada Limited for a Fellowship from 1960 to 1963.

REFERENCES

1. S. N. Ghoshal. Phys. Rev. **80**, 939 (1950).
2. S. Meghir. Ph.D. Thesis, McGill University, Montreal, Que. 1962.
3. R. M. Sternheimer. Phys. Rev. **115**, 137 (1959).
4. K. A. Kraus and G. E. Moore. J. Am. Chem. Soc. **75**, 1460 (1953).
5. N. H. Furman and K. J. Jensen. National Nuclear Energy Series. Div. VIII, Vol. I. McGraw-Hill, New York. 1950. p. 400.
6. E. B. Sandell. Colorimetric metal analysis. 3rd ed. Interscience, Inc., New York. 1959. p. 503.
7. T. D. Price and R. E. Telford. National Nuclear Energy Series. Div. VIII, Vol. I. McGraw-Hill, New York. 1950. p. 404.
8. F. J. Welcher. Analytical uses of ethylenediaminetetra-acetic acid. D. van Nostrand Co., New York. 1957. p. 149.
9. Nuclear Data Sheets. National Academy of Sciences, National Research Council (U.S. Government Printing Office, Washington, D.C.). 1962.
10. C. D. Broyles, D. A. Thomas, and S. K. Haynes. Phys. Rev. **89**, 715 (1953).
11. J. R. Huizenga and R. Vandenbosch. Phys. Rev. **120**, 1305 (1960); **120**, 1313 (1960).
12. L. F. Hansen, R. C. Jopson, H. Mark, and C. D. Swift. Univ. Calif. Rept. UCRL-6582. 1961.
13. G. Wilkinson. Phys. Rev. **75**, 1019 (1949). T. M. Kavanagh. Private communication.
14. T. M. Kavanagh and R. E. Bell. Can. J. Phys. **39**, 1172 (1961).
15. J. W. Meadows, R. M. Diamond, and R. A. Sharp. Phys. Rev. **102**, 190 (1956).
16. S. M. Bailey. Univ. Calif. Rept. UCRL-8710. 1959.
17. T. Matsuo. Ph.D Thesis, Clark University, Worcester, Mass. 1961.

NUCLEAR MAGNETIC RESONANCE STUDIES OF THE PROTONATION OF WEAK BASES IN FLUOROSULPHURIC ACID

II. AMIDES, THIOAMIDES, AND SULPHONAMIDES[1]

T. BIRCHALL AND R. J. GILLESPIE
Department of Chemistry, McMaster University, Hamilton, Ontario
Received May 27, 1963

ABSTRACT

The proton magnetic resonance spectra of solutions of amides in fluorosulphuric acid confirm previous results which indicated that protonation of amides occurs on the carbonyl oxygen. A similar study of solutions of thioacetamide, thioacetanilide, thiourea, and *N*-methylthiourea provides conclusive evidence that the sulphur atom is protonated in these bases. In the case of *N*-methyl- and *N,N'*-dimethyl-*p*-toluenesulphonamide and sulphamide protonation occurs on nitrogen rather than on oxygen. It was not possible to obtain any conclusive evidence on the site of protonation of urea and *N,N'*-dimethylurea. Evidence is presented which indicates that thiourea and *N*-methylthiourea are diprotonated in solution in strong acids such as fluorosulphuric acid, and diprotonation of urea and *N,N'*-dimethylurea under the same conditions also seems very likely.

Can. J. Chem. Downloaded from www.nrcresearchpress.com by 210.87.254.105 on 09/05/12
For personal use only.

In Part I (1) it was shown that a new peak appears at approximately −10 p.p.m. from an external tetramethylsilane reference in the proton magnetic resonance spectrum of certain amides in fluorosulphuric acid at low temperatures. It was shown that this peak can be attributed to the $C{=}\overset{+}{O}{-}H$ group. The low basicity of the solvent and the low temperature (approx. −80°) are together sufficient to reduce the rate of proton exchange between the conjugate acid of the amide and the solvent so that they give rise to separate peaks in the n.m.r. spectrum. Hence it was established unambiguously that acetamide and formamide and their *N,N*-dimethyl derivatives protonate on the carbonyl oxygen and not on nitrogen. The same conclusion has also been reached somewhat less directly by other workers from measurements of the areas of the NH or NH_2 peaks in the n.m.r. spectra of neutral and acid solutions of formamide, acetamide, benzamide, and their *N*-methyl derivatives (2–5). We have now extended our previous measurements to include the *N*-methyl derivatives of formamide and acetamide and also benzamide and its *N*-methyl and *N,N*-dimethyl derivatives. We have also studied thioacetamide, thioacetanilide, urea, *N,N'*-dimethylurea, thiourea, *N*-methylthiourea, sulphamide, and *N*-methyl- and *N,N*-dimethyl-*p*-toluenesulphonamide in order to determine the site of protonation.

RESULTS AND DISCUSSION

Amides

The results of our measurements are summarized in Table I. In every case at a sufficiently low temperature the signal from the $C{=}\overset{+}{O}{-}H$ proton is observed at approximately −10 p.p.m. from the external reference of tetramethylsilane and it is clear therefore that protonation occurs on the carbonyl oxygen. In each case (except *N,N*-dimethylbenzamide) this peak is somewhat broad even at −85°, indicating that even at this low temperature there is a slow proton exchange between the solvent and the conjugate acid of the amide. If the basicity of the solvent is reduced by the addition of antimony pentafluoride the

[1]*Reference 1 is regarded as Part I of this series.*

TABLE I

Chemical shifts of amides in fluorosulphuric acid

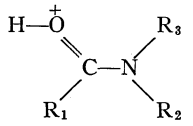

Amide	Temperature (°C)	−δ (p.p.m.) from external T.M.S. O—H	C—R_1	N—R_2	N—R_3	J (c/s)	
N-Methylformamide	25	—	8.50	~8.58	3.44	J_{R_2,R_3}	4.4
						J_{R_1,R_3}	1.0
						J_{R_1,R_2}	4.5
	−85	10.49	8.48	8.66	3.33		
	−69*	10.39	8.57	8.76	3.46	$J_{R_1,OH}$	3.5
N-Methylacetamide	25	—	2.69	8.31	3.36	J_{R_2,R_3}	5.0
	−85	10.15	2.58	8.27	3.25		
Benzamide	25	—	8.08	8.59	8.59		
	−85	10.20	8.03	8.72	8.72		
N-Methylbenzamide	25	—	7.93	8.61	3.54	J_{R_2,R_3}	5.4
	−71	10.37	7.97	8.72	3.50		
	−86	10.34	7.93	8.73	3.47		
N,*N*-Dimethyl-benzamide	25	—	7.85	3.72	3.56		
	−72	9.91	7.84	3.61	3.49		
	−85	9.95	7.85	3.63	3.51		

*Solution in 10 mole% SbF_5 in fluorosulphuric acid.

$C{=}\overset{+}{O}{-}H$ line width decreases, indicating a further reduction in the rate of proton exchange and in the case of *N*-methyl formamide splitting of the $C{=}\overset{+}{O}{-}H$ peak into a doublet is then observed which can be attributed to spin–spin coupling with the formyl proton (J = 3.5 c/s).

Thioamides

As some previous workers have presented evidence for protonation on sulphur (6–9) while others have concluded that protonation occurs on nitrogen (10–11) we have examined the proton magnetic resonance spectra of solutions of thioacetamide and thioacetanilide in fluorosulphuric acid. The results given in Table II clearly establish that protonation occurs on sulphur.

The spectrum of the thioacetamide solution at 25° contained, in addition to the solvent and tetramethylsilane peaks, three peaks A, B, and C of relative areas 1.98:0.9:3.0 which may be assigned to the NH_2, $C{=}SH^+$, and CH_3 groups respectively (Fig. 1). It is interesting to note that the $C{=}SH^+$ peak (B) is quite sharp, indicating that proton exchange with the solvent is quite slow even at 25°. The NH_2 peak (A) is a broad triplet due to N^{14}—H coupling. Reduction of the temperature causes this triplet to collapse to a single line as has also been found to occur in the case of acetamide and formamide (1).

A solution of thioacetanilide in acetone gives a spectrum with three peaks, in addition to the solvent and reference peaks, that may be attributed to the NH, C_6H_5, and CH_3 protons. In fluorosulphuric acid at 25° an additional peak appears that may be assigned to the $C{=}\overset{+}{S}H$ group. The spectrum at −40° (Fig. 2) is essentially the same except that the NH peak is sharper and is more clearly resolved from the solvent peak: the four peaks A, B, C, and D may be attributed to the NH, C_6H_5, $C{=}SH^+$, and CH_3 groups respectively.

Can. J. Chem. Downloaded from www.nrcresearchpress.com by 210.87.254.105 on 09/05/12
For personal use only.

TABLE II

Chemical shifts for solutions of thioamides

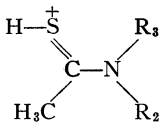

Amide	Temperature (°C)	Solvent	−δ(p.p.m.) from external T.M.S. S—H	C—CH_3	N—R_2	N—R_3	J (c/s)
Thioacetamide	25	Acetone	—	2.35	8.47	8.47	
	25	Water	—	2.94	9.48	9.48	$J_{N^{14},R}$ 50±8
	25	Fluorosulphuric acid	5.75	3.00	9.25	9.25	
	−50	"	5.69	2.89	9.21	9.21	
	−81	"	5.72	2.92	9.29	9.29	
Thioacetanilide	25	Acetone	—	2.47	10.55	7.19	
	25	Fluorosulphuric acid	5.45	3.17	~10.5*	7.72	
	−40	"	5.39	3.09	10.64	7.68	

*N—H peak broad and very close to solvent.

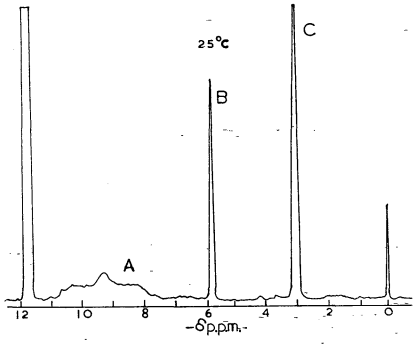

FIG. 1. Thioacetamide in fluorosulphuric acid.

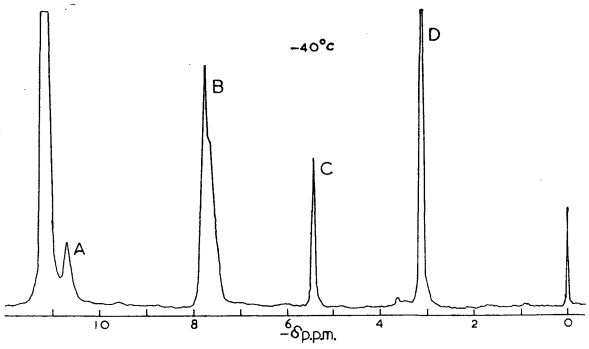

FIG. 2. Thioacetanilide in fluorosulphuric acid.

We note that the C═SH^+ resonance occurs at approximately −5.5 p.p.m. from tetramethylsilane, which is at considerably higher field than the C═OH^+ resonance (approx. −10 p.p.m.). The chemical shifts for the S—H group in thiophenol and thiolacetic acid are −3.2 and −4.73 p.p.m. respectively (12, 13). The sharpness of the C═SH^+ resonance

Can. J. Chem. Downloaded from www.nrcresearchpress.com by 210.87.254.105 on 09/05/12
For personal use only.

Can. J. Chem. Downloaded from www.nrcresearchpress.com by 210.87.254.105 on 09/05/12
For personal use only.

TABLE III

Chemical shifts for solutions of ureas and thioureas

Urea	Temperature (°C)	Solvent	−δ (p.p.m.) from external T.M.S.†				J (c/s)
			Solvent	X—H	N—H	N—CH_3	
Thiourea	25	Water	5.12	—	7.66	—	
	25	Trifluoracetic acid	11.95 (22)	—	7.83	—	
	25	Sulphuric acid	10.89 (29)	5.25 (44)	—	—	
	25	Fluorosulphuric acid	10.30 (15)	4.87 (21)	—	—	
	−50	"	10.63 (46)	4.81 (∼5)	—	—	
	−73	"	11.05 (69)	4.84 (∼5)	—	—	
N-Methylthiourea	25	Water	—	—	8.07, 7.59	3.33	J_{H,CH_3} 3.8
	25	Trifluoracetic acid	11.45 (21)	—	8.02, 7.55	3.16	J_{H,CH_3} 4.2
	25	Sulphuric acid	11.21 (29)	5.21 (broad)	7.84	3.56	No coupling observed
	−47.5	Fluorosulphuric acid	11.11 (33)	4.79 (sharp)	7.29	3.24	
	−67.5	Fluorosulphuric acid*	10.81 (29)	4.86	8.19, 7.32	3.35	
Urea	25	Water	5.13	—	6.08	—	
	25	Trifluoracetic acid	10.11 (13)	—	—	—	
	25	Sulphuric acid	10.81 (∼4)	—	—	—	
	25	Fluorosulphuric acid*	9.10 (∼5)	—	—	—	
	−60	"	9.38 (16)	—	—	—	
	−80	"	9.52 (34)	—	—	—	
N,*N*′-Dimethylurea	25	Water	5.32	—	—	3.08	
	25	Trifluoracetic acid	11.09 (8)	—	—	2.97	
	25	Sulphuric acid	10.94	—	—	3.43	
	−86	Fluorosulphuric acid	11.67 (64)	—	—	3.33 (31)	
	25	Fluorosulphuric acid*	9.97	—	—	3.34	
	−88	"	11.94 (93)	—	—	3.59 (∼130)	

*Fluorosulphuric acid containing 4.47 mole% SbF_5.
†Values in parentheses denote line width in c/s.

at 25° indicates that proton exchange is very much slower than for the C═OH^+ group under the same conditions.

Thiourea and N-Methylthiourea

The results for these substances are shown in Table III. The spectrum of thiourea in water or trifluoracetic acid contains only one line due to the NH_2 group in addition to the solvent peak. The fact that the trifluoracetic acid peak is quite broad suggests that although protonation occurs in this medium proton exchange is rapid at 25°. In the more acidic (and less basic) medium sulphuric acid a new peak appears in the spectrum at approximately −5 p.p.m. that can be attributed to the C═SH^+ group, and the NH_2 peak disappears. In fluorosulphuric acid the spectrum is essentially the same except that the C═SH^+ peak is somewhat narrower, indicating that proton exchange with the solvent is slower than in sulphuric acid. Decreasing the temperature causes a further narrowing of this line as expected. At the same time the solvent peak increases in width with decreasing temperature. This observation and the disappearance of the NH_2 peak can only be reasonably interpreted as being due to diprotonation, the first proton being attached to sulphur and exchanging only very slowly with the solvent and the second proton being attached to nitrogen and exchanging rather rapidly with the solvent.

The behavior of *N*-methylthiourea is similar. In water and trifluoracetic acid the spectrum consists of three peaks A, B, and C, due to the NH, NH_2, and N—CH_3 groups respectively. The latter peak is a doublet due to spin–spin coupling with the NH proton (J = 4 c/s) (Fig. 3). Area measurements gave a ratio (A+B):C = 2.8:3.0. Figure 4

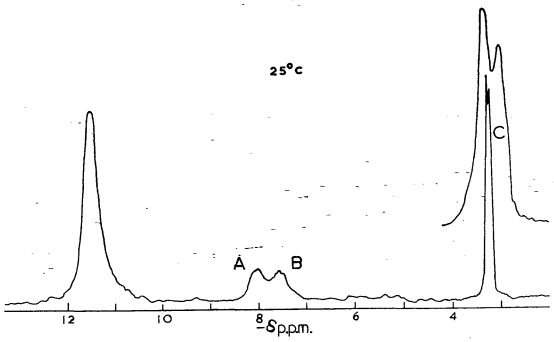

FIG. 3. *N*-Methylthiourea in trifluoracetic acid.

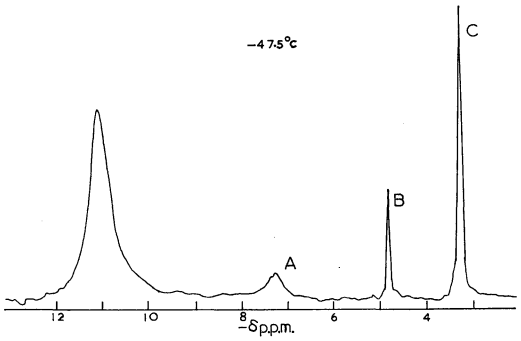

FIG. 4. *N*-Methylthiourea in fluorosulphuric acid.

Can. J. Chem. Downloaded from www.nrcresearchpress.com by 210.87.254.105 on 09/05/12
For personal use only.

shows the spectrum of a fluorosulphuric acid solution at −47.5°. A C=SH^+ peak (B) has appeared, the NH peak has disappeared, and the N—CH_3 peak (C) has collapsed to a single line. The relative areas were found to be A:B:C = 1.81:0.95:3.00. It must be concluded that a second protonation occurs on the nitrogen of the $NH \cdot CH_3$ group but proton exchange between the $\overset{+}{N}H_2 \cdot CH_3$ group and the solvent is quite rapid even at −80°. By using a less basic SbF_5–HSO_3F mixture as solvent it was found possible to reduce the rate of this exchange sufficiently that at −67° a new peak was observed in the spectrum at −8.19 p.p.m. which can presumably be attributed to the two protons on the methylated nitrogen atom. The N—CH_3 peak was found to have a width of 15 c/s which must be at least partly due to slow proton exchange: in the absence of exchange this peak would be expected to be a triplet due to coupling with the $\overset{+}{N}H_2$ protons. At low temperatures these solutions became very viscous and this is also partly responsible for the broadness of the signals.

Our conclusion that protonation of thiourea and its *N*-methyl derivative occurs first on sulphur is in agreement with ultraviolet and infrared spectroscopic studies (6, 7) and wide line n.m.r. (9) studies on thiourea salts. It appears that a second protonation occurs on the nitrogen atom in very strong acid solution.

Urea and N,N′-Dimethylurea

In dilute aqueous solution the spectrum or urea consists of an NH_2 peak. In sulphuric and fluorosulphuric acids this peak disappears and no peak was observed for urea in fluorosulphuric acid even at −86° or in fluorosulphuric acid containing 10% SbF_5 at −88°. However, in both these latter cases the solvent peak was quite broad, indicating that proton exchange is fairly slow but not slow enough for a separate peak from the conjugate acid of urea to be observed.

We observed only a single peak due to the N—CH_3 group in the spectrum of a 6 mole% solution of *N,N*-dimethylurea in water. Thus it appears that in this case the NH protons exchange with the solvent even in dilute aqueous solution. Redpath and Smith (9) however, observed both an NH peak (width = 23 c/s) and a doublet due to the $N \cdot CH_3$ group (J = 4.3 c/s) in a 0.6 weight fraction of the *N,N′*-dimethylurea in water. This doublet collapses in sulphuric acid solution. Although, as in the case of urea, the solvent peak became very broad at low temperatures, it was not possible to slow down exchange sufficiently even at −88° in HSO_3F containing 10% SbF_5 to observe peaks due to NH_2^+ or C=OH^+. Unfortunately our present results do not enable us to draw any definite conclusions concerning the site of protonation in urea and *N,N*-dimethylurea. In simple amides by decreasing the basicity of the solvent the rate of proton exchange with the solvent can be decreased sufficiently that a separate n.m.r. signal from the conjugate acid can be observed. However, in the case of urea and its derivatives decreasing the basicity (and therefore increasing the acidity) of the solvent probably leads to a second protonation of the amide and the diprotonated species exchanges more rapidly with the solvent than the conjugate acids of simple amides. Evidence for the diprotonation of tetraethylurea has been obtained from freezing-point measurements in 100% sulphuric acid (14). Evidence that the site of the first protonation is on the oxygen atom is given by the results of an X-ray diffraction study (15) of the crystal structure of *N*-methylurea nitrate in which a short hydrogen bond was found between the carbonyl oxygen and an oxygen of the nitrate ion. Redpath and Smith (9) have also obtained evidence from the line widths in the n.m.r. spectra of various crystalline urea salts that the conjugate acid of urea has a proton on the carbonyl oxygen. The infrared and ultraviolet spectra of urea

Can. J. Chem. Downloaded from www.nrcresearchpress.com by 210.87.254.105 on 09/05/12
For personal use only.

hydrochloride have also been interpreted (7) on the basis of protonation on the carbonyl oxygen.

Sulphonamides

Our results are summarized in Table IV. The conjugate acids of these bases undergo

TABLE IV

Chemical shifts of sulphamide and some sulphonamides in fluorosulphuric acid

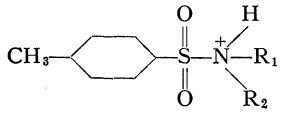

Sulphonamide	Temperature (°C)	−δ (p.p.m.) from external T.M.S. Phenyl	N—H	N—CH_3	C—CH_3	J (c/s)
N-Methyl-*p*-toluenesulphonamide	25	8.06	~7.79	3.30	2.77	
	−5		~7.79	3.29	2.74	J_{H,CH_3} 5.4
	−70		~7.79	3.26	2.68	
N,*N*-Dimethyl-*p*-toluenesulphonamide	25	8.06	~7.56	3.32	2.76	J_{H,CH_3} 5.2
	−50	8.04	~7.56	3.29	2.74	
			NH_3^+	NH_2		
Sulphamide	25		8.21	7.68		

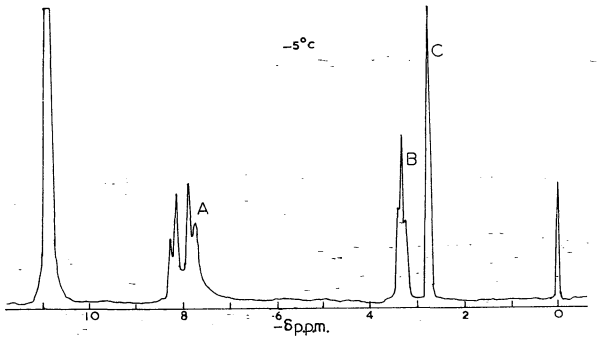

FIG. 5. *N*-Methyl-*p*-toluenesulphonamide in fluorosulphuric acid.

extremely slow proton exchange with the solvent even at room temperature. Figure 5 shows the spectrum of *N*-methyl-*p*-toluenesulphonamide in fluorosulphuric acid at −5°: A is assigned to the C_6H_4 and $\overset{+}{N}H_2$ protons, B to the N—CH_3 group, and C to the *p*-CH_3 group. This assignment is confirmed by the relative areas of the peaks, which were found to be A:B:C = 6.13:3.05:3.00, and the fact that B is a poorly resolved triplet due to spin–spin coupling with the NH_2 protons. Figure 6 shows the spectrum of *N*,*N*-dimethyl-*p*-toluenesulphonamide in fluorosulphuric acid at 25°. A is assigned to the C_6H_4 and $\overset{+}{N}H$ protons, B to the N—CH_3 group, and C to the *p*-CH_3 group. This assignment is confirmed by the relative areas of the peaks, which were found to be A:B:C = 4.87:6.30:3.00, and the fact that B is a doublet due to spin–spin coupling with the $\overset{+}{N}H$ proton. It is clear that in both these cases protonation is on nitrogen.

Sulphamide

A solution of sulphamide in fluorosulphuric acid at 25° gave the spectrum shown in

Can. J. Chem. Downloaded from www.nrcresearchpress.com by 210.87.254.105 on 09/05/12
For personal use only.

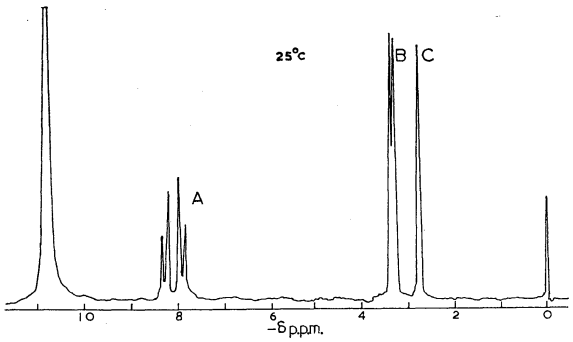

FIG. 6. *N,N*-Dimethyl-*p*-toluenesulphonamide in fluorosulphuric acid.

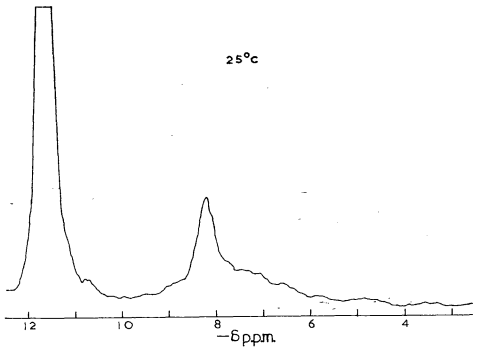

FIG. 7. Sulphamide in fluorosulphuric acid.

Fig. 7, consisting of a moderately broad peak superimposed on a very broad peak. The former is assigned to the NH_3^+ group and the latter to the NH_2 group in the conjugate acid of sulphamide $O_2S(NH_2)(NH_3^+)$. No peaks other than the solvent peak were visible in the spectrum of a sulphuric acid solution at room temperature presumably because of relatively rapid proton exchange between the conjugate acid of sulphamide and the solvent.

EXPERIMENTAL

The solutes were all commercial samples except for the *p*-toluenesulphonamides, which were prepared from *p*-toluenesulphonyl chloride and the corresponding amine. All the solids were recrystallized before use. Other experimental details have been described in Part I (1).

ACKNOWLEDGMENTS

We thank the Petroleum Research Fund of the American Chemical Society for generous financial assistance and Dow Chemical of Canada, Limited, for a Postgraduate Fellowship (to T. B.).

REFERENCES

1. T. BIRCHALL and R. J. GILLESPIE. Can. J. Chem. **41**, 148 (1963).
2. G. FRAENKEL and C. NIEMANN. Proc. Natl. Acad. Sci. U.S. **44**, 688 (1958).
3. A. BERGER, A. LOEWENSTEIN, and S. MEIBOOM. J. Am. Chem. Soc. **81**, 62 (1959).
4. C. A. BUNTON, B. N. FIGGIS, and B. NAYAK. Private communication.
5. R. A. Y. JONES and A. R. KATRITZKY. Chem. Ind. (London), 722 (1961).
6. M. J. JANSSEN. Spectrochim. Acta, **17**, 475 (1961).
7. W. KUTZELNIGG and R. MECKE. Spectrochim. Acta, **17**, 530 (1961).

Can. J. Chem. Downloaded from www.nrcresearchpress.com by 210.87.254.105 on 09/05/12
For personal use only.

8. J. SANDSTROM. Acta Chem. Scand. **16**, 1616 (1962).
9. C. R. REDPATH and J. A. S. SMITH. Trans. Faraday Soc. **58**, 462 (1962).
10. E. SPINNER. Spectrochim. Acta, **15**, 95 (1959).
11. H. HOSAGA, J. TANAKA, and S. NAGAKURA. Bull. Chem. Soc. Japan, **33**, 850 (1960).
12. L. H. MEYER, A. SAIKA, and H. S. GUTOWSKY. J. Am. Chem. Soc. **75**, 4567 (1953).
13. VARIAN HIGH RESOLUTION N.M.R. SPECTRA CATALOGUE. Varian Assoc., Palo Alto, Calif., U.S.A.
14. A. HANTZSCH. Ber. **63B**, 1782 (1930).
15. J. H. BRYDEN. Acta Cryst. **10**, 714 (1957).

Can. J. Chem. Downloaded from www.nrcresearchpress.com by 210.87.254.105 on 09/05/12
For personal use only.

THE INCORPORATION OF PUTRESCINE INTO HYOSCYAMINE[1]

J. KACZKOWSKI[2] AND LÉO MARION
Division of Pure Chemistry, National Research Council, Ottawa, Canada
Received July 3, 1963

ABSTRACT

Putrescine-1,4-^{14}C was fed to the excised root cultures of *Datura metel* L., and the alkaloids subsequently isolated. These consisted of hyoscyamine, hyoscine, and a base of undetermined constitution designated as alkaloid X. All three bases were radioactive. Degradation of the hyoscyamine revealed that ca. 8% of the radioactivity was present in the tropic acid moiety, but that all the radioactivity of the tropine moiety was located in the pyrrolidine ring. The implications of these results are discussed.

INTRODUCTION

Earlier attempts to ascertain whether putrescine was a precursor of hyoscyamine failed (1) although it has been established that ornithine is the precursor of the pyrrolidine ring of that alkaloid in *Datura stramonium* L. (2). Since preliminary experiments carried out by one of us (J. K.) seemed, however, to indicate that root cultures of *Datura metel* L. when fed unlabelled putrescine produced a slightly higher yield of alkaloid, it was decided to repeat the experiments with labelled putrescine.

MATERIALS AND METHODS

Since the biosynthesis of tropane alkaloids is known to take place mostly if not exclusively in the roots (3), isolated root cultures of *D. metel* L. grown in a nutrient as described by Robbins and Bartley Schmidt (4) were used in all the experiments. The cultures were developed from one seed as previously described by Kaczkowski *et al.* (5).

The nutrient solution in which the roots had grown was removed after 30 days and replaced by fresh nutrient solution containing putrescine-1,4-^{14}C, purchased from New England Nuclear Corporation. The times of incubation in contact with the radioactive putrescine in different experiments were 2, 4, 6, and 4 days respectively.

After the incubation period the roots were removed from the nutrient solution, washed thoroughly with water, and dried at 60°. The dried roots, mixed with sodium carbonate, were ground and extracted with chloroform for 12 hours in a Soxhlet apparatus. The crude extract was purified, and an aliquot was chromatographed on paper. The alkaloids which separated on the chromatogram were determined by a nephelometric micromethod, all as previously described by Kaczkowski and Reifer (6). Three alkaloids were thus detected, i.e., hyoscyamine, hyoscine, and an unidentified third base which has been reported previously (7) and will be designated alkaloid X. The radioactivity of the alkaloids eluted from the paper strips was measured with a Baird Atomic end-window gas flow counter against a blank prepared by elution of a paper strip cut from a space on the chromatogram between alkaloid spots.

The bulk of the radioactive alkaloids was separated by thin-layer chromatography on silica gel G (Merck) using a mixture of chloroform, cyclohexane, diethylamine, and acetone in the ratio 5:3:1:1. The hyoscyamine eluted from the silica gel was diluted with inactive hyoscyamine to 600 mg and degraded by hydrolysis and then oxidation with chromic acid as previously described (2). The very small quantity of radioactive hyoscyamine obtained did not permit a higher dilution and consequently the degradation could not be taken further than the formation of N-methylsuccinimide. The diluted hyoscyamine, as well as the products of its degradation were, before counting, ignited to carbon dioxide which was collected as barium carbonate. In each case the radioactivity was determined with an efficiency of ca. 20% and an average background of 10 c.p.m.

RESULTS AND DISCUSSION

Four different experiments were carried out with four different lots of roots, each being fed a different concentration of labelled putrescine and each being allowed a different incubation period. The data concerning these experiments are given in Table I.

[1]*Issued as N.R.C. No. 7553.*
[2]*The University of Agriculture, Warsaw, Poland.*

Can. J. Chem. Downloaded from www.nrcresearchpress.com by 210.87.254.105 on 09/05/12
For personal use only.

TABLE I

Expt. No.	Wt. of roots (mg)	Time of incubation (days)	Amt. of putrescine (mg)	Sp. activity of putrescine (d.p.m./mmole)	Amt. of alkaloid (μg)		
					Hyoscyamine	Hyoscine	Alkaloid X
I	84	2	2.64	4.84×10^8	74	295	267
II	132	4	3.79	9.42×10^8	148	261	213
III	232	6	4.92	7.76×10^8	119	253	269
IV	186	4	5.28	1.32×10^9	129	223	133

TABLE II

Expt. No.	Specific activities of alkaloids (d.p.m./mmole$\times10^6$)		
	Hyoscyamine	Hyoscine	Alkaloid X
I	16.6	1.18	10.4
II	19.0	4.90	18.8
	20.6	3.42	19.5
Ave.	19.8	4.16	19.2
III	40.0	6.90	21.2
	39.2	5.78	22.9
Ave.	39.6	6.34	22.0
IV	95.0	23.7	91.3
	96.5	24.0	93.0
Ave.	95.7	23.9	92.2

Table II contains the specific radioactivities of the isolated alkaloids. In all cases, the activity of the blank was only 1–2 c.p.m. In the first experiment this figure represents but 2% of the activity of hyoscine and a much smaller proportion of the activity of the other two alkaloids. Hence it has not been taken into account in the calculations concerning the remaining experiments.

The results given in Table II show that putrescine-1,4-^{14}C was incorporated into the alkaloids.[3] The extent of incorporation was highest in hyoscyamine and lowest in hyoscine while it was intermediate in base X. This could indicate that the last base, of unknown constitution, might be an intermediate product in the transformation of hyoscyamine into hyoscine, rather than the direct precursor of hyoscyamine as previously suggested (7). In the mature *D. stramonium*, however, it has been shown that when hyoscyamine is being synthesized, hyoscine no longer is being formed (2, 8). Hence either the biosynthesis of the alkaloids in *D. metel* under the conditions used follows a different pattern than in *D. stramonium* or, in the latter, the synthesis of hyoscine gradually decreases as that of hyoscyamine increases so that at maturity the synthesis of hyoscine no longer takes place, although it still does in the isolated root system of *D. metel.*

The values of the specific activities of the alkaloids isolated in the four experiments do not vary regularly with regard to concentration or incubation time, and this irregularity may be attributable to the sensitivity of the root cultures towards small changes in experimental conditions, as well as to the different ages of the subcultures of roots used in each experiment.

The specific activities of hyoscyamine and its degradation products listed in Table III indicate that the incorporation of labelled putrescine is largely specific. Almost all the activity was present in the tropine moiety of hyoscyamine. Furthermore, all the specific

[3]*In a footnote in a recent review of the biosynthesis of alkaloids (K. Mothes and H. R. Schütte. Angew. Chem.* **75,** *268 (1963)), Professor Mothes states that he has found that putrescine-1,4-*^{14}C *is incorporated into hyoscyamine in D. metel.*

Can. J. Chem. Downloaded from www.nrcresearchpress.com by 210.87.254.105 on 09/05/12
For personal use only.

TABLE III

Compound	Amt. (mg)	Specific activity (d.p.m./mmole×10⁴)		M.p. (°C)
Hyoscyamine	600	1.34		
Tropine	245	1.20	51	63 (lit.)
Picrate			293	290–295 (lit.)
Tropic acid	260	0.11	115	117 (lit.)
N-Methylsuccinimide	21	1.22	65	66 (lit.)

activity of the tropine was present in the N-methylsuccinimide derived from it. Although paucity of material did not permit further degradation it is most probable that the label was located at positions 1 and 5 of the tropane skeleton.

About 8% of the total activity of hyoscyamine was located on the tropic acid moiety. This is explainable only by the breakdown of some of the putrescine to simpler products before incorporation into the alkaloids.

The results obtained do not agree with those of Diaper, Kirkwood, and Marion (1), who fed putrescine-1,4-^{14}C (by hydroponic solution) to 7-, 8-, and 9-month-old *D. stramonium* plants kept in the darkness, and found very little radioactivity in the isolated hyoscyamine. There is reason to believe, however, that this finding may not be reliable.[4] On the other hand, ornithine-2-^{14}C fed to mature *D. stramonium* plants is incorporated into hyoscyamine (2) and all of the activity is located on one only of the bridgehead carbons (9). Hence the biosynthetic pathway cannot involve an intermediate which is symmetrical. Putrescine, therefore, does not appear to represent an intermediate step in the incorporation of ornithine-2-^{14}C into the pyrrolidine ring of hyoscyamine since symmetrical putrescine-1-^{14}C (i.e., the product of the decarboxylation of ornithine-2-^{14}C) should produce labelling at both bridgeheads.

It appears probable, then, that although putrescine when fed to the plant can be a precursor of hyoscyamine, it does not represent an intermediate step in the normal incorporation of ornithine into the alkaloid.

REFERENCES

1. D. G. M. Diaper, S. Kirkwood, and L. Marion. Can. J. Chem. **29**, 964 (1951).
2. E. Leete, L. Marion, and I. D. Spenser. Can. J. Chem. **32**, 1116 (1954).
3. S. M. Peacock, Jr., D. B. Leyerle, and R. F. Dawson. Am. J. Botany, **31**, 463 (1944).
4. W. J. Robbins and M. Bartley Schmidt. Botan. Gaz. **99**, 671 (1938).
5. J. Kaczkowski, H. R. Schütte, and K. Mothes. Biochim. Biophys. Acta, **46**, 588 (1961).
6. J. Kaczkowski and I. Reifer. Bull. Acad. Polon. Sci. Ser. Sci. Biol. **9**, 247 (1961).
7. J. Andrzejczuk and J. Kaczkowski. Acta Soc. Botan. Polon. **31**, 461 (1962).
8. L. Marion and A. F. Thomas. Can. J. Chem. **33**, 1853 (1955).
9. E. Leete. J. Am. Chem. Soc. **84**, 55 (1962).

[4]*Dr. E. Leete (private communication) has been able to show by using the wick feeding method that putrescine is indeed incorporated into hyoscyamine in D. stramonium.*

Can. J. Chem. Downloaded from www.nrcresearchpress.com by 210.87.254.105 on 09/05/12
For personal use only.

Can. J. Chem. Downloaded from www.nrcresearchpress.com by 210.87.254.42 on 09/05/12
For personal use only.

LYCOPODIUM ALKALOIDS

XIII. MASS SPECTRA OF REPRESENTATIVE ALKALOIDS[1]

D. B. MacLean
Department of Chemistry, McMaster University, Hamilton, Ontario
Received April 29, 1963

ABSTRACT

The mass spectra of a number of *Lycopodium* alkaloids are recorded and schemes proposed for their fragmentation. The loss of the bridge dominates the fragmentation process in the structural types examined.

The *Lycopodium* alkaloids have been the subject of many studies in the past few years, but there are still many alkaloids of unknown constitution. Those alkaloids whose structures have been elucidated are, for the most part, the most abundant while those whose structure still await solution have been found in smaller quantity. The mass spectrometric method, which has been used in many recent investigations, is particularly well suited to structural studies on substances available in small amount.[2] It was of interest, therefore, to record the spectra of the *Lycopodium* alkaloids of known structure and to study their fragmentation in order that the information so obtained might be applied to the study of those alkaloids whose structures are yet unresolved and to those alkaloids yet to be isolated.

The *Lycopodium* alkaloids which are now known may be conveniently classified for the purposes of this discussion into four groups: those related in skeletal structure to lycopodine (2), by far the largest group; those related in skeletal structure to lycodine (3, 4),

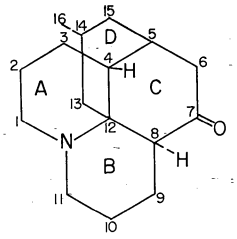

Lycopodine

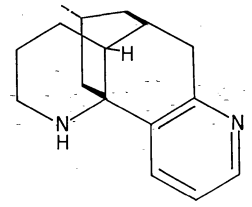

Lycodine

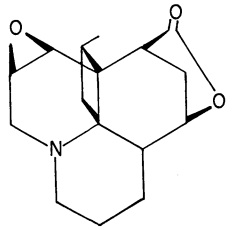

Annotinine

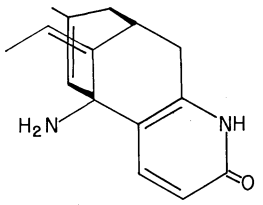

Selagine

[1]*This work was carried out in the laboratories of Professor K. Biemann, where the author spent the academic year 1962–1963 as a guest of the Department of Chemistry, Massachusetts Institute of Technology.*

Financial support of this work from a grant to Professor Biemann from the Petroleum Research Fund of the American Chemical Society is gratefully acknowledged.

[2]*The reader is referred to the recent book by Biemann (1) for a review of the application of the mass spectrometric method to structural problems.*

the next most abundant group; annotinine (5, 6); and selagine (7, 8). At the time of writing, annotinine and selagine are the sole reported representatives of their groups. The alkaloids whose spectra are discussed in this paper are mostly from the lycopodine group and comprise, besides lycopodine and simple derivatives of it, some alkaloids carrying substituents on the bridge and others with substituents on ring C. From an examination of the spectra of these alkaloids it has been possible to formulate a fragmentation mechanism which applies to the lycopodine group and which, with minor modifications, may be applied to the other groups.

The spectra of lycopodine, dihydrolycopodine (2, 9), anhydrodihydrolycopodine (2, 9), and acetyldihydrolycopodine (2, 9) are shown in Fig. 1. A common feature of all these

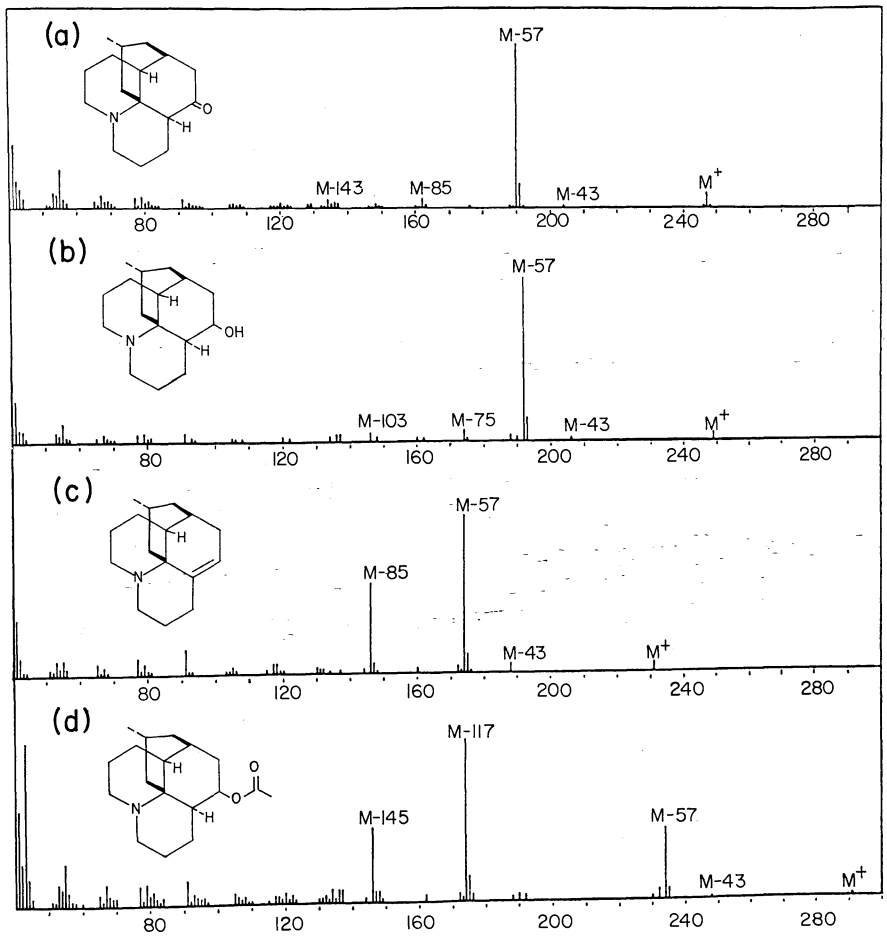

FIG. 1. Mass spectra of lycopodine and simple derivatives of it: (*a*) lycopodine, (*b*) dihydrolycopodine, (*c*) anhydrodihydrolycopodine, (*d*) acetyldihydrolycopodine. Peaks with an intensity $\geqslant$ 2% of the most intense peaks are shown in this and subsequent spectra.

spectra is the presence of a peak at M-57, which corresponds to loss of the bridge plus a hydrogen atom. With the exception of the acetyldihydrolycopodine spectrum, this peak is the strongest in the spectrum. In addition, a peak is found in all the spectra at M-43, the origin of which is adumbrated from the labeling experiments and will be discussed in a

Can. J. Chem. Downloaded from www.nrcresearchpress.com by 210.87.254.42 on 09/05/12
For personal use only.

later section. It will be noted with the exception of lycopodine the spectra all show a peak at *m/e* 146. A fragmentation scheme, compatible with these findings, is shown in Scheme I for dihydrolycopodine.[3] The neutral fragment eliminated in the transformation

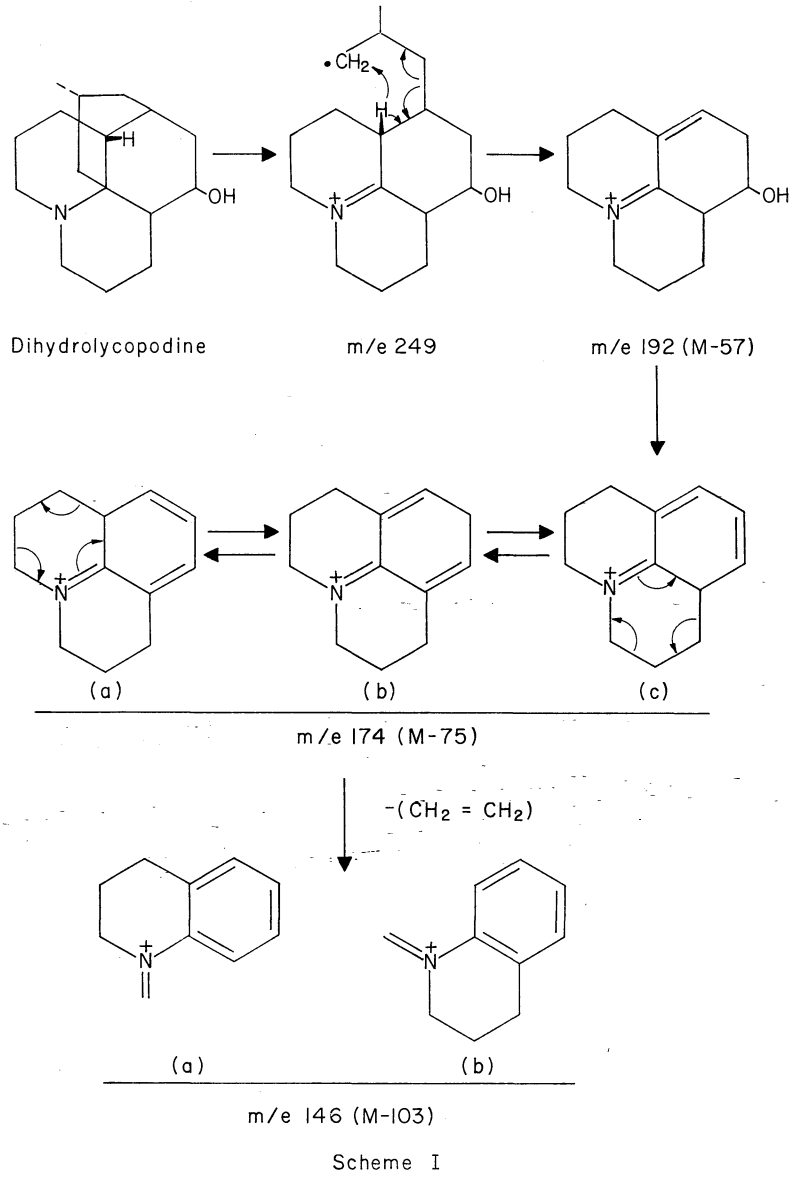

Scheme I

m/e 249 to *m/e* 192 is postulated to be $(CH_3)_2CHCH_2$. In the case of acetyldihydrolycopodine, a molecule of acetic acid rather than one of water is lost, and in anhydrodihydrolycopodine the double bond is already present in the 7,8-position. In the ion of *m/e* 174 it is unlikely that the double bonds are fixed, but instead may assume any of the positions shown in formulas *a*, *b*, and *c*. Thus, a fluid rather than static situation

[3]*For a general discussion of the fragmentation of organic molecules upon electron impact, the reader is referred to ref. 1, Chapter 3.*

Can. J. Chem. Downloaded from www.nrcresearchpress.com by 210.87.254.42 on 09/05/12
For personal use only.

with respect to the unsaturation is considered to pertain. The loss of ethylene to yield the ions of *m/e* 146 may proceed as shown by the arrows. Ions *a* and *b* of mass 146 are identical as written but a distinction would arise if ring A or B carried a label.

Lycopodine, which cannot form the double bond at the 7,8-position, shows peaks at *m/e* 190, 162, and 134, corresponding to the loss of 57, 85, and 113 mass units, respectively. The consecutive losses of 28 mass units are very likely associated with the loss of carbon monoxide and of ethylene, but the order in which they are lost cannot be ascertained by this method although the question could be resolved by a high-resolution spectrum.

In Table I the observed positions of the metastable peaks[4] associated with the loss of

TABLE I

Metastable peaks in the spectra of lycopodine and its derivatives

	m^*_{obs}	m^*_{calc}	
Lycopodine	147.0	247 → 191	147.7
		247 → 190	146.2
Dihydrolycopodine	148.5	249 → 193	149.6
		249 → 192	148.0
Acetyldihydrolycopodine	189.5	291 → 235	189.8
		291 → 234	188.2
Anhydrodihydrolycopodine	131.5	231 → 175	132.6
		231 → 174	131.1
Lycopodine-d_3	150.0	250 → 194	150.5
		250 → 193	149.0

the bridge are recorded along with the values calculated for a loss of 56 and 57 mass units from the molecular ions. In all cases, including that of lycopodine-d_3, the position of the metastable peak is in agreement with the loss of 57 rather than of 56 mass units, and a concerted rather than a stepwise process apparently pertains. A stepwise process in which the molecular ion first loses hydrogen and then isobutylene cannot be ruled out with the data available. It seems less likely, however, because of the low intensity of the ions at M-1 in the five examples discussed.

In Scheme I the hydrogen lost with the bridge is postulated to come from C_4. No direct evidence is at hand to support this postulate, but its origin from C_6, the other likely position for its abstraction, is precluded by a labeling experiment with lycopodine. The spectrum of lycopodine-d_3, in which the C_6- and C_8-hydrogens have been exchanged for deuterium, was examined. It was found that the major peak in the spectrum fell at *m/e* 193, corresponding to loss of 57 mass units from the molecular ion at *m/e* 250. The more intense peak at *m/e* 192 in the deuterated compound, relative to the peak at *m/e* 189 in the undeuterated lycopodine, arises from some lycopodine-d_2 present in the sample. Calculation shows that no more than 5% of the peak at *m/e* 192 can be ascribed to loss of 58 mass units from the molecular ion. Table II records the relative intensities of the peaks in the region of M-57 and of the molecular ion in the spectra of deuterated and undeuterated lycopodine.

In the spectra of dihydrolycopodine and acetyldihydrolycopodine metastable peaks are

[4]*Metastable peaks are observed in a spectrum when ions of mass m_1 decompose in the accelerating region near the exit slit to ions of mass m_2. The approximate value of m/e, m*, at which such ions are recorded in the spectrum may be calculated by applying the relation $m^* = (m_2)^2/m_1$ (10). In practice, in the type of instrument used in this study, the observed values are higher, but usually by not more than one mass unit, than those calculated by the relation above. The metastable peaks are observed as broad peaks of low intensity and it is the intensity maximum which is reported. The presence of a metastable peak is evidence that the transformation m_1 to m_2 is a concerted rather than a stepwise process. In the text following, the symbolism $m_1 \rightarrow m_2$ will be used to denote such a transformation.*

Can. J. Chem. Downloaded from www.nrcresearchpress.com by 210.87.254.42 on 09/05/12
For personal use only.

TABLE II

Relative intensity vs. *m/e* of deuterated and natural lycopodine

	Intensity			Intensity	
m/e	Lycopodine	Deuterated lycopodine	*m/e*	Lycopodine	Deuterated lycopodine
251	—	2.0	194	—	14.0
250	—	10.5	193	—	100.0
249	—	2.3	192	1.0	12.0
248	1.8	0.3	191	15.0	1.4
247	9.0	—	190	100.0	0.4
246	1.8	—	189	0.8	—
195	—	2.0			

present corresponding to the loss of water and of acetic acid, respectively, from the fragment ions. Thus, in dihydrolycopodine a metastable peak is found at *m/e* 159.5 (*m** calc. (192 → 174) = 157.7), and in acetyldihydrolycopodine at *m/e* 131 (*m** calc. (234 → 174) = 129.4). A strong metastable peak is present in each of spectra 1*b*, 1*c*, and 1*d* at *m/e* 124. The loss of 28 mass units from the ion 174 is common to all these spectra, but the calculated position for a metastable peak corresponding to this change is 122.5. The observed value is higher than expected, but there is no other fragmentation process which can give rise to this strong metastable peak.

Three alkaloids–lofoline (11, 12), clavolonine (12, 13), and annofoline (14, 15)—each bearing a substituent on the bridge as well as at position 7, are now examined. The spectra of the three alkaloids, shown in Fig. 2, may be interpreted along the same lines as those outlined in Scheme I. In clavolonine (Fig. 2) the major peak occurs at M-73, corresponding to the loss of the bridge plus hydrogen. This is followed by loss of 28 mass units yielding a peak at *m/e* 162 (M-101) and a further loss of 28 mass units yielding a peak at *m/e* 134 (cf. Fig. 1*a*). The spectrum of lofoline, Fig. 2*b*, resembles that of acetyldihydrolycopodine (Fig. 1*d*), from, which it differs by virtue of the presence of a hydroxyl group on the bridge. Major peaks occur in the spectrum at *m/e* 234 (M-73), 174 (M-133), and 146 (M-161), corresponding, respectively, to the loss of the bridge plus hydrogen, followed by loss of acetic acid and of ethylene.

The fragmentation of annofoline (Fig. 2*c*) follows the same pattern, with peaks appearing at M-71, M-89, and M-117, corresponding respectively to the loss of the bridge plus hydrogen, followed by loss of water and of ethylene. The annofoline spectrum, however, has additional features commented upon later.

The most significant feature of the three spectra of Fig. 2 is the fact that the substituents on the bridge do not alter appreciably the fragmentation pattern exhibited by lycopodine and its derivatives. Both the presence and the nature of the substituents on the bridge are immediately evident from an examination of the spectra. In the investigation of new alkaloids, it will be of great advantage to obtain such information readily and with very little material.

Returning now to the annofoline spectrum, it is observed that the peak at *m/e* 193 (M-70) is somewhat stronger than expected of a normal isotope peak. The fragment ion contributing to this peak may arise by loss of methylcyclopropanone from the molecular ion to give the ion–radical shown below. Alternatively, the bridge might be lost as carbon monoxide and propylene. The ion–radical (M-70) may lose a hydroxyl radical with hydrogen migration to give the ion observed at *m/e* 176 (M-87). Perhaps the most striking

Can. J. Chem. Downloaded from www.nrcresearchpress.com by 210.87.254.42 on 09/05/12
For personal use only.

Can. J. Chem. Downloaded from www.nrcresearchpress.com by 210.87.254.42 on 09/05/12
For personal use only.

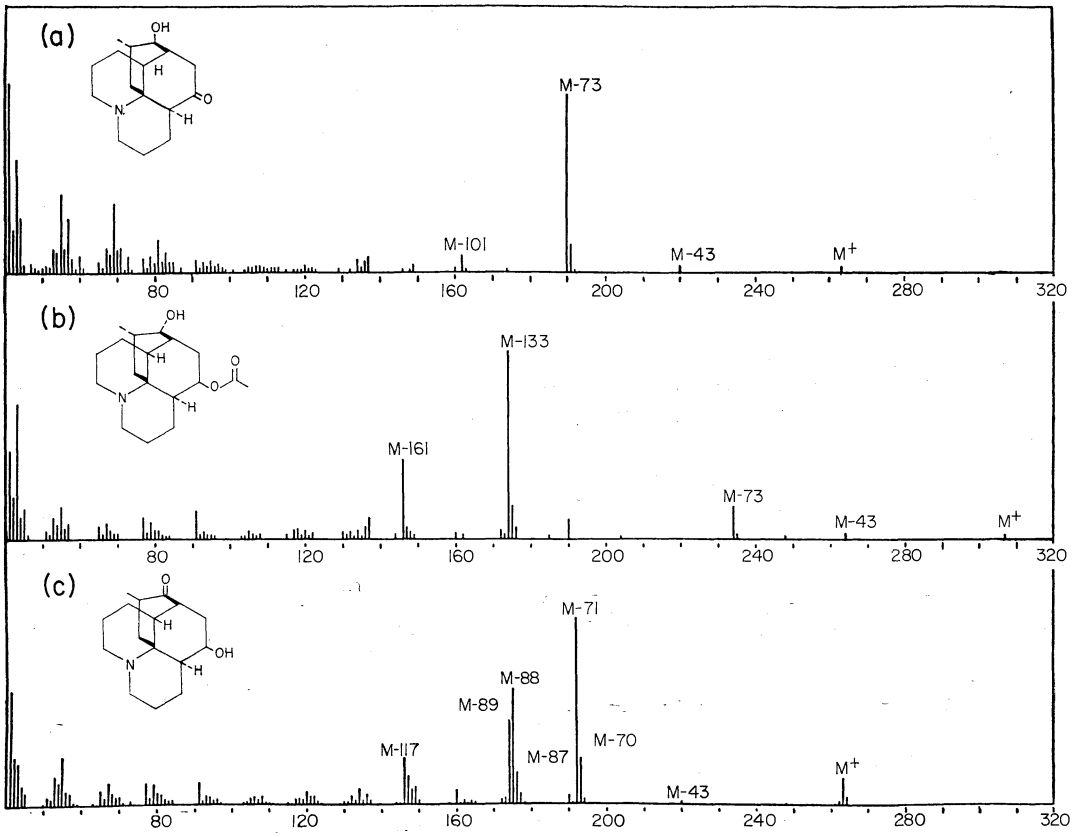

FIG. 2. Mass spectra of alkaloids of the lycopodine group with a substituent on the bridge: (*a*) clavolonine, (*b*) lofoline, (*c*) annofoline.

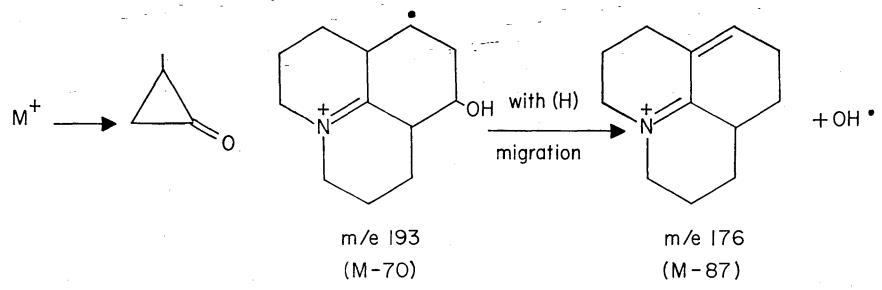

feature in the spectrum of annofoline is the enhanced intensity of the peak at *m/e* 175 (M-88) relative to that at *m/e* 174 (M-89). The ion of *m/e* 174 must arise, at least partly, by loss of water from the ion of *m/e* 192. It is conceivable that the ion of *m/e* 175 arises by loss of OH from the ion of *m/e* 192 although this pattern is not observed in the fragmentation of dihydrolycopodine. It seems more likely that it forms directly from the molecular ion. Annofoline is known to exist as an equilibrium mixture of hemiketal and hydroxy ketone (14, 15), and a mechanism for formation of the fragment M-88 from the hemiketal form is postulated below:

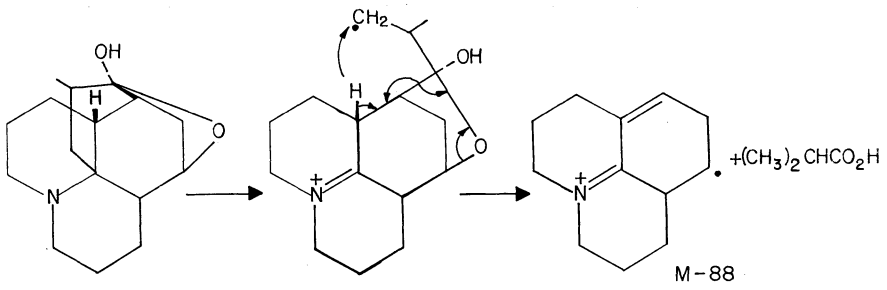

A metastable peak at m/e 117.0 (m^* calc. (263 → 175) = 116.4) is in accord with this postulate. The conversion of 175 → 174 by loss of hydrogen is also supported by a metastable peak at m/e 173.5. Besides the metastable peaks noted above, others are observed at m/e 141 and 124, corresponding, respectively, to the transformations 263 → 192 and 174 → 146.

The spectrum of deuterated annofoline corroborates the findings above and yields information regarding the origin of the M-43 peak. Details of the exchange of annofoline and the recording of the spectrum of deuterated annofoline are found in the experimental section, but it should be pointed out here that the two hydrogens alpha to the carbonyl group differ greatly in behavior, as might be expected. The hydrogen at C_5 exchanges relatively slowly with deuterium but once introduced is stable. The hydrogen at C_{14} exchanges rapidly but surprisingly is lost to a large extent in the heated inlet system of the spectrometer. Only when the inlet system is given a prior treatment with CH_3OD is a satisfactory spectrum of the fully deuterated compound obtained, and even then the intensity of the peak at m/e 265 owing to the dideuterated species decreases rapidly, as Table III illustrates.

TABLE III

Deuterated annofoline; relative intensity vs. m/e at different times

	Intensity				Intensity		
m/e	$t = 0$	$t \approx 30$ min	$t \approx 60$ min	m/e	$t = 0$	$t \approx 30$ min	$t \approx 60$ min
266	8	6	3	191	3	6	10
265	15	14	12	178	8	10	9
264	10	17	16	177	24	26	26
263	3	4	5	176	100	100	100
195	16	14	12	175	68	75	77
194	78	67	60	174	12	16	17
193	95	114	115	173	3	6	8
192	15	17	17				

The major fragment peaks in the spectrum of deuterated annofoline appear at m/e 193, 176, 175, and 147, one mass unit higher than in the undeuterated species, and correspond to loss of 72, 89, 90, and 118 mass units from the molecular ion at m/e 265. Thus one deuterium atom is lost with the bridge and one is retained in the fragment ions. Metastable peaks corresponding to the changes 265 → 193, 265 → 176, and 175 → 147 are observed and lend support to the fragmentation mechanism already proposed. The M-43 peak appearing at m/e 220 in annofoline becomes an M-44 peak appearing at m/e 221 in the spectrum of dideuterated annofoline. One must infer that the bridge carbons are responsible for this peak in the annofoline spectrum and possibly are responsible for it or

Can. J. Chem. Downloaded from www.nrcresearchpress.com by 210.87.254.42 on 09/05/12
For personal use only.

contribute to it in the spectra of the other alkaloids of the lycopodine group where an M-43 peaks is invariably present.

We come now to two alkaloids which have a functional group instead of a hydrogen atom at C_4 and which might, therefore, be expected to differ in their fragmentation from those already examined if the postulated fragmentation be correct. The first of these to be discussed is the alkaloid lycodoline (16), which differs in structure from lycopodine by virtue of the presence of a hydroxyl group at C_4, but its stereochemistry is the same. The spectrum is shown in Fig. 3*a* and it is observed to undergo a more complex fragmentation than other alkaloids previously examined. The molecular ion peak is now the most intense peak while the peak at M-57 is less intense than several others in the spectrum. It is worthy of mention that the peak at M-56 has approximately 50% the intensity of M-57, a reflection of the lack of hydrogen at C_4. The M-17 and M-28 peaks most likely arise by loss of hydroxyl and carbon monoxide, respectively. An M-43 peak is present as in the other spectra examined, but in this case for the first time is more intense than the M-57 peak. The M-71 peak is probably due to loss of 28 mass units from the ion M-43 while that at M-73 may be attributed to loss of the bridge plus the hydroxyl group. Scheme II depicts a possible fragmentation mechanism for two of the fragment ions. The formation of the M-73 fragment is considered to proceed in a stepwise rather than a concerted manner, although the latter possibility cannot be excluded from the evidence at hand.

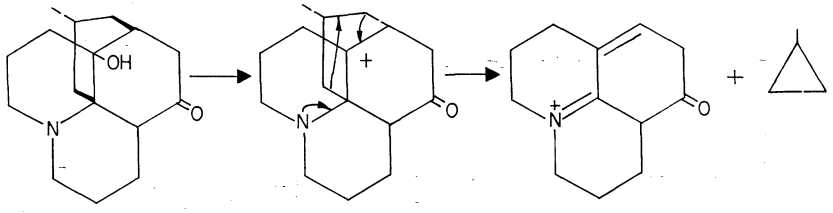

Scheme II

The overall result agrees with the proposition that the hydrogen removed with the bridge is normally derived from the C_4-position. When a hydrogen is absent at C_4, a hydrogen is lost from another position in the molecule, but the particular fragmentation proceeds much less readily.

Acrifoline (17), with a $\Delta^{3,4}$-double bond, is another example of a system lacking a hydrogen at C_4, and an examination of its spectrum, Fig. 3*b*, again shows a divergence from the normal fragmentation pattern. The spectrum exhibits two intense peaks at M-70 and M-87 and has peaks of lesser intensity at M-28, M-43, M-71, and M-89. The M-28 peak may be attributed to loss of carbon monoxide while the M-43 peak is characteristic of this group of alkaloids and may come from the bridged atoms, as previously noted. The M-71 and M-89 peaks are expected and the mechanism shown for their formation in Scheme III[5] needs no further elaboration. The greater intensity of M-70 (loss of bridge) than M-71 (loss of bridge + H) is unique among the spectra examined. (An M-70 peak is present in the spectrum of annofoline, but it is weak in comparison to the M-71 peak and in lycodoline the peak at M-56 is still only 50% as intense as that at M-57.) In acrifoline a hydrogen is not available at C_4 for a concerted elimination, and it is postulated that

[5]*The double bond in the ion distinguished by * may occupy a 5,6- or 6,7-position as indicated by the broken line.*

Can. J. Chem. Downloaded from www.nrcresearchpress.com by 210.87.254.42 on 09/05/12
For personal use only.

Can. J. Chem. Downloaded from www.nrcresearchpress.com by 210.87.254.42 on 09/05/12
For personal use only.

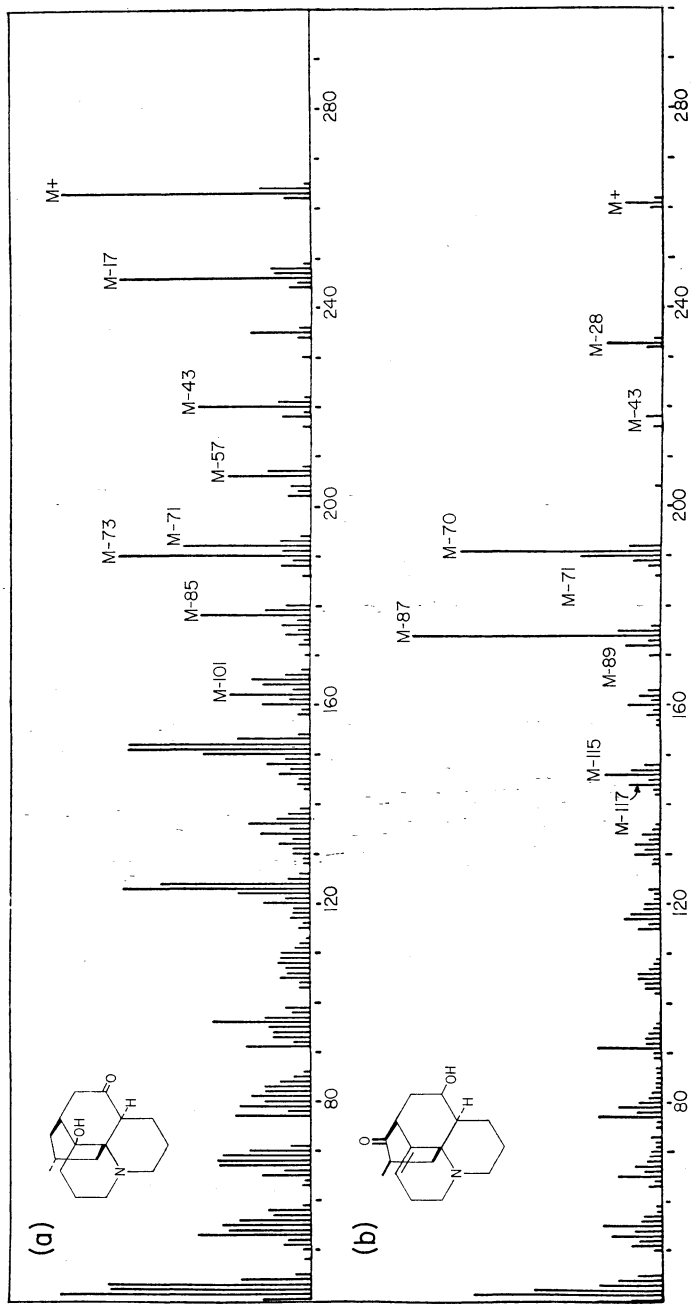

FIG. 3. Mass spectra of alkaloids of the lycopodine group with a functional group at C_4: (*a*) lycodoline, (*b*) acrifoline.

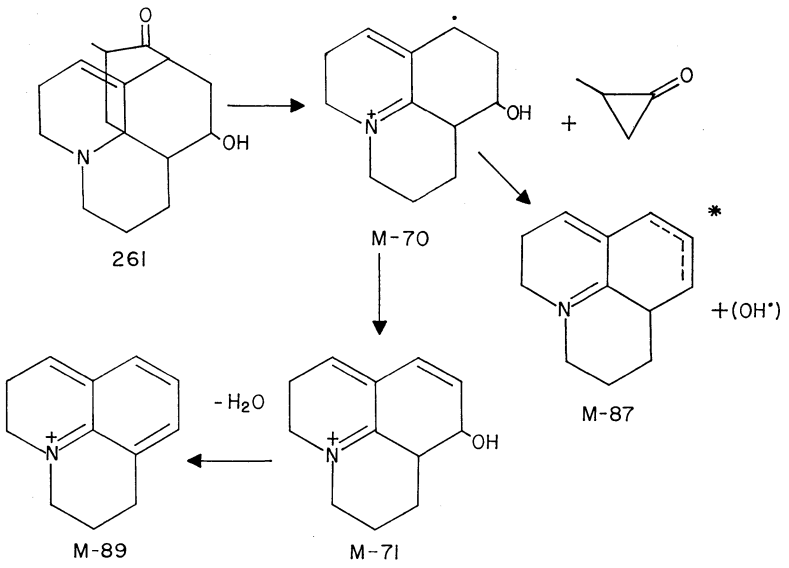

Scheme III

the bridge is lost as methylcyclopropanone or as carbon monoxide and propylene from the molecular ion to leave the stable conjugated ion–radical 191 (M-70). The peak at M-87, the most intense in the spectrum, may be due to an ion formed by loss of hydroxyl radical from the ion *m/e* 191, or alternately may form directly from the molecular ion. Acrifoline like annofoline is an equilibrium mixture of hydroxyketone and hemiketal isomers (17). A concerted elimination from the molecular ion involving the hemiketal form is shown below:[5]

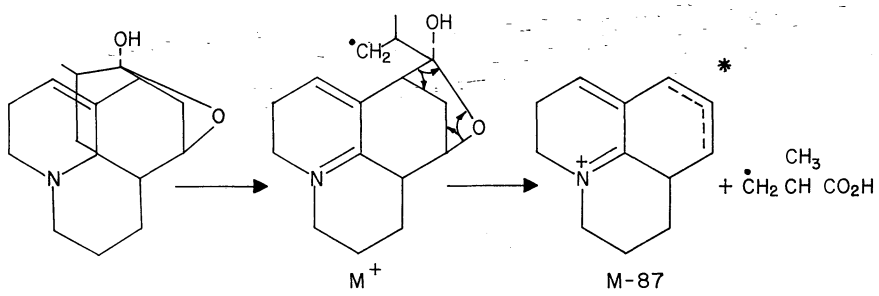

Metastable peaks at *m/e* 159.0 corresponding to the transformation 191 → 174 (m^*_{calc} = 158.5) and at 117.0 corresponding to the transformation 261 → 174 (m^*_{calc} = 116.0) imply that the ion of M-87 may form by both pathways.

The acrifoline spectrum demonstrates again that the absence of a hydrogen at C_4 results in a departure from the fragmentation pattern normally observed.

Two alkaloids, flabelliformine (18) and lycoclavine (19) with oxygen functions at C_7 and C_8 and at C_6 and C_7, respectively, will now be discussed. The spectrum of flabelliformine (Fig. 4*a*) follows the expected fragmentation with peaks at M-57, M-75, and M-103 as well as a weak M-43 peak. In addition to these peaks, there is a peak of high intensity at M-99 which is not observed in other spectra and which is, therefore, characteristic of this

Can. J. Chem. Downloaded from www.nrcresearchpress.com by 210.87.254.42 on 09/05/12
For personal use only.

Can. J. Chem. Downloaded from www.nrcresearchpress.com by 210.87.254.42 on 09/05/12
For personal use only.

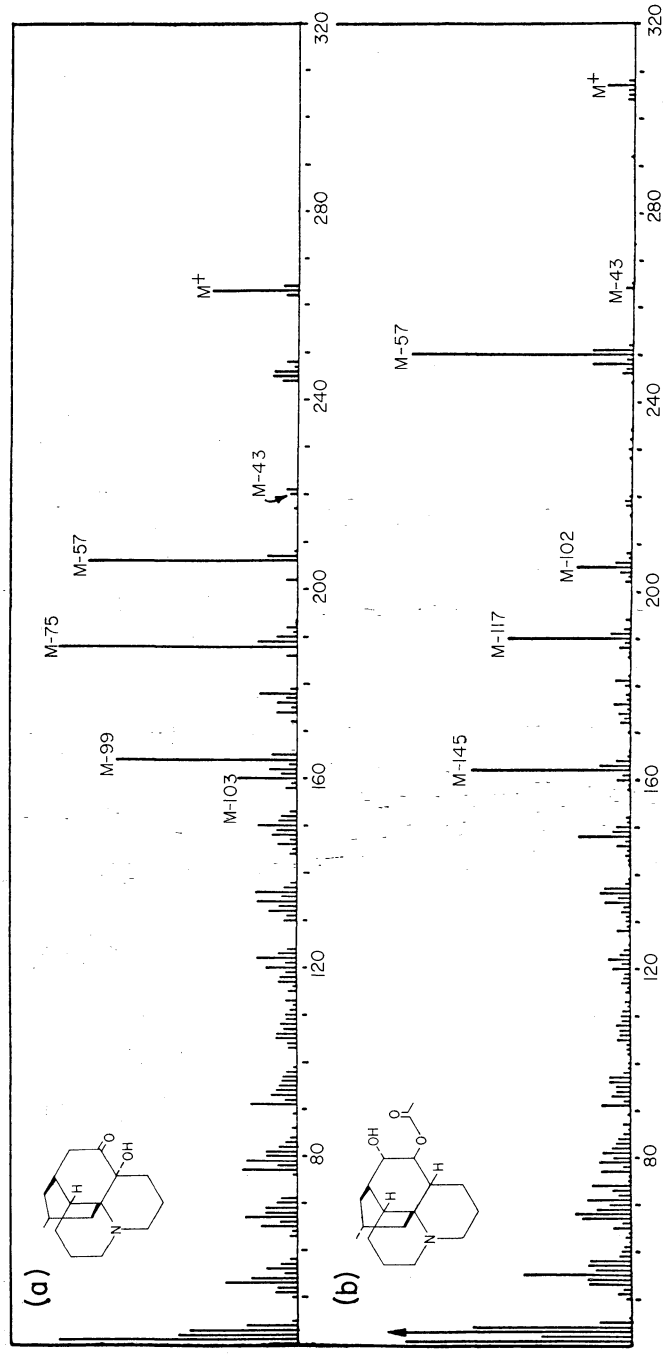

FIG. 4. Mass spectra of alkaloids of the lycopodine group with a substituent in ring C: (*a*) flabelliformine, (*b*) lycoclavine.

compound. A mechanism accounting for the formation of the ion (M-99) is offered below:

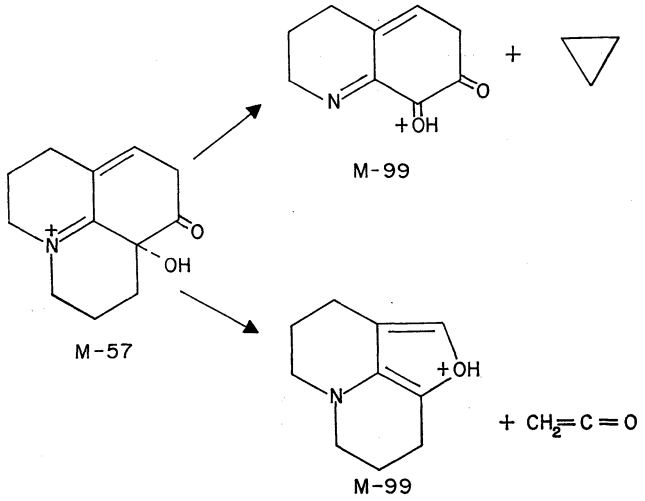

Lycoclavine (Fig. 4*b*) fragments in the expected manner with the peaks at M-57, M-117, and M-145 dominating the spectrum. With the exception of the peak at M-102, the spectrum of lycoclavine is very similar to that of acetyldihydrolycopodine (Fig. 1*d*), from which it differs in structure only by the presence of a hydroxyl group at C_6. The only major difference between the two is the peak at M-102, which is not found in other spectra examined and which is characteristic of this compound. A possible route whereby it might be formed from the molecular ion is shown below:

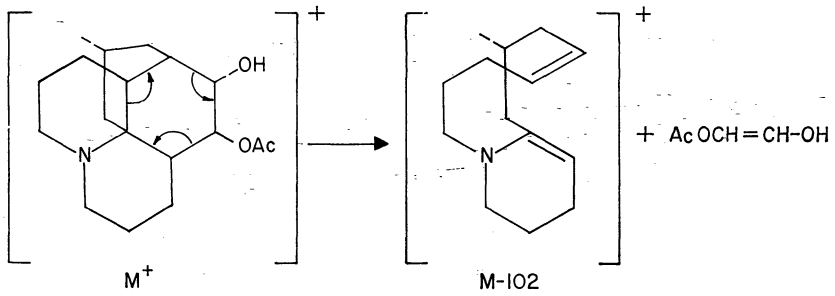

In summary it can be said that the alkaloids of the lycopodine group undergo a fragmentation which is dominated by loss of the bridge atoms and that substituents on the lycopodine skeleton have very little effect on the fragmentation process except when they are situated at C_4. The mass spectrometric method, therefore, should prove valuable in the study of new alkaloids of this group.

The second most abundant group of alkaloids are those related in structure to lycodine. In this category are found lycodine, its N-methyl derivative (20), α- and β-obscurine (20), and de-N-methyl-α-obscurine (20). The spectra of two of these are shown in Fig. 5. The fragmentation of the two substances is very similar with major peaks appearing at M-43, M-57, and M-85. The M-57 and M-85 peaks undoubtedly arise by a mechanism similar to that shown for dihydrolycopodine in Scheme I. The spectra of β-obscurine and of de-N-methyl-α-obscurine were recorded and follow the same fragmentation pattern. For the sake of clarity a fragmentation mechanism for α-obscurine is shown in Scheme IV.

Can. J. Chem. Downloaded from www.nrcresearchpress.com by 210.87.254.42 on 09/05/12
For personal use only.

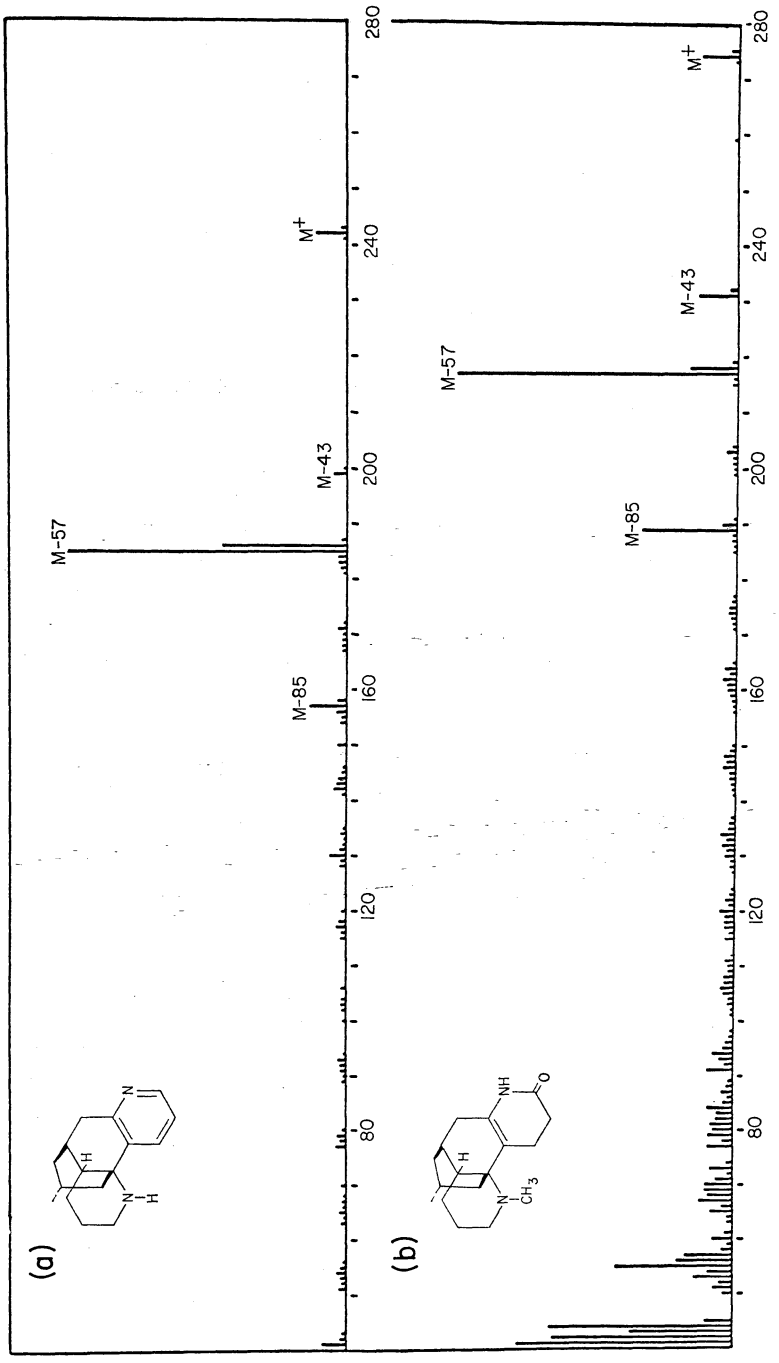

FIG. 5. Mass spectra of alkaloids of the lycodine group: (*a*) lycodine, (*b*) α-obscurine.

Can. J. Chem. Downloaded from www.nrcresearchpress.com by 210.87.254.42 on 09/05/12
For personal use only.

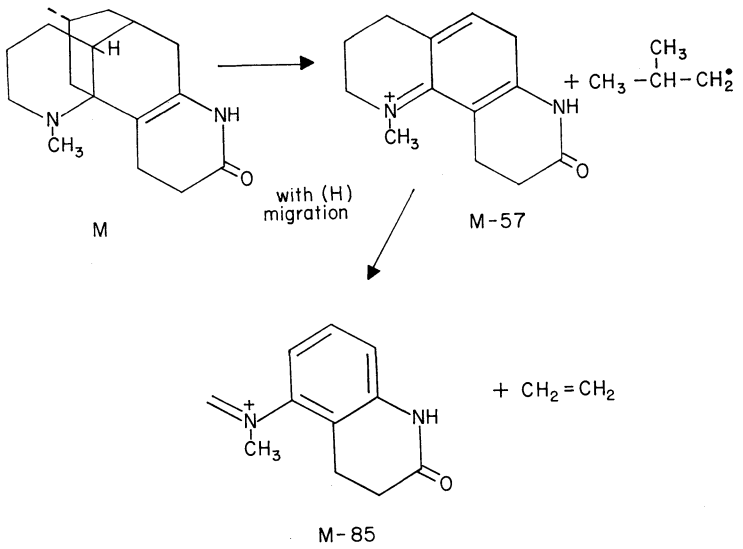

Scheme IV

The most noteworthy feature of these spectra is their very remarkable resemblance to those of the lycopodine group. The bridge is the dominant structural feature affecting the fragmentation in both ring systems. Its loss leads to the major fragment ions, and other modes of fragmentation are usually of minor importance. Although alkaloids of the two ring systems yield very similar spectra, the alkaloids with two nitrogen atoms can be easily differentiated because their molecular weight is always an even number. Confusion can arise only when the lycopodine skeleton carries a nitrogenous substituent group.

Substituted alkaloids of the lycodine group are not known, but if encountered they might be expected to fragment along lines similar to their analogues in the lycopodine group.

Annotinine differs from the other *Lycopodium* alkaloids in that the bridge carries one less carbon and forms a four-membered rather than six-membered ring. It has, however, the hexahydrojulolidine system characteristic of the lycopodine group and might be expected to show some similarity to this group in its fragmentation. The spectrum of annotinine and of a derivative of it, deoxodihydroannotinine (21), are shown in Figs. 6*a* and 6*b*, respectively. Figure 6*b* is simple and can be interpreted by assuming that fragmentation proceeds by expulsion of the bridge to give the ion at M-42. Loss of CO_2 then gives the ion at M-86, which loses hydrogen to yield the fragment M-87. Loss of 28 mass units leads to the ion of *m/e* 146 (M-115). Metastable peaks associated with the changes 219 → 175, 175 → 174, 174 → 146 are observed at *m/e* 141.0, 173.5, and 124.0 (m^*_{calc} = 139.8, 173.0, and 122.5) respectively. It is interesting to note here that the same fragment ions of *m/e* 174 and 146 are derived from deoxodihydroannotinine as from annofoline, lofoline, dihydrolycopodine, anhydrodihydrolycopodine, and acetyldihydrolycopodine, and that in all of the spectra a strong metastable peak appears at 124.0.

In contrast to its deoxo derivative, the spectrum of annotinine, Fig. 6*a*, is much more complex, and a detailed interpretation of it would require a more detailed study. The appearance of peaks at M-42, M-86, M-87, and M-115 is clearly evident, corresponding

Can. J. Chem. Downloaded from www.nrcresearchpress.com by 210.87.254.42 on 09/05/12
For personal use only.

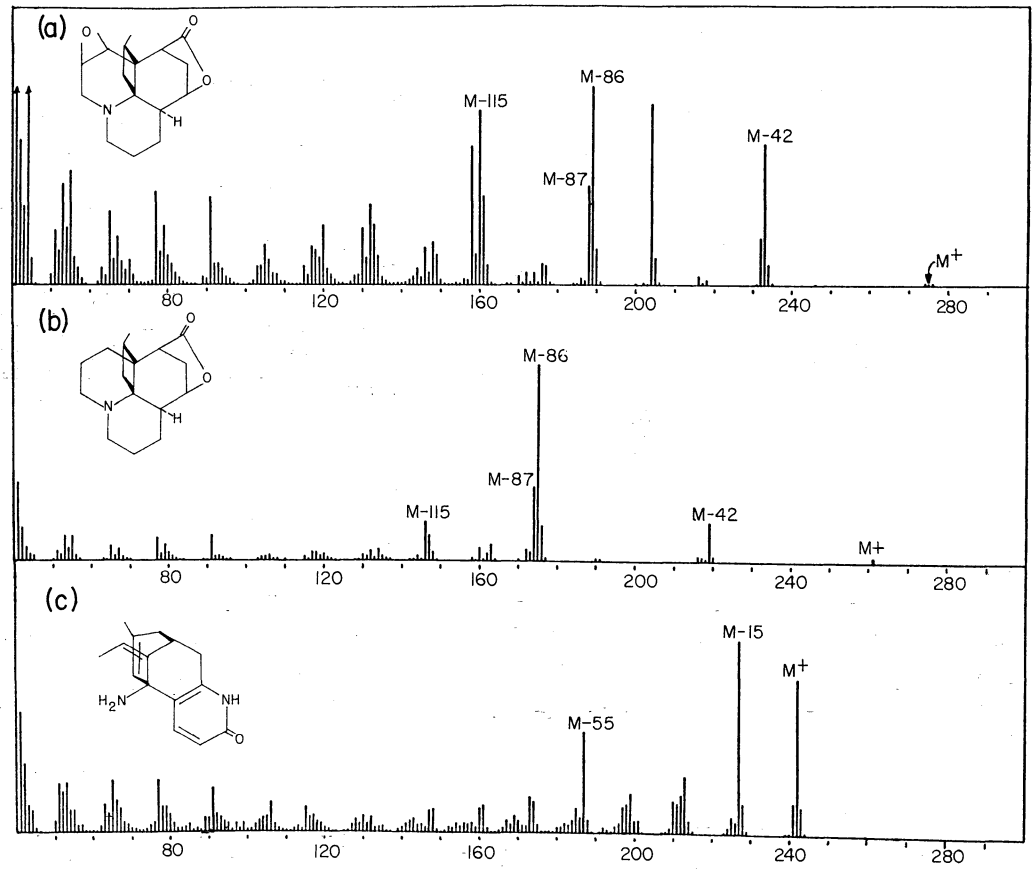

FIG. 6. Mass spectra of alkaloids of the annotinine and selagine groups: (*a*) annotinine, (*b*) deoxodihydroannotinine, (*c*) selagine.

to the changes chronicled above. The M-42 peak is the most significant from the structural viewpoint since it differentiates this structural type from the other two types examined before.

A comparison of the spectrum of annotinine and of deoxodihydroannotinine provides a striking example that the removal of a single functional group greatly simplifies the spectrum.

The selagine spectrum is recorded in Fig. 6*c*. Since it is the only example of its class and since no derivatives of it were at hand for study, a detailed interpretation of its spectrum will not be attempted. It is worthwhile to note, however, the peak at M-55 which arises from the ion formed by loss of the bridge + H. In this respect, at least, the spectrum of selagine is characteristic of *Lycopodium* alkaloids.

This study has shown that the mass spectrometric method can be of considerable value in establishing the structural group to which a *Lycopodium* alkaloid belongs and in the case of alkaloids of the lycopodine group in aiding in the location of a substituent group. The mechanisms for fragmentation which have been proposed must be considered tentative. A more detailed study with specifically labeled compounds would be required to test the mechanistic proposals.

Can. J. Chem. Downloaded from www.nrcresearchpress.com by 210.87.254.42 on 09/05/12
For personal use only.

EXPERIMENTAL

Apparatus, Methods, and Materials

The mass spectra were determined on a CEC-103C mass spectrometer at an ionizing potential of 70 ev and an ionizing current of 50 μa. Samples were introduced through the heated inlet system, which was maintained at 140°. Annotinine, selagine, and α-obscurine, when introduced by this method, gave complex spectra in the low-mass region, probably owing to pyrolytic decomposition. Accordingly, the spectra recorded for these compounds were taken with samples introduced directly into the ion source through a vacuum lock system.

The alkaloids, with the exception of selagine and lycoclavine, were taken from samples isolated in the author's laboratory over the past few years. Their infrared spectra and melting points were in accord with those reported in the literature. The sample of selagine was supplied by Dr. Z. Valenta and that of lycoclavine by Dr. W. A. Ayer, to each of whom my thanks are extended.

Deuterium Exchange Experiments

(a) Lycopodine.—A solution of sodium methoxide in deuteromethanol was prepared by dissolving approximately 50 mg of sodium in 1 ml of CH_3OD. To this solution, 30 mg of lycopodine was added and the mixture heated under reflux for 4 hours. The deuteromethanol was evaporated under reduced pressure, the residue treated with 1 ml of D_2O and extracted with ether. The dried ether extract was evaporated to dryness and the solid residue subjected to a second exchange exactly as above. The residue from the second exchange was recrystallized from dry petroleum ether (30–60°) before its mass spectrum was recorded.

(b) Annofoline.—The exchange was carried out in the same fashion as that described above for lycopodine. The crystalline product was used without further recrystallization.

The Spectrum of Deuterated Annofoline

When the deuterated annofoline prepared above was introduced into the heated inlet system and its spectrum recorded, the most intense peak in the molecular ion region was observed at *m/e* 264 and not at *m/e* 265, as expected. It seemed at first that exchange had not been complete, but closer examination of the spectrum showed that this could not be the case since peaks corresponding to almost complete exchange of deuterium for hydrogen at the bridgehead carbon were present. It appeared more likely that exchange of the deuterium on the bridge with moisture in the inlet system occurred very rapidly. Accordingly the inlet system was given a prior treatment with CH_3OD, the sample introduced, and the spectrum scanned repetitively over the mass region of *m/e* 160 to 270. The results of this experiment are shown in Table III, where the relative intensity of the major peaks in the spectrum of deuterated annofoline are shown at the time of introduction, after approximately 30 minutes, and after approximately 1 hour.

The peak at *m/e* 176 is assigned an arbitrary intensity of 100 and other peaks related to it. The peak at *m/e* 176 was selected as a standard of reference since the ion has no hydroxyl function and its intensity, unlike that of peaks in the region of mass 190 and of the molecular ion, will not be affected by the relative proportion of hydroxyl to deuteroxyl groups in the sample of annofoline.

Table III shows that the intensity of the peak of *m/e* 266 decreases rapidly and, after 60 minutes, it is only slightly stronger than expected of a normal isotope peak, indicating that virtually all of the —OD originally present has reverted to —OH. The peak of *m/e* 265 diminishes rapidly in intensity, too. Initially it is the most intense peak in the molecular ion region but is less intense than the 264-peak after 30 minutes and continues to decrease in intensity relative to the 264-peak.

These results are in accord with the proposition advanced above that the deuterium at C_{14} is easily exchanged but that the deuterium at the bridgehead position is stable in the inlet system.

Deoxodihydroannotinine

This substance was prepared by the method of Betts and MacLean (21).

ACKNOWLEDGMENTS

The author wishes to express his appreciation to Professor Klaus Biemann for the hospitality of his laboratory and for many helpful suggestions in the prosecution of this work and in the preparation of the manuscript. The granting of a year's leave of absence by McMaster University and the award of a Senior Research Fellowship by the National Research Council are gratefully acknowledged.

REFERENCES

1. K. Biemann. Mass spectrometry: organic chemical applications. McGraw-Hill, New York. 1962.
2. W. A. Harrison, M. Curcumelli-Rodostamo, D. F. Carson, L. R. C. Barclay, and D. B. MacLean. Can. J. Chem. **39**, 2086 (1961).
3. W. A. Ayer and G. G. Iverach. Can. J. Chem. **38**, 1823 (1960).

Can. J. Chem. Downloaded from www.nrcresearchpress.com by 210.87.254.42 on 09/05/12
For personal use only.

4. F. A. L. ANET and M. V. RAO. Tetrahedron Letters, No. 20, 9 (1960).
5. K. WIESNER, Z. VALENTA, W. A. AYER, L. R. FOWLER, and J. E. FRANCIS. Tetrahedron, **4**, 87 (1958).
6. M. PRZYBYLSKA and F. R. AHMED. Acta Cryst. **11**, 718 (1958).
7. Z. VALENTA, H. YOSHIMURA, E. F. ROGERS, M. TERNBAH, and K. WIESNER. Tetrahedron Letters, No. 10, 26 (1960).
8. H. YOSHIMURA, Z. VALENTA, and K. WIESNER. Tetrahedron Letters, No. 12, 14 (1960).
9. B. DOUGLAS, D. G. LEWIS, and L. MARION. Can. J. Chem. **31**, 272 (1953).
10. J. A. HIPPLE and E. U. CONDON. Phys. Rev. **68**, 54 (1953).
11. F. A. L. ANET and N. H. KHAN. Can. J. Chem. **37**, 1589 (1959).
12. R. H. BURNELL and D. R. TAYLOR. Tetrahedron, **15**, 173 (1961).
13. R. H. BURNELL and D. R. TAYLOR. Chem. Ind. (London), 1239 (1960).
14. F. A. L. ANET and N. H. KHAN. Chem. Ind. (London), 1238 (1960).
15. F. A. L. ANET. Tetrahedron Letters, No. 20, 13 (1960).
16. W. A. AYER and G. G. IVERACH. Tetrahedron Letters, No. 3, 87 (1962).
17. W. N. FRENCH and D. B. MACLEAN. Can. J. Chem. **39**, 2100 (1961).
18. M. CURCUMELLI-RODOSTAMO and D. B. MACLEAN. Can. J. Chem. **40**, 1068 (1962).
19. W. A. AYER and D. A. LAW. Can. J. Chem. **40**, 2088 (1962).
20. W. A. AYER, J. A. BEREZOWSKY, and G. G. IVERACH. Tetrahedron, **18**, 567 (1962).
21. E. E. BETTS and D. B. MACLEAN. Can. J. Chem. **36**, 473 (1958).

Can. J. Chem. Downloaded from www.nrcresearchpress.com by 210.87.254.42 on 09/05/12
For personal use only.

THE REDUCTIVE CLEAVAGE OF 1,3-OXATHIOLANES WITH LITHIUM ALUMINUM HYDRIDE IN THE PRESENCE OF ALUMINUM CHLORIDE OR BORON TRIFLUORIDE[1]

B. E. LEGGETTER AND R. K. BROWN
Department of Chemistry, University of Alberta, Edmonton, Alberta
Received May 10, 1963

ABSTRACT

A number of 1,3-oxathiolanes and 1,3-dithiolanes were subjected to reduction in ether solution by lithium aluminum hydride in the presence of either aluminum chloride or boron trifluoride. Both of these Lewis acids not only isomerized 1,3-oxathiolanes but also catalyzed their hydrogenolysis to the hydroxy thioethers. Under the same conditions neither aluminum chloride nor boron trifluoride had any effect upon 1,3-dithiolanes. However, in methylene chloride solution, 1,3-dithiolanes are isomerized by both Lewis acids although their hydrogenolysis was not achieved, probably due to the insolubility of the hydride in methylene chloride.

A mechanistic interpretation is discussed to explain the results obtained.

INTRODUCTION

Recently Eliel and co-workers (1, 2) reported the reduction of 13 cyclic hemithioacetals and ketals (1,3-oxathiolanes) with a mixture of lithium aluminum hydride and aluminum chloride in ether solution. They found that in every case cleavage of only the carbon–oxygen bond occurred. Extended reaction times gave further reduction of the hydroxy thioether to the dialkyl sulphide (equation (*a*)).

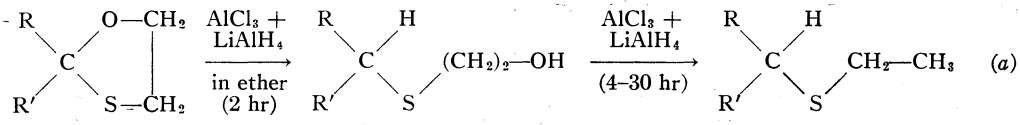

(*a*)

Attempts by the same authors to reduce a hemithioketal with a mixture of *boron trifluoride* and lithium aluminum hydride were unsuccessful, resulting in practically complete recovery of the hemithioketal.* Thus, boron trifluoride – lithium aluminum hydride reduction of 4-*t*-butylcyclohexanone ethylene hemithioketal gave, in 2 hours, less than 1% of the hydrogenolyzed product, whereas the combination of aluminum chloride and lithium aluminum hydride, under otherwise identical conditions, yielded 85 to 90% of the hydrogenolyzed products, which consisted mainly of the hydroxy thioether along with some dialkyl sulphide.

Although *reduction* of the 4-*t*-butylcyclohexanone ethylene hemithioketal failed to occur with the BF_3–$LiAlH_4$ combination, *isomerization* of the two individual isomers of this ketal *did* take place readily and cleanly with the mixture BF_3–$LiAlH_4$ *or* with BF_3 etherate alone (equation (*b*)). Such isomerization was also obtained by $AlCl_3$ alone in ether solution but accompanied by some further decomposition (1).

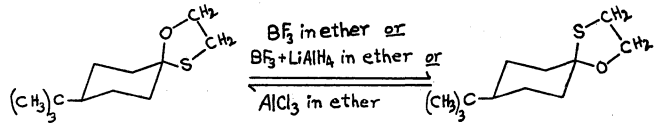

(*b*)

[1]*Taken in part from the thesis of B. E. Leggetter submitted to the Graduate School, University of Alberta, in partial fulfillment of the requirements for the degree of Doctor of Philosophy.*

Reduction of a dioxyketal (a 1,3-dioxolane) with* BF_3–$LiAlH_4$*, however, is readily accomplished (Note 18 in ref. 1). Compare also A. R. Abdum-Nur and C. H. Issidorides, J. Org. Chem.,* **27, *67 (1962).*

Can. J. Chem. Downloaded from www.nrcresearchpress.com by 210.87.254.40 on 09/05/12
For personal use only.

On the basis of this information, a mechanism for the hemithioketal reduction was proposed (1) involving first the formation of the resonance-stabilized sulphocarbonium ion *which could not be reduced by the hydride but did permit isomerization.* Reaction of this ion with the more nucleophilic chloride ion from the aluminum chloride, but not with the less nucleophilic fluoride ion from BF_3, gave the α-halo thioether which in turn could be reduced easily by the hydride to the hydroxy thioether (equation (*c*)).

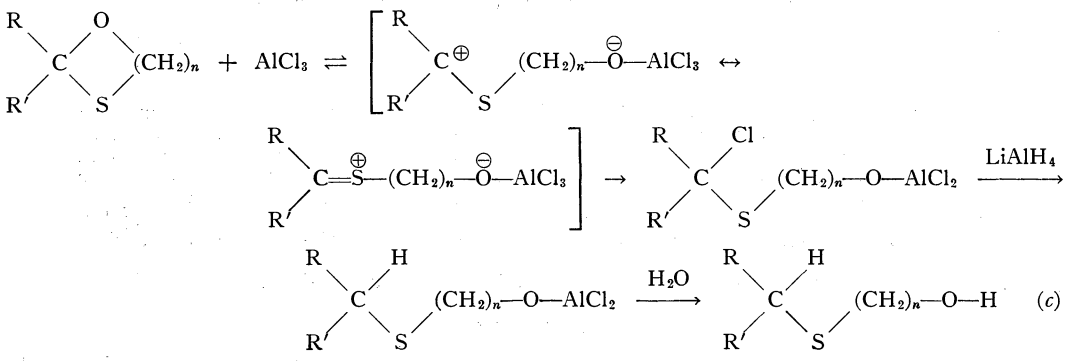

As part of a program of research in this laboratory it had become necessary to examine the selective cleavage of 1,3-dioxolanes (ketals or acetals), and 1,3-oxathiolanes (hemithioketals or acetals) using as one of the reducing agents lithium aluminum hydride along with a Lewis acid. This paper reports the results obtained and gives data which cast some doubt on the mechanism of reductive cleavage suggested by Eliel (1).

RESULTS AND DISCUSSION

A number of 1,3-oxathiolanes in ether solution were treated with the combination of lithium aluminum hydride – aluminum chloride or lithium aluminum hydride – boron trifluoride. The results of these experiments are shown in Table I.

Cleavage of C—O but not C—S Bonds

Our results corroborate the findings of the previous workers (1, 2) that in the reduction of 1,3-oxathiolanes the C—O but not the C—S bond is ruptured. No base-soluble mercaptans were isolated. Analyses by v.p.c. and infrared spectroscopy of the individual products as well as the mixtures of products failed to reveal evidence of the presence of the mercapto group. Furthermore, 1,3-*di*thiolanes failed to reduce at all even when the normal reduction time of 2 hours was extended to 48 hours. Only unchanged 1,3-dithiolanes were recovered, and these nearly quantitatively (experiments 6–9).

Hydrogenolysis with BF_3–$LiAlH_4$

As clearly shown in Table I, boron trifluoride *will* catalyze the reductive cleavage of 1,3-oxathiolanes by lithium aluminum hydride in diethyl ether solution (experiments 10–12, 14–15). However, the yield of reduction products is dependent upon the mode of addition of the reagents and upon the physical state of the hydride. In previous work on the reduction of dioxolanes and oxathiolanes using aluminum chloride as catalyst, we have found that when the Lewis acid is added to an ether solution of the dioxolane or oxathiolane *prior* to the addition of hydride, some resinous material was obtained, resulting in a reduced yield of the hydroxy ether. The same occurred but to a much lesser extent when BF_3 was used as the Lewis acid. Our experience in the reduction of these acetals and ketals with $LiAlH_4$–$AlCl_3$ mixture has been that this loss due to resin formation

Can. J. Chem. Downloaded from www.nrcresearchpress.com by 210.87.254.40 on 09/05/12
For personal use only.

TABLE I

Reduction of 1,3-oxathiolanes with lithium aluminum hydride in the presence of aluminum chloride or boron trifluoride (solvent, diethyl ether at room temperature)*

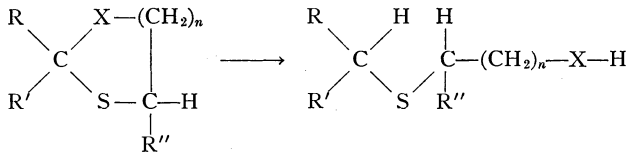

Expt. No.	R	R′	R″	X	*n*	Lewis acid	Total†† product recovery, %	Amount of thioether in the product, %	Amount of recovered 1,3-oxathiolane in product, %
1	H	C_6H_5	H	O	2	$AlCl_3$	—	54	0
2	H	C_6H_5	H	O	1	$AlCl_3$	—	72	0
3	H	*n*-C_3H_7	H	O	1	$AlCl_3$	—	89†	0
4	CH_3	CH_3	H	O	1	$AlCl_3$	—	87	0
5	C_6H_5	C_6H_5	H	O	1	$AlCl_3$	—	73	0
6	H	C_6H_5	H	S	1	$AlCl_3$	—	0	⩾96‡
7	CH_3	CH_3	H	S	1	$AlCl_3$	—	0	⩾96
8	CH_3	H	CH_3	S	1	$AlCl_3$	—	0	92
9	C_6H_5	H	CH_3	S	1	$AlCl_3$	—	0	78
10	CH_3	CH_3	H	O	1	BF_3	95	39	61§
11	CH_3	CH_3	H	O	1	BF_3	73	50	50‖
12	CH_3	CH_3	H	O	1	BF_3	75	56	44¶
13	CH_3	CH_3	H	O	1	BF_3	90	0	100**
14	C_6H_5	H	H	O	1	BF_3	29‡‡	100	0
15	C_6H_5	H	H	O	1	BF_3	90	73	27

*Unless otherwise stated, equimolar mixtures of $LiAlH_4$, Lewis acid, and oxathiolane or dithiolane in ether were used. The Lewis acid was added slowly over a period of 5 minutes to an ether solution of oxathiolane and hydride and then the mixture was stirred 2 hours. After work-up the products were analyzed by distillation and/or v.p.c.

†The solution was stirred for 3.5 hours before work-up.

‡The same result was obtained when the solution was allowed to stand 48 hours.

§The BF_3 etherate was added to the solution of hydride and oxathiolane and then the mixture stirred 3 hours.

‖Solid, finely ground $LiAlH_4$ was added to the stirred solution of BF_3 and oxathiolane in ether and the mixture stirred 3 hours.

¶Some resinous product formed. Here solid lumps of hydride in an ether suspension were added to the stirred ether solution of oxathiolane and BF_3.

**Here a solution of the oxathiolane was added to a stirred ether solution of $LiAlH_4 + BF_3$ as in Eliel's procedure (1), except that equimolar proportions of reagents were used. Eliel used a 4:1 ratio of BF_3:$LiAlH_4$. Our reduction time was 3 hours.

††Total product recovery includes both the recovered oxathiolane (or dithiolane) *and* the thioether.

‡‡Much resinous (polymeric) material remained in the flask after removal of volatile products.

could be avoided, and good control of reduction along with quite satisfactory results could be achieved by careful addition of an ether solution of the Lewis acid to the stirred ether solution of the dioxolane or oxathiolane containing the requisite amount of hydride.* Accordingly this procedure was employed initially in the BF_3-catalyzed reductions of the oxathiolanes. It was found that when equimolar quantities of the oxathiolane and lithium aluminum hydride were treated with ethereal BF_3, 39% of the total isolated product was the hydroxy thioether and the remainder (61%) was unchanged material (experiment 10). However, further investigation showed that if the BF_3 and oxathiolane were mixed *first* and then the hydride added in a finely divided state, a greater proportion of the product was found to be the reduced material (experiment 11). If the hydride was added as in experiment 11, but in the form of small lumps, an even greater proportion of the product was the hydroxy thioether (experiment 12). In both experiments 11 and 12, wherein the oxathiolane and BF_3 were first mixed together, somewhat better reduction did occur, though now with resin formation, than by the method of Lewis acid addition to the

**Addition of an ether solution of the ketal or acetal to a mixture of* $LiAlH_4$ *and* $AlCl_3$ *in ether was the procedure employed by Eliel et al. (1, 2).*

Can. J. Chem. Downloaded from www.nrcresearchpress.com by 210.87.254.40 on 09/05/12
For personal use only.

mixture of hydride and oxathiolane—the procedure found to be much the better when $AlCl_3$ was the Lewis acid.* Finally, a repetition of the procedure used by Eliel and co-workers in the reduction of 4-*t*-butylcyclohexanone ethylene hemithioketal (1), in which 0.05 mole of oxathiolane in ether was added to a 4:1 mixture of BF_3 etherate and $LiAlH_4$ in ether which had been stirred for 5 minutes, gave less than 1% of the reduction product and 99% of the starting material, thus duplicating these authors' results.

The failure of a previously prepared 4:1 mixture, in ether, of BF_3–$LiAlH_4$ to effect reductive cleavage of the oxathiolane might be due to destruction of the reducing species before the oxathiolane could be attacked. The work of Shapiro *et al.* (3) on the preparation of diborane indicates that the addition of excess BF_3 to $LiAlH_4$ in ether produces diborane and aluminum fluoride according to the overall reaction given by equation (*d*). Because

$$3LiAlH_4 + 4BF_3 \xrightarrow{\text{ether}} 2B_2H_6 + 3LiF + 3AlF_3 \qquad (d)$$

of its low solubility in diethyl ether, diborane is evolved (4), and in fact the collection of diborane was used as a measure of the rate of formation of diborane (3) from these reagents.

The practically complete loss of the hydride as diborane from the ether solution thus would account for the absence of significant reduction as reported (1),* and as found in the present work when similar experimental conditions were employed.

Shapiro and co-workers (3) observed that no diborane was evolved until the ratio of BF_3 added to $LiAlH_4$ was greater than 1:1, thus indicating a two-step sequence shown by equations (*e*) and (*f*). Complete failure of reduction found in our experiment (No. 13)

$$BF_3 + LiAlH_4 \rightarrow LiBH_4 + AlF_3\downarrow \qquad (e)$$

$$BF_3 + 3LiBH_4 \rightarrow 2B_2H_6 + 3LiF\downarrow \qquad (f)$$

wherein the ratio of BF_3 to $LiAlH_4$ was only 1:1 could thus be attributed to the total conversion of BF_3 to AlF_3. Since the insolubility of AlF_3 makes it an ineffective Lewis acid (5), no reduction of the oxathiolane would occur even though the reducing species, lithium borohydride, was present (equation (*e*)).

In the addition of BF_3 etherate to a mixture of 1,3-oxathiolane and $LiAlH_4$, a competitive reaction must take place between the acetal and the hydride for the Lewis acid. Coordination of the Lewis acid with the oxathiolane would result in subsequent hydrogenolysis while reaction with the hydride would lead to the formation of AlF_3 and B_2H_6. Such a competitive reaction might explain the variability in reduction due to the physical condition of the hydride.

The much faster reduction of 1,3-dioxolanes as compared to that of the 1,3-oxathiolanes (see latter portion of this discussion), and the concept of competition of the dioxolane (or oxathiolane) with the lithium aluminum hydride for the Lewis acid, BF_3, could explain why 1,3-dioxolanes are quite readily reduced by BF_3–$LiAlH_4$ in ether (see first footnote in this paper) but 1,3-oxathiolanes reduce with more difficulty (1) and depend much more upon the order of addition of the reagents than do the dioxolanes.

**It is interesting that a new batch of* $LiAlH_4$, *which was quite finely divided and appeared light grey in color as compared with the darker grey color and lumpy texture of the batch of hydride used for all our experiments, gave reduction to the hydroxy thioether comparable to that of the darker grey material when the hydride was added to a mixture of the 1,3-oxathiolane and* BF_3 *etherate, but gave only unchanged material if the* BF_3 *was added to the previously mixed hydride and oxathiolane in ether.*

**The small amount of reduction, <1%, reported (1) could be due to the residual* B_2H_6 *remaining in the ether solution or to the presence of some unreacted hydride.*

Can. J. Chem. Downloaded from www.nrcresearchpress.com by 210.87.254.40 on 09/05/12
For personal use only.

Comparison of the Ease of Reduction of 1,3-oxathiolanes and 1,3-dioxolanes

A number of reductions were carried out with 2-*n*-propyl-1,3-dioxolane and 2-*n*-propyl-1,3-oxathiolane. Equimolar proportions of reagents were employed and conditions were identical in all cases except for the length of time that each experiment was allowed to proceed. The results are shown in Table II.

TABLE II

Comparison of the ease of reduction of 2-*n*-propyl-1,3-dioxolane and 2-*n*-propyl-1,3-oxathiolane by $LiAlH_4$ in the presence of $AlCl_3$ (solvent, diethyl ether)

Expt. No.	Total reduction time, min	Total recovery,* %	Yield of β-hydroxy thioether, %	Amount of recovered unreacted acetal, %
		For 2-*n*-propyl-1,3-oxathiolane		
1	20	89	51	49
2	40	84	81	19
3	60	91	91	9
4	210	80	>99.8	<0.2
		For 2-*n*-propyl-1,3-dioxolane		
5	20	88	100	0

*Total recovery includes the unreacted acetal *and* the β-hydroxyalkyl thioether reduction product. The dialkyl thioethers which Eliel found on continued reduction of the hydroxyalkyl thioethers apparently were not formed during the time of our reduction since v.p.c. analyses failed to reveal their presence.

It is clear that under identical conditions 2-*n*-propyl-1,3-dioxolane is reduced considerably faster than is 2-*n*-propyl-1,3-oxathiolane. The dioxolane had disappeared completely within 20 minutes and it is quite likely that the time for complete reduction is less than this. On the other hand, the oxathiolane was approximately 50% hydrogenolyzed in 20 minutes.

Mechanistic Interpretation

Any mechanistic scheme to explain the reductive cleavage, in ether solution, of these acetals or ketals by lithium aluminum hydride in the presence of a Lewis acid must account for: (i) the direction of ring opening of cyclic acetals (6, 7); (ii) the cleavage of the C—O bond but not the C—S bond in oxathiolanes; (iii) the slower rate of cleavage of oxathiolanes as compared with that of the dioxolanes; (iv) the complete failure of reductive cleavage of dithiolanes.

The two reasonable mechanisms which have been advanced (1, 7, 8) are: (A) direct reduction of the initially formed resonance-stabilized oxocarbonium or sulphocarbonium ion as in equation (*g*).

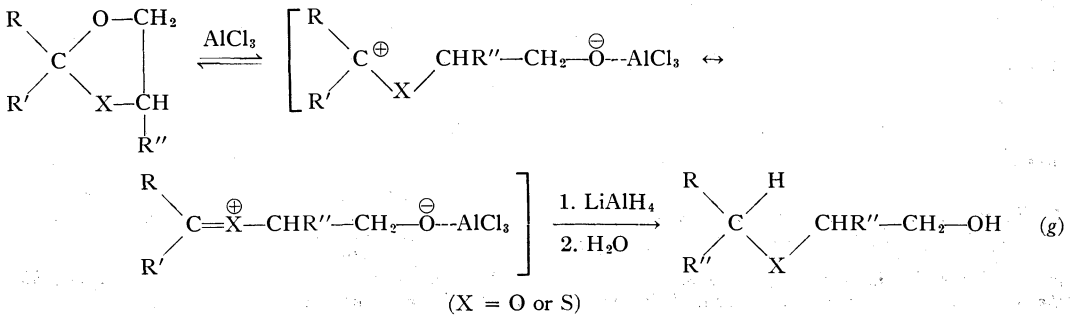

(*g*)

Can. J. Chem. Downloaded from www.nrcresearchpress.com by 210.87.254.40 on 09/05/12
For personal use only.

(B) formation of the α-halo ether from the oxo- or sulpho-carbonium ion followed by reduction of the α-halo ether by the hydride as in equation (*c*).

In view of our observation that BF_3–$LiAlH_4$ causes reduction as does $AlCl_3$–$LiAlH_4$, the argument used as the support for the necessary formation of the α-halo ether is no longer valid. However, this does not mean that the concept of prior α-halo ether formation is disproved. It still *may* be, but is not *necessarily*, the pathway of the reaction.

It is noteworthy that both isomers of 4-*t*-butylcyclohexanone ethylene hemithioketal, when reduced by $AlCl_3$–$LiAlH_4$, were found to give a high (86 to 92%) yield of the same isomer, *trans*-4-*t*-butylcyclohexyl β-hydroxyethyl sulphide (1). This indicates that if α-halogenation were in fact a preliminary step, then *either* the α-halo ether must lose the halogen to become a carbonium ion, a common intermediate from both isomers, which is then reduced stereospecifically, *or* a rapid equilibration of the oxathiolanes occurs (cf. equation (*b*) wherein approximately a 1:1 mixture was found at a slowly attained equilibrium (1)) from which only one of the isomeric α-chloro ethers is formed, and this nearly quantitatively, which is then reduced stereospecifically. In the latter case, if the α-halo ether reacts with $LiAlH_4$ via an S_N1 mechanism, as is likely in view of the known S_N1 character of the solvolysis reactions of α-halo ethers (9),* then initial cleavage of the C—Cl bond must occur to form the readily reducible sulphocarbonium ion.

In view of the fact that the sulphocarbonium ion formation is necessary in the isomerization of the oxathiolane, in the formation of the preferred α-halo ether and also in the reduction (S_N1) of the α-halo ether, it is more logical to assume that prior α-halogenation isn't necessary and that the initially formed sulphocarbonium ion (made with the assistance from the Lewis acid) is the species reduced. The α-halogenation might then occur only as a competitive reaction, with the transient α-halo ether being immediately reduced. No evidence has been obtained in our work (cf. Table II) in the partial reduction of oxathiolanes of α-halo ether formation. No carbonyl compound was found in the products after work-up under alkaline conditions, suggesting α-halo ether formation.

As pointed out by Eliel, Pilato, and Badding (1) "only those functional groups are subject to hydrogenolysis (by $LiAlH_4$) which upon departure leave a stabilized carbonium ion". By and large this seems to be the guiding principle in nearly all the reductive cleavages of 1,3-dioxolanes or 1,3-oxathiolanes encountered in our laboratory. The very few exceptions can be rationalized within the framework of the above statement. This, and other aspects of the problem will be reported upon in a subsequent publication.

Regarding the Selective Cleavage of the C—O Bond Rather than the C—S Bond

There is considerable evidence that association of $AlCl_3$ with thioethers is more difficult than similar association of $AlCl_3$ with oxygen ethers. Harnish and Tarbell found in their study of the cleavage of ethers (10–12) that thioethers are more resistant to cleavage by acidic reagents than are their oxygen analogues. Suter and Hanson (13) found that alkyl *p*-methoxyphenyl thioethers were cleaved by an acetic acid solution of HBr to form only alkyl *p*-hydroxyphenyl thioethers with no evidence of cleavage of the C—S bond. Furthermore, when dry aluminum bromide was added to pure phenyl benzyl sulphide, cleavage occurred to give thiophenol and benzyl bromide, but when electron donor solvents such as ethers or nitrobenzene were used as diluents for this reaction, aluminum bromide failed

**The reviewer kindly pointed out that α-halo ethers can also react very rapidly by the S_N2 mechanism (P. Ballinger, P. B. D. de la Mare, G. Kohnstam and B. M. Prestt, J. Chem. Soc. 3641 (1955). However, since the work done by Ballinger et al. involved* primary *alkyl halides in the α-halo ether structure, while our work concerned itself with* secondary *and* tertiary *alkyl halides of α-halo ether structure, and as well involved the presence of aluminum chloride which could promote dissociation of the halogen as the halide ion, we prefer to consider the S_N1 reaction of our α-halo ethers as being more likely, even in the ether solutions employed.*

Can. J. Chem. Downloaded from www.nrcresearchpress.com by 210.87.254.40 on 09/05/12
For personal use only.

to cause any cleavage of the thioether (10). The explanation offered was that of preferential coordination of the $AlBr_3$ with the electron donor solvents.

For diethyl ether solutions of 1,3-dioxolanes the acetal oxygen atom can compete quite effectively with the solvent oxygen atoms for the Lewis acid, thus leading to Lewis acid catalysis of the reduction with $LiAlH_4$. Dithiolanes in diethyl ether solution would fail to experience effective association between the Lewis acid and the sulphur atoms and hence would be resistant to $LiAlH_4$ reduction, as has been found. If then the *first* and *necessary* step in the reductive cleavage of the 1,3-oxathiolanes is coordination of the oxathiolane with the Lewis acid, then one must have the reaction shown in equation (*h*) in which the sulphocarbonium ion is formed. This could then undergo isomerization accompanied by some polymerization or be reduced if $LiAlH_4$ is present.

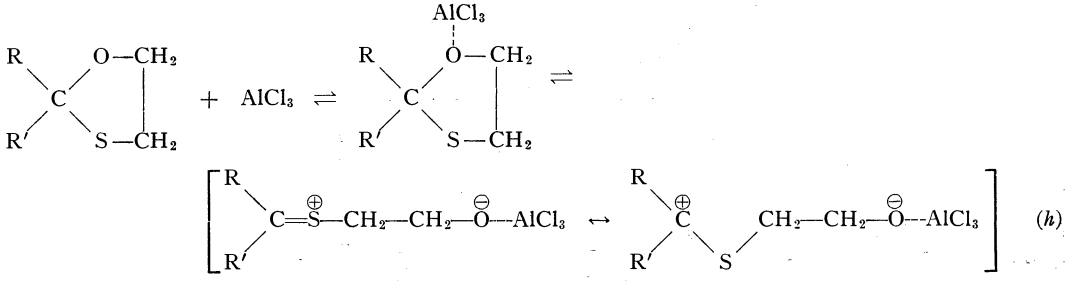

(*h*)

Support for the concept of the inability of the Lewis acid to associate with the sulphur atom of the oxathiolane or dithiolane in diethyl ether solution is obtained from the observation that the high-melting isomer *cis-* (or *trans-*) 4-chloromethyl-2-phenyl-1,3-dithiolane* treated with either BF_3 or $AlCl_3$ in *ether solution* did not isomerize detectably even when the solution was allowed to stand at room temperature for as long as 20 hours. On the other hand, in the solvent methylene chloride, in which the Lewis acids and the dithiolane were quite soluble, equilibration occurred quite readily. Boron trifluoride gave complete equilibration within 90 minutes unaccompanied by polymerization, but aluminum chloride gave equilibration accompanied by extensive gum formation. Detection of isomerization was easily accomplished by n.m.r. analysis of the individual isomers and the mixtures produced, since the signal for the lone proton on C_2 of the dithiolane occurred as a sharp singlet at $\tau = 4.48$ for the low-melting isomer (m.p. 60–62°) and at $\tau = 4.43$ for the high-melting isomer (m.p. 68–69°).

On the assumption that if reduction is to occur there must be prior association of the Lewis acid with the dithiolane, and now knowing that isomerization of dithiolanes does occur in CH_2Cl_2 solution through the agency of a Lewis acid, we attempted to reduce several 1,3-dithiolanes at our disposal. However, the failure of $LiAlH_4$ to dissolve in the CH_2Cl_2 thwarted attempts in this direction and there were obtained only the unchanged dithiolanes. That failure of reduction can be attributed to the insolubility of the $LiAlH_4$ in CH_2Cl_2 is borne out by complete lack of reduction of 2,2,4-trimethyl-1,3-dioxolane in CH_2Cl_2 by the mixture $LiAlH_4$ and $AlCl_3$. This dioxolane is very readily reduced under these conditions if the solvent is ether.

It is possible to explain the more rapid reduction of the dioxolanes as compared with the oxathiolanes. The formation of the stabilized oxocarbonium ion is easier because of the better overlap of the *p*-orbitals of the oxygen atom with the vacant *p*-orbital of the carbonium ion. Similar stabilization of the sulphocarbonium ion in the oxathiolane occurs

*See Note in the experimental section on the preparation of the chloromethyl compounds.

Can. J. Chem. Downloaded from www.nrcresearchpress.com by 210.87.254.40 on 09/05/12
For personal use only.

by the less facile overlap of the *d*-orbitals of the sulphur atom. The *formation* of the stabilized carbonium ion then must be involved in the rate-controlling step or steps of the reaction.

EXPERIMENTAL

All compounds mentioned were made by authentic and reported procedures or were newly prepared and characterized. Except where otherwise stated, all v.p.c. analyses were done with a Burrell K-2 Kromotog using a 2-m column packed with 25% of carbowax 20 M on gas-chrom P as the solid stationary phase. Helium, at a flow rate of approximately 80 ml/min was the carrier gas. The column temperature was dependent upon the boiling point of the products. Products were identified by comparison of their retention times with those of authentic samples, and/or by means of infrared spectroscopy as well as n.m.r. analyses with a Varian A-60 spectrometer. Quantitative measurements were made by comparison of v.p.c. peak areas with those obtained from known quantities of authentic reagents.

Typical Reduction Procedure. Reduction of 2-Phenyl-1,3-oxathiane

The compound, 2-phenyl-1,3-oxathiane, was prepared according to published directions (1). However, the boiling point reported was 166° at 1.2 mm while that found by us is 92° at 1.0 mm. Elemental analysis of our preparation agreed closely for the assigned structure.

To a stirred mixture of 2-phenyl-1,3-oxathiane (12.0 g, 0.067 mole) and lithium aluminum hydride (2.7 g, 0.067 mole) in ether (150 ml) at room temperature was added, over a period of 5 minutes, a solution of dry aluminum chloride (8.9 g, 0.067 mole) in 100 ml of ether. The exothermic reaction which took place during the addition required the slow admixture of the $AlCl_3$. The resulting mixture, first stirred 2 hours, was then cautiously diluted with cold water to destroy the aluminum chloride complexes and the excess hydride. In all cases the excess hydride was employed deliberately so that on treatment with water the solution remained basic at all times to avoid isomerization or hydrolysis of any unreacted acetal. The inorganic material was removed by filtration and the ethereal filtrate was dried over magnesium sulphate. Removal of the ether and distillation of the oil under reduced pressure gave a total yield of 6.5 g (54%) of material boiling at 126° at 1.6 mm. Lit. b.p., 185° at 19 mm (14). The infrared spectrum of this material was identical with that of a sample of benzyl γ-hydroxy-*n*-propyl sulphide prepared from benzyl chloride and 3-mercaptopropan-1-ol (14).

The oxathiolanes reduced by this procedure, along with authentic reduction products and their yields, are shown in Table III.

TABLE III

1,3-Oxathiolanes reduced by $LiAlH_4$ and $AlCl_3$ and product yields

1,3-Oxathiolane	Ref.	Reduction product	% yield	Ref.
2-Phenyl-1,3-oxathiolane	15	Benzyl β-hydroxyethyl sulphide	72	18
2-*n*-Propyl-1,3-oxathiolane	(See expt.)	*n*-Butyl β-hydroxyethyl sulphide	89*	18
2,2-Dimethyl-1,3-oxathiolane	16	*i*-Propyl β-hydroxyethyl sulphide	87	1
2,2-Diphenyl-1,3-oxathiolane	17	Diphenylmethyl β-hydroxyethyl sulphide	73	19

*The reaction time in this case was 210 minutes rather than the usual 2 hours.

Attempted Reduction of 2-Phenyl-1,3-dithiolane

To a stirred mixture of 2-phenyl-1,3-dithiolane (18.3 g, 0.1 mole) (20) and lithium aluminum hydride (1.9 g, 0.05 mole) in ether (120 ml) at room temperature was added a solution of dry aluminum chloride (13.4 g, 0.1 mole) in 60 ml of ether over a period of 3 to 5 minutes. The mixture was then stirred for 2 hours. Following treatment of the mixture as for the 1,3-oxathiolanes or 1,3-oxathiane above, there was obtained, by fractional distillation, 17.5 g (96%) of material whose infrared spectrum was identical with that of the original 2-phenyl-1,3-dithiolane.

A second attempt at reduction using the same conditions but with twice the amount of hydride and also with a reaction time of 48 hours gave 96% recovery of the original material. No evidence of reduction was found.

The 1,3-dithiolanes whose reductive cleavage was attempted by the above procedure are shown in Table IV.

Comparative Rates of Reduction of 2-n-Propyl-1,3-dioxolane and 2-n-Propyl-1,3-oxathiolane

The following specific procedure was used for *four* separate reductions of 2-*n*-propyl-1,3-oxathiolane and

Can. J. Chem. Downloaded from www.nrcresearchpress.com by 210.87.254.40 on 09/05/12
For personal use only.

TABLE IV

1,3-Dithiolanes subjected to reduction by $LiAlH_4$ and $AlCl_3$

1,3-Dithiolane	Ref.	Recovered 1,3-dithiolane, %	Reduction product, %
2,2-Dimethyl-1,3-dithiolane	21	96	0
2,4-Dimethyl-1,3-dithiolane	(See expt.)	92	0
2-Phenyl-4-methyl-1,3-dithiolane	22	78*	0

*The low recovery was due to accidental loss.

one for 2-*n*-propyl-,13-dioxolane. These differed only in the length of time that the reaction was allowed to proceed after admixture of all reagents. Times of 20, 40, 60, and 210 minutes were chosen for the oxathiolane experiments while a 20-minute reduction time was allowed for the dioxolane.

To a stirred mixture of acetal (0.05 mole) and lithium aluminum hydride (0.05 mole) in 70 ml of ether was added at room temperature over a period of *one* minute a solution of aluminum chloride (0.05 mole) in ether (30 ml). The mixture was then stirred for the requisite time at room temperature and then diluted carefully with cold water. After removal of the inorganic material by filtration, the ether extract was dried ($MgSO_4$). The residual oil obtained on removal of the ether was analyzed by v.p.c. The results are shown in Table II.

2-n-Propyl-1,3-oxathiolane was prepared according to modifications of the general procedure recommended in the literature (16) by condensation of *n*-butyraldehyde with 2-mercaptoethanol. *n*-Butyraldehyde (40 g) and 36 g of 2-mercaptoethanol were dissolved in 200 ml of dry benzene. To this was added 0.3 g of *p*-toluenesulphonic acid and 20 g of anhydrous magnesium sulphate. The solution, which became warm upon the addition of these reagents, was allowed to stand for 20 hours and then poured into aqueous sodium carbonate. The organic layer was separated and dried ($MgSO_4$) and then fractionally distilled. There was obtained 50 g (82%) of 2-*n*-propyl-1,3-oxathiolane boiling at 84° at 34 mm. Calc. for $C_6H_{12}OS$: C, 54.54; H, 9.09; S, 24.24. Found: C, 54.63; H, 9.17; S, 24.01.

2,4-Dimethyl-1,3-dithiolane was prepared according to the above procedure by condensation of acetaldehyde with 1,2-dimercaptopropane. Yield 77%. B.p. 81° at 25 mm. Calc. for $C_5H_{10}S_2$: C, 44.78; H, 7.46; S, 47.76. Found: C, 44.55; H, 7.47; S, 47.91.

n-Butyl β-hydroxyethyl thioether was prepared according to the procedure of Klamann and Bertsh (18). B.p. 68° at 3 mm. Lit. b.p. 106–107° at 14 mm.

Reduction of 1,3-Oxathiolanes with $LiAlH_4$–BF_3

In these reductions 2,2-dimethyl-1,3-oxathiolane (16) was used as starting material for experiments 10–13 and was prepared most conveniently in 86% yield by condensation of 2-mercaptoethanol and acetone in the presence of anhydrous magnesium sulphate and a catalytic amount of *p*-toluenesulphonic acid. Excess acetone was removed and the residual oil fractionally distilled, affording 2,2-dimethyl-1,3-oxathiolane. B.p. 57° at 45 mm; lit. b.p. 70° at 65 mm (16).

(a) Experiment 10

A mixture of 2,2-dimethyl-1,3-oxathiolane (0.15 mole) and finely divided lithium aluminum hydride (0.05 mole) in 75 ml of anhydrous ether was stirred while boron trifluoride etherate (0.05 mole) was added dropwise. After the addition, the solution was stirred for 3 hours at room temperature. After cautious addition of water, followed by removal of inorganic precipitate, the ether layer was separated and dried ($MgSO_4$). Removal of the ether left an oil (95% yield) which v.p.c. analysis showed to consist of 39% *i*-propyl β-hydroxyethyl sulphide and 61% of unchanged 2,2-dimethyl-1,3-oxathiolane.

(b) Experiment 11

In this experiment, a mixture of 2,2-dimethyl-1,3-oxathiolane (0.05 mole) and boron trifluoride etherate (0.05 mole) in ether (75 ml) was stirred whilst powdered hydride (0.05 mole) was added in small batches. The remainder of the procedure followed that for experiment 10. Total yield of material was 73%, of which 50% was the hydrogenolized product, *i*-propyl β-hydroxyethyl sulphide, and 50% the unchanged oxathiolane. The low yield (73%) was due to the occurrence of considerable resinous material.

(c) Experiment 12

The same procedure as in experiment 11 was followed except that the hydride was added in the form of lumps. The overall total yield was 75%, 56% of which was *i*-propyl β-hydroxyethyl sulphide and the remainder (44%) unreacted starting material. Here again the formation of resinous material lowered the yield.

(d) Experiment 13

The procedure of Eliel *et al.* (1) was used to reduce 2,2-dimethyl-1,3-oxathiolane with the modification that equimolar proportions of reagents were employed and the reaction time extended to 3 hours. During the

Can. J. Chem. Downloaded from www.nrcresearchpress.com by 210.87.254.40 on 09/05/12
For personal use only.

mixing of the hydride and boron trifluoride a vigorous evolution of gas took place. This had not been noted in the previous experiments. Presumably the gas was B_2H_6. The overall yield of recoverable material was 90%, of which <1% was the hydroxy sulphide and the remainder unchanged oxathiolane.

(e) Experiment 14

A quantity of 2-phenyl-1,3-oxathiolane was reduced by the procedure used in experiment 12. All of the product (29% yield) was benzyl β-hydroxyethyl sulphide. The residual material in the flask was resinous. No starting material was recovered. Analyses by v.p.c. were done with a 2-m column of 25% silicone rubber on Gas-Chrom P at a temperature of 250°. The n.m.r. spectrum agreed with the structure.

(f) Experiment 15

Reduction of 2-phenyl-1,3-oxathiolane by the procedure used in experiment 10 gave a 80% yield of material of which 73% was benzyl β-hydroxyethyl sulphide and 27% was starting material.

Preparation of cis- and trans-2-Phenyl-4-chloromethyl-1,3-dithiolane.

The method of Roberts and Cheng (22) was employed to prepare the 3,5-dinitrobenzoate of 4-hydroxymethyl-2-phenyl-1,3-dithiolane. The method of separation of the cis and trans isomers of this ester devised by Roberts and Cheng proved to be unsatisfactory. However, good separation was achieved by fractional crystallization from benzene. The higher-melting isomer, 118–119° (lit. 112–113° (22)), precipitated, leaving the lower-melting isomer, 99–100° (lit. 100–101° (22)), in solution. Concentration of the mother liquor afforded the latter in 15% yield based upon the hydroxymethyldithiolane used. A 33% yield was obtained for the 118–119° melting isomer.

Both isomeric 3,5-dinitrobenzoates were hydrolyzed to the *cis*- and *trans*-4-hydroxymethyl-2-phenyl-1,3-dithiolanes most satisfactorily by refluxing the esters for 45 minutes in a 1:1 mixture of aqueous ethanol containing 8% of potassium hydroxide. Use of only aqueous KOH as advocated by Roberts and Cheng gave less satisfactory results since much of the material remained unhydrolyzed. The high-melting isomeric ester gave a 77% yield of crude alcohol which was purified by chromatography on alumina with ether as eluant. Subsequent crystallization from benzene–skellysolve afforded the pure alcohol, m.p. 90°; lit. m.p. 88.5–89° (22). The low-melting ester gave a 74% yield of crude alcohol which after purification as above melted at 88°. Lit. m.p. 87.5–88° (22).

Conversion of the 4-hydroxymethyl-2-phenyl-1,3-dithiolane to the 4-chloromethyl-2-phenyl-1,3-dithiolane was accomplished by treatment of the alcohol with an equivalent quantity of thionyl chloride in the presence of a catalytic amount of pyridine, all in refluxing diisopropyl ether. Removal of the ether and other volatile substances gave a pale yellow solid which was purified by chromatography on alumina using skellysolve as eluant. Crystallization from skellysolve gave an analytical sample.

The isomeric alcohol melting at 90° gave the 4-chloromethyl-2-phenyl-1,3-dithiolane in 46% yield based on the alcohol used. An analytical sample melted at 68–69°. Calc. for $C_{10}H_{11}ClS_2$: C, 52.06; H, 4.77; Cl, 15.40; S, 27.77. Found: C, 51.74; H, 4.52; Cl, 15.17; S, 28.01.

The isomeric alcohol melting at 88° gave, by the same procedure, a 58% yield of the 4-chloromethyl-2-phenyl-1,3-dithiolane, melting at 60–62°. Calc. for $C_{10}H_{11}ClS_2$: C, 52.06; H, 4.77; Cl, 15.40; S, 27.77. Found: C, 51.80; H, 4.64; Cl, 15.61; S, 27.61. The n.m.r. spectrum in CS_2 with tetramethylsilane as reference compound supported the structure assigned and gave a sharp singlet for the C_2 proton at $\tau = 4.48$.

(Note: The possibility arises that during the conversion of the 4-hydroxyethyl-2-phenyl-1,3-dithiolanes to the chloromethyl compounds, expansion of the 1,3-dithiolane ring may occur as illustrated by the following scheme.

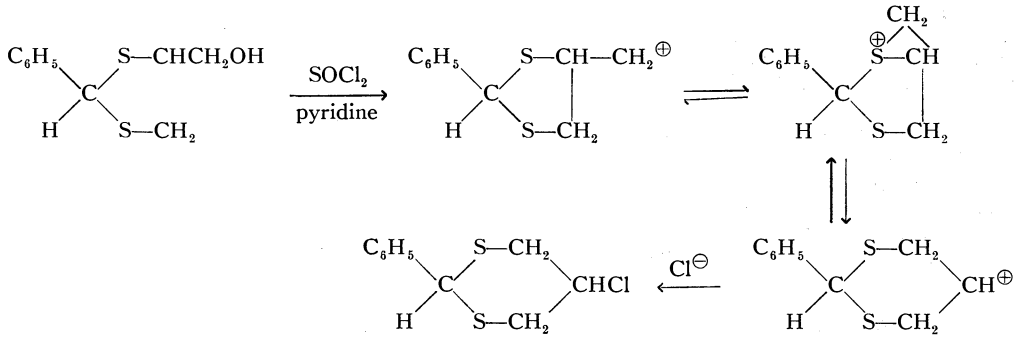

However, it is significant that the two isomeric hydroxymethyl-dithiolanes afforded different chloro derivatives upon treatment with thionyl chloride. This observation would argue against ring expansion. The n.m.r. spectrum also favors the 5-membered ring structure. *Absolute* identification however must await the synthesis of authentic 6-membered ring structures for comparison. However, the main point of the use of these dithiolanes is not affected.)

Can. J. Chem. Downloaded from www.nrcresearchpress.com by 210.87.254.40 on 09/05/12
For personal use only.

The unresolved mixture of *cis*- and *trans*-4-hydroxymethyl-2-phenyl-1,3-dithiolane gave a 65% yield of a mixture of *cis*- and *trans*-chloromethyl compounds which melted over the broad range of 57–62°. Elemental analysis of this mixture gave the following results. Calc. for $C_{10}H_{11}ClS_2$: C, 52.06; H, 4.77; Cl, 15.40; S, 27.77. Found: C, 51.83; H, 4.44; Cl, 15.59; S, 27.90. The integrated areas for proton absorption in the n.m.r. spectrum obtained in CS_2 supported the structural designation. The signal position of the C_2-proton, using tetramethylsilane as internal standard, indicated the expected mixture of the two isomers by the presence of the two singlets at 4.44 τ and 4.49 τ. The relative areas of these two signals indicated a 4:1 ratio of high-melting isomer to low-melting isomer which had occurred as result of a 3-fold crystallization from skellysolve. Further crystallization from the same solvent decreased the content of low-melting isomer in the mixture.

Attempted Reduction of 1,3-Dithiolanes by $LiAlH_4$–$AlCl_3$

A mixture of the dithiolane (0.05 mole) and lithium aluminum hydride (0.05 mole) in 60 ml of dry ether was stirred while a solution of aluminum chloride (0.05 mole) in 20 ml of ether was added dropwise. The reaction mixture was then stirred under nitrogen until a total reaction time of 2 hours had elapsed. Decomposition and subsquent treatment of the reaction mixture in the usual manner afforded only the original unchanged material in at least 90% yield. No alkali-soluble materials were obtained. Vapor phase chromatographic analyses gave no indication of a product other than starting material. Increase in reaction time to 24 hours also failed to yield any hydrogenolyzed products. The compounds subjected to this treatment are shown in Table I, experiments 6–9, and in Table IV.

Equilibration of cis- and trans-4-Chloromethyl-2-phenyl-1,3-dithiolane

In Diethyl Ether as Solvent

A solution of 230 mg of the isomer melting at 68–69° in 20 ml of ether was treated with 135 mg of anhydrous aluminum chloride in 10 ml of ether. The reaction mixture was allowed to stand at room temperature for 20 hours and then poured into aqueous sodium bicarbonate. The ether layer was separated and dried. Evaporation of the solvent afforded 100 mg of product melting sharply at 67–68°. Nuclear magnetic resonance analyses indicated that no equilibration had occurred since only one sharp singlet occurred at $\tau = 4.43$ characteristic of the C_2-proton of the high-melting isomer.

When boron trifluoride etherate was used as the Lewis acid, the same results were obtained.

In Methylene Chloride as Solvent

A quantity (290 mg) of the isomer melting at 68–69° was dissolved in methylene chloride previously dried for 48 hours over $CaCl_2$. Anhydrous boron trifluoride was bubbled into the solution for several minutes and the resulting solution allowed to stand for 90 minutes. The solution was then poured into aqueous sodium bicarbonate. The organic layer was separated, washed with aqueous bicarbonate, then with water, and finally dried (Na_2CO_3). Evaporation of the solvent gave 225 mg of material melting at 51–54°. An n.m.r. spectrum (CS_2) of this product indicated a mixture of *cis*- and *trans*-4-chloromethyl-2-phenyl-1,3-dithiolane in which the high-melting isomer predominated slightly over the low-melting isomer as determined by the integrated areas and by visual inspection of the two singlets at $\tau = 4.43$ and 4.48.

The same reaction was carried out using $AlCl_3$ as the catalyst rather than BF_3, and allowing the reaction mixture to stand for 20 hours. When the mixture was worked up as before, a resinous material was obtained. An n.m.r. spectrum of this substance indicated extensive decomposition and nothing definite concerning isomerization.

A repetition of the reaction with $AlCl_3$ as catalyst, but for a period of 4 hours, gave a resinous oily product whose n.m.r. spectrum showed a somewhat broader and poorly resolved signal at 4.46 τ, indicating that isomerization had occurred along with decomposition.

ACKNOWLEDGMENT

The authors wish to express their appreciation for the generous financial assistance given by the National Research Council of Canada throughout the course of this work.

REFERENCES

1. E. L. Eliel, L. A. Pilato, and V. G. Badding. J. Am. Chem. Soc. **84**, 2377 (1962).
2. E. L. Eliel and V. G. Badding. J. Am. Chem. Soc. **81**, 6087 (1959).
3. I. Shapiro, H. G. Weiss, M. Schmick, S. Skolnik, and G. B. L. Smith. J. Am. Chem. Soc. **74**, 901 (1952).
4. J. R. Elliot, W. L. Roth, G. F. Roedel, and E. M. Boldebuck. J. Am. Chem. Soc. **74**, 5211 (1952).
5. N. O. Calloway. J. Am. Chem. Soc. **59**, 1474 (1937).
6. E. L. Eliel, V. G. Badding, and M. N. Rerick. J. Am. Chem. Soc. **84**, 2371 (1962).
7. E. L. Eliel. Record Chem. Progr. **22**, 129 (1961).
8. E. L. Eliel and M. N. Rerick. J. Org. Chem. **23**, 1088 (1958).
9. J. Hine. Physical organic chemistry. McGraw-Hill Book Co., Inc., New York. 1956. p. 150.
10. D. P. Harnish and D. S. Tarbell. J. Am. Chem. Soc. **70**, 4123 (1948).

Can. J. Chem. Downloaded from www.nrcresearchpress.com by 210.87.254.40 on 09/05/12
For personal use only.

11. D. S. TARBELL and D. P. HARNISH. J. Am. Chem. Soc. **74**, 1862 (1952).
12. D. S. TARBELL and D. P. HARNISH. Chem. Rev. **49**, 1 (1951).
13. C. M. SUTER and H. L. HANSON. J. Am. Chem. Soc. **54**, 4100 (1932).
14. E. ROTHSTEIN. J. Chem. Soc. 684 (1934).
15. F. KIPNIS and J. ORNFELT. J. Am. Chem. Soc. **71**, 3555 (1949).
16. C. DJERASSI and M. GORMAN. J. Am. Chem. Soc. **75**, 3704 (1953).
17. J. R. MARSHALL and H. A. STEVENSON. J. Chem. Soc. 2361 (1959).
18. D. KLAMANN and H. BERTSCH. Ber. **88**, 201 (1955).
19. Z. J. VEJDELEK, V. TRCKA, H. CHYBOBA, and L. TUMA. Chem. Listy, **47**, 49 (1953); Chem. Abstr. **49**, 337 (1955).
20. H. FASBENDER. Ber. **20**, 461 (1887). F. K. BEILSTEIN. Handbuch der organischen Chemie. Vol. 19. Springer-Verlag, Berlin. p. 24.
21. H. FASBENDER. Ber. **21**, 1476 (1888). F. K. BEILSTEIN. Handbuch der organischen Chemie. Vol. 19 Springer-Verlag, Berlin. p. 9.
22. R. M. ROBERTS and C. CHENG. J. Org. Chem. **23**, 983 (1958).

Can. J. Chem. Downloaded from www.nrcresearchpress.com by 210.87.254.40 on 09/05/12
For personal use only.

INVESTIGATION OF THE SELF-ASSOCIATION OF PHENOLS AND ANILINES BY ULTRAVIOLET SPECTROSCOPY

J. C. DEARDEN[1]

Department of Chemistry, Memorial University of Newfoundland, St. John's, Newfoundland

Received February 25, 1963

ABSTRACT

Equations are derived for the calculation of the extent of self-association from ultraviolet absorption spectra. The spectra of a number of phenols and anilines have been taken over wide concentration ranges, and are discussed in terms of association. Association constants for four of the compounds have been calculated. An explanation of the spectral effects of self-association is offered.

Can. J. Chem. Downloaded from www.nrcresearchpress.com by 210.87.254.5 on 09/05/12
For personal use only.

INTRODUCTION

A compound capable of forming a hydrogen bond may associate either with itself or with another hydrogen bonding compound, and such association manifests itself in the ultraviolet absorption spectrum of the compound. The electronic spectral effects of hydrogen bonding between unlike molecules have been widely studied (1), but ultraviolet spectroscopic investigation of self-association has been limited, partly because of the difficulty of obtaining spectra of highly concentrated solutions. Qualitative ultraviolet studies of self-association have recently been made by Ungnade and Lamb (2) on benzoic acids, Forbes *et al.* on benzoic acids (3) and phenols and anilines (4), Rao and Murthy (5) on phenol, Arvan and Zaitseva (6) on dyes, and Lippert and Oechssler (7) on acetic acids. Attempts to determine degrees of association by ultraviolet spectroscopy have been made by von Keussler (8) on phenol, Ito (9) on substituted phenols, and Kaye and Poulson (10) on methanol. Levshin *et al.* (11, 12) have calculated degrees of association and hydrogen bonding energies in dyes, from measurements of the concentration and temperature dependences of their spectra.

In the present paper, equations representing monomer–dimer, monomer–trimer, and monomer–polymer equilibria have been developed.

THE ASSOCIATION OF PHENOL

The evidence for the mode of association of phenol is conflicting. Various workers consider that it forms a dimer (13) or a cyclic dimer (9), a trimer (14, 15), or a polymer (9, 16).

The formation of a cyclic dimer is unlikely for two reasons. Firstly, the hydrogen bonds in such a structure would be strained; secondly, further association would be inhibited, since approach to the proton-accepting sites in the dimer would be sterically hindered. Now, it has been shown (17) that the apparent molecular weight of phenol increases continually with concentration; it is therefore probable that phenol associates first into open dimers and then into open trimers and polymers with increasing concentration (see also ref. 18).

The method developed below for the calculation of the monomer fraction (α) from ultraviolet spectra requires prior knowledge of the relation between the association constant (K) and α, and necessitates the assumption of constant K.

[1]*Present address: "Shell" Research Limited, Thornton Research Centre, P.O. Box 1, Chester, England.*

THE CALCULATION OF MONOMER FRACTION

Three equations are considered, each of which involves a single association constant K:

(i) $$K = \frac{1-\alpha}{2\alpha^2 C}$$ representing dimer formation,

(ii) $$K = \frac{1-\alpha}{3\alpha^3 C^2}$$ representing trimer formation,

(iii) $$K = \frac{1-\sqrt{\alpha}}{\alpha C}$$ representing polymer formation (16),

where C denotes molar concentration.

Ito (9) has shown that, in a spectrum containing monomer and dimer bands, the apparent molar absorptivity ϵ at any wavelength is given by:

(iv) $$\epsilon = \epsilon_M\alpha + \tfrac{1}{2}\epsilon_D(1-\alpha),$$

where ϵ_M and ϵ_D are the true molar absorptivities of monomer and dimer, respectively.

From (iv)

(v*a*) $$\epsilon_1 = \epsilon_M\alpha_1 + \tfrac{1}{2}\epsilon_D(1-\alpha_1)$$

and

(v*b*) $$\epsilon_2 = \epsilon_M\alpha_2 + \tfrac{1}{2}\epsilon_D(1-\alpha_2),$$

where subscripts 1 and 2 refer to concentrations C_1 and C_2.

From (v*a*)

$$\alpha_1 = \frac{\epsilon_1 - \frac{1}{2}\epsilon_D}{\epsilon_M - \frac{1}{2}\epsilon_D}$$

so that

(vi*a*) $$1-\alpha_1 = \frac{\epsilon_M - \epsilon_1}{\epsilon_M - \frac{1}{2}\epsilon_D}.$$

Similarly, from (v*b*)

(vi*b*) $$1-\alpha_2 = \frac{\epsilon_M - \epsilon_2}{\epsilon_M - \frac{1}{2}\epsilon_D}.$$

Combination of (vi*a*) and (vi*b*) gives

(vii) $$\frac{1-\alpha_1}{1-\alpha_2} = \frac{\epsilon_1 - \epsilon_M}{\epsilon_2 - \epsilon_M} = Q, \text{ say.}$$

Similarly, from (i)

(viii) $$\frac{1-\alpha_1}{\alpha_1^2 C_1} = \frac{1-\alpha_2}{\alpha_2^2 C_2}.$$

From (viii)

(ix) $$\alpha_2 = \pm\alpha_1\sqrt{(C_1/QC_2)}.$$

Substituting (ix) in (vii),

$$Q = \frac{1-\alpha_1}{1\pm\alpha_1\sqrt{(C_1/QC_2)}}.$$

Can. J. Chem. Downloaded from www.nrcresearchpress.com by 210.87.254.5 on 09/05/12
For personal use only.

Hence

$$Q \pm \alpha_1 \sqrt{(QC_1/C_2)} = 1-\alpha_1.$$

This is rearranged to give

$$\alpha_1 = \frac{1-Q}{1 \pm \sqrt{(QC_1/C_2)}}.$$

However, only the solution

(x) $$\alpha_1 = \frac{1-Q}{1-\sqrt{(QC_1/C_2)}}$$

is valid, since α must lie between 0 and +1.*

A similar expression for α_1 is obtained if monomer–trimer equilibrium is assumed. In this case, (iv) is replaced by

$$\epsilon = \epsilon_M \alpha + \tfrac{1}{3}\epsilon_T(1-\alpha),$$

where ϵ_T is the true molar absorptivity of the trimer. The expression for α_1 is then given by

$$\alpha_1 = \frac{1-Q}{1-\sqrt[3]{(Q^2C_1^2/C_2^2)}}.$$

The case of monomer–polymer equilibrium cannot be so easily solved; treatment as above yields a complicated expression containing α^6. A simple graphical solution may, however, be obtained as follows. From (iii)

$$\frac{1-\sqrt{\alpha_1}}{\alpha_1 C_1} = \frac{1-\sqrt{\alpha_2}}{\alpha_2 C_2}.$$

Arbitrary values of α_1 and α_2 between 0 and +1 are substituted in $(1-\sqrt{\alpha_1})/\alpha_1 C_1$ and $(1-\sqrt{\alpha_2})/\alpha_2 C_2$ respectively, using the experimental values of C_1 and C_2. From plots of α_1 versus $(1-\sqrt{\alpha_1})/\alpha_1 C_1$ and of α_2 versus $(1-\sqrt{\alpha_2})/\alpha_2 C_2$ corresponding values of α_1 and α_2 are obtained for a range of values of $(1-\sqrt{\alpha_1})/\alpha_1 C_1$. The intersect of a plot of α_1 versus α_2 with the line

(xi) $$\alpha_2 = 1 - \frac{1-\alpha_1}{Q}$$

derived from (vii) yields both α_1 and α_2.

Equation (xi) involves the assumption that the molar absorptivities of all complexes are equal. This is probably only approximately true; as will be shown later, each complex probably has a slightly different spectrum.

RESULTS AND DISCUSSION

The ultraviolet spectra of several phenols and anilines in cyclohexane solution have been obtained over wide concentration ranges. The results have been published previously (4) and so only the spectral curves for phenol are reproduced here (Fig. 1). (Spectral data for the other compounds studied can, if required, be obtained from the author.)

**Ito (9) obtains the equation*

$$1-\alpha = \frac{C_2-C_1}{QC_2-C_1} \pm \sqrt{\left(\frac{(3Q+1)C_1C_2}{QC_2-C_1}\right)},$$

which appears to be incorrect.

Can. J. Chem. Downloaded from www.nrcresearchpress.com by 210.87.254.5 on 09/05/12
For personal use only.

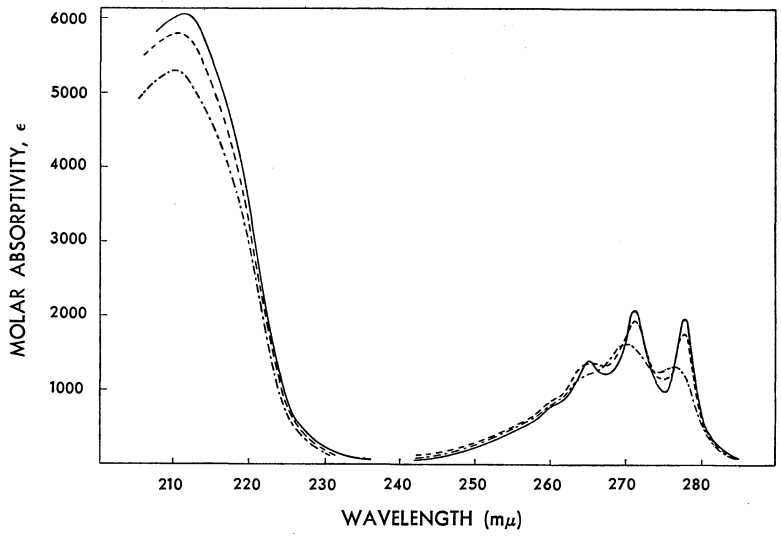

FIG. 1. The spectrum of phenol in cyclohexane at various concentrations. *K*-Band: 0.924×10^{-4} *M* (—); 2.88×10^{-2} *M* (- - -); 0.499 *M* (-·-). *B*-Band: 2.31×10^{-4} *M* (—); 0.104 *M* (- - -); 2.44 *M* (-·-).

The spectra of these compounds show upon self-association slight hypsochromism and hypochromism in both the *K*- and *B*-bands,* together with loss of fine structure in the latter.

Isosbestic points do not occur in the spectra. Ito (9) also observed this, but believed it to be due to experimental inaccuracies, and corrected his spectra so as to obtain isosbestic points. However, it is here considered that the absence of isosbestic points in the spectra is real and is caused by the existence of a number of different complexes, each with its own spectrum (cf. refs. 12, 19).

Phenol

There is wide disparity between the present results for the concentration dependence of the phenol spectrum and those of von Keussler (8) and Ito (9). The present results agree closely, however, with those of Rao and Murthy (5). The spectrum of anisole, which compound is incapable of self-association through hydrogen bonding, also shows a hypochromic effect with increasing concentration. It does not, however, display a hypsochromic shift; such a shift may therefore be taken as evidence of hydrogen bonding. Anisole probably associates slightly (see ref. 20) through dipole–dipole interaction, but this in no way affects the validity of the calculation of α as described above, since the mechanism of association is immaterial to the calculation.

From the spectra obtained, the variation of α with concentration, and the association constant *K*, have been calculated for the cases of dimer, trimer, and polymer formation. The values of *K* are shown in Table I, and of α in Fig. 2. These values are the means of values calculated at several wavelengths. Agreement amongst individual values was reasonably good. In Fig. 2 a comparison is made with the data of Mecke (16) in carbon tetrachloride solution. Since carbon tetrachloride is a weak proton acceptor, it would be expected that self-association in this solvent would be less than in cyclohexane. Hence the values of α determined in the present work are rather high, and those of *K* rather low,

**Referred to in ref. 4 as B- and C-bands, respectively.*

Can. J. Chem. Downloaded from www.nrcresearchpress.com by 210.87.254.5 on 09/05/12
For personal use only.

TABLE I

Association constants of the self-association of phenols and aniline, calculated from ultraviolet spectra

Compound	Assuming dimer formation (liters/mole)	Assuming trimer formation (liters²/mole²)	Assuming polymer formation (liters/mole)
Phenol	1.28	15.4	1.45
m-Cresol	1.87	30.7	2.68
p-Cresol	1.93	34.0	2.30
Aniline	2.02	80.0	2.71

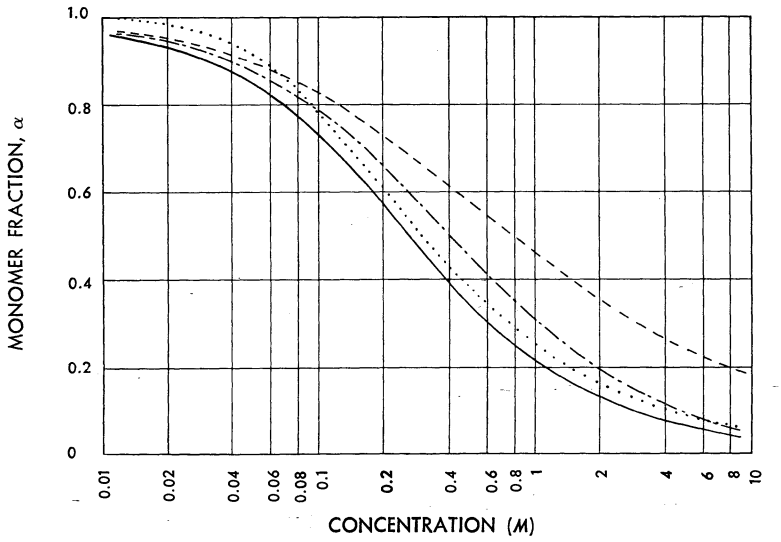

FIG. 2. The change of monomer fraction of phenol in cyclohexane with concentration, assuming dimeric (- - -), trimeric (· · ·), and polymeric (-·-) association, and the data of Mecke in carbon tetrachloride (—).

due probably to experimental error (see Experimental). However, it is important to note that Mecke's curve shows a marked disparity in shape with the dimer curve, but quite good agreement with the trimer and polymer curves, with the latter having the best overall fit.

The effect of association on the *B*-band of phenol is shown in Fig. 3; the polymer spectrum was calculated assuming $\alpha = 0.1$ at a concentration of 2.44 M in cyclohexane. The value of $\alpha = 0.1$ is rather less than that calculated from the present ultraviolet data, and was estimated from Mecke's value of $\alpha = 0.11$ in carbon tetrachloride. The polymer spectrum has slightly more pronounced fine structure, and a slightly smaller band width, than has von Keussler's (8) spectrum of pure liquid phenol. These features are consistent with the concept of the size of the associated molecule increasing continually with concentration.

The Cresols

The present results for the concentration dependence of the spectrum of *o*-cresol were not sufficiently accurate for values of α and K to be calculated. The values of K for *m*- and *p*-cresol are given in Table I, and the variation of α with concentration in Figs. 4 and 5.

Can. J. Chem. Downloaded from www.nrcresearchpress.com by 210.87.254.5 on 09/05/12
For personal use only.

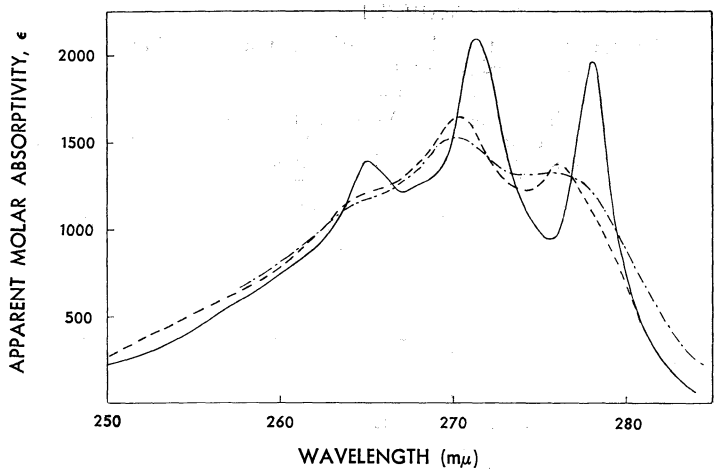

FIG. 3. The *B*-band of phenol in cyclohexane: monomer (—), polymer at 2.44 *M* (- - -) and the data of von Keussler for pure liquid (···).

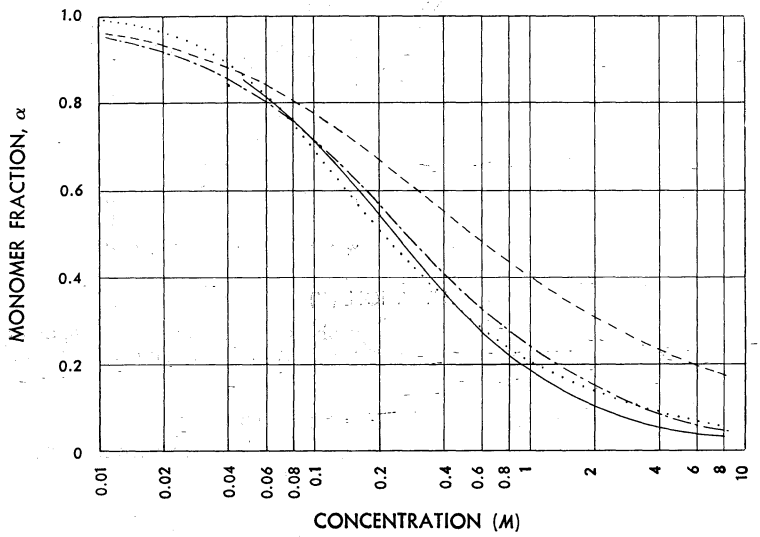

FIG. 4. The change of monomer fraction of *m*-cresol in cyclohexane with concentration, assuming dimeric (- - -), trimeric (···), and polymeric (-·-) association, and the data of Azimi-Pour in carbon tetrachloride (—).

Figure 4 also includes the data of Azimi-Pour (21) for *m*-cresol in carbon tetrachloride, determined by infrared spectroscopy. The data are seen to be in fair agreement, with the present α values again slightly high. The same may be said of the present results for *p*-cresol (Fig. 5) compared with those of Bono (22) from infrared spectra. For both these compounds the assumption of a monomer–trimer or monomer–. . .–polymer equilibrium gives a much better fit with the infrared data than does that of a monomer–dimer equilibrium.

2,6-Di-tert-butylphenol

There appears to be no significant concentration dependence of the spectrum of this compound (4), save for a slight hypsochromic shift at high concentrations. This is consistent with the concept of the very bulky *tert*-butyl groups' preventing the formation

Can. J. Chem. Downloaded from www.nrcresearchpress.com by 210.87.254.5 on 09/05/12
For personal use only.

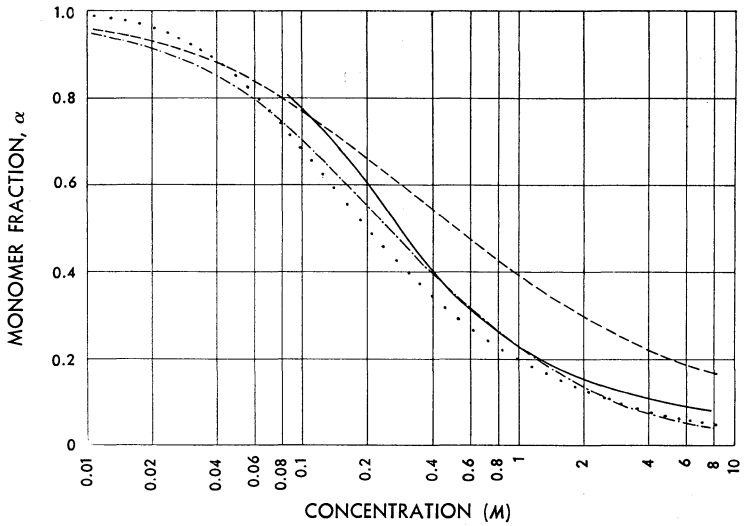

FIG. 5. The change of monomer fraction of *p*-cresol in cyclohexane with concentration, assuming dimeric (- - -), trimeric (· · ·), and polymeric (-·-) association, and the data of Bono in carbon tetrachloride (—).

of an intermolecular hydrogen bond. This phenomenon has been demonstrated in infrared studies by Bellamy and Williams (23), who have shown that the compound is monomeric even as a pure liquid.

Aniline

The *B*-band of aniline displays no appreciable concentration dependence (4), in contrast to the *K*-band, whilst no significant effect is observed on either band in N,N-dimethylaniline. Since the *K*-band of aniline is well clear of any strong high-frequency band absorption, an attempt was made to calculate α and K for aniline from its change in molar absorptivity (see Table I and Fig. 6). The results give α values which are too low, since

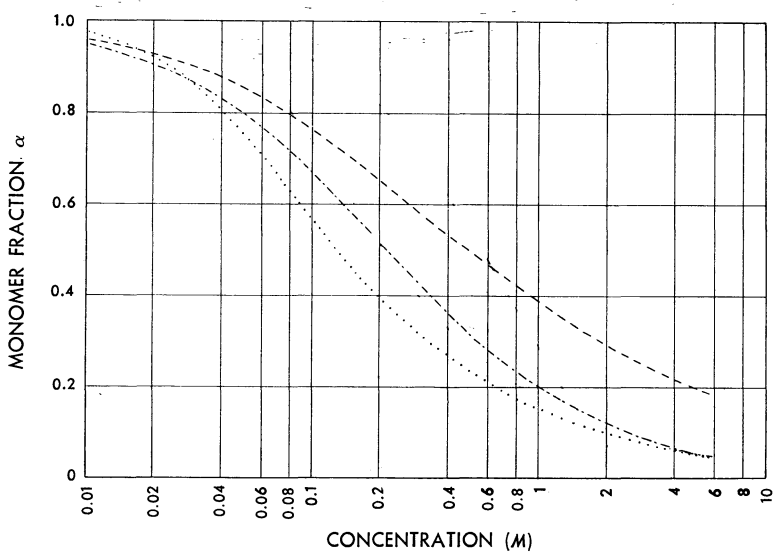

FIG. 6. The change of monomer fraction of aniline in cyclohexane with concentration, assuming dimeric (- - -), trimeric (· · ·), and polymeric (-·-) association.

Can. J. Chem. Downloaded from www.nrcresearchpress.com by 210.87.254.5 on 09/05/12
For personal use only.

it is well known that aniline associates to a lesser degree than, say, phenol. So far as is known, no data have previously been published giving α as a function of concentration for aniline. Fuson *et al.* (24) attempted to determine this by infrared methods but obtained inconclusive results.

THE NATURE OF THE HYPSOCHROMIC SHIFT

Pimentel (25) has differentiated between the spectral effects of two types of hydrogen bond in the case of a compound such as a substituted benzene in which the substituent is ortho,para-directing. A bathochromic shift occurs when the absorbing species acts as proton donor, and a hypsochromic shift occurs when it acts as proton acceptor. In the self-association of phenol (and aniline) both types of hydrogen bonding occur, whether cyclic or open polymers are involved, and so it is difficult to say a priori whether the spectra should shift to longer or shorter wavelengths.

The hydroxyl group in phenol is an electron-donating group, and in the monomeric molecule electron migration is into the ring. When the hydroxyl group acts as proton donor, migration into the ring is increased. Conversely, when the groups acts as proton acceptor, migration into the ring is decreased. If the group acts as both proton donor and proton acceptor, as in I, increased migration, not to the ring, but to the adjacent hydrogen bond,

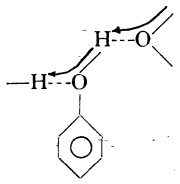

I

will occur, which incidentally may have the effect of strengthening that bond. Thus the shift of the spectrum of I will be similar to that of the spectrum of phenol behaving only as a proton acceptor. Although this latter spectrum has not been isolated, it probably corresponds closely to that of phenol in water. Evidence for this comes from the 1 mμ hypsochromic shift of the phenol spectrum on going from cyclohexane to water solution (26), and from the almost complete absence of K-band absorption corresponding to proton donating molecules, in water solution (4). The shift caused by self-association (1–2 mμ) is thus, as predicted above, similar to that caused by phenol's acting as proton acceptor.

EXPERIMENTAL

Spectra were obtained in spectroanalyzed cyclohexane (Fisher) at ca. 25° C on a Unicam SP 500 spectrophotometer, with a wavelength accuracy of ca. $\pm$0.5 mμ and repeatability of ca. 0.1 mμ in the relevant spectral region. For determinations at high concentrations, two specially constructed cells (Research and Industrial Instruments Co., London, England) were used, with path lengths of 25.1 μ and 2.91 μ. These lengths were measured by the manufacturers to an accuracy of $\pm$1%. However, the spacers in the cells were made of "Teflon", which compresses under load, and so it is probable that the path lengths were slightly different each time the cells were assembled, which would cause slight errors in the determination of apparent molar absorptivity.

The compounds used were commercial materials, and were purified by vacuum distillation or recrystallization.

ACKNOWLEDGMENTS

The author wishes to thank Professor W. F. Forbes, of the University of Waterloo, Ontario, and Drs. W. T. Thorneycroft and E. G. Vaal, of Thornton Research Centre, for helpful discussion.

Can. J. Chem. Downloaded from www.nrcresearchpress.com by 210.87.254.5 on 09/05/12
For personal use only.

REFERENCES

1. G. C. PIMENTEL and A. L. MCCLELLAN. The hydrogen bond. W. H. Freeman & Co., San Francisco. 1960. p. 159.
2. H. E. UNGNADE and R. W. LAMB. J. Am. Chem. Soc. **74**, 3789 (1952).
3. W. F. FORBES and A. R. KNIGHT. Can. J. Chem. **37**, 334 (1959). W. F. FORBES, A. R. KNIGHT, and D. L. COFFEN. Can. J. Chem. **38**, 728 (1960).
4. J. C. DEARDEN and W. F. FORBES. Can. J. Chem. **38**, 896 (1960).
5. C. N. R. RAO and A. S. N. MURTHY. J. Sci. Ind. Res. (India), **20B**, 290 (1961).
6. KH. L. ARVAN and N. E. ZAITSEVA. Opt. Spectry. (USSR) (Engl. Transl.), **11**, 38 (1961).
7. E. LIPPERT and D. OECHSSLER. Z. Physik. Chem. (Frankfurt), **29**, 403 (1961).
8. V. VON KEUSSLER. Z. Elektrochem. **58**, 136 (1954).
9. M. ITO. J. Mol. Spectry. **4**, 125 (1960).
10. W. KAYE and R. POULSON. Nature, **193**, 675 (1962).
11. V. L. LEVSHIN and E. G. BARANOVA. Opt. Spectry. (USSR) (Engl. Transl.), **6**, 31 (1959).
12. V. L. LEVSHIN and V. K. GORSHKOV. Opt. Spectry. (USSR) (Engl. Transl.), **10**, 401 (1961).
13. F. A. PHILBRICK. J. Am. Chem. Soc. **56**, 2581 (1934).
14. K. ENDO. Bull. Chem. Soc. Japan, **1**, 25 (1926).
15. M. SAUNDERS and J. B. HYNE. J. Chem. Phys. **29**, 1319 (1958).
16. R. MECKE. Discussions Faraday Soc. **9**, 161 (1950). H. KEMPTER and R. MECKE. Naturwiss. **27**, 593 (1939); Z. Physik. Chem. **B46**, 229 (1940).
17. C. R. BURY and H. O. JENKINS. J. Chem. Soc. 688 (1934).
18. T. CAIRNS and G. EGLINTON. Nature, **196**, 535 (1962).
19. N. I. SHISHKIN and I. I. NOVAK. Zh. Tekhn. Fiz. **23**, 1485 (1953).
20. C. HEATHCOCK. Can. J. Chem. **40**, 1865 (1962).
21. H. AZIMI-POUR. Rev. Inst. Franc. Petrole Ann. Combust. Liquides, **15** (4), 1 (1960).
22. D. BONO. Ann. Chim. (Paris), **1**, 588 (1956).
23. L. J. BELLAMY and R. L. WILLIAMS. Proc. Roy. Soc. (London), Ser. A, **254**, 119 (1960).
24. N. FUSON, M.-L. JOSIEN, R. L. POWELL, and E. UTTERBACK. J. Chem. Phys. **20**, 145 (1952).
25. G. C. PIMENTEL. J. Am. Chem. Soc. **79**, 3323 (1957).
26. J. C. DEARDEN and W. F. FORBES. Can. J. Chem. **37**, 1294 (1959).

Can. J. Chem. Downloaded from www.nrcresearchpress.com by 210.87.254.5 on 09/05/12
For personal use only.

Can. J. Chem. Downloaded from www.nrcresearchpress.com by 210.87.254.6 on 09/05/12
For personal use only.

NOTES

π-BONDING IN INORGANIC COMPOUNDS
PART 5. DELOCALIZATION OF *d*-ORBITALS IN K_2RuCl_6 AND K_2OsCl_6

A. D. WESTLAND

In a previous article it was shown that the molar magnetic susceptibility of K_2OsCl_6 is much increased when it is diluted with K_2PtCl_6 (1). This was interpreted as a consequence of spin–spin interaction operating by the delocalization of metal *d*-orbitals through ligand *p*-orbitals (2). A similar behavior was observed by Johannesen and Candela for $(NH_4)_2OsBr_6$ dissolved in $(NH_4)_2PtBr_6$ (3). These authors related the spin coupling in a variety of chloro- and bromo-osmates to the mean distance between nearest osmium atoms.

As the bond system of K_2RuCl_6 differs from that of K_2OsCl_6 only in such respects as may be affected by the principal quantum numbers of the metal orbitals and, moreover, as the two compounds possess the same geometry with very nearly the same interatomic distances, it was considered of interest to examine the magnetic behavior of the mixed-crystal system K_2RuCl_6/K_2PtCl_6.

Measurements of the magnetic susceptibility of K_2RuCl_6 have yielded values which are considerably higher than the corresponding values for K_2OsCl_6 (3, 4). This seems to indicate that there is less spin coupling in the case of the ruthenium compound but dilution experiments are required to verify this.

Theoretical estimates of χ have been made by several workers. In 1949, Kotani examined the effect of spin–orbit coupling on calculations of magnetic susceptibility and derived an expression for strong field $(t_{2g})^n$ complexes assuming *inter alia* that coulomb energies are much stronger than spin–orbit coupling (5). This predicts for $(t_{2g})^4$ a singlet ground state with a large intraconfigurational temperature-independent paramagnetism provided that $\zeta \gg kT$ where ζ is the spin–orbit coupling constant. Figgis and his collaborators have shown that this description is not very satisfactory for $OsCl_6^{2-}$ for it leads to a value of ζ_{5d} which is much too large (6). Also they noted that assuming *jj*-coupling overcompensates for the discrepancy. The susceptibility of K_2RuCl_6 was found to exhibit some temperature dependence. Griffith improved the calculation for Ru^{4+}, Os^{4+}, and Ir^{5+} by assuming intermediate coupling (7). He obtained good agreement with experiment by employing the spin–orbit coupling constant and the Racah parameters $3B+C$, obtained from spectroscopic data for the free ions. Kamimura and co-workers came independently to the same result (8). These calculations did not take into account the possibility of spin–spin interaction and since this was shown in the preceding papers of this series to have a very great influence, the agreement between theory and experiment is somewhat deceptive. We proceed also to show that previous work on K_2RuCl_6 was in error.

EXPERIMENTAL

Magnetic measurements were carried out using the Gouy method. Corrections for diamagnetism were based on the measured value for K_2PtCl_6 prepared in a manner identical with that followed for the ruthenium samples.

The solid solutions were prepared by mixing solutions of H_2RuCl_6 and H_2PtCl_6 in various proportions,

the solutions at no time being allowed to become less acid than 9 *N* in HCl. The ruthenium solution was prepared as described by Howe (9) by the oxidation of H_2RuCl_5OH with chlorine in strongly acid (HCl) solution. An equal volume of a saturated solution of KCl in 8 *N* HCl was added to the first solution. Mixed crystals varying in color from black to red-brown, depending upon the ratio of the components, appeared rapidly. These were separated on a fritted-glass filter, washed with 9 *N* HCl and sucked as dry as possible. The products so obtained were dried in a stream of dry hydrogen chloride gas at 35° C. Analysis for K_2RuCl_6: Calc.: Cl, 54.27; Ru, 25.89. Found: Cl, 54.1; Ru, 26.01. Drying at 100° C resulted in hydrolyzed products even when a hydrogen chloride atmosphere was employed. Evidence of hydrolysis was obtained from the infrared absorption spectrum obtained from a nujol mull. Absorption in the region ~3600 cm^{-1}, taken to be due to O—H stretching, was associated with a low magnetic susceptibility. A similar absorption band was exhibited by K_2PtCl_5OH and $K_4Ru_2Cl_{10}O \cdot H_2O$.

X-Ray powder diffraction photographs did not indicate any detectable inhomogeneity.

The preparations were analyzed by distillation and gravimetric estimation of the ruthenium following the method of Thiers *et al.* (10). Platinum was precipitated with zinc after distillation of the ruthenium. Chlorine was determined gravimetrically as silver chloride after treatment of a separate sample with magnesium.

RESULTS AND DISCUSSION

Values of the molar magnetic susceptibility of K_2RuCl_6 in solid solution with K_2PtCl_6 are presented in Table I. The data for the pure salt are in close agreement with those of

TABLE I

Magnetic susceptibility data for the system K_2RuCl_6–K_2PtCl_6
(Values for molar susceptibilities include an estimate, $\chi_d = 0.2\times10^{-3}$, for the molar diamagnetism of K_2RuCl_6)

Mole% K_2RuCl_6	Temperature (°K)	$\chi_g\times10^3$	$\chi_M\times10^3$	μ_{eff}
0.0	90	−0.43	−0.21	
(K_2PtCl_6)	195	−0.43	−0.21	
	300	−0.40	−0.20	
5.93	90	0.161	4.6	1.8
	195	0.011	3.6	2.4
	300	−0.025	3.1	2.7
31.6	90	2.51	4.24	1.75
	195	2.34	4.02	2.50
	300	2.17	3.73	2.98
63.1	90	4.73	3.92	1.68
	195	4.55	3.82	2.44
	300	4.29	3.60	2.94
71.5	90	5.51	3.99	1.70
	195	5.34	3.90	2.46
	300	4.83	3.54	2.92
100.0*	90	9.84	4.06	1.71
	195	9.59	3.96	2.48
	300	8.79	3.65	2.96
100.0†	91.3		3.65	
	288.1		3.11	
100.0‡	63	9.42	3.89	
	78	9.36	3.87	
	298	8.30	3.45	

*Present work.
†Reference 4.
‡Reference 3.

Johannesen and Candela (3). The values given by Earnshaw *et al.* are somewhat lower (4). We found that low values were obtained unless the samples were dried at a low temperature in a stream of dry hydrogen chloride gas (see experimental section).

It is apparent that the results for mixed crystals are not appreciably dependent upon concentration of ruthenium.

This is a sharp contrast to the behavior of K_2OsCl_6, where there is nearly a doubling of the room-temperature susceptibility upon diluting to ~5 mole%.

Can. J. Chem. Downloaded from www.nrcresearchpress.com by 210.87.254.6 on 09/05/12
For personal use only.

It must be concluded that there is no significant degree of spin superexchange in K_2RuCl_6 despite the fact that it is isoelectronic and isostructural with K_2OsCl_6. It follows that there is much less pronounced p_π–d_π orbital overlap between chlorine and ruthenium than between chlorine and osmium. It may be argued instead that there is less overlap between the chlorine atoms of neighboring $RuCl_6^{2-}$ groups than between chlorines in $OsCl_6^{2-}$ groups. This would be the case if the Cl—Cl distance were greater. This possibility cannot be ruled out, as sufficiently accurate X-ray diffraction data are not available. However, as the lattice constants of K_2RuCl_6 and K_2OsCl_6 are nearly identical, there are strong grounds for supposing that all corresponding interatomic distances are very nearly the same in both compounds.

Our evidence for greater *d*-orbital extension in the osmium compound is in accord with other evidence of a pronounced difference in the bonding to members of the second and third transition series, respectively. For example, back coordination of metal *d*-electrons to vacant *d*-orbitals on ligand atoms is apparently more extensive for third-row elements. As an instance of this we note the stability of the sulphoions of Os, Ir, and Pt while the corresponding ions of Ru, Rh, and Pd are not formed. Similarly, complexes containing organic sulphides or phosphines etc. and elements of the former group of metals are generally more stable than corresponding complexes of the latter group.

Griffith's estimate of the low-temperature susceptibility of K_2RuCl_6, viz. $\chi_M = 3650\times10^{-6}$ c.g.s. units/mole, is rather low compared to our value of $\chi_M = 4100\times10^{-6}$ obtained by extrapolation of the data to 0° K. An improved estimate would include the effect of orbital reduction. The theory for this was worked out by Griffith although it was not made use of by him in the case of ruthenium as existing experimental data did not seem to require it. He gives

$$\chi_M = \frac{2N\beta^2(1+\cos\theta)(k+2)^2}{3\delta(1/4\sqrt{2}\tan\theta - 1 + \sec\theta)} \qquad [1]$$

where $\delta = 1/2(15B+5C+\zeta)k$ and $\tan\theta = \sqrt{2}\zeta/\theta$. The parameters B, C, and ζ refer to the free ion and k allows for electron delocalization onto the ligands. When our value for the susceptibility at 0° K is inserted into equation [1], a value $k = 0.74$ is obtained. Allowance was made for the temperature-independent paramagnetism of about 60×10^{-6} c.g.s. units/mole which arises from elements outside the ground configuration. This value of k is in close agreement with that, $k = 0.7_6$, found previously for K_2IrCl_6 (11). There is no reason to suppose that k should be nearly identical for various hexachloro complexes, but an approximate agreement is at least reasonable.

An examination of the temperature dependence provides an independent verification of the treatment. Earnshaw and co-workers (4) provide the relation

$$\chi = \chi^0 \tanh(a/2kT), \qquad [2]$$

where χ^0 is the limiting susceptibility at zero temperature, and a is the energy separation of the ground and first higher level. If we assume that the free ion parameters are reduced by the factor 0.74 and insert these into the expressions of Kamimura and co-workers for the levels concerned (labelled by them W_1 and W_3), a separation $a = 625$ cm^{-1} is obtained. The best fit of the experimental values of χ is provided by $a = 570$ cm^{-1}. This reasonably good agreement is considered strong support for the correctness of the theories of Griffith and Kamimura and his co-workers for Ru^{4+}. We cannot, however, account quantitatively for the behavior of Os^{4+} using these theories.

Can. J. Chem. Downloaded from www.nrcresearchpress.com by 210.87.254.6 on 09/05/12
For personal use only.

The author is indebted to Miss L. Thomson for experimental assistance. Financial support of the Ontario Research Foundation is also gratefully acknowledged.

1. A. D. Westland and N. C. Bhiwandker. Can. J. Chem. **39**, 1284 (1961).
2. B. R. Judd. Proc. Roy. Soc. (London), Ser. A, **250**, 110 (1959).
3. R. B. Johannesen and G. A. Candela. Inorg. Chem. **2**, 67 (1963).
4. A. Earnshaw, B. N. Figgis, J. Lewis, and R. D. Peacock. J. Chem. Soc. 3132 (1961).
5. M. Kotani. J. Phys. Soc. Japan, **4**, 293 (1949).
6. B. N. Figgis, J. Lewis, R. S. Nyholm, and R. D. Peacock. Discussions Faraday Soc. **26**, 103 (1959).
7. J. S. Griffith. Discussions Faraday Soc. **26**, 173 (1959).
8. H. Kamimura, S. Koide, H. Sekiyama, and S. Sugano. J. Phys. Soc. Japan, **15**, 1264 (1960).
9. J. L. Howe. J. Am. Chem. Soc. **26**, 544 (1904).
10. R. E. Thiers, W. Graydon, and F. E. Beamish. Anal. Chem. **20**, 831 (1948).
11. A. D. Westland and N. C. Bhiwandker. Can. J. Chem. **39**, 2353 (1961).

Received May 27, 1963.
Department of Chemistry,
University of Ottawa,
Ottawa, Canada.

Can. J. Chem. Downloaded from www.nrcresearchpress.com by 210.87.254.6 on 09/05/12
For personal use only.

DESULPHURIZATION WITH RANEY NICKEL
III. BENZYL N-ALKYL-N-BENZENESULPHONYLCARBAMATES[1,2]

George R. Pettit and Raymond E. Kadunce

Alkylation of sodium saccharin followed by Raney nickel desulphurization has been found useful for converting certain alkyl halides to N-alkylbenzamides or N-alkylcyclohexylcarboxamides. In addition, Raney nickel desulphurization of N-alkylated dibenzenesulphonamides has been briefly considered for converting alkyl halides to amines. However, alkylation of sodium dibenzenesulphonamide generally proved inefficient, and this route was not further investigated.[1]

The present study was undertaken to evaluate benzyl N-alkyl-N-benzenesulphonylcarbamates (I) as amine precursors. The anion derived from benzyl N-benzenesulphonylcarbamate (I*a*) was predicted[3] to be a stronger nucleophilic agent than its dibenzenesulphonamide counterpart. Alkylation of sodium salt I*b* by normally reactive alkyl

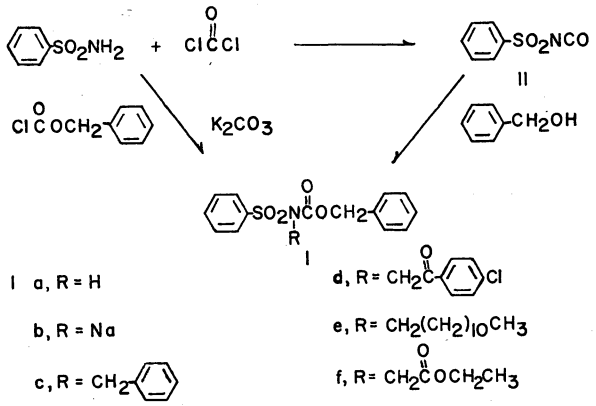

[1]*Part II, G. R. Pettit and R. E. Kadunce, J. Org. Chem.* **27**, *4566 (1962).*
[2]*Abstracted in part from the Master of Science thesis submitted by R. E. Kadunce to the Graduate School, University of Maine, June, 1961.*
[3]*Compare Part II, footnote 7.*

The author is indebted to Miss L. Thomson for experimental assistance. Financial support of the Ontario Research Foundation is also gratefully acknowledged.

1. A. D. Westland and N. C. Bhiwandker. Can. J. Chem. **39**, 1284 (1961).
2. B. R. Judd. Proc. Roy. Soc. (London), Ser. A, **250**, 110 (1959).
3. R. B. Johannesen and G. A. Candela. Inorg. Chem. **2**, 67 (1963).
4. A. Earnshaw, B. N. Figgis, J. Lewis, and R. D. Peacock. J. Chem. Soc. 3132 (1961).
5. M. Kotani. J. Phys. Soc. Japan, **4**, 293 (1949).
6. B. N. Figgis, J. Lewis, R. S. Nyholm, and R. D. Peacock. Discussions Faraday Soc. **26**, 103 (1959).
7. J. S. Griffith. Discussions Faraday Soc. **26**, 173 (1959).
8. H. Kamimura, S. Koide, H. Sekiyama, and S. Sugano. J. Phys. Soc. Japan, **15**, 1264 (1960).
9. J. L. Howe. J. Am. Chem. Soc. **26**, 544 (1904).
10. R. E. Thiers, W. Graydon, and F. E. Beamish. Anal. Chem. **20**, 831 (1948).
11. A. D. Westland and N. C. Bhiwandker. Can. J. Chem. **39**, 2353 (1961).

Received May 27, 1963.
Department of Chemistry,
University of Ottawa,
Ottawa, Canada.

Can. J. Chem. Downloaded from www.nrcresearchpress.com by 210.87.254.105 on 09/05/12
For personal use only.

DESULPHURIZATION WITH RANEY NICKEL
III. BENZYL N-ALKYL-N-BENZENESULPHONYLCARBAMATES[1,2]

George R. Pettit and Raymond E. Kadunce

Alkylation of sodium saccharin followed by Raney nickel desulphurization has been found useful for converting certain alkyl halides to N-alkylbenzamides or N-alkylcyclohexylcarboxamides. In addition, Raney nickel desulphurization of N-alkylated dibenzenesulphonamides has been briefly considered for converting alkyl halides to amines. However, alkylation of sodium dibenzenesulphonamide generally proved inefficient, and this route was not further investigated.[1]

The present study was undertaken to evaluate benzyl N-alkyl-N-benzenesulphonylcarbamates (I) as amine precursors. The anion derived from benzyl N-benzenesulphonylcarbamate (I*a*) was predicted[3] to be a stronger nucleophilic agent than its dibenzenesulphonamide counterpart. Alkylation of sodium salt I*b* by normally reactive alkyl

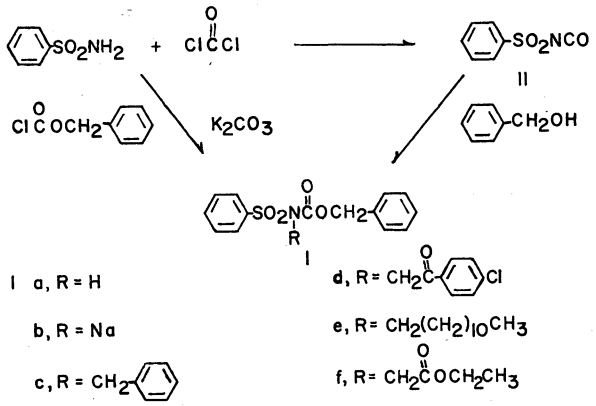

[1]*Part II, G. R. Pettit and R. E. Kadunce, J. Org. Chem.* **27**, *4566 (1962).*
[2]*Abstracted in part from the Master of Science thesis submitted by R. E. Kadunce to the Graduate School, University of Maine, June, 1961.*
[3]*Compare Part II, footnote 7.*

halides was, therefore, expected to proceed satisfactorily. Subsequent cleavage of the N-alkyl derivative with hydrogen bromide (1) or by concomitant desulphurization and hydrogenolysis using Raney nickel might then yield the corresponding amine.

Synthesis of carbamate I*a* was accomplished by condensing (e.g., ref. 2) benzenesulphonamide with carbobenzoxy chloride or, more conveniently and in good yield (91%), by treating benzenesulphonyl isocyanate (II) with benzyl alcohol. The isocyanate was prepared (cf. ref. 3) from benzenesulphonamide and phosgene. Generally, the carbobenzoxy chloride procedure led to carbamate I*a* (72%) accompanied by benzyl N-benzenesulphonyl-N-benzylcarbamate (I*c*). The N-benzyl derivative apparently arises from N-alkylation of initially formed carbamate (I*a*) by benzyl chloride, already present, or generated (4) during partial decomposition of carbobenzoxy chloride. Comparison of the N-benzyl derivative (I*c*) with a specimen prepared from benzyl chloride and the sodium salt of benzyl N-benzenesulphonylcarbamate (I*b*)[4] confirmed the structural assignment.

In contrast to our prior experience with dibenzenesulphonamide, the sodium salt of carbamate I*a*, in dimethylformamide, was easily N-alkylated by *p*-chlorophenacyl bromide, *n*-dodecyl bromide, and ethyl bromoacetate. Interestingly, the principal products (I*d-f*, 68 to 87% yield) were usually accompanied by small quantities of another N-alkyl derivative: subsequently identified as benzyl N-benzenesulphonyl-N-benzylcarbamate (I*c*). Formation of N-benzyl derivative I*c* apparently proceeds by competitive intermolecular condensation of carbamate I*b*.

Both the N-dodecyl (I*e*) and N-α-acetate (I*f*) carbamates were selected for cleavage studies. Treating the N-dodecyl (I*e*) derivative with Raney nickel (W-4) under mild conditions (70° in dioxane) afforded only the product of hydrogenolysis, N-dodecylbenzenesulphonamide. A variety of more vigorous desulphurization techniques (5) also proved unsatisfactory. These experiments led to mixtures of nitrogen-containing products bonded to the nickel residues. Isolation required continuous extraction with benzene and/or dissolution of the nickel components in hydrochloric acid. Raney nickel desulphurization of N-α-acetate I*f* was similarly unrewarding. However, carbamates I*e* and I*f* were readily converted by hydrogen bromide in acetic acid to, respectively, *n*-dodecylamine and glycine ethyl ester hydrobromides.

Although hydrogen bromide cleavage of N-alkyl-N-benzenesulphonylcarbamates appears to offer a practical route to amines, concurrent N-benzylation of carbamate I*b* during the alkylation step limits the overall usefulness of this approach.[5]

EXPERIMENTAL

Before evaporation, all solvent extracts were dried over magnesium or sodium sulphate. Melting points are uncorrected and were observed employing a silicone oil bath and open Kimble glass capillaries. Reaction products were shown to be identical with known specimens by mixture melting point determination and infrared spectral comparison (in potassium bromide). Dr. R. A. Hill of this laboratory recorded the infrared spectra and Dr. A. Bernhardt, Max-Planck Institute, Mülheim, Germany, provided the microanalyses.

Benzenesulphonyl Isocyanate (II)

Phosgene (38 ml) was condensed in a dry-ice trap and then slowly distilled into a refluxing solution of benzenesulphonamide (41 g) in 1,2,4-trichlorobenzene (85 ml). Heating and stirring (in a nitrogen atmosphere) was continued 2 hours. The reaction mixture was next swept with dry nitrogen and distilled through an 8-in. Vigreux column. The fraction boiling at 69–75° (0.5 mm) weighed 31 g and was sufficiently pure for subsequent work. Billeter (6) reported a b.p. of 129.6° at 9 mm.

[4]*Benzenesulphonyl isocyanate may occasionally be a useful reagent for separating alcohols from neutral substances, since reaction between the isocyanate and alcohols may yield carbamates soluble in aqueous base.*

[5]*For example, selection of t-butyl N-benzenesulphonylcarbamate for alkylation might improve this alkyl halide → amine sequence.*

Can. J. Chem. Downloaded from www.nrcresearchpress.com by 210.87.254.105 on 09/05/12
For personal use only.

Benzyl N-Benzenesulphonylcarbamate (Ia)

A. From Benzenesulphonyl Isocyanate

In a typical experiment, benzenesulphonyl isocyanate (3.3 g) was added to benzyl alcohol (2 g) and the mixture was allowed to remain 2 hours at room temperature, in a flask protected from moisture. The viscous oil was triturated with petroleum ether and the colorless needles (m.p. 90–96)° which separated were collected; yield, 4.8 g (91%). Purification was achieved by reprecipitation (at pH 6 using dil. hydrochloric acid) of the amide from 15% sodium hydroxide solution and then recrystallization from chloroform – petroleum ether. A pure colorless crystalline sample of carbamate I*a* melted at 104.5–105.5°; ν_{max} 3290, 1750, 1720, 1350, and 1165 cm^{-1}. Anal. Calc. for $C_{14}H_{13}NO_4S$: C, 57.72; H, 4.47; N, 4.81; S, 11.01. Found: C, 57.78; H, 4.52; N, 4.78; S, 10.72.

B. From Benzenesulphonamide

Carbobenzoxy chloride (14 g, 0.08 mole) was added to a mixture of benzenesulphonamide (10 g, 0.06 mole) and anhydrous potassium carbonate (25 g) in dry acetone (100 ml). Following an overnight period of stirring and heating at reflux the mixture was cooled and filtered. Solid material was treated with 10% hydrochloric acid (200 ml) and extracted with benzene (2×100 ml). Concentration of the benzene extract to ca. 25 ml and dilution with petroleum ether gave 12.5 g (72%) of colorless crystals, m.p. 102.5–105°. Recrystallization from benzene – petroleum ether raised the melting point to 104.5–106°. The carbamate (I*a*) prepared by this method was identical with the substance descibed in procedure A.

Diluting the filtrate (acetone solution), from the original reaction mixture, with water gave 3.4 g, m.p. 106–109°, of benzyl N-benzenesulphonyl-N-benzylcarbamate (I*c*). Six recrystallizations from chloroform – petroleum ether yielded a pure specimen as colorless prisms, m.p. 111.5–112.5°; ν_{max} 1725, 1365, and 1170 cm^{-1}. Anal. Calc. for $C_{21}H_{19}NO_4S$: C, 66.13; H, 5.02; N, 3.67; S, 8.41. Found: C, 65.94; H, 5.01; N, 3.93; S, 8.49.

The benzyl derivative (I*c*) was identical with an authentic specimen obtained by the following method:

Benzyl N-Benzenesulphonyl-N-benzylcarbamate (Ic)

A solution of sodium methoxide in ethanol was added to an equivalent quantity of benzyl N-benzenesulphonylcarbamate in a minimum quantity of absolute ethanol. The sodium derivative (I*b*) which separated was collected and washed with benzene; 95% yield, colorless crystals, d.p. 298–300°. One recrystallization from dimethylformamide – ethyl ether gave microcrystals decomposing at 299–300°.

A mixture of the sodium salt of benzyl N-benzenesulphonylcarbamate (I*b*, 3.14 g, 0.01 mole), benzyl chloride (1.25 g, 0.01 mole), and dimethylformamide (25 ml) was heated (steam bath) 45 minutes. Solvent was removed *in vacuo* and the residue washed with chloroform and filtered. The filtrate was evaporated to a yellow solid (1.6 g, 42%) melting at 110–112°. Recrystallization from acetone – petroleum ether gave large colorless prisms, m.p. 110.5–113°. The product (I*c*) was characterized as noted above (cf. I*a*, procedure B).

Benzyl N-Benzenesulphonyl-N-(p-chlorophenacyl)carbamate (Id)

The preceding experiment was repeated using *p*-chlorophenacyl bromide (1.23 g, 0.05 mole), excess carbamate (I*b*, 2.5 g, 0.08 mole) and a 1.5-hour reaction period. The product recrystallized from benzene – petroleum ether as colorless needles; yield 2.0 g, m.p. 136–140°. Several recrystallizations from the same solvent raised the melting point to 141.5–143°; $\nu_{max}^{CHCl_3}$ 1730, 1705, 1355, 1220, and 1170 cm^{-1}. Anal. Calc. for $C_{22}H_{18}ClNO_5S$: C, 59.51; H, 4.09; S, 7.22. Found: C, 59.12; H, 4.00; S, 7.34.

Benzyl N-Benzenesulphonyl-N-dodecylcarbamate (Ie)

The experimental procedure described for synthesis of N-benzylcarbamate I*c* was repeated using dodecyl bromide (2.49 g, 0.01 mole) in place of benzyl chloride. In this case, a 2-hour reaction period was employed. A petroleum ether solution of the crude oily product slowly (24 hour) deposited benzyl N-benzensulphonyl-N-benzylcarbamate (I*c*, 0.15 g), m.p. 108–110.5°, which was identified by comparison with an authentic specimen. Concentrating and cooling the filtrate led to a waxy solid (2.8–3.4 g, 50–68%) melting at 40–46°. Five recrystallizations from ethyl ether provided an analytical sample of benzyl N-benzenesulphonyl-N-dodecylcarbamate as colorless needles, m.p. 47.5–49.5°; $\nu_{max}^{CHCl_3}$ 1712, 1355, and 1175 cm^{-1}. Anal. Calc. for $C_{26}H_{37}NO_4S$: C, 67.94; H, 8.12; N, 3.05; S, 6.98. Found: C, 67.44; H, 7.89; N, 3.30; S, 6.95.

Cleavage of Benzyl N-Benzenesulphonyl-N-dodecylcarbamate (Ie)

A. By Raney Nickel

A mixture of carbamate I*e* (0.50 g), Raney nickel (4 ml, W-4, 2 weeks old, ref. 7), and dioxane (25 ml) was stirred for 50 minutes at 70±2°. After collecting residual nickel the filtrate was concentrated (*in vacuo*) to 0.15 g of colorless solid, m.p. 45–53°. Recrystallization from methanol–water yielded a pure specimen of N-dodecylbenzenesulphonamide melting at 57–58.5° (ref. 8, m.p. 59°). The product was identical with an authentic specimen prepared from dodecylamine and benzenesulphonyl chloride.

A variety of more vigorous experimental conditions using dioxane as solvent and variously aged samples of W-2 and W-4 Raney nickels gave unsatisfactory results. The mixtures (evidenced by thin-layer chromatograms) obtained were not considered of further interest.

Can. J. Chem. Downloaded from www.nrcresearchpress.com by 210.87.254.105 on 09/05/12
For personal use only.

B. By Hydrogen Bromide (8)

A solution composed of carbamate I*e* (1.4 g), 35% hydrogen bromide in acetic acid (12 ml), and phenol (0.7 g) was allowed to remain at room temperature 48 hours. Dilution with ethyl ether precipitated 0.31 g (74%) of *n*-dodecylamine hydrobromide, d.p. 190° (sintering from 140°). Both the hydrobromide and *p*-toluenesulphonamide (m.p. 74–75°, ref. 9) derivatives were identical with authentic specimens.

Ethyl α-Aminoacetate Hydrobromide

The sodium salt of benzyl N-benzenesulphonylcarbamate (5.5 g) in dimethylformamide (20 ml) was alkylated with ethyl α-bromoacetate (2.9 g) as described using benzyl chloride (cf. I*c*). In this example, a 1-hour reaction period was employed and the crude reaction residue was extracted with benzene. Following removal of benzene, *in vacuo*, a petroleum ether solution of the resulting oily product (6.3 g) was maintained at room temperature 2 days. The benzyl N-benzenesulphonyl-N-benzylcarbamate (0.2 g, m.p. 103–109°) which separated was recrystallized (to m.p. 111–112°) from acetone–water and shown to be identical with an authentic sample (I*c*). Concentrating the petroleum ether filtrate afforded an impure specimen of N-benzenesulphonyl-N-carbobenzoxyglycine ethyl ester. A portion (0.70 g) of the crude oily mixture was treated with 35% hydrogen bromide in acetic acid (7 ml, containing 0.5 g of phenol) as reported using *n*-dodecylcarbamate I*e*. The crude semisolid hydrobromide of glycine ethyl ester weighed 0.22 g. Four recrystallizations from ethanol – ethyl ether led to colorless needles decomposing at 177–178°. Comparison with an authentic specimen of ethyl α-aminoacetate hydrobromide (d.p. 175–176°, ref. 10) confirmed the structural assignment.

ACKNOWLEDGMENTS

This investigation was supported by National Science Foundation Research Grants G-9585 and G-19500.

1. S. Searles and S. Nukina. Chem. Rev. **59**, 1077 (1959). W. F. Erman and H. C. Kretschmar. J. Org. Chem. **26**, 4841 (1961).
2. H. L. Yale and F. Sowinski. J. Org. Chem. **25**, 1824 (1960).
3. C. King. J. Org. Chem. **25**, 352 (1960).
4. J. Thiele and F. Dent. Ann. **302**, 245 (1898).
5. G. R. Pettit and E. E. van Tamelen. *In* Organic reactions. Vol. 12. *Edited by* A. C. Cope. John Wiley and Sons, Inc., New York. 1962.
6. O. C. Billeter. Ber. **37**, 690 (1904).
7. A. A. Pavlic and H. Adkins. J. Am. Chem. Soc. **68**, 1471 (1946).
8. H. R. Snyder and R. E. Heckert. J. Am. Chem. Soc. **74**, 2006 (1952). D. Ben-ishai and A. Berger. J. Org. Chem. **17**, 1564 (1952).
9. R. Sasin, W. A. Butte, Jr., A. L. Borror, and G. S. Sasin. J. Am. Oil Chemists' Soc. **34**, 358 (1957); Chem. Abstr. **51**, 16346 (1957).
10. E. Fischer and H. Schrader. Ber. **43**, 525 (1910).

Received March 29, 1963.
Department of Chemistry,
University of Maine,
Orono, Maine, U.S.A.

NUCLEAR SPIN–SPIN COUPLING CONSTANTS INVOLVING THE GROUP IV ELEMENTS

L. W. Reeves and E. J. Wells

Consideration of correlations involving coupling constants between different nuclei has been mostly confined to those involving C^{13} and hydrogen (1–4). The interest has centered around the following topics: dependence of $J_{C^{13}-H}$ on *s* character (1–4), the variation of $J_{C^{13}-H}$ in molecules of the type CHXYZ (5–8), and the use of $J_{C^{13}-H}$ in conjunction with chemical shift data to indicate diamagnetic anisotropy (9). $J_{Si^{29}-H}$ coupling constants have been measured (16) but these are influenced by polar effects besides being dependent on hybridization (6). Long range $J_{C^{13}-C-H}$ and $J_{C^{13}-C-C-H}$ coupling constants have been

Can. J. Chem. Downloaded from www.nrcresearchpress.com by 210.87.254.105 on 09/05/12
For personal use only.

B. By Hydrogen Bromide (8)

A solution composed of carbamate I*e* (1.4 g), 35% hydrogen bromide in acetic acid (12 ml), and phenol (0.7 g) was allowed to remain at room temperature 48 hours. Dilution with ethyl ether precipitated 0.31 g (74%) of *n*-dodecylamine hydrobromide, d.p. 190° (sintering from 140°). Both the hydrobromide and *p*-toluenesulphonamide (m.p. 74–75°, ref. 9) derivatives were identical with authentic specimens.

Ethyl α-Aminoacetate Hydrobromide

The sodium salt of benzyl N-benzenesulphonylcarbamate (5.5 g) in dimethylformamide (20 ml) was alkylated with ethyl α-bromoacetate (2.9 g) as described using benzyl chloride (cf. I*c*). In this example, a 1-hour reaction period was employed and the crude reaction residue was extracted with benzene. Following removal of benzene, *in vacuo*, a petroleum ether solution of the resulting oily product (6.3 g) was maintained at room temperature 2 days. The benzyl N-benzenesulphonyl-N-benzylcarbamate (0.2 g, m.p. 103–109°) which separated was recrystallized (to m.p. 111–112°) from acetone–water and shown to be identical with an authentic sample (I*c*). Concentrating the petroleum ether filtrate afforded an impure specimen of N-benzenesulphonyl-N-carbobenzoxyglycine ethyl ester. A portion (0.70 g) of the crude oily mixture was treated with 35% hydrogen bromide in acetic acid (7 ml, containing 0.5 g of phenol) as reported using *n*-dodecylcarbamate I*e*. The crude semisolid hydrobromide of glycine ethyl ester weighed 0.22 g. Four recrystallizations from ethanol – ethyl ether led to colorless needles decomposing at 177–178°. Comparison with an authentic specimen of ethyl α-aminoacetate hydrobromide (d.p. 175–176°, ref. 10) confirmed the structural assignment.

ACKNOWLEDGMENTS

This investigation was supported by National Science Foundation Research Grants G-9585 and G-19500.

1. S. Searles and S. Nukina. Chem. Rev. **59**, 1077 (1959). W. F. Erman and H. C. Kretschmar. J. Org. Chem. **26**, 4841 (1961).
2. H. L. Yale and F. Sowinski. J. Org. Chem. **25**, 1824 (1960).
3. C. King. J. Org. Chem. **25**, 352 (1960).
4. J. Thiele and F. Dent. Ann. **302**, 245 (1898).
5. G. R. Pettit and E. E. van Tamelen. *In* Organic reactions. Vol. 12. *Edited by* A. C. Cope. John Wiley and Sons, Inc., New York. 1962.
6. O. C. Billeter. Ber. **37**, 690 (1904).
7. A. A. Pavlic and H. Adkins. J. Am. Chem. Soc. **68**, 1471 (1946).
8. H. R. Snyder and R. E. Heckert. J. Am. Chem. Soc. **74**, 2006 (1952). D. Ben-ishai and A. Berger. J. Org. Chem. **17**, 1564 (1952).
9. R. Sasin, W. A. Butte, Jr., A. L. Borror, and G. S. Sasin. J. Am. Oil Chemists' Soc. **34**, 358 (1957); Chem. Abstr. **51**, 16346 (1957).
10. E. Fischer and H. Schrader. Ber. **43**, 525 (1910).

Received March 29, 1963.
Department of Chemistry,
University of Maine,
Orono, Maine, U.S.A.

NUCLEAR SPIN–SPIN COUPLING CONSTANTS INVOLVING THE GROUP IV ELEMENTS

L. W. Reeves and E. J. Wells

Consideration of correlations involving coupling constants between different nuclei has been mostly confined to those involving C^{13} and hydrogen (1–4). The interest has centered around the following topics: dependence of $J_{C^{13}-H}$ on *s* character (1–4), the variation of $J_{C^{13}-H}$ in molecules of the type CHXYZ (5–8), and the use of $J_{C^{13}-H}$ in conjunction with chemical shift data to indicate diamagnetic anisotropy (9). $J_{Si^{29}-H}$ coupling constants have been measured (16) but these are influenced by polar effects besides being dependent on hybridization (6). Long range $J_{C^{13}-C-H}$ and $J_{C^{13}-C-C-H}$ coupling constants have been

Can. J. Chem. Downloaded from www.nrcresearchpress.com by 210.87.254.40 on 09/05/12
For personal use only.

measured in both enriched compounds (10, 11) and in natural abundance (12). The unfavorable magnetic properties of Ge^{73} make it unlikely that parameters will be available for germanium (17). Recent reports of coupling constants for Sn^{119}, Sn^{117}, and Pb^{207} (13–20) are available for comparison with measurements made by us recently (21). As a minor point we find coupling constants measured in reference 13 to be 3% lower than ours in dimethyltin dihydride.

In the accompanying table are listed coupling constants involving group IV elements

Coupling constant J	Value, c.p.s.	Compound measured	References	J/μ
C^{13}—H	125	Many sp^3 type	1, 3	178
Si^{29}—H	202.5	SiH_4	16	289
Sn^{119}—H	1797	$(CH_3)_2SnH_2$	21	1727
Pb^{207}—H	2380	$(CH_3)_3PbH$	13	4075
C^{13}—C—H	3.8	$(C_2H_5)_3COH$	11	5.4
Si^{29}—C—H	6.57	$(CH_3)_4Si$	15	11.8
Si^{119}—C—H	60.2	$(CH_3)_2SnH_2$	21	57
Pb^{207}—C—H	66.7	$(CH_3)_3PbH$	13	114
C^{13}—F	257	CF_4	14	366
Si^{29}—F	274.8	$SiHF_3$	16	495
C^{13}—C—F	38.5	CF_3CH_2Br	14	54.8
Sn^{119}—C—F	251	$(CH_3)_2Sn(C_2F_4H)_2$	21	239

in situations where hybridization is near sp^3 for the group IV elements. The neighboring atoms are also chosen so as to eliminate the possibility of back donation of charge into the unfilled d orbitals of a group IV atom.

In order to eliminate the contribution to $J_{NN'}$ arising from nuclear constants it is necessary to divide by the dissimilar magnetogyric ratios. In the series C^{13}, Si^{29}, Sn^{119}, and Pb^{207} all have spin 1/2 properties so division by the nuclear moment in nuclear magnetons is sufficient. It is to be noted that $\mu_{C^{13}}$ and $\mu_{Pb^{207}}$ are positive and $\mu_{Si^{29}}$ and $\mu_{Sn^{119}}$ are negative.

The underlying prerequisite of the present discussion is a knowledge of the electronic contribution to J_{X-H} and this is represented in column 5 of the table. We will presume that $J_{C^{13}-H}$ and $J_{Pb^{207}}$ have opposite sign to $J_{Si^{29}-H}$ and $J_{Sn^{119}-H}$ merely because of a change in the sign of the gyromagnetic ratio of the group IV nucleus. This assumption has yet to be tested. Since we assume the electronic contribution to J_{X-H} has the same sign down the group we shall use for our purpose $|J/\mu|$. Discussions regarding absolute magnitudes of coupling constants should compensate for nuclear dependence.

We have found a most satisfactory linear correlation of $\sqrt{|J_{X-H}/\mu_X|}$ with the atomic number Z_X for group IV element X, with the conditions specified earlier. This is shown in Fig. 1. A similar relationship $\sqrt{|J_{X-C-H}/\mu_X|}$ versus Z_X also holds and is shown in Fig. 1. Data for long-range couplings $J_{X-C-C-H}$ are too sparse but the data for J_{X-F} (14–16) is partially available as are some values of J_{X-C-F} (14, 21). The square root law can be tested in this case by taking values of $\sqrt{(J_{X\ldots F}\times\mu_{C^{13}}/J_{C^{13}\ldots F}\times\mu_X)}$ versus atomic number. Three available points give good linear relationship. This is shown in Fig. 2.

The above correlations may be represented analytically:

$$[1] \qquad \sqrt{|J_{X-H}/\mu_X|} = 0.676\,Z_X+8.0$$

$$[2] \qquad \sqrt{|J_{X-C-H}/|\mu_X|} = 0.107\,Z_X+1.95$$

$$[3] \qquad \sqrt{(J_{X\ldots F}\times\mu_{C^{13}}/J_{C^{13}\ldots F}\times\mu_X)} = 0.0245\,Z_X+0.84.$$

Can. J. Chem. Downloaded from www.nrcresearchpress.com by 210.87.254.40 on 09/05/12
For personal use only.

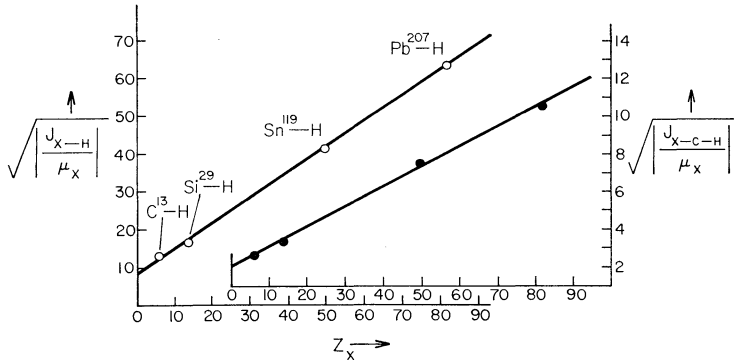

FIG. 1.

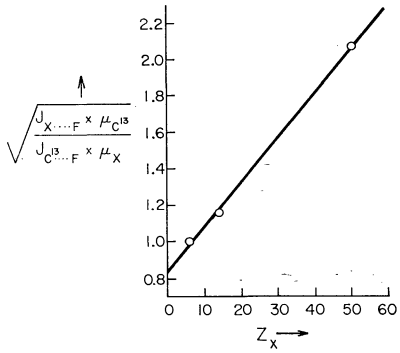

FIG. 2.

In a recent paper using the valence bond approach, Gutowsky and Juan (6) have formulated the contact contribution to J_{X-H} (X = C^{13} or Si^{29}) in sp^3 molecules of the type we are considering. Their expression can be generalized, in their notation, as:

$$[4] \qquad J_{X-H} = \frac{\gamma_H \gamma_X}{h\Delta E_X}\left(\frac{16\pi\beta\hbar}{3}\right)^2 \eta_X^2 \alpha_H^2 |ns_X(0)|^2 |1s_H(0)|^2.$$

The assumptions are that the contact term is the dominant one as has already been shown for C^{13} (22), that the perfect pairing approximation may be used for all the ground-state wave functions down the group, and that the product of the contact matrix elements over all excited triplet states may be replaced by the diagonal element over the ground state, coupled with a mean triplet excitation energy, ΔE_X. The terms which depend on the group IV atoms X are ΔE_X, the normalization term η^2, and the atomic s electron charge density at the nucleus $|ns_X(0)|^2$. An estimate of the dependence of this latter on Z may be obtained from the hyperfine splitting of the ^2S ground states of the atomic alkali metals, where the only **I.S** interaction mechanism is through the scalar contact term. The most accurate hyperfine splitting energies are from atomic microwave measurements and have been tabulated by Ramsey (23, p. 89). The hyperfine structure separation for a single s electron ($L = 0$) is (23, p. 10; 24)

$$[5] \qquad \Delta E = \frac{8\pi\beta}{3}\mu_X |ns_X(0)|^2 \frac{(2I_X+1)}{I_X}.$$

Can. J. Chem. Downloaded from www.nrcresearchpress.com by 210.87.254.40 on 09/05/12
For personal use only.

Thus the contact charge density of the alkali metals may be obtained from knowledge of the splittings ΔE, the nuclear magnetic moments, and the nuclear spins I_X. Figure 3

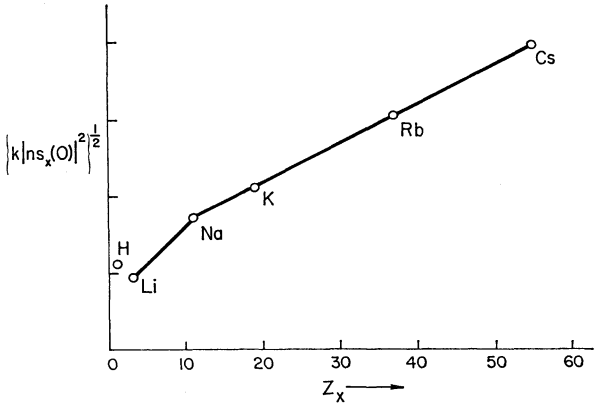

FIG. 3.

shows the correlation of the square root of the contact charge against the atomic number.

Although this correlation fails for small Z values, it is sufficient to allow a qualitative explanation of the J_{X-H} dependence in terms of equation [4]. In moving from group I of the alkalis to group IV*b* without increasing the principal quantum number, we should tend to increase the slope of Fig. 3, and also to iron out the Li–Na irregularity. The conclusion is that most of the Z dependence noted in J_{X-H} is contained in $|ns_X(0)|^2$. Were the atomic wave functions hydrogenic, this dependence would be as Z^3, but is reduced to approximately Z^2 by the inner filled shells. It appears reasonable that the screening by the increasing number of core electrons should leave ΔE_X roughly independent of Z. Thus any Z dependence in η_X^2 caused by the changing ionicity of the X—H bond must be slight.

ACKNOWLEDGMENTS

We wish to thank Dr. J. A. R. Coope for several enlightening discussions. This work was generously supported by the National Research Council of Canada and the Petroleum Research Fund of the American Chemical Society.

1. N. MULLER and D. E. PRITCHARD. J. Chem. Phys. **31**, 768 (1959).
2. N. MULLER and D. E. PRITCHARD. J. Chem. Phys. **31**, 1471 (1959).
3. J. N. SHOOLERY. J. Chem. Phys. **31**, 1427 (1959).
4. N. MULLER. J. Chem. Phys. **36**, 359 (1962).
5. E. R. MALINOWSKI. J. Am. Chem. Soc. **83**, 4479 (1961).
6. H. S. GUTOWSKY and C. S. JUAN. J. Am. Chem. Soc. **84**, 307 (1962); J. Chem. Phys. **37**, 2198 (1962).
7. E. R. MALINOWSKI, L. Z. POLLARA, and J. P. LARMANN. J. Am. Chem. Soc. **84**, 2649 (1962).
8. N. MULLER and P. I. ROSE. J. Am. Chem. Soc. **84**, 3973 (1962).
9. G. S. REDDY and J. H. GOLDSTEIN. J. Chem. Phys. **36**, 2644 (1962).
10. G. J. KARABATSOS. J. Am. Chem. Soc. **83**, 1230 (1961).
11. G. J. KARABATSOS, J. D. GRAHAM, and F. VANE. J. Am. Chem. Soc. **83**, 2448 (1961); J. Phys. Chem. **65**, 1657 (1961).
12. D. R. MCADAMS. J. Chem. Phys. **36**, 1948 (1962).
13. N. FLITCROFT and H. D. KAESZ. J. Am. Chem. Soc. **85**, 1377 (1963).
14. N. MULLER and D. T. CARR. J. Phys. Chem. **67**, p. 112 (1963).
15. G. VAN DYKE TIERS. J. Phys. Chem. **65**, 1916 (1961).
16. E. A. V. EBSWORTH and J. J. TURNER. J. Chem. Phys. **36**, 2628 (1962).
17. J. E. DRAKE and W. L. JOLLY. J. Chem. Phys. **38**, 1033 (1963).
18. D. W. MOORE and J. A. HAPPE. J. Phys. Chem. **65**, 224 (1961).

Can. J. Chem. Downloaded from www.nrcresearchpress.com by 210.87.254.40 on 09/05/12
For personal use only.

19. D. SEYFORTH, T. WADA, and G. F. MACIEL. Inorg. Chem. **1**, 232 (1962).
20. H. KAESZ. J. Am. Chem. Soc. **83**, 1514 (1961).
21. H. C. CLARKE, J. T. KWON, L. W. REEVES, and E. J. WELLS. To be published.
22. M. KARPLUS and D. M. GRANT. Proc. Nat. Acad. Sci. U.S. **45**, 1269 (1959).
23. N. F. RAMSEY. Nuclear moments. John Wiley and Sons Inc., New York. 1953.
24. E. V. CONDON and G. H. SHORTLEY. Theory of atomic spectra. Cambridge University Press. 1957. p. 422.

RECEIVED JUNE 10, 1963.
DEPARTMENT OF CHEMISTRY,
UNIVERSITY OF BRITISH COLUMBIA,
VANCOUVER, BRITISH COLUMBIA.

Can. J. Chem. Downloaded from www.nrcresearchpress.com by 210.87.254.40 on 09/05/12
For personal use only.

MERCURY PHOTOSENSITIZED DECOMPOSITION OF LIQUID CYCLOHEXANE*

CORNELIUS E. KLOTS AND R. H. JOHNSEN

A statement in the recent literature (1) to the effect that alkyl radicals do not undergo normal disproportionating reactions in condensed media gained superficial support from the calculations of Bradley (2) which were compatible with a dimer-like structure to the transition state. The exothermic dissociation to disproportionation products would presumably be quenched by rapid collisional cooling. This model is not inevitable from the calculations, however (3), and the liquid phase disproportionation of ethyl radicals has since been demonstrated (4). The extent to which the larger alkyl radicals disproportionate is crucial in the elucidation of radiation chemistry mechanisms. We have thus adapted the technique of mercury photosensitization as a means of investigating their reactions in condensed phases.

EXPERIMENTAL

Several grades of liquid cyclohexane were used either as received or after washing with sulphuric acid followed by drying over sodium carbonate. Five milliliter samples were saturated with mercury, thoroughly degassed in a Vycor tube equipped with constrictions and break-off seals, thermostatted in water at room temperature, and photolyzed with an AH-4 mercury lamp. In the absence of dissolved mercury no decomposition ensued. The presence of mercury, however, does permit photosensitization via its medium-broadened resonance line (5). Gaseous products were measured manometrically and identified by uptake on hot copper oxide or by gas–solid chromatography as hydrogen. Liquid products were measured, using 4 λ injections on columns similar to those described by Dyne (6), with a flame ionization detector. At conversions less than 0.02% (about ½ hour illumination) only cyclohexene and dicyclohexyl were obtained. Calibration standards were prepared from genuine materials or, conveniently, by X-irradiation of pure cyclohexane using published G-values (6). The two classes of standards were in excellent agreement.

RESULTS AND DISCUSSION

We assume the following mechanism adequately encompasses our results:

$$\mathrm{Hg^* + C_6H_{12} \rightarrow C_6H_{11} + H + Hg}$$

$$\mathrm{H + C_6H_{12} \rightarrow H_2 + C_6H_{11}}$$

$$\mathrm{2C_6H_{11} \xrightarrow{k_c} C_{12}H_{22}}$$

$$\mathrm{2C_6H_{11} \xrightarrow{k_d} C_6H_{10} + C_6H_{12}}$$

In Fig. 1 the yield of cyclohexene is presented as a function of the dicyclohexyl obtained.

*This work was supported in part by the U.S. Atomic Energy Commission under Contract AT-(40-1)-2001.

19. D. SEYFORTH, T. WADA, and G. F. MACIEL. Inorg. Chem. **1**, 232 (1962).
20. H. KAESZ. J. Am. Chem. Soc. **83**, 1514 (1961).
21. H. C. CLARKE, J. T. KWON, L. W. REEVES, and E. J. WELLS. To be published.
22. M. KARPLUS and D. M. GRANT. Proc. Nat. Acad. Sci. U.S. **45**, 1269 (1959).
23. N. F. RAMSEY. Nuclear moments. John Wiley and Sons Inc., New York. 1953.
24. E. V. CONDON and G. H. SHORTLEY. Theory of atomic spectra. Cambridge University Press. 1957. p. 422.

RECEIVED JUNE 10, 1963.
DEPARTMENT OF CHEMISTRY,
UNIVERSITY OF BRITISH COLUMBIA,
VANCOUVER, BRITISH COLUMBIA.

Can. J. Chem. Downloaded from www.nrcresearchpress.com by 210.87.254.42 on 09/05/12
For personal use only.

MERCURY PHOTOSENSITIZED DECOMPOSITION OF LIQUID CYCLOHEXANE*

CORNELIUS E. KLOTS AND R. H. JOHNSEN

A statement in the recent literature (1) to the effect that alkyl radicals do not undergo normal disproportionating reactions in condensed media gained superficial support from the calculations of Bradley (2) which were compatible with a dimer-like structure to the transition state. The exothermic dissociation to disproportionation products would presumably be quenched by rapid collisional cooling. This model is not inevitable from the calculations, however (3), and the liquid phase disproportionation of ethyl radicals has since been demonstrated (4). The extent to which the larger alkyl radicals disproportionate is crucial in the elucidation of radiation chemistry mechanisms. We have thus adapted the technique of mercury photosensitization as a means of investigating their reactions in condensed phases.

EXPERIMENTAL

Several grades of liquid cyclohexane were used either as received or after washing with sulphuric acid followed by drying over sodium carbonate. Five milliliter samples were saturated with mercury, thoroughly degassed in a Vycor tube equipped with constrictions and break-off seals, thermostatted in water at room temperature, and photolyzed with an AH-4 mercury lamp. In the absence of dissolved mercury no decomposition ensued. The presence of mercury, however, does permit photosensitization via its medium-broadened resonance line (5). Gaseous products were measured manometrically and identified by uptake on hot copper oxide or by gas–solid chromatography as hydrogen. Liquid products were measured, using 4 λ injections on columns similar to those described by Dyne (6), with a flame ionization detector. At conversions less than 0.02% (about ½ hour illumination) only cyclohexene and dicyclohexyl were obtained. Calibration standards were prepared from genuine materials or, conveniently, by X-irradiation of pure cyclohexane using published G-values (6). The two classes of standards were in excellent agreement.

RESULTS AND DISCUSSION

We assume the following mechanism adequately encompasses our results:

$$Hg^* + C_6H_{12} \rightarrow C_6H_{11} + H + Hg$$

$$H + C_6H_{12} \rightarrow H_2 + C_6H_{11}$$

$$2C_6H_{11} \xrightarrow{k_c} C_{12}H_{22}$$

$$\xrightarrow{k_d} C_6H_{10} + C_6H_{12}$$

In Fig. 1 the yield of cyclohexene is presented as a function of the dicyclohexyl obtained.

*This work was supported in part by the U.S. Atomic Energy Commission under Contract AT-(40-1)-2001.

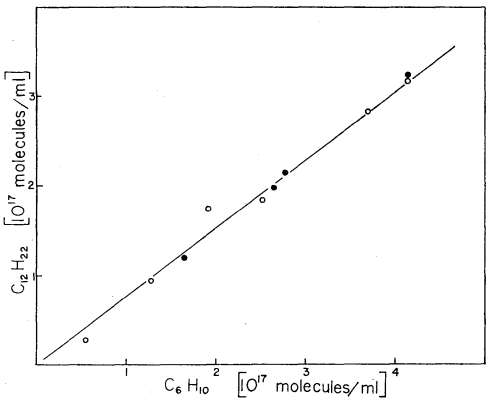

FIG. 1. Yield of cyclohexene as a function of dicyclohexyl. Filled circles obtained with highly purified cyclohexane.

The data, *en toto*, indicate a value of $k_d/k_c = 1.31 \pm .04$. Filled circles represent experiments using Phillips Research Grade cyclohexane with acid treatment, for which an excellent mass balance with the hydrogen yield was obtained. Other materials gave up to 15% too little of the hydrocarbon products but the same apparent k_d/k_c. This speaks against the possible significant role of hydrogen atom – cyclohexyl cage disproportionation producing cyclohexene and non-scavengeable hydrogen gas. There are other indications in the literature that hydrogen atoms are sufficiently mobile so as not to be subject to cage restrictions.

At higher conversions, cyclohexene yields are decreased and cyclohexylcyclohexene appears as a secondary product, as in X-irradiation (6). This is most simply attributed to addition of a cyclohexyl radical to cyclohexene followed by sterically favored disproportionation. Thus, while comparison with gas phase studies of the disproportionation–combination reactions of cyclohexyl radicals is invited, the often-quoted value $k_d/k_c \sim 0.5$ is almost certainly vitiated by the degree of conversion obtained (7). Similar considerations probably also apply to the single previously reported condensed phase adaptation (in *n*-decane) of the mercury photosensitization technique (5).

Prior to the completion of this work we learned of similar studies in other liquid aliphatic media by Professor Gilbert Mains (8). He finds a quantum yield of unity for hydrogen production and draws mechanistic conclusions similar to ours. We are grateful to him for access to his results before their publication. The relevance of our present data to the interpretation of radiation chemistry yields (6) will be discussed, along with additional results, in another place.

1. C. D. WAGNER. J. Phys. Chem. **64**, 231 (1960).
2. J. N. BRADLEY. J. Chem. Phys. **35**, 748 (1961).
3. J. N. BRADLEY and B. S. RABINOVITCH. J. Chem. Phys. **36**, 3498 (1962).
4. M. MATSUOKA, P. S. DIXON, A. P. STEFANI, and M. SZWARC. Proc. Chem. Soc. 304 (1962).
5. M. K. PHIBBS and B. DEB. DARWENT. J. Chem. Phys. **18**, 679 (1950).
6. P. J. DYNE and J. A. STONE. Can. J. Chem. **39**, 2381 (1961).
7. P. W. BECK, D. V. KNIEBES, and H. E. GUNNING. J. Chem. Phys. **22**, 672 (1954).
8. GILBERT J. MAINS and R. R. KUNTZ. J. Am. Chem. Soc. In press.

RECEIVED MAY 21, 1963.
DEPARTMENT OF CHEMISTRY,
FLORIDA STATE UNIVERSITY,
TALLAHASSEE, FLORIDA, U.S.A.

Can. J. Chem. Downloaded from www.nrcresearchpress.com by 210.87.254.42 on 09/05/12
For personal use only.

SECONDARY PROCESSES IN THE PHOTOLYSIS OF CYCLOPENTANONE: THE PHOTOLYSIS OF 4-PENTENAL

JAMES N. BUTLER,[1] ARTHUR T. DRAKE, J. CHRISTOPHER MITCHELL, AND PRITAM SINGH

The primary processes in the photolysis of cyclopentanone have been studied extensively (1). Srinivasan (2) has presented evidence that three primary processes of decomposition occur from different vibrational levels of the same excited singlet state of cyclopentanone:

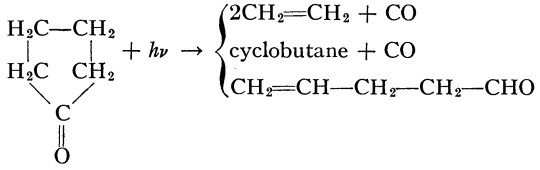

In an attempt to detect the possible isomerization of vibrationally excited cyclobutane molecules to ethylene, we have performed some experiments at very low pressures.

Cyclopentanone (Eastman Kodak), which had been purified by gas chromatography, was photolyzed at room temperature with 3130 Å radiation to approximately 1% decomposition. The pressure ranged from 7 mm to 0.003 mm. The products were analyzed by gas chromatography on a silica gel column at 100° C. The results are listed in Table I.

TABLE I

Variation of ethylene/cyclobutane ratio with pressure in the photolysis of cyclopentanone

Pressure (mm)	Ethylene/cyclobutane ratio	Pressure (mm)	Ethylene/cyclobutane ratio
7.07	2.32	0.24	2.98
2.96	2.29	0.022	3.25
1.30	2.53	0.015	3.38
0.55	2.73	0.003	3.10

It can be seen that the ethylene/cyclobutane ratio increases as the pressure is decreased. A plot of the ethylene/cyclobutane ratio as a function of reciprocal pressure would be expected to give a straight line if part of the ethylene was being formed by isomerization of excited cyclobutane. However, such a plot showed a marked curvature, the slope decreasing as pressure decreased. While it might be possible to interpret this by a complex deactivation mechanism, it seemed much more likely that a systematic error was causing the variation of the ratio with pressure.

The reaction vessel was constructed with the lamp immersed in a well in a 5 liter flask. At high pressure most of the light was absorbed near the central well and relatively little was absorbed at the outer portions of the flask. At low pressure, however, absorption took place throughout the vessel. Although the degree of decomposition could not be accurately estimated in the small samples, it was probably greater at low pressures than at high pressures, even though the time of exposure was the same.

[1]*To whom correspondence should be addressed. Present address: TYCO Laboratories Inc., Bear Hill, Waltham 54, Mass.*

Can. J. Chem. Downloaded from www.nrcresearchpress.com by 210.87.254.5 on 09/05/12
For personal use only.

TABLE II

Variation of ethylene/cyclobutane ratio with degree of decomposition, in the photolysis of cylopentanone (pressure 6–10 mm)

Degree of decomposition (%)	Ethylene/cyclobutane ratio	Degree of decomposition (%)	Ethylene/cyclobutane ratio
0.025	3.41	0.25	2.96
0.075	3.17	0.34	2.35
0.14	2.83	0.75	2.32
0.17	2.86		

The effect of degree of decomposition was studied at pressures from 6 to 10 mm. The results are listed in Table II. The ethylene/cyclobutane ratio decreases as the degree of decomposition increases. Thus, the increasing degree of decomposition at low pressures cannot completely explain the pressure dependence, but could possibly account for the curvature observed in the plot. A different reaction vessel geometry which does not cause the absorbed intensity to change with pressure might give better results.

An alternative explanation is that the other primary product, 4-pentenal, is itself undergoing photolysis, and is also producing ethylene. 4-Pentenal was prepared by the thermal isomerization of vinyl allyl ether (3, 4), and was photolyzed to about 3% decomposition under the same conditions that cyclopentanone had been studied. The major portion (94.5%) of the products of decomposition was produced by the reaction

$$CH_2{=}CH{-}CH_2{-}CH_2{-}CHO \rightarrow 2C_2H_4 + CO.$$

In addition, approximately 1.5% of 1-butene, 0.75% of *cis*-2-butene, and 0.25% of *trans*-2-butene were formed. The remaining 3% of the material was not accounted for, and presumably polymerized. Less than 0.05% of ethane or propylene was formed, which seems to rule out the participation of methyl or allyl radicals in the reaction. 1-Butene may be formed in the primary process if a cyclic transition state is invoked, and similar transition states can be devised to produce the 2-butenes (5).

The quantum yield for the decomposition of 4-pentenal was not measured accurately, but was approximately the same as the quantum yield for the decomposition of cyclopentanone. Thus, the secondary photolysis of 4-pentenal could account for at least part of the ethylene produced from cyclopentanone, even at small degrees of decomposition. However, this predicts that the ethylene/cyclobutane ratio would increase with increasing degree of decomposition, which is contrary to the results given in Table II. Possibly this ratio is influenced by the reactions of free radicals formed in the photolysis of cyclopentanone or 4-pentenal.

The photolysis of cyclopentanone to about 20% decomposition shows a very large number of secondary products. Using a 150 ft capillary column coated with polypropylene glycol, at 0° C, and a flame ionization detector, many of the products of such a photolysis were separated. In addition to ethylene, cyclobutane, and carbon monoxide, which are produced in the primary process, small amounts of 1-butene and smaller amounts of *cis*- and *trans*-2-butene were observed. These presumably resulted from the secondary photolysis of 4-pentenal. More than 40 other products also appeared, including ethane, propane, propylene, acetaldehyde, and numerous C_4, C_5, and C_6-hydrocarbons. Flowers and Frey (6) have reported the formation of cyclohexane when cyclopentanone is photolyzed in the presence of a large excess of ethylene. We observed no appreciable amount of cyclohexane

Can. J. Chem. Downloaded from www.nrcresearchpress.com by 210.87.254.5 on 09/05/12
For personal use only.

under the conditions of our experiment. Clearly, many simultaneous free-radical reactions are taking place in this system, and could account for some of the ethylene formed.

In summary, the secondary processes in cyclopentanone photolysis have been shown to be extremely complicated, and no simple explanation for the pressure dependence of the ethylene/cyclobutane ratio is readily apparent.

ACKNOWLEDGMENTS

The authors gratefully acknowledge the financial assistance of the National Research Council of Canada and the University of British Columbia President's Fund. They also thank Dr. D. E. McGreer for his help and suggestions.

1. R. SRINIVASAN. J. Am. Chem. Soc. **81**, 1546 (1959). F. E. BLACET and A. MILLER. J. Am. Chem. Soc. **79**, 4327 (1957).
2. R. SRINIVASAN. J. Am. Chem. Soc. **83**, 4344, 4348 (1961).
3. C. D. HURD and M. A. POLLACK. J. Am. Chem. Soc. **60**, 1905 (1938).
4. F. W. SCHULER and G. W. MURPHY. J. Am. Chem. Soc. **72**, 3155 (1950).
5. C. A. MCDOWELL and S. SIFNIADES. J. Am. Chem. Soc. **84**, 4606 (1962).
6. M. C. FLOWERS and H. M. FREY. J. Chem. Soc. 2758 (1960).

RECEIVED MAY 22, 1963.
DEPARTMENT OF CHEMISTRY,
UNIVERSITY OF BRITISH COLUMBIA,
VANCOUVER, BRITISH COLUMBIA.

Can. J. Chem. Downloaded from www.nrcresearchpress.com by 210.87.254.5 on 09/05/12
For personal use only.

DETERMINATION OF RELATIVE SIGNS OF H—F COUPLING CONSTANTS IN FLUOROBENZENES BY NUCLEAR MAGNETIC DOUBLE RESONANCE

W. G. PATERSON* AND H. SPEDDING

The discovery (1–3) that the relative signs of n.m.r. coupling constants could be ascertained by nuclear magnetic double resonance has proved to be a valuable aid in the analysis of high-resolution spectra of liquids. This communication summarizes double-resonance experiments with 2,3-difluoro-5,6-dibromonitrobenzene (I), 2,4-dichloro-3,5-difluoronitrobenzene (II), and 2-chloro-4,5-difluoronitrobenzene (III), which yield the relative signs of J_{HF}^{o}, J_{HF}^{m}, and J_{HF}^{p}. The F^{19} n.m.r. spectra of these compounds at 94.1 Mc/s are first order, and the relative signs of the H—F coupling constants were determined by the method of Freeman (3). The decoupling apparatus is such that no other relative signs could be obtained (4). The n.m.r. parameters of the single-resonance spectra are listed in Table I.

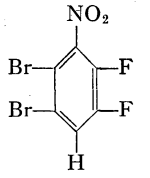

I

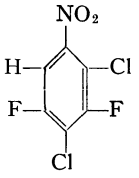

II

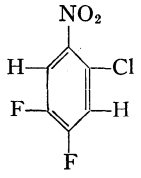

III

Present address: Central Research Laboratories, Minnesota Mining and Manufacturing Co., St. Paul 19, Minn., U.S.A. Correspondence should be addressed to W. G. P.

under the conditions of our experiment. Clearly, many simultaneous free-radical reactions are taking place in this system, and could account for some of the ethylene formed.

In summary, the secondary processes in cyclopentanone photolysis have been shown to be extremely complicated, and no simple explanation for the pressure dependence of the ethylene/cyclobutane ratio is readily apparent.

ACKNOWLEDGMENTS

The authors gratefully acknowledge the financial assistance of the National Research Council of Canada and the University of British Columbia President's Fund. They also thank Dr. D. E. McGreer for his help and suggestions.

1. R. SRINIVASAN. J. Am. Chem. Soc. **81**, 1546 (1959). F. E. BLACET and A. MILLER. J. Am. Chem. Soc. **79**, 4327 (1957).
2. R. SRINIVASAN. J. Am. Chem. Soc. **83**, 4344, 4348 (1961).
3. C. D. HURD and M. A. POLLACK. J. Am. Chem. Soc. **60**, 1905 (1938).
4. F. W. SCHULER and G. W. MURPHY. J. Am. Chem. Soc. **72**, 3155 (1950).
5. C. A. MCDOWELL and S. SIFNIADES. J. Am. Chem. Soc. **84**, 4606 (1962).
6. M. C. FLOWERS and H. M. FREY. J. Chem. Soc. 2758 (1960).

RECEIVED MAY 22, 1963.
DEPARTMENT OF CHEMISTRY,
UNIVERSITY OF BRITISH COLUMBIA,
VANCOUVER, BRITISH COLUMBIA.

Can. J. Chem. Downloaded from www.nrcresearchpress.com by 210.87.254.6 on 09/05/12
For personal use only.

DETERMINATION OF RELATIVE SIGNS OF H—F COUPLING CONSTANTS IN FLUOROBENZENES BY NUCLEAR MAGNETIC DOUBLE RESONANCE

W. G. PATERSON* AND H. SPEDDING

The discovery (1–3) that the relative signs of n.m.r. coupling constants could be ascertained by nuclear magnetic double resonance has proved to be a valuable aid in the analysis of high-resolution spectra of liquids. This communication summarizes double-resonance experiments with 2,3-difluoro-5,6-dibromonitrobenzene (I), 2,4-dichloro-3,5-difluoronitro-

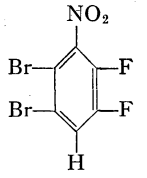

I

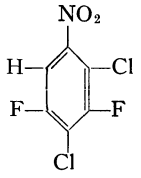

II

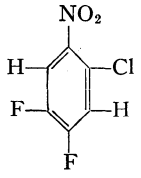

III

benzene (II), and 2-chloro-4,5-difluoronitrobenzene (III), which yield the relative signs of J_{HF}^{o}, J_{HF}^{m}, and J_{HF}^{p}. The F^{19} n.m.r. spectra of these compounds at 94.1 Mc/s are first order, and the relative signs of the H—F coupling constants were determined by the method of Freeman (3). The decoupling apparatus is such that no other relative signs could be obtained (4). The n.m.r. parameters of the single-resonance spectra are listed in Table I.

**Present address: Central Research Laboratories, Minnesota Mining and Manufacturing Co., St. Paul 19, Minn., U.S.A. Correspondence should be addressed to W. G. P.*

TABLE I

Nuclear magnetic resonance parameters (c.p.s.)
(All errors: ±0.2 c.p.s.)

Compound	J_{HF}^{o}	J_{HF}^{m}	J_{HF}^{p}	J_{FF}^{o}	J_{FF}^{m}	δ_{FF}
I	9.2	7.4	—	20.7	—	1178.7
II	8.3	—	2.2	—	4.2	370.9

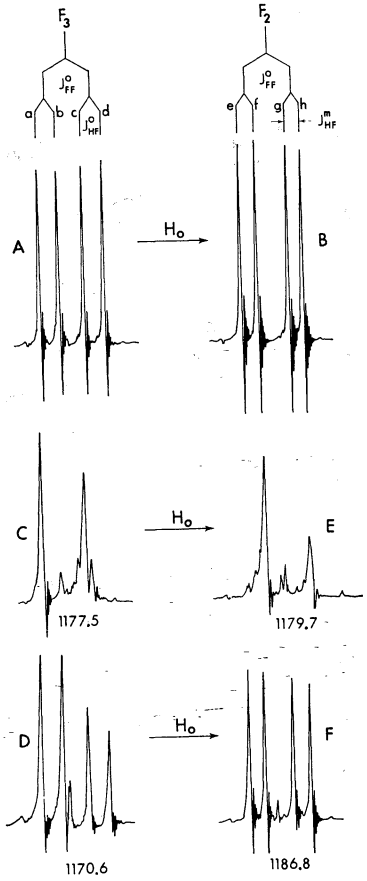

FIG. 1. F^{19} spectra of I dissolved in acetone. The separations in c.p.s. between H_1 and H_2 are shown below the double-resonance spectra. The magnetic field increases from left to right for all spectra. A. Single-resonance spectrum of F_3. B. Single-resonance spectrum of F_2. C. Double-resonance spectrum of F_3 with irradiation at $\frac{1}{2}(f+h)$ with "like-signs" arrangement. D. Double-resonance spectrum of F_3 with irradiation at $\frac{1}{2}(e+g)$ with "opposite-signs" arrangement. E. Double-resonance spectrum of F_2 with irradiation at $\frac{1}{2}(a+c)$ with "like-signs" arrangement. F. Double-resonance spectrum of F_2 with irradiation at $\frac{1}{2}(a+c)$ with "opposite-signs" arrangement.

The F^{19} spectrum and typical double-resonance spectra of I are shown in Fig. 1. Irradiation with a moderately weak r.f. field at a frequency $\frac{1}{2}(a+c)$ in the F_3 spectrum should collapse lines e and g in the F_2 spectrum if J_{HF}^{o} and J_{HF}^{m} are of the same sign, or collapse lines f and h if they are of opposite sign. Analogous arguments apply to irradiation at frequencies $\frac{1}{2}(b+d)$, $\frac{1}{2}(e+g)$, and $\frac{1}{2}(f+h)$. The possibilities are summarized in Table II.

Can. J. Chem. Downloaded from www.nrcresearchpress.com by 210.87.254.6 on 09/05/12
For personal use only.

TABLE II

Separations between r.f. fields H_1 and H_2 required for determination of relative signs of J_{HF}^{o} and J_{HF}^{m} in I

	Location in spectrum of H_2	Separation (c.p.s.) between H_1 and H_2 required for collapse of:			
		a and c	b and d	e and g	f and h
Like signs	$\frac{1}{2}(a+c)$	—	—	1179.6 c.p.s.	—
" "	$\frac{1}{2}(b+d)$	—	—	—	1177.8
" "	$\frac{1}{2}(e+g)$	1179.6	—	—	—
" "	$\frac{1}{2}(f+h)$	—	1177.8	—	—
Opposite signs	$\frac{1}{2}(a+c)$	—	—	—	1187.0
" "	$\frac{1}{2}(b+d)$	—	—	1170.4	—
" "	$\frac{1}{2}(e+g)$	—	1170.4	—	—
" "	$\frac{1}{2}(f+h)$	1187.0	—	—	—

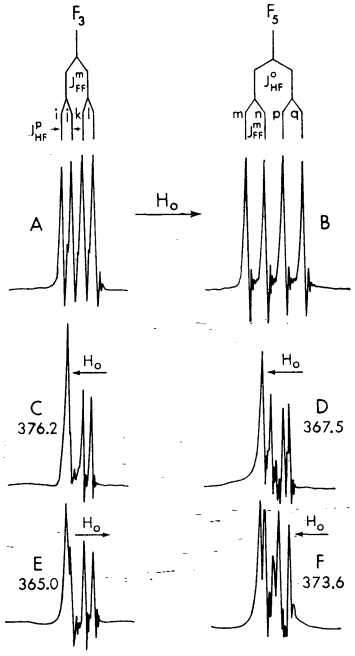

FIG. 2. F^{19} spectra of II as neat liquid. The separations in c.p.s. between H_1 and H_2 are shown beside the double-resonance spectra. The double-resonance spectra, which are all of F_5, were recorded at a substantially faster sweep rate than the single-resonance spectra. The direction of increasing magnetic field is shown for each spectrum. A. Single-resonance spectrum of F_3. B. Single-resonance spectrum of F_5. C. Double-resonance spectrum of F_5 with irradiation at $\frac{1}{2}(i+k)$ with "opposite-signs" arrangement. D. Double-resonance spectrum of F_5 with irradiation at $\frac{1}{2}(i+k)$ with "like-signs" arrangement. E. Double-resonance spectrum of F_5 with irradiation at $\frac{1}{2}(j+l)$ with "opposite signs" arrangement. F. Double-resonance spectrum of F_5 with irradiation at $\frac{1}{2}(j+l)$ with "like-signs" arrangement.

Typical spectra are shown in Fig. 1. It is clear that optimum collapse of the signals is obtained when a decoupling frequency is used which corresponds to like signs for J_{HF}^{o} and J_{HF}^{m}.

The F^{19} spectrum and representative double-resonance spectra of II are shown in Fig. 2. Irradiation at a frequency $\frac{1}{2}(i+k)$ in the F_3 spectrum should collapse lines m and n in the F_5 spectrum if J_{HF}^{o} and J_{HF}^{p} are of the same sign, or collapse lines p and q if they are of opposite sign. Analogous arguments apply to irradiation at frequencies $\frac{1}{2}(j+l)$, $\frac{1}{2}(m+n)$,

Can. J. Chem. Downloaded from www.nrcresearchpress.com by 210.87.254.6 on 09/05/12
For personal use only.

TABLE III

Separations between r.f. fields H_1 and H_2 required for determination of relative signs of J_{HF}^{o} and J_{HF}^{p} in II

	Location in spectrum of H_2	Separation (c.p.s.) between H_1 and H_2 required for collapse of:	
		m and n	p and q
Like signs	$\frac{1}{2}(i+k)$	367.8	—
" "	$\frac{1}{2}(j+l)$	—	374.0
Opposite signs	$\frac{1}{2}(i+k)$	—	376.2
" "	$\frac{1}{2}(j+l)$	365.3	—

and $\frac{1}{2}(p+q)$. A summary of the different arrangements is given in Table III, and experimental spectra are shown in Fig. 2. The data suggest convincingly that J_{HF}^{o} and J_{HF}^{p} are of opposite sign, which implies that J_{HF}^{m} and J_{HF}^{p} are also of opposite sign. These conclusions are in agreement with those obtained from studies of single-resonance spectra (5).

Further experiments of the type just described were also done with compound III, for which each F^{19} multiplet consisted of eight lines. Although the decoupling patterns were complex, the regions of the spectra which were perturbed in the double-resonance measurements left no doubt that all H—F coupling constants in III were of the same sign.

EXPERIMENTAL

The H^1 and F^{19} n.m.r. spectra were obtained with a Varian spectrometer operating at 100 Mc/s and 94.1 Mc/s respectively. The spectra were calibrated by the usual side-band method (6), using a Hewlett–Packard Model 200AB audio-oscillator and a Hewlett–Packard Model 521C frequency counter. The double-resonance experiments were carried out as described by Johnson (4). With the center-band signal phased out, the first modulation side band H_1 of the V3521 Integrator is used to record the n.m.r. spectrum while a second, stronger side band H_2, provided by an audio-oscillator, is applied to the system under investigation such that $|\omega_2-\omega_1|$ is equal to the separation required for the double-resonance experiment. The oscillator output is critical (3). The ratios of the chemical shifts to the coupling constants in the present instance were large enough that second-order corrections to the modulation frequency were unnecessary (7). The frequency of the first modulation side band (nominally 2 kc/s) of the Integrator varied slightly from day to day and was checked before each experiment. Measurements of the foregoing type have been previously reported (8). The compounds were very kindly supplied by Dr. G. C. Finger of the Illinois State Geological Survey, Urbana. The samples were thoroughly degassed by the nitrogen bubbling technique prior to the n.m.r. measurements.

ACKNOWLEDGMENTS

The financial support of the National Research Council of Canada is gratefully acknowledged. The authors wish to thank Mr. G. Bigam for his careful maintenance of the n.m.r. equipment.

1. D. F. Evans and J. P. Maher. Proc. Chem. Soc. 208 (1961).
2. R. Freeman and D. H. Whiffen. Mol. Phys. **4**, 321 (1961).
3. R. Freeman. Mol. Phys. **4**, 385 (1961).
4. L. F. Johnson. Varian Associates Publication No. 87-100-082. Palo Alto, California. August, 1962.
5. H. S. Gutowsky, C. H. Holm, A. Saika, and G. A. Williams. J. Am. Chem. Soc. **79**, 4596 (1957).
6. J. T. Arnold and M. E. Packard. J. Chem. Phys. **19**, 1608 (1951).
7. D. W. Turner. J. Chem. Soc. 847 (1962).
8. W. G. Paterson and G. Bigam. Can. J. Chem. **41**, 1841 (1963).

Received May 24, 1963.
Department of Chemistry,
University of Alberta,
Edmonton, Alberta.

Can. J. Chem. Downloaded from www.nrcresearchpress.com by 210.87.254.6 on 09/05/12
For personal use only.

THE MIXED COMPLEXES OF COPPER(II) AND NICKEL(II) WITH NITRILOTRIACETATE AND GLYCINATE AND THE FORMATION CONSTANT OF THESE AND OTHER MIXED COMPLEXES

Y. J. Israéli

Can. J. Chem. Downloaded from www.nrcresearchpress.com by 210.87.254.40 on 09/05/12
For personal use only.

We found previously that the nitrilotriacetates of copper(II) and nickel(II) can react with other bidentate ligands and form mixed complexes with them (1).

The composition of the mixed complexes formed by the reaction of glycine with the nitrilotriacetates of copper(II) or nickel(II) was determined by Job's method of continuous variations (2). The measurements were taken at several pH values and at the λ_{max} of the solutions containing equimolecular amounts of cation (Me), of nitrilotriacetate (X), and of glycinate (Glyc). At pH = 9 the solutions containing nickel(II) have maxima at 385 mμ and at 590 mμ and the corresponding copper solutions have a single maximum at 685 mμ. For the copper(II) solutions additional measurements were made at 625 mμ. The results of the Job experiments are shown in Fig. 1.

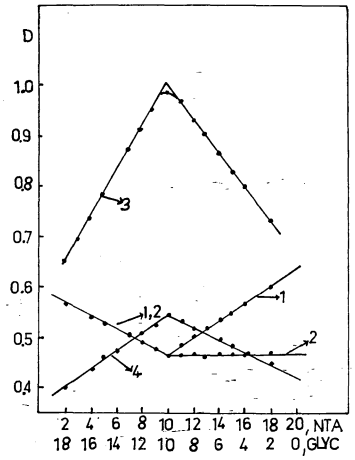

FIG. 1. Composition of the solutions: 5 ml Cu (2×10^{-2} M) + x ml NTA (1×10^{-2} M) + (20−x) ml Glyc (1×10^{-2} M): (1) pH = 10, λ = 685 mμ, (2) pH = 6, λ = 625 mμ; 5 ml Ni (1×10^{-1} M) + x ml NTA (5×10^{-2}) M + (20−x) ml Glyc (5×10^{-2} M): (3) pH = 7, λ = 385 mμ, (4) pH = 9, λ = 590 mμ.

From the curves of Fig. 1 we concluded that, at all the pH values measured, only one complex is formed of composition MeXGlyc.

The formation constant of the mixed complexes, formed by the reaction of nitrilotriacetate of copper(II) or nickel(II) (MeX) with bidentate ligands (BH), was determined by the Martell–Chaberek method (3). The bidentate ligands were glycine (Glyc), sodium salycilate (Salyc), and pyridine aldoxime (PA).

The reaction leading to the formation of the mixed complexes is:

$$MeX + BH \rightarrow MeXB + H^+ \qquad [1]$$

and the formation constant of the mixed complex is:

$$K_f = \frac{[MeXB]}{[MeX][B]}. \qquad [2]$$

To determine K_f, a solution containing equimolecular amounts of cation, trisodium nitrilotriacetate, and bidentate ligand (BH) was titrated with NaOH. All titrations were carried out at an ionic strength of 0.5, kept constant with $NaNO_3$.

In the following equations, a is the number of moles of NaOH added per mole of bidentate ligand (BH):

$$C_A = [MeX]_t = [MeX]+[MeXB] \quad [3]$$

$$C_B = [BH]_t = [HB]+[B^-]+[MeXB] \quad [4]$$

$$C_A = C_B \quad [5]$$

$$aC_B = [B]+[MeXB]+[OH]-[H]. \quad [6]$$

From equations [4], [5], and [6] it follows that:

$$[B] = \frac{K\{(1-a)C_B+[OH]-[H]\}}{[H]}, \quad [7]$$

where K is the acid dissociation constant of the bidentate ligand (BH). For glycine, pK = 9.7 (see ref. 4). For the other bidentate ligands the pK values were redetermined and found to be:

pK of NaSalyc = 11.6; pK of pyridine aldoxime = 9.9.

From equations [3] and [4] it follows that:

$$[MeX] = [B]\left\{1+\frac{[H]}{K}\right\} \quad [8]$$

$$[MeXB] = C_A-[MeX]. \quad [9]$$

From equations [2], [7], [8], and [9] it is easy to calculate K_f.

Table I shows a selection of data obtained in two typical titrations. Table II shows the formation constants of other mixed complexes.

We assert the hypothesis that in these complexes the cation is probably hexacoordinated.

TABLE I

(5 ml Me (0.1 M) + 5 ml Na_3X (0.1 M) + 5 ml Glyc (0.1 M) + 10 ml H_2O + y ml NaOH (0.5 M); μ = 0.5 M, $NaNO_3$)

Me	a	pH	10^7[Glyc]	10^2[MeX]	10^{-3}[MeXGlyc]	$10^{-5}K_f$
Cu	0.2	5.5	9.32	1.58	4.06	2.75
Cu	0.5	6.3	36.40	0.98	9.85	2.78
Cu	0.8	7.3	144.00	0.39	15.53	2.76
Ni	0.2	6.5	93.00	1.58	4.06	0.26
Ni	0.6	7.6	580.00	0.79	11.69	0.26
Ni	0.8	8.3	1440.00	0.41	15.40	0.26

TABLE II

Compound	K_f
CuX,Salyc	2.10×10^5
NiX,Salyc	1.06×10^3
CuX,PA	1.60×10^6
NiX,PA	1.50×10^5

Can. J. Chem. Downloaded from www.nrcresearchpress.com by 210.87.254.40 on 09/05/12
For personal use only.

1. Y. J. Israéli. Bull. Soc. Chim. France. In press.
2. P. Job. Ann. Chim. (Paris), **9**, 113 (1928).
3. A. Martell and S. Chaberek. J. Am. Chem. Soc. **74**, 5052 (1952).
4. H. Flood and V. Loras. Tidsskr. Kjemi, Bergvesen Met. **5**, 83 (1945).

Received May 6, 1963.
Department of Inorganic and Analytical Chemistry,
The Hebrew University,
Jerusalem, Israel.

Can. J. Chem. Downloaded from www.nrcresearchpress.com by 210.87.254.40 on 09/05/12
For personal use only.

THE OCCURRENCE OF D-*glycero*-D-*manno*-HEPTOSE IN THE EXTRACELLULAR POLYSACCHARIDE PRODUCED BY AZOTOBACTER INDICUM

J. K. N. Jones, M. B. Perry, and W. Sowa

Knight and his co-workers (1) showed that *Azotobacter indicum* produced an extracellular polysaccharide containing D-glucose, uronic acid, and an unidentified aldoheptose. In an earlier study of this organism it was found that a fructoglycan was produced when sucrose was used as a substrate, but a polysaccharide containing D-glucose and uronic acid was produced when D-glucose was used as a substrate (2). The occurrence of aldoheptoses in bacterial polysaccharides is well established (3); however, little is known about the fine structure of such polysaccharides or of the sereological specificity of the component aldoheptoses. This note records the identification of D-*glycero*-D-*manno*-heptose in the extracellular polysaccharide produced by *A. indicum* and some preliminary structural investigations.

A. indicum (syn. *Beijerinckia indica* Starket and De) was grown in shake culture on a 5% D-glucose medium supplied with peptone and mineral salts to give after 38 days' growth a 4.5% yield of a crude polysaccharide which was obtained by acetone precipitation from the culture medium. Moving-boundary electrophoresis showed the preparation to be at least a two component mixture containing a major electrophoretically mobile component and an immobile minor fraction. The major component was an acidic glycan which was isolated from the mixture by Cetavlon precipitation (4) leaving a neutral glycan composed of glucose, mannose, rhamnose, and arabinose.

The acidic glycan had an equivalent weight of 1030 corresponding to a uronic anhydride content of 17.1% and was shown to be essentially homogeneous by electrophoresis in veronal buffer (pH 8.6) and in phosphate buffer (pH 7.4).

Hydrolysis of the acidic glycan followed by chromatographic fractionation of the neutral and acidic sugars afforded D-glucose characterized as its *N*-*p*-nitrophenylglycosylamine derivative, D-mannose characterized as its phenylhydrazone derivative, and D-*glycero*-D-*manno*-heptose which was characterized as its acetate and by its reduction to give crystalline D-*glycero*-D-*manno*-heptitol. Chromatographic examination of the uronic acid monosaccharide fraction indicated it to be composed mainly of glucuronic acid and a small amount of galacturonic acid. On reduction of the methyl ester, methyl glycoside preparation from this fraction with borohydride, and hydrolysis of the resulting methyl glycosides, paper chromatography revealed the presence of glucose and small amounts of galactose and a sugar tentatively identified as gulose. The presence of this latter sugar indicates the possible occurrence of small amounts of guluronic acid in the polysaccharide. Quantitative analysis of the uronic acid in the polysaccharide by the

1. Y. J. Israéli. Bull. Soc. Chim. France. In press.
2. P. Job. Ann. Chim. (Paris), **9**, 113 (1928).
3. A. Martell and S. Chaberek. J. Am. Chem. Soc. **74**, 5052 (1952).
4. H. Flood and V. Loras. Tidsskr. Kjemi, Bergvesen Met. **5**, 83 (1945).

Received May 6, 1963.
Department of Inorganic and Analytical Chemistry,
The Hebrew University,
Jerusalem, Israel.

Can. J. Chem. Downloaded from www.nrcresearchpress.com by 210.87.254.105 on 09/05/12
For personal use only.

THE OCCURRENCE OF D-*glycero*-D-*manno*-HEPTOSE IN THE EXTRACELLULAR POLYSACCHARIDE PRODUCED BY AZOTOBACTER INDICUM

J. K. N. Jones, M. B. Perry, and W. Sowa

Knight and his co-workers (1) showed that *Azotobacter indicum* produced an extracellular polysaccharide containing D-glucose, uronic acid, and an unidentified aldoheptose. In an earlier study of this organism it was found that a fructoglycan was produced when sucrose was used as a substrate, but a polysaccharide containing D-glucose and uronic acid was produced when D-glucose was used as a substrate (2). The occurrence of aldoheptoses in bacterial polysaccharides is well established (3); however, little is known about the fine structure of such polysaccharides or of the sereological specificity of the component aldoheptoses. This note records the identification of D-*glycero*-D-*manno*-heptose in the extracellular polysaccharide produced by *A. indicum* and some preliminary structural investigations.

A. indicum (syn. *Beijerinckia indica* Starket and De) was grown in shake culture on a 5% D-glucose medium supplied with peptone and mineral salts to give after 38 days' growth a 4.5% yield of a crude polysaccharide which was obtained by acetone precipitation from the culture medium. Moving-boundary electrophoresis showed the preparation to be at least a two component mixture containing a major electrophoretically mobile component and an immobile minor fraction. The major component was an acidic glycan which was isolated from the mixture by Cetavlon precipitation (4) leaving a neutral glycan composed of glucose, mannose, rhamnose, and arabinose.

The acidic glycan had an equivalent weight of 1030 corresponding to a uronic anhydride content of 17.1% and was shown to be essentially homogeneous by electrophoresis in veronal buffer (pH 8.6) and in phosphate buffer (pH 7.4).

Hydrolysis of the acidic glycan followed by chromatographic fractionation of the neutral and acidic sugars afforded D-glucose characterized as its *N*-*p*-nitrophenylglycosylamine derivative, D-mannose characterized as its phenylhydrazone derivative, and D-*glycero*-D-*manno*-heptose which was characterized as its acetate and by its reduction to give crystalline D-*glycero*-D-*manno*-heptitol. Chromatographic examination of the uronic acid monosaccharide fraction indicated it to be composed mainly of glucuronic acid and a small amount of galacturonic acid. On reduction of the methyl ester, methyl glycoside preparation from this fraction with borohydride, and hydrolysis of the resulting methyl glycosides, paper chromatography revealed the presence of glucose and small amounts of galactose and a sugar tentatively identified as gulose. The presence of this latter sugar indicates the possible occurrence of small amounts of guluronic acid in the polysaccharide. Quantitative analysis of the uronic acid in the polysaccharide by the

colorimetric carbazole method (5) and analysis of the neutral sugars by the gas–liquid partition chromatographic method (6) indicated the composition of the polysaccharide to be: uronic acid 18.8%; D-*glycero*-D-*manno*-heptose 15.9%; D-glucose 32.8%; D-mannose 25.6%; and unidentified components 6.9%.

A spray reagent for the tentative identification of aldoheptoses on paper chromatograms is described. The test is based upon the condensation of the formaldehyde, released by the oxidation of the aldoheptose with buffered (pH 3.6) metaperiodate solution, with acetylacetone in the presence of ammonium salts to form the yellow highly fluorescent 3,5-diacetyl-1,4-dihydrolutidine (7). Under the oxidation conditions used, aldoheptoses liberate 1 mole formaldehyde per mole sugar whereas aldohexoses do not liberate formaldehyde and do not therefore give a positive reaction with the acetylacetone – ammonium acetate spray reagent. The difference in behavior of the aldoheptoses and aldohexoses noted above allows aldoheptoses to be detected on chromatograms even when they overlap with aldohexoses. The reagent is not specific since some other compounds (e.g. glycitols and ketoses) can also liberate formaldehyde on treatment with acidified metaperiodate solution; however, despite the lack of specificity of the test, its application has in several cases shown the presence of aldoheptoses in mixtures where they would otherwise have been overlooked or been identified as aldohexoses.

EXPERIMENTAL

Paper chromatography was performed by the descending method on Whatman No. 1 filter paper, using the following solvent systems: (A) ethyl acetate – acetic acid – formic acid – water (18:3:1:4 v/v); (B) butan-1-ol–ethanol–water (3:1:1 v/v); (C) butan-1-ol–pyridine–water (10:3:3 v/v); and (D) ethyl acetate – pyridine – water (10:4:3 v/v).

The following sprays were used to detect the compounds on the paper chromatograms: (A) 2% solution of *p*-anisidine hydrochloride in butan-1-ol; (B) 1% solution of silver nitrate in acetone, followed by 2% ethanolic sodium hydroxide; and (C) heptose spray—the chromatograms were first lightly sprayed with 0.03 *M* sodium metaperiodate in pH 3.6, 0.2 *M* acetate buffer followed after 1 minute by a 1% aqueous solution of inositol. The chromatograms were next sprayed with a solution of ammonium acetate (15 g), acetic acid (0.2 ml), and acetylacetone (1 ml) in methanol (50 ml) and the papers were examined after standing at room temperature for 30 minutes. The heptoses were located as yellow spots which were intensified when examined under ultraviolet light. The lower limit for the detection of aldoheptoses was found to be 1 γ/sq. cm in daylight and 0.5 γ/sq. cm under ultraviolet light.

Production of the Extracellular Polysaccharide

A. indicum (National Research Council Culture Collection) was kept in subculture on agar slopes having the same composition as the medium used for the liquid growth. The organism was grown at 25° in shake culture and 1 liter conical flasks each containing 300 ml of a medium having the following composition: D-glucose (50 g), peptone (1 g), dipotassium hydrogen phosphate (0.5 g), magnesium sulphate hydrated (0.2 g), sodium chloride (0.2 g), calcium sulphate (0.1 g), ferric chloride (trace), and calcium carbonate (20 g), in water 1 liter. The yield of crude extracellular polysaccharide based on the D-glucose supplied was: 2% (6 days), 2.3% (14 days), 7.5% (19 days), 17.8% (27 days), 18.3% (36 days), and 27.6% (9 months). The main bulk of the culture medium was harvested after 38 days' growth, and after adjustment to pH 4 with acetic acid, the crude polysaccharide was precipitated by pouring the solution into 6 volumes of acetone. The polysaccharides were collected by centrifugation and then precipitated four times in the same way. The polysaccharides were deionized by passage through columns of IR 120 (H^+) and IR 45 (OH^-) ion-exchange resins and the concentrated solution was freeze-dried to give the product in 4.5% yield based on the D-glucose supplied.

Some Properties of the Polysaccharide Preparation

Tiselius electrophoresis of the polysaccharide preparation (1% w/v) in veronal buffer (pH 8.6, $\mu = 0.1$) and in phosphate buffer (pH 7.4, *M*/20) indicated that it was a mixture of a major electrophoretically mobile fraction and a minor immobile fraction. Trial small-scale experiments showed that the polysaccharide preparation could be fractionated into the two electrophoretically identified components by precipitation of the major component with either cetyltrimethylammonium bromide (Cetavlon) or with barium hydroxide solution.

The polysaccharide preparation (10 g) was fractioned by treating its aqueous solution (4 l.) with Cetavlon (80 ml, 10% w/v) to give an insoluble complex of the major component which was collected by centrifugation

Can. J. Chem. Downloaded from www.nrcresearchpress.com by 210.87.254.105 on 09/05/12
For personal use only.

and dissolved in dilute acetic acid (500 ml, 50% w/v); the polysaccharide was then obtained by pouring the solution into ethanol (4 l.). The polysaccharide was twice further precipitated with Cetavlon and regenerated in the same way to give the acidic glycan which was freeze-dried from its aqueous solution (4.66 g).

The supernatant (4 l.) from the first Cetavlon treatment of the original polysaccharide preparation was concentrated to ca. 100 ml and since it did not give any further precipitate on treatment with Cetavlon it was poured into ethanol (1 l.) to give a precipitate of the electrophoretically immobile polysaccharide which contained glucose, mannose, rhamnose, and a trace of arabinose.

Some Properties of the Acidic Glycan

The acidic glycan had $[\alpha]_D^{19}$ +38° (*c*, 0.4 water). Anal. sulphate ash 1.3%; N, 0.2%. It gave a highly viscous solution in water and had a neutralization equivalent of 1030 determined by titration with standard sodium hydroxide solution. Tiselius electrophoresis examination of 1% w/v solution of the glycan in phosphate buffer (pH 7.4, *M*/20) gave a single sharp peak corresponding in behavior to the mobile peak observed in the electrophoresis of the original polysaccharide preparation.

Component Sugars of the Acidic Glycan

A portion of the glycan (20 mg) was hydrolyzed by heating its solution in *N* sulphuric acid (8 ml) at 100° for 10 hours. The hydrolyzate was neutralized ($BaCO_3$), filtered, and the concentrated filtrate was examined by paper chromatography in solvent systems A, B, C, and D and detection was made using the three spray reagents described previously. The polysaccharide hydrolyzate was indicated to contain uronic acid, heptose, glucose, and mannose in the visual ratio 1:1:2:2 together with trace amounts of arabinose and rhamnose.

The acidic glycan (8.6 g) was hydrolyzed with 0.5 *N* sulphuric acid (450 ml) at 100° for 9 hours. The cooled hydrolyzate was neutralized ($BaCO_3$) and ethanol was added to the concentrated filtrate to precipitate the barium uronates (3.3 g) which were removed by filtration. The filtrate was deionized by passage through IR 120(H^+) and IR 45(OH^-) ion-exchange resins and the effluent and washings containing the neutral sugars were concentrated to a syrup (2.7 g).

The neutral sugars (2.5 g) were fractionated by cellulose column chromatography using propan-1-ol – ethyl acetate – water (7:2:1 v/v) as the mobile phase. The isolated sugars were characterized as follows: D-Glucose, $[\alpha]_D^{23}$ +51.6° (*c*, 1.2 water), which gave *N*-*p*-nitrophenylglucosylamine having m.p. and mixed m.p. 182–183°; D-mannose, $[\alpha]_D^{23}$ +9.5° (*c*, 1.1 water), which gave a crystalline phenylhydrazone derivative having m.p. and mixed m.p. 186–187°; D-*glycero*-D-*manno*-heptose, a syrup which had $[\alpha]_D^{20}$ +21.4° (*c*, 2.8 water) and was chromatographically indistinguishable from an authentic specimen of the heptose in all the solvent systems used. The heptose had $R_{glucose}$ 0.90 (solvent A) and $R_{glucose}$ 0.82 (solvent B). The heptose (60 mg) was acetylated in acetic anhydride (6 ml) containing sulphuric acid (0.1 ml) to give hexa-*O*-acetyl-D-*glycero*-α-D-*manno*-heptose which after two recrystallizations from ether – petroleum ether (b.p. 40–60°) had m.p. 135–136° and did not depress the melting point of the authentic acetate on admixture with it (m.p. 138–139°). The derivative and an authentic specimen of the acetate had identical X-ray diffraction patterns. Reduction of the heptose (40 mg) with aqueous sodium borohydride solution afforded D-*glycero*-D-*manno*-heptitol which had m.p. and mixed m.p. 154° and an infrared spectrum (KBr disk) indistinguishable from that of an authentic specimen of the heptitol.

The barium uronates (3.3 g) were dissolved in water and passed down a column of IR 120(H^+) ion-exchange resin. The concentrated solution was fractionated by cellulose column chromatography using solvent A as the mobile phase. A portion of the monosaccharide fraction (50 mg) was treated with 1% w/v methanolic hydrogen chloride solution in a sealed tube at 100° for 3 hours. The cooled solution was neutralized with a solution of diazomethane in ether and the solution was left in contact with a slight excess of diazomethane at 5° overnight to complete the esterification of the acid groups. The concentrated solution was dissolved in 0.4 *M* boric acid (1 ml), and sodium borohydride (50 mg) in 0.4 *M* boric acid (10 ml) was added to the cooled solution followed after 1 hour by sodium borohydride (100 mg) in water (10 ml). The excess borohydride was destroyed by the addition of acetic acid, the solution was deionized by passage through columns of IR 120(H^+) and IR 45(OH^-) ion-exchange resins, the boric acid was removed from the dried solution as methyl borate by repeated distillations with methanol. Examination of the residue by paper chromatography revealed spots corresponding to glucose, galactose, and gulose having $R_{glucose}$ 1.00, 0.83, and 1.26 (solvent B) and 1.00, 0.84, and 1.18 (solvent C) respectively. The components corresponding to galactose and gulose were present in very minor amounts. The original uronic acid monosaccharide fraction on paper chromatography showed a minor component corresponding to galacturonic acid, a large elongated spot corresponding to glucuronic acid, and a large spot corresponding to glucuronolactone.

Quantitative Analysis of the Component Sugars of the Acidic Glycan

The uronic acid content of the acidic glycan determined by the Dische (5) colorimetric carbazole method was found to be 18.8%. The composition of the neutral sugars was determined after complete hydrolysis of the glycan (17.3 mg) with *N* sulphuric acid (7 ml) at 100° for 10 hours. D-Xylose (3 mg) was added to the hydrolyzate as an internal standard and the solution was neutralized ($BaCO_3$), filtered, and the filtrate was treated with sodium borohydride (30 mg) to reduce the aldoses to their corresponding glycitols. The acidified (acetic acid) reaction mixture was concentrated to dryness and the glycitols were acetylated by heating them with acetic anhydride (5 ml) containing sulphuric acid (0.1 ml) at 40° for 5 hours. The resulting

Can. J. Chem. Downloaded from www.nrcresearchpress.com by 210.87.254.105 on 09/05/12
For personal use only.

mixture of glycitol acetates was separated by gas–liquid partition chromatography using a Pye Argon Chromatograph fitted with an ionization detector (80 μc radium D) employing a glass column (117×0.5 cm I.D.) packed with an intimate (1:1 v/v) mixture of 20% w/w Dow Corning stopcock grease on Chromosorb W (60–80 mesh) and 20% w/w butanediol succinate polyester on Chromosorb W (60–80 mesh). Using a column temperature of 215° and an argon flow rate of 125 ml/min, excellent resolution of the glycitol acetates was obtained, and their molar ratios were calculated by direct measurement of peak areas. The composition of the polysaccharide based on the xylose internal standard was: uronic acid 18.8%; D-*glycero*-D-*manno*-heptose 15.9%; D-glucose 32.8%; and D-mannose 25.6%.

We thank Dr. N. K. Richtmyer for a specimen of D-*glycero*-D-*manno*-heptose and the National Research Council for financial assistance (Grants T39 and 706).

1. C. M. QUINNELL, S. G. KNIGHT, and P. W. WILSON. Can. J. Microbiol. **3**, 277 (1957).
2. J. P. MARTIN. J. Bacteriol. **50**, 349 (1945).
3. D. A. L. DAVIES. Advan. Carbohydrate Chem. **15**, 271 (1960).
4. A. S. JONES. Biochim. Biophys. Acta, **10**, 607 (1953).
5. Z. DISCHE. J. Biol. Chem. **183**, 489 (1950).
6. S. W. GUNNER, J. K. N. JONES, and M. B. PERRY. Chem. Ind. (London), 255 (1961).
7. T. NASH. Biochem. J. **55**, 416 (1953).

RECEIVED April 12, 1963.
DEPARTMENT OF ORGANIC CHEMISTRY,
QUEEN'S UNIVERSITY,
KINGSTON, ONTARIO.

PREPARATION AND PROPERTIES OF ISOMERIC 2,4-DINITROPHENYL DERIVATIVES OF ALPHA–EPSILON DIAMINOPIMELIC ACID[1]

D. JUŠIĆ, C. ROY, A. J. SCHOCHER, AND R. W. WATSON

Mono- and di-dinitrophenyl (DNP) derivatives of the LL and meso isomers of diaminopimelic acid (Dap) have been prepared in pure crystalline form for the first time. Chromatographically pure mono- and di-DNP derivatives of DD-diaminopimelic acid have also been prepared, although the amounts were too small to crystallize. Isomeric DNP derivatives of diaminopimelic acid may be separated chromatographically (1) and the free isomers may be regenerated by catalytic hydrogenolysis of the dimethyl esters (2).

Infrared (IR) spectra of the crystalline mono- and di-DNP derivatives, automatically recorded from Nujol mulls using a Perkin–Elmer double-beam spectrophotometer (NaCl prism), have been deposited with Documentation of Molecular Spectroscopy, 4 and 5 Bell Yard, London, W.C.2, England. Differences between IR spectra of mono-LL and mono-meso derivatives include a shoulder at 3440, a small peak at 3400 and shoulders at 1675±20, 1492, 880–910, and 730 present in the meso and absent in the LL-form. Peaks at 3590, 3470, 1140, 1085, and 822 are present in the spectrum of mono-DNP-LL-diaminopimelic acid and absent in the related mono-meso compound. Differences in the IR spectra of di-DNP-LL-diaminopimelic and di-DNP-meso-diaminopimelic acid comprise (*a*) a small peak at 1672 present in the LL-derivative and absent in the meso form and (*b*) two small peaks at 996 and 777 present in the di-DNP-meso derivative and absent in di-DNP-LL-diaminopimelic acid. Besides these main differences a single peak at 3310 in the curve for di-DNP-LL-diaminopimelic acid is replaced by two small peaks at 3335 and 3290 in the spectrum of the di-DNP-meso derivative: two medium peaks at 1230 and

[1]*Issued as N.R.C. No. 7517.*

Can. J. Chem. Downloaded from www.nrcresearchpress.com by 210.87.254.105 on 09/05/12
For personal use only.

mixture of glycitol acetates was separated by gas–liquid partition chromatography using a Pye Argon Chromatograph fitted with an ionization detector (80 μc radium D) employing a glass column (117×0.5 cm I.D.) packed with an intimate (1:1 v/v) mixture of 20% w/w Dow Corning stopcock grease on Chromosorb W (60–80 mesh) and 20% w/w butanediol succinate polyester on Chromosorb W (60–80 mesh). Using a column temperature of 215° and an argon flow rate of 125 ml/min, excellent resolution of the glycitol acetates was obtained, and their molar ratios were calculated by direct measurement of peak areas. The composition of the polysaccharide based on the xylose internal standard was: uronic acid 18.8%; D-*glycero*-D-*manno*-heptose 15.9%; D-glucose 32.8%; and D-mannose 25.6%.

We thank Dr. N. K. Richtmyer for a specimen of D-*glycero*-D-*manno*-heptose and the National Research Council for financial assistance (Grants T39 and 706).

1. C. M. QUINNELL, S. G. KNIGHT, and P. W. WILSON. Can. J. Microbiol. **3**, 277 (1957).
2. J. P. MARTIN. J. Bacteriol. **50**, 349 (1945).
3. D. A. L. DAVIES. Advan. Carbohydrate Chem. **15**, 271 (1960).
4. A. S. JONES. Biochim. Biophys. Acta, **10**, 607 (1953).
5. Z. DISCHE. J. Biol. Chem. **183**, 489 (1950).
6. S. W. GUNNER, J. K. N. JONES, and M. B. PERRY. Chem. Ind. (London), 255 (1961).
7. T. NASH. Biochem. J. **55**, 416 (1953).

RECEIVED April 12, 1963.
DEPARTMENT OF ORGANIC CHEMISTRY,
QUEEN'S UNIVERSITY,
KINGSTON, ONTARIO.

Can. J. Chem. Downloaded from www.nrcresearchpress.com by 210.87.254.42 on 09/05/12
For personal use only.

PREPARATION AND PROPERTIES OF ISOMERIC 2,4-DINITROPHENYL DERIVATIVES OF ALPHA–EPSILON DIAMINOPIMELIC ACID[1]

D. JUŠIĆ, C. ROY, A. J. SCHOCHER, AND R. W. WATSON

Mono- and di-dinitrophenyl (DNP) derivatives of the LL and meso isomers of diaminopimelic acid (Dap) have been prepared in pure crystalline form for the first time. Chromatographically pure mono- and di-DNP derivatives of DD-diaminopimelic acid have also been prepared, although the amounts were too small to crystallize. Isomeric DNP derivatives of diaminopimelic acid may be separated chromatographically (1) and the free isomers may be regenerated by catalytic hydrogenolysis of the dimethyl esters (2).

Infrared (IR) spectra of the crystalline mono- and di-DNP derivatives, automatically recorded from Nujol mulls using a Perkin–Elmer double-beam spectrophotometer (NaCl prism), have been deposited with Documentation of Molecular Spectroscopy, 4 and 5 Bell Yard, London, W.C.2, England. Differences between IR spectra of mono-LL and mono-meso derivatives include a shoulder at 3440, a small peak at 3400 and shoulders at 1675±20, 1492, 880–910, and 730 present in the meso and absent in the LL-form. Peaks at 3590, 3470, 1140, 1085, and 822 are present in the spectrum of mono-DNP-LL-diaminopimelic acid and absent in the related mono-meso compound. Differences in the IR spectra of di-DNP-LL-diaminopimelic and di-DNP-meso-diaminopimelic acid comprise (*a*) a small peak at 1672 present in the LL-derivative and absent in the meso form and (*b*) two small peaks at 996 and 777 present in the di-DNP-meso derivative and absent in di-DNP-LL-diaminopimelic acid. Besides these main differences a single peak at 3310 in the curve for di-DNP-LL-diaminopimelic acid is replaced by two small peaks at 3335 and 3290 in the spectrum of the di-DNP-meso derivative: two medium peaks at 1230 and

[1]*Issued as N.R.C. No. 7517.*

1202 in the di-meso derivative are replaced by a single medium peak with shoulders at 1230, 1205, and 1185 in the di-LL compound. Ultraviolet (UV) spectra of mono- and di-DNP derivatives of the LL and meso isomers are similar to those of DNP-L-valine and DNP-L-arginine (3) and closely resemble the recorded spectrum of di-DNP-diaminopimelic acid (4).

The electrophoretic behavior of the DNP derivatives of diaminopimelic acid is compared with that of DNP-alanine and DNP-glutamic acid in Table I. Mono-DNP-LL-diaminopimelic acid and the mono-DNP-meso derivative have equivalent electrophoretic mobilities. In 1 hour at pH 6.4 these compounds run about 2 cm behind the three di-DNP derivatives, whose net charges are sufficiently alike to prevent their separation from each other. Qualitatively similar differences were observed at pH 3.5.

TABLE I

High-voltage electrophoresis* of dinitrophenyl derivatives of amino acids

	Distance travelled toward anode (cm)		
	pH 6.4		
Derivative	I	II	pH 3.5
Mono-DNP-LL-Dap	6.5	—	4.5
Mono-DNP-meso-Dap	6.5	—	4.5
Di-DNP-LL-Dap	8.4	9.5	—
Di-DNP-DD-Dap	—	9.6	—
Di-DNP-meso-Dap	8.4	9.5	(?)
DNP-alanine	8.8	8.5	(?)
DNP-glutamic acid	13.2	14.1	6.1

*40 v/cm length; 2 ma/cm breadth; 1 hour; pyridine acetate buffers (10); paper immersed in Varsol (11).

Separation of di-DNP-LL-diaminopimelic acid from the di-DNP-meso derivative by paper chromatography was achieved in four solvent systems (Table II). In solvent I(a) on unbuffered paper the di-DNP derivative of each of the three isomers tends to separate. In solvent II(a) on unbuffered paper mono-DNP-LL-diaminopimelic acid runs ahead of the mono-DNP-meso derivative.

TABLE II

Chromatographic separation of dinitrophenyl derivatives of amino acids

	$R_{DNP\text{-}Ala}$*						
		Solvent I(a)†		Solvent II†		Solvent II(a)†	
Derivative	Solvent I†	6 hr	16 hr	5 hr	22.5 hr	17 hr	17 hr
Mono-DNP-meso-Dap	0.13	0.10	0.12	1.55	1.66	1.63	1.77
Mono-DNP-LL-Dap	0.13	0.11	0.14	1.56	1.69	1.80	1.81
Di-DNP-meso-Dap	0.30	0.25	0.24	0.50	0.54	0.52	0.56
Di-DNP-LL-Dap	0.39	0.47	0.44	0.33	0.40	0.31	0.42
Di-DNP-DD-Dap	—	0.33	0.37	0.34	0.39	—	0.42
DNP-alanine	1.00	1.00	1.00	1.00	1.00	1.00	1.00
DNP-glutamic acid	0.13	1.24	1.24	0.76	0.78	0.80	0.83

*Distance run by DNP-derivative/distance run by DNP-alanine.
†Descending chromatograms on Schleicher and Schuell paper (2043B). Solvent systems (buffered paper): I: n-propanol:0.2 N ammonia 85:15 (12); II: 1.5 M Na_2SO_4 in 0.05 M phthalate at pH 6 (13). Solvents I(a) and II(a) on unbuffered paper; buffer: 0.05 M phthalate at pH 6.

Can. J. Chem. Downloaded from www.nrcresearchpress.com by 210.87.254.42 on 09/05/12
For personal use only.

EXPERIMENTAL

Di-DNP-LL-diaminopimelic Acid

Five grams of LL-enriched Calbiochem[2] diaminopimelic acid ($[\alpha]_D^{24-26} = +33.1°$, containing approximately 73% of the LL isomer), treated with 18.3 g of β-naphthalenesulphonic acid yielded 4.8 g of the crystalline LL-nasylate on cooling (5). From this material chromatographically pure LL-diaminopimelic acid was released by the addition of pyridine (6). LL-diaminopimelic acid (1 g) was dissolved in 80 ml of a 1% solution of trimethylamine in water, and 4 g of 1-fluoro-2,4-dinitrobenzene (FDNB) was added (7). After the aqueous solution was stirred for 3 hours in subdued light (8) at 40° C, with addition of 1% trimethylamine at intervals to maintain the pH close to 9, it was extracted: (*a*) with ether until the extracts were colorless (4×80 ml); (*b*) with benzene (3×; discard); and (*c*) again with ether (2×; discard). The water layer was then acidified to pH 1.2 with *N* HCl and extracted with ether until colorless (extract A). Evaporation of extract A to dryness, solution of the residue in a small amount of acetone, and addition of petroleum ether to first turbidity yielded crystals of di-DNP-LL-diaminopimelic acid on standing at 0° C. Recrystallization from (*a*) acetone – petroleum ether (2×) and (*b*) from acetone–water (2×) took place on cooling to 0° C in each solvent. Found: C, 43.70; H, 3.51; N, 15.87. Calculated for $C_{19}H_{18}N_6O_{12}$: C, 43.67; H, 3.45; N, 16.09. M.p. 87° C (decomp.).[3] $[\alpha]_D^{24-26} = -85 \pm 5°$ C.[4] $[M]_D^{24-26} = -444$ (9). Chromatographically pure di-DNP-DD-diaminopimelic acid was prepared in the same way from the pure DD isomer.

Di-DNP-meso-diaminopimelic Acid

This derivative was prepared from pure meso-diaminopimelic acid (1) by the procedure outlined for di-DNP-LL-diaminopimelic acid. Found: C, 43.63; H, 3.72; N, 16.22. Calculated for $C_{19}H_{18}N_6O_{12}$: C, 43.67; H, 3.45; N, 16.09. M.p. 220° C (decomp.)[3]. $[\alpha]_D^{24-26} = 0.0$.

Mono-DNP-LL-diaminopimelic Acid

In the preparation of mono-DNP-LL-diaminopimelic acid the yield was increased by adding one-half of the stoichiometric amount of FDNB to the reaction mixture. After extraction of the acidified aqueous layer with ether (extract A), further extraction of the water layer (pH 1.2) with ethyl acetate (10×) removed the mono-DNP-LL derivative (extract B). Evaporation of extract B to dryness and solution of the residue in a small amount of water gave the crystalline derivative on standing at 15° C. Occasionally the monoderivatives crystallized spontaneously from the aqueous layer after extraction with ether, but they were obtained more consistently after ethyl acetate extraction. Mono-DNP-LL-diaminopimelic acid was chromatographically pure after one recrystallization from water. Found: C, 43.92; H, 4.40; N, 15.51. Calculated for $C_{13}H_{16}N_4O_8$: C, 43.82; H, 4.49; N, 15.73. M.p. 164° C (decomp.).[3] $[\alpha]_D^{24-26} = -65 \pm 5°$ C.[4] $[M]_D^{24-26} = -231$. From the DD isomer a small amount of chromatographically pure mono-DNP-DD-diaminopimelic acid was prepared in the same way.

Mono-DNP-meso-diaminopimelic Acid

The mono-meso derivative is not internally compensated but is a racemic mixture of optically active enantiomorphs. It was prepared from pure meso-diaminopimelic acid by the procedure outlined for mono-DNP-LL-diaminopimelic acid. Both monoderivatives were chromatographically pure after one recrystallization from water. Found: C, 44.23; H, 4.33; N, 15.69. Calculated for $C_{13}H_{16}N_4O_8$: C, 43.82; H, 4.49; N, 15.73. M.p. 198° (decomp.).[3] $[\alpha]_D^{24-26} = 0.0$.

ACKNOWLEDGMENTS

The authors wish to thank Dr. E. Work for kindly providing a sample of the pure DD isomer and to acknowledge the expert assistance of Mr. A. Castagne with the elemental analyses and of Mr. F. Rollin and Mr. R. W. Rowsome in the preparation of infrared spectra.

1. D. JUŠIĆ, C. ROY, A. J. SCHOCHER, and R. W. WATSON. Can. J. Biochem. Physiol. **41**, 817 (1963).
2. D. JUŠIĆ, M. KATES, C. ROY, and R. W. WATSON. Arch. Biochem. Biophys. **99**, 534 (1962).
3. K. R. RAO and H. A. SOBER. J. Am. Chem. Soc. **76**, 1328 (1954).
4. T. FUJIWARA and S. AKABORI. J. Chem. Soc. Japan. **75**, 990 (1954).
5. C. GILVARG. J. Biol. Chem. **234**, 2955 (1959).
6. M. BERGMANN and W. STEIN. J. Biol. Chem. **129**, 609 (1939).
7. F. SANGER and E. O. P. THOMPSON. Biochem. J. **53**, 353 (1953).
8. D. W. RUSSELL. Biochem. J. **83**, 8 P (1962).
9. J. P. GREENSTEIN, S. M. BIRNBAUM, and M. C. OTEY. J. Biol. Chem. **204**, 307 (1953).
10. B. KICKHÖFEN and O. WESTPHAL. Z. Naturforsch. **7b**, 655 (1952).

[2]*California Corporation of Biochemical Research.*

[3]*Temperatures are those at which the compounds began to melt and decompose.*

[4]*Specific rotations ($[\alpha]_D^{24-26}$, C = 0.2% in glacial acetic acid, 1 dm tube) were multiplied by the appropriate molecular weight and divided by 100 to give molar rotations ($[M]_D^{24-26}$).*

Can. J. Chem. Downloaded from www.nrcresearchpress.com by 210.87.254.42 on 09/05/12
For personal use only.

11. A. M. KATZ, W. J. DREYER, and C. B. ANFINSEN. J. Biol. Chem. **234**, 2897 (1959).
12. J. PRIMOSIGH, H. PELZER, D. MAASS, and W. WEIDEL. Biochim. Biophys. Acta, **46**, 68 (1961).
13. F. W. PAIRENT and M. B. WILLIAMSON. J. Chromatog. **4**, 80 (1960).

RECEIVED MARCH 22, 1963.
DIVISION OF APPLIED BIOLOGY,
NATIONAL RESEARCH COUNCIL,
OTTAWA, CANADA.

Can. J. Chem. Downloaded from www.nrcresearchpress.com by 210.87.254.42 on 09/05/12
For personal use only.

PYROLYSIS OF 3-HEXENEDIOIC ACID

GARSON P. SHULMAN AND JEAN OSTERAAS

A recent publication (1) describes the formation of 4-pentenoic acid during attempted preparation of 3-cyclopentenone by pyrolysis of *cis*- or *trans*-3-hexenedioic acid and their barium salts. We required a reference sample of 4-pentenoic acid in this laboratory and chose this method for convenience. Analysis of the crude pyrolyzate by gas chromatographic and infrared techniques showed the presence of three other products, 4-valerolactone (29%), 3-cyclopentenone (3%), and an unidentified minor (<.01%) component. The 68% yield of 4-pentenoic acid is in good agreement with the 66–72% reported by Benington and Morin.

The valerolactone must result from addition of the carboxyl group to the double bond of 4-pentenoic acid. Since the pyrolysis of 3-hexenedioic acid would be expected to produce 3-cyclopentenone, failure to demonstrate the presence of even a trace leads to the erroneous conclusion that the cyclization does not occur in competition with the decarboxylation. Obviously, this is not true; rather, the rate of decarboxylation accompanying double bond migration must be several times that leading to ring closure (97% 4-pentenoic acid – 4-valerolactone to 3% cyclopentenone or 32:1).

Identification of products was by infrared analysis of fractions separated by gas chromatography. The 3-cyclopentenone showed a carbonyl absorption at 1710 cm^{-1}, C—H bands at 2900 cm^{-1} (aldehyde), 1660 cm^{-1} (olefinic), and 1440 cm^{-1} (methylene), with absence of the methyl C—H band at 1375 cm^{-1}. The 4-valerolactone was identified by comparison of the spectrum with that of commercially available material. The 4-pentenoic acid showed typical carboxyl OH bands at 2300–2700 cm^{-1}, a carbonyl band at 1720 cm^{-1}, and terminal olefin bands at 1655, 998, and 912 cm^{-1}. To confirm the presence of 3-cyclopentenone, the 2,4-dinitrophenylhydrazone precipitate was ozonized. Comparison by mixed melting point with the 2,4-dinitrophenylhydrazone of β-ketoglutaric acid showed them to be identical.

EXPERIMENTAL

Pyrolysis of 3-Hexenedioic Acid

A sample of 3-hexenedioic acid* was placed in a micro distillation apparatus and heated until decomposition was complete (flask temperature 280–295°). The distillate gave a positive 2,4-dinitrophenylhydrazone test (m.p. 148°) and a neutralization equivalent of 132 (calculated, 100).

Analysis of Distillate

A Perkin–Elmer Model 154 Vapor Fractometer with a 6 ft silicone column was employed for the analysis. Analytical scale (10 μl) chromatography showed four peaks (<.01%, 3%, 29%, and 68%). Fractions from

**K. & K. Laboratories, Jamaica, New York.*

11. A. M. KATZ, W. J. DREYER, and C. B. ANFINSEN. J. Biol. Chem. **234**, 2897 (1959).
12. J. PRIMOSIGH, H. PELZER, D. MAASS, and W. WEIDEL. Biochim. Biophys. Acta, **46**, 68 (1961).
13. F. W. PAIRENT and M. B. WILLIAMSON. J. Chromatog. **4**, 80 (1960).

RECEIVED MARCH 22, 1963.
DIVISION OF APPLIED BIOLOGY,
NATIONAL RESEARCH COUNCIL,
OTTAWA, CANADA.

Can. J. Chem. Downloaded from www.nrcresearchpress.com by 210.87.254.6 on 09/05/12
For personal use only.

PYROLYSIS OF 3-HEXENEDIOIC ACID

GARSON P. SHULMAN AND JEAN OSTERAAS

A recent publication (1) describes the formation of 4-pentenoic acid during attempted preparation of 3-cyclopentenone by pyrolysis of *cis*- or *trans*-3-hexenedioic acid and their barium salts. We required a reference sample of 4-pentenoic acid in this laboratory and chose this method for convenience. Analysis of the crude pyrolyzate by gas chromatographic and infrared techniques showed the presence of three other products, 4-valerolactone (29%), 3-cyclopentenone (3%), and an unidentified minor (<.01%) component. The 68% yield of 4-pentenoic acid is in good agreement with the 66–72% reported by Benington and Morin.

The valerolactone must result from addition of the carboxyl group to the double bond of 4-pentenoic acid. Since the pyrolysis of 3-hexenedioic acid would be expected to produce 3-cyclopentenone, failure to demonstrate the presence of even a trace leads to the erroneous conclusion that the cyclization does not occur in competition with the decarboxylation. Obviously, this is not true; rather, the rate of decarboxylation accompanying double bond migration must be several times that leading to ring closure (97% 4-pentenoic acid – 4-valerolactone to 3% cyclopentenone or 32:1).

Identification of products was by infrared analysis of fractions separated by gas chromatography. The 3-cyclopentenone showed a carbonyl absorption at 1710 cm^{-1}, C—H bands at 2900 cm^{-1} (aldehyde), 1660 cm^{-1} (olefinic), and 1440 cm^{-1} (methylene), with absence of the methyl C—H band at 1375 cm^{-1}. The 4-valerolactone was identified by comparison of the spectrum with that of commercially available material. The 4-pentenoic acid showed typical carboxyl OH bands at 2300–2700 cm^{-1}, a carbonyl band at 1720 cm^{-1}, and terminal olefin bands at 1655, 998, and 912 cm^{-1}. To confirm the presence of 3-cyclopentenone, the 2,4-dinitrophenylhydrazone precipitate was ozonized. Comparison by mixed melting point with the 2,4-dinitrophenylhydrazone of β-ketoglutaric acid showed them to be identical.

EXPERIMENTAL

Pyrolysis of 3-Hexenedioic Acid

A sample of 3-hexenedioic acid* was placed in a micro distillation apparatus and heated until decomposition was complete (flask temperature 280–295°). The distillate gave a positive 2,4-dinitrophenylhydrazone test (m.p. 148°) and a neutralization equivalent of 132 (calculated, 100).

Analysis of Distillate

A Perkin–Elmer Model 154 Vapor Fractometer with a 6 ft silicone column was employed for the analysis. Analytical scale (10 μl) chromatography showed four peaks (<.01%, 3%, 29%, and 68%). Fractions from

**K. & K. Laboratories, Jamaica, New York.*

chromatography of 100 μl samples were collected in a dry ice trap and the infrared spectra of the second, third, and fourth peaks determined. Details of the spectra are given in the discussion.

Identification of 3-Cyclopentenone

Ten drops of the reaction product was added to 20 ml of 0.5% aqueous 2,4-dinitrophenylhydrazine hydrochloride, giving a precipitate, m.p. 153–156° decomp.

Ozonolysis of the precipitate in ethyl acetate solution gave an oily solid which crystallized from water, m.p. 112–118°. The 2,4-dinitrophenylhydrazone of β-ketoglutaric acid, previously unreported, was prepared from the acid, m.p. 118–120°. A mixture melted at 113–118°.

1. F. BENINGTON and R. D. MORIN. J. Org. Chem. **26**, 5210 (1961).

RECEIVED MARCH 29, 1963.
RESEARCH LABORATORIES,
ARCHER-DANIELS-MIDLAND COMPANY,
MINNEAPOLIS, MINNESOTA.

Can. J. Chem. Downloaded from www.nrcresearchpress.com by 210.87.254.6 on 09/05/12
For personal use only.

THE DETERMINATION OF SELF-ASSOCIATION EQUILIBRIUM CONSTANTS BY INFRARED ABSORPTION SPECTROSCOPY

SERGE N. VINOGRADOV*

Infrared absorption spectroscopy is one of the most widely used methods in the investigation of hydrogen-bonded equilibria in solution (1). The increase in intensity of the absorption band assigned to a X—H (X = N, O, S, etc.) stretching vibration of the "free" or "monomeric" molecule with decrease in concentration in an inert solvent is an important criterion for the existence of self-association through hydrogen bonding. Detailed quantitative data on the variation of the X—H band intensity with concentration can be used to deduce the mode of self-association and hence to calculate the pertinent equilibrium constants; from the latter it becomes possible to evaluate the thermodynamic parameters of the specific hydrogen bond formations.

Milestones in the development of such treatments of infrared absorption intensity data are the Mecke–Kempter relationship, first proposed to describe early data on the self-association of alcohols (2) and since then used in the determination of parameters governing the self-association of α-keto pyrroles (3), 4(5)-methylimidazole (4), and of several oximes (5); the Coggeshall–Saier scheme for the self-association of phenols (6) which has been used by Bono in the study of xylenols and cresols (7); and the recent, very elegant treatments by Rossotti *et al.* of the self-associations of imidazole (8), pyrazole (9), and several pyrazole derivatives (10) based on general methods for the determination of stability constants (11). The systematization by Rossotti and Rossotti of the methods of determination of self-association equilibrium constants (12) relies heavily on graphical procedures.

In the specific case where the absorption band, whose intensity is measured as a function of the concentration, is due only to the "free" molecules and does not include contributions from free "end" X—H groups, it becomes possible to calculate the stepwise self-association equilibrium constants β_{q0}, in the terminology of Rossotti and Rossotti (11), in a slightly more rigorous manner as follows. Assuming the validity of Beer's law, the concentration of the "free" molecules b_1 is given by $b_1 = \epsilon B/\epsilon_1$, where ϵ_1 is the absorptivity of the

*Present address: Biochemistry Department, Yale University, New Haven, Connecticut, U.S.A.

chromatography of 100 μl samples were collected in a dry ice trap and the infrared spectra of the second, third, and fourth peaks determined. Details of the spectra are given in the discussion.

Identification of 3-Cyclopentenone

Ten drops of the reaction product was added to 20 ml of 0.5% aqueous 2,4-dinitrophenylhydrazine hydrochloride, giving a precipitate, m.p. 153–156° decomp.

Ozonolysis of the precipitate in ethyl acetate solution gave an oily solid which crystallized from water, m.p. 112–118°. The 2,4-dinitrophenylhydrazone of β-ketoglutaric acid, previously unreported, was prepared from the acid, m.p. 118–120°. A mixture melted at 113–118°.

1. F. BENINGTON and R. D. MORIN. J. Org. Chem. **26**, 5210 (1961).

RECEIVED MARCH 29, 1963.
RESEARCH LABORATORIES,
ARCHER-DANIELS-MIDLAND COMPANY,
MINNEAPOLIS, MINNESOTA.

Can. J. Chem. Downloaded from www.nrcresearchpress.com by 210.87.254.5 on 09/05/12
For personal use only.

THE DETERMINATION OF SELF-ASSOCIATION EQUILIBRIUM CONSTANTS BY INFRARED ABSORPTION SPECTROSCOPY

SERGE N. VINOGRADOV*

Infrared absorption spectroscopy is one of the most widely used methods in the investigation of hydrogen-bonded equilibria in solution (1). The increase in intensity of the absorption band assigned to a X—H (X = N, O, S, etc.) stretching vibration of the "free" or "monomeric" molecule with decrease in concentration in an inert solvent is an important criterion for the existence of self-association through hydrogen bonding. Detailed quantitative data on the variation of the X—H band intensity with concentration can be used to deduce the mode of self-association and hence to calculate the pertinent equilibrium constants; from the latter it becomes possible to evaluate the thermodynamic parameters of the specific hydrogen bond formations.

Milestones in the development of such treatments of infrared absorption intensity data are the Mecke–Kempter relationship, first proposed to describe early data on the self-association of alcohols (2) and since then used in the determination of parameters governing the self-association of α-keto pyrroles (3), 4(5)-methylimidazole (4), and of several oximes (5); the Coggeshall–Saier scheme for the self-association of phenols (6) which has been used by Bono in the study of xylenols and cresols (7); and the recent, very elegant treatments by Rossotti *et al.* of the self-associations of imidazole (8), pyrazole (9), and several pyrazole derivatives (10) based on general methods for the determination of stability constants (11). The systematization by Rossotti and Rossotti of the methods of determination of self-association equilibrium constants (12) relies heavily on graphical procedures.

In the specific case where the absorption band, whose intensity is measured as a function of the concentration, is due only to the "free" molecules and does not include contributions from free "end" X—H groups, it becomes possible to calculate the stepwise self-association equilibrium constants β_{q0}, in the terminology of Rossotti and Rossotti (11), in a slightly more rigorous manner as follows. Assuming the validity of Beer's law, the concentration of the "free" molecules b_1 is given by $b_1 = \epsilon B/\epsilon_1$, where ϵ_1 is the absorptivity of the

*Present address: Biochemistry Department, Yale University, New Haven, Connecticut, U.S.A.

"free" molecules and ϵ is the absorptivity measured at a stoichiometric concentration B. The latter can then be expressed as

$$B = \sum_1^q qb_q = \sum_1^q q\beta_{q0}b_1{}^q = \epsilon B/\epsilon_1 + 2(\epsilon B/\epsilon_1)^2\beta_{20} + \ldots + q(\epsilon B/\epsilon_1)^q\beta_{q0}.$$

Dividing through by ϵB we obtain

$$1/\epsilon = 1/\epsilon_1 + (2\beta_{20}/\epsilon_1{}^2)(\epsilon B) + \ldots + (q\beta_{q0}/\epsilon_1{}^q)(\epsilon B)^{q-1}.$$

It is evident that a least-squares fit of the experimental data in terms of $1/\epsilon$ versus ϵB to the polynomial $f(x) = \sum_{k=0}^{k=n} a_{nk}x^k$ for different n starting with $n = 1$ will give several analytical functions from which the most valid polynomial can be selected on the basis of the two criteria all $a_{nk} > 0$ and best fit to the experimental data. If ϵ_1 is known experimentally the foregoing equation can be transposed to

$$\frac{1}{\epsilon B}\left(\frac{1}{\epsilon} - \frac{1}{\epsilon_1}\right) = 2\beta_{20}/\epsilon_1{}^2 + (3\beta_{30}/\epsilon_1{}^3)(\epsilon B) + \ldots + (q\beta_{q0}/\epsilon_1{}^q)(\epsilon B)^{q-2}.$$

In this case the experimental data in terms of $(1/\epsilon B)(1/\epsilon - 1/\epsilon_1)$ versus ϵB can be fitted by the method of least-squares to the foregoing general polynomial. In either case it becomes possible to calculate the β_{q0} from the a_{nk} of the selected polynomial. The latter thus defines a physically plausible self-association model.

Only recently has data of sufficient accuracy been published to warrant a calculation on the basis outlined above. Rossotti and his collaborators have investigated the self-association of pyrazole and some of its derivatives in CCl_4 over the concentration range 1×10^{-4} to 1×10^{-2} M at about 20° C and found them to self-associate to "closed" dimers and trimers (9, 10). Their published results were: pyrazole: $\epsilon_1 = 220\pm3$ mole^{-1} liter cm^{-1}, $\beta_{20} = 47.4\pm1.0$ mole^{-1} liter, $\beta_{30} = 7540\pm240$ mole^{-2} liter; 3,5-dimethylpyrazole: $\epsilon_1 = 295\pm2$, $\beta_{20} = 285\pm4$, $\beta_{30} = 45900\pm280$; 3,5-diethylpyrazole: $\epsilon_1 = 225\pm1$, $\beta_{20} = 110\pm1$, $\beta_{30} = 5940\pm360$.

The data of Rossotti *et al.* (9, 10) as plots of $1/\epsilon$ and $(1/\epsilon B)(1/\epsilon - 1/\epsilon_1)$ versus ϵB were fitted to the polynomial $f(x) = \sum_{k=0}^{k=n} a_{nk}x^k$, $n = 1, 2, 3, 4$, by the method of least-squares, using an IBM 1620 computer.* Some of the results are shown in Tables I and II. The standard deviation for each fit is given by $S = (\sum_{i=1}^{i=N} (y_i - \bar{y}_i)^2/(N-n-1))^{\frac{1}{2}}$, where N is the number of points and n is the order of the polynomial. This type of standard deviation gives a better comparison between polynomials of different orders (13).

Generally polynomials of order higher than second or third had at least one negative coefficient. The results of $1/\epsilon$ versus ϵB plots agreed fairly well with the results of Rossotti *et al.*, except in the case of 3,5-dimethylpyrazole, which is still appreciably self-associated even at 1×10^{-4} M (10) and where a procedure which gives ϵ_1 by extrapolation would be expected to give incorrect answers. The results of fitting the $(1/\epsilon B)(1/\epsilon - 1/\epsilon_1)$ versus ϵB plots agreed very well with those of Rossotti *et al.*; for some sets of data two or three equilibrium constants gave almost equally good fits. Hence in these systems there is no experimental evidence for or against the existence of cyclic tetramers.

The equilibrium constants higher than β_{20} varied appreciably with the number of points, i.e. with the concentration range used in the calculations. Although, admittedly, at the lowest concentrations, where the percentage of trimers and (or) higher polymers is small, the appropriate equilibrium association constants can not be too reliable, this

**The least-squares program used was file No. 7.0.002, IBM 1620 program library.*

Can. J. Chem. Downloaded from www.nrcresearchpress.com by 210.87.254.5 on 09/05/12
For personal use only.

Can. J. Chem. Downloaded from www.nrcresearchpress.com by 210.87.254.5 on 09/05/12
For personal use only.

TABLE I

Results of least-squares fitting of $1/\epsilon$ versus ϵB to $f(x) = \sum_{k=0}^{k=n} a_{nk}x^k$, $n = 1, 2, 3$

		Pyrazole					3,5-Dimethylpyrazole					3,5-Diethylpyrazole				
Concn. range, $\times 10^4 M$:		1–8	1–14	1–22	1–50	1–100	1–8	1–14	1–22	1–30	1–100	1–8	1–14	1–25	1–45	1–80
N:		8	12	16	30	43	8	12	16	20	31	8	12	16	20	24
First order $n = 1$	$S\times 10^5$	5.06	4.81	5.19			1.69	3.47	6.31			1.10	1.10	2.78	4.68	
	ϵ_1	227	226	227			302	305	311			225	226	227	230	
	$\beta_{20}\times 10^3$	83.9	75.3	79.5			354	384	423			117	120	128	139	
Second order $n = 2$	$S\times 10^5$	5.43	4.79	5.24	6.22	6.42	1.53	2.54	3.46	3.53	3.70	0.84	0.887	1.49	1.56	2.28
	ϵ_1	226	228	226	224	223	305	298	296	299	299	224	225	224	225	224
	β_{20}	60.6		68.5	59.1	50.9		303	286	307	308	97.1	109	105	109	108
	$\beta_{30}\times 10^3$	18.4	Neg.	3.71	6.47	7.69	Neg.	4.45	5.12	4.19	4.34	15.5	5.43	7.61	6.03	6.15
Third order $n = 3$	$S\times 10^5$					5.89										
	ϵ_1					226										
	β_{20}					72.9										
	$\beta_{30}\times 10^3$	Neg.	Neg.	Neg.	Neg.	1.01	Neg.	Neg.	Neg.	Neg.	Neg.	Neg.	Neg.	Neg.	Neg.	Neg.
	$\beta_{40}\times 10^6$					0.991										

TABLE II

Results of least-squares fitting of $(1/\epsilon B)(1/\epsilon - 1/\epsilon_1)$ versus ϵB to $f(x) = \sum_{k=0}^{k=n} a_{nk}x^k$, $n = 1, 2$

		Pyrazole*				3,5-Dimethylpyrazole†				3,5-Diethylpyrazole			
Concn. range, $\times 10^4 M$:		5–20	5–30	5–36	5–100	2–9	2–16	2–24	2–100	1–8	1–14	1–25	1–80
N:		12	16	20	39	8	12	16	30	8	12	16	24
First order $n = 1$	$S\times 10^5$	15.1	14.6	14.5	11.7	7.95	9.62	11.7	10.2	17.2	13.8	13.0	10.9
	β_{20}	47.5	46.5	47.2	46.9	285	283	281	284	115	114	112	111
	$\beta_{30}\times 10^3$	7.25	7.87	7.51	7.64	41.9	45.9	48.0	45.5	4.57	2.75	4.75	5.51
Second order $n = 2$	$S\times 10^5$	14.5	13.9	14.9	11.7	7.36	9.65	11.7	9.83	16.5	13.6	12.1	10.7
	β_{20}			47.6	47.9		289	287					113
	$\beta_{30}\times 10^3$	Neg.	Neg.	7.02	6.90	Neg.	29.3	35.3		Neg.	Neg.	Neg.	3.85
	$\beta_{40}\times 10^6$			1.17	1.10		10.9	6.60	Neg.				3.40

*Of the 43 points the first four were rejected because of the appreciable uncertainty in the magnitude of $(1/\epsilon B)(1/\epsilon - 1/\epsilon_1)$.
†The first four points were rejected for the same reason as above.

fact raises some suspicion concerning the physical validity of the higher self-association equilibrium constants. It is possible that the assumption concerning the ideality of dilute solutions of self-associating substances in inert solvents, which underlies the calculation of the equilibrium constants, may be invalid oftener than thought. This seems unlikely in the present case where concentrations are under 0.01 M; moreover 3,5-dimethylpyrazole, for example, begins to approach the limit of its solubility in CCl_4 at 20° C only above 0.1 M (14). The final possibility may be that some "open" polymers are present in some concentration ranges as intimated by Mirone and Lorenzelli in the case of 3,5-dimethylpyrazole (3), although the results of two other independent investigations (9, 10, 14) do not support it. Coexistence of "open" and "closed" dimers and (or) trimers as in the case of the dimers of caprolactam (15) is at present outside the scope of the proposed treatment.

1. G. C. Pimentel and A. L. McClellan. The hydrogen bond. W. H. Freeman & Co., San Francisco, Calif. 1960.
2. H. Kempter and R. Mecke. Z. Physik. Chem. (Leipzig), B, **46**, 229 (1940). R. Mecke. Discussions Faraday Soc. **9**, 161 (1950). I. Prigogine and R. Defay. Thermodynamique chimique. Desoer, Liege. 1950. pp. 449–453. B. Ya. Levin. Zh. Fiz. Khim. **28**, 1399 (1954).
3. P. Mirone and V. Lorenzelli. Ann. Chim. (Rome), **49**, 59 (1959).
4. H. Zimmermann. Z. Elektrochem. **63**, 608 (1959).
5. S. Califano and W. Luttke. Z. Physik. Chem. **5**, 240 (1955). W. Luck. Z. Elektrochem. **65**, 355 (1961).
6. N. Coggeshall and E. Saier. J. Am. Chem. Soc. **73**, 5414 (1951).
7. D. Bono. Compt. Rend. **242**, 637 (1956); Bull. Soc. Chim. France, 1368 (1956); Ph.D. Thesis, Univ. of Paris. 1956.
8. D. M. W. Anderson, J. L. Duncan, and F. J. C. Rossotti. J. Chem. Soc. 2165 (1961).
9. D. M. W. Anderson, J. L. Duncan, and F. J. C. Rossotti. J. Chem. Soc. 140 (1961).
10. D. M. W. Anderson, J. L. Duncan, and F. J. C. Rossotti. J. Chem. Soc. 4201 (1961).
11. F. J. C. Rossotti and H. Rossotti. The determination of stability constants. McGraw-Hill Co., New York. 1961.
12. F. J. C. Rossotti and H. Rossotti. J. Phys. Chem. **65**, 926, 930 (1961).
13. P. G. Guest. Numerical methods of curve fitting. Cambridge University Press. 1961. p. 251.
14. S. N. Vinogradov. Ph.D. Thesis, Illinois Institute of Technology. 1960.
15. R. C. Lord and T. J. Porro. Z. Elektrochem. **64**, 672 (1960).

Received May 29, 1963.
Department of Chemistry,
University of Alberta,
Edmonton, Alberta.

Can. J. Chem. Downloaded from www.nrcresearchpress.com by 210.87.254.5 on 09/05/12
For personal use only.

THE FLASH PHOTOLYTIC REDUCTION OF 2-ACETONAPHTHONE IN SOLUTION

W. A. Bryce and C. H. J. Wells

INTRODUCTION

The excited intermediate responsible for the photolytic reduction of aromatic ketones is believed to be the triplet state (1, 2). The initial stages of the mechanism can be represented by the following sequence of reactions:

$$R_2CO + h\gamma \rightarrow R_2CO_S^* \quad [1]$$

$$R_2CO_S^* \rightarrow R_2CO \quad [2]$$

$$R_2CO_S^* \rightarrow R_2CO_T^* \quad [3]$$

$$R_2CO_T^* \rightarrow R_2CO \quad [4]$$

$$R_2CO_T^* + DH \rightarrow R_2COH + D^\cdot \quad [5]$$

fact raises some suspicion concerning the physical validity of the higher self-association equilibrium constants. It is possible that the assumption concerning the ideality of dilute solutions of self-associating substances in inert solvents, which underlies the calculation of the equilibrium constants, may be invalid oftener than thought. This seems unlikely in the present case where concentrations are under 0.01 M; moreover 3,5-dimethylpyrazole, for example, begins to approach the limit of its solubility in CCl_4 at 20° C only above 0.1 M (14). The final possibility may be that some "open" polymers are present in some concentration ranges as intimated by Mirone and Lorenzelli in the case of 3,5-dimethylpyrazole (3), although the results of two other independent investigations (9, 10, 14) do not support it. Coexistence of "open" and "closed" dimers and (or) trimers as in the case of the dimers of caprolactam (15) is at present outside the scope of the proposed treatment.

1. G. C. Pimentel and A. L. McClellan. The hydrogen bond. W. H. Freeman & Co., San Francisco, Calif. 1960.
2. H. Kempter and R. Mecke. Z. Physik. Chem. (Leipzig), B, **46**, 229 (1940). R. Mecke. Discussions Faraday Soc. **9**, 161 (1950). I. Prigogine and R. Defay. Thermodynamique chimique. Desoer, Liege. 1950. pp. 449–453. B. Ya. Levin. Zh. Fiz. Khim. **28**, 1399 (1954).
3. P. Mirone and V. Lorenzelli. Ann. Chim. (Rome), **49**, 59 (1959).
4. H. Zimmermann. Z. Elektrochem. **63**, 608 (1959).
5. S. Califano and W. Luttke. Z. Physik. Chem. **5**, 240 (1955). W. Luck. Z. Elektrochem. **65**, 355 (1961).
6. N. Coggeshall and E. Saier. J. Am. Chem. Soc. **73**, 5414 (1951).
7. D. Bono. Compt. Rend. **242**, 637 (1956); Bull. Soc. Chim. France, 1368 (1956); Ph.D. Thesis, Univ. of Paris. 1956.
8. D. M. W. Anderson, J. L. Duncan, and F. J. C. Rossotti. J. Chem. Soc. 2165 (1961).
9. D. M. W. Anderson, J. L. Duncan, and F. J. C. Rossotti. J. Chem. Soc. 140 (1961).
10. D. M. W. Anderson, J. L. Duncan, and F. J. C. Rossotti. J. Chem. Soc. 4201 (1961).
11. F. J. C. Rossotti and H. Rossotti. The determination of stability constants. McGraw-Hill Co., New York. 1961.
12. F. J. C. Rossotti and H. Rossotti. J. Phys. Chem. **65**, 926, 930 (1961).
13. P. G. Guest. Numerical methods of curve fitting. Cambridge University Press. 1961. p. 251.
14. S. N. Vinogradov. Ph.D. Thesis, Illinois Institute of Technology. 1960.
15. R. C. Lord and T. J. Porro. Z. Elektrochem. **64**, 672 (1960).

Received May 29, 1963.
Department of Chemistry,
University of Alberta,
Edmonton, Alberta.

Can. J. Chem. Downloaded from www.nrcresearchpress.com by 210.87.254.6 on 09/05/12
For personal use only.

THE FLASH PHOTOLYTIC REDUCTION OF 2-ACETONAPHTHONE IN SOLUTION

W. A. Bryce and C. H. J. Wells

INTRODUCTION

The excited intermediate responsible for the photolytic reduction of aromatic ketones is believed to be the triplet state (1, 2). The initial stages of the mechanism can be represented by the following sequence of reactions:

$$R_2CO + h\gamma \rightarrow R_2CO_S^* \quad [1]$$

$$R_2CO_S^* \rightarrow R_2CO \quad [2]$$

$$R_2CO_S^* \rightarrow R_2CO_T^* \quad [3]$$

$$R_2CO_T^* \rightarrow R_2CO \quad [4]$$

$$R_2CO_T^* + DH \rightarrow R_2COH + D^\cdot \quad [5]$$

The ketone molecule is excited initially to an upper singlet state which will decay back to the ground state or form a triplet state by internal conversion. The triplet state will either decay to the ground state or abstract a hydrogen atom from the solvent DH to form a ketyl radical, $R_2\dot{C}OH$. The ketyl radical forms the final products by reacting with the solvent, DH, with the radical, $\dot{D}$, or by dimerization.

Since the photolysis of an aromatic ketone can result in the formation of both the triplet state of the ketone and the ketyl radical as intermediates care must be exercised in the assignment of transient absorption spectra. McClure and Hanst (3) observed the triplet absorption in the flash photolysis of benzophenone in a rigid medium. The close similarity between this absorption and the transient absorption in solution originally led Porter and Windsor (4) to believe that the transient observed in solution was also the triplet state. The absorption was subsequently assigned (5) to the relatively long-lived ketyl radical $C_6H_5\dot{C}OHC_6H_5$. The triplet absorption was not observed in solution, presumably because of the rapidity of the hydrogen transfer occurring in reaction [5].

It has been reported (6) that certain naphthoyl ketones, including 2-acetonaphthone, are not photoreduced in the presence of a weak hydrogen donor such as a secondary alcohol. The reduction of 2-acetonaphthone does occur, however, if a more active hydrogen donor, such as tributylstannane, is added to the system (7). This suggests that the corresponding ketyl radical for 2-acetonaphthone can only be formed in the presence of active hydrogen donors, and that any transient absorption observed when 2-acetonaphthone is photolyzed in the presence of a weak donor must be that of the triplet state. The present work was undertaken to study the decay of the triplet absorption of 2-acetonaphthone in an 'inert' solvent and to characterize any transient absorption that may be observed when 2-acetonaphthone is photolyzed in the presence of tributylstannane. The effect of the addition of 1-naphthol and triphenylene as quenching or energy-transfer agents in the system was also studied.

EXPERIMENTAL

2-Acetonaphthone (Eastman Kodak White label) was recrystallized three times from petroleum ether (60–80°). 1-Naphthol (Eastman Kodak White label) was vacuum sublimed, recrystallized three times from spectroscopic grade benzene, and resublimed. Triphenylene (Aldrich Chemical Corp.) was zone refined. Tributylstannane was prepared from tributyltin chloride (Metal and Thermit Corp.) by the method of Van der Kerk and Luitjen (8). The solutions were all made up in spectroscopic grade benzene (Eastman Kodak) and were thoroughly degassed before flashing. This was done by a freeze–pump–melt–freeze–pump procedure combined with trap-to-trap distillation under high vacuum.

The flash apparatus was of conventional design, the photolysis lamp consisting of a quartz tube of 42-cm length and 3.8-cm O.D., araldited into cylindrical stainless steel electrodes of a design developed by Claesson and Lindqvist (9). Discharge occurred between 1/4-in. tungsten rods mounted in the centers of the electrodes. The lamp was mounted coaxially in a cylindrical brass can coated on the inside with magnesium oxide, and was generally filled with nitrogen to a pressure of 5 cm. The duration of the flash on discharging a 66 μf condenser bank through the lamp at 10 kv was approximately 12 microseconds. The spectroscopic lamp was similar in design to the photolysis lamp but with a quartz capillary of 3-cm length and 2-mm bore. It was filled with nitrogen to a pressure of 4 mm and had a flash-time of 5 microseconds for a 50 joule flash. The timing of the spectroscopic flash was controlled by an electronic delay unit and checked by means of an oscilloscope. The discharge was focused through the reaction vessel onto the slit of a Hilger-Watts E 742 Automatic quartz spectrograph.

The reaction vessel was a quartz tube 21 cm long and 15 mm in diameter located beside the photolysis lamp. It was surrounded by a double quartz cylindrical vessel with an annular space 6 mm wide which could be filled with filter solutions. The absorption spectra were photographed on either Kodak 103-F or Ilford HP3 plates. The plates were scanned with a Hilger-Watts recording microdensitometer and the deflection readings at each wavelength converted to optical density of transient from a previously constructed calibration graph. Each plate was calibrated by inserting alumina-on-quartz neutral density filters between the reaction vessel and the spectrograph, firing the photolamp and the spectroscopic lamp with the delay set at 14 microseconds, and measuring the corresponding plate density.

Can. J. Chem. Downloaded from www.nrcresearchpress.com by 210.87.254.6 on 09/05/12
For personal use only.

RESULTS AND DISCUSSION

The transient absorption observed when a 1.01×10^{-3} M solution of 2-acetonaphthone in benzene was flashed is given by curve A in Fig. 1. The concentration of 2-aceto-

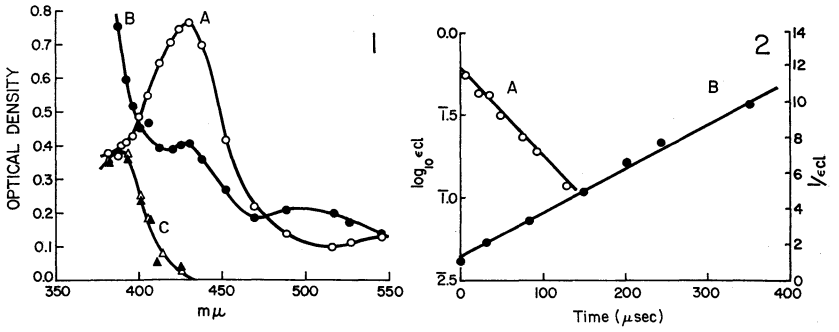

FIG. 1. Transient absorption spectra following photolysis in benzene solution of (A) 1.01×10^{-3} M 2-acetonaphthone; (B) 1.01×10^{-3} M 2-acetonaphthone + 0.17 M tributylstannane; (C) ▲, 0.90×10^{-4} M 1-naphthol, no filter present; △, 1.01×10^{-3} M 2-acetonaphthone + 0.90×10^{-4} M 1-naphthol; filter solution, 0.5 M 1-naphthol. Flash energy, 2220 joules; delay, 11 microseconds.

FIG. 2. (A) Logarithm of the optical density of the triplet state of a 1.01×10^{-4} M solution of 2-acetonaphthone in benzene, against time. (B) Reciprocal of the optical density of the triplet state of a 0.90×10^{-2} M solution of 2-acetonaphthone in benzene, against time. Flash energy, 2220 joules.

naphthone and the absorption spectrum of the solution were unchanged after 30 flashes at 2220 joules per flash, showing that the transient absorption was that of the triplet state. When a solution 1.01×10^{-3} M in 2-acetonaphthone and 0.17 M in tributylstannane was flashed under the same conditions a transient absorption was obtained (curve B, Fig. 1) which differed from that of the triplet state. The peak maximum of this absorption band lies below 385 mμ, and is hidden by the singlet–singlet absorption band of 2-acetonapthone. The new absorption band had a relatively long lifetime as compared to the triplet absorption band and could be detected some 10 milliseconds after flashing. This long lifetime, plus the observation that 20% of the 2-acetonaphthone had been decomposed after 20 flashes, indicates that the transient absorption spectrum was that of the ketyl radical $C_{10}H_7\dot{C}OHCH_3$. The maximum in the absorption in curve B at 430 mμ may be caused by simultaneous triplet–triplet absorption of 2-acetonaphthone, and hence it was not possible to decide whether the spectrum in this region is due to the ketyl radical only, or to a combination of triplet and ketyl radical absorption.

The kinetics of the decay of the triplet state was investigated for different initial concentrations of 2-acetonaphthone. For a 1.01×10^{-4} M solution a plot of the logarithm of the optical density against time was linear within the limitations of plate photometry (Fig. 2, curve A). The first-order rate constant, k_1, had a value of $1.27\pm0.25\times10^{4}$ sec^{-1}, and thus the triplet-state lifetime was $0.75\pm0.25\times10^{-4}$ sec. When the concentration of 2-acetonaphthone was increased to 0.90×10^{-2} M, the decay was second order (Fig. 2, curve B) with a rate constant k_2 of $5.5\pm0.9\times10^{5}$ $(\epsilon C)^{-1}$ sec^{-1}, where ϵ is the molar extinction coefficient and C is the molar concentration. The transition from primarily first-order kinetics at low concentrations to second-order kinetics at the higher concentrations suggests that at the lower concentrations there will be some contribution to the decay from second-order quenching, and hence the value obtained for the rate constant, k_1, is a maximum.

Can. J. Chem. Downloaded from www.nrcresearchpress.com by 210.87.254.6 on 09/05/12
For personal use only.

It has been shown (10, 11) that selective excitation of the triplet level of one molecule in the presence of another molecule with a lower-lying triplet level can lead to energy transfer from the upper triplet to the lower triplet. It was therefore of interest to see if the triplet state of 2-acetonaphthone could be quenched by the addition to the solution of a molecule with a lower-lying triplet level, and to examine the consequent effect on the extent of photoreduction. As illustrated schematically in Fig. 3, the energy levels of 1-naphthol relative to those of 2-acetonaphthone made it suitable for use as a quencher.

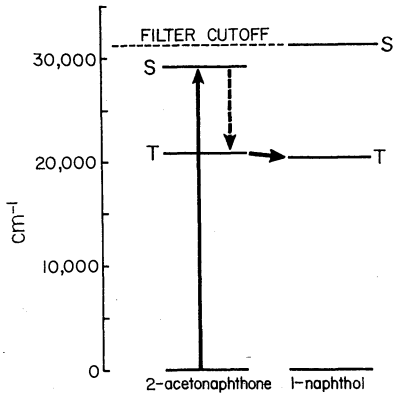

FIG. 3. Energy level diagram of the first excited states of 2-acetonaphthone and 1-naphthol.

Selective excitation of the 2-acetonaphthone in the presence of 1-naphthol was achieved by surrounding the solution to be flashed with a concentrated solution of 1-naphthol. The transfer of energy between the 2-acetonaphthone triplet and the 1-naphthol triplet is shown by the results presented in Fig. 1. Curve A illustrates the triplet-state absorption for a 1.01×10^{-3} M 2-acetonaphthone solution. Curve C shows the triplet absorption of a 0.90×10^{-4} M 1-naphthol solution with no filter in the system, and also shows the transient absorption of a solution which is 0.90×10^{-4} M in 1-naphthol and 1.01×10^{-3} M in 2-acetonaphthone with the 1-naphthol filter present. When a 0.90×10^{-4} M solution of 1-naphthol was flashed with the filter solution present no transient absorption could be detected.

Transfer of energy from the first excited singlet of 2-acetonaphthone to the corresponding state in 1-naphthol is unlikely since this state is higher in 1-naphthol than in 2-acetonaphthone. Direct transfer from the first excited singlet state of 2-acetonaphthone to the triplet of 1-naphthol is also unlikely as this is a spin-forbidden process and, for many donor–acceptor pairs, has been shown to be unimportant compared with triplet–triplet energy transfer (10–12).

The quenching effect of 1-naphthol on the photoreduction of 2-acetonaphthone is shown by the results given in Fig. 4(*a*). Solutions which were 1.01×10^{-3} M in 2-acetonaphthone and 0.42 M in tributylstannane were flashed in the presence of various amounts of 1-naphthol. The results show that the decomposition of the 2-acetonaphthone decreased as the concentration of 1-naphthol increased. The observation that 1-naphthol removes triplet excitation energy from 2-acetonaphthone and also quenches the photoreduction provides convincing evidence that the triplet state is the active intermediate in the photoreduction.

The possibility that 1-naphthol reacted with the tributylstannane on flashing, or that a complex was formed between the 1-naphthol and 2-acetonaphthone was ruled out by the

Can. J. Chem. Downloaded from www.nrcresearchpress.com by 210.87.254.6 on 09/05/12
For personal use only.

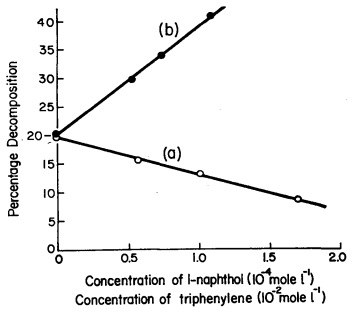

FIG. 4. Percentage decomposition of 2-acetonaphthone against concentration of 1-naphthol and triphenylene in benzene solution: (*a*) 1.01×10^{-3} *M* 2-acetonaphthone + 0.42 *M* tributylstannane + 1-naphthol; filter solution, 0.5 *M* 1-naphthol. (*b*) 5.2×10^{-4} *M* 2-acetonaphthone + 0.21 *M* tributylstannane + triphenylene; no filter present. Flash energy, 2220 joules; number of flashes, 20.

observation that the absorption spectrum of a solution containing 1-naphthol and tributylstannane was the same before and after being flashed, and by the fact that the absorption spectrum of a solution of 2-acetonaphthone and 1-naphthol after flashing was identical with the combined spectra of the two solutes in separate solutions.

Since the action of 1-naphthol as a quencher was to remove triplet-state energy it follows that a molecule which could transfer energy to the 2-acetonaphthone triplet should sensitize the photoreduction. The requirements for an ideal sensitizer are: (1) a first triplet level lying above that of 2-acetonaphthone; (2) a first excited singlet lying below that of 2-acetonaphthone; and (3) a triplet–triplet absorption band lying in a region of the spectrum different from that for 2-acetonaphthone to enable the energy transfer between triplets to be followed by plate photometry. Unfortunately it was not possible to obtain a molecule with all three requirements. Triphenylene, however, does meet the first requirement and was used as a sensitizer. The results presented in Fig. 4(*b*) show that the addition of triphenylene to a solution of 2-acetonaphthone and tributylstannane greatly increases the rate of removal of 2-acetonaphthone from the system. The absorption spectra of triphenylene and 2-acetonaphthone are so similar that it was not possible selectively to excite the triphenylene. However the concentration of 2-acetonaphthone was 5.2×10^{-4} *M* while the lowest concentration of triphenylene used was 5.0×10^{-3} *M* so that it is safe to assume that most of the light was absorbed by the triphenylene. Owing to the closeness of the energies of the first excited singlet states of 2-acetonaphthone and triphenylene it was not possible to decide whether the 2-acetonaphthone was excited to its triplet state by direct energy transfer from the triphenylene triplet or by singlet–singlet energy transfer between the two molecules followed by internal conversion of the singlet of 2-acetonaphthone to the triplet state.

Experiments similar to those carried out with 1-naphthol gave no indication that triphenylene and 2-acetonaphthone formed a complex in solution, or that triphenylene reacted with tributylstannane on flashing.

ACKNOWLEDGMENTS

We are greatly indebted to the National Research Council for financial support for this investigation, and to Dr. D. A. Ramsay for a blueprint of the design of the flash-lamp electrodes.

Can. J. Chem. Downloaded from www.nrcresearchpress.com by 210.87.254.6 on 09/05/12
For personal use only.

1. G. S. HAMMOND and W. M. MOORE. J. Am. Chem. Soc. **81**, 6334 (1959). W. M. MOORE, G. S. HAMMOND, and R. P. FOSS. J. Chem. Phys. **32**, 1594 (1960). W. M. MOORE, G. S. HAMMOND, and R. P. FOSS. J. Am. Chem. Soc. **83**, 2789 (1961). G. S. HAMMOND, W. P. BAKER, and W. M. MOORE. J. Am. Chem. Soc. **83**, 2795 (1961).
2. H. L. J. BACKSTROM and K. SANDROS. Acta Chem. Scand. **14**, 48 (1960).
3. D. S. MCCLURE and P. L. HANST. J. Chem. Phys. **23**, 1772 (1955).
4. G. PORTER and M. W. WINDSOR. Proc. Roy. Soc. (London), Ser. A, **245**, 238 (1958).
5. G. PORTER and F. WILKINSON. Trans. Faraday Soc. **57**, 1686 (1961).
6. F. BERGMANN and Y. HIRSCHBERG. J. Am. Chem. Soc. **65**, 1429 (1943).
7. G. S. HAMMOND and P. A. LEERMAKERS. J. Am. Chem. Soc. **84**, 207 (1962).
8. G. J. M. VAN DER KERK and J. G. A. LUITJEN. J. Appl. Chem. (London), **7**, 369 (1957).
9. S. CLAESSON and L. LINDQVIST. Arkiv. Kemi, **11**, 535 (1957).
10. A. TERENIN and V. ERMOLAEV. Trans. Faraday Soc. **52**, 1042 (1956).
11. G. PORTER and F. WILKINSON. Proc. Roy. Soc. (London), Ser. A, **264**, 1 (1961).
12. H. L. J. BACKSTROM and K. SANDROS. Acta Chem. Scand. **12**, 823 (1958).

RECEIVED MARCH 20, 1963.
DEPARTMENT OF CHEMISTRY,
UNIVERSITY OF BRITISH COLUMBIA,
VANCOUVER, BRITISH COLUMBIA.

Can. J. Chem. Downloaded from www.nrcresearchpress.com by 210.87.254.6 on 09/05/12
For personal use only.

THE OXIDATION OF SODIUM FORMATE BY SODIUM HYPOCHLORITE

M. W. LISTER AND P. ROSENBLUM

The present note describes the measurements of the oxidation of formate ions by sodium hypochlorite solutions, a reaction that in fact turns out to be a reaction of hypochlorous acid.

RESULTS AND DISCUSSION

Table I shows that in a typical experiment the sodium hypochlorite and formate reacted in a precisely 1:1 ratio without any side reaction.

TABLE I

Time (min)	[NaOCl]$\times 10^2$ (M)	[HCOONa]$\times 10^2$ (M)	Difference$\times 10^2$ (M)
0	4.71	12.11	7.40
60.0	4.67	12.07	7.40
121.2	4.60	12.03	7.43
181.1	4.54	11.97	7.43
241.3	4.45	11.89	7.44
300.0	4.37	11.81	7.44
361.3	4.27	11.68	7.41
421.1	4.10	11.52	7.42

NOTE: Initial [NaOH) = 0.00782 M; 60° C; ionic strength 0.653.

Preliminary runs showed that the rate of reaction increased with time. This was attributed to the fact that sodium hydroxide was used by the reaction

$$OCl^- + HCOO^- + OH^- \rightarrow Cl^- + CO_3^{=} + H_2O,$$

and that the rate was faster in less alkaline solutions. In fact the reaction was found to obey the rate equation

$$\text{rate} = k[OCl^-][HCOO^-]/[OH^-].$$

1. G. S. HAMMOND and W. M. MOORE. J. Am. Chem. Soc. **81**, 6334 (1959). W. M. MOORE, G. S. HAMMOND, and R. P. FOSS. J. Chem. Phys. **32**, 1594 (1960). W. M. MOORE, G. S. HAMMOND, and R. P. FOSS. J. Am. Chem. Soc. **83**, 2789 (1961). G. S. HAMMOND, W. P. BAKER, and W. M. MOORE. J. Am. Chem. Soc. **83**, 2795 (1961).
2. H. L. J. BACKSTROM and K. SANDROS. Acta Chem. Scand. **14**, 48 (1960).
3. D. S. MCCLURE and P. L. HANST. J. Chem. Phys. **23**, 1772 (1955).
4. G. PORTER and M. W. WINDSOR. Proc. Roy. Soc. (London), Ser. A, **245**, 238 (1958).
5. G. PORTER and F. WILKINSON. Trans. Faraday Soc. **57**, 1686 (1961).
6. F. BERGMANN and Y. HIRSCHBERG. J. Am. Chem. Soc. **65**, 1429 (1943).
7. G. S. HAMMOND and P. A. LEERMAKERS. J. Am. Chem. Soc. **84**, 207 (1962).
8. G. J. M. VAN DER KERK and J. G. A. LUITJEN. J. Appl. Chem. (London), **7**, 369 (1957).
9. S. CLAESSON and L. LINDQVIST. Arkiv. Kemi, **11**, 535 (1957).
10. A. TERENIN and V. ERMOLAEV. Trans. Faraday Soc. **52**, 1042 (1956).
11. G. PORTER and F. WILKINSON. Proc. Roy. Soc. (London), Ser. A, **264**, 1 (1961).
12. H. L. J. BACKSTROM and K. SANDROS. Acta Chem. Scand. **12**, 823 (1958).

RECEIVED MARCH 20, 1963.
DEPARTMENT OF CHEMISTRY,
UNIVERSITY OF BRITISH COLUMBIA,
VANCOUVER, BRITISH COLUMBIA.

Can. J. Chem. Downloaded from www.nrcresearchpress.com by 210.87.254.105 on 09/05/12
For personal use only.

THE OXIDATION OF SODIUM FORMATE BY SODIUM HYPOCHLORITE

M. W. LISTER AND P. ROSENBLUM

The present note describes the measurements of the oxidation of formate ions by sodium hypochlorite solutions, a reaction that in fact turns out to be a reaction of hypochlorous acid.

RESULTS AND DISCUSSION

Table I shows that in a typical experiment the sodium hypochlorite and formate reacted in a precisely 1:1 ratio without any side reaction.

TABLE I

Time (min)	[NaOCl]$\times 10^2$ (M)	[HCOONa]$\times 10^2$ (M)	Difference$\times 10^2$ (M)
0	4.71	12.11	7.40
60.0	4.67	12.07	7.40
121.2	4.60	12.03	7.43
181.1	4.54	11.97	7.43
241.3	4.45	11.89	7.44
300.0	4.37	11.81	7.44
361.3	4.27	11.68	7.41
421.1	4.10	11.52	7.42

NOTE: Initial [NaOH) = 0.00782 M; 60° C; ionic strength 0.653.

Preliminary runs showed that the rate of reaction increased with time. This was attributed to the fact that sodium hydroxide was used by the reaction

$$OCl^- + HCOO^- + OH^- \rightarrow Cl^- + CO_3^{=} + H_2O,$$

and that the rate was faster in less alkaline solutions. In fact the reaction was found to obey the rate equation

$$\text{rate} = k[OCl^-][HCOO^-]/[OH^-].$$

This gives the integrated equation

$$(x_0-z_0)\ln(x/x_0) + (z_0-y_0)\ln(x-x_0+y_0)/y_0 = -k(x_0-y_0)t,$$

and k was calculated from this equation and found to remain constant. Here $[OCl^-] = x$, $[HCOO^-] = y$, and $[OH^-] = z$, and x_0, y_0, and z_0 are the initial concentrations. Since there is a small spontaneous decomposition of sodium hypochlorite, a small correction for this was applied to the observed rate (and hence to the rate constant) using values of the rate constant for this decomposition obtained by Lister (1, 2). The average correction was 2.2%. The rate constants, which are given in Table II, have been corrected in this way.

TABLE II

Run	Temp. (°C)	Initial ionic strength	Initial [NaOCl]	Initial [$NaHCO_2$]	Initial [NaOH]	$k\times10^5$ (min^{-1})
1	60.0	0.653	0.0472	0.1215	0.00782	1.49
2	"	0.653	0.0473	0.1215	0.00782	1.41
3	"	1.05	0.0496	0.1215	0.00782	1.55
4	"	1.05	0.0497	0.1215	0.00782	1.62
5	"	1.10	0.0460	0.1620	0.01534	1.60
6	"	1.10	0.0460	0.1620	0.01534	1.57
7	"	1.17	0.1219	0.0405	0.00826	1.59
8	"	1.17	0.1221	0.0405	0.00826	1.57
9	"	1.84	0.0481	0.1215	0.00782	1.70
10	"	1.84	0.0482	0.1215	0.00782	1.70
11	"	1.85	0.0468	0.1215	0.01534	1.72
12	"	1.85	0.0468	0.1215	0.01534	1.73
13	50.0	1.04	0.0907	0.1221	0.00816	0.77
14	"	1.04	0.0908	0.1221	0.00816	0.77
15	70.0	1.05	0.0449	0.1209	0.01526	3.81
16	"	1.05	0.0449	0.1209	0.01526	3.82

The inverse dependence of the rate on concentration presumably shows that this is really a reaction of hypochlorous acid:

$$OCl^- + H_2O \rightarrow HOCl + OH^- \quad \text{(fast)}$$
$$HOCl + HCOO^- \rightarrow Cl^- + H_2CO_3 \quad \text{(slow)}$$
$$H_2CO_3 + 2OH^- \rightarrow CO_3^{=} + 2H_2O \quad \text{(fast).}$$

The extra proton is presumed to be attached to the hypochlorite rather than the formate ions, since formic acid is over 4000 times stronger than hypochlorous acid.

For the above mechanism the true rate constant of the slow step (k_T), defined by

$$\text{rate} = k_T[HOCl][HCO_2^-],$$

is related to the apparent rate constant, k, by

$$k_T = kK_a/K_W,$$

where K_a is the ionization constant of hypochlorous acid and K_W the ionic product of water. Using the known values of K_a and K_W at 60° C ($K_a/K_W = 1.93\times10^{-6}$ at 60° C), we get $k_T = 8.2$ (g-mol/l.)$^{-1}$ min^{-1} at 60° C, and an ionic strength of 1.05.

The apparent activation energy obtained from k is 17.7 kcal/g-mol. As ΔH for the hydrolysis of hypochlorite ions is about 11.0 kcal, this means that the true activation energy of the slow stage is only 6.7 kcal/mole. If k_T is given by the usual relation, $k_T = Ae^{-E\ddagger/RT}$, then $\log A = 3.53$ (time in seconds). This is unusually small, but similar

Can. J. Chem. Downloaded from www.nrcresearchpress.com by 210.87.254.105 on 09/05/12
For personal use only.

low values have been found for the reaction of hypochlorous acid with bromide ions (3) or nitrite ions (4). Also somewhat analogous oxidations by hydrogen peroxide have low values of log A, which are explained by Edwards (5) in terms of a transition complex requiring rather special orientation. If the same idea is applied to the present case the transition complex would be

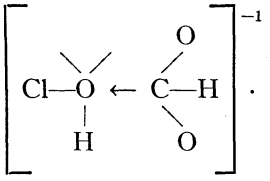

The effect of ionic strength is to give a rather small increase in the rate of reaction with increasing ionic strength, as is to be expected for a reaction between an ion and a neutral molecule. Finally it may be noted that in acid solution the rather similar oxidations of formate ions by halogens have been shown (6, 7, 8) to be reactions of free halogen molecules, $HCOO^- + X_2 + H_2O \rightarrow CO_2 + H_3O^+ + 2X^-$, and are not due to hypohalous acid.

EXPERIMENTAL

Mixtures of aqueous solutions of sodium hypochlorite, sodium hydroxide, and sodium formate of known concentration were made up. Sodium chloride was added to control the ionic strength. The solutions were kept in a thermostat; samples were taken at frequent intervals, quenched in an ice bath, and analyzed as described below.

Sodium hypochlorite was estimated by measuring the absorbance of the solution on a Beckmann DU spectrophotometer. The extinction coefficient of OCl^- at 292 mμ is 350, while sodium formate, and other constituents of the solution, absorb negligibly at this wavelength. For the estimation of formate, a 5-ml aliquot was mixed with 25 ml of water containing 2 g, of sodium carbonate. Hydrogen peroxide (10 ml; 3%) was added to destroy the hypochlorite. Potassium permanganate (0.1 ml; 0.1 N) was added, and the mixture was boiled for 5 minutes to decompose excess peroxide. The solution was cooled, 25 ml of standard potassium permanganate (0.1 N) was added, and the solution was heated on a steam bath for 10 minutes. The sodium formate is quantitatively oxidized by the permanganate under these conditions. The excess potassium permanganate was estimated by acidifying the solution, adding 3 g of potassium iodide, and titrating the iodine with sodium thiosulphate.

1. M. W. Lister. Can. J. Chem. **34**, 465 (1956).
2. M. W. Lister and R. C. Petterson. Can. J. Chem. **40**, 729 (1962).
3. L. Farkas, M. Lewin, and R. Bloch. J. Am. Chem. Soc. **71**, 1988 (1949).
4. M. W. Lister and P. Rosenblum. Can. J. Chem. **39**, 1645 (1961).
5. J. O. Edwards. Peroxide reaction mechanisms. Interscience Publishers. 1962. p. 69.
6. D. L. Hammick, W. K. Hutchinson, and R. F. Snell. J. Chem. Soc. 2715 (1925).
7. D. L. Hammick and M. Zvegintzov. J. Chem. Soc. 1105 (1926).
8. B. F. Chow. J. Am. Chem. Soc. **57**, 1437 (1935).

Received April 22, 1963.
Department of Chemistry,
University of Toronto,
Toronto, Ontario.

Can. J. Chem. Downloaded from www.nrcresearchpress.com by 210.87.254.105 on 09/05/12
For personal use only.

Canadian Journal of Chemistry

Issu[illegible]HE NATIONAL RESEARCH COUNCIL OF CANADA

VOLUME 41 NOVEMBER 1963 NUMBER 11

LYCOPODIUM ALKALOIDS

XIV. FLABELLINE

J. C. F. YOUNG[1] AND D. B. MACLEAN

Department of Chemistry, McMaster University, Hamilton, Ontario

Received May 27, 1963

ABSTRACT

A new alkaloid, $C_{18}H_{28}ON_2$, designated flabelline, has been isolated by countercurrent distribution from the extract of *Lycopodium flabelliforme*. The structure and stereochemistry of flabelline have been established by its conversion to and preparation from lycopodine.

Can. J. Chem. Downloaded from www.nrcresearchpress.com by 210.87.254.105 on 09/05/12
For personal use only.

The investigation of the alkaloids of *Lycopodium flabelliforme* was undertaken by Manske and Marion in 1942 (1). They reported the isolation of lycopodine, the bases L1 to L6, and nicotine. Base L1 has since been shown to be dihydrolycopodine (2), L2 to be acetyldihydrolycopodine (3), and L6 to be a mixture of two compounds, α- and β-obscurine (4). The structures of lycopodine and its derivatives (2) and the obscurines (5) are now known.

Flabelliformine, a hydroxy derivative of lycopodine, was recently isolated from this plant, and its structure elucidated (6).

In this communication we wish to report the isolation and structural elucidation of flabelline, another minor alkaloid of *L. flabelliforme*. The separation procedure used in working up the alkaloids is given in some detail since some fractions are still being investigated and will be reported upon in a subsequent paper.

The alkaloid was extracted according to the procedure of Manske and Marion (1) and the bulk of the lycopodine separated by the method of Barclay and MacLean (7). The residual alkaloids from a number of extractions collected over a period of several years were combined and subjected to a preliminary purification as described in the experimental section. The bases were then subjected, on a large scale, to column chromatography on alumina and divided into three fractions—those eluted with chloroform, those eluted with 2% methanol in chloroform, and a residue eluted with 5% methanol in chloroform. From the chloroform fraction, flabelliformine containing some dihydrolycopodine separated upon treatment with ether. The mother liquor from the separation of flabelliformine was concentrated and the residual bases distributed between chloroform and pH 6.0 citrate–phosphate buffer in a 12-funnel distribution. The distribution was carried out on a large scale and served merely to separate the weak from the strong bases. Many more transfers with a much smaller amount of base would have been necessary to achieve discrete separation of individual bases.

Fractions 1 and 2 from the distribution were almost pure dihydrolycopodine; fractions 3 and 4, a mixture of dihydrolycopodine and flabelline; and fraction 5, a mixture of

[1]*Holder of a National Research Council Bursary 1960–1961 and a Studentship 1961–1962.*

flabelline, flabelliformine, and α-obscurine. The dihydrolycopodine–flabelline mixture was separated by subjecting it to a 49-tube countercurrent distribution. The flabelline after recrystallization from ether–acetone melted at 185–187.5°, and its analysis was in agreement with the formula $C_{18}H_{28-30}ON_2$. The perchlorate of flabelline melted at 280–282° with decomposition. This is the same melting point as that reported by Manske and Marion for L5 perchlorate (1). A comparison of the two substances revealed that they were not identical. The investigation of fractions 6 to 12 has not been completed.

The presence of a secondary amide function in flabelline may be inferred from its infrared spectrum. In Nujol mull the presence of an >NH group is indicated by the split peak at 3180–3250 cm^{-1}. In dilute solution in chloroform the >NH absorption appears at 3415 cm^{-1}. As the concentration of the solution increases, a band shifting from 3315 cm^{-1} to 3270 cm^{-1} appears. This band has been assigned to trans intermolecular hydrogen bonding (8). The Nujol spectrum shows bands at 1645, 1550, and 1300 cm^{-1} which appear at 1656, 1475, and 1308 cm^{-1} in the chloroform spectrum. These peaks are the amide I, II, and III bands, respectively (9).

The ultraviolet spectrum of flabelline does not exhibit any strong absorption above 220 mμ but has strong end absorption.

The n.m.r. spectrum (60 Mc/sec) of flabelline in deuterochloroform shows a broad singlet of intensity corresponding to one proton shifting continuously from $\tau = 2.72$ at high concentration to $\tau = 3.39$ at lower concentration. This has been assigned to the amide >NH, and the chemical shift is assumed to be associated with the change in degree of intermolecular hydrogen bonding with the change in concentration. A singlet at $\tau = 7.98$ with intensity corresponding to three protons has been assigned to the methyl of an acetamide group. A doublet centered at $\tau = 9.11$ ($J = 6$ cycles/sec) indicates a >CH—CH_3 group. Because of underlying absorption, the integrated area of this peak is somewhat greater than three protons. Other peaks in the spectrum have not been assigned to specific groups in the molecule. The absence of absorption (other than that of the >NH group) below $\tau = 6$ precludes the presence of ethylenic protons.

The spectroscopic data are compatible with the presence of an acetamide group in flabelline. The formation of a methiodide by interaction with 1 mole of methyl iodide implies that the basic nitrogen is tertiary. Since the n.m.r. spectrum does not have a peak corresponding to an >N—CH_3 group, one must conclude that the basic nitrogen is part of two rings. It seemed, therefore, that structure I, embodying those features and based upon the structure of lycopodine, II, was a reasonable representation for flabelline. Apparent confirmation of structure I for flabelline was obtained through the following series of reactions. Lycopodine was converted to its oxime, dissolved in acetic anhydride, and treated with hydrogen at 75 atm pressure and at 100°. The product of this reaction proved to be identical with flabelline. The melting points of synthetic and natural flabelline and a mixture of the two were identical. The infrared spectra of synthetic and natural flabelline, as well as those of their perchlorates, were superimposable. Thus structure I was apparently established as the structure of flabelline.

The mass spectrum of flabelline shows that the alkaloid has a mass of 288 and not 290, as required of structure I, and thus flabelline must contain one additional center of unsaturation. By placing a double bond at the 7,8-position of ring C, a structure, III, of the proper mass is obtained which is still compatible with the spectroscopic and chemical data cited above. Confirmation of structure III was obtained by treating flabelline with aqueous hydrochloric acid. Lycopodine was the sole hydrolysis product and was isolated in quantitative yield. It should be pointed out that the 6,7-position for the double bond,

Can. J. Chem. Downloaded from www.nrcresearchpress.com by 210.87.254.105 on 09/05/12
For personal use only.

although compatible with the hydrolysis reaction, is not compatible with the n.m.r. data.

An explanation for the formation of the enamine III rather than the saturated amine I in the reduction reaction is offered below. Reduction of the oxime to the hydroxylamine, followed by dehydration and rearrangement to the enamine and acetylation of the latter would yield the desired product:

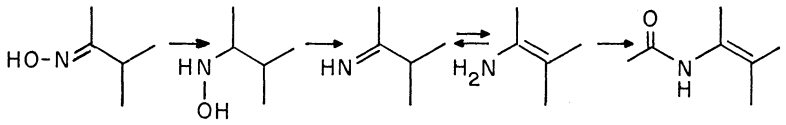

The fact that the reduction does not proceed further is not unexpected, for a double bond in the 7,8-position in the lycopodine skeleton is known to resist the addition of hydrogen. Thus it has been reported that anhydrodihydrolycopodine IV and the enol ether V are not affected at this site under conditions as stringent as those used here (2).

The ultraviolet spectrum of flabelline is worthy of comment. It does not exhibit an absorption band above 220 mμ, although its cyclic analogue, α-obscurine, VI, has an intense peak at 255 mμ. The intense absorption in α-obscurine at higher wavelength may be a consequence of the rigidity imposed upon the chromophore in the cyclic system. Although the preparation of acetylated enamines has recently been reported (10), their ultraviolet spectra were not recorded and thus no analogous cases were available for comparison.

The stereochemistry of flabelline depicted in III follows from its conversion to and preparation from lycopodine, the configuration of which is known (11, 12).

The biogenesis of flabelline can be accommodated by the proposal of Conroy (13). This is the first example of an alkaloid with the lycopodine skeleton carrying a second nitrogen atom, and in this respect its formation is an interesting variation in the usual biogenetic pathway.

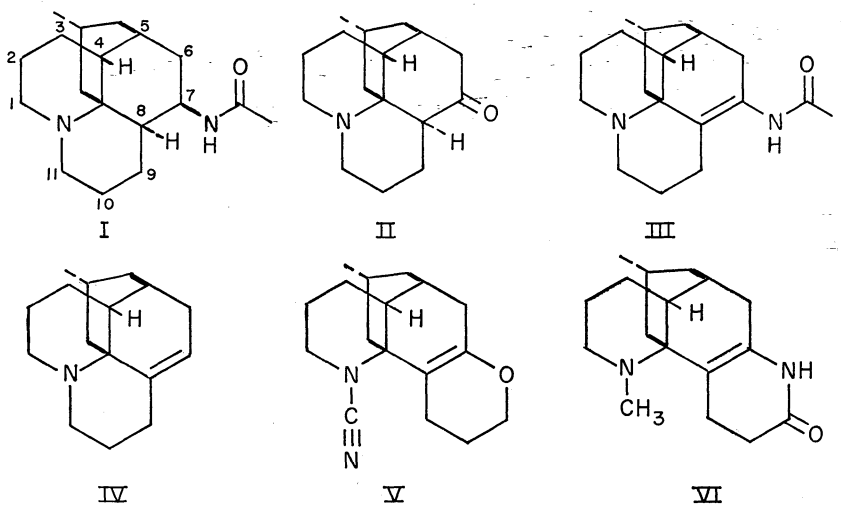

EXPERIMENTAL

Apparatus, Methods, and Materials

All melting points were taken on a Kofler Micro Hot Stage. Infrared spectra were measured in Nujol mull unless otherwise specified and were determined on a Beckman Model IR-5 recording spectrophotometer with a sodium chloride prism. Ultraviolet spectra were measured in methanol on a Perkin–Elmer Model

Can. J. Chem. Downloaded from www.nrcresearchpress.com by 210.87.254.105 on 09/05/12
For personal use only.

4000 Spectrocord. The nuclear magnetic resonance spectra were measured on a Varian V-4300 B high-resolution spectrometer at a frequency of 60 Mc/sec. The n.m.r. spectra were measured in concentrated deuterochloroform solutions with tetramethylsilane as an internal standard. Chemical shifts are given on the τ scale of Tiers. The mass spectrum was run on a CEC 21–103C mass spectrometer equipped with a heated inlet system at an ionizing voltage of 70 ev and an ionizing current of 50 μa.

The crude extract used in these experiments was isolated in these laboratories over a period of several years from *L. flabelliforme* collected in the Wentworth Valley of Nova Scotia. The dry, ground plant material was extracted by the procedure of Manske and Marion (1). Lycopodine was isolated by column chromatography as described by Barclay and MacLean (7). The other more strongly adsorbed alkaloids were eluted and combined to give the mixture of crude alkaloids used in these experiments.

Preliminary Purification of Crude Alkaloids

To a collection of the crude alkaloids obtained after removal of lycopodine were added several liters of water and several hundred grams of tartaric acid. The resultant solution was steam-distilled to remove organic solvents used in the original extractions. Several more liters of water were added to the distillation residue, and the aqueous solution was shaken with about 60 g of powdered celite. Suction filtration through a pad of celite yielded a dark red filtrate which was then extracted twice with ether to remove fatty, non-basic material. The aqueous solution was basified with ammonia and extracted with chloroform. The chloroform extract was washed with water, and evaporated to dryness, yielding about 200 g of a black, tar-like residue.

First Chromatography of Crude Alkaloids

About 75 g of the crude alkaloid extract was taken up in a minimum of warm chloroform and adsorbed on a 5×45 cm column of alumina. The column was eluted with chloroform until the eluate was almost colorless. The eluates were combined and evaporated to dryness, yielding 50 g of dark resinous material. The column was then eluted with 2% methanol in chloroform and 5% methanol in chloroform, yielding dark resinous fractions weighing 14 g and 3 g, respectively.

Isolation of Flabelliformine

The mixture of crude bases obtained by elution with chloroform partially crystallized and the semisolid mas was shaken with cold ether. The insoluble crystalline material (13.0 g) which separated was worked up as described by Curcumelli-Rodostamo and MacLean (6) to yield flabelliformine as the major and dihydrolycopodine as the minor component.

First Separatory Funnel Distribution of Crude Bases

The mother liquor obtained from the separation of crude flabelliformine was evaporated to dryness and the resultant residue was dissolved in 350 ml of chloroform. The chloroform solution was then shaken with 350 ml of a pH 6.00 citrate–phosphate buffer solution for 15 minutes in a 1-liter separatory funnel. The chloroform phase, after separation was complete, was transferred to a second separatory funnel containing 350 ml of fresh buffer solution, and 350 ml of fresh chloroform was added to the first separatory funnel. Both funnels were then shaken for 15 minutes each. This procedure was continued until 12 transfers had been completed.

The resulting extracts were worked up as outlined below. The chloroform fractions were separated from their respective buffer fractions and each washed with ammonia to basify any salts which may have formed. The chloroform extracts were then dried over anhydrous sodium sulphate and evaporated to dryness in tared flasks. The buffer fractions were basified with ammonia and extracted with chloroform. The chloroform extracts were then dried over anhydrous sodium sulphate and evaporated to dryness in tared flasks. Each flask was weighed, the weights of the bases in each flask being recorded (see Table I).

TABLE I

Distribution of alkaloids

Flask No.	Buffer fraction (wt. in g)	Chloroform fraction (wt. in g)	Flask No.	Buffer fraction (wt. in g)	Chloroform fraction (wt. in g)
1	3.631	0.155	7	0.531	0.386
2	4.426	0.365	8	0.529	0.831
3	4.021	0.365	9	0.778	2.361
4	2.622	0.347	10	1.273	3.704
5	1.56	0.186	11	1.5*	5.3*
6	0.972	0.235	12	0.670	6.867

*Estimated value.

Resolution of Fraction 1

Crystalline material formed on treatment with acetone. Recrystallization from acetone yielded 3.0 g of dihydrolycopodine.

Can. J. Chem. Downloaded from www.nrcresearchpress.com by 210.87.254.105 on 09/05/12
For personal use only.

Resolution of Fraction 2

This fraction was worked up in the same manner as fraction 1, yielding 4.0 g of dihydrolycopodine.

Resolution of Fraction 3

Crystalline material formed on treatment with acetone. Recrystallization from acetone yielded two crops of dihydrolycopodine weighing 2.0 and 0.5 g. The filtrate was evaporated to dryness, dissolved in a minimum of chloroform, and adsorbed on a column of alumina. Elution with 0.5% methanol in chloroform effected removal of a yellow band, giving 1.26 g of a yellow oil which resisted all attempts at crystallization. The oil was taken up in acetone, made slightly acid with perchloric acid, and treated with water until the solution was turbid. The crystals which separated were recrystallized from acetone–methanol to give small white crystals melting above 258° (with decomposition and effervescence). The infrared spectrum showed bands at 3480 cm^{-1}, 3300 cm^{-1}, a shoulder at 3150 cm^{-1}, and bands at 1650 cm^{-1} and 1515 cm^{-1}. The mixture of salts was taken up in water, basified with ammonia, and extracted with chloroform. The combined extract was dried over anhydrous sodium sulphate and evaporated to dryness. The residue was combined with fraction 4 and distributed between chloroform and buffer solution (*vide infra*).

Resolution of Fraction 4

This fraction was taken up in a minimum of chloroform, adsorbed on a column of alumina, and eluted with 0.5% methanol in chloroform. A yellow band passed through the column from which a yellow oil was obtained. Treatment with acetone–methanol gave yellow crystals which melted at 150–163°. The infrared spectrum showed bands in the NH region at 3250 cm^{-1}, and in the amide carbonyl region at 1650 cm^{-1} and 1515 cm^{-1}. The crystalline material and filtrates were combined with the residue from fraction 3 and distributed as described in the next section.

Countercurrent Distribution of Fraction 3 and Fraction 4

The residues remaining after removal of dihydrolycopodine from fraction 3 and fraction 4 were combined and dissolved in 50 ml of chloroform. The chloroform solution was divided and placed in the first two tubes of a 49-tube Craig countercurrent extractor. The alkaloid mixture was then distributed between chloroform and pH 6.0 citrate–phosphate buffer solution. The machine was agitated for 15 minutes for each transfer, the buffer layer being the moving phase. When the 49 transfers had been completed, the contents of each tube were made alkaline with ammonia, shaken, and the chloroform layer removed. The remaining aqueous layers were then extracted with fresh chloroform. The chloroform extract for each tube was dried over anhydrous sodium sulphate and evaporated to dryness in tared flasks.

Fractions 35–38 were taken up in acetone and combined. After initial concentration of the solution, ether was added and the solution further concentrated. Yellow rhombic crystals formed on cooling. These crystals (250 mg), after filtering and washing with 2:1 ether–acetone, melted at 185–187.5°. Calc. for $C_{18}H_{28}ON_2$: C, 75.00; H, 9.72; N, 9.72. Found: C, 75.11; H, 9.89; N, 9.45.

The infrared spectrum of flabelline showed a split band at 3250 cm^{-1} and 3180 cm^{-1} in the NH region, and absorption at 1645 cm^{-1}, 1550 cm^{-1}, and 1300 cm^{-1} attributed to the amide I, II, and III bands. The infrared spectra of fractions 39–43 showed the presence of flabelline, and they were combined, adsorbed on a column of alumina, and eluted with 1:1 benzene–chloroform. A wide yellow band passed through the column from which was obtained a yellow oil which crystallized on treatment with 2:1 ether–acetone. Recrystallization from 2:1 ether–acetone yielded about 400 mg of flabelline.

Fractions 44–48 had similar infrared spectra and were combined, adsorbed on a column of alumina, and eluted with 1.5% methanol in benzene. A fluorescent band quickly passed through the column from which light yellow crystals were obtained. Recrystallization from ether – petroleum ether gave about 250 mg of dihydrolycopodine.

Resolution of Fraction 5

This fraction was taken up in benzene, adsorbed on a column of alumina, and successively eluted with 1:1, 1:2, and 1:3 benzene–chloroform. The resultant 15 fractions were collected into three groups on the basis of their infrared spectra. Treatment of the first group with ether gave an amorphous precipitate which was then crystallized from 2:1 ether–acetone, yielding flabelline. The filtrate was taken up in 10% aqueous acetic acid and treated with excess perchloric acid. A dark solid and a crystalline material came down on standing in a refrigerator. Filtration yielded 125 mg of dark solid and 108 mg of crystals, both showing infrared spectra similar to that of flabelline perchlorate. After the filtrate was concentrated and allowed to stand, flabelliformine perchlorate (59 mg) separated. The second group resisted all attempts to obtain a crystalline compound. The third group was taken up in a 2:1 ether–acetone and yielded long needles on standing in a refrigerator. Several recrystallizations from 2:1 ether–acetone gave needle-like crystals of α-obscurine.

Preparation of Flabelline Methiodide

A solution of flabelline (79 mg) in 4 ml of acetone and an excess of methyl iodide was heated under reflux for 3 hours. Crystallization was induced by concentration and scratching. After filtration and recrystallization from acetone–methanol, flabelline methiodide melted sharply at 281–282°. Calc. for $C_{18}H_{28}ON_2 \cdot CH_3I$: C, 53.02; H, 7.20; N, 6.51%. Found: C, 53.15; H, 7.34; N, 6.14%.

Can. J. Chem. Downloaded from www.nrcresearchpress.com by 210.87.254.105 on 09/05/12
For personal use only.

The infrared spectrum had N—H absorption at 3200 cm^{-1} and carbonyl absorption at 1653 cm^{-1}.

Preparation of Flabelline Perchlorate

Several drops of perchloric acid were added to a solution of flabelline (40 mg) in a minimum of warm 10% acetic acid. The resultant 37 mg of short white needles was removed by filtration and melted at 280–282° (with decomposition). Calc. for $C_{18}H_{23}ON_2 \cdot HClO_4$: C, 55.60; H, 7.46; N, 7.20%. Found: C, 55.44; H, 7.30; N, 7.00%.

Preparation of Lycopodine Oxime

To lycopodine (600 mg) dissolved in 10 ml of 95% aqueous ethanol was added a solution of hydroxylamine hydrochloride (600 mg) in 10 ml of 95% aqueous ethanol. Addition of potassium hydroxide pellets (3.0 g) and more ethanol (20 ml) resulted in formation of a white precipitate. The reaction mixture was heated under reflux for 3 hours and then cooled. After the ethanol had been removed, the residue was taken up in water and treated with dilute hydrochloric acid until the solution was only slightly basic. The resultant precipitate was filtered to give 440 mg of lycopodine oxime. Recrystallization from ethanol gave crystals melting at 275–277°. Douglas, Lewis, and Marion (3) report a melting point of 262–264°. Calc. for $C_{16}H_{26}ON_2$: C, 73.24; H, 9.99; N, 10.68. Found: C, 73.01; H, 9.79; N, 10.76.

Hydrolysis of Flabelline

Flabelline (50 mg) was dissolved in 10 ml of concentrated hydrochloric acid and the solution heated under reflux for 12 hours. The solution was made basic and extracted with ether. The dried ether extract upon evaporation yielded lycopodine, identified by comparison of its melting point and infrared spectrum with an authentic sample. The yield was quantitative.

High-pressure Reduction and Acetylation of Lycopodine Oxime with Raney Nickel and Acetic Anhydride

Lycopodine oxime (248 mg), dissolved in 40 ml of redistilled acetic anhydride, was treated with hydrogen (1160 p.s.i.g.) and Raney nickel (several hundred milligrams) at 100° for 24 hours. Excess acetic anhydride was destroyed with ice, and the catalyst removed by filtration. The filtrate was made alkaline with ammonia and extracted with chloroform. The extract was dried over anhydrous sodium sulphate and evaporated to dryness under reduced pressure, leaving a yellow oil which showed an infrared spectrum almost identical with that of flabelline. The residue was adsorbed on a column of alumina and eluted with 1:1 benzene–chloroform. A small amount of lycopodine quickly passed through the column, whereas the major product passed very slowly through the column. The eluates containing the bulk of the product were evaporated to dryness under reduced pressure to give about 100 mg of crystalline material showing an infrared spectrum identical with that of flabelline. Recrystallization from acetone–ether gave rectangular plates which showed no depression of the melting point on admixture with naturally occurring flabelline. The infrared spectrum of the crystalline product was identical with that of natural flabelline.

ACKNOWLEDGMENTS

One of us (D. B. M.) spent the academic year 1962–1963 as a guest of the Department of Chemistry, Massachusetts Institute of Technology, in the laboratories of Professor K. Biemann, where a part of this work was carried out, and wishes to thank Professor Biemann for his hospitality during the year.

We are indebted to the National Research Council and the Ontario Research Foundation for financial support of this work. We wish to thank Dr. L. Marion for a sample of L5 perchlorate.

REFERENCES

1. R. H. F. Manske and L. Marion. Can. J. Res. B, **20**, 87 (1942).
2. W. A. Harrison, M. Curcumelli-Rodostamo, D. F. Carson, L. R. C. Barclay, and D. B. MacLean. Can. J. Chem. **39**, 2086 (1961).
3. B. Douglas, D. G. Lewis, and L. Marion. Can. J. Chem. **31**, 272 (1953).
4. B. P. Moore and L. Marion. Can. J. Chem. **31**, 952 (1953).
5. W. A. Ayer, J. A. Berezowski, and G. G. Iverach. Tetrahedron, **18**, 567 (1962).
6. M. Curcumelli-Rodostamo and D. B. MacLean. Can. J. Chem. **40**, 1068 (1962).
7. L. R. C. Barclay and D. B. MacLean. Can. J. Chem. **34**, 1519 (1956).
8. S. Mizushima, T. Simanouti, S. Nagakura, K. Kuratani, M. Tsuboi, H. Baba, and O. Fujioka. J. Am. Chem. Soc. **72**, 3490 (1950).
9. L. J. Bellamy. The infrared spectra of complex molecules. 2nd ed. Methuen and Co. Ltd., London. 1960. p. 220.
10. C. Djerassi, N. Crossley, and M. A. Kielczewski. J. Org. Chem. **27**, 1112 (1962).
11. F. A. L. Anet. Tetrahedron Letters, No. 20, 13 (1960).
12. K. Wiesner, J. E. Francis, J. A. Findlay, and Z. Valenta. Tetrahedron Letters, No. 5, 187 (1961).
13. H. Conroy. Tetrahedron Letters, No. 10, 34 (1960).

Can. J. Chem. Downloaded from www.nrcresearchpress.com by 210.87.254.105 on 09/05/12
For personal use only.

THE EFFECT OF PHENOLS AND AROMATIC THIOLS ON THE POLYMERIZATION OF METHYL METHACRYLATE[1]

S. C. BARTON, R. A. BIRD, AND K. E. RUSSELL
Department of Chemistry, Queen's University, Kingston, Ontario
Received June 11, 1963

ABSTRACT

Chain transfer constants of a number of phenols in the polymerization of methyl methacrylate have been determined. They are small compared with the corresponding transfer constants with styrene, a maximum value of 0.0026 being observed with pyrogallol. Three deuterated phenols do not have a measurable effect on the rate and degree of polymerization, showing that attack takes place mainly at the O—H group.

The aromatic thiols investigated have transfer constants in the range 2.6 to 7.4. They cause only slight retardation of polymerization, and efficiencies of reinitiation by aromatic thiol radicals are estimated to be at least 95%. The transfer constants of meta-substituted thiols do not differ greatly from that of benzenethiol showing that inductive effects are small. A wider range of reactivities is observed with the para-substituted thiols, indicating the existence of small but significant resonance effects.

Can. J. Chem. Downloaded from www.nrcresearchpress.com by 210.87.254.6 on 09/05/12
For personal use only.

A study of the effect of phenols on the polymerization of styrene (1) has shown that most simple phenols do not retard the polymerization significantly and that their transfer constants are less than 0.008. Some phenols, such as 1-naphthol and 4-methoxyphenol, decrease the rate and degree of polymerization to an intermediate extent while catechol, *t*-butylcatechol, and pyrogallol act as fairly strong retarders with transfer constants approaching 1. The present work gives results of a comparable study using polymethyl methacrylate radicals as the hydrogen acceptors. These radicals differ in reactivity and polarity from polystyryl radicals and it is of interest to compare their rates of reaction with phenols of varying structure. Caldwell and Ihrig (2) have suggested that an addition complex is formed between a polymethyl methacrylate radical and hydroquinone prior to hydrogen abstraction. Information on this point has been obtained by comparison of the transfer activities of phenols and deuterated phenols.

The investigation was extended to the aromatic thiols because simple phenols are too unreactive to show detailed effects of meta and para substitution. An estimate of the influence of electron withdrawal on the transfer process was made from the results for certain meta-substituted thiols. Transfer constants were also determined for deuterated 4-chlorobenzenethiol and 2-naphthalenethiol.

EXPERIMENTAL

Materials

Methyl methacrylate was washed several times with sodium hydroxide solution and water and dried over calcium chloride at 0°. It was distilled at reduced pressure in an atmosphere of nitrogen and degassed on the high-vacuum line. After being stirred with calcium chloride for 1 hour it was subjected to two vacuum distillations and was stored at −78.5°. The phenols were either recrystallized and dried in a vacuum desiccator or sublimed at reduced pressure. Hydroquinone (Matheson, Coleman and Bell) was used without further purification since recrystallization from benzene–acetone mixtures in an atmosphere of nitrogen led to a more strongly retarding product. The deuterated phenols were prepared by dissolving them in a mixture of heavy water and deuterated methanol, followed by removal of the water and methanol at reduced pressure. Infrared analysis showed that conversion to deuterated phenol was greater than 85%.

Benzenethiol, 3- and 4-methylbenzenethiol, 4-chlorobenzenethiol, and 2-naphthalenethiol were commercial products which were purified by distillation or recrystallization. The remaining thiophenols were prepared

[1]*Presented in part at the Eleventh Canadian High Polymer Forum, Assumption University of Windsor, Windsor, Ontario, September 1962.*

by the xanthate method (3): 3-chlorothiophenol, b.p. 203–205° and n_D^{20} 1.6028; 3-bromothiophenol, b.p. 130–132° at 40 mm and n_D^{20} 1.6322; 3-acetylthiophenol, b.p. 143–144° at 12 mm and n_D^{20} 1.6012; 4-bromothiophenol, m.p. 74.5–75.2°; 4-acetylthiophenol, m.p. 27–28.5°.

Azobisisobutyronitrile was recrystallized from ether and stored at 0°.

Procedure

Azobisisobutyronitrile (0.02 g) was weighed into the reaction tube, a known amount of phenol or deuterated phenol up to a maximum of 0.25 g was added and the tube was evacuated. About 5 ml methyl methacrylate was distilled into the tube and, after sealing off, the reaction tube and contents were quickly weighed and placed in a bath at 45.00±0.04°. After approximately 3% of the monomer had been converted to polymer the tube was cooled and the polymer precipitated in methanol and dried *in vacuo* at 60°.

The thiols were added in small glass vials in quantities of the order of 0.001 g to about 15 ml monomer. Significant exchange occurred when deuterated thiols were used and 0.05 g heavy water was added to the reaction mixture to maintain the thiol almost entirely in the deuterated form. This procedure was suggested by Howard and Ingold after its successful use in their autoxidation studies (4). The heavy water has no significant effect on the polymerization in the absence of phenol.

Intrinsic viscosities of the polymethyl methacrylate samples were determined at 20° with chloroform as solvent, and degrees of polymerization were calculated using the relationship (5)

$$\log \bar{P}_n = 3.261 + 1.256 \log [\eta].$$

This relationship between $\bar{P}_n$, the number-average degree of polymerization and $[\eta]$, the intrinsic viscosity, was determined for unfractionated samples and it is probable that the polymer produced in these experiments with phenols and thiols has a similar molecular weight distribution. O'Brien and Gornick (6) state that their equation relating degree of polymerization and intrinsic viscosity in benzene solution applies to polymer samples produced with and without transfer agent; in general, however, it gives somewhat lower values of the number-average degree of polymerization than the above relationship.

Densities of solutions of phenols in methyl methacrylate were determined at 45°.

RESULTS AND DISCUSSION

Transfer Reaction with Phenols

The phenols investigated caused little or no retardation of the polymerization of methyl methacrylate at 45° and there was no evidence for induction periods. The maximum retardation observed was only 8% and this occurred with 0.28 *M* pyrogallol. In some solutions, e.g. of 4-methoxyphenol, the rate of polymerization was slightly greater than that predicted from the rate of polymerization of pure methyl methacrylate. Azobisisobutyronitrile decomposes more rapidly in solutions of phenols in benzene (1) and the increased rate of polymerization may be in part due to a more rapid breakdown of the initiator. It is probable that all phenols are potential retarders but in some cases the retarding influence is so weak that it is masked by another effect of the phenol, e.g. on the initiation process.

The measured retardation by hydroquinone at concentrations up to 0.2 *M* was less than 1%. Caldwell and Ihrig (2) observed a retardation of 13.7% with a 0.169 *M* solution of hydroquinone in methyl methacrylate. They show that the polymerization is extremely sensitive to traces of benzoquinone and it is probable that the retardation was due to the presence in their system of benzoquinone at a concentration of approximately 2×10^{-5} *M*.

The degree of polymerization of the polymethyl methacrylate was decreased only to a slight extent by the addition of phenols. Since the rate of polymerization is largely unaffected by phenols, transfer constants have been calculated using the simple transfer equation

$$\frac{1}{\overline{P}_n} = \frac{k}{k_p^2}\frac{R_p}{[M]^2} + C_X\frac{[X]}{[M]} + C_M,$$

where k is a function of the rate constants for termination by disproportionation and combination, k_p is the propagation rate constant, R_p is the rate of polymerization, X and M

Can. J. Chem. Downloaded from www.nrcresearchpress.com by 210.87.254.6 on 09/05/12
For personal use only.

represent phenol and monomer, and C_X and C_M are the transfer constants for phenol and monomer respectively. The constant k/k_p^2 was determined experimentally using solutions containing initiator and monomer only. C_M was determined from the variation of $\overline{P_n}$ with initiator concentration and was found to be approximately 5×10^{-6} at 45°; this compares with a value of 7×10^{-6} at 60° determined by O'Brien and Gornick (6). Transfer constants for a number of phenols are given in Table I. The reproducibility of the results suggests

TABLE I

Transfer constants of phenols in the polymerization of methyl methacrylate and styrene

Phenol	Transfer constant with methyl methacrylate (45°)	Transfer constant with styrene (60°)
4-Methoxyphenol	<0.0005	0.026
1-Naphthol	<0.0005	0.048
Catechol	<0.0005	0.134
4-*t*-Butylcatechol	0.0009	0.36
2,3,4,6-Tetramethylphenol	0.0011	0.058
Pyrogallol	0.0026	1.04
Hydroquinone	0.0007	—

a maximum error of 0.0005 in C_X but since the experimental values of C_X for deuterated phenols were in the range 0 to −0.0008, results calculated from the above equation may be lower than the true values. It is possible that all the transfer constants quoted should be increased by as much as 0.001; a similar conclusion was reached in the investigation of the effect of phenols on the polymerization of styrene (1).

The reactivities of phenols towards polymethyl methacrylate radicals are relatively low but the significant retardation of polymerization and decrease in degree of polymerization caused by 2,3,4,6-tetramethylphenol, 4-*t*-butylcatechol, and pyrogallol indicate that a transfer reaction between polymer radical and phenol can occur. The corresponding deuterated phenols do not retard the polymerization and their transfer constants are smaller than those of undeuterated phenols. The main transfer reaction must therefore involve the attack of a polymethyl methacrylate radical on a phenol molecule at the O—H group:

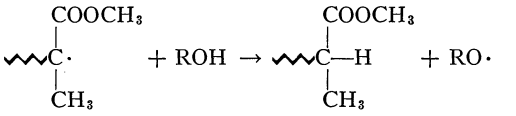

[1]

Caldwell and Ihrig (2) have interpreted their results on the polymerization of methyl methacrylate in the presence of hydroquinone in terms of a preliminary complex formation between the polymer radical and the phenol. If complex formation occurs with 2,3,4,6-tetramethylphenol, 4-*t*-butylcatechol, or pyrogallol, it does not prevent the observation of a significant isotope effect.

The phenoxy radicals formed in reaction [1] can either reinitiate polymerization or be lost by reaction with a polymethyl methacrylate or phenoxy radical. Analysis of the rate measurements by the method of Allen, Merrett, and Scanlan (7) indicates that with pyrogallol, for example, over half the phenoxy radicals reinitiate polymerization by reaction with monomer molecules. If however the pyrogallol causes a significant increase in rate of decomposition of the initiator, the efficiency of reinitiation may well be considerably less than 50%.

Can. J. Chem. Downloaded from www.nrcresearchpress.com by 210.87.254.6 on 09/05/12
For personal use only.

Table I shows a comparison of transfer constants of phenols in the polymerization of methyl methacrylate and styrene. The transfer constants with styrene were obtained at 60° while those for methyl methacrylate were obtained at 45°, but preliminary results indicate that transfer constants of phenols vary only slightly with temperature. The observation of a great difference in transfer activity is not confined to phenols as hydrogen donors. Walling has noted that whereas polymethyl methacrylate radicals have a higher reactivity than polystyryl radicals towards toluene, the reverse is true for the substrate 1-butanethiol (8). Both he and Bamford (9) conclude that the difference in relative reactivity has its origin in a polar effect. Bamford has shown that rate constants for abstraction reactions can be correlated by the equation

$$\log k_s - \log k_{3,T} = \alpha\sigma + \beta,$$

where k_s and $k_{3,T}$ are the rate constants for the reactions of a polymer radical with substrate and toluene respectively, σ is an estimated Hammett σ constant for the radical and α and β are constants for a given substrate. Approximate α values of -9.5 for pyrogallol and 4-*t*-butylcatechol and -6.5 for 2,3,4,6-tetramethylphenol are obtained if it is assumed that the transfer constants for phenols in methyl methacrylate are the same at 45° and 60°. These α values are unusually large and they indicate that the rate constants for hydrogen abstraction from phenols are strongly influenced by polar substituents in the radical. Phenols appear to belong to the same class of substrates as 1-butanethiol and ferric chloride, and Walling and Bamford suggest that the high reactivity of polystyryl radicals towards these substrates is due to contributions to the transition state of polar structures involving donation of an electron from the radical to the substrate. Electron-attracting groups in the radical impede electron donation, and the relatively low reactivity of polymethyl methacrylate radicals towards phenols can therefore be ascribed to smaller contributions of polar structures to the transition state.

Transfer Reaction with Thiols

Transfer constants for a number of aromatic thiols in the polymerization of methyl methacrylate at 45° are given in Table II. The main attack of the polymer radical occurs

TABLE II

Transfer constants of thiols in the polymerization of methyl methacrylate

Thiol	Transfer constant (45°)	Thiol	Transfer constant (45°)
Benzenethiol	4.7	4-Methylbenzenethiol	7.4
3-Methylbenzenethiol	4.7	4-Chlorobenzenethiol	4.6
3-Chlorobenzenethiol	3.5	4-Bromobenzenethiol	5.6
3-Bromobenzenethiol	3.8	4-Acetylbenzenethiol	2.6
3-Acetylbenzenethiol	4.2	2-Naphthalenethiol	6.3

at the S—H group as is shown by the considerable decrease in transfer constant when deuterated thiols are used as substrates. Ratios of the transfer constants for deuterated and undeuterated 4-chlorobenzenethiol and 2-naphthalenethiol are 0.41 ± 0.1 and 0.33 ± 0.1 respectively. Wall and Brown (10) obtained a value of 0.25 for the ratio of transfer constants in the reaction of polystyryl radicals with 1-butanethiol at 60°. The observed isotope effects are smaller than those predicted by simple theory (11) but such a result is often observed when processes with low activation energies are involved.

Can. J. Chem. Downloaded from www.nrcresearchpress.com by 210.87.254.6 on 09/05/12
For personal use only.

The polymerization is only slightly retarded by the thiols, the maximum observed retardation being 15% with 2-naphthalenethiol and 4-methylbenzenethiol at a concentration of 0.001 *M*. The simple transfer equation has been used in the calculation of transfer constants because the correction for retardation is small and requires a knowledge of the fate of the thiol radicals in the termination reaction (1). A correction in the opposite direction of approximately equal magnitude due to loss of thiol during the first 3% polymerization has also been omitted. The overall error in the transfer constants from these causes is less than 5%. The extent of retardation can be used to estimate the efficiency of reinitiation of polymerization by the thiol radicals (7) assuming that the thiols have no effect on the rate of decomposition of the initiator. Approximately 95% of the 2-naphthalenethiol radicals reinitiate polymerization at a thiol concentration of 0.001 *M*, and the efficiencies with other thiol radicals are greater.

The transfer constants for the meta-substituted thiols yield a Hammett ρ value of -0.23 ± 0.1. This is a measure of the extent to which the inductive contribution of a substituent affects the reactivity of a thiol with polymethyl methacrylate radicals (12). The value is only about 10% of that for the ionic dissociation of the corresponding thiols in 48.9% ethanol (13) and is of opposite sign, and it is clear that inductive effects are of only minor importance. The negative Hammett ρ value suggests that there is a weak contribution to the transition state by polar structures in which the thiol is now the electron donor and the polymethyl methacrylate radical is the acceptor. Substituents such as methyl and bromo, which release charge by resonance interaction, favor polar contributions to the transition state when in the para position; 4-methyl and 4-bromobenzenethiol are thus slightly more reactive than the corresponding meta-substituted thiols. The reverse is true for the acetyl substituent which withdraws charge by resonance interaction, and 4-acetylbenzenethiol has a lower transfer constant than 3-acetylbenzenethiol.

A rough estimate of the difference between the activation energies of the transfer and propagation steps can be obtained by comparing the result of O'Brien and Gornick for the transfer constant of benzenethiol at 60° (6) with the present result of 45°. The result at 60° may be low because of the relatively high conversions used but it is probable that the activation energy for the transfer reaction is at least 2 kcal/mole smaller than that for the propagation reaction. Assuming an activation energy of 6.3 kcal/mole for the propagation reaction (14) the activation energy for the abstraction of a hydrogen atom by a polymethyl methacrylate radical from benzenethiol is estimated to be less than 4.3 kcal/mole.

ACKNOWLEDGMENTS

The authors are grateful to the National Research Council for a grant and a bursary, and to Queen's University for a Milton Hersey Fellowship.

REFERENCES

1. M. P. Godsay, G. A. Harpell, and K. E. Russell. J. Polymer Sci. **57**, 641 (1962).
2. R. G. Caldwell and J. L. Ihrig. J. Polymer Sci. **46**, 507 (1960).
3. F. G. Bordwell and H. M. Anderson. J. Am. Chem. Soc. **75**, 6019 (1953).
4. J. A. Howard and K. U. Ingold. Can. J. Chem. **40**, 1851 (1962).
5. B. Baysal and A. V. Tobolsky. J. Polymer Sci. **8**, 529 (1952).
6. J. L. O'Brien and F. Gornick. J. Am. Chem. Soc. **77**, 4757 (1955).
7. P. W. Allen, F. M. Merrett, and J. Scanlan. Trans. Faraday Soc. **51**, 95 (1955).
8. C. Walling. Free radicals in solution. John Wiley and Sons, New York. 1957. p. 157.
9. C. H. Bamford, A. D. Jenkins, and R. Johnston. Trans. Faraday Soc. **55**, 418 (1959).

Can. J. Chem. Downloaded from www.nrcresearchpress.com by 210.87.254.6 on 09/05/12
For personal use only.

10. L. A. WALL and D. W. BROWN. J. Polymer Sci. **14**, 513 (1954).
11. L. MELANDER. Isotope effects on reaction rates. Ronald Press, New York. 1960. p. 20.
12. R. W. TAFT, JR. and I. C. LEWIS. J. Am. Chem. Soc. **81**, 5343 (1959). R. W. TAFT, JR. J. Phys. Chem. **64**, 1805 (1960).
13. G. SCHWARZENBACH and E. RUDIN. Helv. Chim. Acta, **22**, 360 (1939). H. H. JAFFÉ. Chem. Rev. **53**, 191 (1953).
14. M. S. MATHESON, E. E. AUER, E. B. BEVILACQUA, and E. J. HART. J. Am. Chem. Soc. **71**, 497 (1949).

Can. J. Chem. Downloaded from www.nrcresearchpress.com by 210.87.254.6 on 09/05/12
For personal use only.

GLYCOSIDATION OF SUGARS

II. METHANOLYSIS OF D-XYLOSE, D-ARABINOSE, D-LYXOSE, AND D-RIBOSE[1]

C. T. BISHOP AND F. P. COOPER

Division of Applied Biology, National Research Council of Canada, Ottawa

Received April 30, 1963

ABSTRACT

Rates of methanolysis reactions of D-xylose, D-arabinose, D-lyxose, and D-ribose have been determined. It was found that methanolysis of a pentose proceeds to equilibrium through four distinguishable, competing reactions: (1) pentose → furanosides; (2) anomerization of furanosides; (3) furanosides → pyranosides; (4) anomerization of pyranosides. The glycoside compositions at equilibrium are interpreted in terms of stabilities of each of the four glycosides from each sugar as influenced by steric and ionic effects; a system of conformational analysis of furanoside rings is presented. The free energies of reaction in anomerization of pyranosides were in excellent agreement with values calculated from previously reported interaction energies in the pyranoid ring. The relative rates of the reactions were consistent with the view that non-bonded interactions in the methyl glycosides are relieved in the transition states for their interconversions.

Can. J. Chem. Downloaded from www.nrcresearchpress.com by 210.87.254.42 on 09/05/12
For personal use only.

The first paper (1) in this series described a study of the reactions of D-xylose in methanolic hydrogen chloride; the four methyl D-xylosides, products of the reaction, were analyzed at different times by gas–liquid chromatography of their fully methylated derivatives. The resulting rate data showed that four reactions could be distinguished: (1) xylose → methyl furanosides, (2) anomerization of furanosides, (3) furanosides → pyranosides, (4) anomerization of pyranosides; a tentative mechanism was proposed.

The present paper describes an extension of this work to the other pentoses, D-arabinose, D-lyxose, and D-ribose; some of the reactions in the D-xylose series were repeated to obtain comparable data. It is shown that the methanolysis of each pentose proceeds via the reactions given above. The equilibrium compositions can be interpreted in terms of relative stabilities of each of the four glycosides from each sugar and the relative reaction rates indicated that non-bonded interactions in the methyl glycosides are relieved in the transition states for their interconversions.

The conditions cited for the reactions were carefully controlled and products in the D-xylose and D-arabinose series were analyzed by gas–liquid chromatography of their fully methylated derivatives as described previously (1). Reaction products in the D-lyxose and D-ribose series were analyzed by gas–liquid chromatography of their fully acetylated derivatives because of the better separations obtained. The rate at which reducing sugar disappeared was measured by gas–liquid chromatography of the acetylated reaction mixture; the pentopyranose tetraacetates, arising from the reducing sugars, were widely separated from the methyl tri-*O*-acetyl pentosides. Separation of individual methyl tri-*O*-acetyl pentosides in this procedure, although not always complete, was sufficient to provide information about the early products of reaction. The use of acetylation avoided the correction required (1) when the methylation procedure was used on reaction mixtures in which reducing sugars were present. The retention volumes (R_v) in Tables I and II illustrate the separations pertinent to this work. The R_v values of derivatives from a single pentose are made relative to the fastest moving component ($R_v = 1.00$) in that series and are not related to the values in another pentose series. For example, the R_v values for the methyl tri-*O*-methyl-D-xylosides are related only to each other.

[1]*Issued as N.R.C. No. 7542.*

TABLE I

Retention volumes of methyl tri-*O*-methyl-D-pentosides[a]

	D-Xylose	D-Arabinose		D-Xylose	D-Arabinose
α-Furanoside	1.95	1.00	α-Pyranoside	1.40	2.26
β-Furanoside	1.60	1.31	β-Pyranoside	1.00	2.10

[a]Gas–liquid chromatography on column (4 ft×4 mm) of 10% Carbowax 6000 on Gas-Chrom A, 100–120 mesh; 125° C; 100 ml argon/min. Methyl tri-*O*-methyl-D-ribosides not resolved completely.

TABLE II

Retention volumes of methyl tri-*O*-acetyl-D-pentosides and pentopyranose tetraacetates

	D-Xylose[a]	D-Ribose[a]	D-Lyxose[b]
α-Furanoside	1.24	1.00	1.57
β-Furanoside	1.00	1.32	1.28[c]
α-Pyranoside	1.33	1.08	1.00
β-Pyranoside	1.33	1.48	1.13
Tetraacetates (α, β)	2.67, 2.89	3.35, 3.73	2.47, 3.19

[a]Gas–liquid chromatography on column (8 ft×4 mm) of 13% OF-1-0065 on Chromosorb W, 100–120 mesh (packing prepared by Applied Science Laboratories, State College, Pennsylvania, U.S.A.); 200° C; 80 ml helium/min. Separation of D-arabinose derivatives not attempted.
[b]Column (4 ft×4 mm) of 10% ethylene glycol isophthalate polyester on Gas-Chrom Z, 100–120 mesh; 195° C; 60 ml argon/min.
[c]Identified by inference as the only peak not corresponding to one from an authentic sample.

Methanolysis of a sugar proceeds to equilibrium through four distinguishable, competing reactions and a unified kinetic treatment of the complete process is therefore very complicated. However, it has been possible to establish conditions under which a single reaction predominated. Since the observations were made at constant hydrogen ion concentrations the bimolecular reaction could be expressed in terms of first-order rate kinetics. Compositions of reaction products at different times under specific conditions are given in Tables VIII–XI (see Experimental). Inspection of these results shows that a single reaction was predominant during the early periods and was characterized reasonably well by a first-order rate constant. Minor variations in these rate constants for the initial reactions were probably within experimental error. At later stages deviations from first-order kinetics became noticeable and analysis of the products showed that other reactions were occurring to a significant extent. The rate constants indicated in Table VIII–XI were averaged to give the k_1 values in Table III. To give measurable rates reactions 3 and 4 required 10 and 100 times respectively the concentration of hydrogen chloride used for reactions 1 and 2. No Hammett acidity functions have been reported for the methanol – hydrogen chloride system but it had been found (1) that the rates of all methanolysis reactions of D-xylose were approximately proportional to the acid concentrations. The average first-order rates for reactions 3 (Table X) and 4 (Table XI) were therefore reduced to 1/10 and 1/100 respectively to provide comparable k_1 values (Table III) all relative to 0.01% of hydrogen chloride in methanol. This undoubtedly introduced inaccuracies as far as absolute values were concerned; however, the relative orders of reactivity, of major interest in this work, were probably not disturbed. The equilibrium constants (K) in Table III were obtained from glycoside compositions after prolonged reaction periods (Table V) and the k_2 values were calculated from k_1 and K.

Non-bonded interactions impose certain conformations upon molecules and the principles of conformational analysis have been of considerable assistance in interpreting the physical and chemical properties of the pyranoid sugars (2–5). Although Kilpatrick *et al.*

Can. J. Chem. Downloaded from www.nrcresearchpress.com by 210.87.254.42 on 09/05/12
For personal use only.

Can. J. Chem. Downloaded from www.nrcresearchpress.com by 210.87.254.42 on 09/05/12
For personal use only.

TABLE III

Rate constants of methanolysis reactions[a]

Reaction	D-Xylose				D-Arabinose				D-Lyxose				D-Ribose			
	k_1	k_2	k_1+k_2	K	k_1	k_2	k_1+k_2	K	k_1	k_2	k_1+k_2	K	k_1	k_2	k_1+k_2	K
1. Pentose $\xrightarrow{k_1}$ furanosides	57	—	—	—	—	—	—	—	19	—	—	—	226	—	—	—
2. Furanoside: $\alpha \underset{k_2}{\overset{k_1}{\rightleftarrows}} \beta$	49	29	78	1.69	1.39	4.35	5.74	0.32	Very small	Very large	—	—	11.3	3.4	15.2	3.3
3. Furanosides $\underset{k_2}{\overset{k_1}{\rightleftarrows}}$ pyranosides	0.12	0.0004	—	320	0.088	0.011	—	7.9	0.84	0.001	—	650	0.069	0.008	—	8.8
4. Pyranoside: $\beta \underset{k_2}{\overset{k_1}{\rightleftarrows}} \alpha$	0.031	0.014	0.04	2.2	0.093	0.18	0.27	0.52	0.62	0.072	0.64	8.6	0.02	0.11	0.13	0.176

[a]Reaction 2: $K = [\beta]/[\alpha]$; reaction 3: $K = [\alpha\text{-pyr}][\beta\text{-pyr}]/[\alpha\text{-fur}][\beta\text{-fur}]$; reaction 4: $K = [\alpha]/[\beta]$. Concentrations of products for these calculations were taken from the equilibrium values given in Table V.

(6) showed in 1947 that the cyclopentane ring is puckered, the furanoid sugars have been regarded as essentially planar molecules. However, the fructofuranosyl portion of crystalline sucrose (7) and the ribofuranosyl moiety of crystalline cytidine (8) were both found to have non-planar ring structures. More recently specific conformations, based upon nuclear magnetic resonance spectroscopy, have been proposed for D-ribofuranose in purine and pyrimidine nucleosides (9), in thymidine (10), in certain deoxyribonucleosides (11) and nucleotides (12), and in 1,3,5-tri-*O*-benzoyl-α-D-ribofuranose, methyl 2,3-anhydro-α-D-ribofuranoside, and its β-anomer (13). A specific conformation has also been proposed for a furanose ring having a cis-fused *O*-isopropylidene ring (14). However, no system of conformational analysis has been proposed for furanose sugars that permits the prediction of a preferred conformation and accounts for the chemical properties of the compounds concerned. The system shown in Fig. 1 was derived from a consideration of the non-bonded interactions which should be operative in these molecules.

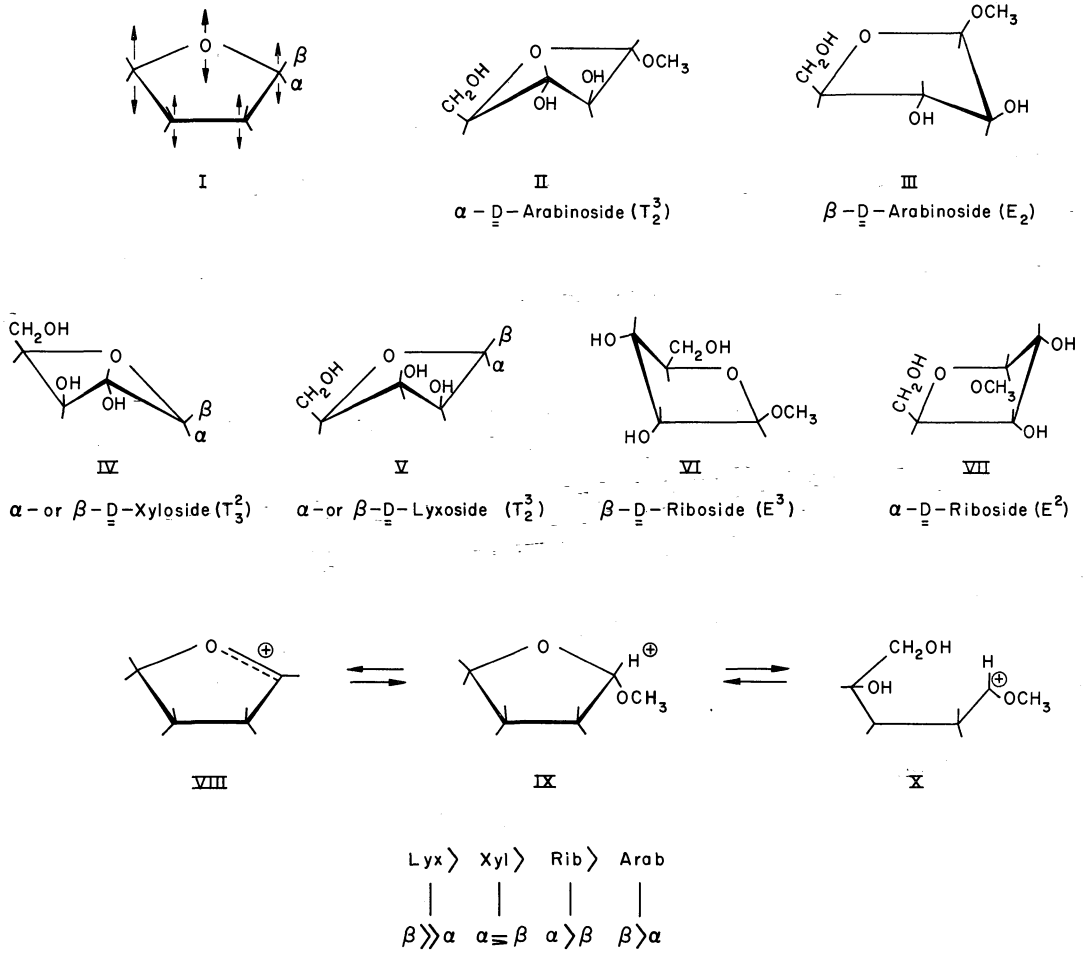

FIG. 1.

The strain inherent in a five-membered ring, cyclopentane or furanoid (I), can be relieved by a slight puckering brought about by movement of one or two atoms out of the plane of

Can. J. Chem. Downloaded from www.nrcresearchpress.com by 210.87.254.42 on 09/05/12
For personal use only.

the ring. For cyclopentane, in which all atoms are equivalent, this results in two possible conformations (6): (*a*) the C_s conformation in which a single atom is displaced from the plane of the other four, (*b*) the C_2 conformation in which two atoms are displaced, one above and the other below the plane of the remaining three adjacent atoms. In the furanoid sugars a more definitive designation of conformation is required because of the specific stereochemistry of the carbon atoms in the ring. Jardetzky (12) used a system for the ribofuranose ring in which the carbon atoms displaced from the plane were designated by number and the direction of displacement was related to the orientation of the C_4—C_5 bond by the terms *endo-* or *exo-*. Hall (13) has proposed a system in which the conformation with four atoms coplanar is designated by E (envelope), that with three atoms coplanar by T (twist). The atoms out of plane can then be indicated as subscripts or superscripts to show respectively displacement below or above the plane of reference; carbon atoms are given as numbers, the ring oxygen by "o". This system is simple, fully descriptive, adaptable to general use, and will be used in the present publication.

In the furanoside ring the effective interactions are those between eclipsed groups on adjacent carbon atoms and the most favored conformations will allow maximum staggering. Conformations with C_1, C_4, or O displaced have a fully or nearly fully eclipsed pair of carbon atoms and should be less stable than those in which C_2 or C_3 or both are displaced from the plane. Methyl α-D-arabinofuranoside (II) has all of its large substituents in trans orientation and the strain in the ring can therefore be relieved by the maximum staggering afforded by a T_2^3 or T_3^2 conformation. In methyl β-D-arabinofuranoside (III) there is an eclipsed interaction between the C_1- and C_2-substituents which should force them away from each other, giving an E_2 conformation. The methyl-D-xylofuranosides have large eclipsed groups at C_3 and C_4 with the bulky hydroxymethyl group at C_4 contributing to a greater repulsive force. The net result of the deformation in which the hydroxymethyl group forces the C_3-hydroxyl down and away will be that C_2 is pushed up, giving the conformation T_3^2 (IV). An important consequence of this conformation is that the C_2-hydroxyl is oriented in an almost ideal skew position with respect to the anomeric substituents and is only slightly closer to the C_1-α than the C_1-β bond angle in a projection along the C_2—C_1 bond. A possible alternate conformation for the methyl β-D-xylofuranoside is E_3. The methyl-D-lyxofuranosides have eclipsed interactions between C_2–C_3 and C_3–C_4 substituents. The molecule should therefore adopt a T_2^3 conformation V which provides for the maximum distance between the *O*-substituents within an ideally staggered form. An alternative for the methyl α-D-lyxofuranoside could be E_3. The interaction between the C_2- and C_3-hydroxyls in the methyl-D-ribofuranosides should result in an E^3 conformation (VI) or its equivalent E^2. The latter should be preferred for the methyl α-D-ribofuranoside (VII) because it would also relieve the interaction between the C_2-hydroxyl and the anomeric substituent. Table IV contains the preferred conformations for the methyl pentofuranosides and the hydroxyl interactions in each compound. On present evidence it is impossible to decide between alternative conformations for a single furanoside.

Analyses of products showed that furanosides were the first compounds formed in the methanolysis of a pentose (Table VIII). This reaction must be regarded as essentially irreversible because of the large excess of methanol present. The quantitative data obtained for three of the sugars showed that higher k_1 values for this reaction were associated with higher furanoside concentrations at equilibrium (Table V). The k_1 for D-arabinose in reaction 1 could not be measured because of the low solubility of that sugar in methanol. However, D-arabinose showed the largest amount of furanoside at equilibrium

Can. J. Chem. Downloaded from www.nrcresearchpress.com by 210.87.254.42 on 09/05/12
For personal use only.

TABLE IV
Preferred conformations of methyl pentofuranosides

Methyl-D-pentofuranoside		Conformation	Hydroxyl interactions (total)	
Arabinoside	α	T_2^3 T_3^2	—	0
	β	E_2	C_1–C_2	(1)
Riboside	β	E^3	C_2–C_3	(1)
	α	E^2	C_1–C_2, C_2–C_3	(2)
Xyloside	α	T_3^2	C_3–C_4	(1)
	β	T_3^2 (E_3)	C_3–C_4	(1)
Lyxoside	α	T_2^3 (E_3)	C_2–C_3, C_3–C_4	(2)
	β	T_2^3	C_1–C_2, C_2–C_3, C_3–C_4	(3)

and should have the largest k_1 based on the correlation observed for the other three sugars. The relative rates in reaction 1 therefore reflected the relative stabilities of the pentofuranosides. In reactions 2, 3, and 4 the rate-controlling steps may be assumed to be the formation of ionic intermediates; since the anomerization of furanosides (reaction 2) and the furanoside to pyranoside conversion (reaction 3) proceed from the same initial products at different rates it is likely, although not proved, that the reaction routes are different. Possible intermediates for the furanoside anomerization (VIII) and for the furanoside to pyranoside conversion (X), both arising from the protonated furanoside (IX), are shown in Fig. 1. The non-bonded interactions between large eclipsed groups in the furanosides (II–VII) will be relieved in X by the opening of the ring. These same interactions will be relieved in VIII if it has a puckered form with C_3 being above or below the plane of the other four atoms. Thus, in VIII, dissociation at C_1 removes any interaction between C_1- and C_2-substituents and displacement of C_3 in an E_3 or E^3 conformation relieves interactions between substituents on that carbon atom and those on C_2 and C_4. The relative orders of reactivity for the four pentoses should therefore be the same for reactions 2 and 3 and should depend on the strength and number of eclipsed interactions in the furanosides. The same argument holds if reactions 2 and 3 proceed through a common intermediate which decomposes at different rates into furanoside and pyranoside. The order predicted from the proposed furanoside conformations is given in Fig. 1. The experimental values confirm this prediction. Thus, the lyxofuranosides, with two adjacent eclipsed interactions, should be the most reactive furanosides (see k_1 values, reaction 3). The xylofuranosides, also with only one eclipsed interaction, should be less reactive than the lyxofuranosides but more reactive than the ribofuranosides because the C_3–C_4 eclipsed interaction involving the hydroxymethyl group is stronger than the C_2–C_3 eclipsed interaction. The arabinofuranosides are free of eclipsed interactions, except at the anomeric position in the β-glycoside, and therefore should be the least strained and slowest reacting of the pentofuranosides.

A similar prediction of the reactivities of the anomeric forms in reaction 2 is shown in Fig. 1 and this was also in complete agreement with the experimentally determined rates (see k_1 and k_2, reaction 2). Starting with the most reactive pentose, the methyl β-D-lyxofuranoside should anomerize at a much faster rate than the α-anomer because of the extra interaction at C_1–C_2. In fact, no methyl β-D-lyxofuranoside could be detected in any of the reactions and the rate of reaction 2 for lyxose could not be determined experimentally. It is apparent, then, that k_1 for this reaction must be smaller and k_2 larger than any of the other rate constants in Table III. In the methyl-D-xylofuranosides (IV) the C_2-hydroxyl bond very nearly bisects the angle made by the bonds of the anomeric substituents being

Can. J. Chem. Downloaded from www.nrcresearchpress.com by 210.87.254.42 on 09/05/12
For personal use only.

oriented slightly more toward the α- than the β-position. This accounts for the slightly greater (1.69 times) rate of anomerization of the α-form. In the D-ribofuranosides the α-glycoside has one more eclipsed interaction than the β- and should therefore be more reactive; for the same reason methyl β-D-arabinofuranoside should anomerize at a faster rate than its α-anomer. It is noteworthy that the one additional eclipsed interaction causes a 3-fold increase in the rate of anomerization in both the ribofuranosides and the arabinofuranosides. Another comparison which substantiates the predicted behavior of these compounds is the approximately equal rates of anomerization of methyl β-D-arabinofuranoside and methyl β-D-ribofuranoside, each having one eclipsed interaction in an envelope (E) conformation. This indicates that the eclipsed interactions at C_1–C_2 and at C_2–C_3 are of nearly the same strength. The rates for reaction 2 are greater than those for reaction 3 for each pentose. It should be emphasized that VIII and X are given only as possible intermediates for reactions 2 and 3 respectively. They are offered primarily to illustrate that any intermediate considered must be of a form that permits relief of the non-bonded interactions in the methyl pentofuranosides.

The differences in rates of pyranoside anomerization (reaction 4) can be explained by principles that are already familiar (2–5). If the pyranoside anomerization proceeds through a cyclic, half-chair carbonium ion, as postulated earlier for the xylopyranosides (1), the conformational changes shown in Fig. 2 must be involved (15). Formation of the

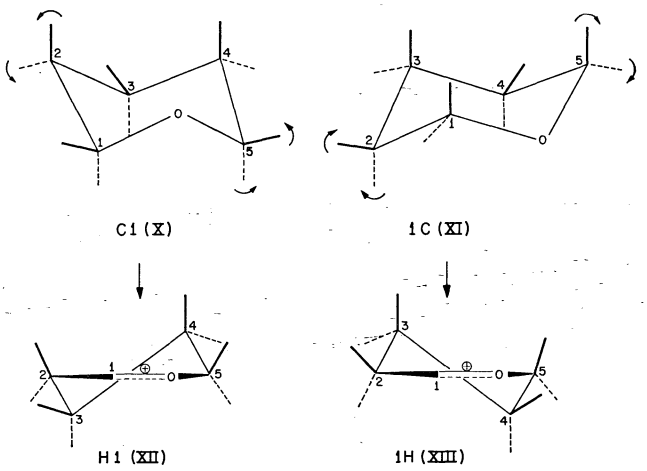

FIG. 2.

H1 (XII) or 1H (XIII) (4) carbonium ions from the C1 (X) or 1C (XI) chair forms (2) respectively requires rotation about the C_2—C_3 and C_4—C_5 bonds as shown. This will be hindered by increased opposition of C_2–C_3 substituents and of C_4—C_5 substituents but these will be of the same magnitude for all pentosides. However, the change will be helped by recession of an axial group on C_2 away from one on C_4 and by the recession of the C_5-axial group from that on C_3. The preferred conformations of the pentopyranosides (2) are shown in Fig. 3 together with the predicted order of reactivity. The xylosides, with no axial substituents, should anomerize at the slowest rate; the ribosides and arabinosides, each with one axial hydroxyl, should anomerize more rapidly than the xylosides but more slowly than the lyxosides, which have either two axial hydroxyls (1C conformation) or one axial hydroxyl and Reeves' $\Delta 2$ effect (2) (axial hydroxyl at C_2 bisects the

Can. J. Chem. Downloaded from www.nrcresearchpress.com by 210.87.254.42 on 09/05/12
For personal use only.

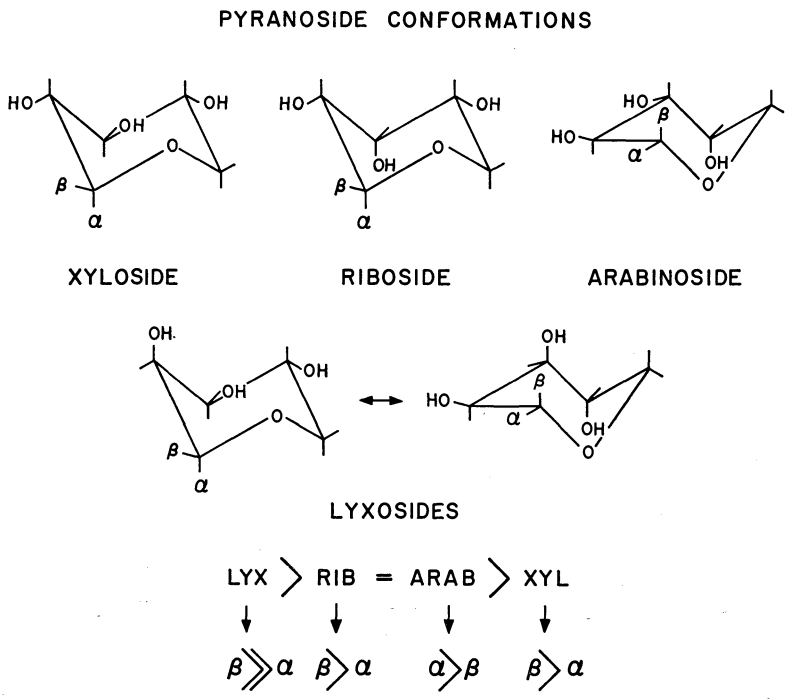

FIG. 3.

angle of the two C—O bonds at C_1). The rates in Table III (k_1+k_2, reaction 4) agree with this interpretation. The ribosides anomerize more slowly than the arabinosides because formation of the H_1 carbonium ion from the former causes increased eclipsing of the hydroxyls on C_2 and C_3.

The relative rates of anomerization of the anomeric pairs can be explained by principles enunciated by Edward (15). The unshared pair of electrons on the ring oxygen of the pyranosides impart a polar character to the C_5-ring oxygen bond and the negative end of this dipole is oriented so that the electrostatic repulsive forces with the C_1-*O*-substituent are stronger when that substituent is equatorially oriented. Those anomers should therefore be less stable and should display a faster rate of reaction; the predicted order of reactivity of anomeric pairs is given in Fig. 3. The k_1 and k_2 values for each pentopyranoside in reaction 4, Table III, confirm the prediction for the anomeric lyxopyranosides, arabinopyranosides, and xylopyranosides. The difference in rate between anomers is greater for the lyxopyranosides because of the additional repulsive force applied to the β-anomer by the axial hydroxyl at C_2. The anomeric ribopyranosides showed reactivities which were the reverse of those predicted on the basis of dipole interaction. Probably the axial–axial interaction between the C_3-hydroxyl and the C_1-α-substituent of anomeric ribopyranosides is stronger than the dipole interaction at the β-position and results in greater reactivity of the α-anomer.

Table V shows the glycoside compositions at equilibrium of the four pentoses and of some *O*-methyl derivatives of D-xylose and D-arabinose. Substitution of the C_2- and C_3-hydroxyl groups in D-xylose or D-arabinose by *O*-methyl groups greatly increased the concentrations of furanoside forms at equilibrium. This can be explained by considering the projections (Fig. 4) of the C_2—C_3 bond with trans *O*-substituents for pyranoside and

Can. J. Chem. Downloaded from www.nrcresearchpress.com by 210.87.254.42 on 09/05/12
For personal use only.

TABLE V

Glycoside compositions at equilibrium[a]

Sugar	α-Furanoside	α+β	β-Furanoside	α-Pyranoside	α+β	β-Pyranoside
D-Xylose	1.9		3.2	65.1		29.8
3-*O*-Methyl-D-xylose		9.0			91.0	
2-*O*-Methyl-D-xylose		12.8			87.2	
2,3-Di-*O*-methyl-D-xylose		16.4			83.6	
D-Arabinose	21.5		6.8	24.5		47.2
3-*O*-Methyl-D-arabinose		50.7			49.3	
2-*O*-Methyl-D-arabinose		66.7			33.3	
2,3-Di-*O*-methyl-D-arabinose		75.4			24.6	
D-Lyxose	1.4		Not detected	88.3		10.3
D-Ribose	5.2		17.4	11.6		65.8

[a]Sugar (2%) in 1% methanolic hydrogen chloride at 35° C.

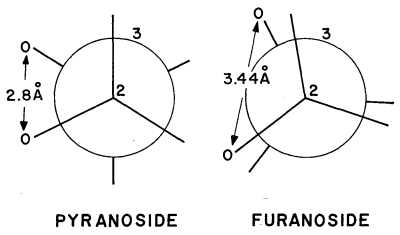

FIG. 4.

furanoside ring forms. Equatorial–equatorial *O*-substituents at C_2 and C_3 in the pyranoside ring are 2.8 Å apart while trans *O*-substituents on a furanoside ring are 3.44 Å apart. An increase in the size of the *O*-substituents will therefore result in a stronger repulsive interaction in the pyranoside than in the furanoside form and the equilibrium will be shifted toward the latter.

The free energies (Table VI) calculated from the equilibrium constants reflect the relative stabilities of the compounds concerned. In the conformation T_3^2 proposed for the

TABLE VI

Free energies for methanolyses of pentoses

	Δ*F* (reaction) (cal/mole)		Δ*F* (reaction) (cal/mole)
Xylose		Lyxose	
α-Furanoside ⇄ β-furanoside	− 320	α-Furanoside ⇄ β-furanoside	Very large
Furanoside ⇄ pyranoside	−3530	Furanoside ⇄ pryanoside	−4080
α-Pyranoside ⇄ β-pyranoside	480	α-Pyranoside ⇄ β-pyranoside	1310
Arabinose		Ribose	
α-Furanoside ⇄ β-furanoside	695	α-Furanoside ⇄ β-furanoside	− 740
Furanoside ⇄ pyranoside	−1260	Furanoside ⇄ pyranoside	−1330
α-Pyranoside ⇄ β-pyranoside	− 400	α-Pyranoside ⇄ β-pyranoside	−1060

xylofuranosides anomerization involves the substitution of one skew orientation for another and no strong interactions. The small Δ*F* for this reaction is consistent with this proposal. Anomerization of arabinofuranosides and of ribofuranosides introduces or removes an eclipsed interaction between the C_1- and C_2-*O*-substituents which can be relieved somewhat because the ring is free to adopt a less strained conformation. The Δ*F* of reaction for these two anomerizations should therefore be nearly the same, greater

Can. J. Chem. Downloaded from www.nrcresearchpress.com by 210.87.254.42 on 09/05/12
For personal use only.

Can. J. Chem. Downloaded from www.nrcresearchpress.com by 210.87.254.42 on 09/05/12
For personal use only.

than for the xylofuranoside anomerization, but less than that of the lyxofuranosides where the C_1–C_2 interaction in the β-anomer cannot be relieved because of the fixed conformation imposed by the other interactions in the ring.

The ΔF of reactions for the furanoside to pyranoside conversions reflect the relative stabilities of the two ring forms in these sugars. In arabinose and ribose the furanoside forms have only one or two easily relieved cis interactions while the pyranoside forms each have an axial hydroxyl group. The ΔF for the ring conversions is therefore less for these two pentoses than for xylose or lyxose because the former has the best possible conformation in the pyranoside form and the latter has the worst possible furanoside conformation.

Similarly, the energy differences between the anomeric pyranosides of xylose and arabinose are very nearly the same; this indicates that the axial C_4-hydroxyl of arabinose has little effect on the relative stabilities of the two anomers. In lyxose and ribose the differences between the anomeric pyranosides are larger than for xylose or arabinose. These larger differences were undoubtedly caused by increased repulsions at the β-anomeric position in lyxose by the axial C_2-hydroxyl and at the α-anomeric position in ribose by the axial C_3-hydroxyl.

Angyal (16) has proposed a system of quantitative conformational analysis for the pyranoid sugars based on interaction energies derived from the equilibrium reactions of cyclitols (17, 18) and the anomeric equilibria of glucopyranose and mannopyranose (19). A similar system was given for acetylated sugars by Lemieux and Chu (20). Total interaction energies for the pyranoid pentoses in the two chair forms are shown in Table VII and were calculated from the following values in kcal/mole: O_1:O_2 = 0.50 (skew

TABLE VII

Interaction energies (kcal/mole) in pyranoid pentoses

	α		β		$\Delta F\ \alpha \rightleftarrows \beta$	
	C1	1C	C1	1C	Calc.[a]	Found
Lyxose	2.2	3.4	3.5	4.3	1.3	1.31
Xylose	2.3	5.0	2.7	5.0	−0.4	−0.48
Arabinose	3.8	3.1	3.8	2.7	−0.4	−0.40
Ribose	4.4	5.2	3.5	3.9	−0.9	−1.06

[a]For the more stable chair forms.

interaction between *O*-substituents on adjacent carbon atoms): O_a:H_a = 0.40 (axial–axial interaction between a hydrogen and an *O*-substituent); O_a:O_a = 2.1 (interaction between two axial *O*-substituents); $\Delta 2$ effect (2) = 0.40 (interaction of axial *O*-substituent at C_2 on equatorial anomer); anomeric effect (15, 21) = 1.20 (interaction of C_5-ring oxygen dipole on equatorial anomer). These values have been reported by Angyal *et al.* (17–19) for aqueous systems and agree substantially with those given by Lemieux and Chu (20) for acetates in an acetic acid – acetic anhydride system. The value for the anomeric effect has been given as 1.45 kcal/mole for methyl glycosides (19) and as 1.3–1.5 kcal/mole for different aglycons in sugar acetates (21). We have found that a value of 1.20 kcal/mole for the anomeric effect gave calculated differences in free energy between anomers that were in excellent agreement (see Table VII) with those found from the glycoside compositions at equilibrium.

The results of the present work are in general support of the sequence of reactions and the mechanism proposed earlier for the methanolysis of D-xylose (1). Only for D-lyxose

was there any evidence for pyranosides being formed early in the reaction (Table VIII. C). It is possible that lyxopyranosides were formed directly from the free sugar as has been proposed by Mowery (22) for D-mannose and L-arabinose. The highly unfavorable conformations of the furanoside forms of lyxose and mannose would be expected to favor the direct formation of some pyranosides from the free sugars. The only example of the reverse reaction, furanoside → pentose, occurred in the D-lyxose series with methyl α-D-lyxofuranoside as the initial compound (see Table X.C), a further indication of the instability of the furanoside forms of this pentose. Although rate data could not be obtained for the reaction of D-arabinose, qualitative examination of the early products of reaction showed that only arabinofuranosides were present.

The present results are also consistent with the proposed mechanisms for the anomerizations of furanosides and pyranosides for which two different cyclic carbonium ion intermediates were postulated. However, the mechanism tentatively proposed earlier for the furanoside → pyranoside ring expansion in D-xylose, which has been criticized (23), must still be regarded as an open question. Further work on this aspect of glycosidation is in progress.

EXPERIMENTAL

Reagents

Sugars were purified products obtained from commercial sources; no impurities were detected by paper chromatography. Methanol was reagent grade and was distilled from magnesium–iodine immediately before use. Hydrogen chloride was dried by passage through calcium chloride.

Apparatus

An F and M Model 500 Chromatograph or a Pye Argon Chromatograph were employed for gas–liquid partition chromatography. Conditions used are cited in Tables I and II.

Preparation of Methyl Pentosides

Methyl pentosides were prepared by methods described in the literature. The physical properties of these compounds and the reported values were as follows:

	Found		Reported		
	m.p. (°C)	$[\alpha]_D$	m.p. (°C)	$[\alpha]_D$	Ref.
Methyl α-D-xylofuranoside	83–84	+181°	84	+182°	24
Methyl β-D-xylofuranoside	Sirup	− 80°	45	− 89.5°	24
Methyl α-D-xylopyranoside	89–91	+151°	91–92	+153.9°	25
Methyl β-D-xylopyranoside	155.5–156.5	− 65°	156–157	− 65.5°	26
Methyl α-D-ribofuranoside	Sirup	+146°	Sirup	+146.8°	27
Methyl β-D-ribofuranoside	80	− 63°	80 (ref. 28)	− 62.4°	27
Methyl α-D-ribopyranoside	25	+103°	Sirup	+103.3°	27
Methyl β-D-ribopyranoside	83–84	−105°	83	−105.0°	29
Methyl α-D-arabinofuranoside	64–66	+123°	65–67	+123°	24, 30
Methyl β-D-arabinofuranoside	56	−117°	56–57	−119°	24
Methyl α-D-arabinopyranoside	131	− 17°	131	+ 17.3°	31[a]
Methyl β-D-arabinopyranoside	169	−242°	169	+245.5°	31[a]
Methyl α-D-lyxofuranoside	94.5–96	+160°	97	+129°	32
Methyl β-D-lyxofuranoside[b]					
Methyl α-D-lyxopyranoside	108–109	+ 59°	108–109	+ 59.4°	33
Methyl β-D-lyxopyranoside	116.5–117.5	−127°	118	−128.1°	34

[a]For the L-enantiomorphs.
[b]Not isolated in amounts sufficient for characterization. The fully acetylated or methylated derivative of each glycoside gave only one peak on gas–liquid chromatography.

Reactions and Analysis of Products

Reaction vessels were screw-capped bottles fitted with silicone rubber septums and maintained at 35±0.01°. Samples (0.4–0.5 ml) were removed by a hypodermic syringe, neutralized by sodium methoxide, and evaporated to dryness. Fully methylated derivatives were prepared from these samples as described previously

Can. J. Chem. Downloaded from www.nrcresearchpress.com by 210.87.254.42 on 09/05/12
For personal use only.

(1). When acetylated derivatives were required (lyxosides, ribosides, and all samples containing reducing sugar) the dry residues were dissolved in 0.3 ml of a mixture of pyridine – acetic anhydride (1:1) at room temperature; acetylation was complete after 1 hour. The solutions from methylation and acetylation were analyzed directly by gas–liquid chromatography, the components being identified by comparison with authentic samples prepared from the glycosides listed above. Amounts of individual components were determined by tracing the peaks from the chromatogram onto glassine paper from which they were then cut out and weighed.

Results

The following tables show the percentage compositions at various times from which the rate constants used in the discussion were obtained. The tables are grouped according to reaction, the conditions for which are specified at the beginning of each section. For each reaction the initial compound is cited as the title of the table. The k values are based on the rate of decrease of initial product except for reaction 3, where they are based on decrease of total ($\alpha+\beta$) furanoside. The rate constants marked with an asterisk (*) were used to give the average values cited in the discussion (Table III).

Reaction 1.—Pentose → furanosides (Table VIII). Conditions: 2% of initial compound in 0.01% methanolic hydrogen chloride at 35±0.01° C.

TABLE VIII

Time (hr)	Unreacted pentose	Methyl glycoside: Furanoside α	Furanoside β	Pyranoside α	Pyranoside β	$k\times10^6$ (sec^{-1})
		A. D-Xylose				
0.25	95.2	3.2	1.7	0.0[a]		*56
0.75	84.7	9.4	5.9	0.0		*61
1.66	72.4	15.7	11.9	0.0		*54
3.0	63.9	20.7	15.5	0.0		42
6.0	35.5	34.5	29.4	0.6		48
22	12.7	40.8	43.7	2.8		26
		B. D-Ribose				
0.25	79.7	2.9	17.4	0.0	0.0	*253
0.50	64.4	4.2	28.3	0.0	0.0	*244
1.0	52.3	6.6	41.0	0.0	0.0	*180
1.5	20.0	10.7	69.3	0.0	0.0	*298
4.5	8.1	14.8	77.2	0.0	Trace	*155
6.0	Trace	18.5	81.5	Trace	Trace	—
24.0	0.0	24.2	73.3	0.5	2.0	—
		C. D-Lyxose				
0.5	96.4	2.1	0.4	1.1	—	*21
1.0	94.8	4.9	Trace	0.2	Trace	*15
1.5	91.2	7.8	—	0.9	Trace	*17
2.0	85.0	13.1	—	1.2	0.8	*23
4.5	71.2	24.7	—	2.7	1.5	*21
7.5	66.4	29.5	—	2.8	1.5	*15
24	12.4	75.8	—	8.1	3.7	
48	1.3	84.9	—	10.4	3.5	
120	1.1	76.8	—	15.6	6.5	
216	—	70.0	—	21.2	8.8	

[a]For α- plus β-pyranoside.

Can. J. Chem. Downloaded from www.nrcresearchpress.com by 210.87.254.42 on 09/05/12
For personal use only.

Reaction 2.—Anomerization of furanosides (Table IX). Conditions: 2% of initial compound in 0.01% methanolic hydrogen chloride at 35±0.01° C.

TABLE IX

Time (hr)	Methyl glycoside: Furanoside α	Furanoside β	Pyranoside α	Pyranoside β	$k\times10^6$ (sec^{-1})
	A. Methyl α-D-xylofuranoside				
0.2	96.5	1.4	0.8	1.3	*48
1.0	80.4	16.1	1.4	2.0	*60
2.0	67.2	30.5	0.6	1.7	*56
3.0	59.8	40.2	Trace	Trace	*48
4.0	54.4	45.6	0.0	0.0	*42
6.0	49.0	51.0	0.0	0.0	33
8.0	44.2	55.8	0.0	0.0	28
12	41.5	58.5	0.0	0.0	12
24	41.1	57.9	0.6	0.4	10
48	40.7	57.5	1.0	0.9	5
	B. Methyl β-D-ribofuranoside				
2	3.1	96.9	0.0	0.0	*4.2
7	10.4	89.6	0.0	0.0	*4.3
24	23.3	76.7	Trace	Trace	*3.1
48	23.6	74.2	0.5	1.6	1.7
72	23.1	74.6	0.6	1.7	1.1
96	22.7	74.1	0.8	2.5	0.9
	C. Methyl α-D-arabinofuranoside				
1	99.8	0.2	0.0	0.0	—
2	99.4	0.6	0.0	0.0	0.67
3	99.3	0.7	0.0	0.0	0.58
5	97.9	2.1	0.0	0.0	*1.10
8	96.7	3.3	0.0	0.0	*1.20
24	92.5	7.5	0.0	0.0	*1.89
48	87.1	12.8	Trace	Trace	0.80
79.5	83.0	17.0	Trace	Trace	0.65
120	79.3	19.2	1.0	0.5	0.56
168	77.9	19.8	1.5	0.8	0.41
216	77.7	19.4	2.0	0.9	0.33
288	73.6	23.5	2.2	0.8	0.25
360	72.6	23.2	2.8	1.4	0.25

Can. J. Chem. Downloaded from www.nrcresearchpress.com by 210.87.254.42 on 09/05/12
For personal use only.

Reaction 3.—Furanosides → pyranosides (Table X). Conditions: 2% of initial compound in 0.1% methanolic hydrogen chloride at 35±0.01° C.

TABLE X

Time (hr)	Methyl glycoside: Furanoside α	Methyl glycoside: Furanoside β	Methyl glycoside: Pyranoside α	Methyl glycoside: Pyranoside β	Lyxose	$k\times10^6$ (sec^{-1})
	A. Methyl α-D-xylofuranoside					
2	43.7	55.3	0.4	0.6		*1.34
4	43.7	54.2	0.7	1.4		*1.41
6	45.7	52.4	0.7	1.1		*0.94
8	42.7	53.9	1.3	2.1		*1.13
24	41.7	48.3	4.9	5.2		*1.10
96	26.6	35.5	14.9	23.1		*1.38
	B. Methyl β-D-ribofuranoside					
4	24.2	74.5	0.6	0.7		*0.85
24	23.4	70.5	1.4	4.7		*0.72
48	22.3	67.0	2.2	8.6		*0.65
72	20.2	64.7	3.1	12.0		*0.63
108	20.0	60.1	3.9	16.0		*0.57
144	18.9	57.7	4.5	18.9		0.51
192	18.0	52.6	5.8	23.7		0.50
	C. Methyl α-D-lyxofuranoside					
1	97.0	—	1.4	0.2	1.4	*8.3
2	94.2	—	3.6	1.2	1.0	*8.3
3	91.2	—	5.5	2.2	1.2	*8.9
5	85.9	—	9.9	3.2	1.0	*8.3
8	78.5	—	14.7	5.7	1.1	7.3
24	48.2	—	38.8	12.2	0.8	4.8
	D. Methyl α-D-arabinofuranoside					
1	93.9	6.1	0.0	0.0		—
3	83.1	15.9	0.5	0.5		*0.92
5	78.4	20.1	0.7	0.8		*0.87
24	70.7	22.1	2.8	4.5		*0.88
48	63.9	20.8	5.2	10.2		*0.96
79.5	60.7	19.5	6.8	13.0		*0.77
120	50.0	17.7	11.0	21.4		*0.90
168	47.4	15.6	12.9	24.1		0.77
216	45.4	15.5	13.8	25.4		0.64
288	43.2	14.2	14.7	27.8		0.54

Can. J. Chem. Downloaded from www.nrcresearchpress.com by 210.87.254.42 on 09/05/12
For personal use only.

Reaction 4.—Anomerization of pyranosides (Table XI). Conditions: 2% of initial compound in 1.0% methanolic hydrogen chloride at 35±0.01° C.

TABLE XI

Time (hr)	Methyl glycoside: Furanoside α	Furanoside β	Pyranoside α	Pyranoside β	$k\times10^6$ (sec^{-1})
	A. Methyl β-D-xylopyranoside				
3	0.0	0.0	3.2	96.8	*3.0
7	0.4	0.3	6.5	92.9	*3.0
30	1.3	1.3	28.8	68.5	*3.5
72	1.2	1.8	49.0	47.9	*2.8
144	1.3	2.0	59.3	37.4	1.9
240	1.9	3.2	65.1	29.8	1.4
	B. Methyl β-D-ribopyranoside				
4	0.4	2.3	1.7	95.6	*3.2
24	2.4	7.6	6.0	83.9	*2.0
48	3.5	12.8	8.3	75.5	*1.6
72	4.2	14.8	8.9	72.1	*1.3
108	5.2	15.0	9.4	70.5	0.9
144	4.9	16.0	10.2	68.9	0.7
192	5.2	17.4	11.6	65.8	0.6
	C. Methyl β-D-lyxopyranoside				
0.25	0.4	—	4.7	94.9	*58
0.5	1.3	—	9.3	89.5	*61
0.75	1.8	—	14.1	84.1	*64
1.0	1.4	—	18.2	80.4	*61
1.5	2.2	—	28.1	69.8	*64
2	3.0	—	35.9	61.1	*69
3	2.5	—	49.3	48.1	*58
4	2.5	—	57.2	40.6	*64
7	2.3	—	61.7	35.9	42
24	1.8	—	84.6	13.6	
192	1.4	—	88.3	10.3	
	D. Methyl β-D-arabinopyranoside				
8	9.8	3.0	15.3	71.9	*11.4
24	16.2	6.1	24.5	53.2	*7.3
79.5	21.3	6.6	23.8	48.4	2.5
120	21.5	6.5	24.3	47.8	1.7
216	21.5	6.8	24.5	47.2	1.0

Can. J. Chem. Downloaded from www.nrcresearchpress.com by 210.87.254.42 on 09/05/12
For personal use only.

ACKNOWLEDGMENTS

We are very grateful to Dr. E. Berner, University of Oslo, Blindern-Oslo, Norway, for seed crystals of a number of the methyl pentofuranosides.

REFERENCES

1. C. T. Bishop and F. P. Cooper. Can. J. Chem. **40**, 224 (1962).
2. R. E. Reeves. Advan. Carbohydrate Chem. **6**, 107 (1951).
3. R. U. Lemieux. Advan. Carbohydrate Chem. **9**, 1 (1954).
4. R. J. Ferrier and W. G. Overend. Quart. Rev. (London), **13**, 265 (1959).
5. B. Capon and W. G. Overend. Advan. Carbohydrate Chem. **15**, 11 (1960).
6. J. E. Kilpatrick, K. S. Pitzer, and R. Spitzer. J. Am. Chem. Soc. **69**, 2483 (1947).
7. T. R. R. McDonald and C. A. Beevers. Acta Cryst. **3**, 394 (1950).
8. S. Furberg. Acta Cryst. **3**, 325 (1950).
9. C. D. Jardetzky. J. Am. Chem. Soc. **82**, 229 (1960).
10. R. U. Lemieux. Can. J. Chem. **39**, 116 (1961).
11. C. D. Jardetzky. J. Am. Chem. Soc. **83**, 2919 (1961).
12. C. D. Jardetzky. J. Am. Chem. Soc. **84**, 62 (1962).
13. L. D. Hall. Chem. Ind. (London), 950 (1963).
14. R. J. Abraham, L. D. Hall, L. Hough, and K. A. McLauchlan. J. Chem. Soc. 3699 (1962).
15. J. T. Edward. Chem. Ind. (London), 1102 (1955).
16. S. J. Angyal. Abstracts of Scientific Papers, 18th International Congress of Pure and Applied Chemistry, Montreal. 1961. D7, p. 275.
17. S. J. Angyal and D. J. McHugh. Chem. Ind. (London), 1147 (1956).
18. S. J. Angyal, P. A. J. Gorin, and M. Pitman. Proc. Chem. Soc. 337 (1962).
19. S. J. Angyal. Personal communication.
20. R. U. Lemieux and P. Chu. Abstracts of Papers, 133rd Meeting of the American Chemical Society. 1958. 31N.
21. R. U. Lemieux. Abstracts of Papers, 135th Meeting of the American Chemical Society. 1959. 5E.
22. D. F. Mowery. J. Org. Chem. **26**, 3484 (1961).
23. B. Capon, G. W. Loveday, and W. G. Overend. Chem. Ind. (London), 1537 (1962).
24. I. Augestad and E. Berner. Acta Chem. Scand. **8**, 251 (1954).
25. E. Fischer. Ber. **28**, 1145 (1895).
26. E. Fischer. Ber. **28**, 1157 (1895).
27. G. R. Barker and D. C. C. Smith. J. Chem. Soc. 2151 (1954).
28. I. Augestad and E. Berner. Acta Chem. Scand. **10**, 911 (1956).
29. E. L. Jackson and C. S. Hudson. J. Am. Chem. Soc. **63**, 1229 (1941).
30. E. D. Montgomery and C. S. Hudson. J. Am. Chem. Soc. **59**, 992 (1937).
31. C. S. Hudson. J. Am. Chem. Soc. **47**, 265 (1925).
32. S. Zurberg and S. Hammer. Acta Chem. Scand. **15**, 1190 (1961).
33. F. P. Phelps and C. S. Hudson. J. Am. Chem. Soc. **48**, 503 (1926).
34. H. S. Isbell and H. L. Frush. J. Res. Natl. Bur. Std. **24**, 125 (1940).

Can. J. Chem. Downloaded from www.nrcresearchpress.com by 210.87.254.42 on 09/05/12
For personal use only.

INDUCTIVE AND MESOMERIC EFFECTS IN SUBSTITUTED FULVENE AND PYRIDINE DERIVATIVES

J. P. CARTIER AND C. SANDORFY
Département de Chimie, Université de Montréal, Montréal, Que.
Received May 21, 1963

ABSTRACT

The electronic charge distribution in substituted fulvene and pyridine derivatives is examined using the simple Hückel molecular orbital method. Parameters characterizing the electronegativity of the substituent and the carbon to which it is linked are varied in order to cover actually existing substituents.

It is found that the nature of the inductive and mesomeric effects is not basically different from that in the case of benzene. The most negative sites in fulvene show a certain variation with the place of substitution. In pyridine they are the ortho and para carbons for meta substitution and the meta carbons for ortho and para substitution.

INTRODUCTION

The inductive and mesomeric effect of substituents on the electronic charge distribution in benzene has been the subject of many theoretical treatments. In the simple Hückel approximation the extent of the mesomeric effect due to the addition of two more π-electrons to the system, as it occurs in phenol or aniline for example, depends on the difference between the Coulomb integral α_R associated with the substituent, R, and the Coulomb integral α_C of a carbon atom. This difference can be taken to be proportional to the corresponding difference in electronegativities (1, 2). The smaller it is the easier the penetration of the electrons of the substituent into the benzene π-orbitals.

The inductive effect is due to the alteration of the potential field in the benzene ring because of the presence of the substituent. The main consequence of this is an increase in the electronegativity of the carbon linked to the substituent (or decrease if the electronegativity of the substituent is lower than that of carbon) which may be represented by a supplement α_{C_R} to its Coulomb integral, generally taken as a fraction of α_R.

One of the present authors published a series of diagrams of electronic charge distributions in monosubstituted benzene derivatives of the phenol or aniline type (3). The quantity $(\alpha_R-\alpha_C)$ was given values of -2, -1, 0, 1, 2, and 3 in units of the carbon–carbon resonance integral, β. The value of α_{C_R} was taken to be 1/10 of that of the respective value of $(\alpha_R-\alpha_C)$. When α_{C_R} is taken as zero we obtain a series of diagrams representing the purely mesomeric effect. The purely inductive effect was obtained by cutting off the substituent from the ring by setting β_{C-R} equal to zero but giving α_{C_R} values equal to $\alpha_R/10$. The combined effect of the two was then computed with the appropriate values of α_R and α_{C_R} and with $\beta_{C-R} = \beta$. The substituents —NH_2, —OH, —F are examples for the positive values of α_R; —PH_2, —AsH_2 for the negative ones.

Recent developments in quantum chemistry (4–6) have given new justification to the simple Hückel method through its resemblance to the Pariser and Parr method (7). This fact encouraged us to undertake similar work on substituted fulvene and pyridine molecules. The former is an isomer of benzene although it contains a five-membered ring while the latter results from the substitution of one of the benzene carbon atoms by the more electronegative nitrogen atom. Comparisons with benzene derivatives were expected to be interesting.

Can. J. Chem. Downloaded from www.nrcresearchpress.com by 210.87.254.105 on 09/05/12
For personal use only.

The computational work for both molecules is more considerable than for benzene since for each of them there are three non-equivalent places for substitution. The simple Hückel approximation was used throughout with all resonance integrals taken as equal and all overlap integrals neglected. In the case of pyridine the supplemental Coulomb integral for the nitrogen atom, $\alpha_N - \alpha_C$, was taken equal to β and for the two ortho carbon atoms, $\alpha_{C_N} - \alpha_C = 0.1\beta$. These values are not indicated in the tables, which only show the variable parameters due to substitution on the pyridine molecule.

RESULTS AND DISCUSSION

Fulvene

Tables I, II, and III contain the electronic charge densities (q) and bond orders (p) for fulvene as used by Coulson and Longuet-Higgins (8). (See also earlier papers by Wheland and Pauling (9) and by Coulson (10).) In the first columns of these tables R, 1, 2, 3, and 4 correspond to the charges, R–1, 1–2, 2–3, 3–4, and 4–5 to bond orders.

The tables refer to substitution in 1, 3, and 4 respectively.

In drawing conclusions from these tables we must remember that in fulvene itself the electronic charge densities are different from unity, all the ring carbons having negative charges and the extracyclic carbon a large positive charge. The numerical values of these charges were shown to be much too high and lead to a dipole moment by far exceeding the experimental value (11–14). It is assumed, however, that this does not affect our comparative conclusions. The charges and bond orders of fulvene itself are in the column corresponding to $\alpha_{C_R} = 0$ among the columns related to the purely inductive effect. The + and − signs after the numbers indicate that the charge density was decreased or increased respectively with respect to fulvene. When the variation is less than 0.005 no signs were given. All the observations follow directly from the tables and therefore only some general features will be outlined.

The largest variations of q occur on the substituent (R) itself. For $\alpha_R = -2$, from the two electronic charges originally on R there only remains 0.15 to 0.30 according to the place of substitution. This great positive charge decreases rapidly with increasing α_R and for $\alpha_R = +3$ we have about 1.90 or 1.95 remaining from 2.00. This behavior is very similar to that obtained for benzene.

The corresponding variations for the carbon linked to the substituent also follow a pattern as in the case of benzene. The inductive effect moderately diminishes q for negative parameters and increases it for positive parameters. The mesomeric effect increases q very substantially for negative parameters, then it decreases it slightly for positive parameters so that the two effects always act in opposite directions. The combined effect is not obtained by addition of the two but it still is intermediate between them. This is so whether the substitution takes place in 1, 3, or 4.

The quaternary carbon 2 is significantly affected by substitution in 1 but the effect of substitution in 3 or 4 on carbon 2 is negligible.

Substitution in 1 increases the negative charge in both 3 and 4 for all values of the parameters. The combined effect is close to the mesomeric effect except for large positive parameters when it is about half way between the inductive and the mesomeric effects.

Substitution in 3 or 4 has an interesting effect on the charge density on carbon 1, which is the extracyclic carbon atom. The inductive effect is very slight for all parameters but the mesomeric effect, which is almost identical with the combined effect, sends large negative charges to 1 for negative values of α_R and slight negative charges for positive values of α_R.

Can. J. Chem. Downloaded from www.nrcresearchpress.com by 210.87.254.105 on 09/05/12
For personal use only.

TABLE I

Electronic charge densities and bond orders of 1-substituted fulvene derivatives

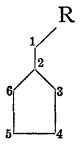

A. Inductive effect

α_1	-0.2β	-0.1β	0	0.1β	0.2β	0.3β
R	2.000	2.000	2.000	2.000	2.000	2.000
R–1	0.000	0.000	0.000	0.000	0.000	0.000
1	0.519+	0.569+	0.622	0.680−	0.742−	0.807−
1–2	0.716	0.738	0.759	0.778	0.795	0.810
2	1.094−	1.072−	1.047	1.020+	0.991+	0.959+
2–3	0.473	0.461	0.449	0.437	0.424	0.412
3	1.099−	1.096	1.092	1.089	1.087	1.085+
3–4	0.763	0.770	0.778	0.786	0.794	0.803
4	1.095−	1.084−	1.073	1.061+	1.047+	1.033+
4–5	0.542	0.532	0.521	0.508	0.494	0.480

B. Mesomeric effect

α_R	-2β	-1β	0	1β	2β	3β
R	0.275+	0.570+	1.120+	1.591+	1.803+	1.891+
R–1	0.641	0.832	0.898	0.714	0.520	0.393
1	1.586−	1.371−	0.984−	0.693−	0.590+	0.564+
1–2	0.380	0.369	0.426	0.540	0.620	0.663
2	1.131−	1.148−	1.164−	1.154−	1.131−	1.114−
2–3	0.609	0.609	0.584	0.540	0.509	0.491
3	1.286−	1.249−	1.188−	1.139	1.117−	1.108
3–4	0.607	0.628	0.671	0.714	0.738	0.750
4	1.218−	1.206−	1.178−	1.144−	1.121−	1.108
4–5	0.665	0.654	0.625	0.591	0.568	0.556

C. Combined effect

α_R α_1	-2β -0.2β	-1β -0.1β	0 0	1β 0.1β	2β 0.2β	3β 0.3β
R	0.303+	0.672+	1.120+	1.573+	1.794+	1.889+
R–1	0.663	0.844	0.898	0.720	0.517	0.376
1	1.539−	1.337−	0.984−	0.727−	0.667−	0.698−
1–2	0.402	0.376	0.426	0.549	0.653	0.721
2	1.134−	1.150−	1.164	1.145−	1.102−	1.054−
2–3	0.602	0.607	0.584	0.535	0.492	0.461
3	1.293−	1.250−	1.118−	1.137−	1.112−	1.099−
3–4	0.604	0.628	0.671	0.717	0.749	0.770
4	1.219−	1.206−	1.178−	1.140−	1.107−	1.081−
4–5	0.666	0.653	0.625	0.588	0.555	0.528

Substitution in 3 sends additional negative charges into 4 and 6, the combined effect being only roughly additive. Carbon 5 is only slightly affected.

Substitution in 4 sends additional negative charges into 3. Except for negative values of the parameters, 5 and 6 are less affected.

Other regularities may be found on examination of the tables.

The "meta" positions (the next-nearest carbons to the place of substitution) are less affected than the others for substitution in 1 and 3. For substitution in 4, 5 and 6 are

Can. J. Chem. Downloaded from www.nrcresearchpress.com by 210.87.254.105 on 09/05/12
For personal use only.

TABLE II

Electronic charge densities and bond orders of 3-substituted fulvene derivatives

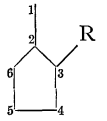

A. Inductive effect

α_3	-0.2β	-0.1β	0	0.1β	0.2β	0.3β
R	2.000	2.000	2.000	2.000	2.000	2.000
R–3	0.000	0.000	0.000	0.000	0.000	0.000
1	0.631−	0.626	0.622	0.620	0.618	0.618
1–2	0.768	0.763	0.759	0.755	0.751	0.748
2	1.055−	1.051	1.047	1.043	1.039+	1.034+
2–3	0.444	0.447	0.449	0.450	0.450	0.448
3	0.989+	1.041+	1.092	1.142−	1.191−	1.237−
3–4	0.783	0.781	0.778	0.772	0.765	0.755
4	1.133−	1.103−	1.073	1.044+	1.016+	0.990+
4–5	0.512	0.516	0.520	0.526	0.532	0.539
5	1.065+	1.069	1.073	1.076	1.079−	1.082−
5–6	0.781	0.780	0.778	0.776	0.773	0.769
6	1.129−	1.110−	1.092	1.074+	1.057+	0.040+
6–2	0.442	0.445	0.449	0.453	0.458	0.463

B. Mesomeric effect

α_R	-2β	-1β	0	1β	2β	3β
R	0.175+	0.405+	1.134+	1.747+	1.895+	1.943+
R–3	0.469	0.655	0.757	0.484	0.319	0.237
1	1.671−	1.564−	1.134−	0.748−	0.667−	0.646−
1–2	0.544	0.608	0.757	0.798	0.785	0.776
2	1.073−	1.050	1.028+	1.046	1.053−	1.054−
2–3	0.507	0.451	0.361	0.380	0.410	0.424
3	1.349−	1.267−	1.028+	0.939+	0.965+	0.988+
3–4	0.497	0.457	0.510	0.681	0.740	0.759
4	1.221−	1.248−	1.321−	1.263−	1.198−	1.166−
4–5	0.718	0.728	0.660	0.548	0.522	0.516
5	1.175	1.128−	1.035+	1.032+	1.049+	1.057+
5–6	0.577	0.584	0.660	0.752	0.772	0.777
6	1.336−	1.338−	1.321−	1.226−	1.173−	1.150−
6–2	0.587	0.577	0.510	0.450	0.442	0.442

C. Combined effect

α_R / α_3	-2β / -0.2β	-1β / -0.1β	0 / 0	1β / 0.1β	2β / 0.2β	3β / 0.3β
R	0.183+	0.420+	1.134+	1.749+	1.901+	1.949+
R–3	0.467	0.659	0.757	0.473	0.296	0.206
1	1.685−	1.567−	1.134−	0.736−	0.651−	0.629−
1–2	0.528	0.604	0.757	0.795	0.776	0.763
2	1.089−	1.055−	1.028+	1.044	1.048	1.044
2–3	0.523	0.455	0.361	0.384	0.418	0.433
3	1.288−	1.238−	1.028+	0.981+	1.059+	1.135−
3–4	0.517	0.464	0.510	0.688	0.744	0.757
4	1.231−	1.251−	1.321−	1.241−	1.143−	1.077
4–5	0.705	0.724	0.660	0.546	0.524	0.526
5	1.188−	1.131−	1.035+	1.036+	1.058+	1.070
5–6	0.578	0.583	0.660	0.755	0.774	0.775
6	1.337−	1.338−	1.321−	1.213−	1.141−	1.096−
6–2	0.585	0.576	0.510	0.451	0.447	0.452

Can. J. Chem. Downloaded from www.nrcresearchpress.com by 210.87.254.105 on 09/05/12
For personal use only.

TABLE III

Electronic charge densities and bond orders of 4-substituted fulvene derivatives

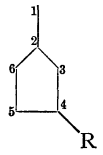

A. Inductive effect

α_4	-0.2β	-0.1β	0	0.1β	0.2β	0.3β
R	2.000	2.000	2.000	2.000	2.000	2.000
R–4	0.000	0.000	0.000	0.000	0.000	0.000
1	0.648−	0.635−	0.622	0.611+	0.600+	0.590+
1–2	0.767	0.763	0.759	0.755	0.751	0.747
2	1.045	1.046	1.047	1.048	1.049	1.049
2–3	0.442	0.446	0.449	0.453	0.457	0.462
3	1.152−	1.122−	1.092	1.063+	1.035+	1.008+
3–4	0.781	0.781	0.778	0.774	0.768	0.762
4	0.985+	1.029+	1.073	1.116−	1.158−	1.199−
4–5	0.517	0.519	0.520	0.520	0.519	0.517
5	1.086−	1.080−	1.073	1.066+	1.059+	1.053+
5–6	0.776	0.777	0.778	0.779	0.781	0.783
6	1.084+	1.089	1.092	1.096	1.099−	1.101−
6–2	0.445	0.447	0.449	0.451	0.452	0.454

B. Mesomeric effect

α_R	-2β	-1β	0	1β	2β	3β
R	0.149+	0.355+	1.208+	1.790+	1.907+	1.947+
R–4	0.419	0.598	0.705	0.440	0.302	0.229
1	1.725−	1.670−	1.208−	0.784−	0.699−	0.670−
1–2	0.495	0.534	0.705	0.774	0.773	0.770
2	1.099−	1.077−	1.027+	1.032+	1.039+	1.042
2–3	0.611	0.617	0.540	0.457	0.446	0.444
3	1.329−	1.362−	1.436−	1.296−	1.219−	1.183−
3–4	0.509	0.468	0.540	0.703	0.747	0.762
4	1.269−	1.220−	1.027+	0.966+	0.980+	0.994+
4–5	0.603	0.540	0.419	0.453	0.484	0.498
5	1.152−	1.105−	1.047+	1.083−	1.089−	1.088−
5–6	0.657	0.719	0.832	0.803	0.787	0.782
6	1.278−	1.212−	1.047+	1.058+	1.068+	1.077+
6–2	0.547	0.509	0.419	0.424	0.435	0.441

C. Combined effect

α_R α_4	-2β -0.2β	-1β -0.1β	0 0	1β 0.1β	2β 0.2β	3β 0.3β
R	0.152+	0.365+	1.208+	1.791+	1.910+	1.951+
R–4	0.413	0.599	0.705	0.431	0.285	0.206
1	1.729−	1.672−	1.208−	0.768−	0.669−	0.630−
1–2	0.490	0.532	0.705	0.772	0.766	0.759
2	1.104−	1.078−	1.027+	1.034+	1.042+	1.046
2–3	0.600	0.614	0.540	0.458	0.450	0.453
3	1.341−	1.365−	1.436−	1.272−	1.164−	1.096
3–4	0.528	0.474	0.540	0.707	0.748	0.759
4	1.206−	1.190−	1.027+	1.003+	1.059+	1.118−
4–5	0.618	0.545	0.419	0.457	0.490	0.503
5	1.177−	1.113−	1.047+	1.079−	1.078−	1.070+
5–6	0.634	0.713	0.832	0.802	0.786	0.783
6	1.292−	1.217−	1.047+	1.054+	1.078+	1.089
6–2	0.557	0.512	0.419	0.427	0.440	0.447

Can. J. Chem. Downloaded from www.nrcresearchpress.com by 210.87.254.105 on 09/05/12
For personal use only.

comparable from this point of view. As in the case of benzene, for negative parameters the charge distribution undergoes more profound changes than for positive ones.

In conclusion we can say that the influence of inductive and mesomeric effects on the electronic charge distribution in the case of fulvene is not substantially different from what is found for benzene.

Looking at the absolute values of the charges in Tables I, II, and III, it is seen that in fulvene itself the most negative sites are the fields of carbons 3 and 6, 4 and 5 being somewhat less negative. This is still so after substitution in 1 with the apparent exception of $\alpha_R = 1\beta$. For substitution in 3 the most negative sites are 4 and 6 for $\alpha_R = 0$, 1, and 2, which would correspond to the cases of substituents occurring in practice.

For other values of α_R we refer to Table II. Substitution in 4 shows an even greater variety and only 3 is always negatively charged (Table III).

In general the negative charges in the ring become larger as a consequence of substitution. For negative parameters the extracyclic carbon is the most negative site.

Pyridine

Our work on pyridine was less extensive. Only $\alpha_R = 0$, 1, and 2 were used with the corresponding inductive parameters. The respective charge distributions have to be compared with that of pyridine itself, which is found in the third line of Tables IVA, B, and C.

Substitution in 2 (ortho to the nitrogen atom) increases the negative charge on the nitrogen appreciably and sends more negative charges to all the carbons. Carbon 5 will be the most negative, then carbon 3. The meta positions are the least positive in pyridine itself but now we have net negative charges there. The inductive effect diminishes q on N, 3, 5, and 6, increases it on 2, and leaves it unchanged on 4. The mesomeric effect increases it on N, 3, 4, 5, and 6 and decreases it on 2. The combined effect is seen to be intermediate between the two.

Substitution in 3 (meta) only affects q_N slightly, increases charges, rendering them negative in 2, 4, and 6 whereas in 3 and 5 it causes only a slight increase. This is a complete reversal in the charge distribution of the ring, the most negative sites being now the ortho and para carbons, not the meta. The inductive effect increases q on 3, decreases it on 2, 4, and 6, and leaves it practically unchanged on N and 5. The mesomeric effect increases charges in 2, 4, and 6, decreases them in 3, and leaves them unchanged on N and 5. The combined effect is again intermediate.

Substitution in 4 (para) increases q_N appreciably and also increases q in 2, 3, 4, 5, and 6; 3 and 5 become the most negative sites. This is a situation similar to that of the substitution in 2. The inductive effect slightly decreases q_N, increases q on 4, decreases it on 3 and 5, and leaves it unchanged on 2 and 6. The mesomeric effect increases q_N slightly, also increases q in 3 and 5, decreases it in 4, and leaves it unchanged in 2 and 6. Again the combined effect is intermediate.

We may summarize our observations by pointing out that the inductive and mesomeric effects are opposed for positive values of the parameters whatever the place of the substitution. Furthermore, whereas in pyridine itself the charge is positive on all carbons, in the substituted derivatives there are negative sites, namely the meta carbons for ortho or para substitution and the ortho and para carbons for meta substitution. This is likely to lead to acceleration of electrophilic reactions with respect to pyridine itself for all three types of substitution.

No attempt is made in this paper to make comparisons with experimental data. We only refer to reviews by Day (15) and by Bergmann (16) and to the work of Thiec and

Can. J. Chem. Downloaded from www.nrcresearchpress.com by 210.87.254.105 on 09/05/12
For personal use only.

TABLE IV

Electronic charge densities of substituted pyridine derivatives

A. Substitution on carbon 2

α_R	α_2	q_N	q_2	q_3	q_4	q_5	q_6	q_7
	+0.2	1.320	0.976	0.949	0.904	0.963	0.889	2.000
	+0.1	1.332	0.935	0.966	0.904	0.973	0.892	2.000
	0	1.345	0.894	0.982	0.904	0.982	0.894	2.000
+2		1.406	0.837	1.039	0.901	1.024	0.900	1.884
+1		1.442	0.860	1.059	0.918	1.048	0.903	1.769
0		1.528	0.977	1.077	0.954	1.104	0.912	1.449
+2	+0.2	1.383	0.907	1.013	0.909	1.008	0.897	1.883
+1	+0.1	1.433	0.892	1.049	0.918	1.042	0.902	1.764
0	0	1.528	0.977	1.077	0.954	1.104	0.912	1.449

B. Substitution on carbon 4

α_R	α_4	q_N	q_2	q_3	q_4	q_5	q_6	q_7
	+0.2	1.327	0.893	0.952	0.984	0.952	0.893	2.000
	+0.1	1.336	0.893	0.967	0.944	0.967	0.893	2.000
	0	1.345	0.894	0.982	0.904	0.982	0.894	2.000
+2		1.388	0.899	1.039	0.846	1.039	0.899	1.888
+1		1.419	0.908	1.063	0.865	1.063	0.908	1.774
0		1.503	0.944	1.100	0.975	1.100	0.944	1.435
+2	+0.2	1.372	0.898	1.014	0.916	1.014	0.898	1.888
+1	+0.1	1.412	0.908	1.053	0.897	1.053	0.908	1.770
0	0	1.503	0.944	1.100	0.975	1.100	0.944	1.435

C. Substitution on carbon 3

α_R	α_3	q_N	q_2	q_3	q_4	q_5	q_6	q_7
	+0.2	1.346	0.861	1.061	0.874	0.984	0.875	2.000
	+0.1	1.345	0.877	1.022	0.889	0.983	0.884	2.000
	0	1.345	0.894	0.982	0.904	0.982	0.894	2.000
+2		1.341	0.954	0.917	0.964	0.980	0.938	1.905
+1		1.340	0.979	0.926	0.993	0.981	0.968	1.812
0		1.340	1.013	0.994	1.061	0.990	1.059	1.544
+2	+0.2	1.343	0.926	0.988	0.937	0.982	0.920	1.905
+1	+0.1	1.340	0.967	0.957	0.982	0.982	0.961	1.811
0	0	1.340	1.013	0.994	1.061	0.990	1.059	1.544

Wiemann (17) on fulvene derivatives and to the review found in Streitwieser's book (18) on pyridine derivatives.

It is hoped that the results presented in this paper will prove useful in establishing correlations between the electronic charge distribution in fulvene and pyridine derivatives and kinetic data related to these molecules.

The spectra of fulvene and pyridine derivatives were extensively studied (19–24) as were the dielectric properties of the latter (25, 26).

ACKNOWLEDGMENTS

The eigenvalues and eigenvectors of the molecules treated in this paper were computed with the help of the Computation Centre, McLennan Laboratory of the University of Toronto. Our sincere thanks are due to Dr. C. C. Gotlieb and Mr. I. Farkas for their valuable assistance.

One of us (J. P. C.) was a holder of a scholarship from the Province of Quebec for which he expresses his gratitude.

Can. J. Chem. Downloaded from www.nrcresearchpress.com by 210.87.254.105 on 09/05/12
For personal use only.

REFERENCES

1. R. S. MULLIKEN. J. Chim. Phys. **46**, 497, 675 (1949).
2. A. LAFORGUE. J. Chim. Phys. **46**, 568 (1949).
3. C. SANDORFY. Can. J. Chem. **36**, 1739 (1958).
4. J. A. POPLE. Trans. Faraday Soc. **49**, 1375 (1953).
5. A. D. MCLACHLAN. Mol. Phys. **2**, 271 (1959).
6. W. T. SIMPSON. J. Chem. Phys. **28**, 972 (1958).
7. R. PARISER and R. G. PARR. J. Chem. Phys. **21**, 466, 767 (1953).
8. C. A. COULSON and H. C. LONGUET-HIGGINS. Proc. Roy. Soc. (London), Ser. A, **191**, 39 (1947).
9. G. W. WHELAND and L. PAULING. J. Am. Chem. Soc. **57**, 2086 (1935).
10. C. A. COULSON. Proc. Roy. Soc. (London), Ser. A, **169**, 413 (1939).
11. G. W. WHELAND and D. E. MANN. J. Chem. Phys. **17**, 264 (1949).
12. J. I. FERNANDEZ ALONSO. Compt. Rend. **233**, 56 (1951).
13. A. PULLMAN, B. PULLMAN, and P. RUMPF. Bull. Soc. Chim. France, **15**, 757 (1948).
14. C. SANDORFY, N. Q. TRINH, A. LAFORGUE, and R. DAUDEL. J. Chim. Phys. **46**, 655 (1949).
15. J. H. DAY. Chem. Rev. **53**, 167 (1953).
16. E. D. BERGMANN. *In* Progress in Organic Chemistry. J. W. Cook. Vol. 3. Academic Press, New York. 1955. p. 81.
17. J. THIEC and J. WIEMANN. Bull. Soc. Chim. France, 177 (1956); 102, 366 (1957); 207 (1958).
18. A. STREITWIESER, JR. Molecular orbital theory for organic chemists. Wiley, New York. 1961. pp. 351–356.
19. B. PULLMAN, M. MAYOT, and G. BERTHIER. J. Chem. Phys. **18**, 257 (1950).
20. C. A. COULSON. Proc. Phys. Soc. (London), Ser. A, **65**, 933 (1952).
21. H. C. LONGUET-HIGGINS and R. G. SOWDEN. J. Chem. Soc. 1404 (1952).
22. A. K. CHANDRA and S. BASU. J. Chem. Soc. 1623 (1959).
23. S. F. MASON. Quart. Rev. (London), **15**, 287 (1961).
24. R. J. L. ANDON, J. D. COX, and E. F. G. HERINGTON. Trans. Faraday Soc. **50**, 918 (1954).
25. J. BARASSIN and H. LUMBROSO. Bull. Soc. Chim. France, 492 (1961).
26. H. LUMBROSO and P. ROSSETTI. J. Chim. Phys. **56**, 844 (1959).

Can. J. Chem. Downloaded from www.nrcresearchpress.com by 210.87.254.105 on 09/05/12
For personal use only.

TOSYLATED PEPTIDES AND *p*-NITROPHENYL ESTERS[1]

CASIMIR BERSE, THOMAS MASSIAH,[2] AND LUCIEN PICHÉ
Department of Chemistry, University of Montreal, Montreal, Que.

Received February 11, 1963

ABSTRACT

The tosyl group causes interference with mixed carbonic anhydride and *p*-nitrophenyl ester formation in certain instances. Several protected peptide sequences, occurring in the insulin molecule, and some tosylated *p*-nitrophenyl esters, have been prepared in the course of investigating this interference.

INTRODUCTION

At the inception of this work, we were interested in preparing certain peptide sequences which occur in the insulin molecule (1). Specifically, we were interested in preparing three peptides which occur in the vicinity of the interchain disulphide bridge of insulin, namely tyrosyl-cysteinyl-asparagine, cysteinyl-glycyl-glutamic acid, and cysteinyl-glycyl-serine, hereinafter abbreviated respectively as H-Tyr-Cy(SH)-Asp(NH_2)-OH, H-Cy(SH)-Gly-Glu-OH, H-Cy(SH)-Gly-Ser-OH, according to the system of Brand (2). A portion of the insulin molecule is reproduced in I. We were particularly interested in

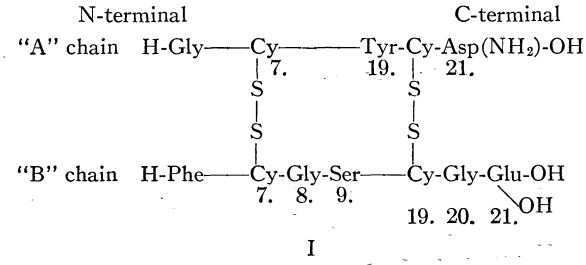

I

these peptides, because we believed, for reasons which will not be delineated here, that the site of the hypoglycemic activity of insulin might be those peptides sequences in the vicinity of the interchain disulphide bridge (3).

In our search for a suitable method of "blocking" the amino group of the various amino acids, we were attracted to the tosyl blocking group, because of the general ease of preparation of tosylamino acids, and the ready crystallinity of such derivatives (4), particularly N-tosylated glutamic acid (5). Furthermore, it seemed desirable to attempt to limit ourselves to one amino blocking group and one method of forming the peptide bond. Indeed such an objective has been achieved in at least two syntheses of oxytocin (6, 7). For our purpose, we chose to use the tosyl blocking group, and to form the peptide bond by the mixed carbonic anhydride method (8). Later, we were forced to modify our original plan, such that we had to use other blocking groups, such as the well known "carbobenzoxy" (9) group, and other methods of forming peptide bonds, such as the N,N′-dicyclohexylcarbodiimide (10) method, because of the failure of the mixed anhydride method with N^{α}-tosylamino acids in certain instances, reported previously (11).

[1]*This paper was presented in abridged form at the 29th meeting of l'ACFAS at Ottawa (Canada), October 27–29, 1961.*

[2]*Present address: Ayerst, McKenna and Harrison Limited, Montreal, Que.*

Can. J. Chem. Downloaded from www.nrcresearchpress.com by 210.87.254.105 on 09/05/12
For personal use only.

Ultimately, therefore, our main interest became the investigation of the factors influencing peptide bond formation, by various methods, with N^{α}-tosylamino acids.

In this paper, we report on the formation of peptide bonds and *p*-nitrophenyl esters of N-tosylamino acids and peptides, and propose a general basis for predicting when either of the foregoing reactions will occur.

DISCUSSION

In Table I, we have tabulated the results of our own work and those of other workers, in the formation of certain peptide sequences and derivatives, using various amino blocking groups. It can be seen that in the case of the tosyl blocking group, as contrasted with the carbobenzoxy and phthaloyl groups, peptide bond or *p*-nitrophenyl ester formation fails in every instance where the tosyl group is alpha to the carboxyl group being reacted with, except in the case of N-tosyl-L-pyroglutamic acid, II, and N-tosyl-L-proline, III. The significance of the structure of these two tosylamino acids

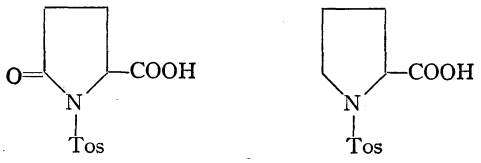

II III

(Tos = tosyl = CH_3—C$_6$H$_4$—SO_2—)

will be discussed later. In order to rule out the possibility of steric hindrance being a factor in the failure of the mixed anhydride method with the N^{α}-tosylamino acids, we prepared (or report numerous instances from the literature) sequences in which the amino acid residues are C-terminal in one instance and N-terminal in another. It is clear, from a study of Table I, that the failure of the desired reactions, in the case of tosylamino acids is ascribable to the tosyl group.

If one examines the structure of the tosylamino derivatives in which mixed anhydride or *p*-nitrophenyl ester formation *fails*, one will see that, in general, the derivatives have the structure IV. On the other hand, those instances where these reactions are successful,

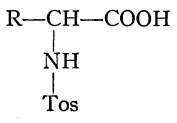

IV

have the structure II, III, or V. It is evident, therefore, *that if the tosyl group is alpha*

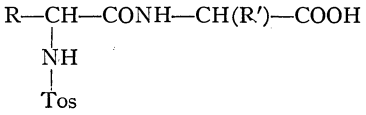

V

to the carboxyl group undergoing activation, and if there is a hydrogen atom on the nitrogen atom to which the tosyl group is attached, there will be interference with *both* of the aforementioned reactions; otherwise the tosyl group does *not* cause interference with *either* of the reactions. This represents, in our view, an important extension of the conclusion

Can. J. Chem. Downloaded from www.nrcresearchpress.com by 210.87.254.105 on 09/05/12
For personal use only.

Can. J. Chem. Downloaded from www.nrcresearchpress.com by 210.87.254.105 on 09/05/12
For personal use only.

TABLE I

No.	Sequence attempted	Protecting group: Amino	Protecting group: Carboxyl	Method	Result	Reference
IX	Cy(SBz)*Asp(NH_2)	Cbz	Na salt	$ClCO_2Et$	+ve	This paper, 15
		Tos	Na salt	$ClCO_2Et$	−ve	T.M.
		Tos	Mg salt	Acid chloride	−ve	T.M.
X	Glu(NH_2)*Asp(NH_2)	Tos	Mg salt	Pyroglutamyl chloride	+ve	16
XI	Cy(SBz)-Tyr*Phe-Glu(NH_2)-Asp(NH_2)	Tos	Et_3N salt	$ClCO_2Et$	+ve	17
XII	Cy(SBz)*Gly	Tos	Et	$ClCO_2Et$	−ve	11
		Cbz	Et	$ClCO_2Et$	+ve	T.M., 18
		Tos	Et	DCC	+ve	11
		Tos	Et	Acid chloride	+ve	11
		Tos	PNB	DCC	+ve	This paper
XIII	Phe*Cy(SBz)	Phth	Et	$ClCO_2Et$	+ve	11
XIV	Tyr*Cy(SBz)	Tos	Et	$ClCO_2Et$	−ve	11
		Tos	Et	DCC	+ve	11
XV	π-Glu*Gly	Tos	Et	$ClCO_2Et$	+ve	This paper
		Tos	Et	Pyroglutamyl chloride	+ve	5
XVI	π-Glu*Cy(SBz)	Tos	Et	$ClCO_2Et$	+ve	This paper
		Tos	Et	Pyroglutamyl chloride	+ve	19
XVII	Cy(SBz)-Gly*Glu(OMe)	Tos	Na salt	$ClCO_2Et$	+ve	T.M.
XVIII	Cy(SBz)-Gly*Ser	Tos	Et	$ClCO_2Et$	+ve	This paper
XIX	Gly*PNP	Tos	Free	DCC	−ve	This paper
		Phth	Free	DCC	+ve	T.M.
XX	Cy(SBz)*PNP	Tos	Free	DCC	+ve	This paper
		Tos	Free	$ClCO_2Et$	−ve	T.M.
		Cbz	Free	DCC	+ve	7
XXI	π-Glu*PNP	Tos	Free	DCC	+ve	This paper
XXII	Pro*PNP	Tos	Free	DCC	+ve	This paper
XXIII	Cy(SBz)-Gly*PNP	Tos	Free	DCC	+ve	This paper

NOTE: Asterisk (*) denotes formation of a new bond; T.M. = unpublished results of one of the authors; Bz = benzyl; Cbz = carbobenzoxy; DCC = N,N′-dicyclohexylcarbodiimide; Et = ethyl; Me = methyl; PNB = *p*-nitrobenzyl; Phth = phthaloyl; PNP = *p*-nitrophenyl; Tos = tosyl = *p*-toluenesulfonyl; +ve denotes a successful reaction; −ve denotes an unsuccessful reaction.

See reviews by Fruton (20), Shapiro (21), Wieland (22), du Vigneaud (23), Springall and Law (24), Goodman and Kenner (25).

which Zaoral and Rudinger (12) had made regarding the *mixed carbonic anhydride method*. Furthermore, to the best of our awareness, the case of tosylated *p*-nitrophenyl ester formation does not seem to have been dealt with in the published literature.

From the present work, and that of others (12, 13), we know, now, that we can form mixed carbonic anhydrides, and thence peptides, of N-tosylamino acids and peptides such as II, III, or V in the conventional manner (8), while mixed anhydrides of tosylamino acids such as IV may be prepared using pivaloyl chloride (13).

Each of the N^{α}-tosylamino acids investigated reacted with an ester of another amino acid to form dipeptides, in the presence of N,N′-dicyclohexylcarbodiimide (10). In contrast to this, only *certain* N^{α}-tosylamino acids formed *p*-nitrophenyl esters, even though the expected coproduct, N,N′-dicyclohexylurea (10), was observed to have formed in *every* case. The reaction of N-tosylglycine, IV (R = H), and N,N′-dicyclohexylcarbodiimide, alone and in the presence of an equimolar amount of each of these ingredients and *p*-nitrophenol, was investigated. In the former instance, N,N′-dicyclohexylurea and the diketopiperazine, VI, arising from N-tosylglycine, IV (R = H), were isolated in essentially quantitative yield. In the latter instance, the same two products were isolated, and 90% of the initial amount of *p*-nitrophenyl was recovered, unreacted. Since diketopiperazines were never detected among the reaction products, in the case of dipeptide formation, it would seem that they are *not* precursors of the dipeptides. Diketopiperazine formation appears to compete successfully with tosylated *p*-nitrophenyl ester formation, however, in those cases where one would predict interference with the desired reaction on the basis of the hypothesis enunciated previously.

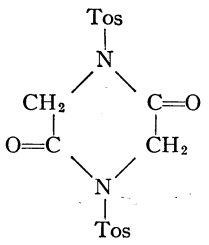

VI

The divergent behavior of N-tosyl-S-benzyl-L-cysteinyl chloride, VII, and N-tosyl-L-pyroglutamyl chloride, VIII (see Table I), towards the magnesium salt of L-asparagine

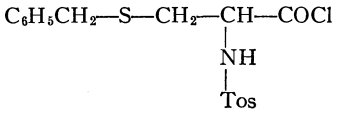

VII

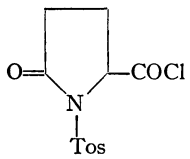

VIII

is unexplained, but it may represent another aspect of the peculiar role of the amino hydrogen atom (12) under the influence of the tosyl group. Since the mechanism of Beecham (14) does not appear to be applicable to the foregoing case, it seems likely that the probable product from VII was the diketopiperazine analogous to VI. No attempt was made to identify the reaction product, however, once it was shown to be a product other than the one expected.

Can. J. Chem. Downloaded from www.nrcresearchpress.com by 210.87.254.105 on 09/05/12
For personal use only.

Can. J. Chem. Downloaded from www.nrcresearchpress.com by 210.87.254.105 on 09/05/12
For personal use only.

EXPERIMENTAL[3, 4]

N-Carbobenzoxy-S-benzyl-L-cysteinyl-L-asparagine, IX

This compound was prepared from N-carbobenzoxy-S-benzyl-L-cysteine (26) (10.35 g; 0.03 mole) and L-asparagine (3.96 g; 0.03 mole) by the mixed carbonic anhydride method, as reported by Leach and Lindley (15). The yield of the product was 6.5 g (47%), after recrystallization from boiling methanol (150 ml); m.p. 157–158° C (lit. (15): 180° C), $[\alpha]_D^{22}$ −32.7 (*c*, 2.43; *N,N*-dimethylformamide). Anal. Calc. for $C_{22}H_{25}O_6N_3S$ (459.5): C, 57.50; H, 5.48; N, 9.15%. Found: C, 57.87; H, 5.47; N, 9.21%.

N-Tosyl-S-benzyl-L-cysteinyl-glycine p-Nitrobenzyl Ester, XII

Glycine *p*-nitrobenzyl ester hydrobromide (27) (5.39 g; 18.5 mmoles) was dissolved in chloroform (75 ml) containing triethylamine (2.59 ml; 18.5 mmoles), and the solution was stirred for 10 minutes. N-Tosyl-S-benzyl-L-cysteine (17) (6.76 g; 18.5 mmoles) was added, the reaction mixture was cooled to 0° C, treated with a solution of *N,N*-'dicyclohexylcarbodiimide (3.82 g; 18.5 mmoles) in dry tetrahydrofuran (25 ml) and stirred for 30 minutes in the cooling bath. The viscous suspension was then transferred to a Burrell wrist action shaker, and agitated for 16 hours at room temperature. The precipitated N,N'-dicyclohexylurea (2.24 g; 57% of the theoretical) was filtered, and the filtrate was concentrated to a semisolid oil *in vacuo*. This oil was dissolved in chloroform (75 ml), and the resulting solution was washed successively with water, 1 *N* sodium bicarbonate, 1 *N* hydrochloric acid, water, and then it was dried over sodium sulphate. Petroleum ether (b.p. 65–110° C) was added to opalescence, and the product was allowed to crystallize at room temperature. The product, thus obtained, weighed 5.57 g (54%), m.p. 116–117° C. Further recrystallizations raised the melting point to a constant value of 118–119° C. $[\alpha]_D^{25}$ −3.12 (*c*, 1.41 in chloroform). Anal. Calc. for $C_{26}H_{27}O_7N_3S_2$ (557.6): C, 56.00; H, 4.88; N, 7.54%. Found: C, 55.62; H, 4.64; N, 7.16%.

N-Tosyl-L-pyroglutamyl-glycine Ethyl Ester, XV

To a stirred solution of N-tosyl-L-pyroglutamic acid (28) (2.83 g; 0.01 mole) in chloroform (30 ml), cooled to 0° C, was added triethylamine (1.4 ml; 0.01 mole) and ethyl chloroformate (0.95 ml; 0.01 mole). After 10 minutes a precooled solution of glycine ethyl ester (prepared from 1.39 g, 0.01 mole, of the hydrochloride and 1.4 ml; 0.01 mole, of triethylamine) in methylene chloride (40 ml) – chloroform (10 ml) was added. The solution was stirred for 30 minutes at 0° C, and 1.5 hours at room temperature, then it was washed to neutrality in the usual way, and dried over magnesium sulphate. The washed and dried solution was evaporated to an oil *in vacuo*, and the oily residue was taken up in 95% ethanol (5 ml) with slight warming. The yield of recrystallized product was 2 g (54%), m.p. 131–132° C (lit. (5): 132–133° C); $[\alpha]_D^{28}$ −21.8 (*c*, 1.19 in dioxane).

N-Tosyl-L-pyroglutamyl-S-benzyl-L-cysteine Ethyl Ester, XVI

This compound was prepared exactly as in the preceding case, from N-tosyl-L-pyroglutamic acid (28) (2.83 g; 0.01 mole) and S-benzyl-L-cysteine ethyl ester (20) (from 2.77 g; 0.01 mole of the hydrochloride).

The crude product was recrystallized from boiling absolute ethanol (2.0 ml) to give 2.21 g (43.8%) of the pure product, m.p. 145–146° C (lit. (19): 142–145° C), $[\alpha]_D^{28}$ −16.7 (*c*, 1.19; dioxane) (lit. (19): $[\alpha]_D^{21.5}$ −17 (*c*, 1.8; dioxane)).

N-Tosyl-S-benzyl-L-cysteinyl-glycyl-L-serine Ethyl Ester, XVIII

A solution of the mixed anhydride of N-tosyl-S-benzyl-L-cysteinyl-glycine (11) (2.12 g; 5 mmoles) in dry tetrahydrofuran (20 ml) was prepared as in XV. To this solution was added a precooled suspension of L-serine ethyl ester (prepared from 0.857 g; 5 mmoles of the hydrochloride (29), on treatment with triethylamine). After being stirred for 30 minutes in the cooling bath and overnight at room temperature, the reaction mixture was evaporated to dryness in a rotary evaporator. The residue was dissolved in boiling ethyl acetate, the resulting solution was filtered, and the filtrate was evaporated to dryness. The semicrystalline oil was dissolved in 10 ml each of warm absolute ethanol and ether. Petroleum ether (b.p. 30–52° C) was added to the solution until it became opalescent. Crystallization of the product was induced by scratching. The yield of crude product was 1.76 g (65%).

For analysis, the product was recrystallized from ethanol–water; m.p. 147.5–148.5° C, $[\alpha]_D^{23.5}$ −30.6 (*c*, 1.37 in ethanol). Anal. Calc. for $C_{24}H_{31}O_7N_3S_2$ (537.6): C, 53.61; H, 5.81; N, 7.82%. Found: C, 53.12; H, 5.78; N, 7.97%.

Products from the Attempted Preparation of p-Nitrophenyl-N-tosylglycinate, XIX

N-Tosylglycine (30) (2.29 g; 0.01 mole) and *p*-nitrophenol (1.39 g; 0.01 mole) were dissolved in a mixture of methylene chloride (100 ml) – dimethylformamide (10 ml), and the solution was cooled to 0° C. N,N'-Dicyclohexylcarbodiimide (2.06 g; 0.01 mole) was then added. The reaction mixture was stirred for 30 minutes at 0° C, and overnight at room temperature, prior to being filtered. The residue (3.6 g) "r_1" was

[3] *Melting points were determined in capillary tubes and are uncorrected.*

[4] *Microanalyses were performed by Dr. C. Daesslé, Organic Microanalyses, 5757 Decelles St., Montreal, Que.*

[5] *We were unable to obtain the melting point reported in reference 15, despite repeated recrystallization of the product or repetition of the preparation.*

retained. On concentrating the filtrate, *in vacuo*, there was obtained a semicrystalline residue "r_2", which was treated with anhydrous ether (50 ml) and filtered. The ether-insoluble residue "r_3" was combined with "r_1". These combined residues ("r_1"+"r_3") were treated with hot absolute ethanol (50 ml), filtered, and the alcohol-insoluble portion "r_4" was weighed (1.7 g; 80%), m.p. 260° C. For analysis, "r_4" was recrystallized from either pyridine or dimethylformamide–ether, m.p. 262° C (lit. (12, 31): 295–296, 275° C), then dried *in vacuo* at 100° C for at least 4 hours. The analysis of the fraction "r_4" corresponded to that for 1,4-ditosylpiperazine-2,5-dione, VI. Anal. Calc. for $C_{18}H_{18}N_2O_6S_2$: N, 6.63%. Found: N, 6.83%.

From the hot alcoholic solution, there separated in an essentially quantitative yield (2.1 g), a product, m.p. 213–215° C, raised to 230–232° C (undepressed by admixture with authentic N,N-'dicyclohexylurea), on recrystallization from hot dimethylformamide. The product gave the correct analysis for N,N'-dicyclohexylurea. Anal. Calc. for $C_{13}H_{24}ON_2$: N, 12.49%. Found: N, 12.61%.

p-Nitrophenol was recovered on evaporation of the ether solution, followed by recrystallization of the residue from toluene. Alternatively, the isolation was achieved by extracting the *initial* filtrate with three portions of 1 *N* sodium hydroxide, acidifying the aqueous alkaline extract with 1 *N* hydrochloric acid, and extracting the acidified solution with ether. Evaporation of the ether, followed by recrystallization of the residue from toluene, gave 1.2 g (86%) of *p*-nitrophenol, m.p. and mixed m.p. 114° C.

N-Tosyl-L-pyroglutamic Acid p-Nitrophenyl Ester, XXI

N-Tosyl-L-pyroglutamic acid (28) (2.83 g; 0.01 mole) and *p*-nitrophenol (1.39 g; 0.01 mole) were dissolved in dry tetrahydrofuran (50 ml). The solution was cooled to 0° C. N,N'-Dicyclohexylcarbodiimide (2.06 g; 0.01 mole) was added, and the reaction mixture was stirred for 30 minutes at 0° C, and for 16 hours at room temperature. The precipitated N,N'-dicyclohexylurea was filtered, and the filtrate was concentrated to a semicrystalline oily residue, *in vacuo*, at about 40° C. The residue was dissolved in a minimum of absolute ethanol, and the resulting solution was filtered. Crystallization of the product was allowed to proceed at room temperature. The yield of recrystallized product was 1.82 g (45%), m.p. 126–128° C (colorless needles), $[\alpha]_D^{24}$ −19.8 (*c*, 1.21 in dimethylformamide). Anal. Calc. for $C_{18}H_{16}O_7N_2S$ (404.4): N, 6.93%. Found: N, 7.16%.

N-Tosyl-L-proline p-Nitrophenyl Ester, XXII

This compound was prepared exactly as in the above case, from N-tosyl-L-proline hemibenzenate (32) (3.06 g; 0.01 mole) and *p*-nitrophenol (1.39 g; 0.01 mole). The yield of the product was 2.90 g (74.8%), m.p. 105–106° C (from ethanol), $[\alpha]_D^{27}$ −106 (*c*, 1.43 in dioxane). Anal. Calc. for $C_{18}H_{18}O_6N_2S$ (390.4): N, 7.18%. Found: N, 7.24%.

N-Tosyl-S-benzyl-L-cysteinyl-glycine p-Nitrophenyl Ester, XXIII

To a stirred, ice-cooled solution of N-tosyl-S-benzyl-L-cysteinyl-glycine (11) (2.12 g; 5 mmoles) and *p*-nitrophenol (0.84 g; 6 mmoles) in dry tetrahydrofuran (20 ml) was added N,N'-dicyclohexylurea (1.24 g; 6 mmoles). The reaction mixture was stirred for 30 minutes in the cooling bath, and 3.5 hours at room temperature. The precipitated dicyclohexylurea was filtered, and the filtrate was evaporated to dryness *in vacuo*. The residue was triturated under ether, then it was dissolved in a minimum of boiling absolute alcohol (5 ml). Almost immediately, the product crystallized out. It was washed with ether then dried at the water pump. The yield of the product was 1.40 g (52%), m.p. 144–145° C, $[\alpha]_D^{26}$ +17.5 (*c*, 1.66; dimethylformamide). Anal. Calc. for $C_{25}H_{25}O_7N_3S_2$ (543.6): C, 55.23; H, 4.64; N, 7.73%. Found: C, 54.91; H, 4.86; N, 8.00%.

ACKNOWLEDGMENTS

One of the authors (T. M.) would like to thank the Office of Scientific Research, Que., for financial support in the form of two research scholarships, 1959–1960, 1960–1961.

We would also like to acknowledge the technical assistance of Mr. Penio Penev.

REFERENCES

1. F. SANGER. Brit. Med. Bull. **16**, 183 (1960).
2. E. BRAND. Ann. N.Y. Acad. Sci. **47**, 187 (1946). E. BRAND and J. T. EDSALL. Ann. Rev. Biochem. **16**, 223 (1947).
3. T. F. MASSIAH. Ph.D. thesis, University of Montreal, Montreal, Que. 1962.
4. J. HONZL and J. RUDINGER. Collection Czech. Chem. Comm. **20**, 1190 (1955).
5. J. RUDINGER. Collection Czech. Chem. Commun. **19**, 375 (1954).
6. L. VELLUZ, G. AMIARD, V. BARTOS, B. GOFFINET, and R. HEYMES. Bull. Soc. Chim. France, 1464 (1956).
7. M. BODANSZKY and V. DU VIGNEAUD. J. Am. Chem. Soc. **81**, 5688 (1959).
8. R. A. BOISSONNAS. Helv. Chim. Acta, **34**, 874 (1951). J. R. VAUGHAN. J. Am. Chem. Soc. **73**, 3547 (1951).
9. M. BERGMAN and L. ZERVAS. Ber. **65**, 1192 (1932).
10. J. C. SHEEHAN and G. P. HESS. J. Am. Chem. Soc. **77**, 1067 (1955).

Can. J. Chem. Downloaded from www.nrcresearchpress.com by 210.87.254.105 on 09/05/12
For personal use only.

11. C. BERSE, T. MASSIAH, and L. PICHÉ. J. Org. Chem. **26**, 4514 (1961).
12. M. ZAORAL and J. RUDINGER. Collection Czech. Chem. Commun. **26**, 2316 (1961).
13. M. ZAORAL. Collection Czech. Chem. Commun. **27**, 1273 (1962).
14. A. F. BEECHAM. J. Am. Chem. Soc. **79**, 3257, 3262 (1957).
15. S. J. LEACH and H. LINDLEY. Australian J. Chem. **7**, 173 (1954).
16. J. M. SWAN and V. DU VIGNEAUD. J. Am. Chem. Soc. **76**, 3110 (1954).
17. V. DU VIGNEAUD, M. F. BARTLETT, and A. JÖHL. J. Am. Chem. Soc. **79**, 5572 (1957).
18. K. C. HOOPER, H. N. RYDON, J. A. SCHOFIELD, and G. S. HEATON. J. Am. Chem. Soc. **78**, 3148 (1956).
19. J. M. SWAN, W. E. SAVIGE, and J. A. MACLAREN. Australian J. Chem. **11**, 345 (1958).
20. J. S. FRUTON. Advan. Protein Chem. **5**, 1 (1949).
21. B. L. SHAPIRO. Chem. Ind. (London), 1119 (1952).
22. T. WIELAND. Angew. Chem. **63**, 7 (1951); **66**, 507 (1954); **69**, 362 (1957).
23. V. DU VIGNEAUD. Chem. Soc. (London), Spec. Publ. No. 2, 49 (1955).
24. H. D. SPRINGALL and H. D. LAW. Quart. Rev. (London), **10**, 230 (1956).
25. M. GOODMAN and G. W. KENNER. Advan. Protein Chem. **12**, 465 (1957).
26. C. R. HARINGTON and T. H. MEADE. Biochem. J. **30**, 1598 (1936).
27. H. SCHWARZ and K. ARAKAWA. J. Am. Chem. Soc. **81**, 5691 (1959).
28. J. RUDINGER. Collection Czech. Chem. Commun. **19**, 370 (1954).
29. C. H. STAMMER, A. N. WILSON, C. F. SPENSER, F. W. BACHELOR, F. M. HOLLY, and K. FOLKERS. J. Am. Chem. Soc. **79**, 3236 (1957).
30. E. FISCHER and M. BERGMANN. Ann. **398**, 96 (1913). E. W. MCCHESNEY and W. K. SWANN. J. Am. Chem. Soc. **59**, 1116 (1937).
31. R. ENGER. Z. Physiol. Chem. **119**, 117 (1930).
32. Z. PRAVDA and J. RUDINGER. Collection Czech. Chem. Commun. **20**, 1 (1955).

Can. J. Chem. Downloaded from www.nrcresearchpress.com by 210.87.254.105 on 09/05/12
For personal use only.

THE PROTON MAGNETIC RESONANCE SPECTRUM OF CYCLOPROPYLAMINE

THE $A_2A_2'X$ CASE WITH STRONG CROSS-COUPLING: A PSEUDO FIRST-ORDER SPECTRUM WITH COMBINATION LINES

H. M. HUTTON[1] AND T. SCHAEFER

Department of Chemistry, University of Manitoba, Winnipeg, Manitoba

Received July 2, 1963

ABSTRACT

By means of the anisotropic solvent effect of benzene on the ring protons of cyclopropylamine the proton spectrum is converted to $A_2A_2'X$. Since the cross-coupling from the A_2 to the A_2' protons is large the spectrum does not approximate to a *pseudo* first-order AX_4 spectrum. Instead, it is one which may be described as *pseudo* first-order with combination lines. The presence of the latter allows a fairly complete set of coupling constants to be derived in a simpler way than by a computer attack on the general A_2B_2X spectrum. Conversely, the approach developed here, when applicable, allows the derivation of reliable input parameters for a computer program. From the temperature dependence of the $A_2A_2'X$ case the A_2 and A_2' protons can be distinguished and it is found that the protons trans to the amino group are preferentially shifted to high field by the benzene molecules.

Can. J. Chem. Downloaded from www.nrcresearchpress.com by 210.87.254.105 on 09/05/12
For personal use only.

INTRODUCTION

Sometimes many of the theoretical transitions in high-resolution n.m.r. spectra effectively coalesce or may be too weak to be observed. Since the analysis of the spectra usually reduces to the problem of assigning the observed peaks, there may then be more than one assignment and, therefore, more than one set of coupling constants which fits the observed spectrum. Abraham and Bernstein have discussed this situation for the ABX, A_2X_2, and ABXY spectra in some detail (1). In practice it is usually found that only sums or differences of coupling constants can be obtained from the observed *pseudo* first-order spectra. In general, such deceptively simple spectra are expected for the ABC...XYZ... systems when quantities of the type $J_{AB'}$ J_{XY} are large compared to the chemical shift differences $\delta_{AB'}$ δ_{XY} plus quantities of the type $J_{AX}-J_{AY}$. Separations between the lines in each group are then given by the average of constants of the type $J_{AX'}$ J_{AY}. When the system has some symmetry the general statements have to be modified slightly (1).

Examples of deceptively simple spectra are discussed in reference 1 and misinterpretations in the literature are also discussed. A similar discussion for the ABX case was given by Schaefer (2), by Grant and Gutowsky for the A_2B_2 case (3), and by Musher and Corey for the three-spin system (4).

We discuss here the ring-proton spectrum of cyclopropylamine. The proton on the substituted carbon atom is shifted far enough to low field by the inductive effect of the amino group that, in general, an A_2B_2X system is obtained at 60 Mc/s. This case was first discussed by Richards and Schaefer (5). By means of solvent effects we bring about a zero shift between the A and B protons and hence obtain an $A_2A_2'X$ system. A *pseudo* first-order spectrum is not found, however, but rather what may be described as a *pseudo* first-order spectrum with combination lines. As we shall show, this is due to a strong cross-coupling between A and A′ protons. Such a situation could have been qualitatively

[1]*Holder of a C.I.L. Fellowship, 1962–1963.*

predicted from the discussion in reference 1. It appears that our example is the first of this type. It will also appear that the existence of the few extra lines in the $A_2A_2'X$ spectrum allows one to place quite stringent limits on the values of the coupling constants. This is important in obtaining good starting values for the parameters in the computer solutions for systems as complex as a strongly coupled A_2B_2X.

EXPERIMENTAL

Proton spectra were taken on a Varian DP60 n.m.r. Spectrometer and calibrations were carried out by the side-band technique relative to internal tetramethylsilane (TMS). Spectra were taken in a number of solvents but in none of them except benzene were they strikingly different from the standard spectrum in $CDCl_3$ recorded by Bhacca *et al.* (6). In benzene it was possible to obtain a spectrum of simple appearance at a concentration of about 1:4 by volume. This concentration was very critical and the collapsed peaks were found to separate rapidly with concentration on *either* side of the critical one.

Spectra of this critical solution in benzene were run at various temperatures up to 131° C. Dissociation of the very weak complex formed with benzene (7) allowed the separation of the collapsed peaks to be followed in a sensitive way. In this way the assignments of the peaks could be checked and it was also possible to obtain the relative order of the shifts of the two sets of equivalent protons in the uncollapsed region.

RESULTS AND DISCUSSION

The proton spectrum of the critical solution in benzene is shown together with calculated spectra in Fig. 1. In Fig. 2 the spectrum of the same solution at 64° C is shown.

1. *The Case $A_2A_2'X$*

The critical solution spectrum of the ring protons corresponds to the case $A_2A_2'X$.* The limiting case where the couplings from A_2 and A_2' to X are equal has already been discussed by one of us (8). None of the possible 46 combination lines were considered in that treatment. Because some of these play a major role in our discussion and for reasons of clarity we discuss here a rather general case, including the combination lines.

The ring-proton system for the critical solution can be characterized as in I:

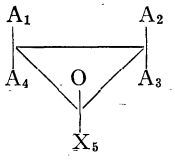

$$H_A = H_{A'} = H_0(1-\sigma_A);$$
$$J_{12} \approx J_{34};\ J_{14} = J_{23};\ J_{15} = J_{25};$$
$$J_{35} = J_{45};\ J_{13} = J_{24}$$

I

We shall assume that $J_{12} = J_{34}$. This is the only approximation we make and from the analysis of cyclopropylcarboxylic acid (9, 10) this approximation is considered to be valid to at least 0.5 c.p.s. Thirty-six of the line positions are independent of J_{12} and J_{34} and from the analysis it is clear that the error in many other line positions will be about half that of the difference in J_{12} and J_{34} or about 0.25 c.p.s.

The matrix elements in the F_z representation are given in reference 8. In the $A_2A_2'X$ case the matrix is factored to eight 1×1, eight 2×2, and two 4×4 submatrices.

Positive quantities A, B, C, D and angles θ, ϕ, ψ, γ are defined by

[1]
$$4A\cos 2\theta = J_{35}-J_{15} \qquad 4B\cos 2\phi = J_{15}-J_{35}$$
$$2A\sin 2\theta = J_{23}+J_{13} \qquad 2B\sin 2\phi = J_{23}+J_{13}$$
$$4C\cos 2\psi = J_{35}-J_{15} \qquad 4D\cos 2\gamma = J_{15}-J_{35}$$
$$2C\sin 2\psi = J_{23}-J_{13} \qquad 2D\sin 2\gamma = J_{13}-J_{23}$$

**The amine protons gave a broad peak. Apart from a slight broadening of the neighboring proton there was no evidence of any coupling with the ring protons by either the amine protons or the nitrogen nucleus.*

Can. J. Chem. Downloaded from www.nrcresearchpress.com by 210.87.254.105 on 09/05/12
For personal use only.

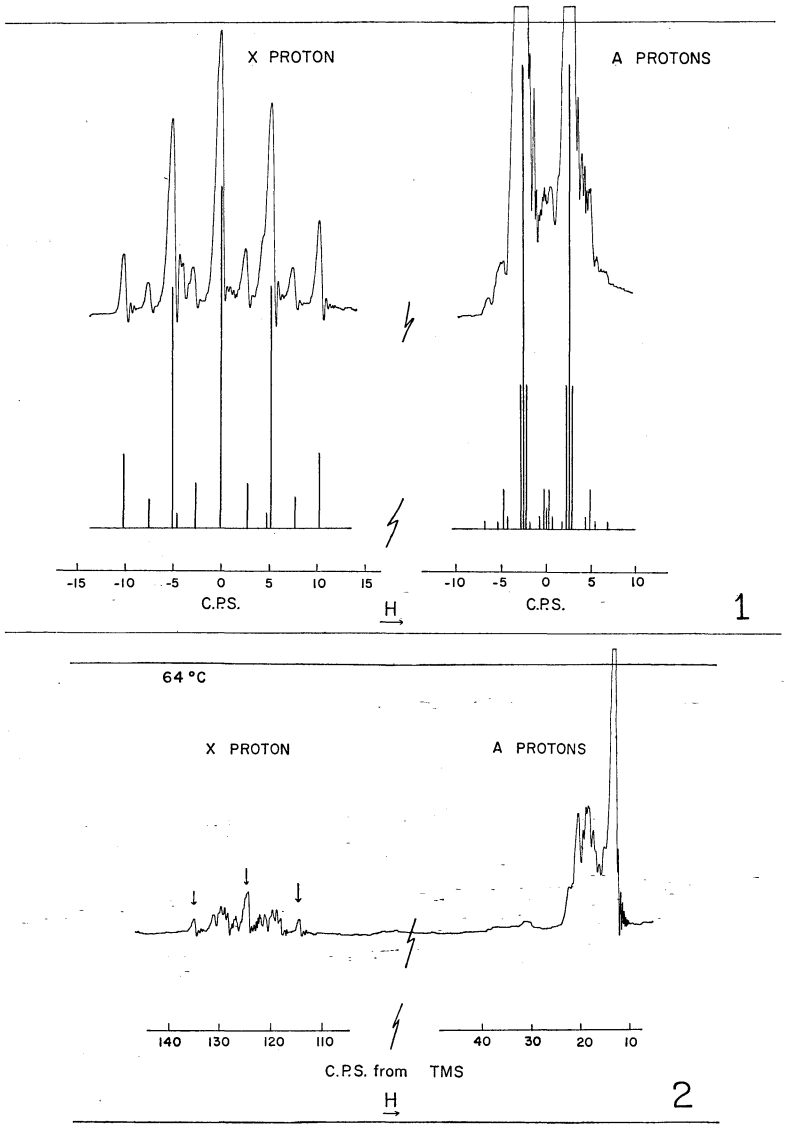

FIG. 1. Proton magnetic resonance spectrum at 60 Mc/s of cyclopropylamine in benzene at room temperature. Calibration is in c.p.s. with respect to $\nu_0(1-\sigma_A)$ and $\nu_0(1-\sigma_X)$, which are at 16.2 c.p.s. and 123.2 c.p.s. to low field of internal TMS, respectively. In the calculated spectrum, the two large *pseudo* triplets in the A region are drawn to one-third the intensity of the other transitions. The amino group resonance at 84.8 c.p.s. to low field of internal TMS is not shown.

FIG. 2. Proton magnetic resonance spectrum at 60 Mc/s of cyclopropylamine in benzene at 64° C; calibration is to low field of internal TMS. The amino group resonance at 90 c.p.s. is not shown. The transitions of the X proton which do not vary in position on introduction of a shift between A_2 and A_2' are indicated by the arrows.

The indicated orthogonal transformations were carried out on the eight 2×2 matrices and the stationary spin functions and energies are given in Tables III and IV of reference 8.*

**Reprint requests for this paper will also receive a reprint of reference 8.*

Can. J. Chem. Downloaded from www.nrcresearchpress.com by 210.87.254.105 on 09/05/12
For personal use only.

Selection rules allow a maximum of 110 transitions for the five nuclei. Of these, 46 are combination lines which were not considered in reference 8 but which will be taken into account here. Of the 46 combination lines, 18 are zero under all circumstances. This leaves 92 transitions for the general case. At this point we cease to distinguish between combination and other lines since for strong cross-coupling there is no longer a real distinction in the $A_2A_2'X$ limit.

The X protons give rise to a maximum of 36 lines of which 16 involve the two 4×4 submatrices. For the other 20, explicit energies and intensities are given in Table I. The A_2 and A_2' protons give rise to 56 lines of which 32 involve the 4×4 submatrices. Explicit energies and intensities for the other 24 are given in Table II.

TABLE I

Transitions and intensities of proton X

	Energy, relative to $\nu_0(1-\sigma_X)$	Relative intensity
1.	$J_{15}+J_{35}$	1
2.	$1/2(J_{15}+J_{35})-A+B$	$(\cos\theta\cos\phi+\sin\phi\sin\theta)^2$
3.	$1/2(J_{15}+J_{35})+A-B$	$(\cos\theta\cos\phi+\sin\phi\sin\theta)^2$
4.	$-1/2(J_{15}+J_{35})+A-B$	$(\cos\theta\cos\phi+\sin\phi\sin\theta)^2$
5.	$-1/2(J_{15}+J_{35})-A+B$	$(\cos\theta\cos\phi+\sin\phi\sin\theta)^2$
6.	$-(J_{15}+J_{35})$	1
7.	$1/2(J_{15}+J_{35})-C+D$	$(\cos\gamma\cos\psi-\sin\gamma\sin\psi)^2$
8.	$1/2(J_{15}+J_{35})+C-D$	$(\cos\gamma\cos\psi-\sin\gamma\sin\psi)^2$
9.	0	1
10.	0	1
11.	$-1/2(J_{15}+J_{35})+C-D$	$(\cos\gamma\cos\psi-\sin\gamma\sin\psi)^2$
12.	$-1/2(J_{15}+J_{35})-C+D$	$(\cos\gamma\cos\psi-\sin\gamma\sin\psi)^2$
13.	$1/2(J_{15}+J_{35})+A+B$	$(\sin\theta\cos\phi-\sin\phi\cos\theta)^2$
14.	$1/2(J_{15}+J_{35})-A-B$	$(\sin\phi\cos\theta-\sin\theta\cos\phi)^2$
15.	$-1/2(J_{15}+J_{35})-A-B$	$(\sin\phi\cos\theta-\sin\theta\cos\phi)^2$
16.	$-1/2(J_{15}+J_{35})+A+B$	$(\sin\theta\cos\phi-\sin\phi\cos\theta)^2$
17.	$1/2(J_{15}+J_{35})+C+D$	$(\sin\gamma\cos\psi+\sin\psi\cos\gamma)^2$
18.	$1/2(J_{15}+J_{35})-C-D$	$(\sin\psi\cos\gamma+\sin\gamma\cos\psi)^2$
19.	$-1/2(J_{15}+J_{35})-C-D$	$(\sin\psi\cos\gamma+\sin\gamma\cos\psi)^2$
20.	$-1/2(J_{15}+J_{35})+C+D$	$(\sin\gamma\cos\psi+\sin\psi\cos\gamma)^2$

NOTE: Transitions 21–36 involve the 4×4 submatrices.

2. The Proton Spectrum of Fig. 1

(a) The X Region

If the six weakest lines in the region are disregarded there are left five equally spaced lines with a separation of 5.10 c.p.s.* Comparison with Table I indicates that we have $|J_{15}+J_{35}| = 10.2$ c.p.s. In a *pseudo* first-order spectrum these five lines would be expected to have intensities in the ratio of 1:4:6:4:1. It is obvious that this is not so and, clearly, the six weak lines derive their intensitis from the inner three of the main lines.

In Table I eight lines are listed (lines 13–20) which become combination lines in the limit of a large shift between the A_2 and A_2' protons. We assign lines 13–16 to the two pairs flanking the main peaks at ±5.10 c.p.s. From equation [1] it immediately follows that $A = B = 1.25$ c.p.s., and using the experimental intensities in Fig. 1 we can place the following limits on the parameters: $1/4(J_{35}-J_{15}) = 0.7 \rightarrow 0.8$ c.p.s., $1/2(J_{23}+J_{13}) = 1.0 \rightarrow 0.9$ c.p.s., $\phi-\theta = 41^\circ \rightarrow 44^\circ$.

**The intensities of these lines increase slightly towards high field, indicating that the X approximation is not quite valid. However, $\nu_0(\sigma_A-\sigma_X) = 107.0$ c.p.s. compared with the largest off-diagonal element, expected to be no larger than about 12 c.p.s. It is well known that the line positions are not nearly as sensitive to the spin functions as are the intensities and we can proceed with the analysis with some confidence.*

Can. J. Chem. Downloaded from www.nrcresearchpress.com by 210.87.254.105 on 09/05/12
For personal use only.

TABLE II

Transitions and intensities of A and A′ protons

	Energy, relative to $\nu_0(1-\sigma_A)$	Relative intensity
37.	$1/4(2J_{13}+2J_{23}+J_{15}+J_{35})-A$	$2(1+\sin 2\theta)$
38.	$1/4(-2J_{13}-2J_{23}+J_{15}+J_{35})-A$	$2(1-\sin 2\theta)$
39.	$1/4(-2J_{13}-2J_{23}-J_{15}-J_{35})-B$	$2(1-\sin 2\phi)$
40.	$1/4(2J_{13}+2J_{23}-J_{15}-J_{35})-B$	$2(1+\sin 2\phi)$
41.	$1/4(-2J_{13}+2J_{23}+J_{15}+J_{35})-C$	$1+\sin 2\psi$
42.	$1/4(2J_{13}-2J_{23}+J_{15}+J_{35})-C$	$1-\sin 2\psi$
43.	$1/4(-2J_{13}+2J_{23}-J_{15}-J_{35})-D$	$1-\sin 2\gamma$
44.	$1/4(2J_{13}-2J_{23}-J_{15}-J_{35})-D$	$1+\sin 2\gamma$
45.	$1/4(-2J_{13}+2J_{23}+J_{15}+J_{35})-C$	$1+\sin 2\psi$
46.	$1/4(2J_{13}-2J_{23}+J_{15}+J_{35})-C$	$1-\sin 2\psi$
47.	$1/4(2J_{13}-2J_{23}+J_{15}+J_{35})-D$	$1+\sin 2\gamma$
48.	$1/4(-2J_{13}+2J_{23}-J_{15}-J_{35})-D$	$1-\sin 2\gamma$
49.	$1/4(2J_{13}+2J_{23}+J_{15}+J_{35})+A$	$2(1-\sin 2\theta)$
50.	$1/4(2J_{13}+2J_{23}-J_{15}-J_{35})+B$	$2(1-\sin 2\phi)$
51.	$1/4(-2J_{13}-2J_{23}+J_{15}+J_{35})+A$	$2(1+\sin 2\theta)$
52.	$1/4(-2J_{13}-2J_{23}-J_{15}-J_{35})+B$	$2(1+\sin 2\phi)$
53.	$1/4(-2J_{13}+2J_{23}+J_{15}+J_{35})+C$	$1-\sin 2\psi$
54.	$1/4(2J_{13}-2J_{23}+J_{15}+J_{35})+C$	$1+\sin 2\psi$
55.	$1/4(-2J_{13}+2J_{23}-J_{15}-J_{35})+D$	$1+\sin 2\gamma$
56.	$1/4(2J_{13}-2J_{23}-J_{15}-J_{35})+D$	$1-\sin 2\gamma$
57.	$1/4(2J_{13}-2J_{23}+J_{15}+J_{35})+C$	$1+\sin 2\psi$
58.	$1/4(-2J_{13}+2J_{23}+J_{15}+J_{35})+C$	$1-\sin 2\psi$
59.	$1/4(-2J_{13}+2J_{23}-J_{15}-J_{35})+D$	$1+\sin 2\gamma$
60.	$1/4(2J_{13}-2J_{23}-J_{15}-J_{35})+D$	$1-\sin 2\gamma$

NOTE: Transitions 61–92 involve the 4×4 submatrices.

We have assumed here that J_{23} is smaller than and of opposite sign to J_{13} and that J_{15} and J_{35} are of the same sign with $J_{35} > J_{15}$. This agrees with a considerable set of data (10–13). The same sign of J_{23} and J_{13} would simply interchange the constants A, B with C, D so that the relative signs of J_{23} and J_{13} cannot be obtained from the spectrum at this point. Opposite signs of J_{15} and J_{35} can, however, be ruled out at this point. If they did have opposite signs then the spectrum would not be simple unless $1/4(|J_{35}|+|J_{15}|) \ll 1/2|J_{23}+J_{13}|$, which is hardly likely. On the other hand, if J_{13} were very small (cross-coupling small) and $1/4|J_{35}-J_{15}| \ll 1/2|J_{23}|$ then the spectrum would be completely *pseudo* first-order as has been shown, in effect, in reference 8.

From the additional demand that C and D be large enough to have $\sin^2(\psi+\gamma) \lesssim 0.01$ (lines 17–20 in Table I are then unobservable), it follows that $C = D = 6.5 \rightarrow 6.6$ c.p.s. with $1/2|J_{13}-J_{23}| = 6.5-6.6$ c.p.s. Hence we obtain $J_{23} = -5.5\pm0.1$ c.p.s. and $J_{13} = 7.5\pm0.1$ c.p.s.

With this set of data the intensities and positions of all the lines in Table I can be calculated. The positions of the two weak lines overlapping the main lines at ±5.10 c.p.s. are still to be accounted for. We note that the pairs of lines at ±10.2 c.p.s. are of unit intensity and should not vary in position on introduction of a shift between A_2 and A_2'. The same holds for the position of the six lines falling at 0 c.p.s. In Fig. 2 the spectrum verifies these statements. The separation of the three peaks in the X region is temperature independent.

(b) The A Region

The partial set of parameters derived from the X region allows the calculation of intensities and positions of the 24 lines in Table II. None of the intense lines deviate by more than 0.2 c.p.s. from the expected positions at $\nu_0(1-\sigma_A)\pm2.55$ c.p.s.

Can. J. Chem. Downloaded from www.nrcresearchpress.com by 210.87.254.105 on 09/05/12
For personal use only.

(c) The 4×4 Submatrices and J_{12}

We must now solve the two 4×4 submatrices. The energy levels of the one will differ from the energy levels of the others only by $\nu_0(1-\sigma_X)$. Hence four transitions between the two sets will fall at $\nu_0(1-\sigma_X)$, no matter what parameters are used for the solution, but the other transitions involving these eight energy levels will depend on the input parameters. J_{15} and J_{35} enter in the same way as in equation [1]. J_{23} and J_{13} enter separately and we take the values obtained above. J_{12} enters also, for the first time, and we chose it as an adjustable parameter. The 4×4 submatrices were solved for the values of J_{12} = 8.0, 9.0, 10.0, 11.0, and 12.0 c.p.s. The positions of the weak lines at ±4.6 c.p.s. in the X region were smooth and fairly sensitive functions of J_{12}, although their intensities were not very sensitive to J_{12}. In this way we found $J_{12} = 12.5\pm0.5$ c.p.s., a reasonable value (10).

The complete calculated spectrum of 92 lines is shown in Fig. 1. Note that additional intensity accrues to the lines at $\nu_0(1-\sigma_X)\pm2.7$ c.p.s. from transitions involving the 4×4 submatrices. Note also that all lines separated by 0.25 c.p.s. or less have been collapsed in order to take the finite resolution of the observed spectrum into account. The agreement found is thought to be satisfactory. It indicates also that J_{23} is indeed negative since it enters diagonally and off-diagonally into the 4×4 submatrices. In Fig. 1 it is seen that the lines in the A region which fall off the ±2.55 c.p.s. doublet calculated in *pseudo* first-order are relatively weak compared to the analogous lines in the X region. If the A region is run at an instrument gain such that the doublet just fills the paper no evidence of any other lines is noticeable.

(d) Summary of Results

We feel that the following sets of parameters in c.p.s. are reliable within the limits stated:

$$\begin{aligned}
\nu_0(\sigma_A-\sigma_X) &= 107.0,\\
J_{34} \approx J_{12} &= J_{cis} = 12.5\pm0.5,\\
J_{14} = J_{23} &= J_{gem} = -5.5\pm0.3,\\
J_{24} = J_{13} &= J_{trans} = 7.5\pm0.3,\\
(J_{15}+J_{35}) &= 10.2\pm0.1,\\
J_{25} = J_{15} &= J_{trans} = 3.6\pm0.5,\\
J_{45} = J_{35} &= J_{cis} = 6.6\pm0.5.
\end{aligned}$$

The last two values have been derived by considering the data in references 10–13, which suggest that the ratio of J_{cis} to J_{trans} falls between 1.5 and 1.8, increasing as the electronegativity of the substituent increases. The geminal coupling constant is designated as negative with respect to the vicinal coupling constants.

3. The Solvent and Temperature Dependence of the Shift of the A and A′ Protons

The effect of the benzene is to shift one pair of protons to high field more effectively than the other. For steric reasons (7, 14) we would expect the protons trans to the NH_2 group to be shifted most rapidly to high field by the anisotropic benzene molecules. If this is actually an association effect, similar to the one we studied for bis(2,2-dichlorocyclopropyl) ether (7), then increasing temperature should cause the fastest low-field shift for these protons. In Fig. 2 the low-field line of the intense doublet in the A region has split up while the high-field line has not. In equation [1] each of the cosine expressions has added to it a shift term on the right-hand side for the A_2B_2X case. From the values of the coupling constants given above we can calculate the values of A, B, C and D as

Can. J. Chem. Downloaded from www.nrcresearchpress.com by 210.87.254.105 on 09/05/12
For personal use only.

a function of the shift between the A and A′ protons. It follows easily that only A changes rapidly in the region of small shift. For instance, when the shift is 1 c.p.s., A has changed from 1.3 to 2.1 c.p.s. while the others have changed by about 0.2 c.p.s. We expect lines like 37 and 51 in Table II to change their positions most rapidly and these are both originally centered on the low-field line of the intense doublet.

Now it is clear that in the limit of large shift the splitting in the group of lines arising from the protons trans to the amino group, i.e., cis to the X proton, will be largest: $J_{cis} > J_{trans}$. Hence, as the shift decreases to zero this group of lines will collapse last. This set of lines appears at low field as shown above and moves to low field as the temperature increases. We have shown, therefore, that it is the protons trans to the amino group which are most solvent dependent and experience the largest high-field shift on dilution in benzene. This is consistent with a preferred interaction with benzene molecules at this position.

The low-field shift of the trans protons can be understood in terms of Buckingham's electric field calculations (15). The cis protons would also be shifted to low field by the dipole whose negative end points in the C—N direction but, due to the angular factor, would be expected to be less, as observed. A quantitative estimate demands a knowledge of the magnitude of this dipole and also, perhaps, whether the contribution of the lone pair on the nitrogen is important.

ACKNOWLEDGMENTS

One of us (H. M. H.) would like to thank Canadian Industries Limited for fellowship support. The financial support of the National Research Council was essential to this study.

REFERENCES

1. R. J. Abraham and H. J. Bernstein. Can. J. Chem. **39**, 216 (1961).
2. T. Schaefer. Can. J. Chem. **40**, 1678 (1962).
3. D. Grant and H. S. Gutowsky. J. Chem. Phys. **34**, 699 (1961).
4. J. I. Musher and E. J. Corey. Tetrahedron, **18**, 791 (1962).
5. R. E. Richards and T. Schaefer. Proc. Roy. Soc. (London), Ser. A, **246**, 429 (1958).
6. N. S. Bhacca, L. F. Johnson, and J. N. Shoolery. NMR Spectra Catalog, Varian Associates. Spectrum No. 37. 1962.
7. H. M. Hutton and T. Schaefer. Can. J. Chem. **41**, 1857 (1963).
8. T. Schaefer. Can. J. Chem. **37**, 882 (1959).
9. K. Wiberg. Private communication.
10. H. M. Hutton and T. Schaefer. Can. J. Chem. **41**, 684 (1963).
11. H. M. Hutton and T. Schaefer. Can. J. Chem. **41**, 1623 (1963).
12. D. Seyferth, H. Yamazaki, and D. L. Alleston. J. Org. Chem. **28**, 703 (1963).
13. J. D. Graham and M. T. Rogers. J. Am. Chem. Soc. **84**, 2249 (1962).
14. T. Schaefer. Can. J. Chem. **39**, 1864 (1961).
15. A. D. Buckingham. Can. J. Chem. **38**, 300 (1960).

Can. J. Chem. Downloaded from www.nrcresearchpress.com by 210.87.254.105 on 09/05/12
For personal use only.

THE TRANSMISSION OF POLAR EFFECTS

KEITH BOWDEN
Department of Chemistry, University of British Columbia, Vancouver, British Columbia
Received June 6, 1963

ABSTRACT

The transmission of polar effects by various groups is assessed by means of the reaction constants ρ or ρ''. The results are critically discussed in terms of the various polar, steric, and solvent effects. Conclusions are drawn as to the importance of the inductive and direct field effects.

Can. J. Chem. Downloaded from www.nrcresearchpress.com by 210.87.254.6 on 09/05/12
For personal use only.

INTRODUCTION

The processes which have been postulated to account for the polar influences of substituents are the direct field, inductive, and resonance effects. The direct field effect is the coulombic action on a reaction center of a charged or dipolar substituent. The inductive effect is the effect due to the polarization of the bonds connecting the substituent to the reaction center. The bonds so affected may be either the strong σ-bonds, which determine the skeletal geometry of the system, or the weaker, fluid π-bonds. In systems involving π-bonds a resonance effect may occur. If the substituent has electrons in suitable atomic orbitals, these can participate in the molecular orbital of a conjugated system (interaction of the π-electron cloud with a lone pair of the substituent), to displace electrons within the system.

Ingold (1) considered the first two effects separable. Other workers have thought this view to be mistaken and have either considered the two effects to be inseparable or one effect to predominate. Kirkwood and Westheimer (2) attempted to calculate the transmission of polar effects by considering the direct field effect alone. Later workers (3, 4, 5) have used their methods to give fair correlations of observed and calculated effects in a number of systems. Dewar and Grisdale (6) in recent studies have attempted an empirical relation on this basis. Jaffé (7) has used a M.O. method to calculate the transmission by π-bonded systems by assuming that only the π-inductive effect is important (cf. ref. 8). Taft (9) regards polar effects as separable into inductive and resonance contributions, in a similar manner to the earlier contributions by Branch and Calvin (10).

The Hammett equation (i) and similar linear free energy relations (4, 5, 9, 11) can be used to correlate reaction rates and equilibria. The substituent constant σ was considered

$$\log (k/k_0) = \rho\sigma \qquad \text{(i)}$$

to be independent of the nature of the reaction, and is a measure of the polar effect of a meta or para substituent relative to the unsubstituted compound. The reaction constant ρ for a reaction series is thus a measure of the susceptibility of the reaction to polar effects.

The relay of polar effects by 23 aryl and alkyl systems has been studied in an attempt to determine the relative importance of the various mechanisms of transmission. Linear free energy relations have been used to assess the efficiency of transmission without confusion caused by exalted resonance effects. Also a model system has been constructed to estimate the direct field effect and the apparent inductive transmission factors have been calculated. The transmission was then interpreted in terms of the direct field and

inductive effects. The steric effects of ortho substitution on the solvation and the transmission of polar effects are discussed. Substituent effects in benzene are related to these results and an analysis of the proposed model systems of benzene is given.

CALCULATIONS AND RESULTS

The correlations were made using the statistical methods of Jaffé (12). The ideals of Wepster and his co-workers (13) were observed, as closely as possible, in choosing the substituents to be studied, which were those in which extra-resonance interactions could be considered negligible, and the substituent constants σ were used (see ref. 13 and p. 000). In a limited number of reactions (Table I, reaction series 8; Table II, reaction series 6 and 8) it was necessary to use substituents (*p*-methyl, *p*-chloro, or *p*-bromo) which might exhibit exalted resonance effects. However, these substituents show only small variations in resonance effect and the σ^n values used should have general applicability.

Three reactions were chosen: ionization of carboxylic acids, esterification of carboxylic acids with diazodiphenylmethane, and alkaline hydrolysis of carboxylic esters, for which sufficient data are available. In Table I the Hammett reaction constants ρ are given for systems where a group Y separates the aromatic phenyl group from the reactive function. Table II shows the Hammett reaction constants for systems in which the ortho substituents of the aryl group are varied. The reaction constants ρ'' in Table III are based on the ionization of *trans* 4-substituted cyclohexanecarboxylic acids (5). The substituent constants σ'' for the hydrogen, chloro, hydroxy, cyano, carbomethoxy, and methoxy groups (5) are used.

Correlation coefficients are in all cases greater than 0.95 and are usually (70% of them) between 0.98 and 1.00. The number of substituents studied, n, is shown and the reference given. Where Wepster's work (13) is indicated, his value of ρ has been used.

Polar Effects

Kirkwood and Westheimer have proposed the equation (ii) to calculate the direct field effect of a substituent group on ionization constants and the relative rates of alkaline

$$[ii] \qquad \log K/K_0 = \frac{e\mu \cos\theta}{2.303kTD'r^2}$$

hydrolysis of esters (2), where μ is the dipole moment, e the electronic charge, k the Boltzmann constant, T the absolute temperature, r the distance between the center of the dipole and the reaction center, and D' the effective dielectric constant. θ is the angle between the line joining the reaction center and the center of the dipole and the axis of the dipole. The effective dielectric constant is difficult to calculate. Molecules are considered to be cavities of low dielectric ($D = 2.0$) embedded in the solvent, which has commonly a very high dielectric constant.

The transmission of the substituent effect is determined by the factor $\cos\theta/r^2D'$. A simple model of the systems studied was used to calculate the readily computable angle and distance. The center of the dipole was considered to be situated at the "para" carbon atom of the phenyl group for the systems involving aromatic and arylaliphatic groups. The direction of the dipole vector was then taken as the line generated by joining the "para" carbon atom to the carbon atom linked to the functional group. The chloro-substituted molecules were used as models for the systems shown in Table III (i.e. aliphatic and alkylaromatic). The reactive center was sited 0.89 Å beyond the carbon of the carboxyl group on the extension of the bond joining the carboxyl carbon to the rings.

Can. J. Chem. Downloaded from www.nrcresearchpress.com by 210.87.254.6 on 09/05/12
For personal use only.

Can. J. Chem. Downloaded from www.nrcresearchpress.com by 210.87.254.6 on 09/05/12
For personal use only.

TABLE I

Hammett reaction constants ρ for systems 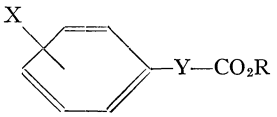

		Ionization						Esterification			Ester hydrolysis		
		Water at 25°			50% ethanol–water at 25°			Diphenyldiazomethane, ethanol at 30°			Alkaline, ethyl esters, ethanol–water at 25° or 30°		
Series	Y	ρ	Ref.	n	ρ	Ref.	n	ρ	Ref.	n	ρ	Ref.	n
1	—	1.000	13	10	1.570	13	4	0.947	13	4	2.558,[d] 2.545,[e] 2.468[f]	13	5, 8, 8
2	CH_2	0.562	13	5	—			0.403	17	4	1.029,[d] 0.964[g]	19, 20	4, 5
3	$(CH_2)_2$	0.237	13	4	0.417	16	3	0.218	17	4	0.635[e]	21	3
4	OCH_2	0.341	14	8	—			0.247	17	4	—[k]		
5	*trans*-C_3H_4	0.190	15	4	0.542	16	5	—			0.846[e]	21	4
6	*cis*-C_3H_4	—			0.517	16	3	—			1.098[e]	21	4
7	*trans*-CH=CH	0.418	13	4	—			0.416	17	4	1.242,[d] 1.255[e, i]	13, 21	5, 5
8	*cis*-CH=CH	—[k]			—			—			1.093[e]	21	3
9	C≡C	—			0.625,[a] 0.417	13, 18	4, 4	0.310	18	4	2.051[e, h]	18	3
10	C_6H_4[c]	—			0.437[b]	13	3	0.224	17	4	0.600[e]	22	4
11	CH=CHCO	—			—[k]			—			0.352[j]	13	3

[a] ρ at 24°.
[b] 50% 2-*n*-Butoxyethanol–water in presence of 0.05 *M* LiCl; ρ (benzoic acids) is 1.438.
[c] *p*-Phenylbenzoic acids.
[d] 85% ethanol–water at 25°.
[e] 88% ethanol–water at 30°.
[f] 56% acetone–water at 25°.
[g] 60% acetone–water at 25°.
[h] ρ at 20°.
[i] Mean ρ from references 13 and 21.
[j] Methyl esters in 12% methanol–water at 25°; ρ (methyl benzoates) is 1.666 (23).
[k] Data insufficient in number or range.

Can. J. Chem. Downloaded from www.nrcresearchpress.com by 210.87.254.6 on 09/05/12
For personal use only.

TABLE II

Hammett reaction constants ρ for systems 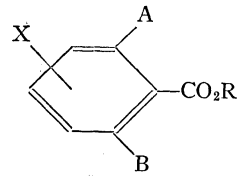

Series	Ortho substituents A	Ortho substituents B	Ionization: Water at 25° ρ	Ref.	n	Ionization: 50% ethanol–water at 25° ρ	Ref.	n	Esterification: Diphenyldiazomethane, ethanol at 30° ρ	Ref.	n	Ester hydrolysis: Alkaline, ethyl esters, 85% ethanol–water at 25° ρ	Ref.	n
1	H	H	1.000	13	10	1.570	13	4	0.947	13	4	2.558	13	5
2	Cl	H	1.146	24	3	—			—			—		
3	OH	H	1.150	25	5	1.778[b]	27	3	—			—		
4	NO_2	H	0.905	13	5	—			—			—		
5	Me	H	1.248[a]	13	6	1.773	13	5	0.887	13	5	2.334[c, f]	13	6
6	Me	Me	—			1.354[i]	28	4	0.642[i]	28	4	2.197[d, f]	30	4
7	C_4H_4	H[g]	1.142	26	3	1.311	6	3	—			2.403[e, f]	31	5
8	C_4H_4	C_4H_4[h]	—			1.924[b]	29	4	0.697	17	4	—		

[a] 1% Ethanol–water at 20°.
[b] 80% 2-methoxyethanol–water at 25°; ρ (benzoic acids) is 1.709 (27).
[c] ρ at 45° is 2.187.
[d] Methyl esters in 60% aqueous dioxane, ρ at 125° is 1.645; ρ (ethyl benzoates) at 25° in 70% aqueous dioxane is 2.470 (32).
[e] ρ at 50° is 2.217.
[f] Using $\rho_{25} = T \times \rho_T/298.2$ (12). This relation seems to be approximately obeyed by this reaction.
[g] 3- or 4-Substituted 1-napthoic acid derivatives; those substituents at 4-position which are affected by steric inhibition of resonance (e.g. nitro (31)) are excluded.
[h] 9-Substituted 10-anthroic acid derivatives; those substituents at 9-position which are affected by steric inhibition of resonance (e.g. nitro (29)) are excluded.
[i] σ^n (p-CO_2Me) is 0.484; incorrect value given in reference 13.

Can. J. Chem. Downloaded from www.nrcresearchpress.com by 210.87.254.6 on 09/05/12
For personal use only.

TABLE III

Reaction constants ρ'' for systems X—Y—CO_2R

		Ionization						Esterification			Ester hydrolysis		
		Water at 25°			50% ethanol–water at 25°			Diphenyldiazomethane, ethanol at 30°			Alkaline, ester in various conditions		
Series	Y	ρ''	Ref.	n	ρ''	Ref.	n	ρ''	Ref.	n	ρ''	Ref.	n
1	C_6H_{10}[a]	1.000	5	6	1.490	5	6	0.540	5	6	1.586[d]	5	5
2	C_8H_{12}[b]	—			2.022[e]	4	5	0.964[e]	4	5	3.094[e, f]	4	5
3	CH_2	5.664	24	4	5.922	33	4	3.999[g]	35	4	—[i]		
4	$(CH_2)_2$	2.188	24	3	—			—[h]			—[i]		
5	$CH_2(C_6H_4)$[c]	—			1.232	34	4	—			—		

[a]4-Substituted *trans*-cyclohexanecarboxylic acid system.
[b]4-Substituted bicyclo(2.2.2)octane-1-carboxylic acid system.
[c]α-Substituted *p*-toluic acid system.
[d]Methyl esters in 50% methanol–water at 25°.
[e]Bromo used in place of chloro substituent.
[f]Ethyl esters in 88% ethanol–water at 30°.
[g]At 25°.
[h]Insufficient data.
[i]Linear free energy relation breaks down, due to variation in steric environment of reaction site (see ref. 9).

TABLE IV
Direct field calculations[a]

Acid system	r (Å)	$\theta°$	$10^2 \cos\theta/r^2$ (Å^{-2})	ϕ[b]
Benzoic	5.17	0	3.74	1.00
Phenylacetic	5.60	24	2.91	0.78
β-Phenylpropionic "anti"	7.39	11	1.80	0.48
β-Phenylpropionic "eclipsed"	4.19	45	4.03	1.08
Phenoxyacetic	7.17	11	1.91	0.51
trans-Phenylcyclopropanecarboxylic	6.19	32	2.22	0.60
cis-Phenylcyclopropanecarboxylic	5.18	41	2.82	0.75
trans-Cinnamic	7.41	9	1.80	0.48
cis-Cinnamic	4.96	41	2.66	0.71
Phenylpropiolic	7.79	0	1.65	0.44
p-Phenylbenzoic	9.45	0	1.12	0.30
Benzylidenepyruvic	8.26	23	1.35	0.36
trans-4-Chlorocyclohexanecarboxylic	6.16	14	2.56	1.00
4-Chlorobicyclo(2.2.2)octane-1-carboxylic	5.87	0	2.90	1.13
Chloracetic	2.83	53	7.44	2.91
β-Chloropropionic "anti"	4.08	21	5.61	2.19
α-Chloro-*p*-toluic	7.04	64	0.894	0.35
p-Chlorobenzoic	6.04	0	2.74	1.07

[a]Calculations were made using "Tables of Interatomic Distances and Configurations in Molecules and Ions", The Chemical Society, London, 1958, Special Publication No. 11.
[b]ϕ is equal to $\cos\theta/r^2$ divided by the same factor for reference system.

Table IV shows the distance r, the angle θ, and $\cos\theta/r^2$. Only for systems 3, 4, 11 (Table I), and 4 (Table III) do conformational considerations affect the calculation. The calculation for both the "anti" and "eclipsed" conformational models (see ref. 40) is shown for the β-phenylpropionic system. However, the "anti" conformer (I) is sterically preferred and can be assumed to be that existing in solution. The benzylidenepyruvic acid system

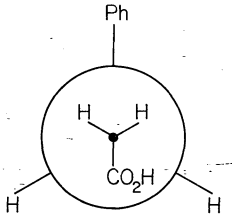

I

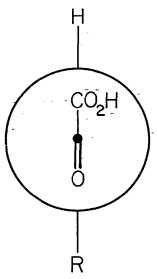

II

(Table I, series 11) is also assumed to occur as the sterically preferred conformer. This molecule can be assumed to be nearly planar (fully conjugated) and have the conformation II where R is *trans*-PhCH.

The inductive effect can be transmitted by the successive polarization of the σ-bonds and the π-bonds. The σ-inductive effect will decrease progressively by transmission through the bonds. The magnitude of the π-inductive effect will depend on the position of the substituent in the same way as does a resonance effect (para substituents having a very much greater effect than meta substituents) and will also be progressively reduced by transmission (6). Inductive transmission of the polar effect can be represented by the relation (iii), where A is a constant, σ the substituent constant, and ϵ the transmission

(iii) $$\log K/K_0 = A\sigma \text{ II } \epsilon_t$$

Can. J. Chem. Downloaded from www.nrcresearchpress.com by 210.87.254.6 on 09/05/12
For personal use only.

factor of the ith atom (see ref. 34). Each type of atom transmitting the effect will have a unique transmission factor. Different estimates of the transmission factors have been given by several workers, mainly on empirical grounds. The factors vary quite widely, with ϵ estimated in the range 0.1 to 0.6 (9, 34, 41).

The ratio ρ/ρ_0 has been used to evaluate the transmission of polar effects by groups (7, 39), where ρ_0 is the reaction constant of the reference system at the same temperature and in the same solvent. These ratios are given in Table V. The apparent transmissive factors, ϵ, for several transmission centers have been calculated from the reaction constants and are given in Table VI.

TABLE V

Ratio of reaction constants, ρ/ρ_0 or ρ''/ρ_0''

Series	Y[a]	Ionization		Esterification	Ester hydrolysis	Mean
		Water	50% ethanol–water			
1	—	1.000	1.000	1.000	1.000	1.000
2	CH_2	0.562	—	0.426	0.397	0.462±0.067
3	$(CH_2)_2$	0.237	0.266	0.230	0.250	0.246±0.012
4	OCH_2	0.341	—	0.261	—	0.301±0.040
5	*trans*-C_3H_4	0.190[b]	0.345	—	0.332	0.338±0.007
6	*cis*-C_3H_4	—	0.329	—	0.431	—
7	*trans*-CH=CH	0.418	—	0.439	0.489	0.449±0.029
8	*cis*-CH=CH	—	—	—	0.429	0.429
9	C≡C	—	0.332	0.327	0.806[b]	0.330±0.003
10	C_6H_4	—	0.304[d]	0.237	0.236	0.259±0.030
11	CH=CH CO	—	—	—	0.211	0.211
	A B[a]					
2	Cl H	1.146	—	—	—	—
3	OH H	1.150	1.040[c]	—	—	—
4	NO_2 H	0.905	—	—	—	—
5	Me H	1.248	1.129	0.937	0.912	—
6	Me Me	—	0.862	0.678	0.88	—
7	C_4H_4 H	1.142	0.835	—	0.939	—
8	C_4H_4 C_4H_4	—	1.126[c]	0.736	—	—
	Y[a]					
1	C_6H_{10}	1.000	1.000	1.000	1.000	1.000
2	C_8H_{12}	—	1.360	1.785	—	1.573±0.213
3	CH_2	5.664	3.974	7.406	—	5.681±1.150
4	$(CH_2)_2$	2.188	—	—	—	2.188
5	$CH_2(C_6H_4)$	—	0.827	—	—	0.827

[a]See Tables I, II, III for full details.
[b]Excluded from calculation due to extreme deviation from other values. These deviations are probably due to large experimental uncertainty in data.
[c]80% 2-methoxyethanol–water.
[d]50% 2-*n*-butoxyethanol–water in presence of 0.05 *M* LiCl.

TABLE VI

Apparent transmission factors (ϵ)[a]

Transmission link center	ϵ	n[b]
C (sp^3)	0.48±0.04	7
C (sp^2 ethylenic)	0.67±0.02	3
C (sp^2 aromatic)	0.60±0.02	2
C (sp)	0.57±0.01	2
C (sp^2 carbonyl)	0.43	1
O	0.61±0.00	2

[a]Calculated from data of Table I; mean deviation shown.
[b]Number of results.

Can. J. Chem. Downloaded from www.nrcresearchpress.com by 210.87.254.6 on 09/05/12
For personal use only.

DISCUSSION

The effects of resonance and medium must be considered before an assessment of the relative importance of the various polar effects can be made.

Resonance Effects

The work of Wepster and Taft has demonstrated the variable resonance effects of substituents (13, 36). Three resonance effects must be considered:

(*a*) conjugation of the substituent and the reaction site through a π-electron system;

(*b*) Resonance interaction of the substituent and the aromatic π-electron system;

(*c*) Resonance interaction of the π-electron system and the functional group.

Reaction systems which allow exalted interactions of the first type to occur should be excluded as they will give rise to anomalous ρ values. Apart from the exceptions noted previously (see p. 000), the reaction constants obtained in this study are free from these effects.

Medium Effects

Reaction constants depend on the reaction medium. The reaction constant, ρ, has been considered to vary with the dielectric constant (D) of the medium according to the

$$\rho = (A+B/D)/RT \qquad \text{(iv)}$$

relation (iv), where the constants A and B respectively describe the susceptibility of the reaction to polar effects independent of and dependent on the medium (37). The polar effect appears to be transmitted through the molecule (term A) and the solvent medium (term B). However it is very likely that ρ is also determined by the solvating power of the medium (33, 38).

The ratio ρ/ρ_0 has been used to evaluate the transmission of polar effects. This ratio will be solvent dependent. The medium in the reactions studied varies from water ($D = 81.1$) to ethanol ($D = 24.3$). Any evidence from this ratio of the ability of a system to transmit polar effects must be considered carefully. As a first approximation, the mean value of the reaction constant ratio can be evaluated and discussed, but the variation of the ratio with both reaction and medium must be considered.

Substituent constants may also depend on the medium (12). This appears to be important only for systems where solvation either enhances the contribution of resonance of the exalted type, or when the substituent is very prone to protonic solvation (e.g. hydroxyl and amino substituents) (48). Such resonance systems have been excluded and the solvation character of the media in this study does not greatly vary.

The Reaction Constants

The results presented in Table I, II, and III lead immediately to certain conclusions. The existence of linear free energy relations of high precision between different series implies that the variable conformational factors present for certain series (e.g. Table I, series 2, 3, 4, and 11; Table III, series 3 and 4) must be unimportant in the change from reactant to transition or product state (9). Likewise these relations indicate that, for a significant direct field effect to operate, the effective dielectric constant must be constant for a series of substituted molecules. Several workers (5, 42) have suggested that a single value of the effective dielectric constant should be used in calculations on such series.

Aliphatic and Alkylaromatic Systems

The systems presented in Table III have the substituent bonded to an sp^3 hybridized

Can. J. Chem. Downloaded from www.nrcresearchpress.com by 210.87.254.6 on 09/05/12
For personal use only.

carbon atom and usually the functional group bonded to a similarly hybridized carbon atom.

A choice of a reference system was necessary for the analysis of the data. The 4-substituted *trans*-cyclohexanecarboxylic acids have the advantage of data being available for several reactions and substituents, without the possibility of variable proximity effects. As reaction series 3 and 4 (α-substituted acetic and β-substituted propionic acids) give good linear relations, no significant primary steric effects of the type associated with alkaline hydrolysis (9) can occur for the ionization and esterification reaction.

Although the results are limited in scope, the significant medium dependence of ρ'' where the substituent is distant from the reaction center (Table III, reaction series 1: the ionization of substituted cyclohexanecarboxylic acids) contrasts sharply with the relative insensitivity to medium when the substituent is proximate to the reaction site (Table III, reaction series 3: the ionization of substituted acetic acids). Any explanation which neglects the transmission of polar effect through the medium must be unsatisfactory. As a solvent-induced change in the polarizability of the system appears very unlikely, the importance of the direct field effect seems confirmed.

The reaction constant ratios presented in Table V summarize the available evidence. If a dominant inductive effect occurs, a ratio of 1.50 must be ascribed to the bicyclo-(2.2.2)octane system, which has three dimethylene links compared to the two of cyclohexane. A mean value of 1.57 ($\pm$0.21) is observed. The mean ratio of 5.68 ($\pm$1.15) for the methylene group would require a transmissive relay ($\epsilon(C_{sp^3})$) equal to 0.45 ($\pm$0.03). Fair correlations have previously been made by direct field calculations (4, 5). The increasing size of the low-dielectric cavity, and the proximity of the dipole to the reactive site increases transmission. This can be seen in Table IV.

An interesting system, α-substituted *p*-toluic acids, has been studied recently by Exner and Jonáš (34). The efficient transmission of polar effects ($\rho''/\rho_0'' = 0.83$) by this system cannot be easily explained by a direct field calculation (using the results in Table IV and an effective dielectric constant which cannot be very much greater than that for the reference system). It is significant that the transmission coefficient for the *p*-phenylene link in Table III (0.21; from ρ'' for α-substituted *p*-toluic and acetic acids) approximates to that of the *p*-phenylene link in Table I (0.26; from ρ for *p*-phenylbenzoic and benzoic acids).

Aromatic and Arylaliphatic Systems

Table I presents the systems where the substituent is bonded to an sp^2 hybridized aromatic carbon atom and the functional group is bonded to a carbon atom which is either sp^1, sp^2, or sp^3 hybridized.

The interpolation of a single methylene group results in a reduction in the transmission, and a second methylene group reduces this further. This can be understood in terms of an inductive effect ($\epsilon(C_{sp^3}) = 0.48$) or a direct field effect (reduction caused by the change in dipole orientation and the higher effective dielectric constant). The increase in ρ observed for transmission by the oxygen atom, compared to the methylene group, can similarly be understood in terms of an inductive effect ($\epsilon(O) = 0.63$) or a direct field effect (see Table IV; for similar conformers $\cos\theta/r^2$ slightly increases, and D' is very similar).

The transmission of a polar effect by the *trans*-ethylenic link ($\rho/\rho_0 = 0.449$) is much greater than that of the dimethylene group ($\rho/\rho_0 = 0.246$). The β-phenylpropionic acids probably exist in the sterically preferred conformation (see p. 000). The direct field effect for this system would be very similar to that for the *trans*-cinnamic acids (see Table IV).

Can. J. Chem. Downloaded from www.nrcresearchpress.com by 210.87.254.6 on 09/05/12
For personal use only.

As the σ-inductive effect will be similar, it is probable that a π-inductive effect causes the observed increase in transmission. The lower value of ρ observed for the *cis*-cinnamic acids compared to the *trans*-cinnamic acids could not be due to a change in a σ-inductive effect. The π-inductive effect is damped in the cis isomer, where steric interaction of the phenyl and carboxyl group is relieved by twisting. This results in a loss of conjugation. Cos θ/r^2 is much greater for the cis than for the trans isomer (ϕ = 0.71, 0.48 respectively; see Table IV). However, the effective dielectric constant will also be greater because of the change in spatial configuration. The field effect may well be greater for the proximate cis isomer (see below for cyclopropane). The decrease in ρ shown for the *cis*- compared with the *trans*-cinnamic acid system would then be due to a reduction in the π-inductive effect.

The markedly reduced transmission observed for the acetylenic link (ρ/ρ_0 = 0.330), compared to the ethylenic link, is very probably due to a reduction in the π-inductive effect, the triple bond being less polarizable (40). The σ-inductive effect should be similar in both cases. The electrostatic field effect would be expected to be greater for this system where the low-dielectric cavity is directly between the substituent and the functional group, and where cos θ/r^2 is comparable to that for the *trans*-cinnamic isomer.

Transmission by the *p*-phenylene system appears very efficient (ρ/ρ_0 = 0.259), considering the length of the carbon chain connecting the substituted phenyl group to the reactive site. If an inductive effect operates, a high transmissive factor ($\epsilon(C_{sp^2}$ aromatic) = 0.60) can be calculated. This system must have an effective dielectric comparable with and possibly slightly less than that of the phenyl group itself. The direct field effect calculations appear to show that a very reasonable estimate (0.30) of the reaction constant ratio (0.26) can be made.

The cyclopropane system seems to be very complex, but permits a number of observations. The magnitude of ρ/ρ_0 (0.338) for the trans isomers makes the occurrence of a π-inductive effect extremely unlikely (see ref. 21); e.g., the ratio can be calculated as 0.34 for an inductive transmission using $\epsilon(C_{sp^3})$ equal to 0.48 (Table VI). The results for the cis isomer ionization equilibria may be anomalous due to a steric effect on solvation (see below). The increase in ρ shown by the ester hydrolysis reaction for the *cis*- compared to the *trans*-phenylcyclopropane system (ρ = 1.098, 0.846 respectively) appears to be due to the direct field effect being much greater for the cis isomer (see Table IV).

Effect of Ortho or "Ortho" Fused Ring Substituents

The possible effects of ortho substituents and "ortho" fused ring substituents on the reaction constants are shown in Table VII.

TABLE VII

Effect of ortho groups on the reaction constants

	Effect on ρ
Polar facilitation of steric inhibited solvation	Increase
Steric inhibition of resonance of functional group (π-inductive effect)	Decrease
Increase in size of low dielectric cavity (field effect)	Increase
Increase in transmissive relay routes (σ- or π-inductive effect)	Increase

The importance of steric inhibition of solvation in the ionization equilibria has been demonstrated (43, 44). The reduced solvation will preferentially decrease the stability of the anion with respect to the acid. Polar facilitation of solvation will then become

Can. J. Chem. Downloaded from www.nrcresearchpress.com by 210.87.254.6 on 09/05/12
For personal use only.

important and will increase the susceptibility of the system to polar effects. The increase in the reaction constant (ρ = 1.15 to 1.25, see Table II) for the ionization reaction in water is very probably due to this effect (see ref. 30). The reaction constant for the ionization in water of the system having an ortho nitro group (ρ = 0.905) alone does not show this increase. This must be due to an effect operating in the opposite direction, to decrease the reaction constant. This decrease is probably due to the steric inhibition of the resonance interaction between the functional group and the aromatic system. The carboxylate group is twisted out of the plane of the aromatic ring by the bulky ortho group. The π-inductive effect will be greatly reduced in these circumstances and ρ will fall. The intense dipole–dipole interaction present in the anion of the *o*-nitrobenzoic acids will intensify this reduction.

Steric effects on solvation appear to be unimportant in the esterification of the acids with diazodiphenylmethane in ethanol (17, 45). The importance of the reduction in the π-inductive effect is then apparent. All other effects would be expected to increase ρ by increasing the transmitting power of the relaying molecule compared to the benzene molecule itself. Changes in the π-electron distribution, especially for the naphthalene or anthracene molecules, may affect these considerations. However, this would only emphasize the importance of the relay of the polar effect by the π-electron system. The results for the alkaline hydrolysis, though less certain and comprehensive, appear to confirm the conclusions for the esterification reaction. The ionization reaction in mixed solvents is more complex. The situation will be complicated by solvent-sorting which occurs in mixed-solvent media (46). However, the results can be understood in terms of a competition between the two effects, the polar facilitation of solvation and the steric inhibition of resonance.

Substituent Effects in Benzene

The polar effect of the substituent group $-NMe_3^+$ is greater at the meta than at the para position (47). It is accepted that this substituent has no resonance interaction with the aromatic ring. The observed ratio of the effects, σ_m/σ_p (1.14±0.02), can be accounted for either by an inductive effect or a direct field effect. The ratio is given as 1.17, using an inductive transmission factor, $\epsilon(C_{sp^2}$ aromatic), of 0.60 (see Table VI), while a direct field effect calculation gives 1.15 as the ratio, assuming the effective dielectric of the isomers to be the same. The ratio σ_m/σ_p^n for dipolar substituents having a negligible exalted resonance effect is 0.89±0.06 (see ref. 13). This ratio, calculated as above, is 1.17 for transmission by an inductive effect and approximately 1.09 for a direct field effect. The decrease in the ratio apparently results from the π-inductive effect, which is much greater from the para than from the meta position. These dipolar substituents have a polar effect from the para position which includes a π-inductive effect amounting to about 20% of the total.

Models of the Benzene System

Roberts and Moreland (4) have attempted to construct a model of the benzene system without the π-electron system. A number of criteria must be satisfied for such a model to be perfect:

(1) The model must be geometrically sound, having a reasonably correct dipole-reactive site distance (r) and angle (θ).

(2) The factors involved in relaying polar effects must remain constant, i.e. the number of chains connecting substituent and reactive site, and the size of low-dielectric cavity.

Can. J. Chem. Downloaded from www.nrcresearchpress.com by 210.87.254.6 on 09/05/12
For personal use only.

(3) The steric environment of reactive center must be similar to that in the benzene system.

Two further factors can be cited which appear impossible to include in a model system:

(4) The substituent group should be bonded to a similar carbon atom (C_{sp^2}).

(5) The functional group should be the same, being a carboxyl group in resonance with an aryl group as in benzoic acid.

The model chosen by Roberts and Moreland, the bicyclo(2.2.2)octane system, fully satisfies only the first of the criteria. The similarity in the effects of substituent groups in both systems does not justify the conclusion that a π-inductive effect does not occur, because the transmissive relay factors (see 2 above) change as between the bicyclo-(2.2.2)octane-1-carboxylic and benzoic acids. The *trans*-cyclohexane system studied by Siegel and Komarmy (5) appears to be a more satisfactory model in terms of the first three criteria. The variation of reaction constants ρ'' with reaction type for the bicyclooctane or *trans*-cyclohexane systems does not parallel that for the benzene system. This throws serious doubt on the applicability of either system as a means of estimating the various transmissive effects in the benzene system.

CONCLUSIONS

The transmission of the polar effect of a substituent is at present best understood in terms of both the inductive and direct field effects. The polar effect is mainly conveyed through the molecular cavity. The direct field effect is an important feature of the polar effect. The σ-inductive effect, in comparison, seems to be less important. For aromatic and conjugated systems, the π-inductive effect is significant.

It is unlikely that an absolute separation of these two effects can be made, though model systems can be devised to attempt this.

ACKNOWLEDGMENTS

The author is indebted to Professor N. B. Chapman, Dr. J. Shorter, and Dr. Ross Stewart for valuable advice and suggestions.

REFERENCES

1. C. K. Ingold. Chem. Rev. **15**, 225 (1934).
2. J. G. Kirkwood and F. H. Westheimer. J. Chem. Phys. **6**, 506 (1938). F. H. Westheimer and M. W. Shookhoff. J. Am. Chem. Soc. **62**, 269 (1940).
3. C. Tanford. J. Am. Chem. Soc. **79**, 5348 (1957).
4. J. D. Roberts and W. T. Moreland. J. Am. Chem. Soc. **75**, 2167 (1953).
5. S. Siegel and J. M. Komarmy. J. Am. Chem. Soc. **82**, 2547 (1960).
6. M. J. S. Dewar and P. J. Grisdale. J. Am. Chem. Soc. **84**, 3539, 3548 (1962).
7. H. H. Jaffé. J. Chem. Phys. **21**, 415 (1953).
8. K. B. Everard and L. E. Sutton. J. Chem. Soc. 2821 (1951).
9. R. W. Taft. *In* Steric effects in organic chemistry. Edited by M. S. Newman. John Wiley and Sons, Inc., New York. 1956. Chap. 13.
10. G. E. K. Branch and M. Calvin. The theory of organic chemistry. Prentice-Hall, Inc., New York. 1941.
11. L. P. Hammett. Physical organic chemistry. McGraw-Hill Book Co., Inc., New York. 1940. Chap. 7.
12. H. H. Jaffé. Chem. Rev. **53**, 191 (1953).
13. H. van Bekkum, P. E. Verkade, and B. M. Wepster. Rec. Trav. Chim. **78**, 815 (1959).
14. N. V. Hayes and G. E. K. Branch. J. Am. Chem. Soc. **65**, 1555 (1943).
15. E. N. Trachtenberg and G. Odian. J. Am. Chem. Soc. **80**, 4018 (1958).
16. R. Fuchs, C. A. Kaplan, J. J. Bloomfield, and L. F. Hatch. J. Org. Chem. **27**, 733 (1962).
17. K. Bowden, N. B. Chapman, and J. Shorter. Unpublished results.
18. J. D. Roberts and R. A. Carboni. J. Am. Chem. Soc. **77**, 5554 (1955).
19. K. Kindler. Ann. **452**, 90 (1927).
20. R. O. C. Norman, G. K. Radda, D. A. Brimacombe, P. D. Ralph, and E. M. Smith. J. Chem. Soc. 3247 (1961).

Can. J. Chem. Downloaded from www.nrcresearchpress.com by 210.87.254.6 on 09/05/12
For personal use only.

21. J. J. Bloomfield and R. Fuchs. J. Org. Chem. **26**, 2991 (1961). R. Fuchs and J. J. Bloomfield. J. Am. Chem. Soc. **81**, 3158 (1959); J. Org. Chem. **28**, 1910 (1963).
22. E. Berliner and L. H. Liu. J. Am. Chem. Soc. **75**, 2417 (1953).
23. E. D. Stecher, F. Dunn, and E. Gelblum. J. Am. Chem. Soc. **79**, 4748 (1957).
24. G. Kortum, W. Vogel, and K. Andrussow. Pure Appl. Chem. **1**, 190 (1960).
25. J. Shorter and F. J. Stubbs. J. Chem. Soc. 1180 (1949).
26. L. K. Creamer, A. Fischer, B. R. Mann, J. Packer, R. B. Richards, and J. Vaughan. J. Org. Chem. **26**, 3148 (1961).
27. W. Simon, A. Morikofer, and E. Heilbronner. Helv. Chim. Acta, **40**, 1918 (1957).
28. J. D. Roberts and C. M. Regan. J. Am. Chem. Soc. **76**, 939 (1954).
29. R. O. C. Norman and P. D. Ralph. J. Chem. Soc. 2221 (1961).
30. H. L. Goering, T. Rubin, and M. S. Newman. J. Am. Chem. Soc. **76**, 787 (1954).
31. A. Fischer, W. J. Mitchell, G. S. Ogilvie, J. Packer, J. E. Packer, and J. Vaughan. J. Chem. Soc. 1426 (1958).
32. C. C. Price and R. H. Michel. J. Am. Chem. Soc. **74**, 3652 (1952).
33. E. Grunwald and B. J. Berkowitz. J. Am. Chem. Soc. **73**, 4939 (1951).
34. O. Exner and J. Jonáš. Collection Czech. Chem. Commun. **27**, 2296 (1962).
35. R. W. Taft and D. J. Smith. J. Am. Chem. Soc. **76**, 305 (1954).
36. R. W. Taft and I. C. Lewis. J. Am. Chem. Soc. **81**, 5343 (1959).
37. L. P. Hammett. J. Am. Chem. Soc. **59**, 96 (1937).
38. B. Gutbezahl and E. Grunwald. J. Am. Chem. Soc. **75**, 559 (1953). C. D. Ritchie and E. S. Lewis. J. Am. Chem. Soc. **84**, 591 (1962).
39. M. Charton. J. Org. Chem. **26**, 735 (1961).
40. E. L. Eliel. Stereochemistry of carbon compounds. McGraw-Hill Book Co., Inc., New York. 1962. Chap. 6.
41. J. C. McGowan. J. Appl. Chem. (London), **10**, 312 (1960).
42. S. Winstein, E. Grunwald, and L. L. Ingraham. J. Am. Chem. Soc. **70**, 821 (1948).
43. J. F. J. Dippy, S. R. C. Hughes, and A. Rozanski. J. Chem. Soc. 1441 (1959).
44. K. Bowden, N. B. Chapman, and J. Shorter. J. Chem. Soc. In press.
45. N. B. Chapman, J. Shorter, and J. H. P. Utley. J. Chem. Soc. 1824 (1962).
46. J. B. Hyne. J. Am. Chem. Soc. **82**, 5129 (1960).
47. J. D. Roberts, R. A. Clement, and J. J. Drysdale. J. Am. Chem. Soc. **73**, 2181 (1951).
48. R. W. Taft, R. E. Glick, I. C. Lewis, I. R. Fox, and S. Ehrenson. J. Am. Chem. Soc. **82**, 756 (1960). R. W. Taft, E. Price, I. R. Fox, I. C. Lewis, K. K. Andersen, and G. T. Davis. J. Am. Chem. Soc. **85**, 709 (1963).

Can. J. Chem. Downloaded from www.nrcresearchpress.com by 210.87.254.6 on 09/05/12
For personal use only.

PROTONATED CARBONYL GROUPS

III. ANTIPYRINE SALTS[1]

DENYS COOK

Exploratory Research Laboratory, Dow Chemical of Canada, Limited, Sarnia, Ontario

Received July 17, 1963

ABSTRACT

Salts of antipyrine (2,3-dimethyl-1-phenyl-5-pyrazolone) with halogen acids have been prepared and their infrared spectra from 4000 to 650 cm^{-1} recorded. Stoichiometrically they are normal 1:1 salts. Identification of bands due to vibrations of the protonating hydrogen atom has been aided by replacement with deuterium atoms. It is concluded that protonation occurs at the carbonyl group from the presence of a doublet (due to correlation field splitting) at 1320 and 1220 cm^{-1}, attributed to the in-plane hydrogen-bending mode. The OH stretching vibration gives rise to bands between 2278 and 2720 cm^{-1} in the different salts. Out-of-plane hydrogen-bending mode absorptions are observed between 840 and 770 cm^{-1}.

More complex acids ($HAsF_6$ etc.) give the anomalous 2 base:1 acid salts, characterized by strong absorption below 1400 cm^{-1}, which probably contain strong, possibly symmetrical, hydrogen bonds.

Can. J. Chem. Downloaded from www.nrcresearchpress.com by 210.87.254.105 on 09/05/12
For personal use only.

INTRODUCTION

Infrared spectroscopic methods have been used recently to ascertain the protonation site in compounds containing carbonyl groups. 4-Pyrones (1) and 4-pyridones (2) were shown to protonate at the carbonyl group oxygen atom, and not at the heterocylic atom. The bending mode of the O^+—H group gives rise to absorption bands near 1260 cm^{-1} (mean value of two components ascribed to correlation field splitting). Thus, while the OH stretching vibration absorption, which can be observed between about 2400 and 3400 cm^{-1} depending on the anion, is diagnostically of little use, except to indicate that protonation has taken place, the bending mode, δ_{OH}, shows increasing dependable utility as an indication of the site of protonation.

A recent study of the infrared spectra of N,N-dicyclohexylacetamide salts (3) showed the bending mode to absorb near 1287 cm^{-1}, a rather higher value than in γ-pyrones (1) and γ-pyridones (2), and with a smaller shift on deuteration. The mesomeric system in amides which is responsible for much vibrational coupling (4) may also give rise to the same effects in the salts. It is of interest therefore to investigate further systems containing the —NRCO— grouping. The salts of antipyrine (2,3-dimethyl-1-phenyl-5-pyrazolone) are described at this time.

RESULTS

The infrared spectrum of the HCl salt of antipyrine is shown in Fig. 1, the broken line being the DCl salt. The bands in the spectra are collected in Table I, and the bands associated with vibrations of the protonating hydrogen atom are summarized in Table II.

DISCUSSION

The broad strong band in the spectra near 2300 cm^{-1} is associated with the OH stretching vibration of the protonated carbonyl group as in I. As Y^- gets larger and the effect of its force field diminishes ν_{OH} gets larger, indicative of a decreasing interaction in the hydrogen bond O^+—H$\cdots Y^-$. In the deuterium substituted salts (I, H = D) the isotopic

[1]*Contribution No. 107.*

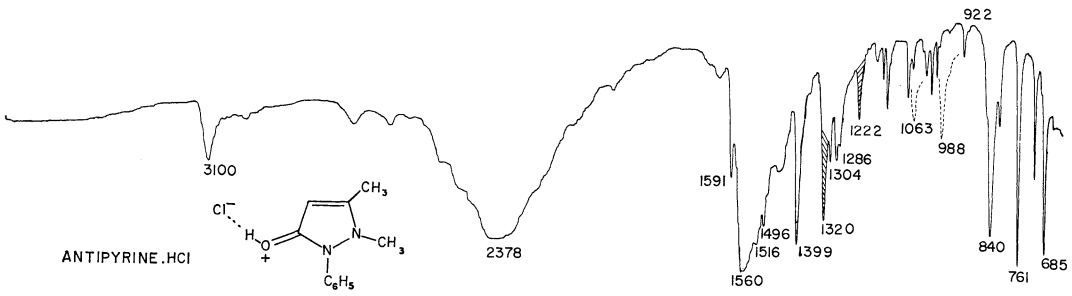

FIG. 1. Infrared spectrum of antipyrine.HCl.

TABLE I

Absorption bands in spectra of antipyrine salts

	HCl	DCl	HBr	DBr	HI	DI
ν_{CH}	3100m		3055m		3052w	
ν_{OH}	2278vs, b*	1814s	2380s, b	1908m, b	2720s, b	2110 m, b
	1591m	1590m	1592s	1590m	1590m	1589m
ν_{CC}	1560s	1558s, sh	1560s, sh	1560s, sh	1570s	1561s
ν_{CN}	1552s, sh	1542vs	1540s	1545s		1550s
	1516s	1517s	1514s	1515s, sh	1530m	1525m
ν_{CO}	1496s	1493s	1496s	1492s	1496s	1492s
	1486m, sh		1490s, sh			
δ_{CH_3}	1452m	1450m	1465m, sh	1458m	1465m	1455m
		1440m	1455m, sh			1448m
	1399s	1398s	1410m	1410w	1409m	1406m
			1390m	1390m	1388m	1390m
					1370m, sh	1382m, sh
δ_{CH_3}	1365w, sh	1365w	1363w	1368m, sh	1362m	1355w
					1310m, sh	
δ_{OH}	1320m	1063m	1315s	1068m	1302m	1063m
	1304m	1302w	1302m, sh			
	1286m	1287m	1293m, sh	1291m	1290m, sh	1292m
	1278m	1276m	1280w	1280m, sh	1280m, sh	1280m, sh
δ_{OH}	1222m	988m	1220m	972m	1211m	964m
	1172w	1182w, sh	1163m	1160w, sh	1160w	1160w, sh
	1153w	1157m	1155w, sh	1150m	1152w, sh	1148w
	1141m	1135w, sh	1139w		1136vw	
	1082m	1083w	1081vw	1080m		
	1070w	1068m, sh	1068vw		1068w	1075w, sh
	1030w	1030m	1032m	1025m	1030w	
	1016w	1015vw	1017m	1010w	1013w	1015w
	1000w	999w	998vw	997vw	988vw	995vw
			985w	980w, sh		
	922w	921w	930m	925vw	929vw	925vw
	853m, sh		857w		859w	
γ_{OH}	840s	706m	795s		770s	
	818m, sh	810m				
			768m, sh			
γ_{CH}	761s	750s	760s	752s	761m	752s
	715m	720m	714m	715m	715m	710m
	685s	684s	688s	690s	688s	689s
			683s, sh			

*The main peak only is listed.

shifts are as expected, with the ratios ν_{OH}/ν_{OD} varying from 1.25 to 1.29. These are normal values for salts of hydrogen halides.

It could perhaps be emphasized at this point that there is nothing in the shape or contour of the absorption band due to the OH stretching vibration to differentiate it from similar bands in other protonated bases. γ-Pyrones (1), γ-pyridones (2), amides (3),

Can. J. Chem. Downloaded from www.nrcresearchpress.com by 210.87.254.105 on 09/05/12
For personal use only.

TABLE II

OH and OD stretching and bending frequencies in antipyrine salts

	HCl		DCl	HBr		DBr	HI		DI
ν_{OH}	2278	(1.26)*	1814	2380	(1.25)	1908	2720	(1.29)	2110
$\Delta\nu_{1/2}$†	250		180	210			270		170
δ_{OH}	1320	(1.24)	1063	1315	(1.23)	1068	1302	(1.22)	1063
δ_{OH}	1222	(1.24)	988	1220	(1.26)	972	1211	(1.26)	964
γ_{OH}	840			794			770		

*The numbers in parentheses are the ratios of the frequencies for the hydrogen and deuterium species.
†Half band-width.

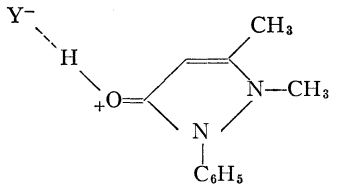

I

pyridine (5), amine oxides (6), etc. all show a similar band with minor variations in contour. They vary in position for the same anion, naturally, due to the different degree of interaction in the hydrogen bond $X^+—H\cdots Y^-$. Consequently such an absorption band is of little diagnostic use in deciding what type of donor atom has been protonated.

An investigation of the in-plane hydrogen-bending mode has shown, by contrast, that it can be diagnostically very useful in determining the type of atom protonated. In the present series of carbonyl donors, γ-pyrones (1) and γ-pyridones (2) were both found to have δ_{OH} near 1260 cm^{-1} (mean value of split components). The known values of δ_{OH} and the splittings, $\Delta\delta_{OH}$, are summarized in Table III. The antipyrine salts reported here

TABLE III

Average OH and OD bending frequency, splitting, and carbonyl stretching frequency in protonated carbonyl compounds

Compound	δ_{OH} (av)	$\Delta\delta_{OH}$	δ_{OD} (av)	$\Delta\delta_{OD}$	δ_{OH}/δ_{OD}	$\nu_{C=O^+H}$
4-Pyrone (1)	1274	135	1025	59	1.24	1490
2,6-Dimethyl-4-pyrone (1)	1253	92	971	57	1.29	1480
1,2,6-Trimethyl-4-pyridone (2)	1245	48	959	73	1.30	1485
1-Ethyl-2,6-dimethyl-4-pyridone (2)	1261	69	964	68	1.31	1475
N,N-Dicyclohexylacetamide (3)	1282	0	1086	0	1.18	1400
Antipyrine (I)	1265	94	1020	90	1.24	1496
1,3-Dimethyluracil (17)	1278	0	962	0	1.33	1515
N,N-Dimethylacetamide (17)	1273	98	1006	72	1.27	1386
N-Methyl-2-pyrrolidone (17)	1265	74	972	60	1.29	1478
Average	1265					

are no exception and their spectra reveal two bands near 1312 and 1218 cm^{-1} (average 1265 cm^{-1}) which shift on deuteration to near 1065 and 975 cm^{-1} (average 1020 cm^{-1}). These values for δ_{OH} are so typical of protonated carbonyl groups that 1265±20 cm^{-1} could be considered a useful group frequency. The values at the higher end of the scale are for salts containing the stronger hydrogen bonds. The ratio δ_{OH}/δ_{OD} (average values) varies from 1.18 to 1.33, but most are close to the higher figure. It seems that the low ratios are found in salts with high δ_{OD}, suggesting that if mechanical effects are concerned in these ratios, they will be more active in the deuterium salts.

Can. J. Chem. Downloaded from www.nrcresearchpress.com by 210.87.254.105 on 09/05/12
For personal use only.

Splitting of the bending mode into two components is usually, but not universally, observed. In N,N-dicyclohexylacetamide salts (3) there was only one component near 1280 cm^{-1}; and in some unpublished data on 1,3-dimethyluracil salts only one component at 1278 cm^{-1} is observed. These values may seem a little high when compared with the average δ_{OH} in Table III. This is because only the hydrohalides have been studied for these two compounds which have stronger hydrogen bonds and therefore slightly higher δ_{OH}.

The doubling in the bending mode has been attributed (1, 2, 6) to correlation field splitting in the solid phase (7, 8). This occurs when two identical molecules having different orientations in the crystal are permitted, by coupling, to split certain vibrational modes. In the general case, the number of components is determined by the various symmetry groups involved, namely, the point group of the molecule, the site group, and the space group of the lattice, subject to a maximum equal to the number of molecules in the unit cell. Some of the components may be active under Raman selection rules, others may have infrared activity. The size of the splittings seems to vary, the larger values being associated with systems in which hydrogen bonding is important (see, for example ref. 9). The fact that in most of the carbonyl salts studied a doublet is common is not unexpected. Two or four is quite a common number of molecules per unit cell. This, in conjunction with a low symmetry for the protonated base and a site group of low symmetry, requires only a slightly higher space group symmetry to permit doubling. The higher the symmetry of the space group the more components will be possible. Naturally these higher symmetry space groups are rarer and therefore structures with more than two components will be more infrequently observed.

Two other atoms in antipyrine which can be considered to have basic character in certain circumstances are the two nitrogen atoms. Protonation of N_1 would give II and of N_2 would give III. Both of these structures have a protonated tertiary sp^3 amine group

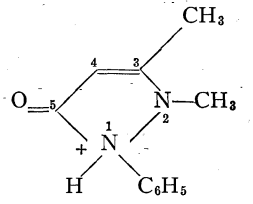

II

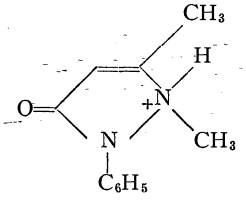

III

which is well known to have a deformation mode near 1420 cm^{-1} (see refs. 1–3 for details). Such a band is not observed in the spectra of antipyrine salts. A further count for rejection of II arises from a consideration of carbonyl frequencies. Antipyrine itself has a strong band at 1670 cm^{-1} associated with the carbonyl stretching mode. A carbonyl group adjacent to a protonated sp^3 nitrogen atom (10) or a quaternized nitrogen atom carrying a positive charge (3, 11) has a much higher carbonyl frequency, close to 1800 cm^{-1}. Protonation at N_1 is therefore discounted from this evidence. This band at 1670 cm^{-1} in the neutral antipyrine, the strongest in the whole spectrum, is replaced by one near 1560 cm^{-1} in the salts, though another strong band is seen near 1496 cm^{-1}. While it has not been conclusively shown that the high-frequency band in amide salts is due exclusively to a C=N vibration, this mode probably makes the largest contribution. In the antipyrine salts there is probably even more coupling of these vibrational modes, so that four bands near 1590, 1560, 1552, and 1516 cm^{-1} are associated chiefly with CC and CN vibrations of the ring, and the 1496 cm^{-1} band predominantly with CO stretching. These

Can. J. Chem. Downloaded from www.nrcresearchpress.com by 210.87.254.105 on 09/05/12
For personal use only.

assignments, though almost certainly oversimplifications, nevertheless help to interpret vibrational modes in different salts. Thus the 1496 cm^{-1} band is close in frequency to other bands due to a protonated carbonyl stretching vibration (1, 2). These are listed under the heading $\nu_{C=O^+H}$ in Table III. With the exception of the two non-cyclic amides they are all close to 1500 cm^{-1}.

Salts Containing 2 Base:1 Acid

The salts of antipyrine and the more complex protonating acids such as $HAsF_6$ and $HSbF_6$ are not of the same stoichiometry as those of the hydrogen halides. The new salts contain two base units to one acid and examples are being more frequently discovered. The infrared spectrum of this type of salt, first observed by White (12), but interpreted correctly for acetamide hemihydrochloride by Albert and Badger (13), does not have an absorption band around 2400 cm^{-1} typical of HCl salts of organic bases, but instead shows very broad absorption below 1500 cm^{-1}; in the case of the antipyrine salts this absorption is centered near 900 cm^{-1}. Furthermore, the split bending mode at 1320 and 1220 cm^{-1} is not observed in the 2:1 salts, nor is there a band near 1270 cm^{-1} where the uncoupled bending mode should absorb. The structure of these salts must be quite different from that of the 1:1 salts. The structure derived from X-ray diffraction studies of acetamide hemihydrochloride (14), $(base\cdots H\cdots base)^+MX_{n+1}^-$, is also suggested for these salts, as it has been for other 2:1 salts (15, 16). (See ref. 15 also for details and further references to similar phenomena in certain acid salts of the type $(anion\cdots H\cdots anion)^-M^+$.)

EXPERIMENTAL

Antipyrine was obtained from Matheson, Coleman and Bell and was used without further purification. The HCl salt was made by passing anhydrous HCl into a solution of antipyrine in a little $CHCl_3$ and excess ether, m.p. 158–159° C. Found: C, 58.99%; H, 5.85%; N, 12.49%; HCl, 15.8%. Calc. for $C_{11}H_{12}N_2O.HCl$: C, 58.79%; H, 5.83%; N, 12.47%; HCl, 16.2%.

The HBr salt was made in the same way, m.p. 184–185°. Found: C, 49.20%; H, 4.78%; N, 10.37%; HBr, 29.6%. Calc. for $C_{11}H_{12}N_2O.HBr$: C, 49.09%; H, 4.87%; N, 10.41%; HBr, 30.0%.

The hydrated HI salt was made from aqueous solutions of each component, m.p. 94–96°. Found: C, 39.76%; H, 4.45%; N, 8.53%; HI, 37.8%. Calc. for $C_{11}H_{12}N_2O.HI.H_2O$: C, 39.53%; H, 4.52%; N, 8.38%; HI, 38.2%. The anhydrous salt was obtained from the hydrate by gentle heating *in vacuo*, m.p. 160–162°. The deuterated salts were prepared by exchange with an excess of D_2O followed by removal of the excess D_2O *in vacuo*. The $HSbF_6$ salt crystallized when 2.35 g antipyrine in 5 ml H_2O was mixed with 4.57 g aqueous (60%) $HSbF_6$, m.p. 271°, decomp. Found: C, 41.96%; H, 3.99%; N, 8.92%. Calc. for $(C_{11}H_{12}N_2O)_2.HSbF_6$: C, 43.09%; H, 4.11%; N, 9.14%.

ACKNOWLEDGMENTS

The assistance of Miss C. D. Anderson with the experimental work is gratefully acknowledged. Dr. L. E. Swim and his associates (The Dow Chemical Company, Midland, Michigan, U.S.A.) are thanked for the microanalyses.

REFERENCES

1. D. Cook. Can. J. Chem. **41**, 505 (1963).
2. D. Cook. Can. J. Chem. **41**, 2575 (1963).
3. D. Cook. Can. J. Chem. **40**, 2362 (1962).
4. T. Miyazawa, T. Shimanouchi, and S. Mizushima. J. Chem. Phys. **29**, 611 (1958).
5. D. Cook. Can. J. Chem. **39**, 2009 (1961).
6. D. Cook. Can. J. Chem. **41**, 1127 (1963).
7. R. S. Halford. J. Chem. Phys. **14**, 8 (1946).
8. D. F. Hornig. J. Chem. Phys. **16**, 1063 (1948).
9. D. F. Hornig. Discussions Faraday Soc. **10**, 115 (1950).
10. H. Pracejus. Chem. Ber. **92**, 988 (1959).
11. R. Gompper and P. Altreuther. Z. Anal. Chem. **170**, 205 (1959).
12. E. H. White. J. Am. Chem. Soc. **77**, 6215 (1955).

Can. J. Chem. Downloaded from www.nrcresearchpress.com by 210.87.254.105 on 09/05/12
For personal use only.

13. N. ALBERT and R. M. BADGER. J. Chem. Phys. **29**, 1193 (1958).
14. W. TAKEI. Ph.D. Thesis, California Institute of Technology, Pasadena, Calif. 1957.
15. D. HADŽI. J. Chem. Soc. 5128 (1962).
16. D. COOK. Chem. Ind. (London), 607 (1963).
17. D. COOK. Unpublished results.

Can. J. Chem. Downloaded from www.nrcresearchpress.com by 210.87.254.105 on 09/05/12
For personal use only.

THE INHIBITED AUTOXIDATION OF STYRENE

PART III. THE RELATIVE INHIBITING EFFICIENCIES OF ORTHO-ALKYL PHENOLS[1]

J. A. HOWARD[2] AND K. U. INGOLD
Division of Applied Chemistry, National Research Council, Ottawa, Canada
Received May 31, 1963

ABSTRACT

The relative rates of reaction of a large number of ortho-alkyl phenols with styrylperoxy radicals have been measured at 65° C. These groups have both an accelerating effect owing to their electron-donating character and a retarding effect which arises from steric factors. With two ortho-alkyl groups both the reaction rate and the overall polar contribution to the transition state decrease as the size of the alkyl groups is increased. A single *o-t*-butyl group produces a small enhancement of the reaction rate over and above its polar effect but this is not observed with any other alkyl groups.

INTRODUCTION

In Part II of this series (1), it was shown that the relative rates of hydrogen abstraction by styrylperoxy radicals from meta- and para-substituted phenols at 65° C could be correlated with Brown's electrophilic substituent constants (2). That is, the relative rates of the reaction

$$RO_2\bullet + XC_6H_4OH \rightarrow ROOH + XC_6H_4O\bullet \qquad [6]$$

can be correlated by the relation

$$\log_{10}\frac{k_6}{(k_6)_0} = a+\rho\sigma^+ = -0.010-1.49\sigma^+. \qquad [1]$$

The influence of ortho-alkyl substituents on k_6 at 65° C is described in the present paper. It is shown that these substituents exert two opposing effects on the rate, i.e., an accelerating effect due to electron release from the substituents and a retarding effect due to steric factors. The relative reactivities and ρ factors for 2,6-dialkyl phenols can be correlated with the degree of hindering of the phenolic hydroxyl group as determined by infrared spectroscopy (3, 4).

EXPERIMENTAL

The experimental techniques and the kinetic treatment of the results have been described previously in Parts I (5) and II (1). Many of the phenols used in this work were carefully purified commercial products. With one exception, the preparation of the remaining phenols is described in the literature. The exception, 2-*t*-butyl-4-cyanophenol (white needles from *n*-hexane, m.p. 163–164° C), was prepared from 2-*t*-butyl-4-bromophenol by the Rosenmund – von Braun nitrile synthesis (6). All the phenols were checked for purity by gas chromatography before use. None contained more than 0.5% impurities.

RESULTS

Under conditions where the self-termination reaction between two peroxy radicals is unimportant, theory predicts (1, 5) that

$$P = \rho-(2e-1)k_1[I_2] = \frac{ek_1k_3[RH][I_2]}{k_6[AH]},$$

[1]*Issued as N.R.C. No. 7537.*
[2]*N.R.C. Postdoctoral Fellow 1961–1963.*

Can. J. Chem. Downloaded from www.nrcresearchpress.com by 210.87.254.105 on 09/05/12
For personal use only.

Can. J. Chem. Downloaded from www.nrcresearchpress.com by 210.87.254.105 on 09/05/12
For personal use only.

where ρ is the measured inhibited rate, e is the efficiency of radical production from the initiator I_2, k_1 is its rate constant for decomposition, k_3 is the propagation rate constant, RH represents the styrene, and AH the phenol. Although this equation fits the data for inhibition by 2,6-di-*t*-butyl-4-methylphenol (BMP) fairly well (5) it does not fit the data for simple meta- and para-substituted phenols (1). Instead, with these phenols, k_6 appears to decrease as the phenol concentration is increased. It was suggested (1) that this was due either to intermolecular hydrogen bonding of the phenols (which would decrease the availability of free phenol for the inhibition reaction) or to a chain transfer reaction between the initially formed phenoxy radical and the styrene. Although the kinetics applicable to inhibited autoxidations with chain transfer depend on the initial assumptions, a very complete analysis by Waters and Wickham-Jones (7) reveals that $P \propto [I_2]^{1/2}$ under almost all conditions.* It was shown previously (1) that P is approximately proportional to $[I_2]^{1.0}$ for the simple phenols and, therefore, the dependence of k_6 on [AH] would appear to be due to intermolecular hydrogen bonding rather than to chain transfer. It was surprising, therefore, to find that at high concentrations there was a similar variation in k_6 with the ortho-alkyl phenols (including 2,6-di-*t*-alkyl phenols), since it is known from infrared evidence that these phenols do not hydrogen bond very readily. Figure 1 shows a plot of $\log_{10}(P/[I_2])$ against $\log_{10}[AH]^{-1}$ for phenol and Fig. 2 shows a similar plot for 2,6-di-*t*-butylphenol and its 4-methyl derivative.† It can be seen that, at sufficiently low concentrations, the order in [AH] is 1.0 for all three phenols, i.e., k_6 is independent of the phenol concentration. However, as the concentration increases the order decreases and hence k_6 will appear to decrease, this effect being more marked for phenol than for the hindered phenols. The experimental points at high phenol concentrations show considerable scatter because the reaction is no longer exactly first order in $[I_2]$, e.g., with 1.0 mole/l. phenol, $P \propto [I_2]^{0.90}$. However, the order increases towards unity as the phenol concentration is reduced. This suggests that at high concentrations there may be some chain transfer with phenol and therefore, possibly, with some of the other simple phenols. For the hindered phenols, $P \propto [I_2]^{1.0}$ over the entire concentration range and chain transfer is therefore unlikely. Since hydrogen bonding is also of little importance with these phenols the reason for their curvature in Fig. 2 is not clear at present.

The lower the reactivity of a phenol the more difficult it is to obtain k_6. This is because an unreactive phenol will tend to be used at fairly high concentrations in order to obtain easily measurable effects and it is then that intermolecular hydrogen bonding and chain transfer are of importance. On the whole, this difficulty was greater for the simple meta- and para-substituted phenols studied previously (1) than in the present work since the simple phenols are generally less reactive than the ortho-alkyl phenols. Values of k_6 for the simple phenols were obtained by extrapolation of the measured values to zero phenol concentration. It is now clear that this extrapolation is not linear. However, additional experiments have shown that any corrections to the previous results are within the limits of the experimental error which is introduced by the extrapolation (approx. $\pm 25\%$).‡ Most of the present work was done in the range where k_6 was independent of the phenol concentration, extrapolation being necessary only for the least reactive ortho-alkyl

*The most likely assumptions lead to $P \propto [RH]^{3/2}[I_2]^{1/2}/[AH]^{1/2}$ (7, 8).

†All the data in these figures were obtained under conditions where the self-termination reaction could be neglected. Some of the data in Fig. 1 have been given previously (Fig. 1 of ref. 1). With the additional data obtained at very high and very low phenol concentrations the original linear plot of $1/k_6$ against [AH] is found to be a curve. The data at low concentrations of BMP have also been given previously (5).

‡For example, the new data for phenol at low concentrations where $P \propto [AH]^{-1}$ give $k_6 = 2.3 \times 10^3$ l./mole sec compared with a value of 2.9×10^3 l./mole sec reported previously (1).

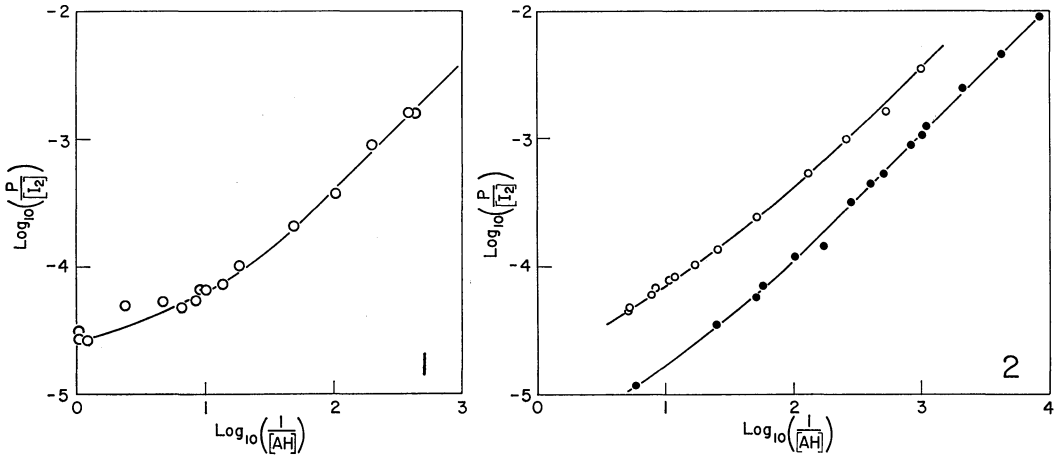

FIG. 1. $\log_{10}(P/[I_2])$ plotted against $\log_{10}[AH]^{-1}$ for phenol.
FIG. 2. $\log_{10}(P/[I_2])$ plotted against $\log_{10}[AH]^{-1}$. Key: ○ 2,6-di-*t*-butylphenol; ● 2,6-di-*t*-butyl-4-methylphenol.

TABLE I

k_6 for *ortho*-alkyl Phenols at 65° C

(Based on k_6(BMP) = 7.95×10^3 l./mole sec)

Phenol	$\sum\sigma^+$	$k_6\times10^{-3}$ (l. mole sec)	Phenol	$\sum\sigma^+$	$k_6\times10^{-3}$ (l. mole sec)
2,6-Me_2	−0.622	8.9	2,4-Me_2	−0.622	18.5
4-Me	−0.933	28	2,4,5-Me_3	−0.688	21.5
4-Cl	−0.508	11.5	2,3-Me_2	−0.377	9.3
4-CN	+0.037	1.3	2,3,5,6-Me_4	−0.754	13.5
2-Bu^t	−0.256	7.47	2,3,4,5,6-Me_5	−1.065	38.4
4-MeO	−1.034	107	2,6-Et_2	−0.590	9.8
4-Me	−0.567	24	2-Pr^i-4-Me	−0.591	17.5
5-Me	−0.322	10.9	2,6-Pr_2^i	−0.560	9.5
4-CN	+0.403	0.87	2,6-Pr_2^i-4-Me	−0.871	26.3
2,6-Bu_2^t	−0.512	2.25	2-Am^t-4-Me	−0.561	18.8
4-MeO	−1.290	31.2	2,6-Am_2^t-4-Me	−0.811	7.3
4-Me	−0.823	7.95	2-Oct^{tt}-4-Me	−0.559	16.5
4-Bu^t	−0.768	7.30	2,6-Oct_2^{tt}-4-Me	−0.807	5.1
4-Am^t	−0.762	7.30	2-Et_3C-4-Me	−0.551*	14.8
4-Cumyl	−0.732*	6.1	2,6-$(Et_3C)_2$-4-Me	−0.791*	7.2
4-Oct^{tt}†	−0.760	6.48	2-Bu^t-6-Me	−0.567	7.2
4-Cl	−0.398	3.24	2-Bu^t-5,6-Me_2	−0.633	16.2
4-CN	+0.147	0.77	2-Bu^t-4-Me-6-Oct^{tt}	−0.815	6.57
4-NO_2	+0.278	~0.48	4,4′-Bis-2,6-Bu_2^t		18.9
4-CHO		~0.80	4,4′-CH_2-bis-2,6-Bu_2^t		13.5
			α,α'-Bis-4-CH_2-2,6-Bu_2^t		15.3

*Assumed.
†Oct^{tt} is $(CH_3)_3CCH_2(CH_3)_2C$.

phenols. The collected rate constants (referred to k_6 for 2,6-di-*t*-butyl-4-methylphenol (1)) are given in Table I together with the sum of the σ^+ constants for all the substituents on the phenol ($\sum\sigma^+$). In calculating ($\sum\sigma^+$) it has been assumed that $\sigma^+_{ortho} = \sigma^+_{para}$. The relative rate constants obtained in this work are in fairly good agreement with the relative rate constants for the reaction of tetralyl peroxy radicals with ortho-alkyl phenols (9).

The values of k_6 for substituted 2,6-dimethyl-, 2-*t*-butyl- and 2,6-di-*t*-butyl-phenols*

**2,6-Di-t-butyl-4-formylphenol has not been included in Fig. 3 owing to the possibility of side reactions between the radicals and the* CHO *group (cf. ref. 10).*

Can. J. Chem. Downloaded from www.nrcresearchpress.com by 210.87.254.105 on 09/05/12
For personal use only.

have been plotted against $\sum \sigma^+$ in Fig. 3. The slopes of the best straight lines through the three sets of points, i.e., the ρ factors, are -1.36 (std. dev. 0.059), -1.46 (std. dev. 0.012), and -1.11_5 (std. dev. 0.026), respectively. The best straight line which was obtained previously for simple meta- and para-substituted phenols ($\rho = -1.49$ (1)) is also shown for comparison as the heavy line in Fig. 3.

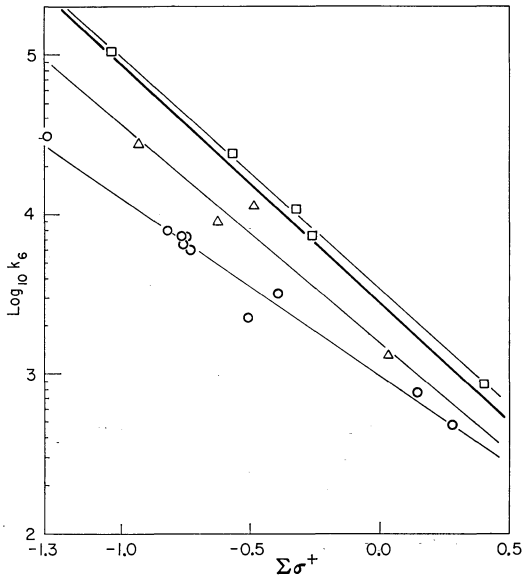

FIG. 3. $\log_{10} k_6$ plotted against $\sum \sigma^+$. Key: Heavy line, simple 3- and 4-substituted phenols (1); △ 2,6-dimethyl phenols; □ 2-*t*-butyl phenols; ○ 2,6-di-*t*-butyl phenols.

The deuterium isotope effect, $(k_6)_H/(k_6)_D$, for 2,6-di-*t*-butylphenol was measured by the technique described previously (5). It was found to be 10.5, which is in good agreement with the value obtained for its 4-methyl derivative (5).

The 2,6-di-*t*-butyl-4-substituted phenols all reacted with two peroxy radicals per molecule of phenol (5). 4,4′-Bis-2,6-di-*t*-butylphenol also reacted with two radicals per molecule but the other two bis-phenols both reacted with four radicals per molecule. The k_6 values of all three bis-phenols are about twice the values obtained for comparable 2,6-di-*t*-butylphenols presumably because they contain two OH groups per molecule.

DISCUSSION

In the two following papers we report on the reaction of *t*-butoxy radicals with hindered and non-hindered phenols (10). To a large extent, the present results can be interpreted along the same general lines and the following discussion has, therefore, been reduced to a minimum. Several points to which only brief reference is made in this paper are discussed in greater detail in the two following papers (10).

Following the suggestion of Russell (11) the transition state for reaction 6 can be considered to consist of three resonance forms:

$$[XC_6H_4O{:}H\bullet OOR \leftrightarrow XC_6H_4O^{+}\bullet H{:}\bar{O}OR \leftrightarrow XC_6H_4O\bullet H{:}OOR]$$
$$\text{I} \qquad\qquad \text{II} \qquad\qquad \text{III}$$

Can. J. Chem. Downloaded from www.nrcresearchpress.com by 210.87.254.105 on 09/05/12
For personal use only.

Structure I resembles the reactants and structure III resembles the products. The importance of polar effects will increase in the order III < I < II. The correlation of the present results with σ^+ constants indicates that structure II contributes to the transition state but the magnitude of the ρ factors suggests that there is only a moderate degree of charge separation in the transition state.

For a given $\sum \sigma^+$, the decrease in k_6 produced by two ortho-alkyl groups is probably due largely to steric factors. That is, the alkyl groups prevent the peroxy radical from approaching the phenolic hydrogen quite as closely as it approaches the hydrogen in a non-hindered phenol. The two groups therefore tend to make the transition state resemble the products to an increasing extent as their size increases. This means that structure III will become of increasing importance and therefore ρ should decrease, as is, in fact, observed.*

The decrease in k_6 and in ρ factors produced by two ortho-alkyl substituents should be related to the degree of steric protection they afford the phenolic hydrogen. A rough measure of this protection is possibly given by the difference in free energy (ΔG) between the cis and trans isomers of ortho-alkyl phenols as determined by infrared spectroscopy in CCl_4 (3). In the reaction of *t*-butoxy radicals with phenols it was shown that the log of the relative reactivities could be correlated with ΔG (10). A similar correlation is shown in Fig. 4 for the reaction of styrylperoxy radicals with 2,6-dialkyl-4-methyl phenols. The circles represent the experimental points and the crosses the values calculated for $\sum \sigma^+ = -0.811$ (i.e., $\sum \sigma^+$ for a 4-CH_3 group ($\sigma^+ = -0.311$) and two *t*-alkyl groups ($\sigma^+ \approx -2\times0.250$).† The results can be represented by,

$$\log_{10} \frac{k_6}{(k_6)_0} = \alpha \Delta G, \qquad [2]$$

where $(k_6)_0 = 46\times10^3$ l./mole sec and $\alpha = -0.5$ mole/kcal. This value of α is significantly smaller than the value obtained with the *t*-butoxy radicals (i.e., -1.23 mole/kcal) presumably because the secondary styrylperoxy radicals are much less subject to steric factors than are the *t*-butoxy radicals. Incidentally, two *o*-ethyl or isopropyl groups appear to have about the same steric effect as two *o*-methyl groups. Moreover, both 2-*t*-butyl-6-methylphenol and 2-*t*-*t*-octyl-6-*t*-butyl-4-methylphenol appear to fit roughly on the line in Fig. 4 at the average ΔG for the two ortho substituents. However, 2-*t*-butyl-5,6-dimethylphenol is rather more reactive than would be expected.

In view of the similarity between equation [2] and the Hammett equation, the direct correlation between ρ and ΔG shown in Fig. 5 is not entirely unexpected.

The excellent agreement between the 4-*t*-alkyl-2,6-di-*t*-butyl phenols and the other phenols in this series indicates that there is little or no hindrance by the 4-substituent towards the attack of a styrylperoxy radical at the 4-position of the initially formed phenoxy radical (1, 12).

It is known from infrared studies of 2-alkyl phenols that these compounds exist as cis and trans isomers in which the phenolic hydrogen points towards the alkyl group and away from it, respectively (3, 4). Provided the alkyl substituent only exerts its normal

**The negative deviations of 2,6-dimethylphenol and 2,6-di-t-butylphenol and the positive deviations of their 4-chloro derivatives from the best straight lines are probably due to differences in the stabilities of the resulting phenoxy radicals which affect k_6 to an increasing extent as structure III becomes of progressively greater importance in the transition state (10).*

†The phenol point ($\Delta G = 0$) was calculated from equation [1]. 2,4,6-Trimethylphenol was corrected for the decreased polar effect of two t-alkyl groups compared with two methyl groups and pentamethylphenol was also corrected for the polar effect of two meta-methyl groups. In the last case ρ was taken to be -1.3 from Fig. 5.

Can. J. Chem. Downloaded from www.nrcresearchpress.com by 210.87.254.105 on 09/05/12
For personal use only.

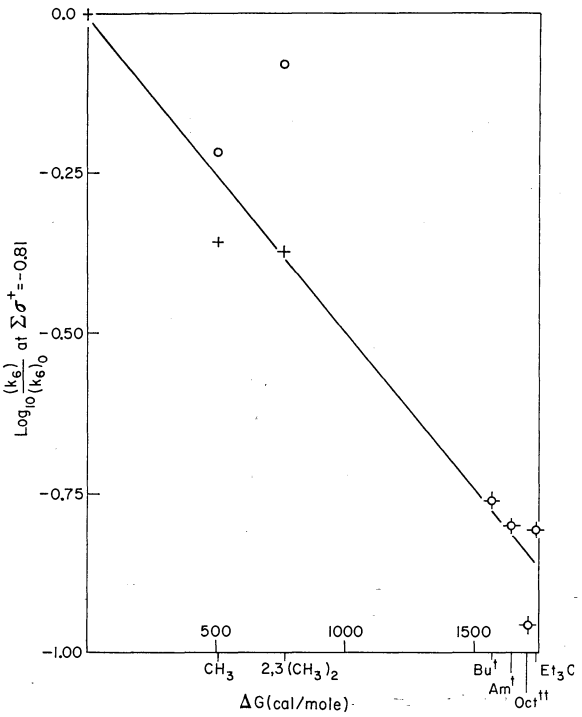

FIG. 4. $\log_{10}(k_6)/(k_6)_0$ for 2,4,6-trialkyl phenols plotted against ΔG. Key: ○ experimental points; + calculated points at $\sum \sigma^+ = -0.81$.

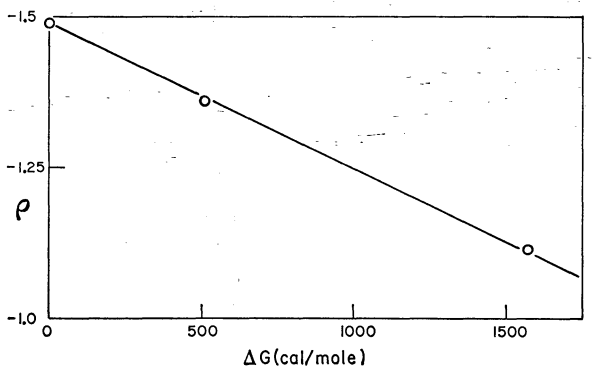

FIG. 5. The ρ factor as a function of ΔG for 2,6-dialkyl phenols.

polar effect on the *trans*-hydroxyl group we might expect to be able to calculate k_6 for a 2-alkyl phenol from equation [1] and the equation for the corresponding dialkyl phenol together with the proportions of the trans and cis isomer present, respectively, under the experimental conditions. Unfortunately, the calculation must be restricted to 2-methyl and 2,3-dimethyl phenols since the infrared evidence indicates that a 2-*t*-alkyl group has effects other than its polar effect on the *trans*-hydroxyl group (see below). A second difficulty is that the [trans]/[cis] ratio depends on the solvent and temperature as well as on the size of the alkyl group. However, the solvent effect is small for a non-polar

Can. J. Chem. Downloaded from www.nrcresearchpress.com by 210.87.254.105 on 09/05/12
For personal use only.

solvent (4) and the ratio can probably be taken to be the same in styrene as in CCl_4. The percentage of the trans isomer of 2,4-dimethylphenol at 65° C should therefore be about 67%. From equation [1], $(k_6)_{trans} = 0.67 \times 24 \times 10^3 = 16 \times 10^3$ l./mole sec. From k_6 for 2,4,6-trimethylphenol, $(k_6)_{cis} = 0.33 \times 10.57 \times 10^3 = 3.5 \times 10^3$ l./mole sec. The calculated k_6 for 2,4-dimethylphenol is, therefore, $= 19.5 \times 10^3$ l./mole sec, which is in excellent agreement with the measured value of 18.5×10^3 l./mole sec. Similarly, the percentage of the trans isomer of 2,3-dimethylphenol should be about 76% at 65° C, leading to a calculated k_6 of 8.9×10^3 l./mole sec in excellent agreement with the measured value of 9.3×10^3 l./mole sec.

The ρ factor for 2-*t*-butyl phenols is only slightly smaller than the ρ factor for the simple phenols, which suggests that a single ortho-alkyl group does not significantly increase the importance of structure III in the transition state. Of particular interest is the fact that the 2-*t*-butyl group causes a slight enhancement of k_6 over that for a simple phenol at the same $\sum \sigma^+$, whereas a slight depression of k_6 is observed with all the other 2-alkyl phenols. Therefore, even if σ^+_{ortho} is greater than σ^+_{para}, a single *o*-*t*-butyl group must exert a specific accelerating effect on the reaction relative to the other alkyl groups. This enhanced reactivity suggests the occurrence of an interaction between the *t*-butyl group and the *trans*-hydroxyl group. A similar conclusion was also derived from the infrared spectra of 2-*t*-alkyl phenols (3, 4).

In conclusion, the maximum rate of hydrogen abstraction from mononuclear phenols by peroxy radicals, i.e., the maximum inhibiting efficiency, will be achieved when the phenolic substituents have the largest possible negative $\sum \sigma^+$ consistent with a minimum of steric protection afforded to the hydroxyl group. In particular, the phenol should contain a *t*-butyl group in the 2-position, groups with large negative σ^+ constants in the 3,4- and 5-positions, and a vacant 6-position. Among mononuclear phenolic autoxidation inhibitors, the well-known commercial antioxidants 2-*t*-butyl-4-methoxyphenol, 2,5-di-*t*-butyl-4-methoxyphenol, and 2,5-di-*t*-butylhydroquinone are of almost optimum efficiency.

REFERENCES

1. J. A. Howard and K. U. Ingold. Can. J. Chem. **41**, 1744 (1963).
2. H. C. Brown and Y. Okamoto. J. Am. Chem. Soc. **80**, 4979 (1958).
3. K. U. Ingold and D. R. Taylor. Can. J. Chem. **39**, 471 (1961).
4. K. U. Ingold. Can. J. Chem. **40**, 111 (1962).
5. J. A. Howard and K. U. Ingold. Can. J. Chem. **40**, 1851 (1962).
6. C. F. Koelsch and A. G. Whitney. J. Org. Chem. **6**, 795 (1941).
7. W. A. Waters and C. Wickham-Jones. J. Chem. Soc. 812 (1951).
8. A. F. Bickel and E. C. Kooyman. J. Chem. Soc. 2215 (1956).
9. D. S. Davies, H. L. Goldsmith, A. K. Gupta, and G. R. Lester. J. Chem. Soc. 4926 (1956).
10. K. U. Ingold. Can. J. Chem. This issue.
11. G. A. Russell. J. Am. Chem. Soc. **78**, 1047 (1956); J. Org. Chem. **23**, 1407 (1958); Tetrahedron, **5**, 101 (1959).
12. K. U. Ingold. J. Phys. Chem. **64**, 1636 (1960).

Can. J. Chem. Downloaded from www.nrcresearchpress.com by 210.87.254.105 on 09/05/12
For personal use only.

THE REACTION OF *tert*-BUTOXY RADICALS WITH 2,6-Di-*tert*-BUTYL-4-METHYLPHENOL AND 2,6-Di-*tert*-BUTYLPHENOL[1]

K. U. INGOLD
Division of Applied Chemistry, National Research Council, Ottawa, Canada
Received May 25, 1963

ABSTRACT

The products of the reaction of *t*-butoxy radicals with 2,6-di-*t*-butyl-4-methylphenol and 2,6-di-*t*-butylphenol in carbon tetrachloride have been analyzed quantitatively. There is a satisfactory agreement between the measured and calculated yields of *t*-butanol with both phenols. The deuterium isotope effect (k_H/k_D) for abstraction of the phenolic hydrogen from 2,6-di-*t*-butyl-4-methylphenol is about 6.4.

INTRODUCTION

The abstraction of hydrogen atoms by alkoxy radicals from substrates in the liquid phase is of particular interest in relation to autoxidation phenomena (1). These radicals are produced in the chain branching decomposition of the initially formed hydroperoxides and are therefore responsible for the autocatalytic nature of most autoxidations.

$$ROOH \rightarrow RO\bullet + \bullet OH \qquad [1a]$$

$$2ROOH \rightarrow RO\bullet + H_2O + RO_2\bullet \qquad [1b]$$

$$RO\bullet + RH \rightarrow ROH + R\bullet. \qquad [2]$$

The *t*-butoxy radical is particularly suitable for studying the relative rates of reaction [2] with different substrates since it may either abstract a hydrogen to give *t*-butanol or decompose to give acetone and a methyl radical. The ratio, [*t*-butanol]/[acetone], produced in different substrates therefore gives a measure of the relative rates of hydrogen abstraction from the substrates. These radicals are readily prepared by the decomposition of di-*t*-butyl peroxide and the reactions can be represented by,

$$(CH_3)_3COOC(CH_3)_3 \rightarrow 2(CH_3)_3CO\bullet \qquad [3]$$

$$(CH_3)_3CO\bullet + RH \rightarrow (CH_3)_3COH + R\bullet \qquad [2a]$$

$$(CH_3)_3CO\bullet \rightarrow CH_3COCH_3 + CH_3\bullet. \qquad [4]$$

This technique has been employed by a number of workers in recent years to measure the relative rates of hydrogen abstraction by *t*-butoxy radicals from a variety of substrates such as hydrocarbons (2–9), ethers, (10, 11), alcohols (12), and amines (13, 14). As a part of our general program for studying the inhibition of autoxidation by phenols (15–17) we considered that an examination of the reaction of *t*-butoxy radicals with phenols might throw considerable light on the overall mechanism of inhibition. In particular, we were interested to see whether the phenolic hydrogen was abstracted by the *t*-butoxy radical in the rate-determining step.

In view of the comparative ease with which an isotope effect was detected in the reaction of peroxy radicals with 2,6-di-*t*-butyl-4-methylphenol (BMP) (15, 16) this compound was chosen for the present investigation. There have also been numerous studies in recent years of the products of oxidation of this phenol by a variety of oxidizing agents (18–25). Some results on the reaction of *t*-butoxy radicals with 2,6-di-*t*-butylphenol (BP) are also reported.

[1]*Issued as N.R.C. No. 7555.*

Can. J. Chem. Downloaded from www.nrcresearchpress.com by 210.87.254.5 on 09/05/12
For personal use only.

EXPERIMENTAL

Reagent grade carbon tetrachloride was chosen as the solvent to eliminate all possibility of the formation of *t*-butyl alcohol by abstraction from the solvent. In general, 14 ml solutions of the peroxide or peroxide + phenol (25 to 200 m*M**) were placed in glass bombs of 16–17 ml capacity. The dissolved air was carefully removed by freezing in liquid nitrogen and evacuating and repeating this procedure at least four times before the bombs were sealed off under vacuum. The peroxide was thermally decomposed at 122° C, at which temperature the half-life was about 16 hrs. and the dead space over the solution was between 1 and 2 ml. For some runs, from which the products were to be isolated, bombs of 40 ml capacity were used. All results represent the average of at least two experiments.

Methane yields were obtained by breaking the bombs in a vacuum system and measuring the volume of gas which could be pumped off at liquid nitrogen temperatures. Mass spectrometric analysis showed that this gas was entirely methane. All the other volatile products were analyzed by gas chromatography. The low-boiling compounds (mainly methyl chloride, *t*-butyl chloride, unreacted peroxide, *t*-butyl alcohol, chloroform, and acetone) were analyzed on a β,β'-thiodipropionitrile column at 70° C. The high-boiling compounds were analyzed on a polyester succinate column (chlorinated products such as hexachlorethane at 125°, and the phenols at 185° C). The identification of all volatile products was confirmed by mass spectrometry and, or, infrared spectroscopy. Since methyl chloride is a gas at room temperature chromatographic analyses were made on samples separate from those in which the methane was analyzed. The samples were injected into the low-temperature column immediately after the bombs were opened.

The three major products resulting from the oxidation of BMP by *t*-butoxy radicals are the following non-volatile dimers;

I. 3,5,3′,5′-tetra-*t*-butyl-4,4′-dihydroxy-1,2-diphenylethane

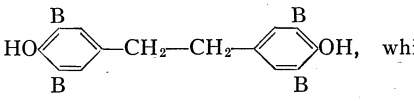

white needles from ethanol, m.p. 174–175°

II. 3,5,3′,5′-tetra-*t*-butyl-4,4′-dihydroxy-1,2-diphenylethylene

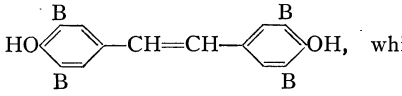

white crystals from ligroin, m.p. 241–242°

III. 3,5,3′,5′-tetra-*t*-butylstilbene-4,4′-quinone†

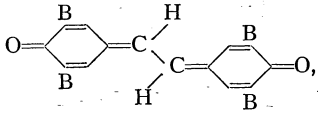

reddish needles from ethanol, m.p. 316–317° (decomp.)

Since these products could not be analyzed by gas chromatography, pure samples were prepared by the oxidation of BMP with benzoyl peroxide in refluxing chloroform (18, 22) to assist in analyses by other techniques. Compounds I (22) and III (18, 22) have been identified previously in this reaction. The present work showed that II is also formed in very small amounts. However, since III is most readily separated and purified it is much simpler to prepare I and II in pure form from III than to isolate them from the reaction mixture. Reduction of III with hydrogen over platinum in dimethoxyethane yields pure I after 1 hour at room temperature. Reduction of III with zinc and acetic acid in benzene yields II (18, 20, 21). Both I and II tend to go slightly yellow on standing in air and, in solution, II is fairly rapidly oxidized by air to III, and a quinhydrone of II and III is precipitated (21).

The n.m.r. spectra of compounds I, II, and III have been described in an earlier publication from this laboratory (26). The ultraviolet spectra showed band maxima (in order of decreasing intensity) at 283 and 277 mμ for compound I; 307, 325, and 295 mμ for II; 448, 420, and 395 mμ for III; 283 and 277 mμ for BMP; and 456, 439, and 307 mμ for 2,6-di-*t*-butylbenzoquinone. Compound I was analyzed by n.m.r. spectroscopy in CCl_4 and compounds II and III by ultraviolet spectroscopy in cyclohexane. At the end of a run, the volatiles were removed under vacuum at room temperature and the residue was dissolved in a known volume of deaerated CCl_4 or cyclohexane. The quantitative analysis of II is much less accurate than that of I and III but it appears to be only a minor product. In some cases unreacted BMP was removed by sublimation under vacuum at 40–50° before analysis. Compound III could be isolated almost quantitatively by washing the evaporated residues with a small quantity of ligroin, CCl_4, or ethanol.

**All concentrations are given in millimoles/liter (m*M*).*

†*The corresponding tetra-t-amyl compound was also prepared from 2,6-di-t-amyl-4-methylphenol. Red plates from ethanol, m.p. 219–220°, with a change to red needles above 200° and some decomposition.*

Can. J. Chem. Downloaded from www.nrcresearchpress.com by 210.87.254.5 on 09/05/12
For personal use only.

The oxidation of 2,6 di-*t*-butylphenol by *t*-butoxy radicals yields two dimeric products: IV, 3,3′,5,5′-tetra-*t*-butyl-4,4′-dihydroxydiphenyl, white needles from ethanol, m.p. 185°, and V, 3,3′,5,5′-tetra-*t*-butyldiphenoquinone, reddish plates from ethanol, m.p. 245–246°. Authentic V was prepared by oxidizing BP with nitric acid (23, 27, 28) and its reduction with hydrogen over platinum gave IV. The keto tautomer of IV (28) was not identified among the products, possibly because it rapidly isomerizes to the enol form (i.e., IV) under the reaction conditions. Compound IV was analyzed by infrared spectroscopy in the O—H fundamental stretching region (calibrated with known mixtures of IV and V) after removal of unreacted BP by sublimation or by extraction with a small quantity of ethanol. Compound V was analyzed by ultraviolet spectroscopy (band maxima at 423 mμ).

RESULTS AND DISCUSSION

The decomposition of di-*t*-butyl peroxide in CCl_4 at 122° C is first order within the limits of experimental accuracy over an initial concentration range from 25 to 200 m*M*. This suggests that the free radical induced decomposition of the peroxide is relatively unimportant compared with reaction [3]. The composition of the main products varies slightly with the initial peroxide concentration and with the extent of its decomposition (see Table I). In addition to the products listed in this table traces of isobutylene oxide, isobutyraldehyde, and chloro-*t*-butanol were also identified.

TABLE I

Reaction products in m*M* from the decomposition of di-*t*-butyl peroxide in CCl_4 at 122° C

[DTBP]	100	100	100	100	100	25	50	200
Reaction time (hr)	4	8	16	24	168	16	16	16
2×[DTBP] decomposed	34	60	96	128	199	23	48	193
Acetone	32	57	89	115	172	22	46	179
1-Chloroacetone	—	0.3	0.5	1	8	—	0.1	2
t-Butanol	0.5	2.5	4	6	0.0	0.5	2	15
t-Butyl chloride	—	—	1	2	12	—	—	1
$(CH_3)_3COCCl_3$	—	0.2	0.2	0.5	3	—	0.1	0.7
$(CH_3)_2CClCH_2CCl_3$	—	0.1	0.1	0.2	6	—	—	0.3
Total	32.5	60.1	94.8	124.7	201	22.5	48.2	198
Methane	1	4	6	9	25	1	2	12
Methyl chloride	29	54	91	110	174	23	46	182
Chloroform	1	2	4	7	22	1	2	10
Hexachloroethane	15	25	44	57	86	11	22	82

Excellent product balances were obtained under all conditions. That is, the sum of the products from acetone to $(CH_3)_2CClCH_2CCl_3$ in Table I is roughly equal to twice the amount of peroxide decomposed. Furthermore,

$$[CH_4]+[CH_3Cl] = [CH_3COCH_3]+[CH_2ClCOCH_3]$$

and

$$[CHCl_3]+2[C_2Cl_6]+[(CH_3)_3COCCl_3] = [CH_3Cl]+[CH_2ClCOCH_3].$$

The major products obviously arise from reaction [5] and subsequent reactions of the methyl radical. These radicals are mainly converted to methyl chloride by reaction with the solvent and the resulting trichloromethyl radicals are mainly destroyed by dimerization. A small fraction of the $CH_3\bullet$, $CCl_3\bullet$, and *t*-butoxy radicals abstract hydrogen from

$$CH_3\bullet + CCl_4 \rightarrow CH_3Cl + CCl_3\bullet \quad [5]$$

$$2CCl_3\bullet \rightarrow C_2Cl_6 \quad [6]$$

the products. Some abstraction from the unreacted peroxide may also occur since it could account for the production of isobutylene oxide and isobutyraldehyde, i.e.,

$$X\bullet + (CH_3)_3COOC(CH_3)_3 \rightarrow XH + (CH_3)_3COOC(CH_3)_2CH_2\bullet \quad [7]$$

Can. J. Chem. Downloaded from www.nrcresearchpress.com by 210.87.254.5 on 09/05/12
For personal use only.

$$(CH_3)_3COOC(CH_3)_2CH_2\bullet \rightarrow (CH_3)_3CO\bullet + \begin{cases} (CH_3)_2C\overset{O}{\triangle}CH_2 \\ (CH_3)_2CHCHO \end{cases} \quad [8]$$

However, the hydrogen balance is not quite as good as the carbon balance since the yield of CH_4, $CHCl_3$, and *t*-butanol is larger than can be accounted for by the products which have obviously lost hydrogen (i.e., chloroacetone, chloro-*t*-butanol, isobutylene oxide, and isobutyraldehyde). This difference may be due to hydrogen loss by several other chlorinated compounds which were present in such small quantities that they could not be identified. The presence of *t*-butyl chloride suggests that some *t*-butyl radicals are formed. They might be produced either by the deoxygenation of *t*-butoxy radicals or by an assymetric decomposition of the peroxide.

The addition of BMP or BP at a comparable concentration to the peroxide greatly simplifies the products since reaction [2] now predominates over reaction [4] and the yield of methyl radicals is thereby greatly reduced. The decomposition of the peroxide is still a first-order reaction but the rate of decomposition is slightly increased by an excess of the phenol (see Fig. 1). This may be due to a direct reaction between the phenol and the peroxide (29) or to some indirect solvation phenomena. However, it is also possible that the increased rate is due to a reduction in the rate of recombination of *t*-butoxy radicals to re-form the peroxide (i.e., the reverse of reaction [3]) since the phenol will reduce the steady-state concentration of these radicals. The major products under varying conditions are given in Fig. 1 and in Tables II and III. Small traces of the following compounds were

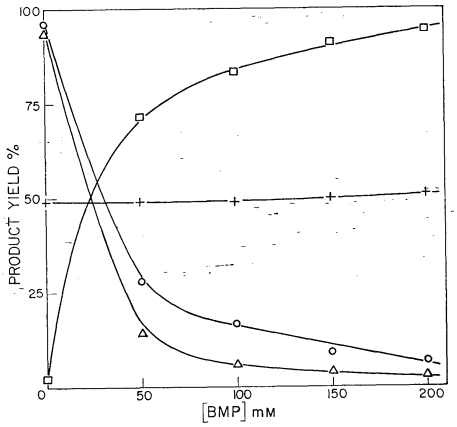

FIG. 1. Percentage composition of the products arising from the 16 hour decomposition of 100 m*M* di-*t*-butyl peroxide as a function of the 2,6-di-*t*-butyl-4-methylphenol concentration. Key: △ methyl chloride; ○ acetone; □ *t*-butanol; + percentage decomposition of the peroxide.

also identified: formaldehyde, trimethylacetic acid, $(CH_3)_2CClCH_2CCl_3$,* $(CH_3)_3COCCl_3$* and, in the presence of BP, traces of water, isobutylene oxide, isobutyraldehyde, and chloro-*t*-butanol were also present. Chloroform and hexachloroethane were not formed. The color of the 100 m*M* peroxide – 100 m*M* phenol mixtures after 16 hours was yellow for BMP and a deep red for BP.

With both BMP and BP the sum of [acetone]+[*t*-butanol]+[*t*-butyl chloride] is roughly equal to twice the amount of peroxide decomposed, but the $[CH_4]+[CH_3Cl]$ is significantly smaller than the amount of acetone produced. Since the yields of methane and chloroform

**Tentative identification by mass spectrometry.*

Can. J. Chem. Downloaded from www.nrcresearchpress.com by 210.87.254.5 on 09/05/12
For personal use only.

TABLE II

Reaction products in mM from equimolar mixtures of di-*t*-butyl peroxide and a phenol

	2,6-Di-*t*-butyl-4-methylphenol						2,6-Di-*t*-butylphenol	
Initial concn. of reactants	50	100	100	100	100	100	50	100
Reaction time (hr)	16	4	7	16	24	168	16	16
2×[DTBP] decomposed	48	32	55	96	124	199	48	96
Methane	—	—	0.1	0.2	0.3	1	—	1
Methyl chloride	4	2	3	6	7	15	7	17
Isobutene	1	—	0.5	1	2	9	1	2
t-Butyl chloride	—	—	—	—	—	1	2	6
Acetone	12	5	8	15	22	38	17	24
t-Butanol	36	27	46	82	98	162	23	65
[*t*-Butanol]/[acetone]	3.0	5.4	5.75	5.5	4.45	4.26	1.35	2.7
[Phenol] reacted	23	23	32	47.5	53.5	66	22	50
[*t*-Butanol]/[phenol] reacted	1.57	1.17	1.44	1.73	1.83	2.45	1.04	1.30

TABLE III

Reaction products in mM from di-*t*-butyl peroxide (200 mM) and a phenol (200 mM)

	2,6-Di-*t*-butyl-4-methylphenol			2,6-Di-*t*-butylphenol		
Reaction time (hr)	5	14	168	6.75	16	168
2×[DTBP] decomposed	80	178	398	104	200	398
Methyl chloride	1	2	7	6	14	40
Isobutene	0.2	2	15	0.1	2	7
t-Butyl chloride	—	—	2	7	15	76
Acetone	8	17	46	18	37	98
t-Butanol	72	158	328	79	148	224
[*t*-Butanol]/[acetone]	9.0	9.3	7.1	4.4	4.0	2.3
[Phenol] reacted	54	100	134	50	87	180
[*t*-Butanol]/[phenol] reacted	1.33	1.58	2.45	1.58	1.70	1.25
2×[I]; 2×[IV]	40	78	60	15	27	25
2×[II]; 2×[V]	1	3	12	28	56	120
2×[III]	3	12	45			
2,6-Bu_2^t-4-CHO phenol	1	2	4	—	—	1
2,6-Bu_2^t-4-CCl_3 phenol	—	1	4	—	2	16
Σ phenolic products	45	96	125	43	85	162
Calculated [Bu^tOH]	53	124	227	71	139	267

are extremely small neither the methyl radical nor the trichloromethyl radical abstracts a significant amount of hydrogen from the phenols, probably for steric reasons. However, the absence of C_2Cl_6 and the unexpectedly small yield of methyl chloride indicates that both radicals must react very rapidly with the phenols or, more probably, with the phenoxy radicals by some mechanism not involving abstraction. The formation of isobutylene (which is not formed in the absence of the phenols) and the identification among the phenolic products of BMP and 2-*t*-butyl-6-methylphenol from BP and 2,6-di-*t*-butyl-4-trichloromethylphenol from both BMP and BP suggest that radical replacement reactions occur rather readily at both the ortho and para positions, for example,

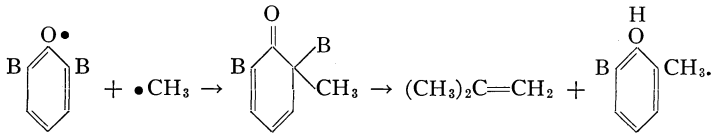

[9]

The radicals may also add to the quinone products III and V (30). The presence of traces of trimethylacetic acid among the products indicates that some rupture of the aromatic ring also occurs during the reaction.

For an equimolar peroxide–phenol mixture the [*t*-butanol]/[acetone] ratio increases approximately linearly with the increase in concentration and, at a given concentration,

Can. J. Chem. Downloaded from www.nrcresearchpress.com by 210.87.254.5 on 09/05/12
For personal use only.

the ratio remains roughly constant until about half of the peroxide has been decomposed (see Tables II and III). At a constant peroxide concentration the ratio increases with increasing phenol concentration (see Fig. 1). Incidentally, no significant fraction of the acetone is produced by decomposition of the peroxide in the vapor above the liquid since increasing the dead space from 1 ml to 10 ml in bombs of 16 ml capacity had no effect on the product composition. Moreover, in the absence of peroxide, BMP is completely stable for 1 week under the reaction conditions and BP produces only minute traces of isobutene.

The ratio [*t*-butanol]/[BMP] reacted varies between a lower limit of 1.0 when there is a large excess of BMP and an upper limit which approaches 3.0 when there is insufficient BMP to react with all the *t*-butoxy radicals produced. The variation in this ratio is due to the formation of the three dimeric phenolic products in which 1, 2, and 3 atoms of hydrogen have been lost per component molecule of BMP. The reaction sequence can be represented as:

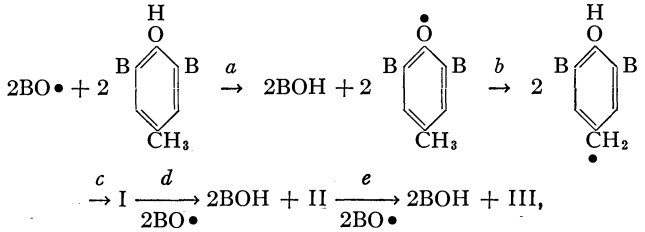

[10]

where B represents the *t*-butyl group. Reaction [10*a*] must involve abstraction of the phenolic hydrogen because of the large deuterium isotope effect found in this work (see below). The formation of I from two phenoxy radicals probably involves hydrogen migration from the 4-methyl group and dimerization of the resulting benzyl radicals. The alternative mechanism via the quinone methide seems less likely but cannot be completely ruled out (31). Reactions [10*d*] and [10*e*] probably also involve abstraction of the

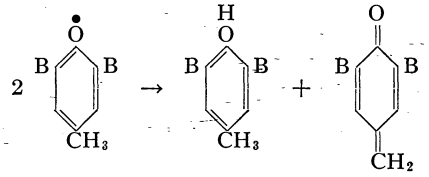

[11]

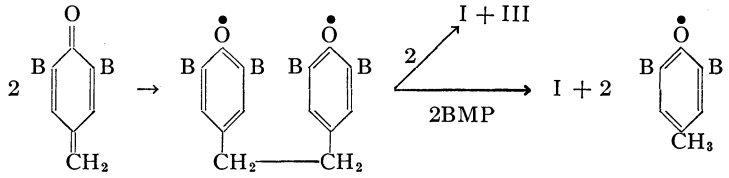

[12]

phenolic hydrogen followed by hydrogen migration since the intermediate radicals have been identified by e.s.r. during the oxidation of BMP with lead dioxide (32, 33).

The reaction of BMP with *t*-butyl peroxy radicals results in the formation of 1-methyl-1-*t*-butylperoxy-3,5-di-*t*-butyl-2,5-cyclohexadienone-4 (24):

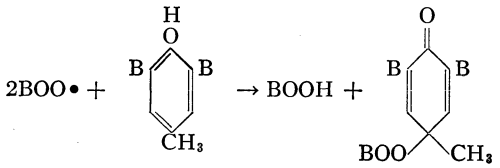

[13]

Can. J. Chem. Downloaded from www.nrcresearchpress.com by 210.87.254.5 on 09/05/12
For personal use only.

and a similar compound is obtained with 2-cyano-2-peroxy propyl radicals (34). The absence of this type of product under the present experimental conditions is probably due both to a reduced probability of addition of the *t*-butoxy radical at the 4-position (because of increased steric effects) and to the instability of the resulting product. That is, at 122° C equilibrium

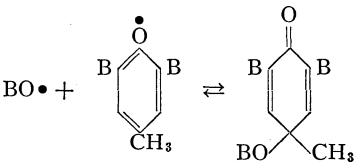

[14]

probably lies largely towards the left and favors the dissociated radicals. This difference in the behavior of alkoxy and peroxy radicals probably accounts for the observation of Moore and Waters (19) that the oxidation of cumene containing BMP at 80–100° C initiated by α,α'-azodiisobutyronitrile yields only traces of I, whereas initiation by 0.1% ferric stearate (which catalyzes the decomposition of cumene hydroperoxide to cumyloxy radicals) yields about 10 times as much I. Both I and III have also been identified as products from the oxidation of oil containing BMP at 120° C catalyzed by iron and copper (20).

As complete product analyses as possible were made on 200 m*M* peroxide – 200 m*M* phenol mixtures at three different extents of peroxide decomposition. The results are given in Table III. With both BMP and BP the products from approximately 90% of the phenol which reacted were identified. 2,6-Di-*t*-butyl-4-formyl- and 4-trichloromethyl-phenol were estimated by gas chromatography. Traces of 2,4,6-tri-*t*-butylphenol, 2,6-di-*t*-butyl-4-*t*-butoxyphenol, and 2,6-di-*t*-butylbenzoquinone were also identified on the chromatograph as products from both BMP and BP. In addition, traces of BMP and 2-*t*-butyl-6-methyl-phenol were formed from BP. Extraction of the products with aqueous sodium carbonate and acidification yielded a very small amount of a white precipitate from BMP but not from BP. This was identified by its melting point (134–135°) as DL-*trans*-1,4-dioxo-5,6-di-*t*-butyl-2-hydroxy-2-cyclohexene (23). The ultraviolet spectra of the 168 hour BMP sample showed a small unknown band at 474 mμ. The e.s.r. spectra of unopened bombs indicated that the phenoxy radicals from BMP and BP were present in only very small amounts.

The concentrations of *t*-butanol which should be expected on the basis of the identified phenolic products, i.e., 2I + 4II + 6III + 2(2,6-Bu_2^t-4-CHO phenol) with BMP and 2IV + 4V + 2(2,6-Bu_2^t-4-CHO phenol) with BP, are also given in Table III. With BMP the calculated [*t*-butanol] is about 70% of the measured concentration, which is not unsatisfactory considering the difficulties involved in obtaining quantitative analyses of the phenolic products (particularly II). The remaining 30% of the *t*-butanol may arise from the unidentified phenolic products if their precursors donate hydrogen atoms very readily to *t*-butoxy radicals. With BP the agreement between the calculated and measured [*t*-butanol] is rather better. However, the large yields of *t*-butyl chloride and the fact that the calculated *t*-butanol is larger than the measured amount after 168 hours both suggest that the *t*-butoxy radical can be deoxygenated to give the *t*-butyl radical which then abstracts a chlorine atom from the solvent. The rapid increase in the yield of *t*-butyl chloride with increasing decomposition of the peroxide suggests that this reaction may involve an oxidation product of BP such as, for example, the keto tautomer of IV.

The occurrence of a large deuterium isotope effect in the reaction of *t*-butoxy radicals

Can. J. Chem. Downloaded from www.nrcresearchpress.com by 210.87.254.5 on 09/05/12
For personal use only.

with BMP was readily demonstrated by adding 1 ml of H_2O and D_2O to bombs containing 14 ml of a 50 mM peroxide – 50 mM BMP mixture. After 16 hours at 122° C the former bomb showed the deep yellow color of compound III while the latter was nearly colorless. The yields of *t*-butanol and acetone in the CCl_4 layer were, respectively, 18 and 11 mM with BMP-H and 0.6 and 26 mM with BMP-D. With 500 mM of BMP-D and 50 mM of peroxide the yields were 28 and 6 mM, respectively. Obviously a significant fraction of the products had dissolved in the aqueous layer and these results are, therefore, not suitable for the calculation of the magnitude of the isotope effect.

Ideally, in order to obtain the true isotope effect without the complication introduced by the addition of D_2O or H_2O, a large excess of the deuterated BMP should be used relative to the amount of peroxide decomposed in order to reduce to negligible importance the loss of deuterium by hydrogen transfer from the 4-methyl group. That is, the initially formed phenoxy radicals will dimerize to give compound I (and then II) containing two OH groups. Since there is obviously a large isotope effect an increasing proportion of the *t*-butoxy radicals will abstract H from these products rather than D from the unreacted BMP as the reaction progresses. However, it can readily be calculated that the BMP-D concentration cannot be raised sufficiently nor the peroxide concentration reduced sufficiently to eliminate this hydrogen-transfer process and still obtain accurately measurable quantities of *t*-butanol and acetone. It is, therefore, necessary to add D_2O to the bombs containing BMP-D and H_2O to the bombs containing BMP-H and measure the products in both the CCl_4 and the aqueous phases.

The following procedure was employed. Solutions of BMP in CCl_4 at various concentrations were shaken with H_2O or D_2O for 24 hours at room temperature (16). 50 mM of peroxide was added to these solutions and the mixtures were shaken for an additional hour to saturate all the CCl_4 with water. The bombs were washed with H_2O or D_2O and dried under vacuum. Fourteen milliliters of the CCl_4 layer of the mixtures was sealed in the bombs by themselves and with the addition of 0.1 and 1.0 ml of water. The yields of *t*-butanol and acetone were measured after 16 hours at 122° C in the CCl_4 layer and also in the water layer for the bombs containing 1.0 ml water. A correction based on the latter figure was used for the bombs containing 0.1 ml water. In every case, the total yields of the two products were the same with both 0.1 and 1.0 ml water. The [*t*-butanol]/[acetone] ratios obtained in this way are shown plotted against the BMP concentration in Fig. 2.

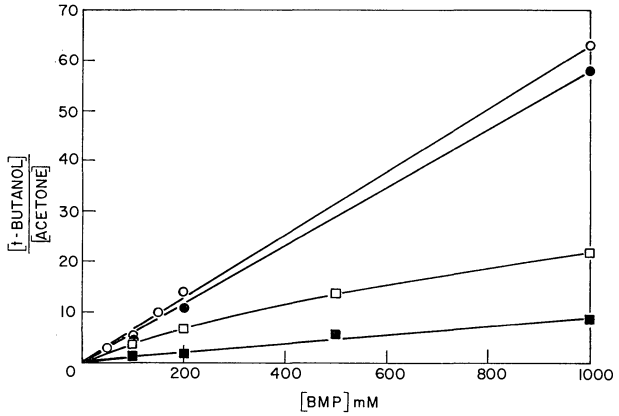

FIG. 2. [*t*-Butanol]/[acetone] ratio resulting from the decomposition of 50 mM of di-*t*-butyl peroxide for 16 hours at 122° C as a function of BMP concentration. Key: ○ saturated with H_2O; ● 14 ml H_2O saturated solution + 0.1 and 1.0 ml H_2O; □ saturated with D_2O; ■ 14 ml D_2O saturated solution + 0.1 and 1.0 ml D_2O.

Can. J. Chem. Downloaded from www.nrcresearchpress.com by 210.87.254.5 on 09/05/12
For personal use only.

The results with H_2O suggest that saturating the CCl_4 with water may reduce the [*t*-butanol]/[acetone] ratio slightly compared with the values obtained in dry CCl_4 and a further slight reduction is produced by excess water. These small effects are quite possibly due to hydrogen bonding between the *t*-butoxy radicals and the water. This would produce a less reactive radical which would show an increased tendency to decompose rather than to abstract hydrogen.

The results with D_2O show that H migration is fairly important in determining the [*t*-butanol]/[acetone] ratio even with a large excess of BMP-D, but that its importance does tend to decrease as the phenol concentration is increased.* The true isotope effect should be roughly proportional to the slopes of the lines through the points obtained with excess H_2O and D_2O provided it is assumed that there is no significant difference in the ability of H_2O and D_2O to stabilize *t*-butoxy radicals. With this assumption, the isotope effect is:

$$k_H/k_D = 6.4.$$

This value can be compared with values of 3.3 at 135° C (3) and 3.8 to 5.3 at 107–116° C (8) for hydrogen abstraction from toluene by *t*-butoxy radicals. The larger isotope effect for hydrogen abstraction from BMP is to be expected because the hydrogen atom is transferred between two identical atoms and, its zero-point energy will probably, therefore, be lost in the transition state (35). In addition, the hindering effect of the *t*-butyl groups will also tend to increase the isotope effect (36) (see also following paper).

REFERENCES

1. K. U. INGOLD. Chem. Rev. **61**, 563 (1961).
2. J. H. T. BROOK. Trans. Faraday Soc. **53**, 327 (1957); J. Inst. Petrol. **44**, 333 (1958).
3. J. H. T. BROOK and R. W. GLAZEBROOK. Trans. Faraday Soc. **56**, 1014 (1960).
4. A. L. WILLIAMS, E. A. OBERRIGHT, and J. W. BROOKS. J. Am. Chem. Soc. **78**, 1190 (1956).
5. E. L. PATMORE and R. J. GRITTER. J. Org. Chem. **27**, 4196 (1962).
6. K. M. JOHNSTON and G. H. WILLIAMS. Chem. Ind. (London), **328** (1958); J. Chem. Soc. 1446 (1960).
7. C. WALLING and B. B. JACKNOW. J. Am. Chem. Soc. **82**, 6113 (1960).
8. S. H. WILEN and E. L. ELIEL. J. Am. Chem. Soc. **80**, 3309 (1958).
9. R. L. HUANG and S. SINGH. J. Chem. Soc. 891 (1958).
10. R. L. HUANG and O. YEO. J. Chem. Soc. 3190 (1959).
11. H. B. HERBERT, J. A. W. REID, and C. J. M. STIRLING. J. Chem. Soc. 5239 (1961).
12. K. SCHWETLICK, W. GEYER, and H. HARTMAN. Angew. Chem. **72**, 779 (1960).
13. R. L. HUANG. J. Chem. Soc. 1816 (1959).
14. M. J. W. STRATFORD. U.S. Dep. Com. Office Tech. Serv. P.B. Rept. 144, 250 (1959).
15. K. U. INGOLD and J. A. HOWARD. Nature, **195**, 280 (1962).
16. J. A. HOWARD and K. U. INGOLD. Can. J. Chem. **40**, 1851 (1962).
17. J. A. HOWARD and K. U. INGOLD. Can. J. Chem. This issue.
18. S. L. COSGROVE and W. A. WATERS. J. Chem. Soc. 388 (1951).
19. R. F. MOORE and W. A. WATERS. J. Chem. Soc. 243 (1954).
20. C. D. COOK. J. Org. Chem. **18**, 261 (1953).
21. C. D. COOK, N. G. NASH, and H. R. FLANAGAN. J. Am. Chem. Soc. **77**, 1783 (1955).
22. G. R. YOHE *et al.* J. Am. Chem. Soc. **75**, 2688 (1953).
23. G. R. YOHE *et al.* J. Org. Chem. **21**, 1289 (1956); **24**, 1251 (1959).
24. T. W. CAMPBELL and G. M. COPPINGER. J. Am. Chem. Soc. **74**, 1469 (1952).
25. H. R. GERSMAN and A. F. BICKEL. J. Chem. Soc. 2711 (1959).
26. S. BROWNSTEIN and K. U. INGOLD. J. Am. Chem. Soc. **84**, 2258 (1962).
27. K. U. INGOLD. J. Phys. Chem. **64**, 1636 (1960).
28. M. S. KHARASCH and B. S. JOSHI. J. Org. Chem. **22**, 1439 (1957).
29. W. J. FARISSEY, JR. J. Am. Chem. Soc. **84**, 1002 (1962).
30. R. P. BUCKLEY, A. REMBAUM, and M. SZWARC. J. Chem. Soc. 3442 (1958).
31. L. J. FILAR and S. WINSTEIN. Tetrahedron Letters, No. 25, 9 (1960).
32. A. L. BUCHACHENKO and M. B. NEIMAN. Dokl. Akad. Nauk SSSR, **139**, 916 (1961).
33. V. D. POKHODENKO, L. N. GANYUK, and A. I. BRODSKII. Dokl. Akad. Nauk SSSR, **145**, 815 (1962).
34. C. E. BOOZER, G. S. HAMMOND, C. E. HAMILTON, and J. N. SEN. J. Am. Chem. Soc. **77**, 3233 (1955).
35. C. A. BUNTON and V. J. SHINER, JR. J. Am. Chem. Soc. **83**, 3214 (1961).
36. E. BACIOCCHI, G. ILLUMINATI, and G. SLEITER. Tetrahedron Letters, No. 23, 30 (1960).

**Part of the curvature for the D_2O-saturated solution and also the slight curvature observable with some of the other experimental points may be due to the increasing aromatic character of the solvent as the phenol concentration is increased (see following paper).*

Can. J. Chem. Downloaded from www.nrcresearchpress.com by 210.87.254.5 on 09/05/12
For personal use only.

THE EFFECT OF SUBSTITUENTS ON THE RELATIVE RATES OF REACTION OF *tert*-BUTOXY RADICALS WITH PHENOLS IN CARBON TETRACHLORIDE AND IN CHLOROBENZENE[1]

K. U. INGOLD
Division of Applied Chemistry, National Research Council, Ottawa, Canada
Received May 25, 1963

ABSTRACT

The relative rates of hydrogen abstraction from substituted phenols by *t*-butoxy radicals can be correlated with the σ^+ constants of the substituents. The effects of an aromatic solvent (chlorobenzene) and of ortho-alkyl substituents on the reactivities of the phenols and on the transition state of the reaction are discussed.

INTRODUCTION

In the previous paper (1) it was shown that *t*-butoxy radicals abstract the phenolic hydrogen from 2,6-di-*t*-butyl-4-methylphenol (BMP). As a continuing part of our investigation into the inhibition of autoxidation by phenols, the influence of substituents on the relative rates of hydrogen abstraction by *t*-butoxy radicals from a number of substituted phenols has been examined both in CCl_4 and in chlorobenzene.

RESULTS

The experimental and analytical procedures were described in the previous paper (1). The present work involved decomposition of equimolar peroxide–phenol mixtures (generally 50 m*M*) in CCl_4 and in chlorobenzene for 16 hours at 122° C (i.e., decomposition of approximately 50% of the peroxide). Only volatile products were analyzed and the consumption of the phenols in chlorobenzene was not measured.

Many of the phenols used in this work were commercial products. The preparation of the remainder is described in the literature. They were all checked for purity by gas chromatography before use and none contained more than 0.5% impurities.

The main investigation centered on the ratio [*t*-butanol]/[acetone] since this gives a measure of the relative rates of hydrogen abstraction from different phenols by *t*-butoxy radicals. This ratio was measured for 3- and 4-substituted phenols and for 4-substituted 2,6-di-*t*-butylphenols. The effect of 2,6-dialkyl substituents on this ratio in CCl_4 was also examined. The main results of this work are given in Table I.

With the notable exception of 4-hydroxybenzaldehyde and 2,6-di-*t*-butyl-4-formylphenol the sum of the [*t*-butanol] plus [acetone] is approximately equal to twice the amount of peroxide decomposed. Moreover, this product balance generally tends to be rather better for phenols containing electron-donating substituents than for those containing electron-attracting substituents, i.e., this balance is better for the more reactive phenols. It should be noted that in chlorobenzene the [*t*-butanol]/[acetone] ratios given in Table I have been corrected to allow for the fact that the decomposition of 50 m*M* of peroxide by itself for 16 hours yields 7 m*M* [*t*-butanol] in this solvent, (2×[DTBP] decomposed = 60 m*M*, [acetone] = 53 m*M*). The corrected [*t*-butanol] has therefore been taken to be the measured value minus (7/53)[acetone.] The reaction is still approximately first order in chlorobenzene but its rate is slightly greater than that in CCl_4, possibly because the

[1]*Issued as N.R.C. No. 7554.*

Can. J. Chem. Downloaded from www.nrcresearchpress.com by 210.87.254.5 on 09/05/12
For personal use only.

Can. J. Chem. Downloaded from www.nrcresearchpress.com by 210.87.254.5 on 09/05/12
For personal use only.

TABLE I

Decomposition of 50 m*M* di-*t*-butyl peroxide in presence of 50 m*M* phenol for 16 hours in carbon tetrachloride and in chlorobenzene

Phenol substituents	Carbon tetrachloride					Chlorobenzene			
	[Phenol] reacted (m*M*)	2×[DTBP] decomposed (m*M*)	[*t*-Butanol] (m*M*)	[Acetone] (m*M*)	[*t*-Butanol] / [Acetone]	2×[DTBP] decomposed (m*M*)	Uncorrected [*t*-Butanol] (m*M*)	[Acetone] (m*M*)	Corrected [*t*-Butanol] / [Acetone]
4-CH_3O						53	52	2.5	20.7
3,4,5-$(CH_3)_3$	44	38	35	0.5	70				
4-CH_3	28	46	44	0.6	73	55	49	5.5	8.8
4-$(CH_3)_3C$	20	44	38	0.7	54	53	51	6	8.4
3,5-$(CH_3)_2$	30	40	44	1.2	37				
3-CH_3	20	42	38	2	19				
None	15	48	43	1.6	27	54	45	10	4.4
3-CH_3O	22	44	40	2	20				
4-Cl	36	42	38	2	19	52	42	9	4.5
3-F	19	42	32	3	9.6				
3-Cl	25	40	32	3	9.6	54	41	13	3.0
4-CN		40	22	5	4.4	56	38	19	1.9
4-CHO*		56	0	Trace	—				
2,6-Bu_2^t-4-CH_3O	23	46	39	4.3	9.0	52	40	11	3.5
2,6-Bu_2^t-4-CH_3	23	48	36	12	3.0	54	33	21	1.44
2,6-Bu_2^t-4-$(CH_3)_3C$	24	46	34	12	2.8				
2,6-Bu_2^t-4-$C_6H_5(CH_3)_2C$	23	46	34	12	2.8				
2,6-Bu_2^t	22	48	23	17	1.35	54	24	30	0.67
2,6-Bu_2^t-4-Cl	26	44	24	13	1.8	52	24	23	0.91
2,6-Bu_2^t-4-CN	16	48	13	27	0.48	57	17	43	0.26
2,6-Bu_2^t-4-CHO	40	54	2	11	0.18				
2,4-$(CH_3)_2$	21	42	36	0.7	51				
2,4,6-$(CH_3)_3$	36	75	74	1.1	67				
2,3,5,6-$(CH_3)_4$	21	43	41	1.2	34				
2,3,4,5,6-$(CH_3)_5$	47	42	40	1	40				
2,6-Pr_2^i-4-CH_3	23	40	35	0.8	44				
2,4,6-Bu_3^s	20	38	31	1	31				
2,6-Am_2^t-4-CH_3	19	48	28	12	2.3				
2,6-Oct_2^{tt}-4-CH_3†	21	44	30	13	2.3				

*$[(CH_3)_3CCl] = 23$; $[CHCl_3] = 28$.
†The Oct^{tt} group is $(CH_3)_3CCH_2(CH_3)_2C$.

transition state for decomposition is stabilized by the aromatic solvent. In CCl_4 the ratio of [*t*-butanol]/[phenol] consumed varies from slightly under 1.0 for 3,4,5 trimethylphenol, pentamethylphenol, 2,6-di-*t*-butyl-4-chlorophenol, and 2,6-di-*t*-butyl-4-cyanophenol to slightly more than 2.0 for phenol.

The most complete product analyses were made with the 4-substituted 2,6-di-*t*-butylphenols in CCl_4 since these phenols give greater yields of secondary products than the much more reactive unhindered phenols. The products, other than acetone and *t*-butanol, resulting from 16 hours' reaction between 50 m*M* peroxide and 50 m*M* of the phenols are given in Table II. These products can be compared with those given previously (1) for 2,6-di-*t*-butylphenol and its 4-methyl derivative.

TABLE II

Products from the 16 hour reaction of 50 m*M* di-*t*-butyl peroxide with 50 m*M* 2,6-di-*t*-butyl-4-substituted phenols in CCl_4

	4-Substituent					
Product (m*M*)	4-CH_3O	4-$(CH_3)_3C$	4-$C_6H_5(CH_3)_2C$	4-Cl	4-CN	4-CHO
Methyl chloride	0	2	2	3	17	1
Isobutene	6	4	4	9	—	2
t-Butyl chloride	—	0.5	0.5	1	0.5	36
Chloroform	—	—	—	—	—	12
$(CH_3)_3COCCl_3$	—	Trace	Trace	1.5	2	1
$(CH_3)_2CClCH_2CCl_3$	—	—	—	—	—	6
$(CH_3)_2C(OH)CH_2Cl$	—	—	—	—	—	2
2,6-Bu_2^t-4-CH_3 phenol	6	3	1	4	—	—
2,6-Bu_2^t-4-Bu^tO phenol	—	1	1	2	1	1
2,6-Bu_2^t-4-CCl_3 phenol	Trace	Trace	Trace	Trace	Trace	Trace
$(CH_3)_3CCOOH$	Trace	Trace	Trace	Trace	Trace	Trace

As was pointed out in the previous paper, the production of isobutene and 4-methyl-, 4-trichloromethyl- and 4-*t*-butoxy-2,6-di-*t*-butyl-phenols indicates that ring substituents can be displaced by the various free radicals present in solution. Further confirmation for such reactions was provided by the identification of 3 m*M* of α-methylstyrene among the products from 2,6-di-*t*-butyl-4-cumylphenol. These displacement reactions appear to become of greatly increased importance with the tri-*t*-alkyl phenols as the concentration of the peroxide and phenol is increased. For example, the yields of most secondary products are slightly more than doubled in the same reaction time with 100 m*M* mixtures but the yields of isobutene rise to 20 m*M* for 2,4,6-tri-*t*-butylphenol and to 30 m*M* for 2,6-di-*t*-butyl-4-cumylphenol. Since these two phenols give the most stable phenoxy radicals (see below) these results suggest that the displacement reactions occur more readily on phenoxy radical than on the free phenol (1).

The reaction of 50 m*M* of 2,6-di-*t*-butyl-4-formylphenol with 50 m*M* of peroxide for 16 hours gives 10 m*M* CH_4, 7.2 m*M* CO, and 2.1 m*M* CO_2 as well as traces of isobutylene oxide. Small amounts of C_2Cl_6 were detected among the products from 2,6-di-*t*-butyl-4-cyanophenol only.

The color of the solutions after reaction is a pale yellow in all cases except for 2,6-di-*t*-butyl-4-chlorophenol where it is orange and 2,4,6-tri-*t*-butylphenol where it is a light greenish blue which changes to a pale yellow after 30 minutes' exposure to the air. The e.s.r. spectra of unopened bombs were measured shortly after the reaction was stopped by cooling the bombs to room temperature. Tri-*t*-butylphenol contained at least 10 m*M* of the free phenoxy radical, the 4-cumylphenol contained a very much lower concentration, and only traces of free radicals were detected with the other phenols.

Can. J. Chem. Downloaded from www.nrcresearchpress.com by 210.87.254.5 on 09/05/12
For personal use only.

Can. J. Chem. Downloaded from www.nrcresearchpress.com by 210.87.254.5 on 09/05/12
For personal use only.

TABLE III

Products from the 16 hour reaction of 25 m*M* di-*t*-butyl peroxide with 25 m*M* 2,6-di-*t*-butyl-4-methylphenol plus 25 m*M* of a 4-substituted 2,6-di-*t*-butylphenol

Products (m*M*)	No second phenol	4-Substituent of second phenol							
		CH_3	CH_3O	$(CH_3)_3C$	$C_6H_5(CH_3)_2C$	H	Cl	CN	CHO
2×[DTBP] decomposed	24	28	28	28	28	29	24	23	29
Methyl chloride	7	3	3	3	3	4	3	6	5
Acetone	7.5	4	3	4	4	6	4	7	5
t-Butanol	18	24	24	24	24	22	20	12	12
[*t*-Butanol]/[acetone]	2.4	6	8	6	6	3.7	5	1.7	2.4
[BMP] reacted	12	7.5	6.5	15	16	10	11	12	14
[Second phenol] reacted	—	7.5	10.5	0	0	2.5	3.5	0.8	6
[Second phenol] reacted/ [BMP] reacted	—	1.0	1.6	0	0	0.25	0.32	0.07	0.43

In principal, there is a second method of measuring the relative rates with which phenols react with *t*-butoxy radicals. It consists of decomposing the peroxide in the presence of two phenols and then measuring the amount of each that is consumed. In order to compare the rates of the primary hydrogen abstraction process without the interference of hydrogen abstraction processes from secondary phenolic products the concentrations of both phenols should be as large as possible relative to the peroxide concentration. However, the phenol concentrations must not be so large that the amounts reacted cannot be measured accurately. The results of some experiments in which 25 m*M* of peroxide was decomposed for 16 hours in CCl_4 in the presence of 25 m*M* of a 4-substituted 2,6-di-*t*-butylphenol plus 25 m*M* of the 4-methyl compound as the reference phenol are given in Table III.

In practice, it is obvious that this method of obtaining relative rates is complicated by a hydrogen-transfer reaction between one phenol and the phenoxy radical of the other. This type of reaction has been frequently observed in the past (2–4) and is known to be rapid* and to have a low activation energy (6). This process is very obvious with the 4-*t*-butyl and 4-cumyl phenols, both of which have about the same reactivity towards *t*-butoxy radicals as the 4-methyl phenol, and yet neither is consumed to any measurable extent. The reaction can be represented as the equilibrium

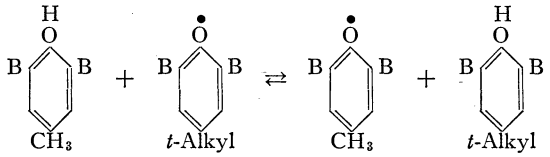

which lies strongly towards the right because the 4-methyl phenoxy radicals dimerize readily (1) whereas the 4-*t*-alkyl phenoxy radicals are rather unreactive towards one another and towards *t*-butoxy radicals. The importance of this equilibrium with the other 4-substituted phenols, which presumably give more reactive phenoxy radicals, cannot be estimated from the present data. However, both the amount of the second phenol consumed and the [*t*-butanol]/[acetone] ratio decrease as the 4-substituent becomes more strongly electron attracting, as is expected. This suggests that this equilibria is not of overriding importance with these other phenols. A comparison of the reactivities of 2,6-di-*t*-butyl-4-methylphenol and its two dimeric phenolic products (i.e., the ethane and ethylene dimers (1)) was also made by the same procedure but by following the consumption of the 4-methyl phenol only. The results indicate that the ethane dimer is slightly more reactive, and the ethylene dimer much more reactive, than the parent phenol.

DISCUSSION

Like many other similar hydrogen-abstraction reactions (7), the relative reactivities of both the simple phenols and the 2,6-di-*t*-butyl 4-substituted phenols towards *t*-butoxy radicals (i.e. [*t*-butanol]/[acetone] ratios) can be correlated with Brown's σ^+ substituent constants (8). That is,

$$\log\left(\frac{[t\text{-butanol}]}{[\text{acetone}]}\cdot\frac{[\text{acetone}]_0}{[t\text{-butanol}]_0}\right) = \rho\sigma^+.$$

With the exception of the 4-formyl phenols, the data given in Table I have been plotted against the σ^+ constants of the 3- and 4-substituents in Fig. 1. For the simple phenols the slopes of the best straight lines, i.e. the ρ values, are -1.19 and -0.74 in CCl_4 and

**The tri-t-butyl phenoxy radical can, in fact, abstract hydrogen from n-decane at 90° C (5).*

Can. J. Chem. Downloaded from www.nrcresearchpress.com by 210.87.254.5 on 09/05/12
For personal use only.

in chlorobenzene respectively, and for the 2,6 di-*t*-butyl-4 substituted phenols the slopes are −0.86 and −0.78. It should be added that there is, of course, considerable experimental uncertainty in the [*t*-butanol]/[acetone] ratios which are greater than about 20. The correlation of the simple phenols in CCl_4 with their σ^+ substituent constants is therefore surprisingly good. As was mentioned in the previous paper (1), for an equimolar peroxide–phenol mixture the [*t*-butanol]/[acetone] ratio increases with increasing concentration of the reactants. The results obtained with 100 m*M* peroxide – 100 m*M* 2,6-di-*t*-butylphenol mixtures in CCl_4 (16 hours) are also shown in Fig. 1. The ρ value in this case is −0.79, which is, within experimental error, the same as the value found with 50 m*M* mixtures. Accurate ρ factors cannot be obtained from the data in Table III on phenol consumption and on the [*t*-butanol]/[acetone] ratios because the experimental points show too much scatter, presumably because of the phenoxy radical – phenol equilibria.

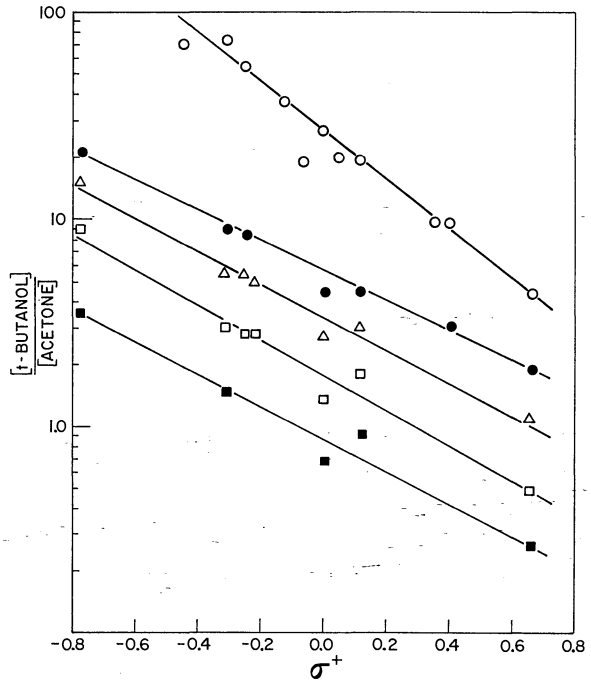

FIG. 1. The [*t*-butanol]/[acetone] ratio after 16 hours at 122° C for equimolar peroxide–phenol mixtures plotted against σ^+ for the 3- and 4-substituents. Key: ○, 50 m*M* of 3- and 4-substituted phenols in CCl_4; ●, 50 m*M* of 3- and 4-substituted phenols in C_6H_5Cl; □, 50 m*M* of 2,6-di-*t*-butyl-4-substituted phenols in CCl_4; ■, 50 m*M* of 2,6-di-*t*-butyl-4-substituted phenols in C_6H_5Cl; △, 100 m*M* of 2,6-di-*t*-butyl-4-substituted phenols in CCl_4.

Following the suggestions of Russell (9), the transition state for the attack of a *t*-butoxy radical on the phenolic hydrogen can be considered to consist of three resonance forms.

$$XC_6H_4OH + \bullet OB \rightarrow$$
$$[XC_6H_4O{:}H\bullet OB \leftrightarrow XC_6H_4O^{+}\bullet H{:}^{-}OB \leftrightarrow XC_6H_4O\bullet H{:}OB]$$
$$\text{I} \qquad\qquad \text{II} \qquad\qquad \text{III}$$
$$\rightarrow XC_6H_4O\bullet + HOB$$

The importance of polar effects will increase in the order III < I < II. In general, the greater the electronegativity of the attacking radical the more will structure II be favored

Can. J. Chem. Downloaded from www.nrcresearchpress.com by 210.87.254.5 on 09/05/12
For personal use only.

and the more important will be the polar effect. Structure I should be important when the attacking radical is very reactive and there is little bond breaking in the transition state so that it resembles the reactants. Structure III should be important when the attacking radical is comparatively unreactive and there is considerable bond breaking in the transition state with the formation of a resonance-stabilized free radical. In this case, the transition state resembles the products. Therefore, if the electron density of the bond being broken determines reactivity, then substituent effects should be correlated by σ constants and the transition state will resemble I, but if polar effects predominate, substituent effects will be correlated by σ^+ constants and the transition state will resemble II.

The correlation of the present results with σ^+ constants indicates that structure II contributes strongly to the transition state. However, the difference in the ρ values between the simple phenols and the dibutyl phenol in CCl_4, the solvent effect, and the deviations of some of the phenols from the best straight lines in Fig. 1 can, tentatively, be accounted for by also taking account of structures I and III.

The sign and magnitude of the ρ factor of a reaction is generally considered to be a measure of the charge separation in the transition state (10). The values of ρ found in the present work (-1.19 and smaller) therefore indicate that there is only a moderate degree of charge separation in the transition state. The excellent correlation of the present results with σ^+ constants is somewhat fortuitous since an exact correlation need not exist for reactions in which a positive center is stabilized by resonance from an aromatic ring. Applying Yukawa and Tsuno's equation (11), i.e.,

$$\log k/k_0 = \rho(\sigma + r(\sigma^+ - \sigma)),$$

to our results we find that the resonance contribution to the reaction (r) is about 1.0. Therefore, the amount of resonance stabilization of the transition state is about the same as that in the solvolysis of cumyl chlorides (where $\rho = -4.62$ (8)). The reason for the absence of a quantitative correlation between r and ρ is at present unclear but it may possibly be connected with the differing effects of solvents upon different reactions (10, 11).

We have recently shown that the majority of radical hydrogen abstraction reactions of the same general type as the present reaction can be correlated with σ^+ substituent constants (7). In particular, it is interesting to compare the present ρ factors with those we have obtained in styrene at 65° C for hydrogen abstraction by polystyryl peroxy radicals from simple phenols ($\rho = -1.49$ (7)) and from 2,6-di-*t*-butyl phenols ($\rho = 1.11_5$ (12)). Although the data are not directly comparable owing to the different solvents and temperatures employed, the smaller ρ factors for the di-*t*-butyl phenols compared with the simple phenols and their decreased reactivity towards both peroxy and alkoxy radicals is of particular significance. The results suggest that two *o*-*t*-butyl groups prevent both radicals from approaching the phenolic hydrogen quite as closely as they approach the phenolic hydrogen of a simple phenol. The activation energy is thereby increased and the probability of reaction will be decreased. Compared with the simple phenols, the transition state for the di-*t*-butyl phenols will tend to resemble the products to a greater extent than it resembles the reactants, i.e., the contribution of structure III to the transition state will become of increasing importance as the phenolic hydrogen becomes sterically better protected.* Further support for this view comes from the fact that 2,6-di-*t*-butylphenol shows a negative deviation from the best line and 2,6-di-*t*-butyl-4-chlorophenol shows a positive deviation† although, in CCl_4, both phenol and 4-chlorophenol fall very close to

**The rather large deuterium isotope effect for the reaction of t-butoxy radicals with 2,6-di-t-butyl-4-methylphenol (1) may also be partly due to the importance of structure III in the transition state of this phenol. That is, the isotope effect will tend to be larger the greater the extent of bond breaking in the transition state.*

†Similar deviations also occur with the peroxy radicals (12).

Can. J. Chem. Downloaded from www.nrcresearchpress.com by 210.87.254.5 on 09/05/12
For personal use only.

the best straight line through the other simple phenols. The deviations of the di-*t*-butyl phenols can, perhaps, be explained if the increased importance of structure III is such that the stability of the resulting phenoxy radical has a significant effect on the reaction rate. That is, both electron-attracting and, to a lesser extent, electron-repelling substituents are known to increase the stability of radicals of the general type $XC_6H_4Y\bullet$ relative to the stability of $C_6H_5Y\bullet$ (13, 14). In particular, the 4-chloro atom has about the same stabilizing influence as a 4-methyl group (14). A positive deviation of the 4-chloro compound in a hydrogen-abstraction reaction therefore suggests that radical stabilization to some extent overcomes the opposing polar effect. Positive deviations with the 4-chloro derivative have been observed in the reaction of *t*-butoxy radicals with dibenzyl ethers (15, 16) and with toluenes at 110° (17) but not at 40° (18). The excellent correlation of phenol and 4-chlorophenol with the other simple phenols in CCl_4 suggests that when steric effects are absent structure III does not contribute significantly to the transition state.

Provided the decreases in reactivity and, in CCl_4, the ρ factor, for the di-*t*-butyl phenols compared to the simple phenols are due to steric effects we might expect a steady change in both quantities as the degree of steric protection afforded the phenolic hydrogen is increased. Although the ρ factors have not been measured, the reactivity data in Table I for 4-methyl-2,6-dialkylphenols certainly suggest such a trend. We have recently determined the difference in free energy (ΔG) between the cis and trans isomers of some ortho-alkyl phenols in CCl_4 by means of infrared spectroscopy (19). This quantity gives a measure of the steric repulsion of the phenolic hydroxyl group by an ortho-alkyl group and should therefore give a rough measure of the steric protection afforded the hydroxyl group by two ortho-alkyl substituents. In Fig. 2 the $\log_{10}$ of the measured and calculated ratios of [*t*-butanol]/[acetone] at a $\sum \sigma^+ = -0.811$* have been plotted against ΔG for the 2,6-dialkyl-4-methyl phenols in CCl_4. The phenol point ($\Delta G = 0$) was calculated from the best line through the simple phenols in Fig. 1. In calculating the points for the methyl phenols it was assumed that there is a linear relation between ρ and ΔG (12). The ρ factor was therefore taken to be -1.08 for 2,4,6-trimethylphenol and -1.03 for both 2,3,5,6-tetramethylphenol and pentamethylphenol.† The results can be represented by

$$\log_{10}\left(\frac{[t\text{-butanol}]}{[\text{acetone}]}\cdot\frac{[\text{acetone}]_0}{[t\text{-butanol}]_0}\right) = \alpha\Delta G,$$

where $[t\text{-butanol}]_0/[\text{acetone}]_0 = 249$ and $\alpha = -1.23$ mole/kcal.

The [*t*-butanol]/[acetone] ratio for 2,6-di-isopropyl-4-methylphenol suggests that the hydroxyl group in this compound is slightly less hindered than the one in pentamethylphenol, a conclusion which has also been reached from studies of the autoxidation of these phenols in alkaline media (20). On the other hand, two *o-s*-butyl groups apparently exert a greater hindering effect than five methyl groups.

In general, there is a small decrease in the reactivity of *t*-butoxy radicals towards hydrogen atom abstraction from hydrocarbons on changing from an aliphatic solvent (including CCl_4) to an aromatic or olefinic solvent (18, 21–24). By analogy to a similar, but much larger,‡ effect which has been observed with chlorine atoms (25, 26) it has been

That is, it has been assumed that $\sigma^+_{\text{ortho}} = \sigma^+_{\text{para}}$ and therefore $\sum \sigma^+ = -0.311$ (4-CH_3) $- 2\times 0.250$ (two o-t-alkyl groups) $= -0.811$.

†*The tetra- and penta-methyl phenols have been plotted at the ΔG value for the 2,3-dimethyl grouping. In actual fact, ΔG will be slightly greater for the latter phenol because of the additional buttressing effect of the 4-methyl group on the 2,3- and 5,6-dimethyl groups.*

‡*It has been suggested (21) that the smaller solvent effect observed with t-butoxy radicals may be due to a lower stability of the π complex owing both to the lower electron affinity of the t-butoxy radical compared with the chlorine atom and the higher temperatures employed in studying the reactions of the t-butoxy radicals. In addition, there may be some steric hindrance to complex formation from the bulky methyl groups (18).*

Can. J. Chem. Downloaded from www.nrcresearchpress.com by 210.87.254.5 on 09/05/12
For personal use only.

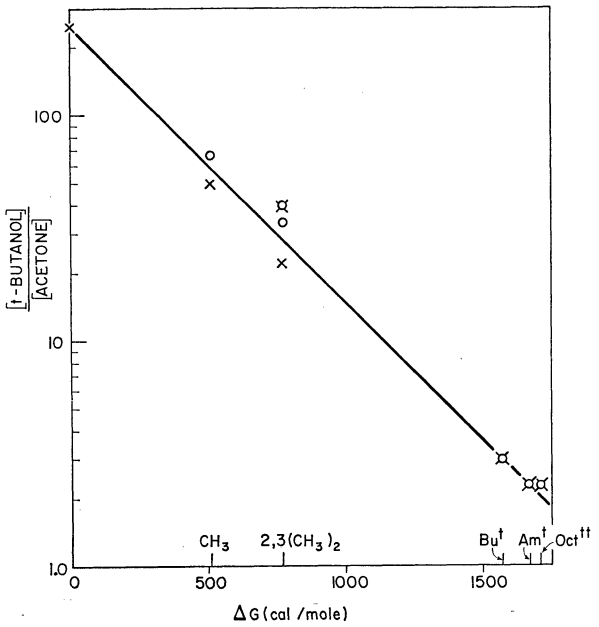

FIG. 2. The [*t*-butanol]/[acetone] ratio for 2,4,6-trialkyl phenols plotted against ΔG. The circles represent the experimental points and the crosses the points calculated for a $\sum \sigma^+ = -0.811$.

concluded that a π complex is formed between the *t*-butoxy radical and the aromatic π electrons. The complexed radical is apparently less reactive and it therefore tends to decompose rather than to abstract hydrogen. It is possible that the same explanation applies to the present results although the observed effects are so large as to suggest that other factors may also be involved. For example, it has been suggested (21) that the solvent may affect the rate of decomposition of the radical as well as its rate of hydrogen abstraction. That is, the large solvent effects observed in this work on changing from CCl_4 to chlorobenzene might be mainly due to an increase in the rate of decomposition of the radical rather than to a decrease in its rate of hydrogen abstraction.

The decrease in the ρ factors for both the simple phenols and the di-*t*-butyl phenols on changing from CCl_4 to chlorobenzene can be attributed to an increase in the relative contribution of structure III to the transition state.* The essentially identical ρ factors in chlorobenzene imply that there is about the same degree of charge separation in the transition state in this solvent for both types of phenols. However, the lower reactivities of the di-*t*-butyl phenols shows that the steric effects of the two *t*-butyl groups are still important. Incidentally, the similarity of the ρ factors suggests that the partially aliphatic character of the local environment surrounding the phenolic hydroxyl group in the 2,6-di-*t*-butyl phenols does not destabilize the charge separation relative to the charge separation in the simple phenols where the local environment is entirely aromatic (7). These decreases in ρ are much greater than have been observed for the reactions of *t*-butoxy radicals with substituted cyclohexanes (22) and of chlorine atoms with substituted toluenes (27).

It has recently been pointed out (25) that for hydrogen abstraction by chlorine atoms

**In this connection, it is interesting that in chlorobenzene the point for phenol falls below the best line through the other simple phenols.*

Can. J. Chem. Downloaded from www.nrcresearchpress.com by 210.87.254.5 on 09/05/12
For personal use only.

there is no consistency in the direction of small solvent effects on relative reactivities determined chiefly by polar factors. This is presumably because a complexed chlorine atom may have either a higher electron affinity (owing to the increased electron affinity of structures such as $Ar^{-}ClH^{+}R$) or a lower electron affinity (since polarization is in the same direction in the complex as in the transition state) than a free chlorine atom (26). In the case of the bulky *t*-butoxy radical a decrease in the electron affinity for the complexed radical seems most likely and this may therefore be the cause of the decreased ρ factors observed in chlorobenzene.

The large amounts of *t*-butyl chloride, chloroform, and carbon monoxide produced from 4-hydroxybenzaldehyde and 2,6-di-*t*-butyl-4-formylphenol might be due to the occurrence of a modified Dakin reaction (28). However, the reaction must involve free *t*-butoxy radicals rather than the peroxide since the consumption of peroxide is not much greater than that in reactions with the other phenols. We are indebted to the referee for suggesting the following radical mechanism to account for the products:

$$Bu^tO\bullet + RCHO \rightarrow Bu^tOH + R\dot{C}O$$
$$R\dot{C}O \rightarrow R\bullet + CO$$
$$R\dot{C}O + CCl_4 \rightarrow RCOCl + CCl_3\bullet \ (\rightarrow CHCl_3)$$
$$RCOCl + Bu^tOH \rightarrow RCO_2H + Bu^tCl.$$

REFERENCES

1. K. U. Ingold. Can. J. Chem. This issue.
2. E. Müller, K. Ley, and G. Schelte. Chem. Ber. **90**, 2660 (1957).
3. K. Ley, E. Müller, R. Mayer, and K. Scheffler. Chem. Ber. **91**, 2670 (1958).
4. C. D. Cook, C. B. Depatie, and E. S. English. J. Org. Chem. **24**, 1356 (1959).
5. M. B. Neiman and A. L. Buchachenko. Izv. Akad. Nauk SSSR Otd. Khim. Nauk, 1742 (1961).
6. R. W. Kreilick and S. I. Weissman. J. Am. Chem. Soc. **84**, 306 (1962).
7. J. A. Howard and K. U. Ingold. Can. J. Chem. **41**, 1744 (1963).
8. H. C. Brown and Y. Okamoto. J. Am. Chem. Soc. **80**, 4979 (1958).
9. G. A. Russell. J. Am. Chem. Soc. **78**, 1047 (1956); J. Org. Chem. **23**, 1407 (1958); Tetrahedron, **5**, 101 (1959).
10. R. Taylor, G. G. Smith, and W. H. Wetzel. J. Am. Chem. Soc. **84**, 4817 (1962).
11. Y. Yukawa and Y. Tsuno. Bull. Chem. Soc. Japan, **32**, 971 (1959).
12. J. A. Howard and K. U. Ingold. Can. J. Chem. This issue.
13. C. Walling. Free radicals in solution. John Wiley and Sons, Inc., New York. 1957. p. 139.
14. R. L. Huang and S. Singh. J. Chem. Soc. 3183 (1959).
15. R. L. Huang and O. K. Yeo. J. Chem. Soc. 3190 (1959).
16. R. L. Huang, H. H. Lee, and S. H. Ong. J. Chem. Soc. 3336 (1962).
17. K. M. Johnston and G. H. Williams. J. Chem. Soc. 1446 (1960).
18. C. Walling and B. B. Jacknow. J. Am. Chem. Soc. **82**, 6108, 6113 (1960).
19. K. U. Ingold and D. R. Taylor. Can. J. Chem. **39**, 471 (1961).
20. H. R. Gersmann and A. F. Bickel. J. Chem. Soc. 2356 (1962).
21. G. A. Russell. J. Org. Chem. **24**, 300 (1959).
22. E. L. Patmore and R. J. Gritter. J. Org. Chem. **27**, 4196 (1962).
23. C. Walling and A. Padwa. J. Am. Chem. Soc. **84**, 2845 (1962).
24. W. V. Sherman and G. H. Williams. J. Chem. Soc. 1442 (1963).
25. G. A. Russell. J. Am. Chem. Soc. **79**, 2977 (1957); **80**, 4987, 4997, 5002 (1958); Tetrahedron, **8**, 101 (1960).
26. C. Walling and M. F. Mayahi. J. Am. Chem. Soc. **81**, 1485 (1959).
27. G. A. Russell and R. C. Williamson. Private communication.
28. H. D. Dakin. J. Am. Chem. Soc. **42**, 477 (1909).

Can. J. Chem. Downloaded from www.nrcresearchpress.com by 210.87.254.5 on 09/05/12
For personal use only.

THE STRUCTURE OF THE EXTRACELLULAR POLYSACCHARIDE OF AZOTOBACTER INDICUM

V. M. PARIKH AND J. K. N. JONES
Department of Chemistry, Queen's University, Kingston, Ontario
Received June 10, 1963

ABSTRACT

The extracellular polysaccharide of the *Azotobacter indicum* has been shown to be a mixture of two polymers of which the acidic polymer was a major fraction. The acidic polymer contained D-*glycero*-D-*manno*heptose in the molar ratio of 1:1:1 plus traces of mannose. It consumed 1 mole of sodium metaperiodate per mole of an average anhydroaldose unit and released 0.95 moles of formaldehyde per anhydroheptose unit. Reduction of the oxidized polymer followed by hydrolysis yielded D-glucose, glycerose, glycolaldehyde, and glycerol. Complete fission of the methylated polymer yielded 2,3-di-*O*-methyl-D-glucuronic acid, 2,4,6,-tri-*O*-methyl α-D-glucose and 3,4,6,7-tetra-*O*-methyl D-*glycero*-D-*manno*heptose. Partial hydrolysis of the methylated polymer produced a methylated aldotriouronic acid composed of 1 mole each of 2,3-di-*O*-methyl-D-glucuronic acid, 2,4,6-tri-*O*-methyl-D-glucose and 3,4,6,7-tetra-*O*-methyl D-*glycero*-D-*manno*heptose. A methylated aldobiouronic acid was also produced and was shown to be composed of 2,3-di-*O*-methyl-D-glucuronic acid and 2,4,6-tri-*O*-methyl D-glucose.

On the basis of these results it is proposed that the polysaccharide is a linear molecule composed of repeating units of D-glucuronic acid, D-glucose, and D-*glycero*-D-*manno*heptose.

DISCUSSIONS

The presence of aldoheptoses in the lipopolysaccharides of a number of microorganisms has been reported in the literature (1) in the past decade; however, very little appears to be known about the mode of their linkages with other units in the polysaccharides. Heptose residues in the polysaccharides of some microorganisms such as *Pasteurella pestis* and *Chromobacterium violaceum* 7917 (1*a*) have been shown to contain free hydroxyl groups at C_6 and C_7 by the action of sodium metaperiodate on the polysaccharides and the detection of formaldehyde thus produced. The microorganism *Azotobacter indicum* produces a polysaccharide rich in aldoheptose and the structural investigations of this polysaccharide form the basis for the present communication.

The presence of a heptose in the extracellular polysaccharide of *A. indicum* was first reported by Quinell and coworkers (2). The identity of the heptose was established by Sowa (3) as D-*glycero*-D-*manno*heptose. Stoodley and coworkers (4) made a detailed study of the factors affecting the production of the polysaccharide by *A. indicum*-446* and reported that the rate of production, the yield, and the composition of the polysaccharide varied largely with the variations in the conditions of growth of these organisms. The yield of the polysaccharide in the present work was 25% (based on D-glucose). The extracellular material was shown (3) to be a mixture of two polymers, the acidic fraction of which was a major constituent (85–90%) and contained D-glucose (33%), D-mannose (26%), D-*glycero*-D-*manno*heptose (16%), uronic acids (19%), and traces of arabinose, rhamnose, and unidentified sugars.

The crude polysaccharide isolated in the present work was a mixture of at least two polysaccharides. The major constituent was an acidic polymer (88%) which could be precipitated with "cetavlon". The acidic polymer contained D-glucuronic acid, D-*glycero*-D-*manno*heptose, and D-glucose, in the approximate molar ratio 1:1:1 (with traces of D-mannose), whereas the non-complexing fraction was a neutral polymer containing

**Gift of the Division of Applied Biology, National Research Council, Ottawa.*

Can. J. Chem. Downloaded from www.nrcresearchpress.com by 210.87.254.6 on 09/05/12
For personal use only.

D-glucose, D-mannose, L-arabinose, and L-rhamnose. The acidic polysaccharide, which contained less mannose than the one isolated by Sowa (3) was obtained in higher yield possibly because the organism was grown in an unbuffered medium.

Experiments such as (*i*) acetolysis, (*ii*) partial degradation of the polymer by dilute acids, and (*iii*) degradation by Fenton's reagent (5) failed to yield oligosaccharides from the acidic polymer. However, isolation of methylated oligosaccharides by the partial degradation of the methylated polymer helped to establish the order of the sugar residues (see below). On oxidation with sodium metaperiodate, the acidic polysaccharide consumed exactly 1 mole of the oxidant per an average anhydroaldose unit, but no significant production of formic acid was observed. The amount of formaldehyde released during the oxidation was found to be 0.95 moles of formaldehyde per anhydroheptose unit, indicating that at least 95% of the anhydroheptose units in the polymer had free hydroxyl groups at C_6 and C_7 and hence were responsible for the consumption of at least 1 mole of the oxidant per an anhydroheptose unit. Hydrolysis of the oxidized polymer gave D-glucose and the Smith-type degradation (6, 7) of the polymer gave glycolaldehyde, D-glucose, glycerol, and glycerose and a trace of arabinose. The proposed structure (see Fig. 1) of the polymer demands liberation of tetronic acid in addition to the compounds mentioned above. This would be absorbed on an ion-exchange resin during the deionization of the hydrolyzate and thus be lost. The presence of a trace of arabinose, however, cannot be explained.

A crude mixture of the acidic and neutral polysaccharides was used for the methylation studies. Isolation of the acidic fraction from the mixture was achieved by extracting an aqueous solution of the partially methylated mixture with chloroform at pH 8.5. This treatment left the sodium salt of the acidic polymer in the aqueous solution. The aqueous solution was acidified and the acidic polymer was isolated. Further methylation of the product was carried out by Kuhn's method (8). The methylated polymer, after fractionation with chloroform–petrol, was subjected to methanolysis followed by hydrolysis. Hydrolysis was later found to be incomplete, and some methyl glycosides were recovered. Considerable decomposition of the methylated sugar units, as evidenced by the dark brown color and the poor yield (approximately 70%) of the hydrolyzate, had taken place. The chromatographic examination of the hydrolyzate showed it to be a mixture of three major and four minor components. Five of the seven fractions were isolated; the remaining two very minor components of the mixture were lost during chromatography. These two minor components were tentatively identified as 3,4-di-*O*-methyl mannose and 4-*O*-monomethyl mannose respectively, on the basis of chromatographic evidence only.

Two (fractions III and IV) of the five fractions isolated after chromatography were found to be methylated oligosaccharides, whereas the remaining three fractions (I, II, and V), which were obtained in relatively low proportions, were found to be methylated derivatives of the monosaccharide units of the polymer (see Table I).

Fraction III proved to be a trisaccharide comprising 1 mole each of 2,3-di-*O*-methyl D-glucuronic acid, 2,4,6-tri-*O*-methyl D-glucose and 3,4,6,7-tetra-*O*-methyl D-*glycero*-D-*manno*heptose. The methylated uronic acid and methylated hexose were identified by the preparation of specific derivatives. The crystalline methylated heptose, a compound which is not reported in the literature, was identified as follows:

(i) The analysis of the sugar indicated that it was a tetramethyl heptose.

(ii) Hydrolysis of the unmethylated polysaccharide with dilute acid was very slow. This suggested that all the heptose was in the pyranose form in the polymer and that it possessed a potential hydroxyl group on C_5.

(iii) Liberation of 0.95 moles of formaldehyde per 1 mole of anhydroheptose unit during

Can. J. Chem. Downloaded from www.nrcresearchpress.com by 210.87.254.6 on 09/05/12
For personal use only.

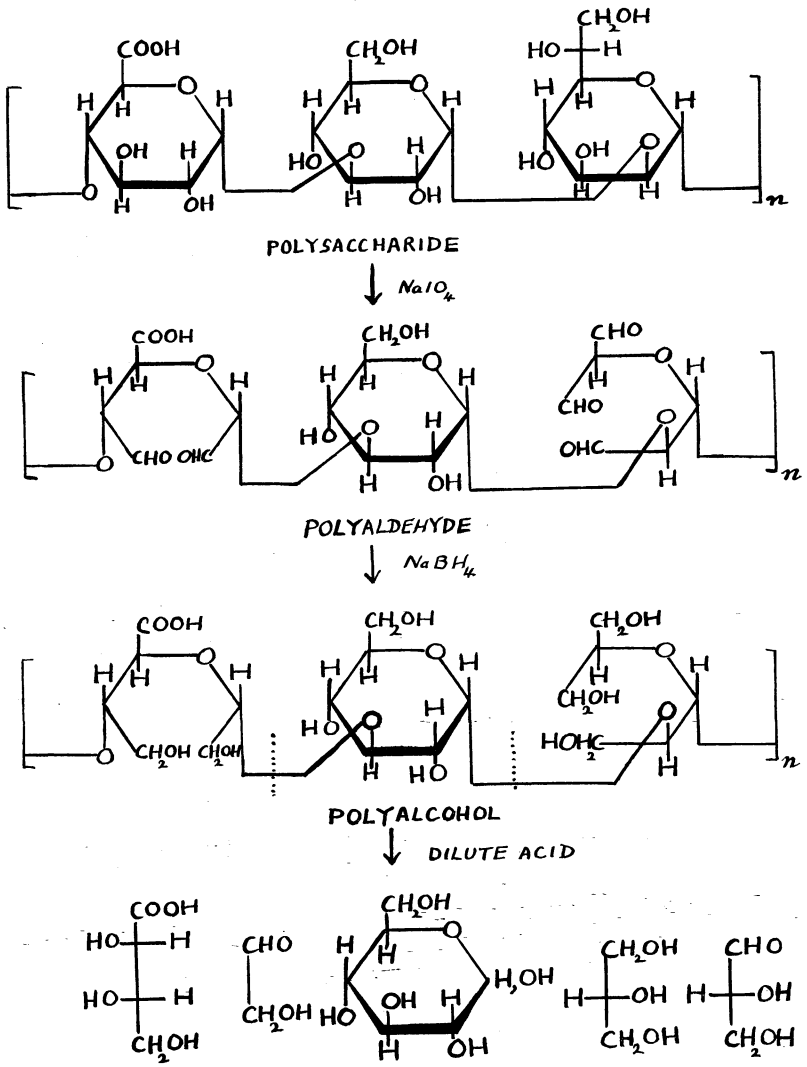

FIG. 1. Smith-type degradation of the polysaccharide.

TABLE I

Sugars produced on hydrolysis of the methylated acidic polysaccharide

Fraction	Name of sugar	Weight, mg	Ref. to proof of structure
I	Methyl $\alpha+\beta$-2,4,6-tri-*O*-methyl-D-glucoside	34	15
II	3,4,6,7-Tetra-*O*-methyl D-*glycero*-D-*manno*heptose	120	—
III	Methylated aldotriouronic acid	475	—
III_A*	2,3-Di-*O*-methyl D-glucuronic acid	76	16, 17
III_B*	2,4,6-tri-*O*-methyl D-glucose	98	18
III_C*	Same as II	109	—
IV	Methylated aldobiuronic acid	325	—
IV_A†	Same as III_A	80	
IV_B†	Same as III_B	103	
V	Same as III_A	12	

*Produced on acid hydrolysis of III.
†Produced on acid hydrolysis of IV.

Can. J. Chem. Downloaded from www.nrcresearchpress.com by 210.87.254.6 on 09/05/12
For personal use only.

the sodium metaperiodate oxidation of the polymer suggested that at least 95% of the heptose residues in the polymer had free hydroxyl groups at positions C_6 and C_7, and thus the tetramethyl heptose isolated from the methylated polymer had methyoxyl groups on C_6 and C_7, leaving C_2, C_3, and C_4 as possible points of attachment.

(iv) When treated with sodium metaperiodate, the tetra-*O*-methyl heptose (II) rapidly consumed 1.0 mole of the oxidant per mole of methylated heptose, and did not liberate either formic acid or formaldehyde, indicating thereby the presence of two adjacent groups in the methylated heptose, possibly at C_1 and C_2.

(v) The methylated heptose was reduced to the corresponding heptitol by reduction with sodium borohydride. The methylated heptitol thus obtained consumed 1 mole of periodate per mole of heptitol and liberated formaldehyde, proving the presence of free hydroxyl groups at C_1 and C_2 in the sugar. The identity of the tetra-*O*-methyl heptose was thus established as 3,4,6,7 tetra-*O*-methyl-D-*glycero*-D-*manno*heptose.

(vi) This identity was further confirmed by the demonstration of a free hydroxyl group at C_2 in the methylated heptose by a positive test with a specific tetrazolium red spray (9).

Fraction IV was proved to be 3-*O*-α-D-2,3-di-*O*-methyl glucuronosyl-2,4,6-tri-*O*-methyl D-glucose on the basis of its equivalent weight, optical rotation, and the identification of its hydrolysis products.

In view of the facts (*a*) that a large quantity (30%) of the material decomposed during the hydrolysis of the methylated polymer, (*b*) that an infrared spectrum of the partially methylated polymer gave a doublet peak in the carboxylic region of the spectrum, and (*c*) that Sowa (3) reported the possible presence of three uronic acids in the polymer, further investigations were undertaken. The methylated polysaccharide was treated with lithium aluminum hydride to reduce the carbomethoxy groups of the uronic acid residues in the polymer. The reduced product showed very little decomposition during methanolysis and hydrolysis. Again hydrolysis was incomplete and some glycosides were detected. Examination of the hydrolyzate indicated the presence of 2,3-di-*O*-methyl D-glucose, 2,4,6-tri-*O*-methyl D-glucose and its methyl glycoside, and 3,4,6,7-tetra-*O*-methyl D-*glycero*-D-*manno*heptose, together with traces of 3,4-di-*O*-methyl mannose (?) and 4-*O*-monomethyl mannose (?). The dimethyl derivatives of glucose and mannose could not be separated chromatographically from one another because of their close R_f values in a number of developing mixtures, but on demethylation of the mixture with boron trichloride (10) a mixture of glucose and mannose in the approximate proportion of 6:1 was obtained. The fact that no methylated sugar other than the three mentioned above was present in the hydrolyzate of the reduced methylated polymer, and that the ratio of glucose to mannose (6:1) in the mixture of dimethyl sugars was approximately the same as that of glucuronic acid (31%) to mannose (4.5%) in the unmethylated acidic polymer, proved that D-glucuronic acid was the only acidic component of the polysaccharide.

Thus, on the basis of these observations, it can be proposed that the acidic polysaccharide isolated from the extracellular material of *Azotobacter indicum*, grown in an unbuffered medium, is a linear, large molecular weight molecule containing several repeating units of the trimer as shown in Fig. 1. The observed optical rotation of the polymer, and of the methylated aldotriouronic acid, together with the fact that it gave a negative precipitin reaction with *Pneumococcus* type III antiserum, as reported by Sowa (3), suggested that the monosaccharide units in the polymer were all α-linked.

EXPERIMENTAL

Methods

Paper chromatography was carried out on Whatman No. 1 filter paper using the following solvent systems (v/v):

Can. J. Chem. Downloaded from www.nrcresearchpress.com by 210.87.254.6 on 09/05/12
For personal use only.

(a) butan-1-ol, ethanol, water (3:1:1);
(b) butan-1-ol, ethanol, water (5:1:4), (top layer clarified with a little ethanol);
(c) ethyl acetate, acetic acid, formic acid, water (18:3:1:4);
(d) butan-1-ol, pyridine, water, benzene (10:6:6:2);
(e) benzene, ethanol, water (169:47:15), (top layer clarified with a little ethanol).

Whatman 3MM paper and columns packed with Whatman cellulose powder by the wet method were used for separations of sugar mixtures. All solutions were concentrated under reduced pressure at 40–45°. Demethylation of methylated sugars was carried out by the procedure of Allen *et al.* (10). All infrared spectra were made in chloroform solutions (6%) using a Perkin–Elmer model 21 infrared spectrophotometer.

Growth of Azotobacter indicum and Isolation of the Polysaccharide

The following ingredients in the quantities given were used to prepare the growth medium: calcium sulphate (0.22 g), magnesium sulphate heptahydrate (0.44 g), dipotassium hydrogen phosphate (1.10 g), peptone (8.80 g), glucose (88.00 g), and distilled water (2200 ml). The medium was equally distributed between each of 11 conical flasks (1 liter), and the flasks were steam-sterilized for 15 minutes at a pressure of 15 p.s.i. They were cooled and innoculated with large doses (4.5 ml) of a highly viscous and fresh growth of *A. indicum*. The flasks were swirled on a mechanical shaker at 23±2° for 19 days, after which the culture medium had become extremely viscous.

The combined solution from 10 of the above flasks (equivalent to 80 g glucose) was diluted with water (2 vol) and centrifuged (12,000 r.p.m. for 90 minutes) to remove suspended cells. The supernatant was filtered through a bed of Celite and the filtrate was concentrated (800 ml). The solution was then poured into ice-cold ethanol (2 vol) containing 0.5% hydrogen chloride, with vigorous stirring. The polysaccharide precipitated in the form of a long continuous thread which was separated by centrifugation and washed repeatedly with ethanol until free from chloride ions, then with acetone (200 ml), and ether (200 ml). The material, on drying *in vacuo* over silica gel for several days, contained moisture (9.6%), ash (0.64%), and had $[\alpha]_D^{23}$ +35±2° (yield 20 g, 25% based on D-glucose). The dried material could not be redissolved completely in water.

Free Boundary Electrophoresis of the Polysaccharide

Electrophoresis of the polysaccharide in veronal or in borate buffer was not possible because the polysaccharide was insoluble in these buffers. A solution of the polysaccharide at a concentration of 1.0% could, however, be prepared in phosphate buffer (pH 7.4), which was then dialyzed twice against the phosphate buffer, 24 hours each time, to gain full equilibration of the ionic concentrations prior to electrophoresis. It was then subjected to moving boundary electrophoresis, and the polysaccharide was found to be a mixture of a major mobile component and a minor stationary component.

Fractionation of the Polysaccharide with "Cetavlon"

Since the dried polysaccharide could not be redissolved completely in water, the fractionation was carried out using an aqueous cell free extract of the *A. indicum*.

A growth from one of the conical flasks was diluted with water (2 volumes), centrifuged, and filtered, and to the filtrate (200 ml) was then added a 10% solution of "cetavlon" with stirring, until no further precipitate formed (11). The acidic polysaccharide complex thus precipitated was collected by centrifugation, and the polysaccharide (800 mg) was recovered from it in the usual way. The non-complexing neutral fraction was recovered from the filtrate by precipitation with alcohol (yield 76 mg). Chromatographic examination of the hydrolyzate of the acidic polymer indicated the presence of uronic acid, D-*glycero*-D-*manno*heptose, and D-glucose in the approximate molar ratio 1:1:1 (with a trace of D-mannose), whereas that of the neutral polysaccharide indicated the presence of glucose, mannose, arabinose, rhamnose, and a trace of heptose or galactose, and possibly a trace of ribose. The equivalent weight of the acidic polymer was found to be 591. This corresponds to the presence of 31.1% hexuronic acid.

Quantitative Analysis of the Component Sugars of the Acidic Polysaccharide

The acidic polysaccharide (138 mg dry wt.) was hydrolyzed by sulphuric acid (*N*, 10 ml) for 10 hours and the hydrolyzate was neutralized ($BaCO_3$), deionized (IR-120 ion exchange resin), and concentrated to a yellow syrup (127.2 mg). The syrup was examined by paper chromatography in solvents (*a*), (*c*), and (*d*) and the chromatograms were sprayed with *p*-anisidine hydrochloride or with silver nitrate/sodium hydroxide. The areas of various spots obtained on heating the chromatograms at 110° for 90 seconds were carefully measured using a compensating polar planimeter, model 4236 (Keuffer and Essex, Germany). The optical densities of these spots were then measured with the help of an optical densichron (Welch Manufacturing Company, Chicago, U.S.A.), and the percentages of the four constituent sugars were calculated to be, uronic acid (31±2), D-glycero-D-*manno*heptose (33±2), D-glucose (32±2), and mannose (4.5±2). A synthetic mixture containing the three sugars in the proportions indicated was prepared and analyzed by this procedure. The results obtained were within the ranges indicated.

Sodium Metaperiodate Oxidations of the Acidic Polysaccharide

Accurately weighed samples of the acidic polysaccharide (51.2 mg dry weight of each) were dissolved in carbon dioxide free distilled water and the solutions were adjusted to pH 7 with sodium hydroxide solution

Can. J. Chem. Downloaded from www.nrcresearchpress.com by 210.87.254.6 on 09/05/12
For personal use only.

(0.01 *N*). Sodium metaperiodate solution (0.03 *M*, 25 ml) was added to each sample and the solutions were made up to volume (100 ml) and kept in the dark. The periodate uptake was determined by the thiosulphate method (12), and the formic acid by the usual procedure (see Table II). Extrapolation of the overoxidation part of the periodate uptake curve gave an uptake of exactly 1.0 mole of the oxidant per mole of anhydrohexose unit. No significant production of formic acid was observed.

TABLE II

Periodate oxidation of the acidic polysaccharide of *A. indicum* moles uptake per $C_6H_{10}O_5$

Time (hours)	0.25	4	8	12	24	30	48	72
Periodate uptake								
Sample I	0.55	0.92	1.03	1.06	1.14	1.20	1.31	1.38
Sample II	0.55	0.91	1.02	1.05	1.13	1.19	1.25	1.37

Formaldehyde released during oxidations of the polysaccharide was estimated by the method of O'Dea and Gibbons (13). The experiment was carried out on three samples (5 mg each, dry weight) of the polysaccharide; each was dissolved in 25 ml of distilled water containing 1 ml of 0.6 *M* sodium metaperiodate solution. Curves were plotted with the optical densities obtained from the polysaccharide solutions as ordinates and duration of oxidation as abscissae. The portions of the curves along the abscissae were extrapolated to zero time to obtain the optical densities corrected for overoxidation of the polysaccharide. The numbers of moles of formaldehyde released per anhydroheptose unit were calculated from these figures. The heptose was considered to be 33.2% of the polysaccharide on the basis of previous chromatographic estimations. The results for the three samples were 0.96, 0.95, and 0.95 moles of formaldehyde per anhydroheptose unit.

Smith-type Degradation of Acidic Polysaccharide (6, 7)

The acidic polysaccharide (250 mg) in water (375 ml) was oxidized with sodium metaperiodate solution (0.03 *M*, 125 ml) for 24 hours. Ethylene glycol (25 ml) was added to destroy excess periodate. After dialysis to remove formaldehyde, ethylene glycol, and salts, a small quantity (ca. 10 mg) of the polyaldehyde was hydrolyzed with *N* sulphuric acid on a boiling water bath for 12 hours, and the hydrolyzate, after neutralization and chromatographic examination, was found to contain D-glucose as a major component together with a trace of arabinose. No uronic acid, heptose, or mannose was found to be present.

The remaining portion of the polyaldehyde (ca. 230 mg) was reduced with sodium borohydride solution (1%, 25 ml) for 18 hours. The excess borohydride was destroyed with dilute acetic acid and the solution was dialyzed three times against distilled water, each time for a period of 12 hours. The solution of polyalcohol thus obtained was concentrated under reduced pressure to yield a white, brittle solid (212 mg) which was hydrolyzed with sulphuric acid (*N*, 20 ml) for 10 hours. The solution was neutralized ($BaCO_3$), filtered, deionized [Amberlite IR-120 (H) and Duolite A-4 (OH) resins], and concentrated to a small volume (5 ml). Chromatographic examination of the hydrolyzate in solvents (*a*), (*b*), (*c*), and (*d*), and spraying with silver nitrate or with *p*-anisidine hydrochloride spray reagents, showed five components which were indistinguishable from D-glucose (major constituent), arabinose, glycerose, glycerol, and glycolaldehyde.

Methylation of the Polysaccharide

A crude mixture of acidic and neutral polysaccharides (18 g) was stirred overnight in water (360 ml) to obtain a highly viscous suspension of the polysaccharide in water. The polysaccharides were then methylated three times by the Haworth procedure. At the end of the third methylation, a separation of the acidic and neutral fractions of the mixed polysaccharides was achieved. The mixture was neutralized and concentrated to a suitable volume (800 ml). It was then rendered alkaline (pH 8.5) and extracted with chloroform (4×400 ml). This removed the neutral fraction of the methylated mixed polysaccharides leaving the sodium salt of the acidic polysaccharide in the aqueous solution. The chloroform solution was washed twice with a solution of sodium sulphate (20%), dried over anhydrous sodium sulphate, and concentrated to give a yellow solid (yield 2.15 g).

The residual aqueous layer (above) was cooled (0°) and acidified with ice-cold 2 *N* sulphuric acid to pH 2, when the acidic polysaccharide separated in the form of a viscous yellowish oily layer. It was isolated by extraction with chloroform (4×400 ml). The chloroform extracts were combined, washed four times with a solution of sodium sulphate (20%), and dried over anhydrous sodium sulphate. The extract was concentrated to a suitable volume (500 ml) and the residual polysaccharide was esterified with an ethereal solution of diazomethane (3%, 40 ml). The neutral solution was concentrated after it had been kept overnight to give a yellow solid (yield 13.2 g; OMe, 36.2%).

A comparative study of the chloroform solutions (6% w/v) of the neutral and acidic partially methylated polysaccharide fractions by infrared spectroscopy showed no absorption at 1755 cm^{-1} in the case of the neutral fraction, but the acidic fraction had a strong doublet peak at frequencies 1755 cm^{-1} and 1730 cm^{-1}. The neutral fraction showed a relatively greater absorption in the frequency range 3550–3500 cm^{-1} indicating thereby that it was more resistant to methylation than was the acidic fraction.

Can. J. Chem. Downloaded from www.nrcresearchpress.com by 210.87.254.6 on 09/05/12
For personal use only.

The partially methylated acidic fraction (13 g) was treated twice with Purdie's reagents (14). However, little further methylation was achieved (yield 12.0 g, OMe, 36.5%) and no significant decrease was observed in the peak at 3500 cm^{-1} in the infrared spectrum of the material. The partially methylated acidic polymer was therefore methylated further by Kuhn's method (8). The methylated material thus obtained [yield, 10.4 g; OMe, 39.8%; $[\alpha]_D^{22}$ +42.3 (*c*, 6 in chloroform)] displayed a negligible hydroxyl peak in the infrared spectrum. A second treatment of the product by the Kuhn procedure did not increase the methoxyl content of the product.

Fractionation of the Methylated Acidic Polysaccharide

The methylated acidic polymer (9.5 g) was dissolved in chloroform (15 ml) and was fractionally precipitated by adding petrol (boiling range 40–60°). Four different fractions were collected (Table III).

TABLE III

Fractionation of the methylated acidic polysaccharide

Amount of petrol, ml	Fraction number	Yield, g	Methoxyl content, %	$[\alpha]_D^{22}$ *c*, 6 in $CHCl_3$
120 ml	A	0.20	Not studied	
130 ml	B	3.50	39.6	+42.5°
140 ml	C	5.40	39.7	+42.5°
Unprecipitated	D	0.36	42.5	+47.0°

Fractions B and C gave infrared spectra indistinguishable from one another and on hydrolysis they gave the same pattern of reducing sugars on paper chromatograms. Fractions B and C were therefore mixed and used for further investigations.

Partial Hydrolysis of the Methylated Polysaccharide

The methylated polymer (1.8 g) was heated with anhydrous methanolic hydrogen chloride (7%, 100 ml) in sealed tubes for 6 hours at 100°. The dark brown solution was diluted with water (50 ml) and the mixture was heated a further 3 hours. It was then neutralized with silver carbonate, filtered, and the filtrate was deionized by passage through Amberlite IR-120 ion exchange resin and concentrated to a dark brown gummy syrup (yield 1.28 g). Chromatographic examination of the syrup in solvents (*a*), (*b*), (*c*), and (*d*) showed the presence of seven components, three of which were major and four minor. The syrup was fractionated on a cellulose column (45×12 cm) using solvent (*c*) as the eluting mixture. Only five fractions could be isolated from the column. The two very minor fractions lost on the column had R_g values in solvent (*b*) of 0.58 and 0.32 respectively, which are the same as those of 3,4-di-*O*-methyl mannose and 4-*O*-methyl mannose.

Identification of the Methylated Fragments (see Table I)

Fraction I: Methyl α+β-2,4,6-Tri-O-methyl D-*glucoside*

This pale yellow syrup (34 mg) did not reduce Fehling's solution and gave only glucose on demethylation. It had R_g, 0.93 in solvent (*b*); OMe, 50.6%; $[\alpha]_D^{22}$ +106.5°, (*c*, 4.44 in methanol). Calculated for tetra-*O*-methyl hexose or methyl tri-*O*-methyl hexoside $C_{10}H_{20}O_6$; OMe, 52.5%. On hydrolysis with aqueous hydrochloric acid (*N*) it gave a crystalline material, indistinguishable from fraction $III_{(B)}$, which was identified as 2,4,6-tri-*O*-methyl D-glucose. It was concluded that fraction I was a mixture of α- and β-methyl glucosides of 2,4,6-tri-*O*-methyl D-glucose, the α-form predominating. The literature (15) value for the β-glucoside is $[\alpha]_D$ −27.4°. The α-glucoside is unknown but is certainly more than +106.5°.

Fraction II: 3,4,6,7-Tetra-O-methyl D-*glycero*-D-*mannoheptose*

This fraction (0.120 g) upon investigation was found to be indistinguishable from the component fraction $III_{(C)}$. A detailed investigation of this sugar is therefore reported at a later stage.

Fraction III: A Methylated Aldotriouronic Acid Containing Uronic Acid, Glucose, and Heptose

This pale yellow reducing syrup (0.475 g) was chromatographically pure and gave a brownish yellow spot on the chromatograms when sprayed with *p*-anisidine hydrochloride. It contained 40.8% methoxyl and had R_g, 0.74 in solvent (*b*). On demethylation, it produced a mixture of D-glucose, D-*glycero*-D-*manno*heptose and D-glucuronic acid. Hydrolysis of fraction III (0.450 g) with aqueous hydrochloric acid (2 *N*, 25 ml) for 17 hours on a boiling water bath gave rise to three fractions which were separated on sheets of Whatman 3MM paper. The three fractions were, fraction $III_{(A)}$ (76 mg); fraction $III_{(B)}$ (98 mg); and fraction $III_{(C)}$ (109 mg).

Fraction $III_{(A)}$: 2,3-Di-O-methyl D-*Glucuronic Acid*

This brown reducing syrup was chromatographically pure, gave a cherry red color on chromatograms sprayed with *p*-anisidine hydrochloride, and had $[\alpha]_D^{22}$ +39.0° (*c*, 2 in water); eq. wt. 221; OMe, 27.1%. Calculated for dimethyl glucuronic acid, $C_8H_{14}O_7$, eq. wt. 222; OMe, 27.9%. Hirst and Jones (16) gave

Can. J. Chem. Downloaded from www.nrcresearchpress.com by 210.87.254.6 on 09/05/12
For personal use only.

the following figures for 2,3-di-*O*-methyl D-glucuronic acid; $[\alpha]_D^{22}$, +36° (*c*, 1.7 in water); eq. wt. 224; OMe, 32.6%. Identification of this fraction $III_{(A)}$ was further confirmed by preparing a crystalline methyl ester of 2,3-di-*O*-methyl D-glucosaccharo-1,4-lactone according to the procedure described by Smith (17). The crystalline methyl ester had melting point and mixed melting point with an authentic specimen, of 101°. Found: OMe, 39.2%; eq. wt. 118. Calculated for $C_9H_{14}O_7$; OMe, 39.75%; eq. wt. 117. Figures reported by Smith are m.p., 101°, OMe, 40.4%; eq. wt. 120.

Fraction $III_{(B)}$: 2,4,6-Tri-O-methyl-α-D-glucose

This fraction crystallized during the concentration of the eluate, in the form of colorless fine needles (yield, 98 mg). On recrystallization from a mixture of benzene–ethanol the crystals had m.p. 123–125°, which was not depressed when mixed with an authentic sample of 2,4,6-tri-*O*-methyl-α-D-glucose. The crystals reduced Fehling's solution, gave only D-glucose on demethylation, and had R_g, 0.76 in solvent (*b*), $[\alpha]_D^{22}$ +110°→ +69.4° (*c*, 3.6 in dry methanol) and OMe, 41.6%. Calculated for $C_9H_{18}O_6$: OMe, 41.9%. Barker, Hirst, and Jones (18) have reported the following figures for 2,4,6-tri-*O*-methyl-α-D-glucose, m.p. 123–126°; $[\alpha]_D^{22}$ +110°→ +70° (*c*, 1 in methanol). Identification of this fraction $III_{(B)}$ was further confirmed by preparing a crystalline amide of 2,4,6-tri-*O*-methyl-D-gluconolactone from it according to the procedure described by Barker, Hirst, and Jones (18). The crystals had m.p. 96–98°; $[\alpha]_D^{22}$ +54° (*c*, 2 in methanol); OMe, 39.1%. The figures reported by Barker *et al.* for the amide are m.p. 98°; $[\alpha]_D$ +54° (*c*, 1.1 in methanol); OMe, 39.2%.

Fraction $III_{(C)}$: 3,4,6,7-Tetra-O-methyl-D-glycero-D-mannoheptose

This fraction (109 mg), obtained by the chromatographic fractionation of the hydrolyzate of fraction III, crystallized. Recrystallization from ether, gave colorless large square plates, with m.p. 108–109°; $[\alpha]_D$ +49.7° (*c*, 2.5 in methanol, no mutarotation) and R_g, 0.855 in solvent (*b*). Found: C, 49.2; H, 8.1; OMe, 44.9%. Calculated for tetramethyl heptose, $C_{11}H_{22}O_7$: C, 49.6; H, 8.27; OMe, 46.6%. On demethylation of the crystals with boron trichloride, only D-*glycero*-D-*manno*heptose was obtained. Fraction $III_{(C)}$ gave a positive tetrazolium red test (9).

Periodate Oxidation of 3,4,6,7-Tetra-O-methyl-D-glycero-D-mannoheptose

Duplicate samples of fraction $III_{(C)}$ (15 mg each), accurately weighed, were dissolved in aqueous methanol (10 ml, 50% v/v). Sodium metaperiodate solution (0.03 *M*, 10 ml) was added to each flask and the solution was made up to 25 ml with distilled water. The oxidation of heptose and the estimation of periodate consumption were carried out according to the usual procedure. The molar periodate consumption per mole of tetramethyl heptose ($C_{11}H_{22}O_7$) was as shown in Table IV.

TABLE IV

Consumption of periodate during the oxidation of tetramethyl heptose

Time (hours)	0.25	1	2	3	6
Periodate uptake					
Sample I	0.26	0.83	1.01	1.02	1.05
Sample II	0.25	0.83	1.02	1.03	1.05

Extrapolation of the overoxidation part of the periodate uptake curve gave an uptake of exactly 1.0 mole of the oxidant per mole of tetramethyl heptose. Neither formic acid nor formaldehyde was found to be liberated during the oxidation.

Reduction of 3,4,6,7-Tetra-O-methyl-D-glycero-D-mannoheptose

Fraction $III_{(C)}$ (30 mg) was dissolved in aqueous methanol (7 ml, 50% v/v) and the solution was added dropwise to a vigorously stirred solution of sodium borohydride (0.1 g) in water (4 ml) at 0°. After 18 hours the excess borohydride was destroyed with dilute acetic acid. The solution was then neutralized and evaporated to dryness. The residue was extracted with dry ether (3×10 ml) and the ethereal extracts on evaporation left a white solid residue (18.5 mg) which was free from the original methylated heptose. The 3,4,6,7-tetra-*O*-methyl-D-*glycero*-D-*manno*heptitol thus obtained was oxidized by sodium metaperiodate in a manner exactly similar to that described for the oxidation of tetramethyl heptose. The molar periodate consumption per mole of tetramethyl heptitol, $C_{11}H_{24}O_7$ was as follows: 0.89 (15 minutes); 1.0 (1 hour), constant value, unchanged even after 9 hours. No formic acid was liberated, but when the mixture was tested qualitatively by the method of O'Dea and Gibbons (13) a deep violet color was formed indicating the liberation of formaldehyde.

Fraction IV: 3-O-α-D-2,3-Di-O-methyl glucuronosyl-2,4,6-tri-O-methyl-D-glucose

This brown colored syrup (0.325 g) reduced boiling Fehling's solution and gave a dark reddish brown spot on the chromatograms when sprayed with *p*-anisidine hydrochloride. It had an R_g value of 0.69 in solvent (*b*), was acidic to litmus, and showed a strong absorption at 1740 cm^{-1}, indicating the presence of uronic acid. Found: OMe, 41.6%; $[\alpha]_D^{22}$ +116.6° (*c*, 3.5 in methanol); eq. wt. 417. Calculated for a disaccharide containing a dimethyl hexuronic acid and a trimethyl hexose, $C_{17}H_{30}O_{12}$: OMe, 42.2%; eq. wt. 426. D-Glucose and D-glucuronic acid were produced on demethylating the disaccharide with boron trichloride. Hydrolysis

Can. J. Chem. Downloaded from www.nrcresearchpress.com by 210.87.254.6 on 09/05/12
For personal use only.

of fraction IV (250 mg) with aqueous hydrochloric acid (2 *N*, 15 ml) on a boiling water bath for 12 hours and subsequent neutralization, deionization, and concentration gave a syrup which on chromatographic examination gave two spots which were indistinguishable from 2,3-di-*O*-methyl D-glucuronic acid (fraction $III_{(A)}$) and 2,4,6-tri-*O*-methyl-α-D-glucose (fraction $III_{(B)}$). The two components of the syrup were separated on Whatman 3MM chromatographic paper using solvent (*a*). The strips of paper containing uronic acid were extracted in cold with dilute formic acid solution to give a syrup $IV_{(A)}$; the yield was 80 mg, after concentration and repeated distillation with methanol to remove all the formic acid. Strips containing neutral sugar were extracted with boiling ethanol and gave a pale yellow syrup $IV_{(B)}$ (103 mg), which crystallized on seeding with crystals of 2,4,6-tri-*O*-methyl-α-D-glucose. A detailed examination of fractions $IV_{(A)}$ and $IV_{(B)}$ showed that they were the same as fractions $III_{(A)}$ and $III_{(B)}$ described earlier.

Fraction V: 2,3-Di-O-methyl D-*glucuronic Acid*

A detailed investigation of fraction V (12 mg) could not be carried out because only a very small quantity of the sugar was isolated. However, this dark brown gummy syrup was believed to be 2,3-di-*O*-methyl D-glucuronic acid as it moved on the paper with the same speed as fractions $III_{(A)}$ and $IV_{(A)}$ in solvent (*c*) and gave a cherry red spot with *p*-anisidine hydrochloride. In view of the fact that some methylated monosaccharides (fractions I and II) were isolated from the column, along with tri- and di-saccharides containing 2,3-di-*O*-methyl D-glucuronic acid, isolation of some 2,3-di-*O*-methyl D-glucuronic acid was anticipated.

Reduction of the Methylated Polysaccharide

The methylated polysaccharide (3 g) was dissolved in dry ether (35 ml) and the solution was added dropwise to a vigorously stirred suspension of lithium aluminum hydride (0.7 g) in dry ether (100 ml), at room temperature. At the end of 24 hours, excess of hydride was destroyed with ethyl acetate (10 ml), the mixture was filtered, and the filtrate (A) was dried over anhydrous magnesium sulphate. The yellowish white residue on the filter paper was dissolved in ice-cold dilute sulphuric acid solution (20%, 50 ml) and the solution was extracted with ether. The ethereal extract was washed with sodium bicarbonate (5%, 50 ml) and then with water (2×20 ml). The extract was dried over anhydrous magnesium sulphate and then was mixed with filtrate (A). The combined filtrate and extracts gave on concentration a colorless amorphous solid (yield 2.4 g).

Examination of Reduced, Methylated Acidic Polysaccharide

Examination of the reduced, methylated acidic polysaccharide by infrared spectroscopy showed practically no absorption in the carboxyl region (1755 cm^{-1} to 1605 cm^{-1}) of the spectrum but showed a remarkable increase in the absorption at 3400 cm^{-1} in place of the very poor peak in that region which was shown by the unreduced polymer. Hydrolysis of the polymer (2 g) with anhydrous methanolic hydrogen chloride (7%, 100 ml) at 80° for 12 hours, and subsequent neutralization, deionization, and concentration of the hydrolyzate, gave a syrup (1.8 g) which, after hydrolysis with aqueous acid, showed the presence of five components on its chromatographic examination in solvents (*a*) and (*d*). One of these five components formed a very minor fraction of the mixture and travelled on chromatograms with a rate corresponding to that of 4-*O*-methyl mannose (R_g, 0.32 in solvent (*b*)). This fraction was lost on the cellulose column (45×12 cm) during the chromatographic fractionation of the mixture using solvent (*e*) as the eluant. The four fractions isolated from the column were examined as follows.

Fraction VI:

This pale yellow, non-reducing, chromatographically pure syrup (0.22 g) had R_g, 0.93 in solvent (*b*). Found: OMe, 50.5%; $[\alpha]_D$ +107° (*c*, 3 in methanol). It gave glucose on demethylation and on hydrolysis 2,4,6-tri-*O*-methyl-α-D-glucose (m.p. and mixed m.p. with $III_{(B)}$, or with $IV_{(B)}$ 124–125°) was obtained. It was thus the same as fraction I.

Fraction VII:

This fraction (0.505 g) was crystalline and was found to be the same as fraction $III_{(C)}$ on the basis of its melting point, mixed melting point with fraction $III_{(C)}$, R_g value, demethylation, and optical rotation. It was thus 3,4,6,7-tetra-*O*-methyl D-*glycero*-D-*manno*heptose.

Fraction VIII:

This fraction (0.350 g) crystallized immediately and was found to be the same as fraction $III_{(B)}$ on the basis of its melting point, mixed melting point with fraction $III_{(B)}$, R_g value, demethylation, and mutarotation. It was thus 2,4,6-tri-*O*-methyl-α-D-glucose.

Fraction IX:

This was a brown syrup (0.430 g) and gave only one brown spot on chromatographic examination in solvents (*a*), (*b*), (*c*), and (*d*). The R_g value of the spot in solvent (*b*) was 0.58. Found: OMe, 29.0%; $[\alpha]_D^{22}$ +66° → +33.2° (*c*, 2 in acetone). Calculated for dimethyl hexose, $C_8H_{16}O_6$: OMe, 29.8%. Irvine and Scott (19) reported the optical rotation of 2,3-di-*O*-methyl-α-D-glucose as $[\alpha]_D^{20}$ +81.9° → +48.3° (*c*, 1 in acetone). Demethylation of fraction IX produced a mixture of D-mannose and D-glucose which were estimated chromatographically to be in the approximate molar proportion of 1:6. Fraction IX was thus a mixture of a dimethyl glucose and dimethyl mannose. The glucose derivative was considered to be 2,3-di-*O*-methyl D-glucose as its formation by reduction, with lithium aluminum hydride, of the 2,3-di-*O*-methyl D-glucuronic acid unit of the polymer was expected.

Can. J. Chem. Downloaded from www.nrcresearchpress.com by 210.87.254.6 on 09/05/12
For personal use only.

The second dimethyl hexose derivative could not be firmly identified because of the difficulty in isolating it in the pure form. However, on the basis of its R_g value, 0.58 in solvent (*b*), and on the basis of the evidence obtained by the periodate oxidation of the polysaccharide, its identity could be tentatively established as 3,4-di-*O*-methyl mannose.

ACKNOWLEDGMENT

The authors are indebted to the National Research Council of Canada for grants (N.R.C. T-19).

REFERENCES

1. D. A. L. Davies. Advan. Carbohydrate Chem. **15**, 271 (1960), and references cited therein.
1*a*. D. A. L. Davies, A. B. Foster, and M. J. Crumpton. Nature, **181**, 412 (1958).
2. C. M. Quinnell, S. G. Knight, and P. W. Wilson. Can. J. Microbiol. **3**, 277 (1957).
3. J. K. N. Jones, M. B. Perry, and W. Sowa. In press.
4. R. J. Stoodley. Ph.D. Thesis, Queen's University. 1962.
5. P. S. O'Colla, J. J. O'Donnell, and T. M. D. Felly. Proc. Chem. Soc. 68 (1962).
6. F. Smith and J. W. Van Cleve. J. Am. Chem. Soc. **77**, 309 (1955).
7. M. Abdel Akher, J. E. Cadotte, B. A. Lewis, R. Montgomery, F. Smith, and J. W. Van Cleve. Nature, **171**, 474 (1953).
8. R. Kuhn, H. Trischmann, and I. Low. Angew. Chem. **67**, 32 (1955).
9. W. E. Trevelyan, D. P. Procter, and J. S. Harrison. Nature, **166**, 444 (1950).
10. S. Allen, T. G. Bonner, E. J. Bourne, and N. M. Saville. Chem. Ind. 630 (1958).
11. A. S. Jones. Biochem. Biophys. Acta, **10**, 607 (1953).
12. G. Neumuller and E. Vasseur. Arkiv Kemi, **5**, 235 (1953).
13. J. F. O'Dea and R. A. Gibbons. Biochem. J. **55**, 580 (1953).
14. T. Purdie and J. C. Irvine. J. Chem. Soc. **83**, 1021 (1903).
15. D. J. Bell. J. Chem. Soc. 859 (1936).
16. E. L. Hirst and J. K. N. Jones. J. Chem. Soc. 506 (1946).
17. F. Smith. J. Chem. Soc. 1035 (1940).
18. C. C. Barker, E. L. Hirst, and J. K. N. Jones. J. Chem. Soc. 1695 (1938).
19. J. C. Irvine and J. P. Scott. J. Chem. Soc. 575 (1913).

Can. J. Chem. Downloaded from www.nrcresearchpress.com by 210.87.254.6 on 09/05/12
For personal use only.

A NEW MUSTARD OIL GLUCOSIDE SYNTHESIS

THE SYNTHESIS OF GLUCOTROPAEOLIN

M. H. BENN

Chemistry Department, University of Alberta, Calgary, Alberta

Received July 2, 1963

ABSTRACT

A new synthesis of mustard oil glucosides is described, illustrated by the synthesis of glucotropaeolin. This synthesis, based on the reaction of thiols with nitrile oxides, leads to a conclusion concerning the stereochemistry about the carbon–nitrogen double bond in the mustard oil glucosides.

In connection with an investigation of their biogenesis and metabolism, it became necessary to synthesize some mustard oil glucosides (VIII). The addition of thiols to nitrile oxides, in the presence of base, has been demonstrated to yield thiohydroxamates (1, 2), and the reaction of 2,3,4,6-tetra-O-acetyl-β-D-glucopyranosylthiol* (V) with the appropriate nitrile oxide (IV) appeared to represent an attractively simple method of constructing the S-glucosyl thiohydroxamate skeleton which characterizes the mustard oil glucosides (3, 4). We wish to report here the successful application of this approach in the synthesis of glucotropaeolin (VIII, R = $PhCH_2$), so establishing a synthesis of the mustard oil glucosides alternative to that described by Ettlinger and Lundeen (5).

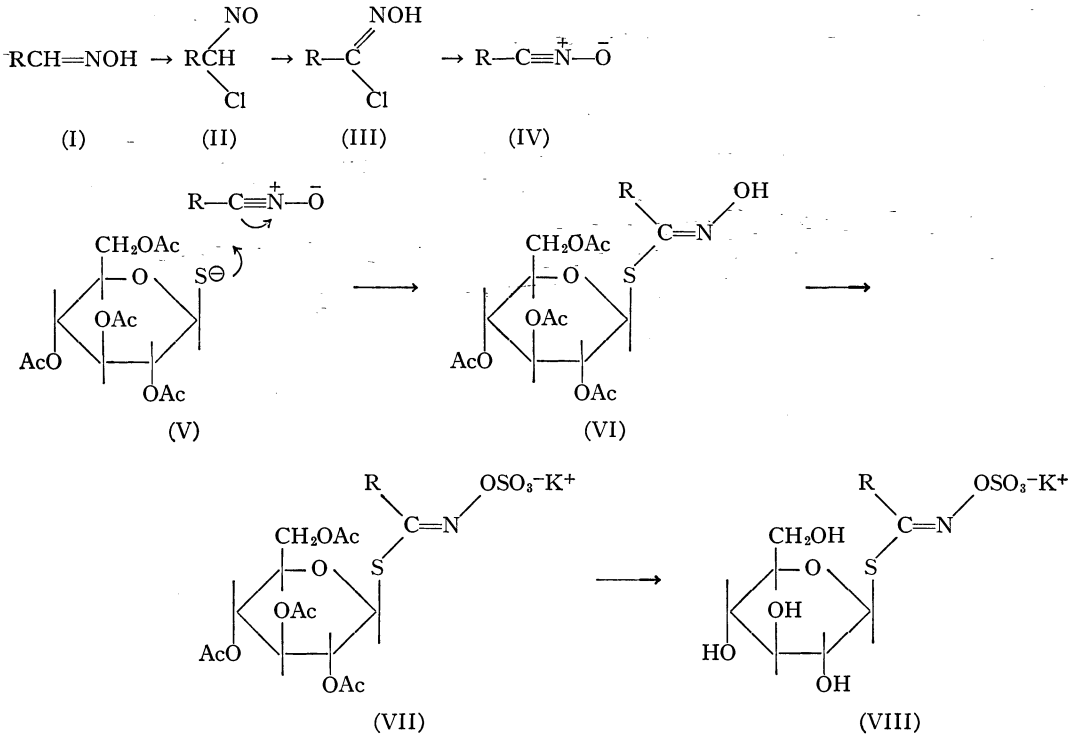

The acetylated sugar was used, in preference to the free thiose, since it afforded a product in which the hydroxyls of the sugar moiety were protected from sulphonation.

Can. J. Chem. Downloaded from www.nrcresearchpress.com by 210.87.254.6 on 09/05/12
For personal use only.

Nitrile oxides are usually unstable compounds, best prepared *in situ* by treating a hydroxamic chloride (III) with base (6). The hydroxamic chloride is conveniently prepared by chlorination of the corresponding aldoxime (I), followed by the spontaneous rearrangement of the initially formed, blue chloronitroso compound (II) (6).

Phenylacetaldoxime (I, R = $PhCH_2$—) was chlorinated in chloroform solution and phenylmethylhydroxamic chloride (III, R = $PhCH_2$—) isolated as a crystalline solid. When excess triethylamine was added to an ethereal solution of tetra-O-acetyl-β-D-glucopyranosylthiol and this hydroxamic chloride, S-tetra-O-acetyl-β-D-glucopyranosyl phenylmethylthiohydroxamate (VI, R = $PhCH_2$—) was formed in excellent yield. Sulphonation of this material with sulphur trioxide – pyridine (5) afforded the tetra-O-acetylglucotropaeolate anion, isolated as the crystalline potassium salt (VII, R = $PhCH_2$—), identical in all respects with an authentic specimen of this salt. Deacetylation with ammoniacal methanol produced glucotropaeolin itself.

The compound (VI, R = $PhCH_2$—) was identical in all its physical properties with those recorded for this compound by Ettlinger and Lundeen (5). A stereochemical feature of the present synthesis is that the addition of the thiol to the nitrile oxide would be expected to produce by "trans" addition, a thiohydroxamate with the *syn-* configuration (of R and OH) about the oxime carbon–nitrogen double bond. This is the configuration opposite to that normally accepted and inferred from the enzyme-induced rearrangement of the mustard oil glucosides to isothiocyanates, a reaction analogous to the Lossen rearrangement (3, 4). It seems improbable that rearrangement about the oxime occurred during the isolation of (VI) and we therefore suggest that the natural mustard oil glucosides in fact have the *syn*-configuration. The enzyme present in the plant is known to be a thioglucosidase (4) and it presumably cleaves the glucoside to the *syn*-thiohydroxamic acid (IX) plus glucose. The *syn*-acid may isomerize to the *anti*-acid (X) as shown and this then undergoes the Lossen type rearrangement to produce the isothiocyanate (XI).

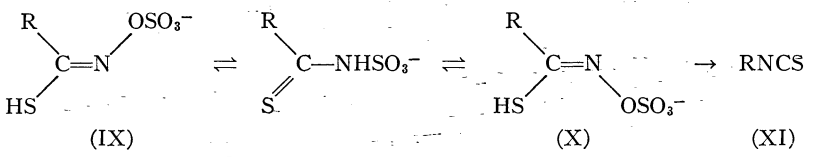

(IX) (X) (XI)

EXPERIMENTAL

Phenylmethylhydroxamic Chloride

Dry chlorine gas was bubbled slowly through an ice-cold solution of phenylacetaldoxime (3.0 g) in chloroform for 30 minutes. The initially blue, now green solution was concentrated under reduced pressure (bath ⩾ 40°) to a pale azure oil, which was crystallized and recrystallized from hexane–ether to give almost colorless prisms, m.p. 89–91°, (1.82 g). Found: C, 59.77; H, 6.52; N, 8.10; S, 17.99. Calc. for $C_9H_{11}NOS$: C, 59.61; H, 6.11; N, 7.73; S, 17.68%. The crude solid product is satisfactory for the subsequent reactions.

S-2′, 3′, 4′, 6′-Tetra-O-acetyl-β-D-glucopyranosyl Phenylthiohydroxamate

Anhydrous triethylamine (0.60 g) dissolved in ether (10 ml) was added in one portion to a gently stirred solution of 2,3,4,6-tetra-O-acetyl-β-D-glucopyranosylthiol (7) (1.19 g) and phenylmethylhydroxamic chloride (0.70 g) in dry ether (50 ml). A copious precipitate of triethylamine hydrochloride was immediately formed. After 30 minutes at room temperature, the reaction mixture was poured into ice-cold, dilute sulphuric acid (ca. 0.5 *N*, 25 ml), the ether layer separated, and the aqueous phase re-extracted with ether (20 ml). The combined ether extracts were dried ($MgSO_4$) and evaporated to a slurry of crystals, (1.32 g), m.p. 159–160°. Recrystallization from ethanol gave the pure compound as colorless needles (1.08 g), m.p. 163–164°, $[\alpha]_D^{26}$ −9.5° (*c*, 2.3 in $CHCl_3$). Lit. (5) records m.p. 163.8–164.1°, $[\alpha]_D^{32}$ −9.6° ($CHCl_3$).

Potassium 2,3,4,6-Tetra-O-acetylglucotropaeolate (5)

The thiohydroxamate (0.25 g) in dry pyridine (5 ml) was stirred with pyridine – sulphur trioxide (0.25 g) overnight, at room temperature. A solution of potassium bicarbonate (0.5 g) in water (15 ml) was then added and after effervescence had ceased, the reaction mixture was shaken with ether (2×20 ml), the ether

Can. J. Chem. Downloaded from www.nrcresearchpress.com by 210.87.254.6 on 09/05/12
For personal use only.

extracts combined and washed with water (2×20 ml), and the combined aqueous extracts freeze-dried. The residual salts were extracted with hot 95% ethanol (3×30 ml) and the combined extracts concentrated to small volume (ca. 10 ml) and filtered, hot. Crude potassium tetra-O-acetyl glucotropaeolate monohydrate crystallized on cooling, and recrystallization from 95% ethanol gave the pure salt (52 mg), m.p. 197–199° (decomp.), $[\alpha]_D^{25}$ $-19\pm1°$ (*c*, 0.5 in H_2O); infrared spectrum in KBr disk superimposable on that of an authentic specimen of the salt. The mixed melting point was undepressed. Lit. (4) m.p. 186–187°; 197–198°, $[\alpha]_D^{20}$ $-20°$ (*c*, 1.0 in H_2O). The melting point of these compounds is known to be dependent on the rate of heating (4).

Glucotropaeolin

The tetraacetate of glucotropaeolin (30 mg) was dissolved in anhydrous methanol, saturated with ammonia (1 ml), and kept at 0° overnight. The reaction mixture was taken to dryness under reduced pressure (bath temp. $\gtrsim$ 40°) and the residue extracted with ether (5 ml), taken up in water (2 ml), and freeze-dried to yield glucotropaeolin as a white amorphous powder (21 mg) chromatographically homogenous when examined on Whatman No. 1 paper in *n*-butanol – acetic acid – water (4:1:5) (8).

ACKNOWLEDGMENTS

We are grateful to Professor Anders Kjaer for the gift of an authentic specimen of potassium tetraacetylglucotropaeolate and to the National Research Council for financial support of this research.

REFERENCES

1. T. Bacchetti and A. Alemagna. Rend. Ist. Lombardo Sci. Lettere, A, **91**, 30 (1957).
2. M. H. Benn. In preparation.
3. M. G. Ettlinger and A. J. Lundeen. J. Am. Chem. Soc. **78**, 4172 (1956).
4. A. Kjaer. Fortschr. Chem. Org. Naturstoffe, **18**, 122 (1960).
5. M. G. Ettlinger and A. J. Lundeen. J. Am. Chem. Soc. **79**, 1764 (1957).
6. A. Quilico. Gazz. Chim. Ital. **67**, 589 (1937) and subsequent papers. R. H. Wiley and B. J. Wakefield. J. Org. Chem. **25**, 546 (1960) and references therein.
7. W. Schneider and A. Bansa. Ber. **64**, 1321 (1931).
8. O. E. Schultz and R. Gmelin. Z. Naturforsch. **8b**, 151 (1953).

Can. J. Chem. Downloaded from www.nrcresearchpress.com by 210.87.254.6 on 09/05/12
For personal use only.

THE BARIEAU–LI CONTROVERSY AND ITS SIGNIFICANCE FOR GENERAL THERMODYNAMICS

G. A. ELLIOTT[1]
Chemistry Department, University of Western Australia, Nedlands, Western Australia
Received January 2, 1963

ABSTRACT

The Barieau–Li controversy shows the need for a general method of discussing conditions of validity of thermodynamic equations. Such a method is here developed and illustrations of its usefulness are given. It is shown how Barieau's principle can be applied in all cases.

Can. J. Chem. Downloaded from www.nrcresearchpress.com by 210.87.254.42 on 09/05/12
For personal use only.

The papers by Barieau (1, 2) and by Li (3, 4) on the E.M.F.'s of cells having phases of varying concentrations have shown very clearly in at least one case (that of the Gibbs–Helmholtz equation) that exact knowledge of the conditions of validity of a thermodynamic relation is not readily available by reference to any established doctrine or method. To that serious extent thermodynamics must be regarded as not sufficiently understood, especially since it is not likely that the Gibbs–Helmholtz equation differs in this respect from other thermodynamic results. Barieau founded his first paper on the principle that the Gibbs–Helmholtz equation must be true for all (closed) systems. From this was derived Barieau's principle for calculating the correct cell reaction. Li (3) then intervened and submitted for consideration a cell which he claimed and Barieau incorrectly admitted could not be treated by Barieau's method. Later, Barieau was able to publish an *ab initio* proof of the Gibbs–Helmholtz equation and it became evident that it is true for all closed systems. Li's method, on the other hand, was based on the idea that the Gibbs–Helmholtz equation could only be proved for systems 'without a concentration variable'. Stout (5) then showed that the methods of Barieau and of Li are equivalent, though that of Barieau has advantages of convenience. Li (4) then pointed out that certain cells are essentially open systems and that Barieau's method would not hold for them.

As a result of this, the precise conditions of validity of the Gibbs–Helmholtz equation still remain a little doubtful, and the occurrence of this controversy and of these doubts confirms the initial statement that there exists no general method of discussing conditions of validity in thermodynamics. A very considerable time has elapsed, however, since the pioneer work of Gibbs (6), who by introducing the concept of molar or chemical potential (μ) first gave an analytical form to chemical thermodynamics, and it is the main object of the present paper to show that the method of Gibbs can easily be used for the solution of validity problems in thermodynamics.

The use of the Gibbs potential makes it possible to put the fundamental energy change equation of reversible thermodynamics in the now familiar form

$$[1] \qquad dE = TdS + \sum \mu \cdot dn - \sum X \cdot dx.$$

(E = energy; T = absolute temperature; S = entropy; μ = chemical potential; n = molar number; and $X \cdot dx$ is a generalized work term.) Gibbs, however, by his method of derivation, left the persisting impression among some scientists that the formulae of thermodynamics apply only to isolated systems. See, for example, the summary by

[1] *Visiting Lecturer to the School of Chemistry, University of Leeds, England, during 1961.*

Can. J. Chem. Downloaded from www.nrcresearchpress.com by 210.87.254.42 on 09/05/12
For personal use only.

Margenau and Murphy (7). However, most scientists will now agree that [1] is not restricted to isolated systems but is quite general, and any attempt to prove this generalization, although instructive, would now be considered too obvious for publication. We must therefore simply assume that (1) is universally valid for reversible changes.* Consequently, the conditions of validity of any thermodynamic relation that can be derived from (1), as most can, are simply the conditions imposed by the derivation. To use this idea, however, it is essential to define clearly the chemical potential and the work terms and to use more developed symbols adequate for a clear and unambiguous formulation of the problem which as far as possible will not allow any implicit assumption to pass unnoticed.

Essentially a work term represents work done by a definable generalized force which acts in definite directions normal or parallel to a macroscopically observable surface such as the wall of a vessel or the surface of a drop of liquid or else in the direction of a force field. The $\mu \cdot dn$ or chemical terms are, however, essentially without directional properties. It is clear that if any work term is not explicitly mentioned in the equation [1] it must be hidden in the chemical terms and we can learn nothing explicitly about it from [1] and its existence may even be overlooked. It is therefore strongly recommended that whenever possible the work terms should be mentioned explicitly. Since it is, strictly speaking, impossible to define a single electric potential difference between two phases there is therefore good reason in this one case to include the corresponding work term in the chemical term forming what Guggenheim (8) has termed an electrochemical potential. This is fully discussed by Guggenheim and those who follow him will find no alteration is necessary in the following general treatment since they will of necessity omit the, for them, undefinable single electric potentials and interpret μ as the electrochemical potential when that term is relevant. Alternatively one may use conventional values as explained in reference 10. Further this case emphasizes the point that the n's and the x's are not always independent variables and a definition of the process of differentiation which applies equally when the variables are dependent is needed. This has been given in a recent publication (9).

It is also necessary to distinguish those parts of the whole change dE which involve the surroundings from those which do not. It will be convenient to attach to a differential the suffix 'i' when it signifies an element of change which is internal and therefore possible for an isolated system; the suffix 'e', however, indicates that the change is external in the sense that it is not possible for an isolated system. For this purpose an isolated system is defined as one which satisfies $dE = 0$ for all changes together with $dS = 0$ for all reversible changes. The same suffixes will also be used when attached to the generalized forces to distinguish those which operate internally from those which operate on the surroundings. We assume T is uniform throughout and the term dS_i is omitted since its value is zero for reversible changes. It is also desirable to write the work of expansion ($P \cdot dV$) as a separate term; this we do by replacing $\sum X \cdot dx$ by $P \cdot dV + \sum' X \cdot dx$ and the meaning of the primed sum is obvious. Equation [1] now becomes

$$[2] \qquad dE = T \cdot dS - P \cdot dV + [\sum \mu \cdot dn_i - \sum X_i \cdot dx_i] + \sum \mu \cdot dn_e - \sum' X_e \cdot dx_e.$$

The quantities in brackets represent those parts of the change which are possible for an isolated system. They represent what is happening inside the 'black box', and the first

It is also applicable under certain conditions to irreversible processes but these will not be discussed in the present paper.

law of course requires that these terms shall sum to zero. Without any significant loss of generality we have transformed equation [1] into two equations [3] and [3*a*] of which the latter has been termed the general chemical condition of equilibrium (10).

$$[3] \qquad dE = T\cdot dS - P\cdot dV + \sum \mu\cdot dn_e - \sum' X_e dx_e$$

$$[3a] \qquad \sum \mu\cdot dn_1 = \sum X_1\cdot dx_1$$

On these two equations we base the new validity principle:

> The conditions of validity of any thermodynamic relation derivable from [3] or [3*a*] or from both are simply those conditions which are necessary for the derivation, plus the usual requirement of thermodynamic reversibility.

For example, since the Gibbs Free Energy is defined by $F = E - T\cdot S + P\cdot V$, we can at once obtain from [3] the result

$$[4] \qquad dF = -S\cdot dT + V\cdot dP + \sum \mu\cdot dn_e - \sum' X_e\cdot dx_e.$$

It follows that the equation

$$[5] \qquad \partial F/\partial T = -S$$

will be valid provided all terms on the right-hand side of [4], except the first one, sum to zero. In practice, this means we must have constant pressure, open circuit for a cell (since $\sum' X_e\cdot dx_e = 0$) during the temperature change, and we must also have $\sum \mu\cdot dn_e = 0$. This last requirement, except in certain rather contrived cases (v.i.), will be satisfied only by closed systems. Further, we may derive from [4] by cross-differentiation between the terms $S\cdot dT$ and any $X_e\cdot dx_e$ of that equation, the result

$$[6] \qquad \partial X_e/\partial T = \partial S/\partial x_e,$$

subject, as is usually stated, to the conditions that for each side of [6] all the variables of [4] except F and those actually involved in the differential coefficient concerned are to be constant. Each of the differential coefficients of [6] is in fact equal to the second partial differential $\partial^2 F/(\partial T\cdot \partial x_e)$ and the order of differentiation makes no difference. According to the true definition (9) of partial differentiation, however, individual constancy of the variables concerned is not required and it will be sufficient if the corresponding terms of [4] sum to zero. The molar conditions of validity of [5] and [6] are therefore identical, namely $\sum \mu\cdot dn_e = 0$. Since in the case of galvanic cells X_e must be identified with the E.M.F. of the cell on open circuit and dx_e with the number of equivalents of electricity transferred, equation [6] readily transforms to $\partial(-\Delta F)/\partial T = \Delta S$, the delta form of [5]. Equation [6], since it contains directly the temperature coefficient of the E.M.F., is in fact the basic form of the Gibbs–Helmholtz equation and [5] is closely related to it, being frequently quoted as such.

In either form, the Gibbs–Helmholtz equation is always valid when $\sum \mu dn_e = 0$. This includes closed systems and since almost any system can become closed simply by expanding the boundaries to include all changes, most cases are in this category. There remain, however, as Li (4) has pointed out, certain systems which are necessarily open; for example, those for which we insist, needlessly no doubt, that volume concentrations shall remain unchanged on heating despite thermal expansion. For such cases material must be

Can. J. Chem. Downloaded from www.nrcresearchpress.com by 210.87.254.42 on 09/05/12
For personal use only.

added or removed during the heating process and the system is then unavoidably open. If during this process $\sum \mu \cdot dn_e = 0$, the material exchanges with the surroundings, as may be seen from [4], do not contribute to dF and the Gibbs–Helmholtz equation is still valid. If this condition is not satisfied, the Gibbs–Helmholtz equation no longer holds without correction. This correction is, however, easily made as we shall now show. Since, when the cell is heated at constant pressure on open circuit, we may omit from [4] $V \cdot dP$ and all the work terms, rearranging and dividing by dT we then obtain

$$[7] \qquad \partial F/\partial T - \sum \mu \cdot dn_e/dT = -S.$$

Hence the Gibbs–Helmholtz equation will effectively hold if we subtract from the $\partial(\Delta F)/\partial T$ calculated from the observed temperature coefficient of the E.M.F. of the cell the quantity $\Delta \sum \mu \cdot dn_e/dT$ by calculation or, more practically, by simply using the temperature coefficient of E.M.F. of the corresponding cell defined only at the lower temperature and heated without altering the material content.

After this correction has been made we can obtain a ΔS value for the correct cell reaction which can *always* be computed by Barieau's principle, since any departure from the Gibbs–Helmholtz equation has been allowed for. This cell reaction is, of course, the one which actually would occur on normal reversible discharge of the cell; that is if it were discharged as a closed system, isothermally and isopiestically, and in a sufficiently large system to prevent appreciable concentration changes during the reaction.

The 'conditions of equilibrium' do not differ in nature from other thermodynamic relations, and they also can usefully be discussed by the new method. Thus, we can see directly from [3] that $dE = T \cdot dS$ will be true for reversible changes provided the remaining terms of [3] vanish. Hence the condition of equilibrium favoured by Gibbs (essentially $dE = 0$ for a change at constant entropy) will be true when no external work is done and whenever $\sum \mu \cdot dn_e = 0$. Certainly, as Li (11) has recently ventured to point out (but without formal proof) it is not necessary for the system to be enclosed in a thermally insulating envelope. Similarly, equation [4], derived unconditionally from [3], reminds us that the much favored condition $dF_{T,P} = 0$ is only true if no net work ($\sum' X_e \cdot dx_e$) is done and if $\sum \mu \cdot dn_e = 0$. Strictly, it is not necessary in either case for the system to be closed. As a concluding example, we discuss the validity of the well-known and frequently misunderstood equation $\sum \mu \cdot dn = 0$. We note first that $\sum \mu \cdot dn = \sum \mu \cdot dn_i + \sum \mu \cdot dn_e$. A glance at [3*a*] now shows that $\sum \mu \cdot dn = 0$ is true provided no internal work is done which is not implicit in the $\sum \mu \cdot dn_i$ term, and provided $\sum \mu \cdot dn_e = 0$. If this latter condition is satisfied, which almost always means the system is closed, it is true for ordinary phase equilibria, but not for systems involving membrane potentials (Donnan equilibria) or in presence of, for example, a gravitational field whereby internal work can be done storing up potential energy within the system, unless the relevant work terms are implicit in the definitions of μ.

All these illustrations show that the usefulness of the Gibbsian method can be increased and precision gained by incorporating the new validity principle which this article describes. The full utilisation of this method requires the adoption of symbols which are clearly defined and adequate to express all relevant matters.

REFERENCES

1. R. E. Barieau. J. Am. Chem. Soc. **72**, 4023 (1950).
2. R. E. Barieau. J. Chem. Phys. **21**, 1827 (1953).
3. J. C. M. Li. J. Chem. Phys. **19**, 1059 (1951).
4. J. C. M. Li. J. Chem. Phys. **23**, 2012 (1955).

Can. J. Chem. Downloaded from www.nrcresearchpress.com by 210.87.254.42 on 09/05/12
For personal use only.

5. J. W. STOUT. J. Chem. Phys. **21**, 1829 (1953).
6. J. W. GIBBS. Collected Works. Vol. I. Longmans, Green, 1928.
7. H. MARGENAU and G. M. MURPHY. The mathematics of physics and chemistry. Van Nostrand, New York. 1944. p. 1.
8. E. A. GUGGENHEIM. Thermodynamics. North-Holland Publishing Company, Amsterdam. 1959. p. 374.
9. G. A. ELLIOTT. Nature, **198**, 1191 (1963).
10. G. A. ELLIOTT. Nature, **167**, 865 (1951).
11. J. C. M. LI. J. Chem. Phys. **29**, 747 (1958).

Can. J. Chem. Downloaded from www.nrcresearchpress.com by 210.87.254.42 on 09/05/12
For personal use only.

STRUCTURAL STUDIES ON AN ARABINOXYLAN FROM PEA SKIN (PISUM SATIVUM)

PART I. METHYLATION STUDIES

N. BANERJI AND C. V. N. RAO

Department of Macromolecules, Indian Association for the Cultivation of Science, Calcutta-32, India

Received April 4, 1963

ABSTRACT

The polysaccharide extracted by 4% sodium hydroxide solution from pea skin (*Pisum sativum*) was shown to be composed of D-xylose and L-arabinose in a ratio of 5:1. Hydrolysis of the fully methylated arabinoxylan yielded 2,3,5-tri-*O*-methyl-L-arabinose, 2,3-di-*O*-methyl-D-xylose, and 2-*O*-methyl-D-xylose in the molar ratio of 1:4.2:1.1 and traces of 2,3,4-tri-*O*-methyl-D-xylose and D-xylose. From these results and those of periodate oxidation studies, a structural formula for the arabinoxylan has been proposed.

Substantial work has been done in the identification of carbohydrate constituents of pea (1), but no polysaccharide has been isolated from pea skin. The present paper describes the isolation and structural chemistry of an arabinoxylan that is present in pea skins.

Powdered pea skins were extracted successively with a boiling mixture of benzene and alcohol, hot water, and 0.4% and 4% alkali solutions. The polysaccharide extracted by hot water gave a blue color with iodine and yielded only glucose on hydrolysis, indicating it to be a starch. The polysaccharides, extracted by 0.4% and 4% alkali solutions, gave on hydrolysis arabinose and xylose in the same ratio together with trace quantities of galactose. As the former one was obtained in very poor yield the later was selected for structural studies.

The polysaccharide extracted from pea skin by 4% sodium hydroxide solution, having specific rotation −86.9°, gave on hydrolysis D-xylose and L-arabinose in the ratio of 5:1 respectively.

The polysaccharide was purified (2) by repeated complex formation with Fehling's solution. After three treatments the material obtained had specific rotation −87.6° and gave arabinose and xylose in the ratio of 1:5. Galactose and uronic acid originally present in traces were removed during purifications. As there was no change in specific rotation or the ratio of arabinose to xylose after repeated purifications, the material was considered to be homogeneous.

The arabinoxylan was methylated to yield a fully methylated derivative, having a weight-average molecular weight 5.12×10^5.

Hydrolysis of the fully methylated arabinoxylan yielded three major components, viz., 2,3,5-tri-*O*-methyl-L-arabinose, 2,3-di-*O*-methyl-D-xylose, and 2-*O*-methyl-D-xylose, which were characterized by their crystalline derivatives. Trace amounts of 2,3,4-tri-*O*-methyl-D-xylose and D-xylose were also obtained. Column chromatographic analysis showed that tri-*O*-methyl-L-arabinose, di-*O*-methyl-D-xylose, and mono-*O*-methyl-D-xylose were present in the ratio of 1:3.81:1.

A small quantity of the mixture was resolved by quantitative paper chromatography and the sugars were estimated by alkaline hypoiodite method (3). The ratio of trimethylarabinose to dimethylxylose to monomethylxylose was 1:4.2:1.1, which is in close agreement with column chromatographic results.

The above results indicate that the main chain of the arabinoxylan from pea skin is

composed of D-xylopyranose molecules joined through $1 \rightarrow 4$ linkages, with branching mainly through position 3 of certain xylose units. The majority of non-reducing end positions are occupied by L-arabinofuranosyl residues. Trace amounts of 2,3,4-tri-*O*-methyl-D-xylose probably originated from a few end points of the macromolecules. The trace quantities of D-xylose present in the mixture are of uncertain structural significance.

The simplest structure of the repeating unit of the arabinoxylan which can accommodate the above facts is given below:

$$\rightarrow (X_p)1 \underset{4}{\rightarrow} 4(X_p) \rightarrow$$
$$\underset{3}{\uparrow}$$
$$A_f1$$

X_p—D-xylopyranose residues; A_f—L-arabinofuranose residues

From the negative rotation of the polysaccharide and its methylated derivative, it is concluded that the majority of the linkages are of β-type.

The above structure is supported by the fact that during periodate oxidation, 0.84 mole of periodate was consumed per anhydro pentose unit, the theoretical value being 0.83 assuming the above structure. As the non-reducing end groups were arabinofuranose residues, no formic acid was liberated but an equal number of xylose residues (16.2%) at the branch points should remain unoxidized. The periodate-oxidized polysaccharide on hydrolysis yielded 14.2% of xylose, a figure in agreement with that expected theoretically.

The fact that the arabinofuranose residues were present as single-unit side chains was further confirmed by subjecting the arabinoxylan and its methylated derivative to mild hydrolysis, taking advantage of the labile linkage of non-reducing arabinofuranose residues. Hydrolysis of the polysaccharide with dilute oxalic acid solution for 1.5 hours yielded a degraded polysaccharide and the supernatant liquid contained arabinose only. The degraded polysaccharide on hydrolysis afforded xylose (80.2%) and arabinose (5.4%) (these and subsequent values are expressed as percentages of the undegraded polysaccharide). The degraded polysaccharide was oxidized with sodium metaperiodate and the xylose residues unattacked by periodate were estimated to be 6.1%.

The fully methylated polysaccharide was heated with dilute aqueous methanolic hydrochloric acid under controlled conditions (4) and the degraded methylated polysaccharide was precipitated, remethylated, and subjected to methanolysis and hydrolysis. The hydrolyzate was found to contain 2,3,5-tri-*O*-methyl-L-arabinose, 2,3-di-*O*-methyl-D-xylose, 2-*O*-methyl-D-xylose, and traces of 2,3,4-tri-*O*-methyl-D-xylose and D-xylose. Quantitative estimation of tri-*O*-methylarabinose, di-*O*-methylxylose, and mono-*O*-methylxylose showed that the length of the repeating unit is about 16 pentose units and the ratio of 2,3,5-tri-*O*-methylarabinose to 2,3,4-tri-*O*-methylxylose is 12:1. Removal of arabinose residues from the methylated polysaccharide did not result in any substantial increase in the amount of trimethylxylose in the hydrolyzate of the degraded and remethylated product. These results together with those of periodate oxidation studies on the original and degraded polysaccharides show that arabinose is present as single-unit side chain in the arabinoxylan. The arabinoxylan obtained from pea skin is structurally similar to the arabinoxylan obtained from other sources, viz., from wheat (5, 6), rye flour (7), barley flour (4), but the length of the repeating unit varies from source to source.

EXPERIMENTAL

Methods

The following solvent systems (v/v) were used for partition chromatography: (A) ethyl acetate – pyridine – water (8:2:1); (B) *n*-butanol – acetic acid – water (4:1:5), upper layer; (C) *n*-butanol–benzene–pyridine–

water (5:1:3:3), upper layer; (D) benzene–ethanol–water (169:47:15), upper layer; (E) methyl ethyl ketone – water azeotrope; and (F) *n*-butanol–ethanol–water (4:1:5), upper layer. The spray reagents used were: (*a*) saturated solution of aniline oxalate in water (8); (*b*) aniline hydrogen phthalate; and (*c*) *p*-anisidine hydrochloride (3% solution in butanol).

All specific rotations are equilibrium values. Unless otherwise stated all evaporations were carried out *in vacuo* at 30–40°. Whatman No. 1 filter papers were used for paper partition chromatography. Large quantities of sugar mixture were separated by Whatman No. 3MM papers.

Isolation of the Polysaccharide

Peas were kept under water overnight and the skins were separated by hand. They were dried in an oven at 35–40° and powdered. The powder (200 g) in batches was extracted for 24 hours with a boiling mixture of benzene and ethanol (2:1, v/v), to remove fats and coloring matter.

The material (200 g), which was free from fats and coloring matter, was extracted with hot water (4 l.) and the polysaccharide, precipitated by alcohol, was triturated and dried. Yield 0.4%, moisture 9.2%, ash 0.05%, nitrogen 0.25%, $[\alpha]_D^{30}$ +98° (*c*, 0.5 in 4% sodium hydroxide solution). The polysaccharide developed a blue color with iodine solution and yielded only glucose when hydrolyzed. The remaining material was subjected to extraction twice with 0.4% sodium hydroxide solution (750 ml each time) at room temperature in an atmosphere of nitrogen for 16 hours. The polysaccharide was precipitated by addition of the acidified extract to twice its volume of acetone. Yield 0.6%. The polysaccharide on hydrolysis gave xylose and arabinose in the ratio of 5:1, with traces of galactose.

The material left after the above treatment was extracted four times with 4% sodium hydroxide solution (1500 ml) and the polysaccharide was isolated as described above. The product was dialyzed for 7 days, reprecipitated, and dried to yield an amorphous powder. Yield 2%, moisture 11.2%, ash 1.2%, $[\alpha]_D^{29}$ −86.9° (*c*, 0.5 in 4% sodium hydroxide solution), pentosan (9) 96.7%, methoxyl 0.34%, uronic acid (9) 0.84%. Intrinsic viscosity 0.89 dl/g (in 4% sodium hydroxide solution).

Hydrolysis, Identification, and Estimation of Xylose and Arabinose

The polysaccharide (1 g) on complete hydrolysis yielded xylose and arabinose together with a trace quantity of galactose. D-Xylose and L-arabinose were separated by paper chromatography.

The dry sirup containing D-xylose was crystallized from dry ethanol; m.p. and mixed m.p. 144–145°; $[\alpha]_D^{30}$ +19° (*c*, 1 in water), lit. +18° (11).

The dry sirup corresponding to L-arabinose was crystallized from dry ethanol; m.p. and mixed m.p. 155–157°; $[\alpha]_D^{30}$ +105° (*c*, 1 in water), lit. +103° (12).

The polysaccharide (0.1002 g) was hydrolyzed with 2 *N* sulphuric acid and the component sugars were estimated quantitatively by the periodate method (10), using D-ribose as reference sugar. Xylose and arabinose were found to be present in the ratio of 5:1.

Purification of the Polysaccharide

The crude polysaccharide was purified by complexing with Fehling's solution (2). The arabinoxylan (20 g) was dissolved in 4% sodium hydroxide solution (1.5 l.) in an atmosphere of nitrogen, and freshly prepared Fehling's solution (1.5 l.) was added whereupon the copper complex precipitated. The precipitate was washed with ice-cold water (1 l.), and cold hydrochloric acid (0.5 *N*) was added to a suspension of the precipitate in water with stirring, until the copper complex decomposed giving, a slightly opalescent solution. The polysaccharide was precipitated by the addition of an equal volume of acetone and was isolated in the usual way. Yield 15 g, $[\alpha]_D^{29}$ −87.6° (*c*, 1 in 4% sodium hydroxide solution). Intrinsic viscosity 1.02 dl/g in 4% sodium hydroxide solution. Xylose and arabinose, estimated in the above manner, were found to be present in the ratio of 5:1; galactose and uronic acid were absent.

Methylation of the Arabinoxylan

The arabinoxylan (5 g) was methylated by treatment first with dimethyl sulphate and alkali and then with methyl iodide and silver oxide according to the method of Falconer and Adams (15, 16) to yield a fully methylated derivative (3.2 g) showing no hydroxyl absorption band in the infrared spectrum. OMe 38.05%; intrinsic viscosity 0.35 dl/g in chloroform; $[\alpha]_D^{29}$ −58° (*c*, 1 in chloroform).

Molecular Weight Determination of the Methylated Arabinoxylan

All measurements of the intensity of scattered light for molecular weight determination of the methylated arabinoxylan were carried out with a Brice-Phoenix light-scattering photometer (Model OM 1000A) using a semioctagonal cell. The concentration used was over a range of $(1–4)\times10^{-3}$ g/ml. The molecular weight was found to be 5.12×10^5, calculated by the dissymmetry method (17).

Methanolysis and Hydrolysis of the Methylated Arabinoxylan and Separation of Methyl Sugars

The methylated arabinoxylan (1 g) was refluxed with 3% methanolic hydrogen chloride (80 ml) till the rotation reached a constant value (18 hours). The resulting mixture of methyl glycosides was hydrolyzed with *N* hydrochloric acid (80 ml) till the rotation reached a constant value (16 hours). After neutralization

and deionization by passing through Amberlite I.R. 120(H)* and Amberlite I.R. 45(OH)* the hydrolyzate was concentrated to a sirup.

The sirup (600 mg), containing the methyl sugars, was resolved on a cellulose column (13) (40×2 cm) using solvent E (14) as eluant to give five fractions.

Fraction I.—On evaporation, this fraction yielded a chromatographically homogeneous sirup (82 mg) having $[\alpha]_D^{29}$ −35.5° (*c*, 0.5 in water), lit. −35° (4). Calculated for $C_8H_{16}O_5$: OMe, 48.4%. Found: OMe, 48.2%. The sirup (5 mg), on demethylation (18), gave arabinose only along with some partially demethylated sugars. The identity of 2,3,5-tri-*O*-methylarabinose was confirmed by preparing the crystalline 2,3,5-tri-*O*-methyl-L-arabonamide through its lactone in the usual way, m.p. and mixed m.p. 129–131°, lit. 130–132° (19).

Fraction II.—The sirup (15 mg), on demethylation, gave arabinose and a trace of xylose. Paper partition chromatography using solvent D, showed the sirup to contain 2,3,5-tri-*O*-methyl-L-arabinose and 2,3,4-tri-*O*-methyl-D-xylose. A small portion of the mixture was separated by paper chromatography and the sugars were estimated by alkaline hypoiodite (3). The ratio of 2,3,5-tri-*O*-methyl-L-arabinose to 2,3,4-tri-*O*-methyl-D-xylose was approximately 2:1.

Fraction III.—On evaporation, this fraction gave a sirup (370 mg) which had $[\alpha]_D^{29}$ +24.2° (*c*, 0.45 in water), lit. +22.6° (19) and which was chromatographically homogeneous. Calculated for $C_7H_{14}O_5$: OMe, 35.0%. Found: OMe, 34.6%. On demethylation it gave xylose only. The 2,3-di-*O*-methyl-D-xylose was characterized through its crystalline N-phenyl-2,3-di-*O*-methyl-D-xylosylamine, m.p. and mixed m.p. 120–122°, lit. 123–124° (4).

Fraction IV.—This fraction yielded a sirup (96 mg) having $[\alpha]_D^{29}$ +34° (*c*, 0.5 in water) lit. +35° (19). Calculated for $C_6H_{12}O_5$: OMe, 18.8%. Found: OMe, 18.2%. It was chromatographically homogeneous and on demethylation gave only xylose. The 2-*O*-methyl-D-xylose was crystallized from methanol–water, m.p. and mixed m.p. 128–129°, lit. 130° (19).

Fraction V.—The sirup (about 7 mg) had the same mobility as that of an authentic D-xylose on a paper chromatogram and had $[\alpha]_D^{29}$ +19° (*c*, 0.25 in water).

From the column chromatographic results the molar ratio of 2,3,5-tri-*O*-methyl-L-arabinose, 2,3-di-*O*-methyl-D-xylose, and 2-*O*-methyl-D-xylose was 1:3.81:1.

Estimation of O-Methyl Sugars

A small quantity (10 mg) of the mixture of methyl sugars was separated quantitatively by paper chromatography using solvent E and the amounts of sugars were estimated by alkaline hypoiodite (3). The molar ratio of 2,3,5-tri-*O*-methyl-L-arabinose to 2,3-di-*O*-methyl-D-xylose to 2-*O*-methyl-D-xylose was 1:4.2:1.1. D-Xylose and 2,3,4-tri-*O*-methyl-D-xylose were present in negligible amounts.

Periodate Oxidation of the Arabinoxylan

The arabinoxylan (94.6 mg) was dispersed in water (50 ml) and oxidized by shaking with 0.1 *M* sodium metaperiodate (50 ml) in the dark at 15°. The amount of periodate consumed during the reaction was estimated by Fleury and Lange's method (20) and at regular intervals. The periodate uptake became constant after 95 hours, corresponding to 0.84 mole of the oxidant per anhydro pentose residue.

Estimation of Sugar Residues Unattacked by Periodate

The polysaccharide (350 mg) in water (25 ml) was oxidized for 4 days with sodium metaperiodate (792 mg) at room temperature in the dark. After removal of the iodate and periodate ions as insoluble barium salts the solution was dialyzed to remove the remaining ions and the periodate-oxidized polysaccharide was precipitated. Yield 180 mg. A portion (119.7 mg) of this precipitate on hydrolysis yielded xylose, which was estimated, in the usual way, to be 14.2%.

Preparation of Degraded Polysaccharide by Mild Acid Hydrolysis (19)

The polysaccharide (2.04 g) was heated with oxalic acid solution (100 ml of 0.02 *N*) on a boiling-water bath for 1.5 hours, cooled quickly, and an equal volume of acetone was added to precipitate the degraded polysaccharide. On paper chromatographic examination, the supernatant liquid was found to contain arabinose and a trace of xylose.

The degraded polysaccharide (166.6 mg) was hydrolyzed quantitatively and estimation of the component sugars of the hydrolyzate, using D-ribose as reference sugar, showed xylose and arabinose to be present in the percentages of 80.1 and 5.4 respectively (these and subsequent values are expressed as percentages of undegraded polysaccharide). The periodate-oxidized degraded polysaccharide (270 mg) was prepared as in the case of original polysaccharide and the amount of xylose unattacked by periodate was estimated, in the usual way, to be 6.1%.

Partial Hydrolysis of Fully Methylated Arabinoxylan

The fully methylated arabinoxylan (100 mg) was dispersed in methanol (25 ml), and 0.2 *N* hydrochloric acid (10 ml) was added and the mixture was refluxed on a boiling-water bath for 4 hours. The solution was cooled and poured into petroleum ether (100 ml) to precipitate the degraded methylated polysaccharide. After removal of the precipitate at the centrifuge, the supernatant liquid was neutralized (silver carbonate),

**A product of Rohm and Hass Company, Pennsylvania, U.S.A.*

filtered, and deionized. Chromatographic examination of the resulting solution showed the presence of 2,3,5-tri-*O*-methyl-L-arabinose and a trace of 2,3-di-*O*-methyl-D-xylose.

The degraded methylated product, obtained in the above treatment, was remethylated twice by Purdie's method (21) to yield a degraded and fully methylated arabinoxylan (52 mg). OMe 38.7%, $[\alpha]_D^{29}$ −52.4° (*c*, 0.5 in chloroform).

After methanolysis and hydrolysis of the methylated degraded polysaccharide followed by the usual treatments, the hydrolyzate afforded a sirup containing 2,3,5-tri-*O*-methyl-L-arabinose, 2,3-di-*O*-methyl-D-xylose, and 2-*O*-methyl-D-xylose with trace amounts of 2,3,4-tri-*O*-methyl-D-xylose and D-xylose as revealed by paper chromatography. The mixture was separated by quantitative paper chromatography and the amount of each sugar was estimated by alkaline hypoiodite. The ratio of trimethylarabinose, dimethylxylose, and monomethylxylose was 1.1:14.5:1.05. The tri-*O*-methyl pentose fraction was resolved chromatographically by solvent D into 2,3,5-tri-*O*-methyl-L-arabinose and 2,3,4-tri-*O*-methyl-D-xylose and quantitative estimation, by the alkaline hypoiodite method, showed them to be present in the ratio of 12:1.

ACKNOWLEDGMENT

The authors are thankful to Dr. P. Bagchi, Director of Research, East India Pharmaceutical Works Ltd., for suggesting the problem and his valuable advice and interest in the work reported in this paper.

REFERENCES

1. A. POTTER, V. SILVEIRA, R. M. MCCREADY, and H. S. OWENS. J. Am. Chem. Soc. **75**, 1335 (1953).
2. C. P. J. GLAUDEMANS and T. E. TIMELL. J. Am. Chem. Soc. **80**, 1209 (1958).
3. E. L. HIRST, L. HOUGH, and J. K. N. JONES. J. Chem. Soc. 928 (1949).
4. G. O. ASPINALL and R. J. FERRIER. J. Chem. Soc. 638 (1958).
5. R. MONTOGOMERY and F. SMITH. J. Am. Chem. Soc. **77**, 3325 (1955).
6. A. S. PERLIN. Cereal Chem. **28**, 370, 382 (1951).
7. G. O. ASPINALL and R. J. STURGEON. J. Chem. Soc. 3519 (1954).
8. R. H. HORROCKS and G. B. MANNING. Lancet, **256**, 1042 (1949).
9. CHARLES DOREE. The methods of cellulose chemistry. 2nd ed. Chapman and Hall Ltd., London. 1947.
10. E. L. HIRST and J. K. N. JONES. J. Chem. Soc. 1659 (1949).
11. J. K. GILLHAM and T. E. TIMELL. Can. J. Chem. **36**, 410 (1958).
12. G. O. ASPINALL, E. L. HIRST, and A. WICKSTROM. J. Chem. Soc. 1160 (1955).
13. L. HOUGH, J. K. N. JONES, and W. H. WADMAN. J. Chem. Soc. 2511 (1949).
14. L. BOGGS, L. S. CUENDET, I. EHRENTHAL, R. KOCH, and F. SMITH. Nature, **166**, 520 (1950).
15. E. L. FALCONER and G. A. ADAMS. Can. J. Chem. **34**, 338 (1956).
16. G. A. ADAMS. Can. J. Chem. **36**, 755 (1958).
17. P. DEBYE. J. Phys. Chem. **51**, 18 (1947).
18. L. HOUGH, J. K. N. JONES, and W. H. WADMAN. J. Chem. Soc. 1702 (1950).
19. G. O. ASPINALL and R. J. STURGEON. J. Chem. Soc. 4469 (1957).
20. P. FLEURY and J. LANGE. J. Pharm. Chim. **17**, 107 (1933).
21. T. PURDIE and J. C. IRVINE. J. Chem. Soc. **83**, 1021 (1903).

THE REACTION OF *t*-BUTYL ALCOHOL VAPOR WITH Hg 6($^3P_1$) ATOMS[1]

ARTHUR R. KNIGHT AND HARRY E. GUNNING
Department of Chemistry, University of Alberta, Edmonton, Alberta
Received June 26, 1963

ABSTRACT

The nature of the decomposition of *t*-butyl alcohol vapor, photosensitized by Hg 6($^3P_1$) atoms in a static system at room temperature, has been examined under a variety of conditions of continuous and intermittent illumination. The inhibiting effect of nitric oxide has also been studied, as well as the influence of added inert gas.

In the decomposition of pure substrate, the reaction products, with the initial quantum yields, Φ^o, under continuous illumination in parenthesis, were: H_2 (0.045), Me_2CO (0.090), CO (0), CH_4 (0.015), C_2H_6 (0.030) together with lesser amounts of C_3H_8, Me_3CH, Me_3CMe, and Me_3COMe. On addition of nitric oxide, Me_3CONO, Me_2CO, N_2O, N_2, H_2O, and trace quantities of H_2 and CO were the only products observed.

The reaction

$$Me_3COH + Hg\ 6(^3P_1) \rightarrow Me_3CO + H + Hg\ 6(^1S_0)$$

is proposed as the primary process in the decomposition and kinetic evidence is presented that the initially formed *t*-butoxy radicals possess excess energy and that their principal subsequent reaction is unimolecular cleavage into acetone and methyl. The results furthermore indicate that the substrate itself is quite inert to abstractive attack by the primary radicals.

INTRODUCTION

Recent investigations of the vapor-phase reactions between Hg 6($^3P_1$) atoms and methanol (1, 2, 3), ethanol (4), and isopropanol (5, 6) have shown that scission of the O—H bond in each case is the dominant primary step in the reaction. What is more, the rate of abstraction of H-atoms from the substrate, by both primary fragments, rises with decreasing strength of the α(C—H) bond, the site of abstractive attack. Thus, $\Phi(H_2)$ increases in the series MeOH, EtOH, *i*-PrOH, with values of 0.45 (2), 0.53 (4), and 0.72 (5) respectively. In the systems inhibited by nitric oxide, a similar trend is shown in the nitrite yield Φ(RONO), in that as the rate of abstraction by RO increases with decreasing $D(C—H)_\alpha$ in the substrate, there is a concomitant drop in Φ(RONO). The foregoing predicts a marked change in the complexion of the reaction when no α(C—H) bonds are present in the alcohol, suggesting the present study of *t*-butyl alcohol.

The photochemical decomposition of *t*-butyl alcohol has not been investigated previously. However, the photolysis of di-*t*-butyl peroxide has been the subject of several studies (7, 8, 9). It has been unequivocally demonstrated that the *t*-butoxy radical decomposes via

$$Me_3C\dot{O} \rightarrow Me_2CO + CH_3, \qquad [2]$$

for which activation energies of 11.2±2 kcal/mole (9) and 13.2±2.4 kcal/mole (10) have been reported. McMillan and Wijnen re-investigated the photolysis (11), taking into account the reaction

$$Me_3C\dot{O} + (Me_3CO)_2 \rightarrow Me_3COH + \dot{R} \qquad [9']$$

and obtained an activation energy difference of 3 kcal/mole for E_2–$E_{9'}$.

Recently, however, McMillan (12) has found evidence for the formation of excited *t*-butoxy radicals in the photolytic system, thereby rendering uncertain the activation

[1]*Presented in part at the 45th Chemical Institute of Canada Conference, Edmonton, May, 1962.*

Can. J. Chem. Downloaded from www.nrcresearchpress.com by 210.87.254.6 on 09/05/12
For personal use only.

energy calculations previously reported. This author has also reported (13) the presence of vibrationally excited $Me_3C\dot{O}$ radicals in the photolysis of *t*-butyl nitrite, and has shown that such species can be collisionally deactivated by the addition of inert gas. Finally, in a recent study of the Hg-photosensitized decomposition of isopropanol (6) carried out in this laboratory, evidence was obtained for excited isopropoxy radicals in the reaction. Thus the formation of vibrationally excited alkoxy radicals appears to be a common characteristic of RȮ-generating systems where the excitation energy exceeds the minimum required for primary bond-scission. For *t*-butyl alcohol, the exothermicity of the primary interaction with Hg $6(^3P_1)$ atoms is very close to the activation energy for the decomposition of the *t*-butoxy radical (*vide infra*) and the presence of excited species might be expected to have a profound effect on the system.

In the present investigation, the decomposition of *t*-butyl alcohol, photosensitized by Hg $6(^3P_1)$ atoms, has been studied to determine the mechanism and the role of energy-rich species in determining the course of the reaction.

EXPERIMENTAL

The essential details of apparatus, procedures, and purification techniques have been given in earlier papers in this series (2, 3, 6).

t-Butyl alcohol (British Drug Houses) was fractionally distilled, and a small, constant-boiling fraction was retained, prior to trap-to-trap distillation and degassing *in vacuo*. Analysis by gas liquid chromatography of the refined material proved the absence of impurities.

At the end of each experiment with pure substrate, products non-condensable at liquid nitrogen temperature were measured in a gas burette and analyzed by gas liquid chromatography, on a molecular sieves column, for CO and CH_4, with hydrogen being determined by difference. The remaining fraction was treated in one of two ways: (*a*) removal of the fraction non-condensable at −98° (methanol slush) for hydrocarbon product analysis on a silica gel column, or, (*b*) analysis of the complete fraction via didecyl phthalate, $\beta\beta'$-oxydipropionitrile, or Carbowax 20M columns, for acetone and methyl *t*-butyl ether. Duplicate runs were carried out at each exposure period (*t*) to allow both procedures to be used.

For the NO-inhibited reaction, products non-condensable at liquid nitrogen temperature, consisting largely of NO, were pumped off (except at $t = 30$ minutes where mass spectrometric analysis was performed). Subsequently, the fraction non-condensable at −130° (*n*-pentane slush) was removed and analyzed on the silica-gel column for N_2O. Finally, the remainder of the products was withdrawn and acetone and *t*-butyl nitrite yields determined with a didecyl phthalate or Carbowax 20M column.

In the intermittent illumination studies, the total yield of products non-condensable at −196° was determined, after which the sample was analyzed by mass spectrometry. In these runs the condensable products were not examined.

An attempt was made to determine the nature of any cell deposit formed in the reaction. In contrast to the alcohol systems previously studied (2, 4, 5), where the formation of a non-volatile product on the walls of the reaction cell could be readily discerned visually after approximately 2 to 4 hours of irradiation, none was apparent in the present system. Infrared spectra of chloroform washings of the cell were taken, but only after about 36 hours of reaction could a weak OH-bond absorption be detected. When the complicating effects of prolonged exposure are considered, however, these results must be regarded as inconclusive with respect to the formation of any glycol, although the results obtained in general indicate that the production of a small amount of glycol is likely.

Light intensities were determined with propane as actinometer (14), using the differential method of Back (15) to obtain a constant value for $d[H_2]/dt$. The values obtained, in μeinsteins/minute were: 1.08 (intermittent illumination) and 2.62 and 2.53 (steady illumination).

In experiments where both NO and CF_4 were added, special precautions were necessary to avoid the complicating effects of the dark reaction previously found in the isopropanol system under the same conditions (6). Blank runs showed that unless NO and CF_4 are stored together for at least 12 hours and subsequently distilled into the reaction cell containing the alcohol, at a temperature at which NO_2 has negligible vapor pressure, i.e. −130°, the NO_2 formed by reaction of NO with trace quantities of oxygen present in the CF_4, reacts with the alcohol to form *t*-butyl nitrite in appreciable quantities. Fairlie *et al.* (16) have studied the kinetics of this reaction in the liquid phase and these authors suggest that the overall reaction can be represented by

$$2NO_2 + ROH \rightarrow HNO_3 + RONO.$$

In the present study, as in the isopropanol work (6), it was found that the reaction could be eliminated by ensuring the absence of NO_2 in any gas admixed with pure *t*-butyl alcohol vapor.

Can. J. Chem. Downloaded from www.nrcresearchpress.com by 210.87.254.6 on 09/05/12
For personal use only.

Can. J. Chem. Downloaded from www.nrcresearchpress.com by 210.87.254.6 on 09/05/12
For personal use only.

RESULTS

As reaction products for the decomposition of *t*-butyl alcohol, at a pressure of 35 mm and at room temperature, H_2, CO, CH_4, Me_2CO, C_2H_6, C_3H_8, Me_3CH, Me_4C, and Me_3COMe were observed. A detectable yield of water was not observed. A specific search was made for isobutylene oxide and di-*t*-butyl peroxide but these products apparently do not form in this system. When the reaction was run in the presence of nitric oxide, the products, Me_3CONO, N_2O, H_2O, N_2, Me_2CO, as well as trace quantities of CO and H_2 were found, and at the same time the yields of hydrocarbon products and methyl *t*-butyl ether were completely suppressed. No search was made for products of the methyl radical-nitric oxide reaction.

The uninhibited reaction was first examined under continuous illumination and the results, as a function of duration of exposure, are summarized as follows: Fig. 1, $\Phi(H_2)$, $\Phi(CO)$, $\Phi(CH_4)$; Fig. 2, $\Phi(Me_2CO)$, $\Phi(C_2H_6)$; Fig. 3, $\Phi(Me_4C)$, $\Phi(Me_3CH)$, $\Phi(Me_3COMe)$, $\Phi(C_3H_8)$.

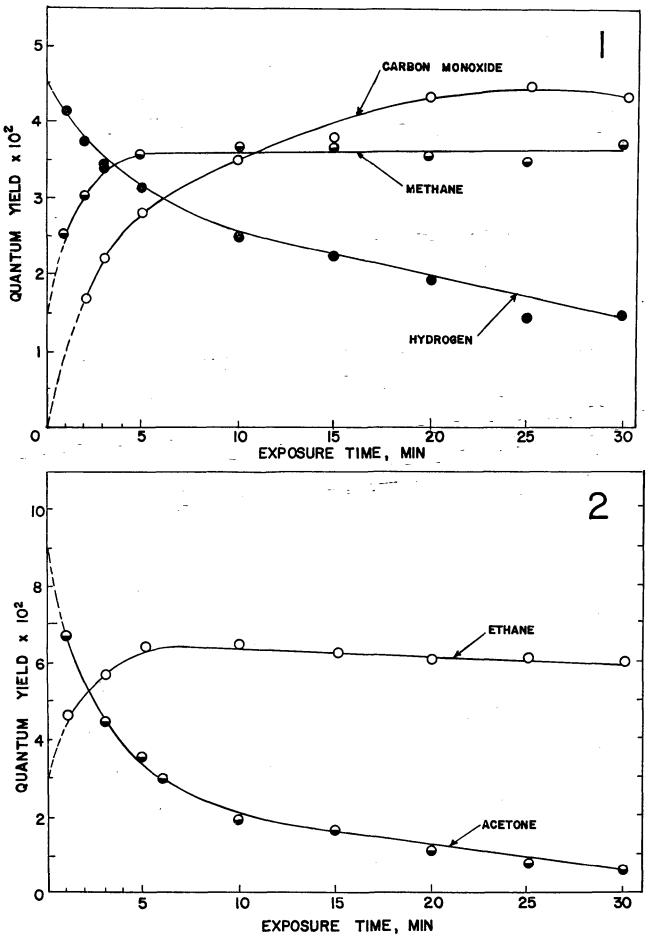

FIG. 1. Mean quantum yield of hydrogen, ●, carbon monoxide, ○, and methane, ◒, as a function of exposure time for 35 mm pure *t*-butyl alcohol.

FIG. 2. Mean quantum yield of acetone, ◒, and ethane, ○, as a function of exposure time for 35 mm pure *t*-butyl alcohol.

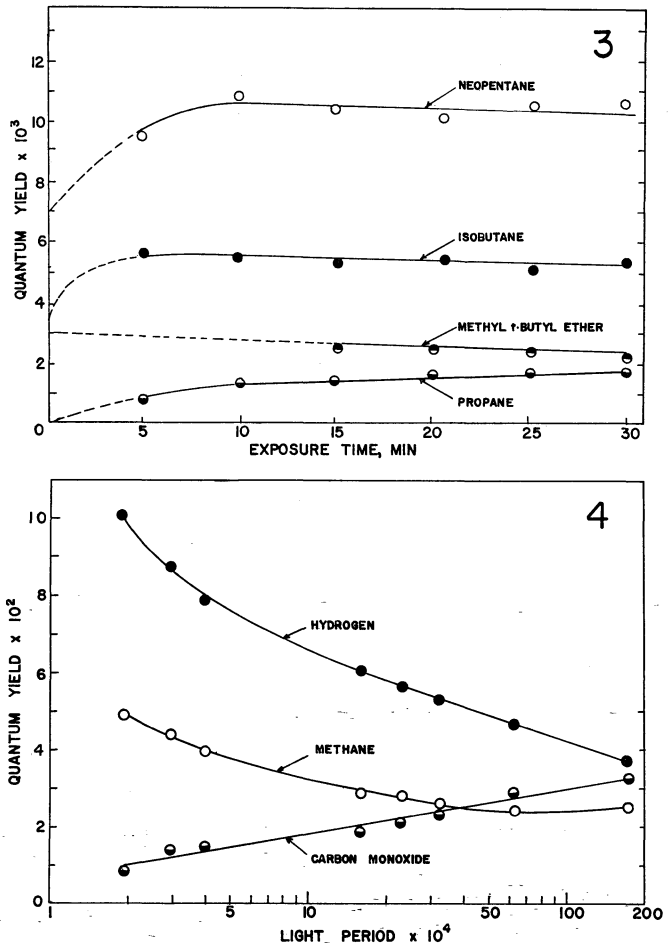

FIG. 3. Mean quantum yield of neopentane, ○, isobutane, ●, methyl *t*-butyl ether, ◓, and propane, ◒, as a function of exposure time for 35 mm pure *t*-butyl alcohol.

FIG. 4. Quantum yield of hydrogen, ●, methane, ○, and carbon monoxide, ◒, as a function of light period, t_L, for a constant dark period of 160 msec for 35 mm pure *t*-butyl alcohol under intermittent illumination.

Under intermittent illumination, the effect of varying the light period, t_L, at a constant dark period, t_D, of 160 msec, on the yields of hydrogen, carbon monoxide, and methane was determined and the results are presented in Fig. 4.

The results obtained in the NO-inhibited reaction are given in Fig. 5. The reported quantum yields have been corrected for competitive quenching by nitric oxide, which was present at a pressure of 10 mm, assuming a quenching cross section, $\sigma_{Q'}^2$ of 15 Å^2 for *t*-butyl alcohol. The resulting correction factor was 1.7. For 30 minutes of exposure, the other products, water excepted, were determined by mass spectrometry and the values found were: $\Phi(N_2) = 2.7\times10^{-2}$, $\Phi(CO) = 8.8\times10^{-3}$, and $\Phi(H_2) = 7.6\times10^{-4}$.

The effect of adding the inert gas, CF_4, on the uninhibited reaction is shown in Figs. 6 and 7. Figure 6 gives the results of a series of runs wherein the yield of acetone was determined as a function of $P(CF_4)$. Here, a short exposure time of 3.0 minutes was employed to minimize the complicating effects of secondary acetone decomposition. One additional

Can. J. Chem. Downloaded from www.nrcresearchpress.com by 210.87.254.6 on 09/05/12
For personal use only.

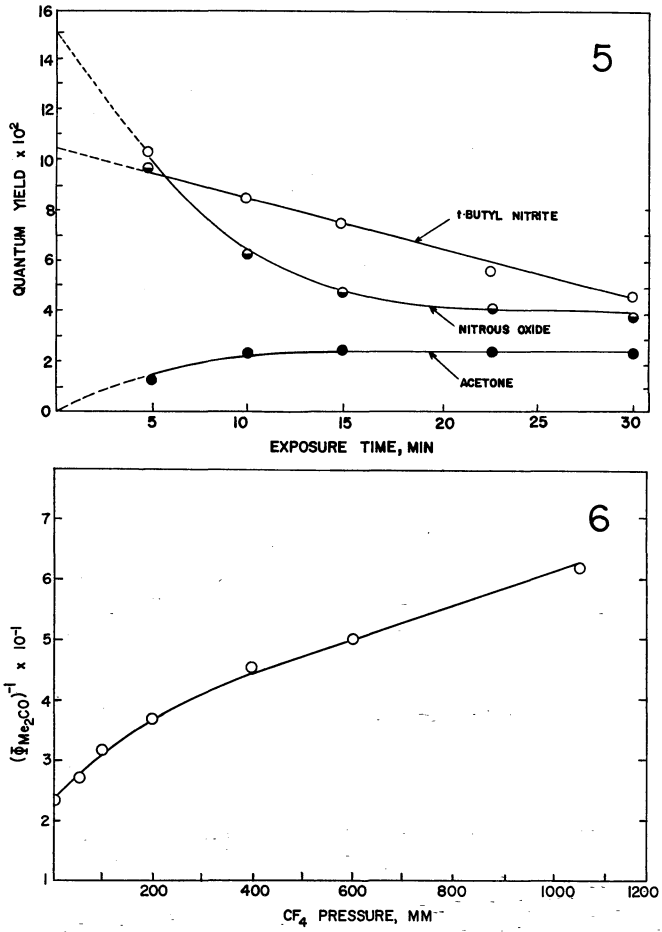

FIG. 5. Mean quantum yield, corrected for competitive quenching by NO, for *t*-butyl nitrite, ○, nitrous oxide, ◒, and acetone, ●, as a function of exposure time for 10 mm NO and 35 mm *t*-butyl alcohol.

FIG. 6. The reciprocal of the acetone quantum yield as a function of carbon tetrafluoride pressure for 35 mm *t*-butyl alcohol at an exposure time of 3 minutes.

run was performed with the *t*-butyl alcohol–CF_4 system, at an exposure time of 10 minutes, in which $\Phi(H_2)$ was determined by mass spectrometry to be 1.4×10^{-2}, for $P(CF_4) = 444$ mm. The addition of inert gas causes a marked decrease in the acetone yield, but the plot of $1/\Phi(Me_2CO)$ vs. $P(CF_4)$ does not give the expected straight line (Fig. 6). In a separate series of experiments, the influence of CF_4 pressure on the yields of isobutane and neopentane was determined. These results are given in Fig. 7. In this series an exposure time of 12 minutes was employed to allow product yields to attain levels consistent with accurate analysis. As shown in the figures, however, even under these conditions, the yields drop off to very small but finite values at $P(CF_4) > 150$ mm. The experimental error in the minute yields at high pressures is unfortunately too large to allow a meaningful plot of reciprocal quantum yields over the entire pressure range.

Finally, the yields of *t*-butyl nitrite and acetone, from the decomposition of a mixture of 35 mm *t*-butyl alcohol and 10 mm nitric oxide, were determined in a series of runs with exposure time = 5 minutes, as a function of CF_4 pressure up to $P(CF_4) = 900$ mm. The results are presented graphically in Fig. 8.

Can. J. Chem. Downloaded from www.nrcresearchpress.com by 210.87.254.6 on 09/05/12
For personal use only.

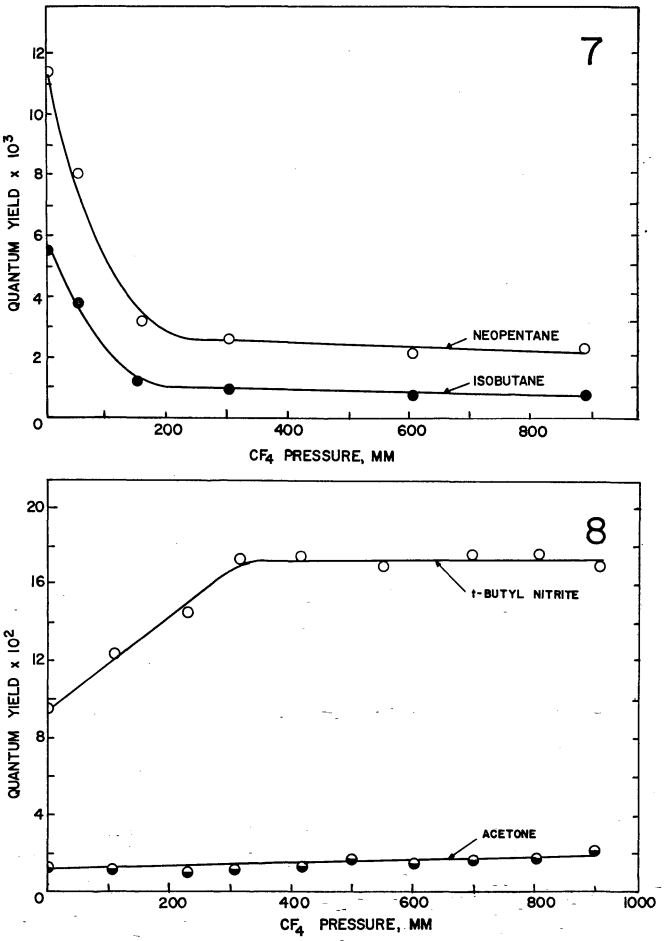

FIG. 7. The quantum yields of neopentane, ○, and isobutane, ●, as a function of carbon tetrafluoride pressure, for 35 mm *t*-butyl alcohol at an exposure time of 12 minutes.

FIG. 8. The quantum yields of *t*-butyl nitrite, ○, and acetone, ◒, as a function of carbon tetrafluoride pressure, for 35 mm *t*-butyl alcohol and 10 mm nitric oxide at an exposure time of 5 minutes. The yields have been corrected for competitive quenching by nitric oxide.

DISCUSSION

The results obtained are consistent with the occurrence of O—H bond scission in the primary process. The appearance of *t*-butyl nitrite as the major heavy product in the NO-inhibited system, the formation of methyl *t*-butyl ether in the uninhibited decomposition, and the close correspondence of the products to those found in the photolysis of the peroxide, where the production of *t*-butoxy radicals has been unequivocally established, all indicate the formation of *t*-butoxy radicals in the decomposition of *t*-butyl alcohol. The fact that nitrous oxide, nitrogen, and water are formed when NO is added, is evidence for the presence of HNO (*vide infra*) and thus, for the formation of hydrogen atoms. The formation of an excited molecule in the primary step can be ruled out, since increasing inert gas pressure in the NO-inhibited reaction results in an increased nitrite yield, whereas an excited molecule would be collisionally deactivated and reduction of product yields would occur.

Can. J. Chem. Downloaded from www.nrcresearchpress.com by 210.87.254.6 on 09/05/12
For personal use only.

The following mechanism is proposed to account for the observed results.

$$Me_3COH + Hg\ 6(^3P_1) \rightarrow Me_3CO^* + H + Hg\ 6(^1S_0) \quad [1]$$

$$Me_3CO^* \rightarrow Me_2CO + CH_3 \quad [2]$$

$$Me_3CO^* + M \rightarrow Me_3CO + M \quad [3]$$

$$H + H + M \rightarrow H_2 + M \quad [4a]$$

$$H + H \xrightarrow{\text{wall}} H_2 \quad [4b]$$

$$CH_3 + H + M \rightarrow CH_4 + M \quad [5]$$

$$CH_3 + CH_3 \rightarrow C_2H_6 \quad [6]$$

$$CH_3 + Me_3CO \rightarrow Me_3COCH_3 \quad [7]$$

$$R + Me_3COH \rightarrow RH + Me_2(\dot{C}H_2)COH \quad [8]$$

$$R + R'H \rightarrow RH + R' \quad [9]$$

$$Me_3CO + H \rightarrow Me_3COH^* \quad [10]$$

$$Me_3COH^* + M \rightarrow Me_3COH + M \quad [11]$$

$$Me_3COH^* \rightarrow Me_3C + OH \quad [12]$$

$$Me_3C + H \rightarrow Me_3CH \quad [13]$$

$$Me_3C + CH_3 \rightarrow Me_3CCH_3 \quad [14]$$

$$2Me_2(\dot{C}H_2)COH \rightarrow \text{glycol} \quad [15]$$

where, R = Me_3CO, CH_3, H, Me_3C, OH; and R'H = Me_2CO, C_2H_6.

Since acetone and methyl radicals are the known decomposition products of *t*-butoxy radicals, and since the presence of this radical has been confirmed, reaction [2] is proposed. The following stoichiometric considerations show [2] to be the sole source of CH_3. In the initial stages of the reaction, methyl radicals evidently give rise to methane, ethane, methyl *t*-butyl ether, and neopentane, and thus their initial quantum yield is given by

$$\Phi^o(CH_3) = \Phi^o(CH_4) + 2\Phi^o(C_2H_6) + \Phi^o(Me_3COCH_3) + \Phi^o(Me_3CCH_3). \quad [16]$$

Substitution of the appropriate values from Figs. 1, 2, and 3 gives a value of 8.5×10^{-2} for $\Phi^o(CH_3)$. On the basis of reaction [2] alone, $\Phi^o(Me_2CO)$ should have the same value. Figure 2 shows that the value is 9.0×10^{-2}, which is in agreement with the value for $\Phi^o(CH_3)$ from equation [16], within experimental error.

Although the results showed that abstraction reactions involving the substrate were apparently minor, this does not preclude abstraction from products or the formation of $Me_2(\dot{C}H_2)COH$ radicals, which give rise to other products or reform the substrate in a step analogous to reaction [10]. It is thus important to establish the contribution of abstraction reactions.

Considering first abstraction by CH_3 radicals, McMillan (11) found in the photolysis of di-*t*-butyl peroxide that only ca. 3% of the methyl radicals formed resulted in methane. Since no H-atoms were present in that system, it is only this fraction which arose by abstraction from substrate or products. In the present system, however, if equation [16] is applied at t = 30 minutes, the data show that 21% of CH_3 radicals give rise to methane. Thus, if the abstraction reaction proceeds, as may be expected, at the same rate here as in the peroxide case, only approximately 14% of the observed methane yield arises via the abstraction of an H-atom by CH_3 radicals. On this basis and evidence presented below for a high H-atom concentration, reaction [5] is the proposed principal mode of methane formation.

Can. J. Chem. Downloaded from www.nrcresearchpress.com by 210.87.254.6 on 09/05/12
For personal use only.

For *t*-butoxy radicals, McMillan and Wijnen (11) found that ca. 5% of this species resulted in *t*-butyl alcohol when the peroxide was photolyzed. However, in view of recent evidence (12) for excited radicals which decompose before abstraction can occur, the estimate of the fraction abstracting may be low when applied to Me_3CO radicals of normal energies. Nevertheless, such radicals react very slowly with primary C—H bonds. In the pyrolysis of di-*t*-butyl peroxide, the relative rates of the reactions

$$Me_3CO \rightarrow Me_2CO + CH_3, \qquad [2]$$

$$Me_3CO + RH \rightarrow Me_3COH + R \qquad [19]$$

have been determined for a large number of hydrogen donors. Relevant to the present argument, k_{19}/k_2 has a value of 0.47 l mole^{-1} for RH = isopropyl benzene (17) but is only 0.06 l mole^{-1} for RH = *t*-butyl benzene (18). An important point here is the possible effects of the residual energy possessed by Me_3CO^*, on the $(k_8+k_9)/k_2$ ratio (analogous to the k_{19}/k_2 ratio in the peroxide case). The energy of the Hg $6(^3P_1)$ atom is 112 kcal/mole, while D(O—H) for *t*-butyl alcohol is reported to be 104 (19) and 102 (20) kcal/mole. If D(O—H) is taken as 103±1 kcal/mole, the maximum excess energy which could be taken by Me_3CO^* is 9±1 kcal/mole. Activation energies of 11.2±2 kcal/mole (9) and 13.2±2.4 kcal/mole (10) have been reported for reaction [2]. Thus the energetic probability of unimolecular decomposition is marginal and no meaningful prediction of the decomposition/abstraction ratio can be made. The results, however, indicate that unimolecular decomposition predominates.

Abstraction by hydrogen atoms may also be important. The reduction of $\Phi(H_2)$ from a value of 1.5×10^{-2} at t = 30 minutes to 7.6×10^{-4} when 10 mm nitric oxide is added indicates that at least 95% of the molecular hydrogen produced arises from H-atoms. A material balance requires that one hydrogen atom be formed along with each acetone molecule and methyl radical, since the latter products are formed in equal quantities initially. $\Phi^0(Me_2CO)$ is 9.0×10^{-2} and this must also be the minimum value for the initial yield of H-atoms. The value is minimal, since any abstraction by Me_3CO radicals results in less acetone being formed than H-atoms. Since the initial yield of molecular hydrogen is 4.5×10^{-2} it first appears that most, if not all, of the hydrogen atoms produced recombine. We have seen, however, that ca. 86% of the methane is arising from CH_3—H combination in [5]. Similarly, reaction [13] accounts for 86% of the isobutane formed. One this basis, the total yield of hydrogen atoms is given by

$$\Phi^0_{\text{H-atoms}} = 2(\Phi^0_{H_2}-\alpha\Phi^0_{H_2})+\alpha\Phi^0_{H_2}+0.86\Phi^0_{CH_4}+0.86\Phi^0_{Me_3CH} \qquad [20]$$

where α is the fraction of molecular hydrogen arising through abstraction by H-atoms. Substitution of the appropriate values from Figs. 1 and 3 yields

$$\Phi^0_{\text{H-atoms}} = 0.107+\alpha 0.045. \qquad [21]$$

Considering the derivation of an analogous equation for Me_3CO radicals, if β is defined as the fraction of Me_3CO abstracting H-atoms, then $(1-\beta)$ will be the fraction yielding acetone. Thus,

$$(1-\beta)\Phi^0_{Me_3CO} = \Phi^0_{Me_2CO}, \qquad [22]$$

$$\Phi^0_{Me_3CO} = \Phi^0_{Me_2CO}/(1-\beta). \qquad [23]$$

Since the initial yields of *t*-butoxy radicals and hydrogen atoms must be the same, [23]

Can. J. Chem. Downloaded from www.nrcresearchpress.com by 210.87.254.6 on 09/05/12
For personal use only.

and [21] may be equated, and after substitution of the value for Φ_{Me_2CO} from Fig. 2, the resulting equation is:

$$0.107-\alpha 0.045 = 0.090/(1-\beta). \quad [24]$$

Now the values of α and β cannot be determined from this single equation, but maximum values can be established. A reasonable assumption is that the minimum fraction of Me_3CO radicals that are abstracting is that observed for the decomposition of the peroxide (see above), thus $\beta = 0.05$. This value corresponds to a maximum of 13% of all H-atoms abstracted. Similarly, it would be unlikely that the amount of H-atom abstraction would be less than that for CH_3 radicals, i.e. 3% (and thus $\alpha = 0.07$). Substitution of this value into equation [24] yields 14% for the extent of abstraction by Me_3CO. Thus limits can be set on the contribution of abstraction reaction by H and Me_3CO as follows: 3% <% H-atoms abstracting <13%; 5% <% Me_3CO radicals abstracting <14%. Thus an estimate of the initial quantum yield of *t*-butyl alcohol disappearance can be obtained. The initial quantum yield of H-atoms and *t*-butoxy radicals is 0.100 ± 0.005 (from limiting values calculated above) and if the quantum yield of decomposition giving isobutyl radicals, 0.010, is added, we have that:

$$\Phi^0_{-ROH} = 0.110\pm0.005.$$

The accumulated evidence points to a very high radical concentration in the system. Thus the reaction resulting in substrate reformation, observed with the other alcohols (2, 4, 5), should also be operative. Since the concentration of H-atoms is considerably higher here, reaction [10] should play an even more important role. Considering first the results of the sector experiments, as illustrated in Fig. 4, the observed increase in $\Phi(H_2)$ and $\Phi(CH_4)$ as the light period is made progressively shorter, is evident for the importance of reaction [10] in lowering the observed yields under steady illumination. As the mean concentration of H-atoms and *t*-butoxy radicals is decreased, the probability of reaction [2] will rise, and hence the concentration of H and CH_3, relative to that of Me_3CO, will be increased, leading to an increased rate for reactions [4] and [5]. The similarity of the $\Phi(H)$ and $\Phi(CH_4)$ curves in Fig. 4 also suggest similar modes of formation of these products.

Further evidence for the importance of the back reaction derives from the fact that when 444 mm CF_4 is added to the system (cf. Results) the hydrogen quantum yield for $t = 10$ minutes drops from a value of 2.49×10^{-2} (for $P(CF_4) = 0$) to 1.36×10^{-2}. As will be seen later, the main effect of added CF_4 is to quench excited *t*-butoxy radicals before decomposition occurs and thus raise their steady-state concentration. Under such conditions the rate of reaction [10] should increase and $\Phi(H_2)$ would be diminished.

The formation of isobutane and neopentane is also related to the occurrence of step [10]. In the decomposition of methanol (2), CH_3 radicals apparently resulted from the decomposition of energy-rich MeOH, in the reaction analogous to [12]. In that case, where the amount of back reaction was less than in the present system (because of the high rate of abstraction from the substrate) the atomic cracking reaction amounted to ca. 5% of the total decomposition at 50 mm methanol pressure (2) and 18% at 8 mm (1). With 35 mm *t*-butyl alcohol, the *t*-butyl radicals produced in reaction [12] account for ca. 10% of the total decomposition. The results of the series of runs with added CF_4, shown in Fig. 6, also indicate that isobutane and neopentane result from $(Me)_3\dot{C}$ radicals formed in step [12] in that, as the partial pressure of CF_4 is increased, there is evidently increased collisional deactivation of Me_3COH^*, thereby reducing the rates of [12], [13], and [14]. The

Can. J. Chem. Downloaded from www.nrcresearchpress.com by 210.87.254.6 on 09/05/12
For personal use only.

residual yield of Me_3CH and Me_4C may be due to a small fraction of the primary process yielding OH and $Me_3\dot{C}$ radicals. However, this fraction cannot exceed ca. 3%.

Figure 2 shows that acetone is undergoing very rapid secondary decomposition in the early stages of the reaction. As in the case of isopropanol (5), acetone may be decomposing by Hg-photosensitization or by photolysis, or both. The overall reaction can be expressed as

$$Me_2CO + Hg^* \text{ and (or) } h\nu \rightarrow 2CH_3 + CO. \qquad [25]$$

Using the mean quantum yield of acetone production for the first minute of exposure, $\Phi(Me_2CO) = 0.067$ (Fig. 2), there should be $0.067 \times 2.53 \times 30 = 5.09$ μmoles of this product after 30 minutes. Only 0.55 μmoles were actually found, indicating that 4.45 μmoles suffered secondary decomposition. Thus, in addition to the 5.09 μmoles CH_3 produced in reaction [2], there should be an additional yield of 2×4.54 μmoles from reaction [25], in all, a total of 14.2 μmoles of methyl radicals. Calculating from the observed yields, we found a value for the CH_3 yield at 30 minutes of 13.8 μmoles. The accountability in CO is not as satisfactory, in that, of the 4.54 μmoles predicted by the calculation, only 3.5 were found after 30 minutes of reaction. In view of the high H-atom concentration in the system, however, some of the missing CO may have disappeared in reactions with H-atoms, and this would likely be followed by dilution of the 1 μmole of HCO radicals among indetectable quantities of minor products.

Two factors may determine the decrease in $\Phi(H_2)$ with time, shown in Fig. 1. Secondary quenching by hydrogen itself, in addition to lowering the rate of reaction [1], will increase the concentration of hydrogen atoms, resulting in increasing importance of [10]. Secondary quenching by reaction products other than hydrogen will also diminish the rate of primary decomposition.

Methane and ethane, as shown in Figs. 1 and 2, increase in yield very rapidly with exposure time during the first ca. 5 minutes of reaction, and thereafter remain essentially constant. In the initial stages of the reaction, methyl radicals result solely from reaction [2], but as reaction [25] increases in importance, it will provide an additional source of methyl radicals. Thus the yields of CH_4 and C_2H_6 would be expected to rise rapidly as $\Phi(Me_2CO)$ falls off (cf. Fig. 2), but level off when acetone had attained a steady-state concentration. Although the rate of the overall reaction [25] decreases very rapidly with time, this condition does not obtain until ca. 15–20 minutes. The fact that $R(CH_4)$ and $R(C_2H_6)$ reach constant values earlier may arise from their rate of formation in reaction [2] being diminished through a general decrease in the rate of step [1] with time, as the concentration of products capable of quenching a detectable fraction of the incident energy increases.

The following mechanism is proposed to account for the observed results in the presence of 10 mm nitric oxide: reactions [1] through [3] will be followed by the following reactions.

$$Me_3CO^* + NO \rightarrow Me_3CO + NO \qquad [26]$$

$$Me_3CO + NO \rightarrow Me_3CONO \qquad [26']$$

$$CH_3 + NO \rightarrow \text{products} \qquad [27]$$

$$H + NO \xrightarrow{M} HNO \qquad [28]$$

$$2HNO \rightarrow N_2O + H_2O \qquad [29]$$

$$2NO + HNO \rightarrow N_2 + HNO_3? \qquad [30]$$

$$Me_3CO + HNO \rightarrow Me_3COH + NO \qquad [31]$$

Can. J. Chem. Downloaded from www.nrcresearchpress.com by 210.87.254.6 on 09/05/12
For personal use only.

The reaction of H-atoms with nitric oxide has been discussed previously (6). There is probably, however, an additional step giving rise to N_2O, since the yield of H-atoms calculated from the stoichiometry of reactions [28] to [30] is inordinately high, and the water yield, though not determined quantitatively, was clearly smaller than that of N_2O.

Since the yields have been corrected for competitive NO quenching, using an assumed value of the quenching cross section for *t*-butyl alcohol, $\sigma_Q^2 = 15$ Å^2, an attempt to obtain a quantitative correlation between yields in the inhibited and NO-free systems does not appear justified.

The marked decrease in $\Phi(Me_2CO)$ with increasing CF_4 pressure shown in Fig. 7 indicates that excited *t*-butoxy radicals are the precursors of acetone. The observed results cannot be interpreted in terms of an excited molecule mechanism, since increased collisional deactivation would decrease the yield of Me_3CO radicals, and when NO is present (cf. Fig. 8 and discussion below), the nitrite yield would drop. Now if there is a simple competition between reactions [2], unimolecular decomposition, and [3] deactivation of Me_3CO^*, the plot of $1/\Phi(Me_2CO)$ vs. $P(CF_4)$ should be linear, whereas the curve of Fig. 10 is not, particularly at low CF_4 pressures. This suggests (*a*) a second acetone-producing step only slightly affected by inert gas pressure, or (*b*) collisional deactivation of Me_3CO^* by a third body is not a simple function of the collison frequency. The latter is more attractive, since the results appear to exclude any acetone-producing reaction other than [2]. Hershenson and Benson (21) have recently suggested that the unimolecular decomposition of Me_3CO, produced in pyrolysis or photolysis, is pressure dependent. Thus the results here may be a combination of this effect and the "normal" removal of vibrational energy through collision.

The observed increase in nitrite yield as the pressure of CF_4 is increased, as shown in Fig. 8, can be ascribed to the dual effect of CF_4 in deactivating excited *t*-butoxy radicals and in removing excess energy from any nitrite formed by the combination of Me_3CO^* radicals and nitric oxide.

Since $\Phi(Me_2CO)$ is essentially invariant with increasing inert gas pressure, the *t*-butoxy radicals giving rise to the "additional" nitrite formed under these conditions, must participate in a reaction other than unimolecular decomposition in the absence of inert gas, where the reaction mixture consists of 35 mm *t*-butyl alcohol and 10 mm nitric oxide. The two alternatives are abstraction and substrate reformation. However, the contribution of the latter reaction would not be expected to *decrease* with rising inert gas pressure since we have seen that with pure *t*-butyl alcohol $\Phi(H_2)$ decreases with increasing CF_4 pressure under these conditions, indicating an *increasing* role for the back reaction. Furthermore, it has been shown that a maximum of 14% Me_3CO^* radicals take part in the abstraction reaction in the absence of both nitric oxide and carbon tetrafluoride. Thus it is apparent that the addition of just 10 mm nitric oxide, greatly facilitates H-atom abstraction by *t*-butoxy radicals. The nitric oxide must cause a partial deactivation of Me_3CO^* to an energy level below the minimum required for reaction [2], but sufficiently high to overcome part of the activation energy requirement for abstraction from the substrate. A similar behavior was found by McMillan (13) in the photolysis of *t*-butyl nitrite – nitric oxide mixtures, where it was found that nitric oxide had an unexpectedly high efficiency in quenching excited alkoxy radicals. From these results, it is apparent that the quenching of excited *t*-butoxy radicals is not a simple collisional deactivation, and further investigation is evidently required to uncover the exact nature of this process.

In summary, the reaction of *t*-butyl alcohol vapor with Hg $6(^3P_1)$ atoms produces excited *t*-butoxy radicals and hydrogen atoms in the primary interaction of substrate and

Can. J. Chem. Downloaded from www.nrcresearchpress.com by 210.87.254.6 on 09/05/12
For personal use only.

sensitizer. The principal mode of disappearance of *t*-butoxy radicals is unimolecular decomposition into acetone and methyl radicals. The alcohol is relatively inert to abstractive attack with the result that radical concentrations are high in the system and combination reactions are thus of considerable importance.

ACKNOWLEDGMENT

This research was supported in part by the National Research Council under Grant No. NRC T-162, which support is gratefully acknowledged.

REFERENCES

1. R. F. POTTIE, A. G. HARRISON, and F. P. LOSSING. Can. J. Chem. **39**, 102 (1961).
2. A. R. KNIGHT and H. E. GUNNING. Can. J. Chem. **39**, 1231 (1961).
3. A. R. KNIGHT and H. E. GUNNING. Can. J. Chem. **39**, 2251 (1961).
4. A. R. KNIGHT and H. E. GUNNING. Can. J. Chem. **39**, 2466 (1961).
5. A. R. KNIGHT and H. E. GUNNING. Can. J. Chem. **40**, 1134 (1962).
6. A. R. KNIGHT and H. E. GUNNING. Can. J. Chem. **41**, 763 (1963).
7. E. R. BELL, F. F. RUST, and W. E. VAUGHAN. J. Am. Chem. Soc. **72**, 337 (1950).
8. L. M. DORFMAN and Z. W. SALSBURG. J. Am. Chem. Soc. **73**, 255 (1951).
9. D. H. VOLMAN and W. M. GRAVEN. J. Am. Chem. Soc. **75**, 3111 (1953).
10. F. W. BIRSS, C. J. DANBY, and C. HINSHELWOOD. Proc. Roy. Soc. (London), Ser. A, **239**, 154 (1957).
11. G. R. MCMILLAN and M. H. J. WIJNEN. Can. J. Chem. **36**, 1227 (1958).
12. G. R. MCMILLAN. J. Am. Chem. Soc. **84**, 2514 (1962).
13. G. R. MCMILLAN. J. Am. Chem. Soc. **84**, 4007 (1962).
14. S. BYWATER and E. W. R. STEACIE. J. Chem. Phys. **19**, 319 (1951).
15. R. A. BACK. Can. J. Chem. **37**, 1834 (1959).
16. A. M. FAIRLIE, JR., J. J. CARBERRY, and J. C. TREACY. J. Am. Chem. Soc. **75**, 3786 (1953).
17. J. H. T. BROOK. Trans. Faraday Soc. **53**, 327 (1957).
18. J. H. RALEY, F. F. RUST, and W. E. VAUGHAN. J. Am. Chem. Soc. **70**, 88 (1948).
19. P. GRAY and A. WILLIAMS. Chem. Rev. **59**, 240 (1959).
20. T. L. COTTRELL. The strengths of chemical bonds. Butterworth, London. 1958.
21. H. HERSHENSON and S. W. BENSON. J. Chem. Phys. **37**, 1889 (1962).

Can. J. Chem. Downloaded from www.nrcresearchpress.com by 210.87.254.6 on 09/05/12
For personal use only.

REARRANGEMENT STUDIES WITH C^{14}

XVII. A REINVESTIGATION OF THE REACTION OF 2-PHENYLETHYL-1-C^{14} BROMIDE WITH MAGNESIUM AND COBALTOUS BROMIDE IN REFLUXING ETHER

D. P. THORNHILL[1] AND C. C. LEE

Department of Chemistry, University of Saskatchewan, Saskatoon, Saskatchewan

Received April 22, 1963

Can. J. Chem. Downloaded from www.nrcresearchpress.com by 210.87.254.40 on 09/05/12
For personal use only.

ABSTRACT

Treatment of 2-phenylethyl-1-C^{14} bromide with magnesium and cobaltous bromide in refluxing ether gave ethylbenzene and styrene with no isotope position rearrangement. The results are contrary to those reported by Smith and Anderson. It was also found that oxidation of styrene-β-C^{14} with concentrated nitric acid gave *p*-nitrobenzoic acid containing 3–4% of the original styrene activity. Nitric acid oxidation of "regenerated styrene" from labeled styrene dibromide under different conditions gave 5.7–37.8% rearrangement. The mechanistic implications of the experimental results are discussed.

INTRODUCTION

Studies in this laboratory on isotope position rearrangement induced by γ-irradiation of 2-arylethyl-1-C^{14} halides (1, 2) have led our attention to the possible extents of 1,2-phenyl shift in the 2-phenylethyl radical. Slaugh (3) has found that the peroxide-catalyzed decarbonylation of 3-phenylpropionaldehyde-2-C^{14} produced the 2-phenylethyl radical which showed 2–5% rearrangement of the C^{14} label in forming ethylbenzene. On the other hand, Smith and Anderson (4) have reported that the 2-phenylethyl radical from reaction of 2-phenylethyl-1-C^{14} bromide with magnesium and cobaltous bromide in refluxing ether gave ethylbenzene and styrene with about 20% isotope position rearrangement. The magnitude of rearrangement for the latter reaction appears to be extraordinarily high in comparison to the results of Slaugh (3). As Smith and Anderson (4) reported the data from apparently only a single experiment with 2-phenylethyl-1-C^{14} bromide, it was decided to repeat this work so as to obtain a confirmation, or otherwise, of their finding. Smith and Anderson (4) degraded their products, ethylbenzene and styrene, by oxidation with concentrated nitric acid. While Roberts, Ropp, and Neville (5) have shown that oxidation of C^{14}-labeled ethylbenzene by concentrated nitric acid does not cause any rearrangement, the applicability of this method for the degradation of C^{14}-labeled styrene has not been studied. The present paper also reports observations on the absence or occurrence of isotope position rearrangements in the oxidation, under various conditions, of styrene-β-C^{14} and *p*-nitrostyrene-β-C^{14}.

RESULTS AND DISCUSSION

2-Phenylethyl-1-C^{14} bromide (2) was treated with magnesium and cobaltous bromide in refluxing ether as described by Smith and Anderson (4). The monomeric products were obtained in 65% and 58% yields for duplicate runs which were found by v.p.c. analysis to consist of 65% ethylbenzene, 35% styrene and 62% ethylbenzene, 38% styrene, respectively. Part of each product mixture was hydrogenated to give pure ethylbenzene. The remainder was separated into ethylbenzene and styrene dibromide, and from the latter, styrene was regenerated by refluxing it with sodium iodide in acetone (4, 6). Each of these fractions was oxidized with alkaline permanganate to give benzoic

[1]*Holder of a Commonwealth Scholarship, 1961–63.*

TABLE I

Activities from reaction of 2-phenylethyl-1-C^{14} bromide with magnesium and cobaltous bromide in refluxing ether

		Activity (mμc/mmole)	
		Run 1	Run 2
Reactant	$C_6H_5CH_2CH_2Br$	640	640
Product	$C_6H_5C_2H_5$	635	
	$C_6H_5CHBrCH_2Br$	645	
C_6H_5COOH	From hydrogenated product	0±0.1	0±0.1
	From ethylbenzene	0±0.1	0±0.1
	From regenerated styrene	0±0.1	0±0.1

acid. As shown in Table I, all samples of benzoic acid were inactive, indicating that, contrary to the report of Smith and Anderson (4), no isotope position rearrangement was involved in the formation of ethylbenzene and styrene.

Although certain details of the mechanism for the Kharasch reaction between an alkyl halide and a Grignard reagent in the presence of cobaltous halide are still in doubt (7–9), the free alkyl radical is generally believed to be involved as an intermediate. In the present studies with 2-phenylethyl bromide, the products, ethylbenzene and styrene, may well be derived from the 2-phenylethyl radical as suggested by Smith and Anderson (4). The excess of ethylbenzene over styrene could be due to a greater amount of hydrogen abstraction over disproportionation reactions. Another possibility is that unreacted 2-phenylethylmagnesium bromide might be present, which on hydrolysis would result in ethylbenzene (9). In an inactive trial, the reaction with 2-phenylethyl bromide and magnesium and cobaltous bromide in refluxing ether was effected as before and the resulting mixture was treated with Dry Ice before hydrolysis by dilute hydrochloric acid. The monomeric products, consisting of 59% ethylbenzene and 41% styrene, were obtained in 63% yield. This yield and product composition were not very different from those obtained in the active runs when no Dry Ice was used. Moreover, no 3-phenylpropionic acid could be isolated after the treatment with Dry Ice. These findings, therefore, suggest that unreacted 2-phenylethylmagnesium bromide was not present in significant amounts when the reaction mixtures were hydrolyzed.

The fact that there was no isotope position rearrangement in the ethylbenzene and styrene indicated that under the conditions used in the present studies, 1,2-phenyl shift in the 2-phenylethyl radical did not occur before the formation of stable products. Seubold (10) has noted that the extent of rearrangement in the neophyl radical increased with increasing dilution in a solvent which was stable towards radical attack. This finding indicated that the longer the lifetime of the radical the greater the opportunity for 1,2-phenyl shifts. In the present case, radical attack on the solvent, ether, is quite feasible, thus decreasing the chance of 1,2-phenyl shift in the 2-phenylethyl radical. Another factor, which may even be more important, is the fact that Slaugh (3) has shown a temperature dependency, which indicated an appreciable activation energy, for the 1,2-phenyl shift in the 2-phenylethyl radical derived from the decarbonylation of 3-phenylpropionaldehyde-2-C^{14}. The rearrangement of 2–5% resulted from decarbonylation carried out at temperatures ranging between 145 and 175° C. The present studies with 2-phenylethyl-1-C^{14} bromide were effected in refluxing ether, a temperature which may be too low to give any measurable extent of 1,2-phenyl shift before the formation of ethylbenzene and styrene.

Can. J. Chem. Downloaded from www.nrcresearchpress.com by 210.87.254.40 on 09/05/12
For personal use only.

Can. J. Chem. Downloaded from www.nrcresearchpress.com by 210.87.254.40 on 09/05/12
For personal use only.

In an attempt to find some probable explanation for the discrepancy between the present results and those reported earlier (4), degradations of C^{14}-labeled ethylbenzene and styrene by various methods of oxidation were investigated. 2-Phenylethyl-1-C^{14} bromide was converted to the Grignard reagent and then treated with water to give ethylbenzene-β-C^{14}, which was oxidized by concentrated nitric acid to practically inactive *p*-nitrobenzoic acid, thus confirming the finding of Roberts, Ropp, and Neville (5). The results from the oxidation of styrene-β-C^{14}* are given in Table II. It can be seen that oxidation with alkaline potassium permanganate or with potassium dichromate in 38% sulphuric acid produced inactive benzoic acid indicating no rearrangement. On the other hand, oxidation with concentrated nitric acid resulted in *p*-nitrobenzoic acid containing about 3–4% of the original styrene activity. These observations suggest that concentrated nitric acid is not the proper reagent for the degradation of C^{14}-labeled styrene.

Smith and Anderson also used concentrated nitric acid to oxidize the styrene regenerated from styrene dibromide. In order to ascertain whether the regeneration procedure will affect the extent of rearrangement, labeled styrene dibromide, prepared from styrene-β-C^{14} and bromine, was refluxed with sodium iodide in acetone for 0.5, 1.5, or 4.0 hours and the resulting material was oxidized. While the use of alkaline permanganate again gave inactive benzoic acid, oxidation of the regenerated material with concentrated nitric acid showed rearrangements varying between 5.7% and 37.8%. The results, also included in Table II, clearly indicate that the shorter the time of refluxing of the dibromide with sodium iodide in acetone, the greater will be the extent of rearrangement as measured by the activity of the *p*-nitrobenzoic acid. Apparently, nitric acid oxidation of incompletely regenerated styrene resulted in further rearrangements which probably directly involved styrene dibromide. An attempt to oxidize pure styrene dibromide with concentrated nitric acid gave a very impure product. Consequently, possible rearrangements in the oxidation of labeled styrene dibromide alone were not investigated.

The rearrangements observed in these nitric acid oxidations, which eventually led to radioactive *p*-nitrobenzoic acid, must involve an overall 1,2-shift of the phenyl group of styrene. A question that arises is whether the *p*-nitro group is introduced before or after the phenyl shift. Starting with 2-phenylethyl-1-C^{14} bromide, nitration (11) gave 2-*p*-nitrophenylethyl-1-C^{14} bromide which was treated with triethanolamine (12) to give *p*-nitrostyrene-β-C^{14}. Oxidation of this compound with alkaline permanganate or with concentrated nitric acid caused no rearrangement (Table II). Conversion of *p*-nitrostyrene-β-C^{14} to the corresponding dibromide followed by refluxing with sodium iodide in acetone for 0.5 hour gave regenerated materials which on nitric acid oxidation showed only very small amounts of rearrangement (Table II). These findings indicate that in the nitric acid oxidation of styrene-β-C^{14}, the fraction of the reaction that is accompanied by rearrangement likely involved nitration after the 1,2-phenyl shift. This is in accord with expectation as nucleophilic migration of the *p*-nitrophenyl group is much less favorable than phenyl migration (13).

While the mechanistic paths responsible for the rearrangements in the nitric acid oxidation of pure styrene or incompletely regenerated styrene are not clear, the observed results suggest that the rearrangement reported by Smith and Anderson (4) for the reaction of 2-phenylethyl-1-C^{14} bromide with magnesium and cobaltous bromide in refluxing ether could be related to their method of degradation of the products. By the nitric acid oxidation of regenerated styrene, with the reaction time in the regeneration process unspecified, Smith and Anderson reported a 20.6% rearrangement, which is well within

**Supplied by the New England Nuclear Corp., Boston, Mass.*

Can. J. Chem. Downloaded from www.nrcresearchpress.com by 210.87.254.40 on 09/05/12
For personal use only.

TABLE II

Data from oxidation of styrene-β-C^{14} or p-nitrostyrene-β-C^{14}

Material oxidized	Reagent	Activity (mμc/mmole)				% rearrangement	
		Parent compound*		Oxidation product†			
		Run 1	Run 2	Run 1	Run 2	Run 1	Run 2
$C_6H_5CHC^{14}H_2$	$KMNO_4$–Na_2CO_3	1280	1280	0±0.07	0±0.07	0.0	0.0
"	$K_2Cr_2O_7$–38% H_2SO_4	1280	1280	0±0.07	0±0.07	0.0	0.0
"	Conc. HNO_3	1280	1280	34.0	55.0 (49.6)‡	2.7	4.3 (3.9)‡
p-$NO_2C_6H_4CHC^{14}H_2$	$KMNO_4$–Na_2CO_3	98.2	98.2	0±0.07	0±0.07	0.0	0.0
"	Conc. HNO_3	98.2	98.2	0±0.07	0±0.07	0.0	0.0
Regenerated styrene (4 hr reaction time)	$KMnO_4$–Na_2CO_3	1280	1280	0±0.07	0±0.07	0.0	0.0
"	Conc. HNO_3	1280		72.8		5.7	
Regenerated styrene (1.5 hr reaction time)	Conc. HNO_3	723§		78.7		10.9	
Regenerated styrene (0.5 hr reaction time)	Conc. HNO_3	67.7§	67.7§	25.6‖	21.7‖	37.8	32.0
Regenerated p-nitrostyrene (0.5 hr reaction time)	Conc. HNO_3	98.2	98.2	0.3	1.3	0.3	1.3

*Styrene-β-C^{14} or p-nitrostyrene-β-C^{14}.
†Benzoic acid or p-nitrobenzoic.
‡From mother liquor after fractional crystallization of p-nitrobenzoic acid, presumably containing a high proportion of o-nitrobenzoic acid.
§Assayed as styrene dibromide.
‖Not as pure as other p-nitrobenzoic acid samples because of difficulties in recrystallization (see experimental part).

the range of rearrangements presently observed for such an oxidation of incompletely regenerated styrene. It is, however, not possible to rationalize the claim of these workers (4) that after hydrogenation of the mixed products to ethylbenzene, nitric acid oxidation gave 18.9% rearrangement.

EXPERIMENTAL

Reaction of 2-Phenylethyl-1-C^{14} Bromide

To a stirred mixture of 1.7 g of magnesium and 20 ml of anhydrous ether under reflux, a few drops of a solution of 10.0 g of 2-phenylethyl-1-C^{14} bromide in 90 ml of anhydrous ether were added. After the start of the typical Grignard reaction, an additional 250 ml of anhydrous ether and 14.5 g of anhydrous cobaltous bromide were introduced into the reaction vessel. Dropwise addition of the 2-phenylethyl-1-C^{14} bromide solution was then continued while the mixture was maintained at a gentle reflux by heating. When the addition of the bromide solution was completed, the mixture was refluxed overnight and then hydrolyzed with dilute hydrochloric acid. The ether layer was separated, washed with water, and dried over anhydrous magnesium sulphate. Fractionation through a 20-inch Dufton column gave, for duplicate runs, 3.7 g (65%) and 3.3 g (58%) of monomeric products boiling between 45–55° C at 20 mm. Vapor phase chromatographic analysis (2) showed the product mixtures from the two runs to consist of 65% ethylbenzene, 35% styrene and 62% ethylbenzene, 38% styrene, respectively.

In another trial using inactive 2-phenylethyl bromide, the reaction was carried out in exactly the same way with the exception that at the end of the reaction, Dry Ice was introduced into the reaction mixture before the addition of dilute hydrochloric acid. The resulting ether layer was washed with diluted sodium hydroxide solution besides water, and then worked up as before. Monomeric products, b.p. 45–55° C at 20 mm, were obtained in 63% yield (3.6 g) which consisted of 59% ethylbenzene and 41% styrene according to v.p.c. analyses. No 3-phenylpropionic acid could be isolated from the sodium hydroxide washings.

Treatment of the Active Monomeric Products

A portion (0.7 g) of the monomeric product mixture from each of the two active runs above was hydrogenated in 50 ml of ethyl acetate using platinum oxide as catalyst. The hydrogen absorbed corresponded to 97% of theoretical and the resulting material was shown by v.p.c. to contain ethylbenzene, but no styrene. After removal of the catalyst and solvent, the residue was oxidized with alkaline permanganate.

To the remainder of each monomeric product mixture, a solution of bromine in chloroform was added dropwise, with stirring. When a slight bromine color persisted, the solvent was distilled off through a small helix-packed column and the residue distilled under reduced pressure. The distillate boiled at 45° C at 20 mm and was identified as ethylbenzene by v.p.c. This fraction was also oxidized with alkaline permanganate.

After the distillation of the ethylbenzene, the residual styrene dibromide solidified on cooling. Recrystallized from pentane, it melted at 73° C (lit. (4) m.p. 73–74° C). About 1.5 g of this dibromide and 50 ml of a saturated solution of sodium iodide in acetone were refluxed with stirring for 5 hours. The resulting material was worked up to give regenerated styrene as described by Smith and Anderson (4). This regenerated styrene was also oxidized by alkaline permanganate.

Permanganate Oxidation

Ethylbenzene was oxidized to benzoic acid with potassium permanganate in the presence of sodium hydroxide according to the procedure previously used for the oxidation of 2-phenylethylamine (14). For the oxidation of styrene-β-C^{14}, *p*-nitrostyrene-β-C^{14}, or regenerated styrene, sodium carbonate was used instead of sodium hydroxide. In a typical run, a mixture of 0.8 g of styrene-β-C^{14}, 4.5 g of potassium permanganate and 1.0 g of sodium carbonate in 50 ml of water was heated under reflux for 3 hours. The resulting material was worked up to give benzoic acid, m.p. 121° C, as previously described (14). Similarly, *p*-nitrobenzoic acid, m.p. 240° C, was obtained from *p*-nitrostyrene-β-C^{14}.

Dichromate Oxidation

To a cooled solution of 4.0 g of potassium dichromate in 25 ml of 38% sulphuric acid was added 0.5 g of styrene-β-C^{14}. The mixture was heated under reflux, and after the initial vigorous reaction had subsided, it was refluxed for 1 hour. On cooling, about 0.5 g of product crystallized. The product was collected by filtration, redissolved in sodium carbonate solution, washed with chloroform, reprecipitated by acidification, and then recrystallized and sublimed to give benzoic acid, m.p. 121° C.

Nitric Acid Oxidation

A mixture of 1.5 g of styrene-β-C^{14} and 9.0 ml of concentrated nitric acid was heated gradually under reflux in an oil bath. After an initial vigorous reaction accompanied by the evolution of copious amounts of fumes, the mixture was maintained at about 100° C for 30 hours. On cooling and with the addition of water, about 2.0 g of crude product was precipitated. This product was taken up in sodium carbonate solution, filtered, repeatedly washed with carbon tetrachloride, and then reprecipitated by acidification. The desired product was then recovered by fractional crystallization. After about 10 recrystallizations from aqueous

Can. J. Chem. Downloaded from www.nrcresearchpress.com by 210.87.254.40 on 09/05/12
For personal use only.

ethanol, pure *p*-nitrobenzoic acid, m.p. 240–241° C (lit. (15) m.p. 241° C) was obtained. In one of the runs, all the filtrates from the recrystallizations were combined and evaporated giving a residue which, after sublimation under high vacuum, melted at 113–118° C. Presumably, this crude material contained a high proportion of *o*-nitrobenzoic acid (lit. (15) m.p. of *o*-nitrobenzoic, 146° C).

p-Nitrostyrene-β-C^{14} was oxidized by concentrated nitric acid in a similar manner. The *p*-nitrobenzoic acid, m.p. 240–241° C, was recrystallized from a mixture of ethyl acetate and pentane. It was not necessary to subject the product to extensive fractional crystallization.

Regeneration of Styrene or p-Nitrostyrene from the Dibromides

Styrene-β-C^{14} or *p*-nitrostyrene-β-C^{14} was treated with the calculated amount of bromine. Styrene dibromide, recrystallized from pentane, melted at 73° C, and *p*-nitrostyrene dibromide, recrystallized from ether-pentane, melted at 74° C (lit. (16) m.p. 72–73° C).

A mixture of 4.0 g of the labelled styrene dibromide and 100 ml of a saturated solution of sodium iodide in acetone, while stirred with a magnetic stirrer, was refluxed for 0.5, 1.5, or 4.0 hours. The resulting material was decolorized with sodium bisulphite solution and then extracted with ether. The extract was washed with water, dried over anhydrous magnesium sulphate, and then the ether was removed by distillation through a helix-packed column. The residual material was used for oxidation.

A similar reaction was carried out with *p*-nitrostyrene dibromide using a refluxing time of only 0.5 hour.

Oxidation of Regenerated Materials

The regenerated materials obtained above were oxidized in alkaline permanganate or in concentrated nitric acid in the same manner as described earlier. However, in the case of the nitric acid oxidation of regenerated styrene obtained after 0.5 hour of refluxing, purification of the *p*-nitrobenzoic acid proved to be more difficult and the product, after repeated recrystallizations, melted over the range of 210–220° C. In an inactive trial, oxidation of pure styrene dibromide with concentrated nitric acid gave a product melting over the range of 130–160° C.

Radioactivity Assays

Samples weighing 10–20 mg were dissolved in toluene containing the appropriate scintillators and counted in a liquid scintillation counter as previously described (17). In the case of *p*-nitrobenzoic acid, its low solubility in toluene necessitated the use of 20% ethanol–80% toluene as solvent. Absolute counting efficiencies were determined using standards containing known amounts of C^{14}. Considerable quenching was observed in the counting of *p*-nitrostyrene and *p*-nitrobenzoic acid. In these cases, corrections for quenching were made with the aid of known quantities of toluene-C^{14} as internal standard.

ADDENDUM

Having learned of our results, Dr. W. B. Smith has repeated the reaction of 2-phenylethyl-1-C^{14} bromide with magnesium and cobaltous bromide and obtained results which are in agreement with ours regarding the lack of rearrangement in this system.

ACKNOWLEDGMENT

The financial support given by the National Research Council of Canada is gratefully acknowledged.

REFERENCES

1. C. C. Lee, D. G. Lee, and I. S. Bhardwaj. Radiation Res. **17**, 536 (1962).
2. D. P. Thornhill and C. C. Lee. Can. J. Chem. **41**, 000 (1963).
3. L. H. Slaugh. J. Am. Chem. Soc. **81**, 2262 (1959).
4. W. B. Smith and J. D. Anderson. J. Am. Chem. Soc. **82**, 656 (1960).
5. R. M. Roberts, G. A. Ropp, and O. K. Neville. J. Am. Chem. Soc. **77**, 1764 (1955).
6. H. Finkelstein. Ber. **43**, 1528 (1910).
7. C. Walling. Free radicals in solution. John Wiley and Sons, Inc., New York. 1957. pp. 588–589.
8. W. B. Smith. J. Org. Chem. **24**, 703 (1959).
9. L. H. Slaugh. J. Am. Chem. Soc. **83**, 2734 (1961).
10. F. H. Seubold, Jr. J. Am. Chem. Soc. **75**, 2532 (1953).
11. R. H. Wiley and W. A. Trinler. J. Polymer Sci. **12**, 113 (1960).
12. R. W. Strassburg, R. A. Gregg, and C. Walling. J. Am. Chem. Soc. **69**, 2141 (1947).
13. J. D. Roberts and C. M. Regan. J. Am. Chem. Soc. **75**, 2069 (1953).
14. C. C. Lee and J. W. T. Spinks. Can. J. Chem. **31**, 761 (1953).
15. R. L. Shriner and R. C. Fuson. The systematic identification of organic compounds. 3rd ed. John Wiley and Sons, Inc., New York. 1948. pp. 224–225.
16. A. Basler. Ber. **16**, 3001 (1883).
17. C. C. Lee, D. Newman, and D. P. Thornhill. Can. J. Chem. **41**, 620 (1963).

Can. J. Chem. Downloaded from www.nrcresearchpress.com by 210.87.254.40 on 09/05/12
For personal use only.

THE EFFECT OF TIME AND TEMPERATURE ON THE HYDROGENATION OF ASPEN LIGNIN

J. M. Pepper and Warren Steck
Department of Chemistry, University of Saskatchewan, Saskatoon, Saskatchewan
Received July 15, 1963

ABSTRACT

A study has been made of the hydrogenation of preextracted aspen sapwood meal under conditions whereby the lignin is degraded to identifiable products. By gas liquid chromatography, guaiacol, 4-methylguaiacol, 4-ethylguaiacol, 4-*n*-propylguaiacol, dihydroconiferyl alcohol, syringol, 4-methylsyringol, 4-ethylsyringol, 4-*n*-propylsyringol, and dihydrosinapyl alcohol were separated and identified.

The relative abundance of these 10 compounds was determined in the chloroform-soluble product after hydrogenation using a dioxane–water (1:1) solvent medium, Raney nickel catalyst, an initial hydrogen pressure of 500 p.s.i. and temperatures of 150°, 165°, 185°, 195°, 210°, and 220° for a reaction time of 5 hours and a temperature of 195° for times of 0, 1.3, 5.0, and 24 hours. The best yield (52.2% of the Klason lignin) of such phenolic derivatives was obtained at a reaction temperature of 195° for 5 hours.

The significance of the observed variation in the yields of these compounds with time and temperature and the relationship of these yields to the structure of lignin is discussed. Evidence is presented in support of both γ-alkyl ether and β-aryl ether linkages in the lignin substance.

INTRODUCTION

In 1938, Harris, D'Ianni, and Adkins (1) reported a successful catalytic hydrogenolysis of an isolated aspen lignin and isolated and identified lignin derivatives of a cyclohexylpropyl nature. Since that time this technique has been applied to the study of various wood and straw meals and isolated lignins, under a variety of conditions involving different catalysts, solvents, times, temperatures, and initial pressures of hydrogen (2, 3). A significant contribution was made in 1948 by Brewer, Cooke, and Hibbert (4), who reported the degradation of maple wood lignin under much milder conditions of hydrogenation than those used by earlier workers and obtained phenylpropyl lignin derivatives, thus providing direct evidence for the aromatic nature of the lignin substance. Subsequently, other workers (5–9) have extended these studies to other lignified materials and various isolated lignins and have thereby added to the variety of aromatic compounds that have been isolated and identified. Of particular interest is the recent work of Coscia, Schubert, and Nord (10) and of Olcay (11), who obtained aromatic lignin derivatives by the hydrogenation of the milled wood lignins from birch, oak, pine, and spruce under conditions which, when applied earlier to other isolated lignins, had given rise to cyclohexyl derivatives. These workers introduced the use of gas–liquid chromatography for the separation and quantitative estimation of the lignin derivatives.

Earlier, in these laboratories, a study had been made of the conditions affecting the isolation, as a chloroform-soluble fraction, of the lignin derivatives resulting from the catalytic hydrogenation of aspen wood meal (8). It was thus found that at temperatures of 170°–180° for a reaction period of 3 hours, using a dioxane–water (1:1) medium, Raney nickel catalyst, and an initial hydrogen pressure of 500 p.s.i., essentially all the lignin was removed from the wood and recovered as a choloroform-soluble fraction. It was of interest, therefore, to apply the technique of gas–liquid chromatography to a detailed study of the products of such a hydrogenation of aspen wood meal and to compare the results with those reported by the earlier workers (10, 11), who used different lignins, copper chromite catalyst, and much higher temperatures of around 225°.

Can. J. Chem. Downloaded from www.nrcresearchpress.com by 210.87.254.105 on 09/05/12
For personal use only.

To this end extractive-free aspen wood meal was subjected to 5 hours contact with dioxane–water (1:1), Raney nickel, and hydrogen, at a temperature of 195±3°. The resulting bomb contents were separated as described in the Experimental section to yield a chloroform-soluble fraction containing the lignin degradation products. By gas–liquid chromatography the major part of this fraction was separated and the identity and relative abundance of the compound represented by each peak was determined. A 10% Apiezon N on Fluoropak column, of a type that had been shown of value for the separation of phenolic lignin oxidation products (12) was found to be equally useful for the separation of phenolic hydrogenation products. All compounds represented by peaks on the chromatogram were identified by comparison of their relative retention times with those obtained for pure reference samples. For the major components, the products were collected and the identity confirmed by infrared and refractive index measurements. Neither 2-(4-hydroxy-3-methoxyphenyl)ethanol nor 2-(4-hydroxy-3,5-dimethoxyphenyl)ethanol, which had been reported as lignin hydrogenation products (9), was found. The relative abundance data were obtained by the measurement of peak areas. The nature and yield of the products so obtained are given in Table I under the column headed 195°.

The significantly large percentage of original wood lignin that could thus be recovered as small molecular weight degradation products capable of being analyzed by gas–liquid chromatography, prompted a more detailed study of this reaction with a view to obtaining maximum yields of structurally important products. To approach this goal two of the important variables were studied, namely, temperature and time of reaction. In the first instance, similar hydrogenations to that described at 195° were effected at 150°, 165°, 185°, 210°, and 220°, and the respective chloroform-soluble fractions studied as before. These results are also found in Table I. From these data it would appear that the initially chosen temperature of 195° was optimum. No appreciable increase in total yield occurs above this temperature and, indeed, at 210°, the important arylpropanols are being further reduced and cracked and at 220° aliphatic ring-saturated compounds began to appear. For these reasons a temperature of 195° was chosen for a subsequent study of the effect of a variation in the time of reaction. A series of hydrogenations was made under conditions similar to those discussed earlier but for times of 0, 1.3, 3.0, and 24 hours. Reaction times are defined as the time at the stated temperature and are exclusive of heating and cooling times which were approximately 1.5 and 6 hours respectively. The resulting chloroform-soluble fractions were treated as before and the results are given in Table II.

DISCUSSION OF RESULTS

This study has again demonstrated the effectiveness of the hydrogenation technique as a prime method of lignin isolation and subsequent degradation to readily identifiable phenolic products. The application of gas–liquid chromatography has made it possible to characterize derivatives which heretofore have been unnoticed, and to do so in such a way that the relative abundance of each product had real meaning. If, as a criterion of value to the study of lignin structure, the maximum yield of oxygen-bearing, phenylpropanoid derivatives be chosen, then the conditions for such a study have been optimized for a reaction temperature of 195° for a period of 5 hours. Under these conditions, 52.2% of the original lignin in the wood (Klason lignin) has been recovered in the form of identifiable derivatives having either a 4-hydroxy-3-methoxyphenyl (type A) or a 4-hydroxy-3,5-dimethoxyphenyl (type B) nucleus. This represents a marked increase in the amount of such aromatic lignin derivatives over that obtained by earlier hydrogenation studies and is now comparable with the recovery of phenolic products obtained by means of oxidation.

Can. J. Chem. Downloaded from www.nrcresearchpress.com by 210.87.254.105 on 09/05/12
For personal use only.

Can. J. Chem. Downloaded from www.nrcresearchpress.com by 210.87.254.105 on 09/05/12
For personal use only.

TABLE I

Effect of temperature on the hydrogenation products of aspen lignin*

			Abundance of chromatographable product†									
			165°		185°		195°		210°		220°	
Compound	R.R.T.	150°§	Yield‡, %	moles ×10⁴	Yield, %	moles ×10⁴	Yield, %	moles ×10⁴	Yield, %	moles ×10⁴	Yield, %	moles ×10⁴
Guaiacol	5.1		Trace	Trace	Trace	Trace	2.2	8.1	Trace	Trace	—	—
4-Methylguaiacol	7.3		—	—	—	—	—	—	—	—	—	—
4-Ethylguaiacol	11		—	—	0.8	2.1	1.9	5.4	0.8	2.2	2.2	7.6
4-*n*-Propylguaiacol	16		2.1	1.8	2.0	4.8	0.6	1.8	7.9	19.8	9.4	29.7
Dihydroconiferyl Alcohol	44		28.4	22.0	26.7	59.3	19.8	59.5	15.9	36.2	11.2	32.4
Total			30.5	23.8	29.5	66.2	24.5	74.8	24.6	58.2	22.8	69.7
Syringol	14		—	—	Trace	Trace	0.7	2.2	Trace	Trace	—	—
4-Methylsyringol	20		—	—	—	—	3.5	9.5	0.5	1.2	1.7	5.4
4-Ethylsyringol	25		—	—	0.9	2.0	7.1	18.0	0.8	1.8	3.7	10.7
4-*n*-Propylsyringol	35		13.8	10.2	13.7	38.2	5.6	6.5	45.5	96.0	48.2	129.0
Dihydrosinapyl alcohol	100‖		55.3	37.2	55.9	106.0	59.4	127.5	28.1	54.7	21.5	53.2
Total			69.1	47.4	70.5	146.2	76.3	163.7	74.9	153.7	75.1	198.3
% of Klason lignin identified		0	16.0		45.5		52.2		46.5		59.1	
% of Klason lignin as $CHCl_3$-soluble fraction		0	18.4		52.8		61.0		72.1		79.3	

*Aspen wood meal (50 g), dioxane–water (1:1) (400 ml), Raney nickel (10 g), initial hydrogen pressure (500 p.s.i.), time (5 hours).
†6 foot, 10% Apiezon N on Fluoropak column. At 150°, no $CHCl_3$-chromatographable product.
‡Based on calculated weight of original Klason lignin. Used as standard to determine relative retention times (R.R.T.).
§No $CHCl_3$-soluble product.
‖Used as standard to determine relative retention times (R.R.T.).

Can. J. Chem. Downloaded from www.nrcresearchpress.com by 210.87.254.105 on 09/05/12
For personal use only.

TABLE II

Effect of time on the hydrogenation of aspen lignin*

Compound	Abundance of chromatographable product							
	0 hr†	1.3 hr		3.0 hr		5.0 hr		24.0 hr	
		Yield, %	moles×10^4	Yield, %	moles×10^4	Yield, %	moles×10^4	Yield, %	moles×10^4
Guaiacol		Trace	Trace	1.3	3.2	2.2	8.1	2.2	7.2
4-Methylguaiacol		—	—	—	—	—	—	0.4	1.3
4-Ethylguaiacol		—	—	—	—	1.9	5.4	0.9	2.2
4-*n*-Propylguaiacol		3.0	1.2	2.5	4.8	0.6	1.8	1.1	2.7
Dihydroconiferyl alcohol		27.5	6.0	28.8	52.2	19.8	59.5	15.7	35.0
Total		30.5	7.2	32.6	60.2	24.5	74.8	20.3	48.4
Syringol		—	—	—	—	0.7	2.2	0.8	2.3
4-Methylsyringol		—	—	—	—	3.5	9.5	9.8	23.8
4-Ethylsyringol		—	—	—	—	7.1	18.0	5.7	12.6
4-*n*-Propylsyringol		15.2	2.5	16.1	27.0	5.6	6.5	7.9	16.1
Dihydrosinapyl alcohol		54.3	8.5	51.3	79.6	59.4	127.5	55.3	107.0
Total		69.5	11.0	67.4	106.6	76.3	163.7	79.5	161.8
% of Klason lignin identified	0		4.0		37.0		52.2		46.8
% of Klason lignin as $CHCl_3$-soluble fraction	0		4.4		51.2		61.0		58.0

*Aspen wood meal (50 g), dioxane–water (1:1) (400 ml), Raney nickel (10 g), initial hydrogen pressure (500 p.s.i.), reaction temperature (195°).
†No $CHCl_3$-soluble product

Of significance, too, is the fact that the major portion of the chloroform-soluble products is capable of being separated by gas–liquid chromatography and that no unidentified peaks appear in the chromatograms. It would thus appear that for that fraction of the protolignin which is released and degraded by this catalytic hydrogenolysis, the cleavage process is quite selective and that the lignin substance itself is joined together in a uniform manner.

From the separate study involving the effect of temperature, some interesting observations may be made. If the chloroform-soluble faction be accepted as a crude lignin fraction (carbohydrates being chloroform-insoluble), than a rapid release of lignin occurs with increasing lower temperatures but levels off to about an 80% recovery at the higher temperatures. Similar results have been reported as a result of a study of the liberation of lignin by an acid-catalyzed solvolysis (13) and the suggestion has been made that the more easily isolated fraction is that associated with the middle lamella whilst the lignin in the cell walls requires more drastic conditions for isolation and degradation to chloroform-soluble fragments. The extraction of the lignin was reflected in the recovery of the residual wood meal which was essentially complete at 150°, dropped steadily through 195°, at which temperature the residue was pulpy and gave a negative Maule reaction. At 210° only a fraction of the meal remained and at 220° the entire sample was solubilized.

The nature and relative abundance of the lignin degradation products have structural significance. No fragments were identified that had other than the type A or type B nucleus. Only at temperatures greater than 150° was there any significant degradation, and initially those compounds with a propanol side chain were in great excess. With increasing temperature, the decrease in the yield of the phenylpropanol derivatives, paralleled as it was for both types of nuclei, was accompanied by an increase in products of a higher state of reduction and even products resulting from a carbon–carbon fission. These secondary effects were checked by studying a similar hydrogenolysis of pure samples of each of dihydroconiferyl alcohol and of dihydrosinapyl alcohol. In each case there was unchanged starting material, but the former gave rise to all of 4-*n*-propylguaiacol, 4-ethylguaiacol, and guaiacol itself; whilst the latter yielded the analogous 4-*n*-propyl-, 4-ethyl-, and 4-methylsyringol and syringol as well as small amounts of the corresponding guaiacol derivatives. This observed conversion of syringol and guaiacol derivatives, by the loss of methoxyl, must not be overlooked in assigning any significance to the relative abundance of each of these types of lignin derivatives.

The molar abundance data of Table I may best be interpreted on the basis of two rather independent lignin substances, one a polymer of essentially type A units and the other of essentially type B units but in each case involving a similar mode of linkage which may be cleaved by catalytic hydrogenolysis. The greater abundance of the syringyl (type B) compounds over the guaiacyl (type A) analogues by a factor of at least two may actually be indicative of the amounts of each such nucleus in the lignin or it may reflect some more basic difference in the ease of liberation of such units. The results also indicate that the increasing molar ratio of type B to type A compounds with increasing temperature is really due to a relative decrease in the latter type since the molar abundance of the former remains more constant. This may result from some as yet unproved condensation reaction involving the free 5-position of type A compounds but for which a similar reaction is impossible for type B compounds.

From a consideration of the data given in Table II many similar conclusions may be drawn regarding the effect of increasing the reaction time on the nature of the products

Can. J. Chem. Downloaded from www.nrcresearchpress.com by 210.87.254.105 on 09/05/12
For personal use only.

of hydrogenation of aspen lignin. The very rapid increase in the yield of chloroform-soluble material from the 1.3-hour to the 3-hour reaction time may be due to the autocatalytic effect of the released phenolic compounds. It is well known that the addition of even traces of mineral or organic acids aid markedly in any lignin isolation procedure (13) With increasing time of reaction there is a similar total increase in aromatic derivatives but less secondary reduction or cracking than in the case of those runs with temperatures over 195°. Again the increasing molar ratio of type B over type A compounds, with increasing time, is a result of a relative decrease in compounds of the latter type since there is no significant decrease in the yield of compounds of the former type.

It may also be of some significance that in none of the hydrogenations was any direct evidence found for the liberation of lignin fragments having molecular weights lying in the range between the monomers and the polymers. As earlier stated, the major part of the chloroform-soluble fraction was chromatographable and was shown to be composed of low molecular weight (monomeric) compounds. The chloroform-soluble portion of one run was, therefore, investigated to determine if dimeric or slightly higher molecular weight lignin fragments might be found in the non-chromatographable part. After removal of the chloroform and precipitation into water, a cream-colored solid was collected and dried over P_2O_5. This material analyzed for C, 63.23; H, 6.59; ash, 0.81; methoxyl, 21.8%, had an average molecular weight above 2480, and gave an infrared spectrum typical of that of an isolated dioxane aspen lignin (13). Similarly, the chloroform-insoluble lignins were examined for the presence of any medium molecular weight substances. From the 1.3-hour run, an ash-free sample analyzed for C, 66.5; H, 6.53; OCH_3, 22.0%, and two similarly isolated fractions had average molecular weights of 6230 and 6800. Rehydrogenation of this polymeric lignin for a further 5 hours at 195° degraded it, in part, to the same kind of monomeric products given in Table I and having no significant variation in their relative abundance as that obtained from other runs conducted for 5 hours.

Finally some comments may be made regarding the nature of aspen protolignin and its mode of isolation by means of the catalytic hydrogenation technique. For the isolation, four distinct phases may be involved: *primary hydrogenolysis*, by which the lignin polymers are freed from other plant constituents; *secondary hydrogenolysis*, by which partial degradation occurs to produce phenylpropanoid derivatives; *cracking*, by which carbon–carbon cleavage occurs with loss of hydroxyl and even methoxyl groups; and finally *ring saturation* to produce cyclohexyl derivatives. An attempt has been made in this investigation to find the conditions which minimize any major reaction beyond the secondary hydrogenolysis stage. During the early stages of the reaction there was some evidence for the simultaneous release of a carbohydrate fraction along with the lignin. From the chloroform-insoluble fraction of the runs conducted for 0, 1.3, and 3.0 hours, it was possible, by an extraction with acetic acid to remove soluble lignin, to isolate a substance which analyzed closely for $(C_6H_{10}O_5)_x$ and which had an average molecular weight of 3860 and 1350 for the 0- and 1.3-hour runs respectively. The parallel increase in the amount of this fraction with the increase in the amount of chloroform-soluble lignin derivatives supports the concept of a lignin-carbohydrate linked substance. Indeed under conditions of low temperatures or short reaction times, relatively stable emulsions were obtained during the chloroform extraction process, which may be the result of the presence of a lignin-carbohydrate substance acting as a surface active agent.

The ready release of arylpropanols, by a hydrogenolysis reaction and in yields representing over 40% of the original lignin, can only be interpreted to mean that a major portion of the lignin has a γ-oxygen function, most likely as either a free primary alcohol

Can. J. Chem. Downloaded from www.nrcresearchpress.com by 210.87.254.105 on 09/05/12
For personal use only.

group or as an ether. However, since aryl alkyl ethers are known to be cleaved, under similar conditions, with aryl retention of the oxygen as a phenolic fragment (14), it would appear that if an ether linkage be present it is of the dialkyl type. The absence of any products bearing α- or β-oxygen functions does not exclude the possibility that such do occur in the lignin. Indeed, the β-aryl ether type of linkage, for which much evidence exists, would, as indicated above, cleave to release the phenolic portion and the β-methylenic group.

Mention has already been made of the absence of lignin derivatives with molecular weights between the isolated monomeric and polymeric substances. Two possible explanations are herein presented, but with no experimental support. It may be that the protolignin consists of a basic polymeric core structure attached to which are much smaller fragments which represent that part of the lignin substances which is separated from the core and degraded into identifiable products by processes of hydrogenolysis, oxidation, or acid-catalyzed hydrolysis. On the other hand, the release of the stabilized monomeric units may result by a process which is in competition with another in which reactive lignin precursors in the wood readily polymerize. The yields resulting from each competitive process would be dependent on the conditions of the reaction.

EXPERIMENTAL

Aspen sapwood (*Populus tremuloides* Michx.) was ground to 20 mesh in a Wiley mill, extracted 48 hours with ethanol–benzene (1:1), and air-dried. Anal: Klason lignin, 17.7%; moisture, 6.1%.

Raney nickel catalyst was prepared according to Pavlic and Adkins (14) with the exception that the washing under a hydrogen atmosphere was deleted. The catalyst was stored under cold dioxane. The dioxane was purified according to Fieser (15).

General Reaction Procedure

Preextracted, air-dried aspen wood meal (50 g), Raney nickel (10 g), and 50% aqueous dioxane (400 ml) were stirred together in a 1410-ml capacity Aminco hydrogenator. The sealed bomb was flushed twice with hydrogen and then filled with hydrogen to 500 p.s.i.g. The temperature was raised (about 120° per hour) and controlled automatically at the desired value for the required time. During this heating period the bomb was rocked continuously but allowed to cool overnight without rocking.

The bomb contents were suction-filtered. The residual wood meal and nickel were washed with 90% aqueous dioxane until the washings were colorless. These washings and the original filtrate were combined, gravity-filtered (if cloudy), concentrated under reduced pressure just beyond the point at which sludge began to form, then extracted with chloroform (3×80 ml or until colorless).

The chloroform solution was back-extracted with 100 ml water, dried over anhydrous sodium sulphate, filtered, and concentrated free of chloroform below 50° at reduced pressure. The resulting reddish oil was termed the chloroform extract; it contained residual dioxane besides lignin degradation products.

The residual nickel and wood meal from the initial filtration were finally soaked in warm water, refiltered, and dried overnight at 100°. The weight of cooled material was recorded and, if desired, a Maule test was performed.

Gas–Liquid Chromatographic Analysis of the Chloroform Extracts

An Aerograph chromatograph, Model A–90P, was used. All separations were made using a 6-foot, 1/4 in. O.D. copper column packed with 10% Apiezon N grease on Fluoropak at 205° (injector and detector at 232°), the helium flow rate being 36 ml/min at 50 p.s.i.g. with a filament current of 200 milliamperes.

Analytical Procedure

The general method consisted of the injection of the crude chloroform-soluble fraction with subsequent progressive calculated corrections for unidentified and for non-lignin material in that fraction.

In preliminary work a large forepeak was always encountered. The collection and determination of the boiling point (100°/730 mm), the refractive index (1.4180 at 25°) and the infrared spectrum indicated this peak to be dioxane (b.p. 101°/760 mm; n_D^{25} 1.4178).

The Aerograph was calibrated as follows for the subsequent determination of dioxane. Measured volumes, of between 0.5 and 7.0 microliters, of dioxane were injected into the column under the same conditions as were used for the analysis of the lignin products, and the height was recorded in each case. A curve of the peak height versus the volume of dioxane injected was drawn so that in the lignin hydrogenation runs the measurement of forepeak height, from a measured volume of chloroform extract, would permit direct reading of the volume of dioxane present in the extract. This volume of dioxane was then subtracted from the

Can. J. Chem. Downloaded from www.nrcresearchpress.com by 210.87.254.105 on 09/05/12
For personal use only.

measured volume of the injected chloroform extract to give the actual volume of lignin products that had been injected. Only a certain portion of these products passed through the column. To discover what fraction of the injected lignin was represented by this portion, a second calibration was made.

This was done as for dioxane using a representative phenol (4-*n*-propylguaiacol) but for which peak area rather than peak height was plotted against the injected volume. This was a straight line plot, the slope of which represented the peak area to be expected from each microliter of chromatographable products. The total peak area from all degradation products in an analysis was measured. The fraction of the original solvent-free chloroform extract detected in the chromatogram was calculated as the found total peak area divided by the theoretical peak area as read from the 4-*n*-propylguaiacol calibration curve.

Finally, by knowing the volume and weight of the whole chloroform-soluble fraction it was possible to apply the gas–liquid chromatography results to find the amount of dioxane in the extract, the percentage of the Klason lignin isolated as chloroform-soluble material, and the percentage of the Klason lignin identified as monophenols.

Peak Identification

Initially samples of the four compounds represented by the major peaks were collected. The infrared spectra, refractive indices, and retention times were compared with those of authentic samples of probable hydrogenation monomers. In this way the presence was established of 4-*n*-propylguaiacol, 4-*n*-propylsyringol, dihydroconiferyl alcohol, and dihydrosinapyl alcohol. Other components were identified by matching retention times and relative retention times with those of authentic reference compounds.

The correctness of the assignments was demonstrated when a synthetic mixture and a hydrogenated lignin sample gave traces superposable with regard to peak positions when run using a 3% SE-30 on firebrick column at 190°.

Preparation of Reference Compounds

All melting points are uncorrected.

Guaiacol, creosol, and syringol (2,6-dimethoxyphenol) were obtained commercially. Prior to use, the former two were redistilled and the last recrystallized from dilute ethanol.

4-Ethylguaiacol.—Acetoguaiacone was reduced in methanol using 10% palladium on charcoal and a trace of hydrochloric acid. The product distilled at 62–64°/0.4 mm.

4-n-Propylguaiacol.—Eugenol was hydrogenated for 1 hour at 150° in ethanol using Raney nickel catalyst. The product distilled at 245–246°/730 mm; reported, b.p. 246°/760 mm (16).

Dihydroconiferyl Alcohol.—The synthesis reported by Coscia, Schubert, and Nord (10) was modified as follows. Ferulic acid was prepared according to Brewer, Cooke, and Hibbert (4) and then converted to ethyl dihydroferulate before reduction with lithium aluminum hydride. This final reduction was effected in 83% yield by using an 18-hour reaction period. The final product distilled at 154–158°/0.2 mm.

4-Methylsyringol.—Syringaldehyde was reduced by the method of Coscia *et al.* (10). The final product distilled at 80–83°/0.16 mm.

4-Ethylsyringol.—The procedure reported by Arlt, Gross, and Schuerch (9) was used. The final product distilled at 85–88°/0.2 mm.

4-n-Propylsyringol.—The synthesis reported by Coscia *et al.* (10) was used. The final product distilled at 118–121°/0.3 mm.

Dihydrosinapyl Alcohol.—Syringaldehyde was converted to sinapic acid in 81% yield by the method of Vorsatz (17). The remainder of the synthesis was similar to that used for the preparation of dihydroconiferyl alcohol. The final product was distilled at 158–162°/0.5 mm.

4-(β-Hydroxyethyl)guaiacol.—2-(4-Hydroxy-3-methoxyphenyl) acetic acid was reduced with lithium aluminum hydride in tetrahydrofuran. A 20% yield of the alcohol was obtained, m.p. 40–42°.

4-(β-Hydroxyethyl)syringol.—A sample that had been prepared by Pepper and Hibbert (5) was available.

ACKNOWLEDGMENTS

The authors wish to thank the National Research Council for financial assistance and for the award of scholarships to one of them (W. S.). Grateful acknowledgment is made of the kindness of Mr. M. Mazurek, who performed the analyses.

REFERENCES

1. E. E. Harris, J. D'Ianni, and H. Adkins. J. Am. Chem Soc. **60**, 1467 (1938).
2. F. E. Brauns. The chemistry of lignin. Academic Press, Inc., New York, N.Y. 1952. Chap. XVIII.
3. F. E. Brauns and D. A. Brauns. The chemistry of lignin. Supplement Volume. Academic Press, Inc., New York, N.Y. 1960. Chap. XVIII.
4. C. P. Brewer, L. M. Cooke, and H. Hibbert. J. Am. Chem. Soc. **70**, 57 (1948).
5. J. M. Pepper and H. Hibbert. J. Am. Chem. Soc. **70**, 67 (1948).
6. E. E. Harris, J. F. Saeman, and C. B. Bergstrom. Ind. Eng. Chem. **41**, 2063 (1949).
7. J. M. Pepper, C. J. Brounstein, and D. A. Shearer. J. Am. Chem. Soc. **73**, 3316 (1951).

Can. J. Chem. Downloaded from www.nrcresearchpress.com by 210.87.254.105 on 09/05/12
For personal use only.

8. J. M. PEPPER and D. C. HAGERMAN. Can. J. Chem. **32**, 614 (1954).
9. H. G. ARLT, S. K. GROSS, and C. SCHUERCH. Tappi **41**, 64 (1958).
10. C. J. COSCIA, W. J. SCHUBERT, and F. F. NORD. J. Org. Chem. **26**, 5085 (1961).
11. A. OLCAY. J. Org. Chem. **27**, 1783 (1962).
12. J. M. PEPPER, M. MANOLOPOULO, and R. BURTON. Can. J. Chem. **40**, 1976 (1962).
13. J. M. PEPPER and M. SIDDIQUEULLAH. Can. J. Chem. **39**, 1454 (1961).
14. A. A. PAVLIC and H. ADKINS. J. Am. Chem. Soc. **68**, 1471 (1946).
15. L. F. FIESER. Experiments in organic chemistry. 3rd ed. D. C. Heath and Co., Boston. 1955.
16. V. IPATIEFF. Ber. **46**, 3591 (1913).
17. F. VORSATZ. J. Prakt. Chem. **145**, 265 (1936).

Can. J. Chem. Downloaded from www.nrcresearchpress.com by 210.87.254.105 on 09/05/12
For personal use only.

GAS–LIQUID CHROMATOGRAPHY OF TERPENES

PART IX. THE VOLATILE OIL OF THE LEAVES OF JUNIPERUS SABINA L.[1]

E. VON RUDLOFF

Prairie Regional Laboratory, National Research Council of Canada, Saskatoon, Saskatchewan

Received July 15, 1963

ABSTRACT

The chemical composition of the volatile oil of the leaves of local savin juniper and of commercial oil of savin was determined by an improved gas chromatographic technique. Both oils contain *d*-sabinyl acetate (38, 37.5%) and *d*-sabinene (30.5, 26%) as the major constituents. Smaller amounts of *d*-α-pinene, *d*-myrcene, *d*-limonene, γ-terpinene, *p*-cymene, *d*-isothujone, *d*-terpinen-4-ol, *d*-sabinol, *d*-citronellol, *d*-cadinene, and *l*-elemol were isolated. Trace amounts of α-thujene, camphene, α-terpinene, 1,8-cineole, terpinolene, thujone, geraniol, a cadinene isomer, and δ-cadinol were tentatively identified. A fraction having the typical pungent odor of juniper leaves was isolated, but it was found to consist mainly of the methyl ester of *d*-citronellic acid. Several unidentified oxygenated sesquiterpenes and a phenol ether were isolated in trace amounts.

Some phylogenetic relationships with other thujone-bearing oils analyzed in this series are discussed.

As part of a systematic study of phylogenetic relationships, the volatile oil of the leaves of *Juniperus sabina* L. and commercial oil of savin have been analyzed by means of the improved technique described in the previous paper of this series (1). Fromm (2) found the main constituent of this oil to be *d*-sabinyl acetate and Semmler (3) obtained *d*-sabinene from the hydrocarbon fraction. Other early reports (4) indicate that minor amounts of α-pinene, α-terpinene, *n*-decanal, dihydrocuminyl alcohol, citronellol, geraniol, and an aldehyde (cuminaldehyde ?) are present. More recently, the oil was examined by fractional distillation by Booth (5), who reported the presence of *d*-sabinene (20%), *d*-sabinyl acetate (40%), and minor constituents (40%), including α-pinene, myrcene, limonene, *p*-cymene, *cis*- and *trans*-thujones, sabinol, terpinen-4-ol, and carvacrol. Bruno (6) identified α-pinene, *d*-sabinene, limonene, and sabinyl acetate by gas–liquid chromatography (GLC).

In contrast, the improved technique used in this study revealed the presence of at least 37 components (see Fig. 1). The average composition, as determined on a variety of columns, is shown in Table I. Little qualitative and quantitative difference was found between the commercial oil and that obtained from local savin juniper plants, except that the sesquiterpene content of the latter was higher. The results obtained confirm that *d*-sabinyl acetate is the major constituent, although an almost equal amount of *d*-sabinene was recorded. Goryaev and Dzhalilov (7) found that the leaf oil of a central Asian savin juniper contained as much as 40% sabinene, which is considerably higher than found in European varieties. GLC analysis of the sabinene isolated in this study did not reveal the presence of any β-pinene, but trace amounts may be present. In the monoterpene hydrocarbon range (peaks 1 to 11) appreciable amounts (2 to 7%) of *d*-α-pinene, *d*-myrcene, *d*-limonene, and γ-terpinene (peaks 2, 5, 7, and 9) as well as smaller amounts (up to 1%) of α-thujene, camphene, α-terpinene, 1,8-cineole, terpinolene, and *p*-cymene (peaks 1, 3, 6, 8, 10, and 11) were recorded.

Amongst the oxygenated monoterpenes thujone, *d*-isothujone, *d*-methyl citronellate, *d*-terpinen-4-ol, *d*-sabinyl acetate, *d*-sabinol, and *d*-citronellol were isolated (peaks 13,

[1]*Issued as N.R.C. No. 7574.*

Can. J. Chem. Downloaded from www.nrcresearchpress.com by 210.87.254.5 on 09/05/12
For personal use only.

14, 17, 18, 20, 21, and 23). Peak 25 was tentatively identified as geraniol by comparison of retention data. The trace components 15, 16, and 19 were not identified. The typical pungent juniper odor was associated with peak 17, but methyl citronellate prepared by mild oxidation of citronellal (8) had only the mild and pleasant odor expected for this type of ester. Comparison of the infrared and n.m.r. spectra of the isolated and synthetic materials showed no significant difference. However, the former did have a weak ultraviolet absorption (λ_{max}^{EtOH} approx. 280 and 240–230 mμ), indicating contamination with a small amount of an aromatic compound. No reference of which component is responsible for the typical juniper odor was found in the literature.

The oil of savin was found to contain many sesquiterpenes (peaks 22, 24, 27 to 37) and isolation of individual compounds proved difficult, not only because of the small amounts present (see Table I), but because some components decomposed readily. Also, there was some overlap between some of the sesquiterpene hydrocarbons and oxygenated monoterpenes when the more efficient polyester or polyethylene glycol columns were used. Prefractionation on a silicone polymer (SE-30) column did separate the oxygenated monoterpenes from sesquiterpenes (9), but some decomposition was encountered in this study. Similar results were obtained by column chromatography on silicic acid. By a combination of these techniques peaks 22, 24, 27, 33, and 37 were isolated fairly pure and peaks 35 and 36 were obtained as a mixture. Peak 22 was found to correspond to the cadinene isomer, which is obtained when δ-cadinol is dehydrated with pyridine-modified alumina (10). Since its infrared spectrum showed the presence of a terminal methylene group, this is not δ-cadinene (11). Peak 24 was found to be another *d*-cadinene isomer having a terminal methylene group. This may be identical with the major hydrocarbon found in the oil of cade and could be *d*-γ_1-cadinene. Wallach (12) identified cadinene in the oil of savin by formation of the crystalline dihydrochloride, but did not establish the position of the double bonds.

Amongst the oxygenated sesquiterpenes, *l*-elemol (peak 33) was isolated and δ-cadinol (peak 36) was tentatively identified. Juniperol and γ-eudesmol have the same relative retention times as peak 35, but their presence could not be confirmed. Peak 37 had the same retention time as eudesmol (mixture of α- and β-isomers) and the infrared spectrum showed some similarities with that of β-eudesmol, but did not agree in all respects. Sorm *et al.* (13) reported the presence of elemene, junipene, juniperol, juniper camphor, and α- and δ-cadinol in juniper berry oil. In this study a very small amount of β-elemene was obtained by chromatography on silicic acid, but this compound appeared to be derived rather by dehydration of elemol than from the oil itself. Juniper camphor was not found to be present. An attempt was made to classify some of the sesquiterpenes into cadinene or eudalene types by means of dehydrogenation with selenium or palladium-on-charcoal (14), but this technique failed to give positive results on a milligram scale. This aspect and other possible means of identifying or classifying such small amounts of sesquiterpenes are being studied further.

Comparison of retention times showed that aromatic compounds of the allyl benzene type may be present. Peak 26 has the retention time (on PEG 20M) of anethole and peak 27 has that of safrole. Peak 27 was isolated and appears to be a mixture containing mainly a phenol ether. The infrared spectrum differed from that of safrole and it is possible that the compound is estragole (methyl chavicol). Cuminaldehyde, carvacrol and its methyl ether, eugenol, and isoeugenol were not detected.

In previous papers of this series the analysis of the oils of the leaves of *Thuja occidentalis* L. (15), *Thuja plicata* D. Don (16), and *Tanacetum vulgare* L. (1) was described. These

Can. J. Chem. Downloaded from www.nrcresearchpress.com by 210.87.254.5 on 09/05/12
For personal use only.

three oils contain thujone or isothujone as the major constituent. A certain biogenetic relationship between these oils and the oil of savin juniper is discernible in that all contain the thujones and several other compounds having a cyclopropane ring. Common to all four oils are also most of the monoterpene hydrocarbons and terpinen-4-ol. However, little or no taxonomic value may be attached to the latter compounds since it is conceivable that they are formed by a non-specific rearrangement or hydroxylation of a common precursor, such as the carbonium-ion derived from geraniol (geranyl pyrophosphate) as proposed by Ruzicka (17). The oil of savin differs from the other three oils in that it contains sabinyl acetate and sabinene as major constituents and several minor components having a terminal methylene group. Also, certain of the oxygenated monoterpenes, including sabinol, methyl citronellate, citronellol, and perhaps geraniol, are specific constituents of the juniper leaves, whereas, for example, carvone and carvotanacetone (besides major amounts of the thujones) are characteristic of the oil of tansy. Thus, it appears that the formation of at least some of the oxygenated monoterpenes may be subject to genetic control and these constituents may therefore have considerable phylogenetic value. Several authors have attempted to find genetic relationships on the basis of the chemical composition of essential oils (18). However, most of the earlier analyses of volatile oils were incomplete and thus do not lend themselves to critical comparison. Other oils will be analyzed by the gas chromatographic technique to determine the scope of the above conclusions.

EXPERIMENTAL

The same gas chromatographic instruments and procedures as described previously (1) were used. Optical rotations of the oils were measured undiluted at 25±2° and those of individual fractions in chloroform solution (1 to 5%). Infrared spectra were recorded with a Perkin–Elmer model 21 double beam spectrophotometer as films between sodium chloride plates and n.m.r. spectra with a Varian 60 spectrograph, using tetramethyl silane as internal standard.

Materials

The commercial oil (Fritzsche Bros., Inc., New York) had n_D 1.4702, $[\alpha]_D$ +65.0°. Steam distillation of the leaves (240 g) of locally grown savin juniper gave a light yellow oil (11.0 g) having n_D 1.4714, $[\alpha]_D$ +47.7°. Reference compounds were either purified commercial samples or those obtained from other plant sources (1). Cadinene was kindly donated by Messrs. Fritzsche Bros., Inc. and elemol, δ-cadinol, juniperol, juniper camphor, and ledol were gifts from Prof. F. Sorm.

Analytical Chromatograms

Temperature-programmed chromatograms were obtained with 1–5 μl aliquots on 6 ft × 1/4 in. O.D. coiled stainless steel column using polyethylene glycol (Carbowax, PEG 20M) (see Fig. 1), Apiezon N, silicone polymer (SE-30) and adipate polyester (NGA) as liquid phases. *n*-Decane, limonene, camphor, terpinen-4-ol and (or) *n*-decanol were used as internal standards in the quantitative measurements. Area measurement (triangulation method) of the peaks accounted for 98±2% of the oils (1).

Isothermal runs were carried out on the same columns and those containing rapeseed oil and ethylene glycol bis-(propionitrile) (EGPN) as liquid phase. Fractions obtained from preparative runs were analyzed for purity on these columns and the identity of essentially pure fractions was confirmed by comparison of spectral properties and retention data. The average percentage composition, as well as some of the physical data of the isolated components, are shown in Table I. Relative retention times of monoterpene hydrocarbons were measured with respect to limonene, those of oxygenated monoterpenes and sesquiterpene hydrocarbons with respect to camphor, and those of oxygenated sesquiterpenes with respect to cedrol.

Prefractionation

The commercial oil (100 ml) was fractionally distilled *in vacuo* (42 mm Hg; takeoff ratio 1:90) through a Podbielniak spinning band column (100×0.8 cm) to give the following fractions:

I (b.p. 63–74° C, 10.5 ml) monoterpene hydrocarbons,
II (b.p. 74–81° C, 17.0 ml) mainly monoterpene hydrocarbons,
III (b.p. 81–123° C, 12.5 ml) mixture of monoterpenes,
IV (b.p. 123–128° C, 6.0 ml) mixture of oxygenated monoterpenes,
V (b.p. 128–132° C, 18.0 ml) mainly sabinyl acetate.

Can. J. Chem. Downloaded from www.nrcresearchpress.com by 210.87.254.5 on 09/05/12
For personal use only.

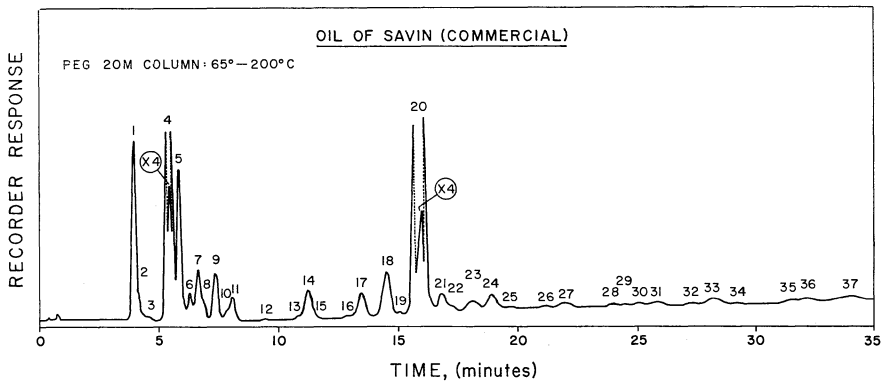

FIG. 1. Gas chromatogram of the oil of savin (6 ft×¼ in. O.D. polyethylene glycol 20M column). (Temperature-programmed from 65 to 200° C.)

TABLE I

Composition of the oil of savin juniper leaves

Peak No.	Compound*	n_D	$[\alpha]_D$	RRT†	Oil from local plants, %	Commercial oil, %
1	α-Pinene	1.4619	+16.9	0.30	2.2	6.8
2	(α-Thujene)	—	—	0.32	0.9	1.0
3	(Camphene)	—	—	0.42	Trace	0.1
4	Sabinene	1.4661	+100.6	0.62	30.5	26.0
5	Myrcene	1.4690	+9.7	0.82	4.5	4.0
6	(α-Terpinene)	—	±0.0	0.94	0.4	1.1
7	Limonene	1.4713	+59.4	*1.00*	1.6	2.7
8	(1,8-Cineole)	—	—	1.07	1.2‡	0.6
9	γ-Terpinene	—	±0.0	1.40	0.7	2.5
10	(Terpinolene)	—	—	1.63	0.7	0.5
11	*p*-Cymene	—	±0.0	1.79	0.4	1.2
12	Unidentified	—	—	0.45	0	Trace
13	(Thujone)	—	—	0.61	Trace	0.5
14	Isothujone	1.4521	+53.3	0.67	0.5	1.9
15	Unidentified	—	—	0.80	0.1	0.2
16	Unidentified	—	—	1.08	Trace	0.2
17	Methyl citronellate	1.4422	+8.1	1.20	1.7	1.8
18	Terpinen-4-ol	1.4762	+22.3	1.40	2.0	3.2
19	Unidentified	—	—	1.60	Trace	0.2
20	Sabinyl acetate	1.4687	+75.9	1.91	38.0	37.5
21	Sabinol	1.4822	+11.1	2.20	0.9	1.1
22	Cadinene isomer	—	—	2.46	0.3	0.5
23	Citronellol	1.4822	+12.0	2.95	1.8	0.8
24	Cadinene	1.5140	+16.5	3.30	4.5	1.5
25	(Geraniol)	—	—	4.85	0.2	Trace
26	(Anethole ?)	—	—	5.40	0.1	Trace
27	(Estragole ?)	1.5100	+3.7	0.40	0.1	0.4
28	Unidentified	—	—	0.45	0.2	Trace
29	Unidentified	—	—	0.55	0.1	Trace
30	Unidentified	—	—	0.58	Trace	Trace
31	Unidentified	—	—	0.61	0.1	Trace
32	Unidentified	—	—	0.66	1.3	0.3
33	Elemol§	1.5070	−9.1	0.84	0.5	0.7
34	Unidentified	—	—	1.05	0.0	0.1
35	(γ-Eudesmol ?)	1.5054	−23.4	1.18	0.8	0.1
36	(δ-Cadinol)			1.25	1.5	0.1
37	(β-Eudesmol ?)	1.5050	−17.2	1.45	2.8	0.2

*Names in parentheses are tentatively identified compounds.
†RRT = relative retention times on 6 ft×¼ in. PEG 20M column: (*a*) monoterpene hydrocarbons at 65° C (limonene = 1.00), (*b*) oxygenated monoterpenes and sesquiterpene hydrocarbons at 120° C (camphor = 1.00), (*c*) oxygenated sesquiterpenes at 180° C (cedrol = 1.00).
‡Could contain another component.
§Melting point 44–50° C.

Can. J. Chem. Downloaded from www.nrcresearchpress.com by 210.87.254.5 on 09/05/12
For personal use only.

At this stage some decomposition appeared to take place, and the vacuum was reduced to 10 mm Hg. Distillation was continued rapidly (takeoff ratio 1:20) to give:

VI (b.p. 95–105° C, 20 ml) sabinyl acetate and higher boiling terpenes,

VII (b.p. 105–145° C, 8 ml) mainly sesquiterpenes.

The distillation residue (6–7 ml) was a black tar which was not further investigated.

The oil from the local plants was prefractionated by preparative GLC (3/8 in. O.D. SE-30 column (1)) and fractions of approximately the same composition were collected by operating the collector manually.

Monoterpene Hydrocarbons

Preparative GLC of fraction I on a 6 ft × 3/8 in. O.D. PEG 20M column (30–50 μl aliquots, repeated injection, 65–90° C in 12 minutes) gave two fractions. The first was impure *d*-α-pinene (peak 1), which contained α-thujene (peak 2). The second was essentially pure *d*-sabinene (peak 4). Analytical runs showed no signs of β-pinene, although up to 2% would not be detectable in the sabinene fraction because of the close retention times.

Similar fractionation of fraction II gave *d*-sabinene, *d*-myrcene (peak 5), impure α-terpinene (peak 6), impure limonene (peak 7), γ-terpinene (peak 9), and impure *p*-cymene. Peaks 3, 8, and 10 were tentatively identified by retention characteristics as camphene, 1,8-cineole, and terpinolene respectively.

Almost identical results were obtained with corresponding fractions from the oil obtained from local plants.

Oxygenated Monoterpenes

Fraction IV was fractionated on a 20 ft × 3/8 in. O.D. PEG 20M column (60 μl aliquots, 170° to 200° C in 25 minutes). Peaks 14, 17, 18, and 20 were isolated practically pure and found to be *d*-isothujone, an unknown ester, *d*-terpinen-4-ol, and *d*-sabinyl acetate (see below) respectively. Peak 13 was obtained only impure but GLC and infrared spectra confirmed that it contained mainly thujone.

Methyl Citronellate

The unknown ester (peak 17) had the typical pungent smell of juniper leaves. Strong infrared absorption bands were recorded at 2970–2860, 1735, 1440, 1380, 1362, 1195, and 1153 cm^{-1}, and medium intensity bands at 1010 and 827 cm^{-1}. Saponification confirmed it to be an ester. Found: C, 71.69; H, 10.97; COOH, 23.38%. Calculated for $C_{11}H_{20}O_2$: C, 71.69; H, 10.94; COOH, 24.43%. The n.m.r. spectrum (trimethyl silane = 0.00) contained the following:

Band	Protons	δ	Assignment
Triplet	1	5.18	$\diagdown C{=}CH-$
Singlet	3	3.67	$-OCH_3$
Complex	3	2.20–2.00	—
Singlet	2	1.92	—
Doublet	6	1.65	$\diagdown C{=}C(CH_3)_2$
Complex	2	1.50–1.10	—
Doublet	3	0.95	$-C-CH_3$

The data were those expected for methyl citronellate, or a closely related compound. Citronellic acid was synthesized by shaking citronellal with a suspension of silver oxide in very dilute aqueous ammonium hydroxide for 5 hours (8). The synthetic acid was converted to the methyl ester with diazomethane and purified by GLC. The synthetic ester had identical infrared and n.m.r. spectra as well as retention characteristics as those of peak 17. However, the smell was only the faint pleasant odor of an unsaturated aliphatic ester. The ultraviolet spectrum of peak 17 showed only very weak, broad absorption bands near 280, 240, and 230 mμ, indicating that a very small amount of an aromatic aldehyde may be present. This impurity could not be detected by GLC.

Sabinyl Acetate

Fraction V contained better than 95% of peak 20. The infrared spectrum suggested this to be an acetate (1737, 1242 cm^{-1}). Saponification gave essentially pure *d*-sabinol, n_D 1.4868, $[\alpha]_D$ +11.2°, *p*-nitrobenzoate m.p. 75–76° C. The ester was obtained almost pure (cf. Table I) by preparative GLC from fractions IV, V, and VI.

From fraction V of the oil from the leaves of the local plants, pure sabinyl acetate, with n_D 1.4675, $[\alpha]_D$ +78.9°, was isolated.

Higher Oxygenated Monoterpenes

Fraction VI was found to be a mixture of *d*-sabinyl acetate, higher boiling monoterpene alcohols, and

Can. J. Chem. Downloaded from www.nrcresearchpress.com by 210.87.254.5 on 09/05/12
For personal use only.

sesquiterpene hydrocarbons. Preparative GLC gave peaks 21, 23, and 24 fairly pure and these were found to be *d*-sabinol, *d*-citronellol, and *d*-cadinene (see below) respectively. Peak 22 appeared to be a cadinene isomer but it was not obtained pure by this technique. The concentration of peaks 25 and 26 was still very low in either fraction VI or VII and could not be isolated in sufficient amounts to record satisfactory infrared spectra.

Sesquiterpenes

To obtain larger amounts of the two cadinene isomers (peaks 22 and 24, see above), aliquots (1.0 g) of fractions VI and VII were chromatographed on silicic acid (30 g). Elution with hexane gave a hydrocarbon fraction which was separated further into three components by preparative GLC. The first was found to have the same infrared spectrum as β-elemene (RRT 1.30). The latter was prepared in small amounts by dehydration of elemol with the pyridine-modified alumina reagent (10). The second component (peak 22) had a similar infrared spectrum and the same retention times as the major hydrocarbon obtained on dehydration of δ-cadinol with the alumina reagent. Typical absorption bands for terminal methylene groups (3070, 1645, and 880 cm^{-1}) were recorded. The third component (peak 24) was obtained in comparatively large amounts; n_D 1.5072, $[\alpha]_D$ +41.6°, infrared bands at 3080, 1645 cm^{-1} (weak), 883, 830, 798 cm^{-1} (medium intensity). It had the same retention times as the major hydrocarbon of the oil of cade.

Elution of the silicic acid chromatogram with chloroform gave a complex mixture of oxygenated mono- and sesqui-terpenes, which was not resolved by preparative GLC. Several decomposition peaks were recorded.

Preparative GLC (6 ft × 3/8 in. O.D. PEG 20M, 115 to 220° C in 30 minutes) of fraction VII gave fairly pure sabinyl acetate (peak 20), *d*-cadinene (peak 24), and peaks 27, 33, and 37; peaks 35 and 36 were collected as one fraction. Peak 27 had a strong ultraviolet absorption (λ_{max}^{EtOH} 276, 235–205 mμ) but no characteristic odor. The aromatic character was confirmed by a sharp, strong band at 1516 cm^{-1} in the infrared spectrum. In addition, the latter showed strong bands at 2930, 1465, 1260, 1235, 1153, 1140, and 1030 cm^{-1}, and medium bands at 3520, 3070, 1725, 1700, 1633, 1605, 1592, 907, and 800 cm^{-1}. Peak 33 had an infrared spectrum which was very similar to that of elemol. The viscous material crystallized on seeding with elemol; m.p. 44–50° C, $[\alpha]_D$ −9.7°. The mixture of peaks 35 and 36 had n_D 1.5054, $[\alpha]_D$ −23.4°, and strong infrared bands at 3440, 2940, 1460, 1375, 1130, 906, and 885 cm^{-1}, and weaker ones at 3090, 1640, 1592, 1505, 1260, 1240, and 800 cm^{-1}. Superimposition of the infrared spectrum of δ-cadinol showed that this compound could be present whereas that of juniperol differed extensively. The infrared spectrum of peak 37 had bands at 3500, 3090 (weak), 2930, 2860, 1710 (weak), 1642, 1592 (weak), 1470–1440, 1385–1370, 1260, 1120 (broad), 1030, 1010, 950 (weak), 932, 910, 885, 875 (weak), 812, and 798 cm^{-1}, and resembled that of β-eudesmol.

ACKNOWLEDGMENTS

The gift of sesquiterpenes by Prof. F. Sorm, Prague, and the technical help of Mr. M. Granat are gratefully acknowledged. The spectra were recorded by Mr. M. Mazurek and Mr. W. C. Haid.

REFERENCES

1. E. VON RUDLOFF. Can. J. Chem. **41**, 1737 (1963).
2. E. FROMM. Ber. **31**, 2025 (1898).
3. F. W. SEMMLER. Ber. **33**, 1463 (1900).
4. E. GUENTHER. *In* The essential oils. Vol. VI. D. Van Nostrand Co., Inc., New York. 1952. p. 388.
5. A. B. BOOTH. Am. Perfumer Aromat. **69**, 45 (1957); Chem. Abstr. **51**, 7658a (1957).
6. S. BRUNO. Farmaco (Pavia) Ed. Prat. **16**, 481 (1961); Chem. Abstr. **56**, 7450b (1962).
7. M. I. GORYAEV and D. R. DZHALILOV. Chem. Abstr. **54**, 23203d (1960).
8. F. W. SEMMLER. Ber. **24**, 208 (1891).
9. E. VON RUDLOFF. Tappi, **45**, 181 (1962).
10. E. VON RUDLOFF. Can. J. Chem. **39**, 1860 (1961).
11. F. SORM, V. HEROUT, and V. SYKORA. Perfumery Essent. Oil Record, **50**, 679 (1959).
12. O. WALLACH. Ann. **238**, 82 (1887).
13. O. MOTL, V. SYKORA, V. HEROUT, and F. SORM. Collection Czech. Chem. Commun. **23**, 1297 (1958).
14. G. CHIURDOGLU and M. DESCAMPS. Ind. Chim. Belge, **26**, 33 (1961).
15. E. VON RUDLOFF. Can. J. Chem. **39**, 1200 (1961).
16. E. VON RUDLOFF. Phytochemistry, **1**, 195 (1962).
17. L. RUZICKA. Experientia, **9**, 357 (1953).
18. A. J. HAAGEN-SMIT. Ann. Rev. Plant Physiol. **4**, 305 (1953).

Can. J. Chem. Downloaded from www.nrcresearchpress.com by 210.87.254.5 on 09/05/12
For personal use only.

REACTIONS OF ORGANOTIN COMPOUNDS

I. THE STABILITY OF DIMETHYLTIN DIHYDRIDE, AND ADDITIONS TO SOME FLUORO-OLEFINS[1]

H. C. CLARK, SHARON G. FURNIVAL, AND J. T. KWON

Department of Chemistry, University of British Columbia, Vancouver, British Columbia

Received July 22, 1963

ABSTRACT

The effect of heat and ultraviolet irradiation on dimethyltin dihydride is reported. At 120°, the major decomposition products are $(CH_3)_3SnH$, Sn, and H_2, with a small amount of $(CH_3)_6Sn_2$. At 130° under ultraviolet light, decomposition is much more rapid giving $(CH_3)_3SnH$, Sn, and H_2, and an appreciable quantity of $(CH_3)_4Sn$. If the dihydride is maintained under these conditions for a longer period (40 hours), $(CH_3)_6Sn_2$ is formed in place of $(CH_3)_3SnH$, and other products are $(CH_3)_4Sn$, Sn, and H_2. Negligible decomposition occurs at 25° even under irradiation.

The ready addition of C_2F_4 to $(CH_3)_2SnH_2$ gives the first reported mono-addition product of an organotin dihydride, $(CH_3)_2SnH(C_2F_4H)$, as well as $(CH_3)_2Sn(C_2F_4H)_2$. Physical and chemical properties of these compounds are described. The additions of $(CH_3)_2SnH_2$ to CF_2CFH, CF_2CH_2, and CF_2CFBr are reported and the results interpreted in terms of the formation of unstable mono-addition products, $(CH_3)_2SnH(C_2F_nX_mH_p)$. Surprisingly, these species decompose through the exchange of halogen and hydrogen between $(CH_3)_2SnH_2$ and the olefin. Thus, usual products from the reaction of $(CH_3)_2SnH_2$ with CF_2CFBr are $(CH_3)_2SnBr_2$ and CF_2CFH, with some $(CH_3)_3SnBr$.

Can. J. Chem. Downloaded from www.nrcresearchpress.com by 210.87.254.42 on 09/05/12
For personal use only.

INTRODUCTION

Since the initial discovery in 1956 by van der Kerk and co-workers (1–3), many studies have been made of the non-catalyzed addition of the Sn–H group across an olefin or acetylene bond. These additions, which generally take place at 80–100° in the absence of solvent, give excellent yields, and have been applied to the preparation of functionally substituted organo-tin compounds (4), and of organometallic polymers (5). Most work has been related to the preparation and characterization of new derivatives, and no systematic studies have yet been made to elucidate the mechanism of these addition reactions. From the qualitative evidence so far available, it has been concluded (5) that (*i*) the mechanism is ionic, (*ii*) predominantly steric factors determine the course of the reaction, and (*iii*) polar effects only influence the rate of the addition.

A noticeable feature of previous studies is that the olefins and acetylenes employed all contain large substituent groups (e.g. phenyl-acetylene, styrene, methyl acrylate). There are no reports of additions to ethylene or acetylene, and in particular, Noltes and van der Kerk have stated (4, p. 39) that aliphatic organotin dihydrides do not react with simple olefins, so that dienes such as butadiene or hexadiene could not be used in polymer-forming reactions. Our own interest originated in a preliminary study of the addition of tetrafluoroethylene to hexamethylditin and to diphenyltin (6), in which the fluoro-olefin is added across the Sn—Sn bond. As a related investigation, we have now examined the addition of several fluoro-olefins to dimethyltin dihydride, $(CH_3)_2SnH_2$.

DISCUSSION

The organotin hydrides, particularly the aryl derivatives, possess only moderate stability towards heat and oxidizing agents. However, in reports of the addition of these hydrides to unsaturated compounds, no mention is usually made of decomposition products of the hydride, nor has any attempt been made to ascertain the importance of this

[1]*Presented at the Symposium on Current Trends in Organometallic Chemistry, Cincinnati, 12–15 June, 1963.*

decomposition to the general mechanism of the addition reaction. Initially, therefore, it seemed desirable to determine the extent of decomposition of dimethyltin dihydride, and to identify the products formed, under the influence of heat and radiation.

Although dimethyltin dihydride is stable indefinitely at 25° in the dark *in vacuo*, decomposition is moderately rapid at 120° in the dark. Some estimate of the rate of decomposition can be obtained from the fact that 6 hours at this temperature was required to give a visible deposit of metallic tin. After 45 hours, decomposition was complete, the products being trimethyltin hydride (50.7%), hexamethylditin (6.1%), metallic tin (39%), and hydrogen (~60%) containing a small quantity of methane. These results are consistent with decomposition according to the equation

$$3(CH_3)_2SnH_2 \rightarrow 2(CH_3)_3SnH + Sn + 2H_2 \quad [1]$$

followed, to a lesser extent, by the reaction

$$2(CH_3)_3SnH \rightarrow (CH_3)_6Sn_2 + H_2. \quad [2]$$

The influence of ultraviolet irradiation can be seen from a similar experiment at 130° when after only 6 hours, decomposition was virtually complete, the products being tetramethyltin (20%), trimethyltin hydride (40%), hydrogen (53%), and metallic tin (49.1%). Under similar conditions (110° and ultraviolet irradiation) but for a period of 40 hours, there was a marked difference in the products obtained. No trimethyltin hydride was isolated, although there was little change in the yields of tetramethyltin (21.9%), metallic tin (69%), and hydrogen (55%, containing a small amount of methane). Instead, hexamethylditin was formed. In the presence of ultraviolet radiation, it therefore appears that two reactions take place, reaction [1] and

$$2(CH_3)_2SnH_2 \rightarrow (CH_3)_4Sn + Sn + 2H_2. \quad [3]$$

Over long periods of time (40 hours) further decomposition occurs to form hexamethylditin, so that reactions [1], [2], and [3] are all involved. For appreciable decomposition of dimethyltin dihydride, a high temperature is necessary, since a sample exposed to ultraviolet light for 40 hours at 25° was very largely (92%) recovered unchanged.

The mechanism of decomposition is clearly complex. Presumably, the first step involves the loss of hydrogen to form $(CH_3)_2HSn\bullet$, which in turn must be responsible directly or indirectly for the cleavage of the CH_3—Sn bond, but detailed kinetic studies are very necessary. In the present investigation, to minimize decomposition effects of the dihydride, reactions were performed at 50° or lower, either with or without ultraviolet radiation.

When equimolar quantities of dimethyltin dihydride and tetrafluoroethylene were allowed to react at 25° in the dark, 63% of the dihydride was consumed giving a 52.3% total yield of *dimethyl(tetrafluoroethyl)tin hydride*, $(CH_3)_2SnH(C_2F_4H)$, and a 9.2% total yield of dimethylbis(tetrafluoroethyl)tin, $(CH_3)_2Sn(C_2F_4H)_2$. The small amount of involatile residue (10% of total mass) was composed of metallic tin and polymerized tetrafluoroethylene. This is only the second instance in which a simple olefin such as C_2F_4 has been found to add readily across the Sn—H bond, and it is the first time that the addition has been found to occur in a stepwise fashion. Previous attempts to isolate the mono-addition product from the reaction of an olefin with an organotin dihydride (e.g. dipropyltin dihydride and methyl acrylate (4, p. 38)) were unsuccessful, only the bis-addition compound being isolated. Similarly, in the only other reported addition of a fluoro-olefin to a tin hydride (7), $(C_4H_9)_2Sn(C_2F_4H)_2$ was the only product obtained from the reaction of dibutyltin dihydride with tetrafluoroethylene. It seems reasonable to suggest, therefore, that the overall reaction can be described in terms of the three equations [4], [5], and [5*a*]:

Can. J. Chem. Downloaded from www.nrcresearchpress.com by 210.87.254.42 on 09/05/12
For personal use only.

$$(CH_3)_2SnH_2 + C_2F_4 \rightarrow (CH_3)_2SnH(C_2F_4H), \quad [4]$$

$$2(CH_3)_2SnH(C_2F_4H) \rightarrow (CH_3)_2SnH_2 + (CH_3)_2Sn(C_2F_4H)_2, \quad [5]$$

$$(CH_3)_2SnH(C_2F_4H) + C_2F_4 \rightarrow (CH_3)_2Sn(C_2F_4H)_2. \quad [5a]$$

There is no evidence at present which allows us to distinguish between [5] and [5*a*].

A series of experiments was performed under different experimental conditions to determine some of the factors influencing the rate of the reaction, and the yields. It is not suggested that these studies elucidate the reaction mechanism, for which considerably more detailed and more systematic studies would be required. Firstly, the effect of ultraviolet light was determined. As can be seen from the experimental results below, the rate of the reaction is increased markedly; for instance after only 20 hours at 25° with ultraviolet irradiation, the yield of dimethyl(tetrafluoroethyl)tin hydride was 23.2% and of $(CH_3)_2Sn(C_2F_4H)_2$, approximately 2%, so that the relative proportions of the two products was unchanged. If the time was increased to 50 hours under the same conditions, the yield of $(CH_3)_2SnH(C_2F_4H)$ was almost the same (22.4%), but the yield of $(CH_3)_2Sn(C_2F_4H)_2$ was raised considerably to 40%. For a 20 hour reaction period, the effect of increasing the temperature from 25° to 50° was to give an excellent yield (75%) of $(CH_3)_2SnH(C_2F_4H)$, and only 1 to 2% of $(CH_3)_2Sn(C_2F_4H)_2$. When the ratio olefin:tin dihydride was changed from 1:1 to 2:1 and the reaction performed at 50° with ultraviolet irradiation for 20 hours, a 77% total yield of $(CH_3)_2Sn(C_2F_4H)_2$, and a 13% total yield of $(CH_3)_2SnH(C_2F_4H)$ was obtained.

Dimethyl(tetrafluoroethyl)tin hydride is a colorless liquid, b.p. 124°, which when sealed *in vacuo*, is stable at 25° for at least 3 months. At higher temperatures, disproportionation is extensive; thus, 72.6% of a sample decomposed at 140° over a 26-hour period to give an almost quantitative yield of $(CH_3)_2Sn(C_2F_4H)_2$. For simple disproportionation to occur, according to equation [5], dimethyltin dihydride should also be formed, but as already described, extensive decomposition of the dihydride occurs at this temperature. As in other tin hydrides, the Sn—H group in $(CH_3)_2SnH(C_2F_4H)$ is reactive, so that chlorination gives a quantitative yield of hydrogen chloride and forms *dimethyl(tetrafluoroethyl)tin chloride* $(CH_3)_2SnCl(C_2F_4H)$, m.p. 18.7–19.1°, b.p. 220°.

$$(CH_3)_2SnH(C_2F_4H) + Cl_2 \rightarrow HCl + (CH_3)_2SnCl(C_2F_4H). \quad [6]$$

The infrared spectrum of $(CH_3)_2SnH(C_2F_4H)$ shows the expected strong absorption at 1877 cm^{-1} due to the Sn—H stretching vibration, and also shows strong bands at 1182, 1102, 1046, and 1028 cm^{-1} due to C—F vibrations. In the spectrum of $(CH_3)_2Sn(C_2F_4H)_2$, the Sn—H band is, of course, absent, and the C—F vibrations give very similar bands although at slightly different frequencies. A detailed study of the proton and F^{19} nuclear magnetic resonance spectra of $(CH_3)_2SnH_2$, $(CH_3)_2SnH(C_2F_4H)$, and $(CH_3)_2Sn(C_2F_4H)_2$ is reported elsewhere (8).

The problem of the mechanism of these additions is of considerable interest. Earlier workers (1) have shown that the reactions are unaffected by free radical inhibitors and have concluded that an ionic mechanism is probable. This would presumably involve hydride-ion attack of the olefin, but it is not possible to exclude a molecular, four-center type of mechanism. From the present results, ultraviolet radiation markedly affects the course of the reaction and more detailed kinetic studies are clearly necessary. Further qualitative information might well result from an investigation of the addition of unsymmetrical fluoro-olefins to dimethyltin dihydride, since any polar influence of the olefin, as well as any steric effect, might then become apparent. For this reason, reactions with trifluoroethylene, 1,1-difluoroethylene, and trifluorobromoethylene were examined.

Can. J. Chem. Downloaded from www.nrcresearchpress.com by 210.87.254.42 on 09/05/12
For personal use only.

Can. J. Chem. Downloaded from www.nrcresearchpress.com by 210.87.254.42 on 09/05/12
For personal use only.

Surprisingly, trifluoroethylene did not react readily with dimethyltin dihydride in a reaction at 25° in the dark for a period of 94 hours; using a 1:1 molar ratio, 95.5% of the dihydride was recovered, and 88% of the olefin; the remainder was apparently lost as polymer. Very similar results were obtained in an identical experiment performed at 50° for 44 hours. However, reaction was much more extensive when carried out in ultraviolet light. When the reaction was performed at 25° for 20 hours with ultraviolet irradiation, using a 1:1 molar ratio, approximately 90% of the dihydride was consumed, hydrogen and a mixture of CF_2=CFH and CHF=CHF were produced, leaving a large quantity of involatile residue which contained metallic tin and dimethyltin difluoride. Moreover, a small quantity of less volatile material, was condensed at −45° *in vacuo*. This was unstable and on standing changed from a liquid to an involatile solid. The infrared spectrum of a freshly prepared sample showed the presence of Sn—H and C—F groups, and the n.m.r. spectrum also indicated two different types of CH_3—Sn groupings. All the evidence indicated that this fraction contained tetramethyltin and $(CH_3)_2SnH(C_2F_3H_2)$. Similar results were obtained in a reaction carried out at 50° for 17 hours with ultraviolet irradiation. In this case it was possible to separate and identify some pure $(CH_3)_4Sn$ as one of the products, although pure $(CH_3)_2SnH(C_2F_3H_2)$ could not be isolated.

Hence, ultraviolet radiation appears necessary to cause reaction with trifluoroethylene. The observations can be interpreted in terms of the initial reaction of equation [7]

$$(CH_3)_2SnH_2 + C_2F_3H \rightarrow (CH_3)_2SnH(C_2F_3H). \qquad [7]$$

However, this product spontaneously decomposes, and

$$(CH_3)_2SnH(C_2F_3H) \rightarrow [(CH_3)_2SnHF] + CFH{=}CFH,$$

rearrangement, and decomposition of the dihydride follow;

$$2[(CH_3)_2SnHF] \rightarrow (CH_3)_2SnF_2 + (CH_3)_2SnH_2, \qquad [8]$$

$$2(CH_3)_2SnH_2 \rightarrow 2H_2 + Sn + (CH_3)_4Sn.$$

The reaction between dimethyltin dihydride and 1,1-difluoroethylene likewise occurred to a negligible extent in the dark, even at 50°. However, under ultraviolet radiation at 25° for 19 hours, consumption of the dihydride was virtually complete, only a small amount (9%) of hydrogen was evolved, and fluoroethylene was a major volatile product. The involatile residue did not appear to contain metallic tin and was composed essentially of dimethyltin difluoride, and fluorocarbon polymer. Again, in some experiments, there was evidence for the existence of $(CH_3)_2SnH(C_2F_2H_3)$ as an unstable −45° fraction which underwent immediate decomposition, and the results can again be interpreted in terms of its transient formation and decomposition,

$$(CH_3)_2SnH_2 + C_2F_2H_2 \rightarrow (CH_3)_2SnH(C_2F_2H_3), \qquad [9]$$

$$(CH_3)_2SnH(C_2F_2H_3) \rightarrow [(CH_3)_2SnHF] + CH_2{=}CHF, \qquad [10]$$

$$2[(CH_3)_2SnHF] \rightarrow (CH_3)_2SnF_2 + (CH_3)_2SnH_2. \qquad [11]$$

When 1,1-difluoroethylene and dimethyltin dihydride were allowed to react in a 2:1 molar ratio, under identical conditions, the products were the same and also included trimethyltin fluoride, as well as dimethyltin difluoride.

Trifluorobromoethylene reacted much more readily with $(CH_3)_2SnH_2$ than either C_2F_3H or CF_2CH_2; after 21 hours in the dark at 50°, at a 1:1 molar ratio, only approximately 2% and 4% of the dihydride and olefin respectively were recovered. Most of the olefin (77%) was converted to trifluoroethylene. A small −45° fraction was unstable and decomposed to a white solid. Approximately half of the total material from the reaction

Can. J. Chem. Downloaded from www.nrcresearchpress.com by 210.87.254.42 on 09/05/12
For personal use only.

was either involatile or was condensed at −10° and contained a small quantity of metallic tin but consisted chiefly of a mixture of dimethyltin dibromide and trimethyltin bromide. When a similar reaction, using a 1:1 molar ratio of reactants, was carried out at 25° for 20 hours under ultraviolet irradiation, the identity and distribution of products was unchanged, except that very little $(CH_3)_3SnBr$ was formed, the major tin-containing product being $(CH_3)_2SnBr_2$.

Again, therefore, the experimental results are consistent with the formation of a mono-addition compound, and indeed the evidence clearly indicates that this was the major component of the −45° fractions described above. The mono-addition compound is unstable and decomposes as shown:

$$(CH_3)_2SnH_2 + C_2F_3Br \rightarrow (CH_3)_2SnH(C_2F_3BrH), \quad [12]$$

$$(CH_3)_2SnH(C_2F_3BrH) \rightarrow [(CH_3)_2SnHBr] + C_2F_3H, \quad [13]$$

$$2[(CH_3)_2SnHBr] \rightarrow (CH_3)_2SnBr_2 + (CH_3)_2SnH_2.$$

Hydrogen, metallic tin, and trimethyltin bromide may result from decomposition of $(CH_3)_2SnH_2$,

$$2(CH_3)_2SnH_2 \rightarrow (CH_3)_4Sn + Sn + 2H_2, \quad [14]$$

$$(CH_3)_4Sn + (CH_3)_2SnBr_2 \rightarrow 2(CH_3)_3SnBr. \quad [15]$$

The results, therefore, indicate low stability of the $Sn(C_2F_3BrH)$ group, and this was confirmed by the reaction of dimethyltin dihydride with trifluorobromoethylene in a 1:2 molar ratio at 50° in the dark for 19 hours. The formation of metallic tin, hydrogen, C_2F_3H, dimethyltin dibromide, and trimethyltin bromide can be interpreted in terms of equations [12–15] (i.e. through the formation of an unstable mono-addition compound). In addition, however, there was a small quantity (13%) of *dimethylbis(2-bromotrifluoro)tin*, $(CH_3)_2Sn(C_2F_3BrH)_2$, identified by its infrared and n.m.r. spectra. This colorless liquid decomposed at approximately 100°, the only products being C_2F_3H and $(CH_3)_2SnBr_2$. A simple decomposition therefore occurs,

$$(CH_3)_2Sn(C_2F_3BrH)_2 \rightarrow 2C_2F_3H + (CH_3)_2SnBr_2, \quad [16]$$

again indicating the inherent instability of the $Sn(C_2F_3BrH)$ group.

The question of the direction of addition of C_2F_3Br to the Sn—H bond is also of considerable interest. That is, is the $Sn—CF_2—CFBrH$ group formed, or is it the $Sn—CFBr—CF_2H$ group? The proton magnetic resonance spectrum shows a pair of triplets for the single proton, as distinct from the methyl protons and this is consistent only with the $Sn—CF_2—CFBrH$ arrangement.

The importance of the present work lies in the fact that it establishes (*a*) that simple olefins can be added directly and easily across the Sn—H bond, and (*b*) that such addition occurs in a stepwise fashion, forming first the mono-addition compound, $R_2SnH(R'H)$. A number of puzzling questions remain. Firstly, the mechanism of addition is most uncertain. Our results indicate that in certain instances, appreciable reaction only occurs under ultraviolet irradiation. On the other hand, all previous evidence argues against a free radical mechanism, and, moreover, there is no evidence for the formation of products of the type $R_2SnH[(C_2F_4)_nH]$, similar to those observed in the free-radical addition of olefins to silanes (9).

Secondly, it is not at all clear why groups such as $>SnC_2F_3H_2$, $>SnC_2F_2H_3$, and $>SnCF_2CFBrH$ should be unstable; the isolation of stable compounds such as $(CH_3)_2Sn(C_2F_2H_3)_2$ would normally be predicted. The high stability and inertness of methyltin

fluorides (e.g. ref. 10) may well favor the formation of dimethyltin difluoride and trimethyltin fluoride, but this argument cannot apply to the formation of $(CH_3)_2SnBr_2$ and C_2F_3H from the $>Sn(CF_2CFBrH)$ group. Further investigation of these reactions and of additions with other olefins, which may throw some light on these questions, is now in progress.

EXPERIMENTAL

General

All reactions were carried out in sealed pyrex Carius tubes of approximately 80-ml capacity. The manipulation and separation of volatile compounds were performed using standard high-vacuum techniques. Volatile products were identified by molecular-weight determinations by the Regnault method, by elemental analysis, by vapor pressure measurements, by the determination of infrared spectra, and in some instances by nuclear magnetic resonance spectra.

Preparation of Dimethyltin Dihydride

The procedure described by Finholt *et al.* (11) was used; this required the reduction of dimethyltin dichloride with lithium aluminum hydride. The apparatus consisted of a three-necked flask fitted with a stirrer, a low temperature condenser (−78°), and dropping funnel, and the reaction was carried out in an atmosphere of dry nitrogen. When dioxane was used as the solvent, the maximum yield of the dihydride was 55% of the theoretical, and it was not possible to remove completely the dioxane from the product. Hence, *n*-butyl ether was used as solvent. In a typical reaction, dimethyltin dichloride (66.1 g, 0.30 mole) was reduced with lithium aluminum hydride (21.1 g, 0.56 mole) in 150 ml *n*-butyl ether to give dimethyltin dihydride (36.3 g) in 81% yield.

Dimethyltin dihydride [M.W. obs. 150, calc. 151; b.p. 35.9°, lit. value 35° (1)] was also characterized by its proton magnetic resonance spectrum (8, 12), and by its infrared spectrum. The principal absorption bands in the latter were: a strong doublet at 1858, 1871 (Sn—H stretch), an intense band at 700–780 cm^{-1} with subsidiary maxima at 776, 759, 748, 727, and 711 cm^{-1}, a broad peak at 670–680 cm^{-1}, and a triplet at 536, 526, 517 cm^{-1}. The active hydrogen of the dihydride was readily determined by reaction with aqueous nitric acid, to give a quantitative yield of hydrogen.

Decomposition of Dimethyltin Dihydride

(*a*) The dihydride (2.193 g, 14.5 mmole) was heated in a sealed tube at 120° in the dark for 45 hours. After 6 hours, metallic tin had formed, and appreciable amounts had been deposited after 20 hours. Vacuum fractionation of the volatile products gave approximately 9 mmole of permanent gas (mainly hydrogen), a white solid (0.287 g) melting at 25°, which was hexamethylditin, and trimethyltin hydride (1.213 g, M.W. obs. 165, calc. 164). This last product was further characterized by its proton magnetic resonance (12) and infrared spectra. Metallic tin (0.670 g) remained in the reaction tube.

(*b*) A sample (2.141 g, 14.2 mmole) was heated at 130° under ultraviolet irradiation (100-watt lamp) for 6 hours, to give hydrogen (approximately 7.5 mmole), a fraction (1.216 g) which condensed *in vacuo* at −45° and which had a molecular weight of 180 and vapor pressure at 25° of 90 mm, unreacted dimethyltin dihydride (0.132 g), and metallic tin (0.777 g). In accord with the observed molecular weight, the −45° fraction was shown spectroscopically to contain tetramethyltin and trimethyltin hydride in an approximately 1:2 ratio.

(*c*) Dimethyltin dihydride (2.550 g, 16.9 mmole) was heated at 110° under ultraviolet irradiation for 40 hours. Hydrogen (approximately 11 mmole) containing a small amount of methane, hexamethylditin (0.466 g; m.p. 25°), tetramethyltin (0.679 g; M.W. obs. 178, calc. 178), and trimethyltin hydride (0.008 g) were the volatile products. Pure metallic tin (1.375 g) in mirror form was the only involatile product. The hexamethylditin and tetramethyltin were shown to be pure from their infrared spectra, and in the latter case by its n.m.r. spectrum.

(*d*) When the dihydride (2.220 g, 14.7 mmole) was subjected to ultraviolet irradiation at 25° for 40 hours, 92% was recovered unchanged. Hydrogen (0.3 mmole), a fraction (0.103 g, M.W. obs. 73) which was condensed at −64°, and metallic tin (0.067 g) were the other products. The −64° fraction was not characterized unambiguously but its infrared spectrum and molecular weight, indicated that only hydrocarbons were present.

Reactions with Tetrafluoroethylene

Typical reactions were as follows.

(*a*) Dimethyltin dihydride (1.650 g, 11.0 mmole) and tetrafluoroethylene (1.100 g, 11.0 mmole) were allowed to react in a sealed tube at 25° in the dark for 160 hours. Vacuum fractionation gave hydrogen (0.04 mmole), unreacted tetrafluoroethylene (0.177 g, 1.77 mmole), unreacted dimethyltin dihydride (0.614 g, 4.06 mmole), and two volatile fractions which were condensed at −10° and −46°. The former was

Can. J. Chem. Downloaded from www.nrcresearchpress.com by 210.87.254.42 on 09/05/12
For personal use only.

dimethylbis(tetrafluoroethyl)tin, $(CH_3)_2Sn(C_2F_4H)_2$, (0.176 g, 0.503 mmole) [calc. for $C_6F_8H_8Sn$: C, 20.6; H, 2.6%. obs: C, 20.3; H, 2.2%. M.W. obs. 349; calc. 351], which has a boiling point of 124.0° and $\Delta H_v = 8.3$ kcal mole^{-1}. The −46° fraction was *dimethyl(tetrafluoroethyl)tin hydride*, $(CH_3)_2(C_2F_4H)SnH$, (1.443 g, 5.75 mmole) [calc. for $C_4F_4H_8Sn$: C, 19.2; H, 3.2%. obs: C, 18.8; H, 2.7%. M.W. obs. 252; calc. 251], which boils at 77.9° and has $\Delta H_v = 9.20$ kcal mole^{-1}. Further characterizations of these compounds are given below. An involatile residue (0.340 g), composed partly of tin, remained in the reaction tube.

(*b*) A similar reaction of the dihydride (0.538 g, 3.60 mmole) and tetrafluoroethylene (0.361 g, 3.61 mmole) at 25° for 22 hours with ultraviolet irradiation, gave a trace of dimethylbis(tetrafluoroethyl)tin, dimethyltetrafluoroethyltin hydride (0.209 g, 0.83 mmole, 23.2%), unreacted dihydride (0.367 g), and unreacted olefin (0.303 g), as well as some involatile residue (0.021 g).

(*c*) With dihydride (1.205 g, 8.03 mmole) and C_2F_4 (0.803 g, 8.03 mmole) at 25° for 50 hours with ultraviolet irradiation, a 40.0% yield of dimethylbis(tetrafluoroethyl)tin (0.934 g, 2.65 mmole) and a 22.4% yield of dimethyl(tetrafluoroethyl)tin hydride (0.373 g, 1.49 mmole) was obtained. The only other products were unreacted starting materials, and an involatile residue (0.387 g) which, from its appearance and infrared spectrum, contained metallic tin and polymerized olefin.

(*d*) Dimethyltin dihydride (1.452 g, 9.62 mmole) and C_2F_4 (0.874 g, 8.74 mmole), after 20 hours at 50° with ultraviolet irradiation, gave dimethyl(tetrafluoroethyl)tin hydride (1.801 g, 7.17 mmole), unreacted dihydride (0.271 g, 1.73 mmole), unreacted olefin (0.052 g, 0.52 mmole), hydrogen (1.1 mmole), and an involatile residue (0.161 g) composed largely of tin and polymerized tetrafluoroethylene.

(*e*) Dimethyltin dihydride (1.145 g, 7.58 mmole) and C_2F_4 (2.200 g, 22.00 mmole), under the same conditions as (*d*), gave hydrogen (0.07 mmole), unreacted olefin (0.611 g, 6.11 mmole), unreacted dihydride (0.314 g), which also appeared to contain small amounts of fluorocarbon material other than C_2F_4, dimethyl(tetrafluoroethyl)tin hydride (0.144 g, 0.960 mmole), dimethylbis(tetrafluoroethyl)tin (2.038 g, 5.83 mmole), and the same involatile residue (0.179 g) as observed in all other reactions.

Pyrolysis of $(CH_3)_2SnH(C_2F_4H)$

A sample (0.260 g) was heated at 140° for 26 hours. The volatile products were hydrogen (0.22 mmole), a fraction (0.032 g) which condensed *in vacuo* at −196°, and which from its infrared spectrum was a mixture of fluorocarbons, unreacted dimethyl(tetrafluoroethyl)tin hydride (0.071 g, M.W. obs. 249, calc. 251), and dimethylbis(tetrafluoroethyl)tin (0.120 g, M.W. obs. 350, calc. 351). An involatile residue (0.037 g) of tin and polymeric material remained.

Chlorination of Dimethyl(tetrafluoroethyl)tin Hydride

The reaction of $(CH_3)_2SnH(C_2F_4H)$ (0.127 g, 0.508 mmole) with chlorine (0.040 g, 0.57 mmole) occurred readily at room temperature to give hydrogen chloride (0.0018 g, 0.51 mmole), and *dimethyl(tetrafluoroethyl)tin chloride* (0.144 g, 0.507 mmole, M.W. obs. 284, calc. 285.5), which has m.p. 18.7–19.1°, b.p. 220°, $\Delta H_v = 6.2$ kcal mole^{-1}.

The infrared spectrum of $(CH_3)_2SnH(C_2F_4H)$ in the vapor phase showed absorption (cm^{-1}) at 2980 (m), 2920 (m) (C—H stretch); 1877 (s) (Sn—H stretch); 1418 (w) (CH_3 asymmetric, deformation); 1368 (m), 1343 (w), 1210 (w) (CH_3 symmetric deformation); 1182 (m), 1102 (s), 1046 (s), 1028 (w, sh), (C—F stretch); 980 (w); 775 (s) (CH_3 rocking); 724 (m); 640 (m); 583 (m); 551 (m); and 521 (m). Infrared absorption bands of $(CH_3)_2Sn(C_2F_4H)_2$ (liquid film) were observed at 2970 (w), 2915 (w) (C—H stretch); 1402 (w, sh), 1384 (w, sh), 1362 (s), 1341 (w, sh); 1274 (w); 1205 (w, sh) (CH_3 symmetric deformation); 1177 (s), 1088 (s), 1042 (s) (C—F stretch); 974 (m); 785 (s) (CH_3 rocking); 736 (w, sh); 638 (m); 580 (m); 549 (m); and 520 (s). The infrared spectrum of $(CH_3)_2SnCl(C_2F_4H)$, as a liquid film, showed absorption at 2970 (w), 2915 (w) (C—H stretch); 1609 (w); 1402 (w) (CH_3 asymmetric deformation); 1382 (w, sh), 1366 (s), 1342 (w, sh); 1282 (w); 1205 (w, sh) (CH_3 symmetric deformation); 1178 (s), 1088 (s), 1046 (s) (C—F stretch); 971 (m); and 790 (s) (CH_3 rocking).

The proton and F^{19} magnetic resonance spectra of $(CH_3)_2SnH(C_2F_4H)$ and $(CH_3)_2Sn(C_2F_4H)_2$ are fully consistent with these formulations and are described in detail elsewhere (8).

Reactions with Trifluoroethylene

(*a*) Dimethyltin dihydride (0.810 g, 5.36 mmole) and trifluoroethylene (0.437 g, 5.33 mmole) were allowed to react at 25° in the dark for 94 hours. Nearly all the dihydride (0.773 g, 95.4%) was recovered, as well as much of the olefin (0.382 g, 87.5%). There remained a white, involatile solid (0.090 g).

(*b*) A similar reaction with equimolar quantities at 50° in the dark for 44 hours led to the recovery of 96% of the dihydride and 86% of the olefin. The infrared spectrum of the involatile residue (9% of total mass) showed the presence of CH_3—Sn groups (strong 780 cm^{-1} band) and C—F groups.

(*c*) Dihydride (1.715 g, 11.4 mmole) and C_2F_3H (0.934 g, 11.4 mmole) were allowed to react under ultraviolet irradiation for 20 hours at 25°. Hydrogen (1.92 mmole, 23.4%) was recovered and a fraction (0.038 g) of low volatility condensed at −45°. The remaining products, apart from an involatile residue (1.540 g), were very volatile and only partial separation into −125° (0.406 g, M.W. 84) and −196° (0.643 g, M.W. 75.5) fractions could be achieved. Infrared examination showed that only the former contained unreacted dimethyltin dihydride, the remaining components of this fraction and those of the latter being unreacted

Can. J. Chem. Downloaded from www.nrcresearchpress.com by 210.87.254.42 on 09/05/12
For personal use only.

trifluoroethylene (M.W. 82), and 1,2 difluoroethylene [M.W. 64]. The infrared spectra of these two compounds allows unambiguous identification in terms of the triplets observed (13) for CHF=CHF at 1117, 1128, and 1138, and 762, 769, and 778 cm^{-1}, which are distinct from absorption bands of CF_2=CHF. The involatile residue contained some metallic tin, and dimethyltin difluororide identified by its infrared spectrum and an X-ray powder photograph.

The −45° fraction was identical with a similar fraction obtained in experiment (*d*) below. Both materials were originally separated as clear liquids, but on standing at 25° decomposed with gas evolution to leave a white involatile solid. Because of this decomposition, molecular weights could not be determined. However, the infrared spectra showed the presence of Sn—H and C—F bonds, although absorption attributable to the latter in the 1000–1200 cm^{-1} region was of much lower intensity in relation to absorption due to Sn—H at approximately 1850 cm^{-1} than would be expected for $(CH_3)_2SnH(C_2F_3H_2)$. Moreover, a proton magnetic resonance spectrum showed two types of CH_3 peaks, in accord with the distinct CH_3—Sn rocking absorptions at 780 and 730 cm^{-1} in the infrared, and these results can be interpreted in terms of a mixture of $(CH_3)_4Sn$ and $(CH_3)_2SnH(C_2F_3H_2)$.

(*d*) Dimethyltin dihydride (1.189 g, 7.98 mmole) and C_2F_3H (0.660 g, 8.03 mmole), after 17 hours at 50° under ultraviolet radiation, gave 4.58 mmole of hydrogen (57%), a −45° fraction (0.172 g) having the properties described above, a −64° fraction (0.339 g, M.W. 170), and fractions which condensed at −125° (0.134 g) and −196° (0.568 g). The involatile residue (0.648 g) was again composed largely of metallic tin with some $(CH_3)_2SnF_2$. The −64° fraction, from its molecular weight and infrared spectrum, was almost pure tetramethyltin (M.W. 178), while the −125° and −196° fractions again contained unreacted dihydride (−125° only), unreacted C_2F_3H, and CHF=CHF.

Reactions with 1,1-Difluoroethylene

(*a*) Dimethyltin dihydride (1.529 g, 10.1 mmole) and CF_2CH_2 (0.647 g, 10.1 mmole) were allowed to react at 25° for 19 hours under ultraviolet irradiation. A small amount of hydrogen was formed (0.95 mmole, 9%), and the only other volatile products were unreacted dihydride (0.085 g) and a fraction which condensed at −196°. The latter (0.420 g) had molecular weight 56, and its infrared spectrum showed the presence of unreacted CF_2=CH_2 (M.W. 64) and of $CHFCH_2$ (M.W. 46). The latter was clearly identified by characteristic triplets (14) at 1142, 1156, 1170, and 913, 929, 949 cm^{-1} and sharp peaks at 863 and 711 cm^{-1}, all of which are absent from the spectrum of CF_2CH_2. The remaining involatile residue (1.671 g) was a clear, white solid which gave an analysis corresponding to $C_{3.0}H_{7.5}SnF_{2.5}$, and whose infrared spectrum showed the presence of fluorocarbon groups. An X-ray diffraction powder photograph identified dimethyltin difluoride, so that this solid was composed of a fluorocarbon polymer, probably of $CHFCH_2$, and $(CH_3)_2SnF_2$, in an approximately 1:2 ratio.

(*b*) When equimolar quantities of $(CH_3)_2SnH_2$ and CF_2CH_2 were allowed to react at 50° in the dark for 21 hours, 90% of the dihydride was recovered unchanged. Most of the olefin (97%) was recovered, although its spectrum indicated the presence of a small amount of $CFHCH_2$. A small quantity of material condensed at −45° but rapidly changed from a clear liquid to a non-volatile white solid with gas evolution.

(*c*) The dihydride (0.931 g, 6.17 mmole) and CF_2CH_2 (0.788 g, 12.3 mmole) were subjected to ultraviolet irradiation for 17 hours at 25°. Hydrogen (0.17 mole, 3%) was obtained, and 12% of the dihydride (0.113 g) was recovered. The fraction (0.510 g) collected at −196° had a molecular weight of 59.6 and was shown spectroscopically to contain unreacted CF_2CH_2, and $CFHCH_2$. The only other product was the white involatile residue which contained a small amount of metallic tin. Elemental analysis, as well as infrared spectroscopic, and X-ray powder photographic examination showed the presence of some fluorocarbon polymer, and considerable amounts of dimethyltin difluoride and trimethyltin fluoride, these two being in an approximately 2:1 ratio.

Reactions with Trifluorobromoethylene

(*a*) Dimethyltin dihydride (1.831 g, 12.1 mmole) and C_2F_3Br (1.950 g, 12.1 mmole) were allowed to react at 50° in the dark for 21 hours. Hydrogen (5.10 mmole, 42%) was recovered, and the fraction (0.722 g) which condensed at −196° (M.W. 83) was shown by its infrared spectrum to be C_2F_3H (M.W. 82). Only 2% of the dihydride (0.030 g) was recovered. Other fractions condensed at −45° (0.024 g) and −10° (1.256 g) leaving a residue (1.693 g). The small −45° fraction showed infrared absorption expected for the presence of Sn—H, C—F, and CH_3—Sn groups, but decomposed on standing to form a white solid, identified as dimethyltin dibromide.

The −10° fraction, which melted at ca. 25°, was separated into trimethyltin bromide (1.192 g) and dimethyltin dibromide (0.060 g) which were readily identified by their spectra and by melting point determinations. Similarly, the remaining grey reaction residue was found to contain some metallic tin, but to consist chiefly of dimethyltin dibromide.

(*b*) When $(CH_3)_2SnH_2$ (1.585 g, 10.5 mmole) and C_2F_3Br (1.694 g, 10.5 mmole) were allowed to react at 25° for 20 hours under ultraviolet irradiation, the products were hydrogen (2.25 mmole, 22%), trifluoroethylene (0.550 g, M.W. 83), unreacted dimethyltin dihydride (0.05 g), and unreacted C_2F_3Br (0.05 g), a −45° fraction (0.037 g) which again decomposed on standing to give involatile, white dimethyltin dibromide, a −10° fraction (0.366 g) which was almost pure trimethyltin bromide, and a grey residue (2.217 g) composed of metallic tin, some trimethyltin bromide, and chiefly dimethyltin dibromide.

Can. J. Chem. Downloaded from www.nrcresearchpress.com by 210.87.254.42 on 09/05/12
For personal use only.

(*c*) Dimethyltin dihydride (3.597 g, 23.8 mmole) and C_2F_3Br (7.791 g, 47.8 mmole) were allowed to react in the dark at 50° for 19 hours. Hydrogen (1.58 mmole, 6.7%) was formed, together with CF_2CFH (1.812 g, 22.1 mmole, 46.5%), and unreacted C_2F_3Br (1.571 g, 20.4%) was recovered. A very small fraction was collected at −45° but again this decomposed on standing at 25° to form $(CH_3)_2SnBr_2$. A clear liquid was condensed in each of a series of traps cooled at +10°, 0°, and −10°; spectroscopic examination showed these fractions (total 1.531 g) to be identical. There remained in the reaction tube, a white solid, m.p. 75° whose infrared spectrum showed it to be $(CH_3)_2SnBr_2$ (m.p. 74°).

A sample of the clear liquid, left to stand *in vacuo* at 25° for 16 days, decomposed completely leaving a residue of dimethyltin dibromide. An attempt to measure the vapor pressure of the liquid showed that slow decomposition occurred above 80°, and above 105° decomposition was rapid and complete. Extrapolation from the vapor pressure readings below 80° gave an approximate b.p. 192°. From a sample decomposed above 105° the only products were C_2F_3H (M.W. 81 and infrared spectrum) and involatile $(CH_3)_2SnBr_2$.

The infrared spectrum of the original liquid showed absorption at 3000 (w), 2920 (w) (C—H stretch), 2335 (w), 1710 (w), 1645 (w), 1605 (w), 1455 (w), 1405 (w), 1375 (m), [1258 (m), 1245 (m), 1152 (s), 1108 (s), 1080 (sh), 1045 (s) (C—F vibrations)], 952 (m), 895 (s), 780 (s) (CH_3—Sn rock), 760 (w, sh). This spectrum, together with the proton magnetic resonance spectrum, and the above evidence, identified the compound as *dimethylbis(2-bromotrifluoroethyl)tin*, $(CH_3)_2Sn(CF_2CFBrH)_2$. The n.m.r. spectrum, which will be discussed more fully elsewhere, showed a single peak at −0.95 and a pair of triplets at −4.65 p.p.m. with respect to tetramethylsilane, the areas being in the ratio 3:1. Such a spectrum is consistent with a formula $(CH_3)_2Sn(CF_2CFBrH)_2$ and not with $(CH_3)_2Sn(CFBrCF_2H)_2$, dimethylbis(1-bromotrifluoroethyl)tin.

ACKNOWLEDGMENT

The financial support of the Office of Naval Research is gratefully appreciated.

REFERENCES

1. G. J. M. VAN DER KERK, J. G. A. LUIJTEN, and J. G. NOLTES. Chem. Ind. (London), 352 (1956).
2. G. J. M. VAN DER KERK, J. G. A. LUIJTEN, and J. G. NOLTES. J. Appl. Chem. (London), **7**, 356 (1957).
3. G. J. M. VAN DER KERK, J. G. A. LUIJTEN, and J. G. NOLTES. Angew. Chem. **70**, 298 (1958).
4. J. G. NOLTES and G. J. M. VAN DER KERK. Functionally substituted organotin compounds. Tin Research Institute, Greenford. 1958.
5. J. G. NOLTES and G. J. M. VAN DER KERK. Chimia (Aarau), **16**, 122 (1962).
6. M. A. A. BEG and H. C. CLARK. Chem. Ind. (London), 140 (1962).
7. C. G. KRESPAN and V. A. ENGELHARDT. J. Org. Chem. **23**, 1565 (1958).
8. H. C. CLARK, J. T. KWON, L. W. REEVES, and E. J. WELLS. Can. J. Chem. In press. 1963. 14, 42, 941
9. A. M. GEYER and R. N. HASZELDINE. Nature, **178**, 808 (1956).
10. H. C. CLARK, R. J. O'BRIEN, and J. TROTTER. Proc. Chem. Soc. 85 (1963).
11. A. E. FINHOLT, A. C. BOND, JR., K. E. WILZBACH, and H. I. SCHLESINGER. J. Am. Chem. Soc. **69**, 2692 (1947).
12. N. FLITCROFT and H. D. KAESZ. J. Am. Chem. Soc. **85**, 1377 (1963).
13. R. N. HASZELDINE and B. R. STEELE. J. Chem. Soc. 2800 (1957).
14. B. BAK and D. CHRISTENSEN. Spectrochim. Acta, **12**, 355 (1958).

Can. J. Chem. Downloaded from www.nrcresearchpress.com by 210.87.254.42 on 09/05/12
For personal use only.

THE RELATIVE ACCEPTOR POWER OF BORON TRIHALIDES AND BORANE TOWARD TRIMETHYLAMINE[1]

J. M. MILLER[2] AND M. ONYSZCHUK
Inorganic Chemistry Laboratory, McGill University, Montreal, Quebec
Received July 15, 1963

ABSTRACT

Gas phase displacement reactions of boron trihalides from their trimethylamine adducts show that the order of acceptor power is: $BBr_3 > BCl_3 > BF_3 > 1/2(B_2H_6)$. This order agrees with recent theoretical calculations and dipole moment, calorimetric, and infrared measurements on boron trihalide complexes with other reference bases.

INTRODUCTION

On the basis of electronegativities and steric requirements of the halogens, the classically accepted order of acceptor power of the boron trihalides was $BF_3 > BCl_3 > BBr_3$ (1). Recent work, however, has indicated the reverse order to be correct. Calorimetric studies by Brown and Holmes (1) on the pyridine complexes of boron trihalides in nitrobenzene solution first revealed the new order. This order was confirmed by Bax, Katritzky, and Sutton (2), who measured dipole moments of boron trihalide and borane (BH_3) adducts of pyridine and trimethylamine. Lappert (3), using ethyl acetate as reference base and taking the shift of the carbonyl stretching frequency in the infrared as an indication of donor–acceptor bond strength, concluded that BBr_3 is a stronger acceptor than BCl_3. Similar studies by Cook (4) on boron trihalide–xanthone complexes also confirm the new order, as do the theoretical calculations of Cotton and Leto (5).

The same order, if correct, should be evident from a study of the displacements of boron trihalides from their molecular addition compounds. Displacement reactions, although complicated by lattice energy and volatility effects, are often used to determine qualitatively the relative stability of a series of closely related complexes in which lattice energies do not vary significantly (6). From such data the relative acceptor strengths of a series of related Lewis acids can be inferred. In all cases where this has been done, the conclusions have not had to be changed when quantitative data have subsequently been reported for gas phase dissociation of the same complexes (6).

Graham and Stone (7) using trimethylamine as reference base found no displacement of BF_3 from $(CH_3)_3N \cdot BF_3$ by B_2H_6 at 80° C. Dutton *et al.* (8) reported that BCl_3 almost quantitatively displaced BF_3 from $(CH_3)_3N \cdot BF_3$ at 205° C, and the reverse reaction was not detected. We have now extended this work by investigating gas phase displacements of BH_3, BF_3, BCl_3, and BBr_3 from their trimethylamine adducts.

RESULTS AND DISCUSSION

It is evident from the results summarized in Table I that BCl_3 almost quantitatively displaced BF_3 from $(CH_3)_3N \cdot BF_3$ while the reverse reaction was not detected. Similarly, BBr_3 displaced BCl_3 and BF_3 from their trimethylamine adducts, while the reverse reaction occurred to a negligible extent. All three boron trihalides displaced BH_3 from

[1]*This work was supported by a grant from The Defence Research Board of Canada (Grant number 9530-20, Project D46-95-30-20). Presented at the 46th Conference of the Chemical Institute of Canada, Toronto, Ontario, June 6–8, 1963.*
[2]*Holder of an N.R.C. Bursary, 1961–62, and N.R.C. Studentships, 1962–64.*

Can. J. Chem. Downloaded from www.nrcresearchpress.com by 210.87.254.5 on 09/05/12
For personal use only.

TABLE I
Displacement data

Reaction	Time (hr)	Temp	Average displacement (%)
$(CH_3)_3N \cdot BF_3 + BCl_3$	3	205	96.4[a]
$(CH_3)_3N \cdot BCl_3 + BF_3$	3	205	0.0[a]
$(CH_3)_3N \cdot BH_3 + BCl_3$	12	130	77.5
$(CH_3)_3N \cdot BF_3 + BBr_3$	2/3	250–300	89.2
$(CH_3)_3N \cdot BBr_3 + BF_3$	3/4	250–300	0.0
$(CH_3)_3N \cdot BCl_3 + BBr_3$	1/2	250–300	72.6[b]
$(CH_3)_3N \cdot BCl_3 + BBr_3$	3/4	250–300	91.3[b]
$(CH_3)_3N \cdot BCl_3 + BBr_3$	3	263–265	95.6[b]
$(CH_3)_3N \cdot BBr_3 + BCl_3$	3/4	250–300	14.7[b]
$(CH_3)_3N \cdot BH_3 + BBr_3$	1	250–300	90.2
$(CH_3)_3N \cdot BH_3 + BF_3$	3/4	130–140	83.3
$(CH_3)_3N \cdot BF_3 + 1/2(B_2H_6)$	3/4	130–140	23.4

[a]Values in reference 8.
[b]Based on BCl_3.

$(CH_3)_3N \cdot BH_3$ with the evolution of diborane which decomposed at the temperatures used. The reverse reaction of B_2H_6 with $(CH_3)_3N \cdot BF_3$ occurred only to a small extent. These results lead us to conclude that the order of acceptor power of boron trihalides and diborane toward trimethylamine is: $BBr_3 > BCl_3 > BF_3 > 1/2(B_2H_6)$.

Brown and Holmes (1) suggested that the order of acceptor power of boron trihalides depends mainly on the extent of p_π—p_π back bonding between the vacant $2p$-orbital of boron and a doubly occupied p-orbital of the halogen.

During adduct formation the hybridization of boron changes from sp^2 to sp^3 with resultant breaking of the p_π—p_π bonds. Cotton and Leto (5) have shown that the strength of boron–halogen p_π—p_π bonding decreases in the order $BF_3 > BCl_3 > BBr_3$, and that the reorganization energy required for adduct formation is also in the same order (48.3, 30.3, and 26.2 kcal mole^{-1} respectively). These reorganization energies provide the most satisfactory explanation of the relative acceptor power of boron trihalides; the larger the reorganization energy, the weaker the acceptor power. The observation that BBr_3 displaced BF_3 to a greater extent than BCl_3 from their trimethylamine adducts may be due to the fact that the difference in reorganization energy between BBr_3 and BF_3 is much greater than that between BBr_3 and BCl_3. Similarly, the great difference between BF_3 and BCl_3 could account for the nearly quantitative displacement of BF_3 by BCl_3 and the absence of the reverse displacement. In the case of BCl_3 and BBr_3 where the difference in reorganization energy is small, the reverse reaction occurred to a significant extent (14.7%).

Since displacement reactions probably occur in the following two steps* (where X and X′ represent different halogen atoms)

$$(CH_3)_3N \cdot BX_{3(g)} \rightleftarrows (CH_3)_3N_{(g)} + BX_{3(g)}$$
$$(CH_3)_3N_{(g)} + BX'_{3(g)} \rightleftarrows (CH_3)_3N \cdot BX'_{3(g)}$$

it might be argued that the least volatile complex would always be formed. In general, volatility and stability of adducts are inversely related, and only if stabilities were equal

The mechanism of this type of reaction is being investigated by Coyle, who has reported, in a recent preliminary communication (Proc. Chem. Soc. 172 (1963)), that the heterogeneous reaction of BCl_3 with $(C_2H_5)_3N \cdot BF_3$ below 60° occurs by halogen exchange without appreciable boron–nitrogen bond cleavage. However, he finds that at 60° boron–nitrogen bonds are broken and reformed.

Can. J. Chem. Downloaded from www.nrcresearchpress.com by 210.87.254.5 on 09/05/12
For personal use only.

would the heavier and presumably less volatile complex be formed in preference. However, the volatility of an adduct is not always determined by its molecular weight. For example, in trimethylamine complexes of germanium and silicon tetrahalides, $(CH_3)_3N \cdot GeF_4$ is more stable and less volatile than $(CH_3)_3N \cdot GeCl_4$ despite the latter's higher molecular weight (9). Similarly, $(CH_3)_3N \cdot SiF_4$ is more stable and less volatile than the heavier $(CH_3)_3N \cdot SiCl_4$ (9). Also, ammonia displaces tetrahydrofuran from its BH_3 complex forming a less volatile adduct (10), even though ammonia is lighter and more volatile than tetrahydrofuran.

Dipole moment measurements on trimethylamine and pyridine adducts (2) indicate that BH_3 is a slightly stronger acceptor than BF_3 but weaker than BCl_3. Although there is no possibility of supplementary π-bonding in the BH_3 group, there is the reorganization energy of BH_3 from sp^2 to sp^3 hybridization and the dissociation energy of diborane to be considered in displacement reactions involving diborane. No calculations have yet been made of the reorganization energy, but the dissociation energy of diborane is known to be 28.4 ± 2 kcal mole^{-1} (11). Thus in displacement reactions involving the BH_3 group, additional energy (14.2 kcal mole^{-1} of BH_3) is produced by dimerization of BH_3 groups. It appears that this extra energy makes the displacement of BH_3 by BF_3 energetically favorable even though $(CH_3)_3N \cdot BH_3$ is thermodynamically more stable than $(CH_3)_3N \cdot BF_3$. Thermochemical data (11) show that although the heat of reaction for $BF_3 + (CH_3)_3N$ is 26.6 kcal mole^{-1} and 17.3 kcal mole^{-1} for $1/2(B_2H_6) + (CH_3)_3N$, the calculated heat of reaction for $BH_3 + (CH_3)_3N$ is 31.5 kcal mole^{-1}. These values indicate that if BH_3 existed as a stable monomer it would be a stronger acceptor than BF_3 toward $(CH_3)_3N$ by about 5 kcal mole^{-1} (11).

EXPERIMENTAL

Methods and Apparatus

Volatile substances were manipulated in a standard high vacuum apparatus made of Pyrex glass (12). Stopcocks and ground glass joints were lubricated with Kel-F 90 grease which is not appreciably attacked by boron trihalides. Molecular weights (M) were determined by vapor density. The purities of volatile components were checked by vapor pressure, molecular weight, and gas phase infrared spectra measurements. The purities of solid adducts were checked by melting point (m.p.) determinations.

The reaction vessel was a pyrex tube, 40 cm long and 4.1 cm diameter, which had at one end a capillary constriction and a magnetically operated break-seal. The other end of the reaction vessel was fused to 20 cm of 2.5 cm tubing through which the weighed solid was inserted in a fused solica boat. This end was then sealed off about 8 cm from the larger diameter tube. After the vessel and its contents were evacuated, a measured amount of the volatile component was condensed in, and the capillary constriction was sealed off. Reactions were carried out by heating the reaction vessel in a tube furnace so that one end of the reaction vessel projected slightly. When all the material had sublimed to this cool end, the reaction tube was pushed into the furnace so that the hot end emerged and cooled, and the sublimation process reversed. This procedure was repeated until the desired reaction time had elapsed. Several reactions were done by placing the entire reaction vessel in a closed oven, but there were no significant differences between these results and those obtained by the multiple pass procedure. On completion of a displacement reaction the vessel was cooled with liquid air and then opened to the vacuum system through the magnetic break seal. Volatile products were removed and analyzed in the vacuum apparatus. The reaction tube was then cut open and the solid material examined, usually by infrared spectroscopy.

Observations of the infrared spectra of solid complexes in KBr discs revealed that each complex had at least one unique peak; these were: 690 cm^{-1} for $(CH_3)_3N \cdot BF_3$; 790 cm^{-1} for $(CH_3)_3N \cdot BCl_3$; 730, 714, and 672 cm^{-1} for $(CH_3)_3N \cdot BBr_3$ and 2357 cm^{-1} for $(CH_3)_3N \cdot BH_3$.

Materials

Diborane was prepared by the reaction of sodium borohydride with sulphuric acid (13). Commercial samples of boron trifluoride (Matheson), boron trichloride (Matheson), boron tribromide (Anderson), and trimethylamine (Matheson) were purified by several vacuum distillations and their purities were checked by vapor pressure, molecular weight, and infrared spectra measurements. Borane-trimethylamine (Callery) was purified by several vacuum sublimations (found m.p. 93–95°; lit. (14) m.p. 94°). Boron trifluoride-trimethylamine was prepared by bubbling trimethylamine and boron trifluoride into a flask of cooled dry

Can. J. Chem. Downloaded from www.nrcresearchpress.com by 210.87.254.5 on 09/05/12
For personal use only.

benzene. This method proved to be more satisfactory than that described in Inorganic Syntheses (15). The crude product was recrystallized from pure ethanol and dried under vacuum (found m.p. 141°; lit. (15) m.p. 138°). Boron trichloride-trimethylamine was prepared from boron trichloride and trimethylamine as described in Inorganic Syntheses (15) (found m.p. 238–240°; lit. (15) m.p. 242–243°). Boron tribromide-trimethylamine was prepared by bubbling trimethylamine into boron tribromide in cooled dry benzene. The white precipitate was recrystallized from hot ethanol (found m.p. 239°; lit. (16) m.p. 238°). The infrared spectra of the trimethylamine complexes were identical to those of Katritzky (17).

Reaction of BBr_3 with $(CH_3)_3N \cdot BF_3$

The reaction of $(CH_3)_3N \cdot BF_3$ (4.85 mmole) with BBr_3 (10.21 mmole) at 250–300° for 40 minutes produced, after distillation at −130°, BF_3 (4.32 mmole) and BBr_3 (5.87 mmole), corresponding to 89.2% displacement. The solid product was shown by its infrared spectrum to be mainly $(CH_3)_3N \cdot BBr_3$, with only a trace of $(CH_3)_3N \cdot BF_3$. After recrystallization once from hot ethanol the solid melted at 234–239° (lit. (15) m.p. for $(CH_3)_3N \cdot BBr_3$: 238°).

Reaction of BF_3 with $(CH_3)_3N \cdot BBr_3$

When $(CH_3)_3N \cdot BBr_3$ (3.69 mmole) and BF_3 (9.24 mmole) were brought together for 45 minutes at 250–300°, the volatile products, separated by distillation at −120°, consisted of BF_3 (9.35 mmole) and BBr_3 (0.25 mmole), indicating that no significant reaction had occurred. The observed BBr_3 probably resulted from slight thermal decomposition of $(CH_3)_3N \cdot BBr_3$. The infrared spectrum of the solid was that of $(CH_3)_3N \cdot BBr_3$ with no sign of $(CH_3)_3N \cdot BF_3$.

Reaction of BBr_3 with $(CH_3)_3N \cdot BCl_3$

After 30 minutes at 250–300°, $(CH_3)_3N \cdot BCl_3$ (4.16 mmole) and BBr_3 (6.79 mmole) yielded a volatile product the infrared spectrum of which contained bands characteristic of BBr_3 and BCl_3 in addition to bands at 878, 916, 918, and 954 cm^{-1}. The first two bands are characteristic of BCl_2Br and the last two of $BClBr_2$; both molecular species are present in a mixture of BCl_3 and BBr_3, and are impossible to isolate (18). Since it was not possible to separate the BCl_3–BBr_3 mixture quantitatively, its composition was estimated from the molecular weight of the gaseous mixture; the results were, BCl_3 (3.02 mmole) and BBr_3 (3.03 mmole). The BCl_3 value indicated 72.6% displacement, while the BBr_3 value indicated 90.0% displacement. The infrared spectrum of the solid showed $(CH_3)_3N \cdot BBr_3$ together with a small amount of $(CH_3)_3N \cdot BCl_3$. A mixed halide analysis of the solid indicated that 71.7% displacement had occurred, which is in excellent agreement with the value indicated by the BCl_3 recovery.

A second reaction of $(CH_3)_3N \cdot BCl_3$ (4.18 mmole) with BBr_3 (8.47 mmole) at 250–300° for 45 minutes produced BCl_3 (3.81 mmole), corresponding to 91.3% displacement.

The same reaction was repeated a third time with $(CH_3)_3N \cdot BCl_3$ (2.57 mmole) and BBr_3 (5.22 mmole) at 263–265° for 3 hours. In this case the reaction was carried out in an oven with more accurate temperature control. The amount of BCl_3 recovered (3.46 mole) indicated 95.6% displacement.

The three experiments show that displacement becomes almost quantitative as the reaction time is increased.

Reaction of BCl_3 with $(CH_3)_3N \cdot BBr_3$

The reaction of $(CH_3)_3N \cdot BBr_3$ (2.52 mmole) with BCl_3 (6.31 mmole) at 250–300° for 45 minutes produced BBr_3 (0.56 mmole) and unconsumed BCl_3 (5.94 mmole), corresponding to displacements of 22.2 and 14.7% based on BBr_3 produced and BCl_3 consumed, respectively.

The solid was mainly $(CH_3)_3N \cdot BBr_3$ as evident from its infrared spectrum which also indicated a small amount of $(CH_3)_3N \cdot BCl_3$.

Reaction of BF_3 with $(CH_3)_3N \cdot BH_3$

Boron trifluoride (6.18 mmole) and $(CH_3)_3N \cdot BH_3$ (3.32 mmole) reacted at 130–150° for 45 minutes to yield a yellow non-volatile oil which solidified on cooling. This solid was probably polymeric $(BH)_x$ produced by thermal decomposition of diborane formed from the displaced BH_3: $xB_2H_6 \rightarrow 2xH_2 + 2(BH)_x$. This decomposition, if quantitative, should yield 1 mole of hydrogen per mole of $(CH_3)_3N \cdot BH_3$ decomposed. The volatile products from the displacement and simultaneous decomposition were hydrogen (2.78 mmol) and BF_3 (3.58 mmole). On the basis of BF_3 consumed, displacement had occurred to 80.5%, while, on the basis of hydrogen produced, the displacement reaction was 86% complete. The infrared spectrum of the solid showed $(CH_3)_3N \cdot BF_3$ with a small amount of $(CH_3)_3N \cdot BH_3$.

Reaction of B_2H_6 with $(CH_3)_3N \cdot BF_3$

Diborane (3.90 mmole, i.e. 7.80 mmole BH_3) and $(CH_3)_3N \cdot BF_3$ (2.64 mmole) were kept at 130–140° for 45 minutes. Then, while all the solid material was at one end of the reaction vessel, the other end was heated to 200° for 1 hour to decompose excess B_2H_6. This procedure was adopted because B_2H_6 cannot be easily separated quantitatively from BF_3 by vacuum distillation. The volatile products consisted of hydrogen (6.84 mmole), boron trifluoride (0.84 mmole), and diborane (0.42 mmole). The displacement based on the amount of BF_3 recovered was 31.8%, and 14.9% based on hydrogen produced. The infrared spectrum of the solid showed it to be mainly $(CH_3)_3N \cdot BF_3$ with a small amount of $(CH_3)_3N \cdot BH_3$.

Can. J. Chem. Downloaded from www.nrcresearchpress.com by 210.87.254.5 on 09/05/12
For personal use only.

Reaction of BCl_3 with $(CH_3)_3N \cdot BH_3$

The reaction of $(CH_3)_3N \cdot BH_3$ (5.82 mmole) with BCl_3 (6.38 mmole) in an oven at 130° for 12 hours produced hydrogen (4.46 mmole) and BCl_3 (1.84 mmole) as the only volatile products. The percentage displacement was 76.9 calculated on the amount of hydrogen produced, and 78.0 on the basis of BCl_3 produced. Infrared measurements revealed that the solid was $(CH_3)_3N \cdot BCl_3$ contaminated with some $(CH_3)_3N \cdot BH_3$.

Reaction of BBr_3 with $(CH_3)_3N \cdot BH_3$

Boron tribromide (6.12 mmole) reacted with $(CH_3)_3N \cdot BH_3$ (4.18 mmole) at 250–300° for 60 minutes to produce hydrogen (3.85 mmole) and BBr_3 (2.42 mmole). The BBr_3 consumed indicated 88.5% displacement while the hydrogen produced indicated 92%. The solid was almost entirely $(CH_3)_3N \cdot BBr_3$, as evident from its infrared spectrum.

Effect of Heat on the Trimethylamine Adducts

The pure complexes were heated separately under the same conditions used in the displacement reactions. In the case of $(CH_3)_3N \cdot BF_3$, $(CH_3)_3N \cdot BCl_3$, and $(CH_3)_3N \cdot BBr_3$ there was no detectable decomposition in 45 minutes at 250–300°, and the infrared spectra of each was unchanged. However, $(CH_3)_3N \cdot BH_3$ decomposed, with formation of hydrogen and $(CH_3)_3N$, to an extent of 30.0% based on the amount of hydrogen evolved.

ACKNOWLEDGMENTS

We are grateful to the Defence Research Board for financial assistance and to the National Research Council for the award of scholarships to one of us (J. M. M.).

REFERENCES

1. H. C. Brown and R. R. Holmes. J. Am. Chem. Soc. **78**, 2173 (1956).
2. C. M. Bax, A. R. Katritzky, and L. E. Sutton. J. Chem. Soc. 1258 (1958).
3. M. F. Lappert. J. Chem. Soc. 542 (1962).
4. D. Cook. Can. J. Chem. **41**, 522 (1963).
5. F. A. Cotton and J. R. Leto. J. Chem. Phys. **30**, 993 (1959).
6. F. G. A. Stone. Chem. Rev. **58**, 101 (1958).
7. W. A. G. Graham and F. G. A. Stone. J. Inorg. Nucl. Chem. **3**, 164 (1956).
8. W. Dutton, W. G. Paterson, and M. Onyszchuk. Proc. Chem. Soc. 149 (1960).
9. J. E. Fergusson, D. R. Grant, K. H. Hickford, and C. J. Wilkins. J. Chem. Soc. 99 (1959).
10. F. G. A. Stone. *In* Advances in inorganic and radiochemistry. *Edited by* H. J. Emeleus and A. G. Sharpe. Vol. 2. Academic Press, New York. 1960. p. 279.
11. R. E. McCoy and S. H. Bauer. J. Am. Chem. Soc. **78**, 2061 (1956).
12. R. T. Sanderson. Vacuum manipulation of volatile compounds. Wiley, New York. 1948.
13. H. G. Weiss and I. Shapiro. J. Am. Chem. Soc. **81**, 6167 (1959).
14. A. B. Burg and T. C. Tatlow. J. Am. Chem. Soc. **59**, 780 (1937).
15. T. Moeller (*Editor*). Inorganic syntheses. Vol. V. McGraw-Hill, New York. 1957. p. 26.
16. R. C. Osthoff, C. A. Brown, and F. H. Clarke. J. Am. Chem. Soc. **73**, 4045 (1951).
17. A. R. Katritzky. J. Chem. Soc. 2049 (1959).
18. L. P. Lindeman and M. K. Wilson. J. Chem. Phys. **24**, 242 (1956).

Can. J. Chem. Downloaded from www.nrcresearchpress.com by 210.87.254.5 on 09/05/12
For personal use only.

NOTES

SYNTHESIS OF DIKETOPIPERAZINES[1]

L. C. VINING[2]

A number of diketopiperazines derived from amino acids have recently been found as metabolic products of microorganisms (1–5). Several (2–4) are reported to possess biological activity against plants or insects, and it has been suggested (5) that compounds of this type are intermediates in the biosynthesis of related microbial metabolites containing the 1:4-diazine ring.

Diketopiperazines have received attention in the past as intermediates in the synthesis of peptides as well as hydrolytic fragments from proteins. They have frequently been prepared by the self-condensation of two molecules of an amino acid ester (6). However, the rate of diketopiperazine formation decreases with increasing molecular size of both the amino acid and the ester substituent (7, 8) and for the less reactive compounds relatively high temperatures are required and yields are poor. Unsubstituted amino acids also afford the dimeric anhydride when heated in a high-boiling solvent (9), and similar conditions can be used to cyclize a dipeptide (10). Need for the more drastic conditions which may lead to racemization (e.g. ref. 5) can be avoided by preparing a dipeptide ester which cyclizes with extreme ease (11). Use of this intermediate also has the obvious advantage of permitting the synthesis of diketopiperazines derived from two different amino acids.

As part of a study in this laboratory of the biosynthesis of aspergillic acid and related compounds it became necessary to prepare certain C^{14}-labeled diketopiperazines. Since no satisfactory procedure was available in the literature a number of methods for the synthesis of dipeptide esters were examined for their convenience and adaptability to the preparation of diketopiperazines on a small scale in good yield. The route selected involved the coupling of an N-carbobenzoxyamino acid with an amino acid ester via the mixed carbonic acid anhydride (12). The protecting carbobenzoxy group was removed by hydrogenation and the resulting dipeptide ester hydrochloride cyclized by treatment with methanolic ammonia (13).

C^{14}-Labeling is most efficiently introduced into the diketopiperazine from the synthetic route outlined above by using the methyl ester hydrochloride derivative of the appropriate C^{14}-labeled amino acid. This derivative can be conveniently prepared in high yield on a small scale. Use of a 10% excess of the N-carbobenzoxy-substituted moiety in the coupling reaction is then advisable. Synthesis of the diketopiperazine has been carried out without isolation of intermediates with an overall yield of 62%.

EXPERIMENTAL

N-Carbobenzoxy-L-isoleucine was prepared in a yield of 92% by the procedure of Fox and co-workers (14). D- and L-Leucine were esterified with methanol using thionyl chloride as catalyst (15). The yields of methyl D- and L-leucinate hydrochlorides were 95 and 93% respectively.

[1]*Issued as N.R.C. No. 7540.*

[2]*Present address: Atlantic Regional Laboratory, National Research Council, Halifax, Nova Scotia.*

Methyl N-Carbobenzoxy-L-isoleucyl-L-leucinate

N-Carbobenzoxy-L-isoleucine (0.26 g = 1 mmole) in dry acetone (2 ml) containing triethylamine (0.14 ml = 1 mmole) was cooled to −10° C in an ice–salt bath, and ethyl chloroformate (0.7 ml = 1 mmole) added slowly, with stirring. After 25 minutes a solution prepared by neutralizing methyl L-leucinate hydrochloride (0.18 g = 1 mmole) in chloroform (1 ml) at −10° C with triethylamine (1 mmole) was added and rinsed in with two 0.5 ml washes of cold chloroform. The temperature of the reaction mixture was allowed to rise to ambient, and after a further 4 hours the solution was evaporated to dryness *in vacuo*. The residue was redissolved in ethyl acetate (25 ml) and the solution extracted successively with 0.1 *N* HCl (2×5 ml) and 0.1 *N* $NaHCO_3$ (2×5 ml), washed with water (3×5 ml), then dried over anhydrous sodium sulphate. The solvent was removed to give methyl N-carbobenzoxy-L-isoleucyl-L-leucinate which, after one crystallization from an ethyl acetate – light petroleum mixture had m.p. 143.5–145° C, $[\alpha]_{D^{26}} = -37.4°$ ($c = 0.3$ in ethanol). Found: C, 64.44; H, 8.25; N, 7.21%. Calc. for $C_{21}H_{32}O_5N_2$: C, 64.26; H, 8.22; N, 7.14%. The yield was 86%.

Methyl N-carbobenzoxy-L-isoleucyl-D-leucinate, m.p. 113–115° C, $[\alpha]_{D^{26}} = -21.6°$ ($c = 0.3$ in ethanol) was prepared similarly in a yield of 79%. Found: C, 64.27; H, 8.10; N, 7.14%.

Methyl L-Isoleucyl-L-leucinate Hydrochloride

Methyl N-carbobenzoxy-L-isoleucyl-L-leucinate (274 mg) was dissolved in glacial acetic acid (20 ml) containing Adams catalyst (300 mg). A slow stream of dry hydrogen was passed through the stirred reaction mixture at room temperature. The effluent gas was led through a trap containing 0.2 *N* barium hydroxide. After 24 hours when no further carbon dioxide was being evolved the catalyst was removed. The product recovered by evaporation of the solvent was crystallized from an ether–methanol mixture as needles (175 mg, 78%), m.p. 163–164° C, $[\alpha]_{D^{26}} = -3.4°$ ($c = 0.5$ in ethanol). Found: C, 52.69; H, 9.07; N, 9.44; Cl, 11.80%. Calc. for $C_{13}H_{27}O_3N_2Cl$: C, 52.96; H, 9.23; N, 9.50; Cl, 12.03%.

Methyl L-isoleucyl-D-leucinate hydrochloride could be prepared in a similar manner, or alternatively by hydrogenation of a solution of methyl N-carbobenzoxy-L-isoleucyl-D-leucinate (0.27 g) in methanol (20 ml) containing *N* hydrochloric acid (1.0 ml) over 5% palladium on charcoal (100 mg) for 16 hours at room temperature and atmospheric pressure. The product after one crystallization from ether–methanol gave prisms, m.p. 204–205° C, $[\alpha]_{D^{26}} = +64.6°$ ($c = 0.5$ in ethanol), in 82% yield. Found: C, 52.78; H, 9.08; N, 9.32; Cl, 11.88%.

Attempts to prepare methyl L-isoleucyl-L-leucinate hydrochloride by the latter procedure gave a product which could not be crystallized.

L-Isoleucyl-L-leucyl Anhydride

A solution of methyl L-isoleucyl-L-leucinate hydrochloride (0.25 g) in dry methanol (50 ml) cooled to −10° C in an ice–salt bath was saturated with dry ammonia. After 30 minutes the reaction mixture was allowed to warm to room temperature and kept for 18 hours. The solvent was evaporated and the residue crystallized from aqueous ethanol to give fine needles (0.14 g = 74%), m.p. (sealed capillary) 283° C, $[\alpha]_{D^{26}} = -83.0°$ ($c = 0.1$ in chloroform). Found: C, 63.86; H, 9.86; N, 12.11%. Calc. for $C_{12}H_{22}O_2N_2$: C, 63.68; H, 9.80; N, 12.38%.

L-Isoleucyl-D-leucyl anhydride, prepared similarly in a yield of 72%, had m.p. (sealed capillary) 289.5–290.5° C $[\alpha]_{D^{26}} = +16.1°$ ($c = 0.1$ in chloroform). Found: C, 63.82; H, 9.70; N, 12.34%.

ACKNOWLEDGMENT

The author thanks Miss M. J. A. Gates for competent technical assistance.

1. J. L. Johnson, W. G. Jackson, and T. E. Eble. J. Am. Chem. Soc. **73**, 2947 (1951).
2. Y. Koaze. Bull. Agr. Chem. Soc. Japan, **22**, 98 (1958).
3. Y. S. Chen. Bull. Agr. Chem. Soc. Japan, **24**, 372 (1960).
4. Y. Kodaira. Agr. Biol. Chem. (Tokyo), **25**, 261 (1961).
5. J. H. Birkenshaw and Y. S. Mohammed. Biochem. J. **85**, 523 (1962).
6. T. Curtius and F. Goebel. J. Prakt. Chem. **37**, 173 (1888).
7. E. Fischer and U. Suzuki. Ber. **38**, 4173 (1905).
8. E. Abderhalden and S. Suzuki. Z. Physiol. Chem. **176**, 101 (1928).
9. C. Sannie. Bull. Soc. Chim. France, **9**, 487 (1942).
10. E. Abderhalden and E. Komm. Z. Physiol. Chem. **139**, 417 (1924).
11. E. Fischer and E. Forneau. Ber. **34**, 2868 (1901).
12. J. R. Vaughan, Jr. and R. L. Osato. J. Am. Chem. Soc. **74**, 676 (1952).
13. E. Fischer and H. Scheibler. Ann. **363**, 136 (1908).
14. S. W. Fox, M. Fling, H. Wax, and C. W. Pettinga. J. Am. Chem. Soc. **72**, 1862 (1950).
15. M. Brenner and W. Huber. Helv. Chim. Acta, **36**, 1114 (1953).

Received May 30, 1963.
Prairie Regional Laboratory,
National Research Council,
Saskatoon, Saskatchewan.

THE STRUCTURE OF CYCLOHEXYLIDENEMALONONITRILE DIMER

M. R. S. Weir and J. B. Hyne

The reaction between cyclohexanone and malononitrile in the presence of base was reported (1) to form cyclohexylidenemalononitrile, described as a crystalline solid of m.p. 173.5–174.5°. A second group of investigators (2) showed that cyclohexylidenemalononitrile is in fact a liquid of b.p. 137–138° at 10 mm, and they suggested that the crystalline solid previously reported was a dimer or polymer of this substance.

Reinvestigation of the solid product, prepared either by treatment of a mixture of cyclohexanone and malononitrile with base (Corson and Stoughton's method (1)) or by treatment of cyclohexylidenemalononitrile with base, has shown it to be a dimer of cyclohexylidenemalononitrile, and we suggest that it has structure I(*a*), I(*b*), existing as a tautomeric mixture. An analogous base-catalyzed dimerization of isopropylidenemalononitrile to give a cyclic product has recently been reported (3). The mechanism for the formation of cyclohexylidenemalononitrile dimer is outlined in Chart I.

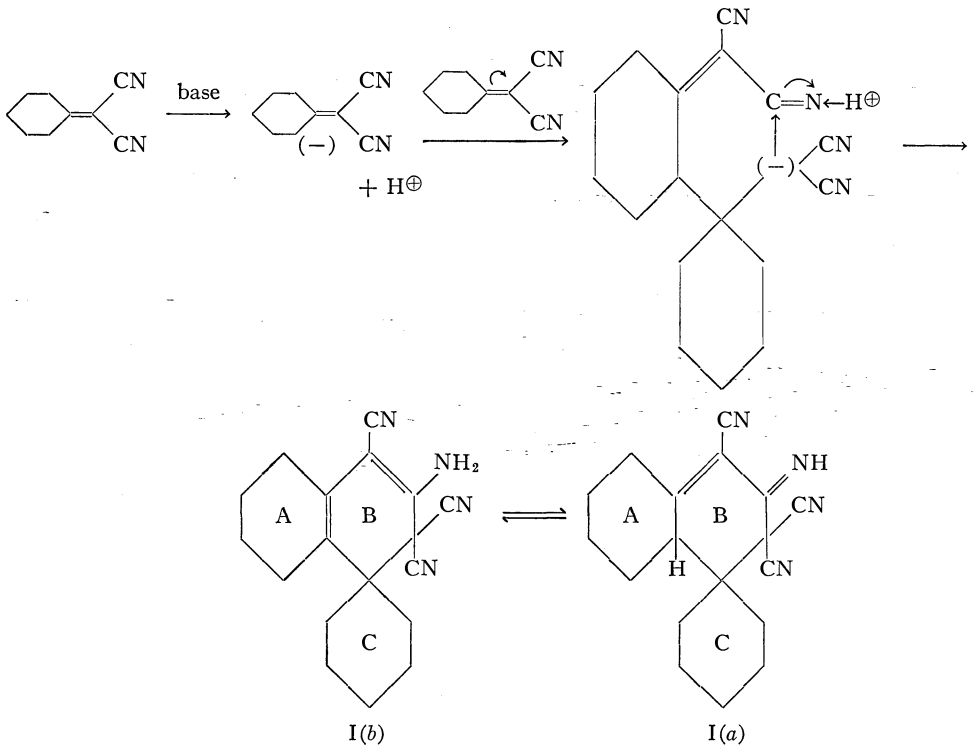

Chart I.

The dimer has the following infrared absorption pattern: 2.79, 2.85 μ (doublet, s, —NH_2); 3.00 μ (w, =NH); 3.30, 3.41 μ (doublet, s, C—H); 4.45 μ (s, conjugated CN); 6.08, 6.22 μ (doublet, s, C=N and C=C).

The positions and areas of the five peaks in the n.m.r. spectrum of the dimer can be assigned as shown in Table I, (I).

Can. J. Chem. Downloaded from www.nrcresearchpress.com by 210.87.254.5 on 09/05/12
For personal use only.

TABLE I

	τ, p.p.m. (T.M.S. = 10)	Rel. area (exptl.)	Theoret. area if tautomeric mixture were 50:50	Assignment
(I)	3.90	0.7	0.5	=N*H*
	4.95	1.3	1	—NH_2
	7.45	0.4	0.5	Bridgehead hydrogen between rings A & B in imino form
	8.00*	8	8	A ring hydrogens
	8.42*	9.5	10	C ring hydrogens
(II)	6.80	0.6	0.5	B ring hydrogen
	7.00	0.7	0.5	Bridgehead hydrogen between rings A & B in imino form
	8.00*	8	8	A ring hydrogens
	8.45*	9.5	10	C ring hydrogens

NOTE: Both spectra were run in $CDCl_3$ (~20% solutions).
*The bands at 8.00 and 8.42 τ are broad and overlap very considerably, making area estimation difficult. Consequently, it is also difficult to *accurately* relate these areas, which will be fixed and not upset by the tautomeric equilibrium, to the areas of the other peaks.

When the dimer is subjected to gentle acid hydrolysis the ketones II(*a*), II(*b*) are formed:

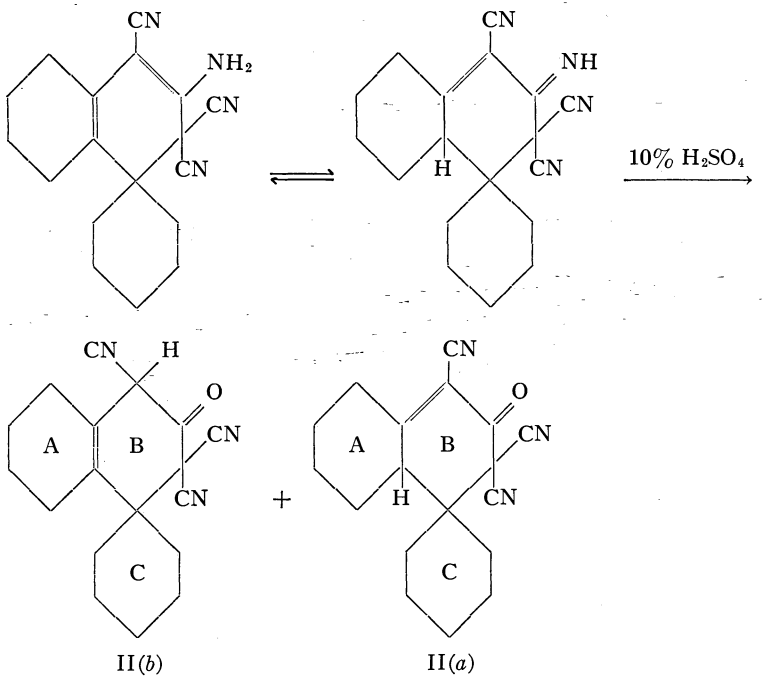

II(*b*) II(*a*)

The infrared spectrum of the hydrolysis product showed no absorption in the N—H stretching region; the characteristic bands were the following: 3.31, 3.42 μ (doublet, s, C—H); 4.50 μ (m, C≡N); 5.80, 5.85 μ* (doublet, s, C=O); 6.20 μ (s, C=C).

The n.m.r. spectrum of the hydrolysis product also showed complete absence of bands corresponding to =NH and —NH_2 groups. The bands are listed in Table I, (II).

**The carbonyl band showed distinct splitting into a doublet, when the spectrum was run in nujol: in a KBr pellet it appeared as one peak at 5.80 μ, with a shoulder at 5.85 μ.*

Can. J. Chem. Downloaded from www.nrcresearchpress.com by 210.87.254.5 on 09/05/12
For personal use only.

Dimerizations of alkylidenemalononitriles to give *acyclic* products has also been suggested by earlier workers (2, 4). Cyclohexylidenemalononitrile could conceivably dimerize to give the acyclic products shown in Chart II.

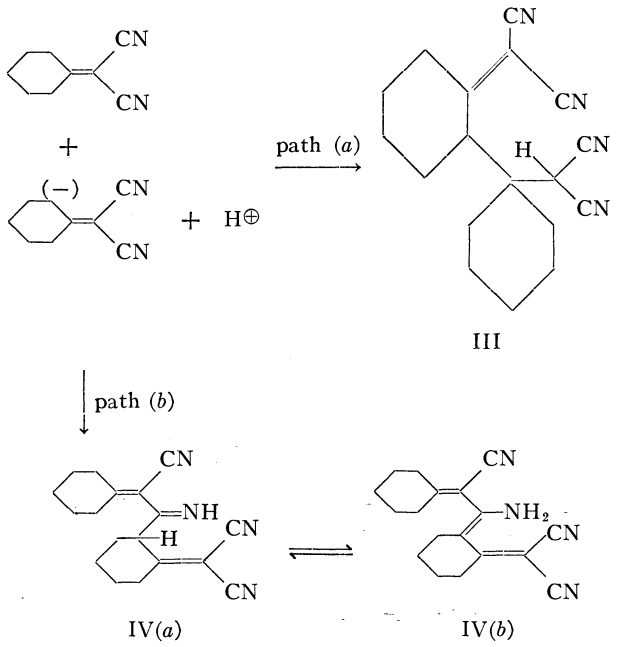

CHART II.

Structure III can be rejected since it does not contain an $—NH_2$ or an =NH group. Structures IV(*a*), IV(*b*) have been rejected in favor of I(*a*), I(*b*) after consideration of the following points. (*a*) If the dimer had this open-chain structure then the ratio of the intensity of the CN to CH absorption in the infrared would be expected to be greater than this ratio for the monomer. We find, in fact, that the ratio is significantly less for the dimer than for the monomer. (*b*) The ultraviolet absorption spectrum of the monomer has one intense band at 235 mμ ($\epsilon \simeq 59{,}000$), while that of the dimer has two bands, one at 300 mμ ($\epsilon = 12{,}400$) and one at 245 mμ ($\epsilon = 7{,}500$). An acyclic dimer with the triene structure IV(*b*) would be expected to absorb at longer wavelength and to have a significantly more intense absorption than the monomer. The reduction in the intensity of the absorption in the dimer relative to the monomer is consistent with the cross-conjugated systems I(*a*), I(*b*). (*c*) The n.m.r. spectra of both the dimer and its hydrolysis product show undisturbed cyclohexane hydrogen absorptions (τ for cyclohexane = 8.5 p.p.m.), consistent with the cyclic spiro structure, where the C ring hydrogens would be expected to be undisturbed. (*d*) The close analogy between this reaction and the dimerization of isopropylidenemalononitrile (3) to give a dimer of the structure

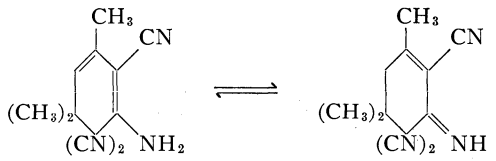

strongly suggests a cyclic product rather than an acyclic one.

Can. J. Chem. Downloaded from www.nrcresearchpress.com by 210.87.254.5 on 09/05/12
For personal use only.

It is also noteworthy that Anderson, Bell, and Duncan (4) showed that the reaction of acetophenone with malononitrile in the presence of base gave two products: (*a*) 1,1-dicyano-2-methyl-2-phenylethylene, and (*b*) a high-melting yellow solid, described as an isomer of the above. The authors state that the infrared spectrum of this yellow compound did not agree with the expected 4-amino-1,1,5-tricyano-2,6-diphenylhepta-1,3,5-triene. It seems probable that this material was in fact the cyclic dimer

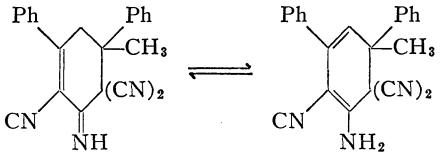

produced by a mechanism analogous to the one given above for the dimerization of cyclohexylidenemalononitrile.

EXPERIMENTAL

Preparation of Cyclohexylidenemalononitrile (2)

Malononitrile (20 g, 0.26 m) was dissolved in 30 g (0.3 m) of cyclohexanone, and 0.5 ml of piperidine was added. The mixture was allowed to stand for about 1 hour, then was dissolved in benzene, washed with 2% hydrochloric acid and then with water. The benzene solution was dried over anhydrous magnesium sulphate and the product distilled, b.p. 85–90° at 1–0.7 mm, n_D^{25} 1.5098. Lit. b.p. 137–138° at 10 mm, n_D^{25} 1.5110.

Preparation of Cyclohexylidenemalononitrile Dimer

When cyclohexylidenemalononitrile was treated with a few drops of piperidine and the mixture allowed to stand at room temperature overnight it solidified to a glass, which on treatment with solvent (95% ethanol) gave a pale yellow crystalline solid, m.p. 172–173°. Recrystallization from 95% ethanol gave pale yellow plates of m.p. 174°. Lit. (1) m.p. 173.5–174.5°. Anal.: Calc. for $C_{18}H_{20}N_4$: C, 74.00; H, 6.86; N, 19.27 mol. wt., 292. Found: C, 73.69; H, 7.00; N, 19.28; mol. wt., 304.

Identical material was obtained by leaving the mixture of malononitrile, cyclohexanone, and piperidine in contact overnight and recrystallizing the resultant glass from 95% ethanol.

Sulphuric Acid Hydrolysis of Cyclohexylidenemalononitrile Dimer

The dimer (100 mg) was stirred overnight with gentle warming in 10 ml of 10% aqueous sulphuric acid. The resulting white solid was washed with water and dried, m.p. 170–175°. Recrystallization from 70% aqueous ethanol gave needles, m.p. 170–173°. Anal.: Calc. for $C_{18}H_{19}N_3O$: C, 73.75; H, 6.49; N, 14.31. Found: C, 73.80; H, 6.52; N, 14.06.

1. B. B. Corson and R. W. Stoughton. J. Am. Chem. Soc. **50**, 2825 (1928).
2. A. C. Cope and K. C. Hoyle. J. Am. Chem. Soc. **63**, 733 (1941).
3. J. K. Williams. Abstracts, Meeting of the American Chemical Society, Los Angeles, Calif. April, 1963.
4. D. M. W. Anderson, F. Bell, and J. L. Duncan. J. Chem. Soc. 4705, (1961).

Received June 20, 1963.
Department of Chemistry,
University of Alberta, Calgary,
Calgary, Alberta.

Can. J. Chem. Downloaded from www.nrcresearchpress.com by 210.87.254.5 on 09/05/12
For personal use only.

LES DIMÉTHYL-6,6 ET DIMÉTHYL-7,7 DÉCALONES-2 *cis* ET *trans*

Hélène Bruderlein,[1] N. Dufort,[2] H. Favre et A. J. Liston

Les diméthyl-6,6 décalones-2 *cis* et *trans* ont été préparées par réduction de la diméthyl-6,6 $\Delta^{1(9)}$-octalone-2 (I). Nous avons obtenu cette cétone α,β-éthylénique, point

[1]*Boursière de l'Office de la Recherche Scientifique de la Province de Québec, 1956–1959.*
[2]*Boursier du Conseil National de Recherches du Canada, 1959–1963.*

It is also noteworthy that Anderson, Bell, and Duncan (4) showed that the reaction of acetophenone with malononitrile in the presence of base gave two products: (*a*) 1,1-dicyano-2-methyl-2-phenylethylene, and (*b*) a high-melting yellow solid, described as an isomer of the above. The authors state that the infrared spectrum of this yellow compound did not agree with the expected 4-amino-1,1,5-tricyano-2,6-diphenylhepta-1,3,5-triene. It seems probable that this material was in fact the cyclic dimer

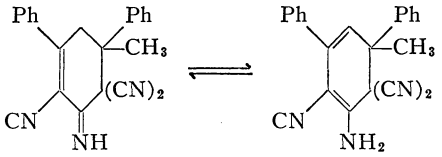

produced by a mechanism analogous to the one given above for the dimerization of cyclohexylidenemalononitrile.

EXPERIMENTAL

Preparation of Cyclohexylidenemalononitrile (2)

Malononitrile (20 g, 0.26 m) was dissolved in 30 g (0.3 m) of cyclohexanone, and 0.5 ml of piperidine was added. The mixture was allowed to stand for about 1 hour, then was dissolved in benzene, washed with 2% hydrochloric acid and then with water. The benzene solution was dried over anhydrous magnesium sulphate and the product distilled, b.p. 85–90° at 1–0.7 mm, n_D^{25} 1.5098. Lit. b.p. 137–138° at 10 mm, n_D^{25} 1.5110.

Preparation of Cyclohexylidenemalononitrile Dimer

When cyclohexylidenemalononitrile was treated with a few drops of piperidine and the mixture allowed to stand at room temperature overnight it solidified to a glass, which on treatment with solvent (95% ethanol) gave a pale yellow crystalline solid, m.p. 172–173°. Recrystallization from 95% ethanol gave pale yellow plates of m.p. 174°. Lit. (1) m.p. 173.5–174.5°. Anal.: Calc. for $C_{18}H_{20}N_4$: C, 74.00; H, 6.86; N, 19.27 mol. wt., 292. Found: C, 73.69; H, 7.00; N, 19.28; mol. wt., 304.

Identical material was obtained by leaving the mixture of malononitrile, cyclohexanone, and piperidine in contact overnight and recrystallizing the resultant glass from 95% ethanol.

Sulphuric Acid Hydrolysis of Cyclohexylidenemalononitrile Dimer

The dimer (100 mg) was stirred overnight with gentle warming in 10 ml of 10% aqueous sulphuric acid. The resulting white solid was washed with water and dried, m.p. 170–175°. Recrystallization from 70% aqueous ethanol gave needles, m.p. 170–173°. Anal.: Calc. for $C_{18}H_{19}N_3O$: C, 73.75; H, 6.49; N, 14.31. Found: C, 73.80; H, 6.52; N, 14.06.

1. B. B. Corson and R. W. Stoughton. J. Am. Chem. Soc. **50**, 2825 (1928).
2. A. C. Cope and K. C. Hoyle. J. Am. Chem. Soc. **63**, 733 (1941).
3. J. K. Williams. Abstracts, Meeting of the American Chemical Society, Los Angeles, Calif. April, 1963.
4. D. M. W. Anderson, F. Bell, and J. L. Duncan. J. Chem. Soc. 4705, (1961).

Received June 20, 1963.
Department of Chemistry,
University of Alberta, Calgary,
Calgary, Alberta.

Can. J. Chem. Downloaded from www.nrcresearchpress.com by 210.87.254.40 on 09/05/12
For personal use only.

LES DIMÉTHYL-6,6 ET DIMÉTHYL-7,7 DÉCALONES-2 *cis* ET *trans*

Hélène Bruderlein,[1] N. Dufort,[2] H. Favre et A. J. Liston

Les diméthyl-6,6 décalones-2 *cis* et *trans* ont été préparées par réduction de la diméthyl-6,6 $\Delta^{1(9)}$-octalone-2 (I). Nous avons obtenu cette cétone α,β-éthylénique, point

[1]*Boursière de l'Office de la Recherche Scientifique de la Province de Québec, 1956–1959.*
[2]*Boursier du Conseil National de Recherches du Canada, 1959–1963.*

du fusion 69–71°, en mettant en œuvre la méthode de Stork (1): condensation de la méthyl-vinyl-cétone avec l'ène-pyrrolidine issue de la diméthyl-4,4 cyclohexanone, suivie de la cyclisation et de l'hydrolyse habituelles. Le spectre infrarouge montre la présence de quelques pourcents de la cétone correspondante β,γ-éthylénique; le spectre ultraviolet présente un maximum à 239 mμ, log ϵ = 4.20.

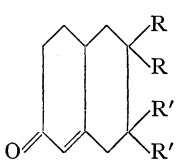

I: R = CH_3; R′ = H
II: R = H; R′ = CH_3

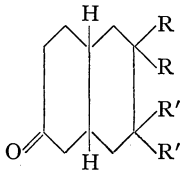

III: R = CH_3; R′ = H
IV: R = H; R′ = CH_3

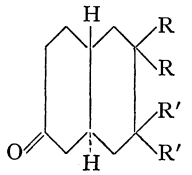

V: R = CH_3; R′ = H
VI: R = H; R′ = CH_3

Nous avons réduit l'octalone I sur palladium/charbon en présence d'acide chlorhydrique et par le lithium dans l'ammoniac liquide et obtenu deux décalones différentes, auxquelles, par analogie avec la série diméthylée en -7,7 (2), nous attribuons les configurations *cis* (III) et *trans* (V) respectivement. Brutes, les décalones ne sont pas pures: la *trans* contient de l'alcool correspondant et la *cis* 9% d'isomère *trans*, décelé par chromatographie en phase gazeuse. La décalone *trans* pure fut obtenue par oxydation chromique de la décalone *trans* brute et la décalone *cis* par chromatographie en phase gazeuse à grande échelle qui permet d'éliminer l'isomère *trans*. Les dinitro-2,4 phénylhydrazones fondent à 193–194° (*trans*) et 170–172° (*cis*).

Augustine et Broom (2) ont réduit l'octalone II sur palladium/charbon en présence d'acide chlorhydrique en diméthyl-7,7 décalone-2 *cis* (IV) qu'ils décrivent comme liquide; dans nos mains, cette décalone est un solide, p.f. 43°, homogène en chromatographie en phase gazeuse. La réduction de l'octalone II par le lithium dans l'ammoniac liquide en décalone VI *trans*, conduit à une décalone *trans* brute qui contient de 10–20% de diméthyl-7,7 décalol-2 *trans* (la configuration du groupe —OH n'a pas été établie). Par oxydation chromique de la décalone brute nous avons obtenu la décalone *trans* VI pure, homogène en chromatographie en phase gazeuse. Les dinitro-2,4 phénylhydrazones que nous avons préparées à partir de nos échantillons de décalones *cis* et *trans* n'ont pas les points de fusion donnés par Augustine et Broom (2).

L'octalone II que nous avons préparée selon la méthode de Stork est en tout point semblable à celle que décrivent Augustine et Broom (2). L'ène-pyrrolidine issue de la diméthyl-3,3 cyclohexanone ne conduit, à la cyanoéthylation, qu'à la diméthyl-3,3 cyanoéthyl-5 cyclohexanone (3): nous pouvions ainsi prévoir la formation exclusive de l'octalone II.

PARTIE EXPÉRIMENTALE[3]

1. Diméthyl-6,6 $\Delta^{1(9)}$-octalone-2 (I)

L'ène-pyrrolidine correspondant à la diméthyl-4,4 cyclohexanone, p.é. 116–117° sous 13 mm, n_D^{22} = 1.5031, a été préparée avec un rendement de 91.1% selon (1). L'octalone I, p.f. 69–71° (cristallisation dans l'éther

[3]*Les points de fusion ont été déterminés en tubes capillaires, en utilisant un thermomètre étalonné avec des substances de points de fusion connus. Les spectres infrarouges ont été déterminés avec un spectromètre Perkin–Elmer, modèle 221, optique* NaCl, *les spectres ultraviolets avec un appareil Beckman DK1. La chromatographie en phase gazeuse fut effectuée avec un appareil Kromo-tog K-2 de Burrell Corporation, pour les déterminations analytiques, et un appareil Fisher Prep-Partitioner, pour les séparations à grande échelle. DNP: dinitro-2,4 phénylhydrazone. SEM: semicarbazone. CPG: chromatographie en phase gazeuse. Les analyses sont de W. Manser, Herrliberg (Suisse) et de C. Daesslé, Organic Microanalyses, Montréal.*

Can. J. Chem. Downloaded from www.nrcresearchpress.com by 210.87.254.40 on 09/05/12
For personal use only.

de pétrole) a été préparée selon la méthode II, 2 de Stork *et al.* (1), avec un rendement de 39.5% à partir de la cétone. Calc. pour $C_{12}H_{18}O$: C, 80.84; H, 10.18%. Trouvé: C, 80.82; H, 10.21%. SEM, p.f. 223–225° (EtOH–dioxanne). Calc. pour $C_{13}H_{21}ON_3$: C, 66.36; H, 8.99; N, 17.86%. Trouvé: C, 66.12; H, 8.94; N, 17.88%.

2. Diméthyl-6,6 décalone-2 cis (III) (cf. réf. 2)

Un mélange de 17.6 g d'octalone I, 1.76 g de palladium sur charbon 10%, 88 ml d'éthanol anhydre et 8 ml de HCl 3 *N* est agité en atmosphère d'hydrogène pendant 12 heures. Une mole d'hydrogène est absorbée. Le catalyseur est essoré et lavé avec un peu d'acétone. Le filtrat et les solvants de lavage sont réunis et évaporés à 11 mm. Le résidue est repris par de l'éther; on lave avec une solution aqueuse saturée de NaCl, sèche sur sulfate de sodium et évapore. Le résidu est distillé: 14.6 g de décalone, p.é. 142° sous 20 mm, n_D^{22} = 1.4858. Rendement: 82%. La CPG (2.5 m, 20% polyester succinique de Craig sur brique) révèle la présence de 9% d'isomère *trans* décrit en 3. L'ordre d'élution est *trans*, *cis*. L'isomère *cis* pur fut obtenu par CPG, à l'échelle du gramme (une colonne de 45×5 cm, suivie de trois colonnes en série de 45×3 cm, 20% huile de silicone No. 200, 1000 cs de Dow Corning sur brique). Calculé pour $C_{12}H_{20}O$: C, 79.94; H, 11.18%. Trouvé: 79.92; H, 11.07%. SEM, p.f. 207–208° (EtOH). Calculé pour $C_{13}H_{23}ON_3$: C, 65.77; H, 9.76; N, 17.70%. Trouvé C, 65.69; H, 9.80; N, 17.61%. DNP, p.f. 170–172° (EtOH). Calculé pour $C_{18}H_{24}O_4N_4$: C, 59.98; H, 6.71; N, 15.55%. Trouvé: C, 59.91; H, 6.66; N, 15.59%.

3. Diméthyl-6,6 décalone-2 trans (V)

A 100 ml d'ammoniac liquide on ajoute 3 g d'octalone I dans 23 ml d'éther anhydre, puis 0.136 g de lithium coupé en petits morceaux jusqu'a ce que la couleur bleue persiste; après 15 minutes, la coloration bleue disparaissant, on ajoute 30 mg de lithium. La solution est agitée pendant 3 heures. On ajoute alors 3.64 g de NH_4Cl et laisse l'ammoniac s'évaporer à température de la pièce. Le résidu est repris par de l'eau et extrait par de l'éther; la solution éthérée est lavée par HCl 3 *N*, puis par de l'eau saturée de NaCl, séchée et évaporée. Le résidu est distillé: 1.1 g, p. é. 74° sous 0.5 mm, n_D^{21} = 1.4880. Rendement: 37%. La décalone brute contient de l'alcool et de l'octalone de départ (décelés par spectroscopie infrarouge). La réduction par NH_3/Li est répétée. Puis 5.3 g de décalone brute sont mis en solution dans 50 ml de pyridine anhydre; cette solution est ajoutée, goutte à goutte, à température de la pièce, à 50 ml de pyridine contenant 5 g de CrO_3. Le tout est agité pendant 12 heures à température de la pièce. On extrait à la manière habituelle la décalone *trans* pure, n_D^{22} = 1.4892 (rendement 31%); un seul pic en CPG, dans les conditions décrites en 2.

Calculé pour $C_{12}H_{20}O$: C, 79.94; H, 11.18%. Trouvé: C, 80.06; H, 11.14%. SEM, p.f. 217–219° (EtOH–dioxanne). Calculé pour $C_{13}H_{23}ON_3$: C, 65.77; H, 9.76; N, 17.70%. Trouvé: C, 65.61; H, 9.69; N, 17.79%. Donne une dépression de p.f. en mélange avec la SEM de la décalone *cis* décrite en 2. DNP, p.f. 193–194° (EtOH–$CHCl_3$). Calculé pour $C_{18}H_{24}O_4N_4$: C, 59.98; H, 6.71; N, 15.55%. Trouvé: C, 59.93; H, 6.65; N, 15.34%. Donne une dépression de p.f. en mélange avec la DNP de l'isomère *cis* décrite en 2.

4. Diméthyl-7,7 $\Delta^{1(9)}$-octalone-2 (II)

Elle fut préparée selon la méthode décrite plus haut en 1, avec un rendement de 43% à partir de la diméthyl-3,3 cyclohexanone, en passant par l'ène-pyrrolidine décrite en réf. 3. P. é. 94° sous 0.15 mm, n_D^{25} = 1.5050. DNP, p.f. 196–197°. Augustine et Broom (2) donnent: DNP, p.f. 196–197°.

5. Diméthyl-7,7 décalone-2 cis (IV)

Elle fut préparée, avec un rendement de 95%, à partir de l'octalone décrite en 4, selon la méthode décrite en 2. Il n'est pas nécessaire de chromatographier en phase gazeuse, la décalone brute cristallisant d'elle-même. P.f. 43° (éther de pétrole). Calculé pour $C_{12}H_{20}O$: C, 79.94; H, 11.18%. Trouvé: C, 79.94; H, 11.18%. SEM, p.f. 186–187° (EtOH 95%). Calculé pour $C_{13}H_{23}ON_3$: C, 65.77; H, 9.76; N, 17.70%. Trouvé: C, 65.57; H, 9.82; N, 17.55%. DNP, p.f. 161.0–162.0° (MeOH). Calculé pour $C_{18}H_{24}N_4O_4$: C, 59.98; H, 6.71; N, 15.65%. Trouvé: C, 59.88; H, 6.63; N, 15.63%. Augustine et Broom (2) donnent: liquide; DNP, p.f. 129–130°.

6. Diméthyl-7,7 décalone-2 trans (VI)

Elle fut préparée avec un rendement de 52% à partir de l'octalone décrite en 4, selon la méthode détaillée en 3. P.é. 69–70° sous 0.45 mm, n_D^{20} = 1.4786. Calculé pour $C_{12}H_{20}O$: C, 79.94; H, 11.18%. Trouvé: C, 79.87; H, 11.15%. SEM, p.f. 195°. Calculé pour $C_{13}H_{23}ON_3$: C, 65.77; H, 9.76; N, 17.70%. Trouvé: C, 65.64; H, 9.85; N, 17.73%. DNP, p.f. 141.5°. Calculé pour $C_{18}H_{24}N_4O_4$: C, 59.98; H, 6.71; N, 15.55%. Trouvé: C, 59.75; H, 6.61; N, 15.63%. Augustine et Broom (2) donnent: liquide; DNP, p.f. 164–165°.

REMERCIEMENTS

Nous remercions le Conseil National de Recherches du Canada d'une subvention de recherches (H. F.) et d'une bourse d'études (N. D.), ainsi que l'Office de la Recherche Scientifique de la Province de Québec d'une bourse d'études (H. B.).

Can. J. Chem. Downloaded from www.nrcresearchpress.com by 210.87.254.40 on 09/05/12
For personal use only.

1. G. STORK, A. BRIZZOLARA, H. LANDESMAN, J. SZMUSZKOVICZ, et R. TERRELL. J. Am. Chem. Soc. **85**, 207 (1963).
2. R. L. AUGUSTINE et A. D. BROOM. J. Org. Chem. **25**, 802 (1960).
3. F. BRUDERLEIN, H. BRUDERLEIN, H. FAVRE, R. LAPIERRE, et Y. LEFEBVRE. Can. J. Chem. **38**, 2085 (1960).

REÇU LE 4 JUILLET, 1963.
DÉPARTEMENT DE CHIMIE,
UNIVERSITÉ DE MONTRÉAL,
MONTRÉAL, QUÉ.

Can. J. Chem. Downloaded from www.nrcresearchpress.com by 210.87.254.40 on 09/05/12
For personal use only.

THE MOLECULAR STRUCTURE OF HETERATISINE HYDROBROMIDE MONOHYDRATE*

MARIA PRZYBYLSKA

The HBr salt of heteratisine, prepared by Dr. O. E. Edwards, was found to be unstable, but its monohydrate, $C_{22}H_{33}O_5N.HBr.H_2O$, which crystallized from water in the form of large colorless prisms, was satisfactory for the X-ray analysis. The space group is $P2_1$ with two molecules per unit cell of the following dimensions: $a = 8.96$, $b = 14.54$, $c = 8.55$ Å, $\beta = 90° 40'$.

Thirteen b axis levels were scanned with filtered Mo radiation and a scintillation counter using the Hilger and Watts' automatic linear diffractometer designed by U. W. Arndt and D. C. Phillips. Close to 1300 intensities were measured.

Two-dimensional Patterson projections along each of the three axes gave two possible locations for the bromine atom. An additional P(UVW) synthesis, however, carried out only for the section at $V = \frac{1}{2}$, led to the unambiguous positioning of bromine at $x = 0.236$ and $z = 0.080$. The y coordinate was taken as 0.250 and a Fourier summation was carried out for sections perpendicular to the b axis, using the phases calculated on the basis of the heavy atom alone. The interpretation of the perspex model of this three-dimensional synthesis gave the position of 13 light atoms of the molecule. These atoms, all treated as carbons, were used in the subsequent calculation of structure factors. The two Fourier syntheses, which followed, yielded the additional 13 and finally the last 3 light atoms. Once all the atoms were located, it became obvious that heteratisine has a similar carbon–nitrogen skeleton to lycoctonine (1) and other related highly oxygenated *Aconitum* and *Delphinium* alkaloids.

There was no difficulty in distinguishing the oxygen peaks from those of carbon, as they were considerably higher, whereas the nitrogen atom was identified on comparison with other structurally similar alkaloids.

The six-membered ring carrying the methoxy group is of appreciably distorted 'boat' form. The methoxyl has the same configuration as the corresponding hydroxyl in delcosine (2), in which the six-membered ring is also in the 'boat' form.

A photograph of the molecule together with its structural formula is given in Fig. 1.

The absolute configuration represented in Fig. 1 has not been determined in this study, but conforms to that of other known diterpenoid alkaloids with the same basic skeleton (3). Evidence from optical rotation† of heteratisine derivatives is also consistent with this absolute stereochemistry.

Issued as N.R.C. No. 7583.
†*Personal communication from Dr. O. E. Edwards.*

1. G. STORK, A. BRIZZOLARA, H. LANDESMAN, J. SZMUSZKOVICZ, et R. TERRELL. J. Am. Chem. Soc. **85**, 207 (1963).
2. R. L. AUGUSTINE et A. D. BROOM. J. Org. Chem. **25**, 802 (1960).
3. F. BRUDERLEIN, H. BRUDERLEIN, H. FAVRE, R. LAPIERRE, et Y. LEFEBVRE. Can. J. Chem. **38**, 2085 (1960).

REÇU LE 4 JUILLET, 1963.
DÉPARTEMENT DE CHIMIE,
UNIVERSITÉ DE MONTRÉAL,
MONTRÉAL, QUÉ.

Can. J. Chem. Downloaded from www.nrcresearchpress.com by 210.87.254.105 on 09/05/12
For personal use only.

THE MOLECULAR STRUCTURE OF HETERATISINE HYDROBROMIDE MONOHYDRATE*

MARIA PRZYBYLSKA

The HBr salt of heteratisine, prepared by Dr. O. E. Edwards, was found to be unstable, but its monohydrate, $C_{22}H_{33}O_5N.HBr.H_2O$, which crystallized from water in the form of large colorless prisms, was satisfactory for the X-ray analysis. The space group is $P2_1$ with two molecules per unit cell of the following dimensions: $a = 8.96$, $b = 14.54$, $c = 8.55$ Å, $\beta = 90° 40'$.

Thirteen b axis levels were scanned with filtered Mo radiation and a scintillation counter using the Hilger and Watts' automatic linear diffractometer designed by U. W. Arndt and D. C. Phillips. Close to 1300 intensities were measured.

Two-dimensional Patterson projections along each of the three axes gave two possible locations for the bromine atom. An additional P(UVW) synthesis, however, carried out only for the section at $V = \frac{1}{2}$, led to the unambiguous positioning of bromine at $x = 0.236$ and $z = 0.080$. The y coordinate was taken as 0.250 and a Fourier summation was carried out for sections perpendicular to the b axis, using the phases calculated on the basis of the heavy atom alone. The interpretation of the perspex model of this three-dimensional synthesis gave the position of 13 light atoms of the molecule. These atoms, all treated as carbons, were used in the subsequent calculation of structure factors. The two Fourier syntheses, which followed, yielded the additional 13 and finally the last 3 light atoms. Once all the atoms were located, it became obvious that heteratisine has a similar carbon–nitrogen skeleton to lycoctonine (1) and other related highly oxygenated *Aconitum* and *Delphinium* alkaloids.

There was no difficulty in distinguishing the oxygen peaks from those of carbon, as they were considerably higher, whereas the nitrogen atom was identified on comparison with other structurally similar alkaloids.

The six-membered ring carrying the methoxy group is of appreciably distorted 'boat' form. The methoxyl has the same configuration as the corresponding hydroxyl in delcosine (2), in which the six-membered ring is also in the 'boat' form.

A photograph of the molecule together with its structural formula is given in Fig. 1.

The absolute configuration represented in Fig. 1 has not been determined in this study, but conforms to that of other known diterpenoid alkaloids with the same basic skeleton (3). Evidence from optical rotation† of heteratisine derivatives is also consistent with this absolute stereochemistry.

Issued as N.R.C. No. 7583.
†*Personal communication from Dr. O. E. Edwards.*

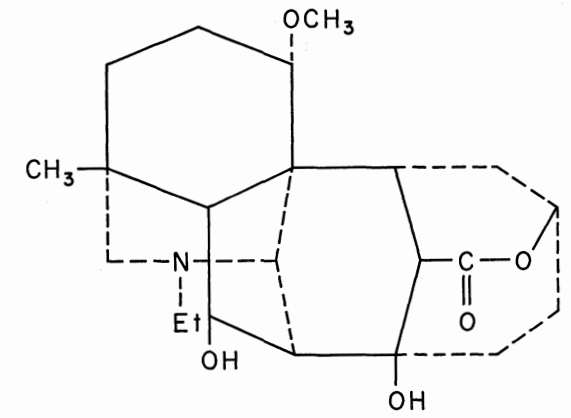

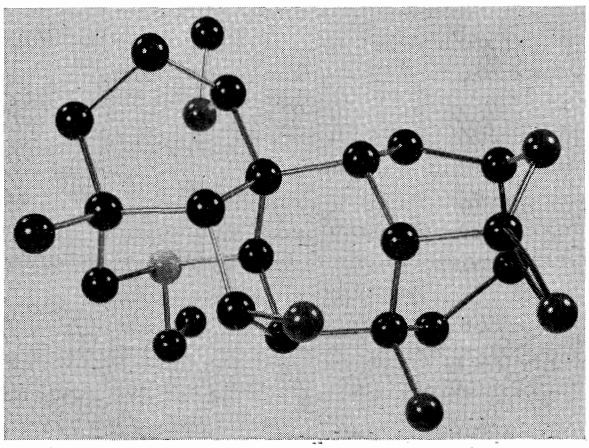

FIG. 1. The stereochemical configuration of heteratisine.

The R factor is 0.19 for the observed data. The fourth three-dimensional electron-density model is completely free from any spurious peaks and leaves no doubt about the correctness of the structure.

Additional intensity measurements and further refinement of the atomic parameters will be carried out and the results will be published in full detail in a different journal.

Grateful acknowledgment is made to Dr. O. E. Edwards for suggesting this problem for a detailed X-ray study and to Dr. L. Marion for his continued encouragement. I also wish to thank Drs. F. R. Ahmed and G. A. Mair for their programs for the IBM 1620 computer and Mrs. C. Mackey for her valuable assistance.

1. M. PRZYBYLSKA. Acta Cryst. **14**, 424 (1961).
2. G. A. MAIR and M. PRZYBYLSKA. In preparation.
3. M. PRZYBYLSKA and L. MARION. Can. J. Chem. **37**, 1843 (1959).

RECEIVED AUGUST 14, 1963.
DIVISION OF PURE CHEMISTRY,
NATIONAL RESEARCH COUNCIL,
OTTAWA, CANADA.

Can. J. Chem. Downloaded from www.nrcresearchpress.com by 210.87.254.105 on 09/05/12
For personal use only.

N.M.R. SOLVENT STUDIES: HYDRAZINE AS A SOLVENT

H. AGAHIGIAN, H. GAUTHIER, H. HOBERECHT, AND L. RAPHAELIAN

The studies of hydrogen bonding (1, pp. 400–407; 2–4, 5 and references cited therein) with respect to proton chemical shifts have shown effects the order of magnitude of which was dependent on causes such as concentration, solvent–solute interactions, and the nature of the solvents, to mention a few. It is interesting to note that, for none of the solvent systems studied, has work been done with anhydrous hydrazine as a solvent. In most cases, the solvent systems used are polar to non-polar with varying concentrations of solute. No study concerning groups such as amino or hydroxyl groups in aromatic systems has been done and the hope is that some information might be obtained which will lead to a better understanding of hydrogen bonding.

Recently, the methyl resonances (6) in steroids were assigned by using pyridine as a solvent, and from the published spectra, a dramatic change was effected which made the assignment possible. In addition, a study of pyrrole and N-substituted pyrroles (7), as well as substituted quinolines (8), and a study of interactions in benzene (9) have shown that the solvent effects are not a function of the extent of hydrogen bonding but require an explanation which involves a preferred orientation of solvent–solute interaction. The scope of this study embodies the use of hydrazine as a solvent in nuclear magnetic resonance (n.m.r.) studies and its effects on the various aromatic protons in systems where the substituents are electron-donating, and will themselves be more susceptible to hydrogen bonding or association with the solvent. The spectra of the saturated heterocyclics, 2-pyrrolidone, and N-methyl 2-pyrrolidone were observed in anhydrous hydrazine using tetramethylsilane as an external standard, as well as in deuterochloroform with external tetramethylsilane, and the spectra were identical. A similar experiment with about 10% solution *dl*-2,3 diphenyl-2,3-butanediol yielded spectra which were essentially unchanged, indicating little or no effect on the aromatic protons in this type of system. The aromatic proton resonance of *dl*-2,3-diphenyl-2,3-butanediol in hydrazine was 456 c/s from external tetramethylsilane; in deuterochloroform the phenyl resonance was 457 c/s from external tetramethylsilane, i.e., essentially unchanged in the two solvents. Although hydrazine is a compound which has applicability in synthetic chemistry it appears to be of value as a solvent for some organic compounds.

The spectrum of *o*-phenylenediamine in deuterochloroform was a single peak; however, in anhydrous hydrazine the aromatic protons were a typical A_2B_2 case similar to *o*-dichlorobenzene (1).* The spectrum of 1,3-phenylenediamine was obtained in both deuterochloroform and hydrazine and marked low field displacement of the ortho protons (H_4 and H_6) in hydrazine compared to the deuterochloroform solution suggested a change in the amino functions possibly due to association.

The spectrum of 2,4-dichlorophenol was obtained in deuterochloroform, deuterochloroform and hydrazine mixtures, and anhydrous hydrazine (Table I). Since the use of an external standard was needed for the anhydrous hydrazine, more reliable data was obtained by viewing the 2,4-dichlorophenol in deuterochloroform while anhydrous hydrazine was added dropwise to effect the changes in line positions of the aromatic protons. While the protons at positions 5 and 6 shifted to high field, the proton at position

*In the terminology of D. R. Whitman, J. Mol. Spectry. **10**, 250 (1963), the aromatic protons should be designated as an AA'BB' type.*

Can. J. Chem. Downloaded from www.nrcresearchpress.com by 210.87.254.40 on 09/05/12
For personal use only.

TABLE I

Chemical shifts of aromatic protons
(c/s from internal TMS)

Compound		Solvent $CDCl_3$	Solvent N_2H_4	Δ
2,4-Dichlorophenol 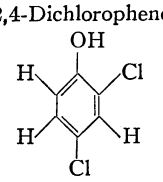	H_3	436±2	436	—
	H_5	430	418	+12
	H_6	413	395	+18
2,5-Dichloroaniline 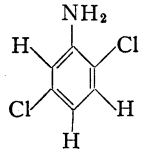	H_3	425	428	− 3
	H_4	399, 393	393	—
	H_6		408	—(11–13)
m-Nitrocresol 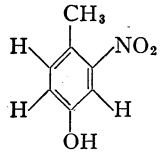	H_3	470	457	+13
	H_5	443	420	+23
	H_6	420	395	+25

3 remained essentially unchanged. The possibility of hydrogen bonding with the halogens would not sufficiently explain this phenomenon and a more reasonable explanation is the contributing resonance forms, which might be drawn for ortho and para quinoid types. The high field shift of the other aromatic protons are most likely due to hydrazine salt formation yielding a phenoxide-type ion. In order to establish that no reaction had occurred, the 2,4-dichlorophenol was dissolved in anhydrous hydrazine and allowed to stand, at which time the hydrazine was removed by vacuum. The proton resonance spectrum of the isolated material indicated it was the starting compound.

The study of a 2,5-dichloroaniline yielded some interesting data concerning the chemical shifts of the three ring protons (Table I). The proton spectrum in deuterochloroform consisted of a doublet at 425 c/s (ortho coupled) from internal tetramethylsilane and two unresolved resonances at 399 and 393 c/s. Successive dropwise addition of hydrazine resulted in a spectrum which consisted of ortho-coupled, ortho- and meta-coupled, and meta-coupled protons (Fig. 1); the ortho coupled proton moving to low field by 3 c/s, the ortho and meta coupled remaining essentially unchanged, and the meta-coupled proton resonance appearing at low field by 11–13 c/s. This low-field shift is most likely due to association of the amino group on the aromatic ring with the hydrazine.

In *m*-nitrocresol, a limitation existed in that, upon addition of a drop of hydrazine to the deuterochloroform solution, a red–orange solid separated. As a result, the chemical shifts (Table I) were obtained by the addition of a drop of deuterochloroform, containing tetramethylsilane, to the anhydrous hydrazine solution. The high-field shifts imply association or interaction with the hydroxyl function and the nitro group.

This study not only applied to amino and phenolic functions on aromatic rings but

Can. J. Chem. Downloaded from www.nrcresearchpress.com by 210.87.254.40 on 09/05/12
For personal use only.

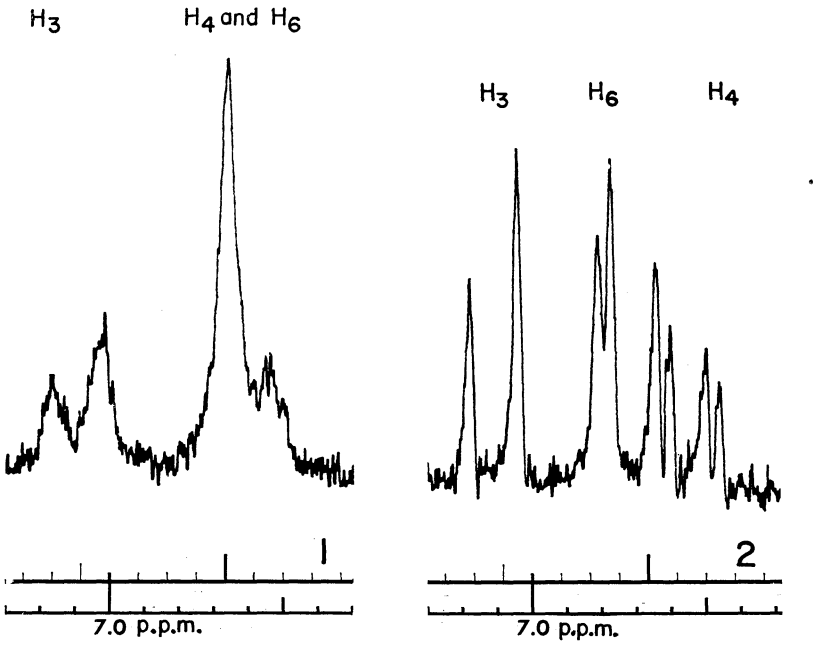

FIG. 1. The aromatic protons of 2,5-dichloroaniline in deuterochloroform using internal $(CH_3)_4Si$.
FIG. 2. The spectrum of 2,5-dichloroaniline in hydrazine demonstrates the effect of hydrazine on the ring protons.

also to systems such as indoles and substituted indoles with the only limitation being the solubility of the organic material in the anhydrous hydrazine. Some of the aromatic compounds studied were *p*-amino-N,N-dimethylaniline, 3-ethoxyaniline, 2-fluoroaniline, and aniline, as well as the various toluenediamine isomers.

EXPERIMENTAL

The n.m.r. spectra were obtained by means of the Varian Associates A-60 spectrometer. The chemical shifts were measured relative to internal tetramethylsilane and in the case of anhydrous hydrazine, a drop of chloroform containing tetramethylsilane was added. In addition, the spectra were obtained in anhydrous hydrazine and no changes were observed which might be due to the addition of a drop of tetramethylsilane in deuterochloroform.

ACKNOWLEDGMENT

The authors wish to thank Mr. G. D. Vickers for his part in this study and the determination of the purity of the anhydrous hydrazine and Dr. Allan P. Gray for his comments and observations.

1. J. A. POPLE, H. J. BERNSTEIN, and W. G. SCHNEIDER. High resolution nuclear magnetic resonance. McGraw-Hill, New York. 1959.
2. A. D. BUCKINGHAM, T. SCHAEFER, and W. G. SCHNEIDER. J. Chem. Phys. **32**, 1227 (1960).
3. T. SCHAEFER and W. G. SCHNEIDER. J. Chem. Phys. **32**, 1218 (1960).
4. G. O. DUDEK. Spectrochim. Acta, **19**, 691 (1963).
5. R. E. KLINCK and J. B. STOTHERS. Can. J. Chem. **40**, 2329 (1962).
6. G. SLOMP and F. MACKELLAR. J. Am. Chem. Soc. **82**, 999 (1960).
7. T. SCHAEFER and W. G. SCHNEIDER. J. Chem. Phys. **32**, 1224 (1960).
8. T. SCHAEFER. Can. J. Chem. **39**, 1864 (1961).
9. W. G. SCHNEIDER. J. Phys. Chem. **66**, 2653 (1962).

RECEIVED APRIL 29, 1963.
OLIN RESEARCH CENTER,
OLIN MATHIESON CHEMICAL CORPORATION,
NEW HAVEN 4, CONNECTICUT.

Can. J. Chem. Downloaded from www.nrcresearchpress.com by 210.87.254.40 on 09/05/12
For personal use only.

Canadian Journal of Chemistry

Issued by THE NATIONAL RESEARCH COUNCIL OF CANADA

VOLUME 41 DECEMBER 1963 NUMBER 12

HALOGEN MIGRATION AND ELIMINATION IN THE CLAISEN REARRANGEMENT OF ALLYL 2,6-DIHALOPHENYL ETHERS[1]

E. PIERS AND R. K. BROWN

Department of Chemistry, University of Alberta, Edmonton, Alberta

Received June 17, 1963

ABSTRACT

A study has been made of some factors affecting the migration or elimination of halogen in the Claisen rearrangement of allyl 2,6-dihalophenyl ethers.

In the thermal rearrangement of allyl 2,6-dichlorophenyl ether, carried out in a number of solvents of different dielectric constant, halogen migration proceeds somewhat better in highly polar solvents. However, a competitive reduction to the monohalogenated allylphenol occurs in the presence of oxidizable solvents and/or products. The reaction is also complicated by the catalytic effects of certain solvents and the phenolic products, which give results similar to those obtained with Lewis acids. Stannous chloride acts as a Lewis acid and catalyzes the rearrangement of allyl 2,6-dichlorophenyl ether with simultaneous halogen rearrangement. As well, a competitive reductive removal of the halogen takes place. Results from the rearrangement of allyl 2,6-dibromophenyl ether with zinc chloride and of allyl 2,6-dichlorophenyl ether with zinc bromide, as well as those from the stannous chloride reactions indicate that the halogen *migration* takes place not only by an allylic shift but also via a competitive halogen *substitution* probably occurring by an S_N2' pathway possibly assisted by a zinc halide bridge mechanism and/or an ionic species such as $ZnX_2Y^{\ominus}$.

INTRODUCTION

In a recent publication (1) it was shown that the thermal Claisen rearrangement of allyl 2,6-dichlorophenyl ether gave not only the previously reported products, 4-allyl-2,6-dichlorophenol and 2-allyl-6-chlorophenol (2), but also a small yield (2%) of the halogen migration product, 2-allyl-4,6-dichlorophenol. The proportion of the halogen migration product increased to 7% and 11% respectively if the thermal rearrangement was conducted in nitrobenzene and in nitrobenzene containing lithium chloride. Addition of the Lewis acid, anhydrous zinc chloride, to a nitrobenzene solution of allyl 2,6-dichlorophenyl ether not only accelerated the rate of rearrangement but also increased the proportion of 2-allyl-4,6-dichlorophenol to as much as 91% of the product (1). It was suggested that the migration of the halogen occurred during the dienone intermediate stage partly by an allylic rearrangement assisted by increased polarity of solvent and/or the presence of the Lewis acid, and partly by a zinc halide bridge mechanism (Fig. 1, routes *a* and *b*). The work reported in the present paper was designed to give additional information concerning the mechanism of rearrangement of the halogen atom.

RESULTS AND DISCUSSION

Thermal Rearrangement of Allyl 2,6-Dichlorophenyl Ether in Various Solvents

To determine the effect of polarity of solvent on the extent of halogen migration, the

[1]*Taken in part from the thesis of E. Piers submitted to the Graduate School, University of Alberta, in partial fulfillment of the requirements for the degree of Doctor of Philosophy.*

Can. J. Chem. Downloaded from www.nrcresearchpress.com by 210.87.254.105 on 09/05/12
For personal use only.

thermal rearrangement of allyl 2,6-dichlorophenyl ether was carried out in a number of solvents* whose polarity, as indicated by their dielectric constant, differed widely. The results are shown in Table I. Although the dielectric constant of a substance generally decreases with increase in temperature, it is reasonable to assume that the *relative* dielectric constants, and hence relative polarity, of a number of solvents would be roughly the same at 170–190° (the temperature of our reaction) as they are at 20° (the temperature at which the dielectric constants are usually measured). Some support for this view is obtained by comparison of the dielectric constant values of several organic liquids at various temperatures (3).

A. Occurrence of Ether Cleavage

In phenol, 10% of the total product of the rearrangement was the ether cleavage material 2,6-dichlorophenol, and 5% of the product was a substance identified as 2-methyl-7-chlorocoumaran, obviously obtained by the cyclization of 2-allyl-6-chlorophenol. Both of these products are characteristic of the zinc chloride catalyzed rearrangement (1) and indicate that phenol not only catalyzes the Claisen rearrangement as has been shown by Goering and Jacobson (5) but also acts in a manner somewhat like that of a Lewis acid by causing ether cleavage as well as coumaran formation. In both N,N-diethylformamide and N-methylformamide the cleavage product also occurred (to the extent of 8% and 6% respectively) but unaccompanied by coumaran formation. A great deal of decomposition took place in these two solvents. The cause of the formation of the cleavage product is not known.

B. Occurrence of Reductive Removal of Halogen

The reduction product, 2-allyl-6-chlorophenol, was found in larger amount in those solvents most easily oxidized. Thus, in decalin, a non-polar solvent wherein considerable decomposition took place during the reaction, 64% of the product was 2-allyl-6-chlorophenol. It is possible that the phenolic products could act as reducing agents under the reaction conditions to yield the monochlorophenol, as is likely in the case of experiment No. 4 where no solvent was used, or in benzonitrile (experiment 6) or in nitrobenzene solutions (experiments 8 and 9). However, for the decalin solution, the fact that the reduction product, 2-allyl-6-chlorophenol, appeared even at a very early stage of the reaction when relatively little phenolic product was present, and that it was present in such a large proportion at the end of the reaction, indicates that the solvent decalin did participate as a reducing agent. Due to the extensive decomposition it was impossible to isolate oxidation products of decalin, such as tetralin etc. to support this view. In N-methylformamide and N,N-diethylformamide, much decomposition took place and the proportion of reduction product was 59% and 23% respectively, presumably also as result of facile oxidation of the solvent and/or its decomposition products.

C. Occurrence of Halogen Migration

In non-acidic solvents of low polarity (diphenyl ether, *o*-dichlorobenzene, allyl 2,6-dichlorophenyl ether) little or no halogen migration occurred (0–2%). The exception to this was decalin wherein 6% of the product was 2-allyl-4,6-dichlorophenol. Since very little of this compound appeared *before 50%* of the original ether had disappeared, it is likely that the phenolic products, associating minimally with the non-polar solvent decalin, and therefore to a greater extent with the remaining unreacted ether, aided the rearrangement of the halogen via a protonation or hydrogen bonding of the acidic proton in the

**The number of solvents was necessarily limited to those of suitable physical characteristics and chemical inertness.*

Can. J. Chem. Downloaded from www.nrcresearchpress.com by 210.87.254.105 on 09/05/12
For personal use only.

Can. J. Chem. Downloaded from www.nrcresearchpress.com by 210.87.254.105 on 09/05/12
For personal use only.

TABLE I

Solvent effect on the halogen migration in the thermal rearrangement of allyl 2,6-dichlorophenyl ether

Expt. No.	Solvent and reaction conditions*	Dielectric constant of solvent†	Composition of reaction mixture, %‡				Character of the reaction
			2,6-Dichloro-phenol	2-Allyl-6-chlorophenol	2-Allyl-4,6-dichlorophenol	4-Allyl-2,6-dichlorophenol	
1	Decalin, 180–185°, 8 hr	?	Nil	64§	6§	30	Considerable decomposition
2	Diphenyl ether, 180–185°, 6 hr	3.6	Nil	3	Nil	97	Very little decomposition
3	*o*-Dichlorobenzene, 178°, 9 hr	7.5	Nil	Trace	Nil	~100	Clean, no decomposition
4	No solvent, 193–200°, 90 min	?	Nil	7	2	91	A small amount of decomposition
5	Phenol, 175–180°, 2 hr	9.9	10	9‖	11	65	Moderate amount of decomposition
6	Benzonitrile, 180–185°, 4.5 hr	25.2	Nil	2	3	95	Very little decomposition
7	N,N-Diethylformamide, 177°, 4.5 hr	?	8	23	38	31	Much decomposition
8	Nitrobenzene, 180–185°, 4 hr	36	Nil	14	7	79	Moderate amount of decomposition
9	Nitrobenzene + LiCl, 180–185°, 3 hr	?	Nil	15	11	74	Moderate amount of decomposition
10	N-Methylformamide 180°, 2.7 hr	190	6	59	25	10	Very much decomposition

*In all cases the reaction time was extended until all of the original ether had disappeared.

†The solvents were arranged in order of increasing dielectric constant (at 20°). Those whose dielectric constants are unknown to us were placed in the order expected, e.g. N,N-diethylformamide is expected to have a dielectric constant not too much different from that of dimethylformamide (37.6). Values of the dielectric constants were obtained from A. A. Maryotte and E. R. Smith, Table of dielectric constants of pure liquids, Natl. Bur. Std., Circ. 514, 1951; reference 3; and reference 4, p. 43. Those for N-methylformamide and N,N-dimethylformamide were obtained from G. R. Leader and J. F. Gormley, J. Am. Chem. Soc., **73**, 5731 (1951).

‡Separate tests showed that in all cases the products were stable under the reaction conditions.

§Analysis of samples of the reaction mixture showed that 2-allyl-6-chlorophenol was formed very early in the reaction (10% after 0.5 hour) and that only very little (1%) of 2-allyl-4,6-dichlorophenol was formed before 50% of the original ether had disappeared.

‖Experiment 5 also gave 5% of a substance which was found to be 2-methyl-7-chlorocoumaran, no doubt derived from the cyclization of some of the 2-allyl-6-chlorophenol in the presence of the acidic phenol solvent. No coumaran was found in any of the other cases.

phenol with the allylic halogen in the intermediate dienone stage, thus promoting the ionization of the allylic halogen. Similarly, rearrangement of halogen in the solvent phenol no doubt is assisted not only by the polarity of the solvent but probably more so by the same effect mentioned above, resulting in the products characteristically produced in the presence of Lewis acids.

In the more highly polar but non-acidic solvents, those of dielectric constant greater than 30 (nitrobenzene, nitrobenzene + LiCl, N,N-diethylformamide, and N-methylformamide) there is a larger extent of halogen migration (7% to 38%). However, the amount of halogen migration does not parallel the polarity of the solvent as expressed by dielectric constant (D.C.) values since N-methylformamide (D.C. = 190) yields 25% of the product as 2-allyl-4,6-dichlorophenol while N,N-diethylformamide (D.C. = 38) yields 38% of the product as halogen-migrated material. However, this can be rationalized if one considers that at the dienone stage there are two competing reactions, one in which the halogen undergoes allylic rearrangement and the other in which the allyl group migrates to the C_4 position. At this stage the halogen migration from C_2 to C_4 is assisted by the greater polarity of solvent while allyl migration from C_2 to C_4 is influenced only minimally if at all by increased solvent polarity (5). Thus the ratio of chlorine migration to allyl rearrangement should give an indication of the effect of polarity of solvent on the extent of halogen migration. In N-methylformamide the ratio is 25/10 while in N,N-diethylformamide it is 38/31. The larger ratio in N-methylformamide parallels its larger dielectric constant. The reductive removal of halogen, greater in the case of N-methylformamide than for N,N-diethylformamide, also must occur at the dienone stage and thus competes with halogen migration. It is likely that if this reductive removal of halogen were not present, the difference in the ratios of halogen to allyl migration in the solvents N-methylformamide and N,N-diethylformamide would be even greater.

Benzonitrile (D.C. = 25.2) is considered to be a polar solvent, yet very little of either the halogen migration product, 2-allyl-4,6-dichlorophenol (3%), or the reduction product, 2-allyl-6-chlorophenol (2%), was formed.

D. Summary re Factors which Affect Halogen Migration and Reductive Removal of Halogen

From the experiments shown in Table I it is seen that a highly polar solvent (expt. 7–10) does assist in the halogen migration as well as in the reductive removal of one of the halogen atoms, with the latter reaction depending upon the presence of an oxidizable substance. However, acidic solvents of lower polarity (and this includes phenolic products of the reaction to some extent) can accomplish the same thing. From the results with benzonitrile it appears that a moderate polarity of the solvent does not promote rearrangement significantly, but requires some additional factor. There is thus no linear comparison between rearrangement of halogen and polarity of solvent due to the complicating effects of solvent and product acidity as well as the effects of the decomposition products.

The Rearrangement of Allyl 2,6-Dichlorophenyl Ether in the Presence of Stannous Chloride

Carlin *et al.* (6) had found that several 2,6-dichlorophenylhydrazones, heated to 260° with a large excess of anhydrous stannous chloride, gave only the corresponding 7-chloroindoles, and these only in small yield (3–17%). Apparently no 5,7-dichloroindole, the result of halogen migration, was obtained. In view of the observation that the presence of oxidizable substances did cause a competitive reductive removal of one halogen atom during the Claisen rearrangement, it was of interest to discover whether stannous chloride

Can. J. Chem. Downloaded from www.nrcresearchpress.com by 210.87.254.105 on 09/05/12
For personal use only.

would yield only the monohalo product, 2-allyl-6-chlorophenol, analogous to the finding by Carlin concerning the Fischer indole synthesis (6). The results of the rearrangement of allyl 2,6-dichlorophenyl ether in the presence of stannous chloride are shown in Table II.

A. Stannous Chloride as a Lewis Acid

There is no doubt that the presence of stannous chloride accelerates the Claisen rearrangement since, for example, in 8 hours 30% of the original ether was left when stannous chloride was used, whereas without stannous chloride under otherwise identical conditions 60% of the ether remained after 8 hours' time (Table II columns 1 and 2, compare sections A and B). Furthermore, both the ether cleavage product, 2,6-dichlorophenol, and the coumaran were formed in the presence but not in the absence of stannous chloride. These products are characteristic of Lewis acid catalyzed rearrangements of the allyl phenyl ethers and do not appear in the purely thermal rearrangement. Thus stannous chloride does behave as a Lewis acid.*

B. Halogen Rearrangement and Reductive Removal

Both the reduction product, 2-allyl-6-chlorophenol, and the halogen migration product, 2-allyl-4,6-dichlorophenol, are formed, the former in somewhat larger amount in the first 6 hours of reaction but in a relatively lesser amount by the end of the reaction.†

The possibility that a large excess of stannous chloride might increase the amount of reduction product was examined. The solubility of stannous chloride in *o*-dichlorobenzene is quite limited, hence relatively dilute solutions of reagents were employed in this experiment. A mixture of 1.25 g (0.006 mole) of allyl 2,6-dichlorophenyl ether and 2.5 g (0.012 mole) of stannous chloride‡ in 125 ml of *o*-dichlorobenzene, when heated to 150–155° for 24 hours, gave only two products, the 2-allyl-6-chlorophenol (reduction product), 37%, and 2-allyl-4,6-dichlorophenol (rearrangement product), 63%. Thus, an increase in the proportion of stannous halide enhanced the proportion of halogen rearrangement. This is in contrast to the findings of Carlin, Wallace, and Fisher (6), who added their hydrazones to an excess of fused (260°) stannous chloride. Such vigorous conditions might account for their failure to find any dihalogenated indole.

The Rearrangement of Allyl 2,6-Dichlorophenyl Ether in the Presence of Anhydrous Zinc Bromide and of Allyl 2,6-Dibromophenyl Ether in the Presence of Anhydrous Zinc Chloride

It was suggested (1) that the halogen migration in the zinc chloride catalyzed Claisen rearrangement of allyl 2,6-dichlorophenyl ether might occur via a zinc chloride§ bridge as shown below (Fig. 1, route *a*). Alternatively, the Lewis acid could promote ionization and create an ion pair which could then rearrange more readily (route *b*) in a manner similar to that which takes place in the thermal rearrangement of the halogen. Route *b* might also be modified to give a species such as $ClZnX_2^{\ominus}$ which could then cause substitution at C_4 by $X^{\ominus}$ as well as enhance migration of $Cl^{\ominus}$. In addition to these routes,

**It is possible that the accumulating stannic chloride is responsible at least in part for the acceleration of reaction. However, it cannot be completely so, since if stannous chloride were not a Lewis acid, some 4-allyl-2,6-dichlorophenol (the product from thermal rearrangement) would have been formed at least in the early stages of the reaction. No 4-allyl-2,6-dichlorophenol was detected.*

†It is possible that the accumulating stannic chloride from the reduction process could be responsible for the increasing proportion of migration product as compared with the reduction product as the reaction progressed.

‡Nearly all of this quantity of stannous chloride went into solution.

§The state of the zinc halides under the conditions of our reactions is not certain. In an organic solvent which only partially dissolves the zinc halides, there might exist a mixture of monomeric, dimeric, and higher aggregate species possibly existing in part, for example, as $ZnX^{\oplus}ZnX_3^{\ominus}$. *Because of the lack of more precise information, the designation* ZnX_2 *is used for simplicity.*

Can. J. Chem. Downloaded from www.nrcresearchpress.com by 210.87.254.105 on 09/05/12
For personal use only.

Can. J. Chem. Downloaded from www.nrcresearchpress.com by 210.87.254.105 on 09/05/12
For personal use only.

TABLE II

Rearrangement of allyl 2,6-dichlorophenyl ether in *o*-dichlorobenzene

Reaction time, hr	Composition of reaction mixture, %*						
	Allyl 2,6-dichlorophenyl ether	2,6-Dichlorophenol	2-Allyl-6-chlorophenol	2-Methyl-7-chlorocoumaran	2-Allyl-4,6-dichlorophenol	2-Methyl-5,7-dichlorocoumaran	4-Allyl-2,6-dichlorophenol
	A. With $SnCl_2$ at 150–155° (ratio of $SnCl_2$ to ether† = 1:1) (0.05 mole of halide and ether in 50 ml of solvent)						
1	90	Nil	6	Nil	4	Nil	Nil
2	79	Trace	12	"	9	"	"
4	59	2	23	"	16	"	"
6	48	2	28	"	22	"	"
8	30	3	34	"	33	"	"
10	19	4	38	"	39	"	"
24	Nil	7	35	8	46	4	"
	B. Without $SnCl_2$, at 150–155° (0.05 mole of ether in 50 ml of solvent)						
6	74	Nil	Nil	Nil	Nil	Nil	26
8	60	"	"	"	"	"	40
24	23	"	"	"	"	"	77
	C. With $SnCl_2$ at 150–155° (ratio of $SnCl_2$ to ether = 2:1) (0.012 mole of $SnCl_2$‡ and 0.006 mole of ether in 125 ml of solvent)						
24	Nil	Nil	37	Trace	63	Trace	Nil

*Separate tests showed that in all cases the products were stable under the reaction conditions, except that in the presence of stannous chloride the 2-allylphenols were converted partly to their respective 2-methylcoumarans.

†A considerable portion of the stannous chloride remained undissolved.

‡Nearly all the stannous chloride dissolved.

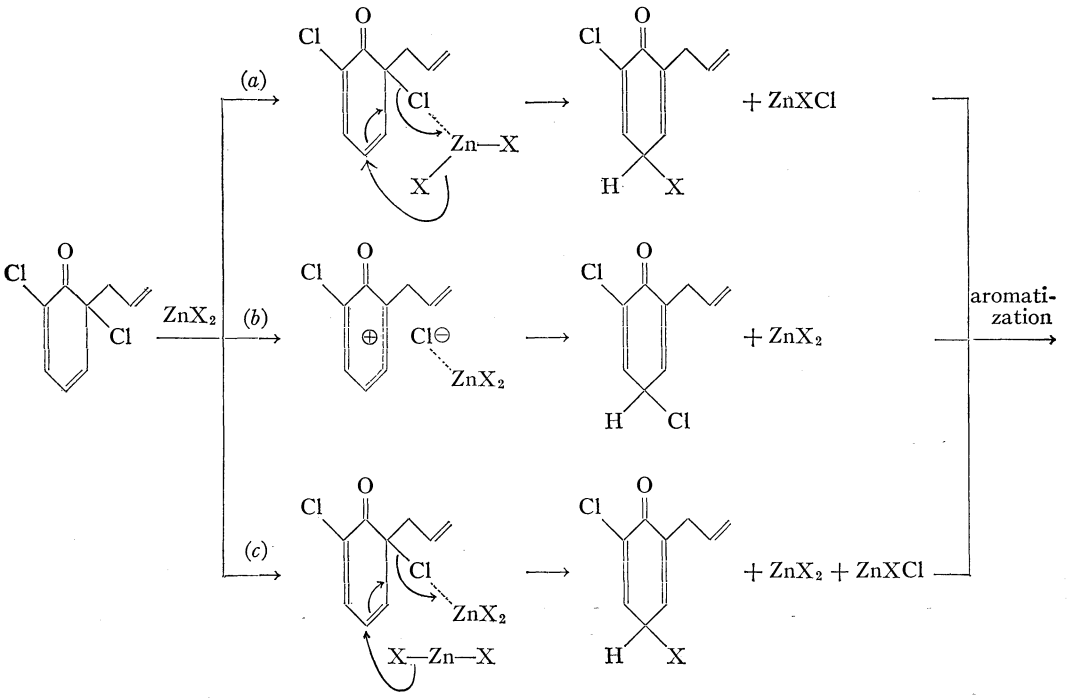

FIG. 1. Mechanistic routes for halogen migration.

halogen rearrangement might be accomplished by an S_N2' mechanism (reference 4, pp. 127–131) involving attack by the metal halide, with or without assistance of the Lewis acid, on the allylic system (route *c*).

In an effort to determine whether all or some of these schemes contribute in the rearrangement of the 2,6-dihalophenyl ethers in the presence of a Lewis acid, the rearrangement of allyl 2,6-dichlorophenyl ether was carried out in the presence of anhydrous zinc bromide. As well, allyl 2,6-dibromophenyl ether was rearranged in the presence of anhydrous zinc chloride. A high proportion of 2-allyl-4-bromo-6-chlorophenol in the first case and of 2-allyl-4-chloro-6-bromophenol in the second would favor the zinc halide bridge concept (Fig. 1, route *a*) and/or the S_N2' mechanism (Fig. 1, route *c*). The results of these experiments are shown in Tables III and IV.

A number of observations can be made from the information in Tables III and IV.

(i) No Rearrangement of the Allyl Group to the Para Position

In neither case was there any indication of the formation of 2,6-dihalo-*p*-allylphenol, the product found in large amount in the purely thermal rearrangement (Table I). Apparently the presence of the Lewis acid was sufficient to cause, at the dienone intermediate stage, reaction exclusively with the halogen atom.

(ii) Little or No Reductive Removal of Halogen

The zinc bromide catalyzed reaction of the dichloro ether (Table III) showed no evidence of reductive removal of a chlorine atom. On the other hand, approximately 3% of the product of the zinc chloride catalyzed reaction of the di*bromo* ether (Table IV, columns 3 and 4) was the monobromo reduction product. Thus, the carbon–bromine bond is more susceptible to the competitive reductive cleavage than is the carbon–chlorine bond.

Can. J. Chem. Downloaded from www.nrcresearchpress.com by 210.87.254.105 on 09/05/12
For personal use only.

Can. J. Chem. Downloaded from www.nrcresearchpress.com by 210.87.254.105 on 09/05/12
For personal use only.

TABLE III

Zinc bromide catalyzed rearrangement of allyl 2,6-dichlorophenyl ether in nitrobenzene solution
(concentration of ether: 0.15 mole of ether in 1 mole of nitrobenzene) (molar ratio of zinc bromide* to ether = 2:1)

Reaction time and temperature‡	Composition of the reaction mixture, %†					Ratio of bromine substitution to chlorine migration§
	2,6-Dichlorophenol	2-Allyl-4,6-dichlorophenol	2-Methyl-5,7-dichlorocoumaran	2-Allyl-4-bromo-6-chlorophenol	2-Methyl-5-bromo-7-chlorocoumaran	
100–110°						
200 hr	16	30	4	45	5	1.5
130–135°						
28 hr	28	21	12	24	15	1.2
30 hr	40	7	20	9	24	1.2
26 hr‖	47	Trace	23	Trace	30	1.3
140–145°						
18 hr	47	Trace	24	Trace	29	1.2
18 hr	51	Nil	23	Nil	26	1.1
150–155°						
12 hr	52	Nil	23	Nil	25	1.1
12 hr	55	Nil	21	Nil	24	1.1

*Not all of the zinc bromide dissolved.
†Separate tests showed that the products were stable under the reaction conditions, except that the 2-allylphenols were partly or completely converted to their respective coumarans.
‡Time of reaction was sufficient for complete disappearance of the original ether.
§The ratios are obtained by comparisons of the sums of the 4,6-dihalophenol and 5,7-dihalocoumaran in each case, i.e. the sums of columns 3 and 4 vs. 5 and 6.
‖A drop of water was deliberately added to the reaction mixture.

Can. J. Chem. Downloaded from www.nrcresearchpress.com by 210.87.254.105 on 09/05/12
For personal use only.

TABLE IV

Zinc chloride catalyzed rearrangement of allyl 2,6-dibromophenyl ether in nitrobenzene solution
(concentration of ether: 0.15 mole of ether in 1 mole of nitrobenzene) (molar ratio of zinc chloride* to ether = 2:1)

Reaction time and temperature‡	Composition of the reaction mixture, %†							Ratio of chlorine substitution to bromine migration§
	2,6-Dibromo-phenol	2-Allyl-6-bromo-phenol	2-Methyl-7-bromo-coumaran	2-Allyl-4,6-dibromo-phenol	2-Methyl-5,7-dibromo-coumaran	2-Allyl-4-chloro-6-bromophenol	2-Methyl-5-chloro-7-bromo-coumaran	
130–135° 30 hr	8	3	Nil	55	2	30	2	0.56
140–145° 26 hr	16	2	1	38	6	31	6	0.84
150–155° 22 hr	26	1	2	25	10	24	12	1.03

*Not all of the zinc chloride dissolved.
†Separate tests showed that the products were stable under the reaction conditions except that the 2-allylphenols were partly converted to their respective coumarans.
‡Sufficient time for complete disappearance of the original ether.
§The ratios are obtained by comparing the sums of the 4,6-dihalophenol and 5,7-dihalocoumaran in each case, i.e. the sums of columns 5 and 6 vs. 7 and 8.

(iii) Ether Cleavage, Dependent upon Temperature and the Presence of Water

Cleavage of the ether to the 2,6-dihalophenol in both instances increased with increase in temperature of the reaction, but was more pronounced when zinc bromide was the catalyst. It is noteworthy that, in contrast to the results obtained with zinc chloride as catalyst, those for the zinc bromide catalyzed reactions were difficult to reproduce in duplicate reactions. Commercial anhydrous zinc bromide* itself was particularly bad in this regard, hence it was heated to its melting point (as was done for zinc chloride) to drive off traces of water. If one prepared zinc bromide in this way and then allowed it to cool in a desiccator containing P_2O_5 and dry nitrogen, and as well stored the desiccator in a dry box (P_2O_5) flushed with dry nitrogen and then carried out all weighings, transfers, and mixing manipulations in this dry box, considerable improvement in reproducibility was found, although the results even then were not entirely satisfactory. Traces of water could be the cause of this difficulty in variability of results. Zinc bromide from our observations was found to be considerably more hygroscopic than was zinc chloride. Furthermore, the addition of one drop of water to the reaction mixture containing zinc bromide catalyst (Table III, 26 hour run at 130–135°) increased the amount of ether cleavage. It is already known that addition of a small amount of water to anhydrous boron trifluoride does enhance the catalytic power of this Lewis acid, probably by production of a proton according to the reaction $BF_3 + H_2O \rightleftarrows BF_3(OH)^{\ominus} + H^{\oplus}$ (7–10).

The greater effectiveness of zinc bromide as compared with zinc chloride in causing cleavage of the ether and also in promoting cyclization of the *o*-allyl-4,6-dihalophenols to the coumarans (a distinctly acid-catalyzed reaction) might be due to a somewhat stronger Lewis acid character of zinc bromide. Analogously, aluminum bromide is considered to be a more effective catalyst in the Friedel and Crafts reaction than is aluminum chloride (11). Also, it has been shown that the electrophilicities of the boron halides towards pyridine or nitrobenzene are in the order $BF_3 < BCl_3 < BBr_3$ (12). To our knowledge no such comparison has yet been reported concerning the aluminum halides (or zinc halides) although such work has been under consideration (12). If one can extrapolate these results to the zinc halides, support is thus obtained for the view that zinc bromide is a stronger Lewis acid than is zinc chloride. The greater solubility of zinc bromide in nitrobenzene as observed in our work indicates greater coordinating power with the solvent. On the other hand, the greater solubility of the bromide in nitrobenzene, as well as that of aluminum bromide in benzene in the Friedel and Crafts reaction (11), could well explain the greater catalytic effect observed. The limited amount of information available precludes any definite conclusion as yet concerning the cause of the greater activity of the zinc bromide.

(iv) Allylic Halogen Migration in Competition with Halogen Substitution by Halide Ion

The ratio of halogen *substitution* to halogen *migration* increased with temperature for the zinc chloride catalyzed rearrangement of allyl 2,6-dibromophenyl ether but decreased slightly for the zinc bromide catalyzed rearrangement of allyl 2,6-dichlorophenyl ether. Under the same conditions, more bromine (from $ZnBr_2$) replaced chlorine than chlorine (from $ZnCl_2$) replaced bromine in the dihalo ethers, but the difference was nearly eliminated at the higher temperature (150–155°). It is clearly seen that predominant substitution, which must occur if the zinc halide bridge concept and/or S_N2' mechanism is 100% operative, does not take place. Hence halogen "migration" can occur only partially, if at all, by one or both of these processes. Alternatively, simple allylic rearrangement of the

**Reagent grade material obtained from Matheson, Coleman and Bell, Norwood, Ohio, U.S.A.*

Can. J. Chem. Downloaded from www.nrcresearchpress.com by 210.87.254.105 on 09/05/12
For personal use only.

halogen atom at the dienone stage, with the assistance of the zinc halide, and involving a rather tight ion pair (route *b*) is also not completely operative since halogen substitution is quite substantial.

Conclusions as to Possible Mechanistic Routes in Halogen Migration and/or Substitution in the Zinc Halide Catalyzed Rearrangement of Allyl 2,6-Dihalophenyl Ethers

Unquestionably, the Lewis acids exert a marked control over these reactions. The absence of *para*-allyl rearrangement must mean that the zinc halide must first be associated with the allylic halogen of the dienone intermediate stage in every case. Subsequently, only halogen substitution and halogen migration, and in some cases reductive halogen elimination, take place.

The results shown in Tables III and IV might be interpreted in terms of the modified route *b* involving the species $ZnClBr_2^{\ominus}$ and $ZnBrCl_2^{\ominus}$ respectively. Thus, in the rearrangement of allyl 2,6-dichlorophenyl ether in the presence of $ZnBr_2$, the carbonium ion could abstract from $ZnClBr_2^{\ominus}$ either a chloride ion to form the dichloro "migration" product or a bromide ion to give the chlorobromo "substitution" product. One would expect that more bromide than chloride ion would be extracted on the basis of both the greater nucleophilicity and greater amount of bromine atoms in the species $ZnClBr_2^{\ominus}$, hence giving rise to a high ratio of bromine substitution to chlorine migration. The ratio actually found is only about 1.2 to 1.3 at 130–135°. On the other hand, for the $ZnCl_2$ catalyzed rearrangement of the di*bromo*ether, where the involvement of the species $ZnBrCl_2^{\ominus}$ is suggested, the ratio of bromine "migration" to chlorine "substitution" at C_4 is 1.8 (i.e. 1/0.56) at the same temperature. One would expect the reverse on the basis of relative amount and nucleophilicity of the halogen. Furthermore, the decrease of these ratios to nearly 1.0 in both cases as the temperature of reaction rose from 130° to 150–155° cannot readily be explained solely by this reaction path. Hence the modified route *b* can contribute only partly to the reaction.

The formation of a greater amount of the product, 2-allyl-4,6-dichlorophenol, as compared with the reduction product, 2-allyl-6-chlorophenol rather than the reverse when the proportion of stannous chloride to the dichloroether was increased (Table II) can be taken as support for the participation of a second molecule of stannous chloride in an S_N2' reaction (route *c*) in competition with reduction. However, from the results of the zinc bromide and zinc chloride catalyzed reactions (Tables III and IV) it is clear that substantial amounts of migration product occurred and therefore a scheme such as *c* can contribute only partly to the reaction.

The results of the zinc bromide catalyzed rearrangement of allyl 2,6-dichlorophenyl ether (Table III) in which the ratio of halogen substitution product to halogen migration product decreases from 1.5 at 100–110° to 1.1 at 150–155° can be rationalized as a competition between the slower allylic migration of chlorine and the reaction by an S_N2' pathway (route *c*) and/or zinc halide bridge (route *a*). Higher temperatures facilitate the breaking of the carbon–chlorine bond and hence route *b* becomes more important, decreasing the ratio of bromine to chlorine attachment at C_4.

The more readily ionizable carbon–bromine bond in the dibromoether (Table IV, catalysis by $ZnCl_2$) would permit greater contribution of allylic halogen migration (route *b*) even at the lower temperature of 130°. Higher temperatures could cause the formation of the species $ZnBrCl_2^{\ominus}$ and modified mechanism *b* could become predominant, thus decreasing the amount of bromine relative to chlorine attachment at C_4.

It is clear that the zinc halide catalyzed reactions of the allyl 2,6-dihalophenyl ethers

Can. J. Chem. Downloaded from www.nrcresearchpress.com by 210.87.254.105 on 09/05/12
For personal use only.

are quite complex and that the results obtained so far cannot be explained solely on the basis of any one of the suggested routes. It is likely that contributions from several or all might be involved in the halogen migration and substitution reactions.

EXPERIMENTAL

Analyses by Gas Chromatography

A Burrell Model K-2 Kromo-Tog, equipped with an integrator and with helium as the carrier gas, was used for all analyses. A 2 m column, packed with 20% Apiezon L on Gas Chrom P (60–80 mesh), afforded good separation of components of the mixtures into clearly resolved peaks. Analyses of carefully weighed authentic mixtures of the reaction products showed that the paper areas of the peaks could be used as a direct measure of the molar compositions of the reaction mixtures. Products were identified by comparison of their retention times with those of authentic samples and/or by means of infrared spectroscopy as well as n.m.r. analyses (Varian H-60).

2,6-Dibromophenol

Decarboxylation of 3,5-dibromo-4-hydroxybenzoic acid (148 g, 0.5 mole) (13) according to the procedure used by Tarbell and co-workers for the corresponding dichloro compound (14) afforded 112 g (89%) of 2,6-dibromophenol, m.p. 55–56° (from hexane). Lit. m.p. 56–57° (15).

Preparation of Ring-Halogenated Allyl Phenyl Ethers

The method previously described (1) for the preparation of allyl 2,6-dichlorophenyl ether was employed to obtain a number of ethers necessary for the present work. The required phenols were all commercially available. A summary of the properties and yields of the ethers is given in Table V.

TABLE V

Allyl phenyl ethers

Ring substituents	Yield, %	Boiling point, °C (mm) Found	Reported	Ref.
2-Chloro	89	100–102 (11)	108–110 (15)	2
2-Bromo-	85	66–67 (0.8)	130–134 (20)	16
2,4-Dichloro-	86	73–73.5 (0.55)	144–145 (20)	17
2,4-Dibromo-	95	90 (0.4)	127–134 (0.5)*	16
2,6-Dibromo-	90	73 (0.4)	112–113 (2)	18
2-Bromo-4-chloro	88	82 (0.5)	New compound†	
2-Chloro-4-bromo-	92	84–85 (0.7)	New compound‡	

*The reported boiling point is in disagreement with that observed, and appears to be too high.
†Anal. Calc. for C_9H_8BrClO: C, 43.67; H, 3.26; Br, 32.29; Cl, 14.32. Found: C, 43.93; H, 3.26; Br, 32.61; Cl, 14.17. n_D^{25} 1.5737.
‡Anal. Calc. for C_9H_8BrClO: C, 43.67; H, 3.26; Br, 32.29; Cl, 14.32. Found: C, 43.68; H, 3.19; Br, 32.14; Cl, 14.51. n_D^{25} 1.5752.

Preparation of Ring-Halogenated 2-Allylphenols

Several 2-allylphenols were obtained from the correspondingly substituted allyl phenyl ethers by rearrangement according to the following general procedure.

A solution of the allyl phenyl ether (0.2 mole) in 80 ml of diphenyl ether was heated with stirring, under an atmosphere of nitrogen, to 205–210° and kept at this temperature for 3 hours. When the solution had cooled, it was diluted with 400 ml of commercial pentane and extracted thrice with Claisen's alkali (19). The combined alkaline extracts were washed several times with pentane, thoroughly cooled in an ice-water bath, acidified with concentrated hydrochloric acid and then twice extracted with pentane. The combined extracts were washed with saturated salt solution and dried with anhydrous sodium sulphate. Removal of the solvent gave an oil which was distilled under vacuum through a short Vigreux column, thus giving the desired phenol. The results are tabulated in Table VI.

Preparation of Halogenated 2-Methylcoumarans

The general procedure reported in the literature (18) was employed to obtain the halogenated 2-methylcoumarans from the corresponding halogen-substituted 2-allylphenols. The results are shown in Table VII.

Thermal Rearrangement of Allyl 2,6-Dichlorophenyl Ether in Various Solvents. General Procedure

Dried and redistilled solvent (50 ml) was stirred and heated, under an atomsphere of purified dry nitrogen, to the desired temperature and then allyl 2,6-dichlorophenyl ether (10 g, 0.05 mole) slowly added over a period of approximately 30 minutes. The resulting solution was then heated for the required time, cooled,

Can. J. Chem. Downloaded from www.nrcresearchpress.com by 210.87.254.105 on 09/05/12
For personal use only.

TABLE VI

Ring halogenated 2-allylphenols

Ring substituents	Yield, %	Boiling point, °C (mm) Found	Boiling point, °C (mm) Reported	Ref.
6-Chloro	90	71–72 (2)	215–220 (750)	2
6-Bromo-	77	59–60 (0.7)	87–88 (2)	16
4,6-Dichloro-	87	77 (0.9)	264 (759)	20
4,6-Dibromo-	60	88 (0.4)	118–122.5 (1.0)	16
4-Chloro-6-bromo-	75	80–81 (0.6)	New compound*	
4-Bromo-6-chloro-	76	80 (0.4)	New compound†	

*Anal. Calc. for C_9H_8BrClO: C, 43.67; H, 3.26; Br, 32.29; Cl, 14.32. Found: C, 43.82; H, 3.36; Br, 32.20; Cl, 14.07. n_D^{25} 1.5838.
†Anal. Calc. for C_9H_8BrClO: C, 43.67; H, 3.26; Br, 32.29; Cl, 14.32. Found: C, 43.60; H, 3.31; Br, 32.08; Cl, 14.43. n_D^{25} 1.5855.

TABLE VII

Halogenated 2-methylcoumarans

Substituents	Yield, %	Boiling point, °C (mm) Found	Boiling point, °C (mm) Reported	Ref.
7-Chloro-	56	74 (1.8)	New compound*	
7-Bromo-	57	71 (0.75)	New compound†	
5,7-Dibromo-	68	90 (0.3)	129–134 (1.0)	18
5-Chloro-7-bromo-	73	95 (0.9)	New compound‡	
5-Bromo-7-chloro-	73	99 (0.8)	New compound§	
5,7-Dichloro-	48	81 (0.7)	New compound‖	

*Anal. Calc. for C_9H_9ClO: C, 64.10; H, 5.38; Cl, 21.03. Found: C, 64.17; H, 5.21; Cl, 21.24. n_D^{25} 1.5496.
†Anal. Calc. for C_9H_9BrO: C, 50.73; H, 4.26; Br, 37.51. Found: C, 50.97; H, 4.21; Br, 37.26. n_D^{25} 1.5735.
‡Anal. Calc. for C_9H_8BrClO: C, 43.67; H, 3.26; Br, 32.29; Cl, 14.32. Found: C, 43.71; H, 3.22; Br, 32.17; Cl, 14.53. n_D^{25} 1.5863.
§Anal. Calc. for C_9H_8BrClO: C, 43.67; H, 3.26; Br, 32.29; Cl, 14.32. Found: C, 43.47; H, 3.39; Br, 32.51; Cl, 14.42. n_D^{25} 1.5863.
Anal. Calc. for $C_9H_8Cl_2O$: C, 53.23; H, 3.97; Cl, 34.92. Found: C, 52.91; H, 4.08; Cl, 35.20. n_D^{25} 1.5640.

and then analyzed directly for products by vapor phase chromatography (v.p.c.) by injecting aliquots of the reaction solution into the Kromo-Tog. The results are recorded in Table I.

Zinc Halide Catalyzed Rearrangement of Allyl 2,6-Dihalophenyl Ethers. General Procedure

A quantity (0.1 mole) of anhydrous zinc halide (prepared by heating the salt to the molten state, cooling it in a desiccator in a dry box flushed with nitrogen, and then grinding it under anhydrous conditions in the dry box) was stirred into 50 ml of dry ether. The mixture was then gently heated to permit evaporation of the ether while dried, redistilled nitrobenzene (41 g) was slowly added. The resulting mixture was heated to the desired rearrangement temperature. Much of the zinc halide remained undissolved as a suspension. After slow addition of the allyl 2,6-dihalophenyl ether (0.05 mole), the resulting mixture was stirred and heated under an atmosphere of purified, dry nitrogen for the specified time. The reaction mixture was then cooled and poured into a mixture of ether and water (1:1). When the resulting solution was filtered, the ether layer was separated, washed twice with saturated salt solution, and then dried (Na_2SO_4). Removal of the ether gave a mixture of reaction products which was analyzed directly by v.p.c. The results are recorded in Tables III and IV.

Rearrangement of Allyl 2,6-Dichlorophenyl Ether in the Presence of Stannous Chloride

(*a*) Anhydrous powdered stannous chloride (9.5 g, 0.05 mole) (21) was stirred into 50 ml of dried, redistilled *o*-dichlorobenzene. After the mixture had been heated to 150–155° under an atmosphere of purified, dry nitrogen, allyl 2,6-dichlorophenyl ether (10 g, 0.05 mole) was slowly added. The reactants were then heated at 150–155° for 24 hours. The cooled material was treated as described above for the zinc halide catalyzed rearrangements and product analysis carried out directly by v.p.c. The results are recorded in Table II.

(*b*) Procedure (*a*) was repeated, employing 1.25 g (0.006 mole) of allyl 2,6-dichlorophenyl ether and 2.5 g (0.012 mole) of stannous chloride in 125 ml of dried, redistilled *o*-dichlorobenzene. After treatment of the cooled reaction mixture as described above, 50 ml of *o*-dichlorobenzene was removed by careful fractional distillation under vacuum. The distillate was shown by v.p.c. to be pure solvent, containing no phenolic products. The residual solution was analyzed by v.p.c. and the results recorded in Table II, section C.

Stability Tests on Products under Reaction Conditions

In all cases synthetic mixtures of the products of the reactions were shown, by the use of an internal

Can. J. Chem. Downloaded from www.nrcresearchpress.com by 210.87.254.105 on 09/05/12
For personal use only.

standard (*n*-tetradecane) in the v.p.c. analysis, to be stable within the limits of experimental error. However, in the case of the metal halide catalyzed reactions the 2-allylphenols were converted in part or completely to the corresponding stable 2-methylcoumarans and to no other product.

ACKNOWLEDGMENT

The authors gratefully acknowledge the generous financial assistance given by the National Research Council of Canada throughout the course of this work. One of us (E. P.) thanks the National Research Council for the award of a Studentship.

REFERENCES

1. E. PIERS and R. K. BROWN. Can. J. Chem. **41**, 329 (1963).
2. D. S. TARBELL and J. W. WILSON. J. Am. Chem. Soc. **64**, 1066 (1942).
3. LANDOLD-BÖRNSTEIN. Zahlenwerte und Funktionen. Band II, Teil 6. Springer-Verlag, Berlin, Germany. 1959.
4. J. HINE. Physical organic chemistry. McGraw-Hill Book Co., Inc., New York. 1956.
5. H. L. GOERING and R. R. JACOBSON. J. Am. Chem. Soc. **80**, 3277 (1958).
6. R. B. CARLIN, J. G. WALLACE, and E. E. FISHER. J. Am. Chem. Soc. **74**, 990 (1952).
7. J. M. CLAYTON and A. M. EASTHAM. J. Chem. Soc. 1636 (1963).
8. A. G. EVANS and M. POLANYI. J. Chem. Soc. 252 (1947).
9. G. F. HENNION and R. A. KURTZ. J. Am. Chem. Soc. **65**, 1001 (1943).
10. P. H. GORE. Chem. Rev. **55**, 234 (1955).
11. C. A. THOMAS. Anhydrous aluminum chloride in organic chemistry. Reinhold Publishing Corp., New York. p. 875.
12. H. C. BROWN and R. R. HOLMES. J. Am. Chem. Soc. **78**, 2173 (1956).
13. E. GROVENSTEIN, JR. and U. V. HENDERSON, JR. J. Am. Chem. Soc. **78**, 569 (1956).
14. D. S. TARBELL, J. W. WILSON, and P. E. FANTA. Organic synthesis. Coll. Vol. III. John Wiley and Sons, Inc., New York. 1955. p. 267.
15. F. G. POPE and A. S. WOOD. J. Chem. Soc. 1823 (1912).
16. C. D. HURD and C. N. WEBB. J. Am. Chem. Soc. **58**, 941 (1936).
17. L. C. RAIFORD and L. H. HOWLAND. J. Am. Chem. Soc. **53**, 1051 (1931).
18. C. D. HURD and C. N. WEBB. J. Am. Chem. Soc. **58**, 2190 (1936).
19. L. F. FIESER. Experiments in organic chemistry. 3rd ed. D. C. Heath and Co., Boston. 1957. p. 310.
20. L. CLAISEN. Ann. **418**, 84 (1919).
21. H. STEPHEN. J. Chem. Soc. 2786 (1930).
22. L. C. RAIFORD and G. R. MILLER. J. Am. Chem. Soc. **55**, 2125 (1933).

Can. J. Chem. Downloaded from www.nrcresearchpress.com by 210.87.254.105 on 09/05/12
For personal use only.

THE METHYL 3-NITRO-3-DEOXY- AND 3-AMINO-3-DEOXY-ARABINOPYRANOSIDES[1]

HANS HELMUT BAER AND ALAUDDIN AHAMMAD[2]
Department of Chemistry, University of Ottawa, Ottawa, Canada
Received July 16, 1963

ABSTRACT

The nitromethane cyclization of L′-methoxy-diglycolic aldehyde was shown to furnish methyl 3-nitro-3-deoxy-α-L-arabinopyranoside and methyl 3-nitro-3-deoxy-β-D-arabinopyranoside as coproducts of the previously obtained β-D-*ribo* isomer. As expected, the enantiomorphic dialdehyde, D′-methoxy-diglycolic aldehyde, afforded the corresponding α-D- and β-L-*arabino* derivatives in addition to the β-L-*ribo* isomer. Catalytic hydrogenation of the four new nitroglycosides gave the corresponding aminoglycoside hydrochlorides. The 3-amino-3-deoxy-D- and L-arabinose hydrochlorides were obtained from their glycosides by hydrolysis and crystallized as mutarotating β-forms.

The spontaneous epimerization, in aqueous solution, of *aci*-nitropentoside sodium salts was investigated.

In the cyclization (1), with nitromethane and sodium methoxide, of L′-methoxy-diglycolic aldehyde (I) a methyl *aci*-nitrodeoxy pentoside sodium salt had been isolated in crystalline condition in a yield of about 40%. This salt had been shown to possess formula II and must therefore be denoted as methyl 3-*aci*-nitro-3-deoxy-β-D-*erythro*-pentopyranoside sodium.[3] Manifold experiences gathered subsequently in similar nitromethane condensations and recorded in papers of this series have borne out the hardly surprising fact that this type of reaction does not proceed in a stereospecific way, although a notable stereoselectivity is always observed. It was of interest, therefore, to investigate whether, and to which extent, stereoisomers of II were formed in the reaction which produced the latter as the apparent main product. The three possible stereoisomers of II which might arise from the dialdehyde I are the corresponding α-L-*threo* (III), β-D-*threo* (IV), and α-L-*erythro* (V) 3-deoxypentose derivatives. The present study was intended, furthermore, to uncover the cause of the previously observed mutarotation of II; i.e. to verify in the pentose series that glycoside nitronates in solution are liable to undergo spontaneous epimerizations, as has been found to be the case with nitronates derived from hexosides (2, 3).

We are now able to demonstrate that when dialdehyde I is cyclized with nitromethane, the α-L-*threo* and β-D-*threo* forms of methyl 3-*aci*-nitro-3-deoxypentopyranoside sodium (III and IV, respectively) indeed occur in the reaction mixture as minor components beside the chief product, β-D-*erythro* salt II. Although the salts III and IV could not be isolated as such, their presence was indicated by the isolation of two new, free nitroglycosides that arose upon deionization of the mixture. Thus, methyl 3-nitro-3-deoxy-α-L-arabinopyranoside (VI), originating from III, and methyl 3-nitro-3-deoxy-β-D-arabinopyranoside (VII), arising from IV, were obtained in yields of approximately 5% each. These crystalline nitroglycosides were hydrogenated to furnish the corresponding aminoglycosides, which crystallized as hydrochlorides: methyl 3-amino-3-deoxy-α-L-arabinopyranoside hydrochloride (VIII) and methyl 3-amino-3-deoxy-β-D-arabinopyranoside

[1]*Part XI in the series Cyclizations of dialdehydes with nitromethane. For Part X see reference 3.*
[2]*A recipient of a Canadian Commonwealth Scholarship; this work was done as part of a research project leading to a degree of Doctor of Philosophy.*
[3]*This notation replaces the older nomenclature, methyl 3-aci-nitro-3-deoxy-β-D-ribopyranoside sodium, which was used in reference 1.*

Can. J. Chem. Downloaded from www.nrcresearchpress.com by 210.87.254.42 on 09/05/12
For personal use only.

hydrochloride (IX). Proof of the structure and configurations of VIII and IX was afforded by acid hydrolysis yielding reducing amino sugars. Glycoside IX gave 3-amino-3-deoxy-D-arabinose hydrochloride (XI), which has been described by Baker, Schaub, and Williams, (4). We obtained an upward-mutarotating β-form ($[\alpha]_D$ $-147° \rightarrow -113°$). Glycoside VIII afforded the hitherto unknown enantiomorph of XI, namely 3-amino-3-deoxy-L-arabinose hydrochloride (X). Belonging to the L-series and exhibiting downward mutarotation ($[\alpha]_D +145° \rightarrow +110°$), the crystalline compound has to be designated as β-form.

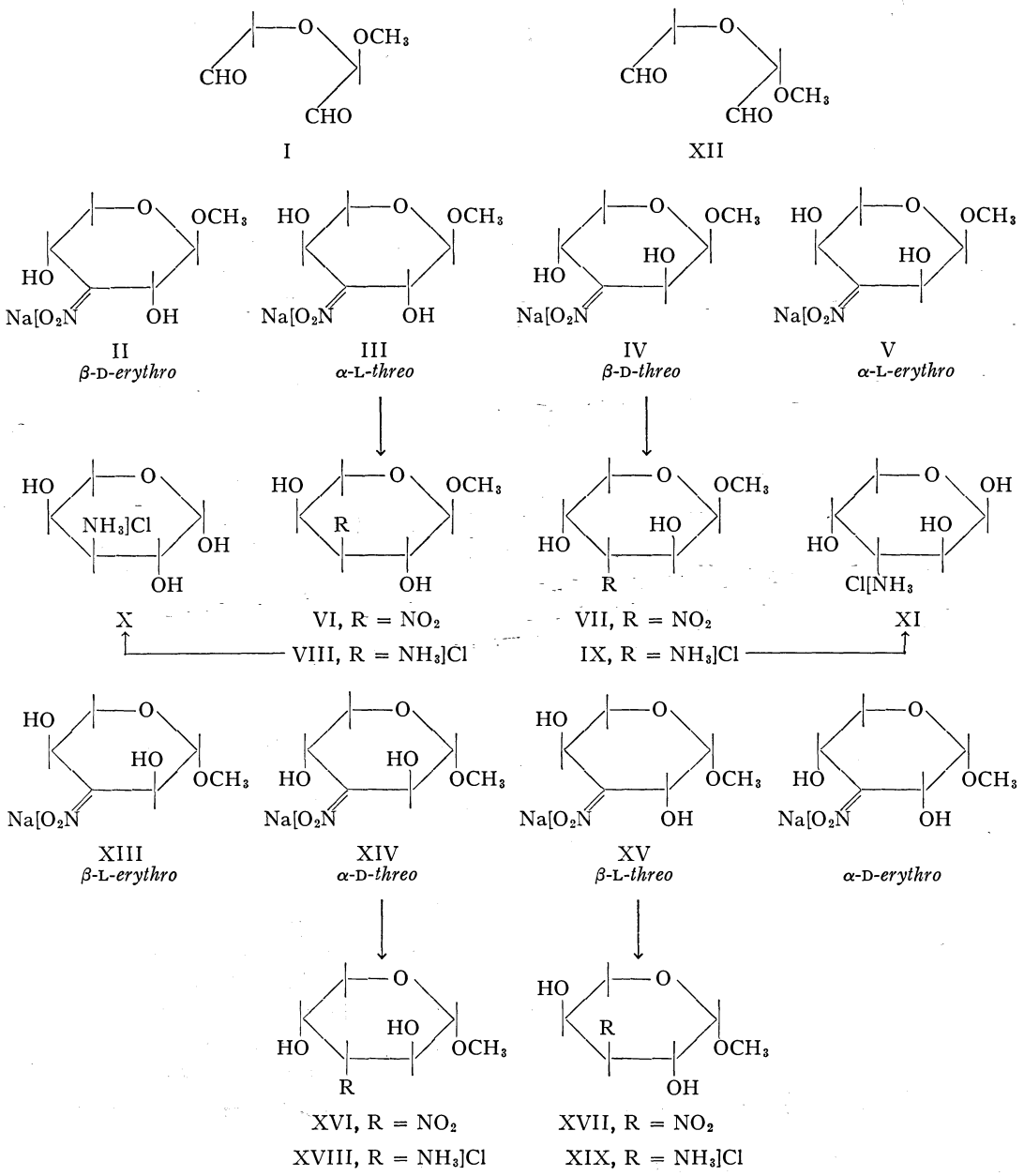

Can. J. Chem. Downloaded from www.nrcresearchpress.com by 210.87.254.42 on 09/05/12
For personal use only.

In the earlier paper (1) there has also been described a parallel nitromethane condensation using D′-methoxy-diglycolic aldehyde (XII; i.e. the enantiomorph of I) and, accordingly, furnishing methyl 3-*aci*-nitro-3-deoxy-β-L-*erythro*-pentopyranoside sodium (XIII; i.e. the enantiomorph of II). Obviously, then, the α-D-*threo* salt XIV and the β-L-*threo* salt XV, being the enantiomorphs of III and IV, respectively, had to be expected to arise as coproducts in this parallel case. This has, in fact, proved true as we have now isolated the corresponding free nitroglycosides, methyl 3-nitro-3-deoxy-α-D-arabinopyranoside (XVI) and methyl 3-nitro-3-deoxy-β-L-arabinopyranoside (XVII). Hydrogenation furnished methyl 3-amino-3-deoxy-α-D-arabinopyranoside hydrochloride (XVIII) and methyl 3-amino-3-deoxy-β-L-arabinopyranoside hydrochloride (XIX), respectively. The physical constants of the new glycosides are shown in Table I.

TABLE I

Physical data of the new glycosides

Compound	Configuration	m.p.	$[\alpha]_D$ in water
(Nitro)			
VI	α-L-*arabino*	180–182°	+85.5°
XVI	α-D-*arabino*	179–180°	−86°
XVII	β-L-*arabino*	179–180°	+278°
VII	β-D-*arabino*	178.5–179.5°	−278°
(Amino)		m.p. (decomp.)	
VIII	α-L-*arabino*	164–165°	+24.7°
XVIII	α-D-*arabino*	165°	(−24.7°)*
XIX	β-L-*arabino*	180–183°	+202°
IX	β-D-*arabino*	181–183°	−205°

*By reversal of the sign of rotation of the enantiomorph (VIII). The amount of substance available was insufficient for measurement of the rotation.

The compounds obey Hudson's rule of isorotation. Thus, the value A for the molecular rotational contribution of the glycosidic carbon atom in a pair of nitro anomers, e.g. VI and XVII, is 18,525; the value is 18,015 for the corresponding amino derivatives VIII and XIX, and 18,710 (5) for the nitrogen-free, parent methyl α- and β-L-arabinopyranosides. The values B for the cores of the molecules are +35,125 for the pair of nitroglycosides VI:XVII; +22,915 for the pair of amines VIII:XIX; and +21,550 for the anomeric methyl L-arabinopyranosides. The latter set of figures exemplifies anew that substitution of an amino group for a hydroxyl in glycosides has little influence upon the optical rotation (3, 6,[4] 7[5]). Introduction of a nitro group, on the other hand, can produce a considerable change in the molecular rotation, as is seen in the present case and in various earlier examples (3, 7).

The course of the cyclization with nitromethane of I in methanol was followed by paper chromatography. It was found that even at 0° the dialdehyde disappeared within about 10 minutes. Already, after 3 minutes, the three nitronates II, III, and IV were present, as was revealed by chromatographic detection of the corresponding free nitroglycosides following deionization. There appeared to be a preponderance of IV during the first few minutes of the reaction, but the final pattern, with II as the chief product, was largely established after 15 minutes; and small changes, if any, in the proportions of II, III, and IV in solution occurred thereafter over a period of 48 hours. The salt II began to crystallize

[4]*Further literature in support of this rule is cited there.*

[5]*In reference 7, tentative configurational assignments for two new amino sugars were based on this rule. They have now been confirmed by nuclear magnetic resonance studies (8).*

Can. J. Chem. Downloaded from www.nrcresearchpress.com by 210.87.254.42 on 09/05/12
For personal use only.

out after an induction period of 10 to 15 minutes, a circumstance which evidently furthered its formation as main product.

The β-D-*erythro* nitronate II had been found (1) to exhibit, in aqueous solution, an unexpected mutarotation (Fig. 1). We have now converted the isolated nitroarabinosides

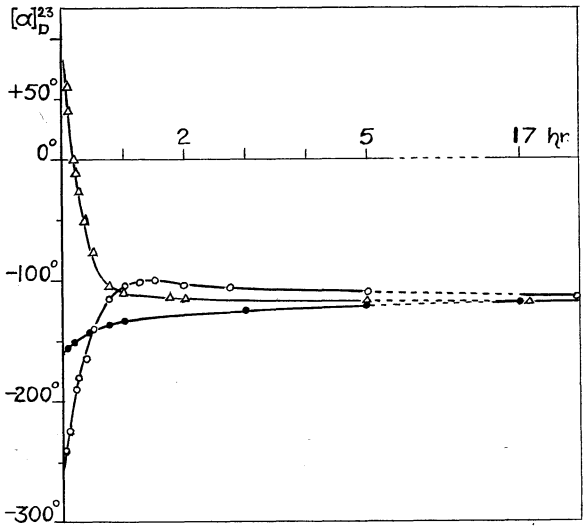

FIG. 1. The mutarotations of the nitronates II (●), III (△), and IV (○) in water.

VI and VII into their respective sodium nitronates, III and IV, by the addition of equivalent amounts of sodium hydroxide in water. Immediately there commenced mutarotations leading to the same final $[\alpha]_D$ value. When, after attainment of the end value, the solutions were deionized, they all showed identical chromatographic patterns, indicating that an equilibration had taken place. In the equilibrium the levorotatory β-D-*erythro* salt II greatly predominated. On account of the rotation value of the equilibrated solution the remainder was judged to consist largely of the dextrorotatory α-L-*threo* salt III. It was in fact possible to isolate the crystalline product of deionization of III, methyl 3-nitro-3-deoxy-α-L-arabinopyranoside (VI), in a yield of 6% from an equilibrated solution of II. An estimate based on the initial rotations of II and III and on the final rotation would indicate a ratio of 85:15 of the two salts, which was consistent with the chromatographic picture. This calculation neglects a possible participation in the equilibrium of the strongly levorotatory β-D-*threo* salt IV; however, since no evidence for its presence was found, it could have been present in negligible amount only. The apparent failure of IV to play a significant part in the composition of the epimerization equilibrium in water is not necessarily inconsistent with the fact that in a kinetically controlled condensation reaction in methanolic medium it does arise to an appreciable extent. The spontaneous epimerization is represented by the following scheme:

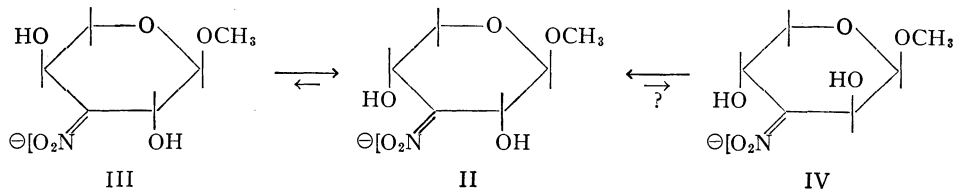

Can. J. Chem. Downloaded from www.nrcresearchpress.com by 210.87.254.42 on 09/05/12
For personal use only.

As for the fourth possible isomer, the α-L-*erythro* salt V, no sign of its formation has thus far been observed either in cyclization or in epimerization experiments. The present results, then, lead to the conclusion that the thermodynamic stabilities of the *aci* nitro salts decrease in the order II > III > IV > V, and hence confirm the conformational considerations which were discussed previously (1).

EXPERIMENTAL

The melting points were taken in an aluminum block. All evaporations were done *in vacuo* at 35–40° (bath temperature). Paper chromatography was performed as described previously (3).

Methyl 3-Nitro-3-deoxy-α-L-arabinopyranoside (VI) and Methyl 3-Nitro-3-deoxy-β-D-arabinopyranoside (VII)

L′-Methoxy-diglycolic aldehyde (I) was prepared (1) from 8.2 g (0.05 mole) of methyl β-D-xylopyranoside, and was dissolved in 75 ml of methanol. Nitromethane (2.8 ml, 1 molar equivalent) was added and the solution was chilled in an ice bath. With swirling, 38.5 ml of a chilled, methanolic sodium methoxide solution (containing 3 g of sodium per 100 ml) was dropped in at a moderately rapid rate. After 15 minutes the reaction mixture was deionized, with efficient magnetic stirring at 0°, by addition of 75 ml of Amberlite IR–120 (H^+) which had been prewashed with methanol. The solution was decanted from the resin and, to ensure complete deionization, slowly passed over a column which contained another 25 ml of fresh Amberlite. The first batch of resin was washed repeatedly with methanol and the washings were also passed over the column. The colorless effluent was evaporated to a sirup that was further evaporated with two successive additions of ethanol. The residue was then taken up in about 10 ml of dichloromethane. Upon inoculation[6] with VI and scratching with a glass rod, crystallization occurred and was allowed to proceed at room temperature for 1 hour. The crystals were collected and washed with ice-cold dichloromethane; yield, 391 mg; $[\alpha]_D^{23}$ +83.7° (*c*, 1.05 in water). Recrystallization from ethyl acetate afforded rectangular platelets of m.p. 180–182° and $[\alpha]_D^{23}$ +85.5° (*c*, 1.1 in water). The product was chromatographically uniform (R_f 0.64) methyl 3-nitro-3-deoxy-α-L-arabinopyranoside (VI). Anal. Calc. for $C_6H_{11}O_6N$ (193.2): C, 37.31; H, 5.74; N, 7.25. Found: C, 37.25; H, 5.63; N, 7.27.

From the above dichloromethane mother liquor a second crop of crystals separated in the course of 24 hours at 0°. This material (379 mg; $[\alpha]_D^{23}$ −149°) was revealed by paper chromatography to be a mixture giving a double spot (R_f 0.64–0.68) corresponding to the two nitroarabinosides VI and VII, and a spot (R_f 0.80) corresponding to methyl 3-nitro-3-deoxy-β-D-ribopyranoside (1).

Now petroleum ether (b.p. 30–60°) was added dropwise to the mother liquor to incipient cloudiness. Upon standing overnight in a refrigerator the solution deposited crystals, the amount of which could be augmented by careful addition of carbon tetrachloride and by keeping the flask first at room temperature, then at 4° for 24 hours. The crystals were isolated and washed with ice-cold dichloromethane; yield, 325 mg, m.p. 160–167°, $[\alpha]_D^{23}$ −218° (*c*, 1.1 in water). After one recrystallization from ethyl acetate the product was not yet chromatographically uniform but showed two spots of R_f 0.68 and R_f 0.80. A pure product, methyl 3-nitro-3-deoxy-β-D-arabinopyranoside (VII), was obtained after three recrystallizations from 1-propanol. It had m.p. 178.5–179.5°, R_f 0.69, and $[\alpha]_D^{23}$ −278° (*c*, 0.5 in water). Anal. Calc. for $C_6H_{11}O_6N$ (193.2): C, 37.31; H, 5.74; N, 7.25. Found: C, 37.58; H, 5.89; N, 7.16.

With a theoretical yield of 9.66 g, the combined nitroglycosides isolated up to this stage amounted to 11.3%. Clearly, the bulk of reaction products was still contained in the main mother liquor. Chromatography showed the presence of both VI and VII, with the latter being in preponderance. The chief component, however, was the β-D-*ribo* isomer (R_f 0.80). An additional weak spot (R_f 0.83) was judged, on the basis of previous experience (1), to be due to the β-D-*xylo* isomer.[7]

An experiment conducted in the same way as described above, except for a reaction time of 50 rather than 15 minutes, gave essentially the same results. When in a further experiment the reaction was interrupted by deionization after 3 minutes, no VI could be isolated but only a levorotatory mixture ($[\alpha]_D$ −222°) of VII and the β-D-*ribo* isomer.

Methyl 3-Nitro-3-deoxy-α-D-arabinopyranoside (XVI) and Methyl 3-Nitro-3-deoxy-β-L-arabinopyranoside (XVII)

D′-Methoxy-diglycolic aldehyde (XII) was prepared (1) from 2.46 g of methyl α-D-xylopyranoside. It was cyclized with nitromethane exactly as described above for I. The yield of crude XVI was 140 mg. It showed m.p. 178–179° and $[\alpha]_D^{23}$ −78° (*c*, 1 in water) after one, and m.p. 179–180° and $[\alpha]_D^{23}$ −86° (*c*, 1 in water) after a second recrystallization from ethyl acetate. Anal. Calc. for $C_6H_{11}O_6N$ (193.2): C, 37.31; H, 5.74; N, 7.25. Found: C, 37.11; H, 5.64; N, 7.09.

The mother liquor furnished 268 mg of a crystalline product of $[\alpha]_D^{23}$ +228.5°. It was XVII accompanied

[6]*Seed crystals were obtained when in a preliminary experiment the sirup was treated with ether and left for several days in an unevacuated desiccator over concentrated sulphuric acid.*

[7]*A pair of poorly resolved spots with R_f 0.80 (strong) and R_f 0.83 (weak) was seen when the crystalline β-D-erythro nitronate II was chromatographed following acidification.*

Can. J. Chem. Downloaded from www.nrcresearchpress.com by 210.87.254.42 on 09/05/12
For personal use only.

by the β-L-*ribo* isomer. Several recrystallizations, first from ethyl acetate, then from 1-propanol, afforded pure XVII with m.p. 179–180° and $[\alpha]_D^{23}$ +278° (*c*, 0.5 in water). Anal. Calc. for $C_6H_{11}O_6N$ (193.2): C, 37.31; H, 5.74; N, 7.25. Found: C, 37.07; H, 5.68; N, 7.17.

The infrared spectra of the two anomeric glycosides XVI and XVII showed marked differences, but they were, as expected, identical with those of the enantiomorphs, VI and VII.

Methyl 3-Amino-3-deoxy-α-L-arabinopyranoside Hydrochloride (VIII)

A sample of 200 mg of the nitroarabinoside VI in 5 ml of water was hydrogenated with a platinum catalyst (200 mg of PtO_2, prehydrogenated) in the presence of 11 ml of *N*/10 hydrochloric acid. The hydrogen uptake was 77 ml at 23° and 757 mm Hg. After filtration and removal of excess acid with Amberlite IR-45(OH^-) to pH 6, the solution was evaporated leaving a colorless sirup which was crystallized from ethanol – ethyl acetate. The yield of colorless needles of VIII showing $[\alpha]_D^{23}$ +21.5° (*c*, 0.5) and m.p. 167–169° was 160 mg (77.5%). For analysis, the product was recrystallized from the same solvents and then exhibited m.p. 164–165° decomp. and $[\alpha]_D^{23}$ +24.7° (*c*, 1 in water). Anal. Calc. for $C_6H_{14}O_4NCl$ (199.6): C, 36.09; H, 7.07; N, 7.02. Found: C, 36.51; H, 7.37; N, 6.80.

Methyl 3-Amino-3-deoxy-β-D-arabinopyranoside Hydrochloride (IX)

A sample of 300 mg of the nitroarabinoside VII in 10 ml of water was hydrogenated with addition of 16.5 ml of *N*/10 hydrochloric acid as described in the preceding section. There was obtained 150 mg of recrystallized, pure IX as colorless needles of m.p. 181–183° decomp. and $[\alpha]_D^{23}$ −205° (*c*, 0.5 in water). Anal. Calc. for $C_6H_{14}O_4NCl$ (199.6): C, 36.09; H, 7.07; N, 7.02. Found: C, 35.65; H, 7.09; N, 6.86.

Methyl 3-Amino-3-deoxy-α-D-arabinopyranoside Hydrochloride (XVIII)

A sample of 14 mg of the nitroarabinoside XVI in 3 ml of water was hydrogenated with the use of 20 mg of platinum dioxide in the presence of 0.72 ml of *N*/10 hydrochloric acid. The hydrogenation product was isolated analogously to VIII. The yield was 7 mg of colorless needles of XVIII. The product was confirmed, by its melting point of 165° (decomp.) and by its infrared spectrum, to be the enantiomorph of VIII.

Methyl 3-Amino-3-deoxy-β-L-arabinopyranoside Hydrochloride (XIX)

Nitroarabinoside XVII (75 mg) in water (5 ml) was hydrogenated with 80 mg of platinum dioxide in the presence of 3.9 ml of *N*/10 hydrochloric acid. The hydrogen uptake was 28 ml (23°, 763 mm Hg) after 1 hour. Work-up of the reaction mixture (as described above for VIII and IX) afforded 46 mg of crystals of XIX, which showed $[\alpha]_D^{25}$ +202° (*c*, 0.5 in water). Although this was in good agreement with the expected value, the melting point of 150–151° did not match that of the enantiomorph IX and could not be raised by simple recrystallization. There were noticeable, if slight, differences in the infrared spectra in nujol of IX and XIX, too. These discrepancies were resolved, however, when XIX was recrystallized, from ethanol – ethyl acetate, with inoculation of the supersaturated solution with a trace of the antipode (IX). The crystals so obtained melted at 180–183° (decomp.) and gave an infrared spectrum identical with that of IX. It appears, therefore, that these aminoglycosides are capable of existing in different crystal modifications.

3-Amino-3-deoxy-β-L-arabinose Hydrochloride (X)

A sample of 104.3 mg of methyl 3-amino-3-deoxy-α-L-arabinopyranoside hydrochloride (VIII) in 10 ml of 2*N* hydrochloric acid was heated in a sealed container for 19 hours at 95–98°. After cooling, the rotation of the yellowish solution was α_D +2.06° in a 2-dm tube, corresponding to a specific rotation for the free sugar of +106.5°. The solution was decolorized with activated carbon and evaporated repeatedly with water to remove excess acid, and the remaining sirup was crystallized by trituration with 1 ml of glacial acetic acid. There could be isolated 80 mg (83%) of X whose infrared spectrum was identical with that of the known enantiomorph (see next section). The product decomposed on being heated at about 150°. On the grounds of a downward mutarotation, the β-configuration was assigned to the crystalline sugar. $[\alpha]_D^{23}$ +145° (2 1/2 minutes) → +110° (20 minutes, final; *c*, 0.5 in water).

3-Amino-3-deoxy-β-D-arabinose Hydrochloride (XI)

A sample of 146 mg of methyl 3-amino-3-deoxy-β-D-arabinopyranoside hydrochloride (IX) was hydrolyzed as described in the preceding section. The hydrolyzate showed α_D −2.77° in a 2-dm tube, which corresponded to $[\alpha]_D^{23}$ −101.8° for the free sugar (XI). Of the latter, an amount of 83 mg could be isolated as crystals showing decomposition at about 150°. The upward mutarotation, $[\alpha]_D^{23}$ −147.4° (2 minutes), → −113° (20 minutes, final; *c*, 0.5 in water) alllowed the assignment to XI of β-configuration. The equilibrium rotation value of XI agreed well with that given in the literature ($[\alpha]_D$ −112°, in water), although a mutarotation had not been recorded previously (4).

The Partial Epimerization of Methyl 3-aci-Nitro-3-deoxy pentopyranoside Sodium Salts

β-D-erythro Salt II

A sample of 1.231 g of II (1) was dissolved in 100 ml of carbon-dioxide-free water at 22°. After 17 hours the mutarotation had reached a final value of $[\alpha]_D^{23}$ −117.9° (Fig. 1). The solution was then deionized with 25 ml of Amberlite IR-120(H^+) and evaporated. The colorless, sirupy residue was evaporated twice with dichloromethane, and finally taken up in a small amount of the latter solvent. Upon scratching with a glass

Can. J. Chem. Downloaded from www.nrcresearchpress.com by 210.87.254.42 on 09/05/12
For personal use only.

rod, crystallization of the nitroarabinoside VI occurred and was allowed to proceed in a refrigerator for 1 hour. The isolated material was washed with ice-cold dichloromethane and amounted to 59 mg; $[\alpha]_D^{22}$ +70.8° (*c*, 0.5 in water). In a parallel experiment the yield was 66 mg; $[\alpha]_D^{23}$ +73.4°. Upon recrystallization from ethyl acetate the product showed m.p. 180° and $[\alpha]_D^{23}$ +85.5° (*c*, 0.5 in water). Identity with VI described in a preceding paragraph was confirmed by the infrared spectra as well as by a mixed melting point that was undepressed.

Paper chromatography of the mother liquor revealed the presence of some residual nitroarabinoside VI (R_f 0.64) besides a large amount of methyl 3-nitro-3-deoxy-β-D-ribopyranoside (R_f 0.80). There was also a little of the slightly faster-moving *xylo* isomer (R_f 0.83). This pattern of composition was confirmed when the corresponding amino glycosides appeared on a chromatogram after hydrogenation of the mother liquor. In addition to these there were detected traces of several slow-moving as well as fast-moving, ninhydrin-positive by-products. The chief component of the hydrogenated mother liquor was isolated in crystalline form and identified as methyl 3-amino-3-deoxy-β-D-ribopyranoside hydrochloride (1); it had m.p. 167–168° decomp. and $[\alpha]_D^{23}$ −119° (*c*, 0.5 in water) after one recrystallization from 95% ethanol.

α-L-threo Salt III

To a sample of 38.75 mg of methyl 3-nitro-3-deoxy-α-L-arabinopyranoside (VI) there was added 2 ml of *N*/10 sodium hydroxide, and the volume of the solution was made up to 5 ml by the addition of carbon dioxide free water. Thus 43.16 mg of the sodium salt III was present. The mutarotation was measured in a 2-dm tube and was found to be $[\alpha]_D^{23}$ +57.9° (3 minutes) → −116.4° (5 hours, constant) (Fig. 1). After deionization, the same chromatographic pattern of nitro compounds, and after hydrogenation, the same pattern of amino compounds were observed as in the partial epimerization of the salt II.

β-D-threo Salt IV

To a sample of 14.78 mg of methyl 3-nitro-3-deoxy-β-D-arabinopyranoside (VII) there was added 0.77 ml of *N*/10 sodium hydroxide and water to make up a volume of 3 ml. Thus 16.45 mg of the salt IV was present. Mutarotation readings were taken with a 2-dm tube and are recorded in Fig. 1. $[\alpha]_D^{23}$ −239° (3 minutes) → −100.3° (90 minutes) → −115.1° (18 hours, final). The chromatograms obtained after deionization as well as after hydrogenation of the equilibrated solution showed the same patterns as those obtained above from III and IV.

ACKNOWLEDGMENTS

This work was supported by grants No. A 1350 from the National Research Council of Canada and No. AI 4697 from the National Institute of Allergy and Infectious Diseases, United States Public Health Service. One of us (A. A.) wishes to thank the Canadian Commonwealth Scholarship and Fellowship Committee for the award of a Scholarship.

REFERENCES

1. H. H. BAER and H. O. L. FISCHER. J. Am. Chem. Soc. **81**, 5184 (1959).
2. H. H. BAER. J. Am. Chem. Soc. **84**, 83 (1962).
3. H. H. BAER and F. KIENZLE. Can. J. Chem. **41**, 1606 (1963).
4. B. R. BAKER, R. E. SCHAUB, and J. H. WILLIAMS. J. Am. Chem. Soc. **77**, 7 (1955).
5. J. K. DALE and C. S. HUDSON. J. Am. Chem. Soc. **52**, 2534 (1930).
6. A. C. RICHARDSON and H. O. L. FISCHER. J. Am. Chem. Soc. **83**, 1132 (1961).
7. H. H. BAER. J. Org. Chem. **28**, 1287 (1963).
8. H. H. BAER, L. D. HALL, and F. KIENZLE. J. Org. Chem. To be published.

Can. J. Chem. Downloaded from www.nrcresearchpress.com by 210.87.254.42 on 09/05/12
For personal use only.

OXIDATION OF N,N-DIMETHYLANILINE

I. THE REACTION WITH BENZOYL PEROXIDE[1]

DONALD M. GRAHAM[2] AND ROBERT B. MESROBIAN[3]

The Polymer Research Institute, Polytechnic Institute of Brooklyn, Brooklyn, New York

Received June 25, 1963

ABSTRACT

The reaction of *N,N*-dimethylaniline (A) with benzoyl peroxide (P) has been shown to exhibit complex kinetics. The observed rates of peroxide decomposition between 0° and 25° C could be described by the relation $-d[P]/dt = k_a[A][P]+k_b[A]^{1/2}[P]^{3/2}$. An unstable Würster salt of tetramethylbenzidine was shown to be one of the main products of the reaction, and a mechanism has been postulated which is consistent with the observed kinetics, involving tetramethylbenzidine as a reaction intermediate.

Can. J. Chem. Downloaded from www.nrcresearchpress.com by 210.87.254.42 on 09/05/12
For personal use only.

INTRODUCTION

The oxidation of *N,N*-dimethylaniline by benzoyl peroxide has been extensively studied (1–13), and much of the work has been reviewed by Walling (14). This system is of particular interest since it produces free radicals which can initiate polymerization. According to Horner and his students (2, 5), when the reaction is carried out at 0° C under nitrogen, in chloroform as a solvent, the main products which can be isolated are an almost quantitative yield of benzoic acid, and from the amine, formaldehyde and methylaniline. In addition, small amounts of *p*-benzoyloxydimethylaniline, and *p,p*-methylene-bis-*N,N*-dimethylaniline were isolated. The mechanism suggested for the reaction involves the initial polar formation of a quaternary hydroxylamine derivative which subsequently decomposes to give radical products. In order to explain the existence of formaldehyde and methylaniline, it is supposed that dealkylation of the tertiary amine plays an important role in the oxidation sequence, although the exact way in which this occurs has not been substantiated.

There still exists a good deal of confusion about the kinetics of the reaction. Horner and Scherf (3, 4) have attempted to make comparative studies of the effect of a large number of substituted dimethylaniline derivatives on the rate of decomposition of benzoyl peroxide. However, it becomes apparent that the rate measurements are quite difficult and unreliable, since the reported rates may vary from paper to paper for a particular amine. Also, although it has been reported that the reaction is second order, the published data are not consistent with this generalization. The results obtained by following the initiation of polymerization by this system also exhibit complex kinetics (9, 13), and the low initiation efficiencies obtained (2–25% (13–16)) indicate side reactions.

EXPERIMENTAL

Reagents

Dimethylaniline (Mallinckrodt reagent grade) was refluxed with acetic anhydride for 12 hours, and then fractionated under 7 mm of nitrogen at least three times, middle cuts being taken each time. The amine was immediately degassed by successive freezing and evacuating, and stored under its own vapor at dry ice temperature. The amine was vacuum-distilled from the storage flask into a transfer pipette when the reaction tubes were charged. *Benzoyl peroxide* (Fisher C.P. grade) was recrystallized twice from chloroform and stored

[1]*Taken from a thesis submitted by D. M. Graham in partial fulfillment of the requirements for a Ph.D. degree, June 1958.*

[2]*Present address: Department of Chemistry, University of Western Ontario, London, Ontario.*

[3]*Present address: Continental Can Company Inc., Chicago, Ill.*

at 0° C. *Toluene* (Fisher reagent grade) was distilled over sodium. *Acetonitrile* (Fisher reagent grade) was purified according to the method of Mann and Saunders (17) and fractionally distilled.

Procedure

The reactions were carried out in a container consisting of two test tubes sealed at the top to a common ground joint which could be attached to a vacuum manifold. Dimethylaniline and solvent were placed in one arm, and a solution of benzoyl peroxide in the other. The contents were degassed by successive freezing, pumping, and melting until no gas was evolved in the last step; this usually required three to four repetitions. The double-tubes were then sealed under vacuum, above the common juncture, and placed in a brine bath regulated to ±0.05° C.

When sufficient time had elapsed for the contents to reach bath temperature, all of the tubes were quickly inverted and shaken, mixing the contents, and reimmersed in the thermostat. After successive time intervals, the tubes were removed, and were quickly immersed in liquid nitrogen to stop the reaction. Each tube was then opened, and, while the contents were still frozen, flushed with a stream of prepurified nitrogen. It was then inverted over a flask containing glacial acetic acid, a few crystals of potassium iodide, and several pieces of dry ice. After all the contents had melted and passed into the flask, the tube was rinsed with cold glacial acetic acid, and the liberated iodine was titrated with sodium thiosulphate.

Although this may appear to be a rather unnecessarily laborious procedure, it was found that all of the steps indicated were required in order to obtain reproducible results. The amine–peroxide system is so susceptible to reaction with oxygen that complete exclusion of the latter during titration is imperative. It was found to be quite impossible to obtain any order of reproducibility when the method reported by Horner and co-workers (1–7) was used.

Reaction Products

Dimethylaniline (79.0 mmole) and benzoyl peroxide (0.94 mmole) in 20 ml toluene were mixed at about −25° C in the absence of oxygen by the procedure described above. When they were mixed, a yellow color was instantaneously formed. This changed slowly to a fluorescent blue-green color and then a bright green precipitate separated, leaving a yellow-orange solution. After filtering and washing the precipitate with cold toluene and drying it *in vacuo*, the yield of green solid was 0.13 g. This compound decomposed rapidly at 60° C and more slowly at room temperature to a yellow-brown solid. Addition of 50% potassium hydroxide to a methanol solution of the green solid deposited a yellow precipitate which, when recrystallized from petroleum ether – toluene, was identified as *N,N,N′,N′*-tetra-methylbenzidine by mixed melting point and elemental analysis. Acidification of the filtrate precipitated white crystals identified as benzoic acid by mixed melting point analysis. Elemental analysis on a fresh sample of the green solid gave: C, 74.9%; H, 6.2%; N, 7.1%. The solid can therefore be tentatively identified as the Würster salt:

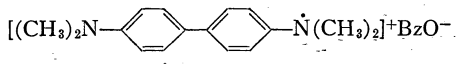

Calc.: C, 76.5%; H, 6.9%; N, 7.7%. On this basis, the observed yield would be 0.36 mmole or 38% based on benzoyl peroxide.

In order to estimate the relative yield of formaldehyde, dimethylaniline (79 mmole) and benzoyl peroxide (2.6 mmole) in 20 ml toluene were allowed to react for 5 hours at 0° C in the absence of oxygen. The reaction mixture was extracted several times with water, and from the extracts 0.36 mmole of the 2,4-dinitrophenylhydrazone of formaldehyde was obtained. The yield of formaldehyde is therefore 14% based on peroxide.

Reaction of tetramethylbenzidine (2.5 mmole) and benzoyl peroxide (0.94 mmole) in toluene at 0° C in the absence of oxygen yielded 0.19 g of green solid. The reaction was much faster than for dimethylaniline and precipitation appeared to be complete after about 30 seconds. The solid exhibited the same properties as those obtained from dimethylaniline and analyzed as: C, 74.3%; H, 6.0%; N, 7.8%. The two green compounds may therefore be assumed to be identical. The corresponding bromide salt having similar properties has been isolated from the bromine oxidation of tetramethylbenzidine (18).

When the green compound was stored, its oxygen content was found to increase (from the results of several attempts at elemental analysis); this may account for the lack of agreement in the above analyses. When tetramethylbenzidine was reacted with benzoyl peroxide in the presence of air, the toluene-washed green solid formed was found capable of oxidizing iodide ion, while the product formed in the absence of oxygen did not, indicating the possible presence of peroxide bonds in the former.

An attempt to polymerize styrene (4.3 mole/l.) in toluene at 0° C with tetramethylbenzidine (6.24×10^{-2} mole/l.) and benzoyl peroxide (2.28×10^{-2} mole/l.) in the absence of oxygen produced only a very small amount of apparently low molecular weight polymer soluble in methylethylketone.

It was also established that no carbon dioxide was evolved in the reaction between benzoyl peroxide and dimethylaniline. Degassed solutions of these compounds were allowed to react at 0° C under prepurified nitrogen in a closed system containing an oil manometer. No pressure change was detected during a period in which 85% of the peroxide should have decomposed. Conditions of the experiment were such that as little as 0.5 mole% yield of carbon dioxide evolved would be detectable.

Can. J. Chem. Downloaded from www.nrcresearchpress.com by 210.87.254.42 on 09/05/12
For personal use only.

RESULTS AND DISCUSSION

Kinetics

Benzoyl peroxide was found to react with dimethylaniline extremely rapidly. Although several authors have reported that the reaction is second order (1–12), this was found not to be strictly true over the concentration range studied here (Fig. 1). In fact, the initial

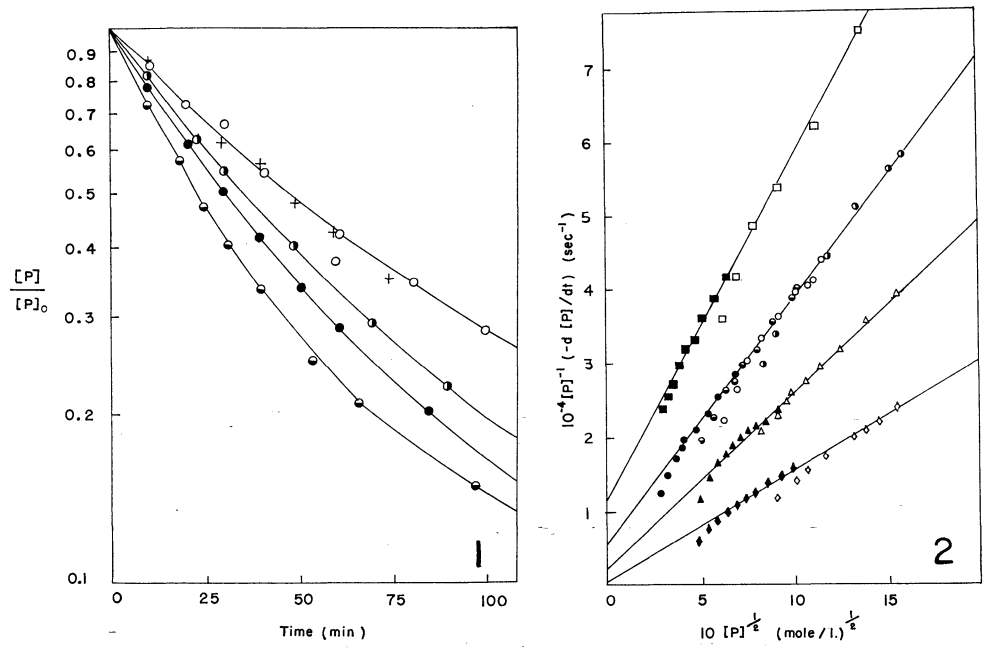

FIG. 1. Decomposition of benzoyl peroxide catalyzed by dimethylaniline at 0° C; initial amine concentration 0.395 mole/l.; initial peroxide concentrations (mmole/l.) in toluene ○ 4.11, ◑ 9.75, ● 13.7, ◒ 25.1, in acetonitrile, + 4.09.

FIG. 2. Differential plots for the catalyzed decomposition of benzoyl peroxide at 0° C; initial amine concentrations (mole/l.) ■ □ 0.790, ● ◒ ○ ◑ 0.395, ▲ △ 0.197, ◆ ◇ 0.079.

slopes of the first order decomposition plots are dependent upon the initial peroxide concentrations; the initial rates were about 4/3 order with respect to peroxide, and about 2/3 order with respect to amine. This probably indicates the presence of an additional decomposition reaction with an order dependence on peroxide greater than unity and, on amine, less than unity.

It was found that plotting $[P]^{-1}(d[P]/dt)$ against $[P]^{1/2}$, where [P] is the peroxide concentration, gave linear plots up to at least 65% decomposition. Some of the plots are shown in Fig. 2, for different peroxide and amine concentrations. In addition, the intercept and the slope are proportional to the initial amine concentration and to its root, respectively; this is evident from the summary of the peroxide decomposition results given in Table I. All measurements were made in toluene solution, but, on the basis of the one run carried out in acetonitrile, it may be tentatively concluded that the nature of the solvent has no great effect on the rate of the reaction, in agreement with the polymerization studies (13).

The rate of peroxide decomposition in the presence of dimethylaniline can therefore be described by the equation

$$-d[P]/dt = k_a[A][P]+k_b[A]^{1/2}[P]^{3/2} \qquad [1]$$

Can. J. Chem. Downloaded from www.nrcresearchpress.com by 210.87.254.42 on 09/05/12
For personal use only.

TABLE I

Dimethylaniline-catalyzed decomposition of benzoyl peroxide

Temp., °C	$[A]_0$, mmole/l.	$[P]_0$, mmole/l.	From $[P]^{-1}(d[P]/dt)$ vs. $[P]^{1/2}$ plot: 10^4 intercept/$[A]_0$, l./mole sec	From $[P]^{-1}(d[P]/dt)$ vs. $[P]^{1/2}$ plot: 10^3 slope/$[A]_0^{1/2}$, l./mole sec
0	79	9.75	1.3	5.41
0	79	24.0		
0	197	9.80	1.4	5.04
0	197	24.0		
0	395	4.11		
0	395	9.75	1.5	5.20
0	395	13.7		
0	395	25.1		
0	790	4.18	1.5	5.16
0	790	18.5		
10	79	13.5	3.9	5.91
10	395	9.75	3.3	6.12
20	79	9.62	8.6	7.02
20	395	4.36	7.9	7.19
25	39	4.62	15	7.64
25	79	9.90	18	5.12
25	395	4.22	16	7.50

NOTE: $[A]_0$ and $[P]_0$ are, respectively, the initial amine and peroxide concentrations.

and the constants k_a and k_b can be determined from the results. The temperature dependence of the rate constants are given in Table II from which is obtained:

$$k_a = 1.1 \times 10^8 \exp(-14800/RT)$$

and

$$E_b = 2.3 \text{ kcal.}$$

The low activation energy of the induced decomposition term compared to E_a is undoubtedly responsible for the reported first order (with respect to peroxide) behavior of the initial rate at high temperatures and low amine concentrations (12).

Mechanism

The following free radical scheme is not intended to be definitive. The evidence available indicates that the overall reaction is complex and that ionic mechanisms likely play a competitive role, at least in the more advanced stages. This sequence, however, does explain the behavior of the system in what must be essentially free radical reactions such as vinyl polymerization and oxidation.

[0] $A + Bz_2O_2 \rightarrow \dot{A}^+ + BzO^- + Bz\dot{O}$

[1*a*] $Bz\dot{O} + A \rightarrow \dot{A}^+ + BzO^-$

[1*b*] $2\dot{A}^+ \rightarrow T + 2H^+$

[1*c*] $T + Bz_2O_2 \rightarrow \dot{T}^+ + BzO^- + Bz\dot{O}$

[4] $2\dot{T}^+ \rightarrow$ dimer

[5] $\dot{T}^+ + Bz_2O_2 \rightarrow T^{++} + BzO^- + Bz\dot{O}$

Can. J. Chem. Downloaded from www.nrcresearchpress.com by 210.87.254.42 on 09/05/12
For personal use only.

A, T, $\dot{T}^{+}$, T^{++} represent dimethylaniline, tetramethylbenzidine, and its semiquinone and quinone, respectively. The reasons for deciding on this particular reaction sequence will become more apparent if the reactions are discussed individually.

Reaction [0].—Spectrophotometric evidence indicates that the primary step occurs through the reversible formation of a molecular complex between the amine and benzoyl peroxide (16). In order to explain the presence of free radicals which do not contain nitrogen and which can initiate vinyl polymerization (2), it is necessary to suppose that benzoyl radicals are produced by decomposition of this complex or perhaps of the hydroxylamine derivative $[(BzO)(CH_3)_2NC_6H_5]^{+}BzO^{-}$, which has been suggested as a further intermediate (13). The overall process has been represented by a single reaction which is kinetically indistinguishable from the detailed sequence.

Reaction [1a].—The benzyol radicals once formed must react rapidly with amine in order that no carbon dioxide be evolved. A reaction similar to [1*a*] has been suggested for hydroxyl radicals formed from hydrogen peroxide and peroxidase in the presence of dimethylaniline (18). The extreme ease of this reaction is very likely responsible for the inhibitory ability of dimethylaniline in certain free radical reactions (19).

Reaction [1b].—The isolation of a tetramethylbenzidine derivative as a major product indicates a para coupling reaction. Such reactions are well known for phenols and aromatic amines under oxidizing conditions, and in this case likely occurs through the intermediate $[(CH_3)_2\dot{N}C_6H_5]^{+}BzO^{-}$ in either a one- or a two-step process (although the absence of *p*-benzoyldimethylaniline in the products would indicate the former). In the mechanism suggested by Horner *et al.* it was postulated that the proton was lost exclusively from one of the *N*-methyl groups on the basis of isolation of formaldehyde and methylaniline from the reaction products. However from the results reported here and by Goode and Gratch (10), it would appear that, in the absence of oxygen and at low temperatures, formaldehyde is formed only in small quantities. It is suggested therefore that methylaniline and formaldehyde are produced primarily during the isolation procedure or in the advanced stages of the oxidation reaction (27).

Reaction [1c].—In order to explain the observed kinetics, it is necessary to postulate an additional reaction involving peroxide and some reactive intermediate. Induced decomposition has usually been explained in terms of attack on peroxide by secondary radicals formed by reaction of the primary radicals (BzO or $\dot{\emptyset}$) with the solvent. In this case, however, this type of mechanism is incompatible with the product analysis. As mentioned previously, the reaction of tetramethylbenzidine with benzoyl peroxide is extremely rapid; this reaction then, along with [5], is very likely responsible for the 4/3 order dependence of the rate on peroxide.

Reaction [4].—According to Michaelis and Granick (20), the semiquinones of tetramethylated diamines do not dimerize, but exist as free radicals even in the solid state. Later work (21, 22), however, indicates that polymerization can indeed occur under certain conditions. It was found that in precipitating semiquinone salts, a solid with a low magnetic susceptibility was associated with a low dielectric constant of the precipitating medium. In the case of tetramethylbenzidine a diamagnetic solid was obtained in all cases. It is very probable therefore, that the green tetramethylbenzidine derivative isolated is the semiquinone dimer, and that the equilibrium favors reaction [4] and not the reverse reaction.

Reaction [5].—According to the theory of hydroquinone oxidation (23), the semiquinone is much more readily oxidizable than the corresponding hydroquinone; hence, reaction [5] might be expected to be a great deal faster than reaction [1*c*].

Can. J. Chem. Downloaded from www.nrcresearchpress.com by 210.87.254.42 on 09/05/12
For personal use only.

Therefore, from these equations, and assuming that the steady-state approximation is applicable, the rate of peroxide decomposition is given by

$$-d[\mathrm{P}]/dt = 3k_0[\mathrm{A}][\mathrm{P}] + 2k_5(k_0/k_4)^{1/2}[\mathrm{A}]^{1/2}[\mathrm{P}]^{3/2}. \qquad [2]$$

If semiquinone dismutation (quinone catalysis (23)), i.e.,

$$\mathrm{T} + \mathrm{T}^{++} \xrightarrow{k_s} 2\dot{\mathrm{T}}^{+} \text{ (or dimer)},$$

is included, and if k_s, the rate constant, is sufficiently large so that the concentration of T^{++} has a steady-state value, the rate of peroxide decomposition will be given by the first term of equation [2]. However, if k_s is small, as appears to be the case for tetramethylbenzidine (18), so that the concentration of T^{++} increases during the reaction, the reaction will be autoinhibited in the late stages, i.e., as the rate $k_s[T][T^{++}]$ approaches $k_4[T][P]$. Such inhibition was observed after about 65% decomposition.

Comparing equations [1] and [2] it is seen that $k_a = 3k_0$ and $k_b = 2k_5(k_0/k_4)^{1/2}$. The calculated rate constants are given in Table II; and from their temperature dependence is obtained:

$$k_0 = 3.7\times10^7 \exp(-14{,}800/RT), \text{ and, } \tfrac{1}{2}E_4 - E_5 = 5.1 \text{ kcal.}$$

TABLE II

Rate constants

Temp., °C	10^4k_a, l./mole sec	10^3k_b, l./mole sec	10^5k_0, l./mole sec	$k_5k_4^{-1/2}$ (l./mole sec)$^{\frac{1}{2}}$
0	1.5	5.2	5.0	0.37
10	3.6	6.0	12	0.27
20	8.2	7.1	27	0.22
25	16	7.4	53	0.17

It is difficult to compare the rate constants evaluated in this work with the results obtained from measurements of the rate of initiation of styrene polymerization. It would appear that the kinetic behavior reported here to a certain extent invalidates the method by which the "apparent second order rate constants" and initiation efficiencies were obtained in the polymerization work. The values of the "apparent rate constants" reported are, however, of the same order of magnitude as k_a and their variation with initial peroxide concentration is consistent with the kinetic analysis presented here. The low efficiency of this system in initiating polymerization is likely due to reaction [1*a*] being able to compete for BzȮ radicals even in the presence of a much higher concentration of styrene than amine. With the tetramethylbenzidine benzoyl peroxide system, the reaction corresponding to [1*a*] would be extremely fast, and as observed, very little initiation of polymerization can occur.

The activation energy, E_0, is of the same order as the activation energies for metal-catalyzed peroxide decomposition (24) but is higher than that observed in the polymerization work. The low temperature independent factor indicates a negative entropy of activation, which might be expected in this case. E_5 is the activation energy for electron transfer between a semiquinone radical and peroxide, and may well be close to zero; this would set a lower limit of about 10 kcal for E_4. The magnitude of E_4 seems perhaps rather high for a radical–radical reaction, and it likely reflects the fact that it was obtained from the difference in temperature dependence of two terms, one of which was relatively

Can. J. Chem. Downloaded from www.nrcresearchpress.com by 210.87.254.42 on 09/05/12
For personal use only.

insensitive to temperature. This high activation energy may also only be apparent, since results from the autoxidation of dimethylaniline indicate that the intermediates involved in the induced decomposition reactions are likely unstable at higher temperatures.

ACKNOWLEDGMENTS

This research was supported in part by the Office of Naval Research, and in part by a grant from the Thiokol Corporation. One of the authors (D. M. G.) would like to express his appreciation to the Thiokol Corporation for a fellowship in 1955–56.

REFERENCES

1. L. Horner and E. Schwenk. Angew. Chem. **61**, 411, 442 (1949).
2. L. Horner and E. Schwenk. Ann. **566**, 69 (1950).
3. L. Horner and K. Scherf. Ann. **573**, 35 (1951).
4. L. Horner and K. Scherf. Ann. **574**, 202 (1951).
5. L. Horner and C. Betzel. Ann. **579**, 175 (1953).
6. L. Horner and W. Kirmse. Ann. **597**, 66 (1956).
7. L. Horner and H. Junkermann. Ann. **591**, 53 (1955).
8. L. Horner. J. Polymer Sci. **18**, 438 (1955).
9. T. H. Meltzer and A. V. Tobolsky. J. Am. Chem. Soc. **76**, 5178 (1954).
10. W. E. Goode and S. Gratch. Abstracts of Papers, 126th Meeting of the American Chemical Society. September, 1954. p. 73.
11. M. Imoto, O. Takayuki, and K. Kimura. J. Polymer Sci. **15**, 485 (1955).
12. M. Imoto and K. Takemoto. J. Polymer Sci. **19**, 579 (1956).
13. C. Walling and N. Indictor. J. Am. Chem. Soc. **80**, 5814 (1958).
14. C. Walling. Free radicals in solution. John Wiley and Sons Inc., New York, N.Y. 1957. p. 590.
15. M. Imoto, T. Otsu, and K. Kimura. J. Polymer Sci. **15**, 475 (1955). M. Imoto and K. Takemoto. J. Polymer Sci. **18**, 377 (1955).
16. K. F. O'Driscoll and E. V. Ricchezza. J. Polymer Sci. **46**, 211 (1960).
17. F. G. Mann and B. C. Saunders. Practical organic chemistry. Longmans, Green and Co., New York, N.Y. 1952. p. 93.
18. F. T. Naylor and B. C. Saunders. J. Chem. Soc. 3519 (1950).
19. G. S. Hammond, C. E. Boozer, C. E. Hamilton, and J. N. Sen. J. Am. Chem. Soc. **77**, 3238 (1955).
20. L. Michaelis and S. Granick. J. Am. Chem. Soc. **65**, 1747 (1943).
21. G. K. Hughes, N. Hush, and D. P. Mellor. Nature, **159**, 612 (1947).
22. G. K. Hughes and N. Hush. J. Proc. Roy. Soc. N.S. Wales, **81**, 48 (1947).
23. J. E. LuValle and A. Weissberger. J. Am. Chem. Soc. **69**, 1567 (1947).
24. A. V. Tobolsky and R. B. Mesrobian. Organic peroxides. Interscience, Inc., New York, N.Y. 1954. pp. 97–99.
25. A. V. Tobolsky and R. B. Mesrobian. Organic peroxides. Interscience, Inc., New York, N.Y. 1954. p. 107.
26. W. Huckel. Theoretical principles of organic chemistry. Vol. I. Elsevier Co., New York, N.Y. 1955. p. 230.
27. D. M. Graham and R. B. Mesrobian. Can. J. Chem. This issue.

Can. J. Chem. Downloaded from www.nrcresearchpress.com by 210.87.254.42 on 09/05/12
For personal use only.

OXIDATION OF N,N-DIMETHYLANILINE

II. THE REACTION WITH OXYGEN CATALYZED BY BENZOYL PEROXIDE[1]

DONALD M. GRAHAM[2] AND ROBERT B. MESROBIAN[3]
The Polymer Research Institute, Polytechnic Institute of Brooklyn, Brooklyn, New York

Received June 25, 1963

Can. J. Chem. Downloaded from www.nrcresearchpress.com by 210.87.254.40 on 09/05/12
For personal use only.

ABSTRACT

When benzoyl peroxide was used to initiate the reaction of oxygen with *N,N*-dimethylaniline, a chain reaction was shown to occur, resulting in an almost quantitative yield of hydrogen peroxide. The reaction was inhibited by mercaptan and benzoquinone, but not by hydroquinone, and was shown to be autoinhibited as well. The rate of oxidation was observed to be much greater in polar solvents, such as acetonitrile or methanol, than in non-polar solvents such as toluene and benzene. Diethyl- and dipropyl-aniline exhibited no chain characteristics under similar conditions, whereas dimethylbenzylamine and dimethyldodecylamine did not react at all.

A mechanism has been postulated involving both semiquinone and peroxide chain carriers which is consistent with all of these observations. From an analysis of the oxidation rates in the presence and absence of mercaptan inhibition, the appropriate rate constants have been determined.

INTRODUCTION

The research described in this series of papers was originally undertaken in an attempt to clear up some of the confusion concerning the mechanism by which tertiary aromatic amines act as inhibitors in hydrocarbon oxidation. In studying the inhibition of cumene autoxidation by dimethylaniline, it became apparent that the amine was being rapidly and preferentially oxidized in the initial stages of the reaction. As the reaction progressed, the amount of retardation increased, indicating that the autoxidation products of the amine are very effective antioxidants. Accordingly, it was realized that in order to understand the antioxidant action of tertiary amines, it was first necessary to investigate the mechanism of their autoxidation.

It was found that highly purified dimethylaniline autoxidized extremely rapidly at 60° C. The highest maximum rate observed for freshly purified dimethylaniline was 2×10^{-4} mole/l. per sec; the corresponding rate measured for pure tetralin was 5×10^{-6} mole/l. per sec. The reaction was initially autocatalytic, and appeared to be also autoinhibited. The maximum degree of oxidation that could be obtained before the rate began to approach zero was about 2 mole%.

Unfortunately, in all cases the measured rates were irreproducible within an order of magnitude and there appeared little prospect of obtaining useful information under such conditions. It therefore appeared desirable to work at lower temperatures using benzoyl peroxide as an initiator in the hope of minimizing side reactions. Some time after the inception of this work, Horner and Junkermann (2) published some semiquantitative results on this system; however, their postulated mechanism was based primarily on the products isolated in the presence of oxygen and of nitric oxide, and differs in detail from that indicated by the results presented in this paper.

[1]*Taken from a thesis submitted by D. M. Graham in partial fulfillment of the requirements for a Ph.D. degree, June 1958.*
[2]*Present address: Department of Chemistry, University of Western Ontario, London, Ontario.*
[3]*Present address: Continental Can Co., Inc., Chicago, Illinois.*

EXPERIMENTAL

Reagents

Dimethylaniline, *benzoyl peroxide*, *toluene*, *acetonitrile*, and *tetramethylbenzidine* were purified as in Part I (1). *Hydroquinone* (Eastman) was recrystallized from benzene under nitrogen. *Benzoquinone* (Eastman) was recrystallized from methanol. *1-Dodecanethiol* (Humphrey-Wilkinson) was fractionally distilled; a middle cut boiling at 126° C and 6 mm (of nitrogen) was used. *Diethyl-*, *Dipropyl-*, *methylethyl-*, and *methylaniline* were Eastman White Label grade, and were purified by fractional distillation under vacuum, in a nitrogen atmosphere.

Oxygen Absorption Measurements

Oxygen absorption was measured with an apparatus of the constant pressure type, slightly modified from that described by Cooper and Melville (3). The reaction flask was first cleaned with alcoholic sodium hydroxide, concentrated nitric acid, rinsed five times with distilled water, and flamed while under a pressure of less than 10^{-5} mm. The amine to be studied was transferred to the reaction flask using an all-glass apparatus in the absence of oxygen. Benzoyl peroxide and the inhibitors were added to the flask immersed in liquid nitrogen as solutions in the solvent to be used. The flask was then evacuated and filled with oxygen. It was then placed in a thermostat and shaken at a rate of 200 strokes per minute; zero time was taken as the time at which the pressure stopped increasing (usually 2–3 minutes).

Measurements at different oxygen pressures indicated that the initial rate was independent of the oxygen pressure above about 150 mm; accordingly, most of the results reported were made at an oxygen pressure of 750 mm in order to minimize the possibility of oxygen diffusion controlled kinetics.

RESULTS

Rate Measurements

Highly purified dimethylaniline exhibited no measurable autoxidation at 0° C; however, the addition of a small amount of benzoyl peroxide caused an extremely rapid uptake of oxygen. On oxidation, the solution changed from light yellow to deep red; at very high concentrations of peroxide and amine, a green solid was observed to precipitate. The catalyzed reaction was much less sensitive to the purity of the dimethylaniline than was the high temperature autoxidation reaction. For example, the catalyzed rate of oxidation of a sample taken from a freshly opened bottle was 5.02×10^{-5} mole/l. per sec, while for the highly purified material, the rate was 6.15×10^{-5} mole/l. per sec; the corresponding autoxidation rates were 0 and 2×10^{-4} mole/l. per sec respectively, at 60° C.

The data are summarized in Table I, and some representative oxygen absorption curves are shown in Fig. 1. No induction period was detected; although if it were less than 2–3 minutes, the time required for the reaction mixture to warm to 0° C, it would not have been observable.

The order dependence of the initial rate on peroxide concentration was between 0.5 and 1.0, and increased with increasing amine concentration. With respect to amine concentration, it was between 1.0 and 1.5, and decreased with increasing peroxide concentration. It was found by plotting $(-d[O_2]/dt)_0/[A]_0[P]_0$ vs. $([A]_0/[P]_0)^{1/2}$, where $(-d[O_2]/dt)_0$ is the initial rate of oxygen uptake, and $[A]_0$ and $[P]_0$ are the initial concentrations of amine and peroxide respectively, that the data are closely fitted by an equation of the form:

$$(-d[O_2]/dt)_0 = k_c[A]_0[P]_0+k_d[A]_0^{3/2}[P]^{1/2}. \qquad [1]$$

The values obtained for k_c and k_d at 0° C and 25° C from least square plots are given in the second and fifth columns of Table VI.

It was also observed that when acetonitrile is used as a solvent, the rate is increased about sevenfold with no apparent change in the order dependence of the rate on peroxide. This is further substantiated by the fact that, for solvent mixtures of acetonitrile and toluene, the ratios of the rates in the mixed solvents to that in the pure toluene (plus amine), when plotted against solvent composition, all fell on a smooth curve, irrespective of the initial concentrations of reactants (Fig. 2). No difference was noted between the

Can. J. Chem. Downloaded from www.nrcresearchpress.com by 210.87.254.40 on 09/05/12
For personal use only.

TABLE I

Benzoyl peroxide initiated oxidation of dimethylaniline in toluene

$[A]_0$, mole/l.	$[P]_0$, mmole/l.	$(-d[O_2]/dt)_0$, mole/l. sec × 10^6		$[O_2]_T$, mmole/l.		$[P]_T$, mmole/l.
		Obs.	Calc.*	Obs.	Calc.†	
			At 0° C			
0.213	129	2.99	3.08			
0.371	196	8.11	8.31			
0.479	129	9.21	8.69			
0.500	177	12.0	11.4			
0.631	177	15.5	15.5			
0.631	129	12.4	12.5			
0.631	98.8	9.87	10.5			
0.631	54.0	6.87	7.07			
0.835	36.0	8.14	8.01			
0.972	129	23.0	22.4			
0.982	24.0	7.66	7.94	62	65.5	54
0.982	24.0	7.72	7.94	63	65.5	48
1.14	121	27.1	26.3			
1.50	24.0	14.2	14.7	73	79.0	54
1.97	24.0	21.8	21.8	88	89.4	
2.54	24.0	31.3	31.6	98	100	
2.80	98.8	90.9	82.7	160	230	
2.80	61.0	61.5	61.2	136	175	
2.80	24.0	37.3	36.2	106	105	
2.80	12.0	25.8	25.0	67	72.6	
2.80	8.83	20.4	21.1	64	61.7	55
3.38	24.0	48.5	48.0	117	115	
3.38	12.0	30.8	32.8			
3 38	8.83	28.3	27.9	65	67.7	
3.38	4.40	18.5	19.4	51	47.2	43
4.58	24.0	75.1	74.4			
4.58	12.0	49.6	51.9			
4.58	8.80	45.5	43.7	93	78.2	
4.58	4.40	31.5	30.5	54	54.8	
			At 25° C			
0.526	8.45	11.2	11.1	24	23	
0.526	33.1	24.7	25.5	50	51	
0.526	54.7	34.0	35.3	67	69	
0.526	91.1	51.1	49.8	90	95	
0.526	151	76.5	71.2	131	131	
0.721	8.45	16.8	17.6	28	27	
1.15	8.45	35.4	36.6			
1.50	8.45	51.6	50.4	40	38	
1.97	8.45	76.9	75.6	46	44	
2.79	8.45	124	125	49	52	

NOTE: $[A]_0$, $[P]_0$, $[O_2]_T$, $[P]_T$ are, respectively, the initial amine concentration, the initial benzoyl peroxide concentration, the total oxygen absorbed, and the concentration of the peroxide produced.
*From equation [1].
†From equation [7].

rate in benzene and that in toluene at 25° C, but an increase in rate was observed in a mixture of methanol (55 mole%) and toluene at 0° C, and this increase is almost exactly equivalent to that which would be observed in the corresponding acetonitrile–toluene mixture.

The rate of oxidation was shown to be autoinhibited by an inhibitor formed in the reaction with oxygen; whereas the reaction of benzoyl peroxide in the absence of oxygen appeared to produce a compound which accelerates the rate. This is apparent from the following two sets of experiments. Solutions of amine (1–2 mole/l.) and peroxide (24 mmole/l.) were allowed to react to completion in the presence of oxygen; a known concentration of peroxide was then added and the rate of oxygen uptake measured. The

Can. J. Chem. Downloaded from www.nrcresearchpress.com by 210.87.254.40 on 09/05/12
For personal use only.

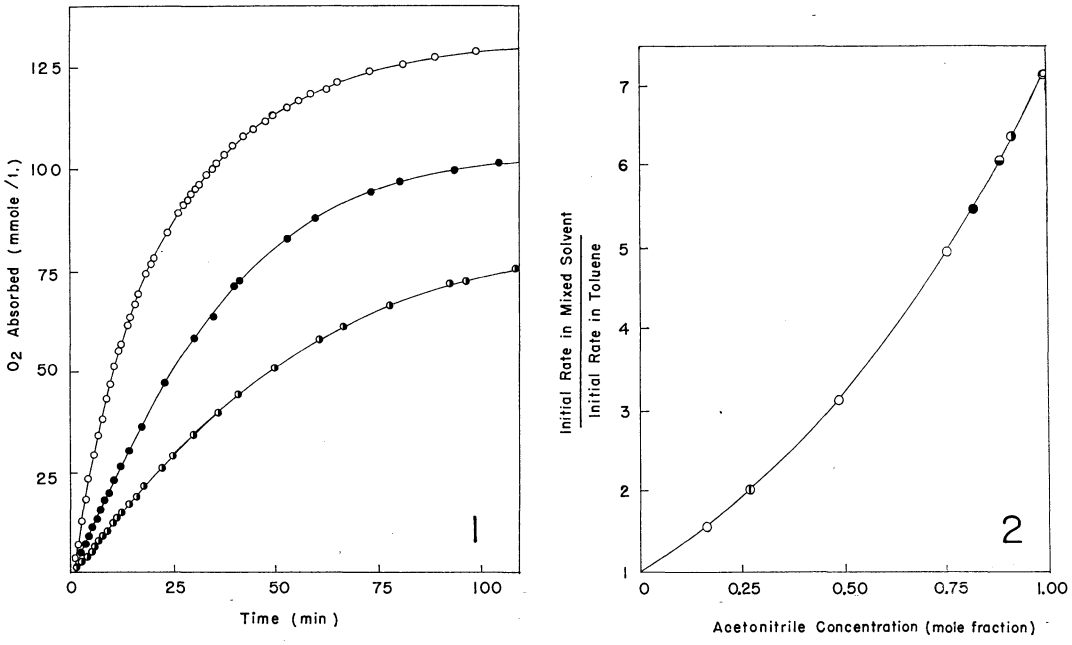

FIG. 1. Benzoyl peroxide initiated oxidation of dimethylaniline in toluene at 0° C; initial amine concentration, 2.80 mole/l.; initial peroxide concentrations, ○ 98.8, ● 24.0, ◑ 8.8 mmole/l.

FIG. 2. Dependence of the initial rate of oxidation on solvent composition for toluene–acetonitrile mixtures. Initial amine (mole/l.) and peroxide (mmole/l.) concentrations, respectively: ○ 0.835, 36.0; ◑ 1.50, 24.0; ◒ 1.94, 12.0; ● 2.80, 8.75; ◐ 2.80, 24.0.

observed rate was in all cases about one-half that estimated from equation [1] after allowing for the decrease in amine concentration by the initial reaction. These experiments were repeated; however, in this case the solutions were degassed before mixing and the preliminary reaction was carried out in the absence of oxygen. The reacted mixture was then placed in an oxygen atmosphere. No oxygen uptake was observed until more peroxide was added; and then the rate of oxidation was about 1.5 times that estimated from equation [1].

Stoichiometry

The total amount of oxygen that reacted, $[O_2]_T$, in any given run appeared to approach a maximum which was dependent on the initial concentrations of reactants. In fact when $[O_2]_T/[P]_0$ was plotted against $([A]_0/[P]_0)^{1/2}$ linear relations were obtained.

It would be particularly desirable to supplement the oxidation uptake measurements with simultaneous measurements of the total peroxide content of the reacting mixture. Unfortunately, due to the extreme lability of the system, the results obtained varied so widely as to be meaningless. It was possible though, to determine the peroxide present at the end of the reaction, $[P]_T$, and to obtain reproducible results; these are given in Table II. Thus, most of the oxygen which is absorbed is in the form of peroxide at the completion of the reaction.

Inhibition

In contrast to its ability to inhibit completely the rate of autoxidation of dimethylaniline, hydroquinone was found to have no effect on the peroxide-catalyzed reaction. Also, although it has been stated (2) that benzoic acid, "by virtue of its acidic function",

Can. J. Chem. Downloaded from www.nrcresearchpress.com by 210.87.254.40 on 09/05/12
For personal use only.

TABLE II

Peroxide production

$[A]_0$, mole/l.	$[P]_0$, mmole/l.	$[O_2]_T$, mmole/l.	$[P]_T$, mmole/l.	$[P]_T/[O_2]_T$
0.982	24.0	62	54	0.87
0.982	24.0	63	48	0.76
1.50	24.0	73	54	0.74
2.80	8.83	64	55	0.78
3.38	4.40	51	43	0.84

retards the decomposition of benzoyl peroxide in dimethylaniline, its presence produced no diminution in rate, nor did the presence of a much stronger acid, toluenesulphonic acid.

Dodecanethiol-1 (RSH) and benzoquinone (Q) were found to retard the reaction considerably, and both proved quite useful in elucidating the reaction mechanism. With both inhibitors the rate was retarded, but no induction period was observed; in addition, the total oxygen absorbed appeared to be decreased.

The results obtained in the presence of benzoquinone are given in Table III. It is

TABLE III

Inhibition by benzoquinone

$[A]_0$, mole/l.	$[P]_0$, mmole/l.	$[Q]_0$, mmole/l.	Oxygen press., mm Hg	$(-d[O_2]/dt)_0$, mole/l. sec $\times 10^6$	$[O_2]_T$, mmole/l.	$(-d[O_2]/dt)_0[Q]_0/[A]_0[P]_0$, $sec^{-1}\times 10^6$
2.80	99.2	59.0	729	2.8	8.7	59
2.80	98.6	11.4	719	8.29	27	34.2
2.80	98.8	9.14	730	12.7	37	42.0
2.80	98.6	5.68	731	20.0	62	41.2
2.80	98.7	3.04	730	35.2	110	38.7
2.80	102	2.27	720	49.1	132	39.1
1.17	102	9.08	731	5.69		43.2
2.80	36.0	9.10	728	4.43		39.9
3.82	98.8	9.14	728	17.4		42.2
2.80	98.6	9.10	579	10.7	29	
2.80	98.8	9.10	313	7.32		
2.80	98.6	9.10	220	3.80		
2.80	98.8	9.11	134	1.81		

apparent from the last column that the initial inhibited rate is proportional to the product of the initial concentrations of amine and peroxide, and is inversely proportional to the initial quinone concentration. This rate is also a function of the oxygen pressure; however, the direct proportionality suggested by the results cannot be assumed, since no correction has been made for the vapor pressure of the solution, and the rate might well be diffusion-controlled at low pressures. The initial rate of oxidation, in the presence of quinone, is therefore given by the relation: $(-d[O_2]/dt)_0 = 4.01\times 10^{-7}[A]_0[P]_0/[Q]_0$, at 726 mm, 0° C, in toluene.

In contrast to inhibition by benzoquinone where the rate approaches zero as the inhibitor concentration is increased, in the presence of mercaptan the rate appears to approach a limiting minimum value as the concentration of inhibitor is increased. This minimum rate is proportional to both the initial amine and peroxide concentrations. These results are given in Table IV. Another striking thing about the values obtained for the inhibited rate is that, when they are divided by the product $[A]_0[P]_0$ the result

Can. J. Chem. Downloaded from www.nrcresearchpress.com by 210.87.254.40 on 09/05/12
For personal use only.

TABLE IV

Inhibition by mercaptan

$[A]_0$, mole/l.	$[P]_0$, mmole/l.	$[RSH]_0$, mole/l.	$(-d[O_2]/dt)_0$, mole/l. sec $\times 10^6$	$(-d[O_2]/dt)_0/[A]_0[P]_0$, l./mole sec $\times 10^6$
		In toluene at 0° C		
0.482	129	0.78	6.64	107
0.478	129	0.18	6.14	99.5
1.50	98.8	0.20	16.2	109
1.50	98.8	1.7	15.4	106
1.50	98.8	0.86	15.5	105
2.80	98.8	0.98	30.0	108
2.80	98.0	0.01	54.3	198
		In toluene at 25° C		
2.80	8.45	1.1	18.7	792
1.50	8.45	1.0	9.80	774
		In acetonitrile at 0° C		
0.835	124	0.72	12.8	124
0.835	61.0	0.79	6.40	126
1.50	98.8	0.98	19.6	132

is almost exactly equal to twice the rate constant k_c. As will be seen later, k_c is the initiation rate constant, k_0, and this equality can be predicted from the postulated mechanism. The values of k_0 in the third column of Table VI are $(-d[O_2]/dt)_0/2[A]_0[P]_0$ and are equal to the corresponding values in the second column, within experimental error. This makes it possible to determine the rate constants k_c and k_d from two initial rate measurements, one in the presence of mercaptan and one in its absence. The rate constants for the four other temperatures given in Table VI were obtained in this way from the data in Table V.

TABLE V

Determination of rate constants by the inhibitor method

Temp., °C	$[A]_0$, mole/l.	$[P]_0$, mmole/l.	$[RSH]_0$, mole/l.	$(-d[O_2]/dt)_0$, mole/l. sec $\times 10^6$	$(-d[O_2]/dt)_0/[A]_0[P]_0$, l./mole sec $\times 10^6$
10	2.80	8.45	1.0	5.37	227
10	1.50	8.45	1.0	2.74	216
10	2.80	8.45	—	44.8	—
10	1.50	8.45	—	13.6	—
15	2.80	8.45	1.0	7.44	314
15	1.50	8.45	1.0	4.18	330
15	2.80	8.45	—	66.7	—
15	1.50	8.45	—	24.5	—
20	2.80	8.45	1.0	13.6	574
20	1.50	8.45	1.0	7.45	588
20	2.80	8.41	—	97.0	—
20	1.50	8.41	—	36.3	—

DISCUSSION

Mechanism

In determining a mechanism for this reaction, it is necessary to account for the chain character of the oxidation (which is evident from the kinetics and from the stoichiometry), and for the products formed. The former is readily explained in terms of the mechanism used to describe hydrocarbon oxidation (4); this mechanism is, however, not compatible with the products isolated, nor can it easily explain quinone inhibition. Hence, a reaction

Can. J. Chem. Downloaded from www.nrcresearchpress.com by 210.87.254.40 on 09/05/12
For personal use only.

sequence has been suggested which is superficially similar to the hydrocarbon mechanism, but which can account for these other observations. The following mechanism is necessarily an oversimplification of the entire process, but is, at least, consistent with the information presently available concerning the initial stages of the reaction. The separate steps have been numbered in such a fashion so as to emphasize the similarities between this chain mechanism and that postulated for hydrocarbon oxidation.

[0] $A + Bz_2O_2 \rightarrow \dot{A}^+ + BzO^- + Bz\dot{O}$

[1a] $Bz\dot{O} + A \rightarrow \dot{A}^+ + BzO^-$

[1b] $2\dot{A}^+ \rightarrow T + 2H^+$

[1c] $T + Bz_2O_2 \rightarrow \dot{T}^+ + BzO^- + Bz\dot{O}$

[2] $\dot{T}^+ + O_2 \rightarrow T^{++} + \dot{O}_2^-$

[3] $\dot{O}_2^- + A \rightarrow \dot{A}^+ + O_2^{=}$

[6] $2\dot{O}_2^- \rightarrow O_2 + O_2^{=}$

The symbols used have been defined in Part I (1).

Reactions [0] and [1_{a-c}] have been discussed in Part I. The following considerations are important in the choice of the remaining three reactions.

Reaction [2]

There is no direct evidence available concerning the step involving the reaction of molecular oxygen. Isolation of formaldehyde, hydrogen peroxide, and methylaniline led Horner and Junkermann (2) to postulate the formation of a peroxide which hydrolyzed to these products on contact with water. All attempts to synthesize this peroxide failed, although a peroxidic solid was obtained from dimethylmesidine with performic acid as an oxidizing agent. The existence of this peroxide is therefore questionable, and an alternative mechanism would seem desirable.

One of the distinguishing features of hydroquinone oxidation, as contrasted with the oxidation of hydrocarbons, is the nature of the peroxides formed; in the former case, hydrogen peroxide is exclusively produced, while, in the latter, hydroperoxides and diperoxides are the main products. This difference undoubtedly arises because of the ability of non-hydrocarbon compounds to enter into electron transfer reactions. Hence, as the results reported here seem to indicate, it is likely that the peroxide formed in this reaction is hydrogen peroxide, probably existing in equilibrium with $[C_6H_5N(CH_3)_2OH^+]OH^-$.

Since it was observed that highly purified *N*-methylaniline is a very effective retarder for both the benzoyl peroxide catalyzed oxidation and the high temperature autoxidation reactions, it appears likely that this compound is responsible, at least in part, for the observed autoinhibition. The results indicate that it is formed only in the reaction sequence involving oxygen and not in the reactions with benzoyl peroxide. Thus, methylaniline and formaldehyde are likely produced mainly in the later stages of the reaction, possibly by rearrangement of dimethylaniline oxide (5–7) or its hydrate, or, by a similar mechanism, from hydrolysis of the unstable diimine of tetramethylbenzidine* (8).

The kinetics of benzoquinone inhibition also favors a semiquinone oxidation mechanism. Benzoquinone is a very poor inhibitor of hydrocarbon oxidation (10), where its action is presumably due to free radical addition. Here, though, it was found to be an extremely efficient inhibitor, and the inhibited rate of oxidation is dependent on the oxygen as well

**It is probably due to this instability that quinone catalysis (9) does not play an important part in the reaction mechanism.*

Can. J. Chem. Downloaded from www.nrcresearchpress.com by 210.87.254.40 on 09/05/12
For personal use only.

as on the inhibitor concentration. This immediately suggests that the inhibitor is competing with oxygen for some reactive intermediate. The fact that hydroquinone is formed quantitatively from the quinone that reacts (11) is analogous to the formation of hydrogen peroxide from oxygen, and further suggests the similarity of action of these two oxidizing agents here.

It seems probable, therefore, that benzoquinone, and hence oxygen, are acting, in a sense, as electron acceptors. Also, since no low temperature oxidation of dimethylaniline in the absence of benzoyl peroxide was detected, and because of the known susceptibility of the semiquinones of diamines to reaction with oxygen, reaction [2] has been postulated to explain the absorption of oxygen.

Reaction [3]

This reaction is analogous to reaction [1*a*] and involves electron transfer between the peroxide radical $\dot{O}_2^-$ and dimethylaniline.

Reaction [6]

Chain termination occurs by electron transfer between two peroxide radicals to a diperoxide and oxygen. This reaction follows from the independence of the rate with respect to oxygen pressure, and it is equivalent to disproportionation of two $R\dot{O}_2$ radicals, which appears to be the main mode of termination in the oxidation of many hydrocarbons at high oxygen pressures (12).

Assuming the applicability of the steady state approximation, this mechanism leads to the following expression for the rate of oxidation at high pressures:

$$-d[O_2]/dt = nk_0[A][P]+k_3(k_0/k_6)^{1/2}[A]^{3/2}[P]^{1/2} \qquad [2]$$

If, as written in reaction [6], oxygen is produced in the termination reaction, then $n = 1$, otherwise $n = 2$, assuming 100% initiation efficiency.

There are three main ways in which reaction with inhibitor might occur:

[7] $$\dot{O}_2^- + I \rightarrow \text{products}$$

$$-d[O_2]/dt = 2k_0[A][P]+2k_0k_3[A]^2[P]/k_7[I] \qquad [3]$$

At high inhibitor concentrations,

$$-d[O_2]/dt = 2k_0[A][P] \qquad [4]$$

If $Bz\dot{O}$ reacts with inhibitor as well, the inhibited rate will be 1/2 this.

[8] $$\dot{T}^+ + I \rightarrow \text{products}$$

$$-d[O_2]/dt = 2k_0[A][P]k_2[O_2]/k_8[I] \qquad [5]$$

[9] $$T + I \rightarrow \text{products}$$

$$-d[O_2]/dt = k_0[A][P]k_{1c}[P]/k_9[I] \qquad [6]$$

In deriving the expression for the rate, in each case the assumption has been that termination occurs predominantly by reaction with inhibitor, that oxygen is not one of the products of the inhibition reaction, and that the primary radical, $Bz\dot{O}$, does not react with inhibitor as rapidly as with amine.

It is apparent from the data given in Table IV that mercaptan inhibition occurs, in this case, by reaction [7]. The initial rate is proportional to the initial peroxide and amine concentrations. In addition, the ratio $-d[O_2]/dt[A]_0[P]_0$ is, within experimental error, equal to twice the rate constant obtained from the intercept of the rate plot. Therefore, oxygen is released in the termination step (i.e., $n = 1$), and the rate constants can be evaluated from equations [2] and [4], and are reported in Table VI.

Can. J. Chem. Downloaded from www.nrcresearchpress.com by 210.87.254.40 on 09/05/12
For personal use only.

TABLE VI

Rate constants

Temp., °C	$10^5k_c = 10^5k_0$* From equation [2]	From mercaptan inhibition	From peroxide decomposition (1)	10^5k_d*	$10^3k_3/k_6^{1/2}$†
		Dimethylaniline in toluene			
0	5.3±0.2	5.35±0.15	5.0	4.51±0.02	6.2±0.1
10	—	11±3	12	9±3	9±3
15	—	16±2	—	14±4	11±3
20	—	29±2	27	20±5	12±3
25	38±3	39±3	53	26.9±0.2	13.6±0.7
10^{-6} A		1.3±0.1	37		
E (kcal)		13.0±0.3	14.8	11.5±0.3	5.0±0.3‡
		Dimethylaniline in acetonitrile			
0	11±12	6.4±0.2	—	36±1	45±2
25	90±60	—	—	247±7	82±40
E (kcal)					7‡
		Methylethylaniline in toluene			
0	—	4.5	—	4.0	6.0
		Diethyl- and dipropyl-aniline in toluene			
0	—	3	—	0(?)	0(?)

*l./mole sec.
†(l./mole sec.)$^{1/2}$.
‡$E_3-\frac{1}{2}E_6$.
NOTE: All precision indices are 90% confidence limits (t test).

The k_0 values are surprisingly close to those obtained from peroxide decomposition in the absence of oxygen, with the exception of the 25° C value. The difference in the E_0 results are due to this discrepancy. This may reflect either the poorer precision that is obtainable from the peroxide decomposition results, or a real decrease in initiation efficiency with increasing temperature. The latter could be due to the instability of one of the intermediates involved in reactions [1] to [4].

There is very little useful information that can be inferred from the ratio $k_3/k_6^{1/2}$ without knowing the magnitude of one of the constants. Since the activation energy, E_6, is usually close to zero, the value obtained for the energy difference, $E_3-\frac{1}{2}E_6$, places dimethylaniline between the highly susceptible aldehydes and the less readily oxidizable hydrocarbons with respect to "dehydrogenation".

On comparing equation [5] and the relation obtained for the rate of oxidation in the presence of benzoquinone, it appears likely that quinone inhibition occurs by reaction [8]. This reaction is readily understood either in terms of a semiquinone–quinone complex, or in terms of electron transfer. Both would lead to the formation of hydroquinone from the inhibitor. Unfortunately, since the solubility of oxygen in mixtures of dimethylaniline and toluene is not known, the rate constants involved in inhibition can not be determined.

The observed stoichiometry can also be explained by this mechanism. If equation [2] describes the entire reaction, the ratio of total oxygen absorbed to peroxide initially present will be given by the relation:

$$\frac{[O_2]_T}{[P]_0} = \frac{n}{3} + \frac{6-2n}{9}\frac{k_3^2}{k_0k_6}\frac{[A]_0}{[P]_0}. \qquad [7]$$

Can. J. Chem. Downloaded from www.nrcresearchpress.com by 210.87.254.40 on 09/05/12
For personal use only.

Values of $[O_2]_T$ calculated from this relation and the measured rate constants are given in Table I and agree quite well with the observed results. This agreement does not necessarily conflict with the observation that the reaction is autoretarded, since it might be expected that the stoichiometry would be much less sensitive than the rate to this type of inhibition.

The increase in rate observed in going from toluene to acetonitrile (or methanol) is likely a result of the increase in dielectric constant. Such an effect should be very small in purely free radical reactions, and it was for this reason that a mechanism involving charged species seems most likely, particularly since the increase appears to occur mainly in the second term of the rate equation, i.e. in k_3 or k_6. This may mean that the sensitive reaction is the termination reaction, since reactions [0] and [3] are similar, and reaction [6] involves the reaction of two anions, or, at least, two strongly polarized radicals. The order of magnitude of the effect is only explainable in terms of the reaction of two like-charged species. The fact that there are probably other reactions involved in polar solvents than those considered in deriving equation [7] is apparent from the $[O_2]_T$ values obtained in acetonitrile. These are much larger than the corresponding values observed in toluene, but much less than would be predicted on the basis of equation [7]. It may be that the apparent continuity of mechanism is fortuitous.

Oxidation of Related Compounds

Tetramethylbenzidine is of particular interest since it is apparently an intermediate in the oxidation of dimethylaniline. It proved impossible to obtain any accurate kinetic data, since at 0° C the reaction is much too fast to follow, and only a rough estimate of its relative overall reactivity could be made. It was found that, for a toluene solution of tetramethylbenzidine (53.2 mmole/l.) and benzoyl peroxide (99.6 mmole/l.), the initial rate was at least 7×10^{-5} mole/l. per sec; the corresponding rate for dimethylaniline would be 4.0×10^{-7} mole/l. per sec. Hence, tetramethylbenzidine oxidizes at least 200 times as fast as dimethylaniline. The reaction may be retarded by mercaptan, but not sufficiently to allow accurate rate measurements.

Results obtained for several other compounds are given in Table VII. *Methylethylaniline*

TABLE VII

Oxidation rates of related compounds

Compound	$[RSH]_0$, mole/l.	$(-d[O_2]/dt)_{max}$, mole/l. sec $\times 10^6$	$[O_2]_T$, mmole/l.
Dimethylaniline	—	57.0	164
Methylethylaniline	—	50.4	100
	1.0	13.5	—
Diethylaniline	—	4.48	20
	1.0	5.06	30
Dipropylaniline	—	4.65	30
	1.0	4.87	30
Dimethylbenzylamine	—	0.0085	0
Dimethyldodecylamine	—	0.015	0

NOTE: The initial amine and peroxide concentrations were, respectively, 2.80 mole/l., and 54.4 mmole/l. The reactions were carried out at 0° C, in toluene.

appears to oxidize by the same mechanism as dimethylaniline; the estimated rate constants are given in Table VI. *Diethylaniline* and *dipropylaniline*, however, do not exhibit a corresponding similarity. Their oxidation rates are much less than for dimethylaniline, and the reaction is not inhibited by mercaptan; if anything, it is slightly accelerated. In

Can. J. Chem. Downloaded from www.nrcresearchpress.com by 210.87.254.40 on 09/05/12
For personal use only.

addition, although it was difficult to estimate accurately the total oxygen absorbed, because of the low rates, it appeared to be equal to about 0.3 to 0.5 times the initial peroxide concentration.

These results would seem to indicate the almost complete absence of a chain reaction, with the initial rate of oxidation being approximately equal to $2k_0[A]_0[P]_0$. The values of k_0 reported in Table VI are based on this assumption.

If oxidation occurred by the *N*-alkyl dehydrogenation mechanism of Horner and Junkermann (2), a diminution in rate might be expected as the size of the alkyl group is increased, although, perhaps not as great as observed here. On the other hand, increasing the size of the alkyl group will undoubtedly sterically hinder the formation of the complex which precedes electron transfer in reaction [3]. In addition, there might be expected to be a limit, beyond which, increasing the size of the alkyl group would not further influence the reaction, as was observed with diethyl- and dipropyl-aniline. If this is the case, the rate of reaction [3] should be greater in solvents of high dielectric constant, where the separation of the cationic quinone and anionic oxygen should be greater.

The other two amines listed in Table VII showed no tendency to react, and the rate limits are those imposed by the experimental conditions.

ACKNOWLEDGMENTS

This research was supported in part by the Office of Naval Research, and in part by a grant from the Thiokol Corporation. One of the authors (D.M.G.) would like to express his appreciation to the Thiokol Corporation for a fellowship in 1955–56.

REFERENCES

1. D. M. Graham and R. B. Mesrobian. Can. J. Chem. This issue.
2. L. Horner and H. Junkermann. Ann. **591**, 53 (1955).
3. H. R. Cooper and H. W. Melville. J. Chem. Soc. 1984 (1951).
4. J. L. Bolland. Proc. Roy. Soc. (London), Ser. A, **186**, 218 (1949); Trans. Faraday Soc. **44**, 669 (1948); Quart. Rev. (London), **3**, 1 (1949).
5. H. Tsuyuki, M. A. Stahmann, and J. E. Casida. Biochem. J. **58**, iv (1955).
6. R. F. Kleinschmidt and A. C. Cope. J. Am. Chem. Soc. **66**, 1929 (1944).
7. A. C. Cope and P. H. Towfe. J. Am. Chem. Soc. **71**, 3423 (1949).
8. L. Michaelis, M. P. Schubert, and S. Granick. J. Am. Chem. Soc. **61**, 1981 (1939).
9. J. E. LuValle and A. Weissberger. J. Am. Chem. Soc. **69**, 1567 (1947).
10. J. L. Bolland and P. ten Have. Trans. Faraday Soc. **43**, 201 (1947).
11. L. Horner and C. Betzel. Ann. **579**, 175 (1953).
12. C. E. Boozer, B. W. Ponder, J. C. Trisler, and C. E. Wrightman III. J. Am. Chem. Soc. **78**, 1506 (1956).

Can. J. Chem. Downloaded from www.nrcresearchpress.com by 210.87.254.40 on 09/05/12
For personal use only.

THE KINETICS OF THE THERMAL REACTIONS OF ETHYLENE OXIDE[1,2]

M. Lynne Neufeld and Arthur T. Blades
Research Council of Alberta, Edmonton, Alberta
Received July 19, 1963

ABSTRACT

The thermal reactions of ethylene oxide in the presence of an excess of propylene have been studied as a function of pressure and it has been found that there are two sets of products, acetaldehyde and free radicals, presumably methyl and formyl. These products are believed to arise from an excited acetaldehyde intermediate. Some evidence has been obtained for the occurrence of a surface-catalyzed rearrangement to acetaldehyde but the free radical products are uninfluenced by surface.

INTRODUCTION

Ethylene oxide decomposes homogeneously in the gas phase at 400° C to give hydrogen, carbon monoxide, methane, ethane, ethylene, formaldehyde, ketene, and acetaldehyde; it has been suggested that the latter product arises by rearrangement while the others result from a free radical chain reaction (1). Mueller and Walters (2) have shown that the addition of sufficient propylene reduces the rate of ethylene oxide disappearance to a constant value and reduces the pressure increase to zero, and it may be inferred that the free radical reaction is a minor primary mode of decomposition. They do, however, suggest that the primary radicals which initiate the chain reaction in the absence of propylene are methyl and formyl (3).

Lossing, Ingold, and Tickner (4), using a high temperature, low pressure flow system coupled to a mass spectrometer, confirmed the production of methyl radicals but were unable to observe acetaldehyde although this compound was stable under their experimental conditions. They proposed only two primary reactions

$$\begin{array}{ll} CH_2\text{—}CH_2 & \rightarrow CH_4 + CO \\ \quad\diagdown\ \diagup & \\ \quad\ O & \rightarrow CH_3 + CHO. \end{array}$$

It has recently been suggested that acetaldehyde may also arise from a free radical chain reaction (5):

$$R\cdot + C_2H_4O \rightarrow C_2H_3O\cdot + RH$$
$$C_2H_3O\cdot \rightarrow \cdot CH_2\text{—}CHO$$
$$\cdot CH_2CHO + C_2H_4O \rightarrow CH_3CHO + C_2H_3O\cdot.$$

The present study was designed to re-examine the pyrolysis of ethylene oxide under conditions such that the origin and contribution of the primary free radical reaction might be assessed and the mechanism and energetics of the rearrangement further elucidated.

EXPERIMENTAL

Ethylene oxide was obtained from Eastman Organic Chemicals and was distilled on a four-foot pyrex helices-packed column with a vapor take-off. Deuterated ethylene oxide was supplied by Merck, Sharp and Dohme, Montreal, and was used without further purification. The propylene was Phillips Research Grade (99.4+ %). Mixtures of these gases were shown to be free of the compounds which were later found to be products of the reaction.

[1]*Contribution No. 221 from the Research Council of Alberta, Edmonton, Alberta.*
[2]*This paper was presented in part at the Chemical Institute of Canada Annual Meeting in Toronto, Ontario, June 6, 1963.*

Can. J. Chem. Downloaded from www.nrcresearchpress.com by 210.87.254.40 on 09/05/12
For personal use only.

Quantitative analyses were carried out for only three of the reaction products, carbon monoxide, methane, and acetaldehyde. The non-condensible products were separated on a 2 ft charcoal gas chromatographic column at 0° and the carbon monoxide and methane estimated from the response of a thermal conductivity detector. The acetaldehyde was determined by the *p*-hydroxybiphenyl colorimetric method (6). Qualitative analysis of the condensible reaction products was carried out on a 20 ft polypropylene glycol gas chromatographic column at 60° and on a 2 ft silica gel column at 25°.

A conventional static pyrolysis system was used for all experiments, two reactors of 75 and 875 cc volume being used for the high and low pressure experiments respectively. The reactors were enclosed in large aluminum block furnaces and the temperatures monitored by a Pt, Pt-Rh thermocouple.

In order to limit the importance of chain reactions, all pryolyses herein reported were carried out in a 4- to 10-fold excess of propylene.

RESULTS

Qualitative analyses revealed carbon monoxide, methane, ethane, ethylene, propane, 1-butene, *cis*- and *trans*-2-butene, acetaldehyde, and diallyl as the major products of the reaction. Since only two oxygen-containing products were observed, the rates of production of these were assumed to be indicative of the rates of two reactions. At conversions up to 10%, these two products were found to increase linearly with time (Fig. 1),

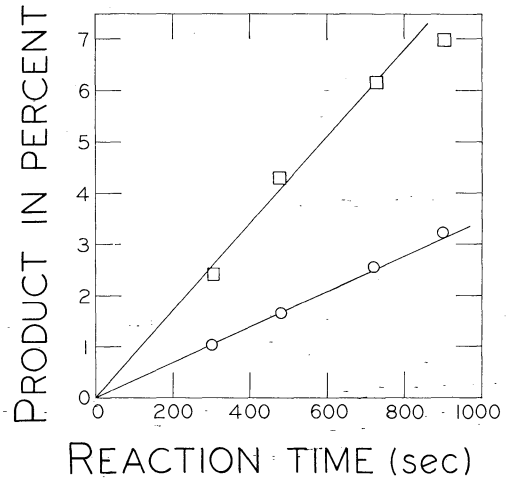

FIG. 1. Percentage yield of the products acetaldehyde □ and carbon monoxide ○ vs. reaction time at 690° K and 31 cm Hg. pressure, 22.6% oxide.

but above this conversion, the ratio of the acetaldehyde to carbon monoxide began to fall rapidly, indicating the onset of a chain decomposition of the acetaldehyde to carbon monoxide. A series of experiments was then carried out at 30 cm Hg pressure in the temperature range 643.5 to 702.3° K, with the conversion limited to 10%, to determine the initial rates of disappearance of ethylene oxide as a function of temperature. These gave a rate expression:

$$k = 10^{14.13} \exp(-56{,}900/RT) \text{ sec}^{-1}$$

which agrees favorably with the expression of Mueller and Walters (2)

$$k = 10^{14.34} \exp(-57{,}400/RT) \text{ sec}^{-1}.$$

Changing the concentration of the oxide in the propylene had no effect on the rates.

Maintaining the total conversion at less than 6%, the rates of production of carbon monoxide and acetaldehyde were measured at constant temperature in the pressure

Can. J. Chem. Downloaded from www.nrcresearchpress.com by 210.87.254.40 on 09/05/12
For personal use only.

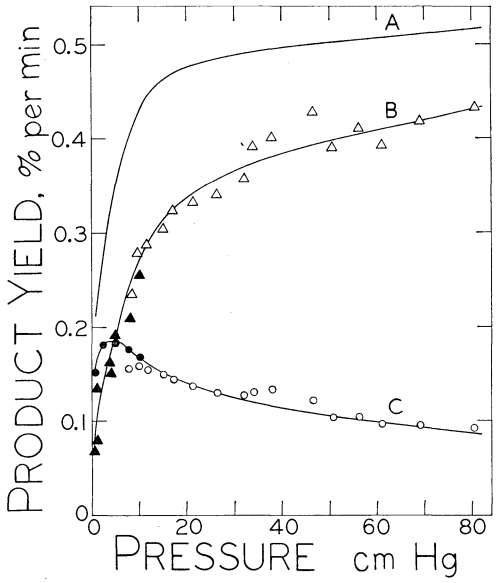

FIG. 2. Rate of reaction in percent per minute vs. pressure. A, total rate; B, acetaldehyde; C, carbon monoxide at 685° K. ○ and △, 12% oxide; ● and ▲, 22.6% oxide.

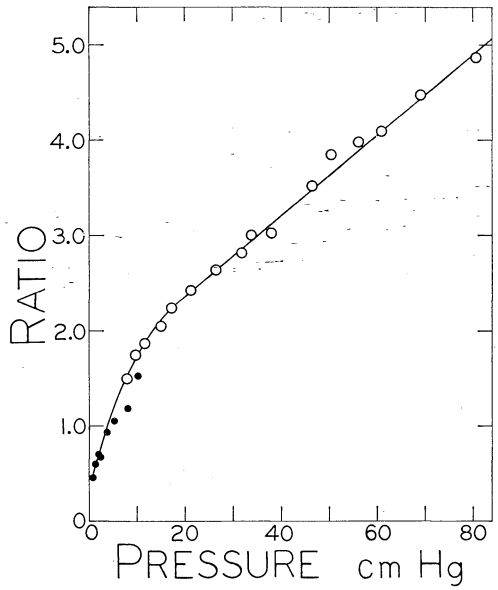

FIG. 3. Ratio of product yields, acetaldehyde: carbon monoxide vs. pressure. ○ small reactor, 12% oxide; ● large reactor, 22.6% oxide; at 685° K.

range 0.6 – 80 cm Hg. These data are displayed as total and individual rates in percent per minute in Fig. 2, and in Fig. 3 as the ratio of rates as a function of the total pressure. In these experiments, two standard mixtures of the oxide and propylene were used (22.6% and 12.0% oxide).

A number of pyrolyses were carried out in variously treated glass reactors and a wide

Can. J. Chem. Downloaded from www.nrcresearchpress.com by 210.87.254.40 on 09/05/12
For personal use only.

range of total rates were obtained. Conditioning by repeated reaction tended to decrease rates only to a limited extent and the lowest rates were obtained with reactors which had been conditioned only by prolonged evacuation at 500° C. It was also observed that despite the conditioning procedure, the rates of production of carbon monoxide remained constant and only the rate of acetaldehyde production was variable.

The hydrogen isotope effects in the production of acetaldehyde and carbon monoxide were measured at 664° K and 30 cm Hg total pressure and were found to be 3.1 ± 0.1 for each product.

DISCUSSION

The production of acetaldehyde, carbon monoxide, diallyl, and a number of other hydrocarbon products in the pyrolysis of ethylene oxide – propylene mixtures confirms the previous observations of a rearrangement reaction and a free radical decomposition of ethylene oxide. The variety of hydrocarbon products gives no reliable clue to the identity of the primary free radical fragments. They do show, however, that even with "totally inhibiting" concentrations of propylene, chain reactions are occurring and that useful information on the free radical reaction must be obtained at low concentrations of the product acetaldehyde. These points are particularly accented by the observation of both butene-1 and butene-2 in the products at high conversions. Butene-1 is believed to arise from allyl and methyl radicals; the butene-2 then arises from the sequence

$$C_3H_5^{\cdot} + 1\text{-}C_4H_8 \rightarrow C_3H_6 + C_4H_7^{\cdot}$$
$$C_4H_7^{\cdot} + C_3H_6 \rightarrow 2\text{-}C_4H_8 + C_3H_5^{\cdot}.$$

Under the conditions of low conversion used for rate measurements, the unimportance of the chain decomposition of acetaldehyde was demonstrated by the linear increase in product yields with time. This was further shown in experiments where acetaldehyde yields were abnormally high because of heterogeneous reaction without any corresponding increase in the carbon monoxide yield. At higher conversions, this situation was not maintained as evidenced by the decrease of the acetaldehyde – carbon monoxide ratio.

The unusual variation in the rate of production of carbon monoxide with pressure and the interrelation of the two products demonstrated by Fig. 3 suggest a mechanism for this pyrolysis involving an excited acetaldehyde intermediate which either collides to become stable acetaldehyde or unimolecularly decomposes to carbon monoxide and free radical fragments, presumably hydrogen atoms and methyl radicals. The possibility of such a mechanism has been discussed before (7) but no evidence has been obtained to support it. The exothermicity (27.6 kcal/mole) (8) and the activation energy (57.4 kcal/mole) (2) provide just about the energy required to break the carbon–carbon bond in acetaldehyde (9). In terms of the Rice, Ramsperger, and Kassel theory (9), this 85 kcal/mole of excess energy in the acetaldehyde is the minimum energy of the product molecules, and the total energy of excitation is greater by an amount determined by the Maxwell-Boltzmann distribution of energy of the reactant molecules and the variation of the specific rate constant with energy. According to this theory, the energy distribution of the product acetaldehyde has a maximum at $(85+(s-1)RT)$ kcal/mole and a substantial fraction have energies in excess of $(85+2(s-1)RT)$ kcal/mole. The value of s is determined from the quasi-unimolecular decrease of the first order rate constant with pressure, and from Fig. 2 s can be estimated to have a value of 11–12 by comparison with the similar effect in cyclopropane (10). This results in an energy of excitation of from 85 to something in excess of 115 kcal/mole (with the most abundant species at 100 kcal/mole)

Can. J. Chem. Downloaded from www.nrcresearchpress.com by 210.87.254.40 on 09/05/12
For personal use only.

for the product acetaldehyde. That such highly excited molecules of acetaldehyde should unimolecularly decompose at about 1 atm pressure seems entirely reasonable, and the following mechanism is proposed for the thermal reactions of ethylene oxide:

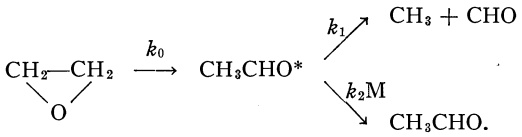

On the basis of this mechanism, the percentage yield curves in Fig. 2 can be explained as follows. At high pressure, a reduction in pressure tends to increase the CO yield at the expense of the acetaldehyde yield; as the pressure is further reduced, the total rate begins to fall because of the onset of quasi-unimolecular behavior, and the individual rates are affected in that the acetaldehyde decreases more rapidly than previously while the CO increases more slowly, and then it too, gradually decreases with decreasing pressure, having become in the process the major product.

The curvature in the product ratio vs. pressure plot is to be expected in this system because of the wide variation in the excess energy of the excited intermediate, the exact curvature being determined by both the energy of excitation distribution curve and the variation of the specific rate constant k_1 with energy. Unfortunately, in the present system this is further complicated by a tendency of the energy distribution curve to shift somewhat to lower energies at very low pressures.

The mechanism proposed above for the production of free radicals in this system explains the failure of Lossing, Ingold, and Tickner (4) to observe the product acetaldehyde. At a pressure of 15 mm Hg of helium, whose collision efficiency of 0.06 compared with cyclopropane (10) would imply an effective pressure of 1 mm Hg, according to Fig. 3, the free radical products would be expected to predominate tenfold over the acetaldehyde; the combination of the high radical concentration and relatively poor discrimination of the two isomers in the mass spectrometer suggest that this minor product would be difficult to detect.

The one unsatisfactory aspect of the mechanism proposed above is the possibility of a considerable contribution from heterogeneous rearrangement reactions. The pressure effects certainly imply that a major portion of the reaction is homogeneous, and this view is supported by the large hydrogen isotope effects observed. All of the data herein recorded were obtained with reaction vessels which had been maintained free from air or water for considerable periods and no lower rate values were obtained. The fact that the free radical reaction was completely uninfluenced by the activity of the surface as indicated by the acetaldehyde production implies that this reaction is not heterogeneous. Unfortunately, no method presently exists for unequivocably determining the extent of the residual contribution of heterogeneous reaction to the acetaldehyde products.

The thermal reactions of ethylene oxide appear to represent a limited class of unimolecular gas phase rearrangements wherein an excited product species is formed of sufficient energy to decompose unimolecularly. It is regrettable that the complications of chain and surface reactions impede the acquisition of more reliable data on this unusual reaction.

ACKNOWLEDGMENTS

The authors wish to acknowledge the assistance of Mr. D. Morrison in some of the experimental work and useful discussions with Mr. P. W. Gilderson and Dr. R. Klemm.

Can. J. Chem. Downloaded from www.nrcresearchpress.com by 210.87.254.40 on 09/05/12
For personal use only.

REFERENCES

1. C. J. M. Fletcher and G. K. Rollefson. J. Am. Chem. Soc. **58**, 2135 (1936).
2. K. H. Mueller and W. D. Walters. J. Am. Chem. Soc. **73**, 1458 (1951).
3. K. H. Mueller and W. D. Walters. J. Am. Chem. Soc. **76**, 330 (1954).
4. F. P. Lossing, K. U. Ingold, and A. W. Tickner. Discussions Faraday Soc. **14**, 34 (1953).
5. M. Flowers, L. Batt, and S. W. Benson. J. Chem. Phys. **37**, 2662 (1962).
6. E. Stotz. J. Biol. Chem. **148**, 585 (1943).
7. H. W. Thompson and M. Meissner. Trans. Faraday Soc. **32**, 1451 (1936).
8. M. S. Kharasch. J. Res. Natl. Bur. Std. **2**, 359 (1929).
9. S. W. Benson. Foundations of chemical kinetics. McGraw-Hill Book Co. Inc., New York. 1960.
10. H. O. Pritchard, R. G. Sowden, and A. F. Trotman-Dickenson. Proc. Roy. Soc. (London), Ser. A, **217**, 563 (1953).

Can. J. Chem. Downloaded from www.nrcresearchpress.com by 210.87.254.40 on 09/05/12
For personal use only.

ANTINEOPLASTIC AGENTS

IX. N-BENZYL-N-BIS(2-HALOETHYL)AMINES[1,2]

GEORGE R. PETTIT, DAVID S. BLONDA, AND ERNEST C. HARRINGTON
Department of Chemistry, University of Maine, Orono, Maine, U.S.A.

Received June 28, 1963

ABSTRACT

A number of N-bis(2-chloroethyl)amines and three N-bis(2-iodoethyl)benzylamines have been prepared for cancer chemotherapy studies. The chloro-nitrogen mustards were readily obtained by aluminum chloride – lithium aluminum hydride reduction of the corresponding N-bis(2-chloroethyl)amides. A convenient procedure for converting N-bis(2-chloroethyl)-benzylamine hydrochlorides to N-bis(2-iodoethyl)benzylamine hydroiodides, employing sodium iodide, was also developed.

Can. J. Chem. Downloaded from www.nrcresearchpress.com by 210.87.254.42 on 09/05/12
For personal use only.

A substantial increase in the survival time of Fischer F-344 rats with Dunning leukemia following treatment with N-bis(2-chloroethyl)-3,4,5-trimethoxybenzylamine hydrochloride or N-bis(2-chloroethyl)-3,4-methylenedioxybenzylamine hydrochloride was reported in a prior study (1). The encouraging chemotherapeutic properties of these benzylamines (see also ref. 2) led us to consider a number of related benzyl groups (Table I) as nitrogen mustard carriers (1, 3, 4).

The amines summarized in Table I were prepared by aluminum chloride – lithium aluminum hydride reduction of the corresponding nitrogen mustard amides. Conversion of 3,5-dimethoxybenzoyl chloride to N-bis(2-chloroethyl)-3,5-dimethoxybenzamide and subsequent reduction (I*a* → II*a*) illustrates the general synthetic route. Although several of the water-sensitive (1) amide intermediates (e.g., I*a* and I*b*) were carefully isolated and purified before reduction, it generally proved more efficient to employ the crude products. The amides were very sensitive to trace amounts of water and readily rearranged to 2-(2′-chloroethylamino)ethyl esters. A number of the N-bis(2-chloroethyl)amides were further characterized by quantitative conversion (5–30 minutes in 95% ethanol) to ester (III*a–d* and IV) hydrochlorides.[3] Interestingly, Popp and colleagues (5) have reported that a related series of N-bis(2-chloroethyl)amides were "very hygroscopic" and gave analytical results consistent with 1–3 moles of water in each case. While "no evidence for rearrangement of the mustard amides was noted" we suggest that these observations are in better accord with an amide → ester rearrangement reaction (1, 6). The latter transformation may generally provide a useful route to stable derivatives of nitrogen mustard amides.

Synthesis of the methyl- and dimethyl-benzylamines noted in Table I was suggested by the favorable action of embitol[4] upon certain human lymphomas (7). Recently, embitol and N-bis(2-chloroethyl)-4-fluorobenzylamine (cf. Table I) were reported (8) to markedly inhibit growth of both sarcoma 45 in rats and Guerin carcinoma in rabbits.

An initial attempt to evaluate the utility of N-bis(2-chloroethyl)amines related to substances with central nervous system activity led to preparation of N-bis(2-chloroethyl)-3,4,5-trimethoxyphenethylamine (V) hydrochloride: a mescaline derivative.

[1]*Refer to G. R. Pettit and J. A. Settepani, J. Org. Chem.* **27**, *2962 (1962), for part VIII of this study.*
[2]*Abstracted in part from the Master of Science thesis submitted by D. S. Blonda to the Graduate School, University of Maine, August, 1962.*
[3]*Refer to ref. 1 and footnote 13 of the same contribution for other examples of this unusual intramolecular transformation.*
[4]*Embitol is a mixture of N-bis(2-chloroethyl)-2- and 4-methylbenzylamine hydrochlorides.*

Can. J. Chem. Downloaded from www.nrcresearchpress.com by 210.87.254.42 on 09/05/12
For personal use only.

TABLE I

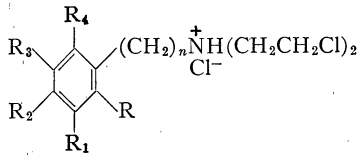

n	R	R1	R2	R3	R4	Yield,[a] %	Solvent[b]	M.P.,[c] °C	Formula	Carbon Calc.	Carbon Found	Hydrogen Calc.	Hydrogen Found	Chlorine Calc.	Chlorine Found	Fluorine Calc.	Fluorine Found	Nitrogen Calc.	Nitrogen Found
1	CH_3					85	1	152–154 (146–147)[e]	$C_{12}H_{18}Cl_3N$	51.00	51.17	6.42	6.25	37.65	37.70			4.95	5.09
1		CH_3				87	1	139–141	$C_{12}H_{18}Cl_3N$	51.00	51.09	6.42	6.32	37.65	37.82			4.95	4.82
1			CH_3			79	1	149–151 (148.5–149)[e]	$C_{12}H_{18}Cl_3N$	51.00	51.24	6.42	6.58	37.65	38.05			4.95	4.84
1[d]	CH_3		CH_3			55	1	145.5–146	$C_{13}H_{20}Cl_3N$	52.63	52.66	6.79	6.72	35.87	35.20			4.72	4.70
1[d]	CH_3			CH_3		69	2	148–149	$C_{13}H_{20}Cl_3N$	52.63	53.11	6.79	6.70					4.72	4.81
1			CH_3	CH_3		34	3	171–172	$C_{13}H_{20}Cl_3N$	52.63	52.82	6.79	6.66					4.72	4.61
1			CH_3		CH_3	78	3	164–165	$C_{13}H_{20}Cl_3N$	52.63	52.52	6.79	6.89	35.87	35.94			4.72	4.85
1			CH_3O			65		108–109 (105–107)[f]											
1		CH_3O		CH_3O		75	1	137–138	$C_{13}H_{20}Cl_3NO_2$	47.50	47.36	6.13	6.34	32.37	32.10			4.26	4.18
2		CH_3O	CH_3O	CH_3O		59	1	145–147	$C_{15}H_{24}Cl_3NO_3$	48.33	48.19	6.49	6.53	28.56	28.45			3.76	3.67
1		CH_3CH_2O	CH_3CH_2O	CH_3CH_2O		87	1	168–169	$C_{17}H_{28}Cl_3NO_3$	50.94	51.17	7.04	6.91	26.54	26.49			3.50	3.65
1			F			30	3	102–103	$C_{11}H_{15}Cl_3FN$	46.09	46.12	5.28	5.62			6.63	6.97	4.89	5.18
2			F			60	1	103–104	$C_{12}H_{17}Cl_3FN$	47.94	48.09	5.70	5.77			6.32	6.67		
1		I	I	I		67	4	193–194	$C_{11}H_{13}Cl_3I_3N$	20.44	20.67	2.03	2.20					2.17	2.12

[a]Yield based on the crystalline hydrochloride which precipitated from ethereal solution.
[b]The hydrochloride was recrystallized from methanol–ether (1), methanol (2), ethanol – ethyl ether (3), 95% ethanol (4).
[c]Melting point of the analytical sample.
[d]Prepared by K. N. Rangammal.
[e]Melting point reported by L. B. Rapp and K. A. Kornev. Ukr. Khim. Zh. **23**, 637 (1957); Chem. Abstr. **52**, 9979 (1958).
Melting point reported by K. V. Levshina and S. I. Sergenshaza, Zh. Obsch. Khim. **24**, 902 (1954); Chem. Abstr. **49**, 8160 (1954).

Nitrogen mustards of this type, capable of penetrating the brain (9) without producing bizarre mental effects, might prove useful in treating brain tumors. Two other N-alkyl-N-bis(2-chloroethyl)amines, N-bis(2-chloroethyl)-4-fluorophenethylamine (Table I), and hexadecylamine VI, were prepared for comparison purposes. The amide (VII) precursor of amine VI was of particular interest since N-(2-hydroxyethyl)hexadecanamide is the antiallergic factor of egg yolk (10).

Another phase of the present study was devoted to preparing the diiodo-derivative[5] of N-bis(2-chloroethyl)-3,4-methylenedioxy- and 3,4,5-trimethoxybenzylamine (1). For this purpose, a procedure employing sodium iodide in acetone (compare refs. 13 and 14) was developed for directly converting the nitrogen mustard hydrochlorides to N-bis(2-iodoethyl)amine hydroiodides. Model experiments were conducted with N-bis(2-chloroethyl)amine II*b* hydrochloride, and eventually N-bis(2-iodoethyl)-3,4,5-triethoxybenzylamine (II*c*) hydroiodide was prepared in 87% yield. Subsequently the required N-bis(2-iodoethyl)amines, II*d* and VIII, were also obtained by this method.

Each of the N-bis(2-haloethyl)amine derivatives arising from this investigation has been submitted to the Cancer Chemotherapy National Service Center (National Institutes of Health, U.S. Public Health Service) for biological studies.

EXPERIMENTAL[6]

Acyl Chlorides

The following acid chlorides were prepared with appropriately adjusted quantities of the corresponding carboxylic acids and phosphorus pentachloride as illustrated (*vide infra*) for 3,5-dimethoxybenzoic acid: 2-methylbenzoyl chloride (15), b.p. 48–49° (2 mm); 3-methylbenzoyl chloride (16), b.p. 52–53° (2 mm); 4-methylbenzoyl chloride (17), b.p. 54–55° (2 mm); 2,4-dimethylbenzoyl chloride (18), b.p. 86–88° (2–3 mm); 2,5-dimethylbenzoyl chloride (19), b.p. 89–90° (2 mm); 3,4-dimethylbenzoyl chloride (19), b.p. 66–70° (2 mm); 3,5-dimethylbenzoyl chloride (20), b.p. 70–72° (2.5 mm); 4-methoxybenzoyl chloride (21), b.p. 96–97° (3 mm); 3,4-dimethoxybenzoyl chloride (21), m.p. 69–71°, b.p. 95–98° (1 mm); 4-fluorobenzoyl chloride (22); b.p. 27–32° (1 mm); and 4-fluorophenylacetyl chloride (23), b.p. 54–58° (1.5 mm).

N-bis(2-Chloroethyl) Amides

Amide precursors of the N-bis(2-chloroethyl)amine hydrochlorides summarized in Table I were prepared according to the method described below for N-bis(2-chloroethyl)-3,5-dimethoxybenzamide (I*a*). Isolation of the amides was most favorable during periods of low laboratory humidity. Solvents used to purify the nitrogen mustard amides were redistilled and stored over sodium. Although several of these *water-sensitive* amides were carefully purified, as noted in the sequel, the crude oily amides were generally employed in the reduction sequence. All glass apparatus used for preparation and subsequent reduction of the amides was dried at 120° for ca. 24 hours.

N-bis(2-chloroethyl)amine Hydrochlorides (Table I)

With one exception, (II*e*), the nitrogen mustard hydrochlorides noted in Table I were obtained by the general experimental methods described (below) for conversion of 3,5-dimethoxybenzoic and 3,4,5-trimethoxyphenylacetic acids to, respectively, benzylamine II*a* and phenethylamine V hydrochlorides. Preparation of N-bis(2-chloroethyl)-3,4,5-triiodobenzylamine (II*e*) was accomplished by employing an amide to lithium aluminum hydride ratio of 1:0.5. Reduction of amide I*c* by an approximately 1:1 molar ratio led to amines containing ca. 6% less iodine than calculated for triiodo-derivative II*e*. Tetrahydrofuran used in the reduction step was first heated at reflux over sodium for 2 hours, then distilled, and stored over sodium wire.

The infrared spectrum of each pure hydrochloride (in potassium bromide) was consistent with the assigned structure.

3,5-Dimethoxybenzoyl Chloride

A mixture of 3,5-dimethoxybenzoic acid (55 g, 0.30 mole) and phosphorus pentachloride (63.5 g, 0.30 mole) was cautiously warmed. After the initial exothermic reaction subsided, heating (steam bath) was

[5]*Decreased toxicity and increased antineoplastic activity with iodo- as compared to chloro-nitrogen mustards has been observed: see refs. 11 and 12.*

[6]*Melting points were observed with open Kimble glass capillaries (silicone oil bath) unless otherwise noted, and are uncorrected. Dr. R. A. Hill of this laboratory recorded the infrared data. Elemental analyses were provided by the microanalytical laboratories of: Dr. A. Bernhardt, Max-Planck Institute, Mülheim (Ruhr), Germany; Dr. C. Janssen, Beerse, Belgium; and Drs. Weiler and Strauss, Oxford, England.*

Can. J. Chem. Downloaded from www.nrcresearchpress.com by 210.87.254.42 on 09/05/12
For personal use only.

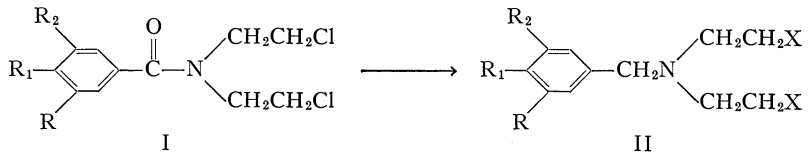

I

a, R = R_2 = OCH_3, R_1 = H
b, R = R_2 = H, R_1 = F
c, R = R_1 = R_2 = I

II

a, R = R_2 = OCH_3, R_1 = H, X = Cl
b, R = R_1 = R_2 = OCH_2CH_3, X = Cl
c, R = R_1 = R_2 = OCH_2CH_3, X = I
d, R = R_1 = R_2 = OCH_3, X = I
e, R = R_1 = R_2 = I, X = Cl

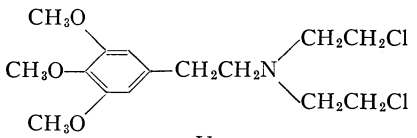

V

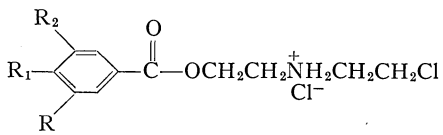

III

a, R = R_2 = OCH_3, R_1 = H
b, R = R_1 = OCH_3, R_2 = H
c, R = R_1 = R_2 = OCH_2CH_3
d, R = R_1 = R_2 = I

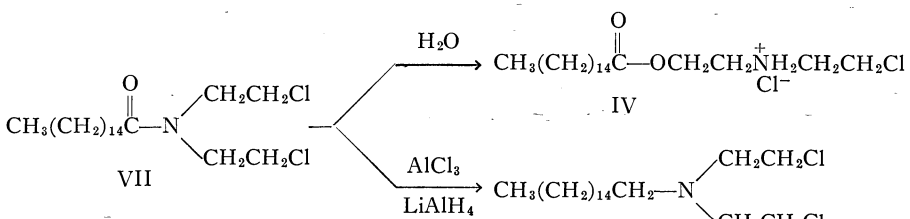

VII

IV

VI

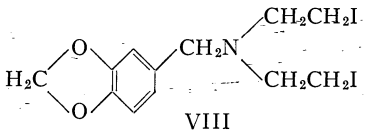

VIII

continued 1 hour. The phosphorus oxychloride was then removed *in vacuo*. Rapid distillation of the reddish brown residue yielded 52 g (86%) of colorless liquid boiling at 91–100° (0.7 mm). An analytical specimen (b.p. 90° at 0.7 mm, ν_{max}^{pure} 1770 cm^{-1}) was prepared by distillation through a 15-cm Vigreux column. Calc. for $C_9H_9ClO_3$: C, 53.90; H, 4.52; Cl, 17.68. Found: C, 53.70; H, 4.82; Cl, 17.81.

Conversion of 3,5-dimethoxybenzoic acid to the acid chloride derivative (b.p. 163–165° at 19–20 mm) with thionyl chloride has been reported (24).

N-bis(2-chloroethyl)-3,5-dimethoxybenzamide (Ia)

A solution of 3,5-dimethoxybenzoyl chloride (21.7 g, 0.108 mole) in *dry* benzene (200 ml) was slowly added (1 hour) to a *dry* benzene (150 ml) solution (ice-bath cooling) of the free amine from 44.4 g (0.248 mole) of N-bis(2-chloroethyl)amine hydrochloride (see ref. 1, footnote 23). The mixture was heated at reflux for 2 hours before collecting N-bis(2-chloroethyl)amine hydrochloride (19.5 g). Removal of solvent from the filtrate led to 31.2 g (98%) of colorless viscous oil. Crystallization from benzene – petroleum ether gave 24.8 g of amide I*a* melting at 58–60°. Three recrystallizations from the same solvent yielded an analytical sample; colorless prisms, m.p. 59–60°, ν_{max}^{KBr} 1650–1600 (broad) cm^{-1}. Calc. for $C_{13}H_{17}Cl_2NO_3$: C, 50.98; H, 5.60; Cl, 23.16; N, 4.58. Found: C, 51.25; H, 5.54; Cl, 23.47; N, 4.49.

2-(2'-Chloroethylamino)ethyl-3,5-dimethoxybenzoate Hydrochloride (IIIa)

A solution of N-bis(2-chloroethyl)-3,5-dimethoxybenzamide (I*a*, 1.0 g) in 95% ethanol (25 ml) was heated at reflux for 5 minutes. Concentrating (*in vacuo*) the solution to dryness afforded a quantitative yield of ester III*a* melting at 123–126°. Five recrystallizations from acetone gave a pure specimen as colorless

Can. J. Chem. Downloaded from www.nrcresearchpress.com by 210.87.254.42 on 09/05/12
For personal use only.

crystals; m.p. 125–126°, ν_{max}^{KBr} 2900–2450 (broad) and 1715 cm^{-1}. Calc. for $C_{13}H_{19}Cl_2NO_4$: C, 48.16; H, 5.91; Cl, 21.87; N, 4.32. Found: C, 48.02; H, 6.00; Cl, 21.40; N, 4.21.

Saponification of 2-(2'-Chloroethylamino)ethyl-3,5-dimethoxybenzoate Hydrochloride (IIIa)

A 0.75-g sample of ester III*a* was saponified in refluxing (3 hours) methanol (20 ml) – aqueous potassium hydroxide (10 ml of 10%) solution. Following removal of solvent and dilution with water (20 ml), the mixture was filtered and neutralized with 5% hydrochloric acid. The 3,5-dimethoxybenzoic acid which separated weighed 0.35 g (100%) and melted at 180–185°. The structural assignment was confirmed by mixture melting point determination and infrared spectral comparison (in potassium bromide) with an authentic sample (m.p. 182–183.5°) of 3,5-dimethoxybenzoic acid.

N-bis(2-chloroethyl)-3,5-dimethoxybenzylamine (IIa) Hydrochloride

To a cold (ice-bath) mixture of aluminum chloride (14.0 g, 0.105 mole), lithium aluminum hydride (4.0 g, 0.105 mole), and tetrahydrofuran (300 ml), under nitrogen, was slowly added (1 hour) a solution of crude amide I*a* (31.2 g, 0.101 mole) in tetrahydrofuran (200 ml).[7] Stirring and cooling were continued 2 hours (total reaction time) before cautiously adding 30-ml portions of acetone, moist ether, and water. After removing the solvent *in vacuo* at 35–40° the residue was diluted with 40% sodium hydroxide solution (250 ml) and extracted with benzene (3 × 100 ml). The combined solvent was dried (magnesium sulphate) and treated with a saturated solution of hydrogen chloride in ethyl ether. The hydrochloride which separated weighed 25.3 g and melted at 135–137°. Four recrystallizations from methanol – ethyl ether afforded an analytical specimen as colorless crystals (see Table I); ν_{max}^{KBr} 2900–2300 (major absorption at 2900 and 2650) cm^{-1}.

2-(2'-Chloroethylamino)ethyl-3,4-dimethoxybenzoate Hydrochloride (IIIb)

The crude amide derived (cf. I*a*) from 3,4-dimethoxybenzoyl chloride (9.0 g) and the amine corresponding to 19.3 g of bis(2-chloroethyl)amine hydrochloride was obtained as a viscous oil. Crystallization from benzene – petroleum ether yielded 9.1 g (81%), m.p. 79–80°, of N-bis(2-chloroethyl)-3,4-dimethoxybenzamide. The corresponding benzylamine derivative has been described by Kravchenko (2).

Conversion of the amide to ethyl ester III*b* was easily accomplished (see III*a*). Three recrystallizations from ethanol – ethyl ether gave pure colorless crystals melting at 144–146°. Calc. for $C_{13}H_{19}Cl_2NO_4$: C, 48.16; H, 5.91; Cl, 21.88; N, 4.32. Found: C, 48.01; H, 5.95; Cl, 21.43; N, 4.28.

3,4,5-Triethoxybenzoyl Chloride

Conversion of 3,4,5-triethoxybenzoic acid (50 g) to the corresponding acid chloride was accomplished essentially as described for preparation of 3,5-dimethoxybenzoyl chloride. In this example, excess phosphorus pentachloride (45 g) and a 1.5 hour reaction period were employed. The fraction (48.5 g, 90%), boiling at 120–124° (1.1 mm), was collected and allowed to crystallize, m.p. 64–67°. Five recrystallizations from benzene – petroleum ether gave pure colorless crystals melting at 70–71° (Feist *et al.*, ref. 25, report a m.p. of 68°), ν_{max}^{KBr} 1745 cm^{-1}. Calc. for $C_{13}H_{17}ClO_4$: C, 57.24; H, 6.28; Cl, 13.00. Found: C, 57.13; H, 6.25; Cl, 12.72.

2-(2'-Chloroethylamino)ethyl-3,4,5-triethoxybenzoate Hydrochloride (IIIc)

A crude oily sample (1.0 g) of N-bis(2-chloroethyl)-3,4,5-triethoxybenzamide prepared as reported for benzamide I*a* was readily rearranged to ester III*c* (1.0 g, m.p. 154–157°) as described using amide I*a*. Five recrystallizations from acetone yielded pure colorless crystals melting at 157–158°, ν_{max}^{KBr} 2900–2450 (broad) and 1715 cm^{-1}. Calc. for $C_{17}H_{27}Cl_2NO_5$: C, 51.52; H, 6.87; Cl, 17.89; N, 3.54. Found: C, 51.64; H, 6.99; Cl, 18.08; N, 3.61.

N-bis(2-chloroethyl)-4-fluorobenzamide (Ib)

The crude product prepared (refer to I*a*) from *p*-fluorobenzoyl chloride (5.0 g) and 11.6 g of bis(2-chloroethyl)amine hydrochloride crystallized from benzene – petroleum ether as colorless needles; yield, 7.1 g (81%); m.p. 69–70°. Recrystallization from the same solvent afforded an analytical specimen melting at 69.5–70.5°, ν_{max}^{KBr} 1640–1620 cm^{-1}. Calc. for $C_{11}H_{12}Cl_2FNO$: C, 50.01; H, 4.58; Cl, 26.85; N, 5.30. Found: C, 50.21; H, 4.81; Cl, 26.78; N, 5.34.

N-bis(2-chloroethyl)-3,4,5-triiodobenzamide (Ic)

Conversion of 3,4,5-triiodobenzoyl chloride (9.0 g, ref. 26) to oily amide I*c* (10.9 g) was readily accomplished (cf. I*a*). The crude amide eventually crystallized (m.p. 113–115°) from benzene – petroleum ether. Three recrystallizations from the same solvent led to an analytical sample in the form of pale yellow plates; m.p. 115–116°,[8] ν_{max}^{KBr} 1630 cm^{-1}. Calc. for $C_{11}H_{10}Cl_2I_3NO$: C, 21.18; H, 1.62; N, 2.25. Found: C, 21.46; H, 1.77; N, 2.08.

A crystalline sample of amide I*c* (0.5 g) was converted to *2-(2'-chloroethylamino)ethyl-3,4,5-triiodobenzoate* (0.5 g) as described for preparation of ester III*a*. A pure specimen recrystallized from methanol – ethyl ether as pale yellow crystals; m.p. 203–204°, ν_{max}^{KBr} 2300–3000 (broad) and 1720 cm^{-1}.

[7]*The aluminum chloride and lithium aluminum hydride were separately dispersed in 150-ml portions of tetrahydrofuran and mixed just before adding the amide solution.*

[8]*Kofler melting point apparatus.*

Can. J. Chem. Downloaded from www.nrcresearchpress.com by 210.87.254.42 on 09/05/12
For personal use only.

N-bis(2-chloroethyl)-3,4,5-trimethoxyphenethylamine (V) Hydrochloride

The acyl chloride (13.4 g, ref. 27) from 3,4,5-trimethoxyphenylacetic acid was converted to N-bis(2-chloroethyl)-3,4,5-trimethoxyphenylacetamide (18.5 g) by using the general procedure described above (see I*a*). Several attempts to crystallize this moisture-sensitive amide were unsuccessful. The crude amide exhibited infrared absorption at ν_{max}^{pure} 1740 (weak) and 1660–1640 (broad) cm^{-1}. Weak absorption at 1740 cm^{-1} was attributed to a small amount (10%) of the corresponding 2-(2′-chloroethylamino)ethyl ester.

Reduction of the amide (11.0 g) to amine V was accomplished as described for preparation of benzylamine II*a* with proportionally adjusted reagent quantities. The crude hydrochloride weighed 6.84 g and melted at 143–146° following recrystallization from methanol – ethyl ether. Four recrystallizations from the same solvent mixture gave pure colorless plates (see Table I); ν_{max}^{KBr} 2700 and 2600 cm^{-1}.

Hexadecanoyl Chloride

Technical grade palmitic acid (30.0 g) was treated with excess phosphorus pentachloride (37 g) as described using 3,5-dimethoxybenzoic acid. The acid chloride boiling at 132–138° (4 mm) was collected: yield, 28.7 g (89%). Ralston (28) has reported a boiling point of 194° at 15 mm. An analytical specimen, distilled through a 15-cm Vigreux column, boiled at 127° (0.8 mm). Calc. for $C_{16}H_{31}ClO$: C, 69.90; H, 11.37; Cl, 12.90. Found: C, 69.97; H, 11.18; Cl, 12.90.

N-bis(2-chloroethyl)hexadecanamide (VII)

The crude amide prepared (see I*a*) from palmitoyl chloride (17.2 g) and N-bis(2-chlorethyl)amine hydrochloride (25.6 g) crystallized following removal of solvent *in vacuo*: yield, 19 g (80%). A small aliquot (ca. 0.5 g) recrystallized from benzene (5 ml) – petroleum ether (20 ml) as colorless microcrystals, m.p. 48–51°. Three recrystallizations from the same solvent led to a pure specimen melting at 55–57°, ν_{max}^{KBr} 1660 cm^{-1}. Calc. for $C_{20}H_{41}Cl_2NO$: C, 63.14; H, 10.33; Cl, 18.64; N, 3.68. Found: C, 63.24; H, 10.11; Cl, 18.38; N, 3.86.

2-(2′-Chloroethylamino)ethyl-hexadecanoate Hydrochloride (IV)

A solution of N-bis(2-chloroethyl)hexadecanamide (VII, 1.0 g) in 95% ethanol (30 ml) was heated at reflux for 30 minutes. After cooling, the colorless crystals (1.0 g) were collected. Three recrystallizations from methanol provided an analytical sample as colorless needles melting[8] at 135–136°, ν_{max}^{KBr} 2700, 2400, and 1715 cm^{-1}. Calc. for $C_{20}H_{41}Cl_2NO_2$: C, 60.28; H, 10.37; Cl, 17.80; N, 3.52. Found: C, 60.48; H, 10.58; Cl, 18.15; N, 3.89.

N-bis(2-chloroethyl)hexadecylamine (VI) Hydrochloride

The crude amide (VII, 16.9 g, 0.044 mole) was reduced using a mixture of aluminum chloride (6.54 g, 0.049 mole) and lithium aluminum hydride (1.85 g, 0.049 mole) as described for preparation of nitrogen mustard II*a*. After cooling[9] the ethereal solution to ca. −10°, the hexadecylamine (VI) hydrochloride (13.9 g, 78%) was collected. Three recrystallizations from methanol – ethyl ether yielded a pure sample as long colorless needles; m.p. 80–81°, ν_{max}^{KBr} 2800–2300 (broad) cm^{-1}. Calc. for $C_{20}H_{42}Cl_3N$: C, 59.63; H, 10.50; Cl, 26.40; N, 3.48. Found: C, 59.95; H, 10.55; Cl, 26.57; N, 3.43.

Wilson and Tishler have reported (29) an alternate route to amine IV hydrochloride (m.p. 76.4–77.2°).

N-bis(2-iodoethyl)-3,4,5-triethoxybenzylamine (IIc) Hydroiodide

A solution of N-bis(2-chloroethyl)-3,4,5-triethoxybenzylamine hydrochloride (1.2 g, 0.003 mole, Table I) in reagent grade acetone (30 ml) was added to 1.35 g of sodium iodide (0.009 mole) in the same solvent (30 ml). The reaction mixture was sealed and stored (with occasional shaking) in the dark at room temperature for 4 days. After removing sodium chloride by filtration, the red filtrate was diluted with ethyl ether. The light-sensitive iodide (1.77 g, 87.5%), m.p. 153–154°, was collected and recrystallized three times from methanol – ethyl ether. Two additional recrystallizations from methanol afforded an analytical sample as pale yellow plates, m.p. 158–159°. Calc. for $C_{17}H_{28}I_3NO_3$: C, 30.24; H, 4.18; I, 56.40; N, 2.08. Found: C, 30.31; H, 3.99; I, 56.40; N, 2.13.

The hydroiodide salt of II*c* exhibited a series of infrared absorption bands (ν_{max}^{KBr} 1290, 1220, 1090, 975, 920, and 955 cm^{-1}) not shown by the hydrochloride derivative of its precursor (II*b*).

N-bis(2-iodoethyl)-3,4,5-trimethoxybenzylamine (IId) Hydroiodide[10]

Conversion of N-bis(2-chloroethyl)-3,4,5-trimethoxybenzylamine hydrochloride (3.6 g, ref. 1) to the hydroiodide salt of nitrogen mustard II*d* was accomplished essentially as outlined in the preceding experiment (cf. II*c*). The iodide crystallized from methanol – ethyl ether as colorless crystals; yield, 4.2 g (66%), m.p. 131–135°. Four recrystallizations from the same solvent gave an analytical sample melting at 151–152° (with decomposition).[8] Calc. for $C_{14}H_{22}I_3NO_3$: C, 26.57; H, 3.50; N, 2.21. Found: C, 26.74; H, 3.77; N, 2.32.

N-bis(2-iodoethyl)-3,4-methylenedioxybenzylamine (VIII) Hydroiodide

A 2.5-g sample of N-bis(2-chloroethyl)-3,4-methylenedioxybenzylamine hydrochloride (1) was treated with sodium iodide as described for preparation of N-bis(2-iodoethyl)-3,4,5-triethoxybenzylamine (II*c*)

[9]*The hydrochloride was relatively soluble in ethyl ether.*
[10]*R. L. Smith performed this experiment.*

Can. J. Chem. Downloaded from www.nrcresearchpress.com by 210.87.254.42 on 09/05/12
For personal use only.

hydroiodide. The pale yellow iodo mustard (VIII) hydroiodide weighed 3.7 g (78%), m.p. 162–164°. Following four recrystallizations from methanol, a colorless analytical specimen (needles) melted at 166–167° (darkening from 162°). Calc. for $C_{12}H_{16}I_3NO_2$: C, 24.55; H, 2.75; I, 64.87; N, 2.39. Found: C, 24.91; H, 3.10; I, 65.33; N, 2.15.

ACKNOWLEDGMENTS

This investigation was aided by Grants number T-79B and T-79C from the American Cancer Society. We are also indebted to Dr. R. B. Ross, Cancer Chemotherapy National Service Center, United States Public Health Service, for recent information concerning embitol.

REFERENCES

1. G. R. PETTIT, M. F. BAUMANN, and K. N. RANGAMMAL. J. Med. Pharm. Chem. **5**, 800 (1962).
2. A. I. KRAVCHENKO. Vopr. Onkol. **1**, 84 (1955); Chem. Abstr. **51**, 3836 (1957).
3. R. C. ELDERFIELD and R. N. PRASAD. J. Org. Chem. **26**, 3863 (1961).
4. G. R. WHEELER. Cancer Res. **22**, 651 (1962).
5. F. D. POPP, S. ROTH, and J. KIRBY. J. Med. Chem. **6**, 83 (1963).
6. W. C. J. ROSS and J. G. WILSON. J. Chem. Soc. 3616 (1959).
7. M. S. KARACHUNSKII. Vrachebnoe Delo, **10**, 100 (1960); Cancer Chemotherapy Abstr. **2**, 306 (1961).
8. L. B. RAPP and K. A. KORNEV. *In* Methods of synthesis and discovery of antitumor preparations. *Edited by* A. I. Berlin. Moskva, Medgiz. 1962; Cancer Chemotherapy Abstr. **3**, 762 (1962).
9. A. H. SOLOWAY, E. NYILAS, R. N. KJELLBERG, and V. H. MARK. J. Med. Pharm. Chem. **5**, 1371 (1962).
10. W, G. SMITH. J. Pharm. Pharmacol. **13**, 1 (1961).
11. J. F. ALLEN and N. B. CHAPMAN. J. Chem. Soc. 1482 (1960).
12. F. KAGAN, R. BIRKENMEYER, and R. STRUBE. J. Am. Chem. Soc. **81**, 3026 (1959).
13. J. L. EVERETT and W. C. J. ROSS. J. Chem. Soc. 1972 (1949).
14. W. C. J. ROSS. J. Chem. Soc. 2589 (1949).
15. I. G. HINTON, F. G. MANN, and A. VANTERPOOL. J. Chem. Soc. 610 (1959).
16. F. BENINGTON, R. D. MORIN, L. CLARK, and R. P. FOX. J. Org. Chem. **23**, 1979 (1958).
17. E. I. DU PONT DE NEMOURS AND CO. Brit. Patent 705,950, March 24, 1954; Chem. Abstr. **49**, 2233 (1955).
18. E. ADOR and F. MEIER. Ber. **12**, 1968 (1879).
19. B. VAN ZANTEN and W. T. NAUTA. Rec. Trav. Chim. **79**, 1211 (1960).
20. M. WEILER. Ber. **32**, 1908 (1899).
21. H. MEYER. Monatsh. Chem. **22**, 428 (1901).
22. J. B. COHEN. J. Chem. Soc. **99**, 1058 (1911).
23. G. OLAH, A. PAVLATH, J. ALAH, and F. HERR. J. Org. Chem. **22**, 879 (1957).
24. J. P. LAMBOOY. J. Am. Chem. Soc. **76**, 133 (1954).
25. K. FEIST, F. KLATT, and W. AWE. Arch. Pharm. **272**, 221 (1934); Chem. Abstr. **28**, 4045 (1934).
26. C. KLEMME and J. HUNTER. J. Org. Chem. **5**, 508 (1940).
27. F. BENINGTON, R. MORIN, and L. CLARK, JR. J. Org. Chem. **22**, 227 (1957).
28. A. RALSTON and W. SELBY. J. Am. Chem. Soc. **61**, 1019 (1939).
29. E. WILSON and M. TISHLER. J. Am. Chem. Soc. **73**, 3635 (1951).

Can. J. Chem. Downloaded from www.nrcresearchpress.com by 210.87.254.42 on 09/05/12
For personal use only.

POSSIBLE INTRAMOLECULAR VAN DER WAALS CONTRIBUTIONS TO PROTON AND CARBON-13 SHIFTS IN ALIPHATIC AND AROMATIC HALOGEN COMPOUNDS

T. SCHAEFER, W. F. REYNOLDS,[1] AND T. YONEMOTO[2]
Department of Chemistry, University of Manitoba, Winnipeg, Manitoba
Received June 9, 1963

ABSTRACT

The chemical shifts of protons and carbon-13 nuclei in aliphatic and aromatic halogen compounds are considered on the basis of inductive, magnetic anisotropy, and intramolecular dispersion effects. It is suggested that a model based on all three effects is more consistent with experiment than a model based on the first two effects only. The dispersion effects in general cause a low-field shift and seem to outweigh magnetic anisotropy effects in some cases.

I. INTRODUCTION

Chemical shifts of protons and carbon-13 nuclei in compounds of the type CH_3X and CH_3CH_2X have been interpreted in terms of the electronegativity of X (a charge density effect), together with contributions due to magnetic anisotropy of the C—X bond and of the group X itself and (or) anisotropy of the C—C bond (1, 2). As noted by Spiesecke and Schneider contributions from other origins also are indicated (1). Similarly, the neighboring proton and carbon-13 shifts of the phenylhalides have also been attributed to anisotropy effects (3).

Now it is undoubtedly true that anisotropy does play an important role in determining chemical shifts in many instances. The most famous cases are perhaps the low-field shifts of the ring protons in aromatic systems and the high-field shift of the acetylenic protons. The former is the "ring-current" effect (4) and the latter can be thought of as due to the large magnetic susceptibility of the cylindrically symmetrical triple bond in the direction of the bond axis.

A classical formula based on the point-dipole approximation has been given by McConnell (5) and has been widely invoked (1, 2, 3). It is $\Delta\sigma = \Delta\chi/3\mathbf{R}^3 (1 - 3\cos^2\theta)$ where θ is the angle between the vector $\mathbf{R}$ to the point of interest and the bond axis on which the dipole lies; the bond having a magnetic anisotropy of $\Delta\chi$. $\Delta\chi$ is presumably large and negative for bonds C—X where X is a halogen (1). $\Delta\sigma$ is the change in the screening constant σ. When $\mathbf{R}$ is of the order of the radius r of the charge distribution giving rise to the anisotropy, the point-dipole approximation breaks down. However, from considerations of the potential due to a non-ideal dipole it can be said that when $\mathbf{R} \approx r$ the error in the formula will be much less than 100% (6). As long as we accept McConnell's formula and do *not* go over to a quantum-mechanical formulation, we must demand of it a consistent interpretation of low- or high-field shifts. It appears, however, that this is not so for the alkyl and aromatic halogen compounds. An indication of discrepancies is the work of Dailey and Cavanaugh (2) who were led to attribute the shielding in the alkyl halides to a "varying C—C bond anisotropy" because the assumption of a C—X bond anisotropy led to contradictions. Measurements of Diehl (7) on the *ortho* methyl protons of the mesitylene halides showed that these shifts are proportional to and less than those of the *ortho* ring protons of the aromatic halides. This is difficult to explain on an anisotropy

[1]*N.R.C. Studentship holder 1962–63.*
[2]*N.R.C. Postdoctoral Fellow 1962–63.*

Can. J. Chem. Downloaded from www.nrcresearchpress.com by 210.87.254.5 on 09/05/12
For personal use only.

basis. We suggest that intramolecular van der Waals or dispersion forces may also be important in causing anomalous low-field shifts.

II. VAN DER WAALS SHIFTS

Shifts due to dispersion forces are certainly important in intermolecular solvent effects (8). First, interaction in the equilibrium configuration causes a distortion of the electronic environment of the nucleus. This distortion is probably an expansion and leads to a low-field shift. Second, the motion of the molecules at moderate temperatures leads to a time-dependent distortion of the symmetry of the C—H bonds and hence to a negative shift. For molecules whose C—H bonds are exposed to a "sideways" attack this second effect could be important. Now both of these effects could presumably also operate on an intramolecular basis. Certainly the first is possible and the second may arise from internal rotations and vibrations of the molecule. These effects should increase as the number of electrons in the perturbing atom increases (8).

For instance, a plot of the β-methyl proton shifts found by Spiesecke and Schneider (1) for the ethyl halides versus the cube of the van der Waals radius of the halogen atom is a straight line. There is a slight deviation for the chloride but it is much less than 10% of the shift range. The total range is over 30 c.p.s. and the other three shifts lie right on the line. The greatest shift to low field is found for the iodide, as expected. It is true that anisotropy effects might also cause a low-field shift, increasing in that order.

In order to estimate the approximate magnitude of such intramolecular dispersion shifts we assume that they are comparable in magnitude to the known intermolecular dispersion shifts in liquids. Linder and co-workers (9) have given a continuum model treatment of the latter and have considered, in particular, the experimental gas-to-solvent shifts of methane (8). They found that no type of interaction other than dispersion need be invoked to explain the solvent shifts of nonpolar solutes (like methane) in reasonably isotropic solvents. Thus the gas-to-solvent shift for methane in *n*-hexane was about -0.2 p.p.m. and increased rapidly with the number of electrons in the solvent molecule, becoming as large as -0.7 p.p.m. for methylene iodide. On this basis it would be possible to expect intramolecular proton dispersion effects as large as -1 p.p.m.

Another estimate may be obtained as follows. On the basis of London's calculations, Stuart has estimated the dispersion interaction energy of two molecules in a vacuum at various separations (10). He uses average values for the molecular parameters and finds about 2 kcal/mole at a distance of 3 Å. This is very nearly the same as the dipole–dipole interaction energy of two molecules having a dipole moment of 1.6 D. Cresswell and Allred (11) have measured a hydrogen-bond shift with tetrahydrofuran of from -0.5 to -0.8 p.p.m. for the haloforms. The enthalpies of formation were of the order of 2.5 kcal/mole. If we make the assumption that weak hydrogen bond shifts are due to fluctuating electric fields in the immediate vicinity of the acceptor atom and that a somewhat similar effect causes intramolecular low-field dispersion shifts, we again arrive at an expected magnitude of the latter of 0 to -1 p.p.m. depending on the properties of the bonded atom perturbing the C—H bond in the same molecule.

We examine below the shifts of a series of halogen compounds, especially the extensive and accurate data of Spiesecke and Schneider, with a view to establishing the importance of dispersion shifts. We choose the halides because of the large atomic number and radius range, important in dispersion interactions, and also because the anisotropy will be expected to be centered somewhere along the C—X bond in a regular fashion. Groups like the nitro and carboxyl groups would not serve our purpose nearly as well.

Can. J. Chem. Downloaded from www.nrcresearchpress.com by 210.87.254.5 on 09/05/12
For personal use only.

III. PROTON AND CARBON-13 SHIFTS IN ALKYL HALIDES

Table I gives the proton and carbon-13 shifts of the gaseous methyl and ethyl halides relative to gaseous methane and liquid benzene respectively. They are taken from the paper by Spiesecke and Schneider (1).

TABLE I*

Proton chemical shifts of gaseous compounds in c/s at 60 Mc/s relative to CH_4 gas

			α	β
CH_4	0			
CH_3F	−239.8	CH_3CH_2F	−253.7	−68.5
CH_3Cl	−162.6	CH_3CH_2Cl	−193.3	−77.5
CH_3Br	−138.9	CH_3CH_2Br	−187.3	−88.0
CH_3I	−111.0	CH_3CH_2I	−178.1	−99.6

Carbon chemical shifts of liquid compounds referred to liquid benzene in p.p.m.

			α	β
CH_4	130.8			
CH_3F	53.3	CH_3CH_2F	49.4	114.1
CH_3Cl	103.8	CH_3CH_2Cl	89.3	110.8
CH_3Br	119.3	CH_3CH_2Br	100.3	108.3
CH_3I	151.0	CH_3CH_2I	126.7	105.5

	Proton chemical shifts in c/s for phenyl halides and mesitylenes†			Carbon-13 chemical shifts of phenyl halides in p.p.m.		
	ortho	meta	CH_3	C—X	ortho	meta
H	0	0	7.81	0	0	0
F	18.5	1.4	7.85	−35.1	14.3	−0.9
Cl	−1.2	1.5	7.74	−6.4	−0.16	−1.0
Br	−13.4	5.1	7.68	+5.4	−3.3	−2.2
I	−24.0	15.0	7.62	32.3	−9.9	−2.6

*Positive numbers indicate greater screening than for the reference nucleus. Data are from references 1, 3, 7.
†The shifts are for the *ortho* methyl protons and are given on the τ-scale.

(a) Methyl Halides

Spiesecke and Schneider plotted the carbon-13 and proton shifts of a whole series of CH_3X compounds against the electronegativity of X and found deviations to low field for the proton shifts of the chloride, bromide, and iodide. Deviations to high field were found for the carbon-13 shifts for all four halides. These deviations were put down to anisotropy effects of the halide. In Fig. 1(*a*) a scale model for the ethyl halides is shown. Tetrahedral angles have been assumed and internuclear distances were taken from the compilation by Sutton *et al.* (12). Before we can apply the point-dipole formula we must decide where to put the dipole. The proper place is at the electrical center of gravity of the C—X bond. At any rate it would be somewhere between the mid-point of the C—X bond and the X nucleus. In Fig. 1(*a*) lines are drawn connecting these extreme points with the relevant nuclei.

Consider the α-carbon nuclei. The angle θ is zero and the formula predicts a relatively large high-field anisotropic shift after electronegativity (charge density) effects are allowed for. This Spiesecke and Schneider found with the largest high-field shift for the iodide, as expected from a consideration of Pascal's constants and ionic susceptibilities (13).

Can. J. Chem. Downloaded from www.nrcresearchpress.com by 210.87.254.5 on 09/05/12
For personal use only.

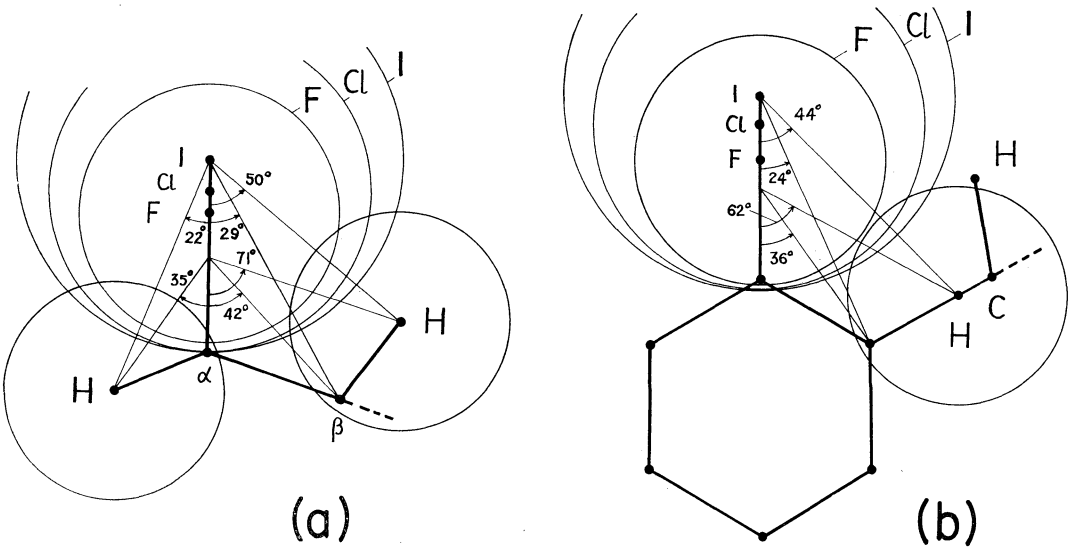

FIG. 1. The figure represents scale models of an ethyl halide molecule (*a*) and of a phenyl halide (or halo-mesitylene) (*b*). Bonds are indicated by heavier lines. The circles represent the van der Waals radii approximately. In (*a*) note that the model should be looked at as representing the halogen-α-carbon-α-hydrogen spatial relationships and, independently, the halogen-α-carbon-β-carbon relationships.

Consider now the α-proton, corresponding to the methyl protons in CH_3X. The angle θ lies between 35° and 22° and remains constant over the rotation of the methyl (or methylene) group. According to McConnell's formula a *high-field* shift should result after allowance for inductive effects. This was not found by Spiesecke and Schneider (1). They found a *low-field* shift and attributed this to inaccuracies of the point-dipole approximation (the finite volume of the electron cloud is ignored). However, the excess low-field shift is quite large (over 1 p.p.m. for CH_3I) and we would expect at least qualitative agreement with the formula.

Whether this is so or not we suggest that dispersion interactions arising from bond vibrations and (or) rotations will cause a low-field shift also and that this explanation is consistent with other data to be considered below. In Fig. 1 circles representing the van der Waals radii of the halogens and the hydrogen atom have been drawn. The values are from Pauling (14). These circles represent a crude attempt to show that electrical interactions between the relevant charge clouds could be large enough to affect bond symmetries and hence cause a low-field shift. For a better approximation the circles should be replaced by "pear-shaped" or other types of contours. However, the overlap of the circles is large enough to indicate that vibrations (perhaps especially bending motions) would be large enough to give rise to dispersion effects.

At this point we may well ask why the proton shift in dimethyl sulphide is displaced to low field by an amount comparable to that of methyl iodide (Fig. 4 of ref. 1). A similar situation is found in the corresponding ethyl compounds. Part of the explanation may go as follows. It has been argued by Linnet and co-workers (15) and very recently by Clementi (16) that there is, at least instantaneously, a pronounced directional character in the pair distribution of atoms. If the pairs in methane can be considered to be strongly localized and directional, the pairs in the neon atom have as much localization and direction (16). While in methane the protons stabilize the directional and localized character of the pairs, in neon there is a large directionality instantaneously. The lone pairs in bonded atoms should have a similar directionality and the spatial extension of these lone pairs would,

Can. J. Chem. Downloaded from www.nrcresearchpress.com by 210.87.254.5 on 09/05/12
For personal use only.

of course, become larger as the screening by the inner shells increases, that is, as the atomic number increases. The electric fields from these lone pairs could presumably lead to a dispersion shift, which would increase in importance as the lone pairs increase in number and spatial extension. Even in the absence of intramolecular vibrations and rotations, then, the electric fields from the lone pairs could cause a low-field shift. This effect would be augmented and perhaps outweighed by favorable vibrational and rotational configurations.

Since the points for dimethylether and trimethylamine lie on the electronegativity correlation line in Fig. 4 of ref. 1, on this basis it would then follow that for these compounds, both in row 2, the spatial extension of the lone pairs is not large enough to result in appreciable "lone pair dispersion" effects. In this connection we note that the point for methyl fluoride also lies on the correlation line. In third row compounds this is no longer so and the two lone pairs of sulphur then give rise to an appreciable low-field shift; augmented, perhaps, by intermethyl dispersion effects. In tetramethylsilane there are no lone pairs and its point lies almost on the line: perhaps intermethyl group effects account partly for the small deviation to low field. On this basis dimethyl selenide should exhibit a greater low-field shift for the protons than dimethylsulphide, *given* that bond pair – lone pair angles do not change. This is a further complication which would have to be considered in a quantitative theory.

(b) Ethyl Halides

The argument presented above for the methyl halides holds also for the carbon and proton shifts of the methylene group in the ethyl halides.

We assume that the inductive effect of the substituent is largely absent at the methyl group (1). Consider the β-carbon. The angle θ varies between 42° and 29° for the extreme positions of the magnetic dipole for the iodide. The anisotropy effect should be a high-field shift, although smaller than for the α-carbon because of the larger separation. A low-field shift is found and can again be attributed to dispersion interactions, the low-field shift being largest for the iodide. In the case of the β-proton a low-field shift was found (Table I). For the position shown in Fig. 1 both anisotropy and dispersion forces would cause a shift to low field. For an average position indicated by the dotted line* the anisotropy contribution would now be to high field. The dispersion interaction would be at a maximum for the position shown in Fig. 1 and would presumably drop off rapidly with distance becoming small in other rotational configurations.

After correction for inductive effects the α-carbon shifts in methyl and ethyl halides can be attributed to magnetic anisotropy effects of the C—X bond. We suggest that the α-proton, β-proton, and β-carbon shifts can also be qualitatively described as due to dispersion interactions which result in an asymmetry of the chemical bond. On this model the dispersion interactions outweigh the anisotropic shifts for the α-protons and β-carbons. The dispersion effects should in general fall off more rapidly with distance than the magnetic effects but it is hard to put this on a quantitative basis, especially since internal motions of the molecule would have to be considered.

IV. PROTON AND CARBON-13 SHIFTS IN AROMATIC HALIDES

The ring proton chemical shifts of substituted benzenes have been a subject of considerable study (17, and references therein; 18–20). Additivity relationships of substituent

**This is a very rough way of estimating the effect but should indicate the approximate extent of the rotational averaging. An accurate averaging process would involve some intransigent integrals hardly necessary in a qualitative discussion of this type.*

Can. J. Chem. Downloaded from www.nrcresearchpress.com by 210.87.254.5 on 09/05/12
For personal use only.

effects in polysubstituted benzenes have been established (17, and references therein; 18, 19). The *para* proton shifts are understood insofar as they correlate with Hammett sigma constants, as do the *para* carbon-13 shifts (3, 17, and references therein). At this position anisotropy, inductive, and, we suggest, dispersion contributions to the shifts will be very small; and, as suggested by Spiesecke and Schneider, the shifts will mirror the π-electron density at the *para*-carbon (3). For strongly electron-withdrawing or electron-releasing substituents the *ortho* shifts should also reflect this effect. This is found for the nitro and amino group, for instance (3). At the *ortho* positions of the halides magnetic and dispersion effects may be large enough, compared to resonance effects, to affect the shifts considerably. In Table I the carbon-13 and proton shifts relative to benzene are given for the phenyl halides. They are taken from reference 3.

(a) Carbon-13 Shifts

In Fig. 1(*b*) a scale model is shown for the aromatic halides. The construction is analagous to that in Fig. 1(*a*) as described above. Consider the C—X carbon-13 shifts. After correction for anisotropy effects as estimated from the α-carbon shifts in the alkyl halides, a rough correlation with electronegativity was found by Spiesecke and Schneider (3). This is very reasonable.

Consider now the *ortho* carbon-13 shifts. The high-field shift for the fluoride is reasonably explained as indicating the predominant effect of the $=F^+$ resonance structures. In this connection it is important to remember that, of all the halogens, fluorine will most easily form a double bond with the ring carbon. Also, the dispersion and anisotropy effects should be smallest for fluorine. The *ortho* carbon-13 shifts for the other halogens progressively decrease as the halogen atom increases in size. From the angles in Fig. 1(*b*), it appears that the anisotropy should cause a high-field shift. An increasing dispersion interaction would cause an increasing low field shift, as observed.*

(b) Ortho Proton Shifts

For the *ortho* proton in fluorobenzene we can again invoke the predominance of the resonance effect. The resonance structure above predicts a high-field shift for this proton as indicated by a large series of measurements (21, and references therein). Anisotropy and dispersion effects are again presumably too small to offset the resonance effect.

For the other compounds there is once more an increasing shift to low field as the size of the halogen increases. If the point dipole is placed at the halogen nucleus a high-field shift is predicted while a small low-field shift is predicted if the dipole is placed at the mid-point of the bond. The dispersion interaction predicts an increasing shift to low field with increase in size of halogen atom, as observed.

(c) Estimation of the Magnitudes of the Dispersion Shifts

In the absence of quantitative information on the magnitude of the anisotropy shifts, only a very crude estimate of the dispersion shifts can be made. If we accept the correlation plots of shift versus electronegativity of Spiesecke and Schneider (1) the deviations to low field may be taken as rough estimates of the dispersion shifts. If the anisotropy formula above is taken as exact these must be regarded as minimum values. These range from about -1.0 to -1.5 p.p.m. for α-protons in the iodide to -0.7 to -1.0 p.p.m. for the chloride. For β-protons the values are correspondingly less by about 0.5 p.p.m. For *ortho* protons in the phenyl halides these shifts seem to be still less but in view of the

**A very small low-field shift is also observed for the meta carbon-13 nuclei but if this is attributed to anisotropy then the high-field shift for the meta protons remains unexplained. Resonance effects are expected to be small at the meta position.*

Can. J. Chem. Downloaded from www.nrcresearchpress.com by 210.87.254.5 on 09/05/12
For personal use only.

added complications due to possible mesomeric effects it is hard to say how much. Presumably dispersion effects are almost negligible for the fluorides. For β-carbons the dispersion shift may be as much as -20 p.p.m. in the iodide and as large as -10 p.p.m. for the *ortho* carbon in the phenyl iodide. Again, estimates of the anisotropy and mesomeric shifts are needed.

V. *ORTHO* METHYL PROTON SHIFTS IN MESITYLENE

Diehl has measured the *ortho* methyl proton shifts in the mesitylene halides (7). He finds the shifts are proportional to those of the *ortho* proton in the phenyl halides. They are smaller by a factor of 0.35. The τ-values are given in Table I. In Fig. 1(*b*) the methyl group is indicated with the proton in the configuration nearest the halogen. The dotted line running through the methyl carbon represents an average position of the proton. With the methyl proton near the halogen it is seen that **R** is virtually the same as for an *ortho* proton in the phenyl halide. The angle is very nearly 90° resulting in a predicted low-field shift for the methyl proton of about 3 times that of the ring proton if the dipole is put at the bond center. Otherwise the difference would be even greater. On the other hand, in the averaged position the increase in **R** is roughly offset by the decrease in θ. At any rate, it is hard to reconcile the greatly reduced effect on the methyl protons with an anisotropy contribution only, as noted by Diehl (7).

In the situation shown in Fig. 1(*b*) there is very strong overlap and therefore, perturbation of the methyl hydrogen electron cloud by the electron cloud of the larger halogen atoms. But in the rotational configuration related to this one by 180° there will be no appreciable overlap. In this case the low-field dispersion shift would therefore be much smaller than for the *ortho* proton in the phenyl halide. After rotational averaging it may be that the smaller low-field methyl proton shift becomes understandable.

On this assumption the high-field shift of 0.04 p.p.m. for the *ortho* methyl group in fluoromesitylene as compared to mesitylene is to be explained as in the corresponding *ortho* proton case. The effect is reduced as would be expected. Whether this argues for hyperconjugation of the methyl group with the ring is questionable.

VI. CONCLUSIONS

As mentioned above, it is hard to put intramolecular dispersion shifts on a quantitative basis. However, we consider that they are present, that they lead in general to low-field shifts of nuclear resonances, and that they may in certain situations be at least as important as anisotropy effects. Various experiments suggest themselves as a check on these considerations. At any rate, we feel that the possibility of the importance of intramolecular dispersion shifts cannot be rejected out of hand.

ACKNOWLEDGMENTS

We thank Dr. W. G. Schneider for his comments and the National Research Council for financial assistance.

REFERENCES

1. H. Spiesecke and W. G. Schneider. J. Chem. Phys. **35**, 722 (1961).
2. J. R. Cavanaugh and B. P. Dailey. J. Chem. Phys. **34**, 1099 (1961).
3. H. Spiesecke and W. G. Schneider. J. Chem. Phys. **35**, 731 (1961).
4. J. A. Pople. J. Chem. Phys. **24**, 1111 (1956).
5. H. M. McConnell. J. Chem. Phys. **27**, 226 (1957).
6. C. J. F. Böttcher. Theory of electric polarization. Elsevier Publishing Company, Amsterdam. 1952. Chap. 1.

Can. J. Chem. Downloaded from www.nrcresearchpress.com by 210.87.254.5 on 09/05/12
For personal use only.

7. P. DIEHL and C. SVEGLIADO. Helv. Chim. Acta, **46**, 461 (1963).
8. A. D. BUCKINGHAM, T. SCHAEFER, and W. G. SCHNEIDER. J. Chem. Phys. **32**, 1227 (1960).
9. B. B. HOWARD, B. LINDER, and M. T. EMERSON. J. Chem. Phys. **36**, 485 (1962).
10. H. A. STUART. Die Physik der Hochpolymeren. Band I. Springer-Verlag, Berlin. (1952). p. 72.
11. C. J. CRESWELL and A. L. ALLRED. J. Am. Chem. Soc. **85**, 1723 (1963).
12. TABLES OF INTERATOMIC DISTANCES and configuration in molecules and ions. Spec. Publ. No. 11. The Chemical Society, London. 1958.
13. P. W. SELWOOD. Magnetochemistry. 2nd ed. Interscience Publishers, Inc., New York. 1956.
14. L. PAULING. Nature of the chemical bond. 3rd ed. Cornell University, Ithaca, New York. 1960.
15. J. W. LINNET and A. J. POE. Trans. Faraday Soc. **47**, 1033 (1951).
16. E. CLEMENTI. J. Chem. Phys. **39**, 487 (1963).
17. B. P. DAILEY and J. MARTIN. J. Chem. Phys. **37**, 2594 (1962).
18. P. DIEHL. Helv. Chim. Acta, **44**, 829 (1961).
19. W. F. REYNOLDS and T. SCHAEFER. Can. J. Chem. **41**, 2339 (1963).
20. J. C. SCHUG and J. C. DECK. J. Chem. Phys. **37**, 2618 (1962).
21. T. SCHAEFER and W. G. SCHNEIDER. Can. J. Chem. **41**, 966 (1963).

Can. J. Chem. Downloaded from www.nrcresearchpress.com by 210.87.254.5 on 09/05/12
For personal use only.

Can. J. Chem. Downloaded from www.nrcresearchpress.com by 210.87.254.5 on 09/05/12
For personal use only.

SYNTHESES AND POLYMERIZATION OF α-TRIMETHYLSILYL ACRYLIC MONOMERS

ARIEL OTTOLENGHI, MATI FRIDKIN, AND A. ZILKHA
Department of Organic Chemistry, The Hebrew University of Jerusalem, Jerusalem, Israel
Received July 24, 1963

ABSTRACT

α-Trimethylsilyl acrylic acid and its methyl ester were prepared in good yield starting from 1,2-dibromoethyltrimethylsilane. These monomers were polymerized with difficulty by free radicals to viscous polymers, but gave solid copolymers with styrene. The methyl ester was also a weak monomer in anionic polymerization. This non-reactivity is due to the steric effect of the α-trimethylsilyl group adjacent to the double bond.

In the present work the preparation and polymerization of α-trimethylsilyl acrylic acid and its methyl ester were investigated. Apart from their intrinsic interest as new monomers, they permit the study of the steric and electric effects of bulky groups attached directly to reactive double bonds, on free radical and anionic polymerization.

Petrov, Mironov *et al.* (1, 2) prepared α-trimethylsilyl acrylic acid by carbonation of the Grignard reagent prepared from α-bromovinyltrimethylsilane (II), and also mentioned its polymerization without giving any details.

We prepared the α-trimethylsilyl acrylic derivatives according to the following scheme:

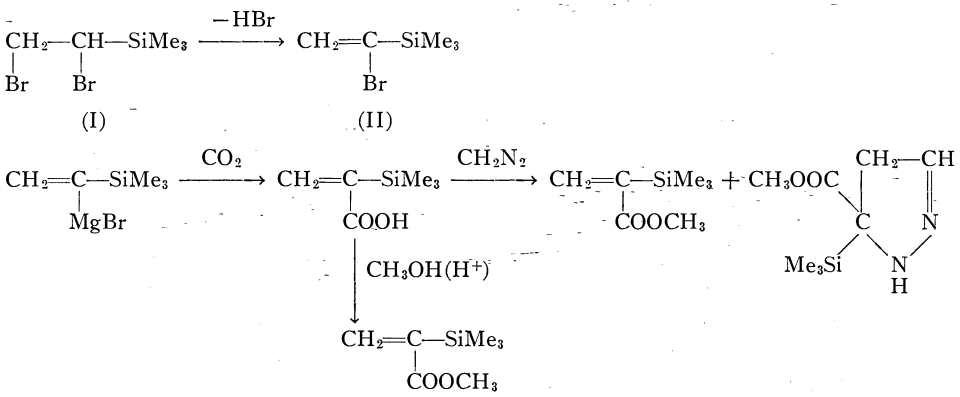

Agre and Hilling (3) have prepared α-bromotrichlorovinylsilane by bromination of vinyl trichlorosilane and subsequent dehydrobromination with quinoline. This last step was realized in 40% yield only due to decomposition of the dibromoderivative with the formation of silicon tetrachloride. This same procedure was later reported (2) to give the α-bromo derivative in 65% yield. α-Bromovinyltrimethylsilane (II) was prepared in 74% yield from this derivative by reaction with methyl magnesium bromide.

We tried to obtain α-bromovinyltrimethylsilane (II) in higher yield starting from 1,2-dibromoethyltrimethylsilane (I) which is obtained in 90% yield from vinyltrimethylsilane (4). Dehydrobromination of this derivative by quinoline gave 10% yield of (II). Since the lower yield of the dehydrobromination in this case may be due to the lower activating effect of the adjacent trimethylsilyl group as compared to the trichlorosilyl group, stronger bases were tried to determine the effect on the yield. Reaction of the dibromo derivative

with sodium methoxide, both solid and in methanol solution, caused an immediate β-elimination reaction, similar to that found by Sommer *et al.* (4), leading to the formation of trimethylsilyl methoxide. Use of sodium butoxide in butanol led to a similar elimination reaction with formation of trimethylsilyl butoxide. Diethylamine in ether, which is a stronger base than quinoline, gave a 70% yield of (II). The reaction was slow and required several days. However, it was found that with diethylamine alone yields of more than 90% were obtained in a relatively short reaction time.

From α-trimethylsilyl acrylic acid (1, 2) the methyl ester was prepared either by direct esterification with absolute methanol in the presence of mineral acid, or by reaction with diazomethane. The latter reaction carried out at 0° in ether, led to the formation of appreciable amounts of probably 5-trimethylsilyl 5-carbomethoxypyrazoline, formed by addition of diazomethane to the double bond, together with a 50% yield of the methyl ester. However, on carrying out the reaction at −70°, a 75% yield of ester was realized and only traces of the pyrazoline derivative were formed.

Reaction of α-trimethylsilyl acrylic acid with thionyl chloride at room temperature, followed by heating the reaction mixture under reflux, resulted in the formation of an acid chloride which had a lower chlorine content than that required by α-trimethylsilyl acrylyl chloride. This acid chloride was converted to the amide derivative by reaction with gaseous ammonia in ether solution. The amide did not analyze for α-trimethylsilyl acrylamide. The infrared spectrum showed absorptions for a carbon–carbon double bond, as well as for the trimethylsilyl group and for the amide group. Its n.m.r. spectrum indicated nine protons of the trimethylsilyl group at 10 τ, four aliphatic protons at 7.5–7.8 τ, two vinyl protons at 4.7–4.8 τ and 4.5 τ (doublet), and two amino protons at 3.8–4.8 τ. The n.m.r. spectrum and the analytical results are in accordance with the following formula:

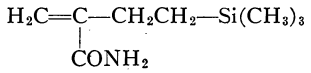

It is difficult to establish the mechanism by which the acid chloride (starting material for the amide derivative) was obtained, but it may be formed by joining two molecules of α-trimethylsilyl acrylic acid, one which has undergone decarboxylation, and the other which has undergone cleavage of the trimethylsilyl group, due to the strongly acidic medium and the heating. Such cleavages of α-trimethylsilylvinyl derivatives by strong acids have been found to occur easily (5, p. 140).

From the analytical and physical data, the following formula is also possible for the amide derivative.

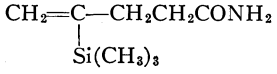

However, this structure contains a trimethylsilyl group adjacent to a vinyl double bond, which is difficult to obtain because of acid cleavage.

In an attempt to prepare β-amino acids substituted in the α position by trimethylsilyl groups, α-trimethylsilyl acrylic acid was heated with benzylamine in pyridine. No addition of benzylamine to the double bond occurred, but β elimination did, resulting in splitting off of the silicon residue and formation of acrylic acid, which on reaction with benzylamine led to the formation of *N*-benzyl-β-alanine (6) as follows:

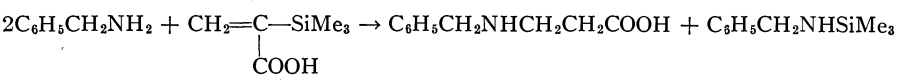

Can. J. Chem. Downloaded from www.nrcresearchpress.com by 210.87.254.5 on 09/05/12
For personal use only.

In an attempt to prepare other vinylsilicon monomers, we tried the reaction of α-trimethylsilylvinyl magnesium bromide in tetrahydrofuran with benzophenone. The reaction did not lead to the addition of the Grignard reagent to the carbonyl double bond but to the formation of benzopinacol, as seen from analyses, melting point, and mixed melting points with an authentic sample. Such a reaction can occur if the Grignard reagent acted as an electron transfer agent leading to the formation of intermediate ketyl derivatives. This seems to have been the case as a blue color, similar to that shown by benzophenone sodium, developed in the reaction mixture during the addition of benzophenone.

Polymerization Experiments

The free radical polymerizations of α-trimethylsilyl acrylic acid and its methyl ester were investigated. These monomers polymerized only with great difficulty even in the presence of relatively high concentrations of benzoyl peroxide and required long reaction times. Irradiation with ultraviolet light in the presence of azo-bis-isobutyronitrile did not cause significant polymerization. The polymers obtained, were highly viscous.

On the other hand, free radical copolymerization of these monomers with styrene was much easier, and solid copolymers were obtained.

The anionic polymerization of the methyl ester was also investigated with phenyl and butyl lithium as catalysts in tetrahydrofuran and petroleum ether. Only partial polymerization occurred even when high catalyst concentrations were used. In all cases, side reactions occurred leading to the formation of liquid products, having relatively low boiling point, which might be formed on addition of the alkyl lithium to the double bond (7), or to the ester group as found in the case of methylmethacrylate (8).

In contrast, it was found that trimethylsilylmethylvinylketone in which the trimethylsilyl group is in a β-position to the active double bond polymerized easily on heating. This is illustrated by the direct preparation of solid polymer in the synthesis of the ketone by reaction of trimethylsilyl methyl magnesium bromide and acrylyl chloride.

The unreactivity of the α-trimethylsilyl acrylic derivatives both in free radical and anionic polymerizations is due to the presence of the trimethylsilyl group in the α position to the vinyl double bond. The silicon atom is more electropositive than carbon. It has vacant *d* orbitals that can hybridize with the π electrons of the adjacent vinyl double bond ($d\pi$—$p\pi$ interaction) (5, p. 100), and thus cause an electron withdrawing effect ($-T$) which is contrary to the $+I$ effect of the methyl groups attached to the silicon atom. There is evidence that the $-T$ effect is stronger than the $+I$ effect, as is seen, for example, from the anti-Markownikoff addition of hydrogen halides to vinyl trimethyl silane (9). From this electric consideration, it would be expected that the trimethylsilyl group should favor the anionic polymerization of the methyl ester by contributing to the reactivity of the double bond by making it more acidic. Since the monomers were not sufficiently reactive it must be that the steric hindrance of the bulky trimethylsilyl group is the governing factor in determining the reactivity of the monomers.

EXPERIMENTAL

*Vinyltrimethylsilane**

Into a three-necked flask fitted with a high speed stirrer, a dropping funnel, and a reflux condenser magnesium metal filings (26.4 g, 1.1 mole), tetrahydrofuran (800 ml), and an iodine crystal were added. Vinyl bromide (107 g, 1 mole) dissolved in tetrahydrofuran (200 ml) was added dropwise so that there was a

**This compound was previously prepared in about 60% yield starting from methyl magnesium halide and vinyltrichlorosilane, or by the Wurtz reaction between vinyl chloride and trimethylchlorosilane (10). The following method starting from vinyl magnesium bromide and trimethylchlorosilane gives higher yields.*

Can. J. Chem. Downloaded from www.nrcresearchpress.com by 210.87.254.5 on 09/05/12
For personal use only.

gentle reflux. The addition required about 3 hours, and the reaction mixture was refluxed for another hour. Trimethylchlorosilane (108 g, 1 mole) dissolved in tetrahydrofuran (100 ml) was added dropwise during 2 hours, and the reaction mixture refluxed for 1 hour more. The reaction mixture was fractionally distilled with an efficient column, and the material boiling up to 60° was collected. This distillate contained tetrahydrofuran together with vinyltrimethylsilane. The tetrahydrofuran was separated by successive washings with water, in which the vinyltrimethylsilane is insoluble. The substance was dried over anhydrous calcium chloride and fractionally distilled. The vinyltrimethylsilane was collected at 55–56°; yield 90 g (90%); n_D = 1.390 (11).

Reaction of 1,2-Dibromoethyltrimethylsilane with Potassium Methoxide

To 1,2-dibromoethyltrimethylsilane (10.4 g, 0.04 mole), prepared by bromination of vinyltrimethylsilane (4), was added with stirring and exterior cooling potassium methoxide solution in methanol (0.78 N, 51 ml) (0.04 mole). Potassium bromide precipitated immediately. It was filtered, and the filtrate was washed with water to remove methanol, dried, and distilled. The compound distilled at 55° and 690 mm, n_D = 1.367, the infrared spectrum showed a (Si—O—C) bond at 9.2 μ, and the compound is therefore trimethylsilylmethoxide (11).

Similar results were obtained on reaction of 1,2-dibromoethyltrimethylsilane with solid sodium methoxide.

Reaction of 1,2-Dibromoethyltrimethylsilane with Potassium Butoxide

This was carried out as before using potassium butoxide in butanol. Trimethylsilyl butoxide (11) was obtained, b.p. 118° at 690 mm, n_D = 1.392.

α-Bromovinyltrimethylsilane

1,2-Dibromoethyltrimethylsilane (217 g, 0.83 mole) and diethylamine (121 g, 1.66 mole), dried over sodium hydroxide, were shaken in a flask for 5 hours at room temperature. The precipitate of diethylamine hydrobromide was filtered and washed with ether. The filtrate was washed several times with cold 5% hydrochloric acid to remove diethylamine, followed by water and dried over magnesium sulphate. α-Bromovinyltrimethylsilane (2) was collected at 26–27° and 15 mm, n_D = 1.458; yield 137 g (92%).

The same reaction carried out in ether (200 ml), with 1,2-dibromoethyltrimethylsilane (200 g) and diethylamine (2 equiv.), with stirring under reflux gave only 70% yield of the α-bromovinyltrimethylsilane after 30 hours, the unreacted dibromo derivative being recovered unchanged.

Methyl α-Trimethylsilyl Acrylate

α-Trimethylsilyl acrylic acid (16 g), prepared by carbonation of the Grignard reagent obtained from α-bromovinyl trimethylsilane (1, 2), was dissolved in absolute methanol (35 ml), concentrated sulphuric acid (0.9 ml) added, and the reaction mixture refluxed for 15 hours. Excess methanol was removed at room temperature *in vacuo*, the residue was taken up in ether (30 ml) and washed with bicarbonate. The ether extract was dried and distilled. The ester was collected at 75° and 50 mm or at 152° and 690 mm, n_D = 1.436, yield 12 g (68%). The infrared spectrum showed absorptions at 5.8 μ (ester group), at 6.2 μ (C=C), and at 8.0 μ and 11.9 μ (trimethylsilyl).

Anal. Calc. for $C_7H_{14}SiO_2$: C, 53.2; H, 8.9; Si, 17.7. Found: C, 54.0; H, 9.0; Si, 17.6.

Methyl α-Trimethylsilyl Acrylate and 5-Trimethylsilyl-5-Carbomethoxy Pyrazoline

Into a three-necked flask fitted with a mechanical stirrer, a dropping funnel and a reflux condenser, α-trimethylsilyl acrylic acid (31.7 g, 0.22 mole) and dry ether (50 ml) were added. An ethereal solution of diazomethane (0.25 mole) was added dropwise at 0°. Nitrogen gas was evolved and a precipitate formed. After addition of the diazomethane the reaction mixture was stirred for another hour. The precipitate (7 g) was filtered, and the ethereal solution fractionally distilled. The methyl ester was collected at 75° and 50 mm, n = 1.436; yield 18.5 g (53%).

The yellowish precipitate, consisting of 5-trimethylsilyl-5-carbomethoxy pyrazoline, was recrystallized from ether – petroleum ether, m.p. 65°. The pyrazoline was soluble in water, acetone, and alcohol. It darkened on exposure to light.

Anal. Calc. for $C_8H_{16}N_2O_2Si$: C, 48.0; H, 8.0. Found: C, 47.4; H, 7.9.

Reaction of α-Trimethylsilyl Acrylic Acid with Thionyl Chloride

Redistilled purified thionyl chloride (50 g, 0.44 mole) was added dropwise at 0° to α-trimethylsilyl acrylic acid (22 g, 0.15 mole). The reaction mixture was left at 0° for 30 minutes and then for several hours at room temperature. The reaction mixture darkened considerably and was refluxed for 2 hours. Excess thionyl chloride was distilled at atmospheric pressure, and the acid chloride was collected at 45–50° and 1 mm; n_D = 1.48; yield 6 g. It contained 19.1% chlorine as compared to 21.8% required by α-trimethylsilyl acrylyl chloride and 18.7% required by 2-methylene-4-trimethylsilyl butyryl chloride. The acid chloride was dissolved in dry ether (50 ml) and cooled to 0° while dry ammonia gas was passed in for 15 minutes. The ethereal solution was washed with water followed by dilute hydrochloric acid, water, and dried over sodium sulphate. The ether was stripped off and the amide derivative recrystallized from dilute ethanol, m.p. 67°. The substance analyzed for 2-methylene-4-trimethylsilyl butyramide.

Anal. Calc. for $C_8H_{17}NOSi$: C, 56.1; H, 9.9; N, 8.2; Si, 16.4. Found: C, 56.1; H, 9.9; N, 8.3; Si, 16.2.

Can. J. Chem. Downloaded from www.nrcresearchpress.com by 210.87.254.5 on 09/05/12
For personal use only.

Reaction of α-Trimethylsilyl Acrylic Acid with Benzylamine

α-Trimethylsilyl acrylic acid (0.8 g) was dissolved in pyridine (2 ml) and benzylamine (1 g) added. The solution was heated at 100° for 3 hours. The reaction mixture was cooled, acetone added, and the resulting precipitate was filtered and recrystallized from water–acetone, m.p. 196°. It did not contain silicon. From analysis, infrared spectrum, and mixed melting point with an authentic sample, the substance was found to be *N*-benzyl-β-alanine (6).

Reaction of α-Trimethylsilylvinyl Magnesium Bromide with Benzophenone

α-Bromovinyltrimethylsilane (10 g, 0.055 mole) was added dropwise with stirring to magnesium filings (1.32 g, 0.055 mole) and dry tetrahydrofuran (50 ml), so as to keep a gentle reflux. (If necessary, a few drops of ethylene dibromide were added to start the reaction.) Refluxing was continued for 1 hour after addition. Benzophenone (10 g) in ether (30 ml) was dropped in during 30 minutes with exterior cooling, and the reaction mixture was heated for 1 hour. During addition, a deep blue color appeared in the solution. The reaction mixture was cooled, ice-cold dilute sulphuric acid was added, and the organic layer separated. The aqueous layer was further extracted with ether. The tetrahydrofuran and ether were driven off from a water bath and the residue recrystallized from alcohol–water. The compound melted at 185°; yield, 3 g. From analyses, infrared spectrum, and mixed melting points it was found to be benzopinacol.

Free Radical Polymerization of α-Trimethylsilyl Acrylic Acid and its Methyl Ester

Monomer (1 g) was placed in an ampoule together with 5% benzoyl peroxide, purified oxygen-free nitrogen was passed in for 10 minutes, and the ampoule was closed and heated at 80°. The acid polymerized to a very viscous mass after 3 days while the ester polymerized only partially after 2 weeks.

Copolymerization experiments with styrene were carried out under the same general conditions at 90°. The copolymers were ground and purified by extraction with methanol. Generally the yields were quantitative. The results are summarized in Table I.

TABLE I

Copolymerization of α-trimethylsilyl acrylic acid and its methyl ester with styrene

Acid (mmole)	Ester (mmole)	Styrene (mmole)	Benzoyl peroxide (mmole)	% Si in copolymer	Time of solidification (days)
—	1.45	9.62	0.19	2.5[a]	1.5
—	2.91	9.62	0.19	5.0[b]	1.5
—	2.91	4.81	0.19	7.4[c]	2
—	1.45	9.62	0.02	3.0[d]	7
1.74	—	9.62	0.13	4.0[e]	1
3.47	—	9.62	0.21	6.1[f]	1
6.95	—	9.62	0.21	[g]	1

[a]Copolymer is insoluble in methanol; m.p. 110–115°.
[b]Melting point of copolymer 100–110°.
[c]Melting point of copolymer 95–100°; a small part of the polymer is soluble in methanol.
[d]Melting point of copolymer 115–120°; copolymer is insoluble in methanol.
[e]Copolymer is partially soluble in methanol.
[f]Copolymer is partially soluble in methanol.
[g]The polymer is partially soluble in methanol. The soluble fraction melted about 120° and contained 7.9% Si (acid in copolymer 40.5%), while the insoluble fraction melted at 185–195° and contained 12.5% Si (acid in copolymer 64%).

Polymerization of Methyl α-Trimethylsilyl Acrylate with Butyl Lithium

(*a*) Methyl α-trimethylsilyl acrylate (4 g) was dissolved in dry ether (10 ml) and butyl lithium in toluene (6×10^{-3} mole) was added at 0° under nitrogen. The reaction mixture was left overnight and was washed with dilute hydrochloric acid. The organic layer was dried over magnesium sulphate, and fractionally distilled. A fraction (0.5 g) was collected at 100° and 5 mm, $n_D = 1.455$. In the infrared it showed absorptions for the trimethylsilyl group and it may be a product of addition of butyl lithium to the ester. A viscous polymer residue (2 g) remained which did not distill up to 200° at 1 mm. In the infrared it showed absorptions for ester groups for trimethylsilyl groups but essentially no carbon–carbon double bond.

(*b*) The reaction between butyl lithium and the ester was carried out under the same conditions as above except that the polymerization temperature was 20°. Fractional distillation gave 1 g unreacted ester and 1.5 g of the product boiling at 100° and 5 mm, $n_D = 1.455$. A polymeric viscous residue (1 g) remained which behaved similarly as before.

Polymerization of Methyl α-Trimethylsilyl Acrylate with Sodium Naphthalene

To freshly distilled methyl α-trimethylsilyl acrylate (4 g) dissolved in dry ether (10 ml), sodium naphthalene in tetrahydrofuran (6×10^{-3} mole) was added at 0° under nitrogen. The reaction mixture was left overnight, and was worked up as before. Fractional distillation gave a fraction boiling at 190–200° and 5 mm, $n_D = 1.490$, and a polymeric viscous residue (1 g) which was similar to the above polymers.

Can. J. Chem. Downloaded from www.nrcresearchpress.com by 210.87.254.5 on 09/05/12
For personal use only.

Attempted Preparation of Vinyltrimethylsilylmethylketone

Trimethylsilylmethyl iodide (7 g, 0.033 mole) dissolved in dry ether (20 ml) was added dropwise with stirring during 30 minutes to magnesium filings (0.8 g, 0.033 mole) and 30 ml ether. The reaction mixture was refluxed gently for 30 minutes, cooled, and added dropwise during 1 hour to acrylyl chloride (3 g, 0.033 mole) in ether (30 ml). The reaction mixture was refluxed for 1 hour and the ether was driven off from a water bath. The residue was heated *in vacuo* to continue the distillation, but nothing distilled and the residue became very viscous. It was purified by trituration with methanol. The polymer was insoluble in acetone but soluble in tetrahydrofuran. It softened around 120° and melted at about 150°. Its infrared spectrum showed absorptions at 5.8 μ (carbonyl) and 8.9 μ and 11.9 μ (trimethylsilyl). It gave a dinitrophenylhydrazone showing the presence of the carbonyl group. The material obtained is, as indicated by analysis, polymeric trimethylsilylmethyl vinyl ketone contaminated with polyacrylic acid.

Anal. Calc. for $(C_7H_{14}SiO)_n$: Si, 19.7. Found: Si, 17.0.

REFERENCES

1. A. D. Petrov, V. F. Mironov, V. A. Ponomarenko, S. I. Sadykh-Zade, and E. A. Chernyshev Izv. Akad. Nauk SSSR Otd. Khim. Nauk, 787 (1958).
2. V. F. Mironov, A. D. Petrov, and N. G. Maksimova. Izv. Akad. Nauk SSSR Otd. Khim. Nauk, 954 (1958).
3. C. L. Agre and W. Hilling. J. Am. Chem. Soc. **74**, 3899 (1952).
4. L. H. Sommer, D. L. Bailey, G. M. Goldberg, C. E. Buck, T. S. Bye, F. J. Evans, and F. C. Whitmore. J. Am. Chem. Soc. **76**, 1613 (1954).
5. C. Eaborn. Organosilicon compounds. Butterworth Scientific Publications, London. 1960.
6. A. Zilkha, E. S. Rachman, and J. Rivlin. J. Org. Chem. **26**, 376 (1961).
7. L. F. Cason and H. G. Brooks. J. Org. Chem. **19**, 1278 (1954).
8. H. Schreiber. Makromol. Chem. **36**, 86 (1959).
9. L. H. Sommer, D. L. Bailey, G. M. Goldberg, C. E. Buck, T. S. Bye, F. J. Evans, and F. C. Whitmore. J. Am. Chem. Soc. **76**, 1613 (1954). E. Larson. Chalmers Tek. Hogskol. Handl. **115**, 25 (1951). M. Kanazashi. Bull. Chem. Soc. Japan, **28**, 44 (1955).
10. S. Murahashi, S. Nozakura, and M. Sumi. Bull. Chem. Soc. Japan, **32**, 670 (1959). M. Kanazashi. Bull. Chem. Soc. Japan, **26**, 493 (1953).
11. P. D. George, M. Prober, and J. R. Elliot. Chem. Rev. **56**, 1065 (1956).

Can. J. Chem. Downloaded from www.nrcresearchpress.com by 210.87.254.5 on 09/05/12
For personal use only.

STEREOCHEMISTRY OF ARSENIC

PART XII.[1] BIS(DIPHENYLARSENIC) OXIDE

W. R. CULLEN AND J. TROTTER

Department of Chemistry, The University of British Columbia, Vancouver, British Columbia

Received July 26, 1963

ABSTRACT

Crystals of bis(diphenylarsenic) oxide are monoclinic, with four molecules in a unit cell of dimensions $a = 11.48$, $b = 30.2$, $c = 5.97$ Å, $\beta = 93.8°$, space group $P2_1/n$. The structure has been determined from projections along the a and c axes, using Fourier and difference syntheses. The As—O—As angle is 137°, the increase from the normal oxygen valency angle probably being a result of $p\pi$—$d\pi$ bonding involving arsenic $4d$ orbitals. The As—O distance is 1.67 Å, and all the other bond lengths and angles are normal. The orientations of the substituent phenyl groups have been determined.

INTRODUCTION

The crystal and molecular structure of bis(diphenylarsenic) oxide, $(C_6H_5)_2As.O.As(C_6H_5)_2$, has been determined as part of a series of investigations of arsenic compounds (1).

EXPERIMENTAL

Crystals of bis(diphenylarsenic) oxide are colorless prisms elongated along c. The density was measured by flotation in aqueous silver nitrate, and the unit cell dimensions and space group were determined from various rotation, oscillation, and Weissenberg films (Cu$K\alpha$ radiation, $\lambda = 1.5418$ Å).

Crystal Data

Bis(diphenylarsenic) oxide, $C_{24}H_{20}OAs_2$; $M = 474.2$; m.p. = 95° C.

Monoclinic, $a = 11.48 \pm 0.03$, $b = 30.2 \pm 0.1$, $c = 5.97 \pm 0.02$ Å, $\beta = 93.8° \pm 0.5°$.

Volume of the unit cell = 2065 Å^3.

$D_m = 1.514$, $Z = 4$, $D_x = 1.516$ g cm^{-3}.

Absorption coefficient for X-rays, $\lambda = 1.5418$ Å, $\mu = 45$ cm^{-1}. $F(000) = 952$.

The intensities of the $hk0$ reflections were recorded on Weissenberg films and estimated visually. The $0kl$ intensities were measured with a G.E. Spectrogoniometer, using a scintillation counter, Cu$K\alpha$ radiation (nickel filter and pulse height analyzer), and the moving crystal–moving counter technique (2). The crystals used had fairly uniform cross-sections and no absorption corrections were applied. The relative structure amplitudes were derived as usual, the absolute scale being established later by correlation with the calculated structure factors. 253 $hk0$ and 114 $0kl$ reflections were observed.

Structure Analysis

The projection along the short c-axis was examined first, and the coordinates of the arsenic atoms were determined from a Patterson synthesis. Structure factors were calculated for the $hk0$ reflections with the arsenic contributions only, using the scattering factor of the International Tables (3), corrected for thermal vibration as usual with $B = 4.5$ Å^2. R for the observed reflections was 0.42. A Fourier series was summed by using as coefficients measured structure amplitudes and calculated signs, but the resulting electron-density map was difficult to interpret. The arsenic atoms and the oxygen atom were well resolved, and one six-membered ring was reasonably well defined and a second rather poorly resolved, but the other two rings could not be located. Inclusion of the contributions of the oxygen and 12 carbon atoms, again with the International Tables' scattering curves (3) with $B = 4.5$ Å^2, reduced R, but only to 0.37. Two more successive Fourier syntheses revealed the third and then the fourth rings, R being reduced to 0.36 and then 0.28. A fourth electron-density distribution, with signs based on all the atoms, gave improved resolution and better positional parameters ($R = 0.21$). The positional and isotropic thermal parameters were then further refined by $(F_o - F_c)$ syntheses. The first difference map suggested small shifts in positional parameters, changes in the isotropic thermal parameters, and the need for anisotropic temperature factors for the arsenic atoms, the directions of maximum thermal vibration being parallel to b. The thermal anisotropy was treated by splitting each arsenic into two half-atoms (4), and application of the various changes reduced R to 0.18.

[1]*Part XI. N. Camerman and J. Trotter, J. Chem. Soc. In press.*

Can. J. Chem. Downloaded from www.nrcresearchpress.com by 210.87.254.40 on 09/05/12
For personal use only.

A second (F_o–F_c) synthesis suggested smaller changes, giving $R = 0.16$, and a third (F_o–F_c) synthesis showed no further significant changes in parameters.

The arsenic positions in the *a*-axis projection were determined by Patterson methods, and location of the other atoms and refinement of the parameters proceeded as for the *c*-axis projection. Since the resolution was poorer, no account was taken of thermal anisotropy, and the final R value was 0.18.

The measured and calculated structure factors for both zones are not listed here to save space but are available from the authors. Electron-density projections are shown in Figs. 1 and 2.

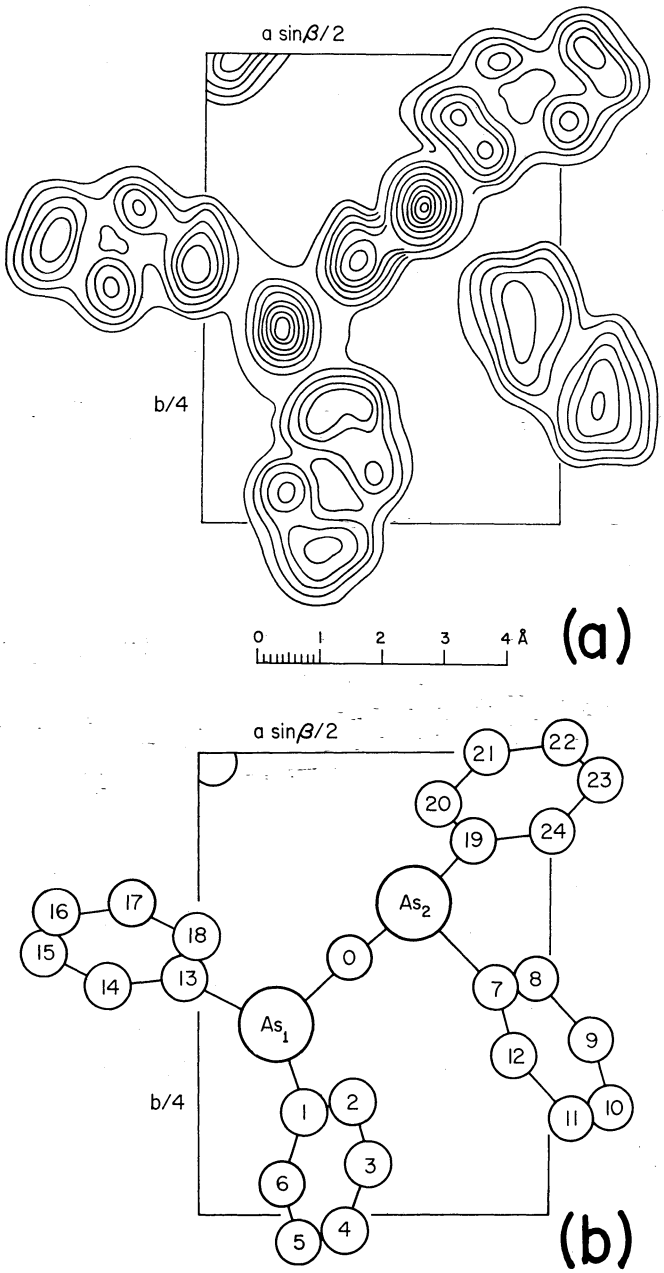

FIG. 1. (*a*) Electron-density projection along *c*. Contours start at 2 eÅ^{-2} and are at intervals of 1 eÅ^{-2}, except at the As atoms, where they start at 5 eÅ^{-2} and are at intervals of 5 eÅ^{-2}. (*b*) Projection of the molecule along ***c***.

Can. J. Chem. Downloaded from www.nrcresearchpress.com by 210.87.254.40 on 09/05/12
For personal use only.

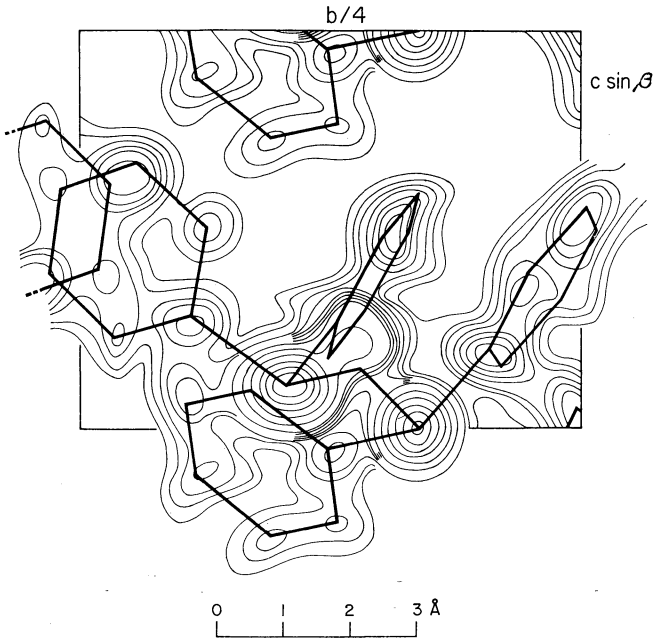

FIG. 2. Electron-density projection along *a*. Contours start at 2 eÅ^{-2} and are at intervals of 1 eÅ^{-2}, except above 10 eÅ^{-2}, where the interval is 5 eÅ^{-2}.

Coordinates and Molecular Dimensions

The final positional parameters are listed, as fractions of the unit cell edges, in Table I; the final temperature factor is $B = 6.0$ Å^2 for all the atoms. The coordinates of the half-atoms used to allow for anisotropic thermal motion of the arsenic atoms in the *c*-axis projection are included in the table. The standard deviations (5) are given in Table II.

The best planes through the four separate phenyl groups have equations:

I. C_1–C_6: $-0.8886\,X' + 0.1759\,Y + 0.4236\,Z' + 0.4598 = 0$,

II. C_7–C_{12}: $-0.6659\,X' - 0.5401\,Y - 0.5147\,Z' + 5.1276 = 0$,

III. C_{13}–C_{18}: $-0.1211\,X' - 0.8669\,Y + 0.4836\,Z' + 2.5522 = 0$,

IV. C_{19}–C_{24}: $+0.2170\,X' - 0.8098\,Y + 0.5451\,Z' + 3.3592 = 0$,

where X', Y, and Z' are coordinates in Å referred to orthogonal axes *a*, *b*, and *c**. None of the carbon atoms deviates significantly from the appropriate plane (maximum displacement 0.03 Å), and each arsenic atom also lies close to the planes of the groups to which it is bonded.

The bond lengths and valency angles in the molecule are given in Table III.

All the intermolecular contacts correspond to van der Waals interactions.

DISCUSSION

The standard deviations (Table II) indicate that the atomic positions (particularly for the carbon atoms) have not been determined very precisely, and only mean values of bond lengths and valency angles are quoted in Table III. Apart from the As—O distances and As—O—As angle, none of the dimensions require special comment: the means are 1.9 Å for As—C, 1.4 Å for C—C, 100° for C—As—C, 104° for C—As—O, and 120° for As—C—C and C—C—C. The mean As—O length is 1.67±0.03 Å, close to the distance in *o*-phenylenediarsine oxychloride (1.69 Å) (6). The As—O—As angle (137°±2°) is considerably larger than the usual valency angle at oxygen (e.g. 105° in H_2O (7)), but is rather similar to corresponding angles in other arsenic compounds, for example about 130° in As_4O_6 (7) and 151° in *o*-phenylenediarsine oxychloride (6) (the last angle is probably influenced by the fact that the As—O—As unit is part of a five-membered ring). The large

Can. J. Chem. Downloaded from www.nrcresearchpress.com by 210.87.254.40 on 09/05/12
For personal use only.

Can. J. Chem. Downloaded from www.nrcresearchpress.com by 210.87.254.40 on 09/05/12
For personal use only.

TABLE I

Fractional positional parameters. The coordinates of the half-atoms used to simulate thermal anisotropy in the *c*-axis projection are appended

Atom	*x*	*y*	*z*
As_1	0.1105	0.1034	0.1100
As_2	0.3075	0.1688	0.0000
O	0.216	0.141	0.154
C 1	0.153	0.056	0.284
2	0.221	0.062	0.502
3	0.246	0.028	0.668
4	0.210	−0.011	0.602
5	0.146	−0.017	0.390
6	0.118	0.017	0.228
7	0.426	0.123	−0.049
8	0.484	0.128	−0.234
9	0.565	0.095	−0.268
10	0.592	0.058	−0.117
11	0.532	0.053	0.065
12	0.452	0.086	0.099
13	−0.020	0.129	0.270
14	−0.131	0.124	0.175
15	−0.225	0.142	0.290
16	−0.207	0.163	0.492
17	−0.095	0.169	0.587
18	−0.003	0.151	0.483
19	0.394	0.203	0.200
20	0.345	0.223	0.392
21	0.413	0.251	0.555
22	0.528	0.257	0.502
23	0.575	0.236	0.320
24	0.507	0.210	0.155
As_1'	0.1105	0.0984	$B = 5.5$ Å^2
As_1''	0.1105	0.1084	5.5
As_2'	0.3075	0.1638	5.2
As_2''	0.3075	0.1738	5.2

TABLE II

Standard deviations (Å)

Atom	$\sigma(x)$	$\sigma(y)$	$\sigma(z)$
As	0.0048	0.0033	0.0058
O	0.049	0.033	0.059
C	0.079	0.054	0.096

TABLE III

Bond lengths (Å) and valency angles (degrees)

	Å		Degrees
As_1—C_1	1.82	C_1—As—C_{13}	102
As_1—C_{13}	1.99	C_7—As—C_{19}	98
As_2—C_7	1.98	Mean C—As—C	100
As_2—C_{19}	1.82		
Mean As—C	1.90	C_1—As—O	106
		C_{13}—As—O	103
As_1—O	1.67	C_7—As—O	101
As_2—O	1.67	C_{19}—As—O	105
Mean As—O	1.67	Mean C—As—O	104
		Mean As—C—C	120
24 C—C	1.28–1.48	Mean C—C—C	120
Mean C—C	1.40		
		As_1—O—As_2	137

angle in the present case is probably again a result of a change in the usual hybridization of the oxygen orbitals to form $p\pi$—$d\pi$ bonds involving donation of oxygen lone-pair electrons to vacant $4d$ orbitals on the arsenic atoms (6).

The orientations of the substituent phenyl groups, which depend on the equations of the mean planes, have been established more reliably than the individual bond lengths and angles. The shape of the molecule is illustrated in Fig. 3. It is seen that the two

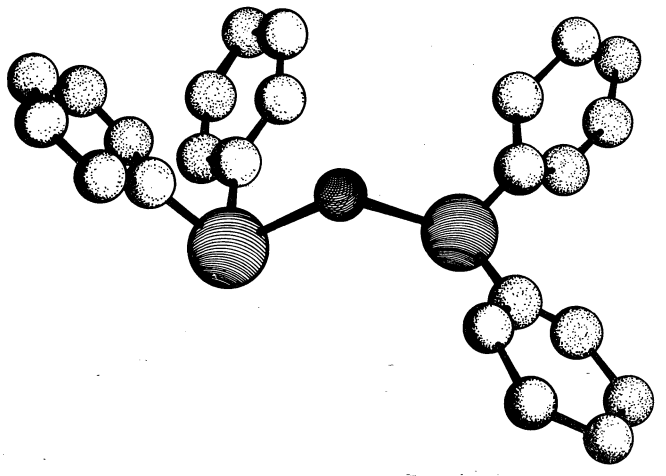

FIG. 3. Perspective drawing of the molecule.

Ph_2As units are not identical and are not related by any symmetry. The orientations of the separate phenyl groups are probably influenced to some extent by intermolecular interactions, and for this reason it is not considered useful to make comparisons with an ideal model as in the diphenylhalogenoarsines (8) and triarylarsines (9). Comparisons with various models can readily be made from the data in Table I.

We are indebted to the National Research Council of Canada and to the President's Research Fund, University of British Columbia, for financial support. We thank Dr. F. R. Ahmed for making available his IBM 1620 programs, and the staff of the UBC Computing Centre for assistance.

REFERENCES

1. W. R. CULLEN and J. TROTTER. Can. J. Chem. **39**, 2602 (1961).
2. T. C. FURNAS. Single crystal orienter instruction manual. General Electric Company, Milwaukee. 1957.
3. International tables for X-ray crystallography. Vol. III. Kynoch Press, Birmingham. 1962.
4. G. KARTHA and F. R. AHMED. Acta Cryst. **13**, 532 (1960).
5. D. W. J. CRUICKSHANK. Acta Cryst. **2**, 65 (1949).
6. W. R. CULLEN and J. TROTTER. Can. J. Chem. **40**, 1113 (1962).
7. TABLES OF INTERATOMIC DISTANCES and configuration in molecules and ions. Chem. Soc. Special Publ. No. 11. 1958.
8. J. TROTTER. Can. J. Chem. **40**, 1590 (1962).
9. J. TROTTER. Can. J. Chem. **41**, 14 (1963).

Can. J. Chem. Downloaded from www.nrcresearchpress.com by 210.87.254.40 on 09/05/12
For personal use only.

A LINEAR RELATIONSHIP BETWEEN BOND ORDERS AND STRETCHING FORCE CONSTANTS

E. A. ROBINSON AND M. W. LISTER
Department of Chemistry, University of Toronto, Toronto, Ontario
Received March 22, 1963

ABSTRACT

A linear correlation between the bond orders and stretching force constants of bonds, which appears to have general application, is derived on the basis of a potential energy function previously used by Pauling in a correlation of C—C bond length with bond order. The relationship is shown to be consistent with predicted bond orders and experimentally determined force constants of C—C, C—O, N—N, and N—O bonds.

The possible effects of anharmonicity and resonance energy on the force constant and equilibrium C—C bond distance are considered for the case of the benzene molecule, and it is concluded that the best agreement with experiment is obtained if we postulate a low degree of anharmonicity and allow for the change of resonance energy with bond distance.

INTRODUCTION

In a recent paper (1) one of us established a linear correlation between S—O stretching force constants and S—O bond orders; and a linear relationship between carbon single, double, and triple bond stretching constants and bond order has been suggested previously by Siebert (2) and by Somayajula (3). A similar relationship has been derived and discussed by Warhurst (4), who applied it to bonds in hydrogen halides. The object of the present paper is to examine the validity of this correlation, namely that the force constant of a bond between any two atoms is a linear function of the order of the bond, and to suggest a reason for it.

Pauling (5) examined the lengths of bonds with fractional bond orders in molecules such as benzene. He noted that the observed bond lengths were close to what one would calculate on the assumption that the observed structure was formed by distorting a conventional, nonresonating molecule (e.g. a Kekulé structure for benzene) to a shape with the symmetry of a resonance hybrid (a regular hexagon for benzene), and that the observed bond lengths were those corresponding to the minimum distortion energy. If the bonds are harmonic oscillators, the distortion energy per bond will be given by

$$V = \tfrac{1}{2}(2 - n)k_1(r - r_1)^2 + \tfrac{1}{2}(n - 1)k_2(r - r_2)^2, \qquad [1]$$

where V is the distortion energy, n is the total bond order, k_1 and r_1 are the force constant and length of a single bond, and k_2 and r_2 are the force constant and length of a double bond.

This assumes that the bond is between a single and double bond; a similar equation could be written for a bond between a double and triple bond. If we put $dv/dr = 0$, equation [1] leads to

$$r = \frac{(2 - n)k_1r_1 + (n - 1)k_2r_2}{(2 - n)k_1 + (n - 1)k_2}, \qquad [2]$$

which is the correlation between bond length and bond order obtained by Pauling; *or*

$$r = r_1 - \frac{r_1 - r_2}{1 + \dfrac{(2 - n)k_1}{(n - 1)k_2}}$$

Can. J. Chem. Downloaded from www.nrcresearchpress.com by 210.87.254.42 on 09/05/12
For personal use only.

as obtained by Coulson (6). Observed distances for C—C bonds agree moderately well with this equation. However, the precise degree of agreement depends on the value used for k_1/k_2, and for the bond order, n. As regards the latter, this can be most simply defined as the average number of electron pairs available per bond, which would make $n = 1.5$ in benzene if only the Kekulé structures are considered; or n may be derived from the coefficients of the atomic orbitals in the molecular orbital treatment of benzene. The latter treatment gives n (defined by $n = 1+\sum c_i c_j$) equal to 1.67 for benzene; Coulson (6, 7) has applied the molecular orbital method to carbon–carbon bonds in a variety of compounds; however, he gets agreement with equation [2] if $k_1/k_2 = 0.765$, which seems to be rather high for this ratio. Experimentally k_1/k_2 is about 0.46; and in fact if we take this value, and $n = 1.5$ for benzene, the calculated bond length is 1.403 Å, as compared with an observed 1.397 Å. Since the present paper is concerned primarily with the force constants, the question of bond lengths will not be pursued further, except in so far as they throw light on treatments of force constants.

The equation given above for V immediately leads to a linear relation between bond order and force constant, since if k is the force constant for the bond of intermediate order n, then

$$k = \frac{d^2V}{dr^2} = (2 - n)k_1 + (n - 1)k_2, \qquad [3]$$

which is the required relation. It is evident that similar considerations applied to a bond with n between 2 and 3 give

$$V = \tfrac{1}{2}(3 - n)k_2(r - r_2)^2 + \tfrac{1}{2}(n - 2)k_3(r - r_3)^2, \qquad [4]$$

whence

$$k = (3 - n)k_2 + (n - 2)k_3. \qquad [5]$$

It should be noted that these equations do not justify writing

$$k_2 = \tfrac{1}{2}(k_1 + k_3); \qquad [6]$$

which is the requirement that equations [3] and [5] represent the same straight line; however, there seems to be experimental evidence for equation [6], and we will therefore now consider this evidence. The question of the approximations made in assuming the above simple function for V will be left until later.

VALUES OF FORCE CONSTANTS

Values of stretching force constants are available in the literature for a fair number of molecules containing C—C, C—O, C—N, N—N, and N—O bonds. Since a variety of bond orders is exhibited by bonds between each pair of atoms these form the most suitable group for testing the proposed linear relation between force constant and bond order.

Only for diatomic molecules are values for the force constants easily and unequivocally calculated from the observed spectral frequencies, and even in these cases anharmonicity should be allowed for. For polyatomic molecules the values of the force constants, quite apart from errors due to neglect of anharmonicity, depend on the force field assumed. Generally, calculations in the past have been based on a simple valency force field (S.V.F.F.), or a S.V.F.F. plus one or more interaction terms. More recently the calculation of force constants has been based by some workers on a more general force field suggested by Urey and Bradley (8). This assumes in addition to a S.V.F.F. that there is a repulsive potential between all non-bonded atoms. Although this is probably a realistic

Can. J. Chem. Downloaded from www.nrcresearchpress.com by 210.87.254.42 on 09/05/12
For personal use only.

force field, it is difficult to apply in practice. For most of the fairly simple molecules considered in this paper, the S.V.F.F. plus some interaction terms is probably the most useful approach. More approximate and simpler methods have also been used quite successfully in cases when group frequencies can be assigned to a diatomic or triatomic group in a more complex molecule (1). At least it is to be hoped that the S.V.F.F. approach will remain useful in aiding our understanding of molecular structure. In the present paper we show that force constants obtained by the S.V.F.F. method can be correlated with bond orders.

Values of the force constants for C—C, C—N, C—O, N—N, and N—O bonds in a variety of molecules have been collected in Table I. Force constants for polyatomic groups are probably not accurate to better than 5–10%, since the values obtained are dependent

TABLE I

Bond lengths and bond orders for some C—C, C—N, C—O, N—N, and N—O bonds

Molecule	Bond	n	$k \times 10^{-5}$ (dynes cm^{-1})	Ref.
C_2H_6	C—C	1.0	4.5	*a*
C_2H_4	"	2.0	9.7	*a*
C_2H_2	"	3.0	15.6	*a*
C_6H_6	"	1.5	7.6	*b*
RNH_2	C—N	1.0	5.0	*c*
R_2NH	"	1.0	5.0	*c*
$C(NH_2)_3^+$	"	1.33	7.1	*d*
RCH=NR′	"	2.0	10.6	*e*
HCN	"	3.0	17.9	*f*
ClCN	"	3.0	16.7	*f*
BrCN	"	3.0	16.9	*f*
ICN	"	3.0	17.4	*g*
FCN	"	3.0	17.5	*f*
CN^-	"	3.0	17.5	*h*
CCl_3CN	"	3.0	17.7	*i*
CO	C—O	3.0	18.7	*j*
H_2CO	"	2.0	12.1	*a*
$CO_3^=$	"	1.33	8.2	*k*
HCO_3^-	"	1.5	9.1	*r*
CH_3OH	"	1.0	5.0	*g*
N_2	N—N	3.0	22.9	*l*
N_3^-	"	2.0	13.7	*j*
N_2H_4	"	1.0	3.6	*m*
NO^+	N—O	3.0	23.0	*n*
NOCl	"	2.0	14.0	*o*
NOBr	"	2.0	14.0	*o*
NO_2Cl	"	1.5	9.7	*p*
NO_2F	"	1.5	9.7	*p*
NO_3^-	"	1.33	8.4	*k*
$N_2O_2^{--}$	"	1.0	4.6	*n*
$(CH_3)_3NO$	"	1.0	4.4	*q*

REFERENCES
a. G. HERZBERG. Infra-red and raman spectra. Van Nostrand, New York. 1945. p. 193.
b. R. C. LORD and D. H. ANDREWS. J. Phys. Chem. **41**, 149 (1937).
c. J. E. STEWART. J. Chem. Phys. **30**, 1259 (1959).
d. L. KELLNER. Proc. Roy. Soc. (London), Ser. A, **177**, 456 (1940).
e. W. GORDY. J. Chem. Phys. **14**, 305 (1946).
f. G. R. HUNT and M. K. WILSON. J. Chem. Phys. **34**, 1301 (1961).
g. H. W. THOMPSON and J. N. LINNETT. J. Chem. Soc. 1291 (1937); 1399 (1937).
h. G. E. LEROI and W. KLEMPERER. J. Chem. Phys. **35**, 774 (1961).
i. W. F. EDGELL and C. J. ULTEE. J. Chem. Phys. **27**, 543 (1957).
j. P. GRAY and T. C. WADDINGTON. Trans. Faraday Soc. **53**, 901 (1957).
k. C. W. F. T. PISTORIUS. J. Chem. Phys. **29**, 1174 (1958).
l. G. R. SOMAYAJULA. J. Chem. Phys. **28**, 814 (1958).
m. P. A. GIGUERE and I. D. LIEU. Can. J. Chem. **30**, 948 (1952).
n. D. J. MILLEN, C. N. POLYDOROPOULOS, and D. WATSON. J. Chem. Soc. 687 (1960).
o. W. G. BURNS and H. J. BERNSTEIN. J. Chem. Phys. **18**, 1669 (1950).
p. M. G. KRISHNA-PILLAI. Z. Physik. chem. (Leipzig), **218**, 334 (1962).
q. J. GOUBEAU. Z. Anorg. Chem. **258**, 18 (1949).
r. This paper.

Can. J. Chem. Downloaded from www.nrcresearchpress.com by 210.87.254.42 on 09/05/12
For personal use only.

on the number of interaction constants in the potential function used in the calculation. Most of the bond orders in this table are those obtained by simple considerations of resonance structures. In the case of CO, NO^+, and CN^-, which are isoelectronic with the N_2 molecule, bond orders of 3 have been assumed.

Some of the numbers in Table I deserve special comment. The force constant for the C—N double bond in compounds of the type RHC=NR′ is taken as 10.7×10^5 dynes cm^{-1} calculated from the carbon–nitrogen stretching frequency in acetoxime CH_3CH=NOH. The guanidinium ion $C(NH_2)_3^+$ is assigned a bond order of 4/3 on the assumption that there are eight electrons round the carbon atom. The azide ion is predominantly $\overset{-}{N}=\overset{+}{N}=\overset{-}{N}$, and although structures such as $N\equiv\overset{+}{N}-\overset{2-}{N}$ must contribute somewhat, these still leave the average bond order as 2.0. The nitrate ion is presumably a resonance hybrid of structures of type $O=\overset{+}{N}\begin{matrix}\diagup O^-\\ \diagdown O^-\end{matrix}$, making the bond order 1.33.

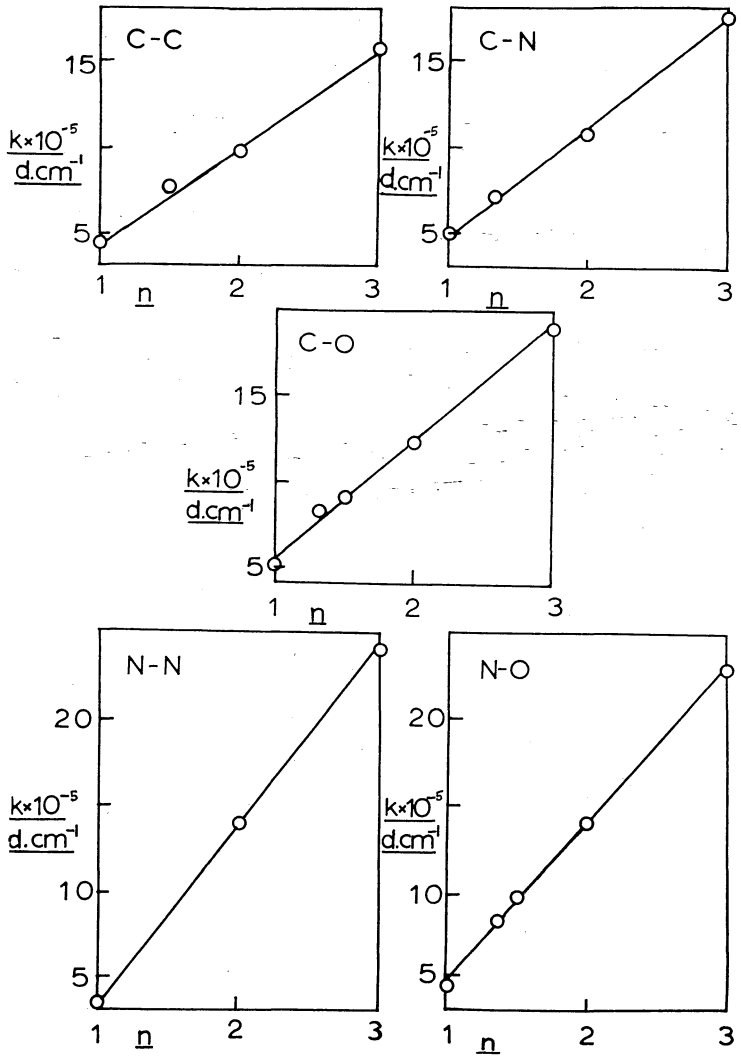

FIG. 1. Bond order – force constant relationships for C—C, C—N, C—O, N—N, and N—O bonds.

Can. J. Chem. Downloaded from www.nrcresearchpress.com by 210.87.254.42 on 09/05/12
For personal use only.

Figure 1 shows the force constants plotted against bond order and in every case a fairly good straight line is obtained. Hence there is experimental justification for the proposed linear relation of force constant and bond order.

DISCUSSION

Two aspects of this correlation deserve further comment. Firstly, as mentioned above neither equation [3] nor [5] requires that $2k_2 = k_1+k_3$, and in fact at present this can be only justified experimentally, as is shown in Table II. It might be suggested that any bond

TABLE II

Constants of single and multiple C—C, C—N, C—O, N—N, and N—O bonds $k\times10^{-5}$ (dynes cm^{-1})

	k_1	k_2	k_3	k_1+k_3	$2k_2$
C—C	4.5	9.7	15.6	20.1	19.4
C—N	5.0	10.7	17.5	22.5	21.4
C—O	5.0	12.1	18.7	23.7	24.2
N—N	3.6	13.7	22.9	26.5	27.4
N—O	4.5	14.0	23.0	27.5	28.0

intermediate between a single and a triple bond should be considered in terms of them, in which case the corresponding potential would be

$$V = \frac{1}{2}\frac{(3-n)}{(2)}k_1(r-r_1)^2+\frac{1}{2}\frac{(n-1)}{(2)}k_3(r-r_3)^2,$$

which gives $k = \frac{1}{2}(3-n)k_1+\frac{1}{2}(n-1)k_3$, and if $n = 2$ then $k_2 = \frac{1}{2}(k_1+k_3)$, as is observed. The distance calculated for intermediate bonds will be

$$r = \frac{(3-n)k_1r_1+(n-1)k_3r_3}{(3-n)k_1+(n-1)k_3}$$

and if $n = 2$

$$r_2 = \frac{k_1r_1+k_3r_3}{k_1+k_3}.$$

Putting in the appropriate values for C—C bonds unfortunately makes $r_2 = 1.28$, which is much too short. Hence the relation $2k_2 = k_1+k_3$ cannot be justified in this way.

Secondly, when we consider compounds containing non-integral double bonds, and benzene in particular, it is evident that a simple potential function like [1] above ignores the effect of certain factors, particularly resonance energy and anharmonicity. Somewhat more detailed considerations were attempted, as follows, using the benzene molecule as a test case.

Suppose we rather artificially consider converting a Kekulé structure for benzene into a resonance hybrid by the steps

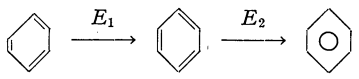

I II III

Here I is a Kekulé structure; in II it is deformed to a regular hexagon, and in III delocalization of the π bonds is included. If the energy change for the transition from I to

Can. J. Chem. Downloaded from www.nrcresearchpress.com by 210.87.254.42 on 09/05/12
For personal use only.

III can be calculated for different ring sizes, then the equilibrium distance, r_e, will correspond to the minimum (i.e. most negative) value for this energy; and from the variation of energy with distance, we can calculate the force constant.

If the bonds are harmonic oscillators, E_1 is given by

$$E_1 = \frac{3}{2}k_1(r - r_1)^2 + \frac{3}{2}k_2(r - r_2)^2.$$

If this is the sole energy term $6k = d^2E_1/dr^2 = 3k_1 + 3k_2$. This gives $k = 7.1 \times 10^{-5}$ dynes cm^{-1} and $r_e = 1.403$ Å for the equilibrium distance. However, the bonds are presumably anharmonic oscillators. No reliable data seem to be available for the anharmonicity of a carbon–carbon bond in a state that is directly applicable to benzene. Spectral data on the C_2 molecule (10) make its potential energy

$$V = 1179.4\frac{(\delta r)^2}{(r_e)} - 2176.8\frac{(\delta r)^3}{(r_e)}$$

where $\delta r = r - r_e$, and r_e is the equilibrium distance. V is in kcal/g-mole. Data of this sort were examined for a variety of diatomic molecules (9); in general we can write

$$V = c_1\frac{\delta r^2}{r_e} - c_2\frac{\delta r^3}{r_e}$$

and it was found that the ratio c_2/c_1 varied only over a small range. Some typical values of c_2/c_1 are given below:

Molecule	Br_2	BrF	I_2	ICl	Cl_2	HF	HCl	HBr	HI	Na_2	
c_2/c_1	2.51	2.00	2.80	2.47	2.80	1.43	1.52	1.59	1.69	1.22	
Molecule	OH	O_2	S_2	Se_2	SO	N_2	P_2	As_2	CN	CO	NO
c_2/c_1	1.44	2.17	2.15	2.36	2.03	1.85	2.10	2.06	1.81	1.82	1.87

There is no particular drift of c_2/c_1 with bond order, or with the position of the atoms in the Periodic Table, though the halogens seem to give rather higher values than other diatomics. Probably a value for carbon between 1.5 and 2 would be correct, and the equilibrium distance and force constant of benzene were calculated with these two values of c_2/c_1. Again this is at present considering only the step I to II. The results were

c_2/c_1	1.5	2.0	Benzene
r_e	1.417	1.423 Å	
k	6.67	6.67×10^5 dynes cm^{-1}	

The effect of including anharmonicity is to make both r_e and k agree less well with experiment.

Another factor that should be considered is that the resonance energy will vary with distance. An estimate of this can be made as follows. If we use the Hückel molecular orbital treatment (10), but do not assume that S, the overlap integral between nearest neighbors is zero, the roots of the secular determinant give for the energy of various molecular orbitals

$$\epsilon = \frac{\alpha - n_i\beta}{1 - n_iS}$$

Can. J. Chem. Downloaded from www.nrcresearchpress.com by 210.87.254.42 on 09/05/12
For personal use only.

where α is the coulomb integral, β the exchange integral, and n_i can have the values -2, -1, -1, 1, 1, and 2. For six electrons in benzene this makes the resonance energy,

$$\Delta\epsilon = \frac{2(\beta - \alpha S)}{(1+S)(1+2S)}.$$

β will vary with distance, and as a first approximation we may take $\beta = \beta_0 S$, as is often done (11). Here β_0 is a constant. This makes the resonance energy

$$\Delta\epsilon = \frac{2S}{1+3S+2S^2} \cdot (\beta_0 - \alpha).$$

The S integrals have been evaluated by Mulliken, Rieke, Orloff, and Orloff (12) for a variety of wave functions and distances, and S can be obtained from their tables. The quantity $(\beta_0 - \alpha)$ can be selected to give the observed effective resonance stabilization of benzene (36 kcal) at the equilibrium distance.

The results of this calculation, on the assumption of harmonic potentials for the bond distortions, are $r_e = 1.395$ Å, $k = 7.22\times10^5$ dynes cm^{-1}. Inclusion of anharmonicity, with $c_2/c_1 = 1.5$, gives $r_e = 1.408$ Å and $k = 6.84\times10^5$ dynes cm^{-1}. If a Morse curve

$$V = D_e(1 - e^{-a(r-r_e)})^2,$$

where D_e is the dissociation energy of the bond, and a is a constant, is used for the distortion of the single and double bonds, the results are $r_e = 1.423$ Å, and $k = 7.22\times10^5$ dynes cm^{-1}. These are to be compared with the experimental $r_e = 1.397$ Å and $k = 7.6\times10^5$ dynes cm^{-1}. The results are summarized in Table III.

TABLE III

Calculated r_e and k for benzene

$k_1 = 4.5\times10^5$ $k_2 = 9.7\times10^5$ $r_1 = 1.54$ Å $r_2 = 1.34$ Å

Vibrational terms	Resonance	r_e(Å)	$k\times10^{-5}$ (dynes cm^{-1})
Harmonic	No	1.403	7.10
"	Yes	1.395	7.22
Morse function	Yes	1.423	7.22
Anharmonic $c_2/c_1 = 1.5$	No	1.417	6.67
" $c_2/c_1 = 1.5$	Yes	1.408	6.84
" $c_2/c_1 = 2.0$	No	1.423	6.67
" $c_2/c_1 = 2.0$	Yes	1.413	6.65

Hence the best agreement comes if we postulate a very low anharmonicity in the bonds, and allow for the resonance energy varying with distance. This explains qualitatively the fact that k for benzene is somewhat above $1/2(k_1+k_2)$, but does not make it enough above this average value. It gives fairly good agreement with the observed distance.

In the above calculations the distance for the single bond was taken to be 1.54 Å as in diamond or ethane. However, these contain σ-bonds with sp^3 hybridization, while in benzene the σ-bonds are sp^2 hybrids. The distance between two carbon atoms with sp^2 hybridization, but joined by a single bond has been derived and found to be 1.504 Å (ref. 5, p. 236), 1.50 Å (13), and 1.503 Å (14). If a mean value of 1.503 Å is used in the calculations, the slightly modified results given in Table IV are obtained. There is now good agreement with the observed distance on the assumption of a moderate degree of anharmonicity ($c_2/c_1 = 2.0$), with due allowance for the effect of resonance. However, the calculated force constants are in general below the observed value, and usually below

Can. J. Chem. Downloaded from www.nrcresearchpress.com by 210.87.254.42 on 09/05/12
For personal use only.

TABLE IV

Calculated r_e and k for benzene

$k_1 = 4.5\times10^5$ $k_2 = 9.7\times10^5$ $r_1 = 1.503$ Å $r_2 = 1.34$ Å

Vibrational terms		Resonance	r_e(Å)	$k\times10^{-5}$ (dynes cm^{-1})
Harmonic		No	1.392	7.10
"		Yes	1.385	7.21
Morse function		Yes	1.404	7.01
Anharmonic	$c_2/c_1 = 1.5$	No	1.401	6.83
"	$c_2/c_1 = 1.5$	Yes	1.394	7.08
"	$c_2/c_1 = 2.0$	No	1.404	6.81
"	$c_2/c_1 = 2.0$	Yes	1.397	6.95

$\frac{1}{2}(k_1+k_2)$. Only for a harmonic bond is k for benzene above $\frac{1}{2}(k_1+k_2)$, and then the bond length is a little too short.

In every other case noted in Table I for fractional bond orders the observed k is a little higher than that calculated from the simple linear relation. These deviations can be at least partially explained by allowing for variation of resonance energy with distance, though, as with benzene, it is necessary to assume very little anharmonicity. In contrast to the behavior of fractional bonds, it is found that when only single, double, and triple bonds are considered, the deviations from $k_2 = \frac{1}{2}(k_1+k_3)$ are small, and occur in both directions.

ACKNOWLEDGMENT

The National Research Council of Canada is thanked for generous financial support.

REFERENCES

1. R. J. Gillespie and E. A. Robinson. Can. J. Chem. **41**, 2074 (1963).
2. H. Siebert. Z. Anorg. Allgem. Chem. **273**, 170 (1953).
3. G. R. Somayajula. J. Chem. Phys. **29**, 814 (1959).
4. E. Warhurst. Trans. Faraday Soc. **40**, 26 (1944).
5. L. Pauling. Nature of the chemical bond. 3rd ed. Cornell, Ithaca, New York. 1960. p. 235.
6. C. A. Coulson. Proc. Roy. Soc. (London), Ser. A, **168**, 413 (1939).
7. C. A. Coulson. Proc. Roy. Soc. (London), Ser. A, **207**, 306 (1951).
8. H. Urey and C. A. Bradley. Phys. Rev. **38**, 1969 (1931).
9. G. Herzberg. Spectra of diatomic molecules. 2nd ed. Van Nostrand, New York. 1950. p. 502.
10. E. Hückel. Z. Physik, **70**, 204 (1931).
11. R. S. Mulliken. J. Phys. Chem. **56**, 295 (1952).
12. R. S. Mulliken, C. A. Rieke, D. Orloff, and H. Orloff. J. Chem. Phys. **17**, 1248 (1949).
13. H. C. Longuet-Higgins. Proc. Roy. Soc. (London), Ser. A, **251**, 172 (1959).
14. H. J. Bernstein. Trans. Faraday Soc. **57**, 1649 (1961).

Can. J. Chem. Downloaded from www.nrcresearchpress.com by 210.87.254.42 on 09/05/12
For personal use only.

TERPENOIDS

IV. THE STRUCTURE AND STEREOCHEMISTRY OF HELMINTHOSPORAL[1]

P. DE MAYO
Department of Chemistry, University of Western Ontario, London, Ontario

AND

E. Y. SPENCER AND ROBERT W. WHITE
Agricultural Research Institute,[2] Canada Department of Agriculture, London, Ontario

Received June 28, 1963

ABSTRACT

Helminthosporal has been converted into the anhydride (X), which has been dehydrogenated to give (VI): this compound has been synthesized. Spectroscopic study of a number of derivatives of helminthosporal has enabled a decision to be made in favor of (XXVI; R = CHO) as a representation of the structure and stereochemistry of the dialdehyde.

In an earlier publication (3) the isolation and characterization of helminthosporal, the toxin from *Helminthosporium sativum* responsible for widespread cereal crop damage, was reported. It was established that this substance contained, as functional groups, a saturated aldehyde and a fully substituted $\alpha\beta$-unsaturated aldehyde, as summarized in the part formulae (I), and that, furthermore, it contained two carbocyclic rings with no

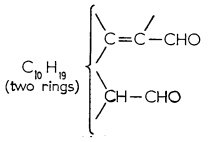

(I)

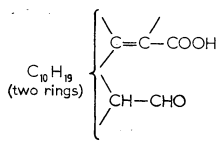

(II)

other centers of unsaturation. The presence of a methyl group as one of the substituents on the ethylenic linkage was shown by the presence of a singlet (3H) at τ 7.91 in the dialdehyde and 8.0 in the corresponding unsaturated acid (II) (3): in the oxime from this acid (3) the band appeared at τ 8.3. The next objective was to ascertain the size and mode of fusion of the two carbocyclic rings.

Reduction of (II) with sodium borohydride has been shown to give a γ-lactone (3). This lactone is not formed, however, by simple closure between the carboxyl and the newly formed alcoholic function. No indication was found, in the appropriate region of the n.m.r. spectrum, of the presence of the methylene protons in a —C$\underline{H_2}$—O—CO— grouping. On the other hand the peak at τ 8.0, already attributed to the vinyl methyl group, moved in the reduction and lactonization to τ 8.6. The infrared spectrum (bands at 3080, 1615, and 905 cm^{-1}) and n.m.r. spectrum (doublets at τ 4.74, 5.03; $J \sim 2$ c.p.s.) gave indication of the presence of an exocyclic methylene group, and this was confirmed by the obtention of formaldehyde (3) on ozonolysis. These observations led to the conclusion that the formation of the lactone involved an allylic rearrangement, as indicated

[1]*Part of the following constituted a preliminary communication (1). Reference 2 is considered part III in this series.*
[2]*University sub Post Office, London, Ontario.*

Can. J. Chem. Downloaded from www.nrcresearchpress.com by 210.87.254.42 on 09/05/12
For personal use only.

in (III), and this conclusion was substantiated when it was found that, by reduction with lithium aluminum hydride, a crystalline diol, characterized as the acetate, was obtained which was different from that obtained by lithium aluminum hydride reduction of helminthosporal itself.

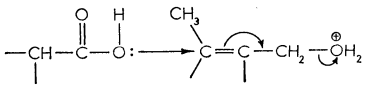

(III)

This lactone gave the expected diol with osmium tetroxide (3), which has been further characterized as the monoacetate. On cleavage with periodic acid a ketone was obtained with the concomitant loss of one carbon atom as formaldehyde. This ketone showed maxima in the infrared at 1802 and 1767 cm^{-1}, one of which was to be attributed to the γ-lactone carbonyl and the other to that of the new cyclanone. It was presumed that these high values were associated with α-oxygen substitution of the cyclic ketone, and this view was confirmed when it was found that zinc and acetic acid reduction gave a keto acid with maxima at 1745 and 1703 cm^{-1}. Since the band at 1703 is to be attributed to the carboxyl carbonyl the new carbonyl was revealed as being present in a five-membered ring. These results may be expressed in terms of the part formulae (V), *a*, *b*, or *c* for the keto lactone and the corresponding (IV), *a*, *b*, or *c* for helminthosporal.

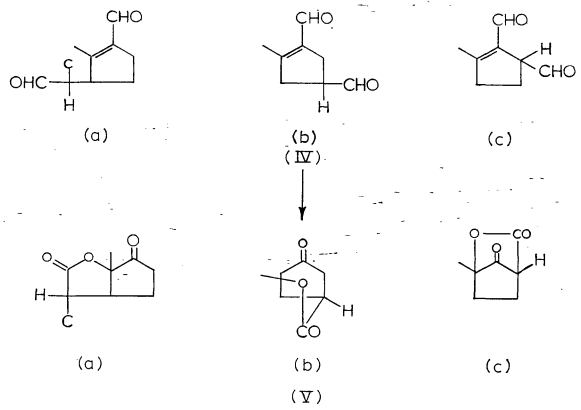

(IV)

(V)

The nature of the second carbocyclic ring was elucidated directly. Ozonolysis of helminthosporal, of (II), or of the borohydride reduction product of (II), gave, after heating, a substance to which the empirical formula $C_{14}H_{20}O_4$ is attributed. The nature of this substance will be discussed below; however, at this point, it may be noted that the loss of only one carbon atom in the ozonolysis excludes (IV*c*), since by the oxidative cleavage a β-dicarbonyl compound would be produced which should suffer a further loss of carbon dioxide or equivalent.

Dehydrogenation of the substance, $C_{14}H_{20}O_4$, gave a crystalline anhydride, $C_{12}H_{12}O_3$, the infrared spectrum of which was similar to that of phthalic anhydride. Its ultraviolet absorption (λ_{max} 253, 307, 318, ϵ_{max} 3000, 3100, 3100 respectively) was also similar to that of phthalic anhydride, but displaced to somewhat longer wavelengths. The n.m.r. spectrum contained a doublet (6H) at τ 8.67 ($J \sim 9.6$ c.p.s.), which bespoke the presence of an

Can. J. Chem. Downloaded from www.nrcresearchpress.com by 210.87.254.42 on 09/05/12
For personal use only.

isopropyl group, whilst a band (singlet, 3H) at τ 7.32 indicated the attachment of a methyl group to the aromatic ring. Two barely resolved singlets at τ 2.4 were to be attributed to two aromatic hydrogen atoms in a nearly identical physical environment. These facts were accommodated by the structure (VI) which also enjoyed inherent biogenetic plausibility. The substance represented by this formula was therefore synthesized.

Isobutyl bromide was converted to the Wittig reagent and condensed with crotonaldehyde. The resultant mixture of dienes was heated with maleic anhydride under the conditions of the Diels-Alder reaction; from the products the crystalline anhydride (VII) was readily isolated. Dehydrogenation then gave (VI), identical in every respect with the product obtained from helminthosporal.

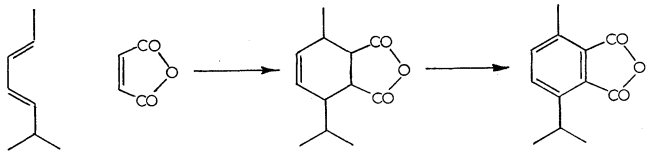

(VII) (VI)

The anhydride (VI) contains 12 of the original carbon atoms present in helminthosporal. Of the two potential carboxyl groups constituting the anhydride, one must be derived, eventually, from the saturated aldehyde in helminthosporal whilst the other must be derived from the α-keto aldehyde formed by cleavage of the ethylenic linkage. Since the two carboxyl functions are vicinal a decision can now be made between (IV*b*), which would permit this feature, and (IV*a*), which would not.

The complete structure of helminthosporal may be arrived at by the combination of the skeleton represented by (VI) and that represented by (IV*b*). This may be accomplished in two ways only leading to (VIII) and (IX) as possible representations of helminthosporal. A decision between these alternatives was possible from a study of the compound $C_{14}H_{20}O_4$ already mentioned, and, for simplicity, further discussion will be in terms of (IX), the formulation finally arrived at.

This substance, $C_{14}H_{20}O_4$, had maxima in the infrared spectrum at 1790 and 1820 cm^{-1}, both absorption bands being strong and broad: it was not, therefore, the expected keto anhydride (X). On mild hydrolysis, however, a dibasic acid, $C_{14}H_{22}O_5$, was formed (XI, R = H) which gave an oily dimethyl ester (XI, R = Me). In this substance, in addition to the ester carbonyl absorption at 1740 cm^{-1}, there could be observed the required acetyl carbonyl at 1715 cm^{-1}. In agreement, reduction with sodium borohydride gave rise to the γ-lactone (XII).

From these results it was concluded that a dilactonic structure (XIII) must be ascribed to the compound $C_{14}H_{20}O_4$. This interpretation was supported by the n.m.r. spectrum which exhibited, in addition to the required two singlet methyl bands (at τ 8.4 and 8.85), a doublet (1H) at τ 7.6 ($J \sim 3.6$ c.p.s.) and a multiplet (1H) at τ 6.89; this and the spectra of other derivatives (4) (see below) exclude formulations based on (VIII) for these substances. In addition, the presence of two doublets (6H) in the methyl region (see also Fig. 1) reveals the presence of the isopropyl group in (XIII), and, therefore, in helminthosporal itself, and excludes the possibility that ring contraction or rearrangement had taken place on dehydrogenation.

The dilactonic structure (XIII) has ample analogy: such a formulation has been established, for instance, for a derivative of δ-ketopimelic acid. For the latter we have

Can. J. Chem. Downloaded from www.nrcresearchpress.com by 210.87.254.42 on 09/05/12
For personal use only.

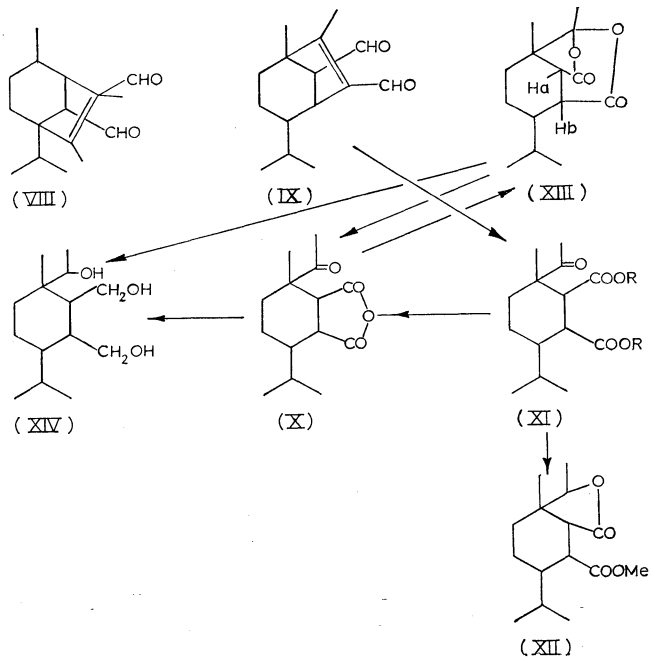

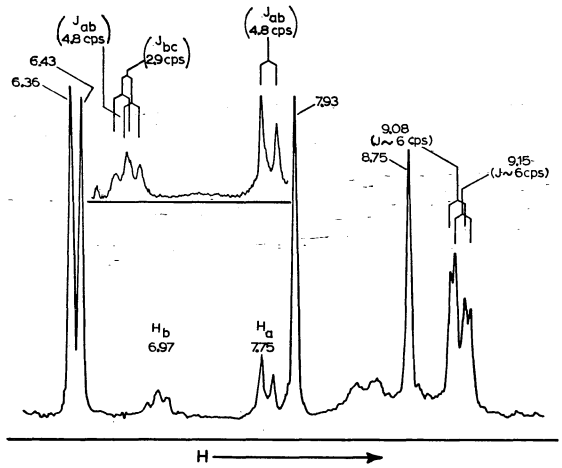

FIG. 1. Nuclear magnetic resonance spectrum of the dicarboxylic ester (XI, R = Me).

observed a broad maximum in the infrared spectrum at 1790 cm^{-1}. However, to complete the structural proof it was desirable to obtain the keto anhydride (X) itself. This was achieved by heating (XI, R = H) with acetic anhydride. At a higher temperature (X) was converted into (XIII). Both compounds gave the same triol (XIV) on reduction with lithium aluminum hydride precluding the possibility of thermal rearrangement of the carbon skeleton at the higher temperature.

With the gross structure of helminthosporal established as (IX) it remains to consider how the dilactone (XIII) is formed, together with the keto lactone [now to be formulated

Can. J. Chem. Downloaded from www.nrcresearchpress.com by 210.87.254.42 on 09/05/12
For personal use only.

as (XV)], by ozonolysis of the borohydride reduction product (XVI) of the aldehyde acid (XVII). This may most simply be explained by postulating the intermediate formation of the ozonide followed by decomposition in the manner indicated in (XVIII).

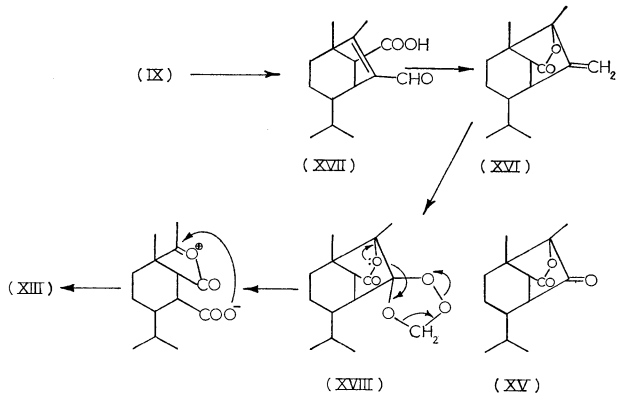

The bridged system in helminthosporal defines the stereochemistry in all but two points: the configuration of the isopropyl group with respect to the carbon bridge, and the configuration of the saturated aldehyde. In the derived aldehyde–acid (XVII) the configuration of the corresponding carboxyl group is defined by the formation of the lactone (XVI). The stereochemistry of the diester (XI, R = Me) may therefore be represented by the alternatives (XIX) and (XX). In the former case the most probable conformation is that depicted, but in the epimer (XX) conformational inversion to (XXI) (mirror image represented) must be expected.

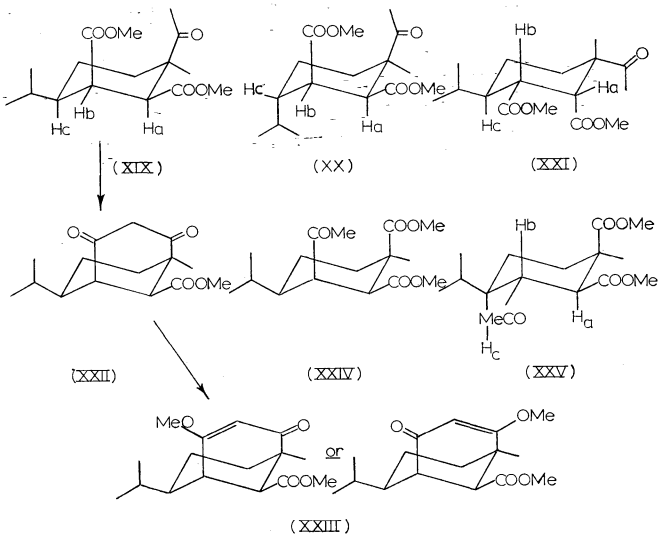

In (XIX) both H_a and H_b would be expected to be weakly coupled since interactions are between axial and equatorial hydrogen atoms. In (XXI) H_b undergoes both a diaxial and an axial–equatorial coupling. Inspection of the n.m.r. spectrum of (XI, R = Me) [see Fig. 1] shows that J_{ab} is ~4.8 c.p.s. and that J_{bc} is smaller, probably about 3 c.p.s.

Can. J. Chem. Downloaded from www.nrcresearchpress.com by 210.87.254.42 on 09/05/12
For personal use only.

The spectrum also shows the isopropyl group at τ 9.15 and 9.08 ($J \sim 6$ c.p.s.) and the singlet methyl (at τ 8.75). This evidence therefore supports the assignment of (XIX) as the steric representation of (XI, R = Me).

In (XIX) one carbomethoxyl group and the acetyl group are situated 1:3 and diaxial. In consequence the ketone may be expected to be hindered (even for a *t*-butyl ketone) and bridging reactions may be expected to be facile. Indeed no derivative of the ketone could be made even under forcing conditions, but treatment with potassium *t*-butoxide readily induced cyclization with the formation of a β-diketone (XXII) characterized as the crystalline enol ether (XXIII).

Using sodium methoxide, followed by hydrolysis, (XIX) was converted into a dicarboxylic acid monomethyl ester which resisted attempts at further hydrolysis. This substance gave, with diazomethane, a diester different from (XIX). Since the monoester could not be hydrolyzed it must be presumed that the intermediate (XXII) has opened in the opposite sense from its formation to give a tertiary carbomethoxyl group as in (XXIV). But under the conditions of formation the acetyl group would now be expected to invert from its axial configuration to the more stable equatorial arrangement. The final diester may thus be formulated as (XXV).

In this keto diester, from which a 2,4-dinitrophenylhydrazone could now be derived, the couplings between H_a, H_b, and H_c are all those of diaxial protons. They should be considerably larger than those in (XIX) (5); in fact J_{ab} was about 11 c.p.s. and J_{bc} was also large though the pattern did not permit the assignment of an exact figure.

It is concluded that (XI, R = Me) is correctly designated by (XIX) and thus that (XXVI, R = COOH) is a steric representation of (XVII). Provided no inversion of the aldehyde has taken place in the formation of (XVII) from (IX), helminthosporal may be represented by (XXVI, R = CHO). That this condition has been fulfilled has been shown by the reduction of (XVII) with lithium aluminum hydride to give the same diol, characterized as the 3,5-dinitrobenzoate, as was obtained from helminthosporal (3).[3]

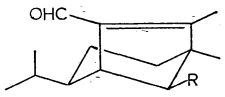

(XXVI)

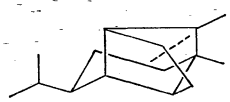

(XXVII)

Inspection of the helminthosporal skeleton reveals that, although constructed from three isoprene units, it is not to be formed by simple cyclization of a farnesyl precursor. We have shown elsewhere (2) that it is most probably derived from a tricyclic precursor with a carbon skeleton such as (XXVII) by oxidative cleavage at the bond indicated.

EXPERIMENTAL

Infrared spectra and n.m.r. spectra were determined in carbon tetrachloride solution, ultraviolet spectra in ethanol, and rotations in chloroform. Light petroleum refers to the fraction of b.p. 35–60°. Melting points were determined on the Köfler hot stage.

The n.m.r. spectra were determined using 1% tetramethylsilane as internal standard using a Varian D.P. 60 spectrometer. The peak positions were determined using an audio oscillator calibrated with a Hewlett Packard 522-B frequency counter.

[3]*The remaining possibility, that epimerization may occur during hydride reduction, whilst not an unknown phenomenon (6), is exceedingly improbable since, in such a delicately balanced situation the aldehyde would certainly have epimerized during isolation.*

Can. J. Chem. Downloaded from www.nrcresearchpress.com by 210.87.254.42 on 09/05/12
For personal use only.

Preparation of the Keto Lactone (XV)

To the diol from the unsaturated lactone (3) (69 mg) in ethanol (4 ml) was added aqueous periodic acid solution (0.01 *N*; 5 ml). After 24 hours, titration of an aliquot indicated an uptake of 0.95 atoms of oxygen. Dilution of the mixture with water, filtration, and crystallization from light petroleum ether gave the keto lactone (XV), m.p. 123–124°, $[\alpha]_D$ +40° (*c*, 1.14), ν_{max} 1802, 1767 cm^{-1}. Calc. for $C_{14}H_{20}O_3$: C, 71.16; H, 8.53. Found: 71.16; 8.49%. The ketone was not brominated in bromine/acetic acid.

Lithium Aluminum Hydride Reduction of the Lactone (XVI)

The lactone (50 mg) was refluxed in ethereal solution containing an excess of lithium aluminum hydride. The diol, isolated in the usual way, was crystallized from light petroleum, m.p. 113.5–114°, $[\alpha]_D$ +38° (*c*, 1.02). Calc. for $C_{15}H_{26}O_2$: C, 75.58; H, 11.00. Found: C, 75.38; H, 10.63%. The monoacetate (acetic anhydride – pyridine at room temperature overnight) had m.p. 80.5–82° (crystallized from light petroleum). Calc. for $C_{17}H_{28}O_3$: C, 72.82; H, 10.06. Found: C, 72.77; H, 9.73%.

Reduction of the Keto Lactone (XV)

The keto lactone (720 mg) was dissolved in glacial acetic acid (100 ml) and activated zinc (30 g) added. The mixture was refluxed for 96 hours, the acetic acid removed by evaporation and the acidic material isolated with aqueous sodium bicarbonate. After crystallization from ether – light petroleum the keto acid was obtained, m.p. 140–142°, $[\alpha]_D$ −66° (*c*, 1.02) ν_{max} 1746, 1703 cm^{-1}. Calc. for $C_{14}H_{22}O_3$: C, 70.55; H, 9.31. Found: C, 70.88; 9.28%.

The Nordilactone (XIII)

(*a*) The aldehyde–acid (XXVI, R = COOH) (100 mg) in ethyl acetate (15 ml) was cooled to −70° and ozone passed until disappearance of the peak at 265 mμ. After evaporation of the solvent, aqueous sodium hydroxide (5%: 10 ml) and hydrogen peroxide (30%: 1 ml) were added and the mixture heated on the steam bath for 1 hour. Isolation of the acidic product in the usual way gave a glass which was heated for 15 hours at 130° under nitrogen. Chromatography of this product on silica gel gave, on elution with benzene, the nordilactone (XIII). Crystallization from light petroleum (b.p. 60–80°) afforded material of m.p. 76.5–77° (56 mg), $[\alpha]_D$ +70° (*c*, 1.01) ν_{max} 1820, 1790 cm^{-1}. Calc. for $C_{14}H_{20}O_4$: C, 66.64; H, 7.99; M.W. 252. Found: C, 66.66; H, 8.06%, M.W. (mass spectrum) 252.

(*b*) Similar ozonolysis of the lactone (XVI) gave formaldehyde, the keto lactone (XV) (identical in every way with the material obtained from periodic acid cleavage), and the nordilactone, the latter two substances in poor yield.

Hydrolysis of the Nordilactone (XIII)

The nordilactone (50 mg) was dissolved in alcoholic alkali (50% aqueous: 5% sodium hydroxide) and refluxed for 1 hour. Isolation of the acidic material gave, on crystallization from light petroleum, the nordiacid (XI, R = H) m.p. 143.5–145°, $[\alpha]_D$ −70° (*c*, 1.01). Calc. for $C_{14}H_{22}O_5$: C, 62.20; H, 8.20. Found: C, 62.10; H, 8.17%.

Treatment with ethereal diazomethane gave the corresponding dimethyl ester (XI, R = Me), n_D^{25} 1.4785. Calc. for $C_{16}H_{26}O_5$: C, 64.40; H, 8.78; OMe (2), 20.80. Found: C, 64.70; H, 8.41; OMe, 19.90%.

Reduction of the Nordilactone (XIII)

The dilactone (25 mg) was added to a solution of lithium aluminum hydride (100 mg) in ether and the mixture allowed to stand overnight. After decomposition of the excess reagent with ethyl acetate and sodium potassium tartrate the product was isolated with ether and crystallized from ether – light petroleum (b.p. 60–80°) to give the triol (XIV), m.p. 158.5–159.5°, $[\alpha]_D$ ±0° (*c*, 0.55). Calc. for $C_{14}H_{28}O_3$: C, 68.81; H, 11.55. Found: C, 68.47; 11.62%.

The Norketo Anhydride (X)

The nordiacid (from 100 mg nordilactone) was heated with acetic anhydride for 5 hours at 150° (bath temperature). The acetic anhydride was then removed *in vacuo* and the residue crystallized from chloroform – light petroleum (60–80°) to give the anhydride (70 mg) m.p. ca. 140° and 156–158°, $[\alpha]_D$ −31° (*c*, 0.93), ν_{max} 1850, 1780, 1720 cm^{-1}. Calc. for $C_{14}H_{20}O_4$: C, 66.64; H, 7.99. Found: C, 67.14; H, 8.05%.

Reduction of the anhydride as described for the dilactone gave the same triol, m.p. and mixed m.p. 158.5–159.5°.

Reduction of the Nordimethyl Ester (XI, R = Me) with Sodium Borohydride

To the ester (200 mg) in 50% aqueous ethanol (40 ml) was added sodium borohydride (1 g). After 3 hours at room temperature the product was isolated in the usual way. Chromatography on silica gel (10 g) afforded a partial separation of the mixture so obtained, elution with benzene giving an oil which gradually solidified. Crystallization from light petroleum (b.p. 60–80°) gave the lactone ester (XII) m.p. 72.5–73.5°, $[\alpha]_D$ −71° (*c*, 0.96), ν_{max} 1770, 1725 cm^{-1}. Calc. for $C_{15}H_{24}O_4$: C, 67.13; H, 9.02. Found: C, 67.67; H, 8.79%.

Dehydrogenation of the Nordilactone

The lactone (300 mg) and powdered selenium (600 mg) were intimately mixed and heated in a sealed

Can. J. Chem. Downloaded from www.nrcresearchpress.com by 210.87.254.42 on 09/05/12
For personal use only.

tube at 325° for 24 hours. After cooling the contents of the tube were extracted with light petroleum. This solution was applied to a column of silica gel and elution continued with the same solvent. After evaporation of the petroleum eluates the product was crystallized from the same solvent to give 3-isopropyl-6-methylphthalic anhydride (26 mg) (VI) m.p. 100.5–101°. Calc. for $C_{12}H_{12}O_3$: C, 70.57; H, 5.92. Found: C, 70.64; H, 5.69%. The material was identical in every respect with the material obtained by synthesis.

Synthesis of 3-Isopropyl-6-methylphthalic Anhydride

(a) Isobutyl Triphenyl Phosphonium Bromide

Triphenylphosphine (25 g) and isobutyl bromide (14.3 g) were heated in a sealed tube at 125° for 15 hours. The resultant white solid was boiled in benzene, filtered, and dried. It had m.p. 210–220°.

(b) 6-Methylhepta-2,4-diene

n-Butyl lithium in pentane was prepared from *n*-butyl chloride. Titration with standard hydrochloric acid indicated 1.19 mmole butyl lithium per ml.

To 10 ml of this solution, under nitrogen, was added pentane (50 ml) and, over 30 minutes, the phosphonium bromide (3.99 g). The solution turned orange, darkened, and a precipitate formed. Anhydrous ether (100 ml) was added and the mixture stirred at room temperature for 3 hours. Crotonaldehyde (0.7 g) was then added and the mixture stirred and refluxed for 7 hours. After removal of the phosphine oxide by filtration the hydrocarbon fraction was isolated in the usual way. This material (1.02 g), λ_{max} 227, $\epsilon \sim 12{,}000$, was used directly in the following experiment.

(c) 3-Isopropyl-6-methylcyclohex-4-ene-1,2-dicarboxylic Acid (VII)

The diene (1.0 g), maleic anhydride (1.2 g), a few crystals of hydroquinone, and benzene (2 ml) were sealed in a tube which was then heated at 150° for 17 hours. The acidic products were extracted with 5% sodium carbonate solution (charcoal) and after acidification the diacid was crystallized from ethyl acetate when it had m.p. 194.5–195° (119 mg). Calc. for $C_{12}H_{18}O_4$: C, 63.70; H, 8.02. Found: C, 63.99; H, 7.96%.

(d) 3-Isopropyl-6-methylphthalic Anhydride (VI)

The diacid (100 mg) was heated at 210° for 45 minutes and then sulphur (50 mg) was added and the temperature increased to 240–260°. After 1 hour the mixture was cooled and extracted with light petroleum. This was filtered through a column of silica gel and the column eluted with the same solvent. Repeated crystallization from light petroleum gave a product identical in every way with the selenium dehydrogenation product of the nordilactone.

Alkali Treatment of the Nordimethyl Ester

A solution of the ester (100 mg) in methanol (1 ml) was added to a solution of sodium methoxide (*N*; 30 ml) and the mixture refluxed for 15 hours. Water (20 ml) was then added and heating continued for a further 3 hours.

The acidic material was isolated and filtered through silica gel in ether–benzene (1:3) solution. After evaporation of the solvent the product was crystallized from light petroleum (b.p. 60–80°) to give the allonordiacid monomethyl ester m.p. 122–123.5°, $[\alpha]_D$ +15° (*c*, 1.25), ν_{max} 3300, 1715, 1730, 1710 cm^{-1}. Calc. for $C_{15}H_{24}O_5$: C, 63.36; H, 8.51; OMe (1), 10.91. Found: C, 63.42; H, 8.75; OMe, 10.77%.

Treatment of the monoacid with ethereal diazomethane, followed by crystallization from light petroleum, gave the dimethyl ester (XXV), m.p. 60–62.5°, $[\alpha]_D$ +32° (*c*, 0.87). Calc. for $C_{16}H_{26}O_5$: C, 64.40; H, 8.78, OMe (2) 20.80. Found: C, 65.18; H, 8.80; OMe, 20.57%. A 2,4-dinitrophenylhydrazone was obtained (steam bath for 1 hour) which crystallized from light petroleum (b.p. 60–80°), m.p. 150.5–152.5°. Calc. for $C_{22}H_{30}N_4O_8$: C, 55.22; H, 6.32; N, 11.70. Found: C, 55.44; H, 6.30; N, 11.51%.

Cyclization of the Nordiester (XIX)

The ester (50 mg) was dissolved in *t*-butanol (10 ml) containing 4% potassium *t*-butoxide, and left at room temperature for 15 hours. The mixture was then diluted with water and acidified and the products isolated with ether. After application to a column of silica gel elution with ether–benzene (1:3) gave the mono ester described above (10 mg). Further elution then afforded an oil which had ν_{max} 1740, 1700, and 1603 cm^{-1}, λ_{max} (neutral) 257 mμ ($\epsilon \sim 11{,}000$), λ_{max} (alkaline) 285 mμ ($\epsilon \sim 10{,}000$).

The oil was treated with an excess of ethereal diazomethane and the residue after evaporation applied to a column of silica gel. Elution with ether–benzene (1:19) yielded the enol ether (XXIII), which, after crystallization from light petroleum (b.p. 60–80°) had m.p. 170–172°, λ_{max} 255 mμ (ϵ, 12,000), λ_{max} 1740, 1660, 1600 cm^{-1}. Calc. for $C_{16}H_{24}O_4$: C, 68.54; H, 8.63. Found: C, 68.20; H, 8.93%.

Reduction of the Monoacid (XXVI, R = COOH)

To lithium aluminum hydride (400 mg) in dioxan (50 ml) was added a solution of the monoacid (400 mg) in dioxan (50 ml). The mixture was refluxed for 12 hours, the excess hydride decomposed with ethyl acetate, and the diol isolated in the usual way. An acidic fraction was obtained which gave 114 mg of starting acid. The glycol (200 mg) was converted directly to the bis-3,5-dinitrobenzoate, m.p. and mixed m.p. 149–151° identical in every respect with material obtained by reduction of the aldehyde (XXVI, R = CHO).

Can. J. Chem. Downloaded from www.nrcresearchpress.com by 210.87.254.42 on 09/05/12
For personal use only.

ACKNOWLEDGMENTS

The authors would like to thank Mr. L. G. Crawford for able assistance, Mr. R. E. Klinck for the n.m.r. spectra, and the National Research Council for financial support.

REFERENCES

1. P. DE MAYO, E. Y. SPENCER, and R. W. WHITE. J. Am. Chem. Soc. **84**, 494 (1962).
2. P. DE MAYO, J. R. ROBINSON, E. Y. SPENCER, and R. W. WHITE. Experientia, **18**, 359 (1962).
3. P. DE MAYO, E. Y. SPENCER, and R. W. WHITE. Can. J. Chem. **39**, 1608 (1961).
4. F. A. L. ANET. Can. J. Chem. **39**, 2262 (1961).
5. R. U. LEMIEUX, R. K. KULLNIG, H. J. BERNSTEIN, and W. G. SCHNEIDER. J. Am. Chem. Soc. **79**, 1005 (1957).
6. S. J. CRISTOL. Abstracts of Papers, 18th American Chemical Society Organic Symposium, Ohio. 1963. p. 21.

Can. J. Chem. Downloaded from www.nrcresearchpress.com by 210.87.254.42 on 09/05/12
For personal use only.

N.M.R. SPECTRA OF TIN COMPOUNDS

I. H^1 AND F^{19} MAGNETIC RESONANCE SPECTRA OF DIMETHYL-1,1,2,2-TETRAFLUOROETHYLTIN HYDRIDE, DIMETHYLBIS(1,1,2,2-TETRAFLUOROETHYL)TIN, AND DIMETHYLTIN DIHYDRIDE

H. C. Clark, J. T. Kwon, L. W. Reeves, and E. J. Wells
Chemistry Department, University of British Columbia, Vancouver, British Columbia
Received June 14, 1963

Can. J. Chem. Downloaded from www.nrcresearchpress.com by 210.87.254.40 on 09/05/12
For personal use only.

ABSTRACT

The H^1 and F^{19} magnetic resonance spectra of three tin compounds have been examined. Taking advantage of C^{13}, Sn^{117}, and Sn^{119} being magnetic nuclei in small natural abundance, it has been possible to obtain 31 coupling constants from the spectra.

INTRODUCTION

Some considerable work has now been devoted to nuclear magnetic resonance spectra (n.m.r.) of organometallic derivatives of group IV elements. First reported values of chemical shifts in methyl and perfluoromethyl tin derivatives showed relatively small variation of methyl and perfluoromethyl chemical shifts (1). Tetravinyltin shows a collapsed ABC proton resonance spectrum which was analyzed by use of the Sn^{119} side bands. These side bands appear due to Sn^{119} indirect spin coupling with protons (2). Parameters obtained from the side bands make possible an exact fit of the main resonance lines. Large differences between the F^{19} chemical shifts of perfluoro transition metal compounds and those of non-transition metals such as tin have been reported (3). Sn^{119} spectra have been studied by Lauterbur and Burke (4) and chemical shifts of a variety of tin compounds obtained. The F^{19} magnetic resonance spectra of triethylfluoroethyl and triethylperfluorovinyl derivatives, of Si, Ge, and Sn (5) reveal smaller metal–fluorine coupling constants in the perfluorovinyl compounds than obtained earlier for metal–H^1 coupling in tetravinyltin (3).

H^1–H^1, H^1–Si^{29}, H^1–F^{19}, and Si^{29}–F^{19} coupling constants have been evaluated from spectra of deuterated silicon derivatives (6). Metal–proton coupling in the methyltin compounds reported earlier (1) has been studied by Kaesz (7, 9). Chemical shifts and some coupling constants have now been reported for mixed hydrides of silicon, phosphorus, germanium, and arsenic (8).

EXPERIMENTAL

Proton magnetic resonance spectra were recorded at 28° C on both Varian A60 and H.R. 60 spectrometers. Peak positions were determined in both cases by bracketing peaks to be measured with audio side bands generated by a Hewlett Packard wide band audio oscillator and calibrated by a Hewlett Packard 522 B electronic counter. Proton resonance peaks were compared to an internal tetramethyl silane reference and fluorine chemical shifts obtained with respect to an external trifluoroacetic acid sample. Fluorine magnetic resonance spectra were recorded at 40 Mc/sec with a Varian V4300 spectrometer.

The preparation and purification of these compounds will be described elsewhere (10).

RESULTS

The magnetic nuclei in the compounds studied are H^1, F^{19}, Sn^{119}, Sn^{117}, and C^{13}; of these H^1 and F^{19} have been observed directly. All the nuclei studied have spin 1/2, and the isotopic abundances are Sn^{117}, 8.68; Sn^{119}, 7.67; and C^{13}, 1.108%. Deuterium, present to a small extent in hydrogen, together with 0.35% abundant Sn^{115} with a moment of

−0.9132 and spin 1/2, do not contribute observable effects in the n.m.r. spectra obtained here.

Spectra of Dimethyltin Dihydride

The proton resonance spectrum of this compound is shown in Fig. 1. The main features are a simple septet for the two hydrogens directly bonded to tin, chemically shifted −4.39 p.p.m. from the internal TMS reference, and a triplet for the hydrogens of the two methyl groups at −0.2 p.p.m. The coupling constants and chemical shifts for this

TABLE I

	CH_3, CH_3, H^a, H^a on Sn; neat	CH_3, CH_3, $CF_2{}^a$—$CF_2{}^b$—H^b, H^a on Sn; neat		CH_3, CH_3, $CF_2{}^a$—$CF_2{}^b$—H^b, CF_2—CF_2—H on Sn; neat	
		H^1 spectrum	F^{19} spectrum	H^1 spectrum	F^{19} spectrum
δ_{CH_3} (p.p.m.)	−0.20	−0.31		−0.63	
δ_{H^a} "	−4.39	−5.53			
δ_{H^b} "		−5.39		−5.63	
δ_{F^a} "			+38.2		+37.9
δ_{F^b} "			+51.2		+51.2
$J_{CH_3-H^a}$ (c.p.s.)	2.65±0.1	2.25±0.1			
$J_{Sn^{119}-H^a}$	1797.1±0.6	1976.6±1			
$J_{Sn^{117}-H^a}$	1717.4±0.8	1889.4±1			
$J_{Sn^{119}-CH_3}$	60.2±0.2	62.8±0.3		64.5±0.5	
$J_{Sn^{117}-CH_3}$	57.6±0.3	60.1±0.3		61.5±0.5	
$J_{C^{13}-CH_3}$	129.9±0.2	132.1±0.4		137.3±0.5	
$J_{H^a-F^a}$		8.4±0.5	8.3±0.2		
$J_{H^a-F^b}$		2.65±0.3	2.65±0.2		
$J_{H^b-F^a}$		5.48±0.1	5.6±0.2	5.1±0.1	5.1±0.3
$J_{H^b-F^b}$		56.9±0.2	57.0±0.5	56.5±0.2	56.7±0.7
$J_{H^b-CH_3}$		Not resolved		Not resolved	
$J_{Sn^{119}-H^b}$	}	27±1		} 32±1	
$J_{Sn^{117}-H^b}$	}			}	
$J_{Sn^{119}-F^a}$			251±2		} 274±10
$J_{Sn^{117}-F^a}$			240±2		}
$J_{Sn^{119}-F^b}$			} 20±1		} 8±1
$J_{Sn^{117}-F^b}$			}		}
$J_{CH_3-F^a}$		Not resolved	Not resolved	Not resolved	1.1±0.1?
$J_{CH_3-F^b}$		Not resolved	Not resolved	Not resolved	Not resolved
$J_{F^a-F^b}$			0.5±0.1?		Not resolved?
$J_{C^{13}-F^a}$		Below noise			Below noise
$J_{C^{13}-F^b}$		Below noise			Below noise
$J_{C^{13}-H^a}$	Not seen	Below noise			
$J_{C^{13}-H^b}$		Below noise		Below noise	
$J_{H^a-H^b}$		0.45±0.1			

[a]Summary of coupling constants obtained from the first order analysis of the spectra of compounds listed.
[b]Summary of chemical shifts obtained for protons. 'δ' is expressed in p.p.m., with respect to an internal TMS reference. For fluorine resonance positions the standard is an external trifluoroacetic acid sample.

compound are listed in Table I. In addition to the main peaks, subsidiary peaks appear because of the detectable amounts of the following:

I H_3C^{13}, H_3C, H, H on Sn

II CH_3, CH_3, Sn^{117}, H, H

III CH_3, CH_3, Sn^{119}, H, H

In I the Sn nucleus is magnetically inactive, but side bands, $\frac{1}{2}\%$ of the height of the methyl peaks, appear on each side of the methyl triplet with a separation $J_{C^{13}-H}$. The relatively low intensity side bands are shown in Fig. 2; $J_{C^{13}-CH_3}$ was measured as 129.9 c.p.s. In addition the molecules II and III contribute to side bands shown in Fig. 2 as

Can. J. Chem. Downloaded from www.nrcresearchpress.com by 210.87.254.40 on 09/05/12
For personal use only.

$J_{Sn^{119}-CH_3}$ and $J_{Sn^{117}-CH_3}$. The *I.I* coupling of nuclear spins in high resolution spectra generally decreases markedly as the number of bonds between the two magnetically active nuclei increases, thus $J_{C^{13}H_3-SnH_2}$ is expected to be much smaller than $J_{C^{13}-CH_3}$ but

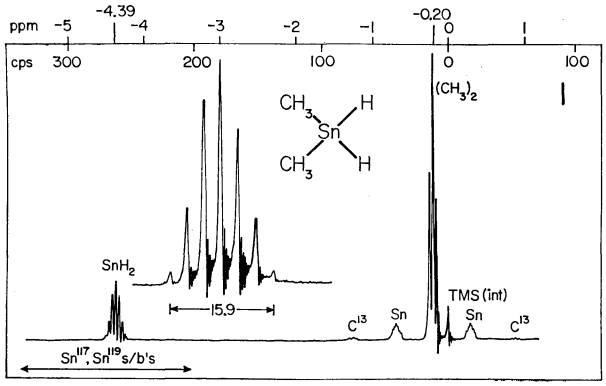

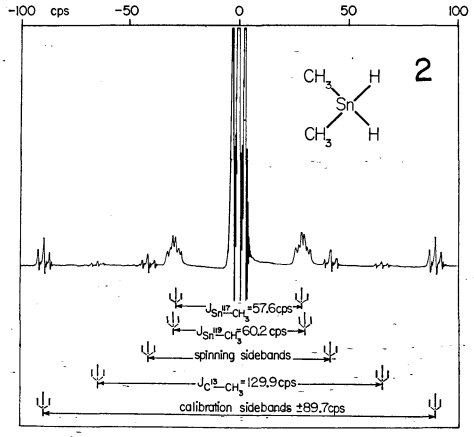

FIG. 1. 60 Mc/s proton spectrum of dimethyltin dihydride, showing main features of the spectrum. Chemical shifts are given with respect to the internal TMS standard. The Sn^{117} and Sn^{119} side bands are located at ±900 from the SnH_2 septet. (See Fig. 3.)

FIG. 2. Expanded 60 Mc/s proton spectrum of dimethyltin dihydride near the methyl resonance region, showing Sn^{117}, Sn^{119}, and C^{13} side bands.

because of the much lower intensity of the main resonance it could not be observed. The coupling of the SnH_2 protons to the magnetically active Sn^{117} and Sn^{119} in molecules II and III produces a very large splitting, the high field component of which exceeds the range of the A60 spectrometer. Figure 3 shows the spectra for determination of $J_{Sn^{117}-H}$ and $J_{Sn^{119}-H}$, with calibrating side bands from the main peak. The low field component of the tin doublets was bracketed repeatedly between calibrated side bands from the main SnH_2 peak on the A60 spectrometer. The precise position of the high field component was obtained by using the same oscillator and electronic counter for the calibrating side bands, on an HR 60 spectrometer. As far as could be determined there was no difference in chemical shift of $>SnH_2$ protons in molecules II and III, that is to say we could detect no isotope shift.

The $I \cdot I$ coupling between magnetically active Sn nuclei in molecules II and III and

Can. J. Chem. Downloaded from www.nrcresearchpress.com by 210.87.254.40 on 09/05/12
For personal use only.

the methyl protons is shown in Fig. 2. Two overlapping triplets due to two tin isotopes are shown. The coupling constant between two nuclei is proportional to the product of the gyro-magnetic ratio of the two nuclei (11) and thus the splitting $J_{Sn^{119}-H^1}$ and $J_{Sn^{117}-H^1}$ are in the ratio of the gyromagnetic ratios of the two tin isotopes. This factor is 1.046, so

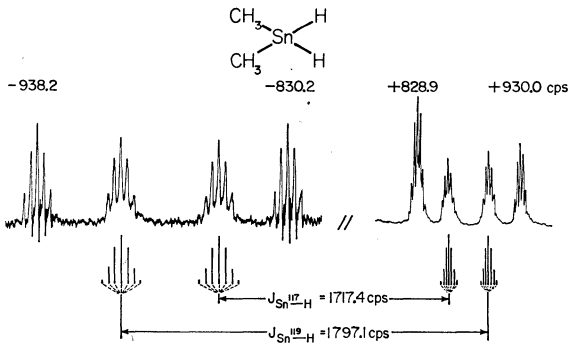

FIG. 3. Side bands from the two magnetic tin isotopes Sn^{117} and Sn^{119} of the SnH_2 group in the 60 Mc/s proton spectrum of dimethyltin dihydride.

that the larger splitting results from 8.68% of Sn^{119} and the smaller splitting from 7.67% of Sn^{117}. Intensities of appropriate side bands were found to be proportional to isotopic abundances, and coupling constants to gyromagnetic ratios within experimental error.

Dimethyl-1,1,2,2-tetrafluoroethyltin Hydride—Proton Magnetic Resonance

The compound contained a small amount of $(CH_3)_2Sn(C_2F_4H)_2$ the peaks of which are assigned in Fig. 4, together with the proton resonance spectrum of the desired compound. The main methyl proton resonance is a doublet and the C^{13}, Sn^{117}, and Sn^{119} side bands are shown with values of the appropriate coupling constants. Proton *a* attached to the tin and proton *b* geminal to the CF_2 group produce overlapping signals. The spectra are all first order and are complete with Sn^{117} and Sn^{119} side bands. The main splitting of the hydrogen H^b signal is the triplet due to coupling with geminal fluorine nuclei, and there is further splitting due to coupling with vicinal fluorine nuclei and interproton coupling H^a—H^b. The central component of the main triplet is overlapped by the signals of H^a. This region in expanded form is the subject of Fig. 5.

The spectrum of H^a is very complex because of a large number of first order splittings. The contributing coupling constants are $J_{H^a-CH_3}$, (seven lines), $J_{H^a-CF_2{}^a}$ (three lines), $J_{H^a-CF_2{}^b}$ (three lines); $J_{H^a-H^b}$ (two lines) and since these are multiplied together to give the total number of lines, we expect 126 components. These are constructed below the spectrum on the same scale. Although all lines are not completely resolved, it is evident that computed spectrum and measured spectrum are in good agreement.

The center component of the triplet for proton H^b is indicated above the spectrum in Fig. 5. This comprises lines due to $J_{H^b-F_2{}^a}$ and $J_{H^b-H^a}$ with corresponding Sn^{117} and Sn^{119} side bands. The agreement of the measured and computed spectrum in the region of overlap is also apparent.

The main peaks for H^a overlap those for H^b but the tin side bands are well separated because J_{Sn-H^a} is such a large coupling constant. The tin side bands of H^a are shown in Fig. 6 between calibrating side bands of the main peak. The center component of the main triplet for H^b was used for calibration purposes and the low field component of this tripleted

Can. J. Chem. Downloaded from www.nrcresearchpress.com by 210.87.254.40 on 09/05/12
For personal use only.

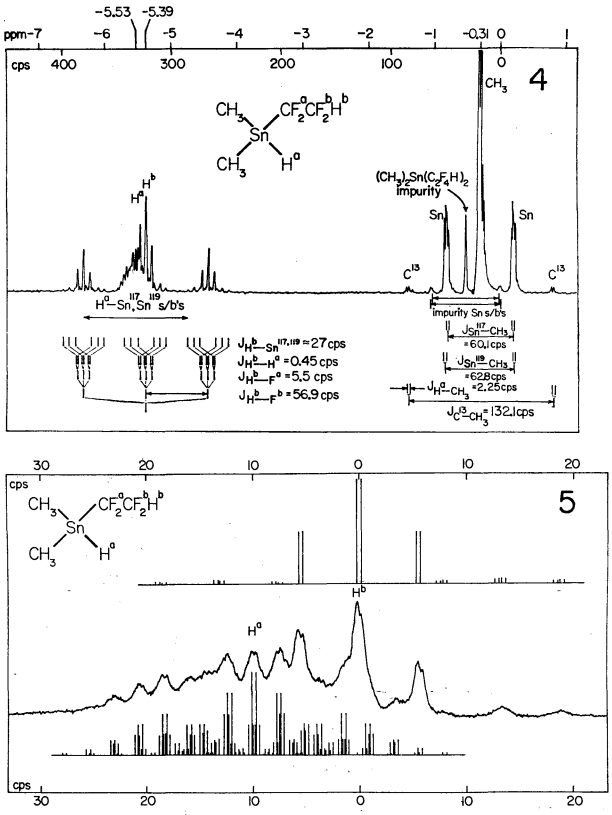

FIG. 4. 60 Mc/s proton magnetic resonance spectrum of $(CH_3)_2SnH(CF_2CF_2H)$, showing main features of the spectrum. Chemical shifts are relative to external TMS standard.

FIG. 5. Comparison of the observed and calculated 60 Mc/s PMR spectrum for the H^a proton in $(CH_3)_2SnH^a(CF_2CF_2H^b)$.

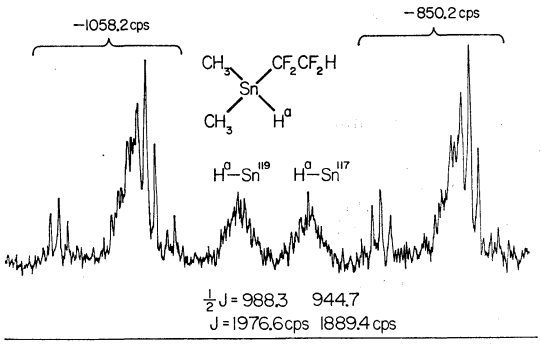

FIG. 6. Low-field tin side bands of the H^a-resonance in $(CH_3)_2SnH^a(CF_2CF_2H^b)$, from an A60 spectrum.

triplet also shows up in the audio modulations of the main resonance in Fig. 5. These spectra were run on the A60 and the high field Sn side bands were ignored since no isotopic shift was observed for the $>SnH_2$ protons in dimethyltindihydride.

Can. J. Chem. Downloaded from www.nrcresearchpress.com by 210.87.254.40 on 09/05/12
For personal use only.

Dimethylbis(1,1,2,2-tetrafluoroethyl)tin—Proton Magnetic Resonance

The proton magnetic resonance spectrum of the above compound is shown in Fig. 7. A very small impurity of the compound whose spectrum is illustrated in Fig. 4 is present and identified in the diagram. The methyl peak of the dimethylbis(tetrafluoroethyl)tin appears to be a single peak but displays some evidence of unresolved couplings since the

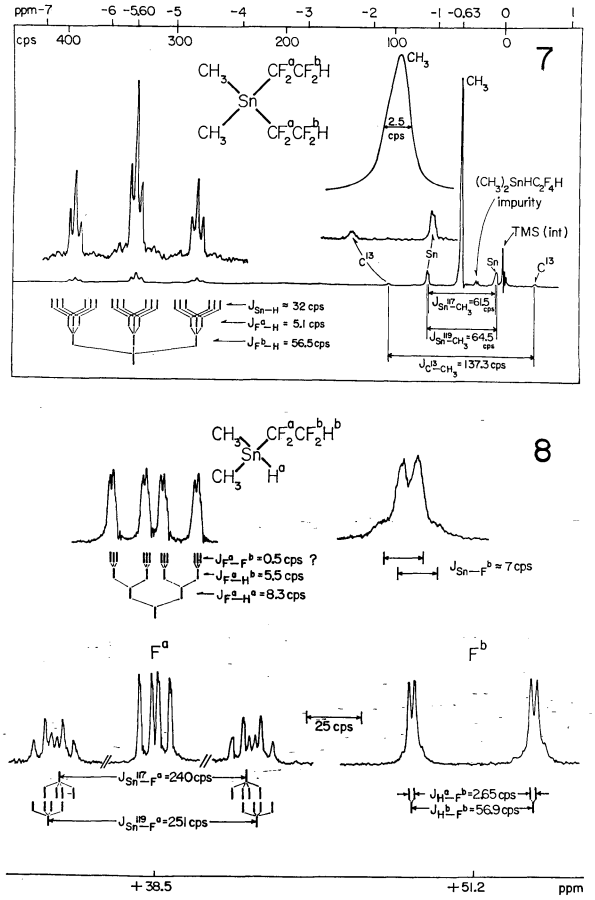

FIG. 7. 60 Mc/s proton resonance spectrum of $(CH_3)_2Sn(CF_2CF_2H)_2$. Chemical shifts are given relative to internal tetramethyl silane.

FIG. 8. 40 Mc/s F^{19} magnetic resonance spectrum of $(CH_3)_2SnH(CF_2{}^aCF_2{}^bH)$. The F^a quartet, with tin side bands, and the two F^b doublets are drawn to the same (broken) frequency scale, though not to the same intensity scale. The chemical shifts are quoted in p.p.m. from an external CF_3COOH standard (not shown). The assignment of each of the F^a quartets as a hyperfine triplet is uncertain (see text).

half width was unusually high, 2.5 c.p.s. C^{13}, Sn^{117}, and Sn^{119} side bands are clearly observed and couplings have been noted. The proton geminal to two fluorine atoms in this compound is a tripleted triplet due to coupling with $F_2{}^b$ and $F_2{}^a$. A remote coupling to the active tin nuclei was observed but the difference in coupling constant H—Sn^{117} and H—Sn^{119} is too small to resolve. The value quoted is a good average of the two values.

Fluorine Magnetic Resonance Spectra

The F^{19} spectrum of the compound with one tin hydrogen is shown in Fig. 8. The peaks due to $F_2{}^a$ are doubleted due to coupling with H^a, doubleted again due to coupling with

Can. J. Chem. Downloaded from www.nrcresearchpress.com by 210.87.254.40 on 09/05/12
For personal use only.

H^b, and then further split. The assignment of splittings to numerical coupling constants is ambiguous here but knowledge of the proton spectrum allows a unique assignment. The smaller splittings assigned as a triplet of 0.5 c.p.s. separation is somewhat doubtful. An alternative assignment might be an incompletely resolved septet, a little distorted due to lack of resolution. However, no hyperfine structure could be detected in the relatively sharp doublet in the proton spectrum of the methyl group. Below the expanded spectrum of $F_2{}^a$ is shown the Sn^{117} and Sn^{119} side bands.

The spectrum of $F_2{}^b$ is a doublet due to coupling $F_2{}^b$—H^b and a smaller doublet structure due to $F_2{}^b$—H^a interaction. Above this on Fig. 8 the tin side bands are resolved for each doubleted component.

Figure 9 illustrates the fluorine magnetic resonance spectrum of dimethylbis(tetrafluoroethyl)tin. The peaks of $F_2{}^b$ are very similar to those in Fig. 8 but lack the splitting

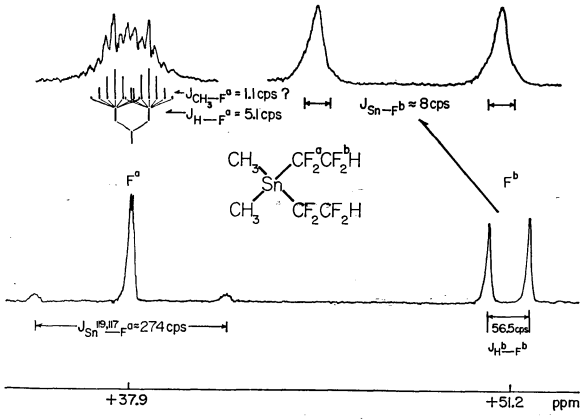

FIG. 9. 40 Mc/s F^{19} spectrum of $(CH_3)_2Sn(CF_2CF_2H)_2$. The relationship of the F^a and F^b resonance on a linear frequency scale is shown below, and the F^a fine structure above. Chemical shifts of the mean frequencies are quoted relative to an external standard of CF_3COOH.

due to the proton on the tin. The peaks due to the fluorine nuclei $F_2{}^a$ do not fit the doubleted septet pattern indicated very well, since the intensities of peaks seem distorted. The double tin side bands are not resolved but an average $J_{Sn^{117,119}-F^a}$ can be evaluated.

We note here that the arrangement of fluorine atoms in this molecule is analogous to that in the compounds studied by Petrakis and Sederholm (12). A good example for comparison would be the molecule

IV 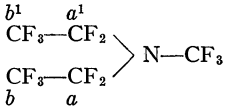 with V 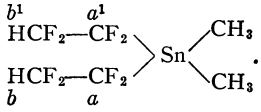

Musher (13) has noted that coupling interpreted by previous authors (12) as being equal, i.e. *ba* and *ba*^{1}, was, in fact, not equal and the mechanism of the simple multiplet spectra observed has been labelled 'virtual coupling'. In the extreme case of two strongly coupled inequivalent sets of spins B_n and C_m (all $I = 1/2$) coupling to a third group of spins, A appears as a simple multiplet of $(n+m+1)$ lines. Petrakis and Sederholm (14) concur with this explanation and some further work has been published by Musher and Corey (15). The multiplet for our fluorines $F_2{}^a$ may well be an intermediate case of virtual coupling (15) where simple multiplets are not observed.

A summary of all coupling constants and chemical shifts is given in Table I.

Can. J. Chem. Downloaded from www.nrcresearchpress.com by 210.87.254.40 on 09/05/12
For personal use only.

DISCUSSION

A consideration of the $I \cdot I$ coupling constants, for compounds containing group IV elements with favorable nuclear spin, is made in a recent note by two of the authors (16). A qualitative extension of factors which influence the coupling in C^{13}—H and Si^{29}—H bonds (17, 18) can be applied to the values $J_{Sn^{119}-H}$ in the compounds studied here. In all three compounds studied, we expect approximately sp^3 hybridization on the tin and no back donation of charge into the empty d orbitals of tin. Recent theoretical work (17) suggests that the sharing of s character amongst the four bonds is uneven and electropositive groups have more s character in the bonding electrons than electronegative groups; thus the Fermi contact term at the group IV nucleus is enhanced. This is illustrated well by the Sn^{119}—H coupling in $(CH_3)_2SnH_2$ and in $(CH_3)_2SnH(C_2F_4H)$. The more electronegative —C_2F_4H group replaces hydrogen in dimethyl tin dihydride with a consequent increase in $J_{Sn^{119}-H}$ from 1797 to 1976 c.p.s. This effect is also seen (Table I) in the $J_{C^{13}-H}$ coupling in the methyl groups, which increases progressively in the series $(CH_3)_2SnH_2$, $(CH_3)_2SnH(C_2F_4H)$, $(CH_3)_2Sn(C_2F_4H)_2$. The group attached to the carbon 13 becomes more and more electronegative with the more distant addition of —C_2F_4H groups. The increase of $J_{Sn^{119}-CH_3}$ follows a similar trend. Hydrogen to fluorine coupling constants via geminal atoms $J_{H^b-F^b}$ are unaffected by changes in the molecules.

This research was supported by grants to (L. W. R.) from the Petroleum Research Fund and the National Research Council of Canada and a grant (to H. C. C.) from the Office of Naval Research.

REFERENCES

1. R. D. Chambers, H. C. Clark, and C. J. Willis. Can. J. Chem. **39**, 131 (1961).
2. D. W. Moore and J. A. Happe. J. Phys. Chem. **65**, 224 (1961).
3. E. Pitcher, A. D. Buckingham, and F. G. A. Stone. J. Chem. Phys. **36**, 124 (1962).
4. P. C. Lauterbur and J. J. Burke. J. Am. Chem. Soc. **83**, 326 (1961).
5. D. Seyferth, T. Wada, and G. E. Maciel. Inorg. Chem. **1**, 232 (1962).
6. E. A. V. Ebsworth and J. J. Turner. J. Chem. Phys. **36**, 2628 (1962).
7. H. Kaesz and J. R. Holmes. J. Am. Chem. Soc. **83**, 3903 (1961).
8. J. E. Drake and W. L. Jolly. J. Chem. Phys. **38**, 1033 (1963).
9. H. Kaesz. J. Am. Chem. Soc. **83**, 1514 (1961).
10. H. C. Clark, S. Furnival, and J. T. Kwon. Can. J. Chem. **41**, 2889 (1963).
11. J. A. Pople, W. G. Schneider, and H. J. Bernstein. High resolution nuclear magnetic resonance. McGraw-Hill, New York. 1959.
12. L. Petrakis and C. H. Sederholm. J. Chem. Phys. **35**, 1243 (1961).
13. J. I. Musher. J. Chem. Phys. **36**, 1086 (1962).
14. L. Petrakis and C. H. Sederholm. J. Chem. Phys. **36**, 1087 (1962).
15. J. I. Musher and E. J. Corey. Tetrahedron, **18**, 791 (1962).
16. L. W. Reeves and E. J. Wells. Can. J. Chem. **41**, 2698 (1963).
17. H. S. Gutowsky and C. S. Juan. J. Am. Chem. Soc. **84**, 307 (1962).
18. J. Malinowsky. J. Am. Chem. Soc. **83**, 4479 (1961).

Can. J. Chem. Downloaded from www.nrcresearchpress.com by 210.87.254.40 on 09/05/12
For personal use only.

RATES OF REACTION OF HYPOCHLORITE IONS WITH SULPHITE AND IODIDE IONS

M. W. Lister and P. Rosenblum
Department of Chemistry, University of Toronto, Toronto, Ontario
Received June 7, 1963

Can. J. Chem. Downloaded from www.nrcresearchpress.com by 210.87.254.40 on 09/05/12
For personal use only.

ABSTRACT

The rates of reaction of sodium hypochlorite with sodium iodide and sodium sulphite have been measured by means of a rapid-flow technique. The measurements were made over a range of temperature and hydroxide concentrations, and show that the actual slow steps of the reactions are

(i) $OCl^- + SO_3^{-2} \rightarrow Cl^- + SO_4^{-2}$

with $K = 2.7\times10^9 \exp(-7.5 \text{ kcal}/RT)$,

and

(ii) $HOCl + I^- \rightarrow HOI + Cl^-$

with $K = 1.6\times10^{-9} \exp(-0.9 \text{ kcal}/RT)$,

with time in seconds.

The decomposition of hypoiodite ions was also measured.

These results, and those for other reactions of hypochlorite ions, or hypochlorous acid, form a series similar to the reactions of peroxides. It is found that the regularities observed for peroxides apply to some extent to the present reactions, and other possible regularities are also examined.

INTRODUCTION

The present work is part of a study on the oxidations effected by hypochlorite ions or hypochlorous acid. The oxidations of sulphite and iodide ions were measured by means of a rapid-flow technique. These reactions, together with those previously reported, form a moderately extensive series, and it is of interest to discover whether the rates of these reactions can be correlated with other properties of the reducing agent. A similar sequence of reactions consists of the oxidations by hydrogen peroxide, which have been particularly studied by Edwards (1, 2, 3), who was able to observe regularities in their rate constants. These reactions of hydrogen peroxide have been used as a basis for comparison in the present work.

EXPERIMENTAL

The rapid-flow technique used in the present work is based on that developed by Hartridge, Roughton, and Millikan (4–7). Briefly, the two reagents are driven by syringe into a Plexiglas mixing chamber. From here the reacting solution passes into a quartz observation tube. The absorbance of the solution is measured at various points along the tube by means of a Beckmann DU spectrophotometer. If d is the distance in cm between the mixing chamber and the point of measurement, and v is the linear rate of flow in cm/sec, then the time for which the reaction has proceeded in the fluid is d/v seconds.

In greater detail, the apparatus is as follows. The reactants are brought to correct temperature in 100 ml syringes held in a thermostat box. A continuously variable speed motor drives a trolley carrying both syringes and observation tube while a second motor drives a block which pushes forward the plungers of the syringes. The mixing chamber and jets are constructed from a drilled-out block of Plexiglas, each jet being 2.5 cm long and 1 mm in diameter, while the mixing chamber is 2 mm long and 1 mm in diameter. A 16-inch long piece of Corning, Vycor 96% silica glass No. 7910 serves as the observation tube; the inside diameter of the capillary is 2 mm while the outer diameter is 7 mm. Both mixing chamber and observation tube are mounted inside a cover similar to that used by Dalziel (8) in his rapid-flow apparatus, but refined to include copper tubing for heating or cooling purposes. A jacket mounted between the Beckmann body and photocell allows the tube to slide smoothly through the light path of the spectrophotometer. The voltage from the photocell is amplified by a Beckmann 5800 Energy Recording Adapter and the amplified voltage is then applied to a Sargent model SR chart recorder. To ensure that a deflection of 100 units on the chart

corresponds to a transmission of 100%, the recorder pen is adjusted to read 100% with the blank solution in the capillary and to indicate zero with the shutter closed. Narrow strips of black tape on the observation tube permit a correlation between distances on the chart paper and the actual distance on the observation tube.

REACTION OF HYPOCHLORITE AND SULPHITE IONS

A study of the kinetics of the oxidation of sulphite ions by hypochlorite ions has not previously been reported; all that was known about the rate was that the reaction is a rapid one.

Experimental Method

The hypochlorite solutions were made up by mixing known volumes of stock hypochlorite (analyzed as in a previous paper) (9), sodium hydroxide, and sodium chloride solutions. Sodium sulphite solutions were analyzed immediately before the run in the following way. A 50 ml aliquot was added to a solution containing a 10 ml aliquot of standard iodine solution and 10 g of sodium bicarbonate. Then the unreacted iodine was titrated with standard arsenious oxide solution, 5 ml of 0.2% starch solution being added just before the end-point.

Since the only absorbing species at 292 mμ in the reaction mixture is the hypochlorite ion (extinction coefficient = 350), this wavelength was used for following the course of the reaction.

For a run the sodium hypochlorite solution was first drawn into one syringe, after the syringe had first been carefully rinsed with the same solution. Next, the sodium sulphite solution was drawn into the other syringe and some ejected in order to displace any hypochlorite in the capillary tube. After allowing the solutions to come to temperature equilibrium, the recorder was adjusted to read 100% as previously described, and the whole length of the observation tube was scanned. This blank served to correct for the effect of fluctuations in the transmission of the glass. A reaction graph was next made with both trolley and syringes moving, then the capillary, filled only with hypochlorite, was scanned in order to determine the extinction coefficient of hypochlorite in the capillary. A fourth scan was made, using the sulphite solution only, to check for drift of the zero setting.

The rate of flow was determined by measuring the volume of water delivered in a certain time interval; this flow rate was found constant to within 1% over the time of the experiment. From the volume rate of flow the linear flow rate was calculated. The diameter of the capillary was determined by measuring the exact length of a weighed 1 cm plug of mercury at various positions along the capillary.

For the constant flow method to give valid results, all parts of the reacting solution should reach the place of observation at the same time. This occurs only in the case of ideal or mass flow. In practice, the central parts of the fluid always move faster than the edges. Such deviations from mass flow are much greater in the case of streamline flow than with turbulent flow (8). Consequently the flow rates used in the present work were always well in excess of the streamline flow region (3 ml/sec). The flow velocity used in most of the present work was approximately 210 cm/sec (6 ml/sec).

A physical test for the efficiency of mixing, i.e., the approach to optical homogeneity of a solution of ammonium sulphate (10), was applied and showed that mixing was complete before the first reading on any run. As an added check to ensure that deviations from mass flow and mixing errors were negligible, some runs were performed at a slower flow rate. These gave the same rate constant as the other runs.

The liquid flowing from the end of the observation tube was a little closer to room temperature than the liquid in the syringes. Measurements performed on water by means of an iron–constantan thermocouple placed in the capillary showed that there was no temperature gradient along the capillary. This meant that the main source of heat loss or gain came from the connecting tubing. The temperature of the reacting fluid was therefore taken to be the same as that of the emerging fluid.

Preliminary tests showed that there are no side reactions in the conversion of sulphite to sulphate by hypochlorite. Consequently the reaction is simply

$$OCl^- + SO_3^{--} \rightarrow Cl^- + SO_4^{--}$$

and the rate constant was found as follows. If the reaction is second order, and if we write $[OCl^-] = x$, and $[SO_3^{--}] = y$, then $dx/dt = -kxy$. Integration gives: $\ln (xy_0/yx_0) = kt(x_0-y_0)$. If A is the absorbance (at 292 mμ) and ϵ the extinction coefficient of OCl^-, then $A/\epsilon = x$, and

$$\ln(A/[A + \epsilon(y_0-x_0)]) = \ln(x_0/y_0) + k(x_0-y_0)t.$$

It was found that a plot of $\ln (A/[A + \epsilon(y_0-x_0)])$ against time was a straight line as required. The rate constant was calculated from the slope of this line. Results from a typical run are given in Table I. The last column gives $\log (A/[\epsilon(y_0-x_0) + A])$. The values of the rate constant, k, are given in Table II.

Inspection of Table II shows that there is no significant change of rate constant with hydroxide concentration.

Can. J. Chem. Downloaded from www.nrcresearchpress.com by 210.87.254.40 on 09/05/12
For personal use only.

TABLE I

(Run 2; at 30.0° C; $[NaOCl]_0 = 0.003967\ M$; $[Na_2SO_3]_0 = 0.002753\ M$; $[NaOH] = 0.102\ M$; ionic strength = 0.621)

Time, millisec	A	log β
11.4	0.150	0.3502
14.3	0.147	0.3617
15.9	0.144	0.3729
18.9	0.133	0.4249
28.0	0.129	0.4472
31.7	0.123	0.4886
39.2	0.118	0.5276
50.4	0.111	0.5977

TABLE II

Run	Temp., °C	Ionic strength	Initial $[OCl^-]$, M	Initial $[SO_3^{--}]$, M	Initial [NaOH], M	$k \times 10^{-4}$ (g-mole/l.)$^{-1}$sec^{-1}
1	30.0	0.621	0.003967	0.002759	0.102	1.26
2	"	"	"	0.002753	"	1.19
3	"	0.623	0.004660	0.001712	0.102	0.90
4	"	"	"	0.001710	"	0.83
5	"	0.632	0.006458	0.004487	0.102	0.91
6	"	"	"	0.004481	"	0.95
7	"	0.613	0.002354	0.001731	0.102	1.19
8	"	"	"	0.001727	"	0.97
9	"	1.12	0.004077	0.002561	0.102	0.93
10	"	"	"	0.002558	"	1.04
11	"	1.62	0.004172	0.002993	0.102	0.83
12	"	"	"	0.002989	"	0.83
13	"	0.620	0.003868	0.002810	0.0510	1.11
14	"	"	"	0.002807	"	0.91
15	"	0.623	0.004066	0.002766	0.204	1.27
16	"	"	"	0.002763	"	1.05
17	16.9	0.623	0.003700	0.002899	0.102	0.72
18	"	"	"	0.002889	"	0.53
19	"	0.619	0.003158	0.001943	0.102	0.60
20	"	"	"	0.001937	"	0.57
21	"	0.620	0.003262	0.002496	0.102	0.57
22	"	"	"	0.002487	"	0.60
23	42.4	0.616	0.004007	0.002952	0.101	1.62
24	"	"	"	"	"	1.77
25	"	0.615	0.003429	0.002825	0.101	1.80
26	"	"	"	"	"	1.68

The temperature dependence of rate constant gives an activation energy of 7.5 kcal mole^{-1}, log A is 9.43 (time in seconds).

REACTION OF HYPOCHLORITE AND IODIDE IONS

Chia and Connick (11, 12) have studied the oxidation of iodide ion by hypochlorite ions in alkaline solution. They found the rate law to be $d[IO^-]/dt = k[I^-][ClO^-]/[OH^-]$ and the rate constant at 25° C and an ionic strength of 1.00 to be 61 sec^{-1}. Since this rate constant has been measured at one temperature only, the present work was undertaken in order to determine the variation of rate constant with temperature and thereby obtain the activation energy.

Can. J. Chem. Downloaded from www.nrcresearchpress.com by 210.87.254.40 on 09/05/12
For personal use only.

Experimental Method

The sodium hypochlorite solutions were made up as in the study of the oxidation of sulphite. Sodium iodide solutions were analyzed as follows. A 25 ml aliquot of the stock iodide solution was transferred to a 250 ml glass-stoppered flask. One gram of urea (to destroy excess nitrous acid), 8 ml of 0.5 *M* sodium nitrite solution, and 5 ml of 4 *N* sulphuric acid were added. The flask was immediately stoppered to prevent the escape of iodine vapor and allowed to stand for about 10 minutes with frequent shaking. It was then cooled in an ice bath, 2 g of potassium iodide were added, and the solution was shaken well to dissolve all the iodine. The iodine was titrated with standard sodium thiosulphate solution, starch solution being added just before the end-point.

At 400 mμ the extinction coefficient for IO^- is 38.5 (12), while that for OCl^- is only 0.52. Therefore, this wavelength was chosen as the one for following the course of the reaction.

The method of carrying out the run was the same as in the oxidation of sulphite ions. A blank was run on the sodium iodide, a reaction graph on the recorder was made, and then another blank was run on the iodide to check for drift. A determination of the extinction coefficient of IO^- was carried out as follows. The chart recorder was started and the syringes were given a short push with the pusher block. Immediately the stopcocks were closed. A graph, made in this way, showed a sharp rise to a maximum, which corresponded to the maximum amount of hypoiodite formed, and then a slow decay, due to formation of iodate.

Chia showed that the rate expression is:

$$-d[OCl^-]/dt = k[OCl^-][I^-]/[OH^-]$$

or

$$dx/dt = -kxy/[OH^-]$$

which on integration leads to

$$\ln xy_0/yx_0 = (kt/[OH^-])(x_0-y_0).$$

If IO^- is the only absorbing species at 400 mμ, $x = A\epsilon$, where A is the absorbance (actually corrected), and

$$\ln x/y = \ln (x_0\epsilon-A)/(y_0\epsilon-A).$$

A plot of log $[(x_0\epsilon-A)/(y_0\epsilon-A)]$ against time gives a straight line of slope equal to $k(x_0-y_0)/[OH^-]$ 2.303, from which the rate constant can be calculated. Results from a typical run are given below.

TABLE III

(Run 43; at 17.7° C; $[NaOCl]_0$ = 0.04084 *M*; $[NaI]_0$ = 0.05103 *M*; [NaOH] = 0.2955 *M*; ionic strength = 1.00)

Time, millisec	*A''*, abs. corrected for drift	*A'*, abs. corrected for I_2OH^-	*A*, abs. corrected for OCl^-	log β
25.2	0.031	0.030	0.026	0.1048
32.9	0.053	0.051	0.048	0.1123
40.9	0.067	0.064	0.061	0.1168
50.5	0.092	0.088	0.085	0.1271
60.8	0.108	0.104	0.101	0.1348
66.8	0.118	0.113	0.110	0.1399
71.3	0.125	0.120	0.118	0.1443
77.4	0.133	0.128	0.126	0.1492
82.3	0.141	0.136	0.134	0.1544
90.4	0.147	0.142	0.140	0.1587
101.0	0.162	0.157	0.155	0.1703

Column 2 indicates the absorbance corrected for drift in the chart recorder. According to Chia and Sigalla (13), I_2OH^- is formed in the reaction mixture as

$$IO^- + I^- + H_2O \rightleftarrows I_2OH^- + OH^-,$$

although they differ as to the size of the equilibrium constant. Chia quotes a value of 0.13 at 25° C for $K = [I_2OH^-][OH^-]/[IO^-][I^-]$ while Sigalla's value is 0.03 for the same constant. Column 3 gives the absorbance corrected for the presence of I_2OH^-, the correction being applied in the following manner. Using Chia's value for K of 0.13, the $[I_2OH^-]$ was calculated. From this the contribution to A'' of the I_2OH^- was calculated at each point by using an extinction coefficient of 100 found for I_2OH^- by Chia. The contribution of I_2OH^-

Can. J. Chem. Downloaded from www.nrcresearchpress.com by 210.87.254.40 on 09/05/12
For personal use only.

was then subtracted from A'' to obtain A'. Column 4 gives the absorbance corrected for the presence of unreacted OCl^-, which absorbs only slightly at 400 mμ. The last column shows the values of log $[(x_0\epsilon - A)/(y_0\epsilon - A)]$. This varies linearly with time, as required by the proposed rate equations.

Table IV contains all the values of the rate constant determined for the hypochlorite–iodide reaction.

TABLE IV

Run	Temp., °C	Ionic strength	Initial [OCl^-], M	Initial [I^-], M	Initial [NaOH], M	k, sec^{-1}
27	25.0	1.00	0.02827	0.05034	0.2043	91.2
28	"	"	0.03131	0.05094	0.1627	91.1
29	"	"	"	"	"	95.0
30	"	"	0.04283	0.02036	0.1406	87.8
31	"	"	"	"	"	87.1
32	"	"	0.04273	0.05094	0.4570	90.9
33	"	"	"	"	"	88.8
34	"	"	0.04244	0.04876	0.3021	95.6
35	"	"	"	"	"	93.9
36	34.3	"	0.04184	0.04861	0.2941	174
37	"	"	"	"	"	173
38	"	"	0.02791	0.04861	0.5933	178
39	"	"	"	"	"	182
40	"	"	0.04166	0.02429	0.4164	164
41	"	"	"	"	"	175
42	17.7	"	0.04084	0.05103	0.2955	59.7
43	"	"	"	"	"	57.0
44	"	"	0.02715	0.04925	0.1989	60.0
45	"	"	"	"	"	60.3
46	"	"	0.04005	0.02461	0.1967	54.3
47	"	"	"	"	"	53.5

As in the case of the oxidation of nitrite (9) and formate ions (14) by sodium hypochlorite, the rate of the oxidation of iodide is also inversely proportional to the hydroxide concentration as shown by the relative constancy of k in Table IV over a wide range of NaOH concentration. Similarly, this reaction is probably one of the undissociated hypochlorous acid and the rate is given by

$$\text{rate} = k_T[HOCl][I^-],$$

where k_T is the rate constant of the slow step. If the mechanism is given by

$$OCl^- + H_2O \overset{K_h}{\rightleftharpoons} HOCl + OH^-$$

$$HOCl + I^- \overset{k_T}{\rightarrow} HOI + Cl^- \text{ (slow step)}$$

$$HOI + OH^- \rightleftharpoons IO^- + H_2O$$

where steps 1 and 3 are rapid equilibria and step 2 is rate-determining, then

$$-d[OCl^-]/dt = k_T K_h([OCl^-][I^-]/[OH^-])$$

and

$$k_T = k/K_h.$$

K_h, calculated from the known values of K_w and K_A for the dissociation of HOCl, is 2.8×10^{-7} at 25° C, and therefore k_T is 3.3×10^8 liters $mole^{-1}$ sec^{-1} at an ionic strength of 1.00 at 25° C. The apparent activation energy, E_a, calculated from the variation of k with temperature, is 11.9 kcal $mole^{-1}$. Data on the heats of formation of the compounds (in aqueous solution) in the reaction

$$NaOCl + H_2O \rightarrow HOCl + NaOH$$

make the heat of hydrolysis of the hypochlorite ion to be 11.0 kcal $mole^{-1}$. Hence, the energy of activation for the reaction of iodide ions and hypochlorous acid is only 0.9 kcal $mole^{-1}$.

Can. J. Chem. Downloaded from www.nrcresearchpress.com by 210.87.254.40 on 09/05/12
For personal use only.

Hypoiodite decomposes at a much faster rate than does hypobromite or hypochlorite. However, the decomposition of hypoiodite could be disregarded in the calculation of rate constant, since the oxidation of iodide is much faster than the decomposition of hypoiodite. Li and White (15) have studied the decomposition, the overall reaction being

$$3OI^- \rightarrow IO_3^- + 2I^-,$$

and have found that the decomposition can proceed along two paths.

$$-d[OI^-]/dt = k'[OI^-]^2 + (k''[OI^-]^2[I^-]/[OH^-])$$

At 25° C they have determined a k'' of 104 (time in minutes) and a k' of 2.9 (time in minutes).

In the present work it was an easy matter to check the rate constants by a simple stopped-flow method. A k'' of 180 (time in minutes) was obtained at 25° C.

In applying the correction for I_2OH^-, Chia's value for the equilibrium constant was used, as well as his value for the extinction coefficient of I_2OH^-. Chia states that this is a rapidly established equilibrium, though there is no evidence, at present, to show whether it is really fast relative to the times involved in the present measurements. If further work shows that the formation of I_2OH^- is in fact slow, the rate constant would be about 6% too high.

The mean value of k at 25° C and an ionic strength of 1.0 is 91.3. This is appreciably higher than Chia's value of 61, and at present the cause of the discrepancy is unknown.

DISCUSSION OF RESULTS

The present results, together with others from earlier work, cover a series of oxidations by hypochlorite ions, or hypochlorous acid. These results are summarized in Table V. The rate constants in this table are all second order constants, with time measured in seconds. E_a is the activation energy, and A in column 5 is the pre-exponential factor in the usual equation, $k = A \exp(-E_a/RT)$.

It will be noted that the reactions in Table V are either due to OCl^- or HOCl. In the mildly alkaline solutions on which these measurements were made, the pH dependence of the reactions showed that one or the other species (but not both) was responsible for the reaction. It does not at present seem possible to explain why certain reducing agents favor one path rather than the other. Reactions of hydrogen peroxide, on the other hand, often follow a rate equation, which is interpreted by Edwards (16) as showing that both H_2O_2 and $H_3O_2^+$ contribute appreciably to the total reaction.

It was mentioned at the beginning of this paper that peroxides give a series of reactions whose rates can be correlated with other properties of the reagents. In particular, Edwards (16) has observed that if different peroxides, of formula ROOH ,where R is any group of atoms (or hydrogen) react with the same reducing agent (e.g. Br^-), then the rates are related to the stability of the ion RO^-. This is explained by the mechanism:

$$R\text{—}O\text{—}O\text{—}H + Br^- \rightarrow R\text{—}O\text{—}O(Br)\text{—}H \xrightarrow{\text{slow}} RO^- + HOBr,$$

$$HOBr + H_3O^+ + Br^- \rightarrow Br_2 + 2H_2O \text{ (fast)},$$

$$RO^- + H_3O^+ \rightarrow ROH + H_2O \text{ (fast)},$$

the suggestion being that if RO^- is stable, the products are formed more rapidly. The relevant stability of RO^- is assumed to be its stability compared with ROH; that is, if pK_a of ROH is low, RO^- is relatively stable. In fact if log k (where k is the rate constant) is plotted against pK_a of ROH a straight line is obtained, with slope, $d \log(k/dpK_a)$, of about −0.4. The reactions of HOCl with Br^- or I^- fall on nearly the same line as do the peroxide reactions, if we take RO^- to be Cl^-, and pK_a for HCl as −7 (17). The data are shown in Fig. 1. This agreement may be partly coincidental, since we are comparing breaking O—O and O—Cl bonds, but these are similar in strength.

Can. J. Chem. Downloaded from www.nrcresearchpress.com by 210.87.254.40 on 09/05/12
For personal use only.

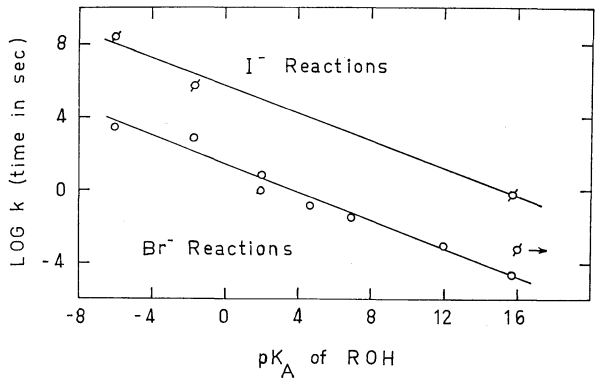

FIG. 1.

Many reactions of peroxides have a relatively low value of log A (16, p. 71); or, in other words, a negative entropy of activation, the values falling between -15 and -35 cal/degree. This is explained on the supposition that the activated complex requires rather careful orientation of the incoming reducing agent. This should also apply to reactions of hypochlorite ions (or HOCl) when the mechanism would be

$$\text{Cl—O(H)} + X^- \rightarrow \text{Cl—O(H)—}X^- \rightarrow Cl^- + XOH.$$

The atoms ClOX are roughly linear in the activated complex. The values of $\Delta S^{\ddagger}$ given in Table V mostly fall in the same range of -15 to -35 cal/degree. The relatively high values with iodate and oxalate ions cannot be explained at present.

A correlation between the activation energy and the heat of reaction ($\Delta H°$) seems to exist. This might reasonably be expected, since if a strong bond is being formed the maximum of energy in the transition state will probably be reached earlier. Other factors, such as the energy of hydration of the various ions, will, of course, modify the results, but the heat of reaction is bound to be an important factor. Figure 2 shows a plot of $\Delta H°$ against activation energy for reactions of OCl^- and HOCl. In both cases the graph is roughly linear with a slope, $dE_a/d\Delta H°$ of 0.22 for OCl^-, and roughly the same for HOCl.

TABLE V

Oxidizing agent	Reducing agent	Log K (25° C)	E_a, kcal	Log A	$\Delta S^{\ddagger}$, cal/deg	Ref.
OCl^-	IO_3^-	−5.04	26.1	14.1	4	*a*
"	OCl^-	−7.63	24.8	10.6	−12.5	*b*
"	ClO_2^-	−5.48	20.8	9.8	−16	*b*
"	SO_3^{-2}	3.93	7.5	9.4	−17.5	—
HOCl	NO_2^-	0.82	6.5	5.6	−35	*a*
"	$HCOO^-$	−1.38	6.7	3.5	−44.5	*c*
"	Br^-	3.47	4.5	6.8	−29.5	*d*
"	OCN^-	−0.55	15.1	10.5	−12.5	*e*
"	$HC_2O_4^-$	1.20	15.0	12.2	−5	*f*
"	I^-	8.52	0.9	9.2	−18.5	—

REFERENCES
a. M. W. LISTER and P. ROSENBLUM. Can. J. Chem. **39**, 1645 (1961).
b. M. W. LISTER. Can. J. Chem. **34**, 465 (1956).
c. M. W. LISTER and P. ROSENBLUM. Can. J. Chem. 41, 2727 (1963).
d. L. FARKAS, M. LEWIN, and R. BLOCH. J. Am. Chem. Soc. **71**, 1988 (1949).
e. M. W. LISTER. Can. J. Chem. **34**, 489 (1956).
f. R. O. GRIFFITH and A. MCKEOWN. Trans. Faraday Soc. **28**, 518 (1932).

Can. J. Chem. Downloaded from www.nrcresearchpress.com by 210.87.254.40 on 09/05/12
For personal use only.

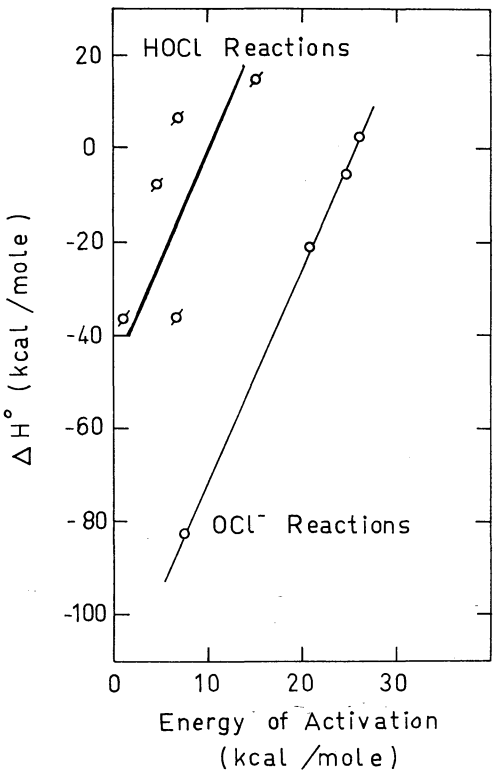

FIG. 2.

REFERENCES

1. J. O. EDWARDS. J. Am. Chem. Soc. **76**, 1540 (1954).
2. J. O. EDWARDS. J. Am. Chem. Soc. **78**, 1819 (1956).
3. J. O. EDWARDS. J. Phys. Chem. **56**, 279 (1952).
4. H. HARTRIDGE and F. J. W. ROUGHTON. Proc. Roy. Soc. (London), Ser. A, **104**, 395 (1923).
5. F. J. W. ROUGHTON and G. A. MILLIKAN. Proc. Roy. Soc. (London), Ser. A, **155**, 260 (1936).
6. F. J. W. ROUGHTON. Proc. Roy. Soc. (London), Ser. A, **155**, 269 (1936).
7. G. A. MILLIKAN. Proc. Roy. Soc. (London), Ser. A, **155**, 277 (1936).
8. K. DALZIEL. Biochem. J. **55**, 79 (1953).
9. M. W. LISTER and P. ROSENBLUM. Can. J. Chem. **39**, 1645 (1961).
10. D. DUBOIS. J. Biol. Chem. **137**, 123 (1941).
11. Y. T. CHIA and R. E. CONNICK. J. Phys. Chem. **63**, 1518 (1959).
12. Y. T. CHIA. U.S. Atomic Energy Comm. UCRL–8311. 1958.
13. J. SIGALLA. J. Chim. Phys. **58**, 602 (1961).
14. M. W. LISTER and P. ROSENBLUM. Can. J. Chem. **41**, 2727 (1963).
15. C. H. LI and C. F. WHITE. J. Am. Chem. Soc. **65**, 335 (1943).
16. J. O. EDWARDS. Peroxide reaction mechanisms. Interscience Publishers, New York. 1962. p. 67.
17. R. P. BELL. The proton in chemistry. Cornell Univ. Press, Ithaca, N.Y. 1959. p. 87.

Can. J. Chem. Downloaded from www.nrcresearchpress.com by 210.87.254.40 on 09/05/12
For personal use only.

CHARACTERISTIC VIBRATIONAL FREQUENCIES OF OXYGEN COMPOUNDS OF SILICON, PHOSPHORUS, AND CHLORINE: CORRELATION OF STRETCHING FREQUENCIES AND FORCE CONSTANTS WITH BOND LENGTHS AND BOND ORDERS

E. A. ROBINSON
Department of Chemistry, University of Toronto, Toronto, Ontario
Received June 25, 1963

Can. J. Chem. Downloaded from www.nrcresearchpress.com by 210.87.254.40 on 09/05/12
For personal use only.

ABSTRACT

For oxygen compounds of chlorine, phosphorus, and silicon, respectively, correlations are established between stretching frequencies and force constants of Cl—O, P—O, and Si—O bonds, and their bond lengths.

By deducing bond orders on the assumption that only $3d_{x^2-y^2}$ and $3d_{z^2}$ orbitals on the central chlorine, phosphorus, or silicon atom are utilized in the formation of double bonds with lone pairs of electrons on oxygen, linear correlations between bond orders and force constants are established.

The present treatment leads to the conclusion that the presence of a maximum of 12 electrons in the valency shells of chlorine, phosphorus, and silicon is required to best explain the bond length and force constant data, when highly electronegative ligands such as oxygen or fluorine are attached to the central silicon, phosphorus, or chlorine atom.

INTRODUCTION

In a previous paper (1) we have obtained a correlation between the lengths and stretching frequencies, or force constants, of S—O bonds, and the problem of defining and measuring the bond orders of S—O bonds was also discussed. It was shown that there is a linear correlation between bond order, simply defined as the number of electron pairs in the bond, and the stretching force constant. The general validity of a linear relationship between bond order and stretching force constant was discussed in a recent paper (2).

The assignment of spectral frequencies to the symmetric and asymmetric stretching modes of PO_2 and ClO_2 groups was discussed recently (3). It was shown that there are straight line correlations between the symmetric and asymmetric frequencies and these correlations are useful in assigning the frequencies of P—O and Cl—O stretching vibrations in species of the type $X_2PO_2^-$, XPO_3^{2-}, PO_4^{3-}, and $XClO_3$, ClO_3^-, ClO_2, ClO_2^-, and ClO_4^-, respectively. The frequencies assigned previously (3) are used as the basis of this paper.

It was shown previously (1) that Lehmann's approximate method of reducing the symmetric and asymmetric A—B stretching frequencies of AB_2, AB_3, and AB_4 groups to the vibrational frequency of an 'equivalent' AB group (4) can be successfully used to calculate the force constants of S—O bonds in SO_2, SO_3, and SO_4 groups. In this paper the same method is applied to PO_2, PO_3, and PO_4, and ClO_2, ClO_3, and ClO_4 groups. The force constants so obtained are compared with those obtained by more rigorous methods, where such data are available.

CHLORINE–OXYGEN BONDS

The Cl—O stretching frequencies and observed bond lengths for various species containing this bond are shown in Table I, which also shows the Cl—O stretching frequency of an equivalent Cl—O group calculated by the method of Lehmann (4), and the force constant calculated from it by treating the Cl—O group as a simple diatomic molecule.

TABLE I

Bond-lengths, stretching frequencies, and force constants for oxygen compounds of chlorine

	ν_{sym}	ν_{asym} (cm^{-1})	ν_{Cl-O}	r_{Cl-O} (Å)	$k\times10^{-5}$ (dynes cm^{-1}) (i)[a]	(ii)[b]
ClO^-	713	—	713	—	3.30	3.30[d]
Cl_2O	—	—	—	1.68 ±0.02[h] 1.70 ±0.02[h]	—	4.96[d], 3.74[f]
ClO_2^-	860	952	906	1.57 ±0.03[g]	5.33	4.18[d], 4.4[e]
ClO_3^-	930	1087	1035	1.46 ±0.01[g]	6.96	6.62[d], 6.76[e]
ClO_2	943	1110	1026	1.49 ±0.014[h] 1.47_3 ±0.01	6.83	7.4[d], 6.76[e]
ClO_4^-	935	1110	1066	1.46[g]	7.30	8.2[d], 6.68[e]
Cl_2O_7	1034 1057	1270 1295	1198	1.424±0.01[i]	9.32	—
$HO.ClO_3$	1050	1326 1263	1213	1.42[g]	9.55	8.02[e]
	740[c]	—	740[c]	1.64[g]	3.79	4.04[e]
$FOClO_3$	1049	1298	1215	—	9.58	—
$FClO_3$	1061	1260 1315	1230	—	9.82	—

[a](i) = Present results.
[b](ii) = Other workers.
[c]Cl—OH (corrected for mass of —OH).
[d]See ref. 17.
[e]H. Siebert. Z. Anorg. Allgem. Chem. **275**, 225 (1954).
[f]K. Venkateswarlu and P. Thirugnanasambandam. Z. Phys. Chem. **212**, 138 (1954).
[g]See ref. 9.
[h]See ref. 8.
[i]See ref. 7.

These force constants are compared with those obtained by other workers using more sophisticated methods. Figure 1 shows the plot of ν_{Cl-O} against bond length, and the

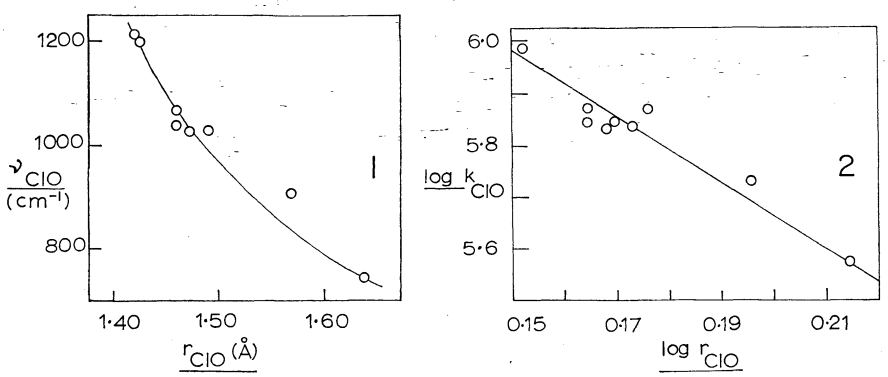

FIG. 1. r_{Cl-O} plotted against bond length.
FIG. 2. log r_{Cl-O} plotted against log k_{Cl-O}.

logarithm of bond length is plotted against the logarithm of force constant in Fig. 2. The latter plot is a straight line which is given by the equation

$$\log k_{Cl-O} = -6.45 \log r_{Cl-O} + 7.0$$

or

$$k_{Cl-O}\, r_{Cl-O}^{6.45} = 1.00\times10^{7} \qquad [1]$$

Can. J. Chem. Downloaded from www.nrcresearchpress.com by 210.87.254.40 on 09/05/12
For personal use only.

which is the form of the relationship suggested by Linnett (5) on the basis Clark's relationship between bond length and force constant (6).

Force Constant – Bond Order Relationship

The longest Cl—O bonds reported in the literature are 1.64 Å for in perchloric acid (7), 1.70 Å in Cl_2O (8), and 1.725±0.03 Å for th in Cl_2O_7 (9). It therefore seems likely that the Cl—O single-b 1.70 Å. Equation [1] enables the value of the stretching force c of length 1.70 Å to be calculated. The value obtained is 3. is very close to the force constant calculated for the Cl—C (10).

We assume, as we did previously in the case of S—C $3d_{z^2}$ orbitals on chlorine are used in π-bonding with and then predicted bond orders are easily calculate electrons in the valency shell of chlorine. For ex as perchloryl fluoride the maximum Cl—O bor to resonance structures such as I.

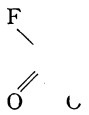

I

The Cl—O stretching force constant in this compound ues cm^{-1} which is the highest Cl—O force constant observed for the Cl—O compound. This is consistent with the fact that there are four highly electroneg groups attached to the central chlorine atom. The force constant is to be compared with that of the S—O bonds in the fluorosulphate ion (structure II), which has the value 8.8×10^5 dynes cm^{-1}

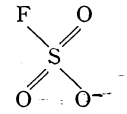

II

(1). Similarly we might expect the Cl—O bond order in the perchlorate ion to be 1.50 (structure III), and the most reliable value for the Cl—O force constant is probably 8.2×10^5 dynes cm^{-1} (11) (cf. $k = 7.1\times10^5$ dynes cm^{-1} for the sulphate ion (1)).

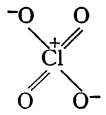

III

On the basis of the force constants 3.3×10^5, 8.2×10^5, and 9.8×10^5 dynes cm^{-1} for bond orders 1.00, 1.50, and 1.67, respectively, a linear force constant – bond order relationship is suggested as is shown in Fig. 3. This is theoretically justifiable (2) and consistent with the similar relationship obtained for S—O bonds (1). It is interesting to note that the linear force constant – bond order curve for Cl—O bonds is almost

Can. J. Chem. Downloaded from www.nrcresearchpress.com by 210.87.254.40 on 09/05/12
For personal use only.

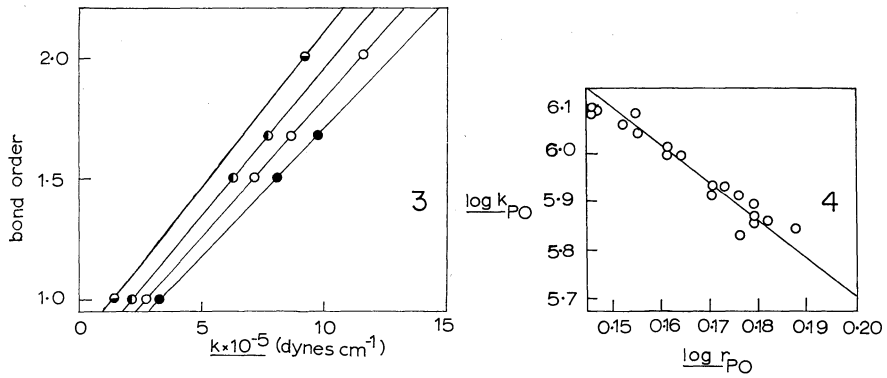

FIG. 3. Bond order – force constant relationships. Key: Cl—O, ●; S—O, ○; P—O, ◐; Si—O, ◒.
FIG. 4. log r_{P-O} plotted against log k_{P-O}.

parallel to that obtained for S—O bonds (Fig. 3). The bond order – force constant relationship fits the equation

$$n_{Cl-O} = 1.02\times10^{-6}\, k_{Cl-O} + 0.66, \qquad [2]$$

where n_{Cl-O} is the bond order.

Bond Order – Bond Length Relationship

Combination of equations [1] and [2] gives a relationship between bond order and bond length.

$$n_{Cl-O} = 10.2/r_{Cl-O}^{6.45} + 0.66 \qquad [3]$$

Bond lengths calculated from this equation for various values of the bond order, n_{Cl-O}, are shown in Table III.

TABLE II

Bond orders and calculated P—O and Cl—O bond lengths

Bond order, n	Bond length			
	r_{P-O} (Å)		r_{Cl-O} (Å)	
	(*a*)	(*b*)	(*c*)	(*d*)
1.0	1.760	(1.76)*	1.698	(1.70)*
1.1	1.689	1.697	1.628	1.634
1.2	1.636	1.646	1.577	1.580
1.33	1.587	1.592	1.525	1.525
1.4	1.565	1.569	1.502	1.501
1.5	1.538	(1.54)*	1.472	1.471
1.6	1.514	1.516	1.447	1.445
1.67	1.500	1.499	1.431	(1.43)*
1.7	1.494	1.492	1.424	1.423
1.8	1.474	1.472	1.405	1.403
1.9	1.458	1.455	1.387	1.386
2.0	1.446	(1.45)*	1.370	(1.37)*

NOTE: (*a*) calculated from equation [3]; (*b*) calculated from equation [4]; (*c*) calculated from equation [7]; (*d*) calculated from equation [8].
*Assumed value.

We have shown (1) that the Pauling relationship between bond length and bond order (12) can also be applied to S—O bonds. It therefore seems appropriate to apply

Can. J. Chem. Downloaded from www.nrcresearchpress.com by 210.87.254.40 on 09/05/12
For personal use only.

TABLE III

Calculated bond orders and bond lengths for oxygen compounds of chlorine

	$k\times10^{-5}$ (dynes cm^{-1})	Bond order,* n	Bond length (Å)	
			r_{obs}	r_{calc}†
ClO^-	3.30	1.00	(1.70)	1.70
Cl_2O	4.96	1.17 (?)	1.70	1.59
ClO_2^-	5.33	1.20	1.57 ±0.03	1.57
ClO_3^-	6.96	1.38	1.48 1.46 ±0.01	1.50
ClO_2	6.83	1.36	1.49 ±0.014 1.47_3±0.01	1.50
ClO_4^-	8.20	1.50	1.46 ±0.01 1.45_2±0.005	1.47
Cl_2O_7‡	9.32	1.62	1.42_4±0.01	1.44
$HOClO_3$	9.55	1.64	1.42	1.43
	3.79§	1.05	1.64	1.66
$FOClO_3$	9.58	1.65	—	1.43
$FClO_3$	9.82	1.67	—	1.43

*Calculated from force constant.
†Calculated from equation [3].
‡Terminal bonds.
§Cl—OH.

the same relationship to Cl—O bonds. On the basis of the Cl—O single-bond length of 1.70 Å and the lengths of bonds of order 1.67 and 2.00, which can be calculated from equation [3] as 1.43 Å and 1.37 Å, respectively, the constants in the Pauling equation may be calculated. The equation takes the form

$$r_{Cl-O} = 1.70 - \frac{0.33}{1+0.44\left[\frac{2-n}{n-1}\right]}. \qquad [4]$$

Bond lengths calculated from this equation for given bond orders are compared with those obtained from equation [3] in Table II. Both equations give very similar values.

Table III shows the bond orders obtained from the stretching force constants, the observed bond lengths, and the bond lengths calculated from the bond orders by means of equation [3].

PHOSPHORUS–OXYGEN BONDS

Phosphorus–oxygen stretching frequencies, bond lengths, and stretching force constants are collected in Table IV. Figure 4 shows the plot of the logarithm of force constant against the logarithm of the bond length. As was found to be the case for S—O bonds (1) and for Cl—O bonds, this plot is a straight line given by the equation

$$\log k_{P-O} = -8.0 \log r_{P-O} + 7.30$$

or

$$k_{P-O} r^{8.0} = 2.0\times10^7 \qquad [5]$$

Extrapolation to the sum of the Pauling covalent radii of phosphorus and oxygen (r_{P-O} = 1.76 Å) gives the value $k_{P-O} = 2.2\times10^5$ dynes cm^{-1} for the force constant of a single bond.

Force Constant – Bond Order Relationship

On the basis of the assumption that only the $3d_{x^2-y^2}$ and $3d_{z^2}$ orbitals of phosphorus

Can. J. Chem. Downloaded from www.nrcresearchpress.com by 210.87.254.40 on 09/05/12
For personal use only.

TABLE IV

Stretching frequencies and force constants for some oxygen compounds of phosphorus

	ν_{sym}	ν_{asym}	ν_{P-O}	$k\times10^{-5}$ (dynes cm^{-1}) (i)[a]	$k\times10^{-5}$ (dynes cm^{-1}) (ii)[b]
$PO_2(OH)_2^{-3}$	870	927[e]	927[d]	5.34	
$C_6H_5PO(OH)_2$[c]	920	1000[e]	990[d]	6.09	
PO_4^{3-}	948	1025[f]	987	6.33	5.65,[m] 5.93[n], 5.80[n]
	980	1082[e]	1057	6.94	
HPO_3^{2-}	980	1100[e]	1060	6.98	6.03[m]
$CH_3OPO_3^{2-}$	985	1100[e]	1062	7.00	
$PO_2(OH)^-$	1014	1106[e]	1065	7.05	
$P_2O_8^{4-}$	998	1115[e]	1076	7.19	
$P_2O_6^{4-}$	1002	1128[e]	1086	7.33	
$P_2O_7^{4-}$	1018	1128[e]	1091	7.40	
$(CH_3)_2PO_2^-$	1028	1168[e]	1098	7.49	
$H_3N^+PO_3^-$	994	1158[e]	1103	7.56	
FPO_3^{2-}	1005	1175[e]	1118	7.77	
$H_2PO_2^-$	1050	1200[e]	1125	7.86	7.43[m]
$P_3O_9^{3-}$	1075	1250[g]	1162	8.40	
$H_2P_2O_7^{2-}$	1087	1253[e]	1170	8.51	
$PO(CH_3)_3$	1170	—	1170	8.51	
$(HO)_2PO_2^-$	1065	1284[e]	1174	8.57	
$P_4O_{12}^{4-}$	1100	1250[g]	1175	8.58	
$F_2PO_2^-$	1125	1262[h]	1194	8.86	
$POBr_3$	1261[i]		1261	9.89	9.59[m]
$POCl_3$	1290[i,j]		1290	10.35	9.98[m]
$PO(CF_3)_3$	1328[k]		1328	11.00	
$POFCl_2$	1331[i]		1331	11.02	
POF_2Cl	1358[i]		1358	11.47	
P_4O_{10}	1400[l]		1400	12.19	11.0[m]
POF_3	1415[j]		1415	12.45	11.39[m]

[a](i) = Present values.
[b](ii) = Other workers.
[c]P—OH.
[d]ν_{P-O} corrected for mass of —OH.
[e]See ref. 3.
[f]See ref. 12.
[g]J. V. Pustinger, W. T. Cave, M. L. Nielsen. Spectrochim. Acta, **15**, 909 (1959).
[h]E. A. Robinson and D. Lavery. Unpublished experiments.
[i]J. V. Bell, J. Heisler, H. Tannebaum, and J. Goldeson. J. Am. Chem. Soc. **76**, 5185 (1954).
[j]J. S. Ziomek and E. A. Pietrowski. J. Chem. Phys. **34**, 1087 (1961).
[k]R. C. Paul. J. Chem. Soc. 574 (1955).
[l]L. W. Daasch and D. C. Smith. Anal. Chem. **23**, 853 (1951).
[m]H. Siebert. Z. Anorg. Allgem. Chem. **275**, 225 (1954).
[n]C. W. F. T. Pistorius. J. Chem. Phys. **28**, 514 (1958).

are available for π-bonding, the maximum bond orders expected are 1.50 in the phosphate ion (structure IV), 1.67 in ions of the type XPO_3^{2-} (structure V), 2.00 in ions of the type $X_2PO_2^-$ (structure VI), and 3.00 in compounds of the type X_3PO (structure VII).

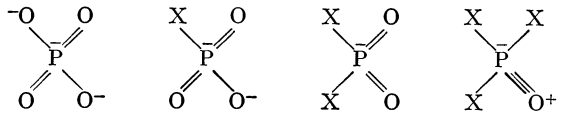

IV V VI VII

The maximum possible bond orders are expected to be approached when the substituents X are highly electronegative ligands such as oxygen or fluorine.

The P—O stretching frequencies are 6.3×10^5 dynes cm^{-1} (12), for the bonds in the phosphate ion ($n_{P-O} = 1.50$), and 7.8×10^5 dynes cm^{-1} for the monofluorophosphate ion ($n_{P-O} = 1.67$), where the maximum possible bond orders might be expected to be achieved. These force constants and bond orders, together with the force constant for a single bond ($n_{P-O} = 1.00$; $k_{P-O} = 2.2\times10^5$ dunes cm^{-1}), fit a straight line correlation

Can. J. Chem. Downloaded from www.nrcresearchpress.com by 210.87.254.40 on 09/05/12
For personal use only.

between P—O bond order and stretching force constant, as is shown in Fig. 3. The straight line is given by

$$n_{P-O} = 1.19\times10^{-6}\, k_{P-O} + 0.74 \quad [6]$$

and is nearly parallel to the linear bond order – force constant plots obtained for Cl—O and S—O bonds.

Bond Order – Bond Length Relationship

Combination of equations [5] and [6] gives a correlation between bond order and bond length,

$$n_{P-O} = 23.8/r^8_{P-O} + 0.74. \quad [7]$$

Equation [7] gives bond lengths of 1.54 Å and 1.44 Å for P—O bonds of order 1.5 and 2.0, respectively, and the single bond length is 1.76 Å. These distances allow the parameters in the Pauling equation (12) to be evaluated, giving

$$r_{P-O} = 1.76 - \frac{0.32}{1+0.45\left[\frac{2-n}{n-1}\right]}. \quad [8]$$

Calculated bond lengths obtained from equations [7] and [8] are shown in Table II. Both equations give comparable values.

Bond orders calculated from the stretching force constants of P—O bonds in various

TABLE V

Bond orders and bond lengths for oxygen compounds of phosphorus

	$k\times10^{-5}$ (dynes cm^{-1})	Bond order n	Bond length[a] (Å)	
			r_{obs}	r_{calc}
$PO_2(OH)_2^{-2}$	5.34	1.38	1.58[d]	1.57
$C_6H_5PO(OH)_2$[b]	6.09	1.47	—	1.54
PO_4^{3-}	6.34	1.50	1.54[d]	1.54
HPO_3^{2-}	6.98	1.58	1.51 ±0.05[e]	1.52
$CH_3OPO_3^{2-}$	7.00	1.58	1.50 ±0.01[d]	1.52
$PO_2(OH)^-$	7.05	1.58	—	1.52
$P_2O_8^{4-}$	7.19	1.60	—	1.51
$P_2O_6^{4-}$	7.33	1.62	—	1.51
$P_2O_7^{4-}$	7.40	1.64	1.51 ±0.15[d]	1.50
$(CH_3)_2PO_2^-$	7.49	1.64	1.50 ±0.02[e]	1.50
$H_3N^+.PO_3^-$	7.56	1.66	1.522±0.011[d]	1.50
FPO_3^{2-}	7.77	1.67	1.49[f]	1.50
$H_2PO_2^-$	7.86	1.69	1.51[e]	1.49
$P_3O_9^{3-}$	8.40	1.75	1.48[d]	1.48
$H_2P_2O_7^{2-}$	8.51	1.76	—	1.48
$PO(CH_3)_3$	8.51	1.76	—	1.48
$(HO)_2PO_2^-$	8.57	1.76	1.538±0.005[e]	1.48
$P_4O_{12}^{4-}$	8.58	1.78	1.49[d]	1.47
$F_2PO_2^-$	9.15	1.84	—	1.46
$POBr_3$	9.89	1.92	1.41 ±0.07[e]	1.46
$POCl_3$	10.35	1.95	1.45 ±0.03[e]	1.45
$PO(CF_3)_3$	11.00	2.00	—	1.44
$POFCl_2$	11.02	2.05	1.54 ±0.03[e]	1.44
POF_2Cl	11.47	2.11	1.55 ±0.02[e]	1.43
P_4O_{10}	12.19	2.18	1.40 ±0.02[d]	1.42
POF_3	12.45	2.22	1.45 ±0.02[e]	1.42

[a]Calculated from equation [7].
[b]P—OH bonds.
[c]This is the P—O distance in calcium thymidylate (see ref. 9).
[d]See ref. 8.
[e]See ref. 9.
[f]M. T. Robinson (J. Chem. Phys. **62**, 925 (1958) reports two P—O distances in K_2PO_3F of 1.44±0.16 and 1.53±0.10 Å, respectively (mean 1.49 Å).

Can. J. Chem. Downloaded from www.nrcresearchpress.com by 210.87.254.40 on 09/05/12
For personal use only.

species are shown in Table V, which also gives P—O bond lengths calculated from these bond orders by means of equation [7].

The bond lengths reported for the P—O bonds in the phosphoryl halides (8) require some comment. The bond length reported for the P—O bond in POF_3 is 1.45±0.02 Å, which is the same as the length of the P—O bond in $POCl_3$ (1.45±0.03 Å), while that in POF_2Cl is 1.55±0.02 Å and the length of the P—O bond in $POBr_3$ is given as 1.41 ±0.07 Å. These bond lengths are clearly inconsistent with, e.g., the P—O stretching frequencies which increase from $POBr_3$, to $POCl_3$, to POF_2Cl, to POF_3, and show a definite correlation with the electronegativities of the ligands attached to phosphorus. It is thus clear that there is inconsistency in the observed values whereas the calculated values of both bond length and bond order show the expected trend with the sum of the electronegativities of the attached ligands.

SILICON–OXYGEN BONDS

Unfortunately very little data is available for the bond lengths and force constants of Si—O bonds but it seems justifiable to assume that the relationship between bond order and stretching force constant is linear as it is for S—O, P—O, and Cl—O bonds, so that just two pairs of bond orders and force constants are required to define the correlation.

We have seen previously that there are linear correlations between logarithms of bond lengths and logarithms of stretching force constants for P—O, Cl—O, and S—O (1) bonds, respectively. The available data for Si—O bonds are given in Table VI and plotted

TABLE VI

Stretching frequencies, force constants, and bond lengths, for silicon–oxygen compounds

	ν_{sym}	ν_{asym}	ν_{Si-O}	Ref.	$k_{Si-O}\times10^{-5}$ (dynes cm^{-1})	r_{Si-O} (Å)	Ref.
$(CH_3)_3Si.OH$	881	—	908*	*a*	4.95	1.63†	—
$(C_2H_5)_2Si(OH)_2$	830	840	847*	*a*	4.48	1.63	*c*
SiO	1242	—	1242	*b*	9.25	1.51	*b*
	851	—	851	*b*	4.35	1.62	*b*

*Corrected for mass of —OH group.
†Assumed same as distance in $(C_2H_5)_2Si(OH)_2$.
REFERENCES: (*a*) Barraclough, Bradley, Lewis, and Thomas. J. Chem. Soc. 2601 (1961). (*b*) Herzberg. Molecular spectra and molecular structure. Vol. 1. D. van Nostrand, New York. 1950. p. 570. (*c*) See ref. 8.

in Fig. 5, assuming a linear correlation between $\log r_{Si-O}$ and $\log k_{Si-O}$. If the length of a single Si—O bond is taken as 1.83 Å (the sum of the Pauling covalent radii of Si and O), extrapolation of the straight line in Fig. 5 gives a value of 1.5×10^5 dynes cm^{-1} for the force constant of a single Si—O bond. This value seems reasonable in comparison with the values 2.2, 2.7, 3.3×10^5 dynes cm^{-1} for the force constants of single P—O, S—O (1), and Cl—O bonds, respectively.

We could assume that the bond order of the Si—O bonds in the silicate ion are 1.50; however, unfortunately, no reliable values seem to be available for the vibrational frequencies of this species. For example, the values given by Siebert (13) for SiO_4^{4-} are the same as those attributed to the $(HO)_2SiO_2^{2-}$ ion by Fortnum and Edwards (14).

Analysis of the spectrum of the diatomic species SiO leads to a value of 1.51 Å for the bond length and 9.25×10^5 dynes cm^{-1} for the force constant (15). The bond length of 1.51 Å suggests that the bond in SiO may be a double bond (cf. the double bond lengths Cl=O, 1.37; S=O, 1.40; and P=O, 1.45 Å). On the basis of the assumed double

Can. J. Chem. Downloaded from www.nrcresearchpress.com by 210.87.254.40 on 09/05/12
For personal use only.

TABLE VII

Bond angles in some halides, oxyhalides, and oxides*

Br_3P:	$\overset{\frown}{BrPBr}$	106±3°	$Cl_2\ddot{S}O$	$\overset{\frown}{ClSCl}$	114±2°	$\overset{\frown}{OSCl}$	106±1°
Br_3PO	$\overset{\frown}{BrPBr}$	108±3°	Cl_2SO_2	$\overset{\frown}{ClSCl}$	111.2±2°	$\overset{\frown}{OSCl}$	106.5±2°
Cl_3P:	$\overset{\frown}{ClPCl}$	100.1±0.3°	$F_3\ddot{S}O$	$\overset{\frown}{FSF}$	92.8±0.1°	$\overset{\frown}{OSF}$	106.8±1°
Cl_3PO	$\overset{\frown}{ClPCl}$	103.6±2°	F_2SO_2	$\overset{\frown}{FSF}$	92.8±0.5°	$\overset{\frown}{OSF}$	—
F_3P:	$\overset{\frown}{FPF}$	104±4°	$:SO_2$	$\overset{\frown}{OSO}$	119.5°		
F_3PO	$\overset{\frown}{FPF}$	102.5±2°	SO_3	$\overset{\frown}{OSO}$	120±2°		

*Data taken from ref. 8.

bond in SiO, and the single bond force constant of 1.5×10^5 dynes cm^{-1}, the bond order – force constant linear relationship may be deduced and is plotted in Fig. 3. It is almost parallel to the corresponding curves for P—O, S—O, and Cl—O bonds and fits in with their relative trends.

The bond order – force constant correlation fits the relationship

$$n_{Si-O} = 1.29\times10^{-6}\, k_{Si-O} + 0.81. \qquad [9]$$

Bond Order – Bond Length Relationship

The bond order in the silicate ion is 1.5 (structure VIII), if it is assumed that there are 12 electrons in the valency shell of silicon. The bond length is 1.63 Å (16) and the corresponding bond lengths for P—O, S—O, and Cl—O bonds of order 1.50 in the PO_4^{3-}, SO_4^{2-}, and ClO_4^- ions are 1.54, 1.49, and 1.47 Å, respectively. On the basis of

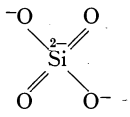

VIII

the single bond length of 1.83 Å, the double bond length of 1.51 Å, and the length of 1.63 Å for a bond of order 1.50 the Pauling formula (12) gives

$$r_{Si-O} = 1.83 - \frac{0.32}{1+0.60\left[\frac{2-n}{n-1}\right]} \qquad [10]$$

Bond lengths calculated from the bond orders obtained from stretching force constants are compared with observed bond lengths in Table VI. Single and double bond lengths and force constants for Si—O, P—O, S—O, and Cl—O bonds are summarized in Table VIII.

DISCUSSION

The formation of double bonds in compounds containing Si—O, P—O, S—O, and Cl—O bonds has recently been discussed by Cruickshank (9) on the basis of evidence obtained from a study of bond lengths, and Wagner (17, 18) has carried out l.c.a.o. – m.o. calculations for species containing Cl—O and P—O bonds, on the basis of a similar approach

Can. J. Chem. Downloaded from www.nrcresearchpress.com by 210.87.254.40 on 09/05/12
For personal use only.

TABLE VIII

Bond lengths and force constants for single and double bonds

	Si—O	P—O	S—O	Cl—O
$n = 1$ $k \times 10^5$ (dynes cm^{-1})	1.5	2.2	2.7	3.3
$n = 1$ r (Å)	1.83	1.76	1.70	1.70
$n = 2$ $k \times 10^5$ (dynes cm^{-1})	9.2_5	11.0	11.7_5	13.0
$n = 2$ r (Å)	1.51	1.45	1.40	1.37

to that used by Moffitt (19) in the case of, e.g., S—O bonds. Both Cruickshank and Wagner concluded that $3d$ orbitals participate significantly in π-bonding between lone pairs of electrons on oxygen and phosphorus or chlorine. Cruickshank's paper (9) has been discussed previously (1). He concluded that for tetrahedrally coordinated silicon, phosphorus, sulphur, and chlorine atoms significant delocalization of lone pairs on atoms

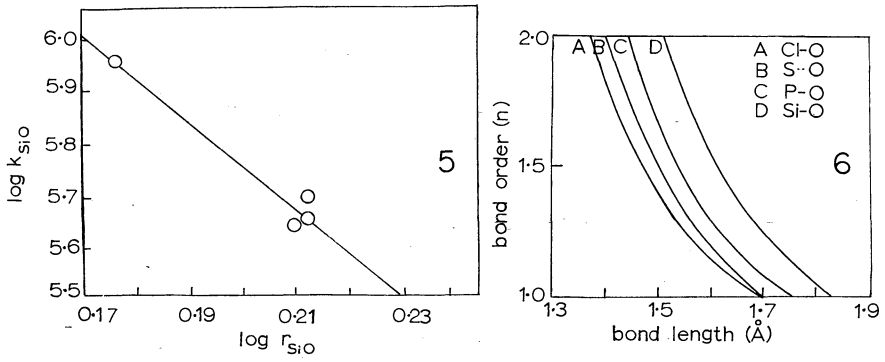

FIG. 5. log r_{Si-O} plotted against log k_{Si-O}.
FIG. 6. Relationships between Cl—O, P—O, and Si—O bond lengths and bond orders.

such as nitrogen or oxygen into the $3d_{x^2-y^2}$ and $3d_{z^2}$ orbitals of the second row element can occur. He assumed a linear correlation between bond length and bond order but the bond length – bond order relationships obtained in this work for Si—O, P—O, and Cl—O bonds are not linear (Fig. 6), but show the same kind of trend that is shown by, for example, C—C bonds.

Wagner (17) concluded that there is no double bond character in the Cl—O bonds in Cl—O$^-$ or ClO_2, and that the π-bond order in ClO_2 is about 0.74, and that 52% of this is of d character. His calculations showed that the extent of participation of $3d$ orbitals in π-bonding increases in the series Cl—O$^-$, ClO_2^-, ClO_3^-, and ClO_4^-, which is in qualitative agreement with the present results. The actual bond orders calculated by Wagner do not agree with those obtained in the present paper. In particular, he obtained very high values for the π-bond orders of ClO_3^- and ClO_4^- of 0.61 and 0.91, respectively. Because of the difficulties encountered in m.o. calculations of this kind the disagreement with the present results is not surprising or unexpected. Also the definition of bond order appropriate for the molecular orbital approach is different from that of the valence bond approach used in the present paper which, at least in part, explains the discrepancies between these results and those of Wagner.

Can. J. Chem. Downloaded from www.nrcresearchpress.com by 210.87.254.40 on 09/05/12
For personal use only.

Chantry and Plane (20) have concluded from Raman intensity studies that the important resonance structures for ClO_3^- and ClO_4^- are IX and X, respectively,

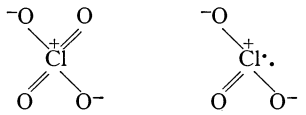

IX X

corresponding to bond orders of 1.50 and 1.33. The conclusions of Chantry and Plane are in excellent agreement with those obtained from the linear force constant – bond order relationship.

In the case of compounds containing P—O bonds Wagner (18) has considered only the bonding in phosphoryl compounds (XYZ)PO. He concludes from his m.o. calculations that the π-bond character of the P—O bonds decreases as the sum of the electronegativities of the attached groups X, Y, and Z decrease; a trend which is consistent with the change in the values of the P—O stretching frequencies and force constants (21). However, his calculated bond orders decrease from 2.98 in F_3PO (essentially a triple bond) to 1.00 in $(CH_3)_3PO$ (a single bond), suggesting valence bond structures such as XI and XII.

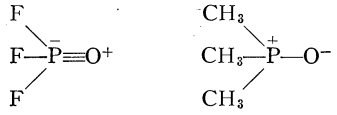

XI XII

The P—O stretching frequencies or force constants in oxyphosphorus ions, for example, suggest longer P—O bond lengths than in $(CH_3)_3PO$, which is inconsistent with the conclusion that the latter contains a single P—O bond. The present correlations between the character of P—O bonds and their force constants and bond lengths are clearly more satisfactory than those of Wagner.

Very few previous estimates of the double bond character of Si—O bonds appear to be available (9). The present results lead to the conclusion that Si—O bonds in all oxysilicon compounds have a large amount of double bond character.

It is thus apparent that the bond lengths and stretching force constants of compounds containing Si—O, P—O, and Cl—O bonds can be very satisfactorily accounted for by assuming that there is a tendency for the valency shell of the central atom to contain 12 electrons, rather than 8, as the Lewis Octet Rule assumed. The $3d_{x^2-y^2}$ and $3d_{z^2}$ orbitals are fully utilized in forming π-bonds in all cases where there are no lone pairs of electrons on the central atom and the attached ligands have high electronegativities. The presence of lone pairs of electrons on the central atom tends to prevent maximum delocalization into the *d* orbitals presumably because they reduce the electronegativity of the central atom. In the case of, e.g., POF_3 and $F_2PO_2^-$, even the presence of highly electronegative fluorine atoms is insufficient to achieve maximum multiple bonding to oxygen, but the calculated bond orders of 2.22 and 1.84, respectively, indicate important contributions from the resonance structures $F_3\bar{P}\equiv\overset{+}{O}$ and $F_2\bar{P}\!\!<\!\!\begin{matrix}O\\O\end{matrix}$, respectively. In this paper no consideration will be given to the likely possibility of double bonding between lone pairs of electrons on fluorine atoms and *d* orbitals on phosphorus or chlorine.

Can. J. Chem. Downloaded from www.nrcresearchpress.com by 210.87.254.40 on 09/05/12
For personal use only.

It should be noted that, although the discussion of double bonding has been couched in the familiar language of atomic orbitals and valence bond resonance structures, so as to conform to current conventions, the fundamental idea involved is that there is space for six pairs of electrons in the valency shells of silicon, phosphorus, sulphur, and chlorine, if these electron pairs are used to bond to highly electronegative ligands. This is most clearly shown in molecules such as SiF_6^{2-}, PF_6^-, and SF_6, where there are six pairs of electrons in single bonds, but 12 electrons in the valency shell is also clearly possible in species such as SiO_4^{4-}, PO_4^{3-}, SO_4^{2-}, and ClO_4^-, and SO_2F_2 and $FClO_3$, etc., where some of the electrons are in multiple bonds. The same idea can also be used to account for the approximately 90° bond angles in molecules such as PH_3 and H_2S (22). The fundamental concept is that the number of localized orbitals that can be fitted around a central atom is a function of their shape and of the space available. In the case of Si, P, S, and Cl there appears to be sufficient space for six pairs of electrons in single bonds if they bond highly electronegative ligands, or the equivalent of six pairs, if some of them are in multiple bonds, in the case of ligands of somewhat smaller electronegativity. It is reasonable to regard the electron pairs in single bond orbitals as occupying less space, or a smaller solid angle, than a pair of electrons in a lone pair orbital (22, 23), since the bond pair is under the influence of two nuclei whereas the lone pair is influenced largely by only one nucleus. Presumably, also, two electron pairs in a double bond orbital occupy more space than a single bond orbital. In the case of oxygen compounds of phosphorus and sulphur it appears that a double bond orbital occupies about the same amount of space as a lone pair orbital, as can be seen by comparing the very similar bond angles in species such as PCl_3 and $POCl_3$, SO_2F_2 and SOF_2, and SO_2 and SO_3 (Table VII). Thus it is very reasonable from this point of view that various combinations of single bond, double bond, and lone pair orbitals around a second row element will occupy *all* the space available.

Can. J. Chem. Downloaded from www.nrcresearchpress.com by 210.87.254.40 on 09/05/12
For personal use only.

ACKNOWLEDGMENTS

Professor R. J. Gillespie of McMaster University is thanked for stimulating discussion and for his contribution to the clarification of the ideas expressed in this paper. The National Research Council of Canada and the Ontario Research Foundation are thanked for generous financial support.

REFERENCES

1. R. J. Gillespie and E. A. Robinson. Can. J. Chem. **41**, 2074 (1963).
2. E. A. Robinson and M. W. Lister. Can. J. Chem. This issue.
3. E. A. Robinson. Can. J. Chem. **41**, 173 (1963).
4. W. J. Lehmann. J. Mol. Spectry. **7**, 261 (1961).
5. J. W. Linnett. Quart. Rev. (London), **1**, 73 (1947).
6. C. H. Douglas-Clark. Phil. Mag. **18**, 459 (1934); **22**, 1137 (1936).
7. P. A. Akishin, N. Rambidi, and E. Zasorin. Kristallografiya, **4**, 360 (1959).
8. L. Sutton. Chem. Soc. (London), Spec. Publ. **11** (1958).
9. D. W. J. Cruickshank. J. Chem. Soc. 5486 (1961).
10. R. A. Durie and D. A. Ramsay. Can. J. Phys. **36**, 35 (1958).
11. K. Venkateswarlu and S. Sandaram. J. Chem. Phys. **23**, 2365 (1955).
12. C. W. F. T. Pistorius. J. Chem. Phys. **29**, 1174 (1958).
13. H. Siebert. Z. Anorg. Allgem. Chem. **275**, 210 (1954).
14. D. Fortnum and J. O. Edwards. J. Inorg. Nucl. Chem. **2**, 264 (1956).
15. G. Herzberg. Spectra of diatomic molecules. Van Nostrand, New York. 1950. p. 570.
16. D. W. J. Cruickshank. J. Chem. Soc. 5487 (1961).
17. E. L. Wagner. J. Chem. Phys. **37**, 751 (1962).
18. E. L. Wagner. J. Am. Chem. Soc. **85**, 161 (1963).
19. W. Moffitt. Proc. Roy. Soc. (London), Ser. A, **200**, 409 (1950); Proc. Roy. Soc. (London), Ser. A, **196**, 510 (1949).

20. G. W. CHANTRY and R. A. PLANE. J. Chem. Phys. **32**, 319 (1960); J. Chem. Phys. **34**, 1268 (1961).
21. J. V. BELL, J. HEISLER, H. TANNEBAUM, and J. GOLDESON. J. Am. Chem. Soc. **76**, 5185 (1949).
22. R. J. GILLESPIE. J. Am. Chem. Soc. **82**, 5978 (1960).
23. J. W. LINNETT and C. E. MELLISH. Trans. Faraday Soc. **50**, 665 (1954).

Can. J. Chem. Downloaded from www.nrcresearchpress.com by 210.87.254.40 on 09/05/12
For personal use only.

SOLVENT EFFECTS ON THE PROTON RESONANCE SPECTRA OF THE DICHLORO- AND DIBROMO-ETHYLENES

REACTION FIELD EFFECTS IN ALIPHATIC SOLVENTS AND SPECIFIC INTERACTIONS IN AROMATIC SOLVENTS[1]

F. HRUSKA,[2] E. BOCK, AND T. SCHAEFER
Department of Chemistry, University of Manitoba, Winnipeg, Manitoba

Received July 12, 1963

ABSTRACT

The proton resonance shifts relative to internal cyclohexane and tetramethylsilane of *cis* and *trans* dichloro- and dibromo-ethylenes were measured in dioxane–water solutions, aliphatic solvents, and aromatic solvents. The dielectric constants of the dioxane–water solutions could be smoothly varied between 2 and 10 and, by taking Δ = *cis*−*trans* shifts as containing only the dipolar reaction field effect, the data for these solutions were treated as a test of the Buckingham reaction field equation. Linear plots were obtained and reasonable values of the coefficients of the E term confirmed the usefulness of this equation. An equation based on a nonspherical cavity was also used. It was also shown that quadrupolar reaction fields affected the proton shifts. Sizeable deviations from the dioxane–water standards were found for halogenated aliphatic solvents and those containing double or triple bonds. These deviations are interpreted in terms of the shape of the solute molecules and dispersion and anisotropic interactions. The much larger deviations found for aromatic solvents are harder to rationalize but specific interactions were found for both *cis* and *trans* forms, indicating an inadequacy in a simple dipole-induced dipole model.

Can. J. Chem. Downloaded from www.nrcresearchpress.com by 210.87.254.6 on 09/05/12
For personal use only.

INTRODUCTION

The effect of the medium on the proton shift may involve magnetic and electrical interactions. The former include bulk susceptibility effects which will not be considered further because in this study we use internal references. Magnetic anisotropy effects are well known, especially for disc-like and rod-like molecules (1). The former usually cause a shift to high field of the solute molecule while the latter give rise to a low-field shift (1).

Electrical interactions are often attributed to orientation effects between permanent dipoles or between permanent and induced dipoles and to interactions arising from dispersion effects (2). These effects tend to expand the electron cloud about a resonating nucleus, thereby decreasing the diamagnetic shielding; they also reduce the symmetry of the electronic environment of the nucleus which reduces the shielding too (1). Shifts due to dispersion interactions are often smaller than those produced by dipolar interactions.

1. Dipolar Effects

The electric dipole of a solute molecule polarizes the surrounding medium. This polarization results in a secondary electric field, the reaction field, at the dipole. It, in turn, polarizes the solute dipole to an extent depending on the polarizability of the solute molecule. In the Onsager treatment (3) the solute molecule is represented by a point dipole at the center of a spherical cavity of radius r in a continuous medium with uniform dielectric constant. The reaction field R is then (3)

$$R = \frac{2(\epsilon-1)(n^2-1)}{3(2\epsilon+n^2)}\frac{\mu}{\alpha} \qquad [1]$$

where n is the refractive index of the solute for sodium D light, μ is the permanent dipole moment of the solute molecule and α is its polarizability, taken as $(n^2-1)r^3/(n^2+2)$.

[1]*Presented in part at the C.I.C. Symposium on Solvation Phenomena at Calgary, Alberta, in August, 1963.*
[2]*Holder of an N.R.C. bursary 1962–63.*

In the treatment of Marshall and Pople (4) the reduction in shielding of a proton in a hydrogen atom is proportional to the square of the applied electric field E. The dependence on E^2 is reasonable for symmetry reasons. A field along an X—H bond will either increase or decrease the electron density at the proton depending on the direction of E. Shifts proportional to E are then expected. A field perpendicular to the X—H bond destroys the axial symmetry of the bond and results in low-field shifts proportional to E^2.

Buckingham's treatment (3) gives a calculated contribution to the shielding of a proton in an X—H bond of

$$\sigma_E = -\chi\times10^{-12}E\cos\theta-10^{-18}E^2, \qquad [2]$$

where θ is the angle between the X—H axis and E and χ are a constant. He suggests a value of $\chi = 2$ while Musher (5) lists values of $\chi = 2$ to 3.4 obtained by several methods. Equations [1] and [2] yield a contribution to the shielding of the X—H proton due to the reaction field R of

$$\sigma_R = -\chi\times10^{-12}\frac{2}{3}\frac{(\epsilon-1)(n^2-1)}{2\epsilon+n^2}\frac{\mu}{\alpha}\cos\theta. \qquad [3]$$

The E^2 term has been neglected since even for the nitrobenzene molecule, as an extreme example, the reaction field in the pure liquid is 0.14×10^6 e.s.u./cm and the E^2 term is then only 8% of the linear term.

Equation [3] predicts a linear variation of the proton shielding as a function of $(\epsilon-1)/(2\epsilon+n^2)$ with a slope of $-2/3\ \chi(n^2-1)\mu\cos\theta\times10^{-12}/\alpha$. Buckingham *et al.* (1) measured the proton shift of CH_3CN in a variety of solvents. The experimental points lay on or near the line of theoretical slope. The scatter was attributed to inaccuracies in bulk susceptibility corrections and to dispersion effects.

Diehl and Freeman (6) utilized a model based on an ellipsoidal cavity and wrote

$$\sigma_R = -\chi\times10^{-12}\frac{3\mu}{abc}\cos\theta\xi_a[1+(n^2-1)\xi_a]\frac{\epsilon-1}{\epsilon+\beta} \qquad [4]$$

where $\beta = n^2\xi_a/(1-\xi_a)$, a, b, c, are the axes of the ellipsoid, and ξ_a is a shape factor. Ross and Sack (7) have evaluated ξ_a for cavities of various shapes. The observed shifts of CH_3CN and paraldehyde yielded values for χ of 3.4 and 3.0, respectively. The spherical cavity model required 1.9 and 7.1, respectively. These results appear encouraging but it is difficult to see why the simple Onsager model could be improved in this way.

2. Quadrupolar Effects

In the presence of two equal and opposed bond dipoles a quadrupolar reaction field may arise. The reaction field gradient of a quadrupolar moment, R^1, is given by (8)

$$R^1 = [6(\epsilon-1)/(3\epsilon+2)]r^{-5}\Phi \qquad [5]$$

where the symbols have been defined above except for Φ, which is the molecular quadrupole moment. For a molecule with two opposed dipoles of moment μ separated by a distance d we have $\Phi = 2\mu d$. The magnitude of r^{-5} is readily obtained if the assumption is made that the molecule is spherical and completely fills the cavity.

3. The Present Measurements

The difficulty in obtaining the reaction field shift lies in the correction necessary for the other factors contributing to the total shift. For our study of polar interactions *cis* and

Can. J. Chem. Downloaded from www.nrcresearchpress.com by 210.87.254.6 on 09/05/12
For personal use only.

trans dichloro- and dibromoethylene* were chosen. All four have single peak proton spectra. The two *cis* forms are dipolar and experience a reaction field. The *trans* forms are nonpolar and a change in ϵ of the medium is not expected to alter the proton shift in the first instance (higher order polar interactions may, however, be present). The shapes of the corresponding *cis* and *trans* forms are very similar and we anticipate the magnetic and dispersion interactions with any one medium to be nearly the same. Then subtraction of the chemical shift of the *trans* from *cis* form isolates the contribution of the reaction field to the total proton shift of the *cis* form. On the other hand, intermolecular dispersion shifts and nonspecific interactions with magnetically anisotropic solvent molecules may well be accounted for by using, as we did, a nonpolar internal reference.

EXPERIMENTAL

Chemical shift measurements were made on 5% solutions in a series of dioxane–water solutions with dielectric constants ranging from about 2 to 10 (see Table III), and also in a variety of aliphatic and aromatic solvents. A Varian DP-60 spectrometer was employed using cyclohexane and tetramethylsilane as internal references. The shift values are estimated to be accurate to at least 0.2 c.p.s. and normally to 0.1 c.p.s.

RESULTS AND DISCUSSION

In Table I the measured shifts of the four compounds in about 40 solvents are given. Also included are the differences Δ = *cis*−*trans* for each pair. In Table II the relevant physical constants are given. In Table III the dielectric functions for the various 5% solutions are presented. Note that these functions were calculated taking the *amount and dielectric constant of the solute and reference into consideration*, assuming an additivity law. In Fig. 1 the Δ values from Table I are plotted against the dielectric functions A and B from Table III.

1. Dioxane–Water Solutions

Since the dielectric constants of these solutions could be varied smoothly between about 2 and 10, and since the weight per cent of water only changed from 0 to 15 in this range, we propose to treat their Δ values as a test of the reaction field model. A least squares treatment of the points 6 and 32 to 38 in Fig. 1 yielded values of χ = 1.3 and 1.6 for Cl and Br, respectively, on substitution of appropriate values from Table II into Equation [3]. We take this as a confirmation of Buckingham's model, although an ideal model would have the same value of χ for Cl and Br. In view of the many unavoidable approximations in the molecular parameters the agreement is perhaps satisfactory.

The shifts from internal cyclohexane for the two *cis* forms were also plotted vs. the dielectric functions A and B. The graphs were accurately linear and yielded χ = 1.9 and 3.0 for *cis* Cl and *cis* Br, respectively. From the smaller slopes for the Δ plots above it follows that the *trans* forms also show a negative slope. Such plots were constructed and on the basis of a quadrupolar effect using Equation 5, trigonometric evaluation of the C—Cl and C—Br bond dipole moments and estimation of the r^{-5} factor from the molecular volume yielded χ = 1.3 for *trans* Cl and χ = 2.2 for *trans* Br. It appears that quadrupole effects are indeed present and can be estimated in this way.

We assume that subtraction of the *trans* from the *cis* shifts corrects for most of the quadrupolar reaction field shifts of the *cis* forms. The quadrupole moments of the *cis* forms are hard to evaluate but are estimated to be slightly smaller than those of the *trans* forms. We are, of course, also assuming that any small changes in dispersion shifts, as the composition of dioxane–water solutions varies, will be the same for the solute and internal reference.

**Hereafter to be called cis* Cl, *trans* Br *etc.*

Can. J. Chem. Downloaded from www.nrcresearchpress.com by 210.87.254.6 on 09/05/12
For personal use only.

TABLE I

Chemical shifts in c.p.s. at 60 Mc.p.s. of *cis* and *trans* chloro- and bromo-ethylenes relative to internal cyclohexane or tetramethylsilane*

	Solvent	*cis* Cl	*trans* Cl	Δ (c.p.s.)	*cis* Br	*trans* Br	Δ (c.p.s.)
1.	Cyclohexane	−288.2	−287.1	−1.1	−324.9	−304.4	−20.5
2.	*n*-Hexane			−0.9*			−20.4*
3.	*n*-Pentane			−0.8*			−20.1*
4.	*n*-Octane			−1.1*			−20.6*
5.	Acetonitrile			−3.7*			
6.	Dioxane	−309.7	−308.2	−1.5	−344.4	−325.3	−19.1
7.	Ethyl ether			−2.4*			
8.	Ethyl acetate			−4.4*			−22.4*
9.	Ethylene bromide	−304.9	−301.4	−3.5			
10.	1-Bromo-2-chloroethane	−304.5	−300.4	−4.1			
11.	Tetrachloroethane (sym)	−301.3	−297.3	−4.0			
12.	Tetrabromoethane (sym)	−307.3	−302.1	−5.2			
13.	Tetrachloroethylene	−294.7	−293.5	−1.2	−331.6	−310.8	−20.8
14.	Dibromomethane	−305.8	−300.8	−5.0	−341.3	−317.3	−24.0
14*a*.	Hexachloro-1,3-butadiene			−2.2			−21.4
15.	Chloroform	−299.7	−295.7	−4.0	−335.2	−312.5	−22.7
16.	Carbon tetrachloride	−298.9	−294.5	−3.4			
17.	Methyl iodide				−342.5	−318.5	−24.0
18.	Carbon disulfide	−296.8	−292.5	−4.3	−333.4	−310.4	−23.0
19.	Benzene	−249.8	−257.8	8.0	−286.4	−273.6	−12.8
20.	Ethynyl benzene	−277.4	−278.6	1.2	−313.4	−294.9	−18.5
21.	Toluene	−251.0	−255.6	4.6	−286.9	−271.0	−15.9
22.	*o*-Xylene	−251.7	−254.2	2.5	−285.4	−267.4	−18.0
23.	Mesitylene			0.0	−287.4	−265.4	−22.0
24.	Aniline	−266.1	−270.2	4.1			
25.	*o*-Toluidine	−263.2	−266.8	3.6			
26.	Bromobenzene	−276.2	−275.5	−0.7			
27.	Chlorobenzene				−309.9	−289.5	−20.4
28.	*o*-Dibromobenzene	−290.8	−286.6	−4.2			
29.	Phenyl isocyanate	−280.8	−276.5	−4.3	−314.6	−289.7	−25.9
30.	Benzonitrile	−308.4	−297.2	−11.2	−342.2	−312.4	−30.8
31.	Pyridine	−319.7	−315.0	−4.7			
32.	Dioxane–water No. 1	−310.7	−308.9	−1.8	−345.6	−325.9	−19.7
33.	Dioxane–water No. 2	−310.9	−308.9	−2.0	−345.9	−326.0	−19.9
34.	Dioxane–water No. 3	−311.4	−309.0	−2.4	−346.3	−326.2	−20.1
35.	Dioxane–water No. 4				−346.9	−326.6	−20.3
36.	Dioxane–water No. 5	−312.5	−309.5	−3.1	−347.4	−326.8	−20.6
37.	Dioxane–water No. 6	−312.9	−309.4	−3.3	−347.7	−326.7	−21.0
38.	Dioxane–water No. 7	−313.3	−309.7	−3.6	−347.9	−326.8	−21.1

An attempt at an improvement in the consistency of the experimental χ values can be based on Equation [4] using an ellipsoidal cavity. Plots of Δ vs. the dielectric functions C and D of Table III are straight lines with slopes of −6.3 c.p.s. for Cl and −4.2 c.p.s. for Br. These shape-corrected slopes yield $\chi = 0.6$ and 0.7, respectively. Whether this consistency indeed argues for small values of χ for the C—H bond is questionable, however.

2. Aliphatic Solvents

(a) The Chloroethylenes

From Fig. 1*a* it is clear that the line through the dioxane–water points also passes through the points for the hydrocarbons (points 1 to 4). Sizeable deviations of up to 2.5 c.p.s. do occur for some of the halogenated solvents and those containing double or triple bonds, e.g., points 5, 8, 12, 14, 15, 16, and 18. Most of these deviations are to negative values of Δ, indicating an excess low-field shift for *cis* Cl. This might be expected on the basis of a stronger van der Waals or anisotropy interaction at the C—H bond for *cis* Cl and this appears reasonable on the basis of the structures of the two forms.

Can. J. Chem. Downloaded from www.nrcresearchpress.com by 210.87.254.6 on 09/05/12
For personal use only.

TABLE II

Relevant physical constants of the dichloro- and dibromo-ethylenes

	cis Cl	*trans* Cl	*cis* Br	*trans* Br
Molecular weight[a]	96.95	96.95	185.87	185.87
Refractive index[a]	1.452	1.449	1.528	
Density[a]	1.291	1.265	2.271	
Dielectric constant[b,c]	9.2	2.14	7.1	2.9
Dipole moment[c]	1.89 D(gaseous)	0	1.35 D (in benzene)	0
Polarizability[d]	0.71×10^{-23} cm^3		1.17×10^{-23} cm^3	
μ_{C-Cl}, μ_{C-Br}[e]	1.13 D		0.79 D	
Quadrupole moment[f]		5.33×10^{-26} esu		3.84×10^{-26} esu
γ^5		2.96×10^{-38} cm^5		3.3×10^{-38} cm^5
Shape factor[g]	0.34		0.32	
C—H length[h]	1.08 Å		1.08 Å	
C—X length[h]	1.67 Å		1.91 Å	
C=C length[h]	1.38 Å		1.34 Å	
XCC angle[h]	123.5°		121°	
HCC angle[h]	120°		120°	

[a]Handbook of Chemistry and Physics. 39th Ed. Chemical Rubber Publishing Company, Cleveland, 1958.
[b]Table of Dielectric Constants . . . , National Bureau of Standards Circular 514. Washington, D.C., 1951.
[c]H. A. Stuart. Die Struktur Des Freien Moleküls. Springer Verlag, Berlin, 1952.
[d]Calculated using an empirical equation, a modified Debye equation, found to give fairly accurate results with a variety of liquids (discussed in Ref. *c*).
[e]Calculated from the total dipole moment of the *cis* form by vectorial addition.
[f]Calculated from the formula $\Phi = 2\mu d$ with d estimated from models.
[g]Calculated using the methods of reference 7.
[h]Table of Interatomic Distances and Configuration of Molecules and Ions. Special Publication No. 11, Chemical Society, London, 1958.

TABLE III

The dielectric functions[a] for the 5% solutions in Table I

No.[b]	ϵ[c]	A[d]	B[e]	No.	ϵ[c]	A[d]	B[e]
1.	2.02	0.202	0.176	16.	2.23	0.217	
2.	1.89	0.191	0.164	17.	6.91		0.362
3.	1.84	0.188	0.159	18.	2.63	0.242	0.215
4.	1.95	0.197	0.169	19.	2.28	0.221	0.198
5.	37.05	0.470		20.	2.98	0.261	0.244
7.	4.28	0.311		21.	2.38	0.227	0.205
8.	6.08	0.353	0.346	22.	2.56	0.239	0.218
9.	4.79	0.326		23.	2.27	0.217	0.197
10.	7.08	0.370		24.	6.84	0.367	
11.	8.02	0.385		25.	6.3	0.358	
12.	7	0.369		26.	5.43	0.341	0.333
13.	2.30	0.221	0.199	27.	5.6	0.344	0.336
14.	7.41	0.374	0.369	28.	7.35	0.374	
14a.	2.55	0.237	0.217	29.	8.8	0.391	0.387
15.	4.76	0.325	0.315	30.	25.4	0.457	0.456
				31.	12.3	0.418	0.415

No.	ϵ[i]	A[d]	B[e]	C[f]	D[g]	E(Cl)[h]	E(Br)[h]
6.	2.21	0.215	0.192	0.426	0.304	0.161	0.150
32.	2.82	0.252	0.235	0.500	0.477	0.185	0.179
33.	3.18	0.270	0.254	0.536	0.516	0.197	0.192
34.	3.76	0.294	0.281	0.583	0.569	0.212	0.209
35.	5.00	0.331	0.322	0.657	0.651	0.235	0.234
36.	5.83	0.349	0.342	0.694	0.690	0.247	0.246
37.	7.24	0.372	0.367	0.741	0.740	0.261	0.261
38.	9.56	0.398	0.394	0.793	0.794	0.276	0.277

[a]Note that they have been calculated assuming additivity of the dielectric constants of the components.
[b]Numbering refers to solutions in Table I.
[c]Dielectric constants of pure solvents taken from reference *b* in Table II.
[d] $A = (\epsilon - 1)/(2\epsilon + 2.10)$ for dichloroethylene in equation 3.
[e] $B = (\epsilon - 1)/(2\epsilon + 2.37)$ for dibromoethylene in equation 3.
[f] $C = (\epsilon - 1)/(\epsilon + 1.09)$ for dichloroethylene in equation 4.
[g] $D = (\epsilon - 1)/(\epsilon + 1.12)$ for dibromoethylene in equation 4.
[h] $E = (\epsilon - 1)/(3\epsilon + 2)$ in equation 5.
[i] F. E. Critchfield, J. A. Gibson, and J. L. Hall. J. Am. Chem. Soc. **75**, 1991 (1953).

Can. J. Chem. Downloaded from www.nrcresearchpress.com by 210.87.254.6 on 09/05/12
For personal use only.

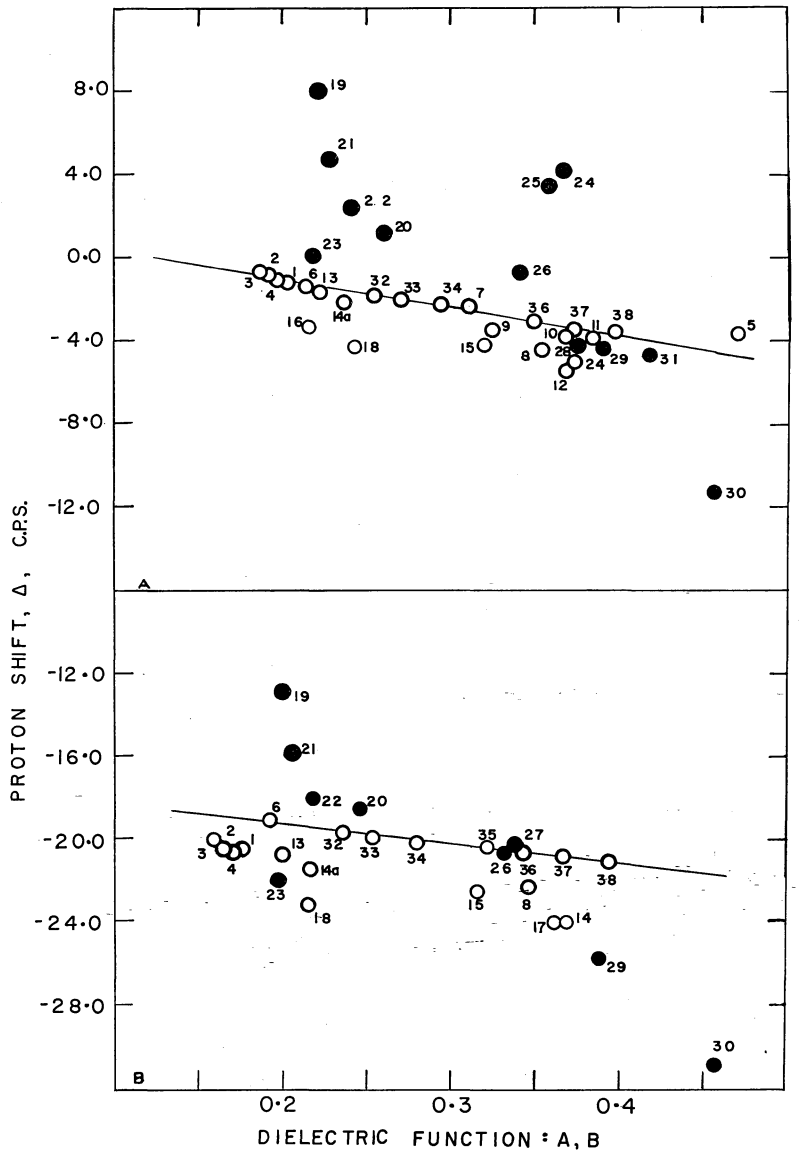

FIG. 1. Δ values from Table I are plotted against the dielectric functions *A* and *B* from Table III for dichloroethylene in *a* and for dibromoethylene in *b*. Open circles indicate dioxane–water solutions (points 6, 32–38) and aliphatic solvents. Solid circles indicate aromatic solvents.

(b) The Bromoethylenes

Here, in Fig. 1*b* the points for the hydrocarbons fall below the Δ line, which is disturbing, and the excess shifts to low field for the *cis* form are also larger for the halogenated solvents and those containing double bonds. These larger excess shifts are understandable on the basis of the somewhat larger size of the bromine atoms. This leads to increased hindrance to approach of the solvent molecule to the *trans* form. We have, however, no explanation for the 1 c.p.s. deviations to low field for the hydrocarbon solvents points 1 to 4.

Can. J. Chem. Downloaded from www.nrcresearchpress.com by 210.87.254.6 on 09/05/12
For personal use only.

3. Aromatic Solvents

It is immediately clear from the solid points in Fig. 1*a* that the Δ values for the aromatic solvents contain large effects other than the reaction field effects. Thus Δ is positive for benzene (point 19) while a reaction field would, of course, shift *cis* Cl to low field of *trans* Cl. The points for *o*-dibromobenzene, phenyl isocyanate, and pyridine, however, appear almost normal for Cl. Only for benzonitrile is Δ large and negative (point 30) for both Cl and Br.

(a) Benzene Solutions

In Table IV the shifts of the four compounds are given relative to their shifts in

TABLE IV

The proton shifts in c.p.s. at 60 Mc.p.s. of the haloethylenes in aromatic solvents relative to their shifts in cyclohexane. Positive values indicate shifts to high field

Solvent	*cis* Cl	*trans* Cl	*cis* Br	*trans* Br
Benzene	38.4	29.3	38.5	30.8
Toluene	37.2	31.5	38.0	33.4
o-Xylene	36.5	32.9	39.5	37.0
Mesitylene			37.5	39.0
Ethynyl benzene	10.8	8.5	11.5	9.5
Aniline	22.1	16.9		
o-Toluidine	25.0	20.3		
Phenyl isocyanate	7.4	10.6	10.3	14.7
Bromobenzene	12.4	11.6	12.5	13.5
Chlorobenzene			15.0	14.9
o-Dibromobenzene	−2.6	0.5		
Pyridine	−31.5	−27.9		
Benzonitrile	−20.2	−10.1	−17.3	−8.0

cyclohexane. The excess shifts are 0.5–0.6 p.p.m. to high field in benzene. They are less for the *trans* than for the *cis* compounds but about the same for Br and Cl.

The work of Schneider (9) is of particular interest in this regard. His measurements indicate a specific interaction of vinyl-X compounds with benzene. The two molecular planes are thought to assume a parallel orientation, with the polar group off the ring. The proton *trans* to the group X is then expected to have the largest shift to high field, as is the case (9). If we think of this as indicating that the benzene avoids electron-rich or bulky groups (10) the smallest high-field shift would be expected for the bromide. This is roughly borne out by the results (9).

Specific interactions are no doubt also present in our aromatic solutions. However, the unmodified dipole – induced dipole model used by Schneider for the alkyl-X and vinyl-X shifts in benzene is not quite compatible with our measurements for the *trans* forms. Also since μ/v, where v is the molecular volume, is less for *cis* Br than for *cis* Cl this should result in a lower excess shift for the former, contrary to the data in Table IV.

A quadrupole – induced quadrupole model will cause excess high-field shifts for the *trans* forms but it is then difficult to see why *trans* Br should have a higher shift than *trans* Cl and, indeed, why the *trans* shifts are almost as large (in one case larger) as the *cis* shifts.

As mentioned by Schneider, experiments with aromatic solutes and aromatic solvents indicate extensive polarizations of the interacting molecules. If we extend this idea to our solutes we note that the polarizability of the bromo compounds is considerably larger (by about 50%) than that of the chloro compounds. We therefore postulate extensive mutual polarization by dispersion interactions of the haloethylene and benzene. A simple

Can. J. Chem. Downloaded from www.nrcresearchpress.com by 210.87.254.6 on 09/05/12
For personal use only.

van der Waals interaction leads to low-field shifts (1) but in this case it is also assumed to lead to a parallel orientation of the solute and solvent molecules. It appears that the large anisotropy of the benzene thus leads to a net high-field shift. Since the van der Waals radii of the Cl and Br are not very different (1.81 and 1.95 Å) the larger polarizability of Br appears to compensate for its larger size and we find comparable excess shifts for the Cl and Br in benzene.

On the other hand, a simpler but related picture in which the larger bromine atoms force the benzene molecules to sit closer to the protons, on an average, might also appear reasonable. Whether, in that case the shift of *trans* Cl may be expected to be larger than the *trans* Br shift in the bulkier solvent molecule, mesitylene, is not clear.

(b) Ethynylbenzene and Benzonitrile Solutions

For ethynylbenzene a similar excess shift is expected since its dielectric constant is only a little larger than that of benzene and its methyl homologues. There is a decrease of from 20–30 c.p.s., however, in the excess shift for both *cis* and *trans* forms. A rationalization assumes a model in which the triple bond is close to the protons, causing a low-field shift by virtue of its cylindrical magnetic anisotropy. The proper orientation may be brought about in an admittedly obscure way by dispersion interactions or, perhaps, by hydrogen bonding of the polar C—H bonds to the triple bond (11, 12).

A somewhat similar effect is then predicted for benzonitrile solutions and, after correction for the triple bond shift using the ethynylbenzene shifts as a reference, we obtain $\Delta = -4.4$ c.p.s. for Cl and $\Delta = -24.1$ c.p.s. for Br. The points 30 are then brought into much closer agreement with the reaction field lines in Fig. 1, the discrepancy being about zero for Cl and about 4 c.p.s. for Br.

(c) Other Aromatic Solvents

The Δ values of Cl for aniline and toluidine also show positive deviations comparable in size to those for the benzenes. Presumably a similar interaction is present. The chloro- and bromo-benzene points fall much closer to the reaction field lines in Fig. 1, as does the point for pyridine. Why this should be so we hesitate to speculate further. From the discussion in this section it is clear, however, that while reaction fields no doubt play their part, there are equally important specific interactions whose magnitude is not predictable a priori. It may well be that each case will have to be individually studied using temperature and concentration techniques.

ACKNOWLEDGMENT

The financial assistance of the National Research Council is very much appreciated.

REFERENCES

1. A. D. BUCKINGHAM, T. SCHAEFER, and W. G. SCHNEIDER. J. Chem. Phys. **32**, 1227 (1960).
2. B. LINDER. J. Chem. Phys. **33**, 668 (1960).
3. A. D. BUCKINGHAM. Can. J. Chem. **38**, 300 (1960).
4. T. W. MARSHALL and J. A. POPLE. Mol. Phys. **1**, 199 (1958).
5. J. I. MUSHER. J. Chem. Phys. **37**, 34 (1962).
6. P. DIEHL and R. FREEMAN. Mol. Phys. **4**, 39 (1961).
7. I. G. ROSS and R. A. SACK. Proc. Phys. Soc. (London), B, **63**, 893 (1950).
8. A. D. BUCKINGHAM. J. Chem. Phys. **30**, 1580 (1959).
9. W. G. SCHNEIDER. J. Phys. Chem. **66**, 2653 (1962).
10. T. SCHAEFER. Can. J. Chem. **39**, 1864 (1961).
11. D. COOK, Y. LUPIEN, and W. G. SCHNEIDER. Can. J. Chem. **34**, 957 (1956).
12. L. W. REEVES and W. G. SCHNEIDER. Can. J. Chem. **35**, 251 (1957).

Can. J. Chem. Downloaded from www.nrcresearchpress.com by 210.87.254.6 on 09/05/12
For personal use only.

EFFECT OF NON-ZERO EXTINCTION COEFFICIENT ON ABSTRACTION–RECOMBINATION RATE RATIOS IN PHOTOCHEMICAL SYSTEMS[1]

H. O. PRITCHARD
University of Manchester, Manchester, England

AND

G. O. PRITCHARD
University of California, Santa Barbara, California, U.S.A.

Received April 22, 1963

ABSTRACT

The data of Marjury and Steacie on the photolysis of acetone and acetone-d_6 in the presence of H_2 and D_2 respectively have been re-analyzed in terms of the integrated rate equations. It is concluded that only part of the discrepancy between the results for the methyl and hydrogen reaction can be accounted for in this way.

In an appendix, it is shown that for high extinction coefficients, the integrated rate expression reaches a limit which may sometimes be attainable experimentally without undue complication from diffusion effects.

Can. J. Chem. Downloaded from www.nrcresearchpress.com by 210.87.254.40 on 09/05/12
For personal use only.

The results of Marjury and Steacie (1) for the reaction of CH_3 and CD_3 with H_2 and D_2, and of Whittle and Steacie (2) for the reaction of CH_3 and CD_3 with HD are shown in Table I. There is a pattern about these results in that activation energies obtained by what Steacie and co-workers call "method I" are consistently about 0.7 kcal below those obtained by "method II". In "method I" the methane formed in the reaction under consideration is deduced from the difference between the total methane obtained and an

TABLE I
Reactions of methyl radicals with hydrogen

Reactant	Radical	Ref.	E	Method	Adjusted E
H_2	CH_3	1	9.2	I	9.9
H_2	CD_3		10.2	II	10.2
D_2	CD_3	1	10.9	I	11.6
D_2	CH_3		11.7	II	11.7
$\underline{\underline{H}}D$	CH_3	2	10.0	I	10.7
$\underline{\underline{H}}D$	CD_3		10.7	II	10.7
$H\underline{\underline{D}}$	CD_3	2	10.7	I	11.4
$H\underline{\underline{D}}$	CH_3		11.3	II	11.3

estimate of the methane produced by abstraction from the radical source. In "method II" the methane formed in the particular reaction has an isotopic constitution different to any of the other methanes produced, and is determined directly mass-spectrometrically.

In the final column in Table I, we have added 0.7 kcal to all the "method I" results. Assuming no isotope effect in the attacking radical, this suggests that there may be some

[1]*Paper presented at the International Symposium on Photochemistry held at the University of Rochester, March 27–29, 1963.*

flaw in the method of correcting for the methane produced by radical attack on the photolytic source.[2]

A similar pattern can be found amongst the abstraction reactions of methyl radicals with other substrates. The data are collected in Table II, and again indicate that a

TABLE II

Reactions of methyl radicals with hydrocarbons

Substrate	Source	Ref.	E (kcal)	Method	Adjusted E
Acetone	Acetone	4	9.7±0.1	II	9.7
	D.T.B.P.	4	9.5±0.3	II	9.5
Diethylketone	Azomethane	4	7.0±0.1	I	8.0
	D.T.B.P.	4	8.0±0.2	II	8.0
Toluene	$HgMe_2$	4	7.3±0.3	I	8.3
	Acetone	5	7.4±0.3	I	8.4
	Acetone-d_6	4[a]	9.3±0.3	II	9.3
2,2-Dimethyl-propane	$HgMe_2$	4	10.4±0.3	I	11.4
	Acetone	4	10.0±0.3	I	11.0
	Acetone-d_6	4[a]	11.0±0.3	II	11.0
2,3-Dimethyl-butane	$HgMe_2$	4	6.8±0.2	I	7.8
	Acetone	4	6.9±0.2	I	7.9
	Acetone-d_6	4[a]	8.8±0.4	II	8.8
Cyclopropane	$HgMe_2$	4	10.2±1.0	I	11.2
	Acetone-d_6	4[a]	11.3±0.4	II	11.3
	Acetone-d_6	6	13.1	II	13.1
Cyclobutane	Acetone-d_6	4[a]	10.3±0.4	II	10.3
	Acetone-d_6	6	10.3	II	10.3
Cyclopentane	Acetone	4	8.3±0.2	I	9.3
	Acetone-d_6	4[a]	9.3±0.2	II	9.3
	Acetone-d_6	6	9.3	II	9.3
Cyclohexane	$HgMe_2$	4	8.3±0.3	I	9.3
	Acetone	4	8.3±0.2	I	9.3
	Acetone-d_6	6	9.7	II	9.7

[a]The figures quoted for these reactions are based on the data compiled in ref. 4, but recalculated on the basis of an activation energy of 11.3 kcal for $CD_3 + CD_3COCD_3 \rightarrow CD_4 + CD_2COCD_3$ used by Gordon and Smith (6).

systematic error of about 1 kcal low occurs whenever correction has to be made to the CH_4 formed due to abstraction from the radical source. (Di-*t*-butyl-peroxide (D.T.B.P.) is regarded as a "method II" source since it is very resistant to methyl radical attack.) It is also significant that no such variation occurs in the values of activation energies for abstraction by CF_3 radicals using different sources (3). In this paper, we confine our attention to the results of Marjury and Steacie since they appear to be a good example of this discrepancy.

An obvious source of possible error is that the experimental data are always reduced according to the local rate equations instead of the correct integrated form of these equations. In the case of the abstraction–recombination system, the integration can be performed analytically for the steady state in the absence of diffusion, as was shown by

[2]*Marjury and Steacie also observed, in agreement with this postulate, that their results obtained by "method II", when calculated by "method I", tended to yield lower values for the activation energy. Whittle and Steacie observed the same behavior for the* $CH_3 + D_2$ *and* $CD_3 + H_2$ *reactions; these results are not included in Table I. The value obtained for* $CH_3 + D_2$ *by Marjury and by Whittle are in exact agreement; however, Whittle obtained a value of 11.1 kcal for* $CD_3 + H_2$, *calculated by "method II".*

Can. J. Chem. Downloaded from www.nrcresearchpress.com by 210.87.254.40 on 09/05/12
For personal use only.

Cvetanović and Whittle (7). Using the photolysis of a ketone as an example, we have

$$X_2CO + h\nu \rightarrow 2X + CO$$

$$X + X_2CO \xrightarrow{k_3} XH + \text{etc.}$$

$$X + X \xrightarrow{k_2} X_2$$

$$X + RH \xrightarrow{k_1} XH + R \text{ etc.},$$

where locally,

$$R_{XH}/R_{X_2}^{\frac{1}{2}} = (k_3[X_2CO]+k_1[RH])/k_2^{\frac{1}{2}}. \qquad [1]$$

If we put $u = (k_3[X_2CO]+k_1[RH])^2$, $v = 8k_2m\phi I_0$, and $w = 2.3\epsilon c$ ($c \equiv [X_2CO]$) we have, per unit volume, etc.,

$$R_{XH} = \frac{B\sqrt{u}}{4k_2wL} \quad \text{and} \quad R_{X_2} = \frac{vw(1-e^{-wL})-2B\sqrt{u}}{16k_2wL}$$

where

$$B = 2\sqrt{u+vw} - 2\sqrt{u+vwe^{-wL}} - 2\sqrt{u}\ln\frac{(\sqrt{u+vw}+\sqrt{u})}{(\sqrt{u+vwe^{-wL}}+\sqrt{u})}$$

and m, ϕ, ϵ, and I_0 have their usual meanings. Equation [1] therefore becomes

$$\delta\cdot\frac{R_{XH}}{R_{X_2}^{\frac{1}{2}}} = (k_3[X_2CO]+k_1[RH])/k_2^{\frac{1}{2}}, \qquad [2]$$

where $\delta = L^{\frac{1}{2}}\left(\int_0^L [X]_l^2 dl\right)^{\frac{1}{2}} \Big/ \int_0^L [X]_l dl = L^{\frac{1}{2}}w^{\frac{1}{2}}[vw(1-e^{-wL})-2B\sqrt{u}]^{\frac{1}{2}}/B$;

putting $\beta = wL$ and $s = vw/u$ gives the expression quoted in reference 7.

If we photolyze acetone (Ac) on its own, the correct form of equation [1] is

$$\frac{k_3}{k_2^{\frac{1}{2}}} = \frac{R_{CH_4}}{R_{C_2H_6}^{\frac{1}{2}}[Ac]}\cdot\frac{L^{\frac{1}{2}}w^{\frac{1}{2}}[vw(1-e^{-wL})-2B\sqrt{u}]^{\frac{1}{2}}}{B} \qquad [3]$$

where $u = (k_3[Ac])^2$. We can find k_3 by trial and error. In the presence of RH we have

$$\frac{k_1}{k_2^{\frac{1}{2}}} = \frac{R_{CH_4}}{R_{C_2H_6}^{\frac{1}{2}}[RH]}\cdot\frac{L^{\frac{1}{2}}w^{\frac{1}{2}}[vw(1-e^{-wL})-2B'\sqrt{u'}]^{\frac{1}{2}}}{B'} - \frac{k_3[Ac]}{k_2^{\frac{1}{2}}[RH]}, \qquad [3']$$

where $u' = (k_3[Ac]+k_1[RH])^2$, and if k_3 is already known, k_1 can now be found by trial and error. Note that the dependence of k_1 on ϵ is slightly different from the dependence of k_3 on ϵ.

In applying these equations to the data of Marjury and Steacie, some assumptions have to be made since the intensity distribution of the mercury lamp used is not known. Also, the extinction coefficient of acetone increases with temperature and decreases with pressure between room temperature and 150° C (see Table III and ref. 8). It was therefore necessary to assume a reasonable value for the average light intensity ($\bar{I}_0$), and derive the mean extinction coefficient ($\bar{\epsilon}$) of acetone for each run from the yield of CO, on the assumption of unit quantum yield for all temperatures. It was also necessary to assume that this light intensity remained constant throughout the series of experiments, and that raising the furnace temperature did not indirectly increase $\bar{I}_0$ by causing the lamp to

Can. J. Chem. Downloaded from www.nrcresearchpress.com by 210.87.254.40 on 09/05/12
For personal use only.

TABLE III

Extinction coefficient of acetone

Temperature °K	ϵ in liter mole^{-1} cm^{-1} at 3130 Å	2775 Å	2537 Å	Pressure
296	2.85	12.5	7.88	4.99 cm at 32.8° C
350	3.27	14.0	8.69	
424	4.52	15.1	8.84	
298	2.32	12.4	7.75	13.1 cm at 24.1° C
364	3.25	13.6	7.89	
410	3.75	14.3	7.95	

run hotter (this seems most unlikely). Calculations were performed for three values of the average incident light intensity, $\bar{I}_0$, of 0.8×10^{15}, 1.0×10^{15}, and 1.2×10^{15} quanta/cm^2 sec; the true value must lie somewhere in this range. The result of the application of equation [3] to the photolysis of acetone and acetone-d_6 is shown in Table IV. The effect is to

TABLE IV

Analysis of the results of Marjury and Steacie for the photolysis of acetone and acetone-d_6

Reaction	Run	T, °K	$k_3/k_2^{\frac{1}{2}}$ uncorr.	$\bar{I}_0 = 1.2\times10^{15}$ $\bar{\epsilon}$	$k_3/k_2^{\frac{1}{2}}$	$\bar{I}_0 = 1\times10^{15}$ $\bar{\epsilon}$	$k_3/k_2^{\frac{1}{2}}$	$\bar{I}_0 = 0.8\times10^{15}$ $\bar{\epsilon}$	$k_3/k_2^{\frac{1}{2}}$
CH_3 + acetone	A1	413	7.01	5.4	7.02	6.9	7.04	9.6	7.07
	A2*	405	5.59	5.3	5.61	6.8	5.62	9.5	5.65
	B1	409	6.19	5.6	6.20	6.8	6.20	8.9	6.20
	C1	409	6.00	5.5	6.00	6.7	6.00	8.6	6.00
	D3	498	48.5	6.7	48.7	8.6	48.9	12.0	49.2
	D4	499	49.5	7.2	49.7	9.2	49.9	13.0	50.3
	D5*	494	42.9	7.0	43.3	9.0	43.5	12.8	44.0
	F1	494	50.3	7.4	50.3	9.0	50.3	11.5	50.3
	G1	565	147.0	8.4	149.0	10.8	150.0	15.4	152.0
	I2	564	165.0	8.5	165.0	10.4	165.0	13.3	165.0
	$A_3/A_2^{\frac{1}{2}}$ =		7.36×10^{-8}	7.46×10^{-8}		7.53×10^{-8}		7.71×10^{-8}	
	$E_3-\frac{1}{2}E_2$ =		9.56	9.57		9.58		9.60	
CD_3 + acetone-d_6	54	407	1.48	7.2	1.49	9.5	1.49	18.0	1.51
	64	433	2.87	8.1	2.89	10.8	2.90	16.4	2.93
	62	461	5.77	8.8	5.81	11.7	5.83	17.8	5.90
	60	485	10.8	8.9	10.8	11.7	10.9	17.6	11.0
	58	529	27.7	9.3	27.9	12.3	28.0	18.2	28.4
	56	569	61.6	10.6	62.1	14.0	62.5	21.1	63.6
	$A_3/A_2^{\frac{1}{2}}$ =		7.04×10^{-8}	7.15×10^{-8}		7.23×10^{-8}		7.46×10^{-8}	
	$E_3-\frac{1}{2}E_2$ =		10.72	10.73		10.73		10.75	

NOTE: $\bar{\epsilon}$ is in liter mole^{-1}cm^{-1} units, $\bar{I}_0$ in quanta/cm^2 sec. $A_3/A_2^{\frac{1}{2}}$ and $k_3/k_2^{\frac{1}{2}}$ in cc$^{\frac{1}{2}}$ molecule$^{-\frac{1}{2}}$ sec$^{-\frac{1}{2}}$ except that all k values are multiplied by 10^{13}.

The two runs marked * were carried out with a filter which transmitted 27% of the incident light at 2537 Å. If this value for $\bar{I}_0$ is used, the mean extinction coefficients are considerably out of line, and can only be reconciled with the other values by choosing a mean transmission of 18.5%; this indicates that much of the photolysis is brought about by radiation, other than at 2537 Å, as was assumed by Marjury and Steacie.

Some of the uncorrected values for the rate constants are not the same as those given by Marjury and Steacie; this is because their rate constants do not always agree with the rates of formation of methane and ethane which they quote.

increase the rate constants slightly, particularly in those runs with high acetone concentration. It is seen that the mean extinction coefficient calculated from the CO yield rises with temperature, and this tends to make the correction factor δ larger at higher temperatures. Thus, the overall effect is to raise both the activation energy and frequency factor somewhat over the uncorrected values. It is this variation of ϵ with T that is more

Can. J. Chem. Downloaded from www.nrcresearchpress.com by 210.87.254.40 on 09/05/12
For personal use only.

important than just the simple correction of the rate constants[3] for light absorption since, as shown in the Appendix, δ is fairly insensitive to everything except ϵ and the acetone concentration.

With these rate constants k_3 for acetone and acetone-d_6, it is now possible to apply equation [3′] to the reactions of CH_3 with H_2 and CD_3 with D_2, as is done in Table V. It is

TABLE V

Analysis of the results of Marjury and Steacie for $CH_3 + H_2$ and $CD_3 + D_2$

Reaction	Run	T, °K	$k_1/k_2^{\frac{1}{2}}$ uncorr.	$\bar{I}_0 = 1.2\times10^{15}$ $\bar{\epsilon}$	$k_1/k_2^{\frac{1}{2}}$	$\bar{I}_0 = 1.0\times10^{15}$ $\bar{\epsilon}$	$k_1/k_2^{\frac{1}{2}}$	$\bar{I}_0 = 0.8\times10^{15}$ $\bar{\epsilon}$	$k_1/k_2^{\frac{1}{2}}$
$CH_3 + H_2$	6	412	4.16	5.0	4.17	6.4	4.29	8.8	4.34
	4	454	12.6	5.7	12.6	7.2	13.0	10.0	13.1
	8	506	37.4	6.3	37.6	8.0	38.7	11.1	39.3
	11	523	58.1	6.5	58.6	8.2	60.0	11.4	61.1
	5	566	85.2	7.3	86.4	9.3	89.2	12.9	91.7
	10	571	87.3	7.4	88.9	9.4	92.0	13.1	95.0
	1	409	3.70	5.2	3.72	6.7	3.75	9.2	3.78
	3	453	12.1	6.0	12.1	7.6	12.2	10.6	12.4
	7	504	35.9	6.6	36.2	8.5	36.6	11.8	37.2
	$A_1/A_2^{\frac{1}{2}}$ =		3.56×10^{-8}		3.73×10^{-8}		3.98×10^{-8}		4.28×10^{-8}
	$E_1-\frac{1}{2}E_2$ =		9.33		9.37		9.41		9.46
$CD_3 + D_2$	66	412	1.44	7.5	1.46	9.8	1.46	14.7	1.47
	67	432	2.19	(8.0)	2.22	(10.6)	2.21	(15.8)	2.23
	68	458	4.77	8.4	4.83	11.0	4.81	16.4	4.85
	71	481	8.53	9.5	8.66	12.6	8.64	19.5	8.82
	70	514	17.2	10.8	17.5	14.5	17.6	22.8	18.2
	69	567	50.7	11.5	51.9	15.4	52.4	24.0	54.9
	$A_1/A_2^{\frac{1}{2}}$ =		6.98×10^{-8}		7.35×10^{-8}		7.68×10^{-8}		8.87×10^{-8}
	$E_1-\frac{1}{2}E_2$ =		10.87		10.90		10.95		11.06

NOTE: Units as in Table IV.

seen that the δ-correction leads to an activation energy which, at most, is only 0.2 kcal greater than the uncorrected value. It is worth noting, however, that when $k_1 \approx k_3$, as is the case here, a rise of 0.1 kcal in E_3 causes a fall of ~0.4 kcal in E_1, and it seems likely that the discrepancies in Table I can largely be accounted for by the δ-correction *and* the sharp dependence of E_1 on small errors in E_3; it is indicative that Whittle's results (2) did not always agree with those of Marjury (1) in those cases where the investigations overlapped. Similar considerations must apply to Table II.

APPENDIX

The behavior of the function δ was investigated for a series of typical reaction mixtures. A basic reaction was considered in which

$$L = 10 \text{ cm}; I_0 = 10^{15} \text{ quanta/cm}^2 \text{ sec}; m\phi = 2;$$

$$k_3[X_2CO]/k_2^{\frac{1}{2}} = k_1[RH]/k_2^{\frac{1}{2}} = 10^6 \text{ molecules}^{\frac{1}{2}} \text{ cc}^{-\frac{1}{2}} \text{ sec}^{-\frac{1}{2}}$$

(i.e. equivalent to $k_3/k_2^{\frac{1}{2}} = k_1/k_2^{\frac{1}{2}} = 10^{-12} \text{ cc}^{\frac{1}{2}} \text{ molecule}^{-\frac{1}{2}} \text{ sec}^{-\frac{1}{2}}$ and

$$[X_2CO] = [RH] = 10^{18} \text{ molecules/cc});$$

$$k_2 = 3.63\times10^{-11} \text{ cc molecule}^{-1} \text{ sec}^{-1}$$

and the correction factor δ was calculated as a function of extinction coefficient.

[3]*J. Caldwell and D. E. Hoare, J. Am. Chem. Soc.* **84**, *3987 (1962), have suggested that the rise in* CO *yield with temperature is not solely due to a rise in* $\bar{\epsilon}$*; in this case, our calculations will exaggerate the error involved in ignoring the* δ*-correction. (The same comment applies to our assumption that* $\bar{I}_0$ *does not increase with* T.)

Can. J. Chem. Downloaded from www.nrcresearchpress.com by 210.87.254.40 on 09/05/12
For personal use only.

The following variations were also tested:

L and I_0 by a factor of 10 each way;

k_2 reduced by a factor of 10^4, keeping $k_3/k_2^{\frac{1}{2}}$ and $k_1/k_2^{\frac{1}{2}}$ fixed, also keeping k_1 and k_3 fixed;

$k_3[X_2CO]/k_1[RH]$ from 0 to ∞, the two extremes corresponding to zero attack on the source [e.g. with CF_3COCF_3] and the absence of RH respectively.

With the exception of the length L of the reaction vessel, the correction δ was virtually independent of all these variations, and the results are shown in Fig. 1 (cf. also Fig. 3 of reference 7, which shows the bottom 2% of these curves on a highly magnified scale). ϵ and c are complementary quantities; ϵ and L are complementary to an acceptable degree of accuracy.

Placing a mirror at the end of the reaction vessel to reflect the light has little effect and, for all practical purposes, the curves with and without the mirror are indistinguishable. The dotted curves in Fig. 1 represent the improvement gained by having two light sources of equal intensity, one at either end of the reaction vessel. The integration of the steady state equations for these two cases was performed numerically.

It would be logical experimentally to make use of the fact that δ tends to a limit of 10.95 (7.75 for two light sources) at very high ϵcL values. Two examples may be cited: (i) the use of a very long vessel would keep δ constant even though the source was being consumed; (ii) in the photolysis of mercury diphenyl (9), one of the products is diphenyl, whose extinction coefficient is even higher by a factor of 10; if L were such that δ already had its limiting value, the accumulation of this strongly absorbing product could not affect the results, provided that its concentration was not allowed to become so large as to cause diffusion problems.

There are two diffusion effects. One is diffusion to the walls, which has been discussed by Hill (10), and the other is diffusion along the concentration gradient. To include these effects one would need to solve an equation of the kind

$$\mathscr{D}(\partial^2[X]_l/(\partial l^2) + m\phi I_0(2.3\,\epsilon c)e^{-2.3\epsilon c l} - (k_3[X_2CO] + k_1[RH])[X]_l - k_2[X]_l^2 = 0,$$

where $\mathscr{D}$ is the diffusion coefficient for the radicals in the reaction mixture; Hill has considered the solution of this equation in the absence of the exponential factor.

It is not likely that the diffusion coefficient $\mathscr{D}$ for any radical will exceed 5 cm^2/sec for any normal reaction mixture: this can be seen by assuming reasonable values for the Lennard-Jones potential between a methyl radical (taken to be like methane) and acetone, and evaluating equation 8.2–44 of Hirschfelder, Curtiss, and Bird (11). The term $\partial^2[X]_l/\partial l^2$ was obtained for our series of model reactions by calculating the radical concentration distributions, as shown in Fig. 2, and differentiating numerically (for simplicity, k_3 was assumed to be zero). Table VI compares, for representative positions in the vessel, the rate of photochemical production of radicals with the net increase in concentration due to diffusion, both in units of molecules/cc sec in the vicinity of the representative point. Clearly longitudinal diffusion has quite an unimportant effect on δ in normal reaction mixtures until ϵ exceeds 1000 liter $mole^{-1}$ cm^{-1} (note that ϵ and c are no longer complementary quantities since $\mathscr{D}$ is concentration-dependent). At the same time, Hill's data show that for $\epsilon > 1000$ liter $mole^{-1}$ cm^{-1}, the diffusion path of the radicals is of the order of 0.1 cm, and Fig. 2 shows that further complications must arise if there is significant removal at the wall.

Can. J. Chem. Downloaded from www.nrcresearchpress.com by 210.87.254.40 on 09/05/12
For personal use only.

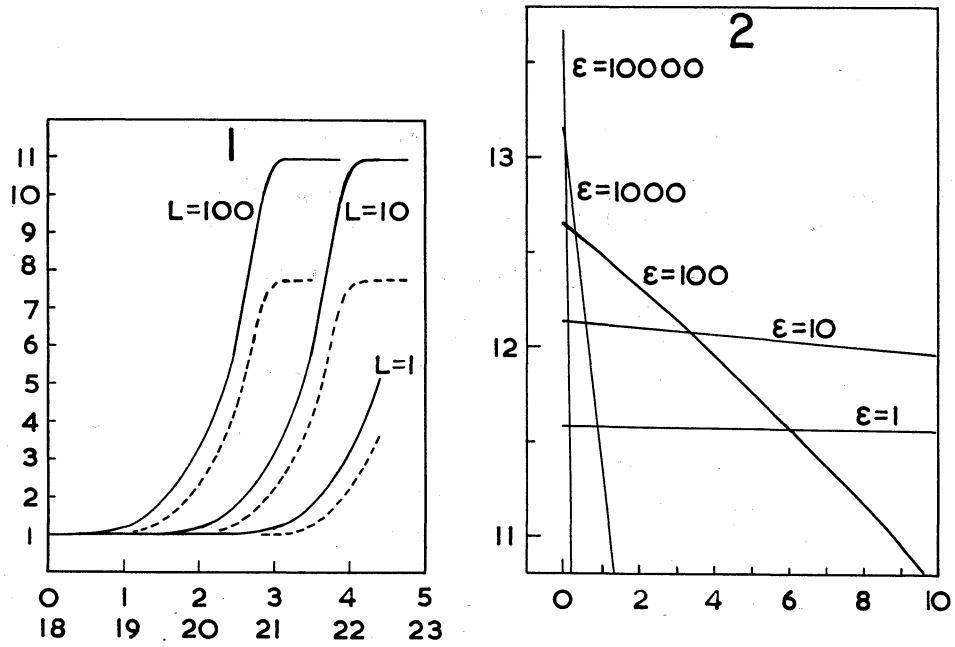

FIG. 1. Variation of correction factor δ with extinction coefficient and concentration. Vertical axis: correction factor δ. Horizontal axis: (upper set) $\log_{10} \epsilon$ for source concentration of 10^{18} molecules/cc, ϵ in liter mole^{-1}cm^{-1}; (lower set) $\log_{10} \epsilon c$, where ϵ is in liter mole^{-1}cm^{-1} and c is in molecules/cc.

FIG. 2. Variation of radical concentration with extinction coefficient and path length; ϵ in liter mole^{-1} cm^{-1}. See text for source concentration, etc. Vertical axis: $\log_{10}$ (radical concentration, molecules/cc). Horizontal axis: length, l, cm.

TABLE VI

ϵ (liter mole^{-1}cm^{-1})	Position l (cm)	Photochemical production (molecules/cc sec)	Accumulation by diffusion* (molecules/cc sec)	Ratio
1	1	8×10^{12}	$\sim10^{7}$	10^{6}
10	1	7.7×10^{13}	2×10^{9}	4×10^{4}
100	1	5.4×10^{14}	5×10^{11}	10^{3}
1,000	1	1.4×10^{14}	5×10^{12}	30
	0.1	5.4×10^{15}	1.5×10^{14}	
10,000	0.1	1.4×10^{15}	1.5×10^{15}	1
	0.01	5.4×10^{16}	4.6×10^{16}	

*Assuming the extreme value of $\mathscr{D} = 5$ cm^2/sec. Hill uses a more realistic value of $\mathscr{D} = 1$ cm^2/sec, which would improve the ratios in the final column by a factor of 5.

ACKNOWLEDGMENTS

We wish to thank Professor G. H. Miller and Mr. J. K. Foote for their assistance in measuring the extinction coefficients of acetone, and the National Science Foundation for financial assistance to one of us (G).

REFERENCES

1. T. G. MARJURY and E. W. R. STEACIE. Can. J. Chem. **30**, 800 (1952).
2. E. WHITTLE and E. W. R. STEACIE. J. Chem. Phys. **21**, 993 (1953).
3. G. O. PRITCHARD and G. H. MILLER. J. Chem. Phys. **35**, 1135 (1961).

Can. J. Chem. Downloaded from www.nrcresearchpress.com by 210.87.254.40 on 09/05/12
For personal use only.

4. A. F. TROTMAN-DICKENSON. Gas kinetics. Butterworths, London. (1955).
5. I. B. BURKLEY and R. E. REBBERT. J. Phys. Chem. **67,** 168 (1963).
6. A. S. GORDON and S. R. SMITH. J. Phys. Chem. **66,** 521 (1962).
7. R. J. CVETANOVIĆ and E. WHITTLE. Can. J. Chem. **32,** 63 (1954).
8. G. W. LUCKEY and W. A. NOYES. J. Chem. Phys. **19,** 227 (1951).
9. W. FIELDING and H. O. PRITCHARD. J. Phys. Chem. **66,** 821 (1962).
10. T. L. HILL. J. Chem. Phys. **17,** 1125 (1949).
11. J. O. HIRSCHFELDER, C. F. CURTISS, and R. B. BIRD. Molecular theory of gases and liquids. Wiley, New York. 1954.

Can. J. Chem. Downloaded from www.nrcresearchpress.com by 210.87.254.40 on 09/05/12
For personal use only.

THE PREPARATION OF SOME THIOSEMICARBAZONES CONTAINING THE *s*-TRIAZINE RING[1]

B. A. GINGRAS, T. SUPRUNCHUK, AND C. H. BAYLEY
Division of Applied Chemistry, National Research Council, Ottawa, Canada

Received July 23, 1963

ABSTRACT

The reaction between cyanuric chloride and aliphatic thiosemicarbazones results in the formation of 1:1 adducts containing a dichloro-*s*-triazine ring. Chemical evidence, infrared spectroscopy, and microbiological studies indicate that the addition of the triazine ring takes place at the N^2 atom of thiosemicarbazones. Since cyanuric chloride failed to react similarly with aromatic thiosemicarbazones, a different type of condensation product was obtained by another method, in which cyanuric chloride was first condensed with *o*-, or *p*-hydroxybenzaldehyde to give 1:3 adducts containing free carbonyl groups. Reaction of these compounds with thiosemicarbazide gave the corresponding tri-thiosemicarbazones.

Can. J. Chem. Downloaded from www.nrcresearchpress.com by 210.87.254.5 on 09/05/12
For personal use only.

Continuing our work on thiosemicarbazones (tscs) as possible fungistatic agents (1), it became interesting to study the reaction of these compounds with cyanuric chloride for the following reasons: firstly, a number of cyanuric chloride derivatives have been described in which addition of the cyanuric chloride molecule enhances the antifungal activity of the original compounds (2–5); secondly, the *s*-triazines thus formed usually contain one or two chlorine atoms which can be used for further condensation reactions. Since it has been reported earlier (1) that aliphatic tscs with chain lengths ranging from C_7 to C_{12} were the most active fungistatic agents in this class, this particular series was used in the present study. Under the various experimental conditions used, it was found that only one chlorine atom was replaced so that the products, in all cases, were substituted 4,6-dichloro-1,3,5-triazines of the general formula (I).

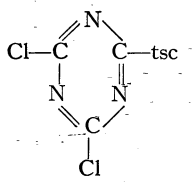

(I)

The products are listed in Table I together with their melting points and analyses.

Thiosemicarbazones (II) are bifunctional compounds containing a thioamide and a thiocarbohydrazide residue, and it was of interest to find out the site of reaction with cyanuric chloride, hence which hydrogen atom was being replaced.

$$RR^1C{=}N^1{-}N^2H{-}C^3S{-}N^4H_2$$

(II)

Since the $-NH_2$ group is known to react easily with cyanuric chloride (6), the possibility of this group being the reactive site in tscs was the first one to be considered. It was found, however, that this was not the case and that tscs reacted with cyanuric chloride even when the terminal $-NH_2$ was replaced by $-NMe_2$; thus, *n*-undecanal-4,4-dimethyl tsc reacted normally with cyanuric chloride to give the 1:1 condensation product. The

[1]*Issued as N.R.C. No. 7565.*

TABLE I

tscs	m.p., °C	Yield, %	Formula	Required, %	Found, %
n-Heptanal	179	75	$C_{11}H_{16}Cl_2N_6S$	C, 39.4 H, 4.77 Cl, 21.18 N, 25.05 S, 9.56	C, 40.32 H, 4.66 Cl, 20.60 N, 24.80 S, 9.48
n-Octanal	189	43	$C_{12}H_{18}Cl_2N_6S$	C, 41.25 H, 5.16 Cl, 20.33 N, 24.05 S, 9.16	C, 41.55 H, 5.32 Cl, 19.50 N, 24.60 S, 9.30
n-Nonanal	170	52	$C_{13}H_{20}Cl_2N_6S$	C, 43.00 H, 5.51 Cl, 19.55 N, 23.13 S, 8.82	C, 42.83 H, 5.03 Cl, 20.02 N, 23.20 S, 8.98
n-Decanal	167	50	$C_{14}H_{22}Cl_2N_6S$	C, 44.6 H, 5.85 Cl, 18.87 N, 22.32 S, 8.52	C, 44.59 H, 5.87 Cl, 19.06 N, 21.95 S, 8.65
n-Undecanal	156	65	$C_{15}H_{24}Cl_2N_6S$	C, 46.2 H, 6.16 Cl, 18.20 N, 21.52 S, 8.20	C, 46.43 H, 6.09 Cl, 18.24 N, 21.40 S, 8.48
9-Undecanal	160	38	$C_{15}H_{22}Cl_2N_6S$	C, 46.4 H, 5.68 Cl, 18.30 N, 21.62 S, 8.25	C, 46.39 H, 5.49 Cl, 18.24 N, 21.60 S, 8.59
n-Dodecanal	160	94	$C_{16}H_{26}Cl_2N_6S$	C, 47.45 H, 6.42 Cl, 17.51 N, 20.75 S, 7.90	C, 47.18 H, 6.57 Cl, 17.59 N, 20.39 S, 8.14

infrared spectrum of this product had no —N—H band indicating that the N^2 hydrogen atom had been substituted. It was also found that, with the terminal $—NH_2$ present but replacing the N^2 hydrogen atom by Me, the resulting 2-methyl tscs failed to react with cyanuric chloride. This shows the importance of the N^2 hydrogen atom and this is in complete agreement with earlier findings that 2-methyl tscs are quite stable, do not dissolve in alkali, and do not form complexes with copper (7, 8). There remains the possibility of reaction at the sulphur atom since tscs may undergo the following tautomeric change:

$$=N—NH—CS—NH_2 \rightleftharpoons =N—N=CSH—NH_2.$$

It is difficult to discriminate between addition of the triazine ring at the N^2 or at the sulphur atoms, since in both cases the hydrogen atom at the N^2 position would be involved. Of course, replacement of this hydrogen atom by a methyl group prevents the tautomerism and the possibility of reaction at either N^2 or S. Two reactions were carried out using the S-sodium salt of acetone tsc and the corresponding S-benzyl derivative with cyanuric chloride, but no condensation products were formed. It should be pointed out that the

Can. J. Chem. Downloaded from www.nrcresearchpress.com by 210.87.254.5 on 09/05/12
For personal use only.

S-substituted derivatives also lacked the N^2 hydrogen atom. In spite of this difficulty, however, it is felt that the addition probably takes place at the N^2 atom, since the tautomerism discussed above is not likely to take place in acetone or dioxane solution in which these reactions were carried out. It was shown that the thione form was the only existing species in the solid state (9) and that the thiol form would be predominant in alkaline solution. Furthermore, infrared spectroscopy provides evidence in favor of the reaction at N^2. The C=S vibration in tscs has been shown to be in the 1080–1130 cm^{-1} region (7) and the spectra of tsc – cyanuric chloride adducts show this band, although it is shifted to higher frequencies by 4 to 20 cm^{-1}. Table II shows this particular region of the spectrum for some compounds.

TABLE II

C=S absorption bands (cm^{-1}) for tscs and their corresponding *s*-triazine derivatives

Carbonyl compounds	tscs (cm^{-1})	Triazines (cm^{-1})
n-Heptanal	1100	1120
n-Octanal	1103	1115
n-Nonanal	1106	1110
n-Decanal	1104	1120
n-Undecanal	1112	1118
9-Undecenal	1105	1120
n-Dodecanal	1110	1120

The probable structure for the condensation products is thus as follows:

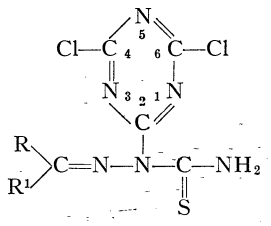

(III)

A second chlorine atom can be substituted on heating (III) with methanol in the presence of sodium bicarbonate. Thus, 2-(*n*-decanal-tsc)-4,6-dichloro-1,3,5-triazine gave the corresponding monomethoxy derivative. The third chlorine atom was not replaced.

We failed to obtain 1:1 adducts between cyanuric chloride and benzaldehyde or the chlorobenzaldehyde tscs. However, aromatic tscs with a primary amino group on the ring gave compounds in which the triazine group is added onto the amino group. Thus, *m*-aminoacetophenone tsc afforded the corresponding substituted 2-amino-4,6-dichloro-1,3,5-triazine (IV). Similar reactions were carried out with the three isomeric hydroxybenzaldehyde tscs but without success. However, an indirect route led to triazine derivatives containing the hydroxybenzaldehydes which gave the corresponding tscs upon further reaction with thiosemicarbazide. The trisubstituted triazines (V*a*, V*b*, V*c*) were described by Allan (10) who obtained them from cyanuric chloride and *o*-, *m*-, and *p*-hydroxybenzaldehyde. The corresponding tri-tscs (V*f*, V*g*) were obtained by the usual method in fair yields (11). The reaction with the *m*-isomer (V*b*) gave a product which could not be purified satisfactorily.

Can. J. Chem. Downloaded from www.nrcresearchpress.com by 210.87.254.5 on 09/05/12
For personal use only.

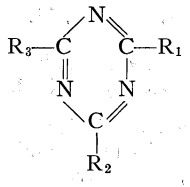

(V)

(V*a*), $R_1 = R_2 = R_3 = o\text{-}OC_6H_4CHO$
(V*b*), $R_1 = R_2 = R_3 = m\text{-}OC_6H_4CHO$
(V*c*), $R_1 = R_2 = R_3 = p\text{-}OC_6H_4CHO$
(V*d*), $R_1 = Cl; R_2 = R_3 = o\text{-}OC_6H_3BrCHO$
(V*e*), $R_1 = Cl; R_2 = R_3 = o\text{-}OC_6H_3ClCHO$
(V*f*), $R_1 = R_2 = R_3 = o\text{-}OC_6H_4CH{=}NNHCSNH_2$
(V*g*), $R_1 = R_2 = R_3 = p\text{-}OC_6H_4CH{=}NNHCSNH_2$

5-Bromo- and 5-chlorosalicylaldehyde were found to be somewhat less reactive and 2:1 adducts containing one chlorine atom were obtained (V*d* and V*e*). Thiosemicarbazones have not as yet been obtained from these last two derivatives.

The fungistatic activities of all compounds described in this work were examined against two organisms and by two methods previously described (1). It was found that the triazines were generally less active than the original tscs so that addition of the cyanuric chloride ring did not enhance the fungistatic activities in this case. This is an interesting finding in itself since it supports the theory that the reaction between cyanuric chloride and tscs takes place at the N^2 atom of the latter. Indeed, it has been shown in this laboratory (12) that the N^2 hydrogen atom must be present for the tscs to have any fungistatic activity. This is related to the fact that N^2-substituted tscs do not form complexes with metals. This phase of the work is being examined further and will form the subject of a separate publication.

EXPERIMENTAL

Thiosemicarbazones and their derivatives not described in the following preparations were reported earlier (7, 11). Reactions between five 2-methyl tscs (from octanal to undecanal), and two *s*-substituted acetone tscs with cyanuric chloride were attempted but are not reported since no tractable products could be obtained. Cyanuric chloride was from commercial sources and was used without further purification. Melting points were taken on a Fisher-John apparatus and are corrected. Infrared spectra are from KBr pellets.

General Procedure for the Preparation of 2-(n-Alkyl tsc)-4,6-dichloro-1,3,5-triazines (III)

A solution of tsc (0.02 mole) in acetone (40 ml) was added slowly to a solution of cyanuric chloride (0.02 mole) in acetone (300 ml). After stirring for 15 minutes, a saturated aqueous solution of sodium bicarbonate was added to bring the pH to 7. The precipitated material was separated by filtration, freed from inorganic salts by washing with water, and after drying, was crystallized from benzene – *n*-hexane. The product was recrystallized from cyclohexane. The various compounds obtained are listed in Table I.

2-(n-Decanal tsc)-4-methoxy-6-chloro-1,3,5-triazine

A mixture of 2-*n*-decanal tsc-4,6-dichloro-1,3,5-triazine (3.56 g, 0.01 mole), methyl alcohol (35 ml), and sodium bicarbonate (1.68 g, 0.02 mole) was stirred for 15 minutes at room temperature, followed by heating under reflux for 30 minutes. After cooling, water was added until the mixture turned cloudy, and the methoxy derivative crystallized out overnight. It was collected and recrystallized twice from ethyl alcohol and finally from *n*-hexane. Yield, 3.2 g, 86.5%; m.p. 114° C. Required for $C_{15}H_{25}ClN_6OS$: C, 48.32; H, 6.71; Cl, 9.68; N, 22.55; S, 8.59%. Found: C, 48.21; H, 7.12; Cl, 9.53; N, 22.90; S, 8.46%.

n-Undecanal-4,4-dimethyl tsc

A solution of *n*-undecanal (6.12 g, 0.036 mole) in ethyl alcohol (150 ml) was added to a warm solution of 4,4-dimethyl thiosemicarbazide (13) (4.32 g, 0.036 mole) in water (100 ml). After addition of glacial acetic acid (5 ml) the resulting mixture was heated on a steam bath for 15 minutes. The mixture was then cooled in ice and enough sodium hydroxide solution to neutralize the acid was added. The 4,4-dimethyl tsc precipitated out, was collected, dried, and recrystallized twice from *n*-hexane. Yield, 8.75 g, 90%; m.p. 49° C

Can. J. Chem. Downloaded from www.nrcresearchpress.com by 210.87.254.5 on 09/05/12
For personal use only.

Required for $C_{14}H_{28}N_3S$: C, 62.8; H, 10.22; N, 15.33; S, 11.67%. Found: C, 61.50; H, 10.65; N, 15.75; S, 12.15%.

The infrared spectrum of this compound is of requisite character and shows only one —NH band at 3200 cm^{-1}. This band disappears in the 1:1 adduct with cyanuric chloride described below.

2-(n-Undecanal-4',4'-dimethyl tsc)-4,6-dichloro-1,3,5-triazine

To a solution of cyanuric chloride (3 g, 0.016 mole) and *n*-undecanal-4,4-dimethyl tsc (4.5 g, 0.016 mole) in acetone (150 ml) was added slowly, with stirring, a saturated aqueous solution of sodium bicarbonate in order to keep the pH of the mixture at 7. After 30 minutes, the acetone was distilled off and the product was extracted from the aqueous solution with chloroform. The chloroform extract was dried, the solvent evaporated, and the residue was dissolved in benzene and passed through a chromatographic column containing silica. A mixture of benzene–ether (4:1) eluted the required material which was further recrystallized from *n*-hexane. Yield, 3.2 g, 47%; m.p. 73° C. Required for $C_{17}H_{28}Cl_2N_6S$: C, 48.68; H, 6.68; Cl, 16.94; N, 20.05; S, 7.64%. Found: C, 48.23; H, 6.72; Cl, 17.45; N, 20.55; S, 7.65%.

2-(m-Aminoacetophenone tsc)-4,6-dichloro-1,3,5-triazine (IV)

A solution of cyanuric chloride (5.35 g, 0.03 mole) in acetone (150 ml) was poured onto crushed ice (ca. 600 ml). To this mixture were added slowly a solution of *m*-aminoacetophenone tsc in acetone (100 ml) and sufficient aqueous sodium hydroxide to keep the mixture neutral, the temperature being maintained between 0 and 5° C. A precipitate was formed and the mixture was stirred until the temperature reached 20° C. The precipitate was collected and recrystallized successively from acetone–water, dimethyl formamide – water, and finally twice from methyl alcohol. Yield, 97%; m.p. > 300° C. Required for $C_{12}H_{11}Cl_2N_7S$: C, 40.45; H, 3.09; Cl, 19.94; N, 27.53; S, 8.99%. Found: C, 39.43; H, 3.17; Cl, 20.20; N, 27.40; S, 9.29%.

Reactions between the three 2,4,6-Tri(formylphenoxy)-1,3,5-triazines (Va, Vb, Vc) and Thiosemicarbazide

Compounds (V*a*), (V*b*), and (V*c*) were prepared by the method of Allan and Allan (10). The reaction of (V*a*) and (V*c*) with thiosemicarbazide gave the corresponding tri-thiosemicarbazones (V*f*) and (V*g*). The procedure described below was used.

A solution of the triazine (8.8 g, 0.02 mole) in dioxane (180 ml) was added to thiosemicarbazide (5.82 g, 0.06 mole) dissolved in hot water (180 ml) containing acetic acid (12 ml). The resulting mixture was heated on the steam bath for 15 minutes and finally allowed to cool. The tri-tsc crystallized out and, after being collected, was recrystallized twice from dimethyl formamide – acetone. (V*f*): Yield, 8.5 g, 64%, m.p. 231° C. Required for $C_{27}H_{24}N_{12}O_3S_3$: C, 49.09; H, 3.64; N, 25.45; S, 14.55%. Found: C, 48.82: H, 3.84; N, 25.45; S, 14.20%. (V*g*): This was best recrystallized from dimethyl formamide – ethyl alcohol. Yield, 8.1 g, 60%; m.p. 243° C. Found: C, 48.20; H, 4.07; N, 25.35; S, 14.80%.

2,4-Di(2-formyl-5-bromophenoxy)-6-chloro-1,3,5-triazine (Vd)

A solution of cyanuric chloride (4.61 g, 0.025 mole) in dioxane (75 ml) was added dropwise to a mixture of 5-bromosalicylaldehyde (15.2 g, 0.075 mole) and sodium hydroxide (3 g, 0.075 mole) in dioxane (100 ml) and water (150 ml). After stirring the mixture for 1.5 hours, a precipitate formed. It was collected and treated with ethyl alcohol from which the unreacted 5-bromosalicylaldehyde (12.1 g) was recovered. The alcohol left a residue which, after recrystallization from dimethyl formamide – water, was shown to be the disubstituted triazine V*d*. Yield, 1 g, 7.8%; m.p. 225° C. Required for $C_{17}H_8Br_2Cl\,N_3O_4$: C, 39.73; H, 1.56; Br, 31.16; Cl, 6.91; N, 8.18%. Found: C, 39.66; H, 1.70; Br, 31.80; Cl, 7.33; N, 8.39%.

2,4-Di(2-formyl-5-chlorophenoxy)-6-chloro-1,3,5-triazine (Ve)

This was prepared as above and the disubstituted triazine V*e* was obtained in a 20% yield; m.p. 212° C. Required for $C_{17}H_8Cl_3N_3O_4$: C, 48.05; H, 1.88; Cl, 25.09; N, 9.89%. Found: C, 47.66; H, 1.82; Cl, 25.20; N, 10.50%.

REFERENCES

1. B. G. Benns, B. A. Gingras, and C. H. Bayley. Appl. Microbiol. **8**, 353 (1960).
2. W. B. Ligett and C. N. Wolf. Can. Patent No. 546,027 (September, 1957).
3. C. N. Wolf. U.S. Patent No. 2,824,823 (February, 1958).
4. K. G. Nolan and W. B. Hardy. U.S. Patent No. 2,822,313 (February, 1958).
5. P. H. Schuldt and C. N. Wolf. Contribs. Boyce Thompson Inst. **18**, 377 (1956).
6. J. T. Thurston, J. R. Dudley, D. W. Kaiser, I. Hechenbleikner, F. C. Schaefer, and D. Holm-Hansen. J. Am. Chem. Soc. **73**, 2981 (1951).
7. B. A. Gingras, R. L. Somorjai, and C. H. Bayley. Can. J. Chem. **39**, 973 (1961).
8. B. A. Gingras, T. Suprunchuk, and C. H. Bayley. Can. J. Chem. **40**, 1053 (1962).
9. S. G. Bogomolov, E. A. Postovski, and U. H. Scheinker. Dokl. Akad. Nauk SSSR, **91**, 1111 (1953).
10. F. J. Allan and G. G. Allan. Rec. Trav. Chim. **69**, 1545 (1959).
11. B. A. Gingras, R. W. Hornal, and C. H. Bayley. Can. J. Chem. **38**, 712 (1960).
12. Unpublished data.
13. K. A. Jensen. J. Prakt. Chem. **159**, 189 (1941).

Can. J. Chem. Downloaded from www.nrcresearchpress.com by 210.87.254.5 on 09/05/12
For personal use only.

THE STRUCTURE OF BIKHACONITINE[1]

Y. TSUDA[2] AND LÉO MARION
Division of Pure Chemistry, National Research Council, Ottawa, Canada
Received August 19, 1963

ABSTRACT

Aconitum spicatum Stapf has been found to contain two major alkaloids, pseudaconitine and bikhaconitine. The latter ($C_{36}H_{51}O_{11}N$) contains one free hydroxyl, four aliphatic methoxyl groups, one acetic and one veratric ester group, while the former ($C_{36}H_{51}O_{12}N$) contains the same substituents plus a second free hydroxyl. Like pseudaconitine, which forms a pyro-derivative hydrolyzable to pyropseudaconine, which can be isomerized to isopyropseudaconine, bikhaconitine gives rise to pyrobikhaconitine, pyrobikhaconine, and isopyrobikhaconine. Bikhaconitine was assumed to differ from pseudaconitine in lacking one secondary hydroxyl. The correctness of this assumption was proved by the conversion of pseudaconitine into bikhaconitine and further to triacetylbikhaconine. This correlation establishes the structure of bikhaconitine and also, since pseudaconitine had previously been correlated with aconitine, establishes its absolute configuration.

Can. J. Chem. Downloaded from www.nrcresearchpress.com by 210.87.254.5 on 09/05/12
For personal use only.

In 1905 Dunstan and Andrews (1) isolated from *Aconitum spicatum* Stapf an alkaloid, $C_{36}H_{51}O_{11}N.H_2O$, $[\alpha]_D$ +12.21 (EtOH) which they named bikhaconitine from the Indian trivial name of the plant, i.e., bikh. They described the base as a solid with a variable melting point (113–116° from dilute ethanol, 118–123° from ether) because of solvation, but they obtained a hydrobromide of constant m.p. 173–175°, $[\alpha]_D$ −12.4 (H_2O). The base which contained six methoxyl groups was saponifiable into acetic acid, veratric acid, and the amorphous bikhaconine $[\alpha]_D$ +33.9 (EtOH). Furthermore, on heating to 180° bikhaconitine lost the elements of acetic acid and formed pyrobikhaconitine, $C_{34}H_{47}O_9N$.

In order to study this base further, a quantity of the root of *A. spicatum* Stapf[3] was procured and the crude alkaloids isolated. There were present two major and several minor alkaloids. The two major alkaloids were separated by chromatography on alumina. The first was eluted from the chromatogram with benzene while the second was eluted afterwards with benzene–chloroform. The latter crystallized readily from methanol. It proved to be identical with pseudaconitine, $C_{36}H_{51}O_{12}N$ (I, R = Et, R_1 = OH, R_2 = $C_6H_3(OCH_3)_2$) (2). The amorphous base obtained from the benzene eluate was characterized as the crystalline perchlorate, m.p. 240–242°. The free base, recovered from the

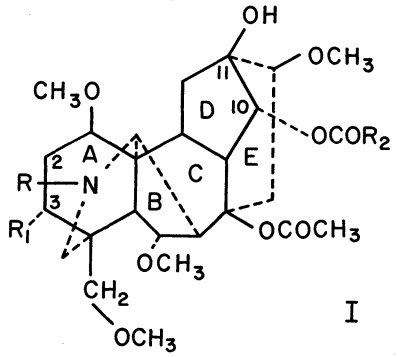

I

[1]*Issued as N.R.C. No. 7599.*
[2]*National Research Council of Canada Postdoctoral Fellow. Present address: School of Pharmacy, Osaka University, Osaka, Japan.*
[3]*We express our gratitude to S. B. Penick and Company, who kindly obtained the plant material, and to Dr. H. R. Schmidt, of that firm, who identified it.*

purified perchlorate, crystallized readily from ethanol–water or from ether with one mole of water of crystallization, $C_{36}H_{51}O_{11}N.H_2O$, $[\alpha]_D$ +16° (EtOH). It did not have a sharp melting point (105–115°) and even after 10 hours at 100° at 10^{-2} mm still retained its water of crystallization (see footnote 4). The base formed a crystalline hydrobromide which after drying melted at 174–176°, $[\alpha]_D$ −8.5° (H_2O).

Although they could be separated readily by chromatography and their mobilities in thin layer chromatography were quite different, yet the IR spectrum of the benzene-eluted base was hardly different from that of pseudaconitine and the n.m.r. spectra of both bases were also very similar.

The infrared spectrum of the perchlorate of the benzene-eluted alkaloid revealed the presence of a hydroxyl (3500 cm^{-1}), two ester carbonyls (1727, 1713 cm^{-1}), and a substituted benzene ring (1600, 1518 cm^{-1}). The n.m.r. spectrum of the free base contained signals indicating the presence of an N-ethyl group (triplet centered at δ 1.08); four aliphatic methoxyls (δ 3.13, 3.24, 3.27, 3.51); a veratroyl group (two aromatic methoxyls δ 3.90, 3.93; three aromatic protons δ 6.8 ∼ 7.8); an acetoxy group (δ 1.30) (3); and a signal at δ 4.87, $J \sim 4.5$ c/s, which will be referred to later.

When treated with alkali the alkaloid was hydrolyzed to veratric acid, acetic acid, and an amorphous alkamine, $[\alpha]_D$ +33.4° (EtOH), the n.m.r. spectrum of which showed the presence of an N-ethyl and four aliphatic methoxyl groups, but no longer contained the signals corresponding to the veratroyl and the acetoxy groups.

The agreement between the properties already described of the benzene-eluted alkaloid and those of bikhaconitine is such as to establish the identity of the two.

The bikhaconitine isolated from *A. spicatum* when acetylated with acetic anhydride and *p*-toluenesulphonic acid gave a quantitative yield of a monoacetate, m.p. 197–199°, while the complete acetylation of the hydrolytic bikhaconine produced the dimorphous triacetylbikhaconine, m.p. 149–151° or 159–162° depending on the rate of crystallization. Under the same conditions pseudaconitine and pseudaconine gave rise to diacetylpseudaconitine and tetraacetylpseudaconine respectively (2). Hence bikhaconitine contains one free hydroxyl only, and as a working hypothesis, it will be assumed to have structure I (R = Et, R_1 = H, $R_2 = C_6H_3(OCH_3)_2$) which lacks the ring A hydroxyl of pseudaconitine.

Dunstan and Andrews (1) had described the pyrolysis of bikhaconitine in which the base lost the elements of acetic acid and formed an amorphous pyro-derivative. In repeating this work it has now been found that bikhaconitine when heated *in vacuo* at 190–195° lost acetic acid very readily and produced pyrobikhaconitine $C_{34}H_{47}O_9N$ (II, R = $COCH_3(OCH_3)_2$) which crystallized from ether, m.p. 155–157°. The n.m.r. spectrum of this product contained a doublet (δ 5.56, $J \sim 6$ c/s) corresponding to one olefinic proton. Alkaline hydrolysis of pyrobikhaconitine gave rise to the amorphous pyrobikhaconine (III, R = H) which also showed in its n.m.r. spectrum a doublet (δ 5.54, $J \sim 8$ c/s) corresponding to one olefinic proton. Pyrobikhaconine when warmed in methanol in the presence of a trace of acid, like pyrodelphonine (4), underwent an allylic rearrangement and gave crystalline isopyrobikhaconine, $C_{25}H_{39}O_6N$, m.p. 189–192°, IV, the n.m.r. spectrum of which showed the presence of four methoxyl groups and contained a broad peak (δ 5.90) corresponding to two olefinic protons. It can be concluded, therefore, that bikhaconitine contains the sequence $\diagdown$C(OAC)—CH_2—CH(OMe)—, just like pseudaconitine (2) and delphinine (4).

Can. J. Chem. Downloaded from www.nrcresearchpress.com by 210.87.254.5 on 09/05/12
For personal use only.

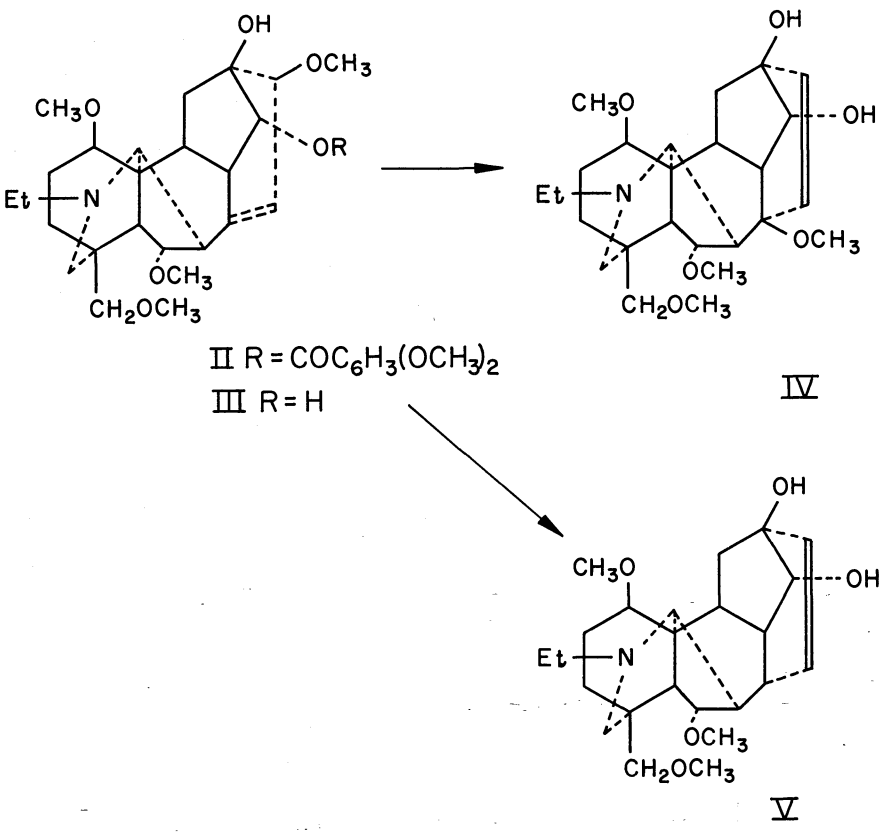

Pyrobikhaconitine on treatment with lithium aluminum hydride, just like pyropseudaconitine (2), underwent reductive cleavage and a rearrangement with accompanying loss of a methoxyl. Under these conditions the product was demethoxyisopyrobikhaconine V, $C_{24}H_{37}O_5N$, m.p. 147–150°, which had an n.m.r. spectrum containing signals indicative of three methoxyl groups, and a poorly resolved signal centered at δ 5.68 attributable to two olefinic protons. Demethoxyisopyrobikhaconine V formed a diacetyl derivative, m.p. 161–163°, indicating the presence of two free hydroxyls. A monoacetyl derivative was also obtained as a by-product which could be converted into the diacetyl compound by further acetylation. The double bond present in V according to the n.m.r. spectrum was confirmed by hydrogenation of the diacetyl derivative which gave rise to dihydrodiacetyldemethoxyisopyrobikhaconine, $C_{28}H_{43}O_7N$, m.p. 172–174°.

Just like the n.m.r. spectra of pseudaconitine and of delphinine, the spectrum of bikhaconitine contains a doublet at δ 4.87 (J = 4.5 c/s) and a signal at δ 1.30 indicating a single proton split by a single neighboring proton, and a shielded acetoxy group respectively. These signals indicate (cf. ref. 3) that the two ester groups of bikhaconitine must be located as in pseudaconitine and be similarly oriented. The fact that the C_{10} proton has one neighboring proton only is evidence that the C_{11} position must be substituted by an oxygenated function. Consequently rings D and E of bikhaconitine must be substituted exactly as rings D and E of pseudaconitine.

Since bikhaconitine contains one free hydroxyl only while pseudaconitine contains two

Can. J. Chem. Downloaded from www.nrcresearchpress.com by 210.87.254.5 on 09/05/12
For personal use only.

and since position 11 is known to be substituted, it is apparent that the C_3 hydroxyl of pseudaconitine must be absent in bikhaconitine as required by structure I (R = Et, R_1 = H, R_2 = $C_6H_3(OCH_3)_2$). This structure accounts well for the formation of monoacetylbikhaconitine and triacetylbikhaconine. It is also in agreement with the formation of an olefinic pyrobikhaconine (II).

If this assumed structure of bikhaconitine is valid, then it should be possible to convert pseudaconitine into bikhaconitine by substitution of hydrogen for the C_3 hydroxyl and thereby prove the structure.

Pseudaconitine was dehydrated with thionyl chloride by a procedure already described (5) and converted into anhydropseudaconitine (perchlorate, m.p. 235–236°). The presence of complex peaks at δ 5.9 corresponding to two olefinic protons in the n.m.r. spectra of both anhydropseudaconitine and its hydrolytic product anhydropseudaconine confirmed that loss of water had occurred at C_2–C_3. A similar pattern has been observed in the n.m.r. spectrum of anhydroindaconitine (5).

Hydrogenation of anhydropseudaconitine (VI) over Adams' catalyst gave a saturated compound which failed to crystallize but had the same mobility as bikhaconitine in thin layer chromatography. It was isolated as its crystalline perchlorate, m.p. 227–233°. Although the melting point was lower than that of bikhaconitine perchlorate, it was not depressed on admixture. The infrared spectra of the two were only very slightly different in the fingerprint region. The base proved to be a mixture of bikhaconitine and the corresponding demethoxy-base, e.g. bikhaconitine, in which one methoxyl had been eliminated. A small quantity of the latter was isolated in pure condition and its n.m.r. spectrum showed the presence of three aliphatic methoxyl groups only (δ 3.16, 3.28, 3.52) together with two aromatic methoxyls (δ 3.10, 3.92). Since many examples of the hydrogenolysis of an allylic-methoxyl have been reported (cf. ref. 6) it is reasonable to assume that it is the methoxyl of ring A which has been removed during hydrogenation and that the base can therefore be represented by partial formula VII.

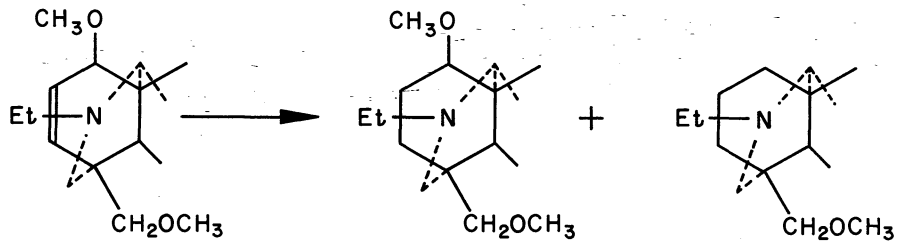

VI VII

Deoxypseudaconitine (bikhaconitine), however, was not obtained in pure form from the mixture although it was the major component. Hence, some of the crude product was hydrolyzed by alkali into the alkamine which in thin layer chromatography showed a strong spot which had the same mobility as bikhaconine, accompanied by a close but weak spot. The crude hydrolytic product was acetylated with acetic anhydride and *p*-toluenesulphonic acid. The product of this last reaction was chromatographed on alumina. A fraction was obtained from the chromatogram which crystallized from hexane, m.p. 147–150°, $[\alpha]_D$ −8.0°, which was identical in melting point with that of the mixture, optical rotation, infrared spectrum, and mobility in thin layer chromatography with triacetylbikhaconine.

This correlation of bikhaconitine with pseudaconitine proves the correctness of the

Can. J. Chem. Downloaded from www.nrcresearchpress.com by 210.87.254.5 on 09/05/12
For personal use only.

assumed structure I (R = Et, R_1 = H, R_2 = $C_6H_3(OCH_3)_2$) and at the same time establishes its absolute configuration, since pseudaconitine has been correlated previously with aconitine (2).

EXPERIMENTAL

All n.m.r. spectra were measured in $CDCl_3$ solution with tetramethylsilane as an internal reference. In each column chromatography Woelm grade IV neutral alumina was used. The melting points were taken on a Kofler hot stage, and are uncorrected. For thin layer chromatography, silica gel G was used as an adsorbent, cyclohexane–chloroform–diethylamine as the solvent system.

Separation of the Alkaloids

The powdered root of *A. spicatum* Stapf (36 kg) was percolated with 95% ethanol. The concentrated extract was diluted with water, acidified with hydrochloric acid, and extracted repeatedly with methylene chloride. The liquor was alkalized with sodium carbonate to liberate the weak bases and extracted with chloroform (Extract A). Sodium hydroxide was then added to liberate the strong bases and the liquor again extracted with chloroform (Extract B).

The methylene chloride extract was evaporated and the residue taken up in dilute hydrochloric acid. Filtercel was added to the acid solution which was filtered and the filtrate extracted with ether. The liquor was then made basic with sodium hydroxide and extracted exhaustively with chloroform. This chloroform extract when evaporated to dryness left a residue of crude bases (340 g). The crude residue consisted of bases forming methylene-chloride-soluble hydrochlorides. A thin layer chromatography test showed two strong spots accompanied by several weak spots indicating the presence of two major alkaloids and several minor ones.

A quantity (130 g) of the crude basic residue was dissolved in benzene containing some chloroform and the solution filtered. The filtrate was poured through a column (6 × 33 cm) of alumina (800 g) which was eluted first with benzene and then with benzene–chloroform. The first two fractions (benzene, 1 l.) yielded a pale yellow gum (84 g). Fractions 3–8 (benzene, 1.5 l., and benzene–chloroform 1.7 l.) gave pseudaconitine (14 g), m.p. 203–205°, after crystallization from methanol (cf. ref. 2).

The yellow gum (84 g) obtained from the first two fractions of the eluate was rechromatographed over alumina (1 kg) in a column (6 × 42 cm) and eluted as follows. Fraction 1 (benzene, 500 ml) was discarded. Fractions 2–15 (benzene, 3.2 l.; benzene–chloroform, 8:2, 1.1 l.; benzene–chloroform, 1:1, 1.1 l.) yielded a gummy base which was dissolved in ethanol. The solution was made just acid to Congo red by the careful addition of 70% perchloric acid, and after it had stood some time at room temperature it deposited the salt as colorless needles (30 g). Fractions 16–18 (benzene–chloroform, 1:1, 250 ml; chloroform, 500 ml) gave a mixture of the base already obtained as its perchlorate and pseudaconitine. Fractions 19–21 (chloroform, 1.4 l.) left on evaporation a residue (28 g) which when crystallized in methanol produced pseudaconitine (13 g). Total yield of crystalline pseudaconitine, 27 g.

Bikhaconitine

The crystalline perchlorate obtained from the first base eluted from the chromatogram was recrystallized from ethanol from which it separated as colorless needles, m.p. 240–242°, $[\alpha]_D$ −5.2° (*c*, 1.6 in $CHCl_3$). Found: C, 55.75; H, 6.62. Calc. for $C_{36}H_{51}O_{11}N.HClO_4$: C, 55.83; H, 6.77%.

The base recovered from the purified perchlorate crystallized from ether or dilute ethanol as colorless needles. From either solvent the crystalline base was hydrated, m.p. 105–110°,[4] $[\alpha]_D$ +16° (*c*, 1.6 in EtOH). For bikhaconitine the literature (1) gives m.p. 118–123° or 113–116°, $[\alpha]_D$ +12.21°, in EtOH. Found: C, 62.34; H, 7.66; N, 2.29. Calc. for $C_{36}H_{51}O_{11}N.H_2O$: C, 62.50; H, 7.72; N, 2.02%.

Bikhaconitine formed a hydrobromide which crystallized from ethanol as colorless prisms, m.p. 174–175°, and the air-dried sample had $[\alpha]_D$ −8.5° (*c*, 1.2 in H_2O). The literature (1) gives m.p. 173–175°, $[\alpha]_D$ −12.4°, in water.

Acetylbikhaconitine

Bikhaconitine (150 mg) in acetic anhydride (3 ml) containing *p*-toluenesulphonic acid (100 mg) was heated on a steam-bath for 1 hour. The reaction mixture was poured into ice water, alkalized, and repeatedly extracted with ether. The combined ether extract was washed, dried, and evaporated to dryness. The residual crystalline acetylbikhaconitine (150 mg) was crystallized from methanol from which it separated as colorless prisms, m.p. 197–199°, $[\alpha]_D$ +21.6° (*c*, 1.5 in $CHCl_3$). Found: C, 63.70; H, 7.28; N, 2.11. Calc. for $C_{38}H_{53}O_{12}N$: C, 63.77; H, 7.46; N, 1.96%. In the n.m.r. spectrum, δ 1.30, 2.04 ($COCH_3$).

[4]*Bikhaconitine can be converted, by oxidative dealkylation followed by methylation, into the N-methyl-N-desethyl derivative which crystallizes readily. Seeding a solution of bikhaconitine in n-hexane with a small crystal of the derivative induced crystallization of bikhaconitine as stout prisms which were not hydrated and melted at 163.5–164°. Found:* C, *63.69;* H, *7.47;* N, *2.11. Calc. for* $C_{36}H_{51}O_{11}N$: C, *64.09;* H, *7.57;* N, *2.08%. We are indebted to Dr. O. Achmatowicz, Jr. for this observation.*

Can. J. Chem. Downloaded from www.nrcresearchpress.com by 210.87.254.5 on 09/05/12
For personal use only.

Hydrolysis of Bikhaconitine

Bikhaconitine perchlorate (75 mg) in 5% methanolic sodium hydroxide (10 ml) was refluxed for 1½ hours. The methanol was evaporated under reduced pressure, the residue was dissolved in water, and the solution extracted with chloroform. The extract was washed, dried, and evaporated to dryness. There was left a gummy residue of bikhaconine (46 mg) which in thin layer chromatography appeared to be homogeneous and showed no carbonyl absorption in the infrared spectrum; n.m.r. triplet centered at δ 1.07 (N—Et) and $4OCH_3$ at δ 3.22, 3.28 (6H), 3.40, $[\alpha]_D$ +33.4° (*c*, 3.2 in EtOH). For bikhaconine the literature (1) reports $[\alpha]_D$ +33.9° in ethanol.

The aqueous solution that had been extracted with chloroform was acidified with hydrochloric acid and extracted repeatedly with ether. The combined ether extract yielded a solid acid which was crystallized from aqueous ethanol from which it separated as colorless prisms, m.p. 184–186°, either alone or in admixture with an authentic sample of veratric acid. The infrared spectra of the two were superimposable.

Triacetylbikhaconine

Bikhaconine (100 mg) and *p*-toluenesulphonic acid (100 mg) in acetic anhydride (5 ml) were heated on a steam bath for 1½ hours. The mixture was poured into ice water, rendered alkaline with sodium carbonate, and the solution extracted with ether. Evaporation of the dried extract left a solid which was dissolved in benzene, and chromatographed on a column of alumina. The eluate on evaporation left the solid triacetylbikhaconine (95 mg) which crystallized from *n*-hexane as colorless needles, m.p. 149–150°, $[\alpha]_D$ −8.1° (*c*, 1.7 in $CHCl_3$). Found: C, 62.65; H, 7.81; N, 2.54. Calc. for $C_{31}H_{47}O_{10}N$: C, 62.71; H, 7.98; N, 2.36%. In the n.m.r. spectrum the signals δ 1.96, 2.05, 2.09 designate the acetyl group protons. Triacetylbikhaconine is dimorphous and, when kept for some time in contact with *n*-hexane, melts at 159–161°. Slow crystallization from *n*-hexane gives the high-melting form as colorless prisms. Either form can be obtained by cross seeding.[5]

Pyrobikhaconitine

Bikhaconitine (2.2 g) was heated *in vacuo* (10^{-2} mm) at 190–195° (air bath) for 5 minutes. The cooled product was dissolved in benzene, and chromatographed on a column (2 × 7 cm) of alumina. The pyrobikhaconitine (1.81 g) obtained by evaporation of the benzene eluate was crystallized from ether from which it separated as clusters of colorless needles, m.p. 155–157°, $[\alpha]_D$ +198.4° (*c*, 1.3 in $CHCl_3$). Found: C, 66.39; H, 7.65. Calc. for $C_{34}H_{47}O_9N$: C, 66.54; H, 7.72%.

Pyrobikhaconine

Pyrobikhaconitine (0.29 g) was refluxed in 3% methanolic sodium hydroxide (10 ml) for 2 hours. The methanol was evaporated, the residue dissolved in water, and the solution extracted with chloroform. Evaporation of the extract left the product as a gum (0.21 g) which by thin layer chromatography was homogeneous. Infrared spectrum of this product showed no carbonyl absorption, and had an absorption at 1620 cm^{-1} attributable to a double bond.

Isopyrobikhaconine

Pyrobikhaconine (90 mg) in methanol (10 ml) containing a few drops of 70% perchloric acid was heated under reflux for 1 hour. The reaction mixture was evaporated under reduced pressure, the residue was dissolved in water, and the solution alkalized with sodium hydroxide and extracted with chloroform. Evaporation of the extract after washing with water and drying gave isopyrobikhaconine (90 mg) which crystallized on trituration. When recrystallized from methanol it consisted of colorless prisms, m.p. 189–192°, $[\alpha]_D$ +33.8° (*c*, 0.7 in $CHCl_3$). Found: C, 66.82; H, 8.67. Calc. for $C_{25}H_{39}O_6N$: C, 66.79; H, 8.75%.

Demethoxyisopyrobikhaconine

A mixture of pyrobikhaconitine (1.8 g) and lithium aluminum hydride (1.2 g) in tetrahydrofuran (30 ml) was stirred for 16 hours at room temperature. After decomposition of the excess hydride by the addition of a few drops of water, the mixture was diluted with methylene chloride and filtered. The material on the filter was washed repeatedly with methylene chloride and the combined filtrate and washings evaporated to dryness. The residue was dissolved in 5% hydrochloric acid, the solution washed with ether, made alkaline with sodium carbonate, and extracted with chloroform. The dried chloroform extract on evaporation left a colorless gum (1.2 g) which was dissolved in benzene and chromatographed over alumina. Elution with methylene chloride and chloroform gave demethoxyisopyrobikhaconine which crystallized from ether–*n*-hexane as colorless fine needles, m.p. 147–150°, $[\alpha]_D$ +66.7° (*c*, 0.8 in $CHCl_3$). Found: C, 68.68; H, 8.58. Calc. for $C_{24}H_{37}O_5N$: C, 68.70; H, 8.89%. Those fractions of the eluate which did not yield a pure product were chromatographed again and an additional crop of the pure compound was obtained. Total yield, 1.0 g.

Acetylation of Demethoxyisopyrobikhaconine

Demethoxyisopyrobikhaconine (1.0 g) in acetic anhydride (5 ml) and pyridine (10 ml) was kept overnight at room temperature. The mixture was poured into ice water, the solution made basic with sodium carbonate, and extracted with methylene chloride. The extract was washed with water, dried over magnesium sulphate, and evaporated under reduced pressure. A residual gum (1.0 g) was left which was dissolved in benzene–

[5]*We are indebted to Dr. O. Achmatowicz, Jr. for this observation.*

Can. J. Chem. Downloaded from www.nrcresearchpress.com by 210.87.254.5 on 09/05/12
For personal use only.

hexane (1:2) and chromatographed over alumina. The benzene–hexane and benzene eluates yielded the diacetyl compound (0.175 g) which crystallized from *n*-hexane–ether as colorless prisms, m.p. 161–163°, $[\alpha]_D$ +31.9° (*c*, 1.2 in $CHCl_3$). Found: C, 66.35; H, 7.84. Calc. for $C_{28}H_{41}O_7N$: C, 66.77; H, 8.21%. In the n.m.r. spectrum the signals at δ 2.01, 2.06 indicated the protons of the two acetyl groups.

Further elution of the chromatogram with benzene and methylene chloride yielded a monoacetyl derivative (0.75 g) which crystallized from pentane as colorless prisms, m.p. 94–97°, $[\alpha]_D$ +66.1° (*c*, 1.1 in $CHCl_3$) Found: C, 67.83; H, 8.70. Calc. for $C_{26}H_{39}O_6N$: C, 67.65; H, 8.52%; (n.m.r., δ 2.07). When further acetylated with acetic anhydride and pyridine, the monoacetyl derivative gave rise to diacetyl-demethoxyisopyrobikhaconine, m.p. 161–163°.

Dihydrodiacetyl-demethoxyisopyrobikhaconine

Diacetyl-demethoxyisopyrobikhaconine (60 mg) in ethanol (10 ml) containing a few drops of acetic acid was hydrogenated over platinum oxide (50 mg) for 10 hours at room temperature. The catalyst was filtered off and the filtrate evaporated to dryness. The residual gum was dissolved in water, the solution made basic with sodium carbonate and extracted with ether. The extract was concentrated to a small volume and allowed to stand at room temperature. It deposited the crystalline dihydro-compound which was recrystallized from ether-*n*-hexane from which it separated as colorless prisms, m.p. 172–174°, $[\alpha]_D$ −57.8° (*c*, 0.9 in $CHCl_3$). Found: C, 66.66; H, 8.62. Calc. for $C_{28}H_{43}O_7N$: C, 66.51; H, 8.57%.

Anhydropseudaconitine

Pseudaconitine (5 g) in thionyl chloride (30 ml) was heated on a steam bath for 4 hours. The excess thionyl chloride was evaporated off under reduced pressure and the residue dissolved in water. The solution was made basic with ammonia and extracted with ether. The extract was washed with water, dried over magnesium sulphate, and evaporated to dryness. It left a gum which was dissolved in benzene and chromatographed on alumina. The benzene eluate yielded an amorphous product which formed a crystalline perchlorate. After several recrystallizations from ethanol, the salt consisted of colorless needles (3.9 g), m.p. 235–236° (decomp.), $[\alpha]_D$ +16.1° (*c*, 1.8 in $CHCl_3$). Found: C, 56.11; H, 6.52. Calc. for $C_{36}H_{49}O_{11}N.HClO_4$: C, 55.99; H, 6.53%. Anhydropseudaconitine recovered from the pure salt remained amorphous and could not be induced to crystallize.

Anhydropseudaconine

Anhydropseudaconitine perchlorate (70 mg) was hydrolyzed in 5% methanolic sodium hydroxide (10 ml) by refluxing for 1 hour. The solvent was evaporated, water added, and the solution extracted with chloroform. The extract yielded anhydropseudaconine as a gum (48 mg) having no carbonyl absorption in the infrared spectrum that failed to crystallize, but was shown by thin layer chromatography to be homogeneous. In the n.m.r. spectrum it showed the complex signal for two olefinic protons (δ 5.9).

Hydrogenation of Anhydropseudaconitine

Anhydropseudaconitine recovered from the pure perchlorate (1.04 g) was dissolved in ethanol (35 ml) and stirred at room temperature for 10 hours in a hydrogen atmosphere in contact with platinum oxide (0.165 g). The catalyst was removed by filtration and the filtrate evaporated to dryness under reduced pressure. There was left a colorless gum which failed to crystallize; in thin layer chromatography it showed only one spot which had the same mobility as bikhaconitine.

The colorless gummy product was dissolved in ethanol and converted to the perchlorate which separated as colorless needles (0.93 g). This perchlorate (A), recrystallized once from ethanol, melted at 227–233°, either alone or in admixture with bikhaconitine perchlorate (m.p. 242°). Further recrystallization did not improve the melting point and in some cases lowered it.

A quantity of perchlorate (A) (0.6 g) was recrystallized three times and converted into the free base which crystallized from ethanol–water. After several recrystallizations from the same solvent, the base consisted of colorless leaflets (50 mg), m.p. 175–182°. The n.m.r. spectrum of this base showed the presence of only three aliphatic methoxyl groups (δ 3.16, 3.28, 3.52) and two aromatic methoxyls (δ 3.90, 3.92). This base was again converted to a perchlorate (perchlorate B); it was crystallized twice from ethanol from which it separated as colorless elongated prisms, m.p. 170–175° (decomp.). Found: C, 53.93; H, 6.45. Calc. for $C_{35}H_{49}O_{10}N.HClO_4.2H_2O$: C, 53.87; H, 6.97%. The salt is that of the new base demethoxydeoxypseudaconitine (demethoxybikhaconitine) which has the same R_F value as bikhaconitine.

The remainder of perchlorate A (which had been crystallized twice only) was refluxed with 5% methanolic sodium hydroxide for 1½ hours. The alkamine isolated from the reaction mixture was acetylated as described above for the preparation of triacetylbikhaconine. The product (0.625 g) was chromatographed in benzene on an alumina column (2 × 15 cm). The first eluate (102 mg) showed two spots in thin layer chromatography and remained amorphous. Further elution with benzene gave a crystalline substance (402 mg) which was homogeneous in thin layer chromatography. This fraction, after crystallization in *n*-hexane, consisted of colorless needles, m.p. 147–150°, $[\alpha]_D$ −8.0° (*c*, 1.9 in $CHCl_3$). Admixture with triacetylbikhaconine failed to depress the melting point, and the infrared spectra of the two samples were superimposable. Both the acetylated product and triacetylbikhaconine had the same mobility in thin layer chromatography.

Can. J. Chem. Downloaded from www.nrcresearchpress.com by 210.87.254.5 on 09/05/12
For personal use only.

ACKNOWLEDGMENTS

We acknowledge our indebtedness to Mr. A. Knoll who prepared the crude extracts from the plant material; also to Mr. H. Seguin for the analyses, Mr. R. Lauzon for the infrared spectra, and Mr. M. Lesage for n.m.r. spectra.

REFERENCES

1. W. R. DUNSTAN and A. E. ANDREWS. J. Chem. Soc. **87**, 1636 (1905).
2. Y. TSUDA and L. MARION. Can. J. Chem. **41**, 1485 (1963).
3. Y. TSUDA and L. MARION. Can. J. Chem. **41**, 1634 (1963).
4. K. WIESNER, F. BICKELHAUPT, D. R. BABIN, and M. GÖTZ. Tetrahedron Letters, No. 3, 11 (1959).
5. R. E. GILMAN and L. MARION. Tetrahedron Letters, No. 20, 923 (1962).
6. H. IRIE, Y. TSUDA, and S. UYEO. J. Chem. Soc. 1446 (1959).

Can. J. Chem. Downloaded from www.nrcresearchpress.com by 210.87.254.5 on 09/05/12
For personal use only.

QUADRUPOLE RELAXATION FOR A SPIN $I = 3/2$

THE F^{19} N.M.R. SPECTRA OF BF_3 AND ClO_3F

J. BACON, R. J. GILLESPIE, AND J. W. QUAIL
Department of Chemistry, McMaster University, Hamilton, Ontario
Received July 23, 1963

ABSTRACT

An expression is derived for the broadening of the components of the quartet obtained for the n.m.r. spectrum of nuclei coupled to a nucleus of spin 3/2 undergoing electric quadrupole relaxation. It is shown that the F^{19} spectra of BF_3 and ClO_3F at various temperatures may be satisfactorily interpreted by means of this expression. Activation energies for molecular reorientation of 1.4 kcal/mole for BF_3 and 1.0 kcal/mole for ClO_3F are obtained.

Can. J. Chem. Downloaded from www.nrcresearchpress.com by 210.87.254.42 on 09/05/12
For personal use only.

INTRODUCTION

In general, the spectra of protons or fluorine nuclei spin–spin coupled to a nucleus of spin I (where $I > 1/2$) would be expected to have a multiplet structure of $2I+1$ lines. Often, however, since nuclei with a spin I greater than 1/2 have quadrupole moments which usually couple strongly, by means of molecular reorientations, to local electric fields, relaxation of the nucleus having the quadrupole moment occurs and the multiplet structure of the H^1 or F^{19} resonance is collapsed to a single line. The expected multiplet structure will therefore be seen only if the high-spin nucleus has a small quadrupole moment or if the high-spin nucleus is in an environment which is highly symmetric electrically. Examples of the first case are the proton spectra of diborane (1, 2) and ammonia (3), B^{11} and N^{14} having relatively small nuclear quadrupole moments (4); examples of the second case are the fluorine spectra of MoF_6 (5) and of SF_6 (6), Mo^{95}, Mo^{97}, and S^{33} having relatively large quadrupole moments but being situated in highly symmetric environments.

While the general cases of very slow relaxation and very rapid relaxation have been treated by various authors (7, 8, 9), the case of an intermediate rate of relaxation which gives rise to a partially collapsed multiplet has been treated only for $I = 1$ (8).

THEORY

A spin of 3/2 can exist in the states $m = 3/2, 1/2, -1/2, -3/2$. Pople (8) has derived a series of expressions for the transition probabilities due to quadrupole relaxation which can be summarized as follows: the probability that a nucleus in state m will undergo a 1 quantum transition (i.e., to state $m\pm1$) is

$$[1] \qquad P_{m,m\pm1} = \frac{3}{20}\frac{(2m \pm 1)^2(I \pm m + 1)(I \mp m)}{4I^2(2I-1)^2}\left(\frac{e^2qQ}{\hbar}\right)^2\tau_q$$

and for the 2 quantum transition the probability is

$$[2] \qquad P_{m,m\pm2} = \frac{3}{20}\frac{(I \mp m)(I \mp m - 1)(I \pm m + 1)(I \pm m + 2)}{4I^2(2I-1)^2}\left(\frac{e^2qQ}{\hbar}\right)^2\tau_q,$$

where e = the charge on an electron
eq = the electric field gradient at the nucleus
eQ = the quadrupole moment of the nucleus
τ_q = the correlation time for molecular reorientation

and $e^2qQ/\hbar$ is the quadrupole coupling constant in radians/sec. Transitions due to electric quadrupole moments occur only for $\Delta m = \pm 1$ or ± 2. For $I = 3/2$ we find from the above expressions that

$$[3] \qquad P_{3/2,\pm 1/2} = P_{\pm 1/2,3/2} = P_{-3/2,\pm 1/2} = P_{\pm 1/2,-3/2} = \frac{1}{20}\left(\frac{e^2qQ}{\hbar}\right)^2 \tau_q$$

and

$$[4] \qquad P_{3/2,-3/2} = P_{-3/2,3/2} = P_{1/2,-1/2} = P_{-1/2,1/2} = 0.$$

The inverse lifetime of each state m is given by

$$[5] \qquad \frac{1}{\tau_m} = \sum_{\substack{n \\ n \neq m}} P_{m,n}.$$

For $I = 3/2$ we find therefore that

$$[6] \qquad \frac{1}{\tau_{3/2}} = \frac{1}{\tau_{1/2}} = \frac{1}{\tau_{-1/2}} = \frac{1}{\tau_{-3/2}} = \frac{1}{\tau} = \frac{1}{10}\left(\frac{e^2qQ}{\hbar}\right)^2 \tau_q,$$

a result also obtained by Pople (8). It has been shown (9) that in the extreme narrowing case the nuclear spin – lattice relaxation time T_1, due to quadrupole coupling for a nucleus of spin $I = 3/2$ is given by

$$[7] \qquad \left(\frac{1}{T_1}\right) = \frac{1}{10}\left(\frac{e^2qQ}{\hbar}\right)^2 \tau_q.$$

If the quadrupole moment is small, or if the high-spin nucleus is in a symmetrical environment (eq small), then τ will be long and the resonance of the spin 1/2 nucleus will be a quartet of equal intensities, each line having width $1/\pi\tau$. The line width of the individual components of the resonance of the high-spin nucleus should be $1/\pi T_1$, which is equal to $1/\pi\tau$ in this case.

It has been shown (9) that the line shape for intermediate rates of quadrupole relaxation (assuming other relaxation mechanisms to be insignificant) is given by the following expression:

$$[8] \qquad I(\omega) \propto \text{Re}\ \{\mathbf{W}.\mathbf{A}^{-1}.\mathbf{1}\}$$

where Re { } denotes "the real part of"

$\mathbf{W}$ is the vector $\begin{bmatrix} 1 \\ \vdots \\ 1 \end{bmatrix}$

$\mathbf{1}$ is the vector $[1, \ldots, 1]$

$\mathbf{A}^{-1}$ is the inverse of the complex matrix $\mathbf{A}$ that is defined by the relationships

$$[9] \qquad A_{m,m} = i[(\omega_0 - \omega) + m \cdot 2\pi J] - \frac{1}{\tau_m},$$

$$[10] \qquad A_{m,n} = P_{m,n}, \qquad m \neq n,$$

ω_0 being the center of the unperturbed multiplet and J the coupling constant in c/sec. Using the previously derived relationship [6] for $1/\tau_m$ and expressing the transition probabilities $P_{m,n}$ in terms of τ we obtain the following expression:

Can. J. Chem. Downloaded from www.nrcresearchpress.com by 210.87.254.42 on 09/05/12
For personal use only.

$$\mathbf{A} = \begin{bmatrix} i[(\omega_0-\omega)+3\pi J]-\frac{1}{\tau} & \frac{1}{2\tau} & \frac{1}{2\tau} & 0 \\ \frac{1}{2\tau} & i[(\omega_0-\omega)+\pi J]-\frac{1}{\tau} & 0 & \frac{1}{2\tau} \\ \frac{1}{2\tau} & 0 & i[(\omega_0-\omega)-\pi J]-\frac{1}{\tau} & \frac{1}{2\tau} \\ 0 & \frac{1}{2\tau} & \frac{1}{2\tau} & i[(\omega_0-\omega)-3\pi J]-\frac{1}{\tau} \end{bmatrix}$$

Inserting the inverse of **A** in equation [7], we find that the line shape is given by the expression

[11] $$I(x) \propto \tau f(\eta,x)$$

where $$f(\eta,x) = \frac{320+16\eta^2(25x^2+17)+\eta^4(80x^4+56x^2+45)}{1024x^2+64\eta^2(36x^4-20x^2+25)+16\eta^4(96x^6-160x^4+110x^2+45)+\eta^6(256x^8-1280x^6+1888x^4-720x^2+81)}$$

$$\eta = 2\pi J\tau, \quad x = \frac{\omega_0-\omega}{2\pi J}$$

Line shapes calculated from equation [11] with various values of η^2 from 100 to 0.1 are shown in Fig. 1. In the collapse of the quartet the outer lines move inward, but the inner lines move outward, resulting in a broad doublet-like structure at values of η^2 near 2. Finally, the "doublet" collapses to a single line.

RESULTS AND DISCUSSION

The Spectrum of Boron Trifluoride

The F^{19} n.m.r. spectrum of BF_3 at room temperature has previously been reported by Muetterties and Phillips (5) and by Coyle and Stone (10) as a broad 1:1:1:1 quartet with $J = 15$ c/sec due to coupling of the fluorine with the 81.2% abundant B^{11}. The F^{19} on the 18.8% abundant $B^{10}(I = 3)$ gives some unresolved underlying structure. We have observed both the F^{19} and B^{11} n.m.r. spectra of BF_3 in the gas phase at room temperature. Since both the F^{19} 1:1:1:1 quartet and the B^{11} 1:3:3:1 quartet are only slightly collapsed at room temperature, the multiplet separations are taken as $J_{B^{11}F}$. The F^{19} resonance gives a value for $J_{B^{11}F}$ of 18.3±0.6 c/sec and the B^{11} resonance gives $J_{B^{11}F} = 18.5\pm0.2$ c/sec.

The BF_3 sample used condensed to a liquid at about −17° C. The F^{19} spectrum of the liquid at four lower temperatures is shown in Fig. 2. At −21° C the value of $J_{B^{11}F}$ (allowing for the partial collapse of the spectrum) was found to be 20.0±0.5 c/sec. Since the quadrupole moment of B^{10} is three times as large as that of B^{11} and since $J_{B^{10}F}$ is much smaller than $J_{B^{11}F}$ (due to the smaller magnetogyric ratio of B^{10}), the spectrum of the fluorine on B^{10} is more collapsed than that of fluorine on B^{11}. By matching spectra calculated from equation [11] with the experimental spectra and making due allowance for the underlying broad fluorine on B^{10} lines, approximate values of η have been obtained for temperatures in the range − 100° to −21° C.

If the suggestion of Moniz and Gutowsky (11) that the reorientation is a thermally activated process described by the usual rate equation

12] $$\tau_q = \tau_q^0 \exp(E_a/RT)$$

Can. J. Chem. Downloaded from www.nrcresearchpress.com by 210.87.254.42 on 09/05/12
For personal use only.

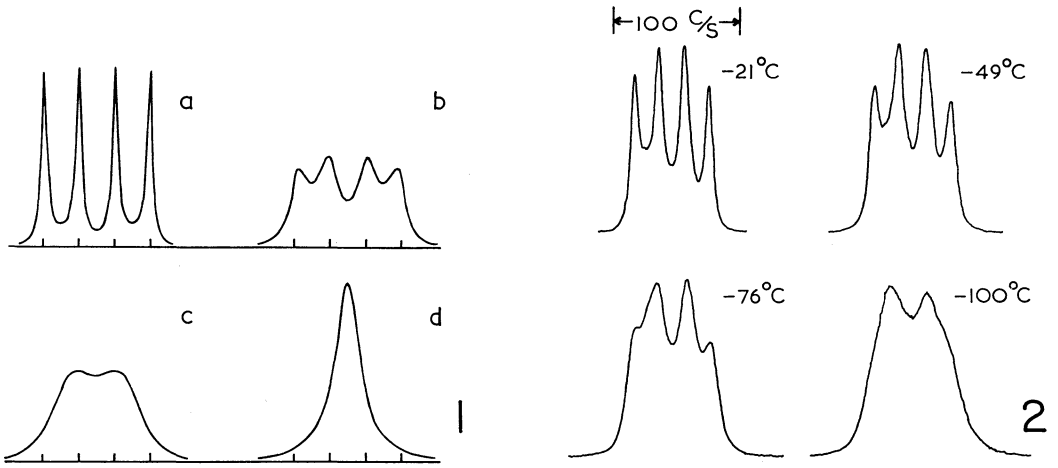

FIG. 1. Theoretical line shapes for the spectra of nuclei of spin 1/2 coupled to a nucleus of spin 3/2 according to equation [11]. (*a*) $\eta^2 = 100$, (*b*) $\eta^2 = 10$, (*c*) $\eta^2 = 1$, (*d*) $\eta^2 = 0.1$. The vertical lines indicate the positions of the quartet in the absence of quadrupole relaxation.

FIG. 2. F^{19} resonance spectra of liquid BF_3.

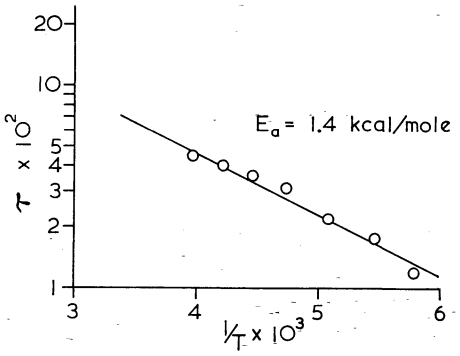

FIG. 3. The temperature dependence of the B^{11} τ estimated from the F^{19} resonance of liquid BF_3.

is accepted, we find from equations [6] and [12] that a plot of log τ vs. $1/T$ should be a straight line of slope $-E_a/2.3R$. The plot of the experimental data is shown in Fig. 3. The plot does not appear to be linear. Nevertheless, a straight line was drawn through the points as shown in Fig. 3. The slope of the line gave a mean activation energy of 1.4 kcal/mole.

The line widths of the F^{19} and B^{11} resonances of BF_3 in the gas phase at room temperature were pressure dependent. However, for any one sample the F^{19} and B^{11} line widths were the same, as predicted by equations [6] and [7].

It is clear from the asymmetry of the BF_3 spectra that there is an isotope effect associated with the two boron isotopes. As would be expected (12), the fluorine on B^{11} resonance occurs at slightly higher field than that of fluorine on B^{10}. The isotope effect was estimated as approximately 3 c/sec at 56.4 Mc/sec or approximately +0.05 p.p.m.

The Spectrum of Perchloryl Fluoride

Studies of the infrared vibrational and rotational spectra (13, 14) and the microwave spectrum (15) indicate that the perchloryl fluoride molecule possesses a nearly regular

Can. J. Chem. Downloaded from www.nrcresearchpress.com by 210.87.254.42 on 09/05/12
For personal use only.

tetrahedral structure about the central chlorine atom, the fluorine atom being bonded directly to chlorine. The molecule possesses no observable dipole moment (16) and it is evident therefore that the electrical environment of the chlorine is highly symmetric: hence a slow rate of quadrupole relaxation would be expected.

The F^{19} n.m.r. spectrum of perchloryl fluoride has previously been recorded by Brownstein (17) and by Agahigian *et al.* (18). Both authors found the F^{19} resonance at room temperature to have a broad, poorly resolved doublet-like structure. Brownstein interpreted the spectrum using a rough qualitative treatment only.

The F^{19} n.m.r. spectrum of perchloryl fluoride recorded at six temperatures over the range −131° C to 24° C is shown in Fig. 4. The theory given above can be used to inter-

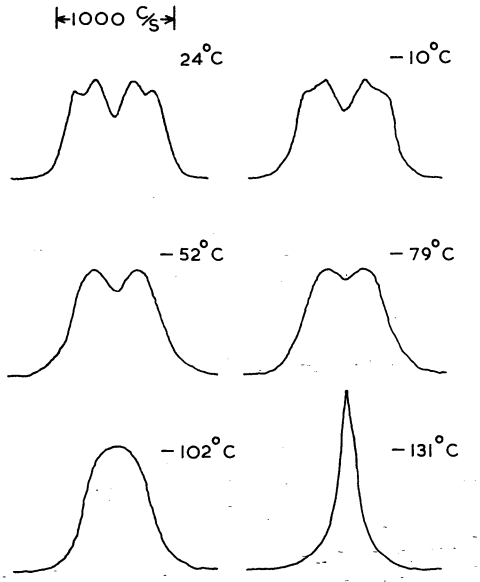

FIG. 4. F^{19} resonance spectra of liquid ClO_3F.

pret these spectra. This task is complicated by the fact that two chlorine isotopes are present, both with spin 3/2. We have therefore considered the ClO_3F spectrum as the sum of two spectra: one due to the molecule $Cl^{35}O_3F$ and the other to the molecule $Cl^{37}O_3F$. The equation to describe this system takes the form

$$I(ClO_3F) = I(Cl^{35}O_3F)+I(Cl^{37}O_3F)$$

and therefore

$$I(ClO_3F) \propto A_{35}\tau_{35}f(\eta_{35},x_{35})+A_{37}\tau_{37}f(\eta_{37},x_{37}),$$

where

$$A_{35} = \text{relative abundance of } Cl^{35}$$
$$A_{37} = \text{relative abundance of } Cl^{37}$$
$$\eta_{35} = 2\pi J_{35}\tau_{35}$$
$$\eta_{37} = 2\pi J_{37}\tau_{37}$$
$$x_{35} = \frac{\omega_0-\omega}{2\pi J_{35}}$$

Can. J. Chem. Downloaded from www.nrcresearchpress.com by 210.87.254.42 on 09/05/12
For personal use only.

and $$x_{37} = \frac{\omega_0 - \omega}{2\pi J_{37}}$$

Since $$\frac{J_{35}}{J_{37}} = \frac{\mu_{35}}{\mu_{37}}$$

in this case, where μ_{35} and μ_{37} are the magnetic moments of the Cl nuclei, it follows that

$$x_{37} = \frac{\mu_{35}}{\mu_{37}} x_{35}.$$

Assuming that the electrical asymmetries (eq) and the correlation times (τ_q) are the same for both molecules, and applying equation [6], we obtain

$$\tau_{37} = \left(\frac{Q_{35}}{Q_{37}}\right)^2 \tau_{35}$$

and $$\eta_{37} = \frac{\mu_{37}}{\mu_{35}} \left(\frac{Q_{35}}{Q_{37}}\right)^2 \eta_{35}$$

Substituting the known values (4) for μ and Q, the final expression for the line shape becomes

[13] $$I(ClO_3F) \propto f(\eta_{35}, x_{35}) + .537\, f(1.371\eta_{35}, 1.201x_{35})$$

where $f(\eta,x)$ is given in equation [11].

Equation [13] was evaluated at small intervals of x over the range $x = 0 \rightarrow x = 3.0$ for different values of η_{35}. The calculated line shape for $\eta_{35}^2 = 5.15$, showing the individual contributions of the two isotopes, is reproduced in Fig. 5. This was the closest fit that could

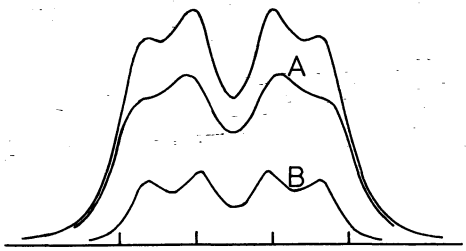

FIG. 5. Calculated line shape for $\eta_{35}^2 = 5.15$, showing the individual contributions of the two isotopes, Cl^{35} (A) and Cl^{37} (B), and their sum. The vertical lines indicate the positions of the Cl^{35} quartet in the absence of quadrupole relaxation.

be obtained for $T = 24°$ C. The splitting between the inner peaks in the experimental spectrum at this temperature was observed to be 289±5 c.p.s. From a comparison of the observed and calculated spectra a value of $J_{Cl^{35}F} = 278 \pm 5$ c.p.s. was obtained. Using this value and by comparing experimental and calculated spectra, values for τ_{35} at each temperature were found.

A plot of log τ_{35} vs. $1/T$ is shown in Fig. 6. It is a reasonably good straight line with a slope corresponding to an activation energy of approximately 1.0 kcal/mole. This energy is less than the corresponding activation energy for any of the 12 nitrogen compounds studied by Moniz and Gutowsky (11). Such a result is expected for perchloryl fluoride, due to the high symmetry and relatively small size of the molecule.

Can. J. Chem. Downloaded from www.nrcresearchpress.com by 210.87.254.42 on 09/05/12
For personal use only.

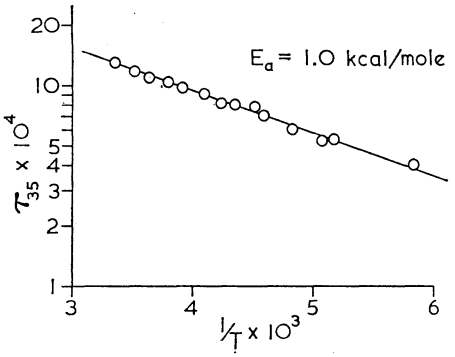

FIG. 6. The temperature dependence of the Cl^{35} τ estimated from the F^{19} resonance of liquid ClO_3F.

EXPERIMENTAL

The boron trifluoride used was obtained from Matheson of Canada, Ltd., Whitby, Ontario. The gas was distilled into 5 mm O.D. silica n.m.r. tubes on a vacuum line and the tubes sealed off under vacuum. The samples were gaseous at room temperature, but condensed to give an adequate volume of liquid for n.m.r. studies at temperatures from −17° C to −25° depending on the pressure of the sample.

Perchloryl fluoride was obtained from Pennsalt Chemicals Corporation, Philadelphia 2, Pa. The gas was distilled into 5 mm O.D. pyrex n.m.r. tubes and the tubes were sealed under vacuum. The compound was a liquid at room temperature under its own vapor pressure (about 12 atm at 24° C). Spectra of ClO_3F were obtained with non-spinning samples, because at the high power level required to observe the F^{19} resonance (50 db below 0.5 w) the noise induced by spinning the sample actually decreased resolution.

The fluorine n.m.r. spectra were obtained using a Varian Associates' high resolution n.m.r. spectrometer and electromagnet operating at a frequency of 56.4 Mc/sec. B^{11} n.m.r. spectra were obtained at 10.3 Mc/sec. The spectra were calibrated using audio sidebands generated with a Muirhead Wigan D-890-A Decade Oscillator.

The low temperature F^{19} studies were performed using a Varian V-4340 variable temperature n.m.r. probe cooled by means of cold air from a liquid air boiler. A copper–constantan thermocouple and a Leeds and Northrup No. 8692 temperature potentiometer were used to measure the sample temperature. After each change in temperature, about one half hour was allowed for thermal equilibrium to be reached. The temperature of the sample was maintained constant to ±0.5° C while each spectrum was recorded.

The mathematical expressions for the line shapes were evaluated using a Bendix G-15 computer.

ACKNOWLEDGMENTS

We thank the Directorate of Chemical Sciences of the United States Air Force Office of Scientific Research for financial support of this work. One of us (J.W.Q.) thanks the National Research Council of Canada for the award of a Studentship.

REFERENCES

1. R. A. OGG. J. Chem. Phys. **22**, 1933 (1954).
2. J. N. SHOOLERY. Discussions Faraday Soc. **19**, 215 (1955).
3. R. A. OGG and J. D. RAY. J. Chem. Phys. **26**, 1515 (1957).
4. J. A. POPLE, W. G. SCHNEIDER, and H. J. BERNSTEIN. High-resolution nuclear magnetic resonance. McGraw-Hill, New York, 1959. p. 480.
5. E. L. MUETTERTIES and W. D. PHILLIPS. J. Am. Chem. Soc. **81**, 1084 (1959).
6. R. J. GILLESPIE and J. W. QUAIL. J. Chem. Phys. In press. 1963.
7. H. S. GUTOWSKY, D. W. MCCALL, and C. P. SLICHTER. J. Chem. Phys. **21**, 279 (1953).
8. J. A. POPLE. Mol. Phys. **1**, 168 (1958).
9. A. ABRAGAM. The principles of nuclear magnetism. Oxford University Press, London. 1961.
10. T. D. COYLE and F. G. A. STONE. J. Chem. Phys. **32**, 1892 (1960).
11. W. B. MONIZ and H. S. GUTOWSKY. J. Chem. Phys. **38**, 1155 (1963).
12. G. V. D. TIERS. J. Inorg. Nucl. Chem. **16**, 363 (1961).
13. D. R. LIDE, JR., and D. E. MANN. J. Chem. Phys. **25**, 1128 (1956).
14. R. P. MADDEN and W. S. BENEDICT. J. Chem. Phys. **25**, 594 (1956).
15. D. R. LIDE, JR., and D. E. MANN. J. Chem. Phys. **25**, 595 (1956).
16. BOOKLET DC-1819. Pennsalt Chemicals Corporation, Philadelphia, Pa.
17. S. BROWNSTEIN. Can. J. Chem. **38**, 1597 (1960).
18. H. AGAHIGIAN, A. P. GRAY, and G. D. VICKERS. Can. J. Chem. **40**, 157 (1962).

Can. J. Chem. Downloaded from www.nrcresearchpress.com by 210.87.254.42 on 09/05/12
For personal use only.

Can. J. Chem. Downloaded from www.nrcresearchpress.com by 210.87.254.5 on 09/05/12
For personal use only.

TETRAHYDROFURANS

II. SPIRO COMPOUNDS CONTAINING THE TETRAHYDROFURAN RING

B. K. Wasson, J. A. Kernan, and J. M. Parker
Research Laboratories, Charles E. Frosst and Co., Montreal, Que.

Received June 26, 1963

ABSTRACT

2-Allyl-2-methallyl-1,3-propanediol (IV) and 2,2-dimethallyl-1,3-propanediol (V) were cyclized in the presence of mineral acid to give 3,3,8-trimethyl-2,7-dioxaspiro(4.4)nonane (VIII) and 3,3,8,8-tetramethyl-2,7-dioxaspiro(4.4)nonane (IX), respectively. Similarly, 2-methallyl-2-(3-methyl-2-butenyl)-1,3-propanediol (VI) afforded 3,3,8,8-tetramethyl-2,7-dioxaspiro(4.5)decane (X). The diol VI was derived from diethyl methallylmalonate by condensation with 3-methyl-2-butenyl bromide, followed by reduction of diethyl methallyl(3-methyl-2-butenyl)malonate (III) with lithium aluminum hydride. The assigned structures of the spiro compounds were supported by infrared and nuclear magnetic resonance spectral analyses.

DISCUSSION

In a previous paper (1), the synthesis of 2,2-dimethyl-4-allyl-4-hydroxymethyltetrahydrofuran (VII) from 2-allyl-2-methallyl-1,3-propanediol (IV) was described. It was noted that during the distillation of VII a forerun contained material which exhibited no infrared absorption for the primary hydroxyl groups or the terminal double bonds present in IV and VII. It would appear that further cyclization occurred between the allyl and

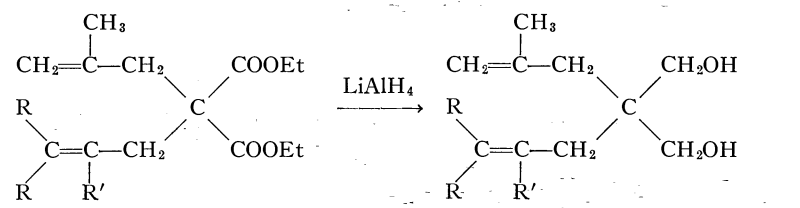

I. R,R′ = H
II. R = H; R′ = CH_3
III. R = CH_3; R′ = H

IV. R,R′ = H
V. R = H; R′ = CH_3
VI. R = CH_3; R′ = H

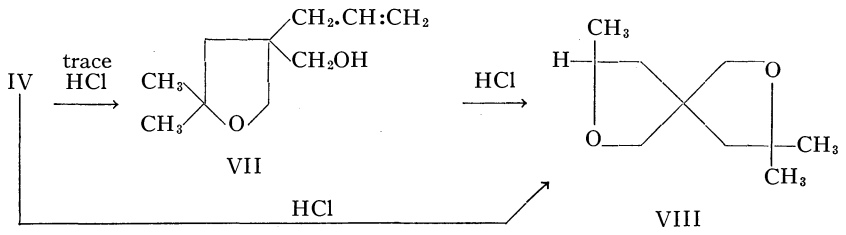

VII

VIII

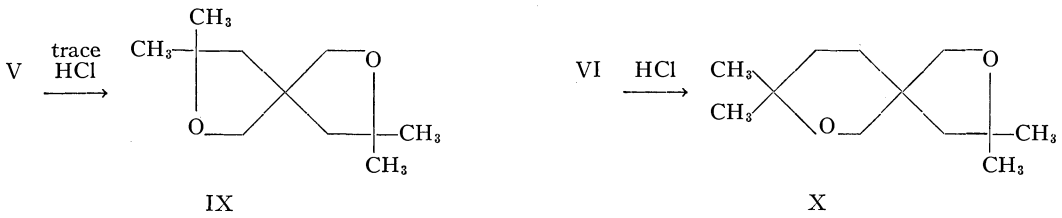

IX

X

the hydroxymethyl group of VII affording the bicyclo compound 3,3,8-trimethyl-2,7-dioxaspiro(4.4)nonane (VIII). This has now been confirmed. A sample of VII was heated 20 hours on the steam bath with concentrated hydrochloric acid to afford an excellent yield of VIII. Furthermore, VIII was obtained directly in high yield when IV was treated with 0.6 molar equivalents of concentrated hydrochloric acid.

A search of the literature failed to reveal a prior synthesis of methylsubstituted-2,7-dioxaspiro(4.4)nonanes. The Patterson, Capell, and Walker Ring Index (2) lists the parent 2,7-dioxaspiro(4.4)nonane but the actual reference (3) described the preparation of the dilactone 1,6-dioxo-2,8-dimethyl-2,7-dioxaspiro(4.4)nonane by treatment of diallylmalonic acid with hydrobromic acid.

3,3,8,8-Tetramethyl-2,7-dioxaspiro(4.4)nonane (IX), a second member of this series, has now been prepared in excellent yield by the acid-induced ring-closure of 2,2-dimethallyl-1,3-propanediol (V). The diol V was obtained by reduction (4) of diethyl dimethallylmalonate (II) with lithium aluminum hydride (5). The ring-closure was vigorously exothermic, even with only a trace of acid present, requiring a solvent to modify the reaction temperature. This confirms the greater activity of the methallyl double bond over that of the allyl double bond. It has already been shown (1) that a molecule containing a methallyl group and a hydroxymethyl group attached to the same carbon atom will condense, according to Markownikoff's rule, to form a tetrahydrofuran rather than a tetrahydropyran ring. Therefore, during the cyclization of 2,2-dimethallyl-1,3-propanediol (V) two tetrahydrofuran rings are formed yielding the 2,7-dioxaspiro(4.4)nonane ring system.

Investigation of the above cyclization was extended to include one member of the methylsubstituted-2,7-dioxaspiro(4.5)decanes. The preparation of 3,3,8,8-tetramethyl-2,7-dioxaspiro(4.5)decane (X) was accomplished by treating the sodio derivative of diethyl methallylmalonate with 3-methyl-2-butenyl bromide to give diethyl methallyl-(3-methyl-2-butenyl)malonate (III). Reduction of III with lithium aluminum hydride afforded 2-methallyl-2-(3-methylbutenyl)-1,3-propanediol (VI) and acid treatment of VI gave X. The crystalline dicarbamate was obtained from VI in high yield.

No information is available concerning the methyl derivatives of 2,7-dioxaspiro(4.5) decane. The literature of related compounds is very scanty, however, one reference (6) was discovered which described a ketolactone, 9,9-bis(hydroxymethyl)-2,7-dioxaspiro-(4.5)decane-3,10-dione. 3,3,8,8-Tetramethyl-2,7-dioxaspiro(4.5)decane (X) represents the first member of this series to be synthesized. The structure X was assigned rather than the isomeric 3,3-dimethyl-8-isopropyl-2,7-dioxaspiro(4.4)nonane or 3,9,9-trimethyl-2,8-dioxaspiro(5.5)undecane, since the ring-closure between the 3-methyl-2-butenyl- and hydroxymethyl groups would follow the normal Markownikoff rule of addition.

Assignment of structures to the cyclized products was supported by infrared absorption and nuclear magnetic resonance (n.m.r.) data. The cyclization of each of the three diols, IV, V, and VI, to the dioxaspiro compounds, VIII, IX, and X, required an increase in the number of methyl groups, the formation of cyclic ether, and the loss of terminal unsaturation and of hydroxyl groups. An inspection of the infrared spectra of IV, V, VI, VIII, IX, and X showed that these changes did occur. They were exhibited by the appearance of a doublet (*gem*-dimethyl) in the 7.25–7.35 μ region in place of the single band at 7.3 μ attributed to each starting diol, by the loss of the two bands at 3.25 and 6.1 μ (terminal unsaturation), the loss of the band at 11.2 μ (methallyl), the absence of the band at 10.95 μ (allyl) from the spectrum of VIII which was originally present in that of IV, the loss of the band at 3 μ (hydroxyl) and the shifting and narrowing of the

Can. J. Chem. Downloaded from www.nrcresearchpress.com by 210.87.254.5 on 09/05/12
For personal use only.

9.6–9.8 μ band (hydroxyl) to 9.5 μ (cyclic ether) (7). In addition, the spectra of VIII, IX, and X possessed a strong band at 12.9–13.0 μ (believed to be *gem*-dimethyl). The infrared spectrum of X showed a strong band at 9.25 μ. This was attributed to the C—O vibration in the tetrahydropyran ring, since the C—O vibration for the tetrahydrofuran ring occurred at 9.5 μ for VIII, IX, and X. It is believed that the above-described cyclizations have general application and will be discussed in future publications.

Nuclear magnetic resonance data, given for 3,3,8-trimethyl-(VIII) and 3,3,8,8-tetramethyl-2,7-dioxaspiro(4.4)nonanes (IX) in the experimental section, has proved that only tetrahydrofuran rings were formed to provide spiro compounds containing methyl groups. Similarly the n.m.r. spectrum of X confirmed the presence of the 2,7-dioxaspiro-(4.5)decane skeletal system containing one tetrahydrofuran and one tetrahydropyran ring. Since this spectrum has shown that neither two tetrahydrofuran nor two tetrahydropyran rings were present, the two alternate isomeric structures 3,3-dimethyl-8-isopropyl-2,7-dioxaspiro(4.4)nonane and 3,9,9-trimethyl-2,8-dioxaspiro(5.5)undecane are eliminated.

3,3,8-Trimethyl-2,7-dioxaspiro(4.4)nonane (VIII) was effective as an anticonvulsant. The pharmacological activities of the 2,7-dioxaspiro(4.4)nonanes and the 2,7-dioxaspiro-(4.5)decanes will be reported elsewhere.

EXPERIMENTAL

Boiling points and melting points (Fisher–Johns apparatus) are uncorrected. Analytical samples of liquids were prepared by distillation through a 24-in., 8-mm diameter Nester and Faust spinning band column. Infrared absorption spectra were obtained with a Beckman IR-5 spectrophotometer equipped with a sodium chloride prism. Solids were examined as potassium bromide pellets, and liquids as thin films. The n.m.r. spectra were taken on a Varian 60 Mc high resolution spectrophotometer. In all cases integration of areas was carried out and the number of protons corresponding to each signal is indicated. Values are given in parts per million (p.p.m.) with tetramethylsilane used as the standard.

Preparation of Diethyl Mono- and Di-substituted Malonates

Diethyl methallylmalonate and diethyl allylmethallylmalonate (I) were prepared by standard methods from the literature (5). Methallyl chloride and diethyl methallylmalonate afforded diethyl dimethallylmalonate (II) in an 80% yield, b.p. 153–158° at 15–20 mm. 3-Methyl-2-butenyl bromide and diethyl methallylmalonate gave diethyl methallyl(3-methyl-2-butenyl)malonate (III) in an 84% yield. Redistillation afforded an analytical sample, b.p. 149–150° at 14 mm, n_D^{25} 1.4581. Anal. Calc. for $C_{16}H_{26}O_4$: C, 68.05; H, 9.28. Found: C, 67.67; H, 9.14. Infrared: λ_{max} 3.25, 6.1 (terminal unsaturation), 5.75 (carbonyl), 7.25–7.32 (methyl), 8.3–8.5 (ester), 11.15 μ (methallyl).

Preparation of 3,3,8-Trimethyl-2,7-dioxaspiro(4.4)nonane (VIII)

Method A

From 2,2-Dimethyl-4-allyl-4-hydroxymethyltetrahydrofuran (VII).—Distilled VII (25 g) was treated dropwise with 6.5 ml of concentrated hydrochloric acid. The temperature of the reaction mixture rose from 25° to 35° and was accompanied by faint discoloration. The mixture was allowed to stand for 30 minutes and was warmed overnight on a steam bath. After it had been cooled, the reaction mixture was made alkaline with 6 *N* sodium hydroxide and extracted with ether. The ethereal extract was washed with water, dried, and evaporated to give 23 g of a liquid residue. Distillation of this residue afforded 20.8 g (83%) of VIII, b.p. 68–74° at 6–8 mm, n_D^{25} 1.4439. An analytical sample had a boiling point of 70.5–71.0° at 6 mm, n_D^{25} 1.4436. Anal. Calc. for $C_{10}H_{18}O_2$: C, 70.55; H, 10.66. Found: C, 70.29; H, 10.64. The infrared spectrum of VIII showed the presence of two bands in the methyl region and the absence of bands associated with unsaturation and hydroxyl groups. N.m.r. signals: multiplet centered at 3.60 p.p.m. (—CH—O—CH_2—C—CH_2—O—, area = 5H), multiplet centered at 1.77 p.p.m. (—C—CH_2—C—CH_2C—, area = 4H), triplet at 1.20, 1.16, 1.10 p.p.m. (methyls, area = 9H).

Method B

From 2-Allyl-2-methallyl-1,3-propanediol (IV).—Distilled IV (25 g) was treated with 6.5 ml of concentrated hydrochloric acid. The temperature of the cooled solution rose rapidly to 80°. The reaction mixture was warmed 7 hours on the steam bath and was worked up as described in method A. Distillation afforded 20.2 g (81%) of VIII, b.p. 77–83° at 8–10 mm, n_D^{25} 1.4438. The infrared absorption of this product was identical with that from the product obtained by method A.

Can. J. Chem. Downloaded from www.nrcresearchpress.com by 210.87.254.5 on 09/05/12
For personal use only.

Preparation of 2,2-Dimethallyl-(V) and 2-Methallyl-2-(3-methyl-2-butenyl)-1,3-propanediol (VI)

A solution of 214.5 g of diethyl dimethallylmalonate (II) in 500 ml of anhydrous ether was added dropwise to a vigorously stirred mixture of 45.6 g of lithium aluminum hydride in 1250 ml of anhydrous ether maintained at 5–20°. The reaction mixture was stirred for 2 hours, cooled, and decomposed by successive additions of methanol–ether, methanol–water, and water. The solids were triturated several times with ether. The combined ethereal extracts were washed with water and evaporated to give an oily residue. Distillation of this residue afforded 136.5 g (93%) of V, b.p. 162.5–172° at 15–20 mm. Infrared: λ_{max} 3.0 (hydroxyl), 3.25, 6.1 (terminal unsaturation), 9.6–9.8 (hydroxyl), 11.2 μ (methallyl).

A similar reduction of diethyl methallyl(3-methyl-2-butenyl)malonate (III) with lithium aluminum hydride gave a 94% yield of VI, b.p. 148–165° at 9 mm, which crystallized as white needles, m.p. 54.5–55.0°. Anal. Calc. for $C_{12}H_{22}O_2$: C, 72.68; H, 11.18. Found: C, 72.74; H, 11.22. Infrared: λ_{max} 3.0 (hydroxyl), 3.22, 6.1 (terminal unsaturation), 6.9 (methylene), 7.25 (methyl), 9.5–9.8 (hydroxyl), 11.25 μ (methallyl). The dicarbamate of VI was prepared (1) in an 85% yield as white crystals, m.p. 140.5–146°. Recrystallization from aqueous methanol afforded an analytical sample having a melting point of 145–146°. Anal. Calc. for $C_{14}H_{24}N_2O_4$: C, 59.13; H, 8.51; N, 9.85. Found: C, 59.17; H, 8.24; N, 9.95. Main infrared bands: λ_{max} 2.93, 2.97, 5.9, 6.25, 7.1, 7.45, 9.4, 11.1, and 12.75 μ.

Preparation of 3,3,8,8-Tetramethyl-2,7-dioxaspiro(4.4)nonane (IX)

A solution of 83.9 g of the diol V in 59.5 ml of tetrahydrofuran was treated with 1.9 ml of concentrated hydrochloric acid. The temperature of the solution rose spontaneously to 60°. The solution was cooled, left 1 hour at room temperature, and refluxed for 2 hours. The solvent was evaporated and the residue dissolved in ether. The ethereal solution was washed with dilute alkali, then with water, and dried. The solvent was evaporated to give 73.7 g of a pale yellow residue. Distillation of this residue afforded 68.3 g (81%) of IX, b.p. 115–121° at 21 mm. An analytical sample of IX had a boiling point of 109–110° at 30–31 mm, n_D^{25} 1.4404. Another specimen had a boiling point of 207.5–208° at atmospheric pressure. Anal. Calc. for $C_{11}H_{20}O_2$: C, 71.69; H, 10.94. Found: C, 72.05, 72.13; H, 11.43, 11.19. The infrared spectrum of IX showed the absence of unsaturation and of hydroxyl groups and the presence of two bands in the methyl region. N.m.r. signals: quartet centered at 3.73 p.p.m. (—O—CH_2—C—CH_2—O—, area = 4H), 1.81 p.p.m. (C—CH_2—C—CH_2—C—, area = 4H), doublet at 1.19 and 1.16 p.p.m. (methyls, area = 12H).

Preparation of 3,3,8,8-Tetramethyl-2,7-dioxaspiro(4.5)decane (X)

A solution of 30 g of the diol VI in 110 ml of tetrahydrofuran was treated dropwise during 15 minutes with 28 ml of 6 *N* hydrochloric acid. The temperature of the solution rose from 22° to 33°. The solution was refluxed for 3 hours and the solvents evaporated to give 31.9 g of crude X. An analytical sample had a boiling point of 94.0–94.5° at 6 mm, n_D^{25} 1.4505. Anal. Calc. for $C_{12}H_{22}O_2$: C, 72.68; H, 11.18. Found: C, 72.66; H, 11.14. The infrared spectrum indicated the absence of unsaturation and hydroxyl groups and the presence of methyl groups (7.25, 7.35 μ). N.m.r. signals: quartet centered about 3.63 and 3.41 p.p.m. (—O—CH_2—C—CH_2—O—, area = 4H), multiplet centered at 1.50 p.p.m. (—C—CH_2—CH_2—C—CH_2—C—, area = 6H), doublet at 1.17 and 1.12 p.p.m. (methyls, area = 12H).

ACKNOWLEDGMENTS

The authors are indebted to Dr. A. Taurins and Dr. C. Stammer of McGill University for n.m.r. analyses, and E. Frank and M. Dillon of our laboratory for elemental analyses. We also wish to acknowledge the capable assistance of A. Franck and O. Kristiansen.

REFERENCES

1. B. K. Wasson, C. H. Gleason, I. Levi, J. M. Parker, L. M. Thompson, and C. H. Yates. Can. J. Chem. **39**, 923 (1961).
2. A. M. Patterson, L. T. Capell, and D. F. Walker. The ring index. 2nd ed. American Chemical Society, Washington. 1960.
3. R. Fittig and E. Hjelt. Ann. **216**, 52 (1883).
4. R. F. Nystrom and W. G. Brown. J. Am. Chem. Soc. **69**, 1197 (1947).
5. W. J. Doran and H. A. Shonle. J. Am. Chem. Soc. **59**, 1625 (1937).
6. S. Olsen. Acta Chem. Scand. **9**, 101 (1955).
7. L. J. Bellamy. Infra-red spectra of complex molecules. 2nd ed. Methuen & Co. Ltd., London. 1958.

Can. J. Chem. Downloaded from www.nrcresearchpress.com by 210.87.254.5 on 09/05/12
For personal use only.

A NEW TYPE OF CARBOHYDRATE ORTHOESTER

SIDE REACTIONS OF THE KÖNIGS-KNORR SYNTHESIS[1]

C.-S. GIAM,[2] H. R. GOLDSCHMID,[3] AND A. S. PERLIN

National Research Council of Canada, Prairie Regional Laboratory, Saskatoon, Saskatchewan

Received August 6, 1963

ABSTRACT

A trisaccharide orthoester (IV) is one of the products formed by decomposition of 2,3,4,6-tetra-*O*-acetyl α-D-mannopyranosyl bromide in the presence of silver oxide. This new type of carbohydrate derivative contains three units of D-mannose linked together through the functional groups of a molecule of acetoacetic acid. The carboxyl group of the latter takes part in the orthoester structure of IV, with one D-mannose unit closing a 1,2-orthoester ring, and another unit comprising the —OR group through its anomeric center; the keto group of the acetoacetate forms a 1,2-ketal structure with the third D-mannose unit. The n.m.r. spectra characteristics of the trisaccharide and some related compounds are described. The following sequence of reactions is consistent with formation of the trisaccharide: 1,2-*trans*-acetoxyl bromide $\xrightarrow{Ag^+}$ 1,2-cyclic acetoxonium ion (IX) $\xrightarrow{-H^+}$ 1,2-cyclic ketene-acetal; ion IX and 2,3,4,6-tetra-*O*-acetyl D-mannose then added to the ketene derivative.

Selective degradation of trisaccharide IV yields a novel type of ketal, i.e., 1,2,*O*-[1-(carbomethoxymethyl)-ethylidene]-β-D-mannose.

Can. J. Chem. Downloaded from www.nrcresearchpress.com by 210.87.254.42 on 09/05/12
For personal use only.

Glycosyl halides decompose readily in the presence of silver oxide or carbonate under conditions generally used for the Königs-Knorr synthesis (1) of glycosides and oligosaccharides (2). This "side reaction" therefore adversely affects the yield of the desired condensation product, particularly when formation of the glycosidic linkage involves an unreactive hydroxylic component. Several products have been isolated (2) from a reaction mixture of 2,3,4,6-tetra-*O*-acetyl α-D-mannopyranosyl bromide (I) and silver oxide in benzene, including 2,3,4,6-tetra-*O*-acetyl D-mannose (II) and a 1,2,1′-linked disaccharide orthoacetate heptaacetate (III). Also isolated, in 10% yield, was a product (IV) which appeared to be a second dimeric orthoester. This last product has now been found to be a novel type of trisaccharide, the structure of which is represented by formula IV. It contains three units of D-mannopyranose linked together through the functional groups of a molecule of acetoacetic acid (the carbon chain of which is shown in heavy type). The carboxyl group of the acid and two D-mannose units (A and B) are combined in the form of a 1,2,1′-orthoester structure, and a 1,2-ketal structure serves to bind the ketone group with the third D-mannose unit (C). Evidence for the structure proposed is presented below.

Deacetylation of IV yielded a crystalline material (V) which on reacetylation, with acetic anhydride – pyridine or – sodium acetate, afforded the original product (IV). In this way a more highly purified sample of IV was obtained, as shown by an increase in the estimated molecular weight from the earlier value (2) of 700 to the value of about 1000 required by the trimeric structure. This procedure showed also that none of the interunit linkages was of the normal ester type. On methylation of V a crystalline derivative (VI) was obtained which on methanolysis gave a 2:1 mixture of 3,4,6-tri- and 2,3,4,6-tetra-*O*-methyl methyl glycoside. When V was treated with lead tetraacetate in pyridine

[1]*Presented before the Division of Organic Chemistry, Chemical Institute of Canada, Toronto, June 8, 1963. Issued as N.R.C. No. 7600.*

[2]*National Research Council of Canada Postdoctoral Fellow, 1962–1963.*

[3]*National Research Council of Canada Postdoctoral Fellow, 1958–1960.*

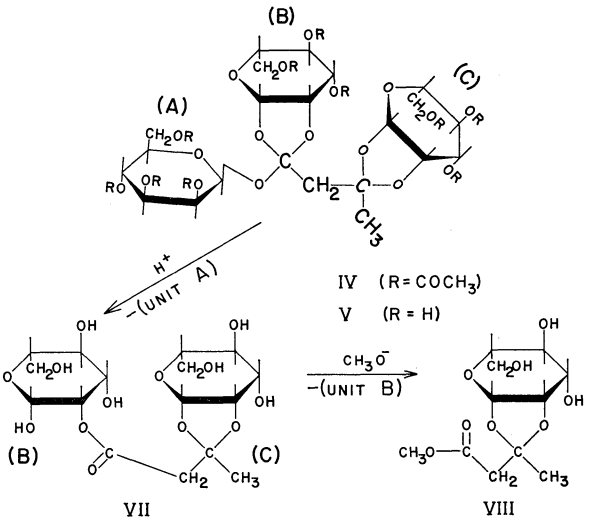

(3, 4), it consumed 4.9 moles of oxidant per mole in 1.5 hours, this uptake being consistent with the presence of four *vic*-diol groups and the release of about 1 mole of formic acid, as seen from comparative oxidations of orthoesters of known structure (5, and experimental section).

Compounds IV and V showed the marked acid-lability of orthoesters (6). As found with other 1,2-orthoesters of D-mannose triacetate, IV was rapidly degraded in cold acidic methanol yielding 3,4,6-tri-*O*-acetyl D-mannose, among other products (2). Treatment of V with dilute sulphuric acid resulted in the release of D-mannose (presumably unit A), and also the formation of an amorphous ester the properties of which correspond to those of structure VII. Both of these products are to be expected from the hydrolysis of V, by analogy with the known behavior of mono- and di-saccharide D-mannose orthoesters (6, 7). A second D-mannose unit (presumably B) was then liberated on addition of sodium methoxide to VII, and the methyl ester of ketal VIII was isolated and characterized as a crystalline triacetate.*

Evidence for the presence of the acetoacetate structure in trisaccharide IV was obtained first by the isolation of acetone from an acid hydrolyzate of the deacetylated material (V). Although acetoacetic acid is very easily decarboxylated to yield acetone, the well-known ethyl ester appears to be substantially more stable, and direct evidence for the acetoacetate moiety was provided by ethanolysis of IV. Ethyl acetoacetate produced in this way was detected in 38% yield by gas–liquid phase chromatography, and characterized as the dinitrophenylhydrazone.

Proton magnetic resonance characteristics of IV and V are consistent with the structures proposed. For example, three non-equivalent anomeric proton signals are evident in the region 5.0 to 6.0 p.p.m. (9) (Figs. 1A and 2A). Other signals in this region are due to protons located α- to secondary acyloxy groups, as shown by their absence from the spectrum of the deacetylated compound (V) (Fig. 2A). The doublet at about 5.7 p.p.m. is close to that expected for the anomeric proton of a D-mannose 1,2-orthoester (5), and is

**Cyclic ketals of type VIII have not been prepared previously. Although analogous ketal derivatives are formed readily by acid-catalyzed condensation, the reaction of acetoacetate and other β-keto esters with a sugar leads under similar conditions to elimination of an extra mole of water and the formation of a 2-substituted furoic acid derivative, the heterocyclic ring of which incorporates C-1 and C-2 of the sugar (8).*

Can. J. Chem. Downloaded from www.nrcresearchpress.com by 210.87.254.42 on 09/05/12
For personal use only.

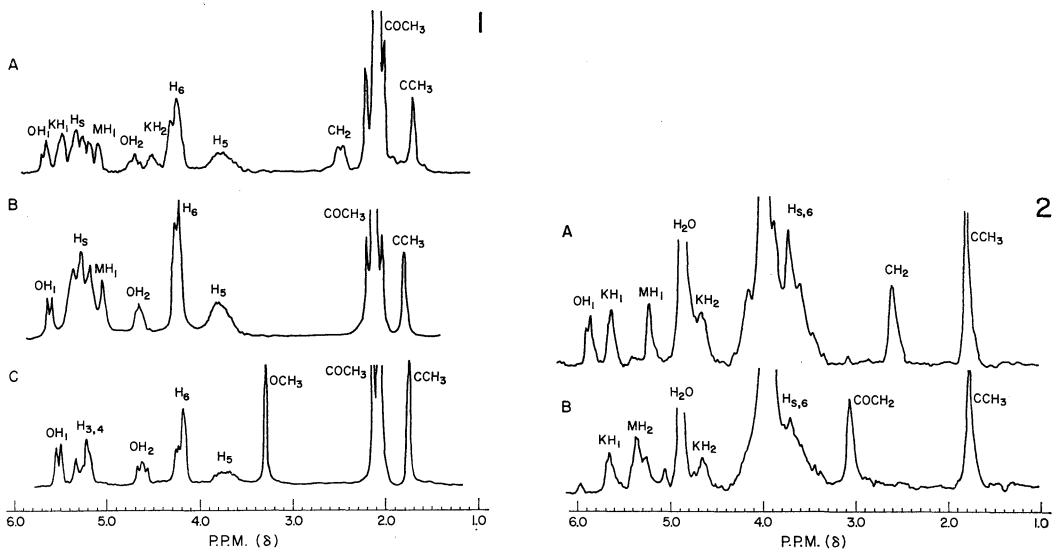

FIG. 1. Proton magnetic resonance spectra (chloroform solution) of (A) trisaccharide acetate IV; (B) disaccharide acetate III; (C) β-D-mannose-1,2-(methyl orthoacetate) 3,4,6-triacetate (*exo*-diastereomer (5)). OH, proton of orthoester unit; KH, proton of ketal unit; MH, proton of mannosyl unit; H_s, proton on secondary carbon atoms.

FIG. 2. Proton magnetic resonance spectra (deuterium oxide solution) of (A) trisaccharide V; (B) hydrolysis product VII. OH, proton of orthoester unit; KH, proton of ketal unit; MH, proton of mannosyl unit; H_s, protons on secondary carbon atoms.

ascribed to H_1 of unit B(OH_1); this assignment is supported by the fact that when acid is added to a solution of V, the signal (OH_1, Fig. 2A) disappears and is replaced by a doublet at lower field (MH_2 in Fig. 2B). The same properties are shown by D-mannose 1,2-orthoacetates on acid hydrolysis (7) and are consistent with opening of the 1,2-orthoester ring of unit B and formation of an *O*-acyl derivative (VII). The doublet (Fig. 1A) having a chemical shift of about 5.5 p.p.m. is ascribed to the anomeric proton (KH_1) of the 1,2-ketal unit, since it is affected neither by deacetylation (Fig. 2A) nor by the acid treatment (Fig. 2B). Although the one-proton signal at 5.1 p.p.m. (Fig. 1A) is not disturbed by removal of neighboring acetyl groups (Fig. 2A), it may no longer be detected after acid hydrolysis (Fig. 2B), and hence can be ascribed to the anomeric proton (MH_1) of the D-mannosyl unit.

Presence of the C-methyl group in IV and V is clearly evident in the three-proton signal at about 1.8 p.p.m., and of the methylene group, in the two-proton signal at about 2.6 p.p.m. (Figs. 1A and 2A). Although the chemical shift for the C-methyl group is the same as that for the C-methyl group of the dimeric orthoacetate (III) (Fig. 1B), it is not materially affected by acid (Fig. 2B) and hence is not indicative of an *orthoacetate* structure in IV and V. By contrast, the acid hydrolysis results in a considerable paramagnetic shift in the signal for the methylene protons (Fig. 2B), consistent with generation of a carbonyl group α- to the methylene on formation of VII from V. In VI, the *O*-acyl linkage likely is through the 2-position of the D-mannose unit, by analogy with the hydrolysis of D-mannose 1,2-orthoacetates to 2-*O*-acetyl D-mannose (7). Thus signal MH_2 (Fig. 2B) which becomes detectable after hydrolysis is closely equivalent to that of H_2 in the *O*-acetate (7), but probably is at relatively too high field for a 1-*O*-acyl derivative (9).

A possible route to formation of IV, consistent with generally-accepted mechanisms,

Can. J. Chem. Downloaded from www.nrcresearchpress.com by 210.87.254.42 on 09/05/12
For personal use only.

could be as follows: on dissociation of the 1,2-*trans*-acyl bromide (I), participation of the 2-*O*-acetyl group leads to the cyclic 1,2-carbonium ion (IX) (10, 11) which, by loss of a proton, may give the cyclic ketene-acetal (X) (12, 13). The latter can then suffer electrophilic attack by IX, as in the normal addition reactions of ketenes and related ketene-acetals (14), with elaboration of the four-carbon chain of the acetoacetate portion (e.g., as in XI). Addition of the elements of a tetra-*O*-acetyl D-mannosyloxy residue to the electron-deficient center of XI then leads to completion of the trimeric structure IV.

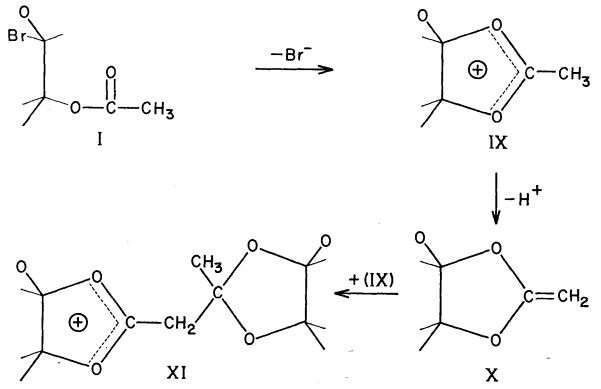

Most probably, the latter step involves 2,3,4,6-tetra-*O*-acetyl D-mannose (II), a major constituent of the reaction mixture (2).

The stereochemistry of three asymmetric centers in the trisaccharide remains to be considered, i.e., of the tertiary carbons in the orthoester and ketal rings and of the D-mannosyl anomeric carbon. The 1,2-orthoester unit appears to be related sterically to the corresponding unit of the disaccharide orthoacetate (III) and to D-mannose 1,2-orthoacetates in which the OR group is thought to be oriented *exo-* to the fused ring system (5). Thus, as noted earlier, protons OH_1 and OH_2 of the trisaccharide (Fig. 1A) are closely equivalent to those of the pertinent diastereoisomeric methyl derivative (Fig. 1C) and of the disaccharide (Fig. 1B). Hence, insofar as the assignment of an *exo*-orientation for the —OR group of the mono- and di-saccharide orthoesters is valid (5), the same orientation may be tentatively assigned for the orthoester structure of the trisaccharide. An *exo*-orientation for the mannosyloxy residue in IV and II is favored also on kinetic grounds, since a group of this magnitude in attacking X or XI is more likely to approach from the side *exo-*, rather than *endo-*, to the fused ring structure (15). Consistent with this possibility is the apparent absence of isomers of the tri- and di-saccharide in the reaction mixture, making it likely that diastereoisomers of only one type predominate.

The molecular rotation of the disaccharide (III) (M_D −16,000), when compared with additive M_D values (16, 17) for β-D-mannose 1,2-(methyl orthoacetate) 3,4,6-triacetate (having −OR *exo* (5)) and penta-*O*-acetyl β-D-mannopyranose (−7860 − 9840 = −17,700) or penta-*O*-acetyl α-D-mannopyranose (−7860 + 21,470 = +13,600) is strongly indicative of a β-configuration for the D-mannosyl unit.* A similarly strongly negative M_D value for the trisaccharide (IV) (−29,200) is clearly consistent with a β-configuration for the D-mannosyl unit in this compound as well. Allowance for the rotatory contribution

**The additive M_D value for the syrupy —OR endo-diastereoisomer of the methyl orthoacetate (5) and penta-O-acetyl-β-D-mannopyranose (+ 4350 − 9840 = − 5490) is less satisfactory than if the —OR exo-orientation is considered.*

Can. J. Chem. Downloaded from www.nrcresearchpress.com by 210.87.254.42 on 09/05/12
For personal use only.

by the third, ketal, unit is provided by degradation product VIII. The sum of the molecular rotations for VIII, β-D-mannose pentaacetate and the pertinent methyl 1,2-orthoacetate (−1370 − 9840 − 7860 = −19,070) is then in reasonable agreement with the observed value for IV.

The absence of model compounds having a closely related type of structure eliminates the possibility at present for considering the relative orientation of the C-methyl and C-methylene groups of the cyclic 1,2-ketal structure.

A further item of note in the n.m.r. spectrum of IV is the splitting of the signal for the methylene protons. This inference of restricted rotation about the carbon–carbon bonds involving the methylene group is not unexpected, in view of the presence of three bulky groups in close proximity. However, splitting of the methylene protons' signal is not detected in the spectrum of the deacetylated material, although its absence may be due here to inadequate resolution or, perhaps, to solvent effects. The chemical shift for the methylene group in IV or V also may be noted. In the absence of adjacent free carbonyl groups its location is at relatively high field (2.45 p.p.m.). On release of the carboxyl–carbonyl group by hydrolysis of V to VII a paramagnetic shift of 0.6 p.p.m. is observed, as noted above. With both carbonyl groups present, i.e., in acetoacetate itself, the chemical shift for the methylene group is found an additional 0.5 p.p.m. towards lower field (at 3.5 p.p.m.).

EXPERIMENTAL

Melting points are corrected. Optical rotations were measured at 25±2° C. Evaporations were carried out *in vacuo* at 40–45° C. The n.m.r. spectra were prepared with a Varian A-60 high-resolution spectrometer. The concentration of solute was generally about 10%, and tetramethylsilane was used as the reference standard internally (for chloroform) or externally (for deuterium oxide).

Trisaccharide IV

Penta-*O*-acetyl α-D-mannopyranose (17.1 g) in ethylene chloride (10 ml) was treated for 12 hours with hydrogen bromide in acetic acid (35 ml, 30–35%). Benzene (100 ml) was added, the solution was washed thoroughly with ice water and cold sodium bicarbonate, and dried with anhydrous calcium sulphate. This crude preparation of 2,3,4,6-tetra-*O*-acetyl α-D-mannosyl bromide (I) was added to a suspension of silver oxide (50 g) and anhydrous calcium sulphate (90 g) in sodium-dried benzene (100 ml), the mixture was shaken for 12 hours, filtered, and the filtrate concentrated. The syrupy residue, on being taken up in ethanol–ether, deposited a white powder (1.2 g), m.p. 198–201° C. Recrystallized from acetone–hexane, the product had m.p. 213–215° C, undepressed by admixture with IV prepared from crystalline I; $[\alpha]_D$ −29° (*c*, 1, $CHCl_3$). Calculated for $C_{42}H_{56}O_{28}$: C, 50.00%; H, 5.59%; acetyl, 43.5%; C-methyl, 27.2%; mol. wt., 1008. Found: C, 50.09%; H, 5.57%; acetyl, 42.8%; C-methyl, 27.5%; mol. wt., 980 (by thermometric vapor pressure measurement in acetone solution of a sample prepared by acetylation of V). The n.m.r. spectrum is reproduced in Fig. 1A.

Deacetylated Trisaccharide (V)

Compound IV was deacetylated catalytically with sodium methoxide under reflux, as described previously (2), affording a crystalline product; m.p. 156–157° C, $[\alpha]_D$ −5.4° (*c*, 1.1, H_2O). Calculated for $C_{22}H_{36}O_{18}$: C, 44.90%; H, 6.18%; C-methyl, 4.6%. Found: C, 45.15%; H, 6.42%; C-methyl, 5.8%. The product obtained in another experiment was hygroscopic and, after equilibration with atmospheric moisture, had m.p. 180° C. Calculated for $C_{22}H_{36}O_{18}.H_2O$: C, 43.60%; H, 6.32%. Found: C, 43.68%; H, 6.42%. The n.m.r. spectrum is reproduced in Fig. 2A. On acetylation with acetic anhydride, using either pyridine or sodium acetate as catalyst, IV was regenerated as shown by mixed melting point tests.

Lead Tetraacetate Oxidation of V and Deacetylated III

Trisaccharide IV (15.6 mg) and disaccharide III (2) (12.0 mg) were each deacetylated catalytically in methanol, and the solutions were neutralized with carbon dioxide. After removal of the methanol, pyridine (3 ml) was added and the solution treated at 0° C with lead tetraacetate (50 mg) in pyridine (3 ml). The uptake of oxidant in moles/mole min) measured iodometrically as described elsewhere (4) was: 3.1 (10), 3.9 (50), and 4.9 (90) for the trimer; 2.3 (15), 3.1 (30), and 3.7 (80) for the dimer. Required for cleavage of four and three *vic*-diol groups (trisaccharide and disaccharide, respectively) and oxidation of 1 mole of formic acid released: 5 moles/mole and 4 moles/mole, respectively.

Can. J. Chem. Downloaded from www.nrcresearchpress.com by 210.87.254.42 on 09/05/12
For personal use only.

Methylated Trisaccharide (VI)

(*a*) To a solution of acetate IV (120 mg) in acetone (5 ml) potassium hydroxide (3 ml, 10%) and dimethyl sulphate (1 ml) were added slowly, excess of the alkali always being present. A second treatment with these reagents was then carried out, the solution was extracted with chloroform, and the extracted material was methylated twice with methyl iodide and silver oxide. The final syrupy product (60 mg) was found by thin-layer chromatography to contain three components, one of which corresponded to methyl tetra-*O*-methyl-D-mannoside and a second, travelling on the chromatogram at a rate expected for a methylated disaccharide. The third, slowest-moving, component (12 mg) was obtained in crystalline form from a solution of the mixture in hexane and, after recrystallization from ether–hexane, had m.p. 163–164° C. Calculated for $C_{32}H_{56}O_{18}$: C, 52.74%; H, 7.75%. Found: C, 52.51%; H, 7.72%.

(*b*) Product V (150 mg) was taken up in liquid ammonia (7 ml) and potassium was added until a stable blue coloration of the solution resulted. The ammonia was evaporated off, methyl iodide (5 ml) was added, the suspension was refluxed for 3 hours, and concentrated. This methylation treatment was repeated twice and the final syrupy product extracted into chloroform. Removal of the solvent afforded crystalline material (150 mg) which was recrystallized from *n*-hexane, m.p. 165–166° C, undepressed by admixture with the product described in section (*a*).

Methanolysis of VI

The methylated trisaccharide (5 mg) was refluxed with methanolic hydrogen chloride (0.6 ml, 1%) for 19 hours, excess ethereal diazomethane was added, and the solution was concentrated. The syrupy residue was examined by gas–liquid phase chromatography using temperature programming (50–205° C in 11 minutes), a column (8 ft × 1/4 in.) of ethylene glycol – *o*-phthalate (18) on firebrick (C-22, 60–80 mesh) (1:4.5) and helium as the carrier gas (60 ml/min). Only two methyl ethers were detected as significant components of the methanolyzate, their retention times being the same as those of methyl 2,3,4,6-tetra-*O*-methyl α-D-mannoside and methyl 3,4,6-tri-*O*-methyl α-D-mannoside. Using the known methyl ether methyl glycosides as standards the ratio of the two products was estimated to be 1:2. After acid hydrolysis of the methanolyzate, products corresponding to 2,3,4,6-tetra-*O*-methyl D-mannose and 3,4,6-tri-*O*-methyl D-mannose were detected by paper chromatography, the latter being readily oxidized by lead tetraacetate in acetic acid.

3,4,6-Tri-O-acetyl-1,2-O-[1-(carbomethoxymethyl)-ethylidene]-β-D-mannose (VIII)

Trisaccharide V was hydrolyzed with 0.1 *N* sulphuric acid yielding mannose and an amorphous product (VII), as described previously (2). The n.m.r. spectrum of the hydrolyzate is reproduced in Fig. 2B; the spectrum of isolated VII is closely similar, differing mainly in that the relative intensity of signals for secondary and C_6 protons (H_s, H_6) is lower than for that of the mixture. When treated with a slight excess of sodium methoxide in methanol, VII yielded mannose and a non-reducing product. (In the earlier experiment (2) two non-reducing products having closely similar R_F appeared to be detectable by paper chromatography.)

The latter product (99 mg), isolated as a syrup by preparative paper chromatography, was treated with acetic anhydride (3 ml) and sodium acetate (100 mg) for 1 hour on the steam bath, the reaction mixture was decomposed with ice-water, and benzene-extractable, neutral, material was recovered: yield, 130 mg of syrup. The latter, on being distilled (120–140° C at 0.01 mm, bath temperature) afforded a solid product which was recrystallized from *n*-hexane; m.p. 100.5–101.5° C, $[\alpha]_D$ −3.4 (*c*, 1.1, $CHCl_3$). Calculated for $C_{17}H_{24}O_{11}$: C, 50.49%; H, 5.98%; saponification equivalent, 101. Found: C, 50.64%; H, 6.08%; saponification equivalent, 100.

Formation of Acetone by Hydrolysis of IV

Trisaccharide IV (5 mg), suspended in 10% sulphuric acid (2 ml), was heated at 100° C for 1 hour under a stream of nitrogen, the effluent gas being passed through a solution of sodium bisulphite (2%). Color tests with sodium nitroprusside or salicylaldehyde on portions of the bisulphite solution were positive for the presence of acetone. On addition of 2,4-dinitrophenylhydrazine in 2 *N* hydrochloric acid to the bisulphite solution a crystalline precipitate was obtained, m.p. 124–126° C, indistinguishable by infrared spectroscopy and by paper chromatographic behavior from acetone-2,4-dinitrophenylhydrazone.

Ethyl Acetoacetate by Ethanolysis of IV

Trisaccharide IV (15 mg) was heated under reflux for 2 hours with ethanolic hydrogen chloride (0.1 ml, 5%). The solution was examined by gas–liquid phase chromatography, using a column (2 ft × 1/4 in.) of butanediol-succinate on Celite (1:6) (18), a column temperature of 108° C, and helium as the carrier gas (40 ml/min). A compound having the same emergence time as ethyl acetoacetate was detected; based on the chromatographic behavior of the authentic ester, the yield was found to be 38%.

Trisaccharide IV (0.54 g) was heated under reflux for 2 hours with ethanolic hydrogen chloride (4 ml, 5%). Ether (200 ml) was added to promote precipitation of methyl mannoside, the filtrate was concentrated to a small volume, and the residue treated with 2,4-dinitrophenylhydrazine in 2 *N* hydrochloric acid. The acid solution was extracted with carbon tetrachloride, and a concentrate of the extract was chromatographed preparatively on thin layers of Silica Gel G (Stahl) using benzene (containing about 1.5% of ether). A major

Can. J. Chem. Downloaded from www.nrcresearchpress.com by 210.87.254.42 on 09/05/12
For personal use only.

zone, corresponding to the hydrazone of ethyl acetoacetate (R_F 0.33) was extracted with ethanol, the extract affording crystalline material, m.p. 94–95° C, undepressed by admixture with the 2,4-dinitrophenylhydrazone of ethyl acetoacetate; the X-ray powder diagram was indistinguishable from that of the authentic specimen. A second zone, corresponding on the chromatogram to the acetone 2,4-dinitrophenylhydrazone (R_F 0.58), also was extracted with ethanol, affording acetone 2,4-dinitrophenylhydrazone, m.p. 126–127° C, undepressed.

ACKNOWLEDGMENTS

The authors express their thanks to Mr. M. Mazurek and Mr. W. C. Haid for microanalyses and for preparation of proton magnetic resonance spectra, infrared spectra and X-ray powder diagrams. Facilities for determining proton magnetic resonance spectra were kindly made available by the Chemistry Department, University of Saskatchewan.

REFERENCES

1. W. KÖNIGS and E. KNORR. Ber. **34**, 957 (1901).
2. H. R. GOLDSCHMID and A. S. PERLIN. Can. J. Chem. **39**, 2025 (1961).
3. R. C. HOCKETT and D. F. MOWERY, JR. J. Am. Chem. Soc. **65**, 403 (1943).
4. H. R. GOLDSCHMID and A. S. PERLIN. Can. J. Chem. **38**, 2280 (1960).
5. A. S. PERLIN. Can. J. Chem. **41**, 399 (1963).
6. E. PACSU. Advan. Carbohydrate Chem. **1**, 77 (1945).
7. A. S. PERLIN. Can. J. Chem. **41**, 555 (1963).
8. F. GARCIA GONZALEZ. Advan. Carbohydrate Chem. **11**, 97 (1956).
9. R. U. LEMIEUX, R. K. KULLNIG, H. J. BERNSTEIN, and W. G. SCHNEIDER. J. Am. Chem. Soc. **80**, 6098 (1958).
10. S. WINSTEIN and R. E. BUCKLES. J. Am. Chem. Soc. **64**, 2780, 2787 (1942).
11. R. U. LEMIEUX. Advan. Carbohydrate Chem. **9**, 1 (1954).
12. S. WINSTEIN. Bull. Soc. Chim. France, **18**, C55 (1951).
13. K. FREUDENBERG and H. SCHOLZ. Ber. **63**, 1969 (1930).
14. F. BAYERSTEDT and S. M. MCELVAIN. J. Am. Chem. Soc. **58**, 529 (1936).
15. R. U. LEMIEUX and J. D. T. CIPERA. Can. J. Chem. **34**, 906 (1956).
16. C. S. HUDSON. J. Am. Chem. Soc. **31**, 66 (1909).
17. C. S. HUDSON. J. Am. Chem. Soc. **38**, 1566 (1916).
18. B. M. CRAIG. Chem. Ind. (London), 1442 (1960).

Can. J. Chem. Downloaded from www.nrcresearchpress.com by 210.87.254.42 on 09/05/12
For personal use only.

ELECTROPHILIC DISPLACEMENT REACTIONS

XV. KINETICS AND MECHANISM OF THE BASE-CATALYZED PROTODEBORONATION OF ARENEBORONIC ACIDS[1]

HENRY G. KUIVILA, JOSEPH F. REUWER, JR., AND JOHN A. MANGRAVITE
Department of Chemistry, University of New Hampshire, Durham, New Hampshire, U.S.A.

Received June 7, 1963

Can. J. Chem. Downloaded from www.nrcresearchpress.com by 210.87.254.40 on 09/05/12
For personal use only.

ABSTRACT

An investigation of the kinetics of the protodeboronation of benzeneboronic acid in water in the pH range 2.0 to 6.7 is described. In addition to the acid-catalyzed reaction studied earlier a reaction whose rate is independent of pH and one whose rate increases linearly with hydroxide ion concentration have been observed. The effect of malonate buffer concentration at low pH confirms the earlier observations of general acid catalysis. Changes in buffer concentration at pH 6.70 have no effect on rate indicating specific hydroxide ion catalysis. Effect of substituents in the ortho, meta, and para position of the benzene ring on the rate of protodeboronation have been examined. Ortho–para ratios for this reaction are high; possible reasons for this are discussed. The Hammett equation using σ correlates the rates for meta and para substituents.

Among the reactions of areneboronic acids in which the dihydroxyboron group is subjected to electrophilic displacement the simple hydrolysis or protodeboronation (eq. [1]) is particularly interesting. Ainley and Challenger (1)

$$ArB(OH)_2 + H_2O \rightarrow ArH + B(OH)_3 \qquad [1]$$

showed that the hydrolysis of boronic acid proceeds in water at 150°, and is catalyzed by concentrated sodium hydroxide, concentrated hydrochloric acid, as well as zinc and cadmium bromides. Ammoniacal silver nitrate has been shown to be an effective catalyst for the protodeboronation of benzeneboronic acid and others of the arene series (2, 3, 4). An understanding of the mechanisms by which these catalysts function would be desirable, and we have embarked upon a series of kinetic investigations toward this end.

A fairly extensive and detailed study of the kinetics of acid-catalyzed protodeboronation has been described (5, 6, 7). Observation of the variation of rate constants in several acidic media, and in deuterium, as well as protium, solvents, along with determination of substituent effects led to the conclusion that the reaction is an electrophilic displacement in which the rate-determining step is the transfer of a proton from an acid to the boronic acid. In view of this an examination of the same reaction catalyzed by base was in order, especially because the strongest electrophile which might be present in significant concentration in aqueous base might well be water. The possibility that a SE1 type of reaction (eqs. [2–4]) might be involved also provided some attraction.

$$ArB(OH)_2 + HO^- \rightleftarrows ArB(OH)_3^- \qquad [2]$$

$$ArB(OH)_3^- \xrightarrow{\text{slow}} Ar^- + B(OH)_3 \qquad [3]$$

$$Ar^- + H_2O \rightarrow ArH + HO^- \qquad [4]$$

[1]*Presented at the Symposium of Organometallic Compounds, sponsored by the Inorganic Chemistry Division of the Chemical Institute of Canada, and the University of British Columbia, in Vancouver, B.C., September 5, 1962. Preceding paper in this series: H. G. Kuivila, L. E. Benjamin, C. J. Murphy, A. D. Price, and J. H. Polevy. J. Org. Chem.* **27**, *825 (1962).*

RESULTS AND DISCUSSION

Exploratory kinetic experiments were carried out with *o*-methoxybenzeneboronic acid at 60° in aqueous borate buffers at pH 8.7. Several difficulties were encountered. First-order rate plots indicated very rapid initial reaction followed by a pronounced decrease to what appeared to be a linear plot. Rate plots could not be reproduced with satisfactory precision. In the presence of oxygen the expected product, anisole, was accompanied by guaiacol, formed by oxidative replacement of the dihydroxyboron group by hydroxyl. When the pH was decreased below 7, it was possible to eliminate these difficulties provided appropriate precautions described in the Experimental part were taken.

Most of the kinetic runs were conducted in aqueous malonate buffer solutions at pH 6.70 at 90°. At this temperature the buffers showed a detectable change in pH after about six days due, presumably, to decarboxylation of the malonic acid. Agreement of the ultraviolet spectrum of the product with that expected was taken as confirmation that the reaction took the expected course. In the cases of *o*-methoxy-, 2,6-dimethoxy-, and *p*-methoxy-benzeneboronic acids a small amount of brown material appeared in the reaction mixture after several half-lives. It apparently functioned as a catalyst for the reaction, but generally made its presence felt in this way late enough in the course of the kinetic run so that satisfactory rate constants could be obtained from initial slopes. Figure 1 shows a typical first-order rate plot for 2,6-dimethoxybenzeneboronic acid;

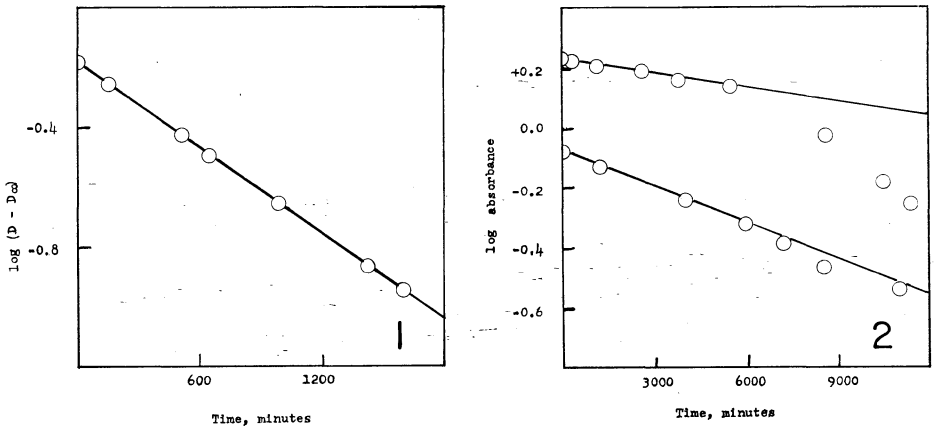

FIG. 1. Pseudo first-order rate plot for the base-catalyzed protodeboronation of 2,6-dimethoxybenzeneboronic acid at 90.0°, pH 6.70; ionic strength 0.14; malonate buffer.

FIG. 2. Pseudo first-order rate constants for base-catalyzed protodeboronation at 90.0°, pH 6.70; ionic strength 0.14; malonate buffer. Upper curve *p*-methoxybenzeneboronic acid. Lower curve *o*-methoxybenzeneboronic acid.

Fig. 2 shows a curved plot for *o*-methoxybenzeneboronic acid and the most extreme case of curvature observed with *p*-methoxybenzeneboronic acid. The other boronic acids gave good linear plots. As shown in Table I (runs 130 and 131), the first-order rate law is valid over at least a 10-fold variation in initial concentration of 2,6-dimethoxybenzeneboronic acid.

Effect of pH and Buffer Concentration

As a test of general base catalysis versus specific lyate ion catalysis the effects of variation of buffer concentration and pH on the rate coefficients were examined. Pertinent results are presented in Tables II and III. The data in Table II are at pH 6.70 and clearly

Can. J. Chem. Downloaded from www.nrcresearchpress.com by 210.87.254.40 on 09/05/12
For personal use only.

Can. J. Chem. Downloaded from www.nrcresearchpress.com by 210.87.254.40 on 09/05/12
For personal use only.

TABLE I

Protodeboronation of 2,6-dimethoxybenzeneboronic acid

Run	Addend	Addend moles/l.	$k_{obs}\times10^6$ sec^{-1}
116*	—	—	17.4
117*	—	—	18.0
130†	—	—	18.2
131‡	—	—	18.3
139§	H_3BO_3	3.45×10^{-3}	9.20
138§	—	—	9.36

*Run under "anaerobic" conditions.
†Initial concentration of 2,6-dimethoxybenzeneboronic acid = 4.45×10^{-3} *M*.
‡Initial concentration of 2,6-dimethoxybenzeneboronic acid = 5.25×10^{-4} *M*.
§pH = 6.42; for all other runs in this table, pH = 6.70.

TABLE II

Run	10^3. conc. malonate anion, moles/liter	Ionic strength	pH_{meas}	$10^6\ k_{calc}$* sec^{-1}	$10^6\ k_{obs}$ sec^{-1}	$10^6\ k_{corr}$† sec^{-1}
—	0.543	0.14	6.70	18.1	18.1	18.1
93m	0.155	0.04	6.70	18.1	22.0	22.0
92m	0.764	0.20	6.70	18.1	20.2	18.8
91m	1.55	0.40	7.15	52.2	53.4	17.9

*Rate of base-catalyzed reaction at pH indicated and $\mu = 0.14$, see Table V.
†Corrected to pH 6.70 and ionic strength 0.14, see Table V.

TABLE III

Variation of the rate of hydrolysis of 2,6-dimethoxybenzeneboronic acid with malonic acid concentration, 90°, ionic strength 0.14, corrected to pH 3.60; buffer ratio (H_2A/HA^-) = 0.155

Run	Conc. malonic acid 10^3 moles/liter	pH_{meas}	$10^6\ k_{calc}$* sec^{-1}	$10^6\ k_{obs}$ sec^{-1}	$10^6\ k_{corr}$† sec^{-1}
—	None	3.60	5.13	—	5.13
75m	0.27	3.70	4.37	5.11	5.87
74m	0.58	3.67	4.58	6.12	6.67
73m	1.17	3.67	4.58	8.60	9.15
70m	1.38	3.59	5.21	8.92	8.84
67m	1.90	3.54	5.66	9.64	9.11
71m	2.74	3.59	5.21	12.5	12.4
69m	3.16	3.72	4.24	7.25	8.14
68m	3.66	3.56	5.47	14.0	13.7
83m	3.90	3.76	3.94	9.27	10.5
72m	6.00	3.39	7.89	18.1	15.3
77m	6.00	3.55	5.56	12.9	12.5
85m	6.00	3.58	5.31	11.8	11.6
76m	11.7	3.61	5.05	21.9	22.0
86m	18.0	3.65	4.73	29.9	30.3
88m	47.4‡	3.62	5.01	55.7	54.2†
87m	50.4§	3.50	5.11	57.5	54.6†
84m	56.0‖	3.55	5.56	46.9	45.1†
89m	74.6¶	3.58	5.31	76.6	75.0†

*Rate of H_3O^+ catalyzed reaction at pH indicated.
†Corrected to pH 3.60 and ionic strength 0.14, see Table V.
‡Ionic strength 0.23.
§Ionic strength 0.26.
‖Ionic strength 0.30.
¶Ionic strength 0.46.

indicate that there is no noticeable effect of malonate ion concentration on rate. Phosphate buffers, on the other hand, revealed an increase in rate with buffer concentration. This was attributed to the presence of catalytic impurities in the buffers because buffers of the same pH at the same concentration made from different reagents gave different rate coefficients.

The data presented in Table III were obtained with a buffer containing the malonate monoanion and malonic acid in a ratio of about 7, resulting in a pH of 3.60. A very pronounced increase in rate results as the buffer concentration is increased. This is a clear-cut indication of general acid catalysis, and confirms the results obtained earlier in the study of the acid-catalyzed reaction. A plot of the data is shown in Fig. 3. A linear relationship between rate and buffer concentration would be expected. The reason for the non-linear plot is not clear at this time.

The effect of pH on the rate of reaction was examined, providing the data presented in Table IV and plotted in Fig. 4. Above pH 6.0 the plot has unit slope as would be

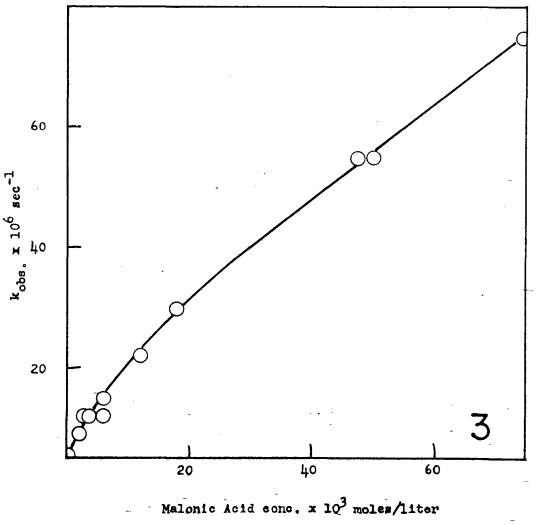

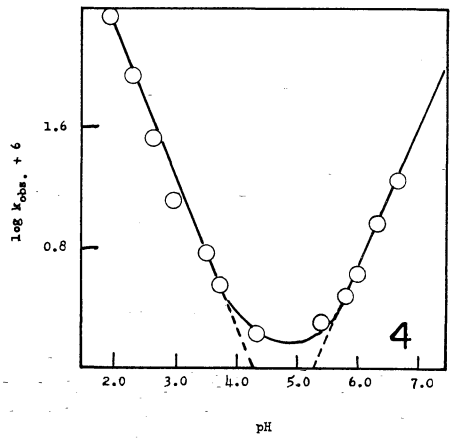

FIG. 3. Test of Brönsted catalysis law for 2,6-dimethoxybenzeneboronic acid at 90.0° with malonate buffers; pH 3.60; ionic strength 0.14.

FIG. 4. pH – log k profile for protodeboronation of 2,6-dimethoxybenzeneboronic acid at 90.0°; ionic strength 0.14.

required for a reaction whose rate is directly dependent upon hydroxide ion concentration. Below this value the slope drops to a minimum near pH 4.85 and then rises again to a negative unit slope below pH 3.5 as the acid-catalyzed reaction comes into prominence. In the pH region around the minimum the rate constants are larger than the sum of the expected contributions from the base- and acid-catalyzed reactions. This means that there is also a pH-independent reaction which predominates in this region. The value of the uncatalyzed rate constant is 0.630×10^{-6} sec^{-1}. This value has been used in constructing the solid line between pH 3.8 and 5.8.

In the pH range between about 6.0 and 6.7 the linear relationship between pH and log k_{obs} suggests the following two-step mechanism as a reasonable working hypothesis.

$$ArB(OH)_2 + H_2O \underset{\text{fast}}{\overset{K_a}{\rightleftharpoons}} ArB(OH)_3^- + H^+ \qquad [5]$$

$$ArB(OH)_3^- + H_2O \xrightarrow[\text{slow}]{k'} ArH + B(OH)_3 + OH^- \qquad [6]$$

Can. J. Chem. Downloaded from www.nrcresearchpress.com by 210.87.254.40 on 09/05/12
For personal use only.

TABLE IV

Effect of pH on the hydrolysis of 2,6-dimethoxybenzeneboronic acid in aqueous malonic acid – sodium malonate buffer at 90.0° C, ionic strength 0.14

Run	pH	$k_{obs} \times 10^6$ sec^{-1}	log k_{obs} +6
118, 119	6.70	18.1	1.258
138	6.42	9.36	0.971
137	6.05	4.25	0.628
136	5.85	3.05	0.484
140	5.45	2.04	0.310
141	4.42	1.78	0.250
82m	3.81	3.66	0.563
78m	3.55	5.96	0.775
20m, 22m	3.00*	20.7	1.316
26m	2.70*	34.5	1.538
24m, 21m	2.40*	90.2	1.955
23m	2.00*	230	2.362

*These runs were carried out in the absence of buffer; perchloric acid was used to adjust acidity.

Now,

[7] $$K_a = \frac{[BA^-][H^+]}{[BAH]} = \frac{[BA^-][H^+]}{[BAH]_S - [BA]^-}$$

where $[BA^-]$ is the concentration of boronate anion, [BAH] and $[BAH]_S$ are the actual and stoichiometric concentrations of boronic acid. Solving for $[BA^-]$,

[8] $$[BA^-] = \frac{K_a[BAH]_S}{[H^+]+K_a} = \frac{K_a[BAH]_S}{[H^+]}$$

if K_a is much smaller than the hydronium ion concentration. This is true, since pH in these experiments is below 6.8 and the pK_a values for the boronic acids are greater than 8.25. The expression for the overall reaction velocity is given by

[9] $$V = k_{obs}[BAH]_S = k'[BA^-][H_2O] = k'[H_2O]\frac{K_a}{[H^+]}[BAH]_S.$$

Whence

[10] $$k_{obs} = 55.5\, k'\frac{K_a}{[H^+]} \text{ or } \log k_{obs} = \text{pH} + \text{const.}$$

and

[11] $$k' = k_{obs}[H^+]/55.5\, K_a.$$

The logarithmic form of eq. [10] describes the linear portion of the rate profile in Fig. 4, indicating that this analysis is reasonable. If the mechanism is correct, knowledge of the pH and the value of pK_a in conjunction with the experimentally determined rate coefficient, k_{obs}, permits evaluation of the specific rate constant k' for reaction [6].

Effect of Ionic Strength

When the ionic strength is increased beyond 0.140 by the addition of sodium perchlorate, the specific rate constant decreases as can be seen from the last column in Table V. This would imply a negative salt effect. However, addition of the salt has the effect of decreasing the pK_a of the acid; the rate constant expected as a result of the change in

Can. J. Chem. Downloaded from www.nrcresearchpress.com by 210.87.254.40 on 09/05/12
For personal use only.

TABLE V

Effect of ionic strength on the base-catalyzed hydrolysis of 2,6-dimethoxybenzeneboronic acid in aqueous malonic acid – sodium malonate buffer (pH 6.70) at 90.0° C

Run	$NaClO_4$ moles/l.	Total μ	pH_{meas}	$k_{calc} \times 10^6$* sec^{-1}	$k_{obs} \times 10^6$ sec^{-1}
118, 119	0.0	0.140	6.70	(18.1)	18.1
128	0.036	0.176	6.67	17.0	18.7
127	0.076	0.216	6.63	15.5	17.1
124	0.120	0.260	6.57	13.5	14.9
126	0.240	0.380	6.54	12.6	14.1
123	0.360	0.500	5.49	11.1	13.8

*Calculated by assuming that $k_{obs} = 18.1 \times 10^{-6}$ at pH 6.70 and that the reaction is first order in hydroxide ion.

pH is shown in the penultimate column. Comparison of the values in the two columns shows that the primary kinetic salt effect is actually positive since the observed rate constants are larger than those calculated at each pH.

Effect of Added Boric Acid

The possibility that boric acid formed in the reaction might have an effect on the rate was tested. The result of run 139 in Table I reveals that no effect is observed when the acid is present in concentration of the order of magnitude of the initial boronic acid.

Effect of Oxygen

In view of the difficulties encountered in preliminary work at high pH values when oxygen was in contact with reaction solutions, its effect was tested at the lower pH. The reaction solutions of runs 116 and 117, Table I, were thoroughly degassed by alternate freezing and thawing at reduced pressure and sealed *in vacuo* before being placed in the constant temperature bath. Oxygen clearly has no effect on the reaction under these conditions.

Effects of Substituents

Rates of protodeboronation of several meta- and para-substituted benzeneboronic acids were measured at pH 6.70. In order to ascertain whether the reaction followed was only the one whose rate coefficient increases linearly with hydrogen ion concentration the rates were also measured at pH 6.42 in several cases. The values found at these two pH values are shown in Table VI, second and third columns. In the fourth column are shown the values which would be expected at the lower pH assuming linear dependence of rate coefficient on hydroxide ion concentration. The agreement between the expected and observed values is satisfactory, and assures that the rate of the same reaction is being measured in each case. Because of the very slow reactions in the case of meta substituents it was not practical to make the same check, but it is probably safe to assume that the result would be the same.

Examination of the values in the second column of Table VI reveals that all substituents increase the value of k_{obs}. Obviously no simple linear free energy relationship will correlate these data with other electrophilic aromatic substitutions. However, if values of k' of equation [11] are estimated, the pattern changes, as seen below.

It is not feasible to determine pK_a values of many boronic acids in water because of their limited solubility. However, values in 25% methanol have been determined by Polevy (8). Another limitation is that the pK_a values were determined at 25° while the

Can. J. Chem. Downloaded from www.nrcresearchpress.com by 210.87.254.40 on 09/05/12
For personal use only.

TABLE VI

Effect of substituents on the rate of hydrolysis of benzeneboronic acid in aqueous malonic acid – sodium malonate buffer at 90.0° C, ionic strength 0.14

Substituent	$10^6 k_{obs}$ (sec^{-1}) pH 6.70	pH 6.42	$10^6 k_{calc}$ pH 6.42	$10^{10} K_a$	$10^6 k'$ (l./mole sec)	log (k'/k'_0)
H	0.145	0.08	0.076	7.59	0.688	0
p-CH_3O	0.610	0.322	0.320	2.57	8.54	1.09
p-CH_3	0.260	0.145	0.137	3.02	3.10	0.654
p-Cl	0.187	0.10	0.098	20.9	0.322	−0.330
p-F	0.250	0.141	0.131	9.33	0.966	0.149
o-CH_3O	1.53	0.772	0.803	2.14	25.8	1.58
o-CH_3	0.360	0.208	0.189	1.02	12.6	1.27
o-Cl	8.60	4.76	4.52	26.9	12.0	1.24
o-F	11.1	—	—	56.2	7.14	1.02
m-CH_3O	0.343	—	—	16.6	0.744	0.034
m-CH_3	0.294	—	—	7.08	1.50	0.338
m-Cl	0.217	—	—	51.3	0.152	−0.656
m-F	0.332	—	—	57.5	0.208	−0.520
2,6-diCH_3O	18.1	9.36	9.47	0.295	2200	3.51

kinetic experiments were conducted at 90°. Thus, absolute values of k' cannot be accurately obtained with the data at hand, but relative values should be significant, and sufficient for our purposes. The last three columns in Table VI contain, respectively, values of K_a, k', calculated according to equation [11], and log (k'/k_0'). Inspection of these values shows that the normal pattern for electrophilic aromatic substitution emerges. When these are plotted against Brown's σ^+ values (9) the point for *p*-methoxy falls considerably below the line; when they are plotted against $\sigma + 0.5\ (\sigma^+ - \sigma)$ (10) the plot is improved somewhat, but considerable scatter results. On the other hand, when the ordinary σ values are used in the plot a good line with a slope of −2.32 results as can be seen in Fig. 5.

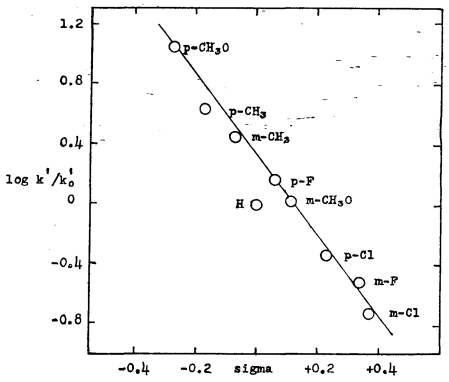

FIG. 5. Hammett plot for protodeboronation of benzeneboronate anions at 90.0°; ionic strength 0.14.

Interestingly enough, the only pronounced deviation from the line is the point for benzeneboronic acid. The negative value of rho indicates that a positive charge develops in the benzene ring in the transition state. The magnitude of the charge is a relatively small one for electrophilic aromatic substitutions which generally have rho values larger than four (11). Displacements of silicon, germanium, tin, and lead from the benzene ring by the proton have rho values of −5.0, −4.6, −3.8, and −2.5, respectively (12–15). Protodeboronation of benzeneboronic acid in 6.3 *N* sulphuric acid at 60° has a rho value of

Can. J. Chem. Downloaded from www.nrcresearchpress.com by 210.87.254.40 on 09/05/12
For personal use only.

−5.0, and the rates are correlated best by σ^+ (7). The decrease in rho when the more reactive boronate anion is the substrate would be expected because the negative charge on the boronate anion decreases the electron demand at the seat of reaction.

The Taft equation for ortho-substituted benzenes (16) can be used as a device for detecting influences on reactivity other than inductive and resonance effects. A plot of k' for the ortho-substituted benzeneboronic acids is not linear; therefore, other factors do indeed play a role in this series.

The methyl and chloro substituents, which have similar steric but opposite electronic effects, produce about the same rate acceleration. Although *o*-fluoro usually has a larger partial factor than *o*-chloro in electrophilic aromatic substitution the reverse is true in the present case.

The ortho–para ratios shown in Table VII are striking in that no simple trend is dis-

TABLE VII

Ortho–para ratios (k'_{ortho}/k'_{para}) for protodeboronation of areneboronic acids in aqueous malonic acid – sodium malonate buffers (pH 6.70) at 90.0° C

Substituent	k'_{ortho}/k'_{para}
CH_3O	3.02
CH_3	4.06
F	7.34
Cl	37.3

cernible. In each case the value is greater than the statistical value of two, in marked contrast to acid-catalyzed protodeboronation in which case only *o*-methyl has a value greater than two (8). Furthermore, methyl and chloro have different values although they have similar bulk; chloro and fluoro have different values although they have similar electronic effects.

These observations may be interpreted as resulting from a combination of steric effects, hydrogen bonding, and electrostatic interactions and will be discussed in terms of the transition state for the formation of a pentadienate intermediate (B) by the attack of a water molecule on a boronate anion (A). Thus the carbon to which the proton becomes

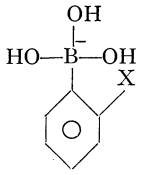

(A)

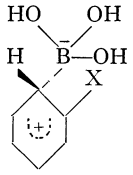

(B)

attached is in the process of changing hybridization from sp^2 to sp^3. Since the C—X and C—B bonds are eclipsed in (A), but staggered in (B), release of strain accompanying this change in dihedral angle in the order methyl > chloro > methoxy ≃ fluoro would be expected. This may be a major factor for all substituents but the fluoro. The distance between the negative charge and the C—X dipole will increase in going from (A) to (B), with a resultant decrease in electrostatic repulsion. The introduction of a positive charge into the ring will decrease the magnitude of the C—X dipoles involving chlorine and fluorine, because the negative end is toward the halogen in the ground state. This will

Can. J. Chem. Downloaded from www.nrcresearchpress.com by 210.87.254.40 on 09/05/12
For personal use only.

lead to further decrease in electrostatic repulsion. The carbon bonded to boron decreases in electronegativity due to decreasing *s* character in the orbital involved, but increases in electronegativity due to the positive charge developing in the ring. The net result is probably a negligible change in the magnitude of charge on boron, and the electrostatic effect is very probably rate-enhancing for chloro and fluoro.

The oxygen in the methoxy group has a relatively high electron density and is at the the negative end of two dipoles. The electrostatic effect should be similar to that for chloro and fluoro. It is to be noted that the introduction of one methoxy group ortho to the boronic acid function increases the rate of reaction by a factor of 38.7 and the introduction of second methoxy increases the rate by a factor of 85.3 beyond that of the first. This kind of enhancement is frequently encountered in steric effects.

The methyl group is at the positive end of the X—C dipole in the boronic acid. As a result the electrostatic repulsion due to change in the bond moment will increase in going to the transition state. This will be counteracted by the change in dihedral angle and leads to the conclusion that the deactivating effect of the methyl group due to electrostatic factors will be smaller than the activating effect of fluoro and chloro.

The effects of hydrogen bonding are difficult to evaluate. Polevy (8) has shown that intramolecular hydrogen bonding occurs to ortho-methoxy, -chloro, and -fluoro in the free boronic acids. Loss of conjugation between substituent and boron, and development of the negative charge on boron in conversion to the anion must diminish the strength of the hydrogen bonds substantially. Whatever remains can be expected to be decreased further due to the electrostatic and geometric changes occurring in going to the transition state.

The resultant of these effects for the four substituents may be summarized as follows. Fluoro activates because of the electrostatic effect; methyl activates mainly because of the relief of steric strain; chloro and methoxy activate because of both effects. In the case of methoxy the reason for activation is not quite clear, since only the steric effect would seem to activate and this should be little larger than that for fluoro.

Mechanism

In the earlier papers of this series on acid-catalyzed protodeboronation it was established that the reaction involves a rate-determining proton transfer from acid to boronic acid. This conclusion was based primarily on the observation of a kinetic isotope effect and general acid catalysis. The base-catalyzed reaction, on the other hand, appears not to be subject to general base catalysis. The mechanism represented by equations [5] and [6] with reaction [6] rate-determining is consistent with this observation. An increase in base concentration results in an increase in rate only when it leads to an increase in the concentration of the boronate anion through an increase in pH. Reaction [6] might very well be subject to general acid catalysis, but this possibility has not yet been examined explicitly. Satisfactory correlation of the rate constants by the "normal" sigma constants and the small value of rho suggests that the positive charge in the benzene ring is not highly developed.

The SE1 type of mechanism (equations [2–4]) can be eliminated as a possibility because it would be expected to have a positive value of rho, whereas a negative value is actually observed.

The uncatalyzed reaction must have a transition state which is neutral overall. This could result from attack on a boronic acid molecule by water, or from attack on a boronate anion by hydronium ion. Rate constants for 2,6-dimethoxybenzeneboronic acid at 90° have

Can. J. Chem. Downloaded from www.nrcresearchpress.com by 210.87.254.40 on 09/05/12
For personal use only.

been calculated assuming these two possibilities, and these are given below along with those for the acid- and base-catalyzed reactions. Perhaps the only conclusions which can

$$ArB(OH)_2 + H_3O^+: \quad 2.12\times10^{-2}\ \text{l. mol}^{-1}\text{sec}^{-1}$$
$$ArB(OH)_2 + H_2O: \quad 1.15\times10^{-8}$$
$$ArB(OH)_3^- + H_3O^+: \quad 2.35\times10^{4}$$
$$ArB(OH)_3^- + H_2O: \quad 2.23\times10^{-3}$$

be drawn from these data with any confidence are that the boronate anion is about a million times as reactive as the boronic acid molecule and the hydronium ion is about a million times as powerful an electrophile as water in aromatic protodeboronation.

EXPERIMENTAL

Materials

All of the boronic acids used in this investigation have been described previously, and the wavelength at which the analytical determinations were made have also been reported (5–8). In view of the sensitivity of the reaction to adventitious materials dissolved in ordinary distilled water all of the water used was redistilled. Recrystallization of the boronic acids and of the buffer substituents were from redistilled water. All pH measurements were made at 25° and are reported as measured.

Kinetics

(A) Base-catalyzed hydrolysis.—An appropriate amount of areneboronic acid was transferred to a 100-ml volumetric flask. The malonate buffer solution was added and the solution diluted to the mark with redistilled water. After all of the areneboronic acid was dissolved, aliquots were transferred to ampoules, which were sealed and placed in the constant-temperature bath at 90.0±0.02° for appropriate intervals. The ampoules were removed from the bath and chilled in ice water, the contents were transferred to a volumetric flask containing sufficient hydrochloric acid to neutralize the buffer base and analyzed spectrophotometrically.

(B) Acid-catalyzed hydrolysis.—The procedure was substantially the same with the exception that sodium acetate was used in the final dilution procedure to neutralize the perchloric acid.

ACKNOWLEDGMENT

It is a pleasure to express our appreciation for support of this research by the U.S. Air Force Office of Scientific Research (Contract AF 49(638)-312).

REFERENCES

1. A. D. Ainley and F. Challenger. J. Chem. Soc. 2171 (1930).
2. A. Michaelis and P. Becker. Ber. **15**, 180 (1882).
3. A. Michaelis and M. Behrens. Ber. **27**, 244 (1894).
4. J. R. Johnson, M. G. van Campen, Jr., and O. Grummitt. J. Am. Chem. Soc. **60**, 111 (1938).
5. H. G. Kuivila and K. V. Nahabedian. J. Am. Chem. Soc. **83**, 2159 (1961).
6. H. G. Kuivila and K. V. Nahabedian. J. Am. Chem. Soc. **83**, 2164 (1961).
7. K. V. Nahabedian and H. G. Kuivila. J. Am. Chem. Soc. **83**, 2167 (1961).
8. J. H. Polevy. Ph.D. Dissertation, University of New Hampshire, 1960.
9. H. C. Brown and Y. Okamoto. J. Am. Chem. Soc. **79**, 1913 (1957).
10. Y. Yukawa and Y. Tsuno. Bull. Chem. Soc. Japan, **32**, 971 (1959).
11. H. C. Brown and L. M. Stock. J. Am. Chem. Soc. **84**, 3298 (1962).
12. C. Eaborn. J. Chem. Soc. 4858 (1956).
13. C. Eaborn and K. C. Pande. J. Chem. Soc. 297 (1961).
14. C. Eaborn and J. A. Waters. J. Chem. Soc. 542 (1961).
15. C. Eaborn and K. C. Pande. J. Chem. Soc. 3715 (1961).
16. R. W. Taft, Jr. *In* Steric effects in organic chemistry. John Wiley, New York. 1956. p. 556.

Can. J. Chem. Downloaded from www.nrcresearchpress.com by 210.87.254.40 on 09/05/12
For personal use only.

LYCOPODIUM ALKALOIDS

PART VIII. NEW ALKALOIDS FROM JAMAICAN LYCOPODIUM SPECIES[1]

R. H. BURNELL, C. G. CHIN, B. S. MOOTOO, AND D. R. TAYLOR
Instituto Venezolano de Investigaciones Científicas (IVIC) Apartado 1827, Caracas, Venezuela
and
University of the West Indies, Kingston, Jamaica
Received June 25, 1963

ABSTRACT

Four more alkaloids have been isolated from *Lycopodium fawcettii*. Lycodine and des-N-methyl-α-obscurine have been found in other *Lycopodium* species but base L, $C_{18}H_{31}NO_4$, and base R, $C_{16}H_{24}N_2O_2$, are new. Some transformations of base L are described including its conversion to the previously described base O. An unstable base from *L. clavatum* has been characterized as the picrate $C_{15}H_{25}NO_3.C_6H_3N_3O_7$. Further characterization of the two bases fawcettidine (base F) and fawcettimine (base A) is reported.

Many alkaloids have been reported (1 (*a*,*b*)) from *L. fawcettii*; most of these possess the lycopodine (2) type of skeleton, although neither lycopodine itself nor any of its simple relatives (those with one or no oxygen functions) have been isolated. Three bases have more recently been isolated from this Jamaican plant, all of which contain two nitrogen atoms. Two of these (from the weaker bases), lycodine (3) and des-N-methyl-α-obscurine (4), have been previously isolated and are of known structure but the other, obtained from countercurrent distribution of the stronger base fraction, is not previously described. The latter, base R, $C_{16}H_{24}N_2O_2$, forms only a monoperchlorate (B. $HClO_4$) and from infrared spectra its structure includes carbonyl and secondary amino groups. Acetylation of base R affords a neutral oily compound showing N-acetyl absorption in the infrared.

Another new strong base containing only one nitrogen atom has also been found. Base L, which analyzes best for $C_{18}H_{31}NO_4$, is shown from its infrared spectrum to contain an O-acetyl residue and two hydroxyl groups. Since the methiodide prepared from base L is normal (B. MeI) the nitrogen is presumably tertiary and this is confirmed by acetylation which gives the diacetate $C_{20}H_{33}NO_5$, identical with base O described elsewhere (1 (*b*)). Further acetylation of base O is ineffective so the other hydroxyl grouping was thought to be tertiary and this suspicion is strengthened by the chromium trioxide oxidation of base L to the hydroxy-keto-acetate, $C_{18}H_{29}NO_4$. The latter is readily hydrolyzed to the dihydroxy-ketone (desacetyldehydro-base L), $C_{16}H_{27}NO_3$, which shows infrared absorption attributable to a six-membered (or larger) ring ketone. Neither hydroxyl in desacetyl-dehydro-base L is suitably placed relative to the ketone for ready elimination.

Base L hydrolyzes to a trihydroxy compound, desacetyl-base L, $C_{16}H_{29}NO_3$, which consumes no periodic acid implying that it contains no cis α-glycol system. Acetylation of desacetyl-base L at room temperature gives rise to the diacetate, base O, but at low temperature (5°) a monoacetate is obtained which is not base L and must be the positional isomer, isobase L (cf. fawcettimine (5) and lycofoline (6)), since on further acetylation it also affords base O. These preliminary results suggest that base L is a tricyclic tertiary base possessing a tertiary hydroxyl, a secondary equatorial hydroxyl, and a secondary axial O-acetyl grouping.

[1]*Part VII. R. H. Burnell and D. R. Taylor. Tetrahedron,* ***18****, 1467 (1962).*

Can. J. Chem. Downloaded from www.nrcresearchpress.com by 210.87.254.40 on 09/05/12
For personal use only.

Further characterization of fawcettimine (7), $C_{16}H_{25}NO_2$, shows that both oxygen atoms are present as carbonyl groups. While the base itself shows only one carbonyl peak in the infrared, the crystalline neutral N-acetyl derivative, the N-nitrosamide, and the fawcettimine methiodide all show two peaks attributable to carbonyls (the N-acetyl derivative also shows the amide peak at 1620 cm^{-1}).

The action of sodium borohydride on N-acetylfawcettimine results in the reduction of only one of the carbonyls; the product, dihydro-N-acetylfawcettimine, $C_{18}H_{29}NO_3$, must contain a hindered carbonyl, the N-acetyl group, and a secondary hydroxyl. Reduction of N-acetylfawcettimine with sodium and isobutanol gives rise to this same dihydro compound.

Fawcettidine, base F (1(*a*)), $C_{16}H_{23}NO$ has been reduced to dihydrofawcettidine with sodium borohydride. The infrared spectra of these compounds (and that of acetyldihydrofawcettidine) show that the ketone in the parent base is in a six-membered (or larger) ring, the molecule contains a carbon–carbon double bond and that the secondary hydroxyl is probably axial. From the n.m.r. spectra only one olefinic proton is shown to be present as well as a secondary C-methyl group. The pK_a of fawcettidine is low (6.2) and that of the reduction product is still low (7.9) for a tertiary lycopodium base. The inference drawn is that both the double bond and the carbonyl are sufficiently close to the nitrogen as to greatly affect its basicity.

The unstable base referred to in an earlier report on the bases obtained from Jamaican *L. clavatum* (7) has now been obtained as the picrate, $C_{15}H_{25}NO_3.C_6H_3N_3O_7$. The free base, however, is extremely labile and rapidly develops a brown color in air.

EXPERIMENTAL

Melting points are uncorrected. Infrared spectral values are for Nujol mulls unless otherwise stated and pK_a determinations were done in 50% methanol.

Bases from L. fawcettii Lloyd and Underwood

The mixture of weak bases from *L. fawcettii* (1(*b*)) (2.2 g) was chromatographed over alumina in benzene affording first fawcettidine (base F: 150 mg), pK_a 6.2, $[\alpha]_D$ 161° (*c*, 0.6 EtOH).

Fawcettidine Methiodide

From methanol–acetone, m.p. 223–225°. Calc. for $C_{16}H_{23}NO.CH_3I$: C, 52.7; H, 6.8; I, 32.8; $(N—Me)_1$ 3.9%. Found: C, 52.6; H, 6.6; I, 32.8; N—Me, 4.1%.

Dihydrofawcettidine

A methanolic solution of $NaBH_4$ was added to fawcettidine (40 mg) in methanol and the mixture was left standing at room temperature for 6 hours. Dilution with water and chloroform extraction gave the dihydro base (40 mg) $[\alpha]_D$ 137° (*c*, 1.0 EtOH) which showed hydroxyl (3200 cm^{-1}) and double bond (1666 cm^{-1}) absorption in the infrared but no carbonyl peak. A sample was sublimed for analysis, m.p. 153–156°, pK_a 7.9. Calc. for $C_{16}H_{25}NO$ requires: C, 77.7; H, 10.2%. Found: C, 77.6; H, 10.5%.

Acetyldihydrofawcettidine

Acetylation of dihydrofawcettidine in acetic anhydride – pyridine gave the O-acetate in the normal manner. The base was converted to the perchlorate, m.p. 220–221°. Calc. for $C_{18}H_{27}NO_2.HClO_4$: C, 55.5; H, 7.2; N, 3.6%. Found: C, 55.9; H, 7.5; N, 3.9%.

Lycodine

The next fraction (180 mg) eluted with benzene gave a crystalline hydrochloride which was recrystallized from methanol–acetone. Calc. for $C_{16}H_{22}N_2.2HCl.H_2O$: C, 57.7; H, 7.9; N, 8.4; Cl, 21.3%. Found: C, 57.7; H, 8.1; N, 8.4; Cl, 21.3%.

The base, m.p. 117–118°, regenerated from the salt showed ultraviolet absorption at 268 mμ (log ϵ = 3.73) and 276 mμ (log ϵ = 3.61). On comparison (mixed melting point, infrared and ultraviolet spectra) with authentic lycodine (for which we thank Dr. W. A. Ayer, Alberta) the two were shown to be identical.

Des-N-methyl-α-obscurine

Closely associated with base I (1(*b*)) in the weak base mixture was a small amount of a crystalline base,

Can. J. Chem. Downloaded from www.nrcresearchpress.com by 210.87.254.40 on 09/05/12
For personal use only.

m.p. 270–272° (sealed tube), showing ultraviolet absorption at 252 mμ (log ε = 3.75). Calc. for $C_{16}H_{24}N_2O$: C, 73.8; H, 9.3; N, 10.8%. Found: C, 74.1; H, 9.3; N, 10.7%.

The infrared spectrum, with a peak at 3250 (NH)cm^{-1} and a complex band centered at 1675 cm^{-1}, was identical with that of des-N-methyl-α-obscurine. A mixed melting point with the latter showed no depression (we thank Dr. W. A. Ayer for the authentic sample).

Base R

The fraction (4.25 g) of the *L. fawcettii* strong bases (1(*b*)) containing fawcettiine was distributed between chloroform and aqueous phosphate buffer, pH 7.4 for 20 transfers. The first five fractions contained weaker bases, including fawcettimine (base A: 140 mg perchlorate). Fractions 6–10 contained fawcettiine (1.24 g) and fractions 11–14 gave a new crystalline perchlorate (101 mg) which crystallized from acetone, m.p. 198–199°. Calc. for $C_{16}H_{24}N_2O_2.HClO_4$: C, 51.0; H, 6.7; O, 25.4; N, 7.4; Cl, 9.4%. Found: C, 51.2; H, 6.7; O, 25.5; N, 7.4; Cl, 9.2%.

The base crystallized from a concentrated acetone solution, m.p. 129–130°, pK_a 7.05. Calc. for $C_{16}H_{24}N_2O_2$: C, 69.5; H, 8.8; O, 11.6; $(C—Me)_1$, 5.4%. Found: C, 69.8; H, 8.8; O, 11.9; C—Me, 4.5%.

The infrared spectrum showed peaks at 3420, 3310, 3120, and 1720 cm^{-1}.

Base L

Fractions 19–20 of the distribution (above) gave a crystalline perchlorate, m.p. 290–294° (decomp.). Calc. for $C_{18}H_{31}NO_4$: C, 50.8; H, 7.6; O, 30.1; N, 3.3; Cl, 8.3%. Found: C, 50.6; H, 7.7; O, 30.4; N, 3.3; Cl, 8.1%.

The base, pK_a 9.7, obtained from the perchlorate, was an oil showing infrared absorption at 3450 (OH), 1723, and 1250 cm^{-1} (OAc).

The *methiodide*, m.p. 281–282° (from acetone). Calc. for $C_{18}H_{31}NO_4.CH_3I$: C, 48.8; H, 7.3; N, 3.3; O, 13.7%. Found: C, 48.6; H, 7.3; N, 3.3; O, 13.6%.

Acetylation of Base L (Base O)

Base L (108 mg) was acetylated in acetic anhydride (4 ml) and pyridine (4 ml) at room temperature for 20 hours. The mixture was then poured into iced water, basified with ammonia, and chloroform extracted giving a white solid (103 mg) which was sublimed twice for analysis, m.p. 179°. Admixture with base O (1(*b*)) (m.p. 180–181°) caused no depression in melting point and the two samples have identical infrared spectra. Calc. for $C_{20}H_{33}NO_5$: C, 65.4; H, 9.0; O, 21.8; $(OAc)_2$, 23.4%. Found: C, 65.5; H, 8.6; O, 21 9; OAc, 23.4%.

Desacetyl-base L

To base L perchlorate (92 mg) in methanol (5 ml) was added 3 *N* sodium hydroxide solution (1 ml). After 21 hours at room temperature the mixture was diluted with water and the chloroform was extracted, affording a crystalline solid (58 mg). Recrystallization was from acetone, m.p. 189–190°, pK_a 9.4. Calc. for $C_{16}H_{29}NO_3$: C, 67.8; H, 10.3; O, 16.9%. Found: C, 67.9; H, 10.4; O, 17.0%.

The base showed no carbonyl absorption in the infrared.

Acetylation of Desacetyl-base L (Isobase L)

Desacetyl-base L (106 mg) was acetylated in acetic anhydride and pyridine at 5° C. The white solid (100 mg) obtained by extraction was sublimed for analysis, m.p. 189–192°. Calc. for $C_{18}H_{31}NO_4$: C, 66.4; H, 9.6; O, 19.7; $(O—Ac)_1$, 13.2%. Found: C, 66.5; H, 9.4; O, 19.7; O—Ac, 12.9%.

The infrared spectrum differed from that of base L and seeding concentrated solutions of the latter with this product caused no crystallization.

Oxidation of Base L (Dehydro-base L)

To a cooled solution of base L (250 mg) in pyridine (5 ml) was added a cold mixture of chromium trioxide (1 g) in pyridine (5 ml). After 90 minutes at 5° the mixture was poured into ice water and made basic with ammonia. Chloroform extraction and evaporation gave a pale brown solid, affording crystals from acetone. A sample was sublimed for analysis, m.p. 196–197°. Calc. for $C_{18}H_{29}NO_4$: C, 66.9; H, 9.0%. Found: C, 66.9; H, 9.1%.

Desacetyldehydro-base L

Dehydro-base L (187 mg) was hydrolyzed in methanol with sodium hydroxide (75 mg) at room temperature for 5 hours. Extraction gave a white solid (124 mg) which was recrystallized from acetone and sublimed for analysis, m.p. 199–200°. Calc. for $C_{16}H_{27}NO_3$: C, 68.6; H, 9.6; O, 16.8%. Found: C, 68.3; H, 9.7; O, 17.0%.

L. clavatum—weak base

The weak base residues from *L. clavatum* (7) were chromatographed over alumina in benzene. The first eluate proved to be extremely labile, colored rapidly when exposed, but afforded a relatively stable picrate, m.p. 125–127°. Calc. for $C_{15}H_{25}NO_3.C_6H_3N_3O_7$: C, 50.8; H, 5.7; N, 11.3; O, 32.2%. Found: C, 51.1; H, 5.7; N, 11.1; O, 32.2%.

Can. J. Chem. Downloaded from www.nrcresearchpress.com by 210.87.254.40 on 09/05/12
For personal use only.

Further elution of the column gave the previously described weak bases (7) and then a substantial amount of fawcettimine (base A).

Acetylation of Fawcettimine (N-Acetylfawcettimine)

To fawcettimine (950 mg) in pyridine (11 ml) was added acetic anhydride (11 ml). After 20 hours at room temperature the volatile materials were removed on a rotary evaporator and the residue taken up in chloroform. After washing thoroughly with dilute hydrochloric acid, dilute ammonium hydroxide, and water, the neutral product (856 mg), obtained on evaporation of the solvent, was recrystallized from acetone–ether, m.p. 144–145°. Calc. for $C_{18}H_{27}NO_3$: C, 70.8; H, 8.9; N, 4.6; O, 15.7%. Found: C, 70.7; H, 9.1; N, 4.7; O, 15.7%.

Infrared peaks were at 1735 (C=O), 1710 (C=O), and 1620 (N—$COCH_3$) cm^{-1}.

Sodium–Isobutanol Reduction of N-Acetylfawcettimine

N-Acetyl fawcettimine (400 mg) was dissolved in toluene (40 ml) containing isobutanol (1 ml) and the solution added to a fine dispersion of sodium (600 mg) in toluene (50 ml) under purified nitrogen. The mixture was stirred for 24 hours, the undissolved sodium decomposed with ethanol, and then the solution was poured into water, shaken, and separated. The aqueous portion was extracted with chloroform. The organic layers were combined, washed with dilute hydrochloric acid and then water, dried, and evaporated to give an oil (359 mg). A crystalline product (90 mg), which was obtained by being dissolved in a small volume of acetone and then cooled, was sublimed for analysis, m.p. 205–206°. Calc. for $C_{18}H_{29}NO_3$: C, 70.3; H, 9.5; O, 15.6; N, 4.6%. Found: C, 70.6; H, 9.5; O, 15.4; N, 4.5%.

The infrared spectrum (Nujol) showed peaks at 3370 (OH), 1735 (C=O), and 1620 (N—$COCH_3$) cm^{-1}.

The material from the mother liquors above slowly crystallized when they were left standing and gave an infrared spectrum identical with that of the sublimed dihydro-N-acetylfawcettimine.

This same reduction product was obtained when N-acetylfawcettimine was treated with sodium borohydride in methanol, but crystallization was only possible after chromatography over alumina.

ACKNOWLEDGMENTS

The authors are indebted to Dr. W. R. Chan (University of the West Indies) for the n.m.r. spectra and one of us (D. R. T.) thanks Geddes Grant Ltd., Kingston, for a Postgraduate Scholarship during part of this work.

REFERENCES

1. (*a*) R. H. Burnell. J. Chem. Soc. 3091 (1959).
   (*b*) R. H. Burnell, B. S. Mootoo, and D. R. Taylor. Can. J. Chem. **38**, 1927 (1960).
2. K. Wiesner. Sci. Rept. Ist. Super. Sanita, **1**, 560 (1961).
3. F. A. L. Anet and C. R. Eves. Can. J. Chem. **36**, 902 (1958).
4. W. A. Ayer. Personal communication.
5. R. H. Burnell and D. R. Taylor. Tetrahedron, **15**, 173 (1961).
6. R. H. Burnell and D. R. Taylor. Tetrahedron, **18**, 1467 (1962).
7. R. H. Burnell and B. S. Mootoo. Can. J. Chem. **39**, 1090 (1961).

Can. J. Chem. Downloaded from www.nrcresearchpress.com by 210.87.254.40 on 09/05/12
For personal use only.

PHASE TRANSITIONS OF WATER AND XENON ADSORBED IN POROUS VYCOR GLASS[1]

G. LITVAN[2] AND R. MCINTOSH[3]
Department of Chemistry, University of Toronto, Toronto, Ontario
Received June 14, 1963

ABSTRACT

Measurements of the expansion of porous Vycor glass containing fixed quantities of adsorbed water indicate that in every instance a phase transition starts below −50° C, with the main change occurring below −160° C. Two other anomalies of the length variation were observed near −22° C and −7° C when the amount of adsorbed water exceeded the value equivalent to two monolayers. The length of the adsorbent after completion of a temperature cycle was different from the initial length. This is thought to be due to damage suffered by the glass and to the fact that the length of the adsorbent is different for adsorption and desorption although the quantity adsorbed may be the same.

The phase transition of adsorbed xenon takes place below the normal triple point and is a function of surface concentration as shown by length variations and equilibrium pressures for fixed quantities adsorbed. All transitions are gradual and hysteresis is exhibited by the isosteres. The adsorption isotherms for xenon – Vycor glass show a decreasing adsorptive capacity and a contraction of the hysteresis loop with lower temperature. The inadequacy of the capillary condensation theory of adsorption in relation to these results is discussed.

The capillary condensation theory assumes that the free energy of the adsorbate is less than that of bulk material at the same temperature because it is held under concave menisci in the pores of the adsorbent. The vapor pressure of the condensed substance is calculated by the relationship due to Kelvin. The theory implies that the adsorbent is inert, and only the shape and size of the pores play any role in determining the adsorptive characteristics. It follows also that the adsorbate has bulk properties except the lowered free energy arising from the presence of the concave meniscus.

There is, however, ample experimental evidence to the contrary. The observed dimensional changes of the adsorbents (0.3% in the case of Vycor glass – water system (1)) during the adsorption process indicate that the solid is perturbed by the presence of the adsorbate. Similarly, the infrared spectra of the adsorbate contain lines caused by forbidden transitions normally observable only in the Raman spectra (2, 3) showing that the adsorbed liquid is in a state different from the bulk state. The crystal structure of the frozen adsorbate, too, has been found by X-ray diffraction methods to differ from the one of the bulk crystal (4). Accordingly, solidified adsorbates failed to nucleate undercooled bulk liquid of the same composition (5).

These findings are to be expected in view of the fact that adsorption is the result of molecular interaction between adsorbate and adsorbent, and this interaction perturbs both.

On applying the equation due to Kelvin the question arises: is it permissible to use the relationship even as an approximation when most of the quantities involved are not only unknown quantitatively but are meaningless on a molecular scale? Surface tension (or even the term surface itself) of a liquid consisting of 30–40 molecules, the radius of an irregularly shaped void, the wetting angle formed by a few molecules on an irregular surface, the molar volume of the adsorbate, and so on, have no significance and one has to

[1]*Based upon a thesis by G. Litvan submitted in partial fulfillment of the requirements for the degree of Doctor of Philosophy.*
[2]*Present address: Division of Building Research, National Research Council, Ottawa, Ontario.*
[3]*Present address: Department of Chemistry, Queen's University, Kingston, Ontario.*

Can. J. Chem. Downloaded from www.nrcresearchpress.com by 210.87.254.6 on 09/05/12
For personal use only.

conclude that the relationship deduced and valid for macroscopic systems cannot be applied for microscopic systems without important reservations.

The contradictions of the capillary condensation theory were realized at an early stage although some of the experimental evidence supporting the criticism was obtained only recently. In spite of this fact some phenomena are explained by the theory. The hysteresis exhibited by the adsorption isotherms of porous adsorbents is probably the most important. In addition, the concept has been applied to explain the features of the expansion isotherms, the freezing point lowering of adsorbates, etc. The lack of another general concept and the apparent success of the theory have helped it to survive on a pragmatic rather than on a theoretical basis. But even so, the number of experimental results not explicable by the theory is growing and it seems desirable to examine its applicability under various conditions. One means of testing the theory has been shown to be the study of phase transitions of adsorbates (6, 7). The present work is a continuation of that investigation.

EXPERIMENTAL

The measurements were carried out using a volumetric adsorption apparatus incorporating a capacitance-type extensometer (1) which was redesigned in order to decrease the 1500 ml dead space of the chamber to 134 ml. Length changes of ± 0.01 to 0.4 μ could be detected depending on the separation of the plates with an estimated error of less than 2%. The temperature of the cell could be varied between -190 and $+200°$ C, and controlled from liquid nitrogen temperature to $+8°$ C. The system was pumped down to less than 10^{-6} mm pressure. Only soft annealed pure gold o-rings sealed satisfactorily throughout the wide temperature range.

The pressure was measured using either a mercury or a dibutyl phthalate manometer (depending on the range) which were isolated from the cell by a bellows type pressure gauge (8) used as a null instrument so that contamination of the adsorbent by the vapors of the manometer fluids was avoided.

Completely metal valves were used to avoid distillation of stopcock grease vapors to the cold adsorbent. During pumping the system was protected by a liquid air trap.

The porous Vycor glass (No. 7930) was supplied by Corning Glass Works and was in the form of an 11.5 cm long rod of 0.70-cm diameter. The effective length of the rod for expansion was 10.0 cm.

Before a run was started the cell containing the adsorbent was heated to above $+150°$ C and pumped at this temperature until "stick vacuum" was obtained.

The water before adsorption was purified several times by vacuum distillation. The xenon used was supplied by the Matheson Co. The research grade gas had less than 0.05 mole% total impurities and was used as obtained.

Because of the large range of the experimental temperatures it was necessary to take into account the coefficient of thermal expansion of the extensometer. The data given are corrected accordingly unless stated otherwise.

The results of the expansion isosteres are expressed in terms of fractional length changes, relative to the length of the rod at $+5°$ C. After the temperature was changed, the system was allowed to come to apparent equilibrium, and this took about 12 to 24 hours. The duration of a run was between 3 and 6 weeks.

RESULTS

Water Expansion Isosteres

The water isosteres (Figs. 1–4) show anomalies mainly in three temperature regions: (*a*) below $-50°$ C the length of the rod does not change in spite of the decrease of temperature and below $-150°$ C it increases. Above a critical water concentration the anamolous variation of length occurs at (*b*) around $-22°$ C, and (*c*) around $-7°$ C. The absence of any discontinuity indicates that the phase changes are gradual. The anomalies occur at higher temperatures on warming than the corresponding ones on cooling. The cooling and warming curves do not coincide. Pronounced hysteresis is exhibited even on repeated cycling. The length of the glass rod at $+5°$ C before and after a freezing–thawing cycle is, in general, not the same.

Xenon Vapor Pressure and Expansion Isosteres

The changes observed in the dimensions of the adsorbent and in the pressure of the

Can. J. Chem. Downloaded from www.nrcresearchpress.com by 210.87.254.6 on 09/05/12
For personal use only.

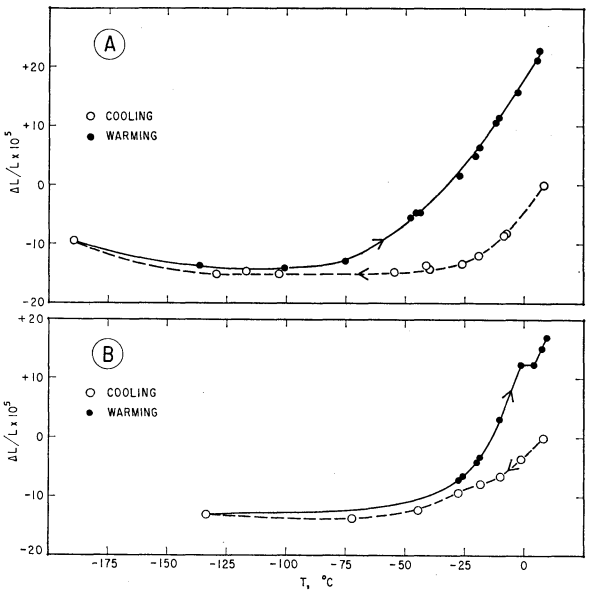

FIG. 1. Expansion isostere. Water content *A* 0.0263 g/g; *B* 0.0480 g/g.

adsorbate due to temperature variation are represented in Figs. 5 and 6. The diagrams in these cases show not only the "corrected" values computed by considering the coefficient of thermal expansion of the extensometer, but the "uncorrected" values as well which represent the apparent length changes of the system.

In order to eliminate the effect of condensation from the vapor phase on cooling or evaporation from the adsorbent on warming, thus maintaining isosteric conditions, in run 17 (Fig. 6) appropriate amounts were withdrawn from or admitted to the system. The amount of xenon to be withdrawn or admitted for a given change of temperature was computed from the values of the isotherms taken at different temperatures (Fig. 7).

The isosteres show that, on cooling, expansion takes place below the freezing point of bulk xenon. The temperature region of the length anomaly seems to be a function of the amount adsorbed, as at smaller concentrations the anomaly occurs at a lower temperature. The peak of the expansion versus temperature plot is at −114.0° C with 600 ml S.T.P. xenon adsorbed and at −128.5° C with 514 ml S.T.P., adsorbed. The log p versus $1/T$ plot consists of two linear sections. The sudden changes of the slope take place at −114.5 and −134.0° C, respectively. The cooling and warming branches of the expansion isosteres are displaced in the temperature region of the expansion anomaly. Below this region the two curves coincide and indicate expansion of the adsorbent. In the case of xenon as with water, the transition is gradual. The lengths of the glass rod at −109° C before and after the temperature cycle are the same.

Isothermal Expansion and Isotherms Using Xenon

The isotherms obtained above and below the bulk freezing temperature of xenon are shown in Fig. 7. The adsorption isotherms indicate a sharp decrease of the adsorptive capacity with decreasing temperature and at the same time a narrowing of the hysteresis loop. The inception of the hysteresis loop occurs essentially at the same value of relative pressure for all temperatures. The amount adsorbed approaches the line for $p/p^0 = 1$

Can. J. Chem. Downloaded from www.nrcresearchpress.com by 210.87.254.6 on 09/05/12
For personal use only.

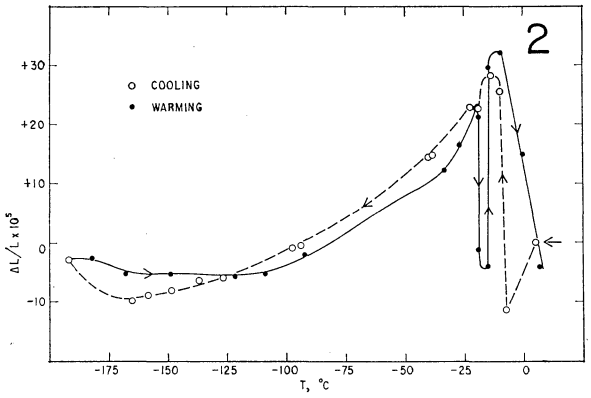

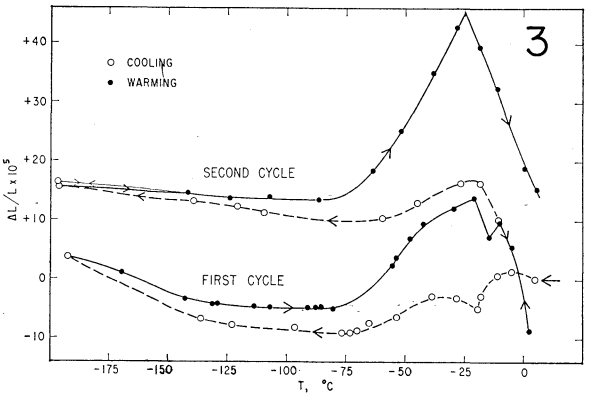

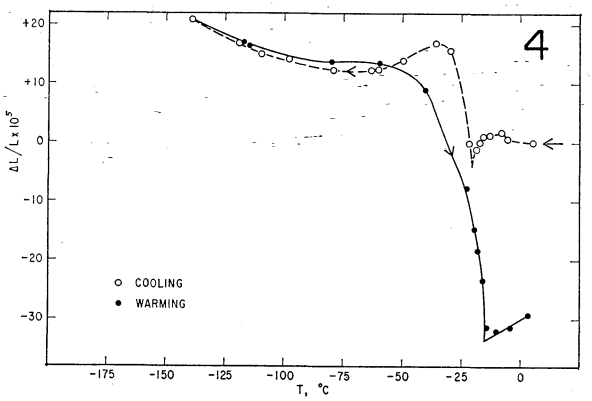

FIG. 2. Expansion isostere. Water content 0.0839 g/g.
FIG. 3. Expansion isostere. Water content 0.1389 g/g.
FIG. 4. Expansion isostere. Water content 0.1754 g/g.

asymptotically at the temperature of −110.1° C, when p^0 is the value (p_l^0) of the vapor pressure of the liquid at that temperature. At −136.3° C and −143.4° C the same is true if (p_s^0), the vapor pressure of the solid, is employed. At −125.6° C the isotherm is considered to cut the $p/p_s^0 = 1$ axis. These facts are interpreted as showing liquid adsorbate down to −125.6° C, but solid adsorbate at −136.3° C and below. The concomitant expansion isotherms indicate small dimensional changes even at relatively high temperatures

Can. J. Chem. Downloaded from www.nrcresearchpress.com by 210.87.254.6 on 09/05/12
For personal use only.

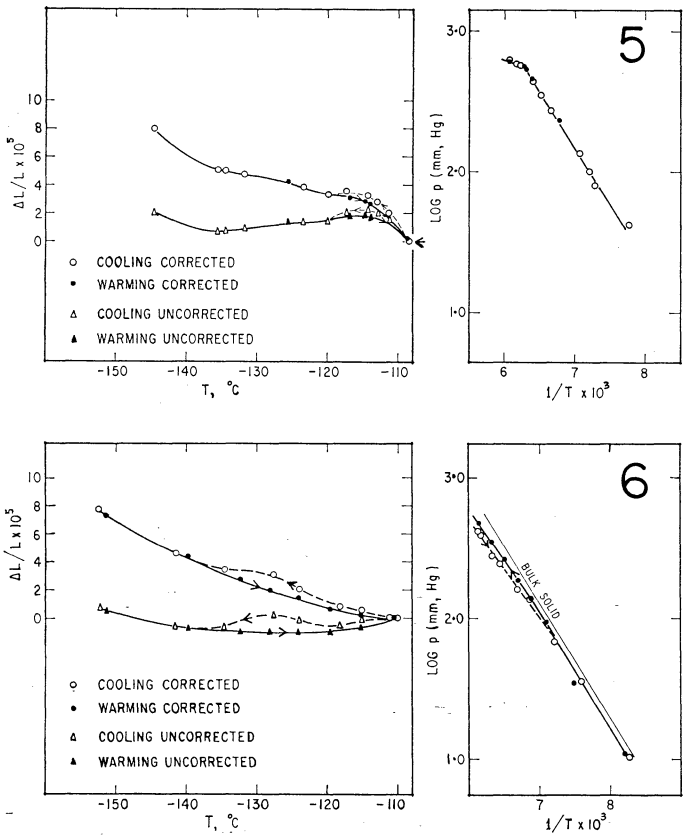

FIG. 5. Isosteric expansion and isostere. Xenon content 600 ml S.T.P.
FIG. 6. Isosteric expansion and isostere. Xenon content 514 ml S.T.P.

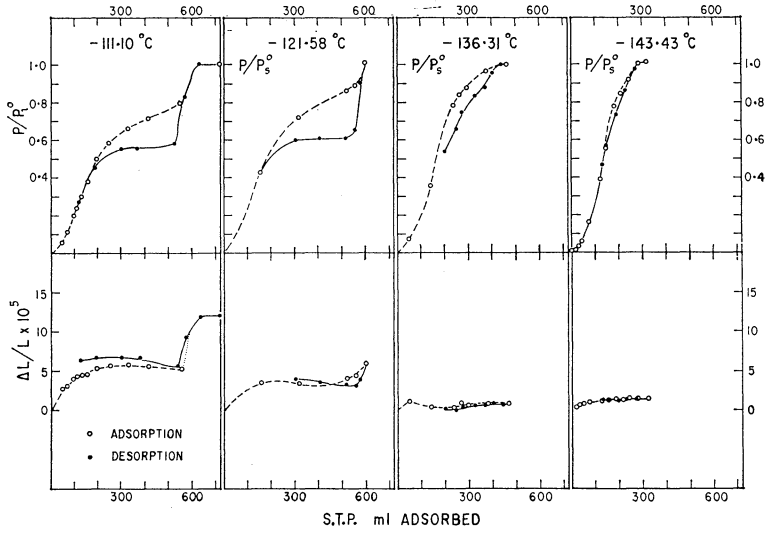

FIG. 7. Isothermal expansion and isotherms for xenon.

Can. J. Chem. Downloaded from www.nrcresearchpress.com by 210.87.254.6 on 09/05/12
For personal use only.

when compared with other systems investigated, and become even smaller with decreasing temperatures. The hysteresis loop of the high temperature isotherm narrows and finally vanishes at low temperature. No pronounced contraction can be detected on desorption as was observed with other adsorbates on Vycor glass.

DISCUSSION

Water Expansion Isosteres

It is apparent at once that the results obtained with the water – Vycor glass system do not support the capillary condensation concepts. According to this theory a sharp freezing point should be observed which is a function of the amount adsorbed. The opposite of these predicted facts is found; that is, the transition is not sharp nor much dependent upon the quantity absorbed. The results, however, can be explained by considering the possible events taking place in the adsorbed layer during the phase transition of the adsorbate.

Freezing in a bulk phase occurs when the kinetic energy of the molecules decreases to such an extent that an order of the species favored by the crystal lattice of the forming solid can develop. If the molecules in the liquid are subjected to external forces which are not present under ordinary conditions the phase transition will take place at a different and lower temperature than the normal freezing point. Adsorbate molecules on the surface are in such a force field. Since the field is not homogeneous its value varies from site to site and from layer to layer. The individual adsorbate molecules are perturbed in different ways depending on their location in the surface. The strongest interaction can be assumed to exist between the sorbent and the first layer and therefore the phase transition of such a layer is expected to occur, if it does at all, at very low temperatures. The transition temperature of the second and subsequent layers approaches the value of the bulk freezing temperature.

Length Anomalies below −50° C

Hodgson and McIntosh (6) found no length anomaly with the water – Vycor glass system between 0° C and −50° C if the water content was less than 0.138 g/g. The present investigation confirms this result (Fig. 1). On further cooling, however, some sort of solidification of the adsorbate seems to take place if indicated by the horizontal portion of the isosteres (Figs. 1 to 4) beginning around −50° C. The contraction of the system due to cooling is compensated for and at around −150° C, is overcome by an expansion effect. It seems reasonable to associate the continuous expansion with the gradual redistribution of the firmly bound molecules in the first layers. The phase transition was prevented from taking place by the strong interaction between the sorbate and substrate at high temperatures but at very low temperatures crystalline or, more probably, amorphous solid forms.

This observed expansion could not have been caused by condensation of water from the vapor phase since, in the case depicted in Fig. 1, 0.54×10^{-4} g water/g glass condensed on the adsorbent during cooling, which could cause only an estimated $\Delta L/L = 1\times10^{-6}$ expansion compared with the observed fractional expansion of 6×10^{-5}. Furthermore, it has to be noted that the condensation process was practically complete at around −100° C, at which temperature ice has a vapor pressure of about 10^{-5} mm. Another possible cause of expansion will be discussed in a later paragraph.

Length Anomalies at −22 and −7° C

It has been reported previously that the adsorbed water begins to freeze at around −22° C regardless of the water concentration if it is higher than a critical value. It can

Can. J. Chem. Downloaded from www.nrcresearchpress.com by 210.87.254.6 on 09/05/12
For personal use only.

be seen from Figs. 1 and 2 that this value is between 0.0480 and 0.0839 g/g water content, which is equivalent to 1.3 and 2.3 monolayers.

Several workers have observed sudden changes in the properties of the adsorbate at a critical surface concentration. Morrison and Drain (10) found the onset of the large increase of heat capacity in the argon–rutile system occurring between 1.6 and 2.2 V_m. Similar results were obtained by other authors (11, 12) with various systems. Studies of the dielectric properties showed that a plot of the dielectric loss versus adsorbed amounts had a discontinuity of slope at a value corresponding to $V_m = 1$ (Ebert and Langhammer (13)). Karagounis (5) observed that organic substances adsorbed on metal oxide powder will not seed the undercooled liquids in bulk state unless V_m is greater than 2. The heat of adsorption usually falls rapidly with coverage and approaches the heat of liquification at twice the monolayer coverage (14).

The results obtained by the various methods show that the first layer or layers of the adsorbate are in a distinctly different state from that of higher layers or of the substance in bulk phases, which explains why adsorbates in these layers have unusual properties, among others a very low freezing point.

The results of the present investigation indicate the existence of two length anomalies above −50° C, namely at around −22° C and −7° C. Since the temperature of the beginning of phase transition is −22° C, and since it is independent of the quantity adsorbed, comparison of the mechanism of the transition is invited with that of the transition water – ice I – ice III. To do so, however, requires the postulate of a pressure in the adsorbed layer of 2115 atm and, if that is assumed, an explanation of why such a pressure exists and does not destroy the glass.

If the pores are blocked by some means the approximate 10% increase of volume occurring on formation of ice I from water can be considered to be the cause of the existence of high pressures as has been assumed by Powers and Helmuth (15) who explained the expansion of porous adsorbents on cooling by this mechanism. Expansion on freezing, however, has been observed with other systems, in which the solid specific volume is less than that for liquid, e.g. the xenon – Vycor glass system (see Figs. 5 and 6).

There are indications that high pressures do exist in the adsorbate layers and are caused not by mechanical reasons but by the force field of the adsorbent which pulls the sorbate molecules toward the surface. The adsorbate molecules are perturbed as though under externally applied pressure.

Several authors such as Goldman and Polanyi (16), Mastrangelo (17), Long and Meyer (18), Schaeffer, Smith, and Wendell (19) have assumed high pressures to exist in the adsorbed layers.

The expansion occurring at −7° C was observed previously (6) in one instance and was suspected to be caused by condensation of water from the vapor phase on cooling. Since the decrease of the dead space did not eliminate this result it can be concluded that it is caused by changes in the adsorbate.

Although the scarcity of experimental data prevents generalization, it seems that the height of the peak at −7° C is inversely proportional to the amount adsorbed (Figs. 2, 3, 4) and disappears on repeated cycling (Fig. 3). These facts suggest that the expansion may be associated with the formation of an amorphous type of ice.

Burton and Oliver (20) detected by X-ray diffraction that semicrystalline—(neither hexagonal nor cubic)—ice formed on a cooled metal surface at below −90° C. It recrystallized into ordinary ice at high temperatures. Recently these findings were confirmed (21) and it was shown by Brazhan (4) that water adsorbed on silica gel froze at

Can. J. Chem. Downloaded from www.nrcresearchpress.com by 210.87.254.6 on 09/05/12
For personal use only.

−9° C in a well defined but unusual structure as determined by X-ray diffraction methods.

The presence of amorphous ice or water with unusual structure in the surface layers is suggested by the dielectric measurements of Dransfield, Frisch, and Wood (22) and Ebert and Langhammer (13).

Such results, obtained by employing various experimental methods, demonstrate the existence of amorphous ice and it seems reasonable to associate the expansion occurring at −7° C with the formation of this structure.

Xenon Vapor Pressure and Expansion Isosteres

The xenon isosteres are similar to the ones obtained for other systems, for example benzene, inasmuch as the temperature at which the phase transition occurs is a function of the amount adsorbed. It is noteworthy, however, that the freezing of the adsorbate caused the system to expand, demonstrating that other factors than an increase of the molar volume can be responsible for this effect.

For both the xenon and water systems the transitions were gradual, which fact contradicts the capillary condensation theory in its usual form. The sharp change of slope of the vapor pressure isosteres does not prove that the transition is sharp as has been pointed out (7). The existence of a freezing range is to be expected according to the molecular picture of phase changes in adsorbed layers.

Both the xenon and water systems exhibited marked hysteresis; the water – Vycor glass system over the entire experimental temperature range; the xenon – Vycor glass, however, only in the region where the phase transition takes place. On examining the experimental results on the basis of the capillary condensation theory the following may be noted.

According to the theory the menisci are the sole reason for the lowering of the freezing point. Because of the equilibrium with the vapor phase the curvature of every meniscus is the same and the liquid in every capillary should freeze at the same temperature. For the solidified adsorbate one may assume either flat (meniscus destroyed) or curved surface (meniscus retained).

In the first case, on warming, the melting should take place at the bulk melting temperature since no concave menisci are present. Although there are indications that the melting point of the adsorbate is usually higher than the freezing point, it is still very much lower than the bulk transition temperature. Furthermore, one should not observe hysteresis in the adsorption isotherm below the adsorbate transition temperature. This is the case for xenon but not for water. In addition, the relative vapor pressure of the solid adsorbate should be unity, which condition is not met by the xenon–glass system according to Fig. 6.

If one assumes the second case to be valid, i.e. concave menisci exist, the freezing and melting points of the adsorbate should coincide and no hysteresis is to be expected in any region. The experimental findings are not in accordance with these predictions. Thus, the capillary condensation theory does not explain the hysteresis phenomenon of the isostere.

$\Delta(\Delta L/L)$ *at* $+5°$ *C*

In the case of the water isosteres the Vycor glass rod exhibits a different length after a temperature cycle than it did before. It is apparent that the length difference $\Delta(\Delta L/L)$ at +5° C is a function of the water content (Table I).

The fact that with zero water content and with xenon adsorbate $\Delta(\Delta L/L) = 0$ establishes that the results are not due to a mechanical error of the extensometer.

Can. J. Chem. Downloaded from www.nrcresearchpress.com by 210.87.254.6 on 09/05/12
For personal use only.

TABLE I

$\Delta(\Delta L/L)$, the difference in the rod length, before and after a temperature cycle, at +5° C for various amounts of adsorbed water

Water content, g/g	$\Delta(\Delta L/L)\times10^5$
0.0000	0
0.0263	+25
0.0480	+15
0.0839	0
0.1389	−15
0.1754	−28

On the other hand, the data in Table II show that the glass rod suffered a permanent

TABLE II

The effect of a temperature cycle on the apparent length of the rod measured under standard conditions, no water present

Run	Water content in run, g/g	$(\Delta L/L)\times10^5$
1	0.1389	+109
2	0.0263	+ 62
4	0.0000	0
5	0.0839	+ 79
8	0.0480	+128
9	0.1754	+120
12	Xenon	0

change during the temperature cycle. The values given represent the change in length of the rod with no water present, under standard conditions, measured between runs.

If the rod suffered permanent damage in every instance, presumably due to the formation of microfissures, resulting in greater length, negative $\Delta(\Delta L/L)$ at +5° C with high water contents would have been obtained only if an opposing contraction occurred. One explanation may be the following.

In spite of the fact that the dead space of the cell was small some adsorption took place during cooling due to lowering of the vapor pressure. Although the amount adsorbed in itself was not sufficient to cause any observable change in length the process took place and the system could be described as being on the adsorption branch of the water isotherm. On warming, the opposite effect, desorption, occurred and the system was on the desorption branch. Since lengths corresponding with the desorption branch are less than those of the adsorption branch it can be understood why $\Delta(\Delta L/L)$ is negative for systems with higher water content than at the inception of the hysteresis loop. Thus reversing the direction of the temperature change results in altering the state of the system from the one of adsorption to the one of desorption.

In order to test this assumption the following experiment was carried out. With a fixed amount of water adsorbed the length of the rod was measured at +2.50° C. After the temperature of the system was changed (raised, lowered, or both) the original temperature, +2.50° C, was restored as closely as possible (within 0.5° C) and the length measured again. The results are shown in Table III. The $\Delta L/L$ data at temperatures other than the reference are omitted being non-equilibrium values. The observed changes were of the order of -30 to $+20\times10^{-5}$.

It can be seen that when the reference temperature was restored by heating (desorption

Can. J. Chem. Downloaded from www.nrcresearchpress.com by 210.87.254.6 on 09/05/12
For personal use only.

TABLE III

Length changes due to temperature variation with fixed amount of water

Point number	Temperature, °C	$\Delta L/L \times 10^5$
1	+2.50	0
2	+25.0	
3	−6.5	
4	+2.30	−1.01
5	+30.0	
6	+2.07	+13.33
7	−31.5	
8	+2.85	−3.60
9	+22.0	
10	0.0	
11	+2.92	−0.12
12	+20.0	
13	+2.02	+10.25

branch), as in points No. 1, 4, 8, and 11, the rod appears to have the same length and about $\Delta L/L = -11\times10^{-5}$ units lower than in cases when the temperature was restored by cooling (adsorption branch), points No. 6 and 13.

Xenon Isotherms

Since the heat of adsorption is always positive the adsorptive capacity should increase with decreasing temperature and, in fact, this is the case in general. There are only a few exceptions known. Kiselev and Kulichenko (23) obtained the isotherms for the benzene – silica gel and benzene–charcoal systems and found a decrease in the adsorptive capacity at temperatures below the bulk freezing point of the adsorbate. Amberg, Everett, Ruiter, and Smith (24) observed the same phenomenon with CO_2 – Vycor glass and N_2O – Vycor glass systems. An explanation of the phenomenon which has already been advanced by several authors (23, 24) is the following. If the state of the adsorbed film resembles that of an undercooled liquid, the saturation pressure of the liquid will exceed that of the solid by an increasing margin as temperature is decreased below the transition temperature. In the experimental assembly, however, the upper limit of pressure which can be generated is the vapor pressure of solid which would form on the walls of the adsorption vessel. In practice, therefore, a relatively smaller part of the adsorption isotherm can be examined as the temperature is lowered. Indeed, it may come about that relative pressures above the value for the inception of the hysteresis loop (about 0.45 p/p^0 at ordinary temperatures) cannot be generated. Thus the adsorptive capacity will decrease with decreasing temperature, the pore spaces may appear to be inactive, and the phenomenon of adsorption hysteresis may disappear. This is essentially the case with xenon. However, this explanation does not explain all the facts. On the basis of what has been said, one would expect that the beginning of the hysteresis loop would be found at higher values of the relative pressure based upon the saturation pressure of solid, that is, at higher values of p/p_s^0, as temperature is decreased. There is no evidence of this.

In addition, the drastic change in the shape of the xenon isotherms is apparent at and below −136.3° C in which case $p/p_s^0 = 1$ was reached with 450 ml S.T.P. adsorbed. The expansion isostere with 514 ml S.T.P. xenon content (Fig. 6) indicates freezing at −128.5° C and the vapor pressure isostere at −134° C, which facts contradict the assumption that the adsorbate is in a liquid state. The isotherms at −136.3° C and

Can. J. Chem. Downloaded from www.nrcresearchpress.com by 210.87.254.6 on 09/05/12
For personal use only.

−143.4° C approach $p/p_s^0 = 1$ asymptotically and this too—as pointed out by Hodgson and McIntosh—suggests the presence of solid adsorbate.

The decrease of adsorptive capacity raises the question as to what conditions obtain during isosteric cooling. On the basis of the low temperature isotherms, much more adsorbed matter is contained within the porous solid for certain conditions of cooling than one would expect. Moreover, the film, although containing more matter than predicted by the isotherms, has a lower equilibrium pressure than the bulk phase. It would seem that some adsorbate is "locked" into the adsorbent on cooling. Such a situation may be the reason for the expansion which is noted in the case of xenon, and at very low temperatures in the case of water. No direct evidence of decreased adsorptive capacity of water at lower temperatures has been obtained by us, but the decreased capacity may be anticipated by analogy with the behavior of xenon.

Xenon Expansion Isotherms

The xenon – Vycor glass system shows, even at high temperatures above the bulk freezing point, relatively small dimensional changes compared to other adsorbate – Vycor glass systems (9). Particularly important is the absence of a pronounced contraction along the desorption branch of the isotherm. Since the surface tension of liquid xenon is estimated to be 15 dynes/cm, a value comparable to those of other adsorbates investigated such as butane, the small dimensional changes are unexpected, and seem to contradict the proposed mechanism of dimensional changes based on the meniscus theory. The fact that the system does not contract on desorption indicates that either there are no menisci present or the contractive forces of the menisci are not the reason for the contraction as assumed in explaining the behavior of butane (9).

The differentiation of the expression for the spreading force ϕ with respect to temperature T gives the following result

$$\left(\frac{\partial \phi}{\partial T}\right)_{A,P,n_s} = \frac{Rn_s}{A}\left(\frac{\partial \ln p}{\partial \ln T}\right)_{A,P,n_s},$$

where the symbols n_s, A, p, P stand for the number of moles adsorbed, the surface area of the adsorbent, the vapor pressure of the adsorbate and the hydrostatic pressure respectively. Since the temperature coefficient of the vapor pressure is positive, such should be the case for the spreading force. Because $\Delta L/L$ is directly proportional to the spreading force, the observed decrease of the length changes with decreasing temperature is expected.

CONCLUSION

The capillary condensation theory in conjunction with assumptions concerning the shape of the voids has been used extensively to explain adsorption hysteresis, to analyze pore sizes, and to explain dimensional changes of the adsorbate–adsorbent system, e.g. (1). It has been employed also to predict the temperature of phase transitions, e.g. (25). However, the amount of experimental evidence which has accumulated and which cannot easily be fitted into the framework of the theory is becoming substantial. It is worthwhile to summarize this evidence, as well as other unexplained results characteristic of porous adsorbents. First, phase transitions are found not to be sharp. Second, the temperature of the beginning of a phase transition depends upon the amount adsorbed for some adsorbates, but not for others. Third, the marked contraction associated with the reversible part of the desorption branch of the isotherm, explained by the decreasing radius of curvature of the menisci, is not found in the case of xenon. The adsorption isotherms are

Can. J. Chem. Downloaded from www.nrcresearchpress.com by 210.87.254.6 on 09/05/12
For personal use only.

similar to those of water, butane, ethylchloride, and so on, but the contraction in the appropriate pressure range is not found.

Under the classification of unexplained results for porous adsorbents may be placed the following observations. The adsorptive capacity of the adsorbent in several cases is known to diminish with decreasing temperature. Although this fact might be explained on the basis of the similarity of the film near saturation to an undercooled liquid, there is evidence that the film is more likely to resemble solid. Second, the expansion of the system found with water on Vycor glass, and which might be anticipated by knowing the densities of bulk ice and water, is revealed also in the case of xenon. The density of solid xenon is, of course, greater than that of liquid. Additionally, a transition of adsorbed benzene brings about contraction of the glass–benzene system. Third, it has been shown that the measured expansion of glass–benzene, glass–water, glass–ethylchloride, etc., is not dependent solely upon the calculated spreading force derived from the Gibbs adsorption equation (9). If the viewpoint is adopted that changes of the chemical potential of the solid are being evaluated rather than spreading forces, the finding is then that expansion is not equal in the various systems for equal changes of the chemical potential of the solid (see Table IV). It is clear that this isolated fact may be rationalized by supposing that the sites of

TABLE IV

Proportionality constants for variation of ϕ with $\Delta L/L$

Adsorbate	K, cal
Water	-2.96×10^4
Butane	-1.06×10^4
Ethylchloride	-0.238×10^4
Xenon	-20×10^4

NOTE: K is defined by the equation $\Delta F_{S_0} = \phi = K\Delta L/L$.

adsorption vary from one adsorbate to the other, and thus the point of application of internal stress also varies. However, there is no independent confirmation of this view.

Thus we find that the capillary condensation theory and the behavior, both reversible and irreversible, which might be considered to result from the presence of menisci, will explain some of the known phenomena admirably. Other findings are not consistent with that theory. In addition there are experimental facts which remain unsatisfactorily explained on the basis of all current theories. The situation is not surprising in view of the complex nature of the adsorbent structure, but it is becoming clear that other theoretical bases must be established before an understanding of physical adsorption in porous bodies can be regarded as achieved.

ACKNOWLEDGMENTS

We would like to acknowledge financial assistance for this work from the National Research Council and the Advisory Committee on Scientific Research of the University of Toronto.

REFERENCES

1. C. AMBERG and R. MCINTOSH. Can. J. Chem. **30**, 1012 (1952).
2. N. SHEPPARD and D. J. C. YATES. Proc. Roy. Soc. (London), Ser. A, **238**, 69 (1956).
3. G. KARAGOUNIS and O. Z. PETER. Z. Elektrochem. **61**, 827 (1957).
4. V. S. BRAZHAN. Kolloidn. Zh. **21**, 645 (1959).
5. G. KARAGOUNIS. Helv. Chim. Acta, **36**, 282, 1681 (1953); Helv. Chim. Acta, **37**, 805 (1954).
6. C. HODGSON and R. MCINTOSH. Can. J. Chem. **37**, 1278 (1959).

Can. J. Chem. Downloaded from www.nrcresearchpress.com by 210.87.254.6 on 09/05/12
For personal use only.

7. C. HODGSON and R. McINTOSH. Can. J. Chem. **38**, 958 (1960).
8. R. K. CHAN and R. McINTOSH. Can. J. Chem. **40**, 845 (1962).
9. H. W. QUINN and R. McINTOSH. Proceedings of the Second International Conference of Surface Activity. Butterworth Scientific Publications, London. 1957.
10. J. A. MORRISON and L. E. DRAIN. J. Chem. Phys. **19**, 1063 (1951).
11. W. A. PATRICK and W. A. KEMPER. J. Phys. Chem. **42**, 369 (1938).
12. H. P. R. FREDERIKSE. Physica, **15**, 860 (1949).
13. G. EBERT and G. LANGHAMMER. Kolloid-Z. **174**, 5 (1961); Kolloid-Z. **175**, 159 (1961).
14. L. J. SLUTSKY and W. H. WADE. J. Chem. Phys. **36**, 2688 (1962).
15. T. C. POWERS and R. A. HELMUTH. Highway Res. Board, Proc. **32**, 285 (1953).
16. F. GOLDMANN and M. POLANYI. Z. Physik. Chem. A, **132**, 321 (1928).
17. S. V. R. MASTRANGELO. J. Chem. Phys. **18**, 896 (1950).
18. E. A. LONG and L. MEYER. Phys. Rev. **76**, 440 (1949).
19. W. D. SCHAEFFER, W. R. SMITH, and C. B. WENDELL. J. Am. Chem. Soc. **71**, 863 (1949).
20. E. F. BURTON and W. F. OLIVER. Proc. Roy. Soc. (London), Ser. A, **153**, 166 (1935).
21. R. H. BEAUMONT, H. CHIKARA, and J. A. MORRISON. J. Chem. Phys. **34**, 1456 (1961).
22. K. DRANSFELD, H. L. FRISCH, and E. A. WOOD. J. Chem. Phys. **36**, 1574 (1962).
23. A. V. KISELEV and V. V. KULICHENKO. Zh. Fiz. Khim. **29**, 663 (1955).
24. C. H. AMBERG, D. H. EVERETT, L. H. RUITER, and F. W. SMITH. Proceedings of the Second International Conference of Surface Activity. Butterworth Scientific Publications, London. 1957.
25. P. KUBELKA. Z. Elektrochem. **38**, 611 (1932).

Can. J. Chem. Downloaded from www.nrcresearchpress.com by 210.87.254.6 on 09/05/12
For personal use only.

INVESTIGATION OF THE INFLUENCE OF SPACE CHARGE ON THE ANODIC OXIDATION OF ALUMINUM, A TYPICAL VALVE METAL

M. J. DIGNAM AND P. J. RYAN
Department of Chemistry, University of Toronto, Toronto, Ontario
Received July 16, 1963

ABSTRACT

Measurements of the time derivative of the anodic overpotential of superpurity aluminum during anodic oxidation were made at various constant current densities. The data have been interpreted in terms of the variation of electric field strength with position in the oxide film. The analytic form of the profile of the electric field strength in the oxide film was deduced, assuming the high field Frenkel defect model. The data were found to be incompatible with the theoretical profile, providing, therefore, evidence against this model. The data are only consistent with a model for the transport process in which the concentration of ionic current carriers at a position in the oxide remote from the metal interface is independent of the field strength. A new model, proposed recently by Dignam to explain transient ionic conduction phenomena, is consistent with this conclusion.

Can. J. Chem. Downloaded from www.nrcresearchpress.com by 210.87.254.40 on 09/05/12
For personal use only.

INTRODUCTION

The influence of space charge on the oxidation of metals and semiconductors has been the subject of a number of theoretical and experimental investigations. In a recent paper by Butler (1), the space charge distribution in a metal oxide – oxygen system under equilibrium conditions is discussed in detail. His approach to the problem, however, is not applicable to any case where the conditions depart seriously from those at equilibrium. Such non-equilibrium conditions clearly obtain during the steady-state anodic oxidation of the valve metals, so that consideration of space charge in these systems must rest on kinematic rather than equilibrium arguments. Information concerning the nature of space charge effects within such anodic oxide films can therefore be used to judge the relative merits of different kinematic models.

If a space charge exists, it will give rise to a variation of electric field strength with position in the oxide film, thus providing a means for its detection. The experiments described herein consist of measurements of the time derivative of the aluminum anode potential, $\dot{\varphi}$, under conditions of constant anodizing current. Ignoring for the moment the problem of charging current and transient effects associated with the ionic current, these measurements can provide information concerning the variation of the electric field strength with position in the oxide film. Details of the assumptions involved are discussed in a later section.

Measurements of the influence of space charge on the steady-state anodic oxidation of aluminum have been carried out in the above manner for a range of current densities, and the results interpreted and compared with predictions based on the high field Frenkel defect model (2). The results indicate that the concentration of ionic current carriers is independent of the electric field strength for steady-state conditions, in direct conflict with the fundamental postulate of the above model.

EXPERIMENTAL

Apparatus

The circuit, designed to maintain the anodizing cell current constant and measure the time derivative of the potential of the aluminum anode with respect to that of a reference electrode, is depicted in Fig. 1. The triangular symbols represent high-gain, d.c., inverting, operational amplifiers, number 3101 made by Donner Scientific Co.; the square symbol, a Keithley Instruments Inc., number 610A electrometer amplifier.

The resistors are all 0.1%, wire-wound; the capacitors, high quality polystyrene. The circuit design can be readily understood in terms of conventional electronic analogue computer circuits. Amplifier 1 maintains a constant current of magnitude e_1/R_1 through the anodizing cell. The reference electrode potential is fed from the electrometer amplifier through amplifier 2 which changes the sign of the potential. The output of amplifier 3 is five times the difference between the potentials of the reference and aluminum electrode. Amplifier 4 is connected as a limited frequency response differentiator, R_3 being chosen to give a few hundred millivolts output for the maximum rate of change of the anode potential encountered for the run in question. R_2 and C were chosen to introduce time constants ($R_2 \times 10$ μf and R_3C) of magnitude 0.1 sec to 1 sec, depending on the conditions of the run. The time constants were chosen as large as possible, without sacrificing accuracy, in order to suppress background noise. The error introduced in this way was in no case the limiting factor. The signal from amplifier 4 is fed through amplifier 5 to a 100-mv strip-chart recorder. The 10-turn potentiometer was used to adjust the output calibration for a known rate of voltage rise into amplifier 4, and e_2 was chosen to offset the zero a known amount, hence providing greater sensitivity. With this arrangement, rates of voltage rise in the range 0.1 to 0.005 volt/sec could be measured with an accuracy of 0.1%, and a sensitivity of 0.02%.

The electrolysis cell, constructed of Lucite, is shown diagrammatically in Fig. 1. The electrolyte used

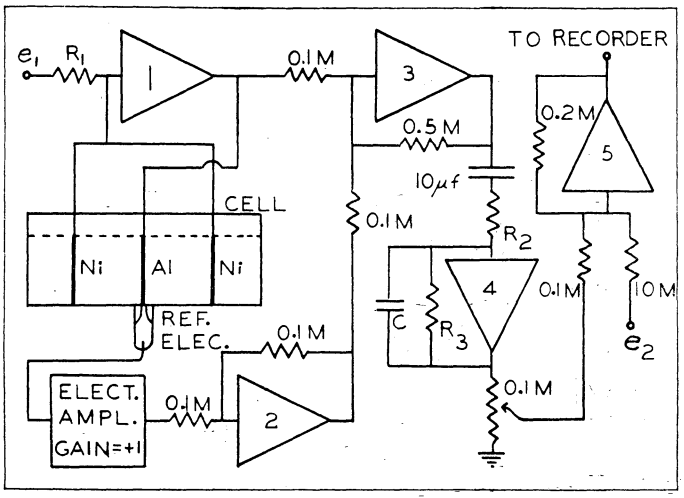

FIG. 1. Electronic circuit employed to measure the time derivative of the anode potential at constant current.

was a 30% solution of ammonium pentaborate in ethylene glycol (3), as it has been shown by Bernard and Cook to lead to 100% current efficiencies for the formation of Al_2O_3. The working cathodes were made of high purity nickel. The reference electrode was a saturated calomel electrode in a cracked glass envelope, which in turn was placed in a tube connected to the cell through a capillary tipped side arm adjacent to the anode.

Experimental Procedure

Superpurity (99.996%) aluminum sheet (0.04 inch thick) was formed into paddle-shaped electrodes of dimensions 1 inch × 0.25 inch for the paddle, 1 inch × 0.06 inch for the tab. Following routine cleaning procedures, the electrodes were electropolished at about 0.2 amp/cm^2 and 25° C in 5 parts ethyl alcohol to 1 part 70% perchloric acid by volume (4). The electrodes were rinsed briefly in ethyl alcohol, then for 1 minute in running distilled water, being dried in a clean air jet and stored in a desiccator over activated alumina. In order to ascertain the influence of surface treatment on the results, a few electrodes were treated by: (*a*) etching in 1:1 nitric acid at 60° C for ½ hour; (*b*) electropolishing, then treated as in (*a*); (*c*) etching in aqueous 10% NaOH at 25° C for 1 minute; (*d*) electropolishing, then treated as in (*c*); (*e*) immersion in chromic-phosphoric acid stripping solution at 25° C for 2 hours; (*f*) electropolishing followed by treatment as in (*e*). In all cases the electrodes were rinsed in distilled water and dried as before.

A typical experimental run was carried out as follows. The cell was filled to just above the shoulders of the paddle-shaped aluminum electrode and was then connected into the circuit with e_1 set at zero and left for 2 to 10 minutes. The appropriate value of e_1 was then switched on and the output of amplifier 5 recorded as a function of time.

A few runs were carried out using electrodes with "tabs" insulated with a thick anodic oxide film.

Can. J. Chem. Downloaded from www.nrcresearchpress.com by 210.87.254.40 on 09/05/12
For personal use only.

Experimental Results

Figure 2 represents the data obtained from a typical run, Δ' being the fractional deviation of the time derivative of the anode potential from its limiting value for thick films ($\Delta' = [\dot{\varphi}(t) - \dot{\varphi}(\infty)]/\dot{\varphi}(\infty)$). The reference point for zero incremental charge passed was chosen as the point at which the aluminum electrode reached a potential of +1.000 volt against the saturated calomel electrode. This potential, although quite arbitrary, was chosen since the data at this point and beyond were quite reproducible. The initial features of the runs, however, were subject to random variations. These features usually resemble in form those depicted by the solid curve, the broken curve representing a limiting case sometimes found.

The most important observation concerning these results is the lack of any appreciable dependence of curve shape, when the results are plotted against charge passed, on the current density employed. A systematic decrease in the height of the broad peak with increasing current density does occur, as can be inferred from the logarithmic plots shown in Fig. 3. It is apparent that the graphs of log Δ' versus charge

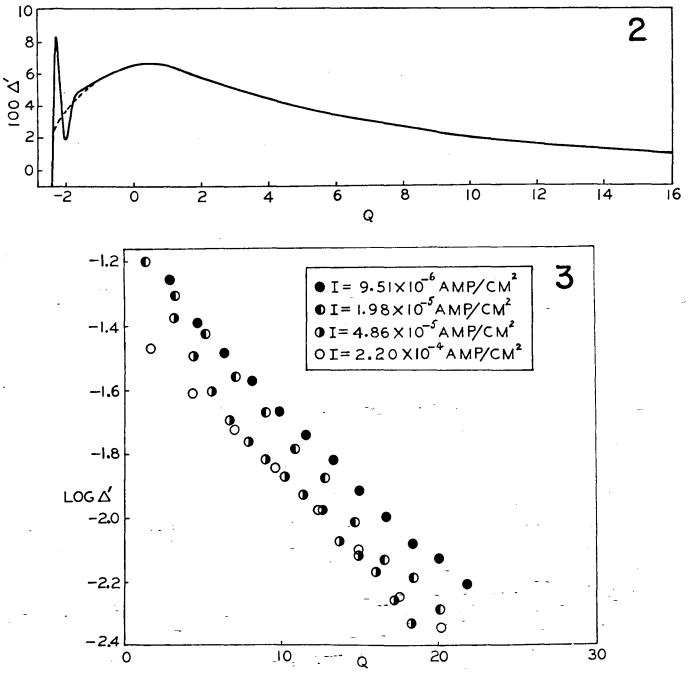

FIG. 2. Experimental data: $100\Delta'$ as a function of total charge passed (Q in mcoul/cm²).
FIG. 3. Dependence of log Δ' vs. Q on current density (Q in mcoul/cm²).

passed are nearly straight lines with the slopes independent of current density. The theoretical significance of these observations will be discussed in the following sections.

INTERPRETATION OF RESULTS

In the introduction it was stated that measurements of the time derivative of the anodic potential against a reference electrode could be interpreted under certain conditions in terms of the variation of field strength with position in the oxide. It is the purpose of this section to examine the arguments leading to this interpretation.

On making the following assumptions:

(1) 100% current efficiency for the formation of the oxide film;
(2) film density independent of the film thickness;
(3) overpotential associated with the reactions at the oxide interfaces independent of the total film thickness;
(4) field strength at a position x in the film is independent of the total film thickness, X; it follows immediately that:

Can. J. Chem. Downloaded from www.nrcresearchpress.com by 210.87.254.40 on 09/05/12
For personal use only.

[1] $$E(x, I) = (F\rho/IW_e)\dot{\varphi}(t,I)$$

where x is calculated from the relation

$$x = (IW_e/F\rho)t + X_0.$$

$E(x, I)$ is the field strength at a distance x from the metal-oxide interface during steady-state formation conditions at a current density I; $\dot{\varphi}(t,I)$ is the time derivative of the anodic potential against a reference electrode measured at time t for steady-state formation conditions at a current density I; W_e is the electrochemical equivalent weight of the oxide; F is Faraday's constant; ρ is the oxide density; and X_0 the film thickness at $t = 0$. Thus, providing the assumptions are valid and that true steady-state conditions can be achieved, the field strength as a function of position in the film may be calculated from $\dot{\varphi}$ as a function of time. Setting aside for the moment the question as to whether true steady-state conditions can in fact be achieved, the four assumptions will be examined.

The first assumption may be examined on the basis of the data of Bernard and Cook (3). These authors measured the weight gain of aluminum anodes anodically oxidized to 150 v at current densities from 10^{-7} to 10^{-3} amp/cm^2. They found that the current efficiencies for oxide formation ranged from 99% to 102%, with the estimated error in their experiments being 1%. Heating the film to 600° C gave no change in weight, indicating the absence of water or glycol in the film. Further, the presence of borates in the film was not detected by chemical analysis, there was no apparent oxygen evolution during formation and no aluminum was detected in the electrolyte after formation. For the present experiments where the same electrolyte was employed, at anode overpotentials well below 150 v, and at current densities of 10^{-5} to 2×10^{-4} amp/cm^2, within the range studied by Bernard and Cook, it is concluded that the current efficiency for oxide formation was not less than about 99%. During an experimental run, the current efficiency can therefore not decrease by more than about 1%, whereas the observed drop in $\dot{\varphi}$ would require more than a 6% decrease in current efficiency with increasing thickness to be explained in this manner.

Concerning the second assumption, significant variation in film density is expected over the first few molecular layers of oxide, but certainly not beyond about 30 Å film thickness.

Concerning the third assumption, if the field strength is a function of position in the film, x, then the defect concentration will also be a function of position. It then follows that the defect concentration in the oxide at the oxide–electrolyte interface will be a function of film thickness. In general, therefore, the overpotential associated with the oxide–electrolyte interface will also be a function of film thickness. Because of the very high field strength ($\sim 10^6$ to 10^7 v/cm) present in the film, however, the contribution of this field to $\dot{\varphi}$ will almost certainly dominate beyond the first few molecular layers of oxide.

Assumption (4) will be valid if all the mobile defects involved in the rate controlling transport process bear a positive charge and are present in low concentration, since for high-field transport conditions diffusion against the field is negligible so that the field strength and defect concentration at x_1 is not influenced by the field or defect concentration at x_2, where $x_2 > x_1$.* If all the mobile defects involved bear a negative charge,

Strictly speaking, we should include the further condition that the dimensions of the oxide–electrolyte interfacial region be small compared with that of the space charge zone, since the above statement is clearly not valid for x_1 within the interfacial region. For the present case, where the space charge zone is about 100 Å thick, this condition is almost certainly fulfilled.

Can. J. Chem. Downloaded from www.nrcresearchpress.com by 210.87.254.40 on 09/05/12
For personal use only.

assumption (4) will still be valid provided that the x-axis direction is reversed, the position $x = 0$ being defined to coincide with the oxide–electrolyte interface. The space charge in this case will be associated with the oxide–electrolyte, rather than with the metal–oxide interface region.

If we define the "excess field", $\Delta = [E(x) - E_\infty]/E_\infty$ where E_∞ is the limiting value for E at large values of x (i.e. the value of E beyond the space charge region), it follows from our previous definition of Δ' and from equation [1] that $\Delta(x,I) = \Delta'(t,I)$ where $x = (IW_e/F\rho)t + X_0$, providing Δ' was obtained from steady-state measurements.

Examining the results from a typical run (Fig. 2) it is apparent that the equality $\Delta = \Delta'$ cannot be applied over the entire curve since electronic charging effects, responsible for the initial rapid rise in Δ', prevent the establishment of a constant ionic current density. The final fall-off of Δ' cannot be ascribed to charging effects, however, since the direction of its change is in the wrong sense. Nor can it be explained by assuming a reduction of true surface area during anodic oxidation, for the same reason. A further possibility eliminated on the same grounds is that the initial oxide film, formed by electropolishing in a chloride-containing solution, causes the current efficiency to be initially low, increasing as anodic oxidation proceeds.

The following possible causes for the final decay of Δ' cannot be eliminated on the above grounds. These are: (1) that the effect is brought about by electrolyte creeping up the electrode tab, thus reducing the current density; and (2) that the effect is the manifestation of transient ionic conduction phenomena. These possibilities will now be examined.

The principal evidence against the acceptance of the first explanation is the fact that the results obtained for electrodes whose tabs were insulated with a thick anodic film did not differ in any systematic way from the results obtained for uninsulated electrodes. In addition, the observed decay of Δ' amounts to over 6%, an effect far too large to be explained in this way.

The possibility that the decay of Δ' arises as a result of transient ionic transport processes must be examined carefully. On interrupting a run at, for example, 10 mcoul/cm^2 (Fig. 2), and starting the run again with the same sample, Δ' assumes values which form a continuation of the previous curve after a time period corresponding to only a fraction of a mcoul/cm^2. The effect of interest does not arise, therefore, as a result of simple ionic transient phenomena. Furthermore, it can be shown that the decay in Δ' is more than a factor of 10 slower than that found for ionic transients. The possibility that some unusual process, associated with the film produced during electropolishing, is responsible for the effect is also ruled out by the results obtained for the different surface treatment procedures. Only electrodes treated finally in chromic-phosphoric acid solutions gave significantly different results, this difference arising almost certainly as a consequence of specific adsorption of chromate ion on the oxide (5).

Finally, the possibility that the effect might arise from the instrumentation was eliminated by conducting suitably designed dummy runs. In addition, runs of a different nature, carried out using independent equipment, produced a very similar phenomenon. In these runs the anodic potential was increased at a constant rate, and the current recorded as a function of charge passed. The current is initially low (as expected) by about 6%, approaching the limiting value in much the same way as $\dot{\varphi}$ approaches its limiting value.

On the basis of the evidence presented, it is eminently reasonable to interpret the final decay of Δ' in terms of a real variation of the field strength with position in the film.

Can. J. Chem. Downloaded from www.nrcresearchpress.com by 210.87.254.40 on 09/05/12
For personal use only.

Assuming the rate controlling transport process to involve mobile defects of one kind only, the equality $\Delta = \Delta'$ may therefore be applied to this region. The initial features of Δ', however, most certainly cannot be interpreted in this way. They probably arise as a result of a combination of a number of the factors which have been discussed.

THEORY AND DISCUSSION

High Field Frenkel Defect Model

For comparison with the data, the theoretical influence of space charge will be calculated on the basis of the above-mentioned model (2). According to this model, interstitial metal ions are transported through the oxide film in accordance with the following equation:

$$I = 2q\, a\, \nu\, n \exp\left[-(U - Eaq)/kT\right] \qquad [2]$$

where I = ion current density in the film;
q = charge on the cation;
ν = vibrational frequency of an interstitial cation;
n = concentration of interstitial cations;
U = activation energy for the migration of interstitial cations in the absence of an electric field;
a = activation distance corresponding to U;
E = electric field strength in the oxide.

To account for transient conduction phenomena, the concentration of interstitial cations is assumed to be a function of the electric field strength and time. The simplest specific model is that suggested by Bean, Fisher, and Vermilyea (6) and by Dewald (7). They proposed that interstitial cation – cation vacancy pairs (i.e. Frenkel defects) are produced by the action of the field on lattice cations, and destroyed by their recombination. The net rate of formation of interstitials and vacancies is given by:

$$\left(\frac{\partial n}{\partial t}\right)_x = \left(\frac{\partial m}{\partial t}\right)_x = (N-m)\nu' \exp\left[-(W - E\lambda q)/kT\right] - I\sigma m/q \qquad [3]$$

where N = concentration of cation lattice sites;
m = concentration of cation vacancies;
t = time;
ν' = vibrational frequency of a lattice cation;
W = activation energy for formation of a Frenkel defect in the absence of an external electric field;
λ = activation distance corresponding to W;
σ = capture cross-section of a vacancy for an interstitial cation.

On applying this theory, it has previously been assumed that n, m, E, and I are independent of position in the film. Although this should be true some distance from the metal–oxide interface, as Dewald points out there must be, in general, a space charge near the metal–oxide interface, thereby making n, m, and E functions of position. The necessity for postulating this space charge can be seen from the following considerations. For steady-state conditions, the ion current density at the interface must be equal to that within the film some distance from the interface. Since transport of ions across the interface and transport within a space charge free oxide are distinct and independent kinetic processes, the rates can in general only be equal providing the field strengths are different. The difference in field strength can only be sustained if the intervening space contains a net charge.

Can. J. Chem. Downloaded from www.nrcresearchpress.com by 210.87.254.40 on 09/05/12
For personal use only.

Profile of Electric Field Strength

Only the cases corresponding to steady-state anodic oxidation will be considered. Under these conditions, the following relations hold:

$$[4] \qquad \left(\frac{\partial I}{\partial x}\right)_t = \left(\frac{\partial I}{\partial t}\right)_x = \left(\frac{\partial n}{\partial t}\right)_x = \left(\frac{\partial m}{\partial t}\right)_x = \left(\frac{\partial E}{\partial t}\right)_x = 0$$

where x is the distance in the oxide measured from the metal–oxide interface. In the zone of the oxide where the space charge is negligible (i.e. at sufficiently large x) we may set $m = n = n_\infty$. The variation of current with field in the space charge free zone, E_∞, under steady-state conditions is then obtained from equations [2] to [4].

$$[5] \qquad I = \alpha \exp \beta E_\infty$$

where $\alpha = q(2aN\nu\nu'/\sigma)^{1/2} \exp\left[-(W + U)/2kT\right]$

and $\beta = q(\lambda + a)/2kT$.

Equation [5] is of the form found experimentally for the valve metals for films thicker than about 100 Å (2).*

An expression for the variation of n with field strength within the space charge zone is obtained from equation [2].

$$[6] \qquad n = n_\infty \exp[(E_\infty - E)\, aq/kT]$$

Similarly, the variation of m with field strength within the space charge zone is obtained from equations [3] and [4], and assuming $N \gg m$.

$$[7] \qquad m = n_\infty \exp[(E - E_\infty)\lambda q/kT]$$

From Poisson's equation we also have:

$$[8] \qquad \frac{dE}{dx} = \frac{4\pi q}{\epsilon}(n - m)$$

where ϵ, the dielectric constant of the oxide, is assumed to be independent of x. Substituting for n and m in equation [8], the resulting equation can be written:

$$[9] \qquad dy/ds = (1 - y^\gamma)/\gamma$$

where y, s, and γ are dimensionless parameters defined as follows:

$$y = \exp\left[-|E - E_\infty|(\lambda + a)\, q/\gamma kT\right]$$

$$s = [4\pi q^2(\lambda + a)n_\infty/kT\epsilon]x$$

for $n_0 > m_0$, $\quad \gamma = (\lambda + a)/a$ and $E_\infty > E$

for $n_0 < m_0$, $\quad \gamma = (\lambda + a)/\lambda$ and $E_\infty < E$

where n_0 and m_0 are the values of n and m at $x = 0 = s$.

Equation [9] can be solved in terms of simple functions for certain values of γ only. Asymptotic solutions for any value of γ, however, can be found. One such solution is easily deduced for the case $y^\gamma \ll 1$. This corresponds, however, to very large deviations of E from E_∞, under which conditions the equations used to obtain equation [9] probably represent poor approximations. In addition, only relatively small deviations of E from

**Strictly speaking, the exponential factor should contain a term in E^2 (8). However, its omission here will cause no serious error.*

Can. J. Chem. Downloaded from www.nrcresearchpress.com by 210.87.254.40 on 09/05/12
For personal use only.

E_∞ are apparent from the experimental results. The asymptotic solution for the other extreme case, $1-y \ll 1$, will be considered in the following development.

The general solution of equation [9] can be expressed as follows:

$$s + s_0 = f(\gamma,y) - \ln (1-y) \quad [10]$$

where

$$f(\gamma,y) = \int_0^y \left(\frac{\gamma}{1-y^\gamma} - \frac{1}{1-y}\right)dy$$

and s_0 is the integration constant.

The important property of $f(\gamma,y)$ is that it approaches a finite value as y approaches unity (see Fig. 4). Equation [10] can be rearranged to give:

$$\ln y = \ln (1-\exp [f(\gamma,y)-(s+s_0)]). \quad [11]$$

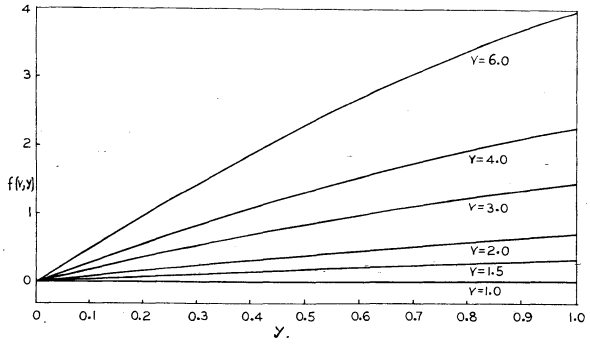

FIG. 4. The function $f(\gamma,y)$ vs. y for various values of γ.

On substituting for y according to its definition, and for E_∞ according to equation [5], equation [11] becomes:

$$|\Delta| = -\gamma \ln (1-\exp [f(\gamma,y)-(s+s_0)])/\ln (I/\alpha) \quad [12]$$

where Δ is $(E-E_\infty)/E_\infty$ as before.

For $1-y \ll 1$ (i.e. E almost equal to E_∞) it follows that $1 \gg \exp [f(\gamma,y)-(s+s_0)]$ and $f(\gamma,y) \simeq f(\gamma,1) = f(\gamma)$, so that equation [12] reduces to the following approximate relation:

$$|\Delta| \simeq \gamma \exp [f(\gamma)-(s+s_0)]/\ln (I/\alpha). \quad [13]$$

Equation [13] represents, therefore, the field profile in the region of the film where the effect of the space charge has almost vanished. In this region, a plot of $-\ln |\Delta|$ versus distance from the metal–oxide interface, x, should yield a straight line:

$$-\ln |\Delta| \simeq \left(\frac{4\pi q^2(\lambda+a)n_\infty}{kT\epsilon}\right)x + \left(\ln\left[\frac{\ln (I/\alpha)}{\gamma}\right] - f(\gamma) + s_0\right) \quad [14]$$

It is seen from equation [14] that the slope, and hence the rate of fall of the space charge effect with distance, is proportional to n_∞, the concentration of defects in the space charge free zone of the film. This is certainly an expected result, which leads to the further expectation that the slope should be an increasing function of current density, since n_∞ increases with increasing current density. Substituting for n_∞ the relation obtained from

Can. J. Chem. Downloaded from www.nrcresearchpress.com by 210.87.254.40 on 09/05/12
For personal use only.

equations [2] and [5], the expression for the slope becomes:

$$[15] \qquad \text{slope} = \left(\frac{2\pi q\alpha^{2a/(\lambda+a)}}{kT\epsilon\nu \exp(-U/kT)}\right)\left(\frac{\lambda+a}{a}\right)\cdot I^{(\lambda-a)/(\lambda+a)}.$$

From the steady-state data for aluminum obtained by Bernard and Cook (3), $\lambda+a \simeq 7.8$ Å, and from transient data obtained in this laboratory (9), $a = 1.25$ Å. For aluminum, therefore, the slope should vary proportionately to $I^{0.7}$, a factor of 20 change in I causing about a factor of 8 change in the slope. The results shown in Fig. 3 clearly do not confirm this prediction, the slope being independent of current density within experimental error. After allowing for the maximum possible errors in the evaluation of $(\lambda+a)$ and a, the results and theory are still irreconcilable. In a recent publication by Ryan and Dignam, a modification of the high-field Frenkel defect model was proposed in order to explain certain transient ionic conduction measurements. It turns out, however, that the modified model leads to identically the same variation of the slope with I as does the original model. The conflict between the results and the theory is basic, in that the results indicate no observable dependence of the concentration of charged defects on the current density (and hence also on the field strength) in contradiction the fundamental postulate of the high-field Frenkel defect model. It is necessary, therefore, either to discard the model completely, or else to reinterpret the data. As the validity of the present interpretation of the data has been carefully examined, the only conclusion justified at present is the rejection of the model.

Further evidence against this model is provided by the calculations illustrated in Fig. 5.

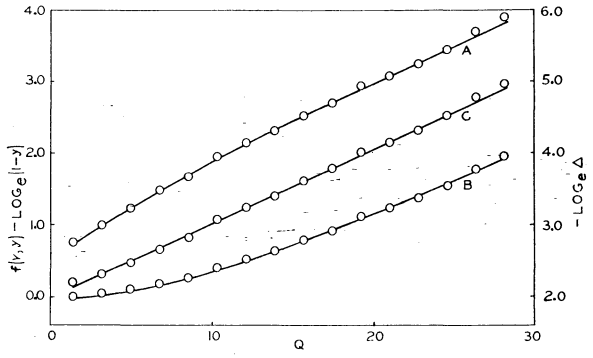

FIG. 5. Space charge data plotted according to: A, equation [14]; B, equation [10] with $\lambda + a = 7.8$ Å and $a = 1.25$ Å; C, equation [10] with $\lambda = a = 7.8/2$ Å. Q in mcoul/cm² in all cases.

The data obtained from one of the most reliable runs is plotted first (curve A) in accordance with the approximate equation [14] (i.e. $-\ln \Delta$ vs. charge passed), then in accordance with the more precise equation [10] (i.e. $f(\gamma,y) - \ln(1-y)$ vs. charge passed), the latter for two sets of values for the parameters ($\lambda+a = 7.8$ Å, $a = 1.25$ Å for curve B, $\lambda = a = 7.8/2$ Å for curve C). In order to calculate the results for curves B and C, the actual field strengths were required. These were calculated from $\dot{\varphi}$ values using the data obtained by Bernard and Cook (3). If the high-field Frenkel defect model were correct, curve B should be linear. It is, in fact, the least linear of the three curves. It is important to determine the significance of the excellent linearity of curve C, calculated assuming only a single activation distance equal to that obtained from steady-state measurements,

Can. J. Chem. Downloaded from www.nrcresearchpress.com by 210.87.254.40 on 09/05/12
For personal use only.

particularly since for $\lambda = a$ the slope of the log Δ' versus Q plots previously discussed will be independent of current density as observed. Its significance, however, is not immediately obvious, since for $\lambda = a$ the high field Frenkel defect model cannot give rise to transient ionic conduction.

One of us (M. J. D.) has recently proposed a new model for the anodic oxidation of the valve metals (10) in which the transient phenomena arise not as a result of a change of defect concentration, but as a result of time dependent polarization phenomena within the film. The theory was proposed initially to explain anomalies relating to conventional steady-state and transient kinetic results, but it appears to contain the essential ingredients to be in accord with the present results, and with recent results relating to transport numbers (11).

The detailed predictions arising from this model have not as yet been worked out, but preliminary investigation has led to a relation formally identical with equation [10], with "λ" and "a" equal to one another and to the empirical steady-state activation distance, which is about 3.9 Å for aluminum (3).

SUMMARY AND CONCLUSIONS

Measurements of the time derivative of the aluminum overpotential versus film thickness during anodic oxidation show no appreciable dependence on formation current density. Analyzed in terms of the high-field Frenkel defect theory, this means that the defect concentration is independent of the steady-state current density, in direct conflict with the basic postulate of this theory. It seems likely, although it is difficult to prove, that these results show the concentration of charged defects in the film to be independent of current density for any assumed mechanism involving mass transport through the film as a rate controlling process. Specifically, therefore, the data are in direct conflict with the high-field Frenkel defect model or any reasonable modification of it, and most likely in conflict with any theory which predicts a dependence of defect concentration on current density.

Alternatively, one can choose to interpret the data in terms of spurious phenomena totally unrelated to space charge effects. All of the data obtained mitigate against such an interpretation. In addition, the data are in excellent accord with a theory already postulated (10) to explain data of an entirely different sort. We prefer at the moment, therefore, to support the above conclusions.

Detailed analysis of space charge effects in relation to the new model (10) will be presented in a future publication.

The authors are grateful to The National Research Council of Canada for supporting this research and for a scholarship (P. J. R.).

REFERENCES

1. J. N. Butler. J. Chem. Phys. **35**, 636 (1961).
2. L. Young. Anodic oxide films. Academic Press, London. 1961. Chap. 3.
3. W. J. Bernard and J. W. Cook. J. Electrochem. Soc. **106**, 643 (1959).
4. P. A. Jacquet. Met. Rev. **1**, 157 (1956).
5. M. J. Pryor. Z. Elektrochem. **62**, 782 (1958).
6. C. P. Bean, J. C. Fisher, and D. A. Vermilyea. Phys. Rev. **101**, 551 (1956).
7. J. F. Dewald. J. Phys. Chem. Solids, **2**, 55 (1957).
8. L. Young. Proc. Roy. Soc. (London), Ser. A, **258**, 496 (1960).
9. P. J. Ryan and M. J. Dignam. Can. J. Chem. **40**, 1875 (1962).
10. M. J. Dignam. In preparation. Presented at meeting of American Electrochemical Society, April, 1963.
11. J. A. Davies. Private communication. Atomic Energy of Canada Limited, Chalk River, Ontario, Canada.

Can. J. Chem. Downloaded from www.nrcresearchpress.com by 210.87.254.40 on 09/05/12
For personal use only.

ENERGETICS AND MECHANISM OF HYDRONIUM ION FORMATION BY ELECTRON IMPACT

D. VAN RAALTE AND A. G. HARRISON[1]
Department of Chemistry, University of Toronto, Toronto, Ontario
Received August 12, 1963

ABSTRACT

The reactions leading to formation of the hydronium ion in the mass spectra of a number of alcohols and formate esters have been elucidated through a study of appearance potentials and metastable transitions and by the use of deuterium labelling. The results lead to $\Delta H_f(H_3O^+) = 157 \pm 3$ kcal/mole corresponding to a proton affinity of the gaseous water molecule of 151 ± 3 kcal/mole.

INTRODUCTION

The generally accepted value for the proton affinity of the gaseous water molecule is 182 kcal/mole (1) based on calculations from crystal lattice energies by Sherman (2). More recently Sokolov *et al.* (3) have recalculated P.A. (H_2O) from lattice energies and, taking into account the effect of hydrogen bonding, have obtained P.A. (H_2O) = 168 ± 7 kcal/mole. This latter value is in essential agreement with an independent estimate obtained by Tal'roze and Frankevich (4) from a study of gas-phase ion–molecule reactions involving H_3O^+ as the product ion. The reaction

$$H_2S^+ + H_2O \rightarrow H_3O^+ + HS \qquad [1]$$

was observed and therefore must be exothermic or thermoneutral. Thermochemical calculations led (4) to a maximum value $\Delta H_f(H_3O^+) \leq 141$ kcal/mole. Using a more recent value (5) for $\Delta H_f(HS)$ this upper limit is raised to 145 kcal/mole, leading to a minimum value P.A. (H_2O) ≥ 163 kcal/mole. On the other hand, the reaction

$$C_2H_2^+ + H_2O \rightarrow H_3O^+ + C_2H \qquad [2]$$

was not observed and was therefore assumed to be endothermic (4). On this basis a minimum value $\Delta H_f(H_3O^+) \gtrsim 136$ kcal/mole (P.A. (H_2O) ≤ 172 kcal/mole) was obtained. This limit must be accepted with reservation, since other factors may be responsible for the non-occurrence of reaction [2].

Although the hydronium ion has been observed as a rearrangement ion in the mass spectra of alcohols (6, 7, 8) and esters (9) no systematic investigation of the energetics and mechanism of formation has been undertaken. An early study (10) of the appearance potential of H_3O^+ from ethyl alcohol has been used (11) to derive $\Delta H_f(H_3O^+) = 172$ or 196 kcal/mole, depending on the mechanism of formation chosen. More recently, Bernecker and Long (12) have measured the appearance potential of H_3O^+ from ethyl formate and have reported $\Delta H_f(H_3O^+) = 207$ kcal/mole, corresponding to P.A. (H_2O) = 100 kcal/mole.

In view of the conflict in the reported values for $\Delta H_f(H_3O^+)$ and the paucity of data concerning the mechanism of formation of this rearrangement ion in the mass spectra of alcohols and esters, we have undertaken a detailed study of the energetics and mechanism of formation of H_3O^+ by electron impact.

[1]*Alfred P. Sloan Research Fellow.*

Can. J. Chem. Downloaded from www.nrcresearchpress.com by 210.87.254.40 on 09/05/12
For personal use only.

Can. J. Chem. Downloaded from www.nrcresearchpress.com by 210.87.254.40 on 09/05/12
For personal use only.

EXPERIMENTAL

All results were obtained using an Associated Electrical Industries MS-2 mass spectrometer. The mass spectra were obtained with 50 volts electron energy, 20 μamp ionizing current and 3 volts repeller (~7 volts/cm field strength). The appearance potentials were obtained as previously described (13), using xenon or krypton as the calibrating gas.

The mass-to-charge ratios of the "low mass" metastables of interest in the present work were measured by comparison with the C^+ ion using electrostatic scanning and making accurate comparison with the voltage necessary to bring the two ion beams into focus. The necessary circuitry and potentiometer are built into the mass spectrometer.

The non-deuterated compounds were commercial samples with the exception of the isopropyl formate which was prepared by standard procedures. All samples were carefully dried and distilled before use to remove traces of water. In all cases the peak attributable to H_2O impurity was scarcely above the normal small instrument background.

The ethyl-1,1-d_2 alcohol, 2-propyl-1,1,1,3,3,3-d_6 alcohol, ethyl formate-*d*, and isopropyl formate-*d* were obtained from Merck, Sharp, and Dohme. The detailed mass spectra of the two esters have been presented previously (14). The deuterated ethyl alcohol initially contained impurities thought to be acetone and diethyl ether. These were removed by careful distillation. The isopropyl-d_6 alcohol also showed diethyl ether impurities which were removed by gas chromatography. Low energy analysis of both alcohols indicated approximately 99% isotopic purity.

RESULTS AND DISCUSSION

The appearance potential of H_3O^+ was measured from ethanol, *n*-propanol, *s*-propanol, *s*-butanol, *s*-pentanol, 3-methyl-2-butanol, diethyl ether, ethyl formate, and isopropyl formate. The measured appearance potentials, postulated neutral products, and the resultant $\Delta H_f(H_3O^+)$ for each compound are given in Table I. The evidence leading to the assignment of the neutral fragments, and thus the details of the ionization mechanism, will be discussed below.

TABLE I

Appearance potentials and heats of formation of H_3O^+

Compound	$A(H_3O^+)$ kcal/mole ±3	Postulated neutral products	$\Delta H_f(H_3O^+)$ kcal/mole ±3
s-Propanol	310	$CH_3 + C_2H_2$	158
s-Butanol	308	$C_2H_5 + C_2H_2$	158
s-Pentanol	308	$n\text{-}C_3H_7 + C_2H_2$	156
3-Me-2-butanol	304	$i\text{-}C_3H_7 + C_2H_2$	154
Ethanol	277	C_2H_3	156
n-Propanol	292	$C_3H_3 + H_2$	155
Diethyl ether	304	$C_2H_5 + C_2H_2$	164
Ethyl formate	302	$HCO + C_2H_2$	159
Isopropyl formate	317	$CH_3 + CO + C_2H_2$	159

The heats of formation of neutral species necessary for the calculations in Table I were taken from the recent compilations of Bernecker and Long (12) and Green (15) with a few exceptions. The heats of formation of the propyl radicals are in some doubt and the values used were based on $D(n\text{-Pr-H}) = 99$ kcal/mole (16) and $D(i\text{-Pr-H}) = 96.5$ kcal/mole, an average of two values 94 kcal/mole (17) and 99 kcal/mole (18). $\Delta H_f(C_3H_3) = 75$ kcal/mole (19) was used in preference to the value quoted by reference (12). The heats of formation of *s*-pentanol, 3-methyl-2-butanol, and isopropyl formate have not been reported and were estimated by comparison with related compounds to be: −75.9, −76.2, and −98 kcal/mole respectively. Calculations using group contributions (20) gave very similar values for the two alcohols; the error for these cases is likely to be small, however the value for isopropyl formate may be in error by ±3 kcal/mole.

Formation of H_3O^+ from $RCH(CH_3)OH$

The most extensive and conclusive evidence for the dissociation mechanism was obtained for secondary alcohols $RCH(CH_3)OH$ where R = CH_3, C_2H_5, *n*-C_3H_7, and *s*-C_3H_7. The mass spectra of these alcohols all show (8) the largest peak at mass 45* (CH_3CHOH^+) corresponding to loss of the group R. For *s*-propanol (21, 22) and *s*-butanol (23) deuterium labelling has shown that the group R is lost without isotopic mixing. Each of the four alcohols showed a pronounced metastable at mass 8.02 corresponding to the transition

$$CH_3CHOH^+ \rightarrow H_3O^+ + C_2H_2 \quad m^* = 19^2/45 = 8.02. \qquad [3]$$

The intensity of the metastable was directly proportional to the sample pressure indicating that reaction [3] was not a collision-induced dissociation. These facts suggest a common mechanism, reaction [4], for the four alcohols.

$$RCH(CH_3)OH \rightarrow R + CH_3CHOH^+ \rightarrow C_2H_2 + H_3O^+ \qquad [4]$$

Calculations assuming this mechanism lead to mutually consistent values for $\Delta H_f(H_3O^+)$ as summarized in the first four rows of Table I.

For *s*-propanol it has been suggested (24) that formation of H_3O^+ would occur by reaction [5] with C_3H_5 (allyl) as the neutral fragment

$$(CH_3)_2CHOH \rightarrow C_3H_5 + H_3O^+. \qquad [5]$$

The experimental appearance potential, 310 kcal/mole, leads to $\Delta H_f(H_3O^+) = 213$ kcal/mole assuming reaction [5]. This value is in disagreement with other values obtained in this work. Furthermore, reaction [5] does not lead to the observed metastable, nor does it explain the observed deuterium labelling to be discussed below.

To provide further information on the detailed mechanism of reaction [4] the mass spectrum of 2-propyl-1,1,1,3,3,3-d_6 alcohol was examined. The spectrum obtained was in good agreement with that previously reported (22). The intermediate mass 45 has moved to mass 48 indicating the formula CD_3CHOH^+. The observed relative intensities for H_2DO^+, HD_2O^+, and D_3O^+ are given in Table II and compared with relative intensities calculated on the following four models:

(i) complete scrambling in parent ion,
(ii) retention of hydroxyl hydrogen and scrambling of remainder in parent ion,
(iii) complete scrambling in CD_3CHOH^+ intermediate,
(iv) retention of hydroxyl hydrogen and scrambling of remainder in CD_3CHOH^+ intermediate.

The results of Table II show that the only model which comes close to predicting the

TABLE II

Relative intensities of labelled hydronium ions in $(CD_3)_2CHOH$

	Relative intensity of:		
	H_2DO^+	HD_2O^+	D_3O^+
Observed	0.492	0.472	0.036
Calculated			
Model (i)	0.100	0.540	0.360
Model (ii)	0.286	0.714	0.000
Model (iii)	0.300	0.600	0.100
Model (iv)	0.500	0.500	0.000

Since only singly charged ions will be discussed, the mass-to-charge ratio will be referred to as the mass.

Can. J. Chem. Downloaded from www.nrcresearchpress.com by 210.87.254.40 on 09/05/12
For personal use only.

observed relative intensities is model (iv) involving retention of the hydroxyl hydrogen and scrambling of the remainder in the CD_3CHOH^+ intermediate. There does not appear to be any reasonable model involving direct decomposition of the parent ion (reaction [5]) which can explain the observed label distribution. A simple interpretation of the label distribution is the formation of a symmetrical protonated ethylene oxide intermediate having the structures I and II for the unlabelled and labelled alcohols respectively.

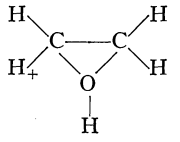

I

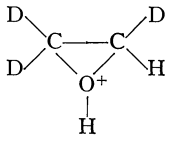

II

Transfer of one hydrogen (or deuterium) from each carbon to the oxygen would explain the product formation and the deuterium labelling. The small ion current for D_3O^+ suggests a small amount of exchange of the hydroxyl hydrogen with the other hydrogens in the intermediate ion. The appearance potentials of the H_2DO^+ and HD_2O^+ ions were identical with the appearance potential of H_3O^+ from the unlabelled alcohol within experimental error. The abundance of the D_3O^+ ion was too low to permit appearance potential measurements.

The deuterium labelling in *s*-butanol (23) provides results in good agreement with those obtained for *s*-propanol. Table III shows the abundance of the relevant ions, as percentage

TABLE III

Partial mass spectra of secondary butanols*

Mass	Ion	*s*-Butanol-d_0	*s*-Butanol-d_5	*s*-Butanol-d_6
18	H_2O^+ or CD_3^+	0.34	2.77	1.11
19	H_3O^+ or HDO^+	1.57	0.17	0.22
20	H_2DO^+		0.70	0.11
21	HD_2O^+		0.64	1.14
22	D_3O^+		0.06	0.26
45	CH_3CHOH	38.60		
48	CD_3CHOH^+		36.50	
49	CD_3CDOH^+			37.60

*From reference 23. Intensities as percentage of total ionization.

of total ionization, for 2-butyl alcohol, 2-butyl-1,1,1,3,3-d_5 alcohol, and 2-butyl-1,1,1,2,3,3-d_6 alcohol. It is obvious that the mass 45 intermediate is formed by loss of the ethyl group without isotopic mixing, appearing as mass 48 in the d_5 alcohol and mass 49 in the d_6 alcohol. The relative intensities of the various labelled hydronium ions in the d_5 alcohol

TABLE IV

Comparison of observed and calculated intensities in *s*-butanol-d_5

	Relative intensity of:		
	H_2DO^+	HD_2O^+	D_3O^+
Observed	0.500	0.460	0.040
Calculated			
Model (i)	0.417	0.417	0.083
Model (ii)	0.556	0.278	0.000
Model (iii)	0.300	0.600	0.100
Model (iv)	0.500	0.500	0.000

Can. J. Chem. Downloaded from www.nrcresearchpress.com by 210.87.254.40 on 09/05/12
For personal use only.

are compared in Table IV with relative intensities calculated on the following four models:

(i) complete scrambling in parent ion,
(ii) retention of hydroxyl hydrogen and scrambling of remainder in parent ion,
(iii) complete scrambling in CD_3CHOH^+ intermediate,
(iv) retention of hydroxyl hydrogen and scrambling of remainder in CD_3CHOH^+ intermediate.

The experimental results are practically identical with the label distribution found for the isopropanol-d_6 and clearly are only in accord with model (iv). The formation of D_3O^+ in low abundance again probably represents a small amount of hydroxyl hydrogen exchange in the intermediate II.

In *s*-butanol-d_6 the intermediate CD_3CDOH^+ should lead only to HD_2O^+ by the mechanism proposed. The partial spectrum in Table III shows, as expected, the largest ion current at mass 21, however, the ion current at mass 22 (D_3O^+) indicates again some scrambling in the intermediate.

Formation of H_3O^+ from Ethyl Alcohol

Two reactions, [6] and [7], must be considered as possibilities for the formation of H_3O^+ from ethyl alcohol.

$$CH_3CH_2OH \rightarrow C_2H_3 + H_3O^+ \quad [6]$$

$$\rightarrow H + CH_3CHOH^+ \rightarrow C_2H_2 + H_3O^+ \quad [7]$$

The mass spectrum of ethyl alcohol shows an appreciable ion current for CH_3CHOH^+ and, in addition, a metastable ion at mass 8.02 (reaction [3]) corresponding to the second step in the overall reaction [7]. However, the measured appearance potential, 277 kcal/mole, leads to $\Delta H_f(H_3O^+) = 115$ kcal/mole assuming reaction [7] and 156 kcal/mole assuming reaction [6]. The agreement of this latter value with the values obtained from the secondary alcohols indicates quite conclusively that the lowest energy process occurring is reaction [6]. Reaction [7], which is of higher energy requirement, is shown to occur by the metastable transition at mass 8.02. Attempts were made to detect breaks in the ionization efficiency curve by the method of Morrison (25). Although a rather large initial curvature was observed, no definite breaks could be identified.

In an attempt to obtain information on the relative importance of reactions [6] and [7] the mass spectrum of CH_3CD_2OH was examined. As has been found previously (26, 27), the mass 45 moves exclusively to mass 46, indicating loss of the α-deuterium. The observed spectrum in the region of the hydronium ion (Table V) is in reasonable agreement with

TABLE V

Partial mass spectra of CH_3CH_2OH and CH_3CD_2OH*

Mass	Ion	CH_3CH_2OH	CH_3CD_2OH (this work)	CH_3CD_2OH (ref. (26))
19	H_3O^+	1.37	0.40	0.47
20	H_2DO^+		0.46	0.49
21	HD_2O^+		0.05	0.06
45	CH_3CHOH^+	16.13		
46	CH_3CDOH^+		10.70	8.71

*Intensities as percentage of total ionization.

that reported by Momigny (26). The appearance potentials for H_3O^+ and H_2DO^+ were 273±3 and 274±3 kcal/mole respectively, in good agreement with the value of 277

Can. J. Chem. Downloaded from www.nrcresearchpress.com by 210.87.254.40 on 09/05/12
For personal use only.

kcal/mole obtained for the undeuterated alcohol. The relative intensities for H_3O^+ and H_2DO^+ are close to that expected for decomposition of the CH_3CDOH^+ intermediate; the small amount of D_2HO^+ must originate by reaction [6]. No significant variation of the ratio H_3O^+/H_2DO^+ was observed as the electron energy was decreased to near the threshold. This probably means that the label distributions obtained from reactions [6] and [7] do not differ significantly. On the basis of the present evidence we cannot assess the relative importance of the two reactions.

Formation of H_3O^+ from n-Propyl Alcohol

The mass spectrum of *n*-propyl alcohol shows only a very small ion current for mass 45 and no metastable corresponding to reaction [3]. The following three reactions must be considered.

$$CH_3CH_2CH_2OH \rightarrow C_3H_5 + H_3O^+ \quad [8]$$

$$\rightarrow C_3H_4 + H + H_3O^+ \quad [9]$$

$$\rightarrow C_3H_3 + H_2 + H_3O^+ \quad [10]$$

The measured appearance potential, $A(H_3O^+) = 292 \pm 3$ kcal/mole leads to $\Delta H_f(H_3O^+) =$ 199 kcal/mole assuming [8], 144 kcal/mole assuming [9] and 155 kcal/mole assuming [10]. Although reaction [10] appears rather unlikely, it gives the best fit for $\Delta H_f(H_3O^+)$ and is, accordingly, the reaction chosen.

Formation of H_3O^+ from Diethyl Ether

The H_3O^+ ion is of moderate abundance (0.8% of total ionization) in the mass spectrum of diethyl ether. A sizeable ion current at mass 45 and a metastable at mass 8.02 (reaction [3]) suggested decomposition through the mass 45 intermediate. $A(H_3O^+) = 304$ kcal/mole leads to $\Delta H_f(H_3O^+) = 164$ kcal/mole assuming reaction [11].

$$C_2H_5OC_2H_5 \rightarrow C_2H_5 + C_2H_2 + H_3O^+ \quad [11]$$

If this reaction is the only one contributing to H_3O^+ formation it must be responsible for the metastable transition, thus suggesting that the mass 45 is $C_2H_5O^+$ formed with C_2H_5 as the neutral fragment. It is probable, however, that the majority of the mass 45 ions are formed by the rearrangement reaction indicated below (28).

$$CH_2{-}CH_2O{-}CH{-}CH_3 \rightarrow H + C_2H_4 + HO\overset{+}{C}HCH_3 \quad [12]$$

The appearance potential of mass 45 was found to be 272 ± 3 kcal/mole in the present work, which leads to an ionic heat of formation of 147 ± 3 kcal/mole, assuming reaction [12], in excellent agreement with best estimates of $\Delta H_f(CH_3CHOH^+) = 145$ kcal/mole derived from simple alcohols. This indicates that reaction [12] is the lowest energy process producing mass 45 and, since decomposition of CH_3CHOH^+ is known to produce H_3O^+ (see above), we conclude that reaction [13], which is of higher energy requirement than reaction [12], also contributes to H_3O^+ formation.

$$C_2H_5OC_2H_5 \rightarrow H + C_2H_4 + C_2H_2 + H_3O^+ \quad [13]$$

Formation of H_3O^+ from Ethyl Formate

The H_3O^+ ion is approximately 1.2% of the total ionization in ethyl formate. In the present work $A(H_3O^+)$ was found to be 302 ± 3 kcal/mole, considerably lower than the value of 334 kcal/mole reported by Bernecker and Long (12). Reactions [14] to [16] must be considered in a discussion of these results.

Can. J. Chem. Downloaded from www.nrcresearchpress.com by 210.87.254.40 on 09/05/12
For personal use only.

$$HCOOC_2H \rightarrow C_2H_3 + CO + H_3O^+ \quad [14]$$

$$\rightarrow C_2H_2 + HCO + H_3O^+ \quad [15]$$

$$\rightarrow C_2H_2 + H + CO + H_3O^+ \quad [16]$$

Table VI records the values calculated for $\Delta H_f(H_3O^+)$ for each of these reactions using

TABLE VI

Appearance potential and calculated $\Delta H_f(H_3O^+)$ in ethyl formate

	$A(H_3O^+)$ (kcal/mole)	$\Delta H_f(H_3O^+)$ (kcal/mole)		
		Reaction [14]	Reaction [15]	Reaction [16]
This work	302	175	159	133
Bernecker and Long	334	207	191	166

both our result and that of Bernecker and Long. It is apparent that the present result gives a satisfactory ionic heat of formation only if reaction [15] is assumed to be the lowest energy process occurring. Reaction [14], which was assumed by Bernecker and Long, does not give results in agreement with other estimates in the present work. The ionization efficiency curve showed a rather large tailing, suggesting that more than one reaction was occurring, and it is possible that Bernecker and Long's appearance potential corresponds to reaction [16].

The mass spectrum of ethyl formate shows a large mass 45 ion current and a metastable at mass 8.02 (reaction [3]). The mass spectrum of ethyl formate-*d* (14) shows that approximately 65% of the mass 45 ion incorporates the formyl hydrogen to give CH_3CHOD^+. In addition, in ethyl formate-*d* a metastable was observed at mass 8.70 indicating the transition

$$DOCHCH_3^+ \rightarrow H_2DO^+ + C_2H_2. \quad [17]$$

Since the mass spectrum of ethyl formate-*d* shows predominantly H_2DO^+ formation (1.2% compared to 0.3% H_3O^+), and since it has been established (14) that the ion CH_3CHOD^+ is formed with H+CO as the neutral fragment, it was thought that the DH_2O^+ formation should give a measure of the fraction of the reaction proceeding by reaction [16]. However, the appearance potential of DH_2O^+ was found to be 306±3 kcal/mole compared to 302±3 kcal/mole for H_3O^+ from the undeuterated ester. One must therefore assume HCO+C_2H_2 (reaction [15]) as the neutral fragments. Obviously, incorporation of the formyl hydrogen in the H_3O^+ ion with formation of HCO as one of the neutrals must involve considerable hydrogen scrambling in the parent ion. The mechanism by which this occurs is unknown.

Formation of H_3O^+ from Isopropyl Formate

The largest peak in the mass spectrum of isopropyl formate is mass 45. In isopropyl formate-*d* the peak moves to mass 46 indicating retention of the formyl hydrogen (14). The rearrangement is given by reaction [18]:

$$HCOOCH(CH)_2 \rightarrow CO + CH_3 + HOCHCH_3^+ \quad [18]$$

The mass spectrum of isopropyl formate also shows a metastable at mass 8.02, moving to mass 8.70 in the formate-*d*. The complete reaction for formation of H_3O^+ would thus appear to be reaction [19] proceeding through the CH_3CHOH^+ intermediate.

$$HCOOCH(CH_3) \rightarrow CO + CH_3 + C_2H_2 + H_3O^+ \quad [19]$$

Can. J. Chem. Downloaded from www.nrcresearchpress.com by 210.87.254.40 on 09/05/12
For personal use only.

$A(H_3O^+) = 317 \pm 3$ kcal/mole leads to $\Delta H_f(H_3O^+) = 159$ kcal/mole assuming this mechanism, in good agreement with other results obtained in this work.

In isopropyl formate-*d* the intermediate hydroxycarbinyl ion contains the formyl deuterium probably attached to the oxygen, i.e. $DOCHCH_3^+$. The labelling results for the secondary alcohols were explained on the basis of retention of the hydroxyl hydrogen in the decomposition of this intermediate. In the present case this should lead exclusively to DH_2O^+ formation. The mass spectrum of isopropyl formate-*d* shows (14) the relative intensities mass 20:mass 19 = 1.86:0.34. It is clear that the major part of the hydronium ion does incorporate the deuterium label as required. The small amount of H_3O^+ probably again represents a small amount of scrambling in the intermediate ion.

SUMMARY

The present results lead to an average value $\Delta H_f(H_3O^+) = 157 \pm 3$ kcal/mole yielding a value of 151 ± 3 kcal/mole for the proton affinity of water. The value of 157 kcal/mole for $\Delta H_f(H_3O^+)$ is considerably higher than the maximum value of 145 kcal/mole indicated by the reported occurrence (4) of the ion–molecule reaction

$$H_2S^+ + H_2O \rightarrow H_3O^+ + HS. \quad [1]$$

The reason for this discrepancy is not obvious. The mechanisms proposed for most of the decomposition reactions in the present work appear to be well substantiated by metastable and labelling evidence. The appearance potentials and resultant ionic heats of formation are therefore not likely to be in error unless excess energy is involved in each ionization process. This would necessitate the same amount of excess energy in each case, and thus appears unlikely. The ion–molecule reactions occurring in the high-pressure mass spectrum of H_2O–H_2S mixtures are numerous and include (4) reactions [20] and [21] in addition to reaction [1].

$$H_2O^+ + H_2S \rightarrow H_3O^+ + HS \quad [20]$$

$$H_2O^+ + H_2O \rightarrow H_3O^+ + OH \quad [21]$$

In these circumstances it is not clear that it has been clearly established that reaction [1] involves an H_2S^+ ion in the ground state. Reaction of an H_2S^+ ion with a minimum of 12 kcal/mole excitational energy could lead to H_3O^+ formation even if reaction of a ground state ion were endothermic.

In any event, the present results combined with the results of Tal'roze and Frankevich (4) clearly indicate that $\Delta H_f(H_3O^+)$ is in the range 145–157 kcal/mole rather than 207 kcal/mole, as had been suggested by previous electron impact work (12).

ACKNOWLEDGMENTS

The authors are indebted to the Advisory Committee on Scientific Research, University of Toronto, and to the National Research Council of Canada for financial support.

REFERENCES

1. R. P. Bell. The proton in chemistry. Cornell University Press, Ithaca, N.Y. 1959.
2. J. Sherman. Chem. Rev. **11**, 164 (1932).
3. S. I. Vetchinkin, E. I. Pshenichnov, and N. D. Sokolov. J. Phys. Chem. Moscow, **33**, 1269 (1959).
4. V. L. Tal'roze and E. L. Frankevich. Dokl. Akad. Nauk SSSR, **111**, 376 (1956).
5. T. F. Palmer and F. P. Lossing. J. Am. Chem. Soc. **84**, 4661 (1962).
6. A. P. Gifford, S. M. Rock, and P. J. Comaford. Anal. Chem. **21**, 1026 (1949).
7. J. Collin. Bull. Soc. Roy. Sci. Liege, **23**, 377 (1954).
8. R. A. Friedel, J. C. Shultz, and A. G. Sharkey. Anal. Chem. **28**, 926 (1956).
9. J. H. Beynon, R. A. Saunders, and R. E. Williams. Anal. Chem. **33**, 221 (1961).
10. M. M. Mann, A. Hustrulid, and J. T. Tate. Phys. Rev. **58**, 340 (1940).

Can. J. Chem. Downloaded from www.nrcresearchpress.com by 210.87.254.40 on 09/05/12
For personal use only.

11. F. H. FIELD and J. L. FRANKLIN. Electron impact phenomena and the properties of gaseous ions. Academic Press, New York. 1957.
12. R. R. BERNECKER and F. A. LONG. J. Phys. Chem. **65**, 1565 (1961).
13. A. G. HARRISON and T. W. SHANNON. Can. J. Chem. **40**, 1730 (1962).
14. D. VAN RAALTE and A. G. HARRISON. Can. J. Chem. **41**, 2054 (1963).
15. J. H. S. GREEN. Quart. Rev. London, **15**, 125 (1961).
16. T. L. COTTRELL. The strengths of chemical bonds. Butterworths, London. 1958.
17. D. P. STEVENSON. Disc. Faraday Soc. **10**, 35 (1951).
18. B. STEINER, C. F. GIESE, and M. G. INGHRAM. J. Chem. Phys. **34**, 189 (1961).
19. J. COLLIN and F. P. LOSSING. J. Am. Chem. Soc. **79**, 5848 (1957).
20. J. D. COX. Tetrahedron, **18**, 1337 (1962).
21. L. FRIEDMAN and J. TURKEVICH. J. Am. Chem. Soc. **74**, 1666 (1952).
22. F. E. CONDON. J. Am. Chem. Soc. **73**, 4675 (1951).
23. W. H. MCFADDEN, M. LOUNSBURY, and A. L. WAHRHAFTIG. Can. J. Chem. **36**, 990 (1958).
24. J. H. BEYNON. Mass spectrometry and its application to organic chemistry. Van Nostrand, Princeton, N.J. 1960.
25. J. D. MORRISON. J. Chem. Phys. **27**, 1767, 2090 (1953).
26. J. MOMIGNY. Bull. Soc. Roy. Sci. Liege, **24**, 111 (1955).
27. J. G. BURR. J. Am. Chem. Soc. **79**, 751 (1957).
28. F. W. MCLAFFERTY. Anal. Chem. **29**, 1782 (1957).
29. L. FRIEDMAN, F. A. LONG, and M. WOLFSBERG. J. Chem. Phys. **27**, 613 (1957).

Can. J. Chem. Downloaded from www.nrcresearchpress.com by 210.87.254.40 on 09/05/12
For personal use only.

AROMATIC SUBSTITUTION

PART V.[1] THE MECHANISM OF THE REACTION OF PHENYLLITHIUM WITH PYRIDINES. DEUTERIUM ISOTOPE EFFECT STUDIES

R. A. ABRAMOVITCH AND CHOO-SENG GIAM
Department of Chemistry, University of Saskatchewan, Saskatoon, Saskatchewan
Received May 17, 1963

ABSTRACT

The ratios of isomers formed in the reaction of 3-alkylpyridines with phenyllithium under various conditions appear to be invariant within the limits of experimental error. A number of experiments, including the reaction of phenyllithium with 3-picoline-2*d* and with an excess of a mixture of pyridine and pyridine-2*d*, are described which establish that the hydride ion elimination stage in these nucleophilic aromatic substitutions is not important in determining the observed orientation and that the addition stage is either virtually irreversible or that the equilibrium lies far on the product side and is not rapidly reversible. A convenient new procedure is described for working up the reaction mixtures.

Can. J. Chem. Downloaded from www.nrcresearchpress.com by 210.87.254.5 on 09/05/12
For personal use only.

In previous parts of this series (1, 2) the reaction of 3-substituted pyridines with phenyllithium has been studied, particular emphasis being placed upon the determination of the orientation of the entering phenyl group and the isomer ratios. It was shown that in the case of most 3-substituents the main product formed was the 2,3-disubstituted pyridine derivative, the 2,5-isomer usually being formed in lesser amounts. In no case was any attack at C_4 of the pyridine ring observed. A number of possible explanations for the observed orientation were considered (1). Among other possibilities it was pointed out that if the second stage in these reactions, the elimination of hydride ion, is rate-determining, and *if it is assumed that the addition step is rapidly reversible* the results might be explained as follows (3-picoline is taken as an example):

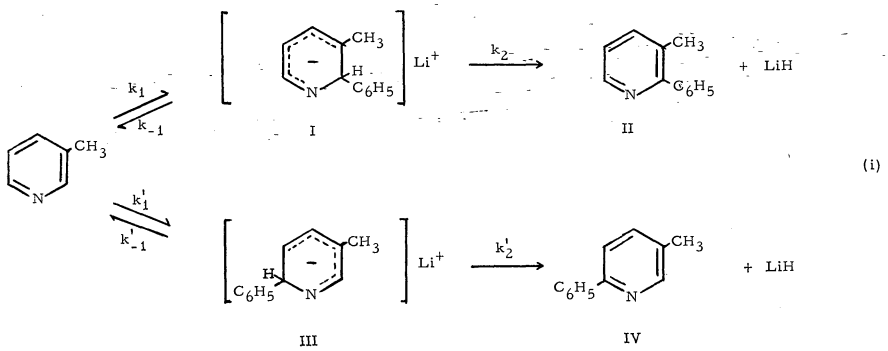

The aromatization step in (i) probably involves the abstraction by the lithium cation of the hydrogen atom with its bonding pair of electrons. The energy of activation for this step would probably be lowered more by an electron-repelling ortho-methyl than by a para-methyl group. This effect might well be greater than the opposing steric effect favoring hydride expulsion from III over that from I.* If this is so, k_2 would be greater

[1]*Part IV: R. A. Abramovitch, W. A. Hymers, J. B. Rajan, and R. Wilson. Tetrahedron Letters, 1507 (1963).*
**If the transition state resembles product there would be appreciable 1,2-alkyl:phenyl repulsion in the case of I → II.*

than k_2' and more II would be formed than IV even though K_1' were greater than K_1, provided the addition step is rapidly reversible. It is to be noted that whereas the addition step is exothermic, heat is required to cause the elimination to take place. In addition, the formation of intermediates such as (I) and (III) finds support in the oxidation of the pyridine–phenyllithium adduct with benzophenone (3), when a by-product, probably 4-diphenylhydroxymethyl-2-phenylpyridine (V), is also formed. This presumably arises by the addition of the 2-phenyl-1,2-dihydropyridyllithium intermediate to benzophenone followed by oxidation and a molecular rearrangement (3).

In order to test the above possibility the reactions of phenyllithium with deuterated pyridine and deuterated picoline were examined. Before doing so, however, it was decided to re-examine the ratios of isomers formed in the reaction between phenyllithium and a 3-alkylpyridine when the phenyllithium solution was added to an excess of the 3-alkylpyridine (which was, therefore, always present in excess throughout the reaction) instead of the other way around (when phenyllithium was present in excess, at least in the initial stages). In this way, it was hoped to get a better indication if possible of the relative discrimination of the attacking reagent towards C_2 and C_6. The results are summarized in Table I. The reaction mixtures were worked up in the usual way by heating with

TABLE I

Addition of phenyllithium to an excess of 3-R-pyridine

R	Overall yield* of phenyl-3-R-pyridine (%)	Ratio of 2,3- to 2,5-isomer
CH_3	48	94:6
C_2H_5	42	87:13
iso-C_3H_7	32	76:24
H	26.7†	—
CH_3	25.6†	96:4
C_2H_5	13.6†	89:11
CH_3	33.8‡	95:5
C_2H_5	23.4‡	87:13

*Based on phenyllithium.
†In the presence of an excess of lithium bromide.
‡Using halide-free phenyllithium.

toluene at ca. 110°. The ratios of the 2,3- to the 2,5-phenylalkylpyridines are the same, within experimental error, as those obtained when the addition was carried out in the reverse order (1).

During the course of this work a much more convenient procedure for the working up of the reaction mixture resulting from the addition of an organo-lithium compound to pyridines was developed. After the addition was completed and the mixture had been stirred at room temperature for varying lengths of time dry oxygen was slowly bubbled through the ethereal suspension: oxidation of the dihydropyridyllithium intermediate occurred readily (3) to give the required reaction products and probably lithium hydroxide. The isomer ratios were essentially unchanged, but the overall yields of products are usually somewhat higher—this may well be due to the fact that extensive polymerization of the dihydropyridyllithium intermediate takes place, particularly when it is heated.

The isomer ratio for the addition of phenyllithium to 3-picoline also remained unchanged when the reaction was carried out in dry light petroleum or in dry benzene instead of in ether. When an ethereal solution of the 3-picoline–phenyllithium adduct was stirred at room temperature for various intervals of time (from 6 to 90 hours) before being worked up, again no change in the isomer ratio was observed but the yield of products rose from

Can. J. Chem. Downloaded from www.nrcresearchpress.com by 210.87.254.5 on 09/05/12
For personal use only.

20.5 to 42.9%. The reactions with 3-picoline and with 3-ethylpyridine with phenyllithium in ether were also carried out in the presence of an excess of anhydrous lithium bromide. The reactions appeared to proceed more slowly under these conditions (as indicated by the evolution of heat) than when one equivalent of lithium bromide was present (which normally arises from the method of preparation of phenyllithium using bromobenzene and lithium in dry ether), and the overall yields of products were somewhat lower; on the other hand, the 2,3- to 2,5-isomer ratios were unchanged within the limits of accuracy of the experiments (±2%). Finally, the reactions were carried out using halide-free phenyllithium from diphenylmercury and lithium metal (6): once again the isomer ratios remained constant.

In order to test whether the possible reversibility of the addition step had any influence upon the isomer ratios observed, the reaction of phenyllithium with an excess of 3-picoline was interrupted by the addition of water after only a small percentage of the addition had occurred. The 1,2-dihydrophenylpicolines (VI) and (VII) thus formed (4) cannot revert to starting material and, if oxidized, should give the isomeric phenylpicolines in a ratio indicative of the actual orientation in the addition step. Thus, one might then expect that if equations (i) hold and $K_1' > K_1$ (the inductive effect of the methyl group would render attack at C_6 more likely than at C_2) one would get more 2,5- than 2,3-isomer. When the suspension of the dihydropyridines obtained after treatment with water was either oxidized directly with chloranil (5) or extracted with ether and the ethereal extract oxidized and the products analyzed by gas chromatography, the ratio of 3-methyl-2-phenylpyridine to 5-methyl-2-phenylpyridine was still found to be about 94:6. These results would indicate that the addition reactions are virtually irreversible, or that the equilibria as in (i) lie far on the side of the addition products and that equilibration of I and III via starting material is so slow as not to be of importance here.

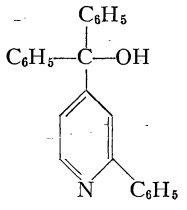

V

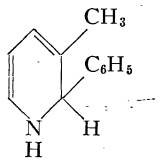

VI

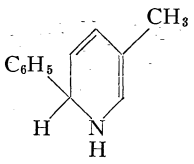

VII

This has been confirmed in two ways. The importance of the hydride ion elimination step upon the orientation of the products formed was determined by measuring the ratio of isomers formed in the reaction of halide-free phenyllithium with 3-picoline-2*d*. Since k_H/k_D in hydride ion eliminations is of the order of 1.8–2.6 (7) then if scheme (i) is applicable one would expect the 2,3- to 2,5-isomer ratio to be substantially higher with 3-picoline than when 3-picoline-2*d* was used. This was not found to be the case, the observed isomer ratio being 95:5 in both cases (under otherwise identical conditions). It is clear, therefore, that the rate of hydride ion elimination is not important in determining the observed orientation.

Finally, an excess of a mixture of pyridine and pyridine-2*d* was allowed to react with a small amount of phenyllithium in the presence of an excess of anhydrous lithium bromide. Unreacted pyridine–pyridine-2*d* mixture was recovered from this competitive reaction and analyzed for pyridine-2*d* using an infrared spectroscopic method (see Experimental). A blank run was carried out using identical conditions except that the phenyllithium was

Can. J. Chem. Downloaded from www.nrcresearchpress.com by 210.87.254.5 on 09/05/12
For personal use only.

left out; the concentration of the pyridine-2*d* in the recovered pyridine–pyridine-2*d* mixture was taken as the "original" concentration in the actual runs. Since the hydride ion elimination step is the slow step in scheme (i) and k_H/k_D should be about 2, one would expect the recovered mixture of starting materials to contain a larger proportion of pyridine-2*d* than it did initially—provided the addition step is readily reversible. In actual practice, the composition of the recovered pyridine–pyridine-2*d* was no different from the initial one.

There seems to be no doubt, therefore, that the second stage in the reactions of phenyllithium with 3-alkylpyridines, namely the elimination of hydride ion does not decide the 'abnormal' orientations observed (1) in these reactions, and that the first step, the addition giving rise to a dihydrophenylpyridyllithium intermediate is not readily reversible. It has been assumed, and the present results, showing the constancy of the isomer ratios produced under various conditions, seem to bear out amply, that there is no, or almost no, selective removal of the isomeric dihydropyridyllithium intermediates due to disproportionation and (or) polymerization but that both isomers undergo these side-reactions at virtually the same rate. It is hoped to submit more evidence supporting this point soon. One must look elsewhere for an explanation of the orienting influence of alkyl groups in such nucleophilic substitution reactions.

EXPERIMENTAL

Starting Pyridines

Commercial 2° pyridine (Reilly Tar and Chemical Co.) was dried (KOH) and fractionally distilled, the fraction, b.p. 110–112° at 720 mm being used. Commercial synthetic 3-picoline was similarly treated; the fraction, b.p. 138–140° at 720 mm was used.

3-Ethylpyridine, b.p. 165–166° at 720 mm, was obtained in 80–87% yield by the reduction of 3-acetylpyridine with hydrazine hydrate and potassium hydroxide according to the procedure of Fand and Lutomski (8). 3-Isopropylpyridine was prepared as described previously (1).

"Ordinary" Phenyllithium

This was prepared as usual and its concentration estimated by titration with 0.1 *N* hydrochloric acid using methyl orange as indicator.

Halide-free Phenyllithium (6)

Diphenylmercury (3.6 g) was added with stirring to a suspension of finely cut lithium (0.4 g) in anhydrous ether (75 ml) under dry, oxygen-free, nitrogen. The mixture was stirred vigorously at room temperature for 24 hours, the clear supernatant liquid was decanted under nitrogen through glass wool, and the clear solution was analyzed for phenyllithium content by acid titration.

Ethereal solutions of anhydrous lithium bromide were prepared either from lithium and 1,2-dibromoethane in ether solution (9) or by dehydrating 'anhydrous' lithium bromide ($LiBr,xH_2O$; Matheson, Coleman, and Bell) at 155° at 1 mm for 12 hours, dissolving it in dry ether and decanting the supernatant liquid from some insoluble material. In either case, the concentration of bromide was determined by Volhard titration.

Addition of Phenyllithium to an Excess of a 3-Alkylpyridine

The procedure will be described only for the case of 3-picoline.

(a) The toluene method.—A solution of 3-picoline (2.79 g, 0.03 moles) in dry ether (25 ml) was treated dropwise and with vigorous stirring in a nitrogen atmosphere with an ethereal solution of phenyllithium (12.5 ml ≡ 0.01 moles of phenyllithium). At the end of the addition the ether was distilled and simultaneously replaced with dry toluene. The mixture was then boiled gently under reflux for 6.5 hours, cooled, treated with water, made strongly alkaline with potassium hydroxide, and extracted with several portions of ether. The ethereal extracts were washed with concentrated hydrochloric acid and the aqueous acid layer was basified and extracted with ether. The combined ether extracts were dried (KOH), evaporated, and analyzed by gas chromatography. The columns, conditions, retention times, and identification of the various peaks have already been described in detail (1).

(b) The oxygen method.—The addition of phenyllithium solution (8.5 ml ≡ 0.01 moles) to 3-picoline (2.79 g, 0.03 moles) was carried out as before. At the end of the addition, the reaction mixture was boiled gently under reflux for 30 minutes and cooled, and oxygen gas was bubbled through until a white suspension had formed. The mixture was then treated with water and worked up as under (*a*) above. The combined yield of 3-methyl- and 5-methyl-2-phenylpyridine was 57% and the molar ratio of these two isomers was 95:5.

Can. J. Chem. Downloaded from www.nrcresearchpress.com by 210.87.254.5 on 09/05/12
For personal use only.

(c) In the presence of an excess of lithium bromide.—The procedure was essentially the same as that described under (*a*) or (*b*), respectively, except that two molar equivalents of anhydrous lithium bromide in dry ether were added per mole of pyridine used. No appreciable evolution of heat was observed when the phenyllithium solution was added. Some typical results are summarized in Table I.

(d) Using halide-free phenyllithium.—The procedure was identical with that used under methods (*a*) or (*b*). A vigorous exothermic reaction took place when the phenyllithium solution was added to the pyridine. A few of the results are given in Table I.

Reaction of Halide-free Phenyllithium with 3-Picoline-2d

The addition of halide-free phenyllithium was carried out as described under (*a*) above except that 3-picoline-2*d* (10) (0.2 g, 0.0021 moles; 11.67 atom % D) was used. To this was added 0.001 moles of phenyllithium in dry ether. The yield of products was 18.6% and the ratio of 2,3- to 2,5-isomer was 95:5.

Oxidation of Dihydrophenylpicolines

(a) A solution of phenyllithium (0.023 moles) in ether (30 ml) was added dropwise with stirring under nitrogen to a solution of 3-picoline (5.58 g, 0.06 moles) in ether (10 ml), at such a rate that the temperature of the reaction mixture did not rise appreciably. It was then immediately cooled to −10°, treated cautiously with an excess of iced water, the ether layer separated, and the aqueous layer extracted with ether. The combined ether extracts were added with stirring to a solution of chloranil (14.6 g) in benzene (600 ml) and filtered. The residue was washed with ether and the combined washings and filtrate were concentrated down to a small volume (2 ml) and analyzed by gas chromatography. The combined yield of 3-methyl- and 5-methyl-2-phenylpyridine was 19.0%; the isomer ratio was 96:4.

(b) In this experiment the mixture obtained above after treatment with water was not extracted with ether but was treated directly with a benzene solution of chloranil and analyzed. The ratio of 2,3- to 2,5-isomer was 94:6 and the combined yield was 22.5%.

Reaction of Phenyllithium with Pyridine–Pyridine-2d Mixture

A solution of 'ordinary' phenyllithium (0.018 moles) in anhydrous ether (66 ml) was added dropwise at 24°, and under oxygen-free dry nitrogen to a well stirred solution of anhydrous lithium bromide (0.076 moles), pyridine (0.0179 moles), and pyridine-2*d* (10) (0.0201 moles) in anhydrous ether (150 ml). At the end of the addition, stirring was continued for another 2 hours, oxygen was bubbled through the mixture for 5–10 minutes, the suspension treated with an excess of water, and the mixture of recovered pyridine and pyridine-2*d* isolated and purified by preparative gas-chromatography on columns of silicone oil (25%) on Fisher Columnpak (60–80 mesh) at 70°. The mixture was then dried (KOH pellets) and distilled.

A blank run was carried out similarly except that the phenyllithium was omitted. The composition of the recovered pyridine–pyridine-2*d* was used for comparison with the recovered material from the actual runs.

The quantitative analyses for pyridine-2*d* were carried out by determining the infrared spectra of authentic mixtures of known concentration of pyridine and pyridine-2*d* (as pure liquids) in matched 1-mm fixed-thickness cells. A calibration curve for the pyridine-2*d* concentration was obtained by plotting log T (where T = % transmission) of the C—D stretching band at 2260 cm^{-1} against the corresponding known concentration of pyridine-2*d*, and was a straight line, thus making it unnecesssary to measure the areas under the C—D band.

In all runs, the composition of the recovered pyridine–pyridine-2*d* mixture was identical with that of the starting material.

ACKNOWLEDGMENTS

This work was carried out during the tenure (by C.-S. G.) of a National Research Council Studentship, and was supported financially by a grant from the National Research Council. Some preliminary experiments were carried out by Dr. B. Staskun.

REFERENCES

1. R. A. Abramovitch and Choo-Seng Giam. Can. J. Chem. **40**, 213 (1962).
2. (*a*) R. A. Abramovitch, Choo-Seng Giam, and A. D. Notation. Can. J. Chem. **38**, 761 (1960).
   (*b*) R. A. Abramovitch and A. D. Notation. Can. J. Chem. **38**, 1445 (1960).
   (*c*) R. A. Abramovitch, C-S. Giam, and K. S. Ahmed. Can. J. Chem. **41**, 1752 (1963).
3. R. A. Abramovitch and B. Vig. Can. J. Chem. **41**, 1961 (1963).
4. K. Ziegler and H. Zeiser. Ber. **63**, 1847 (1930).
5. E. A. Braude, J. Hannah, and R. Linstead. J. Chem. Soc. 3249, 3257 (1960).
6. G. Wittig, F. J. Meyer, and G. Lange. Ann. **571**, 167 (1951).
7. C. G. Swain, R. A. Wiles, and R. F. W. Bader. J. Am. Chem. Soc. **83**, 1945 (1961).
8. T. I. Fand and C. F. Lutomski. J. Am. Chem. Soc. **71**, 2931 (1949).
9. T. V. Talalaeva and K. A. Kocheshkov. Dokl. Akad. Nauk SSSR, **104**, 260 (1955); Chem. Abstr. **50**, 5446*a* (1956).
10. R. A. Abramovitch, D. G. Kroeger, and B. Staskun. Can. J. Chem. **40**, 2030 (1962).

Can. J. Chem. Downloaded from www.nrcresearchpress.com by 210.87.254.5 on 09/05/12
For personal use only.

Can. J. Chem. Downloaded from www.nrcresearchpress.com by 210.87.254.5 on 09/05/12
For personal use only.

NOTES

THE INFRARED AND RAMAN SPECTRA OF CYANOACETYLENE

V. A. Job and G. W. King

The infrared spectrum of cyanoacetylene H—C≡C—C≡N in the vapor, liquid, and solid phases has been investigated by Turrell, Jones, and Maki (1). They were able to assign five of the seven fundamental frequencies of the linear molecule to bands observed in the vapor phase spectrum. Of the two missing fundamentals, $\nu_4(\sigma^+)$ was assigned to a band of medium intensity observed at 875 cm^{-1} in the spectrum of the liquid; $\nu_7(\pi)$ was calculated to be 230 cm^{-1} from the observed combination bands, this frequency being beyond the range of the spectrometer employed in the work.

During the course of a study of the electronic spectrum of cyanoacetylene, we have measured the infrared and Raman spectra of both the hydrogenic and the deuterated compound. The results confirm and extend the assignments of the previous workers. We have also observed in the Raman spectrum the two fundamentals that are missing from the infrared spectrum of the vapor.

The cyanoacetylene was prepared from commercial propiolic acid by the method of Moureu and Bongrand (2), and subjected to repeated trap-to-trap distillation under vacuum until weak bands due to impurities had disappeared from the infrared spectrum. The deuterated compound was prepared by the repeated exchange of propiolamide in slightly alkaline D_2O and the subsequent dehydration of the deuterated propiolamide with phosphorous pentoxide (2). A sequence of 10 exchanges, with D_2O of 99.8% purity being used in the final stages, gave a product estimated to contain ~98% deuterocyanoacetylene from the infrared spectrum. Infrared spectra were recorded in the region 400–4000 cm^{-1} on a Perkin–Elmer model 21 spectrophotometer with CaF_2, NaCl, and KBr optics. The Raman spectrum of the liquid was excited by the filtered 4358 Å line emitted by a spiral Toronto type mercury arc and recorded with a Hilger double prism spectrograph type E612 on Kodak type IIaO photographic plates.

The observed frequencies and their assignments are given in Table I. At a vapor pressure of 290 mm Hg and an absorption path of 10 cm in the vapor, some of the combination bands observed by Turrell, Jones, and Maki only in the spectrum of liquid and solid HCCCN were obtained, as well as some additional weak combination bands which are definitely not due to impurities. A very weak parallel-type band observed at 885 cm^{-1} in the infrared spectrum of HCCCN vapor could possibly be the $\nu_4(\sigma^+)$ fundamental, but a corresponding band was not observed in the DCCCN spectrum and the assignment as the combination $\nu_5+\nu_7$ appears more plausible. The product rule ratios agree well with the theoretical values calculated from the moments of inertia of the molecule (3). The ratios are 1.39 (obs.) and 1.40 (calc.) for the σ^+ stretching vibrations and 1.35 (obs.) and 1.35 (calc.) for the π bending vibrations.

We wish to thank Dr. K. Ramaswamy for assistance in recording the Raman spectra, Dr. R. H. Tomlinson for supplying the deuterium oxide, and the Ontario Research Foundation for financial support.

TABLE I

Observed frequencies (cm^{-1}) and assignments of cyanoacetylene

H—C≡C—C≡N		D—C≡C—C≡N			
Infrared (vapor)	Raman (liquid)	Infrared (vapor)	Raman (liquid)	Assignment	
3979 m ⊥				$\nu_1+\nu_5$	
3549 w ⊥				$\nu_1+\nu_7$	
3386 w ∥				$\nu_3+2\nu_5$	
3328 vs ∥	3256* m	2608 s ∥		ν_1	CH stretch
3136 w ∥	3134* vw	3108 w ∥		$\nu_2+\nu_4$	
3107 w ⊥				$\nu_1-\nu_7$	
2767 w ⊥		2739 w ⊥		$\nu_2+\nu_6$	
2666 w ⊥				$\nu_1-\nu_5$	
2576 w ⊥		2458 w ⊥		$\nu_3+\nu_6$	
2494 w ⊥				$\nu_2+\nu_7$	
2271 s ∥	2270 vs	2250 s ∥	2245 vs	ν_2	CN stretch
2078 m ∥	2070 s	1968 s ∥	1952 s	ν_3	C≡C stretch
1314 s ∥		1045 s ∥		$2\nu_5$	
		1015 m ∥		$\nu_5+\nu_6$	
1010 w ∥	1023 m			$2\nu_6$	
885 vw ∥		732 m ∥		$\nu_5+\nu_7$	
	877 s		860 m	ν_4	C—C stretch
720 m ∥		702 m ∥		$\nu_6+\nu_7$	
663 vs ⊥	684 s	522 s ⊥	~545* w	ν_5	CCH bend
500 s ⊥	502 s	494 s ⊥	~498 m	ν_6	CCN bend
	472 vw			$2\nu_7$	
	230 s		219 w	ν_7	CCC bend

NOTE: v = very; s = strong; m = medium; w = weak; ∥ = parallel-type band; ⊥ = perpendicular-type band; * = diffuse.

1. G. C. TURRELL, W. D. JONES, and A. MAKI. J. Chem. Phys. **26**, 1544 (1957).
2. C. MOUREU and J. C. BONGRAND. Ann. Chim. (Paris), 9e Sér., **14**, 5 (1920).
3. A. A. WESTENBERG and E. B. WILSON, JR. J. Am. Chem. Soc. **72**, 199 (1950).

RECEIVED JULY 31, 1963.
DEPARTMENT OF CHEMISTRY,
MCMASTER UNIVERSITY,
HAMILTON, ONTARIO.

METHYL α-FURANOSIDE DERIVATIVES OF FULLY METHYLATED GALACTOSE AND GALACTURONIC ACID

H. G. WALKER, JR., AND R. M. MCCREADY

It was noted earlier that direct *O*-methylation of D-galactose or D-galacturonic acid by the Kuhn procedure (1) (silver oxide and methyl iodide in dimethyl formamide) gives predominantly α-furanoside product (2). This statement was based on the fact that the main product isolated by gas–liquid chromatography (GLC), was a strongly positive rotating substance whose retention volume did not correspond with that of the α-pyranoside derivative. Hydrolysis of the fully *O*-methylated galactoside gave a substance with a negative rotation similar to that reported for the fully *O*-methylated α-β-D-galactofuranose. In the present work, the furanose structure of the products was confirmed by chemical means.

The fully *O*-methylated β-furano- and α- and β-pyrano derivatives of both D-galactose

Can. J. Chem. Downloaded from www.nrcresearchpress.com by 210.87.254.5 on 09/05/12
For personal use only.

TABLE I

Observed frequencies (cm^{-1}) and assignments of cyanoacetylene

H—C≡C—C≡N		D—C≡C—C≡N			
Infrared (vapor)	Raman (liquid)	Infrared (vapor)	Raman (liquid)	Assignment	
3979 m ⊥				$\nu_1+\nu_5$	
3549 w ⊥				$\nu_1+\nu_7$	
3386 w ∥				$\nu_3+2\nu_5$	
3328 vs ∥	3256* m	2608 s ∥		ν_1	CH stretch
3136 w ∥	3134* vw	3108 w ∥		$\nu_2+\nu_4$	
3107 w ⊥				$\nu_1-\nu_7$	
2767 w ⊥		2739 w ⊥		$\nu_2+\nu_6$	
2666 w ⊥				$\nu_1-\nu_5$	
2576 w ⊥		2458 w ⊥		$\nu_3+\nu_6$	
2494 w ⊥				$\nu_2+\nu_7$	
2271 s ∥	2270 vs	2250 s ∥	2245 vs	ν_2	CN stretch
2078 m ∥	2070 s	1968 s ∥	1952 s	ν_3	C≡C stretch
1314 s ∥		1045 s ∥		$2\nu_5$	
		1015 m ∥		$\nu_5+\nu_6$	
1010 w ∥	1023 m			$2\nu_6$	
885 vw ∥		732 m ∥		$\nu_5+\nu_7$	
	877 s		860 m	ν_4	C—C stretch
720 m ∥		702 m ∥		$\nu_6+\nu_7$	
663 vs ⊥	684 s	522 s ⊥	~545* w	ν_5	CCH bend
500 s ⊥	502 s	494 s ⊥	~498 m	ν_6	CCN bend
	472 vw			$2\nu_7$	
	230 s		219 w	ν_7	CCC bend

NOTE: v = very; s = strong; m = medium; w = weak; ∥ = parallel-type band; ⊥ = perpendicular-type band; * = diffuse.

1. G. C. TURRELL, W. D. JONES, and A. MAKI. J. Chem. Phys. **26**, 1544 (1957).
2. C. MOUREU and J. C. BONGRAND. Ann. Chim. (Paris), 9e Sér., **14**, 5 (1920).
3. A. A. WESTENBERG and E. B. WILSON, JR. J. Am. Chem. Soc. **72**, 199 (1950).

RECEIVED JULY 31, 1963.
DEPARTMENT OF CHEMISTRY,
MCMASTER UNIVERSITY,
HAMILTON, ONTARIO.

METHYL α-FURANOSIDE DERIVATIVES OF FULLY METHYLATED GALACTOSE AND GALACTURONIC ACID

H. G. WALKER, JR., AND R. M. MCCREADY

It was noted earlier that direct *O*-methylation of D-galactose or D-galacturonic acid by the Kuhn procedure (1) (silver oxide and methyl iodide in dimethyl formamide) gives predominantly α-furanoside product (2). This statement was based on the fact that the main product isolated by gas–liquid chromatography (GLC), was a strongly positive rotating substance whose retention volume did not correspond with that of the α-pyranoside derivative. Hydrolysis of the fully *O*-methylated galactoside gave a substance with a negative rotation similar to that reported for the fully *O*-methylated α-β-D-galactofuranose. In the present work, the furanose structure of the products was confirmed by chemical means.

The fully *O*-methylated β-furano- and α- and β-pyrano derivatives of both D-galactose

Can. J. Chem. Downloaded from www.nrcresearchpress.com by 210.87.254.40 on 09/05/12
For personal use only.

and D-galacturonic acid are well known (3, 4). Greene and Pacsu prepared pure methyl 2,3,5,6-α-D-galactofuranoside (5), but preparation of the fully *O*-methylated derivative has not been reported subsequently. The specific rotations of the new compounds, methyl 2,3,5,6-tetra-*O*-methyl-α-D-galactofuranoside (I) and methyl (methyl 2,3,5-tri-*O*-methyl-α-D-galactofuranoside) uronate (II) are reported in Table I, along with that of methyl 2,3,5,6-tetra-*O*-methyl-β-D-galactofuranoside (III) as determined during this study.

TABLE I

Specific rotations of fully *O*-methylated furanoside derivatives

Compound	Rotation[a]
Methyl 2,3,5,6-tetra-*O*-methyl-α-D-galactofuranoside (I)	+108.2
Methyl (methyl 2,3,5-tri-*O*-methyl-α-D-galactofuranoside) uronate (II)	+82.3
Methyl 2,3,5,6-tetra-*O*-methyl-β-D-galactofuranoside (III)	−104.5[b]

[a]All rotations measured in H_2O in a 1-dm tube at 25°. Compound I, C = 1.97; II, C = 2.05; III, C = 1.80.
[b]Reported: −45.2 (*c* 1.42 H_2O), see ref. 7.

The values in Table I were obtained from samples isolated by preparative scale GLC. It is believed that II and III are essentially pure. Analytical scale GLC and thin layer chromatography on silica gel G (TLC) (6), show that I may contain 1–2% of isomeric β-pyranoside impurity. Hydrolysis of I and III leads to the same 2,3,5,6-tetra-*O*-methyl-α,β-D-galactofuranose. Previous data on III would indicate contamination with isomeric impurities (7).

The relationship between I and II was established by reducing and remethylating II to give a product identical with I by GLC and TLC. To confirm the furanose structure, II was converted to the known *N*-methyl-bis-amide of 2,3,5-tri-*O*-methyl mucic acid (4).

Room temperature nuclear magnetic resonance spectral measurements (n.m.r.) on I and III did not reveal useful anomeric conformational information, because of lack of splitting of the resonance from the C-1 proton. Presumably, the methoxyl groups on the furanose ring are not bulky enough to fix the conformation rigidly.

Mass spectrometric analysis of I and the isomeric fully *O*-methylated α-pyranoside isomer showed significant quantitative spectral differences, even though the general fragmentation pattern was similar for both.

EXPERIMENTAL

Preparation and Isolation of Samples

Crude I and II were prepared by direct methylation of D-galactose and D-galacturonic acid, respectively (2). Crude III was prepared by methylation of the reaction product obtained from room temperature glycosidation of galactose using methanolic hydrogen chloride (7).

I, II, and III were obtained by GLC from crude preparations by collecting appropriate peaks with a commercial GLC apparatus; column, 3/8 in. O.D. × 10 ft aluminum tubing; liquid phase, a mixture of fluorosilicone (QF-1) and neopentyl glycol succinate (10 and 12.5 wt% of support, respectively); solid support, Chromosorb W, 60–80 mesh; carrier gas, helium; flow rate, 200 ml per minute; temperature, isothermal, 160–170° range.

Adequate samples were obtained by repeatedly injecting 100–150 mg of crude product and collecting the peak corresponding to the component of interest. Pooled collected fractions were repurified by GLC.

Purity of Samples

Carbon–hydrogen analyses on the purified samples were satisfactory for empirical composition, but indicated nothing about isomeric composition. High isomeric purity of II and III was evident from the homogeneous appearance of these materials on an efficient analytical GLC column (8). Isomeric purity of I was estimated at 98–99%, by analytical scale GLC and TLC. Complete purification of I by GLC was not achieved. Trace amounts of the β-pyranoside isomer persisted as a minor shoulder on the main peak even after several repurifications. Absence of III and the α-pyranoside isomer in purified I was easily shown

Can. J. Chem. Downloaded from www.nrcresearchpress.com by 210.87.254.40 on 09/05/12
For personal use only.

by TLC. The relative retention volumes in the fully methylated galactoside series at 135°, using a 1/8 in. O.D. × 9 ft aluminum column, packed with 5% NPS on Chromosorb W (60–80 mesh) with a flow rate of 25 ml of helium per minute, were as follows: III, 1.00; I, 1.21; methyl 2,3,4,6-tetra-*O*-β-D-galactopyranoside (IV), 1.10; methyl 2,3,4,6-tetra-*O*-methyl-α-D-galactopyranoside (V), 1.16. Relative mobilities by TLC were: III, 1.00; I, 0.66; IV, 0.64; V, 0.48 (6).

Hydrolysis of I and III

Compounds I (39.46 mg) and III (36.03 mg) were hydrolyzed overnight at 100° in sealed tubes in 0.05 *N* H_2SO_4. The $[\alpha]_{25}^{D}$ of product from I was −29.7°; from III, −30.0 (*c* approximately 2, 0.05 *N* H_2SO_4) (reported, −21.2, *c*, 2.12 H_2O) (7). After ion exchange treatment and evaporation, the free 2,3,5,6-tetra-*O*-methyl-α-β-D-galactofuranoside could be purified by GLC at temperatures below 200° C, ($[\alpha]_D^{25} = -30.0$; *c* 1.25 H_2O).

Conversion of II to I

Compound II (264 mg) was reduced with sodium borohydride (152 mg) in methanol at room temperature, overnight, on a mechanical shaker (9). After neutralization of the solution with acetic acid, followed by treatment with Dowex 50 (H^+ form) and Duolite A 4 (OH^- form) ion exchange resins, and evaporation, the residue was methylated. The reduced methylated II was identical with I by GLC and TLC.

Conversion of II to the N-methyl-bis-amide of 2,3,5-tetra-O-methyl-mucic Acid

Compound II (40 mg) was treated with nitric acid and the mucic acid derivative esterified with methanolic hydrogen chloride (4). The product obtained in this manner was not distilled, but was converted to the *N*-methyl-bis-amide which was recrystallized from ethanol; m.p. 228.5–229.5° (micro m.p. (Kofler)); reported m.p. 232° (4). If II had had the pyranose configuration, the *N*-methyl-bis-amide of 2,3,4-tri-*O*-methyl-mucic acid, m.p. 205° (4), would have been obtained.

1. R. Kuhn, H. Trischmann, and I. Löw. Angew. Chem. **67**, 32 (1955).
2. H. G. Walker, Jr., M. Gee, and R. M. McCready. J. Org. Chem. **27**, 2100 (1962).
3. G. C. Maher. Advances in carbohydrate chemistry. Vol. 10. Academic Press, Inc., New York, N.Y. 1955. p. 280.
4. S. Luckett and F. Smith. J. Chem. Soc. 1114, 1506 (1940).
5. J. W. Greene and E. Pacsu. J. Am. Chem. Soc. **59**, 2569 (1937).
6. M. Gee. Anal. Chem. **35**, 350 (1963).
7. W. N. Haworth, D. A. Ruell, and G. C. Westgarth. J. Chem. Soc. 2468 (1924). R. S. Tipson and P. A. Levene. J. Biol. Chem. **129**, 575 (1939).
8. M. Gee and H. G. Walker, Jr. Anal. Chem. **34**, 650 (1962).
9. M. T. Wolfrom and K. Anno. J. Am. Chem. Soc. **74**, 5583 (1952).

Received July 22, 1963.
Western Regional Research Laboratory,
Albany 10, California.

THE PREPARATION OF SOME FLUORO-NITRO-ANTHRAQUINONES AND THEIR REDUCTION TO AMINO-FLUORO-ANTHRAQUINONES

G. Valkanas

Mononitration of 1-fluoro-, 2-fluoro-, and 2,6-difluoro-, and 1,5-difluoro-anthraquinones (1) can be effected by adding the stoichiometric amount of well dried potassium or sodium nitrate to solutions in sulphuric acid (2). Complete reaction of the α-substituted compounds occurs during 12 hours at 0°; higher temperatures lead to partly solvolyzed products. For the β-substituted compounds a further 2 hours heating at 40–45° is necessary to complete the reaction. Satisfactory analyses were obtained except for the nitration product of 1,5-difluoro-anthraquinone. Nitration of anthraquinone itself gives mainly the α-nitro compound together with some β-nitro compounds and some dinitration (3), whereas 1-substituted anthraquinones with *ortho–para* directing substituents appear to

Can. J. Chem. Downloaded from www.nrcresearchpress.com by 210.87.254.40 on 09/05/12
For personal use only.

by TLC. The relative retention volumes in the fully methylated galactoside series at 135°, using a 1/8 in. O.D. × 9 ft aluminum column, packed with 5% NPS on Chromosorb W (60–80 mesh) with a flow rate of 25 ml of helium per minute, were as follows: III, 1.00; I, 1.21; methyl 2,3,4,6-tetra-*O*-β-D-galactopyranoside (IV), 1.10; methyl 2,3,4,6-tetra-*O*-methyl-α-D-galactopyranoside (V), 1.16. Relative mobilities by TLC were: III, 1.00; I, 0.66; IV, 0.64; V, 0.48 (6).

Hydrolysis of I and III

Compounds I (39.46 mg) and III (36.03 mg) were hydrolyzed overnight at 100° in sealed tubes in 0.05 *N* H_2SO_4. The $[\alpha]_{25}^{D}$ of product from I was −29.7°; from III, −30.0 (*c* approximately 2, 0.05 *N* H_2SO_4) (reported, −21.2, *c*, 2.12 H_2O) (7). After ion exchange treatment and evaporation, the free 2,3,5,6-tetra-*O*-methyl-α-β-D-galactofuranoside could be purified by GLC at temperatures below 200° C, ($[\alpha]_D^{25} = -30.0$; *c* 1.25 H_2O).

Conversion of II to I

Compound II (264 mg) was reduced with sodium borohydride (152 mg) in methanol at room temperature, overnight, on a mechanical shaker (9). After neutralization of the solution with acetic acid, followed by treatment with Dowex 50 (H^+ form) and Duolite A 4 (OH^- form) ion exchange resins, and evaporation, the residue was methylated. The reduced methylated II was identical with I by GLC and TLC.

Conversion of II to the N-methyl-bis-amide of 2,3,5-tetra-O-methyl-mucic Acid

Compound II (40 mg) was treated with nitric acid and the mucic acid derivative esterified with methanolic hydrogen chloride (4). The product obtained in this manner was not distilled, but was converted to the *N*-methyl-bis-amide which was recrystallized from ethanol; m.p. 228.5–229.5° (micro m.p. (Kofler)); reported m.p. 232° (4). If II had had the pyranose configuration, the *N*-methyl-bis-amide of 2,3,4-tri-*O*-methyl-mucic acid, m.p. 205° (4), would have been obtained.

1. R. Kuhn, H. Trischmann, and I. Löw. Angew. Chem. **67**, 32 (1955).
2. H. G. Walker, Jr., M. Gee, and R. M. McCready. J. Org. Chem. **27**, 2100 (1962).
3. G. C. Maher. Advances in carbohydrate chemistry. Vol. 10. Academic Press, Inc., New York, N.Y. 1955. p. 280.
4. S. Luckett and F. Smith. J. Chem. Soc. 1114, 1506 (1940).
5. J. W. Greene and E. Pacsu. J. Am. Chem. Soc. **59**, 2569 (1937).
6. M. Gee. Anal. Chem. **35**, 350 (1963).
7. W. N. Haworth, D. A. Ruell, and G. C. Westgarth. J. Chem. Soc. 2468 (1924). R. S. Tipson and P. A. Levene. J. Biol. Chem. **129**, 575 (1939).
8. M. Gee and H. G. Walker, Jr. Anal. Chem. **34**, 650 (1962).
9. M. T. Wolfrom and K. Anno. J. Am. Chem. Soc. **74**, 5583 (1952).

Received July 22, 1963.
Western Regional Research Laboratory,
Albany 10, California.

THE PREPARATION OF SOME FLUORO-NITRO-ANTHRAQUINONES AND THEIR REDUCTION TO AMINO-FLUORO-ANTHRAQUINONES

G. Valkanas

Mononitration of 1-fluoro-, 2-fluoro-, and 2,6-difluoro-, and 1,5-difluoro-anthraquinones (1) can be effected by adding the stoichiometric amount of well dried potassium or sodium nitrate to solutions in sulphuric acid (2). Complete reaction of the α-substituted compounds occurs during 12 hours at 0°; higher temperatures lead to partly solvolyzed products. For the β-substituted compounds a further 2 hours heating at 40–45° is necessary to complete the reaction. Satisfactory analyses were obtained except for the nitration product of 1,5-difluoro-anthraquinone. Nitration of anthraquinone itself gives mainly the α-nitro compound together with some β-nitro compounds and some dinitration (3), whereas 1-substituted anthraquinones with *ortho–para* directing substituents appear to

Can. J. Chem. Downloaded from www.nrcresearchpress.com by 210.87.254.5 on 09/05/12
For personal use only.

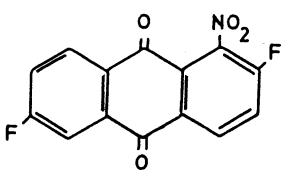

I

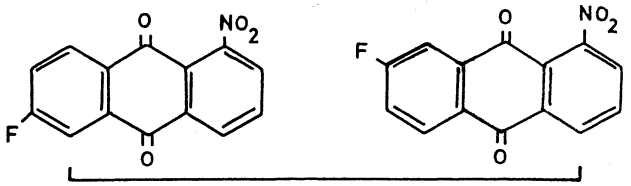

II

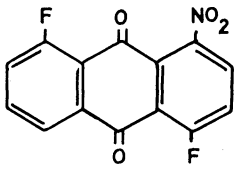

III

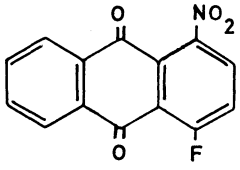

IV

undergo only 4-nitration (4). The nitration product of 2-fluoro-anthraquinone on reduction gives an amine identical with that obtained by the sulphonamide process and described as a mixture of two isomers (II) (5). 1,5-Difluoro-anthraquinone can only give one α-nitration product (III). 2,6-Difluoro-anthraquinone gives a product, presumably (I), from which one fluorine can readily be displaced by treatment with sodium sulphide (Table I); nitration *meta* to fluorine should not give a product with activated fluorine.

TABLE I

Reduction of fluoro-nitro-anthraquinones with sodium sulphide (8) at 70°

	Fluorine, %		
		Found	
Anthraquinone	Calc.*	In 40 min	In 90 min
I 1-Nitro-2,6-difluoro-	14.65	7.25	7.20
II 1-Nitro-6 or 7-fluoro-	7.90	7.55	7.45
III 1-Nitro-4,8-difluoro-	14.65	4.20	None
IV 1-Nitro-4-fluoro-	7.90	1.30	None

*Calculated on the corresponding amine.

1-Fluoro-anthraquinone gives a product different from the fluoro compound prepared from 1-amino-4-nitro-anthraquinone by the fluoroborate process (1). Unlike the reported exclusive 4-nitration of 1-chloro-anthraquinone (6) the nitration of 1-fluoro-anthraquinone seems to lead to a mixture of isomers.

Some typical results concerning the sodium sulphide reduction of the different fluoro-nitro-anthraquinones are included in Table I.

The α-fluoro-compounds (III, IV) readily lose fluorine when reduction with stannous chloride, sodium hydrosulphide (7), or sodium sulphide (8) is attempted. The β-fluoro-compounds (I, II) are more resistant; reduction of compound (II) with all reagents gives 1-amino-6 or 7-fluoro-anthraquinone (5) but compound (I) easily loses the fluorine *ortho* to the nitro group.

Can. J. Chem. Downloaded from www.nrcresearchpress.com by 210.87.254.5 on 09/05/12
For personal use only.

EXPERIMENTAL

The Nitration of 2-Fluoro-anthraquinone

2-Fluoro-anthraquinone (10 g) was dissolved in concentrated sulphuric acid (100 ml). The solution was cooled to 0° and a quantity of well ground, dry sodium nitrate (3.8 g) was added while the solution was well stirred. After 12 hours the solution was heated to 40–45° for 2 hours and then poured onto ice. During the reaction a noticeable change in color to grey-yellow was observed. The grey-yellow precipitate was recrystallized from chlorobenzene to give *1-nitro-6 or 7-fluoro-anthraquinone* (8.2 g, 66.2%), m.p. 222–223°. Anal. Found: C, 62.15; H, 2.2; F, 6.9; N, 5.15%. $C_{14}H_6FNO_4$ requires: C, 62.1; H, 2.25; F, 6.9; N, 5.15%.

Similarly, 2,6-difluoro-anthraquinone (10 g) was nitrated to give *1-nitro-2,6-difluoro-anthraquinone* which on recrystallization from chlorobenzene (7.75 g, 66.3%), had m.p. 207–209°. Anal. Found: F, 13.00; N, 4.9%. $C_{14}H_5F_2NO_4$ requires: F, 13.15; N, 4.85%.

The Nitration of 1-Fluoro-anthraquinone

1-Fluoro-anthraquinone (10 g) was dissolved in sulphuric acid (100 ml) and to the red solution maintained at 0° was added sodium nitrate (3.7 g) with stirring. The reaction mixture was kept at 0° (12 hours) and then poured onto ice to precipitate the grey nitration product (6.7 g, 55.7%), which was recrystallized from chlorobenzene, m.p. 213–214°. Anal. Found: F, 6.95; N, 5.15%. $C_{14}H_6FNO_4$ requires: F, 6.9; N, 5.15%.

Similarly, 1,5-difluoro-anthraquinone (10 g) was nitrated to *1-nitro-4,8-difluoro-anthraquinone.* Recrystallization from chlorobenzene gave a grey product (6.65 g, 60.8%), of m.p. 235–240°. Anal. Found: F, 11.9; N, 4.9%. $C_{14}H_5F_2NO_4$ requires: F, 13.15; N, 4.85%.

1-Fluoro-4-nitro-anthraquinone

1-Amino-4-nitro-anthraquinone (50 g) was converted by treatment with nitrosyl – sulphuric acid solution to *1-diazonium fluoroborate-4-nitro-anthraquinone* (1) (yield, 60.9 g, 89%), decomposition temperature 171-173°. The well dried salt was heated to decomposition in a round-bottomed flask equipped with a reflux condenser. The decomposition was followed by sublimation of the product which was recrystallized from chlorobenzene and further purified by sublimation, m.p. 226–227°. Anal. Found: F, 6.95; N, 5.15%. $C_{14}H_6FNO_4$ requires: F, 6.9; N, 5.15%.

1-Amino-6 or 7-Fluoro-anthraquinone

The nitration product of 2-fluoro-anthraquinone (5 g) was ground to a paste with sodium sulphide nonahydrate (10 g), suspended in hot water at 70–80°, and stirred. The complete reaction occurred in 40 minutes. The solution turned to violet and was filtered hot. The red product recrystallized from anisole gave red needles (yield 4.2 g, 94.2%), m.p. 199–201°. Reduction with sodium hydrosulphide in benzene in the presence of calcium chloride (7) gave similar results; from 5 g of starting material, 4.4 g (98.5%) of amine were obtained which on recrystallization from anisole had m.p. 203–204°. Found: C, 69.6; H, 3.3; F, 7.55; N, 5.8%. Calc. for $C_{14}H_8FNO_2$: C, 69.7; H, 3.3; F, 7.9; N, 5.8%.

1. G. Valkanas and H. Hopff. J. Org. Chem. **27**, 3680 (1962).
2. M. Hill and F. Taylor. J. Org. Chem. **25**, 1037 (1960).
3. H. Olpin, C. Argyle, and F. Brown. U.S. Patent No. (February, 1941) 2,309,708: Chem. Abstr. **37**, 3769 (1943).
4. Ger. Patent No. 137,782: Chem. Zentr. I, 108 (1921).
5. CIBA. Swiss Patent No. (July, 1953) 289,992, 292,690-2: Chem. Abstr. **48**, 11800 (1954).
6. A. Eckert and K. Steiner. Monatsh. **35**, 1138 (1914).
7. R. Haworth and A. Lapworth. J. Chem. Soc. 774 (1921).
8. W. Beisler and L. Jones. J. Am. Chem. Soc. **44**, 2303 (1922).

Received May 13, 1963.
Laboratory of Organic Chemical Technology,
Swiss Federal Institute of Technology,
Zürich, Switzerland.

CONVERSION OF A β-AMIDOESTER TO A PYRIMIDINE: 2-AMINO-4-HYDROXY-5,6,7,8-TETRAHYDRO-1,3,8-TRIAZANAPHTHALENE

Joseph DeGraw and Leon Goodman

As an extension of previous work on the synthesis of folic acid analogs (1), the preparation of 5-deazatetrahydrofolic acid is being investigated. Initially, a study of the preparation of the basic heterocyclic portion of this folic acid analog, 2-amino-4-hydroxy-5,6,7,8-tetrahydro-1,3,8-triazanaphthalene (II), was undertaken. It is hoped that the best general

Can. J. Chem. Downloaded from www.nrcresearchpress.com by 210.87.254.5 on 09/05/12
For personal use only.

EXPERIMENTAL

The Nitration of 2-Fluoro-anthraquinone

2-Fluoro-anthraquinone (10 g) was dissolved in concentrated sulphuric acid (100 ml). The solution was cooled to 0° and a quantity of well ground, dry sodium nitrate (3.8 g) was added while the solution was well stirred. After 12 hours the solution was heated to 40–45° for 2 hours and then poured onto ice. During the reaction a noticeable change in color to grey-yellow was observed. The grey-yellow precipitate was recrystallized from chlorobenzene to give *1-nitro-6 or 7-fluoro-anthraquinone* (8.2 g, 66.2%), m.p. 222–223°. Anal. Found: C, 62.15; H, 2.2; F, 6.9; N, 5.15%. $C_{14}H_6FNO_4$ requires: C, 62.1; H, 2.25; F, 6.9; N, 5.15%.

Similarly, 2,6-difluoro-anthraquinone (10 g) was nitrated to give *1-nitro-2,6-difluoro-anthraquinone* which on recrystallization from chlorobenzene (7.75 g, 66.3%), had m.p. 207–209°. Anal. Found: F, 13.00; N, 4.9%. $C_{14}H_5F_2NO_4$ requires: F, 13.15; N, 4.85%.

The Nitration of 1-Fluoro-anthraquinone

1-Fluoro-anthraquinone (10 g) was dissolved in sulphuric acid (100 ml) and to the red solution maintained at 0° was added sodium nitrate (3.7 g) with stirring. The reaction mixture was kept at 0° (12 hours) and then poured onto ice to precipitate the grey nitration product (6.7 g, 55.7%), which was recrystallized from chlorobenzene, m.p. 213–214°. Anal. Found: F, 6.95; N, 5.15%. $C_{14}H_6FNO_4$ requires: F, 6.9; N, 5.15%.

Similarly, 1,5-difluoro-anthraquinone (10 g) was nitrated to *1-nitro-4,8-difluoro-anthraquinone.* Recrystallization from chlorobenzene gave a grey product (6.65 g, 60.8%), of m.p. 235–240°. Anal. Found: F, 11.9; N, 4.9%. $C_{14}H_5F_2NO_4$ requires: F, 13.15; N, 4.85%.

1-Fluoro-4-nitro-anthraquinone

1-Amino-4-nitro-anthraquinone (50 g) was converted by treatment with nitrosyl – sulphuric acid solution to *1-diazonium fluoroborate-4-nitro-anthraquinone* (1) (yield, 60.9 g, 89%), decomposition temperature 171-173°. The well dried salt was heated to decomposition in a round-bottomed flask equipped with a reflux condenser. The decomposition was followed by sublimation of the product which was recrystallized from chlorobenzene and further purified by sublimation, m.p. 226–227°. Anal. Found: F, 6.95; N, 5.15%. $C_{14}H_6FNO_4$ requires: F, 6.9; N, 5.15%.

1-Amino-6 or 7-Fluoro-anthraquinone

The nitration product of 2-fluoro-anthraquinone (5 g) was ground to a paste with sodium sulphide nonahydrate (10 g), suspended in hot water at 70–80°, and stirred. The complete reaction occurred in 40 minutes. The solution turned to violet and was filtered hot. The red product recrystallized from anisole gave red needles (yield 4.2 g, 94.2%), m.p. 199–201°. Reduction with sodium hydrosulphide in benzene in the presence of calcium chloride (7) gave similar results; from 5 g of starting material, 4.4 g (98.5%) of amine were obtained which on recrystallization from anisole had m.p. 203–204°. Found: C, 69.6; H, 3.3; F, 7.55; N, 5.8%. Calc. for $C_{14}H_8FNO_2$: C, 69.7; H, 3.3; F, 7.9; N, 5.8%.

1. G. Valkanas and H. Hopff. J. Org. Chem. **27**, 3680 (1962).
2. M. Hill and F. Taylor. J. Org. Chem. **25**, 1037 (1960).
3. H. Olpin, C. Argyle, and F. Brown. U.S. Patent No. (February, 1941) 2,309,708: Chem. Abstr. **37**, 3769 (1943).
4. Ger. Patent No. 137,782: Chem. Zentr. I, 108 (1921).
5. CIBA. Swiss Patent No. (July, 1953) 289,992, 292,690-2: Chem. Abstr. **48**, 11800 (1954).
6. A. Eckert and K. Steiner. Monatsh. **35**, 1138 (1914).
7. R. Haworth and A. Lapworth. J. Chem. Soc. 774 (1921).
8. W. Beisler and L. Jones. J. Am. Chem. Soc. **44**, 2303 (1922).

Received May 13, 1963.
Laboratory of Organic Chemical Technology,
Swiss Federal Institute of Technology,
Zürich, Switzerland.

CONVERSION OF A β-AMIDOESTER TO A PYRIMIDINE: 2-AMINO-4-HYDROXY-5,6,7,8-TETRAHYDRO-1,3,8-TRIAZANAPHTHALENE

Joseph DeGraw and Leon Goodman

As an extension of previous work on the synthesis of folic acid analogs (1), the preparation of 5-deazatetrahydrofolic acid is being investigated. Initially, a study of the preparation of the basic heterocyclic portion of this folic acid analog, 2-amino-4-hydroxy-5,6,7,8-tetrahydro-1,3,8-triazanaphthalene (II), was undertaken. It is hoped that the best general

Can. J. Chem. Downloaded from www.nrcresearchpress.com by 210.87.254.5 on 09/05/12
For personal use only.

method for preparing II can be elaborated to provide 6-substituted derivatives of II useful for the synthesis of 5-deazatetrahydrofolic acid.

The condensation of guanidine with a β-keto ester represents probably the most useful general method for preparing 2-amino-4-hydroxypyrimidines. As an extension of this method the condensation of guanidine with 3-carbethoxy-2-piperidone (I) (2) was

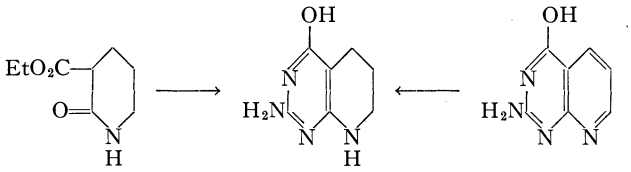

I II III

investigated for the synthesis of II. The reaction, carried out at 150° in methanol with sodium methoxide, afforded the pyrimidopiperideine (II) in 38% yield. This appears to be the first such example of the condensation of guanidine with a β-amidoester to form a pyrimidine ring.

In order to provide a proof of structure for the condensation product and as a second preparative method for II, the catalytic reduction of 2-amino-4-hydroxypyrido[2,3-*d*]-pyrimidine (III) (3) was investigated. When an aqueous suspension of III was treated with hydrogen at atmospheric pressure over platinum oxide, approximately 2 moles of hydrogen were absorbed. The product (II) was identical with that prepared by the condensation method with respect to infrared and ultraviolet spectra and paper chromatographic behavior.

The further utility of these methods for the ultimate synthesis of 5-deazatetrahydrofolic acid is currently under investigation.

EXPERIMENTAL

3-Carbethoxy-2-piperidone (I) was prepared in a two-step reaction sequence as follows. Malonic ester was reacted with acrylonitrile to afford ethyl 2-carbethoxy-4-cyanobutyrate in a 56% yield according to the procedure of Mikeska (4). The cyano ester was catalytically reduced over platinum oxide at atmospheric pressure to yield 3-carbethoxy-2-piperidone (I), essentially following the method described by Koelsch (2). 2-Amino-4-hydroxypyrido [2,3-*d*]pyrimidine (III) was prepared in 51% yield by the procedure of Price *et al.* (3).

2-Amino-5,6,7,8-tetrahydro-4-hydroxypyrido[2,3-d]pyrimidine (II)

A. Condensation of Guanidine and 3-Carbethoxy-2-piperidone

A 1-liter autoclave was charged with 14.4 g (84 mmoles) of 3-carbethoxy-2-piperidone (I), 15.7 g (0.29 mole) of sodium methoxide, 16.4 g (0.172 mole) of guanidine hydrochloride, and 200 ml of absolute methanol. The mixture was stirred at 150° for 8 hours and allowed to cool for another 15 hours. The mixture was evaporated to dryness *in vacuo* and the residue was triturated with 100 ml of water. The insoluble material was collected, washed with water, and dried to leave 5.3 g (38%), m.p. 245–255°. An analytical sample, m.p. 260–270°, was obtained by recrystallization from water; $\lambda_{max(m\mu)}^{pH\,1}$ 280 (ϵ 16150), $\lambda_{max(m\mu)}^{pH\,13}$ 274 (ϵ 8900), R_f 0.70 in *n*-butanol/acetic acid/water, 5/2/3.

Anal. Calc. for $C_7H_{10}N_4O \cdot \frac{1}{4}H_2O$: C, 49.3; H, 6.20; N, 32.8. Found: C, 49.3; H, 6.60; N, 32.6. The material was quite hygroscopic and samples showing various degrees of hydration were encountered; the samples were dried *in vacuo* at 120° for 15 hours prior to analysis.

B. Hydrogenation of 2-Amino-4-hydroxypyrido[2,3-d]pyrimidine

To 10 ml of water were added 0.50 g (2.8 mmoles) of 2-amino-4-hydroxypyrido[2,3-*d*]pyrimidine (III) and 50 mg of platinum oxide. The mixture was stirred under an atmosphere of hydrogen for 21 hours. An uptake of 1.91 moles of gas was observed and the product deposited from solution. The mixture was heated to 95–100° and quickly filtered by suction. The residue was retreated with 5 ml of hot water, filtered, and the combined filtrates were chilled for 30 minutes. The white crystals which formed were collected, washed

Can. J. Chem. Downloaded from www.nrcresearchpress.com by 210.87.254.5 on 09/05/12
For personal use only.

with water, and dried to leave 0.12 g (24%), m.p. 262–273°. This material was identical with that obtained in procedure A with respect to infrared and ultraviolet spectra and paper chromatographic behavior.

ACKNOWLEDGMENTS

This work was carried out under the auspices of the Cancer Chemotherapy National Service Center, National Cancer Institute, National Institutes of Health, Public Health Service, Contract No. SA-43-ph-1892. The opinions expressed in this paper are those of the authors and are not necessarily those of the Cancer Chemotherapy National Service Center.

The authors are indebted to Dr. Peter Lim for infrared interpretations, to his staff for ultraviolet and paper chromatographic data, and to Mr. O. P. Crews for the large-scale preparation of intermediates.

1. J. DeGraw, L. Goodman, B. Weinstein, and B. R. Baker. J. Org. Chem. **27**, 576 (1962).
2. C. Koelsch. J. Am. Chem. Soc. **65**, 2458 (1943).
3. R. Bernetti, F. Mancini, and C. Price. J. Org. Chem. **27**, 2863 (1962).
4. L. Mikeska. U.S. Patent No. 2,461,336 (February 8, 1949): Chem. Abstr. **43**, 4689 (1949).

Received July 15, 1963.
Life Sciences Research,
Stanford Research Institute,
Menlo Park, California.

Can. J. Chem. Downloaded from www.nrcresearchpress.com by 210.87.254.5 on 09/05/12
For personal use only.

THE EFFECT OF ALKYL GROUP VARIATION ON THE RATES OF SOLVOLYSIS OF ALKYL SULPHONIUM HALIDES

J. B. Hyne and H. S. Golinkin

Tertiary butyl and amyl dimethylsulphonium salts have been the standard examples of the sulphonium salt series used in neutral solvolytic rate studies of this type of compound in the past (1). Apart from these cases the apparent hygroscopic nature of the sulphonium salts has limited the study of their solvolytic behavior. In the course of our studies of sulphonium salt solvolysis we have prepared and characterized α-phenethyldimethylsulphonium and benzyldimethylsulphonium bromides. The solvolytic rate behavior of these two compounds together with comparative data on the *t*-butyldimethylsulphonium salt are reported here.

RESULTS

Approximately 10^{-3} M solutions of the various sulphonium salts in the desired solvent media were prepared by weight. Solvolytic kinetics were followed using the conductimetric technique described previously (2) and due to Robertson (3). While the iodide salt was used in the *t*-butyl case the bromides of both the α-phenethyl and benzyl sulphonium ions were employed. Since 0.325 mole fraction ethanol in water was the lowest polarity solvent used the anion does not enter the rate determining step as was shown previously (2, 4). Consequently the change from iodide to bromide does not invalidate the comparison of rates. In both the α-phenethyl and benzyl cases difficulty was encountered in obtaining reproducible results in pure water. In the benzyl case only those rates measured in higher ethanolic compositions were of satisfactory reproducibility. In Table I the rates for the

with water, and dried to leave 0.12 g (24%), m.p. 262–273°. This material was identical with that obtained in procedure A with respect to infrared and ultraviolet spectra and paper chromatographic behavior.

ACKNOWLEDGMENTS

This work was carried out under the auspices of the Cancer Chemotherapy National Service Center, National Cancer Institute, National Institutes of Health, Public Health Service, Contract No. SA-43-ph-1892. The opinions expressed in this paper are those of the authors and are not necessarily those of the Cancer Chemotherapy National Service Center.

The authors are indebted to Dr. Peter Lim for infrared interpretations, to his staff for ultraviolet and paper chromatographic data, and to Mr. O. P. Crews for the large-scale preparation of intermediates.

1. J. DeGraw, L. Goodman, B. Weinstein, and B. R. Baker. J. Org. Chem. **27**, 576 (1962).
2. C. Koelsch. J. Am. Chem. Soc. **65**, 2458 (1943).
3. R. Bernetti, F. Mancini, and C. Price. J. Org. Chem. **27**, 2863 (1962).
4. L. Mikeska. U.S. Patent No. 2,461,336 (February 8, 1949): Chem. Abstr. **43**, 4689 (1949).

Received July 15, 1963.
Life Sciences Research,
Stanford Research Institute,
Menlo Park, California.

Can. J. Chem. Downloaded from www.nrcresearchpress.com by 210.87.254.5 on 09/05/12
For personal use only.

THE EFFECT OF ALKYL GROUP VARIATION ON THE RATES OF SOLVOLYSIS OF ALKYL SULPHONIUM HALIDES

J. B. Hyne and H. S. Golinkin

Tertiary butyl and amyl dimethylsulphonium salts have been the standard examples of the sulphonium salt series used in neutral solvolytic rate studies of this type of compound in the past (1). Apart from these cases the apparent hygroscopic nature of the sulphonium salts has limited the study of their solvolytic behavior. In the course of our studies of sulphonium salt solvolysis we have prepared and characterized α-phenethyldimethylsulphonium and benzyldimethylsulphonium bromides. The solvolytic rate behavior of these two compounds together with comparative data on the *t*-butyldimethylsulphonium salt are reported here.

RESULTS

Approximately 10^{-3} M solutions of the various sulphonium salts in the desired solvent media were prepared by weight. Solvolytic kinetics were followed using the conductimetric technique described previously (2) and due to Robertson (3). While the iodide salt was used in the *t*-butyl case the bromides of both the α-phenethyl and benzyl sulphonium ions were employed. Since 0.325 mole fraction ethanol in water was the lowest polarity solvent used the anion does not enter the rate determining step as was shown previously (2, 4). Consequently the change from iodide to bromide does not invalidate the comparison of rates. In both the α-phenethyl and benzyl cases difficulty was encountered in obtaining reproducible results in pure water. In the benzyl case only those rates measured in higher ethanolic compositions were of satisfactory reproducibility. In Table I the rates for the

TABLE I

Rates of solvolysis of sulphonium salts in EtOH–H_2O mixtures

Mole fraction EtOH	$k \times 10^5$ sec^{-1}				
	t-Bu$\overset{+}{S}Me_2I^-$		PhCHCH$_3\overset{+}{S}Me_2Br^-$		PhCH$_2\overset{+}{S}Me_2Br^-$
	50.3°	78.4°	50.3°	78.4°	78.4°
0.000	0.62_9	$36._1$		$23._5$	
0.125	0.66_4	$39._4$	0.45_4	$26._5$	
0.204	0.73_0	$44._2$	0.47_9	$27._2$	0.10
0.325	0.85_0	$49._8$	0.53_2	$29._6$	0.26

three sulphonium salts studied under various solvent and temperature conditions are recorded.

DISCUSSION

The availability of the rates of solvolysis for the three sulphonium salts in Table I enables a comparison to be made with the rate behavior of the corresponding alkyl chlorides. Using the date of Winstein and Fainberg (5) and Hyne, Wills, and Wonkka (6) the relative rates of solvolysis of the t-butyl, α-phenethyl, and benzyl chlorides and dimethylsulphonium salts may be compared. Conditions chosen for the comparison were 0.204 mole fraction ethanol (approx. 45% ethanol by volume in water) at 50° C for the chloride and 78.4° C for the sulphonium salts. These conditions were dictated largely by the availability of results. The temperature difference is unlikely to have a significant effect since the comparisons are internal within a given set at the same temperature. Use of a mixed solvent medium is perhaps not the best condition in view of the established selective solvation effects (6, 7). Since free energies of activation are being compared, however, the likelihood of gross errors being introduced by such effects is minimized. The rate comparisons are shown in Table II.

TABLE II

Relative rates of solvolysis of alkyl halides and sulphonium salts in 0.204 mole fraction EtOH–H_2O

Leaving group		Alkyl group		
		t-Bu	PhCHCH$_3$	PhCH$_2$
$-S(CH_3)_2$	$k_{78.4°}$ sec^{-1}	4.42×10^{-4}	2.72×10^{-4}	1×10^{-6}
	Relative log k (ΔF^*)	1	1.07	1.79
—Cl	$k_{50.0°}$ sec^{-1} [a]	1.32×10^{-2}	9.80×10^{-3}	1.89×10^{-5}
	Relative log k (ΔF^*)	1	1.07	2.51

[a] NOTE: Rates in this row interpolated from data of refs. 5 and 6.

Comparison of the free energies of activation (ratio of log k) for the two types of solvolysis shows immediately that structural changes in the alkyl group have the same effect on the solvolysis rates of both the halide and the sulphonium salts. Although the two reactions have opposite charge character on activation—one involving charge delocalization while the other requires charge creation—in both cases an incipient alkyl carbonium ion develops on activation.

Can. J. Chem. Downloaded from www.nrcresearchpress.com by 210.87.254.5 on 09/05/12
For personal use only.

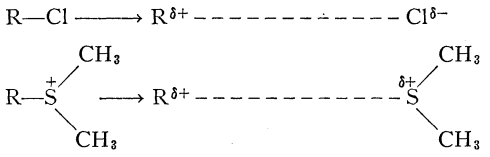

The similar effects of structural change in the alkyl group must imply that the stabilization of the incipient carbonium ion in the transition state is the dominant factor affecting the rate as a function of the alkyl group. This is particularly interesting in view of the fact that we are dealing here with two reactions having leaving groups of entirely different character. Clearly the stabilization of the transition state—or lack of it in the sulphonium case—brought about by solvation of the leaving group does not appear to vary significantly as the nature of the alkyl group is varied. If it did one would imagine that the effect of the alkyl group variation in the case where leaving group solvation was important would be very much different from that in the case where leaving group solvation was minimal.

The data in Table I also shows that the rate dependence on solvent composition is considerably less for the α-phenethylsulphonium salt than for the *t*-butyl compound. This should be compared with the very similar rate dependence on solvent exhibited by the two corresponding alkyl chlorides (5). While the solvent dependence for all three sulphoniums is in the opposite sense from the alkyl halides, as would be expected from the charge character of the activation process, the smaller dependence in the α-phenethyl case probably reflects a smaller change in polarity of the solute on activation. Whether this is due to a lowering of the polarity of the ionic initial state thus approaching the polarity of the transition state or to a more polar transition state closer to the ionic character of the initial state can only be resolved by studies of the relative physical properties of the *t*-butyl and α-phenethyl initial states.

The data recorded in Table I permits the calculation of both enthalpies and entropies of activation for the *t*-butyl and α-phenethyl cases. These parameters are remarkedly insensitive to structural changes. Values of activation energy vary between 32.4 and 33.0 kcal/mole for both salts over the range of solvents used. The entropy values lie in the range of +15 to +18 e.u. in keeping with the charge delocalization on activation resulting in "desolvation" of the transition state compared with the ionic initial state.

Synthesis of Sulphonium Halides

The following refers particularly to the α-phenethyl and benzyl sulphonium salts; the *t*-butyl salt is readily synthesized and isolated from *t*-butyl iodide and dimethyl sulphide in nitromethane. The method is a modified form of that reported by Siegel and Graefe (8). Dimethyl sulphide and the corresponding alkyl halide were mixed in a 1:1 mole ratio. The reaction vessel was stoppered with an aluminum foil covered rubber stopper, and was covered with aluminum foil to omit light. The mixture was allowed to stand at room temperature until the bottom of the flask was covered with crystals. The remaining liquid was deep red in color possibly due to bromine formation. The mixture was washed with 50 ml anhydrous ether to remove any unreacted starting materials. The ether was decanted, but enough was left so that the crystals were not exposed to the atmosphere; 5 to 10 ml absolute ethanol was added to dissolve the crystals. Gentle heating was sometimes necessary for solution to occur. Warm tap water generally sufficed. The solution was then treated with norite A to decolorize it, after which it was filtered over a celite bed on a sintered glass funnel to remove the norite and any undissolved residue. The clear filtrate was placed in a 50-ml standard taper flask, equipped with a vacuum adapter,

Can. J. Chem. Downloaded from www.nrcresearchpress.com by 210.87.254.5 on 09/05/12
For personal use only.

which was previously evacuated and weighed. The flask was then filled with dry ether to precipitate the salt and placed in the refrigerator overnight. The liquor was decanted using an aspirator, but enough was left behind to keep the crystals covered. The remaining liquid was removed under vacuum. The white salt was then dried over phosphorous pentoxide under vacuum. α-Phenethyldimethylsulphonium bromide—reaction time 96 hours; yield 10.1%; m.p. 91.7–92.8° C (lit. m.p. 76–80° C ref. (8)); analysis % C calc. 48.58%, obs. 48.50%; % H calc. 6.12%, obs. 6.09%; % S calc. 12.97%, obs. 12.94%; % Br calc. 32.33%, obs. 32.24%. Benzyldimethylsulphonium bromide—reaction time 120 hours; yield 22.7%; m.p. 100.5–101.5° C; analysis % C calc. 46.36%, obs. 46.69%; % H calc. 5.62%, obs. 5.73%; % S calc. 13.76%, obs. 13.92%; % Br calc. 34.27%, obs. 34.08%.

Copies of infrared potassium bromide pellet spectra of the above salts are available on request.

ACKNOWLEDGMENTS

The authors acknowledge the assistance of Mr. R. E. Wonkka in making certain of the rate measurements and the National Research Council of Canada for financial support.

1. K. A. Cooper, E. D. Hughes, C. K. Ingold, and B. J. MacNulty. J. Chem. Soc. 2038–42 (1948).
2. J. B. Hyne. Can. J. Chem. **39**, 1207 (1961).
3. R. E. Robertson. Can. J. Chem. **33**, 1536 (1955).
4. J. B. Hyne and J. W. Abrell. Can. J. Chem. **39**, 1657 (1961).
5. S. Winstein and A. H. Fainberg. J. Am. Chem. Soc. **79**, 1597, 5937 (1957).
6. J. B. Hyne, R. Wills, and R. E. Wonkka. J. Am. Chem. Soc. **84**, 2194 (1962).
7. E. McC. Arnett, P. McC. Duggleby, and J. J. Burke. J. Am. Chem. Soc. **85**, 1350 (1963).
8. S. Siegel and A. F. Graefe. J. Am. Chem. Soc. **75**, 4519 (1953).

Received July 31, 1963.
Department of Chemistry,
University of Alberta, Calgary,
Calgary, Alberta.

Can. J. Chem. Downloaded from www.nrcresearchpress.com by 210.87.254.5 on 09/05/12
For personal use only.

N.M.R. STUDIES OF BRIDGED RING SYSTEMS. I. CARBON–HYDROGEN SPIN COUPLING CONSTANTS IN BICYCLO[2,2,1]HEPTANE DERIVATIVES

K. Tori, R. Muneyuki, and H. Tanida

The carbon–hydrogen spin coupling constants, $J_{C^{13}-H}$, are considered as useful tools for the investigation of *s*-character of the carbon atomic orbital participating in the C—H bond (1–4). Muller and Pritchard (1) suggested that decrease of the ring size of cycloalkanes with their C—C—C angles increased $J_{C^{13}-H}$ with the percentage of *s*-character of the C—H bond, and, for example, the $J_{C^{13}-H}$ of cyclopropane exhibited the comparable value to that of the sp^2 bond.

It has been known that bicyclo[2,2,1]heptane derivatives have considerably smaller bond angles on their sp^3-tetrahedral and sp^2-trigonal carbons than the respective ordinal angles due to the contribution of ring strain.* Musher (7) proposed that the unusual behavior of the bicyclo[2,2,1]heptane ring toward the magnetic shielding and the proton coupling constant might be due to the π-character in the ring.

**Few data relating to the molecular geometry of this ring system have appeared; however, Schomaker, using an electron diffraction method, has shown the geometry of norbornadiene to be (5): $<C_1C_2C_3 = 109.1°$, $<C_2C_1C_7 = 96.4°$, $<C_2C_1C_6 = 102.2°$, $<C_1C_7C_4 = 96.7°$, $C_1—C_2 = 1.522$ Å, $C_2—C_3 = 1.333$ Å, $C_1—C_7 = 1.558$ Å. There are other data based on the dipole moment studies of bridged bicyclic molecules (6).*

which was previously evacuated and weighed. The flask was then filled with dry ether to precipitate the salt and placed in the refrigerator overnight. The liquor was decanted using an aspirator, but enough was left behind to keep the crystals covered. The remaining liquid was removed under vacuum. The white salt was then dried over phosphorous pentoxide under vacuum. α-Phenethyldimethylsulphonium bromide—reaction time 96 hours; yield 10.1%; m.p. 91.7–92.8° C (lit. m.p. 76–80° C ref. (8)); analysis % C calc. 48.58%, obs. 48.50%; % H calc. 6.12%, obs. 6.09%; % S calc. 12.97%, obs. 12.94%; % Br calc. 32.33%, obs. 32.24%. Benzyldimethylsulphonium bromide—reaction time 120 hours; yield 22.7%; m.p. 100.5–101.5° C; analysis % C calc. 46.36%, obs. 46.69%; % H calc. 5.62%, obs. 5.73%; % S calc. 13.76%, obs. 13.92%; % Br calc. 34.27%, obs. 34.08%.

Copies of infrared potassium bromide pellet spectra of the above salts are available on request.

ACKNOWLEDGMENTS

The authors acknowledge the assistance of Mr. R. E. Wonkka in making certain of the rate measurements and the National Research Council of Canada for financial support.

1. K. A. Cooper, E. D. Hughes, C. K. Ingold, and B. J. MacNulty. J. Chem. Soc. 2038–42 (1948).
2. J. B. Hyne. Can. J. Chem. **39**, 1207 (1961).
3. R. E. Robertson. Can. J. Chem. **33**, 1536 (1955).
4. J. B. Hyne and J. W. Abrell. Can. J. Chem. **39**, 1657 (1961).
5. S. Winstein and A. H. Fainberg. J. Am. Chem. Soc. **79**, 1597, 5937 (1957).
6. J. B. Hyne, R. Wills, and R. E. Wonkka. J. Am. Chem. Soc. **84**, 2194 (1962).
7. E. McC. Arnett, P. McC. Duggleby, and J. J. Burke. J. Am. Chem. Soc. **85**, 1350 (1963).
8. S. Siegel and A. F. Graefe. J. Am. Chem. Soc. **75**, 4519 (1953).

Received July 31, 1963.
Department of Chemistry,
University of Alberta, Calgary,
Calgary, Alberta.

Can. J. Chem. Downloaded from www.nrcresearchpress.com by 210.87.254.6 on 09/05/12
For personal use only.

N.M.R. STUDIES OF BRIDGED RING SYSTEMS. I. CARBON–HYDROGEN SPIN COUPLING CONSTANTS IN BICYCLO[2,2,1]HEPTANE DERIVATIVES

K. Tori, R. Muneyuki, and H. Tanida

The carbon–hydrogen spin coupling constants, $J_{C^{13}-H}$, are considered as useful tools for the investigation of *s*-character of the carbon atomic orbital participating in the C—H bond (1–4). Muller and Pritchard (1) suggested that decrease of the ring size of cycloalkanes with their C—C—C angles increased $J_{C^{13}-H}$ with the percentage of *s*-character of the C—H bond, and, for example, the $J_{C^{13}-H}$ of cyclopropane exhibited the comparable value to that of the sp^2 bond.

It has been known that bicyclo[2,2,1]heptane derivatives have considerably smaller bond angles on their sp^3-tetrahedral and sp^2-trigonal carbons than the respective ordinal angles due to the contribution of ring strain.* Musher (7) proposed that the unusual behavior of the bicyclo[2,2,1]heptane ring toward the magnetic shielding and the proton coupling constant might be due to the π-character in the ring.

**Few data relating to the molecular geometry of this ring system have appeared; however, Schomaker, using an electron diffraction method, has shown the geometry of norbornadiene to be (5): $<C_1C_2C_3 = 109.1°$, $<C_2C_1C_7 = 96.4°$, $<C_2C_1C_6 = 102.2°$, $<C_1C_7C_4 = 96.7°$, $C_1—C_2 = 1.522$ Å, $C_2—C_3 = 1.333$ Å, $C_1—C_7 = 1.558$ Å. There are other data based on the dipole moment studies of bridged bicyclic molecules (6).*

In order to obtain some information about the ring strain and π-character in connection with our work from other standpoints in this ring system, we investigated the proton magnetic resonance spectra of C^{13}—H (in natural abundance) in the bicyclo[2,2,1]heptane series, such as norbornane (I), norbornene (II), norbornadiene (III), benzonorbornene (IV), benzonorbornadiene (V), and quadricyclene (VI). The values of $J_{C^{13}-H}$ determined by the observable C^{13}-satellites are shown in Table II.

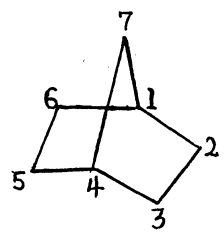

(I)

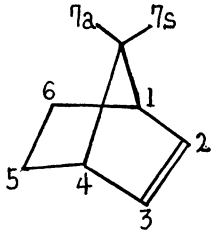

(II)

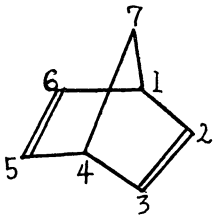

(III)

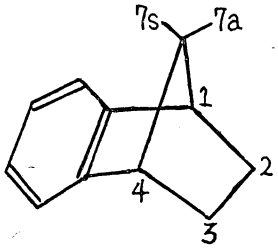

(IV)

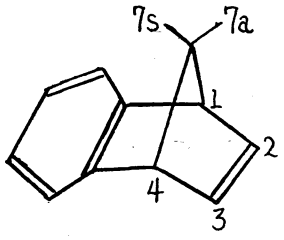

(V)

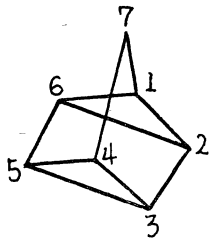

(VI)

TABLE I

$J_{C^{13}-H}$ of some kinds of hydrocarbon, in c.p.s.

Compound	$J_{C^{13}-H}$		Reference
C—H (sp^3) in aliphatic alkyl group	123 ~ 126		1
C—H (sp^3) attached to sp^2-carbon	124 ~ 128		1
Cyclohexane	123		1
Cyclopentane	128		1
Cyclopropane	161		1
Ethylene	156.4	[J_{H-H} (cis) = 11.4]	13
Cycloöctene (sp^2)	153.5	[J_{H-H} (cis) = ca. 10]	This work
Cyclohexene (sp^2)	155.5	[J_{H-H} (cis) = ca. 10]	This work
	171		1
Cyclopentene (sp^2)	160.5	[J_{H-H} (cis) = ca. 5.8]	This work
Cycloöctatetraene (sp^2)	155		14
Cycloheptatriene (sp^2)	156, 154, 161		14
Cyclohexadiene (sp^2)	163		14
Cyclopentadiene (sp^2)	170		14

Since all compounds described are of a hydrocarbon family, it is reasonable to assume that the $J_{C^{13}-H}$ depends only on the percentage of s-character of the bonds. As is clearly shown in the comparison of the data in Tables I and II, $J_{C^{13}-H}$ on the bridge head is much

Can. J. Chem. Downloaded from www.nrcresearchpress.com by 210.87.254.6 on 09/05/12
For personal use only.

TABLE II

Coupling constants in bicyclo[2,2,1]heptane derivatives, in c.p.s.

Compound	$J_{C^{13}-H}$			J_{H-H}					
	Bridge methylene	Bridge head	Double bond	$J_{1,2}$	$J_{2,3}$	$J_{1,3}$	$\lvert J_{7a,7s}\rvert$†	$J_{1,7a}$	$J_{1,7s}$
Norbornane (I)		142±2*	—						
Norbornene (II)		142	165.5	3.2	6.0	1.2	8.2	1.8	1.5
Norbornadiene (III)	135.5	146	172.5	2.8	5.2	1.1		1.6	1.6
Benzonorbornene (IV)		143.5	—				8.7	1.9	1.5
Benzonorbornadiene (V)	135 (av.)	148	175.5	3.0	5.4	1.2	7.2	1.5	1.8
Quadricyclene (VI)	130	178.5 (av.)	—					1.1	1.1

*The presence of impurity which interfered in the signal gave the estimated value.
†Recent observations (15) showed that J_{gem}'s have, in many cases, the opposite sign to the vicinal coupling constants. Since the J_{gem}'s in this table were determined by first order approximation, they are given with no sign.

larger than that of the usual sp^3 bond, so the C—H bonds on these positions should have much increased *s*-character. Also, considerably larger $J_{C^{13}-H}$ values were recognized in the bridge methylene and about the double bond. The introduction of double bonds and (or) benzene ring into the bicyclo[2,2,1]heptane system increased the $J_{C^{13}-H}$ value with the ring strain, as would be expected. From these data, we can reasonably assume that carbon atoms in these series have extraordinary high *s*-character in the C—H bonds and accordingly some π-character in the C—C bonds. The large substituent effect observed by us on a carbonium ion reaction at the 7-position of benzonorbornene derivatives (8) might bear some relation to these results.

The proton spin coupling constants of methylene protons, J_{gem}'s, at the 7-position, which were determined by first order approximation from the C^{13}—H or normal C^{12}—H spectra and listed in a column of $\lvert J_{7a,\,7s}\rvert$ of Table II, were considerably smaller than that of methane (12.4 c.p.s.) (9). This observation may have a relationship to more opening of the corresponding H—C—H angles.*† Non-equivalent values of coupling constants between a proton on the bridge head carbon and a proton on the carbon-7, $J_{1,7a}$, and $J_{1,7s}$ in the compounds, II, IV, and V, were observed. Furthermore, the fact that the coupling constants, $J_{1,2}$, $J_{2,3}$, and $J_{1,3}$, about the protons on the double bond are considerably smaller than usual, would have some relation to the "bent" of the double bond due to the strain in these ring systems.‡

All the spectra were taken with a Varian A-60 spectrometer. Calibration of the spectrometer was checked by using the signal peaks of *p*-anisaldehyde (4.0% solution in carbontetrachloride) (12). The C^{13}—H spectra, except for norbornane and norbornene, were measured in the pure liquid form. For the measurements of the spectra of norbornane and norbornene, a small quantity of deuterochloroform was added to those crystals to make a liquid form, because it is considered that no appreciable errors may be detectable owing to the presence of impurities in this case (1). Technical errors are approximately ±0.5 c.p.s. in $J_{C^{13}-H}$ and ±0.3 c.p.s. in J_{H-H}.

The J_{gem}'s of the bridge methylene in bicyclo[2,1,1]hexane derivatives were about 5.4 ~ 8.4 c.p.s., indicating the angle is much larger (11).

†The relation between J_{gem} and H—C—H angle was discussed by Gutowsky et al. (10). The contrast findings have appeared recently (15).

‡Added in proof: Since the submission of our first draft, the following papers have described the parallel relation between ring size of cycloalkenes and J_{H-H} (cis), and $J_{C^{13}-H}$ of the compounds II and III. O. L. Chapman. J. Am. Chem. Soc. **85**, 2014 (1963); G. V. Smith and H. Kriloff. J. Am. Chem. Soc. **85**, 2016 (1963); P. Laszlo and P. von R. Schleyer. J. Am. Chem. Soc. **85**, 2017 (1963).

Can. J. Chem. Downloaded from www.nrcresearchpress.com by 210.87.254.6 on 09/05/12
For personal use only.

ACKNOWLEDGMENTS

We are indebted to Dr. Y. Hata, Mrs. T. Tsuji, H. Ishitobi, and T. Irie for the preparation of the authentic samples, and to Dr. K. Takeda, Director of this laboratory, for his encouragement.

1. N. Muller and D. E. Pritchard. J. Chem. Phys. **31**, 768, 1471 (1959).
2. J. N. Shoolery. J. Chem. Phys. **31**, 1427 (1959).
3. N. Muller. J. Chem. Phys. **36**, 359 (1962).
4. H. M. Hutton, W. F. Reynolds, and T. Schaefer. Can. J. Chem. **40**, 1758 (1962).
5. C. F. Wilcox, S. Winstein, and W. G. McMillan. J. Am. Chem. Soc. **82**, 5450 (1960).
6. C. F. Wilcox. J. Am. Chem. Soc. **82**, 414 (1960).
7. J. I. Musher. Mol. Phys. **6**, 94 (1963).
8. H. Tanida. J. Am. Chem. Soc. **85**, 1703 (1963).
9. M. Karplus, D. H. Anderson, T. C. Farrar, and H. S. Gutowsky. J. Chem. Phys. **27**, 597 (1957).
10. H. S. Gutowsky, M. Karplus, and D. M. Grant. J. Chem. Phys. **31**, 1278 (1959).
11. K. B. Wiberg, B. R. Lowry, and B. J. Nist. J. Am. Chem. Soc. **84**, 1594 (1962).
12. G. V. D. Tiers and D. R. Hotchikiss. J. Phys. Chem. **66**, 560 (1962).
13. G. S. Reddy and J. H. Goldstein. J. Mol. Spectry. **8**, 475 (1962).
14. H. Spiesecke and W. G. Schneider. Tetrahedron Letters, 468 (1961).
15. R. Freeman and K. Pachler. Mol. Phys. **5**, 85 (1962).

Received July 12, 1963.
Shionogi Research Laboratory,
Shionogi & Co., Ltd.,
Fukushima-ku, Osaka,
Japan.

TRITIUM RECOIL LABELLING OF LITHIUM ALUMINUM HYDRIDE

Constanţa Măntescu and Ana Genunche

Lithium aluminum hydride ($LiAlH_4$) is an extremely powerful reducing agent. Although its violent reaction with water does not permit its use for the reduction of water-soluble compounds, it reacts readily, and in many cases quantitatively, with substances soluble in ethers such as diethyl ether and tetrahydrofuran.

By the preparation of $LiAlH_4$-*t* it was possible to obtain a large variety of tritiated organic compounds; $LiAlH_4$-*t* is usually prepared by the reaction of lithium hydride-*t* (1, 2) and aluminum chloride (3). The direct exchange of $LiAlH_4$ with a hydrogen–tritium mixture at 100° C could not be carried out (1).

We tried to prepare $LiAlH_4$-*t* using the recoil tritium resulting from the $Li^6(n,\alpha)T$ nuclear reaction. Preliminary results are reported in this note. The proportion of $LiAlH_4$ in the samples before the irradiation was established (4) using the hydrolitic and pyrolitic methods for analysis. Samples of 30–50 mg of $LiAlH_4$ sealed in quartz tubes were irradiated in high vacuum in the I.F.A. reactor with an integral thermal neutron flux of 7.2×10^{15} n/cm² to 7.5×10^{17} n/cm². The irradiated samples were again analyzed in order to determine the chemically active $LiAlH_4$ contained in the samples after irradiation.

The total amount of tritium introduced in the sample during irradiation was determined by measuring the activity of the hydrogen gas evolved on hydrolysis and pyrolysis.

The labelling of $LiAlH_4$ was tested by preparing methanol-T and 2-propanol-2T. The reaction of 1 mole carbon dioxide with 0.75 moles of $LiAlH_4$ in ethereal solution was used to prepare methanol-T. Non-labelled methanol was employed for the decomposition of excess $LiAlH_4$ and for the liberation of methanol-T by alcoholysis (5). The average radiochemical yield was 77% as compared with the stoichiometric reaction. 2-Propanol-2T

Can. J. Chem. Downloaded from www.nrcresearchpress.com by 210.87.254.6 on 09/05/12
For personal use only.

ACKNOWLEDGMENTS

We are indebted to Dr. Y. Hata, Mrs. T. Tsuji, H. Ishitobi, and T. Irie for the preparation of the authentic samples, and to Dr. K. Takeda, Director of this laboratory, for his encouragement.

1. N. Muller and D. E. Pritchard. J. Chem. Phys. **31**, 768, 1471 (1959).
2. J. N. Shoolery. J. Chem. Phys. **31**, 1427 (1959).
3. N. Muller. J. Chem. Phys. **36**, 359 (1962).
4. H. M. Hutton, W. F. Reynolds, and T. Schaefer. Can. J. Chem. **40**, 1758 (1962).
5. C. F. Wilcox, S. Winstein, and W. G. McMillan. J. Am. Chem. Soc. **82**, 5450 (1960).
6. C. F. Wilcox. J. Am. Chem. Soc. **82**, 414 (1960).
7. J. I. Musher. Mol. Phys. **6**, 94 (1963).
8. H. Tanida. J. Am. Chem. Soc. **85**, 1703 (1963).
9. M. Karplus, D. H. Anderson, T. C. Farrar, and H. S. Gutowsky. J. Chem. Phys. **27**, 597 (1957).
10. H. S. Gutowsky, M. Karplus, and D. M. Grant. J. Chem. Phys. **31**, 1278 (1959).
11. K. B. Wiberg, B. R. Lowry, and B. J. Nist. J. Am. Chem. Soc. **84**, 1594 (1962).
12. G. V. D. Tiers and D. R. Hotchikiss. J. Phys. Chem. **66**, 560 (1962).
13. G. S. Reddy and J. H. Goldstein. J. Mol. Spectry. **8**, 475 (1962).
14. H. Spiesecke and W. G. Schneider. Tetrahedron Letters, 468 (1961).
15. R. Freeman and K. Pachler. Mol. Phys. **5**, 85 (1962).

Received July 12, 1963.
Shionogi Research Laboratory,
Shionogi & Co., Ltd.,
Fukushima-ku, Osaka,
Japan.

Can. J. Chem. Downloaded from www.nrcresearchpress.com by 210.87.254.40 on 09/05/12
For personal use only.

TRITIUM RECOIL LABELLING OF LITHIUM ALUMINUM HYDRIDE

Constanţa Măntescu and Ana Genunche

Lithium aluminum hydride ($LiAlH_4$) is an extremely powerful reducing agent. Although its violent reaction with water does not permit its use for the reduction of water-soluble compounds, it reacts readily, and in many cases quantitatively, with substances soluble in ethers such as diethyl ether and tetrahydrofuran.

By the preparation of $LiAlH_4$-*t* it was possible to obtain a large variety of tritiated organic compounds; $LiAlH_4$-*t* is usually prepared by the reaction of lithium hydride-*t* (1, 2) and aluminum chloride (3). The direct exchange of $LiAlH_4$ with a hydrogen–tritium mixture at 100° C could not be carried out (1).

We tried to prepare $LiAlH_4$-*t* using the recoil tritium resulting from the $Li^6(n,\alpha)T$ nuclear reaction. Preliminary results are reported in this note. The proportion of $LiAlH_4$ in the samples before the irradiation was established (4) using the hydrolitic and pyrolitic methods for analysis. Samples of 30–50 mg of $LiAlH_4$ sealed in quartz tubes were irradiated in high vacuum in the I.F.A. reactor with an integral thermal neutron flux of 7.2×10^{15} n/cm^2 to 7.5×10^{17} n/cm^2. The irradiated samples were again analyzed in order to determine the chemically active $LiAlH_4$ contained in the samples after irradiation.

The total amount of tritium introduced in the sample during irradiation was determined by measuring the activity of the hydrogen gas evolved on hydrolysis and pyrolysis.

The labelling of $LiAlH_4$ was tested by preparing methanol-T and 2-propanol-2T. The reaction of 1 mole carbon dioxide with 0.75 moles of $LiAlH_4$ in ethereal solution was used to prepare methanol-T. Non-labelled methanol was employed for the decomposition of excess $LiAlH_4$ and for the liberation of methanol-T by alcoholysis (5). The average radiochemical yield was 77% as compared with the stoichiometric reaction. 2-Propanol-2T

Can. J. Chem. Downloaded from www.nrcresearchpress.com by 210.87.254.40 on 09/05/12
For personal use only.

TABLE I

The specific activity of the tritiated compounds versus the contents of chemically active $LiAlH_4$-*t*

Sample A	Nominal flux, n cm^{-2} sec^{-1} $\times 10^{11}$ B	Integral flux, n $cm^{-2} \times 10^{15}$ C	Chemically active $LiAlH_4$[a], % Before irradiation D	Chemically active $LiAlH_4$[a], % After irradiation E	The specific activity of the tritiated compounds dis. sec^{-1} $mol^{-1} \times 10^8$ $LiAlH_4$-*t* F[b]	CT_3OH G[c]	CT_3OH H[d]	$CH_3CTOHCH_3$ I[c]	$CH_3CTOHCH_3$ J[d]	η_r[e] H/G	η_r[e] J/I	Gram-atoms T per mole irradiated $LiAlH_4$ 10^{-6}	Gram-atoms T introduced into $LiAlH_4$ per mole $LiAlH_4$ destroyed 10^{-6}
1	2.0	7.2	87.5	75.8	3.1	2.3	1.8	0.8	0.6	77.5	75.1	0.29	2.15
2	2.0	28.8	87.5	71.2	11.8	8.9	6.9	3.0	2.2	77.2	74.8	1.10	6.00
3	50.0	750.0	87.5	36.0	198.0	149.0	74.5	49.5	25.6	50.1	51.8	18.40	32.00

[a]Chemically active $LiAlH_4$ determined by hydrolysis and pyrolysis.
[b]Determined as HT.
[c]The activity resulting from stoichiometric reaction.
[d]The measured activity.
[e]The average radiochemical yield.

was obtained by reducing 1 mole of acetone with 0.25 moles of $LiAlH_4$, using 2-propanol for the decomposition of excess $LiAlH_4$ and the liberation of 2-propanol-2T by alcoholysis (6). The average radiochemical yield was 75% as compared with the stoichiometric reaction. The fact that tritium was not attached to the hydroxyl groups was established by the alcoholysis of samples of non-labelled $LiAlH_4$ with the methanol-T and 2-propanol-2T prepared by us; the hydrogen evolved was not radioactive.

The activity of the tritiated compounds was determined by introducing them into two compensated Geiger–Müller counters by means of a vacuum line (7). In all experiments reported in this note the fraction of tritium which had left the crystalline lattice of $LiAlH_4$ during irradiation without participating in the labelling process of $LiAlH_4$ was not determined.

The results shown in Table I, indicate a variation of the contents of chemically active $LiAlH_4$ versus the nominal and (or) integral neutron flux, to which the sample had been exposed. The differences between the data given in the columns G and I on one hand, and those given in the columns H and J, on other hand, seem to show an advanced radiation damage of the crystalline lattice of $LiAlH_4$ to a chemical form non-active in the chemical reduction, especially for sample No. 3.

In this note we have succeeded in demonstrating qualitatively the formation of $LiAlH_4$-*t* by irradiation of $LiAlH_4$ with thermal neutrons, and in showing the possibility of tritiation of organic compounds by using $LiAlH_4$-*t* thus prepared. The labelling of $LiAlH_4$ as a result of neutron irradiation via substitution of recoil T atoms from the $Li^6(n,\alpha)T$ nuclear reaction is a simple and fast procedure. The usual methods (1–3) are more complicated requiring two reactions although at the first sight they are more favorable because of the higher specific activities obtained.

In forthcoming experiments we shall try to study the phenomenon quantitatively in order to explain the influence of neutron flux, and of the irradiation temperature etc., and at the same time to find the best conditions for obtaining a maximum specific activity for a minimum damage of the crystalline lattice of $LiAlH_4$.

1. K. E. Wilzbach and L. Kaplan. J. Amer. Chem. Soc., **72**, 5795 (1950).
2. M. Zelinski. Nukleonika, **7**, 789 (1962).
3. A. E. Finholt, A. C. Bond, Jr., and H. J. Schlesinger. J. Amer. Chem. Soc., **69**, 1199 (1947).
4. J. A. Krynitzky. J. Amer. Chem. Soc., **70**, 486 (1948).
5. G. I. Feklisov. Izv. Akad. Nauk SSSR Otd. Khim. Nauk, 587 (1953).
6. A. Murray and D. L. Williams. Organic synthesis with isotopes. Vol. 2. Interscience, New York. 1958.
7. C. Mănțescu and M. Fiti. Commissariat à l'énergie atomique, Saclay, France. No. 31054.

Received June 24, 1963.
Institute of Atomic Physics,
Bucharest, Rumania.

Can. J. Chem. Downloaded from www.nrcresearchpress.com by 210.87.254.40 on 09/05/12
For personal use only.